
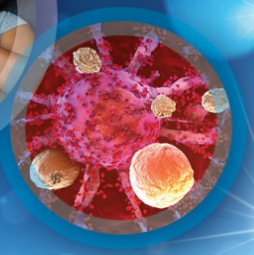


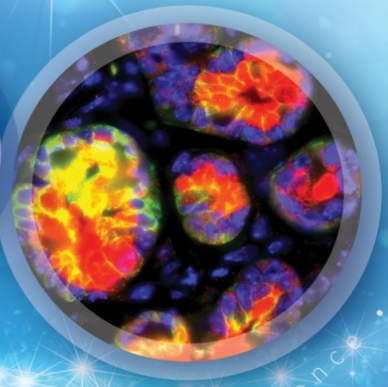
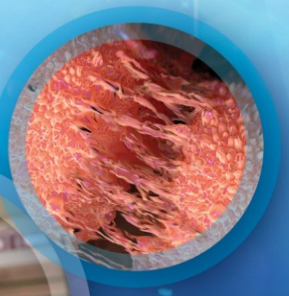

clinical care • translational • immunotherapy

genomics

diversity

drug discovery • patient care • mentoring

data science • policy

equity and inclusion

AACR

American Association for Cancer Research®

ANNUAL MEETING 2023

ADVANCING THE FRONTIERS OF CANCER SCIENCE AND MEDICINE

ORLANDO • APRIL 14-19

#AACR23 • AACR.ORG/AACR2023

PROCEEDINGS

Part B: APRIL 18-19

Continuing Medical Education Activity - *AMA PRA Category 1 Credits*™ available

Proceedings of the AACR
April 2023
Part B: Tuesday, April 18 and Wednesday, April 19, 2023

TABLE OF CONTENTS

PRESENTATIONS: TUESDAY, APRIL 18

- Combination Therapies for Cancer
- Community-based Research and Biobanking Research
- Diagnostic and Prognostic Biomarkers 4
- Immune-based Biomarkers for Prognostic and Predictive Benefit
- Immunomodulatory Agents and Interventions
- Increasing the Clinical Utility of Cell-Free DNA Testing
- Inflammation, Immunity, and Cancer
- Liquid Biopsies: Circulating Nucleic Acids and Circulating Tumor Cells 4
- Molecular Targeted Therapies 2
- New Approaches in Radiodiagnostics and Theranostics
- Precision Oncology in Pediatric Cancer: From Genomics to Databases to Real World Evidence
- Spatial Profiling, Tumor Classification, and Response Assessment
- Spatial Proteomics and Transcriptomics 1
- The Next Wave of Precision Oncology: New Drugs, Databases, and Analytics to Refine Care
- Therapeutic Antibodies, Including Engineered Antibodies

ENDOCRINOLOGY

- Endocrine-related Cancers and Nuclear Receptors: Molecular Biology, Biomarkers, and Genomics

EXPERIMENTAL AND MOLECULAR THERAPEUTICS

- Anticancer Approaches Targeting Signal Transduction Pathways
- Anticancer Approaches: Antibody-Drug Conjugates, Epigenetics, and Tumor Environment
- Drug Resistance in Molecular Targeted Therapies 3

- Drug Resistance in Molecular Targeted Therapies 4 / Regulation of Gene Expression in Drug Resistance
- Identification of Molecular Targets 1
- Identification of Molecular Targets 2 / New Nonclinical Models for Targets
- Molecular Targets
- New Tricks for Known Targets: Novel Approaches to Inhibit Oncogenic Signaling
- Novel Antitumor Agents, PI3K/AKT Inhibitors, Proteasome Inhibitors, and Topoisomerases
- Novel Targets and Pathways
- Oncogenes and Tumor Suppressor Genes as Targets for Therapy 3
- Targeting Protein Kinases and Phosphatases for Therapy 1
- Targeting Protein Kinases and Phosphatases for Therapy 2
- Theranostics and Radionuclides / Pharmacologic Approaches
- Tyrosine Kinase and Phosphatase Inhibitors 1
- Tyrosine Kinase and Phosphatase Inhibitors 2

IMMUNOLOGY

- Adoptive Cell and Natural Killer Cell Therapy
- CAR T-cell Therapy 2
- Combination Immunotherapies 1
- Combination Immunotherapies 2
- Determinants of Immunotherapeutic Effectiveness
- Developments in Anticancer Immunotherapy
- Inflammation and Immunity in the Tumor Microenvironment
- Modifiers of the Tumor Microenvironment
- New Opportunities for Combinatorial Immunotherapies
- Novel Preclinical Models for Cancer Immunotherapy

MOLECULAR/CELLULAR BIOLOGY AND GENETICS

- Cancer and Metabolism 1
- Cancer and Metabolism 2
- Chromatin Structure and Function in Cancer
- Epigenetic Mechanisms as Drivers of Tumorigenesis
- Gene Regulation and Transcription Factors in Cancer
- Gene Regulation in Cancer
- Non-coding RNAs in Brain, Melanoma, Lung, and Head/Neck
- Non-coding RNAs in Breast and Gynecological/Urinary Tract Cancers and New Techniques/Technologies
- Non-coding RNAs in Gastrointestinal, Blood, and Bone Marrow Cancers
- Oxidative Stress, Metabolism, and Cell Senescence
- Responses to Hypoxic, Proteotoxic, and Other Novel Forms of Cell Stress
- Role of Mitochondria and Signaling Pathways in Cancer

MULTIDISCIPLINARY

- AACR Project GENIE Use Cases

POPULATION SCIENCES

- Cancer Screening and Health Equity
- Descriptive Epidemiology and Environmental Risk Factors
- GWAS/Post-GWAS
- Survivorship and Biomarkers of Prognosis

PREVENTION / EARLY DETECTION / INTERCEPTION

- Behavioral and Biological Opportunities to Improve Cancer Prevention, Early Detection, and Disparities
- Diet, Nutrition, Lifestyle, and Environment and Cancer Prevention

- Dietary Derivatives and Repurposed and New Drugs for Cancer Prevention

TUMOR BIOLOGY

- 3D and Tissue Recombinant Models
- Advances in Angiogenesis
- Evaluating Tumor Progression via 3D and Spatial Approaches
- Inflammation and Tumor Progression
- Novel Targets, Biomarkers, and Models for Cancer
- Patient-Derived Xenograft Models
- Pediatric Cancer 2: Biology and Therapeutics
- Pediatric Cancer 3: Genomes and Novel Tumor Models
- PET, MRI, and CT Imaging
- Regulation of Invasion and Migration
- Signaling Pathways That Impact the Tumor Microenvironment
- Single Cell and Spatial Considerations of the Tumor Microenvironment
- Spatial Considerations of the 3D Tumor Microenvironment
- Stem Cells and the Microenvironment

PRESENTATIONS: WEDNESDAY, APRIL 19

BIOINFORMATICS / COMPUTATIONAL BIOLOGY / SYSTEMS BIOLOGY / CONVERGENT SCIENCE

- Bioinformatics Applications in Cancer Biology 3
- Databases, Platforms, and Tools
- Integrative Spatial and Temporal Multi-omics of Cancer

CLINICAL RESEARCH EXCLUDING TRIALS

- Immune Checkpoints

- Immune Monitoring and Responses to Therapy
- Liquid Biopsies: Circulating Nucleic Acids and Circulating Tumor Cells 5
- Preclinical Therapies and Clinical Observations in Pediatric Oncology
- Retrospective Clinical Analyses 2
- Spatial Proteomics and Transcriptomics 2
- Vaccines

EXPERIMENTAL AND MOLECULAR THERAPEUTICS

- Apoptosis and Growth Factor Receptors as Therapeutic Targets
- Cell Death Pathways and Treatment / Molecular Classification of Tumors for Diagnostics, Prognostics, and Therapeutic Outcomes
- DNA Damage Response
- DNA Repair / Molecular Classification of Tumors for Diagnostics, Prognostics, and Therapeutic Outcomes / Others
- DNA-reactive Agents, HDAC and Methyltransferase Inhibitors, and Tubulin Agents
- Epigenetics
- Growth Factor Receptors as Therapeutic Targets

IMMUNOLOGY

- Anticancer Immunotherapeutics
- Immune Checkpoints
- Immune Mechanisms Mediated by Other Therapies
- Immunotherapy Strategies and Mechanisms

MOLECULAR/CELLULAR BIOLOGY AND GENETICS

- Cyclin-dependent Kinases and Cyclin-dependent Kinase Inhibitors
- DNA Methylation Changes in Cancer

- Metabolism and Metabolomics of Cancer
- Multi-omics Tumor Profiling
- Targeting DNA Damage Response and Novel Pathways

POPULATION SCIENCES

- Diet, Alcohol, Tobacco Use, and Other Lifestyle Factors
- Novel Factors Associated with Cancer Mortality

PREVENTION / EARLY DETECTION / INTERCEPTION

- Early Detection and Molecular Markers of Prevention

TUMOR BIOLOGY

- Cancer Stem Cells and Therapeutic Resistance
- Cell Adhesion and Cell Signaling in Cancer and Drug Resistance
- Crosstalk between Cancer Cells, Immune Cells, and Fibroblasts
- Immunotherapy and Cellular Interactions in the Tumor Microenvironment
- Interactions Between the Microbiome, Cancer Cells, and Tumor Stromal Components
- Methods to Measure Clonal Evolution
- Tumor-Stromal Cell (Including Immune Cell) Interactions and Therapy Responses

Tuesday, April 18, 2023

BIOINFORMATICS / COMPUTATIONAL BIOLOGY / SYSTEMS BIOLOGY / CONVERGENT SCIENCE

Algorithms and Statistical Methods

#4270

Prediction of cancer transcriptomes from whole-slide images with Vis-Gene

Yuanning Zheng[1], Marija Pizurica[1], Francisco Carrillo-Perez[1], Christian Wohlfart[2], Wei Yao[3], Nadia Shamout[3], Olivier Gevaert[1], Antoaneta Vladimirova[3]. *[1]Stanford Center for Biomedical Informatics Research (BMIR), Stanford, CA,[2]Roche Diagnostics GmbH, Penzberg, Germany,[3]Roche Molecular Systems, Inc., Santa Clara, CA*

Introduction: Whole slide images (WSIs) are a crucial tool used by pathologists for diagnosing and grading cancers. In recent years, deep learning techniques have revolutionized the area, helping pathologists in the detection and classification of cancers. Earlier studies have related morphological features of tissues to molecular profiles, such as mutations and gene expression, and several machine learning-based approaches have been proposed to use WSIs to predict gene expression. However, most of the established methods treat different parts of the tissues in an isolated manner, not using the spatial relation between the tiles. In this work, we proposed Vis-Gene, a deep learning approach using a vision transformer for predicting gene expression from WSIs.
Methods: WSIs and RNA-seq data of five cancer types from the TCGA project were used for training and evaluation, including brain (GBM, n = 212), lung (LUAD, n = 520), kidney (KIRP, n = 295), colon (COAD, n = 290) and pancreas (PAAD, n = 180). The datasets were split into 80% for training and 20% for testing. In addition, data from healthy lung and brain tissues were obtained from the GTEx project. WSIs were split into tiles of 256 X 256 pixels, and 4,000 tiles of each image were used for training. Image features of each tile were extracted using a pre-trained Resnet-50. We clustered similar tiles using the k-Means algorithm, and the mean feature value of each cluster was used. We then used a vision transformer to “translate” image features to gene expression. To improve accuracy, we leveraged a transfer learning approach by pretraining the vision transformer on data from healthy tissues.
Results: We carried out five-fold cross-validations to assess the performance of Vis-Gene in each cancer type. The root-mean-squared error (RMSE) of the top 500 most accurately predicted genes in GBM was 0.12, and the standard deviation (SD) was 0.007. The RMSE of the top 100 most accurate genes in LUAD was 0.58 (SD: 0.02), KIRP was 0.63 (SD: 0.02), COAD was 0.53 (SD: 0.03), and PAAD was 0.56 (SD: 0.04). In all the tested cancers, Vis-Gene achieved significantly lower RMSE values and higher correlation coefficients (r) compared to a baseline model and existing computational models. Gene set analysis showed that the top accurately predicted genes in GBM were related to neuropeptide signaling pathway, gliogenesis, and inflammatory response. The top accurate genes in LUAD were related to NF-kappaB signaling and regulation of cell adhesion. Using spatial transcriptomic datasets, we further validated the results of Vis-Gene in predicting intra-tumoral heterogeneity of gene expression.
Conclusion: We established a new machine learning framework that can accurately predict gene expression from WSIs. This allows us to link histology features of cancers to molecular phenotype. Vis-Gene has the potential to identify clinically relevant endpoint expressions of the target genes.

#4271

A new methodological approach to discovering biomarkers of mammographic breast density using pathway-guided lipid amalgamation

Chongliang Luo, Jingqin Luo, Kayla R. Getz, Myung Sik Jeon, Adetunji T. Toriola. *Washington University in St. Louis, St Louis, MO*

Introduction: High mammographic breast density (MBD) is a risk factor for breast cancer. Studies are evaluating the associations of various multi-omic biomarkers, in well-defined pathways with MBD, but the existing methodological approaches have drawbacks. For example, multivariate association analysis adjusting for covariates may identify too many biomarkers and lacks proper biological interpretation. On the other hand, simple amalgams (e.g., combination or sum) of species within pathways may result in few associated pathways, as the species within a pathway could have different directions of associations. Variable selection approaches such as the least absolute shrinkage and selection operator **(**Lasso) select individual species without considering prior knowledge of the pathway structure. We propose a new pathway-guided amalgamation method to form species clusters that could enhance biological interpretation.
Methods: The plasma concentration of 982 lipid species in 14 super-pathways was measured in the blood samples of 705 premenopausal women drawn during their annual screening mammogram. We aimed to identify amalgams of lipid species that are associated with the volumetric percent density (VPD, in log scale). The proposed method utilizes the fused Lasso algorithm which penalizes the differences between effects for the lipid species within the same pathway and hence induces equality among similar effects. The lipid species with the same effects can be amalgamated to form clusters of species as new biomarkers. The number of clusters was chosen by cross-validation. Besides amalgamation, the method also facilitates variable selection by singling out influential individual species.
Results: The proposed method identified 11 amalgams formed by 744 species, with 3 amalgams in Cholesteryl Esters (CE), and 1 amalgam each in Phosphatidylcholines (PC), Lysophosphatidylcholines (LPC), Phosphatidylinositols (PI), Dihydroceramides (DCER), Hexosylceramides (HCER), Lactosylceramides(LCER), Diacylglycerols (DAG), and Triacylglycerols (TAG). Amalgams in the same pathway can have opposite directions of association: 2 of the 3 amalgams in CE had negative associations with VPD while the third showed a positive association. Species with small effects in the same direction of associations may be combined: an amalgam comprising 518 species in the TAG pathway was identified with each presenting a small negative association with VPD but collectively, forming one amalgam with a large effect.
Conclusions: The proposed amalgamation method provides a flexible and interpretable variable selection and clustering approach to discover lipidomic biomarkers for MBD. The amalgamation is especially preferred when multiple biomarkers species within one pathway share similar effects, or species within one pathway show opposite directions of associations.

#4272

Pan-cancer analysis of intra-tumor heterogeneity in 9,116 cancers using a novel regularized likelihood model

Yujie Jiang[1], Kaixian Yu[2], Matthew D. Montierth[3], Shuangxi Ji[2], Seung Jun Shin[4], Shuai Guo[2], Shaolong Cao[2], Yuxin Tang[5], Scott Kopetz[2], Pavlos Msaouel[2], Jennifer R. Wang[2], Marek Kimmel[5], Peter Van Loo[2], Hongtu Zhu[6], Wenyi Wang[2]. *[1]The University of Texas MD Anderson Cancer Center/Rice University, Houston, TX,[2]The University of Texas MD Anderson Cancer Center, Houston, TX,[3]The University of Texas MD Anderson Cancer Center/Baylor College of Medicine, Houston, TX,[4]Korea University, Seoul, Korea, Republic of,[5]Rice University, Houston, TX,[6]University of North Carolina at Chapel Hill, Chapel Hill, NC*

Subpopulations of tumor cells characterized by mutation profiles may confer differential fitness and consequently influence the prognosis of cancers. Understanding subclonal architecture has the potential to provide biological insight in tumor evolution and advance cancer precision treatment. Recent subclonal reconstruction methods require heavy computational resources, prior knowledge of the number of subclones, and extensive postprocessing. These drawbacks can be addressed by using a regularized likelihood modeling approach, which is novel to the field. Therefore, we propose a model-based method, **Cl**onal structure **i**dentification through pair-wise **P**enalization, or CliP, to address these drawbacks. To evaluate the performance of CliP against other methods, we generated a benchmark dataset of 4,050 simulated samples with varied tumor purity, read depth, copy number alteration rate, and true numbers of clusters. Our results suggest that CliP outperforms popular methods such as PhyloWGS in accuracy and shows similar robustness in most scenarios. We further compared CliP performance against 10 other subclonal reconstruction methods to the consensus subclonal reconstruction results on whole-genome sequencing (WGS) data from the Pan-Cancer Analysis of Whole Genomes (PCAWG, n = 1,993). Our result shows that of all 11 methods, CliP achieves the highest correlation with the consensus calls. In terms of speed, CliP can finish running a sample with 5,000 SNVs within one minute, which is ~1,000 times faster than MCMC-based algorithms. Next, we profiled the subclonal structures of 7,711 patient samples with well-annotated clinical outcomes from The Cancer Genome Atlas (TCGA) across 32 cancer types applying CliP to the whole-exome sequencing (WES) data. This is the largest and most complete pan-cancer characterization of intratumor heterogeneity (ITH) through the lens of subclonal reconstruction. We further used CliP outputs to address a commonly asked question on which sequencing platform to use for cancer evolution studies: the cost-effect WES data at higher read depth versus the more comprehensive WGS data at lower read depth. There were a total of 588 tumor samples from 21 cancer types, for which both PCAWG and TCGA have profiled using the WGS and WES platform, respectively. Using both datasets to compare results from these samples as benchmark, we observed that for most cancer types, subclonal reconstruction from WES is as informative as that from the matched WGS data. In summary, our study represents a significant methodological advancement in subclonal reconstruction and highlights the importance of measuring tumor subclone structure.

#4273

Integration with benchmark data of paired bulk and single-cell RNA sequencing data substantially improves the accuracy of bulk tissue deconvolution

Shuai Guo[1], Xuesen Cheng[2], Andrew Koval[1], Shuangxi Ji[1], Qingnan Liang[2], Yumei Li[2], Leah A. Owen[3], Ivana K. Kim[4], John Weinstein[1], Scott Kopetz[1], John Paul Shen[1], Margaret M. DeAngelis[3], Rui Chen[2], Wenyi Wang[1]. *[1]UT MD Anderson Cancer Center, Houston, TX,[2]Department of Molecular and Human Genetics, Baylor College of Medicine, Houston, TX,[3]SUNY University at Buffalo, Buffalo, NY,[4]Harvard Medical School, Boston, MA*

The accuracy of current deconvolution methods largely relies on the quality of cell-type expression references. However, single-cell (sc) and single-nuclei (sn) RNA-seq data used for building the reference are usually generated from independent studies that are distinct from the bulk RNA-seq data to be deconvolved. This study design inherently introduces technical confounding factors as unwanted variations, which is not fully addressed by current methods. To evaluate the impact of this variation on deconvolution accuracy, we generated a benchmark dataset where bulk and snRNA-seq profiling were performed from the same aliquot of single-nuclei that were extracted from 24 healthy retina samples. All donor eye samples were collected within six hours post-mortem and were absent of any disease. This study design guarantees the matched sequencing data to present the same cell-

type compositions, so that cross-platform technical artifacts become the remaining confounding factor. We used the benchmark dataset to evaluate the performance of seven current deconvolution methods and found they performed much worse in matched real-bulk data than in matched pseudo-bulks that were summations of the single-cell data. This finding suggests that none of these methods have fully addressed the major technical artifacts between bulk and single-cell sequencing platforms. We therefore propose DeMix.SC, a new deconvolution framework that optimizes deconvolution parameters using a small set of matched bulk and sc/snRNA-seq data from the same tissue type. DeMix.SC includes two major steps. First, we measure the technical variations across genes and across platforms using the benchmark data. Second, we introduce a new weight function for each gene that produces a ranking order that accounts for both the platform-specific technical variations and cell-type specific expressions at gene level. Using the benchmark data for retina, we applied DeMix.SC to previously published human retinal RNA-seq data from 523 individuals with different stages of age-related macular degeneration (AMD). We observed that DeMix.SC can accurately capture the cell-type composition shifts in the AMD retina. DeMix.SC revealed a significant drop of rod cells as well as increased astrocytes, bipolar cells, and Müller cells in the AMD retina compared to the non-AMD group. The proportion changes of the later three minor cell types were not identified by other methods, while DeMix.SC could reveal such tendency. In summary, DeMix.SC integrates benchmark data to improve the deconvolution accuracy in retina samples. Our method is generic and can be applied to other disease conditions, such as deciphering the cell-type heterogeneity in cancer. We expect DeMix.SC will help revolutionize the downstream cell-type specific analysis of bulk RNA-seq data and identify cellular targets of human diseases.

#4274

Functional dissection of complex tissue microenvironment using spatial transcriptomics data

Xinyu Zhou[1], Alexander White[2], Tingbo Guo[3], Pengtao Dang[3], Yuhui Wei[2], Xiao Wang[1], Kaman So[4], Chi Zhang[4], Sha Cao[4]. *[1]Indiana University Bloomington, Bloomington, IN,[2]Indiana University, Indianapolis, IN,[3]Purdue University, Indianapolis, IN,[4]Indiana University, School of Medicine, Indianapolis, IN*

Spatial transcriptomics (ST) data holds enormous potential to provide new perspectives for biologists seeking to understand the tumor tissue microenvironments. Cells in the same microenvironment are always exposed to biochemical conditions displacing specific spatial patterns. To truly dismantle the tissue microenvironment heterogeneity as well as cells' diverse responses to the variable microenvironment, we rely on spatial information to dissect the tissue into different functional regions, which are spatially dependent and biologically meaningful.
We have developed a statistical method, smooth Low Rank approximation and Clustering (smoothLRC) to model the spatial transcriptomic data as its low-rank approximation with spatial smoothness. smoothLRC accomplishes this by extracting the latent low-rank structure of the expression profiles. We present a regularized maximum likelihood estimator approximating the noisy observed expression matrix. This estimator incorporates spatial information and addresses expression dropout. It uses a low-rank Poisson distribution to account for the noise that plagues ST-based gene expression data with severe dropout events and a spatial smoothness penalty to encourage neighboring cells to fall into the same functional region. A dropout is an event where genes expressed in a given cell or region are incorrectly measured as unexpressed.
SmoothLRC has the following key features: 1) it is a statistically rigorous method; 2) the spatially smooth low-rank subspace could enable meaningful functional dissection, which is an unprecedented capability; 3) the low-rank structures could be used to recover the original expression, saving many expression values that are not captured.

#4275

Averon: informatics platform to discover Actionable Vulnerabilities Enabled by Rewired Oncogenic Networks

Andrey A. Ivanov, Haian Fu. *Pharmacology and Chemical Biology, Emory University School of Medicine, Atlanta, GA*

Missense mutations can change protein structure, cellular localization, and functions. Such changes lead to the rewiring of protein-protein interaction (PPI) networks, activation of oncogenic pathways, and acquisition of cancer hallmarks. However, the translation of the landscape of oncogenic mutations into clinically actionable biological models for cancer target discovery remains a major challenge. We address this challenge by leveraging the power of computational systems biology supported by high-throughput screening technologies. While some mutations can disrupt the PPIs, others may induce new PPIs that are not natural for the wild-type counterparts. Recently, we have established a quantitative High Throughput differential Screening (qHT-dS) platform [1] to discover such mutant-enabled or neomorph PPIs (neoPPIs). The screening of more than 13,000 mutant interactions revealed a landscape of gain-of-interactions encompassing both oncogenic and tumor suppressor mutations. This emerging neoPPI landscape may offer new mutant-directed therapeutic approaches for precision medicine. However, to infer clinically actionable mechanistic insights into how neoPPIs promote tumorigenesis special computational tools are needed. To inform the neoPPI-based target discovery, we develop a set of innovative informatics tools for discovering Actionable Vulnerabilities Enabled by Rewired Oncogenic Networks (Averon). Implemented in a widely-used Jupyter Notebook format, the Averon streamlines the identification of the oncogenic programs and clinically significant genes that are regulated by neoPPIs in cancer patients. The Averon can recapitulate well-established connectivity between known mutant-dependent PPIs and specific oncogenic pathways and reveal new, previously unknown mechanisms of neoPPI-mediated oncogenic signaling. To inform new therapeutic strategies in neoPPI-dependent cancers, Averon connects neoPPI-regulated genes with available approved drugs and clinical compounds. Together, the Averon provides a powerful informatics environment to determine therapeutically actionable vulnerabilities created by mutant-regulated protein-protein interactions to inform new personalized therapeutic strategies in cancer.

Acknowledgments: This work was supported in part by NCI's Informatics Technology for Cancer Research (ITCR) Program (R21CA274620, A.A.I.), Winship Cancer Institute #IRG-17-181-06 from the American Cancer Society (A.A.I.). Cancer Target Discovery and Development (CTD^2) Network (U01CA217875, H.F.), NCI Emory Lung Cancer SPORE (P50CA217691, H.F.), Career Enhancement Program (A.A.I., P50CA217691), Winship Cancer Institute (NIH 5P30CA138292).

References: 1. Mo X, et al., Systematic discovery of mutation-directed neo-protein-protein interactions in cancer. *Cell.* 2022, 185, 1974-1985.

#4276

Recovering false negatives in CRISPR fitness screens with JLOE

Merve Dede, Traver Hart. *Department of Bioinformatics and Computational Biology, The University of Texas MD Anderson Cancer Center, Houston, TX*

It is widely accepted that pooled library CRISPR-Cas9 knockout screens offer greater sensitivity and specificity than prior technologies in detecting essential genes whose disruption leads to fitness defects, a critical step in identifying candidate cancer targets. However, the assumption that CRISPR screens are saturating has been largely untested and it is still poorly understood whether possible systematic biases in CRISPR screens affect our understanding of human cell-intrinsic gene

essentiality. In the absence of a ground truth, the actual true positive, false positive and false negative rates of a typical genome-wide CRISPR-Cas9 knockout screen are still unknown. Through integrated analysis of screen data in hundreds of cancer cell lines generated by the Cancer Dependency Map, we examine some of the biases characteristic of genome-wide CRISPR-Cas9 knockout screening. With our computational modeling approaches, we estimate the true positive rate, false positive rate and show that a typical CRISPR screen has a ~20% false negative rate, in addition to library-specific false negatives. Furthermore, replicability of essential gene hits falls sharply as gene expression decreases, while cancer subtype-specific genes within a tissue show distinct profiles compared to false negatives. With our cumulative analyses across tissues, we identified an improved new set of core essential genes, which, like the previous set, can be used as a metric for the quality control of genome-wide CRISPR-Cas9 knockout screens. Our results also suggest only a small number of lineage-specific essential genes, with the overwhelming majority of genes showing overlap between related tissues and are enriched for transcription factors that define pathways of tissue differentiation. To recover false negatives in these genome- wide CRISPR knockout screens, we introduce a method called Joint Log Odds of Essentiality (JLOE), which extends fundamental concepts from our Bayesian framework of BAGEL algorithm to improve analysis across multiple cell line screens. JLOE uses information derived from previous screens to update the probability of essentiality of each screen based on prior observations. We show that JLOE selectively rescues the false negatives without an increased false discovery rate and improves screen concordance with the Sanger dataset, reducing the number of background-specific essential genes. Overall, our methods offer a significantly improved analysis of genome-wide CRISPR-Cas9 knockout screens, detecting and correcting for the previously unidentified false negatives and enhancing our identification of cancer-specific vulnerabilities as therapeutic targets.

#4277

Measuring proliferation rates of distinct tumour clones using single-cell DNA sequencing

Olivia Lucas[1], Sophie Ward[2], Rija Zaidi[1], Mark Hill[2], Emilia Lim[2], Haoran Zhai[1], Abigail Bunkum[1], Sonya Hessey[1], Michelle Dietzen[1], Andrew Rowan[2], Cristina Naceur-Lombardelli[1], Nnenna Kanu[1], Mariam Jamal-Hanjani[1], Charles Swanton[1], Simone Zaccaria[1]. *[1]Cancer Institute, University College London, London, United Kingdom,[2]Francis Crick Institute, London, United Kingdom*

Background**:**
Tumour proliferation rate is a key phenotypic feature of cancer, with higher rates linked to poorer clinical outcomes. Thus far, proliferation rates have been measured using pathological or experimental techniques on bulk tumour samples. However, while tumours are heterogeneous compositions of distinct clones with varying levels of fitness, measuring the proliferation of individual clones has not been possible to date. We hypothesise that enabling the identification of the most proliferative clones would reveal genomic hallmarks of aggressive clones, or the prediction of their potential phenotype, e.g., metastatic potential.

Methods:
We have developed SPRINTER (Single-cell Proliferation Rate Inference in Neoplasms Through Evolutionary Routes), a novel computational method to measure proliferation rates in individual tumour clones using single-cell whole-genome DNA sequencing. To assess the accuracy and power of SPRINTER, we have also developed an experimental approach to DNA sequence >18,000 single cells, accurately separated in different DNA-replication phases. We have sequenced and applied SPRINTER to >10,000 non-small cell lung cancer cells from longitudinal and metastatic tumour samples within the TRACERx study and PEACE autopsy programme. We have further analysed published data from >10,000 breast cancer cells.

Results:
We demonstrate that SPRINTER can accurately identify subpopulations of cells with different proliferation rates using relatively small numbers of cells, in contrast to previous preliminary approaches. While our estimates are concordant with previous bulk experimental studies (5-40%), we importantly have identified clonal heterogeneity in proliferation rates. Using bulk analysis, we have identified patterns of dissemination of tumour clones in non-small cell lung cancer. Integrating this with single-cell data, our results indicate that more widely disseminating tumour clones have higher proliferation rates, suggesting a link between proliferation and dissemination potential. We additionally find that clones are more proliferative in the metastatic versus the primary setting. Furthermore, we have identified high proliferation clones that may have a selective advantage in a breast tumour, and have inferred that they likely arose recently in cancer evolution.
Conclusions:
We have developed a novel method that enables accurate identification of proliferation rates of individual tumour clones using single-cell DNA sequencing data, allowing the investigation of genomic hallmarks in highly proliferative clones that might lead to higher fitness.

#4278
Transcriptome-driven combination design: A computational approach
Christina Gavazzi, Mikhail G. Grushko, Jeremy M. Goldstein, Mahta Samizadeh, Zakary Y. ElSeht, Katherine Arline. *Shepherd Therapeutics, Boston, MA*

While rational drug combination design seeks to improve patient outcomes by leveraging biological synergy, outcomes from combination trials often fail. Only 12.4% of phase 1 trials eventually achieve regulatory approval. *In vitro* evidence has provided the rationale for the drug combinations in 36.6% of phase 1 combination trials, but none of those trials progressed past phase 3 (from a study by Paller CJ et al., 2019). A review of DrugCombDB, a publicly available database of experimental synergy results, supports the idea that such outcomes are mirrored in preclinical data. Analysis of the similarity of synergy scores within indication-specific subsets of cell lines from data in a 2022 paper by Douglass, et al. show that in both breast and lung cancer, combinations predicted to be synergistic in at least one cell line from that indication failed to be synergistic in the majority of indication cell lines more than half of the time.
SHEPHERD's Gene Cluster Voting Algorithm (GCVA) was adapted to improve upon current drug combination design and anticipate transcriptome changes as the result of drug treatment. GCVA relates drug sensitivity to the transcriptome by calculating a list of biomarkers that contribute to sensitivity and resistance for specific drugs, enabling the prediction of drug sensitivity on patient transcriptomic data captured via bulk RNAseq.
Via this method, 15,137 publically available synergy data points in the Douglass paper were compared to predictions by our computational approach. For all synergy metrics contained within the dataset (ZIP, Bliss, Loewe, and HSA), the synergistic predictions made by application of GCVA have significantly higher synergy scores compared to the antagonistic predictions made by GCVA ($p < .001$). These test results support the potential for the application of GCVA to intelligent combination design with the ultimate goal of deployment on a patient-by-patient basis.In addition, analysis of GCVA's drug efficacy predictions for the cell line DU145 showed that treatment with 9 kinase inhibitors consistently potentiated the predicted efficacy of between 5 and 11 additional drugs. Dasatinib, temsirolimus, and cabozantinib were newly predicted effective after treatment with each and every kinase inhibitor. This data suggests an avenue for the design of intelligent drug combinations based on anticipated transcriptomic changes that may improve on existing synergy prediction methods.

#4279

Method for identifying microsatellite instability high DNA abnormality samples

Dilmi Perera, Sahand Khakabi, Ka Mun Nip, Sonal Brahmbatt, Adrian Kense, Kevin Tam, David Mulder, Melissa McConechy, David Huntsman, Ruth Miller, Rosalía Aguirre-Hernández. *Imagia Canexia Health, Vancouver, BC, Canada*

Introduct**ion:** Tissue samples with high microsatellite instability (MSI-H) can be indicators of cancerous tumors that are sensitive to certain types of cancer treatments (e.g., immune modulation-checkpoint inhibitor treatment). MSI-H regions can be identified with Polymerase Chain Reaction (PCR) based assays and next-generation sequencing (NGS). However, these MS regions are susceptible to PCR and sequencing errors. We developed a computational method for detecting microsatellite instability high (MSI-H) tumors using next-generation sequencing (NGS) data to accurately identify true MSI-H samples from MS-Stable samples based on an analysis of these MS regions.

Methods: We developed a method for classifying a tissue sample as being microsatellite instability high (MSI-H) without using normal tissue from the same person which doubles the sequencing cost. Furthermore, the algorithm was designed for amplicon targeted assays where it is not always feasible to choose the most predictive MS sites. The machine learning classifier (ML) algorithm is a random forest algorithm with a training set of known MSI-H and MS-Stable samples to learn the relationship between the MSI status and the distribution of repeats in microsatellite regions of genomes using 21 MS loci. A negative control was used to normalize the ML features and therefore reduce the effects of PCR and sequencing errors in noisy MS sites.

Results: The MSI detection algorithm was validated in analytical and clinical samples achieving an accuracy greater than 98%. Analytical samples consist of commercial reference standard samples and well characterized FFPE treated cell-lines. Clinical samples consists of clinical FFPE tumor samples from cancer patients that were orthogonally validated using immunohistochemistry (expression of mismatch repair genes, i.e., MMRnormal vs MMRd) on tumor tissue and/or the Promega MSI PCR using matched tumor/normal. All experiments were performed in the Imagia Canexia Health CAP, CLIA, DAP certified laboratory using the Find It assay standard operating procedures for detecting genomic mutations in solid tumor tissue.

Conclusions: The MSI detection algorithm can accurately identify samples with MSI-H tumors. When used in a clinical setting, these patients can then be directed to treatments such as immune-checkpoint inhibitors.

#4280

Automatic identification of cancer cell-cell interfaces at the pixel level

Jie Zhou, Jan Martinek, Zichao Liu, Ali Foroughi pour, Te-Chia Wu, Santhosh Sivajothi, Paul Robson, Karolina Palucka, Jeffrey Hsu-Min Chuang. *The Jackson Laboratory for Genomic Medicine, Farmington, CT*

Deciphering cell-cell interactions is critical for understanding the role of the tumor immune microenvironment. Although multiplex imaging methods are increasingly used for spatial characterization of cell communities and tissue morphologies, quantification of the interface between contacting cells has been mostly unexplored. Here we design an unsupervised pixel-level clustering method that accurately detects the contacting interface between cells. First, we observed pixel-level clusters with cell type specific phenotypes including tumor, immune infiltrates and extracellular structures in two independent melanoma datasets using cytometry time-of-flight (CyTOF) imaging mass cytometry (IMC) images. More importantly, our pixel-level approach identified clusters with mixed phenotypes, which are demonstrated to be direct contacts between T

cells and myeloid cells. Specifically, pixels in the interface clusters simultaneously express T cell ($CD3^+$, $CD4^+$ or $CD8^+$) and myeloid cell ($CD68^+$) phenotypic markers at comparable levels. Spatial mapping of the pixels in interface clusters shows that interface pixels are in the physical contact regions between T cells and myeloid cells. In addition, the abundance of T cell and myeloid cell interface clusters is correlated with positive response to immune checkpoint inhibitors (ICIs) ($p<0.05$). We also identified other clusters indicating interfaces between the stroma, tumor cells, and immune infiltrates. Our work enables reliable delineation of cell interactions at high resolution, and therefore can unravel new information about how cancer cells interact with their environment.

#4281

Data driven refinement of gene signatures for enrichment analysis and cell state characterization

Alexander T. Wenzel, Pablo Tamayo, Jill P. Mesirov. *UC San Diego, San Diego, CA*

The use of gene expression data has been crucial to the functional characterization of changes in molecular pathway activity and for identifying targets for novel treatments. However, the interpretation of this data is complicated by its high dimensionality and the difficulty of identifying biological signals within a list of differentially expressed genes. Gene Set Enrichment Analysis (GSEA) is a standard method for identifying pathway enrichment in gene expression data by testing whether a set of genes whose expression would indicate the activity of a specific process or phenotype are coordinately up- or downregulated more than would be expected by chance. As GSEA relies on high quality gene sets with coordinately regulated member genes, we maintain the Molecular Signatures Database (MSigDB) which contains 9 collections of curated gene sets representing different biological pathways and processes. Over time, we have observed that some of the MSigDB gene sets, especially those that are manually curated or defined in a very specific biological context, may not provide a sensitive and specific enough co-regulation signature. In response, we have created a data-driven, matrix-factorization-based refinement method to build more sensitive and specific gene sets. This method incorporates large-scale datasets from multiple sources such as the Cancer Dependency Map as well as curated protein-protein interaction networks. We will present the initial results of this refinement method and our ongoing work which will yield a new collection of refined gene sets that will be made freely available in MSigDB for use with GSEA and many other applications.

#4282

Total RNA sequencing of frozen biopsies combined to *k*-mer sequence analysis identify new hallmarks of immune checkpoint therapy response in melanoma

Hugues Hermann[1], Séverine Roy[2], Sandrine Agoussi[1], Emilie Routier[3], Céline Boutros[3], Djaouida Belkadi[3], Haoliang Xue[4], Antoine Lainé[4], Stephan Vagner[5], Daniel Gautheret[4], Caroline Robert[6].
[1]INSERM U981, Gustave Roussy, Villejuif, France,[2]INSERM U981 & Department of Cancer Medicine, Gustave Roussy, Villejuif, France,[3]Department of Cancer Medicine, Gustave Roussy, Villejuif, France,[4]Institute for Integrative Biology of the Cell (I2BC), Université Paris-Saclay, CNRS, CEA, Université Paris-Saclay, Gif-sur-Yvette, France,[5]CNRS UMR3348 & INSERM U1278, Curie Institute, Orsay, France,[6]INSERM U981 & Department of Cancer Medicine, Gustave Roussy & Paris Saclay University, Villejuif, France

Introduction: Predicting response to immune checkpoint inhibitors (ICI) is key for stratifying patients and identifying factors of resistance. The main recognized ICI response biomarkers in melanoma are T-cell gene expression signatures, PD-L1 expression and tumor clonal mutational

burden, all of which are specific of responding tumors but nevertheless not robust enough to guide therapeutic strategies. Biomarkers of progression (eg. TGF-B) are scarce and inconsistent across studies. All current gene expression-based biomarkers of ICT-response are based on formalin-Fixed paraffin-embedded (FFPE) samples, sequenced using RNA capture or polyA+ libraries. This technique is known to incompletely represent RNA populations.
Patients, Material, Methods: Here we introduce the first total RNA-seq dataset from fresh frozen biopsies collected from 80 advanced melanoma patients, prior to treatment with anti PD-1 or combined anti-PD-1/anti-CTA4 therapy. The cohort included 43 responders and 37 non-responders based on RECIST best objective response. To ensure all possible RNA biomarkers are captured, we applied a k-mer based computational protocol that extracts all subsequences of fixed size (31 nt) from the raw RNA-seq reads and performs differential expression statistics on k-mers. This identifies response-specific RNA sequences independently of annotated genes, enabling identification of novel RNAs and RNA isoforms.
Results: In responding patients, this analysis identified a large number of immunoglobulin and HLA mRNA fragments, consistent with an immune-active microenvironment. However, the most remarkable finding was the specific expression in non-responding tumors of centromeric satellite repeats (HSAT-II and ALR elements) and of a set of intergenic loci which independently described the progressor population. Altogether, total RNA-seq biomarkers were found in most non-responding patients, providing the basis for a strong predictor of resistance. This contrasted with results in FFPE/capture seq data that showed few notable k-mers in the progressor group, due to the incomplete RNA sequencing. Our approach revealed a number of other unexpected markers, including a set of circular RNAs in responders and a mutant of the PRAME tumor-specific antigen in progressors. Our main finding is that the combination of frozen sample conservation and total (ribodepleted) RNA sequencing reveals a unique source of non-coding RNAs produced from pervasive transcription of intergenic and repeated regions, likely associated to chromatin derepression, that are not detected by the usual FFPE/capture seq methods.
Conclusion: We argue that these novel RNA sequences will be instrumental in the development of improved ICI-response predictors and a better understanding of resistance to ICI.

#4283

scMSI: Accurately detect the sub-clonal micro-satellite instability by an integrative Bayesian model

Yuqian Liu[1], Yan Chen[1], Huanwen Wu[2], Xuanping Zhang[1], Xin Lai[1], Xin Yi[3], Zhiyong Liang[2], Jiayin Wang[1]. *[1]Xi'an Jiaotong University, Xi'an, China,[2]Chinese Academy of Medical Sciences and Peking Union Medical College, Beijing, China,[3]Geneplus Beijing Institute, Beijing, China*

Microsatellite instability (MSI) is an important genomic biomarker for cancer diagnosis and treatment. For some cancers with high-degree of heterogeneity, e.g. endometrial cancer, the existing approaches always fail to identify the micro-satellite instability on one or multiple sub-clones, which would deprive the chance for patients to benefit from treatments. However, it is a computational challenge to estimate the sub-clonal MSI because multiple sub-clones may share the genomic status. Herein, in this paper, we propose an accurate and efficient algorithm, named scMSI, to estimate the sub-clonal microsatellite status. scMSI adopts an alternating iterative model to de-convolute the length distribution, which is a mixture of sub-clones. During the deconvolution, an optimized division of each sub-clone is achieved by a heuristic algorithm, which is bounded to the clonal proportions best consistent with the known clonal structure. To evaluate the performance, we conducted a series of experiments on simulation datasets. The results supported that scMSI solved the detection problem of MSI on sub-clones. It outperforms the existing approaches on multiple metrics. In addition, we collected a cohort of 16 endometrial cancer patients, who have positive

responses on the treatment but with negative MSI status. We sequenced these patients. scMSI reported MSI on sub-clones according the sequencing data, which are further validated by the conclusions on immunohistochemistry. Thus, scMSI could provide a powerful tool for MSI analysis.

#4284

Enhancing subclonal reconstruction algorithm for resolving complex tumor phylogenies from multi-sample tumor DNA sequencing

Helena Winata[1], Daniel Knight[1], Juber A. Patel[2], Nicholas K. Wang[1], Pier Selenica[2], Stefan E. Eng[1], Caroline Kostrzewa[2], Jaron Arbet[1], Yingjie Zhu[2], Ronglai Shen[2], Jorge Reis-Filho[2], Pedram Razafi[2], Paul C. Boutros[1]. *[1]UCLA Jonsson Comprehensive Cancer Center, Los Angeles, CA,[2]Memorial Sloan Kettering, New York, NY*

Cancer is characterized by the ongoing accumulation of somatic mutations, providing selective advantages that may lead to dysregulated cellular proliferation. While the cancer genome at diagnosis has been extensively studied, many cancer types still lack strong prognostic biomarkers. The continuous acquisition and selection for driver mutations in a population of cancer cells acts as a Darwinian process, resulting in clonal expansions of progressively more aberrant and fit phenotypes. Reconstructing tumor evolution allows us to understand key events that drive cancer progression and patterns of mutation co-occurrence within clones. These evolutionary features guide our understanding of fundamental mechanisms that lead to disease lethality. Inferring tumor evolution from DNA sequencing data is becoming part of routine analysis in cancer research. As sequencing costs drop, sequencing multiple tumor samples from a patient becomes routine. These multiple samples can represent different spatial regions of a tumor, longitudinal samples from a single region or a combination of both. This provides an opportunity to study tumor evolution in much greater detail and accuracy than was previously feasible through single-sample datasets. The most widely used methods to reconstruct the subclonal evolution of a tumor utilize stochastic-search algorithms. These approaches iterate through a parameter space to select phylogenetic solutions that maximize the likelihood of observed sequencing data. They are optimized for low complexity cases, where the size and number or subclones are relatively limited. As tumor subclonal structure increases in complexity, the parameter space grows exponentially, and stochastic-search algorithms become computationally intractable. For instance, recent benchmarking studies have revealed that many methods fail to reconstruct clone trees for data with as few as ten subclones. To circumvent current computational limitations, we developed a deterministic algorithm for subclonal reconstruction that leverages fundamental principles of cancer biology to encode heuristics that reduce the solution space to biologically plausible phylogenies. When applied to samples (4-36 tumors; median 16) from 12 patients with metastatic breast cancer, our method reduced the average runtime ten-fold. We were able to delineate the evolutionary history of up to 57 distinct subclones per patient, which is infeasible with most current methods. Benchmarking using methods developed for the SMCHet DREAM challenge on real and simulated datasets further quantifies the accuracy, resolution, and scalability. We have thus presented a novel method for rapid and optimized reconstruction of tumor evolutionary histories.

#4286

A statistical learning method for simultaneous copy number estimation and subclone clustering with single cell sequencing data

Feifei Xiao[1], Fei Qin[2], Guoshuai Cai[2]. *[1]University of Florida, Gainesville, FL,[2]University of South Carolina, Columbia, SC*

The availability of single cell sequencing (SCS) enables us to assess intra-tumor heterogeneity and identify cellular subclones without the confounding effect from mixed cells. Copy number aberrations (CNAs) have been commonly used to identify subclones in SCS data since cells comprising a subpopulation are found to share genetic profile. However, currently available methods may generate spurious results (e.g., falsely identified CNAs) in the procedure of CNA detection, hence diminishing the accuracy of subclones identification from a large complex cell population. In this study, we developed a CNA detection method based on a fused lasso model, referred to as FLCNA, which can simultaneously identify subclones in single cell DNA sequencing (scDNA-seq) data. Spike-in simulations were conducted to evaluate the clustering and CNA detection performance of FLCNA benchmarking to existing copy number estimation methods (SCOPE, HMMcopy) in combination with commonly used clustering methods. FLCNA was also applied to a real scDNA-seq dataset with breast cancer and clusters identified using FLCNA showed clearly different genomic variation patterns. In conclusion, FLCNA provided superior performance in subclone identification and CNA detection with scDNA-seq data.

#4287

The combination of statistical methods to compare observed and simulated data allowed to assess effectively the validity of mathematical model predictions in a context of a EGFR+ lung adenocarcinoma

Evgueni Jacob, Laura Villain, Nicoletta Ceres, Jean-Louis Palgen, Adele L'Hostis, Claudio Monteiro, Riad Kahoul. *NOVADISCOVERY, Lyon, France*

Introduction

In silico models proved to be a promising tool to complement and optimize clinical trials. These models should be validated to assess their capacity to reproduce real life behaviors. Opposed to real-life clinical trials where the amount of available data might be low, in silico approaches give us the possibility to simulate virtual populations of thousands of patients. This data size heterogeneity might be an issue. Moreover, in real life data, patients are seen at scheduled visits, leading to an observation time uncertainty (OTU), which is not the case in simulated data.In the context of the validation of a EGFR-mutant Lung Adenocarcinoma mathematical model, we depicted the interest of using combined validation methods to assess the capacity of the model to predict the time to tumor progression, from heterogeneous clinical trials datasets.

Methods

In this context, to overcome the limitation of using default log-rank test that could lead to biased results, 4 bootstrapped methods have been used:

- 2 methods based on the log-rank test where the ratio of significant tests at a given alpha risk level is assessed, taking into account the OTU: The “default Log-rank test” and the “modified test” based on a combination of weighted log-rank tests (MaxCombo).
- 2 methods based on prediction intervals. The “raw coverage”, which corresponds to the proportion of the observed time-to-event curve included in the prediction interval and the “juncture metric” which corresponds to the proportion of the observation period where the prediction interval overlaps with an interval bound between the observed data and the same data shifted by the OTU.

Results

As each one of the validation approaches has its own strengths and weaknesses and conditions of application, the validation process has been based on the combination of well selected methods. Validation metrics showed that the model reproduces successfully real life data depending on a given context. When all the metrics give the same result, we were able to easily conclude. But when it was not the case, this led us to investigate the origin of these discrepancies, taking into account method robustness.

Conclusion
The validation process is of the utmost importance to assess the level of credibility of the model. We showed that in order to fully evaluate the model, a combination of validation approaches is preferable. The use of multiple metrics highlights the eventual inconsistencies in model predictions and validation dataset's content that would not have been detected by only a single approach.
The drawback of combining metrics is that it complexifies the decision making, implying that the final decision, regarding whether the model is validated or not, is assumed by the user, without forgetting that the validation is not an end objective per se but a stepwise process.

#4288

Predicting DNA methylation in cervical cancer using somatic mutations in a classified mixed model prediction

Jairo D. Ramos[1], J. Sunil Rao[2]. *[1]Sylvester Comprehensive Cancer Center, University of Miami, Miami, FL,[2]Public Health Sciences - Division of Biostatistics, University of Miami, Miami, FL*

In cervical cancer, the promoter CpG islands of several tumor suppressor genes have been found with abnormal DNA methylation (DNAm) levels, which results in transcriptional silencing. Genetic databases from tumor samples are available without the corresponding DNAm profile. To fulfill this gap and contribute to deciphering the link between genetic variants and DNAm, we performed this study to find a good statistical model for predicting DNAm using genetic data. To address this, we downloaded from the TCGA dataset the genes with significant somatic mutations, as reported by the BROAD Institute, and the DNAm beta values, in known CpG sites, from 307 Cervical Squamous Cell Carcinoma and Endocervical Adenocarcinoma (CESC) samples. Clinical data were also downloaded from patients, including race, age, gender, and cancer stage. We tested five mixed models containing both fixed and random effects to include the unmeasured source of variations in DNAm, for which we used the clustering of samples based on DNAm patterns. Models tested were: Classified mixed model prediction (CMMP), Linear regression model (LM), High dimensional shrinkage estimator based on the elastic net (ENET), a combination of CMMP - ENET, and Random Forest prediction (RF). Besides the significantly mutated genes, the clinical variables were also included as covariates to predict DNAm. We used shared random effects to borrow strength across racial groups, which improves predictive accuracy. Models were enhanced by combining other types of cancers to increase data heterogeneity and the number of samples. Lung Adenocarcinoma (LUAD) and Liver Hepatocellular Carcinoma (LIHC) were selected using Gini and Gap statistics for optimal clustering. Model fitting was evaluated using the average mean squared prediction error (MSPE). Results revealed that the CMMP model with CESC LIHC and LUAD data combined showed the best prediction results (lowest MSPE). The plot of the averaged estimated ENET coefficients indicated that the most important-significantly mutated genes to predict DNAm were *CTNNB1*, *DMD, XIRP2, and PIK3CA*. SNPs in these genes linked to cervical cancer include rs121913396, rs121913403 (*CTNNB1*), rs867262025, and rs121913279 (*PIK3CA*).In summary, we developed a mixed-effects model for accurately predicting DNAm levels in cervical cancer, using genes with significant somatic mutations (SNVs and INDELs). These results also align with growing evidence suggesting that genetic variation plays a role in DNAm.

#4289

Long-read, assembly-based characterization of rearranged cancer karyotypes

Ayse Keskus[1], Tanveer Ahmad[1], Ataberk Donmez[1], Yi Xie[2], Isabel Rodriguez[2], Rose Milano[2], Nicole Rossi[2], Hong Lou[3], Laksh Malik[4], Kimberley Billingsley[5], Cornelis Blauwendraat[5], Michael Dean[2], Mikhail Kolmogorov[1]. *[1]Center for Cancer Research, National Cancer Institute, NCI,*

Bethesda, MD,[2]Division of Cancer Epidemiology and Genetics, National Cancer Institute, NCI, Rockville, MD,[3]Leidos Biomedical Research, National Laboratory for Cancer Research, Frederick, MD,[4]Center for Alzheimer's and Related Demetias, National Institutes of Health, Bethesda, MD,[5]Center for Alzheimer's and Related Dementias, National Institutes of Health, Bethesda, MD

Introduction: Recent pan-cancer whole-genome sequencing studies revealed the rich landscape of structural variants (SV), from simpler indels to complex events involving multiple breakpoints and sequence gain/loss. SVs may contribute to tumorigenesis through direct modification of coding sequence or deregulation from copy number alterations, enhancer hijacking, or topological domain modification.
A substantial part of the variation in the human genome is not accessible to short reads due to mapping ambiguities. Recent benchmarking studies reported that the best short-read methods only have 30-70% SV sensitivity. Long-read sequencing (such as PacBio or Oxford Nanopore) can overcome the limitations of short reads, however the current methods were not designed for the analysis of rearranged cancer genomes with complex copy number profiles.
Methods: We developed BGA (Breakpoint Graph Assembler), a method that combines the ideas from long-read assembly and breakpoint graph frameworks. BGA detects abnormally mapped reads and builds a breakpoint graph that characterizes the structure of derived cancer karyotypes. Complex events with multiple breakpoints form connectivity clusters and are classified based on the subgraph properties. BGA also takes advantage of phased haplotypes and can incorporate multiple related datasets (such as in tumor-normal comparison or multi-site tumor sampling). BGA is freely available at: *https://github.com/KolmogorovLab/BGA*.
Results: We first analyzed three cancer cell lines and corresponding matching normal DNAs (HCC1954, H2009, and COLO829). In each cell line, we identified 8-56 somatic rearrangement clusters involving more than two breakpoints and at least 1kb of sequence. In H2009, we identified a chromoplexy event involving chr13 and chr1, consistent with previous FISH experiments. COLO829 showed the lowest number of somatic rearrangement clusters (n=8), including translocation and inversion events between chr3, chr10, and chr12 within the *RARB*, *BICC1*, and *TRHDE* genes. Homologous recombination deficient HCC1954 has the highest number of complex events including the chr17q arm which hosts ERBB2, chromoplexy between chr8, chr5, and chromothripsis in chr21.
In addition, we analyzed three other HPV-infected cell lines (CaSki, SCC152, SNU1000). In each of them, we observed complex clusters of HPV-HPV and HPV-human breakpoints that formed cycles, suggesting extrachromosomal amplification. The HPV fragments had many interactions with chromosomal DNA in CaSki and SC152, but not in mostly episomal SNU1000 cells. We also observed karyotype-scale changes that did not involve HPV sequences, such as the simultaneous exchange of six chromosome arms of chr2, chr7, and chr17 in CaSki.

#4290

ReCorDE: A novel computational framework to discover potential combinations of anti-cancer drugs

Emily T. Ghose[1], August John[1], Huanyao Gao[2], Krishna R. Kalari[2], Liewei Wang[2]. *[1]Mayo Clinic Graduate School of Biomedical Sciences, Rochester, MN,[2]Mayo Clinic, Rochester, MN*

Background**:** Cancer is usually treated with a combination of drugs rather than a single agent. Treating cancer with a drug combination decreases the likelihood of the cancer acquiring resistance to therapy. It also allows for lower dosages of individual drugs, which reduces the occurrence and severity of side effects. Using public datasets, we investigated potential anti-cancer drug

combinations using a novel framework, ReCorDE (Recurrent Correlation of Drugs with Enrichment), which identifies correlated drug response patterns for drugs with different primary mechanisms of action.
Methods: 250 drugs from CTRPv2, GDSCv2, and PRISM datasets were examined using normalized logIC50 or AUC measurements. ReCorDE consists of a correlation and an enrichment step. For each dataset, we constructed pairwise drug-drug relationships using Spearman's correlation. Combinations significant ($p < 0.05$) in less than two datasets after Benjamini-Hochberg (BH) correction were pruned. To turn each drug combination into a drug class combination, all drugs were mapped to their corresponding fourth-level Anatomical Therapeutic Chemical (ATC) codes. Then, using a hypergeometric test, for each class combination in the subset of significant drug combinations (the "inside" set), we tested for enrichment of that class combination in the inside set compared to the class combination universe, the distribution of class combinations for all unique pairwise drug-drug associations (250 unique drugs; 31,125 distinct drug combinations mapped to 1596 distinct class combinations). Multiple testing during enrichment was corrected using the BH method with a significance cutoff of $p< 0.05$.
Results: We found 2764 pairs to be significant at $a = 0.05$ using the AUC measure. With a correlation coefficient of 0.77, vincristine and YK-4-279, an EWS-FLI1/RNA Helicase A inhibitor, had the lowest computed p-value of of 1.39×10^{-120}. Adjusted p-values for >15% of these combinations had p-values $< 5 \times 10^{-6}$. Class combination enrichment on the same set showed 132 class pairs were enriched in the inside set compared to the class combination universe after BH correction. Taxanes/Plk1 inhibitors (OR = 69.5, adjusted $p = 5.6 \times 10^{-11}$); Aurora Kinase inhibitors/histone modifying agents (OR=9.2, adjusted $p = 6.13 \times 10^{-11}$); and pyrimidine analogues/CDK inhibitors (OR=3.43, adjusted $p = 0.02$) are a few notable enriched class combinations. The enrichment of these class combinations in the inside set suggests that combinations of drugs from these classes may be particularly effective in treating cancer compared to other drug combinations.
Conclusions: Our framework, ReCorDE, demonstrates that finding potential drug combinations and characterizing novel, frequently perturbed pathways outside of a drug's primary mechanisms of action can be accomplished by identifying correlated drug-drug pairs from large, publicly accessible databases.

#4291
Deconvolution of cell type composition in FFPE tissue: Application to benign breast disease
Yuanhang Liu[1], Chen Wang[1], Stacey J. Winham[1], Aditya Bhagwate[1], Robert A. Vierkant[1], Julie M. Cunningham[1], Bryan M. McCauley[1], William A. Jons[1], Derek C. Radisky[2], Amy C. Degnim[1].
[1]Mayo Clinic, Rochester, MN,[2]Mayo Clinic, Jacksonville, FL

Purpose: Benign breast disease (BBD) is viewed as a non-obligate precursor stage in the development of breast cancer (BC). Transcriptome profiling using RNA sequencing (RNA-seq) of bulk formalin-fixed paraffin-embedded (FFPE) tissue blocks has been routinely used in BC research. However, RNA-seq of heterogeneous bulk samples represents an averaged expression profile across all cell mixtures. Downstream analyses, such as biomarker discovery, are likely confounded by differences in cell proportions. There is a lack of research in optimizing strategies for cell type deconvolution especially for FFPE samples. We evaluated and optimized strategies for cell type deconvolution using existing single cell RNA-seq (scRNA-seq) and single nucleus RNA-seq (snRNA-seq) breast tissue references, and applied these to a cohort of BBD FFPE samples to assess risk of subsequent BC.

Methods: 7 scRNA-seq and 3 snRNA-seq public samples from women's breast tissue were normalized using SCTransform, then integrated using Harmony to form a complete reference set. Bioinformatics evaluations examined the performance of existing statistical and deep learning-based deconvolution methods. Computational simulations were conducted to evaluate those methods on three scenarios: 1) baseline; 2) incomplete reference set; 3) FFPE artifacts. FFPE artifacts were simulated based on a generalized additive model using 7 in-house paired FFPE-fresh frozen samples. Finally, we applied the best performing method to our BBD cohort of 62 samples. Differential expression analysis adjusting for cell proportions was performed to identify transcriptomic aberrations in BBD cases.
Results: snRNA-seq was more sensitive in capturing adipocytes, while scRNA-seq was more sensitive in detecting lymphocytes in breast tissue. The median number of detectable genes per cell was higher for scRNA-seq than snRNA-seq before integration (1264 vs 558). Marker gene-based regression methods (e.g. CIBERSORT) displayed higher variance and lower bias compared to methods directly using scRNA-seq data (e.g. SCDC). Incomplete reference data led to increased bias and little effect on variance. FFPE artifacts had a higher impact on performance compared to incomplete reference data. Overall, Scaden, a deep learning-based method, was the top performing method across all simulation scenarios and was especially robust to FFPE artifacts. 59 differential expressed genes (DEGs) were identified with fold change > 1.5 and p value < 0.01. DEGs involved in BC, e.g. S100A8, WNT4 and HIST1H3H, would be left out if cell proportions were not properly adjusted.
Conclusions: We constructed the first complete single cell reference data for women's breast tissue and benchmarked existing cell type deconvolution methods. Compared to analyses not adjusting for cell proportions, we observed substantial differences in perturbed genes and pathways associated with BC risk for BBD patients.

#4292

Gene model correction for PVRIG and TIGIT in single cell sequencing data enables accurate detection and study of its functional relevance

Sergey Nemzer[1], Niv Sabath[1], Assaf Wool[1], Zoya Altber[1], Hirofumi Ando[2], Drew M. Pardoll[2], Sudipto Ganguly[2], Yaron Turpaz[1], Zurit Levine[1], Roy Z. Granit[1]. *[1]Computational Discovery, Compugen Ltd., Holon, Israel,[2]Bloomberg-Kimmel Institute for Cancer Immunotherapy, Sidney Kimmel Comprehensive Cancer Center, Johns Hopkins University School of Medicine, Baltimore, MD*

Single cell RNA sequencing (scRNA-seq) has gained increased popularity in recent years and has revolutionized the study of cell populations; however, this technology presents several caveats regarding specific gene expression measurement. Here we examine the expression levels of several immune checkpoint genes, which are currently assessed in clinical studies. We find that unlike in most bulk sequencing studies, PVRIG and murine TIGIT suffers from poor detection in 10x Chromium scRNA-seq and other types of assays that utilize the GENCODE gene model. We show that the default GENCODE gene model, typically used in the analysis of such data, is incorrect in the PVRIG genomic region and contains also a predicted read-through transcript to which PVRIG reads co-align, causing these to be discarded and hence hindering its proper detection. Moreover, we find that the murine TIGIT 3' UTR is mis-annotated, leading to the loss of legitimate reads. We thus generated a corrected reference genome, by removing the faulty read-through in the case of PVRIG and by extending the TIGIT 3' UTR and demonstrate that by employing these changes we can correctly capture genuine expression levels of these checkpoints, and which align with our findings at the protein level using FACS and CITEseq. Furthermore, we show that specialized read multimap algorithms such as RSEM and STARsolo can also partially improve the detection of PVRIG. Our

study provides means to better interrogate the expression of PVRIG and murine TIGIT in scRNA-seq and emphasize the importance of optimizing gene models and alignment algorithms to enable accurate gene expression measurement in scRNA-seq and bulk sequencing. Moreover, our results support detailed study of the expression of immune checkpoints in clinical and pre-clinical studies towards the development of cancer immunotherapy treatments.

#4293

Strategies and resources for applying a quantitative multiplex IHC imaging workflow to characterize immune contexture in solid tumors

Shamilene Sivagnanam, Courtney M. Betts, Nell Kirchberger, Konjit Betre, Lisa M. Coussens. *Cell, Developmental and Cancer Biology, OHSU Knight Cancer Institute, Portland, OR*

Conventional immunohistochemistry (IHC) is a standardized diagnostic technique used in tissue pathology. However, the capacity to label only one marker per tissue section is a critical limitation. Multiplex immunohistochemistry (mIHC) is a powerful imaging technique used in basic, translational research and clinical settings to simultaneously detect the expression of multiple epitopes in a single formalin-fixed paraffin-embedded (FFPE) tissue section, allowing for characterization and quantification of cells while maintaining their spatial location. This technique allows for a comprehensive view of the immune milieu, expression patterns, and interactions between cell types that can help elucidate the complexity of the tumor-immune microenvironment (TiME). Multiplex imaging has emerged as a powerful tool to better understand tumor progression, response or resistance to therapy, and potentially identify predictive biomarkers. However, this technique requires careful tissue considerations and generates enormous amounts of hierarchical data, including single cell marker expressions, locations, and shape features, resulting in complex and challenging analyses. We previously published a validated platform using nine matched primary and recurrent head and neck squamous cell carcinoma (HNSCC) sections stained sequentially with a panel of 29 antibodies identifying malignant tumor cells, and 17 distinct leukocyte lineages and their functional states[1]. Here, we have optimized and consolidated important considerations, including tissue quality and QC steps necessary for generating high quality data from multiplex imaging studies. We demonstrate strategies for a streamline analytic pipeline using our quantitative workflow developed to characterize immune cells and infiltration patterns within spatial compartments of solid tumors in FFPE tissues, and herein, provide strategies and resources to practically adapt and utilize our analytic mIHC pipeline.

1. Banik, G., et al., Methods Enzymol., 2020

#4294

Bridging the gap between targeted NGS and FISH gene-level CNV detection capabilities in hematologic malignancies

Christophe N. Magnan[1], Hyunjun Nam[2], Shashikant Kulkarni[3], Segun C. Jung[4]. *[1]NeoGenomics Laboratories, Carlsbad, CA,[2]NeoGenomics Laboratories, San Diego, CA,[3]NeoGenomics Laboratories, Houston, TX,[4]NeoGenomics Laboratories, Aliso Viejo, CA*

Background: Copy Number Variations (CNVs) are prominent features of cancer cells. From a clinical standpoint, their accurate detection at a low cost is a priority. With regular increases in the number of markers to be tested, the cost effectiveness and practicality of gold standard techniques like Fluorescence In Situ Hybridization (FISH) are slowly decreasing. Cost-efficient Next Generation Sequencing (NGS) targeted gene panels can be scaled up but accurately detecting CNVs from the resulting data remains challenging. We demonstrate large amounts of data and machine learning can help bridge the gap between the two techniques.

Methods: We collected the sequencing data of 6,277 patients tested using a custom amplicon based NGS assay designed to detect somatic alterations in 297 hematological cancer relevant genes such that at least one concurrent FISH test was also performed. FISH results were used to infer the gain, loss, or normality information for each corresponding gene. The annotated genes were then used to curate a training set by extracting 20 features per gene from the alignment results. A 3-class random forest classifier was trained using this dataset. The selected model was evaluated on a distinct set of 2,738 patients.
Results: Evaluation results are provided in Table 1 for 8 genes for which the FISH probe used to infer the gain, loss, or normality information directly spanned the gene region. The predicted CNVs are almost a perfect match with FISH for 6 of these genes with a limit of detection at 20% abnormal cells. In most cases, the model reduces discordant calls by over 50% compared to using existing CNV detection software only.
Conclusion: We show the CNV detection capabilities of a targeted NGS assay can closely match the gold-standard FISH technique by analytically correcting the biases introduced by the targeting procedures. The model presented here is used to detect CNVs in ALL patients after a successful formal validation in our laboratory.

Table 1: Evaluation results.

Gene	FISH Positive Cases (Gain/Loss)			FISH Negative Cases (Normal)			All FISH Cases		
	Total	**Concordant**	**Sensitivity**	**Total**	**Concordant**	**Specificity**	**Total**	**Concordant**	**Accuracy**
ATM	72	72	**100.00%**	641	629	**98.13%**	713	701	**98.32%**
CBFB	23	22	**95.65%**	517	506	**97.87%**	540	528	**97.78%**
EGR1	171	169	**98.83%**	1,541	1,538	**99.81%**	1,712	1,707	**99.71%**
KMT2A	27	25	**92.59%**	474	472	**99.58%**	501	497	**99.20%**
MET	113	113	**100.00%**	1,593	1,582	**99.31%**	1,706	1,695	**99.36%**
NF1	15	15	**100.00%**	908	908	**100.00%**	923	923	**100.00%**
TERT	10	10	**100.00%**	1,723	1,709	**99.19%**	1,733	1,719	**99.19%**
TP53	76	73	**96.05%**	1,567	1,556	**99.30%**	1,643	1,629	**99.15%**

#4295

Streamlining the reconstruction of subclonal evolution in DNA sequencing data

Gage Black, Yi Qiao, Xiaomeng Huang, Gabor Marth. *Human Genetics, University of Utah, Salt Lake City, UT*

In many cancer types, the evolution of subclonal malignant cells leads to a diverse tumor population that can affect treatment efficacy. In addition, evolution throughout treatment can lead to resistant subclonal populations and eventual relapse. To effectively treat these cancers, it is essential to understand the subclonal architecture of the tumor, including the somatic mutations that differentiate each population. Many tools have been developed to attempt to cluster mutations or reconstruct the clonal architecture of a given tumor sample. However, few can accommodate multiple samples, which is common in longitudinal or metastasis studies. In addition, these tools typically focus on just one of the steps necessary for a full analysis (e.g., variant clustering, subclone hierarchical tree reconstruction, and tree visualization). Many require non-standard data formats, necessitating data format conversion between each step. These requirements make it very challenging for investigators without a deep understanding of each tool to perform a full subclonal analysis. To make the

identification of temporal and spatial heterogeneity more streamlined and accessible to analysts with basic programming knowledge, we have developed a pipeline that takes somatic mutations in standard VCF file format as input and produces meaningful results that are easy to interpret. Variant data is extracted and formatted for the input to PyClone-VI (Gillis and Roth, 2020), which is used to cluster somatic variants based on their allele frequencies at each time point. SuperSeeker, an improvement on the SubcloneSeeker method developed within our lab (Qiao et al., 2014), implements advanced tumor subclone reconstruction algorithms to jointly analyze multiple samples and construct hierarchical trees that account for all subclones observed in a patient. A sample trace, or the cellular fraction of each subclone found in each sample, is also provided. The output of SuperSeeker is an updated VCF file with the tree and sample trace information added to the header. Finally, a GraphViz rendering of the hierarchical tree is made for easy visualization. In addition to this rendering, the final VCF file can also be used for interactive analysis and visualization of the results using our Oncogene.iobio web tool. This pipeline makes identifying temporal and spatial heterogeneity more efficient, requiring only standard file types as input, and basic command line knowledge. In a recently published study, we investigated subclonal evolution in 38 patients with CLL being treated with a BTKi. The initial subclonal architecture analysis for each patient in this study was laborious and time intensive. Using this pipeline, we can now identify subclonal evolution in these patients and create an interactive visualization more efficiently. This approach can streamline analyses, increase efficiency, and lead to a deeper understanding of a tumor's subclonal evolution.

#4296

Fast de novo antibody structure prediction with atomic accuracy

Yining Wang, Xumeng Gong, Shaochuan Li, Bing Yang, Yiwu Sun, Yujie Luo, Hui Li, Le Song.
BioMap, Beijing, China

Background: In the field of antibody engineering, an essential task is to design a novel antibody whose paratopes bind to a specific antigen with correct epitopes. Understanding antibody structure and its paratope can facilitate a mechanistic understanding of its function. Therefore, antibody structure prediction from its sequence alone has always been a highly valuable problem for de novo antibody design. AlphaFold2 (AF2), a breakthrough in the field of structural biology, provides a solution to this protein structure prediction problem by learning a deep learning model. However, the computational efficiency and undesirable prediction accuracy on antibody, especially on the complementarity-determining regions limit its applications in de novo antibody design.
Methods: To learn informative representation of antibodies, we trained a deep antibody language model (ALM) on curated sequences from observed antibody space database via a well-designed transformer model. We also developed a novel model named xTrimoABFold++ to predict antibody structure from antibody sequence only based on the pretrained ALM as well as efficient evoformers and structural modules. The model was trained end-to-end on the antibody structures in PDB by minimizing the ensemble loss of domain-specific focal loss on CDR and the frame aligned point loss.
Results: xTrimoABFold++ outperforms AF2 and OmegaFold, HelixFold-Single with 30+% improvement on RMSD. Also, it is 151 times faster than AF2 and predicts antibody structure in atomic accuracy within 20 seconds. In recently released antibodies, for example, cemiplimab of PD-1 (PDB: 7WVM) and cross-neutralizing antibody 6D6 of SARS-CoV-2 (PDB: 7EAN), the RMSD of xTrimoABFold++ are 0.344 and 0.389 respectively.
Conclusion: To the best of our knowledge, xTrimoABFold++ achieved the state-of-the-art in antibody structure prediction. Its improvement on both accuracy and efficiency makes it a valuable tool for de novo antibody design, and could make further improvement in immuno-theory.

Experimental results on immune antibody dataset with 95% confidence interval.				
Method	RMSD	TMScore	GDTTS	GDTHA
AlphaFold2	3.1254 ± 0.1410	0.8385 ± 0.0055	0.7948 ± 0.0057	0.6548 ± 0.0063
OmegaFold	3.2610 ± 0.1463	0.8384 ± 0.0057	0.7925 ± 0.0059	0.6586 ± 0.0063
HelixFold-Single	2.9648 ± 0.0997	0.8328 ± 0.0055	0.7805 ± 0.0057	0.6225 ± 0.0060
ESMFold	3.1549 ± 0.0067	0.8390 ± 0.0003	0.7952 ± 0.0003	0.6551 ± 0.0003
xTrimoABFold++	**1.9594 ± 0.0805**	**0.8986 ± 0.0052**	**0.8694 ± 0.0057**	**0.7456 ± 0.0066**

#4297

OFFONOME: a new notion of genes' on/off

Wonyoung Choi[1], Hyo Young Choi[2], Daivd Neil Hayes[3]. *[1]Center for Cancer Research, University of Tennessee Health Science Center, Memphis, TN,[2]Department of Preventive Medicine, University of Tennessee Health Science Center, Memphis, TN,[3]Department of Medicine, University of Tennessee Health Science Center, Memphis, TN*

Background: RNA-seq is now the most widely used technique for gene expression profiling, which generates nucleotide level genome coverage as well as summary gene expression values. In general, low-expressed genes are excluded in the data processing due to their low signal-to-noise ratio. Nonetheless, it has been shown that low-expressed genes can provide crucial information such as presence of rare cells in bulk tissue samples. To optimize signal to noise in low-expressed genes, we applied a novel approach in which we transform low-expressed genes to a robust dichotomized state of being either "on" or "off".
Methods: To determine the status of genes, we use the shape of base-level read coverage which is expected to be homogeneous across the samples if they are "on", whereas appear to be random noise if they are "off". We model base-resolution RNA-seq data as vectors in high dimensional data space and measure their level of shape similarity (LSS) using angles between samples with lower angles indicating higher similarity which is more likely to be "on" status. Applying this approach to 3 human cancer samples (head and neck squamous cell carcinoma (HNSC), lung adenocarcinoma (LUAD) and lung squamous cell carcinoma (LUSC)) from the Cancer Genome Atlas (TCGA), we identified lists of genes, the OFFONOME, that were either always or sometimes "off". Differential OFFONOME genes were queried to address supervised and unsupervised analyses.
Results: Using our technique, we characterized the OFFONOME of HNSC (5851 genes), a set which would typically have been filtering for removal because of low expression. In the HNSC OFFONOME, we observed five gene clusters, each of which was strongly associated with specific gene ontology. One of the clusters identified a rare population of normal myocytes infiltrating otherwise invasive tumors. For the OFFONOME of LUAD (5435 genes) and LUSC (5292 genes), we found clusters enriched with cilia and keratinization-related genes. In the result of integrated analysis, we observed that squamous cell carcinoma (SCC) tumor types shared "on" status for keratinization-related genes known for the cause of SCC. By comparison, LUAD had "on" status genes related to microtubule-based movement related with cilia structure. Strikingly, clustering the OFFONOME with the LSS distinguished 3 tumor types with almost perfect separation, outperforming several competing gene expression measures.
Conclusion: In this study, we applied a new notion of gene expression. This approach enables a robust characterization of "on" and "off" status which can be especially effective for the genes expressed at low level. The OFFONOME from 3 cancer types revealed not only the tissue-specific genes but also the genes shared in similar tumor types. Collectively, OFFONOME can provide new

insights into genes expressed at vanishingly low levels, such as from minor cell populations within bulk tumor analysis.

#4298

Machine learning-based model for survival prediction after immunotherapy in patients with solid tumor

Salma Y. Fala[1], Mohamed Osman[2]. *[1]Suez Canal University, Portsaid, Egypt,[2]Zaazig University, AL-Sharqia, Egypt*

Background: Immune checkpoint inhibitors (ICIs) have led to a paradigm shift in solid tumors treatment. However, not all patients respond favorably to these drugs, highlighting the need for reliable predictions to achieve more personalized care and better management. This study aimed to create and validated ML model to predict survival in solid tumors patients receiving ICIs.
Methods: We obtained clinical and genomic data from cBio Cancer Genomics Portal. Data were randomly divided into a training set (80%) and a validation set (20%). light gradient boosting algorithm was trained to predict patients' survival at different time points.
Results: We identified 1660 patients with a median survival of 18 months. LGB yielded AUCs of 67.91% at 1 year, 79.89.6% at 2 years, and 79.75% at 3 years, respectively. The most important predictors that influenced the performance of the model in predicting 3-year-survival were: Age (22.89%), tumor mutational burden (18.24%), and tumor purity (13.23%). Moreover, multivariate analysis was performed and drug type was identified as an independent prognostic indicator (P< .001). So, a Subgroup analysis was done and the OS rates were: 98.57%, 75.55%, 33.84% in patients who received CTLA-4, 98.57%, 75.55%, 33.84% with PD-1/PD-L1, and 97.99%, 9.94%, 4.62% with combo treatment, at 1-, 3-, and 5 years, respectively.
Conclusion: Our ML-based model that integrates both clinical and genomic data is an improved tool for survival prediction, enabling an accurate risk classification and leading to a more precise decision-making. Moreover, this study highlights the importance of age and tumor microenvironment as the main contributors in making survival prediction in patients receiving ICIs.

Table. Performance in survival prediction among training and testing sets

Survival	Average AUC	Average Accuracy	Survival Duration	Positive Predictive Value (Precision)	Sensitivity (Recall)
1-year	67.91%	63.18%	**<12 months**	58%	54%
			>=12 months	67%	70%
2-years	79.89%	78.70%	**<24 months**	86%	84%
			>=24 months	62%	65%
3-years	79.75%	86.02%	**<36 months**	95%	89%
			>=36 months	45%	65%

#4299

Gene expression based machine learning classifier to predict and validate cancer type in patient derived xenograft (PDX) models

Warren Andrews, Long Do, Jonathan Nakashima. *Certis Oncology Solutions, San Diego, CA*

Patient derived xenografts (PDX) are increasingly utilized in translational research and drug development. Characterizing the genomic features of PDX is essential to establishing reliable models for cancer research. Despite great interest, problems remain in PDX tumor data banks

including improper cancer type diagnosis and sample mix-ups. In an effort to improve annotation and quality of PDX models, we developed a machine learning model trained on gene expression data from The Cancer Genome Atlas (TCGA). We then applied the model to corresponding data collected from nearly 300 Certis PDX models plus publicly available data from NCI's Patient-Derived Models Repository (PDMR). The model shows high precision and variable recall and provides a fast and accurate method for cancer type diagnosis.

Artificial Intelligence and Machine/Deep Learning 1

#5352

Targeting DNA methylation in T cells to improve the efficacy of immunotherapy

Pengtao Dang[1], Xiao Wang[2], Haiqi Zhu[3], Jia Wang[2], Tingbo Guo[4], Xinyu Zhou[2], Paveethran Swaminathan[2], Chi Zhang[5], Sha Cao[5]. *[1]Deparment of Electrical Computer Engineering, Purdue University, Indianapolis, IN,[2]Deparment of Computer Science, Indiana University, Bloomington, IN,[3]Department of Computer Science, Indiana University, Bloomington, IN,[4]Deparment of Mathematics, Purdue University, Indianapolis, IN,[5]School of Medicine, Indiana University, Indianapolis, IN*

T-cells are critical mediators of immunity and immunologic memory. Their cell fates are regulated in part through epigenetic mechanisms, including DNA methylation. Recent genome-wide methylation analyses have revealed dynamic alterations in the methylome at various stages of development and differentiation of T cells. At single cell level, it is not easy to simultaneously collect RNA-seq and RBBS methylation profiling. An important task is to understand the expression change of which genes and pathways are regulated by DNA methylations, especially for the ones that are associated with functional variations in the T cells from tumor microenvironment.In this study, we developed a computational approach based on our recently developed metabolic flux estimation to estimate cell-wise global DNA methylation activity level by using scRNA-seq data. We also hypothesize that the global DNA methylation activity level in one cell determines most of the DNA methylation level in gene-specific DNA methylations. Hence, the dependency between gene-specific DNA methylation and expression could be imputed by the dependency between predicted global DNA methylation input level and the gene expression. We validated our method to impute cell-wise global DNA methylation level by using four independent sets of paired gene expression and DNA methylation data. Noted, our prediction of global DNA methylation activity is from a pure metabolic perspective. We found that two metabolic reaction rates, named metabolic flux from methionine to SAM and SAM to SAH, purely predicted by using gene expression data can accurately impute DNA methylation activity in all validating data sets. Our method enables further identification of the disease/cell context specific contributor of DNA methylation, i.e., the genes high contribution to DNA methylations in each individual cell or cell groups. We applied our method on scRNA-seq data of different T cell types extracted from TME of lung, liver, and colon cancer. We have seen that exhausted T cells, especially the ones with decreased Granzymes and PRF1 are associated with increased global DNA methylation level and related genes, suggesting the potential clinical implications in targeting DNA methylation to improve the efficacy of immunotherapies.

#5353

Graph representation learning of tumor topology from spatial imaging data

Nicholas Ceglia, Samuel S. Freeman, Maryam Pourmaleki, Andrew McPherson, Sohrab P. Shah. *Memorial Sloan Kettering Cancer Center, New York, NY*

Recently, novel technologies have enabled spatially resolved multiplexed protein profiling of tumors; however, there is an unmet need for unbiased detection of spatial structures within the tissue. By encoding multiplexed images as a graph, we produce an efficient and well-studied graph representation that allows for the application of sophisticated machine learning methods, particularly graph neural networks (GNNs) and graph autoencoders (GAE). While GNNs have recently become popular tools in the analysis of spatial data, current GNN methods are limited by production of cell-level representations rather than graph-level representations. To understand patterns of local tissue structure and protein expression, we implemented a generalizable GAE framework that summarizes marker intensity and morphological values with the local topology of neighboring cells. In this way, each local cellular graph is represented as a single point in the lower dimensional space. We show that our framework generates low-dimensional features that reflect both cellular attributes and tissue structure. We demonstrate that clustering local structure in 318 fields of view from 22 tumor lesions across 7 patients with in-transit melanoma captured using multiplexed immunofluorescence (mpIF) can produce spatial motifs predictive of response to intralesional interleukin-2 (IL-2) immunotherapy. Additionally, we applied our framework to mpIF data of 146 high grade serous ovarian cancer tumors across 50 patients. We identify clusters with higher CD8+ T cell infiltration that associate with homologous recombination deficiency. Our method can be readily applied to various spatially resolved multiplexed imaging platforms, and the resulting embeddings provide a compressed representation of subgraphs that can be used in further classification or regression analysis of patient- and/or image-level histological, clinical, or genomic labels.

#5354

Prediction of OncotypeDX high risk group for chemotherapy benefit in breast cancer by deep learning analysis of hematoxylin and eosin-stained whole slide images

Gil Shamai[1], Ran Schley[1], Ron Kimmel[1], Nora Balint-Lahat[2], Iris Barshack[3], Chen Mayer[3].
[1]Technion-Israel Institute of Technology, Haifa, Israel,[2]Institute of Pathology Sheba Medical Center, Ramat Gan, Israel,[3]Institute of Pathology, Sheba Medical Center, Ramat Gan, Israel

Introduct**ion:** Breast cancer is the most common cancer in women, with most patients diagnosed with early-stage disease. While adjuvant therapy should be considered in all fit patients, in many low-risk patients drug toxicity may out-weigh the potential benefit, therefore, identifying these patients is desired. Hematoxylin and eosin (H&E) is the basic staining routinely performed for biopsies. It allows visual examination of the tissue and cells. Such manual examination, however, does not provide information about the molecular profile of the cancer, which is essential for diagnosis and guidance of treatment. The OncotypeDX assay is recommended for patients with node-negative, estrogen receptor-positive invasive breast cancer for determining chemotherapy benefit. It is based on RT-PCR gene expression profiling and provides a recurrence score (RS) that enables patient stratification to non-high risk (RS < 26) and high risk (RS ≥ 26). It was shown that high risk patients are likely to benefit from chemotherapy, while non-high risk are not. Unlike H&E staining, the OncotypeDX assay is costly, time consuming, and inaccessible in low-income countries. Here, we sought to evaluate whether analysis of scanned H&E-stained slides by convolutional neural networks (CNNs) could predict the RS risk group (high versus non-high), which determines eligibility for chemotherapy.
Methods: 684 H&E-stained slides were collected from 430 invasive breast cancer patients who were assayed for OncotypeDX between 2014 and 2020 at Sheba medical center, Israel. The slides were scanned at 0.25 micron/pixel, and automatically segmented and split to 256x256 non-overlapping tiles, resulting in overall 339,986 tile images containing tissue. The patients were randomly split into training (75%) and test (25%) sets, and a CNN model was trained and validated on the training set to classify each tile to non-high risk (RS < 26) versus high risk (RS ≥ 26), in 5-

fold cross-validation. The final model was then applied to the held-out test set, and tile scores were aggregated to produce per-patient prediction scores. The final CNN prediction scores on the test set were compared to the ground truth risk group and the AUC performance was calculated.
Results: The AUC performance of the model on the held out test set for high-risk versus non-high-risk classification based on the H&E images alone was high (0.798, 95% CI: 0.689 - 0.875, P value < 0.001), showing that the H&E image analysis could predict the high risk group.
Conclusions: These results show, for the first time, that CNN-based analysis of H&E images could predict benefit from chemotherapy, thus implying distinct tumor morphologies differing between RS groups. Utilizing such a system may enable physicians in countries that lack genetic profiling capabilities to refine chemotherapy stratification based on H&E images alone.

#5355
Elraglusib response prediction and mechanistic discovery using iterative machine learning
Joseph McDermott[1], Taylor Weiskittel[2], Daniel Billadeau[2], Benedito Carneiro[3], Hu Li[2], Andrew Mazar[4]. *[1]Lantern Pharma Inc., Dallas, TX,[2]Mayo Clinic, Rochester, MN,[3]Brown University, Providence, RI,[4]Actuate Therapeutics Inc, Fort Worth, TX*

Elraglusib is a selective GSK-3 inhibitor that has activity on a broad array of neoplasms as well as their immune microenvironment. However the determinants of tumor response have not been elucidated. Here, we use genomic panels of cancer driver genes to predict patient response to elraglusib therapy as measured by RECIST criteria. Patient response in the Phase I 1801 trial (NCT03678883) was matched to genomic data from patient tumors, with 80 cases used to train Machine Learning models and 26 cases reserved as a test set for model evaluation. When predicting response from mutation status alone our models reached a modest accuracy of 65% in the test set, which we attributed to the sparsity of genomic data. To remedy this, we engineered pathway-based features to provide combinatorial information while ensuring feature stability. To select the optimal combination of features, we designed an iterative design process that first randomized feature combinations and then created refined models from the highest performing pathway features. This resulted in several final models with greater than 88% accuracy. We retained several models of similar accuracy to more comprehensively identify potential biomarkers and combinatorial relationships. These models were then interpreted using SHapley Additive exPlanations (SHAP) where we were able to identify highly predictive features for both the entire pan-cancer cohort and specific histologies. We found the feature constructed from the Reactome pathway “Chromatin Modifying Enzymes” frequently occurred in high performing models with a high-ranking SHAP value. This feature included genes such as *SMARCA4*, *HDAC2*, and *KDM5A*, and was negatively associated with patient response. Another frequently observed high-ranking pathway feature with a negative response association was based on the “Innate Immune System” Reactome pathway. Many of the features highlighted in our models were negatively associated with elraglusib response and thus could be general markers of poor prognosis. To address this, we altered our pipeline to test only positively associated features which substantially reduced our feature pool to only 285 features but still produced models with accuracies of up to 81%. Analysis of key features used by these models identified several positive markers of elraglusib including mutations in the *POLE* gene, which previously has been linked to DNA-damage response deficiency and anti-tumor immune response. In sum, we forecast elraglusib response for a variety of tumor histologies and simultaneously reveal potential mechanisms of elraglusib sensitivity and biological action. In future work we will investigate the utility of using POLE and other identified biomarker candidates to predict the likelihood of patient response to elraglusib, as well as whether our machine learning models will be an effective tool to guide patient stratification.

#5356

Collaborating to ensure data-driven drug discovery on the Cancer Genomics Cloud: Realizing the possibilities for MoDaC and ATOM

Soner Koc[1], Vojislav Varjacic[1], Miona Rankovic[1], Marijeta Slavkovic-Ilic[1], Aleksandar Danicic[1], Sean Black[2], Naomi Ohashi[2], Titli Sarkar[2], Zelia Worman[1], Jack DiGiovanna[1], Brandi Davis-Dusenbery[1], Dennis A. Dean[1]. *[1]Seven Bridges Genomics Inc., Boston, MA,[2]Fredrick National Laboratory for Cancer Research, Frederick, MD*

Introduct**ion**. The NCI-funded Cancer Genomics Cloud (CGC) and the NCI Predicative Oncology Model and Data Clearinghouse (MoDaC) advance NCI computing infrastructure and tools that aim to reduce the burden of cancer on patients. The CGC provides a collaborative cloud base computation infrastructure that collocates computation, bioinformatics workflows, and 3+ PB data to researchers. MoDaC provides a publicly available resource generated from the Joint Design of Advanced Computing Solutions for Cancer (JDACS4C) Program and the Accelerating Therapeutics for Opportunities in Medicine (ATOM Consortium). The NCI-sponsored MoDaC program aims to add machine learning toolsets to identifying novel treatments for Cancer Patients. We present our progress collaborating with MoDaC to make machine learning models available on the Cancer Genomics Cloud.

Methods. Our Bioinformatics teams migrated MoDaC tools on the CGC, defined standards for releasing models, and collected recommendations for decreasing the time required to make MoDaC tools available on the Cancer Genomics Cloud. We mirrored the ATOM Modeling Pipeline (AMPL), a drug discovery platform, on the CGC by making the GIT repository cloud accessible through Jupyter Notebook access, supporting interactive analysis. We translated AMPL and JDACS4C models into CWL. Converting these ML models into CWL supports reproducible execution, scalable deployment, and computational portability.

Results. The AMPL drug discovery platform on the CGC includes data ingestion & curation, featurization, model training & tuning, prediction generation, visualization & analysis functionality as Jupyter notebooks and CWL workflows. The release consists of chemo-informatics tools for integrating cancer treatment features in deep-learning graph models. JDACS4C ML Models ported to the CGC include classifiers (tumor and normal-tumor pairs), autoencoders (Gene Expression), drug response predictors (single and combination), and Multitask Convolutional Neural Networks (extract information from cancer pathology reports).

Conclusion. We optimized the MoDaC Drug Discovery and Machine Learning tools into cloud-native resources on the CGC, supporting interactive and GUI-driven analysis. The release supports technical and newer users to machine learning, allowing access to a broader user base than those who traditionally have access to ML toolsets. These MoDaC toolsets will support pre-clinical study evaluation, treatment identification, and experimental design. Moreover, existing MoDaC-AMPL tutorials on the CGC support distributed ML-Drug Discovery training. Lastly, collaborating with MoDaC teams identified standardization approaches that can reduce the time and effort to make these tools widely available across the NIH-NCI computational infrastructure.

#5357

Estrogen receptor gene expression prediction from H&E-stained whole slide images

Anvita A. Srinivas[1], Ronnachai Jaroensri[1], Ellery Wulczyn[1], James H. Wren[2], Elaine E. Thompson[2], Niels Olson[3], Fabien Beckers[4], Melissa Miao[4], Yun Liu[1], Cameron Chen[1], David F. Steiner[1]. *[1]Google Health, Palo Alto, CA,[2]Henry M Jackson Foundation, Bethesda, MD,[3]US Navy, Washington, DC,[4]Verily, South San Francisco, CA*

Gene expression profiling (GEP) represents an important approach to inform breast cancer treatment. However, access to GEP involves challenges associated with cost, tissue transportation, and turn around time. In this work, we explore the prediction of estrogen receptor gene (*ESR1*) expression directly from images of hematoxylin and eosin (H&E) stained, formalin-fixed paraffin-embedded (FFPE) breast cancer tissue. Since H&E staining is a fast and inexpensive component of the standard tissue preparation in pathology, this approach is tissue preserving and requires no additional tissue processing. Our method uses a deep multiple instance learning approach to process cropped image patches from whole-slide images (WSI) into a numeric embedding vector summarizing the information in each patch. A gated attention mechanism then aggregates these embeddings into a single prediction for the WSI. We train and tune the model on a site-based split of The Cancer Genome Atlas (TCGA) BRCA dataset, and evaluate it on both a heldout split of TCGA (independent sites) and a separate dataset from a tertiary teaching hospital (TTH). All splits of TCGA have *ESR1* value, immunohistochemistry (IHC) estrogen receptor (ER) status, and limited clinical outcome data. The TTH dataset has IHC-based ER status and clinical outcome, but not *ESR1* expression. On the TCGA heldout test split, our model's root mean square error (RMSE) for predicting normalized gene expression counts (TPM) was 2.90 [95% CI: 2.57, 3.23], and the Pearson correlation was 0.57 [95%CI; 0.46, 0.67]. For predicting IHC-based ER status on the same TCGA split, this weakly-supervised *ESR1*-predicting model had an area under the receiver-operator curve (AUROC) of 0.81 [0.74, 0.87]. This was comparable to a strongly-supervised method directly predicting ER status (AUROC: 0.85 [0.77, 0.92]). Lastly, when evaluated for association with patient outcomes (progression-free interval; PFI) using the independent TTH dataset, this *ESR1*-predicting model had a concordance index (c-index) of 0.59 [0.52, 0.65]. For comparison, the c-index for PFI using the IHC-based ER status for these cases was 0.61 [0.54, 0.66]. This work further demonstrates the potential to infer gene expression from H&E stained images in a manner that shows meaningful associations with clinical variables. Because obtaining H&E stained images is substantially easier and faster than genetic testing, the capability to derive molecular genetic information from these images may increase access to this type of information for patient risk stratification and provide research insights into molecular-morphological associations. Future work incorporating more comprehensive sets of genes remains a valuable next step.

#5358

Digital SP263 PD-L1 tumor cell scoring in non-small cell lung cancer achieves comparable outcome prediction to manual pathology scoring

Hen Prizant[1], John Shamshoian[2], John Abel[2], Andrew Beck[2], Laura Chambre[2], Stephanie Hennek[2], Hartmut Koeppen[1], Daniel Ruderman[1], Meghna Das Thakur[1], Michael Montalto[2], Benjamin Trotter[2], Ilan Wapinski[2], Wei Zou[1], Minu K. Srivastava[1], Jennifer Giltnane[1]. *[1]Genentech, Inc., South San Francisco, CA,[2]PathAI, Boston, MA*

Background: Tumor cell (TC) PD-L1 expression is predictive of response to PD-L1-targeted immunotherapy, and accurate scoring is crucial for treatment selection. Scoring relies on manual assessment of immunohistochemically labeled tissue and is subject to subjective variation due to pathologist assessment. As a digital alternative, a clone-agnostic AI-based model for PD-L1 quantification in non-small cell lung cancer (AIM-PD-L1 NSCLC) was developed[1]. AIM-PD-L1 was deployed on samples from a Phase 3 study of anti-PD-L1 atezolizumab combination therapy with carboplatin and paclitaxel, and/or bevacizumab in Stage IV NSCLC (IMpower150; NCT02366143). Digital and manual PD-L1 TC scores were compared and interrogated for their respective potential to predict efficacy to atezolizumab combination treatments.

Methods: AIM-PD-L1 was deployed on images (n=768) digitized from SP263-labeled slides with available manual pathologist TC scores to quantify tissue regions and individual TCs. PD-L1 expression status was determined for each tumor cell and a slide-level TC score was computed. Overall survival (OS) and progression free survival (PFS) analyses of patients at selected cutoffs of 1%, 50%, and across a continuum of cutoffs from 0% to 100% PD-L1 TC by digital and manual methods were conducted, comparing groups treated with or without atezolizumab in combinations with carboplatin and paclitaxel, and/or bevacizumab. Digital and manual scores were compared using agreement rates, Lin's concordance and Spearman's correlation coefficients, and hazard ratios (HRs) were calculated for OS and PFS analysis.
Results: At the slide level, correlation between continuous digital and manual scores was high (r 0.84 [95% CI 0.81-0.86]). Digital assessment of PD-L1 positivity at the 1% cutoff identified more positive patients than manual scoring (70% vs. 55% prevalence, respectively), with comparable treatment benefit (digital OS HR 0.69 [0.53-0.9], and manual OS HR 0.72 [0.54-0.98], digital PFS HR 0.67 [0.54-0.83], and manual PFS HR 0.66 [0.52-0.84]). Continuous digital PD-L1 TC scores showed that treatment benefit improved for patients with scores ≥50% compared to manual scoring. At the ≥50% PD-L1 TC cutoff, numerical improvement was observed in OS and PFS by digital scoring compared to manual (digital OS HR 0.5 [0.29-0.86] compared to manual OS HR 0.64 [0.4-1.02], and digital PFS HR 0.37 [0.24-0.57], compared to manual PFS HR 0.53 [0.37-0.76]).
Conclusions: AIM-PD-L1 scoring was as effective at predicting outcomes as manual using the ≥1% PD-L1 TC expression and at the ≥50% TC cutoff, digital scoring identified a subgroup with enriched efficacy compared to manual. Further evaluation of the accuracy and reproducibility of PD-L1 scoring by digital pathology as well as its potential use for patient enrollment or stratifications in clinical trials is needed.
[1]Griffin et. al. AACR (2022)

#5359
Translating state-of-the-art deep learning predictions of treatment efficacy to clinical practice
Gustavo Arango-Argoty, Etai Jacob. *Oncology Data Science, AstraZeneca, Waltham, MA*

Despite the clinical success of immune checkpoint blockade therapies, in many patients the disease becomes unresponsive or resistant to treatment. Attempts to predict treatment efficacy and identify determinants of response have suffered from limited accuracy. Here, we introduce a state-of-the-art deep learning method that better captures the complex relationships among the host, the immune system, and tumor biology. Our method, an explainable deep learning framework, is based on transformer architecture that combines data with different feature sets and clinical endpoints for survival prediction or classification. The framework includes(1) a new loss function based on Harrell's concordance-index, (2) an explainability module providing importance score between features based on mutual contribution to predictions, and (3) a transfer learning strategy that enables leveraging diverse clinical data sets in the public or private domain. Using seven data sets comprising more than 140,000 patients from immunooncologic (IO), targeted, and chemotherapy treatments, our method consistently outperformed other methods previously described in the literature, including CoxPH and random survival forest (RF). For example, our framework achieved a concordance index of 0.66 (±0.04) vs. 0.60 (±0.04) of the second-best method (RF) on MYSTIC IO arms using only clinical data. Utilizing our explainability module, we identified key features driving response prediction that are consistent with those in previous publications. For example, in the Chowell et al. data set, we identified albumin, neutrophil-to-lymphocyte ratio, prior-chemo-treatment, and tumor mutation burden as the most important features. We also identified in sparse mutation calls of 469 genes from the Samstein et al. data set, functional modules of several genes, each with a strong predictive power. For example, the functional module with the highest hazard

ratio (HR) (1.43) was the gene pair KEAP1 and STK11, which are well-established drivers of resistance to multiple therapies. We further validated these results across multiple data sets: The Cancer Genome Atlas HR = 1.23), GENIE/anti-PD-L1 (HR = 1.06), and MYSTIC/anti-PD-L1/CTLA-4 (HR = 1.39). Another example is a functional module related to adaptive immunity, comprising the genes AKT2, BTK, CDC73, HLA-B, IKBKE, INPPL1, RFWD2, TRAF2, and WHSC1. This module stratified patients with an HR of 0.58 within the Samstein et al. data set and 0.42 within the independent validation data set. We describe a new deep learning method with state-of-the-art performance in survival prediction and the potential to uncover biological and clinical insights related to disease response and resistance. Our framework simplifies the process of translating complex AI models to clinical practice and may accelerate the identification of targetable drivers of resistance and response.

#5360

Improved identification of CHIP mutations from cell-free DNA without matched normal samples using machine learning

Gustavo Arango-Argoty[1], Gerald Sun[1], Aleksandra Markovets[1], Carl Barrett[2], Zhongwu Lai[1], Etai Jacob[1]. *[1]Oncology Data Science, AstraZeneca, Waltham, MA,[2]Translational Medicine Oncology, AstraZeneca, Waltham, MA*

Blood-based liquid biopsies are becoming the standard for noninvasive profiling of tumors from circulating tumor DNA (ctDNA) to facilitate treatment decisions. However, it is known that non-tumor-derived mutations, such as those from clonal hematopoietic (CH) lineage, are also present in cell-free DNA (cfDNA) and can complicate tumor mutation detection and interpretation. Filtering alterations associated with CH can reduce the risk of false positives in ctDNA analysis. Current strategies for filtering CH mutations are based on prior knowledge of those in canonical CH genes, sequencing a matched peripheral blood mononuclear cell sample, or using multiple time points to evaluate changes in allele frequency (AF), with the assumption that AF of CH of indeterminate potential (CHIPs) are unlikely to be impacted by treatments; however, these approaches are either insufficient or cost prohibited. We present a machine learning framework that incorporates prior knowledge from tumor and blood-derived mutations to improve the classification of CH and tumor variants from plasma-only cfDNA samples and that greatly outperforms a simple rule-based approach. We developed a classification framework composed of three main modules to maximize the information gain from ctDNA as non-ctDNA samples: (1) a sequence context-based model where each variant is represented by 128 mutational signatures extracted using a bag-of-words-like modeling (using normal and tumor samples) along with mutational function effect scores from SnpSift and cancer type origin. In total 6,745 CH and 57,210 somatic tumor-derived mutations are used to train a model to distinguish CH, CH-putative cancer driver , and tumor mutations; (2) a ctDNA-context model that includes patient-level information (age, mutational signatures, and variant allele frequencies) from 392 tumor and 481 CH blood-derived mutations extracted exclusively from ctDNA samples to predict blood or tumor origin; and (3) a meta-classifier where models 1 and 2 are aggregated into a single score for predicting the origin of a given mutation. We compared our models against a baseline strategy where mutations were predicted as CH if they fell into a list of 27 canonical CH-related genes. Our proposed metaclassifier that integrates sequence- and ctDNA-based features improved the overall performance of CH detection (AUC = 0.83, compared with the baseline model, AUC = 0.72), highlighting the value of adding ctDNA-derived and mutation-context features to profile somatic mutations. As ctDNA assays and technologies rapidly progress and gain adoption for precision oncology, we anticipate that our work, combined with existing benchmarking efforts, will enable more robust analyses on critical applications such as

early disease detection, minimal residual disease, and mutational profiling to ultimately best inform clinical decision-making.

#5361

Deep learning models capture high dimensional features for cell morphology analysis

Kevin B. Jacobs, Kiran Saini, Nianzhen Li, Senzeyu Zhang, Ryan Carelli, Amy Wong-Thai, Stephane C. Boutet, Anastasia Mavropoulos, Andreja Jovic, Jeanette Mei, Mahyar Salek, Maddison Masaeli. *Deepcell Inc., Menlo Park, CA*

Many methods for imaging and sorting tumor cells require biomarker labels that perturb cells and may create a selection bias. The Deepcell platform can characterize and sort cells using only brightfield images of unlabeled single cells, thereby enabling more comprehensive and unbiased assessment of tumor cell morphology and heterogeneity. Cells are imaged with a high-speed camera during microfluidic flow and brightfield images are analyzed in real-time by deep learning models to generate quantitative embeddings, which are reproducible and multi-dimensional descriptions of cell morphology. One of the key technical challenges in building this platform was the development of an AI model to extract features from cell images from diverse human cells without prior knowledge of specific cell types, cell preparation, or other application-specific knowledge for an exploratory approach.

Deepcell's 'Human Foundation Model' (HFM) is a feature encoder that transforms cell images into 128 dimensional embedding vectors. The model backbone, responsible for extracting image features, is based on the ResNet18 convolutional deep neural network architecture. Training utilizes a multi-task semi-supervised training framework that combines the VicReg self-supervised learning model, which learns images features without labels, along with supervised auxiliary models using labeled data. These sub-models enable the backbone model to recognize specific cell attributes such as granulation, pigmentation, characteristics of malignancy, attributes related to cellular states like apoptosis and necrosis. We augment the deep learning embeddings with computer vision derived cellular features, such as area, perimeter, intensity, and texture features to improve model interpretability and accuracy.

Here, we describe how the HFM self-supervised backbone model was trained, the discriminatory power added by the supervised tasks, and validation of the reproducibility and generalization capabilities of the resulting model. We also demonstrate how the resulting embeddings can be visualized using the Deepcell Cloud software and how clusters of cells in our embedding space can be related to cell images, interpretable morphological features, and actionable biological characteristics. Potential applications of the Deepcell platform are diverse and promising, such as label-free enrichment of malignant cells and discovery of morphologically distinct subpopulations of heterogeneous cancer cell samples.

#5362

AI-enabled novel workflow to evaluate T-cell activity *in vitro* using 3D spheroid models

Zhisong Tong, Oksana Sirenko, Misha Bashkurov, Angeline Lim. *Molecular Devices, LLC (Moldev), San Jose, CA*

T-cell therapies are designed to help our immune system eliminate cancer cells. Those include CAR T-cells (Chimeric Antigen Receptor engineered T-cells), tumor infiltrating lymphocytes (TIL), and other genetically modified T-cells. In recent years, the field of cell therapy has started to expand, including the launch of the first CAR T-cell therapies to treat blood cancer in 2017, which was a critical milestone in this field. Despite its boom, the discovery of novel immunotherapies that specifically enhance T-cell response against cancer cells remains a challenging task, limited by the

absence of robust in vitro models to evaluate these immunotherapies throughout their development. The use of CAR T-cells on solid tumors has been lagging due to challenges that include tumor heterogeneity, immunosuppressive microenvironments, and the lack of unique tumor antigens that can be recognized by the CAR-T cells. As such, the ability to screen for CAR T-cells (e.g. with CRISPR) that effectively target and kill tumors is an area of active research. Here we describe a method for assessment of T-cell effect and penetration into the multi-cellular 3D tumor spheroids as a proof-of-concept model for in vitro CAR T assays. Spheroids were formed from Hela cell lines in 96-well round bottom plates. We activated the human peripheral blood mononuclear (PBMC) cells with PMA/ionomycin for 6 hours, then treated the spheroids with stimulated PBMC for 72 hours. Samples were imaged with a confocal imager every 2 hours for a 72 hour period. High-content imaging and analysis allowed us to observe and measure phenotypic changes in cancer spheroids and the process of T-cell penetration over a period of 72 hours. To optimize the workflow, we developed an image analysis approach that uses a deep learning-based segmentation model and a machine learning-based classification model to quantify the T-cell induced phenotypic changes in the spheroids using brightfield images. Our results show clear distinct phenotypic changes among different treatment groups and the feasibility of using AI-based analysis workflows to accurately predict the efficacy of T-cells in an in vitro assay. Moreover, the information associated with the penetration of T-cell into the 3D spheroids was explored by calculating the coordinates of the penetrated T-cells and T-cell movements from the nearest edge of the spheroids where the T-cell penetration speed was estimated. Our results show that the stimulated T-cells have much greater penetration speed compared to non-stimulated T-cells. Image analysis also allowed us to measure and quantitate the deterioration of cancer spheroids and changes in their morphology. Overall, our results show that the 3D spheroid models and the high-content analysis workflow may potentially be used as a metric to evaluate the efficacy of cell therapy in vitro.

#5363

MicroArray-based MethylationToActivity: Advancing biological knowledges from DNA methylation profiles of patient tumors

Karissa Dieseldorff Jones[1], Waise Quarni[2], Daniel Putnam[1], Shivendra Singh[2], Qiong Wu[2], Jun Yang[3], Xiang Chen[1]. *[1]Computational Biology, St. Jude Children's Research Hospital, Memphis, TN,[2]Department of Surgery, St. Jude Children's Research Hospital, Memphis, TN,[3]Department of Surgery & Department of Pathology, St. Jude Children's Research Hospital, Memphis, TN*

DNA methylation (DNAm) is a relatively stable regulatory epigenetic mechanism. Although accurate DNAm classifiers have been built for early detection of cancer and subtype classifications, its transcriptional regulatory roles remain unclear. To address this challenge, we developed a deep-learning framework MethylationToActivity (M2A) that accurately predicts individual promoter activity from WGBS methylomes. As array-based methylome is the most common epigenetic data from patients' tumor samples, we redesigned M2A's raw features and model topology for array methylomes, which shows an accurate prediction of the promoter activity (R2 = 0.74), approaching its WGBS counterpart (R2 = 0.79). Transfer learning improves the prediction accuracy to 0.77. In a primary rhabdomyosarcoma cohort, M2A prioritized candidate genes with strong subtype-specific alternative promoter usage (APU) and identified distinct isoforms of a subgroup of APU genes including NAV2 expressed in the two major subtypes (aRMS and eRMS). Molecular experiments revealed that PAX3-FOXO1 directly binds to the aRMS-specific promoter and is required for its active transcription. Genetic deletion of PAX3-FOXO1 leads to NAV2 APU. Overexpression of aRMS-specific NAV2 isoform significantly promoted cell proliferation, supporting its oncogenic function. These data indicate that PAX3-FOX1 is critical for APU in aRMS. We conclude that the

new M2A provides vast insight into downstream functional interpretation of differential DNAm patterns.

#5364

Language modeling of peptide-HLA interactions achieves state-of-the-art performance on prediction of peptide presentation by HLA Class II

Daniel Sprague, Joshua Klein, Italo Faria do Valle, Olivia Petrillo, Melissa Rotunno, Matthew Davis, Monica Lane, Karin Jooss, Ankur Dhanik. *Gritstone Bio, Inc., Emeryville, CA*

Precise and sensitive prediction of neoantigen presentation to the immune system via human leukocyte antigen (HLA) class II molecules remains a challenge despite the early success of neural networks applied to HLA class I. However, it is necessary to address this modeling challenge because presentation of a neoantigen epitope by both classes of HLA molecules may be valuable to induce a sustained immune response with therapeutic cancer vaccines.
Previously we have developed a machine-learning based platform, EDGE^{TM}, that provides a state-of-the-art model to predict presentation of peptides by HLA Class I. Here we propose a new addition to our EDGE^{TM} platform: a model that leverages structural information of putative epitopes and HLA class II alleles from their *in-situ* context to predict presentation of peptides by HLA class II. Our model achieves this by leveraging the Evolutionary Scale Model pre-trained protein language model (LM), which has been demonstrated to embed protein sequences with rich structural information. The input to the model is a linear peptide consisting of an epitope and its flanking amino acids, concatenated with structurally relevant amino acids from each HLA allele. This allows our model to treat the modeling problem entirely as a natural language processing task, which minimizes imputation of covariates found in prior approaches when performing inference in the context of vaccine design, while maximizing the richness of the LM embeddings on longer linear peptides. Crucially, this also allows our model to generalize to any allele that has a known sequence. Additionally, DR-, DP-, and DQ-specific immunoaffinity purified mass spectrometry multi-allelic (MA) presentation data were generated per tumor or cell line sample, spanning 89 alleles in aggregate. We demonstrate that incrementally decreasing HLA class II allele MA resolution during training results in substantially improved predictions for situations where MA presentation data has completely ambiguous epitope presentation across DR/DP/DQ alleles. Our model achieves an Average Precision (AP) of 0.92 and ROC-AUC of 0.98 on the same benchmark validation data as the current state-of-the-art model BERTMHC, which achieved an AP of 0.81 and ROC-AUC of 0.95. These are the best AP and ROC-AUC for an HLA Class II presentation model on this benchmark dataset to the best of our knowledge. Our model is a significant advancement in HLA class II epitope prediction that allows our EDGE^{TM} platform to bring neoantigen vaccine design optimized for both class I and class II presentation within reach.

#5365

Extracting novel knowledge from scientific literature to build a web portal for cancer researchers to keep up with the latest scientific discoveries

Feng Pan[1], Yuan Zhang[1], Xin Sui[2], Donghu Sun[2], Menghan Chung[2], Jinfeng Zhang[1]. *[1]Florida State University, Tallahassee, FL,[2]Insilicom LLC, Tallahassee, FL*

Millions of new papers are published in biomedical sciences every year. In many disciplines, it has become impossible to read all the published new papers to learn what is happening in the frontier of a particular area. This gap is widening as the publishing speed has been accelerating in recent years. To address this challenge, one can convert unstructured text data into a structured form, which can

then support highly accurate information retrieval, information integration, and automated knowledge discovery. A plausible approach for such a task is to use named entity recognition (NER) and relation extraction (RE) methods to identify important biological entities and extract their relations to construct knowledge graphs (KGs). The LitCoin Natural Language Processing (NLP) Challenge was recently organized by NCATS of NIH and NASA to spur innovation by rewarding the most creative and high-impact uses of biomedical text to create KGs. In addition to entities and relations, the manually annotated LitCoin dataset also contains the annotations of relations being new discoveries or background knowledge. Our team participated in the challenge and ranked first place. The novelty prediction model of our pipeline has achieved an F1 score of 0.90. We have applied our model to all the PubMed abstracts published previously and the newly published ones to extract the novel discoveries in each article. A web portal has been created to allow scientists to view the latest discoveries in cancer research. The web portal is updated daily with versatile visualization tools for cancer researchers to quickly grasp the latest discoveries in a particular area. It also offers powerful functions to explore the existing literature and make sophisticated inferences about causal and indirect relationships.

#5366

Constructing the largest-scale biomedical knowledge graph using all PubMed articles and its application in automated knowledge discovery

Yuan Zhang[1], Feng Pan[1], Xin Sui[2], Donghu Sun[2], Menghan Chung[2], Jinfeng Zhang[1]. *[1]Florida State University, Tallahassee, FL,[2]Insilicom LLC, Tallahassee, FL*

The number of biomedical publications is growing at an accelerated speed. This ever-increasing amount of scientific literature has made reading all the published articles regularly impossible even for a very specific research area. A solid grasp of existing literature is essential for coming out with novel and plausible scientific ideas. To bridge the gap between the published scientific findings and our incapability of manually processing them, we need to convert the unstructured text into structured form to enable automated methods to use the structured, machine-readable information to generate novel hypotheses, which can then be manually validated. A plausible approach for converting unstructured text into structured form is to use named entity recognition (NER) and relation extraction (RE) methods to identify the biological entities and extract their relations to construct knowledge graphs (KGs). KGs can link concepts within existing research to allow researchers to find connections that may have been difficult to discover without them. The LitCoin Natural Language Processing (NLP) Challenge was recently organized by NCATS of NIH and NASA to spur innovation by rewarding the most creative and high-impact uses of biomedical, publication-free text to create KGs. Our team participated in the challenge and ranked first place. Using the pipelines developed for the LitCoin NLP challenge, we have constructed the largest-scale biomedical KG using all PubMed articles. We further develop advanced deep-learning methods to predict new links from the constructed KG. We demonstrate the power of this new framework using several examples important for drug discovery.

#5367

Deep neural networks using protein-protein network information predict multiple myeloma survival

Jiening Zhu[1], Jung Hun Oh[2], Anish K. Simhal[2], Rena Elkin[2], Larry Norton[3], Joseph O. Deasy[2], Allen R. Tannenbaum[4]. *[1]Department of Applied Mathematics & Statistics, Stony Brook University, Stony Brook, NY,[2]Department of Medical Physics, Memorial Sloan Kettering Cancer Center, New*

York, NY,[3]Department of Medicine, Memorial Sloan Kettering Cancer Center, New York, NY,[4]Stony Brook University, Stony Brook, NY

The modern development of sequencing technologies provides a comprehensive molecular portrait of human cancers. There is a strong need to develop methods to not only improve patient prognosis predictions but also to understand the driving factors for treatment. However, the high-dimension, low-sample size nature of the genomic data poses challenges for typical machine learning algorithms. The systematic understanding of genes with respect to a network (protein-protein interaction (PPI) network) is a way to handle the limit and the nonparametric analysis of geometric properties such as Ollivier-Ricci curvature and associated invariant measure developed by our group have proven to be successful for the prediction of survival in multiple cancers. In this work, we propose a novel supervised deep learning approach combining the aforementioned geometric methods, which benefit from the flexibility provided by deep learning techniques while still preserving much of the interpretability of the geometric analysis. We take advantage of a state-of-the-art graph neural network approach. Sparse connections between layers were inspired by the known biology of the PPI network from the Human Protein Reference Database (HPRD) and pathway information from the Kyoto Encyclopedia of Genes and Genomes (KEGG) database, supplemented with geometric network features which are fed into the network in corresponding layers. The prediction is based on a local-global principle, where highly predictive features are selected from early layers of the network and fed directly to the final layer to produce a multivariable Cox regression. We applied our method to RNA-Seq gene expression data from the CoMMpass study of multiple myeloma (MM). More specifically, 657 patients in the data set were randomly divided into training, validation and set-aside testing sets by a ratio of 6:2:2. We obtained an average C-index 0.66 of the prediction in the testing set from a 10-fold data split. Dichotomizing the testing set by its mean value to define high-risk vs. low-risk yielded a significant p-value of the log-rank test in the set-aside data (p-value =3e-4). We observed that geometric protein network information not only improved the outcome prediction (vs. 6% worse without geometric feature inputs), but was also more robust to fold splitting. From our model, we identified WEE1, CENPE and CENPF as top genes driving survival differences (higher expression of WEE1 increased risk and lower negative curvature between CENPE and CENPF increased risk). WEE1 is a cell cycle-related gene that regulates DNA repair and CENPE and CENPF are components of a fibrous layer of mitotic kinetochores, which have been indicated in the literature to be related to the prognosis as well as possible targets for treatment. While it is therefore logical that these genes would be implicated in the natural history of MM, they were identified entirely on the basis of network analysis.

#5368

AI-enabled prediction of lung cancer specific hot spot gene alterations from histology images

Gowhar Shafi[1], Shiva Shivamurthy[2], Anand Ulle[2], Chongtham Cha Chinglemba[1], Sumit Haldar[2], Fauzul Moubeen[2], Mohan Uttarwar[1]. *[1]OneCell Dx Inc, Cupertino, CA, USA and India, Cupertino, CA,[2]Indx.AI Inc, Cupertino, CA, USA and India, Cupertino, CA*

Background**:** The clinical intervention relies on molecular testing of primary biomarkers. We developed an AI enabled platform to predict NCCN guidelines recommended hot-spot genomic alterations from the image analysis using H&E slide.

Methods: AI engine was trained using clinically observed hot spot genomic alterations present in lung cancer patients as a ground truth based on histological FFPE whole-slide images. The H & E stained histological images of the tumor having matching pathogenic mutations were downloaded from the TCGA database for the training and testing purpose. The program extracted

histopathological features, followed by pattern mapping to predict genomics status based on the results of NGS testing from 480 samples. ResNet AI algorithm was trained to predict lung specific hot spot genomic alterations. An H & E stained slide was imaged with a 40x objective lens to obtain a brightfield image as an input data. The input image was segmented into 65 x 10^3 tiles, each of 64 μm^2 in size for an individual pathological class. 80% of the data set was used for training the engine while validation and blinded study was respectively performed on remaining 10% data.
Results: Using single blinded clinical samples. AI model analyzed whole slides. Table 1 summarize parameters for clinically significant variants. Higher sensitivity and specificity was observed for variants encoding mutated cell surface proteins compared to variants encoding intracellular mutant targets when compared on similar training and testing parameters.
Conclusions: AI-enabled prediction of hotspot genomic alterations resulted comparable to NGS with shortest TAT, cost and resources. It predicted actionable gene alterations with high positive and negative prediction values. Table 1

Gene	Sample (n = 480)		Evaluation parameters for tested samples					
	Training	Testing	Sensitivity (%)	Specificity (%)	PPV (%)	NPV (%)	F1-score (%)	Accuracy (%)
KRAS	248	62	100	94	94	100	97	97
ALK	16	4	100	100	100	100	100	100
EGFR	72	18	88	100	100	90	94	94
MET								

16	4	50	100	100	66	66	75	
ROS	16	4	100	100	100	100	100	100
STK11	88	22	82	73	75	80	78	77
RET	24	6	50	100	100	60	50	67
BRAF	14	2	100	100	100	100	100	100
NTRK	92	24	78	56	64	71	70	67
ERBB2	12	4	50	50	50	50	50	50

#5369

Detection of ERG:TMPRSS2 gene fusion in prostate cancer from histopathology slides using attention-based deep learning

Mohamed Omar[1], Zhuoran Xu[1], Sophie B. Rand[1], Daniela C. Salles[2], Edward M. Schaeffer[3], Tamara L. Lotan[2], Massimo Loda[1], Luigi Marchionni[1]. *[1]Department of Pathology and Laboratory Medicine, Weill Cornell Medicine, New York, NY,[2]Department of Pathology, Johns Hopkins University, Baltimore, MD,[3]Department of Urology, Feinberg School of Medicine, Northwestern University, Chicago, IL*

ERG:TMPRSS2 fusion is present in almost 50% of prostate cancer (PCa) cases of European ascent and plays an important role in carcinogenesis and disease progression. ERG status is detected using fluorescence in situ hybridization (FISH) or reverse transcription-polymerase chain reaction (RT-PCR), and since these tests are costly and require special training, there is need for innovative tools to decrease the cost and streamline the diagnostic process. For this reason, we have developed a deep learning (DL) system capable of inferring ERG fusion status using only digitized hematoxylin and eosin (H&E)-stained slides from PCa patients, and detecting tissue regions of high diagnostic relevance. To develop the model, we used the PCa TCGA dataset which includes 436 formalin-fixed paraffin-embedded (FFPE) H&E-stained whole slide images (WSIs) from 393 PCa patients who underwent radical prostatectomy. Subsequently, we evaluated the model's performance on an independent cohort of 314 WSIs provided by the Johns Hopkins University (natural history cohort). Slides were divided into tiles of 500X500 px from which feature extraction was performed using a pre-trained ResNet50 model. Feature vectors were then used to train attention-based multiple instance learning framework to predict the slide-level label as either ERG-positive or negative, and to score slide regions based on their contribution to the slide-level representation. Our model can predict the ERG fusion status with an Area Under the ROC Curve (AUC) of 0.84 and 0.73 in the training data and the independent testing cohort, respectively. Also, the model detects tissue regions with high attention score for each class. To decipher the cellular composition in these highly relevant regions for the cases predicted as ERG-positive or negative, we used HoVer-Net model to perform nuclear segmentation and classification into five categories: benign epithelial, tumor, stroma, immune, and necrotic. Notably, we found that the cellular composition of the highly relevant patches can capture prognostic information. Specifically, In the TCGA dataset, a high ratio of neoplastic cells in the relevant patches was significantly associated with worse progression free survival (PFS), while high ratios of necrotic, stromal, and stromal to neoplastic cells were significantly associated with better PFS. Similar findings were also obtained in the natural history cohort in which a high ratio of neoplastic cells was significantly associated with worse overall survival (OS) and metastasis free survival (MFS), while high ratios of immune, stromal, and stromal to neoplastic cells were significantly associated with longer OS and MFS. These results show that ERG fusion status can be inferred from H&E-stained WSIs, ultimately demonstrating the

benefit of DL systems in extracting tissue morphological features of high diagnostic and prognostic relevance.

#5370

New oncology target identification and validation platform combining artificial intelligence and preclinical pharmacology

Sebastien Vachenc[1], Nicolas Ancellin[2], Didier Grillot[2], Kenji Shoji[1], Joanna Giemza[1], Nathalie Jeanray[1], Leila Outemzabet[1], Salvatore Raieli[1], Lamine Toure[1], Olivier Duchamp[2], Fabrice Viviani[2], Philippe Genne[1], Jan Hoflack[1], Stéphane Gerart[1]. *[1]Oncodesign Precision Medecine, Dijon Cedex, France,[2]Oncodesign Services, Dijon Cedex, France*

Despite major advances in cancer therapy in the last decades, treatment resistance can develop over time. Precision medicine allows for the successful implementation of targeted therapies and stratification of patients, but treatment resistance remains a major obstacle in patient management. The identification and validation of new targets associated with cancer resistance remains a major challenge. The great diversity of molecular mechanisms involved in treatment resistance phenomena, whether intrinsic (de novo or primary) or acquired (secondary), constitutes a real therapeutic challenge for patient care. A better understanding of resistance mechanisms would allow to explore new therapeutic strategies to circumvent these phenomena in different types of cancer. The OncoSNIPE® project was developed in this context as part of a multicenter and collaborative clinical study (NCT04548960) in more than 800 chemo-naive adult patients. The objective of this project was to identify early and/or late markers of treatment resistance in three different pathologies for which resistance problems are encountered: triple negative breast cancer (TNBC) or luminal B, locally advanced or metastatic non-small cell lung cancer (NSCLC) and pancreatic ductal adenocarcinoma (PDAC). The program included traditional clinical and whole exome sequencing (WES) monitoring of patient biopsies (Exom-seq and RNA-seq) at diagnosis and relapse, monitoring of blood markers (RNA-seq and Proteomics – Cytokine) at diagnosis, and the evaluation of best therapeutic responses and relapse. The program used bioinformatics, artificial intelligence, statistical learning and semantic enrichment approaches to discover the diversity of mechanisms involved in these resistances and to identify new therapeutic targets, through hetero-modal data including clinical, genomic, transcriptomic, immunological and radiomic dimensions. Subsequently, a specific flowchart for target validation was applied to the resulting list, considering the target's developmental potential, its essentiality, prior knowledge (database mining) and home-made score of the link between the target and the disease. Finally, new targets were prioritized using weighting parameter and heuristic approximation based on the Crank algorithm. Experimental work on multiple targets began in the laboratory, initially in vitro, using 2D and 3D cell culture (including cells from patient-derived xenografts) and molecular interference. A wide variety of intrinsic or acquired molecular mechanisms involved in treatment resistance are being evaluated as candidates for diagnostic and therapeutic development.

#5371

Modeling single-cell dynamics using stochastic generative models based on neural differential equations

Michael E. Vinyard[1], Anders W. Rasmussen[2], Ruitong Li[1], Luca Pinello[3], Gad Getz[4]. *[1]Chemistry & Chemical Biology, Harvard University, Cambridge, MA,[2]Klarman Cell Observatory, Broad Institute MIT and Harvard, Cambridge, MA,[3]Molecular Pathology Unit, Center for Cancer Research, Massachusetts General Hospital, Charlestown, MA,[4]Broad Institute of MIT and Harvard, Cambridge, MA*

Hematopoietic malignancies arise from driver alterations acquired during specific, often intermediate and transient, differentiation states. When adequately sampled, “snapshot” single-cell measurements can capture dynamic biological processes, including transient states. While there are effective computational modeling solutions to order and capture the relationships among these cell states (often projecting onto a lower dimensional manifold with directionality), methods to infer the causal gene regulatory mechanisms driving cell state transitions remain limited.
Recently, a mathematical framework for modeling cell dynamics from snapshot data using a physics-based drift-diffusion equation was proposed. This drift-diffusion equation framework describes the dynamics of cell distributions with respect to time, wherein stereotypical driving forces (e.g., hematopoietic development) are captured by the drift term, and biological stochasticity is attributed to the diffusion term. The existing modeling solutions within this framework are forced to assume a fixed diffusion parameter across cell states, ascribing all observed dynamics to drift alone. Here, we expand on current drift-diffusion models to learn both the drift and diffusion terms that describe every observed cell state. These models are constructed from stochastic neural differential equations, continuous deep neural networks that approximate the theoretically complex differential equations underlying gene regulatory networks in hematopoiesis.
Lineage-barcoded, multi-time point single-cell RNA sequencing experiments can approximate ground truth cellular dynamics. Using such data, we demonstrate the predictive accuracy of our proposed approach through benchmarking against the state-of-the-art methods. Through our drift-diffusion model, we can now distinguish, for the first time, between the deterministic and stochastic contributions to cell fate decision making. In doing so, we identify genes whose expression is associated with cellular drift and indeed show that they correspond to well-known markers of specific cell types; moreover, we identify genes that are associated with cell states that exhibit notable diffusion. Finally, we demonstrate the potential of such models to capture the essence of the dynamic processes through prediction on out-of-distribution data (referred to as “transfer learning” in the machine learning field). For example, when the model is trained on *in vitro* hematopoiesis data, our model is able to accurately predict cell trajectories in the corresponding *in vivo* mouse model. We anticipate that such insights will be useful in identifying key dynamic and time-dependent regulatory processes in normal development and cancer.

#5372
Supervised manifold learning and classification; application to expression data visualization and cancer prediction
James Webber, Kevin Elias. *Brigham and Women's Hospital, Boston, MA*

Background: Manifold Learning (ML) has become essential in recent years for expression data visualization and dimension reduction. ML operates under the assumption that the data points lie on a manifold embedded in Euclidean space. The goal of ML is to learn an inverse embedding function to decipher the manifold structure. Cancer classification is a widely investigated application of expression profile data (e.g., miRNA) currently in the literature. The non-linear ML techniques commonly applied to expression data, such as *t*-distributed Stochastic Neighborhood Embedding (TSNE), Isomap, and Locally Linear Embedding (LLE), are intended for visualization, and cannot easily be applied to classification or unseen data, more generally. Such methods are also unsupervised, and do not factor in class information. Conventional linear ML methods, such as Principal Component Analysis (PCA), while applicable to unseen data and easy to use, are limited and can learn only linear manifolds.

Results: We introduce a novel, non-linear ML technique, which incorporates class memberships, and is readily applicable to unseen data and classification. Specifically, we construct a series of neighborhood graphs which describe the manifold structure locally within each cluster and among the cluster centroids. Our objective function uses the neighborhood graph information to preserve the class separations and manifold structure in reduced dimension space, and we train a neural network to learn an explicit, inverse embedding function. This allows for fast visualization and classification of unseen data. The technique is compared against similar methods from the literature which use neural networks for ML, and is shown to offer improved cancer classification performance on expression data from The Cancer Genome Atlas (TCGA) and The Cancer Proteome Atlas (TCPA).
Conclusion: We present a new, supervised ML technique designed specifically for classification, which can be efficiently applied to unseen data. The results show promise on multiple, large-scale expression data sets, and thus warrant further research into supervised ML methods for cancer classification and expression data visualization.

#5373

Autoencoder-based multimodal prediction of survival for non-small cell lung cancer

Jacob G. Ellen[1], Etai Jacob[2], Nikos Nikolaou[2], Natasha Markuzon[2]. *[1]University College London, London, United Kingdom,[2]AstraZeneca Oncology, Waltham, MA*

Most non-small cell lung cancer (NSCLC) prognosis prediction approaches use one data type and do not take advantage of the large amount of multimodal data available. To evaluate and explore the benefits of multimodal data integration, we present a combined feature selection and denoising autoencoder pipeline for NSCLC survival prediction and survival subtype identification using microRNA (miRNA), mRNA, DNA methylation, long non-coding RNA (lncRNA) and clinical data. Survival performance for both lung adenocarcinoma (LUAD) and squamous cell carcinoma (LUSC) patients was compared across modality combinations, data integration time and training data types. Multimodal data combinations outperformed single data modalities, with the early integration of all data modalities achieving concordance indexes (C-indexes) of 0.67 (±.04) and 0.63 (±.02) for LUAD and LUSC, respectively versus corresponding C-index of 0.64 (±.02) and 0.59 (±.03) for the best single cell modality (clinical). Notably, combining just lncRNA and clinical data facilitated effective survival discrimination, with C-indexes of 0.69 (±.03) for LUAD and 0.62 (±.03) for LUSC. Overall, higher performance was achieved by using a single denoising autoencoder for all biological data (early integration) and by training on both LUSC and LUAD patient data together. Two survival subtypes (log rank test p-value=1e-9) were identified, with 991 differentially expressed transcripts in the poorer survival group. Our analysis shows the value of multimodal data integration for predicting NSCLC progression, with especially good performance using the combination of lncRNA and clinical data. Early integration of biological data, with an initial linear feature selection technique and a denoising autoencoder for dimensionality reduction, showed effective survival performance and survival subtype identification. Further research is underway to expand analysis to different cancer types and data modalities and extract more biological interpretability from autoencoder models.

#5374

Why only focus on the tumor?: The crucial role of the extra-tumor environment to predict poor responders for locally advanced rectal cancer

Rumi Shin[1], Byunho Jo[1], Inyeop Jang[1], Cheong-Il Shin[2], Jin Sun Choi[3], Seung-Yong Jeong[3], Seung Chul Heo[3], Ji Won Park[3], Min Jung Kim[3], Tae Hyun Hwang[1]. *[1]Department of Artificial*

Intelligence and Informatics, Mayo Clinic, Jacksonville, FL,[2]Department of Radiology, Seoul National University College of Medicine, Seoul, Korea, Republic of,[3]Department of Surgery, Seoul National University College of Medicine, Seoul, Korea, Republic of

Introduction As total neoadjuvant therapy for locally advanced rectal cancer (LARC) emerged, the possibility of skipping radiotherapy for poorly responsive patients arose. Machine-learning algorithms have focused on the radiopathologic features of tumor segmentation in order to predict responsiveness to radiotherapy. However, in addition to the tumor itself, there are several factors related to responsiveness, such as vasculature affecting hypoxia or MRI-detected extramural vascular invasion status. We aimed to predict poor responders using pretreatment rectal MRI images without segmentation and to identify which factors mainly contribute to the prediction algorithm.
Methods Between Jan 1, 2000, and Dec 30, 2020, 689 consecutive patients were retrospectively included in two hospitals. Poor responders were defined by tumor regression grades (TRG) 2 and 3 that were determined through surgical resection. The ResNet-50 model was trained to predict poor responders from pretreatment rectal MRIs (T2-weighted axial, sagittal, and coronal images). We adopted a tenfold cross-validation for training and testing the model and used Gradient-weighted Class Activation Mapping (Grad-CAM) to highlight the important regions in the MRI scans that help predict poor responders.
Results The number in each group of TRG was 108 (15.7%), 250 (36.3%), 265 (38.5%), and 66 (9.6%) for TRG0, TRG1, TRG2, and TRG3, respectively. There were 618 patients in the training cohort and 71 patients in the validation cohort. In the training and validation cohort, the accuracy for the prediction of poor responders was 85.6% (area under the curve (AUC) 0.856 [95% CI 0.761-0.950]) and 70.2% (AUC 0.703 [0.682-0.724]), although without segmentation. Our prediction model achieved a sensitivity of 0.724 (95% CI 0.700-0.748), a specificity of 0.684 (0.658-0.710), a positive predictive value of 0.697 (0.656-0.737), and a negative predictive value of 0.708 (0.666-0.751) in the validation cohort. Grad-CAM showed that the most important part of the accurately predicted images to contribute to the prediction was not the tumor (7/355, 1.9%) but the pelvic vasculature (353/355, 99.4%), including iliac vessels, femoral vessels, and presacral plexus, and followed by the mesorectum (38/355, 10.7%).
Conclusion The pelvic vasculature contributes more to predicting poor responders to radiotherapy than the tumor itself. Therefore, when creating a prediction model for responsiveness to radiotherapy in LARC, this should be considered.

#5375
Learned phenotypic embeddings enable scalable imputation of high-content molecular data elucidating prognostic chromatin signatures
Christopher S. Probert, Zachary R. McCaw, Navami Jain, Daphne Koller. *Insitro, South San Francisco, CA*

Emerging high-content data modalities like functional genomics and spatial proteomics have enormous potential to reveal determinants of phenotypic plasticity that underlie variability in clinical outcomes, but to date these modalities are only collected in modestly sized research cohorts (< 200-400 patients), where we lack power to detect subtype-specific or prognostic signatures.
To study intertumor heterogeneity on a much larger scale (>10,000 patients), we developed a machine learning framework based on self-supervised embeddings that allows scalable imputation of high-content data on large standard of care datasets. Our framework starts by learning a phenotypic embedding of tumor state based solely on H&E histology images, allowing the

embedding to be trained on large patient cohorts regardless of availability of molecular covariates. It then learns to predict genomic or proteomic labels from the lower-dimensional phenotypic embeddings. This model can be used for imputation in much larger cohorts, where only clinical outcome and histology are available.
To demonstrate our method, we use the TCGA ATAC-seq data, which is available for 400 patients across 23 cancer types. By learning self-supervised embeddings of histology, our framework was able to impute ATAC-seq for 5,000 peaks in 11,000 patients across 31 cancer types, with high accuracy in held out samples (R2 = 0.61). To our knowledge, this represents the broadest available pan-cancer chromatin landscape.
The imputed ATAC-seq reveals a subset of peaks that are significantly associated with overall survival (OS) in multiple cancer types (e.g., Breast (BC) ATAC-only HR 1.75, p: 8.6E-3). Genes proximal to these peaks are strongly enriched for well characterized oncogenes, and also several novel genes with functions in cellular metabolism and chromatin remodeling whose expression is not known to be prognostic in our disease settings.
Finally, we developed models to predict OS from H&E slide embeddings and from imputed ATAC-seq, both pan-cancer and in specific tumor types. Both models significantly outperform baseline stage and molecular subtype clinical risk predictors (e.g., BC baseline HR: 2.44, p: 3E-6 vs. embedding/imputed ATAC HR 3.78, 2E-9, p for improvement 2E-9) and, interestingly, we find that adding an ATAC-seq based risk score to an embedding-based risk score significantly improves disease-specific survival prediction (HCC embedding-only HR: 2.13, p: 8E-5 vs. HCC embedding/imputed ATAC HR: 2.65, p: 1E-6). This suggests that histopathology images are a rich source of prognostic information beyond that which is captured by traditional pathologist grading. Overall, our work highlights the ability to use self-supervised embeddings of histopathology to impute biological covariates on large, standard-of-care cohorts, empowering novel insights into disease mechanisms and patient outcome.

#5376

Protein structure-based modeling to improve MHC class I epitope predictions

Eric A. Wilson[1], John Kevin Cava[2], Diego Chowell[1], Abhishek Singharoy[3], Karen S. Anderson[4].
[1]Precision Immunology Institute, Icahn School of Medicine at Mount Sinai, New York City, NY,[2]School of Computing and Augmented Intelligence, Arizona State University, Tempe, AZ,[3]School of Molecular Sciences, Arizona State University, Tempe, AZ,[4]School of Life Sciences, Arizona State University, Tempe, AZ

The ability to accurately identify peptide ligands for a given major histocompatibility complex class I (MHC-I) molecule has immense value for targeted anticancer therapeutics. However, the highly polymorphic nature of the MHC-I protein makes universal prediction of peptide ligands challenging due to lack of experimental data describing most MHC-I variants. To address this challenge, we have developed a deep convolutional neural network, HLA-Inception, capable of predicting MHC-I peptide binding motifs using electrostatic properties of the MHC-I binding pocket. By approaching this immunological issue using molecular biophysics, we measure the impact of sidechain arrangement and topology on peptide binding, feature not captured by sequence-based MHC-I prediction methods. Through a combination of molecular modeling and simulation, 5821 MHC-I alleles were modeled, providing extensive coverage across human populations. Predicted peptide binding motifs fell into distinct clusters, each defined with different degrees of submotif heterogeneity. Peptide binding scores generated by HLA-Inception are strongly correlated with quantitative MHC-I binding data, indicating predicted peptides can be ranked, both within and between alleles. HLA-inception also showed high precision when predicting naturally

presented peptides and can be used for rapid proteome-scale MHC-I peptide binding predictions. Finally, we show that the binding pocket diversity measured by HLA inception predicts response to checkpoint blockade.

#5377

An integrative prognostic machine learning model in mantle cell lymphoma

Holly A. Hill[1], Preetesh Jain[2], Michael L. Wang[2], Ken Chen[1]. *[1]Bioinformatics and Computational Biology, UT MD Anderson Cancer Center, Houston, TX,[2]Lymphoma and Myeloma, UT MD Anderson Cancer Center, Houston, TX*

Background: Mantle cell lymphoma (MCL) is an uncommon B-cell lymphoma. The clinical course is highly variable: some patients have aggressive disease and relapse after treatment, while others have indolent disease or respond exceptionally to frontline therapy. Prognostication of MCL patients is dynamic and continues to evolve as novel therapies develop. Current prognostic indicators, such as the MCL international prognostic index (MIPI), were primarily designed with patients treated with chemo-immunotherapies. Using machine learning (ML) and molecular data, we provide a novel predictive method to improve upon conventional clinical markers.
Methods: We studied 785 MCL patients diagnosed at MD Anderson since 2014 and retrospectively classified them as “aggressive MCL” (n=311): relapsed or refractory to frontline treatment, and “mild MCL” (n=474): those who did not relapse after the first treatment (exceptional response) or had indolent disease never requiring treatment. After data extraction and feature engineering, 195 baseline features comprised of clinical, genomic, pathology, and cytogenetic data were integrated into an extreme gradient-boosted ensemble ML model (XGBoost). The dataset containing all patients was split (75/25) into a training and test set. Hyperparameters for the model were tuned using a grid-based, space-filling (Latin hypercube) technique and resampled 10-fold cross-validation from the training set. Training, validation, and testing sets were split using stratification of the classification variable to avoid class imbalance.
Results: Our integrative model achieved area under the curve (AUC) = .82 and accuracy = .76 on the test set and outperformed an XGBoost model using only clinical features (AUC = .78, accuracy = .68). Additionally, the fully integrated model improved on metrics from a similar multivariate logistic model including all patients (AUC = .72, accuracy =.72). Univariate logistic models were fit on the classification variable using the MIPI and other prognostic indices. The integrated ML model significantly outperformed the MIPI (AUC = .62, accuracy = .60) and other indices in predicting patient class. Clinical, pathological, cytogenetic, and genomic data were all represented as impactful features in a variable importance plot (VIP) and Shapley (SHAP) additive values of the fully integrated ML model. This model was used to launch a rest application programming interface (API) in which important features could be entered and a prediction returned.
Conclusion: Our study demonstrates that the current paradigm of using limited features in disease prognostics should be replaced with more advanced ML models that utilize genomic and other molecular data. Future work will include expanding the features included in the model and using the rest API to construct a graphical user interface accessible to clinicians and other researchers to make treatment decisions in precision oncology.

#5379

Deep learning enables label-free tracking of heterogeneous subpopulations

Tyler Jost, Andrea Gardner, Amy Brock. *University of Texas at Austin, Austin, TX*

Observing and quantifying the proliferation of subpopulations in cancer is key to understanding how heterogeneous groups of cells interact and respond to therapy, their environment, and each other. Prior research has demonstrated that cell-state properties such as metastatic potential and genotype perturbation are encoded in cellular morphology and can be identified with various machine-learning approaches. This encoding spans multiple imaging modalities such as brightfield, phase contrast, and stained whole-slide images, and phenotype prediction can be accomplished using both classical and deep machine learning methods. Here we show that not only do these prediction capabilities extend to transcriptomic subpopulations, but that they can be used to track these populations in high throughput longitudinal live-cell imaging experiments. Using single-cell RNA sequencing, we observed that, among untreated MDA-MB-231 triple negative breast cancer cells, there exist two transcriptomically distinct populations of cells. Using fluorescence-activated cell sorting based on the differentially expressed surface marker ESAM, we isolated these subpopulations and fluorescently labeled them with mCherry or GFP depending on their transcriptomic cluster. Cells were then grown in monoculture or coculture and imaged every 4 hours at 20x resolution. To identify the associated transcriptomic cluster, we trained an instance segmentation algorithm, Mask R-CNN, to both segment and classify cells. We find that, despite being derived from the same cell line, these phenotypes can be predicted using phase contrast images alone. These results demonstrate that cellular phenotypes manifested by distinctive RNA expression signatures can now be surveilled in a high-throughput manner across multiple samples and conditions without further RNA sequencing or biomarker labeling. We anticipate that this methodology of high throughput tracking will be applicable to other heterogeneous subpopulations, such as isolated therapy-resistant or sensitive cells. Tracking transcriptomically distinct populations using only high-throughput imaging will increase the granularity of population analysis and enable more rapid assessment of cancer cell evolutionary dynamics.

#5380

Systematic evaluation and comparison of drug response prediction models: a case study of prediction generalization across cell lines datasets

Alexander Partin[1], Thomas S. Brettin[1], Yitan Zhu[1], Jamie Overbeek[1], Oleksandr Narykov[1], Priyanka Vasanthakumari[1], Austin Clyde[1], Sara E. Jones[2], Satishkumar Ranganathan Ganakammal[2], Justin M. Wozniak[1], Andreas Wilke[1], Jamaludin Mohd-Yusof[3], Michael R. Weil[2], Alexander T. Pearson[4], Rick L. Stevens[1]. *[1]Argonne National Laboratory, Lemont, IL,[2]Frederick National Laboratory for Cancer Research, Frederick, MD,[3]Los Alamos National Laboratory, Los Alamos, NM,[4]Hematology/Oncology, Department of Medicine, University of Chicago, Chicago, IL*

Predictive modeling holds great promise for improving personalized cancer treatment and efficiency of drug development. In recent years**,** deep learning (DL) has been extensively explored for drug response prediction (DRP), outperforming classical machine learning in prediction generalization to new data. Despite the considerable interest in DRP, no agreed-upon methodology for evaluating and comparing the diverse DL models yet exists. Existing papers generally demonstrate the performance of proposed models using cross-validation within a single cell line dataset and compare with baseline models of their choice, substantially limiting the scope and validity of model evaluation and comparison. In this work, we investigate the ability of DRP models for generalizing predictions across datasets of multiple drug screening studies, a more challenging scenario mimicking practical applications of DRP models. Five cell line datasets and six community DRP models with advanced DL architectures have been explored.
Public cell line drug screening datasets have been curated and processed for this analysis, including CCLE, CTRP, GDSC1, GDSC2, and GCSI. For each dataset, the same preprocessing pipeline was

used to generate cell line gene expressions, drug representations, and drug response values. The six DRP models include advanced architectures and feature engineering methods such as transformer, graph neural network, and image representation of tabular data. Systematic model curation and training have been applied, including consistent training and testing data splits across models and hyperparameter optimization (HPO). To cope with the large-scale model training and HPO, automatic workflows have been implemented and executed on high-performance computing systems.
A 5-by-5 matrix of prediction scores, corresponding to the five datasets in both row and column dimensions, has been generated for each model, with off-diagonal values representing the cross-dataset generalization. Despite the advanced DL techniques, all models exhibit substantially inferior performance in cross-dataset analysis as compared with cross-validation within a single dataset.
This result demonstrates the challenge of cross-dataset generalization for DRP and motivates the need for rigorous and systematic evaluation of DRP models, which simulates real-world applications.

#5381

A broad-use deep learning model based on multi-dimensional morphology to identify and characterize tumor cell heterogeneity

Emilie C. Schneider, Stephane C. Boutet, Anastasia Mavropoulos, Andreja Jovic, Jeanette Mei, Nianzhen Li, Kiran Saini, Senzeyu Zhang, Chassidy Johnson, Vivian Lu, Ryan Carelli, Kevin B. Jacobs, Mahyar Salek, Maddison Masaeli. *Deepcell Inc., Menlo Park, CA*

Technological advances have ushered in a new multi-omics era that has elucidated more granular information on cell types and functions at single-cell resolution. Integrating morphology as a multi-dimensional readout of cell identity, state, and function is an area of broad interest, since it has been historically difficult to quantify morphological properties. Here, we apply artificial intelligence (AI) and multi-dimensional morphology to characterize a variety of human cell types and states using the Deepcell platform. Captured brightfield images of cells flowing inside a microfluidic channel are analyzed by AI models in real-time and cells of interest can be sorted for downstream molecular or functional analyses.
We developed an AI model, termed ‘Human Foundation Model’ (HFM), for broad use that combines machine learning with computer vision for multi-dimensional morphology analysis to provide interpretable features on a broad range of human cells and diverse sample types. The HFM training and validation datasets, comprising 1.18 million and 4.05 million cell images, respectively, were chosen to capture a comprehensive range of visual features and cover a wide spectrum of biological diversity. Samples included 6μm polystyrene beads (as controls) and multiple immune and carcinoma cell lines. Subsets of these images were labeled for specific cell features then included in the supervised portion of the model training.
We apply the HFM as part of the Deepcell system to identify and characterize the morphological heterogeneity of tumor cells in different types of cancers such as melanoma, non-small cell lung carcinoma, and malignant pleural effusions. We further demonstrate the ability of the platform to distinguish different cell types (epithelial, stromal, immune, and endothelial cells) commonly found in tumors that typically require complex antibody panels.
With the Deepcell platform and the HFM, we determined cell identities using morphological features associated with distinct processes characterized by granules, vesicles, cell size, pigmentation and others. Furthermore, sorted cells of interest are unlabeled and can be retrieved for

further analysis. This AI-powered technology can be applied to diverse areas including drug screenings/mechanism of action, tumor biology, and functional genomics.

Artificial Intelligence and Machine/Deep Learning 2

#5387

Discovery of plasma protein biomarkers associated with overall survival in R/R DLBCL patients treated with loncastuximab tesirine

Francesco Vallania[1], Victoria Cheung[1], Anupriya Tripathi[1], Maggie Louie[1], Thomas Snyder[1], Jimmy Lin[1], Karin Havenith[2], Yajuan Qin[2], Serafino Pantano[2], Jens Wuerthner[2], Patrick H. van Berkel[2]. *[1]Freenome, Inc., South San Francisco, CA,[2]ADC Therapeutics SA, Epalinges, Switzerland*

Plasma proteomics is a non-invasive source of potential biomarkers associated with cancer treatment outcomes, including disease progression and overall survival (OS). Loncastuximab tesirine (lonca) is an antibody-drug conjugate, composed of a humanized anti-CD19 antibody conjugated to a pyrrolobenzodiazepine dimer cytotoxin, for the treatment of relapsed/refractory (R/R) diffuse large B-cell lymphoma (DLBCL). Here, we investigated the association of plasma protein biomarkers with OS of R/R DLBCL patients prior to treatment with lonca (phase 2 trial, NCT3589469, LOTIS-2).Abundances of 888 plasma proteins, including inflammation, cancer and DNA repair associated markers, were measured for 69 patients with R/R DLBCL from plasma samples collected at baseline. Protein markers predictive of OS were selected using a L1 regularized Cox proportional hazards model (CoxPH) incorporating survival time and censoring status. Protein modules associated with OS were discovered by performing principal component analysis (PCA) on scaled protein abundances. Gene Set Enrichment Analysis (GSEA) was performed using Molecular Signatures Database (MSigDB) sets. We initially applied a regularized COX proportional hazards model to our proteomics dataset to identify proteins associated with OS, which revealed 5 protein markers (associated with decreased survival = REG3A, LAP3; associated with increased survival = NPTXR, C1QTNF1, FLT3) which stratified patients into distinct survival groups (p = 2.3e-4). As a complement to this approach and to extend our biological understanding of this cohort, we then applied PCA to the proteomics data to reveal underlying protein modules associated with survival. Our analysis identified principal component 3 (PC3) to have the strongest association to OS (rho= -0.63, FDR = 8.7e-07); with its top loadings consisting of known markers of cancer progression (top 3 proteins: SIGLEC10, IL6, TNFRSF6B). GSEA on PC3 loadings identified 68 significantly enriched gene sets (FDR < 5%). Gene sets reflective of changes in immune activation, increased cytokine activity and interleukin mediated activation (IL6, IL10) were negatively associated with OS, including activation of the following Hallmark pathways: IL6/JAK/STAT3 signaling and inflammatory response pathways.Overall, our results identify proteomics markers associated with DLBCL survival upon treatment with lonca, highlighting the potential of plasma proteins as a source of relevant biomarkers pending additional validation. [FV and VC contributed equally to this work]

#5388

A unified computational pathology method to quantify HER2 expression from raw IHC and IF images in breast cancer

Nicolas Brieu[1], Joshua Z. Drago[2], Ansh Kapil[1], Zonera Hassan[1], Anatoliy Shumilov[1], Claire Myers[3], Fatemeh Derakhshan[2], Fresia Pareja[4], Fanni Ratzon[2], Dana Ross[4], Jorge Reis-Filho[4], Thomas Padel[1], Andreas Spitzmuller[1], Christian C. Sachs[1], Felix Fegerer[1], Sihem Khelifa[1], J. Carl Barrett[5], Günter Schmidt[1], Hadassah Sade[1], Mark Gustavson[3], Sarat Chandarlapaty[6]. *[1]AstraZeneca*

Computational Pathology, Munich, Germany,[2]Memorial Sloan Kettering Cancer Center, New York, NY,[3]AstraZeneca Pharmaceuticals LP, Gaithersburg, MD,[4]Pathology, Memorial Sloan Kettering Cancer Center, New York, NY,[5]AstraZeneca Pharmaceuticals LP, Waltham, MA,[6]Medecine, Memorial Sloan Kettering Cancer Center, New York, NY

Background**:** The development of automated quantitative methods to measure biomarker expression such as HER2 aims at reducing the subjective variability of pathologist-performed biomarker assessment of immunohistochemically (IHC) stained tissue slides. As an example, the deep learning-based Quantitative Continuous Scoring (QCS) algorithm [1] enables the objective measurement of biomarker expression based on the detection of individual tumor cells in the tumor regions and - for each cell, on the instance segmentation of its nucleus, cytoplasm, and membrane compartments.
Methods: In order to extend the QCS image analysis to similarly analyze tissue slides stained with immunofluorescence (IF), we re-trained the fully supervised deep-learning models, adjusted the normalization of images on tissue controls to account for variability between different staining batches, and finally used the normalized signal in IF instead of the Optical Density (OD) signal in IHC as a 8-bit grayscale image on which the biomarker expression is estimated. We performed QCS on HER2 IF images (HER2 clone 29D8 [CST], imaged with Vectra [Akoya] in parallel with HER2 IHC clone 4B5 [Roche Tissue Diagnostics]) performed on 26 primary and metastatic breast cancer samples representing the full range of HER2 expression, from null to highly overexpressed.
Results: Our analysis demonstrated that the QCS-based scoring on IHC-HER2 images correlates with the QCS-based scoring on IF-HER2 images. We observed a Pearson correlation of R=0.92 between the median membrane OD in IHC and the median normalized membrane signal in IF. Defining a positive cell as having an estimated membrane expression higher than a given so-called positivity threshold, we found a median Pearson correlation of R=0.85 between the percentage of positive cells detected in IHC and the percentage of positive cells detected in IF for increasing values of positivity thresholds. Correlation of the QCS median normalized membrane signal in IF was R=0.91 with mRNA (ERBB2 transcript levels [Nano String]) and R=0.88 with IHC-based H-scores, against R=0.83 and R=0.87 respectively for the QCS median membrane OD signal in IHC.
Conclusion: We describe the extension of a computational pathology-based approach for biomarker quantification in IHC to IF stained tissue slides. The consistency of the image analysis method translates into the consistency of the measurements in the two imaging methods. The use of IF could enable the improved quantification of expression, co-localization and spatial distribution of multiple proteins on the tissue sample.
References: [1] Gustavson et al., abstract PD6-01, Cancer Research *81*, PD6-01, 2021

#5389

Micron-resolution spatial analysis near the tumor-stromal border reveals a distinct density distribution of tumor-infiltrating lymphocytes and related genomic features

Sanghoon Song[1], Gahee Park[1], Sukjun Kim[1], Sangjoon Choi[2], Seokhwi Kim[3], Wonkyung Jung[1], Mingu Kang[1], Mohammad Mostafavi[1], Heon Song[1], Aaron Valero[1], Sérgio Pereira[1], Donggeun Yoo[1], Seulki Kim[1], Seunghwan Shin[1], Ken Nesmith[1], Chan-Young Ock[1]. *[1]Lunit, Seoul, Korea, Republic of,[2]Department of Pathology and Translational Genomics, Samsung Medical Center, Sungkyunkwan University School of Medicine, Seoul, Korea, Republic of,[3]Ajou University School of Medicine, Suwon, Korea, Republic of*

Tumor-infiltrating lymphocytes (TILs) play a major role in predicting response to immunotherapy in solid tumors. However, few studies have analyzed TIL distribution and associated genomic

signatures based on proximity to the tumor-stromal border (TSB). Here, we describe TIL density, *IFN-γ* signature, and tumor mutational burden (TMB), according to set distances from the TSB, in The Cancer Genome Atlas (TCGA) pan-carcinoma dataset. For spatial TIL analysis, we used Lunit SCOPE IO, an AI-powered H&E whole-slide image analyzer, which identifies and quantifies tumor and lymphocyte cells within cancer or stroma area. In TCGA pan-carcinoma (n=7,468) dataset, the median values of cancer area and cancer stroma were 46.8 (interquartile range [IQR] 21.6-87.0) and 26.6 (IQR 10.9-54.5) mm^2, respectively, and those of TIL density in each area were 72.1 (IQR 34.1-160.1) and 747.2 (IQR 330.4-1575.9) /mm^2, showing 10-fold enrichment in stromal TIL (sTIL) compared to intratumoral TIL (iTIL). Subdividing the cancer area in 10 micron-wide steps from the TSB toward the tumor core, the median proportions of 0-10, 10-20, 20-30 (IT 0-10, IT 10-20, IT 20-30), and greater than 30 microns (IT 30-core) were 17.7%, 20.8%, 13.6%, and 47.9%, respectively. For subdividing the cancer stroma outwards from the TSB, the median proportions of 0-10, 10-20, 20-30 (ST 0-10, ST 10-20, ST 20-30), and greater than 30 microns (ST 30-outside) were 13.6%, 19.4%, 13.5%, and 53.5%, respectively. From the tumor core to TSB, median values of TIL density were 53.4 (IT 30-core), 59.3 (IT 20-30), 69.3 (IT 10-20), 127.4 (IT 0-10) /mm^2, respectively. From the TSB to the remaining stroma, median values of TIL density were 98.7 (ST 0-10), 567.6 (ST 10-20), 708.8 (ST 20-30), and 896.1 (ST 30-outside) /mm^2, respectively. Hence, the density of TIL generally increased from the tumor core to the outside of cancer stroma. Of note, *IFN-γ* signature showed the highest level of correlation with TIL density in IT 10-20 (Spearman's rho [ρ] 0.5146) or IT 0-10 (ρ 0.5143), compared with other subdivided cancer areas (ρ 0.4567-0.4924), and cancer stromas (ρ 0.1454-0.4529). However, TMB was highly correlated with TIL density in ST 20-30 (ρ 0.3162) or ST 30-outside (ρ 0.3278), compared with other subdivided cancer stromas (ρ 0.0588-0.2843) and cancer areas (ρ 0.0784-0.1208). In conclusion, AI-powered analysis of the tumor micro-environment reveals that iTIL density increases from the tumor core to the outside of tumor-stromal border. *IFN-γ* signature is high in the area of the tumor-stromal border on the tumor side, while tumor mutational burden is associated with sTIL far from the tumor-stromal border.

#5390

Robust prediction of pan-cancer immune checkpoint blockade response using machine learning

Tiangen Chang[1], Saugato R. Dhruba[1], Yingying Cao[1], Luc G. T. Morris[2], Eytan Ruppin[1]. *[1]NIH-NCI, Bethesda, MD,[2]Memorial Sloan Kettering Cancer, New York, NY*

Immune checkpoint blockade (ICB) has revolutionized our approach to cancer treatment. However, the response rate is still low. With the accumulation of data, efforts to use these data to build machine learning predictors of ICB response are rising. However, as most datasets are still quite small, pertaining machine learning models may often 'overfit' the data, i.e., have a much weaker performance on independent test data than on the data they were learned upon. Here we analyzed ~2000 patient samples from multiple cohorts across 16 solid tumor types. Based on 10 genomic & clinical features, we built different machine learning models, comparing their performance in terms of the Area Under ROC Curve (AUC) and importantly, in terms of the AUC difference between training vs validation sets, using a standard cross validation procedure. As a result, the Linear LASSO Regression (LLR) model outperformed all other models by having the highest AUC on the validation set (0.74) and notably, the smallest AUC difference between training and validation sets (0.02). In contrast, these two AUC values for the FDA approved tumor mutational burden (TMB) biomarker are 0.63 and 0.03. The highest predictive features were, receiving chemotherapy before ICB treatment or not, TMB, cancer type, blood albumin level, blood neutrophil-to-lymphocyte

ratio, and patient age. The LLR score also consistently predicted overall survival and progression-free survival across all individual cancer types. More importantly, ICB response probability increased near-monotonically from 0% to > 43% with the LLR score, which is an important feature for patient exclusion. In contrast, ICB response probability is ~25% when TMB = 0 and not always higher with higher TMB. In summary, the LLR model identifies key features predicting pan-cancer ICB response and survival. The use of combined genomic and clinical features holds potential to further facilitate clinical ICB patient stratification beyond TMB.

#5391

Machine learning of cancer type and tissue of origin from proteomes of 1,277 human tissue samples and 975 cancer cell lines

Zhaoxiang Cai[1], Zainab Noor[1], Adel T. Aref[1], Emma L. Boys[1], Dylan Xavier[1], Natasha Lucas[1], Steven G. Williams[1], Jennifer M. Koh[1], Rebecca C. Poulos[1], Peter G. Hains[1], Phillip J. Robinson[1], Rosemary Balleine[2], Roger R. Reddel[1], Qing Zhong[1]. *[1]ProCan, Children's Medical Research Institute (CMRI), Sydney, Australia,[2]The University of Sydney, Sydney, Australia*

Introduct**ion** Cancer type is determined through tumor morphology, aided by immunohistochemical staining. The development of machine learning (ML) models using histology slides has powered the image-based prediction of the site of origin in cancer of unknown primary (CUP). Here, we used ML on proteomic data to predict cancer types and tissue of origin from a sample cohort consisting of 1,277 human tissue samples spanning 44 cancer types. The training proteome datasets included two independent sets of proteomes acquired from a pan-cancer cell line collection and a subset of the tissue cohort for online ML.

Methods All samples were processed using data-independent acquisition mass spectrometry (DIA-MS). Two proteomic profiles from the pan-cancer cell line cohort were generated using two independent sample preparation methods. These were normalized by Combat and merged by averaging the protein abundance, yielding a single training set (D1) with 975 cell lines and 9,688 proteins. Similary, 1,277 tissue samples were processed by DIA-MS, quantifying 9,501 proteins. Celligner was used to align the cell lines (D1) with the tissue cohort. Half of the tissue proteomes were used as a second training set (D2) for online ML and a hold-out test set was constructed by taking the other half of the tissue cohort (T1). A multinomial logistic regression was used to predict cancer and tissue types. Top-k accuracy, as the evaluation metric, computes how often the correct cancer and tissue type class is among the top k classes predicted.

Results As a proof of concept, we defined six cancer types (adenocarcinoma, sarcoma, squamous carcinoma, lymphoma, melanoma and small cell carcinoma) and seven adenocarcinoma tissues of origin (breast, colorectal, liver, lung, ovary, stomach/esophagus and pancreas) for an ML experiment. We learned a classifier using the cell lines (D1) as the baseline training set, and consecutively added 10% of D2 to D1 for online ML. We tested the baseline model and each subsequent new model on the test set T1. We observed a monotonic performance increase from 0.89 (baseline; Top-1 accuracy) to 0.97 (all D2 were used) when predicting the six cancer types. We observed an analogous trend when predicting the seven tissue types (from 0.64 to 0.84). These results suggest that cancer cell lines can be used to predict cancer type and adenocarcinoma tissue of origin.

Conclusion Our proteomic-based ML model can predict cancer type and adenocarcinoma tissue of origin in concordance with existing histopathological classification. It can also assign multiple probabilities to tumor type and tissue of origin, potentially enabling the classification of CUP in future work. By adding tissue samples stepwise to the existing model, its predictive performance

can be further enhanced. This reflects a real-world knowledgebase that will continue to increase in predictive power as additional data are added.

#5392

Universal immunohistochemistry positivity classification of cancer cells across multiple cancer types and antibodies using artificial intelligence

Biagio Brattoli[1], Mohammad Mostafavi[1], Sangjoon Choi[2], Taebum Lee[3], Seokhwi Kim[4], Wonkyung Jung[1], Soo Ick Cho[1], Jinhee Lee[1], Keunhyung Chung[1], Jeongun Ryu[1], Seonwook Park[1], Sergio Pereira[1], Seunghwan Shin[1], Chan-Young Ock[1]. *[1]Oncology, Lunit, Seoul, Korea, Republic of,[2]Department of Pathology and Translational Genomics, Samsung Medical Center, Sungkyunkwan University School of Medicine, Seoul, Korea, Republic of,[3]Department of Pathology, Chonnam National University Hospital, Chonnam National University Medical School, Gwangju, Korea, Republic of,[4]Department of Pathology, Ajou University School of Medicine, Suwon, Korea, Republic of*

Background: Novel cancer therapeutic antibodies targeting tumor-specific antigens are in development. However, precise quantification of target protein expression on Tumor Cells (TC) from immunohistochemistry (IHC) is challenging. Here, we developed an artificial intelligence powered image analyzer, called Universal IHC (UIHC), which robustly detects and quantifies targets of interest expressed in multiple untrained cancer types and antibodies.
Methods: UIHC model can detect TCs and classify IHC positivity across many antibody-cancer pairs, called “domains”. UIHC is trained on four domains: lung cancer (569K/107K) (No. of negative TC / positive TC), bladder cancer (270K/116K), and breast cancer stained with PD-L1 22C3 pharmDx (270K/96K), and breast cancer stained with HER2 4B5 (307K/256K); all annotated by board-certified pathologists. For comparison, we developed four AI models using only a single domain (SD). All models were evaluated on hold-out test sets divided in three groups: “in-domain” included the four training domains; “near-out-domain” contained PD-L1 SP142 and SP263 on lung cancer; “far-out-domain” contained 7 antibodies on 15 cancer types.
Results: For cell detection, the harmonic means of the precision and recall (F1 score) averaged on TC- and TC+ (mF1), formatted as (UIHC; avg-SD [min, max]) were: “in-domain” (72.5%; 68.9% [67.1%-69.9%]), “near-out-domain” (64.8%; 61.6% [59.7%-65.2%]), and “far-out-domain” (70.3%; 62.5% [59.0%-65.9%]).
At image level, cutoffs at 1% and 50% of TPS are applied for PD-L1 22C3 and SP263, thus 3-way accuracy is computed*. In far-out-domain, the mean TPS per antibody is used as a cutoff.
UIHC outperforms SD on most antibodies (Table 1).
Conclusion: We demonstrated that a UIHC, built by merging multiple domains during development, can be effective on untrained domains. UIHC can be applied to novel targets in future clinical research with minimal or no adaptation needed.

Model performance of the proposed UIHC model and four SD models. *3-way acc 1%-50% TPS cutoff

Hold-out test-set				Cell detection performance **(mF1)**		Tumor Proportion Score (TPS) classification performance **(accuracy)**	
Test set group	**Staining(antibodies)**	**Cancer type**	**Number of**	**UIHC model**	**SD models Average [min-max]**	**UIHC model**	**SD models Average [min-max]**

			negative TC / positive TC				
In-domain test set	**PD-L1 22C3**	**Lung**	37716 / 13792	76.7%	71.5%* [65.6%-75.9%]	80.8%*	77.3%* [75.7%-78.7%]
Near-out-domaintest set	**PD-L1 SP263**	**Lung**	524 / 485	64.1%	64.0% [57.6%-72.6%]	80.0%*	72.5%* [60.0%-80.0%]
Far-out-domain test set	**TROP2**	**Pan-cancer**	1243 / 3289	78.9%	70.7% [63.7%-78.4%]	94.0%	87.8% [87%-90%]
	MET		3493 / 1134	80.5%	77.7% [75.1%-80.4%]	96.0%	96.0% [92.0%-100.0%]
	Claudin18.2		2927 / 74	72.7%	63.4% [55.1%-73.3%]	94.0%	93.8% [81.3%-100.0%]
	DLL3		2973 / 3	68.9%	42.5% [40.3%-43.8%]	100%	92.4% [87.5%-94.0%]
	HER3		2768 / 138	60.9%	54.2% [44.0%-71.3%]	94.0%	93.9% [87.5%-88.0%]
	FGFR2		2358 / 438	50.8%	58.9% [52.8%-58.9%]	81.0%	87.9% [87.5%-88.0%]
	Ecadherin		443 / 912	79.2%	74.6% [72.1%-76.7%]	90.0%	82.5% [80.0%-90.0%]

#5393

Comparison of deep learning approaches applied to hematoxylin and eosin-stained whole slide images from women with benign breast disease to predict risk of developing invasive breast cancer

Monjoy Saha[1], Mustapha Abubakar[1], Thomas E. Rohan[2], Ruth M. Pfeiffer[1], Máire A. Duggan[3], Kathryn Richert-Boe[4], Jonine D. Figueroa[5], Jonas S. Almeida[1], Gretchen L. Gierach[1]. *[1]Division of Cancer Epidemiology and Genetics, National Cancer Institute, National Institutes of Health, Rockville, MD,[2]Department of Epidemiology and Population Health, Albert Einstein College of Medicine, Bronx, NY,[3]Department of Pathology and Laboratory Medicine, University of Calgary,*

Calgary, AB, Canada,[4]Kaiser Permanente Center for Health Research, Vancouver, WA,[5]Usher Institute of Population Health Sciences and Informatics, The University of Edinburgh, Scotland, United Kingdom

Purpose: To compare deep learning (DL) approaches applied to hematoxylin and eosin (H&E)-stained whole slide images (WSIs) from women with benign breast disease (BBD) to predict risk of developing invasive breast cancer (BC).
Method: Two deep convolutional neural networks (CNNs) based on a customized 16-layer CNN (known as VGG-16 by Visual Geometry Group, University of Oxford) and an automated CNN (Google's AutoML) were trained using H&E-stained WSIs to identify distinct histological features on diagnostic BBD biopsies that characterize BBD patients who were (cases, n=347) and were not (controls, n=347) subsequently diagnosed with invasive BC. The CNNs consisted of multiple convolutions, max pooling, fully connected, etc., layers. To incorporate our data into the VGG network, we customized the network architecture and hyperparameters to enhance the classification performances. For AutoML, we used the system's default network with standard hyperparameters. The trained model was then tested on a held-out set of 140 patients (70 cases and 70 controls). The quantitative performance was evaluated using accuracy (ACC), sensitivity (SE), precision (PR), area under the receiver operating characteristic curve (AUROC), etc. For qualitative results, we generated heatmaps using weights and feature maps from the final convolution layer of our customized CNN. Heatmaps were superimposed onto original H&E images to highlight different unique features (such as pattern, texture, color, and morphology).
Results: We found both deep learning methods to demonstrate remarkable ability in predicting case-control status in the held-out set (AUROC= 90% and 89% for customized CNN and AutoML, respectively). However, our customized CNN outperformed AutoML in terms of ACC (83.57% (95% confidence interval (CI): 76-89%) vs 77.86% (95%CI: 70-84%), respectively); SE (82.85% (95%CI: 72-91%) vs 77.86% (95%CI: 70-84%), respectively); PR (84.05% (95%CI: 73-92%) vs 81.97% (95%CI: 70-91%), respectively); F1 score (83.45% (95%CI: 76-89%) vs 76.34% (95%CI: 68-83%), respectively); as well as error rates (0.16% (95%CI: 0.11-0.24%) vs 0.22% (95%CI: 0.16-0.30%), respectively). Heatmaps revealed specific stromal and epithelial features that were distinct between case and control images.
Conclusion: By using routinely available H&E-stained WSIs, we developed a customized CNN that outperformed AutoML in distinguishing future BC cases from controls in a BBD population. The qualitative results identified stromal and epithelial regions in the BBD biopsies that were highly predictive of being a case versus control and vice versa thereby providing etiologic clues into breast cancer development following BBD. Future research will focus on leveraging DL to better understand the histologic basis of BBD progression to invasive BC.

#5394
Detecting pulmonary malignancy against benign nodules using non-invasive cfDNA fragmentomics assay
Shun Xu[1], Ji Luo[1], Wanxiangfu Tang[2], Hua Bao[2], Jiajun Wang[1], Shuang Chang[2], Haimeng Tang[2], Zifang Zou[1], Xiaoxi Fan[1], Yang Liu[1], Changrui Jiang[1], Xue Wu[2], Yang Shao[2]. *[1]The Department of Thoracic Surgery, The First Hospital of China Medical University, Shenyang, China,[2]Nanjing Geneseeq Technology Inc., Nanjing, China*

Background: Early screening using Low-Dose Computed Tomography (LDCT) can reduce mortality by non-small-cell-lung cancer (NSCLC), which contributed the most cancer-related death worldwide. Yet ~25% of the "suspicious" nodules identified by LDCT are confirmed to be benign

through resection surgery, which adds to patients' discomfort and the burden of the healthcare system. In this prospective study, we set to develop a non-invasive liquid biopsy assay for distinguishing pulmonary malignancy from benign lung nodules using cfDNA fragmentomic profiling.
Methods: An independent training cohort, which consisted of 193 patients with malignant nodule and 44 patients with benign nodule, was used to construct a machine learning model. Base models employing 4 different fragmentomics profiles were optimized using an automated machine learning (autoML) approach before being ensemble stacked to create the final predictive model. An independent validation cohort included 96 malignant nodules and 22 benign nodules, as well as an external test cohort containing 58 malignant nodules and 41 benign nodules, were used to assess the performance of the ensemble stacked model.
Results: Our machine learning models showed excellent performances in detecting patients with malignant nodules. The AUCs reached 0.857 (0.782 - 0.932) and 0.860 (95% CI: 0.788 - 0.933) in the independent validation cohort and the external test cohort, respectively. The validation cohort achieved an excellent 68.2% specificity (95% CI: 45.1-86.1%) at the targeted 90% sensitivity (89.6%, 95% CI: 81.7-94.9%). An equivalently good performance was observed while applying the cutoff to the external cohort, which reached a specificity of 63.4% (95% CI: 46.9-77.9%) at 89.7% sensitivity (95% CI: 78.8-96.1%). Subgroup analysis for the independent validation cohort showed that the sensitivities for detecting various subgroups of nodule size (< 1cm: 91.7%; 1 - 3cm: 88.1%; > 3cm: 100%; Unknown: 100%) and smoking history (Yes: 88.2%; No: 89.9%) all remained high among the lung cancer group. Additionally, the specificities for successfully identifying the benign nodules among different subgroups decrease as the size increase (< 1cm: 80.0%, 1 - 3cm: 66.7%, > 3cm: 33.3%).
Conclusions: Our cfDNA fragmentomics assay can provide a non-invasive approach to distinguish malignant nodules from the radiographically suspicious but pathologically benign nodules.

#5395

Improving survival prediction using flexible late fusion machine learning framework for multi-omics data integration

Nikos Nikolaou[1], Domingo Salazar[2], Harish RaviPrakash[1], Miguel Goncalves[2], Gustavo Alonso Arango Argoty[1], Nikolay Burlutsky[2], Natasha Markuzon[1], Etai Jacob[1]. *[1]AstraZeneca Oncology, Waltham, MA,[2]AstraZeneca Oncology, Cambridge, United Kingdom*

Improving cancer patients Overall Survival (OS) prognosis is critical for personalization of treatment using model-identified drivers of cancer progression. Current cancer prognosis models largely rely on clinical and demographic patient characteristics. Adding 'omics'-based modalities can help improve patient OS prediction and lead to better disease categorization and understanding. We introduce a data driven methodology for combining multi-omics and clinical data, including clinical/demographics, mutations, gene expression, long non-coding and micro-RNA expression, DNA methylation, and proteomics for improving prediction of OS in cancer patients. High dimensionality of 'omics' modalities present challenges to combining them into one model. We propose a late stage modalities fusion where we construct a separate data driven model for OS prediction for each modality, later combining individual predictions in a final linear OS prediction model. With a limited number of patients to develop the model, such an approach helps to better protect against overfitting, and allows to account for different degrees of informativeness of modalities by weighting them according to individual success. We introduce a robust machine learning pipeline with rigorous training, testing and evaluation capabilities, and demonstrate its effectiveness on a suit of TCGA data. When comparing early vs. late fusion of omics and clinical

modalities for survival prediction using NSCLC TCGA data, we observe the C-index improvement from 0.57±.04 to 0.61±.01. Best individual modality performance was at 0.59±.02 using clinical modality. Dominant modalities in unimodal survival analysis varied between cancers, with clinical, RNA, and miRNA for LUAD, and clinical, RNA, and RPPA for LUSC. Using pan-cancer TCGA data for survival prediction, the best C-index = 0.77 was achieved using multi-omics model, followed by 0.76±.01 for clinical, 0.75±.01 for RNA seq, and 0.73±.01 for RPPA unimodal models.

#5396

Early detection of ovarian cancer using mRNA sample data to investigate the correlation of specific gene mutations with ovarian cancer

Zahra Saghaie, Christine Richardson, M. Taghi Mostafavi. *UNC Charlotte, Charlotte, NC*

Introduct**ion:** Ovarian cancer (OC) is the second most common gynecologic cancer in the U.S, and is the deadliest cancer of the female reproductive system. Because of the complex nature of OC, diagnoses are often by display of symptoms at late stages of disease. Identifying OC at early stages can increase the 5-year survival rate from 40% in stage IV to 94% in stage I. Therefore, effective screening and detection of OC at early stages is imperative. The main objective of this study is to develop a diagnostic panel of markers that correlate with early-stage OC, and ultimately, improve the survival rate of patients.

Background: Approaches in the past several years to detect malignant OC have focused on processing relevant images or screening genomic data. These studies use liquid-based biopsies, sonographic images, cyst images, CT images, MR imaging and genomics data. Some studies have focused on distinguishing malignant tumors versus benign tumor cells. In addition to statistical methods to examine available genomic datasets, Machine Learning models including K-Nearest Neighbor, K-means, Convolutional Neural Networks, Deep Learning, Support Vector Machine, Random Forest, and Fuzzy algorithms have been used.

Methods: In this study we proposed a method to determine a possible correlation between some actively expressed genes and OC, using publicly available mRNA data sets. The samples were retrieved from the GSE106817 dataset via the NCBI GEO site, with 333 cancerous and 2759 Non-cancerous samples. The objective is to define a set of genes which is able to illustrate prediction of correlation through the use of PCA, NMF and SVD. We further verified our findings by testing on one additional different mRNA datasets. For this, we compared several machine learning algorithms to potentially correlate active genes and OC stages, from the available data.

Results and Discussions: Through our study we have developed Machine Learning models valuable to identify patterns of disease at different stages, thus, potentially be useful in developing predictive models. Our initial experimental results have been demonstrated with a set of mRNA signatures, which may be used to create a panel of biomarkers valuable for detecting early-stage OC. Our results confirm the correlation between OC and PAX8, PEG3, and BIRC5, and MYB and RAC2. Continuation of this study highlights methods towards the early detection of OC and to improve disease identification outcome.

#5397

Prediction of conversion surgery completion following neoadjuvant modified FOLFIRINOX in borderline resectable and locally advanced pancreatic adenocarcinoma: machine learning algorithm analysis

Hyunseok Yoon[1], Kyu-Pyo Kim[2], Inkeun Park[2], Jae Ho Jeong[2], Heung-Moon Chang[2], Baek-Yeol Ryoo[2], Changhoon Yoo[2]. *[1]Department of Internal Medicine, Asan Medical Center, University of*

Ulsan College of Medicine, Seoul, Korea, Republic of,[2]Department of Oncology, Asan Medical Center, University of Ulsan College of Medicine, Seoul, Korea, Republic of

Background: Neoadjuvant modified (m) FOLFIRINOX is a standard therapy for medically fit patients with borderline resectable pancreatic cancer (BRPC) and locally advanced unresectable pancreatic cancer (LAPC). Completion of conversion surgery following mFOLFIRINOX is an important prognostic factor. In this study, we evaluated multiple machine learning models to predict completion of conversion surgery following neoadjuvant mFOLFIRINOX in BRPC and LAPC.
Methods: Between January 2017 and December 2020, a total of 647 patients with BRPC and LAPC treated with neoadjuvant mFOLFIRINOX at Asan Medical Center, Seoul, South Korea were enrolled. All demographic and clinicopathological data were retrospectively collected; age, ECOG performance status, BMI, resectability as per the NCCN guidelines, tumor location, tumor size, maximum standardized uptake value assessed by 18F-FDG PET/CT, number of cycles of mFOLFIRINOX, tumor response to mFOLFIRINOX, and serum CA 19-9. Several machine learning models, such as logistic regression and random forest classifier, were trained to predict curative-intent resection and were then internally validated. The relative importance of each variable was analyzed using both Gini importance and permutation importance.
Results: Among 647 patients, 173 (26.7%) underwent curative-intent conversion surgery (R0 or R1) following mFOLFIRINOX. The patients who underwent surgery showed significantly better overall survival (median 42.1 vs 17.2 months, P<0.0001) than those who did not. In multivariable analysis using logistic regression, age, resectability as per the NCCN guidelines, tumor size, number of cycles of mFOLFIRINOX, tumor response to mFOLFIRINOX, and CA 19-9 change rate (percentage change in CA 19-9 after mFOLFIRINOX) were significantly correlated to tumor removal with curative-intent conversion surgery. Random forest classifier showed the best predictive capability with AUC at 0.832. The most important feature was the CA 19-9 change rate.
Conclusions: In this large cohort-based analysis, completion of conversion surgery could be predicted successfully in BRPC and LAPC patients treated with neoadjuvant mFOLFIRINOX using machine learning models. Further external validation is necessary for generalization.

#5398

Optimization generator app (OpGen) for radiotherapy treatment planning using case-based reasoning

Reza Reiazi[1], Surendra Prajapati[1], Abdallah Sherif Radwan Mohamed[2], Clifton David Fuller[2], Mohammad Salehpour[1]. *[1]Radiation Physics, The University of Texas MD Anderson Cancer Center, Houston, TX,[2]Radiation Oncology, The University of Texas MD Anderson Cancer Center, Houston, TX*

Case-based reasoning (CBR) means adopting previous experiences (i.e, data from previous patients) to meet new demands (new patients). In this scenario, we developed an application named OpGen to generate optimization objective values for head and neck radiotherapy inverse treatment planning, using the previously treated patient with an acceptable outcome. OpGen will be helpful in radiotherapy treatment planning automation and efficiently reducing the required time to reach the target goals and improving the quality and safety of the treatment.OpGen has been developed in Python and has four main modules: 1- Analyzing radiotherapy treatment planning parameters of the previous patients in the database. We have developed (a) a powerful graphical user interface (GUI) that allows quantitative and qualitative analysis of the previous knowledge, including the type of frequently used objective parameter (Min Dose, Max Dose, Min DVH dose, etc.); (b) The

range of values used for each specific objective type, and (c) Histogram of the number of patients vs. values used for a specific objective type. 2- Importing patients from treatment planning and retrieving a user-defined number of treatment planning information from the previously treated patients in the database corresponding to the given patient using the user-defined quantitative features (geometrical, distance or geo-distance) and retrieval algorithms (k-Nearest Neighbor and Random Forest). 3- Generating optimization objective values based on the following available options: (a) The most similar patient in the database; (b)- Average or median value over the number of patients retrieved from the database; and (c) Deep learning generated values using a model trained over 100 similar cases retrieved from the database. 4- Generate a portable database of the objective values and patient geometric information for any inter- or intra-institutional usage of the algorithm. OpGen is compatible with RayStation (RaySearch Laboratories™) treatment planning and can retrieve, analyze and generate treatment planning optimization parameters in less than 3 minutes. OpGen can potentially increase the quality and safety of radiotherapy treatment planning by improving the efficiency of the optimization process.

#5399

Deep learning-based ensemble model using H&E images for the prediction of KRAS G12C mutations in non-small cell lung cancer

Sehhoon Park[1], Jongchan Park[2], Minuk Ma[2], Hyun-Ae Jung[1], Jong-Mu Sun[1], Yoon-La Choi[1], Jin Seok Ahn[1], Myung-Ju Ahn[1], Sanghoon Song[2], Gahee Park[2], Sukjun Kim[2], Huijeong Kim[2], Seunghwan Shin[2], Chan-Young Ock[2], Se-Hoon Lee[1]. *[1]Samsung Medical Center, Seoul, Korea, Republic of,[2]Lunit, Seoul, Korea, Republic of*

Background: As the KRAS G12C mutation became targetable in non-small cell lung cancer (NSCLC), tissue based KRAS mutation test is now an essential practice for the treatment decision. Recently, predicting KRAS mutations using deep-learning models with H&E images to potentially increase the pre-test probability has been reported with modest performance. Herein, we conducted a novel approach to improve the performance of KRAS G12C prediction based on an ensemble model trained not solely on H&E images, but also with multi-layered semantic content produced by a pre-trained artificial-intelligence (AI) analyzer, Lunit SCOPE IO.
Methods: The Cancer Genome Atlas LUAD and LUSC (TCGA-Lung) samples were used for model development. A self-supervised vision transformer was used to extract deep features from raw H&E images; and an AI-based pathology profiling analyzer extracted semantic contents such as the spatial information of tumor cells, lymphocytes, cancer epithelium, and cancer stroma. A set of classifiers was trained based on the two features, and the ensemble of these features was used to improve robustness. The final model was evaluated through cross-validation and assessed on independent NSCLC samples from Samsung Medical Center (SMC) who tested KRAS mutation by various methods including whole exome sequencing or target sequencing.
Results: TCGA-Lung dataset (n = 930) includes 150 (16.1%) KRAS driver mutations, and 62 (6.7%) KRAS G12C. The best cross-validation performances of the models predicting KRAS G12C, measured by mean area-under-the-curve (AUC), were 0.768 trained by only H&E images (HE-only), 0.714 by AI semantic content (AISC) with MLP classifier (AI-MLP), and 0.697 by AISC with random forest (AI-RF), respectively. An ensemble of the three models showed an increased AUC of 0.787 in TCGA-Lung by cross-validation. These models were applied to an independent SMC dataset (n = 363), including 54 (14.9%) KRAS driver mutations, and 22 (6.1%) KRAS G12C. The mean AUC to predict KRAS G12C by HE-only, AI-MLP, and AI-RF models were 0.599, 0.644, and 0.678, respectively, implying limited robustness. However, the AUC of an ensemble of the 3 models was 0.745 in the SMC dataset, showing 71.0% sensitivity and 72.7%

specificity. Similar results were observed regardless of the KRAS testing method (TruSight Oncology 500 panel; n = 249; AUC 0.787, other tests; n = 114; AUC 0.720), the tissue size (surgical resection; n = 138; AUC 0.724, biopsy n = 225; AUC 0.763), and histology (excluding squamous cell carcinoma, n = 286; AUC 0.697).
Conclusions: An AI-based ensemble model combining H&E images with semantic contents extracted from pre-developed AI model significantly improved the accuracy and the robustness of KRAS G12C mutation prediction using H&E sample in NSCLC.

#5400

Predicting disease progression in inoperable localized NSCLC patients using cfDNA fragmentomics assay

Yin Yang[1], Tao Zhang[1], Jingbo Wang[1], Jianyang Wang[1], Wanxiangfu Tang[2], Hua Bao[2], Haimeng Tang[2], Xue Wu[2], Yang Shao[2], Xin Wang[1], Yuqi Wu[1], Linfang Wu[1], Xin Xu[1], Kunpeng Xu[1], Jingjing Zhao[1], Luhua Wang[1], Nan Bi[1]. *[1]Department of Radiation Oncology, National Cancer Center/National Clinical Research Center for Cancer/Cancer Hospital, Chinese Academy of Medical Sciences and Peking Union Medical College, Beijing, China,[2]Nanjing Geneseeq Technology Inc., Nanjing, China*

Background: There is an urgent clinical need to accurately predict the risk for disease progression in post-treatment NSCLC patients. However, the current ctDNA mutation profiling approaches were limited by low sensitivity, while the cfDNA fragmentomics profiling has shown an excellent capability for cancer early detection in NSCLC and therefore exhibits great potential for predicting disease progression. In this retrospective study, we aim to develop a non-invasive liquid biopsy assay utilizing cfDNA fragmentomics profiling for predicting disease progression in inoperable localized NSCLC patients.
Methods: The study cohort retrospectively enrolled 44 patients diagnosed with inoperable localized NSCLC who received first-line chemoradiotherapy/radiotherapy (including 23 disease progression during follow-up). Plasma samples were collected during or post-treatments, including 39 at the fourth week of treatment (TP1), 33 and 25 at 1 (TP2) and 3 (TP3) months post-treatment, respectively. cfDNA fragmentomic profiling, generated based on target sequencing data, was used to fit Regularized Cox Regression models. For each time point, a leave-one-out cross-validation (LOOCV) was performed to evaluate the models' predictive performances, which was subsequently compared against the ctDNA status determined by the mutation-based method.
Results: Our cfDNA fragmentomics assay showed excellent performance detecting patients with a high risk for disease progression. At TP1, the high-risk patients detected by our model showed an increased risk of 3.62 times (hazard ratio [HR] = 3.62, $p = 0.0026$) for disease progression, compared to 3.91 times (HR = 3.91, $p = 0.0022$) and 4.00 times (HR = 4.00, $p = 0.019$) for TP2 and TP3, respectively. These fragmentomics determined HRs were higher compared to the ctDNA mutation-based results (HR = 2.08, $p = 0.074$; HR = 1.49, $p = 0.61$) at TP1 and TP3, albeit being lower at TP2 (HR = 9.47, $p < 0.0001$). At TP1, the predictive model reached 40% sensitivity at 92.9% specificity, which was higher than the mutation-based method (40% sensitivity at 78.6% specificity), while the combination of the two methods reached a higher sensitivity (60%). Finally, a subset of the cohort (N = 19) with data for all three time points (TP1, TP2 and TP3) was examined, and the patients were labelled as high-risk for having a positive prediction or ctDNA status at any time point. The combined methods could predict disease progression with an excellent sensitivity of 88.9% at 80% specificity.
Conclusions: We developed a cfDNA fragmentomics assay for predicting disease progression in inoperable NSCLC patients. This assay showed increased predicting power during and post

treatment compared to the ctDNA mutation-based method, thus illustrating a great clinical potential to guide treatment decisions in inoperable NSCLC patients.

#5401

Computational cancer cell gene expression deconvolution from tumor bulk RNA-seq via the machine learning algorithm Helenus

Valentina Beliaeva[1], Ekaterina Ivleva[2], Boris Shpak[2], Daniil Litvinov[2], Anastasia Zotova[2], Krystle Nomie[2], Daniiar Dyikanov[2], Alexander Kuznetsov[2], Maria Savchenko[2], Aleksandr Zaitsev[2], Nathan Fowler[1], Alexander Bagaev[1]. *[1]Bostongene, Corp., Waltham, MA,[2]BostonGene, Corp., Waltham, MA*

Background**:** Biomarker gene expression is becoming more commonly utilized for clinical decision-making in oncology clinical practice. However, complex tumor tissue comprises a population of cancer cells (CC) and the tumor microenvironment (TME), causing expression signals belonging to the CC and TME calculated from bulk RNA-seq of the tumor tissue to be indistinguishable. To circumvent this, Helenus, a gene expression deconvolution tool, was developed to estimate TME-specific gene expression, consequently, providing precise CC-specific gene expression.

Methods: Helenus performs the "subtraction" of TME gene expression from the total expression calculated from bulk RNA-seq of the tumor tissue. To accurately reconstruct the CC expression profile, LightGBM gene models were trained on artificial transcriptomes created from > 1,000 different solid tumor cancer cell lines and > 3,000 samples of various TME cellular proportions. The LighGBM gene models included genes expressed predominantly in the TME (e.g., *CD3E*), both the TME and the CC (e.g., *BCL6*), or in the CC (e.g., *HER2*). The input features included: 1) RNA percentages of TME cell types predicted by the cell deconvolution tool Kassandra (Zaitsev et al., 2022); 2) evaluation of TME target gene expression *via* the estimation of its weighted average expression profile in TME cell populations; and 3) a set of TME- and CC-specific genes. The resulting predictions were adjusted based on the CC cell fraction. To evaluate Helenus' performance, CC and TME RNA were mixed at different ratios using various cancer cell lines and peripheral blood-derived TME cell populations and suspensions of tumor cells prepared from cancer tissue across multiple tumor purity dilutions.

Results: Helenus deconvolution resulted in an increased concordance correlation value from 0.73 to 0.98 between the real gene expression profile of pure CC and the reconstructed CC expression from bulk RNA-seq. Helenus showed high concordance between the gene expression profile of sorted cancer cell lines and the deconvolved gene expression across a wide range of CC RNA concentrations (20-90%) mixed with imitated TME RNA at varying concentrations. Helenus demonstrated high performance calculating gene expression of multiple clinically relevant biomarkers in the TME:cancer cell line mixes: *CD274* (PD-L1) (mean absolute error [MAE] ~3.5-fold reduction); *HLA-A* (~2.8-fold MAE reduction); *MKI67* (Ki-67, ~2.2-fold MAE reduction), *ERBB2* (HER2, ~1.7-fold MAE reduction). Helenus deconvolved CC expression and found significant correlations with CC gene amplifications and deletions (e.g., *BCL-2*, *VNN3*) independent of tumor purity ($p < 0.003$).

Conclusion: Helenus, the CC gene expression deconvolution tool, was developed with high accuracy to contribute to tumor diagnosis, disease monitoring, treatment decisions, and clinically relevant biomarker identification.

#5402

Using computer vision to resolve proliferative dynamics within therapeutic responses in large scale screens of patient derived models

Madhavi Kannan, Brian Larsen, Chi-Sing Ho, Jagadish Venkataraman, Martin Stumpe, Ameen Salahudeen. *Tempus Labs, Chicago, IL*

IC50, Emax, and AUC values are commonly used to assess susceptibility for a given therapeutic candidate but are subject to the number of cell divisions for a given in vitro model. When comparing multiple in vitro models and especially patient-derived models such as patient-derived tumor organoids, the degree of intrinsic cell proliferation or doubling time substantially differs and therefore limits conventional metrics as above. Furthermore, assays that directly measure cellular viability can oftentimes overlook therapeutic agents that have cytostatic, versus cytotoxic mechanisms of action and require assays with similar sensitivity and precision to account for this phenotype. Finally, terminal endpoint assays can require tedious temporal optimization to capture the full dynamic range of a given therapeutic which makes cross-therapeutic and cross-model comparisons difficult to interpret. An assay that incorporates these multiple features and in vitro specific doubling time would lead to highly accurate measurements of drug effects and allow the calculation of growth-adjusted IC50 values i.e. GI50 values.

We, therefore, sought to develop a computer vision model that utilizes label-free longitudinal light microscopy images as input to report the total number of nuclei present within a given experimental well, allowing for the monitoring of cell division and any cytostatic effects. To train the neural network, we use Hoechst-stained images as our ground truth. The model used is an extension of the Regularized Conditional Adversarial Network (PMID: 34320344). It takes as input Brightfield images along with the registered Hoescht stained wells. The label for each well is obtained using commercial image processing software to count the total number of nuclei present in each well from the Hoescht stained channel. The model was trained to predict the virtually stained Hoescht well for every Brightfield, as well as the aggregate nuclei count for all organoids present inside the well. The model was trained on 29000 individual sites across 9 distinct cancer types.

Five experiments were conducted during training to test for bit depth and tonality effects of the input training data. Inference on 9240 images showed a pearsonR score of 0.81 on the best-performing model. Results show that the model performs well and can be applied in real-time using only experimental data to correct for differing cell division rates and measure cytostatic phenotypes all while using simple light microscopy. The tool will enable cross-comparison of different therapeutic MoAs as well as enable cross-cancer type/indication comparison for a therapeutic in development to inform early development clinical strategy.

#5403

Predicting cancer cell response to TEAD auto-palmitoylation inhibitor using bulk RNA-seq data and a random-forest based algorithm

Adam Kurkiewicz[1], Sebastian Y. Müller[1], Oliver Gibson[1], Sara Castellano[1], Germán Stark[1], Pol A. Vecino[1], Shuirong Zhou[2], Tracy T. Tang[3]. *[1]BioMage Ltd., Edinburgh, United Kingdom,[2]Bio-Research Innovation Center Suzhou, Suzhou, China,[3]Vivace Therapeutics, San Mateo, CA*

TEAD transcription factors are the major effectors of the Hippo-YAP/TAZ pathway essential in controlling organ size and maintaining tissue homeostasis. Upon coactivator YAP/TAZ binding, TEAD transcription factors are activated to induce expression of genes involved in cell proliferation and survival. It has been shown that auto-palmitoylation is required for TEAD interaction with YAP/TAZ and hence activation of transcriptional activity. Potent small molecule

TEAD auto-palmitoylation inhibitors have been reported (Tang *et al*, 2021, *Mol Cancer Ther*.). These TEAD inhibitors disrupt YAP/TAZ-TEAD protein interaction, suppress TEAD transcriptional activity, and selectively block proliferation of *NF2*-deficient mesothelioma *in vitro* and inhibit *NF2* mutant xenograft tumor growth *in vivo*. Although genetic alterations of pathway components (such as, *NF2*) leading to YAP/TAZ constitutive nuclear localization and TEAD activation have been reported in a variety of human malignancies, these alterations are infrequent in most cancers, and increased accumulation of nuclear YAP has been reported in cancers (e.g., hepatocellular carcinoma) that do not harbor pathway mutations. Utilizing *in vitro* efficacy data from cell line screens, gene expression (RNA-Seq) datasets, and a custom bioinformatics data-processing and normalization pipeline, we sought to elucidate gene expression patterns by using a random-forest based classifier. Our classifier, which aims to predict the response (efficacy) of treatment using normalized gene expression of selected genes, was originally trained on the public bulk RNA-seq pan-cancer *in vitro* dataset available in the Cancer Cell Line Encyclopedia (CCLE) from the Broad Institute, as well as a privately obtained TEADi response data for corresponding CCLE cell lines. Binary response labels (responder/non responder) for each cell line were obtained by thresholding efficacy measures. The classifier - evaluated using cross-validation - achieved an average AUC of 0.80. Then from our screen of 50 patient-derived Chinese liver cancer (CLC) cell models (Qiu *et al*, 2019, *Cancer Cell*), both as single agent and in combination with mTOR inhibitor everolimus, we found that TEAD inhibitors (TEADi) were efficacious in several of these liver cancer models. This allowed us to verify the classifier without any re-training on an independent dataset (CLC). In this independent validation scenario, the classifier achieved the AUC of 0.82. Having established efficacy of predictions on both *in vitro* datasets, we re-trained the classifier using both CCLE and CLC datasets as input to achieve maximum predictive performance, and we predicted, post-hoc, response status of 99 responders out of 2056 patient-derived xenograft models. The algorithm showed early promise by retrospectively classifying a model with *in vivo* efficacy as the most likely to respond.

#5404

Predicting protein receptor status from H&E-stained images in breast cancer

Geongyu Lee[1], Chungyeul Kim[2], Tae-Yeong Kwak[1], Sun Woo Kim[1], Hyeyoon Chang[1]. *[1]Deep Bio Inc., Seoul, Korea, Republic of,[2]Department of Pathology, Korea University Guro Hospital, Seoul, Korea, Republic of*

Correct prediction of cancer molecular subtype plays a very important role in determining the treatment of cancer patients. In determining the molecular subtype of breast cancer, protein receptors such as estrogen receptors (ER), progesterone receptors (PR), and human epidermal growth factor receptor type 2 (HER2) are used as key factors. These protein receptors also play an important role in determining the treatment method or predicting the prognosis of breast cancer. To confirm this, a test should be performed by immunohistochemical (IHC) staining. In this study, we investigated the morphological relationship between the molecular subtypes and hematoxylin and eosin (H&E) stained whole slide images (WSIs) without IHC stained images, and performed an experiment to evaluate that the protein receptors can be predicted by these morphological features. The TCGA-BRCA data were utilized in this study. There were 728 cases out of the total 1097 cases where the IHC status for ER, PR, and HER2 was either positive or negative. Each individual case is scanned using different scanners and magnifications. In some cases with multiple slides, we use only the first scanned image. The entire WSI was randomly split into 3:1:1, and used for training, tuning, and test, respectively. Individual WSIs was tiled into 1024x1024 patches for this study. The multi-task deep learning model predicts the protein receptor status of individual patches. In this

study, a confidence measure was added to remove the uncertainty of the deep learning model. When learning WSIs, patches of less than 70% based on these confidence scores did not affect WSIs. Specifically, when learning morphological features, we used strong augmentation such as grayscale, gaussian blur, color jitter, and posterization to ensure that predictions were not biased by color alone. Based on individual patches, ER accuracy of 76%, PR accuracy of 65%, and HER2 accuracy of 79% are shown. As a result of prediction by majority voting on WSI images through patch predicted results, ER accuracy of 74.6% PR accuracy of 66%, and HER2 accuracy of 76.6% Through this study, it was confirmed that the sufficiently trained deep learning model predicted ER, PR, and HER2, which are important factors of molecular subtype, relatively well. Through this, it was found that there was some correlation between morphological characteristics and molecular subtypes in H&E stained WSIs. If more data are collected through future experiments, a molecular subtype prediction model can be developed.

#5405

An ML-based tool for predicting tissue of origin for cancer of unknown primary (CUP) based on genomic and transcriptomic data

Zoia Antysheva, Daria Kiriy, Anton Sivkov, Alexander Sarachackov, Alexandra Boyko, Naira Samarina, Nara Shin, Jessica H. Brown, Ivan Kozlov, Viktor Svekolkin, Alexander Bagaev, Nathan Fowler, Nikita Kotlov. *BostonGene, Corp., Waltham, MA*

The ability to locate a tumor primary site for patients with a cancer of unknown primary (CUP) is a major obstacle in providing personalized therapeutic options and access to clinical trials. Despite the recent use of molecular-based tools to identify the tumor tissue-of-origin (TOO), overall survival for CUP patients remains low. Here, we present an AI-based tool that predicts the TOO by using genomic and transcriptomic data to classify CUP tumors into hierarchically-organized molecular subgroups. The TOO predictor was composed of DNA, RNA, and Consensus classifiers that were hierarchically organized with respect to molecular diagnosis with upper level clusters based on common molecular features reflecting similar cell of origin, and lower levels containing specific diagnoses for further classification. The ML-based DNA classifier was trained on a dataset of publicly available genomic data generated from 8,000 samples, and independently validated using more than 5,500 samples. The ML-based RNA classifier was trained on a dataset of publicly available transcriptomic data created from more than 10,100 samples with tumor- and normal-specific features for each cancer type, and independently validated using 20,000 samples. The Consensus classifier, combining outputs from both DNA and RNA algorithms, was trained on a dataset of genomic and transcriptomic data from 1,000 samples, and validated on an independent dataset of 2,000 samples. Each classifier contained features selected based on data analysis according to the weighted F1-score, and the best hyperparameters for the final model. The 3-classifier algorithm predicts TOO for 33 cancer types and subtypes belonging to solid neoplasms, independently of sample source, sequencing methods, and cohort. Validation of the Consensus classifier showed a higher accuracy (95% f1-score) compared to the DNA and RNA classifiers (79% and 93% f1-scores, respectively), along with a high sensitivity (95%), specificity (99%), and precision (96%), as it takes into account both genomic events and expression patterns. The TOO predictor was prospectively validated on approximately 298 clinical samples with a known diagnosis using all classifiers. The diagnosis was identified in 90% of clinical cases (295/297) by the Consensus classifier with 90% sensitivity and 94% precision. The call rate for the DNA and RNA classifiers was above 95%. Of note, sensitivity of the top 4 predicted diagnoses was > 90% for all 3 classifiers, and the calculated rule-out accuracy of the Consensus classifier was 97%. In conclusion, an ML-based algorithm was developed that utilizes genomic and transcriptomic data to

accurately predict the TOO for CUP tumors. Utilizing the Consensus classifier after DNA and RNA classifiers helps to identify the TOO of the tumor with high specificity, which can guide precision oncology therapeutic options.

#5406

A deep learning enabled digital pathology platform for characterization of cancer-associated thrombosis of ovarian cancer

Ju Young Ahn[1], Wendolyn Carlos-Alcalde[2], Matthew Vasquez[3], Min Soon Cho[2], Vahid Afshar-Kharghan[2], Stephen T. Wong[3]. *[1]Department of Biomedical Engineering, Texas A&M University, College Station, TX,[2]Division of Internal Medicine, Benign Hematology, The University of Texas MD Anderson Cancer Center, Houston, TX,[3]Systems Medicine and Bioengineering Department, Houston Methodist Neal Cancer Center, Houston, TX*

Purpose: Cancer-associated thrombosis (CAT), characterized by activation, extravasation, and aggregation of platelets in tumor microenvironment, is a common complication observed in ovarian cancer patients. A third of ovarian cancer patients have elevated platelet counts that are associated with poor prognosis. However, the exact mechanism by which platelets preferentially extravasate into tumor microenvironment is unknown, partly owing to lack of tools that can accurately segment and measure platelet counts found in tumor tissues. In this study, we hypothesize that tumor secreted SDF-1 interacts with CXCR4 receptors on platelets and initiates platelet chemotaxis towards tumor microenvironment. We developed a digital pathology (DP) platform with automated whole tissue confocal imaging and deep learning (DL) model that can be used to automatically segment out platelets and calculate platelet density with high precision and consistency in the mouse ovarian cancer tissue sections for supporting hypothesis evaluation.
Methods: A DL algorithm to accurately segment out platelets was developed based on the U-Net structure using our original datasets from the murine ovarian cancer model. Tumor-bearing mice were injected with 5 mg/kg of Plerixafor, a CXCR4 inhibitor, daily for 4 weeks. Then, tumor nodules were resected, stained with CD41a antibody, and imaged using the whole slide confocal microscopy. Using these high-resolution images, we performed manual annotation of platelets to generate the mask dataset and performed further data augmentation to increase the diversity of datasets. We trained our model using 85% of these images and performed validation using the remaining 15%.
Results: Using our DLDP platform, the validation dataset achieved pixel-wise accuracy of 98.7%. A receiver operating characteristic (ROC) curve demonstrated an area under the ROC curve (AUC) of 0.99 with high sensitivity and specificity. Intersection over union (IoU) score of 0.724 was obtained. A statistically significant ($p=0.0467$), 7.03% reduction in the platelet density was shown in the Plerixafor-treated mouse ovarian tumor tissues ($n=8$) compared to the control tumor tissues ($n=9$). Note that the traditional threshold method was not able to find the statistical significance ($p=0.0966$) in the same dataset.
Conclusions: We developed a DLDP platform to segment and quantitate tens of thousands of platelets from whole slide mouse ovarian cancer tissues automatically with high accuracy and consistency. Applying the DLDP platform, we demonstrated that treatment with Plerixafor leads to overall reduction in platelet infiltration within ovarian murine tumors. With high-throughput, accurate, and automated detection of platelets, our DLDP platform can serve as a powerful tool for characterization of CAT by evaluation of platelet density as a potential prognostic biomarker for ovarian cancer.

#5407

A pan-cancer PDX histology image repository with genomic and pathological annotations for deep learning analysis

Brian S. White[1], Xing Yi Woo[2], Soner Koc[3], Todd Sheridan[4], Steven B. Neuhauser[5], Shidan Wang[6], Yvonne A. Evrard[7], John David Landua[8], R. Jay Mashl[9], Sherri R. Davies[9], Bingliang Fang[10], Maria Gabriela Raso[10], Kurt W. Evans[1], Matthew H. Bailey[11], Yeqing Chen[12], Min Xiao[12], Jill Rubinstein[4], Ali Foroughi pour[4], Lacey Elizabeth Dobrolecki[8], Maihi Fujita[13], Junya Fujimoto[10], Guanghua Xiao[6], Ryan C. Fields[9], Jacqueline L. Mudd[9], Xiaowei Xu[12], Melinda G. Hollingshead[14], Shahanawaz Jiwani[7], PDXNet consortium, Tiffany A. Wallace[14], Jeffrey A. Moscow[14], James H. Doroshow[14], Nicholas Mitsiades[8], Salma Kaochar[8], Chong-xian Pan[15], Moon S. Chen[15], Luis G. Carvajal-Carmona[15], Alana L. Welm[13], Bryan E. Welm[13], Ramaswamy Govindan[9], Shunqiang Li[9], Michael A. Davies[10], Jack A. Roth[10], Funda Meric-Bernstam[10], Yang Xie[6], Meenhard Herlyn[12], Li Ding[9], Michael T. Lewis[8], Carol J. Bolt[5], Dennis A. Dean[3], Jeffrey H. Chuang[1]. *[1]The Jackson Laboratory for Genomic Medicine, Seattle, WA,[2]Bioinformatics Institute, Agency for Science, Technology and Research (A*STAR), Singapore, Singapore,[3]Seven Bridges Genomics, Inc, Charlestown, MA,[4]The Jackson Laboratory for Genomic Medicine, Farmington, CT,[5]The Jackson Laboratory, Bar Harbor, ME,[6]University of Texas Southwestern Medical Center, Dallas, TX,[7]Leidos Biomedical Research Inc., Frederick National Laboratory for Cancer Research, Frederick, MD,[8]Baylor College of Medicine, Houston, TX,[9]Washington University School of Medicine, St. Louis, MO,[10]The University of Texas MD Anderson Cancer Center, Houston, TX,[11]Brigham Young University, Provo, UT,[12]The Wistar Institute, Philadelphia, PA,[13]Huntsman Cancer Institute, University of Utah, Salt Lake City, UT,[14]National Cancer Institute, Bethesda, MD,[15]University of California - Davis, Davis, CA*

Patient-derived xenografts (PDXs) model human intra-tumoral heterogeneity in the context of the intact tissue of immunocompromised mice. Histological imaging via hematoxylin and eosin (H&E) staining is performed on PDX samples for routine assessment and, in principle, captures the complex interplay between tumor and stromal cells. Deep learning (DL)-based analysis of large human H&E image repositories has extracted inter-cellular and morphological signals correlated with disease phenotype and therapeutic response. Here, we present an extensive, pan-cancer repository of nearly 1,000 PDX and paired human progenitor H&E images. These images, curated from the PDXNet consortium, are associated with genomic and transcriptomic data, clinical metadata, pathological assessment of cell composition, and, in several cases, detailed pathological annotation of tumor, stroma, and necrotic regions. We demonstrate that DL can be applied to these images to classify tumor regions with an accuracy of 0.87. Further, we show that DL can predict xenograft-transplant lymphoproliferative disorder, the unintended outgrowth of human lymphocytes at the transplantation site, with an accuracy of 0.97. This repository enables PDX-specific investigations of cancer biology through histopathological analysis and contributes important model system data that expand on existing human histology repositories. We expect the PDXNet Image Repository to be valuable for controlled digital pathology analysis, both for the evaluation of technical issues such as stain normalization and for development of novel computational methods based on spatial behaviors within cancer tissues.

#5408

AI powered-platform to predict gene modifications from prostate and breast cancer whole slide images

Wei Huang[1], Parag Jain[2], Chensu Xie[2], Hassan Muhammad[2], Hirak Basu[3], George Wilding[2], Rajat Roy[2]. *[1]University of Wisconsin-Madison, Madison, WI,[2]PathomIQ, Cupertino, CA,[3]Department of Genitourinary Medical Oncology, MD Anderson Cancer Center, Houston, TX*

There is little published evidence of predicting cancer genotypes directly from tissue histology, especially for breast and prostate cancers. Artificial intelligence (AI) enables discriminating and extracting morphological features reflective of the underlying genomic alterations at visual and subvisual levels. We have built a morphology-based and AI-powered platform for cancer genotyping, risk stratification and outcome prediction that addresses the needs for treatment decision-making in a cost effective and timely fashion. A cohort of 390 prostate and 742 invasive breast cancer patients with known molecular status of key genes, such as TP53, PIK3CA, MYC, ERBB2, TMPRSS2-ERG and PTEN from The Cancer Genome Atlas were included in this study. Hematoxylin and eosin (H&E) stained whole slide images (WSI) of the cancer tissue sections were available at 20x or 40x. The WSI from the two cancer cohorts were split 2:1 into a training and test dataset, respectively. Our platform involved two different deep Convolutional Neural Network (DCNN) architectures. The platform first divided each WSI into multiple tiles. Each tile was then analyzed using a DCNN that graded the tile and generated a high dimensional vector to provide a mathematical representation of the morphology. The combination of high dimensional vectors across the WSI was then fed into a second DCNN that generated a morphological score, which predicted whether the gene under consideration was wild type or modified. Our platform has achieved 70 - 80% accuracy as defined by the Area under the Curve for the receiver operating characteristics curves for the genetic markers on the test cohorts (Table 1). Our platform can predict genotypes/molecular alterations directly from H&E stained WSI with high accuracy. This technology presents a novel, practical and cost-effective approach for cancer molecular classification and risk stratification, enabling timely and optimal treatment decision-making for positive clinical outcomes.

Genotype Prediction for Breast Cancer (BrCa) and Prostate Cancer (PCa) from WSI

Cohort	Molecular Biomarker	Training Dataset (n)		Test Dataset (n)		Test ROC AUC Score (%)
		Gene Modification/Loss	Intact/Wild type	Gene Modification/Loss	Intact/Wild type	
BrCa	TP53	196	302	96	149	80
	PIK3CA	153	344	75	170	74
	MYC	68	414	33	204	77
	ERBB2	66	416	32	205	78
PCa	TMPRSS2-ERG	104	157	51	78	70
	PTEN	57	201	28	99	73

#5409

NuKit: a deep learning platform for histopathological Images

Ching-Nung Lin[1], Christine H. Chung[2], Aik Choon Tan[1]. *[1]University of Utah Huntsman Cancer Institute, Salt Lake City, UT,[2]Head and Neck Endocrine Oncology, Moffitt Cancer Center, Tampa, FL*

Hematoxylin and eosin (H&E) staining is the most common type of histopathological images used for quantitative data analysis. For histopathological image analysis, nucleus segmentation represents one of the initial steps in quantitative data analysis pipelines. Recently, deep learning methods for nucleus segmentation on histopathological images become the mainstream in digital pathology. However, adopting these pre-trained models in digital pathology or clinical research remains limited. Two main factors limit the usage of deep learning methods in routine research: 1) many models required some technical background to execute the programs, and 2) the speed of returning the results to the users. To overcome these limitations, we have developed and implemented NuKit, a deep learning platform which accelerates nucleus segmentation and provides prompt results to the users. NuKit platform consists of two deep learning models coupled with an interactive graphical user interface (GUI) to provide fast and automatic nucleus segmentation “on the fly”. The two deep learning models are: 1) the whole image segmentation model and 2) the click segmentation model. Both deep learning models provide complementary tasks in nucleus segmentation in the NuKit platform. The whole image segmentation model performs whole image nucleus whereas the click segmentation model supplements the nucleus segmentation with user-driven input to edits the segmented nuclei. We used PanNuke as the training data set which contains 160,368 nuclei extracted from 7,901 image tiles. The sources of this data set were curated from The Cancer Genome Atlas (TCGA) and included a very few in-house data. For test sets, we used several popular data sets such as TCGA (not used in the training set). We used DICE coefficient as the metric for comparisons of NuKit with other deep learning methods. For the results, we observed that NuKit achieved comparable results with the state-of-the-art deep learning methods and outperforms those non-deep learning methods. For TNBC and CoNSeP data sets, NuKit achieved DICE 0.793 and 0.854 comparing to HoVer-Net 0.749 and 0.664. For CoNSeP test data set, NuKit achieved DICE 0.860 comparing to Cell Profiler 0.434 and QuPath 0.588. In addition, both pre-trained models were embedded in the NuKit GUI, which provides interactive and prompt response to users in analyzing their histopathological images. The outputs of NuKit are interoperable with other quantitative image analysis tools to facilitate the ecosystem of computational pathology to many formats to combine with other software to construct pipelines. In summary, we have introduced NuKit, an innovation platform which combines two deep learning models coupled with interactive GUI to accelerate nucleus segmentation task in histopathological images. We believe that NuKit provides a new platform to bridge the pre-trained deep learning models into digital pathology and clinical usage.

#5410

Predictive biomarker discovery method to bridge the gap between preclinical disease model dose-response and clinical trials

David Futorian, Oren Fischman, Gali Arad, Nitzan Simchi, Omri Erez, Eran Seger, Rozanne Groen, Kirill Pevzner. *Protai, Tel Aviv, Israel*

The translational gap of drug and biomarker discovery remains one of the biggest challenges in the pharmaceutical industry. On one hand high throughput screening and omics methods facilitate the generation of in-vitro and in-vivo data of dose-response for a particular drug or combinations. On

the other hand, clinical omics techniques allow for the creation of large scale treatment-naive clinical datasets, with the TCGA and CPTAC as prominent examples. However, the question of which disease model best represents the response/ resistance mechanisms of an oncology patient remains challenging.
In this study we present a machine learning (ML) based computational technique for integrating omics from preclinical dose-response studies with clinical treatment-naive samples to create putative predictive biomarkers, and exemplify its application 2 case studies - PARP or AKT inhibitors.
We utilize the Cancer Cell Line Encyclopedia (CCLE) and Genomics of Drug Sensitivity in Cancer (GDSC) as a resource for in-vitro dose response data for PARPi and AKTi, coupled with multi-omic molecular data. We utilize the treatment naive molecular characterization from the Clinical Proteomic Tumor Analysis Consortium (CPTAC) data of Breast cancer patients. Multi-omic analysis of these datasets derived 2 putative predictive biomarkers for PARPi and AKTi. The multi-omic analysis resembles the data availability at the critical drug development stage of transition from preclinical response models to a clinical trial. These biomarkers are tested on a validation dataset obtained from the iSPY adaptive clinical trial and achieve superior results compared to the original enrolment biomarkers and even the retrospectively derived biomarkers.
This study presents a novel computational approach to bridge the gap between preclinical dose-response and clinical datasets and suggests an efficient way to discover predictive biomarkers based on data accessible in a preclinical setting.

#5411

Efficient development of prognostic tests for detecting cancer risk using proteomic technology

Yolanda Hagar, Leigh Alexander, Jessica Chadwick, Gargi Datta, Joe Gogain, Rachel Ostroff, Clare Paterson, Laura Sampson, Caleb Scheidel, Sama Shrestha, Amy Zhang, Michael Hinterberg.
SomaLogic, Inc., Boulder, Co, CO

Background**:** Prognostic models for assessing future health outcomes can be developed using time-to-event (also known as “survival”) data. This methodology is ubiquitous in statistical literature and in the analysis of cancer outcomes, but its use in high-dimensional analyses tends to be limited as the methods are difficult to implement in a machine learning environment. Additionally, development of certified prognostic clinical tests using proteomic biomarkers for detecting future cancer risk can be time-consuming, prone to overfitting issues, and difficult to navigate. We demonstrate the utility of combining SomaScan® proteomic data with pipeline machine learning tools and survival analysis methodology to identify powerful and robust LDT-certifiable prognostic tests for assessing future risk of cancer.
Methods: Data pipeline and analysis tools were developed using R. In addition to standard machine learning techniques, statistical methods include elastic net AFT models, subsampling survival techniques, and metrics for assessing predictive survival models. The pipeline takes the analyst from data processing and QC through identification of optimal models for prediction of clinical endpoints, and then through validation on a hold-out test set. The tools include an assessment of model robustness against sample handling issues, longitudinal stability, the impacts of assay noise on model performance, effects of putative interferents, and risk of failure during CLIA validation in the lab. We demonstrate the utility of the tools and methods for development of a lung cancer risk model.
Results: Analysis time for validation of an optimal clinical model was reduced by at least 80%, resulting in the development of 7 LDT-certified tests within 3 years, including a test for lung cancer risk. Inclusion of methods that allow for subsampling and penalized regression using AFT models

show improved predictive performance and identification of top features related to clinical endpoints.
Conclusion: Not only are powerful, prognostic tests do-able, but they can be LDT certified in an efficient manner and made to be robust to real-life lab settings. Survival analysis in a machine-learning setting allow us to leverage proteomic technology in new ways, leading to tests that assess future cancer risk, which can be used for precision medicine applications.

#5412

Redefined chronic inflammatory responses as prognostic markers in glioma: an explainable artificial intelligence model

Debajyoti Chowdhury[1], Hiu Fung Yip[1], Hao Liu[2], Xuecheng Tai[3], Aiping Lu[1]. *[1]Hong Kong Baptist University, School of Chinese Medicine, Hong Kong SAR, Hong Kong,[2]Department of Mathematics, Hong Kong Baptist University, Hong Kong SAR, Hong Kong,[3]Hong Kong Centre for Cerebro-Cardiovascular Health Engineering, Hong Kong SAR, Hong Kong*

Introduction: Glioma is an aggressive brain tumor. Many inflammatory mediators within the tumor microenvironment (TME) determine its progression. Unfortunately, no ubiquitous prognostic markers reveal the intricacy between TME and chronic inflammatory responses (CIRs). CIRs used to vary among individuals affecting prognosis. And opting for the best-optimized treatment remains challenging.
Methods: We proposed an explainable artificial intelligence (XAI) approach to redefine CIRs as prognostic markers for glioma using 694 and 693 patients' data derived from The Cancer Genome Atlas (TCGA) and the Chinese Glioma Genome Atlas (CGGA), respectively. First, using five curated databases, we identified CIR-related genes those enriched nine HALLMARK pathways using gene set variation analysis (GSVA). Then, we trained the XAI model to characterize the personalized inflammatory mediators (PIMs) using multimodal factors such as transcription factors (TFs) network and cell infiltration markers. It resulted in rationalized typified CIRs. Finally, we used overall survival (OS) analyses to validate them as potential prognostic markers and showed a personalized co-drug discovery strategy by optimizing CIRs.
Results: The proposed XAI model deciphered the PIMs and endorsed the typified CIRs as efficient prognostic markers. It characterized five unique CIR types (p-value<0.0001). The OS analyses indicated the differential prognostic ability of the typified CIRs for glioma, lower-grade glioma (LGG) at p-value<0.0001, and glioblastoma (GBM) at p-value<0.22. We found that patients with higher CIRs had significantly shorter OS than those with lower CIRs. We showed that CIR type 4 and type 2 were highly inflamed and had poor OS for LGG, and GBM, respectively. Chronic pro-inflammatory responses were positively correlated with the poor OS of glioma patients. GSVA indicated lower activation of apoptotic pathways and higher activation of the hypoxia pathway as likely causes. We identified the effector genes within the personalized CIR networks, which demonstrated prognostic ability and may offer potential targets for optimizing the patient-specific CIRs through co-drug intervention. Additionally, we identified their transcriptional regulatory networks comprising TFs (e.g., SMAD3, HIF1A, NFKB1, GATA3, RORA, JUN) contributing to the inflammatory pathways (e.g., TNFα, NF-kβ, IFN-γ, hypoxia).
Conclusions: Our findings highlight a new strategy to redefine CIRs as prognostic markers for glioma and show that optimizing CIRs improves the OS. It opened a new avenue for co-drug discovery to ensure better survival.
Acknowledgments: HK GRF (12102722, 12101018, 12102518, 12100719), HK Theme-based Scheme (T12-201/20-R), IRMS-HKBU (RC-IRMS/15-16/01), TISSF (Guangdong-Hong Kong-Macau Joint Lab, 2020B1212030006) and NSFS (ZR2020QH219).

#5413

AIVE, an artificial intelligence protein miner based on omics data to discover new cancer druggable candidates

Dongwan Hong. *Catholic University of Korea, College of Medicine, Seoul, Korea, Republic of*

Recently, AI software including Alphafold, RoseTTAFold and ESMFold, can predict protein structures based on amino acid sequences, and DeepMind (Alphafold2) and Meta (ESMFold) opened hundreds of millions of protein structures to world-wide clinical researchers. These tools are possible to generate protein structures in a shorter time and less cost than traditional protein study methods. Finally, they can lead to the advent of the *protein rush generation*. To evaluate accurately and quickly the prediction of structures of mutations embedding in protein sequences, we developed an *Artificial Intelligence analytics toolkit for predicting Virus mutation in protEin (AIVE; http://ai-ve.org)* that clinical researchers can use easily on web. An amino acid property eigen selection score (APESS) defined in AIVE is a comprehensive mathematical analysis model, andit was calculated basically by below: 1 artificial intelligence base clustering (AIBC) using predicted aligned error (PAE) and per-residue confidence (pLDDT) values, 2 base level change rate (BLCR)using the probability of occurrence of mutation in each amino acid sequence or nucleotide sequence, 3chemical property eigen score (CPES) using amino acid properties (PH, Residue and Hydrophobic),and 4polarity based feature selection (PBFS) using continuous position of polar amino acids including S, C, N, Q, T, and Y [*APESS = AIBC ´ BLCR ´ CPES ´ PBFS*]. AIVE also calculated the docking score using AlphaFold to estimate protein to protein interaction (PPI) among hosts (or mutations) and provided a graph as final report showing APESS distribution among mutation group, and evaluation of APESS and docking score. For example, according to APESS score in lung cancer, we can find out the feasibility of structure transformation of H-bond in EGFR protein (L858R) tyrosine kinase and also show the differences of tyrosine kinase affinity between each lung cancer patients. However, for the T790M mutation of EGFR protein, there was no significant difference compared with the wild type (790). The execution time of AIVE (GPU based web server platform) depends on the length of the input sequence, and it completes such an example case in an average of 2-3 hours. AIVE can suggest anti-cancer candidates in protein-level and present a precision medicine model which is available to implement close to real time.

#5414

Automated detection of high-grade urothelial carcinoma from urine cytology slides using attention-based deep learning

Mohamed Omar[1], David Kim[2], Luigi Marchionni[3], Momin T. Siddiqui[3]. *[1]Weill Cornell Medicine, New York, NY,[2]Department of Pathology and Laboratory Medicine, Memorial Sloan Kettering Cancer Center, New York, NY,[3]Department of Pathology and Laboratory Medicine, Weill Cornell Medicine, New York, NY*

Urine cytology has long been an effective and non-invasive test for the detection of bladder urothelial carcinomas (UC) routinely performed in cases of unexplained hematuria or for monitoring patients with UC. In cytopathology practice, urine cytology specimens are examined manually with a light microscope to identify morphologic features associated with different diagnostic categories based on the Paris System (TPS) for Reporting Urinary Cytology. Specifically, the diagnosis of high-grade urothelial carcinoma (HGUC) requires the identification of > 5-10 cells with a nuclear/cytoplasm ratio of 0.7 or greater and hyperchromasia together with coarse chromatin or irregular nuclear membranes. However, the task of identifying HGUC involves

a substantial degree of manual review and is often associated with intra-and inter-observer variability. To address this, we have designed an accurate and efficient deep learning system capable of automatically distinguishing between HGUC and non-HGUC using digitized cytology slides. Our model has been developed using a retrospective cohort of 158 digitized urine ThinPrep cytology slides consisting of HGUC (n=98) and negative for HGUC (n=60). The model was then prospectively validated on a cohort of 105 urine cytology slides that were also independently reviewed prospectively in a blinded manner by a cytopathologist and cytotechnologist. Our system uses Otsu's method for automatic image thresholding followed by dividing images into non-overlapping tiles of 500X500 pixels at the highest magnification. Subsequently, we use a pre-trained ResNet50 model to extract features which are used for training our attention-based multiple instance learning framework. For the training task, our retrospective cohort (158 slides) has been divided into 10 different splits each consisting of training (70%), validation (15%), and testing (15%) sets. The training and validation sets were used for the model training and optimalization, respectively, while the testing set was used for assessing the performance. This process yielded 10 different models with an average Area Under the ROC Curve (AUC) of 0.80 in the testing set. The best performing model had an AUC of 0.90 and an accuracy of 0.88. This model was subsequently validated prospectively in an independent testing cohort with 105 slides. In the prospective testing cohort, the model was able to accurately distinguish between HGUC and non-HGUC with an AUC of 0.83, accuracy of 0.76, sensitivity of 0.89, and specificity of 0.62. Additionally, our system can detect slide regions with high attention score for HGUC which are enriched in atypical urothelial cells. These findings show that our system can be utilized to assist cytopathologists in assessing urine cytology slides and to detect regions with high-diagnostic relevance for further assessment which is expected to reduce the time needed for manual review.

Artificial Intelligence: From Pathomics to Radiomics

#5418

AI-driven image analysis enables simplified, label-free cytotoxicity screening

Gillian Lovell[1], Daniel A. Porto[2], Jasmine Trigg[1], Nevine Holtz[2], Nicola Bevan[1], Timothy Dale[1], Daniel Appledorn[2]. *[1]Sartorius, Royston, United Kingdom,[2]Sartorius, Ann Arbor, MI*

The increasing use of precious, patient-derived cells has driven the need for non-perturbing and label-free cell measurements, particularly in the oncology field. To address this we developed the Incucyte® AI Cell Health Analysis Software Module, which uses two pre-trained deep neural networks to perform automated, unbiased analysis of Phase contrast images to segment individual cells and perform label-free Live/Dead cell classification. The neural networks which perform cell instance segmentation and infer cell viability were trained on a wide diversity of cell types with varied morphologies, ensuring that the analysis is applicable across a variety of adherent and suspension tumor cell types. Here, we demonstrate the application of this analysis across diverse and commonly used biological models of breast cancer, glioblastoma, and B-cell lymphoma. In each case, cells were treated with chemotherapeutic compounds or biosimilar antibodies and Phase contrast images were acquired at regular intervals over 3 - 4 days using the Incucyte® Live-Cell Analysis System. Using the Incucyte® AI Cell Health Analysis cells were accurately segmented and the percentage of dead cells were quantified over time without the requirement for a fluorescent reporter or other exogenous label, and with limited user input. Four breast cancer cell lines were treated with a panel of chemotherapeutics designed to target specific expression patterns. AI Cell Health analysis showed that Estrogen receptor (ER) inhibitor Tamoxifen selectively induced >60% cell death only in ER positive cell lines BT474 and MCF7; dual epidermal growth

factor receptor (EGFR/ HER2) inhibitor Lapatinib induced cell death in AU565, BT474 and MCF7 which express these surface markers. In contrast, Lapatinib and Tamoxifen induced morphological change - but minimal cell death - in triple negative MDA-MB-231 cells. Three glioblastoma cell lines A172, U87 and T98G were treated with a larger panel of chemotherapeutic compounds and for four of the active compounds, efficacy was also determined. Cisplatin, doxorubicin, vinblastine and taxol induced concentration-dependent cell death in A172 and T98G cells; U87 cells displayed resistance to each of these compounds with a maximal 46.5% cell death induced by doxorubicin. Ramos B-cell lymphoma cells were exposed to increasing concentrations of monoclonal antibody Rituximab and the biosimilar Truxima®. The antibodies induced specific cell death via the surface marker CD20 in a time and concentration-dependent manner with similar efficacy (IC_{50} Rituximab 94.7 ng/mL; Truxima® 110.3 ng/mL), while antibody control IgG1 remained non-perturbing to cells. These results demonstrate that the Incucyte® AI Cell Health Analysis is applicable to a broad range of cancer types cultured in 2D monolayer. This unbiased method enables accurate, label-free quantification of cytotoxic effects induced by clinically relevant therapeutics.

#5420

Deep learning-based mapping of tertiary lymphoid structure scores from H&E images of renal cell carcinoma trained by spatial transcriptomics data

Seungho Cook[1], Haenara Shin[2], Mi-Kyoung Seo[1], Dae Seung Lee[1], Hongyoon Choi[3]. *[1]Portrai, Inc, Seoul, Korea, Republic of,[2]Kim Jaechul Graduate School of AI, Korea Advanced Institute of Science and Technology (KAIST), Daejeon, Korea, Republic of,[3]Department of Nuclear Medicine, Seoul National University Hospital, Seoul, Korea, Republic of*

Purpose Tertiary lymphoid structures are organized aggregates of immune cells present in the tumor microenvironment (TME) in which novel targets as well as beneficial biomarkers for immunotherapy in cancer were found. Here, we have developed and validated a deep learning model by integrating H&E images of renal cell carcinoma and spatial transcriptomics data to infer spatial mapping of tertiary lymphoid structure scores in TME only using hematoxylin and eosin (H&E) images.

Methods A total of 20 H&E images combined with spatial transcriptomics data of renal cell carcinoma were used to develop a model. Tertiary lymphoid structure scores can be acquired for each spot in spatial transcriptomics by geometric mean of the specific gene expression relevant to B cell, T cell, immunoglobulin, fibroblast, complement, and others. A convolutional neural network using H&E image patches as inputs was developed to predict the tertiary lymphoid structure scores from H&E-stained tissue image patches of renal cell carcinoma acquired by different patients. For the external validation, the model estimated the tertiary lymphoid structure scores from H&E-stained tissue image patches of renal cell carcinoma of The Cancer Genome Atlas (TCGA-RCC).

Results The tertiary lymphoid structure scores inferred by the model using H&E image patches were significantly correlated with those derived by spatial transcriptomics data as an internal validation ($r = 0.68$, $p < 1e\text{-}10$) . The mean value of the deep learning-based tertiary lymphoid structure scores estimated by the TCGA-RCC tissue images was significantly correlated with the tertiary lymphoid structure scores, T cell enrichment scores and immune cell enrichment scores estimated by bulk RNA-seq data from the corresponding TCGA data.

Conclusions A deep learning model to infer spatial tertiary lymphoid structure in the tumor microenvironment using H&E images was developed. As the tertiary lymphoid structure is a key to predict responsiveness of immune checkpoint inhibitors, mapping the score only using H&E images could be clinically translated into image-based biomarkers. This approach can provide

objective and flexible deep learning-based models for characterizing tumor microenvironment related to spatial immune distribution.

#5421

Constructing the largest-scale knowledge graph using all PubMed abstracts and its application for highly specific and accurate knowledge retrieval

Xin Sui[1], Yuan Zhang[2], Feng Pan[2], Donghu Sun[1], Menghan Chung[1], Jinfeng Zhang[2]. *[1]Insilicom LLC, Tallahassee, FL,[2]Florida State University, Tallahassee, FL*

Most of the biomedical knowledge the research community has acquired during the past few decades has been deposited in scientific literature as unstructured text. Converting the unstructured text into the structured form will enable novel methodologies and applications for scientific discovery that can fully harness the power of the existing knowledge. To this end, two fundamental questions need to be addressed: named entity recognition (NER) and relation extraction (RE). NER deals with identifying the concepts or entities in texts, such as diseases, genes/proteins, chemical compounds, etc. while RE aims to extract the relations among these entities. Together, the extracted information forms a knowledge graph (KG) where the nodes are entities in the texts and the edges represent their relationships. KGs can link concepts within existing research to allow researchers to find connections that may have been difficult to discover without them. The LitCoin Natural Language Processing (NLP) Challenge was recently organized by NCATS of NIH and NASA to spur innovation by rewarding the most creative and high-impact uses of biomedical text to create KGs. Our team participated in the challenge and ranked first place. We have applied the methods we developed for the LitCoin NLP challenge to all PubMed abstracts and constructed the largest-scale biomedical KG to date. We show that powerful and versatile query functions can be implemented on top of the KG to enable highly specific and accurate knowledge retrieval and inference of causal and indirect relationships.

#5422

Machine learning models identify key histological features of renal cell carcinoma subtypes

Samuel Vilchez, Isaac Finberg, Miles Markey, Shima Nofallah, Kathleen Sucpito, Fedaa Najdawi, Geetika Singh, Ben Trotter, Victoria Mountain, Jake Conway, Robert Egger, Chintan Parmar, Ilan Wapinski, Stephanie Hennek, Jonathan Glickman. *PathAI, Inc., Boston, MA*

Renal cell carcinoma (RCC) is a heterogeneous disease with 16 different subtypes identified and diagnosed by assessment of tumor histology, and specific molecular and genetic markers. Three major subtypes - clear cell, papillary, and chromophobe carcinoma - have different prognoses and treatment regimens. Treatment response has been associated with mutations that may affect the tumor microenvironment (TME). Here, machine learning (ML) models quantified histologic features of the TME directly from RCC hematoxylin and eosin (H&E)-stained whole slide images (WSI). The potential for model outputs to predict clinically-relevant biomarkers was investigated. Machine learning models based on convolutional neural networks were trained using RCC and non-RCC kidney WSI of biopsies and resections from the cancer genome atlas (TCGA), proprietary, and commercial sources (tissue model N=3208; cell model N=789; vessel model N=839) to classify and quantify histologic features of the TME including cells, tissues, and blood vessels. Thousands of human interpretable features (HIFs) were extracted from model predictions that precisely describe the TME across each WSI (e.g., cell density within a tissue region). Associations between HIFs and PBRM1 loss of function (LOF) mutations and VEGFA mRNAseq expression in clear cell RCC were determined using univariate logistic regressions and Spearman

correlations, respectively. False discovery rate in multiple hypothesis testing was controlled using an Empirical Brown's Method and the Benjamini-Hochberg procedure.
ML-models generated 3390 HIFs from 692 TCGA RCC WSI. After quality control to remove features with missing values, outlier slides and de-duplication, 237 HIFs (657 WSI) remained. Major RCC subtypes could be extracted directly from these HIFs using hierarchical clustering ($p<10-6$, chi-squared test). Individual RCC subtypes were distinguished by features describing immune cells and vascularization. A mixed subcluster enriched for higher stage ($p<10-6$, chi-squared test) papillary and clear cell RCC tumors was associated with increased prevalence of sarcomatoid regions and immune cells. In clear cell RCC, significant associations were found between HIFs describing a spatially specific increase in lymphocytes in the cancer epithelium (FDR-corrected $p=0.004$) and decrease in macrophages (FDR-corrected $p=0.004$) in the entire tumor area and PBRM1MUT, a mutation associated with response to immunotherapy; VEGFA expression, predictive of angiogenesis, positively associated with an increased abundance of lymphocytes near erythrocytes (Spearman $r=0.37$).
ML model quantified RCC TME histology allowed identification of spatially specific differences that correlate with histological subtypes, mutations, and vascularization. Complementary ML-based TME assessment and genomic analyses may be used, after further validation, to explore novel biomarkers.

#5423

AI powered quantification of mitotic rate in H&E stained tissue detects significant differences between treatment groups of preclinical pancreas cancer xenografts

Sharon Ruane[1], Lukas Ruff[1], Brian Reichholf[2], Christina Aigner[1], Emil Barbuta[1], Stephan Tietz[1], Olivér Atanaszov[1], Rosemarie Krupar[1], Simon Schallenberg[3], Maximilian Alber[1], Francesca Trapani[2], Frederick Klauschen[4]. *[1]Aignostics GmbH, Berlin, Germany,[2]Boehringer Ingelheim RCV GmbH & Co KG, Vienna, Austria,[3]Institute of Pathology, Charité Universitätsmedizin Berlin, Berlin, Germany,[4]Institute of Pathology, Ludwig Maximilian University, Munich, Germany*

Background: Mitotic rate is a readout routinely used for characterization of tumor samples. Standard methods to quantify cell division include manual pathologist counts based on hematoxylin and eosin (H&E) staining and either manual or automated assessment of immunohistochemistry (IHC) staining using phospho-histone H3 (pHH3). These suffer the drawbacks of high inter-pathologist variability in the case of H&E assessment and time inefficiency and false positive calls in case of pHH3 staining. Aiming to overcome these issues, we developed a mitosis detection model based on H&E-stained tissue sections alone.
Methods: To develop and evaluate the model, we used 1032 H&E-stained tissue sections (156 used for model training) of pre-clinical pancreas cancer xenografts originating from mice that have undergone a series of experiments conducted to examine the pharmacodynamic effect of several anti-cancer protocols. We trained (i) a tissue segmentation model (segmenting tissue regions into 'carcinoma', 'stroma', 'necrosis', and 'other') and (ii) a segmentation model for pixel-level mitosis detection (segmenting 'mitosis' vs. 'non-mitosis'). Regions predicted as mitosis were post-processed to represent individual dividing cells. The tissue segmentation model served as a filter to predict mitotic rate for carcinoma tissue areas only, which has not been accounted for in previous AI-based methods for mitotic rate prediction on H&E tissue. To evaluate the model on detecting mitotic events, the model was compared against a 5-pathologist consensus of mitotic count. The mitotic rates predicted by the model were used to infer differences between treatment groups (various treatments and dosages vs. control).

Results: The mitosis detection model for quantifying rates of cell division in carcinoma regions of H&E-stained tissue sections showed a notable agreement with the 5-pathologist mitotic count consensus (Pearson correlation 0.92). Furthermore, the model correlated well with mitosis counts based on pHH3 IHC staining (Pearson correlation 0.78), which were available for 63 cases. Finally, when used to characterize the entire CDX cohort, the case level mitotic rate predicted by the model showed significant differences between treatment groups in line with or better than using a pHH3 IHC stain.
Conclusion: This study demonstrates the efficacy and scalability of AI-based models for the quantification of mitotic rate based on H&E-stained tissue alone, presenting a time- and cost-efficient approach that also mitigates inter-annotator variability.

#5424

A deep learning approach (AI) which accurately identifies breast tumor cells, tumor infiltrating lymphocytes (TILS) and fibroblasts from H&E slides

Luiz Augusto Zillmann da Silva[1], Alistair R. W. Williams[2], Aidan Kubeyev[3], Andrea Giorni[1], Jordan Laurie[1], Prabu Sivasubramaniam[3], Matthew Foster[3], Matthew Griffiths[3], Uzma Asghar[4].
[1]Concr Pty Ltd, Brisbane, Australia,[2]Division of Pathology, The University of Edinburgh, Edinburgh, United Kingdom,[3]Concr Ltd, Cambridge, United Kingdom,[4]Technical, Concr Ltd, Cambridge, United Kingdom

Background: Histopathology assessments of cancers require highly skilled pathologists, are labor intensive and prone to errors without proper training or fatigue. Machine learning can assist pathologists by increasing efficiency and minimizing individual variability. This study adapted a deep learning model to reliably identify 3 cell types from triple negative breast cancers fixed on H&E slides and verified performance with an expert pathologist.
Methods: We apply the U-Net architecture to analyse pathology slides fixed with triple negative breast cancer (TNBC) tissue. The public dataset NuCLS was used for training. Semantic segmentation was used to identify single cells of 3 types: tumor cells, fibroblasts, and tumor infiltrating lymphocyte (TILs). For validation, the pathologist annotated 8 random H&E tiles. The 3 cell types accuracy for NuCLS and the model was evaluated by our pathologist.
Results: Overall, there was a 73% agreement with the pathologists (Pathologist *vs*. NuCLS). A set of 1,555 (90%) TNBC slides were used for training and 173 for validation (10%; unseen data). Table 1 outlines the accuracy metrics for each cell type and for each comparison. Compared to our pathologist, the model accurately identified TILs (62%), followed by fibroblasts (42%) and lastly tumor cells (26%). A significant source of discrepancy was variation in labeled single cell boundaries. The model was better at identifying TILs. The pathologist took 1.5 hours to annotate 8 tiles for the 3 cells and our model 644ms.*Table 1 - Accuracy metrics.*

Quality assessment8 H&E tiles	**Pathologist *vs.* NuCLS**	**U-Net model *vs.* NuCLs**	**U-Net model *vs.* Pathologist**	**U-Net model *vs.* NuCLs (Full)**
Background	86%	71%	62%	73%
Tumour	43%	35%	26%	71%
Fibroblast	45%	39%	42%	31%
TILs	34%	96%	62%	87%
Overall	73%	74%	61%	71%

Conclusion: It is possible to develop a deep learning model to identify breast cancer cells, fibroblasts and TILs from H&E stained slides, with similar accuracy levels as a trained pathologist. The model performed better than a pathologist in identifying TILs, but both struggled with fibroblasts. Accuracy of 71% overall and 87% for TILs, motivates expansion to further datasets and other cancer types.

#5425

Analysis of cancer patients' molecular and clinical data using artificial intelligence and machine learning approaches

Ali Firooz[1], Avery T. Funkhouser[2], Julie C. Martin[3], W. Jeffery Edenfield[3], Homayoun Valafar[1], Anna V. Blenda[2]. *[1]Computer Science & Engineering, University of South Carolina, Columbia, SC,[2]Biomedical Sciences, University of South Carolina School of Medicine Greenville, Greenville, SC,[3]Prisma Health Cancer Institute, Greenville, SC*

Background: Development and clinical course of cancer is multifactorial with influences from the general health status of the patient, germline and neoplastic mutations, co-morbidities, and environment including lifestyle. For effective and individualized treatment of each patient, such multifactorial data must be easy-to-access and easy-to-analyze.
Purpose Statement: Cancers are characterized on a molecular level by the presence of complex gene mutations and other specific molecular markers. Moreover, special importance is placed on so-called cancer-critical genes, mutations of which are involved in the development and progression of various cancers. However, not all detected sequence alterations in these genes are known as cancer-causing mutations; thus, a more detailed and sensitive analysis is prudent. In addition, there is a limited number of established and reliable cancer biomarkers of sera. To that end, a complete analysis of molecular basis of cancer needs to include additional biomarkers such as galectins and glycans, since patients' galectin and glycomic profiles have promising cancer differentiating and diagnostic potential.
Methods: We utilized a Relational Database Management System populated by clinical data from the Prisma Health Cancer Institute Biorepository of ~6,000 cancer patients with at least 66 different cancer diagnoses. Molecular data is available for gene mutations, serum galectin proteins, and glycomic profiles of cancer patients. Mutation status of 50 cancer-critical genes in 1,500 patients, 320 individual patient profiles of 5 serum galectin proteins, and serum and tissue glycomic profiles of 60 patients have been included and will be expanded. In addition, healthy control values for galectin and glycomic profiles were obtained and added for reference. We performed statistical and AI models of Data Analytics using R, Python, and TensorFlow platforms. A comprehensive set of patient data was used to develop a predictive model of patient outcome using the clinical observations as the desired outcome.
Results: The use of typical statistical analyses (linear and logistic regression) revealed insignificant correlation between the predictors and the cancer type of patient outcome. However, the use of the Decision Tree revealed some interesting relationships that can be used for explainability and reliability of the Machine Learning approaches. Finally, Artificial Neural Network approaches provided the best performance in classification of cancer types from the given information.
Conclusion: Our studies provide predictive models that could potentially be used to improve the diagnostic and prognostic power of data collected from patients at presentation. However, the dichotomy of black box AI approaches that perform better than explainable approaches, complicate deployment of these techniques in the domain of medicine and healthcare.

#5426

Multi-omic characterization and predictive features of advanced ovarian cancer patients in a large phase III cohort

Cyril Ramathal[1], David Masica[1], Peter Ansell[1], Bridget Riley-Gillis[1], Jacob Degner[1], Thanh Bui[1], Priya Narayanan[1], Josue Samayoa[1], Xin Huang[1], Robert F. Coleman[2], Jeffrey F. Waring[1]. *[1]AbbVie Inc., North Chicago, IL,[2]US Oncology Research, The Woodlands, TX*

Discovery and validation of biomarkers derived from multi-dimensional clinico-genomic datasets have become critical in precision medicine and oncology drug development. The integration of multi-dimensional genomic and imaging datasets from patients in late-stage oncology clinical trials can be difficult, in part due to limited patient enrollment and sample collection, especially tumor tissue biopsies. The objective of this project was to conduct predictive biomarker discovery on integrated clinico-genomics data spanning tumor genomics, germline genetics, tumor imaging, and circulating blood-based biomarkers for a cohort of 800+ advanced ovarian cancer patients enrolled in the phase III trial of the PARP-1 inhibitor Veliparib (VELIA). Genomic (DNA & RNA) and imaging datasets were generated from 800+ patient-matched tumor biopsies, liquid biopsies and whole blood to enable various biomarker analyses for this study, notably in BRCA-deficient and HRD+ subgroups. Pairwise analysis of individual features with clinical outcomes shows that increased tumor-mutation burden (TMB), RNA-based estimates of immune activity (ICR and MIRACLE scores), CA-125 elimination constant (KELIM score), and image-based estimates tumor-infiltrating lymphocytes (TILs) were each significantly associated with longer PFS and less progressive disease (PD). Similarly, homologous recombination deficiency (HRD) and BRCA alteration were associated with better clinical outcomes, while high CA-125 was associated with worse outcomes. To understand the concerted impact of these features on clinical outcome, we developed multivariate classifiers of PD and regressors (Cox Proportional Hazards) of PFS using XGBoost; using a train-test split of 75/25, we trained the models with 500 rounds of 10-fold cross validation hyperparameter tuning, which resulted in fit models. The PD classifier achieved a validation accuracy of 0.71 and F1-score of 0.78, with high immune activation, high TMB, high KELIM, and HRD and BRCA alteration predicting better outcomes. The PFS survival model achieved a validation C-index of 0.61, with a rank importance of features similar to that of PD classification models; for both models, patients receiving Veliparib had clear benefit relative to that of control arms. Collectively, this study illustrates the value of integrating multi-dimensional datasets with predictive machine learning to identify clinically-relevant biomarkers. CR, DM, PA, BR, JD, TB, PN, JS, XH, and JFW are employees of AbbVie. RLC an employee at The University of Texas MD Anderson Cancer Center and has no funding to disclose. The design, study conduct, and financial support for this research were provided by AbbVie. AbbVie participated in the interpretation of data, review, and approval of the publication.

#5427

Improving non-small cell lung cancer segmentation on a challenging dataset

Yi Wei[1], Balaji Selvaraj[2], Mayank Patwari[1], Qin Li[3], Meng Xu[4], Konstantinos Sidiropoulos[1], Zhenning Zhang[4], Leon Fedden[1], Anant Madabhushi[5], Mohammadhadi Khorrami[6], Vidya Sankar Viswanathan[6], Amit Gupta[7]. *[1]AstraZeneca, Cambridge, United Kingdom,[2]AstraZeneca, Chennai, India,[3]Translational Medicine Oncology, AstraZeneca, Waltham, MA,[4]AstraZeneca, Gaithersburg, MD,[5]Georgia Institute of Technology and Emory University and Atlanta Veterans*

Administration Medical Center, Atlanta, GA,[6]Emory University School of Medicine, Atlanta, GA,[7]University Hospitals Cleveland Medical Center, Cleveland, OH

When applied to different datasets, performance of the same deep learning tumor segmentation model can greatly vary. In a non-small cell lung cancer CT scan segmentation study that consists of two datasets, we found that the SwinUNETR model achieves state-of-the-art DICE score on a public dataset NSCLC but performs badly on a private dataset of curated data collected clinically. This performance variation reduces the applicability of such models. To mitigate this gap, through experimentation, we identified a set of techniques and applied them in the following order: (1) normalize a dataset to reduce differences between images. (2) stratify a dataset according to tumor sizes to form a more diverse training set. (3) isolate the lung area before training to help the model focus on the right area. (4) before training, initialize models with self-supervised pre-training weights (5) use a new loss function to give more weights on the cancerous area (6) after a model is trained, perform 3-axis test time flipping augmentation and ensemble the final predictions. In our experiments, our set of techniques improved the test DICE score for both datasets we tested on, where the best improvement was a 53% improvement from 0.32 to 0.49 DICE score.

#5428

Skeletal muscle gauge prediction by a machine learning model in patients with colorectal cancer

Jeonghyun Kang. *Surgery, Yonsei University College of Medicine, Seoul, Korea, Republic of*

Background: Skeletal muscle gauge (SMG) was recently introduced as an imaging indicator of sarcopenia for the prediction of clinical outcomes, including chemotherapy toxicity and prognosis, in patients with cancer. Computed tomography (CT) is essential for measuring SMG; thus, the use of SMG is limited to patients who undergo CT.
Objective: We aimed to develop a machine learning algorithm using clinical and inflammatory markers to predict SMG in patients with colorectal cancer (CRC)
Methods: The least absolute shrinkage and selection operator (LASSO) regression model was applied for variable selection and predictive signature building in the training set. The predictive accuracy of the LASSO model, defined as LP-SMG was compared using the area under the receiver operating characteristic (AUROC) and decision curve analysis (DCA) in the test set.
Results: A total of 1,094 patients with CRC were enrolled and randomly categorized into training (n=656) and test (n=438) sets. Low SMG was identified in 142 (21.6%) and 90 (20.5%) patients in the training and test sets, respectively. According to multivariable analysis of the test sets, LP-SMG was identified as an independent predictor of low SMG (OR: 1329.431, CI: 271.684-7667.996, p<.001). Its predictive performance was similar in the training and test sets (AUROC: 0.846 vs. 0.869, p=.427). In the test set, LP-SMG showed better outcomes in predicting SMG than single clinical variables, such as sex, height, weight, and hemoglobin, as measured by AUROC and DCA.
Conclusions: LP-SMG, incorporating clinical variables and serum inflammatory indicators, showed superior performance compared to single variables in predicting low SMG. This machine learning model can be used as a screening tool to detect sarcopenic status without using CT during the treatment period. Applying a machine learning model might be beneficial in reducing the effort, cost, and radiation exposure from conventional CT-based diagnosis.

#5429

Using machine learning to predict tissue of origin from somatic mutation features

Andrea Giorni[1], Prabu Sivasubramiam[2], Aidan Kubeyev[2], Jordan Laurie[1], Luiz Silva[1], Matthew Foster[1], Uzma Asghar[2], Matthew Griffiths[2]. *[1]Concr Pty Ltd, Brisbane, Australia,[2]Concr Ltd, Cambridge, United Kingdom*

Background: Predicting tissue of origin (ToO) using clinical and molecular data improves diagnostic accuracy up to 95% in patients with Cancer of Unknown Primary (CUP). It is hypothesized that better treatment stratification of CUP patients using omics and machine learning (ML) classifiers may improve prognosis.

Methods: We used publicly available whole exome somatic mutation data from 4733 primary solid tissue samples, across 11 tumor types from the TCGA database, and employed a ML classifier to predict their ToO. We used 5 sets of modeling features:

1) Non-silent somatic mutation burden of 230 cancer-related genes 2) Frequency of SNP substitution type 3) Trinucleotide mutation frequency 4) Copy number variation of the 230 cancer-related genes 5) Presence of hotspot mutations.

We trained a Support Vector Machine on a training subset (80% of samples) and tuned the hyperparameters maximizing a 5-fold cross-validation F1-score. We then tested the model performance on a validation subset (20% of samples) and on a limited (n=6) dataset of metastatic samples present in the TCGA database.

Results: On the primary tumor validation set, we achieved an average AUC of 0.98(std: 0.02) and top 1, top 2 and top 3 accuracies of 80%(std: 0.11), 90%(std: 0.08) and 95%(std: 0.04) respectively, across 11 tumor types. The classification accuracy plateaus after ~300 samples, suggesting further data collection may benefit low performing tumor types. The 2 worst performers: esophageal and stomach cancers were mostly misclassified with colorectal cancers, reflecting their relative similarity. On metastatic samples (n=6) the model achieved a 67% accuracy, this is work in progress.

Conclusion: Our study confirms the potential for a DNA-based machine learning approach to improve prognosis in CUP patients by aiding diagnosis of ToO. To this end, we plan to take this study further by applying this approach to large, independent datasets derived from metastatic samples and liquid biopsies from CUP patient cohorts.

	Top_1_acc	**Top_2_acc**	**Top_3_acc**	**Precision**	**Recall**	**F1_score**	**Training_size**
Breast	0.88	0.97	0.99	0.88	0.84	0.86	756
Colorectal	0.85	0.97	0.98	0.83	0.83	0.83	460
Oesophagus	0.5	0.75	0.89	0.51	0.5	0.51	144
Liver	0.83	0.92	0.96	0.82	0.89	0.85	288
Lung	0.86	0.91	0.94	0.98	0.81	0.88	396
Ovary	0.87	0.94	0.97	0.77	0.9	0.83	312
Pancreas	0.73	0.79	0.85	0.62	0.7	0.66	132
Prostate	0.88	0.94	0.98	0.75	0.88	0.81	380
Sarcoma	0.78	0.84	0.96	0.8	0.82	0.81	180
Stomach	0.73	0.91	0.95	0.68	0.58	0.62	340
Endometrial	0.9	0.97	0.99	0.86	0.87	0.87	400
Mean	**80.09%**	**90.09%**	**95.09%**	**0.77**	**0.78**	**0.78**	**344**
	Top_1_acc_n	**Top_2_acc_n**	**Top_3_acc_n**	**n**			

				samples			
Metastatic breast	2	2	2	2			
Metastatic prostate	0	0	0	1			
Metastatic pancreas	0	0	0	1			
Metastatic sarcoma	1	1	1	1			
Metastatic oesophagus	1	1	1	1			
Mean accuracy	**67%**	**67%**	**67%**				

#5430

Improved colorectal cancer survival prediction with deep learning-based WSI analysis on PETACC8 and PRODIGE13 cohorts

Jean-Eudes Le Douget[1], Julien Taïeb[2], Paul Jacob[1], Frédéric Bibeau[3], Karine Le Malicot[4], Jean-François Emile[5], Aurélien de Reyniès[5], Mehdi Morel[1], Simon Jégou[1], Côme Lepage[6], Pierre Laurent-Puig[7]. *[1]Owkin, Paris, France,[2]Georges Pompidou European Hospital, Paris, France,[3]Centre Hospitalier Universitaire de Besançon, Besançon, France,[4]FFCD, Dijon, France,[5]AP-HP, Paris, France,[6]INSERM, Dijon, France,[7]INSERM, Paris, France*

Colorectal cancer (CRC) is the third most common cancer worldwide and represents the third leading cause of cancer deaths. Robust postoperative prediction of CRC patient prognosis may prove useful to better stratify patients, guide therapeutic choices and improve clinical trial designs. Deep learning-based analysis of whole slide images (WSI) has recently proved successful at various prediction tasks, including for example survival prediction for malignant pleural mesothelioma.

We developed a deep learning model that predicts overall survival (OS) of CRC patients, using WSI stained with haematoxylin/eosin as input, and also evaluated the difference in prognostic power obtained when combining our model prediction with other clinical factors, namely tumor grade, sex and age. The model was trained on PETACC8 cohort, constituted of 1939 WSI from patients with stage III colon cancer. The PRODIGE13 cohort, constituted of 1155 WSI from patients with stage II and III colon and rectal cancers, was used for validation; only stage III colon cancers (N=428) were selected. Patients from both cohorts received standard chemotherapy treatment, with half of the PETACC8 population also receiving CETUXIMAB antibody treatment. Both cohorts were provided by the FFCD.

Our model first extracts information on small tiles of size 112µm from the WSI, using a deep learning network trained in a self-supervised fashion, then aggregates the information of these tiles using a Multiple Instance Learning model (MIL) at the slide level to establish the final prediction. Our model was able to predict OS from WSI, reaching a c-index of 0.63 [0.61 - 0.66] in cross-validation over the PETACC8 cohort and a c-index of 0.59 [0.53 - 0.65] when transferring the PETACC8-trained model onto the PRODIGE13 cohort. The model was also able to significantly stratify patients into high and low risk groups [HR: 2.67; $p<0.0001$]. We observed

a significant c-index gain when combining our prediction and the pT classification in a linear Cox model as compared to pT alone, with c-index increasing from 0.61 to 0.66 (p=0.03). Overall, we demonstrated that our model is able to robustly predict OS from WSI in stage III colon cancers and provides increased prognostic power, on top of more traditional clinical markers such as tumor grading. Further investigation of the WSI regions targeted by our model could provide valuable insights into postoperative histopathological features of prognostic significance.

#5431

3D multiplexed tissue imaging reconstruction and optimized region-of-interest (ROI) selection through deep learning model of channels embedding

Erik Burlingame, Luke Ternes, Eun Na Kim, Joe W. Gray, Young Hwan Chang. *Biomedical Engineering, Oregon Health & Science University, Portland, OR*

Tissue-based sampling and diagnosis is the extraction of information from specifically limited spaces and its diagnostic significance of a certain object. Pathologists deal with issues related to tumor heterogeneity since analyzing a single sample does not necessarily capture a representative depiction of cancer, and a tissue biopsy usually only presents a small fraction of the tumor. Many multiplex tissue imaging platforms (MTIs) make the assumption that tissue microarrays (TMAs) containing small core samples of 2-dimensional (2D) tissue sections are a good approximation of bulk tumors although tumors are not 2D. However, emerging whole slide imaging (WSI) or 3D tumor atlases that employ MTIs like cyclic immunofluorescence (CyCIF) strongly challenge this assumption.
In spite of the additional insight gathered by measuring the tumor microenvironment in WSI or 3D, it can be prohibitively expensive and time-consuming to process tens or hundreds of tissue sections with CyCIF. Even when resources are not limited, the criteria for region-of-interest (ROI) selection in tissues for downstream analysis remain largely qualitative and subjective as stratified sampling requires the knowledge of objects and evaluates their features. Although TMAs fail to adequately approximate whole tissue features, a theoretical subsampling of tissue exists that can best represent the tumor in the whole slide image. To address these challenges, we propose deep learning approaches to learn multi-modal image translation tasks from two aspects: 1) generative modeling approach to reconstruct 3D CyCIF representation and 2) co-embedding CyCIF image and Hematoxylin and Eosin (H&E) section to learn multi-mappings by a cross-domain translation for minimum representative ROI selection. We demonstrate that generative modeling enables a 3D virtual CyCIF reconstruction of a colorectal cancer specimen given a small subset of the imaging data at training time. By co-embedding histology and MTI features, we propose a simple convex optimization for objective ROI selection. We demonstrate the potential application of ROI selection and the efficiency of its performance with respect to cellular heterogeneity. The key takeaway is that this pipeline allows for intelligent representation from H&E images, which enables a plethora of subsequent analyses on this representation space with other multiplexed imaging platforms such as Multiplexed ion beam imaging (MIBI), Imaging Mass Cytometry (IMC) or NanoString GeoMX as only a few ROIs could be selected and analyzed using these platforms.

#5432

Validation of spatial gene expression patterns predicted by deep convolutional neural networks from breast cancer histopathology images

Kathy Ton[1], Yinxi Wang[2], Liuliu Pan[1], Kimmo Kartasalo[2], Balazs Acs[3], Philippe Weitz[2], Liang Zhang[1], Yan Liang[1], Johan Hartman[4], Masi Volkonen[5], Christer Larsson[6], Pekka Ruusuvuori[7], Joseph Beechem[1], Mattias Rantalainen[2]. *[1]NanoString Technologies, Inc., Seattle, WA,[2]Karolinska Institute, Stockholm, Sweden,[3]Karolinska Institute, Seattle, WA,[4]Karolinska Instutitute, stockholm, Sweden,[5]Turku University Hospital, Turku, Finland,[6]Lund University, Lund, Switzerland,[7]University of Turku, Turku, Finland*

Molecular profiling is central in cancer precision medicine but remains costly and is only based on tumor average profiles. Morphologic patterns observable in histopathology sections from tumors are determined by the underlying molecular phenotype and therefore have the potential to be exploited for the prediction of molecular phenotypes. Transcriptome-wide expression morphology (EMO) analysis with deep convolutional neural networks (CNN) enables the prediction of mRNA expression and proliferation markers from routine histopathology whole slide images in breast cancer. The NanoString GeoMx® Digital Spatial Profiler (DSP) platform has capabilities of associating crucial spatial information with intratumor variabilities of gene expression, serving as an ideal tool to characterize and validate the prediction of intratumor heterogeneity. The GeoMx platform also provides functionalities of overlaying and aligning hematoxylin and eosin (H&E) whole slide scans on serial tissue sections with morphology marker staining to facilitate region of interest (ROI) selection to match relevant image tiles from the model input, which is a key step to ensure accuracy for the evaluation of the model predictions. The GeoMx RNA Immune Pathways Panel contains 84 gene targets including key genes involved in immune pathways and tumorigenesis and was used to validate the prediction of mRNA expression output from deep CNN models.

#5433

Representation learning for histological profiling of lung squamous premalignant lesions and tumors

Rushin Gindra[1], Yi Zheng[2], Regan Conrad[2], Emily Green[2], Sarah Mazzilli[2], Ehab Billatos[2], Mary Reid[3], Eric Burks[4], Vijaya Kolachalama[2], Jennifer E. Beane[2]. *[1]Helmholtz Munich and TranslaTUMedicine, Munich, Germany,[2]Boston Univ. School of Medicine, Boston, MA,[3]Roswell Park Comprehensive Cancer Institute, Buffalo, NY,[4]Boston Medical Center, Boston, MA*

Lung squamous cell carcinoma (LSCC) is preceded by the development of bronchial premalignant lesions (PMLs). PMLs progress through a series of histologic grades characterized by molecular and morphologic alterations. To enhance our understanding of PML progression to lung cancer, we are developing deep learning methods to quantitate PML histologic features and localize PML severity along the histologic disease spectrum.
We leveraged whole slide images (WSIs) of lung tumors (lung adenocarcinoma, LUAD and LSCC) and non-involved adjacent (referred to as ‘normal’) tissue from the Clinical Proteomic Tumor Analysis Consortium (CPTAC), the National Lung Screening Trial (NLST) and the Cancer Genome Atlas (TCGA). The NLST WSIs were used for training a self-supervised contrastive learning (simCLR) model. A graph isomorphism network (GIN) trained on CPTAC WSIs was developed using the features from simCLR and perform WSI-level predictions on tissue subtype (LUAD, LSCC, normal). Model performance was assessed using area under the receiver operating curves (AUC). The model was used to learn WSI-level features of endobronchial biopsies of PMLs from two datasets (PCGA, n=365 samples spanning all histologic grades, and CIS, n=112, only high-grade samples). The features from the final layer of the GIN were used to

compute principal components (PCs) and visualize the relationships between samples using t-SNE and UMAP. To interpret how the GIN processes WSI data, we performed gradient-based class activation mapping (Grad-CAMs) on the graphs.
High model performance was observed on the CPTAC test dataset (Accuracy = 87%, AUC >= 0.89) but dropped slightly on the TCGA dataset (Accuracy = 72%, AUC >= 0.75). The GIN-CAMs identified WSI regions that were highly associated with the output label based on expert pathologist annotation on TCGA cases. Clustering revealed distinct groupings of normal, LUAD and LSCC subtypes (PC1 & PC2, $p<0.01$). Most WSIs from the PCGA data clustered with normal tissues (PC1 & PC2: $p<0.01$ for PCGA v LUAD, PCGA v LSCC). However, a portion of the CIS samples were closely grouped with LSCC tumor cases (74% of CIS WSIs were classified as LSCC tumors. PC1 & PC2: $p<0.01$ for CIS v LUAD; PC1: $p<0.01$ for CIS v LSCC). Additionally, the feature distribution of CIS samples that progressed towards LUSC tumors were significantly different than those that regressed (PC1 & PC3: $p < 0.05$ for Progressive v Regressive).
The GIN recognizes and generates robust features that are distinctly and consistently observed in the different histologic groups across multiple cohorts. These features are also able to stratify progressive and regressive high-grade lesions. The stratification of PMLs is an important step in designing novel interception strategies to prevent the development of lung cancer, and our results suggest that pathology data may be efficacious to include in future biomarkers.

#5434

Machine-learning-based epigenetic detection of early-stage lung cancers using the EpiCheck liquid biopsy platform

Dvir Netanely[1], Stephen Lam[2], Anna McGuire[3], Stephen Deppen[4], Eric Grogan[4], Fabien Maldonado[4], Michael Gieske[5], Joseph Seaman[6], Kimberly Rieger-Christ[7], Satish Kalanjeri[8], Luis Herrera[9], Nichole Tanner[10], Garrett B. Sherwood[11], Orna Savin[1], Shacade Danan[1], Sarah Zaouch[1], Nimrod Axelrad[1], Revital Knirsh[1], Ofir Shliefer[1], Keren Manor[1], Radha Duttagupta[12], Aharona Shuali[1], Peter J. Mazzone[13], Gerard A. Silvestri[10], Catherine A. Schnabel[12], Danny Frumkin[1], Adam Wasserstrom[1]. *[1]Nucleix, Rehovot, Israel,[2]Respiratory Medicine, University of British Columbia, Vancouver, BC, Canada,[3]Surgery, University of British Columbia, Vancouver, BC, Canada,[4]Thoracic Surgery, Vanderbilt University, Nashville, TN,[5]Family Medicine, St. Elizabeth Healthcare, Mitchell, KY,[6]Sarasota Memorial Hospital, Sarasota, FL,[7]Lahey Hospital & Medical Center, Burlington, MA,[8]Pulmonary and Critical Care Medicine, Harry S. Truman Memorial Veterans' Hospital, Columbia, MO,[9]Orlando Health, Orlando, FL,[10]Medical University of South Carolina, Charleston, SC,[11]Novant Health, Winston-Salem, NC,[12]Nucleix, San Diego, CA,[13]Pulmonary Medicine, Cleveland Clinic, Cleveland, OH*

Alterations in DNA methylation are one of the earliest, most common signatures of cancer development, making them ideal biomarkers for early detection. Methylation profiling of plasma cell-free DNA (cfDNA) has significant potential to expand the use of liquid biopsies to cancer screening. The EpiCheck platform combines methylation-sensitive restriction endonuclease (MSRE) digestion with whole genome sequencing to comprehensively map genome-wide DNA methylation changes with high fidelity. In this proof-of-concept study, MSRE-NGS was used to interrogate a liquid biopsy atlas focused on early-stage lung cancers to i) identify informative NGS methylation biomarkers in plasma, and ii) develop a machine learning method to discriminate between cancer and high-risk, non-cancer controls. The EpiCheck lung cancer atlas was constructed using biospecimens from academic (UBC, Vanderbilt, Cleveland Clinic) and

commercial biobanks, and from a prospective multi-center study (NCT04968548). Plasma samples were collected from 93 high-risk primary lung cancer patients (62% stage I) and 90 high-risk individuals without cancer. Extracted DNA was digested with methylation-sensitive endonucleases and sequenced at an average depth of 600x. Methylation levels of ~6 million genomic loci were rank ordered using Student's t-test. Gene set enrichment analysis (GSEA) was performed on the top ranking 1000 differentially methylated loci. A logistic regression classifier with Lasso regularization was trained on 100,000 loci, and performance was examined by mean AUC using 5-fold cross-validation. A total of 23,130 loci exhibited significant differential methylation patterns between cancers and controls ($p<0.01$, FDR corrected). Of these, 20,159 and 2,971 lung cancer loci were hypermethylated and hypomethylated, respectively. Biological characterization using GSEA identified enrichments in transcriptional regulation and developmental control. In particular, loci were enriched for Polycomb Repressive Complex regulated genes, suggesting a possible connection to abnormal epigenetic regulation via histone modification in lung cancer. Construction of a machine learning logistic regression model based on the five training folds utilized 224 loci on average, and achieved a mean cross-validation AUC of 0.93 when distinguishing plasma cancer cases vs controls. Our findings demonstrate that the MSRE-NGS EpiCheck platform identified putative biomarkers within the plasma methylome for detecting early-stage lung cancer. A machine learning model trained on methylation targets performed with high accuracy in discriminating lung cancer patients from high-risk healthy individuals. Additional studies are required for defining the strength of the approach and for validating its use in non-invasive lung cancer screening.

#5435

Correlating and combining computational radiomics, deep radiomics and transcriptomics data in soft-tissue sarcomas (STS) patients highlight complementary prognostic information

Amandine Crombe[1], Carlo Lucchesi[2], Frédéric Bertolo[2], Michèle Kind[1], Raul Perret[3], Francois Le Loarer[3], Mariella Spalato-Ceruso[4], Maud Toulmonde[4], Audrey Laroche[5], Vanessa Chaire[3], Aurelien Bourdon[2], Antoine Italiano[4]. *[1]Radiology, Institute Bergonié, Bordeaux, France,[2]Bioinformatics, Institute Bergonié, Bordeaux, France,[3]Biopathology, Institute Bergonié, Bordeaux, France,[4]Medical oncology, Institute Bergonié, Bordeaux, France,[5]Sarcoma unit, Institute Bergonié, Bordeaux, France*

Introduction: STS are mostly prognosticated through nomograms relying on age, size, histotype and grade. Radiomics approaches, complemented with deep-learning, deep-radiomics and gene-expression profiling, could help understanding the bridge between STS radiophenotypes and molecular features and provide more efficient prognostic tools. Our goals were to investigate correlations between imaging and transcriptomics patterns, and to develop supervised prognostic models for STS patients.
Methods: We included all consecutive adult patients with newly-diagnosed locally-advanced STS managed at our sarcoma reference center between 2008 and 2020, with contrast-enhanced baseline MRI. After MRI dataset homogenization, we reduced the dimensions of the MRI data space by extracting 138 radiomics features (RFs) and 1024 deep-RFs with computational approach and autoencoder neural networks. Patient RNA was extracted from untreated samples. Following transcriptomic sequence analysis, gene expression levels for each patient were calculated. Complexity Index in Sarcoma (CINSARC) signature was extracted. Unsupervised classifications of patients based on radiomics, deep-radiomics and transcriptomics datasets were built using consensus hierarchical clustering. Differential Gene Expression and oncogenetic

pathways analyses were performed. Associations between the 3 classifications, CINSARC, grade, histotypes and SARCULATOR were explored, as well as their prognostic value. The main outcome was the metastatic-relapse free survival (MFS). The SARCULATOR nomogram and prognostic semantic-radiological features were extracted for benchmarking and understanding models outputs.
Results: 220 patients were included (111 men, median age: 62 years); 60 patients developed metastases after completing curative treatments (data are being updated with 2 additional follow-up years). Transcriptomic analysis was achieved in 54 patients and is being updated with 56 additional samples.
So far, no significant associations were found between the radiomics-based classifications and the transcriptomics-based (including CINSARC).
Nevertheless, the computational radiomics, deep-radiomics, and transcriptomics classifications were associated with MFS, though transcriptomic significance was dampened by the small sample size (P=0.008 [N=220], 0.006 [N=220] and 0.070 [N=54], respectively), suggesting complementary prognostic information.
Supervised models using data-splitting, cross-validated algorithms training, and various combinations of input data are being elaborated to improve the MFS prediction.
Conclusion: Integrating complementary multiomics datasets with computational and deep radiomics should pave the way for better performing and personalized prognostications in STS patients.

#5436
Developing artificial intelligence algorithms to predict response to neoadjuvant chemotherapy in HER2-positive breast cancer
Zhi Huang[1], Anil V. Parwani[2], Kun Huang[3], Zaibo Li[2]. *[1]Purdue University, West Lafayette, IL,[2]The Ohio State University Wexner Medical Ctr., Columbus, OH,[3]Indiana University, Indianapolis, IN*

Increasing implementation of whole slide image (WSI) and advances in computing capacity enable the use of artificial intelligence (AI) in pathology, such as quantification of biomarkers, aids in diagnosis and detection of lymph node metastasis. However, predicting therapy response in cancer patients from pre-treatment histopathologic images remains a challenging task, limited by poor understanding of tumor immune microenvironment. In this study, we aimed to develop AI models using multi-source histopathologic images to predict neoadjuvant chemotherapy (NAC) response in HER2-positive (HER2+) breast cancers. First, pretreatment tumor tissues were stained with Hematoxylin and Eosin (H&E) and multiplex immunohistochemistry (IHC) including tumor immune microenvironment markers (PD-L1: immune checkpoint protein; CD8: marker for cytotoxic T-cells; and CD163: marker for type 2 macrophages). Next, we developed an AI-based pipeline to automatically extract histopathologic features from H&E and multiplex IHC WSIs. The pipeline included: A) H&E tissue segmentation based on DeepLabV3 model to generate stroma, tumor, and lymphocyte-rich regions. B) IHC marker segmentation to segment CD8, CD163, and PD-L1 stained cells. C) H&E and IHC non-rigid registration to match H&E and IHC images since they were stained from different levels of tissue. D) Image-based registration and segmentation histopathologic feature construction. A total of 36 histopathological features were constructed to represent tumor immune microenvironment characteristics such as ratios of PD-L1, CD8 and CD163 in tumoral, stromal or lymphocyte-rich regions. They were used to train machine learning (ML) models to predict NAC response in a training dataset with 62

HER2+ breast cancers (38 with complete and 24 with incomplete response). The ML model using logistic regression demonstrated the best performance with an area under curve (AUC) of 0.8975. We also tested ML models using pathologists-derived histopathologic features, but the best performed model showed an AUC of 0.7880. Finally, the developed logistic regression ML model was tested on an external validation dataset with 20 HER2+ breast cancers (10 with complete and 10 with incomplete response) and yielded an AUC of 0.9005. In summary, we described an automatic, accurate and interpretable AI-based pipeline to extract histopathologic features from H&E and IHC WSIs and then used these features to develop machine learning model to accurately predict NAC response in HER2+ breast cancers. The ML model using AI-based extracted features outperformed the model using features manually generated by pathologists.

#5437

Vision transformers for breast cancer human epidermal growth factor receptor 2 (HER2) expression staging without immunohistochemical (IHC) staining

Gelan Ayana, Eonjin Lee, Se-woon Choe. *Kumoh National Institute of Technology Education Organization, Gumi, Korea, Republic of*

Purpose: Staging of human epidermal growth factor receptor 2 (HER2) expression is crucial for evaluating the effectiveness of breast cancer treatment. However, it involves an expensive and challenging immunohistochemical (IHC) staining in addition to hematoxylin and eosin (H&E) staining. Here, we argue that customized vision transformers are effective in breast cancer HER2 expression staging using only H&E-stained images.
Methods: Our algorithm has three modules: a localization module to weakly localize the necessary features of an image via spatial transformers, an attention module to learn global features from the image using vision transformers, and a loss module that determines the closest one to a HER2 expression level from input images by calculating the ordinal loss. We utilized a publicly available breast cancer HER2 expression dataset, the breast cancer immunohistochemical image (BCI) dataset, which contains paired H&E and IHC stained images. Results were calculated with 95% confidence intervals and t-test was used to evaluate the significance of the proposed model against other models.
Results: Our approach achieved area under receiver operating characteristics curve (AUC), precision, sensitivity, and specificity of 0.9202±0.01, 0.922±0.01, 0.876±0.01, and 0.959±0.02, respectively, averaged over five-fold cross-validation, in staging HER2 expression. The proposed method showed better performance than the conventional vision transformer model and state-of-the-art convolutional neural network models with statistical significance of $p<0.01$ in all cases.
Conclusion: Our findings are important in assisting HER2 expression staging in breast cancer treatment, while avoiding the need for an expensive and time-consuming IHC staining procedure.

Comparison of the proposed model with state-of-the-art models. CNN-convolutional neural network

Study	Neural network	Model	AUC
Couture et al. (2018)	CNN	VGG16	0.75
Shamai et al. (2019)	CNN	ResNet50	0.74
Yang et al. (2021)	CNN	ResNet50	0.76
Naik et al. (2020)	CNN	ResNet50	0.78
Khater et al. (2021)	CNN	ShuffleNet	0.75
Conde-Sousa et al. (2022)	CNN	EfficientNet	0.88

Farahmand et al. (2022)	CNN	InceptionV3	0.90
Proposed	Vision transformer	vitb_16	0.92

#5438

The combination of artificial intelligence and BLEACH&STAIN multiplex fluorescence immunohistochemistry facilitates automated prostate and breast cancer detection

Tim Mandelkow[1], Gisa Mehring[1], Elena Bady[1], Maximilian Lennartz[1], Christoph Fraune[1], Frank Jacobsen[1], Natalia Gorbokon[1], Till Krech[1], Eike Burandt[1], Anne Menz[1], Ria Uhlig[1], Till S. Clauditz[1], Guido Sauter[1], Markus Graefen[2], Sarah Minner[1], Niclas C. Blessin[1]. *[1]University Medical Center Hamburg-Eppendorf, Hamburg, Germany,[2]Martini-Clinic Hamburg-Eppendorf, Hamburg, Germany*

Background: Automated prognosis marker assessment in prostate and breast cancer using immunohistochemistry is currently hampered by the lack of a reliable differentiation between benign and malignant glands. To evaluate the patient's risk in routine clinical practice in prostate cancer prognosis parameters such as the Gleason grading, that are accompanied by a high interobserver variability are used. In breast cancer multi-gene panels are used that are influenced by fluctuating tumor purity. A reproducible prognostic evaluation is lacking in both tumor entities.
Design: To enable automated prognosis marker quantification, we have developed and validated a framework for automated prostate and breast cancer detection that comprises three different artificial intelligence analysis steps and an algorithm for cell-distance analysis of multiplex fluorescence immunohistochemistry. Pan-cytokeratin (panCK) antibodies were used to detect epithelial cells and antibodies directed against Myosin and p63 were used to identify basal cells.
Results: The optimal distance between $Myosin^+$ and $p63^+$ basal cells and benign $panCK^+$ cells was identified as 25 µm in breast and 23 µm in prostate cancer and used to exclude benign glands from the analysis combined with several deep learning-based algorithms. Our framework discriminated normal glands from malignant glands with an AUC of 0.96 in breast and 0.98 % in prostate cancer. The approach for automated prostate and breast cancer detection, by excluding benign gland from the analysis, improved the predictive performance of prognosis markers significantly ($p<0.001$). To compare the multiplex fluorescence immunohistochemistry-based (mfIHC) automated prognosis marker assessment with "classical" bright field-based automated prostate cancer detection for prognosis marker assessment in a cohort of 30 biopsies from routine clinical practice prognosis markers were manually assessed and set as gold standard. An excellent agreement between the mfIHC-based automated cancer detection and the reference manual cancer identification was found (intraclass correlation [ICC]: 0.94 [95% CI 0.87 - 0.97]).
Conclusion: Automated prostate and breast cancer identification enables fully automated prognosis marker assessment in routine clinical practice using deep learning and multiplex fluorescence immunohistochemistry. BLEACH&STAIN as well as other multiplex fluorescence immunohistochemistry approaches that enable the simultaneous analysis of 20+ biomarkers can be used to established prognosis panels that can be now assessed in an automated manner.

#5439

Deep understanding of medication events from clinical narratives is essential to building a holistic picture of cancer patient medication history

Jacob Hoffman, Neehar Mukne, Daniela Weiss, Christine Swisher, Max Kaufmann. *The Ronin Project Inc, San Mateo, CA*

MOTIVATION: One of the most complex aspects of providing care to cancer patients is building an accurate list of medications a patient is taking. Medication lists need to capture the necessary clinical context about how the patient uses the drug, such as if they can no longer afford a medication or decide to change the frequency at which they take it due to side effects. While hidden from the medication list, these changes are significant to medical decision making. Moreover, many studies focus on providing cancer medication safely. Still, providers are often not aware of other medications, which clinicians may administer in a different practice than the one providing cancer care. While many solutions attempt to improve the medication list, they frequently ignore one of the highest quality sources of medication information: clinical narratives. In this work, we propose utilizing Natural Language Processing (NLP) to extract medications and medication change events from clinical narratives.
METHODS & DISCUSSION: In this work, we utilize NLP to extract medications and medication change events from clinical narratives. We use the medication event extraction schema from the N2C2 2022 Challenge to train and evaluate various models for two classification tasks. The first is Event Classification (EC), to identify if a medication was changed. The second is Event Context Classification (ECC) to understand the nature of any change.
Using this schema, we can parse a sentence from a clinical note such as “She was experiencing a bad episode of dry cough, so stopped taking lisinopril.” Parsing such a note helps us understand an actor (the patient) initiated an action (stopping the medication) with a temporality (in the past) and with a certainty (not hypothetical).
Our approach for both tasks involved using a pre-trained clinical language model while varying the context window around a medication, masking extraneous drugs, and using mark-up tokens around events. The most performant experiments utilized more extended context around a drug, with irrelevant drug masking. We also note that longer-range encoders had better F1 performance than the original BERT architectures.
We achieved a 92% performance (micro F1) for EC when detecting a medication change. For ECC, we achieved scores of 74%, 90%, 73%, and 88% (micro F1) over the categories of Action, Certainty, Temporality, and Actor.
CONCLUSION: Given the performance observed, this approach could allow clinicians to incorporate additional extracted medication context to improve patient care and provide high-quality treatment plans. Furthermore, we can aggregate this information across patients to give more insights to clinicians and researchers about the actual use of medications.

#5440

Deep-learning model for tumor type classification enables enhanced clinical decision support in cancer diagnosis

Madison Darmofal[1], Shalabh Suman[2], Gurnit Atwal[3], Jie-Fu Chen[4], Anna Varghese[5], Jason C. Chang[4], Anoop Balakrishnan Rema[4], Aijazuddin Syed[4], Quaid Morris[6], Michael Berger[4]. *[1]Weill Cornell Medicine, Memorial Sloan Kettering Cancer Center, New York, NY,[2]Memorial Sloan Kettering Cancer Center, New York, NY,[3]Department of Molecular Genetics, University of Toronto, Toronto, ON, Canada,[4]Department of Pathology, Memorial Sloan Kettering Cancer Center, New York, NY,[5]Department of Medicine, Memorial Sloan Kettering Cancer Center, New York, NY,[6]Computational and Systems Biology, Memorial Sloan Kettering, New York, NY*

Background: Knowledge of a patient's tumor type is essential for guiding clinical treatment decisions in cancer, but histologically-based diagnosis remains challenging for a subset of cancers. Genomic alterations are highly indicative of tumor type and can be used to build classifiers that predict diagnoses, but most genomic-based classification methods use whole genome sequencing (WGS) data which is not feasible for widespread clinical implementation at present. Clinical sequencing is typically performed using cancer gene panels that target individual mutations, often drivers, but previous tumor type classifiers developed using driver-based features alone perform poorly. We hypothesize that a classifier developed using state-of-the-art deep-learning methods and a sufficiently large training cohort would be able to overcome previous accuracy limitations and support the development of a clinically-relevant tumor type prediction model.
Methods: We present Deep Genome-Derived Diagnosis (GDD-ENS), an ensemble-based deep-learning tumor type classification method trained using data from cancer gene panel sequencing. We specifically use data from MSK-IMPACT, an FDA-authorized clinical sequencing assay that reports genomic alterations including mutations, indels, copy number alterations, and gene fusions across 505 cancer-associated genes. We aggregated a discovery cohort of 35,372 patients with solid tumors profiled with MSK-IMPACT across 38 common cancer types and used this set to generate 4,487 somatic mutation features for development.
Results: GDD-ENS achieves 78.8% accuracy on a held out validation cohort of 6971 patients. For the 71.9% of predictions assigned a high confidence by the model, accuracy increases to 92.7%, rivaling WGS-based models. We use Shapley Values to report prediction-specific feature importance, and aggregate them across cancer types to show GDD-ENS identifies known cancer type-genomic alteration trends. GDD-ENS also, with high accuracy, identifies patients with cancer types not included in the 38 common types using metrics derived from ensemble statistics. For patients where non-genomic information could further guide predictions, we implement a customizable prediction-specific adaptive prior distribution and report improved accuracy after adjusting predictions to account for features such as metastatic sample biopsy site. Finally, we apply GDD-ENS to a set of 1,123 patients with Cancers of Unknown Primary (CUP) and return high confidence predictions for 49% of these patients, in some cases matching predictions on CUP samples with diagnoses that were later confirmed through additional sampling and disease progression.
Conclusions: Integrating GDD-ENS into prospective clinical sequencing workflows will enable clinically-relevant tumor type predictions that can guide treatment decisions in real-time.

#5441

Cell cycle arrest status predicted from H&E stained images using deep learning

Christina Aigner[1], Brian Reichholf[2], Maxime Emschwiller[1], Marija Pezer[1], Tobias Winterhoff[1], Simon Schallenberg[3], Rosemarie Krupar[1], Lukas Ruff[1], Sharon Ruane[1], Maximilian Alber[1], Frederick Klauschen[4], Francesca Trapani[2]. *[1]Aignostics GmbH, Berlin, Germany,[2]Boehringer Ingelheim RCV GmbH & Co KG, Vienna, Austria,[3]Institute of Pathology, Charité – Universitätsmedizin Berlin, Berlin, Germany,[4]Institute of Pathology, Ludwig Maximilian University, Munich, Germany*

Background: Cyclin-dependent kinase inhibitor p21 is a regulator of cell cycle progression. Due to its capacity to induce cell cycle arrest (CCA) when expressed in the nucleus, it is also considered a tumor suppressor and its presence can be used to evaluate the efficacy of anti-cancer treatment. Since pathologists cannot assess nuclear p21 status of cells using hematoxylin & eosin

(H&E) stained tissue alone, the current state-of-the-art approach requires evaluation using immunohistochemistry (IHC). This process is time-consuming, adds additional cost and usually requires a separate section of the sample tissue. Further, manual evaluation of IHC stainings typically shows high inter-pathologist variability. In this study, we developed a deep learning model that predicts cell-level nuclear p21 status on H&E-stained tissue alone, aiming to bypass the IHC-staining step and all drawbacks associated with it.
Methods: 99 tissue sections of pancreas cancer xenografts were stained by H&E, then restained for p21 (IHC). The samples originated from mice that had undergone experiments conducted to examine the pharmacodynamic effect of anti-cancer treatments. H&E and IHC image pairs were coregistered to micrometer level precision. A tissue segmentation model was trained to detect regions of 'carcinoma' in H&E. This model was used as a filter and only cells within the tumor region were considered for analysis. Individual cells were detected in the H&E image and these locations were transferred to the IHC image. A deep learning model was trained using IHC-informed labels to extract labels at scale from each IHC image. These labels were then transferred to the H&E image and used to train a second deep learning model which predicted nuclear p21 status from H&E alone.
Results: IHC-informed labels were extracted with a balanced accuracy (BA) of 0.93. The resulting 'H&E only' nuclear p21 model achieved a cell-level BA of 0.83. A case level comparison of the share of predicted p21+ nuclei showed a Pearson correlation of 0.72 with the share of p21+ nuclei determined by the IHC-informed extracted labels. Further, when used to characterize all samples, the model detected significant differences between treatment groups.
Conclusion: Nuclear p21 status can be detected at a cellular level in H&E images alone, using a deep learning model. This provides an opportunity to assess samples for cell cycle arrest status at scale in a standardized manner, without the need for IHC staining.

#5442

SlideQC: An AI-based tool for automated quality control of whole-slide digital pathology images

Daniela Rodrigues[1], Stefan Reinhard[2], Therese Waldburger[2], Daniel Martin[3], Suzana Couto[4], Inti Zlobec[2], Peter Caie[1], Erik Burlingame[1]. *[1]Indica Labs, Albuquerque, NM,[2]Institute of Pathology, University of Bern, Bern, Switzerland,[3]Genmab, New York, NY,[4]Pathology, Genmab, Princeton, NJ*

Introduction: Artifacts are often introduced during tissue collection and processing, slide preparation, and/or when generating whole slide images (WSI). The presence of artifacts has a negative impact on the digital pathology workflow as artifacts may hinder diagnostic reporting and can lead to false positive and false negative results when using image analysis algorithms or computer-aided diagnosis systems. Manual quality control of WSI is a time-consuming procedure and therefore automated quality control tools, which report and exclude artifacts, are highly desirable to streamline digital pathology workflows. To automate the quality control step, we developed SlideQC, an AI-based quality control tool that automatically detects, reports, and outlines artifacts such as air bubbles, dust/debris, folds, out-of-focus,and pen marks, in both research and clinical workflows. Methods: SlideQC was trained with a DenseNet-based network using 1984 annotations for artifacts including air bubbles, dust/debris, folds, out-of-focus, and pen markers, across 254 Haematoxylin and Eosin (H&E) stained WSI from more than 9 tissue types. A set of 2048 annotations from synthetically generated out-of-focus images was added to supplement the training data. The performance of the SlideQC was evaluated on an external test

cohort of 49 WSI H&E images sourced from the open-source database 'HistoQCRepo', across 375 annotations (tissue and artifact), and compared with the performance of HistoQC, an open-source quality control tool for digital pathology slides. Results: On the external test cohort, SlideQC showed high sensitivity, specificity, and F1-score with average values of 0.93, 0.99, and 0.93, across the five artifact types. In the same cohort, HistoQC attained an average sensitivity, specificity, and F1-score of 0.65, 0.79, and 0.54, respectively. Conclusions: SlideQC achieved high sensitivity, specificity, and F1-score on an external test cohort. SlideQC can add efficiency gains to a workflow by performing quality control on 100% of slides rather than the currently manually performed on only a subset of the slides in clinical pathology departments. SlideQC can allowthe triaging and alerting of slides containing a high level of artifact within a digital pathology workflow. The tool can also be used to exclude the artifact region from downstream analysis by subsequent image analysis algorithms.

#5443

Pathomics reveals the molecular and immune evolution from lung preneoplasia to invasive adenocarcinoma

Pingjun Chen[1], Frank Rojas[2], Xin Hu[3], Junya Fujimoto[2], Alejandra Serrano[2], Bo Zhu[4], Lingzhi Hong[1], Rukhmini Bandyopadhyay[1], Muhammad Aminu[1], Maliazurina B. Saad[1], Morteza Salehjahromi[1], Sheeba J. Sujit[1], Neda Kalhor[5], Harvey I. Pass[6], Andre L. Moreira[7], Ignacio I. Wistuba[2], Don L. Gibbons[4], John V. Heymach[4], Luisa M. Solis Soto[2], Jianjun Zhang[4], Jia Wu[1].
[1]Imaging Physics, The University of Texas MD Anderson Cancer Center, Houston, TX,[2]Translational Molecular Pathology, The University of Texas MD Anderson Cancer Center, Houston, TX,[3]Genomic Medicine, The University of Texas MD Anderson Cancer Center, Houston, TX,[4]Thoracic/Head and Neck Medical Oncology, The University of Texas MD Anderson Cancer Center, Houston, TX,[5]Pathology, The University of Texas MD Anderson Cancer Center, Houston, TX,[6]Surgery, NYU Langone Health, New York, NY,[7]Pathology, NYU Langone Health, New York, NY

Introduction: Atypical adenomatous hyperplasia (AAH) is the only recognized preneoplasia of lung adenocarcinoma, which can progress to adenocarcinoma in situ (AIS), minimally invasive adenocarcinoma (MIA) and eventually to invasive adenocarcinoma (ADC). A more complete understanding of the early carcinogenesis of lung cancer is critical for lung cancer early detection and interception. However, studying these lung cancer precursors is challenging because these lesions are often insufficient for molecular and immune profiling. Artificial intelligence (AI)-based studies on H&E histopathology images, termed pathomics, have achieved substantial progress in revealing heterogeneous phenotypic characteristics of various cancers. However, pathomics on lung precancerous progression and their correlation with genomic features remain underexplored.
Methods: We curated FFPE H&E slides from two ethnic groups, including the Caucasian cohort containing 46 lesions with 170 regions of interest (ROI) (74 AAH, 10 AIS, 21 MIA, and 65 ADC) and the Asian cohort containing 128 lesions with 369 ROIs (59 AAH, 84 AIS, 77 MIA, and 149 ADC). We adopted the expert-in-the-loop strategy to develop a deep learning pipeline to segment and annotate the cells within ROI into three categories: epithelial, lymphocyte, and other. Next, we measured the ratio and density of epithelial cells and lymphocytes inside each ROI as pathomics features. Finally, we interrogated ROI-level features and examined their correlation with molecular and immune features in the Asian cohort.

Results: We observed a progressive increase in the ratio and density of epithelial cells and a progressive decrease in the ratio and density of lymphocytes defined by the AI model from AAH to AIS, MIA, and ADC, consistent with the same trends defined by T cell receptor (TCR) sequencing and multiplex immunofluorescence (mIF). When correlating pathomics features with molecular/immune features, the epithelial cell ratio exhibited prominent positive correlations with the frequency of allelic imbalance (rho=0.588, p=4.71e-13) and nonsynonymous mutation burden (rho=0.453, p=1.03e-7). In contrast, the lymphocyte ratio showed a notable negative correlation with copy number variation burden (rho=-0.412, p=1.61e-6).
Conclusion: Employing AI tools to analyze HE images of lung precancerous lesions, we revealed that molecular and immune evolution during early lung carcinogenesis is consistent with the results from complicated, time-consuming, and expensive molecular/immune profiling, which requires a large number of tissue specimens, highlighting the potential of pathomics in the study of cancer biology, particularly in diseases having limited tissue specimens.

#5444

Integrated analysis of gene expression signatures and AI-based detection of tertiary lymphoid structures and stromal tumor-infiltrating lymphocytes in breast cancer H&E samples

Nadezhda Lukashevich, Vladimir Kushnarev, Daniil Dymov, Anastasia Zotova, Anna Belozerova, Ivan Valiev, Lev Popyvanov, Anna M. Love, Nathan Fowler, Alexander Bagaev, Ekaterina Postovalova. *BostonGene, Corp., Waltham, MA*

Background: Transcriptomic and morphological features of the tumor microenvironment (TME) are associated with favorable prognosis and can serve as surrogate markers for immune checkpoint inhibitor response in certain breast cancer subtypes. Tertiary lymphoid structures (TLS) and stromal tumor-infiltrating lymphocytes (sTILs) are integral components of the TME. New techniques for TLS characterization could improve reproducibility and automate the current workflow. Here, we correlated AI-based imaging platform predictions of TLS and sTILs on breast cancer H&E whole slide images (WSIs) with expression data.
Design: WSIs from 390 TCGA breast cancer samples were used to detect normalized tumoral TLS and tumor stroma infiltration areas by a convolutional neural network (CNN). High and low groups were defined by IQR1 and IQR3. Gene counts were compared using differential expression analysis followed by gene set enrichment analysis (GSEA) with hallmark gene sets. Kassandra's cell type percentage predictions, functional gene signature (Fges) single-sample GSEA, and PROGENy pathway activity median-scaled scores were compared with the Mann-Whitney U test. The Fges consisted of 4 TLS and 29 TME signatures and were clustered into 4 groups: fibrotic, myeloid, T cell, and TLS. Group medians were analyzed. Somatic deep amplifications, deletions, and missense mutations of cancer pathways were compared with Fisher’s exact test. The FDR method was used to adjust p-values.
Results: *FDCSP, CXCL13, CD79A, CCL19,* and *IGLL5* were upregulated in the TLS-high group (logFC > 1.5, p < 0.003), and *CXCL13, CXCL9, CCL19, CD3E,* and *CD79A* were upregulated in the sTIL-high group (logFC > 2, p < 4e-9). GSEA identified interferon γ and α response and allograft rejection signatures in TLS- and sTIL-high groups (p = 0.006, NES > |2.5|). sTIL-high samples expressed high levels of E2F targets, while the sTIL-low group was enriched with myogenesis and epithelial-mesenchymal transition gene sets.
The TLS-high group was enriched in the TLS Fges cluster (p = 1e-5) and contained high B, $CD4^+$ T, and $CD8^+$ T cell content (p < 2e-4). sTIL samples expressed high levels of B, $CD4^+$ T, $CD8^+$ T,

and myeloid cells ($p < 0.001$) and TLS and myeloid clusters ($p < 1e-5$). TGFβ and VEGF pathways were more active in sTIL-low samples ($p < 0.001$), while JAK-STAT was most active in the sTIL-high group ($p = 0.0006$). In the basal subtype ($p < 0.001$), the TLS-high group was associated with *NOTCH2* amplification; the sTIL-low group had increased *NRG1* deletions; and the sTIL-high group contained *BRCA2* mutations.
Conclusions: RNA-based methods used were concordant with AI-based methods of TLS and sTIL detection. Our CNN-based method of identifying immune structures in the TME with morphological features on H&E WSIs may automate traditional pathology workflows with additional validation.

#5445

Segmentation-free analysis of multiplexed images with unbiased spatial analytics and explainable AI for predicting disease outcomes

Filippo Pullara, Brian Falkenstein, Bruce Campbell, Samantha Panakkal, Akif Burak Tosun, Jeffrey Fine, S. Chakra Chennubhotla. *SpIntellx, Inc., Pittsburgh, PA*

Background: The spatial intratumor heterogeneity (ITH) is widely acknowledged as driving therapeutic response and providing fuel for drug resistance. Currently, patient selection for immunotherapy is driven mostly by PD-1/PD-L1 based IHC tests and mutational analysis. These oversimplified approaches fail to predict the risk of recurrence, therapeutic response and drug resistance with high accuracy. We hypothesize that functional responses of heterogeneous non-random spatial arrangements of tumor, stromal and immune cells in the tumor microenvironment are determined by distinct combinations of their internal states and spatial interactions within neighborhoods. The interactions generate distinct cell-cell communication networks forming functional spatial configurations of cells, termed microdomains, as organizational units of spatial ITH. Deriving the spatial networks within each microdomain with unbiased spatial analytics and the underlying network biology through explainable AI, is key to understanding tumor initiation, tumor progression, and response to therapy.
Problem: There has been an explosion of spatial imaging technologies using immunofluorescence and/or mass spectrometry for intact tissues measuring protein expressions, DNA and RNA probes. To extract high-value knowledge from these multiplexed datasets, a key first step is to segment cells accurately. Despite decades of research, this step remains elusive due to imaging artifacts arising from issues with tile stitching, incorrect registration, signal oversaturation, non-uniform illumination, poor or high-background nuclei signal, defocus, varying cell and nuclear shapes, fluorescence emission efficiency variation, overlapping and/or superimposed nuclei and low resolution (e.g., mass cytometry). Those artifacts may lead to incorrect cell phenotypes, incomplete cell phenotype atlases, and missing rare cell, fusion cell or transition cell types.
Solution: We present TumorMapr™, a segmentation-free, unbiased spatial analytics and explainable AI platform that extracts information and creates knowledge from patient disease pathology samples imaged with any technology including fluorescence, mass spectrometry etc.
Results: We apply TumorMapr on hyperplexed immunofluorescence dataset of colorectal cancer and hyperplexed imaging mass cytometry dataset of triple negative breast cancer to discover functional cell prototypes involving spatial collections of neighboring pixels highly predictive of disease progression and response to therapy, tumor promoting and tumor restraining microdomains and microdomain-specific network biology predictive of disease outcomes. We further compare these results with segmentation-based approaches to showcase the discovery of novel cell prototypes.

#5446

Immune phenotypes classified by deep learning-based H&E tissue analyzer demonstrate distinct immune landscape and transcriptomic features in ovarian cancer

Horyun Choi[1], Youjin Oh[2], Chan-Young Ock[3], Kyunghyun Paeng[3], Young Kwang Chae[2].
[1]University of Hawaii John A. Burns School of Medicine, Honolulu, HI,[2]Northwestern University Feinberg School of Medicine, Chicago, IL,[3]Lunit, Seoul, Korea, Republic of

Introduction: Deep learning-based H&E slide analyzer, Lunit-SCOPE IO can classify the tumor microenvironment as three immune phenotypes (IPs): inflamed, immune-excluded and immune-desert. In our previous study, the IPs demonstrated distinct survival outcome and immunologic landscape in endometrial cancer. To further explore the application of IPs in other type of cancer, we applied Lunit-SCOPE in ovarian cancer (OV) and compared tumor microenvironments based on the IPs.
Methods: H&E slide images, RNA-sequencing data, and clinical data were obtained from TCGA OV cohort. Lunit-SCOPE IO is a H&E slide analyzer using deep learning algorithm and was trained with 1,824 H&E slides of advanced NSCLC. We used the analyzer to classify H&E slide images from TCGA OV cohort to three IPs. Cibersort was used to assess immune cell infiltration across the IPs. The cytolytic activity score was obtained from geometric mean of GZMA and PRF1 RNA expression. We further assessed transcriptomic characteristics across IPs via differentially expressed genes analysis and gene set enrichment analysis (GSEA). Additionally, we compared CD274 gene expression across IPs. Finally, survival analysis was performed to evaluate survival outcome based on IPs. We used Mann-Whitney method to compare non-parametric variables between the IPs.
Results: The proportion of inflamed, immune-excluded and immune-desert group in TCGA OV were 7 (10.2%), 13 (18.8%), and 49 (71%), respectively. Inflamed group showed significantly higher proportion of M1 macrophage compared with immune-desert group (6.6% vs. 2%, P=.012). We observed higher cytolytic activity score in inflamed group compared to immune-desert group (7.21 vs. 5.27, P=.016). In GSEA, inflamed group is significantly enriched in IL6 JAK STAT3 signaling, interferon gamma response, KRAS signaling up, and inflammatory response pathway (NES 2.19; adjusted P=.021, NES 1.70; adjusted P=.021, NES 1.62; adjusted P=.037, and NES 1.52; adjusted P=.037, respectively). Immune-desert is related to upregulated MYC target V2 pathway (NES -1.95; adjusted P=.037). Inflamed group did not show significant difference in CD274 expression, compared with others (Inflamed vs. immune-excluded, 4.97 vs. 4.19, P=.115 and Inflamed vs. immune-desert, 4.97 vs. 3.95, P=.058). Inflamed group did not show any significant difference in overall survival, compared with non-inflamed group (Inflamed vs. non-inflamed, HR 0.98; 95% CI 0.45 - 2.14; P=.958).
Conclusion: Deep learning-based H&E slide analyzer can be used to classify tumor H&E slide images with OV into three IPs. In this study, the classification demonstrated distinct immunologic traits and transcriptomic characteristics in tumor microenvironment. The enrichment of interferon gamma response pathway in inflamed OV group may indicate opportunities for targeted immunotherapy.

#5447

Artificial intelligence (AI)-based classification of stromal subtypes reveals associations between stromal composition and prognosis in NSCLC

Fedaa Najdawi, Sandhya Srinivasan, Neel Patel, Michael G. Drage, Christian Kirkup, Chintan Parmar, Jacqueline Brosnan-Cashman, Michael Montalto, Andrew H. Beck, Archit Khosla, Ilan

Wapinski, Ben Glass, Murray Resnick, Matthew Bronnimann. *PathAI, Inc., Boston, MA*

Background**:** Many cancers are known to involve a desmoplastic stromal reaction. While cancer-associated stroma (CAS) has long been appreciated histologically, single-cell molecular analyses have revealed its heterogeneity, and the cellular composition of CAS has been linked to prognosis in several cancer types, including NSCLC. While pathologists have sought to manually classify CAS based on collagen architecture or nuclear density, this approach has not sufficiently captured the heterogeneity of CAS. To this end, we have developed an artificial intelligence (AI)-based model to predict stromal composition in NSCLC from hematoxylin and eosin (H&E)-stained tissue.
Methods: We developed a convolutional neural network-based model to classify CAS as immature, mature, densely inflamed, densely fibroblastic, or elastosis. This model was trained using manual pathologist-derived annotations (N=3019) of H&E-stained whole slide images (WSIs) of PDAC obtained from the TCGA (N=126). This stromal subdivision model was deployed on H&E-stained LUAD (N=468) and LUSC (N=430) WSIs. Model performance was assessed by qualitative review by expert pathologists. Human interpretable features (HIFs) were extracted from the stromal subdivision model (e.g., proportional area of mature relative to total stroma) and were assessed to identify associations with overall survival (OS) using univariate Cox regression analysis after adjusting for age, sex, and tumor stage.
Results: The stromal subdivision model successfully predicted areas of immature, mature, densely inflammatory, and densely fibrotic stroma, as well as elastosis, in LUAD and LUSC. In LUAD, higher combined proportional areas of mature and fibroblastic stroma relative to total cancer stroma was associated with poor OS (p=0.007), while higher combined proportional areas of densely inflamed stroma and elastosis relative to total cancer stroma was associated with improved OS (p=0.007). These findings were validated by stratified tertile analysis based on the corresponding risk direction. Notably, while the average stromal compositions did not differ significantly between NSCLC subtypes, the stromal HIFs were only prognostic in LUAD but not in LUSC.
Conclusions: We developed a first of its kind model to characterize CAS subtypes in NSCLC tissue. Features extracted from this model are related to prognosis in LUAD, but not in LUSC, further confirming the importance of CAS to tumor biology and the importance of considering histologic subtypes. Work is ongoing to identify relationships between stromal HIFs and treatment response in NSCLC as well as other cancer indications.

Clinical Applications of Artificial Intelligence and Mathematical Oncology

#5693
Cancer cells subvert fibroblast function to promote a growth factor enriched tumor microenvironment in endocrine therapy resistant ER+ breast cancer
Jason I. Griffiths[1], Patrick A. Cosgrove[1], Eric Medina Castaneda[1], Aritro Nath[1], Jinfeng Chen[1], Frederick R. Adler[2], Jeffrey T. Chang[3], Qamar J. Khan[4], Andrea H. Bild[1]. *[1]City of Hope National Medical Center, Duarte, CA,[2]University of Utah, Salt Lake City, UT,[3]UT Health Sciences Center at Houston, Houston, TX,[4]The University of Kansas, Kansas City, KS*

While endocrine therapy (ET) has considerably improved Stage II/III ER+ breast cancer survival rates, resistance emerges in 30-50% of patients. Recent advances have uncovered numerous cancer intrinsic and tumor-microenvironment mediated mechanisms contributing to ET

resistance. However, the predominant mechanisms that prevent cure and ultimately lead to development of terminal metastatic cancer remain unknown. To reveal the leading causes of ET resistance in early-stage ER+ breast cancers, we used single-cell RNA sequencing to profile serial tumor biopsies from a larger cohort of patients. Patients received either endocrine therapy (letrozole) alone or in combination with a CDK4/6 cell cycle inhibitor (ribociclib). We examined the evolution of tumor composition, cellular communication, and the phenotypic diversity of tumor-associated cancer and non-cancer cells throughout treatment. Our analyses reveal that ET-resistant tumors are fibroblast- and endothelial-enriched and consistently exhibit broad upregulation of growth factor signaling to cancer cells, with consistent activation of ERBB communication across patient tumors. Fibroblasts emerged as the primary source of these additional growth factor signals. Upregulation of fibroblast growth factor signaling (via NRG1/2, EGF and IGF) was commensurate with differentiation to a mesenchymal cancer-associated-fibroblast (myCAF) phenotype, which was itself stimulated by cancer cells through EGF and TGF signaling. In response to growth factor enrichment, cancer cells of ET-resistant tumors showed activation of MAPK signal transduction and downstream transcription factors promoting proliferation including FOS, JUN and TRIB1. These results indicate that ET resistance emerges in patient tumors when cancer cells subvert fibroblast function to promote a growth factor enriched tumor microenvironment permitting estrogen independent cancer proliferation.

#5694

Adaptive treatment scheduling of PARP inhibitors in ovarian cancer: Using mathematical modeling to assess clinical feasibility and estimate potential benefits

Maximilian A. R. Strobl[1], Alexandra L. Martin[2], Christopher Gallagher[3], Mehdi Damaghi[4], Mark Robertson-Tessi[5], Robert Gatenby[6], Robert M. Wenham[7], Philip K. Maini[3], Alexander R. A. Anderson[5]. *[1]Moffitt Cancer Center, Tampa, FL,[2]Division of Gynecologic Oncology, West Cancer Center and Research Institute, Memphis, TN,[3]Mathematics, University of Oxford, Oxford, United Kingdom,[4]Stony Brook Cancer Center, Stony Brook, NY,[5]Integrated Mathematical Oncology, Moffitt Cancer Center, Tampa, FL,[6]Cancer Biology and Evolution Program, Moffitt Cancer Center, Tampa, FL,[7]Gynecologic Oncology Program, Moffitt Cancer Center, Tampa, FL*

PARP inhibitors (PARPis) are revolutionizing the treatment of ovarian cancer. Yet for many patients these improvements come at the cost of physical and financial toxicity and responses are typically temporary due to emerging drug resistance. A growing body of pre-clinical and clinical work suggests that when cure is unlikely, it is possible to delay progression and reduce drug use through patient-specific drug scheduling. So-called 'adaptive therapy' dynamically adjusts treatment to preserve drug-sensitive cells which interfere with resistant cells through competition. In a prior study, we developed a mathematical model to describe the treatment response of ovarian cancer cells to the PARPi olaparib in vitro, and we proposed a candidate adaptive PARPi algorithm. Here, we extend our model to capture the dynamics in patients and use it to study the feasibility and potential benefit of adaptive PARPi administration in practice.
Our prior model posited that treatment induces cell cycle arrest that moves cells from the proliferating subset of the population to an arrested compartment. The model predicted that while there is scope for treatment reductions, these need to be carefully timed and prolonged treatment breaks should be avoided. Based on these results we proposed an adaptive treatment algorithm in which the olaparib dose is switched between high and low doses, depending on the tumor's growth rate. To test the translational potential of this strategy, we retrospectively collected data from 53 ovarian cancer patients who received olaparib at the H Lee Moffitt Cancer Center

between 2014 and 2021. Using serum CA-125 as a proxy for tumor burden, we first examined whether our mathematical model could capture the patients' longitudinal dynamics. While the response of some patients was consistent with what we had observed in vitro, in others there was evidence of the emergence of a distinct drug-resistant population, and we extended our mathematical model to account for this. After calibrating and validating the model with the patient data, we tested whether these patients would have benefited from adaptive PARPi treatment. Our simulations suggest that our proposed algorithm is feasible and provides a means for reducing treatment in a patient-specific manner. In addition, in a subset of patients we predict that adaptive therapy could delay progression. Overall, this work corroborates the potential for adaptive PARPi therapy and helps to identify outstanding challenges on the way to clinical translation.

#5695

Deep learning risk prediction model of distant recurrence from H&E endometrial cancer slides

Sarah Fremond[1], Sonali Andani[2], Jurriaan Barkey Wolf[1], Gitte Ørtoft[3], Estrid Høgdall[4], Jouke Dijkstra[5], Jan J. Jobsen[6], Ina M. Jürgenliemk-Schulz[7], Ludy CHW Lutgens[8], Melanie E. Powell[9], Naveena Singh[10], Linda R. Mileshkin[11], Helen J. Mackay[12], Alexandra Leary[13], Dionyssios katsaros[14], Hans W. Nijman[15], Stephanie M. de Boer[16], Remi A. Nout[17], Vincent T.H.B.M Smit[1], Carien L. Creutzberg[1], Nanda Horeweg[16], Viktor H. Koelzer[18], Tjalling Bosse[1]. *[1]Pathology, Leiden University Medical Center (LUMC), Leiden, Netherlands,[2]Pathology and Molecular Pathology and Computer Science, ETH Zurich, University Hospital, University of Zurich, Zurich, Switzerland,[3]Gynaecology, Copenhagen University Hospital, Copenhagen, Denmark,[4]Gynaecology, Herlev Hospital, University of Copenhagen, Copenhagen, Denmark,[5]Vascular and Molecular Imaging, Leiden University Medical Center (LUMC), Leiden, Netherlands,[6]Radiation Oncology, Medisch Spectrum Twente, Enschede, Netherlands,[7]Radiation Oncology, University Medical Center Utrecht, Utrecht, Netherlands,[8]Radiation Oncology, Maastricht UMC+, Maastricht, Netherlands,[9]Clinical Oncology, Barts Health NHS Trust, London, United Kingdom,[10]Pathology, Vancouver General Hospital, Vancouver, BC, Canada,[11]Medical Oncology, Peter MacCallum Cancer Center, Melbourne, Australia,[12]Medical Oncology and Hematology, Odette Cancer Center Sunnybrook Health Sciences Center, Toronto, ON, Canada,[13]Medical Oncology, Gustave Roussy Institute, Villejuif, France,[14]Gynecologic Oncology, University of Torino, Torino, Italy,[15]Obstetrics & Gynecology, University Medical Center Groningen, Groningen, Netherlands,[16]Radiation Oncology, Leiden University Medical Center (LUMC), Leiden, Netherlands,[17]Radiation Oncology, Erasmus University Medical Center, Rotterdam, Netherlands,[18]Pathology and Molecular Pathology, University Hospital Zurich, University of Zurich, Zurich, Switzerland*

Accurate risk prediction of distant recurrence (DR) is crucial for personalized adjuvant systemic therapy of endometrial cancer (EC) stage I-III patients, as DR is associated with a 5-year overall survival of 10-20%. Risk stratification and treatment recommendation are currently based on histopathological and molecular markers, which is challenging due to high inter-observer variability and testing costs respectively. Deep Learning (DL) models can predict prognosis by identifying relevant visual features from H&E whole slide images (WSIs) at different resolutions without prior assumptions. Here, we developed and tested the first interpretable state-of-the-art DL model for WSI-based risk prediction of DR of stage I-III EC (DeREC) from the randomized

PORTEC-1/-2/-3 trials and three clinical cohorts with long-term follow-up data. We used one representative H&E WSI each from 1761 EC patients, excluding those who received adjuvant chemotherapy as it lowers the risk of DR. We randomly sampled 20% as a held-out internal test set (N=353 with 62 events; 8.45 year median follow-up) and performed a 5-fold cross-validation on the training set (N=1408). WSIs were partitioned into 360 micron patches at 40x magnification. DeREC combined self-supervised representation learning of patches using a multi-resolution vision transformer and a WSI-level graph attention-based time-to-event prediction model. The model performance of correctly ranking patients by predicted risk scores and true time to DR was measured with the concordance-index and compared with a Cox' Proportional Hazards (CPH) model fitted on histopathological variables (histotype, grade, lymphovascular space invasion, stage). Discriminative quality of the predicted risk groups was investigated with Kaplan-Meier analysis and the log-rank test. Most predictive patches by predicted risk groups were reviewed by an expert gynecopathologist for identification of prognostic morphological features. DeREC achieved a concordance-index of 0.764 [95%CI 0.754-0.773] on 5-fold cross validation and 0.757 on the test set, as compared to 0.704 [95%CI 0.662-0.746] with CPH. Predicted risk groups around quartiles 1 and 3 accurately stratified patients between low (N=89), intermediate (N=175), high (N=89) risk of DR ($p<0.0001$). Among the predicted low-risk group only 3 (3.37%) patients relapsed whereas intermediate and high-risk groups counted 27 (15.43%) and 32 (35.96%) events respectively. DeREC is the first DL model accurately distinguishing EC patients at high risk of DR from those at low risk using one H&E WSI, which would aid decisions on adjuvant treatment. DeREC outperformed standard statistical prediction methods using histopathological variables, indicating that it identified prognostic visual features which can be further investigated. Future development includes the integration of clinicopathological and molecular information.

#5696

A prognostic machine learning model for early breast cancer which combines clinical and genetic data in patients treated with neo/adjuvant chemotherapy

Aidan (Amanzhol) Kubeyev[1], Andrea Giorni[2], Prabu Siva[1], Luiz Silva[2], Jordan Laurie[2], Matthew Foster[2], Matthew Griffiths[1], Uzma Asghar[1]. *[1]Concr, Cambridge, United Kingdom,[2]Concr, Brisbane, Australia*

Background: Accurate modelling of the impact of patient-specific features and cancer treatments on survival allows the assignment of targeted therapy. There has not been any effort to build a multi-source model for the survival analysis of breast cancer. We show in this study a prognostic model, which integrates genetic (DNA), clinical and therapy inputs to predict survival for early breast cancer (stages 1-3) for all breast cancer subtypes.
Methods: We used a data-driven Random Survival Forest approach, a statistical non-parametric ensemble learning method, that incorporates censor and time-to-event data. The learning is performed by creating numerous decision trees and selecting the model based on the correct responses in unseen data. We used The Cancer Genome Atlas Breast Cancer (TCGA) dataset and observed improvements in the accuracy when more sources of data were used, in line with the previous research. Integrating the impact of non-silent somatic tumor mutations (whole exome) and gene copy number variation (CNV) were analyzed on all mutations and per particular mutation.
Results: Data from 1096 women with stage 1-3 early breast cancer were inputs to the model n=437 ER+ve HER2-ve, n=123 HER2+ve ER+ve, n=40 HER2+ ER-ve and n=126 TNBC.

Pathological stage 1, n=183; stage 2, n=620; and stage 3, n=249. The following chemotherapy and hormonal treatments were used in the analysis: anthracycline, taxanes, platinum, alkylating and anti-metabolite agents, anti-oestrogen, aromatase inhibitors, ovarian suppression and HER2 antibody treatment.
The model accuracy for predicting survival for early breast cancer using only clinical data was 0.78 for Area Under Curve (AUC) and c-index. The predictive accuracy improved stepwise by adding hormone, genetic and treatment data to AUC of 0.86 and c-index to 0.85. We observed the same trend if the proportion of test data increased from 0.25 to 0.75. Changes in median genes FGFR2 and CDKN2A copy number were strongly prognostic with p=0.0001 and p=0.002, and weaker signals for CBFB p=0.05, HRAS p=0.06, AKT p=0.07.
Conclusion: Using public datasets, we developed a predictive survival model for an individual with early breast cancer up to 5 years from diagnosis using multi-source and patient-specific data. We show that using this approach for survival analysis yields good accuracy.

#5697

Predicting response to PD-L1 inhibition in NSCLC using a quantitative systems pharmacology model guided by immunogenomic data

Hanwen Wang, Theinmozhi Arulraj, Aleksander S. Popel. *Johns Hopkins University School of Medicine, Baltimore, MD*

Introduction: Non-small cell lung cancer (NSCLC) is the most common subtype of lung cancer with an overall 5-year survival rate of 26%, which varies by the disease stage. Novel drug combinations involving immune checkpoint inhibitors are being investigated in clinical trials in NSCLC. In this study, we generated about 450 virtual patients that resembled actual patients with NSCLC and simulated tumor growth during PD-L1 inhibition using a quantitative systems pharmacology (QSP) model.
Methods: We recalibrated a previously developed QSP model of the cancer-immunity cycle (1) to NSCLC with parameters estimated by published experimental data. Proportions of CD8, CD4, and regulatory T cells (Tregs), M1 and M2 macrophages in lung adenocarcinoma and lung squamous cell carcinoma were downloaded from iAtlas database and used to calculate the ratios of CD8/CD4, Tregs/CD8, and M1/M2. The three immune subset ratios (observed data) were used to guide the virtual patient generation. We first randomly generated deviations around the baseline model parameters to account for inter-patient variability and then selected virtual patients with model-predicted immune subset ratios statistically matching the observed data. Finally, we simulated tumor growth during PD-L1 inhibition and predicted clinical response in the virtual patient cohort.
Results: Our model predicted an overall response rate of 16.3% with a 95% bootstrap confidence interval of (11.8, 22.4)% for the overall virtual patient cohort. It also showed that CD8 T cells, PD-L1 expression, CD8/CD4, CD8/Tregs, M1/M2 ratios, and the number of NSCLC-specific T cell clones were significantly higher in responders to PD-L1 inhibition. Furthermore, Tregs/CD8 and CD8/CD4 ratios were predicted to be the best predictive biomarkers according to ROC analysis with areas under ROC curve of 0.71 and 0.66.
Conclusion: Immunogenomic analysis of RNA-seq data on iAtlas allowed generation of realistic virtual patients using QSP models in immuno-oncology. With a virtual patient cohort guided by immunogenomic data, our model provided reliable efficacy prediction for immunotherapy and a tool to identify predictive biomarkers in NSCLC. 1. Wang H, Zhao C, Santa-Maria CA, Emens LA, Popel AS. Dynamics of tumor-associated macrophages in a quantitative systems

pharmacology model of immunotherapy in triple-negative breast cancer. iScience. 2022;25:104702.

#5698

A multicenter study validated an integrated deep learning model for precision malignancy risk assessment and reducing unnecessary biopsies in BI-RADS 4 cases

Chika F. Ezeana[1], Tiancheng He[1], Tejal A. Patel[2], Virginia Kaklamani[3], Maryam Elmi[3], Erica Ibarra[3], Pamela M. Otto[3], Kenneth A. Kist[3], Heather Speck[4], Lin Wang[1], Joe Ensor[5], Ya-Chen T. Shih[6], Bumyang Kim[6], I-Wen Pan[6], David Spak[7], Wei T. Yang[7], Jenny C. Chang[5], Stephen T. C. Wong[8]. *[1]Department of Systems Medicine and Bioengineering, Houston Methodist Neal Cancer Center, Houston Methodist Hospital, Houston, TX,[2]Department of General Oncology, The University of Texas MD Anderson Cancer Center, Houston, TX,[3]The University of Texas Health Science Center, San Antonio, TX,[4]The University of the Incarnate Word School of Osteopathic Medicine, San Antonio, TX,[5]Houston Methodist Neal Cancer Center, Houston Methodist Hospital, Houston, TX,[6]Department of Health Services Research, The University of Texas MD Anderson Cancer Center, Houston, TX,[7]Department of Radiology, The University of Texas MD Anderson Cancer Center, Houston, TX,[8]Department of Systems Medicine and Bioengineering, Department of Radiology and Pathology, Houston Methodist Neal Cancer Center, Weill Cornell Medicine, Houston Methodist Hospital, Houston, TX*

Introducti**on:** BI-RADS category 4 is associated with a wide variability in probability of malignancy, ranging from 2 to 95% while biopsy-derived positive predictive value (PPV3) for this category's lesions remains low at 21.1% in the US. A major fallout of these facts is that we have way very high false positive rate leading to too many unnecessary biopsies and their associated costs and emotional burden. We improved our in-house intelligent-augmented Breast cancer RISK calculator (iBRISK), an integrated deep learning (DL) based decision support app and assessed its performance in a multicenter IRB-approved study.

Methods: We improved iBRISK by retraining the DL model with an expanded dataset of 9,700 patient records of clinical risk-factors and mammographic descriptors from Houston Methodist Hospital (HMH) and validated using another 1,078 patient records. These patients were all seen between March 2006 and December 2016. We assessed the model using blinded, independent retrospective BI-RADS 4 patients who had biopsies subsequently after mammography and seen January 2015 - June 2019 at three major healthcare institutions in Texas, USA: MD Anderson Cancer Center, the University of Texas Health Sciences Center at San Antonio, and HMH. We dichotomized and trichotomized the data to evaluate precision of risk stratification and probability of malignancy (POM) estimation translated into biopsy decision augmentation. The iBRISK score as a continuous predictor of malignancy and possible cost savings was also analyzed.

Results: The multicenter validation dataset had 4,209 women, median age (interquartile) was 56 (45, 65) years. The use of iBRISK score as a continuous predictor of malignancy yielded an AUC of 0.97. Among "low" and "moderate" POM patients, only two out of 1,228 patients (0.16%) and 118 out of 1788 (6.6%) were malignant respectively. This translates to an even better precision when compared to newly introduced BI-RADS 4 subcategories 4A and 4B, with associated PPV3s of 7.6% and 22%, respectively. The "high" POM group had a malignancy rate of 85.9% (1,025/1,193). Estimated potential cost savings in the US was over $260 million.

Conclusion: The iBRISK app demonstrated high sensitivity in malignancy prediction and can potentially be used to safely obviate biopsies in up to 50% of patients in low/moderate POM-

groups. This would result in significant healthcare quality improvement, cost savings, and help reduce patient anxiety.

#5699

Development and validation of a quantitative systems pharmacology model for prediction of preclinical efficacy of PARP inhibitors rucaparib and talazoparib combined with the ATR inhibitor gartisertib (M4344)

Claire C. Villette[1], Frances Brightman[1], Nathalie Dupuy[1], Astrid Zimmermann[2], Florianne Lignet[2], Frank T. Zenke[3], Nadia Terranova[4], Jayaprakasam Bolleddula[3], Samer El Bawab[2], Christophe Chassagnole[1]. *[1]Physiomics Plc, Oxford, United Kingdom,[2]Merck KGaA, Darmstadt, Germany,[3]EMD Serono, Billerica, MA,[4]Merck Institute of Pharmacometrics an affiliate of Merck KGaA, Darmstadt, Germany*

Introduction: Poly (ADP-ribose) polymerase (PARP) and ataxia telangiectasia and Rad3-related (ATR) inhibitors target key DNA damage response (DDR) kinases. PARP inhibitors (PARPi) suppress the catalytic activity of PARP and trap PARP in a complex with damaged DNA, resulting in the accumulation of unrepaired single-strand breaks (SSBs) and stalled replication forks. Loss of ATR activity blocks cell cycle arrest induced by single-stranded DNA and sensitizes cancer cells to agents that induce DNA replication stress. Thus, PARP inhibition synergizes (through synthetic lethality) with concurrent ATR inhibition by inducing replication fork collapse, double-strand breaks (DSBs), and PARP-DNA complex formation, with simultaneous loss of intra-S and G2/M checkpoints and suppression of DNA-damage repair, leading to mitotic catastrophe. Four PARPi are currently approved for the treatment of various cancers and several ATR inhibitors (ATRi) are in clinical trials either as monotherapies or in combination with other chemotherapeutic agents. We developed and validated a semi-mechanistic quantitative systems pharmacology (QSP) model that represents the mechanisms of action of PARPi and ATRi with minimal parameters, which could be used to inform the optimization of combination regimens.

Methods: A QSP model of a growing cancer cell population was developed by considering SSBs and DSBs, and parallel DNA repair pathways relying on PARP and ATR. PARPi and ATRi mediated saturable inhibitory effects on their respective DDR pathways, while PARP-DNA trapping was represented as an increased conversion rate from SSBs to DSBs. Phenotypic impairments of the DDR such as BRCA mutations were embedded as DDR pathway deficiencies. The model was calibrated using experimental data derived from rucaparib and talazoparib combination studies with gartisertib.

Results: The calibrated model captured well the tumor-growth inhibition observed in the HBCx9 PDX model for rucaparib and gartisertib, either alone or in combination, over average daily doses ranging from 50 mg/kg to 200 mg/kg (QD/BID) of rucaparib and 1-3 mg/kg (QD/BIW/QD alternate weeks) of gartisertib. The model was also able to predict the wide range of responses (from shrinkage to progressive disease) observed in a panel of triple-negative breast cancer PDX models (BRCA-mutant and wild type) treated with talazoparib and gartisertib in combination. The complete DDR model utilized 9 variable parameters, and the mechanisms of action of PARP and ATR inhibition were described by 4 parameters each.

Conclusion: This newly developed QSP model provides a framework that can be applied to optimize the dosing regimens of PARP and ATR inhibitor combinations and help with clinical dosing strategy.

Integrative Cancer Systems Biology

#4303

High-throughput 3D tumoroid models for immunotherapy and drug discovery

Duy Nguyen[1], Alexander McGhee[1], Diego Pedro[1], Alfonso Pepe[1], Matthew Schaller[1], Ryan Smolchek[2], Jack Famiglietti[2], Stephanie Warrington[2], W. Gregory Sawyer[1]. *[1]University of Florida, Gainesville, FL,[2]Aurita Bioscience, Gainesville, FL*

The tumor microenvironment (TME) is a complex 3D cellular system comprised of a diverse amalgam of cells. To characterize the TME, we developed a 3D cell culture platform which facilitates imaging-based analysis and cell viability for extended durations. We used this platform to collect in-situ spatiotemporal measurements of cytokine concentrations in the tumor vicinity, track cellular activity, and model local tumor invasion of glioblastoma (GBM) using fast-scanning confocal microscopy. The mechanism by which we achieve long-term 3D culture is perfusion, modeled as flow through a porous medium. Perfusion facilitates regulated transport of nutrients and waste within the soft microgel medium: Liquid-Like Solids (LLS). The interstitial space is tuned to mimic a capillary bed, and surface bioconjugation of the microgels promotes cellular adhesion and migration. To measure cytokine concentrations, GBM tumoroids were grown in LLS and printed into a dispersion of ELISA beads in LLS. The mechanical stability of LLS ensures the tumor and ELISA beads remain stationary without impeding cellular activity. Cytokine on and off-rates were referenced alongside measured bead fluorescence intensities and positions to fit spatiotemporal reaction-diffusion models. Fast-scanning confocal microscopy facilitated in-situ observation of the evolutionary dynamics of tumor progression. Co-culture of patient-derived tumor explants and autologous PBMCs printed into type I collagen-bioconjugated LLS enabled studies of cancer-immune interactions. In-situ cytokine measurements revealed local IL-8 concentrations reached a maximum value of 2 ng ml^{-1} after 10 hours. A cellular production rate was estimated at 2 molecules $cell^{-1}$ s^{-1}. Invasive behavior into the proximal space was determined to be super-diffusive; off-lattice agent-based simulations indicated this behavior is a result of the confinement of invasive fronts to the microgel interstitium. The invading glioblastoma cells used anchorage-dependent migration and were guided by geometric cues to traverse the porous bioconjugated LLS network. Cancer-immune interaction studies revealed average CD8+ speeds greater than 2.8 μm min^{-1} and both chemotaxis and chemokinetic behavior. CD8+ T-cell killing rates were estimated at approximately 3 cancer cells hr^{-1} initially, monotonically falling over 12 hours to roughly 1 cell hr^{-1}. The development of the in-situ 3D ELISA assay and imaging-based analysis techniques have enabled the tracking of tumor-immune cell interactions, observation of dynamic tumor progression, and local cytokine concentration profiling at appreciable spatiotemporal resolutions. The combination of a physiologically relevant 3D culture platform with the capacity for in-situ qualitative and quantitative observation may lead to new, powerful, preclinical models that allow for interrogation of the TME and decrease the rate of false discovery.

#4304

Network-based inference identifies cell state-specific drugs targeting master regulator vulnerabilities in diffuse midline glioma

Ester Calvo Fernandez[1], Junqiang Wang[2], Xu Zhang[3], Hong-Jian Wei[4], Hanna E. Minns[5], Aaron T. Griffin[1], Lukas Vlahos[1], Timothy J. Martins[6], Pamela S. Becker[6], John Crawford[7], Robyn D. Gartrell[5], Luca Szalontay[5], Stergios Zacharoulis[8], Zhiguo Zhang[3], Robert Wechsler-Reya[9],

Cheng-Chia Wu[4], Andrea Califano[10], Jovana Pavisic[5]. *[1]Department of Systems Biology, Department of Pathology and Cell Biology, Columbia University Irving Medical Center, New York, NY,[2]Department of Systems Biology, Columbia University Irving Medical Center, New York, NY,[3]Department of Genetics and Development, Columbia University Irving Medical Center, New York, NY,[4]Department of Radiation Oncology, Columbia University Irving Medical Center, New York, NY,[5]Department of Pediatrics, Columbia University Irving Medical Center, New York, NY,[6]Department of Medicine and Institute for Stem Cell and Regenerative Medicine, University of Washington, Seattle, WA,[7]Department of Pediatrics, University of California Irvine & Children's Hospital Orange County, Orange, CA,[8]Department of Pediatrics, Columbia University Irving Medical Center & Bristol Myers Squibb, New York, NY,[9]Department of Neurological Sciences, Columbia University Irving Medical Center, New York, NY,[10]Departments of Systems Biology, Medicine, Biomedical Informatics, Biochemistry & Molecular Biophysic, Columbia University Irving Medical Center, New York, NY*

Diffuse Midline Glioma (DMG) are fatal pediatric brain tumors with no therapies. We leveraged network-based methodologies to dissect the heterogeneity of DMG tumors and to discover Master Regulator (MR) proteins representing pharmacologically accessible, mechanistic determinants of molecularly distinct cell states. We produced the first DMG regulatory network from 122 publicly available RNAseq profiles with ARACNe (Basso et al. Nat Genet 2005), and inferred sample-specific MR protein activity with VIPER (Alvarez et al. Nat Genet 2016) based on the differential expression of their targets. 7 of the top 25 most active MRs found comprise a well-characterized MR block (MRB2) (Paull et al.Cell 2021), frequently activated across aggressive tumors, and enriched in DMG patient MR signatures (Fisher's Exact Test $p=4.4x10^{-18}$). A CRISPR/Cas9 KO screen across 3 DMG patient cell lines identified a set of 73/77 essential genes that were enriched in the MR signature of 80% of patient samples (GSEA p=0.000034). FOXM1 emerged as an essential MR, significantly activated across virtually all patients.

We then generated RNAseq profiles following perturbation with ~300 oncology drugs in 2 DMG cell lines most representative of patient MR signatures, and used this to identify drugs that invert patient MR activity profiles using the NYS/CA Dept. of Health approved OncoTreat algorithm (Alvarez et al. Nat Genet 2018). OncoTreat predicted sensitivity to HDAC, MEK, CDK, PI3K, and proteosome inhibitors in subsets of patients, overlapping with published DMG drug screens. Importantly, 80% of OncoTreat-predicted drugs ($p<10^{-5}$) from 3 DMG patient tumor biopsies showed *in vitro* sensitivity in cultured tumor cells from the respective patients, with overall 68% accuracy among 223 drugs evaluated by both OncoTreat and *in vitro* (Fisher's Exact Test p=0.0449).

Further analysis of DMG intra-tumor heterogeneity via protein activity inference across DMG single cells from 6 published scRNAseq profiles identified 6 tumor clusters with unique MR signatures co-existing in virtually all patients representing distinct cellular states (2 astrocyte-, 1 oligodendrocyte-, and 3 oligodendrocyte precursor cell-like states). Targetable MRs and OncoTreat-predicted drugs were distinct between these states. Bulk RNAseq analysis recapitulated predictions seen in the more prevalent OPC-like states, but failed to capture MR and drug predictions for the AC-like states (*e.g.* JAK1/Ruxolitinib and STAT3/Napabucasin). We are currently validating cell state-specific drug predictions *in vivo* at single-cell resolution in subcutaneous patient-derived xenograft and orthotopic syngeneic DMG models that we have shown recapitulate patient tumor heterogeneity, including with focused ultrasound-mediated drug delivery. This provides a platform to nominate much-needed novel drugs and drug combinations to treat DMG.

#4305

Germline structural variants shape prostate cancer clinical and molecular evolution

Nicholas K. Wang[1], Alexandre Rouette[2], Kathleen E. Houlahan[1], Takafumi N. Yamaguchi[1], Julie Livingstone[1], Chol-Hee Jung[3], Peter Georgeson[3], Michael Fraser[2], Yu-Jia Shiah[2], Cindy Q. Yao[2], Vincent Huang[2], Natalie S. Fox[1], Natalie Kurganovs[3], Katayoon Kasaian[2], Veronica Y. Sabelnykova[2], Jay Jayalath[2], Kenneth Weke[2], Helen Zhu[4], Theodorus van der Kwast[5], Tony Papenfuss[3], Housheng H. He[4], Niall M. Corcoran[6], Robert G. Bristow[4], Alexandre R. Zlotta[7], Christopher Hovens[3], Paul C. Boutros[1]. *[1]Human Genetics, UCLA - University of California Los Angeles, Los Angeles, CA,[2]Ontario Institute for Cancer Research, Toronto, ON, Canada,[3]Australian Prostate Cancer Research Centre Epworth Richmond, Richmond, Australia,[4]Medical Biophysics, University of Toronto, Toronto, ON, Canada,[5]Pathology and Laboratory Medicine, University of Toronto, Toronto, ON, Canada,[6]Surgery, University of Melbourne, Melbourne, Australia,[7]Princess Margaret Cancer Center, Toronto, ON, Canada*

Inherited genetic variation profoundly influences cancer risk and outcome. While the impact of germline single nucleotide polymorphisms has been well-studied in several cancer types, the effects of germline structural variants (gSVs) on cancer biology and clinical outcomes is largely unknown. From our cohort of 300 men with localized, intermediate risk prostate cancer, we identified 6,003 gSVs present in at least 3% of patients; 48 were associated with recurrent somatic alterations or clinical outcome. Of these, approximately 50% were associated with expression of nearby genes or intersected with exons or regulatory regions. Using external cohorts, we validated three gSVs that were strongly associated with poor clinical outcomes, including an inversion at chr14q24.1 present in ~20% of patients. Notably, a strong synergistic effect on outcome was observed in patients with somatic TP53 alterations or high genomic instability, defining a new aggressive prostate cancer subtype with chr14INV as a novel, recurrent biomarker.

#4306

Identifying genetic dependencies of replication stress using interpretable artificial intelligence

Xiaoyu Zhao, Akshat Singhal, Trey Ideker. *UC San Diego, La Jolla, CA*

Rapid proliferation is a hallmark of tumor cells, associated with sensitivity to chemicals that cause DNA replication stress (RS). Due to sustained proliferative signaling and/or defective DNA repair, cancer cells undergo persistent RS making them strongly dependent on the replication stress response (RSR). A consequence of this dependency is that RS becomes an exploitable therapeutic vulnerability in cancer treatment. Classical RS drugs work predominantly by interfering with DNA replication in dividing cells. Recently, an increasing number of drugs have been designed to specifically target RSR proteins. However, molecular pathways responsible for drug response are incompletely understood. Here we build an interpretable deep-learning model aimed at understanding mechanisms of susceptibility and resistance to replicative stress. Instead of associating genetic alterations with drug responses directly, our approach is to project individual mutations on a map of protein complexes and larger molecular assemblies with prior evidence for involvement in cancer. This approach is prompted and supported by the concept that cancer is a network-based disease arising from the action of hallmark cancer pathways. Through systematic interpretation, the model identifies 37 complexes that integrate rare alterations in hundreds of genes for accurate response prediction. The complexes, which cover roles in

transcription, DNA repair, cell-cycle checkpoint, and immunity, are further investigated by directed genetic perturbations, validating 24 for which RS effects are phenocopied by CRISPR guide RNAs. For complexes with poorly characterized functions, further insights are obtained via their profiles of in-silico activation across RS agents. This study creates a library of system-level genetic vulnerabilities governing replication stress, with implications for drug selection and combination.

#4307

Integrative molecular subtypes of acute myeloid leukemia

Qianxing (Quincy) Mo, Seongseok Yun, David A. Sallman, Nicole Vincelette, Guang Peng, Ling Zhang, Jeffrey E. Lancet, Eric Padron. *H. Lee Moffitt Cancer Center and Research Institute, Tampa, FL*

Introduction: Acute Myeloid Leukemia (AML) is a heterogenous disease characterized by distinct clinical course and prognosis based on genomics, epigenomics or transcriptomics profile. However, the multi-omics profiles have not been systematically integrated to define the integrative molecular subtypes of AML. There is a great clinical interest to identify the patterns across multi-omics profiles that could be used for prognosis and guiding targeted therapy in AML.
Methods: To identify integrative molecular subtypes (iSubtypes) of AML, we performed an integrative clustering (iCluster) analysis of the AML multi-omics data (n=160) generated by The Cancer Genome Atlas (TCGA), which consisted of somatic mutation, DNA copy number, DNA methylation and RNA-seq gene expression data for 160 AML samples. We identified the multi-omics signatures that drove the molecular classification of AML. Based on the methylation and gene expression signatures, we derived a gene panel for classification of AML and verified the prognostic power of the gene panel using three independent AML datasets (n=1382).
Results: We identified four iSubtypes of AML that featured distinct multi-omics signatures. At the DNA level, the iSubtype 1 was characterized by chromosomal abnormalities and high-frequency mutation of *TP53* (30%) and *RUNX1* (27%); the iSubtype 2 was characterized by chromosomal abnormalities and high-frequency mutation of *CEBPA* (20%) and *FLT3* (26%); while the iSubtypes 3 and 4 were characterized by chromosomal normality and high-frequency mutation of *FLT3* (34%, 41%), *NPM1* (37%, 57%) and *DNMT3A* (20%, 41%). At the epigenomics level, the iSubtypes 1, 3 and 4 were characterized by hypomethylation of subtype driver genes, while the iSubtypes 2 was characterized by hypermethylation of subtype driver genes. At the transcriptomics level, the 4 iSubtypes were distinguished by differentially expressed genes involved in immune process, regulation of immune process, angiogenesis, leukocyte cell activation and migration, wound healing and cell structure organization, etc. The iSubtypes 1 and 4 had the worse overall survival (OS), while the iSubtype 3 had the best and the iSubtype 2 had the middle OS. Based on the subtype-driving methylation and transcription signatures, we derived a 571-gene panel for classification of AML. Using 3 independent AML transcriptomics datasets, we demonstrated that the excellent power of the gene panel in classifying AML into 4 gene expression subtypes with similar survival outcomes.
Conclusions: iSubtypes of AML are jointly determined by multi-omics profiles. The subtype-driving methylation and transcription signature have excellent power in classifying AML into clinically relevant subtypes. This integrative analysis provides insights into the biological processes underling AML.

#4308

Cancer as a disease of information

Adam Julian Goldstein. *University of Oxford, Oxford, United Kingdom*

The causes and symptoms of cancer are often described in physical terms, for example as DNA mutations leading to increased cell proliferation. These understandings have been immensely informative, but physical changes are only one of several ways to understand what cancer is and why it behaves the way it does. An alternative perspective builds upon Claude Shannon's work in information theory, and sees cancer as a result of missing, noisy, and/or distorted information. In this talk I summarize existing research and discuss the implications for understanding cancer as a disease of information. I then explain how detecting and treating cancer look different when viewed through this lens. In particular, I discuss how this approach offers the hope for rehabilitating cancer cells by restoring expected information flows, in contrast to some current treatments which exacerbate information disruptions.

#4309

Early apoptotic measurements of patient-derived organoids predict patient response to therapy

Kelley E. McQueeney[1], Patrick Bhola[1], Sarah J. Hill[2], Anthony Letai[3]. *[1]DFCI/Harvard Medical School, Boston, MA,[2]DFCI/Brigham and Women's Hospital, Boston, MA,[3]Medical Oncology, DFCI/Harvard Medical School, Boston, MA*

The use of imperfect models and ex vivo culture systems to try to predict patient drug response represents an enormous bottle neck in cancer treatment. Nonetheless, determining how effective an approved drug will be for an individual cancer patient, as well as identifying novel compounds that may be beneficial to a specific population often requires the use of primary tumor cells. Patient-derived organoids represent an intermediate between primary tumor cells, whose limited supply may hinder reliable drug testing, and cell lines, which often do not reflect what happens in vivo. Herein, we describe the development of a novel assay platform, termed 3D-DBP (3D dynamic BH3 profiling), to detect early apoptotic measurements in ovarian cancer patient-derived organoids and present evidence that this method can be used to predict patient response to therapy. We have optimized the use of patient-derived organoids from 16 individual tumors in a microscopy-based imaging assay. We image the BH3 peptide-induced release of cytochrome c from mitochondria, which indicates permeabilization of the outer mitochondrial membrane, in intact organoids. The less cytochrome c retained in each organoid, the more primed that organoid is for apoptosis. By comparing results of drug-treated and untreated cells, we can identify drugs that cause a significant increase in apoptotic priming in organoids. In the 16 patient-derived organoids investigated this 3D DBP technique was an effective means of predicting patient response to carboplatin therapy. In summary, we have not only created a means of visualizing drug response in intact organoids, but also have demonstrated its clinical utility.

#4310

Ultra high-plex spatial proteogenomic investigation of giant cell glioblastoma multiforme immune infiltrates reveals distinct protein and RNA expression profiles

Shilah Bonnett, Alyssa Rosenbloom, Giang Ong, Mark Conner, Daniel Newhouse, Felicia New, Hiromi Sato, Chi Pha, Saskia Ilcisin, John Lyssand, Gary Geiss, Joseph M. Beechem. *NanoString Technologies, Inc., Seattle, WA*

The advancement of spatially resolved, multiplex proteomic and transcriptomic technologies has revolutionized and redefined the approaches to complex biological questions pertaining to tissue heterogeneity, tumor microenvironments, cellular interactions, cellular diversity, and therapeutic response. Most spatial technologies yield single analyte proteomic or transcriptomic datasets from separate formalin-fixed paraffin-embedded (FFPE) tissues sections. Multiple studies have demonstrated a poor correlation between RNA expression and protein abundance owing to transcriptional and translational regulation, target turnover, and post-translational protein modifications. Therefore, a workflow that accurately measures RNA and protein simultaneously within a single tissue section with distinct spatial context is critical to a more complete biological understanding of cellular interactions and activities. Such multimodal omic datasets of protein and DNA or RNA have been termed “spatial proteogenomics”. Here we present a novel spatial proteogenomic (SPG) assay on the GeoMx® Digital Spatial Profiler platform with NGS readout that enables ultra high-plex digital quantitation of proteins (147-plex) and RNA (whole transcriptome, > 18,000-plex) from a single FFPE sample. We demonstrated high concordance, $R > 0.85$, and minor change in sensitivity (<11%) between the SPG assay and the single analyte GeoMx Whole Transcriptome Atlas and GeoMx NGS Protein assays. We used the SPG assay to interrogate 23 different glioblastoma multiforme samples across 4 pathologies. We observed clustering of both RNA and protein based on cancer pathology and anatomic location. The in-depth investigation of giant cell glioblastoma multiforme (gcGBM) revealed distinct protein and RNA expression profiles compared to that of glioblastoma multiforme (GBM). Spatial proteogenomics allowed

simultaneous interrogation of critical protein post-translational modifications alongside whole transcriptomic profiles within the same distinct cellular neighborhoods. Within our dataset, we observed >2-fold higher protein expression levels of phospho-GSK3β (Ser9) in gcGBM compared to GBM. Inactivation of GSK3β through phosphorylation has been shown to enhance proliferation of GBM cells. We also observed differential protein expression phosphorylated Tau variants. Phospho-Thr231 Tau was >2-fold higher in GBM compared to gcGBM. Associated with neurodegenerative Alzheimer's disease, changes in Tau expression and phosphorylation have also been observed in glioblastoma. Our study exemplifies the utility of the SPG assay in expanding our understanding of glioblastoma multiforme molecular pathology.

#4311

Using multiomics analysis to identify dysregulated transcription factors in non-small cell lung cancer (NSCLC) to drive the expression of a cancer-activated synthetic biomarker

Yue Wendy Zhang, Shireen Rudina, Dariusz Wodziak, Chloe Xia, Maggie Louie, Albert Park, David Suhy. *Earli Inc., Redwood City, CA*

Early detection of cancer is an important driver of increased survival, quality of life and reduced healthcare costs. Earli is developing a highly sensitive, orthogonal approach that uses a genetic construct that usurps dysregulated pathways and actively forces cancer cells to drive the expression of a detectable 'synthetic' biomarker. Identification of abnormally elevated transcription factors (TF) in cancer is crucial when developing a cancer-activated expression platform. Evaluating TF function in a genome wide fashion is a challenge, especially since TF activity is not solely reflected by just its RNA expression or even by protein abundance, but also its post-translational modification including phosphorylation. In this study, we use the publicly available multiomics dataset from Clinical Proteomic Tumor Analysis Consortium (CPTAC) which includes RNA-seq based transcriptional profiling, MS based protein abundance and phosphorylation from 211 paired tumor and normal adjacent samples derived from NSCLC patients. Performing Multiomics Factor Analysis (MOFA) analysis, we identified a short list of 34 dysregulated TFs in NSCLC that displayed high expression levels in at least two of the three

omics platforms relative to normal tissues, six of which scored highly across all three. A subset of candidate TF binding sequences were subcloned as multimers into expression constructs with a basal promoter and empirically evaluated in multiple cancer cell lines, including patient-derived xenograft (PDX) cell lines and normal cell lines.Transfection experiments demonstrated that these novel chimeric synthetic promoters could produce robust levels of expression in PDX-derived cell lines that was 10-20x higher than expression mediated by known cancer-activated promoters such as the endogenous survivin (BIRC5) promoter. Furthermore, levels achieved were only 3-4 fold lower than a control EF-1a promoter, one of the strongest promoters, typically used to drive constitutive expression in mammalian cells. Currently, a small subset of these chimeric constructs is being tested in murine tumor models and in large animal cancer models such as oncopigs. These experiments will further drive the development of this approach for use in early cancer detection.

#4312

Identification of shared mutations across many parallel human and canine cancers based on comprehensive survey of canine cancer mutations and the “caninization” of human mutations from COSMIC

Sharadha Sakthikumar, Salvatore Facista, Derick Whitley, Manisha Warrier, William Hendricks, Guannan Wang. *Vidium Animal Health, a TGen subsidiary, Phoenix, AZ*

Introduction: Vidium Insight™ is a canine cancer genomic biomarker database built from exhaustive curation of peer-reviewed literature describing genomic mutations in canine cancers. This repository catalogs the ever-increasing abundance of cancer mutations and their diagnostic, prognostic, and therapeutic biomarker associations in canine oncology. However, the design of cancer research/clinical studies in dogs and the interpretation of the data, still rely heavily on inferences from human cancers. To leverage the wealth of well-annotated human mutation data and close the canine cancer genomics knowledge gap, we recently "caninized" ~ 400K cancer mutations from the largest human mutation database, COSMIC. Here, we aim to systematically assess the cross-species

conservation status of mutations found in parallel human and canine cancers.
Methods: Human mutations from the COSMIC Cancer Gene Census (CGC) dataset were “caninized”, i.e. structured analysis of protein sequence conservation and conversion of human cancer mutations to their canine homologous sites. Caninized point and indel mutations, as well as copy number alterations, were subsequently intersected with curated primary canine data in Vidium Insight™ to determine if they have been previously reported in canine cancers. Cancer-wise mutation data were also parsed and assessed for any shared mutations in equivalent human and canine cancers.
Results: Over 90% of the coding point and indel mutations in COSMIC CGC were successfully converted to the canine genome, i.e. caninized. We found 436 unique caninized mutations reported in 27 primary canine cancers across 78 studies. Of these, 410 were predicted pathogenic mutations that likely contribute to oncogenesis. Genes affected by copy number alterations in human cancers have published evidence in canine cancers as well. We then assessed concordance in putative cancer driver mutations recorded in both species. Of the 27 primary canine cancers that have mutation data to date, 26 have been shown to share somatic mutations with corresponding human cancers.
Conclusion: It has long been recognized that human and canine cancers share similar etiology, histopathology, clinical manifestations, and treatment responses. We have demonstrated high-level conservation of mutation profiles across many parallel human and canine cancers. Our work suggests that pathogenic mutations found in one species can inform the other's genomic and molecular underpinnings, guide basic/clinical research, drive drug development, facilitate clinical management, and ultimately, empower genomic-guided precision medicine across species.

#4313

A novel gene regulatory network model identifies master regulators in cancer

Praneeth Reddy Sudalagunta[1], Rafael Renatino Canevarolo[1], Mark Meads[1], Maria Coelho Siqueira Silva[1], Xiaohong Zhao[1], Raghunandan Reddy Alugubelli[1], Joon-hyun Song[2], Erez Persi[3], Mehdi Damaghi[2], Kenneth H. Shain[1], Ariosto Silva[1]. *[1]H. Lee Moffitt Cancer Center, Tampa, FL,[2]Stony*

Brook Cancer Center, Stony Brook, NY,[3]National Center for Biotechnology Information, Bethesda, MD

Small-scale regulatory networks can model known biological processes; while large-scale genome-wide datasets can identify novel mechanisms. We developed a biophysical modeling framework that combines the accuracy of small-scale networks with the power of large-scale datasets. As a proof of principle, we implemented this framework on a cohort of 844 multiple myeloma (MM) patients' (and 1092 TCGA breast cancer patients) z-normalized RNAseq data using t-Distributed Stochastic Neighbor Embedding to construct a disease-specific transcriptomic map, where genes closer to each other co-express within the cohort. Fuzzy c-means clustering is carried out to identify clusters of genes that are likely regulated by a common transcription factor (TF). We construct a gene regulatory network (GRN) for each cluster of co-expressing genes on a disease-specific transcriptomic map by identifying upstream TFs for each cluster using publicly available databases ENCODE and ChEA, and kinases that phosphorylate these TFs using PhosphoSitePlus and PhosphoPoint. An exhaustive list of TFs and kinases are reduced to a few key predictor variables using regression tree modeling for each gene in that cluster. This leads to a cascading network of kinases that phosphorylate TFs, which regulate expression of genes in a cluster. We derived a mechanistic model from first-principles to define functional relationships governing the GRN; where transcription, translation, and post-translational modifications are modeled using first-order reversible reaction kinetic equations. The patient-specific rate constants of the model are parametrized by single sample gene set enrichment analysis scores of key KEGG pathways like ribosome, protein synthesis, RNA degradation, etc. The system of differential equations, under steady-state, reduce to an algebraic equation that can predict the expression of every gene in a cluster from the expression of its upstream TFs and kinases alone, which is fitted to RNAseq data of 422 MM patients to estimate undetermined parameters. The remaining patients' data is used to estimate the accuracy of the model using Pearson's correlation (model predicted vs actual) coefficient, r. Out of 16,738 genes, 7,936 were predicted accurately ($r>0.5$), while the remaining genes were shown to have a significant overlap (hypergeometric test; p-value<1e-48 and representation factor = 7.27) with genes that have high variability in

chromatin accessibility across patients. A reduced GRN with only accurately predicted genes is obtained for each cluster, followed by linking GRNs to each other through TFs and kinases that are featured in other GRNs; where betweenness centrality measures of the resulting directed graph identifies disease-specific master regulators. MYC, STAT3, CREB1, POLR2A, PLK1, and TP53 are found to be key hubs in MM network; similar analyses are being conducted for other cancers featured in TCGA.

#4314

CEACAM7 an early detection biomarker for pancreatic ductal adenocarcinoma

Anupam Dhasmana, Swati Dhasmana, Sheema Khan, Murali M. Yallapu, Meena Jaggi, Subhash C. Chauhan. *Immunology & Microbiology, University of Texas Rio Grande Valley, McAllen, TX*

Background: As per key statistics of American Cancer Society 2021, Pancreatic Cancer (PanCa) affects around 60,430 persons (31,950 men and 28,480 women) a year in the U.S. and is tricky to diagnose and treat. PanCa is the 4th leading cause of cancer death with a 5-year survival rate of only 9%, along with a poor prognosis. Generally (around 85-90%) PanCa are adenocarcinomas, such as Pancreatic ductal adenocarcinomas (PDAC). PDAC is now one of the most challenging tumor entities worldwide, characterized as a highly aggressive disease with dismal overall prognosis with a mortality rate near the incidence rate. For PDAC, no early tumor specific biomarker is available, therefore, novel early detection biomarker strategy is immediately required to upgrade the narrow diagnostic portfolio against PanCa. Considering this alarming situation, our team has identified a novel oncogenic protein, Carcinoembryonic antigen-related cell adhesion molecule 7 (CEACAM7). Our studies suggested high CEACAM7 expression in PDAC tumors and its association with patient survival. In this study we have investigated the potential role of CECAM7 for early PDAC diagnosis and its role in PDAC progression.
Methodology: This study includes bioinformatics pre-screening using publicly available cancer databases followed by molecular biology techniques. To detect the degree of expression of CEACAM7 in normal pancreatic cell (HPNE) and PDAC progressive cellular models, we have minutely scrutinized the PDAC cell panel (HPAF-2, SU86.86 & Panc-1) &

TMAs of PDAC patients, in terms of mRNA & protein expression level of CEACAM7. The confocal microscopy was performed to identify the intensity and localization of CEACAM7 protein. IHC analysis was also performed to identify the protein expressions in the pancreatitis and tumor cores along with their locations, grading and Mean Composite Score.
Results: Bioinformatic results confirmed the relevance of CEACAM7 as a potential early diagnostic and prognostic marker of PDAC. HPAF2 (well differentiated) expressed highest mRNA and protein expression analyses, followed by SU86.86 (moderately differentiated) and very low expression in AsPc1 (poorly differentiated), and Panc1 (poorly differentiated). The IHC analyses of TMAs exhibited negligible or faint staining in pancreatitis (chronic and acute) and most of the positive cases were in tumor grading 1 & 2.
Conclusion: Our observations clearly cite that CEACAM7 can serve as a potential early diagnostic and/or prognostic marker of PDAC and may also potentiate the sensitivity of the existing biomarker panel of PDAC. However, further studies are warranted to determine its clinical significance.
Keywords: Pancreatic cancer, PDAC, CEACAM7, Early detection biomarker, Tumor grading

#4315

Exploring the relationship of SSTR2 immunohistochemical and textural features to neuroendocrine tumor grade

Leah Sherbansky, Patrick Savickas, Sharwari Phanse, Jack Casey, Julie Feldstein. *HistoWiz, Brooklyn, NY*

Due to the heterogeneous nature of neuroendocrine tumors, concrete management poses adversity. A pathologic grading system defined by the World Health Organization (WHO) scaled 1-3 offers a means to guide the course of treatment. While Ki-67 is considered a gold standard tumor grading marker, Somatostatin Receptor 2 (SSTR2) has been strongly associated with low-grade neuroendocrine tumors, as it mediates the effects of somatostatin, an anti-cell-proliferation hormone. This study aims to focus on only SSTR2 and its stratified relationship with tumor grade to perform a similar role as Ki-67, given previous association with low-grade tumors. The main purpose of this study is to extract a variety of features from tumor

histology images including SSTR2 expression, as well as textural features. Textural analysis offers an exhaustive method to extract morphologic characteristics from images and explore patterns unrecognizable to the human eye. This study will be accomplished through 3 objectives: first, to explore the relationship of SSTR2 expressive features to tumor grade. Second, to create a classification task to determine if machine learning models are able to accurately predict tumor grade directly from values of SSTR2 expression. The final objective of this study is to incorporate textural features into the classification task, and determine whether adding textural features to the classification dataset will improve the ML models' ability to predict tumor grade. TMAs were stained for SSTR2, then scanned and analyzed to determine various quantifiable values: percent SSTR2, percent 1+ cells, percent 2+ cells, and percent 3+ cells, and H-score. From the data analysis, percent SSTR2 was the only value with nonconcurrent thresholds per grade: 51-98% for grade 1, 24-47% for grade 2, and .03-20% for grade 3. Textural features local binary pattern (LBP) as well as Grey-level co-occurrence matrix (GLCM) were extracted from the tumor images as well. Four separate machine learning algorithms (logistic regression, random forest, naive bayes, and support vector machine) were run on this collected dataset in 3 separate combinations: SSTR2 alone, Textural features alone, and a combination of SSTR2 and textural features. The dataset with the highest average classification metrics was SSTR2 expression alone, with the random forest classifier yielding 100 percent precision and accuracy. Two of the machine learning models improved in precision and accuracy when textural features were added to the SSTR2 dataset. The lowest-performing dataset was the textural features dataset, due to a heavy class imbalance that impacted the performance of the ML models. The results of this study depict a highly stratified relationship between SSTR2 percentage and tumor grade, and that adding textural features to the SSTR2 dataset will increase grade-classification abilities.

#4316

Identification of tertiary lymphoid structures from H&E slides using deep learning analysis of nuclear morphology is associated with favorable survival in colorectal cancer patients

Becky Arbiv, Tal Dankovich, Sun Dagan, Yuval Shachaf, Tomer Dicker, Ron Elran, Avi Laniado, Amit Bart, Ori Zelichov, Ettai Markovits. *Nucleai,*

Tel Aviv, Israel

Background: Tertiary lymphoid structures (TLS) are organized aggregates of immune cells that develop in non-lymphoid tissues and are associated with better prognosis and immunotherapy response across cancer types. Multiple IHC stainings are required for an accurate detection of TLS, making it challenging to implement as a clinical biomarker. Here, we developed a deep learning (DL) model that extracts nuclear morphology features to detect TLS from H&E slides and demonstrated its prognostic role in colorectal cancer (CRC) patients.
Methods: A publicly available dataset consisting of 140 tissue cores from 35 CRC pts stained with H&E and 56 protein markers using the CODEX multiplex immunofluorescence (mIF) system was analyzed. Immune cell aggregates on the H&E were annotated by expert pathologists as either TLS or lymphocyte aggregates (LA), based on marker expression from the mIF stain on the same core. TLS were defined as dense aggregates of CD3+/CD20+/CD21+ cells, while all other immune cell aggregates were defined as LA. Next, HoVerNet was used to perform nuclear segmentation on cells within the TLS and LA on the H&E. Nuclear features including eccentricity, solidity, convexity, and nuclear intensity per cell were extracted and the mean and variance of each feature was summarized per tissue core. Based on these features, a univariate analysis comparing TLS and LA was performed, and a TLS classifier was trained using multivariate logistic regression. The classifier performance was assessed using 5 repeats of 5-fold cross validation and average accuracy and area under the ROC curve (AUC) were calculated. Overall survival (OS) was compared between patients with predicted TLS and LA using a Cox proportional hazard regression analysis.
Results: From the 140 tissue cores, we identified cores with either TLS (n=18), LA (n=34) or none (n=92). No core presented both TLS and LA. In a Mann Whitney univariate analysis, cells in TLS areas demonstrated a higher mean nuclear eccentricity ($p<0.0001$) and solidity ($p=0.01$) along with lower variance in these features ($p<0.0001$ and $p=0.001$, respectively) compared to cells in LA. The multivariate classifier trained on nuclear features exhibited a 90.4% average accuracy ($p<0.0001$) and 94% AUC ($p<0.0001$) in differentiating between TLS and LA. Median OS was significantly higher in patients with at least one predicted TLS (n=13) vs.

patients with at least one predicted LA (n=13) detected on H&E (NR vs. 19 months, HR=0.21, 95% CI 0.06-0.78; p=0.01).
Conclusions: Nuclear based morphological features can be used to accurately detect the presence of TLS and LA from H&E slides, without the need for mIF or IHC stainings. Given the predictive value of TLS presence, this work demonstrates the potential for H&E slides to be used for patient selection for immunotherapy treatments.

#4317

Comparison of Single-Molecule Flow (SiM-Flow) and qRT-PCR for detection of plasma miR-375 and miR-1290 in metastatic castrate-resistant prostate cancer (mCRPC)

Manish Kohli[1], Siva Nalla[2], Chia-Wei Kuo[3], Claire Hanson[1], Matt Larsen[1], Anna Neibling[1], Jennifer Lloyd[1], Julia Batten[1], Neeraj Agarwal[1], Umang Swami[1], Benjamin Maughan[1], Sumati Gupta[1], Rebecca L. Smith[4], Andrew Smith[5]. *[1]University of Utah Huntsman Cancer Institute, Salt Lake City, UT,[2]University of Illinois, Urbana Champagne, Urbana-Champagne, IL,[3]University of Illinois, Urbana-Champagne, Urbana, IL,[4]University of Illinois, Urbana Champagne, Urbana, IL,[5]University of Illinois, Urbana Champagne, Urbana, UT*

Background**:** Plasma microRNA (miR)-375 and miR-1290 levels have been associated with poor survival and resistance to docetaxel chemotherapy. Detection of plasma miRs is typically performed using qRT-PCR, which is time-intensive and laborious. We developed a novel technique, SiM-Flow, that rapidly and accurately quantifies miRs from low blood volumes (~100 uL). SiM-Flow uses a fluorescence-based flow cytometer to digitally count nucleic acids that have been extended and fluorescently tagged. Our goal was to compare plasma miR detection using SiM-Flow with qRT-PCR assays and determine clinical outcomes in mCRPC stage.
Methods: Forty mCRPC patients undergoing state-specific treatment were enrolled prospectively. Uniform processing of plasma was performed on patient blood samples. Total RNA was extracted from 100 µL of plasma and qRT-PCR was performed using TaqMan miRNA assays for targets miR-375 and miR-1290, endogenous controls miR-30a-5p and miR-16, and exogenous control cel-miR-39. SiM-Flow was conducted using a

commercial flow cytometer to count fluorescent barcoded rolling-circle-amplification-extended miR nanoparticles for the same targets. Target miR-375 and miR-1290 were normalized using the geometric means of endogenous controls miR-30a-5p, miR-16, and miR-39 and compared across the two assays by Spearman's rank correlation analysis. Survival analysis was calculated from date of developing mCRPC to death using Cox Proportional Hazard Regression (CPHR) for association with mean of the miR targets normalized by miR-16.
Results: qRT-PCR assays were optimized to detect native targets, endogenous controls, and spike-in miRs from plasma with ≤100 aM limit of detection (LOD), while SiM-Flow was able to detect miRs from plasma with ≤10 aM LOD. After normalization, target miRs in plasma were detected in 26/40 mCRPC patients by qRT-PCR and in 31/40 patients by SiM-Flow. The Spearman Rho for normalized miR-375 was 0.738 and normalized miR-1290 was 0.130. Survival analysis showed a hazard ratio of 1.03 (95% CI 1.01, 1.05) for the mean of miR-375.
Conclusion: Target miR-375 levels detected with SiM-Flow had higher with qRT-PCR, at lower LOD for SiM-Flow. Mean Normalized miR-375 target levels also were associated with poor prognosis in mCRPC.

#4318
Cancer cell communication with macrophages prevents T cell activation during emergence of cell cycle therapy resistance
Jason I. Griffiths[1], Patrick A. Cosgrove[1], Eric Medina Castaneda[1], Aritro Nath[1], Jinfeng Chen[1], Frederick R. Adler[2], Jeffrey T. Chang[3], Qamar J. Khan[4], Andrea H. Bild[1]. *[1]City of Hope National Medical Center, Duarte, CA,[2]University of Utah, Salt Lake City, UT,[3]UT Health Sciences Center at Houston, Houston, TX,[4]The University of Kansas Medical Center, Kansas City, KS*

By corrupting signals for growth and survival, evolving cancer cells can engineer the tumor microenvironment (TME) to promote treatment resistance. However, the specific interactions between malignant and non-malignant cells that predispose drug resistance and their changes during treatment remain widely unknown. Here we examine the composition, communication, and phenotypic diversity of tumor-associated cell populations in serial biopsies from early-stage ER+ breast cancers. We used

single-cell RNA sequencing to profile over 400 thousand malignant and non-malignant cells from patient tumor samples obtained before, during and after treatment. The patients received either endocrine therapy (letrozole) alone or in combination with a CDK4/6 cell cycle inhibitor (ribociclib). Our analyses reveal that cancer cells from ribociclib-resistant tumors stimulate macrophage differentiation towards an immune-suppressive phenotype through upregulation of a diversity of cytokines and growth factors. The macrophage phenotype shift leads to reduced crosstalk with cytotoxic T-cells via IL-2/15/18 receptors, diminishing T-cell activation and recruitment. These results indicate that cancer communications promoting an immune-cold TME predispose tumors to develop CDK4/6 cell cycle inhibitor resistance, and that the beneficial effects of blocking cancer cell proliferation must be balanced against their inhibitory effect on immune cell division and activation. An optimal treatment strategy will require coupling the prevention of cancer division with activation of an effective cytotoxic T-cell response.

#4319

The need for new publication standards in cancer genomics, lessons from curating COSMIC database

Alexander Holmes[1], Sari A. Ward[2], Zbyslaw Sondka[2]. *[1]COSMIC, Wellcome Sanger Institute, Cambridge, United Kingdom,[2]Wellcome Sanger Institute, Cambridge, United Kingdom*

A consequence of the progress in cancer genomics is the exponential growth in data produced by research and clinical projects. Given the limited capacity within a scientific manuscript to share experimental data, various approaches have been developed: some data are simply excluded from the publication, moved to the supplementary materials, external repositories are used, and big research programmes present their integrated results on dedicated websites. This last approach has been extremely successful in generating comprehensive and unbiased datasets used by legions of scientists to discover new mechanisms driving cancer, biomarkers and drug targets. However, journal publications are still delivering more data globally, especially from rare cancers and underrepresented populations. To bring the full potential of these data and to make all this knowledge fully available, several challenges need to be addressed. COSMIC (Catalogue of

Somatic Mutations in Cancer) has an in-house expert curation team that extracts information about genetic variants, their significance, patients and their response to therapy from publications and integrates it into a standardised cross-referenced database available to the scientific community. Although curators are able to extract data presented in non-standard forms (e.g. manuscript figures), interpret and translate between various data formats, they cannot extract data that are not included in the publication. Approximately one third of manuscripts that are curateable are discarded due to the absence of data generated in the research process but not included in the publication. This clearly shows an urgent need for bringing researchers, publishers, and curators together to develop new publication standards that would allow communities to fully exploit the potential of published data and make them re-usable for further discoveries. We would like to propose several suggestions to start this discussion: - Use accepted naming conventions and standards to make your data interoperable, think about your work as part of the world heritage - Include all data you generate; even if not directly relevant to the manuscript topic, they may be invaluable for somebody else's research - Share full data and use service providers that share all the data with you - When possible, share the data per patient or sample, not per cohort - Publishing a manuscript is not an endpoint, there's a huge potential in your data to be further utilised to fight cancer

#4320

A novel digitally directed tissue microdissection platform integrates digital pathology with molecular analysis: Case study in metastatic colorectal cancer.

John H. Butler[1], Bidhan Chaudhuri[1], Katie Konigsfeld[1], Rish Pai[2].
[1]Quantumcyte, Sunnyvale, CA,[2]Dept of Lab Medicine & Pathology, Mayo Clinic, Scottsdale, AZ

Artificial intelligence (AI) based digital pathology has been getting rapid adoption over the last 2 to 3 years. These AI based digital pathology models can analyze samples at high resolution and scale. Retaining that resolution at scale through molecular analysis is key to the discovery of novel biomarkers. We have developed a technology that can integrate AI-supported digital pathology (DP) algorithms to identify informative tissue

regions for selective microdissection to improve molecular analysis of FFPE material. The system is capable of extracting DNA, RNA or proteins with cellular (10 micron) resolution from FFPE tissue sections. The samples are ready for use in off-the-shelf molecular analysis workflows (qPCR, Next Gen Sequencing, etc). The system decreases the tumor cellularity requirements for clinical analysis by extracting only the area enriched for informative biomarkers. To demonstrate the capability of the system we used an AI based digital pathology model that was developed to identify multiple cellular phenotypes from a H&E stained colorectal cancer FFPE tissue sections. We used the digital pathology output to guide the microdissection of RNA from tumor buds, carcinoma, immature stroma and inflammatory stroma in a paired designed RNA seq experiment. The data showed that the system is capable of enriching the tumor-bud tissue content from<1% in the tissue to ~50% purity in the crude lysate. Bioinformatic analysis of the RNAseq signatures showed that the tumor buds had a distinct RNAseq signature relative to the other three cell types and that the gene expression pattern was consistent with EMT pathways. The methodology is scalable, robust, and simpler than current microdissection techniques. This technology can be used to develop novel tests by integrating with AI algorithms, targeting tissue enriched for predictive biomarkers, and enabling low tumor cellularity samples to be analyzed with high precision.

#4321

Clinical-grade early detection of esophageal cancer on data from a non-endoscopic device using deep learning

Adam G. Berman[1], Ahmad Miremadi[2], Maria O'Donovan[2], Shalini Malhotra[2], Monika Tripathi[3], Rebecca C. Fitzgerald[4], Florian Markowetz[1].
[1]Cancer Research UK Cambridge Institute, University of Cambridge, Cancer Research UK Cambridge Institute, University of Cambridge, Cambridge, United Kingdom,[2]Pathology, Cambridge University Hospitals, NHS Foundation Trust, Cambridge, United Kingdom,[3]Cancer Research UK Cambridge Institute, Cancer Research UK Cambridge Institute, Cambridge, United Kingdom,[4]Early Cancer Institute, University of Cambridge, Early Cancer Institute, University of Cambridge, Cambridge, United Kingdom

Aim: Our goal was to evaluate a novel deep learning system for integrated human-AI review of whole-slide images (WSIs) from the Cytosponge to predict progression from Barrett's esophagus (BE) to esophageal adenocarcinoma (EAC).
Background: Fewer than 1% of BE patients advance to EAC, therefore delineating the patients at elevated risk is crucial for prioritizing their surveillance and treatment. Previous work has shown that the Cytosponge, a non-endoscopic test, coupled with biomarkers (TFF3, atypia, p53) can be used to identify and risk-stratify individuals with BE. However, the Cytosponge workflow to date has required a time consuming pathology review.
Methods: We collected 1,700 BE Cytosponge WSIs from over 800 patients. We hand-drew over 30,000 digital annotations on the WSIs, a 300-hour collaborative effort between a computer scientist and 4 pathologists. Using these data for training, validation, and testing, we developed a deep learning system to determine whether cellular atypia and/or p53 overexpression is present. We used this system in a machine-assisted (MA) review process to highlight the most diagnostically interesting regions of WSIs for pathologist review. In our proposed system, patients are automatically triaged into high or low confidence positive, and high confidence negative classes for both atypia and p53 status, and only low confidence cases are sent for MA review.
Results: Out of 23 architectures, the best atypia model achieves an accuracy of 0.90, and the best p53 model 0.96. The model was concordant with pathologists in 342/425 (80.5%) validation and 301/330 (91.2%) test-set patients. The system also identified 83 validation cases with atypia and/or p53 that were not previously reported by the pathologists. Of these, 29 (35%) were confirmed abnormal with the ground truth endoscopy biopsies (11 high grade dysplasia or intramucosal carcinoma, 14 low grade dysplasia, 5 indefinite for dysplasia). In the test set 29 results were discordant with pathology including 6 (21%) confirmed abnormal on endoscopy biopsies (3 HGD/IMC, 2 LGD, 1 IND). We used the models' outputs to localize where these "missed" regions lie in the WSIs, and pathologist MA review confirmed the presence of focal abnormalities (cellular atypia +/- p53 aberrance) correctly identified by the algorithm. If pathologists only review cases for which the model had low confidence, this preserves overall performance while reducing pathologist workload

over twenty-fold. MA review on the remaining WSIs is 4.7 times faster than standard review for atypia screening and 16.0 times faster for p53. Conclusion: This work shows the potential of an integrated human-AI WSI review process to drastically expedite a time consuming task and improve on pathologist performance when abnormal regions are easy for human eyes to miss. This work therefore lays the groundwork for similar machine-doctor approaches in other areas of medicine.

#4322

AI assisted detection and characterization of tertiary lymphoid structures in patients with colorectal cancer

Samantha Burg[1], Nathaniel Hart[1], Astin Powers[2], Wenjun Zhang[1]. *[1]Pharma Services Assay Development, Ventana Medical Systems, Inc., Tucson, AZ,[2]Pathology, Ventana Medical Systems, Inc., Tucson, AZ*

Tertiary Lymphoid Structures (TLSs) are ectopic immune cell aggregates that form in response to abnormal physiology and inflammation. TLS presence in the tumor environment has been associated with positive clinical outcomes and response to immune checkpoint inhibition therapy. Using a fluorescent multiplex panel consisting of Pan-cytokeratin (PanCK), Programmed Death Ligand-1 (PD-L1), cluster of differentiation (CD) 8, CD3, and CD68 we developed a HALO-based artificial intelligence (AI) classifier to detect TLSs in colorectal cancer (CRC) tissue. In conjunction with cell-type and spatial analyses, we used the AI TLS classifier to characterize several features of the TLS and peri-TLS environment. We trained the AI classifier using 51 examples of TLSs from 8 patients, and applied it to images of 21 CRC patient tissues. TLSs were detected in 9/21 patient samples. We then used cellular detection and spatial analysis to characterize features of the TLS, including the germinal center (GC), T cell zone and peri-TLS area. We detected a higher cell density (Mean=12250 ±2039 SD; cells/mm^2) within the interior of AI-detected GCs relative to the 1st 200 μm outside of the AI-defined GC border (8005±1870). In addition, we examined the spatial distribution of CD3+ and CD8+ T cells relative to the TLS GC. We found elevated CD3+ cell density in the interior of the GC (5784±1649) and within 200 μm of the GC border (5126±2239) which decreased at distances >200 μm from the GC border. We found CD8+ density to be elevated within the 1st 200 μm of the GC border (1903±1182)

and declined 400 μm away from the GC border (963±828). The spatial distribution of T cells surrounding an area of high cell density is indicative of a T cell zone surrounding germinal center. Further analysis of the AI-detected TLS GCs indicated that PD-L1+ cell density was highest within the germinal center (355± 534;9) relative to the exterior of the germinal center (1st 150μm outside germinal center:276± 441). We created an AI classifier that can detect TLS(s) within patient tissue in the absence of a B-cell marker and confirmed that our AI classifier was detecting TLSs by characterizing canonical features of TLSs. Further exploration of the TLS and peri-TLS area may offer insights into immune-tumor interaction within the tumor microenvironment, and paired detection of TLSs in a clinical cohort with outcome data may predict patient response to immune checkpoint inhibitor therapy.

CHEMISTRY

Biological Mass Spectrometry and Systems Biology

#5298
Multiplex immunoassay characterization of 48 cytokines, chemokines, and growth factors in colorectal cancer
Wen-Rong Lie, Harold Steiner, Sasha Williams, Munmun Banerjee, Anthony Saporita, Brooke Gilliam, Qiang Xiao. *MilliporeSigma, St. Louis, MO*

Cytokines, chemokines, and growth factors are critical mediators of immune system function capable of signaling through autocrine, paracrine, and endocrine mechanisms. Their pleiotropic immunomodulatory properties allow these biomolecules to react to diverse stimuli and regulate the immune response. We developed a novel immunoassay, using Luminex xMAP technology, for the simultaneous measurement of 48 cytokines, chemokines, and growth factors in serum, plasma, and cell culture supernatant. Many of these proteins have been proposed as biomarkers of colorectal cancer (CRC) and as key regulators of the tumor microenvironment (TME). While this complex milieu can support antitumor immunity, CRC is frequently characterized by chronic inflammation driving disease progression, with the TME serving as a potent

reservoir from which the cytokines, chemokines, and growth factors exert their influence. The MILLIPLEX Human Cytokine/Chemokine/Growth Factor Panel B (HCYTB-60K) assays were performed in 96-well plates and run on the Luminex LX200™ instrument. Data was acquired via xPONENT v. 4.3 software. Data analysis was performed for all immunoassays using the Belysa Immunoassay Curve Fitting Software. Commercially available serum samples obtained from colorectal cancer patients and healthy controls were evaluated for cytokine, chemokine, and growth factor expression. Of the 48 analytes tested, statistically significant increases in BAFF, sFas, SCF, and MPIF-1 were observed in colorectal cancer serum. In contrast, IL-20 and ENA-78 decreased relative to healthy controls. While the immunoassay was verified for measurement of serum and plasma samples, additional sample types may be of interest to cancer researchers. Therefore, we evaluated the ability of the 48-plex immunoassay to measure these biomarkers in CSF, urine, milk, tumor samples and exosomal isolates, establishing a profile for these proteins in each sample type. Altogether, this study uses a novel multiplex immunoassay to characterize the immunological profile of colorectal cancer serum, focusing on 48 cytokines, chemokines, and growth factors. Additionally, alternative sample types were evaluated to establish the utility of this technology for applications beyond serum, plasma, and cell culture supernatant.

#5299

Impact of gut microbial metabolites on colon epithelium

Nobel Bhasin[1], Lakmini Herath Senavirathna[2], Madeline Bresson[1], Lyu Zhe[1], Victoria B. Poplaski[1], Zahraa A. Lami[1], Teresa A. Brentnall,[3], Antone R. Opekun[1], John F. Valentine[4], Britton A. Britton[1], Pan Sheng[2], Ru Chen[1].
[1]Baylor College of Medicine, Houston, TX,[2]University of Texas, Houston, TX,[3]University of Washinton, Seattle, WA,[4]University of Utah School of Medicine, Salt lake city, UT

Inflammatory bowel disease (IBD) is a major risk factor for colorectal cancer (CRC) development. Dysbiosis of the gut microbiome has been implicated in the pathogenesis of IBD and CRC. The gut microbiome and its interaction with the colon may play a significant role in enabling tumor permissive state in an inflammatory environment. However, the functional

impact of colon microbiome on epithelial cells that enables neoplastic transformation under inflammatory condition is not clear. This study seeks to examine the impact of mucosa-adherent microbiota on colon epithelial cells. We used in vitro mini-bioreactor arrays to cultivate mucosa-adherent microbiota from colon biopsies, including biopsies from IBD patients with dysplasia (progressors) and without dysplasia (non-progressors). Paired dysplastic and non-dysplastic tissue from progressors was included in the study. HCT116 cells were exposed to the metabolites derived from the cultivation of microbial communities. Cell lysate and secretome were collected after the treatment of microbial metabolites and analyzed by LC-MS/MS. The differentially expressed proteins were identified using Limma. Over-representation analysis was performed using Reactome in Grofiler. Pathways relating to cell division, mitosis and cell proliferation were enriched in cells treated with microbiome metabolites from progressors. Pathways reflecting a proliferative phenotype were also found enriched in the cell secretomes after treatment with microbiome metabolites from progressors. We functionally verified the proliferative phenotype in cells using BRDU incorporation assay. Microbial metabolites from non-dysplastic biopsy from progressor showed significantly higher cell proliferation compared to non-dysplastic biopsy from non-progressors ($p<0.05$). Furthermore, microbial metabolites from dysplastic tissue showed a significantly higher proliferation compared to non-dysplastic tissue from the same patient ($p<0.01$) and patients without dysplasia ($p<0.0001$). A significantly higher degree of DNA damage was induced by microbial metabolites derived from IBD progressors than non-progressors ($p<0.05$). Together, our findings suggest that microbial metabolites in the dysplastic tissue alter the colon microenvironment to induce higher cellular proliferation and DNA damage, which may contribute to colon neoplastic progression in the IBD patients.

#5300

Mass spectrometry-based protein biomarker analysis in chemoimmunotherapy combinations identifies unique immune signatures in pancreatic cancer

Nigel Beaton, Marco Tognetti, Kamil Sklodowski, Roland Bruderer, Lukas Reiter. *Biognosys AG, Schlieren, Switzerland*

Although the combination of chemotherapy with immunotherapy has led to significant improvements in the treatment of some solid tumors, metastatic pancreatic ductal adenocarcinoma (mPDAC) prognosis has remained largely unaffected by such approaches. Recently, PRINCE, a randomized phase 2 clinical study, reported significantly improved 1-year overall survival (OS) for mPDAC patients treated with nivolumab and chemotherapy (nivo/chemo) compared to historical control but not for sotigalimab and chemotherapy (sotiga/chemo) or a combination of the three. Interestingly, the study identified potential improvement to treatment outcome with patient stratification. Here, we report an unbiased mass spectrometry (MS)-based proteomics profiling of a subset of plasma samples from the PRINCE trial (n = 211, 62 individuals from nivo/chemo and sotiga/chemo longitudinal samples). Briefly, plasma samples were depleted, digested to tryptic peptides, measured by MS/MS and quantified using Spectronaut (Biognosys). Data was investigated for both protein and peptide biomarker with an emphasis on baseline biomarkers associated with clinical outcomes. Plasma profiling identified 1,662 proteins and 17,451 modified peptides across the cohorts. First, we developed a model that identified the pharmacodynamic effects of treatment in individual patients. In accordance with the PRINCE study and among the major model contributors, sotiga/chemo increased proteins associated with innate immunity and chemokines (including CCL15) while proteins aiding in T cell activation and immune cell migration increased with nivo/chemo (including CXCL7 and CD115). Second, we looked for markers in the pretreatment plasma samples that could predict OS. Overall, we found 25 predictive markers ($p < 0.05$), with only six shared among the two arms, including attractin and CD58. Among the seven predictive biomarkers specific to nivo/chemo, we found MEGF10 and GALNT1, which are suggested to play a role in neoantigen generation. For sotiga/chemo, we found 12 predictive biomarkers including IGF2, CD304, and periostin (known to support immune responses). Third, we expanded our predictive biomarker search to the identified peptides, an analysis that is currently only possible using an unbiased mass spectrometry-based approach. Using such an approach we identified predictive peptides, likely cleavage products, as well as predictive post-translational modifications. Herein we demonstrate the value of both an unbiased approach, as well as the use of peptide level data for novel biomarker identification. We identify numerous

proteins and peptides that have the potential to be used for better patient treatment stratification in the case of mPDAC and immunotherapy.

#5301
Detection of arginine posttranslational modifications by single-molecule protein sequencing on the Quantum-Si platform
Kenneth Skinner, David Kamber, Brian Reed. *Quantum-Si, Guilford, CT*

Aberrant post-translational modifications (PTMs) on arginine residues, such as methylation and citrullination, are closely linked to oncogenic processes. Detection of these PTMs is challenging with current technology and can be hampered by low abundance and mass differences that are difficult to resolve by mass spectrometry. To overcome these challenges, we developed methods for PTM detection using Quantum-Si's Platinum single-molecule protein sequencing platform. Proteins are sequenced on Quantum-Si's Platinum instrument using our library prep protocol. Briefly, proteins are digested into peptide fragments, conjugated to linkers, then immobilized at the bottom of nanoscale reaction chambers on a semiconductor chip, resulting in exposed N-termini for sequencing. During sequencing, the immobilized peptides are exposed to a solution of dye-labeled N-terminal amino acid (NAA) recognizers that reversibly bind to their cognate NAAs with distinct kinetic properties. Aminopeptidases sequentially remove NAAs to expose subsequent amino acids for recognition. Fluorescence lifetime, intensity, and kinetic data are collected in real time and analyzed to determine primary sequence and PTM content. The data output consists of distinct pulsing regions called recognition segments (RSs). Each RS corresponds to a period of time between aminopeptidase cleavage events, during which an NAA recognizer binds on/off to its exposed target NAA. Chemical modification to a NAA or to a nearby downstream amino acid can modulate recognizer affinity, resulting in a characteristic change in the average pulse duration (PD) during an RS. To demonstrate the detection and differentiation of arginine PTMs, we applied our platform to distinguish between asymmetric dimethylarginine (ADMA) and symmetric dimethylarginine (SDMA) and between citrulline and native arginine residues. Sequencing traces revealed that arginine and ADMA bind the arginine recognizer (PS621) with similar PD, whereas SDMA exhibited no binding. These results indicate that SDMA, in contrast to ADMA, has

reduced binding affinity with PS621, providing a clear kinetic difference between these isomeric arginine PTMs. Moreover, citrulline and arginine side chains also exhibited distinguishable kinetic signatures. Citrullination eliminated the N-terminal arginine recognized by PS621 and resulted in a large increase in the median PD of preceding amino acid residues. Taken together, single-molecule protein sequencing offers an alternative approach to detection of arginine PTMs that is not based on m/z, but rather on the kinetic signature of binding between recognizers and N-terminal amino acids. The ability to directly detect arginine PTMs offers potential for biomedical research. We envisage applications using Quantum-Si's platform to key areas of cancer research including biomarker development and drug discovery.

#5302

Unmasking aggressive tumor profiles in lung adenocarcinomas through the molecular abundances and catalytic action of serine hydrolases

Tatjana Sajic[1], Stephan Arni[2], Rudolf Aebersold[1], Sven Hillinger[2]. *[1]Swiss Federal Institute of Technology, Zürich, Switzerland,[2]University Hospital Zürich, Zürich, Switzerland*

(a) Current proteomic methods quantify solely the catalytically active portion of enzymes without normalizing the active portion to the total enzyme amount, thus compromising comparison of the results. We take advantage of a SWATH/DIA-MS workflow and describe a method based on depletion-dependent ABPP (dd-ABPP) able to concurrently determine catalytically active enzymes and their total molecular abundances, as well as quantify the contextual sample proteomes.
(b) We monitored high quality peptides of more than 190 SH activities and molecular abundances of around 4000 contextual tissue proteins in advanced lung adenocarcinomas (LUAD). While we found that LUAD tumors display enhanced proteolytic activities compared with control lung tissue, the most prominent characteristic of an aggressive tumor phenotype was enhanced lipolysis of metabolic SHs emphasized by IAH1, ABHD12, LYPLA2 and ABHD10.
(c) Molecular signatures of the activity profiles of 23 SHs and 59 contextual tissue proteins discriminate aggressive tumors at the time of diagnosis. Enhanced detection of S-palmitoylated proteins correlating by active-

enzyme capture uncovers their functional links with the metabolic SHs related to lipoprotein depalmitoylation via enzymes displaying increased de-palmitoylase activities and enhanced fatty acid metabolism in aggressive LUAD. To further validate our findings, we analysed LUAD tumors for panels of saturated and unsaturated fatty acid (C8-C22) levels. Strikingly, we detected a statistically significant increase in monounsaturated palmitoleic acid (C16:1) in the aggressive compared with less-aggressive tumors. Notably, the primary source of palmitoleic acid in the cellular environments results from an excess of free palmitic acid and its conversion by rate-limiting enzyme Stearoyl-CoA desaturase 1 (SCD) that is enhanced in LUAD cancer.
(d) We detected a significant increase in palmitoleic acid levels in aggressive tumors. To a certain extent our data support previous findings on the active process of lipid desaturation in lung adenocarcinoma cells as the main source of energy for cell proliferation. Our approach also revealed that changes in the active lipase fractions between subtypes do not follow changes in enzyme protein quantities, suggesting that lipase regulations are related rather to peculiarities of the enzyme protein sequence, a distorted enzyme-inhibitor equilibrium, or a distorted molecular composition of the tissue itself. Since the inhibitors of serine lipases are promising targets in other RAS-mutant carcinomas, and the inhibitors of a rate-limiting SCD1 enzyme prevent palmitic acid conversion to a monounsaturated form, these metabolic vulnerabilities detected in aggressive LUAD will be helpful for future therapeutic strategies in lung cancer.

#5303

Upregulation of the polycomb group protein SCML2 contributes to aggressive prostate cancer

Ava M. Boston[1], Abdulrahman M. Dwead[1], Marwah M. Al-Mathkour[2], Kezhan Khazaw[1], Bekir Cinar[1]. *[1]Biological Sciences, Clark Atlanta University, Atlanta, GA,[2]Miller School of Medicine, University of Miami, Miami, FL*

Advanced prostate cancer (PC) is the leading cause of death in the US because there is no effective treatment due to the poorly understood disease mechanism. Sex comb on midleg-like-2 (SCML2) is a member of Polycomb repressive complex 1 and regulates homeotic gene expression

during development. Using proteomic approaches, we have identified SCML2 as a binding partner of the YAP1 protein complexes isolated from PC cell lines. Both SCML2 and YAP1 regulate basic cellular biology, including stem cell maintenance and carcinogenesis; however, whether SCML2 and YAP1 cooperate to contribute to the aggressive PC in humans remains unknown. We showed that AR-positive cell lines express high levels of SCML2 with a significant increase in castration-resistant PC cells compared to its castration-sensitive cell counter, suggesting a possible role of SCML2 in PC progression. We also showed that androgens regulated the protein-protein interaction between SCML2 and YAP1, as evaluated by proximity ligation assay. In addition, the GST-pulldown assay revealed that SCML2 interacted with the WW/SH3 domain of YAP1, where AR also binds. Besides, our RNAi-aided gene silencing experiment demonstrated that YAP1 and SCML2 might be functionally antagonistic. Moreover, gene silencing and growth assays showed that SCML2 might act as a growth suppressor in castration-sensitive PC cells while acting as a growth mediator or survival factor in castration-resistant PC cells. Furthermore, our analysis of the cancer genome atlas PC data set has indicated that amplification of SCML2 is associated with reduced progression-free survival. These observations suggest that SCML2 and YAP1 interaction is biologically functional, and the degree of their interaction may play a critical role in PC progression downstream of dysregulated androgen/AR signaling.

#5304

Development of a plasma biomarker panel for gastric cancer detection based on an autoimmune response signature

Rongzhang Dou[1], Ehsan Irajizad[1], Yining Cai[1], Johannes F. Fahrmann[1], Jody V. Vykoukal[1], Yihui Chen[1], Hiroyuki Katayama[1], Ali H. Abdel Sater[1], Melissa Pizzi[2], Kohei Yamashita[2], Matheus Sewastjanow Da Silva[2], Edwin J. Ostrin[1], Jaffer Ajani[2], Samir M. Hanash[1]. *[1]Clinical Cancer Prevention, UT MD Anderson Cancer Center, Houston, TX,[2]Gastrointestinal Medical Oncology, UT MD Anderson Cancer Center, Houston, TX*

Background**:** Gastric cancer is frequently diagnosed at an advanced stage and is associated with poor outcomes. Harnessing the immune response to

tumor antigens which occurs early during tumor development has potential for the early detection of gastric cancer.
Methods: Plasma samples from gastric cancer patients were collected before and after treatment and from healthy controls for identification of immunoglobin (Ig)-bound antigens using mass spectrometry. Ingenuity pathway analysis(IPA) was utilized to investigate networks and pathways associated with Ig bound proteins identified in plasmas from cases. A combined biomarker panel was established based on a logistic-regression model and ROC analysis was used to assess panel performance.
Results: A total of 65 Ig bound proteins were identified that were upregulated in gastric cancer patients' plasma compared with healthy control. Canonical pathways involving these immunogenic proteins included HIF-1α, VEGF, actin cytoskeleton, and immunogenic cell death signaling which play important roles in both gastric cancer development and progression. Four of the top ten performing proteins exhibited high mRNA levels in gastric cancer tissue. The association of these four Ig bound proteins in gastric cancer plasmas was further validated using as controls a cohort of MEN1 patients plasmas. A blood-biomarker panel based on these four biomarkers was established using a logistic-regression model which yielded an area under the curve (AUC) of 0.963 (95% confidential interval [CI] =0.89-1.00) for gastric cancer discrimination with a sensitivity of 0.889 at 95% specificity.
Conclusion: Our data reveal a panel of plasma Ig-bound antigens associated with the development of gastric cancer with potential application for early detection and monitoring.

#5305
Detection and quantification of proteins using protein identification by short-epitope mapping (PrISM)
Torri Rinker[1], Jarrett D. Egertson[1], Steven Tan[1], Aisha Ellahi[2], Jamie Sherman[2], Maria Villancio-Wolter[1], Brittany Nortman[1], Julia Robinson[1], Ahana Dutta[1], Katherine Winters[1], Noah Steiner[1], Elvis Ikwa[1], Hunter B. Boyce[2], James H. Joly[1], Filip Bartnicki[1], Pierre F. Indermühle[1], Christina Inman[1], Shubhodeep Paul[1], Jacinto Villanueva[1], Jennifer McGinnis[1], Aimee A. Sanford[1], Sophia Watts[1], Jessica Nicastro[1], Sonal S. Tonapi[1], Jacob Devine[1], Cara Li[1], Kaitlyn Burke[1], Jonathan Leano[1], Nikola

Kondov[1], Mirella Huber[1], Bilal Ali[1], Carlos Flores[1], Sheri K. Wilcox[1], Parag Mallick[1]. *[1]Nautilus Biotechnology, Inc., San Carlos, CA,[2]Nautilus Biotechnology, Inc., Seattle, WA*

Introducti**on:** Here, we demonstrate Protein Identification by Short-epitope Mapping (PrISM), which aims to provide comprehensive proteome analysis with broad dynamic range at single-molecule resolution by interrogating immobilized, intact proteins in parallel using multi-affinity probes. Improving the dynamic range and scale for protein analyses will enable a deeper understanding of low abundant protein in all stages of cancer progression. In addition, enabling the interrogation of single-molecules will provide a deeper understanding of protein diversity, such as the proteoforms resulting from non-canonical post-translational modifications inherent to cancer[1]. The combination of single-molecule sensitivity with comprehensive proteome coverage could also open the door for highly sensitive and specific diagnostics.
Methods: PrISM uses non-traditional affinity reagents with high affinity and low specificity that bind to short epitopes in multiple proteins. Sample proteins were conjugated to DNA nanoparticles and deposited on a high-density patterned flow cell at optically resolvable locations. Multi-affinity probes were applied to sample proteins over multiple cycles to generate binding patterns for each single-molecule protein, which are translated to protein identifications and quantities using a custom machine learning approach. We acquired PrISM data on native biological and control samples using dozens of multi-affinity probes targeting trimer or tetramer sequences.
Results: We report single-molecule deposition of over 1 billion DNA nanoparticle complexes on a flow cell. We demonstrate how the PrISM methodology identifies individual protein molecules through iterative probing with our multi-affinity probes. Further, we provide an analytical assessment of the sensitivity and specificity of PrISM and demonstrate the ability to accurately estimate the false identification rate of these proteins using a target-decoy based statistical approach.
Conclusions: Combining single-molecule analysis, intact (non-digested) proteins, and iterative probing, PrISM provides a new tool for quantitative proteomics. We demonstrate linear and reproducible quantification of proteins using PrISM, potentially enabling detection of low abundant proteins and proteoforms associated with cancer. The ability to make

comprehensive measurements of intact proteins at single-molecule resolution could accelerate basic cancer research through to the clinic.
References: 1. Alfaro et al., *Nature Methods*, 2021.

#5307

Imaging mass cytometry enables identification of distinct tissue phenotypes in highly autofluorescent lung and colon cancer tissues, producing consistent data across serial sections

Smriti Kala[1], Brenna O' Neill[2], James Pemberton[1], James Mansfield[2], Fabian Schneider[2], Clinton Hupple[1]. *[1]Standard BioTools, Markham, ON, Canada,[2]Visiopharm, Hørsholm, Denmark*

Background**:** Successful implementation of immunotherapy requires a deep understanding of the spatial interactions between various cell types in the tumor microenvironment (TME). Most fixed tissues are autofluorescent and staining with cyclic immunofluorescence methods often produces data that are difficult to analyze due to the challenges of background subtraction. Imaging Mass Cytometry™ (IMC™) is a powerful tool for high-plex imaging, utilizing CyTOF® technology to simultaneously assess 40-plus protein markers at subcellular resolution without spectral overlap or background autofluorescence. This study demonstrates a tissue phenotyping workflow in highly autofluorescent lung and colon cancer tissues using high-plex IMC, which produces reliable data that can be easily analyzed.
Methods: Serial sections of lung and colon cancer tissues were stained with a 30-marker panel comprised of structural, tumor, stroma, immune cell, and immune activation markers as well as the IMC Cell Segmentation Kit, for improved nucleus and plasma membrane demarcation. The data analysis pipeline used Phenoplex™ (Visiopharm®) software for straightforward, accurate, and quantifiable phenotyping. The analysis workflow consisted of tissue segmentation (to define tumor, stroma, extracellular matrix, and regions of necrosis), nuclear detection using a deep-learning algorithm pre-trained on IMC DNA channels, cell segmentation, a threshold-based cellular phenotyping step, and spatial analyses. Statistical analyses of the reproducibility between serial sections were performed using a paired t-test.
Results: In this work, we have shown that analysis of IMC images from highly autofluorescent lung and colon cancer tissues can uncover tissue phenotypic signatures of the TME through the determination of distinct

immune cell types found in the vicinity of cancerous cells. Moreover, cell segmentation generated cell counts that were highly consistent across the serial sections, with only 2.7% variability. This demonstrates the power of IMC in generating robust data across adjacent serial sections, which can be easily analyzed without the need to train the analysis software for background subtraction.
Conclusions: Overall, this work demonstrates that by avoiding autofluorescence, IMC can generate high-quality, reproducible data, consistent across serial sections. The images can be easily and accurately analyzed in a streamlined way using the Phenoplex software, thus empowering IMC users to be confident in biological interpretation of high-dimensional proteomic data. This study demonstrates how systematic digital profiling of the spatial TME using IMC leads to repeatable, quantitative results generated through a simplified workflow.

#5308
Analysis of extracellular vesicle surface markers as small cell lung cancer biomarkers
Patricia M. M. Ozawa[1], Sarah M. Groves[2], Vito Quaranta[2], Alissa M. Weaver[1]. *[1]Cell and Developmental Biology, Vanderbilt University, Nashville, TN,[2]Department of Biochemistry, Vanderbilt University, Nashville, TN*

Small Cell Lung Cancer (SCLC) is an aggressive tumor type, usually metastatic at diagnosis, with a median survival of less than a year. SCLC tumors are heterogeneous and are composed of neuroendocrine (A, A2, N) and non-neuroendocrine (Y) subtypes, with the cooperation by heterogeneous cells being key to drive tumor survival. Unfortunately, the current SCLC treatment approach does not take tumor heterogeneity into consideration. Importantly, there are no consensus markers that can identify SCLC subtypes or early tumors. Extracellular vesicles (EVs), small vesicles known to promote cell to cell communication, have been investigated as non-invasive biomarkers for cancer diagnostics, staging, and treatment monitoring. EVs are attractive candidates for biomarker research due to the selective packaging of RNA, DNA, and proteins that are then secreted in the blood. Therefore, our aim was to identify new biomarkers based on EV surface proteins with potential for early detection and tumor

characterization. We used differential ultracentrifugation to isolate EVs from four SCLC subtypes A, A2, N, and Y, which were submitted to label-free mass spectrometry (EV-proteomics). We identified a total of 3011 proteins, with the two most distinct subtypes being A2 and N, with 786 differentially expressed EV-proteins. Meanwhile, the 2 most similar subtypes were N and A, with only 75 differentially expressed EV-proteins. Gene set enrichment analysis of EVs derived from the A2 subtype showed an association with pathways in cancer, chemokine signaling, and neuronal systems. In addition, PANTHER analysis identified enrichment in nicotine pharmacodynamic pathways on these EVs, which corroborate the association of A2 cell lines with drug resistance. EVs derived from the N and A subtypes were enriched in spliceosome, RNA processing, and metabolism, while EVs from Y cell lines were enriched in extracellular matrix organization and metabolic pathways, similar to pathways from cell line RNAseq data. 13 proteins were differentially expressed in all group comparisons, including proteins involved in PI3K and nicotinic acetylcholine receptor signaling pathways. Further comparison of EV-proteomics with top genes from CIBERSORT analysis using cell line RNAseq data showed an overlap of 9 surface proteins, with 3 possible SCLC pan markers. In conclusion, EV-proteins isolated from SCLC cell lines presented a unique signature for each subtype, especially EVs derived from A2 subtype, which has a signature associated with drug resistance. We identified surface proteins on SCLC EVs with potential as SCLC pan and tumor characterization, which will be validated on EVs derived from cell lines and patient plasma by Western blotting and single-EV microflow cytometry.

#5309

Isolation and validation of small extracellular vesicles from rhabdomyosarcoma cells

Paula R. Quaglietta[1], Ashby Kissoondoyal[1], Ethan Malkin[2], Salvador Mejia[3], Ann Gong[1], David Malkin[1], Reto M. Baertschiger[1]. *[1]The Hospital for Sick Children, Toronto, ON, Canada,[2]Princess Margaret Cancer Centre, Toronto, ON, Canada,[3]Princess Margaret Cancer Center, Toronto, ON, Canada*

Extracellular vesicles (EVs) are nano-sized (30-1000 nm) membranous particles released by nearly all cell types. EV biology is a rapidly growing field, however its relative novelty and the intrinsic heterogeneity of EVs result in a lack of standardized and reproducible protocols. We sought to develop and validate an EV isolation method using rhabdomyosarcoma cell lines, with multiple characterization/validation methods, to improve the reproducibility and reliability of EV research in pediatric cancer research. EVs were isolated and analyzed in triplicate from 4 rhabdomyosarcoma cell lines (RH4, RH18, RH30, RD), of varying clinical characteristics including subtype, TP53 status and FOXO1 fusion status. Cells were grown to 70% confluency in six 175cm^2 flasks, to ensure sufficient EV content for all downstream analyses, then incubated for 48 hours in media containing 10% EV-depleted FBS. The resultant 120mL of conditioned media (CM) per cell line was collected and subject to differential ultracentrifugation to isolate EVs. CM was centrifuged twice, then concentrated to less than 10mL using 3kDa MWCO filter tubes. Concentrated CM was centrifuged twice before passing through a 0.22μm pore-sized syringe filter prior to the final ultracentrifugations. The sample was ultracentrifuged and the EV pellet was carefully washed, re-centrifuged and resuspended in 100μL of PBS. Protein analysis by Western blot confirmed the presence of EV markers (syntenin-1, TSG101) and absence of non-EV markers (calnexin, histone H2Ax). EV quantification and size distributions were evaluated by NanoSight nanoparticle tracking analysis and visualized by transmission electron microscopy. All isolations were positive for EV markers and negative for non-EV markers by Western Blotting. All isolations showed similar size distributions by nanoparticle tracking analysis, within the range of 30-250nm. EVs in each sample with the typical cup-like shape were observed in electron microscope images of EVs. Overall, our method demonstrates good reproducibility of EV isolations from multiple rhabdomyosarcoma cell lines. This methodology can be used as a baseline for other cell lines to provide greater consensus within the field, allowing further discoveries analyzing the secretome of patient-derived cell lines with the potential to translate into more specific diagnostic tools.

#5310
An expanded quantitative protein expression atlas of human cancers

Han Liang. *Bioinformatics and Computational Biology, UT MD Anderson Cancer Center, Houston, TX*

The Cancer Genome Atlas (TCGA) and Cancer Cell Line Encyclopedia (CCLE) are the most widely used and deeply characterized resources for cancer research. Despite rich molecular and phenotypic data available for these cohorts, large-scale proteomic data across cancer lineages remain limited. Here we expanded our previous effort to generate high-quality protein expression data of 447 clinically relevant proteins for ~8,000 TCGA patient samples and ~900 CCLE cell line samples using reverse phase protein arrays. We show that the protein expression profiles provide deeper mechanistic insights into cancer dependency and serve as a sensitive functional readout for the fitness effect of somatic mutations, e.g., BRAF mutations. We develop a protein-centered strategy to identify synthetic lethality pairs with high confidence. We identify pro- and anti-metastasis protein markers and demonstrate their prognostic relevance in patient cohorts. Collectively, this dataset provides a valuable resource for elucidating cancer mechanisms, identifying protein biomarkers, and developing therapeutic strategies.

#5311

Lipidomic profiling of extracellular vesicles derived from cancer cell lines: Lipid species as potential biomarkers and cellular uptake enhancers

Ruben R. Lopez Salazar[1], Prisca Bustamante[1], Chaymaa Zouggari[2], Yunxi Chen[1], Thupten Tsering[1], Ion Stiharu[3], Catherine Mounier[4], Vahe Nerguizian[2], Julia Burnier[5]. *[1]Pathology, RI MUHC McGill, Montreal, QC, Canada,[2]Electrical, École de technologie supérieure ÉTS, Montreal, QC, Canada,[3]Mechanical, Industrial and Aerospace Engineering, Concordia University, Montreal, QC, Canada,[4]Centre de recherche sur les maladies orphelines (CERMO-FC)), Département des sciences biologiques, Université du Québec à Montréal, Montreal, QC, Canada,[5]Pathology and Oncology, RI MUHC McGill, Montreal, QC, Canada*

Introduction: Extracellular vesicles (EVs) are lipid bilayer-made particles shed by cells to the extracellular space. They carry different cargo proteins,

nucleic acids, and other metabolites. EVs play a role in disseminating cancer to distant organs by communicating with the tumor microenvironment to prepare the metastatic niche and also through horizontal transfer of oncogenic traits to recipient cells. The EV surface, which includes proteins and lipids, plays a role in organotropism and cellular uptake. While proteins have been extensively characterized, lipids have not been explored sufficiently. This work aims to evaluate EV lipids as potential biomarkers and their role in enhancing cellular uptake.
Methods: To detect which lipid species (LS) were differentially expressed, we used two cell models of liver metastatic cells: colorectal cancer (HT29) and uveal melanoma (MP41, MP46, MEL 270, OMM 2.5) cell lines. Colon (CCD18-Co) and fibroblast (BJ) immortalized non-cancerous cells were used as controls. EVs were isolated from culture media by ultrafiltration using 100 kDa units filters. Lipids were extracted by methyl-tert-butyl ether for high-throughput lipidomics. High-resolution 'shotgun' mass spectrometry was performed. Data was analyzed using LipidView software (SCIEX), and the lipid % normalized was reported. MarkerView (SCIEX) was used to perform Principal Component Analysis. The LS segregating cancerous vs. non-cancerous cells were identified. To evaluate the influence on cellular uptake, we used liposomes as EV models with lipid formulations containing the segregating LS to compare them with naturally occurring lipids and EVs using Incucyte live cell imaging.
Results: We identified four LS that segregated EV subpopulations. PE 34:1 and PS 36:1 divided cancerous vs non-cancerous cells, uveal melanoma cells were segregated by PE 36:2, and normal colon cells were segregated by LPC 18:0. We validated the effect of PS 36:1 in cellular uptake by producing liposomes with a lipid formulation resembling the lipid profile of naturally occurring EVs lipid profile with an artificially high DOPS concentration (17% of the total molar ratio). We determined that human hepatocytes preferentially internalized liposomes made of naturally occurring EVs, followed by the ones with a high concentration of DOPS and lastly by a control EV lipid formulation.
Conclusion: This study identified EV LS that segregated cancerous, normal, and melanoma cell lines. We showed that LS could be used to distinguish cell populations. Moreover, we demonstrated that LS alone influences cellular uptake and that adding the segregating LS to lipid formulations in

excess effects cellular uptake. These results pave the way to identify EV lipid biomarkers and better understand EV based cancer dissemination.

#5312

Next generation quantitative proteomic analysis of urothelial lesions reveals novel diagnostic biomarkers to distinguish pathologic pitfalls and protein-protein interactions

Han Suk Ryu, Soo Young Park, Da Sol Kim, Cheng Hyun Lee. *Seoul National University Hospital, Seoul, Korea, Republic of*

There are several unmet needs remained to be solved in bladder urothelial lesions. Especially, the molecular biology of inverted urothelial papilloma (IUP) as a precursor disease of urothelial carcinoma is poorly understood. Also, muscle-invasive urothelial carcinoma (MIUC) of the bladder, showing a highly aggressive tumor behavior, has prompted the quest for robust biomarkers associated with invasion. A total of 265 tissue specimens from urinary bladder were enrolled for proteomic analysis and validation. Candidate biomarkers were selected through bioinformatic analysis, followed by validation. The latter comprised 2D and 3D invasion and migration assays, also a selection of external public datasets to evaluate mRNA expression and an in-house patient-derived tissue microarray (TMA) cohort to evaluate protein expression with immunohistochemistry (IHC). From the overall proteomic landscape, we found divergent ‘NU-like’ (low-risk) and ‘PUC-like’ (high-risk) signatures in IUP. The latter were characterized by altered metabolism, biosynthesis, and cell-cell interaction functions, indicating oncologic significance. Further machine learning-based analysis revealed SERPINH1, PKP2, and PYGB as potential diagnostic biomarkers discriminating IUP from PUC. The immunohistochemical validation confirmed PYGB as a specific biomarker to distinguish between IUP and PUC with inverted growth. For biomarkers predicting invasion, our multilayered platform-based analysis identified tubulin beta 6 class V (TUBB6) as a promising prognostic biomarker predicting MIUC of the bladder. The in vitro 2D and 3D migration and invasion assays consistently showed that inhibition of TUBB6 mRNA significantly reduced cell migration and invasion ability in two BUC cell lines with aggressive phenotype (TUBB6 migration, $P = .0509$ and $P < .0001$; invasion, $P = .0002$ and $P = .0044$; TGFBI migration, $P = .0214$ and

P = .0026; invasion, P < .0001 and P = .0001; T24 and J82, respectively). Validation through multiple public datasets, including The Cancer Genome Atlas (TCGA) and selected GSE (Genomic Spatial Event) databases, confirmed TUBB6 as a potential biomarker predicting MIUC. Further protein-based validation with our TMA cohort revealed concordant results, highlighting the clinical implication of TUBB6 expression in BUC patients (overall survival: P < .001). We propose PYGB and TUBB6 as a novel IHC biomarker to predict IUP diagnosis or invasion and poor prognosis in routine practice, also select the optimal treatment in BUC patients.

#5313

The expression of phospho-Rb S249, N-cadherin, E-cadherin, and B-catenin as a prostate proteomic score for the risk classification of prostate cancer tumors

Sheila M. Valle Cortes[1], Pedro Santiago Cardona[1], Carlos Diaz Osterman[1], Jaileene Perez Morales[2], Darielys Maldonado Maldonado[1], Gilberto Ruiz Deya[1]. *[1]Biochemistry, Ponce Health Sciences University, Ponce, PR,[2]Moffitt Cancer Center, Tampa, FL*

Prostate cancer (PCa) ranks as the second leading cause of cancer-related deaths in American men. Most PCa deaths occur due to aggressive, fast-growing tumors that develop into metastasis when cancer cells spread to other body parts, including the lymph nodes, bones, etc. However, men could also be affected by indolent, slow-growing tumors, which may exist for an extended period without causing any symptoms or death. Current prognostic methods, such as Prolaris, or Oncotype, do not precisely specify how aggressive cancer might be, resulting in overtreating patients with indolent PCa. Therefore, improved ways to differentiate indolent from aggressive tumors are needed. In the presented study, we have validated the clinical potential of phospho-Rb S249, N-cadherin, B-catenin, and E-cadherin to discriminate between indolent and aggressive PCa tumors. We hypothesize that the biomarkers phospho-Rb S249, N-cadherin, E-cadherin, and B-catenin expression in PCa will be a clinical tool for the risk classification of PCa tumors when used as part of a prostate proteomic (PPS) that can predict the risk of the tumor of evolving into an aggressive phenotype. We conducted immunohistochemistry staining of these biomarkers on PCa tumor microarrays and correlated it with the patient's

clinical parameters, such as tumor size, lymph node invasion, metastasis, etc. Also, we correlated it with the PSA levels and created a PPS. The combination of our proteomic biomarkers predicts patient staging by 53.83%. Adding clinical data such as the tumor size, lymph node invasion, and metastasis (TNM) increases the precision of the prediction to 83.21%. In addition, the PSA levels increased as the phospho-Rb S249 expression and N-cadherin rise, accompanied by up-regulation of E-cadherin. Also, the PPS showed to distinguish between normal prostate tissue, hyperplasia, and PCa. Results suggest that these biomarkers could serve as a tool for the risk classification of indolent and aggressive PCa tumors.

#5314

A peripheral blood-based glycoproteomic predictor of checkpoint inhibitor treatment benefit in advanced non-small cell lung cancer

Klaus Lindpaintner, Chad Pickering, Alan Mitchell, Gege Xu, Xin Cong, Daniel Serie. *InterVenn, South San Francisco, CA*

Background**:** Protein glycosylation is the most common and complex form of post-translational protein modification. Glycosylation profoundly affects protein structure, conformation, and function. The elucidation of the potential role of differential protein glycosylation as biomarkers has been limited by the technical complexity of generating and interpreting this information. We have recently established a novel, powerful platform that combines liquid chromatography-mass spectrometry with a proprietary artificial-intelligence-based data processing engine that allows, for the first time, highly scalable interrogation of the glycoproteome. Here we report the performance of this platform to predict likely benefit from immune-checkpoint inhibitor (ICI) therapy in advanced non-small cell lung cancer (NSCLC).

Methods: Our platform was utilized to assess 532 glycopeptide (GP) and peptide signatures representing 75 serum proteins in pretreatment blood samples from a cohort of 123 individuals (54 females, 69 males, age range 30 to 88 years). Inclusion criteria were a diagnosis of unresectable stage 3 or 4 NSCLC, treatment with pembrolizumab monotherapy (26 patients), or treatment with combination pembrolizumab-chemotherapy (97 patients). Overall survival (OS) data were available for all patients.

Results: An ensemble multivariable-model-based glycoproteomic classifier consisting of 7 GP and non-glycosylated peptide biomarker features selected from a generalized additive model for OS was developed using ≈2/3^{rds} of the full cohort (n=88) and validated in the remainder of patients (n=35). The classifier yielded similar statistical significance in Cox regression analysis for separating patients who are likely to benefit from ICI therapy from those who are not, to accurately predict likely ICI benefit with a sensitivity of >95% while performing at a specificity of 33% to predict those who are unlikely to benefit. Results were further analyzed in patients with either non-squamous or squamous NSCLC with first-line therapy (n=98). The classifier yielded a hazard ratio (HR) for prediction of likely ICI benefit of 3.6 with median OS of 13.9 vs. 4.2 months, and of 3.5 with median OS of 13.5 vs. 4.5 months in the entire cohort and the first-line treated patients, respectively.
Conclusions: The glycoproteomic classifier described here predicts with high sensitivity which patients are likely to benefit from ICI therapy. In addition to potentially reducing the use of ICIs in a safe manner in patients who would be unnecessarily subjected to possible adverse drug reactions, our classifier simultaneously has the potential of reducing the burden of health care expenditures. Our results indicate that glycoproteomics holds a strong promise as a predictor for ICI treatment benefit which appears to significantly outperform other currently pursued biomarker approaches.

#5315
Identification of urinary proteome signatures associated with triple-negative breast cancer
Michael N. Lombardo[1], Roopali Roy[1], Susan Pories[2], Meg Lotz[2], Rama Aldakhlallah[1], Simon T. Dillon[3], Towia A. Libermann[3], Marsha A. Moses[1].
[1]Vascular Biology Program, Department of Surgery, Harvard Medical School, Boston Children's Hospital, Boston, MA,[2]Hoffman Breast Center, Mount Auburn Hospital, Harvard Medical School, Cambridge, MA,[3]Genomics, Proteomics, Bioinformatics and Systems Biology Center, Beth Israel Deaconess Medical Center, Boston, MA

Triple-negative breast cancer (TNBC), an aggressive breast cancer subtype, accounts for ~15% of all breast cancers and is associated with a poor prognosis and high rates of recurrence and distant metastases. Patients

diagnosed with TNBC have limited treatment options and are often restricted to chemotherapy-based regimens, in stark contrast to patients with other breast cancer subtypes where the development of targeted therapeutics have significantly improved patient outcomes. TNBC is characterized by the loss of estrogen receptor, progesterone receptor and human epidermal growth factor receptor 2. This and the genetic and molecular tumor heterogeneity of TNBC has not only limited advances in the development of targeted therapy but also in the identification of biomarkers that can predict disease status and monitor treatment response. Advances in next-generation sequencing technologies have led to the identification of promising clinically actionable mutations however these tests often require invasive procedures to obtain tumor tissue and lack the ability to monitor treatment efficacy or detect recurrence, highlighting the need for non-invasive markers. A number of serum protein biomarkers have been evaluated in TNBC however none have yet to be successfully deployed in the clinic as indicators of disease. We have previously established that the urinary proteome can serve as a source of highly specific and sensitive biomarkers that can detect disease status and stage of multiple cancer types. Within the context of our global proteomics approach to cancer biomarker discovery, we have utilized the SomaScan discovery platform to identify 281 proteins that are differentially expressed in the urine of patients with TNBC compared to the urine of age- and sex-matched controls. The gene expression profiles of these proteins in TNBC tumor tissue were compared to those of normal breast tissue utilizing the R2 Genomics Platform. Proteins whose gene expression profile was consistent with the proteomic data were validated for the ability to distinguish between TNBC and non-TNBC diagnoses using mono-specific ELISAs of patient urine samples. These results demonstrate that a global proteomics approach coupled with clinical gene expression data can be effectively utilized to identify potential biomarkers for TNBC. These findings identify clinically relevant proteins that should be further explored as potential biomarkers in the development of non-invasive diagnostics for TNBC. (This work was supported by the Breast Cancer Research Foundation and the Nile Albright Research Foundation).

High-throughput Screening, Lead Identification and Optimization, and in Silico Drug Discovery

#5319

EU-OPENSCREEN - An open-access initiative in chemical biology to support anti-cancer drug discovery

Bahne Stechmann, Charlotte Wit. *EU-OPENSCREEN ERIC, Berlin, Germany*

Over the past two decades, an increasing number of small molecule drugs that target unique molecular changes underlying a specific cancer have been approved, and small molecule drugs represent a major therapeutic class for cancer treatment. Chemical ‘probes’ are also indispensable tools to advance our understanding of pathologies at the molecular and cellular level and to validate novel drug targets.

A major bottleneck in identifying and developing these chemical compounds in academia is often access to robust disease-relevant assays, high-throughput screening platforms, comprehensive screening libraries, medicinal expertise for the hit-to-lead optimization. In order to democratize access to these resources for a broader scientific community, the publicly funded EU-OPENSCREEN (www.eu-openscreen.eu) initiative has been established with the aim to accelerate drug discovery efforts in an open-access setting in collaboration with researchers from academia and industry. EU-OPENSCREEN’s 30 expert centers offer access to their cancer target-based and phenotypic drug screening expertise, capabilities in developing disease-relevant assays and hit-to-lead optimization capabilities. The identified bioactive ‘hit’ compounds will be progressed into high-quality chemical starting points to be further developed into drug leads or chemical probes for the elucidation of mechanisms of cancer onset, progression, resistance and effects of drug therapy. All generated tool compounds and associated bioactivity data are made available to the global scientific community.

Here we will present an overview of anti-cancer drug discovery projects of EU-OPENSCREEN and explain the opportunities and benefits for other international scientists to collaboratively develop novel anti-cancer drug leads and chemical probes.

EU-OPENSCREEN receives funding from the European Union's Horizon 2020 and Horizon Europe research and innovation programs under grant agreements No 654248 and 101058620.

#5320

The RenMice™ HiTS (Hyperimmune target specific) Platform facilitates identification of novel therapeutic antibodies for challenging targets

Xiaoqian Zhang[1], Shufang Fu[1], Shujin Zhang[1], Xin Ji[1], Li Hui[2], James Jin[2], Jing Zhang[1]. *[1]Biocytogen Pharmaceuticals (Beijing) Co., Ltd, Beijing, China,[2]Biocytogen Boston Corp, Wakefield, MA*

In recent years, an increasing number of therapeutic antibodies have shown to be effective for the treatment of cancer and other diseases. However, limitations in the traditional discovery process, including immune tolerance of highly homologous genes, challenges with antibody sequence humanization, clone selection, and model selection for drug efficacy and safety evaluation, often hinder the process of identifying new therapeutic antibodies. The RenMice™ HiTS (Hyperimmune Target Specific) Platform is a library of chromosome engineered mice with fully human immunoglobulin variable domains replacing the mouse loci, each with a specific drug target gene knocked out. These mice are designed to establish robust immune responses and generate antibodies that bind to more epitopes of the target protein, including conserved domains. The platform is ideal for challenging targets, such as proteins with high homology across species, or multi-pass transmembrane proteins (e.g. GPCRs/ion channels). Here, we show that the platform can be used to generate antibodies that cross-react with multiple species, like human, monkey, dog, and mouse targets, by immunizing with both human and mouse or dog antigen. We provide examples for newer campaigns, including species cross-reactivity and internalization of novel antibodies targeting NECTIN-4, and high-throughput in vivo efficacy screening of novel anti-PD-1 antibodies in wild-type mice. In the future, we will evaluate the preliminary toxicity of these cross-reactive antibodies in preclinical animal models. Thus, selection of the best antibody candidate based on in vivo efficacy and safety allows for a streamlined and successful preclinical phase. In conclusion, the RenMice™ HiTS platform facilitates the generation of developable antibodies that recognize novel epitopes and challenging targets.

#5321

Large scale pan cancer drug combination screening to identify effective and actionable combinations and biomarker hypothesis

Azadeh Bashi[1], Elizabeth A. Coker[2], Krishna Bulusu[1], Marta Milo[1], Claire Crafter[1], James Lynch[1], David Jenkins[3], Howard Lightfoot[2], Brandon Willis[3], Courtney Andersen[3], Omid Tavana[3], Kevin Mongeon[3], Jacob Gordon[3], Paul Smith[1], Simon Barry[1], Ultan McDermott[1], Lisa Drew[3], Susan Critchlow[1], Mathew J. Garnett[2], Jerome Mettetal[3]. *[1]AstraZeneca Oncology, Cambridge, United Kingdom,[2]Wellcome Sanger Institute, Cambridge, United Kingdom,[3]AstraZeneca Oncology, Waltham, MA*

Drug combinations are highly desirable in oncology as they can improve therapeutic response and overcome drug resistance. However, responses can be context-specific, meaning there is a real need for large-scale studies to fully explore the drug combination response landscape.

We present a screen of 109 drug combinations in over 750 diverse cell lines covering 41 hematological and solid tumor types. Each combination was screened in a full 7x7 matrix format, representing over 2.3 million individual data points, the largest such study to date. We took a novel approach to assess combination benefit. Growth inhibition and highest single agent (HSA) and Bliss excess combination heatmaps were generated for all >68,000 combination-cell line pairs, and each was scored for high activity (combination Emax>0.5) and combination benefit/synergy (HSA>0.1). Out of 4578 combination-cancer type pairs 489 met the filtering criteria. We prioritized combinations based on their efficacy and cancer type selectivity to minimize risk of potential tissue toxicity. We identified several known combination-cancer type pairs (e.g. MCL1 inhibitor AZD5991 plus BCL2 inhibitor venetoclax in AML) as well as novel indications for combinations already known to be active in a different cancer type (e.g. AZD5991 plus AKT inhibitor capivasertib in endometrial cancer or AURKB inhibitor AZD2811 plus venetoclax in DLBCL). We selected 4 combinations based on clinical need and validated them further *in vitro* and *in vivo* (selumetinib plus venetoclax or AZD5991, AZD2811 plus venetoclax, and capivasertib plus AZD5991).

To understand how molecular context affects drug response, we also used GDSC tools ANOVA to perform over 5.4 million statistical tests to identify statistically significant associations between drug response metrics and

multi-omics features including mutations, CNAs, gene expression and methylation. Associations were identified with five response metrics, covering both single agent and combination responses. We looked for significant associations across 21 different subgroups of cell lines and 6 molecular 'baskets' (TP53, KRAS, MLL2/KMT2D, PTEN, PIK3CA, and BRAF). We identified 11,611 biomarkers which met the significance criteria (p<=0.001, FDR<=10%, and both positive and negative Glass deltas >=1). Moreover, we used biomarkers of single-agent response to identify any combination Emax or Bliss associated biomarkers that could not be explained by the action of either drug. This resulted in identification of 1,631 'emergent' biomarkers.
In summary, our screen and pipeline have been designed to optimize preclinical interpretation with a focus on actionability, particularly by our unique approach, and to provide a valuable resource for exploration by the wider research community. As a result of this screen, we identified and validated novel combination-tumor types in multiple cancer types.

#5322

High throughput chemotherapeutic drug screening system for gastric cancer: cure-GA

Jieun Lee[1], Jung Eun Kim[2], Sanjun Lee[3], Tae-Kyeong Lee[1], In Hee Kim[2], So Hee Yoon[2], Mira Yoo[1], Eunju Lee[1], Doo-Young Hwang[1], So Hyun Kang[1], Bo Sung Ku[2], Dong Woo Lee[2], Young Suk Park[1], Ji-Won K[4], Jin Won Kim[4], Sang-Hoon Ahn[1], Keun-Wook Lee[4], Hyung-Ho Kim[1], Hyun Jung Oh[5], Yun-Suhk Suh[1]. *[1]Department of Surgery, Seoul National University Bundang Hospital, Gyeonggi-do, Korea, Republic of,[2]Department of Precision Medicine, Medical & Bio Decision (MBD Co., Ltd.), Gyeonggi-do, Korea, Republic of,[3]Department of Surgery, Kyung Hee University Hospital at Gangdong, Seoul, Korea, Republic of,[4]Department of Internal Medicine, Seoul National University Bundang Hospital, Gyeonggi-do, Korea, Republic of,[5]Department of Pathology, Seoul National University Bundang Hospital, Gyeonggi-do, Korea, Republic of*

To discover clinically applicable anticancer drugs and predict therapeutic response for advanced gastric cancer, we developed a high-throughput drug (HTD) screening system that could rapidly evaluate drug reactivity using

3D cultured primary cells derived from gastric cancer (GC) patients. Primary cancer cells were isolated from fresh surgical specimens that resected from 143 GC patients using Gentle Max tissue dissociation system. Primary cells were mixed with Matrigel, and placed on a micropillar for three-dimensional (3D) culture. After the primary cells were stabilized in the complete culture medium (CCM) than added various chemotherapeutic drugs containing 5-FU, Oxaliplatin, and Paclitaxel in CCM and incubated for 7 days. Cell viability was determined through calcein staining and quantified scanned images. The IC_{50} for each drug was calculated by a sigmoidal dose-response curve, using the GraphPad Prism 9 program. The average weight of gastric cancer tissue used in the experiment was 300 mg (75 mg ~ 1930 mg), and the average number of dissociated viable cells for each tissue was 3.9 x 10^6 cells/case. About 2.4 x 10^5 live cell was required per drug, we were able to obtain an average of 6.4 (Min.2, Max 14) drug reactivity data per tissue using the HTD screening system. GC tissues obtained from the operating room were dissociated within 16 hours and then loaded into the HTS system within 3 hours. Cells were stabilized for 1 day in 3D culture plate and exposed to the drug for 7 days, and then data reports were made within 3 days. As a result, it was possible to obtain within 14 days from fresh surgical GC tissue to drug response data. Additionally, we confirmed that 3D cultured primary cells derived from GC tissues consistently preserved primary characters using IHC. Similar to their parental cancer tissue, GC 3D cultured primary cells derived from adenocarcinoma large glandular patterns and retain the expression of some marker proteins. In this study, we evaluated the drug response data for 101 cases (success rate 71%; 101/143) to 5-FU, Oxaliplatin, and Palitaxel, etc. using the HTD screening system and it was confirmed that individual patient had a difference response to each drug. Here we established the HTD screening system using 3D cultured GC patient derived primary cells. The advantages of this system were that it is the first model system that directly used patient-derived primary cells for drug screening, and it can rapidly evaluate drug reactivity to various anticancer drugs within 10 days. The HTD screening system based on patient-derived primary cells can provide that information to predict drug response and allow for finding more appropriate therapy for each patient.

#5323

Accelerating the drug discovery process with an automated high-throughput protein production and characterization platform for AI-driven antibody development of immunotherapy

Zhehao Xiong, Wei Jiang, Lijun Xia, Jianhua Huang, Cheng-chi Chao.
Biomap, Menlo Park, CA

The demonstrated effectiveness and vast potential of large molecule therapeutics have driven biopharmaceutical companies to change the ways by which they discover and develop novel biologic therapies. While the conventional antibody discovery process via animal immunization and *in vivo* hypermutation can generate sufficient hits for functional screening, this approach can only cover a limited subset of sequence diversity. In silico, artificial intelligence (AI) driven methods, by contrast, have the potential to cover 2-3 orders of magnitude more sequence diversity compared to conventional methods and more rapidly produce a drug candidate with a superior safety and efficacy profile. However, this approach requires wet lab validation of predicted sequences as well as targeted data generation to improve AI-predicted rankings. Traditional wet lab methods for protein generation and characterization are expensive, time consuming, and prone to human error. These limitations restrict the overall potential benefit of the AI-driven antibody discovery process. To accelerate this process, which consists of a complex series of cycles spanning different functional teams, a substantial increase in the throughput of the end-to-end production and characterization workflow is established in-house such that 10^4 antibodies with property data can be generated and analyzed within a short period of time. BioMap has implemented a highly integrated and automated protein expression, purification, and characterization platform linked with a unified informatics system to eliminate as much manual operation as possible. This high-throughput robotic platform interweaves multiple procedures including plasmid preparation, cell dispensing, mammalian transfection, protein purification, and characterization, and it is coupled to our in-house informatics system and database. Empowered by state-of-the-art liquid handling system and well-established experimental protocols, the integrated facility is capable of the delivery of 10^3 protein samples from plasmids in ten days within a single batch. Benefiting from our robust transient expression platform, the production scale ranges from 0.5 to 30 mL with an average antibody yield of 300 mg/L. The high-throughput workflow brings

a challenge to track the provenance of each protein and manage data flow across different stations. To address this bottleneck, a well-defined informatics platform and database have been developed to provide sample registration, interface with lab instruments, experimental process tracking, and automated data recording and analysis. The implementation of this system provides a massive amount of high-quality data available for AI training and validation with a very short turnover time and enables AI-driven development of next-generation biologics.

#5324

Drug repurposing and genetic screening strategies for effective treatment discovery in soft-tissue sarcomas

Mushriq Al-Jazrawe[1], Kathryn Cebula[1], Elisabeth A. Abeyta[1], Haley S. Curtis[2], Jane K. McIninch[2], Jaime H. Cheah[2], James Berstler[2], Lisa Miller[2], James Neiswender[2], Lisa Brenan[2], Mike Burger[2], Francisca Vazquez[2], Jesse S. Boehm[1]. *[1]Koch Institute for Integrative Cancer Research at MIT, Cambridge, MA,[2]Broad Institute, Cambridge, MA*

Treatment advances for soft-tissue sarcomas have been slow. This is, in part, due to their rarity (accounting for 0.7% of all cancers) and heterogeneity (over 50 different diseases fall under this category). Moreover, preclinical models are scarce, often exhibiting slow growth kinetics, which limits their study by large genetic and pharmacological libraries. Here, we present an update on our efforts to harness the power of patient-partnered research to create a platform for rare cancer drug target discovery as a broadly available community resource. We developed a patient-partnered tissue donation pipeline to enable patients anywhere in the United States to participate and piloted our approach for *CTNNB1*-driven desmoid tumors. To overcome challenges in tissue heterogeneity during ex vivo culture, we optimized a multiplexed sequencing protocol to quantitatively track changes in tumor cell fraction across hundreds of media formulations. Following this strategy, we were able to verify and expand three cell lines that preserve the *CTNNB1* mutations at high purity. To identify potential therapeutics, we completed a 6,750-drug repurposing screen, at 2.5uM in duplicate, in two verified cell line models. After extensive quality control assessments and data integration steps to leverage the power of other large scale drug screens, we selected 263 compounds for

follow-up based on potency, selectivity, and association with molecular features associated with desmoid tumors. Approximately 70% of selected compounds were validated by an 8-point, 2-fold dilution, dose-response format with a top concentration of 10uM. Of the confirmed active compounds, 80 showed a strong pattern of selectivity, 20 are FDA approved drugs and 13 investigational compounds show a statistical association with *CTNNB1* hotspot mutation status or transcriptomic features associated with desmoid tumors. To prioritize potential therapeutic targets, we tested an efficient CRISPR/Cas9 all-in-one library design. The reduction of the CRISPR/Cas9 library size was achieved via multiple gene- and guide-level strategies, which enables statistically powered gene essentiality interrogation in slow-growing patient-derived models. We tested several plating and infection parameters and developed an optimized pipeline for the rapid introduction of this library into early patient-derived samples. Established cell lines of mesenchymal and non-mesenchymal origin, which have previously been tested by genome-wide libraries, were used to control for library and lineage effects. We are developing a biologist-friendly web portal that will enable the research community to easily interact with models and data produced by this effort. Our study provides evidence that a systematic patient-powered approach can facilitate discovery of therapeutic hypotheses for these understudied diseases.

#5326

Comparison of CAR-T cell-mediated cytotoxicity assays with suspension tumor cells using high-throughput plate-based image cytometry method

Leo Li-Ying Chan[1], Yu-Jun Sun[2], Yi-Chun Chen[2], Wei-Kai Hua[2], Sariena Chiung-Yuan Wu[2]. *[1]Advanced Technology R&D, Nexcelom from PerkinElmer, Lawrence, MA,[2]Research and Development, GenomeFrontier Therapeutics, Taipei City, Taiwan*

In the recent decade, chimeric antigen receptor (CAR)-T cell therapy has revolutionized strategies for cancer treatments due to its highly effective clinical efficacy and response for B cell malignancies. Currently, there are six CAR-T cell products available in the market including Kymriah, Yescarta, Tecartus, Breyanzi, Abecma, and Carvykt. The success of CAR-T cell therapy has stimulated the increase in the research and development of

various CAR constructs to target different tumor types. Therefore, a robust and efficient in vitro potency assay is needed to quickly identify potential CAR gene design from a library of construct candidates. Traditionally, in vitro CAR-T cell-mediated cytotoxicity is assessed using release assays such as 51Cr (radioactivity), calcein (fluorescence), and LDH (enzymatic). However, release assays indirectly measure cell death via molecules released in supernatant and typically limited to only endpoint assays. In addition, handling and disposing of 51Cr hazardous materials is less preferred. Luciferase reporter assay, although highly sensitive, has similar drawbacks as the release assays. Finally, flow cytometry method can directly measure cell death and viability, but can be time-consuming and requires a large number of CAR-T cells when the effector-to-target (E:T) ratio is high. Furthermore, additional steps are required for adherent cells that require trypsinization. Image cytometry methodologies have been utilized for various CAR-T cell-mediated cytotoxicity assay using different fluorescent labeling methods, mainly due to their ease-of-use, ability to capture cell images for verification, and higher throughput performance. In this work, we employed the Celigo high-throughput plate-based Image Cytometer to evaluate and compare two CAR-T cell-mediated cytotoxicity assays using GFP-expressing or fluorescent dye-labeled myeloma and plasmacytoma cells. Performing time- and E:T ratio-dependent CAR-T cell-mediated cytotoxicity assays, the GFP-based method demonstrated higher sensitivity in detecting the
level of cytotoxicity when compared to the CMFDA/DAPI viability method. We have established the criteria and considerations for the selection of cytotoxicity assays that are fit-for-purpose to ensure the results produced are meaningful for the specific testing conditions.

#5327

Automated organoid alignment for clonal response characterization in pancreatic ductal adenocarcinoma

Ethan Samuel Lin, Md Shahadat Hossan, Austin Stram, Eleanor E. Riedl, Luke J. Koeppel, Jaimie M. Warner, Jeremy D. Kratz. *Department of Medicine, University of Wisconsin-Madison, Madison, WI*

Background**:** Therapeutic screening Pancreatic Ductal Adenocarcinoma (PDAC) relies on well-level assessment for high throughput response

evaluation. Patient-derived cancer organoids (PCOs) model subclonal populations, however the significance of resistant populations is uncertain when characterized with well-level response. Using a high-throughput screening assay, we present an automated alignment algorithm to characterize populations of organoid growth as compared to validated well-level therapeutic response assays.

Methods: High content imaging was performed in low volume (10uL), 96-well angiogenesis plating format (Ibidi, Inc) at 4x objective with 5-frame Z-stack (600um) with brightfield imaging captured at 0h and 72h. Images underwent processing using Gen5 suite (Biotek, Inc) including Z-projection to render organoids into single two-dimensional planes. Baseline objects were defined between 50µm and 750µm, and filtration based on circularity defined as >0.4. Object alignment was performed based on root-mean-square-deviation (RMSD) between all combinations of objects to optimize match determination. This analysis was performed in drug screen of 80 independent agents in early clinical trials in combination with CDK7 inhibitor, SY-5609. Well level viability was performed using standardized 3D CellTiterGlo (CTG, Promega Inc.) (33% v/v). Response was assessed using descriptive statistics, effect size (Glass's Δ), and Therapeutic Sensitivity Index (TSI) defined as the weighted average between elements with growth from media control versus treated population.

Results: Z projection of 600um in Low-volume plating (10µL) of matrix suspension yielded 1.68 organoids per µL relative to the traditional hanging drop design (50µL) 0.75 organoids per µL ($p<0.005$). Organoid alignment across the continuum of RMSD yielded maximum successful matches at 75µm with 66.1% of objects versus 6.7% based on randomly assigned objects across validation experimental sets (n=1380). An optimal circularity value was determined at 0.4; an increase of circularity by 0.1 yielded a >5% reduction in of matched objects, while a decrease in circularity by 0.1 yielded a <5% reduction in unmatched objects. A poor correlation was seen for the percent of growing organoids within a population and well level normalized viability via CTG ($R = 0.37$). The normalized CTG value had improved in correlation when compared to effect size relative to control ($R = 0.54$) and TSI ($R = 0.56$).

Conclusion: We provide a method for high fidelity alignment of PCOs in low-volume format for matrix-based screening applications. These techniques can be adapted to existing staining protocols to characterize

subclonal response in the context of both molecular heterogeneity and clinical outcomes.

#5328

Novel KRAS-specific in-well lysis ELISA for high throughput screening

Hyun Min Park, Jason Poole, Mary Anne Jelinek. *Active Motif, Carlsbad, CA*

RAS is one of the most frequently mutated genes in cancer. Gain–of–function missense mutations promoting oncogenesis cluster at codons 12, 13, and 61 of KRAS, NRAS and HRAS. These result in enhanced GTP binding due to fast exchange of nucleotide and/or impairment of GAP (GTPase Activating Protein) binding. Although these mutants are all activating, they are not equal in their oncogenic potential and differences in patient survival are associated with different RAS mutants and which RAS allele is affected, with KRAS being the most prevalent. Current RAS therapeutic approaches have migrated to be isoform specific. With this in mind, we have developed an activation state specific high throughput screening compatible (HTS) assay that is specific for KRAS. A novel rabbit anti–KRAS recombinant antibody was isolated via cloning of immunoglobulin variable regions from antigen positive B cells isolated from rabbits immunized with a peptide immunogen targeting a region of low homology between the RAS isoforms. Antibody specificity was validated with recombinant HRAS, KRAS and NRAS proteins over a wide concentration range by both immunoblotting and by a bead–based multiplex ELISA where all three RAS isoforms were present. The new assay allows for direct in–well lysis of cells cultured in 96–well plate format, either directly in media or following a PBS wash step. Activated KRAS in the lysate is captured on the assay plate and detected via chemiluminescence using the KRAS specific antibody. Preliminary assay validation has included EGF treatment of HeLa cells to show activation in cells expressing wildtype KRAS and inhibition with the selective non–covalent KRASG12D inhibitor MRTX1133 in Aspc1 cells known to express KRASG12D over a wide range of cell seeding densities. We anticipate that this assay will further the discovery of novel KRAS specific therapeutics.

#5329

High throughput screening strategies in the development of logic gated cell therapies

Li Wang, Sofia Kyriazopoulou Panagiotopoulou, Rona Harari-Steinfeld, Dasmanthie De Silva, Michelle Tan, Laura Lim, Angela Boroughs, Cate Sue, Jon Chen, Jamie Thomas, Mary Chua, Ed Yashin, Christine Shieh, Ryan Fong, Sophie Xu, Grace Zheng, Brendan Galvin, Aaron Cooper, Tarjei Mikkelsen, Nicholas Haining. *Arsenal Biosciences, Inc, South San Francisco, CA*

Chimeric antigen receptor T cell (CAR T) therapy has demonstrated unprecedented therapeutic activity in hematologic malignancies. However, generating potent clinical responses against solid tumors remains a challenge for CAR T therapy. As the field strives to improve the therapeutic efficacy of CAR T cells with novel target antigens and enhanced potency, the risks of on-target toxicity pose a major barrier to progress. To address these challenges, we have developed engineered CAR T cells to target solid tumors through AND logic gates, where CAR expression is conditionally induced by a transcription factor released from a priming receptor (PrimeRTM) upon binding to the PrimeR antigen. The AND gate limits off-tumor toxicity as it requires both CAR and PrimeR antigen expression in the tumor microenvironment.

To ensure PrimeR expression and signal transduction upon antigen binding, while minimizing residual ‘‘leaky’’ CAR induction in the absence of PrimeR antigen, we screened hundreds of PrimeR binders using both arrayed and pooled strategies. In an arrayed strategy, we engineered T cells from four donors in multiwell plates using CRISPR-mediated, non-viral, site-specific integration of logic gates bearing a variable PrimeR binder and a fixed MSLN CAR. In addition, we employed a pooled screening strategy, where we engineered T cells from two independent donors with a pool containing a subset of >300 of the same logic gates.

Engineered T cells from both strategies were co-cultured with cell lines bearing either both CAR and PrimeR antigens or a single antigen, in order to evaluate fidelity and on-target functionality. In the arrayed setting, on-target functionality was quantified based on the levels of CAR induction, cytokine secretion, T cell activation, and target cell killing in the presence of both antigens, while fidelity was assessed based on the absence of these activity signals in the presence of a single antigen. In the pooled setting,

sorting based on functional markers was performed and sequencing was used to quantify the relative abundance of cells with each logic gate in different sorted populations. On-target activity and circuit fidelity were then quantified based on enrichments in different sorted populations.
Results from the pooled and arrayed screens were highly concordant. We combined the screen readouts to nominate a small set of PrimeR binders that exhibited both high fidelity and on-target functionality. We confirmed the desired characteristics of these binders with targeted arrayed screens in additional conditions as well as in in-vivo models. We have applied both screen strategies to select a small set of leads from hundreds of candidate PrimeR binders in the context of a logic-gated MSLN CAR. As pooled and arrayed screens come with different sets of limitations and advantages, both serve as important tools for the effective selection of receptors in the development of novel cell therapies.

#5330

Cell identity, count, and viability for critical quality attributes using the Cellaca PLX image cytometer

Carolina Franco Nitta, Mackenzie Pierce, Aiyana Parker, Sopaul Hem, Timothy Smith, Surbhi Ratnani, Marek Dobrowolski, Srinivas Gundimeda, Bo Lin, Dmitry Kuksin, Leo L. Chan. *Nexcelom Bioscience, Lawrence, MA*

Cell and Gene therapy is one of the fastest growing fields for cancer therapeutics that heavily relies on robust and consistent instrumentations and technologies to verify and validate the critical quality attributes (CQA) that are fit-for-purpose. Some of the key parameters required for satisfying CMC (Chemistry Manufacturing and Controls) criteria standards for cellular therapeutic products are cell identity, count, viability, purity, potency, stability, and microbiological quality, which may be routinely performed using flow cytometry. Some of these critical attributes can be exceedingly trivial for flow cytometric analysis, which can be complex, requires a dedicated user, and may carry a high maintenance cost. In the past decade, affordable image cytometry has been developed for cell characterization and cell-based assays but has not demonstrated the sensitivity required for visualization and analysis of surface markers, cell health, and viability. In this work, we demonstrate the capability of the newly developed Cellaca PLX image cytometry system for population

analysis of surface markers, viability of fluorescent protein expressing cells, and cell health in comparison to flow cytometry. For immunophenotyping assays, PBMCs were stained with anti-human CD3/CD4/CD8 antibodies with Hoechst. Additionally, viability detection of GFP and RFP-containing cell lines was performed by staining with RubyDead and Hoechst. Finally, apoptosis was induced in Jurkat cells with staurosporine and stained with Caspase 3-488, RubyDead, and Hoechst. All assays were imaged and analyzed using the Cellaca PLX image cytometer, and the data generated were compared directly to the CytoFlex flow cytometer. Results show similar percentages of surface marker populations: CD3 (76% and 81%, PLX and CytoFlex, respectively), CD4 (43% and 42%), and CD8 (15% and 17%). RFP and GFP-containing cells showed comparable viabilities on Cellaca PLX and CytoFlex, and the population percentages of Hoechst positive cells stained with Caspase 3 and RubyDead were within 5% of each other. Our experiments demonstrate that the Cellaca PLX can be of significant value to the Cell and Gene Therapy communities providing novel image cytometry methods which may satisfy several CMC criteria including high-throughput, high sensitivity, and low maintenance.

#5331

DNA-encoded macrocyclic compound libraries for challenging targets

Ying Zhang[1], Anthony Keefe[1], Paolo Centrella[1], John Cuozzo[2], Holly Soutter[3], Daniel Resnicow[4], Sevan Habeshian[5], Matt Clark[1]. *[1]X-Chem Pharmaceuticals, Waltham, MA,[2]Relay Pharmaceuticals, Cambridge, MA,[3]Broad Institute, Cambridge, MA,[4]Bonito Biosciences, Waltham, MA,[5]Orbis Medicines, Zurich, Swaziland*

Increasingly drug discovery programs require the development of orally available and cell permeable classes of drugs derived from the chemical space beyond Lipinski's rule of 5 (bRO5). The chameleon-like physicochemical properties and differentiated binding modes of bRO5 compounds make them suitable starting points, especially for difficult-to-drug targets beyond traditional small molecule drug discovery. The synthesis of macrocyclic (MC) peptide DNA-Encoded Libraries (DEL) aligns with these efforts and has been an important addition to the rapidly growing field of DNA-encoded small molecule library screening. DEL screening of *de novo* designed bRO5 compounds will aid the exploration of

bRO5 chemical space. X-Chem's macrocyclic compound libraries apply chemistries beyond traditional peptide formation and extend to the inclusion of diverse building block classes. A case study of a successful screening campaign utilizing these MC DEL for Bcl2 will be presented.

#5332

Characterization and comparison of acridine orange/propidium iodide and acridine/DAPI viability detection methods for cell and gene therapy development

Yongyang Huang, Samir Patel, Mackenzie Pierce, Carolina Franco Nitta, Bo Lin, Leo Chan. *Nexcelom Bioscience, Lawrence, MA*

Cell viability is one of the critical quality attributes (CQAs) for cell and gene therapy products. Characterization of cell viability, in addition to cell identity, cell count and other CQAs, are essential to ensure the quality, safety and efficacy throughout various developmental stages of cell and gene therapies. To determine cell viability, a variety of viability detection methods have been used, such as trypan blue (TB) exclusion assay, and fluorescence-based dyes including acridine orange / propidium iodide (AO/PI), acridine orange / 4′,6-diamidino-2-phenylindole (AO/DAPI), all of which have been employed on flow or image-based cytometry systems. In this work, we employed the Cellaca MX high-throughput cell counter to characterize and compare AO/PI and AO/DAPI viability detection methods. First, we measured the viabilities of different ratios of viable and non-viable Jurkat cells created via two cell dying processes. Next, viabilities of the stained cells were measured multiple times within a 30 min staining time for each method in order to monitor the trend of viability changes. The viability results showed that the AO/DAPI method were generally higher than AO/PI method with differences ranging from 0% to 24%. We also observed the discrepancy of the measured viability differences between naturally-dying and heat-killed Jurkat cells, suggesting that the viability difference might be dependent on the cell dying process. In the time-dependent viability characterization, results from AO/DAPI method showed increasing dead cell counts leading to decreasing viability, revealing an on-going staining process. In contrast, results from AO/PI method showed more consistent cell count and viability measurements, indicating a more instantaneous staining process. Lastly, we conducted a cell proliferation

assay as an orthogonal method to confirm replicability of the low viability cell samples. The proliferation assay results showed no significant increase in cell concentrations within the 4-day time frame. The viability results before the culture were approximately 0% for both naturally-dying and heat-killed Jurkat cells, using the AO/PI staining method, and 12% and 9% using the AO/DAPI respectively. Furthermore, spiked samples of natural-dying and heat-killed cells with healthy cells (>90% viability) were generated and measured, which showed exponential growth. The viability results of these spiked samples before the culture were 11% and 9% by AO/PI and 17% and 18% by AO/DAPI, respectively. Taken together, these results suggest that cell viability methods need to be optimized for different fluorescent stains in order to generate reliable, robust, and fit-for-purpose results for the downstream assays for cell and gene therapy products..

#5333

Combining chemoproteomics with machine learning identifies functionally active covalent fragments for hard-to-drug cancer drivers

Johannes C. Hermann[1], Robert Everley[2], Laura Marholz[2], Matthew Berberich[2], Tzu-Yi Yang[2], Yu-Hsin Chao[2], Abduselam K. Awol[2], Michael Shaghafi[1], Han Yoon[1], Rohan Varma[1], Reed Stein[1], Karsten Krug[1], Emily Lachtara[2], Daniel Erlanson[1], Chris Varma[1], Kevin R. Webster[2]. *[1]Frontier Medicines, South San Francisco, CA,[2]Frontier Medicines, Boston, MA*

a) Many cancer drivers are considered “undruggable” and without targeted treatments because they lack binding sites for conventional small molecules. Here, we introduce The FRONTIER™ Platform applying machine learning (ML), chemoproteomics and covalent chemistry to identify binding sites and cell-active covalent fragments across the human proteome, including against most cancer drivers and previously “undruggable” targets. Molecules tested in functional assays are active and can serve as starting points for new drug discovery initiatives.
b) We are using mass spectrometry and data analysis workflows to perform high-throughput chemoproteomic profiling experiments. These experiments identify hits across the proteome using different cancer-relevant cell backgrounds and characterize binding sites for drug discovery. Customized ML algorithms using chemoproteomic, genomic and structural data to characterize and prioritize identified binding sites for covalent drug

discovery. The performance of the platform allows the profiling of thousands of compounds from a custom-built library that has been optimized by ML for covalent fragment-based drug discovery. The nature of the fragment hits and the ability to map them to and focus on preferred binding sites for covalent drugs enables accelerated lead generation.
c) We show details of the platform highlighting library design concepts and the hotspot map with binding site prioritization algorithms. We show coverage and applicability across important cancer target classes and signaling pathways. Covalent fragment hits have been identified for multiple difficult cancer targets, including KRAS, p53, STAT3, KEAP1, PTPN11 and others. The platform also identifies ligands for novel allosteric binding sites in established oncology targets such as CDK4, PI3KCA and BTK. We will highlight how discovered ligands show functional activity in orthogonal assays, demonstrating their fitness for drug discovery campaigns and target validation experiments.
d) Undruggable targets across a variety of cancer target classes have become druggable.

#5334

Targeting the KIF15-TPX2 PPI to overcome KIF11 inhibitor resistance in epithelial ovarian cancer

Benjamin K. Gibbs[1], Justin T. Douglas[2], Rebecca J. Wates[1], Peter R. McDonald[3], Amy M. Whitaker[4], Cornelius N. Ndi[5], Harsh B. Pathak[1], Laurie A. Harned[2], Sarah A. Neuenswander[2], Melinda A. Broward[6], Bret D. Freudenthal[7], Anuradha Roy[3], Frank J. Schoenen[5], Andrew K. Godwin[1].
[1]Department of Pathology and Laboratory Medicine, University of Kansas Medical Center, Kansas City, KS,[2]Nuclear Magnetic Resonance Lab, University of Kansas, Lawrence, KS,[3]Structural Biology Center, University of Kansas, Lawrence, KS,[4]Department of Biochemistry and Molecular Biology, University of Kansas Medical Center, Kansas City, KS,[5]Higuchi Biosciences Center, University of Kansas, Lawrence, KS,[6]Institute for Advancing Medical Innovations, University of Kansas Medical Center, Kansas City, KS,[7]Department of Biochemistry, University of Kansas Medical Center, Kansas City, KS

Most cases of epithelial ovarian cancer (EOC) exhibit extensive molecular heterogeneity, presenting challenges in developing targeted therapies. Despite extensive efforts and incremental successes in developing targeted drugs and immunotherapies for other cancers, chemotherapies continue to be the most used treatment of ovarian cancer. Although seemingly simplistic, identification of drugs targeting cellular machinery independent of genomic and genetic status continues to be a strong clinical need. Previously, we performed an RNAi-based screen of the druggable genome across a diverse histological panel of EOC cell line representing both platinum-sensitive and -resistant tumors (PMID: 23056589). This screen elucidated KIF11 as essential in maintaining EOC cell viability. KIF11, a mitotic spindle assembly motor protein, has been targeted clinically. Although drugs are well tolerated, potent, and specific, the objective response rates to KIF11 inhibitors in clinical trials were commonly less than 10%. The efficacy of KIF11 inhibitors is blunted via a compensatory motor kinesin, KIF15. The overexpression of KIF15 has been shown to compensate for absent KIF11 in the formation of the bipolar spindle apparatus during mitosis. Silencing KIF15 significantly sensitizes cells to KIF11 inhibitors and resensitizes resistant cells to KIF11 inhibitors. We developed a high throughput screening approach using Alpha technology to identify compounds that inhibit the protein-protein interaction (PPI) between KIF15 and TPX2, a unique approach to inhibiting KIF15 from previous efforts. Of the nearly 200,000 compounds screened, 177 compounds were selected to be further characterized based on assay performance and chemical properties. These compounds were screened for TPX2 or KIF15 binding by STD-NMR and waterLOGSY. Three compounds across two chemotypes were confirmed to bind KIF15. No compounds were found to bind TPX2. Additionally, 168 of the 177 compounds were screened for drug synergism *in vitro*. The synergism assay yielded 32 strongly and 8 weakly synergistic hits. The lead compound in each of the two chemotypes revealed by NMR were classified as strongly synergistic (max. bliss score of 8.0 and 29.9). To expand the potential lead compounds identified for further development, an antibody-free cellular thermal shift assay (CETSA) is being completed with 168 compounds. Preliminarily, CETSA has shown that the two lead compounds significantly stabilize KIF15 (ΔTm = 5.6 °C and 9.6 °C). These two lead compounds behaved in a dose-dependent manner in the AlphaScreen (IC_{50}= 2 μM and

6 μM), a favorable characteristic for further development. To date, two chemotypes have been identified as KIF15 inhibitors uniquely targeting the KIF15-TPX2 PPI. The data indicates KIF15 inhibition in combination with KIF11 inhibition is synergistic, thus demonstrating a potential novel treatment approach for people with EOCs.

#5335

circAde: a circRNA-based system for prolonged and more effective treatment of cancer

Eoghan T. O'leary, Sara Vikberg, Emilie Foord, Erik D. Wiklund, Lone Ottesen, Victor Levitsky, Thomas B. Hansen. *Targovax ASA, Lysaker, Norway*

In recently performed phase I/II clinical studies, we have demonstrated successful delivery of vectorized transgene-encoding mRNA payloads to solids tumors with substantial clinical benefit. In patients, persistent and prolonged transgene expression correlated with positive clinical outcome, and thus temporal expansion of the transgene expression profile is expected to improve the therapeutic benefit even further. Recently, circular RNA (circRNA) has been discovered as a novel class of endogenously expressed RNA. CircRNAs, in contrast to mRNAs, are resistant to exo-nucleolytic decay which results in high intra-cellular stability and persistent expression within cells. Therefore, circRNA-based systems serve as an interesting new technology towards prolonged effects of treatment. Here, we show that our proprietary vector system, circAde, allows high expression of circRNAs through spliceosome-dependent biogenesis. By comparing the protein output from circAde and mRNA-based vectors, we show that the circAde-system out-performs conventional mRNA-based design, both in terms of transgene yield and temporal sustainability of expression. Moreover, using a panel of proof-of-concept-reporters, we show that certain design-features greatly influence the circRNA production and subsequent protein expression from the vector. Without the 5’cap, circRNAs are dependent on IRESs (internal ribosome entry sequences) for effective translation. By conducting two orthogonal IRES screens on 1000+ putative IRES elements, we have identified the most effective IRES sequence in melanoma and lung-cancer cells supporting effective circRNA production and high-yield protein expression, thereby improving our circAde vector system even

further. Our results open a new platform towards development of novel, more effective strategies for the treatment of cancer and other settings in which durable transgene expression is desirable.

#5336

Discovery of a novel activin receptor-like kinases (ALKs) inhibitor targeting TGF-β signaling pathways

Mai Arai[1], Mitsuharu Hanada[1], Hideki Moriyama[1], Hiroshi Ohmoto[1], Kazuhito Naka[2], Masaaki Sawa[1]. *[1]Carna Biosciences, Inc., Kobe, Japan,[2]Department of Stem Cell Biology, Research Institute for Radiation Biology and Medicine, Hiroshima University, Hiroshima, Japan*

Introducti**on:** Transforming growth factor β (TGF-β) plays a key role in promoting tumor progression mainly through facilitating angiogenesis, epithelial-mesenchymal transition (EMT) and also inducing immunosuppression in tumor microenvironment, allowing cancer cells to escape immune surveillance. Activin receptor-like kinases (ALKs) consisting of seven type I receptor serine/threonine kinases are responsible for TGF-β family signal transduction by phosphorylating Smad proteins, which can activate target gene expression. Therefore, ALKs are attractive drug targets for intervention in TGF- β signaling pathways as cancer immunotherapy.

Materials and methods: We have produced seven human recombinant ALK proteins (ALK1-7). The in vitro kinase assays for all ALKs have been developed using TR-FRET system. To evaluated cellular potency, TGF-β-dependent Smad3 phosphorylation assays in A549 (human lung adenocarcinoma cell line) and NMuMG (murine normal mammary gland cell line) cells were established. A TGF-β-mediated Treg differentiation assay was performed as an ex-vivo cellular assay using naive CD4+ T cell isolated from mouse spleen. In vivo anti-tumor efficacies of selected compounds, alone or in combination with anti-PD-1 antibody were assessed in a CT26.WT murine colon carcinoma syngeneic model.

Results: We have implemented a high-throughput screening (HTS) against human ALK5 over our in-house compound library. Hit compound **1** was identified from the HTS, and the subsequent Hit-to-Lead study led to a novel thiazole analog 2 as the starting point of lead optimization. Our lead optimization efforts led to advanced lead compound AL1, which exhibited

strong inhibitory potency for ALK5 with an IC50 value of single digit nanomolar. Unfortunately AL1 showed very low oral bioavailability in dogs, we continued the optimization study and identified compound AL2 having improved ADME property. In cellular assays, AL2 strongly suppressed the TGF-β-dependent Smad3 phosphorylation in A549 cells. In addition, treatment with AL2 decreased in the percentage of mouse CD4+/CD25+/Foxp3+ Treg cells dose-dependently in the ex vivo TGF-β-mediated Treg differentiation assay. As a monotherapy and combined with an anti-PD-1 antibody, oral administration of AL2 demonstrated robust in vivo antitumor efficacy in the CT26.WT murine colon carcinoma syngeneic model.
Conclusions: On the basis of its in vitro potencies, PK profiles, and in vivo efficacies, AL2 is currently being further evaluated in preclinical studies.

#5337
Design, synthesis and evaluation of dual-targeted mEGFR and AURK inhibitors as anticancer agents
Dayna Gesinski, Sonali Kurup. *Ferris State University, Big Rapids, MI*

Mutant epidermal growth factor receptor (mEGFR) inhibitors constitute the recommended therapy for mEGFR-positive cancers. However, resistance has developed to mEGFR inhibitors due to newer mutations within the enzyme pocket and redundant signaling pathways that bypass mEGFR inhibition. Recent studies have shown that resistance to mEGFR inhibitors could be overcome if given in combination with aurora kinase (AURK) inhibitors. Dual EGFR/AURK kinase inhibitors provide a novel approach to overcome resistance to EGFR inhibitors. In a previous study, Kurup *et al.* identified **1** as a nanomolar mEGFR inhibitor. Using a structure-based design approach, novel analogs of **1** that incorporated varied sidechains for dual mEGFR and AURK inhibition were designed. The synthesis of the target compounds involved microwave-assisted, copper and palladium catalyzed coupling reactions. This study led to the identification of dual-targeted mEGFR/AURKA and mEGFR/AURKB inhibitors, and compounds with sub-micromolar cellular potencies. The design, synthesis, kinase inhibitory activities and anticancer effects of these novel analogs will be presented. Structure-activity relationships for mEGFR, AURKA and AURKB inhibition will be defined.

#5338

A novel in vitro assay to evaluate the roles of hepatic metabolism on anticancer drug safety and efficacy

Albert P. Li, Hong Wei. *In Vitro ADMET Laboratories, Discovery Life Sciences LLC, Columbia, MD*

It has been well-established that hepatic drug metabolism may have significant impact on the efficacy and off-target toxicity of anticancer drugs. We present here an in vitro assay, the metabolism-dependent cytotoxicity assay (MDCA), for the evaluation of the roles of specific pathways on the efficacy of anticancer drugs. The assay employs a novel in vitro hepatic metabolic system, the permeabilized cofactor-supplemented human hepatocytes (MetMax Human Hepatocytes, MMHH), as an exogenous metabolic activating system for the evaluation of the in vitro cytotoxicity of anticancer agents towards a designated tumor and nontumor cells. MMHH are derived from cryopreserved human hepatocytes isolated from human livers procured for but not used for transplantation provided to our laboratory from the International Institute for the Advancement of Medicine. We have previously demonstrated that MMHH retained all drug metabolizing enzyme pathways present in human hepatocytes. The advantages of MMHH include the following: 1. Drug metabolizing enzyme activities are not affected by cytotoxicity of the drug substrate, a major limitation of intact human hepatocytes; and 2. Drug metabolism pathways can be selected by cofactor specification (e.g. NADPH/NAD+ for phase 1 oxidation; Uridine 5′-diphosphoglucuronic acid (UDPGA) for glucuronidation; 3'-phosphoadenosine 5'-phosphosulfate (PAPS) for sulfation; N-acetyl coenzyme A for N-acetylation). We present here a proof-of-concept study to evaluate the role of various hepatic metabolic pathways towards the cytotoxicity of cyclophosphamide, a commonly used drug for the treatment of renal carcinoma, towards a renal cancer cell line, HEK293 cells. We observed that NADPH enhanced the cytotoxicity, consistent with the known metabolic activation of cyclophosphamide by P450 isoforms (e.g. CYP2B6; CYP3A4) to the known metabolic activation of cyclophosphamide to 4-hydroxycloophosphamide, followed by the formation of the ultimate cytotoxic metabolites phosphoramide mustard and acrolein, which are responsible for its anticancer properties. In addition, we

found that the addition of L-glutathione attenuated cyclophosphamide cytotoxicity towards the HEK293 cells, an observation consistent with the roles of this cellular detoxification system in the resistance of tumor cells to chemotherapeutic agents. Minimal effects were observed for UDPGA and PAPS, consistent with the known noninvolvement of these phase 2 conjugating pathways in cyclophosphamide metabolism. MDCA represents an in vitro experimental system that can be routinely applied towards the discovery and development of novel anticancer drugs to evaluate the roles of drug metabolism in efficacy and safety, with various cancer cells (e.g. prostate carcinoma, neuroblastoma) and cells from normal tissues (e.g. cardiomyocytes, intestinal mucosal cells), respectively, as target cells.

#5339

4-Amino-*N*-phenylbenzamides as dual-targeted mEGFR and AURK inhibitors and anticancer agents

Brianne Rogers, Nicholas Rohde, Justin Mikitaroff, Joshua Matson, Samantha Satawa, Felix Amissah, Sonali Kurup. *Ferris State University, Big Rapids, MI*

Small molecule, mutant epidermal growth factor receptor kinase (mEGFR) inhibitors are rendered ineffective in NSCLC due to mutations within the enzyme binding sites and redundant signaling pathways. The mEGFR inhibitors were found to retain their anticancer effects in NSCLC cells if given concurrently with AURK inhibitors. Dual-targeted small molecules designed to inhibit both mEGFR and AURK could demonstrate improved anticancer effects compared to monotargeted mEGFR inhibitors. We conducted molecular modeling studies to determine if there were similarities between the kinase pockets of mEGFR and AURK that could be exploited to develop dual-targeted mEGFR and AURK inhibitors. An overlap was observed for the active and allosteric sites of the kinase pocket for mEGFR and AURK. A series of compounds were synthesized and evaluated against mEGFR, AURKA, and AURKB. We found the kinase inhibitory profile to vary significantly depending on the substitution pattern ranging from selective mEGFR inhibitors to dual mEGFR and AURK inhibitors. The 4-substituted amino-*N*-phenylbenzamides were identified as dual mEGFR/AURK inhibitors. Dual mEGFR/AURK inhibitors demonstrated varied modes of binding within mEGFR and AURK. The

most potent dual mEGFR and AURK inhibitors displayed nanomolar inhibition of mEGFR and AURK, and single-digit micromolar inhibition of non-small cell lung cancer cells. Target compounds were further evaluated in a 96-kinase screening assay and demonstrated selectivity for target kinases. The synthesis, structure-activity relationship (SAR) analysis and anticancer effects will be presented and discussed.

#5341

Data mining of PubChem bioassay data reveals OXPHOS inhibitors with anti-cancer activity

Sejal T. Sharma[1], Liping Feng[1], Nicha Boonpattrawong[1], Lisa M. Barroilhet[1], Manish Patankar[1], Spencer S. Ericksen[2]. *[1]Department of Obstetrics and Gynecology, University of Wisconsin-Madison, Madison, WI,[2]UW-Carbone Cancer Center, Drug Development Core, Small Molecule Screening Facility, University of Wisconsin-Madison, Madison, WI*

High Grade Serous Ovarian Cancer (HGSOC) is a fatal disease that is typically detected at an advanced stage when there are limited modalities for effective treatment. Treatment efficacy against cancer is dependent on tumor metabolism and its adaptation for most therapies. Warburg effect is an important adaptation found in tumors where cells primarily catabolize glucose even in presence of sufficient oxygen and nutrients. Nevertheless, recent evidence suggests cells in tumor microenvironments remain dependent on mitochondrial ATP production via oxidative phosphorylation (OXPHOS). OXPHOS also represents a major metabolic pathway in cancer stem cells and tumor cells of relapse patients. Molecular signatures of glycolysis and OXPHOS are both detected in tumors. This points to the OXPHOS pathway as a potential therapeutic target in cancer. Here we apply a data mining approach to identify OXPHOS inhibitors to evaluate as candidates for therapies against HGSOC. High-Throughput Screening (HTS) on mechanistic targets like OXPHOS are cost prohibitive for academic laboratories. As an alternative, we deployed a data mining pipeline to find active chemical classes among 8415 available OXPHOS-related bioassays in the PubChem data repository. Active compound clusters frequently contain α,β-unsaturated carbonyl groups, which are also observed in both endogenous quinone electron carriers and atovaquone–a potent inhibitor of OXPHOS. Out of 312041 unique compounds tested in

the assays, we selected 6 representative molecules from each of the 6 largest active chemical clusters to test for OXPHOS inhibition, ROS production, and reduced cancer cell proliferation. We assayed cell viability (MTT) to check for proliferation of human (OVCAR3, OVCAR5, OVISE) and mouse (ID8) ovarian cancer cells against 6 compounds, Oryzalin, Allylyestrenol, Esbiothrin, Lacidipine, Coumatetralyl, and CID929419 (MLS000713029), 72 h post treatment. ID8 and OVCAR5 significantly decreased cell proliferation after Lacidipine and Oryzalin treatment. Significant increase in intracellular ROS, a frequent consequence of OXPHOS inhibition, was observed in all cell lines after Lacidipine treatment. Elevated ROS was also observed in ID8 and OVISE cells after Esbiothrin treatment. To confirm OXPHOS inhibition as the mechanism of action, we performed Mito Stress Test on the Seahorse Analyzer and measured Oxygen Consumption Rate. Treatment with Oryzalin, Allylyestrenol, Esbiothrin, and Lacidipine significantly decreased basal respiration rate and ATP production in ID8 and OVCAR3 cells. This suggests that 4 of the 6 compound classes prioritized by the data mining pipeline inhibits OXPHOS in ovarian cancer cells. Thus, our pipeline provides an efficient alternative to HTS for identifying OXPHOS inhibitors. Next, we plan to test the *in-vivo* efficacy of these drugs against ovarian tumors in a mouse model and investigate their molecular mechanisms.

#5342

Assessment of polyphenolic secondary metabolites and small molecules against the xenobiotic metabolic and cell cycle regulatory proteins in prostate cancer

Sumit Sheoran[1], Swati Arora[1], Tanmay Basu[2], Naidu Subbarao[3], Atul Kumar Upadhyay[2], Sugunakar Vuree[1]. *[1]Lovely Professional University, Jalandhar, India,[2]Thapar Institute of Engineering & Technology, Patiala, India,[3]Jawaharlal Nehru University, Delhi, India*

Background: Prostate cancer (PCa) is the second most frequent kind of cancer in males globally after Lung Cancer. In clinical practice, medicines that act as antagonists/partial agonists of hormone receptors against prostate tissue are employed in PCa treatment. Cyproterone acetate, Flutamide, and Bicalutamide are prominent medications that induce acute and long-term toxicity and create drug resistance in patients and remission. We

concentrated on flavonoids since they are non-cytotoxic and have substantial showing inhibitory action.
Methodology: We selected 560 flavonoids and small compounds along with 3 targets from the extensive literature review. Three-dimensional (3D) structures of selected proteins were obtained from Protein Data Bank, docked with 560 flavonoids and small molecules 3D structures, obtained from PubChem and CHEMBL database using Gold Docking Software. ADME characteristics were used to determine their bioactivities in the human body and drug-like investigations by using SwissADME and Zinc database, while Lipinski's rule of five was used to evaluate the flavonoids' anti-prostate cancer efficacy. Additionally, we have performed molecular simulation at 100ns and furthermore, we will perform cytotoxicity analysis.
Results: Diosmetin (58.72), Lapatinib Ditosylate (121.61), and Estramustine Phosphate Sodium (143.38) has the highest binding affinity for CDKN2 (4EK3), CYP17A1(3RUK), and CYP19A1(3S79), respectively, and are stable throughout 100ns simulation studies. At present, we are working on cytotoxicity studies on PC3 cell lines. As per the literature review by Ansar et al. 2022 quercetin and thymoquinone induce cytotoxicity in breast, lung, and prostate cancer cells effectively; MCF-7 cells were the most sensitive cells to quercetin with an IC50 value of 50 μM and PC3 cells were more sensitive to thymoquinone with an IC50 value of 20 μM.
Conclusion: As a result of our findings, these four Flavonoids may be viable candidates for additional research into PCa prevention or management.Keywords: Diosmetin, Lapatinib Ditosylatye, Prostate cancer, In-silico, Simulation

#5343

Evaluating the screened polyphenolics molecules as potential chemosensitizers against the oncogenic signalling proteins in lung cancer

Swati Arora[1], Sumit Sheoran[1], Tanmayee Basu[2], Naidu Subbarao[3], Atul Kumar Upadhyay[4], Sugunakar Vuree[1]. *[1]Lovely Professional University, Jalandhar, India,[2]Thapar Institute of Engineering & Technology, Patiala, India,[3]Jawaharlal Nehru University, Delhi, India,[4]Thapar institute of Engineering 7 technology, Patiala, India*

Background: Lung cancer is the most commonly diagnosed cancer globally. There are numerous agonists and antagonistic treatment interventions available for therapy. However, all of them possess different detrimental consequences in addition to resistance and remission in sufferers. Medicinal plants have traditionally been employed to treat a wide range of ailments and problems.
Methodology: A total of 550 flavonoids and small molecules retrieved from literature and databases (Chembl, and PubChem) were analysed for molecular docking, biological activities, ADME, and drug-like properties through SwissADME and PreADMET, Molecular Simulation, and cytotoxicity studies. Simultaneously, review literature is employed to identify the novel protein targets viz. ROS1 (3ZBF) & EGFR (6DUK). Additionally, the crystal structures of the proteins were obtained from PDB and their domains and active sites were predicted using ScanProsite, MOTIF Search, metaPOCKET2, and PrankWeb tools. Finally, the proteins and ligands were energy-minimized using Chimera and open babel tool and subjected to virtual screening and molecular docking using GOLD. Furthermore, the molecular simulation was performed at 100ns by utilizing GROMACS, and cytotoxicity studies were performed by employing the A549 Lung cancer cell line.
Results: Diosmin (64.57) and Hesperidin (60.98) had the greatest binding affinity with the identified targets, i.e., ROS1 (3ZBF) and EGFR(6DUK) respectively against Lung Cancer, and remained stable during 100ns of molecular simulation. Furthermore, we have performed cytotoxicity studies on A549 cell lines that show both the compounds have significant anticancer activity and do not affect healthy cells in the range of, i.e., Diosmin (500 µg/ml to 0.024 µg/ml.) and Hesperidin (500 µg/ml to 125 µg/ml).
Conclusion: After the analyses, we can conclude that it has the potential to be exploited as a novel therapeutic agent in the treatment of lung cancer.Keywords: Diosmin, Hesperidin, In-silico, A549, Lung Cancer, Simulation

#5344
Novel melanoma leads demonstrate efficacy in A375 xenograft model in nude mice

Dmitriy Minond, Sadeeshkumar Velayutham. *Pharmaceutical Sciences, Nova Southeastern University, College of Pharmacy, Fort Lauderdale, FL*

The purpose of this study was to evaluate efficacy of novel anti-melanoma leads for in vivo efficacy. Despite the recent advances in melanoma therapy, the need for new targets and novel approaches to therapy is urgent. We previously reported novel melanoma leads, 2155-14 and 2155-18, that work via binding and downregulating spliceosomal proteins hnRNPH1 and H2. To determine the therapeutic potential of these compounds we tested them in A375 cell-line derived xenograft in nu/nu mice. For determination of 2155-14 and 2155-18 potency in vivo, nude mice were inoculated subcutaneously with A375 cell line and tumors were allowed to reach $100mm^3$. Animals were then randomized into four groups to receive subcutaneous administration of vehicle, 10mg/kg vemurafenib, and 25mg/kg 2155-14 and 2155-18 three times per week for 15 days. The result revealed that both 2155-14 and 2155-18 significantly decreased the growth of A375 tumors, which was comparable to vemurafenib. These results are well correlated with the exposure of leads in plasma. In summary, these results suggest a therapeutic potential of targeting spliceosomal proteins hnRNPH1 and H2 and support potential of 2155-14 and 2155-18 as drug candidates for treatment of melanoma.
Keywords: Melanoma, drug discovery, A375, xenograft.

#5345
The application of CDK16 inhibitors in the treatment of triple-negative breast cancer
Haihua Xiao, Huangyu Jiang, Kunxian Feng, Mengli Yang, Jinping Yang, Chengfang Jian, Yuan Tian, Natalya Vasilevich, Lichun Sun. *Xiao Haihua (Individual), Shenzhen, China*

Triple-negative breast cancer (TNBC) with estrogen receptor (ER), progesterone receptor (PR) and HER2 (c-erbB-2, neu) being negatively expressed in patient cancer tissues displayed its unique clinical pathological difference from other types of breast cancers. TNBC is more common in younger patients and more likely to have a family history of breast cancer. TNBCs more likely have poor prognosis and postsurgical recurrence, with strong invasiveness and metastasis. However, there is lack of effective and

TNBC-targeting drugs. The non-typical CDK16 was found highly expressed in TNBCs and clearly associated with prognosis and survival of patients. CDK16 could promote the progression and metastasis of TNBC by phosphorylating PRC1. Knockdown of CDK16 could significantly suppress tumor growth and metastasis. Furthermore, in our studies, rebastinib acting as a CDK16 inhibitor displayed its strong suppression of TNBC tumor growth in a dose-dependent manner, indicating rebastinib or its analogs could be druggable and likely used to treat TNBC patients.

#5346

Discovery of new targeted protein degraders using DNA-encoded chemistry

Anthony D. Keefe[1], Jeremy S. Disch[2], Jennifer Duffy[3], Esther C. Lee[4], Diana Gikunju[5], Betty Chan[6], Benjamin D. Levin[7], Michael I. Monteiro[8], Sarah A. Talcott[9], Anthony Lau[10], Fei Zhou[1], Anton Kozhushnyan[1], Neil E. Westlund[1], Patrick B. Mullins[1], Yan Yu[1], Moritz von Rechenberg[2], Junyi Zhang[2], Yelena Arnautova[11], Yanbin Liu[12], Ying Zhang[1], Andrew J. McRiner[13], Anna Kohlmann[11], Matthew A. Clark[1], John W. Cuozzo[2], Christelle Huguet[8], Shilpi Arora[14]. *[1]X-Chem Inc., Waltham, MA,[2]Relay Therapeutics, Cambridge, MA,[3]Nirogy Therapeutics, Framingham, MA,[4]AstraZeneca, Cambridge, MA,[5]Exo Therapeutics, Watertown, MA,[6]Auron Therapeutics, Waltham, MA,[7]Stablix Therapeutics, New York, NY,[8]Ipsen, Cambridge, MA,[9]DFCI, Boston, MA,[10]Broad Institute, Cambridge, MA,[11]Black Diamond Therapeutics, Cambridge, MA,[12]Cyteir Therapeutics, Lexington, MA,[13]Auron Therapeutics, Cambridge, MA,[14]Transition Bio, Cambridge, MA*

Bispecific degraders (PROTACs) of ERα are expected to be advantageous over current inhibitors of ERα signaling (aromatase inhibitors/SERMs/SERDs) used to treat ER+ breast cancer. Information from DNA-encoded chemical library screening provides a method to identify novel PROTAC binding features as the linker positioning, and binding elements are determined directly from the screen. After screening ~120 billion DNA-encoded molecules with ERα WT and 3 gain-of-function mutants, with and without estradiol to identify features that enrich ERα competitively, the off-DNA synthesized small molecule exemplars

exhibited nanomolar ERα binding, antagonism, and degradation. Click chemistry synthesis on an alkyne E3 ligase engagers panel and an azide variant that rapidly generated bispecific nanomolar degraders of ERα, with PROTACs inhibiting ER+ MCF7 tumor growth in a mouse xenograft model of breast cancer. This study validates this approach toward identifying novel bispecific degrader leads from DECL screening with minimal optimization.

#5347

Selective targeting deacetylase 3 (HDAC3) and HDAC8 by PROTACs

Yufeng Xiao, Seth Hale, Nikee Awasthee, Xuan Zhang, Yi Liu, Zhiguang Huo, Dongwen Lyu, Lei Wang, Weizhou Zhang, Megan Mosteiro, Daiqing Liao, Guangrong Zheng. *University of Florida, Gainesville, FL*

Histone deacetylases (HDACs) are enzymes that play an essential role in multiple cellular processes such as DNA transcription, translation, replication, recombination, repair, and metabolism, and their dysregulation can be linked to many different diseases. Most commonly, the overexpression of HDACs is found in various cancer types including hematologic cancers, as well as solid malignancies. Of the many HDACs found in the body, class I HDACs, which consist of HDACs 1, 2, 3, and 8, play an essential role in activating oncogenes underlying tumorigenesis, disease progression, and treatment resistance. Several HDAC inhibitors (HDACis) have been approved for cancer treatment, however, they are pan-inhibitors. This lack of specificity poses many disadvantages for HDACis, including toxicity and other off-target effects. Isozyme-selective inhibitors may reduce these off-target effects and thus enhance their safety. Though favorable, selectivity is difficult to achieve from conventional inhibitors due to the highly homologous catalytic domain among HDAC isozymes. In addition, several HDAC isozymes have deacetylase-independent scaffolding functions that cannot be blocked by traditional inhibitors. Recently, there have been advances in Proteolysis Targeting Chimera (PROTAC), an emerging drug discovery technology designed to hijack cell's existing protein degradation machinery, the ubiquitin-proteasome system (UPS) to selectively degrade target proteins. Selective degradation by PROTAC is a potential solution to many of the concerns associated with current HDACis. Previously, we reported an HDAC3-selective PROTAC, XZ9002, and following that we reported the discovery of PROTAC YX968,

which can degrade both HDAC3 and HDAC8 isozymes with single-digit nanomolar DC_{50}, this highly potent dual degrader exhibits distinct effects on modulating gene expression and is much more potent in inhibiting cancer cell proliferation compared to XZ9002. Based on this, we are further modifying the PROTACs to be selective for HDAC8. The HDAC3, HDAC8 selective degrader and HDAC3 and HDAC8 dual degrader we developed could be useful chemical probes to dissect the complex biological function of HDAC3 and HDAC8 and potential therapeutics for treating cancer.

#5348

Targeting MEK, alone and in combination with BRAF, in metastatic $BRAF^{K601E}$-mutated melanoma

Sze Man Chan, Sin Ting Chow, Sai Fung Yeung, Kwok Wing Stephen Tsui.
School of Biomedical Sciences, The Chinese University of Hong Kong, Hong Kong, China

Mitogen-activated protein kinase/ERK signaling pathway has been one of the major mechanisms underlying melanoma haboring BRAF mutation. Of these, K601E mutation belongs to a rare mutation sub-type, comprising only 3% of the BRAF mutations in melanoma. Although patients with BRAF V600E/K mutation respond to MEK inhibitor, whether it also applies to those with BRAF K601E mutation remains elusive. Here, we examined the effects of MEK and BRAF/MEK inhibition on $BRAF^{K601E}$-expressing melanoma cells. Melanoma cell line (MeWo) was transfected with doxycycline-inducible vector encoding wild-type or K601E-mutant BRAF. Subsequently, cells or xenograft-bearing mice were treated with trametinib, dabrafenib plus trametinib or sorafenib plus trametinib. Compared with $BRAF^{WT}$, MTT assay demonstrated that $BRAF^{K601E}$ cells were more sensitive towards drug treatment. The effects of combined treatment were more profound. Tumorigenicity assay showed that trametinib treatment inhibited tumor growth of $BRAF^{K601E}$ xenografts. Our preliminary results demonstrated the therapeutic values of MEK and BRAF/MEK inhibitors against $BRAF^{K601E}$-mutated melanoma. As previous studies report the superior therapeutic effects of BRAF/MEK inhibitors over MEK inhibitor alone, phenotype characterization of the

cells, as well as underlying mechanisms behind such response, worth further investigation.

Natural Products

#3818
Isoandrographolide derivative, (3,19)-4-Bromobenzylidene-isoandrographolide induces apoptosis and causes loss of mitochondrial membrane potential in ER positive Breast cancer

Balasubramanyam Karanam[1], Nitesh Tamang[2], Yashwanth Inabathina[1], Sai Kiran Mavileti[3], Lakshminath Sripada[2], Srinivas Nanduri[4], Nageswara Rao Golakoti[3]. *[1]Tuskegee University, Tuskegee, AL,[2]Sri Sathya Sai Institute of Higher Learning, Puttaparthi, India,[3]Chemistry, Sri Sathya Sai Institute of Higher Learning, Puttaparthi, India,[4]National Institute of Pharmaceutical Education and Research, Hyderabad, India*

Natural product, Andrographolide.is diterpene lactone extracted from Andrographis paniculata. In traditional form of medicine, it is being used in India, China and Malaysia for treating various diseases. While in the last two decades there are many reports on andrographolides and its derivatives with various biological activities such as anti-cancer and anti-inflammatory. We synthesized compounds along with isoandrographolide were characterized and tested for their anticancer activity against 60 cancer cell line at NCI. Most compounds were found to be active against leukemia and breast cancer with (3,19)-4-Bromobenzylidene-isoandrographolide having best growth inhibition of 76.90% and 87.54% against leukemia (MOLT-4) and breast cancer (BT-549) respectively. Upon further testing compound (3,19)-4-Bromobenzylidene-isoandrographolide was found to be more activate than the tamoxifen against MCF-7. Compound (3,19)-4-Bromobenzylidene-isoandrographolide arrested cell cycle at G1-Phase of MCF-7 and was observed to be inducing apoptosis and loss of mitochondrial membrane potential. We discuss our studies on crystal structure, cell cycle progression assay, apoptotic studies on ER-positive breast cancer MCF-7.

#3819

Naringin nanoparticles inhibit metastasis of lung cancer through TGF-β1-smad2/3 signaling pathway

Wen Chen. *Jiangxi Science and Technology Normal University, Nanchang, China*

Lung cancer causes high mortality due to its high metastasis. Naringin is a naturally occurring flavonoid that is widely found in the various citrus fruits. Naringin is known to have several therapeutic effects including anticancer, anti-pulmonary fibrosis, antimicrobial, anti-inflammatory. However, low bioavailability and solubility of naringin limit its application. This project designed a thermosensitive naringin nanoparticle to investigate whether it might inhibit metastasis of lung cancer by inhibiting TGF-β1-smad2/3 signaling pathway. Cells were treated with various concentrations of naringin nanoparticles and unwrapped naringin for 48 hours. Naringin nanoparticles of 100μmol/L showed obvious inhibitory effect on the larger wound surface of cultured human cancer cells. Westerm blot was used to detect the expression of P-Smad2 , Smad2,and α-SMA in A549 cells. The results showed that naringin significantly reduced the expression of EMT-related protein α-SMA in A549 cells in a concentration-dependent manner. Naringin nanoparticles can reverse the EMT process. naringin nanoparticles can inhibit the expression of P-Smad2 protein in A549 cells, which may play a role in inhibiting lung cancer through TGF-β1/Smad signaling pathway.The animal experiment was performed. The mice were given various concentrations of naringin nanoparticles and unwrapped naringin by IV. the protein expression levels of α-SMA, TGF-β1 and P-Smad3 in mice lung tissue were detected by immunohistochemistry. The results showed that naringin nanoparticles 50um/ml,0.2mL/day/time had significant effect on the inhibition of lung cancer tissue migration, and the different doses of naringin nanoparticles showed a certain dose-dependent trend. The expression of TGF-β1 and P-Smad3 in mice treated with naringin nanoparticles was significantly decreased, suggesting that naringin nanoparticles could inhibit the migration of lung cancer cells by inhibiting TGF-β1/Smad pathway.

#3820

Changes in the transcriptome of a triple negative breast cancer cell line following treatment with a water-soluble extract from the leaves of the

indigenous Southern African plant *Tulbaghia violacea*

Zodwa Dlamini[1], Rodney Hull[1], Mohammed Alouna[2], Clement Penny[2].
[1]Pan African Cancer Research Institute, University of Pretoria, Hatfield, South Africa,[2]University of the Witwatersrand, Johannesburg, South Africa

Triple negative breast cancer (TNBC) accounts for approximately 20% of all breast cancer cases. And is defined by the absence of oestrogen, progesterone, and human epidermal growth factor 2 receptors. This makes it difficult to treat and leads to a low five-year survival rate. In South Africa a large percentage of the population still relies on traditional medicine based on the use of medicinal plants. One of these plants, African garlic (*Tulbaghia violacea),* that has been used to treat symptoms similar to that observed in cancer. However, the usefulness of these treatments has yet to be clinically proven. Previous studies have revealed that the water-soluble extract from the leaves of *T. violacea* had anticancer activity against a TNBC cell line. In order to identify the signalling pathways involved in this anti-cancer activity whole transcriptome sequencing was performed using RNA extracted from both TNBC and normal breast cells before and after treatment with the water-soluble *T. violacea* extract. Paired end sequencing was performed at a depth of 10 million bases for 300 cycles. Data analysis was performed using the Galaxy platform/ Sequencing results led us to perform an antibody array assay for proteins involved in the receptor tyrosine kinase pathway. In line with the increased levels of apoptosis previously observed following treatment of the TNBC cell line with the extract, there was an increase in the transcription of genes associated with apoptosis. Decreases were observed in the transcription of genes involved in growth receptor signalling, angiogenesis, and cancer related pathways such as the Wnt, Notch and the PI3K pathway. This work highlights the pathways affected by compounds present within a water-soluble extract of the leaves of *T, violacea.* Combined with the results of our [previous work, this indicates that the compounds isolated from *T, violacea* could serve as lead compounds for the development of future therapeutic treatments for TNBC.

#3821

Berberine and emodin synergistically suppress the EGFR signaling cascade by targeting LAMB3 in pancreatic ductal adenocarcinoma

CAIMING XU[1], SILEI SUI[1], Keisuke Okuno[1], Silvia Pascual-Sabater[2], Cristina Fillat[2], Ajay Goel[1]. *[1]Molecular Diagnostics and Experimental Therapeutics, Beckman Research Institute of City of Hope, Monrovia, CA,[2]Institut d'Investigacions Biomèdiques August Pi i Sunyer, Barcelona, Spain*

Background: Pancreatic cancer is one of the most devastating malignancies due to the development of intrinsic chemoresistance following chemotherapy. Extracellular matrix (ECM) proteins are intimately linked to cellular proliferation, invasion, and acquisition of chemoresistance in PDAC cells, making them promising therapeutic targets in this malignancy. Naturally occurring dietary botanicals, including berberine (BER) and emodin (EMO), have been shown to suppress ECM as one of the mechanism(s) for their anti-tumorigenic activity, along with their time-tested safety and cost-effectiveness. In addition, both BER and EMO are also known to induce apoptosis by modulating different pathways and regulating pro-apoptotic genes. Herein, we hypothesized that combined treatment with BER and EMO might exhibit synergistic anticancer efficacy by targeting the ECM and apoptotic pathways in PDAC cells.
Methods: We undertook genomewide transcriptomic profiling analysis to identify critical ECM-related genes differentially expressed in PDAC. Subsequently, the TCGA dataset was analyzed to identify the prognostic significance of ECM-associated genes with overall survival (OS) and disease-free survival (DFS) in PDAC. A series of cell culture experiments were performed using PDAC cells, followed by their validation in patient-derived organoids to examine the synergistic anti-proliferative and chemopreventive effects of BER and EMO against PDAC.
Results: Transcriptomic profiling identified that LAMB3 expression was significantly upregulated in PDAC tissue ($P < 0.01$) and was significantly associated with poor OS and DFS in PDAC patients ($P < 0.01$). The combination of BER and EMO displayed superior synergistic anti-tumor potential in PDAC cells vs. individual compounds, as revealed by cell proliferation, clonogenicity, migration, and invasion assays. The combination of BER and EMO also altered the expression of key proteins involved in cellular apoptosis, epithelial-mesenchymal-transition, and EGFR/ERK//AKT growth factor signaling pathways. Finally, these findings were successfully validated in PDAC patient-derived 3D organoids.

Conclusions: We provide the first evidence that combined treatment with berberine and emodin exerts synergistic anti-cancer activity in PDAC, primarily regulated through the LAMB3-mediated interaction with other members of the EGFR-signaling pathway.

#3822

Novel evidence for the role of the p53 signaling pathway in mediating the anticancer effects of aronia berry extract in colorectal cancer cells

Yoh Asahi[1], Keisuke Okuno[1], Caiming Xu[1], Aknobu Taketomi[2], Ajay Goel[1]. *[1]Beckman Research Institute of The City of Hope, Monrovia, CA,[2]Department of Gastroenterological Surgery I, Hokkaido University Graduate School of Medicine, Sapporo, Japan*

Background: The development of safe and effective novel agents remains a critical challenge for improving the prognosis of patients with unresectable colorectal cancer (CRC). Natural products containing polyphenols can be a good source of anti-cancer agents for their potential effect on multiple signaling pathways with anti-cancer effect. Due to its rich polyphenols content, Aronia berry extract (ABE) is gaining increased attention as an anti-cancer agent with its protective effect against cancer cells, including CRC, exerting potent antioxidant and antiproliferative effects. Thus, we hypothesized that ABE could be a novel complementary therapeutic option in patients with CRC by virtue of its ability to modulate multiple key cancer-related pathways.
Methods: First, an MTT assay was performed to prove the antiproliferative effect of ABE in two CRC cells, SW480 and HCT116, and IC_{25} and IC_{50} of ABE in both CRC cells were identified. Next, the anti-cancer effects of ABE were examined by wound healing, colony formation, and invasion assays. Apoptosis studies were performed using the Muse Annexin V & Dead Cell Assay Kit on the muse cell analyzer. RNA-sequencing was performed to clarify the critical regulatory genes and pathways modulated by ABE by comparing genome-wide profiling between CRC cells with and without ABE treatment.
Results: Results of the MTT assay revealed that ABE decreased the viability of both CRC cells, and the IC_{25} and IC_{50} of ABE were 80.0 μg/mL and 130.0 μg/mL for SW480 and 80.0 μg/mL and 140.0 μg/mL for

HCT116. ABE inhibited proliferation, migration, cellular survival, and invasion of CRC cells and induced apoptosis in those cells (SW480 control vs. IC_{25}: $p<0.05$, control vs. IC_{50}: $p<0.01$, HCT116 control vs. IC_{25}: $p<0.01$, control vs. IC_{50}: $p<0.01$). After ABE treatment, the genome-wide transcriptomic analysis identified 439 differentially expressed genes ($p<0.05$ and $|log2FC|>0.5$) in both CRC cells. These differentially expressed genes were used for pathway analysis and some critical cancer-related pathways, including the p53 signaling pathway ($p=0.005$, fold enrichment 3.8), NF-kappa B signaling pathway ($p=0.030$, fold enrichment 2.7), Hippo signaling pathway ($p=0.037$, fold enrichment 2.2), and MAPK signaling pathway ($p=0.011$, fold enrichment 2.0), were detected as significantly activated or suppressed pathways.
Conclusions: We have investigated the anti-cancerous effect of ABE in CRC cells and identified multiple critical cancer-related pathways modulated by ABE, with the p53 signaling pathway as the key mediator for growth suppressive anti-cancer efficacy of this naturally occurring phytochemical. Our findings provide evidence for the use of ABE as a safe and effective complementary and integrative medicine approach against CRC.

#3823

Therapeutic potential of plant-derived nanovesicles for neuroendocrine prostate cancer

Amritha Sreekumar, Matthew Simmons, Tae Jin Lee, Ashok Sharma, Sharanjot Saini. *Augusta University, Augusta, GA*

Background: Neuroendocrine prostate cancer (NEPC) is a highly lethal variant of prostate cancer (PCa) that often emerges after androgen receptor (AR)-targeted therapies such as enzalutamide and abiraterone. NEPC arises via trans-differentiation of prostate adenocarcinomas to neuronal lineage, a process referred to as ‘neuroendocrine trans-differentiation’ (NED), wherein prostate cancer cells show an altered expression of lineage markers such as decreased expression of AR and increased expression of neuronal markers. Currently, there is a lack of effective targeted therapies for NEPC. Current treatment options are limited to highly toxic platinum-based drugs. Hence, there is an urgent need to develop novel treatment strategies to treat NEPC. The focused objective of this study is to develop novel, non-toxic

therapeutic intervention against NEPC. Towards this, we exploited the potential of plant-derived nanovesicles/extracellular vesicles as a novel therapeutic. Extracellular vesicles (EVs) are lipid-bilayer-delimited particles that are released from almost all types of cells, including plant cells, typically between 30-150 nm in size.
Methods: EVs/nanovesicles were isolated from plant-derived sources by ultracentrifugation. Isolated nanovesicles were characterized by Nanoparticle Tracking Analyses and electron microscopy. After characterization, the effects of nanovesicles were tested in NEPC cell lines *in vitro.* Effects on cell viability and apoptosis were assessed by MTS assay and flow cytometry, respectively. To understand the mechanistic basis of EV induced alterations, next generation RNA sequencing was performed in control vs EV treated NCI-H660 cells on Illumina HiSeq platform. Significant targets were further validated by real time PCR and Western blot analyses.
Results: Plant-derived nanovesicles reduced viability and induced apoptosis in NEPC cell lines. Genes involved in ECM-receptor interaction, focal adhesion, proteoglycans in cancer and small cell lung cancer genes were significantly impacted by these vesicles in NEPC cell line. Remarkably, nanovesicles led to significantly attenuated levels of key proneural transcription factors including ASCL1, BRN2 and SOX2. In addition, neuronal markers ENO2 and NCAM1 were downregulated suggesting that treatment with nanovesicles reverse the 'cardinal' genetic alterations that drive NEPC.
Conclusion: Plant-derived nanovesicles can be employed as a novel treatment modality in neuroendocrine prostate cancer.

#3824
Remodeling of anaplastic thyroid cancer cell signaling and immune landscape by natural alkaloid berberine
Tara Jarboe, Kaci Kopec, Nicole R. DeSouza, Jan Geliebter, Raj K. Tiwari, Xiu-Min Li. *New York Medical College, Valhalla, NY*

Anaplastic thyroid cancer (ATC) is universally diagnosed as Stage IV with a five-year-survival of 4%, illuminating its dreadful prognosis. ATC is undifferentiated, has an inflammatory tumor microenvironment (TME), and metabolic dysregulation. As it is refractory to all established therapies, we

propose a novel therapeutic - Berberine (BBR), a natural plant alkaloid, with numerous cellular targets that can potentially reprogram ATC's aggressive phenotype. This research comprehensively examines the multitarget efficacy of BBR. Following initial dose response studies, all assays used 100μM concentration of BBR or DMSO vehicle control for 24-hour exposure. To model the ATC tumor microenvironment, monocyte cell line U937 cells were activated and polarized into a proinflammatory macrophage phenotype. In the presence of berberine at the activation and polarization stages, 33 soluble inflammatory mediators were downregulated in the conditioned media compared to controls. Targeting the aggressiveness of anaplastic disease, berberine slowed proliferation by 50% selectively in ATC cells from 48 to 72 hours, while sparing the immortalized normal thyroid cells. BBR also delayed wound healing by 30% in ATC cells after 24, 48, and 72 hours. These observations were substantiated by Western blot analysis of ATC and immortalized normal cells where BBR decreased phosphorylation of MEK, ERK, and ribosomal protein S6, crucial downstream regulators of the pro-proliferative and pro-survival pathways and increased phosphorylation of AMPKα, activating its anti-tumor and regulatory effects. Validation of *in vitro* findings via RNA-Seq was conducted by Genewiz from Azenta Life Sciences and Qiagen's Ingenuity Pathway Analysis was used for *in silico* modeling. Greater than 400 significantly differentially expressed genes were identified suggesting that BBR regulates mitochondrial metabolism, cholesterol biosynthesis, glycometabolism, apoptosis, inflammation, and proliferation. BBR's ability to alleviate inflammatory mediators in the TME, depress overactive cell signaling, and regulate metabolism to make it a more targetable cancer reveals it as an interesting candidate to prime ATC for combination therapy.

#3825

Andrographis reverses gemcitabine-associated chemoresistance by regulating calcium signaling in pancreatic ductal adenocarcinoma

Keisuke Okuno[1], Caiming Xu[1], Masanori Tokunaga[2], Cristina Fillat[3], Haiyong Han[4], Yusuke Kinugasa[2], Ajay Goel[1]. *[1]Molecular Diagnostics and Experimental Therapeutics, Beckman Research Institute of The City of Hope, Monrovia, CA,[2]Gastrointestinal Surgery, Tokyo Medical and Dental University, Tokyo, Japan,[3]Institut d'Investigacions Biomèdiques August Pi i*

Sunyer (IDIBAPS), Barcelona, Spain,[4]Molecular Medicine, The Translational Genomics Research Institute, Phoenix, AZ

Background: Pancreatic ductal adenocarcinoma (PDAC) is one of the lethal malignancies due to the acquisition of intrinsic or acquired resistance to chemotherapeutic drugs, such as Gemcitabine (Gem). Recent evidence revealed that calcium signaling significantly contributes to Gem-associated chemoresistance (Gem resistance) in PDAC cells. Andrographis, a labdane diterpenoid isolated from the traditional herb *Andrographis paniculate*, is known to have a potent calcium channel-blocking potential. Accordingly, we hypothesized that Andrographis might facilitate the reversal of Gem resistance in PDAC.
Methods: The critical regulatory pathways associated with the Gem resistance in PDAC were identified by analyzing publicly available cell line-based transcriptomic profiling. Gem resistant (Gem-R) PDAC cells (Gem-R MIA PaCa-2 and BxPC-3) were established by continuously culturing cells with Gem. A series of cell culture experiments were performed using Gem-R PDAC cells to evaluate the Andrographis-mediated reversal of Gem resistance in PDAC cells. At last, the cell culture findings were validated in patient-derived PDAC organoids.
Results: Transcriptomic profiling identified the calcium signaling pathway as one of the key regulators of Gem resistance (Fold enrichment: 2.8, P =0.002). The combination of Andrographis and Gem revealed a superior anti-cancer potential in Gem-R PDAC cells on cell viability, clonogenicity, and migration compared to individual treatments with Andrographis or Gem. The combined treatment potentiated cellular apoptosis in Gem-R MIA PaCa-2 (Andro, Gem vs. Combination, 20.3%, 10.9% vs. 31.4%) and Gem-R BxPC-3 (Andro, Gem vs. Combination, 11.3%, 6.8% vs. 16.1%). The fluo-4 assay demonstrated that Andrographis decreased intracellular calcium concentration in Gem-R PDAC cells, while the combined treatment with Andrographis and Gem decreased its concentration more in Gem-R MIA PaCa-2 (fold change [FC] =0.79 vs. Andrographis; FC =0.54 vs. Gem) and Gem-R BxPC-3 (FC =0.80 vs. Andrographis; FC =0.73 vs. Gem). Finally, the combined treatment with Andrographis and Gem showed anti-cancer activity in patient-derived PDAC organoids.
Conclusions: We have firstly investigated the Andrographis-mediated reversal of chemoresistance against Gem in PDAC cells, possibly through

the regulation of cellular apoptosis and calcium signaling, using a systematic series of Gem resistant cell cultures and patient-derived tumor organoid models. Our findings could provide evidence of the combined treatment with Andrographis and Gem as a complementary therapeutic modality against PDAC.

#3826

Potency of cardiac glycosides by structure in organotypic models of pancreatic and ampullary carcinomas

Md Shahadat Hossan[1], Ethan Lin[2], Austin Stram[1], Jamie Warner[2], Luke Koeppel[2], Ellie Riedl[2], Jeremy Kratz[1]. *[1]Department of Medicine, University of Wisconsin-Madison, Madison, WI,[2]University of Wisconsin-Madison, Madison, WI*

Background**:** Organotypic models have emerged as an important preclinical model for developmental therapeutics in pancreatic and biliary cancer. Naturally derived cardiac glycoside in 2D monoculture exquisite potency, here we describe their activity in cancer and normal liver with patient-derived cancer organoids (PCOs).

Methods: PCOs of pancreatic and ampullary cancers and normal hepatic tissues were generated. Response was assayed with four structurally different cardiac glycoside (cerberin, neriifolin, digitoxin, digoxin; 72h). Response was characterized by growth inhibition (GI_{50}) using 3D CellTiterGlo (CTG) and subclonal population response by high content imaging using normalized change in diameter (n=1038).

Results: Dose response revealed improved potency for cerberin and neriifolin, versus digoxin and digitoxin across models (see table). In a normal liver organoid model, there was no convergence in dose response observed when extended to 1uM of each cardiac glycoside. Ampullary PCO response was assayed using subclonal population analysis. Cerberin at 10nM achieved growth arrest across the population as assayed by median Δ diameter (growth +4.0±32.0, GΔ=0.94, $p<0.005$). Neriifolin at 10nM had subclonal with residual growth representing 72% of overall population as assayed by Δ diameter (growth +18.3%, GΔ=0.65). Traditional cardiac glycosides of digoxin and digitoxin at 10nM had significant portions with residual growth (94.9% and 84.7%, respectively) as well as did not achieve meaningful effect (GΔ=-0.10 and GΔ=0.05, respectively).

Conclusions: CGs have varied potency for anticancer activity between different structural motifs. Cerberin induce population growth arrest in cancer models which differed from normal liver. This work requires dedicated mechanistic modeling to explain differences in anti-cancer activity that may confer sensitivity and in considering models of cardiac toxicity.

Potency of Cardiac Glycosides in Organoid Models.

	GI_{50} (nM) Ampullary	GI_{50} (nM) Pancreatic	GI_{50} (nM) Normal Liver
Cerberin	7.4	7.20	71.0 (NC)
Neriifolin	10.2	7.4	62.0 (NC)
Digoxin	29.6	47.9	55.5 (NC)
Digitoxin	NC	40.0	85.5 (NC)

#3827

Schinus terebinthifolius extracts impair migration of BT549 triple negative breast cancer cells _in vitro_

Alexis Tapanes-Castillo[1], Mariacira Di Santi[1], Abel Sousa[1], Jonathan M. Brown[1], Paola M. Gonzalez Rodriguez[1], Thiago P. Leal[1], Leticia Saladrigas[1], Vadym Trokhymchuk[1], Leonardo M. Soto Chumpitaz[1], Andrea Peterson[1], Susana Gutierrez[1], Rolando J. Petit[1], Carlos Planchart[1], Christian Del Corro[1], Daniela A. Ramos[1], Valeria Nazaire[2], Sean Mondesire[3], Maria Pina[1]. *[1]College of Health Sciences and Technology, St. Thomas University, Miami Gardens, FL,[2]School of Science, Miami Dade College, Miami, FL,[3]Institute for Simulation and Training, University of Central Florida, Orlando, FL*

Bark extracts, derived from the Brazilian peppertree (*Schinus terebinthifolius*) were tested on BT549 triple negative breast cancer cells, a model system for invasive, metastatic cancers. Crude extracts, prepared with a 50% ethanol-50% water solvent, were investigated for cytotoxicity and effects on cell migration *in vitro*. Extract-treated cells exhibited statistically significant slower migration velocities than untreated control cells. Crude bark extracts, screened at a concentration of 3.15mg/mL in five

independent experiments, produced an approximate 80% decrease in average migration velocity ($p<0.05$ in every experiment). Three independent tetrazolium based MTT cytotoxicity experiments confirmed that cells exposed to the same 3.15 mg/mL crude extract concentrations displayed similar viability as untreated control cells. Interestingly, these data suggest the Brazilian peppertree bark extract harbors bioactivity that impairs BT549 cell migration without cytotoxic side effects. Current experiments aim to discover which bioactive molecules, present in the crude extract, impede cancer cell migration. Silica-based column chromatography was used to separate the crude extract into fractions of increasing polarity. A wet method, which commenced with hexane, followed by dichloromethane, methanol, ethanol, ethyl acetate, and butanol, was employed. Fractions which retained anti-migratory activity were identified. Gas chromatography Mass Spectrometry (GCMS) was performed on crude extracts, samples with strong anti-migratory activity, and samples with weak anti-migratory activity, solubilized with ethanol, methanol, and acetonitrile. Data from two independent, complete sets of experiments, involving column chromatography, cellular assays with fractionated extracts, and GCMS, replicated results. Compounds that were unique to specific samples, as well as compounds that were found in multiples samples were identified. *Rstudio* software was utilized to organize and visualize data. This work lays down the preliminary foundation for future experiments testing specific purified forms of candidate molecules present in Brazilian peppertree bark extracts for the ability to limit BT549 cancer cell migration *in vitro*. Furthermore, Western blotting and immunocytochemistry experiments are underway to determine cellular signaling pathways targeted by the extract. Funding was provided by St. Thomas University's Summer Research Institute and U.S. Dept. of Education STEM grants P03C110190, P031C160161, and P031C210035.

#3828

Herbal extracts from lycii radicis corex and achyranthes japonica prevent multiple myeloma progression

Syed Hassan Mehdi[1], Sun-OK Lee[2], Dam Huh[3], Donghoon Yoon[1].
[1]University of Arkansas for Medical Sciences, Little Rock, AR,[2]Food Science, University of Arkansas, Fayetteville, AR,[3]Dongwoodang Pharmacy Co., Yeongchen, Korea, Republic of

Multiple Myeloma (MM) is a plasma cell malignancy that, despite advances in treatment, remains incurable. In over 90% of MM patients, aberrant bone remodeling occurs and results in osteolytic lesions. Korean traditional medicine has a long-standing interest in healthy foods to enhance the immune system, energy-boost, and Yin-and-Yang balance. Traditional medicine has used herbal extracts (HE) from natural plants with fewer side effects and long-term treatment tolerance. In earlier studies, lycii radices cortex (LRC) and achyranthes japonica (AJ) containing HE have demonstrated the ability to enhance cell growth and mineralization of osteoblast cells while also inhibiting osteoclast differentiation. The current study investigated the effects of LRC+AJ containing HE on murine 5TGM1 MM-bearing mice.This HE significantly increased the mouse survivals of both Treatment before Transplant (TbT) and Treatment after Transplant (TaT) groups with median survivals of undetermined and 52.5 days, respectively, while MM control had a median survival of 42 days. The Mantel-Cox test found that TbT and TaT mice were significantly different from the control group (P=0.0014 and 0.0182, respectively). In histomorphometric analysis, the spines were scanned by micro-CT and revealed that TbT and TaT groups had significantly increased bone volume over total volume (BV/TV) than control. To see if HE affects cell growth of myeloma cells and osteoblast cells, we further investigated the HE on preosteoblast cell line MC3T3-E1, mouse MM cell line 5TGM1-Luc, and human MM cell line U-266. Cells were treated with HE, and viability was assessed at 48 and 96 hours post-treatment. Remarkably, LRC+AJ containing HE increased MC3T3-E1 cell growth while it decreased 5TGM1 and U-266 cell viability. In addition, we found the DAP3G in HE used in this study.Our results demonstrated that LRC+AJ HE prevents MM and promotes bone formation in 5TGM1 engrafted NSG mice. We also found that LRC+AJ HE suppresses myeloma cell growth and enhances osteoblast cell survival. Although it is yet to be defined, a correlation of osteoblast activity and myeloma cell inhibition suggests a possible connection of these events to prevent MM progression.

#3829

Antioxidant and antiproliferative activities of *Ipomoea cairica* extracts on three breast cancer cell lines

Ayodeji Mathias Adegoke[1], Doreen Kulabako Kyagaba[1], Nomonde Hadebe[1], Nandi Mabaso[1], Relebohile Patricia Lefojane[2], Himansu Baijnath[3], Oyeronke Adunni Odunola[4], Mamello Patience Sekhoacha[1].
[1]Pharmacology, University of the Free State, Bloemfontein, South Africa,[2]Department of Health Sciences, Central University of Technology, Bloemfontein, South Africa,[3]School of Life Sciences, University of KwaZulu-Natal, Durban, South Africa,[4]Department of Biochemistry, University of Ibadan, Ibadan, Nigeria

Introducti**on:** Breast cancer was the top cause of cancer deaths in 2020 with a death toll of 685 000 worldwide. Breast cancer treatments are based on drug specificity for unique receptors on the surface of some breast cancer types, there is a search for alternative treatments that are inclusive of different breast cancer types. Evidence suggests that antioxidants offer a protective effect against certain cancers. Studies on *Ipomoea cairica* have reported potential anticancer activity, hence this study aimed to assess the antioxidant and antiproliferative potentials of the extracts of *Ipomoea cairica* on three breast cancer cell lines.
Materials and Methods- The study protocol was approved by the University of the Free State Health Sciences Research Ethics Committee (HSREC), with approval number: UFS-HSD2022/0353/2607-0001. *Ipomoea cairica* stem and leaves were harvested and identified by Prof. H. Baijnath, Department of Conservation Science, School of Life Sciences, University of KwaZulu-Natal, Durban, South Africa, with specimen number 29 30 DD housed at the Ward Herbarium. The dried plant was extracted sequentially using organic solvents ranging from non-polar to polar and water. The extracts were filtered and concentrated using a rotary evaporator and then evaporated to dryness/lyophilized. Cells were cultured according to standard established procedure. The extracts were subjected to phytochemical analyses. FRAP, DPPH, and ABTS assays were done to examine antioxidant activity and MTT assays were used to evaluate the antiproliferative/cytotoxicity of the extracts against normal (Vero) and breast cancer cell lines (MCF-7, MDA-MB-231, and 4T1).
Results and Discussion- Extracts of *Ipomoea cairica* possess alkaloids, saponins, phenols, flavonoids, phytosterols, tannins, triterpenoids, and anthraquinones. The results from the DPPH and ABTS assays revealed that

the methanol and ethyl acetate fractions had significantly the highest antioxidant potentials while the methanol stem extract exhibited the most significant antioxidant activity in the FRAP assay. The DCM stem extract showed the highest antiproliferative activity against all tested cell lines. **Conclusion-** Extracts of *I. cairica* possess significant antioxidant properties and antiproliferative activities against a wide array of breast cancer types including the most challenging triple-negative breast cancer. The plant would make for a strong herbal candidate for adjuvant therapy with breast cancer medication.

#3830

The anticancer activity of a water-soluble extract from the leaves of the indigenous Southern African plant *Tulbaghia violacea* against a triple negative breast cancer cell line

Rodney Hull[1], Zodwa Dlamini[1], Clement Penny[2], Mohammed Alaouna[2].
[1]SA-MRC Precision Oncology Research Unit (PORU); Pan African Cancer Research Institute (PACRI), DSI/N, University of Pretoria, Pretoria, South Africa,[2]Department of Internal Medicine, Faculty of Health Sciences, University of the Witwatersrand, Johannesburg, South Africa

Triple negative breast cancer (TNBC) is difficult to treat and leads to a low five-year survival rate.In South Africa, a sizable percentage of the population still relies on traditional plant-based medicine. One of these plants, *Tulbaghia violacea),* has traditionally been used to treat cancer. In order to establish the usefulness of both methanol and water-soluble extracts from the leaves of this plant, extracts were used to treat a TNBC cell. Cytotoxicity assays were carried out to establish the IC50 values against the TNBC cell line. These concentrations were used to carry out assays to study the ability of these extracts to inhibit cell migration, invasion, as well as the effect of these extracts on the cell cycle and their ability to induce apoptosis in these cells. Finally, the antioxidant activity of these cells was assayed. The IC50 values for the water and methanol soluble extracts was determined to be 400 and 820 µg/mL respectively. Due to the high IC50 value and inconsistent performance of the methanol soluble extract, further studies focussed on the water-soluble extract. Treatment of the TNBC cells with the water-soluble extract led to an increase in apoptosis, with the extract causing approximately 82% of the

TNBC cells to undergo apoptosis compared to only 32% of the normal breast cells. This extract also significantly decreased the ability of the TNBC cells to migrate or penetrate abasement membrane in scratch and invasion assays. These results demonstrate that the water-soluble extract from *T. violacea* leaves contains compounds that are able to preferentially induce apoptosis in TNBC cells while also inhibiting the ability of these cells to metastasize. The exact molecular make up of this extract will need to be determined on order to develop the extract as a potential therapy for TNBC.

#3831

The molecular composition of a water-soluble extract from the leaves of the indigenous Southern African plant *Tulbaghia violacea* that displays anti-cancer activity against a triple negative breast cancer cell line

Mohammed Alaouna[1], Clement Penny[1], Rodney ulll[2], Zodwa Dlamini[2].
[1]Department of Internal Medicine, Faculty of Health Sciences, University of the Witwatersrand, Johannesburg, South Africa,[2]SA-MRC Precision Oncology Research Unit (PORU); Pan African Cancer Research Institute (PACRI), DSI/N, University of tPretoria, Pretoria, South Africa

Approximately 20% of all breast cancer cases are Triple negative breast cancer (TNBC), whichis more difficult to treat and has a higher mortality rate than other types of breast cancer. Thereis an active practice of traditional medicine in in South Africa, in the form of infusions madeusing plant material. Previously we demonstrated that water soluble extracts from the leaves ofone of these plants, African garlic (*Tulbaghia violacea),* is able to induce apoptosis in TNBCcell lines, while also inhibiting the ability of these cells to migrate or penetrate a basementmembrane. In an attempt to isolate the molecular compounds that are present in this extract,water soluble leaf extracts were subjected to Fourier transform infrared spectroscopy (FITR),Gas chromatography–mass spectrometry (GC-MS) and Nuclear magnetic resonance (NMR)spectroscopy. Identified compounds of interest were then used in computational dockingstudies with the anti-apoptotic protein Cox2. The FITR analysis indicated that the extractconsisted of multiple compounds, belonging to a variety of classes. GC-NS and NMRspectroscopy identified 36 and 61 separate compounds respectively. Many of these compoundswere similar in structure to

compounds with known anti-cancer properties. Many compoundswith established medical uses were also identified in the extract. Five compounds identified inthe extract, d-Glycero-d-galacto-heptose, H-Pyran-4-one, 2,3-dihydro-3,5-dihydroxy-6-methyl, and Benzaldehyde and 4-(1-methylethyl)- demonstrated high binding affinity towardsCOX2. With d-Glycero-d-galacto-heptose having a higher docking score than manycommercially available COX2 inhibitors. Based on our findings, the compounds within theextract could be used as the basis for the development of safe and effective drugs for thetreatment of TNBC and other cancers. In order to fulfil this potential, future work shouldexamine the molecular pathways affected by the treatment of TNBC cells with this extract orindividual compounds.

#3832

Apoptotic and cell cycle effects of triterpenes isolated from*Phoradendron wattii* on a chronic myelogenous leukemia cell line

Rosa E. Moo-Puc[1], Shirley A. Calderón Sauri[1], Jairo R. Villanueva-Toledo[2], Sergio R. Peraza-Sánchez[3], Antonieta Chávez-González[4].
[1]Farmacología de productos naturales, Unidad de Investigación Médica Yucatán, Unidad Médica de Alta Especialidad, Instituto Mexicano del Seguro Social, Merida, Mexico,[2]Fundación IMSS, Cátedras CONACyT, Merida, Mexico,[3]Unidad de Biotecnología, Centro de Investigación Científica de Yucatán (CICY), Merida, Mexico,[4]Unidad de Investigación Oncológica, Hospital de Oncología, Centro Médico Nacional, Instituto Mexicano del Seguro Social, ciudad de México, Mexico

Introduction: Medicinal plants have been used in traditional medicine practices since ancient times. Mayan traditional medicine uses herbs as treatment to illness that can be related to cancer disease such as *Phoradendron wattii*. As part of the search for novel cancer treatment two triterpene compounds were isolated from *P. wattii*: 3-*epi*-betulinic acid and lupenone with preliminary activity on leukemias. We investigated the cancer treatment abilities of 3-*epi*-betulinic acid and lupenone on human chronic myelogenous leukemia (K562) cell line and monocytes isolated from peripheral blood using flow cytometry methods.

Results: Lupenone showed low effect on both cells with an IC_{50} of 177.60 ± 5.07 µg/mL and a selectivity index (SI) of 0.10 times more on K-562 cell line than on monocytes. Nevertheless, 3-*epi*-betulinic acid showed a moderate anti-CML activity with an IC_{50} of 38.74 ± 5.07 µg/mL, having a SI of 4.10 on K-562 cells when compared to monocytes. These results indicate that 3-*epi*-betulinic acid was 41 times more selective for K-562 cell line than lupenone and it also was 7.45 more selective than etoposide as positive control. Additionally, 3-*epi*-betulinic acid increased cell population in the G_0/G_1 phase of the cell cycle and apoptotic cells, and it inhibited cell proliferation in a dose-dependent manner. Furthermore, the relative expression of genes associated with apoptosis Bax and caspase 3 increased compared to control.
Conclusion: Combined, these results suggest that 3-*epi*-betulinic acid plays an important regulatory role of cell cycle and apoptosis. Finally, the 3-*epi*-betulinic acid investigated in this work is potentially a cheap, safe, and effective alternative to chemotherapy in cancer treatment.

#3833
Leonurine derivatives as a potential novel therapeutic approach to acute lymphoblastic leukemias (ALL)
Joseph W. Schramm, Melanie Ehudin, Bing He, Chingakham Singh, Daniel Bogush, Jeremy Hengst, Diwakar Bastihalli Tukaramrao, Arati Sharma, Dhimant Desai, Sinisa Dovat. *Penn State Health Milton S. Hershey Med. Ctr., Hershey, PA*

Background: Pre-B cell Acute lymphoblastic leukemia (B ALL) high risk (HR) subgroups continue to result in significant mortality and morbidity of pediatric oncology patients. T cell ALL is higher risk and therapy has made less improvement than B ALL with a higher rate of significant poor outcomes. Novel treatment strategies are required to overcome chemotherapy resistance and improve mortality/morbidity for HR B ALL. Leonurine is a bioactive alkaloid that is naturally occurring only in Herbra Leonuri which has been used in traditional herbal medicine. Traditionally, it has been used for menstrual disorders. Research has further described its ability to scavenge oxygen free radicals, anticoagulation properties, and other anti-inflammatory properties[1]. There are investigations in its role for myocardial infarction, stroke, chronic kidney disease, and other

inflammatory disorders[2]. Our research data that suggests that leonurine and its derivatives have antileukemic effects.Methods/Results: We analyzed multiple derivatives of leonurine and selected a potent candidate based on cell viability assays use for further testing designated as investigational leonurine derivative (ILD). WST1 proliferation studies comparing ILD to vehicle were performed in cell lines Nalm6, 697, Molt4, CEM, and JM1 at multiple time points. The half maximal inhibitory concentration (IC50) values was variable depending on the treatment time and cell line although all values were consistently between 1.2-4.4 uM. Apoptosis activity was determined by flow cytometry Anexin/7AAD assays showed increased apoptosis in cell lines treated with ILD for Nalm6, Molt4, and 697 cell lines. Caspase 3/7 activity was increased in cells treated with ILD when compared to vehicle treatment. DNA damage assays were performed which revealed only an increased frequency in single strand breaks and not double strand breaks. Western blot was performed to determine levels of PI3K, p-AKT, BCL2/BCL-XL and caspases. The blots suggest that apoptosis may be a result of increased activation of PI3K/AKT signaling. We performed RNAseq on cells treated with ILD at the 24-hour time point and present gene ontology data for this analysis. Nalm6, 697, and Molt4 cell lines expressing GFP and Luciferase were injected into NRG mice as means for in vivo pharmacologic testing. NRG mice injected with these cell lines were treated with ILD five days a week for a total of 3 weeks. Nalm 6 leukemia cells showed minimal differences between treatment and control groups.Conclusion: In summary, leonurine derivatives have a promising impact on apoptosis and cell survival. Further investigation into mechanisms and pharmacokinetics/dynamics will be more revealing. Study of leonurine derivatives will result in further translational and therapeutic applications.

#3834

Antiproliferative activity of substituted chromone-2-carboxamides on MDA-MB-231 cells and their 3D pharmacophore models

Kinfe Ken Redda[1], Madhavi Gangapuram[1], Suresh Eyunni[2], Elizabeth Mazzio[1], Karam F. A. Soliman[1]. *[1]College of Pharmacy and Pharmaceutical Sciences, Florida A&M University, Tallahassee, FL,[2]College of Science and Technology, Florida A&M University, Tallahassee, FL*

After lung cancer, breast cancer is the second leading cause of cancer death in women in the United States, accounting for 12.5 % of all new cancer cases globally. Triple-negative breast cancer (TNBC) remains the hardest breast cancer and is difficult to treat. The current treatment option for TNBC is the surgical removal of the tumor, followed by chemotherapy. However, patients with advanced diseases respond poorly to current treatments. Therefore, discovering more effective and less toxic small drug molecules with a unique mechanism of action is one of the top priorities in drug discovery programs. Chromones have a benzo-pyrone skeleton and display interesting pharmacological activities, such as anti-cancer, anti-HIV, antiviral and anti-inflammatory, with low toxicity. In continuation of our current research work, we report the design and synthesis of substituted chromone-2-carboxamides by attaching substituted phenyl, tetrahydropyridine, and tetrahydroisoquinoline groups as anti-breast cancer agents. The starting material, substituted chromone-2-carbonyl chloride, was obtained by the acylation reaction of corresponding carboxylic acids using phosphorous pentachloride in dry cyclohexane. An equimolar amount of acyl chloride was slowly added to a stirred solution of corresponding substituted N-amino salt in dry THF in the presence of triethyl amine and refluxed at 70 ^{o}C that led to the formation of the ylides. The ylides were reduced using sodium borohydride to yield the desired substituted chromone-2-carboxamides in moderate to good yields. The synthesized compounds were characterized by NMR and elemental analysis. These compounds were evaluated for their cytotoxic effects on MBA-MB-231 ER-ve breast cancer cell lines using a Synergy HTX multi-mode reader (Bio-Tek, Winooski, VT, USA) with excitation/emission wavelength settings at 550/580. Compound MG-KKR-5-140A showed the most potent cytotoxicity with an IC_{50} value of 0.82 µg/mL on the MDA-MB-231 cell line. *In-silico* pharmacophore hypotheses were generated using GALAHAD and PHASE, and the best models with probable bioactive conformation(s) for these compounds were proposed. These confirmations and the alignments of the molecular structures give us an insight into designing compounds with better biological activity. *This research was supported by the National Institute on Minority Health and Health Disparities of the National Institutes of Health under Award Number U54 MD007582. The content is solely the responsibility of the authors and does not necessarily represent the official views of the National Institutes of Health.*

Structural and Chemical Biology

#3839

Discovery of GSTZ1 as a novel target for drug refractory non-small cell lung cancer by using fragment-based chemical proteomics

Yi Liao, Sean Chin Chan, Eric A. Welsh, Bin Fang, Luxin Sun, Ernst Schönbrunn, John M. Koomen, Derek R. Duckett, Eric B. Haura, Andrii Monastyrskyi, Uwe Rix. *Moffitt Cancer Center, Tampa, FL*

A subset of non-small cell lung cancer (NSCLC) patients respond poorly to clinical drugs targeting defined oncogenic driver mutations. To improve the efficacy of these drugs in drug refractory NSCLC, the identification of supporting therapeutic targets and discovery of the binding molecules are urgently needed. Photoreactive fragment-like probes can discover target proteins that constitute novel cellular vulnerabilities and provide the chemical basis for drug discovery. However, the rational design of the fragment probe library, target prioritization, and sample throughput are still challenging. We applied a structurally diverse panel of BioCore fragments fully functionalized with orthogonal diazirine and alkyne moieties. These probes were used for protein crosslinking in live cells and subsequent target identification through label-free quantitative LC-MS/MS analysis. High-confidence targets were queried against a pharmacogenomic database (DepMap) and prioritized through multiple cross-comparison with other probes. The top-ranked probe-binding target was validated using a competitive affinity assay, an enzymatic activity assay, and RNA interference. Proteome-wide tyrosine reactivity was profiled using sulfur-triazole exchange chemistry (SuTEx). The tyrosine phosphorylation of proteins was investigated using a pY-100 antibody and western blotting. Using sotorasib-refractory KRAS G12C H1792 lung cancer cells, we identified 932 probe-enriched proteins from panel-wide cross-comparisons suggesting the high potential of exploring the ligandable proteome. We also performed intensive cross-comparison analysis and identified 31 unique high-confidence targets, with glutathione S-transferase zeta 1 (GSTZ1) identified as a unique target of probe 17. We found that high expression of GSTZ1 was significantly associated with poorer NSCLC patient survival. Probe 17 was validated to physically bind to GSTZ1 and inhibit the enzymatic activity of GSTZ1. In addition, *GSTZ1* gene knockdown sensitized drug-refractory NSCLC cells with KRAS G12C, FGFR1 amplification, and DDR2 mutation to clinical targeted drugs and induced more cell apoptosis in combination with these targeted drugs. SuTEx proteomics suggests modulation of drug resistance pathways leading to the identification of altered KRAS and FGFR1 tyrosine phosphorylation by GSTZ1, which provides a functional insight into the mechanism of drug sensitization. We developed a chemical biology workflow for the simultaneous discovery of high-confidence targets and their binding probe molecules, such as probe 17 and GSTZ1. GSTZ1 was found to cooperate with oncogenic alterations in supporting refractory NSCLC cell survival signaling, which may form the biological basis for developing novel GSTZ1 inhibitors to improve the therapeutic efficacy of oncogene-directed targeted drugs.

#3840

High-resolution structural insights into targeting the *MYC* oncogene G-quadruplex with the quinoline derivative PEQ

Jonathan Dickerhoff[1], Jixun Dai[2], Danzhou Yang[1]. *[1]Purdue University, West Lafayette, IN,[2]The University of Arizona, Tucson, AZ*

The transcription of the *MYC* oncogene, a central player of oncogenesis, is strongly controlled by DNA G-quadruplexes in its promoter region (MycG4). Stabilization of MycG4 with small molecules downregulates *MYC* expression and has devastating effects on many cancers. Thus, targeting MycG4 is an attractive anti-cancer strategy especially since the MYC protein is considered a very difficult target. DNA G-quadruplexes are four-stranded secondary structures and enriched in promoters of oncogenes. Their globular shape and high structural diversity distinguishes them from the thread-like and uniform DNA duplex ubiquitously found in the cell. High-resolution structures reveal the molecular interactions between ligands and G-quadruplexes and are the key for structure-based rational design of new and improved drugs. Here, we present the new MycG4 binder PEQ, a

quinoline derivative, and describe its molecular recognition of the MycG4. PEQ is more drug-like than many prominent G-quadruplex binder because it lacks an extensive aromatic moiety. Most of the reported G-quadruplex binding ligands include extended and rigid aromatic moieties with less drug-like properties. We used solution NMR and molecular dynamics calculations to first determine the high-resolution structures of the unbound wild-type MycG4, and next structures of PEQ in complex to wild-type MycG4 or the most commonly studied modified MycG4. This modified MycG4 sequence bears a mutated residue in the binding pocket that is critical for ligand interactions. PEQ binds the MycG4 with a 2:1 stoichiometry and stacks on the G-quadruplex ends. Specific binding pockets are formed in which a flanking residue is recruited by the PEQ to form a joint-plane. The identity of the recruited residue controls the orientation of the ligand and the resulting interactions, as shown by structural comparison of PEQ in complex with either the wild-type or mutated MycG4. Including the PEQ structure, four ligand-MycG4 complexes are now available and we performed the first systematic analysis. We show that despite the dynamic character of the flanking sequences, all ligands recruit DNA bases in a conserved and sequence-specific manner. Moreover, we propose the design of complementary hydrogen bonds to match the recruited DNA base with a drug via structure-based rational design. In conclusion, our work introduces the quinoline PEQ as new lead compound for cancer therapeutics targeting MYC through the MycG4. We present the MycG4-ligand structure with wild-type binding sites as more accurate target and identify important aspects of ligand binding to guide future design of cancer therapeutics.

#3841

Development of p300-targeting PROTAC degraders with enhanced selectivity and onset of degradation

Graham P. Marsh[1], Sean Goggins[1], Darko Bosnakovski[2], Michael Kyba[2], Samuel Ojeda[3], Drew A. Harrison[3], Christopher J. Ott[3], Hannah J. Maple[1]. *[1]Bio-Techne Corporation, Bristol, United Kingdom,[2]Lillehei Heart Institute, Minneapolis, MN,[3]Massachusetts General Hospital Cancer Center, Boston, MA*

CREB-binding protein (CBP, CREBBP, KAT3A) and E1A-binding protein (EP300, p300, KAT3B) are paralogous multi-domain proteins that act as chromatin regulators and transcriptional co-activators. They contain a histone acetyltransferase (HAT) domain that catalyzes the histone H3, lysine 27 acetylation (H3K27ac) mark at regulatory elements such as enhancers and promoters. Transcription factors associate with stretches of H3K27ac marks (known as ‘super-enhancer’ elements) and result in gene transcription that ultimately establishes cell identity and fate. They are implicated in cancer pathology, and small molecule inhibition of the bromodomain (BRD) or HAT domain of CBP/p300 are considered promising therapeutic strategies for a number of cancer types. CBP and p300 are highly homologous but have distinct roles that have to date been hard to delineate, since small molecule inhibitors developed to date are unable to selectively target each protein independently. Additionally, small molecule inhibitors that target individual domains are unable to entirely abrogate the full functionality of CBP/p300. A bromodomain-recruiting dual CBP/p300 PROTAC Degrader ‘dCBP1’ was therefore recently developed to provide a chemical tool to explore the phenotypic consequences of CBP/p300 chemical knockdown. A further study demonstrated that it is possible to degrade p300 with some selectivity by converting a CBP/p300 dual HAT-domain inhibitor into a PROTAC, called ‘JQAD1’.
We have used a different HAT-domain recruiting ligand to develop novel PROTACs that elicit proteasome-mediated degradation of p300 with significantly enhanced selectivity over CBP, compared with JQAD1. We additionally demonstrate a faster onset of degradation for lead PROTAC molecules and present data exploring the consequences of selective p300 degradation in CIC-DIX4 sarcoma.

#3842

Berberine recognition of the dGMP-bound PDGFR-β promoter G-quadruplex: Structural insight into specific drug targeting

Kai-Bo Wang, Jonathan Dickerhoff, Yichen Han, Danzhou Yang. *Purdue University, West Lafayette, IN*

PDGFR-β (Platelet-Derived Growth Factor Receptor beta) is a receptor tyrosine kinase whose overexpression drives the progression and metastasis of many cancers. It is an established anticancer target and PDGFR-β inhibition via kinase inhibitors has been actively sought-after. However, PDGFR-β kinase inhibitors often lack specificity. The PDGFR-β gene promoter forms DNA G-quadruplexes that are transcription silencer whose stabilization by small molecules represses PDGFR-β expression. Therefore, targeting PDGFR-β promoter G-quadruplexes for transcriptional silencing is a promising alternative strategy for cancer therapy. G-quadruplex is an exciting family of non-canonical DNA secondary structures. DNA G-quadruplex within the PDGFR-β gene promoter forms novel vacancy pockets (vG4) that can be filled-in by guanine metabolites such as dGMP and cGMP. This presents an attractive target for small molecule targeting. Herein, we present the binding of the natural product berberine with the unique PDGFR-β dGMP-vG4 binary complex to form a novel ternary complex, the first case observed in DNA G-quadruplexes. Using circular dichroism, fluorescence, and nuclear magnetic resonance (NMR) spectroscopy, we demonstrated that berberine binds with high affinity and strongly stabilizes the dGMP-fill-in PDGFR-β vG4. Our determined high-resolution NMR structure of this ternary complex in K^+-containing solution reveals a 2:1 binding stoichiometry of berberine to the dGMP-fill-in PDGFR-β vG4. Significantly, one berberine directly stacks upon and extensively covers the dGMP. This direct binding mode provides structural basis for targeting the unique PDGFR-β promoter G-quadruplex by small molecules and suggests an intriguing strategy of designing drug-like, guanine-conjugated molecules to selectively silence the PDGFR-β gene. Because vG4 formation and dGMP fill-in is a unique property of the PDGFR-β promoter G-quadruplex, our study provides a structural basis for rationally designing small molecule drugs to specifically target the PDGFR-β promoter G-quadruplex to inhibit oncogenic PDGFR-β for cancer therapeutics.

#3843

Potent human ClpP protease agonists with anticancer properties bind the enzyme with improved structural complementarity and alter the mitochondrial N-terminome

Mark F. Mabanglo[1], Keith S. Wong[1], Marim M. Barghash[1], Lee M. Graves[2], Edwin J. Iwanowicz[3], Walid A. Houry[1]. *[1]Biochemistry, University of Toronto, Toronto, ON, Canada,[2]Department of Pharmacology and the Lineberger Comprehensive Cancer Center, University of North Carolina at Chapel Hill, Chapel Hill, NC,[3]Madera Therapeutics LLC, Cary, NC*

The mitochondrial ClpP protease is responsible for mitochondrial protein quality control through specific degradation of proteins involved in several metabolic processes. ClpP overexpression is also required in many cancer cells to eliminate ROS-damaged proteins and to sustain oncogenesis. Targeting ClpP to dysregulate its function using small molecule agonists is a novel strategy in cancer therapy. Here, we synthesized novel imipridone-derived compounds and related chemicals, which we characterized using biochemical, biophysical, and cellular studies. Using X-ray crystallography, we found that these compounds have enhanced binding affinities due to their greater shape and charge complementarity with the surface hydrophobic pockets of ClpP. N-terminome profiling of cancer cells upon treatment with one of these compounds revealed the global proteomic changes that arise and identified the structural motifs preferred for protein cleavage by compound-activated ClpP.

Together, our studies provide the structural and molecular bases by which dysregulated ClpP affects cancer cell viability and proliferation.

#3844

A biophysical investigation into the binding interactions of novel anti-cancer inhibitors of atypical protein kinase C (aPKCs)

Radwan Ebna Noor[1], Tracess B. Smalley[2], Mildred Acevedo-Duncan[1]. *[1]University of South Florida, Tampa, FL,[2]H. Lee Moffitt Cancer Center and Research Institute, Tampa, FL*

The aim of this study is to address the challenge of the expression of recombinant atypical protein kinase C (aPKCs) in a bacterial system and understand the binding interactions of novel anti-cancer inhibitors of aPKCs. The Protein kinase Cs (PKCs) expression at a high rate is a key indicator of cancer cell proliferation and survival. In particular, the over-expressions of aPKCs were found to be directly associated with various cancer cells in benign and malignant stages. Several cancer growth blockers (inhibitors) are available for targeted therapy. However, these inhibitors had to pass through rigorous *in silico* screening, *in vitro,* and *in vivo* assays before FDA approval. During the characterization studies of the protein, insights into binding interactions between aPKCs and drug molecules are crucial. For successive studies such as for biophysical characterization, the recombinant bioactive full-length PKC- ι (an aPKC) expression in the bacterial system is still a challenge. In addition, the binding interaction studies of aPKCs with inhibitors in physiological conditions providing structural details are limited to some X-ray crystallography structures and computational studies. Here we addressed these two challenges and report a protocol detailing the bioactive full-length and catalytic domain of PKC- ι expression and purification from the bacterial system. The further characterization of the recombinant protein by the determination of melting temperature, functional activity, and circular dichroism reported here provides important information on the characteristics of the protein in its native state. Moreover, we show the chemical interactions of five novel anti-cancer inhibitors ICA-1S (Nucleosidic homolog) 5-amino-1-((1R,2S,3S,4R)-2,3-dihydroxy-4-methylcyclopentyl)-1H-imidazole-4-carboxamide), ICA-1T (Phosphorylated nucleosidic homolog of ICA-1S, [4-(5-amino-4-carbamoylimidazol-1-yl)-2,3-dihydroxycyclopentyl] methyl dihydrogen phosphate), ACPD (2-acetyl-1,3-cyclopentanedione), DNDA (3,4-diaminonaphthalene-2,7-disulfonic acid) and ζ(ZETA)-Stat (8-hydroxy-1,3,6- naphthalenetrisulfonic acid) to locate their regions of binding on the catalytic domain of the aPKCs (PKC- ι and PKC- ζ). We have utilized the chemical shift changes obtained from various multi-dimensional Nuclear Magnetic Resonance (NMR) experiments. Moreover, we have applied the isothermal calorimetry method to understand the biophysical properties of the aPKCs in presence of these inhibitors. The observed biophysical properties of the protein and chemical shift perturbations in the amide backbone of the catalytic domain upon binding shed light on the molecular recognition process, binding characteristics, and atomic-level structural details of the aPKCs.

#3845

Structural mechanisms of how PTEN mutations degrade function at the membrane and life expectancy of carriers of mutations in the human brain

Hyunbum Jang[1], Jiaye Chen[2], Lilia M. Iakoucheva[2], Ruth Nussinov[1]. *[1]Frederick National Laboratory for Cancer Research, Frederick, MD,[2]Department of Psychiatry, University of California San Diego, La Jolla, CA*

PTEN negatively regulates PI3K/AKT/mTOR signaling through dephosphorylation of PIP_3 to PIP_2. PTEN dysfunction triggers disease phenotypes, ranging from cancer and PHTS to NDDs such as ASD. The most common PTEN mutations, nonsense, frameshift, and deletion/insertion, may cause

premature termination of translation. PTEN has a considerable number of missense mutations that may result in loss of protein function through reduced catalytic activity and protein stability. To decipher mechanistic details of the mutations and structural features of the mutant proteins, comprehensive computational studies were performed for PTEN mutants at an anionic lipid bilayer containing PC, PS, PIP_2, and PIP_3. Six PTP mutations (Y68H, H93R, A126T, R130Q, G132D, R173C) and two C2 mutations (F241S, D252G) were considered. The PTP mutations are known to associate with cancer, PHTS, macrocephaly, and ASD, while the C2 mutations are exclusively related to macrocephaly and ASD. Our studies indicate that the PTEN mutants can effectively absorb the anionic lipid bilayer, similar to wild-type PTEN. However, Y68H significantly disrupts the core of PTP domain, reducing protein stability. H93R hijacks the substate PIP_3, interrupting the catalytic site residues recruitment of the substate for catalysis. A126T, R130Q, and G132D in the P loop directly influence the dynamics of the loop, yielding a collapsed loop conformation. The collapsed P loop loses the interaction with the WPD loop, leading to dehydration in the catalytic site. R173C and D252G at the interface between two major domains disrupt the domain-domain interaction, allosterically biasing the P loop dynamics. However, F241S in C2 exhibits less effective allosteric connection to the catalytic site than that observed in the wild type. PCA of the sampled conformations found that the macrocephaly and ASD-related H93R and F241S are likely to sample the conformations present in the wild type. In contrast, the sampled conformations for the cancer and PHTS-related Y68H, A126T, and G132D are different from those for the wild type. These distinct structural features seem to correlate with mutation strength and timing of the expression of the genes that determine the cancer and NDD outcomes. The isoform expression data extracted from the BrainSpan indicate that exon 5 is impacted by NDD or non-NDD mutations. Interestingly, PTEN splicing isoforms that do not carry exon 5 are exclusively impacted by the NDD mutations, F241S and D252G. The increased life expectancy of PTEN variants carriers carrying exons 5 and 7 is highly correlated to increased lifetime risk for certain cancers. Our results underscore the detailed structural and functional mechanisms of PTEN with mutations at the membrane, and suggest that tissue-specific splicing isoform expression should be taken into consideration while predicting the effect of mutations in various diseases.

#3847

Target identification of a multi-pass transmembrane G protein coupled receptor using limited-proteolysis coupled mass spectrometry (LiP-MS)

Martin Soste[1], Dominique Kamber[1], Nadine Dobberstein[2], Mirjam Zimmermann[2], Aurelien Rizk[2], Yuehan Feng[1], Yaroslav Nikolaev[2], Nigel Beaton[1]. *[1]Biognosys AG, Schlieren, Switzerland,[2]InterAx Biotech AG, Villigen, Switzerland*

In drug discovery, target identification (ID) after phenotypic screens is a resource-intensive endeavor aimed to understand compound's mechanism of action. Target ID for membrane proteins is particularly challenging due to hurdles such as poor protein solubility, instability and low expression levels. Addressing these hurdles, recent proteomics-based strategies allow to analyze proteins in their native environment, and do not require compound modification or genetic manipulation of target cell lines.

Limited proteolysis coupled to mass spectrometry (LiP-MS) is a peptide-centric strategy that exploits structural protein alterations and steric hindrances induced by drug to detect drug-protein interactions, estimate potency (EC50) and predict binding sites across the proteome. Our previous reports (AACR 2020 and 2021) showed the applicability of LiP-MS on cytosolic proteins such as kinases and phosphatases. Here, LiP-MS workflow was adapted for multi-pass membrane proteins which are often underrepresented in global, unbiased target ID approaches.

For protein targets in the cytosol or intracellular organelles, LiP-MS deploys a dose-response (DR) analysis recorded by incubating cell lysates with a given compound. Here, to monitor proteins in plasma membrane, live cells were treated with the compound in a DR curve for a short period of time before lysis and subsequent LiP-MS analysis. Live cell treatment allows to achieve target ID by 1) locking the receptor in its native conformation to detect the structural difference between the drug-bound and unbound forms and; 2) detecting structural changes in downstream signaling cascades resulting from changes in protein-protein interactions, post-translational modifications or other mechanisms. We evaluated the performance of this workflow using a tool compound (IAX16840) targeting specific G-protein coupled receptors. Our unbiased LiP scoring identified atypical chemokine receptor 3 (ACKR3), the primary known compound target, among the top 3 hits. Additional 82 proteins were perturbed in drug-treated samples based on the LiP scores. Mapping the altered peptides on the GPCR signaling network showed enrichment of perturbations in ACKR3 downstream pathways, providing additional evidence of ACKR3 binding.
Taken together, we demonstrate that the live cell LiP-MS is applicable for target ID of multi-pass membrane proteins. The approach also provides a system-level view of protein and pathway perturbations downstream of a signaling protein (e.g. GPCR), revealing possible mechanisms of its endogenous action. Further optimization of LiP-MS protocol is sought to accommodate different classes of receptors.

CLINICAL RESEARCH EXCLUDING TRIALS

Biomarkers of Therapeutic Benefit 4

#4326

Predictive value of CXCL10 for the occurrence of immune related adverse events in patient with renal cell carcinoma

Yuji Miura[1], Takanobu Motoshima[2], Toshiki Anami[2], Hiromu Yano[1], Remi Mito[1], Shinji Urakami[3], Keiichi Kinowaki[4], Hirotake Tsukamoto[5], Ryoma Kurahashi[2], Yoji Murakami[2], Junji Yatsuda[2], Yukio Fujiwara[1], Tomomi Kamba[2], Yoshihiro Komohara[1]. *[1]Cell Pathology, Kumamoto Univ Graduate School of Medical Sci, Kumamoto, Japan,[2]Urology, Kumamoto Univ Graduate School of Medical Sci, Kumamoto, Japan,[3]Urology, Toranomon Hospital, Tokyo, Japan,[4]Pathology, Toranomon Hospital, Tokyo, Japan,[5]Clinical Immunology and Cancer Immunotherapy, Kyoto University, Kyoto, Japan*

Background: Immune checkpoint inhibitors (ICIs) have recently improved the prognosis of various cancers. In contrast, some immune-related adverse events (irAEs) caused by ICIs are fatal and have become problematic. The pathogenesis of irAEs remains unknown and must be elucidated to establish biomarkers.
Materials and Methods: Plasma samples were collected prospectively from patients with advanced and metastatic renal cell carcinoma (RCC) prior to initiation of ICI treatment (baseline) and 2 or 3 weeks after the first cycle of ICI treatment (post-dose 1). Plasma cytokines and chemokines (GRO [CXCL1], IL-17A, IL-1β, IL-6, IL-8, IP-10 [CXCL10], MCP-1 [CCL2], TNFα) were measured by Luminex system, and plasma level of CXCL13 and anti-CD74 autoantibody levels were measured by ELISA. Their association with irAEs was analyzed.
Results: In a discovery cohort of 13 patients, plasma levels of CXCL1, IL-17A, IL-1β, IL-6, IL-8, CXCL10, MCP-1, and TNFα were measured at baseline and post-dose 1. Only CXCL10, at post-dose 1 but not at baseline, was significantly associated with grade 2 or higher irAEs (p=0.0413). Plasma CXCL10 levels were then measured at baseline and post-dose 1 in a validation cohort of 43 RCC patients who received ICI-based treatment. Higher plasma CXCL10 levels both at baseline and

post-dose1 were significantly associated with the occurrence of grade 2 or higher irAEs (p=0.0246 and 0.0137, respectively). We evaluated the relationship between plasma levels of CXCL10 and CXCL13, which we measured in a previous study, and the incidence of irAEs. At baseline, the plasma CXCL13 level was positively associated with the CXCL10 level (p=0.0007), but no significant association was observed post-dose 1 (p=0.2678). Plasma CXCL13 levels were significantly higher in patients with grade 2 or higher irAEs at baseline but not at post-dose 1 (p=0.0037 and 0.052, respectively). No significant association between plasma anti-CD74 autoantibody level and both irAE pneumonitis and any grade 2 or higher irAE was observed. Conclusion: Plasma CXCL10 is significantly associated with the occurrence of irAEs in patients with RCC treated with ICIs. CXCL10 is a potential predictive and on-treatment biomarker for irAEs.

#4327

MSI cancer associated DNA (TA)n-dinucleotide repeat expansions and implications for Werner synthetic lethality

Gabriele Picco[1], Shriram Bhosle[1], Maria Kalyva[2], Elena Grassi[3], Freddy Gibson[1], Angham Al Saedi[1], Sara Vieira[1], Mathijs Sanders[4], Livio Trusolino[5], Andrea Bertotti[5], Isidro Cortes-Ciriano[6], Mathew Garnett[1]. *[1]Wellcome Sanger Institute, Hinxton, United Kingdom,[2]European Molecular Biology Laboratory- European Bioinformatics Institute EMBL-EBI, Hinxton, United Kingdom,[3]Candiolo Cancer Institute, Translational Cancer Medicine, Candiolo, Italy,[4]Erasmus University Medical Center, Rotterdam, Netherlands,[5]Candiolo Cancer Institute, Candiolo, Italy,[6]European Molecular Biology Laboratory, Hinxton, United Kingdom*

Microsatellite instability (MSI) is caused by deficient DNA mismatch repair (MMR) and is a ubiquitous feature of cancer. Werner syndrome (WRN) helicase is involved in genome stability and DNA repair. We identified WRN as a synthetic-lethal target in dMMR/MSI cancers and highlighted WRN inhibition as a therapeutic option for dMMR/MSI cancers refractory to available therapies. A previously unappreciated genetic feature of dMMR/MSI cancer cells, DNA (TA)n-dinucleotide repeat expansions, were recently reported to cause vulnerability to WRN depletion. Our mechanistic understanding of TA-dinucleotide repeat expansion biology is limited, and their potential therapeutic implications are unclear. To investigate the landscape of these alterations in cancer, we inferred (TA)-dinucleotide repeat expansions by performing coverage analysis in a collection of hundreds of preclinical cancer models and human tumors (PCAWG) profiled by whole genome sequencing (WGS). We validated our findings in cancer cell lines and organoid cultures by performing long-read WGS. Furthermore, we investigated TA-expansions in single-cell-derived clones from human MSI tumors and cancer organoids. Finally, we inferred TA repeats in laser capture microdissection (LCMB)-derived samples obtained from patients affected by familial cancer predisposition syndromes. Our analysis unveils the landscape of TA-repeats alterations in a large collection of tumors and preclinical models, informing on the level of inter-tumor heterogeneity and their association with variable levels of WRN dependency. In addition, we investigated intra-patient tumor heterogeneity of TA-repeats length both within clonal organoids expanded from normal and neoplastic colorectal stem cells, and within different subclones derived from MSI cancer organoids. Furthermore, analysis of non-neoplastic and neoplastic tissues from patients affected by familial cancer predisposition syndromes revealed the pattern of TA-repeats expansions associated with various DNA-repair pathway alterations. Finally, we will discuss the clinical implications of our findings, as TA-repeats heterogeneity may affect sensitivity and resistance to the future generation of WRN inhibitors. Our data provide fresh insights into the inter and intra-tumoral heterogeneity of TA-dinucleotide repeat expansions in human cancers. These data contribute to understanding the role of MMR in cancer and exploiting Werner as a therapeutic target in cancer.

#4329

Combined extracellular vesicle PD-L1 and radiomics as predictors of response in patients with advanced lung cancer undergoing immunotherapy

Murat Ak[1], Diego De Miguel Perez[2], Priyadarshini Mamindla[1], Alessandro Russo[3], Vishal Peddagangireddy[1], Mehmet E. Er[1], Şerafettin Zenkin[1], Muthukumar Gunasekaran[4], Luis Lara-Mejia[5], Francesco Buemi[3], Feliciano Barron[5], Marisol Arroyo-Hernández[5], Sunjay Kaushal[4], Andres F. Cardona[6], Aung Naing[7], Vincenzo Adamo[3], Oscar Arrieta[5], Rivka R. Colen[1], Christian Rolfo[2].

[1]Hillman Cancer Center, University of Pittsburgh Medical Center, Pittsburgh, PA,[2]Center for Thoracic Oncology, Tisch Cancer Institute, Icahn School of Medicine at Mount Sinai, New York, NY,[3]Medical Oncology Unit, A.O. Papardo & Department of Human Pathology, University of Messina, Messina, Italy,[4]Departments of Surgery and Pediatrics, Ann and Robert H. Lurie Children's Hospital of Chicago, Feinberg School of Medicine, Northwestern University, Chicago, IL,[5]Thoracic Oncology Unit, Instituto Nacional de Cancerología (INCan), Mexico City, Mexico,[6]Luis Carlos Sarmiento Angulo Cancer Treatment and Research Center (CTIC), Universidad El Bosque, Bogota, Colombia,[7]Departments of Investigational Cancer Therapeutics, The University of Texas MD Anderson Cancer Center, Houston, TX

Background: Immune-checkpoint inhibitors (ICIs) have improved the clinical benefit of only a subset of patients with advanced non-small cell lung cancer (NSCLC), since tissue PD-L1 has showed low predictive accuracy. We have previously showed that extracellular vesicle (EV) PD-L1 identified durable responders to ICIs and that the radiomics analysis of baseline CT scans improved the EV PD-L1 predictive model. Here, we aim to validate this combination model to identify non-responders to ICIs.

Methods: We enrolled 3 cohorts of patients, cohort (1) included 27 patients receiving ICIs, cohort (2) 17 on ICIs + chemotherapy (ChT), and cohort (3) with 13 undergoing ChT. Baseline and 3rd cycle plasma samples were collected, EV were isolated by ultracentrifugation, and EV PD-L1 dynamics was analyzed by immunoblot. 800 radiomics features were evaluated in baseline CT scans and a set of 6 features identified in cohort 1, were analyzed in cohort 2 and 3. Early and durable responses were assessed in CT scans after the 3rd and the 6-8 treatment cycle, respectively, using RECIST v1.1.

Results: Increased expression of EV PD-L1 during treatment showed good predictive value at identify non-responders to ICIs and was not associated with ChT response. The addition of radiomics features improved the predictive model for early and durable response to ICIs, while similar AUC was observed in particular for durable response in cohort 2. Moreover, these biomarkers outperformed tissue PD-L1 and were unspecific for response to Docetaxel (Table 1). No predictive models could be evaluated for early response to ChT.

Conclusions: We present for the first time, validated evidence of the combination of EV PD-L1 and radiomics as a highly accurate minimally invasive biomarker for predicting response to ICIs. This combinatorial approach outperformed the current standard-of-care tissue PD-L1 and is a promising tool for the stratification of patients to receive ICIs.

Table 1: Predictive models for early and durable response:

A: Predictive models for early RECIST response (3 treatment cycles)									
Cohort:	**1: ICIs (n=27)**			**2: ICIs + Docetaxel (n=17)**			**3: Docetaxel (n=13)**		
Biomarker:	AUC	Sensitivity	Specificity	AUC	Sensitivity	Specificity	AUC	Sensitivity	Specificity
ΔEV PD-L1 + Radiomics	73.3%	83.3%	73.3%	75.0%	100.0%	75.0%	NA		
ΔEV PD-	61.7%	50.0%	73.3%	71.9%	100.0%	56.3%	NA		

L1									
Radiomics	67.8%	83.3%	53.3%	90.6%	100.0%	87.5%	NA		
Tissue PD-L1 ≥1%	57.5%	75.0%	40.0%	62.5%	100.0%	25.0%	NA		
B: Predictive models for durable RECIST response (6-8 treatment cycles)									
Cohort:	**1: ICIs (n=27)**			**2: ICIs + Docetaxel (n=17)**			**3: Docetaxel (n=13)**		
Biomarker:	AUC	Sensitivity	Specificity	AUC	Sensitivity	Specificity	AUC	Sensitivity	Specificity
ΔEV PD-L1 + Radiomics	81.3%	75.0%	90.9%	76.7%	100.0%	66.7%	53.6%	42.9%	83.3%
ΔEV PD-L1	72.7%	56.3%	81.8%	83.3%	50.0%	100.0%	54.8%	28.6%	83.3%
Radiomics	71.0%	50.0%	90.9%	61.7%	50.0%	80.0%	57.1%	42.9%	83.3%
Tissue PD-L1 ≥1%	60.2%	75.0%	54.5%	63.3%	100.0%	26.7%	52.4%	28.6%	66.6%

#4330

A CD5 signature identifies diffuse large B-cell lymphomas (DLBCLs) sensitive to Bruton's tyrosine kinase (BTK) inhibition

Alan Cooper[1], Sravya Tumuluru[1], Kyle Kissick[2], Girish Venkataraman[2], Nikita Kotlov[3], Aleksander Bagaev[3], Andrew Lytle[4], Gerben Duns[4], David W. Scott[4], Christian Steidl[4], Brendan Hodkinson[5], Srimathi Srinivasan[5], Justin Kline[6], James Godfrey[7]. *[1]University of Chicago, Chicago, IL,[2]Pathology, University of Chicago, Chicago, IL,[3]BostonGene, Waltham, MA,[4]Centre for Lymphoid Cancer, British Columbia Cancer, Vancouver, BC, Canada,[5]Janssen Research & Development, Spring House, PA,[6]Medicine, University of Chicago, Chicago, IL,[7]Hematology and Hematopoietic Cell Transplantation, City of Hope, Duarte, CA*

Introduction: Gene expression profiling has identified DLBCLs that bear transcriptional similarity to either non-malignant germinal center B-cells (GCB-DLBCL) or activated B-cells (ABC-DLBCL, i.e. non-GCB-DLBCL). This cell-of-origin (COO) classification has guided precision medicine strategies, including the use of ibrutinib, a BTK inhibitor (BTKi), with ABC-DLBCLs thought to be sensitive to BTKi due to their constitutive activation of NF-kB downstream of the B-cell receptor (BCR). However, the phase III Phoenix trial testing the addition of ibrutinib to R-CHOP chemoimmunotherapy surprisingly failed to demonstrate a survival benefit in non-GCB-DLBCLs. By employing a newly defined genetic classification algorithm (LymphGen), distinct genetic DLBCL subtypes that benefit from this regimen were identified. However, LymphGen is not utilized in the clinic and fails to classify >40% of DLBCLs. To overcome these challenges, we sought to identify a straightforward biomarker of BTKi sensitivity. CD5 was selected as a potential candidate, given its role as a negative regulator of BCR signaling and expression in other BTKi-responsive B-cell lymphomas.

Methods: CD5 IHC was performed on a cohort of 405 DLBCLs, most with paired RNA and targeted mutational sequencing. Comparison of the transcriptomes of $CD5^+$ and $CD5^-$ DLBCLs was used to construct a 60-gene CD5 signature (CD5sig), which was applied to large genomic DLBCL datasets, including pre-treatment biopsies from the Phoenix trial (n = 584) to evaluate its utility in predicting improved response to R-CHOP + ibrutinib.

Results: Twenty-seven DLBCLs were identified as $CD5^+$ by IHC (6% of cases; 12% of non-GCB). Consistent with previous reports, $CD5^+$ DLBCLs were enriched for a non-GCB COO and exhibited inferior progression-free survival to R-CHOP. $CD5^+$ DLBCLs upregulated genes related to BCR signaling and had a significantly higher incidence of *CD79B* BCR-activating mutations. A CD5 signature (CD5sig) was created from differentially expressed genes between CD5 IHC^+ and CD5 IHC^- non-GCB-DLBCLs. When applied to an external dataset of 349 non-GCB-DLBCLs, $CD5sig^+$ DLBCLs (15% of cases) were enriched for BCR-activating mutations and were majority MCD (*MYD88* and *CD79B*) or unclassified by LymphGen. $CD5sig^+$ DLBCLs were largely devoid of *BCL10* activating mutations known to drive BTKi resistance. When applied to the Phoenix study, $CD5sig^+$ DLBCLs selectively benefitted from R-CHOP + ibrutinib by event-free and overall survival. This survival difference was preserved even among LymphGen-unclassified DLBCLs.
Conclusions: Here, we identify CD5 expression as a simple and useful biomarker to identify high-risk, BCR-driven DLBCLs beyond those identified through genetic classification. Based upon unique transcriptional features of CD5 IHC^+ DLBCLs, we developed a novel CD5 signature that identifies DLBCLs vulnerable to BTKi therapy.

#4331

Comprehensive analysis of copy number variation and sensitivity to targeted therapy in renal cell carcinoma using in-house cancer gene panel testing

Akhito Takeuchi[1], Mayu Takeda[2], Eiji Sugihara[3], Yoshinari Muto[1], Sachio Nohara[4], Shigeki Tanishima[4], Kenji Zennami[5], Kiyoshi Takahara[5], Tetsuya Tsukamoto[6], Ryoichi Shiroki[5], Hideyuki Saya[7], Makoto Sumitomo[1]. *[1]Fujita Cancer Center and Department of Urology School of Medicine, Fujita Health University, Toyoake, Japan,[2]Fujita Cancer Center and Department of Medical Research for Intractable Disease, Fujita Health University, Toyoake, Japan,[3]Fujita Cancer Center and Research Promotion Headquarters, Open Facility Center, Fujita Health University, Toyoake, Japan,[4]Department of Bio Informatics, Communication Engineering Center, Electronic System Business Group, Mitsubishi Electric Software Corp., Tokyo, Japan,[5]Department of Urology School of Medicine, Fujita Health University, Toyoake, Japan,[6]Department of Pathology School of Medicine, Fujita Health University, Toyoake, Japan,[7]Fujita Cancer Center, Fujita Health University, Toyoake, Japan*

Purpose: Immune checkpoint inhibitors (ICIs) and tyrosine kinase inhibitors (TKIs) are the main drugs used to treat metastatic renal cell carcinoma (mRCC), but there are no effective biomarkers to determine their use. In this study, we aimed to identify factors that correlate with staging of RCC and drug sensitivity to mRCC based on the results of an in-house cancer gene panel test at Fujita Health University.
Methods: 133 patients with RCC (70 non-metastatic RCC and 63 mRCC). DNA was analyzed for mutations in 143 cancer genes using the PleSSision Rapid cancer gene panel test. NextSeq2000 was used as the next-generation sequencer. From the curated reports obtained, factors including each gene mutation information and the correlation between copy number (CN) variation (CNV) cluster analysis information, clinicopathological information, and therapeutic response to ICI or TKI was examined. In this study, the therapeutic response was evaluated with RECIST1.1 and complete response and partial response were determined as objective response (OR). The endpoint was progression-free survival 2 (PFS2) defined as the interval between first-line treatment and the second relapse.
Result: Mutational analysis showed no difference in the pattern of genetic variation with or without metastasis. CNV analyses showed a marked trend toward a decrease in CN on homologous recombination repair genes in a part of mRCCs. Cluster analysis of CNV information for each gene

in response to TKI treatment in mRCC revealed multiple regions of decreased or increased CN. The main regions of increased CN were shown to be those formed by CN gain of oncogenes on chromosomes 7 and 12. Detailed analysis of this hot spot showed that when the cutoff value of sum of CN for *KRAS*, *ERBB3*, *CDK4*, and *MDM2.* for chromosome 12 set to 9, 8 (72.7%) of 11 patients with CN 9 or higher were in OR group, while 4 (7.7%) of 52 patients with CN less than 9 were in OR group, showing a significant difference between the two groups ($P < 0.001$). Similarly, when the cutoff value of sum of CN for *EGFR*, *MET*, and *BRAF* for chromosome 7 set to 8, 5 (83.3%) of 6 patients with CN 8 or higher were in OR group, while 7 (12.3%) of 57 patients with CN < 8 were in OR group, showing a significant difference between the two groups ($P < 0.001$). On the other hand, genetic markers predicting susceptibility to ICI could not be identified. Kaplan-Meier analysis showed that the group of patients with higher CN values for either chromosome 7 or 12 had better PFS2 after TKI treatment than the group of patients with lower CN values for either chromosome 7 or 12 ($P < 0.001$).
Conclusion: Our results from in-house cancer gene panel tests successfully showed an association between RCC progression and cancer-related gene alterations. Furthermore, the results showed the possibility of predicting TKI treatment sensitivity in mRCC by focusing on CN gain of oncogenes in specific chromosomal regions.

#4332

Characterizing cancer-associated fibroblasts in prostate cancer using Vizgen's MERSCOPE™ Platform

Ben Patterson, Cheng-Yi Chen, Nicolas Fernandez, Simran Kaushal, Leiam Colbert, Jiang He.
Vizgen, Cambridge, MA

Understanding the spatial complexities within cancer provides crucial information for evaluating individual tumor development and progression; recent research in prostate cancer has shown how critical it is for oncologists to maintain a spatial context while characterizing a highly heterogeneous tumor microenvironment. As more and more research groups acknowledge the need for spatial biology solutions to solve difficult questions surrounding cell identity, heterogeneity, and interaction, Vizgen's MERSCOPE™ Platform provides a powerful tool to illuminate spatial information. Built on Multiplexed Error-Robust Fluorescence in situ Hybridization (MERFISH) technology, Vizgen's MERSCOPE™ enables the direct profiling of the spatial organization of intact tissue with subcellular resolution. Here, we use a 500-gene panel to demonstrate the MERSCOPE's spatial capability, assessing the canonical signaling pathways of cancer, cancer type-specific genes, select immune genes, proto-oncogenes, and tumor-suppressor genes in patient-derived prostate cancer samples. Using the Vizgen Cell Boundary Stain kit, we were able to generate a molecular and cellular atlas of these individual patient tumors by clustering cells based on gene expression and mapping these clusters back onto a spatial representation of the tumor. We found specific clusters relating to prognostic outcomes in cancer-associated fibroblasts (CAFs) and myofibroblasts. Subsequently, we used single-cell RNA-seq datasets to impute related transcriptome data for these various fibroblast clusters to help characterize them more specifically. To understand the heterogeneity intrinsic to CAFs, we performed a neighborhood analysis to determine how proximity to immune cells, tumor cells, and other stromal cells altered gene expression in different CAF clusters. We found gene expression changes associated with inflammation and reactive stromal signaling in CAFs based on their proximity to tumor versus stromal tissue compartments. We also compared the gene expression of tumor cells near CAFs to those more deeply embedded within the tumor compartment. This revealed interesting transcriptional covariations between superficial layers of tumor and their surrounding stromal milieu involved in cell proliferation and signaling. These analyses demonstrate the transcriptional variation possible across fibroblastic stromal cells acting in

tumor-adjacent or stromal contexts. Notably, we were able to map and catalogue different patterns of gene expression relating to inflammation, tumor proliferation, and reactive stromal signaling. These findings demonstrate how the MERSCOPE platform can provide deep insights into the complex heterogeneity observed in the tumor microenvironment.

#4333

Spatial analysis of tumor-infiltrating lymphocytes in tumor microenvironment as biomarker for immune checkpoint inhibition in biliary tract cancer

Yeong Hak Bang[1], Kyunghye Bang[2], Jin Ho Shin[3], Hyunseok Yoon[4], Kyu-Pyo Kim[1], Inkeun Park[1], Jae Ho Jeong[1], Heung-Moon Chang[1], Baek-Yeol Ryoo[1], Chiyoon Oum[5], Seulki Kim[5], Yoojoo Lim[5], Gahee Park[5], Chan-Young Ock[5], Changhoon Yoo[1]. *[1]Department of Oncology, Asan Medical Center, University of Ulsan College of Medicine, Seoul, Korea, Republic of,[2]Division of Hemato-Oncology, Department of Internal Medicine, Chung-Ang University Gwangmyeong Hospital, Gwangmyeong, Korea, Republic of,[3]Department of Pathology, Asan Medical Center, University of Ulsan College of Medicine, Seoul, Korea, Republic of,[4]Department of Internal Medicine, Asan Medical Center, University of Ulsan College of Medicine, Seoul, Korea, Republic of,[5]Lunit, Seoul, Korea, Republic of*

Background: Recently, anti-PD-L1 in combination with cytotoxic chemotherapy has shown significant survival benefit in a randomized phase 3 trial for unresectable or metastatic biliary tract cancer (BTC). However, no biomarker including PD-L1 expression has been established to predict clinical outcomes, and there is an unmet need for a novel predictive biomarker for anti-PD-1 or PD-L1 therapy. Here, we assessed TILs using artificial intelligence (AI)-powered spatial analysis in advanced BTC treated with anti-PD-1 beyond 1st line treatment.
Methods: An AI-powered whole-slide image (WSI) analyzer (Lunit SCOPE IO, Lunit, Seoul, Korea) was used to segment tumor epithelium and stroma, and identification of intratumor TIL (iTIL) and stromal TIL (sTIL). H&E stained WSI from pre-treatment samples was acquired from Asan Medical Center (n =166), and a total of 154 samples (92.8%) after quality control were used for the final analysis. Immune phenotypes (IP) were defined as follow: inflamed as high iTIL and sTIL; immune-excluded as low iTIL and high sTIL; immune-desert as low TIL overall. Among them, 20 patients were available for multi-color flow cytometry analysis (FACS) using peripheral blood mononuclear cells, collected at baseline, C1D8, and C2D1.
Results: All patients (n=154) were treated with anti-PD-1 (pembrolizumab or nivolumab) monotherapy, and 72 of 154 patients (46.8%) were treated as 2nd line. Gemcitabine plus cisplatin (GemCis) was used prior to anti-PD-1 as first-line therapy in all patients. Overall, 15 (9.7%) patients showed inflamed IP. With median follow-up duration of 15.4 months, the inflamed IP group showed better overall survival (17.2 vs. 6.6 months, P=0.03), and progression-free survival (PFS; 4.5 vs. 2.6 months, P=0.09) along with higher PFS rate at 12 months (33.3% vs. 11.5%, P=0.035), and overall response rate (26. 7% vs. 8.6%, P=0.053) than other phenotype groups. There was no significant difference in median PFS with GemCis among IP groups (P=0.74). In the FACS available subgroup, inflamed IP showed higher baseline central memory T (Tcm)+effector memory T (Tem)/Tnaive ratio than other IPs. With the administration of anti-PD-1, Tcm+Tem/Tnaive ratio was increased, while the proportion of PD1+CD8+T, CD39+CD8+T, CD103+CD8+T and Treg were decreased in the inflamed IP group than other phenotype groups.
Conclusions: Immune phenotypes classified by AI-powered spatial TIL analysis was effective to predict the clinical outcomes of patients with advanced BTC treated with anti-PD-1 therapy.

#4334

Clever-1/PD-L1 ratio predicts response to Bexmarilimab, a novel macrophage-guided immunotherapy, in immune deprived cancers

Mari L. Björkman[1], Elisa M. Vuorinen[1], Juho Jalkanen[1], Marie-Louise Fjällskog[1], Jussi Koivunen[1], Teppo Huttunen[2], Maija Hollmén[3], Petri Bono[4]. *[1]Faron Pharmaceuticals, Turku, Finland,[2]Estimates, Turku, Finland,[3]MediCity Research Laboratory and InFLAMES Flagship, University of Turku, Turku, Finland,[4]Terveystalo, Helsinki, Finland*

Introduction**:** Clever-1 is an immunosuppressive scavenger receptor expressed on tumor associated macrophages. High levels of Clever-1 are associated with poor survival, T-cell exclusion and dysfunction, and immunotherapy resistance. Bexmarilimab (FP-1305) is a novel humanized anti-Clever-1 IgG4-antibody capable of promoting an immune switch, potentially leading to intratumoral proinflammatory responses in patients. In a first-in-human all-comer single agent Phase I/II study in advanced solid tumors (NCT03733990) approximately 30% of patients in hepatocellular carcinoma, cutaneous melanoma and cholangiocarcinoma achieved immune activation, characterized by an IFNg response, which led to a survival benefit (ASCO 2022). Here, we show that patients getting a therapy benefit have immunologically cold tumors with low PD-L1 staining and high Clever-1 staining.

Methods: Pre-treatment tumor samples were immunohistochemically stained for Clever-1 (4G9, Santa Cruz) using Ventana platform and scored by % of intratumoral positive cells out of all viable cells and PD-L1 (22C3, Agilent) with combined positivity scoring (CPS). Ratio (PD-L1/Clever-1) at baseline was compared using non-parametric Wilcoxon-test according to clinical benefit.

Results: 23 successful baseline biopsies and stainings were obtained, 6 per cutaneous melanoma, 11 per cholangiocarcinoma and 1 per hepatocellular carcinoma, from patients treated with bexmarilimab. Patients had received an average of three previous lines of therapy. At baseline, patients that saw a clinical benefit (CBR) from bexmarilimab had average PD-L1/Clever-1 ratio of 0.2 compared to 4.4 ($p=0.042$, Wilcoxon nonparametric test) in patients that did not respond to the treatment.

Conclusion: PD-L1/Clever-1 IHC staining ratio may be used to predict bexmarilimab responding patients. These patients have a low PD-L1 staining and low IFNg levels as reported previously, and are often refractory to checkpoint inhibitors and other T cell activating agents. Bexmarilimab provides a novel therapy option for a tumor group that is otherwise poorly responsive to immune therapies.

#4335

Repurposing metformin in early-stage high risk prostate cancer to avoid ADT-induced cardiovascular toxicity

Philip Gregory[1], Beatriz Mateo-Victoriano[2], Ling Zhang[1], Cassie Due[3], Marijo Bilusic[4], Priyamvada Rai[5]. *[1]Radiation Oncology, University of Miami, Miami, FL,[2]Radiation Oncology, Sheila and David Fuente Graduate Program in Cancer Biology, University of Miami, Miami, FL,[3]College of Arts and Sciences, University of Miami, Miami, FL,[4]Department of Medical Oncology/Department of Medicine, University of Miami, Miami, FL,[5]Radiation Oncology, Sylvester Comprehensive Cancer Center, University of Miami, Miami, FL*

Prostate cancer is the second most common cause of cancer-related deaths in American men. About 20-40% of patients with localized castration-sensitive prostate cancer (CSPC) eventually progress, requiring androgen deprivation therapy (ADT). However ADT inevitably fails, giving rise to castration-resistant prostate cancer (CRPC), which is incurable and fatal. A significant fraction of patients undergoing ADT die of treatment-accelerated cardiovascular disease. Pre-existing metabolic

dysfunction has been implicated in PC disease incidence, higher rates of prostatectomy failure, and accelerated progression to CRPC. Thus, there is an unmet need to counter the adverse sequelae of ADT through alternative CSPC treatments that do not exacerbate metabolic syndrome but prevent PC progression. Few studies have evaluated whether targeting the metabolic dysfunction associated with early-stage PC can prevent progression and thus the need for ADT. In a recent clinical trial spearheaded by Dr. Bilusic, metformin, an affordable and well-tolerated insulin-sensitizing diabetes drug, has recently shown promise as monotherapy in biologically-recurrent CSPC, preventing PSA rise in about 40% of high-risk patients. To identify the molecular mechanisms and biomarkers of positive response to metformin in PC patients, we performed preliminary cytokine profiling of responder vs non-responder patient sera. We found that mitigation of inflammatory factors implicated in cardiovascular disease as well as markers of pro-apoptotic response are associated with positive metformin response. We also found that metformin responders exhibited pre-treatment cytokine signatures associated with inflammatory metabolic diseases, including diabetes and hyperinsulinemia, which are conditions known to benefit from metformin treatment. We have been able to model the variability of metformin treatment response in two well-characterized CSPC cell lines, LNCaP (highly responsive) and LAPC4 (minimally responsive). Metformin induced cell death in LNCaP but not in LAPC4, which possesses mutant p53 and high Bcl-2 levels. LAPC4 instead showed markers of senescence, which is associated with an inflammatory phenotype. Metformin also elevated levels of damaging high-potency (short-lived) ROS in LNCaP to a greater extent than in LAPC4. LAPC4 instead exhibited elevated levels of hydrogen peroxide upon metformin treatment, a ROS associated with inflammation. Thus the cell models show congruence with factors of positive response seen in patients. Our findings shed light on the potential mechanism of positive response to metformin in CSPC patients, and lay the groundwork for further investigation, while insight into biomarkers predicting positive response could be immediately useful in the clinic.

#4336

Automation of proximity ligation immunoassay for interaction between PDL1 and PD1 detection in the tumor microenvironment using microfluidic based system

Hampus Elofsson[1], Agata Zieba Wicher[1], Carolina Oses Sepulveda[2], Tony Ullman[2], Maria-Giuseppina Procopio[3], Alix Faillétaz[3], Diego G. Dupouy[3], Charlotte Stadler[2]. *[1]R&D, Navinci Diagnostics AB, Uppsala, Sweden,[2]SciLife Lab, Royal Institute of Technology (KTH), Stockholm, Sweden,[3]R&D, Lunaphore Technologies S.A., Tolochenaz, Switzerland*

The PD-1/PD-L1 signaling pathway is essential for immune control and maintaining immune system balance. PD-1 and PD-L1 proteins exert most functions in cells and tissues by undergoing modifications and forming dynamic complexes – effects that cannot be explored by genomics, transcriptomics, or conventional immunostaining methods. Numerous cancer therapies are being developed that affect PD-1/PD-L1 signaling, and tools to study the PD-1/PD-L1 axis are, therefore, essential. One prerequisite for successfully establishing diagnostic assays is reproducibility, standardization, and, ideally, high sample throughput via automation. Here, we aimed to introduce a new technological solution to allow for the simultaneous detection of PD-L1 and PD-1 interaction and the adjacent immune cell context in tissue samples on the Lunaphore's automated microfluidic staining platform. The assay for detecting PD-1-PD-L1 interaction was developed and technically validated by Navinci Diagnostics. Although the detection of interaction alone provided important information on the immune status in the tumor microenvironment, we believed that PD-1/PD-L1 readout would be most powerful in the context of its cellular ecosystem. Therefore, the PD-1/PD-L1 assay was combined with the analysis of immune and cancer cells to determine their involvement in this signaling. The feasibility of combining multiplex immunofluorescence with proximity ligation assay was conducted and confirmed on human tonsils. The spatial profiling panel included immune

markers for all T-cells (CD3), helper T-cell (CD4), cytotoxic T-cells (CD8), B-cells (CD19/20) and activation/exhaustion markers granzyme B (activated cytotoxic T-cell), Ki67 (proliferating cells), and LAG3 (malignant B cells, CD8 T cells, CD4 T_{regs}). We evaluated, implemented, and optimized the assays on the Lunaphore staining instrument to reduce labor time and cost for the end users. In the next phase, the potential of our assay to be benchmarked as a diagnostic tool in clinical praxis will be thoroughly tested and validated on diagnostic tissue samples from NSCLC patient cohorts. We believe this approach will enable spatial and functional studies of the interface between the tumor and the immune system and provide necessary information about signaling pathway activation in situ, the latest representing a novel state-of-the-art in tissue diagnostics.

#4337

Predicting PD-L1 status in solid tumors using transcriptomic data and artificial intelligence algorithms

Ahmad Charifa[1], Alfonso Lam[1], Hong Zhang[1], Andrew Ip[2], Andrew Pecora[2], Stanley Waintraub[2], Deena Graham[2], Donna McNamara[2], Martin Gutierrez[2], Andrew Jennis[2], Ipsa Sharma[1], Jeffrey Estella[1], Wanlong Ma[1], Andre Goy[2], Maher Albitar[1]. *[1]Genomic Testing Cooperative, Irvine, CA,[2]John Theurer Cancer Center at Hackensack University Medical Center, Hackensack, NJ*

PD-L1 immunohistochemistry (IHC) is routinely used to predict the clinical response to immune checkpoint inhibitors (ICIs); however, multiple assays and antibodies have been used. This study aimed to evaluate the potential of targeted transcriptome and artificial intelligence (AI) to determine PD-L1 RNA expression levels and predict the ICI response compared to traditional IHC. RNA from 396 solid tumors samples was sequenced using next-generation sequencing (NGS) with a targeted 1408-gene panel. RNA expression and PD-L1 IHC were assessed across a broad range of PD-L1 expression levels. The geometric mean naïve Bayesian (GMNB) classifier was used to predict the PD-L1 status. PD-L1 RNA levels assessed by NGS demonstrated robust linearity across high and low expression ranges, and those assessed using NGS and IHC (Tumor cells (TC), Tumor Proportion Score (TPS) and tumor-infiltrating immune cells (ICs) were highly correlated (Tables 1). RNA sequencing provided in-depth information on the tumor microenvironment and immune response, including CD19, CD22, CD8A, CTLA4, and PD-L2 expression status. Sub-analyses showed a sustained correlation of mRNA expression with IHC (TPS and ICs) across different solid tumor types. Machine learning showed high accuracy in predicting PD-L1 status, with the area under the curve varying between 0.988 and 0.920. Targeted transcriptome sequencing combined with AI is highly useful for predicting PD-L1 status. Measuring PD-L1 mRNA expression by NGS is comparable to measuring PD-L1 expression by IHC for predicting ICI response. RNA expression has the added advantages of being amenable to standardization and avoidance of interpretation bias, along with an in-depth evaluation of the tumor microenvironment.

Correlation between PD-L1 expression levels and PD-L1 IHC results

IHC test results	Variable	Cases (N)	Mean	Median	Range	Lower Quartile	Upper Quartile	10th Percentile	90th Percentile	Std. Dev.
TC<1%	CD274	223.00	4.49	2.97	0.00 - 25.99	1.79	5.73	1.07	9.16	4.32
TC>1%	CD274	90.00	14.87	10.11	0.62 - 77.53	4.60	18.62	2.95	32.35	15.75
TC<10%	CD274	267.00	5.17	3.36	0.00 - 72.72	1.94	6.43	1.14	10.71	6.14
TC>10%	CD274	46.00	20.81	14.03	2.90 - 77.53	8.67	26.32	4.21	51.02	17.33

IC<1%	CD274	133.00	3.95	2.66	0.00 - 25.99	1.71	4.03	0.99	7.95	4.56
IC>1%	CD274	129.00	9.38	5.43	0.29 - 77.53	3.21	10.31	1.74	19.05	12.13
IC<10%	CD274	226.00	5.69	3.03	0.00 - 72.72	1.92	6.09	1.15	12.25	8.24
IC>10%	CD274	36.00	12.50	8.52	0.29 - 77.53	4.72	13.80	4.18	31.83	13.95
TPS<1%	CD274	143.00	3.36	2.35	0.00 - 25.99	1.41	3.58	0.53	7.40	3.87
TPS>1%	CD274	207.00	10.19	5.63	0.29 - 133.81	3.03	11.65	1.74	22.25	14.74
TPS<10%	CD274	252.00	4.25	2.87	0.00 - 72.72	1.74	4.96	0.92	8.70	5.81
TPS>10%	CD274	98.00	15.50	9.67	0.29 - 133.81	4.91	18.74	2.90	31.87	18.57
TPS<30%	CD274	319.00	5.35	3.32	0.00 - 72.72	1.94	6.43	1.06	12.00	6.48
TPS>30%	CD274	31.00	28.50	18.62	2.90 - 133.81	11.47	35.94	6.67	52.69	27.31

#4339

Development of new droplet digital PCR method for MSI assessment with automated analysis pipeline shows concordance in FFPE and plasma

Sarah Kreston, Mai Ho, Claire Gould, Ubaradka Sathyanarayana, Brittany D'Alessio, Janice Riley, Gary A. Pestano. *Biodesix, Inc., Boulder, CO*

Introduct**ion**: Microsatellite instability (MSI) arises when short tandem DNA repeat sequences undergo a length change due to impaired mismatch repair (MMR). MSI is present in many cancers and is an approved biomarker for immune checkpoint inhibitor therapy. In this study, we used 71 clinical specimens to evaluate a new droplet digital (ddPCR) method to assess MSI in tissue and in plasma. The ddPCR assay is designed to detect mutations in BAT25, BAT26, NR21, NR24 and Mono27, and is intended for use in FFPE. Our evaluation extended these analyses to cfDNA in plasma.

Methods: DNA was extracted from ten (10) CRC FFPE samples, fifty-two (52) CRC liquid biopsies, and ten (10) Normal Healthy Donors (NHD) and tested using the new assay. DNA extracts were quantified by fluorescence, and duplicate ddPCR reactions were performed using 2.6 ng input DNA per well. MSI status was determined with a pre-commercial release auto-calling analysis software, which makes a positive call (MSI-High) when two or more of the five MSI markers ($\geq$ 40%) are detected. Markers are called positive if the fractional abundance or copy number is greater than the previously established limit of blank (LOB) in FFPE and plasma, respectively. For FFPE, the LOBs (%) are 2.11 (BAT25), 0.34 (BAT26), 2.38 (NR21), 1.51 (NR24) and 0.56 (Mono27) based on analytic specimen evaluation. For plasma, a marker is positive if one (1) mutant copy is detected.

Results: All 10 FFPE samples were deemed to be concordant with the reference Promega PCR assay at the microsatellite evaluation level. Additionally, the 8 cfDNA samples with reference MSI status yielded 87.5% (7/8) concordant results for microsatellite loci status. A survey of 44 plasma

colorectal donor samples and 10 NHD samples with no reference results, yielded various microsatellite status as expected. The auto calling module for microsatellite loci status in these plasma samples accurately called 85.2 status (n = 54). At the marker level, 87% of BAT25, 98.1% of BAT26, 92.6% of NR21, 79.6% of NR24, and 61.1% of Mono27 calls were concordant between auto-calling and expert review.
Conclusion: The new droplet digital MSI assay coupled with an automated calling module for MSI Status provides a convenient, cost-effective, and reproducible laboratory test method to determine MSI status in FFPE specimens. The utility of the test method and auto calling method for detection of MSI in cfDNA is less clear, with heterogenous clusters that require expert review appearing more often than in FFPE samples.

#4340

HLA-B44 motif neoepitope is associated with a favorable tumor immune microenvironment and predicts ICB response in NSCLC

Rui Li[1], Charlene M. Fares[2], Tristan R. Grogan[3], Tianhao Zhang[4], Debory Li[5], Matthew Theisen[6], Maria A. Velez[7], Paige M. Brodrick[7], Jackson P. Lind-Lebuffe[7], Yazeed Radwan[7], Gregory A. Ayzenberg[7], David Elashoff[3], Bin Liu[8], Aaron E. Lisberg[7], Amy L. Cumming[7], Edward B. Garon[7].
[1]Internal Medicine, UCLA David Geffen School of Medicine, Los Angeles, CA,[2]Allina Health Cancer Institute, Saint Paul, MN,[3]General Internal Medicine and Health Services Research, UCLA David Geffen School of Medicine, Los Angeles, CA,[4]Molecular Biology, UCLA David Geffen School of Medicine, Los Angeles, CA,[5]Medicine, Western University of Health Sciences, Los Angeles, CA,[6]Kensho Technologies, Los Angeles, CA,[7]Hematology/Oncology, UCLA David Geffen School of Medicine, Los Angeles, CA,[8]Pulmonary and Critical Care, UCLA David Geffen School of Medicine, Los Angeles, CA

Immune check point blockade (ICB) has recently transformed the treatment of non-small cell lung (NSCLC). However, the majority of patients do not respond to ICB. For ICB to be effective, tumor neoantigens need to be presented in a human leukocyte antigen (HLA) class I-restricted manner. Recent studies by our group and others have shown that HLA-B44 supertype is associated with extended survival in patients treated with ICB. Herein, we hypothesize that HLA-B44-specific motif neoepitopes generate an active tumor immune microenvironment and a favorable ICB response in NSCLC. Utilizing the TCGA database, we found that nearly half of the NSCLC patients have at least one HLA-B44 allele, of whom 36.8% and 37.3% of patients harbor at least one B44 motif neoepitope in lung adenocarcinoma (LUAD) and lung squamous carcinoma (LUSC), respectively. In a pooled analysis of patients with LUAD and LUSC, gene expression of *PD-L1*, *CTLA-4*, *LAG-3*, *CXCL9*, *CXCL10*, *CXCL13*, *CD8A* and cytolytic gene signature (includes *GZMA* and *PRF1*) is elevated in patients with B44 motif neoepitopes compared to those without motif neoepitopes. Immune cell component analysis showed increased infiltration of Th1, Th2 and CD8 T cells in LUAD and regulatory and CD8 T cells in LUSC. Although a linear regression model revealed a positive correlation between tumor mutational burden (TMB) and number of B44 motif neoepitopes, pooled analysis of LUAD and LUSC with similar TMB showed significant elevation of *CTLA-4*, *LAG3*, *CXCL10* and a trend of increased expression of *CXCL9* in motif patients. Upon investigation of possible immune editing, we found a significantly higher proportion of genes containing B44 neoepitope downregulated at the RNA level both in LUAD and LUSC. Lastly, we showed that combining B44 motif with either PD-L1 or TMB improved prediction of progression-free survival in NSCLC patients treated with ICB. In summary, we demonstrate that HLA-B44 motif neoepitopes are associated with a favorable tumor immune microenvironment and can serve as a potential biomarker for ICB benefit in NSCLC patients.

#4341

Indoleamine 2,3-dioxygenase 1 is highly expressed in tertiary lymphoid structures and associated with improved outcome in patients with advanced non-small cell lung cancer treated with anti-PD1/PDL1 inhibitors

Jean-Philippe Guegan[1], Florent Peyraud[2], Christophe Rey[1], Oren Ngouala[1], Ophélie Odin[1], Imane Nafia[1], Isabelle Soubeyran[2], Sylvestre Le Moulec[3], Alban Bessede[1], Antoine Italiano[2]. *[1]Explicyte, Bordeaux, France,[2]Institute Bergonié, Bordeaux cedex, France,[3]Clinique Marzet, Pau, France*

Background**:** Immune checkpoint inhibitors (ICI) has revolutionized the management of patients with non-small cell lung cancer (NSCLC). However, most patients with advanced NSCLC patients displayed primary resistance to ICI. Indoleamine 2,3-dioxygenase 1 (IDO1) may play a role in primary resistance by catabolizing tryptophan to several immunosuppressive metabolites such as kynurenine. The aim of our study was to investigate the role of IDO1 expression in the outcome of NSCLC patients treated with immunotherapy.

Methods: We analyzed the largest NSCLC gene expression (GE) dataset worldwide including 891 pre-treatment tumors from POPLAR and OAK studies, two RCT assessing the efficacy of atezolizumab vs docetaxel in NSCLC. We then confirm our findings with multiplex immunofluorescence (mIF) and digital pathology analysis to investigate the correlation between expression of IDO1 by tumor cells and spatial distribution of CD8+ T cells.

Results: The PFS of $IDO1^{high}$ patients was significantly higher than $IDO1^{low}$ (3.81 vs 1.89months, p=7.13e-09). Strikingly, high IDO1 expression was also associated with better ORR (19.9% vs 5.2%, p=9.93e-05) and improved OS (15.9 vs 9.65 months, p=6.35e-06). When adjusting for covariates (histological subtype, TLS signature, PD-L1 expression), IDO1 remained independently associated with PFS (HR 1.54, p=4.1e-4) and OS (HR 1.43, p=8.2e-3). None of these correlations were observed in the docetaxel arm, suggesting a predictive value of IDO1 GE specifically for response to atezolizumab. Using a deconvolution approach, the tumor microenvironment composition differed significantly between $IDO1^{high}$ and $IDO1^{low}$ tumors. Indeed, $IDO1^{high}$ tumors were characterized by the highest expression of genes specific to immune populations such as interferon-gamma-producing T helper 1 (Th1) cells, CD8+ T cells, natural killer cells, cytotoxic lymphocytes, and B cells. To further validate our findings, we performed mIF on 53 NSCLC tumors. Overall, elevated IDO1 expression by tumor cells was correlated with increased CD8+/PD1+ T cells infiltration (p=0.001). Spatial cell distribution analysis also revealed that the relative distance between tumor cells and CD8+ T cells was significantly lower in $IDO1^{high}$ compared to $IDO1^{low}$ patients. Interestingly, 52% of tumors were characterized by the presence of TLS and IDO1 was observed in most TLS analyzed.

Conclusions: IDO1 expression by tumor cells in NSCLC is associated with improved outcome in patients with NSCLC, independently of PDL1 expression score. IDO1 overexpression in NSCLC is associated with increased immune activity and may represent a negative feedback mechanism to CD8+ T cell infiltration.

#4342

Predictive precision medicine platform accurately predicts individual patient response to AML treatments to maximize outcomes

Meagan A. Jacoby[1], John S. Welch[2], Peter Westervelt[1], Matthew Christopher[1], Geoffrey L. Uy[1], Ravi Vij[1], Keith E. Stockerl-Goldstein[1], Brad S. Kahl[1], Iskra Pusic[1], John F. DiPersio[3], Mark A. Schroeder[1], Miriam Y. Kim[1], Todd A. Fehniger[1], Armin Ghobadi[1], Christine J. Gu[4], Wade Anderson[4], Kathryn Vanderlaag[4], Kamran Ali[4], Camille Pataki[4], Markus D. Lacher[4]. *[1]Department of Medicine, Washington University, Saint Louis, MO,[2]Washington University, Saint Louis,*

MO,[3]Department of Internal Medicine, Washington University, Saint Louis, MO,[4]Notable Labs, Foster City, CA

Introduction: Offering the optimal frontline treatment to a patient with acute myeloid leukemia (AML) requires trading off expected benefit and risk. Typical standard of care intensive induction chemotherapy (e.g., cytarabine plus idarubicin (7+3)) results in high clinical response rates. However, many patients receive a less intensive regimen (e.g., venetoclax plus decitabine (VenDec)) because their individual toxicity risk is high based on lack of medical fitness. Predicting an individual patient's clinical response prior to treatment has the potential to increase the benefit/risk ratio (therapeutic index) for some patients and optimize their treatment selection. Here, we demonstrate the ability of an automated high-throughput, multi-color flow cytometry predictive precision medicine platform (PPMP) to predict response to 7+3 or VenDec.
Methods: To assess correlation between PPMP-predicted and actual clinical response to 7+3 or VenDec in clinical trial NCT04263181, pre-induction blood samples were collected from 31 patients of which 18 received 7+3 (all newly diagnosed (ND) AML) and 13 VenDec (7 ND AML, 5 secondary AML, 1 MDS). We measured drug effects on leukemic blasts by applying a cutoff at the total blast count that optimizes separation between predicted responders and non-responders ("conventional approach") or by a machine learning (ML) approach considering multiple cell populations. For the former approach, training sets represented 13 patients for 7+3 and 8 for VenDec. Both 7+3 and VenDec models were validated with 5 patients. For the ML approach, the model was trained on all 13 VenDec patients and monitored using leave-one-out cross-validation.
Results: For the conventional approach, predicted and true clinical responses were highly correlated for 7+3 (AUC = 0.91) and VenDec (AUC = 0.81), with 100% precision (positive predictive values (PPV)) for both, i.e., all predicted responders were true clinical responders. Some true clinical responders were not identified (negative predictive value (NPV) = 67% for 7+3 and 57% for VenDec), resulting in an accuracy of 94% (7+3) and 77% (VenDec). To maximize NPV and accuracy for predicting VenDec clinical outcomes, we applied a novel ML-based algorithm to integrate the behavior of malignant and non-malignant cell populations, yielding a model with 100% accuracy (100% PPV and NPV). Additional outcome data, including overall survival, are under evaluation.
Summary: Total blast-based predictions yielded accuracies of 94% for 7+3 and 77% for VenDec. An ML algorithm for VenDec considering additional cell populations increased the accuracy to 100%. Further studies will expand patient numbers. We plan to use this platform to inform our frontline decision making with the goal to maximize the therapeutic benefit/risk ratio and ensure that the most appropriate frontline therapy is used for each individual patient.

#4343

Development of an *APC* and *TP53*-based duplex sequencing assay to positively predict colorectal cancer response to EGFR inhibitors

Mingli Yang[1], Michael J. Schell[2], Lance Pflieger[3], Jesse Salk[4], Timothy J. Yeatman[1]. *[1]Department of Surgery, University of South Florida, Tampa, FL,[2]Moffitt Cancer Center and Research Institute, Tampa, FL,[3]Phenome Health, Seattle, WA,[4]TwinStrand Biosciences, Seattle, WA*

Two well-characterized EGFR inhibitor (EGFRi) therapies (cetuximab, panitumumab) have been FDA approved for metastatic colorectal cancer (CRC). Unfortunately, the extended RAS/RAF testing required in the drug labels, identifies only non-responders, and only ~50% of treated patients will respond to therapy. Thus, there is an unmet need to develop additional biomarkers to identify EGFRi sensitive patients. Using an innovative hybrid approach fusing gene expression and DNA sequencing, we recently reported that combined mutations in *APC* and *TP53* were strongly correlated with a validated gene expression signature measuring cetuximab sensitivity in CRC

human tumors (Yang et al. *Cancer Epidemiol Biomarkers Prev.* 2019), suggesting a potential positive biomarker role of *APC* + *TP53* mutations. This finding prompted us to develop a DNA test designed to positively select EGFRi-responsive patients as augmentation to currently used negative predictors for CRC patients. By leveraging the TwinStrand Duplex Sequencing (DS) technology, we recently developed an ultrasensitive custom 6-gene panel (*APC, TP53, KRAS, BRAF, NRAS*, and *HRAS*) CLIA-certified assay for FFPE CRC tissues. The assay has been analytically validated using reference cell lines (n=10) which were individually sequenced to >3,000x Duplex depth. The 6-gene DS assay yielded exceptionally high assay performance: (1) accuracy (passed, $r^2 = 0.98$ for Duplex VAF vs. target VAF for Positive Control mutations); (2) sensitivity (passed, all mutations >1/5,000 were detected in all Positive Control replicates; 1 mutation at 1/5,000 was detected in 2/3 replicates), (3) specificity (passed, 2 mutations detected in the Negative Control at 1 count in 1 replicate; VAF <1/10,000), and (4) precision (passed, <2-fold variation among Positive Control replicates for VAF >1/500). Importantly, the validation analysis on fresh frozen (FF):FFPE paired tissues from 21 CRC patients shows: (1) The 6-gene DS assay performed on FFPE samples faithfully reproduces assay results on FF samples; (2) The ultrasensitive DS assay can accurately detect additional "new" mutations at low allelic frequencies compared to a standard NGS method. TwinStrand DS identified 17 mutations not identified by standard NGS; 13 of these new mutations had < 10% VAF. Furthermore, preliminary Kaplan-Meier analysis of the third-line EGFRi data shows that while the statistical significance was not achieved due to the small simple size (n=28), patients harboring combined *APC* and *TP53* mutations(AP) (vs non-AP patients) tended to have longer progression free survival (6.65 vs 3.95 months, P=0.064) and overall survival (17.80 vs 10.65 months, P=0.14). Additional data acquisition and analysis is ongoing. Thus, there is an opportunity to change clinical practice and standards of care to ultimately improve CRC outcomes if this new, robust, sensitive test is clinically-validated.

#4344

Consensus genomic subtypes of gastric adenocarcinoma and their therapeutic implication

Yun Seong Jeong[1], Young-Gyu Eun[2], Sung Hwan Lee[3], Sang-Hee Kang[4], Sun Young Yim[5], Eui Hyun Kim[6], Joo Kyung Noh[2], Bo Hwa Sohn[1], Ju-Seog Lee[1]. *[1]UT MD Anderson Cancer Center, Houston, TX,[2]Kyung Hee University, Seoul, Korea, Republic of,[3]CHA Bundang Medical Center, Seongnam, Korea, Republic of,[4]Korea University Guro Hospital, Seoulg, Korea, Republic of,[5]Korea University College of Medicine, Seoul, Korea, Republic of,[6]Yonsei University College of Medicine, Seoul, Korea, Republic of*

Background**:** Gastric adenocarcinoma (GAC) is heterogeneous lethal disease in genomic and clinical level. Although the clinical relevance of genomic and molecular subtypes of GAC has been demonstrated, their translation to the clinic has been hindered by discrepancies in classification methods. We aim to examine a consensus of genomic subtypes and correlate them with clinical outcomes.

Method: We collected genomic data from 2527 GAC tumors and divided the data into discovery (n = 1427) and validation sets (n = 1100). By integrating 8 previously established genomic subtype algorithms, we identified 6 clinically and molecularly distinct genomic consensus subtypes (CGSs) in discovery set. For validation of clinical significance of new subtypes, we constructed GAC predictor of integrated consensus subtype with 120 genes (GPICS120) and applied it to validation data set. In systematic analysis of genomic and proteomic data, we estimated potential response rate of each subtype to standard and experimental treatments such as radiation therapy, target therapy, and immunotherapy and further validated their functional significance in cell line models.

Results: Among identified 6 subtypes. CGS1 is characterized by poorest prognosis, very high stem cell characteristics, and high IGF1 expression, but low genomic alterations. CGS2 showed canonical

epithelial gene expression patterns. CGS3 and CGS4 are characterized by high copy number alterations and low immune activity. However, CGS3 and CGS4 are different in high HER2 activation (CGS3) and SALL4 and KRAS activation (CSG4). CGS5 has highest mutation burden and moderately high immune activity that is characteristics of MSI-high tumors. Most of CGS6 tumors are EBV-positive and shows extremely high methylation and high immune activity. Most interestingly, CSG1 is most responsive to immunotherapy while CGS3 is significantly associated with benefit of chemoradiation therapy due to high basal level ferroptosis. In addition, we also identified potential therapeutic targets for each subtype.
Conclusion: Consensus subtype is robust classification system and can be the basis for pre-clinical investigation of subtype-based targeted interventions and future clinical trials.

#4345

Molecular pathology studies reveal PD1+ CD8 T cell density correlates with response to supraphysiological testosterone treatment in pre-treatment biopsies and MYC mRNA and protein correlate with response after treatment

Carolina Gomes Alexandre[1], Jessica Hicks[1], Tracy Jones[2], John T Isaacs[1], Kiara Bowers[1], Alyza Skist[1], Laura Sena[1], Jennifer Meyers[2], Emmanuel Antonarakis[1], David Sanin[1], Hanfei Qi[1], Samuel Denmeade[1], Mark Markowski[1], Srinivasan Yegnasubramanian[1], Angelo De Marzo[1]. *[1]Johns Hopkins University School of Medicine, Baltimore, MD,[2]Pathology, Johns Hopkins University School of Medicine, Baltimore, MD*

While most patients with metastatic prostatic adenocarcinoma respond initially, nearly all develop resistance to multiple lines of androgen deprivation therapies. This is related to overexpression of the androgen receptor (AR), which is frequently driven by AR amplification. In some patients, increased AR renders tumor cells sensitive to high dose androgens which paradoxically inhibits their growth. Bipolar Androgen Therapy (BAT) was introduced in which patients with castration resistant prostate cancer (CRPC) are treated intermittently with high dose testosterone. This produces biochemical and objective responses, and may re-sensitize prostate cancer to subsequent second generation AR inhibitors. This study utilizes samples from a recently performed clinical trial for patients with CRPC that included sequential biopsies of soft tissue metastases before BAT and after 3 cycles of BAT and before patients were treated with nivolumab.Tumor cells were present in FFPE blocks for both the pretreatment and C4D1 time points for 24 of the patients. These FFPE samples were stained using a recently validated iterative multiplex IHC assay containing 6 antibodies including: CD3 (T cells), CD4 (Helper T Cells), CD8 (Cytotoxic T Cells), PD1 (T Cell Checkpoint), FOXP3 (T-Reg cells), and Keratin 8 (epithelial cell marker). Biopsy slides were scanned after each round of staining and whole slide scans were imported into the HALO image analysis where they underwent color deconvolution, image registration and fusion. Regions of tumor were demarcated manually, and computerized automated image analysis was used to determine cell densities for 8 cell phenotypes (total CD3+, CD3+CD4+, CD3+CD8+, CD3+CD4+Foxp3+, CD3+CD4+PD1+, CD3+CD8+PD1+, CD3+CD4+PD1-, CD3+CD8+PD1-). There was a higher density of CD3+CD8+PD1+ cells in the pretreatment biopsies of men who responded (R) (to BAT) as compared with those who did not respond (NR)(p=0.015 Wilcoxon rank-sum test; mean 92.7 [R] vs 13.9 [NR]). The difference in R vs. NR was less and not significant in the CD3+CD8+PD1- population. There was a trend towards a higher density of CD3+CD4+PD1+ cells in the pretreatment samples in responders, but less so in the CD3+CD4+PD1- population. In the C4D1 biopsies, only CD3+ total cells were significantly higher in the R vs. NR (P=0.02), but the other phenotypes were not. We conclude that increased density of CD3+C8+PD1+, but not CD3+CD8+PD1- cells was present in pre-treatment biopsies in responders as compared with non-responders to BAT. These results indicate that men who are likely to respond to high dose testosterone treatment harbor tumors that are immunologically distinct prior to treatment

than those men unlikely to respond. Additional spatial analysis and comparisons with RNAseq data will be presented.

#4346

TFF1 and TFF3 predict response to CDK4/6 inhibitors in breast cancer patients

Linjie Luo[1], Yan Wang[2], Sophia Mastoraki[2], Akshara Singareeka Raghavendra[3], Juliana Navarro-Yepes[2], Nicole M. Kettner[1], Serena Kim[4], Debasish Tripathy[5], Kelly Hunt[6], Khandan Keyomarsi[1].
[1]Experimental Radiation Oncology, The University of Texas MD Anderson Cancer Center, Houston, TX,[2]The University of Texas MD Anderson Cancer Center, Houston, TX,[3]Breast Medical Oncology, The University of Texas MD Anderson Cancer Center, Houston, TX,[4]2School of Social Sciences, Rice University, Houston, TX,[5]Breast Cancer Oncology, The University of Texas MD Anderson Cancer Center, Houston, TX,[6]Breast Surgical Oncology, The University of Texas MD Anderson Cancer Center, Houston, TX

Background**:** Cyclin-dependent kinase 4/6 inhibitors (CDK4/6is) in combination with endocrine therapy (ET) have become the mainstay treatment for patients with hormone receptor (ER)-positive, HER2-negative metastatic breast cancer (BC). However, one-third of patients do not respond to the treatment (intrinsic resistance), leading to early tumor progression and treatment failure, and most patients eventually acquire resistance to therapy. The exact mechanisms of resistance to CDK4/6i are yet to be elucidated, and due to subsequent early (intrinsic) or late progression on CDK4/6i, long-term cures are not achieved.
Methods: Transcriptomic profiles of BC cell lines that were sensitive or resistant to approved CDK4/6i, independent of subtype, were downloaded from the Cancer Cell Line Encyclopedia database. Bioinformatics analysis was performed by integrated Differential Expression and Pathway (iDEP) workflow. In parallel, transcriptomic profiles of metastatic biopsies from pre-CDK4/6i-treated BC patients (n = 54) were generated using RNA-Access technology. Key common biomarkers identified from the BC cell lines and patient tumor samples were validated by immunohistochemistry in formalin-fixed paraffin-embedded (FFPE) metastatic specimens from 73 patients prior to CDK4/6i therapy.
Results: Transcriptomic profile comparisons of BC cell lines (n = 35) that were sensitive versus resistant to CDK4/6is identified Trefoil Factor 1 and 3 (TFF1 and TFF3) secretory proteins as top predictors of response. Correlation analysis showed a strong negative correlation between TFF1 and TFF3 levels to IC50 values of palbociclib and abemaciclib. Knockdown of TFF3 in CDK4/6i-sensitive BT20 cells with shRNA induced drug resistance in the cells. Transcriptomic data from 54 BC patients pre-treated with CDK4/6i showed the expression levels of TFF1 and TFF1/3 receptors (CCR4 and CCR7) were significantly increased in patients who developed late progression (> 6 months) compared to early progressors (< 3 months). In addition, IHC analysis of TFF1 and TFF3 expressions in 73 pre-treated BC patient samples showed significantly higher protein expression levels in late progressors than in early progressors.
Conclusions: Our results identified and validated the common biomarkers, TFF1 and TFF3, as predictors of CDK4/6i response efficacy in ER-positive, HER2-negative BC patients. These findings provide a predictive tool capable of selecting *de novo* metastatic BC patients who will have the greatest benefit from the combination of CDK4/6i with endocrine treatment. Furthermore, our discovery of biomarkers in early versus late progression on CDK4/6i therapy will enable new therapeutic avenues and provide the rationale for future large-scale clinical trials.

#4347

A pivotal clinical trial of cResponse, a functional assay for cancer precision medicine

Seth Salpeter[1], Vered Bar[1], Guy Neev[1], Adi Zundelevich[1], Gil Rosen[1], Sandra Hanks[2], Naoise Costelloe[3], Jonathan Krell[4], Ravid Straussman[5]. *[1]Curesponse Ltd, Rehovot, Israel,[2]Curesponse UK Ltd, Sutton, United Kingdom,[3]Curesponse UK, Sutton, United Kingdom,[4]Imperial College, London, United Kingdom,[5]Weizmann Institute, Rehovot, Israel*

Precision cancer therapy has the potential to revolutionize treatment outcome. While genomic analysis has become central to cancer personalized medicine, recent studies have not shown that it drastically improves the patient's survival as compared to standard drug selection. Additionally, genomic mutations may suggest several treatment protocols without elucidating which approach will yield the best clinical response. To advance cancer precision guidance, we have developed cResponse, a combined genomic-functional drug sensitivity platform to determine individualized patient treatment regimens. Fresh patient cancer samples are taken by biopsy or resection and sectioned into 250uM slices which when cultured in cResponse platform demonstrate similar architecture and tissue proliferation to those found in vivo. An initial clinical study showed that cResponse can preserve human cancer tissue in 3D culture together with its microenvironment, including endothelial and immune cells, at a high viability (>90%) with continued cell division for more than 7 days. On a cohort of 34 patients treated with neoadjuvant therapy or systemic therapy for metastatic disease, the assay was able to predict patient response to drug treatment with a sensitivity of 96% and a specificity of 77.7%. To further validate the capacity of the cResponse platform to predict patient response to cancer therapy, a follow up pivotal clinical study was established at 7 major cancer centers located in the UK with the goal of recruiting a total of 170 patients to provide a large statistical validation of the previous results. Here we report on the outcome of the first 50 patients recruited to the pivotal trial and describe the predictive results correlated to patient response.

#4348

Validation of an integrative pan-solid tumor predictor of pembrolizumab monotherapy benefit

Benjamin J. Bulen, Nickolay A. Khazanov, Laura E. Lamb, Daniel H. Hovelson, Kat Kwiatkowski, D. Bryan Johnson, Daniel R. Rhodes, Scott A. Tomlins. *Strata Oncology, Ann Arbor, MI*

Background: We previously reported the development and validation of an integrative Immunotherapy Response Score (IRS) algorithm, which integrates tumor mutation burden (TMB) and quantitative gene expression of PD-L1, PD-1, ADAM12 and TOP2A, to predict PD-1 or PD-L1 (together PD-[L]1) monotherapy (mono) benefit across solid tumors from routine formalin fixed paraffin embedded samples. Herein, we evaluated IRS performance for predicting pembrolizumab (pembro) mono benefit in a second, independent validation cohort.
Methods: We identified patients from an ongoing observational trial (NCT03061305) integrating molecular profiling with real world treatment data who were 1) treated with systemic pembro mono, 2) not included in the original IRS cohort, and 3) had valid molecular profiling data to generate IRS. IRS status (IRS-High [H] vs. -Low [L] by the previously validated threshold; -H with increased benefit) association with pembro real world progression free survival (rwPFS) by time-to-next therapy was determined by Cox proportional hazard modeling (adjusting for age, gender, line of systemic therapy, and PD-(L)1 mono indicated (microsatellite instable high [MSI-H], TMB-H, or approved tumor type) vs. not indicated. The predictive nature of the IRS biomarker was assessed in the subset of >= 2nd line patients through a case cross-over analysis (pembro rwPFS vs. immediately preceding therapy line rwPFS) as assessed by likelihood ratio test (LRT).
Results: Of the 176 patients in this independent validation cohort (from 25 tumor types), 78 (44%) patients were IRS-H, while 40 (23%) were TMB-H. Pembro mono rwPFS was significantly longer in IRS-H vs. IRS-L patients (median rwPFS 18.7 vs. 6.4 months, adjusted hazard ratio [aHR] 0.46,

p=0.007), while PD-(L)1 mono indicated status was not associated with pembro mono rwPFS (indicated vs. not indicated aHR 1.47, p=0.26). In the case cross-over analysis of 55 (31%) patients treated with systemic therapy prior to pembro mono, pembro rwPFS was significantly longer than preceding therapy in IRS-H patients (median 18.7 vs. 5.5 months) but not IRS-L patients (median 4.9 vs. 5.4 months); the LRT for interaction between IRS status and pembro/prior therapy was significant (p=0.046); results in the TMB-L/non-MSI-H subset (n=45) of patients was similar (LRT p=0.025).
Conclusion: These results confirm the pan-solid tumor PD-(L)1 monotherapy predictive nature of the IRS biomarker.

#4349

C-C chemokine receptor 2-positive monocytic myeloid-derived suppressor cells predicts chemotherapeutic responses of the metastatic lesions in breast cancer patients

Ju Won Kim[1], Jason K. Sa[2], Seung Pil Jung[3], Kyong Hwa Park[1], Serk In Park[4]. *[1]Department of Internal Medicine, Korea University Anam Hospital, Seoul, Korea, Republic of,[2]Biomedical Sciences, Korea University College of Medicine, Seoul, Korea, Republic of,[3]Department of Surgery, Korea University Anam Hospital, Seoul, Korea, Republic of,[4]Biochemistry and Molecular Biology, Korea University College of Medicine, Seoul, Korea, Republic of*

Anti-tumoral T cell immunity is counterbalanced by several types of immunosuppressive cells such as Myeloid-Derived Suppressor Cells (MDSC). Circulating MDSC levels correlate with poor prognosis and metastatic progression of breast cancer patients. However, the value of MDSC in predicting chemotherapeutic treatment responses in the metastatic lesions is not clearly understood. We performed a prospective cohort clinical study to measure MDSC before and after chemotherapy in metastatic breast cancer patients (*N*=64). Multicolor flow cytometry was used to quantitate two major subtypes, i.e. monocytic (M-) and polymorphonuclear (PMN-) MDSC, and one additional subtype, C-C chemokine receptor 2 (CCR2)-positive M-MDSC in the fresh peripheral blood mononuclear cells. M-MDSC were defined as HLA-DR$^{low/-}$CD45^{+}CD11b^{+}CD15^{-}CD14^{+} PBMC, and PMN-MDSC were defined as CD45^{+}CD11b^{+}CD33^{+}CD15^{+} CD14^{-} PBMC. PMN-MDSC and CCR2^{+} M-MDSC, but not M-MDSC, were significantly increased after chemotherapy. Subsequently, we divided the patients by two groups (therapy-sensitive *vs*. -resistant groups) by treatment responses. Treatment-resistant patients had significantly increased CCR2^{+} M-MDSC. Unsupervised clustering of patients based on MDSCs populations dichotomized patients PMN-MDSC high or M-MDSC high groups. M-MDSC high patients had increased bone and lymph node metastasis. In addition, CCR2^{+} M-MDSC levels correlated with the progression-free survival (P<0.05). Altogether, our results showed that CCR2^{+} M-MDSC levels potentially predict the therapeutic responses in the metastatic lesions of breast cancer patients.

#4350

Pharmacodynamic biomarkers: Evaluation of oncology drug target engagement in human plucked scalp and beard hair

Greg Tudor, Frida Ponthan, Adam Boanas, Aude-Marine Bonavita, Catherine Booth. *Epistem Ltd, Manchester, United Kingdom*

We have developed a method to assess target expression changes following exposure of plucked hairs to chemotherapeutic agents and other potential therapeutics. Successful *ex vivo* responses provide proof of concept data prior to clinical studies. Plucked hair is a valuable surrogate biomarker tissue to monitor pharmacodynamic (PD) responses in a clinical trial. The collection of hairs is

minimally invasive, simple and is amenable to frequent sampling. Since hairs are epithelial appendages, many signaling pathways active in other epithelial tissues, including cancers, are also present in hairs. Highly proliferative plucked human scalp hair can be utilized as a surrogate tissue to measure proliferation, phosphorylation and DNA damage responses after treatment. Furthermore, hairs are highly vascularized, suggesting that administered Test Articles may be delivered efficiently to the hair in a similar manner to other highly vascularized tissues, including many tumor types. Human plucked hair (either from the scalp or beard) was placed in maintenance media in the presence of conventional or targeted chemotherapeutic agents, known for their different mechanisms of action (e.g. Gemcitabine, Carboplatin, Tarceva), for a range of time points. Hairs were then fixed post-exposure and longitudinal sections immunohistochemically labelled for various markers including p-ERK1/2, p-AKT, p-Chk1, g-H2AX, Ki67 and androgen receptor. Quantitative image analysis to measure the level of labelling was performed using an Aperio ScanScope. The relative number of positively labelled cell nuclei, or relative tissue area (depending on the labelling pattern of the target), of the hair outer root sheath labelled was analyzed, along with label intensity. In subsequent trial patients, formaldehyde fixed plucked hairs were returned to the lab, similarly sectioned, labelled and quantified. In addition, where antibody labelling is not possible or more detailed information on the modulation of a pathway may be useful, drug treated plucked hairs can be subjected to Next Generation Sequencing (NGS) gene expression analysis. The expected changes in labelling were observed. For example, Gemcitabine, which is linked to DNA polymerase inhibition, increased p-Chk1 labelling 4-fold after 4-8 hours and strongly induced p53 by 24 hours. Tarceva, an inhibitor of the EGF pathway, decreased levels of both p-ERK1/2 and p-AKT 3-fold after only 10 minutes. The alkylating agent carboplatin increased g-H2AX labelling up to 12-fold after 24 hours. We have demonstrated that plucked hair is a valuable PD biomarker tissue for various chemotherapy agents. Proof of concept studies performed *ex vivo* can inform the design of clinical validation studies by indicating optimum markers and timepoints. Further, each hair is an independent unit thereby allowing independent replicate tissues (hairs) to be sampled.

#4351

Multiplex detection of G12/G13 KRAS mutations with an electrochemiluminescent hybridization assay

Annamaria Szabolcs[1], Timothy J. Break[1], Isaac H. Shin[1], Seth B. Harkins[1], Jacob N. Wohlstadter[2].
[1]Assay Development, Meso Scale Discovery, Rockville, MD,[2]Meso Scale Discovery, Rockville, MD

Purpose: Oncogenic Kirsten rat sarcoma virus (KRAS) mutations are the most prevalent cancer mutations in all human tumors. Also, genotyping the KRAS gene has become increasingly important with the emergence of new evidence highlighting differences in downstream signaling pathways, tumor microenvironment composition, treatment responses and prognoses linked to specific single nucleotide polymorphisms (SNPs) in the G12 or G13 codons. FDA approval of G12C-specific anti-KRAS drugs highlights the importance of the development of reliable SNP assays to interrogate the mutation status in a tumor sample. Currently available genotyping assays are based on NGS, PCR, or ddPCR. These methods can be time-consuming, costly, suffer from amplification bias, or require follow-up testing or bioinformatics skills to analyze. Building on Meso Scale Discovery's (MSD) existing technology, we aimed to develop a method for the identification of eight KRAS SNPs located on the G12-G13 codons in a single reaction.
Methods: Ten-spot, 96-well N-PLEX plates were used for the study. SNP-specific upstream probes carrying unique 5′ leader sequences complementary to spot-specific captures on the N-PLEX plates were designed for eight KRAS genotypes (WT, G12R, G12C, G12S, G12A, G12D, G12V, G13D). Locus-specific downstream probes were 5' phosphorylated for ligation and 3' biotinylated for detection. Synthetic DNA targets were used as assay calibrators, and commercially available FFPE

reference samples were tested for validation. DNA (10 ng) was PCR amplified with primers flanking the KRAS mutation sites. A multiplexed mixture of upstream and downstream probes was hybridized to the amplicons, and 30 cycles of ligation was performed using DNA ligase in a thermal cycler. Samples were subsequently hybridized to spot-specific capture oligonucleotides on the surface of the assay plates and detected with SULFO-TAG labeled streptavidin. Electrochemiluminescence readout was collected on an MSD imager.
Results: Optimization of probe concentrations and ligation temperature was performed to maximize signal-to-background ratios and assay specificity. Spike recovery experiments using artificial target DNA showed successful identification of KRAS mutant genotypes at spike levels as low as 0.1% over wild-type background. Validation experiments with gDNA extracted from FFPE reference samples confirmed that the multiplex SNP assay can accurately differentiate eight KRAS genotypes in samples with >0.4% tumor burden.
Conclusion: These data highlight a novel approach to simultaneously identify eight KRAS genotypes from 10 ng of DNA input in a single reaction within 4-5 hours. The assay is capable of identifying double mutants and can provide a semiquantitative assessment of tumor burden without the need for follow-up testing.

#4352

Leveraging deep proteome profiling of plasma- and serum-derived extracellular vesicles for melanoma biomarker discovery and disease dissection

Evelyn Lattmann[1], Luca Räss[2], Marco Tognetti[2], Julia Martinez Gomez[1], Valérie Lapaire[1], Roland Bruderer[2], Lukas Reiter[2], Yuehan Feng[2], Lars M. Steinmetz[3], Mitchell P. Levesque[1]. *[1]Department of Dermatology, University of Zurich, University Hospital Zurich, Schlieren, Switzerland,[2]Biognosys AG, Schlieren, Switzerland,[3]Department of Genetics, Stanford University School of Medicine, Palo Alto, CA*

Extracellular vesicles (EV) play an important role in melanoma progression but their potential as clinical biomarkers has yet to be realized. EVs can be found in most liquid biopsies (e.g., blood, urine, CSF) and exosomes are the most prominent subcategory of EVs. Exosomes are 50-200 nm lipid-bilayer enclosed particles secreted by all body cells, including tumor cells, and serve as mediators of metastasis formation and typically contain several classes of bioactive molecules such as RNA, proteins, lipids, and metabolites.
Blood and its liquid components plasma/serum are the most frequently used matrix for biomarker discovery due to the ease of collection. However, most proteomic platforms for plasma/serum profiling are unable to profile EV proteins due to the high dynamic range of protein concentrations in EV preparations. This is due to 1) EV isolation methods that vary in their potential to separate EVs from free proteins, and 2) the presence of a natural corona of high-abundant blood proteins attached to the EV surface. To tackle this challenge, we developed SEC-DIA-MS an integrated workflow combining size-exclusion chromatography, EV concentration, and optimized mass spectrometry to enable deep profiling of the proteome content of the enriched vesicles.
From 200 µl of plasma or serum from a test melanoma patient cohort (6 patients and 3 matched controls), we quantified 2,242 exosome-associated proteins, achieving a 2.5-fold increase in depth compared to previous melanoma studies. To gain a better understanding of the exosome enrichment efficiency, we extensively characterized the plasma/serum proteome by analyzing native, depleted, and EV-enriched blood from the same donors. We successfully validated well-known exosome markers such as CD9, CD63, CD81, PDCD6IP, and TSG101, and found that EV samples are significantly enriched in intact membrane proteins and those related to T cell biology, further underlining the uniqueness of the EV proteome composition. We further assessed the differences between plasma and serum EVs and suggest the use of plasma samples for future studies due to

better separation of healthy and melanoma samples. Furthermore, known melanoma markers such as MCAM, TNC, and TGFBI were upregulated in melanoma plasma-derived EV but not depleted plasma samples, highlighting the specific information contained in EVs.
Taken together, we demonstrated the applicability and potential of an EV-based proteomic workflow for biomarker discovery in plasma and serum. The ease of automating and scaling up such an approach enables a broader application to other indications and biological matrices.

#4353

Utilizing scRNA sequencing to understand biomarkers of response and resistance to Sacitizumab Govetican in localized TNBC

Nicole Peiris[1], Simona Cristea[2], Mengran Zhang[2], Siang Koh[1], James Coates[1], Ilze Smidt[1], Veerle Bossuyt[1], Laura Spring[1], Aditya Bardia[1], Leif Ellisen[1]. *[1]Harvard Medical School, Massachusetts General Hospital, Boston, MA,[2]Harvard Medical School, Dana Farber Cancer Institute, Boston, MA*

Triple-Negative Breast Cancer (TNBC) is an aggressive breast cancer subset, which lacks expression of estrogen receptors, progesterone receptors, and human epidermal growth factor receptor-2. This subset of breast cancer disproportionately affects Black and African American women and improving TNBC treatment options is vital to reducing breast cancer mortality. The novel antibody-drug conjugate, Sacitizumab Govetican (SG), which targets TROP2 at the cell surface, has shown promising clinical results from the NeoSTAR trial (NCT04230109), a phase II study evaluating neoadjuvant SG therapy in a localized TNBC setting. As part of the NeoSTAR clinical trial, we have collected and processed pre- and post- SG treatment patient samples, with the aim of understanding response to this monotherapy. Herein, we identify biomarkers of response and resistance to SG monotherapy through the use of single cell RNA sequencing of matched pre- and post-treatment patient biopsies combined with exome sequencing these patient samples. Pre-treatment core needle biopsy samples, and if applicable, post-treatment residual disease biopsies were dissociated into single cell suspensions and subjected to single cell RNA sequencing. Additionally, fixed patient tissue samples were processed accordingly for exome sequencing analyses. Overall, we analyzed over 144,000 cells from 37 total scRNA seq libraries with an average of 3800 cells per biopsy sample, demonstrating the feasibility of this method. From these analyses, we observed several cell-type differences between patients who achieved a pathological complete response (pCR) and patients who had residual disease (RD). Specifically, our data shows that tumor infiltrating lymphocytes are a potential prognostic biomarker of response to SG. Furthermore, we detected alterations in among stromal and immune cell subsets, among non-responders, indicating that these cell types maybe indicative of SG resistance. Taken together, we outline biomarkers of response to SG treatment for an improved understanding of resistance mechanisms in the neoadjuvant setting to improve TNBC outcomes among patients.

#4354

An exosome-based *ESR1* monitoring RT-qPCR technology that rapidly and accurately detects circulating tumor acquired resistance variants at ≤0.1% frequency in liquid biopsy samples

Sarah Statt[1], Julie Thibert[1], Kurt Franzen[2], Aquiles Sanchez[2], Liangjing Chen[1], Megan Yociss[1], Elliot Hallmark[1], Melissa Church[1], Stela Filipovic-Sadic[1], Gary Latham[1], Johan Skog[2]. *[1]Asuragen, a bio-techne brand, Austin, TX,[2]ExosomeDx, a bio-techne brand, Austin, TX*

Introduction: Hormone receptor-positive/human epidermal growth factor receptor 2-negative (HR+/HER2-) breast cancer is the most common type of breast cancer. Patients with HR+/HER2- metastatic breast cancer (mBC) often become resistant to aromatase inhibitors commonly used in endocrine therapy (ET). Estrogen receptor (*ESR1*) ligand binding domain mutations are frequently

detected in HR+ mBC and have been reported to be associated with ET resistance, noting up to 60% patients with mBC will develop resistance to treatment via acquired resistance in ESR1. Recent studies have shown that monitoring of *ESR1* mutations in plasma may serve as a predictive biomarker of acquired resistance to ET, showcasing a strong need for sensitive nucleic acid-based assays. We describe a comprehensive methodology for targeted clinical RT-qPCR monitoring of *ESR1* mutations in plasma that utilizes both exosomal nucleic acids and cfDNA to report multiple mutations, provide a streamlined workflow, and accommodate a range of inputs from clinically relevant samples.
Methods: Exosomal nucleic acids (exosomal DNA and RNA) and circulating cell-free DNA (cfDNA) were co-isolated using the ExoLution Plus Isolation Kit (Exosome Diagnostics). RT-qPCR-based target enrichment was performed using modified QuantideX reagents (Asuragen) and mutations were confirmed on the QuantStudio qPCR Platform (ThermoFisher). Bioinformatic analyses were conducted using custom software.
Results: We developed novel technologies and tested greater than samples across key ET resistance mutations, utilizing contrived samples as needed due to availability. Preliminary studies demonstrated that ESR1 exosomal RNA + cfDNA ranged from approximately 9,500 copies to 64,000 copies in a set of 2mL female presumed normal plasma samples; these results suggest that even 2mL plasma could provide sufficient exosomal RNA/DNA + cfDNA for mutation detection at variant frequencies less than or equal to 0.01%. The *ESR1* RT-qPCR showed greater than 90% analytical sensitivity (at less than or equal to 1% mutant allele frequency) and greater than90% analytical specificity. Further, the technology detected less than 10 mutant copies for most tested mutants, showing an LOD of at least 0.1% (5 mutant copies in a background of 5,000 WT copies).
Conclusion: A fast, efficient, and sensitive *ESR1* RT-qPCR panel approach was developed and evaluated, demonstrating the reliable and specific detection of rare variants in liquid biopsy specimens. Importantly, this prototype technology has potential to address several challenges associated with mutation monitoring in liquid biopsies by expanding detection of mutant analytes (exosomal RNA and DNA), improving analytical sensitivity (novel reagents and software), and increasing accessibility (qPCR instrument install base).

#4355

Prediction of cancer treatment response from histopathology images for a broad set of treatments and indications

Danh-Tai Hoang[1], Gal Dinstag[2], Leandro C. Hermida[3], Doreen S. Ben-Zvi[2], Efrat Elis[2], Katherine Caley[1], Sanju Sinha[3], Neelam Sinha[3], Christopher H. Dampier[3], Tuvik Beker[2], Kenneth Aldape[3], Ranit Aharonov[2], Eric A. Stone[1], Eytan Ruppin[3]. *[1]The Australian National University, Canberra, Australia,[2]Pangea Biomed, Tel Aviv, Israel,[3]National Cancer Institute, Bathesda, MD*

Background: Advances in artificial intelligence have paved the way for predicting cancer patients' survival and response to treatment from hematoxylin and eosin (H&E)-stained tumor slides. Extant approaches do so either via prediction of actionable mutations and gene fusions, or directly from the H&E images by training a task-specific model using large treatment outcome data.
Methods: Here we present the first approach for predicting patient response to multiple targeted treatments and immunotherapies directly from H&E slides. It is founded on two conceptual steps: (1) First, we developed DeepPT, a deep-learning framework that trains on formalin-fixed, paraffin-embedded (FFPE) TCGA whole slide images and their corresponding gene expression profiles to predict wide-scale tumor gene expression from the slides. (2) Second, we apply ENLIGHT, a published approach that predicts individual responses to a wide range of targeted and immunotherapies based on the tumor biopsy measured transcriptomics. Here we apply ENLIGHT to

predict patient treatment response from the DeepPT predicted expression values instead of those measured directly from the tumor, notably, without any further training or adaptation of ENLIGHT. Results: First, we find that DeepPT generalizes well to predicting gene expression in all 13 TCGA cohorts tested in cross-validation and importantly, in two independent unseen breast and brain cancer datasets. DeepPT outperforms HE2RNA, a state-of-the-art algorithm for the same task. Second, we demonstrate that the combined DeepPT/ENLIGHT pipeline (termed ENLIGHT-DeepPT) successfully predicts true responders using the original ENLIGHT decision threshold with odds ratios of 1.5 - 4.5, increasing the baseline response rates by 15-85% among predicted responders in five independent unseen cohorts of diverse cancer types and treatments. Remarkably, in one dataset where matched data was available, ENLIGHT-DeepPT has similar performance to that obtained by a supervised learning algorithm that was recently published in Nature, trained on the same cohort. Conclusions: We present for the first time a general framework for predicting patient response to a broad array of targeted and checkpoint therapies from histopathological images, without reliance on treatment outcome data, which are yet scarce and challenging to obtain. Importantly, ENLIGHT-DeepPT offers clinicians real-time treatment recommendations when one cannot wait for sequencing results. Also, and due to its very low cost, we very much hope that it will facilitate the advent of precision oncology in developing countries.

Biomarkers of Therapeutic Benefit 5

#5451
Multiplex immunofluorescence for cancer research
Patrick Savickas, Sharwari Phanse. *R&D, HistoWiz, New York, NY*

Multiplex Immunofluorescence (M-IF) is a technique where multiple antibodies are visualized using unique fluorophores on the same slide. Thus, instead of employing panels of separately stained IHC slides that only reveal regional localization, it enables direct visualization of numerous proteins of interest on the same cell. This enables researchers and clinicians to comprehend precise interactions taking place at the cellular level in their tissue. The challenge of figuring out how to individually link markers with fluorophores without incurring cross contamination has hindered the development of M-IF assays. The first traditional approach was to ensure each marker was generated from a unique host species, and then use secondary antibodies against those host species conjugated to unique fluorophores. As a result, the unique host species that an antibody could be generated in were exhausted forcing the researchers to reach into exotic species. The second generation of technologies attempted to temporally solve this problem by sequentially staining the markers and then stripping off the antibody in between steps; preserving the fluorophores. This system leveraged the interaction of tyramide attached to a fluorophore and its affinity for tyrosine residues in tissue to form a stronger bond then the antibody to the tissue to endure the harsh striping step. This allowed the usage of multiple antibodies from the same host species but added antigen sheltering as the confounding variable due to crowding and exhaustion of antigenic sites. The latest generation technology we are using attempts to solve this linkage problem with DNA barcoding. A lock and key mechanism wherein the primary antibody is pre-conjugated with a unique barcode and the fluorophore with a corresponding inverse barcode. In this technique the primary antibodies can be applied as a cocktail in parallel to the tissue with the dna based linkage easily and gently broken when necessary. We then took this novel technique and applied it in a shotgun approach using Tissue Microarrays (TMAs) to screen against dozens of cores from breast, endometrial, carcinoma and melanoma cases. We then use Inform software to algorithmically categorize each cell and R-Studio to statically prove a significant coefficient of variation. This creates the ability to build panels for signatures that answer key research questions like “Where are the immune cells in the tissue microenvironment” and “is the

tumor hot or cold? Activated, exhausted or proliferating?". This abstract contrasts the operation of the new technology with the earlier approaches and will demonstrate how artificial intelligence-assisted algorithms can analyze and produce statistically significant datasets for cancer researchers.

#5452

Complimentary use of DNA- and RNA-based NGS assays optimizes detection of clinically relevant translocations for comprehensive genomic profiling

Rongqin Ren[1], Jennifer Jackson[2], Jacob Kames[2], David Riles[2], Christopher Coldren[1], Scott Wheeler[1], Pranil Chandra[1], Michelle Shiller[1]. *[1]PathGroup, Nashville, TN,[2]Personal Genome Diagnostics, Baltimore, MD*

Introduction: Detection of gene translocations is a key component of clinical diagnostics to enable precision medicine in oncology. Several methods such as fluorescence in situ hybridization or RT-PCR have historically been employed, however, next-generation sequencing (NGS)-based comprehensive genomic profiling (CGP) including DNA and RNA sequencing approaches have been validated for this purpose. Here we explore the complimentary nature of these methods to enable detection of clinically relevant translocations to guide patient care.
Methods: We utilized Endeavor, a 505 gene DNA-based CGP assay developed by Personal Genome Diagnostics, to assess single nucleotide variants, insertion/deletions, amplifications, translocations, microsatellite instability, and tumor mutation burden as well as a 53 gene RNA-based Invitae NGS FusionPlex Solid Tumor v1 assay. 151 patients with advanced or metastatic solid tumors, including lung, colorectal, esophageal, breast, brain, bladder, and prostate cancers, were consecutively enrolled and only overlapping target regions were evaluated to compare performance.
Results: Of the 151 cases selected for the study, failure rates were 2.0% and 9.9% for Endeavor and FusionPlex, respectively. Translocations were detected in 21/151 (13.9%) cases by Endeavor and 17/105 (11.3%) cases by FusionPlex. For the 133 cases where data was available from both assays, 12 (9.0%) concordant translocation positive cases were detected involving *ALK*, *RET*, *NTRK1*, *NTRK3*, *MET* exon 14 skipping, *EGFR*vIII, and *EWSR1* with 109 (82.0%) cases translocation negative by both assays achieving a concordance rate of 91%. For 7 (5.3%) cases, Endeavor detected translocations events in *FGFR1*, *FGFR2*, *ETV4*, *ETV6*, *MYC*, and *NTRK3* that were not detected by FusionPlex. Conversely, FusionPlex identified 5 (3.8%) cases with translocations in *ROS1*, *NTRK2*, and *EGFR*vIII that were not detected by Endeavor (Table 1). Discrepancies in translocation detection were attributed to variability in assay failure rates, panel design, and underlying biological differences in detectability associated with DNA- and RNA-based methods.
Conclusions: In this study, comparison of translocation detection using DNA and RNA-based NGS approaches revealed a high concordance between the two assays and were equally valuable for identifying actionable targets. These findings provide confirmatory support for the complimentary use of DNA- and RNA-based NGS approaches to most accurately identify clinically relevant translocations thereby providing more comprehensive results to help guide cancer treatment strategies.

#5453

Individualized risk stratification in newly diagnosed multiple myeloma

Arjun Raj Rajanna[1], Francesco Maura[1], Andriy Derkach[2], Bachisio Ziccheddu[1], Niels Weinhold[3], Kylee Maclachlan[2], Benjamin Diamond[1], Faith Davies[4], Eileen Boyle[4], Brian Walker[5], Alexandra Pos[3], Malin Hulcrantz[2], Ariosto Silva[6], Oliver Hampton[7], Jamie K. Teer[6], Niccolò Bolli[8], Graham Jackson[9], Martin Kaiser[10], Charlotte Pawlyn[10], Gordon Cook[11], Dennis Verducci[1], Dickran Kazandjian[1], Fritz Van Rhee[12], Saad Usmani[2], Kenneth H. Shain[6], Marc S. Raab[3], Gareth Morgan[4],

Ola Landgren[1]. *[1]Univ. of Miami Sylvester Comprehensive Cancer Ctr., Miami, FL,[2]Memorial Sloan Kettering Cancer Center, New York, NY,[3]University Hospital, Heidelberg, Germany,[4]NYU Langone, Perlmutter Cancer Center, New York, NY,[5]Indiana University, Indianapolis, IN,[6]Moffitt Cancer Center, Tampa, FL,[7]M2GEN, Tampa, FL,[8]Fondazione IRCCS Ca' Granda Ospedale Maggiore Policlinico, Milano, Italy,[9]The Newcastle Upon Tyne Hospitals NHS Foundation Trust, Newcastle, United Kingdom,[10]The Institute of Cancer Research, London, United Kingdom,[11]University of Leeds, Leeds, United Kingdom,[12]University of Arkansas for Medical Sciences, Little Rock, AR*

Background: Clinical outcomes for newly diagnosed multiple myeloma (NDMM) patients are heterogenous with survival ranging from months to > 10 years. Though several clinical and genomic features predict outcomes, the “one-size-fits-all” treatment paradigm remains dominant for NDMM.
Hypothesis: By integrating clinical, genomic and therapeutic data, using artificial intelligence, an individualized risk-prediction model for NDMM (IRM) can facilitate individually-tailored therapeutic decisions.
Methods: We included 1933 patients with clinical and genomic data from 5 cohorts: MMRF CoMMpass (n=1062), MGP (n=492), Moffit AVATAR (n=177), UAMS (n=93), and MSKCC (n=109). The median follow-up was 43 months. Overall, we considered 160 clinical (e.g., age, ECOG, race), therapeutics, and genomic variables. To correct for time-dependent variables such as autologous stem cell transplant (ASCT) and continuous treatment, a multi-state model was designed across two phases: induction (phase 1), and post-induction (phase 2). Neural Cox Non-proportional-hazards (NCNPH) was used to integrate the data and build the model.
Results: Overall, the 5-year overall survival (OS) c-index for IRM was 0.73, significantly higher than all existing prognostic models: R2-ISS (0.62), ISS (0.61) and R-ISS (0.56). The overall model accuracy was significantly improved by the inclusion of 12 genomic features, including 1q21 gain/amp, *TP53* loss, t(4;14)(*NSD2*;*IGH*), complex copy number signatures, APOBEC mutational signature contribution, and del1p. Prescribed therapy emerged as a key determinant of risk, suggesting that effective combinations may have a different impact in the context of individual patient features, with the potential to significantly change clinical outcomes despite poor historical prognostication (i.e., treatment variance). Leveraging these concepts, we interrogated the clinical impact of ASCT and continuous treatment in the context of NDMM treated with bortezomib, lenalidomide and dexamethasone (VRd). Integrating predicted outcomes and treatment variance for all 4 possible treatment combinations (i.e., VRd +/- ASCT +/- continuous treatment) we identified 3 patient groups. In the first group (n=632), patients were characterized by complex genomic features, older age, high ISS, poor outcomes and limited treatment variance, reflecting aggressive and refractory myeloma. The second group (n=571) was characterized by high treatment variance, with favorable outcomes if ASCT and continuous treatment are provided. The last group (n=730) included patients with favorable clinical and genomic profiles, achieving good outcomes, with minimal advantage from ASCT.
Conclusion: Integrating historical and emerging genomic features with clinical and therapeutic data, we developed the first individualized risk-prediction model for personally-tailored therapeutic decisions in NDMM.

#5454

Peripheral blood biomarkers in Phase II study of pembrolizumab in combination with oral binimetinib in patients with unresectable locally advanced or metastatic triple-negative breast cancer

Saranya Chumsri[1], Joseph J. Larson[2], Daniel L. Adams[3], Kathleen S. Tenner[2], Cha-Mei Tang[3], Morgan T. Weidner[1], Amanda N. Arnold[1], Dana L. Haley[1], Pooja Advani[1], Kostandinos Sideras[1], Alvaro Moreno-aspitia[1], Edith A. Perez[1], Keith L. Knutson[1]. *[1]Mayo Clinic Florida, Jacksonville, FL,[2]Mayo Clinic, Rochester, MN,[3]Creatv Microtech Inc., Potomac, MD*

Background: Activation of the RAS/MAPK pathway is associated with reduced tumor-infiltrating lymphocytes and poor outcomes in triple-negative breast cancer (TNBC). This trial evaluated the efficacy of pembrolizumab and MEK inhibitor, binimetinib. Here we evaluated potential biomarkers in peripheral blood to predict response.

Methods: Patients with unresectable locally advanced or metastatic TNBC with ≤ 3 prior lines of therapy were enrolled. Treatment includes a 2-week run-in with binimetinib followed by pembrolizumab. There were 2 dose levels (DL) with binimetinib at 45 mg at DL 0 and 30 mg at DL -1. A standard 3+3 design was used in phase I, and Simon's two-stage Optimal design was used in phase II. Circulating tumor cells (CTC) and circulating cancer-associated macrophage-like cells (CAML) were isolated using CellSieve microfilters and immunofluorescently labeled with PD-L1 and p-ERK. Wilcoxon rank sum test and Cox regression model were used for analysis.

Results: A total of 22 patients were enrolled, with a median age of 58 years old. Dose-limiting toxicity (DLT) was observed in 2 out of 4 patients in DL 0, with grade 3 ALT abnormality, flank pain, and nausea. In the next 6 patients in DL -1, there was 1 DLT with grade 3 AST/ALT abnormality. There were 17 patients treated with DL -1 and were evaluable for response. The objective response rate (ORR) was 29.41% (95% CI: 10.31-55.9) with 1 complete response (CR) and 4 partial responses (PR). The clinical benefit rate (CBR ≥ 24 weeks) was 35.29% (95% CI: 14.21-61.67). ORR in patients without liver metastases was 55.56% (95% CI: 21.20 - 86.30), and CBR was 66.67% (95% CI: 29.93-92.51). There was no response observed in all 5 patients with liver metastases. Baseline mean CTC count was 1.3 cells, and CAML count was 8.9 cells/7.5 mL. Baseline PD-L1 in CAML (p 0.04) and

decline in CAML size (p 0.02) after 1 cycle were significantly associated with CBR. However, baseline CTC count, CAML count (p 0.64), CAML size (p 0.46), p-ERK in CAML (p 0.23), and changes in CTC count, CAML count (p 0.83), p-ERK (p 0.07), and PD-L1 (p 0.08) in CAML were not significantly associated with responses. Using Cox regression analysis, a reduction in CAML count (p 0.02), CAML size (p 0.01), and PD-L1 in CAML (p 0.03) were associated with significant improvement in overall survival but not the reduction in p-ERK (p 0.6).
Conclusions: Pembrolizumab and binimetinib at 30 mg are safe with manageable toxicities. Promising activity was observed in patients without liver metastases. Baseline PD-L1 expression, early reduction in CAML count, size, and PD-L1 expression were significantly associated with subsequent responses, providing potential noninvasive biomarkers to predict response to this combination. Future larger clinical trials are warranted to further evaluate the efficacy of this combination.

#5455

Large-scale cancer genomic analysis reveals significant disparities between microsatellite instability and tumor mutational burden

Jungyoon Choi[1], Jung Sun Kim[1], Kyong Hwa Park[2], Xingyi Guo[3], Yeul Hong Kim[2]. *[1]Korea University Ansan Hospital, Ansan, Korea, Republic of,[2]Korea University Anam Hospital, Seoul, Korea, Republic of,[3]Vanderbilt University Medical Center, Nashville, TN*

Microsatellite instability (MSI) and tumor mutational burden (TMB) are efficacy biomarkers for cancer immunotherapies, with both MSI-high and TMB-high considered hypermutator phenotypes that predict better drug responses. However, the inter-relationship between these biomarkers has not been well-investigated. Herein, we conducted a large-scale cancer genomic analysis to characterize patterns of distribution between MSI-high and TMB-high across 22 human cancer types, and identify mutated genes that may contribute to MSI-high cancers.We analyzed somatic mutation data from the Genomics Evidence Neoplasia Information Exchange (GENIE; n=49,496) to characterize gene mutations and patterns of distribution between MSI and TMB for each cancer. Associations between TMB and MSI were evaluated using multivariable linear regression models adjusted for age at sequencing report, sex, race, sequencing center, and histological

subtype. Associations between MSI and gene mutations were evaluated using multivariable logistic regression models adjusted for the above mentioned covariates and TMB.Our analysis revealed that considerable differences in the prevalence of MSI-high and TMB-high by cancer types. The moderate differences were observed in cancers with the top prevalence of MSI-high/TMB-high, such as 31.1%/28.7% in endometrial cancer, 18.4%/17.7% in colorectal cancer, and 17.2%/12.2% in stomach cancer, while most other cancers showed high differences of prevalence (>10%). Notably, MSI-high patients were observed to have a substantial proportion of TMB-low phenotypes ranging from 31% to 89% among these cancer types, likely indicating distinct drug responses compared to TMB-high phenotypes. Association analyses between TMB and MSI for these cancers showed the strongest associations in colorectal cancer (P=4.0x10-255) and stomach cancer (P=6.2x10-60), while marginal or no associations were observed in several cancers including head and neck cancer (P=0.08) and hepatocellular carcinoma (P=0.15). In addition, we identified several mutated genes associated with MSI-high phenotypes, including known mismatch repair genes (e.g., MSH3, POLD1, MLH1, and MSH6) and novel mutated genes (e.g., RNF43, ARID1A, ARID1B, NOTCH3, SMARCA4, KMT2C, and CREBBP), in endometrial cancer (n=32 genes), in colorectal cancer (n=29 genes) and in stomach cancer (n=18 genes), at a Bonferroni-corrected $P < 0.05$.Our study revealed large discrepancies in prevalence between MSI-high and TMB-high in many cancer types,, highlighting the need to consider distinct or combined biomarkers for immunotherapies. Our study also identified novel mutated genes associated with MSI-high cancers, providing additional insights into MSI-high carcinogenesis and candidate genetic biomarkers to screen patients for potential immunotherapy.

#5456

Application of a multiplex urinalysis test for predicting treatment response in patients with BCG unresponsive bladder cancer: a pilot study

Hideki Furuya[1], Kaoru Murakami[1], Ian Pagano[2], Runpu Chen[3], Yijun Sun[3], Nari Kim[1], Edward E. Kadel[4], Cheryl V. Wong[4], Nicole Davarpanah[4], Charles J. Rosser[1]. *[1]Cedars-Sinai Medical Center, Los Angeles, CA,[2]University of Hawaii Cancer Center, Honolulu, HI,[3]The State*

University of New York at Buffalo, Buffalo, NY,[4]Genentech, San Francisco, CA

Introduction and Objective: Recently, we reported that Oncuria™, a multiplex urinalysis test, could be predictive of BCG treatment response. Furthermore, high-grade BCG unresponsive bladder cancer have limited treatment options. Such patients are offered either radical cystectomy or systemic therapy. One of the systemic therapies include immune-oncology agents, e.g., PD-1 or PD-L1 inhibitors. In this study, we tested the performance of Oncuria™ in a BCG unresponsive cohort to determine if it could predict response to a PDL1 inhibitor.
Methods: Oncuria™ data was evaluated in voided urine samples obtained from a prospectively collected cohort of 18 subjects who have BCG-unresponsive NMIBC with treatment of atezolizumab monotherapy or atezolizumab BCG combination (provided by Genentech, NCT02792192). The urine samples were collected prior to treatment in both arms. The Oncuria™ test, which measures 10 cancer-associated biomarkers was performed in an independent clinical laboratory. Predictive models were previously developed using supervised learning and cross-validation analyses. Model performance was validated using ROC curves.
Results: Pre-treatment urinary concentrations of MMP9, VEGFA, CA9, SDC1, PAI1, APOE, A1AT, ANG and MMP10 were increased in patients who developed disease recurrence. A combinatorial predictive model of treatment outcome achieved sensitivity and specificity of >90%.
Conclusion: Previous pilot study found that monitoring the urinary levels of a cancer-associated biomarker panel enabled the discrimination of patients who did not respond to intravesical BCG therapy. In this study, we noted the performance of Oncuria™ for the prediction of systemic PDL1 inhibitor treatment response. A limitation of this study includes its small sample size. With further study, the multiplex Oncuria™ test may be applicable for the clinical evaluation of bladder cancer patients who have not previously responded to intravesical BCG treatment and is considering systemic immune-oncology options.

#5457
Prevalence of “low” HER2 expression is frequent in breast cancer but also in cancers of other origin: A tissue microarray study on 131 tumor

types

Maximilian Lennartz[1], Florian Viehweger[1], David Dum[1], Ria Uhlig[1], Andrea Hinsch[1], Doris Hoeflmayer[1], Christoph Fraune[1], Christian Bernreuther[1], Patrick Lebok[1], Soeren Weidemann[1], Guido Sauter[1], Till Sebastian Clauditz[1], Frank Jacobsen[1], Till Krech[1], Andreas H Marx[2], Sarah Minner[1], Ronald Simon[1], Natalia Gorbokon[1], Stefan Steurer[1], Eike Burandt[1]. *[1]University Medical Center Hamburg-Eppendorf, Hamburg, Germany,[2]Academic Hospital Fuerth, Fuerth, Germany*

HER2 is a receptor tyrosine-protein kinase coded by the ERBB2 gene. The HER2 status is routinely assessed to select patients eligible for targeted therapy with anti-HER2 drugs. HER2 positivity was restricted to cancers with a 3+ score at immunohistochemistry (IHC) and/or gene amplification. The successful use of HER2 antibody-drug conjugates in tumors with IHC scores of 1+ (HER2 low) or 0 with incomplete and faint staining in ≤10% of tumor cells (HER2 ultralow) is currently changing the traditional dichotomy of HER2 testing in breast cancer. To determine HER2 expression in neoplastic tissues, a tissue microarray containing one 0.6mm tissue spot each from 7,505 tumor samples from 131 different tumor types and subtypes was analyzed by immunohistochemistry. IHC scoring included 3+, 2+, 1+, and a category "+" (faintly positive in less than 10% of tumor cells; ultralow). The cohort included 310 breast cancers for which the HER2 amplification was also assessed by fluorescence in situ hybridization. Among 555 evaluable breast cancers, HER2 IHC was 3+ in 7.6%, 2+ in 3.2%, 1+ in 14.6%, "+" in 15.9% and 0 in 58.7%. The HER2 amplification rate was in 95.8% of 3+, 61.5% of 2+, 18.2% of 1+, but 0% in "+" and HER2 0 breast cancers. Among 4,912 non-breast cancers, the HER2 status was 3 in 0.6%, 2 in 0.7%, 1 in 3.3%, "+" in 2.3%, and 0 in 93.2%. In these tumors, 3+ positivity was largely restricted to gastric/esophageal adenocarcinoma, urothelial carcinoma, ovarian cancer as well as adenocarcinomas of the lung, colon, and pancreas. A 2+ positivity was mostly seen in tumor entities that had also 3+ cases. A 1+ or "+" HER2 positivity was found in 50 of 147 analyzed non-breast cancer categories. HER2 low and ultralow (1+ or "+") was most commonly seen in basal cell carcinoma of the skin (52.2%), clear cell carcinoma of the ovary (33.3%), urothelial carcinoma of the renal pelvis (33.3%), gallbladder adenocarcinoma (26.7%), muscle-invasive urothelial carcinoma of the

bladder (24.5%), prostatic adenocarcinoma, Gleason 4+4 (23.3%), endometrial serous carcinoma (22.7%), prostatic adenocarcinoma, Gleason 5+5 (19.2%), carcinosarcoma of the ovary (18.8%), renal oncocytoma (17.9%), serous carcinoma of the ovary (17.8%), gastric adenocarcinoma, intestinal type (13.2%), neuroendocrine tumor (NET) of the lung (11.1%), carcinosarcoma of the uterus (11.1%), endometrioid carcinoma of the ovary (11.1%), squamous cell carcinoma of the larynx (10.7%), parathyroid gland adenoma (10%), endometrioid endometrial carcinoma (9.7%), adenocarcinoma of the esophagus (9.5%), cholangiocarcinoma of the liver (9.3%), and pancreatic/ampullary adenocarcinoma (8.6%). While 3+ IHC is limited to only few cancer types, there is a much broader range of tumor entities that can show HER2 low and ultralow expression. HER2 antibody-drug conjugates may therefore be successful drugs in a large variety of different tumor entities.

#5458

TONSL is an immortalizing oncogene of the chromosome 8q24.3 amplicon and new therapeutic target in breast cancer

Aditi S. Khatpe[1], Rebecca Dirks[2], Poornima Bhat-Nakshatri[2], Henry Mang[2], Katie Batic[2], Sarah Swiezy[2], Jacob Olson[3], Xi Rao[4], Yue Wang[4], Hiromi Tanaka[4], Sheng Liu[4], Jun Wan[4], Duojiao Chen[4], Yunlong Liu[4], Fang Fang[5], Sandra Althouse[6], Emily Hilsey[7], Maggie M. Granatir[7], Rebekah Addison[7], Constance J. Temm[7], George Sandusky[7], Audrey Lee-Gosselin[8], Kenneth Nephew Nephew[5], Kathy D. Miller[9], Harikrishna Nakshatri[1]. *[1]Indiana University School of Medicine, Indianapolis, IN,[2]Department of Surgery, Indiana University School of Medicine, Indianapolis, IN,[3]Decatur Central High School, Indianapolis, IN,[4]Department of Medical and Molecular Genetics, Indiana University School of Medicine, Indianapolis, IN,[5]Medical Science Program, Indiana University School of Medicine, Bloomington, IN,[6]Department of Biostatistics and Health Data Science, Indiana University School of Medicine, Indianapolis, IN,[7]Department of Pathology and Laboratory Medicine, Indiana University School of Medicine, Indianapolis, IN,[8]Stark Neurosciences Research Institute, Indiana University School of Medicine, Indianapolis, IN,[9]Department of Medicine, Indiana University School of Medicine, Indianapolis, IN*

Study of genomic aberrations leading to immortalization of epithelial cells has been technically challenging due to lack of an appropriate isogenic model system. To address this technical challenge, we utilized primary breast luminal epithelial cells propagated from healthy donors of different genetic ancestry and their hTERT-immortalized counterparts to identify functional gene expression changes associated with immortalization. We identified elevated expression of TONSL (Tonsoku Like, DNA Repair Protein) as one of the earliest events during immortalization. TONSL is located on chromosome 8q24.3 and amplified in ~20% of breast cancers with significantly higher amplification in metastatic tumors. TONSL forms a complex with FACT and MMS22L1 to modulate multiple cellular pathways including DNA replication, repair through homologous recombination (HR) and functions as a post replicative histone/chromatin reader. TONSL alone immortalized primary breast epithelial cells and increased telomerase activity. While TONSL overexpression alone was insufficient for neoplastic transformation, TONSL-immortalized primary cells modified to overexpress defined oncogenes generated estrogen receptor-positive adenocarcinomas in NSG mice. Analysis of breast tumor microarray with ~500 tumors revealed poor overall and progression free survival of patients with TONSL-overexpressing tumors. TONSL increased chromatin accessibility to pro-oncogenic transcription factors including NF-κB and limited access to the tumor suppressor p53. Most importantly, TONSL overexpression resulted in significant changes in the expression of genes associated with DNA repair hubs, including upregulation of several genes in HR and Fanconi Anemia pathways. Consistent with the effects of TONSL on HR-associated genes, TONSL overexpressing primary cells exhibited upregulated DNA repair via HR. Moreover, TONSL was an essential gene for growth of TONSL-amplified breast cancer cell lines *in vivo*. Breast cancer cell lines with TONSL/chr8q24.3 amplification were sensitive to TONSL-FACT complex inhibitor CBL0137, both *in vitro* and *in vivo*. To our knowledge, TONSL is the only gene other than telomerase with immortalizing function and represents a new therapeutic target for breast cancer with chr8q24.3 amplification.

#5459

Association between stomatitis and treatment efficacy with novel TROP2-directed antibody drug conjugate (ADC), datopotamab

deruxtecan, in patients with metastatic cancer

Rachel O. Abelman[1], Laura M. Spring[1], Phoebe K. Ryan[1], Geoffrey Fell[2], Dejan Juric[1], Rebecca S. Heist[1], Aditya Bardia[1]. *[1]Harvard Medical School/Massachusetts General Hospital, Boston, MA,[2]Harvard Medical School/Dana Farber Cancer Institute, Boston, MA*

Background**:** Incidence of toxicity with immunotherapy has been correlated with likelihood of treatment response (Hussaini, Cancer Treat Rev 2021; Schuell, Br J Cancer 2005). However, this phenomenon has not yet been demonstrated with antibody-drug conjugates. Datopotamab deruxtecan (Dato-DXd) is a novel ADC composed of an anti-Trop2 monoclonal antibody, a stable tetrapeptide-based cleavable linker, and a topoisomerase-I inhibitor payload (Bardia, Annals of Onc 2021). Early phase studies have demonstrated significant activity in heavily pretreated patients with metastatic non-small cell lung cancer (NSCLC) and metastatic breast cancer (MBC). Stomatitis was a common treatment-emergent adverse event (TEAE) observed in clinical trials. We conducted a study to evaluate the association between incidence of stomatitis and treatment response with Dato-DXd and evaluate the impact of steroid mouthwash. We hypothesized that presence and grade of mucositis would correlate with observed treatment efficacy.

Methods: We included all patients treated at one academic institution (Massachusetts General Hospital) with Dato-DXd. Stomatitis was assessed by NCI-CTCAE V5.0. Objective Response Rate (ORR) was assessed by RECIST criteria with independent radiology review. Use of mouthwash was evaluated by secondary review and categorized as primary or secondary prophylaxis. A time-to-event analysis was performed to evaluate the time to onset of stomatitis.

Results: 60 patients, including 19 with MBC and 41 with NSCLC, were treated with Dato-DXd between June 2018-September 2022. The median age of patients was 64 and 41/60 patients were female. The median time to onset of mucositis was 14 days (95% CI 12-42 days). There was no significant difference in incidence of stomatitis between the MBC and NSCLC cohorts. Compared to patients who had progressive disease (PD), patients who had a partial response (PR) or stable disease (SD) were 11 times more likely to have stomatitis (OR 11.0, 95% CI 3.61-44.01, $p<0.001$). Later in the trial (January 2020 onward), 28 patients received

primary steroid prophylaxis - excluding these patients, those who were found to have PR/SD were 8.8 times more likely to develop stomatitis compared to patients who had PD (OR 8.8, 95% CI 1.5-73.3, p=0.023). **Conclusion:** The development of stomatitis may be associated with higher likelihood of therapeutic efficacy. Given that these findings are a hypothesis-generating post-hoc exploratory analysis from a single institution, this requires validation in larger studies before drawing strong conclusions and impacting clinical decision making. Further research is also needed evaluate the relationship between TEAEs and therapeutic efficacy with other ADCs.

#5460

Novel immunohistochemistry-based predictive and prognostic tests for hormone receptor-positive breast cancer

Danira Jaksic[1], Amandeep Kaur[1], Dean Reddick[1], David David Datzkiw[1], Shailly Varma Shrivastav[2], Vijayakrishna Gadi[3], Leigh Murphy[4], Anuraag Shrivastav[1]. *[1]The University of Winnipeg, Winnipeg, MB, Canada,[2]Oncodrex Inc, Winnipeg, MB, Canada,[3]University of Illinois Cancer Center, Chicago, IL,[4]CancerCare Manitoba, Winnipeg, MB, Canada*

Background: Breast cancer (BC) is the most diagnosed cancer worldwide and the most common cancer diagnosed in American women. Despite successes of adjuvant endocrine therapies in treating the most common subtype of hormone receptor-positive (HR+) BC, de novo and emergent resistance to these therapies, i.e., endocrine resistance, remains a significant concern with patients experiencing recurrences during and after adjuvant treatment. We report here unique patterns of expression (UPE) of N-myristoyltransferase 1 (NMT1) protein that are prognostic and predictive markers for HR+ BC. We have discovered that the expression and localization of NMT1 are predictive markers for the endocrine therapy response in HR+ BC. The data from many observational studies suggest that after five years of adjuvant endocrine treatment, the likelihood of distant recurrence continues for the subsequent twenty years. We have developed simple immunohistochemical (IHC)-based tests that could become part of routine first line prognostic and predictive tests and have the potential to be incorporated as necessary tests in the panel of BC tests for designing treatment regimens of BC.

Methods: Expression patterns of NMT1 were determined using IHC analyses on formalin fixed paraffin embedded primary tumor samples from treatment naïve BC patients. The tumor tissues in duplicates were stained with NMT1 monoclonal/polyclonal antibodies on an autostainer (Leica Bond). Stained slides were scored in a blinded manner to outcomes and scored with an "H" index representing the intensity and percent positive cells within each section. The relationship of UPE was correlated with clinical outcomes of RFS (RFS = endpoint recurrence and/or death due to BC) and OS (OS = endpoint death due to breast cancer).
Results: The final cohort was composed of 448 BC cases of primary HR+ tumors from patients who received adjuvant tamoxifen therapy after surgery. UPE2 (defined by > median H score 100) was significantly associated with better clinical outcomes represented by both RFS (HR = 0.70, *P* = 0.0304, 95% CI 0.510 to 0.97, n = 440) and OS (HR = 0.71, *P* = 0.0306, 95% CI 0.530 to 0.97, n = 440), whereas UPE4 strongly predicted worse treatment response for both RFS (HR= 1.49, P = 0.0014, 95% CI 1.08 to 2.04, n=440) and OS (HR = 1.54, P = 0.0055, 95% CI = 1.54 to 2.08, n=440).
Conclusions: We observed that the expression and localization patterns of NMT1 constitute four unique patterns of expression signatures (UPE:1-4) and serve as prognostic and potentially predictive markers for HR+ BC. This assay provides a novel method to stratify cancers that may better enable endocrine treatment and duration optimization in the adjuvant setting for HR+ breast cancer. Moreover, in distinction to genomic assays, fewer logistic and financial barriers to implementation would exist for the UPE:1-4 IHC assay in resource-poor settings.

#5461

Gain early insights from single cell RNA-sequencing of clinical trial needle biopsy cores

Thomas Gallup[1], Sang Yun[1], Dave Gallup[1], Kyuson Yun[2]. *[1]EMPIRI Inc, Houston, TX,[2]Department of Neurology, Houston Methodist Research Institute, Houston, TX*

Single cell RNA-sequencing (scRNA-seq) yields valuable insights into the molecular heterogeneity of multiple cell types in normal and cancer tissues. scRNA-seq approach has the potential to not only answer basic research questions but also enhance clinical studies and clinical trials and accelerate

drug development and testing. However, a consistent and reproducible method for isolating viable single cells and generating high quality single cell data from needle biopsy cores has been challenging to develop. Based on our experience isolating single cells from a large number of surgical tumor tissues, we set out to optimize a dissociation and processing protocol to generate viable single cell suspensions in adequate quantity for scRNA-seq from needle biopsy cores. A total of 17 de-identified 18-gauge needle biopsy samples were collected in collaboration with MD Anderson Cancer Center investigators. Samples were from liver, lymph node, pelvis, abdominal, neck, and lung tissues and included matched pre- and post-treatment samples. Patient biopsies were kept in RPMI medium on ice and transferred to EMPIRI (time to capture ranged from 3 to 6.5 hours after biopsy collection). Samples were dissociated using mechanical and enzymatic methods to achieve a single cell suspension. Cells were washed and viability and cell counts were verified before capture via 10x Chromium Connect. Captured cells were processed through the 10x Genomics Chromium Next GEM Single Cell workflow before sequencing on Illumina NovaSeq 6000 sequencer. Raw sequencing data were processed through EMPIRI's computational pipeline that includes QC steps, doublet removal, and Seurat and other downstream analyses. Recovery of viable cells from individual 18-gauge biopsy cores ranged from 2,000-300,000 cells per core, depending on the tissue type and cellularity. Cell viability was strictly monitored and was maintained above 80% for 16 of 17 samples (most samples >90%). Cell counts after sequencing and pipeline analysis averaged 6,466 cells per sample. The median number of UMI counts per cell was 5,580, and an average of 1,699 genes were identified per cell. Average sequencing saturation was 73%. Here, we demonstrate the feasibility of integrating scRNA-seq analysis into clinical trials or clinical studies to obtain rapid insights into on-target drug effects and anticipated cellular responses to therapies, including immunotherapies, within 3 weeks of biopsy collection. We have established a method for isolating high quality single cells for scRNA-seq from tissue biopsy core, as small as a single 18-gauge needle core. We tested our protocol on 17 human samples and showed successful isolation of highly viable cells from lung, lymph node, pelvis, abdominal, neck, and lung tissues. We were able to generate scRNA-seq data sets from all samples for analysis.

Acknowledgements: We thank our MDACC collaborators, particularly Drs. Scott Kopetz and Van Morris.

#5462

Elevated creatine phosphokinase (CPK) as a strong predictor of aumolertinib (Au) treatment response in patients (pts) with advanced non-small cell lung cancer (NSCLC): post-hoc analysis of AENEAS

Shun Lu[1], Chuan Li[2], Hong Jian[1], Xiaorong Dong[3], Jianhua Chen[4], Gongyan Chen[5], Yuping Sun[6], Yinghua Ji[7], Jiawei Wei[2], Si Sun[2], Zhenzhong Su[2], Qiu Sun[2], Hongying Wei[2], Qiong Wu[2]. *[1]Department of Medical Oncology, Shanghai Chest Hospital, Shanghai JiaoTong University, Shanghai, China,[2]Hansoh Pharmaceutical Group Co. Ltd., Shanghai, China,[3]Cancer Center, Union Hospital Tongji Medical College Huazhong University of Science and Technology, Wuhan, China,[4]Department of Medical Oncology-Chest, Hunan Cancer Hospital & The Affiliated Cancer Hospital of Xiangya School of Medicine, Central South University, Changsha, China,[5]Thoracic Oncology Medicine, Harbin Medical University Cancer Hospital, Harbin, China,[6]Department of Oncology, Jinan Central Hospital, Jinan, China,[7]Department of Oncology, First Affiliated Hospital of Xinxiang Medical University, Xinxiang, China*

Background: In AENEAS trial (NCT03849768), first-line Au for EGFR-mutated, advanced NSCLC showed robust improvement in PFS over gefitinib (G). CPK elevation was the most common AE during Au treatment which may pose safety concerns. To evaluate the relationship between CPK elevation and Au efficacy, we performed a post-hoc analysis of AENEAS.
Methods: AENEAS is a double-blind, randomized controlled phase III trial. Untreated advanced NSCLC pts with EGFR sensitizing mutations were assigned 1:1 to receive Au (110 mg QD) or G (250 mg QD). The primary endpoint was PFS. Secondary endpoints included ORR, DCR, DoR and DepOR. Data cutoff: Aug 1, 2021.
Results: 37.9% (81/214) of pts receiving Au had CPK elevation, among whom the mPFS was 26.3 mos and was significantly longer (HR=0.45; 95% CI: 0.31-0.67; P<.0001) than that of the CPK-normal pts (133/214) at 13.9 mos. PFS benefits remained consistent across all prespecified subgroups. Also for all the secondary endpoints, CPK-elevated pts demonstrated significant benefits over CPK-normal pts (TABLE). Multivariable

regression analysis revealed that CPK elevation was an independent predictor of prolonged PFS for pts receiving Au, with 54% reduced risk of progression or death for CPK-elevated pts compared with CPK-normal pts (HR=0.46; 95%CI: 0.31-0.68; P=.0001). Au demonstrated PFS benefits over G in both CPK-elevated pts (HR=0.40; 95% CI: 0.21-0.79; P=.0059) and CPK-normal pts (HR=0.63; 95% CI: 0.48-0.83; P=.0010), and the benefit was magnified in CPK-elevated pts. Further supported by post-hoc analysis of a phase 1/2 study (NCT02981108), PFS was also significantly prolonged in CPK-elevated pts receiving second or later line Au (17.7 vs 10.9 mos; HR=0.63; 95% CI: 0.46-0.87; P=.0049).
Conclusion: Our study first revealed the predictive value of CPK elevation on improved treatment response of Au, which is of great significance to help guide medical care.

Summary of Endpoints

	Elevated CPK(N=81)	**Normal CPK(N=133)**
PFS, months		
Median (95% CI)	26.3 (20.7-NA)	13.9 (12.4-19.8)
HR (95% CI)	0.45 (0.31-0.67)	
P-value	<0.0001	
12-months PFS rate (95% CI)	84.9 (74.9-91.1)	59.4 (50.2-67.5)
24-months PFS rate (95% CI)	54.3 (42.4-64.7)	30.1 (21.9-38.8)
DoR, months		
Median (95% CI)	23.5 (18.1-NA)	15.2 (10.2-19.2)
HR (95% CI)	0.51 (0.33-0.79)	
P-value	0.0024	
12-months DoR rate (95% CI)	77.7 (65.7-85.9)	55.8 (44.3-65.9)
24-months DoR rate (95% CI)	46.9 (33.7-59.0)	31.0 (20.9-41.6)
ORR (95% CI), %	87.7 (78.5-93.9)	66.9 (58.2-74.8)
OR (95% CI)	3.54 (1.64-7.64)	
P-value	0.0013	
DCR (95% CI), %	98.8 (93.3-100.0)	89.5 (83.0-94.1)

OR (95% CI)	9.59 (1.22-75.54)	
P-value	0.0318	
DepOR, %		
Mean (Std)	-50.5 (17.4)	-42.0 (24.1)
Range	-100.0-3.6	-100.0-50.0
P-value	0.0105	

#5463

The PD-L1 protein expression in Chinese patients with recurrent or metastatic head and neck squamous cell carcinoma: A multi-center retrospective study

Haizhen Lu[1], Dong Kuang[2], Lili Jiang[3], Jingping Yun[4], Qingxin Xia[5], Jian Wang[6], Pei Duan[2], Ping Zhou[3], Shengbing Zang[4], Yiping Jin[5], Xiangnan Jiang[6], Jielin Li[7], Wenmin Tang[7], Jiansong Zhou[7], Jihua Chen[7], Jianming Ying[1]. *[1]National Cancer Center/National Clinical Research Center for Cancer/Cancer Hospital, Chinese Academy of Medical Sciences and Peking Union Medical College, Beijing, China,[2]Tongji Hospital, Tongji Medical College, Huazhong University of Science & Technology, Wuhan, China,[3]West China Hospital, Sichuan University, Chengdu, China,[4]Sun Yat-Sen University Cancer Center, Guangzhou, China,[5]Affiliated Cancer Hospital of Zhengzhou University, Zhengzhou, China,[6]Fudan University Shanghai Cancer Center, Shanghai, China,[7]MSD China, Shanghai, China*

Programmed death-ligand 1 (PD-L1) is a trans-membrane protein and co-inhibitory factor of the immune response. PD-L1 can combine with its receptor (PD-1) to reduce the proliferation of PD-1-positive cells and induce apoptosis. Therefore, PD-L1 was employed as a prognostic marker and a target for anti-cancer immunotherapy in blocking the PD-1 and PD-L1 checkpoints. PD-L1 is highly expressed in various malignancies, including head and neck squamous cell carcinoma (HNSCC). HNSCC is the sixth most common cancer worldwide, with high incidence and mortality rates in China. Although PD-L1 expression has been widely investigated, the PD-L1 expression status in Chinese HNSCC patients (pts) is largely unrevealed. The primary objective of this study was to determine the prevalence of PD-L1 expression with the Combined Positive Score (CPS) ≥20 in Chinese pts

with recurrent or metastatic (R/M) HNSCC. The secondary objectives were to determine the prevalence of CPS≥1 in pts with R/M HNSCC and to study the difference in the demographic characteristics, clinicopathological parameters, treatment status, and other available biomarkers between the PD-L1 CPS≥20 group and the PD-L1 CPS<20 group. This study was a multi-center retrospective analysis of data from six centers in China from August 9, 2021, to February 28, 2022. Pts with histologically/cytologically confirmed diagnoses of R/M HNSCC were included. PD-L1 expression was assessed by IHC using the 22C3 PharmDx assay (Agilent, Santa Clara, CA, USA) and was determined using a CPS. The Chi-square test, Fisher's exact test, or Wilcoxon rank sum test would be used to compare the prevalence of these variables among pts between the PD-L1 CPS≥20 group and the PD-L1 CPS<20 group. Out of 406 enrolled pts with R/M HNSCC, 402 testing pts were included in the final analysis. For all testing R/M HNSCC pts, 168 pts (41.8% [95% CI 36.92-46.78]) had PD-L1 expression with CPS ≥20. In addition, 337 pts (83.8% [95% CI 79.86-87.29]) had PD-L1 expression (CPS≥1). For the testing pts, there were statistically significant differences in variables of gender (P < 0.001), smoking habit (P = 0.0138 for non-smokers versus current smokers), and primary tumor site (P < 0.001 for hypopharynx versus oral cavity and P = 0.0304 for larynx versus oral cavity) between the PD-L1 CPS≥20 group and the PD-L1 CPS<20 group. In summary, in Chinese R/M HNSCC pts, most pts (83.8%) had PD-L1 expression, and two-fifths (41.8%) had PD-L1 expression with CPS ≥20. Prevalence of PD-L1 among Chinese pts with R/M HNSCC was consistent with that reported in the global KEYNOTE-048 study. PD-L1 expression was significantly associated with gender, smoking history and primary tumor site. Our findings of the variables related to the PD-L1 expression levels can supply adjuvant evidence for clinical practice and are a solid basis for future research on immunotherapy.

#5464

Predictive biomarkers for PD-1 and PD-L1 checkpoint inhibitor response in NSCLC: An analysis of clinical trial and real-world data

WeiQing Venus So[1], David Dejardin[2], Eva Rossmann[3], Jehad Charo[4].
[1]Roche Innovation Center New York, F. Hoffmann-La Roche Ltd., New York, NY,[2]Department of Biostatistics, F. Hoffmann-La Roche Ltd., Basel, Switzerland,[3]Roche Innovation Center Basel, Basel, F. Hoffmann-La Roche

Ltd., Basel, Switzerland,[4]Roche Glycart AG, F. Hoffmann-La Roche Ltd., Schlieren, Switzerland

Importance**:** Largest analysis combining clinical trial and real-world data (RWD) to assess the clinical utility of biomarkers for anti-PD-1/PD-L1 checkpoint inhibitors (CPI) in NSCLC patients.
Objective: To assess the association between tumor PD-L1, TMB and blood analytes with clinical outcomes in patients with advanced NSCLC following CPI therapy.
Design: Retrospective cohort study with patients stratified into high and low biomarker groups. Correlation with treatment outcome in the different biomarker groups was investigated and compared between patients treated with CPI versus chemotherapy.
Setting: Data derived from electronic health records mostly from community oncology settings were combined with clinical trial data.
Participants: Starting with 71850 patients with advanced NSCLC who received CPI or chemotherapy, we selected 24152 patients from an electronic health record-derived de-identified NSCLC clinicogenomic database (CGDB) from a real-world cohort and nine Roche atezolizumab trials. Patients were diagnosed between January 2011 and February 2020 (data collection cut-off date).
Main Outcomes and Measures: Drug response was assessed by RECIST criteria for clinical trials and real-world response for RWD. Durable response was defined as having CR/PR without progression during the study period of 270 days. Associations of biomarker levels with treatment outcomes were analyzed using Fisher's exact test.
Results: High expression of PD-L1 on tumors (≥50%) were associated with lower risk of resistance to CPI (odds ratio [OR] 0.21; 95% CI = 0.14, 0.32; P< .001). The association was stronger in patients who had prior chemotherapy than first line CPI, with non-squamous than squamous histology, and smokers than non-smokers. Higher TMB (≥9.57 mut/Mb) was also associated with durable response (OR = 0.41; CI = 0.30, 0.55; P< .001). The combination of high TMB and PD-L1 expression was the strongest predictor of durable response (OR = 0.04; CI = 0.00, 0.20; P< .001). There was no evidence of an association between PD-L1/TMB and response to chemotherapy, suggesting a CPI-specific predictive effect. In contrast, blood

analytes were prognostic, having correlation with clinical outcome irrespective of treatment type.
Conclusion: This study supports the predictive utility of PD-L1 expression and TMB for NSCLC patients receiving CPI therapy and further elucidates their utility in patient sub-populations.

#5465
Immune cell dynamics of patients and mice with hepatocellular carcinoma treated with anti-PD-L1 plus anti-CTLA-4 combination therapy
Yuta Myojin, Benjamin Ruf, Mohamed-Reda Benmebarek, Kylynda Bauer, Rajiv Trehan, Kelley Coffman, Chi Ma, Cecilia B. Monge, Changqing Xie, Tim Greten. *National Cancer Institute Center for Cancer Research, Bethesda, MD*

Background: Hepatocellular carcinoma (HCC) is one of the major causes for cancer-related death. Single agent immunotherapy or combined immunotherapy have become the standard of care in advanced HCC. Recently, the combination of durvalumab (dur) plus a single dose of 300 mg tremelimumab (trem) (STRIDE regimen) have received FDA approval based on results from the HIMALAYA trial. However, immune responses have not been studied in detail. We tested the combination of 4x 75 mg trem plus dur and locoregional therapies in HCC at and conducted correlative studies.
Methods: We enrolled 28 patients with biopsy proven advanced HCC in an open-labeled phase 2 trial using dur and trem combined with ablative therapies (NCT02821754). Patients received four doses of 75mg trem every 4 weeks and 1500mg dur every 4 weeks until progression. Patients underwent an interventional radiologic procedure (RFA/TACE) on day 36. Peripheral blood mononuclear cells (PBMC) and serum from patients enrolled were collected at baseline and after 1 cycle (day 28). PBMC was analyzed by multicolor spectral cytometry using a 17 antibody pan immune cell panel and a 25 antibody T cell panel. Serum samples from patients were collected at baseline and on day 28. Serum samples were analyzed with a 34-plex cytokine/chemokine array. Mice with orthotopically injected HCC (RIL-175 and Hep55.1C) were treated with anti-PD-L1 plus anti-CTLA4 and followed for tumor responses. Hepatic lymphocytes, tumor infiltrating

lymphocytes (TILs), and splenocytes were analyzed by spectral cytometry from mice treated with immune checkpoint inhibitors.
Results: 28 patients with advanced HCC were enrolled in this study. The best clinical response for treatment was the following, partial response (PR, n=5), stable disease (SD, n=12), progressive disease (PD, n=8), and not evaluable (n=3). Median PFS and OS were 4.5 and 20.8 months respectively. Patient PBMC analysis demonstrated an increase of regulatory T cells 1.65 times from baseline after 28 days in all patients. The frequency of $Tbet^{+}CD4^{+}$ T cells showed a non-significant increase in patients demonstrating a PR. Serum cytokine analysis revealed the levels of IL-18, IL-10, CCL-2, and VEGF-a increased in responders after treatment. in contrast, an increase of IL-6 and TNF-alpha after treatment was found only in patients with PD. In animal experiments, the size of liver tumors treated with anti-PDL1 and anti-CTLA4 were significantly smaller than that with isotype controls. The lymphocytes in the adjacent livers and tumor-infiltrating lymphocytes (TILs) were analyzed. $PD1^{+}CD8^{+}$ T cells and $Tbet^{+}CD4^{+}$ T cells in the liver and TILs increased with combination treatment.
Conclusion: Anti-PD-L1 and anti-CTLA4 combination therapy have an anti-tumor effect on HCC. We observed an expansion of $PD1^{+}$ $CD8^{+}$ T cells and $Tbet^{+}$ $CD4^{+}$ T cells.

#5466
Functional status of tumor-associated macrophages impacts clinical outcome of durvalumab in patients with advanced NSCLC as revealed by proteomics mass spectrometry
Anna Margaret Hansen, Vivian Ying Wang, Andrew Chambers, David Chain, Jaime Rodriguez Canales, Jorge Blando, Steve Sweet, Zachary A. Cooper, Ashok Gupta, Carl Barrett, Yeoun Jin Kim, Ikbel Achour.
AstraZeneca US, Gaithersburg, MD

Introduction: Predictive biomarkers of anti–PD-(L)1 therapies have largely focused on the tumor-T cell axis where tumor cell PD-L1 expression has demonstrated its clinical utility in predicting overall survival (OS) in patients with advanced NSCLC. In prior work using computational image analysis of multiplex immunofluorescence (mIF), we have shown the positive impact of CD68+ PD-L1+ macrophages in combination with CD8+

T cells in predicting long-term OS benefit in NSCLC patients treated with durvalumab (anti-PD-L1), highlighting the impact of the myeloid compartment on IO responses. In part, using proteomics mass spectrometry we sought to investigate further the functional impact of myeloid cells on the IO response and in particular, suppressive (M2) tumor associated macrophages (TAMs).
Methods: Pre-treatment tumor samples from 66 patients with advanced NSCLC patients enrolled in durvalumab nonrandomized phase 1/2 trial (10 mg/kg Q2W, CP1108/NCT01693562) were processed for global and targeted proteomics. A pathologist determined the tumor area and a single FFPE tumor tissue section was used for laser-capture macrodissection and protein extraction followed by mass spectrometry analysis using label-free, data-independent and parallel reaction monitoring.
Results: Among the immune associated proteins detected by proteomics mass spectrometry, we evaluated CD163 protein expression, a well-described marker of suppressive (M2) macrophages, and its impact on durvalumab clinical outcomes, alone and in relationship with PD-L1 and immune infiltration. While proteomics-based biomarker evaluable population (BEP) shows shorter median (m) OS compared to intended to treat population, we validated that high expression of PD-L1 as measured by IHC or proteomics associates with greater OS benefit as expected when treating with durvalumab. Building on this, the evaluation of protein associated with suppressive M2 macrophages, revealed that approximately 30% of NSCLC patients with high CD163 protein expression show poor OS benefit (5 months mOS) following durvalumab treatment. In contrast, patients with PD-L1 TC $\geq$50% and low CD163 expression derive greater OS benefit (13.4 months mOS) than those with high CD163 expression (5 months mOS) or with PD-L1 TC <50% regardless of level of CD163 expression (4.1-7.4 months mOS). Moreover, patients with poorer outcome have significantly higher baseline CD163 protein expression as a proportion of total CD45 protein expression.
Conclusion: This analysis further confirms the importance of myeloid cell function within the tumor microenvironment (TME) in determining the outcome to T cell-directed IO therapy and highlights the utility of proteomics mass spectrometry in assessing more broadly and quantitatively the TME complementing findings based on RNAseq and IHC/mIF assays.

#5467

Single-cell analysis of CD34-enriched blood cells reveals early prognostic markers of myelodysplastic syndromes

Zohar Shipony[1], Nimrod Rappoport[2], Gila Lithwick-Yanai[1], Eti Meiri[1].
[1]Ultima Genomics, Newark, CA,[2]Weizmann Institute of Science, Rehovot, Israel

Myelodysplastic Syndromes (MDS) are a group of blood malignancies characterized by aberrant differentiation of hematopoietic stem and progenitor cells (HSPC) in the bone marrow that results in inefficient hematopoiesis and high risk of transformation to acute myeloid leukemia. In order to detect aberrant HSC differentiation in blood samples sensitively and accurately, we explored the use of scRNA-seq of CD34-enriched cells from peripheral blood in identifying differentiation trajectories that are abnormal in patient samples versus expected normal development.
A total of 685,000 CD34-enriched PBMCs from 93 samples were analyzed using 10X 3' v3 scRNA-seq library preparation. For increased efficiency, the samples were multiplexed in groups of 5 individuals and were later identified based on individual natural genetic variation using a custom genotyping assay or low-pass WGS. We then sequenced these 24 libraries on a UG100 sequencer to yield an average of 20,000 reads per cell. Six of these libraries were also sequenced on a NovaSeq. Comparison between scRNA profiles generated on the two different sequencers yielded highly similar results, including a similar ability to demultiplex the patient samples using genetic markers, accurately quantify gene modules and determine cell populations.To analyze the scRNA data, we used a novel computational framework, Metacell, to reconstruct metacell modules for both healthy and disease samples allowing us to find variability in the differentiation process between the disease samples and the normal baseline state. Two patients with MDS which had transformed to acute myelogenous leukemia (AML) demonstrated unique and distinct metacell clusters that were significantly separate from normal HSPC differentiation patterns, demonstrating distinct clusters with elevated levels of BCL2 which is an existing therapy target in secondary AML. Our results demonstrate that scRNA-seq analysis of peripheral blood HSPCs samples can be used to detect aberrations in HSC development in MDS patients and serve as a prognostic tool for stratification of patients with aggressive disease and drug response. Given

the cost-efficiency of the entire process, we believe this is one of the first examples of the potential practical utility of single-cell analysis in a clinical setting.

#5468

Which are the clinicopathological characteristics useful to define the metastatic breast cancer patients that will respond to CDK4/6 inhibitors and hormone therapy? An Italian real-world experience

Sara Bravaccini, Andrea Roncadori, William Balzi, Giovanni Martinelli, Maria Teresa Montella, Michela Palleschi, Roberta Maltoni. *IRCCS Istituto Romagnolo per lo Studio dei Tumori (IRST) "Dino Amadori", Meldola, Italy*

The development of CDK4/6 inhibitors has changed the therapeutic management of hormone receptor positive (HR+) metastatic breast cancer (mBC) by targeting the cell cycle machinery and overcoming endocrine resistance. However, a high proportion of patients will present disease progression due to the resistance of cancer cells to CDK4/6 inhibitors. Loss of retinoblastoma function, dysregulation of several signaling pathways and overexpression of CDK6, CDK7 and cyclin E have been described as main actors in the development of resistance to CDK4/6 inhibitors. Despite these findings on the role of new emerging biomarkers, we wondered if the clinicopathological characteristics could be useful to identify the patients that will respond to CDK4/6 inhibitors by the analysis of a retrospective case series of patients with HR+ mBC treated with hormone therapy plus CDK4/6 inhibitors (ribociclib, palbociclib, abemaciclib) at IRCCS Istituto Romagnolo per lo Studio dei Tumori (IRST) "Dino Amadori" (Meldola, Italy). 177 mBC patients 66 of whom were treated with CD4/6 inhibitors plus letrozole and 111 treated with CDK4/6 inhibitors and fulvestrant were enrolled in the study. The median age was 63 years (range 38-92), of whom 103 younger than 65 years. 152 were in postmenopausal status. Among the clinical characteristics, neutropenia was developed in 80 patients. ki67 was low (<20%) in 85 patients. 21 (23.3%) patients had bone metastases, 36 visceral metastases (23.3%) and 33 (36.7%) in other organs. The multivariable Cox PH model showed that having received a prior adjuvant treatment and the number of metastases were the only factors associated with the progression-free survival (PFS). Furthermore, when introducing the

presence of neutropenia as a potential predictor of PFS in the Cox PH model, it resulted to be a risk predictor of progression. To better describe the mechanism linking PFS and neutropenia a multistate model was developed. Low body surface area and older age were associated with an increased risk of developing neutropenia. High Ki67, the presence of visceral metastases and the absence of a prior adjuvant chemotherapy were prognostic factors of progression/death. As expected, among neutropenic patients, those with multiple previous lines of treatment were at higher risk of disease progression/death. Finally, the neutropenia status was associated with a more than double risk of progression/death with respect to patients without neutropenia (HR=2.311; p=0.025). Given that we identified a set of factors associated with the probability to develop neutropenia and considering that neutropenia itself is associated with an increased risk of progression, these baseline characteristics should be taken into account in order to reduce the occurrence of both neutropenia and disease progression.

#5469

Characterization of *CCNE1* amplifications and associated genomic features in ovarian and uterine cancers

Sunantha Sethuraman[1], Dominik Glodzik[1], Pier Selenica[2], Adrienne Johnson[1], Jorge S. Reis-Filho[2], Artur Veloso[1], Ian M. Silverman[1]. *[1]Repare Therapeutics Inc., Cambridge, MA,[2]Memorial Sloan Kettering Cancer Center, New York, NY*

Amplification of the Cyclin E1 gene (*CCNE1*) is a recurrent genetic alteration in ovarian and uterine cancers. Therapeutic approaches to target cancers harboring *CCNE1* amplification are being developed (e.g. PKMYT1, WEE1, and CDK2 inhibitors). In this study, we report the genomic landscape and architecture of *CCNE1* amplifications using a combination of whole-exome (WES) and whole-genome sequencing (WGS) approaches. WES data from 361 ovarian and 580 uterine cancers was retrieved from TCGA. WGS data from 113 ovarian and 51 uterine cancers was retrieved from PCAWG. For both WES and WGS, amplification was defined as CN minus ploidy (CN-ploidy) >= 4. *CCNE1* amplification was detected in up to 21.2% of ovarian and 13.7% of uterine cancers from both methods. A review of the co-alteration landscape using WES revealed that *TP53* alterations frequently co-occurred with *CCNE1* amplifications in both

ovarian and uterine cancers (ovarian: 95.8% vs 87.6%, OR = 3.24, p=0.1; uterine: 89.6% vs 36.0%, OR = 15.2, p =2.14e-13) and *BRCA1* alterations were mutually exclusive with *CCNE1* amplifications in ovarian cancer (2.1% vs 17.9%, OR=0.2, p = 3.1e-3). In addition, alterations in *ARID1A* (0% vs 40.5%, OR = 0, p = 1.3e-10) and *PTEN* (4.2% vs 60.1%, OR = 0.03, p =2.7e-15) were mutually exclusive with *CCNE1* amplifications in uterine cancer. The number of *CCNE1* copies ranged widely, with median CN-ploidy values of 9.3 (range: 4.0 -35.0) in ovarian and 7.7 (range: 4.0 -40.3) in uterine cancers from the WES cohort, and 7.4 (range: 4.1 -34.3) in ovarian and 11.0 (range: 4.6 - 81.9) in uterine cancers from WGS. We also observed a broad range of *CCNE1* amplicon sizes, from highly focal to chromosome arm-level amplifications. WGS data showed frequent loss of heterozygosity (LOH) of chromosome 19 arms and an enrichment of fold-back inversions proximal to the *CCNE1* amplicon implicating breakage-fusion-bridge in formation of *CCNE1* amplicons. Whole genome duplication (WGD) was detected significantly more frequently in ovarian and uterine cancers with *CCNE1* amplification than the wild-type group (ovarian: 90.9% vs 48.3%, p = 6.4e-10; uterine: 78.7% vs 21.9%, p = 7.1e-15). As compared to *CCNE1* wild-type cancers, *CCNE1*-amplified cancers were found to display an enrichment for certain structural variant signatures: RS1, dominated by 100Kb-1Mb duplications (median = 30, p=0.08); RS2, dominated by translocations (median = 16, p=0.001); and RS7, dominated by 100Kb-1Mb deletions (median=23, p=0.0002). In conclusion, *CCNE1*-amplified ovarian and uterine cancers are enriched for *TP53* alterations and display a high degree of genome instability manifested as WGD and characteristic structural variants. Fold-back inversions and LOH were frequently observed at the *CCNE1* locus in tumors with *CCNE1* amplification, suggesting a potential breakage-fusion-bridge mechanism in the genesis of this amplicon.

#5470

Identification of gene amplification based signature as predictors for chemotherapy in squamous cell carcinoma of the lung

Yuan Tang[1], Yuli Li[1], Ting Hou[2], Lili Jiang[1], Hongjie Liu[2], Chunxiao Pan[2], Weiya Wang[1], Li Qiu[1], Yajing Zhang[1], Guiping Zhang[1], Ke Zheng[1].
[1]Department of Pathology, West China Hospital, Chengdu, China,[2]Burning Rock Biotech, Guangzhou, China

Background: Lung squamous cell carcinoma (LUSC) is the second most popular histologic subtype accounting for 25%~30% of lung cancer. Due to the lack of targeted therapies for LUSC, the prognosis is poor and chemotherapy still plays a full role in the treatment of LUSC patients currently. However, a significant proportion of patients showed a bad response to chemotherapy. The development of predictive biomarkers is urgent. We aimed to identify new chemotherapy biomarkers based on genomic alterations.
Methods: We retrospectively analyzed DNA sequencing data of 317 LUSC patients (pts) at West China hospital. We collected the clinical features and progression-free survival (PFS) of 35 pts with chemotherapy only. Pts were assigned to different subgroups based on genomic alterations using non-negative matrix factorization (NMF) clustering. Based on the characteristics of the cluster, we then explored clear gene signatures to predict the prognosis of chemotherapy. The clinical information and sequencing data of TCGA LUSC with chemotherapy were used to validate the prognostic value of the signature.
Results: The 317 LUSC pts were grouped into 4 clusters characterized by different genomic alterations. Cluster 1 (C1) had 129 pts and was characterized by *TP53* alterations. There were 116 pts in cluster 2 (C2) characterized by *PIK3CA* amplification (amp). Cluster 3 (C3) had 33 pts and was characterized by gene amp of *CCND1*, *FGF3*, *FGF4*, and *FGF19*. Cluster 4 (C4) was characterized by gene amp of *FGFR1*, *KDR*, *KIT*, and PDGFRA. The 35 pts treated with chemotherapy only were also classified into 4 clusters. C1 was associated with the shortest PFS (hazard ratio (HR), 2.87; 95% confidence interval (CI), 1.15-7.13; p = 0.018) independently of the clinical stage, but C2, C3, and C4 showed no significant difference. In addition, we also found that pts with *TP53* loss of function (LOF) alteration had significantly shorter PFS than those without
TP53 LOF (wildtype or not LOF, p = 0.029). So we further modified the clustering by *TP53* alteration from C1 and gene amp from C2, C3, and C4. Therefore, 35 pts were then grouped into 3 subtypes based on *TP53* LOF and gene amp characteristics, and the PFS was significantly different. Pts (n = 8, 23%) with at least one amp of 9 genes (*PIK3CA, CCND1, FGF3, FGF4, FGF19, FGFR1, KDR, KIT,* and *PDGFRA*) but no *TP53* LOF had the longest PFS (HR, 0.12; 95% CI, 0.02-0.66; p = 0.011). Pts (n = 6) with

TP53 LOF but no 9-gene amp had poor survival compared with pts in other subtypes. This gene signature was validated in TCGA pts. The signature of 9-gene amp without TP53 LOF also indicated the best PFS and *TP53* LOF without 9-gene amp indicated the worst PFS ($p = 0.081$).
Conclusion: We develop a biomarker signature that consists of 9-gene amp and *TP53* LOF to indicate the prognosis of chemotherapy. Our results suggest that 9-gene amp without *TP53* LOF in LUSC is a favorable prognostic marker for patients taking chemotherapy.

#5471

Integrating tumor-intrinsic and immunological factors to identify immunogenic breast cancers from a low-risk cohort; results from the randomized SweBCG91RT trial

Axel Stenmark Tullberg[1], Martin Sjöström[2], Emma Niméus[3], Fredrik Killander[3], Laura Chang[4], Felix Y. Feng[2], Corey W. Speers[5], Lori J. Pierce[5], Anokó Kovács[6], Dan Lundstedt[7], Erik Holmberg[7], Per Karlsson[7].
[1]University of Gothenburg, Gothenburg, Sweden,[2]Department of Radiation Oncology, UCSF Helen Diller Family Comprehensive Cancer Center, San Francisco, CA,[3]Lund University, Lund, Sweden,[4]Exact Sciences, Redwood City, CA,[5]Department of Radiation Oncology, University of Michigan, Ann Arbor, MI,[6]Department of Pathology, University of Gothenburg, Gothenburg, Sweden,[7]Department of Oncology, University of Gothenburg, Gothenburg, Sweden

Purpose: The local immune infiltrate's influence on tumor progression may be linked to tumor-intrinsic factors. This study aimed to investigate whether integrating immunological and tumor-intrinsic factors could identify patients who may be candidates for de-escalation of radiotherapy (RT).Experimental Design: The practice-changing SweBCG91RT trial included 1178 patients with stage I-IIA breast cancer, randomized to breast-conserving surgery with or without adjuvant RT with sparse use of systemic therapy (95% without systemic therapy) and followed for a median time of 15.2 years. We developed two gene expression models to capture immunological activity and immunomodulatory tumor-intrinsic qualities, respectively. We then analyzed if combining these two variables could identify a subgroup where RT de-escalation is feasible.

Results: The immunomodulatory model correlated with proliferation and was named Proliferative Index. The immunological model was enriched for T cell signatures and was named Immunescore. Increased Proliferative Index predicted an increased prognostic benefit from Immunescore ($p_{interaction}$=0.01). Combining the two models stratified patients who may be recommended an escalated RT (RT boost) by RT benefit and prognosis. Patients with a low predicted risk benefited from standard RT (HR: 0.28, CI 95% 0.09-0.85, p=0.025) and had a 5.4% 10-year incidence of ipsilateral breast tumor recurrence (IBTR) after radiation. In contrast, the group with a high predicted risk, characterized by rapidly proliferating tumors without an immune infiltrate, had a clinically meaningful high 10-year incidence of IBTR despite RT treatment (19.5% (CI 95% 12.2-30.3)).
Conclusions: Integrating tumor-intrinsic and immunological factors may identify immunogenic tumors in early-stage breast cancer populations and identify patients for whom de-escalated RT may be appropriate. Patients with rapidly proliferating tumors and an immune infiltrate may be candidates for RT de-escalation.

#5472

Utilizing response in immune checkpoint inhibitor treated cohorts improves clinical applicability of neoantigen immunogenicity predictions

Hima Anbunathan, Neeraja Ravi, Rachel Marty Pyke, Steven Dea, Richard O. Chen, Sean Michael Boyle. *Personalis, Inc., Menlo Park, CA*

Introduction: Neoantigen-based biomarkers have improved predictions of response to immune checkpoint blockade (ICB) therapy, highlighting the importance of accurate prediction of immunogenic neoantigen candidates. A challenge in developing robust immunogenicity prediction models is limited availability of sequencing-associated immunogenicity data for evaluating methods due to the complexity of generating such datasets. We propose a novel approach to optimize prediction models of immunogenic neoantigens using a meta-analysis framework based on multiple ICB cohorts.
Methods: To build on the 110 mono-allelic immunopeptidomics-derived SHERPA® MHC binding prediction framework, we engineered T-cell recognition features on two datasets: peptide-centric data aggregated by Schmidt et al. and patient-specific exome and transcriptome sequencing data

from the TESLA consortium. We developed two-tiered models based on the feature landscapes of both datasets to predict peptide-MHC (pMHC) immunogenicity, incorporating features with significant performance gains. We systematically re-processed publicly available DNA and RNA sequencing data from over 500 ICB treated patients spanning 12 different cohorts across five different cancer types with a harmonized bioinformatics pipeline. We then evaluated the performance of each model consisting of a unique combination of immunogenic features across the ICB training (N=7) and validation (N=5) cohorts using a meta-analysis framework.
Results: We evaluated iterations of SHERPA-Immunogenicity (SI) models using the Schmidt et al. and TESLA datasets, resulting in a range of performance metrics (area under the precision recall curves of 0.74-0.84 and positive predictive values of 0.32-0.54). After aggregating pMHC predictions into patient-specific scores based on the most immunogenic peptide present (SHERPA-Immunogenicity Maximum - SIM) or the quantity of immunogenic peptides identified (SHERPA-Immunogenicity Burden - SIB), we observed that responders had higher SIM and SIB scores compared to non-responders across the melanoma training cohorts. We found SIM scores outperformed SIB scores, suggesting the degree of epitope immunogenicity may be a critical factor in predicting response. The model with the most significant meta p-value for ICB response in melanoma cohorts (OR=2.43, p=0.006) also predicted overall survival in 3/5 melanoma cohorts ($p<0.05$).
Conclusions: We developed a novel framework to predict neoantigen immunogenicity utilizing meta-analysis of ICB cohorts to overcome dataset limitations and gain prediction performance confidence. We look forward to supporting personalized cancer vaccine development with our pMHC immunogenicity predictions and applying our predictive biomarker on additional ICB cohorts.

#5473
Genomic profiling of chemotherapy-related clonal hematopoiesis in patients with high-grade serous ovarian cancer
Sara Corvigno, jun yao, Li Zhao, amma asare, Joseph celestino, richard hajek, Ency Arboleda Goette, Elaine Stur, Emine Bayraktar, Mark S Kim, ping song, Qingxiu Zhang, xingzhi song, Mohammad Mohammad, kenna

Shaw, Jianhua zhang, karen lu, amir jazaeri, shannon westin, Sanghoon Lee, anil sood. *UT MD Anderson Cancer Center, Houston, TX*

Background: Clonal hematopoiesis (CH) is identified as the presence of clonal populations of hematopoietic stem cells (HSC). Hematopoietic lineage differentiation is subjected to genetic mutations that, due to fitness advantages, might give rise to clonally expanded populations. Clonal hematopoiesis of indeterminate potential (CHIP) is defined as the outgrowth of a single clone driven by acquired somatic mutation(s) in HSCs, in the absence of hematological abnormalities. Previous studies have been shown the association of CH with aging and a higher risk of developing secondary hematologic malignancies in cancer patients treated with chemotherapy agents. It is therefore of great interest to study CH incidence prior to and post chemotherapy exposure and its association with the evolution of hematologic malignancies. We aimed to characterize CHIP variants of a highly selected group of patients with high-grade serous ovarian cancer (HGSC) who underwent neoadjuvant chemotherapy; moreover, while previous CHIP studies are largely knowledge based and are limited to known hematologic genes or target gene panels, our study discovers novel CHIP mutations.
Methods: Comprehensive ultra-high-depth whole exome sequencing using unique molecular barcode technologies was performed using plasma-derived cell-free DNA and matched white blood cells DNA and tumor DNA from pre-NACT (n=12) and post-NACT (n=12) samples of patients with HGSC who have excellent or poor response to NACT. Using spike-in mutated DNAs as positive controls, we detected variant alleles at 1% variant allele frequency.
Results: We identified on average about 3,000 candidate CHIP variants in one patient. Among these, 1,977 variants affecting 1,375 genes were recurrently found in more than one patient. These CHIP genes include not only previous reported CHIP genes (e.g. DNMT3A, JAK2, TET2, and KMT2D) but also many novel CHIP candidates (such as RPTN, MTCH2, FAM186A, CACNA1A, FCGBP, and MUC3A). A number of CHIP mutations were uniquely found enriched in post-chemotherapy samples (e.g. ARID1A T290P, TP53 G245D, SMARCA4 G495D, and CIC T2456P). Interestingly, there is a strong enrichment of COSMIC cancer census genes in CHIP genes identified in every patient.

Conclusions: Our findings corroborate the notion that CHIP mutations are present in nonmalignant blood cells of patients with HGSC, and some are enriched after chemotherapy. Moreover, our innovative sequencing approach allowed discovery of novel candidate CHIP genes. The systematic identification of CHIP in patients with HGSC might be an important new clinical consideration when establishing chemotherapy protocols.

#5474

Combined use of MRI and TAM analysis in GB monitoring

Carolina Giordano[1], Giuseppe Maria Della Pepa[1], Simona Romano[2], Laura Marrone[2], Carlo Maria Donzelli[1], Maria Fiammetta Romano[2], Simona Gaudino[1]. *[1]Università Cattolica del Sacro Cuore - Fondazione Policlinico Universitario Agostino Gemelli, Rome, Italy,[2]University of Naples Federico II, Napoli, Italy*

Glioblastoma (GB) is the most frequent and aggressive primary brain tumor. It is a highly infiltrating tumor. Complete eradication by surgery is difficult. The probability of survival beyond two years is very low. Magnetic resonance imaging (MRI) is a routine procedure for diagnosing gliomas. However, morphological MRI often fails to identify and quantify the presence of infiltration in peritumoral non-enhanced areas, resulting in inaccuracy in the assessment of invasive margins. Up to 50% of the patients show pseudo-progression. Morphological MRI fails to distinguish the marked enhancement in the tumor bed caused by radionecrosis from actual tumor progression. Diagnosis of GB recurrence through MR morphological sequences has a sensitivity and specificity of about 68% and 77%. Such percentages rise thanks to the use of non-morphological sequences (PWI, DWI, MRS), which are used in routine tumor protocols only in large centers and interpreted by expert neuroradiologists. Biomarkers in conjunction with MRI may help improve the classification, prognosis, and treatment choice. GB is highly infiltrated with monocytic cells, tumor-associated macrophages (TAMs), that invade the peripheral blood. Our group has recently identified a splice isoform of FK506-binding protein 51 (FKBP51) as a reliable TAM marker. We found an expansion in circulating CD163/FKBP51s monocytes in a cohort of GB patients. In patients with an MRI diagnosis of complete surgical tumor removal, these monocytes dramatically decreased. In patients with an MRI diagnosis of residual tumor, most of the peripheral CD163

monocytes that in the preoperative stage were FKBP51s- had turned into FKBP51s+. CD163/FKBP51s+ monocytes helped to distinguish between radionecrosis and actual tumor progression. These results suggest that circulating CD163/FKBP51s+ monocytes are associated with GB and can be helpful in monitoring GB patients.

#5475

Improved prediction of immunotherapy responses by constitutive neoantigen load and LINE-1 methylation

Hyoeun Bang[1], Jeong Yeon Kim[2], Cheolyong Joe[3], Kyeonghui Kim[2], Younghak Bang[3], Hyemin Kim[4], Honghi Cha[4], Eunjoo Oh[4], Naeun Lee[3], Inkyung Shin[1], Seung-Jae Noh[1], Dae-Yeon Cho[1], Se-Hoon Lee[4], Jung Kyoon Choi[2]. *[1]PentaMedix Co., Ltd., Seongnam, Korea, Republic of,[2]Bio and Brain Engineering, KAIST, Daejeon, Korea, Republic of,[3]Health Sciences and Technology, Sungkyunkwan University, Seoul, Korea, Republic of,[4]Medicine, Sungkyunkwan University School of Medicine, Seoul, Korea, Republic of*

Previous biomarkers such as PD-L1 expression, tumor mutation burden (TMB), and neoantigen load have limited accuracy in predicting responses to immune checkpoint inhibitor (ICI) therapy. In this work, we propose an improved predictor of ICI responses on the basis of our previous findings on the role of neoantigen functionality and genomic hypomethylation in tumor immunity. Specifically, we developed a metric of constitutive neoantigen load given the association of constitutive neoantigens derived from genes indispensable for cancer growth with favorable clinical responses to ICI (Clin. Transl. Med. 12:e714). A panel that captures somatic mutations on the 300 most essential genes identified by genome-wide screening in ~1,800 pan-cancer cell lines was used. Our DeepNeo algorithm (Nat. Commun. 11:951; Nat. Genet. 2023) was employed to identify T cell-reactive neoantigens from somatic mutations binding patient-matched HLA proteins. Also, considering the role of genomic hypomethylation in inducing resistance of tumors to ICI therapy (Nat. Commun. 10:4278), we developed an assay that estimates genomic hypomethylation by targeted sequencing of LINE-1 elements. Constitutive neoantigen load and LINE-1 methylation status were evaluated in our cohort consisting of 335 lung cancer patients treated with ICIs. As a result, constitutive neoantigen load (HR=0.671; p-

value=3.13E-03) and LINE-1 methylation (HR=0.597; p-value=0.012) outperformed PD-L1 (HR=0.74; p-value=0.199), TMB (HR=0.917; p-value=0.511), and the combination of PD-L1 and TMB (HR=0.707; p-value=0.218). The combination of constitutive neoantigen load and LINE-1 methylation (HR=0.245; p-value=1.11E-05) showed even better predictive power. In conclusion, our approach can be used as new companion diagnostics for ICI-based immune-oncology.

#5476

Veracyte Biopharma Atlas for colorectal cancer: Combining multi-parameter approach and machine learning to capture the complexity of the tumor immune contexture

laurent vanhille, Alboukadel Kassambara, Chafik Hamdad, Margaux Mercadal, Alexia Papadopoulos, Pernelle Outters, Théo Vasse, Vanina Leca, Jérôme Galon, Jacques Fieschi. *Veracyte, Inc., Marseille, France*

(a) Understanding the immune contribution has deeply modified the standard of care of patients, especially with the advent of immunotherapies (ITs). However, ITs are still efficient only on a minority of the patients, especially for colorectal cancer (CRC), a high-incidence cancer. One hypothesis to explain the heterogeneity of the response to IT is that the presence or absence of immune factors within the tumor micro-environment (TME) may critically impact the efficacy of treatments. In this context, a deeper molecular understanding of the TME could be key to stratify patients. Here, we describe a proof of concept of the Veracyte Biopharma Atlas for CRC based on a multi-omics approach which integrates a unique range of assays allowing to decipher the immune contexture of tumors and offer a personalized and dynamic “fingerprint” of the interactions between the tumor and the immune system.
(b) Veracyte Biopharma Atlas characterizes the tumor microenvironment by analyzing information from 3 different modalities: (i) proteomics (Brightplex® multiplex immunohistochemistry panels), (ii) transcriptomics (RNA sequencing) and (iii) genomics (somatic mutations by exome sequencing). This deep characterization of the tumor and its micro-environment requires the integration of thousands of features. The innovative Veracyte Biopharma Atlas approach relies on linear (multimodal factor analysis) and non-linear (self-organizing map) approaches with

graphical representation of the data to integrate this multi-omics information.
(c) Gene expression profiling, genomics analysis and proteomics by multiplex spatial technology were performed on 47 CRC FFPE samples to characterize the immune contexture of this disease. Multimodal analysis was used to derive a unique atlas map highlighting clusters distinguished by complex features and their immune tumor contexture. Indeed, as examples, the atlas map allows the identification of a group of patients displaying high immune cell infiltration, including T cell and macrophages. They are also characterized by an immune genes signature. By contrast, another group of patients is poorly infiltrated by immune cells but exhibits an elevated M2/M1 ratio, favorable to tumor development.
(d) This proof of concept lays the foundations of an atlas for CRC that will be extended to samples associated with clinical data to build a map of the disease. Later-on, by projecting data from new specimens onto this referential map, it will become possible to establish an Immunogram of the tumor microenvironment of individual patients to define the most appropriate treatment but also facilitate the development of new therapies.

#5477

An investigation to study differential gene expression of lung cancer cells, tumor associated macrophages, and bone marrow derived mesenchymal stems cells in the tumor microenvironment

Hirendra N. Banerjee[1], Joseph Hedley[1], Cheslsey Aurelus[1], Narendra Banerjee[1], Kuldeep Rawat[1], Quentin Reaves[1], Shennel Brown, Darla Gilmartin[1], Makieyah Liverman[1], Jazmine Cuffee[1], Elizabeth Cagle[1], Erik Armstrong[1], Brent lake[1], Santosh Mandal[2], Somiranjan Ghosh[3], Stephen Beebe[4], Kamal Asadipour[4], Christopher Krauss[5], Santanu Bhattacharya[6], Tanmay Kulkarni[7], Zahidur Abedin[8]. *[1]Natural, Pharmacy and Health, Elizabeth City State University, Elizabeth City, NC,[2]Chemistry, Morgan State University, Baltimore, MD,[3]Pediatrics, Howard University Medical School, DC, DC,[4]Bioelectrics, Old Dominion University, Norfolk, VA,[5]IBBR, University of Maryland, Gaithersburg, MD,[6]Biochemistry and Molecular Biology, Mayo Clinic, Jacksonville, FL,[7]Biomedical Engineering and Pathology, Mayo Clinic, Jacksonville, FL,[8]Molecular Biology, Primbio Research, Garnet Valley, PA*

Cancer is a public health crisis affecting approximately 19.3 million globally, annually. Lung cancer has the highest percentage of incidence and is responsible for 27% of cancer-related deaths. The prevalence of lung cancer worldwide led us to investigate differential gene expression in lung adenocarcinoma and small cell lung cancer cell lines in comparison to a healthy lung cell line. We also investigated the effect of lung tumor microenvironment to bone marrow derived pluripotent mesenchymal stem cells (PMSC) and tumor associated macrophages. This research involved cancer and healthy cell line culture with appropriate medium. Whole transcriptomic and small non-coding RNA sequencing and analysis by Ingenuity Pathway Analysis (Qiagen, USA), Quantitative RT-PCR and ELISA assays. We further studied morphological changes and differential gene expression in extracellular vesicles(exosomes) isolated from the TAM and TME exposed PMCs by atomic force microscopy and RNA sequencing techniques. The results of our investigation showed differential gene expression and novel core canonical pathways in the lung cancer cells, TME exposed TAM, and PMSC. We also observed morphological changes in TME derived exosomes from TAM and PMSC. RNA sequencing results showed differential gene expression of both coding and non-coding RNAs including tRNA fragments. Thus, our findings of this investigation led to identification of multiple cancer related genes and small non-coding microRNA, long non-coding RNA, and tRNA fragments which will have potential diagnostic and therapeutic target value that demands further future research. Acknowledgement: This research is supported by a grant from US NIH-NIGMS- 5T34GM100831-08 and US-NIH Grant# U 54 MD007597-31-5959.

#5479

A six-protein signature predicts response and survival in patients with advanced cutaneous melanoma treated with immunotherapy

Srikanth Manda[1], Adel T. Aref[1], Erin K. Sykes[1], Steven G. Williams[1], Jennifer M. Koh[1], Erin M. Humphries[1], Daniel Bucio-Noble[1], Daniela Lee-Smith[1], Natasha Lucas[1], Dylan Xavier[1], Alexander Menzies[2], Ines Da Silva[2], Felicity Newell[3], Rosemary Balleine[4], Peter G. Hains[1], Graham Mann[5], Phil J. Robinson[1], Georgina V. Long[2], James Wilmott[2], Qing Zhong[1], Richard A. Scolyer[2], Roger R. Reddel[1]. *[1]ProCan, Children's*

Medical Research Institute (CMRI), Sydney, Australia,[2]Melanoma Institute Australia, Sydney, Australia,[3]QIMR Berghofer Medical Research Institute, Sydney, Australia,[4]Faculty of Medicine and Health, The University of Sydney, Sydney, Australia,[5]The John Curtin School of Medical Research, Canberra, Australia

Introduction: Cutaneous melanoma (CM) is one of the most aggressive types of skin cancer, with a poor prognosis for advanced stages. Despite the advances in immunotherapy (IO) treatment, robust predictive biomarkers are still required. The aim of this study was to identify a prognostic and predictive protein-based signature for advanced CM.
Methods: A training cohort of 142 pretreatment tumor samples from 71 patients with metastatic CM treated with IO (anti-PD-1) and an independent validation cohort from 67 patients with stage III treatment-naïve CM were analyzed by data-independent acquisition mass spectrometry (DIA-MS). Survival analysis based initially on univariate regression and subsequently on 100 runs of 20-fold cross-validation of multivariate Cox regression with Least Absolute Shrinkage and Selection Operator (LASSO) was performed to obtain a reduced list of candidate proteins associated with melanoma-specific survival. A risk score was built from the final six proteins. The prognostic ability of this 6-protein signature for melanoma-specific survival was demonstrated by a time-dependent receiver operating characteristic curve (AUROC) and validated by four independent datasets. The predictive ability of the 6-protein signature was also explored in the training dataset using response to IO as the outcome of interest. Finally, differential expression analyses were conducted on the training data to identify the top proteins associated with response to IO. Proteins that were highly correlated (Pearson R^2 >0.9) with the 6-protein signature were identified and subjected to pathway enrichment analysis (PEA).
Results: Proteomic analyses identified 4298 and 4577 proteins in the training and validation cohorts respectively, with 81.1% overlap between the two sets. Using LASSO multivariate Cox modeling, six proteins were identified in the training cohort, from which a risk score was calculated that dichotomized patients into high- and low-risk groups (Hazard ratio (HR) 2.7, 95% confidence interval (CI) 1.9-3.9, and, AUROC 0.86). The 6-protein signature's prognostic performance was validated using the RNAseq dataset from the same training cohort (HR 2.7, p<0.001), a second RNASeq dataset

from The Cancer Genome Atlas (HR 1.7, p<0.001), a single-cell RNASeq dataset from patients treated with IO (HR 1.2, p<0.001) and finally a proteomic dataset in an independent cohort (stage III treatment-naïve CM) (HR 2.4, p<0.001). The 6-protein signature was also associated with response to IO (HR 2.3, p=0.005). PEA showed that the highly correlated proteins were mostly related to DNA repair and DNA metabolic pathways. PEA revealed activation of immune-related pathways in patients who achieved a good response to IO.
Conclusion: A 6-protein signature identified a sub-group of patients with advanced CM who are at higher risk of progression on IO and death from melanoma.

Cancer Outcomes 2

#4358
Glucagon-like peptide 1 agonist use and the progression of monoclonal gammopathy of undetermined significance to multiple myeloma in US veterans with diabetes mellitus

Nikhil Grandhi[1], Lawrence Liu[2], Mei Wang[3], Theodore Thomas[3], Akhil Kumar[3], Kristin Vargo[3], Kristen Sanfilippo[1], Grahm Colditz[1], Su-Hsin Chang[3]. *[1]Washington University In St. Louis, St. Louis, MO,[2]City of Hope Comprehensive Cancer Center, Duarte, CA,[3]St. Louis Veterans Affairs Medical Center, St. Louis, MO*

Background: Glucagon-like peptide 1 (GLP-1) agonists are increasingly used in diabetics due to their cardiac and renal benefits along with their actions as antihyperglycemics. They also showed inhibitory effects in ovarian, breast, prostate, and pancreatic cancers in preclinical studies. However, to our knowledge, no studies have examined whether GLP-1 agonists have a similar effect in multiple myeloma. Using a population-based study design, we aimed to assess the association of GLP-1 agonist use in the progression of MGUS to MM in patients with diabetes mellitus (DM).
Methods: Patients diagnosed with MGUS from 1999-2021 in the Veterans Health Administration were identified via ICD codes and further confirmed by a natural language processing (NLP)-based algorithm. Progression to smoldering MM (sMM) or MM was also confirmed by another NLP-based algorithm. Only patients with DM, IgG, IgA, or light chain MGUS, and

black and white patients were included. We excluded patients who experienced progression within 1 year of MGUS diagnosis or within 2 years of DM diagnosis, and patients diagnosed with MGUS before DM diagnosis. We performed 1:2 matching for patients with and without GLP-1 agonist exposure based on their follow-up time. Gray's test was performed to detect the difference between the two cumulative incidence functions (CIF) for progression stratified by GLP-1 agonist use status. The association between GLP-1 agonist use and progression was estimated by multivariable-adjusted hazard ratio (aHR) using Fine-Gray distribution hazard model with death as a competing event and time-varying GLP-1 agonist use. The covariates included age, BMI, monoclonal protein (M-spike) level (≥1.5g/dL), creatinine (>1.5 mg/dL), glycated hemoglobin (HbA1c; < 7%, 7% - 9%, and > 9%) at MGUS diagnosis, metformin and sodium-glucose co-transporter 2 inhibitor (SLGT2i) use, as well as sex, race, MGUS heavy chain subtype, light-chain MGUS, Charlson Comorbidity Index, and months from diagnoses of DM to MGUS.
Results: Our NLP algorithm confirmed 19,551 patients with DM and MGUS. After applying our inclusion and exclusion criteria, we had 14,832 patients, of which 1,303 had GLP-1 agonist use. After matching, our analytic cohort included 1,303 patients with exposure, and 2,606 patients without. There is no evidence to show that CIFs were different between the exposed and unexposed groups. However, the multivariable analysis showed that GLP-1 agonist use was associated with decreased progression to MM: aHR 0.35, 95% confidence interval 0.14-0.90, $p = 0.03$.
Conclusions: For DM patients with MGUS, GLP-1 agonist use is associated with a 65% reduction in risk of progression from MGUS to sMM/MM. Prospective studies examining whether GLP-1 agonists can be used as possible chemoprevention in MGUS patients with DM should be explored.

#4359

Interventions to improve pathologic nodal staging of curatively resected lung cancer: A population-based implementation study

Meredith A. Ray[1], Carrie Fehnel[2], Olawale Akinbobola[2], Andrea Saulsberry[2], Kourtney Dortch[2], Anberitha Matthews[2], Amal Anga[3], Christopher Giampapa[4], Elizabeth Sales[5], Sherry Okun[6], Edward T. Robbins[7], Bradley Wolf[8], Paul Levy[9], Horace L. Wiggins[10], Thomas Ng[11], Vishal Sachdev[12], Ganpat Valaulikar[3], Hetal D. Patel[13], Nicholas R. Faris[2],

Matthew Smeltzer[14], Raymond U. Osarogiagbon[2]. *[1]University of Memphis, Memphis, Memphis, TN,[2]Baptist Cancer Center, Memphis, TN,[3]Veterans Affair Medical Center, Memphis, TN,[4]Jackson-Madison County General Hospital, Jackson, TN,[5]Doctors Anatomic Pathology, Jonesboro, AR,[6]Tupelo Pathology Group, Tupelo, MS,[7]Baptist Memorial Hospital - Memphis, Memphis, TN,[8]Baptist Memorial Hospital - DeSoto, Southaven, MS,[9]Baptist Memorial Hospital - North Mississippi, Oxford, MS,[10]St. Bernard's Regional Medical Center, Jonesboro, AR,[11]Methodist University Hospital, Memphis, TN,[12]North Mississippi Medical Center, Tupelo, MS,[13]Jackson-Madison County General Hospital, Jackson, MS,[14]University of Memphis, Memphis, TN*

Introduction. Despite its importance, pathologic nodal (pN) staging of lung cancer remains poor. We evaluated the quality and survival impact of two interventions to improve pN staging.
Methods. Using a non-randomized stepped-wedge design, we implemented use of a lymph node (LN) specimen collection kit to improve intraoperative LN collection (surgical intervention) and a novel gross dissection method for intrapulmonary LN retrieval (pathology intervention) in 12 hospitals in five contiguous Hospital Referral Regions in AR, MS and TN (2009-2021). With appropriate statistical methods we compared surgical quality and survival of patients among: neither (Group 1), pathology only (Group 2), surgical only (Group 3), and both (Group 4) interventions.
Results. Of 4,019 patients, 50%, 5%, 21% and 24%, were in Groups 1-4 respectively. Rates of non-examination of LNs and non-examination of mediastinal LNs: 11%, 9%, 0% and 0%; 29%, 35%, 2% and 2% respectively in Groups 1-4 ($p<0.0001$). Attainment of American College of Surgeons Operative Standard 5.8: 22%, 29%, 72%, 85%; International Association for the Study of Lung Cancer's stringent definition of 'complete resection': 14%, 21%, 53%, 61% ($p<0.0001$). Compared to Group 1, adjusted hazard ratios, aHR (95% CI), were: Group 2, 0.93 (0.76-1.15); Group 3, 0.91 (0.78-1.03); Group 4, 0.75 (0.64-0.87). Compared to Group 2, Group 4 aHR- 0.72 (0.57-0.91); compared to Group 3, was 0.83 (0.69-0.99). These relationships remained after excluding wedge resections.
Discussion. Combining a LN collection kit and novel gross dissection method significantly improved pN evaluation and survival in a population-

based cohort.

#4360

Opioid, non-opioid, and non-pharmacological pain management in patients with a history of cancer

Oyomoare L. Osazuwa-Peters[1], Justin M. Barnes[2], Eric Adjei Boakye[3], Trinitia Y. Cannon[1], Tammara L. Watts[1], Tomi Akinyemiju[1], Nosayaba Osazuwa-Peters[1]. *[1]Duke University School of Medicine, Durham, NC,[2]Washington University in St. Louis School of Medicine, St. Louis, MO,[3]Henry Ford Health System, Detroit, MI*

Background Pain is highly prevalent among individuals with cancer. Consequently, adequate and equitable pain management are hallmarks of quality cancer care. Unfortunately, up to one-third of patients with cancer consider their pain symptoms poorly managed. Objective To characterize clinical and sociodemographic factors associated with opioid, non-opioid, and non-pharmacological pain management among individuals with a history of cancer. Methods We used the 2018 to 2020 full-year consolidated data files of the Medical Expenditure Panel Survey (MEPS), linked to the medical conditions, prescribed medicines, outpatient visits and office-based medical provider visits files. We estimated adjusted relative risk (aRR) of receipt of opioid, non-opioid, and non-pharmacological pain management (acupuncture, chiropractor, and massage/occupational/physical therapy), based on clinical (cancer site, comorbidities, depression status) and sociodemographic (race, sex, age, marital status, education, insurance, income, English speaking ability) factors, accounting for complex survey design in quasi-Poisson regression models. Results The study cohort was composed of 7,035 individuals with cancer, with 19.2% (0.65%; weighted proportions (standard error) receiving opioids, 51.09% (0.9%) receiving non-opioids, and 20.56% (0.75%) receiving non-pharmacological pain management. In our final models, compared to Other cancers, patients with bladder cancer were more likely to receive opioids (aRR 1.52; 95% CI 1.06, 2.17), while those with lung cancer were less likely to receive non-pharmacological pain management (aRR 0.46; 95% CI 0.25, 0.84). Also, depression was associated with increased risk of both opioid (aRR 1.26; 95% CI 1.09, 1.46) and non-opioid (aRR 1.26; 95% CI 1.18, 1.34) , but not non-pharmacological pain management. There were no statistically

significant differences in risk of opioid prescription between Black vs. White patients with cancer; however, Asian patients were significantly less likely to receive opioids (aRR 0.18; 95% CI 0.05, 0.67) as were patients who did not speak English well (aRR 0.22; 95% CI 0.11, 0.43). Female patients with cancer were significantly more likely to receive non-opioids (aRR 1.21; 95% CI 1.12, 2.31) and non-pharmacological pain management (aRR 1.49; 95% CI 1.27, 1.75) than males. Conclusions There are clinical and sociodemographic factors associated with opioid, non-opioid, and non-pharmacological pain management among individuals with cancer, and those who are depressed are at highest risk for opioid prescription, while those who cannot speak English well are less likely to receive opioids. For equitable pain care in patients with cancer, it is important that barriers associated with pain management are eliminated.

#4361

The plasma proteome as a cardiovascular disease risk assessment tool in cancer survivors

Emma V. Troth[1], Matthew Ayala[1], Jessica Chadwick[1], Erin Hales[1], Michael Hinterberg[1], Jessica N. Kuzma[1], Clare Paterson[1], Rachel Ostroff[1], Joan E. Walter[2], Christian Mueller[2], Josef Coresh[3]. *[1]SomaLogic, Inc., Boulder, CO,[2]Cardiovascular Research Institute, University of Basel, Basel, Switzerland,[3]Johns Hopkins University, Baltimore, MD*

Cardiovascular disease (CVD) is the most common non-cancer cause of death in cancer survivors and there is an unmet clinical need for easy, accurate, and safe CVD prognostic risk-stratification in adult cancer survivors. This study investigated whether a previously validated 27-plasma protein prognostic model for four-year cardiovascular (CV) events could have such a utility. We used the 27-plasma protein model to predict the four-year risk of a CV event (myocardial infarction, stroke, transient ischemic attack, heart failure hospitalization, death) in 906 participants with a prior history or active malignancy of any type of cancer and compared predictive results to follow-up CV outcome data. The participants were from the BASEL VIII or ARIC (visit 3) studies with a medically adjudicated prior diagnosis of cancer. BASEL VIII is an observational cohort study in patients with suspected coronary artery disease. ARIC is a multi-site cohort study funded by the NHLBI, NCI, and NPCR investigating risk factors for CV

health. A subset analysis was conducted to assess model performance in participants with no prior history of CVD and those with stable CVD. The 27-plasma protein model accurately stratified participants into 4 distinct and non-overlapping (95% CI) risk bins. The median time to event for all cancer survivors who had an event in this study was 1.3 years. Observed 4-year event rates across the 4 risk bins (low, medium-low, medium-high, and high) were 10.4%, 16.8%,31.5% and 58.2%, respectively, which were higher than stratified event rates from our previously published metacohort analyses (5.6%, 11.2%, 20.0% and 43.4%, respectively) in participants with elevated CVD risk factors (e.g., prior events, diabetes, kidney disease and suspected coronary artery disease). The plasma protein model accurately predicted 4-year CVD risk with a C-index of 0.71 (0.68, 0.74) and 4-year AUC of 0.74 (0.69, 0.79). Performance of the protein model was comparable between participants with no prior history of CVD (C-Index: 0.69; AUC: 0.71) and stable CVD (C-Index: 0.69; AUC: 0.72), demonstrating the model accurately predicts CV event risk in cancer survivors regardless of cardiovascular history. Cancer survivors in this cohort can be distinguished with 4-year CV event rates as high as 58.2%, underscoring the urgent need for an easy and accurate risk stratification tool for this population. Prognostic protein testing may provide a novel tool for CVD risk assessment in adult cancer survivors.

#4363

Monocyte-specific epigenetic age acceleration and cardiomyopathy risk among survivors of childhood cancer

Cheng Chen[1], Qian Dong[2], Qin Na[3], Nan Song[4], John Easton[2], Heather L. Mulder[2], Emily Walker[2], Geoffrey Neale[2], Emily R. Finch[2], Qian Li[2], Yutaka Yasui[2], Daniel A. Mulrooney[2], Melissa M. Hudson[2], Kirsten K. Ness[2], Jinghui Zhang[2], Xiang Chen[2], Hui Wang[1], Leslie L. Robison[2], Zhaoming Wang[2]. *[1]Shanghai Jiao Tong Univ., School of Med., Shanghai, China,[2]St. Jude Children's Research Hospital, Memphis, TN,[3]Nanjing Medical University, Nanjing, China,[4]College of Pharmacy, Chungbuk National University, Cheongju, Korea, Republic of*

Our assessment of epigenetic age acceleration (EAA), calculated with DNA methylation (DNAm) data generated from bulk DNA derived from peripheral blood mononuclear cells (PBMC), supports accelerated aging in

childhood cancer survivors (CCS). It is challenging to disentangle variation of DNAm at cell-type specific levels from the effects of age-dependent cell type composition, and bulk measurements may obfuscate the links between EAA and age-related outcomes (e.g., cardiomyopathy). Methylation profiling was generated using Infinium EPIC BeadChips on PBMC-derived DNA from CCS in the St. Jude Lifetime Cohort. Tensor composition analysis was employed to deconvolute bulk DNAm and infer DNAm at each leukocyte subtype level, i.e., a single n (individuals) by m (DNAm sites) matrix of observed DNAm data was deconvoluted into multiple n by m matrices of DNAm data. Epigenetic age (EA, using Levine's clock) and EAA (residuals from the fit of a simple linear regression of EA on chronological age at blood draw) were calculated for bulk PBMCs and each cell subtype (CD4T, CD8T, B, natural killer, and monocyte). Cardiomyopathy (CMP) was assessed by echocardiography, and severity graded (2 = moderate, 3 = severe/disabling, 4 = life-threatening and 5 = fatal) using a modified version of the National Cancer Institute Common Terminology Criteria for Adverse Events. Cumulative doses of anthracyclines and mean heart radiation doses (heart-RT) calculated through radiation dosimetry were abstracted from medical records. Associations between EAA and CMP were evaluated by multivariable Cox regression. Cell-type specific EA was highly correlated with bulk EA with Pearson r2 between 0.63 (CD8T) and 0.79 (CD4T), but the linear regression lines of cell-type specific EA against bulk EA differed in both intercept and slope, suggesting heterogeneity across leukocyte subtypes. Cell-type specific EAA was moderately correlated with bulk EAA with Pearson r2 between 0.23 (monocyte) and 0.29 (CD8T). Among 2,044 CCS (median age = 33.7 years), 104 (5.1%) developed CMP (≥grade 3). Among bulk EAA and five cell-type specific EAAs, monocyte EAA was the only one significantly associated with CMP (hazard ratio per standard deviation increase in EAA = 1.25, 95% CI = 1.04-1.50, P = 0.018). Cell sorting of PBMC followed by DNAm is currently underway for further validation. We showed an in-depth view of the variability of EAA across leukocyte subtypes, and more importantly, demonstrated that monocyte EAA was associated with CMP risk. Our novel finding is plausible and consistent with the literature implicating monocyte-derived cardiac macrophages in cardiac remodeling, which can be induced by cardiotoxic cancer treatment exposures in CCS. Therapeutic strategies that prevent deleterious effects of monocytes contributing to adverse cardiac

remodeling, while sparing their essential immune functions, may prevent or ameliorate CMP among CCS.

#4364

Cost-effectiveness analysis of abemaciclib and endocrine therapy combination for the adjuvant treatment of HR+/HER2-, node-positive, high-risk, early breast cancer

Ashna Talwar[1], Ashish Deshmukh[2], Meghana Trivedi[1], Rajender R. Aparasu[1]. *[1]University of Houston, College of Pharmacy, Houston, TX,[2]Medical University of South Carolina, Charleston, SC*

Background**:** Abemaciclib is the only approved cyclin-dependent kinase 4/6 (CDK4/6) inhibitor approved for adjuvant treatment of hormone receptor-positive, human epidermal growth factor receptor-2-negative (HR+/HER2-), node-positive, high-risk early breast cancer (EBC) patients. However, the addition of abemaciclib to the standard of care endocrine therapy (ET, such as tamoxifen or aromatase inhibitors) results in a drastic increase to the overall healthcare costs.

Objective: In this study, we aimed to evaluate the cost-effectiveness of abemaciclib and ET combination versus ET monotherapy for the adjuvant treatment of HR+/HER2-, EBC from the U.S. third-party payer perspective.

Methods: A Markov-based decision analytic model using TreeAge Software was developed. The model simulated lifetime costs and health outcomes over a lifetime. The model incorporated the disease course of the progression-free disease, progressive disease, death due to disease, and mortality due to other causes. All clinical data and utilities were derived from the literature and clinical trial: monarchE. Notable adverse events such as neutropenia, leucopenia, anemia, and diarrhea were included. Age-specific mortality risk was calculated from the U.S. life tables. The outcomes were measured by costs, quality-adjusted life-years (QALYs), and incremental cost-effectiveness ratio (ICER). The willingness-to-pay threshold was set at $100,000 per QALY gained.

Results: We simulated our analysis on patients assigned to either abemaciclib + ET or ET alone groups as per the monarchE trial. The median age of the patients was 51 years. In base case analysis, the total costs for abemaciclib plus ET and ET alone treatment, were USD 122,052.11 and USD 40,344.87, respectively. Abemaciclib plus ET treatment produced 4.5

QALYs, while the ET treatment alone produced 4.31 QALYs. Overall, abemaciclib plus ET was marginally more effective than ET with an additional 0.20 QALYs but much costlier with an ICER of $417,780.18/QALY. For utilities ranging from 0.41 to 0.69, the ICERs ranged from USD 36,5950 to USD 4,463,866.59 per QALY, which exceeded the WTP threshold. Using probabilistic sensitivity analysis, we estimated that the combination of abemaciclib plus ET was a cost-effective strategy at the willingness-to-pay threshold of $500,000 per QALY or higher for the base case population.
Conclusion: At current costs, abemaciclib plus ET is not cost-effective as compared to ET monotherapy for patients with node-positive, high-risk, HR+/HER2- EBC in the US healthcare system from the third-party payer perspective.

#4365
Comorbidities at diagnosis are associated with poor outcomes among pediatric acute lymphoblastic leukemia and lymphoblastic lymphoma patients
Maua Mosha[1], Jennifer Mayer[1], Ernest K. Amankwah[2]. *[1]Johns Hopkins All Children's Hospital, St. Petersburg, FL,[2]Johns Hopkins University School of Medicine, St. Petersburg, FL*

The influence of comorbidities at index diagnosis on outcomes of pediatric leukemia and lymphoma is not well established. We evaluated the association between medical comorbidities and pediatric acute lymphoblastic leukemia (ALL) and lymphoblastic lymphoma (LL) outcomes in a retrospective cohort study using electronic health records from the TriNetX Research Network Database, a global de-identified federated health research network. Study participants included pediatric (≤21 years) patients newly diagnosed with ALL or LL from July 2009-June 2019 and followed through June 2022. The main outcomes included progression/relapse, toxicity, overall mortality and cancer-specific mortality. Comorbidities included chronic lung disease; congenital heart disease; neurologic, immune, hematologic, vascular and genetic disorders; renal disease; gastrointestinal disease; prematurity and hepatobiliary disease. Patients with any comorbidity were matched with patients with no comorbidity on age at diagnosis, gender, race/ethnicity, and treatment using

propensity score matching. We identified 5,375 patients diagnosed with ALL/LL with comorbidities and 5,375 without comorbidities after propensity score matching. The mean age at diagnosis was 9.7 years (standard deviation=6.2). A higher proportion of the patients were male (56.9%), White (63.6%) and Not Hispanic or Latino (63.4%). Patients diagnosed with comorbidities had a higher risk for progression/relapse (73% vs 51%; Relative Risk, RR=1.42, 95% confidence interval (CI)=1.38-1.47) and treatment related toxicity (80% vs 50%; RR=1.59, 95% CI=1.54-1.64), compared to patients diagnosed with no comorbidities. Similarly, overall mortality (Hazard ratio, HR=1.62, 95% CI=1.37-1.91) and cancer-specific mortality (HR=4.39, 95% CI=2.28-8.46) were higher among patients diagnosed with comorbidities than those without comorbidities. Comorbidities among patients diagnosed with ALL/LL is associated with poor outcomes independent of treatment and thus targeted interventions for the proper management of these patients are needed to improve outcomes.

#4367

The MD Anderson Symptom Inventory (MDASI) survey discloses persistent moderate to high-level symptoms in cancer survivors

Katherine Gilmore, Patricia Chapman, Johnny Rollins, Soo-Hyun Lee-Kim, Justine Robinson, Ellen Mullen, Haleigh Mistry, Prachee Singh, Robin Coyne, Ana Nelson, William Osai, Karen Stolar, Susan Knippel, Danielle Fournier, Tamera Plair, Whittney Thoman, Angela Peek, Loretta Williams, Maria A. Rodriguez. *UT MD Anderson Cancer Center, Houston, TX*

Background: We implemented the integration of the MD Anderson Symptom Inventory (MDASI) survey into patient visits in our Survivorship Clinics to help manage long and late effects of cancer and its therapy. Patients are transitioned to Survivorship if they have completed treatment with curative intent, are in remission, and past the period of highest relapse risk, as determined by disease experts [average ~ 3 years past treatment]. Methods: The MD Anderson Symptom Inventory (MDASI) is a validated cancer specific symptom burden questionnaire. It was integrated into the electronic health record (EHR), and sent via the patient portal to patients 7 days prior to their clinic visit. High alerts (>= 7) were set for four key symptoms (pain, distress, sadness, and shortness of breath). Alerts triggered

an automated message to the provider. From November 2019 to October 2022, 4322 patients completed PRO surveys.
Results: Table 1 summarizes the frequency of moderate (4-6) and high (7-10) level responses. Categories with more than 5% of respondents endorsing a moderate symptom value are bolded with those more than 10% bold and italic. There is significant variation of severity for the four key symptoms amongst patients with different disease types. Lymphoma and thyroid cancer patients have higher symptom severity, while prostate cancer patients report relatively low symptom severity. Overall, for this cohort of responders, the totals of moderate and high levels symptoms are: distress =12.5 %; pain = 9.5 %; sadness = 8.7 %; and shortness of breath = 8 %.
Conclusion: A subset of cancer survivors still experience moderate to high level symptoms, as measured by the MDASI survey, even years after treatment. There are notable differences across patient populations. Further study can identify at-risk patient groups who may require additional intervention.

Table 1. Moderate and High Values for Four Symptoms from the Survivorship MDASIs

Clinic	Total PROs	Distress Mod %	Distress High %	Pain Mod %	Pain High %	Sad Mod %	Sad High %	SOB Mod %	SOB High %
Breast	915	**7.65%**	1.97%	**8.96%**	2.95%	**6.56%**	1.09%	**5.79%**	1.64%
H&N	618	**5.99%**	2.27%	**6.63%**	4.21%	4.53%	2.10%	4.69%	3.07%
Lymph	112	***16.96%***	1.79%	**9.82%**	**6.25%**	**8.93%**	0.89%	***10.71%***	1.79%
Prostate	496	3.43%	0.60%	1.81%	1.18%	2.02%	0.40%	2.62%	0.60%
SCT	229	**8.73%**	1.31%	**7.86%**	**5.68%**	**5.68%**	1.31%	**7.86%**	1.31%
Thoracic	103	2.91%	1.94%	**9.71%**	1.94%	3.88%	2.91%	***12.62%***	3.88%
Thyroid	1849	***12.93%***	**5.08%**	**6.00%**	2.49%	**8.82%**	2.97%	**6.54%**	2.11%
Grand Total	4322	**9.37%**	3.15%	**6.52%**	3.01%	**6.66%**	2.01%	**5.99%**	1.97%

#4368
Symptom network identification from anxious and depressive groups in colorectal cancer patients

Jinah Sim[1], Ji Won Yu[1], Nan Song[2], Ae Sun Shin[3], Ji Won Park[4], Seung Yong Jeong[4]. *[1]Hallym University, Chuncheon, Korea, Republic of,[2]College of Pharmacy,, Chungbuk National University, Chungbuk, Korea, Republic of,[3]Seoul National University College of Medicine, Seoul, Korea, Republic of,[4]Seoul National University Hospital, Seoul, Korea, Republic of*

Backgrounds: Colorectal cancer (CRC) is one of the most common cancers in the world, and recently in South Korea, the incidence rates are increasing. CRC patients have a high prevalence of depression and experience various symptoms such as bowel problems. However, previous studies analyzing network analysis has not yet been conducted to understand the association between symptoms with chronic anxiety and depression.
Methods: In this study, symptom network and centrality analysis were conducted to confirm the interaction between symptoms and functioning (e.g., pain, fatigue, physical functioning, etc.) of patients diagnosed with CRC according to the higher risk of anxiety and depressive groups ahead of surgical treatment. In this study, symptom and functioning variables in a total of 939 CRC patients were measured using EORTC QLQ-C30 and EORTC QLQ-CR29. Network analysis, visualization, and centrality analysis were performed to determine the connectivity between anxiety, depression, and other correlated symptoms amongst CRC patients using the qgraph R package.
Results: As a result of confirming the difference in anxiety and depression according to socio-demographic characteristics, there was a significant difference in the education level in the group with anxiety($Ps<0.05$). The group with depression showed significant differences in Fasting blood sugar and education level($Ps<0.05$). There were significant differences in symptoms according to anxiety and depression, the group with high risk of anxiety showed significant differences in 30 symptoms such as urological frequency and physical function. The group having depression showed significant differences in 26 symptoms such as fatigue and physical function. In the result of performing symptom network analysis and centrality analysis without any stratification of anxiety or depression, fatigue was found to be a central symptom in all patients. In both the anxious and depressed groups, pain was estimated as the central symptom.
Conclusion: In conclusion, the study compared and analyzed symptom networks to confirm the interaction between symptoms of CRC patients

according to anxiety and depression. The symptom network of CRC patients showed different patterns according to anxiety and depression. Pain appeared as a central symptom in both the anxious and depressed groups. This indicates that pain is a key role because it is related to other symptoms and affects the flow of the symptom network the most. Therefore, intensive pain management is expected to be important in treating CRC patients with anxiety and depression. It is expected that the basis for the management of colorectal cancer patients and survivors can be prepared toward the long term of cancer treatment and survival.

#4369

The effects of primary hepatocellular carcinoma surgical resection on five year survival rates among different races

Jingwei Song[1], Eric Song[2], Daniel Gharavi[2]. *[1]School of Medicine, Virginia Commonwealth University, Richmond, VA,[2]Honors College, Virginia Commonwealth University, Richmond, VA*

Background: Hepatic surgical resection is the treatment of choice for noncirrhotic HCC patients. Previous studies indicate that Asian patients were proportionally more likely to be treated surgically. However, studies on the outcome of this preference are very limited.
Methods:We examined data from the Surveillance, Epidemiology and End Results (SEER)-Medicare database to identify patients diagnosed with HCC between 2004 and 2017.The disease specific and relative five year survival rates as well as 95% Cl were calculated.
Results:Among the total of 6,716 Asian or Pacific Islander (A/P) patients diagnosed with localized HCC, 45.9% of them received surgical resection. The localized HCC surgical resection rates for White (27,360 total cases) and Black (4,546 total cases) were 35.6% and 33.1% respectively. This pattern remained the same for patients with regional and distant site involved HCC: Highest percentage of A/P patients received surgical resections. For patients with localized HCC, five year cause specific survival rate was statistically higher for A/P patients than White and Black ($P<0.05$) 24 months after the surgery. These trends continued until the end of the study. For patients with regional HCC, surgical resection played no significant role for the five year cause specific survival rate among the different races. However, for patients with distant involved HCC, five year

cause specific survival gap between White and A/P gradually increased after surgery and reached a statistically significant level on month 48 (23.9% with 95% CI 18.6% to 29.6% for White and 9.7% with 95% CI 4.4% to 17.5% for A/P). The pattern remained the same between Black and A/P patients without statistical significance, most likely due to the limited sample size for both.. Our research also indicated that surgical resection may play a similar role for the five year relative survival rate. After localized HCC surgical resection, A/P patients had the highest five year relative survival rate compared to White and Black patients ($P<0.05$). For the patients with regional HCC, surgical resection played no significant role on five year relative survival rate among different races. However, for the patients diagnosed with distant involved HCC, five year relative survival gap between White and A/P gradually increased after surgery and reached a statistically significant level on month 48 (23.7% with 95% CI 18.3% to 29.4% for White and 10.5% with 95% CI 5.2% to 18.0% for A/P). The pattern remained the same between Black and A/P patients without statistical significance due to the limited sample size in both categories. Conclusion: A/P primary HCC patients were more likely to be treated surgically. However, the benefits of surgical resection for A/P patients can only be appreciated for those with localized HCC. For A/P patients diagnosed with distant site node involved HCC, surgical resection may cause more harm than good.

#4370

How much time is needed to complete quality of life assessments in oncology trials? - Metadata analysis

Jowita Marszewska, Lindsay Hughes. *Individual, Philadelphia, PA*

Introduction: Digitalization in clinical trials introduced electronic data collection. Participants in diverse environments can use electronic devices to report their experiences with the drug by completing patient reported outcome assessments (ePROs). Quality of life (QOL) reports describe how a patient feels or functions during a treatment with a new drug. For oncology trials, QOL data is needed to prove the treatment effect and support a labeling claim.
Methods: The literature search in the Web of Science for articles containing QOL keyword found ten articles with the highest number of citations. QOL

instruments relevant to cancer research were identified based on the literature search. Form completion times corresponding to the cancer-specific instruments were identified and analyzed using a metadata of 948 instruments and 17,234,458 assessment submissions.
Results: Three general QOL measures in oncology trials were identified: the EORTC Quality of Life Questionnaire - Core Questionnaire (EORTC QLQ-C30), Functional Assessment of Chronic Illness Therapy - Fatigue (FACIT-F), and SF-36 Health Survey (SF-36). Median times of form completion in seconds (s) increased in the following order: FACIT-F < EORTC QLQ-C30 < SF-36v2 and were equal to 105 s < 213 s < 386 s. Metadata analysis showed that participants spent less than two minutes on completion of the FACIT-F assessment, which is only 18% of the estimated completion time of 10 minutes. Metadata analysis showed that it took participants three and a half minutes to complete the EORTC QLQ-C30 assessment, which is roughly one third of the estimated completion time of 11 minutes. The completion time for SF-36v2 fell within the estimated range of 5 to 10 minutes.
Conclusions: Properly selected QOL instruments facilitate collection of the right data for demonstration of a treatment benefit. It is recommended to include a general oncology and a disease specific QOL instrument to show the treatment's success of improving patient's QOL. At the same time, the completion of the instruments should not be burdensome considering disease progression characteristic for oncology studies.

#4371

iCCaRe: Social determinants of health navigation, psycho-oncology, and emotional support for Black prostate cancer survivors: Review of current practices

Dottington Fullwood[1], AJ Merriweather[1], Che Ngufor[1], Deidre Pereira[2], KC Balaji[3], Roxana Dronca[4], Gerardo Colon-Otero[5], Jennifer Crook[1], Parisa Fathi[1], Emelina Asto-Flores[1], Shannon Pressey[1], Folakemi Odedina[1]. *[1]Mayo Clinic Cancer Center Florida, Jacksonville, FL,[2]Clinical and Health Psychology, University of Florida, Gainesville, FL,[3]Urology, University of Florida - Jacksonville, Jacksonville, FL,[4]Oncology, Mayo Clinic Cancer Center Florida, Jacksonville, FL,[5]Internal Medicine, Mayo Clinic Cancer Center Florida, Jacksonville, FL*

Background: Black men continue to be disproportionately affected by prostate cancer incidence and mortality as compared to their White counterparts, despite worldwide declining prostate cancer diagnosis rates. This complex phenomenon remains poorly understood, especially at the point of a prostate cancer diagnosis. Newly diagnosed Black men report initial feelings ranging from being “shocked,” to “receiving a death sentence,” and both an ineptness of asking questions and a reliance on physicians for treatment options due to lack of knowledge. The psychological distress from prostate cancer uncertainties affects health management and treatment decisions, though it is unclear to what extent the role of social determinants of health factor in making informed healthcare decisions.
Aim: In this scoping review, we examined the influence of the social determinants of health at point of prostate cancer diagnosis among Black men seeking to make an informed decision about their treatment plans.
Methods: We followed the methodological framework: the Preferred Reporting Items for Systematic reviews and Meta-Analyses extension for Scoping Reviews (PRISMA-ScR). Five electronic databases, Emabase, Pubmed, PsycInfo, Scopus, and Web of Science were searched for quantitative and qualitative primary studies from the period 2005 until March 2022. Two authors independently screened titles and abstracts, and full texts, against predefined criteria: empirical research, post 2000, in English-language peer-reviewed journals; participants included Black prostate cancer survivors and research explored social determinants of health at point of prostate cancer diagnosis. Studies were quality assessed for data charting.
Results: The search yielded 283 studies, with 45 included studies for synthesis. Traditional social determinants of health were frequent. However, identification of themes such as social support, masculinity and stigma, fear of abandonment by medical staff, and cost of diagnostic procedures were prominent determinants. Notably, sub-themes emerged that included coping factors such as emotional distress, perceptions of normalcy, and poor prostate cancer knowledge.
Conclusion: Understanding the social determinants of health impact on Black men, especially at point of prostate cancer diagnosis will allow survivors, physicians, and researchers to work at solving these health disparities.

#4372

Hierarchy of prognostic quality markers after curative-intent resection of stage IA non-small cell lung cancer

Huibo Shao[1], Yu-Sheng Lee[2], Carrie Fehnel[1], Olawale Akinbobola[1], Andrea Saulsberry[1], Kourtney Dortch[1], Anberitha T. Matthews[1], Nicholas R. Faris[1], Meredith A. Ray[3], Matthew Smeltzer[3], Raymond U. Osarogiagbon[1].
[1]Baptist Cancer Center, Memphis, TN,[2]University of Memphis, Memphis, TN,[3]School of Public Health, University of Memphis, Memphis, TN

Introduction**.** 5-year disease-free survival after curative-intent resection of stage IA NSCLC approximates 65%. The quality of resection and differences in cancer biology probably account for most curative-intent treatment failure. We evaluated the hazard associated with markers of surgical quality.

Methods. Using the population-based Mid-South Quality of Surgical Resection cohort, we compared outcomes of pathologic IA NSCLC resections from 2009 to 2021. With the stringent International Association for the Study of Lung Cancer complete (R0) resection for reference, we evaluated eight quality benchmarks: wedge resection; resections with positive margins; non-examination of lymph nodes (LN) from anywhere (pNX), mediastinal (pNXmed), intrapulmonary, hilar, low paratracheal and subcarinal stations. We evaluated hazard ratios (HR), adjusted for age, sex, insurance, histology, comorbidity, preoperative staging and technique of resection (95% CI) from Proportional Hazards models.

Results. Of 2,243 resections, 906 (41%) were R0; 1,333 were non-R0, including 3% R1/R2, 13% pNX, 15% wedge resections, 15% pNXmed, 45% without subcarinal, 41% without hilar, 47% without low paratracheal, and 36% without intrapulmonary LNs.Compared to IASLC-R0, adjusted HRs were: 2.04 (1.21-3.44) for R1/R2; 1.75 (1.33-2.31) for pNX; 1.64 (1.26-2.14) for wedge resections; 1.35 (1.12-1.63) for non-examination of intrapulmonary LN; 1.33 (1.03-1.72), pNXmed; 1.25 (1.02-1.53), non-examination of hilar LN; 1.15 (0.95 - 1.39) missing station 4; and 1.11 (0.90-1.37) missing station 7 LNs.

Conclusion. Surgical quality, indicated by markers of LN evaluation, have significant impact on long-term survival and should be required selection criteria or stratification factors in lung cancer surgery trials.

#4373

Venetoclax-based therapy in treatment-naïve and relapsed/refractory acute myeloid leukemia

Aditya Ravindra, Luna Acharya, Bradley Loeffler, Sarah L. Bell, Grerk Sutamtewagul, Prajwal Dhakal. *University of Iowa Hospitals & Clinics, Iowa City, IA*

Background**:** Clinical trials in acute myeloid leukemia (AML) report complete remission (CR) in ~60% of newly diagnosed (ND) pts treated with venetoclax (VEN)-based therapy with hypomethylating agents (HMA, azacitidine [AZA] and decitabine [DEC]) or low-dose cytarabine. However, results from prospective studies in relapsed refractory (R/R) AML remain scarce. Here, we compare the outcomes in ND and R/R pts treated with VEN-based therapy.

Methods: We performed a retrospective analysis of ND and R/R pts with AML diagnosed between 2016 and 2021 who were treated with VEN-based therapy at the University of Iowa. We used ANOVA and chi-square test to compare variables between ND and R/R pts. Logistic regression analyses and Cox regression models evaluated the effects of ND vs. R/R AML on objective response rate (ORR defined as complete remission (CR) + complete remission with incomplete count recovery [CRi]) and overall survival (OS), respectively. OS was estimated using the Kaplan-Meier method.

Results: Of 53 pts, 31 pts had ND AML, and 22 pts had R/R AML. Median age was 67 years (range 26-85). Among total pts, 52% were treated with VEN + AZA, 48% were treated with VEN+ DEC, 25% had prior exposure to HMA, and 19% had an allogeneic transplant before treatment with VEN-based therapy. Eleven pts had *TP53* mutation (7 pts in ND, 4 in R/R group), 13 had *NPM1* mutation (ND- 8, R/R-5), and 7 had *FLT3* mutation (ND-5, R/R-2). ORR was 53% in total pts (CR- 34%, CRi- 19%), of which 11% did not have minimal residual disease. There was no statistically significant difference in ORR between ND and R/R pts (Odds ratio [OR] 2.04, 95% confidence interval [CI] 0.6-6.4, p=0.2). Treatment with VEN + DEC conferred a similar ORR compared to VEN + AZA (OR 0.37, 95% CI 0.1-1.2, p=0.1). Prior HMA use did not affect ORR (OR 0.4, 95% CI 0.08-2.2, p=0.3). ND pts had longer 6-month OS than R/R pts (82% vs. 55%), but 12-

month OS was similar (59% vs. 55%). ND or R/R status did not affect OS (Hazard ratio [HR] 0.7, 95% CI 0.3-1.6, p=0.4). Treatment with VEN + DEC conferred similar OS compared to VEN + AZA (HR 1.6, 95% CI 0.7-3.7, p=0.2). Age, *TP53*, *NPM1,* and *FLT3* mutations, and adverse cytogenetics, did not affect ORR or OS.
Conclusions: Our real-world analysis shows no significant difference in ORR or OS among pts with ND or R/R AML indicating effective response to VEN-based therapy regardless of treatment status. We report similar 12-month OS for ND and R/R pts despite a higher 6-month OS for ND group. Treatment combination with either AZA or DEC had comparable outcomes, and prior HMA use did not predict worse outcomes in our study. These results are important clinically as AZA and DEC are often used interchangeably, and a significant proportion of pts with prior myelodysplastic syndrome are treated with HMA. Subsequent studies are required to understand the similarities and differences in factors predicting response to VEN-based therapy in ND and R/R AML.

#4374
Patient provider communication about the use of medical cannabis for cancer symptoms
Kea Turner[1], Jessica Y. Islam[1], Yessica C. Martinez[1], Omar Garcia Rodriguez[1], Diane Rodriguez Irlanda[2], Oliver T. Nguyen[1], Heather S.L. Jim[1], Kathleen M. Egan[1]. *[1]Moffitt Cancer Center, Tampa, FL,[2]University of South Florida, Tampa, FL*

There has been limited study of patient-provider communication regarding medical cannabis for cancer symptoms. To address this gap, this study assesses the prevalence of patient-provider communication about the use of medical cannabis for cancer symptoms. Three types of communication are examined: 1) patient-provider discussions; 2) provider recommendations; and 3) provider instructions for how to use medical cannabis. We administered a survey from August to November 2021 with adult cancer patients who completed treatment from July 2017 to December 2019 at a National Cancer Institute designated Comprehensive Cancer Center; 1,592 individuals participated (response rate: 17.6%). About half of participants were female (52.1%). The age distribution of participants included 18-44 (9.4%), 45-54 (12.8%), 55-64 (25.3%), 65-74 (35.4%), and 75 and above

(17.3%). Participant's racial and ethnic background included Hispanic/Latinx (6.5%), African American/Black (4.0%), Asian American (1.0%), additional or multiple racial categories (3.5%), and White (91.5%). About a third (33.5%) of participants (530/1584) reported discussing medical cannabis for cancer symptoms with a healthcare provider. Participants who had discussed cannabis with a provider reported discussions with multiple providers including their oncology physician (62.3%), primary care provider (45.7%), oncology advanced practice provider (APP) (34.3%), dietician (7.4%), pharmacist (2.8%), and other healthcare provider (34.3%). Fewer (15.6%) participants (248/1592) reported receiving a recommendation for medical cannabis from a healthcare provider for their cancer symptoms. Participants who had received a recommendation reported recommendations from their oncology physician (32.7%), primary care provider (26.6%), oncology APP (13.7%), dietician (4.8%), pharmacist (1.6%), and other healthcare provider (56.9%). About a third (33.7%) of participants (537/1592) reported using medical cannabis during their cancer treatment and most often reported receiving instructions on how to use cannabis from no one (36.9%) or from a cannabis store or dispensary worker (23.8%). Less commonly, participants reported receiving instructions from their healthcare provider including their primary care provider (3.7%), oncology APP (2.0%), oncology physician (1.5%), pharmacist (<1%), or dietician (<1%). Based on this survey, about a third of cancer patients discuss medical cannabis with a healthcare provider but fewer receive a recommendation and/or instructions for how to use medical cannabis from a healthcare provider. Additional interventions may be needed to ensure that cancer patients interested in or currently using medical cannabis receive guidance from oncology care providers.

#4375

A bootstrapping method to optimize go/no-go decisions from single-arm, signal-finding studies in oncology

Aparna Mohan[1], Raunak Dutta[1], Jacqueline Buros-Novik[2], Omobolaji Akala[3], Brian Gregory Topp[3]. *[1]Vantage Research, Chennai, India,[2]Generable, New York, NY,[3]Merck, Rahway, NJ*

Background: Phase Ib, single-arm trials are common in oncology development. Since these trials are not powered for statistical significance,

Go/No-Go decisions are largely driven by observed trends in ORR relative to historic control. Here we develop a bootstrapping method to systematically compare secondary endponts, such as the waterfall plot, to historic control data. In addition, we identify an actionable Go threshold and estimate the expected false positive and false negative rates associated with that threshold.
Method: A proprietary mathematical model was used to simulate thousands of single-arm trials (n = 30) with a combination of pembrolizumab and a novel agent with miserable (Rx0), modest (Rx1), moderate (Rx2) or magnificent (Rx3) efficacy. A bootstrapping method was used to compare waterfall plots from these trials to a simulated Phase III pembrolizumab monotherapy control arm (n = 511).
Results: The bootstrapping method provides a visualization of the observed waterfall plot for the single-arm combination trial relative to the range of possible outcomes from historic control data (5^{th}, median, 95^{th} percentile). The method also provides a score reflecting the probability that the observed data is different from the historic control. An ROC analysis showed a strong ability to separate drugs with modest (AUROC = 83%), moderate (AUROC = 96%) and magnificent combination efficacy (AUROC = 99%) from drugs with miserable efficacy. The method was shown to effectively move drugs with a range of efficacy through an *in-silico* pipeline while rejecting drugs without combination efficacy.
Conclusion: This bootstrapping method allows comparisons of secondary endpoints from early clinical trials to historic control data. The visualization is intuitive, and the quantification provides an actionable Go-threshold. The method also provides an estimate of the risk associated with that recommendation. We suggest incorporation of this as a component of Go/No-Go decision making in early oncology trials.

#4376

A correlation of soluble HLA serum levels with clinical data and survival in patients with invasive breast cancer after neoadjuvant treatment

Christian M. Tegeler[1], Jonas Rieth[2], André Koch[3], Dominik Dannehl[4], Léa L. Volmer[4], Sabine Matovina[4], Markus Hahn[4], Tobias Engler[4], Andreas D. Hartkopf[5], Sara Y. Brucker[4], Juliane S. Walz[6], Jonas S. Heitmann[7], Annika Nelde[8]. *[1]Department of Obstetrics and Gynecology; Department of Peptide-*

based Immunotherapy, University Hospital and University of Tübingen, Tübingen, Germany,[2]Department of Peptide-based Immunotherapy; Department of Immunology, University Hospital and University of Tübingen; Institute for Cell Biology, Tübingen, Germany,[3]Department of Obstetrics and Gynecology, University Hospital of Tübingen; Research Institute for Women's Health, University of Tübingen, Tübingen, Germany,[4]Department of Obstetrics and Gynecology, University Hospital of Tübingen, Tübingen, Germany,[5]Department of Obstetrics and Gynecology, University Hospital of Ulm; University Hospital of Tübingen, Tübingen, Germany,[6]Department of Peptide-based Immunotherapy; Department of Immunology, University Hospital and University of Tübingen; Institute for Cell Biology; Clinical Collaboration Unit Translational Immunology, German Cancer Consortium (DKTK), Tübingen, Germany,[7]Department of Internal Medicine, Clinical Collaboration Unit Translational Immunology, German Cancer Consortium (DKTK); University Hospital of Tübingen; Cluster of Excellence iFIT (EXC2180), Tübingen, Germany,[8]Department of Peptide-based Immunotherapy; Department of Immunology, University Hospital and University of Tübingen; Institute for Cell Biology; Cluster of Excellence iFIT (EXC2180), Tübingen, Germany

Invasive breast cancer (IBC) is the most common malignant disease in women worldwide. In recent years, the landscape of treatment options has rapidly evolved. With the success of checkpoint inhibitors in triple negative IBC, immunotherapy has become standard of care highlighting the strength of T cell-based strategies for anti-tumor therapy. Naturally, the targets of T cell-mediated immune responses are represented by short peptides presented on human leukocyte antigen (HLA) molecules. For several years, huge effort has been made to analyze and characterize HLA-presented tumor antigens to further understand anti-tumor immunity and to identify suitable targets for novel immunotherapy approaches. Aside from membrane-bound HLA molecules, soluble HLA-peptide complexes (sHLA) can be found in a variety of body fluids. These molecules are suggested to impact cellular immune responses, but it is still a matter of debate, whether shifts in sHLA levels contribute to disease outcome or are observed as a consequence of disease. Whereas the role of the non-classical sHLA-G in IBC has been studied showing elevated levels in patients compared to a healthy cohort, data on classical sHLA class I molecules is not yet available. Here, we

report on sHLA class I serum levels in patients with IBC after neoadjuvant chemotherapy or combined chemotherapy with antibody treatment (n = 52). We observed higher serum levels of sHLA in neoadjuvant-treated IBC patients without histopathological complete response after neoadjuvant therapy (n = 36) compared to healthy volunteers (n = 84). Patients with locally advanced tumors, according to TNM classification, had a tendency towards lower sHLA levels than patients with small size tumors. Furthermore, sHLA levels were decreased in patients with sentinel node or disseminated axillary lymph node metastases compared to non-metastatic patients. Of note, sHLA levels tended to be elevated in patients with Her2-overexpression (based on immunohistochemistry staining and fluorescence in situ hybridization), whereas for histological hormone receptor expression a tendency towards lower sHLA levels in patients with high expression was observed. Furthermore, sHLA levels were reduced in patients with disseminated tumor cells in bone marrow aspiration. No significant difference in sHLA levels were seen in terms of grading of tumor, prevalence of distant metastasis, menopausal status and elevated tumor markers. Interestingly, we observed a tendency to prolonged progression-free survival in patients with high serum concentrations of sHLA, which will be updated with data from additional patients at the AACR meeting. Taken together, these data provides first insights about sHLA class I in patients with IBC after neoadjuvant treatment suggesting an impact of sHLA and T cell-mediated immune surveillance on survival in patients with IBC.

#4377

Economic burden of lung cancer patients in the emergency department

Jayla Hsiung[1], Kamil Taneja[2], Bill Hum[2], Karan Patel[3], Michael Diaz[4], Shreyas Chandragiri[5], Eric M. Toloza[6]. *[1]Highland Park High School, Highland Park, NJ,[2]Renaissance School of Medicine, Stony Brook, NY,[3]Cooper Medical School, Camden, NJ,[4]University of Florida College of Medicine, Gainesville, FL,[5]Sidney Kimmel Medical School, Philadelphia, PA,[6]Thoracic Oncology, Moffitt Cancer Center, Tampa, FL*

Introducti**on:** In 2022, the National Cancer Institute estimated that more than 240,000 individuals will be diagnosed with lung or bronchus cancer. Many patients present to the emergency department (ED) for septicemia and pneumonia, which leads to long hospital stays. However, there is little data

on the annual trends of hospital charges and risk factors for a high charge for these patients.

Methods: We utilized the 2006-2012 Nationwide Emergency Department Sample to analyze the charges of lung cancer patients. Multivariate linear regressions were used to identify factors associated with higher ED and inpatient (IP) costs. The 20 most common primary diagnoses of these patients were included in the analysis to take into account the reason for the ED visit. Charges were corrected for inflation by normalizing to 2012 US Dollars.

Results: During this time period, 1,344,817 lung cancer patients presented to the ED. Lung cancer patients were charged a cumulative of $3.06 billion in the ED and $38.6 billion in the IP setting. Annual cumulative ED charges increased by a factor of 2.5 from $575 million in 2006 to $1.42 billion in 2012 ($p<0.001$). Annual cumulative IP charges increased by a factor of 1.4 from $10.8 billion in 2006 to $14.6 billion in 2012 ($p<0.001$). Furthermore, annual per-patient ED and IP charges increased significantly during this time period. Per-patient annual ED charges increased by a factor of 1.6 from $2,169 in 2006 to $3,522 in 2012 ($p<0.001$). Per-patient annual IP charges increased by a factor of 1.2 from $41,835 in 2006 to $49,051 in 2012 ($p<0.001$). Table 1 shows the top 5 factors associated with higher ED and with higher IP charges, respectively.

Conclusion: The ED and IP charges associated with lung cancer patients are drastically increasing. ED charges have increased by a factor of 2.5 and IP charges have increased by a factor of 1.4 from 2006 to 2012. Furthermore, hospitals in the West and Midwest are associated with higher charges.

Factors Associated with High Emergency Department and Inpatient Charges for Lung Cancer Patients

	Emergency Department			Inpatient	
Factor	Beta (95% Confidence Interval)	p-value	Factor	Beta (95% Confidence Interval)	p-value
Chest Pain	2868 (2628-3109)	<0.001	Septicemia	22251 (19960-24541)	<0.001
Abdominal Pain	2274 (2041-2509)	<0.001	West Hospital	22155 (16220-28090)	<0.001

West Hospital	1434 (1007-1862)	<0.001	Respiratory Failure	19331 (16798-11557)	<0.001
Midwest Hospital	933 (662-1205)	<0.001	Secondary Malignancy	10283 (9009-11557)	<0.001
Lower Respiratory Disease	882 (756-1007	<0.001	Age 30-39	9057 (349-17755)	<0.001

#4378

Risk factors for death in the emergency department for melanoma patients

Jayla Hsiung[1], Kamil Taneja[2], Karan Patel[3], Michael Diaz[4], Jared Wolfe[3], Eric M. Toloza[5]. *[1]Highland Park High School, Highland Park, NJ,[2]Renaissance School of Medicine, Stony Brook, NY,[3]Cooper Medical School, Camden, NJ,[4]University of Florida College of Medicine, Gainesville, FL,[5]Moffitt Cancer Center, Tampa, FL*

Introduction**:** Many cancer deaths are related to melanoma. While there have been many studies that have identified risk factors for death in these patients, very few of them have analyzed the risk factors for death in melanoma patients in the emergency department (ED).
Methods: We utilized the 2006-2012 Nationwide Emergency Department Sample to characterize melanoma patients who die in the ED. Multivariate logistic regression was used to identify patient and hospital characteristics that were significantly associated with a higher chance of death. A p-value ≤0.05 was considered significant.
Results: From 2006 to 2012, 239,956 melanoma patients presented to the ED, and 2.1% of these melanoma patients died. Most melanoma patients who died in the ED were over the age of 70 years (60.0%), male (63.8%), Medicare beneficiaries (65.6%), of the highest income quartile (31.0%), presenting to a hospital in the South (35.3%), presenting to non-trauma hospitals (48.3%), and presenting to metropolitan non-teaching hospitals (43.4%). The most common reasons for patients who died upon presentation to the ED were a secondary malignancy (20.7%), septicemia (10.8%), acute cerebrovascular disease (7.5%), pneumonia (5.2%), and congestive heart

failure (2.6%). The top 3 factors associated with high risk of death were septicemia (odds ratio (OR)=7.39, 95% confidence interval (CI)=5.79-9.43; p<0.001), acute cerebrovascular disease (OR=3.44, 95%CI=2.62-4.51; p<0.001), and age >70 years (OR=2.50, 95%CI=1.24-5.03; p=0.010). Table 1 lists all risk factors associated with a higher risk of death.

Conclusion: Melanoma patients over the age of 70, with septicemia, acute cerebrovascular disease, or pneumonia, and of male sex are at higher risk for death in the ED. Clinicians should be aware of these risk factors when melanoma patients present to the ED.

Risk Factors Associated with Death for Melanoma Patients in the Emergency Department

Risk Factor	Odds Ratio (95% Confidence Interval)	p-value
Septicemia	7.39 (5.79-9.43)	<0.001
Acute Cerebrovascular Disease	3.44 (2.62-4.51)	<0.001
Age >70	2.50 (1.24-5.03)	0.010
Charlson Comorbidity Index of 3 or More	2.32 (1.89-2.84)	<0.001
Pneumonia	1.76 (1.27-2.45)	0.001
Charlson Comorbidity Index of 1	1.64 (1.40-1.93)	<0.001

Charlson Comorbidity Index of 2	1.63 (1.31-2.03)	<0.001
Medicaid	1.63 (1.19-2.23)	0.002
Metropolitan Teaching Hospital	1.33 (1.05-1.68)	0.017

#4379

Survival among adults diagnosed with secondary acute myeloid leukemia

Ephrem Sedeta[1], Ahmedin Jemal[2], Lauren Nisotel[2], Hyuna Sung[2]. *[1]Internal Medicine, Brookdale University Hospital and Medical Center, Brooklyn, NY,[2]Surveillance & Health Equity Science, American Cancer Society, Atlanta, GA*

Background**:** The burden of second primary cancers including secondary acute myeloid leukemia (sAML) is increasing in the United States; however, limited data exist regarding survival among individuals with sAML. This study aims to examine survival differences between sAML and AML arising de novo (dnAML) in relation to antecedent cancer types and the receipt of prior cancer treatment.

Methods: Individuals aged ≥20 years and diagnosed with sAML or dnAML between 2001 and 2018 and followed for vital status through 2019 were identified from Surveillance, Epidemiology, and End Results 17 database, covering 27% of the US population. The differences in AML-specific survival between individuals with sAML and dnAML were examined using multivariable Cox proportional hazards regression. Trends in five-year age-standardized relative survival from 2001-2014 were assessed using Joinpoint survival model for sAML and dnAML, separately.

Results: A total of 7,306 individuals diagnosed with sAML and 40,398 individuals with dnAML were included. During a median follow-up of 6 months, 78% of individuals with sAML died from AML compared to 71% of those with dnAML. In multivariable models, the risk of AML-specific mortality was 8% higher in individuals diagnosed with sAML than in those diagnosed with dnAML (hazard ratio [HR]=1.08, 95%CI=1.05-1.11), with the elevated risk more pronounced among those with younger ages at diagnosis ($HR_{20\text{-}54\ years}$=1.60, 95%CI=1.46-1.75 versus $HR_{65+\ years}$=0.99, 95%CI=0.96-1.03; $P_{interaction}$<0.0001) and those who received chemotherapy ($HR_{chemotherapy\ yes}$=1.14, 95%CI=1.10-1.19 versus $HR_{chemotherapy\ no/unknown}$=0.95, 95%CI=0.90-0.99; $P_{interaction}$=0.0004). Subgroup analysis by antecedent cancer types showed that HRs substantially varied ranging from 0.74 (95%CI=0.57-0.95) for

individuals with a history of thyroid cancer to 1.78 (95%CI=1.04-3.07) for those with a history of soft tissue sarcomas. Further subgroup analysis by the receipt of chemotherapy for antecedent cancers showed that the elevated risk was generally restricted to individuals with a history of chemotherapy receipt with some variations by cancer types. Five-year relative survival significantly increased from 2001 to 2014 for both sAML and dnAML; though the increase was slower for sAML (annual percent change [APC]=0.30%, 95% CI 0.20-0.40) compared with dnAML (APC=0.77%, 95%CI=0.69-0.84). Likewise, five-year survival for the most contemporary period (2010-2018) was substantially lower for sAML (9.8%, 95%CI=9.3-10.3) than for dnAML (22.8%, 95%CI=22.3-23.2).
Conclusion: Individuals with sAML had in general worse AML cause-specific survival compared with their dnAML counterparts, with the differences most pronounced among those diagnosed at younger ages and who received chemotherapy. The findings may inform targeted treatment and survivorship recommendations for cancer survivors who develop sAML.

#4380
Pre- and postoperative fecal microbiota and its association with complications after surgery in colon cancer patients
Dieuwertje E. Kok[1], Jannigje G. Kers[2], Hendriek C. Boshuizen[2], Niels Klaassen[2], Henk K. van Halteren[3], Flip M. Kruyt[4], Marjolein L. Smidt[5], Johannes H. W. De Wilt[6], Annemarie Boleij[6], Ellen Kampman[2], Erwin G. Zoetendal[2]. *[1]Division of Human Nutrition and Health, Wageningen University & Research, Wageningen, Netherlands,[2]Wageningen University & Research, Wageningen, Netherlands,[3]Division of Human Nutrition and Health, Admiraal de Ruyter Hospital, Goes, Netherlands,[4]Division of Human Nutrition and Health, Hospital Gelderse Vallei, Ede, Netherlands,[5]Maastricht University Medical Center & GROW School for Oncology, Maastricht, Netherlands,[6]Radboudumc, Nijmegen, Netherlands*

Introduction: Postoperative complications impact morbidity and mortality of colon cancer patients. Emerging evidence suggests that intestinal microbiota might play a critical role in the development of postoperative complications after gastrointestinal surgery. Here, we studied changes in fecal microbiota composition comparing samples collected before and after colon cancer surgery. Moreover, we examined whether the microbiota composition before surgery was associated with postoperative complications, and we explored potential determinants of the preoperative microbiota in colon cancer patients.

Methods: For this study, two fecal samples were provided by 78 patients with colon cancer. The first (preoperative) sample was collected shortly after diagnosis and before (median and interquartile (IQR) range of 4 (2-6) days) colon cancer surgery. The second (postoperative) sample was collected approximately 6 weeks (median and IQR of 42 (37-47) days) after surgery and before start of adjuvant chemotherapy (whenever applicable). Based on 16S ribosomal RNA gene amplicon sequencing, the fecal microbiota diversity and composition were determined. Preoperative microbiota composition of patients who developed postoperative complications in the 30 days following surgery (n=18, 23%) was compared to those who did not (n=60, 77%) using univariate and multivariate analyses. Explorative random forest analyses were conducted to identify predictors of complication status, with relative abundance of the core genera, sex, age, fecal calprotectin levels, dietary fiber intake, body mass index, smoking status, ASA classification, cancer stage and tumor location being considered as potential predictors.
Results: After surgery, microbial alpha diversity was reduced compared to the preoperative situation, whereas compositional changes over time only reached statistical significance for *Lachnospiraceae NK4A136* and *Coprococcus 1*, which both decreased in relative abundance after surgery. Already before the start of surgery, relative abundance of the genera *Bacteroides* (10% vs 6%) and *Lachnoclostridium* (0.6% vs 0.2%) appeared to be higher in patients with complications versus those with uncomplicated recovery. In a prediction analysis, current smoking and relative abundance of *Lachnoclostridium* were identified as most profound predictors of complication status. Fecal calprotectin levels and current smoking status explained most (together 6%) of the overall variation in microbiota composition before surgery.
Conclusion: In this study, higher relative abundances of the genera *Bacteroides* and *Lachnoclostridium* before surgery were associated with postoperative complications in patients with colon cancer. Future studies should expand on the potential causal and pathogenic routes underlying these observations.

#4381

Predictive risk factors for cancer thrombosis in gastric cancer patients

Song Ee Park[1], Moon Ki Jung[2], In Gyu Hwang[1]. *[1]Division of Hemato-oncology, Department of Internal Medicine, Chung-Ang University, Seoul, Korea, Republic of,[2]Division of Cardiology, Department of Internal Medicine, Chung-Ang University, Seoul, Korea, Republic of*

Background Gastric cancer is strongly associated cancer thromboembolism. We aimed to identify the Khorana risk score (KRS) and other risk factors for cancer thromboembolism in patients with gastric cancer after gastrectomy.
Methods We reviewed 610 gastric patients, who had undergone D2 radical gastrectomy between January 2005 and December 2017. Kaplan-Meier survival analysis and Cox regression models were used to evaluate for independent predictor of cumulative incidence of cancer thromboembolism and survival.
Results The median follow up was 67.0 months. There were 35 (5.7%) caner thromboembolism. The cumulative incidences of thromboembolism were 6.1%, 3.1%, 3.3%, and 20.7% in stages I, II, III, IV. 181 (29.7%) patients were relapsed cancer and 159 (26.1%) patients were died. A high KRS (cumulative incidence 5.8%) was not associated with cancer thromboembolism compared to an intermediate KRS (cumulative 5.7%) (HR=1.005, 95% CI = 0.540-2.061, P= 0.876). After gastrectomy, recurrent cancer (cumulative incidence 9.9%) was associated with cancer thromboembolism compared to no recurrence (cumulative incidence 4.0%) (HR 3.713, 95% CI 1.879-7.335, P < 0.001).
Conclusions Recurrent gastric cancer patients after gastrectomy were significantly increased cancer thromboembolism risk compared to no recurrent cancer patients. Among patients with gastric cancer after gastrectomy, KRS did not stratify the patients at high risk of cancer thromboembolism.

#4382
Evolution of curative-intent lung cancer surgery in a 4 eras in the population-based mid-south quality of surgical resection (MS-QSR) cohort
Olawale Akinbobola[1], Meredith A. Ray[2], Carrie Fehnel[1], Andrea Saulsberry[1], Kourtney Dortch[1], Anberitha T. Matthews[1], Nicholas R. Faris[1], Caroline M. Godfrey[3], Matthew Smeltzer[2], Raymond U. Osarogiagbon[1]. *[1]Baptist Cancer Center, Memphis, TN,[2]University of Memphis, Memphis, TN,[3]Vanderbilt University Medical Center, Nashville, TN*

Background**.** Most patients die within 5 years of curative-intent lung cancer surgery. Differences in surgical quality and cancer biology drive long-term overall survival (OS) differences after curative-intent resection. From 2009 onward, we implemented a sequence of interventions to improve surgical quality and pathologic evaluation in a regional population. We evaluated population-level surgical quality and OS in the MS-QSR cohort.
Methods. We categorized the MS-QSR into 4 (approximately) 5-year eras: 1) 2004-08, baseline; 2) 2009-13 (quality feedback and pilot intervention studies); 3) 2014-18 (surgical intervention with a lymph node collection kit); 4) 2019-22

(dual surgical and pathology intervention with novel gross dissection method). We compared surgical quality and OS across eras using standard statistical methods.
Results. Of 6,701 resections, 15%, 33%, 32%, and 20% were in Eras 1-4, respectively. American College of Surgeons Operative Standard 5.8 quality was attained in 4%, 22%, 45%, and 65% of resections in Eras 1-4, respectively; the International Association for the Study of Lung Cancer's stringent definition of 'complete resection' was achieved in 0%, 9%, 20%, and 31%, respectively; 120-Day mortality rates were 10%, 9%, 7%, and 4%; 3-year OS rates were 49%, 64%, 71%, and 84%; 5-year OS, 34%, 52%, and 61%, in Eras 1-3 (too early for Era 4); $p<0.0001$ for all comparisons.
Conclusion. Population-level surgical quality and OS have improved sequentially in parallel with implementation of interventions to surgical and pathology practices. The higher OS threshold in the MS-QSR creates a platform to interrogate the biologic drivers of surgical outcomes differences.

#4383
Development and validation of the Lung Cancer-Health Index (LC-HI), a clinically-relevant, disease-specific patient-reported outcome measure
Anika Varma[1], Spencer Rosero[1], Jamison Seabury[1], Jennifer Weinstein[1], Charlotte Engebrecht[1], Christine Zizzi[1], Nuran Dilek[2], John Heatwole[3], Megan Baumgart[4], Deborah Mulford[4], Ronald Maggiore[5], Lainie Conrow[6], Jennifer King[7], Jacinta Wiens[7], Chad Heatwole[1]. *[1]Center for Health + Technology, University of Rochester, Rochester, NY,[2]Department of Neurology, University of Rochester, Rochester, NY,[3]Pittsford Sutherland High School, Rochester, NY,[4]Department of Medicine, University of Rochester, Rochester, NY,[5]Hospice of Michigan, Ann Arbor, MI,[6]Wilmot Cancer Institute, University of Rochester Medical Center, Rochester, NY,[7]Go2 Foundation for Lung Cancer, Washington DC, DC*

Study Aim: The goal of this research is to develop and validate a novel, disease-specific patient-reported outcome measure (PRO) for use in clinical monitoring and therapeutic trials in Lung Cancer (LC).
Methods: LC currently accounts for the greatest number of cancer deaths worldwide, driving an increased need for novel therapeutic development in LC. To bolster clinical trial infrastructure, it is critical to have a comprehensive, sensitive and reliable PRO that accurately tracks LC multifactorial disease burden. This research describes the development and validation of the Lung Cancer-Health Index (LC-HI) as an efficient mechanism for assessing how

patients with LC feel and function in response to therapeutic treatment. We conducted semi-structured, qualitative interviews with 15 individuals diagnosed with LC and collected 653 direct participant quotes to determine the most frequent and important symptoms in LC. Based upon participant responses, we designed a survey that inquired about 162 symptoms from 14 symptomatic themes. This survey was implemented in a cross-sectional study with 139 participants with LC. The collected data was used to generate the first version of the LC-HI, which contained symptom questions showing the highest impact to the population and the potential to respond to therapeutic intervention. Symptom questions were grouped into distinct subscales using factor analysis. We beta-tested the LC-HI with 15 patients with LC to evaluate its usability, clarity, and applicability. Based on patient feedback, we modified the instrument and evaluated its test-retest reliability with 22 individuals with LC. Known groups testing was performed with the final instrument.
Results: The final version of the LC-HI contains 45 symptom questions grouped into 10 subscales that measure the following areas of LC health: 1) fatigue, 2) physical function, 3) emotional health, 4) sleep and daytime sleepiness, 5) activity participation, 6) breathing function, 7) gastrointestinal function, 8) cognitive function, 9) social performance, and 10) pain. Total LC disease burden is measured using a weighted composite of these subscale scores. During beta interviews, individuals with LC deemed the instrument to be easy to use, clear, relevant, and comprehensive. Statistical and psychometric analyses confirmed that the LC-HI is reliable, valid, sensitive, specific, of high internal consistency, and able to differentiate between groups with known varying levels of disease burden (based on disability status and smoking history).
Conclusions: Our research demonstrates the validity of the LC-HI as a marker of the multifaceted disease burden in LC. This disease-specific PRO provides researchers and clinicians with a reliable tool to use in patient monitoring, clinical trials, and to support FDA drug labeling claims.

#4384

Does progressive disease justify pembrolizumab discontinuation: a simulation analysis

Kannan Thiagarajan[1], Madhav Channavazzala[1], Brian Gregory Topp[2]. *[1]Vantage Research, Chennai, India,[2]Merck, Rahway, NJ*

Background: With checkpoint inhibition becoming first line therapy in several cancer indications, there is a growing number of patients that are refractory to PD1 therapy. It is unclear if these patients should remain on PD1 inhibitors while

new therapies are added on top or if PD1 should be discontinued when new therapies are initiated. Here we simulate a randomized controlled study comparing pembrolizumab + a checkpoint inhibitor (P+C) to a checkpoint inhibitor (C) in virtual patients that are refractory to PD1 therapy.
Methods: An IO QSP model was developed that includes intra-patient heterogeneity in tumor dynamics (target, non-target, and new metastatic lesions). The model was calibrated to individual lesion data from a large multicentre, open-label phase III study (Keynote-001) in patients with metastatic melanoma. A two year phase III study comparing P+C to C was simulated with 310 virtual patients in each group. Virtual patients were removed from the trial at the time of RECISTv1.1 progression or dropout due to AE or loss to follow-up.
Results: Virtual patients in the P+C arm displayed deeper (-11.5% vs 24.5%) and longer response (186.4 days vs 96.5 days) than virtual patients in the CPI arm. The percent of virtual patients displaying low prevalence progression (< 50% of the target lesions with PD) was 86% vs 52% for P+C vs. C. Median progression free survival was also longer in the P+C arm (3.8 vs 2.1 months). Difference in progression free survival were driven mainly by virtual patients that displayed oligoprogression during the pembrolizumab monotherapy run-in period.
Conclusions: Simulations presented here show that virtual patients that continued pembrolizumab treatment beyond RECISTv1.1 progression (as part of a combination) did better than virtual patients that discontinue pembrolizumab (and switch to a new therapy).

#4385

Unprecedented tumor: immune interaction--clinical and drug-development implications

Farah Mazahreh[1], Liyan Mazahreh[2], Brad Fugere[2], Ahmad Mazin Safar[3].
[1]Medicine, UAMS, Little Rock, AR,[2]CAVHS, Little Rock, AR,[3]UAMS Winthrop P. Rockefeller Cancer Institute, Little Rock, AR

Background: Classic therapeutic (RX) oncology principles demand radiographic response or durable stable disease as surrogates of overall survival (OS) prolongation, the ultimate metric of Rx benefit. Progressive disease (PD), however, is an undisputed indication of treatment failure. Immune Oncology (IO) trials reporting individual patient outcomes using swimmers' plot (SP) suggest substantial OS subsequent to PD, unprecedented pre-IO.
Hypothesis: Unrecognized phenomenon of OS benefit in the setting of radiographic PD, is tissue-agnostic and prevalent (>15%).

Methods: We conducted a retrospective review of IO monotherapy trials in 3 cancers if SP were reported. Percentage of PD patients (Pts) surviving beyond defined time landmarks is reported (Table).
Results: Realizing that 3rd or subsequent Rx lines rarely provide > 6 months OS duration in most cancers, our results indicate that 2/3rd of IO-treated pts, regardless of histology, or line of therapy are performing significantly better than expected; 1/3rd surviving > 1 year beyond PD.
Discussion: In IO, radiographic bulk may increase despite undeniable OS benefit (in years). We likely underestimated this phenomenon since pts with PD at 1st assessment aren't included in the SP, and with longer follow up, OS of PD pts is likely to improve with longer time to manifest it. This phenomenon--we term 'Disguised Responders' (DRs)--challenges an oncology principal. DRs needs to be considered by clinicians and future drug developers to accurately identify putative novel drugs. A plausible mechanism of DRs posits that 'virulence' of a given subclone, regardless of size or bulk, dictates Rx outcome. Virulence may operate through cachexia-induction, propensity to metastasize or metabolic adaptability, to name a few. Novel experimental approaches are desperately awaited to probe and measure virulence of different tumor subclones in future drug evaluations.

Clinical Trials of IO Monotherapy					**Number and (%) of pts surviving beyond clinical PD (months)**					
Tumor	Rx Line	1st Author/Yr	N	PD (n)	<6	6-11	12-23	24-35	36-47	≥48
NSCLC*	2nd +	Topalian "19	22	12	1	2	4	1	4	
	1st +	Fredinandus "21	45	2	1	1				
	1st +	Kim "22	139	22	13	5	3			
	N/A	Bilger "22	18	10	3	4	3			
	2nd	Dart "21	7	3		2	1			
	2nd +	Tozuka (MR) "20	11	11		4	6	1		
	2nd +	Tozuka (PD) "20	51	51	29	12	7	2	1	
	2nd +	Waterhouse "20	39	38	16	14	4			4
Subtotal			**332**	**149**	**63**	**44**	**28**	**4**	**5**	**4 (3%)**

					(42%)	**(30%)**	**(18%)**	**(3%)**	**(3%)**	
Melanoma	1st +	Warburton "20	70	13	1	4	3	4	1	
	2nd +	Topalian "19	34	21		1	2	10	4	4
	2nd +	Weber "15	38	4	2		1	1		
	2nd +	Dimitriou "21	125	9		3	4	2		
Subtotal			**267**	**47**	**3 (6%)**	**8 (17%)**	**10 (21%)**	**17 (36%)**	**5 (11%)**	**4 (8.5%)**
RCC**	2nd +	Topalian 19"	**10**	**7**	1			1	2	3
				7	15%			15%	30%	42%
Total			**609**	203	33%	**25%**	**15%**	**10%**	**6%**	**5.4%**
*Non-small cell lung cancer. ** Renal Cell Carcinoma										

#4386

Comparison of cytotoxicity of anthracycline based antineoplastic drugs in breast cancer

Mitali Singhal[1], Jacobo Elies Gomez[1], Sanjit Nayak[2], Kirsten Riches Suman[2], Amalia Ruiz Estrada[1]. *[1]School of Pharmacy and Medical Science, University of Bradford, Bradford, United Kingdom,[2]School of Chemistry and Biosciences, University of Bradford, Bradford, United Kingdom*

Mitoxantrone (MTX) is used for the chemotherapeutic treatment of breast cancer, but it has a dose-limiting cardiotoxicity. One of the mechanisms of MTX cytotoxicity is by inhibiting the topoisomerase II enzyme, which is crucial for maintaining cellular processes like replication. The aim of the study is to investigate if an alternative analog of MTX, named KP71 would be a suitable antineoplastic drug with reduced cardiovascular side effects. Cytotoxicity of both drugs in breast cancer cell lines MDA-MB-468, MDA-MB-231, MCF7, the non-neoplastic breast cell line MCF10, cardiac human fibroblasts (HFB), and human umbilical vein endothelial cells (HUVEC) was assessed by MTT at 96h. The IC_{50} values (nM) for MTX/KP71 were as shown in table below. DNA decatenation assay demonstrated topoisomerase II inhibition with values of IC_{50}

= 2.9/12.3 μM for topoisomerase IIα, and 2.1/7.0 μM for topoisomerase IIβ for MTX/ KP71 respectively. Western blotting showed DNA damage by the gradation in γH2AX expression at different concentrations of MTX and KP71 at 6 h and 24 h treatment. KP71 was found to retain the ability to inhibit the proliferation of neoplastic cell lines in vitro with a slower profile of cytotoxicity on non-neoplastic cell lines as compared to MTX. KP71 partly exerted cytotoxicity by damaging DNA and inhibiting topoisomerase II enzyme activity. Organotypic HFB-HUVEC co-cultures were used to investigate the effects of anthracycline drugs in angiogenesis. Although both drugs reduced the number of tubules (and branches) compared to control (absence of drug), there were not significant differences between MTX and KP71.

MTT IC50 (nM)		
	MTX	KP71
MDA-MB-468	27	50
MDA-MB231	38	169
MCF7	63	150
MCF10	35	90
HFB	160	1177
HUVEC	56	93

#4387

Total toxicity burden of FDA approved immune checkpoint inhibitors in USA

Fan Yang, Chloe Shay, Zhaohui Qin, Nabil Saba, Yong Teng. *Emory University, Atlanta, GA*

Immune checkpoint inhibitors (ICIs) have revolutionized the treatment landscape for multiple cancers, demonstrating effective and durable responses and becoming the standard of care for a variety of malignancies. However, ICI-based treatment has resulted in the rise of unique immune-related adverse events (irAEs). To date, very little information is available on the frequency, significance, and management of single-organ or multiorgan irAEs in clinic. In this study, the irAEs associated with the treatment of seven FDA-approved ICIs, including three PD-1 inhibitors (cemiplimab, nivolumab and pembrolizumab), three PD-L1 inhibitors (atezolizumab, avelumab and durvalumab), and one CTLA4 inhibitor (ipilimumab), were analyzed based on the data of 149,303 report cases (January 1, 2015 - June 30, 2022) collected from FDA Adverse

Events Reporting System (FAERS) public dashboard. Our data reveal that irAEs associated with the treatment of anti-PD-1 ICIs (e.g., pembrolizumab) require less hospital care resources compared with anti-PD-L1 and anti-CTLA4 ICIs. Tissue and organ toxicity of ICIs are age and gender specific. 'Cardiac disorders' is the main disorder caused by these ICIs in cancer patients aged 65-85, while 'reproductive system and breast disease' is the main disorder in cancer patients aged 18-64. There are risks of respiratory and urinary system toxicity in male patients and reproductive system toxicity in female patients when they receive the treatment of ICIs. Studies such as this one provide the statistical data for understanding patients at risk of developing irAEs, which will underscore the importance of further exploring research strategies to predict, detect, and mitigate toxicities from ICIs.

Clinical Informatics and Data Science / Retrospective Clinical Analyses 1

#4391

Real world data and multi-genomic analysis of non-common mutations in the EGFR mutation-positive non-small cell lung cancer

Seoree Kim[1], Yeoun Eun Sung[2], Joo Ri Kim[2], Chan Kwon Jung[2], Jeong-Oh Kim[2], Jeong-yeon Shin[2], Guk Jin Lee[1], Sang hoon Chun[1], Young Ho Lee[3], Jin Hyoung Kang[2]. *[1]Bucheon St. Mary's Hospital, Bucheon, Korea, Republic of,[2]Seoul St. Mary's Hospital, Seoul, Korea, Republic of,[3]Research Center for Bioconvergence Analysis, Korea Basic Science Institute (KBSI), Daejeon, Korea, Republic of*

Introduction: There are similar and different properties between the epidermal growth factor receptor mutations (mEGFR), which are classified into common, uncommon, and compound mutation subtypes depending on their location and pattern on the EGFR gene. We investigated the RWD and RNA expression profile of non-common mutations (uncommon and compound mutations) in the mEGFR+ NSCLC patients.
Method: We analyzed the NGS data extracted from the Foundation Medicine (FMI) SRC. And, we collected the medical information for stage I-IIIA mEGFR+ NSCLC patients receiving curative surgical resection. In Böehringer Ingelheim (BI) open data access (ODA), we analyzed treatment results in stage IV mEGFR+ NSCLC patients treated with EGFR TKI. We explored the RNA expression profile by High-Plex Digital Spatial Profiling. A total of 18,676 DEG libraries were constructed, and 419 significance genes with > 2-fold changes, 3-log 2 normalized read counts, and p-value = 0.05 (up and down) were identified.

Result: In FMI-SRC cohort, 10,059 mEGFR+ cases of total 78,656 cases consist of common, 6,994 (69.5%), uncommon, 1,966 (19.6%), and compound, 1,099 (10.9%). In hospital cohort, 941 mEGFR+ cases consist of common, 860 (91.4%), uncommon, 60 (7.4%), and compound, 21 (2.2%). Median relapse-free survival (mRFS) in non-common mutations (31.4M and 33.7M) was shorter than common mutations (40.1M, p=0.877). CNS recurrence in the non-common mutations (40.0% and 35.3%) tended to be higher than that of common mutations (27.4%, p=0.361). In BI-ODA, median time on treatment (mTOT) in 163 uncommon mutations (10.0M) and 139 compound mutations (11.5M) were shorter than historical data of common mutations (17.3M). Spatial RNA-seq data of the ratio of deconvolution individual cells showed that genes involved in inflammatory and immune response were relatively lower in non-common mutations. Gene ontology string analysis revealed RNA expression of genes in compound mutations was functionally associated with chemokine production (23.4%), electron transfer activity (14.9%) and T cell selection (8.5%), and, in uncommon mutations, was associated with regulation of oligopeptide transport (26.1%), hypermethylation of CpG island (21.7%), and CD4+ CD25+ regulatory T cell lineage commitment (13.0%), compared to common mutations. Based on the GSEA, relatively highly clustered genes in compound mutations were the protein modification process, G-protein coupled receptor, regulation of cytosolic calcium ion concentration, and IL-5 production pathways, and lower ES levels in oxidative phosphorylation and RNA processing pathways, when compared to common mutations.
Conclusion: Taken together, our results suggest that uncommon and compound mEGFR subtypes exhibiting shorter mRFS and mTOT, and distinguishing RNA expression profile of functional signaling pathways be not same disease entity as common mEGFR subtype

#4392

Expression landscape of trophoblast cell surface antigen 2 (Trop-2) in breast cancer

Kai Song, Oh Kyu Yoon, Luting Zhuo, Emon Elboudwarej, Biao Li, Jillian Boice, Yang Pan, See Phan, Monica Motwani. *Gilead Sciences Inc., Foster City, CA*

Background**:** Antibody-drug conjugates (ADCs) are novel agents linking potent payloads to antibodies targeting antigen-expressing tumors. Sacituzumab govitecan (SG), a Trop-2-directed ADC, is approved for patients with metastatic triple-negative breast cancer (mTNBC) with ≥2 prior therapies (≥1 in metastatic

setting). SG is also being investigated in other breast cancer subtypes, including hormone receptor-positive/human epidermal growth factor receptor 2-negative (HR+/HER2-) metastatic breast cancer and in earlier lines of treatment. To understand the landscape of Trop-2 expression and potential clinical actionability of Trop-2 and other antigens, we evaluated RNA expression data in breast cancer from The Cancer Genome Atlas (TCGA) and Molecular Taxonomy of Breast Cancer International Consortium (METABRIC).
Methods: TCGA and METABRIC datasets were assessed for Trop-2, HER2, and programmed death ligand 1 (PD-L1) expression via processed RNA sequencing (RNA-seq) and microarray data of the corresponding genes *TACSTD2*, *ERBB2*, and *CD274*. Gene expression across clinical parameters was assessed via one-way ANOVA, t-test, or Spearman correlation. HER2 status was classified as HER2 immunohistochemistry (IHC) 0 or HER2-low (IHC1+, or IHC2+ and in situ hybridization-negative). Survival was estimated via Kaplan-Meier method. Neoadjuvant therapy datasets were assessed for effects of aromatase inhibitors on Trop-2 expression.
Results: RNA-Seq data was available from 1030 and 2136 breast cancer patients in TCGA and METABRIC datasets, respectively. Most patients (96%) had high *TACSTD2* expression (>100 transcripts per million [TPM]). *TACSTD2* expression was comparable by breast cancer histology (median log2TPM 6.8-7.5), by disease stages I-IV (median log2TPM 7.0-7.5), or by subtypes (median log2TPM 7.1-7.3). *TACSTD2* expression was not correlated with *ERBB2* (Spearman rho=0.06) or *CD274* (Spearman rho=-0.13) expression. No difference in *TACSTD2* expression was noted between HER2 IHC0 or HER2-low subtypes. *TACSTD2* expression was not associated with survival, though low tertile *TACSTD2* groups had better prognosis in the basal subtype; treatments were heterogeneous. Changes in *TACSTD2* gene expression were not observed post-aromatase inhibitors.
Conclusions: While SG is approved for use in mTNBC, *TACSTD2* is stably expressed across all breast cancer stages and subtypes, including HER2 IHC0 and HER2-low, and across all ranges of PD-L1 expression, suggesting a broad patient population may benefit from Trop-2-directed ADCs.

#4393
Tumor volumetric analysis to correlate disease burden with response to dual immune checkpoint blockade in metastatic NSCLC
Muhammad Aminu, Natalie I. Vokes, Maliazurina B. Saad, Hui Li, Lingzhi Hong, Mohamed S. Mohamed, John Boom, Pingjun Chen, Mehmet Altan, Saumil Gandhi, Stephen Swisher, Mara B. Antonoff, Jenny V. Pozadzides,

George Blumenschein Jr, Don L. Gibbons, Tina Cascone, Yasir Y. Elamin, Xiuning Le, Marcelo V. Negrao, Ferdinandos Skoulidis, Anne S. Tsao, Janet Tu, J.Jack Lee, Jianjun Zhang, John V. Heymach, Jia Wu. *The University of Texas MD Anderson Cancer Center, Houston, TX*

Background: Compared to other well-studied biomarkers, the relationship between overall tumor burden and immune-checkpoint inhibitor (ICI) efficacy is poorly understood.
Methods: We identified patients with stage IV NSCLC without EGFR, ALK or ROS1 alterations treated on the LONESTAR protocol with nivolumab + ipilimumab with formal 3-month radiographic response evaluation. Response was annotated using RECIST 1.1. Manual segmentation of primary and measurable metastatic lesions on pre-treatment CT scans was performed, and tumor volume was calculated from these measurements. Tumor burden was defined as the involvement status, volume, or lesion counts within specific organs (lungs, pleura, lymph nodes, liver, adrenals, bone, and soft tissue) and across whole body. We explored the impact of baseline tumor burden on ICI response and its association with other clinical features.
Results:152 patients were included; patients with progressive disease (PD; n=50) at 3 months were compared to all others (n=102). Overall disease volume correlated to tumor volume at the primary lesion (spearman rho=0.69), lymph node (rho=0.45), soft tissue (rho=0.23), lung metastases (rho=0.22), and pleura (rho=0.20); overall lesion counts correlated to lesion counts in lymph nodes (rho=0.61), lung metastases (rho=0.45), and bone (rho=0.16). On univariate analysis, overall tumor volume (P=2e-53) and lesion counts (P=2e-51) had the strongest association with PD, outperforming PD-L1 (P=0.02), ECOG performance status (PS, P=7e-16), and clinical variables including prior treatment and smoking status. PD correlated with higher disease burden in all individual organs except bone; adrenal metastases inversely correlated with PD. Volumetric features complemented PD-L1 and other clinical risk factors to predict PD; in a composite model (ClinVol) AUC=0.82, sensitivity=66%, specificity=93%, while PD-L1 alone yielded an AUC=0.62, sensitivity=94%, specificity=28%. Similar trends were observed for subgroup analyses stratified by brain metastasis status or smoking history, in which volumetric measures increased the power of PD-L1 to predict PD by a consistent AUC increase of ~0.2. Upon subgroup analysis stratified by PD-L1, volumetric models showed robust stratification of PD, with AUC of 0.97, 0.81, 0.81 respectively for PD-L1 <1%, 1-49%, and ≥50%.

Conclusion: Higher baseline tumor burden was associated with increased likelihood of disease progression on combination ICI therapy. ClinVol modeling improves predictive accuracy of 3-month progression.

#4394

Feasibility analysis of querying EHR databases for cancer clinical trial criteria

Dylan J. Cooper[1], Joseph Herman[1], Nalan Yurtsever[2], Sergio Garza[3], Daniel A. King[4], Yonah Ziemba[2]. *[1]Northwell Health Cancer Institute, Lake Success, NY,[2]Department of Anatomic and Clinical Pathology, Northwell Health, New Hyde Park, NY,[3]Cancer Informatics, Northwell Health Cancer Institute, Lake Success, NY,[4]Medical Oncology, Northwell Health, Lake Success, NY*

Background: In order to enroll patients for clinical trials (CT), it is common to run queries in clinical databases using CT eligibility criteria as filters and specifications. However, CT eligibility criteria are often unavailable as discrete data fields, which can interfere with CT recruitment. The purpose of this study was to identify the most commonly needed eligibility criteria that are specified in cancer CT to investigate whether and how they could be found in clinical databases.
Design: We examined the data elements needed for the trial eligibility criteria that would be used in queries for all the Breast, Gastrointestinal, Genitourinary, Head and Neck, and Cutaneous Cancer treatment trials open for enrollment across our health system. We then performed a sort-rank exercise for these eligibility criteria terms.
Results: The analysis included 33 trials and 12 data elements. Table 1 shows the number of times each eligibility criterion appeared in the 33 CTs and its feasibility for an EHR query. The data elements that appeared most frequently were Organ/Cancer Site (100%), Tumor Morphology (66.7%), Presence of Metastases (51.5%), TN Staging (39.4%), and Days Since Diagnosis (24.2%). Of these, only Organ/Cancer Site and Days Since Diagnosis were accessible as structured datapoints in our clinical databases.
Conclusions: The lack of feasibility for EHR query is likely due to the fact that healthcare information is generally stored in a discrete, structured form as a means of completing care transactions (drug orders or laboratory values) and ensuring billing compliance (ICD and outpatient CPT codes). This presents a critical challenge when data are required for CT enrollment, quality assurance metrics, and prospective and retrospective clinical research. Health systems—and by extension, their patients—would benefit from investing in structured data

schemas involving AJCC staging, tumor morphology, and presence of metastases.

Eligibility criteria with corresponding number of appearances in CTs and feasibility for EHR query		
Eligibility criterion	Number of trials with each criterion	Feasibility for EHR query
Organ/Cancer Site	33 (100%)	Accessible (ICD codes very detailed for site and used consistently for purpose of billing)
Tumor Morphology	22 (66.7%)	Not accessible (Code have not been created in ICD system, SNOMED is not widely adopted, not needed for billing)
Presence of Metastases	17 (51.5%)	Not accessible (Not coded consistently, coded in ICD as a “secondary” malignancy but generally does not affect billing)
TN Staging	13 (39.4%)	Not accessible (Not coded in ICD system)
Days Since Diagnosis	8 (24.2%)	Accessible (Structured data captured for purpose of initial transaction)
Tumor Markers and Other Lab Results	4 (12.1%)	Accessible (Structured data captured by laboratory instrument for purpose of initial transaction)
Immunohistochemical Biomarkers	4 (12.1%)	Not accessible (Pathologist assessment documented as narrative text)
History of Systemic Therapy	3 (9.1%)	Accessible (NDC drug code captured with initial order in order to complete the initial transaction)
Feasibility of Resection	3 (9.1%)	Not accessible (Surgeon assessment documented as narrative text)
Disease progression	3 (9.1%)	Not accessible (Radiologist assessment documented as narrative text)
Surgical Procedure	2 (6.1%)	Accessible as CPT codes for outpatient surgeries as needed for billing. Not accessible for inpatient surgeries where billing is capitated

		as a single fee for entire hospitalization based on disease related groups
Margins	2 (6.1%)	Not accessible (Pathologist assessment documented as narrative text)

#4396

TROP2 expression in non-small cell lung cancer

Peiwen Kuo[1], Emon Elboudwarej[1], Lauri Diehl[1], Jilpa Patel[1], Sabeen Mekan[2], Juliane M. Jürgensmeier[1]. *[1]Gilead Sciences Inc., Foster City, CA,[2]Gilead Sciences Inc., Morris Plains, NJ*

Introduction: Non-small cell lung cancer (NSCLC) is a major cause of cancer-related deaths globally with high unmet need. A variety of novel therapeutic strategies are being explored to improve patient outcomes including the use of antibody drug conjugates (ADCs) to deliver highly potent, cytotoxic payloads to tumors. Trophoblast cell-surface antigen 2 (TROP2), also known as tumor-associated calcium signal transducer 2 (TACSTD2), has emerged as an attractive target for ADCs. Sacituzumab govitecan-hziy is a novel ADC composed of a TROP2 antibody coupled to SN-38 and is being evaluated in NSCLC. High TROP2 mRNA expression is observed in many tumor types, however, TROP2 protein expression in NSCLC is not well-established. Here we characterized TROP2 expression across three independent datasets to explore the TROP2 relationship to baseline characteristics, molecular features of interest, and its prognostic value in NSCLC.
Methods: We analyzed three independent datasets: (1) The Cancer Genome Atlas (TCGA) NSCLC adenocarcinoma (LUAD, N=660) and squamous cell carcinoma (LUSC, N=484) mRNA expression data, (2) a NSCLC adenocarcinoma FFPE tumor sample set (“Translational data set”; N=107), (3) an independent clinical NSCLC adenocarcinoma (N=103) and squamous cell carcinoma (N=37) data set. TROP2 IHC was performed on tumor sample sets (2) and (3) using the SP295 antibody (Robust Prototype Assay, Ventana) with H-Score and assessment of the percentage of membrane-positive tumor cells as readouts. Wilcoxon rank-sum and Kruskal-Wallis tests (continuous variables), Kaplan-Meier method (survival probability curves) and log-rank test (time to event outcome) were used (GraphPad Prism 8.1.2 and R version 4.0.5).
Results: TROP2 mRNA was highly expressed in NSCLC and expression was similar in adenocarcinoma and squamous cell carcinoma in the TCGA data set. TROP2 expression did not vary with patient’s age, gender, race or tumor stage.

Furthermore, TROP2 expression was not associated with TP53, KRAS or driver mutation status (including EGFR, ALK, ROS, RET, MET). TROP2 expression in the Translational sample set was consistent with the findings from the TCGA data analysis: TROP2 mRNA and protein expression were high and independent of patient baseline demographics, tumor stage and TP53 and KRAS mutation status. Finally, in an independent clinical NSCLC dataset, TROP2 protein was highly expressed and there was no relationship between TROP2 and baseline demographics including gender and age. TROP2 membrane H-scores and percentage of membrane-positive tumor cells also highly correlated in the two independent datasets.
Conclusions: Three large independent datasets confirmed high expression of TROP2 in NSCLC both, as mRNA and protein. TROP2 expression in tumors did not differ between histological subtypes, baseline characteristics or clinically relevant driver alterations. Based on the TCGA data set, TROP2 expression was not prognostic for survival.

#4397

Chemotherapy-induced peripheral neuropathy and falls in cancer survivors relate to digital balance and gait impairments

Vrutangkumar Shah[1], Daniel Muzyka[1], Carolyn Guidarelli[2], Kristen Sowalsky[1], Kerri M. Winters-Stone[2], Fay B. Horak[2]. *[1]Clario, Portland, OR,[2]OHSU, Portland, OR*

Background and Aim: Standing postural sway and gait tests with body-worn inertial sensors provide a multitude of objective, digital balance, and gait measures that represent several different domains controlling mobility. However, it is not clear which domains of balance or gait best reflect the impact of treatment-induced peripheral neuropathy on mobility or differentiate fall risk in cancer survivors. This study aimed to determine which domains of balance and gait differed between cancer survivors who reported 1) symptoms of peripheral neuropathy versus asymptomatic survivors and 2) falls in the previous six months versus non-fallers.
Methods: Both postural sway during 30 seconds of quiet stance and gait characteristics from the Instrumented Time-Up-and-Go test (ITUG) were recorded with six synchronous inertial sensors (Opals by APDM Wearable Technology, a Clario company). The sensors were placed on both shanks and wrists, and one on the lumbar spine and sternum in 425 female cancer survivors (age: 62 ± 6 years). A principal component analysis (PCA) approach was used

first to identify independent domains of mobility from 14 balance and gait measures for subsequent analysis.
Results: PCA analysis revealed 5 independent domains (PC1: Sway amplitude, PC2: Gait pace; PC3: Sway frequency; PC4: Gait spatial-temporal and PC5: Turning) that accounted for 81% of the variance of performance across the participants. Cancer survivors who reported neuropathy showed a significantly higher sway frequency (PC3) than asymptomatic survivors. Cancer survivors who reported falls showed a significantly larger sway area (PC1) and slower gait pace (PC2) than non-fallers.
Conclusions: Wearable sensor instrumentation from short balance and gait tests capture objective digital gait and balance outcomes reflective of treatment-related neuropathy and fall risk in women treated with chemotherapy for cancer. Wearable sensors could be used for oncology clinical trials to assess the impact of cancer treatment and symptom mitigation strategies to limit changes in mobility that might lead to excess falls in people with cancer.

#4398

Validation of an updated algorithm to identify non-small cell lung cancer (NSCLC) patients in administrative claims databases

Sandip Pravin Patel[1], Rongrong Wang[2], Summera Qiheng Zhou[3], Daniel Sheinson[2], Ann Johnson[2], Janet Lee[2]. *[1]University of California, San Diego, CA,[2]Genentech Inc, South San Francisco, CA,[3]Genesis Research, Hoboken, NJ*

Purpose: Administrative claims data using the ICD-9-CM or ICD-10-CM coding systems are not detailed enough to distinguish between lung cancer subtypes, which presents challenges for real-world research. This study updated and validated a previous treatment-based algorithm that uses claims data to identify NSCLC vs small-cell lung cancer (SCLC) (Turner RM, et al. Front Pharmacol 2017;8:883).
Methods: This study used Optum's de-identified Market Clarity Data (2007-2021) which deterministically links medical and pharmacy claims with electronic health record (EHR) data from providers across the continuum of care. Included patients had lung cancer diagnosis and histology information available in the EHR, which is the gold standard for validation. Patients were required to have ≥3 months of continuous health plan enrollment before and after the diagnosis date. First, to replicate the Turner algorithm, patients were identified between Jun 2014 and Oct 2015 with any first-line NSCLC treatment and no SCLC treatment (Step 1). Next, the Turner algorithm was applied from Nov 2015 to Dec 2020 to evaluate if performance decreased given the approval

of immunotherapies since 2015 (Step 2). Finally, the Turner algorithm was updated with NSCLC treatments approved since 2015 in concordance with the latest US treatment guidelines. Algorithm performance at each step was measured using sensitivity, specificity, positive predictive value (PPV) and negative predictive value (NPV).
Results: Sample sizes and performance statistics for each step are presented in the Table. From Step 1 to Step 2, specificity and PPV decreased while sensitivity and NPV increased. Algorithm performance improved slightly for all measures from Step 2 to Step 3.
Conclusions: This updated treatment-based algorithm improves validity and accuracy in identifying NSCLC patients in claims databases and supports its use in real-world research using claims databases when histology data is unavailable.

	Step 1: Turner replication	**Step 2: Turner 2015-2020**	**Step 3: Updated Turner 2015-2020**
Date range	Jun 2014-Oct 2015	Nov 2015-Dec 2020	Nov 2015-Dec 2020
Sample size	406	2573	2744
Sensitivity	0.873	0.920	0.932
Specificity	0.933	0.865	0.923
PPV	0.987	0.976	0.988
NPV	0.560	0.640	0.673

#4399

Can technology improve the quality and efficiency of multidisciplinary cancer conferences?

Opuruiche Ibekwe, Carmelo Gaudioso, Kristopher M. Attwood, Ellis G. Levine, Stephen B. Edge, Chukwumere E. Nwogu. *Thoracic Surgery, Roswell Park Comprehensive Cancer Center, Buffalo, NY*

Background: The use of multidisciplinary cancer conferences (MCCs) in cancer patient management is known to lead to improved quality of care and patient outcomes. Applying technology to MCCs may serve to optimize the process and enhance its contribution to patient care. The purpose of this study is to evaluate the impact of a tumor board technology platform on the quality of MCCs.
Methods: Data was collected prospectively from Thoracic, Gynecology (GYN) and Breast Cancer MCCs, September 2020 to February 2022, at a

comprehensive cancer center using an MCC performance assessment tool and a self-administered survey. The Mann Whitney U and X^2 tests were used as appropriate, to compare the quality of information presented and discussed, time per case reviewed, and consensus before and after implementation of the NAVIFY® Tumor Board Solution. Weighted composite scores of 11 of the variables were calculated and averaged between observers. Higher mean scores reflect higher quality and vice versa.

Results: Pre and post NAVIFY® data were collected from 249 and 289 cases, respectively. The overall quality of information presented increased after NAVIFY® implementation (Table 1). This increase was maintained within the Thoracic, Breast and GYN MCC subgroups (mean composite scores: 63.9 vs 82.9; $p < .001$, 63.4 vs 72.3; $p < .001$, and 59.8% vs 63.5%; $p = 0.009$ respectively). Increased participation by surgical, medical and radiation oncologists was also documented for the MCCs (mean score: 3.9 vs 4.1; $p < .001$, 3.4 vs 3.9; $p < .001$, and 3.5 vs 3.6; $p = 0.035$ respectively) as well as increased frequency of consensus (85.9% to 95.5%; $p = 0.001$). No change in discussion time was seen. Pathologists/radiologists surveyed reported greater ease of finding information they needed to prepare for the MCC (76.1% vs 96.7%; $p = 0.048$).

Conclusions: Using technology to organize and convey data at MCCs improves quality of information presented and discussed, clinician participation and the ability to reach a consensus.

Table 1. Comparison of Observational Measures Before and After NAVIFY® Platform Introduction

		Baseline Period	**Post Period**	**P-value**
Total Observed Cases	N	250 (46.4%)	289 (43.6%)	
Observed Cases By MCC	Thoracic	156 (62.4%)	177 (61.2%)	0.963
	Breast	42 (16.8%)	50 (17.3%)	
	GYN	52 (20.8%)	62 (21.5%)	
All MCCs				
Composite Score	Mean/SD	62.9/7.7	76.9/10.6	*<.001*
Composite Score Breakdown	>= 90	-	26 (9.0%)	*<.001*
	80-90	9 (3.6%)	100 (34.6%)	

	70-80	28 (11.2%)	84 (29.1%)	
	60-70	132 (52.8%)	57 (19.7%)	
	< 60	81 (32.4%)	22 (7.6%)	
Surgical Oncologist Contribution	Mean/SD	3.9/0.8	4.1/0.7	*<.001*
Medical Oncologist Contribution	Mean/SD	3.4/1.0	3.9/1.0	*<.001*
Radiation Oncologist Contribution	Mean/SD	3.5/0.9	3.6/1.2	*0.035*
Discussion Time (minutes)	Mean/SD	10.2/4.4	10.3/4.3	0.605
Consensus Reached	Yes	213 (85.9%)	276 (95.5%)	*0.001*

#4400

Machine learning (ML) on real-world data (RWD) of front-line (1L) metastatic castration resistance prostate cancer (mCRPC) patients for dynamic prediction of time to tx discontinuation (TTD)

Prerna Jain, Deep K. Hathi, Hossein Honarvar, Rahul K. Das. *ConcertAI, Cambridge, MA*

Background: Abiraterone (abi) and enzalutamide (enza) are two novel androgen therapies (NAT) for 1L treatment (tx) for mCRPC. As there is no head-to-head randomized controlled clinical trial (RCT) between Abi and Enza, predicting 1L comparative effectiveness of these two drugs for mCRPC, especially in patient groups under-represented in RCTs is critical. ML was performed on electronic health records (EHR) to evaluate risk factors of TTD in 1L mCRPC patients and identify predictive markers of patient subgroups with differential outcomes from enza vs. abi.
Methods: Patients with curated mCRPC diagnosis and 1L tx between Jan 2012-May 2022 were identified in a ConcertAI® oncology EHR database. For dynamic prediction of TTD, survival XGBoost models were built with four different timepoints as index: 1L start, and 30, 60, and 90 days from 1L start. A 60:20:20 split was used for train, validation, and test sets. TTD was defined as either tx end or death. Risk factors and interaction terms were identified using SHapley Additive exPlanations (SHAP) and marginal hazard ratios.
Results: The sample size ranged between 1580-1636 patients (Table 1). Holdout testset cumulative dynamic AUROC for the models ranged between 0.65-0.75. PSA rise from 1L start, elevated PSA, liver enzymes, and platelets to lymphocytes ratio, low hemoglobin and albumin, prior NAT tx, intake of pain

medications, lower BMI, and high comorbidity were risk factors for TTD across all models. Tx with enza or abi was predictive of lower risk of TTD. While enza was better than abi in the overall population, SHAP interaction terms revealed that enza had worse TTD than abi in patients with higher ALP and NATs did not have any TTD benefit over chemo for patients with lower HGB.
Conclusions: ML on RWD identified prognostic markers for 1L mCRPC tx discontinuation and predictive markers of patient subpopulations with different outcomes from enza vs. abi.

Table 1: Summary of TTD Models: Cohort characteristics, model performance, risk factors: Mean HR (95% CI)

	Index of models			
	1L Tx-start	**1L Tx start + 30 days**	**1L Tx start + 60 days**	**1L Tx start + 90 days**
N patients (event prevalence)	1636 (89 %)	1611 (89.8%)	1585 (91.3)	1570 (92.2)
Model performance: hold-out CD-AUC (mean ± SD)	0.65±0.04	0.70±0.03	0.75±0.04	0.75±0.05
Risk factors				
Current Tx: enzalutamide (vs no)	0.81 (0.61, 0.92)	0.82 (0.76,0.86)	0.94 (0.91,0.97)	0.97 (0.96,0.99)
Current Tx: abiraterone (vs no)	0.84 (0.68, 0.94)	0.91 (0.88,0.94)	0.96 (0.94, 0.98)	0.93 (0.87, 0.97)
Current Tx: Count of drugs in regimen ≥ 2 (vs = 1)	0.90 (0.81, 0.97)	0.87 (0.83,0.93)	0.95 (0.92, 0.98)	0.93 (0.85, 0.97)
Tx history: Prior NAT treatment (vs no)	1.27(1.01, 1.57)	1.38 (1.21, 1.54)	1.33 (1.19, 1.52)	1.42 (1.15, 1.85)
Tx history: Analgesics usage (vs no)	1.20 (1.03, 1.39)	1.25 (1.13, 1.40)	1.03 (1.02, 1.06)	1.04 (0.99, 1.02)
PSA based features: Baseline PSA (ng/mL) ≥ 14.0 (vs ≤ 2.0)	1.12 (1.03, 1.22)	1.13 (1.06, 1.20)	1.31 (1.22, 1.44)	1.32 (1.20, 1.5)
PSA based features: PSA rise from 1L start (ng/mL) ≥ 16.5 (vs ≤ -3.5)	NA	1.25 (1.14, 1.37)	1.22 (1.11, 1.31)	1.23 (1.10, 1.41)
Vitals: (BMI) ≥ 32.1 (vs ≤ 25.2)	0.89 (0.78,0.97)	0.95 (0.90, 0.99)	0.93 (0.88, 0.96)	0.88 (0.75, 0.98)
Liver enzymes: ALP (U/L) ≥	1.11 (1.03,	1.3 (1.17,	1.18 (1.13,	1.32 (1.13,

159.0 (vs ≤ 70.0)	1.21)	1.43)	1.25)	1.62)
Liver enzymes: AST (U/L) ≥ 27.0 (vs ≤ 16.0)	1.01 (0.95, 1.07)	1.21 (1.02, 1.44)	1.09 (1.02, 1.15)	1.11 (0.94, 1.55)
CBC panel: WBC counts (103/mL) ≥ 344.7 (vs ≤ 158.2)	1.01 (0.99, 1.03)	1.16 (1.04, 1.3)	1.05 (1.02, 1.08)	1.07 (0.99, 1.16)
CBC panel: Platelets to lymphocytes count ratio ≥ 266.4 (vs ≤ 125.9)	1.09 (0.98, 1.25)	1.07 (0.99, 1.16)	1.01 (0.97, 1.04)	1.08 (1.00, 1.16)
CBC panel: HGB (g/dL) ≥ 13.4 (vs ≤ 10.7)	0.94 (0.81, 0.99)	0.83 (0.78, 0.87)	0.82 (0.77, 0.87)	0.73 (0.63, 0.84)
Comorbidity: Elixhauser Score ≥ 16.0 (vs ≤ 7.0)	1.04 (1.00, 1.11)	1.20 (1.05, 1.33)	1.10 (1.05, 1.16)	1.06 (1.02, 1.17)
Interaction of Tx (Enza vs. others) with HGB (g/dL) ≤ 11.0 (yes vs. no)	log-rank p value = 0.04	NA	NA	NA
Interaction of Tx (Enza vs. others) with ALP (U/L) ≥ 213.0 (yes vs. no)	log-rank p value = 0.02	NA	NA	NA
Footnote: ALP**,** alkaline phosphatase; AST, aspartate aminotransferase; BMI, body mass index; CBC, complete blood count; CI, confidence interval; Enza, enzalutamide; HGB, Hemoglobin; HR, hazard ratio; PSA, prostate specific antigen; Tx, treatment; WBC, white blood cell.				

#4401

The precision chemotherapy to improve the epithelial ovarian cancer prognosis

Seongeun Pak, Youn Jin Choi. *Catholic University of Korea, Seoul, Korea, Republic of*

Purpose: Recurrence is common in ovarian cancer patients, even in those patients who show complete response after first-line chemotherapy, 80% of the patients experience a recurrence. So gynecologic oncologists often have to consider several factors when choosing next chemotherapy regimen. Therefore, this study aimed to find serial chemotherapy regimen choice to anticipate patients' better prognosis.

Materials and Methods: We reviewed 656 patients diagnosed ovary cancer in one tertiary institutional hospital between 2006 and 2020. Patents' clinic-

pathologic characteristics, primary treatment, chemotherapy regimens, survival outcomes were collected. We divided patients into several groups according to their chemotherapy regimen by mechanism of action and compared them. 1st line chemotherapy(CTx) type 1: carboplatin-paclitaxel, carboplatin-docetaxol, cisplatin-paclitaxel, cisplatin-docetaxol2nd line CTx type 1 : carboplatin-paclitaxel, carboplatin-docetaxol, cisplatin-paclitaxel, cisplatin-docetaxol2nd line CTx type 4 : carboplatin-gemcitabine2nd maintenance CTx type 2 : PARP inhibitor(PARPi)2nd line CTx Type 5: Platinum + topoisomerase inhibitor 2nd line CTx Type 6(cisplatin-vinorelbine)2nd line CTx Type 8(topoisomerase inhibitor only) 2nd line CTx Type12 (single taxol) The survival rate of ovary cancer patients decreased from stage 1 to stage 4.Among 1st line CTx type 1 and 2nd line CTx type(1 or 4) patients, those who used PARPi in 2nd line maintenance CTx(n=14) had a higher death rate than those who did not receive maintenance CTx or received that other than PARPi(hazard ratio 1.44). In the 1st line CTx 1~4 group, we divided patients according to 2nd line CTx type. We compare 2nd line CTx type 5 group(n=30) with type 6+8+12 group(n=26). The death rate was of type 5 group was higher than type 6+8+12 group. And Overall survival of 2nd line CTx type 5 group was 22 months, that of 2nd line CTx type 6+8+12 group was 26 months.
Conclusion: When changing the chemotherapy regimen in the recurrence of ovarian cancer, the survival rate or overall survival may vary depending on the order in which the regimen is used. If we collect patients data more broadly, the predictive power will be better.

#4402

Survival impact of post-operative immunotherapy in resected stage III cutaneous melanomas in the checkpoint era

Garo G. Hagopian[1], Christopher Grant[1], Danielle Brazel[1], Priyanka Kumar[1], Maki Yamamoto[2], James Jakowatz[2], Warren Chow[3], Thuy Tran[2], Justin Moyers[3]. *[1]Internal Medicine, UCI Medical Center, Orange, CA,[2]Surgical Oncology, UCI Medical Center, Orange, CA,[3]Hematology and Oncology, UCI Medical Center, Orange, CA*

Introduction: Since 2015, immune checkpoint inhibitors have been approved as post-operative therapy for resected stage 3 cutaneous melanoma. This approval was a result of studies which demonstrated improved recurrence free survival. However, overall survival (OS) benefit has yet to be observed. We examine the

OS of postoperative immunotherapy in stage 3 melanoma using real world data from the National Cancer Database (NCDB).
Methods: Data was collected from the 2020 NCDB Participant Use File (October 2022 release). Patients were staged by both the 7th and 8th version of American Joint Committee on Cancers (AJCC). Those who underwent definitive surgery since 2016 and had sufficient pathologic data for staging were included. Patients who received systemic therapy prior to surgery were excluded. Patients were then sorted by the type of postoperative therapy started within 12 weeks from definitive surgery and classified into the no post-operative systemic therapy (NP) or postoperative immunotherapy (PI) groups. Survival time was calculated from the time of definitive surgery to last contact or death. OS was estimated by Kaplan-Meier method and compared by log-rank method.
Results: 18,167 patients underwent surgery for stage 3 disease between 2016-2020. By AJCC v8 staging, 4,256 had Stage 3A disease, 3,752 stage 3B disease, 9,251 stage 3C disease, and 908 stage 3D disease. Median OS was not met in any stage 3 PI groups. The 36 - month landmark survival of all stage 3 subgroups is shown in Table 1. Only 13.3% of patient received PI in 2016. PI use increased to 24.8% in 2017, 43.8% in 2018, 46.8% in 2019, and 50.8% in 2020.
Discussion: Using a large real-world database, we found that patients receiving post-operative immunotherapy in the checkpoint era have a significant survival benefit compared to those who did not. The benefit was significant in stage IIIB-C in AJCC v7 and Stage IIIC-D in AJCC v8. However, the benefit was not significant in stage 3A melanoma.

Table 1: 36-month Landmark survival reported with 95% confidence interval for both AJCC versions

		No Post-Operative Immunotherapy		**Post-Operative Immunotherapy Given**		
Stage	**Total Patients (n)**	**n (%)**	**36- month survival % (95% CI)**	**n (%)**	**36- month survival % (95% CI)**	**p-value**
AJCC v 7						
Stage 3	**15272**					
Stage 3A	3818	2539 (66.5)	90 (89-91)	1141 (29.9)	91 (90-92)	p=0.737
Stage	4572	2990	78 (77-79)	1461	83 (82-94)	p=0.001

3B		(65.4)		(32.0)		
Stage 3C	6882	4021 (58.4)	64 (63-65)	2637 (38.3)	73 (72-74)	p<0.001
AJCC v 8						
Stage 3	**18167**					
Stage 3A	4256	2981 (70.0)	91 (90-92)	1145 (26.9)	93 (92-94)	p=0.354
Stage 3B	3752	2255 (60.1)	84 (83-85)	1379 (36.8)	87 (86-88)	p=0.057
Stage 3C	9251	5592 (60.4)	65 (64-66)	3372(36.5)	76 (75-77)	p<0.001
Stage 3D	908	550 (60.6)	44 (42-46)	316 (34.8)	59 (56-62)	p<0.001

#4403

The Efficacy of Immune Checkpoint Inhibitors in Advanced Biliary Tract Cancer with KRAS Mutation

Sun Young Jeong, Jaeyeon Jang, Youngkyung Jeon, Ye Ji Jung, Daeho Choi, Joohyun Hong, Seung Tae Kim, Jung Yong Hong, Joon Oh Park, Young Suk Park, Ho Yeong Lim. *Division of Hematology-Oncology, Department of Medicine, Samsung Medical Center, Sungkyunkwan University School of Medicine, Seoul, Korea, Republic of*

BackgroundWith a 15% of incidence, KRAS is one of the most common mutations in biliary tract cancer (BTC) and a poor prognostic factor. In BTC, the immune checkpoint inhibitor (ICI) as salvage therapy has modest activity. There was little data on the efficacy of ICIs according to the status of KRAS mutation in BTC.

MethodWe conducted molecular profiling in BTC patients who received the ICIs as salvage therapy. Programmed death ligand 1 (PD-L1) expression on tumor cells and tumor-infiltrating lymphocytes (TIL) was also assessed. We analyzed overall survival (OS) and progression-free survival (PFS) of ICI in BTC patients according to the status of PD-L1 expression and KRAS mutation.

ResultA total of 62 patients were included in this analysis. The median age was 68.0. 47 patients (75.8%) received pembrolizumab and 15 (24.2%) received

nivolumab as salvage therapy. All patients received gemcitabine plus cisplatin as the frontline therapy, and 53.2% had fluoropyrimidine plus oxaliplatin (FOLFOX) before ICIs. The median lines of prior chemotherapy were 2.5. KRAS mutation was found in 14 patients (22.6%). 28 patients (45.2%) were positive for PD-L1 CPS. There was no statistical correlation between the status of KRAS mutation and PD-L1 expression. The median OS and PFS to ICI were 5.6 (IQR; 3.3 - 8.0) and 3.8 (IQR; 3.0 - 4.5) months, respectively. There were no statistically significant differences in PFS to ICIs according to the status of KRAS mutation (Mutant type vs. Wild type) and PD-L1 expression (Positive vs Negative). In subgroup analysis, patients with both KRAS mutation and PD-L1 positivity had longer PFS as compared to patients with KRAS mutation and PD-L1 negativity (6.5 vs 2.6 months, p=0.047). This finding was not shown in patients with a wild type of KRAS.
ConclusionThis analysis showed that PD-L1 expression might be a novel biomarker for ICIs in BTC patients with KRAS mutation but not the wild type of KRAS.

#4404

Survival impact and trends of immunotherapy use in metastatic merkel cell carcinoma in the checkpoint era: analysis of a large database

Christopher R. Grant[1], Garo Hagopian[1], Danielle Brazel[1], Priyanka Kumar[1], Justin Moyers[2]. *[1]Department of Medicine, University of California Irvine Medical Center, Orange, CA,[2]Division of Hematology and Oncology, Department of Medicine, University of California Irvine Medical Center, Orange, CA*

Introduction: Merkel Cell Carcinoma (MCC) is an aggressive skin cancer that has typically been treated with conventional chemotherapy in the metastatic setting. In 2017, metastatic MCC treatment options expanded when the FDA approved immune checkpoint inhibitors based on single-arm uncontrolled studies. We utilized data from the National Cancer Database (NCDB) to examine the survival benefit of first line immunotherapy (IO) or chemotherapy (CT) in metastatic MCC.
Methods: The NCDB was analyzed to identify patients with metastatic MCC from 2017-2020. Patients who did not have data available on AJCC version 8 staging group, survival status, and treatment details (surgery, radiation therapy, CT, IO) were excluded from the analysis. Patients were divided into cohorts based on first line systemic therapy; those who received chemotherapy and those who received immunotherapy. Survival time was calculated from the time of

initiation of systemic treatment to last contact or death. Overall survival (OS) was estimated by Kaplan-Meier method and compared by log-ranked method. Results: We identified 648 patients with stage IV MCC between 2017-2020. Of those, 15.3% (n=99) received CT, 51.7% (n=335) received IO, and 32.9% (n=213) did not receive systemic therapy. Median OS was 13.2 (95% CI: 10.1-16.2) months for those receiving any systemic therapy. Median OS was 13.8 (95% CI: 7.9-19.7) months for CT and 12.9 (95% CI: 9.6-16.2) months for immunotherapy (p=0.379). In the first year of IO approval in 2017, only 37.4% of patients received IO which increased to 54.5% in 2018, 59.6% in 2019, and 54.9% in 2020. Chemotherapy use decreased throughout the same time period from 23.9% in 2017 to 12.4% in 2020. There was a notable difference in the number of patients less than 65 years old who received IO (66%) relative to the number of patients 65 years and older who received IO (80%) (p=0.006). Discussion: Immunotherapy has supplanted chemotherapy as the first line treatment of choice in MCC, particularly in those 65 and older. However, we did not find first line use of immunotherapy to provide a statistically significant survival advantage over chemotherapy in stage IV Merkel cell carcinoma. Clinical equipoise exists, and a randomized clinical trial is needed.

#4405

Tumor mutational burden, as a potential predictive marker for the efficacy of immunotherapy in advanced gastric cancer

Jaeyeon Jang, Youngkyung Jeon, Sun Young Jeong, Ye Ji Jung, Daeho Choi, Joohyun Hong, Jeeyun Lee, Won Ki Kang, Seung Tae Kim. *Samsung Medical Center, Seoul, Korea, Republic of*

Background: The optimal value of tumor mutational burden (TMB) for predicting treatment response of immunotherapy in advanced gastric cancer (AGC) is still unclear. We aimed to establish the optimal cut-off value of TMB, and evaluate the efficacy of immunotherapy in AGC according to TMB and other markers.
Method: From October 1, 2020, to July 27, 2021, at Samsung medical center in Korea, patients with AGC, who received pembrolizumab or nivolumab were included. TMB was measured by next-generation sequencing (NGS)-based assays, and PD-L1 is tested using immune-histochemical assay 22C3 pharmDx. Based on receiver operating characteristic analysis, the cut-point value of TMB was determined as the point where the Youden's index is maximum.
Result: A total of 53 patients were analyzed. The cut-off value of TMB for predicting the overall response of immune checkpoint inhibitors was defined as

13.31 mutations/megabase (mt/mb), with 56% of sensitivity and 95% of specificity. Under this definition of TMB, 7 patients were TMB-high group (≥13.31 mt/mb), while 46 patients were TMB-low group (<13.31 mt/mb). The overall response rate (ORR) had a statistically significant difference between TMB-low (8.7%, n=4/46) and TMB-high patients (71.4%, n=5/7; *p*=0.001). The progression-free survival (PFS) and overall survival (OS) for 53 patients were 1.93 months (95% CI, 1.600-2.268) and 4.26 months (95% CI, 2.992-5.532). The OS was longer in the TMB-high group with the median of 20.8 months (95% CI, 2.292-39.281) compared to the TMB-low group with the median of 3.31 months (95% CI, 1.604-5.019; *p*=0.049). The ORR of the patients whose PD-L1 CPS was 1 or above was not different from the patients whose PD-L1 CPS was lower than 1.
Conclusion: In this study, the optimal value of TMB for predicting the objective response rate of immunotherapy in AGC was determined as 13.31 mt/mb. TMB-high (≥13.31 mt/mb) was associated with a better objective response rate, and TMB-high patients exhibited better overall survival. TMB has the potential for predicting therapeutic response to immunotherapy in advanced gastric cancer.

#4406

Impact of site of metastases on response to immunotherapy in microsatellite stable (MSS) metastatic colorectal cancer (mCRC)

Marwan Fakih, Jaideep Sandhu, Xiaochen Li, Chongkai Wang. *City of Hope National Medical Center, Duarte, CA*

Background: We have noted that responses to the combinations of regorafenib and nivolumab (REGONIVO) or regorafenib ipilimumab nivolumab (RIN) were limited to MSS mCRC without liver involvement. We sought to delineate the impact of non-liver metastatic sites on the response to these combinations.
Methods: We performed a single center retrospective analysis of MSS mCRC receiving REGONIVO or RIN. To isolate the impact of immunotherapy on metastatic disease sites, we performed a 2-month (mo) analysis of organ specific response using organ specific RECIST assessment.
Results: 96 patients (Pts) (39 RIN and 57 REGONIVO) were evaluated. Overall response rate (ORR), median progression free survival (PFS), and median overall survival (OS) were 0%, 2 mo, and 7 mo in pts with liver metastatic (LM) disease (n = 33). We focused on the impact of other metastatic disease site on OS and PFS within the non-LM group to exclude liver as a confounding variable (n=63). Pts with lung-only mCRC had the best prognosis with an ORR, median PFS, and median OS of 56%, 13 mo, and unreached at 24 mo. Pts with

peritoneal mCRC fared poorly (ORR 0%, median PFS= 1.5 mo, median OS =12 mo). A high ORR (75%) was noted in a small cohort of 4 pts with lymph node only disease. However, concurrent LN with lung only mCRC diminished efficacy outcomes. Differences in PFS and OS by organ involvement were independent of treatment (REGONIVO or RIN) based on estimates from Cox proportional hazard model. 2-mo response rates by metastatic sites are shown in Table 1. Responses at the 2-mo mark in the 96 pt cohort occurred in lung, LN, and soft tissue metastases but were most robust in lung only metastatic disease. Conclusions: Responses to the combination REGONIVO or RIN are most robust in lung-only metastatic disease and appear to be modest in the setting of LN and soft tissue involvement. Liver and peritoneal disease was associated with lack of benefit from these combinations.

Table 1 2-month Response Rates by Site of Metastatic Disease

Sites of mCRC	Number of Pts	PD	SD	PR+CR
Lung	72	33 (45.8%)	21 (29.2%)	18 (25.0%)
Lung response in the setting of liver mets	*27*	*18 (66.7%)*	*7 (25.9%)*	*2 (7.4%)*
Lung response without liver mets	*45*	*15 (33.3%)*	*14 (31.1%)*	*16 (35.6%)*
Lung response in lung only metastatic disease	*16*	*3 (18.8%)*	*4 (25.0%)*	*9 (56.2)*
Liver	33	31 (93.9%)	2 (6.1%)	0 (0%)
Lymph Node (LN)	49	32 (65.3%)	12 (24.5%)	5 (10.2%)
LN in the setting of liver mets	*22*	*20 (90.9%)*	*2 (9.1%)*	*0 (0%)*
LN in the setting of no liver	*30*	*14 (46.7%)*	*11 (36.7%)*	*5 (16.6%)*
LN only	*4*	*1 (25%)*	*0 (0%)*	*3 (75%)*
Peritoneal	15	14 (93.3%)	1 (6.7%)	0 (0%)
Soft tissue	30	11 (39.3%)	15 (53.6%)	2 (7.1%)
Bone	8	4 (50%)	4 (50%)	0 (0%)

Brain	1	1 (100%)	0 (0%)	0 (0%)
Spleen + Adrenal	5	4 (80%)	1 (20%)	0 (0%)

#4407

Clinicopathologic characteristics and mutational analysis of MYC amplified head and neck squamous cell carcinoma (HNSCC)

Thomas Cyberski[1], Alka Singh[2], Mark Lingen[3], Alexander Pearson[2], Nishant Agrawal[4], Evgeny Izumchenko[2], Ari Rosenberg[2]. *[1]The University of Chicago Pritzker School of Medicine, Chicago, IL,[2]Medicine, Section Hematology/Oncology, University of Chicago, Chicago, IL,[3]Pathology, Medicine, University of Chicago, Chicago, IL,[4]Surgery, Section Otolaryngology, University of Chicago, Chicago, IL*

Amplification of MYC proto-oncogene is commonly found in many types of cancer, and frequently associated with poor clinical outcomes. Analysis of the TCGA-HNSCC dataset indicates that MYC amplification is estimated to be present in ~12% of HNSCC cases, and has a significant impact on patients' median survival (32.2 vs 56.9 months for patients with wild-type MYC). While the association between MYC amplification and HNSCC progression was previously reported, its role in regulating mechanisms of acquired resistance to therapy remain under investigated. In this study, we seek to further characterize the clinicopathological features associated with MYC amplified HNSCC, and highlight the molecular changes that may contribute to acquired resistance to treatment.

Seven HNSCC patients with MYC amplification were identified by searching the Oncoplus database at the University of Chicago. A retrospective chart review was conducted to collect demographic and clinical data for each patient, and mutational landscape was characterized. In a single patient, MYC amplification was acquired following treatment with chemoimmunotherapy (nivolumab, carboplatin, paclitaxel), chemoradiation, and maintenance nivolumab resulting in rapidly progressive disease despite an initial response to therapy. RNA sequencing and immunohistochemical staining was performed to compare specimens collected before and after progression.

Seven patients were diagnosed with HNSCC and were found to have MYC amplification on molecular testing of their cancer between 2018 and 2021. Four were male, median age 61 (range 46-71), stage T2-4 (n=6), N2-3 (n=6), p16+ (n=2). All patients (n=7) developed recurrent and/or metastatic disease following

primary therapy with locoregional recurrence (n=3), metastatic recurrence (n=2), or both (n=2). Median survival for the cohort was 3.1 years. Previous therapy included surgery (n=4), radiotherapy (n=7), chemotherapy (n=7), targeted therapy (n=4), and immunotherapy (n=4). The most common mutations co-occurring with MYC amplification were CDKN2A loss (n=5), TP53 loss (n=5), CCND1 amplification (n=2) and KDM6A loss (n=2). Acquisition of MYC amplification and acquired resistance to chemoimmunotherapy was associated with upregulation of glycolysis pathway, WNT/beta-catenin signaling, and significant changes to tumor microenvironment (TME) such as tumor infiltrating lymphocytes repertoire and PD1/PD-L1 expression levels.
Alongside the data from TCGA, the cases described in this study highlight the poor prognosis associated with MYC amplified HNSCC. While loss of function mutations in CDKN2A and TP53, upregulation of glycolysis pathway, and TME reprogramming may contribute to treatment resistance and secondary immune evasion, further studies in larger cohorts are warranted to develop therapies that target MYC mediated mechanisms of resistance in HNSCC.

#4408

Provisional prognostic score for monomorphic epitheliotropic T-Cell lymphoma

Philip A. Haddad, Dinesh Keerty, Neelakanta Dadi. *LSUHSC-S, Feist-Weiller Cancer Center/Overton Brooks VAMC, Shreveport, LA*

Background: Monomorphic Epitheliotropic Intestinal T-cell Lymphoma (MEITL) is a rare extranodal intestinal PTCL. It is an aggressive disease with an overall poor prognosis. However, the disease presents a diverse spectrum of survival outcomes. We conducted this study to develop a provisional MEITL prognostic score (MPS) for this rare disease.
Methods: We used our updated MEITL database, which contains retrospective data on 218 cases. Such data included demographics such as sex, age, and race. It also included disease presentation symptoms, duration of symptoms before diagnosis, site(s) of the disease, stage, blood counts, disease immune and molecular phenotype, types of treatment, quality of response, and survival outcomes. Out of the 218 cases, only 140 cases had complete survival and outcomes data, the sample chosen for this study. Cox proportional-hazards model and Log-rank tests were used to assess the influence of clinicopathologic factors on overall survival (OS). Due to the relatively small training cohort, we included factors that statistically impacted OS as well as factors that numerically trended that way.

Results: The median OS of the cohort was 11 months. The following dichotomous variables were identified as impactful prognostic factors in this cohort: Bone marrow involvement (9 vs. 14 months), Non-biclonal TCR status (10 vs. 17.5 months), CD56+ (10 vs. 26 months), Ki67≥70% (4 vs. 8 months), cMyc expression >15% (7 vs. 12 months). A prognostic model was devised using these variables to identify different levels of risk. Each variable was assigned a score of 1 when present, except for cMyc, which was assigned 2 points for having the highest hazard ratio among all the variables. In this exploratory cohort, low risk was assigned a score of 0, intermediate risk a score of 1-2, and high risk a score of 3-6. This prognostic score system led to our cohort's most optimal risk discriminatory model, where low, intermediate, and high risk had a median OS of 26, 12, and 4 months, respectively (p=0.002). Conclusion: This MPS is a promising new tool for risk-stratifying patients with MEITL. However, it still needs prospective validation.

#4409

Survival determinants of aggressive adult T-cell leukemia/lymphoma (ATLL): analysis of a pooled database

Supriya Gupta, Christopher Graham, Philip A. Haddad. *LSUHSC-S, Feist-Weiller Cancer Center/Overton Brooks VAMC, Shreveport, LA*

Background: Adult T-cell leukemia/lymphoma (ATLL) is a rare Peripheral T-cell Lymphoma subtype caused by Human T-Lymphotropic Virus 1 (HTLV-1). The disease encompasses a vast phenotype ranging from the smoldering and chronic indolent subtypes to the lymphoma and acute aggressive subtypes. Aggressive ATLL which comprise acute/leukemic, lymphoma, and other indolent subtypes with aggressive transformation tend to have poor outcome with conventional chemotherapy rarely achieving durable lasting remission. We conducted this pooled database analysis to identify key factors that affect the clinical outcomes of aggressive ATLL subtypes.
Methods: To study the demographic characteristics, molecular and immunohistochemical signatures, therapeutic interventions, survival, and prognostic factors, we compiled a pooled database of 462 ATLL cases. Kaplan-Meier survival curves were constructed. Cox proportional hazards model and Log-rank tests were used to assess the influence of demographic and clinicopathologic factors on the overall survival (OS).
Results: Three hundred and forty-seven aggressive ATLL patients with survival data were included in this analysis. The median OS of the whole group was 14 months, with a median OS of 12.8, 16, and 12 months for acute, lymphoma, and

transformed subtypes. The median age was 54 years, with a M:F ratio of 1.1. SCT demonstrated superior OS compared to chemotherapy (28 vs. 10 months, $p<0.0001$). Similarly, LSG15 regimens were superior to no chemotherapy and other combinations (29 vs. 1 vs. 15 months, $p<0.0001$). Asians and Afro-Caribbeans lived longer than Whites, Indians, and Hispanics (15.7, 15, 10, 3, 1 months, $p<0.0001$, respectively). The presence of hypercalcemia (Ca>11 mg/dl, Anemia (Hgb<12 g/dl), elevated LDH ($\geq$1000 U/L), and effusions adversely effected OS. Moreover, visceral involvement generally and specifically GI, kidney, lung, and heart were significantly detrimental to OS. However, age, sex and the presence of constitutional symptoms or HAM/TSP did not impact the OS.
Conclusions: This study explored a wide array of clinical factors and their impact on the OS of aggressive ATLL. It identified race, types of treatment, the presence of hypercalcemia, anemia, elevated LDH, effusion and visceral metastases as significant determinants of OS in aggressive ATLL.

#4410
Determinants of progression-free and overall survival of angioimmunoblastic T-Cell lymphoma (AITL): a pooled analysis
Philip A. Haddad, Frankie Powell. *LSUHSC-S, Feist-Weiller Cancer Center/Overton Brooks VAMC, Shreveport, LA*

Background: Angioimmunoblastic T-cell lymphoma (AITL) is a major subtype of peripheral T-cell lymphoma with a T-cell follicular helper phenotype. It accounts for approximately 1-2% of non-Hodgkin's lymphoma and 15-20% of peripheral T-cell lymphoma. AITL has unique clinical features with an aggressive course and poor prognosis. Therefore, it is essential to uncover the clinically significant prognostic factors to chart an optimal treatment strategy for AITL. Currently, AITL prognostic factors are not well established. Several retrospective AITL series with limited numbers reported varying prognostic factors and occasionally discordant results. Consequently, such studies lacked the power to validate factors that influence long-term clinical outcomes. We conducted this meta-analysis to evaluate the pooled impact of selected clinicopathologic factors on progression-free (PFS) and overall survival (OS) in patients with AITL.
Methods: A review of the medical literature was conducted using online databases. Inclusion criteria comprised AITL diagnosis, English language, and studies reporting factors impacting PFS and OS with hazard ratios (HR). A meta-analysis was conducted using an inverse variance method. The pooled

value for the estimate, with 95% CI, was calculated using the Fixed effects model and the Random effects model.
Results: Eight retrospective series with 944 patients were included and analyzed. Factors that impacted both PFS and OS included: Bone marrow involvement (HR 1.51, 95%CI:1.01-2.25; HR 1.58, 95%CI:1.02-2.44), mediastinal involvement (HR 1.44, 95%CI:1.10-1.88; HR 1.48, 95%CI:1.09-2.02), B-symptoms (HR 1.40, 95%CI:1.14-1.71; HR 1.55, 95%CI:1.22-1.96), stage >II (HR 1.50, 95%CI:1.05-2.13; HR 1.74, 95%CI:1.15-2.61), ECOG $\geq$2 (HR 1.74, 95%CI:1.42-2.13; HR 2.39, 95%CI:1.65-3.44), ↑LDH (HR 1.47, 95%CI:1.12-1.94; HR 1.39, 95%CI:1.01-1.91), Albumin<3.5g/dl (HR 1.43, 95%CI:1.10-1.85; HR 1.57, 95%CI:1.01-2.45), sIL2R >530U/ml (HR 1.72, 95%CI:1.12-2.65; HR 1.90, 95%CI:1.29-2.80), and extra-nodal involvement >1 site (HR 1.92, 95%CI:1.53-2.41; HR 2.01, 95%CI:1.48-2.72). Factors that impacted OS only are: effusion (HR 2.60, 95%CI:1.32-5.14), leukocytosis (HR 1.11, 95%CI:1.02-1.22), and PIT >1 (HR 1.83, 95%CI:1.22-2.73). Factors that impacted PFS only are: Age (HR 1.37, 95%CI:1.18-1.59), Anemia (HR 1.63, 95%CI:1.34-1.97), and ↑β2-microglobulin (HR 1.73, 95%CI:1.19-2.52). However, sex, thrombocytopenia, ↓total protein, ↑IgG, ↑IgA, ↑IgM, ↑CRP, and IPI >2 did not significantly impact PFS or OS.
Conclusions: This is the first meta-analysis to explore the impact of clinicopathologic factors on AITL PFS and OS. It delineates factors that impact PFS and OS and those that do not influence either.

#4411
Clinicopathologic determinants of survival in enteropathy-associated T-cell lymphoma (EATL): analysis of a pooled database
Philip A. Haddad, Sai Malireddy. *LSUHSC-S, Feist-Weiller Cancer Center/Overton Brooks VAMC, Shreveport, LA*

Background: EATL is a rare and rapidly progressive extranodal T-cell lymphoma which arises from the intestinal intraepithelial T lymphocytes. It often occurs in the context of untreated or long-standing Celiac disease (CD) or the development of refractory sprue. EATL tends to be less responsive to conventional chemotherapy, often with poor clinical outcomes. We conducted this analysis to explore the clinicopathologic determinants of survival in this rare extranodal T-cell entity.
Methods: To study the demographic characteristics, molecular and immunohistochemical signatures, therapeutic interventions, survival, and prognostic factors, we compiled a pooled database of 220 cases. Kaplan-Meier

survival curves were constructed. Cox proportional-hazards model and Log-rank tests were used to assess the influence of demographic and clinicopathologic factors on overall survival (OS).
Results: A total of 220 patients with confirmed EATL were identified. The median age was 60, with a peak incidence between 64 and 75. There was a slight female predominance with F:M ratio of 1.1. The jejunum was the most involved site (47%). The median OS of the whole group was 10 months. The most common presentations were abdominal pain, followed by perforation, diarrhea, obstruction, and gastrointestinal bleeding. The majority presented at stage I&II (53%). The median duration of symptoms before diagnosis was 2 months. Younger patients (p=0.02) and HLH (p=0.006) had worse OS. The time interval between diagnosing CD and EATL impacted OS, with <1 yr and >20yrs having worse outcomes (p=0.04). Combination chemotherapy and stem cell transplant (SCT) were statistically superior to no treatment, with a median OS of 11, 22, and 0.75 months respectively (p=0.002). Further analysis revealed that surgical resection imparted a survival advantage in combination with chemotherapy and SCT. When surgical resection was incorporated into the analysis, median OS amounted to 0.75, 9, 16, 8, 69 months for surgery alone, chemotherapy, surgery+chemotherapy, SCT, and surgery+SCT, respectively (p=0.003). Combinations that used anthracyclines (p=0.02) and etoposide (p=0.05) had better OS. The quality of response to treatment also seemed to impact the outcome (p=0.0001) with median OS of 9, 9, and 69 months for <PR, PR, and CR, respectively. OS was not impacted by stage, constitutional symptoms, presentation with obstruction or perforation, or CD30+. While male sex, colon and visceral involvement, and null TCR type seemed to impact OS negatively, they did not reach statistical significance.
Conclusions: This study presents updated clinicopathologic data from a pooled cohort of patients with EATL. It identifies age, CD duration, HLH, treatment modalities, and quality of response as major determinants of OS in this rare disease.

Combination Therapies for Cancer

#5483
Combined inhibition of CDK4/6 and AKT is highly active against the luminal androgen receptor (LAR) subtype of triple negative breast cancer (TNBC)
Maria del Rosario Chica-Parrado, Gun Min Kin, Chang-Ching Lin, Kyung-min Lee, Fabiana Napolitano, Dan Ye, Emmanuel Bikorimana, Saurabh Mendirata,

Ariella Hanker, Carlos L. Arteaga. *UT Southwestern Harold C. Simmons Comprehensive Cancer Center, Dallas, TX*

The LAR subtype of TNBC is enriched for targetable biomarkers, including androgen receptor (AR) expression, *PIK3CA* mutations, and intact Rb. The purpose of this study was to investigate the most effective combinations of inhibitors of CDK4/6 (palbociclib), AR (enzalutamide), and PI3K-AKT (alpelisib/capivasertib) against preclinical models of LAR TNBC. MDA-MB-453 and MFM-223 (both AR positive/Rb-intact/*PIK3CA*-mutant) LAR TNBC cells were treated with each inhibitor alone or in different combinations. Drug sensitivity was measured as growth in 2D, colony formation, and CellTiterGlo viability. Synergistic drug effects were expressed as the combination index (CI) calculated by CompuSyn methods. Activation of cell cycle and PI3K-AKT signaling molecules in response to different inhibitors or siRNAs was measured by immunoblot analysis. An androgen response element (ARE) luciferase reporter assay was used to evaluate AR transcriptional activity. MDA-MB-453 and MFM-223 cells were sensitive to single-agent palbociclib, alpelisib, or capivasertib (IC_{50} ~500 nM) but not enzalutamide (IC_{50} 15-25 μM). Palbociclib combined with either the PI3Kαi alpelisib or the AKTi capivasertib synergistically inhibited growth of both cell lines (CI values, 0.07-0.86). AR transcriptional reporter activity was not altered by any of these treatments. Treatment with palbociclib monotherapy (24 h) suppressed p-Rb and increased phosphorylation of AKT^{S473} and its substrates FOXO3A, GSK3β, and PRAS40, suggesting PI3K/AKT signaling mediates an adaptive response to CDK4/6 blockade. In MDA-MB-453 cells, palbociclib-induced phosphorylation of AKT substrates was suppressed by treatment with capivasertib but not with alpelisib alone or with the PI3Kβ/δ inhibitor AZD8186, suggesting that the compensatory activation of AKT was due to a mechanism independent of the PI3K isozymes. We next used RICTOR siRNAs to block mTORC2-mediated phosphorylation AKT^{S473} after palbociclib treatment. Gene silencing of RICTOR reduced levels of the mTORC2 substrate p-$SGK1^{S422}$ but did not block phosphorylation of AKT^{S473} and its substrates in palbociclib-treated cells, suggesting that this adaptative response was mTORC2-independent. Mean CI values showed that the combination of palbociclib/capivasertib was clearly more synergistic than palbociclib/alpelisib in both cells lines (mean CI, 0.29 vs. 0.78). Currently, we are comparing both combinations in mice bearing established MDA-MB-453 xenografts. Further investigation of the mechanisms of adaptive activation of AKT upon blockade of CDK4/6 in TNBC cells are in progress. In sum, addition of an AKT inhibitor, but not PI3K inhibitors, to palbociclib suppressed the

rebound activation of AKT following treatment with the CDK4/6i, supporting a testable therapeutic strategy in LAR TNBC with intact Rb.

#5484

Synergistic antitumor activity of *nab*-sirolimus in combination with *KRAS* inhibitors (KRASis) sotorasib and adagrasib in *KRAS G12C* NSCLC and bladder cancer xenografts

Shihe Hou[1], Andrew Kwon[1], Jorge Nieva[2], Neil Desai[1]. *[1]Aadi Bioscience, Inc., Pacific Palisades, CA,[2]University of Southern California, Los Angeles, CA*

KRAS is frequently mutated in non-small cell lung cancer (NSCLC) and other tumor types, with *KRAS G12C* mutation representing ~12% of patients with NSCLC. Sotorasib (sot) is approved and adagrasib (ada) is under review for the treatment of *KRAS G12C* NSCLC. Mutations in *KRAS* may lead to mTORC1 activation, and mTOR may contribute to adaptive resistance to KRASis. *nab*-Sirolimus (*nab*-S) is a novel albumin-bound nanoparticle form of the mTOR inhibitor sirolimus approved for the treatment of locally advanced unresectable or metastatic malignant perivascular epithelioid cell tumors. This study investigated the antitumor activity of *nab*-s in combination with KRASis in *KRAS G12C* NSCLC and bladder xenograft models. Athymic mice bearing subcutaneous *KRAS G12C*- and *STK11*-mutant NCI-H2030 and NCI-H2122 NSCLC and *KRAS G12C* and *PTEN*-null UMUC3 bladder cancer were treated for 6 weeks with *nab*-s IV at 15 mg/kg/wk, sot or ada (for NCI-H2122 and UMUC3) orally at 30 mg/kg/d alone or in combination. Tumor samples were harvested for analysis of tumor drug levels and biomarkers. In all 3 models tested, single-agent (SA) *nab*-s or KRASis overall showed modest tumor growth suppression. In contrast, *nab*-s in combination with either sot or ada showed greater tumor growth inhibition and a higher meaningful tumor regression rate vs SA (**Table**). There was no significant difference in antitumor activity between combinations of *nab*-s with either sot or ada. High trough intertumoral sirolimus levels were observed in groups treated with *nab*-s alone or in combination with KRASis, indicating sustained presence of sirolimus in the tumor. *nab*-S in combination with either sot or ada showed synergistic antitumor activity compared to the SA. A multicenter, single-arm, open-label Phase 1/2 clinical study is planned to determine the recommended Phase 2 dose, safety, tolerability, and efficacy for the combination of ada and *nab*-s in patients with *KRAS G12C* tumors.

Changes in TGI and Tumor Regression

Tumor	Combination	TGI vs	*P* Value vs	Tumor	*P* Value vs

Model	Treatment	Single Agent (%)		Single Agent for Tumor Growth Curve (ANOVA)		Regression Over 30%	Single Agents for Rate of Tumor Regression Over 30% (Chi-Square)
		vs *nab*-S	vs KRASi	vs *nab*-S	vs KRASi		
NCI-H2030	*nab*-S + Sotorasib	129	111	0.01	0.001	3/6	0.03
NCI-H2122	*nab*-S + Sotorasib	112	106	0.001	<0.001	8/10	<0.001
	nab-S + Adagrasib	101	100	0.001	<0.001	4/10	0.03
UMUC3	*nab*-S + Sotorasib	107	105	<0.001	<0.001	6/6	<0.001
	nab-S + Adagrasib	107	107	<0.001	0.04	6/6	0.001
ANOVA, analysis of variance; KRASi, *KRAS* inhibitor; *nab*-s, *nab*-sirolimus; TGI, tumor growth inhibition.							

#5485

Clinical evaluation of a functional combinatorial precision medicine platform reveals combination-specific sub-populations in t-cell lymphoma

Edward Kai-Hua Chow[1], Masturah Rashid[2], Sanjay Prasad De Mel[3], Jasmine Goh[1], Anand Jeyasekharan[4]. *[1]Cancer Science Institute, National University of Singapore, Singapore, Singapore,[2]KYAN Therapeutics, Singapore, Singapore,[3]2NUS Center for Cancer Research (N2CR), Yong Loo Lin School of Medicine, National University of Singapore, Singapore, Singapore,[4]Cancer Science Institute, National University Singapore, Singapore, Singapore*

T-cell lymphoma (TCL) is a heterogenous subgroup of non-Hodgkin's lymphoma with poor prognosis. Approved targeted monotherapies have seen limited success due to lack of effective combinations or identification of sensitive patient populations. Hence, there is a need to develop alternative strategies to identify effective combinations for individual patients and specific TCL sub-populations. We interrogated the potential for an ex vivo combinatorial drug sensitivity platform, Quadratic Phenotypic Optimization Platform (QPOP), in a clinical study for relapsed/refractory Non-Hodgkin Lymphoma (RR-NHL) to identify effective subtype-specific combinations through a functional combinatorial precision medicine approach.

We analyzed 37 primary samples from patients with RR-NHL of both T- and NK-cell origin in Singapore, with disease amenable to biopsy or blood/ marrow aspiration. Single cell suspensions from tumor samples were treated with a panel of 12 drugs with known preclinical or clinical efficacy against TCL. Post-drug treatment cell viability was used as a phenotypic input for QPOP analysis, which maps experimental data points to a second-order quadratic function to predict cell killing efficacies for all possible permutations of drug combinations. Romidepsin-based combinations appeared among the top ranked QPOP-derived 2-drug combinations with predicted output cutoff < 0.55 in 91.8% of samples treated with similar QPOP drug panel. Among these combinations, combinations with copanlisib, ifosfamide and venetoclax were the most frequently occurring doublet, appearing in 24, 14 and 8 samples, respectively. A total of 10 patients received QPOP-derived romidepsin-based combinations at physicians' discretion. We noted outcomes of stable disease or better in 7/10 (70%) patients, with clinical benefit seen in 2 complete responses and 2 partial responses (40%). Thus, romidepsin-based combinations showed improved outcomes for TCL patients compared to the prior reported overall response rate of 25% that led to romidepsin's approval as monotherapy. This study showed the clinical utility of QPOP in identifying combination therapy-specific sub-populations in TCL. Targeted agents, such as romidepsin, copanlisib and venetoclax, that have previously been explored as single agents in TCL were predicted by QPOP to be more effective in the proper combination for the proper patient. This study demonstrates that functional combinatorial precision medicine platforms, such as QPOP, may improve clinical outcomes through identification of more appropriate combination therapies. This work, as well as additional studies in other cancer types, provide evidence towards the need for optimal combination therapy design and the potential of functional precision medicine to improve precision and personalized cancer treatment.

#5486

Combining bromodomain and extraterminal (BET) protein inhibitor treatment with standard MAPK inhibitors improved MAPK signaling inhibition in colorectal cancer

Hey Min Lee[1], Alexey Sorokin[1], Preeti Kanikarla Marie[1], Saikat Chowdhury[1], Anand Singh[2], Amanda Anderson[1], Jumanah Yousef Alshenaifi[1], Funda Meric-Bernstam[3], Kunal Rai[2], Scott Kopetz[1]. *[1]GI Medical Oncology Department, UT MD Anderson Cancer Center, Houston, TX,[2]Genomic Medicine Department, UT MD Anderson Cancer Center, Houston, TX,[3]Investigational Cancer Therapeutics Department, UT MD Anderson Cancer Center, Houston, TX*

Background: Overexpression and activation of the MAPK signaling pathway is known to play a key role in colorectal cancer (CRC) progression. Substantial efforts have been made to target MAPK signaling pathways in CRC, particularly blocking oncogenic mutations in KRAS or BRAF. However, standard treatments targeting MAPK signaling have demonstrated limited activities in CRC patients and are in strong need of improved efficacies. Thus, we investigated how the combination of BET inhibitor treatment could affect MAPK signaling activation.
Methods: We performed a wide-scale drug combination study testing 15 drug combinations using CRC patient-derived xenograft (PDX) models. PDX models were treated for 21 days, and tumor volume and body weight changes were measured for assessment of treatment responses and toxicities. For the BET inhibitor (iBET-151) plus MEK inhibitor (binimetinib or trametinib) combination, RNA-seq and RPPA was performed on PDX tumor tissues collected after 7 days of treatment for pharmacodynamics study (n=3 per treatment condition). Tumors collected on day 21 were sequenced for H3K27Ac ChIP-seq and IHCs for understanding epigenomic changes in active enhancers and target validations.
Results: Our preliminary screening of 15 drug combinations in CRC PDX models have shown the most promising and active responses in a combination of BETi with MEKi (5 out of 20 PDXs obtained tumor regression). Preclinical H3K27ac ChIP-seq data has shown lost enhancer peaks after BET inhibition were significantly associated with RAS signaling pathways ($q<0.05$). Gene set enrichment analysis on preclinical transcriptomic data also demonstrated downregulation of KRAS-signaling in BETi plus MEKi combination treatment compared to MEKi as monotherapy ($p<0.05$). MAPK activation scores (MPAS) were also significantly downregulated in transcriptomic and enhancer levels under BETi plus MEKi combinations compared to MEKi. Downstream transcription factors of MAPK signaling pathways, such as MYC and FOSL1,

were synergistically downregulated in combination with BETi. Also, we found downregulation of EREG, a member of the epidermal growth factor (EGF) family, under BET inhibition which may play a role in MAPK downregulation together with standard therapy.
Conclusions: Some studies have shown MAPK signaling activation as a resistance mechanism of BET inhibition in multiple cancer types. However, the understanding of the crosstalk between the activity of BET inhibition in a combination with MAPK signaling inhibition is limited in CRC. We found BET inhibition induces deeper inhibition of MAPK pathway activation together with standard targeted therapies. Our data demonstrated transcriptomic and epigenetic levels of the mechanism of BETi activity together with MAPK inhibition in CRC.

#5487

Synergy between FAK and PI3K inhibitors in cervical and pancreatic cancer cells

Chao-Cheng Chen[1], Suyang Wang[1], Jr-Ming Yang[1], Chuan-Hsiang Huang[2].
[1]Pathology, Johns Hopkins Medicine, Baltimore, MD,[2]Johns Hopkins Medicine, Baltimore, MD

The Ras/PI3K/ERK signaling network is frequently mutated in many cancer types including cervical cancer and pancreatic cancer. Our previous study suggested that PI3K and FAK form a positive feedback loop to modulate ERK activation. We tested combined inhibition of FAK and PI3K on the growth of cervical and pancreatic cancer in vitro. We found that FAK and PI3K inhibitors synergistically inhibited the growth of some cervical cancer and pancreatic cancer cell lines. The synergy was due to both increased apoptosis and decreased cell proliferation. Molecularly, FAK inhibition caused downregulation of PI3K and ERK signaling in cervical cancer but not pancreatic cancer cells. Interestingly, PI3K inhibitors induced activation of several RTK including insulin R and IGF-1R in cervical cancer cells, as well as EGFR, Her2, Her3, Axl, and EphA2 in pancreatic cancer cells. Together, our results show the promise of combining FAK and PI3K inhibition for cervical cancer and pancreatic cancer treatment, but biomarkers for sensitivity to the combination are needed, and concomitant RTK inhibition may be required to combat potential resistance to the combination.

#5489

Synergistic activity of SCD1 blockade in combination with tyrosine kinase inhibitors lenvatinib and cabozantinib in hepatocellular carcinoma (HCC)

Justyna J. Gleba[1], Aylin Alasonyalilar-Demirer[1], Matthew L. Pawlush[1], Ahmet Bilgili[1], Peyton G. Hickman[1], Kabir Mody[2], Lewis R. Roberts[3], Steven R. Alberts[4], Mark J. Truty[5], Tushar C. Patel[3], Han W. Tun[6], John A. Copland[1].

[1]Cancer Biology, Mayo Clinic Cancer Center Florida, Jacksonville, FL,[2]IMV Inc, Dartmouth, NS, Canada,[3]Gastroenterology and Hepatology, Mayo Clinic Cancer Center Florida, Jacksonville, FL,[4]Medical Oncology, Mayo Clinic Cancer Center Florida, Jacksonville, FL,[5]General and GI Surgery, Mayo Clinic Cancer Center Florida, Jacksonville, FL,[6]Hematology/Oncology, Mayo Clinic Cancer Center Florida, Jacksonville, FL

Hepatocellular carcinoma (HCC) is the most common type of primary liver cancer. Tyrosine kinase inhibitors (TKIs) are approved as a first-line treatment for unresectable HCC. Lenvatinib and cabozantinib are two of the most used TKIs, but the therapeutic duration is limited due to the development of drug resistance. Therefore, understanding the mechanisms of resistance and combining TKIs with other drugs antagonizing resistance should lead to antitumor synergy, eliminating drug resistance. It turns out that the simultaneous use of TKIs together with an inhibitor of stearoyl-CoA desaturase 1 (SCD1) prevents the development of drug resistance, leading to a durable response. SCD1 is the enzyme responsible for *de novo* fatty acid (FAs) synthesis, converting saturated fatty acids (SFAs) into monounsaturated fatty acids (MUFAs). MUFAs are an alternative energy source to glucose, integral to cellular membranes, and prevent endoplasmic reticulum (ER) stress and other signaling pathways. In our laboratory, we developed a novel, highly specific SCD1 inhibitor - SSI-4. We have tested the biological activity of SSI-4 against different HCC cell lines and patient-derived xenografts (PDX) mouse models. Of the twelve tested HCC cell lines, four were highly sensitive to SSI-4 (IC_{50} 1-50 nM). Other cell lines showed moderate or no sensitivity to SSI-4. We tested the concomitant use of SSI-4 with lenvatinib and cabozantinib, tyrosine kinase inhibitors (TKIs) FDA-approved for HCC, in HCC cell lines *in vitro* and using HCC PDX *in vivo* mouse models. Our studies showed that the combination of the SCD1 inhibitor with both lenvatinib and cabozantinib showed a highly synergistic effect and no development of drug resistance i.e. durable response versus single TKI therapy. Ongoing mechanistic studies are examining whether known molecular targets of tested TKI's such as VEGFR1, 2, and 3, PDGFRα, FGFR, KIT, and RET dominate in HCC drug resistance to lenvatinib and

cabozantinib, and how the use of SSI-4 overcomes the phenomenon of resistance.

#5490

Combination of the PI3k inhibitor Paxalisib with the nucleoside analog Gemcitabine over-activates the integrated stress response and induces atypical teratoid/rhabdoid tumor cell death

Tyler Findlay, Kristen Malebranche, Anupa Geethadevi, Eric Raabe, Charles Eberhart, Jeffrey Rubens. *Johns Hopkins University School of Medicine, Baltimore, MD*

We have previously identified high activation of both mTORC1 and mTORC2 in the aggressive infantile brain tumor, atypical teratoid/rhabdoid tumor (AT/RT). Paxalisib is a highly brain penetrant PI3k inhibitor which acts upstream of mTOR to simultaneously inhibit mTORC1/2. Paxalisib is well-tolerated in ongoing pediatric clinical trials. In murine orthotopic xenograft models of AT/RT, Paxalisib significantly extended survival (CHLA-06: 40 to 54 days, p=0.001; BT12: 21 to 35 days, p=0.02). However, to improve the durability of this single agent therapy, we evaluated the efficacy of rational therapeutic partners. Analysis of RNAseq following mTOR inhibition (mTORi) of 4 cell lines representative of AT/RT showed an upregulation of genes associated with the integrated stress response (ISR), (*ATF4*: CHLA-06, *t*-test $p<0.05$; *CHOP*: CHLA-02, CHLA-06 *t*-test $p<0.001$). The activation of the ISR is further suggested through induction of *PPP1R15A*, a gene whose activation is closely associated with stress events and leads to downstream cell growth arrest and apoptosis (BT37 *t*-test $p<0.001$, CHLA-02, CHLA-06, CHLA-266, *t*-test $p<0.01$). Gemcitabine is a pyrimidine nucleoside prodrug, which inhibits DNA synthesis and induces DNA damage. As a result, Gemcitabine also induces phosphorylation of eIF2α and the activation of the ISR. While the ISR can be protective, intense or prolonged activation leads to cell death. We therefore hypothesized that Paxalisib would combine with Gemcitabine to hyper-activate the ISR and drive AT/RT cell death. Through Western blot analysis, we demonstrate that combination therapy increases phospho-eIF2α, ATF4, and CHOP compared to DMSO control. Furthermore, we demonstrate that combination therapy increases apoptosis (Western blot cPARP, MUSE Annexin V Assay) and synergizes to decrease AT/RT cell growth (SynergyFinder BLISS score CHLA-06: 16.8, BT12: 14.3, CHLA-266: 13.9, BT37: 11.4, CHLA-05: 10.4). Ongoing treatment of mice bearing CHLA06 orthotopic tumors demonstrate that combination therapy further extends median survival. Our

studies suggest that pharmacologically activating the ISR may be an effective strategy to target AT/RT and combination of Paxalisib and Gemcitabine may be an effective treatment to help extend survival in this deadly disease.

#5492

Determining effects of the CD206 positive M2 macrophage depleting engineered exosome in combination with anti PD1 therapy in breast tumor

Mahrima Parvin[1], Mohammad H. Rashid[2], Ahmet Alptekin[2], Ali S. Arbab[3].
[1]Biochemistry and Cancer Biology, Augusta University, Augusta, GA,[2]Georgia Cancer Center, Augusta University, Augusta, GA,[3]Medical College of Georgia, Augusta University, Augusta, GA

Introducti**on:** Triple negative breast cancer (TNBC) subtype of breast cancer, which lacks molecular markers such as HER2 and estrogen/progesterone receptors, has limited treatment options. Exosomes are nano-sized (30-150 nm) spherical vesicles, derived from the endosomal system for intercellular communications, can be engineered to express targeting peptides to target specifically CD206 positive M2 macrophage. Investigators have used either synthetic nanoparticles or fusion protein to deliver Fc-IgG2b to initiate Antibody dependent cellular cytotoxicity (ADCC) but reports are showing a lack of ADCC following tagging with gold nanoparticles. To overcome this, in our lab, we developed engineered exosomes in non-tumorous cells, HEK293, to carry therapeutic Fc-mIgG2b to enhance ADCC and to carry peptide to deplete CD206+ M2 macrophages. We investigated the effectiveness of engineered therapeutic exosomes to target and deplete immunosuppressive CD206+ M2 macrophages in TNBC in combination with anti PD-1.
Methods: In this study, we developed syngeneic metastatic TBNC model (luciferase + 4T1 cells in Balb/c) by implantation of 50K 4T1-luci cells in fat pad. On day 1 of tumor implantation, animals were treated with vehicle, engineered exosomes, anti-PD1 plus engineered exosomes, 2 dose/week for 3 weeks. They were euthanized 1 day after the last dose of treatment. Single-cell suspension was made from the primary TME, lung, and spleen. Using flow cytometry surfaces markers were investigated to determine different T-cell and myeloid cell populations.
Results: We observed very surprising results following three weeks of therapies. Although the number of cytotoxic T-cells was significantly higher in the primary and metastatic TME in exosome-treated animals, there was also an increased number of proliferative T reg cells. The number of CD8+ cells was decreased following concurrent therapy with an anti-PD1 antibody. Most interestingly, lung

tissue macrophages (CD11c) showed significantly increased PD-L1 expression following exosomes and anti PD1 with engineered exosomes therapies.
Conclusion: This study demonstrates that treatment with engineered therapeutic exosome targeting M2 macrophages with anti PD-1 could be utilized effectively. This study will also make a greater impact in exosome engineering based targeted therapy and will open new arena to target and deplete pathogenic cell in different tumors using engineered exosome.

#5493

Novel strategy to make KRAS targeted therapies more effective for PDAC treatment

Ana I. Martinez Bulnes[1], Orlando Garcia[1], poornima Shaji[2], Swathi Holla[3], Nirnoy Dan[4], Anupam Dhasmana[1], Shabnam Malik[1], Murali Yallapu[5], Stephen Behrman[6], Subhash Chauhan[1], Sheema S. Khan[5]. *[1]Immunology and Microbiology, University of Texas Rio Grande Valley, McAllen, TX,[2]UT Southwestern Medical Center, Dallas, TX,[3]Immunology and Microbiology, Baylor College of Medicine, Houston, TX,[4]University of Connecticut, Connecticut, NY,[5]Immunology and Microbiology, University of Texas Rio Grande Valley, edinburg, TX,[6]Medicine, University of Tennessee Health Science Center, Memphis, TN*

Introduction**:** Pancreatic Ductal Adenocarcinoma (PDAC) patients exhibit extremely poor prognosis. KRAS mutation on codon-12 is present in 70-95% of PDAC cases and it drives PDAC growth and progression. Galectin-1 (Gal-1) is present in both PDAC and stromal cells, being involved in tumor microenvironment, immune cell activation and metastasis. Therefore, this study discusses the efficiency of combined inhibition of mutated $KRAS^{G12D}$ and Gal-1 inhibition to effectively suppress PDAC growth and progression. For this we have delivered $KRAS^{G12D}$ inhibiting siRNA ($siKRAS^{G12D}$) using a superparamagnetic iron oxide nanoparticle (SPION) and a galectin inhibitor.
Methods: SPION nano-formulation was used to deliver $siKRAS^{G12D}$ and investigate in conjunction with Gal-1 inhibitor for its anticancer efficacy. Particles were investigated for size, physico-chemical characterization (Dynamic light scattering), hemocompatibility (hemolysis assay) and the complexation of siKRAS (gel retardation assay). Cellular internalization and uptake of the particles were investigated. Anti-cancer efficacy was determined using *in vitro* functional assays for cell viability (MTT), migration (Boyden chambers),

invasion (Matrigel), clonogenicity, tumor spheroid formation, and in a *KrasG12D;LSL-Trp53R172H* syngeneic mouse model.
Results: Our results demonstrate that SP-siKRAS efficiently internalized in PDAC cells and suppressed $KRAS^{G12D}$ as well as its downstream targets, YAP and PDL-1. Combined targeting of siKRAS and Gal-1 inhibited cell proliferation, clonogenicity, migration, and invasion of PDAC cells and tumor spheroid growth in 3D cell models, which recapitulate the heterogeneity and pathophysiology of PDAC. We have used -*KrasG12D;LSL-Trp53R172H* syngeneic mouse model of PDAC for investigating efficacy of combined SP-siKRAS formulation and galectin-1 inhibitor. Our results showed that the combination treatment inhibited the fibrotic tumor growth and increased survival rate. The combined treatment increased infiltration of total T cell population and CD8+T cells, reduced the population of myeloid-derived suppressor cells (MDSCs) by 50%
(CD45+, CD3-, CD11b+, Ly6C high, Ly6G-) and T-Regulatory cells (Treg) by 57% (FoxP3+CD25+CD45+CD3+) and increased memory T cells by 34% in mice.
Conclusion: This gene therapy targeting KRAS G12D mutation with a Gal-1 inhibition has a potential to modulate the oncogenic network and tumor microenvironment resulting in the repression of growth, metastasis, chemoresistance, and improvement in patient survival. This study will develop a novel sustainable therapeutic approach to target PDAC growth and improve patient survivability.

#5494
Preclinical combination of ONC201 with radiotherapy and Temozolomide in a GBM mouse orthotopic model results in reduced tumor burden and prolonged survival
Lanlan Zhou, Laura Jinxuan Wu, Jun Zhang, Andrew George, Marina Hahn, Leiqing Zhang, Attila A. Seyhan, Wafik S. El-Deiry. *Pathology and Laboratory Medicine, Legorreta Cancer Center at Brown University, Providence, RI*

Glioblastoma (GBM) is the most common and lethal primary malignancy of the central nervous system. It is estimated that more than 13,000 new cases of GBM will be diagnosed this year in the United States. Despite multidisciplinary treatments such as surgery, chemotherapy, and radiotherapy, the five-year survival rate for GBM patients is only 6.8 percent and has shown no notable improvement in the last three decades. There have only been five drugs and one device ever approved by the FDA for the treatment of GBM since it was first

identified in the scientific literature in the 1920's. Our *in vitro* studies suggested that first-in-class small-molecule imipridone TIC10/ONC201 can inactivate ERK/AKT, induce the integrated stress response (ISR), upregulate pro-apoptotic TRAIL receptor DR5, deplete cancer stem cells, and induce mitochondrial dysfunction, growth arrest or cell death in GBM cells. Knockdown of ClpP protects GBM cells from ONC201 but not TMZ. ONC201 crosses the blood-brain barrier and has induced durable tumor regressions in adult and pediatric H3K27M-mutant diffuse midline glioma patients. We hypothesized that ONC201 may synergize with radiotherapy and temozolomide in GBM. GBM mouse orthotopic models were established through intracranial injection of luciferase expressing U251 GBM cells with a KOPF model 940 small animal stereotaxic frame and a Stoelting Quintessential Stereotaxic Injector. Tumor formation and growth was confirmed with bioluminescence imaging. Randomized treatment group mice received weekly treatment of ONC201 (100 mg/kg p.o.) and/or radiotherapy (2 Gy local irradiation) and/or TMZ (20 mg/kg i.p.) for four weeks for long term survival and tumor monitoring or one week for short term biomarker studies. We observed that the triple combination of ONC201, radiotherapy and TMZ significantly prolongs survival and reduces tumor burden compared to single treatment and dual combinations. Short term biomarker studies demonstrated that triple combination treatment decreases tumor cell proliferation, induces more apoptosis and inhibits ClpX to unleash mitochondrial ClpP. Our data support further development of the triple combination regimen of ONC201, TMZ and radiation therapy for GBM first-line treatment.

#5495

Combination therapy with poly (ADP-ribose) polymerase inhibitor in endometrial cancer

Conway Xu, Xiaonan Hou, Erik Jessen, Chen Wang, S. John Weroha. *Mayo Clinic, Rochester, MN*

Objective: Endometrial cancer (EC) is the most common gynecologic malignancy and serous histology is the second most common subtype. It is associated with poorer outcomes as recurrent disease tends to be resistant to chemotherapy. Given the dearth of proven targeted therapies in this setting and the tendency for serous ECs to have homologous recombination deficiency (HRD), this study aimed to test the synergy between poly (ADP-ribose) polymerase inhibitors (PARPis) and SN38, an active metabolite of DNA topoisomerase I, irinotecan. PARPis are currently FDA approved in ovarian

cancer and have their greatest efficacy in tumors with HRD while topoisomerase inhibitors are a standard chemotherapy option for recurrent cancer.
Methods: A genomic instability score (GIS) was derived from low-pass whole genome sequencing-based bioinformatics analysis according to three previously reported HRD metrics: telomeric allelic imbalance, large state transitions, and loss of heterozygosity. GIS was calculated for 34 patient derived xenograft (PDX) tumors, of which eight had serous histology. PARPi, rucaparib, and SN38 were used to treat EC PDX tumors in e*x vivo* 3D cell culture experiments using RealTime Glo for viability after 4-5 days of drug exposure. Synergy was assessed by calculating the combination index (CI) using Chou-Talalay method.
Results: GIS ≥ 42 was noted in 62.5% (5/8) of serous EC PDX tumors and only 19.2% (5/26) of non-serous EC PDX tumors. Synergy (CI < 1.0) between rucaparib and SN38 was demonstrated in 85.7% (6/7) of serous EC PDX *ex vivo* 3D cell culture experiments, but only 62.5% (10/16) of non-serous EC PDX tumors.
Conclusions: Most serous EC PDX tumors had a high GIS, consistent with HRD, when compared to a minority of non-serous histologies. Furthermore, combination therapy of rucaparib and SN38 had a synergistic effect in almost all serous EC PDX models, while still being effective in a majority of non-serous models. Additional PDX tumors need to be assessed to establish the predictive value of a GIS on synergy between rucaparib and SN38. Further *in vivo* studies are also needed to confirm these *ex vivo* findings of synergy. Ultimately, the hope is to generate preclinical data which justifies the use of PARPis in serous ECs as monotherapy or in combination with other anticancer therapies.

#5496

Glutaminase inhibition induces replication stress in ovarian cancer cells and inhibition of replication checkpoint causes synthetic lethality

Pamela Luna, Ganesh Acharya, Damieanus Ochola, Swetha Peddibhotla, Chinnadurai Mani, Mark B. Reedy, Komaraiah Palle. *Texas Tech University Health Sciences Center, Lubbock, TX*

Ovarian cancer (OC) is a highly aggressive disease and the most lethal gynecologic malignancy in women. Although the majority of OC patients respond to chemotherapeutic drugs, more than 70% of the patients relapse and die as a result of chemoresistance. Therefore, novel therapeutics are warranted to prevent chemoresistance and treat the relapsed disease to improve prognosis. Many cancer cells depend on Glutamine as major carbon source and these cells have high Glutaminase (GLS) expression, an enzyme that converts Glutamine to

Glutamate. Chemo-resistant OC cells have elevated levels of GLS, which confirms their increased dependency on glutamine metabolism. Based on these observations, we postulated that GLS inhibition may attenuate the aggressive growth of GLS ^{high} OC cells and may sensitize to the agents that can further potentiate these effects. Interestingly, GLS inhibition using a clinical-stage drug CB839 caused replication stress and activated DNA damage checkpoint protein 1 (CHK1) mediated cell cycle arrest. These novel findings suggested a role for CHK1 in protecting GLS inhibition-induced DNA damage by facilitating the timely repair of DNA breaks. Based on these observations, we hypothesized that GLS inhibition in combination with CHK1 inhibition may cause synergistic lethality in chemo-resistant and GLS^{high} OC cells. We evaluated the combination of GLS inhibitor CB839 and CHK1 inhibitor Prexasertib. Our results demonstrate that GLS inhibition-induced CHK1 phosphorylation is significantly attenuated by Prexasertib treatment. Similarly, combined treatment of CB839 and Prexasertib showed significantly elevated levels of DNA damage as measured by COMET assays, replication stress-mediated DNA damage responses, and synergistic OC cell lethality compared to individual drug treatments. Furthermore, CB839 and Prexasertib combination was more synergistic in cells that expressed high GLS compared to low GLS-expressing OC cells indicating the specificity of the combination of these drugs. Together, our studies identified a novel connection between metabolic and DNA damage checkpoint pathways in OC and propose a novel synergistic lethality-based combination therapy to treat chemo-resistant and aggressive OC.

#5497

Venetoclax and dinaciclib elicit synergisticpreclinicalefficacy against high-risk B-cell leukemia

Ernesto Diaz-Flores, Holly Pariury, Mignon Loh. *UCSF - University of California San Francisco, San Francisco, CA*

Hypodiploid acute lymphoblastic leukemia (ALL) is an aggressive blood cancer with a poor prognosis despite intensive chemotherapy or stem cell transplant. Children and adolescents with positive end-of-induction minimal residual disease (MRD) have an overall survival lower than 30%. However, data regarding therapeutic alternatives for this disease is nearly non-existent, emphasizing the critical need for new or adjunctive therapies that can improve outcomes. We previously reported on the therapeutic efficacy of venetoclax (ABT-199) in hypodiploid B-ALL but with limitations as monotherapy *(Diaz-Flores, Cancer Research, 2019)*. Accordingly, hypodiploid B-ALL patient

derived xenografts treated with Venetoclax developed therapeutic resistance over time. To better understand the mechanism of resistance that arises following inhibition of BCL-2, we first generated a hypodiploid cell line (NALM-16) deficient in BCL-2. Given that BCL-2 plays an essential role in B-cell function standard CRISPR/Cas9 knockout strategies greatly impaired survival. We overcame this limitation by using a magnetic levitation system (the LeviCell by LevitasBio). Analysis of the surviving clones identified an increase in MCL1 (**Fig. 1A**). We then harnessed unbiased drug screen (>1800 bioactive compounds) followed by selection of synergistic drug combinations identified Dinaciclib as an efficient drug combination with Venetoclax in eliminating leukemic cells in vitro. Interestingly, mechanistic studies identified that Dinaciclib, through transcription regulation (RNApol II) significantly modulates MCL-1. Data using knock-outs and knock-ins of MCL-1 indicated how MCL-1 only becomes essential for survival when Venetoclax is present. Preclinical studies using patient derived xenografts indicated that, while none of the drug monotherapies achieved complete blast elimination, venetoclax + dinaciblib led to complete resolution of the leukemic burden within all solid organs analyzed (**Fig. 1B**). This combination therapy was relatively well tolerated. This study also indicates that high BCL-2 and MCL-1 levels with concomitant BIM, BAD and/or PUMA levels, represent biomarkers for response to this combination. In summary, our study identified a highly synergistic drug combination, venetoclax and dinaciclib, for the treatment of hypodiploid B ALL, an aggressive leukemia with few effective current therapies. Finally, the promising results presented in this study may prompt further studies to support the inclusion of hypodiploid and other B-ALL patients to clinical trials combining phase I/II drugs against BCL-2 (mainly venetoclax) and CDK9 (dinaciclib, alvocidib, flavopiridol, SNS-032) or MCL-1 (MIK-665).

#5498

SHP2 inhibition enhances antitumor effect of mirdametinib in a pediatric brain tumor model bearing CDC42SE2BRAF fusion by rewiring the proteome and phosphoproteome landscape

Nur P. Damayanti[1], Anthony Alfonso[2], Josue D. Ordaz[1], Erika Dobrota[3], M. Reza Saadatzadeh[3], Pankita Pandya[2], Barbara J. Bailey[1], Khadijeh Bijangi-Vishehsaraei[2], Harlan E. Shannon[2], Kathy Coy[2], Melissa Trowbridge[2], Anthony L. Sinn[2], Rosa Gallager[4], Julia Wulfkuhle[4], Emanuel Petricoin[4], amber mosley[2], Mark S. Marshall[2], Alex Lion[2], Michael J. Fergusson[2], karl balsara[5], Karen E. Pollok[2]. *[1]Neurological Surgery, Indiana University School of Medicine, Indianapolis, IN,[2]Indiana University School of Medicine, Indianapolis,*

IN,[3]Pediatric, Indiana University School of Medicine, Indianapolis, IN,[4]George Mason University, Manassas, VA,[5]Neurological Surgery, University of Oklahoma School of Medicine, Oklahoma, OK

Pediatric gliomas are the most common type of pediatric brain tumors representing wide range of molecularly and clinically heterogenous subtypes. The hyperactivity of mitogen-activated protein kinases (MAPK) pathway has been identified in the majority of pediatric glioma suggesting its therapeutic potential. However, pharmacologic targeting single MAPK pathway's component is limited due to the development of drug resistance and differential response associated with tumor molecular landscape. Therefore, effective combination strategy in the framework of precision medicine is needed. Here we report combination benefit and molecular underpinning therapeutic response of brain penetrant MEK inhibitor (mirdametinib) and SHP2 inhibitor (SHP099) in a pediatric patient derived xenograft (PDX) and xenoline developed at our institution. Our model was derived from a pediatric patient who was diagnosed with rare high-grade subtype of glioma, anaplastic pleomorphic xanthoastrocytoma, and did not respond to MEK inhibitor, trametinib. Integrative multi-omics revealed molecular fidelity between our model and its patient tumor counterpart including the presence of 7q35 fusion, *CDC52SE2-BRAF*, *CDKN2A/B* loss, and MAPK pathway hyperactivation. *In vitro* studies using our xenoline IU-X128 demonstrated synergy between SHP099 and mirdametinib to curtail cell proliferation ($p<0.05$). Moreover, this combination was well tolerated in our PDX, IU-RHT128, and potentiated anti-tumor effect of the single agent within clinically achievable doses. Reverse Phase Proteome Array (RPPA) identified MAPK reactivation via Mushasi RNA binding protein-PI3K-AKT crosstalk as a potential innate resistance mechanism to single agent MEK inhibitor in the PDX tumor. Further, tandem mass tags (TMT)-LC-MS/MS profiling on tumor treated with single agent SHP099 or mirdametinib and their combination revealed that combination therapy does not only revert certain proteome and phosphoproteome reprogramming from single agent treatment but also created a novel landscape which can be associated with anti-tumor effect. In this case, kinase network reprograming leading to MAPK reactivation was identified in mirdametinib treated tumor which was attenuated in the combination treatment. In summary, our results demonstrated that combination SHP099 and mirdametinib is superior to single agent alone in the pediatric A-PXA brain tumor model with proteome and phosphoproteome reprogramming of multiple networks as potential molecular mechanisms underlying therapeutic benefit of combination therapy. Ultimately, clinical translation of this finding

will potentially benefit patient of this malignant rare pediatric glioma subset which currently does not have standard therapy.

#5499

Synergistic effects of the combination of ERK1/2 with EGFR, KRAS^{G12C}, CDK4/6, and PD-L1 inhibition for cancer treatment

Ya Kong[1], Peng Chen[1], Lulu Jiang[1], Bin Jiang[2], Jay Mei[3], Bo Shan[3], Bing Hou[3].
[1]Shanghai Antengene Corporation Limited, Shanghai, China,[2]Antengene Biotech LLC, Shanghai, PA,[3]Antengene Corporation, Shaoxing, China

Background: Mitogen-activated protein kinase (MAPK) cascade is a key pathway that regulates a wide variety of cellular processes, which is frequently activated in cancers. Many nods of the MAPK pathway are considered as promising anti-tumor drug targets, such as RTKs, KRAS^{G12C}, RAF, MEK1/2, and ERK1/2. Multiple inhibitors targeting proteins on MAPK pathway have been developed for cancer treatment. However, the effectiveness of these inhibitors is often limited due to acquired drug resistance via pathway feedback activation, indicating the necessity of combination strategies to help block reactivation or bypass activation of MAPK pathway. ATG-017 is an oral, potent, and highly selective inhibitor of ERK1/2, which is under Phase 1 clinical investigation. This study tested the *in vivo* antitumor effects induced by the combination of ATG-017, with EGFR inhibitor (Osimertinib), KRAS^{G12C} inhibitor (ATG-012), CDK4/6 inhibitor (Abemaciclib) or PD-L1 inhibitor (Atezolizumab), in preclinical tumor models.
Methods: The *in vivo* combinations of the drugs were tested in NCI-H1975, NCI-H358 (non-small cell lung cancer) or EL4 (T cell Lymphoma) CDX mouse models. The tumor bearing mouse were treated with vehicle control, ATG-017 (15 or 25 mg/kg, QD), Osimertinib (1mg/kg, QD), ATG-012 (10mg/kg, QD), Abemaciclib (25mg/kg, QD), Atezolizumab (10mg/kg, BIW) or the combination for 9 to 21 days. The tumor size was measured twice a week and tumor growth inhibition (TGI) was evaluated compared with vehicle group. Tumor tissues were collected for tumor infiltrating lymphocyte (TIL) analysis using Flow cytometry or multiplex IHC.
Results: In the NCI-H1975 CDX *in vivo* study, the monotherapy of ATG-017 and Osimertinib induced TGIs of 61.95% and 79.18%, respectively on day 17 after grouping. The combination of ATG-017 and Osimertinib showed 101.85% TGI. In the NCI-H358 CDX *in vivo* study, the monotherapy of ATG-017, ATG-012, and combination induced TGI of 44.29% ,73.71% and 97.13%, respectively on day 8 after grouping. The monotherapy of ATG-017, Abemaciclib, and the

combination induced TGIs of 91.40% ,63.10% and 108.15%, respectively on day 20 after grouping. In the EL4 syngeneic T cell lymphoma model, neither ATG-017 nor Atezolizumab showed single agent activity, while the combination induced a significant TGI of 21.86% on day 9 after grouping. The percentage of infiltrating CD8+ T cells, CD8:CD4 ratio and M1:M2 macrophage ratio were found increased in the combination group, suggesting the potential role of ATG-017 plus PD-L1 inhibitor in changing a "cold" tumor towards a "hot" phenotype. Conclusion: Strong synergism has been observed for the combination of ATG-017 with EGFR, $KRAS^{G12C}$, CDK4/6, and PD-L1 inhibition, suggesting promising therapeutic strategies for cancer patients that warrants further investigation.

#5500

Patient-derived organotypic cultures (PDOCs) from melanoma metastases as a precision medicine test to improve patient management

Antonella Bresin[1], Fiorenza Lotti[2], Lauretta Levati[1], Pier F. Ferrucci[2], Francesca Ricci[1], Francesco Scicchitano[1], Zorika C. Di Rocco[1], Giandomenico Russo[1], Luisa Lanfrancone[2]. *[1]IDI-IRCCS, Rome, Italy,[2]European Institute of Oncology, Milan, Italy*

INTRODUCTION Despite significant improvements in advanced melanoma therapy, there is still a pressing need for innovative therapies. Here, we optimized a method for testing the drug sensitivity of PDOCs and evaluated whether this preclinical model could be a valid tool for rapidly determining the patient's tumor response profile to approved and alternative therapies.
METHODS PDOCs were generated from melanoma metastases (> 60 specimens) after mechanical or enzymatic dissociation. Tissue fragments (<70um) were harvested, embedded in 3D collagen beads (1.5 mg/mL type I collagen), and cultured in a 96-well plate for 6 days, maintaining tumor and stromal viability. More than 20 primary cell lines from the same samples were also stabilized. The melanoma cells or the PDOCs were left untreated or treated with the patient's own therapy or with alternative drugs, and the efficacy of treatments was evaluated by MTT assay and flow cytometry. CD8+ T cell infiltration and cytokine secretion were also investigated.
RESULTS The first experiments were set up to validate PDOCs as predictive preclinical models of patient response to therapy. We tested approved melanoma therapies (i.e., the combination of BRAF and MEK inhibitors, or anti-PD-1 antibodies) on the same melanoma specimens at the IDI and IEO institutes. More than 10 different samples were compared, finding reproducible results

between the two Institutions. Furthermore, drug response in PDOCs was comparable to the clinical response of matched patients undergoing the tested therapy, demonstrating PDOCs are reliable predictive tools. Then, we used primary cell lines to screen a pool of ten different targeted agents selected through functional screening of a bioactive library of 512 compounds on patient-derived xenografts, and based on known drug resistance mechanisms in melanoma. The three best-performing compounds were subsequently studied in PDOCs as single agents or in combination with immunotherapy. We found high heterogeneity of drug efficacy in different melanoma samples with no obvious correlation to BRAF or NRAS mutations, metastasis type, or patients' prior therapies. Of note, in some cases, the combination with an anti-PD-1 inhibitor significantly improved the efficacy of one or more of the three drugs. CONCLUSIONS We optimized and validated PDOCs as personalized preclinical models suitable for assessing the drug sensitivity/resistance profile of individual patient-derived melanomas. By retaining tumor stromal components and heterogeneity, PDOCs could be used to predict patients' clinical response to currently approved agents, helping oncologists expedite decision-making when several treatment options are possible. Furthermore, the model could be used to evaluate the effectiveness of alternative treatments on tumors resistant to approved therapies, and to explore new drug combinations.

#5501

Vertical inhibition of the MAPK pathway with D3S-002, a potent and selective ERK1/2 inhibitor, to improve anti-tumor activity of and overcome resistance to KRAS G12C inhibitors

Jing Zhang, Jingtao Lu, Zhiqiang Zheng, Jiang Lu, Allison Wang, Jia Wang, Janet Chen, Haopeng Rui, Cheng Chen, Zhi Jian Chen. *D3 Bio (Wuxi) Co. Ltd., Shanghai, China*

While covalent KRAS G12C inhibitors have demonstrated encouraging clinical efficacy in patients with KRAS G12C mutation, the overall response rate and progression-free survival appear to be suboptimal. Achieving deeper and more durable responses in these patients remain as major challenges. Preclinical and clinical translation research highlights adaptive feedback reactivation of the RAS-RAF-MEK-ERK signaling cascade as key molecular mechanisms driving primary and acquired resistance to KRAS G12C inhibitors. Concurrent inhibition of KRAS G12C and downstream MAPK pathway is thus an attractive combination strategy to improve clinical outcomes for KRAS G12C-mutant population.

D3S-002 is a potent and selective kinase inhibitor targeting ERK1/2, the final node of the RAS-MAPK pathway and the central mediator of the feedback activation loop. To investigate the combination effect of D3S-002 with KRAS G12C inhibitor D3S-001, this study utilized multiple preclinical in vivo models including cancer cell line-derived xenograft (CDX) tumors that are sensitive to, or primarily resistant to KRAS G12C inhibitors, and patient-derived xenograft (PDX) tumors that have progressed on KRAS G12C inhibitor treatment in the clinic. In NCI-H358 NSCLC and SW837 CRC models that are sensitive to KRAS G12C inhibitor monotherapy, adding D3S-002 to D3S-001 or to D3S-001 and cetuximab doublet regimen led to faster, deeper, and more durable anti-tumor responses at dose levels that are well tolerated in mice with no body weight loss observed. In NCI-H2122 NSCLC model that is primarily resistant to KRAS G12C inhibitor alone, the addition of D3S-002 resulted in near complete tumor growth inhibition.
Furthermore, CR9537 PDX model was established from tumor biopsy of a CRC patient who had progressed on combination treatment of KRAS G12C inhibitor MRTX849 and a SHP2 inhibitor in a clinical trial. Next generation sequencing (NGS) analysis identified secondary KRAS Q61H mutation as an acquired resistance mechanism. In this PDX model, KRAS G12C inhibitor, D3S-001 or MRTX849, monotherapy only achieved approximately 50% tumor growth inhibition, highlighting the acquired resistant phenotype. Adding D3S-002 to D3S-001 or MRTX849 resulted in over 80% tumor growth inhibition and significantly prolonged survival, suggesting the combination treatment can be beneficial for KRAS G12C inhibitor pre-treated patient population.
Collectively, vertical inhibition by concurrently targeting KRAS G12C and ERK1/2 with respective inhibitor D3S-001 and D3S-002 demonstrated enhanced anti-tumor activity in NSCLC and CRC models with different sensitivity to KRAS G12C inhibitor monotherapy. These results provide a strong rationale for further investigation of the combination strategy of D3S-001 and D3S-002 in KRAS G12C-mutant solid tumors in the clinic.

#5502

Androgen blockade confers sensitivity to PIKfyve inhibition in prostate cancer

Yuanyuan Qiao, Sarah Nicole Yee, Caleb Cheng, Yang Zheng, Jie Luo, Yi Bao, Xia Jiang, Xuhong Cao, Yuping Zhang, Arul M. Chinnaiyan. *University of Michigan Medical School, Ann Arbor, MI*

In 2022, 268,490 American men will be diagnosed with prostate cancer and 34,500 men will succumb to its complications. Despite significant advances in prostate cancer treatment over the past few decades, resistance inevitably develops with certain therapies, including second-generation anti-androgens; new case numbers also keep climbing each year, leading to one in every eight men being diagnosed with prostate cancer during his lifetime. Therapies targeting the androgen receptor (AR) as the main driver of prostate cancer lead to various mechanisms of resistance and promote disease progression to castration-resistant prostate cancer (CRPC), which has a median survival of only 9-36 months. Amongst recurrent CRPC, 17%-30% of patients develop neuroendocrine prostate cancer which is characterized by it's unique histopathology and loss of AR signaling. Our previous study demonstrated that autophagy blockade via PIKfyve inhibition has preferential cytotoxicity in neuroendocrine prostate cancer over prostatic adenocarcinoma leading us to further validate the role of AR signaling in PIKfyve blockade sensitivity. Thus, we postulate that androgen signaling attenuates the dependency of prostate cancer on PIKfyve, while on the other hand, AR antagonist may sensitize prostatic adenocarcinoma to PIKfyve inhibition.

Method

Several AR positive prostate cancer cell lines were examined for combinational effect of AR antagonists and PIKfyve inhibitors *in vitro* with synergistic scores calculated. A pair of isogenic LNCaP cells with proficient AR signaling (LNCaP-parental) and deficient AR signaling (LNCaP AR-null) were used for PIKfyve inhibitor sensitivity. Additionally, two AR positive cell line-derived xenografts (LNCaP and VCaP) were established *in vivo* for combinational assessment of AR antagonist Enzalutamide and PIKfyve inhibitor ESK981. Tumor growth inhibition were monitored pre- and post- treatments. On target assessment were examined for downstream targets of AR antagonist, as well as LC3-lipidation for PIKfyve inhibition. *In situ* cell death events of treated tumors *in vivo* were evaluated by TUNEL assay.

Conclusion

We have discovered that inhibition of AR signaling by Enzalutamide demonstrated strong synergistic anti-proliferative effects with PIKfyve inhibition by ESK981. Similarly, using a pair of isogenic LNCaP cells with proficient (LNCaP-parental) and deficient AR signaling (LNCaP AR-null), we showed that loss of AR signaling notably increased the sensitivity of LNCaP cells to PIKfyve inhibition. Concurrent treatment with Enzalutamide and ESK981 *in vivo* triggered greater tumor inhibition and more robust *in situ* cell death events than either agent alone. Collectively, PIKfyve may have a context-dependent role in

AR signaling-dependent and -independent prostate cancer, so that by co-targeting AR signaling and PIKfyve, therapeutic outcome of prostate adenocarcinoma can be improved.

#5503

Targeting CDK12-mediated DNA damage response to overcome cisplatin resistance in human urothelial carcinoma

Po-Ming Chow[1], Jun-Ren Dong[1], Chung-Sheng Shi[2], Kuo-How Huang[1].
[1]Department of Urology, National Taiwan University College of Medicine, Taipei City, Taiwan,[2]Graduate Institute of Clinical Medical Sciences, Chang Gung University, Tao-Yuan City, Taiwan

Urothelial carcinoma (UC) accounts for more than 90% of bladder cancer. According to the 2019 Surveillance, Epidemiology and End Results (SEER) Program database, the 5-year survival rates of regional and metastatic bladder cancer are 36.3% and 4.6%, respectively. Patients who received radical cystectomy suffer from a high recurrence rate of up to 30%. As for metastatic UC, only half of the patients respond to standard platinum-based chemotherapy, with 20% of 5-year overall survival. CDK12 shows transcription regulatory effects via regulating RNA polymerase II CTD phosphorylation. In our research, we used CDK12 selective inhibitor SR-4835 to treat the UC cell lines including T24, BFTC905, RT4, and cisplatin-resistant T24/R. MTT assay result has demonstrated the cytotoxicity of SR-4835 against UC cells. Using q-RT-PCR and immunoblotting, we have confirmed the reduction of ATM mRNA and protein expression after the treatment of SR-4835. The expression of DNA damage marker gamma-H2AX was also elevated. Flow cytometry data indicated an increase in apoptotic population after treatment. According to these findings, we presume SR-4835 can lead to a DNA damage-induced apoptosis process. Furthermore, we also observed the inhibition of AKT pathway, which is related to cell survival and proliferation. Due to the effects of DNA-repair inhibition, we aim to combine SR-4835 to enhance the anti-cancer effects of cisplatin. The results of UC mice xenograft have confirmed that SR-4835 and cisplatin display a synergistic effect against UC tumor growth *in vivo*. We will further dissect the mechanisms of the *in vitro* synergistic effects between SR-4835 and cisplatin using immunoblotting, RNA-sequencing, comet assay, and various functional assays. Conclusively, our study aims to explore the role of CDK12 in urothelial carcinoma and the therapeutic effects of SR-4835, especially its potential to overcome cisplatin resistance and manage metastatic disease.

#5504

A tumor-promoting senescent secretome triggered by platinum chemotherapy exploits a targetable TGFβR1/Akt-mTOR axis in lung cancer

Estela González-Gualda[1], David Macias[1], Samir Morsli[1], José Ezequiel Martín[1], Hui-Ling Ou[1], Mary Denholm[1], Ioana Olan[2], Reuben Hoffmann[3], Mark Dane[3], Dimitris Veroutis[4], Guillermo Medrano[5], Francisca Mulero[5], Carla P. Martins[6], Mariano Barbacid[5], Vassilis Gorgoulis[7], James E. Korkola[3], Doris M. Rassl[8], Gary J. Doherty[9], Robert C. Rintoul[10], Masashi Narita[2], Daniel Muñoz-Espín[1].
[1]Oncology, University of Cambridge UK, Cambridge, United Kingdom,[2]CRUK Cambridge Institute, Cambridge, United Kingdom,[3]Oregon Health & Science University, Portland, OR,[4]University of Athens, Athens, Greece,[5]Spanish National Cancer Research Centre, Madrid, Spain,[6]AstraZeneca, Cambridge, United Kingdom,[7]University of Athens, Athens, Greece,[8]Royal Papworth Hospital NHS Foundation Trust, Cambridge, United Kingdom,[9]University of Cambridge, Cambridge, United Kingdom,[10]Oncology, Royal Papworth Hospital NHS Foundation Trust, Cambridge, United Kingdom

Background Platinum-based chemotherapy is commonly used for the treatment of non-small cell lung cancer (NSCLC), yet clinical outcomes and survival rates remain very poor and continues to be a cancer of unmet need. Recent evidence points to cellular senescence, a response to oncogenic- and therapy-induced genotoxic stress, and its associated proinflammatroy secretory phenotype (SASP) as an emerging hallmark of cancer. Hence, targeting senescence and its associated tumor-promoting activities is emerging as a novel and promising therapeutic strategy but largely unexplored in lung cancer.
Experimental Procedures Our study includes a variety of methodologies, including: - Functional in vitro analyses: proliferation, colony formation, tumor spheres, migration assays. High throughput unbiased analyses: RNAseq, proteomics and microenvironment microarrays (MEMA). - In vivo models of lung cancer: xenografts, orthotopic and genetically engineered mouse models. Longitudinal tumor burden by IVIS and microCT and mouse survival. - Clinical samples: Histological and in silico analyses.
Results Here we show that cisplatin-derived SASP enhances the malignant phenotype of lung cancer cells. Using xenograft, orthotopic and KrasG12V-driven murine NSCLC models, we demonstrate that cisplatin-induced senescent cells strongly promote tumor progression. Mechanistically, we find that a TGF-β-enriched SASP drives pro-proliferative effects through TGFβR1 and Akt/mTOR pathway activation. We validate the translational relevance of

chemotherapy-induced SASP using clinical NSCLC samples from a trial with patients who received neoadjuvant platinum-based chemotherapy. Importantly, TGFβR1 inhibition with galunisertib or senolytic treatment significantly reduces tumor promotion driven by cisplatin-induced senescence. Finally, we demonstrate, using distinct murine NSCLC models, that addition of TGFBR1 inhibitors to platinum-based chemotherapy reduces tumor burden and improves survival, providing pre-clinical proof-of-concept for future trial designs on combination therapies.

Conclusions and Impact We regard this work as a major conceptual dissection of tumor-promoting activities of therapy-induced senescence, and a preclinical advance in the management of lung cancer with potential wide therapeutic applications in precision medicine. Of note, we expect our findings to have implications for multiple cancer types, including ovarian, breast, mesothelioma, oesophageal, head and neck, bladder and brain cancers, where platinum-based therapies remain important standard-of-care treatments.

#5505

Combination nitazoxanide and auranofin treatment has synergistic anticancer activity in anaplastic thyroid cancer and act by enhanced activation of multiple cell death pathways

Chandrayee Ghosh[1], Viswanath Gunda[1], Jiangnan Hu[1], Lisa Zhang[2], Ya-Qin Zhang[3], Min Shen[4], Electron Kebebew[1]. *[1]General Surgery, Stanford University School of Medicine, Stanford, CA,[2]National Institute of Child Health and Development, National Institutes of Health,, Bethesda, MD,[3]3National Center for Advancing Translational Sciences, National Institute of Health, Bethesda, MD,[4]National Center for Advancing Translational Sciences, National Institute of Health, Bethesda, MD*

Purpose: Anaplastic thyroid cancer (ATC) is one of the most aggressive human cancers, with a median survival time of 6 months and with no current curative treatment. We have used quantitative high-throughput screening (qHTS) of clinically approved or investigational agents to identify candidate compounds for ATC therapy. As monotherapy for most cancers is not effective, we used combination drug matrix screening of highly active compounds from our single agent qHTS to identify compound combinations that may show synergistic effect. In this study, we evaluated the anticancer activity of nitazoxanide and auranofin combination treatment and its mechanism of action and biomarkers of treatment response in *in vitro* and *in vivo* models of ATC.

Experimental Design: We used four (8505C, C643, SW1736, THJ16T) ATC cell lines in *in vitro* and *in vivo* ATC models to evaluate the safety and efficacy of this combination treatment compared to single agent and vehicle control.
Results: Combination nitazoxanide and auranofin treatment synergistically inhibited cellular proliferation ($p<0.001$) and inhibited colony formation and migration ($p<0.001$) in ATC cell lines. We observed cellular oxidative stress with significant increase in ROS levels in the combination treatment group ($p<0.001$). Nitazoxanide treatment alone and in combination with auranofin caused G1/G0 arrest in cell cycle, induced autophagy (increased LC3BII expression) and later apoptosis. Auranofin treatment alone and in combination with nitazoxanide induced ferroptosis (decreased GPX4 expression and intracellular GSH/GSSG ratios). RNA-Seq analysis, to identify biomarkers of response, showed >7-fold increase in HMOX-1 (heme oxygenase 1) with combination treatment which was validated by western blot. Combination treatment significantly inhibited tumor growth as compared to single agents ($p<0.01$) and had no significant treatment-related toxicity *in vivo*. Analysis of tumor samples showed significantly increased LC3BII expression by immunohistochemistry and reduced GPX4 mRNA expression ($p<0.0001$) with combination treatment compared to control *in vivo*.
Conclusions: Combination nitazoxanide and auranofin treatment has synergistic anticancer activity in both *in vitro* and *in vivo* ATC models. The synergistic activity of the combination is due to enhanced G1/G0 arrest, greater activation of autophagy, apoptosis and ferroptosis than single drug treatment. LC3BII, HMOX-1 and GPX4 levels could be useful biomarkers of treatment response to combination nitazoxanide and auranofin.

#5506

Circulating immature neutrophils early detect hyperprogressive disease upon first-line PD-1/PD-L1 inhibitors in non-small cell lung cancer patients selecting best candidates for platinum-based chemotherapy and PD-1/PD-L1 inhibitors combinations

Roberto Ferrara, Giuseppe Lo Russo, Chiara Maura Ciniselli, Annamaria Piva, Barbara Bassani, Elena Jachetti, Giuseppina Calareso, Valeria Duroni, Settimio Di Gregorio, Claudia Proto, Arsela Prelaj, Alessandro De Toma, Mario Occhipinti, Marta Brambilla, Sara Manglaviti, Laura Mazzeo, Arturo Rinaldi, Teresa Beninato, Monica Ganzinelli, Filippo De Braud, Marina Chiara Garassino, Paolo Verderio, Mario Paolo Colombo, Sabina Sangaletti.
Fondazione IRCCS Istituto Nazionale dei Tumori, Milan, Italy

Background: Hyperprogressive disease (HPD) has been described in ≃14-25% of pretreated non-small cell lung cancer (NSCLC) patients upon single-agent (SA) PD-1/PD-L1 inhibitors (ICI) and has not been reported upon platinum-based chemotherapy (PCT) and ICI combinations. So far, no predictive biomarkers are available for HPD early detection.
Methods: NSCLC patients treated with 1st line SA-ICI or PCT-ICI were assessed for HPD and circulating neutrophils. HPD was defined as delta tumor growth rate (TGR) >50% and/or TGR ratio ≥2. Circulating low density neutrophils (LDNs) were assessed by flow cytometry on peripheral blood mononuclear cells (PMBCs). LDNs were defined as $CD66b^{+}CD15^{+}$ cells among $CD11b^{+}$ PBMCs and immature subtypes as $CD10^{-}$ LDNs. The LDNs predictive role was assessed by penalized model-based tests.
Results: 144 NSCLC patients were included: 75 treated with SA-ICI, 69 with PCT-ICI. In the SA-ICI cohort, HPD occurred in 8 (11%) patients, while progressive disease (PD) and response or stable disease (PR/SD) occurred in 33 (44%) and 34 (45%) of patients respectively. Immature circulating $CD10^{-}$ LDNs were significantly higher in baseline blood samples of HPD patients [median (ME): 39.3, interquartile range (IQR): 28.7] compared to PD [ME: 7.4, IQR: 14.9, $p<0.01$] or PR/SD patients [ME: 3.7, IQR: 12.6, $p<0.01$]. Circulating $CD10^{-}$ LDNs were associated with HPD [odds ratio (OR): 1.17, 95% CI: 1.06; 1.29], with a good prediction capability [cross-validated AUC 0.97 (95%CI: 0.94;1.00)]. A 30.5% cut-off value for $CD10^{-}$ LDNs circulating neutrophils was identified by Younden index to discriminate HPD from others. In the PCT-ICI cohort, 14 patients had circulating $CD10^{-}$ LDNs ≥30.5%, being at high risk of HPD. However, no HPD was observed in PCT-ICI cohort and dynamic LDNs evaluation in high HPD risk patients showed 52.3% (IQR: 28.4) median reduction in $CD10^{-}$ LDNs upon PCT-ICI, versus only 8.9% (IQR: 34.6) reduction in HPD patients upon SA-ICI, suggesting that PCT prevents HPD by reducing selectively immature LDNs.
Conclusions: Baseline circulating immature neutrophils characterize HPD upon 1st line SA-ICI and a 30.5% cut-off of immature neutrophils could select NSCLC patients to be addressed to PCT-ICI combinations.

#5507

A potential combinatorial treatment strategy to overcome olaparib resistance in high-grade ovarian cancer

Jie Bao[1], Eva Daniela Mendoza Ortiz[2], Jessica Agudelo[3], Roman Filimonov[3], Anniina Färkkilä[1], Jing Tang[1]. *[1]Faculty of Medicine, University of Helsinki, Helsinki, Finland,[2]Institute of Molecular Medicine Finland, University of Helsinki, Helsinki, Finland,[3]Puissan Biotech Oy, Helsinki, Finland*

PARP1 inhibitors have evolved the treatment of *BRCA*1/2-mutated high-grade serous ovarian cancer. However, its resistance is frequently observed. In our initial combinatorial drug screening, OSU-03012 (AR-12) appeared as a promising drug to be combined with PARP inhibitor Olaparib in multiple ovarian cancer cell lines, regardless of *BRCA* mutation status. OSU-03012 is designed as an orphan drug with anti-microbial activity. It has also shown cell-context-dependent anti-cancer activity. Using imaging-based high-throughput drug sensitivity analysis, we found that OSU-03012 and BX-912, while both classified as 3-Phosphoinositide Dependent Protein Kinase 1 (PDK-1) inhibitors, not only differed in their synergistic effect together with Olaparib, also caused distinct phenotypic changes in ovarian cancer cells. Cell senescence was observed in BX-912 but not OSU-03012 treatment, alone or together with Olaparib. Recently, dihydroorotate dehydrogenase (DHODH) has been identified as a secondary target of OSU-03012, which explains its anti-cancer activity by regulating nucleotide metabolism and thus affecting DNA repair. However, in our study, OSU-03012 did not similarly affect cell viability and phenotype on ovarian cancer cell lines as a DHODH inhibitor BAY2402234. Interestingly, compared to BX-912 and BAY2402234, OSU-03012 showed higher selectivity on ovarian cancer cell lines over normal epithelial carrying *BRCA* and *TP53* mutations; it also exhibited reduced toxicity on a human fibroblast cell line. We are further clarifying the putative targets of OSU-03012 using thermal proteome profiling. To investigate the molecular evidence of OSU-03012 for treating ovarian cancer, we performed a differential gene expression analysis using Genomics of Drug Sensitivity in Cancer (GDSC) database. All ovarian cancer cell lines included in GDSC drug screening are classified as Olaparib- or OSU-03012-sensitive/insensitive, based on the respective IC50 threshold. We found that OSU-03012 sensitivity is positively associated with several known genes regulating ovarian cancer progression, such as *LUM* and *COL3A1,* as well as genes (e.g., *PTPRZ1*) that are associated with Olaparib insensitivity in this analysis. Interestingly, angiogenesis signatures were found to be enriched in both Olaparib and OSU-03012-sensitive cancer cell lines. We are currently establishing a cancer-vascular cell system in a microfluidic setting to study how such combinatorial

drug treatment would connect to tumor microenvironment remodeling. Altogether, we identified a potential non-cancer drug for ovarian cancer treatment and to overcome Olaparib resistance. A multidisciplinary approach highlights the importance of drug target profiling and sensitivity signatures scoring to improve treatment stratification.

#5508

Artesunate increases enzalutamide efficacy in advanced prostate cancer

Xinyi Wang, Fengyi Mao, Jinghui Liu, Yifan Kong, Daheng He, Chi Wang, Zhiguo Li, Xiaoqi Liu. *University of Kentucky, Lexington, KY*

Prostate cancer (PCa) is the most diagnosed worldwide. PCa development and progression require androgen receptor (AR) signaling, which stimulates its downstream gene expressions and cancer progression. While second-generation anti-androgen drugs plus androgen deprivation therapy (ADT) remains the first-line treatment for advanced prostate cancer patients, around one-third of patients will relapse in a short period. Advanced prostate cancer results in more mortalities than primary PCa patients. Evidence shows that the recurrence is caused by AR overexpression, AR variants, AR mutations, and signaling crosstalk. Thus, it is urgently needed to discover a novel therapeutic strategy for treating advanced prostate cancer. The heat shock protein family (HSP), including HSP90 and HSP70, play important roles in refolding aggregated protein for cancer cell proteomic equilibrium. HSP is induced primarily by heat shock factor (HSF1). As AR's chaperone protein, HSP70 and HSP90 increase AR transcription activity. Inhibiting HSP70 and HSP90 promotes STUB1, an E3 ligase, binding to AR and AR - V7, and ubiquitination. Artesunate (ART) is a semi-synthetic ingredient from Artemisia annua and is the most common treatment for malaria throughout the world. It was approved for medical use by the FDA (Food and Drug Administration) (Food and Drug Administration). Recently ART has been unveiled for its anticancer properties. However, the efficacy of ART treatment in advanced prostate cancer and the direct target of ART have not been investigated yet. Herein, we have examined the efficacy of combining Enzalutamide (Enza) and ART in advanced prostate cancer cell lines. We also performed unbiased bioinformatics analysis using RNA seq results in enzalutamide-resistant cell line C4-2R cells and 22RV1 cells to investigate the cell response toward ART treatment. We identified ART could downregulate of AR signaling pathway. Moreover, we determined that ART treatment

induces AR degradation in proteasome dependent manner. Interestingly, we found HSP70 and HSP90 are also decreased in RNA seq results. Taking these together suggests that ART may target HSF1 directly. Our results suggest ART induced AR degradation could be a promising clinical strategy for advanced prostate cancer.

#5509

The PI3K inhibitor Paxalisib combines synergistically with the MEK inhibitor Mirdametinib to target atypical teratoid/rhabdoid tumors

Kristen J. Malebranche, Tyler Findlay, Anupa Geethadevi, Charles Eberhart, Eric Raabe, Jeffrey Rubens. *Johns Hopkins University School of Medicine, Baltimore, MD*

Atypical teratoid/rhabdoid tumors (AT/RT) are aggressive pediatric brain tumors and the most common malignant brain tumors of infancy. The four-year event-free survival rate is only 37%. For patients with relapsed AT/RT there are limited treatment options, but precision therapies may help improve survival for patients with this deadly disease. We have previously identified strong activation of the PI3K-AKT-mTOR (mTOR) signaling pathways in AT/RT. Paxalisib is a highly brain-penetrant PI3K inhibitor acting upstream of mTOR. We find that Paxalisib slows tumor growth in orthotopic xenograft models of AT/RT and extends median survival from 40 to 54 days ($p=0.001$, log-rank test). RNASeq after mTOR pathway inhibition identifies reflexive activation of the RAS-RAF-MEK-ERK (MAPK) pathway as a possible mechanism of therapy resistance (KEGG pathway analysis). The RAS-RAF-MEK-ERK (MAPK) pathway plays a pivotal role in regulating cell growth and survival and activation of the pathway contributes to the aggressive growth of numerous cancers. Mirdametinib is a small, allosteric MEK inhibitor currently used in clinical trials for both pediatric low- and high-grade gliomas (PD0325901). We find that dual inhibition of both the mTOR and MAPK pathways by Paxalisib and Mirdametinib synergize to reduce AT/RT growth and viability (Bliss synergy score 16.77). Paxalisib also combines with Mirdametinib to induce high levels of apoptosis and cell senescence (as determined by western blot: cPARP, pRB, P21, P16). Naïve treatments in mice bearing AT/RT orthotopic tumors suggests the combination therapy decrease mTOR and MAPK pathway activation (as determined by western blot). These data support the use of Paxalisib and Mirdametinib combination therapy as a promising novel combination therapy to treat relapsed AT/RT.

#5510

TAS102 synergizes with regorafenib against colorectal and gastric cancer cells

Jun Zhang, Lanlan Zhou, Shuai Zhao, Wafik S. El-Deiry. *Brown University, Providence, RI*

TAS-102 is an oral formulation consisting of trifluridine (FTD) and thymidine phosphorylase inhibitor tipiracil hydrochloride (TPI). Regorafenib is a multi-targeted tyrosine kinase inhibitor, it inhibits the activities of VEGFR2 and 3, Ret, Kit, PDGFR and Raf kinases and results in the inhibition of tumor angiogenesis and cell proliferation. TAS102 or regorafenib monotherapy can lead to an overall survival benefit in metastatic colorectal cancer (mCRC) patient previously treated with conventional chemotherapy and target therapy (Arnold et al., 2018). TAS102 in combination with bevacizumab, a monoclonal antibody against vascular endothelial growth factor A (VEGF-A), is associated with a significant and clinically relevant improvement in progression-free survival in colorectal cancer (C-TASK FORCE)(Kuboki et al., 2017; Pfeiffer et al., 2020). FTD can synergize with nintedanib to inhibit the growth of colorectal cancer xenografts(Suzuki, Nakagawa, Matsuoka, & Takechi, 2016). We previously reported that regorafenib combined with a fluoropyrimidine can delay disease progression in case reports of multidrug-resistant mCRC patients(Marks et al., 2015). Therefore, we hypothesized that the combination of TAS102 and regorafenib may be active in CRC and other gastrointestinal (GI) cancers, and may in the future provide a treatment option for patients with advanced GI cancer. We investigated the therapeutic effect of TAS102 in combination with regorafenib in preclinical studies employing cell culture, colonosphere assays that enrich for cancer stem cells, and in vivo. We found that TAS102 in combination with regorafenib has synergistic activity against multiple GI cancers in vitro including colorectal and gastric cancer, but not liver cancer cells. TAS102 inhibits colonosphere formation and this effect is potentiated by regorafenib. In vivo anti-tumor effects of TAS102 plus regorafenib appear to be due to anti-proliferative effects, necrosis and angiogenesis inhibition. Growth inhibition by TAS102 plus regorafenib occurs in xenografted tumors regardless of p53, KRAS or BRAF mutations, although more potent tumor suppression was observed with wild-type p53. Regorafenib significantly inhibits TAS102-induced angiogenesis and microvessel density in xenografted tumors, and inhibits TAS102-induced ERK1/2 activation

regardless of RAS or BRAF status in vivo. Collectively, TAS102 plus regorafenib is a
synergistic drug combination in preclinical models of GI cancer, with regorafenib suppressing TAS102-induced increase in microvessel density and p-ERK as contributing mechanisms. The drug combination may be further tested in gastric and other GI cancers.

#5511

Investigating Wee1 and Myt1 combined inhibition as a potential cancer therapeutic strategy

Sargun Sokhi, Joanne D. Hadfield, Jeremy Fung, Gordon K. Chan. *Oncology, University of Alberta, Edmonton, AB, Canada*

Introduction: Cell cycle is under the surveillance of checkpoints to repair any damage before the cell transits between phases. Wee1 and Myt1 kinases prevent premature entry into mitosis by monitoring the G2/M checkpoint by adding an inhibitory phosphorylation on Cdk1. Wee1 is overexpressed in various tumors and MK-1775, a Wee1 small molecule inhibitor, is currently in phase I/II cancer clinical trials. Although MK-1775 was shown to potentiate the effect of other genotoxic therapies, yet clinical resistance has emerged towards it. In examining the mechanism of MK-1775-mediated cytotoxicity, we identified Myt1 as a resistant factor. Emerging evidence suggests that Myt1 is an important cancer therapeutic target. Hence, we are examining a novel Myt1 kinase small molecule inhibitor, RP-6306 in combination with MK-1775 as a potential synthetic lethal cancer therapy. We hypothesize that a combination of MK-1775 and RP-6306, inhibitors against two partially redundant kinases important for adaptation to genotoxic stress, will achieve synthetic lethality while circumventing the issue of resistance development following monotherapies.
Model Systems Used: 1) a cervical cancer cell line that is tetracycline inducible for Myt1 expression; 2) cancer cell lines (breast and cervical) that are resistant to MK-1775 through upregulation of Myt1.
Methods: We established the IC50 of RP-6306 in a panel of tumorigenic and non-tumorigenic cell lines using standard crystal violet viability assay. Following that, we tested the combination effect of MK-1775 and RP-6306 in model cell lines listed above using zero potency model of synergy. The effect of the combination treatment on the clonogenicity was evaluated using clonogenic assay. Timelapse microscopy on a High Content Imaging system

was used to determine the effect of RP-6306 and MK-1775 on mitotic duration and cell fates.
Results: We found that MK-1775 and RP-6306 combination treatment shows synergistic cell killing in a panel of cancer cell lines. Wee1 inhibition shows synergistic cell killing with Myt1 inhibition especially in inducible Myt1 overexpressing cells. Wee1 and Myt1 combined inhibition resists the increase in clonogenic potential of the cancer cells transiently overexpressing Myt1. RP-6306 and MK-1775 combination treatment promotes mitotic arrest leading to cell death in Myt1 overexpressing cells. We also found that the mechanism of cell death in the cells treated with the combination treatment is centromere fragmentation leading to mitotic catastrophe.
Conclusions: The combined Wee1 and Myt1 inhibition leads to synthetic lethality. Hence, our findings strongly suggest that the combined MK-1775 and RP-6306 treatment has promising potential to mitigate MK-1775 resistance. Our research contributes to the development of novel potential combination therapy while optimizing and improving the efficacy of MK-1775 treatment for potential clinical use.

#5512

TIC10/ONC201 in combination with ceralasertib exhibits potent synergy in high grade serous ovarian cancer cells

Maryam Ghandali[1], Kadir Mert Selvi[2], Kelsey E. Huntington[1], Andrew George[1], Anna Ochsner[1], Benedito A. Carneiro[1], Donn S. Dizon[1], wafik S. El-Deiry[1]. *[1]Legorreta Cancer Center at Brown University, Providence, RI,[2]hacettepe University, Ankara, Turkey*

High-grade serous ovarian cancer (HGSOC) is the most common and malignant form of ovarian cancer. Although patients with HGSOC are likely to respond to treatment, it is common for the cancer to recur and become resistant to treatment, therefore there is a need to develop new targets and novel combinations to increase patient survival rates. ATRi's (Ataxia telangiectasia and Rad3 related inhibitors) have shown efficacy in HGSOC. Considering ATRi's have shown moderate efficacy as a single treatment in HGSOC patients, we hypothesized that combining ATRi's with ONC201 would enhance efficacy. ONC201 is a pro-apoptotic TRAIL-inducing compound that activates the integrated stress response and inactivates the Akt pathway which is upregulated in over 70% of HGSOC. Inactivation of the Akt pathway may result in a synergistic effect that could be translated for use in

patients with HGSOC. Three HGSOC cell lines were treated with the novel drug combination of ceralasertib (ATRi) and ONC201 and CellTiterGLO viability assays were performed after 72 hours to evaluate the synergistic effect of combination treatment. Western blots were performed to investigate the synergistic effect of combination treatment on the Akt pathway as well as expression of the cellular metabolic stress protein ATF4. Cytokine profiling using the Luminex 200 technology was performed to study treatment-induced changes in the tumor microenvironment. Cell viability after ceralasertib and ONC201 combination treatment showed synergy in HGSOC cell lines (OVCAR3, KURAMOCHI, TOV21G) . In TOV21G cell line, combination studies of ONC201 and ceralasertib calculated by compusyn software demonstrated a synergistic effect of both drugs, Combination indexes below one were observed at concentration of 0.008-2 μM of ceralasertib with 0.31-5 μM of ONC201 with the best combination index of 0.65. We similarly observed synergy in the two other cell line between ONC201 and ceralasertib. Western blotting showed reduction in total Akt and Erk expression and an increase in ATF4, consistent with the observed synergetic effect of ceralasertib and ONC201 combination. Our ongoing studies are exploring potential mechanisms of synergy between ceralasertib and ONC201 and effects on immune–mediated killing of HGSOC cells. Our results suggest a rational and potentially effective novel therapy combination of ATRi ceralasertib and ONC201 that maybe further developed for HGSOC.

Community-based Research and Biobanking Research

#5516
Identifying DNA methylation biomarkers in Brazilian women of African descent

Lissette Delgado-Cruzata[1], Diego J. Gomes de Paula[2], Jennifer Vieira Gomes[3], Tatiana A. Simão[4], Leonor Gusmão[3], Luis Felipe Ribeiro Pinto[2], Sheila C. Soares-Lima[2]. *[1]The City University of New York, John Jay College, Bronx, NY,[2]National Cancer Institute, Rio de Janeiro, Brazil,[3]Rio de Janeiro State University (UERJ), Rio de Janeiro, Brazil,[4]Biochemistry Department, Rio de Janeiro State University (UERJ), Rio de Janeiro, Brazil*

Breast cancer is the most common cancer, and the leading cause of cancer-related deaths in Brazilian women. Studies have shown that in Brazil while breast cancer mortality has increased in the last decade for all women,

mortality in women of African descent has doubled. A recent study showed that Afro-Brazilian women suffer from higher excess breast cancer mortality even after adjusting for extent of disease, year of diagnosis, age and socioeconomic status, which suggests biological factors also contribute to the differences in the clinicopathological make-up of the disease in women in this group. DNA methylation biomarkers, representing a combination of genetic and non-genetic factors, have the potential to be especially valuable when considering the combined contribution of the environment and genetics in breast cancer etiology. Several groups have found differences in DNA methylation levels associated with race and ethnicity in breast cancer. In addition, research has shown that women of different races/ethnicities with similar breast cancer tumor subtypes have distinct DNA methylation patterns. To explore further the association between race, ancestry and DNA methylation, we conducted a study in paired tumor and non-tumor tissue samples of forty-eight Brazilian women who self-identified as Black or Brown and were treated at National Cancer Institute Breast Cancer Hospital in Rio de Janeiro, Brazil. We carried out a DNA methylation profiling analysis using Illumina EPIC (850k) arrays in bisulfite converted DNA originally extracted from frozen tissue samples. A total of 739,883 differentially methylated probes (DMP) were identified, of which a large proportion 6,241 (78.4%) were hypomethylated. Lower DNA methylation was more common on intragenic regions and gene bodies, while hypermethylation was more commonly found on the promoter regions. DNA methylation was often higher in non-tumor than tumor samples. Among our top hits we found genes previously associated with estrogen receptor negative tumor types, CDH4, CERK, PROX1 and ADHFE1, and with high risk of breast cancer mortality (ST6GAL1, LYN, TFF1 and BMP3). A DPM enrichment pathway analysis predicted effects in known signaling pathways and transcriptional misregulation. We are currently analyzing the associations between the top differentially methylated regions with ancestry informative markers, and the clinicopathological characteristics of disease, to gain a better understanding of the role of DNA methylation marks in this population. This study adds to our current knowledge on epigenetics marks that will ultimately help us address mortality due to this disease in this population.

#5517

Pegaspargase is a viable option in elderly adults with acute lymphoblastic leukemia

Yosef Joseph Rene Amel Riazat-Kesh[1], Hannah Levavi[2], Sangeetha Venugopal[3], Carli Beall[4], Ronald Hoffman[2], Marina Kremyanskaya[2], John Mascarenhas[2], Sara Kim[5], Michal Bar-Natan[2]. *[1]Internal Medicine, Mt. Sinai Morningside and West, New York, NY,[2]Hematology/Oncology, Mt. Sinai Hospital, New York, NY,[3]Sylvester Cancer Center, University of Miami, Miami, FL,[4]Oncology Pharmacy, Northwestern Medicine, Chicago, IL,[5]Oncology Pharmacy, Northwell Health, New York, NY*

Pegaspargase (peg-asp) is a pegylated form of asparaginase with a longer half-life used in pediatric-inspired chemotherapy for treatment of adult acute lymphocytic leukemia (ALL). Peg-asp appears to confer a survival advantage, but use in older adults is limited by concern for toxicity, though incidence and associated factors are poorly characterized. Our primary objective was to compare peg-asp tolerability in different age groups; secondary objectives were assessment of patient- (pt) and disease-dependent factors associated with toxicity. We retrospectively reviewed 58 ALL pts treated with at least 1 dose of peg-asp (500-2500IU/m2) at our institution between 2016-2021. We used χ-squared- and Fisher's test, and multivariable regression analysis to assess relationships between pt-factors and toxicities. Median doses received was 2 (range 1-7). 38 pts were 40 years or older, 20 were >60 years. 18 received PEG during induction only, 8 in consolidation only, 27 in both, and 5 during salvage therapy post-relapse. 17 had Philadelphia (Ph) positive B-ALL; 32 Ph negative B-ALL; 7 T-ALL; and 2 had mixed phenotype acute leukemia. Pts were 19-78 years old (median 48.5). Grade 3 or 4 toxicities observed in >10% of cases included hepatotoxicity (81%, 47/58); antithrombin 3 depletion (72.4%, 42/58); hypofibrinogenemia <100 (58.6%, 34/58); hypertriglyceridemia (20.8%, 10/48); venous thromboembolism (12.1%, 7/58) and hemorrhage (12.1%, 7/58). Acute pancreatitis (8.6%, 5/58) and hypersensitivity (2/58, 3.4%) were less common. On univariate analysis, grade 3 liver injury was significantly associated with younger age groups (18-40 and 40-60 vs >60 years; p=0.025), likely due to older age strongly correlating (p <0.01) with receipt of <2000IU/m2 pegaspargase. No other toxicity was significantly associated with age. Hypofibrinogenemia and hepatotoxicity were significantly associated with initial receipt of pegaspargase during induction vs consolidation (p=0.042, p=0.013, respectively) but age was not. Pts receiving a max dose PEG of <2000IU/m2 had significantly lower odds of developing hepatotoxicity and hypertriglyceridemia than those receiving 2000 IU/m2 or more (p=0.008,

p=0.003, respectively). On multivariate analysis, higher max dose of PEG received (2000 IU/m2 or over) correlated with greater odds of hepatotoxicity, hypertriglyceridemia and acute pancreatitis (OR 1.72, CI 1.23-2.38; OR 1.31, CI 2.18, CI 1.59-3.03; and OR 1.46, CI 1.13-1.88, respectively). Hypertriglyceridemia was also associated with older age and BMI >30 (OR 1.31, CI 1.05-1.62, and OR 1.31, CI 1.09-1.59, respectively). In summary, low dose pegaspargase is a viable option in ALL in adults over 60, with only hypertriglyceridemia associated with older age. Future work might correlate serum pegaspargase activity to intolerance and outcomes, and examine whether prophylactic treatment e.g. with levocarnitine might prevent toxicity.

#5518

Use of antihypertensive drugs and the risk of cancer, findings of a population-based cohort study in Shanghai

Suna Wang[1], Li Xie[1], Ying Qian[1], Jie Wang[1], Guanglu Zhang[1], Lei Li[1], Weituo Zhang[1], Herbert Yu[2], Wensui Zhao[3], Biyun Qian[1]. *[1]School of Public Health and Hongqiao International Institute of Medicine, Shanghai Tongren Hospital, Shanghai Jiao Tong University School of Medicine, Shanghai, China,[2]Cancer Epidemiology Program, University of Hawaii Cancer Center, Honolulu, HI,[3]Shanghai Changning District Center for Disease Control and Prevention, Shanghai, China*

Background: The widespread use of antihypertensive drugs has raised concerns on whether the use increases the risk of cancer. Although multiple studies have addressed this issue, it remains unclear if hypertension patients who are on antihypertensive medications are at higher risk for cancer.
Methods: Between 2013 and 2017, we enrolled 101,370 individuals with hypertension from community healthcare centers in Changning Shanghai, followed through December 31, 2019. Drug administration was defined as the class and number of ever use the major antihypertensives. The main outcomes included the incidences of all cancer and major types of cancer in Shanghai (lung, colorectum, thyroid, and stomach).
Results: During a mean follow-up of 5.1 (SD 1.3) years, 4970 cancer cases were newly diagnosed in the cohort. CCBs were the most frequently used antihypertensives which were associated with a moderately increased risk of all cancer (hazard ratio, HR: 1.11, 95% CI: 1.05-1.18). The second commonly used drug ARBs were also associated with increased risk of all cancer (HR: 1.10, 95%CI: 1.03-1.17) as well as lung and thyroid cancers (HR: 1.21,

95%CI: 1.05-1.39; HR: 1.66, 95%CI: 1.22-2.27, respectively). No cancer association was found with other antihypertensives. Individuals who use more than one class of antihypertensives had a higher risk of all cancer, and a possible dose-response relationship was suggested.
Conclusions: Use of ARBs or CCBs may be associated with an increased risk of cancer. Taking more than one class of antihypertensives appeared to have a higher risk for cancer.

#5519

Biobanking of gastric organoid models from a racially diverse cohort for gastric cancer interception

Priya Alagesan[1], Paula Scotland[2], HannahSofia Brown[1], Shannon J. McCall[3], Meira Epplein[4], Katherine S. Garman[2]. *[1]Duke University School of Medicine, Durham, NC,[2]Department of Medicine – Division of Gastroenterology, Duke University Medical Center, Durham, NC,[3]Duke BioRepository & Precision Pathology Center, Department of Pathology, Duke University School of Medicine, Durham, NC,[4]Department of Population Health Sciences, Duke University School of Medicine, Durham, NC*

Purpose: In the United States, significant disparities exist in gastric cancer incidence and mortality between Black Americans and non-Hispanic White Americans. *Helicobacter pylori* (*HP*) infection is the most important risk factor for developing non-cardia gastric adenocarcinoma (GAC), the most common type of gastric cancer. Non-cardia GAC is thought to occur via progression from *HP*-induced atrophic gastritis to gastric intestinal metaplasia (GIM), dysplasia, and cancer. The purpose of this study was to enroll racially diverse (~50% self-identified as Black) patients from the endoscopy suite across the spectrum of *HP*-associated disease (gastritis, GIM, GAC) in a prospective observational cohort to biobank blood and tissue samples with patient-reported survey data and clinical history from the electronic health record.
Methods: In an ongoing prospective study funded by an NIH P20 disparities project, we enrolled a diverse, racially balanced cohort of research participants undergoing upper endoscopy. We tracked and optimized screening, enrollment, and collection of blood, tissue, and survey data. Organoids were generated from fresh and/or cryopreserved biopsies of normal gastric tissue, gastritis, GIM, or GAC. Gene expression, immunohistochemistry and DNA mutational profiling were performed in a subset of organoids.

Results: To date, 563 patients were identified in screening (47% Black patients) and 250 were successfully included with a 44% enrollment rate (46% Black participants). Rates of successful sample and data collection were: 86% blood, 87% tissue collection, and 89% survey collection. The proportion of Black participants was greater in the *HP*-positive group (65%) vs. known *HP*-negative (46%) (p=0.03). Gastric organoids were generated with >90% success from 49 patients, including paired organoid lines from incomplete, complete, and/or extensive GIM, matched tumor and non-tumor and gastric antrum and body samples. 20 organoid lines were derived from cryopreserved endoscopic biopsies. Ongoing characterization of tumor organoids reflects expected heterogeneity among gastric cancer patients and provides a functional measure of cytokine expression.
Conclusions: To address health disparities related to gastric cancer, diverse patient cohorts must be established with successful biobanking from groups most affected by the disease. Patient-derived gastric organoids can be generated from diverse populations and across different clinical conditions as one approach to understanding and addressing gastric cancer health disparities.

#5520

Research Ready graphic-style story to support future research participation among adolescents

Lauren Bates[1], Susan Gertz[2], Susan Hershberger[2], Melinda Butsch Kovacic[3], We Engage 4 Health Community-Academic Partnership. *[1]Cincinnati Children's Hospital Medical Center, Cincinnati, OH,[2]Miami University, Oxford, OH,[3]University of Cincinnati, Cincinnati, OH*

Historically, marginalized adults are more likely to be mistrustful of health research worrying both about its invasiveness and their own safety. As a result, many decline to participate. Adolescents have a much lower perception of risk compared to adults and are also susceptible to peer pressure and socialized trust or mistrust from their parents and family members, which can influence risk perception. As encouraging equitable participation in research becomes an important tool in the fight against cancer disparities, We Engage 4 Health created a graphic-style story “Research Ready” to help community members learn the 3 P’s: the purpose of cancer research, how they are kept safe while participating, and why people from diverse backgrounds are needed to participate. An accompanying Research Review Activity was also included

to further support participants' decision-making regarding research participation. Two groups of diverse adolescents were asked to read the story aloud together in small groups and then discuss an active research study targeting adolescents using the review activity with a scientist to consider whether the first the teen story character (Vito) and ultimately themselves, should consider participation in the study and to identify what information was needed from study staff to better be able to make a decision based on their values and accurate information provided by study staff. Group 1 included 45 adolescents that were 68% African American and 10% European American. Group 2 included 73 high schoolers that were 78% Asian, 15% European American, and 5% African American. Post-discussion surveys indicated that only 9% and 3% in group 1 and group 2 respectively had previously participated in health research. However, after the story discussion, 83% and 89% indicated they thought it would be safe to participate in research and 76% and 89% indicated a willingness to participate in research in the future. Finally, 60% collectively enjoyed the story's graphic-style format. These data suggest Research Ready to be potentially useful in promoting future research participation and may be especially useful in engaging ethnic/racial groups commonly underrepresented in cancer research.

#5521

Racial and ethnic disparities for intravascular large B-cell lymphoma: A Surveillance, Epidemiology, and End Results (SEER) database analysis with emphasis on Hispanics.

Daniela Urueta Portillo[1], Daniel Rosas[1], Joel E. Michalek[1], Qianqian Liu[1], Adolfo E. Diaz Duque[2]. *[1]UT Health and Sciencer Center San Antonio, San Antonio, TX,[2]Mays Cancer Center UT Health San Antonio MD Anderson, San Antonio, TX*

Background: Intravascular large b-cell lymphoma (IVLBCL) is a rare but highly aggressive subtype of non-Hodgkin lymphoma (NHL). IVLBCL is a clonal proliferation with selective growth within the blood vessel. It has been primarily described in Asian and European populations, and a median age presentation is in the sixth to seventh decades without a sex predilection. The US incidence is 0.95 in 1 million, but is thought to be higher, as the diagnosis is mainly done postmortem. Meanwhile, the incidence rate of IVBCL in Hispanics (HI) remained unknown. This study looks at demographics,

treatment patterns, and outcomes of patients with IVLBCL in the US, examining disparities by HI vs Non-Hispanic (NH).
Methods: Data were analyzed on IVLBCL patients reported to the SEER 18 database between 2000 and 2018. SEER 18 contains the most comprehensive population-based cancer information in the US, covering approximately 27% of the US population and 36% of HI alone. The racial groups analyzed were NH whites, HI whites, blacks, and Asians/PIs (Pacific Islanders). Patient characteristics, age-adjusted incidence rate, and survival rate were compared across ethnic groups. Kaplan-Meier and Cox regression analyses compared overall survival (OS) between HI and NH. Multivariate analysis and propensity score matching were performed, with adjustment for age, stage and B-symptoms.
Results: We identified 164 patients with IVLBCL, of which 10% were HI. 41% of HI were male vs 44% of NH. HI were diagnosed at an older age, 72. vs 69 y.o., compared to NHI (p=0.907). Most of NH and HI were diagnosed between 60-80 y.o. (p=0.322), 53.1% and 47.1%, respectively. Regarding race, HI and NH were mainly identified as whites (88% vs 78%), followed by Asians (6% vs 17%) (p=0.013). For HI, 53% presented B symptoms compared to 16% of NH (p=<0.001). On survival analysis, the survival probability at 2, 5 and 10 years of HI vs NH was (0.540 vs 0.505), (0.432 vs 0.425), and (0.443 vs 0.237), respectively. The median survival time was 0.8 years for HI and 1.9 years for NH. The 10 year OS probability was not significantly different for HI vs NH (p=0.66).On multivariate analysis, when adjusted for age, those patients who were 60 to 80 y.o. had worse OS compared to those younger than 60 y.o., with HR 1.4 (95% CI: 0.7 - 2.1).
Conclusion: In our study, despite a lower percentage of patients identified as Asian in our HI population, there is a significant difference in the presence of B-symptoms between HI and NH, going against the traditional description of an Asian variant with increased systemic symptoms. Despite this finding, it demonstrated similar outcomes in the 10 years survival analysis for HI and NH. Standardized treatment may explain why no variation was reported in OS. Our analysis shows that ethnic variations do not seem to affect oncological outcomes in IVLBCL for HI in the US.

#5522

Does physician-patient language concordance increase clinical trial enrollment in breast cancer patients?: A real-life study in a majority-minority population

Daniela Urueta Portillo[1], Ana M. Mendoza Sanchez[2], Nitzia E. Quilantan[3], Lisa Maria Mendoza Sanchez[4], Marcela Mazo Canola[1], Jonathan Gelfond[1], Julio A. Peguero[2]. *[1]UT Health Science Center at San Antonio, San Antonio, TX,[2]Oncology Consultants, Houston, TX,[3]Oncology Consulants, Houston, TX,[4]Universidad Autonoma de Chihuahua, Chihuahua, Mexico*

Introduction: Clinical trial accrual and enrollment are essential to break disparities seen in minority populations affected by cancer. Despite Hispanics (HI) being 18.9% of the US population and the fastest-growing minority in the US, they only represent 4% of the patients enrolled in clinical trials. These disparities are often explained by different social determinants of health, but could also be due to decreased perceived interest by oncologists in their participation simply due to lack of English proficiency. Effective doctor-patient communication is vital in establishing a healthy doctor-patient relationship, and is vital in delivering high-quality health care. In this study, we explore whether physician-patient language concordance affects clinical trial enrollment.
Methods: We evaluated 233 patients diagnosed with breast cancer who consented to experimental clinical trials in a private Oncology practice in Houston, Texas, from 2008-2022. All trials had approved consent in English and Spanish. We used logistic regression to model the probability of treatment, while adjusting for the effects of cancer type, gender, race, ethnicity, and language concordance.
Results: Of the 233 patients with breast cancer, 191(82%) were enrolled in a clinical trial, and 96% of these patients spoke the same language as their providers. 42 patients were not enrolled, with 95% of patients speaking the same language as their provider. There were 209 (90%) patients who spoke English, 22 (9%) were Spanish speakers and 2 (1%) were Arabic speakers. Of the Spanish speakers, 18 were enrolled, with 13 (72%) having language concordance with their provider. The ethnicity was evaluated, resulting in 72 (31%) patients being Hispanics, 55 (24%) African American, 94 (40%) Caucasian, 7 (3%) Asian, 4 (2%) Middle Eastern and 1 (0.4%) American Indian. It also evaluated the rate of consent withdrawal, showing only 6 (3%) patients. After evaluating the results, it was noted that there was no statistically significant association of physician-patient language concordance with enrollment rate ($p=0.776$). There was also no significant difference in consent withdrawal ($p=0.626$), and no change associated with gender ($p=0.344$) or ethnicity when evaluated ($p=0.13$).

Conclusion: In conclusion, our analysis confirms no significant difference in breast cancer patients' enrollment in clinical trials if there is language concordance between physician and patient. The efforts of the medical workforce to use translators and translated versions of informed consents, surveys or outcome assessments, when available, seem enough for our patients to agree to continue enrollment.

#5523

Impact of COVID-19 on longitudinal breast cancer research studies involving TNBC patients

Cherie Bates[1], Esther Kong[1], Elena Zaikova[1], Samuel Aparicio[1], Karen Gelmon[2]. *[1]Molecular Oncology, BC Cancer Research Institute, Vancouver, BC, Canada,[2]Medical Oncology, BC Cancer, Vancouver, BC, Canada*

Background Triple-negative breast cancer (TNBC) accounts for ~15% of breast cancer diagnoses but is linked to worse outcomes and comprises a disproportionate number of breast cancer deaths. The TNBC pilot study is a prospective longitudinal study to provide a critical resource for understanding TNBC disease. However, the pandemic impacted the collection of samples.
Objective To highlight the impacts of COVID-19 on this longitudinal cancer translational research study including the patient's perspective and to develop recommendations to avoid future disruptions.
Methods 389 participants were enrolled in the prospective longitudinal cohort, which collected serial blood samples for up to 5 years. Due to the pandemic, research was curtailed for 6 months due to concerns about patient safety, halting the collection of blood samples. Missed samples and data gaps were documented. To complement this, we initiated a survey capturing the patient perspective on their experience of the study disruption due to COVID.
Results 217 enrolled participants missed a blood draw or had a collection outside the study window. 158 patients missed 1 time-point collection, and 59 patients missed ≥ 2 collections. Of the 217 participants who missed a collection, 6 disease recurrence diagnoses and 3 deaths occurred during research curtailment. The collection of survey responses from participants is ongoing and will be presented at the AACR Annual Meeting.
Conclusion Missed samples resulted in irreplaceable data gaps critical to monitoring patient outcomes, and reduced cohort sampling during the pandemic. Our current knowledge of the risks suggests that with proper informed consent, collections could have continued. To mitigate disruption in

future clinical studies, clear plans should be part of study design to provide continuity. The participants' experience to be reported will also help researchers understand their issues and help develop policies.

Missed collections and clinical events during COVID-19 research curtailment

	Number of patients
Total with missed or late blood draws	217
Missed 1 collection	158
Missed ≥ 2 collections	59
Diagnosed with disease recurrence	6
Deaths	3

#5524

Persistent patient barriers to genomic testing in ambulatory oncology

Ellana K. Haakenstad[1], Jane Roberts[1], Anna C. Revette[1], Wendy Loeser[1], Joseph Grider[1], Andrea Kruse[1], Alissa Gentile[1], Rachel Freedman[1], Neal I. Lindeman[2], Olga Kozyreva[1], Pedro Sanz-Altamira[1], Christopher S. Lathan[1], Michael Hassett[1], Ethan Cerami[1], Annette S. Kim[2], Danielle K. Manning[2], Jonathan Nowak[2], Marios Giannakis[1], R. Coleman Lindsley[1], William C. Hahn[1], Barrett J. Rollins[1], Levi Garraway[3], Bruce E. Johnson[1], Nadine Jackson McCleary[1]. *[1]Dana-Farber Cancer Institute, Boston, MA,[2]Brigham and Women's Hospital, Boston, MA,[3]Roche and Genentech, San Fransisco, CA*

Purpose: Tumor genomic testing and cancer clinical trial enrollment provide key access to precision cancer therapeutics and supportive care options to enhance the patient experience. However, physician and patient barriers limit participation of patients who are historically underrepresented in genomic studies and clinical trials [historically underrepresented patients (HUP)], thereby decreasing generalizability for those most negatively affected by cancer diagnosis. We interviewed patients to identify factors impacting genomic testing uptake and clinical trial enrollment.

Methods: From 09/2021 - 12/2021 we interviewed 16 patients diagnosed with cancer seen at an ambulatory oncology center. Patients were HUP (Black, American Indian or Alaska Native, Native Hawaiian or other Pacific Islander,

Hispanic/Latinx, or older adult [70 years or older], or from a low-income zip code). From non-inclusive groups, patients identified as: 3 primarily spoke a language other than English, 9 Black, 3 other race, 6 Hispanic, and 3 aged 70 years or older. One-on-one interviews utilized a structured interview guide and lasted approximately 45 minutes. Participants were recruited until thematic saturation was reached then transcripts coded for major patterns and themes.
Results: Regarding tumor genomic testing, many patients were unsure if they received testing or if testing was recommended (citing possible confusion with medical terminology or overwhelm with information). Cited barriers included education (not understanding the benefit of participating, investigational drug/device identity, the procedures and processes involved), mistrust of research (specifically concerns over data privacy); and logistical accessibility (cost, time away from work, transportation). Those tested found it to be an easy process. Several cited that a patient advocate or social worker would be beneficial to navigate the process. Barriers around clinical trial enrollment included education (the risks of participating/side effects, size of the study, investigational drug/device identity), mistrust of research (data privacy, inclusion of HUP in trial, loss of autonomy in decision making), and logistical accessibility (time commitment). HUP who participated in a clinical trial appreciated the additional psychosocial support and clinical monitoring. Patients were emphatically interested in participating in genomic testing and cancer clinical trials when presented as the best course of care, though concerns about side effects from clinical trials persisted.
Conclusion: Patient barriers to tumor genomic testing and cancer clinical trials center around education, mistrust in research, and logistical accessibility. Patients who participated in genomic testing and clinical trials did have a positive experience. Barriers may be addressed with personalized education and coaching, including supportive resources referral.

#5525

Community cancer research advocates: Helping underrepresented minority groups become research ready

Sarah Been[1], Susan Gertz[2], Susan Hershberger[2], Melinda Butsch Kovacic[3], We Engage 4 Health Community-Academic Partnership. *[1]University of Cincinnati, Cincinnati, OH,[2]Miami University, Oxford, OH,[3]University of Cincinnati Cancer Center, University of Cincinnati, Cincinnati, OH*

Even though certain racial/ethnic minority groups get cancer more often, are diagnosed at younger ages, and are at risk for earlier death, clinical trials fail to include adequate proportions of representatives from these groups. Encouraging equitable participation in research becomes an important tool in the fight against cancer disparities. Therefore, we co-created with community representatives a graphic-style story entitled "Research Ready" that is used by trained Community Research Advocates (including some survivors or family of survivors themselves) to hold brief discussions to help eligible hesitant participants to learn the 3 P's: the purpose of cancer research, how they are kept safe while participating, and why people from diverse backgrounds are needed to participate. Importantly, advocates use a Research Review activity to discuss factors that influence their willingness to participate as well as identify questions they have for the research study's staff. Focus group and survey-based evaluation data show these discussions to be useful in increasing hesitant patients' willingness to consider participation in research and increase perception of safety. Advocates too appreciate the opportunity to serve. While this pilot is small, additional partnerships within the University of Cincinnati Cancer Center to expand the program will be developed. Future partnership with a community patient navigator program will also enable additional support and transportation to research appointments. Collectively, we anticipate that this program will ultimately support hesitant patients' decision-making and improve cancer research participation particularly among racial/ethnic minorities.

#5526

State-of-the-art biobanking of gastroesophageal adenocarcinoma samples: Integrating non-viable biospecimens with 3D and 2D cell models and their characterization, validation, and utilization of cell models for precision oncology

Mingyang Iris Kong, Sanjima Pal, Julie Berube, France Bourdeau, Betty Giannias, Nicholas Bertos, Veena Sangwan, Lorenzo Ferri. *McGill University Health Centre Research Institute, Montreal, QC, Canada*

Traditionally, biobanking platforms have collected and stored non-viable biological specimens such as serum, plasma, and fresh-frozen or formalin-fixed paraffin-embedded (FFPE) tissues. These constitute key resources for clinical and contemporary genomics, transcriptomics, and proteomics studies. However, such specimens cannot be used for studies involving drug testing,

high throughput target validation, and implementation for personalized medicine. Next-generation biobanking strategies rectify this issue by combining the collection of non-viable samples from patients with the propagation of viable tissue fractions as *in vitro* 2D and 3D cell models or *in vivo* xenograft models. Such cutting-edge biobanking strategies enable downstream cell-based high-throughput functional assays promoting the discovery of therapeutic targets or assessing treatment responses and resistance to treatment. Here, we provide comprehensive details of our establishment of a state-of-the-art biobanking platform for gastroesophageal adenocarcinoma (GEA) samples (n=389). Our approach opens new directions for understanding disease biology and conducting translational cancer studies. Patient-derived 2D cells (n=376), organoids (PDOs) (n=185), and xenografts (PDXs) (n= 99) included in our pipeline retain crucial features of the original human tumors, serving as valuable tools for clinical and experimental analyses in the context of precision oncology. We also discuss the entire approach of next-generation biobanking and emphasize the importance of integrating the propagation of PDOs and PDXs simultaneously. In addition, we explain each protocol optimized to propagate patient tissue-derived cell models. We validate that these models recapitulate tissue heterogeneity and are relevant preclinical models. Taken together, we described each approach used to develop one of the largest next-level biobanks for GEA.

#5527

Undergraduate cancer research scholars' community field experiences encourage community engagement to curb future disparities in the cancer workforce

Melinda Butsch Kovacic, Rachael D. Nolan, Melissa Loyd, Sharon Sauter, Karen Ramos, John R. Kues. *University of Cincinnati Cancer Center, University of Cincinnati, Cincinnati, OH*

Lack of access to cancer prevention, early screening, and treatment, particularly in low socioeconomic, underserved communities, are cited as substantial barriers to improving survivorship. Overcoming the complexity of this problem will require a larger, diverse, and dedicated workforce. Community engagement can lead to greater awareness of and both access and accrual to research. Encouraging trainees understanding of and participation in community engagement early on is one approach to curb cancer research related disparities. The current pipeline of cancer-focused healthcare

professionals and researchers that understand, appropriately engage, and connect with their target communities and patient populations is dangerously inadequate. To expand our future culturally competent, cancer-focused workforce, the University of Cincinnati Cancer Center has established the Cancer Research Scholars Program which is supported in part by a National Cancer Institute R25. The program offers to 20-23 undergraduate scholars each year, unique and inspiring paid research opportunities across the cancer continuum and educational experiences that included cancer topics, professional development, team science, and both cultural humility and microaggression training. Importantly, all scholars prepare for and participate in one of three community-engaged, cancer-focused summer field experiences offered with our community partners to encourage the supporting of and//or active participation in community-engaged research, education, and outreach in their future cancer careers. Twelve of the 23 summer 2022 Scholars were also invited to continue their research into the academic year either in-person or virtually. After year 1, Scholars and mentors completed surveys and on-camera interviews about the program highlighting the program's successes as well as areas for improvement. Nearly all Scholars appreciated the community engagement opportunities offered and understood their value to their potential careers. Annual tracking of these Scholars will determine the program's longer-term impact on the cancer workforce.

#5528

Palliative and end of life care utilization in Asian and White patients with stage IV lung cancer

Xiao Hu[1], John W. Melson[1], Stacey Pan[2], Yana Salei[2], Yu Cao[1]. *[1]Division of Hematology-Oncology, Department of Medicine, Tufts Medical Center, Boston, MA,[2]Department of Medicine, Tufts Medical Center, Boston, MA*

Background**:** Lung cancer (LC) is the leading cause of cancer death in Asian Americans, the fastest growing racial/ethnic group in the US. Early palliative care (PC) is recommended for patients with stage IV LC. Research on PC and end of life care (EOLC) for Asian patients (AP) with stage IV LC in the US is limited. This retrospective study examines racial influences on PC and EOLC in patients with stage IV LC at an urban academic medical center serving a large proportion of AP.

Methods: Patients newly diagnosed with stage IV LC from 01/01/2014 to 12/31/2019 were identified from Tufts Medical Center cancer registry.

Baseline demographics, disease characteristics, treatment history, PC and hospice use, and EOLC were compared between AP and White patients (WP) by Mann-Whitney U test and Chi-square/Fisher's exact tests for continuous and categorical variables, respectively. Time to palliative care (TTPC) in AP and WP was compared via log-rank test.
Results: Of 89 AP and 197 WP (similar median age: 71 and 68 years old, respectively), AP had significantly more male representation (71.9% vs 48.2%), never-smokers (36.0% vs 7.1%), non-small cell histology (85.4% vs 72.6%), linguistic diversity (non-English languages: 6 vs 2), and interpreter use (43.8% vs 0.5%), with less preference for English (12% vs 99%). No difference in brain metastasis at diagnosis was noted. PC use was similar in AP and WP (38.2% vs 37.6%); relatively more first encounters occurred inpatient vs outpatient in both groups. Median TTPC tended to be longer in AP (15.7 vs 12.4 months, p=0.120). PC evaluation occurred within 12 months after diagnosis in 27 (30.3%) AP and 63 (32.0%) WP. Of those seen by PC, only 7 (20.6%) AP and 16 (21.3%) WP had more than one PC encounter. Of 22 AP and 74 WP with confirmed death, relatively more AP patients died in hospital (68.2% vs 32.4%, p=0.004), more often in ICU (40.9% vs 24.3%); no differences were found in use of mechanical ventilation (18.2% vs 16.2%) or cardiopulmonary resuscitation (0% vs 1.4%) preceding death. Within 6 months of death, outpatient oncologists and AP patients had fewer code status (0% vs 24.3%, p=0.010) but similar rates of health care proxy (18.2% vs 32.4%, p=0.110) and hospice care (18.2% vs 28.4%, p=0.411) discussions. Hospice enrollment (29.2% vs 32.0%, p=0.722), median time from entering hospice to death (16.5 vs 12.5 days, p=0.795) and from last systemic treatment to death (39 vs 55.5 days, p=0.844) were similar in AP and WP.
Conclusion: PC utilization was similarly sub-optimal in AP and WP with newly diagnosed stage IV LC in this study, though TTPC tended to be longer in AP. While hospice utilization was also similar in AP and WP, AP had a higher rate of in-hospital death and fewer code status discussions with their outpatient oncologists in the 6 months preceding death. Whether these findings reflect racial disparities, cultural preferences, or other factors influencing PC and EOLC for AP with advanced LC warrants further study.

#5529

Lung cancer clinical trials in Latin America: A 20-year analysis

Thomas M. Knapp[1], Joseph Nygaard[1], Joshua Cassinat[1], Priya Gopalan[2].
[1]University of Central Florida, Orlando, FL,[2]Orlando VA Medical Center,

Orlando, FL

Background Several multinational cancer research collaborative organizations have been formed recently in Latin America in an effort to increase clinical research and the enrollment of patients in clinical trials, including the Latin American Cooperative Oncology Group (LACOG), established in 2012, and the Latin American Consortium for Lung Cancer Research (CLICaP), established in 2010. The aim of this study is to characterize changes in lung cancer clinical trial participation in Latin America before and after 2012.
Methods Clinical trials were identified in clinicaltrials.gov using the search terms "lung cancer," country filters for 21 Latin American countries, and study start dates 01/01/2001-12/31/2011 and 01/01/2012-12/31/2021. Clinical trials were categorized as either originating in Latin America (LA) or outside Latin America with participation of Latin American countries (non-LA). The number of trials, trial phase, driver mutation studied, and types of intervention were collected for each country. Descriptive statistics and chi-square analysis with 95% confidence intervals were calculated.
Result: Our analysis included 426 clinical trials involving Latin American countries, of which 74% (317/426) were phase 3 trials. Only 6% (26/426) of the trials from 2001-2021 were LA trials. Comparing the period 2001-2011 to 2012-2021, there was a marked increase in total clinical trials (101 v. 325, $p<0.001$), predominantly due to an increase in non-LA trials (87 v. 313, $p<0.001$). The number of LA trials was unchanged between the two periods (14 v. 12, $p=0.69$). There was an increase in the percentage of phase 3 trials (60% v. 79%, $p<0.001$) between the two periods. There was also an 83% increase in studies for patients with specific driver mutations (EGFR, KRAS, ALK, and RET) (53 v. 97, $p<0.001$). The countries with the highest rates of open clinical trials were Brazil, Mexico, and Argentina. In all three countries, the total number of clinical trials increased between the period 2001-2011 and 2012-2021: Mexico (40 v. 88, $p<0.001$, 120% increase), Brazil (61 v. 108, $p=0.003$, 77% increase), and Argentina (50 v. 78, $p=0.013$, 56% increase).
Conclusion Overall, there was a significant (>3-fold) increase in clinical trial participation by Latin American countries, specifically in non-LA trials, from 2012-2021. This increase may correspond to the organization of CLICaP and LACOG, which are multinational cancer research organizations in Latin America. However, there were few LA trials. More LA studies are therefore needed to confidently extrapolate the results of global clinical trials to patients in Latin America.

#5530

A community led approach to addressing disparities in pancreatic cancer care for Native Americans in Oregon

Claymore Kills First, Grace A. McCarthy, Charles D. Lopez, Brett C. Sheppard, Jackilen Shannon, Jonathan R. Brody. *OHSU, Portland, OR*

Pancreatic adenocarcinoma (PDAC) is the third leading cause of cancer-related deaths in the United States (US). Due to unique barriers facing Native Americans (NA) patients, this underrepresented population has worse outcomes and increased mortality. In Oregon, NAs have nearly double the PDAC incidence rate compared to the general US population. Oregon Health & Science University (OHSU) is a leader in PDAC care and research, yet NAs remain underrepresented in pancreatic cancer research at OHSU, and across the country. This highlights the need for a focused and comprehensive research program that collaborates with local tribal communities to identify specific issues and barriers that can be addressed to improve patient care in the NA population. We hypothesize that if we establish a workflow that strengthens existing relationships with tribal communities and leverages established OHSU infrastructure and expertise, we can directly address the unmet need of understanding, preventing and treating PDAC for NA individuals in our local communities. This includes increasing enrollment of NAs in PDAC clinical trials and developing a genetic registry that could help both depict genetic underpinnings that predispose NA individuals to PDAC and potentially guide therapeutic approaches. To build trust within NA communities, we initiated collaborations with Oregon tribes to develop culturally appropriate programs guided by NA community members. Through OHSU's Northwest Native American Center of Excellence, we developed a close relationship with the Confederated Tribes of Warm Springs. Together with our institution's Community Outreach, Research, and Engagement (CORE) team, we are working with the Confederated Tribes of Warm Springs to better understand provider and NA community member attitudes towards and barriers to clinical trial participation. We will incorporate these perceptions into a tribe-specific program that describes the multi-faceted facilitators and barriers that inform decision-making. Moreover, we are implementing a patient navigator program to help NA patients overcome clinical trial barriers by providing culturally appropriate patient education, reimbursement for travel-associated expenses, local administration of

chemotherapy, and telehealth capabilities. Future work includes co-implementing strategies for tribes to review incoming research requests with the goal of implementing a system to promote awareness and enrollment of NAs in PDAC clinical research. This system will be then be utilized to establish the first NA PDAC tissue registry to identifying gene-environment interactions and unique genetic alterations that may predispose NA individuals to PDAC. Overall, this collaborative work will create a roadmap for engagement and a conscientious process to provide awareness and the best in class treatment for NA individuals with PDAC.

#5531

Early detection of cancer disparity and treatment resistance in TNBC

Amy H. Tang[1], Richard A. Hoefer[2], Dasom Lee[3], Emily L. Breeding[4], Mary L. Guye[5], Janet S. Winston[6], Billur Samli[6], Jennifer Koblinski[7], Valentina Robila[8], Michael O. Idowu[9], Rick J. Jansen[10], Harry D. Bear[11]. *[1]Microbiology and Molecular Cell Biology, Leroy T. Canoles Jr. Cancer Center, Eastern Virginia Medical School, Norfolk, VA,[2]Sentara Cancer Network, and George Mason University, Sentara Healthcare Systems, Norfolk, VA,[3]Department of Medicine, Division of Oncology, Stanford University School of Medicine, Stanford,, CA,[4]VUMC Department of General Surgery, Vanderbilt University Medical Center, Nashville, TN,[5]Sentara Surgery Specialists - Surgical Oncology, Sentara CarePlex Hospital, and Sentara Cancer Network, Newport News, VA,[6]Sentara Pathology, and Pathology Sciences Medical Group, Sentara Norfolk General Hospital, Norfolk, VA,[7]Massey Cancer Center, Virginia Commonwealth University, Richmond, VA,[8]Department of Pathology, Division of Anatomic Pathology, Virginia Commonwealth University, Richmond, VA,[9]Department of Pathology, Division of Anatomic Pathology, Virginia Commonwealth University (VCU) Medical Center, Richmond, VA,[10]Department of Public Health, Genomics, Phenomics, and Bioinformatics Program, North Dakota State University, Fargo, ND,[11]Departments of Surgery and Microbiology & Immunology, Division of Surgical Oncology, Virginia Commonwealth University, Richmond, VA*

Triple-negative breast cancer (TNBC) is the most aggressive breast cancer subtype and disproportionately affects BRCA1 mutation carriers and young black women. Black/African American (AA) patients with TNBC have the highest mortality rate and the shortest survival of any racial/ethnic group in

the United States. TNBC challenges our ability to personalize effective therapy. Neoadjuvant chemotherapy (NACT) is the standard-of-care (SOC) to treat T2 or LN+ TNBC. The addition of immune checkpoint blockade (ICB) has revolutionized treatment for these high-risk patients. Pembrolizumab plus chemotherapy is the new SOC for neoadjuvant systemic therapy (NST) in TNBC. Pathologic complete response (pCR) is a reliable indicator that correlates with improved long-term survival. However, clinical uncertainties remain in those who have an incomplete pathologic response (pIR) since many similarly treated TNBC patients with identical stage and comparable residual cancer burden (RCB) demonstrate disparate clinical outcomes. Current methods fall short in predicting tumor recurrence and treatment resistance in the clinic.

Supported by ample evidence in developmental, evolutionary, and cancer biology, we proposed that EGFR-K-RAS-SIAH pathway activation is a major driving force in TNBC and that its most downstream gatekeeper, SIAH, is a tumor-specific, therapy-responsive, and prognostic biomarker for patient risk stratification in TNBC. The persistent high expression of SIAH in residual tumors after neoadjuvant therapy reflects EGFR/K-RAS pathway activation (ON) and resistance to treatment. The loss of expression of SIAH in residual tumors reflects EGFR/K-RAS pathway inactivation (OFF) and response to treatment (i.e. treatment efficacy). Here we propose to establish the power of SIAH as a prognostic biomarker to differentiate high-risk from low-risk tumors and predict “real-time” therapy response, in both pre- and post-neoadjuvant (NACT/NST) setting.

Breast cancer mortality rates in Hampton Roads Virginia and Richmond Virginia are among the worst in the U.S. and demonstrate a major cancer health disparity. Black patients in our region have a 60-70% higher mortality rate than white patients according to CDC/SEER databases. Using a large cohort of 525 racially diverse TNBC patients (246 black and 279 white patients) at Sentara Cancer Network, we conducted Kaplan-Meier survival analyses and detected a major racial disparity, with significantly lower survival among the Black/AA TNBC cohort, compared to national databases. We will expand this TNBC disparity study by using 2 large racially-diverse cohorts of 981 TNBC patients (459 Black and 493 white patients) from the Sentara Cancer Network and VCU Massey Cancer Center to analyze the prognosis of SIAH expression. By focusing on this tumor-driving EGFR-K-RAS-SIAH pathway, we aim to delineate the underlying molecular basis of treatment resistance and racial disparity in high-risk TNBC.

#5532

Increasing racial and ethnic diversity of phase 1 solid tumor clinical trials through enrollment at a safety net hospital

Varun Roy[1], Esther Lee[2], Ming Li[1], Xiomara Menendez[1], Elena Nieves[1], Rebecca Umayam[1], Nicole Jensen[1], Lorraine Martinez[1], Diana Hanna[1], Jorge Nieva[1], Anthony El-Khoueiry[1], Jacob Thomas[1]. *[1]USC Norris Comprehensive Cancer Center, Los Angeles, CA,[2]Georgetown University School of Medicine, Washington DC, DC*

Background: Racial minorities are under-represented in oncology clinical trials. African Americans and Hispanic/Latinos account for 13% and 18% of the US population, respectively, but in 2018 these groups combined were only 8% of oncology trial subjects. Disproportionate enrollment can limit how generalizable trial outcomes may be and can perpetuate healthcare disparities. The majority of clinical trial enrollment occurs at large academic cancer centers that may not reflect the diverse general cancer patient population in the US. Los Angeles County/University of Southern California Medical Center (LAC+USC) is a large safety net hospital that serves a racially and ethnically diverse patient population.

Methods: We developed a database of all adult patients (pts) enrolled in phase I solid tumor trials at LAC+USC from 2015 - 2022. The data collected includes baseline demographics (age, gender, race, ethnicity, primary language, tumor histology), type of therapeutic intervention, radiologic response per RECIST 1.1, duration of treatment, and survival. Progression-free survival was defined as time from enrollment in the study until progression, discontinuation of treatment, or death. Disease control rate (DCR) was defined as pts with best response of CR, PR, or SD.

Results: 120 pts with solid tumors were enrolled in phase 1 trials at LAC+USC from 2015-2022. Median age was 58 (range 26-78); 58% female; ECOG 0-1 (99%), 2 (1%). 73 patients (61%) were Hispanic, 27 (23%) Asian/Pacific Islander, 9 (8%) non-Hispanic (NH) White, 5 (4%) were NH Black, and 6 (5%) were unknown. 70% of pts had a primary language other than English: 56% Spanish. The most common tumor types were colorectal (16%), hepatocellular (13%), non-small cell lung (12%), head and neck (11%), and ovarian (11%). Trial interventions included chemotherapy (19%), immunotherapy (35%), targeted therapy (54%), and 10% required biomarker selection. The disease control rate (DCR) was 58/120 (48%): 2 pts had CR, 9

pts had PR, and 47 pts had SD. 4-month progression-free survival (PFS) was 42/120 (35%), and 6-month PFS was 27/120 (23%). 90-day survival was confirmed in 101/120 (84%) of patients.
Discussion: A racially diverse population can be successfully enrolled in early phase oncology trials at a safety net hospital. Patient populations that are underrepresented nationally in clinical trials had robust enrollment and comprised the majority of participation (88%) in this setting. Almost half of patients derived clinical benefit (48% DCR) from trial participation. Creating an infrastructure to enroll patients to phase 1 clinical trials at a safety net hospital may be a successful strategy to improve racial and ethnic diversity.

#5533

Providing culturally responsible health care to Pacific Islander communities: The creation of a cultural competency training for healthcare professionals

Mark Lee Willingham Jr.[1], Kevin Cassel[2], Angela Sy[3], Munirih Taafaki[4], Tressa P. Diaz[5], Angelina G. Mummert[6]. *[1]Population Sciences in the Pacific - Cancer Prevention, University of Hawai'i Cancer Center, Honolulu, HI,[2]Population Sciences in the Pacific Program, University of Hawai'i Cancer Center, Honolulu, HI,[3]Department of Tropical Medicine, Medical Microbiology & Pharmacology, John A. Burns School of Medicine, Honolulu, HI,[4]Department of Quantitative Health Sciences, John A. Burns School of Medicine, Honolulu, HI,[5]School of Health, University of Guam, Mangilao, Guam,[6]Office of Research & Sponsored Programs, University of Guam, Mangilao, Guam*

Cultural competency is the ability to respectfully engage, understand, and communicate through conscientious interaction, enabling effective work and meaningful relationships in cross-cultural situations. Cultural competency recognizes the importance for organizations of participants' diverse social and cultural values, beliefs, and behaviors, and has gained attention because it can bridge health perspectives, understanding, and respect between health professionals and patients. There remains a need for cultural competency in healthcare as disparities persist across the U.S. in racial and ethnic minority groups who experience worse health outcomes and lower healthcare quality than the general public. Therefore, a cultural competency training curriculum was created using various resources to improve interactions between Pacific Islander patients and healthcare professionals. This training helps to reduce

racial/ethnic disparities in healthcare by encouraging mutual understanding and improving patient satisfaction, adherence to medical instructions, and overall health outcomes by highlighting patient-centered care as a result of utilizing components of cultural competency. To improve patient experiences in Hawai'i, healthcare professionals need the tools to better interact with patients from different cultures, such as Pacific Islanders. This training provides healthcare professionals with culturally-based content for improving cultural competence techniques for interacting with Pacific Island patients. This training was pilot tested with key stakeholders from community organizations and Cancer Center faculty/staff. Local health clinics, providers, and practices will have the opportunity to participate in this training through a Zoom-based electronic training format and be provided with three continuing medical education credits. The initial delivery of the training was intended for in-person sessions; however, a virtual format was adapted due to the COVID-19 pandemic and subsequent social distancing regulations. Healthcare providers are provided pre-training resources, a pre- and post-test, and a course evaluation to determine the validity of training objectives. To date, two Federally Qualified Health Centers have been provided the training , n=60, as well as one Cancer Health Equity Partnerships' Scientific Workshop, n=40. For attendees, the analysis of correct responses from the pretest to post-test showed a significant improvement on 6 of the 12 questions. Respondents also agreed that the training resources aligned with the course objectives. Improved patient interactions from this training can help support better patient outcomes, adherence to medical advice regarding cancer screenings, and many other aspects of improving health equity for Pacific Islanders.

#5534

"Simply ask and explain": perspectives from Black patients with lung cancer on strategies to address racial disparities in biospecimen research participation

Jeenn A. Barreiro-Rosa[1], Oluwatumilara Akeke[1], Annabella Opoku[2], Alison Hilton[3], Jessica Carda-Auten[3], Randall Teal[3], Aaron Carpenter[1], Hayley N. Morris[3], Lauren Matthews[3], Ashley Rankin Collins[3], Marjory Charlot[3]. *[1]UNC School of Global Public Health, Chapel Hill, NC,[2]University of Alabama, Tuscaloosa, AL,[3]UNC Lineberger Comprehensive Cancer Center, Chapel Hill, NC*

Background: Participation of racially diverse populations in research is necessary to advance cancer care. However, representation of Black individuals in biospecimen cancer research remains low and requires being asked to engage in research. We sought to understand the experiences, beliefs, and knowledge about biospecimen research among Black patients with lung cancer.
Methods: Semi-structured interviews with a purposive sample of 15 Black patients diagnosed with lung cancer were conducted between January and August 2022 at a large academic center in North Carolina. Interviews were digitally recorded and transcribed and analyzed using thematic analysis.
Results: Themes related to who should initiate discussions about biospecimen donation, what should be considered before donation, and communication strategies to increase participation of Black patients with cancer in biospecimen research emerged from the interviews. Most participants indicated that discussions about biospecimen donation should be initiated by trusted and knowledgeable members of the medical team and most expressed trusting their providers. Some also expressed the importance of including family members in discussions about medical and research decisions. Some participants felt it was important to consider if donating specimens would cause pain or would require additional procedures. Recommended communication strategies to facilitate participation included use of simple and easily understood language in addition to messaging related to how biospecimen donation would benefit others. Participants also felt cultural humility, respect, and empathy during research recruitment would help enhance enrollment of Black participants in biospecimen research. Of note, all participants reported never being asked to participate in biospecimen research and felt that underrepresentation of Black participants may be due to not being asked.
Conclusion: Black participants in this study have not been asked to participate in biospecimen research but are willing to be engaged in conversations about research from their medical team. Simply being asked, trusting their medical provider, cultural humility, and framing the message on how the research will benefit others are some of the recommended strategies to enhance research participation among Black patients. Future research should incorporate these strategies into an intervention to assess the impact on recruiting Black individuals in biomedical research.
Sponsored by the Lung Cancer Research Foundation Research Grant on Disparities in Lung Cancer

#5535

Research team perspectives on engaging Black patients with cancer in biospecimen research

Aaron Carpenter[1], Hayley N. Morris[2], Annabella Opoku[3], Alison Hilton[2], Jessica Carda-Auten[2], Randall Teal[2], Jeenn A. Barreiro-Rosado[4], Lauren Matthews[2], Oluwatumilara Akeke[2], Ashley Rankin Collins[2], Marjory Charlot[2]. *[1]UNC Gillings School of Global Public Health, Chapel Hill, NC,[2]UNC Lineberger Comprehensive Cancer Center, Chapel Hill, NC,[3]University of Alabama, Tuscaloosa, AL,[4]UNC School of Global Public Health, Chapel Hill, NC*

Background**:** Representation of Black individuals with cancer in biospecimen research remains disproportionately low compared to white counterparts. Clinicians and research staff are responsible for informing, inviting, and consenting patients to participate in such research. We sought to understand clinician and research staff perspectives on engaging Black patients in biospecimen research.

Methods: We conducted 10 in-depth interviews with purposively sampled clinicians and research staff at a large academic cancer center in North Carolina between January and August 2022. Participants underwent semi-structured interviews (duration 45-60 minutes) and were asked open ended questions about biospecimen research barriers in general, barriers specific to people who identify as Black or African American, and considerations when discussing biospecimen research with Black patients. Interview transcripts were analyzed using thematic analysis.

Results: Perceived patient related barriers to biospecimen donation included pain from sample collection, invasive sample collection, lack of to time or transportation, medical research mistrust, health literacy, and limited knowledge of opportunities for involvement. Many felt that these barriers were faced by both Black and non-Black patients. However, some felt for Black patients, these barriers existed within the context of historical injustices in medicine, current bias in health care and socioeconomic inequities, while others felt socioeconomic status not race was more of a concern. Clinician and research staff identified barriers to discussing biospecimen research included lack of time given busy clinical practice and concern with patients' physical and emotional state. Patients' race was not considered a barrier. When asked about considerations for discussing biospecimen research specifically with

Black patients, participants felt time to establish rapport and trust, readiness to discuss historical injustices in biomedical research, reminding participants research is voluntary, and having in person discussions were important. Few felt that patient race was not relevant to these discussions.
Conclusion: Some clinicians and research staff acknowledge that historical injustices and current racial bias in biomedical research and health care contribute to low representation of Black individuals in biospecimen research, while others did not. Further research is needed to assess whether race and/or racism agnostic approaches versus acknowledgement of structural racism's influence on biomedical research and health care have an impact on fair representation of Black individuals in biospecimen research.
Sponsored by the Lung Cancer Research Foundation Research Grant on Disparities in Lung Cancer

#5536

Landscape and analysis of ERBB2 amplification and short variant mutations in large-scale Chinese patients with colorectal cancer

Zhiqin Chen[1], Shijun Yu[1], Yin Wu[1], Bei Zhang[2], Ding Zhang[2], Yong Gao[1], Ming Quan[1]. *[1]Department of Oncology, Shanghai East Hospital, School of Medicine, Tongji University, Shanghai, China,[2]The Medical Department, 3D Medicines Inc, Shanghai, China*

Background**:** Human epidermal growth factor receptor 2 (ERBB2) amplification is a rapidly emerging therapeutic target in CRC, in spite of a relatively low incidence. While ERBB2 amplification has been considered as a critical biomarker to predict the efficacy and safety of anti-ERBB2 therapy of CRC, its point mutation status is largely ambiguous.**Methods:** Blood or tissues samples from 2454 Chinese patients with CRC were collected, and the genomic landscape, clinical characteristics and genetic features of ERBB2 in these samples were retrospectively investigated using next-generation sequencing (NGS) analysis. **Results:** Of the 2454 colorectal cancer patients, 3.46% (85) carried ERBB2 amplification, 2.24% (55) carried ERBB2 mutation, and some patients harbored both ERBB2 amplification and point mutation at the same time. Microsatellite instability high (MSI-H) was found in approximately 32.7% (18/55) of patients with ERBB2-mutated CRC, but almost negative in ERBB2-amplified CRC. The median fold change of ERBB2 amplification was 30 (Range 4 to 245). Among the 16 mutation sites detected from 55 patients with ERBB2 point mutations, p.R678Q was the

most common mutation site (28%), followed by p.V842I (24%) and p.S310F/Y (12%), which appeared to be slightly different from previous reports. ERBB2
mutation was more frequently found in CRC patients aged < 50 years. 50.9% of CRC patients with wild-type ERBB2 carried KRAS mutation, which was significantly higher than those with mutated ERBB2 (25.6%). A higher incidence of BRAF mutation was observed in patients with mutated-ERBB2 (8.5% vs. 2.3%). In addition, CRC patients with ERBB2 CNV showed a higher prevalence of TP53 mutation comparing with those with ERBB2 SNV (92.3% vs. 58.3%), while KRAS mutation exhibited a contrary trend (14.1% vs. 45.8%)**Conclusions:** The overall variation rate of ERBB2 is 5.4% in Chinese patients with CRC, which is accompanied by significantly different molecular pathological characteristics compared to patients with wild-type ERBB2, and different mutation types (CNV or SNV) display different molecular pathological characteristics.

#5537

Prognostic impact of sarcopenia in patients with metastatic castration sensitive prostate cancer

Hiroaki Iwamoto, Kouji Izumi, Atsushi Mizokami. *Department of Integrative Cancer Therapy and Urology, Kanazawa University Graduate School of Medical Science, Kanazawa, Japan*

Background/Aim: Recently, sarcopenia has been reported to be a useful prognostic factor in cancer patients, including prostate cancer patients. Gleason score, the presence or absence of visceral metastases, and the number of bone metastases, which were used in the LATITUDE and CHAARTED trials, are known prognostic factors for metastatic castration-sensitive prostate cancer (mCSPC). Although a large proportion of patients with mCSPC are elderly, the significance of sarcopenia in metastatic castration-sensitive prostate cancer is unknown.
Patients and Methods: Of 193 patients with mCSPC treated at Kanazawa University Hospital between 2000 and 2019, 150 patients with confirmed CT at diagnosis were included. Sarcopenia was determined based on the definition of Martin et al. Overall survival and prognostic factors were retrospectively evaluated.
Results: The median age was 72 years, median PSA 241 ng/mL, Gleason score (GS) ≥ 9 in 91 patients, visceral metastases in 23 patients, and

sarcopenia in 106 patients. 109 patients (72.7%) were diagnosed as high risk by Latitude risk classification and 105 patients (70%) were diagnosed as high volume by Charted risk classification. All cause death was 64 patients, and the median follow-up period was 38.2 months. The median overall survival was 69.6 months. On multivariate analysis, GS ≥9 (P <0.0001, hazard risk =3.78), LDH ≥ 300 U/L (P <0.0001, hazard risk =2.88), and sarcopenia (P=0.04, hazard risk=2.07) were significant independent poor prognostic factors predicting shorter OS. The prognosis could be significantly stratified into a high risk group if two or more of these three factors were met and a low risk group if one or less was met (44 months vs. 106.4 months, P=0.0001, hazard risk=2.91). This classification more clearly stratified prognosis than the LATITUD classification (55.1 months vs. 135 months, P =0.027, hazard risk =1.8) or the CHAARTED trial classification (52.9 months vs. 135 months, P =0.009, hazard risk =1.98).
Conclusion: Sarcopenia that can assess general status was considered useful in the prognostic evaluation of patients with mCSPC.

#5538

Prevalence of factors serving as common cancer clinical trial eligibility criteria by race and ethnicity

Yayi Zhao[1], Rossybelle P. Amorrortu[1], Rachel Howard[2], Kedar S. Kirtane[3], Susan T. Vadaparampil[4], Dana E. Rollison[1]. *[1]Department of Cancer Epidemiology, Moffitt Cancer Center, Tampa, FL,[2]Department of Health Informatics, Moffitt Cancer Center, Tampa, FL,[3]Department of Head and Neck-Endocrine Oncology, Moffitt Cancer Center, Tampa, FL,[4]Office of Community Outreach, Engagement, and Equity; Department of Health Outcomes & Behavior, Moffitt Cancer Center, Tampa, FL*

Background: Racial/ethnic minority patients remain underrepresented in clinical trials potentially due to restrictive trial eligibility criteria that disproportionally affect minority cancer patients.
Objective: To examine the prevalence of existing medical conditions and abnormal lab values that commonly serve as clinical trial eligibility criteria among cancer patients by race and ethnicity.
Methods: A cross-sectional analysis was conducted among patients new to Moffitt Cancer Center in 2011-2021 with multiple myeloma (n=3,967), breast (n=14,348), lung (n=10,492), and prostate (n=7,823) cancers. Demographics, existing medical conditions, and lab values were obtained from the Electronic

Health Record, whereas history of cancer and metastatic disease at diagnosis were obtained from the Cancer Registry. Prevalence of medical conditions and abnormal lab values were reported among all patients and compared by race groups (White, Black, Hispanic, and other races) using age-adjusted logistic regression. For factors with prevalence higher than 5%, stratified analysis was conducted with respect to cancer type and adjusted for multiple comparisons.
Results: Compared to White patients, Black (B) and Hispanic (H) patients were found to have higher prevalence of diabetes (OR [odds ratio] = 2.26 [B]/1.40 [H]), organ transplantation (OR=1.58 [B]/1.77 [H]), hepatitis (OR=1.74 [B]/1.48 [H]), HIV (OR=4.25 [B]/1.92 [H]), and abnormal creatinine value (OR=1.77 [B]/1.23 [H]). In addition, Black patients were more likely to have hypertension (OR=1.41) while patients of other races were more likely to be diabetic (OR=1.36). Similar patterns were observed across cancer types.
Conclusion: Restrictive cancer clinical trial eligibility criteria may post a structural barrier that disproportionately impact racial/ethnic minority patients. Investigators should consider leveraging real-world data to define and design appropriate trial eligibility criteria.

Prevalence of factors commonly included as clinical trial eligibility by race/ethnicity.

Factors	**All**	**White**	**Black**		**Hispanic**		**Other**	
	Prevalence (%)	**%**	**%**	**OR (95% CI)**	**%**	**OR (95% CI)**	**%**	**OR (95% CI)**
Diabetes	6.30	5.90	10.00	2.26 (1.97-2.58)	6.50	1.40 (1.20-1.63)	6.50	1.36 (1.07-1.70)
Chronic obstructive pulmonary disease	10.30	11.40	6.20	0.61 (0.52-0.72)	6.10	0.61 (0.52-0.71)	5.90	0.57 (0.44-0.72)
Hypertension	18.00	18.50	19.80	1.41 (1.27-1.55)	13.40	0.87 (0.78-0.97)	13.50	0.84 (0.71-1.00)
Heart condition	3.00	3.10	2.60	1.10 (0.86-1.39)	2.00	0.80 (0.61-1.03)	1.80	0.70 (0.44-1.05)

Organ transplant	0.90	0.90	1.40	1.58 (1.11-2.20)	1.50	1.77 (1.28-2.41)	0.40	0.46 (0.16-1.00)
Autoimmune disease	2.50	2.60	2.10	0.84 (0.63-1.09)	1.90	0.78 (0.59-1.01)	2.20	0.90 (0.60-1.30)
Hepatitis	0.70	0.70	1.20	1.74 (1.17-2.49)	1.00	1.48 (0.99-2.15)	0.40	0.60 (0.21-1.30)
HIV infection	0.30	0.20	0.90	4.25 (2.62-6.74)	0.40	1.92 (1.01-3.40)	0.20	0.71 (0.12-2.30)
History of any cancer	15.90	17.20	10.30	0.69 (0.60-0.78)	10.30	0.69 (0.61-0.77)	10.90	0.71 (0.59-0.85)
Metastasis at diagnosis	21.20	21.40	22.60	1.13 (1.02-1.24)	19.80	0.96 (0.87-1.05)	18.60	0.88 (0.75-1.02)
Abnormal neutrophil count	19.70	20.10	20.20	1.00 (0.86-1.16)	16.60	0.79 (0.67-0.93)	18.20	0.89 (0.69-1.13)
Abnormal creatinine	14.00	13.50	19.30	1.77 (1.57-1.99)	14.10	1.23 (1.08-1.39)	13.40	1.13 (0.93-1.38)
Abnormal glomerular filtration rate	14.00	13.50	22.40	2.32 (1.99-2.70)	11.20	1.07 (0.88-1.30)	10.10	0.91 (0.66-1.22)
Abnormal bilirubin	2.40	2.50	2.40	1.02 (0.69-1.45)	2.40	1.03 (0.70-1.46)	2.40	0.99 (0.52-1.69)
Abnormal aspartate aminotransferase	9.40	9.40	9.20	0.88 (0.72-1.07)	9.70	0.92 (0.76-1.12)	8.50	0.82 (0.59-1.12)

Assessing knowledge, vaccine hesitancy, and completion rates of free HPV vaccination in uninsured/underinsured low-income patients

Hiram Diaz[1], Gerardo Colon-Otero[2], Laura M. Pacheco-Spann[3], Christopher C. DeStephano[4], Sandra Casanova-Leyva[5]. *[1]University of Puerto Rico, San Juan, PR,[2]Department of Hematology/Oncology, Mayo Clinic, Jacksonville, FL,[3]Quantitative Health Sciences, Mayo Clinic, Jacksonville, FL,[4]Department of Medical and Surgical Gynecology, Mayo Clinic, Jacksonville, FL,[5]Mayo Clinic, Jacksonville, FL*

Background: Human Papillomavirus (HPV) vaccination rates remain low in the U.S., particularly among minorities and low-income patients. In 2014, a Mayo Clinic study of uninsured, low-income, working, Volunteer in Medicine (VIM) Clinic patients in Jacksonville, Florida found a statistically significant lower awareness of HPV (50.3% vs 63.6%) and the HPV vaccine (32.1% vs 62.7%) than the national population. As a result, our team collaborated with Merck to develop a free HPV vaccination program and video education campaign for VIM patients.

Methods: We assessed VIM patients HPV vaccination knowledge, awareness, and prevalence of hesitancy towards receiving the vaccine. VIM patients (ages 18-45) with no previous history of HPV vaccination were invited to participate in this study. The Parents Attitudes about Childhood Vaccines (PACV) survey was used to evaluate vaccine hesitancy. Patients who declined the HPV vaccine were shown an educational video to assess effectiveness in persuading patients' opinion. Each participant received a vaccine hesitancy PACV score, which was compared with their vaccine disposition. Mayo Clinic IRB approval of the study was obtained.

Results: Our analysis included 43 patients (34 females, 9 males) with a median age of 40 (age range 27- 45). Patients had overall knowledge of HPV of 88.4%, with 69.8% having heard of the HPV vaccine. 85.7% PACV survey respondents were deemed non-hesitant (PACV scores 0-49), and 80.6% of the non-hesitant subset (29/36) agreed to undergo vaccination. The average PACV score of vaccine-interested participants was lower (25.2) than the average of participants not interested in the vaccine (36.7). Black participants had a statistically significant higher PACV score than White participants. The PACV scores of individuals who were already familiar with the HPV vaccine were significantly lower than those of participants who were unfamiliar with the HPV vaccine. Only 20% (2/10) of individuals, who had previously declined vaccination, agreed to receive the HPV vaccine after viewing the HPV

educational video. Of the 33 participants who agreed to receive the free HPV vaccine, only 9 (27.3%) completed all three doses.
Conclusions: HPV vaccine awareness and knowledge at VIM increased compared to the 2014 cohort. Vaccine hesitancy was not observed in most patients, yet video education was effective in only a small portion of patients with vaccine hesitancy. Additionally, a minority of patients who agreed to receive the free HPV vaccine series completed all three doses. Our results suggests that free HPV vaccination and video education is not sufficient to achieve adequate vaccination rates among low-income uninsured young adults, nor overcoming vaccine hesitancy. Innovative measures are warranted to improve vaccination rates in this population.

#5540

Spouse caregivers of patients with glioblastoma report unmet needs throughout the disease trajectory

Diana L. Coman[1], Megan Chard[1], Lisa Desautels[2], Barbara J. Lutz[1], Laurie Minns[1]. *[1]University of North Carolina, Wilmington, NC,[2]The Glioblastoma Support Network, Overton, NV*

Glioblastoma (GBM) is a devastating and terminal cancer that results in memory loss, cognitive declines, personality changes, neuropsychiatric symptoms, and physical impairments that greatly affect quality of life of both the patient with GBM and their primary caregiver, who is often a spouse or partner. These caregivers describe feeling unsupported and unprepared to assume the responsibilities associated with addressing the progressive physical, emotional, and psychological support needs of their loved ones with GBM. In this qualitative study, female spouse primary caregivers were recruited through a private Facebook support group to write letters describing their experiences in caring for their loved ones with GBM. Using a reflexive thematic analysis, 101 letters from caregivers were analyzed for unmet needs, challenges, and opportunities for better care and support. Caregivers expressed feeling unsupported and poorly prepared, and described different levels and types of needs and challenges throughout the GBM disease trajectory. The 4 phases of the trajectory included the acute phase (first 2-4 months post diagnosis), living with disease progression, end of life stage, and the bereavement stage. Challenges included difficulties adapting to sudden life changes, the need for more education on what to expect, feelings of sudden loss, relationship strain, and not having enough knowledge about GBM.

Associated emotional responses included feelings of fear, lack of control, agony, disappointment, and exhaustion. These challenges and emotional impact were greatest during the acute and living with disease progression phases. Caregivers also described relying heavily on friends, community supports (such as faith groups), peer-support through the Facebook group during this living with disease progression phase, but still experienced high levels of relationship strain and other unmet needs. These findings on the primary caregivers' experiences provide opportunities to guide more timely and tailored interventions to provide support and improve care for patient/caregiver dyads to help mitigate the burden of this progressive disease and improve quality of life for caregivers.

Diagnostic and Prognostic Biomarkers 4

#5544
Association of circulating markers of gut barrier damage and inflammation with colorectal neoplasia stage

Flavia Genua[1], Petr Holý[2], Pavel Souček[3], Václav Liška[4], David J. Hughes[1].
[1]Cancer Biology and Therapeutics Laboratory, Conway Institute, School of Biomedical and Biomolecular Sciences, University College Dublin, Dublin, Ireland,[2]Faculty of Medicine in Pilsen and Third Faculty of Medicine Charles University, Prague, Czech Republic,[3]Laboratory of Pharmacogenomics, Biomedical Center, Faculty of Medicine in Pilsen, Charles University, Pilsen, Czech Republic,[4]Department of Surgery, Biomedical Center, Faculty of Medicine in Pilsen, Charles University and University Hospital Pilsen, Pilsen, Czech Republic

A disturbance in the microbiome facilitated by gut barrier dysfunction and inflammation can influence the progression of colorectal neoplasia. One of the most studied indicators of gut barrier status is lipopolysaccharide (LPS). Increased permeability of the gut barrier leads to extensive translocation of microbes into the lamina propria, which is associated with higher circulating levels of LPS. Additionally, increased serum concentrations of inflammatory cytokines including IFNy, IL6, IL10, and TNFα have been associated with impaired gut integrity and its progressive dysfunction.
We investigated the role of gut barrier permeability and inflammation in colorectal cancer (CRC) development by assessing markers of intestinal barrier dysfunction and inflammation in two different patient cohorts; Irish

(discovery) and Czech (validation). ELISA assays were used to assess circulating concentrations of lipopolysaccharide binding protein (LBP) and C-reactive protein (CRP) in serum from patients with CRC (n=30), colorectal adenoma (n=40), and negative after colonoscopy/blood donor controls (n=35). Circulating levels of inflammatory cytokines and calprotectin were assessed using an MSD MultiSPOT platform and an MSD R-plex assay (Mesocale Discovery, Rockville, Md, United States), respectively. Differences between pathology groups were assessed using the Kruskal Wallis or Mann-Whitney U test. Receiver operating curve (ROC) analysis was implemented to identify single and combinations of biomarkers capable of discriminating between CRC patients and controls with maximum sensitivity (SE) and specificity (SP) (RStudio, PBC, Boston, MA URL http://www.rstudio.com/).
In the discovery cohort, levels of LBP, TNFα, IL6, calprotectin and CRP were significantly higher in CRC patients than in controls after false discovery rate correction (p=0.02, p=0.03, p=0.006, p=0.01, p=0.006, respectively). The area under the ROC curve (AUC) was 0.76 (95% CI: 0.64-0.87, p = 0.003) for LBP,
0.69 (95% CI: 0.55-0.82, p = 0.007) for calprotectin and 0.87(95% CI: 0.74-1.00, p = 0.003) for CRP. The optimal biomarker combination for discriminating between CRC and controls was the combination of the three markers (SP= 0.75, SE = 0.75). In the validation cohort, levels of calprotectin and TNFα, were significantly higher in cancer compared to control (p=0.05, p=0.02, respectively). Furthermore, IFNγ and IL10 were also significantly elevated in cancer compared to control (p= 0.02, p=0.003, respectively).These results support the hypothesis that a dysfunctional gut barrier and attendant inflammation may influence CRC development and progression. Additionally, LBP, CRP and calprotectin may have potential as diagnostic biomarkers for CRC or for risk stratification. Gut bacterial and barrier wall modulation and stabilization has potential for preventing colorectal adenomas and hence colorectal cancer.

#5545

Assessing LGR5 expression levels on colorectal cancer tissue samples for use in LGR5-targeting CAR-T cell therapy clinical trial

Emma J. Thompson[1], Veronika Bandara[2], Batjargal Gundsambuu[2], Silvana Napoli[2], Stuart Mills[3], Jade Foeng[4], Dylan McPeake[4], Timona Tyllis[4], Caitlin Abbott[4], Allison Cowin[3], Timothy Sadlon[5], Shaun McColl[4], Carmela Ricciardelli[6], Simon C. Barry[5], Claudine S. Bonder[1]. *[1]Centre for Cancer*

Biology, University of South Australia, Adelaide, Australia,[2]Carina Biotech, Adelaide, Australia,[3]Future Industries Institute, University of South Australia, Adelaide, Australia,[4]Chemokine Biology Laboratory, University of Adelaide, Adelaide, Australia,[5]Molecular Immunology, Robinson Research Institute, University of Adelaide, Adelaide, Australia,[6]Adelaide Medical School, University of Adelaide, Adelaide, Australia

Leucine-rich repeat containing G-protein coupled receptor (LGR5) is stem cell marker that potentiates canonical signaling in the Wnt/β-catenin signaling pathway (Barker *et al.* 2007). LGR5 is known to be expressed on several tissues; particularly the stem cells within intestinal crypts and the stem cell niche at the base of hair follicles (Barker *et al.* 2007 and Jaks *et al.* 2008). The plasticity and stem phenotype of LGR5+ cells has led to their identification as a cancer stem cell marker for some solid tumors including colorectal cancer (CRC) (Barker *et al.* 2009). This presents LGR5 as a potential target molecule for CAR-T cell directed specific tumor cell killing. For treatment of CRC with LGR5-directed CAR-T cells, it is critical to gain an understanding of the level of LGR5 expression on normal tissue compared with cancerous tissue. The aim of this study was to develop a screening technique for patient selection, and importantly identify potential responders to LGR5-targeting CAR-T cell therapy.Utilizing commercially purchased tissue microarrays a cohort of patient primary tumor biopsies (n=472) were assessed for LGR5 expression; ~60% displayed moderate to high level LGR5 positivity, with a trend toward higher grade, later stage tumors having higher levels of LGR5. LGR5 expression levels on lymph node metastases showed a positive correlation to LGR5 expression on patient-matched primary tumor tissue. Seven out of ten liver biopsies from metastatic colon cancer lesions showed a medium to high level LGR5 staining, indicating this may be used as a screening tool for metastatic CRC patients. We also observed restricted expression of LGR5 across the many normal tissues, suggesting limited off-target effects of LGR5-targeting CAR-T cells.The data obtained in this study provides evidence that LGR5 IHC of biopsies could be used as a diagnostic screening tool of CRC patients for inclusion into a Phase1a/2 clinical trial.

Barker N, *et al*., 2007, Identification of stem cells in small intestine and colon by marker gene Lgr5. *Nature* 449: 1003–1007 Barker N. *et al*. 2009, Crypt stem cells as the cells-of-origin of intestinal cancer. *Nature* 457**:** 608–611Jaks V. *et al*. 2008, Lgr5 marks cycling, yet long-lived, hair follicle stem cells. *Nat Genet.* Nov;40(11):1291-9.

#5546

Urine metabolomic biomarkers discovery for bladder cancer diagnostics

Andrew J. Schwab, Matthew W. Mitchell, Edward D. Karoly, Rangaprasad Sarangarajan. *Metabolon, Inc., Morrisville, NC*

Current estimates in the United States for 2022 are about 81,180 new cases of bladder cancer diagnosis with about 17,100 deaths from the disease (American Cancer Society). Urothelial carcinoma, also known as transitional cell carcinoma (TCC), is the most common type of bladder cancer, approximately 70% of newly diagnosed TCC patients have non-muscle invasive bladder cancer (NMIBC) tumors. The gold standards for initial diagnosis and recurrence of TCC, cystoscopy and cytology, are both limited by their inability to visualize certain areas within the bladder or detect low grade tumors. Moreover, these tests are associated with false positive profiles, with potential for abnormal readouts even in individuals with no obvious signs of cancer. High recurrence rate predicates the need for constant monitoring of signs and symptoms associated with bladder disease following initial diagnosis, and non-invasive diagnostic modalities to detect both recurrent and primary early-stage tumors are a critical unmet need. In this study, comprehensive metabolomic profiling from human urine samples was used to identify and validate a panel of metabolites as potential biomarkers of bladder cancer. Urine samples from 439 total subjects (comprised of 66 bladder cancer, 119 history of bladder cancer but no bladder cancer at time of urine sampling, 58 hematuria subjects, 48 renal cell carcinoma, 58 prostate cancer, and 89 healthy subjects) were analyzed using a proprietary global untargeted metabolomic platform. A follow-up study to determine the reproducibility of the initial data set was conducted with 162 urine samples from subjects with bladder cancer that were either recurrent or primary, or with a negative diagnosis for bladder cancer with a previous history of bladder cancer or had hematuria or urinary voiding issues. Utilizing both data sets, eight biochemicals (lactate, gluconate, palmitoyl sphingomyelin, acetylcarnitine, choline phosphate, succinate, and adenosine) were identified as potential urine biomarkers for bladder cancer. In addition, 3-hydroxybutyrate (BHBA), 2-hydroxybutyrate (AHB), and adipate were identified as potential urine biomarkers for urological cancers. In total, 37 biochemicals have now been identified with having the potential to serve as urine bladder cancer biomarkers, and the majority of the biochemicals identified as biomarkers

were associated with biochemical pathways previously shown to be perturbed in bladder tumors. The performance characteristics of the identified biochemicals in the detection of bladder cancer will be reported.

#5547

Evaluation of two clinically focused targeted NGS systems for liquid biopsy testing shows a high level of concordance in resulting actionable mutations

Sarah Kreston, Claire Gould, Kylie Blair, Leisa Jackson, Janice Riley, Gary A. Pestano. *Biodesix, Inc., Boulder, CO*

Introduct**ion:** The use of blood-based molecular diagnostics is increasingly becoming routine in clinical oncology practice. The purpose of this study was to evaluate variant resulting concordance for the four major somatic variant classes using two clinical next-generation sequencing (NGS) systems for conducting highly sensitive blood-based analyses. All donor specimens were de-identified remnants from patients previously diagnosed with advanced NSCLC. We utilized two independent panels, systems and bioinformatic pipelines that are focused on clinical testing for key actionable variants. The fifty-gene panel Oncomine Precision Assay (OPA) GX was performed on the Genexus Integrated Sequencer and the 52 gene GeneStrat NGS (GSNGS) test was run as a reference on the Ion GeneStudio S5 PRIME system. The four major classes of mutations evaluated included Single Nucleotide Variants (SNV), Insertions and Deletions (INDEL), copy number amplifications (CNAs) and gene fusions.

Methods: For this study, de-identified reference GSNGS cell-free nucleic acid (cfNA) remnant specimens (n=33 variants) that passed all validated QC bioinformatics thresholds were blinded and tested on the Genexus. DNA concentration was measured by fluorometry, and specimens were diluted to an input of 6.6 ng to 53.4 ng for library preparation. The Genexus system is pre-programmed to process specimens to result generation. Variant calls for all mutation classes were conducted using the on-board bioinformatics pipelines, and results were compared to those generated by the GeneStrat NGS Test. We included specimens harboring somatic variant mutations in KRAS, NRAS, BRAF, EGFR, ERBB2, and FGFR; CNAs; EML4-ALK fusions; and MET exon 14 skipping.

Results: All samples passed the OPA (Genexus) bioinformatic quality control criteria and mapped reads were highly consistent, demonstrating accuracy of

calls between both the Ion Torrent platforms, informatic pipelines and panels. We observed 100% concordance in variant calls for SNVs, INDELs and fusions between the two platforms. There was one CNA variant observed on the S5 that was not called by the Genexus workflow, yielding overall concordance of 97% (32 of 33). Of note, 44 additional somatic variants (SNV and INDELs) and 1 additional fusion were detected using the Genexus workflow. This was due to the lower threshold for variant calling on this system.

Conclusion: The high concordance of the independent workflows for the detection of nucleic acid variants in circulation demonstrates the capability of both systems to be used for testing of clinical specimens. Specifically, actionable variants in the four major mutation classes were successfully detected in the reference and test specimen set. As a part of clinical validation, orthogonal testing of variants will need to be conducted.

#5548

Clinical management and decision making in early ER-positive breast cancers through improved prognosis and pathway directed molecular profiling

John M. S. Bartlett[1], Cheryl Crozier[2], Vinay K. Mittal[3], Dan Dion[2], Angela De Luca[2], Adam E. Sundby[2], Elizabeth Woroszchuk[2], Bradley d'Souza[2], Louis Gasparini[2], Mary Anne Quintayo[2], Mehar Chahal[2], Anna Y. Lee[2], Mathieu Larivière[3], Kyusung S. Park[3], Anupma Sharma[3], Jeffrey M. Smith[3], Seth Sadis[3], Daniel W. Rea[4], Melanie Spears[2], Jane Bayani[2]. *[1]Cancer Research UK Edinburgh Centre, The University of Edinburgh, Edinburgh, United Kingdom,[2]Diagnostic Development, Ontario Institute for Cancer Research, Toronto, ON, Canada,[3]Thermo Fisher Scientific, Carlsbad, CA,[4]Cancer Research UK Clinical Trials Unit, University of Birmingham, Birmingham, United Kingdom*

Hormone receptor positive (HR+ve) breast cancer (BCa) comprises over 80% of all newly diagnosed BCas. While there is an initial good response to anti-hormone therapies, many patients will experience a recurrence. Validated prognostic tests are used to guide chemotherapy decisions, but the goal of precision medicine has yet to be achieved. We developed and validated a 95-gene prognostic signature (Bayani et al 2017) from the TEAM trial (van de Velde et al, 2011), demonstrating this risk classifier performed as well as the 21-gene, 50-gene and 70-gene tests and can be used in HER2+/-ve cases

including only nodal status. RNA profiling has improved decisions regarding adjuvant chemotherapy but is insufficient for stratification to targeted therapies increasingly available in the early setting. The genomic landscape of BCas has identified recurrent patterns of mutation and copy-number changes. Except for HER2, there are few genes for whom mutational or gene dosage are reliable for stratification to targeted therapies. It is increasingly evident that a multi-omic approach to precision medicine is needed to encompass the biological complexity of cancer. Here we present the findings from the RNA profiling of patients from the TEAM trial using a custom diagnostic-grade NGS panel of the 95-gene risk classifier and DNA sequencing using a large (500 gene) comprehensive genomic profiling panel (OCAPlus, Thermo Fisher Scientific). 95-gene prognostic results of 1,182 patients showed prognostic utility using the custom panel with 265 (22%) low-risk patients experiencing >90% relapse free survival (DRFS)(HR=4.47 (95% CI 2.46-8.02, p=5.54e-07)) at 10 years. In 857 cases profiled with OCAPlus, the genes most frequently mutated included PIK3CA (53%), MAPK31 (25%), TP53(17%), CDH1 (17%) and GATA3 (10%). Frequent copy number changes were identified in CCND1 (18%), FGFR1 (12%), and MDM2 (5%). To investigate the potential for stratification to targeted therapies, a pathway approach was taken to identify aberrations in targetable signaling pathways. Among the 788 cases with both OCAPlus and the 95-gene results, the most frequently impacted pathways were PI3K/AKT (67%), HHR Pathway (55%), Chromatin regulation (50%), RAS/RAF/MEK/ERK (40%) and Cell Cycle (37%). To address the clinical need for those patients deemed at risk for recurrence, the consequence of aberrations in those pathways were investigated. Among 95-gene high-risk patients (n=604), those with mutations in genes of the Cell Cycle pathway experienced poorer DRFS (HR=1.95 (95%, CI 1.29-2.95, p= 0.0159), suggesting these patients might benefit cell cycle-targeting therapies. With no reliable biomarkers to predict response, and with associated side effects/ toxicities of these agents, this offers a rational pathway-directed method of decision making for those identified as high-risk of recurrence.

#5549

Normalized platelet splicing junction count is a novel biomarker for diagnosis of ovarian tumors

Eunyong Ahn[1], Se Ik Kim[2], Sungmin Park[1], Sarah Kim[1], Seung Jin Yang[3], Yeochan Kim[3], Dong Won Hwang[2], Heeyeon Kim[4], HyunA Jo[4], Untack Cho[4], Juwon Lee[4], Yong-Sang Song[2], TaeJin Ahn[5]. *[1]Foretell My Health,*

Pohang, Korea, Republic of,[2]Department of Obstetrics and Gynecology, Seoul National University Hospital, Seoul, Korea, Republic of,[3]School of Life Science, Handong Global University, Pohang, Korea, Republic of,[4]Cancer Research Institute, College of Medicine, Seoul National University, Seoul, Korea, Republic of,[5]Handong Global University, Pohang, Korea, Republic of

Owing to a lack of disease-specific symptoms and effective screening tools, most ovarian cancers are diagnosed at an advanced stage, resulting in high recurrence and mortality rates. Recently, there has been an effort to diagnose ovarian cancer utilizing platelets, which are crucial in the immunology of oncogenesis. These transcriptome-wise techniques, however, had two significant drawbacks: utilizing a normalization method that can be altered depending on the content of the samples in the dataset and using an excessive number of features. We, therefore, present a method for assessing the existence of ovarian cancer or benign tumors by utilizing a fewer features with a sampling invariant normalization technique.
First, we downloaded platelet transcriptome data of patients with ovarian cancer (n=28), benign ovarian tumor (n=17), and their healthy counterparts (n=204) from GEO (GSE158508 and GSE89843 - PRJNA353588 and PRJNA353588). Second, for external validation, we prospectively enrolled patients with ovarian cancer (n=4) and benign ovarian tumors (n=9), and healthy women (n=14) at Seoul National University Hospital (SNUH), collected their blood samples, and obtained platelet transcriptome data. The normalization was performed using commonly and invariantly existing 20 splice junctions in the isolated platelet of tumor and normal samples. Herein, 319 splice junctions were selected as features for the SVM model diagnosing the existence of an ovarian tumor. Feature selection and model development were conducted using a training set (n=152) and model performance was assessed from a separate test set (n=97).
SVM classifier that utilized our splice junction-based biomarkers (20 for normalization, 319 for tumor classification) demonstrated 93.8% (71.7 - 98.9%) sensitivity, 100.0% (95.5 - 100.0%) specificity, and 1.0 of AUC in the test data set with a predetermined 0.5 cut-off value. Considering the difference of sequencing raw data between the open source and newly collected sample in terms of read length and read types (single-end vs paired-end), the SVM model from the open source was not suitable to the independent validation set. Thus, we train new SVM models using the same splice junctions with LOOCV in SNUH dataset. As the results, the model showed its diagnostic

performance with 92.3% (66.7 - 98.6%) sensitivity and 92.9% (68.6 - 98.7%) specificity.
We found novel splice junction-based biomarkers for the early detection or diagnosis of ovarian tumors. Although possible confounding factors such as ethnic variance may affect the performance of the models using these biomarkers, since the data preprocessing procedure is sampling invariant, the inclusion of samples from the same population would not affect our classification results. Furthermore, suggested biomarkers can be utilized during medical checkups of women without any symptoms to find women with ovarian tumors, whether benign or malignant.

#5550

Sociodemographic disparities in access to biomarker testing in patients with advanced colorectal cancer

Saad Sabbagh[1], Iktej Jabbal[2], Barbara Dominguez[1], Mira Itani[1], Mohamed Mohanna[1], Arun Nagarajan[1]. *[1]Cleveland Clinic Florida Foundation, Weston, FL,[2]AdventHealth Sebring, Sebring, FL*

Introducti**on** All patients with newly diagnosed colorectal cancer are recommended to undergo microsatellite instability (MSI) testing. In addition, mutational testing using biomarkers such as KRAS, NRAS, and BRAF is recommended for patients with metastatic cancers. Testing for these markers is vital as they guide therapeutic decision-making and serve as prognostic indicators. Our study aims to analyze disparities in testing for MSI and KRAS biomarkers based on sociodemographic factors in patients with metastatic colorectal cancer. Furthermore, we explored the survival characteristics in these patients based on sociodemographic factors and on access to biomarker testing.
Methods The National Cancer Database (NCDB) was queried for patients diagnosed with metastatic colorectal cancer (MCC). At the bivariate level, we performed chi-squared statistics and multivariate logistic regression modeling to explore variables associated with patients undergoing MSI and KRAS testing. In addition, Multivariate Cox regression and Kaplan-Meier analyses were performed for survival analysis.
Results N = 51,913 patients with MCC diagnosed between 2010 to 2017 were included. The median age for Whites was 68.0 years versus 64.0 years for Blacks. Blacks had a lower probability of undergoing MSI testing (OR 0.90, [0.84-0.96] $p< 0.0009$). Factors associated with a lower likelihood for MSI

testing included treatment at a Community Cancer Program (OR 0.61, [0.55-0.66] p<0.0001), residing in areas with people having lower education (OR 0.68, [0.62-0.74] p<0.0001) and in rural areas (OR 0.74, [0.61-0.90] p-value 0024), and a median household income of < $38,000 (OR 0.88, [0.80-0.96] p 0.0040). Patients with no insurance and Medicaid/governmental insurance were also less likely to undergo both MSI and KRAS testing. Blacks had a decreased likelihood of having high MSI levels among patients who underwent testing compared to Whites (OR 0.67, [0.50-0.91] p-value 0.0107). After controlling for confounding variables, survival analysis showed poor survival in patients who did not undergo testing for MSI and KRAS (HR 1.20, [1.17-1.23] p<0.0001 and HR 1.04, [1.01-1.06] p-value 0.0016 respectively). **Conclusion** Our analysis reveals that sociodemographic factors such as being from a minority race, having no insurance, residing in areas with lower education and rural settings were associated with a lower probability of undergoing MSI testing in patients with metastatic colorectal cancer. This is of concern as our study also reveals that not undergoing biomarker testing is associated with poorer survival. Addressing such sociodemographic discrepancies among racial groups is essential in achieving equitable care and narrowing gaps in outcomes.

#5551

Cancer associated PSA-glycoforms as prostate cancer markers

Hannu Koistinen[1], Ruusu-Maaria Kovanen[1], Timo-Pekka Lehto[2], Antti Rannikko[3], Tuomas Mirtti[2]. *[1]Department of Clinical Chemistry, University of Helsinki, Helsinki, Finland,[2]University of Helsinki, Helsinki, Finland,[3]Helsinki University Hospital, Helsinki, Finland*

Changes in protein glycosylation have been observed in several cancers, where they affect cellular growth behavior, invasiveness and acquisition of metastatic potential. Such changes are not random and have been found to associate with cancer aggressiveness. Thus, detection of protein glycosylation may offer novel opportunities for cancer biomarker development. Since prostate-specific antigen (PSA) is glycosylated, assessing different PSA-glycoforms may provide valuable diagnostic and prognostic information. We recently established a novel in situ proximity ligation-based method for the detection of different protein-glycoforms in tissue sections. This method utilizes protein-specific antibody and glycan-binding lectins. We have optimized this method for the detection of different PSA-glycoforms in

formalin-fixed paraffin-embedded prostatic tumor samples. We found that PSA is, indeed, differently glycosylated in prostate cancer (n=23) compared to benign prostate tissue (n=4). Two of the 25 studied lectins showed prominent staining only in cancer tissues ($p<0.0001$ for both), although the total PSA staining was stronger in benign tissues ($p=0.006$). We are currently validating these results in large, well-curated clinical cohorts, with intention to test whether PSA-glycoforms in tissue offer improved detection of clinically significant prostate cancer. These studies facilitate development of tools for identification of cancer-specific PSA-isoforms in serum samples. Detection of such isoforms is likely to provide independent diagnostic and prognostic information.

#5552

MAGE-A3 and MAGE-A4 protein show co-expression in tumor of lung, bladder, and colon cancer

Rachel Gonzalez. *OriGene Technologies, Inc., Rockville, MD*

Melanoma Antigen Gene Family (MAGE-A) are part of the cancer-testis antigens whose limited expression in normal tissues and high expression in cancer make them excellent targets for immunotherapy. Clinical trials have already begun targeting MAGE-A3 and MAGE-A4 proteins in tumors. Should these trials lead to new treatment protocols, it is important to develop a diagnostic immunohistochemistry (IHC) tool for pre-screening patients who would benefit. The MAGE-A family consists of 12 members that share up to 85% sequence homology presenting a challenge for finding highly specific antibodies for IHC. Using CytoSections, a new screening control tool for IHC, ICC, IF, and in-situ hybridization, highly specific IHC MAGE-A3 and MAGE-A4 antibodies were developed and screened. The MAGE-A3 and MAGE-A4 antibodies were assessed on twenty-two lung cancers, twenty-one colon cancer, and more than thirty bladder cancers which resulted in cases that co-express MAGE-A3 and MAGE-A4 proteins in all three types of tumors. Using immunofluorescence, tumors positive for both proteins were double stained for MAGE-A3 and MAGE-A4 to show the proteins were co-expressed in the same tumor cells. Immunohistochemistry continues to be a rapid and reproducible method for the detection of proteins in tumors. Antibodies specific to MAGE-A3 and A4 proteins for IHC may be a useful tool in predicting outcomes or benefits for patients.

#5553

Diagnostic aqueous humor proteome predicts metastatic potential in uveal melanoma

Chen-Ching Peng, Liya Xu, Jesse Berry. *The Vision Center, Children's Hospital Los Angeles, Los Angeles, CA*

Introduction: Approximately half of patients with uveal melanoma (UM), a primary eye cancer, will develop metastatic disease. Gene expression profiling (GEP) is clinically validated to stratify risk of metastasis by assigning UM patients to two highly prognostic molecular classes: class 1 (low metastatic risk) and class 2 (high metastatic risk). However, GEP requires intraocular tumor biopsy which are limited by small tumor size and tumor heterogeneity; furthermore, there are small risks of retinal hemorrhage, bleeding or tumor dissemination. Thus, liquid biopsy has emerged as a significantly less invasive alternative. Blood biopsy has largely been unsuccessful for clinical use in UM due to low detection rates in the setting disease limited to the eye, however eye-specific aqueous humor (AH) liquid biopsy may be a better alternative. In this study, we seek to determine the AH proteome related to the advanced GEP class 2 using the diagnostic AH specimens.

Method: Twenty UM treatment naive AH were collected before plaque brachytherapy. Patients were sub-grouped by GEP classes into GEP 1 (n=12) and GEP 2 (n=5). Three patients were classified as GEP unknown (GEP NA, n=3) due to the unavailability of tumor biopsy. Ten microliters of AH samples were analyzed by proximity extension assay-derived multiplexed Olink platform. Protein expression levels of 1472 targets were analyzed, compared between GEP classes and correlated with clinical features. Significant differentially expressed proteins (DEPs, fold-change (FC) > 2 or FC < 0.5, $P < 0.01$) were subjected to Qiagen ingenuity pathway analysis for cellular pathway and upstream regulator identification.

Results: GEP 2 class was correlated with AJCC stages ($P = 0.012$), advanced clinical tumor stages ($P = 0.007$) and mutated BAP1 ($P = 0.018$). 45 DEPs were identified when comparing GEP classes. Among them, 31 are up-regulated DEPs [fold-change (FC) >2, $P < 0.01$] and 14 are down-regulated DEPs (FC < 0.5, $P < 0.01$) in GEP 2 compared to GEP1. The unsupervised clustering analysis showed that the 45 DEPs well-differentiate AH samples by GEP classes, and the 3 GEP NA samples were clustered with GEP1 class. Pathway analysis showed that 45 DEPs contribute to metastatic-related pathways including cellular movement, cellular proliferation and epithelial to

mesenchymal transition. Two upstream regulators, IL1 receptor and SPRY2, were predicted to regulate 8 out of the 45 DEPs. IL1R2 (FC = 3.4, P = 0.021) and SPRY2 (FC = 0.6, P = 0.052) protein expression levels were found matched as prediction in our Olink dataset.
Conclusions: 45 AH DEPs could differentiate GEP class 1 and 2 at the diagnostic stage and could be detected even when the tumor was too small to biopsy. IL1R and SPRY2 are potential upstream regulators for the 8/45 DEPs that contribute to metastasis-related pathways. AH liquid biopsy offers a new opportunity to determine metastatic potential for patients in the absence of tumor biopsy.

#5554

Mammaglobin-A expression in highly specific for tumors derived from the breast, the female genital tract and salivary gland tumors

Natalia Gorbokon, Patrick Timm, David Dum, Anne Menz, Franziska Büscheck, Cosima Völkel, Andrea Hinsch, Maximilian Lennartz, Andreas Luebke, Claudia Hube-Magg, Christoph Fraune, Christian Bernreuther, Patrick Lebok, Till Clauditz, Frank Jacobsen, Guido Sauter, Ria Uhlig, Stefan Steurer, Sarah Minner, Andreas Marx, Ronald Simon, Eike Burandt, Till Krech. *University Medical Center Hamburg-Eppendorf, Hamburg, Germany*

Background: Human mammaglobin-A (SCGB2A2) is a small epithelial secretory protein with unknown function. Because of its frequent expression in breast epithelial cells, it is used as a diagnostic marker for breast cancer and represents an attractive target for novel therapies involving adaptive T cell transfer and antitumor vaccines for breast cancer patients. However, there is growing evidence that mammaglobin-A expression is not limited to breast cancers.
Methods: In order to comprehensively determine mammaglobin-A expression in normal and neoplastic tissues, a tissue microarray containing 16,328 samples from 128 different tumor types and subtypes as well as 608 samples of 76 different normal tissue types was analyzed by immunohistochemistry.
Results: Mammaglobin-A positivity was found in 37 of 128 tumor categories, 32 of which were derived of one of four organs: breast (6 tumor categories), endometrium (5 tumor categories), ovary (5 tumor categories), and salivary glands (16 tumor categories). Only 5 additional tumor types showed occasional mammaglobin positivity. These tumors mostly exhibited a weak mammaglobin-A staining and included medullary thyroid cancer, teratoma of

the testis, squamous cell carcinoma of skin and the pharynx, and prostatic adenocarcinoma (Gleason 5+5=10). Among 1,139 evaluable invasive breast carcinomas of no special type (NST), low mammaglobin-A immunostaining was linked to high BRE grade ($p=0.0011$), a loss of estrogen and progesterone receptor expression ($p<0.0001$ each), and triple negative status ($p<0.0001$) but not to patient survival. In endometrial cancer, low mammaglobin-A immunostaining was linked to advanced tumor stage ($p=0.0198$). Although a similar trend was seen for endometrioid and serous high-grade carcinomas of the ovary, these associations did not reach statistical significance. Conclusions: Our data characterize mammaglobin-A as a highly specific marker for tumors derived from either female organs or the salivary gland. The potential use of anti-Mammaglobin therapies should be studied also in other mammaglobin-positive tumor types.

#5555

Altered p53/p16 expression is linked to urothelial carcinoma progression but is unrelated to prognosis in muscle-invasive tumors

Simon Schallenberg[1], Henning Plage[2], Sebastian Hofbauer[2], Kira Kornienko[2], Sarah Weinberger[2], Paul G. Bruch[2], Florian Roßner[1], Sefer Elezkurtaj[1], Martina Kluth[3], Maximilian Lennartz[3], Tim Mandelkow[4], Elena Bady[4], Niclas C. Blessin[3], Andreas H. Marx[5], Henrik Samtleben[5], Margit Fisch[6], Michael Rink[6], Marcin Slojewski[7], Krystian Kaczmarek[7], Thorsten Ecke[8], Steffen Hallmann[8], Stefan Koch[9], Nico Adamini[10], Sarah Minner[4], Ronald Simon[4], Guido Sauter[4], David Horst[1], Tobias Klatte[2], Thorsten Schlomm[2], Henrik Zecha[10]. *[1]Institute of Pathology, Charité Berlin, Berlin, Germany,[2]Department of Urology, Charité Berlin, Berlin, Germany,[3]University Medical Center Hamburg-Eppendorf, Hamburg, Germany,[4]Institute of Pathology, University Medical Center Hamburg-Eppendorf, Hamburg, Germany,[5]Department of Pathology, Academic Hospital Fuerth, Fuerth, Germany,[6]Department of Urology, University Medical Center Hamburg-Eppendorf, Hamburg, Germany,[7]Department of Urology, University Hospital Stettin, Stettin, Poland,[8]Department of Urology, Helios Hospital Bad Saarow, Bad Saarow, Germany,[9]Department of Pathology, Helios Hospital Bad Saarow, Bad Saarow, Germany,[10]Department of Urology, Albertinen Hospital, Hamburg, Germany*

Background**:** Most inactivating p53 mutations result in a nuclear accumulation of the defective p53 protein. However, p53 alterations that result in a complete lack of cellular p53 and complete absence of p53 immunostaining do also occur. As p16 is upregulated in p53 inactivated cells, p16 immunohistochemistry may be a surrogate marker for p53 inactivation.

Design: In this study, we investigated p53 and p16 immunostaining on more than 2,500 urothelial bladder carcinomas in a tissue microarray format to better understand their impact in relation to clinicopathological parameters of disease progression and patient outcome.

Results: p16 immunostaining was not observed in normal urothelium but occurred in 1,576 (63.5%) of cancers including 755 (30.4%) with a strong staining. The fraction of p16 positive cases increased markedly from pTaG2

low grade (9.6%) to pTaG3 high grade tumors (46.5% strongly positive, p<0.0001 for pTaG2 low vs. pTaG3) but continuously decreased from pTaG3 to pT2 (41.3% strongly positive), pT3 (36.5%) and pT4 (33.3%; p=0.0030). Within pT2-4 carcinomas, p16 positivity was also linked to high grade (p=0.0005) but unrelated to overall survival. p53 staining has been recorded as negative in 203 (8.4%), very weak in 373 (15.4%), weak in 1,341 (55.3%), strong in 115 (4.7%), and very strong in 393 (16.2%) cancers. The fraction of tumors with negative (potentially p53 null phenotype), strong, and very strong p53 positivity increased markedly from pTaG2 low grade to pTaG3 high grade tumors (p<0.0001) and from pTaG3 to muscle-invasive pT2-4 cancers (p=0.0007). p53 staining pattern was unrelated to histopathological parameters of malignancy or patient prognosis within pT2-4 carcinomas, however. There was a significant overall association between p53 and p16 expression but strong p16 expression predominated in tumors with very strong, strong, and negative p53 staining. Subset analyses showed that the combination of p53 negative/p16 strongly positive cancers was particularly linked to features of tumor aggressiveness.
Conclusion: Our data show that altered function of p53 and p16 immunostaining increases during grade and stage progression although these alterations lack prognostic significance in pT2-4 carcinomas. That high level p16 expression is limited to neoplastic urothelium and that the p53 null phenotype is largely limited to grade 3 and invasive urothelial carcinomas are features with potential diagnostic utility.

#5556
Lemur tyrosine kinase 3 serves as a predictor of patient outcome and a target for the treatment of ovarian cancer
Thea K. Kirsch-Mangu[1], Axel S. Tullberg[2], Anna Portela[3], Khalil Helou[2], Ghassan M. Saed[1]. *[1]Wayne State University School of Medicine, Detroit, MI,[2]University of Gothenburg, Gothenburg, Sweden,[3]Xenopat, Barcelona, Spain*

The objective of these in vitro and in vivo studies was to validate Lemur Tyrosine Kinase 3 (LMTK3) as a specific target and predictor of clinical outcome in ovarian cancer. LMTK3 belongs to a family of regulated tyrosine kinases with three structurally related isoforms, LMTK1, LMTK2,

and LMTK3. Both nuclear and cytoplasmic LMTK3 expressions correlated with tumor grade and patient survival in cancers such as breast and colorectal cancer. We tested the clinical significance of the LMTK3 gene by immunohistochemistry (IHC) using LMTK3 monoclonal antibody on formalin-fixed paraffin-embedded sections (FFPE) collected from 204 early-stage (stage I-II) ovarian cancer patients. Results from this IHC LMTK3 study revealed a higher cytoplasmic to nuclear localization of LMTK3 correlated with worse overall survival ($P<0.01$). Further investigation of LMTK3's prognostic value by screening LMTK3 signaling in 270 stage III-IV ovarian cancer patients is ongoing. We utilized the MTT ((3-(4,5-dimethylthiazol-2-yl)-2,5-diphenyltetrazolium bromide) assay for testing the killing efficacy of targeting LMTK3 by a monoclonal antibody, siRNA, and specific LMTK3 binding peptides (LMTK3BP) in ovarian cancer cell lines SKOV3, MDAH-2774, A2780, and TOV-21G. Treatment with LMTK3 specific monoclonal antibody, siRNA, and LMTK3BP significantly induced killing of both chemosensitive and chemoresistant ovarian cancer cells without affecting normal cells in vitro. Moreover, we observed this killing as synergistic with both Cisplatin and Taxotere treatment in vitro. Lastly, we used an A2780 cell line derived orthotopic xenograft mouse model of ovarian cancer to test the efficacy of specific LMTK3BP in vivo. Strikingly, LMTK3BP 20 mg/kg IV dose given three times a week for three weeks showed a 35% tumor reduction. Furthermore, in vivo safety studies showed no signs of toxicity of the LMTK3BP, even at a very high dose of 40 mg/kg. Thus, with dose optimization in ongoing experiments, we could expect a higher efficacy. In conclusion, this study highlighted the importance of LMTK3 as a predictor of patient clinical outcome and potential target for treatment in ovarian cancer.

#5557

Patterns of oncogene co-expression at single cell resolution influence survival in diffuse large B-cell lymphoma

Michal M. Hoppe[1], Patrick Jaynes[1], Shuangyi Fan[2], Yanfen Peng[1], Shruti Sridhar[1], Phuong Mai Hoang[1], Xin Liu[3], Sanjay de Mel[3], Limei Poon[4], Esther Chan[3], Joanne Lee[3], Choon Kiat Ong[5], Tiffany Tang[6], Soon Thye Lim[6], Chandramouli Nagarajan[7], Nicholas F. Grigoropoulos[7], Soo-Yong Tan[2], Susan Swee-Shan Hue[2], Sheng-Tsung Chang[8], Shih-Sung Chuang[8], Shaoying Li[9], Joseph D. Khoury[9], Hyungwon Choi[10], Pedro Farinha[11],

Anja Mottok[12], David W. Scott[11], Carl Harris[13], Alessia Bottos[14], Gayatri Kumar[15], Kasthuri Kannan[15], Laura J. Gay[16], Hendrik F. P. Runge[16], Ilias Moutsopoulos[16], Irina Mohorianu[16], Daniel J. Hodson[16], Yen-Chee Lin[3], Wee-Joo Chng[1], Siok-Bian Ng[1], Claudio Tripodo[17], Anand D. Jeyasekharan[1]. *[1]Cancer Science Institute of Singapore, Singapore, Singapore,[2]Department of Pathology, Yong Loo Lin School of Medicine, National University of Singapore, Singapore, Singapore,[3]Department of Haematology-Oncology, National University Health System, Singapore, Singapore,[4]Department of Haematology-Oncology,, National University Health System, Singapore, Singapore,[5]Division of Cellular and Molecular Research, National Cancer Centre Singapore, Singapore, Singapore,[6]Division of Medical Oncology, National Cancer Centre Singapore, Singapore, Singapore,[7]Department of Haematology, Singapore General Hospital, Singapore, Singapore,[8]Department of Pathology, Chi-Mei Medical Center, Tainan, Taiwan,[9]Department of Hematopathology, Division of Pathology and Laboratory Medicine, MD Anderson Cancer Center, Houston, TX,[10]Department of Medicine, Yong Loo Lin School of Medicine, National University of Singapore, Singapore, Singapore,[11]BC Cancer Research Centre, Vancouver, BC, Canada,[12]Institute of Human Genetics, University Medical Center and University of Ulm, Ulm, Germany,[13]Hoffmann-La Roche Ltd, Basel, Switzerland,[14]F. Hoffmann-La Roche Ltd, Basel, Switzerland,[15]Translational Molecular Pathology, The University of Texas, MD Anderson Cancer Center, Houston, TX,[16]Wellcome-MRC Cambridge Stem Cell Institute, Cambridge, United Kingdom,[17]Tumor Immunology Unit, University of Palermo, Palermo, Italy*

Background: Cancers often overexpress multiple clinically relevant oncogenes.
However, it is not known if multiple oncogenes within a cancer combineuniquely in specific cellular sub-populations to influence clinical outcome.We studied this phenomenon using the prognostically relevantoncogenes MYC, BCL2 and BCL6 in Diffuse Large B-Cell Lymphoma(DLBCL).
Methods: Quantitative multispectral imaging simultaneously measured oncogene co-expression at single-cell resolution in reactive lymphoid tissue

(n=12)and four independent cohorts (*n*=409) of DLBCL. Mathematically derived co-expression phenotypes were evaluated in DLBCLs with immunohistochemistry (*n*=316) and nine DLBCL cohorts with gene expression data (*n*=3974). Bulk and single-cell RNA sequencing was performed on patient-derived B-cells with induced co-expression of MYC,BCL2 and BCL6.
Results: Unlike in non-malignant lymphoid tissue where the co-expression of MYC, BCL2 and BCL6 in a B-cell is limited, DLBCLs show multiple permutations of oncogenic co-expression in malignant B-cells. The percentage of cells with a unique combination MYC+BCL2+BCL6- (M+2+6-) consistently predicts survival in contrast to that of other combinations (including M+2+6+). An estimated percentage of M+2+6- cells can be derived from any quantitative measurement of the component individual oncogenes, and correlates with survival in immunohistochemistry and gene expression datasets. Comparative transcriptomic analysis of DLBCLs and transformed patient-derived B-cells identifies cyclin D2 (CCND2) as a potential BCL6-repressedregulator of proliferation in the M+2+6- population.
Conclusions: Unique patterns of oncogene co-expression at single-cell resolution affect clinical outcomes in DLBCL. Similar analyses evaluating oncogenic combinations at the cellular level may impact diagnostics and target discovery in other cancers.

#5558

Understanding the molecular mechanism of tumor budding and its relationship with tumor microenvironment in colorectal cancer

Phimmada Hatthakarnkul[1], Holly Leslie[2], Hester Van Wyk[3], Leah Officer-Jones[4], Silvia Cusumano[4], Aula Ammar[5], Kathryn A.F. Pennel[5], Jean A. Quinn[5], Jennifer Hay[6], James Park[3], Noori Maka[3], John Le Quesne[2], Chanitra Thuwajit[7], Nigel Jamieson[5], Joanne Edwards[5]. *[1]Biomedical Science, Mahidol University, Bangkok, Thailand,[2]University of Glasgow, Glasgow, United Kingdom,[3]School of Medicine, University of Glasgow, Glasgow, United Kingdom,[4]Beatson Institute, Glasgow, United Kingdom,[5]School of Cancer Science, University of Glasgow, Glasgow, United Kingdom,[6]Glasgow Tissue Research Facility, University of Glasgow,*

Glasgow, United Kingdom,[7]Immunology, Mahidol University, Bangkok, Thailand

Background: Tumor budding (TB), a single or cluster of up to 4 cells at the tumor-invasive front, is a well-established prognostic marker and an independent predictor of metastasis in colorectal cancer (CRC). Despite that, the underlying molecular mechanism that drives this phenotype and its relationship with the tumor microenvironment (TME) remains unclear.
Methods: The relationship between TME and TB was investigated using multiplex immunofluorescence (mIF) in tissue microarrays (TMAs) of the tumor core and full sections. GeoMx^{TM} digital spatial profiling (DSP) was employed to identify the mechanism underlying TB and its surrounding TME, using the GeoMx Immune-oncology pathway panel in full CRC sections.
Results: In the current study, TB was independently associated with decreased cancer-specific survival (OR 1.856, 95% CI 1.360-2.533, P<0.001) in a cohort of 650 CRC patients. Additionally, TB was significantly associated with the Glasgow microenvironment score (GMS) (P=0.017). mIF performed in TMAs of the tumor core (n=650) showed that high CD3+ (OR0.374, 95% CI0.263-0.533, P<0.001) associated with good prognosis, whereas high CD68+ (OR2.902, 95% CI1.728-4.873, P<0.001) associated with poor prognosis. In addition, eighteen full sections were stained with an immune-related multiplex panel. Interestingly, in the invasive area, CD3+CD8+ was less frequent, while CD3+FOXP3+ was significantly higher compared to the stromal area in a patient with high TB (P=0.06, P<0.01, respectively). Moreover, though no significant difference was found, tumors with high buds showed an increase in neutrophil marker (CD66b) compared to low buds. No association is also found with a myeloid marker (CD68, CD163). The proliferation index of the tumor in the invasive area showed that the tumor with low buds is likely to be more proliferative. Besides, we found that a small subpopulation of budding is KI67+, suggesting the heterogeneity among TB. Furthermore, the mechanism underlying TB was observed using GeoMx^{TM}. Twelve cases, selected from mIF stained, with low (n=6) or high buds (n=6) were utilized, and 96 areas of interest (AOI) were identified from the tumor core, invasive front, and stroma. The results showed the differential expression of genes between the tumor core and the invasive front in patients with high TB. A

significant decrease in immune-related genes (e.g., CD3, NKG7, IL6, CXCR6, CD47, IFNAR1 and VSIR) compared to the stromal area at the invasive front was also observed (P<0.001).
Conclusion: TB is associated with poor prognosis and showed a distinct gene expression characteristic compared to the tumor mass. It may also affect the inflammatory response at the invasive tumor. The underlying mechanism of TB and its relationship with TME warrants future studies to confirm this finding.

#5559

Exploratory analysis of hormone receptor-positive (HR+), human epidermal growth factor receptor 2-negative (HER2-) *PIK3CA* mutated (mut) advanced breast cancer (aBC) treated with taselisib (TAS) and/or fulvestrant (FUL) reveals increased *CCNE2* expression with poor outcome to placebo (PBO) + FUL but not TAS + FUL in SANDPIPER

Radia M. Johnson[1], Bonnie Liu[1], Javier Cortés[2], Susan Dent[3], Nadia Harbeck[4], Ian E. Krop[5], William Jacot[6], Robert L. Yauch[7], Thomas J. Stout[7], Frauke Schimmoller[7], Steven Gendreau[7], Timothy R. Wilson[7].
[1]Genentech, Inc., South San Francisco, CA,[2]International Breast Cancer Center (IBCC), Pangaea Oncology, Quironsalud Group, Madrid Barcelona; Universidad Europea de Madrid, Madrid, Spain,[3]Duke Cancer Institute, Duke University, Durham, NC,[4]Department Gynecology and Obstetrics, Breast Center and Cancer Center (CCC) Munich, Ludwig-Maximilians-University (LMU) Hospital, Munich, Germany,[5]Yale Cancer Center, New Haven, CT,[6]Institut du Cancer de Montpellier (ICM) Val d'Aurelle, Montpellier University, Montpellier, France,[7]Genentech, Inc., San Francisco, CA

PIK3CA mutations occur in ~40% of patients (pts) with HR+/HER2- aBC. TAS is a potent and selective β-sparing PI3K inhibitor that has shown modest clinical benefit when combined with FUL endocrine therapy in patients (pts) with *PIK3CA*mut aBC. To better understand the molecular features associated with response to TAS and/or FUL, we examined the gene expression profiles of archival tissue from pts enrolled in SANDPIPER (NCT02340221). Most patients did not have prior treatment with a CDK4/6i. RNA sequencing was performed on baseline tissue

samples from 456 pts with *PIK3CA*mut tumors. Exploratory biomarker analyses revealed 28 genes associated with worse outcome. Of these, *CCNE2* [HR=1.11 (1.04-1.19), p=0.002], *RRM2* [HR=1.14 (1.07-1.22), p<0.0001] and *TUB4A* [HR=1.15 (1.05-1.26), p=0.004] are involved in the regulation of mitotic cell cycle. *CCNE2* encodes CYCLIN E2, a G1 cyclin that binds and activates CDK2. Elevated expression of *CCNE2* has been associated with poor outcome in ER-positive breast cancer, and has been identified as part of gene signatures that predict disease progression in tamoxifen-resistant breast cancer or advanced breast cancer. Since *CCNE2* expression may be a marker of more proliferative tumors, we assessed whether the inclusion of *CCNE2* gene expression would add value to a prognostic model that already includes cell cycle as a factor. Analysis of deviance after sequential addition of variables into Coxph models with stratification factors showed that elevated *CCNE2* expression is significant, in addition to cell cycle signature scores, for association with worse PFS (*likelihood ratio test p* = 0.001). When we grouped patients based on *CCNE2* expression split by quartile with the highest values (Q4) grouped as *CCNE2* high vs lower values (Q1-Q3), we found that the *CCNE2* high group does worse in the PBO + FUL treatment arm. Median PFS for *CCNE2*-high group in the placebo arm was 3.75 months compared to the other groups (log-rank $p < 0.0001$; PBO, *CCNE2*-low 7.3 months, TAS, *CCNE2*-high 7.6 months; TAS, *CCNE2*-low 7.3 months). A significant statistical interaction was observed between high *CCNE2* gene expression and PBO + FUL treatment arm HR=1.51 (1.03-2.20), p=0.04], suggesting that CCNE2 expression may be associated with poor PFS to in 2L ER+/HER2- *PIK3CA*mut aBC patients that receive PBO + FUL. Our analysis revealed an association between high *CCNE2* expression and worse PFS in patients that received PBO + FUL. Further, this association was not observed in the patients that received the combination of TAS+FUL, which may inform future rational combination strategies for the clinical development of PI3K inhibitors in ER+/HER2- *PIK3CA*mut aBC.

#5560

Prognostic effect of co-mutations on patients with *NPM1*+ acute myeloid leukemia (AML) enrolled in the Connect® Myeloid registry

Jaroslaw P. Maciejewski[1], Daniel A. Pollyea[2], Gail J. Roboz[3], Karen Seiter[4], Bart L. Scott[5], Irene S. DeGutis[6], Pavel Kiselev[6], Edward Yu[6], Ali

McBride[6], Willem Heydendael[6], Harry P. Erba[7]. *[1]Cleveland Clinic, Taussig Cancer Center, Cleveland, OH,[2]University of Colorado, Aurora, CO,[3]Weill Cornell Medicine and NY Presbyterian Hospital, New York, NY,[4]New York Medical College, Valhalla, NY,[5]Fred Hutchinson Cancer Research Center, Seattle, WA,[6]Bristol Myers Squibb, Princeton, NJ,[7]Duke University, Durham, NC*

Introduction: The 2017 World Health Organization classification of myeloid neoplasms and acute myeloid leukemia (AML) recognizes AML with mutated *NPM1* as a distinct entity with favorable prognosis. However, as mutations other than *NPM1* may further influence disease prognosis, here we assess the prognostic effect of *NPM1* co-mutations in patients (pts) with AML enrolled in the Connect® Myeloid Registry (NCT01688011).
Methods: The Registry is a large, US, multicenter, prospective observational cohort study of pts with newly diagnosed AML, myelodysplastic syndromes, idiopathic cytopenia of undetermined significance, or myelofibrosis. In this analysis, pts with AML ≥55 years of age were grouped by known *NPM1* status (*NPM1*+ vs *NPM1*–). The frequency of gene mutations was analyzed among patients with *NPM1*+ AML and *NPM1*– AML. Overall survival (OS) was evaluated using the Cox model adjusted for age and mutations in *TP53* and *RUNX1*.
Results: Overall, 123 pts with *NPM1*+ AML and 360 pts with *NPM1*– AML were included. Most pts were male (*NPM1*+, 61.5%; *NPM1*−, 60.7%) and White (*NPM1*+, 78.0%; *NPM1*−, 85.6%); median (range) age was 67 (55-87) and 71 (55-97) years for the *NPM1*+ and *NPM1*− groups, respectively. After adjusting for age, pts with *NPM1*+ AML had significantly longer median OS than pts with *NPM1*– AML (26 vs 15 months; HR [95% CI]: 0.58 [0.44-0.76]; $P < 0.01$; Table). Pts with *NPM1*+ vs *NPM1*– AML had a lower frequency of certain key mutations such as *TP53* (1.6% vs 18.6%) and *RUNX1* (0.8% vs 14.8%). The significant survival benefit with *NPM1*+ vs *NPM1*– initially observed after adjusting for age was not observed after further adjusting for presence of *TP53* and *RUNX1* mutations (*NPM1*+ vs *NPM1*–; 23 vs 19 months; HR [95% CI]: 0.75 [0.48-1.17]; $P = 0.21$).
Conclusions: *TP53* plus *RUNX1* mutation was identified as a pattern of co-mutational burden that were observed less frequently and potentially contributed to the improved OS of pts with *NPM1*+ AML and poorer OS of pts with *NPM1*– AML.

	***NPM1*+ n = 123**	***NPM1*– n = 210**
Overall survival, months Adjusted for age	26.0	15.0
Hazard ratio (95% CI)	0.58 (0.44-0.76)	
Adjusted for age, *TP53, RUNX1*	23.0	19.0
Hazard ratio (95% CI)	0.75 (0.48-1.17)	
Frequency of gene mutations, n (%) *TP53*	2 (1.6)	39 (18.6)
ASXL1	3 (2.4)	37 (17.6)
FLT3-ITD	44 (35.8)	36 (17.1)
TET2	20 (16.3)	34 (16.2)
DNMT3A	29 (23.6)	33 (15.7)
IDH2	11 (8.9)	33 (15.7)
RUNX1	1 (0.8)	31 (14.8)
NRAS/KRAS	11 (8.9)	30 (14.3)
IDH1	18 (14.6)	18 (8.6)
CEBPA	4 (3.3)	15 (7.1)
WT1	5 (4.1)	14 (6.7)
FLT3-TKD	18 (14.6)	13 (6.2)
PHF6	0	12 (5.7)
PTPN11	4 (3.3)	12 (5.7)
SF3B1	2 (1.6)	8 (3.8)
C-KIT	1 (0.8)	7 (3.3)
EZH2	1 (0.8)	4 (1.9)
ETV6	0	3 (1.4)
MLL-PTD	1 (0.8)	1 (0.5)
Other	30 (24.4)	114 (54.3)

#5561
Molecular imaging of calcification and soft tissue defines prognosis of DCIS to invasive breast cancer

Jayakrupakar Nallala[1], Doriana Calabrese[1], Sarah Gosling[2], Esther Lips[3], Rachel Factor[4], Allison Hall[4], Sarah Pinder[5], Ihssane Bouybayoune[5], Elinor Sawyer[5], Lorraine King[4], Jeffrey Marks[4], Thomas Lynch[4], Donna Pinto[6], Jelle Wesseling[3], Shelley Hwang[4], Keith Rogers[2], Nick Stone[1], Grand Challenge PRECISION consortium. *[1]University of Exeter, Exeter, United Kingdom,[2]Cranfield University, Cranfield, United Kingdom,[3]The Netherlands Cancer Institute, Amsterdam, Netherlands,[4]Duke University School of Medicine, Durham, NC,[5]Kings College London, London, United Kingdom,[6]DCIS411, San Diego, CA*

Introduction: Ductal carcinoma in situ (DCIS) is a non-obligatory precursor to invasive breast cancer (IBC). Currently there are no reliable markers to indicate if DCIS will progress IBC after an initial treatment, or if it will remain as DCIS. Because of this uncertainty, standard treatment for DCIS includes surgery with or without radiotherapy. Breast microcalcifications are a common feature in the mammographic detection of DCIS and occur in around 80% of DCIS and 50% of IBC. Despite this, their potential role in the development of DCIS and with progression to IBC remains largely unexplored. The main aim of the study is to identify novel biomarkers for DCIS prognosis, based on chemical and molecular compositional changes of calcifications and their surrounding soft tissue in DCIS.
Methods: Consecutive tissue section from 422 patients were analyzed using mid-infrared and Raman hyperspectral imaging and X-ray diffraction (XRD) and included (i) ‘DCIS controls’ (DCIS without recurrence) (n=193), (ii) ‘DCIS cases’ (DCIS which subsequently recurred as an invasive disease) (n=123), (iii) ‘synchronous DCIS with invasive cancer’ (n=44) and ‘benign’ (n=62) groups. Both parametrized and data mining approaches including cluster analysis, unsupervised and supervised multivariate statistical analysis and biomodelling based on leave-one-sample-out cross-validation were used to classify the data and develop DCIS prediction models.
Results: Prediction modelling of 314 calcification and soft tissue spectral images from 170 patients (‘DCIS controls’=118 versus ‘DCIS cases’=52) showed an AUROC mean value of 0.85 in distinguishing DCIS that did not recur from DCIS that recurred as IBC. Prediction modelling of XRD data from 124 patients (‘DCIS controls’=67 versus ‘DCIS cases’=57) showed an

AUROC mean value of 0.80. The calcification spectral features showed pathology specific changes in phosphate to carbonate ratio as well as changes in magnesium whitlockite content. The epithelial features showed changes in protein secondary structure and content indicating structural remodeling between the two groups. XRD parametrized data analysis corroborated these observations in terms of difference in whitlockite, as well as crystallinity/unit axis of the measured calcifications. The prediction models are currently being tested independently on the remaining sample data.
Conclusion: Complementary chemical and molecular analysis of breast calcifications and soft tissue using spectroscopy and XRD imaging predicts the likely progression of DCIS to IBC. Subject to the ongoing validation of biomarkers, these approaches appear as promising DCIS risk assessment tools that can inform diagnosis, prognosis and treatment options.

#5562

Prevalence and prognostic significance of malnutrition in patients with brain metastasis

Zheran Liu[1], Yu Zhang[2], Yiyan Pei[1], Yan He[1], Jiayi Yu[3], Renjie Zhang[1], Jingjing Wang[1], Weelic Chong[4], Yang Hai[4], Xingchen Peng[1], Fang Fang[1].
[1]West China Hospital of Sichuan University, Chengdu, China,[2]Affiliated Hospital of Chengdu University, Chengdu, China,[3]Chengdu University of Traditional Chinese Medicine, Chengdu, China,[4]Thomas Jefferson University, Philadelphia, PA

Background: Malnutrition is a severe but modifiable risk factor for cancers. However, the relationship between malnutrition and the survival of patients with brain metastases has not been fully revealed. We aimed to evaluate the prevalence of malnutrition and assess its prognostic value on patients with brain metastases.
Method: We retrospectively recruited 2633 patients with brain metastases between January 2014 and September 2020. Three malnutrition scores were used to evaluate patients' malnutrition status at their first admission, including controlling nutritional status (CONUT), the nutritional risk index (NRI), and the prognostic nutritional index (PNI). The association between malnutrition and overall survival was estimated.

Results: A total of 1984 (75.4%) of patients were assessed as any degree malnourished and 963 (36.6%) of patients were assessed as moderate to severe malnutrition by at least one malnutrition score. The three malnutrition scores were associated with each other and with BMI. Malnutrition assessed by any of the three scores was significantly associated with poor overall survival (adjust hazard ratio [HR] and 95% confidence interval [CI] for CONUT: 1.12 [1.10-1.16]; for NRI: 0.97 [0.97-0.98]; for PNI: 0.96 [0.95-0.97], all p values <0.001). Furthermore, malnutrition was a better indicator than BMI, and adding malnutrition to the Graded Prognostic Assessment scoring system could significantly improve the accuracy of prognosis prediction.
Conclusion: Malnutrition was prevalent in patients with brain metastases and was significantly associated with overall survival. Malnutrition monitoring on patients' first admission could improve the survival prediction ability for brain metastasis.

#5563

Androgen receptor (AR) is frequently found in human cancers and inversely linked to patient outcome in breast and renal cell carcinomas

Florian Viehweger[1], David Dum[1], Anne Menz[1], Ria Uhlig[1], Andrea Hinsch[1], Doris Höflmayer[1], Tim Mandelkow[1], Christoph Fraune[1], Christian Bernreuther[1], Patrick Lebok[1], Sören Weidemann[1], Guido Sauter[1], Maximilian Lennartz[1], Frank Jacobsen[1], Till S. Clauditz[1], Till Krech[1], Andreas H. Marx[2], Ronald Simon[1], Stefan Steurer[1], Eike Burandt[1], Sarah Minner[1]. *[1]Institute of Pathology, University Medical Center Hamburg-Eppendorf, Hamburg, Germany,[2]Pathology, Klinikum Fürth, Fürth, Germany*

Background**:** Androgen receptor (AR) is a nuclear transcription regulator which mediates the growths stimulating effect of androgens. Inhibition of AR signaling is the most important first line therapy in prostate cancer. Clinical trials are ongoing for molecularly defined subsets of breast cancers expressing AR. In surgical pathology, AR immunohistochemistry is used as a marker for prostate cancer.
Design: To comprehensively determine AR expression in normal and neoplastic tissues, a tissue microarray containing 18,234 samples from 141

different tumor types and subtypes as well as 608 samples of 76 different normal tissue types was analyzed by immunohistochemistry.
Results: AR positivity was found in 116 of 141 tumor categories, and 66 of these tumor categories contained at least one case with strong AR staining. AR positivity was most seen in different categories of prostate cancer (87.8-100%), various subtypes of breast cancer (34.3-94.9%) and ovarian cancers (48.7-97.1%), in endometrial cancers (53-61.1%), salivary duct carcinomas (70%), teratomas (60%), renal cell carcinomas (41.8-62.7%), urinary bladder cancers (43.2-48.7%), granular cell tumors (40.7%), leiomyosarcomas (33.3%), gastrointestinal stroma tumors (31.1%) and urothelial carcinomas of the kidney pelvis (30.4%). Seventy-seven additional tumor types showed AR expression in up to 30% of the analyzed samples, but AR expression was typically only weak in these tumors. Among 1,430 evaluable invasive breast carcinomas of no special type (NST), absent or low AR immunostaining was significantly linked to high BRE grade ($p<0.0001$), advanced pT stage ($p<0.0001$), presence of nodal and distant metastasis ($p<0.0001$ each), HER2 overexpression ($p=0.005$), reduced estrogen and progesterone receptor expression ($p<0.0001$ each), triple negative status ($p<0.0001$) and shortened patient survival ($p=0.0024$). Among 1,149 clear cell renal cell cancers (RCC), low AR immunostaining was linked to high ISUP, Fuhrman and Thoenes grades ($p<0.0001$ each), high UICC and pT stage ($p<0.0001$ each), presence of distant metastases ($p=0.0075$), and reduced time to recurrence ($p=0.0007$), overall survival ($p=0.0097$) and tumor-specific survival ($p=0.0129$). In 297 papillary RCC, low AR staining was associated with high ISUP grade ($p=0.0179$), advanced pT stage ($p=0.0055$) and nodal metastasis ($p=0.0044$). Low AR expression was linked to invasive growth ($p<0.0001$) and nodal metastasis in urothelial carcinoma ($p=0.0052$).
Conclusion: The results of our study demonstrate AR expression in a wide range of cancers. AR expression occurs most frequent in cancers of the prostate, breast, and ovary, but can be found in many types of non-prostate and non-gynecological neoplasms. The poor prognosis of breast and kidney cancers with reduced AR expression argues against a tumor promoting role of AR in these tumor types.

#5564
SerpinE2: A potential biomarker for urological cancers

Ruusu-Maaria Kovanen, Netta Koskinen, Timo-Pekka Lehto, Antti Rannikko, Tuomas Mirtti, Hannu Koistinen. *University of Helsinki, Helsinki, Finland*

SerpinE2, also known as protease nexin-1, is an extracellular serine protease inhibitor modulating the activity of serine proteases such as thrombin, plasmin, urokinase-type plasminogen activator and trypsin. Dysregulation between extracellular serine proteases and their cognate inhibitors has been implicated in malignant progression, making serpins promising biomarkers for tumor progression and prognosis. SerpinE2 is upregulated in many cancers and promotes tumor invasion and metastasis. In this study, we analyzed serpinE2 expression by immunohistochemistry on tissue microarrays comprising of samples from prostate, bladder and kidney cancers. The studied samples were clinically hard-to-risk stratify and thus relevant for biomarker studies. We aimed to study the association of serpinE2 expression with survival and clinicopathological features in all three cancers, and evaluate its potential as an immunohistochemical biomarker. In the case of bladder cancer, association of serpinE2 expression with response to neoadjuvant chemotherapy was also assessed. We found that although the strong expression of serpinE2 was related to more aggressive prostate cancers ($p = 0.017$) and high grade bladder cancers ($p = 0.034$), it was not associated with relapse, treatment response or survival of prostate and bladder cancer patients. In renal cancer, on the contrary, serpinE2 expression was significantly lower in patients with tumor relapse ($p = 0.048$) and high expression predicted favorable disease-specific survival ($p = 0.013$). Our findings help understanding the functional role of serpinE2 in cancer progression and guide the prognostic biomarker research of serpinE2, particularly for prediction of renal cancer-specific survival.

#5567

Circulating bacterial DNA is a non-invasive biomarker for early recurrence of NSCLC patients

Haiming Chen[1], Yiming Lu[2], Mantang Qiu[1]. *[1]Peking University People's Hospital, Beijing, China,[2]Beijing Institute of Radiation Medicine, Beijing, China*

Background: Alteration of human microbiota has been implicated in non-small cell lung cancer (NSCLC). However, most metagenomics studies utilized fecal samples, circulating bacteria DNA in patients with respectable NSCLC remain unexplored. This study aimed to characterize bacteria DNA in plasma of respectable NSCLC patients and build a machine-learning model to detect early recurrence of NSCLC.
Methods: We performed whole genome sequencing of plasma from 101 NSCLC patients with (n = 36, R) or without (n = 65, NR) tumor recurrence within three years after surgery. Microbial DNA was obtained by removing the host genome and relative abundance was measured by mapping reads into microbial genomes. Significant microbial features were identified in the discovery set and built into a random forest model, which was tested in the validation set.
Results: We enrolled 22 R and 39 NR patients with matching demographic features in the discovery set. The remaining 14 R and 26 NR patients were included in the validation set. PCoA analysis using Bray-Curtis distance showed significant differences between R and NR patients at genus level and species level in the discovery set. Notably, in the discovery set, 4 genera and 13 species showed significantly lower abundance in R patients, whereas 11 genera and 21 species were conversely enriched. Based on these significant microbial features, the random-forest model obtained the maximal AUC value of 0.9044 (95% CI, 0.8203-0.9886) when 11 features were selected. In the validation set, this model distinguished R from NR patients with an AUC of 0. 8434 (95% CI, 0.7189-0.9679).
Conclusions: This pioneer study characterized alteration of circulating bacterial DNA in NSCLC patients with early recurrence, and illustrated significant difference in microbial composition between R and NR patients. The predictive model constructed with selected circulating microbial features was an accurate and non-invasive tool for prediction in early NSCLC recurrence.

#5569

Quantification of tumor-associated vasculature as an imaging biomarker for monitoring the response of triple-negative breast cancer to neoadjuvant chemotherapy

Chengyue Wu[1], Casey E. Stowers[1], Zhan Xu[2], Ernesto A. B. F. Lima[1], Clinton Yam[3], Jong Bum Son[2], Jingfei Ma[2], Gaiane M. Rauch[4], Thomas E.

Yankeelov[1]. *[1]Oden Institute for Computational Engineering and Sciences, University of Texas at Austin, Austin, TX,[2]Department of Imaging Physics, The University of Texas MD Anderson Cancer Center, Houston, TX,[3]Department of Breast Medical Oncology, The University of Texas MD Anderson Cancer Center, Houston, TX,[4]Department of Breast Imaging, The University of Texas MD Anderson Cancer Center, Houston, TX*

Introduction: Patients with locally advanced, triple-negative breast cancer (TNBC) typically receive neoadjuvant systemic therapy (NAST). However, the response of TNBC to NAST is varied and a prognostic marker is still lacking. Since angiogenesis plays an important role in cancer progression, the quantification of changes in the tumor vasculature during treatment has the potential to provide useful information for characterizing the treatment response. We have recently developed a method to quantify changes in tumor-associated vasculature through a novel analysis of dynamic contrast-enhanced magnetic resonance imaging (DCE-MRI). In this study, we investigated its ability to monitor the response of TNBC to NAST.
Methods: Dynamic contrast-enhanced (DCE) MRI was acquired in TNBC patients (N = 50; 25 pathological complete response (pCR), 25 non-pCR) before, after 2 and 4 cycles of Adriamycin/Cyclophosphamide (A/C), as part of the ARTEMIS trial (NCT02276433). Using DCE-MRI, we identified the tumor-associated vessels *via* a breast vasculature analysis. Specifically, the difference between pre- and post-contrast DCE-MRI images was enhanced by a histogram-based intensity transfer function. The 3D vasculature in the breast was then segmented by applying a Hessian filter. Given the vasculature segmented by the algorithms and the tumor masks segmented by radiologists, a lowest-cost tracking algorithm was used to automatically detect the vessels that are most likely to contact the tumor. These vessels are defined as tumor-associated vessels (TAV). The number of TAVs per patient was tabulated and the Wilcoxon rank sum test compared the TAV values before (V1), after 2 cycles (V2), and after 4 cycles of NAST (V3). Additionally, we compared the percent change of TAV from V1 to V3 between the pCR patients and non-pCR patients. Statistical significance was defined as $P < 0.05$.
Results: A significant decrease in the number of TAVs was observed during the NAST. In particular, the number of TAVs has a median (interquartile range) of 15 (7 - 24), 7 (3 - 14), and 2 (0 - 8) at V1, V2, V3, respectively,

which are (pair-wise) significantly different ($P < 0.01$). Moreover, pCR patients showed a significantly greater decrease in the number of TAVs as compared to non-pCR patients. The percent changes in the number of TAVs from V1 to V3 have a median (range) of -88.89% (-100.00% - -60.00%) and -66.67% (-87.85% - -40.88%) in the pCR and non-pCR patients, respectively ($P < 0.05$).
Conclusion: These preliminary results demonstrate that tumor-associated vasculature may be a valuable imaging biomarker for monitoring the response of TNBC to NAST. Ongoing efforts include additional investigation of the TAVs beyond their number, as well as applying the analysis to more patients.

#5570

Development of prognostic index based on twenty-three genes for predicting superficial-to-invasive progression of non-muscle invasive bladder cancer patients

Jae-Yoon Kim[1], Seong-Hwan Park[1], Seon-Young Kim[1], Seok Joong Yoon[2], Seon-Kyu Kim[1]. *[1]Korea Research Institute of Bioscience and Biotechnology, Daejeon, Korea, Republic of,[2]Chungbuk National University College of Medicine, Cheongju, Korea, Republic of*

Background: Although recent advances in high-throughput technology and data-driven approach have provided many insights into non-muscle invasive bladder cancer (NMIBC), previous studies are still limited in their ability to predict the clinical behavior of NMIBC. Here, using deep learning method with long term follow-up data, we identified a prognostic gene set consisting of a small gene group for precisely predicting NMIBC heterogeneity.
Methods: We sought to identify progression-associated genes in patients with NMIBC using Cox regression analysis and verified their predictive values using a fully connected neural network (FNN) algorithm in five independent cohorts comprising more than 800 NMIBC patients. Based on these genes, a prognostic index (PI) in NMIBC progression was also developed. The association between the PI and prognosis of NMIBC patients was evaluated using Kaplan-Meier plots and log-rank tests.
Results: Gene expression profiling in NMIBC patients identified a prognostic gene set consisting of 1,789 genes for predicting NMIBC

progression in a patient cohort (training set, n = 103). Their prognostic significances were validated based on FNN algorithm in other four independent cohorts (validation sets, n = 722). Pathway enrichment analysis revealed a twenty-three gene signature including known prognostic transcription factors such as FOXM1 and E2F1 along with novel genes. We incorporated these genes into the PI system, which was a significant prognostic indicator of NMIBC progression. The PI system was shown to be an independent risk factor by a multivariate analysis and subset stratification according to stage and grade (each $P < 0.001$). The subset analysis also revealed that the PI system could identify patients who would benefit from BCG immunotherapy.
Conclusions: The twenty-three gene-based PI represents a promising diagnostic tool for the identification of high-risk NMIBC patients who would display different clinical behaviours as well as response to BCG immunotherapy.

#5571
FoxP3 absolute quantification to build an effective risk model for cancer patient survival
Adele Ponzoni, Sandra Delebecq, Melodie Boute, Corinne Ramos, Jonathan Stauber. *ImaBiotech, Loos, France*

Background: Forkhead box protein P3 (FOXP3), belonging to the forkhead/winged-helix family, is of great importance in modulating the differentiation and development of T-regulatory cells (Tregs). The numbers of $FOXP3^+$ Tregs as well as exhaustive subsets of $CD4^+$ and $CD8^+$ T cells have been observed increased in solid tumor tissues of patients with colorectal and breast cancers, which helps to create an immunosuppressive environment and promotes tumor progression. However, the correlation between the presence of $FOXP3^+$ Tregs and patients' survival has been extensively studied in many cancer types, which remains conflicting. The approach presented here aims to absolutely quantify the level of FOXP3 in single cells and constructed effective immune risk models to predict tumor prognosis.
Method: Imaging mass cytometry (IMC) was used to quantify FOXP3 inside each single cell. The indirect quantification used a free-metal titration curve in order to match the level of intensity of the metal-tagged antibodies

to the level of expression of the antigen. Deep learning (StarDist QuPath extension) was used for cell segmentation and expression quantification. FOXP3 quantification in tissue or at the single cell level was validated against ELISA assay that measure FOXP3 in tissue lysate.
Results: Linearity of the metal signals with an average %CV of 17% was observed emphasizing the linear correlation between free metal concentration and intensity. With the IMC technique, the minimum amount of FoxP3 detectable is 0.09 femtogram and its absolute quantification in the different cells in tumor tissues was confronted to disease prognosis in order to start building an effective immune risk model.
Conclusion: With the introduction of new biologics in cancer therapy, it is imperative to follow real quantitative change in the expression of biological marker that are indicator of tumor prognosis. Indeed, although the FOXP3 distribution was already seen to be heterogenous in tumors, its absolute level of expression indicative of disease progression can be directly correlated to gain better understanding of the patient response stratification to biologics.

#5572

A COX-2-based pro-tumourigenic inflammatory signature predicts poor outcome in early-stage non-small cell lung cancer

Victoria Fife[1], Matthew Roberts[1], Christian P. Bromley[2], Derrick Morgan[1], Sophie Atkinson[1], Cong Zhou[1], Anshuman Chaturvedi[3], Steven Bagley[4], Garry Ashton[4], Lisa M. Coussens[5], Philip A. J. Crosbie[6], Caroline Dive[1], Elaine Kilgour[1], Santiago Zelenay[2]. *[1]Cancer Biomarker Centre, Cancer Research UK Manchester Institute (Alderley Park), Manchester, United Kingdom,[2]Cancer Inflammation and Immunity, Cancer Research UK Manchester Institute (Alderley Park), Manchester, United Kingdom,[3]Histopathology, The Christie Hospital, Manchester, United Kingdom,[4]Core Facilities, Cancer Research UK Manchester Institute (Alderley Park), Manchester, United Kingdom,[5]Department of Cell, Developmental & Cancer Biology, Knight Cancer Institute, Oregon Health and Science University, Portland, OR,[6]Division of Infection, Immunity and Respiratory Medicine, University of Manchester, Manchester, United Kingdom*

Lung cancer is the most common cause of cancer-related deaths with Non-Small Cell Lung Cancer (NSCLC) accounting for ~85% of cases. Patients with early-stage NSCLC (stages I-IIIA) undergo surgery with curative intent but up to 30% relapse. Identification of biomarkers that predict outcome at the point of surgery could inform patient management. Here, we explored whether a COX-2-based pro-tumourigenic inflammatory gene signature (PTI), measured in surgically resected samples from early-stage NSCLC patients, can predict patient outcome. Gene expression analysis was performed on 30 formalin fixed paraffin embedded surgical tumour samples from early-stage NSCLC patients with 36-63 months follow-up, using a custom code-set on the NanoString nCounter® platform. Additionally, *in silico* analysis of early-stage NSCLC data from The Cancer Genome Atlas (TCGA) was undertaken. The PTI gene signature and a published signature associated with T cell-inflamed tumours measuring IFNγ activity (IFNG)[1] were assessed in both datasets and correlated with patient outcome. NanoString gene expression data was robust, displaying good correlations with immunohistochemistry (IHC) expression for key proteins such as CD8 and COX-2, $R=0.88$, $p<1x10^{-6}$ and $R=0.83$, $p<1x10^{-6}$, respectively. The IFNG signature score, widely reported to associate with response to checkpoint inhibitors[2], did not correlate with outcome and consistent with this observation neither did CD8 protein expression (by IHC). In contrast, patients with LUSC (n=16) with the highest (upper quartile) PTI score showed significantly worse overall survival ($p<0.01$). Median overall survival for these PTI^{high} patients was <6 months vs 4.5 years for LUSC patients with PTI^{low} scores. Analysis of TCGA data from stage I-IIIA LUAD/LUSC cases confirmed these contrasting findings for the PTI compared with the IFNG signature. A multiplexed IHC panel for immune contexture analysis was successfully transferred from the Coussens Laboratory Oregon to CRUK Manchester[3] and with inclusion of COX-2 in this panel and adaptation of the pipeline for use with the HALO image analysis platform, analysis of the immune contexture in PTI high versus low tumours is underway. Transcriptional profiling of early-stage NSCLC samples revealed that COX-2-associated inflammation predicts patient outcome following surgery. These data highlight the importance of pro-tumourigenic inflammation in early-stage NSCLC. Findings are under validation in a larger cohort, including early-stage NSCLC samples from Manchester's early-detection screening studies and mapping of the immune

contexture of PTI high versus low tumours is underway. 1: Ayers, M., et al., J Clin Invest., 2017 2: Danaher, P., et al., J Immunother Cancer., 2018 3: Banik, G., et al., Methods Enzymol., 2020

#5573

Use of circulating tumor DNA (ctDNA) for early assessment of treatment response in patients with non-small cell lung cancer (NSCLC): A real-world (RW) analysis incorporating baseline ctDNA level and molecular response

Sean Gordon, Bojan Losic, Katie Quinn, Kyle Chang, Jiemin Liao, Han-Yu Chuang. *Guardant Health, Redwood City, CA*

Background: Data suggests that changes in ctDNA quantity correlate with response to therapy in patients with advanced solid malignancies. Furthermore, absolute baseline (pre-treatment) ctDNA level has been shown to be associated with patient prognosis. However, there is little information on how these variables can be combined to better interpret ctDNA results and enhance predictive power of treatment response. Here, we develop a model that incorporates the effects of both baseline ctDNA level as well as linear and nonlinear relative ctDNA change.
Methods: We queried the Guardant INFORM database, which comprises aggregated commercial payer health claims and de-identified records from over 225,000 individuals with comprehensive ctDNA testing via Guardant360 (G360). From September 2018-March 2022, patients with NSCLC treated with immune checkpoint inhibitors (ICI) (monotherapy or in combination) who received a ctDNA test within 15 weeks prior to treatment initiation and a second test 3-15 weeks after treatment initiation were retrospectively evaluated. Cox proportional hazards (CPH) were used for RW time to next treatment (TTNT) and time to treatment discontinuation (TTD) analyses. Gender, age, line of therapy (LOT) and comorbidities were included as covariates. ctDNA change from baseline to on-treatment (using the Guardant360 Response algorithm) was modeled as a continuous variable using a regularized cubic spline and baseline ctDNA level (using maximum variant allele fraction) was modeled as an interaction effect. Model validation and calibration were carried out via bootstrap resampling, ANOVA was used for multiple design hypothesis testing.

Results: 82 patients met the study criteria. 31 patients with large ctDNA decrease (e.g. >=50% decrease), also known as molecular responders, had significantly longer TTNT and TTD compared to other patients, regardless of baseline ctDNA level. 51 patients with small ctDNA decrease or ctDNA increase showed ctDNA level dependent trends in TTNT and TTD, with decreased risk for shorter TTNT and TTD for lower baseline ctDNA level. We found that the interaction between baseline ctDNA level and ctDNA change was significant (TTNT: p = .0069, TTD: p = .0236), and that ctDNA change had a nonlinear effect on both TTNT and TTD (TTNT: p = .0014, TTD: p = .0349). TTNT (TTD) bootstrap-adjusted concordance indices were 0.69 (0.65) and hazard ratios [95% CI] were 5.36 [1.79, 16.10] (2.37 [1.13, 4.98]).
Conclusions: These data demonstrate a statistically significant interaction between baseline ctDNA level and treatment-induced ctDNA level change in association with RW clinical outcomes. This facilitates the development of patient-based models incorporating baseline ctDNA level with ctDNA molecular response for association with RW clinical outcomes.

Immune-based Biomarkers for Prognostic and Predictive Benefit

#5701
Predictive biomarker models of immunotherapy response in patients with metastatic melanoma: genomic, transcriptomic, and immune profiles from the Personalised Immunotherapy Program (PIP)
Tuba N. Gide[1], Nurudeen A. Adegoke[1], Yizhe Mao[1], Monica Lennox[1], Saurab Raj[1], Camelia Quek[1], Ismael A. Vergara[1], Nigel Maher[1], Alison Potter[2], Robyn P. M. Saw[3], John F. Thompson[4], Andrew J. Spillane[1], Kerwin F. Shannon[1], Matteo S. Carlino[1], Maria Gonzalez[1], Serigne N. Lo[1], Alexander M. Menzies[1], Inês Pires da Silva[1], Richard A. Scolyer[1], Georgina V. Long[1], James S. Wilmott[1]. *[1]Melanoma Institute Australia, The University of Sydney, Camperdown, Australia,[2]Royal Prince Alfred Hospital and NSW Health Pathology, Camperdown, Australia,[3]Royal North Shore Hospital, Camperdown, Australia,[4]Royal Prince Alfred Hospital, Camperdown, Australia*

Background: While immune checkpoint inhibitors (ICI) have become the standard-of-care for advanced melanoma patients, only half of treated patients will survive beyond 5-years and many develop significant toxicity. The PIP study is combining pre-treatment clinical, molecular, and immunological profiles of melanoma patients to provide accurate prediction of response to ICI therapies.
Methods: 504 patients with advanced melanoma who received anti-PD-1±CTLA-4 ICI were studied to develop predictive models of resistance to ICI. Resistance was defined as patients with progressive disease as best response, or partial response/stable disease with <6 months progression-free survival (RECIST 1.1). Machine learning models were developed using clinicopathological characteristics, tumor mutation burden (TMB, Qiaseq TMB IO), gene expression profiling ((GEP), Nanostring Pancancer 360 IO) and spatial quantitative pathology immune profiling (multiplex immunofluorescence, (MIF)) of baseline melanoma biopsies. Models were developed in a discovery cohort (n=247), validated in an independent cohort (n=97), with an accruing prospective cohort (n=160). Model predictive performance was assessed using the area under the curve (AUC).
Results: Models were developed and validated using sequential addition of omics features to relevant clinical factors. Baseline clinical data alone achieved an AUC of 68%. Clinical plus three-tier TMB (<10, 10-20, >20 mut/mb) achieved an AUC of 78%. Clinical data plus GEP achieved 79% AUC, inclusive of tumor inflammation, antigen presentation and T-cell related signatures. Clinical and MIF spatial pathology achieved an 82% AUC including the distances between T-cells, CD16+ cells and melanoma cells as features in the model. Finally, the combination of TMB and GEP achieved an 83% AUC. Prospective validation of the models is awaiting follow-up milestones.
Conclusion: Multi-omic models using pre-treatment tissue and clinicopathology can significantly improve the accuracy of predicting patient outcomes to ICI treatments compared to baseline clinical data alone. Several models may be required based on different omic combinations to account for the reality of biopsy suitability and assay failures. These findings prove personalized precision treatment of patients with immunotherapies is possible in the clinical setting and such approaches should become routine care.

#5702

Ovarian cancer tumor microenvironment and atezolizumab (atezo) clinical activity: IMagyn050 sub-study

Venkatesh Krishnan[1], Ching-Wei Chang[2], Habib Hamidi[1], Michael A. Bookman[3], Charles Landen[4], Tashanna Myers[5], Hiroaki Kajiyama[6], Sakari Hietanen[7], Lyndsay Willmott[8], Premal Thaker[9], Cagatay Taskiran[10], Jalid Sehouli[11], Victor Khor[12], Yvonne Lin Liu[12], Sandro Pignata[13], Kathleen Moore[14], Luciana Molinero[1]. *[1]Oncology Biomarker Development, Genentech, Inc., South San Francisco, CA,[2]Personalized Healthcare and Early Development Oncology Biostatistics, Genentech, Inc., South San Francisco, CA,[3]Gynecologic Oncology Group Foundation (GOG-F) and Kaiser Permanente Northern California, San Francisco, CA,[4]Department of Obstetrics and Gynecology, Gynecologic Oncology Group Foundation (GOG-F) and University of Virginia, Charlottesville, VA,[5]Gynecologic Oncology Group Foundation (GOG-F) and Baystate Medical Center, Springfield, MA,[6]Department of Obstetrics and Gynecology, Nagoya University, Nagoya, Japan,[7]Turku University Hospital, Turku, Finland,[8]Arizona Center for Cancer Care, Phoenix, AZ,[9]Gynecologic Oncology Group Foundation (GOG-F) and Washington University School of Medicine, St Louis, MO,[10]Turkish Society of Gynecologic Oncology (TRSGO) and Koc University School of Medicine and VKV American Hospital, Istanbul, Turkey,[11]Arbeitsgemeinschaft Gynaekologische Onkologie (AGO)/Nord-Ostdeutsche Gesellschaft für Gynäkologische Onkologie (North-Eastern German Society of Gynaecologic Oncology; NOGGO) and Charité-Medical University of Berlin (Campus Virchow Klinikum), Berlin, Germany,[12]Product Development Oncology, Genentech, Inc., South San Francisco, CA,[13]Multicentre Italian Trials in Ovarian Cancer and Gynecologic Malignancies (MITO) and Istituto Nazionale Tumori IRCCS Fondazione G Pascale, Napoli, Italy,[14]Gynecologic Oncology Group Foundation (GOG-F) and Stephenson Cancer Center at the University of Oklahoma Health Sciences Center, Oklahoma City, OK and Sarah Cannon Research Institute, Nashville, TN*

Background: Tumor biomarkers such as CD8 density and location (i.e., immune inflamed phenotype) and immune rich molecular subtype have been linked to immune checkpoint blockade (ICB) overall survival (OS) in

different cancers. The IMagyn050 trial (NCT03038100), which evaluated the efficacy of Atezo vs placebo (Pla) with carboplatin, paclitaxel and bevacizumab (CPB) in front line ovarian cancer patient (pts), did not meet its co-primary endpoints of PFS in ITT or PD-L1+ (Moore et al. JCO 2021). In the current IMagyn050 substudy we assessed potential predictive tumor immune biomarkers for Atezo clinical benefit.
Methods: FFPE tumors from the biomarker evaluable population were tested for PD-L1 IHC, CD8/PanCK IHC (total CD8 T cells and immune location phenotypes [inflamed, excluded, desert]) and RNA-seq (to derive molecular subtypes, biological pathways and cellular components [xCELL]) in tissue from baseline (n=860), on-treatment (OT, 9 weeks, n=233), intra- (n=8) and inter-lesion (n=12) matched samples. Hazard ratio (HR) interaction test from multivariate adjusted Cox-regression analysis for PFS and OS was performed to test predictive biomarkers.
Results: While tumors with CD8 T cells, immunoreactive molecular subtypes or immune inflamed phenotype were enriched for PD-L1+, only pts with immune inflamed tumors showed improved OS Atezo benefit (HR 0.67). Improved Atezo PFS/OS benefit was also observed in pts with whose tumors had high oxidative phosphorylation (OXPHOS, HR: 0.72/0.65) and UV Response (UV, HR: 0.64/0.58) but not IFNγ response. Plasma B cells were linked to improved OS Atezo benefit vs Pla (HR 0.53). We leveraged OT samples from pts in the neoadjuvant cohort to assess treatment effect on the tumor microenvironment. Analyses showed that CPB reduced tumor proliferation and increased tumor immune inflammation (CD8 T cells, PD-L1 and IFNα/IFNγ response), further increased by Atezo. Immune inflammation is challenging in ovarian cancer due to extensive tumor heterogeneity. Prevalence of tumor biomarkers varied by anatomic locations: total CD8, CD8 localization and molecular subtypes. Inter- and intra-lesion biomarker status within the same pt showed PD-L1 and plasma B cells as most consistent. Molecular subtypes and immune phenotypes had moderate intra-lesion agreement but discordant between lesions. PD-L1 and OXPHOS were the only biomarkers linked to Atezo benefit regardless of anatomical location.
Conclusion: This comprehensive exploratory study suggests that DNA damage, OXPHOS, plasma B cells and immune inflamed tumors, but not molecular subtypes or total CD8 T cells, may predict Atezo + CPB OS. This treatment promotes immune inflammation in OC tumors. Notably, we

found that several biomarkers are highly heterogeneous. Our findings highlight the challenges of achieving durable clinical benefit from targeted immunotherapy in ovarian cancer pts.

#5703

The immune cell state atlas analysis predicts therapeutic benefits with immune checkpoint inhibitors

Tingyi Li[1], Vineeth Sukrithan[2], Aakrosh Ratan[3], Martin McCarter[4], John Carpten[5], Howard Colman[6], Alexandra P. Ikeguchi[7], Xuefeng Wang[1], Igor Puzanov[8], Susanne Dalton[9], Michelle Churchman[10], Patrick Hwu[1], Paulo C. Rodriguez[1], William S. Dalton[10], George J. Weiner[11], Ahmad Tarhini[1].
[1]Moffitt Cancer Center & Research Inst, Tampa, FL,[2]The Ohio State University, Columbus, OH,[3]University of Virginia, Charlottesville, VA,[4]University of Colorado Cancer Center, Aurora, CO,[5]USC Norris Comprehensive Cancer Center, Los Angeles, CA,[6]Huntsman Cancer Institute, Salt Lake City, UT,[7]Stephenson Cancer Center, Oklahoma City, OK,[8]Roswell Park Comprehensive Cancer Center, Buffalo, NY,[9]Markey Cancer Center, Lexington, KY,[10]M2GEN, ORIEN, Hudson, FL,[11]University of Iowa Holden Comprehensive Cancer Center, Iowa City, IA

Introducti**on:** In this study, we investigated the prognostic role of the immune cell state atlas in predicting therapeutic benefits of patients treated with immune checkpoint inhibitors (ICI) within the ORIEN network of 18 collaborating cancer centers under the Total Cancer Care protocol.
Methods: We utilized RNA-seq data of 926 samples generated from 875 individuals. Gene expression data were deconvoluted for immune cell states using the Carcinoma EcoTyper software. We then conducted a series of survival analyses to test the association between survival outcomes and predicted cell types and states in five malignant tumors: Genitourinary (GU), Gastrointestinal (GI), Thoracic (THO), Cutaneous (CUT), Head & Neck (H&N). The regularized Cox regression model in R package 'glmnet' was then applied to select the complementary pathway signatures (including gene ontology and KEGG pathways) to the immune cell states in predicting survival outcomes. We also explored the immune-related long non-coding RNAs (lncRNA) as potential biomarkers for cell states and patient outcomes.

Results: EcoTyper analysis revealed that 692 (~80%) of patients were assigned to the 10 pre-identified Carcinoma Ecotypes (CE1 to CE10) or cell state atlas group. Overall, two immune deficiency ecotype patient groups (CE1 and CE2) pre-identified based on the independent training data were linked to worse survival, while two proinflammatory ecotype groups (CE9 and CE10) were associated with favorable surxvival. Those ecotype groups showed strong prognostic significance in predicting OS in melanoma and H&N. Meanwhile, CE6, a non-neoplastic tissue enriched cell subtype, was also found to be highly associated with longer OS in H&N and GU. CE7, an age-related mutation patient subgroup, contributed to shorter survival in both melanoma and GI. We also found that a subset of activated B cell state and the exhausted/effector CD4 T cell state were significantly associated with patient survival in melanoma and GU, respectively. The penalized Cox regression model revealed that β-catenin signaling pathway, P53 pathway and heme metabolism in the MSigDB Hallmark gene sets are the most complementary pathways to the ecotype scores in multiple cancer types. In additional, multiple pathways in KEGG such as endocytosis were found to jointly contribute to the ecotype-pathway composite prognostic model. In anazlying immune-related lncRNA biomarkers, we highlighted the prognostic role of NKILA in our dataset, which has been studied to promote tumor immune evasion.
Conclusion: Our analysis has successfully established the utility of immune cell state atlas in predicting therapeutic benefits with ICIs. We expect that the discovered complementary signatures in the cancer-cell compartment will also lead to a novel spectrum of tumor-based biomarkers to ICI.

#5704
An integrated immune signature predictive of adjuvant immunotherapeutic benefits for high-risk melanoma
Alyssa N. Obermayer[1], Timothy I. Shaw[1], Sandra J. Lee[2], F. Stephen Hodi[3], William A. LaFramboise[4], Walter Storkus[5], Arivarasan D. Karunamurthy[6], Patrick Hwu[7], Howard Streicher[8], Dung-Tsa Chen[1], John M. Kirkwood[9], Ahmad A. Tarhini[10]. *[1]Biostatistics and Bioinformatics, H Lee Moffitt Cancer Center and Research Institute, Tampa, FL,[2]Biostatistics, Dana Farber Cancer Institute, Boston, MA,[3]Dana Farber Cancer Institute, Boston, MA,[4]Pathology, Allegheny Health Network Cancer Institute,*

Pittsburgh, PA,[5]Immunology, University of Pittsburgh, Pittsburgh, PA,[6]Pathology, University of Pittsburgh, Pittsburgh, PA,[7]Administration, H Lee Moffitt Cancer Center and Research Institute, Tampa, FL,[8]National Cancer Institute, Rockville, MD,[9]UPMC Hillman Cancer Center, Pittsburgh, PA,[10]Cutaneous Oncology and Immunology, H Lee Moffitt Cancer Center and Research Institute, Tampa, FL

Introduction CTLA4 blockade with ipilimumab was more favorable than interferon-α2b (IFN) in high-risk melanoma in phase adjuvant III trial E1609. Characterization of the pretreatment tumor immune biomarkers and clinical covariates may inform the likelihood of response to ipilimumab and other immune checkpoint inhibitors (ICI), and guide future development of this and other modalities in this patient population.
Methods We utilized PATH-SURVEIOR, a bioinformatics framework developed in-house for associating genes and pathway signatures with clinical endpoints, to perform survival analysis of gene expression levels of 31 candidate immune-related biomarkers based on previous preliminary data. We analyzed microarray gene expression data from 471 melanoma patients treated with ipilimumab (ipi) and 248 melanoma patients treated with IFN as part of E1609. We then developed a LASSO Cox regression model and validated our model in 22 patients treated with neoadjuvant ipi in a separate clinical trial.
Results Using PATH-SURVEIOR, we evaluated 31 candidate immune biomarkers and their association with patient outcome by including treatment group (ipi and IFN) as a multiplicative covariate interaction in the Cox hazard model. Our analysis identified CXCL9, CD8A, CXCL10, and INPP5D as Tier 1 biomarkers (HR > 1 and $P < 0.05$) and IDO1, IGKC, and IL2RB as Tier 2 biomarkers (HR > 1 and $P < 0.1$). Next, we developed an ipilimumab immune-based risk score using LASSO Cox regression (L-IPI7) based on these 7 aggregate biomarkers. We then split our 471 ipi-treated cohort into training (310, 66%) and testing (161, 33%) cohorts and assessed our model for its ability to predict overall survival (OS) and relapse-free survival (RFS). Our risk score was capable of stratifying ipi-treated patients into High-Risk and Low-Risk populations, which correlated with OS. As a negative control, we assessed our risk score in 248 IFN-treated patients and found no significant association with OS. As validation, we applied our L-IPI7 score to a cohort of 22 patients treated with

neoadjuvant ipi and determined that the score was able to predict patients with a high risk of relapse. Interestingly, when we developed an interactive Cox-regression model with colitis status (grade 0-1 vs grade 2+), we found that neoadjuvant ipi patients with low-grade colitis were associated with a higher L-IPI7 risk score for disease relapse. In addition, we determined that: i) higher age and higher L-IPI7 risk score identified patients with the worst OS and RFS And ii) female patients with a low L-IPI7 risk scores had a better OS and RFS.
Conclusions We developed a broadly applicable model based on LASSO Cox Regression predictive of adjuvant ipi treatment outcomes in melanoma. Our L-IPI7 score based on expression of CXCL9, CD8A, CXCL10, INPP5D, IDO1, IGKC, IL2RB effectively predicts survival, with interactions with age, gender and on-treatment development of colitis.

#5705
Digital pathology based prognostic & predictive biomarkers in metastatic non-small cell lung cancer
Aditi Qamra[1], Minu K. Srivastava[2], Eloisa Fuentes[2], Ben Trotter[3], Raymond Biju[3], Guillaume Chhor[3], James Cowan[2], Steven Gendreau[2], Webster Lincoln[2], Lisa McGinnis[2], Luciana Molinero[2], Namrata S. Patil[2], Amber Schedlbauer[2], Katja Schulze[2], Adam Stanford-Moore[3], Laura Chambre[3], Ilan Wapinski[3], David S. Shames[2], Hartmut Koeppen[2], Stephanie Hennek[3], Jane Fridlyand[2], Jennifer M. Giltnane[2], Assaf Amitai[2].
[1]Hoffmann-La Roche Limited, Mississauga, ON, Canada,[2]Genentech, Inc., South San Francisco, CA,[3]PathAI, Boston, MA

Background: In recent years, a relationship between the tumor microenvironment (TME) and patient response to targeted cancer immunotherapy has been suggested. We applied machine-learning algorithms on H&E stained tissue to study the TME in metastatic non-small cell lung cancer (NSCLC) patients. Our goal was to identify digital pathology (DP) features associated with outcome under combination treatment or monotherapy with atezolizumab (atezo), an anti-PD-L1 therapy, and relate those features to other data modalities. We analyzed patient data from two phase 3 clinical trials, OAK (docetaxel versus atezo in 2L+ NSCLC) and IMpower150 (bevacizumab, carboplatin, and

paclitaxel (BCP) versus BCP+atezo (ABCP) in advanced 1L non-squamous NSCLC).
Methods: As part of our effort to build a DP-based tumor-immune microenvironment atlas, digitized H&E images were registered onto the PathAI research platform. Over 200K annotations from 90 pathologists were used to train convolutional neural networks (CNNs) that classify slide-level human-interpretable features (HIFs) of cells and tissue structures from images and deployed on images from OAK and IMpower150. HIFs and PD-L1 status were associated with outcome in all samples in each arm in OAK and results were validated in IMpower150, using Cox proportional hazard models. Bulk RNAseq was run using samples extracted from the same area as the H&E slide.
Results: We identified a composite feature capturing the ratio of immune cells to fibroblasts in the stroma predictive of both overall survival (OS) (HR=0.74 p=0.0046) and progression-free survival (PFS) (HR=0.87 p=0.14). While patients primarily benefit from atezo if they are PD-L1 high, we found that even PD-L1 negative patients benefited from atezo when enriched for this feature (22C3 PD-L1 assay: OS HR=0.59 p=0.015, PFS HR=0.8 p=0.25; SP142 PD-L1 assay: OS HR=0.74 p=0.12, PFS HR=0.88 p=0.45). We thus recognized a DP feature that was predictive for positive outcome with atezo treatment, independent of PD-L1 levels. This association was then validated in IMpower150 comparing ABCP to BCP, both overall (OS HR=0.69 p=0.012) and in PD-L1 negative patients (SP263 assay OS HR=0.56 p=0.034). Integrating with RNAseq, patients enriched for this DP feature showed similar enrichment for B and T gene signatures and depletion in CAF-related gene signatures, thus showing the harmonization of TME between different data modalities.
Conclusions: Using a deep learning-based assay for quantifying pathology features of the TME from H&E images in two NSCLC trials, we identified a novel biomarker predictive of outcome to PD-L1 targeting therapy, even in PD-L1 low & negative patients. Importantly, our work shows how different data modalities (DP, gene expression) can be integrated to further our understanding of the TME.

#5706
ImmunoPROFILE: A prospective implementation of clinically validated, quantitative immune cell profiling test identifies tumor-

infiltrating CD8$^+$ and PD-1$^+$ cell densities as prognostic biomarkers across a 2,023 patient pan-cancer cohort treated with different therapies

James Lindsay[1], Bijaya Sharma[2], Kristen D. Felt[2], Anita Giobbie-Hurder[1], Ian Dryg[1], Jason L. Weirather[1], Jennifer Altreuter[1], Tali Mazor[1], Priti Kumari[1], Joao V. Alessi[3], Ajit J. Nirmal[4], Michael P. Manos[5], Ananth R. Kumar[1], William Lotter[1], Ethan Cerami[1], Burce E. Johnson[4], Neil I. Lindeman[6], Lynette M. Sholl[7], Jonathan A. Nowak[8], Scott J. Rodig[7]. *[1]Data Science, Dana-Farber Cancer Institute, Boston, MA,[2]ImmunoProfile, Brigham and Women's Hospital, Boston, MA,[3]Data Science, Lowe Center for Thoracic Oncology, Dana-Farber Cancer Institute, Harvard Medical School, Boston, MA,[4]Dana-Farber Cancer Institute, Harvard Medical School, Boston, MA,[5]Department of Medical Oncology, Dana-Farber Cancer Institute, Boston, MA,[6]Harvard Medical School, Brigham and Women's Hospital, Boston, MA,[7]Department of Pathology, Brigham and Women's Hospital, Boston, MA,[8]Brigham and Women's Hospital, Harvard Medical School, Boston, MA*

Tumor-infiltrating lymphocyte (TIL) density has been identified as a prognostic and predictive biomarker in select tumors treated with defined therapies. These observations suggest that TILs may be general markers of patient outcomes, but evidence in support of this hypothesis has been limited by small cohorts.

We validated ImmunoPROFILE, a multiplexed immunofluorescence (MIF)-based assay coupled with machine-learning-based image analysis, to identify and quantify tumor cells (cytokeratin, PAX5, PAX8, SOX10), T cells (CD8), T-regulatory cells (FOXP3), exhausted cells (PD-1) and immunosuppressive tumor and immune cells (PD-L1). We applied the MIF panel to specimens from patients collected prospectively over three years and analyzed 2,023 cases across 27 tumor types. The association between biomarkers and overall survival (OS) was investigated using Cox models controlling for patient risk factors such as cancer type, metastatic vs. primary disease, age, and gender. Multivariable biomarker selection was based on likelihood ratios.

The assay was highly robust (success rate 97%), reproducible (inter-scanning and intra-staining density controls within 1 SD, inter-staining PD-

L1 scores ≤11% CV), and operator-independent (R^2 >0.7 to >0.9 for each biomarker and 95% concordance in PD-L1 score-based interpretation between technicians). From whole slide images, a total of 11,932 individual regions of interest were analyzed across the cohort, resulting in >50 million spatially-resolved single cells which were summarized into cell population densities and PD-L1 scores.

High densities of $CD8^+$ (>64/mm^2, p<0.0001), PD-1^+ (>50/mm^2, p<0.0001), and $FOXP3^+$ (>30/mm^2, p<0.0001) T cells were associated with longer overall survival (OS) irrespective of therapy and across all cancer types. PD-L1 metrics were not associated with OS (p=0.43). Compared to patients with low densities of $CD8^+$ and PD-1^+ cells, high densities of at least one of these cell types had better OS (Both high, HR: 0.49, 95% CI: 0.41 - 0.59; $CD8^+$ high, HR: 0.63, (0.48 - 0.82); PD-1^+ high, HR: 0.71, (0.54 - 0.93)). The results were consistent in the subset of patients (N=1572) who did not receive immunotherapy (IO). In patients who received IO therapy (N=451), only PD-1^+ T-cell density associated with OS (HR: 0.48, (0.36 - 0.65)).

To our knowledge, this is the first enterprise-level immune biomarker assay using multiplexed staining, digital imaging, and machine learning to be applied in a prospective manner to clinical specimens at scale. We found that select immune cell densities are prognostic across cancer types and therapies and demonstrated that quantification of multiple cell populations yields better prognostic power than single marker analyses.

#5707

Tumor and immune determinants of response to anti-BCMA CAR T-cell therapy in multiple myeloma using cell-free DNA

Mia Carleton[1], Hitomi Hosoya[2], Kailee L. Tanaka[1], Brian Sworder[1], Vanna Hovanky[2], Bita Sahaf[2], Matthew J. Frank[2], George E. Duran[1], Tian Y. Zhang[3], Sally Arai[2], David Iberri[1], Michaela Liedtke[1], David B. Miklos[2], Michael S. Khodadoust[1], Surbhi Sidana[2], David M. Kurtz[1]. *[1]Department of Medicine, Division of Oncology, Stanford University School of Medicine, Stanford, CA,[2]Division of BMT and Cellular Therapy, Stanford University School of Medicine, Stanford, CA,[3]Department of Medicine, Division of Hematology, Stanford University School of Medicine, Stanford, CA*

Background: Multiple myeloma (MM) is an incurable disease with a heterogenous clinical course and genomic landscape. Autologous anti-BCMA chimeric antigen receptor (CAR) T-cells are a promising new therapy, but determinants of response and resistance are not well known. Cell-free DNA (cfDNA) is a useful tool to study MM as it allows for repeated, non-invasive tumor assessment. We apply a novel method for simultaneously tracking tumor mutations and CAR T-cells from cfDNA using Cancer Personalized Profiling by Deep Sequencing (CAPP-Seq).
Methods: We designed a 480kb CAPP-Seq hybrid capture panel to identify mutations, track tumor burden and minimal residual disease, and detect cfDNA derived from the CAR transgene (CAR-cfDNA) in patients receiving idecabtagene vicleucel (ide-cel). Flow cytometry (FC) for enumeration of CAR T-cells was performed from peripheral blood mononuclear cells (PBMCs) when available.
Results: We profiled 153 biologic samples, including plasma, PBMCs, and bone marrow mononuclear cells, from 15 patients receiving ide-cel and 18 healthy controls. We observed a median of 84 SNVs (range 30-277) prior to therapy. Patients with prolonged responses (>90 days) had significantly lower circulating tumor DNA (ctDNA) at day 28 post-infusion than patients with early progression (<90 days) (0.6 vs. 4.6 log haploid genome equivalents (hGE)/mL; p=0.002). Additionally, higher ctDNA at D28 was prognostic for time to progression (TTP) (HR=1.67, p=0.019). We validated CAR-cfDNA detection by comparison with FC from PBMCs at matched timepoints (n=38), finding a significant correlation (rho=0.79, p=3E-09). CAR-cfDNA typically reached its peak level around D14 (median 332 hGE/mL), with ctDNA declining at the same time-point. Thus, CAR-cfDNA levels and ctDNA burden were inversely correlated (rho= -0.3, p=0.019). Surprisingly, peak CAR expansion was not associated with TTP (HR=1, p=0.463). However, lower CAR-cfDNA at D28 was prognostic for inferior TTP (HR=2.68, p=0.011). This suggests CAR persistence may play a more important role in clinical outcomes. Furthermore, among progressors, time until loss of detectable CAR-cfDNA correlated with TTP (rho=0.81, p=0.02). Patients who progressed before day 90 had a median CAR persistence of 28 days. In contrast, patients who progressed after day 90 had a median of 137 days and often had emergent copy number alterations in ctDNA at relapse. This included one case with emergent loss of chr16, where *TNFRSF17* (*BCMA*), resides. This event was detected 36

days prior to clinical relapse; BCMA loss was validated via whole-genome sequencing and immunohistochemistry staining of the tumor.
Conclusions: Cell-free DNA is a promising biomarker for mutational genotyping, disease monitoring, and tracking CAR T-cells in MM. The persistence of CAR-cfDNA has particular prognostic importance and novel strategies to increase CAR persistence should be explored.

Immunomodulatory Agents and Interventions

#4416
IL-1 blockade prevents cardiac toxicity and improves immunotherapy efficacy

Nilesh P. Talele[1], Heena Kumra[1], Igor L. Gomes-Santos[1], Sylvie Roberge[1], William W. Ho[1], Patrik Andersson[1], Sampurna Chatterjee[1], Marie Siwicki[2], Dan G. Duda[1], Mikael J. Pittet[3], Dai Fukumura[1], Rakesh K. Jain[1]. *[1]Harvard Medical School/Massachusetts General Hospital, Norwood, MA,[2]Center for Systems Biology, Massachusetts General Hospital Research Institute and Harvard Medical School, Boston, MA,[3]Department of Pathology and Immunology, University of Geneva, Geneva, Switzerland*

Background: Immune checkpoint blockers (ICBs) have revolutionized cancer treatment, but they are often associated with severe immune related adverse events (irAEs). These severe irAEs are more often seen in patients with obesity or concomitantly treated with cytotoxic therapies.
Methods: We aimed to understand the mechanisms of ICB-induced irAEs, in the context of obesity and ICB/chemotherapy combinations. We developed a mouse model of cardiac irAEs, which is the most fatal type of irAE in ICB-treated cancer patients, with clinically relevant features: (i) an ICB-resistant cancer (pancreatic ductal adenocarcinoma or PDAC), (ii) obesity induced with high-fat diets, and (iii) a combination treatment of ICB (α-PD1 + α-CTLA4) and chemotherapy (FOLFIRINOX).
Results: Our FDA and single institution retrospective analyses indicate that patients treated with ICB had greater relative risk of developing myocarditis as compared to other anti-cancer therapies. Mice with orthotopic PDAC and obesity developed irAEs after treatment with ICB and chemotherapy as compared to chow diet. These irAEs recapitulated those observed in patients with cancer and obesity, including cardiac dysfunction consistent

with myocarditis, cardiac fibrosis, and increased circulating levels of interleukin-1 beta (IL-1b). IL-1β blockade prevented myocarditis and reduced cardiac fibrosis after immunotherapy. Importantly, IL-1β blockade also enhanced the anti-tumor effects of ICB + FOLFIRINOX combination therapy, and increased mouse survival.
Conclusions: We developed a translationally relevant 'triple hit' mouse model and discovered that IL-1β mediates ICB-induced cardiotoxicity. In addition, we found that IL-1β blockers, which are already used in the clinic for cardiology indications, both reduce adverse events and simultaneously enhance the antitumor effects triggered by immunotherapy.

#4417

Activity of novel RNA therapeutics to overcome resistance to immune checkpoint blockade

Marvin O'Ketch, Jeffrey A. Kiefer, Dnyanesh Rasale, Warren S. Weiner, Lizette A. Castaño, Nathalie A. Azorsa, David W. Lee, Kerry M. Barnhart, Spyro Mousses, David O. Azorsa. *Oligon, Scottsdale, AZ*

T-cells in the tumor microenvironment can often become exhausted and dysfunctional due to chronic and prolonged exposure to antigen. The resulting condition of T cell exhaustion represents an important mechanism of clinical resistance to immune checkpoint blockade. The transcription factor NR4A1 is known to be upregulated in tumor-specific T-cells and is a mediator of T cell dysfunction including driving exhaustion during chronic antigen stimulation of T-cells. Pro-oncogenic activities of NR4A1 have been observed in various solid tumors, including colorectal and breast cancers, and co-expression of NR4A1 with known immune checkpoint markers such as PD-L1 and B7 family members has also been observed in various cancer cell lines. These findings have identified NR4A1 as an important target for overcoming resistance to cancer immunotherapy. We hypothesize that targeted silencing of the NR4A1 and other immunomodulatory genes can reverse T-cell exhaustion and expand the clinical benefit of immune checkpoint blockade in solid tumors resistant to immune therapy. To reverse T-cell exhaustion with a targeted approach, we developed T cell targeting SeekRs^{TM}, which are chimeric RNA therapeutics containing dual-flanking aptamer binders connected by a double-stranded bridge containing siRNA silencers that can target multiple

immunomodulatory genes. First-generation aptamer-siRNA chimeras designed with a CTLA-4 targeting aptamer containing a STAT3 siRNA demonstrated effectiveness in silencing its target. Modifications to the structure included the addition of chemically modified nucleotides to improve serum stability. Additionally, dimerization of the structure to form a SeekR dimer molecule greatly improved internalization and target silencing compared to the monomeric chimera. Newly developed SeekRs targeting T cells and designed to silence NR4A1 have effectively downregulated NR4A1 in model cell lines and activated T cells. These results demonstrate that dual targeting SeekRs can be used to specifically deliver siRNA to T cells for targeted silencing that can reverse exhaustion and potentially overcome resistance to cancer immunotherapy in the clinic.

#4418

Heterogeneity of IFN-γ responsiveness in myeloid malignancies-implication for the possible impact on IFN-γ immunotherapy

Kedwin Ventura, Iuliia Kovalenko, Jui-En Ray Lee, Biswas Neupane, Daniel Stapor, Sawa Ito. *University of Pittsburgh School of Medicine, Pittsburgh, PA*

Introduction: Allogeneic stem cell transplantation (alloSCT) can potentially cure hematologic malignancies through graft-versus-leukemia effect (GVL). Several studies have suggested that IFN-γ pathway is critical for GVL sensitivity or resistance in leukemia cells. In mouse model, acute myeloid leukemia (AML) generated in IFN-γ receptor-deficient mice acquired resistance to GVL (Matte-Martone, Shlomchik WD, J Clin Invest. 2017). Other groups have reported that IFN-γ restores HLA expression on myeloid blasts from patients who relapsed AMLs after alloSCT. These data support the clinical application of IFN-γ to augment GVL in subjects with post-transplant relapse. However, AML is molecularly heterogeneous, and the IFN-γ responsiveness may vary by AML subtypes. We analyzed IFN-γ responsiveness of primary AML cells and investigated the role of IFN-γ on cell death and T-cell recognition of AML cell lines.
Methods: Primary AML cells collected at diagnosis (n=60), at relapse after chemotherapy (n=4), and at post-transplant relapse (n=8) were stimulated with IFN-γ at 1 ng/ml or 50 ng/mL *in vitro*, and IFN-γ responsiveness was analyzed by measuring phosphorylation of STAT1 (pSTAT) after 15

minutes and upregulation of HLA-DR after 48 hours by flow cytometry. U937 and THP-1 cell lines were used to investigate IFN-γ induced cell death and the impact of IFN-γ priming of leukemia cells on the activation of alloreactive T cells. For this, Jurkat cells transduced with anti-HA1 T cell receptor (αHA1-TCR-T) were used, and the activation was analyzed through CD69 upregulation by flow cytometry.
Results: IFN-γ responsiveness was heterogeneous in both pSTAT1 and HLA-DR upregulation of primary AML blasts. IFN-γ responsiveness also varied within the subpopulation of leukemic blasts within the sample at diagnosis and relapse, implying clonal evolution. Compared to THP-1, U937 cells fail to upregulate HLA-DR with IFN-γ despite appropriate pSTAT1 response to IFN-γ, suggesting silencing of downstream IFN-γ activation site (GAS) and transcription of IFN-stimulated genes (ISGs). IFN-γ directly induced cell death in THP-1 *in vitro*, while U937 was resistant to IFN-γ induced cell death. Priming of THP-1 with IFN-γ significantly improved the affinity of αHA1-TCR-T to peptide-stimulated THP-1.
Conclusion: IFN-γ responsiveness of AML blasts was heterogeneous, and cell line data suggest an impact of IFN-γ sensitivity on IFN-γ mediated cell death and alloreactive T cell recognition. Future studies aim to understand the mechanisms underlying IFN-γ sensitivity or resistance in AML, which would help to design clinical trials by selecting the patients who would obtain maximal benefit from IFN-γ therapy in post-transplant relapse (NCT04628338).

#4419

Use of luciferase-labeled target cells to explore immune cell killing in high throughput format in 2D and 3D co-cultures

Carla Castro, Philipp Metzger, Daniel Feger, Sarah Ulrich, Oliver Siedentopf, Jan E. Ehlert, Holger Weber. *Reaction Biology Europe GmbH, Freiburg, Germany*

With the development and approval of cutting-edge immune-based approaches for cancer treatment in recent years, the global immune-oncological (IO) pipelines have dramatically increased. To overcome the challenges of rising treatment resistance, new strategies are being developed pointing towards enhancing and sustaining T cell-mediated

cytotoxicity, exploiting NK, monocytes and γδT cell killing capacity, and combinatorial therapies, among others.

Examples of such strategies are the bispecific antibodies, which are mainly T-cell (BiTE) engagers, but also NK-cell engagers. In addition to the FDA approved immune checkpoint inhibitors, monoclonal antibodies against tumor antigens are being developed to enhance the cytotoxic response of NK and macrophages/monocytes through antibody-induced cell cytotoxicity (ADCC)

To facilitate the efficacy analysis of BiTEs, we developed a 384-well format assay system based on luciferase-labeled tumor cells (advantages: high-throughput capability, non-radioactive, non-toxic, relatively low cost, and easily adaptable to automation). As only the tumor cells are labeled, the specific detection of luciferase exclusively correlates to the number of viable tumor cells, allowing for co-cultures with high excess of effector cells without the effector cells causing interference. Due to high sensitivity, few tumor cells are required for a sufficient signal/noise ratio, keeping the overall need for primary effector cells to a minimum, even at high effector/target cell ratios. This is of great advantage when working with rare cytotoxic subpopulations (e.g. NK cells), precious samples from patients, or simply saves resources when performing large exploratory studies. In addition, combination of low 384-well format volumes with nanodrop agent dispensing technology minimizes the amounts of expensive antibodies and other agents.

Applying this technology, we evaluated the combinatorial effects of Blinatumomab with other clinically relevant agents on the luciferase-labeled GCB-like DLBCL cell line OCI-LY1. Depending on compound combination, we observe synergistic (e.g. Lenalidomide) but also antagonistic effects (e.g. MEK-inhibitor, Selumetinib, and MCL-1-inhibitor, S63845). We also developed CD3-stimulated T cell killer assays either using target cells grown in monolayer or spheroids, with the intent to study checkpoint inhibitors or other T cell activation modulators. In contrast to target cells grown in monolayers, immune cytotoxicity of spheroids by anti-CD3 stimulated T cells was incomplete, showing the additional challenge for effector cells when using 3D cultures as targets. Moreover, we show an ADCC example using NK as cytotoxic cells. Our data supports the outstanding usefulness of this methodological approach for the exploration

of the overall efficiency of a therapy to enhance tumor cell killing by immune effector cells.

#4420

Carbohydrate-CD11b engagement enhances differentiation of tumor-associated myeloid cells in immunotherapy of solid cancers

Mei Zhang. *Biomedical Engineering, Case Western Reserve University School of Medicine, Cleveland, OH*

Background: Methods to perturb tumor-associated myeloid cell function are being actively pursued to overcome these challenges in immunotherapy and search for a cure. CD11b is a potential therapeutic target to modulate suppressive myeloid derived cells and induce tumor-reactive T-cell responses. However, CD11b can bind to multiple carbohydrate ligands that trigger a variety of myeloid cell functions like adhesion, migration, and even phagocytosis and proliferation. This has created a major challenge to understand the molecular basis by which CD11b converts differences in receptor-ligand binding into subsequent immune signaling responses, and to use this knowledge for therapeutic development.

Methods: This study investigated a previously reported carbohydrate ligand, BG34-200, that showed anti-tumor effect through modulating $CD11b^+$ cells. Applying modern approaches of peptide microarray, multi-parameter FACS analysis, cellular/molecular immunological technology, advanced microscopic imaging, and transgenic mouse models of solid cancers, we studied the BG34-200-CD11b carbohydrate-protein engagement and immunological changes it triggered in the context of solid cancers including osteosarcoma, melanoma and pancreatic cancer.

Results: Our results show that BG34-200 can mediate direct, specific, multi-site and multivalent binding to integrin CD11b to trigger cellular differentiation in a suppressive tumor-associated myeloid cell subset. In melanoma, osteosarcoma, and pancreatic cancer, we detected this rare myeloid cell subset in blood, which displayed an inflammatory monocyte phenotype and exhibited immunosuppressive behavior. BG34-200-CD11b engagement could induce differentiation of these tumor-associated inflammatory monocytes into dendritic cells by inducing phagocytosis that effectively trigger F-actin cytoskeletal rearrangement and intrinsic ICAM-1 clustering important for antigen presentation and effector T cell stimulation.

Conclusions: Our findings improve understanding of molecular basis by which CD11b converts difference in carbohydrate ligands into subsequent immune signaling responses, may lead to development of safe and novel therapies modulating myeloid derived cell function for immunotherapy of solid cancers.

#4421

Targeting myeloid-derived suppressor cells with actinium-225 lintuzumab, a CD33 antibody radioconjugate to enhance antitumor immunity

Amanda Chin, Mary Chen, Jason Li, Megan McCloskey, Caroline Jennings, Le-Cun Xu, Monideepa Roy, Denis Beckford, Helen Kotanides. *Actinium Pharmaceuticals, Inc., New York, NY*

Introduction: Myeloid-derived suppressor cells (MDSCs) are a heterogeneous population of myeloid lineage cells with potent immunosuppressive activity found enriched in cancer patients. Crosstalk between MDSCs and the tumor microenvironment can promote tumor immune evasion and thus there is growing interest in developing therapeutic approaches to intervene in the MDSC suppressive function. Both monocytic-MDSC (M-MDSC) and granulocytic-MDSC (G-MDSC) subpopulations express the cell surface CD33 myeloid marker. For well-defined cell surface markers like CD33, there is considerable interest in the use of radionuclides as therapeutic payloads, particularly α-particle emitters such as actinium-225 (^{225}Ac) since they deliver substantially higher decay energies over a much shorter distance than β-emitters, rendering them more suitable for precise, potent, and efficient target cell killing while minimizing toxicity to surrounding bystander cells. Actimab A, the anti-CD33 antibody lintuzumab armed with the ^{225}Ac radioisotope (CD33 ARC), is currently being evaluated in R/R AML and has demonstrated significant anti-leukemic activity in Phase 1/2 clinical trials. We therefore hypothesized that MDSCs can be directly targeted by the CD33 ARC. Hence, we evaluated the therapeutic potential of the CD33 ARC to deplete MDSCs through preclinical studies in vitro and in vivo with humanized mouse model. Methods: CD33 ARC was generated by conjugating lintuzumab with *p*-SCN-Bn-DOTA and subsequently radiolabeled with ^{225}Ac. Primary MDSCs were isolated from cancer patient peripheral blood or healthy donor

PBMCs. The specific binding of CD33 ARC to CD33 positive MDSCs and the decreased viability of MDSCs in response to treatment in vitro was characterized by immunophenotyping using flow cytometry. The therapeutic efficacy of CD33 ARC to deplete MDSC in vivo was evaluated in human CD34 reconstituted humanized NOG-EXL mice.
Results: CD33 positive MDSCs (M-MDSCs and G-MDSCs) were identified in human cancer peripheral blood samples, including colorectal and lung. Significantly more MDSCs were found in the peripheral blood of cancer patients in comparison to healthy donors. CD33 ARC treatment of human cancer MDSCs induced a potent dose-dependent reduction in MDSC viability leading to increased depletion of MDSCs. Furthermore, in the humanized NOG-EXL mouse model, CD33 ARC therapy demonstrated in vivo activity of CD33 ARC to deplete human MDSCs.
Conclusions: In this study, we demonstrate CD33 ARC alpha targeted radiotherapy depletes human CD33 positive immune suppressing MDSCs present in multiple cancer types, to enhance antitumor immunity. These findings present a translatable strategy that supports further evaluation of ^{225}Ac lintuzumab as a MDSC targeting agent to improve the efficacy of antitumor therapies.

#4422

Evaluation of immune response to tumor associated antigens in patients with high grade serous ovarian cancer vaccinated intra-dermally with DCP-001, an allogeneic, cancer cell-based vaccine

Marco De Bruyn[1], Annegé Vledder[1], Rob ten Pas[2], Anneke Eerkens[1], Koen Brummel[1], Hester van Zeeburg[2], Jeroen Rovers[2], Hans Nijman[1].
[1]University Medical Center Groningen, Groningen, Netherlands,[2]Mendus, Leiden, Netherlands

Treatment of high grade serous ovarian cancer (HGSOC) after debulking and chemotherapy remains challenging. This phase 1 trial (NCT04739527) evaluates the use of a cell-based relapse vaccine, DCP-001, to prevent disease recurrence after primary treatment. Previous data in acute myeloid leukemia, has shown that DCP-001 induces an immune responses to tumor associated antigens, like WT1 and PRAME, frequently upregulated in HGSOC. In NCT04739527, DCP-001 is given four times biweekly (week 0, 2, 4 and 6) at a dose of 25 million cells/vaccination (vc), followed by 2

monthly boosters (week 14 and 18) of 10 million cells/vc, after primary debulking and chemotherapy. IFNγ ELISpot is performed on peripheral blood mononuclear cells after restimulation with WT1, PRAME, MAGEA3/4 and NY-ESO1. Vaccine induced T-cell response (VIR) at any point after week 0 are calculated as at least a 2-fold increase of the mock-corrected baseline response. Sustained VIR are counted if a VIR to the same antigen is observed in at least 2 timepoints after start of DCP-001. Flow cytometry is performed using a 40-marker panel to evaluate the immune profiles of innate and adaptive immune system, as well as activation and exhaustion markers and memory profiles. At present, a total of 7 patients have been included and 6 have completed the full vaccination schedule (week 22). DCP-001 is well-tolerated, with only mild to moderate adverse events, mainly related to local injection side reactions, or systemic discomfort with fatigue, diarrhea, temperature elevation and headache. Immune responses have been evaluated in 5 patients by IFNy ELISPOT. VIR were detected in a range of 0-8, and all but 1 patient had at least one sustained VIR to either of the 4 antigens. One patient had no VIR, however this patient had already high baseline responses to all 4 antigens. Flow cytometry showed changes during the vaccination in the immune profiles of these patients, with in general an activation of the innate and adaptive immune system. Detailed analysis is currently ongoing. Finally, at the week 22 visit, 2 patients had progressed during the treatment and 4 had no clinical signs of progressive disease. Taken together, initial data from the phase I trial demonstrate that DCP-001 is safe and well-tolerated and induces durable T-cell responses to tumor associated antigens in OC patients. The study will continue to enroll new patients, follow-up for progression and overall survival and will further analyze the immune responses induced by DCP-001.

#4423

XMT-2056, a HER2-targeted STING agonist antibody-drug conjugate, exhibits ADCC function that synergizes with STING pathway activation and contributes to anti-tumor responses

Jahna Soomer-James, Marc Damelin, Naniye Malli. *Mersana Therapeutics, Inc., Cambridge, MA*

XMT-2056 is a systemically administered Immunosynthen STING agonist antibody-drug conjugate (ADC) that targets a novel HER2 epitope and induces complete tumor regressions with a single dose in multiple tumor models. We have previously shown that XMT-2056 delivers its STING agonist payload into tumor cells and FcγRI (CD64)-expressing myeloid cells, activating STING signaling in both cell types, leading to type I interferon (IFN) and anti-tumor innate immune responses. Here, we demonstrate that XMT-2056 exhibits ADCC (antibody-dependent cell-mediated cytotoxicity) function, which synergizes with STING pathway activation and induces potent cancer cell-killing activity in co-cultures of HER2-expressing cancer cells and FcγRIII$^+$ (CD16$^+$) immune cells. We show that both XMT-2056 and HT-19 (the unconjugated parental antibody) retain significant cancer cell-killing activity in an Fc-dependent manner in PBMC co-cultures depleted of FcγRI-expressing myeloid cells. This activity is abrogated by co-depletion of FcγRIII$^+$ immune cells, illustrating the ADCC function of XMT-2056. In this setting, XMT-2056 cancer cell-killing activity was significantly increased compared to HT-19, suggesting that the STING payload contributes to the differential activity observed with XMT-2056 treatment. Indeed, co-treatment of cancer cell and immune cell co-cultures with HT-19 and free STING agonist payload enhanced the anti-tumor responses, although to a lesser extent than XMT-2056, suggesting a synergy between the ADCC function and STING pathway activation. Consistently, XMT-2056 treatment of HER2-expressing cancer cells co-cultured with unstimulated CD56$^+$/FcγRIII$^+$ NK cells induced granzyme b and IFN-γ cytokine production, expression of NK cell activation markers, and cancer cell-killing activity. The ADCC activity of HT-19 was comparable to that of trastuzumab in NK cell co-cultures. Finally, we found that depletion of FcγRI$^+$ cells inhibited the cancer cell-killing activity of XMT-2056 in cancer cell and PBMC co-cultures more substantially compared to depletion of FcγRIII$^+$ cells or CD56$^+$ NK cells, indicating a greater contribution of myeloid cells to the XMT-2056 mechanism of action in this setting. Notably, XMT-2056 was capable of engaging both FcγRI$^+$ myeloid cells and FcγRIII$^+$ NK cells, activating both STING-mediated innate immune responses and ADCC function in triple cultures with HER2-expressing cancer cells. Collectively, our data reveal a synergy between ADCC function and STING pathway induction both mediated by XMT-2056, which enhances the cancer cell-killing activity of

FcγRIII$^+$ cells. This additional mechanism of action of XMT-2056 can potentially impact the overall anti-tumor immune responses in tumors infiltrated by FcγRIII$^+$ cells.

#4424

Immunoregulatory role of club cell secretory proteins in non-small cell lung cancer

Aakanksha Rajiv Kapoor, Vivek Mittal. *Cardiothoracic Surgery, Weill Cornell Medicine, New York, NY*

Introducti**on.** Immune checkpoint inhibitors (ICI) particularly those targeting the PD-1/PD-L1 axis are approved for NSCLC patients. However, most patients experience little clinical benefit due to immunosuppressive barriers in the tumor microenvironment. Our goal to identify immunomodulatory agents that may overcome these barriers, led to the finding that low dose stereotactic body radiation therapy (SBRT) in combination with ICI resulted in marked tumor regression and improved survival by generating durable anti-tumor immunity (Ban et al., Nature Cancer, 2021). Unexpectedly, we uncovered that the immune-modulating functions of SBRT was acutely dependent on the secretory function of lung resident *Scgb1a1*$^+$ club cells that protect the bronchioles from xenobiotic agents. Blocking club cell secretome *in vivo* blunted the efficacy of the combination treatment and altered myeloid cell phenotypes. These findings led to the hypothesis that radiation-induced club cell factors may synergize with ICI to attenuate immunosuppressive barriers by reducing myeloid suppressive cells.

Methods and Data. Expression of 8 highest expressed club cells secretory factors (CC10, SP-A, SP-B, SP-D, Hp, Secretoglobin 3A1, 3A 2, and 1C 1) in combination with PD-1 blockade elicited significant tumor control and improved survival of NSCLC mice. Mechanistically, the 8 club cell factors inhibit myeloid suppressor cell phenotypes as determined by reduced pSTAT3, pERK and concomitant inhibition of immunosuppressive mediators Arg1, iNOS, etc. Further screening of individual club cell factors showed that CC10 alone effectively blunted myeloid suppression activity as determined by flow cytometry for Arg1 and iNOS. Hence, CC10 can functionally alter the immunosuppressive nature of myeloid suppressor

cells. The ability of CC10 in improving the efficacy of ICI in impairing tumor growth and improving survival is currently being examined.
Conclusions. Myeloid suppressor cells inhibit immune cells like T cells or NK cells leading to poor prognosis in cancer treatment. Increase in their numbers has been linked to tumor aggressiveness and low efficacy of immunotherapy. Hence, there is an unmet clinical need to specifically target these cells. Agents targeting myeloid suppressor cell accumulation and differentiation (e.g., ATRA, Vitamin D, Sunitinib, Gemcitabine, Bevacizumab, Tadalafil), are being tested in human clinical trials. However, these agents lack specificity and selectivity for myeloid suppressor cells *in vivo*. Therefore, our work provides the rationale for the development of CC10 as selective inhibitor of myeloid suppressor cells and has the potential for achieving a robust and durable anti-tumor immunity in NSCLC.

#4425
GlycoConnect™ immune cell engagers (GC™-ICEs). A non-genetic approach to targeted IL-15 immunotherapy
Remon van Geel, Floris van Delft. *Synaffix BV, Oss, Netherlands*

Engagement of T cell or NK cells to harness a patient's immune system is a promising approach in immuno-oncology. An immunocytokine, *i.e.* a tumor-targeting antibody (fragment) genetically fused to an immunostimulatory cytokine, is specifically designed for this purpose. Fusion antibody-IL-15 immunocytokines, based on a variety of molecular architectures, are currently finding their way to the clinic with promising results.
Here we demonstrate how GlycoConnect™, a site-specific conjugation technology anchoring on the native antibody glycan, can be applied for attachment of IL-15 without prior antibody engineering. Moreover, the immunostimulatory activity of these GlycoConnect™ immune cell engagers (GC™-ICEs) can be modulated by tailoring linker design and payload stoichiometry. In particular, we demonstrate how a protease-cleavable mAb-IL-15 conjugate can be used to prevent systemic activation of the immune system, leading to a significantly improved therapeutic index in rodent models. In vitro and in vivo studies will be presented to showcase

the biological activity of these GC™-ICEs in comparison to conventional immunocytokines obtained via genetic engineering.

#4426

Removal of soluble TNF receptors as a novel form of immunotherapy for patients with advanced solid tumors

Piotr J. Wysocki[1], Piotr Tomczak[2], Tomasz Jankowski[3], Tomasz Nowikiewicz[4], Gal Markel[5], Ronnie Shapira[5], Gokhan Demir[6], Mustafa Bozkurt[6], Sameera Bilgrami[7], Annette Marleau[7], Adam Ostrowski[8], Lawrence Florin[9], Victoria Manax[10], Robert Segal[11]. *[1]Szpital Uniwersytecki w Krakowie Oddzial Kliniczny Onkologii, Krakow, Poland,[2]Centrum Medyczne Pratia Poznan, Skorzewo, Poland,[3]Samodzielny Publiczny Szpital Kliniczny nr 4 w Lublinie Klinika Pneumonologii, Onkologii i Alergologii, Lublin, Poland,[4]Centrum Medyczne INTERCOR Sp. z o.o., Bydgoszcz, Poland,[5]Sheba Medical Center, Tel Hashomer, Israel,[6]Acibadem Universitesi Klinik Arastirmalar Etik Kurul, Kayisdagi Caddesi, Kayisdagi Caddesi, Turkey,[7]Research and Development, Immunicom, Inc., San Diego, CA,[8]Clinical Operations, Immunicom, Inc., Krakow, Poland,[9]Clinical Operations, Immunicom, Inc., Philadelphia, PA,[10]Medical Affairs, Immunicom, Inc., Houston, TX,[11]Medical Affairs, Immunicom, Inc., Philadelphia, PA*

Immunicom, Inc. has developed a novel subtractive immunotherapeutic apheresis method (Immunopheresis®) to selectively remove soluble tumor necrosis factor receptors, sTNF-R1 and sTNF-R2 (sTNF-Rs) generated by tumors. sTNF-Rs block the tumoricidal activities, hence their removal restores the anticancer immunotherapeutic activity of native TNF-α. Past use of systemic administration of TNF-α to treat solid tumors resulted in unacceptable toxicities. Immunicom's LW-02 Column contains a bead matrix covalently bonded to a single-chain, TNF-α capture ligand (scTNF) with high affinity and selectivity to remove sTNF-Rs from plasma. Three clinical trials (NCT04004910, NCT04142931, NCT04690686) have been conducted in patients with various advanced-stage breast cancers (BC), melanoma (M), renal cell carcinoma (RCC) and non-small cell lung cancers (NSCLC). Patients were assigned to receive LW-02 Column Immunopheresis® monotherapy or combined with various chemo- or

immunotherapies. Immunopheresis® was administered 3x/week for each trial's 12 or 16-week Primary Treatment period with each procedure processing 2 plasma volumes (2PV). Patients with (at least) clinical stability and/or tumor responses could receive additional treatment. Compared to healthy persons, patients in all 3 trials were noted as having significantly elevated baseline blood concentrations of sTNF-R1 and sTNF-R2. For instance, sTNF-R1 plasma levels were 3.5 ng/mL, 3.5 ng/mL, 2.2 ng/mL and 2.1 ng/mL for BC, M, RCC and NSCLC, respectively, which were 5-8-fold higher than normal values. Likewise, sTNF-R2 plasma concentrations (which can be 4-fold, or more, greater than sTNF-R1) were 4-9-fold higher for BC (16.5 ng/mL), M (19.1), RCC (22.7) or NSCLC (11.1 ng/mL) than normal values. Through the data cutoff, >1,600 LW-02 Column Immunopheresis® procedures were performed. On average, 95% of sTNF-R1 and 80% of sTNF-R2 are removed from plasma at the 30-minute procedure timepoint. At the 2PV timepoint, overall mean reductions of sTNF-R1 and sTNF-R2 in whole blood were 51 and 52%. Further, minimal leaching (mean of 113 ng per procedure), of the scTNF capture ligand was detected, a quantity that is insufficient to cause any meaningful clinical effects. *In vitro* testing determined that the LW-02 Column has no discernable evidence of unintended or "off-target" removal of other cytokines or blood constituents or any non-specific binding. Moreover, the trial results demonstrate Immunopheresis® is safe with minimal side effects determined to be related to treatment with the column. Results from 3 trials indicate that cancer patients with advanced solid tumors present with significantly upregulated levels of immune inhibitory sTNF-Rs. LW-02 Column Immunopheresis® can safely and selectively remove sTNF-Rs thus allowing endogenous TNF-α to instigate its multiple anticancer pathways.

#4427

Cucurbitacin B: A promising drug candidate for targeting tumor immunosuppressive cells

Emmanuel B. Anning[1], Mudassier Ahmad[2], Sahir Alvi[2], Carlos Parez[3], Mehdi Chaib[4], Divyam Bansal[2], Dae Kim[5], Subhash Chauhan[6], Taha Merghoub[7], Bilal Hafeez[2]. *[1]Graduate School of Biomedical Sciences, Baylor School of Medicine, Houston, TX,[2]Immunology and Microbiology, University of Texas Rio Grande Valley, Edinburg, TX,[3]Graduate School of Biomedical Sciences, University of Texas Rio Grande Valley, Edinburg,*

TX,[4]Graduate School of Biomedical Sciences, MD Anderson Cancer Center, Houston, TX,[5]Immunology and Microbiology, University of Texas Rio Grande Valley, Houston, TX,[6]Immunology and Microbiology, University of Texas Rio Grande Valley, McAllen, TX,[7]Memorial Sloan Kettering Cancer Center, New York, NY

Immunotherapy has emerged as a major breakthrough in cancer treatment. However, it showed only a marginal response in pancreatic and liver cancers. Thus, novel strategies are highly desirable to take full advantage of immunotherapy in the treatment of these cancers. One of the critical factors that influence the efficacy of immunotherapy is the increased infiltration of myeloid-derived suppressor cells (MDSCs) and tumor-associated macrophages (TAM) into tumors that alter the immune landscape and serve as facilitators of tumor proliferation, metastatic growth, and immunotherapy resistance. Thus, we believe that selecting a potent molecule that has the ability to suppress the function or revert the phenotypes of TAM and MDSCs will have a more significant impact in enhancing tumor immunotherapy response. Cucurbitacin B (Cuc B) is a potent inhibitor of Stat3, CSF-1R, and PI3Kγ and has shown its chemopreventive and therapeutic effects against various cancers but is limitedly explored for its application in modulating tumor immune response. In this study, we investigated the molecular effects and underlying molecular mechanisms of Cuc B on TAM and MDSCs. Cuc B significantly ($P<0.01$) decreased the expression of M2 markers (Arginase I, YM1 FIZZ1, PPARγ and TGFβ in M2 polarized BMDMs and increased M1 markers (NOS2, IL-6, and CD11C) compared to IL-4 alone treatment group**.** It has been demonstrated that TAMs secrete PDL-1 which neutralizes the function of T-cells. Cuc B treatment significantly ($P<0.001$) decreased PDL-1 expression in IL-4-treated RAW264.7 cells. Surprisingly, we observed that Cuc B treatment abolished the protein levels of PI3Kγ in IL-4 treated macrophages as determined by confocal microscopy and Western blot analysis. Cuc B treatment of bone marrow-derived MDSCs significantly ($P<0.01$) decreased the expression of Arginase-1, IL-10, PDL-1, and Stat3. We observed that IL-4-treated BMDMs inhibited phagocytic capacity which was significantly restored upon Cuc B treatment. We observed that Cuc B is a more potent molecule than a pharmacological inhibitor of PI3Kγ (IPI-549) in suppressing key signaling components of TAM and MDSCs. We are

performing *in vivo* study to investigate Cuc B potential to enhance checkpoint blockade immunotherapy response in clinically relevant mouse models of cancer. These results suggest that Cuc B is a novel therapeutic agent which has the potential to suppress or revert TAMs and MDSCs phenotypes. Cuc B may be used as an adjuvant drug molecule in combination with PD1 or CTLA-4 antibodies for improving immunotherapy response against less responsive tumors.

#4429

'Free' ISG15 acts as an immunoadjuvant to enhance $CD8^+$ T cell-mediated anti-tumor immunity

Mariam Oladejo, Laurence Wood. *Immunotherapeutics and Biotechnology, Texas Tech University Health Sciences Center, Abilene, TX*

Interferon-stimulated gene 15 (ISG15) is a ubiquitin-like molecule that is primarily involved in antiviral responses. ISG15 can either exist in the conjugated form, where it is covalently bound to proteins in a process termed ISGylation or can be released extracellularly in the cytokine-like "free" form. Although conjugated ISG15 often indicates poor prognosis in cancers, 'free' ISG15 is suggested to have immunostimulatory properties, owing to its ability to stimulate the production of IFN-gamma from lymphocytes and natural killer (NK) cells. While the immunomodulatory properties of free ISG15 are known, its ability to improve the antigen-specific T-cell response mediated by tumor immunotherapies has not been fully elucidated. The need for $CD8^+$ T cell-based immunoadjuvant in cancer immunotherapy is underscored by the current failure in the generation of optimum $CD8^+$ T cell response by the multitude of cancer vaccines in clinical trials. In this study, we demonstrated that ISG15 is vital for the generation of antigen-specific adaptive immunity; we showed that ISG15 deficient (ISG15-/-) mice do not develop effective systemic $CD8^+$ T cell response after ovalbumin protein vaccination in non-tumor bearing mice. Upon tumor challenge of ISG15-/- mice and wild type C57/BL6 mice with B16-OVA melanoma tumors, effective OVA-specific $CD8^+$ T cell-mediated anti-tumor immunity was not elicited, and the tumors progressed at a faster rate in the ISG15-/- mice. We then utilized a clinically relevant model to evaluate the therapeutic benefits of 'free' ISG15. We used a synergistic therapeutic approach that involved the concomitant administration of a

DNA-construct encoding ‘free’ ISG15(mutISG15) and a *Listeria-monocytogenes*(Lm)-based cancer vaccine directed against the tumor vasculature (Lm-LLO-CD105A) to intervene in murine models of renal cell carcinoma (Renca) and breast cancer (4T1-Luc). The combination of Lm-LLO-CD105A and mutISG15 led to a significant reduction in tumor burden in both syngeneic models. This tumor control was mediated by the expansion of a population of highly polyfunctional $CD8^+$ T cells in the combinatorial therapy group. These $CD8^+$ T cells were characterized by the robust production of multiple cytokines, including IFN-gamma, IL-2, and TNF-alpha.Moreover, we confirmed that mutISG15 significantly increased the antigen (CD105)-specific anti-tumor response generated by Lm-LLO-CD105A. Not surprisingly, *in-vitro* studies demonstrated that mutISG15 probably potentiates the induction of maturation, activation, and antigen-presentation of dendritic cells to facilitate the activation and effective functionality of tumor-specific T cells. Conclusively, our results positions ‘free’ ISG15 as a powerful T-cell stimulant that may provide a suitable therapeutic option for improving the effectiveness of therapeutic cancer vaccines.

#4430

Sacituzumab-Interferon beta mutein fusion protein, ABN202 (anti Trop2-interferon beta mutein), is a potent therapeutics for Trop-2-positive urothelial cancer

Jiyang Lee[1], Myeung-Ryun Seo[1], Heegeon Park[2], YeongMun Kim[1], Saehyung Lee[2], Na Young Kim[2], Chan Gyu Lee[3], Hae Min Jeong[3], Jun Young Choi[2], Young kee Shin[1]. *[1]Seoul National University, Seoul, Korea, Republic of,[2]ABION INC., Seoul, Korea, Republic of,[3]Genopharm Inc., Seoul, Korea, Republic of*

Background : Trop2, trophoblast cell-surface antigen 2, is a type 1 transmembrane glycoprotein overexpressed in many solid tumors such as breast, lung, pancreatic, gastric, colon, urothelial cancer. Overexpression of Trop2 is associated with aggressive disease progression and poor prognosis. Recently, Trop2 targeting antibody-drug conjugate such as sacituzumab-govitecan (Trodelvy®) was approved for the treatment of triple-negative breast cancer and urothelial cancer (UC) patients. Interferon-beta (IFN-beta), a pleiotropic cytokine, can induce direct/in-direct tumor killing and

activate anti-tumor immune response in tumor microenvironments. However, it is challenging to develop IFN-beta as an anti-cancer agent due to its low biophysical properties, short half-life, and the systemic toxicity. Previously, we developed IFN-beta mutein (ABN102), which showed improved stability and biophysical properties compared to wild-type IFN-beta. We hypothesis to reduce any toxicity of ABN102 by fusing with tumor targeting antibody. In this study, we generated antibody cytokine fusion protein (ABN202), anti Trop2-interferon-beta mutein, and evaluated the efficacy of ABN202 against Trop2-positive UC cell line models. Method & Result : We aimed to determine the direct anti-cancer efficacy of ABN202 using Trop2-positive UC cell lines and the indirect immune cell mediated effect of ABN202 using Trop2-positive UC cell lines co-cultured with human peripheral blood mononuclear cell (PBMC). The in vivo efficacy of ABN202 was further confirmed in Trop2 positive tumor mouse model. Our results revealed that ABN202 directly inhibited proliferation and activates the apoptosis-related signaling mechanisms via Type 1 IFN signaling, showing better efficacy than either anti Trop2 antibody (sacituzumab) or ABN102 alone. ABN202 induces the activation of PBMC subsets and enhanced immune cell-mediated cancer cell killing when UC cell lines were co-cultured with PBMC. The anti-cancer efficacy of ABN202 were confirmed in Trop2-positive tumor mouse model. Conclusion : We evaluated the direct and indirect anti-cancer efficacy of ABN202 (anti Trop2-interferon-beta mutein) in Trop2-positive urothelial cancer. Our results support that ABN202 is a potent drug candidate in Trop2-positive urothelial cancer by directly inhibiting tumor growth and activating anti-cancer immune responses through type 1 IFN signaling.

#4432

A highly differentiated A2AR inhibitor for potential use in cancer therapy

Chandregowda Venkateshappa, Kishore Narayanan, Rashmi Nair, Aravind AB, Ramakishore VP Putta, Jwala Nagaraj, Megha Goyal, Vijay Kamal Ahuja, Amith A Dhudashiya, Samiulla DS, Girish Daginakatte, Thomas Antony, Kavitha Nellore, Susanta Samajdar, Murali Ramachandra.
Aurigene Discovery Technologies Limited, Bangalore, India

As a potent immunosuppressor adenosine is essential for maintaining tissue homeostasis and preventing an overzealous immune response during inflammation and infection. However, adenosine generated within the tumor microenvironment by the action of ectonucleotides hinders the immune reaction towards cancer cells by signaling through adenosine receptors such as high affinity A2AR expressed on immune cells. Tumors evade the immune response by usurping pathways that negatively regulate normal immune responses. Resistance to inhibition of immune checkpoint targets arises because of an upregulation in the expression of the CD39-CD73 axis and the resulting increase in production of adenosine in the tumor microenvironment. Inhibition of either adenosine generation or signaling by inhibition of A2AR along with other immune activation strategies have been shown to be effective therapeutic approaches.
In view of this, we sought to discover and develop novel small molecule inhibitors that dually target A2AR and an immuno-suppressive ligand expressed in the tumor microenvironment. Aurigene's dual inhibitors exhibit potent inhibition of both A2AR and an immuno-suppressive target of relevance in respective biochemical assays. Potent biochemical activity translated into rescue of chemokines and IL-2 in human PBMCs. Lead compounds exhibited desirable drug-like properties and excellent pharmacokinetic exposure in rodents. In a syngeneic tumor model, lead compounds demonstrated significant tumor growth inhibition. Anti-tumor efficacy correlated well with tumor drug levels and modulation of pharmacodynamic markers. In summary, we have identified first-in-class dual inhibitors with good drug like properties, which showed significant antitumor efficacy. Evaluation of these lead compounds in additional tumor models and in vivo toxicity studies will be presented.

#4433

Galectin-3 synergizes with CD47 to suppress phagocytosis and T cell immunity in peritoneal metastases of gastric adenocarcinoma

Yibo Fan, Shumei Song, Yuan Li, Shilpa Dhar, Jiankang Jin, Xiaodao Yao, Ruiping Wang, Ailing Wang, Melissa Pool Pizzi, Jingjing Wu, Katsuhiro Yoshimura, Lang Ma, Samir Hanash, George Calin, Linghua Wang, Michael Curran, Jaffer Ajani. *UT MD Anderson Cancer Center, Houston, TX*

Peritoneal metastasis (PC), the common sites of gastric adenocarcinoma (GAC) metastasis, remains resistant to therapies available in the clinics and new target is strived to be found. CD47 is one of the major players in conveying the “don’t eat me” signal upon binding its receptor SIRPα on myeloid cells which evade innate immune responses. Previously clinical studies on the blockade of CD47 alone resulted in limited clinical benefits suggesting that other target(s) must be inhibited simultaneously with CD47 for gaining advantage. Here, we found that CD47 was highly expressed on peritoneal malignant cells and its overexpression was a poor prognosticator. Additionally, we observed that Galectin-3 (Gal-3) was highly enriched in tumor cluster and was positively correlated with CD47 expression in short survival of patients revealed by scRNA-seq and metastatic GAC samples. Moreover, we found double positive of Gal-3 and CD47 significantly associated with diffuse type, poor differentiation, and tumor relapse. Mechanistically, Depletion of Gal-3 in mouse tumor and human tumor cells reduced the levels of CD47 through inhibition c-Myc expression and its binding to the promoter of CD47. Additionally, tumor-derived Gal-3 were found critical for tumor progression accompanied with protected GAC cells from phagocytosis by macrophages. Gal-3 deficiency resulted in a marked reduction in M2 macrophages and elevated T cell effector activity. Dual blockade of Gal-3 and CD47 significantly decreased tumor growth by promoted phagocytosis, repolarization of macrophage and boosted T cell immune responses in the tumor microenvironment. Our data uncover that Gal-3 synergizes with CD47 to suppress phagocytosis and orchestrates immunosuppressed milieu in the tumor microenvironment warrants combination therapeutic strategy in GAC patients with peritoneal metastases.

#4434

A PD-1-targeted, receptor-masked IL-2 immunocytokine with maintained potential to engage endogenous IL-2Ra drives selective stimulation of PD-1^{+} T cells and robust anti-tumor efficacy

Jiaxi Wu, Nicolin Bloch, Aaron Chang, Ramandeep Bhavsar, Supriya Patel, Qingqing Wang, Hassan Shakil Ahmed, Vidur Garg, Michael Amatulli, Yuetian Yan, Shunhai Wang, Drew Dudgeon, Willy Ramos, Pamela Krueger, Ashique Rafique, Tammy Huang, Erica Ullman, Aynur Hermann,

William Olson, John Lin, Eric Smith, Tong Zhang. *Regeneron Pharmaceuticals, Inc., Tarrytown, NY*

Interleukin-2 (IL-2) is a key cytokine for T cell proliferation, differentiation, and effector function. Recombinant IL-2 has been used for the treatment of metastatic melanoma and renal cell carcinoma, and induced complete, durable tumor regression in some patients. However, its broader use in cancer immunotherapy has been limited by severe toxicity. A new generation of IL-2 therapies with decreased binding to IL-2 receptor α-chain (IL-2Rα) is being developed to reduce toxicity and Tregs expansion yet with limited clinical success so far. Here, we show that the ability to engage IL-2Rα is critical for maximal anti-tumor activity of a systemic IL-2 therapy, and an alternative approach to circumvent systemic toxicity is to deliver IL-2 specifically to tumor-reactive T cells. We developed REGN10597, a PD-1-targeted, receptor-masked IL-2 immunocytokine with attenuated systemic IL-2 activity but maintained capacity to engage endogenous IL-2Rα on PD-1^+ T cells. Compared to WT IL-2, receptor masked IL-2 shows improved PK and diminished systemic toxicity in mice. REGN10597 shows PD1-targeting-dependent IL-2 activity in vitro and drives selective expansion of tumor-infiltrating PD-1^+ CD8 T cells with vigorous effector functions in vivo. In preclinical syngeneic tumor models in PD-1 humanized mice, REGN10597 demonstrates robust anti-tumor efficacy both as a single agent and in combination with PD-1 or PD-L1 blocking antibodies. These findings highlight the therapeutic potential of REGN10597 as a novel targeted and receptor masked WT IL-2 therapy, supporting its clinical development for the treatment of cancer.

#4435

A causal modeling platform for testing lifestyle interventions on the microbiome and response to immunotherapy

Aaditya Pallerla[1], Bailey Conrad[2], Amna Bibi[2], Nyelia Williams[2], Caroline Wheeler[2], Rebecca Hoyd[2], Shankar Suman[2], Joseph Amann[2], Yangyang Liu[2], Marisa Bittoni[2], Shiqi Zhang[3], Madison Grogan[2], Alvin Anand[2], Najma Afrah[2], Carolyn Presley[2], Fred K. Tabung[2], Lang Li[4], Yael Vodovotz[5], Jiangjiang Zhu[3], David P. Carbone[2], Steven K. Clinton[2], Daniel Spakowicz[1]. *[1]Pelotonia Institute for Immuno-Oncology, The Ohio State*

University Comprehensive Cancer Center – James Cancer Hospital and Solove Research Institute, Columbus, OH,[2]Department of Internal Medicine, The Ohio State University College of Medicine, Columbus, OH,[3]Department of Human Sciences, The Ohio State University College of Education and Human Ecology, Columbus, OH,[4]Department of Biomedical Informatics, The Ohio State University College of Medicine, Columbus, OH,[5]Department of Food Science and Technology, The Ohio State University College of Food, Agriculture, and Environmental Sciences, Columbus, OH

Rational manipulation of the gut microbiome by diet or other interventions is a promising approach to improving the efficacy and safety of cancer immunotherapy. However, linking lifestyle variables to specific microbial populations and the host immune response to cancer therapies is challenging due to their complexity. We established an experimental system to examine such complexity by linking a human dietary intervention and fecal biospecimens to mouse models to test the response to immunotherapy. Longitudinal human microbiome samples collected before and after a specific dietary or other intervention allow us to test the hypothesis that an intervention alters the response to immunotherapy via impact on the host microbiome. One set of samples was taken from the BEWELL study, which examined the impact of 2 x 80 mL black raspberry (BRB) drink boxes per day for 4 weeks in people at high risk for lung cancer. Participant samples were chosen based on enrichment of specific taxa. Pre- and post-BRB intervention samples were gavaged into mice. Mouse mc38 cells were injected subcutaneously and treated with anti-PD1 Ab or isotype control. Tumor size was monitored, and at the end of the study, tumor immune cell composition data were collected. Tumor growth over time was modeled using a linear mixed-effects model with tumor volume as the outcome variable and the predictor variables of time and treatment (PD1 vs. IgG) interacting with gavage and quadratic time to accommodate non-linear tumor growth and including random effects by mouse. For sample 68, enriched for *Roseburia* CAG 309, the interaction between time, gavage post-BRB, and Anti-PD1 treatment significantly affected tumor volume ($p < 0.05$) relative control. The same significant effect ($p < 0.05$) was also seen for sample 79, enriched for *Lachnospira pectinoschiza*, and samples 84 and 85, enriched for *Blautia obeum*. To determine the mechanism by which this

might occur, we analyzed the tumor's immune cell composition. Post-BRB mice treated with Anti-PD1 showed a significant increase in tumor-infiltrating CD8+ immune cells relative control, as compared to mice gavaged with pre-BRB stool. Modeling results showed samples whose response was improved slightly after the BRB dietary intervention. These samples were associated with the enrichment of the taxon *Roseburia* CAG 309. A black-raspberry dietary intervention in humans modified the microbiomes of several participants in a way that is hypothesized to improve response to PD1 treatment. Future directions include supplementing individual microbes into pre-intervention gavages to confirm which taxa improve response. These results suggest that this modeling platform is an effective system for testing microbiome modification on tumor growth and assessing mechanisms by which this might occur and is extendable to other lifestyle-based interventions where pre- and post-intervention specimens are collected.

#4436

A novel antibody-enabled dual precision targeted protein stabilization (TPS^2) that augments anti-tumor immune response by targeting CBL-B inhibitor to exhausted T cells while blocking checkpoint molecule, PD-1

Joanne Lim[1], Anna Skaletskaya[1], Uttapol Permpoon[2], Yeonjoon Kim[2], Shikha Saini[1], Khuloud Takrouri[1], Zinaida Ribkovskaia[1], Palash Bhar[1], Nathan Fishkin[1], Dong-Ki Choi[2], Ji Hyun Park[2], James Palacino[1], Peter U. Park[1]. *[1]Orum Therapeutics, Cambridge, MA,[2]Orum Therapeutics, Daejeon, Korea, Republic of*

It is well-established that T cells play a key role in the success of cancer immunotherapies. The goals of T cell-targeting therapies have been to restore the effector function of tumor-specific T cells that are either dysfunctional due to the immunosuppressive mechanisms in the tumor microenvironment, the lack of co-stimulatory signals, or negative regulation by expression of checkpoint molecules such as PD-1. E3 ligase Casitas B-Lineage Lymphoma Proto-Oncogene B (CBL-B) has recently gained attention as a master regulator of multiple immune-activation mechanisms. Inhibition of CBL-B enables the activation of antigen-specific T cells, and has been shown in syngeneic mouse tumor models to be efficacious as a

cancer immunotherapy agent. CBL-B inhibition has also been shown to enhance and prolong the effects of anti-PD-1 antibody (Ab) therapy. However, genetic knockout of CBL-B in mice led to spontaneous autoimmunity characterized by auto-antibody production and infiltration of activated T cells and B cells into multiple organs that could result in tissue damage. In order to mitigate safety issues that could result from systemic CBL-B inhibition, we developed novel antibody-drug conjugates (ADCs) that target CBL-B inhibitors (CBL-Bi) to T cells via binding to PD-1. Using PD-1-expressing Jurkat NFAT reporter cells and mixed lymphocyte reaction assay, we demonstrated that our TPS^2 approach enhanced the activation of T cells *in vitro* compared to treatment with anti-PD-1 Ab alone. Evaluation of pathways downstream of TCR activation in primary exhausted T cells showed increased Notch1, phospho-PLCγ2, and ZAP-70 accumulation following anti-PD-1/CBL-Bi treatment and is correlated with IFNγ induction. When autologous mature dendritic cells were co-cultured with dissociated tumor cells from melanoma patients, the highest magnitude of tumor-infiltrating lymphocyte activation was observed using delivery of CBL-Bi by anti-PD-1 ADC, compared to CBL-Bi alone, anti-PD-1 Ab alone, or combination treatment. The potential of anti-PD-1/CBL-Bi ADC for activation effector T cell function is also evident by increased intratumoral transcript levels of Granzyme B and Perforin following treatment in a humanized mouse model. In conclusion, we validated that the biological activity of CBL-Bi is retained after conjugation with an anti-PD-1 antibody. The use of anti-PD-1 Ab for developing the ADC not only targets the CBL-Bi payload to exhausted T cells but also blocks negative regulation of T cells via PD-1. Together, anti-PD-1/CBL-Bi ADC enhanced T cell activation *in vitro* as well as *in vivo*. Evaluation of safety and efficacy in animal tumor models is ongoing, to support further development of the TPS^2 approach.

#4437

BXQ-350: A novel biologic with an innovative mechanism of action targeting sphingolipid metabolism that induces cancer cell death and repolarizes the tumor microenvironment

Gilles H. Tapolsky, Tim Stephens, Nikhil Wilkins, Robin Furnish, Charlie Cruze, Ray Takigiku. *Bexion Pharmaceuticals, Inc, Covington, KY*

Background: Antineoplastic agents seem to affect tumors by targeting cancer cells via cytotoxic mechanism (traditional cytotoxic agents), an oncogenic pathway that promotes cancer cells proliferation (targeted agents), or immune pathways that are dysregulated in the tumor microenvironment (immune checkpoint inhibitors -ICI-). Clinical results have demonstrated that ICIs led to significant clinical benefits and durable responses in patients that previously had no or limited therapeutic options. Clinical results also demonstrated that combining ICIs or ICI with cytotoxic / targeted agents improved response rate and duration of response. BXQ-350 is a novel biologic simultaneously leading to cancer cells death and rebalancing the tumor microenvironment by targeting sphingolipid metabolism that is dysregulated in cancer cells. Sphingosine-1-phosphate (S1P) is a signaling metabolite known to promote cancer cell survival and proliferation and to favor an immunosuppressor environment; ceramide is a metabolite known to induce cancer cell apoptosis, mitophagy or necrosis and to favor an immunoeffector environment.
Methods: BXQ-350 was investigated preclinically in different *in vitro* and *in vivo* models and clinically in a first-in-human Phase 1 safety and dose escalation study in cancer patients with recurrent advanced solid tumors.
Results: Preclinical results demonstrated that BXQ-350 targets sphingolipid metabolism, decreases S1P levels while it simultaneously increases ceramide levels, leading to cancer cells death across multiple cancer cell lines. By impacting S1P and ceramide, BXQ-350 is additive or synergistic with different classes of antineoplastic agents. In addition, *ex vivo* experiments demonstrated BXQ-350 modulates many of immune-effector / suppressor cells as it repolarizes macrophages towards the antitumoral M1 phenotype, inhibits differentiation and activity of immunosuppressor of MDSCs, and promotes the proliferation of CD4+ and CD8+ Tcells as well as their activity. Clinical results revealed that BXQ-350 was well tolerated in cancer patients and showed signs of single agent activity. Analyses of biomarker samples showed that in patients experiencing a clinical benefit, systemic S1P plasma levels decreased significantly, and ceramide levels increased. Analysis of circulating cytokines revealed that BXQ-350 seemed to induce an increase of antitumoral cytokines (IFNg, TNFa, IL-2) and a decrease in protumoral ones (IL-6, IL-8, IL-10).
Conclusions: Preclinical and clinical results demonstrated that BXQ-350 modulates sphingolipid metabolism leading to cancer cell death and

stimulating the tumor microenvironment. Additional studies are ongoing to further understand BXQ-350's MOA.

#4438

Bypassing immune evasion in colorectal cancer by integrin inhibition-mediated downregulation of PD-L1

William J. MacDonald, Brooke Verschleiser, Lindsey Carlsen, Kelsey E. Huntington, Wafik S. El-Deiry. *Legorreta Cancer Center at Brown University, Providence, RI*

Integrin receptors have long posed a potentially attractive target for disrupting cancer hallmarks. Promising preliminary findings with integrin inhibition as an adjuvant to chemotherapy have not translated to clinical success. However, the effect of integrin inhibition on tumor-immune cell interactions remains largely unexplored. Further investigation could shed light on a connection between integrin signaling and immune checkpoint expression, opening the path for using integrin inhibitors to sensitize otherwise resistant tumors to immunotherapy. Fluorescently labeled wild-type HCT-116 colorectal cancer cells and TALL-104 T-cells were co-cultured and treated with GLPG0187, a small molecule integrin inhibitor, at various doses. Co-cultures were observed at different time points using fluorescence microscopy and cell counts were quantified using ImageJ software. The co-culture included the cell viability marker ethidium homodimer so the number of viable cells of each type could be determined using colocalization. This assay revealed synergistic cancer cell killing, indicating that integrin inhibition may be sensitizing cancer cells to immune cells. The hypothesized mechanism involves TGF-beta-mediated PD-L1 expression in cancer cells. GLPG0187 has been shown to inhibit the αvβ6 integrin receptor, which is responsible for the activation of latent-TGFβ into the active form. By blocking this receptor, there would potentially be a reduction of TGFβ signaling and therefore a reduced expression of PD-L1 leading to an enhanced immune response. To investigate this mechanism, both WT and p53-/- HCT-116 cells were pre-treated with GLPG0187 and subsequently with latent-TGFβ. Western blot analysis demonstrated that the addition of latent-TGFβ increased the expression of PD-L1 in cancer cells. Additionally, a low dose of integrin inhibitor rescued these effects, returning PD-L1 expression back to control levels. However, the higher

dose of the drug did not reduce PD-L1 expression. This could potentially be due to off-target effects conflicting with the proposed pathway, however, these findings are still under active investigation. Ongoing proteomic experiments include a larger range of both drug and latent-TGFβ doses. Probing for additional downstream markers of TGFβ and up-stream markers of PD-L1 will help to further elucidate the mechanism. Further co-culture experiments include anti-PD-L1 and anti-PD-1 therapy to investigate the viability of integrin inhibition as an adjuvant to immune checkpoint blockade.

#4439

Negative impact of the GABA pathway on aPD(L)1 immunotherapy

Svetlana Lyalina[1], Guadalupe Ortiz-Munoz[1], Kobe Yuen[1], Ira Mellman[1], Sanjeev Mariathasan[1], Matthew Albert[2], Deepti Nagarkar[3], Christine Moussion[1]. *[1]Genentech, South San Francisco, CA,[2]HiBio, South San Francisco, CA,[3]Nagarkar (Individual), South San Francisco, CA*

Although gamma-amino butyric acid (GABA) is well characterized as the primary inhibitory neurotransmitter of the central nervous system, its role in the periphery as an immunomodulatory agent is not well understood. Given the widespread use of GABA-A receptor agonists as palliative care in clinical practice, we examined here the impact of GABA on response to immunotherapy in preclinical tumor models and the association of GABA-A receptor agonist usage with outcomes in patients receiving immunotherapy.We show that important genes controlling the GABA pathway are enriched in human tumors versus normal tissue across indications, and tumor cells themselves are able to produce GABA. We found that several key genes of the GABA pathway are upregulated in non-responders to atezolizumab and we derived a 5-gene signature associated with poor outcomes in 2L urothelial cancer patients receiving atezolizumab. Preclinical models further indicated that GABA at the tumor site promotes tumor growth and dampens adaptive immunity preventing response to immunotherapy. Finally, we noted that 45% of urothelial cancer patients received concomitant GABA-A positive allosteric modulators, given as palliative therapy in atezolizumab trials IMvigor-210 and -211. This group exhibited significantly lower OS and PFS as compared to atezolizumab treated patients who did not receive GABA-A positive modulators. A

similar negative impact was seen in patients receiving standard of care anti-PD(L)1 immunotherapy in 2L NSCLC using EHR derived deidentified Flatiron Health - Komodo Health claims linked data. These findings highlight the need for further evaluation of concomitant GABA modulators to understand potential risk associated with palliative care in the setting of cancer immunotherapy.

#4440

Efficacy of Gen-1, an interleukin-12 immune gene therapy, at different dose frequencies

Subeena Sood[1], Jean D. Boyer[2], Jessica Kim[2], Majed M. Matar[2], Olivia Signer[2], Jennifer S. Rice[2], Alanna M. Smith[2], Nicholas Borys[2], Khursheed Anwer[2]. *[1]Research and Development, Imunon Inc, Lawrenceville, NJ,[2]Imunon Inc, Lawrenceville, NJ*

Introduction: The purpose of this study was to investigate the effect of dosing frequency on the antitumor activity of intraperitoneal GEN-1, an interleukin-12 (IL-12) immune gene therapy in a mouse model of peritoneally disseminated ovarian cancer.
Procedures: Three GEN-1 dosing regimens were examined for efficacy in ID-8 tumor-bearing mice: weekly, every 2 weeks and every 3 weeks. 2.5 million cancer cells were bolus injected into 4 groups (B, C, and D) of 10 mice each. A control group (A) of 6 mice had PBS injected IP without tumor and an untreated control (E) of 15 mice were injected with 2.5 million cancer cells. Groups B, C, and D were injected with GEN-1 IP weekly, every 2 weeks, and every 3 weeks respectively. Six animals from each group B, C, and D were harvested for translational research (TR) after 5 weekly, 3 every 2-week and 2 every 3-week treatments respectively. The remaining 4 animals in each group were followed for weight change (tumor burden) and survival. Additionally, TR evaluated change in ascites T-cell, B-cell and myeloid cell populations.
Results: There was a gradual rise in tumor burden and mortality in all treatment groups with comparable rate between once every week and once every 2-week regimens. Once every 3-week regimen had relatively higher

mortality rate and higher tumor burden. There were similar or higher increases in T-cell and B-cells with reduced treatment frequency with lesser increases in myeloid cell density with reduced treatment frequency. Conclusions: Once every 2-week dosing of GEN-1 in human studies is warranted. Future combination studies of Gen-1 with immune checkpoint inhibitors will evaluate the safety and efficacy of this regimen.

#4441

Bifunctional immunotherapeutic HCW9218 facilitates recruitment of immune cells from tumor draining lymph nodes to promote antitumor activity and enhance checkpoint blockade efficacy in solid tumors

Varghese George, Pallavi Chaturvedi, Niraj Shrestha, Leah Kanakraj, Crystal Gilkes, Nicole Encalada, Meng Wang, Xiaoyun Zhu, Bai Liu, Peter Rhode, Hing C. Wong. *HCW Biologics, Inc., Miramar, FL*

Immunotherapeutics that aid in boosting natural immune defenses against cancers have revolutionized cancer treatment. Previously, we reported a novel heterodimeric bifunctional fusion molecule, HCW9218, designed using soluble tissue factor (TF)-based scaffold technology comprising extracellular domains of the human transforming growth factor-β (TGF-β) receptor II and a human interleukin (IL)-15/IL-15 receptor α complex which exhibited both immune cell stimulatory and TGF-β neutralizing properties. Herein, we showed in two different syngeneic murine tumor models (B16F10, 4T1) that subcutaneous treatment with HCW9218 induces a proliferative burst of $CD8^+$ T cells and NK cells in blood and a subsequent infiltration of these cells into established tumors. In vivo imaging of 4T1 tumor-bearing mice after treatment showed that HCW9218 was present both in lymph nodes and established tumors up to 24hr following treatment. Comprehensive analysis of tumor infiltrating lymphocytes (TILs) showed that HCW9218 mediated antitumor activity by expanding TCF^+TIM3^- 'progenitor exhausted' (Tpex) $CD8^+$ T cells in tumors. Sphingosine-1-phosphate receptor blockade resulted in decreased tumor infiltration of $CD8^+$ Tpex in B16F10 and 4T1 tumor-bearing mice indicating that these cells originate from tumor draining lymph nodes (TdLN). Increased 'terminally exhausted' $TCF\text{-}1^-TIM3^+$ (Tex) $CD8^+$ TILs were also observed in tumors of HCW9218-treated mice indicating increased antitumor activity. Tumor transplantation experiments further

confirmed the mechanism of HCW9218 antitumor activity by increasing influx of CD45.1$^+$ CD8$^+$ T cells into transplanted tumors from CD45.2$^+$ mice. Additionally, HCW9218 enhanced the therapeutic efficacy of PD-L1 treatment by increasing the infiltration of activated/memory CD8$^+$ T cells into B16F10 tumors in mice leading to significant reduction in tumor volume. Collectively, the results of this study
demonstrated that HCW9218 treatment of mice bearing solid tumors resulted in modulating the TdLN immune landscape and invigorating T cells for enhanced checkpoint blockade therapy. HCW9218 are currently in two clinical trials (clinicaltrials.org: NCT05322408, NCT05304936) against chemo-resistant/refractory solid tumors.

#4442

Dual benefit of MALT1 blockade in glioblastoma

Juliana Hofstatter Azambuja[1], Saigopalakrishna S. Yerneni[2], Gabriela N. Debom[1], Lisa M. Maurer[1], Hannah E. Butterfield[1], Linda R. Klei[1], Gary Kohanbash[1], Peter C. Lucas[1], Linda M. McAllister-Lucas[1]. *[1]University of Pittsburgh, Pittsburgh, PA,[2]Carnegie Mellon University, Pittsburgh, PA*

Background**:** Glioblastoma multiforme (GBM) is the most common and aggressive malignant primary brain tumor. Despite advances in treatment modalities, GBM remains largely incurable and new treatment approaches are desperately needed. An innovative strategy for cancer therapy is to combine the inhibition of cancer cell-intrinsic oncogenic signaling with cancer cell-extrinsic immunological activation of the tumor microenvironment (TME). MALT1 represents a candidate target whose inhibition may provide this dual benefit. Originally identified as a proto-oncoprotein in lymphoma, MALT1 has recently also been implicated in multiple solid tumors, including GBM, and significant effort has been made to develop MALT1 protease inhibitors as anti-cancer agents. Interestingly, blockade of MALT1 protease has also been shown to selectively reprogram tumor infiltrating Treg cells into antitumor effector cells. Based on these observations, we hypothesized that in GBM, MALT1 acts both within tumor cells and within cells of the TME to promote tumorigenesis and MALT1 inhibitor treatment could thus have dual benefit.
Methods/Results: We assembled a panel of mouse and human GBM cell lines and performed western-blot analysis to show that these cells

demonstrate constitutive MALT1 expression and proteolytic activity. MALT1 blockade in GBM cells, using siRNA or MALT1 protease inhibitors, reduces viability and clonogenic potential, suggesting that inhibition of MALT1 could impair tumor cell survival. Single-cell RNAseq data from public datasets demonstrated that myeloid cells have the highest MALT1 expression in the GBM TME. Our data indicate that co-culture of macrophages with GBM cells induces MALT1-NF-κB activation within the macrophages and this is associated with polarization towards an M2-like immunosuppressive phenotype. Additionally, treating primary human or mouse macrophages with MALT1-protease inhibitor prevents GBM-induced M2-polarization, increases M1-polarization and enhances GBM cell killing. In a syngeneic orthotopic mouse model, GBM tumor growth is impaired, and survival is extended when tumor cells are implanted into MALT1-protease dead (PD) host mice (mice which harbor a point mutation in the MALT1-protease catalytic cysteine) as compared to when implanted into wild-type host mice. MALT1-PD mice demonstrate a less immunosuppressive GBM TME with increased M1-macrophages and decreased M2-macrophages, MDSCs and Tregs. Taken together, our findings suggest that inhibiting MALT1 protease in TME cells promotes anti-tumor immunity against brain tumors.
Conclusions: Our studies suggest MALT1 protease as a new therapeutic target in GBM whose inhibition could have dual benefit via both direct effect on tumor cells and by reversing the immunosuppressive TME.

#4444

Targeting PI3K isoforms to improve the effectiveness of T cell mediated immunotherapy

Ritu Bohat[1], Xiaofang Liang[1], Chunyu Xu[1], Yitao Tang[2], Jiakai Hou[1], Nicholas A. Egan[1], Leilei Shi[3], Ashley Guerrero[1], Roshni Jaffery[1], Elizabeth M. Burton[4], Han Liang[5], Hussein Tawbi[2], Michael A. Davies[2], Weiyi Peng[1]. *[1]Biology and Biochemistry, University of Houston, Houston, TX,[2]Department of Melanoma Medical Oncology, The University of Texas MD Anderson Cancer Center, Houston, TX,[3]Department of Epigenetics and Molecular Carcinogenesis, The University of Texas MD Anderson Cancer Center, Houston, TX,[4]Genomic Medicine, The University of Texas MD Anderson Cancer Center, Houston, TX,[5]Bioinformatics and Computational*

Biology, Systems Biology, The University of Texas MD Anderson Cancer Center, Houston, TX

Hyperactivation of the PI3K pathway has been reported to correlate with resistance to immune checkpoint blockade therapy (ICB) in melanoma, highlighting the therapeutic potential of combining PI3K inhibition (PI3Ki) with ICB. To maximize the clinical benefit of PI3Ki-based immune oncology (IO) combination, we characterized the role of PI3K isoforms in tumor and T cells and determined the immunological impacts of PI3Ki alone or in combination with ICB. Inhibitions of PI3K were achieved by either genetic knockdown (KD) or the bioactive compound in PTEN-present (B16/MC38), PTEN-absent (BP/D4M) tumor cell lines, and CD8+ T cells (Pmel-1). Following PI3Ki, we determined the activation status of the PI3K pathway (p-AKT level), transcriptional profile, and cellular function of these cells. We found both *in vitro* KD and pharmacological inhibition of either PI3Kα or PI3Kβ displayed a dramatic reduction of the PI3K pathway in tumor cells but moderate or no reduction in T cells, whereas the PI3K pathway significantly decreased in T cells with PI3Kγ or PI3Kδ inhibition. KD of PI3Kα or β isoforms drastically sensitized both D4M and MC38 tumors to αPD1 *in vivo*. We also observed that only PI3Kγ or PI3Kδ inhibition profoundly suppressed cytokine production and cytotoxicity of CD8+ T cell, suggesting that PI3Kα or PI3Kβ isoform inhibition can achieve tumor specific PI3Ki with limited impacts on T cell function. Furthermore, we used multiple syngeneic melanoma models to determine whether PI3K isoform inhibition can synergize the antitumor activity of ICB *in vivo*. In PTEN-present tumors, BYL719 (BYL, a PI3Kα inhibitor) synergized with αPD1 to delay tumor growth and extend survival (median survival of MC38-bearing mice in control (Ctrl), BYL, αPD1, and combination (Comb) groups: 30, 36, 33, and >45 respectively; $p<0.05$: Ctrl/BYL/αPD1 vs Comb). However, a limited combinatorial effect between GSK2636771(a PI3Kβ inhibitor) and αPD1 was observed in PTEN-present tumor models. Moreover, the combination of BYL and αPD1 exhibits superior antitumor activity in a spontaneous Braf-mutant, PTEN-loss melanoma model when compared with either reagent. Mechanistically, the combination of BYL and αPD1 improved CD8+ T cells tumor infiltration (14 days treatment, mean CD8+ number/mg of the tumor, Ctrl:1392.9, BYL:2073.9, αPD1:1545.2, Comb:4691.8; $p<0.01$: Ctrl/BYL/

αPD1 vs Comb) and reduced MDSCs in MC38 tumors ($p<0.05$: Ctrl vs Comb). Multi-omics profiling of tumor cells with *in vitro* and in *vivo* PI3K isoform inhibition is ongoing. Collectively, our results demonstrate that PI3Kα inhibitor can potentiate T cell-mediated antitumor immune responses regardless of PTEN status, providing a strong rationale for the clinical development of the BYL-based IO combination. In collaboration with Novartis, MD Anderson Cancer Center will launch a Phase I/II trial of the FDA-approved BYL in combination with αPD1 in advanced melanoma and breast cancer patients.

Increasing the Clinical Utility of Cell-Free DNA Testing

#5709

Whole genome error-corrected sequencing for sensitive circulating tumor DNA cancer monitoring

Alexandre P. Cheng[1], Adam J. Widman[2], Anushri Arora[3], Itai Rusinek[4], William F. Hooper[1], Rebecca Murray[1], Daniel Halmos[1], Theophile Langanay[1], Giorgio Inghirami[1], Soren Germer[3], Melissa Marton[3], Adrienne Helland[3], Rob Furatero[3], Jaime McClintock[3], Lara Winterkorn[3], Zoe Steinsnyder[3], Yohyoh Wang[1], Srinivas Rajagopalan[1], Asrar I. Alimohamed[5], Murtaza S. Malbari[1], Ashish Saxena[1], Margaret K. Callahan[2], Dennie T. Frederick[6], Lavinia Spain[7], Ariel Jaimovich[4], Doron Lipson[4], Samra Turajlic[7], Michael C. Zody[3], Nasser K. Altorki[1], Jedd D. Wolchok[1], Michael A. Postow[2], Nicolas Robine[3], Genevieve Boland[6], Dan A. Landau[1]. *[1]Weill Cornell Medical College, New York, NY,[2]Memorial Sloan Kettering Cancer Center, New York, NY,[3]New York Genome Center, New York, NY,[4]Ultima Genomics, Newark, CA,[5]Dana Farber Cancer Institute, Boston, MA,[6]Massachusetts General Hospital, Boston, MA,[7]The Francis Crick Institute, London, United Kingdom*

In many areas of oncology, we lack sensitive tumor-burden monitoring to guide critical decision making. While circulating tumor DNA (ctDNA) promises to enable disease monitoring, this approach is limited by the sparsity of ctDNA in the plasma. To overcome this challenge, error-corrected deep targeted sequencing has been proposed.

Nonetheless, this framework is limited by the low number of genomic equivalents (GEs, ~10^3 /mL of plasma), imposing a ceiling on effective sequencing depth. We have previously shown that genome-wide mutational integration through plasma whole genome sequencing (WGS) can sever the dependency between available GEs and assay sensitivity (Zviran *et al*, 2020). In this approach, tumor-informed mutational profiles are applied to plasma WGS, allowing detection of tumor fractions as low as 10^{-5}. However, the higher cost of WGS limits practical depth of coverage (20-30X) and may limit broad adoption. Lower costs may thus allow for enhanced ctDNA cancer monitoring via WGS. We therefore applied emerging lower-cost WGS (1USD/Gb, Almogy *et al*, 2022) to plasma from 7 patients with metastatic cancer at ~115x coverage depth. Read depth profiling and error rates were comparable between matched Ultima and standard platform datasets. Integration of deep learning architectures for signal to noise enrichment (Widman *et al*, biorxiv, 2022) with deeper WGS coverage enabled ctDNA detection at the parts per million range.
We reasoned that lower sequencing cost can be harnessed for duplex error-corrected WGS. Proof-of-concept experiments in mouse PDX samples showed ~1,500x decrease in errors. Applied to the plasma of stage IV melanoma patients (n=5), we obtained error rates ~10^{-7}. We used this approach to tackle the challenging context of cancer monitoring in early-stage melanoma without matched tumor sequencing. While in uncorrected WGS, *de novo* mutation calling yielded limited ability to detect melanoma specific mutations, duplex-corrected WGS allowed us to harness melanoma mutational signatures for disease monitoring without matched tumor profiling. Analytic validation of our assay showed sensitive and specific cancer detection when the concentration of ctDNA was at 10^{-4} concentrations. Applied to a cohort of stage III melanoma patients with negative ctDNA detection using previously described methods, we detected ctDNA in all cases (n=4), demonstrating enhanced sensitivity using duplex WGS. These data demonstrate the exciting potential of low cost WGS for ultra-sensitive ctDNA cancer monitoring. In the tumor-informed setting, deeper sequencing increased sensitivity for mutational profile detection. Moreover, the application of duplex error-correction at genome scale allowed for sensitive cancer monitoring without matched tumor profiles. We envision that the era of low-cost sequencing will empower ultra-

sensitive cancer monitoring via WGS, with transformative impact on cancer care.

#5710

Detection and monitoring of t(11;14) in liquid biopsies from patients with relapsed/refractory multiple myeloma treated with venetoclax-based regimens

Xiaotong Li[1], Lao H. Saal[2], Christian Brueffer[2], Yilun Chen[2], Johanna Asklin[2], Saman Alvi[1], Srinivas Venkatram[1], Jeremy A. Ross[1]. *[1]AbbVie Inc., North Chicago, IL,[2]SAGA Diagnostics, Lund, Sweden*

Venetoclax (Ven) is a selective B-cell lymphoma 2 inhibitor being studied in t(11;14)+ relapsed/refractory multiple myeloma (MM) Detection of t(11;14) in MM requires bone marrow (BM) aspiration and evaluation of CD138+ plasma cells by fluorescence in situ hybridization (FISH) Innovative techniques may provide less invasive detection of t(11;14) in liquid biopsies Here we present results of the SAGAsign® integrated approach combining low-coverage whole-genome sequencing (WGS) to characterize t(11;14) breakpoints together with personalized digital polymerase chain reaction (dPCR) assays to efficiently detect and monitor the genomic rearrangements in circulating tumor DNA (ctDNA) Baseline BM aspirates were collected from 270 patients (pts) from Ven clinical trials (NCT02755597, NCT01794520, NCT03314181, NCT02899052) Previously generated WGS to an average coverage ~22× was used Paired samples of peripheral blood mononuclear cell (PBMC) DNA and plasma circulating cell-free DNA (cfDNA) were analyzed by dPCR at timepoints after Ven-based treatment Of the 90 t(11;14)+ pts by FISH, 160 t(11;14) breakpoints were identified by WGS in 74 pts (concordance in Table) At the time of data cutoff, dPCR assays were designed and evaluated in 8 t(11;14)+ pts; 7/8 (88%) and 6/8 (75%) pts had detectable t(11;14) in cfDNA or PBMCs, respectively Higher levels of t(11;14) mutant allele frequency (MAF) were observed in cfDNA compared with PBMCs After Ven-based treatment, t(11;14) MAF in cfDNA became undetectable in pts with a complete response In conclusion, this approach has the capability to reconstruct t(11;14) breakpoints from WGS data that is highly concordant with FISH; translocations appear more readily detectable in cfDNA than PBMC samples from pts with MM SAGAsign assays detected and

monitored t(11;14) in liquid biopsies thus highlighting its potential utility for identifying pts with t(11;14) for targeted therapies

Concordance between WGS and FISH testing for t(11;14)			
Samples, n	FISH+	FISH−	Total
WGS+	74	11	83
WGS−	16	169	187
Total	90	180	270
	Concordance, %	**n/N**	**95% CI**
t(11;14) positive	82.2	74/90	72.7–89.5
t(11;14) negative	93.9	169/180	89.3–96.9
Overall testing	90.0	243/270	85.8–93.3

#5711

Blood-based early detection of non-small cell lung cancer using orphan noncoding RNAs

Mehran Karimzadeh, Jeffrey Wang, Aiden Sababi, Oluwadamilare I. Afolabi, Dung Ngoc Lam, Alice Huang, Diana R. Corti, Kristle C. Garcia, Seda Kilinc, Xuan Zhao, Jieyang Wang, Taylor B. Cavazos, Patrick Arensdorf, Kimberly H. Chau, Helen Li, Hani Goodarzi, Lisa Fish, Fereydoun Hormozdiari, Babak Alipanahi. *Exai Bio Inc., Palo Alto, CA*

Background: Orphan non-coding RNAs (oncRNAs) are a novel category of small non-coding RNAs that are present in the tumor tissue and blood of people with cancer and largely absent in people without cancer. To examine the potential of using oncRNAs for early cancer detection via liquid biopsy, we assessed the oncRNA content of serum from people with and without non-small cell lung cancer (NSCLC) and developed a prediction model for NSCLC.

Methods: A total of 540 serum samples were obtained from Indivumed (Hamburg, Germany) and MT Group (Los Angeles, CA) and divided into cohort A for training (150 NSCLC cases, 219 controls; female: 30.7%/36.1%; mean age: 67.9 ± 8.9/62.4 ± 9.2; ever-smoker: 95.3%/26.9%, respectively) and cohort B for internal validation (88 NSCLC cases, 83 controls; female: 40.9%/54.2%; mean age: 62.7 ± 9.2/54.1 ± 12.4; ever-

smoker: 89.8%/6.0%, respectively). We used RNA isolated from 0.5 mL of serum to generate and sequence libraries at an average depth of 18.5 ± 6.5 million 50-bp single-end reads using next-generation sequencing. Previously, we created a large catalog of NSCLC oncRNAs found in 999 NSCLC tumor tissues and largely absent in 679 normal samples from The Cancer Genome Atlas (TCGA) smRNA-seq database. This catalog was distilled by removing smRNA species found in the serum of an independent cohort of 31 non-cancer donors to yield a final NSCLC oncRNA catalog of 81,004 distinct oncRNA species. This distilled catalog was the reference for identifying NSCLC oncRNAs in the present study. Using oncRNA data we generated by sequencing samples from cohort A, we trained a logistic regression model for predicting NSCLC presence. The model was then validated in cohort B.
Results: From the 540 samples sequenced, we detected 64,379 oncRNAs from the distilled TCGA oncRNA catalog in at least one sample across both cohorts (A: 55,650, B: 47,539).Using 5-fold cross-validation, the AUC of the logistic regression model was 0.95 (95% CI: 0.93-0.97) for the training cohort, and was 0.98 (0.97-0.99) for the validation cohort. Sensitivities for detecting NSCLC at 95% specificity were 0.78 (0.69-0.86) for early stage (I/II) cancer and 0.75 (0.60-0.87) for late stage (III/IV) cancer in the training cohort, and 0.92 (0.83-0.98) and 1.0 (0.85-1.0), respectively, in the validation cohort.
Conclusion: These results demonstrate the potential for accurate, sensitive, and early detection of NSCLC through sequencing the oncRNA content of a routine blood draw. The performance of the model trained on one cohort and internally validated in a separate cohort supports the generalizability of this approach in detecting NSCLC.

#5712

Anti-TIGIT antibody tiragolumab leverages myeloid cells and regulatory T cells to improve PD-L1 checkpoint blockade

Namrata S. Patil[1], Shyam Srivats[1], Yoonha Choi[1], Xiangnan Guan[1], Barzin Nabet[1], Lisa McGinnis[1], Eugene Chiang[1], Alexis Dunkle[1], Bill O'Gorman[1], Patrick S. Chang[1], Ruozhen Hu[1], John Silva[1], Joy Han[1], Amelia Au-Yeung[1], Chikara Takahashi[1], Nandini Molden[1], Pallavi Daggumati[1], Wendy Connolly[1], Melissa Johnson[2], Delvys Rodriguez Abreu[3], Byoung Chul Cho[4], Antoine Italiano[5], Ignacio Gil-Bazo[6], Enriqueta Felip[7], Ira Mellman[1],

Raymond Meng[1], Sanjeev Mariathasan[1], Robert Johnston[1], David S. Shames[1]. *[1]Genentech Inc., South San Francisco, CA,[2]Sarah Cannon Research Institute/Tennessee Oncology, Nashville, TN,[3]Hospital Universitario Insular de Gran Canaria, Las Palmas, Spain,[4]Yonsei Cancer Centre, Yonsei University College of Medicine, Seoul, CA,[5]Institut Bergonie CLCC Bordeaux, Bordeaux, France,[6]Clínica Universidad de Navarra, CIMA Universidad de Navarra Pamplona, Pamplona, Spain,[7]Vall d'Hebron Institute of Oncology (VHIO), Barcelona, Spain*

Background: TIGIT is a co-inhibitory receptor and immune checkpoint associated with T cell and natural killer (NK) cell dysfunction in cancer. Tiragolumab is an anti-TIGIT antibody with an active IgG1/kappa Fc. In a randomized double-blind phase 2 clinical trial in non-small cell lung cancer (NSCLC), tiragolumab + atezolizumab (anti-PD-L1) combination treatment demonstrated significant improvement relative to atezolizumab alone. However, the mechanisms underlying the efficacy of this combination are not well understood.
Methods: In CITYSCAPE (phase 2, NCT03563716), chemotherapy-naïve patients with locally advanced/metastatic NSCLC received either placebo + 1200 mg atezolizumab or 600 mg tiragolumab + 1200 mg atezolizumab q3w IV. We collected tumor pretreatment samples and serum samples (baseline and on-treatment) from patients enrolled in the trial, which were subject to bulk RNA-seq and proteomics, respectively. In the mouse tumor model, BALB/c mice were implanted with syngeneic CT26 tumors. After tumor establishment, mice were randomized by tumor volume and then treated with control IgG2a, anti-PD-L1, anti-TIGIT IgG2a-LALAPG (Fc-inactive) ± anti-PD-L1, anti-TIGIT IgG2b ± anti-PD-L1, or anti-TIGIT IgG2a ± anti-PD-L1. Three days after treatment, CD45+ immune cells were collected from the peripheral blood and tumor from selected treatment groups and underwent single cell RNA sequencing or flow cytometry profiling. Tumor growth was also monitored to determine efficacy.
Results: Here, we show that tiragolumab functions as both a conventional checkpoint inhibitor and, via Fc gamma receptor engagement, as a modulator of immunosuppressive myeloid cells and T regulatory (Treg) cells. Gene expression analysis of patient tumor samples revealed high levels of these cell subsets, were instead associated with treatment benefit

in the tiragolumab + atezolizumab arm but not atezolizumab arm. Analysis of patient serum proteins suggested an association of myeloid cell activation with clinical benefit mediated by the combination therapy. In mouse tumor models, treatment with anti-PD-L1 + anti-TIGIT IgG2a (but not anti-TIGIT IgG2b or Fc-silent anti-TIGIT) led to effective tumor control in mice, suggesting a pivotal role for activating Fc receptors. Phenotypic profiling by single cell RNAseq and flow cytometry revealed that Fc-active anti-TIGIT remodels the tumor microenvironment, most prominently by inducing antigen presentation machinery in myeloid cells, counteracting of anti-PDL1-enforced CD8+ T cell exhaustion, and reducing Treg suppressive capacity.
Conclusions: These findings reveal that FcR engagement is one of several distinct mechanisms by which tiragolumab unleashes antitumor immune responses, and inform further clinical development of anti-TIGIT therapies.

#5713

Assessing the real-world utility of cell-free microbial DNA in diagnosing early-stage lung cancer

Serena Fraraccio[1], Stephen Wandro[1], Akanksha Singh-Taylor[1], Sandrine Miller-Montgomery[1], Eddie Adams[1], Rob Knight[2], Leopoldo N. Segal[3], Harvey I. Pass[4], Gregory D. Sepich-Poore[1]. *[1]Research & Development, Micronoma, Inc., San Diego, CA,[2]Department of Bioengineering, Department of Pediatrics, Department of Computer Science and Eng., University of California San Diego, San Diego, CA,[3]Division of Pulmonary and Critical Care Medicine, New York University School of Medicine, New York, NY,[4]Department of Cardiothoracic Surgery, New York University School of Medicine, New York, NY*

Introduction: Links between cancer and microbes date back four millennia (Sepich-Poore et al. 2021. *Science*). Recently, we found that microbial DNA is detectable in tumor tissues and patient blood from many human cancer types (Poore et al. 2020. *Nature*). These intratumoral and bloodborne microbiomes were distinct between cancer types, between normal and malignant tissues, and present in cell-free plasma samples. However, the practical utility of cell-free microbial DNA (cf-mbDNA) as a bona fide liquid biopsy diagnostic, including its applicability in early-stage disease in treatment-naïve individuals, distinguishing histological subtypes, and

discriminating against non-cancer-but-diseased patients remains unknown. Thus, we constructed an age and sex-matched cohort of >1000 individuals with lung cancer, lung disease, and no disease (healthy) to evaluate the utility of a cf-mbDNA-driven liquid biopsy diagnostic.
Methods: Shallow shotgun metagenomic sequencing with gold-standard positive and negative controls was performed using 400 μL of patient plasma. Direct genome alignments separated human and microbial reads, and generated genome-wide binned and species-level abundances, respectively. Novel taxonomic diversity was captured by additionally performing *de novo* co-assemblies in tandem with tumor and blood samples from The Cancer Genome Atlas (TCGA). Multi-modal, stacked machine learning classifiers then evaluated the diagnostic performance of microbial-only and multi-species (microbial + human) information.
Results: Cf-mbDNA provides strong diagnostic performance in treatment-naïve, cancer-bearing individuals versus age and sex-matched healthy controls, as early as stage I disease (AUROCs≥0.90). Furthermore, cf-mbDNA outperforms histological classification compared to human genomic information. Multi-species models paired with routinely-available clinicodemographic information provided robust discrimination of lung cancer versus lung diseases (AUROC≥0.80). Importantly, the addition of cell-free microbial information produced an integrated model surpassing the diagnostic performance of PET-CT and clinical risk models for lung nodule malignancy determination in a blinded validation cohort of Stage I lung cancer and non-cancer lung disease samples.
Conclusion: Cf-mbDNA features comprise a novel class of biomarkers that are combinable with host analytes, and show promise for real-world, early-stage, lung cancer diagnosis.

#5714

Cell-free DNA fragmentation profiling for monitoring therapeutic response in metastatic colorectal cancer

Bahar Alipanahi[1], Iris van 't Erve[2], Keith Lumbard[1], Laurel K. Millberg[1], Zach Skidmore[1], Lorenzo Rinaldi[1], Jacob Carey[1], Jennifer Tom[1], Cornelis J. A. Punt[3], Nicholas C. Dracopoli[1], Gerrit A. Meijer[2], Robert B. Scharpf[1], Victor E. Velculescu[4], Remond Fijneman[2], Alessandro Leal[1]. *[1]Delfi Diagnostics, Baltimore, MD,[2]Netherlands Cancer Institute, Amsterdam, Netherlands,[3]University Medical Center Utrecht, Utrecht, Netherlands,[4]The*

Sidney Kimmel Comprehensive Cancer Center, Johns Hopkins University School of Medicine, Baltimore, MD

BACKGROUND: Cell-free circulating tumor DNA (ctDNA) assays have been adopted to monitor therapeutic response in both early- and late-stage cancer. However, tests currently available require deep-targeted sequencing to detect cancer-specific mutations at low mutant allele frequency (MAF) levels in the circulation. Recently, we developed a tumor-agnostic approach called DELFI Tumor Fraction (DELFI-TF), a Bayesian probabilistic model designed to predict plasma tumor fractions based on genome-wide fragmentation-related features.
METHODS: Overall, 692 longitudinal plasma samples collected from 153 patients with initially unresectable colorectal cancer (CRC) liver-only metastases participating in the phase III study CAIRO5 (NCT02162563) were split across a training (RAS/BRAF mutant) and a validation cohort (RAS/BRAF wildtype). For all cell-free DNA (cfDNA) samples of patients within the training cohort (n=312), the tumor burden was quantified as the MAF of the tumor-tissue-proven RAS/BRAF variant measured by digital droplet PCR (ddPCR). Using cfDNA fragment-sequencing statistics from low-coverage WGS data, a Bayesian regression model was trained against the MAF of the tumor-specific driver RAS/BRAF variant in all longitudinal timepoints in the training cohort. Changes in DELFI-TF scores during first-line FOLFOX/FOLFIRI and bevacizumab therapy were assessed to predict disease response. A tissue-informed approach was applied to detect minimal residual disease in the subgroup of patients treated with curative intent (complete resection of the primary tumor and liver metastases).
RESULTS: In the training cohort, DELFI-TF scores strongly correlated with RAS/BRAF MAF measured by ddPCR ($r=0.85$, $p<0.001$). DELFI-TF captured plasma tumor fractions associated with copy number changes when ddPCR failed to detect RAS/BRAF mutations. Before treatment initiation, DELFI-TF correlated with the sum of the largest diameters on CT scans according to RECIST1.1 ($r=0.49$, $p<0.001$). Patients with negative and positive changes in DELFI-TF more often exhibited response and progressive disease based on consecutive RECIST assessments, respectively. Median progression-free survival was 9.9 and 12.8 months for patients with DELFI-TF low versus DELFI-TF high, respectively ($p=0.007$). Overall survival was 28.8 and 58.9 months for patients with

DELFI-TF low versus DELFI-TF high, respectively (p=0.001). In patients treated with curative intent, tissue-informed focal and arm-level copy number changes were detected 4-12 weeks after metastasectomy. Most patients presenting molecular relapse were later diagnosed with clinical recurrence by conventional CT imaging.
CONCLUSIONS: DELFI-TF demonstrates the ability to use cfDNA fragmentomes to estimate cfDNA tumor burden with a performance comparable to standard approaches for treatment response monitoring and clinical outcome prediction.

#5715

Circulating tumor DNA in colorectal cancer patients with resectable liver metastases: Preliminary results of the MIRACLE study

Lissa Wullaert[1], Maurice P. H.M. Jansen[2], Jaco Kraan[2], Jan M. van Rees[1], Corine M. Beaufort[2], Yannick M. Meyer[1], Boris Galjart[1], Pieter M. H. Nierop[1], Florian E. Buisman[1], Diederik J. Höppener[3], Erik P. van der Stok[1], Gianmarco Motta[2], Dirk J. Grünhagen[1], Henk M. W. Verheul[2], Stefan Sleijfer[1], Saskia M. Wilting[2], Cornelis Verhoef[1], John W. M. Martens[2].
[1]Surgical Oncology, Erasmus MC Cancer Institute, Rotterdam, Netherlands,[2]Medical Oncology, Erasmus MC Cancer Institute, Rotterdam, Netherlands,[3]Oncological Surgery, Erasmus MC Cancer Institute, Rotterdam, Netherlands

Introducti**on:** Recurrence risk after curative surgery for colorectal liver metastases (CRLM) remains high, underlining the need for novel prognostic markers. Liquid biopsies provide promising biomarkers to detect minimal residual disease (MRD) after local treatment. The aim of this study was to determine and compare the characteristics of cell-free DNA (cfDNA) and circulating tumor DNA (ctDNA) in liquid biopsies taken before and after surgical treatment of CRLM.
Materials & Methods: Patients with isolated CRLM were recruited before undergoing potentially curative hepatic resection. Only patients who did not receive per-operative chemotherapy were selected. Peripheral blood samples were collected in CellSave preservative tubes at four different time points and processed into plasma within 96 hours after withdrawal. Subsequently, cfDNA was isolated from 4mL plasma, in which the total

cfDNA concentration was measured. Mutations characterizing ctDNA were determined before surgery by next generation sequencing (NGS) using a colon-specific targeted panel (Oncomine Colon cfDNA assay, 14 genes). Samples were sequenced at >20.000 average reads depth and variants were called mutations when the variant allele frequency was above their predefined limit of detection. Longitudinal blood samples of ctDNA-positive patients were evaluated by digital PCR (dPCR) using mutation-specific assays, in which samples were considered ctDNA positive when >5 mutant copies were detected.
Results: Blood samples of 231 patients were collected one day before surgery (T0), and were repeated one day (T1), one week (T2), and three weeks (T3) after surgery. The cfDNA yields per mL plasma were higher at T1 and T2 (median 93 ng and 64 ng, respectively) compared to T0 (6 ng, $p<0.001$) and T3 (12 ng, $p<0.001$). NGS at T0 was performed for 196 patients and detected ctDNA in 129 patients (66%). Mutations had a median allele frequency of 6.3% (ranging from 0.28 to 86.4%), and were observed in 12 genes, predominantly in *TP53 (n=69), KRAS (n=57), APC (n=40), and PIK3CA (n=23)*. dPCR analyses were performed for 87 patients out of the 129 patients with ctDNA at T0, and confirmed *TP53, KRAS, PIK3CA,* and *BRAF* mutations in 75 patients, with average ctDNA loads of 9%, 8%, 18% and 4% for these genes. Longitudinal dPCR analyses were performed in 58 patients of whom subsequent post-surgical samples were available, and revealed that ctDNA was detectable in 22 patients (40%) at T1/T2, and in 21 patients (36%) at T3. Nine patients (16%) had detectable ctDNA at both T1/T2 and T3. Average mutation loads were 0.97% at T1/T2 and 1.79% at T3 ($p=0.36$).
Discussion/Conclusion: ctDNA is a potential biomarker to detect MRD after curative treatment for CRLM. Our results demonstrate that out of all patients with detectable ctDNA at baseline (before surgery), ctDNA is still present in 36% of patients three weeks after resection.

Inflammation, Immunity, and Cancer

#4448
Chemokine (C-X-C motif) ligand 17 promotes cutaneous squamous cell carcinoma via modulating tumor-immune evasion

Alok R. Khandelwal, Rema Anisha Kandula, Emily Daniel, Md Maksudul Alam, Henry Craighead, Tara Moore-Medlin, Cherie-Ann O. Nathan. *LSU Health Shreveport, Shreveport, LA*

Cutaneous squamous cell carcinoma (cSCC) is a keratinocyte-derived invasive and metastatic tumor of the skin. It is the second-most commonly diagnosed form of skin cancer, striking 200,000 Americans annually. Further, organ transplant patients are at significantly increased risk of cSCC compared to the general population. Excision of cSCC of the head and neck area results in significant facial disfigurement. An increased understanding of the mechanisms involved in the pathogenesis of cSCC could identify means to prevent, inhibit, and reverse this process. Chemokine (C-X-C motif) ligand 17 (CXCL17) is the latest chemokine family member, and an increased CXCL17 protein expression was observed in both mouse and human cSCC cell lines. Further, deletion of CXCL17 was associated with significant inhibition of tumor cell-intrinsic properties such as proliferation, migration, and motility. CXCL17 is identified as a potent chemoattractant for macrophages, dendritic cells and myeloid-derived suppressive cells. Accordingly, utilizing a syngeneic, tumor-cell xenograft cSCC mouse model, we evaluated the effect of CXCL17 deletion on cSCC tumor-immune evasion and elucidated the underlying mechanism. Deletion of CXCL17 was associated with a significant reduction in tumor volume compared to the wild-type counterparts. Further, CXCL17 deleted cSCC tumor cell xenografts exhibited a significant increase in CD8+, cytotoxic T cells in the tumor microenvironment, suggesting an important role of CXCL17 in mediating tumor-immune evasion. Interestingly, treatment with CXCL17 induced macrophage M2 polarization and promoted macrophage efferocytosis *via* modulating efferocytotic machinery proteins such as MERTK, TIM4, GAS6 and AXL. Our studies have established substantial evidence for the role of CXCL17 in modulating tumor-cell extrinsic properties to affect the progression of cSCC.

#4449

The expression and immune regulation of thymic stromal lymphopoietin in non-small cell lung cancer development and progression

Chung-Yu Chen[1], Ying-Yin Chen[1], Hung-Chueh Peng[1], Yi-Ling Ye[2]. *[1]National Taiwan University Hospital Yunlin Branch, Douliu, Taiwan,[2]National Formosa University, Huwei Township, Taiwan*

Purpose: Previous studies have shown thymic stromal lymphopoietin (TSLP) to be an important driver of type 2 inflammation. A new and unexpected function for TSLP has been found in the induction and progression of a variety of tumors. This study conducted TSLP performance in lung cancer patients and the correlation of the clinical pathological data.
Materials and Methods: The patients with pathological diagnosis of lung cancer were enrolled. The percentage of CD19 + B cells was determined in the lymphocyte gate and counted via flow cytometry. Relevant serum cytokines including TSLP were analyzed using LEGENDplex software. In vitro study was conducted by A549 cell line and the mRNA expression change of TSLP was extracted by Reverse Transcriptase PCR (RT-PCR).
Results: When comparing the frequencies of B cell subsets between early-stage (N = 31) and late-stage lung cancer group (N = 29), the frequency of memory B cell (17.3±6.1% vs 23.4±15.1%, p=0.042), CD27+IgM+ B cell (1.8±1.3% vs 2.9±2.3%, p=0.030), class-switched B cell (15.5±5.5% vs 22.2±14.9%, p=0.023), class-switched memory B cell (69.9±11.3% vs 59.9±19.7%, p=0.017) and plasmablast (8.5±7.3% vs 18.0±20.8%, p=0.019) were significantly different between groups. The patients with higher frequency of class-switched B cell had significantly worse prognosis than low frequency (HR 3.054, 95% CI 1.007-9.262, p=0.049). The level of IL-1B, IL-6, IL-10, IL-12, IL-13, and TSLP were significantly higher in the late-stage cancer patients. Simulation in vitro test with human lung A549 cell line was performed, the expression of short-form TSLP (sfTSLP) level decreased with the higher anti-cancer drug as Pemetrexed concentration.
Conclusions: The increase proportion of CD27+CD38- (class-switched) B cell could be an independent, poor prognostic factor for NSCLC patients. TSLP signaling is addressed to the anti-cancer therapeutic response. Therefore, TSLP and relevant cytokines may be involved directly and indirectly in shaping the inflammatory status of the tumor microenvironment.

#4450

SOX4 promotes tumor development and immune evasion via disruption of zinc homeostasis between nasopharyngeal carcinoma cells and T cells

Yuma Yang[1], Lanqi Gong[1], Jie Luo[1], Xiaona Fang[1], Jiao Huang[1], Lu Bai[1], Qin Liu[1], Beilei Liu[1], Shan Liu[1], Jinlin Huang[1], Ching Ngar Wong[1], Baifeng Zhang[1], Danyang Zheng[1], Yu Zhang[2], Wei Dai[1], Xinyuan Guan[1]. *[1]Clinical Oncology, The University of Hong Kong, Hong Kong, Hong Kong,[2]State Key Laboratory of Oncology in Southern China, Sun Yat-sen University Cancer Center, Guangzhou, China*

Background: Nasopharyngeal carcinoma (NPC) is a highly undifferentiated squamous malignancy with dense infiltration of dysfunctional T cells that is endemic in East and Southeast Asia. Based on multicentral single-cell RNA sequencing (scRNA-seq) analysis, we have identified SRY-Box Transcription Factor 4 (SOX4), an essential developmental transcription factor, is specifically and highly expressed by NPC cells and contributes to tumor growth and distant metastasis. SOX4 upregulation also promotes ZIP14-mediated intracellular zinc uptake, leading to competitive deprivation of free zinc in the tumor microenvironment (TME), which inhibits zinc-dependent T cell receptor (TCR) activation. Thus, our study provides experimental insights into how NPC develops and evades immune surveillance.
Methods: scRNA-seq data and bulk RNA-Seq data from our lab and GEO database were integrated and analyzed on a bioinformatic basis. Immunohistochemistry staining was performed to validate the SOX4 protein level in an independent clinical cohort. Cell lines, patient-derived xenografts, and humanized mouse models were generated to evaluate the *in vitro* and *in vivo* function of SOX4. Flow cytometry was used for T-cell immunophenotyping. Immunoprecipitation was used to study protein-DNA interaction. The dual-luciferase reporter assay was utilized to demonstrate the transcriptional regulation of SOX4 on the ZIP14 promoter. qRT-PCR, immunoblotting, and immunofluorescence staining were also employed for functional studies.
Result: Our transcriptome analysis showed SOX4 was frequently overexpressed by NPC cells, compared to infiltrating immune and stromal cells. Increasing SOX4 expression in normal nasopharyngeal epithelial cells enhanced proliferation, stemness, migration, and invasion. SOX4 also transcriptionally upregulated ZIP14 in NPC

cells which promoted the uptake of free zinc from the TME. Thus, competitive deprivation of zinc between NPC cells and T cells in the TME inhibited TCR signaling and T-cell cytotoxicity, leading to NPC immune evasion. Conclusion: This study reveals the SOX4-ZIP14-Zinc axis as a vital mechanism for simultaneously inducing tumor development and immunosuppression in the NPC microenvironment. Therapeutic inhibition of SOX4 or ZIP14 is a new strategy for NPC patients and potentially synergizes with PD-1/PD-L1 blockades to overcome immunosuppressive signals in the TME.

#4451

Developing a PROTAC-based NR4A1 degrader for melanoma cancer therapy

Rohan Master[1], Yuewan Luo[2], Yufeng Xiao[3], Daohong Zhou[4], Lei Wang[5], Guangrong Zheng[6], Weizhou Zhang[5].
[1]University of Florida, Gainesville, FL,[2]Biotech Research and Innovation Centre, University of Florida, Copenhagen, Denmark,[3]Department of Medicinal Chemistry, University of Florida, Gainesville, FL,[4]Department of Biochemistry & Structural Biology, Joe R. Teresa Lozano Long School of Medicine, San Antonio, TX,[5]Pathology, Immunology, and Laboratory Medicine, University of Florida, Gainesville, FL,[6]Medicinal Chemistry, University of Florida, Gainesville, FL

Introduct**ion:** Melanoma originates from melanocytes within the epidermis and is one of the most common cancers, with nearly 100,000 new cases yearly. Despite numerous advancements in therapies to treat melanoma, a prevalent population of patients still do not respond to currently approved therapies. Recent studies have highlighted the role of transcription factor nuclear receptor subfamily 4 group A member 1 (NR4A1) in melanoma for cancer survival, invasion, and metastasis. NR4A1 is also involved in glucose metabolism. Our project aims to identify an effective degrader of NR4A1 using a PROTAC strategy and then validate its effectiveness in reducing the growth of melanoma. PROTACs consists of three domains: a warhead that binds to the protein of interest, a ligand to an E3 ligase, and a linker that brings both domains in proximity to one another. The PROTAC can recruit an E3 ligase to ubiquitinate NR4A1 and degrade it via the ubiquitin-proteasome system (UPS).
Results: Our first goal was to identify valid PROTAC candidates that can effectively degrade NR4A1. We identified NR-V04, which demonstrated a dose-dependent degradation of NR4A1 in various melanoma cell lines. We further investigated time-dependent degradation, and NR-V04 was able to achieve *in vitro* degradation of NR4A1 16 hours after treatment. Additionally, we validated the mechanism of degradation via the UPS through various models. NR-V04 treatment of cells with a VHL knockout, which removes the E3 ligase recruited, experienced no degradation of NR4A1, and treatment of cells treated with MG132, a proteasome inhibitor, also showed no degradation. We observed degradation *in vitro* of numerous mouse and human cell lines. To investigate the cancer-killing effects of NR-V04, we completed MTS assays on the human melanoma cell lines CHL1 and A375, which showed an EC50 of 0.723 μM and 1.025 μM, respectively. When comparing NR-V04 treated and untreated CHL1 cells, NR-V04 was able to significantly decrease melanoma cell viability. NR4A1 knockout in CHL1 also showed decreased melanoma cell viability, and when comparing NR-V04 treated and untreated in NR4A1 knockout, there was no further decrease in melanoma cell viability. As for *in vivo* models, NR4A1 knockout in CHL1 and A375 exhibited slower tumor growth compared to the wild type. Furthermore, NR-V04 showed suppression of CHL1 and A375 tumor-bearing NSG mice melanoma growth at low dose concentrations of 1 mg/kg after seven days compared to vehicle and warhead treatment. Western blot analysis of tumor tissue provides support for the ability of NR-V04 to degrade tumor-intrinsic NR4A1.
Conclusion: NR-V04 can selectively degrade NR4A1, *in vitro* and *in vivo*, to decrease melanoma cancer cell viability via the UPS. NR-V04 holds promising therapeutic potential as a cancer therapy for patients with melanoma.

#4452

FASN inhibition overcomes immune evasion by upregulating MHC-I in hepatocellular carcinoma

Jiao Huang[1], Wai Ying Tsang[1], Xiaona Fang[1], Yu Zhang[2], Jie Luo[1], Lanqi Gong[1], Baifeng Zhang[1], Ching Ngar Wong[1], Beilei Liu[1], Jinlin Huang[1], Yuma Yang[1], Shan Liu[1], Zhihong Li[1], Xinyuan Guan[1]. *[1]The University of Hong Kong, Hong Kong, China,[2]Sun Yat-sen University Cancer Center, Guang Zhou, China*

Immune evasion is one of the important factors leading to the progression of hepatocellular carcinoma(HCC). Restricted antigen presentation by decrease of MHC-I remains a huge barrier to triggering an immune attack. However, knowledge is limited on how to enhance antigen presentation of cancer cells. Here we identify that FASN inhibition by shRNA and inhibitors could boost MHC-I level on HCC cell surface. FASN deficiency also

promotes antigen presentation and augments $CD8^+$ T cell cytotoxicity. Mechanistically, FASN knock-down decreases the degradation of MHC-I in lysosomes. Moreover, ZDHHC3-mediated palmitoylation participates in this process. In vivo, orthotopic HCC mouse model shows that Fasn knock-down greatly improves the cytotoxicity of tumor-infiltrating $CD8^+$ T cells and suppresses HCC tumor growth, indicating that inhibiting FASN is a promising way to enhance the efficiency of immunotherapy in HCC.

#4453

Neutrophil-to-lymphocyte ratio associates with intratumoral myeloid predominance and clinical outcomes of pembrolizumab in head and neck squamous cell carcinoma

Hiroki Morimoto[1], Takahiro Tsujikawa[1], Aya Miyagawa-Hayashino[2], Alisa Kimura[1], Sumiyo Saburi[1], Junichi Mitsuda[1], Kanako Yoshimura[1], Gaku Ohmura[1], Shigeyuki Mukudai[1], Hikaru Nagao[1], Yoichiro Sugiyama[1], Shibata Saya[3], Hiroshi Ogi[4], Eiichi Konishi[2], Kyoko Itoh[4], Shigeru Hirano[1]. *[1]Otolaryngology–Head and Neck Surgery, Kyoto Prefectural University of Medicine, Kyoto, Japan,[2]Surgical Pathology, Kyoto Prefectural University of Medicine, Kyoto, Japan,[3]SCREEN Holdings Co., Kyoto, Japan,[4]Pathology and Applied Neurobiology, Kyoto Prefectural University of Medicine, Kyoto, Japan*

Neutrophil-to-lymphocyte ratio (NLR) in peripheral blood is an emerging biomarker candidate of immunotherapy in a wide range of cancers. However, little is known about the potential relationships between the tumor immune microenvironment and systemic inflammatory markers including NLR. Here we have explored systemic and tumor-immune microenvironmental characteristics related to treatment outcomes of immune checkpoint inhibition, based on 29 consecutive patients with recurrent/metastatic head and neck squamous cell carcinoma who received pembrolizumab between 2020 and 2021. NLR greater than 4.5 at pretreatment status significantly correlated with short overall survival (OS). Although NLR did not show a significant association with tumor volumes, high NLR exhibited significant correlations with malnutrition status characterized by CONUT (controlling nutritional status), and GNRI (geriatric nutrition risk index). Among the patients whose NLR was greater than 4.5 at pretreatment status, those whose NLR decreased to less than 4.5 at day 21 had a better OS than those whose NLR did not decrease, indicating that longitudinal changes in NLR correlate with prognosis. To investigate association with tumor-immune microenvironment, 14-marker multiplex immunohistochemistry was performed to quantitatively evaluate intratumoral $CD8^+$ T cells, helper T cells, regulatory T cells, B cells, natural killer cells, macrophages, dendritic cells, mast cells, and granulocytes. Notably, NLR at pretreatment status significantly correlated with intratumoral immune cell densities, where high NLR correlated with low lymphoid cells and high tumor associated macrophages in tissue. NLR in peripheral blood significantly correlated with myeloid to lymphoid cell ratios in tissue, suggesting the presence of association between circulating and intratumoral immune complexity profiles. This study highlights that the association between intratumoral myeloid predominance and systemic nutritional and inflammatory status might be a possible factor for resistance to immunotherapy. Understanding immune dynamics in tissue and blood during immunotherapy potentially contributes to the establishment of predictive biomarkers and monitoring for immunotherapy.

#4454

Loss of CX3CL1 expression mediates immune evasion in *STK11* mutated lung adenocarcinomas

Eria Eksioglu[1], Gabriela M. Wright[1], Trent R. Percy[2], Kenneth L. Wright[1], W. Douglas Cress[1]. *[1]Moffitt Cancer Center, Tampa, FL,[2]Arkansas College of Osteopathic Medicine, Fort Smith, AR*

Immunotherapy has improved survival for many cancer patients, especially for immunogenic malignancies such as lung cancer. However, even in lung cancer, the response rate for anti-PD1 therapy (for example) does not exceed 20%. Thus, it is critical to identify mechanisms that block the response to immune checkpoint therapies. STK11 (also known as LKB1) is encoded by the serine threonine kinase 11 gene (*STK11*). Patients harboring tumors with *STK11* mutations have reduced infiltrates of cytotoxic T-cells and clinical studies have shown that they respond poorly to anti-PD1 or anti-PDL-1 therapies regardless of PDL-1 status, which otherwise predicts benefit. Herein, we have used gene expression data from a cohort of 442 lung adenocarcinoma patients to identify CX3CL1 (fractalkine) as a gene silenced in *STK11* mutant tumors with potential to be a key direct modulator of the immune system relevant to STK11 loss. To further explore this hypothesis, we have edited the *STK11* gene in A549 cells back to wild type (*STK11* corrected). As predicted, restoration of STK11 function resulted in modest expression of CX3CL1 as measured by Western blotting. Unexpectedly, exposure of *STK11* corrected cells to human immune cells isolated from the blood of healthy donors resulted in a 5 to 10-fold increase in CX3CL1 suggesting

interactive signaling between tumor and immune cells. Using transwell assays and *STK11* corrected A549 cells we find that restoration of functional STK11 increases immune cell migration, adhesion and invasion in vitro. Finally, cytotoxicity assays demonstrate that *STK11* corrected A549 cells are 3 to 5-fold more sensitive to immune cell killing. Taken together these results suggest the hypothesis that CX3CL1 loss mediates immune evasion in *STK11* mutant lung adenocarcinomas. Future work will further explore the mechanisms underlying this pathway in preclinical models.

#4455

Protein phosphatase 4 inhibition stimulates anti-tumor immunity in ovarian cancer

Remya Raja[1], Christopher Wu[1], Esen Y. Bassoy[1], Thomas Rubino[1], Emma Utagawa[1], Paul Magtibay[2], Kristina Butler[2], Marion Curtis[1]. *[1]Immunology, Mayo Clinic, Scottsdale, AZ,[2]Gynecology, Mayo Clinic, Phoenix, AZ*

Background**:** Increased infiltration of T cells into ovarian tumors has been repeatedly shown to be predictive of enhanced patient survival. However, despite the evidence of an active immune response in OC, immune checkpoint blockade therapy has been ineffective. Recently studies have shown that deficiencies in the DNA damage response (DDR) can drive increased genomic instability and tumor immunogenicity. One target involved in the DDR that has the potential to be of therapeutic value is protein phosphatase 4 (PP4); however, the effect of PP4 deficiency on anti-tumor immunity remain unknown.
Results: Our results show that PP4 inhibition combined with carboplatin leads to increased carboplatin sensitivity, DNA damage, and micronuclei formation. Using a panel of ovarian cancer cells, we show that PP4 inhibition triggers inflammatory signaling via NF-κB and STAT1 activation resulting in increased expression of pro-inflammatory cytokines including IFNβ1, CCL5, CXCL10, and IL-6. Moreover, conditioned media from OC cells treated with the combination of PP4 inhibitor and carboplatin significantly increased migration of both CD8 T cell and NK cells over carboplatin treatment alone. Knockdown of STING in OC cells significantly abrogated the increase in CD8 T cell migration induced by PP4 inhibition. *PPP4C* or *PPP4R3B* knockdown resulted in strong induction of NK cell IFN-γ, increased degranulation, and increased NK cell-mediated cytotoxicity against OC cells. Stable knockdown of PP4C in a syngeneic, immunocompetent mouse model of ovarian cancer resulted in significant reduction of tumor growth *in vivo*. PP4C low tumors had increased infiltration of CD161+ NK cells and CD4+ T cells. Addition of low dose carboplatin treatment in vivo led to increased CD8+ T cell infiltration in PP4C low tumors when compared to the untreated groups.
Conclusions: Our work has identified a role for PP4 inhibition in promoting anti-tumor immune activation. These findings provide the rationale for combining PP4 inhibitors with immunotherapy as a new approach in ovarian cancer treatment.

#4456

Inducible nitric oxide synthase (iNOS) and cycloxygenase-2 (COX2) inhibition reprogram the tumor microenvironment and suppress tumor growth in hepatocellular carcinoma

Ronghua Wang, Christof Kaltenmeier, Ruiqi Yang, Tony Haykal, Hamza Yazdani, Celine Tohme, David Geller, Samer Tohme, Timothy Billiar. *Surgery, University of Pittsburgh School of Medicine, Pittsburgh, PA*

Hepatocellular carcinoma is a common cancer worldwide and a leading cause of cancer-related death. Chronic inflammation, accumulation of genetic changes and alternations of the liver microenvironment are critical during the process of carcinogenesis and development of HCC. Inducible nitric oxide synthase (iNOS or NOS2)-derived NO and cyclooxygenase-2 (COX2) are important parts of the neoplastic inflammatory environment. Continuous exposure to moderate to high concentrations of NO, produced by inducible NO synthase (iNOS) and COX2, promotes neoplastic transformation, chemotherapeutic resistance, enhanced cell proliferation, increased inflammation and immune resistance. Our previous study reported that iNOS promoted stem-like characteristics and activation of liver cancer stem cells through Notch signaling pathway. iNOS activity in both the liver cancer stem cells and the microenvironment contributes to tumor progression in mice, suggesting that targeting iNOS in the entire tumor could have therapeutic benefit in HCC. iNOS-derived NO and COX2-derived prostaglandin E2 (PGE2) were shown to promote feed-forward iNOS/COX2 crosstalk because NO induced COX2 and PGE2 induced NOS2. Our research showed that iNOS inhibition with the iNOS inhibitor (1400W) and COX2 inhibitor (Celebrex) diminished HCC tumor growth. The cytokine analysis revealed considerably lower levels of inflammatory cytokines including, IL-6, tissue inhibitor of matrix metalloproteinase-1 (TIMP1), macrophage inflammatory protein-3alpha (MIP-3alpha), IL-1B, CC chemokine subfamily of eosinophil chemotactic proteins eotaxins (CCL11), M-CSF, thymus and activation-regulated chemokine (TARC, CCL17) and leukemia inhibitory

factor (LIF) in HCC with iNOS/COX2 inhibition. iNOS/COX2 levels influence the polarization and spatial location of lymphoid cells including CD8+ T cells. Targeting iNOS/COX2 blockade improved CD8+ T cell penetration into the tumor core. We also found that iNOS/COX2 blockade result in more CD4+ T helper cells and CD8+ tumor infiltrating lymphocyte (TIL), but reduce the number of exhausted CD4+ T cells and CD8+ T cells (PD1-high, Lag3+, CD39+ Tex). The results suggesting that iNOS/COX2 inhibitor therapy may alleviate HCC growth by promoting a anti-tumorigenic TME, modifying lymphoid spatial localization and gene expression phenotypes and decreasing T-cell exhaustion.

#4457

Post exposure suppression of radiation pneumonitis by TRAIL pathway agonists TLY012 and ONC201

Jillian R. Strandberg[1], Anna Louie[1], Marina Hahn[1], Praveen Srinivasan[1], Andrew George[1], Arielle De La Cruz[1], Leiqing Zhang[1], Liz Hernandez Borrero[1], Kelsey Huntington[1], Christopher Azzoli[2], Abbas E. Abbas[2], Lanlan Zhou[1], Seulki Lee[3], Wafik S. El-Deiry[1]. *[1]Legorreta Cancer Center at Brown University, Providence, RI,[2]Lifespan Cancer Institute, Providence, RI,[3]D&D Pharmatech, Rockville, MD*

Thoracic therapeutic ionizing radiation is limited by toxicities such as pneumonitis and fibrosis of the lungs. Such limitation restricts therapeutic doses and adversely affects patient quality of life while undergoing and following treatment. ONC201/TIC10 is a small-molecule anti-cancer drug that activates the integrated stress response (ISR) and drives the tumor necrosis factor-related apoptosis-inducing ligand (TRAIL) pathway. Pegylated recombinant long-acting TRAIL (TLY012) has been shown in preclinical models to induce the reversal of fibrosis and currently has orphan drug status for systemic sclerosis and chronic pancreatitis. We show a similar effect of both TLY012 and ONC201 in vivo in protecting from radiation pneumonitis and fibrosis of the lungs. WT and TRAIL-/- C57Bl/6 mice receiving a single 20 Gy thoracic radiation dose with shielding of other organs and treated with 10 mg/kg of TLY012 twice a week showed a significantly reduced alveolar wall thickness and lessened inflammation compared to controls and DR5-/- mice receiving the same treatment upon histological analysis of the lungs conducted 13 days post-irradiation. WT and TRAIL-/- C57Bl/6 mice treated with 100 mg/kg of ONC201 once a week showed similar effect to a lesser extent. Further analysis in C57Bl/6 WT mice bearing orthotopic mammary fat pad e0771 TNBC tumors similarly receiving a single 20 Gy thoracic radiation dose revealed the same pattern of protection from radiation pneumonitis upon TRAIL-pathway agonism through treatment with TLY012 and ONC201 both in combination and alone, while also showing a significant reduction in tumor burden at the experimental endpoint (day 9 post-irradiation) in the combination treated mice. Further, pulse oximetry readings of the hind paw revealed a notable reduction in oxygen saturation in all mice except those treated with TLY012. Cytokinomic profiling of mouse serum upon sacrifice revealed a significant reduction in CCL22/MDC levels in the TLY012 cohort. Additional post-hoc analysis including immunophenotyping, immunostaining, and bulk RNA analysis through Nanostring nCounter technologies is underway. Altogether, these findings suggest a role for TLY012, ONC201, or broader modulation of the TRAIL/DR5 pathway in mitigating adverse effects and outcomes of therapeutic radiation, and may serve as a foundation for safer use of radiation in the clinic.

#4458

Single cell landscape of multicentric Castleman disease in identical twins

Jason Yongsheng Chan[1], Jui Wan Loh[1], Jing Quan Lim[1], Herty Liany[1], Elizabeth Chun Yong Lee[1], Jing Yi Lee[1], Bavani Kannan[1], Boon Yee Lim[1], Kerry Lim[1], Jeslin Chian Hung Ha[1], Cedric Chuan-Young Ng[1], Tun Kiat Ko[1], Dachuan Huang[1], Dominique Yuan Bin Seow[2], Chee Leong Cheng[2], Sock Hoai Chan[1], Joanne Ngeow[1], Bin Tean Teh[1], Soon Thye Lim[1], Choon Kiat Ong[1]. *[1]National Cancer Centre Singapore, Singapore, Singapore,[2]Singapore General Hospital, Singapore, Singapore*

Idiopathic Multicentric Castleman Disease (iMCD) is a rare IL-6-driven hematological disorder characterized by systemic lymphadenopathy, elevated immunoglobulin levels, and prominent plasmacytosis in the bone marrow and lymph nodes. An unusual occurrence of iMCD in identical twins provided a unique opportunity to answer genetic and molecular features of this disease, including the cell-of-origin of IL-6 signals, and the immune milieu within affected lymphoid organs and in circulation. Germline whole genome sequencing of the affected twins identified pathogenic homozygous mutations of *NCOA4* c.G1322A and monoallelic mutations of *TRAF3* c.G1504A - both genes recently implicated in IL-6 signaling and B-cell regulation. Their unaffected sister was heterozygous mutant for *NCOA4* and homozygous wildtype for *TRAF3* loci. Via single cell sequencing of 63,519 cells from bone marrow, lymph node, and peripheral blood mononuclear cells, we identified nodal endothelial cells and fibroblastic

reticular cells (FRC) as the source of IL-6 signals. The latter are composed of mainly T-cell zone FRCs (CCL19+/CCL21+/IL7+/PDPN+/MADCAM1-) and a minor population of follicular dendritic cells (FDCs) (CD21+/CD35+/CXCL13+). An “inflammatory” peripheral monocytosis enriched for the expression of S100A family genes was evident in both twins, as well as a group of monocytes expressing cytotoxic gene signatures in the affected twin with milder clinical manifestations. Their unaffected sister mainly carried monocytes enriched for expression of major histocompatibility complex (MHC) class II genes. In conclusion, we provided evidence of a genetic cause of iMCD, identified the putative cell-of-origin of IL-6 signals in this rare disease, and described a distinct monocytic immune response phenotype.

#4459

Spatial profiling of the inflamed tumor microenvironment identifies novel prognostic subclasses in non-metastatic clear cell renal carcinoma patients

Teijo Pellinen[1], Lassi Luomala[1], Kalle Mattila[2], Jenni Säilä[1], Annabrita Hemmes[1], Katja Välimäki[1], Oscar Bruck[1], Lassi Paavolainen[1], Harry Nisen[1], Petrus Järvinen[1], Olli Kallioniemi[1], Paula Vainio[3], Panu Jaakkola[3], Tuomas Mirtti[1]. *[1]University of Helsinki, Helsinki, Finland,[2]University of Turku, Turklu, Finland,[3]University of Turku, Turku, Finland*

INTRODUCTION: Clear cell renal cell carcinoma (ccRCC) is highly vascularized and inflamed, and RNA signatures of angiogenesis/inflammation have been suggested as biomarkers for predicting progression and therapy benefit. Here, we explored as to how the spatial localization of endothelial cells and leukocytes and their mutual interactions contribute to disease progression.
EXPERIMENTAL PROCEDURES: We applied multiplexed fluorescence IHC (mfIHC) to quantify CD45+ leukocytes, CD31+ endothelial cells, D2-40+ lymphatic cells, CD11b+ myeloid cells, CD3+ and CD20+ lymphocytes, as well as PDGFRB+ fibroblasts and epithelial cells (CK+/Ecadherin+/CAIX+) in two cohorts of non-metastatic primary ccRCC. Both the Helsinki (N=178) and Turku cohorts (N=241) contained TMA cores from tumor center, tumor border, and benign areas of each patient. mfIHC data were compared with clinical parameters, such as tumor stage (pT), Fuhrman grade, necrosis, and patient outcome (RFS, recurrence-free survival).
RESULTS: CD31+ endothelial cells were associated with favorable ($p<0.001$) and CD45+ leukocytes with poor prognosis ($p<0.001$), high pT ($p<0.05$), high Fuhrman grade ($p<0.05$), and high necrosis ($p<0.05$) in TMA cores representing the tumor center and tumor border areas. CD45+ cells varied spatially with regards to CD31+ cells and EpiStain+ cells. For example, in tumor center cores, CD45+ cells co-localized with EpiStain+ cells ranging from 0.1 to 97% (median for both cohorts, 70.6% and 72.5%). The association of CD45+ leukocytes with poor prognosis was significant when counting the fraction of CD45+ cells not interacting with CD31+ or EpiStain+ cells, but not when including only the interacting cells. We then categorized patients into three classes based on the quantity of the cell types: 1) $CD45^{+High}/CD31^{+Low}$, 2) $CD45^{+Low}/CD31^{+High}$, and 3) Other. $CD45^{+High}/CD31^{+Low}$ phenotype patients had a significantly lower 5-year RFS rate compared to that of $CD45^{+Low}/CD31^{+High}$ patients (Helsinki: 37.9% vs. 92.0%; Turku: 50.0% vs. 93.5%; $p<0.001$, Log-rank test).
CONCLUSIONS: In ccRCC, both the quantity and spatial localization of inflammatory cells with respect to vascular endothelial cells and tumor cells dictates its association with patient prognosis. Our results suggest that although CD45+ leukocyte infiltration associates with recurrent disease, the higher risk is only observed when CD45+ cells are not in contact with vasculature or tumor cells. This suggests how analysis of well-known prognostic biomarkers by IHC can be refined by using mfIHC and considering the spatial configurations of cells in the TME in ccRCC. Ongoing work is aimed to add further profiling of additional TME cell subset associations with inflammation, prognosis, and therapy response.

#4460

Spatial profiling of immune biomarkers in resected treatment-naïve early stage lung adenocarcinoma

Sharia D. V. Hernandez[1], Wei Lu[1], Alejandra G. Serrano[1], Claudio J. Arrechedera[1], Beatriz Sanchez-Espiridion[1], Nejla Ozirmak[2], Max Molina[1], Larisa Kostousov[1], Sean Barnes[1], Khaja Khan[1], Ximing Tang[1], Junya Fujimoto[1], Edwin R. Parra[1], Gabriela Raso[1], Stephanie T. Schmidt[3], Carmen Behrens[4], John Heymach[4], Jianjun Zhang[4], Ken Chen[2], Boris Sepesi[5], Tina Cascone[4], Don Gibbons[1], Ignacio I. Wistuba[1], Cara Haymaker[1], Luisa M. Solis[1]. *[1]Translational Molecular Pathology, The University of Texas MD Anderson Cancer Center, MD Anderson Cancer Center, TX,[2]Bioinformatics & Computational Biology, The University of Texas MD Anderson Cancer Center, MD Anderson Cancer Center, TX,[3]Genomic Medicine, The University of Texas MD Anderson Cancer Center, MD Anderson Cancer Center, TX,[4]Thoracic-Head & Neck Med Onc, The University of Texas MD Anderson Cancer*

Center, MD Anderson Cancer Center, TX,[5]Thoracic and Cardiovascular Surgery, The University of Texas MD Anderson Cancer Center, MD Anderson Cancer Center, TX

Background**:** Recently, neoadjuvant immunotherapy plus chemotherapy has been approved for treatment of resectable non-small cell lung carcinoma (NSCLC). Defining the immune landscape of these tumors and its spatial distribution will help to understand lung cancer biology. Here, we analyzed the distribution of immune-related biomarkers in tumor-defined regions and its associations with clinicopathological variables in resected lung adenocarcinomas using high-plex profiling approaches.
Methodology: Thirty-three FFPE tumor tissues from surgically resected treatment-naïve lung adenocarcinoma stage I/II were used to construct a tissue microarray from the MD Anderson ICON cohort. We used three 1-mm core per patient [2 from central tumor (CT), and 1 from invasive margin (IM)] and performed the GeoMx Digital Spatial Profiling protein protocol to assess 49 immune biomarkers. Pancytokeratin (panCK; epithelial), CD45 (immune) and SYTO 13 (nuclear) were utilized as morphology biomarkers. Regions of interests were placed in cores containing tumor, and segmented in '"Tumor (Tu)" (PanCK+) and the "tumor microenvironment (TME)" (PanCK-). Digital counts were normalized using background correction. Statistical analysis was performed using linear mixed model. A p value equal or less than 0.05 was considered significant.
Results: We first compared the relative counts of immune biomarkers in the TME in CT and IM. IM had higher CD3, CD8, CD45RO, as well as CD163 and STING (P ranges 0.006 to 0.035), while CT had higher PD1 (P 0.025). Then we analyzed differential biomarker expression by sex and smoking status. Females had higher counts of Immune related biomarkers: CD45, CD3, CD20, immune checkpoints: PD-L1, VISTA, CTLA4, LAG3, and ICOS, and myeloid: CD68, CD11c, CD163, and B2M (P ranges 0.0005 to 0.046). Smokers had higher counts of CD66b (P 0.007) and B2M (P 0.039) while never smokers had higher counts of HLA-DR, CD34, FoxP3, OX40L, Tim-3, and B7-H3 (P ranges 0.001 to 0.049). Finally, we analyzed Tu segments. IM had higher CD66b, VISTA, CD163, OX40L, HLA-DR, GZMB, STING, and CD8 (P ranges 0.007 to 0.045) than CT. Female patients had higher CD45, CD68, CD11c and CD163 (P ranges 0.008 to 0.045) , and males had higher SMA (P 0.005). Smokers had higher CD66b (P 0.007), B2-microglobulin (P 0.043), and never smokers had higher HLA-DR, STING, CD34, CD44, FoxP3 and CD25 (P ranges 0.006 to 0.043).
Conclusions: In this study, biomarker analysis of treatment-naïve adenocarcinoma in CT areas and IM indicates a higher immune response in the IM and presence of inhibitory signaling inside the tumor. Our data also showed that tumors from females have higher immune response than tumors from males, which is concordant with previous studies. Distinct profiling by smoking status was also observed. Further analysis of gene expression analysis of this set is ongoing.

#4461

Optimized human immunophenotyping panels enhance the flexibility for high-dimensional flow cytometry analysis with CyTOF

Lauren J. Tracey, Michael Cohen, Christina Loh. *Standard BioTools Inc, Markham, ON, Canada*

The immune system plays a pivotal role in the pathogenesis of cancer. Beyond its importance in leukemia and lymphoma, scientists now understand that the immune system is involved in virtually all malignancies. Heterogeneity of cell phenotypes within a tumor microenvironment, including blood cell phenotypes, is a hallmark of cancer that is poorly understood. Resolution of these phenotypes is essential to direct therapeutic development. CyTOF® technology has pioneered the field of high-dimensional flow cytometry through the use of isotopically pure metal-tagged antibodies and a highly sensitive mass cytometer to enable 50-plus-parameter analysis. Easy panel design without the need for compensation controls or issues of autofluorescence allows for comprehensive single-cell analysis in complex biological samples and is particularly well suited for revealing the intricacies of oncogenesis. Maxpar® OnDemand reagents were recently introduced for CyTOF to increase flexibility and facilitate larger panel design in a short period of time. To this end, lineage markers that have strong, reliable expression were reassigned to optimal metal isotopes to reserve the high-sensitivity lanthanide channels for more difficult-to-detect markers with low endogenous expression, common in immuno-oncology studies. In this study, we aimed to test the newly released Maxpar OnDemand™ Antibodies to create an optimized immune phenotyping panel and maximize further customization for CyTOF. Individual antibody performance was compared between the new and existing antibodies with different metal tags. Human peripheral blood mononuclear cells (PBMC) and fresh whole blood (WB) were stained to confirm equivalent capabilities for population gating. Importantly, we demonstrated the power of these antibodies to generate reproducible, impactful data by creating functional human immunophenotyping panels. A 20-marker human phenotyping panel was tested in PBMC and WB. We identified

major immune cell populations including T cells, B cells, granulocytes, natural killer (NK) cells, and monocytes. Furthermore, the addition of CD45RO to the panel enhanced the delineation of naive, memory and effector T cell subsets. Additional myeloid markers were included to resolve the complexity within this compartment. With the updated placement of key lineage markers, the optimized phenotyping panel is ideal for future immuno-oncology studies as it can be easily expanded to interrogate cell cycle proteins, cytokines, cell signaling proteins, and oncogenic transcription factors. This work demonstrates the capability of CyTOF for robust, high-parameter immunophenotyping and a high degree of flexibility to expand our understanding of the complex processes underlying carcinogenesis and response to therapy. For Research Use Only. Not for use in diagnostic procedures.

#4462

Immunoregulatory effects of NNMT-expressing cancer-associated fibroblasts

Janna Heide[1], Andras Piffko[2], Agnes J. Bilecz[1], Ethan A. Teich[1], Lisa Schweizer[3], Sayed R. Alhunayan[1], Kaiting Yang[2], Ernst Lengyel[1]. *[1]Department of Obstetrics and Gynecology, University of Chicago, Chicago, IL,[2]Department of Radiation and Cellular Oncology, University of Chicago, Chicago, IL,[3]Max Planck Institute of Biochemistry, Muenchen, Germany*

Nicotinamide N-methyltransferase (NNMT) is highly expressed in the stroma of several malignancies and has been shown to drive the transformation of resting fibroblasts into cancer-associated fibroblasts (CAFs) through epigenetic changes. Given that CAFs can promote immunosuppression in cancer, the aim of our study was to investigate the effect of NNMT-expressing CAFs on the tumor-immune environment.
Using a co-culture system of normal fibroblasts and activated PBMCs, we found that IFN-γ produced by PBMCs upregulates NNMT expression in fibroblasts. We confirmed this mechanism *in vivo* in IFN-γ knockout mice and identified T cells as the main source of IFN-γ in the tumor. Gene expression and protein analysis showed that upregulation of NNMT in CAFs induces the secretion of the chemokine CXCL1, a critical chemoattractant for immunosuppressive myeloid-derived suppressor cells (MDSCs). Upregulation of NNMT induces CXCL1 secretion directly through promoter hypomethylation, and *in vitro* migration assays show that NNMT-expressing CAFs recruit high numbers of MDSCs. Using spectral flow cytometry, we analyzed the tumor-immune cell infiltration in whole-body NNMT-knockout mice and discovered that NNMT knockout of the stroma significantly reduced the abundance of MDSCs and increased the number of functional CD8+ T cells. Increased T cell cytotoxicity was associated with a significant reduction in tumor burden in the syngeneic ID8 ovarian and MC38 colon cancer models. These findings were confirmed after adoptive transfer of NNMT-wildtype immune cells into irradiated whole-body NNMT-knockout mice. Moreover, in scRNA-seq data of various human malignancies, we found a strong correlation between NNMT and CXCL1 expression in CAFs.
In summary, our results support a model in which cancer cells induce IFN-γ secretion by T-cells, thereby upregulating NNMT expression in fibroblasts, leading to CXCL1 secretion. CXCL1 secreted by CAFs recruits MDSCs to the tumor, which in turn suppress the anti-tumor T cell response.

#4463

Prognostic significance of systemic inflammatory markers in recurrent or metastatic head and neck cancer patients treated with nivolumab

Hiroe Tada, Kazuaki Chikamatsu. *Gunma University School of Medicine, Maebashi, Japan*

Treatment strategies for head and neck cancer has been improved with the contribution of immunotherapy. In spite of the fact, the mechanisms underlying the response to immune checkpoint inhibitors (ICIs) remain unclear, and discovery of the biomarker predicting therapeutic efficacy of ICIs is urgently required. Our previous study indicated that in patients with recurrent or metastatic head and neck squamous cell carcinoma treated with nivolumab, circulating T cells showed dynamic alterations depending on treatment efficacy using flow cytometry and mass cytometry. However, these analyses are somewhat complicated to apply each patient in clinical setting. In this study, we focused on systemic inflammatory markers, including inflammatory makers such as blood cell fractions and C-reactive protein(CRP) in peripheral blood. Firstly, we assessed the pretreatment systemic inflammatory markers in 61 recurrent or metastatic head and neck cancer patients treated with nivolumab, and determined whether these markers were associated with treatment responses by Kaplan-Meier method, multivariate analysis, regression analysis and classification and regression trees(CART). Next, we investigated circulating T cell subsets in 36 recurrent or metastatic head and neck cancer patients using flow cytometry. High neutrophil to lymphocyte ratio(NLR), platelet to lymphocyte ratio(PLR), and systemic immune-inflammation index(SII) significantly associated with poor prognosis in overall survival (NLR: p=0.0047, PLR: p=0.0357, SII:

p=0.0011). Furthermore, high albumin, lymphocyte to monocyte ratio(LMR), and prognostic nutritional index(PNI) were significant good prognostic markers of overall survival (albumin: p=0.0037, LMR: p=0.0088, PNI: p=0.037). Overall survival time were estimated the values that were defined systemic inflammatory markers by multivariate analysis. These systemic inflammatory markers were assigned importance by each coefficient. Notably, the number of monocyte and lymphocyte have a strong influence on overall survival time. In addition, the index that were depending on the number of white blood cells and monocyte, the percentage of lymphocyte, platelet count, albumin, and PNI were useful prognostic tools in analyzing regression analysis. Furthermore, the evaluation of PNI were contributed to the predict treatment efficacy in analyzing CART. Moreover, NLR, PLR, and SII were positively correlated with the proportion of Treg (NLR: R^2=0.3622/p=0.0001, PLR: R^2=0.4198/p<0.0001, SII: R^2=0.3654/p<0.0001). We concluded that in recurrent or metastatic head and neck cancer patients treated with nivolumab, systemic inflammatory markers could provide new insight into rational therapeutic strategies in cancer immunotherapy for head and neck cancer.

#4464

Comparison of two DTH models for T cell-mediated immunity in preclinical screen

Yingying Cai. *Yingying Cai (Individual), Shanghai, China*

Introduction: Delayed-type hypersensitivity (DTH) involves the recruitment of T cells into tissues and the activation by antigen-presenting cells to produce cytokines, which further activates local endothelial cells and recruits macrophages, resulting in tissue erythema, swelling and inflammation. DTH models in mice are classical *in-vivo* T cell-mediated immunity screening models for atopic dermatitis, asthma and autoimmune diseases. Different antigens and haptens have been used to establish DTH models with different Th1/Th2 profiles. More immunity characterization of the most widely used DTH models need to be revealed.
Results: We established DNFB, Oxazolone induced DTH models in both BALB/c and C57BL/6 mice with ear thickness as the readout. At the termination, we measured Th1 (ie, IFN-γ) / Th2 (ie, IL-4) profile, pro-inflammatory cytokines including IL-13, TNF, and IL-17 as well as myeloperoxidase (MPO) activity from mice ears as indices to score the degree of inflammation. Oxazolone in BALB/c exhibited more repeatable and robust window in Th1/Th2 balance and cytokines profiles. The comparison of two DTH models were further validated by the pathological analysis for cell infiltration in mouse ears and immune-phenotyping in spleen by FACS.
Conclusion: The comparison of DNFB and Oxazolone induced DTH models characterized the disease progression and established a more comprehensive preclinical DTH model with well-defined Th1/Th2 profile for the drug efficacy evaluation in the T cell-mediated immune response.
Key words: Delayed-type hypersensitivity, mice model, T cell-mediated

#4465

Evaluation of tumor draining lymph nodes in dogs with spontaneously arising osteosarcoma using single-cell sequencing

Samuel A. Brill, Dylan T. Ammons, Anne C. Avery, Douglas H. Thamm. *Colorado State University, College of Veterinary Medicine & Biomedical Sciences, Fort Collins, CO*

Tumor draining lymph nodes (TDLNs) function as an anatomic niche which primes immune cells to generate anti-cancer responses. While tumors are frequently staged based on the presence or absence of TDLN metastasis, mechanisms for how tumors impact the TDLN microenvironment and immunologic responses are incompletely understood. Dogs with spontaneously arising tumors provide an opportune model to study immuno-oncology, sharing many similarities to human patients with their environment, clinical care, and pathobiology. To evaluate how tumors impact TDLN responses, we conducted single cell RNA sequencing (scSeq) on cryopreserved TDLNs of dogs with osteosarcoma (n=4) and healthy controls (n=2). We obtained an average of 3,984 cells per sample (range 1,603-5,259) with a total of 4,780 cells from healthy samples and 19,121 cells from TDLN samples. All samples were integrated into one dataset, then unsupervised clustering was completed. Each unique cell cluster was assigned an identity using canonical markers and reference mapping to human datasets. Following cell classification, we observed notable changes in gene expression across all cells isolated from the LNs, with most differences arising from changes to the transcriptome of myeloid cells. Although still preliminary, the data also demonstrate differences in the abundance of T, B, and myeloid cells between healthy and tumor draining LNs. Taken together, this dataset provides indications of the changes TDLNs undergo in dogs with osteosarcoma.

#4466

Inhibition of ERO1a and IDO1 improves dendritic cell infiltration into pancreatic ductal adenocarcinoma

Apple Tay[1], Andreas Lundqvist[1], Siu Kwan Sze[2]. *[1]Oncology-pathology, Karolinska Institutet, Stockholm, Sweden,[2]School of Biological Science, Nanyang Technological University of Singapore, Singapore, Singapore*

Pancreatic ductal adenocarcinoma (PDAC) is one of the most hypoxic, lethal, and treatment resistant cancers. Due to its desmoplasias along with the hypoxic state and scarce infiltration of T cells, PDAC is considered a cold tumor. Using a proteomic approach, we previously identified that the expression of endoplasmic reticulum oxidoreductase 1 alpha (ERO1α) is induced by hypoxia and correlates with reduced survival in PDAC. Furthermore, we observed an increased kynurenine formation under hypoxia, suggesting a role of indoleamine 2,3-dioxygenases (IDO1) in PDAC. Since ERO1α and IDO are involved in driving immune suppression through influencing the generation of immature myeloid cells, we sought to investigate whether inhibition of these pathways modulates the myeloid cell composition in PDAC. Using MiaPaCa2 as a PDAC spheroid model with hypoxic core grown in serum-free defined media and immune cell infiltration, we assessed the functional role of ERO1a with IDO1 in modulating monocyte infiltration and differentiation into pro- and anti-inflammatory phenotypes, followed by characterizing the immunomodulatory factors secreted using tandem mass spectrometry. Inhibition of ERO1a and IDO1 significantly improved U937 monocyte infiltration (p-value = ****) and differentiation into dendritic cells (p-value = ****). Secretome analysis of proteins identified with high false discovery rate (q-value<0.01) revealed a downregulation of hypoxia and pancreatic cancer pathways in PDAC spheroids. In the presence of monocytes, upregulation of immune-related pathways for antigen presentation (15-fold) and myeloid cell maintenance signaling (2-fold) were observed. Moreover, specific immune-modulatory factors involved in immune infiltration and migration including interleukin 8, lymphocyte cytosolic protein 1 and transgelin-2 were upregulated at 27-, 20-, and 14-fold respectively. Taken together, these results indicate that inhibition of ERO1a and IDO1 drives an inflamed tumor microenvironment associated with improved monocyte infiltration and differentiation into dendritic cells to potentially enable T cell infiltration and killing of PDAC tumors.

#4467

Plasmacytoid dendritic cells, prevalent in the TME of smokers, is associated with a good prognosis and treatment response of LUAD.

Eun Young Kim, Yoon Jin Cha, Yong Jun Choi, Min Kyung Park, Yoon Soo Chang. *Yonsei University College of Medicine, Seoul, Korea, Republic of*

Background: Attempts to find therapeutic biomarkers through investigation of subgroup showing good responses to certain drugs in cancer often yielded meaningful results. Smoker's lung adenocarcinoma has consistently shown a favorable response to immune checkpoint inhibitors (ICIs) than non-smoker's lung adenocarcinoma. Comparing the macrophages (Mϕ) and dendritic cells (DC) constituting the innate immune tumor microenvironment (TME) in lung cancer of smokers and nonsmokers, we tried to figure out the difference in TME and biomarkers that predict the therapeutic response to ICIs.

Methods: The inflammatory TME of current and never smokers' lung cancer was explored by tumor and adjacent normal appearing lung tissues (Tu and NL hereafter) scRNA sequencing and verified by IF, IHC, and open-source dataset.

Results: Compared to lungs of nonsmokers, smokers' lung have an increased proportion of cell populations involved in innate immunity, and the increased cell population was mostly Mϕ, which were enriched in NL. When the number of Mϕ present in the NL of the corresponding individual were taken as the denominator, Tu of smokers has a lower proportion of Mϕ than that of non-smokers. Further sub-clustering of Mϕ and DCs showed that FCN1-mono and CD163-LGMN Mϕ, which correspond to the initial differentiation into the resident cell population within the tissue, and mo-DC, cDC2, and pDC were significantly enriched in the Tu. Among them, pDC is a functionally differentiated tissue resident cell that showed a different tissue distribution pattern between smokers and non-smokers, so it was estimated as one of the causes of the different treatment response to ICIs between the two patient groups. The difference of pDC's distribution was further verified through IHC staining using anti-LILRA4 and anti-TLR9 antibody, showing pDC was significantly enriched in the smokers' TME. A significant increase in TLR9 expression was observed in or around lung cancer immediately after ionizing radiation or cisplatin treatment in LSL-Kras G12D mouse model. The survival analysis of TCGA-LUAD dataset showed that the patients' overexpressing pDC markers such as IRF4 and TLR9 was superior clinical outcomes to the age, gender and smoking matched control group. Comparing the difference in TMB between the top 25% and bottom

25% groups according to the expression of TLR9, it was 5.81/Mb in the upper group and 4.36/Mb in the subgroup, showing a significant difference.
Conclusions: pDC is an innate immune cell population that showed a prominent increase in smokers' TME compared to that of non-smokers, suggesting that its increase may be one the factors that smokers' lung cancer show favorable responses to ICI than that of non-smokers. These findings suggest that the pDC signature can be developed as a biomarker predicting the response to ICIs and increasing the number of pDCs or its activity may improve treatment outcome of ICIs.

#4468

Tumor-derived extracellular vesicles transmit retroelement and pericentromeric RNAs to drive proinflammatory and DNA damage responses in stromal fibroblasts and immune cells

Valentina Evdokimova[1], Peter Ruzanov[1], Hendrik Gassmann[2], Lincoln D. Stein[1], Poul H. Sorensen[3], Stefan Burdach[2], Laszlo Radvanyi[1]. *[1]Ontario Institute for Cancer Research, Toronto, ON, Canada,[2]Technical University of Munich, Munich, Germany,[3]University of British Columbia, Vancouver, BC, Canada*

Chronic cancer-associated inflammation and immunosuppression are common features in most patients with solid malignancies. The causes of this chronic inflammatory-immunosuppressive state are still largely undefined. We hypothesized that selective RNAs can be secreted by cancer cells in extracellular vesicles (EVs) and may trigger proinflammatory responses in target cells, leading to chronic inflammation linked to immune cell dysfunction and immunosuppression. We found that tumor cell lines from pancreatic ductal adenocarcinoma (PDAC), prostate cancer (PCa) and from pediatric cancer such as Ewing sarcoma (EwS) continuously secrete large numbers of small (40-200 nm) EVs. In contrast to non-transformed fibroblasts, cancer cell-derived EVs are enriched with large subsets of retroelement and pericentromeric transcripts, including *LINE*, *SINE* and *HERV* retroelements, and human satellite 2 and 3 (HSAT2,3) RNAs. These virus-like RNAs were highly elevated in plasma EVs from EwS patients but not in healthy donors. Some of them, including *HERV-K* and *HSAT2*, were detected in peripheral blood myeloid cells with $CD33^{+}HLA\text{-}DR^{-}$ immunosuppressive phenotypes, and these cell populations were expanded in EwS patients compared to healthy donors. Using mouse xenografts and *in vitro* models, we also found that at least some of these RNAs, such as *HSAT2*, are transmitted to stromal fibroblasts and immune cells in the tumor microenvironment. They also accumulated in fibroblasts after treatment with EwS EVs, coincident with the induction of proinflammatory and DNA damage responses. Prolonged exposure of fibroblasts to EwS EVs also led to mitotic defects and senescence. Expression and dissemination of these highly immunogenic virus-like RNAs in EVs may thus be a common feature of multiple human malignancies, potentially affecting host cells in the local and systemic tumor environment. This, in turn, may induce chronic inflammation contributing to an overall immunosuppressed state in patients.

#4469

Disruption of ATG9A-dependent basal autophagy sensitizes cancer cells to innate inflammatory signaling

Dasun N. Jayatunge, Tsz-Ming Tsang, Colten M. McEwan, Joshua L. Andersen. *Department of Chemistry and Biochemistry, Brigham Young University, Provo, UT*

Pathogen-derived nucleic acids are recognized by pattern recognition receptors (PRRs), including cGAS and RIG-I, which trigger the innate immune response by activating IRF3-mediated interferon gene expression. In tumors, high levels of chromosomal instability can also lead to DNA fragments leaking into the cytosol to trigger PRR-mediated interferon response, resulting in pro-inflammatory cytokine secretion from the tumor. This could potentially expose tumor cells to immune attack. However, through mechanisms that are not completely understood, tumor cells dampen the interferon response to escape immune recognition. Previous work demonstrated that loss of ATG9A, but not ATG5, increased inflammatory signaling through the STING-IRF3 cascade, suggesting that perhaps an autophagy-independent function of ATG9A regulates inflammation. Here we found that loss of ATG9A or other upstream regulators of basal autophagy (e.g., ATG101), but not core LC3 lipidation machinery (ATG5 or ATG7), sensitizes cells to dsDNA-induced IRF3 activation and interferon gene expression. We also found that loss of ATG9A or ATG101, but not ATG5 or ATG7, increases the basal activity of the ubiquitin-sensing, IRF3-targeted kinase TBK1, which increases further upon dsDNA treatment. In these ATG9A and ATG101 deficient cells, TBK1 is clustered around large p62-positive condensates that previously been shown to contain large accumulations of LC3. Our preliminary data suggest a model in which ATG9A deletion causes the accumulation of LC3-positive membrane at p62 condensates, which may act as a platform for inflammatory signaling. Our current work focuses on identifying the upstream pathways and core mechanism that

regulates IRF3 activation in ATG9A-deficient cells and exploiting this mechanism to improve anti-tumor immunity.

#4470

E-cigarette aerosol exposure increases NF-kB and modulates inflammatory markers in oral epithelial cells

Vengatesh Ganapathy[1], Jimmy Manyanga[1], Dehra McGuire[1], Daniel Brobst[1], Balaji Sadhasivam[1], Mayilvanan Chinnaiyan[1], Constantin Georgescu[2], Jonathan Wren[2], Lurdes Queimado[1]. *[1]The University of Oklahoma Health Sciences Center, Oklahoma City, OK,[2]The Oklahoma Medical Research Foundation, Oklahoma City, OK*

Background**:** E-cigarette use has skyrocketed among youth, in part because e-cigarettes are perceived as a safer substitute for traditional cigarettes. However, the resulting health effects of e-cigarette use are still unclear. E-cigarette aerosols contain harmful and potentially harmful substances such as flavorings, carbonyl compounds, heavy metals, carcinogens and reactive oxygen species (ROS). A recent *in vitro* study from our laboratory showed that e-cigarette aerosols can increase cellular ROS and suppress cellular antioxidant capacity. An imbalance between the ROS production and the availability of antioxidants or free radical scavengers, can lead to chronic inflammation. Here we examine the effect of exposure to e-cigarette aerosols on the expression of the inflammatory regulator NF-kB and its downstream inflammatory targets in oral epithelial cells.
Methods: Human oral epithelial cancer (UM-SCC-1) cells were exposed, every other day for 2 weeks, to e-cigarette aerosol extracts (18 mg/ml of nicotine; tobacco flavor) prepared from two distinct e-cigarette brands. Standard tobacco extracts were used as a positive control. Whole-cell RNA was isolated and processed for RNA-sequencing. The altered gene expression was further validated by western blotting and ELISA using a human cytokine array. Data were analyzed by Student's t-test.
Results: RNA sequencing data showed that a 2-week exposure of oral epithelial cells to e-cigarette aerosol extracts resulted in significant changes in several key cellular signaling pathways, including inflammatory and immune response signals. Exposure to e-cigarette aerosol extracts resulted in a significant increase in the expression of proteins involved in inflammatory pathways, such as TLR3, TGF beta, ERK1/2 and NF-kB. We also observed a significant increase in pro-inflammatory and anti-inflammatory cytokines after exposure to e-cigarette aerosol extracts, including CD54, IL-1a and IL-10.
Conclusion: Our data suggest that chronic exposure to e-cigarette aerosol increases the expression of TLR3, TGF beta, and ERK1/2, which possibly contributed to the observed increase in NF-kB and its down-stream targets (e.g., CD54, IL-1a and IL-10). NF-kB is a pleiotropic transcription factor with key roles in multiple biological processes, such as immune homeostasis and development. Chronic NF-kB activation by e-cigarette aerosol exposure could contribute to chronic inflammation and tumorigenesis.

#4471

Reprogramming “cold” NF1 malignancies into “hot” tumors for immunotherapy

Laasya Madana, Lu Q. Le, Nipunika Somatilaka, Renee McKay. *Dermatology, UT Southwestern Medical Center, Dallas, TX*

Introduction: Neurofibromatosis Type 1 (NF1) results from mutations in the *NF1* gene that inactivate the tumor suppressor, neurofibromin. This leads to hyperactive RAS signaling that predisposes NF1 patients to tumor development. Over time, some of these tumors can develop into malignant peripheral nerve sheath tumors (MPNST) which are currently incurable.Immune checkpoint blocking (ICB) programs a patient’s immune system to enhance tumor destruction. However, MPNSTs are cold tumors characterized by low immune cell presence in the tumor microenvironment. Interestingly, MPNSTs show checkpoint protein PD-L1 expression suggesting ICB as potential therapy for MPNST, given the ability to increase immune cell density in the tumor microenvironment. Activation of the intracellular receptor stimulator of interferon genes (STING) enhances antitumor immunity through the induction of pro-inflammatory cytokines and chemokines, including type I interferons. Cyclic GMP-AMP synthase (cGAS) is an enzyme that once bound to cytosolic DNA, synthesizes cyclic GMP-AMP (cGAMP), which activates STING to induce inflammatory cytokines and other immune mediators. Preclinical studies using mouse tumor models have assessed the efficacy of STING agonists that trigger the cGAS-STING-IFN axis, ultimately leading to augmented innate immunity and a T cell-rich tumor environment. Additionally, combining STING agonists with ICB has a synergistic effect in treating tumors. Therefore, we hypothesize that treatment with STING agonists would turn “cold” MPNSTs into “hot” tumors making them susceptible to targeting with ICB. Methods: We treated MPNST cell lines with synthetic STING agonist ADU-S100 for varying durations of 8, 18, 24, and 48 hours. At the end of the treatment, cells were harvested for qRT-PCR and immunoblot analysis.

Results: We measured STING-IFN pathway activation through immunoblotting and observed that phosphorylation of STING effector proteins - a readout of STING activation -- was increased followingby 8 hours after treatment. qRT-PCR analysis showed that STING target cytokine/chemokine gene expression was also upregulated by 8 hours after ADU-S100 treatment.
Conclusions: Theise data demonstrates that ADU-S100 was able to activate the STING pathway in MPNST cell lines leading to proinflammatory cytokine/chemokine production. We will next test STING agonist in vivo use to determine whether ADU-S100 treatment inin mouse MPNST modelss of MPNST to is able to reprogram the tumor microenvironment into an immune inflamed one amenable to immunotherapy.

#4472

A mouse model for GvHD: an excellent tool for evaluating the efficacy of anti-GvHD drugs and testing mechanisms of immunoregulation

Meirong Wu[1], Shiru Zhang[1], Fang Zhu[1], Hongyan Sun[1], Jianming Xu[1], Cunxiang Ju[1], Hongyu Wang[1], Santi Suryani Chen[2], Zhiying Li[2], Mark Wade Moore[2], Jing Zhao[1], Xiang Gao[1]. *[1]Gempharmatech Co., Ltd., Nanjing, China,[2]GemPharmatech LLC., La Jolla, CA*

Hematological malignancies, including leukemia, lymphoma and multiple myeloma, account for about 7% of all newly diagnosed cancers. Allogeneic hematopoietic stem cell transplantation (HSCT) is a traditional treatment for hematologic malignancies. Currently, CAR-T cell therapy has made a major breakthrough in the treatment of hematologic malignancies. However, the occurrence of acute Graft-versus-Host Disease (GvHD) represents a major obstacle for HSCT and limits the application of CAR-T cell therapy.
GemPharmatech established and characterized two murine models for anti-GvHD drug evaluation. In the first model, bone marrow from C57BL/6 donor mice was transplanted into a sublethally-irradiated BALB/c recipient mouse. In this model, T cell infiltration, tissue damage, and systemic inflammation were observed, similar to the clinical observations of patients receiving allogeneic HSCT. Efficacy evaluation of anti-GVHD drugs have been carried out based on this model. Our results showed that treatment with the anti-GVHD drug Ibrutinib, the survival rate and the lifespan of the mice was significantly prolonged, and the GvHD score was reduced by about 70% compared with the placebo group.
In the second model, human Peripheral Blood Mononuclear cells (PBMCs) were transplanted into irradiated severe immunodeficient NCG mice. The cohort was irradiated to accelerate GvHD occurrence. The reconstructed human T cells will recognize and attack mouse tissues to cause GvHD. Our results showed that hCD45+ cells infiltrated into heart, liver, and spleen of huPBMC-NCG mice. This model has also been successfully used for anti-GvHD efficacy evaluation. Upon treatment with an anti-GVHD drug, the lifespan of huPBMC-NCG mice was significantly extended and weight loss was alleviated.
Overall, the above-mentioned GvHD models show great potential for preclinical evaluation of anti-GvHD drug development in allogeneic HSCT.

Liquid Biopsies: Circulating Nucleic Acids and Circulating Tumor Cells 4

#5577

Detection of RAS mutations in colorectal cancer patients using DNA from extracellular vesicles

Sho Kuriyama, Takeshi Yamada, Hiromichi Sonoda, Seiichi Shinji, Akihisa Matsuda, Kazuhide Yonaga, Takuma Iwai, Kohki Takeda, Koji Ueda, Toshimitsu Miyasaka, Shintaro Kanaka, Hiroshi Yoshida. *Nippon Medical School, Tokyo, Japan*

Introduction: Precision medicine is becoming increasingly important in cancer treatment, and liquid biopsy (LB) is a core technique. Circulating tumor DNA (ctDNA) is the main target for LB; however, in some patients, its sensitivity is inadequate. Detection of post-operative ctDNA, called Minimal Residual Disease (MRD), indicates cancer recurrence; however, some patients experience recurrent disease without being MRD-positive. To improve sensitivity of ctDNA detection, we focused on exosomes, small vesicles of endosomal origin that contain DNA (exoDNA) derived from cells, including cancer cells. In this study, we assayed *KRAS* mutations in patients with colorectal cancer using exoDNA, and analyzed the utility of biomarkers in prognosis, using a machine learning algorithm.
Materials and Methods: Patients who underwent curative surgery for colorectal cancer from November 2018 to December 2020 were recruited prospectively. Blood samples were obtained before surgery, and ctDNA was extracted from 1 mL of plasma. Exosomes were isolated from this plasma, followed by exoDNA extraction. *KRAS*

mutations in ctDNA and exoDNA were analyzed using droplet digital PCR. The Random Survival Forest (RSF) algorithm was used for variable importance analysis.
Results: 300 patients (123 with *KRAS* mutation and 177 without) were included. The median patient age was 71 years (range: 35 - 91). Concentrations of exoDNA were significantly higher in Stage IV patients compared to patients at other stages ($p < 0.01$). Numbers of exosomes did not differ by stage. *KRAS* mutations were detected in exoDNA of 56 patients (45.5%) and in ctDNA of 28 patients with *KRAS* mutation in their tumors (22.7%, $p<0.001$). Sensitivity of exoDNA was higher than that of ctDNA in Stage II/III patients with *KRAS* mutations (Stage II; 33.3% vs 14.2%, p=0.02, Stage III 46.7% vs 13.3%, p=0.001). However, sensitivity of cfDNA was almost equal to that of exoDNA in stage IV patients (53.8% vs 50.0%, $p = 0.78$). Surprisingly, in patients without *KRAS* mutations in their tumors, *KRAS* mutations were detected in exoDNA of 24 patients (13.5%) and in ctDNA of one patient (0.5%). Of 103 stage III patients, 31 (30.1%) experienced recurrence. The RSF algorithm showed that the exoDNA concentration is the most important risk factor for recurrence, followed by a lack of adjuvant chemotherapy.
Conclusion: Sensitivity of *KRAS* mutation detection using exoDNA is excellent. Additionally, the concentration of exoDNA appears to be a superior predictor for recurrence of Stage II/III colorectal cancer after curative surgery.

#5578
Analytical validation of an NGS-based, personalized and tumor-informed liquid biopsy assay for detecting minimal residual disease (MRD) with high sensitivity and specificity
Wei Gao, Wuqiang Cao, Xiaoling Zeng, Zihan Tian, Xue Zhang, Ning Fu, Pansong Li. *Geneplus-Beijing Institute, Beijing, China*

Introduct**ion:** Circulating tumor DNA (ctDNA) based MRD detection has been proven effective for predicting the relapse of various cancers after curative surgery. We developed a custom-built, tumor-informed MRD detection method named OncoWES-MRD. Somatic variants were identified and prioritized by whole-exome sequencing (WES) of tumor tissues and matched peripheral blood samples. Patient-specific panel targeting up to 50 top-ranked single-nucleotide and Indel variants was designed to analyze plasma for assessing the presence of ctDNA. The ctDNA level was also quantified by in-house software. Here, we report the analytical validation results of this assay.
Methods: The analytical validation was performed on a colorectal cancer cell line SW480. The sheared SW480 DNA was titrated to normal DNA from NA12878 cell line to produce samples with a variant allele frequency (VAF) of 0.1%. The dilution accuracy was confirmed by droplet digital PCR (ddPCR). Then the 0.1% samples were serially diluted to VAF of 0.05%, 0.02%, 0.01%, 0.005%, 0.003%, and 0.001%. As for these dilution gradients below the detection limit blank of the ddPCR assay (0.1%), the changes of exogenously introduced viral DNA copies were used as indicators of the dilution ratio. To explore the relations between the number of variants and the limit of detection (LoD), a customized capture panel covering 200 prioritized variants for SW480 was designed. Each gradient was tested 42 times with an average sequencing depth above 100,000X. The analytical specificity assessment was conducted on 20 NA12878 wild-type samples and 44 blood samples from 22 healthy donors. The library prep starting DNA input was 60 ng for each reaction. ctDNA fraction was evaluated using the maximum likelihood method, and also taking allelic copy number and cancer cell fraction into consideration.
Results: The WES-MRD assay by monitoring 50 variants demonstrated a sample-level sensitivity of 97.6% at VAF of 0.003%, and 76.2% sensitivity at VAF of 0.001%, along with a specificity of 98.4%. The LOD of 0.1% VAF was achieved at the single variant level. The assay performed 95.2% analytical sensitivity at 0.02% VAF, even with 6 somatic mutations, therefore defining the minimal monitoring number. Based on WES sequencing data of 514 solid tumors, 96.1% of samples met the assay requirement of variant numbers. The upper limit monitoring variants number was set to 50, as keep increasing the monitoring variants showed limited sensitivity improvement while specificity was impaired. In the quantitative aspect, a strong linear correlation between the theoretical cell line tumor fractions with the estimated ctDNA fractions ($R^2 = 0.98$).
Conclusions: The WES-based personalized MRD assay demonstrated high sensitivity and high specificity to detect tumor-derived variants down to VAF of 0.003% and accurately quantified.

#5579
Single cell characterization of circulating plasma cells and BCMA levels in patients with multiple myeloma
Sonia Maryam Setayesh[1], Stephanie Shishido[1], Libere Ndacayisaba[1], Amin Naghdloo[1], Jeremy Mason[1], Dean Tessone[1], Carli Kaleta[1], Robert Z. Orlowski[2], Elisabet E. Manasanch[2], James Hicks[1], Peter Kuhn[1]. *[1]Convergent*

Science Institute in Cancer, USC - University of Southern California, Los Angeles, CA,[2]Department of Lymphoma/Myeloma, Division of Cancer Medicine, MD Anderson Cancer Center, Houston, TX

Multiple myeloma (MM), a disease caused by the clonal proliferation of plasma cells (PCs), is the second leading hematologic malignancy in the world, with a global incidence rate increase of 126% and mortality rate increasing by 94% in the past decade. Recently, B cell maturation antigen (BCMA) has emerged as a promising biomarker and therapeutic target for MM due to its selective high expression on malignant PCs, improving the treatment landscape. However, the current diagnostic workup relies on bone marrow aspirates (BMA) which are highly invasive and do not allow for the detection of BCMA levels on circulating PCs, severely limiting the options for repeatable assessments and treatment-monitoring. In our study, we report the utility of a blood-based liquid biopsy, using enrichment-free high definition single cell assay (HDSCA) for the detection, quantification, and morphological characterization of circulating PCs and other BCMA+ cells. We applied a previously validated 4-color immunofluorescence assay using DAPI, CD138, BCMA, and CD45 to examine matched peripheral blood and BMAs from 68 patients across the MM disease spectrum (11 monoclonal gammopathy of undetermined significance [MGUS], 21 smoldering MM [SMM], 18 newly diagnosed MM, and 18 relapsed refractory MM [RRMM]) and peripheral blood from 23 normal donors as controls. Our analysis revealed diverse subtypes of circulating CD138(+/-), BCMA(+/-), and CD45(+/-) cells across the patients, representing both normal and abnormal PCs. We detected significantly higher circulating CD138+ BCMA(+/-) cells in MM precursor conditions (MGUS, SMM), compared to the normal donors. Additionally, we were able to detect BCMA+ oncosomes (identified by the lack of a nuclear structure) in the circulation of patients from both precursor and overt disease conditions. Our findings establish the utility of HDSCA blood-based liquid biopsy for early disease detection and anti-BCMA therapy response monitoring in MM and other B-cell malignancies expressing BCMA.

#5580

Circulating tumor DNA (ctDNA) identifies genomic alterations associated with resistance to Nivolumab in combination with other agents in metastatic castration-resistant prostate cancer from the CheckMate 9KD trial

Yu Wang, Jun Li, Jonathan Baden, Saurabh Gupta, Justin M. David. *Bristol Myers Squibb Company (New York), Lawrenceville, NJ*

Introduction**:** Metastatic castration-resistant prostate cancer (mCRPC) is characterized by an immunosuppressive tumor microenvironment resulting in resistance to single agent immunotherapy, and several combination strategies are being clinically evaluated to address this resistance. CheckMate 9KD (NCT03338790) was a nonrandomized, open-label, multicohort, phase 2 trial of nivolumab combined with rucaparib, docetaxel, or enzalutamide for mCRPC, which showed encouraging clinical activity for the nivolumab plus docetaxel combination. To identify genetic factors potentially associated with response or resistance in this trial, we conducted a retrospective analysis of the tumor genomic alteration landscape utilizing circulating tumor DNA (ctDNA) from plasma samples.
Methods: We performed integrated analyses of sequence and structural alterations identified through comprehensive genomic profiling of cell-free DNA (cfDNA) obtained from plasma at baseline using the GuardantOMNI™ assay (500 genes). The analysis was performed on 253 unique samples across all cohorts for which both clinical and OMNI datasets were available. Variant prevalence in ctDNA was compared to that of matched tumor tissue using the FoundationONE® assay (395 genes). Hazard ratios with corresponding two-sided 95% CI were estimated via unstratified multivariable Cox modeling adjusted by subject age and homologous recombination repair deficiency (HRD) status. Odds ratios with corresponding two-sided 95% CI were estimated via unstratified logistic regression modeling adjusted by subject age and HRD status.
Results: Most patients (239/253; 94.5%) were ctDNA(+), with a substantially higher prevalence of most gene variants detected in cfDNA compared to patient-matched tumor tissue. Mutations in the *AR*, *TERT*, *DNMT3A*, *HNF1A*, and *TP53* genes had the highest frequency. Amplifications in a number of genes detected in ctDNA including the androgen receptor (*AR*), PI3K/Akt pathway regulators (*PIK3CA*, *PIK3CB*, *PREX2*), and epigenetic regulators (*DNMT3A*, *EZH2*, *KDM6A*), were positively associated with poorer clinical outcomes (rPFS and/or OS) in the nivolumab + docetaxel arm.
Conclusions: This investigation highlights the utility of liquid biopsy for evaluating tumor genomic alterations in late-stage mCRPC trials and provides translational insights into potential resistance mechanisms to inform patient selection and combination strategies for future clinical development.
Acknowledgements: We acknowledge the patients and families, clinical study teams, and investigators who made the CheckMate 9KD study possible, and acknowledge Guardant Health and Foundation Medicine for the

collaborative development and validation of the GuardantOMNI™ and FoundationOne®CDx assays, respectively.

#5581

Single-cell genomic analysis of patient-derived circulating tumor cells in pancreatic cancer

Harrison Ball[1], Brittany Rupp[1], Sarah Owen[1], Kaylee Smith[1], Valerie Gunchick[2], Evan T. Keller[3], Vaibhav Sahai[2], Sunitha Nagrath[1]. *[1]Chemical Engineering, University of Michigan, Ann Arbor, MI,[2]Internal Medicine, University of Michigan, Ann Arbor, MI,[3]Urology, University of Michigan, Ann Arbor, MI*

Metastatic pancreatic cancer suffers from an extremely low five-year survival rate of only 3%. While patients with localized disease show marginally better survival rates, 52% of pancreatic cancers are not diagnosed until metastases have already developed. There is therefore a critically unmet need in the early diagnoses of pancreatic cancer patients. Liquid biopsies have emerged as a promising tool for cancer diagnosis through the analysis of various blood-based biomarkers. Among these, circulating tumor cells (CTCs) stand out as a promising target of interest. Over the past decade, CTCs have been identified as a precursor to metastasis. CTCs have also been shown to harbor mutations matching those of the primary tumor, making them a potential surrogate for biopsied tissue. However, CTCs are an extremely heterogenous population of cells, making bulk analysis challenging. In this study, we demonstrate a workflow for the isolation and genomic characterization of single CTCs from pancreatic cancer patients. CTCs are first enriched using a size-based microfluidic system, the Labyrinth, developed in the Nagrath lab. Single CTCs are subsequently isolated using the DEPArray Nxt system, followed by whole genome amplification (WGA) and low-pass sequencing. The pipeline was optimized using three commercially available pancreatic cancer cells lines (Panc-1, Capan-2, and BxPC-3) and two pancreatic cancer CTC cell lines previously developed in-house (CTC-CL-1 and CTC-CL-2). Finally, the workflow was validated using a blood sample from a stage IV pancreatic ductal adenocarcinoma patient. Following WGA, the average nucleic material concentration of the cell lines was 26.24 ± 16.28 ng/μL and 14.43 ng/μL for cells isolated from the patient sample. The average fragment size was 746 ± 232.79 bp for cell line cells and 507 bp for patient sample cells. This was within the expected range of 100-2000 bp. Both CTC cell lines show gains on parts of chromosome 8q (Myc), 10q (FGFR2) and 17q. Myc is a known oncogene and FGFR2 has been associated with cell growth, migration, and invasion. There are also noticeable differences between the two CTC-CL-1 cells, with one cell showing a 3p12.3-3p26.3 gain (CTNNB1), and the other showing a loss of 6q12-6q15 and gain of 6q16.1-6q27 (Myb, ESR1). A patient sample CTC and patient-matched WBC were isolated and sequenced. The CTC has a noticeable gain of chromosome 1q and loss of chromosome 5q. A gain in chromosome 1q has been seen previously in pancreatic cancer and chromosome 5q is the location of multiple oncogenes including APC, CSF1R and FGFR4. The loss of APC is known to affect Wnt/β-catenin signaling, causing an increase in CD34 expression which is linked to increase in cell invasion and migration. These results demonstrate an efficient workflow for the single cell genomic analysis of pancreatic CTCs. Further studies can be conducted to characterize the heterogenous landscape of CTCs in pancreatic cancer.

#5582

Liquid biopsy-based comprehensive genomic profiling reveal mutational landscape in real-world patients with unresectable NSCLC

Haoran Tang, Feng Xie, Yue Zhang, Shidong Jia. *Huidu (Shanghai) Medical Sciences, Ltd., Fengxian District, Shanghai, China*

Introduct**ion:** NSCLC accounts for more than 80% of all lung cancer, and has been shown for clinical benefits from targeted therapies, according to tests of multiple genes, such as EGFR, KRAS, ALK, ERBB2. Previous studies revealed molecular characteristics and responses of targeted therapies in NSCLC. However, most studies used tissue biopsies. There is increasing interest to characterize the molecular profile of NSCLC through liquid biopsy. Hence, here we report a comprehensive genomic profiling study in unresectable NSCLC patients using liquid biopsy.

Methods: The prospective study is part of the Predicine's Phoenix Program, a global molecular biomarkers screening program in multiple solid tumors. Currently, the study enrolled 352 unresectable advanced NSCLC patients from 24 centers in China, who were naïve to the 1st line treatment or recurrent after 1st line targeted therapies. 10ml of blood was collected from each patient and delivered to a central lab for ctDNA analysis. The study applied PredicineCARE, an NGS-based liquid biopsy assay, to profile somatic mutations, copy number variations, and gene fusions among these patients.

Results: The study identified 1614 somatic mutations and 202 copy number variants among blood samples from 352 patients. The most common altered genes were TP53(176/352, 50%), EGFR(144/352, 41%), PIK3CA(35/352, 10%), CDNK2A(35/352, 10%), KRAS(28/352, 8%), and RB1(28/352, 8%). Gene copy number gain incidents were identified on MYC(n=22), PIK3CA(n=16), EGFR(n=15), and MET(n=7), etc. Notably, the study also reported gene copy number loss incidents through liquid biopsy, such as CDKN2A(n=16), PTEN(n=11), and RB1(n=10). The study identified 12 gene fusion incidents, including 7 EML4-ALK fusions, 2 RET fusions(KIF5B-RET and NCOA4-RET), 2 NTRK fusions(ETV6-NTRK3 and NOS1AP-NTRK1), and 1 rare CD74-NRG1 fusion.
Conclusions: This study revealed the comprehensive mutational landscape of advanced NSCLC through liquid biopsy, providing novel biomarkers for clinical diagnosis and targeted therapy mechanism studies.

#5583

Pre-radiotherapy ctDNA risk-stratifies non-small cell lung cancer patients with oligometastatic disease

Nicholas P. Semenkovich[1], Yun E. Wang[2], Aadel A. Chaudhuri[3]. *[1]Medicine, Washington University In St. Louis, St. Louis, MO,[2]Tempus Labs Inc., Chicago, IL,[3]Radiation Oncology, Washington University In St. Louis, St. Louis, MO*

Background: Oligometastatic non-small cell lung cancer (NSCLC) patients may uniquely benefit from personalized therapies via liquid biopsy. Widespread metastatic disease is incurable, yet some patients with oligometastatic disease experience prolonged progression-free survival when treated with aggressive local stereotactic body radiotherapy (RT). Distinguishing patients who would benefit from aggressive RT from those who would benefit from systemic therapies remains a challenge. We hypothesized that pre-RT ctDNA can be used to risk-stratify those with oligometastatic NSCLC and enable earlier personalized approaches when considering systemic therapy versus aggressive local RT.
Methods: A retrospective multi-institutional cohort of 1,487 patients (median age: 65 years, 53% female [n=784], 47% male [n=703]) who were diagnosed with oligometastatic NSCLC was selected. Each patient underwent liquid biopsy ctDNA analysis using the Tempus xF assay (v2) at least once, with a subset of patients undergoing serial sampling at 2-8 timepoints for a total of 1,880 ctDNA assays. 309 of the patients (20%) underwent RT after liquid biopsy was obtained and oligometastatic NSCLC was diagnosed. Outcomes for overall survival (OS) and progression-free survival (PFS) were defined with respect to the initiation time of RT (i.e., time from RT to death, time from RT to progressive disease).
Results: Across all ctDNA assays, 3,520 pathogenic or likely pathogenic (P/LP) variants were identified (1.8 variants/sample, mean). Among patients with a liquid biopsy obtained prior to RT, 48% (n=151) experienced progressive disease and 11% (n=34) died during the study period. Focusing on patients with ctDNA obtained pre-RT, P/LP variants were detected in 74% (n=230) while 26% (n=79) had zero variants detected. Of those with detectable variants, 76% (n=175) had 1-3 variants, while 24% (n=55) had ≥4 P/LP variants detected in ctDNA. Both overall survival and progression-free survival were significantly worse in patients with detectable ctDNA from pre-RT liquid biopsy compared to those without (median OS 16.8 months vs. 25 months; p=0.027, HR=1.65; median PFS 5.4 months vs. 8.8 months; p=0.021, HR=1.57). Remarkably, survival correlated inversely with the number of detected variants from pre-RT liquid biopsies; when patients were stratified by variant quantity, both OS and PFS were significant (OS p=0.045, PFS p=0.003; stratified by 0, 1-3, and ≥4 variants). This finding was also significant in a multivariate Cox proportional hazards analysis (OS HR=1.15, CI 1.04-1.24; PFS HR=1.16, CI 1.06-1.25), but was not significant for parameters such as age at diagnosis or squamous histology.
Conclusions: These data suggest that a ctDNA-informed approach may be a powerful pre-RT biomarker to help risk-stratify oligometastatic NSCLC patients and potentially enable personalized decision-making for RT versus systemic therapy.

#5584

Analysis of cell free DNA to predict outcome to Bevacizumab combination therapy in metastatic colorectal cancer patients

Ian S. Miller[1], Valentina Thomas[1], Tom Venken[2], Ingrid Arijs[2], Ana Barat[1], Johannes Betge[3], Tianzuo Zhan[4], Timo Gaiser[5], Matthias P. Ebert[3], Jochen Prehn[1], Rut Klinger[6], Darran P. O'Connor[7], Brian Brian Moulton[8], Verena Murphy[8], Ray McDermott[9], Brian Bird[10], Gregory Leonard[11], Liam Grogan[12], Anne Horgan[13], Nadine Schulte[5], Markus Moehler[14], Nicole Prannikar[15], Judith Franz-Werner[16], Hans-Peter Feustel[16], Diether Lambrechts[17], Annette T. Byrne[1]. *[1]Department of Physiology and Medical Physics, Royal College of Surgeons in*

Ireland, Dublin, Ireland,[2]Department of Human Genetics, VIB Center for Cancer Biology, Leuven, Belgium,[3]DKFZ-Hector Cancer Institute, Mannheim, Germany,[4]Department of Medicine II, Heidelberg University, Mannheim, Germany,[5]University Medical Center Mannheim, Mannheim, Germany,[6]UCD Conway Institute of Biomolecular and Biomedical Science, University College Dublin, Dublin, Ireland,[7]Department of Pharmacy and Biomolecular Sciences, Royal College of Surgeons in Ireland, Dublin, Ireland,[8]Cancer Trials Ireland, Dublin, Ireland,[9]Department of Medical Oncology, St. Vincent's University Hospital, Dublin, Ireland,[10]Bon Secours Cork Cancer Centre, Cork, Ireland,[11]University Hospital Galway, Galway, Ireland,[12]Medical Oncology Department, Beaumont Hospital, Dublin, Ireland,[13]Department of Medical Oncology, University Hospital Waterford, Waterford, Ireland,[14]Department of Medicine, Johannes-Gutenberg University Clinic, Mainz, Ireland,[15]Medical Department I, Klinikum Ludwigsburg, Ludwigburg, Germany,[16]Onkologische Schwerpunktpraxis, Speyer, Germany,[17]VIB Center for Cancer Biology, Leuven, Belgium

Purpose: Cell-free DNA (cfDNA) analysis in plasma is an emerging technique with numerous applications in oncology. We employed cfDNA to determine chromosomal instability (CIN), nucleosome footprints (NF) and methylation profiles in metastatic colorectal cancer (mCRC) patients and to predict outcome to bevacizumab (BVZ) combination therapy.
Experimental Design: Low coverage whole-genome sequencing (LC-WGS) was performed on matched tumor and plasma samples from 74 mCRC patients participating in the CTRIAL-IE 12-16 AC-ANGIOPREDICT Phase II clinical trial (NCT01822444), prior to receiving BVZ, and analyzed for CIN (3 subclusters with low, intermediate and high CIN, respectively) and nucleosomes. For 61/74 mCRC patients, plasma samples before and after BVZ treatment were available and used for targeted methylation sequencing. A validation cohort of mCRC plasma samples (n= 24) from the University Medical Center Mannheim (UMM) was similarly profiled.
Results: Based on cfDNA CIN profiles, we subtyped mCRC patients with 92.3% accuracy of sample distinction into low and high CIN clusters (cluster 1 against cluster 2 and 3), demonstrating concordance between matched plasma and tumor samples. Improved survival outcome was observed in CIN high patients. Plasma-based CIN clustering and improved survival for CIN high patients was also confirmed in the UMM cohort. NF and methylation profiles differed between CIN clusters and healthy individuals, and could reliably separate cluster 1 from cluster 2 and 3 samples (AUC=0.72 and 0.85 respectively). A large methylation score decrease after BVZ treatment was associated with improved overall survival ($p = 0.013$).
Conclusions: cfDNA can be analyzed to predict outcome to BVZ in mCRC patients. Detection of CNAs, NFs and methylation profiles facilitated stratification of samples into CIN clusters and informed patient response to treatment.

#5585

Tissue based next generation sequence is more accurate than ctDNA to detected pathogenic variants in *MTAP* wild type tumors

Andre Luiz De Souza. *Rhode Island Hosp./Brown Univ. Med. School, Providence, RI*

Next generation sequencing (NGS) of circulating tumor DNA (ctDNA) prevents invasive biopsies and captures tumor heterogeneity. In a prior report by Zhang et al (Nat Commun 2021), certain actionable mutations were more prevalent in ctDNA than tissue-based databases (e.g., *EGFR* 48% versus 25.2%). Our group investigated if discrepancies in patterns of pathogenic variants between liquid biopsy and tissue specimens in a subtype of metastatic urothelial carcinoma (*MTAP* deleted) can inform the best approach of utilizing tissue or blood. MTAP (methyl-adenosine phosphorylase) is an enzyme involved in salvage purine biosynthesis and its deletion confers sensitivity to pemetrexed and taxanes, but resistance to immune checkpoint inhibitors. The *MTAP* gene is deleted in 25% of urothelial carcinomas. We report herein the pattern of pathogenic variants from ctDNA in 17 patients with metastatic urothelial carcinoma, 10 with *MTAP*-deletion and 17 with *MTAP* wild-type. Among 10 patients with *MTAP*-deleted urothelial carcinoma with collected ctDNA, 3 had no detected pathogenic variant. The most common pathogenic variants in 7 patients were *TP53* (4/7, 57%), *TERT* (4/7, 57%), *ERBB2* (2/7, 28%); *PIK3CA* (2/7, 28%), and *NFE2L2* (2/7, 28%). The mutations found in paired ctDNA and tissue based NGS were *TP53* in 26.6 % (4/15), *TERT* in 21.0 % (4/19), *ERBB2* in 66.6 % (2/3), *PIK3CA* in 50 % (2/4), and *NFE2L2* in 100% (1/1) of patients. Three of the 10 patients with collected ctDNA had *ELF3* frameshift loss-of- function alterations on tissue not found on ctDNA. Among 54 patients with *MTAP* wild-type urothelial carcinoma, 26 had collected ctDNA. Among these 26 patients, 9 had no detected pathogenic variants. Among the 17 patients with pathogenic variants, the most common mutations were *TP53* (76%, 13/17), *TERT* (47%, 8/17), *ERBB2* (24%, 4/17), *RB1*

(24%, 4/17), and *BRCA1* or *BRCA2* (24%, 4/17). Three of these 17 patients had no or insufficient tissue for NGS. The mutations found in paired ctDNA and tissue based NGS were *TP53* in 100% (14/14), *TERT* in 64% (9/14), *ERBB2* in 43% (6/14), *RB1* in 29% (5/14), and *BRCA1* or *BRCA2* in 36% (5/14) of patients. *MTAP* wild-type patients had a higher frequency of *TERT* alterations (p=0.012), but not *ERBB2*, (p=0.453) than patients with *MTAP*-deleted type tumors. Ongoing evaluation of timing and location of pathogenic variants will inform where (primary tumor, metastatic site) and when (after chemotherapy, immune checkpoint inhibitors, antibody drug conjugates) to biopsy patients on progression after cancer therapies.

#5587

Ultra-deep targeted sequencing of cell-free DNA and patient-matched white blood cells for treatment response evaluation in patients with metastatic colorectal cancer

Iris van 't Erve[1], Jamie E. Medina[2], Alessandro Leal[2], Eniko Papp[3], Jillian Phallen[2], Vilmos Adleff[2], Elaine Jiayuee Chiao[2], Adith S. Arun[2], Karen Bolhuis[4], John K. Simmons[3], Aanavi Karandikar[3], Kenneth C. Valkenburg[3], Mark Sausen[3], Samuel V. Angiuoli[3], Robert B. Scharpf[2], Cornelis J. A. Punt[5], Gerrit J. A. Meijer[1], Victor E. Velculescu[2], Remond J. A. Fijneman[1]. *[1]Department of Pathology, Netherlands Cancer Institute, Amsterdam, Netherlands,[2]Sidney Kimmel Comprehensive Cancer Center, Johns Hopkins University School of Medicine, Baltimore, MD,[3]Personal Genome Diagnostics, Baltimore, MD,[4]Department of Medical Oncology, Amsterdam University Medical Centers, Amsterdam, Netherlands,[5]Julius Center for Health Sciences and Primary Care, University Medical Center Utrecht, Utrecht, Netherlands*

Background: Treatment response monitoring of patients with metastatic colorectal cancer is currently performed by computed tomography (CT) imaging, which assesses tumor volume. Circulating tumor DNA (ctDNA) testing has the potential to replace or complement CT imaging by assessing the presence and abundance of tumor-specific mutations, allowing for personalized treatment and early adaptation of treatment regimens through risk stratification and the emergence of therapy resistance mutations. However, germline and clonal hematopoiesis-associated alterations can confound the identification of tumor-specific alterations in cell-free DNA (cfDNA), often requiring additional sequencing of tumor tissue.
Aim: The present study assessed whether ctDNA-based treatment response monitoring could be performed in a tumor tissue-independent manner by combining ultra-deep targeted sequencing analyses of cfDNA with patient-matched white blood cell (WBC) derived DNA.
Methods: In total, 183 cfDNA and 49 WBC samples, along with 28 tissue samples, from 52 metastatic colorectal cancer patients participating in the prospective phase III CAIRO5 clinical trial were analyzed using an ultra-deep targeted sequencing liquid biopsy assay.
Results: The combined cfDNA and WBC analysis prevented the reporting of false positives due to germline or hematopoietic variants in 40% of patients. Patient-matched tumor tissue sequencing did not provide additional information. Longitudinal analyses of ctDNA were more predictive of overall survival than standard-of-care radiological response evaluation. ctDNA mutations related to primary or acquired resistance to the EGFR inhibitor panitumumab were identified in 42% of patients.
Conclusions: Accurate ctDNA mutation detection by combined cfDNA and WBC genomic DNA analyses in a tumor tissue-independent manner mitigates sample logistics challenges in the clinical setting, and the application of this approach for evaluation of therapeutic response and resistance opens new avenues for early adaptation of treatment regimens.

#5588

Methylated ctDNA dynamics correspond with clinical tumor load in metastatic lung cancer patients on therapy

Patrick Ye[1], Brian Woodward[2], Robb Viens[1], Sydne Langpap[1], Katherine Shelburne[1], Wen Zhou[1], Joyce Zhu[1], Jan Wignall[1], Gary Palmer[1], David Tsao[1], Oguzhan Atay[1], Hatim Husain[2]. *[1]BillionToOne Inc., Menlo Park, CA,[2]UC San Diego Moores Cancer Center, La Jolla, CA*

Treatment monitoring assays are needed to accurately and rapidly assess the efficacy of cancer treatments. While imaging remains the gold standard for monitoring the efficacy of cancer treatment, the use of more sensitive tools, such as liquid biopsy, could be beneficial for the patient's ultimate treatment outcome. Several liquid biopsy-based assays that measure circulating tumor DNA (ctDNA) have been developed to meet this need. However, approaches that rely on quantifying the variant allele fraction (VAF) of somatic variants may be inaccurate or inconsistent due

to a scarcity of detected somatic variants in the ctDNA or may be logistically infeasible if they require a tumor biopsy *a priori*. Methylated ctDNA has shown promise as a biomarker for treatment monitoring without requiring a tumor biopsy, but current efforts are limited in their ability to precisely quantify the amount of methylation present in the ctDNA. We hypothesize that more precise quantification of methylated ctDNA could enable more accurate correspondence with clinical tumor load and cancer treatment outcomes.
Here, we present a retrospective study characterizing how amounts of methylated ctDNA dynamically change through cancer therapy. We tested 75 patient-treatment events, with each event composed of patient samples from one pre-treatment and two post-treatment time points, all from patients with Stage III-IV metastatic lung cancer receiving targeted therapies or immunotherapy. We employed a novel methylation-based, tumor-naive liquid biopsy assay for treatment monitoring by counting the number of methylated molecules in cell-free DNA. We observed methylation amounts ranging from <50 to >50,000 total methylated tumor molecules per 1000 assayed genomic equivalents at individual time points, indicating that the assay can detect a broad range of tumor load in blood. In addition, we measured changes between time points as large as >96% decrease and >2800% increase in methylation. We found that methylation correlated with maximum variant allele fractions as measured by a treatment selection assay ($r^2 = 0.74$). Moreover, in this tumor-naive assay, we identified a median of 58 informative methylated loci, significantly more than a median of ~1-5 informative SNVs identified in VAF-based tumor-naive assays, and ~4-16 informative SNVs identified in VAF-based tumor-informed assays. This ~6-10x increase in the number of informative loci enables much more precise quantification and underlies the assay's robustness and precision across patients, time points, and therapies. Finally, these changes in normalized total tumor molecules correlated with radiographic responses on imaging, duration of response, and time on therapy. Overall, our findings support the utility of methylated ctDNA as a biomarker for monitoring tumor load in cancer patients.

#5589

The effect of morphine-based perioperative analgesia on circulating tumor cells dissemination in colorectal cancer patients

Pavel Stejskal[1], Josef Srovnal[2], Emil Berta[1], Alona Rehulkova[1], Lubomír Večeřa[3], Tomas Gabrhelik[3], Filip Haiduk[4], Jan Maca[4], Jan Bruthans[5], Pavel Michalek[5], Pavla Kourilova[1], Marian Hajduch[1]. *[1]Institute of Molecular and Translational Medicine, Palacky Univ. Faculty of Medicine, Olomouc, Czech Republic,[2]Palacky Univ. Faculty of Medicine, Olomouc, Czech Republic,[3]Tomas Bata Hospital, Zlin, Czech Republic,[4]University Hospital Ostrava, Ostrava, Czech Republic,[5]General University Hospital Prague, Prague, Czech Republic*

Purpose: Circulating tumor cells (CTCs) are primary or metastatic tumor cells shed into the bloodstream and are considered precursors of distant metastatic spread and can act as an independent prognostic and predictive biomarker. Colorectal cancer (CRC) is the leading cause of cancer-related deaths worldwide and metastasis is the major cause of death. Previous studies showed poorer survival in CRC patients treated perioperatively with morphine in comparison to piritramide.
Patients and Methods: In total, 150 CRC stage I-III patients undergoing either radical or laparoscopic surgery were enrolled in this prospective multicentric randomized study (NCT03700411). Patients were randomized into three arms using different perioperative analgesia - morphine, piritramide, and epidural analgesia. Three peripheral blood samples were collected preoperatively, one day and one month after surgery respectively. To preserve the cellular content of specimens, Cell-Free DNA BCT® (Streck, Inc.) blood collection tubes were used. The CTCs were identified using CytoTrack CT11™ (2/C, Denmark), a semi-automated immunofluorescence microscopy detecting the pan-cytokeratin and EpCAM signals. The method recovery rate was analyzed using SW-480 cancer cell line by flow cytometry.
Results: The CTCs recovery rate of the method was 72% and the method was certified by ISO 15189. The analyses of CTC presence revealed the highest positivity rate in the samples collected from patients treated with morphine on the first day after surgery (51.4 %). Also, a significant increase in positivity (from 23.5 % for the perioperatively collected samples) compared to samples from patients treated with epidural analgesia (31.1 % to 33.3 %) and piritramide (44.2% to 41.0%) was observed. The CTC presence was lower in control samples collected after one month irrespective of the analgesia type. The highest positivity among the control samples was in those associated with morphine analgesia (32.1 % versus 25.7% for epidural and 25.0% for piritramide analgesia).
Conclusion: A significant increase in CTC levels was found in postoperative blood samples of CRC patients treated with morphine compared to piritramide and epidural analgesia. Enrollment in the study is ongoing.

Acknowledgments: This study was supported by the Ministry of Health of the Czech Republic (NV18-03-00470), Palacky University Olomouc (LF 2022_012), European Union - Next Generation EU (LX22NPO5102) and European Regional Development Fund (ENOCH CZ.02.1.01/0.0/0.0/16_019/0000868).

#5590

Liquid biopsy testing in metastatic or advanced breast cancer patients during the COVID-19 pandemic

Benjamin L. S. Furman, Ebru Baran, Sonal Brahmbhatt, Betty Chan, Ka Mun Nip, Adrian Kense, Brenda Murphy, Vincent Funari, David G. Huntsman, Ruth Miller, Melissa K. McConechy. *Imagia Canexia Health, Vancouver, BC, Canada*

Objective: During the COVID-19 pandemic, cancer patients had restricted access to standard of care tissue biopsy. Liquid biopsy assays using next generation sequencing technology provides a less invasive method for determining circulating tumour mutations (ctDNA) associated with targeted treatments or prognosis. As part of deploying technology to help cancer patients obtain molecular testing, a clinical program was initiated to offer liquid biopsy testing for Canadian patients with advanced or metastatic breast cancer.
Methods: Blood was drawn in two 10 mL Streck^{TM} DNA BCTs and sent to the CAP/CLIA/DAP accredited Imagia Canexia Health laboratory for testing using the clinically validated Follow It^{TM} liquid biopsy assay. Plasma was isolated using a double spin protocol and plasma cell-free DNA (cfDNA) extracted using an optimized Promega Maxwell RSC method. Extracted cfDNA was amplified using the multiplex amplicon-based hotspot 30 or 38 gene panel and sequenced. An in-house developed bioinformatics pipeline and reporting platform were used to identify pathogenic single nucleotide variants (SNVs), indels (insertions and deletions), and gene amplification. Included in the panel are genes associated with metastatic breast cancer: *AKT1, BRAF, ERBB2, ESR1, KRAS, PIK3CA, TP53.*
Results: To identify biomarkers, 1214 metastatic or advanced breast cancer patient cfDNA samples were tested. There were 15 cases sent for repeat testing. We reported 48% of samples harboring pathogenic ctDNA mutations in *TP53* (22%), *PIK3CA* (19%), *ESR1* (18%), *AKT1* (2%), *ERBB2* (1.5%). Co-occurring variants were identified in samples with *ESR1*/*PIK3CA* as well as *TP53*/*PIK3CA* (both p-values <0.001). Interestingly, 29% of samples with mutated *ESR1* harbored ≥ 2 *ESR1* ctDNA mutations. In 56% of cases, previous molecular testing indicated the cancer subtype as hormone receptor (ER, PR) positive with/without HER2 negative status. In this specific subgroup, 49% harbored ctDNA mutations with 63% of those being *PIK3CA* and/or *ESR1* mutations.
Conclusions: A population of Canadian women with metastatic breast cancer were tested using a liquid biopsy gene panel during the COVID-19 pandemic for identification of biomarkers for targeted therapeutic options. Over 50% of the samples were identified as hormone positive, with greater than 60% harboring *PIK3CA* and *ESR1* ctDNA mutations. Studies have shown that metastatic *PIK3CA* mutated ER-positive/HER2-negative tumors are predictive to respond to alpelisib therapy and have FDA and Health Canada approval. Additionally, *ESR1* mutations are associated with acquired resistance to antiestrogen therapies, and interestingly we identified 29% of *ESR1* mutated samples with multiple mutations possibly indicating resistance subclones. In future studies, longitudinal monitoring for presence of multiple targetable and resistance mutations could be utilized to predict or improve clinical management.

#5591

Circulating tumor DNA for recurrence prediction and efficacy analysis in the ICONIC trial of peri-operative FLOT and avelumab (PD-L1) in localized esophago-gastric adenocarcinoma

Marco Gerlinger[1], Anderley Gordon[2], Louise J. Barber[3], Georgios Laliotis[4], Avani Athauda[2], Benjamin Challoner[5], Andrew Woolston[3], Sonia Mansukhani[5], Matt Dunstan[2], Nikoletta Petrou[2], Komel Khabra[2], Retchel Lazaro-Alcausi[2], Richard Crux[2], Victoria Borja[2], Ruwaida Begum[2], Isma Rana[2], Charuta Palsuledesai[4], Meenakshi Malhotra[4], Minetta Liu[4], Adham Jurdi[4], Shruti Sharma[4], Sheela Rao[2], Sacheen Kumar[2], David Cunningham[2], Ian Chau[2], Naureen Starling[2], M. Asif Chaudry[2]. *[1]Barts Cancer Institute & St Bartholomew's Hospital, London, United Kingdom,[2]Royal Marsden Hospital NHS Foundation Trust, London, United Kingdom,[3]Barts Cancer Institute, London, United Kingdom,[4]Natera, Austin, TX,[5]The Institute of Cancer Research, London, United Kingdom*

Background: The utility of molecular residual disease (MRD) detection by circulating tumor (ct)DNA in early-stage (pT2+ or N+, M0) esophagogastric adenocarcinoma treated with peri-operative systemic therapy has not been assessed in prospective trials.

Methods: This exploratory analysis of the phase 2 ICONIC trial (NCT03399071), assessed whether ctDNA can predict recurrence and determine the efficacy of 4xFLOT+avelumab (FLOT-A) before and after surgery. Exome sequencing of pre-treatment biopsies was successful in 24/26 patients (pts) (92.3%) who had received FLOT-A and had undergone surgery at the time of analysis. All pts had R0 resections. Tumor-informed ctDNA assays (Signatera^{TM}) were designed for these 24 pts and 220 serial plasma samples were analyzed. Pathologic response was assessed using Mandard tumor regression grading (TRG1 complete, 2 excellent, 3 good, 4 poor and 5 no response). The median follow-up was 17.0m from surgery. Progression free survival (PFS) was calculated from surgery to radiological recurrence or death.
Results: ctDNA was detected in 23/24 pts (95.8%) prior to treatment. PFS was significantly shorter for pts with a mean number of tumor DNA molecules per ml plasma in the middle & highest tertile (p=0.049, HR=8.33, 95% CI: 1.01-1083, Firth Correction for Cox regression). 6 pts remained ctDNA-positive post neoadjuvant chemotherapy (NAC). None of these pts had a TRG1/2, 3 (50.0%) had TRG3 and 3 (50%) TRG4/5 in the resection specimen. Of 18 ctDNA-negative pts 5 (27.8%) had TRG1/2, 10 (55.6%) TRG3 and 3 (16.7%) TRG4/5. Post-surgery and prior to adjuvant therapy, 6/24 pts were ctDNA-positive. ctDNA positivity at this time point was associated with significantly shorter median PFS (12.9m) compared to ctDNA-negative status (PFS not reached, p<0.0001, HR=27, 95%CI: 3.0-241). Nodal status and Mandard TRG are routinely used as clinical predictors. Only the former was significantly associated with poor median PFS (pN+: 13.5m, pN-: not reached, p=0.027, HR=11, 95%CI: 1.3-98). Of 6 pts who remained ctDNA positive post-operatively, none achieved ctDNA clearance despite adjuvant FLOT-A. The median lead-time from ctDNA positivity after surgery to recurrence was 11.4 months.
Conclusions: Post-NAC/pre-surgical ctDNA positivity correlated with worse pathological response. Persistent ctDNA after NAC & surgery was a stronger predictor of recurrence than nodal status or TRG in the resection specimen. Post-operative adjuvant therapy failed to clear ctDNA in any of the pts who were ctDNA positive after surgery, indicating that administering more of the same treatment is ineffective. This provides an opportunity to test new adjuvant therapies in pts who remain ctDNA positive after surgery. Whether post-operative therapy can be omitted in pts who are ctDNA negative after surgery should be assessed in future trials.

#5592

Expansion and characterization on ALK positive NSCLC circulating tumor cells isolated using a size based inertial microfluidic Labyrinth device

Yuru Chen, Shamileh Fouladdel, Harrison Ball, Xu Cheng, Liwei Bao, Habib Serhan, Albert Liu, Bryce Vandenburg, Laura Goo, Nathan Merrill, Aaron Udager, Angel Qin, Sofia D. Merajver, Sunitha Nagrath.
University of Michigan, Ann Arbor, MI

Introduct**ion**
Lung cancer (LC) is the leading cause of cancer deaths. 85% of LC are non-small cell lung cancer (NSCLC). Fusions involving anaplastic lymphoma kinase (ALK) are oncogenic drivers in ~ 7% of NSCLC. Previous studies have shown that drug resistance develops within ~2 years after ALK tyrosine kinase inhibitor targeted therapy. Due to resistance mechanisms and the biological heterogeneity that evolves over the treatment of ALK+ NSCLC, it is important to monitor and study those dynamic changes through the clinical treatment course to understand cancer progression.
Circulating tumor cells (CTCs) are rare cells, shed from cancer lesions into the bloodstream. They can be isolated from a patient's peripheral blood sample (~20ml) to enable study of tumor characteristics at multiple time points. They are promising biomarkers that not only offer phenotypic and genotypic information, but also present a potential to expand into patient derived ex vivo tumor models. In this study, we use a high throughput label-free microfluidic device, Labyrinth, developed in the Nagrath lab for cell size based CTC enrichment, followed by expansion of CTCs in organoid models, further molecular characterization, and growth in patient-derived xenograft (PDX) models.
Methods
Blood samples were collected from patients (n=22), three with known ALK status. CTC isolation was performed using Labyrinth at 2.0 mL/min. A part of the isolated CTCs were immunofluorescently stained for pan cytokeratin (pan CK), CD45, DAPI, epithelial cell adhesion molecule (EpCAM), and vimentin markers for enumeration. Others were processed for expansion in ultralow attachment plates with three types of organoid culture media. The rest of the CTCs were used for molecular characterizations.
Growth curves were produced on expanded samples on Day 0, 7, 14, and 21 in different culture conditions. A live/dead assay and in situ hybridization (FISH) were also performed. On Day 7, selected samples were injected

into NSG™ mice. Bulk RNA sequencing was conducted on the original tumor, Day 0 and 7 CTCs, and PDX samples.

Results

The median CTC concentration in this cohort (n=22) was 316.2 CTCs/ ml of blood. Isolated CTCs from ALK+ NSCLC patients showed ALK fusions by FISH. We observed that the number of ALK CTCs was reduced over time consistent with decreased tumor size in CT scans. There were significant differences ($p<0.05$) for vimentin positive CTCs compared to the other three types of CTCs, which indicated a higher prevalence of a mesenchymal state of NSCLC CTCs. One of the two samples successfully developed into PDX after two months. In summary, we demonstrated a successful workflow to enrich and expand CTCs from ALK+ NSCLC patients. The expanded CTCs can be further characterized and can generate tumors in PDX models.

#5593

Clonal mutation burden and evolutionary dynamics analysis in metastatic gastro-esophageal adenocarcinoma (GEA) by error corrected whole-exome circulating tumor DNA sequencing

Neil McCafferty[1], Caroline Fong[2], Louise J. Barber[1], Andrew Woolston[1], Dimitrios Kleftogiannis[3], Taqia Rana[2], Susan Cromarty[2], Shannon Kidd[2], Ruwaida Begum[2], Ian Chau[2], Naureen Starling[2], David Cunningham[2], Marco Gerlinger[4]. *[1]Barts Cancer Institute, London, United Kingdom,[2]Royal Marsden Hospital NHS Foundation Trust, London, United Kingdom,[3]University of Bergen, Bergen, Norway,[4]Barts Cancer Institute & St Bartholomew's Hospital, London, United Kingdom*

Introduction: The evolution of metastatic cancers over time can be assessed in circulating tumor DNA (ctDNA) but sequencing and bioinformatics tools for ultra-deep ctDNA whole-exome sequencing (WES) analysis are lacking.

Methods: We developed ctDNA WES that only requires 15ng DNA to achieve sequencing depths of 1000-2000x. Error correction with molecular barcodes and duplex DNA detection allowed calling of mutations ≥0.5% variant frequency (VF). This pilot study applied ctDNA WES to plasma from 20 EGA patients (pts) and standard WES to matched biopsies in order to assess ctDNA WES performance and whether clonal mutation burden (cMB), a critical immunotherapy biomarker and important for neoantigen vaccine designs, differed between ctDNA and biopsies. We furthermore established a mutation and copy number data analysis pipeline using Bayesian clustering to define subclones and track their evolution during therapy in 3pts.

Results: The median age of pts was 71y, 95% had distant metastases and 5% locally advanced EGAs. At a median sequencing depth of ????x after de-duplication, VFs of mutations in pre-treatment ctDNA was low (<2% VF) in 8 pts, and intermediate (2-10%) to high (>10%) in 12. Whether cMB differed in biopsies vs ctDNA was assessed in 7 pts with high VFs in ctDNA and good cancer purity in matching biopsy WES. The median cMB was 82 in biopsies and 111 in ctDNA. The increase was driven by 3 cases with 30%, 35% and 59% higher cMB in ctDNA vs biopsies. In two pts, most mutations that only appeared clonal in ctDNA were subclonal rather than absent in the primary tumor, indicating the subclonal presence of the metastasis progenitor clone. Subclonal intermixing in primary tumors hence limits the accurate identification of mutations that are clonal in metastatic disease. Evolutionary dynamics analyses in 3 pts who had good responses to chemotherapy before progression showed a major clonal sweep in one, supporting monoclonal resistance, and evolution of small subclones in two, indicating polyclonal resistance. A MEK1 K57T mutation evolved at resistance in a *HER2* amplified EGA treated with trastuzumab+chemotherapy, demonstrating the utility to identify mechanisms of acquired resistance.

Conclusions: ctDNA WES can assess the genetics of entire metastatic cancer cell populations over time and deconvolute their evolutionary trajectories. 43% pts had higher cMB in ctDNA compared to biopsies. Liquid biopsy analyses by WES may be superior to tissue-based WES for mutation burden analysis and neoantigen vaccine designs. ctDNA WES identified distinct evolutionary modes of resistance. A larger cohort is being analyzed to define how these differ clinically and whether they can be predicted from pre-treatment ctDNA WES. Efforts to increase the ctDNA WES sensitivity are ongoing as 8 pts had low ctDNA VFs which increased false negative rates.

#5594

Association of circulating cell-free DNA and prostate cancer risk groups in patients undergoing proton therapy

Andrew Bass[1], Johnny Velasquez[1], Moein Rajaei[2], Curtis Bryant[3], Nancy Mendenhall[3], Luisel J. Ricks-Santi[2]. *[1]University of Florida, Gainesville, FL,[2]Pharmacotherapy and Translational Research, University of Florida,*

Gainesville, FL,[3]University of Florida Health Jacksonville Radiation Oncology, University of Florida Health Proton Therapy Institute, Gainesville, FL

Even after radiation treatment, prostate cancer (PCa) patients receiving radiotherapy (RT) are still at risk for disease progression and recurrence. Predicting outcomes associated with cancer treatment is critical to PCa survivorship given that the 5-year survival rates for local and regional stage PCa is nearly 100%. Radiogenomics is a promising field of research focused on identifying genomic markers that can provide clinically useful prognostic predictions regarding radiation response and can potentially serve as the basis for personalized RT where cancer management is tailored to fit each individual patient. Circulating cell-free (ccfDNA) DNA has been found to 1) be associated with radiation sensitivity or toxicity, 2) relapse or recurrence, and 3) risk for the development of metastases before, during or following photon RT. Proton therapy, alternative to photon therapy, is a promising treatment that can reduce excess radiation dose and, in turn, the risk for adverse events. However, few studies have been done to determine if ccfDNA can predict response in proton radiation, which purports superior dose distribution, avoiding healthy tissues, minimizing the exit dose, and potentially reducing overall toxicity. The overall aim of this study is to determine if the quantity of ccfDNA is associated with PCa risk groups. We hypothesized that PCa patients within the highest risk group have quantitatively increased levels of ccfDNA compared to those in low and intermediate risk groups. This study leveraged the University of Florida Health Proton Therapy Institute Outcomes Tracking Protocol biobank of PCa patients with plasma and serum collected before, during and after proton RT. Isolation of ccfDNA at baseline, during treatment, and following treatment was undertaken and ccfDNA quantities were compared among patients in the low, intermediate and high risk groups using ANOVA. Our results indicate that the quantity difference between baseline and day 14 of treatment ($p=0.055$), 2 weeks post-treatment ($p=0.54$), and 4 weeks post-treatment ($p=0.002$) was associated with risk group. There was trend towards increasing ccfDNA quantity, as risk group increased; however, there was no correlation between risk group and treatment times using the Pearson correlation. Our results were consistent in that high ccfDNA quantity was associated with PCa risk. This is the first study determining the application of ccfDNA quantity on prostate cancer outcomes in patients undergoing proton RT. Identifying the determinants of radiation-related adverse outcomes will help inform impending predictive genomic technologies and improve cancer-related outcomes and survivorship.

#5595

Serial monitoring of circulating tumor cells and circulating tumor DNA in metastatic lobular breast cancer identifies intra-tumor heterogeneity and precision and immuno-oncology biomarkers of therapeutic importance

Andi K. Cani, Emily M. Dolce, Kevin Hu, Chia-Jen Liu, Elizabeth P. Darga, Dan Robinson, Yi-Mi Wu, Dafydd G. Thomas, Costanza Paoletti, Scott A. Tomlins, James M. Rae, Aaron M. Udager, Arul M. Chinnaiyan, Erin F. Cobain, Daniel F. Hayes. *University of Michigan, Ann Arbor, MI*

Precision and immuno-oncology clinical decisions are based on predictive biomarkers. Circulating biomarkers offer a minimally invasive approach to monitor intra-patient tumor heterogeneity and detect in real-time the clinically-relevant evolving clonal architecture. Although currently underutilized, single-cell DNA next generation sequencing of circulating tumor cells (CTC) is a particularly suitable method to complement tissue and circulating tumor DNA (ctDNA). Here we analyzed 113 individual CTC, 21 ctDNA, 15 white blood cells (WBC) samples and 15 tissue biopsies, from 15 CTC-positive lobular breast cancer patients. CTC were enriched with the CellSearch® system and isolated as single cells with the DEPArray™ system. CTC, WBC, and ctDNA underwent scNGS with the Oncomine Comprehensive Assay covering ~500 genes and 1.1Mb of genomic space to detect mutations, copy number alterations, tumor mutation burden (TMB) and microsatellite instability (MSI). 99.1% of single cells and 95.2% of ctDNA samples were informative. Our CTC-based precision medicine reporting platform, MI-CTCSeq, detected CTC in 9 of 15 patients (60%) with FDA-approved actionable alterations including in the oncogenes *PIK3CA* and *FGFR2* and HER2. 3 of these 9 (33%) harbored actionable alterations not shared between all 3 analyte types (tissue, CTC and ctDNA) including 3 actionable mutations found in CTC and ctDNA only, 1 in tissue and ctDNA only, and 1 in ctDNA only. Two of those ctDNA mutations were identified near the limit of detection and with a priori knowledge from tissue or CTC. Interestingly, 1 patient with plentiful CTC had no detectable ctDNA. Another patient's tissue biopsy was inadequate for sequencing while both liquid biopsy analytes were abundant. 13 patients (87%) displayed intra-patient, inter-CTC genomic heterogeneity of driver mutations. 1 of 4 (25%) patients with CTC available in >1 timepoint displayed fluctuations in their CTC subclonal makeup between timepoints. Data from this patient's 2 tissue biopsies, 4 ctDNA samples, and 27 individual CTC over 6

timepoints, combined to reveal in unprecedented detail inter-metastatic lesion and inter-CTC heterogeneity and evolution in response to endocrine, chemo and immunotherapy selective pressures. In a novel approach we show detection of single-cell CTC TMB and MSI. CTC TMB was highly concordant (R 0.81) with the corresponding tissue biopsies. Further, in a novel observation, we detected intra patient, inter-CTC heterogeneity of TMB and MSI, which has potential implications for immunotherapy response and development of resistance. Taken together, these data support the non-invasive biomarker interrogation and monitoring by liquid biopsy that incorporates CTC to complement tissue in informing treatment approaches.

#5596

Cell free DNA levels and fragmentation patterns in different liquid biopsy analytes (blood, urine and vaginal fluid) in cervical cancer patients

Sarah Tadhg Ferrier[1], Erica Mandato[1], Alexandra Bartolomucci[1], Thupten Tsering[1], Shuk On Annie Leung[2], Julia Valdemarin Burnier[1]. *[1]McGill University Health Centre Research Institute, Montreal, QC, Canada,[2]McGill University Health Centre, Montreal, QC, Canada*

Background**:** Cervical cancer (CC) is the 4th most commonly diagnosed cancer among women, with approximately 528,000 new cases annually. Current screening approaches for this disease have certain limitations; Pap tests require dedicated cytopathology infrastructure, while human papillomavirus (HPV) DNA testing may lead to invasive procedures in patients with transient infection. Liquid biopsy has emerged as a minimally invasive approach to detect and monitor disease progression and treatment response. We and others have previously demonstrated the clinical utility of circulating tumor (ct)DNA to monitor HPV+ cancers. Moreover, cell free (cf)DNA fragmentation patterns have been found to be a biomarker of disease burden. This cfDNA is thought to originate largely as a result of cell death, where small fragments of ~167 bp are associated with apoptosis and larger fragments (>1000 bp) are associated with necrosis. Despite advances in liquid biopsy techniques, little is known about the composition of cfDNA from different analytes in CC patients.
Methods: The aim of this study was to compare the presence and composition of cfDNA from different liquid biopsy analytes in patients with CC and high grade cervical intraepithelial neoplasia or dysplasia (CIN/CD). Blood, urine, and vaginal swabs were collected from 20 patients with CC and 9 patients with CIN/CD at the McGill University Health Centre. All samples were centrifuged twice to isolate supernatant. Samples were tested for HPV ctDNA by ddPCR. Analysis of fragment length was performed using the Agilent Bioanalyzer 2100. Dominant fragment was determined as the DNA fragment with the highest concentration, while overall fragment was calculated as the average fragment across all bioanalyzer peaks.
Results: HPV16/18 ctDNA was detectable 14/20 CC patients and 2/6 CIN patients, and 0/3 CD patients in plasma, urine, and vaginal swab. Concordance for all sample types tested was seen in 90% of cases. On average, fragment analysis demonstrated 174, 195, and 183 bp dominant small fragments in plasma, urine and vaginal swab, respectively. Plasma samples showed only smaller fragments (range: 168-187 bp). Other analytes displayed a predominance of larger cfDNA, with an overall fragment size of 3996 and 5194 bp in urine and vaginal swab, respectively.
Conclusions: HPV-DNA was detectable in all analytes sampled in patients with CC and CIN, with a trend of higher detection in CC samples. The fragmentation patterns of cfDNA varied between patients and within patients across analytes, with larger fragments - likely of necrotic origin - seen only in urine and vaginal swab cfDNA. Smaller fragments - likely related to apoptosis - were seen across all sample types studied. Overall, analysis of fragmentation may provide valuable insight into cfDNA origins in different sample types and provide a novel biomarker for diagnosis and surveillance.

#5597

Enhanced detection and classification of cell-free DNA alterations through matched normal analyses with PGDx elio™ plasma complete

Tonya N. Watkins, Paul McGregor, David Riley, Tolga Ayazseven, Kristy Waskiewicz, Kelly M. R. Gerding, Ellen L. Verner, Amy Greer, Aanavi Karandikar, Rami Zahr, Kenneth C. Valkenburg, Jamie Platt, Samuel V. Angiuoli, Mark Sausen. *RESEARCH AND DEVELOPMENT, Personal Genome Diagnostics, Baltimore, MD*

Liquid biopsies represent a transformation in the management of cancer as they have the potential to detect, characterize, and monitor cancers earlier than can be achieved with conventional diagnostic modalities. However, cell-free DNA (cfDNA)-based alterations can be derived from the tumor, germline, or may be associated with clonal hematopoiesis (CH), which can confound non-invasive tumor profiling, molecular response assessment, and

clonal evolution analyses through inaccurate variant classification. To facilitate global access to a decentralized liquid biopsy solution to address this, we developed and validated the 521 gene PGDx elio plasma complete test for paired analysis of cfDNA and matched leukocyte DNA. PGDx elio plasma complete enables detection of single nucleotide variants, insertions and deletions, copy number amplifications, translocations, microsatellite instability, blood tumor mutation burden, and loss of heterozygosity. We first optimized the assay workflow to incorporate genomic DNA derived from leukocytes to facilitate direct detection and characterization of germline alterations as well as those that may be associated with CH, resulting in de-duplicated, error-corrected sequencing coverage of approximately 1,750-fold. A fully automated bioinformatics algorithm was then developed and validated to perform integrated analyses of cfDNA-derived alterations to assign the appropriate biological source of these variants. To assess the impact of these paired sample analyses, we analyzed the blood samples obtained from 24 patients representing seven different solid tumor types (breast, colorectal, gastric, gastro-esophageal junction, lung, and melanoma). Across this cohort, of the alterations detected in cfDNA (n=322), 87.3% were correctly classified as somatic, germline or CH without the patient-matched normal blood sample. Specifically, of the variants that were determined to be associated with CH (n=26), only 35% were appropriately assigned without the paired comparison. Additional sources of discordance for somatic and germline alterations were primarily attributed to patients with high levels of ctDNA where differentiation of these variant sources can be challenging through solely computational-based techniques. Taken together, these data demonstrate that through the integrated analysis of cell-free DNA and matched leukocyte DNA, classification of the source of cfDNA-derived alterations can be achieved, which may improve the accuracy of non-invasive tumor profiling, molecular response assessment, and clonal evolution analyses.

#5598

Microfluidic isolation and capture of circulating tumor cells and clusters from mouse blood

Celine Macaraniag, Jian Zhou, Ian Papautsky, Jing Li, William Putzbach, Nissim Hay. *University of Illinois at Chicago, Chicago, IL*

Background**.** Circulating tumor cells (CTCs) and their clusters have been regarded as potential targets for therapies and subjects for identifying certain mechanisms of cancer metastasis. Mouse models have been especially useful tools to investigate the process of metastasis, since they are easier to control and are less variable compared to clinical patient samples. Therefore, it is of interest to extract and study CTCs and CTC clusters from such mouse models. However, most isolation systems are designed and tested for human blood and cell lines. Sized-based methods of CTC isolation have been optimized for human cell lines, but mouse CTCs are generally smaller in size (i.e., ~14 μm EO771 breast cancer cells). Therefore, mouse cell separation necessitates a varied protocol for CTC isolation. We used mouse blood and EO771, a mouse breast cancer cell line, to demonstrate the isolation of mouse CTCs from mouse blood using a sized-based microfluidic device. We also validated the presence of endogenous CTCs and CTC-neutrophil clusters in a tumor bearing mouse model.
Methods. Our microfluidic device employs inertial migration in a straight channel segment (150 μm × 50 μm × 24 mm) to isolate CTCs from blood samples. We spiked 100 and 1000 ZsGreen-expressing EO771 cells in 5× diluted blood containing tdTomato-expressing neutrophils, easily distinguishing CTCs from the red-colored neutrophils. To enumerate the recovered cells, we used Cytospin to concentrate the cells into a glass slide. Lastly, we used hydrodynamic traps to capture CTC clusters from tumor-bearing mouse blood. The blood was extracted from the posterior vena cava of the mice at the endpoint experiment.
Results. We achieved an overall recovery rate of 22-29%, which combines the recovery of the isolation device and the Cytospin. Here, we enumerate cells only after their extraction from the collection tube outside of the isolation device. Other methods with higher capture efficiency enumerate the recovered CTCs before they are harvested from the isolation device which is not always representative of the number of cells that are analyzed. We were also able to discover endogenous CTC-neutrophil clusters from tumor-bearing mice which we distinguished apart with anti-EpCAM staining of CTCs (green) and anti-Ly6G (red) staining of neutrophils.
Conclusion. We demonstrated and optimized a procedure for isolating mouse-derived CTCs from naïve mice blood and CTC-neutrophil clusters from tumor-bearing mice with our microfluidic isolation devices, as opposed to the isolation of human CTCs as in other sized-based isolation systems. In future studies, we aim to continue to use our microfluidic devices to capture and study CTC and CTC clusters.

#5599

An introduction of a highly sensitive circulating tumor DNA monitoring system for minimal residual disease detection using a library of 1000 digital PCR probes

Satoshi S. Nishizuka, Hayato Hiraki, Masakazu Abe, Akiko Yashima-Abo, Takeshi Iwaya. *Iwate Medical Univ., Yahaba, Japan*

Background: Many patients undergo a next generation sequencing (NGS)-based cancer genome profiling (CGP) test, but it often does not aid in choosing an optimal therapeutic regimen. Therefore, the genomic information should be used for minimal residual disease (MRD) detection, which directly leads to improved post-treatment cancer patient management. Circulating tumor DNA (ctDNA) is a small fraction of DNA present in blood that carries somatic mutations in cancer patients. Our previous studies demonstrated the clinical validity of ctDNA as a tumor marker for MRD detection. However, the variant allele frequency (VAF; reflecting the fraction of somatic mutations) of ctDNA is less than 1%, at which stable detection is difficult for NGS. Instead of NGS, we have established a highly sensitive ctDNA monitoring system for MRD detection using an originally developed library of >1000 digital PCR (dPCR) probes.
Patients and Methods: Using a Clinical Institutional Review Board approval from the Iwate Medical University Hospital, we initiated a dPCR assay system, called off-the-shelf (OTS)-Assay, in April 2022 under a partnership with Quantdetect, Inc (Tokyo, Japan). The OTS-Assay has three main components: OTS-Scan, OTS-Select, and OTS-Monitor. The OTS-Scan can provide an original CGP if a patient comes with no CGP results. The OTS-Select chooses matched somatic mutations from our dPCR probe library. The OTS-Monitor quantifies VAFs of ctDNA periodically in the patient plasma with a sensitivity of 0.05% VAF. There is no strict patient eligibility criteria other than the requirement of previous therapy for treatment of an advanced cancer.
Results: Between April and November 2022, 26 patients visited Iwate Medical University Hospital for the OTS-Assay. Twenty-five patients were referred from other Departments of Iwate Medical University Hospital. The primary cancer types include esophagus (n=21), colorectal (n=2), pancreas (n=2), and breast (n=1). Twenty patients had CGP results at their first visit. OTS-Select were used for 13 patients and picked an average of 11.4 mutations per patient. Among those, each of eight patients were immediately able to start ctDNA monitoring with one of the 1000 dPCR probes. As of November 2022, there are four patients who received OTS-Monitor more than one time. Any unexpected VAF increase of ctDNA has not been noted, although a substantial decrease of ctDNA VAF was found in one patient who received one cycle of chemotherapy.
Conclusion: The OTS-Assay is a practical introduction of our previous clinical research products based on a core technology, which uses an originally developed library of >1000 dPCR probes. The potential of early and accurate MRD detection will improve post-treatment cancer patient management.

#5600

Utility of circulating tumor DNA and transcriptomic profiling in predicting outcome in muscle invasive bladder cancer patients

Sia Viborg Lindskrog[1], George Laliotis[2], Karin Birkenkamp-Demtröder[1], Iver Nordentoft[1], Philippe Lamy[1], Elshaddai Z. White[2], Natalia Pajak[2], Tine G. Andreasen[1], Punashi Dutta[2], Meenakshi Malhotra[2], Shruti Sharma[2], Mark Calhoun[2], Adam ElNaggar[2], Minetta C. Liu[2], Mads Agerbæk[3], Jørgen B. Jensen[3], Lars Dyrskjøt[1].
[1]Department of Molecular Medicine, Aarhus University Hospital, Aarhus, Denmark,[2]Natera, Austin, TX,[3]Aarhus University Hospital, Aarhus, Denmark

Background: Standard treatment of localized muscle invasive bladder cancer (MIBC) is neoadjuvant chemotherapy (NAC) followed by radical cystectomy (RC); however, only 40-50% respond to NAC and approx. 50% experience relapse. Evaluation of treatment efficacy and early detection of relapse are therefore major clinical challenges.
Methods: We present a clinical update of a previously described cohort of 68 patients who received NAC prior to RC (NAC cohort; Christensen et al. JCO 2019; median follow-up (FU) of 58 months) together with evaluation of a retrospectively collected cohort of 120 patients who did not receive NAC (no-NAC cohort; median FU of 71 months). Circulating tumor DNA (ctDNA) was analyzed before NAC (NAC cohort, n=63), prior to RC (NAC cohort, n=67; no-NAC cohort, n=115) and after RC (NAC cohort, n=66; no-NAC cohort, n=37) using Signatera™. RNA-seq was performed on 176 tumors.
Results: Updated clinical FU for the NAC cohort showed that ctDNA-positive patients had significantly worse recurrence-free survival (RFS) compared to ctDNA-negative patients (before NAC: HR=16, 95%CI=3.6-70.5, p=0.0002; during surveillance after RC: HR=27.6, 95%CI=7.9-96.9, p<0.0001). After NAC prior to RC, 84% (52/62) of patients were ctDNA-negative, and of these 81% (42/52) achieved pathological complete response (pCR), while none of the ctDNA-positive patients achieved pCR (PPV 100%; NPV 81%). For the no-NAC cohort, presence of ctDNA was also prognostic at both time points (before RC: HR=2.5, 95%CI=1.4-4.4, p=0.001; single

time point after RC: HR=10.1, 95%CI=3.2-31.6, $p<0.0001$). In both cohorts, transcriptomic pathway analysis showed an enrichment of oncogenic pathways, namely EMT and hypoxia ($q<0.0001$), in tumors from ctDNA-positive patients (n=62/142). This may reflect a more aggressive cancer phenotype of ctDNA shedding tumors. Among those who were ctDNA-positive after NAC (n=7) we found enrichment of EMT ($q<0.0001$) and TGF-β signaling ($q=0.005$), whereas there was enrichment of anti-tumor immune pathways, including IFNα and IFNγ response ($q=0.03$ and $q=0.04$), in patients with ctDNA clearance after NAC (n=11). Similarly, we found upregulation of IFNα and IFNγ response pathways ($q<0.0001$) in ctDNA-negative patients without relapse in the no-NAC cohort (n=34/57). Finally, we classified all tumors according to the MIBC consensus classes and found more Ba/Sq tumors among the ctDNA-positive patients ($p<0.0001$). We are currently investigating the potential clinical benefit of receiving NAC in ctDNA-positive and -negative patients by comparing the NAC and no-NAC treated patients.
Conclusion: Presence of ctDNA was associated with worse prognosis for both NAC and no-NAC treated patients. Transcriptomic analysis of primary tumors showed that anti-tumor immune responses may be associated with a particularly good outcome whereas EMT may be promoting more aggressive disease.

#5601

Oncomine™ dx express CE-IVD liquid biopsy assay for non-small cell lung cancer: Performance review and analytical validation

Nicholas Siepert, Jeoffrey Schageman, Jian Gu, Thilanka Jayaweera, Madhu Jasti, Luming He, Stephen Wunch, Emilia Ostrowska, Tasha Delacour, Diarra Hassell, Thomas Bowden, Daniela Garcia, Stephanie Tong, Swasti Raut, Nader Ezzedine, Elliott Martinez, Kelli Bramlett. *Thermo Fisher Scientific, Austin, TX*

Introduct**ion -** Clinical diagnostics assays for oncology are becoming more readily available due to the advancement and democratization of Next-Generation Sequencing (NGS). Additionally, liquid biopsy can be used in NGS to detect genetic variants in circulating tumor DNA and RNA. Liquid biopsy is a less invasive option compared to traditional biopsy methods for early detection and continuous monitoring of cancer treatment outcomes. Here, we discuss screening of over 3,500 non-small cell lung cancer (NSCLC) samples, and the analytical validation of the Oncomine™ Dx Express Test (ODxET) and Genexus™ Dx Integrated Sequencer for detection of clinically significant variants in liquid biopsy samples.
Methods - Our team screened over 3,500 NSCLC liquid biopsy samples in search of high priority clinical variants. Variants selected for analytical validation studies included ERBB2 exon 20 insertion, EGFR exon 20 insertion, EGFR exon 19 deletion, EGFR T790M, KRAS G12C, BRAF V600E, and RNA fusion isoforms including ALK, NTRK1/2/3, RET, and ROS1 oncogenic drivers. Over 550 screened samples were found to be positive for these variants of interest. This screening was performed on the Genexus™ Dx Integrated Sequencer according to the user guide.
Results - The Genexus™ Dx Integrated Sequencer automates library preparation, sequencing, analysis, and reporting QC metrics and variant calls. Sequencing run setup is quick and straightforward, taking less than 15 minutes to start a run and just over 24 hours to go from nucleic acid to report. Limit of detection (LoD) for DNA SNVs, insertions, and deletions at 5 ng DNA input level ranged from 0.65% to 1.82% allelic frequency (AF), depending on the variant. The higher DNA input of 30 ng resulted in a lower LoD range, from 0.31% to 0.42% AF. RNA fusion and splice variant LoD at 5 ng sample input ranged from 9.9 to 19.6 molecular counts. The higher 30 ng input resulted in a lower LoD range for RNA variants as well, ranging from 6.4 to 8.0 molecular counts. In the analytical accuracy study, the false positive rate was found to be 0.2% for SNVs, 0% for insertions/deletions, and 0% for fusion targets. In the analytical reproducibility study, the average with-in run repeatability call rate (No Calls excluded) was 99.64% for DNA variants and 98.75% for RNA variants.
Conclusion - Here, we demonstrated that the ODxET workflow on Genexus™ Dx Integrated Sequencer is a fast and efficient tool for testing clinical NSCLC liquid biopsy samples with high sensitivity and specificity.
For in vitro diagnostic use. Not available in all regions including the United States.

#5602

Markers of hypoxic cells: Testing a pre-clinical detection assay

Beatriz Zayas, Karoline Rios, Luis Ortiz, Osvaldo Cox. *Science, Technology and Environment, University Ana G Mendez, San Juan, PR*

The proposed project aims to test the applicability of a novel set of patented organic compounds as markers of hypoxic circulating tumor cells (H-CTC) with potential pre-clinical relevance. Circulating tumor cells (CTC) are

individual cells or clusters that can move from tumors to circulation invading other tissues. Often cells in the tumor need to adapt to low oxygen levels, generating a population of cells known as hypoxic cells that can survive low oxygen levels. These hypoxic cells can produce more cell junction proteins, augmenting connections between cells causing them to break away in clusters rather than individually. Clustered CTCs are much more efficient at metastasis formation. Release of CTC can also be stimulated by cancer treatments such as radiation and chemotherapy. To date, our research has generated in-vitro studies with a set of 3-nitrobenzazolo[3,2-a]quinolinium chloride salts (NBQS) demonstrating its capacity as markers of hypoxic human cancer cells in vitro. Comparison with the control Pimonidazole demonstrated the advantages of novel NBQ-TOM compounds as hypoxic marker. We here, aim to test the applicability of NBQS to identify hypoxic cells among circulating tumor cells (H-CTC). To date limited commercially CTC detection methods are available. Our application can be described as pre-clinical detection technology of hypoxic cancer cells serving also in cancer management. To determine the capacity of novel compound, NBQ-345 TOM as hypoxic fluorescent marker, colon tumor cells (COLO 205) are culture under hypoxic and aerobic environment and treated with NBQ-345TOM (25uM) for 24 hours. After treatment fluorescence is measured with an OPTIMA BMG Fluorimeter. Fluorescence emission results demonstrated significant formation of the NBQ-234 TOM fluorescent metabolite on hypoxic tumor cells in contrast to cells treated under aerobic environment. Also, fluorescence microscopy analysis of colon cancer cells treated for 24 hours with NBQ-345 TOM at hypoxic and aerobic conditions confirmed the stronger fluorescence generation at hypoxic conditions in contrast to cells at aerobic conditions.

#5603

Functional studies on viable circulating tumor cells (v-CTCs) and frequent expression of PD-L1 on v-CTCs in pancreatic cancer

Masahiro Tanemura[1], Masaki Kashiwazaki[1], Kenichi Matsumoto[1], Kenta Furukawa[2], Manabu Mikamori[2], Tadafumi Asaoka[2], Daisaku Yamada[3], Shogo Kobayashi[3], Hidetoshi Eguchi[3]. *[1]Department of Surgery, Rinku General Medical Center, Izumisano, Japan,[2]Department of Surgery, Osaka Police Hospital, Osaka, Japan,[3]Department of Surgery, Osaka University Graduate School of Medicine, Suita, Japan*

Introduction: The analysis of CTCs as liquid biopsies provides the possibility to avoid invasive tissue biopsies, with obvious implications in cancer diagnostics and treatments. We tested new methods for v-CTCs detection in patients (pts) with pancreatic cancer (PC), and investigated the clinical potential of v-CTCs in prognosis. We analyzed the PD-L1(L1) expression in primary PC tumors, metastatic lymph nodes (LN) and v-CTCs.
Pts and Methods: 7.5 ml of venous blood was collected from 39 PC pts, either upfront surgery (U group) or pre-treatment, consisted of Gem:800mg/m^2; and S-1:80mg/m^2 given concurrently with IMRT to 60Gy ((NACRT:N group). To detect v-CTCs, we employed a telomerase-specific replication-selective adenovirus expressing GFP. For U group, samples were obtained before/after resection. For N group, samples were obtained before/after NACRT and after resection. To distinguish between leucocyte and cells with either epithelial or mesenchymal origin, cells were stained by anti-CD45, anti-Cytokeratin and anti-Vimentin Abs. GFP-positive and CD45-negative cells were counted as v-CTCs. To assess L1 expression in PC tissues (PC tumors and LN) and on v-CTCs, L1 IHC kit (22C3, for tissues) and anti-human L1 mAb(MIH1, for CTCs) were employed.
Results: U group: 24 pts aged 53~85 years (male/female=12/12) were enrolled. 24 pts underwent curative resection. No v-CTCs were detected in 6 pts at both before and after resection, and 5 of 6 pts survived without recurrence. V-CTCs were identified in 18 of 24 pts, and 13 of 18 pts developed liver metastasis. Marked decrease of CTC counts were seen after resection in 10 of 18 pts, but 9 pts developed recurrences. N group: 15 PC pts aged 44~77 years (male/female=4/11) were enrolled. 15 pts underwent curative resection. No v-CTCs at 3 sampling points were detected in 5 pts, and 5 pts survived without recurrences. V-CTCs was identified in 10 of 15 pts, and 4 out of 10 pts developed disease recurrence. Marked increase in CTC counts was observed after NACRT in 5 of 6 CTC-positive pts before NACRT, and 3 of 5 pts developed liver metastasis and died. NACRT may induce tumor cell dissemination into the blood circulation for CTC-positive pts. PD-L1 expression: L1 expression were assessed for 21 pts (U group:18, N group: 3). For PC tumors, L1 molecules were expressed in 12 pts and expression level of these pts were all low (57%, ≥50% [high]=0 pts, 1-49% [low]=12 pts {10%=6, 20%=4, 40%=2}, <1% [negative]=9 pts). For metastatic LNs, metastatic LNs were observed in 14 pts and L1-positive expression in these LNs were detected in only 4 pts (28%, all low expression). On the contrary, the majority of detected v-CTCs clearly expressed L1 molecule (92 CTCs out of 103 detected CTCs were L1-positive=89 %).
Conclusions: Viable CTC detection appears as a good prognostic marker. Immunotherapy with anti-PD-1/PD-L1 Abs may target v-CTCs, resulted in improvement of poor prognosis.

#5604

Circulating tumor DNA for predicting peritoneal only disease recurrence in colon cancer

Kevin C. Chang[1], Daniel Berg[2], Chandrika Chandrasekharan[2], Kelsey Steckly[2], Saima Sharif[2], Carlos H. F. Chan[2].
[1]Carver College of Medicine, University of Iowa, Iowa City, IA,[2]University of Iowa Hospitals and Clinics, Iowa City, IA

Background: Peritoneal Carcinomatosis in Colon Cancer (PCCC) is a major cause of morbidity. Early detection of PCCC is important for early intervention like systemic chemotherapy and cytoreductive surgery (CRS) +/- hyperthermic intraperitoneal chemotherapy (HIPEC). Circulating tumor DNA (ctDNA) testing is a promising method to assess recurrence not detectable yet on imaging, identifying 87.5% of recurrences in Stage I-III CRC with a mean lead-time of 8.7 months. It is unclear if ctDNA testing is sensitive in detection of recurrent PCCC ahead of clinical/radiological presentation.
We report data from 6 CRC patients with PCCC who underwent complete CRS and were followed with serial ctDNA testing.
Methods: In this single institution study, patients with PCCC were included from our prospectively enrolled GI cancer patient cohort (GIMER: IRB #201202743). Peritoneal carcinomatosis at CRS was determined using the Peritoneal Cancer Index. ctDNA concentration in mean tumor molecules/mL of plasma was assessed using a commercially available tumor-informed, personalized ctDNA assay (Signatera™, Natera, Inc.) that uses patient-specific somatic single-nucleotide variants. Plasma samples for ctDNA analysis were collected before surgery, 1, 2, 4, 6 months post-surgery, then every 3 months until a positive ctDNA test triggered CT imaging. Patients also had routine CT imaging every 6 months after surgery.
Results: 5 of 6 patients met endpoint with median time of 35 days from positive ctDNA to recurrence on imaging. In 4 patients, positive ctDNA prompted CT imaging which was negative, but follow-up PET scan was positive. Patient 6 was ctDNA negative and recurrence-free at last follow-up.
Conclusions: This analysis demonstrated the potential of longitudinal ctDNA monitoring for early detection of PCCC recurrence by prompting early imaging. PET was more sensitive in detecting recurrence than CT, and should be considered when determining PCCC recurrence. Enrollment and further analysis of ctDNA continues.

Table 1

Patient	Pre-op Chemo	Post-chemo, pre-op ctDNA	Peritoneal Cancer Index	Post-op (1m) ctDNA	2m ctDNA	4m ctDNA	6m ctDNA	9m ctDNA	12m ctDNA	15m ctDNA	Recurrence	Days between ctDNA positivity and positive imaging	Imagi Findir
1	Yes	0	5	0	0	0	0	0.48	-	-	Yes	6	CT C Positi
2	Yes	0	4	0	0	0	0.04	-	-	-	Yes	54	CT C Negat PET Positi
3	Yes	0.28	18	0	0	0	0	0.09	-	-	Yes	25	CT C Negat PET Positi
4	Yes	0	0	0	0	0	0	0	0	0.18	Yes	35	CT C Negat PET Positi
5	Yes	0.61	5	0	0	0.17	0	0.32	0.12	-	Yes	274	CT C Negat PET Positi

6	Yes	0	5	0	-	0	0	-	-	-	No	NA	CT C Negat to dat

#5605

Ambient storage and stabilization of proteins and cell-free nucleic acids in whole blood samples

Jing Li, Lisa Bartron, Jordan LaRue, Sama Mehta, Nicholas M. George. *Streck Laboratories, Inc.®, Omaha, NE*

Introduction: Highly anticipated advancements in biotechnology and instrumentation now allows for simultaneous detection of multiple biomarkers. This is accelerating the cancer research field towards the development of multianalyte-based *in vitro* diagnostic tests for early detection and/or monitoring of cancer. These multianalyte liquid biopsy tests are often based on detection of cancer-related proteins and/or tumor-specific genomic and transcriptomic changes (circulating cell-free nucleic acids) in plasma. A specialized and proprietary stabilization reagent has been developed for use in a blood collection tube with the capability to simultaneously stabilize protein biomarkers of interest and cell-free nucleic acids.
Methods: Blood samples from self-proclaimed healthy donors were drawn into evacuated blood collection tubes containing a new stabilization reagent and stored at room temperature. Plasma was isolated using a general double-spin protocol (1800 ×g for 15 min and 2800 ×g for 15 min) and frozen at -80 °C until use. Plasma levels of proteins of interest including cancer markers and immuno-oncology checkpoint markers were measured by Ella Simple Plex Assays (Bio-Techne) and Luminex xMAP® Technology Assays (Bio-Techne, samples tested by LuminexPLORE Lab). Total cell-free nucleic acids were isolated using the QIAamp Circulating Nucleic Acid Kit and the resultant cfDNA or cfRNA was analyzed with fluorometric-based assay (quantitative) and Bioanalyzer / Tapestation (qualitative).
Results: Compared with blood samples collected in EDTA and ACD-A tubes, the new stabilization reagent maintained the draw time levels of plasma proteins of interest such as TGF-β1, MMP-9, IL-8/CXCL8, CCL5/RANTES, Granzyme B, CEA and PD-L1 for up to 5 days of room temperature storage in whole blood. The reagent also effectively maintained draw time levels of plasma cell-free nucleic acids to near draw time levels. In addition, the new reagent also minimized *in vitro* hemolysis during room temperature storage.
Conclusion: This new and breakthrough stabilization reagent simultaneously maintains the draw time levels of proteins of interest and cell-free nucleic acids for an extended period of time in whole blood. It provides cancer researchers and clinical assay developers confidence in blood sample integrity and flexibility in sample storage, transport, and processing at ambient temperature for multianalyte analysis or multiomics profiling.

#5606

Dynamics of sequence and structural cell-free DNA landscapes in small-cell lung cancer during systemic therapy

Lavanya Sivapalan[1], Wade T. Iams[2], Zineb Belcaid[1], Susan C. Scott[1], Noushin Niknafs[1], Archana Balan[1], James R. White[1], Prasad Kopparapu[2], Christopher Cann[2], Blair V. Landon[1], Gavin Pereira[1], Victor E. Velculescu[1], Christine L. Hann[1], Christine M. Lovly[2], Valsamo Anagnostou[1]. *[1]The Sidney Kimmel Comprehensive Cancer Center, Johns Hopkins University School of Medicine, Baltimore, MD,[2]Division of Hematology-Oncology, Department of Medicine, Vanderbilt University Medical Center and Vanderbilt-Ingram Cancer Center, Nashville, TN*

Background: Patients with small-cell lung cancer (SCLC) have an exceptionally poor prognosis and may not always undergo biopsies for molecular testing, necessitating real-time non-invasive biomarkers of early therapeutic response to ultimately enable timely intervention and improve patient outcomes.
Methods: We performed targeted error-correction sequencing on serial plasma cell-free DNA (n=139) and matched white blood cell (WBC; n=32) DNA from 33 patients with metastatic SCLC who received treatment with chemotherapy (n=16) or immunotherapy-containing (n=17) regimens. Tumor-derived sequence mutations and plasma aneuploidy were tracked longitudinally using a tumor-agnostic WBC DNA-informed approach and combined to evaluate changes in total cell-free tumor load (cfTL). Dynamic changes in cfTL were monitored for each patient to determine circulating tumor DNA (ctDNA) molecular response during therapy.
Results: Longitudinal assessment of cfTL dynamics allowed for the evaluation of molecular response in all patients studied. Overall, 9 patients were classified as molecular responders based on sustained complete

elimination of cfTL. For 14 patients, we observed initial molecular responses, followed by cfTL recrudescence. In a subset of 10 patients we observed a distinct pattern of molecular progression characterized by cfTL persistence across all timepoints analyzed. Patients with sustained molecular responses attained longer overall (OS; log-rank p=0.0006) and progression-free (PFS; log-rank p<0.0001) survival, with molecular responses detected on average 4 weeks earlier than imaging. Importantly, ctDNA molecular response remained the most significant predictor of OS (molecular response vs molecular progression HR=0.09, 95% CI=0.02-0.42, p=0.002; molecular response f/b recrudescence vs molecular progression HR=0.14, 95% CI=0.04-0.48, p=0.002) and PFS (molecular response vs molecular progression HR=0.02, 95% CI=0.00-0.16, p<0.001; molecular response f/b recrudescence vs molecular progression HR=0.05, 95% CI=0.01-0.26, p<0.001) after adjustment for clinical covariates in a multivariate cox proportional hazards regression model. Analysis of landmark OS and PFS endpoints revealed that molecular responses more accurately predicted OS at 12 (AUC 78.1% vs 73.3%) and 64 months (AUC 87.3% vs 67.6%) and PFS at 3 (AUC 91.7% vs 82.0%) and 12 months (AUC 83.5% vs 78.8%) compared to conventional imaging. Conclusions: Longitudinal tracking of sequence and structural ctDNA features provide an accurate and rapid approach to track changes in tumor burden and prognosticate outcomes during systemic therapy in patients with SCLC. These findings suggest that therapeutic response monitoring based on combined molecular response criteria may be used to provide guidance on clinical decision making for patients with SCLC.

Molecular Targeted Therapies 2

#4476

BI-732, a novel fourth-generation EGFR-TKI, demonstrates promising activities against the C797S-mediated EGFR-TKI resistance

Eun Ji Lee[1], Jiyun Lee[2], Seung Yeon Oh[1], You Won Lee[3], Ju young Kim[3], Su-Jin Choi[3], Sewon Park[4], Mi Ra Yu[3], Jae Hwan Kim[5], Kyoung-Ho Pyo[6], Jii Bum Lee[7], Min Hee Hong[7], Sun Min Lim[7], Anke Baum[8], Lydia Woelflingseder[8], Harald Engelhardt[8], Mark Petronczki[8], Flavio Solca[8], Mi Ran Yun[9], Byoung Chul Cho[7].
[1]Department of Biomedical Science institute, Graduated School of Medical Science, Brain Korea 21 FOUR Project for Medical Science, Yonsei University College of Medicine, Seoul, Korea, Republic of,[2]Lung Cancer Center, Yonsei Cancer Center, Yonsei University College of Medicine, Seoul, Korea, Republic of,[3]Department of Research Support, Yonsei Biomedical Research Institute, Yonsei University College of Medicine, Seoul, Korea, Republic of,[4]JEUK Institute for Cancer Research, JEUK Co., Ltd., Gumi, Korea, Republic of,[5]Severance Biomedical Science Institute, Yonsei University College of Medicine, Seoul, Korea, Republic of,[6]Yonsei New Ii Han Institute for Integrative Lung Cancer Research, Yonsei University of Medicine, Seoul, Korea, Republic of,[7]Division of Medical Oncology, Department of Internal Medicine, Yonsei Cancer Center, Yonsei University College of Medicine, Seoul, Korea, Republic of,[8]Boehringer Ingelheim RCV GesmbH & Co KG, Vienna, Austria,[9]Severance Biomedical Science Institute, Yonsei University College of Medicine, Seoul, Republic of Korea, Seoul, Korea, Republic of

Introduction: Epidermal growth factor receptor (EGFR) tyrosine kinase inhibitors (TKIs) is a standard modality of the 1st-line treatments for patients with EGFR-mutated non-small-cell lung cancer (NSCLC). The FDA approved osimertinib, a third-generation EGFR-TKI, is highly selective for EGFR-activating mutations (exon 19 deletion [del19] or L858R point mutation in exon 21 [L858R]) as well as EGFR-T790M mutation. Nevertheless, resistance inevitably emerges and leads to disease progression. Acquired EGFR-C797S mutation is the most common on-target resistance mechanism to osimertinib in first- and second-line settings, and there are currently no approved targeted therapies. We aimed to evaluate the efficacy of BI-732, a fourth-generation EGFR-TKI developed to overcome the C797S mutation. Materials and Methods: We constructed several types of Ba/F3 cells expressing EGFR mutations containing the C797S mutation as follows: EGFRdel19/C797S, EGFRL858R/C797S, EGFRdel19/T790M/C797S, and EGFRL858R/T790M/C797S. We also constructed PC9 cells harboring EGFRdel19/C797S (named PC9-DC cells) using the CRISPR/Cas9 system. Furthermore, we generated two patient-derived cells, YU-1097 with EGFRdel19/T790M/C797S and YU-1182 with EGFRL858R/C797S. The in vitro efficacy of BI-732 was tested in several cell lines harboring the EGFR-C797S mutation mentioned above. We further evaluated in vivo antitumor activity of BI-732 in subcutaneous YU-1097 xenograft model and intracranial YU-1097-tumor model.Results: BI-732 effectively inhibited the viability of Ba/F3 cells expressing EGFRdel19/C797S (IC50, 6.8 nM), EGFRL858R/C797S (IC50, 213.4 nM), EGFRdel19/T790M/C797S (IC50, 3.8nM), and EGFRL858R/T790M/C797S (IC50, 15.2 nM), concomitant with marked reduction in EGFR and downstream signal phosphorylation. Moreover, BI-732 exhibited comparable nanomolar in vitro activity to

osimertinib on EGFR activating mutation while sparing wild-type EGFR activity. We further confirmed the superior antiproliferative efficacy of BI-732 in PC9-DC (IC50, 24.9 nM), YU-1182 (IC50, 73 nM) and YU-1097 cells (IC50, 2.9 nM). Oral administration of BI-732 at a concentration of 25 mg/kg as a single agent resulted in significant tumor regression with 183.2% tumor growth inhibition (TGI) in the subcutaneous YU-1097 xenograft model. In a combination treatment strategy with osimertinib, BI-732 showed enhanced antitumor activity at much lower concentrations than monotherapy. BI-732 also demonstrated the ability to penetrate brain-blood barrier (BBB) in the intracranial YU-1097-tumor models.Conclusions: BI-732 is a potent, selective, and orally available fourth-generation EGFR-TKI for EGFR mutations including C797S and has efficient BBB penetration. Our findings suggest that BI-732 can be effective against EGFR mutant NSCLC, especially EGFRDel19/T790M/C797S and EGFRDel19/C797S, that have progressed with previous EGFR inhibitors.

#4477

DIACC3010, optimized inhibitor of S6 kinase, combined with endocrine therapy, has potent antitumor activity in treatment-resistant ER-positive HER2-negative metastatic breast cancer

Christel Navarro[1], Apostolia Maria Tsimberidou[2], Cecile Bougeret[1], Elsa Borghi[1], Dominique Bridon[1], Helene Sicard[1]. *[1]DIACCURATE, Paris, France,[2]Investigational Cancer Therapeutics, The University of Texas, MD Anderson Cancer Center, Houston, TX*

Background: Ribosomal protein S6 kinase (S6K) is a key regulator of estrogen receptor (ER) function, and its high expression is associated with poor clinical outcomes in breast cancer (BC). Recent data have demonstrated that S6K is involved in resistance to CDK4/6 inhibitors in metastatic BC (MBC). DIACC3010 (formerly M2698) is an oral brain-penetrant potent inhibitor of S6K. By design, DIACC3010 also selectively inhibits AKT1 and AKT3, while sparing AKT2. DIACC3010 was previously evaluated in a phase 1 trial (NCT01971515). We performed exploratory correlative analyses of the phase 1 trial in ER+ HER2-negative MBC patients in addition to nonclinical experiments to evaluate its role in the CDK4/6 and endocrine therapy (ET) resistant setting.
Methods: DIACC3010 was evaluated as monotherapy, or combined with either trastuzumab or tamoxifen, in a multicenter phase 1 trial that accrued 101 patients with advanced/refractory solid tumors (Tsimberidou et al, J Hematol Oncol 2021 14(1):127). The current analysis focused on patients with ER+ HER2-negative MBC and aimed to explore the efficacy of DIACC3010 according to *ESR1* mutational status. DIACC3010 was also evaluated in tamoxifen resistant patient-derived xenograft (PDX) mouse models, both alone and combined with tamoxifen.
Results: Twenty patients were evaluable at baseline for their tumor mutational status and included in the analysis. Median age was 60 years and median number of prior lines of therapy was 5.5. Twelve of 20 (60%) patients had received prior treatment with CDK4/6 inhibitors. Nine of 20 patients (45%) had *ESR1* mutations, of whom 4 had received CDK4/6 inhibitor. Median progression free survival was 5.6 months in patients with *ESR1* mutations, and 2.6 months in patients with *ESR1* wild-type tumors. Among the 13 ER+ BC PDX models evaluated, 10 provided interpretable results and 4 were found resistant to tamoxifen. The combination of DIACC3010 and tamoxifen significantly reduced tumor growth in 6/10 (60%) of all PDX models, and in 4/4 (100%) of the tamoxifen-resistant PDX models.
Conclusions: Exploratory analyses from the phase 1 trial, along with nonclinical efficacy in PDX models, demonstrate that DIACC3010 may have antitumor activity in MBC patients with ET resistance. Experiments are underway to assess nonclinical efficacy of DIACC3010 combination with elacestrant or CDK4/6 inhibitors in various models of ER+ MBC, including ET resistant.

#4478

Up284, A small molecule inhibitor of ADRM1 demonstrates significant anti-tumor efficacy in preclinical models of aggressive breast cancer

Balasubramanyam Karanam[1], Ravi Anchoori[2], Yung-Nien Chang[2], Rachel Martini[3], Florencia Madorsky Rowdo[4], Melissa B. Davis[4]. *[1]Tuskegee University, Tuskegee, AL,[2]Up Therapeutics LLC, Frederick, MD,[3]Surgery, Weill Cornell Medicine, New York, NY,[4]Englander Institute for Precision Medicine, Weill Cornell Medicine, New York, NY*

Quadruple-negative breast cancer (QNBCs) is a highly aggressive and metastatic disease and remains clinically challenging breast cancer subtype with worst prognosis. Due to its exceeding heterogeneity, absence of the AR, ER, PR, Her2 receptors and lack of established therapeutic targets, QNBC is hard to treat cancer and recurs rapidly

with standard chemo regimen. QNBC demonstrated vulnerability to proteasome inhibition due to their higher metabolic needs. But FDA approved 20S proteasome inhibitors failed to treat solid tumors including QNBC. Hence, developing an effective strategy to overcome the limitations associated with current 20S proteasome inhibitors is mandated to provide alternate treatment options for QNBC patients. Preclinical, Up Therapeutics lead candidate small molecule inhibitor Up284 has shown significant tumor growth inhibition as a single agent in animal models. To explore potential synergy of Up284 with other therapeutic agents, we conducted the in vivo combination experiments. In this work, we present ADRM1 amplification in QNBC tumors, identification of a small molecule selective inhibitor of ADRM1, Up284 (Up Therapeutics), Up284 demonstrated efficacy against panel of BC cell lines and patient derived organoids. In vivo combination results for Up284 with widely used BC standard-of care chemotherapy regimen demonstrated strong in vivo synergy in tumor mouse syngeneic models. Taken together, these data demonstrated combination synergy of a small molecule ADRM1 inhibitor with other agents. These results pave the road for potential clinical evaluation of combination treatment of QNBC in patients.

#4479

Targeting of eIF4A1 curtails lung metastases in triple-negative breast cancer

Sangita Sridharan[1], Shobhit Srivastava[1], David Terrero[2], Saloni Malla[2], Amit K. Tiwari[3], Dayanidhi Raman[1]. *[1]Cell and Cancer Biology, University of Toledo Health Science Campus, Toledo, OH,[2]Pharmacology & Experimental Therapeutics, University of Toledo, Toledo, OH,[3]Pharmacology and Experimental Therapeutics, University of Toledo, Toledo, OH*

Triple-negative breast cancer (TNBC) is an aggressive type of breast cancer. Patients diagnosed with TNBC benefit less or none from any current targeted therapies and also the standard-of-care neoadjuvant chemotherapies (NACT) which is cytotoxic. TNBC shows an increased risk of tumor relapse, therapy failure, and high proclivity to develop distant metastases. Intrinsic resistance to NACT is mainly due to a small population of breast cancer cells that acquire stem cell-like features (BCSCs). BCSCs are capable of self-renewal, proliferation, plasticity, immune regulation and chemoresistance. These properties mediate tumorigenesis, metastasis, and resistance to NACT and sometimes even to targeted therapy. Overall, FDA-approved drugs that are effective for advanced TNBC are currently unavailable.

The eukaryotic translation initiation factor (eIF4A1) is an mRNA helicase that catalyzes the ATP-dependent unwinding of many oncogenic mRNAs which harbor secondary structures in the 5' leader region. There is preferential reliance on eIF4A1 by tumor cells as many oncogenic mRNAs require the helicase activity of eIF4A1 for their efficient translation. Several eIF4A1-dependent mRNAs (downstream effectors) include: survivin (survival), c-MYC, STAT1 (immunoevasion through transcription and subsequent translation of PD-L1), Rho kinase1 (invasion), and Cyclins D1 and D3. Bioinformatic analyses revealed that higher gene expression of eIF4A1 significantly impacts patient survival. Clinically, an enhanced protein expression of eIF4A1 was evident in histopathologic analyses of drug-resistant human TNBC biospecimens. Importantly, our *in vitro* data indicated that the viability of BCSCs was significantly reduced when eIF4A1 is targeted by nanomolar levels of Rocaglamide A (RocA). Furthermore, in paclitaxel-resistant TNBC cells, there is an upregulation in the total levels of eIF4A1 and its downstream effectors. Pluripotency transcription factors (e.g., SOX2, OCT4 and NANOG) and drug transporters (ABCB1, ABCG2 and ABCC1) were also increased in an eIF4A1-dependent manner. Genetic ablation and pharmacological targeting of eIF4A1 with RocA reversed the drug-resistant profile. Our *in vitro* data implied a key role for eIF4A1 in chemoresistance/therapy failure. Targeting of eIF4A1 may be an effective anti-cancer strategy to overcome drug resistance. To this end, we orthotopically implanted CRISPR-control (CC) and eIF4A1-KO (KO) human TNBC cells and evaluated the primary tumor progression and metastases in NOD/SCID-*beige* mice. Longitudinal tumor progression was followed by IVIS imaging. The tumor volume and the wet weight was significantly higher in CC than KO tumors (n=7 mice). Similarly, the lung metastatic burden is significantly low in KO than CC mice (n=7 mice; $p<0.002$)). Taken together, we propose that eIF4A1 is an actionable molecular target for drug-resistant TNBC using chemotherapy/immunotherapy.

#4480

Treatment of PTEN/PI3K co-mutated endometrial adenocarcinoma with multitarget small molecule inhibitors

Ritchie Delara[1], Cody McHale[2], Dhananjaya Pal[2], Krishnaiah Maddeboina[2], R. Wendel Naumann[1], Erin Crane[1], Jubilee Brown[1], Donald Durden[2]. *[1]Division of Gynecologic Oncology, Levine Cancer Institute, Charlotte, NC,[2]Molecular Targeted Therapeutics Laboratory, Levine Cancer Institute, Charlotte, NC*

Introduction: The objective of this study is to assess the feasibility and safety of treating endometrial adenocarcinoma (EC) with multitarget inhibitors which orthogonally target known oncogenic kinases and epigenetic regulators. The Molecular Targeted Therapeutics Laboratory has developed nanomolar potent multitarget small molecule chemotypes that inhibit the PI3K/Akt/mTOR pathway, cancer-associated kinases, and epigenetic regulatory proteins such as BRD4 *in vitro* and *in vivo*.
Methods: Two EC cell lines (AN3-CA, RL95-2) were treated with varying concentrations of triple PI3K/BRD4/CDK4/6/9 inhibitor LCI132 and dual PI3K/CDK4/6/9 inhibitors LCI133 and LCI136 for 48 hours; and cell viability assays were performed with IC_{50} determination. EC cells were treated with multitarget inhibitors and other indicated inhibitors of PI3K, BET, CDK4/6, and CDK9 for 24 hours; and lysates were prepared accordingly for Western blot (WB) and qRT-PCR analyses. Flow cytometry was conducted for cell cycle and apoptosis assays.
Results: In cell-free assays, LCI132 is a nanomolar inhibitor of PI3K/BRD4/CDK4/6/9, LCI133 is a picomolar inhibitor of CDK9, and LCI136 is a nanomolar inhibitor of PI3K and CDK9. LCI133 demonstrated nanomolar potency towards AN3-CA (IC_{50} 248 nM) and RL95-2 (IC_{50} 105 nM). LCI136 demonstrated nanomolar potency towards AN3-CA (IC_{50} 631 nM) and RL95-2 (IC_{50} 728 nM). WB demonstrated 24-hour treatment of *FBXW7mut* AN3-CA with LCI132 inhibited AKT phosphorylation but an increase in c-MYC protein expression. A corresponding increase in c-Myc gene expression at 24 hours was confirmed on qRT-PCR. In *FBXW7wt* RL95-2, LCI132 decreased c-Myc protein expression. LCI132 demonstrated dose-dependent G1 arrest, and dose-dependent pre-apoptotic and apoptotic activity.
Conclusions: Dual-target inhibitors LCI133 and LCI136 are nanomolar potent in AN3-CA and RL95-2 EC cell lines, suggesting a role of CDK9 inhibition of PTEN/PI3K co-mutated EC. Preliminary studies demonstrate an upregulation of MYC gene and protein expression in *FBXW7mut* EC but not *FBXW7wt*, and the role of FBXW7 as a predictive biomarker in treatment of PTEN/PIK3R1 co-mutated EC warrants further investigation.

#4481
Vrtx153, novel small molecule inhibitor of krasg12d
Prashant Kashinath Bhavar[1], Uday Kumar Surampudi[1], Partha Pratim Sarma[2], Anuj Ramesh Kshirsagar[2]. *[1]VRise Therapeutics Inc., Cambridge, MA,[2]VeGen Therapeutics, Hyderabad, India*

Pancreatic cancer is an intractable malignancy and is the seventh leading cause of global cancer deaths in industrialized countries and the third most common in the USA. Despite advancement in the knowledge of potential risk factors that cause pancreatic cancer and newly available tools for early diagnosis, its incidence is estimated to increase and will include 0.35 mln new cases within 2040. *KRAS* is the predominant isoform mutated in cancer and are found in 92-95% of Pancreatic Cancer patients, dominated by somatic mutations of $KRAS^{G12D}$. $KRAS^{G12D}$, is one of the most frequently mutated oncogenes across adenocarcinoma of *Pancreas (51%), Colon and Rectal (13.4%) and Lung (3%)*. With KRAS mutations found in nearly all PDAC, this cancer type is arguably the most *RAS*-addicted cancer. $KRAS^{G12D}$ is a clinically relevant target but owing to structural complexity of the protein, poses challenges for its effective inhibition. Previously, we reported a series of compound including a proprietary tool compound *VTRX144*, with low nM potency in 2D (<25 nM). Optimized lead from VRise de-novo platform has yielded an unparallel potent, highly selective, inhibitor, namely *VRTX153*. *VRTX153* demonstrated high-affinity for $KRAS^{G12D}$ in a GDP-loaded $KRAS^{G12D}$ assay, with an IC50 value of less than 2 nM and more than1500 -fold selectivity over $KRAS^{WT}$, KRAS mutants and other RAS proteins including HRAS & NRAS. VRTX153 inhibited ERK1/2 phosphorylation (pERK) and cell viability in $KRAS^{G12D}$-mutant cell lines in both 2D and 3D, as evaluated by CellTiter-Glo®. In-vivo translation of activity in a mouse xenograft model representing PDAC is being investigated.

#4482

Discovery of GH2616, a potent and selective KIF18A inhibitor with robust *in vivo* efficacy in p53 mutant cancer

Jie Jack Li, Guiping Zhang, Jiapeng Li. *Suzhou Genhouse Pharmaceutical Co., Ltd., Suzhou, China*

Chromosomal instability (CIN) is one of the hallmarks of cancer. Cancer cells often undergo whole-genome doubling (WGD) and P53 represents a major barrier to the proliferation of WGD+ cells. Therefore, cancer cells with either CIN or WGD often harbor the p53 mutation. Recently, KIF18A has emerged as a potential therapeutic target in CIN or WGD cancer cells. We have identified a potent and selective KIF18A inhibitor, GH2616. *In vitro*, GH2616 inhibited the kinesin motor activity with an IC_{50} less than 50 nM, and with an EC_{50} less than 50 nM in the mitotic index assay using HT29 cells (WGD). *In vivo*, GH2616 inhibited the growth of WGD CDX models with a dose dependent manner. GH2616 has good oral bioavailability in different species and metabolic stability for QD dosing. This compound also showed low potential of DDI thus suitable for drug combinations. In a cell panel with more than 200 cell lines, GH2616 selectively inhibit the growth of cells with p53 mutant and some other specific biomarkers in multiple tumor types. In conclusion, we discovered GH2616 as a novel KIF18A inhibitor with potent *in vivo* efficacy. It is currently under evaluation in IND-enabling studies and IND filing is expected in Q4, 2023.

#4483

Distinct spatial distribution patterns of ALK-inhibitor naïve versus ALK-inhibitor treated ALK-positive NSCLC brain metastases

Tia Cheunkarndee[1], Paola Ganem[2], Kristen A. Marrone[2], Joseph C. Murray[2], Josephine L. Feliciano[2], Christine L. Hann[2], Susan C. Scott[2], David Ettinger[2], Valsamo Anagnostou[2], Patrick M. Forde[2], Julie R. Brahmer[2], Benjamin P. Levy[2], Vincent Lam[2], David O. Kamson[3]. *[1]Johns Hopkins University School of Medicine, Baltimore, MD,[2]Thoracic Oncology, Johns Hopkins University School of Medicine, Baltimore, MD,[3]Neuro-Oncology, Johns Hopkins University School of Medicine, Baltimore, MD*

Background: Non-small cell lung cancer (NSCLC) with anaplastic lymphoma kinase rearrangement (ALK+) has a high affinity to form brain metastases (BrM). The cumulative incidence of BrMs in ALK+ lung cancer is over 50%, despite highly effective ALK tyrosine kinase inhibitors (TKIs) with CNS activity. Pharmacokinetic (PK) data from other CNS-active lung cancer TKIs (e.g., osimertinib) have revealed major brain white vs. gray matter drug concentration differences, raising the possibility of a PK-driven effect on BrM formation and response. This study aims to compare the size and distribution of ALK+ NSCLC BrMs at diagnosis in a TKI-naïve and TKI-exposed cohort.

Methods: We retrospectively reviewed brain MRIs from the date of BrM diagnosis for patients with ALK+ NSCLC at Johns Hopkins. Demographic and clinical information were collected by chart review. Each tumor was marked in a standard space brain model in the corresponding anatomic location represented by a sphere of corresponding diameter using 3D Slicer 4.11. FreeSurfer white-gray matter atlases were used to assess BrM distribution. The data for patients who were on TKI vs TKI-naïve at the time of BrM diagnosis were then analyzed separately. T-tests were used to compare the metastatic burden (sum of BrM diameters), mean BrM diameter per patient, number of BM per patient, per individual mean of *white matter exclusive* (defined as no overlap with gray matter) and *deep white matter* (≥5mm away from gray matter) BrMs between patient groups.
Results: 429 BrMs were identified in 39 patients, with 25 patients being TKI-naïve at the time of BrM diagnosis while 14 patients were on TKI therapy. TKI-exposed patients had significantly smaller BrM diameters than those in the TKI-naïve group (6.1±3.8 vs 10.2±5.5mm, p=0.02). While metastatic burden was very similar between the groups, the mean number of BrM per patient was numerically higher in the TKI-exposed group (10.6±11.9 vs 6.2±9.5; p=0.22). Notably, patients in the TKI-exposed group also had higher numbers of white matter exclusive (3.5±4.4 vs 1.4±2.0, p=0.05) and deep white matter metastases (3.2±4.3 vs 1.3±2.0, p=0.06) than those who were TKI-naïve.
Conclusion: Our data highlight the differences in BrM characteristics among ALK+ NSCLC exposed to ALK TKI. TKI therapy was associated with similar BrM burden but smaller individual lesions that were more likely to be exclusive to the white matter where drug concentrations might be significantly lower. These findings suggest that suboptimal drug CNS distribution in the white matter may underly brain progression of ALK+ NSCLC despite TKI therapy. Spatial analyses evaluating ALK TKIs of varying CNS penetrance and later disease time points in more granular anatomic regions are ongoing.

#4484

HER3 expression after systemic therapy and clinical characteristics in patients with hepatocellular carcinoma

Mao Okada[1], Chigusa Morizane[1], Tomoyuki Satake[1], Mariko Nishioka[1], Nobuyoshi Hiraoka[2], Satoshi Nara[3], Tomoya Kakegawa[4], Maki Kobayashi[4], Kumiko Koyama[5], Minoru Esaki[3], Takuji Okusaka[1].
[1]Department of Hepatobiliary and Pancreatic Oncology, National Cancer Center Hospital - Japan, Tokyo, Japan,[2]Division of Pathology and Clinical Laboratories, National Cancer Center Hospital - Japan, Tokyo, Japan,[3]Department of Hepatobiliary and Pancreatic Surgery, National Cancer Center Hospital - Japan, Tokyo, Japan,[4]Translational Research Department, Daiichi Sankyo RD Novare Co., Ltd., Tokyo, Japan,[5]Translational Science Department I, Daiichi Sankyo Co., Ltd., Tokyo, Japan

Background: In hepatocellular carcinoma (HCC), several standard regimens with angiogenesis inhibitors and immune checkpoint inhibitors have been established; however, novel therapeutic strategies to target key molecules associated with HCC are further required to improve treatment options. ErbB3 (HER3), a member of the HER receptor tyrosine kinase family, has recently emerged as a promising therapeutic target in various cancers. In this study, HER3 expression status after current targeted therapies in HCC was evaluated in order to explore an opportunity for developing anti-HER3 therapy for HCC.
Methods: We collected clinical data and tumor tissue from HCC patients (pts) who received systemic therapy between January 2010 and June 2020 and the tissue samples at post systemic therapy were also obtained. Immunohistochemical staining for HER3 was conducted using HER3/ErbB3 (D22C5) XP Rabbit mAb (Cell Signaling Technology) as a primary antibody. IHC scoring (0, 1+, 2+, 3+) of membranous staining intensity was performed according to HER2 IHC gastric scoring guideline.
Results: Seventeen pts were eligible. Eight pts (47%) were HER3 2+/3+, (2+: 7, 3+: 1,), while nine pts (53%) were 0/1+ (0: 4, 1+: 5). For HER3 2+/3+ and HER3 0/1+ groups, median age (range) was 63(43-71)/69(47-78), median alpha-fetoprotein levels were 6071(4-23620)/19.1(1.2-1138) [ng/ml], and median des-gamma-carboxy prothrombin levels were 1351(135-92650)/302(10-10916) [mAU/ml], respectively. The proportions of patients with HER3 2+/3+ were 67% in HCV+ pts, 25% in HBV+ pts, and 43% in other etiologies. Median overall survival of HER3 2+/3+ and 0/1+ pts after start of first line systemic therapy was 32.3 (95% CI: 8.7-51.4) and 12.9 (95% CI: 6.1-20.7) months, respectively (HR: 0.28, 95% CI: 0.09-0.92,

p=0.036).Paired pre- and post-treatment samples were available for eight pts. The median number of regimens administered between the pre- and post-treatment samples was 2(1-5). Treatment regimens were sorafenib: 7; lenvatinib: 2; ramucirumab: 1; others: 10, including duplicates. At post-treatment, HER3 was upregulated in 4 pts (1 pt: 0 to 1+, 3 pts: 1+ to 2+) and downregulated in 3 pts (all pts: 1+ to 0). Pts with HER3 upregulation had developed resistance after at least one prior tyrosine kinase inhibitor (TKI) with stable disease or partial response as best response.
Conclusion: In this study, 47% of pts were HER3 2+/3+ at post-treatment. In paired analysis, half of pts upregulated HER3 expression after systemic therapy including TKIs, suggesting HER3 might be one of the factors associated with resistance to systemic therapy.

#4485

JPI-547, a novel dual inhibitor of PARP 1/2 and tankyrase 1/2 overcomes olaparib resistance in BRCA 1/2 mutant ovary and breast cancer preclinical model

Min Sil Kang[1], Nar Katuwal[1], Mithun Ghosh[1], Young kyu Jeong[1], Sa deok Hong[1], Sung Min Park[1], John Kim[2], Hyunju Cha[2], Banyoon Cheon[2], Seul-Gi Kim[1], Yong Wha Moon[1]. *[1]CHA University, Seongnam-si, Korea, Republic of,[2]Onconic Therapeutics Inc., Seoul, Korea, Republic of*

PARP inhibitors have prolonged the survival of various cancer patients with homologous recombination (HR) deficiencies. However, most patients eternally acquire resistance. Many attempts have been made, but there are no clear strategies to overcome resistance. We evaluated the efficacy and mechanism of JPI-547, a novel dual inhibitor of PARP1/2 and tankyrase1/2, in olaparib resistant breast and ovary preclinical cancer models. We established olaparib resistance models using mammalian cancer cell lines and patient-derived tumor xenografts (PDTXs). Two olaparib-resistant cells cell lines (BT474-OR/SNU251-OR) were established by exposing parent BRCA1/2 mutation carrying BT474 and SNU251 (breast and ovary cancer) to gradually increasing the concentration of olaparib for 8 months. An olaparib-resistant PDTX model [WJO-003(O2)], the parent BRCA1 mutation carrying ovary cancer PDTX was engrafted and treated with olaparib in 75mg/kg twice daily for 1 month and then 100mg/kg twice daily for 3 months. Using established olaparib resistance models, the anti-tumor efficacy of JPI-547 was compared with olaparib, niraparib, and talazoparib. IC_{50} of BT474-OR and SNU251-OR cell lines showed 5.5 and 6.7 fold increase compared to those of parent cell lines, respectively. While JPI-547 treatment in BT474-OR and SNU251-OR showed similar IC_{50} to the matching parent cells. In the PARPi-sensitive PDTX model, CPDX-013, JPI-547 inhibited tumor growth the greatest among other PARP inhibitors. Remarkably, 4 of 7 mice showed complete regression of the tumors. In the olaparib-resistant PDTX model, WJO-003(O2), JPI-547 inhibited tumor growth the most effectively compared to other PARP inhibitors (at day 60, the mean tumor volume: 2539, 1319, 871, 601, and 29 mm^3 in control, niraparib, olaparib, talazoparib, and JPI-547, respectively; $p<0.01$). Since JPI-547 treated groups suppressed the tumor growth the most effectively both in olaparib-sensitive and resistant PDTX, to test whether JPI-547 is effective in prior PARPi-exposed tumor, we switched a PARPi to JPI-547 when most of PARPi treated tumors slowly retrieved the tumor growth. This subsequent treatment of JPI-547 completely suppressed the growth of tumor compared to a single other PARPi treated groups in both olaparib-sensitive and resistant models. The data suggest that JPI-547 efficiently inhibits growth of the tumor previously exposed to other PAPRi. JPI-547 treated tumors showed a decrease of RAD51 in comparison to other PARPi treated groups, which is likely mediated by inhibition of tankyrase 1/2 by JPI-547 and suppression of TNK1/2-MERIT40 complex. Then this suppression resulted in blockade of HR repair.JPI-547 showed promising efficacy in an olaparib-resistant preclinical model. JPI-547 merits further clinical development in the PARP inhibitor-resistant ovary and breast cancer.

#4486

Proof of principle for pharmacogenomic-guided precision oncology for pediatric malignancy

Gi Ju Lee[1], Seung-Won Choi[2], Seung Ah Choi[3], Hee-Jin Cho[4], Robyn Gartrell[5], Ji Won Lee[6], Joo Whan Kim[3], Nam-Gu Her[1], Raul Rabadan[2], Ki Woong Sung[6], Do-Hyun Nam[6], Seung-Ki Kim[3]. *[1]Aimed Bio Inc., Seoul, Korea, Republic of,[2]Columbia University, New York, NY,[3]Seoul National University Hospital, Seoul,*

Korea, Republic of,[4]Kyungpook National University, Daegu, Korea, Republic of,[5]Columbia University Irving Medical Center, New York, NY,[6]Samsung Medical Center, Seoul, Korea, Republic of

Childhood cancers are rare and clinically diverse. They are typically associated with few driver mutational events than adult cancers, constituting potential targets for patient-specific precision therapy approaches. Here, we evaluated the feasibility of using a patient-derived tumor cell (PDC) based drug screening system and integrated multi-omics data to achieve precision oncology for pediatric patients. We established a PDC library derived from a few passage-cultured tumor cells from surgically resected tumor specimens and conducted chemical screening, which composed of various target agents of major oncogenic pathways (e.g. receptor tyrosine kinase inhibitor, proteasome inhibitor and histone deacetylase etc.). Next Generation Sequencing was performed to characterize the genomic and transcriptomic traits of tumors. Overall, success of establishing PDCs of pediatric cancers was high (80.4%) and comparable to adult cancers. The amount of obtained tissue was an important factor for the success of PDC establishment; the estimated optimal weight for PDC establishment was small (1.14g) and it is noteworthy that a small amount of tumor sample is sufficient to identify the potential hit(s) of parental tumors. The platform provided therapeutic options to pediatric tumors regardless of actionable targets. Our PDC approach identified several potential gene-drug associations, including anti-PI3K/Akt agents for neuroblastomas and anti-SHH agents for sarcomas with EWSR1 fusion. Given that a considerable proportion of pediatric tumors still lack actionable targets with matched treatment options, PDC-based drug screening profiles can be an optimal therapeutic strategy for these cases. Collectively, our analysis confirmed the feasibility of PDC-based in vitro drug screening systems to guide the therapeutic strategy for pediatric patients. This approach will accelerate the preclinical research for pediatric tumors to understand their pathophysiology and investigate the potential therapeutic strategies to fulfill the future precision oncology.

#4487

Effective anti-tumor effect in a rare metastatic Wilms tumor xenograft by inhibition of RAS/PI3K hyperactivation

Mohammad Reza Saadatzadeh[1], Khadijeh Bijangi Vishehsaraei[1], Erika A. Dobrota[1], Barbara J. Bailey[1], Lauren E. Hein[2], Kathryn L. Coy[3], Melissa A. Trowbridge[1], Anthony L. Sinn[3], Troy A. Markel[3], Michael J. Ferguson[3], Pankita H. Pandya[1], Karen E. Pollok[1]. *[1]Pediatrics, Indiana University School of Medicine, Indianapolis, IN,[2]University of Michigan, Ann Arbor, MI,[3]Indiana University School of Medicine, Indianapolis, IN*

Wilms Tumor (WT) is an embryonal renal tumor that accounts for more than 90% of kidney tumors in children. Significant advances in multidisciplinary therapeutic approaches have increased survival rates up to 90%. However, approximately 15% of patients with favorable histology and 50% of patients with anaplastic WT experience recurrence of disease. Thus, there is still a critical need to develop therapies that are effective and safe for these patients with progressive disease. To address this, we have developed a pipeline of patient derived xenograft (PDX) models from single academic institution patients with metastatic and aggressive cancers. Among these we have developed 3 xenograft models derived from patients with WT. To gain a detailed understanding of the complex array of mutations and identify therapeutic targets, molecular signatures were obtained at the DNA and protein levels via whole genome sequencing and reverse phase protein array analyses respectively. While PDX derived from encapsulated WT specimens exhibited basal levels of PI3K and MAPK pathway activation, which are well-known for promoting tumor survival, growth, and metastasis, no mutations that drive hyperactivation of these pathways were identified in these PDX. In contrast, a rare WT xenograft (PDX120) was established from a female patient with recurrent disease and metastatic cancer in the liver. -OMICS data indicated hyperactivation of PI3K (PIK3CA p.H1047R) and MAPK (KRAS p.G12_G10ins) which was validated by qPCR and immunoblotting in original tumor sample and serially passaged PDX120 xenografts. -OMICS data also confirmed the fidelity of the molecular signature between the original tumor sample and the serially passaged PDX120. The metastatic WT model was screened with two FDA approved drugs as single agents: Trametinib (MAPK pathway inhibitor; BID M-F 1mg/kg PO Day 1-35) or Alpelisib (PI3K pathway inhibitor; QD M-F 50mg/kg PO: Mice were dosed Day 1-29, followed by a gap period, and then dosing re-initiated, Day 86-103). Trametinib therapy did not

effectively attenuate PDX120 tumor growth. In contrast, the PI3K inhibitor Alpelisib was well tolerated and significantly decreased PDX120 growth and prolonged survival compared to the vehicle control (Two-way ANOVA, Holm-Sidak, $p<0.05$). At the end of the study, histological analyses indicated a complete lack of Ki67+ and tumorigenic cells in the Alpelisb-treated tumors compared to vehicle controls, indicating a dominant growth dependency on PI3K pathway activation. While efficacy data generated in PDX derived from patients is not used to guide clinical decisions at this time, it can validate therapeutic approaches and provide rationale for future clinical trials. In conclusion, these studies provide critical feasibility data that has high translational value and great potential to improve survival and quality of life for children suffering with progressive WT.

#4488

TY-4028: a novel, targeted therapy for non small-cell lung cancer with EGFR exon 20 or HER2 exon 20 insertion mutations

Jun Li[1], Chengshan Niu[2], Zhongwei Guo[2], Huan Wang[3], Bailu Zheng[3], Yuge Dou[2], Apeng Liang[1], Kaige Ji[2], Shengli Dong[1], Meihua Li[1], Yanchao Zhao[2], Yazhen Zhang[2], Aishen Gong[3], Hao Liu[2], Xinmiao Hu[2], Hui Su[3], Mingyu Jiang[3], Shaoqing Chen[3], Xiugui Chen[3], Yusheng Wu[1]. *[1]TYK Medicines, Inc., Huzhou, China,[2]TYK Medicines, Inc., Zhengzhou, China,[3]TYK Medicines, Inc., Shanghai, China*

Epidermal growth factor receptor (EGFR) activating mutations represent major drivers to the development of non-small cell lung cancer (NSCLC). Among the oncogenic EGFR mutations, a significant cohort, counting for approximately 4-10% of the EGFR mutation spectrum, bear EGFR exon 20ins mutations. Meanwhile, approximately 2% of NSCLC patients bear hotspot mutations in HER2. Strikingly, over 90% of the HER2 mutations occurred in NSCLC are identified as exon 20ins mutations. Despite the successful launch of 1st, 2nd, and 3rd generation of EGFR inhibitory agents in the clinic that inactivate oncogenic EGFR signaling through targeting specific EGFR mutations, de novo or acquired, none of these standard-of-care therapies is specific to EGFR exon 20ins or HER2 exon 20ins. In addition, trastuzumab and EGFR-TKIs have limited effectiveness for NSCLC patients with HER2 exon 20ins mutation. TAK-788 (mobocertinib) and JNJ6372 (amivantamab-vmjw) are the FDA approvals for NSCLC driven by EGFR exon 20ins mutations. Only T-Dxd is used as a second-line treatment for NSCLC patients with HER2 mutation. Considering the large population of lung cancer and the fact that many patients are missed in diagnosis due to the heterogeneous characteristics of EGFR and Her2 exon 20ins, there are probably more than ten thousand lung cancer patients suffering the EGFR or Her2 exon 20ins mutations. There are urgent unmet medical needs to develop target therapeutics for EGFR and Her2 exon 20ins mutations. We discovered and developed TY-4028, which is a novel, potent, and orally available inhibitor targeting EGFR and Her2 exon 20ins mutations and is currently in the IND enabling stage. In EGFR-related tumor cells and genetically engineered Ba/F3 cell lines, TY-4028 showed similar or better antitumor effects than TAK-788, and better antitumor effects than DZD9008. The B/P ratio (brain tissue $AUC_{0\text{-}last}$/plasma $AUC_{0\text{-}last}$) of SD rats was 1.63 and 1.04 respectively after oral administration of TY-4028 in male and female SD rats, which suggested that TY-4028 had good potential to cross Blood Brain Barrier (BBB). Preclinical studies showed a good PK profile and manageable toxicity with TY-4028. TY-4028 has remarkable efficacy in mouse models of EGFR exon 20ins and HER2 exon 20ins. The data showed that all doses of TY-4028 had significant effects, and the tumors nearly demonstrated complete regression in the PDX LU0387 model and PC9 CDX model. At the same dose, the efficacy of TY-4028 was similar to that of TAK-788, while the tolerance of TY-4028 was better than that of TAK-788. At the same dose, the efficacy of TY-4028 was better than that of DZD9008. Taken together, the data demonstrated TY-4028 has great potential to meet the unmet medical needs for NSCLC patients with EGFR exon 20ins mutation or HER2 exon 20ins mutation. #Jun Li and Chengshan Niu contributed equally to this work. *They are the correspondent authors.

#4489

N-Cadherin acts as a predictive biomarker for anti-FGFR therapy in *KRAS* wild-type NSCLC

Santiago G. Borrego[1], Cristina Cirauqui[1], David Gómez-Sánchez[1], Haiyun Wang[2], Alicia Luengo[1], Chiara Ambrogio[3], Luis Paz-Ares[4], Irene Ferrer[1]. *[1]Research Institute (i+12) Hospital 12 de Octubre / Spanish*

National Cancer Research Center (CNIO) / Biomedical Research Cancer Network Center (CIBERONC), Madrid, Spain,[2]Tongji University, Shanghai, China,[3]Department of Molecular Biotechnology and Health Sciences, Molecular Biotechnology Center (MBC), Torino, Italy,[4]Medical Oncology Department, Research Institute (i+12) Hospital 12 de Octubre / Spanish National Cancer Research Center (CNIO) / Biomedical Research Cancer Network Center (CIBERONC) / Complutense University, Madrid, Spain

Background: Lung cancer is the leading cause of cancer-related deaths worldwide. FGFR1 has been associated with tumorigenesis in a variety of tumor types, including lung cancer. As a therapeutic approach, their inhibition has been attempted and was initially focused on FGFR1-amplified tumors, though with limited success. Preliminary data of our group suggests that N-Cadherin play a key role for the oncogenicity of FGFR1 and predict FGFR-targeted therapy efficacy in Non-small cell lung cancer (NSCLC). However, it is possible that other biomarkers, together with N-Cadherin, can determine the response to anti-FGFR therapy. Therefore, it is essential the identification of new biomarkers that could help to predict more accurately those patients that could benefit from anti-FGFR therapy.
Materials and Methods: We have treated 15 NSCLC PDX models with high FGFR1 expression levels and variable N-Cadherin expression levels, with the FGFR inhibitor (FGFRi) AZD4547. Based on their sensitivity to treatment, the PDX models were classified into two groups: Responders and Non-responders. All PDX models were characterized at the proteomic, genomic, and transcriptomic levels by western blot, whole exome sequencing, and RNA-Seq, respectively, and we used this information for defining the responder versus the non-responder group. Subsequently, the GDSC repository was used to validated our data in a cohort of lung adenocarcinoma (LUAD) cell lines.
Results: Responder and non-responder groups revealed a distinct pattern of genomic alterations and gene expression profile. As expected, GSEA identified an enrichment in Responders group of pathways related to FGFR1 signaling and ECM proteins, among them N-Cadherin stands out. Moreover, we observed an enrichment of *KRAS* mutations and genes related to the *KRAS* signature and to the intrinsic resistance to FGFRi in the non-responder group. To validate our findings and using the GDSC repository, we observed an enriched resistance to inhibitors of FGFR1 signaling in a cohort of *KRAS* mutant LUAD cell lines. Furthermore, we confirm a tendency for increased sensitivity in high N-Cadherin expressing cell lines, but only in *KRAS* wildtype context.
Conclusions: In conclusion, previous research had underlined N-Cadherin as a potential biomarker of response to FGFRi, while not successful in all contexts. Transcriptome study of PDXs classified as responder or non-responder to FGFRi revealed a differential gene expression pattern, with an upregulation of N-Cadherin pathway observed in the Responder group, while an enrichment of KRAS signaling and *KRAS* mutations in non-Responders. Furthermore, we validated our finding using a cell line repository that confirm that N-Cadherin could predict FGFR-targeted therapy efficacy but only in the *KRAS* wildtype context .

#4491

TY-0584: A potent, orally available small molecule YAP/TEAD inhibitor, exhibits anti-tumor effects *in vitro* and *in vivo*

Apeng Liang[1], Shengli Dong[1], Guangbin Liu[1], Zhengfei Guo[1], Meihua Li[1], Shuaibo Han[1], Yundi Cao[1], Yian Tu[1], Chao Zhou[1], Yu Yu[1], Linglin Xiao[1], Wei Huang[1], Xinlong Yang[1], Lian Fang[1], Haoyun Li[1], Chengshan Niu[2], Mingyu Jiang[3], Feng Xing[3], Shaoqing Chen[3], Jun Li[4], Yusheng Wu[4]. *[1]TYK Medicines, Inc. (Changxing), Huzhou, Zhenjiang, China,[2]TYK Medicines, Inc. (Zhengzhou), Zhengzhou, Henan Province, China,[3]TYK Medicines, Inc. (Shanghai), Xuhui District, Shanghai, China,[4]TYK Medicines, Inc., Huzhou, Zhenjiang, China*

Hippo/YAP pathway plays an essential role in cell proliferation, tissue regeneration, and tumorigenesis. The emerging evidence shows that hyperactivation of the Hippo/YAP pathway induces metastasis, chemoresistance, and the attribute of cancer stem cells. Dysregulated Hippo/YAP pathway can be a dominant driver of mesothelioma, meningioma, and schwannoma. It has been reported that Hippo/YAP oncogenic activation in mesothelioma is driven by NF2 loss function. In addition, it contributes to 10% of all cancers, including lung, gastric, colon, cervical, ovarian, breast, melanoma, hepatocellular, and squamous cell

carcinoma. Despite the urgent need to develop a therapeutic strategy to curb the dysregulated pathway, YAP/TAZ is difficult to be directly targeted with small molecule inhibitors because of the lack of a catalytic niche. TEADs require auto-palmitoylation to become functional. Therefore, small molecules that target palmitoylation of TEAD have been explored and VT3989 (NCT04665206) and IK-930 (NCT05228015) have success to enter the clinical trials. To target cancers with dysregulated Hippo/Yap pathway, we have discovered and are developing TY-0584, which is a potent and orally available YAP/TEAD inhibitor in the IND enabling stage. The results of PK and toxicity studies of TY-0584 showed a favorable safety profile. TY-0584 had excellent efficacy in the malignant mesothelioma H226 CDX mouse model, which is driven by NF2 deletion mutation. TY-0584 treatment also demonstrated good efficacy in the head and neck cancer PDX tumor mouse model. In previous studies, Hippo/Yap signaling promotes drug resistance to EGFR-targeted therapies in non-small cell lung cancer (NSCLC). To relax the YAP resistance mechanism in EGFR treatment, we asked if combined YAP inhibition grants an extension of responses to EGFR therapy. To this end, we treated EGFR-driven NSCLC cell models with TY-0584 and TY-9591. TY-9591 is a third-generation EGFR inhibitor developed by TYK Medicines and is currently under a pivotal Phase III clinical investigation in China (NCT05382728). The results show that the combination treatment not only offers synergistic effects, but also enhances apoptosis, compared to single drug treatment. Our *in vivo* data further underscores this exciting finding. Our studies showed that TY-9591 had excellent efficacy in the PC9 CDX mouse model, but tumors gradually recurred as many targeted cancer therapies did. In line with the results of the *in-vitro* experiments, another YAP/TEAD inhibitor TY-0536 in combination with TY-9591 significantly delay the tumor regrowth in the PC9 CDX mouse model. In summary, we identified a potent and orally available YAP/TEAD inhibitor TY-0584 which is a promising candidate for further clinical validation. [Shengli Dong and Apeng Liang contributed equally to this work. Jun Li, Shengli Dong, and Apeng Liang are the corresponding authors.]

#4492

A novel and potent FLT3 and IRAK4 dual inhibitor for the treatment of acute myeloid leukemia

Rui Yang[1], Lei Wu[1], Bing Zhang[1], Michael Xiang[2], Suyue Wang[1], Camille Xiang[2], zhijian Lu[2], Jason Xiang[2]. *[1]Polymed Biopharmaceuticals, Inc., Hangzhou, China,[2]Polymed Biopharmaceuticals, Inc., Cambridge, MA*

Several potent FMS-like tyrosine kinase 3 (FLT3) inhibitors have been developed and approved for the treatment of FLT3-mutant acute myeloid leukemia (AML) recently. These inhibitors block the signaling pathways involved in proliferation of leukemic cells, and have shown favorable initial results in early-stage AML patients. However, a significant percentage of patients relapsed with poor prognoses. The relapse is generally caused by a compensatory innate immune stress response, such as Toll-like receptor activation, which induces adaptive resistance to the FLT3 inhibition. Interleukin-1 receptor associated kinase 4 (IRAK4) functions as a mediator of Toll-like receptor and interleukin-1 receptor signaling pathways. Patients harboring a U2AF1 or SF3B1 spliceosome mutation were found to express a longer and more active isoform of IRAK4 kinase, which could result in lasting activation of NF-κB and MAPK in oncogenic and innate immune signaling. Emavusertib (CA-4948), an IRAK4/FLT3 inhibitor, is currently in phase I clinical trials. To address the critically unmet medical needs of myeloid leukemia patients, we have developed a novel and potent FLT3 and IRAK4 dual inhibitor HPB-092 with excellent selectivity to provide durable efficacy in myeloid malignancies by eliminating adaptive resistance .
HPB-092 significantly inhibited MV4-11 tumor cell proliferation at low nanomole concentration. HPB-092 demonstrated good oral bioavailability in several animal species. In a disseminated MV4-11 xenograft mouse model, HPB-092 displayed strong anti-tumor activity at 5mg/kg. HPB-092 was well-tolerated with no obvious adverse events at a dose of 40 mg/kg in two-weeks safety study in SD rats. In addition, no rhabdomyolysis side-effect was observed upon histological analysis. These results underscore the potential therapeutic benefit and safety profile of HPB-092 for the treatment of AML, especially in patients with mutations in U2AF1 or SFF3B1 spliceosome.

#4493

Sudocetaxel Zendusortide (TH1902), a peptide-drug conjugate for the treatment of sortilin-positive (SORT1+) TNBC and Her2-positive breast cancers

Cyndia Charfi[1], Michel Demeule[1], Jean-Christophe Currie[1], Alain Zgheib[2], Bogdan Alexandru Danalache[2], Richard Béliveau[2], Christian Marsolais[1], Borhane Annabi[1]. *[1]Theratechnologies, Montreal, QC, Canada,[2]Université du Québec à Montréal, Montreal, QC, Canada*

Over the last decade, the targeting of specific cell surface receptors such as human epidermal growth factor receptor 2 (Her2) in breast cancer cells has allowed the emergence of innovative strategies for the delivery of anticancer agents. High expression levels of the sortilin receptor (SORT1) have been reported in various tumors of breast cancer patients, including triple-negative breast cancer (TNBC), HR+ and Her2+ breast cancers. Given SORT1 function in ligand internalization, we addressed the sorting and trafficking of the newly designed TH19P01 peptide recognizing SORT1, and of TH1902, an anticancer TH19P01-docetaxel conjugate (PDC), and whether such PDC could target SORT1+ breast cancers. *In vitro*, high expression of SORT1 was found in several TNBC and Her2+ breast cancer cell lines as well as in in more than 88% of cases (H-score >100) from commercial breast cancer tissue microarrays. SORT1-mediated cell surface binding and internalization of TH19P01 was first investigated in TNBC-derived MDA-MB-231 cells. The binding and uptake of Alexa^{488}-labeled TH19P01, at 4 and 37°C respectively, were found significantly reduced upon siRNA-mediated SORT1 silencing. This demonstrates that functional SORT1 processes are required for both cell surface recognition and internalization of TH19P01. Moreover, the internalization of TH19P01 and TH1902 in MDA-MB-231 cells were monitored by fluorescence microscopy using a polyclonal antibody generated against TH19P01. Both TH19P01 and TH1902 showed a rapid uptake and co-localized in the perinuclear region with the late endosomal marker Rab-7 and with the lysosomal marker Lamp-1 within 30 minutes indicating that both compounds are internalized through a receptor-mediated endocytosis pathway. In addition, TH19P01 internalization after 1 hour appeared significantly associated within intracellular compartments of MDA-MB-231 cells whereas Herceptin remained mostly localized at the cell surface of Her2+ BT-474 cells. *In vivo*, weekly administration of intravenous bolus of TH1902 (35 mg/kg) at an equivalent docetaxel MTD dose (15 mg/kg) led to complete tumor regression, while docetaxel only inhibited tumor growth by half in a murine MDA-MB-231 xenograft tumor model. Furthermore, in mice bearing Her2+ HCC-1954 breast tumor xenografts, TH1902 induced complete tumor regression in contrast to docetaxel and Herceptin. Taken together, these preclinical data demonstrate the high anticancer properties of TH1902 against SORT1+ TNBC and Herceptin resistant Her2+ breast cancers. These results demonstrate that TH1902 can be a promising avenue for personalized therapy in the treatment of all SORT1+ breast cancers.

#4494

Multi-specific cMet x EGFR x VEGF antibody for difficult to treat cancers

Mark Chiu. *Tavotek Lab Inc., Springhouse, PA*

Cancers such as TNBC, pancreatic, and gastric are difficult to treat due to diverse etiologies. Several subtypes of these cancers are driven by abnormal EGFR signaling, increased cMET activation, and VEGF linked angiogenesis which are responsible for tumor growth and metastasis. TAVO412, a humanized multi-specific antibody with two distinct anti-EGFR nanobody domains, an anti-cMet Fab arm, and an anti-VEGF ScFv domain, was designed to treat patients with these unmet medical needs. In addition, the Fc domain allows for the heterodimerization, antibody-like pharmacokinetic profile, and additional mutations that enhance the Fc effector functional activity. In preclinical xenograft models, TAVO412 demonstrated strong tumor growth inhibition effects on TNBC, PDAC, GC or NSCLC cell line-derived tumors. The mechanisms of action included selective and potent binding to EGFR, cMet, and VEGF at lower pH values found in the solid tumor environment; effective blocking of EGFR and cMet pathways that drove cancer cell growth and proliferation; shutdown of VEGF mediated angiogenesis; and potent and efficacious Fc effector function that enhanced ADCC, ADCP, and CDC. TAVO412 had better TGI than analogous molecules. TAVO412 also demonstrated strong tumor growth inhibition against NSCLC patient derived xenograft (PDX) models with mutant EGFR and cMet genotypes. Each of the binding arms had cross reactivity with the cynomolgus monkey orthologues allowing the cyno model to be a relevant toxicology model. In the pivotal GLP

toxicology study in cynomolgus monkeys, TAVO412 was well tolerated, had no major organ toxicities, observations were mostly consistent with EGFR-related effects and recoverable. In conclusion, TAVO412 was successfully discovered and developed for hard-to-treat solid tumors. This drug is expected to be safe and efficacious in cancer patients. The IND application was approved by the US FDA in October 2022. A first-in-human, 2-Part Phase 1 study to examine the preliminary efficacy, safety, tolerability, pharmacokinetic / pharmacodynamic parameters; maximum tolerated dose / recommended phase 2 dose of TAVO412 will be starting in the first quarter of 2023.

#4495

A mechanistic study of the TFE3-splicing machinery gene fusions reveals a new druggable target for translocation renal cell carcinoma

Nur Damayanti[1], Sabrina Orsi[2], Ricardo Cordova[3], Christopher Rupert[2], Li Shen[2], William Marston Linehan[4], Kirk Staschke[3], Peter Hollenhorst[5], David Heppner[6], Roberto Pili[2]. *[1]Neurosurgery, Indiana University, Indianapolis, IN,[2]University at Buffalo, Buffalo, NY,[3]Indiana University, Indianapolis, IN,[4]National Cancer Institute, Bethesda, MD,[5]Indiana University, Bloomington, IN,[6]Chemistry, University at Buffalo, Buffalo, NY*

TFE3 is a member of basic helix-loop-helix leucine zipper MiT transcription factor family and its chimeric proteins are associated with translocation renal cell carcinoma (tRCC). Despite the variety of genes fusions, most of *TFE3* fusions partner genes are linked to spliceosome machinery. Dissecting the function of *TFE3* fused to spliceosome machinery factors (TFE3-SF) could direct the development of effective therapies for this lethal disease, which is refractory to standard treatments for kidney cancer. Here, by using a combination of *in silico* structure prediction, molecular cloning, next generation transcriptomics, FRET technology, mutagenesis, proteomics, and high-throughput high-content screening (HTHCS) we interrogated a series of oncogenic mechanisms of TFE3-SF-containing fusions, including spontaneous nuclear translocation, nuclear paraspeckle occupancy, enhanced *in vitro* proliferation and *in vivo* growth, transcriptome remodeling, alternative splicing reprogramming, and novel dimer partner recruitment. Molecular inhibition of TFE3-SF dimerization reverses its oncogenic activity and represents a potential new target for therapeutic intervention. By using HTHCS combined with FRET technology we screened FDA approved drugs library (LOPAC) and small molecule library (Microsource) and identified hits compounds which inhibit TFE3-SF dimerization. Hits compounds were validated in 2D and 3D models utilizing patient derived xenolines expressing TFE3-SF. Ouabain and terfenadine demonstrated decreased cell proliferation, reduced spheroid growth and *in vivo tumor* growth. Overall, our results unmask synthetic vulnerabilities of TFE3-SF dimerization for novel therapeutic strategies in patients with this aggressive type of kidney cancer.

#4496

JPI-547, a dual inhibitor of PARP/Tankyrase, shows promising antitumor activity against pancreatic cancers with homologous recombination repair deficiency or Wnt-addiction

Kyoung-Seok Oh[1], Ah-Rong Nam[1], Ju-Hee Bang[1], Yoojin Jeong[1], Sea Young Choo[1], Hyo Jung Kim[1], Su In Lee[1], Jae-Min Kim[1], Jeesun Yoon[2], Tae-Yong Kim[2], Banyoon Cheon[3], Hyunju Cha[3], John Kim[3], Do-Youn Oh[2]. *[1]Cancer Research Institute, Seoul National University College of Medicine, Seoul, Korea, Republic of,[2]Department of Internal Medicine, Seoul National University Hospital, Seoul, Korea, Republic of,[3]Onconic Therapeutics, Seoul, Korea, Republic of*

Background**:** PARP inhibitors have shown antitumor activities against solid tumors with HRD (homologous recombination deficiency). The definition of HRD and other potential biomarkers besides HRD should be further evaluated for PARP inhibitors. JPI-547 is a novel PARP inhibitor, simultaneously targeting tankyrase1/2, other members of the PARP family, that are involved in the Wnt/β-catenin pathway.
Method: Antiproliferative effect of JPI-547 and a variety of PARP inhibitors (olaparib, veliparib, talazoparib, niraparib, and rucaparib) were determined by MTT assay or clonogenic assay in 9 human pancreatic ductal adenocarcinoma (PDAC) cell lines (Capan-1, HPAF-II, Capan-2, AsPC-1, SNU-410, SNU-213, SNU-324, MIA-PaCa2, and PANC-1). Transcriptome data and gene dependency score of the cell lines

were obtained from the CCLE database and DepMap respectively. DNA damage was monitored by immunofluorescent imaging of γ-H2AX and DR-GFP assay determined the homologous recombination repair (HRR) efficiency. A xenograft tumor model was established to substantiate the in vivo antitumor effect of JPI-547.
Results: JPI-547 more potently blocks Poly(ADP-ribosyl)ation than olaparib, and induces a strong antiproliferative effect on Capan-1, a cell line with BRCA2 del. JPI-547 leads to cell cycle arrest and induces enhanced apoptotic cell death than olaparib. JPI-547 inhibits tumor growth of Capan-1 in vivo, suggesting the potent antitumor activity of JPI-547 against PDAC with HRD. Cell lines harboring RNF43 *LOF* mutations (HPAF-II, AsPC-1, and Capan-2), intrinsically addicted to Wnt/ β-catenin pathway, are more sensitive to JPI-547 than cells with RNF43 wild types. Interestingly, RNF43 mutations could not distinguish the sensitivity of other PARP inhibitors except JPI-547. CTNNB1 gene dependency score and β-catenin levels positively correlate with cellular sensitivity to JPI-547. JPI-547-induced DNA damage was alleviated in HR-proficient PDAC cells. DR-GFP assays confirm that JPI-547 does not directly alter the HRR efficiency of Wnt-addicted PDAC cells. Collectively, these data indicate that the vulnerabilities of Wnt-addicted PDAC cells to JPI-547 were irrelevant to HRD mimicking. Rather, JPI-547 stabilizes AXIN-2 in Wnt-addicted PDAC cells and downregulates the active form of β-catenin level in the nucleus, thereby disrupting the transcription of its target genes. Knockdown of β-catenin neutralized the antiproliferative effect of JPI-547, suggesting that inhibition of the β-catenin pathway is an important mode of action by JPI-547 in Wnt-addicted PDAC cells.
Conclusion: JPI-547 shows promising, preclinical antitumor effects against PDAC cells with HRD or Wnt-addiction, providing a rationale for further biomarker-driven clinical development of JPI-547 for the treatment of patients with PDAC.

#4497
Efficacy of Jak1/2 inhibition in murine myeloproliferative neoplasms is mediated by targeting nonmalignant cells
Sivahari Prasad Gorantla[1], Michael Rassner Rassner[2], Tony Andreas Müller[2], Teresa Poggio[2], Kirstyn Anne Crossley[2], Anna-Lena Denecke[2], Kornelia R Fritsch[2], Geoffroy Andrieux[3], Helen Kleinfelder[2], Shifa Khaja Saleem[2], Sudheer Madan Mohan Gambheer[2], Irene Gonzalez Menendez[4], Detlef Bentrop[5], Rainer Trittler[6], Svetlana Rylova[7], Dietmar Pfeifer[2], Leticia Quintanilla Martinez[4], Christine Dierks[2], Robert Zeiser[2], Anna Lena Illert[2], Nikolas von Bubnoff[1], Justus Duyster[2]. *[1]Department of Hematology and Oncology, UKSH, Luebeck, Germany,[2]Hematology, Oncology and Stem cell transplantation, Faculty of Medicine, Clinic for Internal Medicine, Freiburg, Germany,[3]Medical Center, Faculty of Medicine, University of Freiburg, Institute of Medical Bioinformatics and Systems Medicine, Freiburg, Germany,[4]Department of Pathology and Neuropathology, University Hospital Tübingen & Comprehensive Cancer Center Tübingen, Tübingen, Germany,[5]Albert-Ludwigs-Universität Freiburg,, Institute of Physiology, Freiburg, Germany,[6]Albert-Ludwigs-Universität Freiburg, Institute of Pharmaceutical Sciences, Freiburg, Germany,[7]Department of Nuclear Medicine, University Medical Center Freiburg, Freiburg, Germany*

Ruxolitinib (Jakavi) is a potent JAK1/JAK2 specific inhibitor, approved for the treatment of myeloproliferative neoplasia (MPN) such as primary myelofibrosis (PMF) and polycythemia Vera (PV). The primary clinical benefit of ruxolitinib in MPN patients is reduction in spleen size and alleviation of constitutional symptoms and significant improvement in the quality of life. However, the effect of ruxolitinib on bone marrow fibrosis and $JAK2^{V617F}$ allelic burden is modest. In addition, $JAK2^{V617F}$ negative MPNs also demonstrated clinical benefits, thus, is not clear whether the ruxolitinib primarily blocks the proliferation of the malignant clone or exerts its effects by targeting non-malignant cells. To gain the mechanism of ruxolitinib action in MPNs, we developed two $JAK2^{V617F}$-driven MPN mouse models harboring ruxolitinib resistant mutations $JAK2^{V617F+L902Q}$ and $JAK2^{V617F+L983F}$ in the malignant clone. Similar to $JAK2^{V617F}$ recipients, $JAK2^{V617F+L902Q}$ and $JAK2^{V617F+L983F}$ transplanted mice showed an increase in WBC, HCT, RBC, HB and reticulocyte values. Histopathological analysis revealed that the myeloproliferative phenotype resembles PV with a proliferation of all three lineages albeit with only a moderate increase in megakaryopoeisis. Grade II bone marrow fibrosis was observed in $JAK2^{V617F+L902Q}$

and JAK2$^{V617F+L983F}$ after 2-3 months similar to JAK2^{V617F} mice. Surprisingly, these mice respond to ruxolitinib treatment similar to ruxolitinib sensitive JAK2^{V617F} mice, indicated by reduction of spleen size, leukocyte count and proinflammatory cytokines in the serum. Mechanistically, we could identify a direct role of ruxolitinib in the impairment of inflammatory processes in the bone marrow microenvironment, particularly on the cytokine production of mesenchymal stem cells and endothelial cells. These results suggest that the ruxolitinib mediated effects in MPN patients are mainly due to abrogation of inflammatory signaling processes in non-malignant cells. Therefore, combination treatment of JAK1/2 inhibitors with novel inhibitors, which specifically act on malignant cells might improve the clinical benefit for MPN patients to JAK family inhibitors.

#4499

The peptide-drug conjugate sudocetaxel zendusortide (TH1902) potentiates anti-tumoral activity of the anti-PD-L1 checkpoint inhibitor and induces immune cell infiltration in a B16-F10 syngeneic melanoma model

Michel Demeule[1], Jean-Christophe Currie[1], Cyndia Charfi[1], Alain Zgheib[2], Isabelle Cousineau[2], Richard Béliveau[2], Christian Marsolais[1], Borhane Annabi[2]. *[1]Theratechnologies, Montreal, QC, Canada,[2]Université du Québec à Montréal, Montreal, QC, Canada*

Tumor-infiltrating immune cells are involved in the control of cancer and are closely related to clinical outcomes. Sudocetaxel Zendusortide (TH1902), a peptide-drug conjugate (PDC) of the sortilin (SORT1)-binding peptide TH19P01 ester-linked to two docetaxel moieties, has been shown to exert superior anti-cancer activities in multiple cancer models including melanoma syngeneic and xenograft murine models. Melanomas express elevated levels of SORT1 and are considered as one of the most immunogenic tumors where immune checkpoint inhibitors are among the standard of care treatment used. Here, we first questioned whether TH1902 anti-cancer effects involved infiltration of immune cells in a murine SORT1-positive syngeneic, non-immunogenic and highly aggressive B16-F10 melanoma model in C57BL/6 mice. Weekly administration of docetaxel reduced by half the growth of B16-F10 tumor allografts, while administration of TH1902 as a single agent and at equivalent docetaxel doses, was well tolerated and resulted in tumor regression after only 2 treatments. Surprisingly, in this immunologically cold tumor, immunohistochemistry analysis of tumors for immune cell infiltration showed a net increase in total leukocytes (CD45+) infiltration within TH1902-treated tumors compared with docetaxel-treated tumors, especially with for tumor-infiltrating lymphocytes (TILs) and tumor-associated macrophages (TAMs). Furthermore, the increased staining intensities for Perforin and Granzyme B were indicative of the elevated cytotoxic T and natural killer (NK) cells activity in TH1902-treated tumors. This corroborated with increased caspase-3 apoptotic activity. TH1902 and docetaxel doses were next halved and combined with the checkpoint inhibitor anti-PD-L1. In a first study, the TH1902/anti-PD-L1 combination resulted in increased tumor growth inhibition when compared with both agents alone. Interestingly, TH1902 as a single agent showed better tumor growth inhibition than docetaxel or docetaxel/anti-PD-L1 combination. In a second study, the TH1902/anti-PD-L1 combination significantly increased animal survival over either anti-PD-L1 or TH1902 as single agents (21 days increased median survival compared to 2.5 and 12.5 days respectively). We conclude that the superiority of TH1902 anticancer activity over docetaxel involves, in part, the modulation of infiltrating immune cells within the tumor microenvironment. This is the first demonstration that immune cell infiltration patterns play a pivotal role in the TH1902-associated anti-tumoral response. Combination of TH1902 with checkpoint inhibitors (anti-PD-L1) further reveals that this may lead to improved clinical outcomes in future immunotherapy translational approaches.

#4500

Enedione derivates as a potential cancer treatment through the inhibition of COPZ1

Allana C. F. Martins[1], Barbara Mitsuyasu Barbosa[2], Ingridhy O. Maia Freitas da Silveira[1], Roberto S. Gomes[1]. *[1]Pharmaceutical Sciences, North Dakota State University, Fargo, ND,[2]Chemical and Biological Sciences, Sao Paulo State University (UNESP), Botucatu, Brazil*

Cancer is a leading cause of death worldwide; it was responsible for approximately 10 million deaths in 2020. Besides surgery for tumor removal, the most common treatments available are chemotherapy and radiation, which are not selective, resulting in side effects such as pain, hair loss, nausea, and vomiting. They are also ineffective against stem-like and dormant tumor cells, which could lead to a relapse and/or metastasis. Consequently, the development of drugs with tumor-specific targets is needed. COPI is a coatomer responsible for the retrograde transport from Golgi complex (GC) to the endoplasmic reticulum (ER). In this context, we developed four compounds targeting disruption of GC through inhibition of COPI and previous results showed that compounds 1-4 significantly decrease cell viability of pancreatic cancer cell lines MIA PaCa-2 and AsPC-1, compared to hTERT-HPNE normal pancreatic cell line. In the present work, RT q-PCR confirmed that the two isoforms of the COPI ζ subunit COPZ1 and COPZ2 are expressed at similar levels in normal cells while COPZ2 is downregulated in tumor cell lines. Our *in vitro* results demonstrated that compounds **1-4** decreased cell viability of breast cancer (HCC1143) and melanoma (A-395) cell lines. The tested compounds are able to target COPZ1-dependent tumor cells, therefore they are great candidates for further studies aiming to develop a selective treatment for cancer.

#4501

Novel EHE PDX model used for drug sensitivity

Sandhya Krishnan, Robert Porter, Danh Truong, Salah-Eddine Lamhamedi-Cherradi, Krzysztof Grela, Rafal Zielinski, Sharon Landers, Vinod Ravi, Joseph A. Ludwig. *UT MD Anderson Cancer Center, Houston, TX*

EHE is a low-to-intermediate grade angiocentric non-vasogenic tumor that exhibits a wide survival range dependent upon tumor size, stage, and location. Most tumors originate in the lung (37%), soft tissue (20%), or liver (16%), and those with multifocal peritoneal or pleural spread have a 5-year survival rate of ~22%. Solitary lesions are often resected for curative intent. However, treatment options for those with metastatic disease at diagnosis remain less well-defined. Generally, the chemo-resistant slow-growing soft-tissue EHEs can often be observed off therapy for years or decades. In contrast, pleural or peritoneal tumors required rapid intervention with systemic cytotoxic chemotherapies. Given the lack of effective treatments, there remains a significant unmet need.

Unique among all cancer types, more than 90% of EHEs harbor in-frame chromosomal translocations with WWTR1 (TAZ) or YAP1 in the N-terminal domain. Given that YAP and TAZ are two paralogs, which share numerous epigenetic functions as YAP/TEAD or TAZ/TEAD transcriptional coactivators downstream of the Hippo tumor-suppressor pathway, the oncogenic effect of the resulting EHE-associated TAZ-CAMTA1 (TC) or YAP1-TFE (YT) fusion proteins must, with all certainty, continue to depend on the truncated YAP/TAZ proteins. Since no EHE cell lines exist, one cannot predict if the TC FP behaves similarly in human sarcomas that expose different tissue-specific TEAD binding sites.

Trametinib (a MEK inhibitor) was chosen for initial evaluation. We determined the preclinical efficacy of trametinib in the only available EHE patient-derived tumor explant (PDX) in existence, which genetic testing confirmed harbored a TAZ-CAMTA1 translocation. We propagated EHE PDX tumors in mice, then treated with vehicle or trametinib for more than 80 days. Tumor volumes were measured 2-3 times a week, and tumors were collected for further histology and proteomic analysis. Trametinib demonstrated potent antineoplastic activity, consistent with the limited activity observed in recent clinical studies.

A separate 10-day study was conducted to measure early pharmacodynamic studies of a potent, oral, selective small molecule palmitoylation inhibitor of TEAD provided by Ikena Oncology. Edge-Seq RNA sequencing and western blots were performed to validate the TEAD-dependent gene and protein expression. EdgeSeq analysis demonstrated significant down-regulation of multiple TEAD dependent genes, indicating on-target inhibition of TEAD in this model. Western blot protein analysis of YAP, TAZ, TEAD1, TC FP, CTGF, and CYR61, collected for pharmacodynamic analysis, demonstrated reduced CYR61, indicative of possible TEAD inhibitor activity; CTGF protein levels were unchanged. The use of one EHE PDX was a limitation, as this model may not fully recapitulate human tumor biology. Future research, using additional EHE PDX models, will be required in gauge the effect of different inhibitors.

#4502

Aptamer conjugated prostate specific membrane antigen (PSMA) targeting nanobees for prostate cancer prevention and therapy

Islam Rady[1], Sayed Bakry[2], Fatma Abou El-Azm[3], Hasan Mukhtar[4]. *[1]Molecular Biology, Al-Azhar University, Cairo, Egypt,[2]Center for Genetic Engineering, Faculty of Science, Al-Azhar University, Cairo, Egypt,[3]Pharmacology, Mansoura University, Mansoura, Egypt,[4]Department of Dermatology, School of Medicine and Public Health, University of Wisconsin-Madison, Madison, WI*

Melittin (MEL), a major peptide component of bee venom (BV), has shown chemopreventive as well as chemotherapeutic effects against many cancers in preclinical model systems. However, its applicability to humans has met with limited success due to several issues including its toxicity, nonspecificity, degradation, inefficient systemic delivery and limited bioavailability. Earlier, the concept of "nanochemoprevention" i.e. the use of nanotechnology to improve the outcome of cancer chemoprevention is introduced. Then, "non-targeted nanobees" i.e. nanoformulated mellitin is developed to exhibit excellent anti-prostate cancer efficacy *in vitro* and in animal models coining the concept as 'Nanobee- Chemoprevention'. Here, we are extending this work and developed nanobees targeted with small molecular entities (A10 2′-fluoropyrimidine RNA aptamers (Apt)), able to bind to prostate specific membrane antigen (PSMA), a transmembrane protein that is overexpressed in prostate cancer (PCa) and evaluated their efficacy in preclinical studies. The Apt-Nanobees led to an enhanced anti-proliferative activity in PCa cell lines compared to the free melittin. The behavior of Apt-Nanobees in modulating apoptosis and cell-cycle, was also determined. Then, *in vivo* experiments, in mouse xenograft model of prostatic tumor using nanobees with a model of targeted nanosystems, were conducted. The obtained data supported our hypothesis of targeted nanobees enhanced the bioavailability and limited unwanted toxicity of melittin, thus leading to a significant potential for probable clinical outcome.

#4503

Polyamine blockade therapy: A strategy to block immunosuppression in pancreatic cancer

Joseph A. Goode[1], Sai Preethi Nakkina[1], Manav Gandhi[1], Otto Phanstiel[2], Deborah A. Altomare[1]. *[1]Burnett School of Biomedical Sciences, University of Central Florida, Orlando, FL,[2]Department of Medical Education, University of Central Florida, Orlando, FL*

Pancreatic ductal adenocarcinoma (PDAC) is characterized by dense desmoplasia which contributes to poor prognosis by hindering tumor entry of immune cells and therapeutics. This leads to PDAC being difficult to treat with gemcitabine, a current standard-of-care, with only a 22% 12-month survival rate. Therapeutic modalities are needed to tackle the PDAC tumor microenvironment (TME). An alternative target is polyamine metabolism which is required for tumor growth, survival, metastasis, and also for modulating generation, survival, and activity of immune cells. Myeloid-derived suppressor cells (MDSCs) are immune cells that have a key role in PDAC metastasis, invasion, progression, and in impeding anti-tumor immune response to therapeutics in PDAC. MDSCs include monocyte-like (M-MDSC) and neutrophil-like (PMN-MDSC) cells. Previous studies have shown that polyamine blockade therapy (PBT), consisting of difluoromethylornithine (DFMO) to block polyamine biosynthesis and a polyamine transport inhibitor (Trimer44NMe), elicits anti-tumor immune response, improved survival, and a decrease in MDSCs in other tumor types. This is of interest given our previous findings that PBT improved survival of PDAC-bearing mice. Here, we tested PBT in altering PDAC-stimulated MDSC survival and whether it shifts their immunosuppressive phenotype. Studies were conducted using CD11b+ bone marrow cells that were differentiated into MDSCs via GM-CSF and tumor-conditioned media from PDAC cells derived from a genetic mouse model for pancreatic cancer (KPC-mice). Bulk RNA-sequencing was conducted on MDSCs treated with PBT, gemcitabine or combination. MDSCs exhibited widespread downregulation of expression in the gemcitabine and combination treatment, but PBT alone exhibited more targeted downregulation. Specifically, Gene Ontology (GO) analysis revealed a decrease in genes associated with immune cell migration and chemotaxis, and KEGG analysis showed downregulation of inflammatory pathways. These findings indicate that PBT may modify MDSCs from their tumor-associated immunosuppressive and pro-inflammatory behavior. MDSC subtype-specific markers were investigated by flow cytometry. Results show subsets of immune cells, such as PMN-MDSCs, are reduced upon PBT treatment alone or in combination with gemcitabine, thereby highlighting the dependence of this subtype on polyamine metabolism. In

conclusion, PBT alters the expression of MDSC immunomodulatory genes, decreases MDSC survival and supports the use of PBT for treatment of PDAC in combination with other immunomodulatory therapeutics.

#4504

Targeting cMYC in metastatic castration resistant and neuroendocrine prostate cancer

Chidiebere U. Awah, Olorunseun O. Ogunwobi. *The City University of New York, New York, NY*

Prostate cancer is the most common cancer in men and the second leading cause of cancer death among men in the United States according to the National Cancer Institute. Current treatment modalities involve prostatectomy, androgen receptor blockade and supportive /palliative care. Despite these treatment options, metastatic castration resistant prostate cancer and neuroendocrine prostate cancer still have very dismal clinical outcomes. Therefore, there is a need to understand the biology of the aggressive prostate cancer subtypes to identify novel targetable molecules. The castration resistant prostate cancer, neuroendocrine prostate cancer and the metastatic prostate cancers that recur have c-MYC amplification. These cancers are not responsive to androgen blockade or deprivation therapy. Attempts to target c-MYC have been difficult due to the intrinsic disordered nature of c-MYC. Various approaches have been attempted to control c-MYC; namely RNAi which has high off target effects, anti-sense oligonucleotides (ASO) which have low cellular penetrance and needs phosphorothioate modification, G-quadruplex inhibitors which are unspecific as they block POLII, the BRD4 and CDK inhibitors which are indirect inhibitors of c-MYC. Only OmoMyc a bHLH domain mutant with enhanced leucine zipper dimerization is in phase 1 trials with limited bioavailability. To explore the possibility of targeting c-MYC in these difficult-to-treat prostate cancers, we transfected C4-2B, a cellular model of metastatic castration resistant prostate cancer, with engineered destabilized 3‘UTR AU rich element of c-MYC. We found that we degraded c-MYC transcript and protein and killed the cancer cells. Taken together, we offer preliminary evidence that we can directly target c-MYC and inhibit these difficult-to-treat cancers. *In vivo* studies to validate these findings are ongoing.

New Approaches in Radiodiagnostics and Theranostics

#5610

[^{18}F]FluorThanatrace ([^{18}F]FTT) PET Imaging of PARP-inhibitor drug-target engagement as a biomarker of response in ovarian cancer

Sarah B. Gitto[1], Austin R. Pantel[1], Mehran Makvandi[2], Hyoung Kim[3], Sergey Medvedev[3], Joanna K. Weeks[2], Drew A. Torigian[2], Chia-Ju Hsieh[2], Benjamin Ferman[3], Nawar A. Latif[3], Janos L. Tanyi[3], Lainie P. Martin[3], Shannon M. Lanzo[2], Fang Liu[4], Quy Cao[4], Gordon B. Mills[5], Robert K. Doot[2], David A. Mankoff[2], Robert H. Mach[2], Lilie L. Lin[6], Fiona Simpkins[7]. *[1]Department of Pathology and Laboratory Medicine, Perelman School of Med. Univ. of Pennsylvania, Philadelphia, PA,[2]Department of Radiology, Perelman School of Med. Univ. of Pennsylvania, Philadelphia, PA,[3]Department of Obstetrics and Gynecology, Perelman School of Med. Univ. of Pennsylvania, Philadelphia, PA,[4]Department of Biostatistics, Epidemiology, and Informatics, Perelman School of Med. Univ. of Pennsylvania, Philadelphia, PA,[5]Department of Cell, Developmental and Cancer Biology, Oregon Health & Science University School of Medicine, Portland, OR,[6]Department of Radiation Oncology, MD Anderson Cancer Center, The University of Texas, Houston, TX,[7]Department of Obstetrics & Gynecology, Perelman School of Med. Univ. of Pennsylvania, Philadelphia, PA*

Purpose: Poly(ADP-ribose) polymerase enzyme inhibitors (PARPi) have become the standard-of-care treatment for homologous recombination deficient (HRD) high-grade serous ovarian cancer (HGSOC). However, not all HRD tumors respond to PARPi and biomarkers to predict response are needed. [^{18}F]FluorThanatrace (FTT) is a PARPi-analog PET radiotracer that non-invasively measures PARP-1 expression. Herein, we evaluate the ability of FTT uptake to serve as a biomarker to predict response to PARPi in patient-derived xenograft (PDX) models and patients with HGSOC.
Patients and Methods: In PDX models, FTT-PET was performed before and after PARPi (olaparib), ataxia-telangiectasia inhibitor (ATRi), or both. Changes in FTT were correlated with tumor size changes. Patients

with HRD and HGSOC that were enrolled in CAPRI (PARPi+ATRi), LIGHT (PARPi only), or off-trial (PARPi only) were selected for this single-center, prospective, cohort, IRB-approved study. FTT-PET/CT imagining was obtained from the skull base to the proximal thighs on an Ingenuity TF scanner (Philips Healthcare) 60-90 minutes after intravenous infusion of 8-12 mCi FTT. Subjects were imaged with FTT-PET at baseline and after ~1 week of PARPi monotherapy treatment. Target lesions (primary tumor and/or metastases) were identified at the time of the baseline imaging on correlative anatomic imaging using RECIST 1.1 and maximum standardized uptake value (SUV_{max}) data, normalized by body weight, was collected. Changes in FTT-PET uptake were compared to changes in tumor size, CA-125, and progression free survival (PFS).
Results: A decrease in FTT tumor uptake after 1 week of PARPi treatment correlated with response to PARPi+ATRi treatment in PARPi-resistant PDX models (r=0.81-0.83, P=0.1-0.22). In HGSOC patients (n=13), percent differences in FTT-PET after ~7 days of PARPi compared to baseline correlated with the first RECIST response (r=0.60, P=0.034), best RECIST response (r=0.75, P=0.01), best CA-125 response (r=0.73, P=0.033), and PFS (r=0.67, P=0.027). All patients with >50% reduction in FTT uptake had >6-month PFS and >50% reduction in CA-125 (P=0.004 and P=0.016, respectively). Utilizing only baseline FTT uptake correlated to best RECIST response (r=-0.65, P=0.035) but did not predict response when corelated with other measures. Importantly, a decrease in FTT uptake does not appear to be associated with a reduction in tumor burden or apoptosis in response to drug cytotoxic activity at this early timepoint, indicating specificity for drug-target engagement.
Conclusions: The decline in FTT uptake shortly after PARPi initiation compared to baseline provides an in vivo measure of drug-target engagement and shows promise as an early biomarker to guide PARPi therapy. FTT-PET has both pre-clinical and clinical applications warranting further study, including guiding PARPi combination therapy.

#5611

LAG-3 PET imaging in patients with cancer before immune checkpoint inhibitor therapy

Pim P. van de Donk[1], Lotte M. Smit[1], Joyce van Sluis[2], Wim Timens[3], Adrienne H. Brouwers[2], Marjolijn N. Lub-de Hooge[2], Sjoerd G. Elias[4], Jourik A. Gietema[1], Claudia A. J. van Winkel[1], JuAn Wang[5], Jason Giurleo[5], Thomas Uldrick[5], Hung Kam Cheung[5], Hilde Jalving[1], Sjoukje F. Oosting[1], Daan G. Knapen[1], Derk-Jan A. de Groot[1], Elisabeth G. E. de Vries[1]. *[1]Medical Oncology, University Medical Center Groningen, Groningen, Netherlands,[2]Department of Nuclear Medicine and Molecular Imaging, University Medical Center Groningen, Groningen, Netherlands,[3]Department of Pathology and Medical Biology, University Medical Center Groningen, Groningen, Netherlands,[4]Department of Epidemiology, Julius Center for Health Sciences and Primary Care, Utrecht, Netherlands,[5]Regeneron Pharmaceuticals, Tarrytown, NY*

Background Immune checkpoint inhibitors (ICIs) can induce durable responses in multiple different tumor types. Lymphocyte activation gene-3 (LAG-3) is one of the immune checkpoints for which therapeutic antibodies are being developed. PET imaging with radiolabeled ICIs can visualize whether the drug reaches the tumor, and might serve as a target expression readout. Therefore, we aimed to evaluate the safety of the radiolabeled LAG-3 antibody ^{89}Zr-DFO-REGN3767, to determine the optimal tracer dose and imaging time point, and to get insight into ^{89}Zr-DFO-REGN3767 whole body distribution.
Methods Patients with advanced solid tumors received 37 MBq ^{89}Zr-DFO-REGN3767 together with unlabeled antibody to achieve a 2, 5, 10, 20, or 40 mg total protein dose (NCT04706715). Patients underwent PET/CT scans on days 0, 2, 4, and 7 after injection, followed by a tumor biopsy. After that, they received treatment with cemiplimab alone or combined with platinum-containing chemotherapy. PET scans were analyzed by placing volumes of interest (VOIs) in tumor lesions and normal tissues. Tracer uptake was measured in the VOIs and expressed as the maximum standardized uptake value (SUV_{max}) for tumor lesions and as the mean standardized uptake value (SUV_{mean}) for normal tissues.
Results The 16 included patients experienced no ^{89}Zr-DFO-REGN3767-related side effects. Tumor-to-blood ratios for all dose levels increased from days 0 to 7. Therefore, imaging 7 days after tracer injection was deemed optimal to achieve the highest contrast. The 40 mg tracer dose resulted in the most favorable blood kinetics. At this dose, tracer uptake in tumor lesions (n = 17) varied between patients (geometric mean

SUV_{max} 6.2; SD 1.7). In normal tissues, uptake was seen in the spleen ($\bar{x}$ 11.2; SD 1.6), and bone marrow ($\bar{x}$ 2.2; SD 0.7), which increased from days 0 to 7. Tracer uptake was visually present in regions with inflammation.
Conclusion ^{89}Zr-DFO-REGN3767 PET imaging is feasible and studied patients did not experience tracer related side effects. Optimal imaging results were achieved with the 40 mg protein dose and imaging on day 7. ^{89}Zr-DFO-REGN3767 shows specific accumulation in LAG-3 rich tissues and tumor lesions.

#5612
Shape features of extra-nodal lesions on positron emission tomography identifies responders to CAR-T-cell therapy
Yoganand Balagurunathan[1], Zhouping Wei[1], Jin Qi[1], Erin Dean[1], Zachary Thompson[1], Jung Choi[1], Frederick Locke[2]. *[1]H. Lee Moffitt Cancer Center, Tampa, FL,[2]Bone Marrow Transplant, H. Lee Moffitt Cancer Center, Tampa, FL*

Background: Lymphoma is a common primary malignancy consisting of a heterogeneous collection of lymphoid neoplasms. Diffuse large B-cell lymphoma (DLBCL) is the most common, aggressive disease form that accounts for 30% of all lymphoma cases. The disease spreads systemically to involve organs other than lymph nodes 40% of the time, with 5-year survival of about 38% for intermediate grade disease. Recent development in chimeric antigen receptor (CAR) T-cell therapy has shown tremendous promise in providing a cure to patients with relapsed/refractory (R/R) DLBCL. We propose to develop an image-based biomarker to identify patients that would respond to engineer edcell-based treatments.
Methods: We identified a cohort of 58 patients with R/R DLBCL, whose largest lesions on the baseline positron emission tomography /computed tomography (PET/CT) imaging were identified along with their anatomical sites related to non-lymphatics. The lesion's co-registered PET imaging was used to converge on a regional boundary to obtain the most active part of the lesion, applying Standardized Uptake Value definition with 41% regional threshold. The lesion regions were characterized using imaging metrics (radiomics) broadly categorized into: Size (n=38), Shape (n=9), Texture (n=259),followed by principal component (PC) analysis to reduce the dimensionality in each of the feature categories. These Radiomics metrics along with whole body metabolic tumor volume (MTV) were used both collectively and independently to assess risk to disease progression measured by overall survival using Cox-regression model. We also compared the Radiomic metrics to MTV to identify linear dependency measured by Coefficient of Determination (R^2).
Results: PET scans shape features (extra nodal) that describes compactness to sphericity, represented as a principal component across the samples had a 21% increased risk to disease progression compared to 15% using MTV, with a CI of [1.0487, 1.417] and [1.04, 1.30] respectively. Patients have a median follow up of 1 year after CAR-T treatment. Shape-PC (Non-Lymph) lesions were not related to MTV with a correlation coefficient of 41.8% (R^2 of 0.0725). Most non lymphatic lesions (top three sites) in our cohort were from lung, bone and liver. Patients with no non- lymphatic lesions were not part of this cohort.
Conclusion: We identified Non-Size based features that are prognostic to patient response to treatment. These metrics provide complementary information to MTV and may serve as a surrogate to treatment response. Our features would require a secondary validation in a larger cohort prior to clinical use.

#5613
Tumor glucose metabolism profiles detected via [18F]-FDG PET/CT correlate with the immune landascape in soft-tissue sarcomas
Amandine Crombe[1], Frédéric Bertolo[2], Jean-Philippe Guegan[3], Alban Bessede[3], Raul Perret[4], Mariella Spalato-Ceruso[5], Maud Toulmonde[5], Audrey Laroche[6], Francois Le Loarer[4], Vanessa Chaire[4], Michèle Kind[1], Carlo Lucchesi[2], Antoine Italiano[5]. *[1]Radiology, Institute Bergonié, Bordeaux, France,[2]Bioinformatics, Institute Bergonié, Bordeaux, France,[3]Explicyte, Bordeaux, France,[4]Biopathology, Institute Bergonié, Bordeaux, France,[5]Medical oncology, Institute Bergonié, Bordeaux, France,[6]Sarcoma unit, Institute Bergonié, Bordeaux, France*

Background: Improving the assessment of the immune landscape of soft-tissue sarcoma (STS) through imaging biomarkers could help better selecting and monitoring patients that could benefit from immunotherapy. Our aim was identify whether metabolic patterns of soft-tissue sarcoma (STS) on pre-treatment 18F-Fluorodeoxyglucose (18F-FDG) positron emission tomography (PET/CT) were associated with different immune profiles on molecular and cellular levels.
Methods: This single-center prospective study included consecutive adult patients with newly-diagnosed, non-metastatic, high-grade STS treated in a curative intent with available pre-treatement 18F-FDG-PET/CT. Maximal standardized uptake value (SUVmax), SUVpeak, SUVmean, metabolic tumor volume (MTV) and total lesion glycolysis (TLG) were extracted. A cross-validated principal component analysis (PCA) was developed on the PET/CT metrics. The first two principal components (PC1 and PC2) and an unsupervised metabolic classifications were computed.
Differential gene expression (DGE), oncogenesis pathways analyses, complexity index in sarcoma (CINSARC) molecular signature and immunohistochemistry panels (CD8, CD14, CD20, CD45, CD68, c-MAF) were performed. Correlations between nuclear imaging, immunohistochemistry and transcriptomics data were achieved.
Results: 85 patients were included (median age: 62 years, 37 women) between 2016 and 2021. The robust PCA defined 3 metabolic groups (high [n=21], intermediate [n=15] and low [n=49]). PC1 reflected the tumor metabolism and PC2 the size and amount of necrosis. Transcriptomics and immunohistochemistry data were available in 32 and 31 patients, respectively. PC1 was significantly positively correlated with CINSARC (P=0.0029) and the cellular densities in CD8+, CD14+, CD45+, CD68+ and c-MAF (range of P-values: 0.0175-0.0499). The metabolic-high group was characterized by the upregulation of 13 immune pathways, including ICOS, CD27, IFNG, CXCL9-10/CXCL3 genes.
Conclusion: Metabolic profiles on 18F-FDG-PET/CT of high-grade STS highlights distinct immune profiles, which could pave the way for potential biomarkers of STS immunophenotyping.

#5614

Genomic aberrations in circulating tumor DNA (ctDNA) and clinical outcomes from [^{177}Lu]Lu-PSMA-617 in metastatic castration-resistant prostate cancer (mCRPC)

Heidi Fettke[1], Louise Kostos[1], James Buteau[1], Jason A. Steen[2], Elizabeth Medhurst[1], Mo B. Haskali[1], Declan Murphy[1], Maria Docanto[1], Patricia Bukczynska[1], Nicole Ng[1], Shahneen Sandhu[1], Siavash Foroughi[3], Luc Furic[1], Tu Nguyen-Dumont[2], Michael S. Hofman[1], Arun A. Azad[1]. *[1]Peter MacCallum Cancer Centre, Melbourne, Australia,[2]Monash University, Melbourne, Australia,[3]Walter and Eliza Hall Institute of Medical Research, Melbourne, Australia*

[^{177}Lu]Lu-PSMA-617 (LuPSMA) radionuclide therapy improves overall survival in mCRPC, and was recently approved by the FDA. Nevertheless, owing to the heterogeneous nature of mCRPC, responses to LuPSMA therapy can be variable, and resistance is inevitable. As a result, biomarkers linked to clinical outcome with LuPSMA are urgently required. Using plasma ctDNA, we present the first comprehensive genomic analysis of a prospective cohort of mCRPC patients treated with LuPSMA. Targeted sequencing of 78 genes was performed on baseline plasma and matched buffy coat samples from patients who received LuPSMA on a prospective registry (NCT04769817). Reportable alterations included pathogenic single-nucleotide and copy number variants. Association between alterations and clinical outcomes were assessed using log rank, cox proportional, and chi-squared analyses. Clinical data collected included PSA decline by ≥50% or ≥90% (PSA50-response rate, PSA50-RR; and PSA90-RR), and PSA progression free survival (PSA-PFS). In total, 100 patients (median age 74 years, range 52-90) received a median of 4 cycles of LuPSMA. 83 patients had detectable ctDNA (median fraction 17%, range 0-94%) with PSA50-RR 50%, PSA90-RR 22%, and a median PSA-PFS of 7.2 months. Patients with an *AR* or *PTEN* aberration had significantly shorter PSA-PFS (HR 0.50 and 0.59, respectively; Table), as did patients with any *PI3K* pathway aberration (HR 0.56). Additionally, patients with a high ctDNA burden had significantly worse PSA-PFS (HR 0.42, Table). There were no significant differences in PSA-RR based on deleterious genomic changes. Our data reveal that aberrations in the *AR* and PI3K pathways, along with pre-treatment ctDNA fraction, whilst not linked to PSA-RR, are prognostic for durability of response to LuPSMA. If validated in

larger cohorts, these data will help to optimise the use of LuPSMA by improving patient selection and enhancing prognostication.

Analysis of clinical endpoints based on deleterious genomic changes in ctDNA

	n	PSA-PFS (months, wild type (wt) vs variant)	PSA-PFS HR (95% CI, wt vs variant)	PSA50-RR (wt vs variant)	PSA90-RR (wt vs variant)
Exonic *AR* variants	47	**8.1 vs 6.0 p=0.005**	**0.50 (0.30-0.83) p=0.006**	58% vs 40% p=0.09	23% vs 21% p=0.8
Any *AR* variant (intronic and upstream enhancer regions included)	49	**8.1 vs 6.0 p=0.007**	**0.53 (0.31-0.83) p=0.008**	60% vs 41% p=0.09	24% vs 20% p=0.7
RB1 variant	19	7.9 vs 5.5 p=0.2	0.67 (0.39-1.2) p=0.2	51% vs 42% p=0.5	23% vs 21% p=0.9
PTEN variant	25	**7.8 vs 6.3 p=0.04**	**0.59 (0.36-1.00) p=0.045**	50% vs 48% p=0.9	22% vs 24% p=0.8
TP53 variant	43	8.1 vs 6.7 p=0.1	0.67 (0.42-1.1) p=0.1	52% vs 47% p=0.6	20% vs 26% p=0.5
BRCA2 variant	10	7.7 vs 5.1 p=0.2	0.63 (0.29-1.30) p=0.2	51% vs 40% p=0.7	20% vs 40% p=0.1
PIK3CA variant	8	7.7 vs 4.1 p=0.08	0.48 (0.20-1.1) p=0.09	52% vs 13% p=0.06	23% vs 13% p=0.5
PI3K pathway variant	35	**7.8 vs 5.5 p= 0.02**	**0.56 (0.34-0.91) p=0.02**	55% vs 40% p=0.2	22% vs 23% p=0.9
ctDNA fraction ≥20%	43	**9.0 vs 5.1 p=0.0002**	**0.42 (0.26-0.67) p<0.001**	55% vs 42% p=0.2	21% vs 23% p=0.8

#5615

Novel trop-2-targeted NIR-II fluorescence imaging technique for accurate determination of breast conserving surgery margin *in vivo* and human fresh tissue

Weiling Chen[1], YongQu Zhang[1], LiXin Zhang[1], XiangJie Luo[1], YuanYuan Zhu[1], GuiMei Wang[2], YunZhu Zeng[3], JiaZheng Wang[1], RongHui Li[4], WenHe Huang[5], GuoJun Zhang[5]. *[1]Xiamen University, Xiamen, China,[2]Department of Pathology, Xiang'an Hospital of Xiamen University, Xiamen, China,[3]Department of Pathology, Cancer Hospital of Shantou University Medical College, Shantou, China,[4]Department of Medical Oncology, Xiang'an Hospital of Xiamen University, Xiamen, China,[5]Department of Breast-Thyroid-Surgery and Cancer Center, Xiang'an Hospital of Xiamen University, Xiamen, China*

Purpose Accurate evaluation of tumor boundaries in breast-conserving surgery is very important to reduce the second operation of patients.Near-infrared fluorescence imaging using molecular agents has shown promise for in situ imaging during resection.However, there are very effective probes that can be applied to clinical trials up to now. Here we developed a new technology that can quickly identify the tumor area both in vivo and the resected breast tissue during the operation and distinguish the tumor boundary.
Methods 1. Characterization and biosafety of the probe SG-ICG were performed.2. The targeting of the probe was verified by in vitro fluorescence co-localization and flow cytometry experiment and in vivo fluorescence imaging using tumor-bearing mouse model.3. Fluorescence image-guided surgery in spontaneous breast cancer transgenic mice and transplanted tumor model were to evaluated the specificity and sensitivity of guided tumor resection with the probe.4. The tumors and peritumoral muscle tissues of tumor-bearing mice were surgically removed and incubated with SG-ICG, and then imaged by a NIR-II fuorescence imaging system. 5. Six surgically removed breast tissues were incubated with the probe immediately after intraoperative resection and imaged to identify the tumor area. The accuracy of fuorescence imaging was confirmed by pathological diagnosis.

Results 1. SG-ICG was successfully synthesized with good dispersibility, stability with high intensity of NIR-II fluorescent imaging. 2. SG-ICG could specifically target high expression level of Trop-2 in breast cancer cell lines compared with IgG-ICG.3. SG-ICG was able to detected the MDA-MB-231-luc breast cell tumor-bearing mouse models with tumor-to-background ratios of ~4, correspondingly, nearly 2-fold NIR-II FL signal decrease was detected while blocked by unlabeled SG. 4. SG-ICG was able to detected the minimal residual lesions and the minimum detectable tumor diameter is about 1mm. The NIR-II fluorescence guidance facilitated more complete tumor resection, it has improved the relapse free survival rate, and effectively discriminates between benign and malignant breast tissues in spontaneous breast cancer transgenic mice (AUC= 0.9931; 95% CI: 0.9708, 1.0;P<0.0001)..5. This new technology yielded more than 83.33% specifcity and 100% sensitivity in identifying the tumor area in the resected breast tissue. **Conclusions** By using fuorescently labeled anti-human trop-2 antibody-drug conjugate to incubate freshly isolated tissues during surgery, the probes can quickly accumulate in breast cancer tissues, which can be used to quickly identify tumor areas in the resected breast tissues and distinguish tumor boundaries. This technology is expected to be used for rapid intraoperative pathological detection and margin determination.

#5616

Optical metabolic imaging of treatment-naive human NSCLC to determine long-term outcome

Paola Monterroso Diaz*. University of Arkansas, Fayetteville, AR*

Lung cancer remains the leading cause of cancer deaths in the US and worldwide. The five-year survival rate of patients with non-small cell lung carcinoma (NSCLC) remains significantly low given that over half present with locally advanced or metastatic disease at time of diagnosis, and experience tumor recurrence following therapeutic intervention.Current evaluation techniques to assess treatment response are lacking, given they are implemented several weeks after treatment completion and are solely based on anatomical changes in tumor size, forgoing other criteria such as functional or metabolic changes. There is a critical need to identify markers early on following diagnosis that are indicative of patient long-term outcome. Two photon microscopy (TPM) techniques are well-suited to provide non-invasive high-resolution information on cell metabolism within three-dimensional tissue. Specifically, two-photon excited fluorescence imaging of autofluorescent cofactors, nicotinamide adenine dinucleotide (NADH) and flavin adenine dinucleotide (FAD), can be used to metabolically characterize cancerous tissue. The goal of this study is to utilize the optical redox ratio (ORR) of FAD/[NADH+FAD] autofluorescence and NADH fluorescence lifetime decay to identify measurable differences in optical metabolic endpoints of human NSCLC that are indicative of their long-term outcome. Twenty-nine NSCLC specimens were obtained from the Lung Cancer Biospecimen Resource Network. They were resected from the lung prior to the patient receiving therapy. Clinical detail reports were used to evaluate the follow-up data of each patient and classify them into groups that reflected their eventual outcomes: responder (N=21), non-responder (N=18), non-metastatic (N=25), and metastatic (N=14). TPM was used to determine the ORR for each sample. NADH lifetime images were collected and fit to a biexponential model to separate the short (A1) and long (A2) components of free and bound NADH. We observed a significantly higher optical redox ratio for tumors within the metastatic group compared to non-metastatic. This is consistent with previous findings from our lab that revealed increases in the ORR with increasing metastatic potential in cells, as well as other studies reporting a decrease in NADH concentration in metastatic cancers. Additionally, a significantly shorter mean NADH lifetime in the metastatic tumor group was revealed when compared to non-metastatic. This stands in agreement with other studies highlighting decreases in the average lifetime of NADH in metastatic cells compared to non-metastatic. These results demonstrate the feasibility of using optical imaging of autofluorescence and lifetimes of metabolic cofactors to characterize treatment-naïve primary NSCLC tumors and determine differences in their optical metabolic endpoints that are indicative of their long-term outcome.

#5617

A novel DNA double-strand breaks biosensor based on fluorescence resonance energy transfer

Jung-Soo Suh, Tae-Jin Kim*. Pusan National University, Busan, Korea, Republic of*

Revealing the spatiotemporal behavior of DNA double-strand breaks (DSBs) is crucial for understanding the processes of DNA damage and repair. Traditionally, γH2AX and DNA damage response (DDR) factors have been used to detect DSBs using classical biochemical assays, such as antibody-based immunostaining. However, a reliable method to visualize and assess DSB activity real-time in living cells is yet to be established. Herein, we developed a novel DNA double-strand breaks biosensor (DSBS) based on fluorescence resonance energy transfer (FRET) by employing the H2AX and BRCT1 domains. By applying FRET imaging with DSBS, we show that DSBS specifically reacts to drug- or ionizing radiation (IR)-induced γH2AX activity, allowing for the quantification of DSB events at high spatiotemporal resolutions. Taken together, we provide a new experimental tool to evaluate the spatiotemporal dynamics of DNA double-strand breaks in response to cancer therapies. Ultimately, our biosensor can be useful for elucidating the molecular mechanisms underlying DNA damage and repair processes and applying for cancer therapies.

#5618

Multi-institutional validation of a radiomics-based artificial intelligence method for predicting response to PD-1/PD-L1 immune checkpoint inhibitor (ICI) therapy in stage IV NSCLC

Ravi B. Parikh[1], Petr Jordan[2], Rita J. Ciaravino[2], Ryan A. Beasley[2], Arpan A. Patel[3], Dwight H. Owen[4], Arya Amini[5], Brendan D. Curti[6], Ray Page[7], Aurelie Swalduz[8], Jean-Paul Beregi[9], Jan Chrusciel[10], Eric Snyder[11], Pritam Mukherjee[12], Heather M. Selby[12], Soohee Lee[13], Roshanthi Weerasinghe[14], Shwetha Pindikuri[13], Jakob B. Weiss[15], Andrew L. Wentland[16], Anish Kirpalani[17], An Liu[5], Olivier Gevaert[18], George Simon[19], Hugo JWL Aerts[15]. *[1]Medical Ethics and Health Policy and Medicine, University of Pennsylvania, Philadephia, PA,[2]Onc.AI, San Carlos, CA,[3]Medicine, Hematology/Oncology (SMD), University of Rochester Medical Center, Rochester, NY,[4]Division of Medical Oncology, The Ohio State University, Columbus, OH,[5]Radiation Oncology, City of Hope, Duarte, CA,[6]Clinical Research, Providence Cancer Institute, Portland, OR,[7]The Center for Cancer & Blood Disorders, Fort Worth, TX,[8]Centre Léon Bérard, Lyon, France,[9]CHU Nimes, Nimes, France,[10]Centre Hospitalier de Troyes, Troyes, France,[11]University of Rochester Medical Center, Rochester, NY,[12]Stanford University, Palo Alto, CA,[13]Providence Health & Services, Renton, WA,[14]Providence St. Joseph Health, Portland, OR,[15]Mass General Brigham, Boston, MA,[16]School of Medicine and Public Health, University of Wisconsin, Madison, WI,[17]University of Toronto, Toronto, ON, Canada,[18]Medicine - Biomedical Informatics Research, Stanford University, Palo Alto, CA,[19]Medical Oncology, Moffitt Cancer Center, Tampa, FL*

There is an urgent clinical need to identify patients likely to benefit from immune checkpoint inhibitor ICI treatment. Approaches available in the clinic today, such as PD-L1 immunohistochemistry (IHC) and tumor mutation burden (TMB), are insufficient for this task, in part as differences in microenvironments expressed by individual tumors may lead to heterogeneous response patterns. Recent efforts exploring the utility of quantitative imaging (radiomic) biomarkers to predict response to ICIs have shown promise to provide a more accurate and scalable method. In contrast to previously published models, our work focuses on generalizable models for predicting individual lesion-level as well as patient-level response at 3-month follow-up per RECIST criteria, using a large multi-institutional “real-world” dataset. The models combine radiomics features with demographic, molecular, and laboratory values routinely available in patients’ electronic medical records. We analyzed radiomic characteristics of 6,295 primary and metastatic lesions from 1,206 metastatic NSCLC patients treated with anti-PD-1/anti-PD-L1 ICIs from 8 institutions across the US and Europe. Patients with unavailable PD-L1 IHC, imaging follow-up, or with oncogenic driver mutations were excluded from analysis, resulting in a total dataset of 766 subjects randomly assigned to training (N=514) and validation sets (N=252). Using gradient-boosted decision tree algorithms, we developed a multi-modal predictive model to identify patients responding to ICI therapy at 3-months and evaluated its performance against an imaging-only CT radiomics model and the clinical standard of care, biopsy-based PD-L1 IHC. The multi-modal model contains CT radiomic features capturing lesion heterogeneity and spicularity, patient demographics, PD-L1 TPS, and tumor burden volume in the lung, lymph nodes, and the liver. Under the two-tailed DeLong test, the multi-modal model demonstrated statistically significant benefit over the current standard of care (PD-L1 IHC) in predicting multi-lesion 3-month response: 0.81 (P=.005) area under the receiver operating characteristic curve (ROC-AUC) in first-

line ICI monotherapy patients, 0.72 (P=.044) in all-lines ICI monotherapy, and 0.71 (P=.025) in all-lines ICI-chemotherapy combination. The imaging-only model demonstrated predictive performance comparable to PD-L1 IHC: 0.71 (P=.226), 0.61 (P=.905), 0.62 (P=.674) on the same cohorts respectively. A multi-modal CT radiomics-based approach demonstrated predictive accuracy benefit over the current clinical standard and may provide an opportunity for more personalized patient management, such as risk-based escalation/de-escalation of concurrent chemotherapy in NSCLC patients. We will evaluate this methodology in prospective studies.

#5619

Radiomics-based machine learning models to predict progression and biomarker status in non-small cell lung cancer (NSCLC) patients treated with immunotherapy

Jisang Yu[1], Yury Velichko[2], Hyeonseon Kim[1], Moataz Soliman[2], Nicolo Gennnaro[2], Leeseul Kim[3], Youjin Oh[1], Trie Arni Djunadi[1], Jeeyeon Lee[4], Liam Il-Young Chung[1], Sungmi Yoon[5], Zunairah Shah[6], Soowon Lee[7], Cecilia Nam[8], Timothy Hong[8], Rishi Agrawal[2], Pascale Aouad[2], Young Kwang Chae[1]. *[1]Department of Oncology, Northwestern Univ. Feinberg School of Medicine, Chicago, IL,[2]Department of Radiology, Northwestern Univ. Feinberg School of Medicine, Chicago, IL,[3]Ascension Saint Francis Hospital Evanston, Evanston, IL,[4]School of Medicine, Kyungpook National University, Daegu, Korea, Republic of,[5]New York City Health and Hospitals Corporation North Central Bronx/Jacobi Medical Center, The Bronx, NY,[6]Weiss Memorial Hospital, Chicago, IL,[7]Baylor University, Waco, TX,[8]Northwestern University, Evanston, IL*

Background: Radiomics is an emerging tool that involves the extraction of high-throughput features from medical images. These quantitative values can be used to develop predictive models for clinical characteristics and treatment outcomes. We evaluated radiomic features-based models as imaging biomarkers in NSCLC patients.

Methods: 71 patients with NSCLC treated with immunotherapy who had pretreatment CT chest with contrast were retrospectively evaluated. The main tumor and 1cm-thick peritumoral space surrounding the tumor were manually segmented using LIFEx software (IMIV/CEA, Orsay, France) by four physicians. Of 255 radiomic features collected, those with >0.4 of Fleiss' kappa coefficient were selected. The Random Forest (RF) algorithm with mixed effects was used to develop multi-reader models and assess feature importance. The dataset was divided into a training set (75%) and a test set (25%). Bootstrapping with 1,000 iterations was conducted to estimate the model performance. Durable disease control was defined as having no progression of diseases per RECIST 1.1 up to 24 weeks from starting immunotherapy.

Results: Among 71 patients, 35 (49.3%) are female and 36 (50.7%) are male. The median age was 66. 48 (67.6%) adenocarcinoma, 13 (18.3%) squamous cell carcinoma, and 10 (14.1%) other histologic types were included. 22 radiomic features were included based on importance in the prediction models from both the tumor and peritumoral space. Each model is trained to predict patients' durable disease control, TTF1 expression, PD-L1 expression, histology (adenocarcinoma or not), and Neutrophils Lymphocyte Ratio (NLR; greater than 5 or not) status. The statistical results from the models to predict clinical outcomes are shown in Table.

Conclusion: The radiomic features-based models lack accuracy in predicting clinical characteristics and outcomes. Further validation with larger cohorts is warranted.

Statistics of radiomics-based models in predicting clinical characteristics and treatment outcomes

	Durable Disease Control(Yes/No) (n=64)	TTF1 expression(Yes/No) (n=62)	Histology(Adeno/Other) (n=71)	NLR(>=5/<5) (n=71)	PD-L1 expression(Yes/No) (n=52)
Patient Number(%)	33 (51.56%) / 31 (48.44%)	37 (59.68%) / 25 (40.32%)	48 (67.61%) / 23 (32.39%)	28 (39.44%) / 43 (60.56%)	35 (67.31%) / 17 (32.69%)
Sensitivity (95% CI)	0.63 (0.58, 0.72)	0.62 (0.56, 0.74)	0.69 (0.56, 0.82)	0.55 (0.47, 0.61)	0.57 (0.48, 0.65)
Specificity (95% CI)	0.46 (0.37, 0.52)	0.68 (0.58, 0.76)	0.22 (0.12, 0.34)	0.60 (0.56, 0.68)	0.36 (0.30, 0.45)

Positive Predictive Value(95% CI)	0.52 (0.49, 0.57)	0.44(0.37, 0.60)	0.62 (0.59, 0.64)	0.69 (0.67, 0.74)	0.72 (0.68, 0.77)
Negative Predictive Value(95% CI)	0.58 (0.54, 0.63)	0.79 (0.74, 0.88)	0.28 (0.22, 0.32)	0.46 (0.39, 0.51)	0.25 (0.21, 0.28)

#5620

Radiogenomic analysis in the patients with primary brain tumor using dual time point ^{18}F-FET PET/CT

Dong Yun Lee, Sang Woo Song, Seungjoo Lee, Minyoung Oh, Jungsu S. Oh, Jaeseung Kim. *Asan Medical Center (AMC), Seoul, Korea, Republic of*

Purpose: To evaluate the association between genomic data and imaging features of dual time point ^{18}F-FET PET/CT in patients with primary brain tumor for radiogenomic mapping.
Methods: From June 2021 to July 2022, we prospectively enrolled the patients under suspicious of *de novo* primary brain tumor in Asan Medical Center. Prior to the surgery, contrast-enhanced MRI and ^{18}F-FET PET/CT scans were routinely performed. Twenty minutes after the post-injecting (p.i.) approximately 5 mCi of ^{18}F-FET, patients underwent early PET/CT acquisition (20-40 min p.i.). Delay PET/CT (80-100 min p.i) was subsequently obtained after 40-minute break. SUVmax, maximum tumor-to-brain ratios and PET-positive volumes using different isocontours of SUVmax (I30, I60, I90%) in tumor were calculated in each sum images. Histopathologic results were made based on 2016 WHO classification and, isocitrate dehydrogenase (IDH) mutation, O^6-methylguanine-DNA methyltransferase (MGMT) methylation, telomerase reverse transcriptase (TERT) mutation and co-deletion of 1p19q status were investigated as well. Spearman's correlation coefficient (r), logistic regression and AUC-ROC analysis were employed using aforementioned radiomics information.
Results: A total of 42 patients (median age 55.5 yrs, range 21-84; M:F=31:11) were recruited and, 29 patients had glioblastoma with grade IV. Except TERT mutation (n=25), IDH mutation (n=11), MGMT methylation (n=19) and co-deletion of 1p19q (n=8) had statistically significant correlation each other (IDH vs. MGMT, r=0.55; IDH vs. 1p19q, r=0.53; MGMT vs. 1p19q, r=0.42). Early scan of I60% was closely related with IDH mutation (positive, 3.92 ± 3.04 vs. negative, 7.96 ± 5.36; p=0.005) meanwhile delay scan of I30% had significant association with co-deletion of 1p19q (present, 34.16 ± 18.67 vs. absent, 71.99 ± 38.79; p=0.01). The accuracy of logistic regression and the corresponding AUC-ROC values for IDH/MGMT/TERT/co-deletion of 1p19q status were 0.86/0.73/0.78/0.85, and 0.88/0.76/0.78/0.91, respectively.
Conclusion: Although this is a preliminary and interim analysis during our prospective study being slated to enroll the patients until December 2023, we suggest that the information acquired from both genetics and ^{18}F-FET could be integrated into better characterization of primary brain tumor.

#5621

Multi-parametric MRI maps regional heterogeneity of high grade glioma phenotypes

Matthew Flick[1], Taylor Weiskittel[2], Kevin Meng-Lin[3], Fulvio D'Angelo[4], Francesca Caruso[5], Shannon Ensign[6], Mylan Blomquist[7], Luija Wang[8], Christopher Sereduk[9], Gustavo De Leon[10], Ashley Nespodzany[11], Javier Urcuyo[12], Ashlynn Gonzalez[11], Lee Curtin[12], Kyle Singleton[12], Aliya Anil[13], Natenael Simmineh[14], Erika Lewis[15], Teresa Noviello[16], Reyna Patel[17], Panwen Wang[9], Junwen Wang[18], Jennifer Eschbacher[13], Andrea Hawkins-Daarud[9], Pamela Jackson[9], Kris Smith[13], Peter Nakaji[19], Bernard Bendok[9], Richard Zimmerman[9], Chandan Krishna[9], Devi Patra[9], Naresh Patel[9], Mark Lyons[9], Matthew Neal[9], Kliment Donev[20], Maciej Mrugala[17], Alyx Porter[17], Scott Beeman[21], Yuxiang Zhou[17], Leslie Baxter[22], Christopher Plaisier[23], Jing Li[8], Hu Li[3], Anna Lasorella[24], Chad Quarles[14], Kristin Swanson[9], Michele Ceccarelli[16],

Antonio Iavarone[25], Nhan Tran[9], Leland Hu[26]. *[1]Mayo Clinic Alix School of Medicine, Scottsdale, AZ,[2]Mayo Clinic Alix School of Medicine, Rochester, MN,[3]Mayo Clinic, Rochester, MN,[4]Neurological Surgery, Miller School of Medicine, University of Miami, Miami, FL,[5]Electrical Engineering and Information Technologies, University of Naples, Naples, Italy,[6]Hematology and Oncology, Mayo Clinic Arizona, Phoenix, AZ,[7]Molecular Pharmacology and Experimental Therapeutics, Mayo Clinic, Rochester, MN,[8]Georgia Institute of Technology, Atlanta, GA,[9]Mayo Clinic Arizona, Scottsdale, AZ,[10]Neurological Surgery, Mayo Clinic, Scottsdale, AZ,[11]Neuroimaging Research, Barrow Neurological Institute, Phoenix, AZ,[12]Neurological Surgery, Mayo Clinic Arizona, Scottsdale, AZ,[13]Barrow Neurological Institute, Phoenix, AZ,[14]University of Texas MD Andersen Cancer Center, Houston, TX,[15]Arizona State Univeristy, Tempe, AZ,[16]University of Naples, Naples, Italy,[17]Mayo Clinic Arizona, Phoenix, AZ,[18]The University of Hong Kong, Hong Kong, China,[19]Banner University Medical Center, Phoenix, AZ,[20]Mayo Clinic Ariona, Phoenix, AZ,[21]Arizona State Univesity, Phoenix, AZ,[22]Mayo Clinic, Scottsdale, AZ,[23]Arizona State University, Tempe, AZ,[24]Miller School of Medicine, Miama, FL,[25]Miller School of Medicine, University of Miama, Miama, FL,[26]Radiology, Mayo Clinic, Phoenix, AZ*

High grade glioma (HGG) represents a group of devastating diseases with dismal prognosis. Surgical resection of the contrast enhancing (CE) region of HGG remains the mainstay of treatment, but recurrence inevitably arises from the unresected non-contrast enhancing (NE) region, surgically inaccessible due to cancer cell invasion into healthy brain tissue. Due to its critical role in recurrence, understanding of the NE region is central to the improvement of clinical outcomes. We reveal the biological characteristics of this region through image localized multi-regional sampling. We linked microenvironmental characteristics measured by multi-parametric MRI to genomic mutations and transcriptional phenotypes using mixed effect modeling which allowed us to control for individualized patient effects. We first confirmed that T2 is a significant indicator of IDH mutation status in the NE region, being the first description of such a relationship in a HGG cohort. We found the combination of EGFR amplification and CDKN2A homozygous loss was associated with a significantly lower mean diffusivity (MD) compared to double wild type tumors in the NE region, indicating the presence of greater cellular packing and proliferation in EGFR amplification/CDKN2A loss regions. Finally, using single cell pathway based tumor classifications, we showed that nK2, a DSC-MRI metric representing cell size heterogeneity, correlated positively with neuronal signature and negatively with glycolytic/plurimetabolic signature within the NE tumor, indicating that glycolytic/plurimetobolic tumors possessed a high amount of cell size heterogeneity compared to neuronal samples. This hypothesis was supported using digital reference object (DRO) modeling which confirmed that cell size and heterogeneity drove the differential nK2 signal between neuronal and glycolytic/plurimetabolic samples. We identified immune cell infiltrate as one possible mechanism of increased cell size heterogeneity using transcriptomic signature analysis which found more immune cell signatures within glycolytic/plurimetobolic tumors compared to neuronal. Collectively this study demonstrates the central role of multi-parametric MRI as a non-invasive measure of tumor biology and a tool for understanding the clinically critical NE region which can then inform new therapies targeting this region of HGG recurrence.

#5622

Integrative cross-platform characterisation of mammographic screen-detected breast cancer

Alison M. Cheung[1], Dan Wang[1], Kela Liu[1], Yutaka Amemiya[1], Elzbieta Slodkowska[2], James G. Mainprize[1], Jane Bayani[3], Arun Seth[1], John Bartlett[4], Martin J. Yaffe[1]. *[1]Sunnybrook Research Institute, Toronto, ON, Canada,[2]Anatomic Pathology, Sunnybrook Health Sciences Centre, Toronto, ON, Canada,[3]Ontario Institute for Cancer Research, Toronto, ON, Canada,[4]Cancer Research UK Edinburgh Centre, Edinburgh, United Kingdom*

Mammography screening is widely used for earlier detection of breast cancer and has been shown to contribute to reduction of mortality and morbidity. Most screen-detected breast cancers are early stage, hormonal receptor-positive, HER2-negative (HR+ HER2-) breast cancers. The majority of HR+ HER2- cancers are assigned to molecular intrinsic subtypes of Luminal A and Luminal B, which generally harbour low recurrence risk, with Luminal B cases being more invasive but still less aggressive than HER2-enriched

or Basal-like subtypes. However, some of these Luminal cancers later recur (5+ years after diagnosis) often as advanced and/or metastatic disease. We studied a cohort of screen-detected breast cancers (42 cases) at Sunnybrook Health Sciences Centre (Toronto, ON Canada) with integrated cross-platform radiomics, molecular and proteomic analysis in an attempt to better characterise these cancers and their proclivity for late recurrence. Utilising a Nanostring 200-gene assay, the molecular subtypes (PAM50 and MammaTyper-like) and a range of recapitulated clinical prognostic scores (50-Gene, 70-Gene and 21-Gene Risk) were determined for these cancers. While a majority of cases (29 out of 42) were subtyped as Luminal A cancers by PAM50, a fraction (12 out of 29) of these were either subtyped as Luminal B/HER2+ based on MammaTyper-like results, or measured as intermediate to high risk of recurrence based on the 70-Gene or 21-Gene Risk classification. Although discordant results from multi-parametric assays are not uncommon, we postulate that here, discordance could suggest presence of heterogeneous cellular or molecular elements with invasive phenotype that could lead to aggressive transformations in the long run. Differential expression analysis between Luminal A cases with consistent subtyping and low risk prognostication and those with discordant subtyping or prognostication results revealed a panel of genes with significant changes in expression. Further analysis of RNA expression of these genes via Receiver Operating Characteristic (ROC) curve demonstrated that some genes showed high Area Under the Curve (AUC) scores in the classification between the two groups of Luminal A breast cancers, further supporting the existence of distinct molecular phenotypes. Targeted sequencing with Oncomine Comprehensive Assay V3 did not reveal particular mutational patterns between the two Luminal A groups. Nevertheless, radiomic analysis of mammographic images of the cancer, as well as single cell phenotyping of the tumor microenvironment with protein multiplexing will be incorporated to further characterise elements that are phenotypically different, and potentially identify mechanistic drivers contributing to late recurrence in Luminal A cancers.

Precision Oncology in Pediatric Cancer: From Genomics to Databases to Real World Evidence

#4509

A pan-Canadian precision oncology program for children, adolescents and young adults with hard-to-cure cancer: The PRecision Oncology For Young peopLE (PROFYLE) Program

Stephanie A. Grover[1], Lesleigh Abbott[2], Jason N. Berman[2], Guillaume Bourque[3], Jennifer A. Chan[4], Avram E. Denburg[1], Rebecca J. Deyell[5], Conrad V. Fernandez[6], Cynthia Hawkins[1], Jan-Willem Henning[7], Meredith S. Irwin[1], Nada Jabado[8], Steven J. M. Jones[9], Philipp F. Lange[5], Paul Moorehead[10], Michael F. Moran[1], Daniel A. Morgenstern[1], Sapna Oberoi[11], Antonia Palmer[12], Shahrad R. Rassekh[5], Donna L. Senger[13], Adam Shlien[1], Daniel Sinnett[14], Caron Strahlendorf[5], Patrick J. Sullivan[15], Michael D. Taylor[1], Suzanne Vercauteren[5], Anita Villani[1], Stephanie Villeneuve[6], James A. Whitlock[1], David Malkin[1], on behalf of the PROFYLE Consortium. *[1]The Hospital for Sick Children, Toronto, ON, Canada,[2]Children's Hospital of Eastern Ontario, Ottawa, ON, Canada,[3]McGill University, Montreal, QC, Canada,[4]University of Calgary, Calgary, AB, Canada,[5]BC Children's Hospital, Vancouver, BC, Canada,[6]IWK Health Centre, Halifax, NS, Canada,[7]Tom Baker Cancer Centre, Calgary, AB, Canada,[8]McGill University Health Centre, Montreal, QC, Canada,[9]BC Cancer, Vancouver, BC, Canada,[10]Janeway Health and Rehabilitation Centre, St. John's, NL, Canada,[11]CancerCare Manitoba, Winnipeg, MB, Canada,[12]Advocacy for Canadian Childhood Oncology Research Network (Ac2orn), Toronto, ON, Canada,[13]Lady Davis Institute of Medical Research and McGill University, Montreal, QC, Canada,[14]Centre Hospitalier Universitaire Sainte-Justine, Montreal, QC, Canada,[15]Childhood Cancer Canada, Toronto, ON, Canada*

Background**:** Over 4,300 children, adolescents, and young adults (CAYA) are diagnosed with cancer each year in Canada, 1/3 of whom have refractory/metastatic disease or will relapse. The PRecision Oncology For Young peopLE (PROFYLE) national, collaborative program, was created to provide equitable access to molecular profiling to identify novel targeted treatment options in a clinically relevant timeframe for all CAYA with hard-to-cure cancers in Canada.

Design: Building upon 3 pre-existing regional precision oncology programs, PROFYLE now includes >20 institutions and has united an interdisciplinary team of experts, leaders, research teams, end-users and advocates from across Canada. The program has 14 domain specific nodes that are unified by a shared

governance structure, and has harmonized biobanking, genomics, bioinformatics and reporting procedures. PROFYLE includes genomic and transcriptomic sequencing of paired germline and cancer fresh/frozen samples, proteomic analysis, and cancer modelling. Inclusion criteria: ≤29y; treatment at a Canadian center; diagnosis of a hard-to-cure cancer. Profiling results are reviewed by multidisciplinary Molecular Tumor Boards. A report including a results/recommendations summary of actionable findings (therapeutic, diagnostic, prognostic, cancer predisposition), potential targeted therapy options including available clinical trials, clarification of diagnosis, and genetic counseling recommendations is provided to the treating oncologist.
Results: >1,000 CAYA are included from all of the provinces. Cancer diagnoses: 34% sarcoma, 16% leukemia/lymphoma, 16% CNS tumor, 11% neuroblastoma, 23% other. 17% of participants had a cancer-predisposing pathogenic/likely pathogenic germline variant, 45% had ≥1 potentially actionable somatic alteration, 22.6% had a therapeutically targetable somatic alteration. The most frequent classes of therapeutic alterations were RAS/MAPK (15%), cell cycle (14%), epigenetic (13%), RTK (12%), PI3K/AKT/mTOR (11%), DNA repair (9%), immune checkpoint (8%). Of clinicians who reported the utility of results, 55% indicated the findings were useful for clinical management.
Future Directions: Collaborations with other national and international initiatives and data from this interdisciplinary, multi-institutional research program will inform the development of a framework to innovatively link research, clinical and system considerations with Canadian values relevant to multi-omic profiling and drug access for CAYA. In addition, we believe that with a comprehensive molecular view of cancer, PROFYLE will transform our understanding of underlying disease mechanisms, facilitate and improve diagnostic and prognostic indicators, and identify new therapeutic strategies and targets for CAYA patients with cancer.

#4511
Impact of the comprehensive genomic profiling on the individual therapeutic planning in high-risk/refractory tumors: real-world precision medicine in pediatric oncology
Petra Pokorna[1], Hana Palova[1], Sona Adamcova[1], Vojtech Bystry[2], Michal Kyr[3], Dagmar Al Tukmachi[1], Sona Mejstrikova[1], Peter Mudry[3], Jaroslav Sterba[3], Ondrej Slaby[4]. *[1]CEITEC, Masaryk University, Brno, Czech Republic,[2]Masaryk University, Brno, Czech Republic,[3]Department of Pediatric Oncology, University Hospital Brno, Brno, Czech Republic,[4]CEITEC, Faculty of Medicine, Masaryk University, Brno, Czech Republic*

Background: Despite major improvements in the survival of pediatric cancer patients that were achieved through the intensification of chemotherapy and the perfection of supportive care in the past decades, treatment outcomes for high-risk, relapsed, and refractory solid cancers remain unsatisfactory. Accelerating the progress of pediatric oncology requires both therapeutic advances and attention to reducing the long-term cytotoxic treatment-related side effects. This could be achieved by targeting specific molecular changes that drive pediatric malignancies.
Material and Methods: From September 2016 to August 2020, a total of 192 patients with pediatric high-risk solid tumors successfully underwent comprehensive genomic profiling. Since more than thirty patients had two or more biopsies from recurrent relapses, the total number of samples examined was 295. In the cohort, there were 78 cases of central nervous system tumors, 68 sarcomas, 14 neuroblastomas, 10 lymphomas, and 22 tumors of other histology. Whole-exome sequencing was performed in all patients, fusion gene analysis in 96% of patients, whole-transcriptome profiling in 84% of patients, and CNV analysis in 63% of patients.
Results: The diagnostic yield of therapeutically actionable findings was 40%, with single-nucleotide variants and small insertions/deletions being the most common actionable alteration types. In 23% of patients, a clinically relevant gene fusion was identified. The majority of the identified fusions were of diagnostic significance, and 18% of those were therapeutically targetable gene fusions involving BRAF, RAF1, ALK, FGFR1, or NTRK2. Four patients were eligible for immunotherapy based on high tumor mutational burden (>10 mut/Mb). Lymphomas and CNS tumors showed the highest rate of patients with therapeutically actionable findings (60% and 56%, respectively), followed by neuroblastomas (36%), sarcomas (25%), and other solid tumors (23%). All results and individual treatment plans were discussed at multidisciplinary molecular tumor boards.

Conclusion: Precision medicine in pediatric oncology has rapidly developed over the last decade and resulted in new therapeutic options based on molecular biomarkers and increased our understanding of the complexity of pediatric malignancies. Supported by the Ministry of Health of the Czech Republic, grant nr. NU20-03-00240 and the project National Institute for Cancer Research (Programme EXCELES, ID Project No. LX22NPO5102) - Funded by the European Union - Next Generation EU.

#4512

My Pediatric and Adult Rare Tumor Network (MyPART): integrating longitudinal, clinical, molecular, and patient-reported outcomes for rare tumors

Shadin Ahmed[1], Margarita Raygada[1], Robin Lockridge[2], Mary Frances Wedekind Malone[1], Jaydira Del Rivero[3], John W. Glod[1], Barbara J. Thomas[1], Donna Bernstein[1], Markku M. Miettinen[4], Liqiang Xi[4], Jung Kim[4], Manoj Tygagi[4], Mark Raffeld[4], Kenneth Aldape[4], Ashkan A. Malayeri[5], Abby B. Sandler[1], Brigitte C. Widemann[1], Karlyne M. Reilly[1]. *[1]Pediatric Oncology Branch, National Cancer Institute, Bethesda, MD,[2]Clinical Research Directorate, Frederick National Laboratory for Cancer Research, Frederick, MD,[3]Developmental Therapeutics Branch, National Cancer Institute, Bethesda, MD,[4]Laboratory of Pathology, National Cancer Institute, Bethesda, MD,[5]Radiology and Imaging Sciences, Clinical Center, National Institutes of Health, Bethesda, MD*

Background**:** Rare tumors are defined as <15 cases/100,000 people/year and present an unmet need due to lack of effective medical treatments, paucity of biospecimens and research models, and difficulty accruing to clinical trials. **MyPART** (**My** **P**ediatric and **A**dult **R**are **T**umor Network) was established to: 1) engage patients/advocates as partners in rare tumor research, 2) provide expertise and personalized health care to children and young adults with rare tumors, and 3) build databases and tools to advance research on new treatments for rare tumors. We have developed a natural history and biospecimen acquisition study (NCT03739827), enrolling patients with rare solid tumors, their family members, and participants with germline mutations at increased rare tumor risk.
Method: Participants in our natural history study enroll remotely or come to the National Institutes of Health Clinical Center. Participants complete medical and family history forms, patient reported outcomes (PROs), and provide tumor samples and blood and/or saliva for DNA/RNA analysis. For patients coming to the Clinical Center, blood samples are collected for immune phenotyping and cytokine analysis. Clinical staff extract medical records for downstream analyses. Tumors are analyzed using a 500+ gene panel and genomic analysis. Participants are followed yearly to collect data on recurrence, progression, PROs, development of additional tumors, and response to treatments such as standard of care and any treatment trials they may join.
Results: We report a clinical and molecular summary of the first 200 participants (66% female, 35% male), with neuroendocrine neoplasms (NEN), adrenocortical cancer (ACC), SDH-deficient gastrointestinal stromal tumor (sdGIST), chordoma, medullary thyroid cancer (MTC), and other less commonly enrolled tumors totaling 35 different tumor types. Participants come from 46 US states and 9 countries. Early results show tumor-specific differences in mutations, treatment/management, PROs, and self-reported non-tumor health issues. The most common pathogenic germline mutations are *SDHA/SDHB/SDHC* in sdGIST and *RET* in MTC and other tumors. The most common pathogenic tumor mutations are *TP53* and *CTNNB1* in ACC, *SDHA/B* and *TP53* in sdGIST, *MEN1* in NEN, *RET* and *HRAS* in MTC, and *SMARCB1* in chordoma. Clinically significant levels of anxiety and pain are more frequent in ACC, NEN, and sdGIST.
Conclusions: By developing methods to provide value to rare tumor patients, using a large catchment area and opportunity for remote participation, and collecting data in a tumor-agnostic way, we can learn about multiple rare tumors and share findings more quickly than if each rare tumor was studied alone. We describe the MyPART cohort and challenges to overcome for successful longitudinal rare tumor natural history studies.

#4513

St. Jude Survivorship Portal: A data portal for storing, analyzing, and sharing large and complex cancer survivorship datasets

Gavriel Matt[1], Edgar Sioson[1], Jaimin Patel[1], Jian Wang[1], Robin Paul[1], Colleen Reilly[1], Congyu Lu[1], Kyla Shelton[1], Qi Liu[2], Weiyu Qiu[2], Cindy Im[2], Zhaoming Wang[1], Carmen L. Wilson[1], Nickhill Bhakta[1], Kirsten Ness[1], Gregory T. Armstrong[1], Melissa M. Hudson[1], Leslie L. Robison[1], Jinghui Zhang[1], Yutaka Yasui[1], Xin Zhou[1]. *[1]St. Jude Children's Research Hospital, Memphis, TN,[2]University of Alberta, Edmonton, AB, Canada*

Survivors of childhood cancer are at risk for developing various adverse health conditions as adults that are attributable to the cancer and treatments they were exposed to as children. Cancer survivorship research relies on large-scale, longitudinal studies that generate a wide range of demographic, clinical, and genetic data on cancer survivors at multiple time points. To maximize the utility of these comprehensive datasets, we must be able to store and share these datasets in a web-based environment that can be accessed by the broader survivorship research community. Furthermore, this environment should be integrated with analytical tools for performing statistical analyses on the stored data without needing to download the data and import it into third-party analytical software. To address this need, we have created the St. Jude Survivorship Portal (https://survivorship.stjude.cloud > Clinical Data Browser), a web-based data portal for exploring, sharing, and analyzing data from survivors of pediatric cancer. The portal hosts data from two large cohorts of pediatric cancer survivors: the St. Jude Lifetime Cohort Study and the Childhood Cancer Survivor Study. The data stored on the portal consists of demographic data, clinical data, including cancer diagnosis, cancer treatment, clinical outcomes, and patient-reported data, and genetic data, including whole-genome-sequencing-derived genotypes and published polygenic risk scores computed for >500 traits. This data is organized hierarchically in a data dictionary that can be easily explored by the user. Charts and plots of variables can be quickly created, customized, and stratified with other variables, all within the portal environment. Statistical analyses, including cumulative incidence analysis and regression analysis, may also be performed within the portal. In cumulative incidence analysis, users can analyze the incidence of a variety of CTCAE-graded adverse events (e.g., cardiovascular dysfunction, neurological disorders, subsequent neoplasms) in survivors and can also compare them across different survivor populations defined by other variables. In regression analysis, users have the option to perform either a linear, logistic, or cox regression analysis and may use any of the demographic, clinical, or genetic variables on the portal as outcome or explanatory variables in the analysis. In this way, users can assess any risk factor associations within a survivor cohort and generate predictive models for outcomes of interest. Lastly, we also provide the user with the option to download the data on the portal for use in any future analyses. The St. Jude Survivorship Portal provides a comprehensive, powerful, and easy-to-use interface for sharing and analyzing childhood cancer survivorship data that will serve as a valuable research tool for the broader survivorship research community.

#4514

Variations of blood DNA methylation associated with cancer treatment exposures among childhood cancer survivors of African ancestry

Qian Dong, Sarmistha Das, Cheng Chen, John Easton, Heather L. Mulder, Emily Walker, Geoffrey Neale, Deo Kumar Srivastava, I-Chan Huang, Jinghui Zhang, Melissa M. Hudson, Leslie L. Robison, Kirsten K. Ness, Nan Song, Zhaoming Wang. *St. Jude Children's Research Hospital, Memphis, TN*

We previously showed that cancer treatment associated DNA methylation (DNAm) signatures were present decades following the cancer diagnosis in childhood cancer survivors (CCS) of European ancestry (EA) and that treatment associated DNAm sites mediated the causal pathway from specific treatment exposures to increased risk of chronic health conditions (CHCs). This new analysis further evaluated and compared the treatment and DNAm associations in CCS of African ancestry (AA) from the St. Jude Lifetime Cohort Study. Cancer treatments were abstracted from medical records. DNAm was measured using MethylationEPIC BeadChip with blood-derived DNA. Among 370 AA CCS (53.2% female, median age at blood draw=31.2 [range=18.4-65.1] years), treatments included alkylating agents (54.6%), anthracyclines (48.6%), epipodophyllotoxins (29.2%), corticosteroids (33.0%), and vincristine (61.6%), and radiation therapy (RT) to brain (26.5%), chest (27.6%), abdomen (22.7%), and pelvis (21.6%). Epigenome-wide association study (EWAS) for each treatment, using multivariable linear regression adjusting for sex, age at blood draw, leukocyte cell subtype proportions, genotype principal components and DNAm principal components, showed little inflation with genomic control (GC) factor between 1.1 (brain-RT) and 1.2 (chest-RT). A total

of 93 5′-cytosine-phosphate-guanine-3′ (CpG) was associated with one or more cancer treatments (GC-adjusted $P<9\times10^{-8}$), including epipodophyllotoxins (n=46), alkylating agents (n=38), corticosteroids (n=3), anthracyclines (n=3), abdominal-RT (n=3), chest-RT (n=2), and pelvic-RT (n=1). A total of 60 differentially methylated regions (DMRs) was identified using DMRcate R package, including alkylating agents (n=28), epipodophyllotoxins (n=22), corticosteroids (n=3), abdominal-RT (n=4), chest-RT (n=2), and anthracyclines (n=1). A total of 39 CpGs from EWAS were nested within 21 DMRs. 92.1% (650/706) chemo-associated CpGs in EA were replicated in AA CCS, and 98.9% (86/87) chemo-associated CpGs in AA were replicated in EA CCS. In contrast, 66.7% (4/6) RT-associated CpGs in AA were replicated in EA CCS, and 71.7% (638/890) RT-associated CpGs in EA were replicated in AA CCS. Moreover, the four CpGs that partially mediated the effect of abdominal-RT on hypercholesterolemia in EA were not associated with abdominal-RT in AA CCS, further suggesting substantial difference in RT-associated CpGs as compared to chemo-associated CpGs between AA and EA CCS. Future studies by including a larger sample size of AA CCS are warranted to assess the difference in treatment-associated DNAm alterations and subsequent disparity in risk of treatment-related CHCs between AA and EA CCS. The DNAm sites can be used as predictors for risk management (treatment decision-making) and potential mechanistic targets for intervention for those at the greatest risk of CHCs.

#4515

PIONEER: harnessing multi-omics data to enhance immunotherapeutic target discovery and development

Amber K. Weiner[1], Hemma Murali[2], Rawan Shraim[1], Karina L. Conkrite[1], Alexander B. Radaoui[1], Daniel Martinez[1], Brian Mooney[3], Sandra E. Spencer Miko[3], Gian Negri[3], Alberto Delaidelli[3], Caitlyn de Jong[3], Yuankun Zhu[1], Allison P. Heath[1], Jennifer Pogoriler[1], Yael P. Mosse[1], Deanne M. Taylor[1], Poul H. Sorensen[3], Gregg B. Morin[3], Benjamin A. Garcia[4], John M. Maris[1], Sharon J. Diskin[1]. *[1]Children's Hospital of Philadelphia, Philadelphia, PA,[2]University of Pennsylvania, Philadelphia, PA,[3]BC Cancer, Vancouver, BC, Canada,[4]Washington University, St. Louis, MO*

Introduction: Immunotherapeutic strategies have produced remarkable results in some malignancies. However, optimal cell surface targets in many childhood cancers remain elusive and tools for novel target discovery are limited. We developed a proteogenomic approach to identify high confidence cell surface proteins for immunotherapy development and applied it to neuroblastoma, an often fatal childhood cancer. Through the Pediatric Immunotherapy Discovery and Development Network (PI-DDN), we have extended this approach to 14 high-risk childhood cancers. This effort includes MS-based surfaceome data generation for 175 patient-derived xenograft (PDX) models, 30 primary patient tumors, and 10 human derived cell line models.

Methods/Results: To optimize the utility of our approach and data, we are developing a web-based application called PIONEER (Pediatric Integrative Omics Network Enhancing Early Research). The goal of PIONEER is to disseminate data to the broader scientific community and to provide the necessary analysis, query and visualization tools to make these data accessible to everyone, regardless of computational expertise. A pilot version of PIONEER was developed using R Shiny Dashboard and is derived from our neuroblastoma efforts. The application is comprised of two main categories: (1) target discovery data and prioritization (2) target validation and preclinical development. Modules include proteomics, transcriptomics, epigenomics, multi-omics, validation and pre-clinical drug development. Cancer ‘omics data currently housed in PIONEER include tumor and cancer cell line mass-spectrometry based proteomics, RNA-sequencing, and chromatin immunoprecipitation (ChIP) sequencing. Extensive normal tissue expression data from GTEx and mass spectrometry will be integrated. Surface proteins are prioritized through an integrative multi-omic analysis of tumor and normal tissue data. Users can perform queries and cancer subtype and cross-histotype studies, apply custom cutoffs, and generate plots for visualization. We are currently adding functionality to support automatic data analysis and integration for surface proteins (SPACE: Surface Protein Analysis for Collaborative Efforts). Through the target validation and preclinical development modules, users can view an antibody repository, immunofluorescence, immunohistochemistry, drugs in development

for each protein, and efficacy in patient derived xenograft models. PIONEER will be deployed using R Connect; data for additional histotypes will be incorporated as available.
Conclusion: PIONEER will provide a comprehensive characterization of the surfaceome of high-risk pediatric cancers and a web-based application for data integration, visualization and sharing. This interface facilitates the discovery of optimal immunotherapeutic drug targets in high-risk childhood cancers.

#4516

Rare high-penetrance and common low-penetrance variants associated with risk of pediatric acute lymphoblastic leukemia

Zhaoming Wang[1], Cheng Chen[2], Na Qin[3], Nan Song[4], Hui Wang[5], Gregory T. Armstrong[1], Kirsten K. Ness[1], Melissa M. Hudson[1], Jinghui Zhang[1], Leslie L. Robison[1], Cindy Im[6]. *[1]St. Jude Children's Research Hospital, Memphis, TN,[2]Shanghai Jiao Tong University, Shanghai, China,[3]Nanjing Medical University, Nanjing, China,[4]Chungbuk National University, Cheongju, Korea, Republic of,[5]Shanghai Jiao Tong University, Shanghai, Chile,[6]University of Minnesota, Minneapolis, MN*

Leveraging existing genetic data for survivors of pediatric acute lymphoblastic leukemia (ALL) from the St. Jude Lifetime Cohort Study (SJLIFE) and Childhood Cancer Survivor Study (CCSS; the CCSS original cohort data was downloaded from dbGaP, phs001327.v2), genetic variants across the full allelic spectrum were analyzed for their associations with ALL risk. A total of 2,695 ALL cases with whole-genome or whole-exome sequencing were available for rare variant analyses. Pathogenic/likely pathogenic (P/LP) variants in 60 genes associated with autosomal dominant cancer predisposition syndromes were characterized and classified with "PeCanPIE" - the Pediatric Cancer Variant Pathogenicity Information Exchange, a web- and cloud-based platform. We subsequently carried out an enrichment analysis of P/LP variants by comparing ALL survivors with a general population from the GnomAD database and found seven significant genes after adjustment for multiple testing (P< 8.3x10-4, i.e., 0.05/60) including: BRCA1 (odds ratio [OR]=4.06; 95% CI, 2.00-7.59; P=1.21×10-4), BRCA2 (OR=3.48; 95% CI, 1.82-6.15; P=1.50×10-4), CDKN2A (OR=22.30; 95% CI, 5.13-96.68; P=3.07×10-5), PALB2 (OR=5.12; 95% CI, 2.39-10.00, P=3.77×10-5), PAX5 (OR=44.58; 95% CI, 6.49-490.68; P=4.77×10-5), PTPN1 (OR=66.85; 95% CI, 11.96-670.57, P=1.63×10-7), and TP53 (OR=17.86; 95% CI, 6.12-50.36; P=3.43×10-7). Two of these genes have also been previously linked with pediatric ALL (CDKN2A and TP53). Repeating these analyses with 309 newly diagnosed patients from the Pediatric Cancer Genome Project, we observed similar results for five of these genes (BRCA1, BRCA2, CDKN2A, PALB2, and TP53). To further investigate common germline variants associated with ALL risk, we performed a genome-wide association analysis using 2,777 ALL cases and 6,255 controls (5,881 other pediatric cancer cases and 374 non-cancer controls) with whole-genome sequencing or imputed SNP-array data. In addition to replicating known associations at ARID5B, IKZF1, CDKN2A, BMI1, PIP4K2A, CCDC26 and CEPBE, we identified a novel variant (rs112425636, chr17:82324152:G:A; OR=1.65; 95% CI, 1.42-1.93; P=2.48×10-10) mapped to the intronic region of SECTM1 gene. Based on RNA sequencing data for 164 pediatric hematological cancer samples, we found that the expression of SECTM1 gene was significantly higher among patients with GG genotype than patients with AA or AG genotypes for rs112425636 (FPKM=1.34 vs. 0.71, P<0.01). Among the subset of 32 B-ALL samples, the magnitude of difference was larger (FPKM=1.90 vs. 0.70, P=0.017). In summary, we found statistical evidence for several cancer predisposition genes harboring rare high-penetrance variants and a novel common low-penetrance variant associated with risk of pediatric ALL. Our novel findings add new knowledge to the full allelic spectrum of genetic architecture of pediatric ALL susceptibility.

#4517

Novel prognostic and predictive biomarker for neuroblastoma

Dinesh Babu Somasundaram, Zhongxin Yu, Ashley Baker, Natarajan Aravindan. *University of Oklahoma Health Sciences Center, Oklahoma City, OK*

Recently we showed that Retinal degeneration protein 3 (RD3) is constitutively expressed in healthy adult and fetal tissues beyond retina and, its gradient expression from high to low in ganglioneuroma, ganglioneuroblastoma and neuroblastoma (NB). Crucially, our sequential in *vitro* and *in vivo* studies

identified that RD3 regulates NB progression and metastasis, and its loss prompts the evolution of therapy defying progressive disease (PD). Here we investigated the prognostic significance of RD3 in NB, its predictive benefit and, its association to clinical outcomes. RNA-Seq data mining (4 independent study cohorts, total n = 1013) indicated that high RD3 can predict good NB prognosis. RD3 expression (immunohistochemistry) gauged in our NB patient cohort (n = 100) showed a positive correlation with longer overall survival (OS, P = 1.0E-04) and relapse-free survival (RFS, P = 2.1E-02). Similarly, high RD3 correlated with longer OS (P = 1.2E-03) and RFS (P = 2.1-02) in children presented with high-risk NB (HR-NB), irrespective of MYCN amplification status (MYCN amplified, P = 1.4E-02; non-amplified, P = 5.5E-03) and patient age (<2Y age, P = 2.8E-02; >2Y age, P = 1.0E-04) groups. Significantly, we observed a gradient loss of RD3 with NB progression, from stage 1 through stage 4 disease. Consistently, RD3 loss was substantial in metastatic disease when compared to the primary neuroblastomas, and this loss associated with poor OS in patients presented with metastatic disease (P = 4.0E-02). More importantly, RD3 is significantly lost in therapy resistant progressive NB and corroborated significantly (P = 9.5E-03) with the poor progression free survival. Multivariate analysis identified RD3 as an independent (P = 4.4E-02) prognostic factor for NB. These results demonstrate that RD3-loss can forecast poor prognosis in NB, and further imply that assessing RD3 loss could serve as the good predictor for therapy response and / or PD evolution. Together, these data identify a novel prognostic and predictive factor for neuroblastoma. Funding: This work was partially or in full, funded by Oklahoma Center for the Advancement of Science and Technology, OCAST-HR19-045; National Institutes of Health, NIH-P20GM103639 and Department of Defense DoD-CA210339

#4518

Highlighting the prenatal, natal, and early childhood risk factors of cancer: seeking better opportunities for cancer prevention

Abeer Abd Elmoneim[1], Ayat Roushdy[2], Ehab Metwally[2]. *[1]Sohag University, Cairo, Egypt,[2]Taibah University, Madinah, Saudi Arabia*

Background: Fostering new public health approaches to cancer prevention is required to reduce the number of new cases. Early life exposures, to carcinogens may affect different phases of the multi-tage clonal expansion model of carcinogenesis. Critical development periods, in-utero and puberty, exposures may induce permanent changes in tissue differentiation, metabolism, and gene expression that influence cancer risk. Epigenetic modifications are also critical for regulating cellular processes and responses during development that are maintained overtime. Therefore, promising strategies should develop for cancer prevention mainly on environmental approaches. We aim in this study to assess the prevalence of risk factors of childhood cancer in Almadinah City, a local community in Saudi Arabia, and to address cancer prevention opportunities during prenatal, natal and early children life.
Patients and Methods: The study is a cross section observational study. The population includes convenient samples of pregnant mothers, neonates and preschool children. Data regarding natal, prenatal and early childhood risk factors of cancer collected using a predesigned questionnaire.
Results: Early life exposure to cancer risks increases prevalence of cancer. Risk factors like high birth weight, maternal obesity and smoking are the most frequent risks followed by chromosomal anomalies and genetic syndromes. Prenatal use of folic acid, breastfeeding and allergy, respectively, are the most frequent protective factors against cancer development.
conclusions: Strict approaches should be designed for preventing early life exposures and their cumulative effect that can lead to cancer development.

Spatial Profiling, Tumor Classification, and Response Assessment

#4522

Pathologic complete response rate across triple negative breast cancer subtypes in the IMMUcan study

Andrea Joaquin Garcia[1], Mattia Rediti[1], Abdelkader Benyagoub[2], Stéphanie Tissot[3], Sylvie Rusakiewicz[3], Robin Liechti[4], Flavia Marzetta[4], Nicolas Penel[5], Julio Oliveira[6], Jean-Charles Goeminne[7], Pierre Fournel[8], Andreia Capela[9], Xiaoxiao Wang[10], Delphine Vincent[10], Françoise Rothe[1], Marie Morfouace[11], Henoch

Hong[11], Donald Jackson[12], Christos Sotiriou[10], Laurence Buisseret[10]. *[1]Institut Jules Bordet, Brussels, Belgium,[2]Department of Oncology, Center of Experimental Therapeutics, CHUV, Laussane, Switzerland,[3]Department of Oncology, Center of Experimental Therapeutics, CHUV, Lausanne, Switzerland,[4]Vital-IT Group, SIB Swiss Institute of Bioinformatics, Lausanne, Switzerland,[5]Oscar Lambret Cancer Center, Lille, France,[6]Instituto Português de Oncologia, Porto, Portugal,[7]Service of Medical Oncology, Clinique et Maternité Ste Elizabeth, Namur, Belgium,[8]Institut de Cancérologie Lucien Neuwirth, Saint-Étienne, France,[9]Centro Hospitalar Vila Nova Gaia e Espinho, Vila Nova De Gaia, Portugal,[10]Breast Cancer Translational Research Laboratory, Institut Jules Bordet, Brussels, Belgium,[11]Merck KGaA, Darmstadt, Germany,[12]Acting Head Sanofi, Cambridge, MA*

Background: IMMUcan (SPECTA NCT02834884) is a European public-private effort to generate molecular and cellular profiling data of the human tumor microenvironment (TME) from up to 3,000 patients, to better understand how the immune system and tumors interact. Triple-negative breast cancer (TNBC) is a heterogenous disease with distinct molecular subtypes characterized by different gene expression, genomic profiles, and clinical outcomes. Here, we explored the association between molecular subtypes and response to neoadjuvant chemotherapy as well as levels of immune cell infiltration in the prospective IMMUcan TNBC cohort.
Methods: At the cut-off date on June 29th, 2022, we identified a first cohort of 132 patients to perform preliminary analyses, of which 109 had pre-treatment RNAseq data available. Among those, pathological Complete Response (pCR) information was available for a total of 86 patients. Preliminary data included the density of CD3+, CD20+ and CD8+ immune cells from the stroma and tumor compartments from multiplex-immunofluorescence (mIF) for 69 patients. TNBC subtypes were computed as described by Bareche et al. Association of continuous variables with pCR was evaluated with logistic regression (univariate analysis).
Results: The pCR rates differed across TNBC subtypes (Fisher's test, P = 0.02). In detail, pCR was achieved in 88% (8/9) of basal like (BL), 63% (17/27) of immunomodulatory (IM) and 45% (16/35) of mesenchymal (M) tumors, while lower pCR rates were observed for the mesenchymal stem-like (MSL) and luminal androgen receptor (LAR) subtypes with 37% (3/8) and 14% (1/7), respectively, suggesting differences in the sensitivity to neoadjuvant chemotherapy in line with previous reports. When considered as continuous signature scores, pCR was positively associated to BL levels (OR = 2.7, 95% CI, 1.5-4.8; False Discovery Rate [FDR] = 0.0031), and negatively associated to MSL and LAR signature levels (OR = 0.53, 95% CI, 0.32-0.87; FDR = 0.019; OR = 0.30, 95% CI, 0.12-0.74; FDR= 0.019). In addition, CD3+ cell densities in the tumor and stroma were significantly higher in IM tumors (P = 0.002 and P < 0.001), while lower levels were found in M tumors (P = 0.005, P = 0.002). Similarly, stromal CD20+ levels were higher in IM tumors (P = 0.008) and lower in M tumors (P = 0.006), suggesting a more immunosuppressive TME in the M subtype. CD8+ cells levels were not significantly different between subtypes.
Conclusions: These preliminary results show relevant differences in the pCR rates among TNBC subtypes, to be confirmed on a larger series of patients and further suggesting a substantial TNBC heterogeneity regarding treatment response. Of note, preliminary mIF results suggest a differential role of the immune response across molecular subtypes. Additional analyses integrating mIF and genomic data are currently ongoing.
Funding: IMI2 JU grant agreement 821558, supported by EU's Horizon 2020 and EFPIA.

#4524

Multiparametric characterization of early-stage SCLC human tumors reveals novel patient subgroups based on specific molecular to immune landscape associations

Angel Nunez-Buiza[1], David Gómez-Sánchez[2], Jose Maria Gracia-Rodríguez[1], Esther Conde[3], Jose Luis Solorzano[4], Eva María Garrido-Martín[5], Jose Carlos Machado[6], Susana Guimarães[7], Ernest Nadal[8], Sonia Molina-Pinelo[9], Miguel Ángel Piris Pinilla[10], Nuria Romero-Laorden[11], Fernando Franco[12], Fernando López-Ríos Moreno[3], Álvaro Conrado Ucero[13], Luis Paz-Ares[14]. *[1]Research Institute (i+12) Hospital 12 de Octubre / Spanish National Cancer Research Center (CNIO), Madrid, Spain,[2]Research Institute (i+12) Hospital 12 de Octubre / Spanish National Cancer Research Center (CNIO) / Biomedical Research Cancer Network Center (CIBERONC), Madrid, Spain,[3]Pathology Department, Research Institute (i+12) Hospital 12*

de Octubre / Biomedical Research Cancer Network Center (CIBERONC), Madrid, Spain,[4]Pathology Department, Research Institute (i+12) Hospital 12 de Octubre / Spanish National Cancer Research Center (CNIO) / MD Anderson, Madrid, Spain,[5]Department of Cell Biology, R&D Division, & Oncology Business Unit, Biomedical Research Cancer Network Center (CIBERONC) / PharmaMar, Madrid, Spain,[6]Faculty of Medicine of the University of Porto / i3S – Institute for Research and Innovation in Health of the University of Porto / IPATIMUP - Institute of Molecular Pathology and Immunology of the University of Porto, Porto, Portugal,[7]Pathology Department, Centro Hospitalar Universitário S.João / Faculty of Medicine of the University of Porto, Porto, Portugal,[8]Catalan Institute of Oncology, IDIBELL, Barcelona, Spain,[9]Biomedical Research Cancer Network Center (CIBERONC) / Institute of Biomedicine of Seville (IBIS) (HUVR, CSIC, Universidad de Sevilla), Sevilla, Spain,[10]Pathology Service, Fundación Jiménez Díaz, Madrid, Spain,[11]Division of Medical Oncology, Hospital Universitario La Princesa, Madrid, Spain,[12]Pathology Department, MD Anderson, Madrid, Spain,[13]Departments of Medicine and Physiology, Research Institute (i+12) Hospital 12 de Octubre / Spanish National Cancer Research Center (CNIO) / School of Medicine, Complutense University, Madrid, Spain,[14]Departments of Medicine and Physiology, Research Institute (i+12) Hospital 12 de Octubre / Spanish National Cancer Research Center (CNIO) / Biomedical Research Cancer Network Center (CIBERONC) / School of Medicine, Complutense University / Medical Oncology, Madrid, Spain

Small cell lung cancer (SCLC) is a lethal malignancy with few therapeutic options. Tissue resection or biopsy are unusual, so the scarce sample available has limited our knowledge on the biology of SCLC tumors. Recent advances propose novel molecular subtypes (SCLC-A, SCLC-N, SCLC-P, SCLC-I, NAPI classification) to classify SCLC patients and specific treatment susceptibilities of defined subgroups. In this line, we collected 119 tumor samples from a cohort of early-stage SCLC patients with complete clinical annotation, in order to find specific molecular and immune profiles that define new patient characteristics with potential impact on prognosis or therapy selection. For this, we subjected the tumor tissue to RNA-seq targeted panel of onco-immune-related genes and to immune characterization by IHC. In addition, we analyzed molecular aberrations by whole exome sequencing. All data, including clinical annotations, were integrated by multiparametric computational analysis. Based on the computational analysis of the onco-immune transcriptomic data, we found two major groups of patients with either pro-immunogenic or pro-tumorigenic profiles. The transcriptomic pro-immunogenic group shows better survival and higher infiltration of immune cells (CD4+ T cells, CD8+ T cells, B cells and Macrophages). In contrast, the pro-tumorigenic group presents worse survival and less immune cell infiltration. Using bioinformatics, we described a gene signature that can identify both subgroups. This gene signature includes immune cell markers (MS4A1, CD3D), antigen receptor complex (CD79A), adhesion and migration of T cells (CD2) and immunomodulatory genes (IDO1, TIGIT) expressed in the pro-immunogenic group, and, proliferation (MKI67), transcription regulator (TOP2A) and epithelial and mesenchymal transition-related genes (TWIST1) in the pro-tumorigenic group. Exome sequencing analysis resulted in the expected genomic heterogeneity of SCLC tumors beyond TP53 and RB1 mutations in most patients. However, we found a significant enrichment of XIRP2 gene alterations in the pro-tumorigenic group. Consistent with an early-stage of SCLC, most of the samples were described as SCLC-A subtype by the predominant expression of ASCL1. Interestingly, our findings suggest a relevant biological heterogeneity within SCLC-A tumors that impacts immune infiltrate and disease outcome. Here we show a gene signature that can subclassify early-stage SCLC patients according to their clinical, molecular and immune features, and provides prognostic value independently of the NAPI classification. Since immunogenicity of the tumor impacts response to immunotherapy, we speculate that this gene signature might predict therapy response and therefore contribute to tailored treatment of SCLC.

#4525

YAP1 in relapsed pulmonary high-grade neuroendocrine carcinomas (NEC) is associated with *CDKN2A* loss, intact *RB1*, EMT and therapeutic vulnerability to MEK1 and CDK4/6 inhibition

C. Allison Stewart[1], Lixia Diao[2], Yuanxin Xi[2], Runsheng Wang[3], Kavya Ramkumar[3], B. Leticia Rodriguez[3], Benjamin B. Morris[3], Li Shen[2], Bingnan Zhang[3], Yan Yang[3], Azusa Tanimoto[3], Veronica Y. Novegil[3], Luisa

M. Solis Soto[4], Pedro F. Simoes da Rocha[5], Natalie Vokes[3], Don L. Gibbons[3], Michael Frumovitz[6], Junya Fujimoto[4], Jing Wang[2], Bonnie Glisson[3], Lauren A. Byers[3], Carl M. Gay[3]. *[1]UT MD Anderson Cancer Center, Houston, TX,[2]Department of Bioinformatics and Computational Biology, UT MD Anderson Cancer Center, Houston, TX,[3]Department of Thoracic/Head & Neck Medical Oncology, UT MD Anderson Cancer Center, Houston, TX,[4]Department of Translational Molecular Pathology, UT MD Anderson Cancer Center, Houston, TX,[5]Department of Medical Oncology, Hospital del Mar, Barcelona, Spain,[6]Department of Gynecologic Oncology and Reproductive Medicine, UT MD Anderson Cancer Center, Houston, TX*

Neuroendocrine carcinomas (NECs) are clinically aggressive carcinomas commonly arising from the respiratory and gastrointestinal tracts, typically categorized as large-cell neuroendocrine carcinomas (LCNECs) or small cell carcinomas (most commonly small cell lung cancer (SCLC)). Clinically, pulmonary LCNECs (pLCNECs) mirror the course common to SCLC - initial response followed by rapid and insurmountable resistance to one-size-fits-all approaches. Recently, SCLC has been subdivided into four subtypes with unique vulnerabilities, three of which are defined by the transcription factors ASCL1, NEUROD1, and POU2F3, while a fourth group exhibits an inflamed signature. We hypothesize that pLCNEC may be similarly classified into molecularly distinct subsets with unique therapeutic vulnerabilities - a fundamental step toward personalized medicine. We applied our SCLC 1300 gene signature to pLCNEC patient tumors and, as in SCLC, found three distinct subtypes determined by differential expression of *ASCL1*, *NEUROD1*, and *POU2F3*, but with a unique fourth subtype marked by expression of the transcription factor *YAP1*. Unlike in treatment-naïve SCLC, where YAP1 is absent, *YAP1* expression clearly defines pLCNEC as two, roughly equal subsets with the *YAP1*-low tumors encompassing tumors expressing the other three transcription factors. Conversely, *YAP1*-high pLCNEC is more mesenchymal and inflamed, and less neuroendocrine (NE), reminiscent of inflamed SCLC. Additionally, YAP1-high status is associated with smoking exposure ($P<0.001$, FC=81), high frequency of *CDKN2A* homozygous deletion and *SMARCA4* mutations, as well as intact *RB1*. These features are distinct from SCLC, wherein transcriptional subtypes lack distinct genomic characteristics. Consistent with *CDKN2A* deletion, *YAP1*-high pLCNEC cell lines have increased sensitivity to MEK1 and CDK4/6 inhibition. We also demonstrate that RB1 loss downregulates YAP1 expression, which may account for the absence of YAP1 in treatment-naïve SCLC due to ubiquitous loss of *RB1*. In contrast to treatment-naïve SCLC, where our group and others have been unable to detect YAP1, single-cell RNAseq analysis of biopsies from patients with relapsed SCLC identified emerging *YAP1*-positive cancer cell populations, which are similarly associated with increased EMT, immune cell infiltration (CD8+ T-cells), and loss of NE gene expression. This suggests that the ability for cancer cells to acquire YAP1 expression and, perhaps, pLCNEC-like features, may be a resistance mechanism in relapsed SCLC, contributing to the abundant intratumoral heterogeneity and highlighting potential vulnerabilities to overcome resistance. In summary, YAP1 may be a predictive biomarker of intact *RB1* and response to cellular and checkpoint immunotherapy and MEK1/CDK4/6 inhibition in pLCNEC and relapsed SCLC.

#4526

Molecular landscape of clonal hematopoiesis in patients with lung cancer: First results of the CHIC study

Marco Tagliamento, Christophe Marzac, Mihaela Aldea, Damien Vasseur, Arnaud Bayle, Anas Gazzah, Maud Ngocamus, Claudio Nicotra, Julieta Rodriguez, Antonin Levy, Capucine Baldini, Santiago Ponce, Felix Blanc-Durand, Etienne Rouleau, Antoine Italiano, Ludovic Lacroix, Luc Friboulet, David Planchard, Fabrice Barlesi, Yohann Loriot, Jean-Baptiste Micol, Benjamin Besse. *Gustave Roussy, Villejuif, France*

Introduct**ion:** CHIC (Clonal Hematopoiesis In Lung Cancer) is a retro-prospective study that aims to describe the characteristics of clonal hematopoiesis (CH) in patients with non-small cell lung cancer (NSCLC). We present preliminary results from the retrospective cohort.

Experimental procedures: A retrospective analysis conducted in patients with metastatic or recurrent NSCLC included in the MATCH-R study (NCT02517892) at Gustave Roussy (Villejuif, France). CH was evaluated by a 74-gene targeted NGS panel (HaloPlex - Agilent) performed on DNA extracted by isolated-by-blood leukocytes. The variant allele frequency (VAF) threshold of detection was set at 1%.

Results: 108 consecutive patients with advanced NSCLC included from October 2015 to July 2019 were evaluated, irrespective of the tumor molecular profile. 46% of the patients were female, 67% were former or current smokers. 82% of the patients had adenocarcinoma and 44%, 23%, 33% had bone, liver and/or brain metastases, respectively. Patients had received a median of 2 lines of systemic therapy and 81% were on active anticancer treatment at the time of CH assessment. At least one CH mutation was found in 38 out of 108 patients (35% prevalence), with an increasing with age trend. Patients carrying CH were older as compared to those without CH and had in 29% vs. 11% of cases tumor histology other than adenocarcinoma (p=0.009). No difference in overall survival was observed according to CH detection (log rank p=0.318). We found 64 mutations in 19 different genes: 63% of the patients carried a single mutation, while co-occurrence of two, three, four or five mutations, within the same gene or in more than one, was found in seven (18%), four (11%), one (3%) and two patients (5%), respectively. Epigenetic modifiers (*DNMT3A*, *TET2*, *ASXL1*) were the most frequently mutated genes: 38 mutations with a median VAF of 6.5% detected in 32 patients. DNA repair genes (*PPM1D*, *TP53*, *CHEK2*, *ATM*) were the second most frequently mutated: 11 mutations at a median VAF of 4% were detected in 9 patients. 7 mutations in genes encoding for the cohesin complex (*SMC3*, *SMC1A*, *RAD21*, *STAG2*) were found in 6 patients, with a median VAF of 5%. A non-simultaneous cfDNA sequencing by FoundationOne Liquid CDx assay (324-gene panel) was performed in 9 patients for tumor profiling. In 2 out of 3 tested cases the presence of CH was confirmed in plasma liquid biopsy. 4 patients with no detectable CH by the targeted blood sequencing subsequently were found having CH mutations in plasma NGS, on average 45 months apart. To note, as many as 5 out of the 19 detected mutated genes (*PPM1D, SMC3, SMC1A, PRPF8, ZRSR2*) are not part of the FDA-approved NGS panel used for cfDNA profiling in solid tumors.
Conclusion: We found a consistent prevalence of CH in patients with NSCLC by using a sequencing approach targeted for hematologic disorders. Prognostic implications of CH are under investigation and will be evaluated in the full cohort.

#4527

CD8 T cell-melanoma cell interactions in response and resistance to ipilimumab plus nivolumab: Biopsy analysis of SWOG S1616

Katie M. Campbell[1], Lawrence Kuklinski[1], Zaid Bustami[1], Jessica Maxey[2], Egmidio Medina[1], Sandra Santulli-Marotto[2], Cynthia R. Gonzalez[1], Nataly Naser Aldeen[1], Kari Kendra[3], Sapna Patel[4], Siwen Hu-Lieskovan[5], James Moon[6], Shay Bellasea[6], Christine N. Spencer[2], Marshall A. Thompson[2], Michael Wu[6], Ari Vanderwalde[7], Philip O. Scumpia[1], Antoni Ribas[1]. *[1]UCLA - University of California Los Angeles, Los Angeles, CA,[2]Parker Institute for Cancer Immunotherapy, San Francisco, CA,[3]Ohio State University, Columbus, OH,[4]MD Anderson Cancer Center, Houston, TX,[5]Huntsman Cancer Institute, Salt Lake City, UT,[6]SWOG Statistic and Data Management Center, Seattle, WA,[7]West Cancer Center, Memphis, TN*

Background: In the randomized S1616 trial (NCT03033576), patients with metastatic melanoma refractory to anti-PD-1-based therapy had improved progression free survival (PFS, HR = 0.63, p = 0.037) and objective response to ipilimumab plus nivolumab (ipi/nivo, RR 28%) compared to ipilimumab alone (ipi, RR = 9%). We hypothesized that reversal of resistance to PD-1 blockade with CTLA-4 blockade would result in increased CD8 T-cell infiltration in patient biopsies.
Methods: Multiplex ion beam imaging (MIBI) for 32 protein markers, spanning tumor, immune, and stromal cell types, was used to evaluate the tumor microenvironment in melanoma tumor biopsies collected at baseline (N=21 samples) and one month on-treatment (N=22; N=16 paired timepoints). Tumor-immune cell dynamics were determined by comparing baseline and on-treatment biopsies within clinical groups (ipi/nivo response, N=10; ipi/nivo no-response, N=9; ipi no-response, N=8).
Results: Multiplex analysis in ipi/nivo responsive patients demonstrated increased proportions of CD8 (median 1.6X increase), CD4 (2.1X), regulatory T cells (1.6X), and monocytes (1.4X), with a paralleled 8.1X decrease in melanoma cells over the course of treatment. This was confirmed by histopathologic evidence of tumor regression, necrosis, and immune infiltrate in on-treatment, responding tumor biopsies, as determined by dermatopathologists. Melanoma cells had direct, cell-membrane interactions with CD8 T cells in ipi/nivo responsive patients, both at baseline (median 26%) and on-treatment (median 86%). The shared

interface between melanoma and CD8 T-cells had polarized expression of CD3, CD8, and CD45RO. There was no change in T-cell infiltration nor tumor cell content over the course of treatment in ipi/nivo non-responders nor ipi non-responders; similar proportions of melanoma cells were interacting with CD8 T-cells at baseline (median 24%) and on-treatment (27%).
Conclusion: Reversal of resistance to PD-1 blockade is associated with increased frequency of CD8 T-melanoma cell interactions and pathological response, reflective of different stages of antitumor immune responses. Response to ipi/nivo in the anti-PD-1 refractory setting was further associated with increased tumor-polarized and activated CD8 T cells interacting with melanoma cells, demonstrated by the colocalized expression of immune synapse proteins at tumor-CD8-T-cell membrane interfaces.

#4528

Evaluation of plasma circulating tumor DNA (ctDNA)-based whole genome sequencing (pWGS) and whole exome sequencing (pWES) and concordance with tumor tissue whole exome sequencing (tWES): a pilot study in patients with recurrent or metastatic head and neck squamous cell carcinoma or metastatic urothelial carcinoma

Razvan Cristescu, Andrew Albright, Steven Townson, Cai Chen, Blanca Homet Moreno, Nati Lerman, Z. Alexander Cao, Carol Peña. *Merck & Co., Inc., Rahway, NJ*

Background: The genetic heterogeneity and clonal evolution of tumors is hypothesized to influence disease response and acquisition of resistance during treatment. However, comprehensive analysis of the changing tumor molecular landscape to support evaluation of such a hypothesis is often difficult to quantify due to the lack of accessibility to longitudinal biopsy samples in a large number of patients (pts). Longitudinal analyses using pWGS or pWES may allow the delineation of the genetic evolution of tumors and its impact on treatment outcomes. We conducted a pilot study to evaluate the feasibility of obtaining pWGS and pWES data from ctDNA in pretreatment samples from pts enrolled in 2 phase 3 trials that evaluated second-line pembrolizumab versus chemotherapy/standard-of-care therapy: KEYNOTE-040 (recurrent or metastatic head and neck squamous cell carcinoma; NCT02252042) and KEYNOTE-045 (metastatic urothelial carcinoma, NCT02256436). Concordance between pWES and tWES was also evaluated.
Methods: Cell-free DNA was isolated from 1-3 mL of plasma; pWGS (via low-pass WGS) and pWES were performed on samples from pts with available tWES data generated as part of planned tissue biomarker analyses for the respective studies. Tumor burden in ctDNA was estimated from pWES data using single nucleotide variant (SNV)-based maximum somatic allele frequency (MSAF) and from pWGS data using a copy number variation-based measure of mutational burden in the tumor fraction. Concordance between the pWES and tWES mutational spectrum was determined using the Jaccard index. Concordance of key driver somatic events (*FGFR3, TP53*, and HPV status) was evaluated.
Results: Plasma samples from 47 pts (KEYNOTE-040, n = 24; KEYNOTE-045, n = 23) were analyzed. Tumor burden estimates from pWGS (median coverage, 5.84; range, 4.28-8.18) and pWES (median coverage, 1806; range, 1038-2413) data were highly correlated (Spearman $\rho = 0.94$). A range of 0 to 956 nonsynonymous SNVs (median, 50) per pt was identified in ctDNA. When the ctDNA tumor burden was high (MSAF ≥5%, observed in two-thirds of pts), a relatively high concordance was observed for individual alterations in *TP53*, *FGFR3*, and HPV status (overall agreement: 0.87, 0.97, and 0.96, respectively); between tissue- and plasma-based tumor mutational burden ($R = 0.49$); and in overall mutational landscape overlap (Jaccard index: median, 0.30; range, 0.002-0.53).
Conclusions: These data show that pWES exhibits reasonably high concordance with tWES when the tumor burden in ctDNA is relatively high and may be informative regarding tumor genomic characteristics. Extensive longitudinal studies are still needed to understand tumor genetic evolution using plasma ctDNA.

#4529

The tumor molecular landscape of nasopharyngeal carcinoma (NPC) in endemic and non endemic areas

Deborah Lenoci[1], Carlo Resteghini[1], Mara Serena Serafini[1], Federico Pistore[1], Silvana Canevari[1], Brigette B.Y. Ma[2], Stefano Cavalieri[1], Annalisa Trama[1], Lisa Licitra[1], Loris De Cecco[1]. *[1]Fondazione IRCCS Istituto*

Nazionale dei Tumori, Milan, Italy,[2]Department of Clinical Oncology, The Chinese University of Hong Kong, Hong Kong SAR, Hong Kong

Nasopharyngeal carcinoma (NPC) is an epithelial malignancy with a higher incidence in Asian endemic areas (EA) than in non endemic areas (NEA). Epstein-Barr virus infection is associated with most NPCs in both areas. We dissected the gene expression (GE) and microenvironment of NPC, leading to the identification of molecular subtypes that might explain the differences between EA and NEA NPCs. We retrieved data from NPC-EA transcriptomic repositories: 6 GE datasets, including tumor and normal samples (GSE12452, GSE34573, GSE132112, GSE53819, GSE68799, GSE102349); one validation dataset with both EA and NEA(https://doi.org/10.5281/zenodo.5347891); 4 GE signatures associated with prognosis and treatment prediction (PMID: 24297049, 35262435, 32596151, 33096113); and NPC EBV related genes/pathways and gene sets (PMID: 35846746, 35394843, 35105963; Liu NPC, Wood EBV EBNA1 Down, Sengupta NPC LMP1 UP, REACTOME DNA Repair; Hallmarks). The 6 datasets were integrated using a bioinformatic meta-analysis approach, and the classifier method was applied to the validation dataset in order to identify the subtype with worst prognosis. Furthermore, RNA sequencing was performed on 50 Italian NEA NPC samples (INT188/19; GSE208281). Biological and functional profiling of EA and NEA were performed using xCell, Gene set enrichment analyses, and treatment prediction methods (PMID: 16103067, pRRophetic R, PMID: 28052254). Four clusters (Cl) were identified through a meta-analysis of EA-NPC. Prognostic analyses revealed that Cl3 had the worst prognosis (P=0.0476), confirmed by three of the four prognostic signatures and in the validation dataset (P=0.0368). Based on the biological and functional characterization of these clusters, we arrived at the following GE subtypes: Cl1, Immune-active; Cl2, Defense-response; Cl3, Proliferation; Cl4, Perineural-interaction/EBV-exhaustion. According to the treatment prediction methods, the sensitivity of each cluster was radiotherapy and immunotherapy for immune-active, radiochemotherapy and immunotherapy for defense-response, chemotherapy for proliferation, and cisplatin treatment for perineural-interaction/EBV-exhaustion. In our NEA cohort, only three clusters were expressed (excluding perineural-interaction/EBV-exhaustion). Immune/biological characterization and treatment prediction analyses of NEA partially replicated the EA results. Our study provides a relevant biological overview of EBV-related NPC in both EA and NEA. The immune microenvironment plays a critical role in NPC owing to the viral etiology of this malignancy. The presence of a perineural-interaction/EBV-exhaustion cluster in EA suggests an inactive EBV infection according to the viral related “hit and run theory”; however, further analyses are needed. The immune/biological characterization of EA and NEA may help predict the response to different therapeutic strategies.

#4530

Single-cell analysis of oral squamous cell carcinoma (OSCC) from smoker vs. non-smoker patients highlights two groups of tumors with distinct immune microenvironments

Yannick Le Meitour[1], Béatrice Vanbervliet[1], Sonia Canjura-Rodriguez[1], Cyril Degletagne[1], Laurie Tonon[1], Lucas Michon[1], Jebrane Bouaoud[1], Philippe Zrounba[2], Aude Excoffier[2], Karène Mahtouk[1], Pierre Saintigny[1]. *[1]Univ Lyon, Claude Bernard Lyon 1 University, INSERM 1052, CNRS 5286, Centre Léon Bérard, Cancer Research Center of Lyon, Lyon, France,[2]Department of Surgical Oncology, Centre Léon Bérard, Lyon, France*

Background and Rationale: OSCC is the most frequent head and neck cancer. While it is mainly affecting patients with a smoking and/or alcohol history (SD), 10% to 15% of OSCC are diagnosed in patients with not known risk factors (NSND). We and others have shown that OSCC from NSND patients are characterized by an enrichment in interferon gamma (IFNγ) response and PD-1 signaling pathways together with a higher intratumor T-cell infiltrate. Herein, we seek to gain more insights into the immune and non-immune tumor microenvironment (TME) of OSCC in SD vs. NSND patients.
Material and Methods: We made use of single-cell RNA seq (10x Genomics) from non-sorted and CD45 negative enriched cell suspensions of OSCC biopsies from 11 treatment naïve patients, human papillomavirus negative, including 6 SD and 5 NSND patients.
Results: All samples were characterized by a strong immune cell infiltrate. Consistent with our previous results, the analysis of 51,629 immune cells confirmed that NSND patients’ samples displayed a significantly

higher proportion of T cells (p = 0.005) compared to SD patients. NK cells were also increased, with 2% in SD patients versus 6% in NSND patients (p = 0.008). T cells strongly expressed IFNγ and remarkably, both myeloid cells and tumor cells from NSND patients had an increased enrichment in IFNγ response pathway in NSND as compared to SD patients. The TME of SD patients was characterized by the presence of 15% of plasma cells vs. 3% in NSND patients (p = 0.003). Thus, tumors from NSND versus SD patients represent two distinct groups of tumors characterized by a different immune TME. Moreover, tumors from SD patients displayed 2% vs. 4% Cancer Associated Fibroblasts (CAFs) (p = 0.01). In addition, among CAFs subpopulations, myofibroblast CAFs, defined as the subpopulation producing extracellular matrix proteins were found only in tumors from SD patients, suggesting that distinct CAFs subpopulations may shape the immune TME by affecting the recruitment and function of adaptive immune cells in SD versus NSND patients. Finally, we analyzed tumor cells using non-negative matrix factorization to find Meta Programs (MP), which are set of genes coordinately upregulated. We identified 5 MP associated with different biological functions: epithelial differentiation, stress, cell cycle (G2/M), partial epithelial-to-mesenchymal transition, and epithelial senescence. While the epithelial differentiation MP was found in all patients, the remaining ones were more frequently found in SD patients.
Conclusion: Our results show that the TME of OSCC from NSND vs. SD differs in terms of T, NK, and plasma cells composition, CAFs, and tumor cells MP. Integration with spatial transcriptomics is ongoing. Those biological differences may represent an opportunity to refine the therapeutic approaches in the two populations of patients.

#4531

Clinical translation of biomarkers for ZL-1211, an anti-CLDN18.2 antibody, in patients with advanced solid tumors from a phase I dose-escalation study

Zhen Luo[1], Xiao Wang[1], Xuehuo Zeng[1], Jiaqing Yi[1], Tegan Burns[1], Herman Liu[1], Xinyu Zhang[2], Wenyu Liu[2], Karl Hsu[1], Hua Gong[1]. *[1]Zai Lab (US) LLC, Menlo Park, CA,[2]Zai Lab (Shanghai) Co., Ltd., Shanghai, China*

ZL-1211, a humanized monoclonal IgG1 antibody targeting CLDN18.2, induces cancer cell death through antibody-dependent cellular cytotoxicity (ADCC) and complement-dependent cytotoxicity (CDC). We developed ex vivo ADCC and CDC assays to study the mechanism of actions of ZL-1211. Our preclinical data has demonstrated greater antitumor activities than the clinical leading benchmark via enhanced ADCC by mutation in Fcγ domain and potent CDC activities. We used those ex vivo assays to further profile the clinical specimens from patients collected at baseline (pre-infusion) and the following cycles (post-infusion) in our phase 1 study (NCT05065710). Preliminary results in clinical samples indicated that baseline ADCC and CDC capabilities were correlated with anti-tumor activity of ZL-1211 in patients with CLDN18.2-positive locally advanced or metastatic solid tumors, suggesting probable predictive biomarkers. Results also showed that changes in circulating ZL-1211 mediated ADCC and CDC activities were dose-dependent and in accordance with the pharmacokinetic (PK) profile. In addition, we performed differential gene expression analysis and real-time PCR to compare gene expression in ZL-1211 responder and non-responder PDX models and CCLE cell lines. Our findings reveal that several immune-related genes may serve to predict the responses to ZL-1211 treatment. Other potential predictive biomarkers such as Fcγ receptor CD16A polymorphism and baseline stromal CD8 expression were also evaluated in clinical samples. Taken together, analytical approaches developed and validated from preclinical studies were successfully translated to characterize clinical samples in the current Phase 1 trial. The exploratory analysis indicated the clinical relevance of multiple biomarkers and their potential as predictive biomarkers of ZL-1211.

#4532

Spatial profiling delineates tumor-T-cell dynamics in anti-PD-1-refractory melanoma treated with ipilimumab or ipilimumab plus nivolumab

Nataly Naser Al Deen[1], Katie M. Campbell[1], Egmidio Medina[1], Cynthia R. Gonzalez[1], Philip O. Scumpia[2], Antoni Ribas[1]. *[1]Medicine - Hematology Oncology, UCLA David Geffen School of Medicine, Los Angeles, CA,[2]Medicine, UCLA David Geffen School of Medicine, Los Angeles, CA*

Background**:** Immune checkpoint blockade (ICB) therapies promote anti-tumor activity by facilitating CD8 T-cell activation at the tumor site (e.g., anti-PD-1), or in the lymph node, promoting T-cells trafficking to the tumor site (e.g., anti-CTLA-4). Focusing on patients with metastatic melanoma refractory to anti-PD-1 therapy who received ipilimumab ± nivolumab (ipi±nivo), we hypothesize that combination therapy could overcome anti-PD-1 primary resistance in some patients, by facilitating T-cell trafficking and infiltration into the tumor.
Methods: Visium spatial transcriptomics using 18,000 RNA plex (n=10), multiplexed ion beam imaging (MIBI) using 32 protein plex (n=4), and CosMx single cell imaging using 1000 RNA plex (n=2) were performed on paired baseline (n=5) and on-therapy biopsy samples (n=5). Paired samples were derived from patients with complete response to ipi+nivo (n=3), partial response to ipi+nivo (n=1), and no response to ipi monotherapy (n=1).
Results: Visium spatial transcriptomics revealed a decrease in melanoma gene expression clusters and an increase in expression of immune clusters. Further characterization of the immune clusters revealed signatures of CD4+ and CD8+ T cells displaying stronger activation markers, in particular cytotoxic markers and interferon gamma clusters, along with M1 macrophage transcripts. However, further analysis of the paired biopsies in the ipi monotherapy non-responder revealed a concomitant increase in the immune-suppressive M2 macrophages, tolerogenic DCs, regulatory T cells, and exhausted T cells, which was not observed in the ipi+nivo responders. Confirmatory studies performed in two patients (ipi+nivo responder vs ipi non-responder) using MIBI confirmed a decrease in the tumor burden, and large increases in CD8 (199X in ipi+nivo vs 1.52X in ipi), CD4 (22.3X in ipi+nivo vs 8.56X in ipi), and T cells (26.1X in ipi+nivo vs 2.13X in ipi). Focusing on the non-responder (ipi) paired biopsies, CosMx revealed heterogeneous tumor clusters, with little to no immune infiltration in the baseline biopsy, and a decrease in tumor burden with increased markers of immune response and immune suppression in the on-therapy biopsy.
Conclusion: Integrated single cell spatial analyses, on the RNA and protein levels, revealed increased immune cell recruitment to the tumor site in responders to anti-CTLA-4 + anti-PD-1 therapy compared to a non-responder to anti-CTLA-4 monotherapy, and may provide clues to cancer-immune cell interactions in response to ICB. The presence of immune suppressive clusters at the tumor site in the on-therapy biopsy in the anti-CTLA-4 monotherapy would support our hypothesis that while anti-CTLA-4 facilitates T-cell trafficking and infiltration into the tumor site, anti-CTLA-4 alone without anti-PD-1 may not be sufficient to overcome anti-PD-1 primary resistance in some patients.

#4533
Serum protein changes in patients with desmoid tumors responsive to the TBL1 inhibitor, tegavivint
Stephen Horrigan, Kimberly R. Holloway, David Stenehjem, Casey Cunningham. *Iterion Therapeutics, Houston, TX*

Background: A Phase 1/2 clinical trial (NCT03459469) of the small molecule tegavivint in patients with desmoid tumors (DTs), demonstrated drug safety and tolerability with evidence of clinical activity. Transducin Beta-Like Protein 1 (TBL1) is a necessary co-activator for beta-catenin's oncogenic activity. Wnt-activation promotes formation of a TBL1: beta-catenin complex that protects β-catenin from degradation in the nucleus and promotes Wnt-target gene activation. Tegavivint binds TBL1 preventing the interaction with beta-catenin, which results in nuclear beta-catenin degradation and inhibition of downstream transcription. For patients whose desmoid tumors responded to tegavivint we assayed changes in serum-based proteins, selected based on their cancer-related function and dysregulation by aberrant Wnt/ beta-catenin signaling, to potentially identify suitable biomarkers that may be useful in future studies.
Methods: Whole blood and tumor tissue was collected from desmoid patients before and after administration of tegavivint at dose levels ranging from 1 to 5 mg/kg administered via a 4-hour intravenous (IV) infusion on days 1, 8, and 15 of a 28-day cycle. Collection timepoints were pre-dose and up 1 week (wk.) following the start of the infusion. Secreted protein levels were profiled in the serum using Luminex multiplex technology. Changes in protein levels were compared to the tegavivint pharmacokinetic (PK) profiles. Tissue samples were analyzed for gene expression changes.
Results: Preliminary analyses demonstrated that the majority of tegavivint treated patients with an objective response to tegavivint showed a consistent and expected pattern in serum levels of known Wnt/ beta-catenin

regulated proteins. Decreases in levels of DKK1, FGF-2, MMP-1, PDGF-AA and VEGF-A and an increase in CCL5 levels were observed. In treated patient serum, protein level changes were detected as early as 2 hours (h) following the start of infusion and continued to progress in the predicted direction at 24 h. At the 5 mg/kg dose, all selected biomarkers remained decreased (or in the case of CCL5, increased) during the dosing interval, with a tegavivint half-life of 48.6 h and C_{min} (trough value) 1 wk. post treatment above in vitro IC_{50} values. Gene expression changes were found in tumor tissue in comparing pre- to post-tegavivint treatment.
Conclusion: A panel of beta-catenin regulated proteins and transcripts were identified as candidate pharmacodynamic biomarkers in patients whose desmoid tumor responded to tegavivint. Alterations in these serum proteins continued throughout the dosing interval and, for several proteins, a potential dose response correlation was observed. Further characterization of the relationship between tegavivint plasma levels, serum biomarkers, transcriptional changes and clinical responses in additional patients and time points will be presented.

#4534

National Multidisciplinary Tumor Board improves diagnostic stratification and therapeutic management in Cancers of Unknown Primary: the French Experience

Nicolas Jacquin[1], Maud Kamal[2], Ivan Bieche[2], Célia Dupain[2], Isabelle Guillou[2], Linda Larbi-Chérif[2], Etienne Rouleau[3], Julien Masliah Planchon[2], Isabelle Soubeyran[4], Christelle de la Fouchardière[5], Camille Tlemsani[6], Hélène Blons[7], Fabienne Escande[8], Michel Vidaud[6], Jennifer Wong[2], Pierre Saintigny[5], Sandrine Boyault[5], Adrien Buisson[5], Yves Allory[9], Anne Vincent-Salomon[2], Vincent Cockenpot[5], Janick Selves[10], Christophe Le Tourneau[2], Sarah Watson[2]. *[1]Institut Godinot, Reims, France,[2]Institut Curie, Paris, France,[3]Gustave Roussy, Villejuif, France,[4]Institut Bergonié, Bordeaux, France,[5]Centre Léon Bérard, Lyon, France,[6]Institut Cochin, Paris, France,[7]Hôpital Européen Georges Pompidou, Paris, France,[8]CHU de Lille, Lille, France,[9]Institut Curie, Saint Cloud, France,[10]CHU de Toulouse, Toulouse, France*

Introduction: With the increasing complexity of current diagnostic investigations, the integration of clinical, pathological and molecular characteristics is crucial for the management of patients (pts) with cancers of unknown primary (CUP). A national multidisciplinary tumor board (NatCUPMTB) was created 2 years ago in France to discuss the diagnostic and therapeutic management of CUP pts. The objective of this study was to evaluate its diagnostic, prognostic and therapeutic impact after 2 years of activity. Methods: This was a multicenter retrospective study with prospective follow-up. All pts discussed at least once in the NatCUPMTB between June 2020 and August 2022 were included. Pts and tumors characteristics, pathological and molecular analyses including WGS, WES and RNAseq performed on SEQOIA and AURAGEN national large-scale sequencing platforms, multidisciplinary tumor board (MTB) conclusions, and follow-up after MTB were collected. Results: 76 pts for whom a long-term follow-up was available were included. The median age at diagnosis was 57 yo, 54% were female, and the median number of metastatic sites at diagnosis was 2. The median time between diagnosis and first MTB presentation was 3.8 months (0.2-55). MTB investigations enabled to identify a likely primary origin in 44/76 (58%) pts, and the MTB recommended a personalized therapeutic strategy in 50/76 patients (66%). MTB recommendations were based on the combination of clinical, pathological and molecular investigations in 55% of pts. After a median follow-up of 6.2 months, the median overall survival (OS) was 17.7 months from diagnosis and 11.0 months from the 1st MTB presentation. Pts for which the MTB had a diagnostic impact, and having received a treatment following MTB recommendation (based on putative origin or targetable alteration) had increased OS compared to pts with no diagnostic orientation (median OS 18.4 months vs 5.6 months, p=0.003) or having received other treatments (median OS 18.4 vs 4.4 months, p=0.0001). Conclusion: NatCUPMTB provides significant diagnostic and therapeutic benefit in pts with CUP. Early presentation of pts at NatCUPMTB as soon as CUP diagnosis is suspected should be recommended.

#4535

Clinical outcomes and molecular features of different histopathologic patterns in patients with stage IB non-squamous non-small-cell lung cancer

Dongsheng Yue, Bin Zhang, Chen Chen, Qiang Zhang, Xinyi Wu, Jiping Xie, Changli Wang, Zhenfa Zhang.
Department of lung cancer, Tianjin Medical University Cancer Institute and Hospital, Tianjin, China

Background: About 15% to 20% of patients with stage IB non-small-cell lung cancer (NSCLC) may develop recurrence within 5 years. However, the use of adjuvant therapy for resected stage IB patients remains controversial. This study investigated the differences in prognosis and molecular features between different histopathologic patterns of stage IB non-squamous NSCLC (nsNSCLC) and tried to identify patients who most in need of adjuvant therapy.
Methods: A total of 215 patients with completely resected pathologic stage IB (tumor size 3-4 cm) nsNSCLC from Tianjin Medical University Cancer Institute & Hospital between 2014 and 2018 were included in the study. For 130 patients, genomic profiling of tumor tissues was sequenced by a panel of 9 driver genes (OncoScreen® Focus CDx Tissue Kit, Burning Rock Biotech) and the molecular risk stratification was assessed by 14-gene quantitative PCR (qPCR) assay (DetermaRx™, Burning Rock Biotech).
Results: Among the 215 patients, 67.9% were solid/micropapillary-predominant pattern (S/MP), 40.5% had received platinum-based doublet adjuvant chemotherapy, and 5.1% had received adjuvant targeted therapy with or without chemotherapy. Patients with S/MP pattern had significantly worse DFS than those with lepidic/acinar/papillary-predominant (L/A/P) pattern (hazard ratio [HR]: 2.16, 95% confidence interval (CI): 1.28 to 3.67; P = 0.013). However, neither pattern could benefit from adjuvant therapy. *EGFR* mutation was successfully detected in 75 out of 126 patients (59.5%), and the positive rate in S/MP pattern was significantly lower than that in L/A/P pattern (50.6% vs 79.5%, P = 0.002). However, *EGFR* mutation status was not a prognostic factor for DFS in neither overall population nor different histopathologic patterns. *EGFR*-mutant patients showed the trend to benefit from adjuvant targeted-based therapy in the limited samples. Molecular risk stratification was successfully assessed in 99 patients, of which 37.4%, 26.3%, and 36.4% were predicted as molecularly high-risk, intermediate-risk, and low-risk patients, respectively. There were significant differences in the proportion of high- and low-risk patients between S/MP and L/A/P patterns (for high-risk: 46.2% vs 20.6%; for low-risk: 26.2% vs 55.9%; P = 0.009). The high-risk patients had significantly shorter DFS than the low-risk patients (HR, 2.93, 95% CI: 1.31-6.54; P = 0.012), especially those in S/MP pattern (HR, 3.45, 95% CI: 1.46-8.15; P = 0.017).
Conclusion: Our study confirms that S/MP pattern is a significantly worse prognostic factor for DFS in nsNSCLC and that there are significant differences in molecular features between these two different histopathologic patterns. qPCR-based assay could reliably identify patients with a worse prognosis in S/MP pattern, suggesting that such patients are most likely to benefit from personalized adjuvant therapy.

#4536

Investigating the correlation between molecular diagnostics, targeted therapies and treatment outcomes in Rosai Dorfman disease: a single-institution experience

Samuel B. Reynolds[1], Sabrina R. Wilcox[2], Moshe Talpaz[1], Asra Z. Ahmed[1]. *[1]Hematology and Medical Oncology, University of Michigan, Ann Arbor, MI,[2]Department of Pediatrics, University of Michigan, Ann Arbor, MI*

Introduction: Rosai Dorfman Disease (RDD) is a non-Langerhans cell histiocytic disease whose pathologic features include sinus histiocytosis with variable emperipolesis. Traditional management consists of local therapies (resection, radiation) for limited lesions and myelosuppressive therapies for systemic disease. Recent studies, however, have identified MAP Kinase pathway mutations in RDD, prompting further research into the utility of targeted agents.
Methods: A retrospective analysis was conducted at a single institution over a 20-year period (2002-2022) of 40 patients with RDD. Inclusion criteria included age ≥18 and histopathologic evidence of RDD without obscuring secondary malignancies. Clinical data points included biological gender, age at diagnosis, molecular diagnostics, imaging and therapies administered. Binary data was utilized for statistical analysis and comparison of outcomes by treatment type, time to diagnosis and use of targeted agents.
Results: In this analysis, 72% of patients were female and 28% male with an average age at diagnosis of 45.8 years, over 50% of whom were diagnosed between 1 and 12 months of presentation. Primary disease was most commonly extranodal (>90%), found in cutaneous, osseous and CNS structures (50%, 36% and 16.6%,

respectively). Regarding management, surgery was most common in >36% of patients, followed by steroid and myelosuppressive therapies (25% each), immunotherapy (13.88%) and targeted molecular therapies (11.1%). Disease responses were considered stable if grossly unchanged during serial exam or imaging surveillance, partial if diminished but still present and complete if disease was grossly and radiographically resolved; a partial response or better was observed in >75% of patients. With respect to treatment rendered, stable disease was equally likely between recipients of molecular and conventional (non-molecular) therapy at 25%. Partial responses were higher in molecular therapy recipients (75% as compared to 42%), although complete responses have not yet been observed in this cohort. Patients diagnosed at <1 month from symptom onset had higher rates of disease stability and complete responses compared to those diagnosed at >24 months.
Conclusions: To our knowledge, this study is the largest of its kind in adult Rosai Dorfman Disease. Early recognition and utilization of targeted molecular therapies, based on our preliminary data, are associated with higher rates of achieving disease stability and at least a partial response. The current absence of complete responses in patients receiving targeted molecular therapy is likely attributable to the still-emerging use of these agents and interim response assessments not yet being completed. Higher complete response rates in targeted agents relative to conventional therapies are anticipated in ongoing analyses.

#4537

Erdheim Chester disease: A retrospective study characterizing the molecular and pathologic footprints with clinical presentation and comparative outcomes in the present era of targeted molecular targeted therapy

Sabrina R. Wilcox[1], Samuel B. Reynolds[2], Jennifer Girard[2], Asra Ahmed[2]. *[1]Internal Medicine and Pediatrics, University of Michigan, Ann Arbor, MI,[2]Oncology and Hematology, University of Michigan, Ann Arbor, MI*

Erdheim Chester Disease (ECD) is a rare, non-Langerhans cell histiocytic disease, characterized as a neoplastic disorder in 2016. MAP Kinase and PI3-AKT pathway somatic mutations and/or fusion genes have been shown to play a significant role in disease pathogenesis. Despite this, molecular sequencing at diagnosis has yet to become a standard of practice.
Retrospective analysis of 19 patients diagnosed with ECD at a single institution over a twenty-years (2002-2022) was conducted. Inclusion criteria were patients 18 years or older, histopathologic diagnosis of ECD, and clinical correlation of disease. The following was collected for each patient: biological sex, age at diagnosis, molecular testing (if utilized), immunohistochemistry, imaging results, therapies administered and best treatment outcomes. Information was translated into binary data for statistical analysis.
In this analysis, 47% of patients were females; average age at diagnosis was 51.2 years. 36% of patients were diagnosed within 12 months of symptoms onset. Molecular diagnostics were utilized in 100% of patients, (immunohistochemistry 94%, sequencing 26%). Primary disease was most commonly extranodal (94%), followed by osseous (63%), dermal (52%) and the central nervous system (36%). Treatment consisted of targeted molecular therapy most often (57%), followed by myelosuppressive therapy and steroids (42%), and immunotherapy or radiation (10% each). Disease responses were considered stable if grossly unchanged clinical exam or imaging surveillance, partial (PR) if diminished but still present and complete (CR) if disease was grossly or radiographically resolved. A PR or better was observed in 83% of patients. Stable disease was seen more often in patients treated with conventional therapy (33%) as compared to targeted molecular therapy (11%). PR was higher in targeted therapy recipients (55%). CR was more common with conventional therapy than molecular (66% vs 33%). Patients diagnosed within 1 month of symptom onset had higher rates of disease stability, compared to diagnosis at > 24 months (50% compared to 25%).
To our knowledge, this is one of the largest studies of its kind conducted in adult ECD. Targeted molecular therapy utilization by this analysis is associated with higher rates of partial disease response as compared to conventional therapy. The opposite was observed in complete responders. Use of targeted molecular therapies is very recent and higher CR rates are expected in ongoing analyses and longer patient follow-up. Moreover, molecular diagnostics were not routinely employed at diagnosis which delayed the initiation of treatment. Thus, we strongly advocate for early genetic profiling at the time of ECD diagnosis and utilization of targeted therapies when actionable mutations are observed.

#4538

The heterogeneous immune and molecular landscape of endometrial cancer metastases

Matthew J. Hadfield[1], Sharon Wu[2], Alex Farrell[3], Matthew Oberley[3], Nathaniel Jones[4], Thomas Herzog[5], Premal Thaker[6], Don Dizon[1]. *[1]Medical Oncology, Brown University/Legorreta Cancer Center, Providence, RI,[2]Caris Lifesciences, Phoneix, AZ,[3]Caris Life Sciences, Phoneix, AZ,[4]Gynecological Oncology, University of Southern Alabama, Mobile, AL,[5]Gynecological Oncology, University of Cincinnati, Cincinnati, OH,[6]Gynecological Oncology, Washington University School of Medicine, St. Louis, MO*

Introduction: Endometrial Cancer (EC) is a diverse malignancy with multiple histological subtypes. There is a paucity of data exploring the genomic landscape of endometrial cancer primary lesions (ECP) and endometrial metastatic lesions (ECM.) Correlations with genetic makeup and sites of metastatic disease have not been previously studied.

Methods: Relationships of ECM and alterations detected by NGS (592, NextSeq; WES, NovaSeq) were investigated in 15,489 EC samples (Caris Life Sciences, Phx, AZ). PD-L1 expression was tested by IHC (SP142, >2|5%). Microsatellite instability (MSI) was tested by FA, IHC and NGS. Tumor mutational burden (TMB) was measured by summing somatic mutations per tumor (H: >10 mt/MB). Immune infiltrates estimated by deconvolution of WTS data (NovaSeq) using MCP Counter. Real world overall survival (rwOS) was extracted from insurance claims and calculated using Kaplan-Meier estimates for cohorts defined by biopsy site, using start of treatment to last contact. Statistical significance determined by chi-square and Mann-Whitney U and adjusted for multiple comparisons ($q<0.05$).

Results: ECM had higher HER2 amplification (by CISH) compared to ECP (20.4% vs. 16.9%) but lower PR positivity (45.2% vs. 50.2%) ($q<0.05$). TMB-H was highest in ECM to GI (34.2%) compared to Uterine (22.4%) ($q<0.05$). d-MMR/MSI-H prevalence was highest in ECM to GI (30.3%) and lowest in ECM to lung (11.5%) and liver (10.9%) compared to Uterine (19.5%) ($q<0.05$). Hierarchical clustering of ECM sites by alteration (mutations, amplifications and fusions) frequency revealed ECM to Bone and GU having a distinct pattern compared to Uterine with increased alterations in RTK RAS (Bone vs Uterine: FGF3-amp, 3.45% vs 0.39%, FGF19-amp, 3.36% vs 0.39%), Cell Cycle (Bone vs GU vs Uterine: TP53-mt, 37.6% vs 42.3% vs 53.7%), WNT (GU vs Uterus: RNF43-mt, 15.4% vs 7.06%; CTNNB1-mt, 22.3% vs 12.9%) and Chromatin Remodeling (GU vs Uterine: ASXL1-mt, 23.1% vs 7.64%; KMT2D-mt, 18.9% vs 11.1%, ARID1A, 43.8% vs 33.8%) pathway genes.ECM to Bone had the lowest infiltration of B cells and T cells ($q<0.05$). IFN score was 1.21-fold higher in ECM to Bone compared to ECP of Uterus ($q<0.05$). ECM to GU (n=29, HR: 1.59, 570 days, p=0.04) had worse post-Carboplatin survival than ECP (n=3023, 1096 days) while ECM to Lung had better (n=279, HR: 0.73, 1602 days, p=<0.01). ECM to Liver (PD-1/PD-L1i: n=27, HR: 2.4, 165 days, p=<0.01; Bevacizumab: n=44, HR: 1.5, 286 days, p=0.03) had worse post-tx survival compared to ECP (PD-1/PD-L1i: n=607, 760 days; Bevacizumab: n=693, 463 days). ECM to GI (n=44, HR: 0.56, 1080 days, p=0.003) and Lung (n=86, HR: 0.70, 768 days, p=0.01) had improved post-Gemcitabine treatment compared to ECP (n=533, 452 days).

Conclusions: ECM to Bone and GU organs have unique molecular alterations when compared to ECP of the uterus and have lower infiltration of immune cells. We also highlight differences in OS when comparing different ECM.

#4539

Tumor evolution and immune microenvironment dynamics define response to neoadjuvant treatment of esophageal adenocarcinoma

Melissa Barroux[1], Jacob Househam[2], Eszter Lakatos[2], Tahel Ronel[3], Ann-Marie Baker[2], Henrike Salié[4], Max Mossner[2], Kane Smith[2], Chris Kimberley[5], Salpie Nowinski[2], Alison Berner[5], Vinaya Gunasri[5], Marnix Jansen[6], Giulio Caravagna[7], Julia Slotta-Huspenina[8], Wilko Weichert[8], Markus Alberstmeier[9], Benny Chain[10], Helmut Friess[11], Bertram Bengsch[12], Roland M. Schmid[1], Jens T. Siveke[13], Michael Quante[4], Trevor A. Graham[2]. *[1]Medical Clinic and Polyclinic II, Klinikum rechts der Isar, Technical University of Munich, Munich, Germany,[2]Centre for Evolution and Cancer, The Institute of Cancer Research, London, United Kingdom,[3]Centre for Genomics and Computational Biology, Barts Cancer Insitute, London, United*

Kingdom,[4]Clinic for Internal Medicine II, University Medical Center Freiburg, Freiburg, Germany,[5]Centre for Genomics and Computational Biology, Barts Cancer Institute, London, United Kingdom,[6]Department of Pathology, University College London, London, United Kingdom,[7]Department of Mathematics and Geosciences, University of Triest, Triest, Italy,[8]Institute of Pathology, Technical University of Munich, Munich, Germany,[9]Visceral and Transplantation Surgery, University Hospital, Ludwig-Maximilians-Universität (LMU) Munich, Munich, Germany,[10]Division of Infection and Immunity, University College London, London, United Kingdom,[11]Department of Surgery, Klinikum rechts der Isar, Technical University of Munich, Munich, Germany,[12]Signalling Research Centres BIOSS and CIBSS,, University of Freiburg, Freiburg, Germany,[13]Bridge Institute of Experimental Tumor Therapy and Department of Medical Oncology, West German Cancer Center, University Hospital Essen, Essen, Germany

Introduct**ion:** Locally advanced esophageal adenocarcinoma (EAC) remains difficult to treat, and resistance is common. The ecological and evolutionary dynamics responsible for treatment failure are incompletely understood.
Aim & Methods: We performed a multi-omic study with a multi-timepoint strategy to examine neoadjuvant treatment response at clonal resolution and in the surrounding tumor microenvironment. EAC samples from chemotherapy responding (REs) and chemotherapy non-responding (NRs) patients with locally advanced EAC were collected at three time points (prior, during, and after neoadjuvant therapy) within the multicenter *MEMORI* trial. Whole exome sequencing (mean depth 300x) was performed on 47 samples from 17 REs and on 24 samples from 10 NRs. Matched RNA sequencing was performed on 53 samples from 17 REs and on 26 samples from 10 NRs. To characterize immune response we performed imaging mass cytometry (IMC) with a 18-marker panel on 26 samples from 9 REs and 16 samples from 6 NRs and T-cell receptor sequencing in 18 RE-samples and 9 NR-samples.
Results: We observed profound changes in mutation signatures over time, characterized by C>A transitions after exposure to neoadjuvant chemotherapy (FOLFOX), which is consistent with earlier observed oxaliplatin induced mutational signatures. Phylogenetic analysis showed no major changes in the clonal make-up during treatment, suggesting phenotypic plasticity rather than clonal evolution caused treatment resistance. EAC samples displayed widespread copy number alterations (CNAs), as previously described. CNAs arising during treatment were significantly more likely to be small, focal alterations rather than large alterations. At the transcriptome level neoadjuvant treatment led to significant changes with significant upregulation of immune and stromal pathways and oncogenic pathways such as *KRAS, Hedgehog* and *WNT*. The presence of immune escape mechanisms (defined as LOH or mutations in HLA, B2M mutations or PDL-1 overexpression) and a lack of clonal T-cell expansions were linked to poor clinical treatment response. Moreover, IMC analyses showed a less activated T-cell phenotype in NRs than in REs throughout treatment.
Conclusion: Using a multi-timepoint approach, we integrated genetic analyses with transcriptomic analyses and analyses of the tumor immune microenvironment for a holistic understanding of treatment resistance. This study identifies profound transcriptional changes during treatment with limited evidence that clonal replacement is the cause, suggesting phenotypic plasticity as a mechanism for therapy resistance. The presence of immune escape, a less activated T-cell phenotype and a lack of clonal T-cell expansions in patients with poor clinical treatment response has high pharmacological relevance and could be exploited via combined immune-chemotherapy treatments.

#4540

Multiregional transcriptomics of colorectal cancers define prognostic features less vulnerable to tumor heterogeneity

Jonas Langerud[1], Ina A. Eilertsen[1], Hossein Moosavi[1], Ingeborg F. Backe[1], Merete Hektoen[1], Marine Jeanmougin[1], Ole Sjo[2], Arild Nesbakken[3], Ragnhild A. Lothe[1], Anita Sveen[1]. *[1]Department of Molecular Oncology, Oslo University Hospital, Institute for Cancer Research, Oslo, Norway,[2]Department of Gastrointestinal Surgery, Oslo University Hospital, Oslo, Norway,[3]Institute for Clinical Medicine, Faculty of Medicine, University of Oslo, Oslo, Norway*

Purpose: Tumor heterogeneity compromises the clinical applicability of transcriptomic subtypes of colorectal cancers (CRCs). We performed multiregional tumor sampling to map the intra-tumor heterogeneity of primary CRCs and to evaluate the prognostic relevance of features less vulnerable to heterogeneity.
Methods: Gene expression profiling was performed of 708 primary tumor samples from 515 patients treated by surgery for stage I-IV CRC at Oslo University Hospital (Human Transcriptome 2.0 Arrays). This included 2-4 multiregional samples from each of 97 patients (n=290 samples; mean 2.9 per tumor), and single bulk tumor samples from 418 patients. Intra-tumor heterogeneity was evaluated according to consensus molecular subtype (CMS) classification, including computational assessment in the single samples by CMS enrichment scores. Gene-wise heterogeneity scores were calculated as intra-class correlation coefficients in the multiregional sample set, and genes with low heterogeneity were used as input for subtype discovery by non-negative matrix factorization.
Results: Heterogeneous CMS classification of multiregional samples was found in 40% of tumors. Heterogeneous tumors were enriched with CMS3 (odds ratio 5.0) and CMS4 (odds ratio 12.5), and the most common combinations were CMS2/4 and CMS1/3. Microsatellite instability and *BRAF*^{V600E} mutations were enriched among tumors with a major CMS1 component only. *KRAS*/*NRAS* mutations were most frequent in CMS3 tumors without CMS1. Intra-tumor heterogeneity was primarily driven by mesenchymal-like and stromal signals, but was independently associated with a poor 5-year relapse-free survival among patients with stage I-III CRC (multivariable hazard ratio 1.5 [1.0-2.2]). Heterogeneity explained a larger proportion of variation in survival (14%) than cancer-associated fibroblasts (6%). Genes with low intra-tumor heterogeneity were enriched in cancer cell intrinsic signaling pathways, including cell cycle progression and MYC targets. *De novo* subtyping based on these genes recapitulated the intrinsic iCMS groups identified from single-cell sequencing (Joanito et al., Nat Genet 2022;54:963-75) with high accuracy (Cohen's κ=0.80). Further sub-stratification identified four subtypes with similar biological activity to the original CMS, but lower classification heterogeneity among multiregional samples (25%). The subtypes were called congruent CMS (cCMS) and provided stronger prognostic stratification than CMS in multivariable analysis with clinicopathological and molecular features (cCMS4: hazard ratio 5.9 [2.4-14.7]; cCMS2: 3.4 [1.5-7.6]; cCMS3: 2.0 [0.9-4.3] with cCMS1 as reference).
Conclusion: Multiregional sampling of primary CRCs enabled identification of cancer-intrinsic transcriptomic features robust to intra-tumor heterogeneity and with prognostic relevance.

#4542
Development of a one-step molecular classifier for endometrial carcinoma using an amplicon-based gene panel and next generation sequencing technology

Melissa K. McConechy[1], Amy Jamieson[2], Amy Lum[3], Samuel Leung[3], Adrian Kense[1], Sonal Brahmbhatt[1], Ka Mun Nip[1], Ebru Baran[1], Dilmi Perera[1], Kurt Yakimovich[1], Ruth Miller[1], C. Blake Gilks[4], David Huntsman[1], Jessica N. McAlpine[5]. *[1]Imagia Canexia Health, Vancouver, BC, Canada,[2]Department of Gynecology and Obstetrics, University of British Columbia, Vancouver, BC, Canada,[3]Department of Molecular Oncology, University of British Columbia, Vancouver, BC, Canada,[4]Department of Pathology, University of British Columbia, Vancouver, BC, Canada,[5]Department of Gynecology and Obstetrics,, University of British Columbia, Vancouver, BC, Canada*

Objectives: Molecular classification of endometrial carcinoma (EC) is now recommended by the WHO, ESGO/ESTRO/ESP and NCCN guidelines. The pragmatic molecular classification tool, ProMisE, identifies four molecular subtypes based on next generation sequencing (NGS) for the detection of somatic pathogenic *POLE* mutations, and immunohistochemistry for mismatch repair and p53 proteins. ProMisE provides valuable prognostic and predictive information to direct care, however, multiple molecular results are often received from different time periods and/or from different centers which can cause delays. Therefore, we developed a classifier that relies on a single DNA-based NGS test with the goal of recapitulating the prognostic value of ProMisE by producing concordant results.
Methods: Formalin fixed paraffin embedded (FFPE) EC tumor DNA was sequenced using the clinically validated Imagia Canexia Health Find It™ amplicon-based next generation sequencing gene panel assay. The 38 gene panel assessed single nucleotide variants (SNVs), indels (insertions and deletions), gene amplification and microsatellite instability (MSI) using 21 MSI loci. To compare to the original ProMisE classifier, we identified somatic mutations in *POLE*, *TP53* and MSI-High or MS-Stable for molecular classification. Molecular subtypes assigned by both classifiers were assessed for concordance metrics and Kaplan-Meier survival curves.
Results: The one-step NGS molecular classifier assessed 165 unique patient FFPE EC samples that had previously been assessed by ProMisE. There were 152/165 cases that were concordant between molecular subtype assignment from the original ProMisE and the one-step NGS assay with a

kappa statistic of 0.88 and accuracy of 0.92. There were 13 samples that were discordant (original classifications: 3 *POLE*, 3 MMRd, 2 p53abn, 5 NSMP/p53wt), which will be reviewed in detail. Results were concordant in 14 of 15 cases (93%) when both diagnostic biopsy and hysterectomy specimens were tested. Molecular subtypes maintained their associations with clinical outcomes (progression free survival, disease specific survival, overall survival).
Conclusion: The one-step NGS molecular classifier demonstrates high concordance with the original ProMisE classifier including between biopsy and hysterectomy samples. This shows that reliable molecular testing could be obtained from time of first diagnosis. Prognostic value of this new one-step classification tool is maintained. Appropriate interpretation of results is critical, including limiting *POLE* mutation assignment to a confirmed list of pathogenic mutations and correct order of segregation for ECs with more than one molecular feature. Further validation is needed in a larger cohort to implement into standard of care testing.

#4543

Identification of tumor-specific breast cancer expression subtypes and subtype-specific drug response prediction

Julie Karam[1], Paul Rejto[2], Jadwiga R. Bienkowska[2], Xinmeng J. Mu[2], Whijae Roh[2]. *[1]Brown University, Providence, RI,[2]Pfizer, San Diego, CA*

Breast cancer is a complex disease with a high degree of inter-tumor heterogeneity. Subtyping the disease and identifying the genomic features driving these subtypes are critical for precision oncology for breast cancer. With increasing availability of single cell RNA-seq data and deconvolution methods, there is unmet need for identifying novel tumor-intrinsic subtypes based on deconvoluted tumor-specific expression profiles as well as novel bulk tumor subtypes based on bulk RNA-seq data. Drug response prediction based on tumor-intrinsic subtypes can be also potentially more robust than drug response prediction based on bulk subtypes because currently available CRISPR and drug screening data are mostly based on only cancer cell lines. Therefore, we applied consensus hierarchical clustering, Bayesian Non-negative Matrix Factorization (BayesNMF), and deconvolution methods to 1,058 TCGA breast cancer samples and identified seven bulk expression subtypes (S1-S7) and five tumor-specific expression subtypes

(S1-S5). In order to characterize our subtypes, we first performed subtype association with previously characterized subtypes, including PAM50, HR status, and METABRIC IntClust subtypes. Notably, Luminal A and METABRIC IntClust 4ER+ breast cancer was further partitioned into our S1 and S5 bulk subtypes. We characterized the subtypes with pathway activity, TME deconvolution, and subtype-associated driver mutations. Our BayesNMF bulk and tumor-specific subtypes showed stronger association with prognosis than PAM50 subtypes, suggesting potential clinical utility of our subtypes. We projected BayesNMF to DepMap cell lines and CPTAC breast cancer samples to identify subtype-specific vulnerabilities and proteogenomic characterization of our subtypes, respectively. We also developed the method to predict CDK4 selective and CDK6 selective drug response in human breast tumor tissues by training the NMF models with CDK4 and CDK6 dependency scores and gene expression features in the DepMap cell lines. Our tumor-specific S5 subtype had significantly lower CDK4 response scores and significantly higher CDK6 response scores than others suggesting that this subtype, which is primarily triple-negative breast cancer, might be potentially a good subtype for CDK6 selective inhibitors. Additionally, our tumor-specific S4 subtype had significantly higher CDK4 response scores and significantly lower CDK6 response scores than others suggesting that this subtype might be a promising patient population for CDK4 selective inhibitors. We further applied machine learning methods to identify biomarkers that associate with subtypes and CDK4/CDK6 dependency scores using gene expression, mutations, and CNAs. Overall, our subtyping approach identifies clinically-relevant novel breast cancer subtypes with subtype-specific cancer vulnerabilities and therapeutic targets.

#4544

Genomic, transcriptomic, functional, and mechanistic characterization of rhabdomyosarcoma with FUS-TFCP2 or EWSR1-TFCP2 fusions

Julia Schoepf[1], Sebastian Uhrig[2], Christoph E. Heilig[1], Kwang-Seok Lee[1], Tatjana Walther[1], Alexander Carazzato[1], Anna Maria Dobberkau[1], Dieter Weichenhan[2], Christoph Plass[2], Mark Hartmann[1], Gaurav Diwan[3], Zunamys Carrero[4], Claudia R. Ball[4], Tobias Hohl[1], Thomas Kindler[5], Patricia Rudolph-Hähnel[5], Anna Nilsson[6], Ingrid Øra[7], Roland Imle[2], Ana Banito[2], Robert Russell[3], Barbara C. Jones[8], Daniel B. Lipka[1], Hanno

Glimm[4], Daniel Hübschmann[1], Wolfgang Hartmann[9], Stefan Fröhling[1], Claudia Scholl[1]. *[1]German Cancer Research Center (DKFZ) and National Center for Tumor Diseases (NCT) Heidelberg, Heidelberg, Germany,[2]German Cancer Research Center (DKFZ), Heidelberg, Germany,[3]Heidelberg University Biochemistry Centre, Heidelberg University, Heidelberg, Germany,[4]National Center for Tumor Diseases (NCT/UCC) Dresden, Faculty of Medicine and University Hospital Carl Gustav Carus, Technical University Dresden, Dresden, Germany,[5]University Cancer Center Mainz, Johannes Gutenberg University Mainz, Mainz, Germany,[6]Pediatric Oncology and Coagulation, Karolinska University Hospital, Stockholm, Sweden,[7]Pediatric Oncology and Hematology, Skåne University Hospital, Lund University, Lund, Sweden,[8]Hopp Children's Cancer Center Heidelberg (KiTZ), Heidelberg, Germany,[9]Gerhard Domagk Institute of Pathology, University Hospital Münster, Münster, Germany*

Rhabdomyosarcoma (RMS) is a soft-tissue sarcoma subtype composed of malignant immature precursor cells with myogenic differentiation defined by aberrant expression of the transcription factors MYOD1 and MYOG. Four subtypes are distinguished, characterized by considerable clinical, histologic, and genetic heterogeneity. RMS with fusions of the transcription factor TFCP2 to either FUS or EWSR1 has only recently been observed, but its classification and pathogenesis are unclear. We studied the clinical course, histopathology, and molecular landscape of 12 cases of this new RMS type and determined the functional properties of tumor-specific genetic alterations. Unusually for gene fusion-driven sarcomas, most tumors had highly rearranged genomes, including chromothripsis, and signs of defective homologous recombination DNA repair. All tumors were characterized by extremely high expression of a truncated TERT variant and the receptor tyrosine kinase ALK. The latter was additionally affected by intragenic deletions (33%), which resulted, together with aberrant splicing events, in the expression of shortened ALK variants (58%). Three ALK variants were oncogenic in immortalized cells *in vitro* and after xenotransplantation in mice and responded variably to different ALK inhibitors. Additional recurrent alterations included CDKN2A/MTAP co-deletions (67%) and mutations in PAPPA2 (25%) encoding an IGFBP5-

specific proteinase. DNA methylation analysis of FUS/EWSR1-TFCP2 RMS, along with 19 other soft-tissue sarcoma types, revealed a close relationship with undifferentiated sarcoma but not with other RMS subtypes, suggesting that FUS/EWSR1-TFCP2 RMS is a distinct sarcoma entity possibly arising from a different cell of origin than other RMS types. Transduction of TFCP2 fusions into immortalized human cells conferred anchorage-independent growth and blocked late myogenic differentiation. Genes significantly induced in these cells were also highly expressed in patient tumors, including ALK, TERT, and two known regulators of skeletal muscle cells, IGFBP5 and PTH1R. ACT-seq demonstrated direct binding of FUS-TFCP2 to the ALK and TERT gene loci outside their regular promoters, which correlated with the expression of alternative transcript variants. Finally, FUS-TFCP2 appeared to induce a defect in DNA double-strand repair in immortalized cells, rendering them sensitive to treatment with cisplatin. Together, our study gives insights into the pathogenesis of a new RMS subtype defined by FUS-TFCP2 or EWSR1-TFCP2 fusions and suggests entry points for therapeutic intervention with DNA-damaging agents, ALK inhibitors, and, in the case of additional CDKN2A/MTAP co-deletion, drugs targeting PRMT5.

#4545

Integrative immune-genomic comparison of canonical Ewing sarcoma with Ewing-like mimics identifies potential targets for personalized therapies

Zhusheng Zhang[1], Qiyuan Bao[1], Junxiang Wen[1], Zhuochao Liu[1], Qi Liu[1], Yuhui Shen[1], Lin Shao[2], Bing Li[2], Song-An Chen[2], Weibin Zhang[1].
[1]Shanghai Jiaotong University Ruijin Hospital, Shanghai, China,[2]Burning Rock Biotech, Guangzhou, China

Introduction: Ewing sarcoma (ES) is one of the most common types of small round cell sarcoma (SRCS) from the skeletal origin, characterized by small round blue cell morphology and *FET-ETS* fusions. However, recent NGS-based technology has dramatically increased the characterization of other SRCS entities that share morphological, pathological, and clinical similarity with canonical ES. Currently, these sarcomas are often treated with similar regimens derived from ES. Whether any subsets of these

sarcomas might benefit from personalized anti-cancer strategies remains largely unknown.
Methods: To explore potential therapeutic vulnerabilities, 51 FFPE samples from 49 patients (median age 31 years, 65.3% male) diagnosed as ES or its mimics by conventional pathology review were sent to DNA (OncoScreen®Plus) and RNA sequencing (OncoRNA, Burning Rock Biotech) for genomic and immune signature profiling. Tumor samples were classified into 5 groups based on their similarity with classic ES: (a) Canonical ES (n=12), defined as ES with *EWSR1-FLI1* fusion and a primary bone origin; (b) Non-canonical ES, which were found with either non-*EWSR1-FLI1 FET-ETS* fusion, or ES in extra-skeletal sites (n=11); (c) Non-*FET-ETS* fusion SRCS (n=10), defined as SRCS with gene fusions other than *FET-ETS* family; (d) Fusion-negative SRCS (n=4); and (e) non-SRCS, where the diagnosis was primarily suspected as ES but finally re-diagnosed as another histology (n=12).
Results: The NGS-based diagnosis rectified the pathological diagnosis in 9/51 samples, including ES misdiagnosed as other (n=3), other misdiagnosed as ES (n=4), Non-*FET-ETS* fusion SRCS misdiagnosed as ES (n=1) and ALK fusion sarcoma misdiagnosed as SRCS (n=1). In the remaining 42 samples, 23 diagnoses were confirmed by both NGS and FISH, while 11 SRCS were negative in both NGS and FISH assay, yielding a concordance of 81.0% (34/42). In the 8 samples with discordant diagnosis, a definitive diagnosis was achieved by FISH but not NGS in 1 of 8 (12.5%), and vice versa in 7 of 8 (87.5%). Interestingly, genomic profiling revealed that Non-*FET-ETS* fusion SRCS had high frequencies of *TP53* mutations (40%) and copy number loss (including 30% in *CD274* and *JAK2*; 20% in *PTCH1*, *CDKN2A/B*, and *MTAP*) and featured higher levels of homologous recombination deficiency (HRD) (p=0.024) and chromosome instability (p=0.022) than other groups. Remarkably, non-canonical ES demonstrated upregulated *PDCD1* expression (p=0.034). The distribution of immune hot and cold subtypes was comparable among all groups (p=0.334).
Conclusion: Our study shows that NGS could efficiently facilitate the definitive diagnosis of ES and its mimics. We also revealed a diverse immune-genomic landscape of these SRCS, indicative of potential therapeutic opportunities targeting HRD and immune check-point in specific subtypes of these sarcoma entities.

#4546

Comprehensive analysis using transcriptional factor based molecular subtypes and correlation to clinical outcomes in small-cell lung cancer

Sehhoon Park, Tae Hee Hong, Soohyun Hwang, Hyun-Ae Jung, Jong-Mu Sun, Jin Seok Ahn, Myung-Ju Ahn, Jong Ho Cho, Yong Soo Choi, Jhingook Kim, Young Mog Shim, Hong Kwan Kim, Yoon-La Choi, Se-hoon Lee, Keunchil Park. *Samsung Medical Center, Seoul, Korea, Republic of*

Background: Several studies have reported the predictive and prognostic value of novel transcriptional factor-based molecular subtypes in small-cell lung cancer (SCLC). We conducted an in-depth analysis using multi-omics data to elucidate the underlying characteristics that lead to differences in clinical outcomes between subtypes.

Patients and Methods: Immunohistochemistry (IHC, n=252), target exome sequencing (n=422), and whole transcriptome sequencing (WTS, n=189) data generated from 427 patients with SCLC patients were comprehensively analyzed. The differences in the mutation profile, gene expression profile were analyzed according to the IHC-based molecular subtype. Clinical implication was evaluated based on treatment outcomes of individual patients.

Results: IHC based molecular subtyping revealed a high incidence of ASCL1 subtype (SCLC-A, 56.3%) followed by ASCL1/NEUROD1 co-expressed (SCLC-trans, 17.9%), NEUROD1 (SCLC-N, 12.3%), POU2F3 (SCLC-P, 9.1%), triple-negative (SCLC-TN, 4.4%) subtypes showing high concordance with WTS-based subtyping. We delineated the SCLC-trans subtype resembling SCLC-A rather than SCLC-N in terms of both gene expression profiles and clinical outcomes. SCLC-TN type was defined as non-significant expression of A, N, P. Favorable overall survival (OS) was observed in SCLC-A compared to SCLC-N (adjusted HR 2.4, 95% CI 1.5-3.9, $p < 0.001$) and SCLC-P (adjusted HR 1.7, 95% CI 0.9-2.9, $p = 0.087$). SCLC-TN showed a similar OS with SCLC-A (adjusted HR 1.2, 95% CI 0.6 -2.7, $p = 0598$). The clinical outcome based on inflamed phenotype, clustered by effector cell gene expression profile which are only found in 5% of SCLC-N but 60% of SCLC-P, was more likely to benefit from first-line immunotherapy treatment than non-inflamed phenotype ($p = 0.013$).

Inflammed phenotype demonstrated longer progression-free survival to the first line immunotherapy compared to the non-inflammed phenotype. (10.5 vs 4.3, $p = 0.013$)
Conclusions: This study provides fundamental data, including the incidence and basic demographics of molecular subtypes of SCLC using both IHC and WTS from a comparably large cohort including potential differences in the distribution of subtypes based on ethnicity. Additionally, our results reveal differences in the underlying biological pathway activities and immunogenicity based on molecular subtype, possibly related to the difference in clinical outcomes, including immunotherapy response.

Spatial Proteomics and Transcriptomics 1

#5626
Multiomic spatial profiling of the tumor immune microenvironment at single cell resolution

Niyati Jhaveri[1], HaYeun Ji[1], Anushka Dikshit[2], Jessica Yuan[1], Emerald Doolittle[2], Steve Zhou[2], Maithreyan Srinivasan[2], Bassem B. Cheikh[1], Fabian Schneider[3], James Mansfield[3], Julia Kennedy-Darling[1], Oliver Braubach[1]. *[1]Akoya Biosciences, Menlo Park, CA,[2]Advanced Cell Diagnostics, a Bio-Techne Brand, Newark, CA,[3]Visiopharm A/S, Horsholm, Denmark*

Background**:** It has been well established that the tumor microenvironment (TME), which comprises cancer cells, stromal cells, and surrounding extracellular matrix, plays a critical role in cancer development, progression, and control. The immunological components within tumors, known as the tumor immune microenvironment (TiME), have also been implicated in tumor development, recurrence, and metastasis. Effective strategies for cancer immunotherapies will require a deep understanding of the factors that shape both the TME and TiME. Here, we describe a spatial multiomics approach that utilizes RNAscope™ ISH technology paired with high-plex whole-slide spatial phenotyping with the PhenoCycler™-Fusion platform. This two-step approach is compatible with human FFPE tissues and enables researchers to characterize the spatial biology of the TiME more accurately by detecting RNA and protein markers on serial sections. The resulting multiomic data more accurately reveal the interplay between

TME and TiME by giving insight into cell lineages, surrounding structures, as well as secreted chemokines and cytokines that exist within the TME ecosystem.
Methods: We performed ultrahigh-plex spatial phenotyping on the PhenoCycler-Fusion on FFPE tumor tissue sections, using an antibody panel that is designed for immune cell phenotyping, evaluation of immune contexture and proliferation across the TME. Using serial sections from the same tissue blocks, we then ran the RNAscope HiPlex v2 assay automated on the PhenoCycler-Fusion system. This assay consisted of a 12-plex immuno-oncology panel of RNA target probes, which were selected to detect macrophages, chemokines, and cytokines within tumors. We used Phenoplex software to analyze the protein and RNA datasets and to compute cell phenotypes and spatial associations.
Results and Conclusions: In this proof-of-concept study, we demonstrate the utility of multiomic spatial profiling on the PhenoCycler-Fusion platform. Analysis of the resulting multiplex imaging data not only revealed the structural organization of cells within the TME, but also activation states of immune cells. Together, this information provides a more complete functional map of immune cells within the TME and TiME and thereby enriches our understanding of tumor biology that may be deterministic of immunotherapy responsiveness. This work paves the way for future research that will rely on deep spatial phenotyping with protein biomarkers coupled with accurate quantification of the expression of regulatory cytokines, chemokines, growth factors, or non-coding RNAs that only RNA probes can detect.

#5627
Spatial protein profiling by cyclic immunofluorescence to interpret and improve bulk tumor-based predictor of response to chemotherapy with bevacizumab in neoadjuvant breast cancer treatment
Mads Haugland Haugen[1], David Kilburn[2], Hongli Ma[2], Cameron Watson[2], Allison Creason[2], Dong Zhang[2], Maria Aa Dahle[1], Ole Christian Lingjaerde[3], Marianne L. Smebye[1], Oeystein Garred[4], Mette S. Foersund[4], Mai T. Nguyen[4], Gunhild M. Maelandsmo[1], Gordon Mills[2], Olav Engebraaten[1]. *[1]Tumor Biology, Oslo University Hospital, Institute for Cancer Research, Oslo, Norway,[2]Oregon Health and Science University,*

Knight Cancer Institute, Portland, OR,[3]Informatics, University of Oslo, Oslo, Norway,[4]Pathology, Oslo University Hospital, Oslo, Norway

Introduction: A limited number of drugs are available for use in breast cancer patients, and several are not in practical use due to the lack of adequate biomarkers. We have recently demonstrated the feasibility of using machine learning on molecular data from bulk tumor analysis to create a nine-protein signature named VEGF-inhibition Response Predictor (ViRP) for selecting BC patients for treatment with chemotherapy and bevacizumab. The ViRP score is currently being validated in the NAPEER+ clinical trial (EudraCT 2021-005850-27). Increasing evidence suggests that spatial organization of cells within the tumor microenvironment influences survival and response to therapy in numerous cancer types. In methods based on bulk tumor analysis all tumor cells are profiled simultaneously with both colocalized and distant stroma and immune cells. We are thus pursuing information on spatial organization of cellular phenotypes expressing selected cancer related proteins including our nine ViRP proteins.
Methods: From the NeoAva (NCT00773695) clinical trial evaluating the effect of bevacizumab in combination with neoadjuvant chemotherapy (n=132 pts), FFPE tissue sections from patients before, during, and after treatment were made. Cyclic immunofluorescence (cyCIF) was used to profile the spatial expression of 32 cancer-signaling and 32 immune-related proteins, comprising our nine ViRP proteins, on FFPE tissue sections from selected patients (n = 20). The Galaxy-ME platform was used for image processing and downstream analysis of spatial protein profiling.
Results: Use of cyCIF for spatial analysis enabled for evaluation of malignant cells in the context of surrounding microenvironmental cells, including immune cells. We found that cell type-specific protein abundance and subcellular localization formed a highly heterogenous pattern in the tissue. This was particularly evident for the nine ViRP proteins, and differences in expression between tumor cell populations will be further elucidated. Among the patients selected for cyCIF analysis, 4 were chosen based on misclassification by the ViRP signature. Ongoing studies focus on revealing spatial expression patterns to optimize the ViRP biomarker and explore why misclassification occurs. Furthermore, the observed molecular biology of the evolving tissues under treatment in responding and non-

responding patients may reveal new biomarkers indicative of treatment response or resistance.
Conclusion: We observe that the expression of proteins in tumor tissues is highly heterogeneous, and thus include numerous features not captured by bulk tumor analysis. Future development of new predictive tools and biomarkers that integrate molecular data which is multiparametric and spatial will set the stage for a new class of biomarkers in cancer diagnostics.

#5629

Spatial genomics and proteomics enable multimodal analyses of oral SCC clonal heterogeneity and interactions with tumor microenvironment

Raju Kumar[1], Rana Ibrahim[1], Bassem Ben Cheikh[2], Emma Bailey[1], Hannah Cottom[3], Oliver Braubach[2], Trevor Graham[4], Jun Wang[5], Ines Sequeira[1]. *[1]Barts Centre for Squamous Cancer, Queen Mary University of London, London, United Kingdom,[2]Akoya Biosciences, Menlo Park, CA,[3]Barts Health NHS Trust, London, United Kingdom,[4]Centre for Evolution and Cancer, The Institute of Cancer Research, London, United Kingdom,[5]Barts Cancer Institute, Queen Mary University of London, London, United Kingdom*

Cancer progression is an evolutionary process governed by the clonal evolution of the genetic mutations acquired during tumor growth, together with the co-evolution of the tumour ecosystem. The nature of cancer subclonal mutations and their effects on the tumour microenvironment are the major drivers of intratumor heterogeneity and contribute to cancer progression, metastasis, therapy resistance and disease recurrence. Therefore, a spatially resolved genetic and cellular profiling of tumors is crucial to investigate tumor architecture and cellular diversity. Oral squamous cell carcinoma (OSCC), a subset of head and neck cancer, accounts for 355,000 new cases annually worldwide and has a 5-year survival rate of only 50%. We recently conducted a multi-level analysis of OSCC genetic and microenvironment heterogeneity (Sequeira et al, 2020, NatComms). Computational analysis of tumour clonal dynamics from DNA sequencing data revealed that high genetic heterogeneity to be a feature of early-stage lesions that are likely to progress to more aggressive tumors (Williams et al 2018, NatGen; Sequeira et al, 2020, NatComms). These

tools can be used to predict tumour behavior and for early diagnosis of aggressive lesions. The goal of this study is to elucidate the functional and spatial intratumor heterogeneity, tumor clonal dynamics and evolutionary landscape of human OSCC, and to study the interaction of tumour cells with the microenvironment, in particular the role of specific mutations in promoting epithelial-to-mesenchymal transition and tumor progression, using an interdisciplinary approach that combines spatial integrative genome analysis and deep single-cell phenotyping of tumor microenvironment. We performed whole-exome sequencing from multifocal OSCC tumor regions and matched metastasis, and used computational methods to investigate the tumor subclonal organization, construct phylogenetic trees for each tumor and assess the genetic diversity of the different tumour regions and metastasis. We then combined Single cell Spatial Phenotyping on the *PhenoCycler* platform (Akoya Biosciences) (Black et al, 2021, NatProtocols) with the subclonal genomic analysis to investigate how different mutational landscapes affect tumor microenvironment and metastasis, at unprecedented detail. Together, this multi-modal integrated spatial genomics and proteomics analysis of the tumor ecosystem highlights the importance of spatial cellular organization and provides a comprehensive human OSCC spatial atlas of tumour heterogeneity, providing a foundation for exploring cancer evolution, heterogeneity and progression.

#5630

Robust spatial biomarker discovery through multi-platform multiplex image analysis of breast cancer clinical cohorts

Jennifer R. Eng[1], Elmar Bucher[2], Zhi Hu[3], Melinda Sanders[4], Bapsi Chakravarthy[4], Jennifer Pietenpol[4], Rosalie C. Sears[1], Summer Gibbs[5], Joe W. Gray[5], Koei Chin[6]. *[1]Molecular and Medical Genetics, Knight Cancer Institute, Oregon Health & Science University, Portland, OR,[2]Intelligent Systems Engineering, Indiana University, Bloomington, IN,[3]Knight Cancer Institute, Oregon Health & Science University, Portland, OR,[4]Vanderbilt-Ingram Cancer Center, Vanderbilt University Medical Center, Nashville, TN,[5]Biomedical Engineering, Knight Cancer Institute, Oregon Health & Science University, Portland, OR,[6]Center for Early Detection Advanced*

Research, Knight Cancer Institute, Oregon Health & Science University, Portland, OR

Spatial profiling of tissues promises to elucidate tumor-microenvironment interactions and enable development of spatial biomarkers to predict response to immunotherapy and other therapeutics. However, spatial biomarker discovery is often limited to small patient cohorts and single technologies, limiting statistical power and increasing the likelihood of technical artifacts. We utilized cyclic immunofluorescence, (CyCIF), to profile patient tissues from 102 breast cancer patients, 63 with clinical follow up. We then developed methods for comparative analysis of data from three disparate imaging technologies including our CyCIF images, as well as publicly available imaging mass cytometry and multiplex ion-beam imaging breast cancer data sets. We demonstrate similar single-cell phenotyping results across breast cancer patient cohorts imaged with the three methods, and furthermore, show agreement in the prognostic value of cellular and spatial biomarkers across platforms. We identified T cell infiltration as independently associated with longer survival in high-proliferation breast cancer, which was enriched for activated and spatially clustered T cells. A comparison of six spatial analysis methods revealed robust spatial biomarkers, including tumor-macrophage and tumor-fibroblast proximity associated with poor prognosis in estrogen receptor positive and triple negative tumors, respectively. Our methods enable assembly of larger clinical cohorts from diverse platforms to aid in predictive and prognostic spatial biomarker identification and validation.

#5631

Expanding tools for multiplex mRNA imaging in spatialomics through the ViewRNA tissue assay kits

Nancie Mooney. *Thermo Fisher Scientific, Eugene, OR*

Spatialomics is a rapidly growing field as it allows researchers to gain a deeper understanding of transcriptomes and corresponding protein expression profiles in cells within complex tissue microenvironments. One critical technology for spatialomics is in-situ hybridization (ISH) technology, which enables direct visualization and quantitation of nucleic acid in cells with single molecule resolution. The Invitrogen ViewRNA ISH

assays incorporate branched DNA (bDNA) technology provides tools for interrogating multiple RNA transcripts at the same time, paving the way for improved spatialomics research. This technology is a powerful tool for spatialomics, giving insight into important mechanisms within cells and tissue. With researchers increasingly using spatialomic data in fields like neuroscience, immuno-oncology & single-cell analysis, these scientists will need the rapid and efficient detection of mRNA co-expression profiles that ViewRNA portfolio provides. In our newest offering, ViewRNA fluorescence tissue kits we extended our branched DNA technology, proprietary probe set design and signal amplification technology with Alexa Fluor probes offering a unique, robust, and sensitive in situ hybridization assay for RNA localization in fixed tissues. With fluorescence detection using Alexa Fluor 488, Alexa Fluor 546, Alexa Fluor 594, Alexa Fluor 647, and Alexa Fluor 750, these kits allow multiplexed detection and imaging paving the way for improved spatialomics. This technology lays the foundation for expanded fluorescent profiles to provide scientists additional tools to probe multiple transcripts per sample, allow broader spatialomics research. For Research Use Only. Not for use in diagnostic procedures.

#5632

Evaluating a novel molecular biomarker of angioinvasive lung adenocarcinoma with spatial transcriptomics

Dylan Steiner[1], Lila Sultan[1], Travis Sullivan[2], Emily Green[1], Hanqiao Liu[1], Xiaohui Xiao[1], Gang Liu[1], Avrum Spira[1], Sarah Mazzilli[1], Kimberly Rieger-Christ[2], Eric Burks[1], Jennifer Beane[1], Marc Lenburg[1]. *[1]Boston Univ. School of Medicine, Boston, MA,[2]Lahey Hospital and Medical Center, Burlington, MA*

Microscopic vascular invasion (VI) is predictive of recurrence in stage I lung adenocarcinoma (LUAD) but is difficult to assess in resection specimens and cannot be accurately predicted prior to surgery. Thus, new biomarkers are needed to identify this aggressive subset of stage I LUAD tumors. To assess molecular and tumor microenvironment (TME) features associated with angioinvasive LUAD we profiled 171 resected stage I tumors with and without VI by RNA-seq, including 16 tumors by high-resolution spatial transcriptomics (10x Genomics Visium). Visium capture areas were selected by an experienced thoracic pathologist to include

invasive foci, tumor regions distal to foci, and tumors without invasive foci. We identified a robust molecular signature of VI from the RNA-seq data containing subclusters of genes involved in hallmark programs of tumor suppression, EMT, angiogenesis, growth and metabolism. This VI-associated signature increases across the spectrum of indolent to aggressive stage I LUAD histopathology and is predictive of recurrence-free survival. Analysis of 43,421 Visium spots across 16 tumors revealed high inter-tumor patient heterogeneity, with most spots clustering by tumor identity, suggesting tumor-intrinsic properties. Scoring the Visium data for VI signature expression revealed spatial variability around VI foci, with distinct spatial distributions of different signature subclusters among tumor and stromal compartments within and adjacent to regions of tumor intravasation. We found increased expression of the bulk VI signature in invasive tumors, regardless of whether the capture area contained the invasive focus. We independently verified this finding by performing laser-capture microdissection and RNA-seq from invaded vessel regions and uninvaded parenchyma of 8 additional tumors with VI and tumor regions of non-VI tumors. Given increased signature expression in regions of invasive tumors at a distance from VI foci, we leveraged our bulk RNA-seq dataset to develop a transcriptomic predictor of VI. We applied a nested cross-validation approach within a training cohort to select a machine learning model. We then evaluated the performance of our model in an independent test set. Finally, we generated over 200 pseudo-bulked *in silico* biopsies similar in size to standard transthoracic needle biopsies using the spatial data. The scores from these *in silico* biopsies were similar to predictions from matched bulk RNA-seq data, suggesting robustness to intra-tumor heterogeneity. Our combined bulk and spatial transcriptomics analysis suggests that VI-associated gene expression extends far from the site of intravasation and can be used to predict the presence of VI. This may enable the prediction of angioinvasive LUAD from small biopsy specimens, allowing for more tailored treatment prior to surgery.

#5633

Analysis of the immune microenvironment and tumor-infiltrating immune cells across different solid tumors by combined spatial transcriptomics and proteomics

Julia Femel, Emily Neil, Dongju Park, Fabio El Yassouri, Anijutta Appelshoffer, Erica Lloyd, Michael DiBuono, Henry Sauer, Hanna Lafayette, Hsinyi Smith, Jinling Wang, Dominic Mangiardi, Alex Makrigiorgos, Paurush Praveen, Silvia Rüberg, Werner Müller, Tanya Wantenaar, Robert Pinard, Andreas Bosio. *Miltenyi Biotec B.V. & Co. KG, Bergisch Gladbach, Germany*

With the advent of immunotherapies such as immune checkpoint inhibitors and CAR T cells, the interest in the tumor microenvironment and tumor-infiltrating lymphocytes (TILs) cells has increased in recent years as these play a critical role in predicting response to therapy and clinical outcomes. We have reported on the identification of potential targets for CAR T cell therapies by analyzing a multitude of tumor samples with hundreds of antibodies by flow cytometry and a new spatial proteomics platform, the MACSima Imaging Platform (Schäfer et al. Nat. Commun., 2021; Kinkhabwala et.al. Sci. Rep., 2022). Here we report on the analysis of tumor microenvironment and tumor infiltrating immune cells using a novel combined spatial transcriptomics and proteomics approach. For protein expression analysis we generated a panel of 60 fluorochrome conjugated antibodies (REAscreen Immuno-oncology, human, FFPE, version 01) selected to identify immune cells, cancer associated fibroblasts, matrix, blood vessels, lymphatics and malignant epithelial cell populations. RNA analysis was based on a novel in situ hybridization and amplification method followed by a cyclic spatial decoding of transcripts (RNAsky). To standardize and further ease the process of protein and RNA detection we generated the antigen and RNA detection probes in a ready-to-use format, i.e., dried and sealed in 96 well plates ready to be inserted into the MACSima. FFPE specimens of different tumor entities reviewed by a pathologist were first hybridized to probes, which were amplified, and spatially decoded by fluorochrome conjugated oligonucleotides. Subsequently the same specimen was exposed to fluorescently labeled antibodies by cycles of antibody reaction, image acquisition and erasure of signal. Finally, specimens were stained with H&E to report on tissue integrity and correlate spatial orientation. The 2D image stacks were analyzed for transcript and antigen quantification and pattern recognition using both, pixel and segmented single-cell data (MACS iQ View Analysis Software). Across the specimens we identified more than 20 cell types

including 12 immune cell subsets. The comparison of the tumor microenvironment, tumor-infiltrating immune cells (TILs) and their spatial organization in relation to the tumor cells allowed to identify differences and similarities across the tumor types. In summary we report here on a novel standardized and automated combined spatial RNA and protein expression analysis of the tumor microenvironment and tumor infiltrating immune cells across tumor types. The characterization dataset demonstrates the ability of our platform to perform standardized in-depth phenotyping of sample cohorts. This will enable discovery and further development of predictive and prognostic biomarkers critical to patient stratification for immunotherapy.

#5635

Joint secondary transcriptomic analysis of triple negative breast cancer offers a window into new therapeutic possibilities and biomarkers

Naomi Rapier-Sharman, Jenna Birchall Poulsen, Mauri E. Dobbs, Brett E. Pickett. *Microbiology and Molecular Biology, Brigham Young University, Provo, UT*

Breast cancer is a harmful growth of mutated breast tissue that is diagnosed in 2.3 million women yearly, and kills 685,000 patients (15%) each year around the world. Left unchecked, breast cancer can grow proliferatively and metastasize to new tissue sites, monopolizing the body's energy supply and ultimately causing organ failure and death. Due to increased use of treatments targeting the breast tumor-specific markers Estrogen Receptor (ER), Progesterone Receptor (PR), and Human Epidermal growth factor Receptor 2 (HER2), patient survival of breast cancer has increased in recent years. However, patients with triple-negative breast cancer (TNBC), tumors lacking all three commonly-targeted biomarkers, suffer greater illness, experience more frequent relapse, and enjoy a shorter lifespan compared to other breast cancer patients due to the paucity of tumor-selective treatments for TNBC. Further research on TNBC is needed to understand targetable mechanisms and develop treatments capable of targeting the key mechanisms. To investigate the transcriptomic profiles of TNBC tumors, we performed a joint secondary analysis of publicly available RNA-sequencing data for TNBC, consisting of 214 relevant samples across 11 distinct studies in the NCBI Gene Expression Omnibus (GEO). We found

~12,500 significant differentially expressed genes (FDR p-value <= 0.05) and 67 significantly modulated pathways (FDR p-value <= 0.05). Additionally, our novel findings include candidates for drug repurposing, high-integrity predictive biomarkers, and potential new TNBC molecular mechanisms. We found several TNBC drug targets that have not yet been fully leveraged along with drugs that could likely be successfully repurposed for use in TNBC based on previous target history and our transcriptomic results. This joint secondary analysis opens the door to future therapeutic options that could increase patient survival once validated in the wet lab.

#5636

Multiplex digital spatial profiling (DSP) of proteins in the tumor microenvironment in response to GSK-3 inhibition by 9-ING-41 (elraglusib) correlates with novel immunostimulatory effects observed *in vivo*

Kelsey E. Huntington[1], Christoph Schorl[2], Shaolei Lu[1], Daniel Newhouse[1], Benedito A. Carneiro[3], Wafik S. El-Deiry[1]. *[1]Pathology and Laboratory Medicine, Brown University, Providence, RI,[2]Molecular Biology, Cell Biology and Biochemistry, Brown University, Providence, RI,[3]Medicine, Brown University, Providence, RI*

Glycogen synthase kinase 3 (GSK-3) is a serine/threonine kinase with key roles in myriad biological processes such as tumor progression, and inhibition of GSK-3 using the small molecule elraglusib has shown promising preclinical antitumor activity in multiple tumor types. Our preclinical experiments showed that elraglusib treatment increased tumor cell PD-L1 expression, downregulated angiogenic and immunosuppressive signaling pathways, and increased anti-tumor immune responses *in vitro* and *in vivo*. Subsequent studies showed that several circulating factors were predictive of response to PD-1/PD-L1 blockade and GSK-3 inhibition in a murine model of colorectal cancer. To determine the translational relevance of our prior results we evaluated tumor biopsies and plasma samples from patients with refractory solid tumors of multiple tissue origins enrolled in a Phase 1 clinical trial investigating elraglusib (NCT03678883). Plasma samples were collected from patients at baseline and 24 hours post-IV administration of elraglusib and were analyzed using Luminex technology.

Paired FFPE tumor biopsies from patients with colorectal or pancreatic cancer before and after treatment were selected to analyze the tumor microenvironment using NanoString GeoMx DSP technology. The region of interest (ROI) selection strategy focused on mixed tumor and immune cell segments and ROIs were segmented using panCK+ and CD45+ morphology stains. Cytokine analysis revealed that elevated baseline plasma levels of IL-1 beta and reduced levels of VEGF correlated with improved progression-free survival (PFS) and overall survival (OS). PFS was also found to be positively correlated with elevated plasma levels of immunostimulatory analytes such as Granzyme B, IFN-gamma, and IL-2 at 24 hours post-treatment with elraglusib. CD45+ tumor-infiltrating immune cells had lower expression of VISTA, PD-1, and IDO-1 inhibitory checkpoint proteins and higher expression of OX40L and B7-H3 stimulatory checkpoint proteins in post-treatment biopsies as compared to pre-treatment biopsies. Moreover, time-on-study length negatively correlated with CD39 expression in PanCK+ segments and positively correlated with CD163 expression in CD45+ segments. This ongoing study, to our knowledge, represents the first digital spatial analysis of tumor biopsies from patients treated with elraglusib. These novel circulating biomarkers of response to GSK-3 inhibition could provide significant clinical utility and the spatial proteomics data may give us insights into the immunomodulatory mechanisms of GSK-3 inhibition.

#5637

Path to the holy grail of spatial biology: Spatial single-cell whole transcriptomes using 6000-plex spatial molecular imaging on FFPE tissue

Shanshan He, Michael Patrick, Jason W. Reeves, Patrick Danaher, Julian Preciado, Joseph Phan, Erin Piazza, Zachary Reitz, Lidan Wu, Rustem Khafizov, Haiyan Zhai, Michael Rhodes, David Ruff, Joseph Beechem.
NanoString Technologies, Inc., Seattle, WA

Cancer research across drug development, molecular biomarkers, and patient response depends on understanding biology that is dependent on complex interactions between malignant, immune, and stromal cells. To survive clearance mechanisms, a tumor can rely on a myriad of escape strategies, and the microenvironment is architected around the current path

of escape. To enable a more comprehensive picture of tumor biology, we have developed the CosMx™ Spatial Molecular Imager (SMI) technology to capture a snapshot of thousands of RNA species resolved subcellularly from a single, standard histopathology slide. Building upon the previously released panels, this study tests a new 6,000-plex panel, the highest RNA plex measured *in situ* within human tissue, allowing the imputation of a spatial whole transcriptome in the tissue. We performed an ultra-high-plex RNA assay to detect 6,000 targets simultaneously *in situ* on an FFPE human liver cancer tissue (~1 cm^2 area) using the CosMx SMI. This RNA panel covers broad biological areas with special emphasis on oncology, immunology, and signal transduction, such that all cancer researchers can benefit from the direct detection of targets of interest (*sans* imputation) in intact tissue. Analysis algorithms were developed to allow robust assessments of cell types, cell states, cell-cell interactions, and pathway activation. Imputation based on reference profiles from HCA, TCGA, and other public repositories allows estimation of non-measured transcripts at a ratio of approximately 1:3, compared to the approximate 1:20-1:70 imputations performed previously for spatial data.Thousands of transcripts were simultaneously detected with high sensitivity and specificity on the FFPE liver cancer tissue section at single-cell subcellular resolution. We were able to accurately map known reference profiles from scRNA-seq into this sample while identifying cancer-specific malignant, immune, and stromal cells in this tissue sample using this ultra-high plex RNA panel. In addition, we constructed sample-specific spatial neighborhoods, defined by cell types, cell states, and nearly unlimited sets of biological pathways through the imputed whole transcriptome. Finally, we measured >1,000 ligand-receptor interactions between key cell types of adjacent cells in the tissue, identifying mechanisms for tumor-mediated escape as well as reactive re-architecting of the native stroma which defines the trajectory of cancer's evolution. Single-cell spatial measurements of gene expression at 6,000 plex from a single FFPE slide has the potential to transform our understanding of tumor biology and facilitate the next advances in cancer research by extracting the highest data density possible from rare specimens collected during patient treatment.

#5638

Total-sync ultra-content microscopic opto-biotinylation enables high-sensitivity hypothesis-free subcellular protein discovery

Jung-Chi Liao[1], Chih-Wei Chang[1], Yi-De Chen[1], Chantal Hoi Yin Cheung[1], Chia-Wen Chung[1], Hsiao-Jen Chang[1], Yong-Da Sie[1], You-Pi Liu[1], Yu-Chih Lin[1], Hsiang-Ju Kai[1], Weng Man Chong[1], Hsin-Yi Wu[2]. *[1]Syncell Inc., Taipei, Taiwan,[2]Department of Chemistry, National Taiwan University, Taipei, Taiwan*

High-sensitivity hypothesis-free subcellular proteomics is challenging due to the limited sensitivity of mass spectrometry and the lack of amplification tools for proteins. Without such technology, it is not possible to discover proteins at specific locations of interest in cells or tissue samples. Here, we introduce a total-sync ultra-content microscopic system termed Microscoop^{TM} that integrates microscopy, optics, FPGA-based mechatronics, photochemistry, and deep learning or computer vision to enable high-content in situ photolabeling. Microscoop^{TM} photolabels proteins at user defined regions of interests (ROIs) under a microscope utilizing directed photochemistry in one field of view (FOV) at a time for tens of thousands of FOVs with similar morphological features. With this platform, we are able to photolabel proteins with biotin probes in cellular organelles, granules or cell-cell contact surfaces with a high precision at nanoscale resolution, and obtain sufficient amount of biotinylated proteins for mass spectrometry. We made a robust demonstration in the proteome mapping of human cellular nucleus from single-shot experiment to >1000 nuclear protein identification with > 90% specificity. Further data analysis revealed identification of a hundred of low protein copy number proteins and a high coverage of nuclear complexes. In proteome mapping of the nucleolus, we ranked proteins by order of abundance and revealed that 97 out of the top 100 proteins were annotated as nucleolar proteins. Unexpectedly, in mapping the stress granule (SG) proteome, a relatively low SG specificity (74%) were found in the top 50 abundant proteins, therefore we further characterize the proteins that have no prior SG annotation by immunostaining. Nine out of the thirteen unexplored proteins including PDLIM7, EIF3CL, YWHAE, RPSA, UGDH, DDX17, ANLN, PSMA6, and MCM2 were found to have SG patterns and co-localized with SG marker (G3BP1), raising our top 50 SG specificity to up to 92%. Together, our total-sync ultra-content microscopic platform enables

hypothesis-free, de novo subcellular proteome mapping at user defined ROIs with high sensitivity and specificity, thereby broadly benefits the cell biology field in finding novel proteins or biomarkers.

#5639

High throughput spatially resolved laser-activated cell sorting links the genomic molecules with its spatial information

Sumin Lee, Amos C. Lee, Sunghoon Kwon. *Seoul National University, Seoul, Korea, Republic of*

Spatial omics profiling technologies have been recognized recently for its ability to decipher the genetic molecules that are structurally relevant in pathology. Especially, in tumor biology, tumor is not the group of malignant tumor cells, but rather group of various cells such as tumor cells, immune cells, fibroblasts, etc. gathers together, constructing the tumor microenvironments. Technologies to analyze such microstructures have evolved from bulk sequencing, single cell sequencing to spatial omics profiling technologies. Spatial omics profiling technologies have highly influenced in decoding cancerous mechanisms by questioning the tumor heterogeneity, tumor microenvironment and spatial biomarkers. Most of the spatial omics technologies focus on mapping the spatial omics landscape in a large scale. They rather introduces the spatially-barcoded capture probes or fluorescence labeled target probes to spatially locate the genetic molecules. The information depth and the scalability of the techniques varies according to the purpose of the spatial assay techniques. Such technologies are capable of discovering the spatial heterogeneity and the spatial landscape of the consisting cell types due to relatively low depth of the omics information. To effectively address the target molecules for therapeutics or diagnostics, higher depth of the omics information are required. To meet the needs, region of interest (ROI)-based spatial technologies isolated the target regions and applies chemistries for higher coverage omics data. Conventional cell sorters utilizes microfluidic channels to sort cells of interest which requires cell dissociation in a solution phase. For instance, Fluorescence activated cell sorter (FACS) or Magnetic-activated cell sorting (MACS) uses fluorescence or magnetic particles, respectively, to designate the cells of interest in dissociated cell solutions. Spatially isolating techniques such as laser capture

microdissection (LCM) is able to sort out the ROIs while preserving the spatial context, but it approximately takes an hour for isolating the targets. Also, it uses rather UV laser to dissect out cells or IR-activated melting of polymers to stick out cells which might cause damage to cells. Here, I developed the automated spatially resolved laser activated cell sorter that isolates the cells in target per second while preserving the spatial context of the cells. Specific region of indium tin oxide (ITO) coated slide glass evaporates when illuminated by IR laser pulse, plunging the cells into the desired reservoir. The applicability of the suggested cell sorter are demonstrated in omics profiling chemistries such as DNA sequencing, RNA sequencing, mass spectrometry, etc.

#5640

Identifying pathophysiological features of mouse tumors using imaging mass cytometry

Qanber Raza, Liang Lim, Thomas D. Pfister, Nick Zabinyakov, Christina Loh. *Research and Development, Standard BioTools, Markham, ON, Canada*

Mouse tumor models are widely utilized for cancer studies and preclinical drug development. An obstacle in predicting therapeutic drug efficacy is the ability to quantitatively evaluate the multi-parametric post-treatment response in the tumor microenvironment (TME). Identification of immuno-oncological processes that dictate tumor growth, metastasis, and immune response is essential for selecting promising drug candidates for further clinical evaluation. Imaging Mass Cytometry™ (IMC™) is a vital and proven high-plex imaging technology that enables deep characterization of the complexity and diversity of tumor tissue without disrupting spatial context. The Hyperion™ Imaging System utilizes IMC technology to simultaneously assess 40-plus individual structural and functional markers in tissues, providing unprecedented insight into the organization and function of the TME. We have previously demonstrated the application of IMC in combination with Maxpar® and Maxpar OnDemand™ antibodies to highlight cellular composition of normal mouse tissues. Here, we showcase the Maxpar OnDemand Mouse Immuno-Oncology IMC Panel Kit for application on a variety of mouse tumor tissues. We compiled the antibody panel to quantitatively assess IO-related processes and applied it

to a tissue microarray (TMA) containing a large variety of mouse tumors. Antibodies in panel kits were selected from the Maxpar and Maxpar OnDemand catalogs. We digitized high-plex data from mouse tissues using the Hyperion Imaging System and generated images demonstrating the detailed layout of the TME. We further conducted single-cell analysis to identify specific populations of tumor and immune cells in the TME. The Mouse Immuno-Oncology IMC Panel Kit successfully identified pathophysiological processes such as immune cell infiltration and activation, signaling pathway activation, biomarkers of epithelial-to-mesenchymal transition (EMT), metabolic activity, growth, and the tissue architecture of the TME. Single-cell analysis of several highly relevant tumor types separated distinct cellular clusters representing tumor, immune, stromal, and vascular cells. Activation of cellular processes associated with signaling, growth, and metastasis were identified in tumor cells. In addition, cytotoxic and inflammatory activation in lymphoid and myeloid immune cell subtypes were detected. Application of IMC based multiparametric analysis successfully identified the spatial landscape of the TME at single-cell resolution. Quantitative analysis of tumor composition revealed critical insights regarding prognostic parameters such as metastatic and growth potential of tumors, and identification and activation of immune cell infiltrates. Overall, we demonstrate the power of IMC and provide evidence of its successful application in mouse tumor models. **For Research Use Only. Not for use in diagnostic procedures.**

#5641

Single cell spatial molecular imaging of 76-plex proteins in clinical cancer samples in response to personalized treatment

Zachary R. Lewis[1], Brian Birditt[1], Emily Brown[1], Kan Chantranuvatana[1], Brian Filanoski[1], Chris Corless[2], Tiên Phan-Everson[1], Gary Geiss[1], Tyler Hether[1], Evie Hobbs[3], Brett Johnson[4], Taylor Kelley[4], Charles Lopez[3], Rhonda Meredith[1], Anastasiya Olson[4], Giang Ong[1], Mithra Korukonda[1], Erin Piazza[1], Jason Reeves[1], Alyssa Rosenbloom[1], Kiara Siex[4], Hye Son Yi[1], Edward Zhao[1], Joseph M. Beechem[1], Gordon Mills[4]. *[1]NanoString Technologies, Inc., Seattle, WA,[2]Knight Diagnostic Laboratories, Oregon Health and Sciences University, Portland, OR,[3]Division of Hematology & Medical Oncology, Knight Cancer Institute, Oregon Health and Sciences*

University, Portland, OR,[4]Knight Cancer Institute, Oregon Health and Sciences University, Portland, OR

The power of spatial biology lies in the integration of multiple scales of information from subcellular to tissue scale. Until recently, spatial analysis of protein biomarkers in tissues was limited to a few markers at a time using traditional IHC colorimetric or fluorescent readout. Here, we demonstrate the ability of NanoString's CosMx™ Spatial Molecular Imager (SMI) platform to quantify more than 70 proteins encompassing key targets in immuno-oncology and tumor biology, localize the proteins and analyze protein expression at a single cell level. Key to the technology is the use of fully automated fluidics and imaging systems, short turnaround time, and high sensitivity. The CosMx protein assay has been optimized for FFPE samples, which represent the largest collection of biospecimens available for clinical investigation. To that end, we explored the utility of CosMx spatial proteomics on a series of clinical samples from cancer patients, including the Serial Measurements of Molecular and Architectural Response to Therapy (SMMART) trial, across multiple cancer types. CosMx SMI's high-level protein multiplexing capabilities enabled spatial analysis of metastatic tumors in response to personalized treatment for a single patient over time. Combining spatial data obtained from both CosMx RNA and protein assays on the same sample reveals distinct regions of Tumor Associated Macrophages and their interactions with tumor cells in some samples. Detection of phosphoproteins also allows for analysis of the impact of kinase inhibitor treatment on the spatial environment in longitudinal biopsies. The highly-multiplexed spatial analysis of proteins in longitudinal metastatic breast cancer biopsies under therapeutic pressure provides a unique opportunity to understand evolution of tumors and develop and implement therapeutic approaches that can directly target mutations arising in the tumor cells while effectively engaging the immune system.
FOR RESEARCH USE ONLY. Not for use in diagnostic procedures.

#5642
Validation of a novel multiplex immuno-fluorescence panel for the spatial analysis of the tumor microenvironment

François Rivest, Victor de Gautard, Vytautas Navikas, Saska Brajkovic, Bastian Nicolai. *Lunaphore Technologies SA, Tolochenaz, Switzerland*

IHC counterparts. Subsequently, the panel was transferred on a multi-organ TMA including several tumoral and non-tumoral specimens, showing robust performance across multiple tissue types. The protocol was optimized to achieve high staining quality for all 13 markers in terms of signal specificity Investigation of the tumor microenvironment (TME) by multiplex immunofluorescence (mIF) has accelerated the understanding of the spatial immune context in tumors. mIF has proven to be a powerful technique for the identification of new potential biomarkers and therapeutical targets. Despite increased application of mIF assays to characterize the TME, state-of-the art protocols remain technically challenging. Manual execution and use of dedicated reagents render them lengthy and costly. Moreover, their reproducibility is often questioned together with their transferability between different tissue types.
Here, we show the development and validation of an Immuno-Oncology (IO) Core Panel of 13 clinically relevant biomarkers to enable spatial analysis of the immune TME on the COMET™ platform across various tissue types. Formalin-fixed paraffin-embedded human tissue sections from tonsil and a 24-cores multi-organ tissue microarray (TMA) were stained using the IO Core Panel from Lunaphore on the COMET™ platform by fully automated sequential immunofluorescence (seqIF™), which consists of cycles of staining, imaging, and elution. The panel allows for simultaneous detection of CD3, CD4, CD8, CD45, FoxP3, PD1, PD-L1, CD11c, CD20, CD56, CD68, aSMA and Ki-67 by indirect immunofluorescence using unlabeled primary antibodies and Alexa Fluor™ Plus secondary antibodies. The 13-plex IO Core panel was initially developed and validated on tonsil as positive control tissue. To compare immunofluorescent (IF) and immunohistochemistry (IHC) staining patterns, the sections retrieved from COMET™ after seqIF™, were stained by a histology facility with standard IHC established for routine pathological diagnosis. All markers demonstrate accurate detection with specific IF staining, comparably to gold-standard, sensitivity, ratio to background and dynamic range. The repeatability and reproducibility of the automated IO Core Panel on the COMET™ platform was verified by day-to-day tests on one platform and tests among multiple platforms, respectively.

Our study demonstrated the robustness of the validated IO Core Panel across multiple tissue types with highly specific and reproducible results. The marker detection with standard indirect immunofluorescence on the COMET™ instrument allows for future, rapid expansion and customization of the panel including additional primary antibodies towards the need of the individual underlying scientific question.

#5643

High-spatial-resolution multi-omics analysis of cancer tissues

Emily Neil, Dongju Park, Erica Lloyd, Michael Dibuono, Seiyu Hosono, Reto Muller, Hanna Lafayette, Hsinyi Smith, Robert Pinard. *Miltenyi Biotec, Waltham, MA*

Recent technological breakthroughs in single cell sequencing have revealed that malignant cells and nonmalignant cells are both highly dynamic and in the case of tumor cells, that the intratumoral heterogeneity is quite remarkable. However, several questions remain, especially in a spatial context, and a rapidly growing need has been observed for imaging-based approaches with single-cell resolution to visualize and characterize the tumor microenvironment. In the current study, we used Miltenyi Biotec newly developed spatial gene expression technology and automated imaging platform, to acquire spatial microscopy data for multiple biological analytes and multiple cancer tissues. The approach is based on fluorescence microscopy and the MICS technology principle of cyclic staining (MACSima™ Imaging Cyclic Staining) along with validated fluorochrome-conjugated antibodies and specifically amplified oligonucleotide probes combined with a proprietary signal removal system. FFPE tissue blocks were analyzed and each gene, which display a unique emission spectrum during a single cycle, was decoded. Due to the non-destructive nature of the workflow, H&E staining, immunofluorescence and RNA data can be collected together into a single image and on a single section. Using our antibody and targeted RNA immune-oncology panel coupled with our smart segmentation and flexible gating software suite, we have generated a topographical map of the expression profile level for several cancer tissues i.e.: tonsil, pancreas, kidney and ovary. This technology allows for the analysis of hundreds of protein markers and RNA transcripts on a single tissue, the characterization of the spatial architecture and the expression

topography of tumor tissue sections. A better understanding of tissue microenvironment and implementation of spatial biology approaches will help advance the identification of more suitable biomarkers and for cancer therapy.

#5644

Spatially resolved transcriptomics points to distinct malignant cell populations within primary and castration resistant prostate cancer

Antti Kiviaho, Heini M. L. Kallio, Sini K. Eerola, Elisa M. Vuorinen, Tomi Häkkinen, Sinja Taavitsainen, Ebrahim Afyounian, Teemu Tolonen, Juha Kesseli, Alfonso Urbanucci, Kirsi J. Rautajoki, Teuvo L. J. Tammela, Tapio Visakorpi, Matti Nykter. *Tampere University, Faculty of Medicine and Health Technology, Tampere, Finland*

Background: Prostate cancer (PCa) is the second most common cancer in men. Despite its high prevalence, many patients carry an indolent form of the disease and are thus suspect to overtreatment. Conversely, some cases treated with androgen deprivation therapy can develop into castration resistant prostate cancer (CRPC), for which there is no curative treatment. Understanding why some tumors are more aggressive than others could lead to more accurate patient risk stratification. Here we characterize cancer and normal cell subpopulations within prostate tissue in their spatial context using a multimodal integrative approach.
Methods: We performed spatially resolved transcriptomics (ST) on a set of primary tumor PCa, CRPC and benign prostatic hyperplasia (BPH) patient samples. In addition to ST, we produced RNA-seq, DNA-seq and assay for transposase accessible chromatin using sequencing (ATAC-seq) data, allowing for multiomic integration within and across sample categories. We performed extensive analysis of ST data, employing unsupervised clustering, spot expression signal deconvolution, differential gene expression analysis and copy number variation (CNV) inference.
Main Results: The systematic analysis of spot expression profiles revealed a high degree of variation in nearby tissue regions, as we found up to three unique luminal cell populations inside a one millimeter radius in PCa. Similarly in locally recurrent CRPC, we identified cumulative CNVs in proximal luminal cell populations, with the inferred CNV profiles validated through DNA-seq. A set of marker genes was calculated for each unique

cell population, with multiple PCa associated genes found to be differentially expressed. Although we observed significant variation in the luminal cell populations, the stromal gene expression was markedly similar across all samples.
Conclusions: We discovered shared, similar and unique cell populations both within and across different PCa and CRPC sections. We observed various luminal cell populations with distinct gene expression profiles in samples from both progression stages. The close spatial proximity of these cell clusters suggests that ST can be used to discover and examine finely detailed populations in their original spatial environment.

#5646

Spatial transcriptomic profiling of the human and mouse retina prepared with CryoJane Tape Transfer System using GeoMx and CosMx spatial analysis

Charles Glaser[1], Su Ma[1], Wei Yang[1], Yan Liang[1], Joeseph Beechem[1], Vera L. Bonilha[2], Sujata Rao[2], William Horrigan[2], Bela Anand-Apte[2].
[1]NanoString Technologies, Inc., Seattle, WA,[2]Cole Eye Institute and Cleveland Clinic Lerner College of Medicine-CWRU, Cleveland, OH

The goal of this study is to identify key transcriptomic markers within layers of the retina by individually profiling layers using cellular and subcellular spatial transcriptomics, additionally, comparing the results between each level. Both human and mouse retina samples, prepared fresh frozen and fixed frozen, are analyzed using the GeoMx® Digital Spatial Profiler (DSP) and CosMx® Spatial Molecular Imager (SMI) using the whole mouse transcriptome atlas and 1000-plex mouse neuro panel, respectively. Samples are fixed using Cryo-Jane Taper Transfer system. Samples are mounted on to adhesive coated slides as well as adhesive tape to mount samples to glass slides. This method is used to secure fragile frozen tissue, such as the retina. Human and mouse samples were stained using immunofluorescent microscopy targeting neurofilament H (NF-H), glial fibrillary acidic protein (GFAP) and NeuN on DSP and 18s rRNA, amyloid-beta and GFAP on SMI. Staining allows for identification of structural layers in the retina. Simultaneously, regions of interest (ROI) for spatial profiling are selected based on immunofluorescent stains. On DSP, each sample had 3x ROIs in the photoreceptor layer, inner nuclear layer and

ganglion cell layer, then, oligonucleotides were collected and sequenced. Finally, raw counts were Q3 normalized for analysis. For SMI data analysis, 6 field of views (FOVs) were put on each section to cover most regions with multiple layers. ~8000 genes were detected on human retina samples using DSP. Around 500 unique genes were detected between the photoreceptor and inner nuclear layer using DSP. Preliminary SMI results show we were able to identify cell types (amacrine, horizontal cell, biopolar cell, ganglion cell, etc) and cell specific markers for outer nuclear layer, inner nuclear layer and ganglion cell layer**.** Data between DSP and SMI showed high concordance with one another, identifying many genes in each layer.

#5647

Single cell, multiomic spatial phenotyping of immunotherapy responses in head and neck cancer

HaYeun Ji[1], Niyati Jhaveri[1], Ning Ma[1], Bassem B. Cheikh[1], Aditya Pratapa[1], James Monkman[2], Ken O'Byrne[3], Brett Hughes[4], Arutha Kulasinghe[2], Oliver Braubach[1]. *[1]Akoya Biosciences, Menlo Park, CA,[2]The University of Queensland, Brisbane, Australia,[3]The Princess Alexandra Hospital, Brisbane, Australia,[4]The Royal Brisbane and Women's Hospital, Brisbane, Australia*

Background**:** Immune checkpoint inhibitors (ICI) have proven to be game-changing treatments for mucosal head and neck squamous cell cancer (HNSCC). Emerging successes with anti-PD-1/PD-L1 therapy have led to durable responses and prolonged survival in both human papillomavirus-positive (HPV+) and negative (HPV-) patients. There is now a need for predictive biomarkers to guide patient selection for highly targeted ICI therapies as currently available diagnostic biomarkers have a limited value. The tumor microenvironment (TME) composition, contexture, and cellular architecture are now recognized as key to understanding immune responsive and resistant phenotypes. Here, we are using a spatial biology approach to explore the TME in metastatic/recurrent HNSCC tumors treated with Pembrolizumab / Nivolumab.

Methods: In this study, we used single cell, multiomic spatial phenotyping utilizing the PhenoCycler-Fusion spatial biology platform to characterize the TME of HNSCC tumors from a cohort of n=40 patients. The discovery

cohort consisted of patients who had complete vs. partial vs. stable vs. progressive responses to ICI therapy. We first analyzed tissues using an ultrahigh-plex antibody panel of >60 antibodies that label immune cell lineages, checkpoints, activation markers as well as tissue structure and the stroma. We then conducted whole-slide, single cell resolution RNA detection with complementary markers on serial sections from the same tissue blocks; the combination of these data allowed us to obtain multiomic spatial signatures that offered uniquely comprehensive insight into the TME of our tissue cohorts.
Results: Our study identified highly resolved tissue immune contexture analysis and metabolic tissue signatures associated with resistance and sensitivity to immunotherapy. Most notably, multiomic profiling of HNSCC tumours provided deeper insights into ICI therapy resistance than the single omics based approaches alone.
Conclusions: Our study demonstrates the power of unbiased, multiomic spatial phenotyping with whole-slide imaging to identify biomarkers associated with response to ICI therapy in HNSCC.

#5648
Single cell spatial phenotyping of bladder tumors with a novel mechanism of NKG2A and HLA-E mediated resistance to BCG immunotherapy
Dmytro Klymyshyn[1], Niyati Jhaveri[1], Nadine Nelson[1], Michael Prater[2], Zhenqin Wu[3], Steven Hamel[3], Matthew D. Galsky[4], Nina Bhardwaj[4], John P. Sfakianos[4], Subham Basu[2], Oliver Braubach[1], Amir Horowitz[4]. *[1]Akoya Biosciences, Marlborough, MA,[2]Abcam, Cambridge, United Kingdom,[3]Enable Medicine, Menlo Park, CA,[4]Icahn School of Medicine at Mount Sinai, New York, NY*

Background: ~75% of diagnosed bladder tumors are non-muscle-invasive, requiring instillation of *M. bovis* Bacillus Calmette-Guérin (BCG) with recurrence rates observed in ~50% of patients. Treatments for BCG-resistant bladder tumors have lagged because few studies have tried to understand the relationship between timing of tumor recurrence and the state of immune system at the time of recurrence. Natural Killer (NK) cells are very early responders to tumor cells. HLA-E, like PD-L1, is sensitive to IFN-γ and strongly inhibits $NKG2A^+$ NK and CD8 T cells and is commonly

upregulated on tumors. We observed that BCG exposure results in chronic activation of NK and CD8 T cells and their acquisition of NKG2A and PD-1 phenotypes. Upon tumor recurrence in all patients sampled, a subset of the tumor cells aggregated in nests, were activated in response to NK/CD8 T cell-derived IFN-γ, and upregulate HLA-E and PD-L1. Spatial sequencing revealed *HLA-E*^{Bright} tumor nests with high levels of *CXCL9/10/11* and in significantly closer proximity to NK/CD8 T cells (and Tregs) compared with *HLA-E*^{Dim} tumor nests that lacked *CXCL9/10/11*. Here, we apply single cell spatial phenotyping to study major subsets of NK cells in the TME of bladder tumors obtained from patient matched tumor sections before and after BCG therapy.

Purpose of the study: The goal of this study is to understand the underlying cell-to-cell interactions that promote BCG resistance in non-muscle-invasive bladder cancer (NMIBC).

Methods: The PhenoCycler technology centers around an oligo-based barcoding strategy, in which oligonucleotide-labeled antibodies are imaged in iterative cycles of hybridized/dehybridized complementary oligonucleotide fluorescent reporters. The platform enables (1) whole-slide imaging, (2) single-cell and subcellular resolution, (3) compatibility with a wide range of FFPE tissues, (4) customized content and plexing capability and (5) sophisticated analysis of cell phenotypes and cellular neighborhoods.

Results and conclusions: We developed a comprehensive antibody panel for in-depth analysis of the TME of bladder tumors. Our panel centers around a core of 67 markers for cell lineage, immune checkpoints, immune activation markers, tissue structure and vasculature. This core was supplemented with a module of additional antibodies that define complex NK cell phenotypes, including markers of maturation and differentiation, metabolism, activation and inhibition, trafficking, cytolytic killing, as well as cytokines/chemokines that shape the TME. The power of single cell spatial biology is the ability to visualize all major subsets of NK cells and their associated microenvironment simultaneously in single tissue sections. In doing so, we are defining novel functional interactions as new correlates of BCG resistance and identifying pathways that can be exploited for next-gen immunotherapies.

The Next Wave of Precision Oncology: New Drugs, Databases, and Analytics to Refine Care

#5717

Bridging the gap between clinical-omics and machine learning to improve cancer treatment

Chang In Moon[1], Byron Jia[2], Bing Zhang[1]. *[1]Lester and Sue Smith Breast Center, Baylor College of Medicine, Houston, TX,[2]Chemistry, Carleton College, Houston, TX*

Background: Few omics data-based prediction models have made a clinical impact due to lack of access to real-world, clinically relevant datasets for method development and evaluation. The expanding integration of omics profiling into cancer clinical trials opens a new opportunity to address this problem. Clinical trials ensure high quality of the treatment response information and clinical relevance of the identified molecular features and constructed prediction models. Here we present a python package ClinicalOmicsDB that provides a framework for systematic benchmarking of machine learning algorithms using a compendium of carefully collected and curated clinical omics datasets. The package further leverages interpretable AI to gain biological insights from high-performing models. Approach: We downloaded omics datasets from 28 clinical trials across 7 cancer types, totaling 6127 patients and 60 treatment arms. For each treatment arm, we performed random stratified splitting of the data into 80% for training and the remaining 20% for testing, and this was repeated 30 times to create 30 simulated train-test pairs. Based on all 60 treatment arms, we created 1800 train-test pairs for prediction model development and evaluation. To illustrate the utility of this package, we benchmarked six supervised machine learning algorithms for their ability to distinguish responders from non-responders. For each training dataset, 5-fold cross-validation was used to select the top 20 non-redundant features and to optimize hyperparameters. The optimized pipeline was used to train a full model based on the complete training dataset, which was then applied to the paired testing dataset for performance evaluation using AUROC. Shapley plots were created for models with satisfactory AUROC scores to facilitate biological interpretation.

Results: Among the 6 algorithms tested, random forests had the best overall performance. It achieved an AUROC>0.75 for 11 treatment arms. Shapley plot identified LPIN1 as a top predictive marker for the combination treatment of fluorouracil, doxorubicin, and cyclophosphamide (AC) in unselected breast cancers. The cancer testis antigen MAGEA1 was among the top predictive markers for combination treatment with pembrolizumab, taxane, and AC in HER2- breast cancers. Shapley plot of a protein-based model identified SRC_Y527 and ERBB3 as the top biomarkers for predicting whether HER2+ breast cancer would respond to the combination of trastuzumab emtansine, pertuzumab, and AC.
Conclusion: We created a computational framework that uses real-world omics data to benchmark machine learning algorithms and to identify predictive markers based on best-performing models. More datasets will be continuously added, and new algorithms can be easily benchmarked against existing ones. ClinicalOmicsDB unifies the efforts from the clinical and machine learning communities to improve cancer treatment.

#5718

Additivity predicts the clinical efficacy of most approved combination therapies for advanced cancer

Haeun Hwangbo[1], Sarah Patterson[1], Andy Dai[2], Deborah Plana[3], Adam C. Palmer[1]. *[1]University of North Carolina at Chapel Hill, Chapel Hill, NC,[2]North Carolina School of Science and Mathematics, Chapel Hill, NC,[3]Harvard Medical School, Boston, MA*

Most advanced cancers are treated with drug combinations. Rational designs aim to identify synergistic drug interactions to produce superior treatments. However, metrics of drug interaction (i.e., synergy, additivity, antagonism) apply to pre-clinical experiments, and there has been no established method to quantify synergy versus additivity in clinical settings. Here, we propose and apply a model of drug additivity for progression-free survival (PFS) to assess if the clinical efficacies of approved drug combinations are more than, or equal to, the sum of their parts. This model accounts for the benefit from patient-to-patient variability in the best single drug response, plus the added benefit of the weaker drug per patient. Among all FDA approvals of combination therapies for advanced cancer between 1995 and 2020, we identified 37 combinations across 13 cancer

types (24,723 patients) where the efficacies of monotherapies and combination therapies could be analyzed at matched doses. 95% of combination therapies exhibited progression-free survival times that were additive, or less than additive. Across all trials and follow-up times, the coefficient of determination of the additivity model was R^2=0.90, with no fitting or training, only the operation of addition. While there were deviations from additivity, with several combinations being less than additive, 100% of the approved combinations studied would have been predicted to succeed by the additivity model. This study has two key findings. First, a synergistic effect (more than additive) is neither a necessary nor even common property of clinically effective drug combinations. Second, the predictable efficacy of many of the best drug combinations established over the past 25 years suggests that additivity can be used as a design principle for novel drug combinations and clinical trials, which could be helpful as the number of possible therapies grows and as cancers are increasingly divided into subtypes with distinct drug sensitivities.

#5719

Clinical response to the PDGFRα inhibitor avapritinib in high-grade glioma patients

Lisa Mayr[1], Maria Trissal[2], Kallen Schwark[3], Jenna Labelle[2], Andrew Groves[2], Julia Furtner-Srajer[4], Jeffrey Supko[5], Liesa Weiler-Wichtl[1], Olivia Hack[2], Jacob Rozowsky[2], Joana G. Marques[2], Eshini Pandatharatna[2], Ulrike Leiss[1], Verena Rosenmayr[1], Frank Dubois[2], Noah F. Greenwald[6], Sibylle Madlener[1], Armin S. Guntner[7], Hana Pálová[8], Natalia Stepien[1], Daniela Lötsch-Gojo[9], Christian Dorfer[9], Karin Dieckmann[1], Andreas Peyrl[1], Amedeo A. Azizi[1], Alicia Baumgartner[1], Ondřej Slabý[8], Petra Pokorná[8], Pratiti Bandopadhayay[2], Rameen Beroukhim[10], Keith Ligon[2], Christof Kramm[11], Annika Bronsema[12], Simon Bailey[13], Ana Guerreiro Stücklin[14], Sabine Mueller[15], David T. W. Jones[16], Natalie Jäger[16], Jaroslav Štěrba[17], Leonhard Müllauer[18], Christine Haberler[19], Chandan Kumar-Sinha[20], Arul Chinnaiyan[20], Rajen Mody[21], Mary Skrypek[22], Nina Martinez[23], Daniel C. Bowers[24], Carl Koschmann[21], Johannes Gojo[1], Mariella Filbin[2]. *[1]Pediatrics and Adolescent Medicine, Medical University of Vienna, Vienna, Austria,[2]Pediatric Oncology, Dana-Farber Cancer*

Institute, Boston, MA,[3]University of Michigan, Ann Arbor, MI,[4]Biomedical Imaging, Medical University of Vienna, Vienna, Austria,[5]Medicine, Massachusetts General Hospital, Boston, MA,[6]Cancer Biology, Dana-Farber Cancer Institute, Boston, MA,[7]Analytical Chemistry, Johannes Kepler University, Linz, Austria,[8]Central European Institute of Technology, Brno, Czech Republic,[9]Neurosurgery, Medical University of Vienna, Vienna, Austria,[10]Medicine, Dana-Farber Cancer Institute, Boston, MA,[11]Pediatric Hematology and Oncology, University Medical Center Göttingen, Göttingen, Germany,[12]Pediatric Hematology and Oncology, University Medical Centre Hamburg-Eppendorf, Hamburg, Germany,[13]Pediatric Neuro-Oncology, Newcastle University, Newcastle, United Kingdom,[14]Oncology, University Children's Hospital Zurich, Zurich, Switzerland,[15]Pediatrics, Neurology, and Neurological Surgery, University of California San Francisco, San Francisco, CA,[16]Hopp Children's Cancer Center Heidelberg, Heidelberg, Germany,[17]Pediatric Oncology, Masaryk University, Brno, Czech Republic,[18]Pathology, Medical University of Vienna, Vienna, Austria,[19]Neuropathology and Neurochemistry, Medical University of Vienna, Vienna, Austria,[20]Pathology, University of Michigan, Ann Arbor, MI,[21]Pediatrics, University of Michigan, Ann Arbor, MI,[22]Children's Minnesota, Minneapolis, MN,[23]Neurology and Neurological Surgery, Jefferson University, Philadelphia, PA,[24]Pediatrics, University of Texas Southwestern Medical Center, Dallas, TX

PDGFRA has been shown to be commonly altered in high-grade gliomas (HGGs), including histone 3 lysine 27-mutated diffuse midline gliomas (H3K27M DMG), a disease with almost no long-term survivors. Here, we performed comprehensive genomic and transcriptomic analysis of 260 high-grade glioma cases, which revealed PDGFRA genomic alterations (mutations and/or amplifications) in 13% of patients. H3K27M DMGs had significantly higher PDGFRA expression compared to H3 wild-type tumors, and PDGFRA gene amplification resulted in even higher expression levels in H3K27M DMGs as well as H3 wild-type HGGs. We tested a panel of patient- derived pHGG/H3K27M DMG models against a range of PDGFRA inhibitors, including avapritinib, a potent small molecule inhibitor with relatively selective activity against both wild-type and mutant

PDGFRA. Avapritinib showed supra-micromolar blood-brain barrier penetration in our pre-clinical models and demonstrated significant survival impact in an aggressive patient-derived H3K27M DMG mouse xenograft model. Finally, building on this preclinical activity, we report here the first clinical experience using avapritinib in eight pediatric and young adult patients with high-grade glioma (H3K27M DMG and/or PDGFRA altered). Avapritinib has thus far been well tolerated with no significant acute toxicities. Most importantly, our preliminary data reveal radiographic response evaluated by RAPNO criteria in 50% of patients, a striking outcome rarely seen in this patient population. In summary, we report that avapritinib is a selective, CNS-penetrant small molecule inhibitor of PDGFRA that shows potent activity in preclinical models and produces promising clinical responses with good tolerability in patients with high-grade glioma. This suggests a promising role for avapritinib therapy in this population with previously dismal outcomes.

#5720

Combination therapies in matched 3D in vitro and in vivo preclinical models of rare and recalcitrant cancers from the National Cancer Institute's Patient-Derived Models Repository

Thomas S. Dexheimer[1], Thomas Silvers[1], Rene Delosh[1], Russell Reinhart[1], Chad Ogle[1], Zahra Davoudi[1], Eric Jones[1], Debbie Trail[1], John Carter[1], Justine Mills[1], Kyle Georgius[1], Howard Stotler[1], Michelle Norris[1], Shannon Uzelac[1], Suzanne Borgel[1], Tiffanie Minor[1], Luke Stockwin[1], Michael Mullendore[1], Kevin Plater[1], Keegan Kalmbach[1], Jessica Steed[1], Matthew Murphy[1], Gareth Bliss[1], Carrie Bonomi[1], Kelly Dougherty[1], Marion Gibson[1], Kevin Cooper[1], Dianne Newton[1], Cindy R. Timme[1], Yvonne A. Evrard[1], Melinda G. Hollingshead[2], Nathan P. Coussens[1], Ralph E. Parchment[1], James H. Doroshow[2], Beverly A. Teicher[2]. *[1]Applied and Developmental Research Directorate, Frederick National Laboratory for Cancer Research, Frederick, MD,[2]Division of Cancer Treatment and Diagnosis, National Cancer Institute, Frederick, MD*

There is a major need in oncology drug development to establish predictive preclinical assays with high translational relevance to patient responses. The National Cancer Institute's Patient-Derived Models Repository

(https://pdmr.cancer.gov) offers a collection of highly characterized models from a variety of cancer types including rare and recalcitrant malignancies and tumors from patients of diverse ancestry. This collection includes matched sets of patient-derived cell lines, organoids, and xenografts (PDXs), which allows comparisons of drug responses from *in vitro* and *in vivo* assays performed with the same patient-derived tumor model. A high-throughput screen was conducted using matched sets of patient-derived organoids and cell lines. Patient-derived cell lines were grown as 3D multicellular spheroids mixed with endothelial cells and mesenchymal stem cells. The patient-derived organoids were 100% tumor cells and were plated in 5% basement membrane extract supplemented with growth factors and cytokines. All drugs were tested at concentrations up to their reported clinical C_{max} values and cell viability for individual drug treatments and drug combinations were assayed using CellTiter-Glo 3D after seven days drug exposure. Prior to the endpoint viability measurements, growth curves for spheroid median volume and organoid median surface area were calculated from a series of non-invasive brightfield images collected every 12 hours. For some drug combinations, differential responses were observed between the matched organoids and multicellular spheroids, potentially reflecting the contribution of the stromal component in the spheroids. Overall, the drug-dependent growth responses observed from the two 3D *in vitro* models (i.e., multicellular spheroids and organoids) were frequently comparable to those observed *in vivo* from PDXs. For example, the *in vitro* activities of several drug combinations including: BAY1895344 + temozolomide, erlotinib + cediranib, entinostat + talazoparib, and selumetinib + abemaciclib, demonstrated good agreement with the responses observed *in vivo*. However, among the drug combinations tested ixazomib + panobinostat showed the greatest cytotoxicity *in vitro* but had no activity in the matched PDX models. The availability of matched patent-derived cell lines, organoids and PDXs provides an opportunity to learn about the features of assay methodologies and data analyses that influence the successful translation of preclinical results between *in vitro* and *in vivo* systems. The results of this study are encouraging, but also highlight discrepancies that will be important to investigate, understand and address in order to improve translational capacity of future assays. This project was funded in part with federal funds from the NCI, NIH, under contract no. HHSN261201500003I.

#5721

Automated annotation for large-scale clinicogenomic models of lung cancer treatment response and overall survival

Justin Jee[1], Chris Fong[1], Karl Pichotta[1], Thinh Tran[1], Anisha Luthra[1], Mirella Altoe[1], Steven Maron[1], Ronglai Shen[1], Si-Yang Liu[1], Michele Waters[1], Joseph Kholodenko[1], Brooke Mastrogiacomo[1], Susie Kim[1], A Rose Brannon[1], Michael F. Berger[1], Axel Martin[2], Jason Chang[1], Anton Safonov[1], Jorge S. Reis-Filho[1], Deborah Schrag[1], Sohrab P. Shah[1], Pedram Razavi[1], Bob T. Li[1], Gregory J. Riely[1], Nikolaus Schultz[1]. *[1]Memorial Sloan Kettering Cancer Center, New York, NY,[2]New York University, New York, NY*

The digitization of health records and prompt availability of tumor DNA sequencing results offer a chance to study the determinants of cancer outcomes with unprecedented richness; however, abstraction of key attributes from free text presents a major limitation to large-scale analyses. Using natural language processing (NLP), we derived sites of metastasis, prior treatment at outside institutions, programmed death ligand 1 (PD-L1) levels, and smoking status from records of patients with tumor sequencing to create a richly annotated clinicogenomic cohort. We sought to define whether combining features would improve models of overall survival (OS) and treatment response as validated in a multi-institution, manually curated cohort. We leveraged the manually curated AACR GENIE Biopharma Collaborative (BPC) dataset to train NLP algorithms to abstract the aforementioned features from overlapping records available at Memorial Sloan Kettering (MSK). All models achieved precision and recall > 0.85. We deployed these algorithms to records of all MSK patients with non-small cell lung cancer (NSCLC) and tumor profiling with our FDA-authorized institutional targeted sequencing platform (N=7,015). These labels were combined with genomic, demographic, histopathologic, internal treatment and staging data to train random survival forests (RSF) to predict OS and time-to-next-treatment (TTNT) for molecularly targeted and immunotherapies. RSFs trained on the MSK NSCLC cohort were validated with the curated, non-MSK BPC NSCLC cohort (N=977). The addition of NLP-derived variables to genomic features enhanced RSF predictive power

for OS (c-index, 10x bootstrap 95%CI: 0.58, 0.57-0.59 vs 0.75, 0.74-0.76 combined) and targeted and immunotherapy TTNT. The size of the MSK NSCLC cohort enabled discovery of associations between metastatic sites, PD-L1 status, genomics, and TTNTs not apparent in the smaller BPC cohort. We measured the added predictive value of variables not available in BPC with MSK-only cross-validation analyses. White blood cell differential counts and additional tissue genomic features including tumor mutational burden and fraction genome altered added minimally, while circulating tumor DNA sequencing added prognostic power for OS over other factors including disease burden. Using NLP we present a large NSCLC cohort with rich clinicoradiographic annotation, leading to superior models of patient outcomes. Our data uncovers associations not observed in smaller, manually curated cohorts and provides a foundation for further research in therapy choice and prognostication.

#5722

The mutational signatures of 100,477 targeted sequenced tumors

Donghyuk Lee[1], Min Hua[2], Difei Wang[2], Lei Song[2], Tongwu Zhang[2], Kai Yu[2], Xiaohong R. Yang[2], Jianxin Shi[2], Stephen J. Chanock[2], Maria Teresa Landi[2], Bin Zhu[2]. *[1]Pusan National University, Busan, Korea, Republic of,[2]National Cancer Institute, Bethesda, MD*

Mutational signatures, the footprints of somatic mutations, are associated with the causes of cancer and have been well-studied for tumors with whole exome or genome sequencing. However, due to the low number of detected mutations, mutational signatures were insufficiently explored for many tumors sequenced by targeted panels in clinics. It impedes the clinical application of mutational signatures. Here, we present a new method, SALMON (Signature Analyzer for Low Mutation cOuNts), to identify mutational signatures in targeted sequenced tumors based on tumor mutational burden. SALMON adjusts for panel size differences and uses a large number of targeted sequenced tumors rather than a large number of mutations per tumor (as with whole exome or genome sequencing) to overcome the challenges of mutational signature analysis for targeted sequencing. Extensive simulations and pseudo-targeted sequenced data show that SALMON can accurately detect spiky or common signatures. We applied SALMON to investigate the pan-cancer patterns of mutational

signatures for 100,477 targeted sequenced tumors in AACR Project GENIE, including 14,428 lung and 11,389 breast tumors. We detected well-established signatures in tumor types that have not previously been associated with these signatures, such as the smoking signature in ovarian tumors. Interestingly, analysis of thousands of tumors per cancer type from diverse populations revealed gender discrepancies, self-described race differences, subtype heterogeneity, and metastatic enrichment of mutational signatures. For instance, most sex-biased signatures are more frequently present in males for non-gender-specific cancers. Thiopurine treatment-induced signature in glioma is enriched in Black patients. And endometrioid ovarian or uterine cancers have a higher prevalence of polymerase epsilon (POLE) deficiency-related signatures than non-endometrioid ovarian or uterine cancers, respectively. Our study demonstrates the feasibility and utility of mutational signature analysis for targeted sequenced tumors, enabling precision applications of mutational signatures in the clinical setting.

#5723

An *in vivo* pharmacogenomics platform replicates and extends biomarkers of therapy response identified via causal inference analysis of clinical data

David Amar[1], Erick Scott[1], Ian P. Winters[1], Gregory D. Wall[1], Dmitri A. Petrov[2], Monte M. Winslow[2], Joseph Juan[1], Ian K. Lai[1], Lafia Sebastian[1], Edwin A. Apilado[1], Gabriel Grenot[1], Vy B. Tran[1], Charles Rudin[3], Michael J. Rosen[1]. *[1]D2G Oncology, Mountain View, CA,[2]Stanford University, Stanford, CA,[3]Memorial Sloan Kettering Cancer Center, New York, NY*

Recent development of therapies targeting oncogenes have dramatically improved cancer care for subsets of patients and generated a wave of interest in cancer precision medicine. However, effective targeted therapies are scarce as we have a limited understanding of how drug responses are modulated by tumor genotype. Here, we utilize both human data and in vivo models to identify genetic drivers of therapy response in KRAS-driven non-small cell lung cancer patients treated with chemotherapy. We first present an integrative causal inference analysis of three clinical data resources: (1) the recently released Genomics Evidence Neoplasia Information Exchange, Biopharma Collaboration dataset (GENIE-BPC;

n=197), (2) a selected set of patients from the Tempus Clinico-genomic Database (n=330), and (3) an additional cohort from Memorial Sloan Kettering Cancer Center (n=218). Each dataset was first analyzed separately using a causal inference pipeline. Doubly robust estimators for each variant were inferred within a counting process survival analysis model accounting for time-varying treatments and immortal time bias. Meta-analysis of the results from all three cohorts identified three commonly mutated and highly replicable genes with a significant effect on overall survival: KEAP1, SMARCA4, and CDKN2A.
As further validation, we used our murine in vivo pharmacogenomics (PGx) platform that can quantify the effects of therapies across thousands of tumors of diverse genotypes. These tumors are initiated de novo in the native microenvironmental context in mice with an intact adaptive immune system. We tested a chemotherapy combination of carboplatin and pemetrexed in mice with KrasG12D-driven lung tumors and inactivation of each of 60 putative tumor suppressors. Treatment led to >75% reduction in tumor sizes relative to tumor suppressor inactivated (matched) vehicle-treated controls. These models identified causal effects for two out of the three candidates above: KEAP1 (resistance) and CDKN2A (sensitive). Moreover, our PGx platform identified additional candidate genes beyond those found using the clinical data, which had insufficient sample size for these rarely mutated genes. Together, we demonstrate how leveraging our PGx platform together with human data within a causal inference framework may improve the stratification of patients by their clinical outcomes, profoundly advancing the promise of precision medicine.

Therapeutic Antibodies, Including Engineered Antibodies

#5652
IL-19 blockade reprograms glioblastoma immunosuppressive microenvironment and overcomes chemo-resistance as revealed by single-cell transcriptome analyses

Gilbert A. Lee, Cheng-Yu Chen. *Taipei Medical University, Taipei, Taiwan*

Glioblastoma multiforme (GBM) is the most aggressive brain tumor with chemo-resistant, immunosuppressive, and invasive property. Despite the application of standard therapies which include a combination of surgery,

radiotherapy, and temozolomide (TMZ) chemotherapy, tumor inevitably recurred (in patients) at peritumoral region. Targeting multiple arms of the GBM-mediated immunosuppressive ability and their invasiveness can improve therapeutic efficacy. Genomic screening identified that IL-19 is a predicted immune suppressive cytokine in peritumoral region and was associated with poor survival in patients with GBM. IL-19 blockade inhibited both TMZ-sensitive and resistant tumor progression. Molecular studies revealed that silencing IL-19 markedly abrogated IL-19-WISP1-AKT signaling to inhibit TMZ-resistant GBM cell invasion, as well as weaken its suppressive ability on $CD8^{+}$T cell activation. Single cell transcriptome analysis revealed that IL-19 blockade promoted T cell activation, upregulated effector function of T cell subsets, and reprogrammed tumor-associated macrophage subsets toward a weakened pro-tumoral phenotypes. Thus, Targeting IL-19 can be a novel therapeutic strategy to reverse immunosuppressive microenvironment and restrict invasiveness of chemo-resistant GBM.

#5653

LCB97, an antibody drug conjugate (ADC) targeting a novel tumor antigen for the treatment of multiple solid tumors

Yeojin Jeong[1], Gunther Spohn[2], Flavio Mehli[2], Chul-Woong Chung[1], Changsik Park[1]. *[1]LegoChem Biosciences, Inc, Daejeon, Korea, Republic of,[2]Elthera AG, Schlieren, Switzerland*

LCB97 is an antibody-drug conjugate (ADC) directed against a novel tumor antigen, composed of monomethyl auristatin E (MMAE) as payload (DAR 4) and the humanized IgG1 antibody AFF4 generated by Elthera. AFF4 targets a novel antigen preferentially expressed in various solid tumors including pancreatic cancer, ovarian cancer, colon cancer, breast cancer and melanoma. LCB97 generated by using LCB's *ConjuAll*^{TM} technology with AFF4 showed potent cytotoxicity in various cancer cell lines including breast cancer (BC), ovarian cancer (OC), pancreatic cancer (PaC), small cell lung cancer (SCLC), colorectal cancer (CRC) and melanoma. LCB97 also showed excellent anticancer efficacy in several cell line-derived xenograft (CDX) models, including BC, CRC, OC and melanoma. Preliminary toxicity assessment in cynomolgus monkeys (an AFF4 cross reactive species) demonstrated that LCB97 was well tolerated within the

estimated therapeutic index of ~20 for repeat dosing. In conclusion, LCB97, generated by combining theAFF4 monoclonal antibody of Elthera and the highly innovative *ConjuAll*^{TM} platform technology of LegoChem Biosciences is a promising next-generation ADC for the treatment of various solid cancers, including BC, CRC, melanoma, OC and PaC.

#5654

A therapeutic humanized anti-carcinoma monoclonal antibody (mAb) NEO-201 can also target human granulocytic myeloid-derived suppressor cells (gMDSCs) and regulatory T (Tregs) cells

Massimo Fantini[1], Christina M. Annunziata[2], Philip M. Arlen[3], kwong Y. Tsang[1]. *[1]Precision Biologics, Inc, Bethesda, MD,[2]Women's Malignancy Branch, National Cancer Institute, Bethesda, MD,[3]Precision Biologics, Inc., Bethesda, MD*

Background**:** NEO-201 is a humanized IgG1 mAb reactive against multiple human cancers but not against most normal epithelial tissues. NEO-201 binds to core 1 or extended core 1 O-glycans expressed by its target cells, including neutrophils, various carcinomas, and some human hematological malignancies. NEO-201 can mediate antitumor activity through antibody-dependent cellular cytotoxicity (ADCC), complement dependent cytotoxicity (CDC), and blockade of the CEACAM5/CEACAM1 ICI pathway. A previous study using flow cytometry demonstrated that NEO-201^{+}/CD4^{+} T cells were also CD25^{+}/CD127^{-}/Foxp3^{+}/CD15s^{+} using PBMCs from healthy donors (HD). NEO-201 can kill these Treg cells through CDC *in vitro*. NEO-201 does not bind to the majority of CD4^{+} T cells and to other immune subsets. Human gMDSCs are increased in cancer patients and are a population of immature MDSCs deriving from immature neutrophils and alternative activation of mature neutrophils. gMDSC are characterized by HLA-DR^{-}, CD11b^{+}, CD33^{+}, CD15^{+}phenotype.We have shown that NEO-201 recognizes and kill human neutrophils through ADCC. This current investigation was designed to evaluate whether NEO-201 can target and mediate ADCC activity against human gMDSCs. **Methods:** gMDSCs were generated from human neutrophils from 5 HD isolated using EasySep^{TM} direct human neutrophil isolation kit. Isolated neutrophils were cultured in complete RPMI1640 medium supplemented

with human GM-CSF and human IL-6 for 7 days. Phenotypic analysis by flow cytometry was performed on the generated gMDSCs using NEO-201 and mAbs against human CD33, HLA-DR, CD15, CD14, CD66b. Flow cytometry based ADCC assay was performed using gMDSCs stained with both CD33 and HLA-DR as target. PBMCs from a separate HD were used as effectors at different E:T ratios. The ADCC activity of NEO-201 was evaluated comparing the percentage of $CD33^{+}$/$HLA\text{-}DR^{-}$ viable cells in gMDSCs incubated with medium alone to the percentage of $CD33^{+}$/$HLA\text{-}DR^{-}$ viable cells incubated with PBMCs alone and with PBMCs plus NEO-201.
Results: Flow cytometry analysis revealed that gMDSCs can be generated from human neutrophils after 7 days of culture with GM-CSF and IL-6 and that they express the following phenotype: $HLA\text{-}DR^{-}/CD33^{+}/CD15^{+}/CD14^{-}/CD66b^{+}$. NEO-201 bound to the majority of these gMDSCs. NEO-201 was functional in mediating ADCC to kill these gMDSCs.
Conclusion: This study demonstrated that NEO-201 can be used to identify and kill suppressive gMDSCs in addition to Treg cells. Depletion of suppressive Tregs and gMDSCs in the TME could be an effective strategy to prevent hyperprogressive disease when anti-PD-1 is used in cancer immunotherapy. These data support the rationale for the ongoing phase II clinical trial using NEO-201 in combination with pembrolizumab in checkpoint refractory patients with metastatic solid tumors.

#5655
preclinical development of a novel anti-tslpr bispecific antibody 1b7/cd3 targeting crlf2-rearranged ph-like b-all
Ze Tian, chunhua shi, Amin AI-Shami, GuoJun Yong, Jason K Allen, Jill Wardell Olson, Melinda G Smith, Qing Chang, Qing Shi, Junping You, Michelle A Gonzalez, Timothy E Lofton, Jasbir Kaur, Qi Zhang, DongXing Zha, Nitin Jain, Marina Y Konopleva, Timothy Heffernan, Jeffrey J Molldrem. *UT MD Anderson Cancer Center, Houston, TX*

Acute lymphocytic leukemia (ALL) is the most common form of leukemia in childhood and adolescence. Outcomes of relapsed/refractory adult B-ALL remain dismal with long-term survival of less than 10%. Although targeted therapies such as blinatumomab, inotuzumab ozogamicin, and CD19 CAR T cell therapy are a significant treatment advance for patients

with B-ALL, there is still an unmet medical need for novel therapies for B-ALL. CRLF2-rearranged B-ALL, a subtype of Philadelphia chromosome-like B-ALL, is a high-risk disease subset with poor long-term outcomes. In an effort to identify new therapeutic targets for B-ALL, we validated by flow cytometry that patients with CRLF2-rearranged Ph-like ALL overexpress thymic stromal lymphopoietin receptor (TSLPR) at levels comparable with CD19. We subsequently generated antibodies against TSLPR from immunized H2L2 Harbor mice through single B cell cloning technology. The lead antibody was further engineered to a CD3-redirecting bispecific antibody (BsAb) using Xencor's CD3e bispecific antibody technology to create 1B7/CD3 BsAb with an Fc-silent region. 1B7/CD3 BsAb exhibits high affinity binding to both human and cynomolgus monkey CD3e and TSLPR by BLI. Additionally, UHPLC-SEC analysis of 1B7/CD3 shows that this BsAb is stable without any aggregation or degradation present after five weeks incubation at 37 ^{o}C. In cell-based analyses,1B7/CD3 BsAb demonstrate potent antigen-specific T cell activation and tumor lysis activity against TSLPR^{+}-REH and MHH-CALL4 cell lines as well as a primary B-ALL patient sample, but none against human peripheral blood mononuclear cells (PBMC) collected from healthy donors. Animal tumor models suggest that 1B7/CD3 triggers a dose-dependent tumor regression or growth inhibition in PBMC humanized TSLPR-REH CDX and BOS-1 PDX models across donors. Correspondingly, T cell activation and expansion were examined by CD69 and CD3^{+} T cells with the best effect observed at the 1mg/kg dose. 1B7/CD3 exhibits durable PK with $T_{1/2}$ in NSG mice of up to ten days. Finally, 1B7/CD3 BsAb demonstrated a tolerable safety margin in a two-dose exploratory toxicity study in cynomolgus monkeys with MTD equal to or less than 1mg/kg. Consistent with clinical observation, we observed a transient increase of six major cytokines (IFNγ, IL-6, IL-8, IL-10, MCP-1 and TNFα) 4hr post the initial dosing, but no notable induction of cytokine levels after the second dosing (except for IL-8). Thus, our preclinical data provide the framework for the clinical evaluation of 1B7/CD3 BsAb in patients with CRLF2-rearranged B-ALL.

#5657

HK010, a novel anti-PDL1×CD137 bispecific antibody, exhibits potent anti-tumor immunity and low toxicity

Liangwei Li[1], Wenting Liu[2], Guodong Shen[3], Dayan Zhang[2], Weiming Zhou[2], Fengrong Wang[2], Xiaoli Zeng[2], Yang Huang[1], Liansheng Cheng[2].
[1]Georgia State University, Atlanta, GA,[2]Hefei Hankemab Biotechnology Co., LTD, He Fei, China,[3]The First Affiliated Hospital of University of Science and Technology of China, He Fei, China

Background: Checkpoint inhibitors targeting the PD-1/PD-L1 have changed the treatment and prognosis for patients with advanced solid tumors. There remains a unmet need for additional therapies due to treatment resistance. Tumor-necrosis superfamily members, such as CD137 and CD40, have been shown to synergize with the checkpoint inhibitors in preclinical studies. However, agonists antibodies have exhibited limited clinical activity for severe liver toxicity. Here we have developed a Fc-silenced bispecific antibody targeting PD-L1 and CD137, HK010, which could overcome these limitations by tumor-directed T-cell activation and checkpoint blockade.
Methods: The antigen binding specificity and affinity of HK010 were determined by enzyme-linked immunosorbent assay (ELISA), surface plasmon resonance (SPR) and flow cytometry. The functional activity of HK010 was determined using in vitro cell-based assays and reporter gene assay. Transgenic mice expressing human PD-L1 and 4-1BB were transplanted with human PD-L1-expressing murine MC38 cells to assess in vivo antitumor activity. Cytokine release assay was conducted by incubating HK010 with peripheral blood mononuclear cells (PBMCs) from healthy donors (n=6). The pharmacokinetic (PK) behavior and safety profiles of HK010 were characterized in cynomolgus monkeys.
Results: HK010 is a IgG4 PD-L1x4-1BB bsAb, which was designed to maintain a high affinity for human PD-L1 and a low affinity for human 4-1BB (KD PD-L1: 2.27 nM; KD 4-1BB: 493 nM) to achieve strong blocking of PD-1/PD-L1 and appropriate agonism of 4-1BB. HK010 retained full blockade activity on PD-1/PD-L1 signaling and enhances T-cell proliferation and IFN-γ production in vitro primary cell assays and Mixed lymphoid reaction (MLR). In addition, it led to a dose-dependent increase in the CD137-driven NFκB reporter gene activation through the bridging of PD-L1 on target cells and CD137 on effector cells. In humanized PD-L1/4-1BB transgenic mice bearing with MC38/hPDL1 tumor, HK010 showed robust single agent anti-tumor activity and induced durable antigen-specific

immunological memory that prevents the growth of the same tumor cells in the mice re-challenged. There were no signs of toxicity in human cytokine release assay for HK010. Toxicology data in cynomolgus monkeys showed that HK010 was well-tolerated up to 150 mg/kg (MTD≥150mg/kg) dose without systemic toxicity. Furthermore, HK010 was confirmed to be highly safe in the 5-week repeated-dose toxicity study with no observed treatment-related mortality, abnormality in hematological indexes, important organs. Conclusion: These data demonstrate that HK010, an anti-PD-L1×CD137 bispecific antibody, may exert a strong localized anti-tumor therapeutic efficacy with a low risk of liver toxicity through tumor-directed T-cell activation and checkpoint blockade in tumors.

#5658

MG-Ig (molecularly grafted immunoglobulin): An alternative platform for production of bispecific antibodies

Donglin Liu[1], Li Zeng[1], Berenice E. Liu[2], Chien-Hsing Chang[3]. *[1]FrontAim Biomedicines Inc., Princeton, NJ,[2]Princeton High School, Princeton, NJ,[3]Consultant for FrontAim Biomedicines Inc., Princeton, NJ*

The generation of bispecific molecules, in which two target-specific moieties are engineered into a single entity, offers an attractive approach to optimize biological activity which may improve clinical outcomes. Among various formats of bispecific molecules, the heterodimeric Fc currently is a favorable scaffold for the design of bispecific antibodies because of its structural similarity to the natural antibody. However, development of molecules based on this concept is challenged by the presence of potential homodimer contamination, reduced yield, and stability loss relative to the natural Fc. Here, we report the development of the MG-Ig platform by grafting a single chain fragment variable (scFv) onto the hinge region of a full-size immunoglobulin with a different specificity to produce a trivalent IgG-like bispecific antibody that retains natural homodimer Fc. Whereas the MG-Ig platform is evolved from the Dock-and-Lock (DNL) technology which exploits the interaction between the anchoring domain (AD) of A kinase anchor proteins and the dimerization and docking domain (DDD) of regulatory subunit of cAMP-dependent protein kinase, the main distinctions include 1) the AD-fused scFv monomer is judiciously designed to graft onto the DDD dimer inserted into the hinge region of IgG, forming a bispecific

antibody with three (1+2) binding arms and 2) all modular subunits are expressed in a single host cell and self-assemble to generate the bioactive conjugate *in situ*. To validate the method, bispecific T-cell engagers, designated 3scFv×hL0125C (CD3×Trop2) and 3scFv×hACD20C (CD3×CD20), which redirect T cells to Trop2 and CD20, respectively, have been produced with high yield and purity. Flow cytometry analysis demonstrated the bispecific binding of 3scFv×hL0125C to both CD3 on Jurkat and Trop2 on ME-180 with unaltered affinities. These T-cell redirecting bispecific antibodies mediated dose-dependent killing of target cancer cells when co-incubated with human PBMCs. Based on the 60-h viability assays using MTS, the IC_{50} of 3scFv×hL0125C was about 6 pM for MDA-MB-468, 13 pM for MDA-MB-231, 20 pM for BT-474, and 18 pM for HCT116. In 3D culture of HCT116 cells, the formation of multicellular tumor spheroids was impeded by 3scFv×hL0125C at 19.5 pM or higher, which is consistent with the cytotoxicity assays for tumor cells grown in monolayer. In addition, 3scFv×hL0125C was stable in human plasma for 7 days at 37°C, retaining
bispecific integrity and binding activity. These data are promising and merit further development of MG-Ig bispecific antibodies for preclinical and clinical studies.

#5659

Targeting solid cancers with a cancer-specific monoclonal antibody to surface expressed aberrant O-glycosylated proteins

Mikkel K.M. Aasted[1], Aaron C. Groen[2], John T. Keane[3], Sally Dabelsteen[4], Edwin Tan[2], Julia schnabel[2], Fang Liu[3], Hyeon-Gyu S. Lewis[3], Constantine Theodoropulos[2], Avery D. Posey[3], Hans H. Wandall[5]. *[1]ICMM, University of Copenhagen, Faculty of Health, Copenhagen, Denmark,[2]GO Therapeutics, Natick, MA,[3]Perelman School of Medicine, University of Pennsylvania, Philadelphia, PA,[4]University of Copenhagen, Copenhagen, Denmark,[5]Department of Cellular and Molecular Medicine, University of Copenhagen, Faculty of Health, Copenhagen, Denmark*

The lack of antibodies with sufficient cancer selectivity is currently limiting the treatment of solid tumors by immunotherapies. Most current immunotherapeutic targets are tumor-associated antigens also found in

healthy tissues. Such targets often do not display sufficient cancer selectivity to be used for potent antibody based immunotherapeutic treatments, such as chimeric antigen receptor (CAR) T cells. Many solid tumors, however, display aberrant glycosylation that results in the expression of tumor-associated carbohydrate antigens that are not present on healthy tissues. Targeting aberrantly glycosylated glycopeptide epitopes within existing or novel glycoprotein targets may provide the cancer selectivity needed for immunotherapy of solid tumours, but only a few such glycopeptide epitopes have been targeted. Here, we used *O*-glycoproteomics data from multiple cell lines to identify a glycopeptide epitope in CD44v6, a cancer-associated CD44 isoform, and through a glycopeptide immunization strategy developed a cancer-specific monoclonal antibody, 4C8. 4C8 selectively binds to Tn-glycosylated CD44v6 in a site-specific manner with low nanomolar affinity. 4C8 was shown to be highly cancer selective by immunohistochemistry of sections from multiple healthy and cancerous tissues. 4C8 CAR T cells demonstrated target-specific cytotoxicity *in vitro* and significant tumor regression, and increased survival *in vivo*. Importantly, 4C8 CAR T cells selectively killed target cells in a mixed organotypic skin cancer model without affecting healthy CD44v6+ keratinocytes, indicating tolerability and safety. Targeting aberrantly glycosylated glycopeptide epitopes may provide the cancer selectivity needed for solid tumour immunotherapy.

#5660

IGM-7354, an immunocytokine with IL-15 fused to an anti-PD-L1 IgM, induces NK and CD8+ T cell mediated cytotoxicity of PD-L1-positive tumor cells

Thierry D. Giffon[1], Melanie Desbois[2], Poonam Yakkundi[1], Susan Calhoun[1], Keerthana Sekar[1], Carolyn Denson[1], Tasnim Kothambawala[1], Alexander Pearson[1], Sivani Pandey[2], Deepal Pandya[3], Rodnie Rosete[1], Daniel Machado[1], Pat Raichlen[1], Dean Ng[3], Abhinav R. Jain[4], Roel Funke[5], Eric Humke[5], Paul R. Hinton[3], Beatrice Wang[1], Bruce A. Keyt[6], Maya F. Kotturi[2], Angus M. Sinclair[1]. *[1]Immuno Oncology, IGM Biosciences, Inc., Mountain View, CA,[2]Preclinical Sciences, IGM Biosciences, Inc., Mountain View, CA,[3]Antibody Discovery, IGM Biosciences, Inc., Mountain View, CA,[4]Process Development, IGM Biosciences, Inc., Mountain View,*

CA,[5]Clinical Sciences, IGM Biosciences, Inc., Mountain View, CA,[6]Research and Development, IGM Biosciences, Inc., Mountain View, CA

Immunostimulatory cytokines are a promising immunotherapy for the treatment of advanced malignancies, but generally have been associated with severe toxicities when administered systemically. The recent development of antibody-cytokine fusion proteins, or immunocytokines, aims to localize cytokine activity to the tumor microenvironment and thus improve their therapeutic index. We have developed IGM-7354, a high affinity, high avidity anti-PD-L1 pentameric IgM antibody with an IL-15Rα chain and IL-15 fused to the joining (J) chain. The IGM-7354 immunocytokine was designed to deliver IL-15-mediated stimulation of NK and CD8+ T cells to PD-L1-expressing tumors and antigen-presenting cells, to enhance anti-tumor immune responses. The multivalent binding of IGM-7354 to PD-L1 provided a stronger binding avidity for human PD-L1 than the monovalent binding of IL-15 to IL-15Rb as confirmed in kinetic binding assays. In vitro IGM-7354 induced the proliferation of a cytotoxic T cell line responsive to IL-15 stimulation and enhanced the proliferation of NK and CD8+ T cells from healthy donor human PBMCs. In cytotoxicity assays with human PBMC and PD-L1+ cancer cell lines, IGM-7354 enhanced cancer cell killing through NK and CD8+ T cell expansion and cytotoxic activity, evidenced by Ki67 and Granzyme B upregulation in these cell populations. Next, in vivo pharmacodynamic studies were performed in two humanized mouse models: non-tumor-bearing BRGSF-HIS mice engrafted with human CD34+ cells, and PD-L1+ MDA-MB-231 tumor-bearing MHC-/- NSG mice engrafted with human PBMCs. In the BRGSF model, IGM-7354 increased NK cell activation and Granzyme B expression as well as NK and CD8+ T cell proliferation. In the tumor-bearing mouse model, IGM-7354 dose-dependently increased NK and CD8+ T cell proliferation in blood and infiltration of lymphocytes into the tumor. This pharmacodynamic activity correlated with IGM-7354 anti-tumor activity in the MDA-MB-231 model. Lastly, IGM-7354 increased the proliferation of NK and CD8+ T cells in cynomolgus monkeys and particularly induced the expansion of effector memory CD8+ T cells in the periphery. In summary, IGM-7354 induces NK and CD8+ T cell proliferation in both in vitro and in vivo preclinical models, resulting in the killing of PD-L1+ tumor cells. The strong avidity of IGM-7354 for PD-L1

may enhance IL-15 delivery to tumors and antigen-presenting cells and thus provide a more favorable safety profile. A Phase 1 clinical trial is planned.

#5661

Pre-clinical development of a dopamine receptor 2, PD-1, and CD47 trispecific antibody for the treatment of solid tumors

Shugang Yao[1], Hiba Zahreddine[1], Dominic Hou[1], Elijus Undzys[2], Liying Gong[1], Richard Wargachuk[1], Xiaowei Wang[2], Alex Zhou[2], Lucy Lai[1], Luis A. Da Cruz[1], David Young[1]. *[1]KisoJi Biotechnology, Montreal, QC, Canada,[2]KisoJi Biotechnology, Toronto, ON, Canada*

Multispecific antibodies can have multiple independent mechanisms of action to achieve better clinical outcomes in cancers with high unmet medical needs. Here we describe the preclinical development of a trispecific antibody (KJ-101) targeting dopamine receptor 2 (DRD2), PD-1, and CD47.

DRD2 is a G protein-coupled receptor upregulated in many cancer types where it correlates with decreased patient survival. In pre-clinical studies, DRD2 is associated with cancer cell stemness and tumor growth. Clinical responses were achieved with small molecules targeting DRD2 and dopaminergic drugs for neuroendocrine tumors. In SCLC, representing 15% of lung cancers, 60-70% of patients showed high expression of DRD2. Checkpoint inhibition has shown some efficacy in lung cancer where PD-L1 inhibitors were approved as first-line therapy in SCLC . SCLC patients rapidly fail chemotherapy, develop resistance to treatment and metastases. These observations suggest a link between DRD2 expression and resistance to treatment, making this receptor an attractive target for multispecific antibody therapy.

The VHH components of KJ-101 (anti-DRD2, anti-PD-1 and anti-CD47) produce multiple effects to achieve a strong anti-tumor activity. The anti-DRD2 VHH induces intracellular signaling and suppresses tumor growth via ADCC. Treatment with anti-DRD2 antibody significantly suppressed tumor growth in the DRD2-positive NCI-H510A SCLC model in SCID mice. The anti-PD-1 VHH restores T cell function, and the anti-CD47 VHH recruits T cells without their generalized activation and blocks the interaction between CD47 and SIRPα. The KJ-101 anti-tumor efficacy was tested in several *in vivo* immuno-oncology xenograft models of human SCLC or TNBC, reconstituted with human PBMC or with CD34+ hemopoietic stem cells. KJ-101 treatment led to tumor regression in the TNBC model, blocked metastases formation in CD34+ humanized NCG mice bearing established NCI-H69 tumors, and blocked metastases formation and increased survival in tail vein metastatic models of SCLC. KJ-101 is produced at a high yield (6 g/L) in a manufacturing cell line. Conventional purification yields 99% purity and notably displays high stability under accelerated stability testing.

In conclusion, the trispecific KJ-101 antibody has strong *in vivo* anti-tumor activity mediated via multiple mechanisms of action, is easily expressed

and purified, and is very stable. Together, this data supports the clinical development of KJ-101 in advanced metastatic neuroendocrine cancer indications, including SCLC.

#5662

Early unwanted immunogenicity assessment of immuno oncology drugs

Sofie Pattyn, Martijn Vlaming, Alanah Pieters, Jana Schockaert.
ImmunXperts, a Q2 Solutions Company, Gosselies, Belgium

Bispecifics targeting multiple antigens or epitopes have been showing great promise for treatment of cancer. However, managing unwanted immunogenicity has become a challenge in the development cycle of these promising therapeutics as there is a trend towards higher unwanted immune responses compared with classical monoclonal antibodies. In vitro assays using human primary immune cells can be used to assess the risk of induction of a cytokine release storm or induction of unwanted immunogenicity. For the latter, T cell activation and proliferation assays can be used to assess and predict an unwanted immune response and avoid induction of anti-drug antibodies later on. In order to achieve reliable and consistent results, high quality primary immune cells should be used in combination with sensitive fit-for-purpose in vitro assays.

#5663

Discovery and characterization of anti-LILRB2 antibody SPX-104

Anthony Haight[1], Qian Chen[1], Ernesto Rodriguez[1], Martin Siekierzycki[1], Victoria Hall[1], Brandon Williams[1], Jun Shi[1], Dinh-Duc Nguyen[1], Robert Cai[1], Jichun Ma[1], Michael White[1], Jingdong Qin[1], Jadon Shen[1], Chuanke Zhao[2], Zhuona Rong[2], Lin Meng[2], Chengchao Shou[2]. *[1]Sparx Biopharmaceutical Corp, Mount Prospect, IL,[2]Peking University, Bejing, China*

T-cell based immunotherapies have produced durable remission in certain cancer patients, but owing at least partially to immunosuppression in the tumor microenvironment, response rates with current therapies remains challenging. Reversing the immunosuppression is a recognized pathway for enhancing the activity of existing IO therapies. LILRB2 (ILT4) is a key receptor for macrophage maturation and polarization and an emerging

therapeutic target in immuno-oncology. This research aims to produce anti-LILRB2 antibodies to redirect the polarization of myeloid cells, specifically macrophages, in the tumor microenvironment. The LILRB2 antibodies were generated through the mouse hybridoma method. After humanization and maturation, potent and selective IgG4 anti-LILRB2 antibodies were obtained. Binding affinities were evaluated through ELISA and 293T-LILRB2 cell flow cytometry binding assays which demonstrated sub-nanomolar binding affinity as well as effective blocking of the interaction of LILRB2 with its ligands HLA-G and HLA-A2 for multiple antibodies. SPX-104 was shown to redirect macrophage polarization in primary cultured human PBMC and human monocyte derived macrophage (HMDM) models. SPX-104 treatment induced hTNFa expression and suppressed hIL10 expression in the LPS stimulated PBMC model. In the HMDM model, SPX-104 effectively induced pro-inflammatory cytokine hTNFα expression in M-CSF. Furthermore, an autologous mixed lymphocyte reaction (auto-MLR) assay to evaluate T cell response showed dose-dependent increases in hIFNγ and hGM-CSF expression following SPX-104 treatment. In a CD34-humanized hLILRB2 transgenic mouse efficacy model, SPX-104 in combination with an immune checkpoint inhibitor, effectively inhibited tumor growth. These results confirm enhanced T cell activity following macrophage redirected polarization. The *in vitro* and *in vivo* evaluation, of SPX-104 relative to other anti-LILRB2 antibodies will be presented.

#5664

A novel immunotherapy for relapsed/refractory acute lymphoblastic leukemia (ALL)

Uksha Saini[1], Julie Hixon[2], Gisele Rodrigues[3], Christopher Foley[4], Leniher Castan Chibas[1], Ross Hamilton[1], Wenqing Li[3], Eric S. Schafer[5], Susan Rheingold[6], Michael Heffernan[1], Philip Breitfeld[1], Scott Durum[7], Atul Varadhachary[1]. *[1]Fannin Innovation Studio, Houston, TX,[2]NIH, Bethesda, MD,[3]NIH, Frederick, MD,[4]Bristol Myers Squibb, San Diego, CA,[5]5.Texas Children's Hospital & Baylor College of Medicine, Houston, TX,[6]Children's Hospital of Philadelphia, Philadelphia, PA,[7]National Institutes of Health, Frederick, MD*

Successful treatment of ALL has been a major feat of modern medicine. Overall, 5-year survival in pediatric ALL patients approaches 90%, but 10-15% of patients will relapse. In relapse, ALL is still challenging to cure with 5-year overall survival rates being at or just below 50% and traditional therapies in this space have been highly toxic. Novel immunotherapies such as blinatumomab, inotuzumab and CAR T-cells have improved outcomes and reduced toxicities but are not curated to some of the most vulnerable patients in relapse including T-cell ALL (for which there are no FDA approved immunotherapies) and Philadelphia-like B-ALL. Thus, unmet needs remain in relapsed/refractory (r/r) ALL. The IL-7 and TSLP axes play an important role in B-ALL and T-ALL including in chemotherapy resistance. CD127 (IL7RA) is an attractive target due to limited expression in normal tissues, as confirmed with a GLP.

We are developing 4A10, a novel monoclonal antibody against CD127 which labels ALL cells for degradation via antibody-dependent cell-mediated cytotoxicity (ADCC) and inhibiting IL-7 signaling in T-ALL. 4A10 has demonstrated robust in-vitro and in-vivo anti-cancer activity in pre-clinical PDX models. The antibody substantially reduces circulating tumor burden and organ infiltration, and prolongs overall survival in both naïve and chemotherapy resistant PDX models. Thus, 4A10 holds promise as a novel agent in patients with r/r ALL.

4A10 manufacturing has been successfully scaled up, with a stable master cell bank and good yields at the 200L scale. Our clinical formulation showed no refrigerated or frozen degradation over 3 months and minimal degradation or aggregation at 25°C. In their pre-IND guidance, FDA confirmed that our approach to physicochemical and biological characterization of 4A10 and our proposed analytical methods and tests appear acceptable for early clinical development.

4A10 was well-tolerated in rodent and non-human primate (NHP) toxicological studies with a No Observable Adverse Event Level (NOAEL) in NHPs well in excess of the expected therapeutic dose. Repeat dose NHP pharmacokinetic and pharmacodynamic studies support weekly dosing and do not indicate dose accumulation. Although pivotal GLP toxicology studies have yet to be completed, initial NHP studies do not provide any indications of concern.

We plan to initiate a Phase I/IIA study in 2023 to assess 4A10 in patients with r/r ALL. The Phase I portion of the study will determine the

recommended Phase II dose, and the Phase IIA expansion cohorts have been designed to provide clinical proof of concept. The clinical study will be conducted in partnership with the Therapeutic Advances in Childhood Leukemia and Lymphoma (TACL) consortium and key adult centers. If our Phase I/IIA is successful, we expect to follow with a single pivotal Phase II trial for marketing approval.

#5665

HX301 (ON1232580) a novel kinase inhibitor with potent activity against CSF1R and FLT3, shows strong anti-AML activity in defined preclinical models

Xiaoyu An[1], Henry Li[2], Linda Xue[3], Jinping Liu[4], Lingxin Xiong[1], Hang Ke[2], Cen Chen[2], Bing Gao[4], Jia Zheng[1], Zhengzheng Bao[4], Sheng Guo[3], Lei Zhang[2], Faming Zhang[2]. *[1]Crown Bioscience, Inc., Taicang, China,[2]Hanx Biopharmaceuticals, Ltd, Wuhan, China,[3]Crown Bioscience, Inc., Suzhou, China,[4]Crown Bioscience, Inc., Beijing, China*

Acute myeloid leukemia (AML) is an aggressive leukemia of myeloid lineage with different subtypes of varying treatments/outcomes and a global annual mortality ~150,000. The first-line treatment of AML is usually induction chemotherapy, followed by further chemo-/radiation therapies or stem cell transplant. Targeted therapy tailored for specific driver mutations could be alternative treatment options, *e.g*., new inhibitors targeting IDH mutations and FLT3-ITR CSF1R is a receptor tyrosine kinase (RTK) responsible for the growth, survival and polarization of certain myeloid lineages of cells including macrophages. It is also frequently expressed in certain AML patient populations , thus implicated in the pathogenesis, or a new possible drug target of AML.

To test this hypothesis, a novel kinase inhibitor, HX301 with strong anti-CSF1R activity (IC_{50} of ~0.7nM) as well as anti-FLT3 (IC_{50} of ~7nM), were assessed for anti-AML activity. First, an *in vitro* proliferation assay was performed using primary macrophages and a panel of AML cell lines, confirming that HX-301 has high potency in primary macrophage culture (IC_{50} of ~70nM) and also among cultures of a subsets of AML lines (*e.g*. IC50 < 1μM), such as MV4-11 (medium CSF1R expressing and FLT3-ITD), EOL1, MOL13, *etc*. Next, HX301 was pharmacologically modeled

using four preclinical models to test anti-leukemia activity *in vivo*, including subcutaneous xenograft of MV4-11 cells (CDX) and systemically engrafted PDX models AM8096 (high CSF1R expression but wild type FLT3), AM7577 (FLT3-ITD but little CSF1R expression) and AM5512 (wild-type FLT3 and little CSF1R expression).
Our data demonstrated that HX301 partially inhibited MV4-11 tumor growth as measured by tumor volume, consistent with the *in vitro* observation, possibly due to the inhibition of CSF1R or FLT3-ITD, or both. On the other hand, HX301 completely suppressed leukemogenesis of AM8096, likely due to the inhibition of CSF1R. This observation suggested that CSF1R is likely the driving mechanism for the leukemogenesis of this model; or in another word, for being a PDX, CSF1R likely drives pathogenesis in the original patient. HX301 also suppressed AM7577 growth, likely due to the suppression of FLT3-ITD activity since we previously reported FLT3-ITD being the driver mutation in this model which responded to AC220, a FLT3 TKi. Lastly, HX301 has little activity against AM5512.
All the data suggests that HX301 can potentially be explored for the treatment of AML, at least a subset of the patients with CSF1R and FLT3-ITD as leukemogenic drivers. Further preclinical/translational studies are being conducted in order to reveal predictive biomarkers, in addition to FLT3 mutation and CSF1R expression/mutations. We believe that HX301 could be a potential candidate for treating subset of AML, warranting further clinical investigation.

#5666

NAV-003, a full-length IgG1 bispecific antibody targeting a unique mesothelin epitope and CD3 to improve cytotoxicity against humoral immunosuppressed tumors

Luigi Grasso[1], Qun Jiang[2], Raffit Hassan[2], Nicholas C. Nicolaides[1], J. Bradford Kline[1]. *[1]Navrogen, Cheyney, PA,[2]National Cancer Institute, Bethesda, MD*

Mesothelin (MSLN) is a cell surface protein over-expressed in a number of cancer types. Several antibody- and cellular-based MSLN targeting agents have been tested in clinical trials where their therapeutic efficacy has been moderate at best. Previous studies using antibody and CAR-T based agents

have shown the importance of particular MSLN epitopes for optimal therapeutic response, while other studies have found certain MSLN-positive tumors can produce proteins that can bind to subsets of IgG1-type antibodies and suppress their immune-effector activities. In an attempt to develop a more optimized anti-MSLN targeting agent, we engineered a humanized divalent anti-MSLN/anti-CD3ε bispecific antibody called NAV-003 that targets a MSLN epitope proximal to the tumor cell surface and an anti-CD3ε single-chain antibody capable of effectively binding, activating and directing T-cells to the surface of MSLN-bound tumor cells. NAV-003 has shown significantly improved tumor cell killing against lines producing immunosuppressive proteins *in vitro and in vivo*. Moreover, NAV-003 demonstrated good tolerability and efficacy against patient-derived mesothelioma xenograft models co-engrafted with human peripheral blood mononuclear cells. Together these data support the potential for NAV-003 clinical development and human proof-of-concept studies in patients with MSLN-expressing cancers.

#5667

CYT-303 FLEX-NK^{TM} engager dose response efficacy mechanisms in HCC tumor model and safety in cynomolgus monkey toxicology studies support clinical evaluation in hepato-cellular carcinoma

Vishal Khairnar, Christine Waters, Solgalim Diaz, David De Franco, Jean Kadouche, Daniel Teper, Wei Li, Antonio Arulanandam. *Cytovia Therapeutics, Natick, MA*

BACKGROUND**:** CYT-303 is a multifunctional bispecific NK engager (NKE) targeting NK cell activating receptor NKp46 and tumor antigen Glypican-3 (GPC3) expressed in HCC (hepatocellular carcinoma). Cytovia's proprietary FLEX-NK^{TM} platform utilizes a novel FLEX-linker and human IgG1 back bone to allow for simultaneous binding to targeted cancer cells and NK cells. We evaluated CYT-303 dose response pharmacology efficacy mechanisms in HCC tumor models and conducted safety assessment studies in cynomolgus monkeys to support first in human clinical studies in HCC patients.

METHODS: CYT-303 dose response pharmacology mechanistic studies were conducted in NSG-hIL-15 mice bearing Hep3B tumors and flow cytometry was used to assess bold and tumor NK cells. A 4-week CYT-303

repeat dose GLP toxicology study in cynomolgus monkeys at 6, 20 and 60 mg/kg dose was conducted following weekly intravenous infusions followed by a 6-week recovery period. CYT-303 toxicokinetic and anti-drug antibody (ADA) assessments were conducted using validated immunoassays.
RESULTS: CYT-303 dose response in HCC tumor models showed increased tumor growth inhibition at the lower 2-3 mg/kg doses compared to higher 5-10 mg/kg doses consistent with the dose response previously reported in NK cell redirected cytotoxicity assays against HCC tumors. The increased anti- tumor efficacy observed at the lower doses were associated increased infiltration of PBNK's to the tumor and corresponding reductions in PBNK's in blood suggesting CYT-303 facilitates PBNK entry and retention in HCC tumors expressing GPC3 tumor antigen. CYT-303 safety assessment in the 4-week toxicology study in cynomolgous monkeys showed no treatment related toxicities or cytokine release and the NOAEL was determined to 60 mg/kg/week the highest dose administered in the study. No treatment related clinical signs, clinical pathology (hematology and clinical chemistry) and anatomic pathology (macroscopic, microscopic and organ weights) changes were observed. CYT-303 toxicokinetic analysis showed dose dependent increases in Cmax and AUC's and no evidence for CYT-303 accumulation. CYT-303 anti-drug antibodies in monkeys were minimal and only observed in one low dose animal (1 out of 22) which also showed reduced CYT-303 exposures. Based on these pharmacology and toxicology results a pharmacologically active dose (PAD) based approach together with pharmacokinetic modeling would be utilized to estimate first in human dosing in HCC patients.
CONCLUSIONS: CYT-303 efficacious doses identified in the HCC model together with safety in cynomolgus monkeys and planned human pharmacokinetic modeling studies support clinical evaluation of CYT-303 in first in human HCC clinical trials.

#5668
Using clinical utility index (CUI) to determine the optimal biological dose of a nonfucosylated anti-TIGIT antibody: A proposed alternative to maximum tolerated dose (MTD)
Gabriela Patilea-Vrana, John Harrold, Joseph A. Ware, Shaparak Lonning, Hun Lee, Lisa Brooks, Haley Neff-LaFord, William D. Hanley, Andres

Forero-Torres. *Seagen, Bothell, WA*

SEA-TGT is a human nonfucosylated monoclonal antibody (mAb) targeting the T cell immunoreceptor with immunoglobulin (Ig) and ITIM domains (TIGIT) protein. TIGIT is an immunoregulatory receptor expressed on activated and memory T cells, Tregs, and NK cells. TIGIT binding to CD155 and CD112 on tumor cells drives an inhibitory signal resulting in decreased T cell functionality. TIGIT targeting has been reported to release these inhibitory signals, drive Treg depletion, augment CD8+ T cell generation, and promote anti-tumor responses. SGNTGT-001 (NCT04254107) is a phase 1 clinical trial that evaluated the safety and tolerability of SEA-TGT as monotherapy in solid tumors and lymphomas at doses ranging from 0.01 to 6 mg/kg. Because an MTD was not identified in dose escalation, pharmacokinetic (PK) and pharmacodynamic (PD) endpoints were measured to assess biological activity and inform dose selection. The biological activity of SEA-TGT as monotherapy was compared across different dose levels using a clinical utility index (CUI), which mathematically integrated multiple clinically-meaningful PK and PD endpoints into a single readout. PD endpoints included NK and CD8+ T cell proliferation, maintenance of overall peripheral CD8+ T cell numbers, depletion of peripheral regulatory T cells, and peripheral target engagement. The PK endpoint was pharmacokinetic linearity. Surrogates of predicted tumor efficacy metrics included tumor target engagement and formation of the TIGIT:SEA-TGT:Fc receptor gamma (FcγRIIIa) trimer complexes in the tumor. An increase in the CUI score, representing an increase in biological activity, was observed during dose escalation, with an apparent plateau between the 0.3 and 6.0 mg/kg levels. Based on safety signals at 6 mg/kg and PK variability at lower doses, 1 and 3 mg/kg were of most interest for further evaluation. Both 1 and 3 mg/kg represented biologically active dose levels as they showed PK and PD activity that were within desirable ranges and had similarly high overall CUI scores relative to all doses evaluated. Dose selection for SEA-TGT was based on biological activity as assessed via PK/PD endpoints and integrated into a CUI model. Based on the totality of clinical data and the CUI results from monotherapy dose escalation from SGNTGT-001, the SEA-TGT dose of 1 mg/kg was determined to be the lowest biologically active dose with acceptable safety and tolerability.

#5671

MB201, a CD8+ T cell-selective anti-PD-L1 x IL-2 variant fusion protein, exhibits a potent anti-tumor efficacy without peripheral toxicity

Bom Park, Hyojoo Bang, Youngjun Jung, Sunjung Cho, Mi Seong Kim, Seok Chan Kang, Sungyoub Jung, Youngjin Park. *Mustbio, Suwon, Korea, Republic of*

Interleukin-2 (IL-2), a cytokine with pleiotropic immune effects, is the first approved cancer immunotherapy. However, the clinical application of IL-2 is limited by systemic activation of unexpected immune cells, leading to severe toxicities including vascular leakage syndrome (VLS). These adverse effects were mainly caused by the activation of Treg and endothelial cells bearing IL-2 receptor (IL-2R) αβγ. Recently, studies have mainly focused on the optimization of IL-2Rs binding affinity to selectively invigorate $CD8^+$ T cells in tumors, but the toxicity risk has yet to be solved. To overcome these limitations, we developed MB201, a novel anti-PD-L1 x IL-2v fusion protein, which selectively activates $CD8^+$ T cells by attenuating binding affinity to IL-2Rβγ with no binding to IL-2Rα. MB201 showed a strong binding affinity to PD-L1 (K_D value is 0.5 nM) and a weak binding affinity to IL-2Rβγ and IL-2Rαβγ (K_D value is 23.8 nM and 30.6 nM, respectively), indicating the preferential targeting $PD\text{-}L1^+$ tumor cells. MB201 exhibited a preferential activation of $CD8^+$ T cells than Treg cells, which showed remarkably reduced activation compared to rhIL-2 (more than 100-fold based on EC50). Consistently with the result of T cell activation, MB201 only increased the expansion of CD8+ T cells rather than Treg cells in CD3-stimulated PBMC. Indeed, MB201 induced negligible expansion of immune cells and lower pro-inflammatory cytokine release compared to the rhIL-2 in CD3-unstimulated PBMC, indicating the reduced peripheral toxicity risk. When administered to MC38 syngeneic mice, MB201 showed superior anti-tumor efficacy without both body weight reduction and lung weight gain compared to the avelumab monotherapy or combination therapy with rhIL-2. These preclinical observations support that MB201 has characteristics of a superb safety

profile and excellent anti-tumor efficacy, and it may offer an advantageous therapeutic strategy for the treatment of cancer.

#5672

Comparative mouse pharmacokinetics of matched- and unmatched-isotype anti-PD-L1 antibodies

Breanna Demestichas, Sam Kleeman, Matthew Chvasta, Tobias Janowitz.
Cold Spring Harbor Laboratory, Cold Spring Harbor, NY

Immune checkpoint inhibitors (ICI) are highly effective for a minority of patients with cancer. Pre-clinical research into mechanisms of ICI resistance is reliant upon anti-PD-1 or anti-PD-L1 antibody treatment in mouse models of cancer. Common approaches utilize commercially-available rat isotype anti-PD-L1 antibodies given by intraperitoneal (IP) injection at relatively high doses (5mg/kg every 2-3 days), often for extended periods. However, there has been limited investigation into the pharmacokinetics of these antibodies with single and repeat dosing, which could inform rational dose scheduling. Non-species-matched antibodies are known to induce accelerated anti-drug immune responses, compared to species-matched antibodies. As a result, we hypothesized that matched-isotype anti-PD-L1 (based on the grafting of atezolizumab variable regions onto a mouse IgG2a scaffold) and unmatched-isotype rat IgG2b anti-PD-L1 would be associated with distinct pharmacokinetics on single and repeated dosing. We first confirmed that both matched and unmatched antibodies have nanomolar-range affinity for mouse PD-L1 by surface plasmon resonance (0.85nM and 0.37nM, respectively). Using a single IP injection in 8-week-old male C57BL/6J mice followed by repeated tail-vein plasma sampling and an indirect anti-PD-L1 ELISA, we detected a trend towards prolonged median half-life for the matched (n=17 mice) versus unmatched (n=19) antibody (91.5 versus 39.0 hours). We detected a particularly wide range of half-life measurements for matched antibody experiments (19.8 to 337.7 hours), suggesting that antibody clearance can be highly heterogeneous. Using repeated IP injection (2 doses, 14 days apart), we identified markedly accelerated antibody clearance for both antibodies resulting in comparable antibody half-lives after dose 2 (11.9 versus 12.5 hours, n=13 and n=8 mice, respectively), suggestive of a time-dependent anti-drug adaptive immune response. These findings have significant implications for *in vivo* antibody

treatment experiments, demonstrating that repeat dosing is associated with rapid antibody clearance, irrespective of the antibody species. These data should be taken into consideration when planning longer-term antagonism of PD-1/PD-L1 signaling with antibodies in mice and strengthen the basis for short term window studies that examine the intratumoral immune biology. Furthermore, the high variability in antibody half-life suggests that antibody pharmacokinetics could confound ICI treatment response studies *in vivo*.

#5673

Characterization of AB598, a therapeutic anti-human CD39 antibody for the treatment of cancer

Amy E. Anderson, Angelo Kaplan, Urvi Vani, Enzo Stagnaro, Kaustubh Parashar, Julie Clor, Nigel P. C. Walker, Steve W. Young, Matthew J. Walters, Ester Fernandez-Salas, Christine E. Bowman, Lisa Seitz. *Arcus Biosciences Inc., Hayward, CA*

Background: CD39 catalyzes the conversion of extracellular adenosine triphosphate (ATP) into adenosine monophosphate (AMP), resulting in decreased levels of immunostimulatory ATP and increased levels of immunosuppressive adenosine in the tumor microenvironment (TME). By blocking CD39 in the TME, particularly in combination with immunogenic cell death (ICD)-inducing chemotherapies, local levels of ATP can increase, leading to myeloid cell activation and improved tumor control. AB598 potently binds and inhibits enzymatic activity of human and cynomolgus CD39 but not murine CD39. Human CD39 knock-in (hCD39KI) mice have been employed to determine anti-tumor efficacy of AB598 in animals with competent immune systems.
Methods: Binding affinity and enzymatic inhibition of AB598 were determined in primary human immune cells. ATP-mediated activation of monocyte-derived dendritic cells (moDCs) and macrophages were assayed *in vitro* with and without AB598. Whole blood and tissue-based receptor occupancy (RO) assays were developed using AB598-competitive and non-competitive anti-CD39 reagents. *In vitro* binding of AB598 was determined in samples from human and cynomolgus donors. CD39 protein expression, target engagement, and enzymatic inhibition were assessed in whole blood and tissue samples collected from AB598-dosed animals. CD39 expression

patterns in peripheral immune subsets were confirmed in samples from healthy human donors. CD39 enzymatic activity was evaluated in blood-derived cells and serum from healthy human donors and cancer patients. Results: AB598 binds to CD39-expressing monocytes, B cells, and other immune cell populations in human and cynomolgus whole blood with sub-nanomolar affinity. Following AB598 dosing in preclinical species, decreases in CD39 surface expression on peripheral immune cells were observed, consistent with other anti-CD39 therapeutic antibodies. Target engagement and enzymatic inhibition were evident in tissues collected from AB598-dosed animals. Treatment with AB598/chemotherapy combinations resulted in significant syngeneic tumor control in hCD39KI mouse models. Conclusion: When used in combination with an ICD-inducing chemotherapy agent, AB598 can promote anti-tumor immunity by activation of myeloid cells due to increased local ATP levels. Preclinical characterization of the pharmacodynamic effects of AB598 support our therapeutic rationale and demonstrate target engagement and inhibition both peripherally and intratumorally.

#5674

Anti-CCR8-based bispecific antibodies engineered to preferentially eliminate tumor-infiltrating regulatory T cells: leaving effectors unharmed

Tianhang Zhai[1], Shuang Dai[1], Weifeng Huang[1], Yuanhong Chen[1], Shaogang Peng[1], Shihui Zhou[1], Liandi Chen[2], Jijui Zhang[1], Chao Wang[2], Chao Wang[2], Zhiyuan Li[1], Andy Tsun[2]. *[1]Biotheus (Suzhou) Co., Ltd., Suzhou, China,[2]Biotheus Inc., Zhuhai, China*

Background: Regulatory T cells (Tregs) play a critical role in maintaining homeostasis and self-tolerance and can hamper anti-tumor immunity through multiple mechanisms. Therefore, the targeted depletion of tumor-infiltrating Tregs is sought to promote effective anti-tumor immunity while preserving peripheral homeostasis. CCR8 has been identified as a potential specific target for tumor-infiltrating Tregs. However, CCR8 is also expressed on memory T cell subpopulations and the consequences of their depletion are still unclear. In an attempt to rationally design highly-specific Treg-depleting agents, TIGIT and CTLA-4 were selected as binding targets for engineering CCR8-based IgG-like bispecifics for highly effective

depletion of CCR8/TIGIT or TIGIT/CTLA-4 double-positive Tregs that are enriched in tumors. Here, we detail our results for an anti-CCR8 x TIGIT bispecific as a best-in-class Treg-targeting agent.
Methods: Anti-CCR8/TIGIT bispecific antibody candidates were generated in a 1+1 format and screened using several anti-CCR8 and anti-TIGIT binding arms with a wide range of affinities. CCR8 and TIGIT single-positive cells and CCR8/TIGIT double-positive cells were generated to screen for bispecifics with preferential binding and killing activity towards double-positive cells over single-positive cells *in vitro*. An anti-CCR8/TIGIT surrogate antibody was generated and used to evaluate anti-tumor efficacy as a proof-of-concept study in human-CCR8 knock-in mice, inoculated with CT-26 tumor cells.
Results: An anti-CCR8/TIGIT bispecific antibody, named PM1024, was selected from several candidate pairs that satisfied our screening criteria. PM1024 showed strong binding to CCR8/TIGIT double-positive cells but minimal binding to CCR8 and TIGIT single-positive cells. As such, PM1024 induced strong ADCC activity towards double positive cells but much weaker activity towards CCR8 or TIGIT single positive cells. An anti-CCR8/TIGIT surrogate antibody demonstrated significant anti-tumor efficacy *in vivo*, with similar or better tumor growth inhibition compared to the corresponding monospecific agents.
Conclusion: We successfully generated an anti-CCR8/TIGIT bispecific antibody (PM1024) that preferentially eliminates CCR8/TIGIT double-positive cells over single-positive cells. PM1024 bears the attributes to selectively eliminate tumor-infiltrating Treg cells over CCR8 or TIGIT single-positive lymphocytes, such as effector T cells and NK cells. PM1024 may thus function as a safer, more specific, and highly effective tumor-infiltrating Treg-depleting agent.

#5675

Discovery and development of an asymmetric IgG-like bispecific antibody targeting EGFR and c-MET, engineered through H-H and H-L chain charge-based heterodimerization

Ping Wang[1], Weifeng Huang[2], Zhenting Zhao[1], Xiaoniu Miao[1], Shaogang Peng[2], Chao Wang[1], Yao Yan[1], Tiantian Dong[1], Andy Tsun[1], Yingda Xu[1], Xiaolin Liu[1], Luo Yi[1]. *[1]Biotheus Inc., Zhuhai, China,[2]Biotheus (Suzhou) Co., Ltd., Suzhou, China*

Background: Lung cancer remains the leading cause of cancer mortality and is the most commonly diagnosed cancer with an estimated 2.2 million cases per year. EGFR, a tyrosine kinase receptor, plays a central role in cellular proliferation, survival, differentiation, and migration. Gain-of-function somatic mutations of EGFR significantly drives disease progression. Small molecule tyrosine kinase inhibitors (TKIs), designed to inhibit EGFR signaling specific to these mutations (e.g., L858R and E19del etc.), have achieved excellent clinical outcomes. However, patients carrying TKI-insensitive mutations (e.g., E20ins) and/or those with disease progression after TKI treatment, by the upregulation of complementary signaling pathways (HGF/c-MET, etc.), remain an unmet medical need. Here, we report the discovery of a fully-human afucosylated anti-EGFR x cMET IgG-like bispecific antibody (PM1080).
Methods: PM1080 was generated by introducing unique mutations to the CH1-CL domains of each binding arm to promote correct HC-LC pairing. KIH mutations were also introduced to each CH3 domain to support HC-HC heterodimerization and generate an IgG-like bispecific with one arm binding to EGFR and the other to cMET. PM1080 was expressed via a four-chain expression system in CHO cells carrying a *fut8*$^{-/-}$ knockout to generate afucosylated molecules with enhanced ADCC activity.
Results: Through monovalent affinity measurements, PM1080 interacted with EGFR at single digit nanomolar affinity and at sub-nanomolar affinity to c-MET. PM1080 preferentially bound to EGFR/c-MET double-positive cells rather than EGFR single-positive cells. PM1080 blocked both EGF/EGFR and HGF/c-MET signals via physical blockade of the interaction between EGF/HGF to their corresponding receptors and induced EGFR/c-MET internalization and degradation from the cell surface. Through intricate engineering, PM1080 was expressed via a four-chain system and produced as an afucosylated antibody with significantly improved ADCC function. PM1080 induced potent anti-tumor efficacy against EGFR/c-MET-positive tumor cells as a single agent. Importantly, PM1080 induced anti-tumor activity regardless of EGFR mutations at the intracellular signaling domain, and thus may serve as a promising combinational agent to TKI therapies. As expected, synergistic anti-tumor activity was observed when PM1080 was combined with either 1st or 3rd generation TKIs in both *in vitro* and *in vivo* models.

Conclusion: PM1080, a bispecific antibody targeting EGFR & c-MET was discovered for cancer treatment. PM1080 displayed potent anti-tumor efficacy either as a single agent or in combination with EGFR TKIs. Preclinical PK and toxicity studies have been conducted to support future first-in-human studies.

#5676

SGN-BB228, a CD228-directed costimulatory antibody anticalin® bispecific provides potent and conditional 4-1BB costimulation to T cells *in vivo* and in an *in vitro* model of T cell exhaustion

Barrett Updegraff, Johannes Urban, James Mutschler, Gregory L. Szeto, Brian P. O'Connor, Shyra J. Gardai, Ryan A. Heiser. *Seagen, Bothell, WA*

Agonist antibodies targeting 4-1BB (CD137) effectively costimulate cytotoxic T cells and are active in preclinical models of cancer. However, the clinical development of these agents has been hampered by limited efficacy and/or poor tolerability at active doses. To overcome the efficacy and safety limitations of this approach, SGN-BB228, a first-in-class, investigational CD228 x 4-1BB costimulatory Antibody Anticalin® bispecific (Mabcalin^{TM}) was created. SGN-BB228 is designed to target CD228 (melanotransferrin), a GPI-anchored oncofetal membrane protein with limited normal tissue expression, but high prevalence and expression in melanoma, mesothelioma, lung cancer, and other tumor types. SGN-BB228 is designed to provide a potent costimulatory bridge between tumor-specific T cells and tumor cells, improving and limiting T cell-mediated cytotoxicity to tumors, potentially expanding the therapeutic window for 4-1BB agonism. Here we describe the anti-tumor activity and pharmacodynamic effects of SGN-BB228 in vivo using humanized mouse tumor models, and the in vitro costimulatory effect of SGN-BB228 in a tumor cell line-based model of functional T cell exhaustion. In vivo, SGN-BB228 improved the quality and magnitude of the cytotoxic T cell response within CD228-expressing tumors, augmenting anti-tumor immunity. In vitro, 4-1BB costimulation provided by SGN-BB228 elicited proliferation, and cytokine production from functionally exhausted human T cells when in culture with CD228-expressing tumor cell lines engineered to engage the T cell receptor. Functionally exhausted T cells in this system are a mixed population that share phenotypic markers and single cell transcriptional

signatures associated with either progenitor exhausted T cells (T_{PEX}) or terminally exhausted T cells (T_{EX}). Interestingly, in this system, anti-PD-1 (nivolumab) failed to reinvigorate functionally exhausted T cells despite high PD-L1 expression by tumor cells. The unique ability of 4-1BB costimulation provided by SGN-BB228 to improve T cell activity in this model suggests the potential to drive immunomodulation in circumstances where PD-1 blockade fails. Together these data highlight SGN-BB228, a first-in-class, investigational CD228 x 4-1BB costimulatory Antibody Anticalin® bispecific with potent and CD228-conditional 4-1BB costimulatory activity with therapeutic potential in multiple solid tumor types. These data support the first-in-human phase 1 clinical trial of SGN-BB228 in advanced melanoma and other solid tumors (NCT05571839), which is currently recruiting.

#5677

MB101, a novel PD-L1 x CD3 targeted bispecific antibody, exhibits potent tumor-killing efficacy with minimal off-tumor toxicity

Suna Kim, Hyojoo Bang, Yongjun Jung, Sunjung Cho, Youngsam Kim, Sang-hyun Park, Seok Chan Kang, Youngjin Park, Sungyoub Jung.
Mustbio, Suwon-si, Korea, Republic of

Bispecific antibody (bsAb) which targets tumor-associated antigens and simultaneously induces CD3-mediated T cell activation, is one of the promising therapeutic approaches for cancer treatment. However, despite numerous CD3-based bsAb have been developed, the clinical application faces pronounced hurdles, such as increased on-target off-tumor toxicity and cytokine release syndrome (CRS) by using high-affinity anti-CD3 moieties. Accordingly, there are still needs for the development of CD3-based bsAb with more favorable properties, which are tumor-specific targeting and potent tumor killing activity without excessive cytokine release. Thus, we developed MB101, a novel PD-L1 x CD3 bsAb with low affinity to CD3, which is uncoupled potent tumor cytotoxicity from severe cytokine release. MB101 showed a strong binding affinity to PD-L1 (K_D = 0.4 nM) but a weak binding affinity to CD3 (K_D = 1.0 μM), indicating preferentially targeting to PD-$L1^+$ tumor cells. MB101 showed an effective tumor cell killing activity with higher Emax compared to avelumab mono-

or combination treatment with CD3 mAb in PD-L1$^+$ MDA-MB-231 cells. T cell-mediated cytotoxicity stimulated by MB101 in co-culture with target cells was accompanied by lower secretion of pro-inflammatory cytokines than CD3 mAb and bsAb comparator with high-affinity anti-CD3 arm. Additionally, in the absence of target cells, MB101 treatment to PBMC induced a very low level of pro-inflammatory cytokines, suggesting the possibility of reduced CRS risk. Furthermore, we proved that T cell-mediated cytotoxicity by MB101 was increased in a PD-L1 expression-dependent manner of tumor cells, but not normal cells, indicating minimal on-target off-tumor toxicity. Consistently with *in vitro* results, MB101 effectively regressed tumor volume (TGI=83%) without induction of excessive cytokine release in human CD3 knock-in mouse model. In addition, MB101 showed superior tumor growth inhibition (TGI=70%) than that of avelumab (TGI=44%) in humanized mouse xenograft model. In summary, MB101 selectively triggers robust PD-L1-dependent tumor cytotoxicity while inducing very low cytokine release, suggesting that MB101 might be a promising therapeutic option as CD3-based bsAb for cancer treatment.

#5679

Tetra-specific antibody GNC-035: guidance and navigation control (GNC) molecule development for treatment of ROR1+ malignancies

Jahan Salar Khalili[1], Sa Xiao[2], Yi Zhu[1]. *[1]SystImmune Inc., Redmond, WA,[2]Sichuan Baili Pharmaceutical Co., Ltd., Chengdu, China*

Cancer-intrinsic immune escape mechanisms and immune cell suppression can progressively diminish the curative potential of currently available T cell-based therapies. Barriers to successful T cell checkpoint therapies may be addressed by redirection of T cells toward tumor antigens using T cell engagers that function independently of MHC presented T cell epitopes. Here we demonstrate that an octavalent, tetraspecific Guidance and Navigation Control (GNC) antibody, GNC-035, binds to ROR1, CD3, PD-L1, and 4-1BB and mediates redirected T cell cytolysis of human solid tumor and leukemia and lymphoma cell lines in a ROR1 specific manner. Experiments using GNC-035 to redirect T cell cytotoxicity toward ROR1+ cancer cell targets show the T cells in PBMC are highly functionalized by pre-exposure to GNC-035. This pre-exposure of PBMC to GNC-035 results

in greater tumor cell killing efficacy compared to concurrent exposure of tumor cells in the presence of T cell effectors. This result suggests that the systemic delivery of GNC-035 can condition the T cell compartment to increase the therapeutic impact of T cells migrating to solid tumors, with or without preexisting infiltrating T cells. This beneficial conditioning of T cells by pre-exposure to GNC-035 is not observed with pre-exposure to CD3xROR1 bi-specific T cell engager controls.
To evaluate the potential for GNC-035 to mediate cytokine release syndrome, the molecule is evaluated in soluble formats in the presence of PBMC and the ROR1+ A549 cancer cells, or HUVEC cells. Under these conditions, the cytolysis of A549 target cells is detectable after exposure to GNC-035 at 100 fM concentrations as well as the release of IFN-γ and certain other inflammatory cytokines at 24 or 48 hours post-treatment. However, consistent with Blinatumomab treatment, PBMC exposed to soluble GNC-035 for 24 or 48 hours on a monolayer of HUVEC cells, produced significantly greater amounts of IFN-γ and IL-6 at concentrations greater than 10 pM. These results indicate GNC-035 has a therapeutic window of activity that is ROR1 dependent, spanning cytolytic activity, and IFN-γ release without a production of IL-6 and which is wider than that indicated by Blinatumomab in PBMC.
Collectively, the GNC-035 represents a class of multi-specific and multi-modal immune cell engagers with potential to mediate ROR1+ cancer regression, overcome TCR-based immune escape and reverse T cell immune suppression in tumor microenvironment. The clinical phase I-b study of GNC-035 is under way in breast cancer and hematologic cancers and the available data exhibit strong signals of efficacy with acceptable tolerability.

#5680

Tetra-specific antibody GNC-039: guidance and navigation control (GNC) molecule development for treatment of EGFRvIII+ malignancies

Jahan Salar Khalili[1], Sa Xiao[2], Yi Zhu[1]. *[1]SystImmune Inc., Redmond, WA,[2]Sichuan Baili Pharmaceutical Co., Ltd., Chengdu, China*

One of the primary challenges in the targeting of the tumor specific antigen EGFRvIII is the expression of the antigen among tumor cells in cranial

glioblastoma tumors. The development of GNC-039 is based on the capability of this protein to redirect T cell cytolysis toward the tumor specific antigen EGFRvIII and guide T cells in the tumor microenvironment. Here we demonstrate that the tetraspecific Guidance and Navigation Control (GNC) antibody, GNC-039, binds to EGFRvIII, CD3, PD-L1, and 4-1BB and mediates T cell cytolysis of the human glioblastoma cancer cell line U87 expressing EGFRvIII in the in vitro tumor spheroid model.

When delivered intravenously, the biodistribution of GNC-039 is an important factor in the development of this intracranial tumor targeting biologic. To better understand the biodistribution of GNC-039, Orthotopic Patient Derived Xenograft (PDX) models of Glioma were utilized and vivo-tag680XL-labelled GNC-039 was evaluable by total flux in the Brain area. Multiple IV infusions of GNC-039 were carried out over the study period (29 Days). Groups received either GNC-039 (n=5), GNC-039 with engrafted PBMC (n=5), Temozolomide(n=5), or Vehicle (n=5). The PDX model was sensitive to Temozolomide, 0/5 mice residual tumor, medial overall survival (mOS) of 15 days. In the Vehicle treatment group, 5/5 mice had residual tumor, mOS was 26 days. Mice receiving GNC-039 without PBMC, could partially respond to the treatment, in this group 3/5 animal had residual brain tumors by end of study, but with only a mOS of 15 days. In these animals, the GNC-039 accumulated in the brain region to its maximal level by the third dose on Day 7 and stayed consistently at that level for the duration of the study period. However, in the mouse group with engraft PBMC, the level of GNC-039 in the brain region could exceed that of the drug when infused alone. Mice receiving GNC-039 with engrafted PBMC completely responded to treatment, 5/5 mice in the group had no residual brain tumor, and a mOS of 20 days. In the presence of the engrafted PBMC, the increased level of GNC-039 in the brain region was delayed compared with treatment in the absence of PBMC. As a point of comparison, the Day 7 levels from GNC-039 treatment alone were not reached until Day 15 in presence of PBMC. However, beyond this timepoint, the level of GNC-039 in the brain region was significantly increased due to the engrafted PBMC.

Collectively this data indicates the functionality of GNC-039 as a multi-specific T cell engager with the potential to target EGFRvIII+ cancer cell cytolysis in primary brain disease. The clinical phase I-b study of GNC-039

is under way and the available data exhibit strong signals of efficacy with acceptable tolerability.

#5681

Tetra-specific antibody GNC-038: guidance and navigation control (GNC) molecule development for treatment of CD19+ malignancies

Jahan Salar Khalili[1], Sa Xiao[2], Yi Zhu[1]. *[1]SystImmune Inc., Redmond, WA,[2]Sichuan Baili Pharmaceutical Co., Ltd., Chengdu, China*

B cell malignancies treated with CD19-directed immunotherapies can relapse, in some cases due to clonal selection for reduced CD19 antigen expression or enhancement of immunosuppressive phenotypes. Here we demonstrate that a Guidance and Navigation Control (GNC) tetra-specific antibody, GNC-038, binds to CD19, CD3, PD-L1, and 4-1BB and mediates cytolysis of human leukemia and lymphoma cells by T cells.
Redirected T cell cytolysis (RTCC) occurs in the presence of GNC-038 (Emfizatamab), resulting in the killing of CD19+ leukemia and lymphoma cell lines. The cytolytic functions induced by GNC-038 are similar to Blinatumomab in vitro, as indicated by T cell degranulation and production of IFN-gamma. Human T cells in PBMC exposed to GNC-038 in vitro proliferate in a dose-dependent fashion. Proliferation is further enhanced upon rechallenge with leukemic target cells. Proliferation of T cells from individuals with higher % PD-1+ and Effector polarized compartments is enhanced by GNC-038 compared to Blinatumomab. To evaluate the contribution of each binding domain of GNC-038 in mediating RTCC function, versions of GNC-038 were prepared, replacing each antigen binding domain with anti-FITC binding domains. Under assay conditions using PBMC for RTCC toward the CD19+ target cell line Nalm-6, the results demonstrate the contribution of each domain to the overall, anti-leukemic cytolytic activity.
To evaluate the potential for GNC-038 to mediate cytokine release syndrome, the molecule is evaluated in soluble, and plate bound formats in the presence of PBMC and CD19+ leukemic targets cells. In comparison to Blinatumomab, the production of cytokines is comparable, with some notable differences. PBMC exposed to soluble GNC-038 for 48 hours produced more IFN-γ, IL-2 and TNF-α, while showing no significant difference in production of IL-6. Based on these results, the primary

indicator of CRS, IL-6, does not suggest increased risk compared to Blinatumomab, while the type of T cell activity induced by GNC-038 in PBMC with leukemia cells is distinct.
Collectively, the GNC-038 represents a class of multi-specific and multi-modal immune cell engagers with potential to mediate CD19+ cancer killing, while also increasing the T cell compartment's therapeutic potential to respond to T cell redirection upon subsequent cycles of therapy. The clinical phase I-b study of GNC-038 is under way and the available data exhibit strong signals of efficacy with acceptable tolerability.

ENDOCRINOLOGY

Endocrine-related Cancers and Nuclear Receptors: Molecular Biology, Biomarkers, and Genomics

#5277
Activation of TRPM8 channel suppresses prostate cancer growth and progression
Swapna Asuthkar. *University of Illinois College of Medicine (Peoria), Peoria, IL*

Prostate cancer (PC) is one of the most prevalent male malignancies and a leading cause of cancer-related deaths in men. While androgen-deprivation therapy is successful in the early stages of PC, tumor cells eventually become resistant to its effects. With a median survival of 18 months, the shift to androgen-independent prostate cancer (AIPC) has a poor prognosis. Mechanisms causing this change have yet to be explained, however mounting evidence implicates the loss of transient receptor potential melastatin 8 (TRPM8) as a significant contributor. The prostate epithelium normally expresses the ionotropic receptor TRPM8. Our team has recently shown that testosterone-induced activation of TRPM8 enhances Ca^{2+} absorption and causes apoptosis. This prompted us to propose that increased TRPM8 activity on the plasma membrane is cytotoxic to PC cells and that TRPM8 internalization is a crucial step in the pathogenesis of PC. We examined the amounts of TRPM8 mRNA in benign tumor and metastatic PC patient datasets. TRPM8 mRNA is initially elevated in the early stages of PC but is increasingly lost during the progression to AIPC. In addition,

male and female TRPM8$^{-/-}$ mice exhibited increased serum testosterone levels, heightened AR activity, and activation of cell cycle, invasion, and adhesion-related effectors. In both AR^{+} and AR^{-} xenograft models, our research reveals that TRPM8 possesses potent antitumor properties. Given this, investigating the *in vivo* role of TRPM8 in PC has the potential to significantly enhance patient outcomes by preventing progression to the androgen-independent state.

#5278

Fbxo22 regulates estrogen signaling and suppresses tamoxifen-induced endometrial cancer

Atsushi Goda[1], Satoru Meguro[2], Yoshikazu Johmura[3], Wenwen Wu[4], Ichiro Maeda[5], Yodo Sugishita[6], Nao Suzuki[7], Yasuo Miyoshi[8], Junki Koike[1], Makoto Nakanishi[2], Tomohiko Ohta[4]. *[1]Department of Pathology, St. Marianna University School of Medicine, Kawasaki, Japan,[2]Division of Cancer Cell Biology, Institute of Medical Science, University of Tokyo, Tokyo, Japan,[3]Department of Cancer and Senescence Biology, Cancer Research Institute, Kanazawa University, Kanazawa, Japan,[4]Department of Translational Oncology, St. Marianna University Graduate School of Medicine, Kawasaki, Japan,[5]Department of Pathology, Kitasato University School of Medicine, Sagamihara, Japan,[6]Department of Frontier Medicine, St. Marianna University Graduate School of Medicine, Kawasaki, Japan,[7]Department of Obstetrics and Gynecology, St. Marianna University School of Medicine, Kawasaki, Japan,[8]Division of Breast and Endocrine Surgery, Department of Surgery, Hyogo College of Medicine, Nishinomiya, Japan*

Introduction: Selective estrogen receptor modulators (SERMs), such as tamoxifen, function as agonists or antagonists for estrogen receptors (ERs) in a tissue-specific manner. We have discovered that Fbxo22, a F-box subunit of SCF ubiquitin ligase complex is critical for the functional alteration of SERM (Johmura, et al., *J Clin Invest*, 2018). SCF^{Fbxo22} ubiquitinates and degrades lysine demethylase 4B (KDM4B) complexed with SERM-bound ER, that triggers release of coactivator SRC from ER, thus mediating antagonistic function of SERM. Without Fbxo22, stabilized KDM4B mediates the interaction of SRC with AF1 domain of ER in the

presence of SERM, which only abrogates the interaction of SRC with AF2 domain, resulting in agonistic function. Accordingly, tamoxifen failed to prevent the growth of Fbxo22-depleted, ER-positive breast cancers in vitro and in vivo, and a low level of Fbxo22 in tumor tissues predicted a poorer outcome in ER-positive luminal breast cancers. Hence, Fbxo22 is a critical regulator of estrogen signaling in breast cancer. However, whether it is also important for other estrogen-associated cancers is unknown. To clarify the significance of Fbxo22 in other estrogen-associated cancers, we investigated its role in endometrial carcinogenesis.
Methods: Fbxo22 expression in 22, 30, 29 and 30 cases of normal human endometrium, endometrial hyperplasia (EH), atypical endometrial hyperplasia (AEH) and endometrial cancer (EC), respectively, were analyzed by immunohistochemistry. In addition, we established endometrial epithelium-specific conditional Fbxo22 knockout (Fbxo22-cKO) mice by developing *Fbxo22*-floxed mice and mated them with *Lactoferrin-iCre* mice, and analyzed spontaneous and tamoxifen-induced endometrial neoplasia. Endometrium of the mice in each phase of estrus cycle was also analyzed after PMSG/hCG-induced synchronization.
Results: Fbxo22 was expressed only in secretory phase and was absent in proliferative phase of the human endometrial epithelium, and the expression was inversely correlated with proliferative marker Ki-67. The Fbxo22 expression was down regulated as the endometrium progressed to malignancy (H-score: 124±69, 85±51 and 25±35 for EH, AEH and EC, respectively) (P<0.0001). In consistent with the expression in human menstrual cycle, Fbxo22 was also expressed in diestrus, but not in other phases in mice. Interestingly, the estrus cycle was prolonged in Fbxo22-cKO mice with paradoxical morphology of proliferative epithelial cells with secretory stromal cells. Finally, all five cKO mice developed EH or AEH in four months. The phenotype was accelerated by tamoxifen treatment, with all nine mice developed AEH or EC after one- or two-month tamoxifen treatment whereas wild type mice only developed EH.
Conclusion: Fbxo22 is an essential regulator of estrogen signaling in endometrium and prevents endometrial carcinogenesis including that induced by tamoxifen.

#5279

Molecular analysis of *AMBRA1* as a candidate tumor suppressor in sporadic parathyroid adenomas

Stephanie Chinwo[1], Justin Bellizzi[1], Jessica Costa-Guda[2], Andrew Arnold[3].
[1]Center for Molecular Oncology, UConn Health, Farmington, CT,[2]Center for Molecular Oncology and Dept of Reconstructive Services, UConn Health, Farmington, CT,[3]Center for Molecular Oncology and Division of Endocrinology and Metabolism, UConn Health, Farmington, CT

Primary hyperparathyroidism is a common endocrine disorder that is most often caused by a sporadic single-gland parathyroid adenoma. Currently, the only known and experimentally validated oncoprotein for parathyroid adenomas is cyclin D1. Overexpression of cyclin D1 has been reported in 20-40% of cases; about 8 percent of cases harbor a DNA rearrangement involving the cyclin D1 (*CCND1*) locus. Other molecular mechanisms underlying this cyclin D1 overexpression have yet to be identified. Here, we explored a potential parathyroid tumorigenic mechanism that could increase cyclin D1 stability through a defect in the AMBRA1 E3 ligase adaptor, a molecule responsible for its degradation. Evidence that *AMBRA1* may be a tumor suppressor gene includes: accumulation of cyclin D with hyperproliferation in AMBRA1-deficient cells, context-dependent growth of tumors in Ambra1-deficient mice, and the correlation between low levels of AMBRA1 and poor clinical outcomes in The Cancer Genome Atlas. Therefore, we examined *AMBRA1* for evidence of tumor suppressor-type inactivation in a cohort of 98 typical parathyroid adenomas. Tumor genomic DNA was subjected to PCR-amplification of all 18 coding exons of *AMBRA1*, followed by Sanger sequencing. Sequences were analyzed by comparison to the normal reference sequence (ENST00000683756.1), seeking to assess any observed intragenic or splice-site variants as potential or likely loss-of-function mutations. Thus far, with 97 percent of the coding region for this 1298-amino acid protein fully sequenced, we have identified an inactivating mutation in 1 of 98 tumors (1%): c.126G>A, resulting in an early stop codon p.Trp42. This mutation showed loss of heterozygosity and was confirmed to be somatic by sequencing of the patient's matched germline DNA. We also identified likely non-pathogenic variants in 5 tumors: missense variant c.3385G>T (p.Ala1129Ser), 3' UTR variants c.*576A>T and c.*491T>C and synonymous variants c.579C>T and c.2776C>T, each in a single tumor. 4 of 5 were found as germline variants

in the normal population and the one missense scored as benign by *in silico* criteria. To conclude, our observations suggest that *AMBRA1* may function as a classical tumor suppressor gene in sporadic parathyroid adenomas at very low frequency. Further study may include protein expression analysis of AMBRA1 to investigate influences on gene expression. To further elucidate the mechanisms behind cyclin D1 overexpression in parathyroid adenomas, other molecules that participate in its degradation should be explored as potential tumor suppressors.

#5280

O-GlcNAcylation of progesterone receptor promotes mammary tumorigenesis

Harmony Ivanna Saunders, Sean M. Holloran, Gloria Trinca, Chad Slawson, Christy Hagan. *University of Kansas Medical Center, Kansas City, KS*

The role of hormone receptors in breast cancer has been well established as a key contributor to breast cancer tumorigenesis. Estrogen receptor and progesterone receptors are present in nearly 70% of breast cancers. The role of estrogen receptor and estrogens in breast cancer has been extensively studied and targeted effectively through endocrine therapy, however the impact of progesterone and the progesterone receptor (PR) independent of estrogen is not well understood. We have previously demonstrated that PR promotes tumor growth and drives an immune suppressive environment, therefore understanding the biology of PR in breast cancer is critical. We have also demonstrated that PR attenuates type 1 interferon signaling via inhibition of STAT1 phosphorylation and increased degradation of STAT2. Post-translational modifications such as phosphorylation and SUMOylation can influence PR target gene promoter selectivity thereby altering its function. Our recent work indicates PR is modified by O-GlcNAc, a single N-acetyl-glucosamine sugar that cycles on and off and serine or threonine amino acids in nuclear, cytoplasmic and mitochondrial proteins. Levels of total O-GlcNAc staining are higher in breast cancer tissue compared to adjacent normal tissue. Active O-GlcNAcylation, as evidenced by immunohistochemistry staining of O-GlcNAc-transferase (OGT), is elevated in patients with PR+ tumors compared to PR-. Using T47D breast cancer cells (an ER/PR-positive tumor line), mass spectrometry analysis

revealed an O-GlcNAc site at S499 on PR. We then used a naturally occurring PR-negative variant of T47D cells to introduce stable expression of a mutant PR with serine to alanine substitution at the O-GlcNAc site (S499A), thereby blocking O-GlcNAc flux, in addition to wt PR as a control. RNA-Seq analysis of these cells following treatment with progesterone revealed several significant differential gene expression patterns, including rescue of PR dependent interferon signaling attenuation. T47D-mutant PR cell lines implanted into immune deficient mice had significantly decreased growth as compared to WT-PR control tumors. In syngeneic mice harboring PR-positive and PR-negative tumors, loss of O-GlcNAc flux and increased O-GlcNac levels increased tumor growth only when tumors were expressing PR, corroborating the influence of O-GlcNAc in immunodeficient mice. Together these findings indicate O-GlcNAcylation of PR is potentially a mechanism of PR driven breast cancer tumorigenesis and immune evasion.

#5281

Role of TMEM97/Sigma-2 receptor in prostate cancer

Xiangwei Fang[1], Yuanqin Zhang[1], Jiuhui Wang[1], Paul Cacioppo[1], Michael Crider[2], Daotai Nie[1]. *[1]Southern Illinois University School of Medicine, Springfield, IL,[2]Southern Illinois University Edwardsville, Edwardsville, IL*

Introduction: Prostate cancer is the most common cancer in men. About one in eight men will be diagnosed with prostate cancer in his lifetime, and one in forty-one men will die of it. Sigma 2 receptor (σ2R) has been implicated in carcinogenesis including prostate cancer. Its molecular identity remained elusive until 2017 that transmembrane protein 97 (TMEM97) was identified as the bona fide sigma 2 receptor. Past studies have shown that σ2R is highly expressed in various mammalian tumors and TMEM97 works as an oncogene in different cancers. In this study, we examined the expression of TMEM97/σ2 receptor in prostate cancer, evaluated its interaction with androgen receptor (AR), and determined its functions in tumor cell growth and progression.
Methods: The expression of TMEM97 at mRNA levels and its association with clinical parameters were queried in the TCGA database using cBioportal. Its expression pattern in prostate tumor tissues was examined by IHC using a commercially validated antibody. A correlation analysis of

TMEM97 with AR was conducted utilizing both PCTA and TCGA databases. To determine its roles in tumor proliferation, clonogenicity, and responses to hormone deprivation and chemo-therapy, TMEM97 expression was overexpressed and knocked down, and the subsequent effects were determined by cell proliferation MTS assay, colony formation assay with and without enzalutamide treatment. A xenograft model of nu/nu mice was used to assess the impact of TMEM97 overexpression on tumor formation and growth in vivo. The effects of TMEM97 overexpression and knockdown on AR transcriptional activity were examined.
Results: A significant elevation of TMEM97 mRNA levels, with a Z-Score above 2.0, was found in 5% of the prostate cancer patients and was associated with significantly reduced survival. TMEM97 protein was detected in prostate tumor tissues of all stages and grades. Its expression is highly correlated with the expression of AR in prostate cancer. Prostate cancer cells with TMEM97 overexpression showed growth advantage over the control cells both in normal culture conditions and also under treatment of enzalutamide. TMEM97 knockdown weakened growth, and sensitized castration resistant 22Rv1 toward enzalutamide, which is linked to the decrease of AR-V7. TMEM97 overexpression in LNCaP cells also significantly increased tumor formation and growth when xenografted into nu/nu mice. In LNCaP cells, TMEM97 overexpression elevated AR target genes expression. Parallelly, these genes were all significantly downregulated in TMEM97 knockdown cells. A compound with a high affinity to TMEM97 was found to induce apoptosis of prostate cancer cells with preferential degradation of AR-V7.
Conclusion: The observations suggest that TMEM97/sigma2 receptor plays a role in prostate tumor cell proliferation and the increased expression of TMEM97 can elevate AR activity and stimulate prostate tumor formation and growth.

#5282

Mitotane induces GDF-15 expression *in vitro* and *in vivo:* A potential therapy-induced mechanism of immune escape in adrenocortical carcinoma

Isabel Weigand[1], Tanja Anderlik[2], Jochen Schreiner[1], Hanna Remde[2], Otilia Kimpel[2], Laura-Sophie Landwehr[2], Eva Hoster[3], Florian Wedekink[4], Alexandra S. Triebig[1], Tanja Maier[1], Jörg Wischhusen[4], Martin Reincke[1],

Martin Fassnacht[2], Matthias Kroiss[1]. *[1]Department of Internal Medicine IV, University Hospital LMU Munich, Munich, Germany,[2]Department of Internal Medicine I, Division of Endocrinology and Diabetes, University Hospital Wuerzburg, University of Wuerzburg, Wuerzburg, Germany,[3]Institute for Medical Informatics, Biometry and Epidemiology, Ludwig-Maximilians-University, Munich, Germany,[4]Experimental Tumor Immunology, Department of Obstetrics and Gynecology, University Hospital, University of Wuerzburg, Wuerzburg, Germany*

Context: Adrenocortical carcinoma (ACC) is a rare endocrine malignancy with poor prognosis and limited treatment options. The only approved therapy is mitotane, an adrenal toxicant, alone or in combination with cytotoxic chemotherapy. Response rate is only ~20%. Results of later line immune checkpoint inhibition (ICI) in ACC are disappointing, most likely due to an immunologically cold, immunosuppressive microenvironment. Among the factors induced in mitotane-treated ACC cell lines, we previously found growth/differentiation factor 15 (GDF-15), an anti-inflammatory cytokine physiologically expressed during pregnancy.
Aim: As GDF-15 is an emerging mediator of tumor immune escape, we investigated changes in GDF-15 secretion upon mitotane treatment in ACC *in vitro* and *in vivo,* and explored a potential correlation with response to therapy and survival.
Methods: Four different human ACC cell lines (NCI-H295R, CU-ACC1, CU-ACC2 and JIL-2266) were treated with mitotane. GDF-15 secretion and expression were determined by ELISA and immunoblot. GDF-15 levels in sera of 142 ACC patients (94 prior and 48 during mitotane) were analyzed by ELISA and correlated with survival from the time point of blood collection. GDF-15 serum levels were quantified in three responders and seven non-responders to ICI treatment.
Results: *In vitro*, 24h treatment with 25 µM mitotane-induced GDF-15 secretion and expression in all cell lines by up to one order of magnitude. In 32 patient samples, GDF-15 serum concentrations increased from 0.6±1 ng/l prior mitotane to 2.1 ± 2.7 ng/l after mitotane initiation, $p<0.0001$.Importantly, patients with low serum GDF-15 levels before and during mitotane treatment had a significantly longer overall survival compared to patients with higher GDF-15 serum levels. This association retained statistical significance after adjustment for the known prognostic

factors Ki67 and ENSAT tumour stage in the mitotane treated group (95% CI 1.15-.1.73, HR1.41, p=0.001). In an exploratory cohort of three responders and seven non-responders to ICI we found a trend for higher GDF-15 serum concentrations in the non-responders.
Conclusion: Mitotane induces GDF-15 both *in vivo* and *in vitro* and potentially contributes to the poor response rates to ICI in ACC.

#5283

Glucocorticoid receptor (GR) activity alters invasive lobular breast cancer (ILC) oncogenic properties

Ishrat Durdana[1], Candace Frerich[1], Muriel Laine[2], Smita Rindhe[1], Lynda Bennett[1], Robert Bachoo[1], Geoffrey Greene[2], Suzanne Conzen[1]. *[1]UT Southwestern Harold C. Simmons Comprehensive Cancer Center, Dallas, TX,[2]The University of Chicago, Chicago, IL*

Invasive breast cancer (BC) is commonly divided into two subtypes, invasive ductal carcinoma (IDC) and invasive lobular carcinoma (ILC). ILC makes up 10-15% of all BC cases. Expression of nuclear hormone receptors further define clinical histology and directs treatment; receptors include estrogen (ER), progesterone (PR), androgen (AR), and glucocorticoid receptors (GR). Tumor GR expression activation is associated with good prognosis in ER+ but poor prognosis in ER- BC. The majority of ILC tumors are ER+, and we have found that GR expression in primary ILC tumors correlates with improved overall survival. We hypothesized that GR activity in ILC may play a role in ILC's indolent natural history and could alter its metastatic tendency. We used two isogenic ILC cell lines, each with and without GR expression (MM134-GR+/GR- and SUM44PE-GR+/GR-) to study GR-mediated ILC associated phenotypes. Specifically, we describe GR's effect on proliferation *in vitro* and tumor formation in the *in vivo* MIND model. We also measured GR-mediated ILC adherence to major components of the extra cellular matrix (collagen I, collagen II, laminin, fibronectin, vitronectin, and tenascin). To recapitulate early metastasis, we examined ILC cell movement through a 10 uM microchannel device. We found that GR expression and activation in ILC cell lines cause decreased cell proliferation and decreased adherence to laminin. Preliminary experiments suggest that GR activation altered ILC cell's ability to enter and navigate through restrictive 10 uM microchannels. Given our

preliminary findings, we will investigate the effect of selective GR modulators (SGRMs) on ILC phenotypes and gene expression. We hypothesize that the gene expression changes following GR activation will be different in ILC compared to IDC. In addition, we are examining the genes required for survival of ILC cells on collagen using an *in vitro* CRISPR-Cas9 screen. *In vivo* experiments examining the association of GR expression with tumor growth *in vivo* are ongoing.

#5284

Recurrent Middle Eastern differentiated thyroid carcinoma has worse outcome than persistent disease

Sandeep K. Parvathareddy, Abdul K. Siraj, Padmanaban Annaiyappanaidu, Nabil Siraj, Saeeda O. Ahmed, Zeeshan Qadri, Saud Azam, Khawla S. Al-Kuraya. *King Faisal Specialist Hospital & Research Centre, Riyadh, Saudi Arabia*

Background: Differentiated Thyroid Cancer (DTC) is the most common endocrine malignancy. Despite its excellent prognosis, recurrent and persistent disease remain major challenges after initial treatment. Although most studies have considered persistence and recurrent as a single entity, emerging studies to differentiate recurrent and persistent disease are controversial and study on recurrent and persistent DTC from Middle Eastern ethnicity is lacking.
Methods: We retrospectively analyzed 1822 patients who underwent surgery ± I131 treatment for DTC with a median age of 38.9 years and median follow-up of 90 months.
Results: We found a similar prevalence rate of persistent and recurrent disease (16.4% vs. 16.6%) in Middle Eastern DTC patients. Relative to patients with persistent disease, patients with recurrent disease were significantly older (median age 36.1 vs. 45.8 years; $p < 0.0001$), were more likely to have ATA high risk tumors ($p < 0.0001$) and had a higher rate of distant metastasis ($p < 0.0001$). However, structural disease had an almost similar frequency in both recurrent and persistent disease (72.2% vs 73.3%). On multivariant logistic regression analysis, both T status and N status are independent predictors for both recurrent and persistent disease. However, older age, extrathyroidal extension and the presence of distant metastasis were independent predictors of only recurrent disease. In

addition, patients with recurrent disease had significantly worse overall survival (OS; $p < 0.0001$) and cancer specific survival (CSS; $p < 0.0001$), which remained significant in multivariate Cox proportional hazard model (Hazard ratio = 2.72; 95% confidence interval = 1.20 - 7.01; $p = 0.0153$ for OS and Hazard ratio = 5.09; 95% confidence interval = 2.10 - 15.24; $p = 0.0001$ for CSS).
Conclusion: Although persistent and recurrent disease in Middle Eastern DTC have similar frequencies, recurrent disease had worse outcome compared to persistent disease. This has great potential clinical relevance to differentiate recurrene from persistence for therapeutic and follow-up approach for improving outcomes of DTC patients from Middle Eastern ethnicity.

#5285

Identification of therapeutic targets in poorly differentiated carcinoma through a multimodal molecular analysis

Vanessa Zambelli[1], Marta Fornaro[1], Giulia Orlando[2], Ida Rapa[3], Francesca Napoli[1], Susanna Cappia[1], Lorenzo Daniele[4], Simonetta Piana[5], Mauro Papotti[2], Marco Volante[1]. *[1]University of Turin, San Luigi Hospital, Turin, Italy,[2]University of Turin, Molinette Hospital, Turin, Italy,[3]San Luigi Hospital, Orbassano (TO), Italy,[4]Mauriziano Hospital, Turin, Italy,[5]Arcispedale Santa Maria Nuova Azienda USL- IRCCS, Reggio Emilia, Italy*

Poorly differentiated thyroid carcinoma (PDTC) represents a rare subtype of thyroid cancer with aggressive clinical course and peculiar clinical and pathological characteristics. Recent genetic studies highlighted the main molecular pathways involved in its pathogenesis but data are affected by heterogeneity of case selection and relatively limited sample size. Using a multimodal molecular approach, aim of this project was to implement the PDTC molecular characterization and to identify novel prognostic biomarkers and potential therapeutic targets. A total of 84 cases of PDTC classified according to the Turin proposal were selected from a multi-Institutional series. Fifty-nine samples underwent DNA, RNA and protein analyses. Mismatch repair (MMR) defects were tested using immunohistochemistry for MLH1, MSH2, MSH6 and PMS2. DNA and RNA analyses were performed by means of next generation sequencing

(NGS) using Oncomine Comprehensive assay V3. Due to the high failure rate in RNA analysis, gene fusion analysis was enriched by 25 additional samples. MMR protein loss was observed in 7/59 samples (11.9%). In NGS DNA analyses, 51/59 cases were adequate. The most prevalent mutations were in *NRAS* (13/51, 25%) and *TP53* (13/51, 25%), all mutually exclusive each other. *TERT* promoter (*TERTp*) mutations were detected in 11/51 of cases (21.6%). Other genes with a relevant prevalence were *PTEN* (15.7%), *NF1* (13.7%), *ATM* (13.7%), *NOTCH3* (11.8%) and *BAP1* (11.8%). Mean number of alterations was higher in *TP53*-mutated cases (5.8 mutations/case) than in *RAS*-mutated cases (2.8 mutations/case). *TP53*-mutated samples lacked *TERTp* co-mutations but were associated with mutations in *PTEN* and in genes related to MMR system and/or loss of MMR proteins. *PIK3CA* was the most prevalent co-mutated gene (three samples) in *RAS*-mutated cases. A third group (25 cases) lacked *RAS* or *TP53* mutations, had a low mean number of alterations (2.7 mutations/case) and was enriched for *TERTp* mutations (up to 32%). Copy number variations were not detected. Among the 43 cases adequate for NGS RNA analysis, gene fusions in *PAX8-PPARG* (one case) and *TBL1XR1-PIK3CA* (two cases) were detected. This latter fusion has never been reported in thyroid cancer, and was validated by fluorescence in situ hybridization (FISH). In conclusion, PDTC are genomically clustered into *RAS*-mutated tumors (with low mutational burden and co-mutations affecting genes involved in the same pathway), *TP53*-mutated cancers (with high mutational burden, absence of *TERTp* mutations and strong association with MMR defects) and a third “double negative” group enriched for *TERTp* mutations. Overall, targetable gene fusions have a prevalence of 7%. Moreover, 38% of overall cases harbor mutations in genes coding for tyrosine kinases potentially targetable and/or have defects in the MMR that claim a potential role for immunotherapy.

#5286

Matrix metalloproteinase 14 in associated with poor survival in adrenocortical carcinoma

Liudmila V. Popova[1], Elaine Mardis[2], Katherine Miller[3], Priya H. Dedhia[1].
[1]Department of Surgery, The Ohio State University Wexner Medical Ctr., Columbus, OH,[2]The Steve and Cindy Rasmussen Institute for Genomic Medicine, Natiowide Children's Hospital, Columbus, OH,[3]The Steve and

Cindy Rasmussen Institute for Genomic Medicine, Nationwide Children's Hospital, Columbus, OH

Adrenocortical carcinoma (ACC) is an aggressive malignancy of the adrenal cortex. Five-year survival in Stage IV disease is 6%. Surgical resection is the mainstay of treatment; however, most patients present with unresectable disease or experience tumor recurrence after surgery. No targeted therapies are available for treatment of ACC. Thus, there is a critical need to understand molecular mechanisms driving advanced ACC. Matrix metalloproteinases (MMPs) have been associated with worse prognosis in other human cancers. Although pan-inhibition had limited clinical success, recent studies suggest select inhibition may improve patient outcomes. Here, we use The Cancer Genome Atlas (TCGA) and single nuclei RNA sequencing data (snRNAseq) to evaluate the expression of MMPs in ACC. RNA sequencing data from 77 ACC patients in TCGA was downloaded from UCSC Treehouse Public Data Tumor Compendium v11. Using the Kaplan-Meier estimator, survival was compared between the highest and lowest quartile of RNA expression for each MMP in R v.4.1. For snRNAseq, normal adrenal and adrenal adenoma samples were collected from a patient diagnosed with adrenal hypercortisolism. Seven primary and metastatic ACC samples were collected from patients diagnosed with ACC at time of surgical resection and included one primary tumor-metastasis pair. Single nuclei were isolated from frozen samples. Sequencing libraries were generated and sequenced on the Illumina NovaSeq 6000. Data were preprocessed using the 10x Genomics CellRanger software suite. Downstream analysis was performed using Seurat v.4 for R. ACC specimens in TCGA expressed all 24 MMPs with MMP14 demonstrating the highest expression. MMP14 expression was associated with significantly worse survival with a hazard ratio of 3.6 (95% CI 1.2 - 11.1). In addition, increased MMP14 expression was associated with higher AJCC tumor stage ($p < 0.05$). snRNAseq analysis of our ACC primary and metastatic samples identified 7 adrenal cortex clusters and one cluster each - fibroblasts, macrophages, infiltrating lymphocytes, endothelial, and adrenal medulla cells. Two cell clusters were present in primary and metastatic samples but not benign adrenal samples and were characterized by high KI67 expression or high ribosomal content. MMP14 expression was significantly higher in metastatic versus primary tumors in 2

adrenal cortex clusters with 3.6 and 2 fold increased expression, respectively ($p < 0.05$); and one of these clusters was defined by a 15-fold increase in expression of ZNRF3, which is involved in activation of the Wnt pathway. These data suggest that MMP14 expression is associated with worse survival and may be associated with metastatic progression. Further studies are needed to confirm whether simultaneous targeting of Wnt pathway and MMP14 may result in decreased metastatic progression.

#5287

Is testosterone the male sex hormone responsible for increased male mortality in melanoma? *In-vitro* studies based on human melanoma (BLM) cell model

Pandurangan Ramaraj. *Biochemistry, A.T. Still Univ. - Missouri Campus, Kirksville, MO*

Clinical studies showed that menstruating females were better protected in melanoma than post-menopausal women and men of any age. But, these studies did not correlate with the steroid status of females. Our in-vitro study with progesterone (P), a female sex hormone showed significant inhibition of human melanoma cell growth. A literature survey showed that progesterone levels ranged between 1000-1500 ng/dl in menstruating females compared to post-menopausal women (20-100 ng/dl) and men (27-90 ng/dl), suggesting increased progesterone levels could offer protection to the menstruating females. Moreover, Elisarray showed that progesterone action was mediated by specific suppression of proinflammatory cytokine IL-8. So, it was proposed that a low level of progesterone in males leading to non-suppression of IL-8 in melanoma, could be responsible for increased melanoma cell growth and male mortality. This hypothesis prompted us to check the effect of male sex hormones androstenedione (AD) and testosterone (T) on melanoma cell growth and IL-8 secretion. Both AD and T decreased IL-8 secretion along with a decrease in cell growth. However, when progesterone was added along with androgens, there was a significant decrease in cell growth and in IL-8 secretion. This raised the question of why male mortality was high when androgens also decreased cell growth and IL-8 secretion. In order to address this question, it was decided to induce endogenous IL-8 in melanoma cells by pre-incubating with endothelin (50ng/ml) and then add steroids. AD and P individually

decreased IL-8 secretion and in combination significantly decreased IL-8 secretion and cell growth even in endothelin pretreated cells when compared to their respective control cells. But, T was not able to suppress endogenous IL-8 induced by endothelin and in fact, cell growth also was slightly increased compared to straight T-treated cells.
Conclusion: So, in males 2 reasons 1) a deficiency of progesterone and 2) inefficiency of T to suppress endogenous IL-8 could possibly result in increased IL-8 levels. This increased IL-8 level in males could lead to increased cell growth and metastasis in melanoma (IL-8 had already been shown to stimulate melanoma cell growth and metastasis by us and others) leading to death. So, a situation arising out of male reproductive endocrine physiology could probably be responsible for increased male mortality in melanoma.

#5288
Single-cell multiomics reveal divergent transcriptional and epigenetic cell states in breast cancer
Aysegul Ors[1], Hisham Mohammed[1], Aaron R. Doe[1], Syber Haverlack[1], Mithila Handu[1], Ryan Mulqueen[2]. *[1]Knight Cancer Institute / CEDAR, Oregon Health & Science University, Portland, OR,[2]MD Anderson Cancer Center, University of Texas, Houston, TX*

Over the recent years, single-cell sequencing studies have been used to better describe the highly heterogeneous nature of breast cancers on transcriptional and genetic levels. It is also known that breast cancers are highly driven by estrogen receptor alpha (ER), a transcription factor that's important for mammary tissue homeostasis. However, little is known about how estrogen signaling heterogeneity affects cancer progression and response to anti-estrogen therapy at a single-cell level. Leveraging single-omic and multi-omic single-cell sequencing technologies, we tracked estrogen response in breast cancer cell and organoid models. We developed TITAN, a topic-modeling based analysis tool to reveal signaling gradients in single-cell RNA-seq data. With this approach we showed that distinct cells prioritize distinct gene groups in response to estrogen. We defined two of these gene networks to be driven by either ER or FOXM1. These same networks exist not only in all the models used in the study but also in breast cancer patient datasets. FOXM1 is activated in estrogen treated cells and

the FOXM1 driven gene signature correlates with more aggressive types of disease. Our combined scRNA and scATAC-seq experiments also highlighted distinct chromatin accessibility states associated with either cell group. Using scNMT-seq in patient samples we were able to describe DNA methylation and chromatin accessibility influence on hormone signaling patterns at the single-cell level. Together, our results provide insights into defining transcriptional and epigenetic cell states in ER positive breast cancer.

#5289

Proteomic profile of breast carcinomas with unbalanced levels of progesterone receptor isoforms

Andres M. Elia[1], Jana Sanchez[2], Rui Vitorino[3], Leo Saldain[1], Paula Martinez Vazquez[4], Javier Burruchaga[4], Eunice Spengler[4], Javier Muñoz[2], Paola Rojas[1], Luisa Helguero[3], Claudia Lanari[1]. *[1]IBYME-CONICET (Institute of Biology and Experimental Medicine), Buenos Aires, Argentina,[2]Centro Nacional de Investigaciones Oncológicas (CNIO), Madrid, Spain,[3]Institute of Biomedicine (IBIMED), University of Aveiro, Aviero, Portugal,[4]Hospital de Agudos "Magdalena V de Martínez", Gral Pacheco, Argentina*

Preclinical studies indicate that progesterone receptors (PR) play a relevant role in breast carcinogenesis. Even more, a misbalanced expression of PR isoforms A (PRA) and B (PRB) differentially affect breast cancer progression and only tumors with higher levels of PRA than PRB (PRA-H) respond to an antiprogestin treatment. There are controversial results regarding the prognosis of PRA-H luminal tumors compared with those with the opposite ratio (PRB-H tumors) highlighting the necessity to further understand the role of PR isoforms in tumor progression and to develop novel methods to discriminate these tumors without performing western blot studies. Along this line we have previously studied the transcriptome of PRA-H or PRB-H breast cancer samples, thus our aim is to expand these results and compare the proteome profile of PRA-H and PRB-H samples obtained from postmenopausal breast cancer patients. Nuclear (Nuc) and cytosolic (Cyt) protein fractions were obtained from 18 breast cancer samples classified as PRA-H or PRB-H and they were studied by LC-MS/MS (UltiMate 3000 LC system - Q Exactive HF-X mass spectrometer -

Thermo). We observed 289 differentially deregulated proteins in Cyt (164 down and 125 up) and 301 in Nuc extracts (131 down and 170 up; logFC > 1, pval < 0.05). Gene set enrichment analysis of the Nuc fractions showed biological processes related to Cell junction organization (pval = 8,87e-05), Collagen formation (pval = 0,0005), and Cell-Cell communication processes (pval = 0,0035) in PRB-H tumors; while in PRA-H tumors, pathways related to Innate Immune System (pval = 8,8e-05), Class I MHC mediated antigen processing & presentation (pval = 8e-05) and Stabilization of p53 (pval = 0,0051) processes were enriched. Similar trends were observed in Cyt fractions. Individual candidates that were overrepresented in both fractions in PRB-H tumors are BAG3 and GH3, related to cell proliferation, and VWF, related to the activation of the Akt pathway. Overrepresented proteins in both fractions of PRA-H tumors are BST2, IFT27 related to invasion, and MIF associated with poor prognosis. As we were interested in looking for differential expressed proteins that could be tested in plasma samples to discriminate both tumor types, using the Vertebrate Secretome Database we focused on those that might be secreted. Noteworthy is CBP1 which was overrepresented in the PRB-H tumors and this was in agreement with the RNA-Seq data and with results obtained using preclinical models, repurposing this protein as one candidate of concern in the search for biomarkers. Other secretory proteins of interest are SFRP2 and SERPIND1, both highly expressed in PRA-H Cyt fractions. In conclusion, this study underscores the biological differences between PRA-H and PRB-H breast carcinomas and provides candidates that deserve to be tested as surrogate markers in plasma to discriminate patients that may benefit from an antiprogestin treatment.

#5292

Characterization of androgen receptor properties and interactome in mediating transcriptional condensates in prostate cancer

Nicholas C. Pinette, Shabnam Massah, Sofia Kochkina, Fan Zhang, Maitree Biswas, Joseph Lee, Jörg Gsponer, Nada Lallous. *Vancouver Prostate Center, Vancouver, BC, Canada*

In The United States of America 1 in 8 men will develop prostate cancer (PCa) in their lifetime. The assembly of phase-separated condensates containing players of the transcriptional machinery such as transcription

factors, coactivators (e.g. MED1), and RNA polymerase II enhances the transcription of key oncogenes in various cancer including PCa. Many proteins undergoing phase-separation possess intrinsically disordered regions (IDR) that mediate multivalent intra- and inter-molecular interactions, essential for condensate formation. We recently demonstrated that full-length AR, the main oncogenic driver in PCa, is more prone to form nuclear transcriptional condensates upon androgen stimulation in PCa models than in benign epithelial prostate models. In this study, we investigated the effects of mutating or truncating key residues or regions involved in AR transcriptional activity on its ability to form nuclear condensates in LNCaP cells as visualized by confocal microscopy. We also used various bioinformatics tools to predict additional AR residues and sequences with high propensity for phase-separation. We thus made various truncations and mutations and evaluated their ability to form condensates in LNCaP cells. We also tested the effect MED1 phosphorylation and treatment with various inhibitors targeting different domains of the AR on the ability of full-length protein to form droplets in vitro. We hope by better understanding what drive AR condensates formation in PCa, to elucidate this new mechanism of transcriptional regulation and to identify new therapeutic avenues for patients with advanced forms of the disease.

EXPERIMENTAL AND MOLECULAR THERAPEUTICS

Anticancer Approaches Targeting Signal Transduction Pathways

#4858

Effect of mTOR activity in peripheral blood mononuclear cells with metformin in high-risk prostate cancer patients receiving external beam radiotherapy and androgen deprivation therapy

Febin Antony[1], Anuraag Shrivastav[2], Arbind Dubey[1], Nawaid Usmani[3], Aldrich Ong[1], Rashmi Koul[1], Harvey Quon[4], Gokulan Sivananthan[1], William Hunter[1], Don Yee[5], Lindsay Rowe[5], Brita Danielson[5], Andrew Plesniarski[6], Ruey-Chyi Su[6], Julian O. Kim[1]. *[1]Radiation Oncology, Cancer Care Manitoba, Winnipeg, MB, Canada,[2]Biology, Cancer Care Manitoba Research Institute, Winnipeg, MB, Canada,[3]Radiation Oncology, University of Alberta, Edmonton, AB, Canada,[4]Radiation Oncology, Tom Baker*

Cancer Center, Calgary, AB, Canada,[5]Radiation Oncology, Cross Cancer Institute, Edmonton, AB, Canada,[6]Medical Microbiology & Infectious Diseases, JC Wilt Infectious Diseases Research Centre, Winnipeg, MB, Canada

Introduction: There is considerable interest in the antineoplastic properties of metformin for prostate cancer treatment, however, the underlying mechanism of action of metformin in this setting is poorly understood. It is suspected that metformin's antineoplastic activity is related to inhibition of mTOR (mammalian target of rapamycin), which ultimately inhibits cell proliferation. In this pilot study, we assessed the mTOR activity of peripheral blood mononuclear cells (PBMCs) from high-risk Prostate cancer (PCa) patients treated with androgen deprivation therapy (ADT) and external beam radiotherapy (EBRT) plus metformin versus placebo. We hypothesized decreased mTOR expression in PBMCs from patients receiving metformin versus placebo.
Methods: Normoglycemic adult males with high-risk PCa receiving ADT & EBRT were randomized to metformin 500 mg 3 times daily or placebo. Peripheral blood samples were collected from participants ≥ 6 months after starting study drug, buffy coats were extracted, and PBMCs were isolated ≤2 hours after specimen collection using ficoll-hypaque density gradient method. The mTOR expression was assessed by phosphorylation of serine 2448 (pmTOR; S2448). Activity of mTOR was measured in both unstimulated or stimulated (using CD3/CD28 antibodies) CD4+ and CD8+ T cells.
Results: Samples from 15 patients were analyzed (11 placebo & 4 metformin). We observed lower expression of pmTOR in PBMCs in patients receiving metformin compared to placebo indicating metformin demonstrated inhibition of mTOR activity in PBMCs. A general trend of mTOR inhibition was observed in the metformin group across the cell population and conditions (unstimulated vs. stimulated T cell populations). However, the most pronounced difference was observed in unstimulated CD4+ cells, which is of interest since they represent the closest physiological state to the study participants.
Conclusion: In this pilot study, we observed mTOR inhibition in the PBMCs of PCa patients treated with metformin. Further assessment of

mTOR activity amongst PCa patients receiving metformin is warranted in order to confirm these findings.

#4859

Bi-steric mTORC1 inhibitors are superior to rapamycin and induce apoptotic cell death in tumor models with hyperactivated mTORC1

Heng Du[1], Yu Chi Yang[2], Heng-Jia Liu[1], Min Yuan[3], John Asara[3], Kwok-Kin Wong[4], Mallika Singh[5], David Kwiatkowski[1]. *[1]Brigham and Women's Hospital, Boston, MA,[2]Revolution Medicines Inc., Redwood, CA,[3]Beth Israel Deaconess Medical Center, Boston, MA,[4]New York University Langone Medical Center, New York, NY,[5]Revolution Medicines Inc, Redwood, CA*

The PI3K-mTOR pathway is one of the most commonly dysregulated pathways in human tumors. Rapalogs have been used extensively in human clinical trials but exhibit modest clinical benefit for the most part, possibly due to their lack of effect on 4E-BP1, a key target downstream of mTORC1. ATP-competitive mTOR inhibitors can fully inhibit mTORC1 but are poorly tolerated possibly due to their inhibition of mTORC2. A new class of selective mTORC1 inhibitors has been developed and termed ‘bi-steric’, which comprise a rapamycin-like core moiety covalently linked to an mTOR active-site inhibitor. We report that bi-steric mTORC1-selective inhibitors (RMC-4627 and RMC-6272) have greater activity than rapalogs for tumors with mTORC1 hyperactivation. RMC-4627 and RMC-6272 showed more effective growth inhibition in multiple tumor cell lines with mTORC1 dysfunction compared to rapamycin. Both RMC-4627 and RMC-6272 at ~1 nM showed near complete inhibition of p4E-BP1$^{T37/46}$, which was not seen with rapamycin treatment. Rapamycin and both bi-steric compounds markedly reduced kidney tumor burden and human bladder cancer PDX tumor size after four weeks of treatment. Tumor regrowth assessed after two-month treatment cessation was significantly reduced in the RMC-6272 group as compared to the rapamycin group. Finally, TUNEL staining showed RMC-6272 treatment led to a greater induction of apoptosis in kidney tumor cells and human bladder cancer PDX tumors relative to rapamycin after a single dose of each compound. This is the first time that clear evidence for cell death after mTORC1 inhibition has been seen. Integrative multi-omic analysis reveals differential global rewiring

induced by RMC-6272 in comparison to rapamycin. Genes involved in cell cycle transition were downregulated by RMC-6272 vs. rapamycin. Proteins downregulated by RMC-6272 treatment relative to rapamycin were enriched for translation and ribosome-related proteins, consistent with effects of non-phosphorylated 4E-BP1 on synthesis of those proteins. Multiple purine metabolites were decreased to a greater extent in RMC-6272 treated cells as compared to rapamycin treatment, including deoxyadenosine, AICAR, AMP, IMP, and GMP. Notably, there was no significant change in R5P, suggesting that downregulation of the purine de novo synthesis pathway was the cause of these changes. Strong tumor cell apoptosis was induced by the suppression of de novo purine synthesis through mTORC1-PRPS1 axis. PRPS1, the rate-limit enzyme involving in purine synthesis was regulated by mTORC1 activity. In summary, RMC-4627 and RMC-6272 demonstrate improved *in vitro* and *in vivo* inhibition of mTORC1 in comparison to rapamycin, and induced more cell death in preclinical models, indicating the potential of bi-steric mTORC1-selective inhibitors as a novel therapeutic strategy to treat tumors with mTORC1 dysregulation.

#4860

PI3K inhibition sensitize cancer cells to tumor treating fields (TTFields)

Anat Klein-Goldberg, Tali Voloshin, Efrat Zemer-Tov, Rom Paz, Lilach Koren, Kerem Wainer-Katsir, Alexandra Volodin, Bella Koltun, Boris Brant, Yiftah Barsheshet, Tal Kan, Cfir David, Tharwat Haj Khalil, Adi Haber, Moshe Giladi, Uri Weinberg, Yoram Palti. *Novocure Ltd, Haifa, Israel*

Introduction: Tumor Treating Fields (TTFields) are electric fields that disrupt cellular processes critical for cancer cell viability and tumor progression, ultimately leading to cell death. TTFields therapy is approved for treatment of adult patients with glioblastoma (GBM) or unresectable pleural mesothelioma. Clinical trials are underway in other solid tumors, including ovarian cancer and non-small cell lung carcinoma (NSCLC). The objective of this study is to identify possible mechanisms involved in reduced sensitivity of cancer cell to TTFields, and explore strategies to circumvent them.

Methods: Ovarian cancer A2780, GBM U-87 MG, and NSCLC H1299 cells with reduced sensitivity to TTFields were generated by continuous long-term application of TTFields. Luminex multiplex assay was employed to examine changes in signaling pathways in these cells, and specific pathway markers were validated by Western blot. *In vivo* validation was performed by immunohistochemistry of ovarian cancer, hepatocellular carcinoma, and NSCLC tumor sections from animals treated with TTFields. Next, TTFields concomitant with alpelisib, an isoform specific PI3K inhibitor, was evaluated both *in vitro* and in an *in-vivo* model of ovarian cancer.
Results: TTFields inflicted a continuous cytotoxic effect on the different cancer cells albeit sensitivity to treatment was reduced following prolonged duration of application. Luminex analysis revealed activation of the PI3K/AKT signaling pathway in treated cells, and kinetics experiments showed that amplitude of AKT signaling increased over time, with significant increases in phosphorylation levels of AKT and focal adhesion kinase (FAK). AKT phosphorylation was also demonstrated in tumor sections of animals treated with TTFields. Experiments performed with concomitant alpelisib sensitized the cells to TTFields and enhanced cytotoxicity *in vitro* and treatment efficacy *in vivo*.
Conclusions: The current study demonstrates that the PI3K/AKT signaling pathway is involved in reduced cancer cell sensitivity to TTFields, and that PI3K inhibition can further sensitize cancer cells to TTFields.

#4861

Copanlisib enhances the effectiveness of anti-PD1 therapies for colorectal cancer

Alexa E. Schmitz, Kennedy J. Maduscha, Sarbjeet Makkar, Cheri A. Pasch, Rebecca A. DeStefanis, Philip B. Emmerich, Dustin A. Deming. *University of Wisconsin - Madison, Madison, WI*

Introduction: Immunotherapies are increasingly being used for patients diagnosed with cancer, however, for metastatic colorectal cancer (CRC), more than 95% of patients have shown little to no clinical benefit to immunotherapy. Previous work from our lab has shown that copanlisib, a PI3K inhibitor, was found to enhance MHC class I expression in *Kras* mutant CT26 murine colon cancer cells. Here we examine the potential for

anti-cancer activity with the combination of copanlisib and anti-PD1 treatments using this model.
Methods: The impact of copanlisib on CT26 cells was performed using the WST assay and the expression of MHC class I was assessed using flow cytometry. CT26 flank allografts were generated in Balb/C mice and subsequently treated for 15 days with copanlisib (10 mg/kg), anti-PD1 (0.2 mg, BioXCell) or the combination. An IgG2a antibody (BioXCell) was used as a control. Tumors were measured twice a week using a caliper. Tumors were excised, and prepared for immunohistochemistry for CD8, CD4, perforin, granzyme B, and F480 was performed. Staining was quantified as the number of positive staining cells per 20X field of view (FOV).
Results: CT26 viability in response to 200 nM copanlisib was relatively unchanged as compared with untreated controls. Via flow cytometry, a 75% increase in mean fluorescent intensity (MFI) for MHC class I was observed comparing control to copanlisib ($p=0.003$). *In vivo,* after 15 days there was no difference in the growth rate of those cancers treated with control versus copanlisib or anti-PD1. A significant reduction in growth rate was observed with the combination of anti-PD1 with copanlisib compared to the other arms (median fold change=3.62; control: 7.49, $p=0.002$, copanlisib: 8.88, $p=0.003$; anti-PD1: 8.93, $p=0.002$). There were no differences in CD8 T cell and perforin expression between the treatment groups. Granzyme B expression was higher in the combination compared (median/FOV= 44) to the control (27, $p= 0.01$). Additionally, a significant reduction in F480 expression was seen in the combination compared to the other treatment groups (median/FOV=43; control: 139, $p<0.001$, copanlisib: 110, $p<0.001$; anti-PD1:149, $p<0.001$).
Conclusions: In conclusion, copanlisib in combination with anti-PD1 demonstrated enhanced anti-tumor activity in Balb/c mice that were injected with CT26 CRC cells. This response was correlated with increased granzyme B expression and a reduction in macrophages with the combination treatment. Further studies will expand on the mechanism of this combination therapy.

#4862
Investigation of the JAK/STAT signaling pathway in chemotherapy and PARP inhibitor resistant ovarian cancer

Esther Rodman[1], Michael Emch[1], Elizabeth Bruinsma[2], Xiaonan Hou[2], Scott Kaufmann[2], Saravut J. Weroha[2], John Hawse[1]. *[1]Biochemistry and Molecular Biology, Mayo Clinic College of Medicine and Science, Rochester, MN,[2]Department of Oncology, Mayo Clinic College of Medicine and Science, Rochester, MN*

Ovarian cancer is the 7th most common cancer in women and the most fatal of all female reproductive cancers, with 5-year overall survival of 10-30%. Despite initial responses to first line platinum- and paclitaxel-based chemotherapies, >70% of ovarian cancers recur with increasingly resistant disease; and nearly all of these women die of their disease. Recently, the use of targeted therapies such as bevacizumab and PARP inhibitors have been shown to improve progression-free survival in a subset of patients. However, these agents have thus far failed to improve overall survival in patients without specific genetic signatures, highlighting the continued need for alternative therapies. Through an unbiased drug screen, we have identified lestaurtinib as a potent inhibitor of many sensitive and resistant ovarian cancer cell lines and patient derived organoid models. Lestaurtinib is a known tyrosine kinase inhibitor originally developed to block FLT3, a protein that is not expressed in any of the ovarian cancer cell lines tested. To elucidate the mechanisms by which lestaurtinib inhibits ovarian cancer cells, we have examined its impact on the phospho-proteome in parallel with RNAseq. Results of these studied have identified inhibition of the JAK/STAT signaling pathway as a top hit. Assessment of STAT1 and STAT3 has revealed that these transcription factors are constitutively activated in chemotherapy- and PARP inhibitor-resistant cell lines as reflected by high levels of Tyr701/705 and Ser727 phosphorylation, suggesting that induction of this pathway may drive resistance. Surprisingly, profound differences in the ability of various JAK/STAT inhibitors to block these specific phosphorylation events is observed, which correlates with their potency. Further, STAT1 and STAT3 ChIPseq experiments following cytokine-mediated activation of this pathway reveal that these transcription factors bind to genomic regions encoding genes involved in oncogenic and drug resistance pathways. Genetic knockdown of STAT1 and STAT3 via siRNA, or knockout via CRISPR/Cas9, results in significant growth inhibition of sensitive and resistant models of ovarian cancer, confirming their importance in maintaining cell viability. Finally,

combining lestuartinib with standard-of-care cisplatin or olaparib (a PARP inhibitor) is shown to be synergistic, indicating that pharmacological inhibition of JAK/STAT signaling has the potential to counteract drug resistance. Ongoing studies are aimed at further understanding the role of JAK/STAT signaling in ovarian cancer, elucidating the mechanistic processes by which STAT1/3 mediate progression of this disease, and identifying the most effective pharmacological strategies to study in possible future clinical trials.

#4863
PMCA inhibition induces cytotoxic calcium stress and suppression of Wnt signaling in refractory molecular subtype of gastric cancer

Saeli Ban[1], Jungmin Kim[2], Jonghwan Bae[1], Ki Cheong Park[3], Suji Lee[4], Moon Hwan Kim[1], Jae-Ho Cheong[5]. *[1]VERAVERSE Co., Ltd., Seoul, Korea, Republic of,[2]Department of Surgery, Yonsei University Health System, Yonsei University College of Medicine, Severance Biomedical Science Institute, Yonsei University College of Medicine, Seoul, Korea, Republic of,[3]Yonsei University College of Medicine, Seoul, Korea, Republic of,[4]Department of Surgery, Yonsei University Health System, Yonsei University College of Medicine, Yonsei University College of Medicine, Seoul, Korea, Republic of,[5]Department of Surgery, Yonsei University Health System, Yonsei University College of Medicine, VERAVERSE Co., Ltd.; Severance Biomedical Science Institute, Yonsei University College of Medicine, Seoul, Korea, Republic of*

Background: Gastric cancer (GC) is the fourth leading cause of cancer-related deaths worldwide, but its genetic heterogeneity retards the development of novel therapeutics. Recently, tumor molecular classification identified clinically refractory SEM (i.e., Stem-like, EMT and Mesenchymal) subtype GC which exhibited over-expression of the plasma membrane Ca2+ ATPase (PMCA) whose role is circumventing calcium overload causing ER stress and apoptosis. Here, we showed that PMCA4 is associated with Wnt signaling activity by regulating Secreted Frizzled-Related Protein 2 (SFRP2) expression and demonstrated that PMCA4 inhibition might achieve dual mechanism-specific anti-cancer effect by inducing calcium-mediated apoptosis and restraining oncogenic Wnt activity in SEM subtype GC.
Materials and Methods: GC cell lines and patient-derived organoids (PDOs) were categorized either SEM-subtype (SNU484, SNU668, SK4, MKN1; GA077T, GA265T, GA333T, GA352T) or non-SEM subtype (MKN45, NCIN87, SNU16, SNU601; GA200T, GA247T, GA215T) based on transcriptome signatures or subtype-specific biomarker genes. PMCA4 expression was confirmed using western blot and its calcium clearance function was examined using Fluo-4 AM fluorescent Ca2+ dye. Biological and molecular characteristics of GC cell lines and PDOs upon PMCA4 inhibition were investigated using RT-qPCR, western blot, and TOPflash/FOPflash reporter assay. The target engagement of novel PMCA inhibitor PM058 (bis-indole maleimide derivative) was evaluated by cellular thermal shift assay (CETSA), and the efficacy was determined by

CCK8 cell viability assay for cell lines and by Cell Titer-Glo for PDOs.Results: PMCA4 was highly expressed in SEM subtype GC cell lines and PDOs. The siRNA-mediated PMCA4 knockdown (KD) or pharmaceutical inhibition of PMCA4 suppressed the calcium clearance, the cell viability, and decreased cell invasion/migration. TCF/LEF-responsive reporter assay revealed that pharmaceutical inhibition of PMCA4 suppressed Wnt/beta-catenin signaling activity, proven by decrease in beta-catenin and Wnt target gene expression. PMCA inhibition was mechanistically associated with the increased expression of SFRP2, a Wnt antagonist. Importantly, PM058, a PMCA inhibitor, treatment resulted in highly efficacious anti-cancer effect in PDOs at nano molar range, which correlated with PMCA4 protein expression.Discussion and Conclusion: Our results provide the proof of concept that PMCA4 can be a promising therapeutic target for refractory subtype cancer. The proposed mechanism of PMCA4 inhibition is calcium overload - induced apoptosis and interfering with Wnt signaling activity via SFRP2 in GC. Importantly, we demonstrated a novel potent inhibitor PM058 that blocks PMCA function in clinically intractable SEM subtype GC cancer.

#4864

ALK inhibitors downregulate the expression of death receptor 4 in ALK-mutant NSCLC cells via facilitating Fra-1 and c-Jun degradation and subsequent AP-1 suppression

Wen Zhao[1], Danlei Yu[1], Yifan Zhai[2], Shi-Yong Sun[1]. *[1]Emory University, Atlanta, GA,[2]Ascentage Pharma (Suzhou) Co., Ltd, Suzhou, China*

The successful treatment of patients with advanced non-small cell lung cancer (NSCLC) harboring chromosomal rearrangements of anaplastic lymphoma kinase (ALK) with ALK tyrosine kinase inhibitors (ALK-TKIs) represents a promising targeted therapy. As a result, various ALK-TKIs have been rapidly developed, some of which were already approved while some are being tested in clinical trials. Death receptor 4 (DR4; also called TNFRSF10A or TRAIL-R1) is a cell surface protein, which is supposed to function as a pro-apoptotic protein that transduces TRAIL death signal to trigger apoptosis. Its expression is positively regulated by MEK/ERK signaling and thus can be downregulated by MEK/ERK inhibition. This study thus focused on determining the effects of AKL inhibition on DR4

expression and the underlying mechanisms. ALK-TKIs such as brigatinib and alectinib effectively and preferentially inhibited AKT/mTOR as well as MEK/ERK signaling and decreased cell survival in ALK-mutant (ALKm) NSCLC cells with induction of apoptosis. This was also true to DR4 downregulation, which occurred even at 2 h post treatment. These ALK-TKIs did not affect DR4 protein stability, rather potently decreased DR4 mRNA expression. In parallel, they promoted degradation and decreased the levels of Fra-1 and c-Jun, two critical components of AP-1, and suppressed AP-1 (Fra-1/c-Jun)-dependent transcription/expression of DR4. Hence, it appears that ALK-TKIs downregulate DR4 expression in ALKm NSCLC cells via facilitating Fra-1 and c-Jun degradation and subsequent AP-1 suppression. Our findings thus warrant further investigation on elucidating the biological significance of DR4 downregulation in ALK-targeted cancer therapy.

#4865

Mechanisms of EGFR inhibitor sensitivity and resistance in chordoma

Nindo Punturi, Lee Dolat, Joan Levy, Josh Sommer, Daniel M. Freed.
Chordoma Foundation, Durham, NC

Target discovery studies have identified EGFR inhibition as a promising therapeutic strategy in chordoma, motivating ongoing clinical trials. Yet EGFR is not mutated in chordoma, leaving the mechanisms associated with EGFR inhibitor (EGFRi) sensitivity and resistance unclear. In this study, we profiled a panel of over 10 chordoma cell lines to categorize their sensitivity to afatinib, a second-generation EGFRi with potency against the wild-type receptor. Several cell lines, including U-CHCF365, UM-Chor1, MUG-Chor1, and U-CH1, were highly sensitive to afatinib in cell viability assays, with absolute IC50 values below 50 nanomolar. In contrast, other chordoma cell lines, including UM-Chor5C and U-CHCF359B, exhibited limited response to EGFRi at concentrations exceeding 1 micromolar. Among sensitive cell lines, we found that afatinib promoted cell death in some cases (e.g., U-CH1) whereas in others it induced a profound cell cycle arrest. Moreover, in U-CH1 cells, acute afatinib treatment enriched a population of drug-tolerant persister cells with a fusiform morphology, potentially indicative of an epithelial-mesenchymal transition. Ongoing studies are focused on understanding the mechanisms of afatinib-induced

cell death, drug tolerance, and acquired resistance, with a view to designing rational combination strategies capable of enhancing the magnitude and duration of therapeutic response. In cell lines with matched xenograft models, in vitro responses to afatinib were consistent in vivo. In a panel of 12 chordoma patient-derived xenograft (PDX) models treated with afatinib or cetuximab, differential sensitivity to EGFRi was recapitulated - with EGFRi promoting complete or negligent tumor growth inhibition in sensitive or resistant models, respectively. Finally, we combined drug sensitivity profiling of chordoma cell lines and PDXs with whole-exome and whole-transcriptome sequencing to identify genomic and transcriptomic features associated with sensitivity and resistance to EGFRi in chordoma. Collectively, our data identify a striking degree of differential sensitivity to EGFRi in chordoma, and begin to shed light on factors associated with primary and acquired resistance. These results provide a framework for guiding patient selection and identifying potential combination therapy regimens to improve EGFRi efficacy and address resistance.

#4866

Pharmacological mechanisms of osimertinib in advanced non-small lung cancer bearing the deletion exon 19 of *EGFR* In an original chicken chorioallantoic membrane (CAM) Model.

David Barthelemy[1], Arnaud Vigneron[2], Xavier Rousset[3], Jerome Guitton[1], Emmanuel Grolleau[1], Margaux Raffin[1], Julie Balandier[1], Gaelle Lescuyer[1], Florence Geiguer[1], Sebastien Couraud[1], Jean Vaillet[3], Nazim Benzerdjeb[1], Lea Payen-Gay[1]. *[1]Centre Hospitalier Lyon Sud - HCL, Pierre Benite, France,[2]Université Claude Bernard Lyon 1, INSERM 1052, CNRS 5286, Centre Léon Bérard, Centre de Recherche en Cancérologie de Lyon, Lyon, France,[3]Inovotion, Grenoble, France*

Introduction: NSCLC accounts for about 80-85% of all lung cancers. Approximately 10-50% of patients with NSCLC harbor EGFR activating mutations, such as in-frame deletions in exon 19 (Ex19del). Currently, for patients with advanced NSCLC, testing for sensitizing mutations in *EGFR* is mandatory prior to the administration of anti-EGFR inhibitors such as Osimertinib. The CAM xenograft offers a rich environment in nutrients and embryonic growth factors, favorable for aggressive tumor development,

with its highly vascularized membrane and natural immunodeficiency at engraftment (at EDD9).
Methods: HCC827 Ex19del cells have been engrafted *in ovo*, and treated with various doses of osimertinib for seven days (4 treatments). The xenografts were collected and immunohistopathological, transcriptional and genetic analyses were carried out. Based on human transcriptional data, supervised multivariate discrimination between conditions and ontology analysis was performed through GSEA.
Results: The xenograft growth was inversely dependent on the exposure dose of osimertinib, with a reduction in tumor weight of 58% for 10 µM (corresponding to 8.3 µg/Kg, $T_{1/2}$ =4hr). The histological analysis showed epithelial tumor cells composed of solid sheets. The quantity of tumor cells was significantly lower in the treated group, with an area of tumor necrosis. The immunohistochemistry of tumor cells confirmed the human pulmonary epithelial origin, with TTF1 positive in treated and control groups. As expected, the ontology analysis of transcriptomic findings highlighted a downregulation of the EGFR pathway and its downstream effectors. Furthermore, the transcriptomic responses associated with chemotaxis, immune cell recruitment, and angiogenesis were dampened in the presence of osimertinib. This suggests that therapeutic efficacy was not uniquely guided through cell-autonomous mechanisms, but also takes place at the tissue level. We confirmed this in an independent experiment of *in ovo* HCC827 engraftment, showing a statically significant reduction of 15% in the number of vessels surrounding the xenograft in the osimertinib-treated condition. This demonstrates the advantage of using the *in ovo* model to decipher the regulations associated with therapeutics in a complex tissue context.
Conclusions: For the first time, we have observed that osimertinib modulates angiogenesis and chemotaxis, which apparently reduces immune system recruitment and immune checkpoint responses. The ontologic analysis of transcriptomic findings in the CAM model strongly support the clinical observations of the pharmacological tumoral response to targeted therapy. The fact that immune infiltration was reduced in osimertinib-treated tumors may partially explain the lower response to immunotherapy regimens in osimertinib resistance contexts.

#4867

Effect of FGFR3 activity on Nectin-4 expression in urothelial carcinoma

Sean Clark-Garvey[1], Mi Zhou[2], Andrew Truong[3], Wolfgang Beckabir[4], Michael Sturdivant[3], William Kim[1]. *[1]Lineberger Comprehensive Cancer Center, Division of Oncology, University of North Carolina at Chapel Hill, Chapel Hill, NC,[2]Lineberger Comprehensive Cancer Center, University of North Carolina at Chapel Hill, Chapel Hill, NC,[3]Lineberger Comprehensive Cancer Center, Department of Pharmacology, University of North Carolina at Chapel Hill, Chapel Hill, NC,[4]Lineberger Comprehensive Cancer Center, Department of Microbiology and Immunology, University of North Carolina at Chapel Hill, Chapel Hill, NC*

Bladder cancer is a common malignancy in the U.S. and cause of significant morbidity and mortality. Combination platinum-based chemotherapy has long been the mainstay in the treatment of metastatic urothelial carcinoma (mUC); however, over the last decade there have been significant advances in systemic therapy, which includes the FDA approval of the pan-FGFR inhibitor erdafitinib (approved for tumors with FGFR2/3 alterations) and the antibody drug conjugate (ADC) enfortumab vedotin (which targets the cell surface protein Nectin-4). Despite these advances, most patients with mUC will progress and succumb from their disease, highlighting the need for further therapeutic development. In parallel to therapeutic advances, there have been significant advances in the molecular characterization of UC, including identification of luminal and basal subsets. *NECTIN4* and *FGFR3* alterations are known to be enriched in luminal subtypes and we have found, via query of the TCGA data, that *NECTIN4* expression was significantly higher in *FGFR3* altered tumors. Given this association we sought to investigate the effect of FGFR3 activity on Nectin-4 expression. Using erdafitinib, in select luminal UC cell lines (RT112, RT4, SW780) with FGFR3 fusion proteins, we found, much to our surprise, that FGFR inhibition increased Nectin-4 expression. Western blots, probing for Nectin-4, following 24H, 48H, and 72H of treatment with erdafitinib (50 nM) showed a significant increase in protein expression in all three cell lines. Importantly, we consistently saw increased expression of what we believe corresponds to the membrane bound form of Nectin-4 and have now confirm such by flow cytometry and immunofluorescence probing for Nectin-4 in the RT112 cell line. We have also seen statistically

significant increases in *NECTIN4* on RT-PCR following treatment with erdafitinib; however, we believe that Nectin-4 regulation by FGFR inhibition is not merely transcriptional because the induction of Nectin-4 protein appears significantly greater than the fold increase in mRNA. Notably, in two additional UC cell lines (HT1376 - a luminal cell line with high Nectin-4 expression & UMUC3 - a basal cell line with low Nectin-4 expression), with no alterations in FGFR3, we did not see a significant change in Nectin-4 expression following treatment with erdafitinib. Based on our above results, we hypothesize that FGFR3 inhibition, in tumors harboring FGFR3 alterations, may act as a sensitize agent to Nectin-4 ADC targeted therapy; however, our results are preliminary and further investigation, particularly with in vivo models, is warranted.

#4868

Targeting of ERG positive prostate cancers with ERGi-USU-6 salt derivative

Binil Eldhose[1], Katherine Beck[2], Cyrus Eghtedari[3], Gartrell C. Bowling[2], Mallesh Pandrala[4], Sanjay V. Malhotra[5], Xiaofeng A. Su[6], Albert Dobi[1].
[1]Department of Surgery, Center for Prostate Disease Research, Murtha Cancer Center Research Program, Uniformed Services University of the Health Sciences, The Henry M Jackson Foundation for the Advancement of Military Medicine, Inc, Bethesda, MD,[2]School of Medicine, Uniformed Services University of the Health Sciences, Bethesda, MD,[3]United states Naval Academy, Annapolis, MD,[4]Department of Cell, Development and Cancer Biology, Oregon Health and Science University, Portland, OR,[5]Department of Cell, Development and Cancer Biology, Oregon Health and Science University, Bethesda, OR,[6]David H. Koch Institute for Integrative Cancer Research, Massachusetts Institute of Technology, Cambridge, MA

Introducti**on:** Prostate cancer (PCa) is the second leading cause of cancer deaths among men in the United States. Approximately 50% of patients with PCa harbor an oncogenic TMPRRS2- ERG gene fusion in their primary tumor and 35% of patients with metastatic castration resistant prostate cancers have the gene fusion. We have identified a potent small molecule inhibitor, ERGi-USU-6 salt derivative 7b, that selectively inhibits

the growth of ERG positive tumor. This small molecule inhibitor is also effective in inhibiting the growth of benign and cancerous mouse prostate organoids expressing TMPRSS2-ERG (ERG positive organoids). To gain insights into the cancer-selective properties of ERGi-USU-6 salt 7b we evaluated pathways associated in ERGi-USU induced inhibition.
Methods: The biological activities of salt derivative 7b, were assessed in hormone- refractory metastatic tumor derived ERG positive prostate cancer cell line, VCaP along with organoids. We monitored the pathways associated in the mechanism of drug action through, cell cycle-regulator proteins by immunoblot assays, cell cycle and ferroptosis related analyses in response to 7b treatment. We also monitored the levels of the RIOK2 kinase,
previously shown to bind the parental ERGi-USU compound. The normal primary endothelium derived HUVEC cells were used as normal control due to the normal endogenous expression of ERG in endothelial cells including HUVEC.
Results: Cell growth and immunoblot analysis indicated the inhibition of ERG positive prostate organoid upon ERGi-USU treatments resulting in the downregulation of ERG and RIOK2 protein levels. The cell cycle analyses, pathway mapping by protein assessment and ferroptotic assays suggests that salt derivative 7b treatment inhibits the ERG positive prostate cancer through ferroptosis along with RIOK2 inhibition.
Conclusions: Our results showed that the ferroptosis inducer ATF3 gene is involved in the cancer-selective activity of ERGi-USU-6 salt derivative 7b. Further, based on our observations we hypothesize that ferroptosis, the iron-dependent form of programmed cell-death, may be the mechanism of cancer selective activity of salt derivative 7b.

#4869

Furin and Notch signaling pathway as part of the 2OHOA landscape against glioblastoma

Raquel Rodríguez-Lorca[1], Roberto Beteta-Göbel[1], Ramón Román[1], Manuel Torres[2], Victoria Llado[3], Pablo V. Escribá[2], Paula Fernández-García[1].
[1]R&D, Laminar Pharmaceuticals SA, Palma, Spain,[2]Laboratory of Molecular and Cellular Biomedicine, University of Balearic Islands, Palma, Spain,[3]Laminar Pharma, Inc., Acton, MA

Glioblastoma (GBM) is the most common and aggressive cancer tumor of the central nervous system, with only 12-15 months of patients' median survival. Melitherapy is a novel therapeutic platform based on the regulation of the membrane's structure and organization with the consequent modulation of certain cell signals. In this context, 2-hydroxioleic acid (2OHOA, LAM561, INN: idroxioleic acid) has been developed for the treatment of GBM and is currently running a phase IIB/III clinical trial for newly diagnosed GBM patients. 2OHOA modulates the lipid composition and structure of cancer cells, increasing membranes fluidity and altering the activity of membrane-associated proteins, inhibiting the proliferation, inducing ER stress and differentiation, and finally triggering cell death by autophagy. The Notch signaling pathway has been highly related to tumorigenesis and cell survival driving the pathogenesis of GBM. In this work, we studied whether 2OHOA modulates the Notch pathway and its relevance in its mechanism of action (MoA) as an antitumoral drug. For this purpose, the 2OHOA's effect on different components of the pathway was studied by western-blot, Q-PCR, and confocal microscopy. In addition, Notch receptor processing and NICD formation (final effector) were analyzed by cell fractionation and Notch processing enzymes activity, like furin, was evaluated upon 2OHOA treatment. First, the inhibition of this pathway in GBM cells by 2OHOA was confirmed by (i) lower expression levels of some of its components (Notch1, Notch3, and Jagged) and target genes (Hes1, CD3), (ii) less nuclear presence of NICD and Hes1 after 2OHOA treatment, (iii) accumulation of full-length Notch receptor in the membranes, impairing its processing and the NICD formation. Second, the relevance of Notch pathway in 2OHOA's MoA was determined by the partial hindering of 2OHOA antiproliferative effect by Hes1 overexpression. Moreover, the reduction of Hes1 expression induced by the drug in different GBM cells

correlated positively with their sensitivity to 2OHOA. Finally, 2OHOA downregulated furin-like proteases activity by physical association, an enzyme responsible for the Notch processing first step. All together reveals that the inhibition of Notch pathway by 2OHOA plays a role in its antitumoral effect, and this event is unleashed by the direct furin enzyme inhibition, identifying it as a novel target for this drug in the GBM and other pathologies treatment.

#4871

Dysregulation of MYC-family proteins sensitizes cancers to NMT inhibition: identification of NMTi sensitivity and mechanism

James Zhang[1], Gregor A. Lueg[1], Monica Faronato[1], Evon Poon[2], Andrii Gorelik[1], Andrea G. Grocin[1], Eva Caamano-Gutierrez[3], Francesco Falciani[4], Roberto Solari[5], Robin Carr[5], Andrew S. Bell[1], Edward Bartlett[1], Jennie Hutton[1], Miriam Llorian-Sopena[6], Probir Chakravarty[6], Bernadette Brzezicha[7], Martin Janz[8], Matther J. Garnett[9], Louis Chesler[2], Dinis P. Calado[6], Edward W. Tate[1]. *[1]Department of Chemistry, Imperial College London, London, United Kingdom,[2]Institute of Cancer Research, Sutton, United Kingdom,[3]Institute of Integrative Biology, University of Liverpool, Liverpool, United Kingdom,[4]University of Liverpool, Liverpool, United Kingdom,[5]Myricx Pharma, London, United Kingdom,[6]Francis Crick Institute, London, United Kingdom,[7]EPO Experimentelle Pharmakologie & Onkologie Berlin-Buch GmbH, Berlin, Germany,[8]Max Delbruck Center for Molecular Medicine and Charite - Universitatmedizin Berlin, Berlin, Germany,[9]Wellcome Sanger Institute, Cambridge, United Kingdom*

N-myristoyltransferases (NMTs) catalyze the protein N-terminal modification *N*-myristoylation, a lipidation event which affects >150 proteins and is involved in protein localization, stability, and function. NMT has been suggested as a target in cancers, but there has been a lack of rationale to identify patients who may respond to NMT inhibition. Additionally, the mechanism of action of NMT inhibitors (NMTi) is difficult to dissect, as NMT substrates feature in multiple biological pathways, and many studies have focused only on a single substrate. Here, a combination of bioinformatic, biochemical, proteomic, and cellular biology techniques have been combined to show that deregulation of MYC-family

proteins sensitizes cells to NMT inhibition. Cell lines sensitive to NMTi were identified through screening of hundreds of cancer cell lines, and the transcriptome of sensitive and insensitive lines compared to obtain a "Sensitive to NMTi" gene set. This gene set correlated well with MYC-related gene sets and mutation, amplification, or chromosomal rearrangement in MYC(N) were predictive for NMTi sensitivity, suggesting that MYC deregulated cancer cells are sensitive to NMTi. This was verified by cytotoxicity assays in B-cell lymphoma and neuroblastoma lines, where highly MYC(N) expressing lines exhibited increased NMTi sensitivity, including in the SHEP21N and P493-6 lines, in which MYC(N) levels can be regulated. Furthermore, proteomic profiling identified multiple pathways which are affected by NMTi, and these were further validated. In particular, an impact on Complex I formation was seen, and mitochondrial dysfunction in high MYC(N) cells upon NMTi was seen through the loss of basal and maximal respiration, ATP production and spare respiratory capacity. Loss of Complex I formation was shown to be caused by the loss of the NMT substrate NDUFAF4 upon NMTi treatment. Furthermore, application of an orally bioavailable NMTi eliminated tumors in mouse models of both diffuse large B-cell lymphoma and neuroblastoma and were well tolerated with no changed in body weight, suggesting that NMT inhibitors are well tolerated and efficacious in vivo.

#4872

DCC-3116, a first-in-class selective ULK1/2 inhibitor of autophagy, in combination with the KIT inhibitor ripretinib induces complete regressions in GIST preclinical models

Madhumita Bogdan, Mary J. Timson, Hikmat Al-Hashimi, Bryan D. Smith, Daniel L. Flynn. *Deciphera Pharmaceuticals, LLC, Lawrence, KS*

Background**:** Cancer cells activate autophagy as an adaptive stress response (ASR) mechanism to therapies targeting the RTK/RAS/MAPK/PI3K pathways, limiting antitumor response. Autophagy is initiated through ULK1/2 kinases and is triggered by inhibitors of the MAPK and PI3K pathways. Most gastrointestinal stromal tumors (GIST) are driven by mutations in KIT kinase. KIT signals through MAPK/PI3K pathways, suppressing ULK1/2 kinases and autophagy[1,2,3]. Inhibition of mutant KIT reverses this suppression, activating autophagy and cancer cell survival.

Approved therapies for GIST include imatinib, sunitinib, regorafenib, ripretinib, and avapritinib. Treatment with these inhibitors is initially successful, but drug resistance can develop either through KIT secondary mutations or ASR pathways including autophagy. DCC-3116 is a selective, potent, first-in-class investigational inhibitor of the ULK1/2 in clinical development in combination with targeted therapies that activate the autophagic ASR pathway. Herein we demonstrate that ULK1/2 and autophagy are activated upon treatment with ripretinib in KIT mutant GIST models. A combination of ripretinib with DCC-3116 inhibits autophagy *in vitro* and leads to complete tumor regressions in preclinical models of GIST.

Methods: Inhibition of ULK1/2 in cell assays was measured using an ELISA for the ULK substrate phospho-ATG13 (pATG13). Autophagic flux was measured by monitoring mCherry/GFP tagged LC3 protein in GIST cells. Xenograft studies were performed at CROs.

Results: Ripretinib treatment led to the activation of ULK1/2 by 2-3-fold in mutant KIT GIST cell lines. DCC-3116 inhibited both ripretinib-induced and basal pATG13 with IC_{50} values of 12-32 nM. Treatment of GIST-T1 cells with ripretinib increased autophagic flux 3-fold. DCC-3116 potently inhibited flux with an IC_{50} value of 38 nM. Ripretinib also induced pATG13 and autophagic flux (1.5-2.5-fold) in multiple imatinib-resistant cell lines, which was inhibited by DCC-3116 with IC_{50} values between 8-189 nM. In a GIST T1 PK/PD model, DCC-3116 inhibited ULK1/2-mediated pATG13. The combination of DCC-3116 with ripretinib resulted in complete tumor regressions in comparison to single agent treatment in GIST preclinical models.

Conclusions: These data demonstrate preclinically that, like other receptor tyrosine kinase inhibitors[1], ripretinib activates ULK1/2-mediated autophagy as an ASR resistance mechanism which is inhibited by DCC-3116, providing the rationale to study the combination of DCC-3116 with ripretinib in GIST patients. DCC-3116 is currently in a Phase 1 clinical trial in patients with advanced solid tumors (NCT04892017).

References: 1. Bogdan *et al.* 2021. *Mol Cancer Ther* 20(12 Suppl):Abstract P084. 2. Gupta *et al.* 2010. *PNAS* 107:14333-83.Li *et al.* 2013. *Lung Cancer* 81:354-61

#4873

Pimavanserin suppresses glioblastoma progression by modulating the Akt/FOXO/Bim signaling axis

Manas Yogendra Agrawal, Sharavan Ramachandran, Carson Zabel, Sanjay K. Srivastava. *Department of Immunotherapeutics and Biotechnology, Texas Tech University Health Sciences Center, Abilene, TX*

Glioblastoma multiforme (GBM) is a highly aggressive grade IV malignant brain tumor with an average survival time of around 15 months; and a 5-year survival rate of 5%. Drug resistance, blood brain barrier (BBB) impermeability, and drug toxicity are some caveats in treating this malignancy. Current chemotherapeutic agents fail to address these challenges. In this study, we aim to repurpose an FDA-approved anti-psychotic agent Pimavanserin Tartrate (PVT), for the treatment of GBM and further delineate its mechanism. To unravel the oncolytic effects of PVT, cytotoxicity assay on several human (SF268, SF188, SF295, U251) and murine (CT2A-Luc) GBM cell lines was performed. Our results demonstrate that PVT inhibited the growth of various GBM cells with IC_{50} ranging 5 to 8 μM, contrary to Temozolomide (TMZ), a standard care therapy which has an IC_{50} ranging 600 to 1,300 μM after 48- and 72-hours of treatment. Moreover, PVT treatment enhanced the activity of TMZ when given in combination. Pro-apoptotic proteins such as cleaved caspase-3 and Bax were upregulated by PVT treatment as evaluated confirming apoptosis to be the mode of cell death. The apoptotic cell population increased in a dose-dependent fashion, for example, 10μM PVT exhibited 70% increase in apoptosis as observed in the annexin assay. PVT treatment suppressed the phosphorylation of PI3K and Akt, and increased the expression of FOXO proteins, which are the negative downstream regulators of Akt. FOXO proteins translocate to the nucleus leading to the enhanced transcription of Bim, a pro-apoptotic protein resulting in apoptosis. Oral administration of 10mg/kg PVT significantly suppressed the growth of intracranially implanted GBM tumors without any other organ toxicity. Our observations provide a robust foundation for PVT's anti-cancer efficacy against GBM by modulating Akt/FOXO/Bim pathway.

#4874

Hyperforin induces apoptosis and inhibits invasion via inhibiting AKT/NF-KB signaling pathway in colorectal cancer cells

Ying-Tzu Chen[1], I-Tsang Chiang[2], Yuan Chang[3], Fei-Ting Hsu[4]. *[1]Chine Medical University, (Individual), Taichung, Taiwan,[2]Medical Administrative Center, Show Chwan Memorial Hospital, Changhua, Taiwan,[3]Department of Medical Imaging, Taipei Medical University-Shuang Ho Hospital, Ministry of Health and Welfare, New Taipei City, Taiwan,[4]Department of Biological Science and Technology, China Medical University, Taichung, Taiwan*

Recently, the incidence of colorectal cancer (CRC) has been increasing year by year and has become the first incidence cancer in Taiwan. Epidermal growth factor receptor inhibitor (EGFR inhibitor) has been recognized as an important target of CRC. Therefore, targeting EGFR and its related signaling could be a potential strategy to overcome this disease. Hyperforin is a natural prenylated phloroglucinol and has been identified as the major molecule responsible for the antidepressant effects. Previous studies indicated that hyperforin has other potentially pharmacologically meaningful biological properties, including antibacterial ability and inhibition of inflammatory mediators. Numerous studies have also pointed out the anti-tumor potential of hyperforin is associated with the induction of apoptosis signaling. However, whether hyperforin may regulate CRC progression and its underlying mechanism is unclear. In our study, we used the MTT assay to prove the cytotoxicity of CRC cells (HT29 and HCT116 cells) was induced by hyperforin. We then used the flow cytometry to confirmed that hyperforin may induce both extrinsic/intrinsic apoptotic pathways in CRC cells. We further demonstrated hyperforin-induced apoptosis pathways is associated with mitochondrial-dependent apoptosis and death receptor dependent apoptosis. Then, transwell invasion, migration, and wound healing assay results proved the inhibition effect by hyperforin in HT29 and HCT116 cells. Additionally, we suggested that hyperforin can effectively inhibit EGFR downstream genes MEK-ERK and AKT signaling, as well as inhibit the phosphorylation of NF-KB and the nuclear translocation in CRC cells. In sum, our results show that hyperforin can inhibit the apoptosis and metastasis ability of CRC cells by inhibiting both AKT/NF- KB and ERK/ NF-KB signaling pathway.

#4875

The anti-tumor effects of GSK-3β inhibitor (9-1NG-41) in ETMR and ATRT pediatric brain tumors

Divya Gandra, Lauren Difabio, Kaitlyn H. Smith, Kimberly Q. McKinney, Giselle S. Sholler. *Atrium Health, Charlotte, NC*

Purpose Embryonal brain tumors (EBTs): ETMR (embryonal tumor with multilayered rosettes) and ATRT (atypical teratoid rhabdoid tumor) are aggressive malignancies with poor prognosis necessitating alternative strategies. GSK-3β is a serine threonine kinase often overexpressed in solid tumors and a positive regulator of NF-κB which promotes tumor growth and chemotherapy resistance. 9-ING-41 is a maleimide-based small molecule that crosses the blood brain barrier and selectively inhibits GSK-3β. Previously we demonstrated that 9-ING-41 decreases ETMR and ATRT cell viability through apoptosis and increases p53 signaling, however the exact mechanism leading to its activation is unknown. This study aims to determine the optimal dosing for 9-ING-41 and describe the phenotypic response of these cell lines to 9-ING-41 using cell viability assay, western blotting and neurosphere assay. This information will help further elucidate the mechanism of action for this drug.

Methods ATRT cell lines ATRT 2141, ATRT-787199, ATRT 803499, LCH-091-07 and the ETMR cell line BT-183 were grown for 24hrs prior to 9-ING-41 treatment in DMEM and Neurocult medium, respectively. Cell viability was assessed after 72hrs of treatment using Cell Titer Glo 2.0. Western blots were analyzed for XIAP, cleaved caspase-3, p53, MDM2 after 24 and 48 hours at 200nM, 400nM and 600nM. Neurosphere assays were done by seeding two cells per well in a 96-well plate followed by treatment with 9-ING-41. Neurosphere frequency and size was monitored weekly for up to 4 weeks using Incucyte® S3 software. Pearson's correlation graph was generated to determine the relationship between GSK-3β expression and sensitivity to 9-ING-41. Graph Pad Prism was used for statistical analysis and level of significance set to p=0.05.

Results The IC50s of 9-ING-41 in cell lines ATRT 2141, ATRT-787199, ATRT 803499 and LCH-091-07 were 194nM, 558nM, 730nM & 5353nM, respectively. We observed decreased expression of NF-κB mediated anti-apoptotic marker XIAP and an increase in expression of apoptotic marker cleaved caspase-3 and tumor suppressor p53 in response to 9-ING-41.

MDM2, a negative regulator of p53 had a significant increase in expression indicating it is not responsible for p53 increase which may suggest ATM pathway could be responsible for regulating p53 increase. GSK-3β expression in vitro, correlated with sensitivity to 9-ING-41. There was a dose dependent decrease in frequency and size of neurospheres in response to 9-ING-41.
Conclusion 9-ING-41 decreases cell viability and neurosphere formation in ETMR and ATRT cell lines within clinically relevant doses. p53 stabilization is not mediated by MDM2 and may be downstream of the ATM pathway. Further studies are underway to demonstrate its efficacy in mouse models.

#4876

A systems pharmacology approach to discover synergistic targeted therapy combinations

Cameron T. Flower[1], Chunmei Liu[2], James R. Heath[2], Wei Wei[2], Forest M. White[1]. *[1]Department of Biological Engineering, Massachusetts Institute of Technology, Cambridge, MA,[2]Institute for Systems Biology, Seattle, WA*

The discovery of oncogenic signal transduction in cancer has enabled the development and clinical use of dozens of kinase-directed targeted therapies, but patient response is often transient and resistance invariably develops. In the setting of BRAF-mutant melanoma, for instance, a majority of patients relapse within one year of initiating targeted therapy. Combination therapies blocking compensatory signaling pathways provide a strategy for boosting treatment efficacy and delaying resistance. To find synergistic kinase inhibitor combinations, we used a multimodal systems pharmacology approach to quantify the early adaptive signaling and gene regulatory dynamics in patient-derived $BRAF^{V600E}$-mutant melanoma cells under oncogene inhibition. Cells were treated with vemurafenib or vehicle and sampled longitudinally at timepoints spanning minutes to days. To measure signaling dynamics, thousands of protein phosphorylation sites covering commonly altered signaling axes in cancer were motif-enriched by immunoprecipitation, barcoded with isobaric tandem mass tags (TMT), and quantified by high-resolution mass spectrometry (MS). The resulting time-resolved phosphoproteomics data showed rapid (<15 minutes) and potent (>8-fold) downregulation of ERK1/2, confirming strong BRAF inhibition.

Statistical integration of signaling measurements with time-series RNA-seq data collected at the same timepoints enabled reconstruction of multi-scale regulatory networks governing the adaptive response to oncogene inhibition. In particular, we observed early induction of SRC-family kinase (SFK) signaling and a broad cytoskeletal signaling module, implicating a compensatory prosurvival signaling program. The induction intensified over the 3-day treatment window and was fully reversed following a 6-day drug holiday, suggesting a reversible nature of drug adaptation. Immunoblotting confirmed sustained loss of ERK1/2 activity and concomitant elevated SFK phosphorylation following drug treatment. Accumulation of reactive oxygen species, a known activator of SFKs, strongly correlated with SFK activity, and both were ablated following treatment with the antioxidant precursor N-acetylcysteine. This adaptive response predicted a significant degree of synergy between vemurafenib and the pan-SFK inhibitor dasatinib, which was validated in a panel of patient-derived melanoma cell lines and in melanoma xenograft mouse models. Targeted MS of phospho-ERK1/2 and canonical SFK substrates, including CTTN, PXN, and PAG1, validated the mechanism of action of this combination. Complementary data from patient-derived non small-cell lung cancer (NSCLC) cells under tyrosine kinase inhibitor treatment demonstrates the generality of our integrative approach, and supports the notion that SFK activation may be a hallmark response to oncogenic RTK-RAS-ERK pathway inhibition.

#4877

Mutant or overexpressed SF3B1 facilitates endometrial cancer tumorigenesis

Pooja Popli[1], Xinchao Deng[2], Premal Thaker[2], Ramakrishna Kommagani[1].
[1]Baylor College of Medicine, Houston, TX,[2]Washington University in St. Louis, St. Louis, MO

Aberrant expression or mutations in core splicing factors including U2AF1, SRSF2, ZRSR2, and SF3B1 found to drive tumorigenesis of various malignant tumors e.g., myelodysplastic syndromes, chronic lymphocytic leukemia, uveal melanoma, and breast cancer. Importantly, the amplifications and mutations in SF3B1, the pioneer splicing factor, are reportedly far more common than those in other splicing factors. However,

the functional relevance and underlying mechanisms of dysregulated SF3B1 in endometrial cancer are not investigated. Endometrial cancer is the fourth most common cancer in women in the United States and there will be about 65,950 new endometrial cancer cases in the current year alone with 12,550 estimated cancer deaths in the United States. In this study, we thus investigated the role of SF3B1 in endometrial adenocarcinoma. We found SF3B1 is one of the most frequently amplified or mutated splicing factors in endometrial cancer. Specifically, analysis of The Cancer Genome Atlas (TCGA) uterine pan-cancer dataset revealed that up to 9% of endometrial cancers have SF3B1 mutations or amplification. Additionally, we showed that the SF3B1 protein is overexpressed in human as well as mouse endometrial tumor samples. Further analysis found elevated SF3B1 protein in multiple endometrial cancer cell lines even in the absence of SF3B1 mutations. However, we did not observe any altered expression at the transcript level. Further, we identified a correlation between the over-expressed SF3B1 levels and the tumorigenicity/invasive potential of cancer cell lines. For instance, endometrial cancer cell lines (Ishikawa, AN3CA, KLE) with over-expressed SF3B1 levels were much more tumorigenic and invasive than those with low endogenous SF3B1 levels (normal human endometrial epithelial cells, RL-95-2 cells). Moreover, cell viability assays revealed that Ishikawa, AN3CA, and KLE cells were more susceptible to the loss of SF3B1 or treatment with the SF3B1 inhibitor Pladienolide-B (PLAD-B) than RL-95-2 cells. To further ensure that overexpressed or mutated SF3B1 drives endometrial tumorigenesis, we transiently transfected an empty vector or a vector expressing FLAG-tagged wild-type SF3B1 or vector with mutated SF3B1 construct R957Q into RL-95-2 cells which have minimal endogenous SF3B1. Analysis of proliferation assays revealed that cells overexpressing SF3B1 proliferated significantly more than cells expressing empty vector. Intriguingly, we observed that RL-95-2 cells over-expressing R957Q mutants were even more proliferative than the cells expressing wild-type SF3B1. Together, this data suggest that SF3B1 over-expression and mutation play a crucial oncogenic role in endometrial cancer, and these findings may support the development of SF3B1 inhibitors to treat this disease.

#4878

Transcriptional response to rocaglate translation inhibitors in lymphoma shows cellular adaptation through induction of stress and survival pathways

Paola Manara[1], Tyler Andrew Cunningham[2], Jr Jyun David Ho[3], Olivia B. Lightfuss[1], Abdessamad Youssfi Alaoui[1], Jonathan Harry Schatz[2].
[1]Medicine, University of Miami, Sylvester Comprehensive Cancer Center, Miami, FL,[2]Medicine, University of Miami, Miller School of Medicine, Miami, FL,[3]Medicine, University of Miami, Sylvester Comprehensive Cancer Center, FL

Background**:** 40% of diffuse large B-cell lymphoma (DLBCL) patients do not achieve cure in response to the standard immunochemotherapy. Relapsed and refractory tumors respond poorly to targeted signaling inhibitors due to pathway redundancies in this genetically heterogenous disease. Pharmacologic disruption of the cap-initiation complex eIF4F is an emerging clinical treatment strategy to bypass resistance. In preclinical experiments, B-lymphomas show high susceptibility to rocaglates, natural and synthetic cap-dependent translation inhibitors. Among these compounds, eFT226 (zotatifin), is currently in phase I/II clinical evaluation for solid tumors. Rocaglate mechanisms remain incompletely defined for use in B-cell lymphoma. Recent findings in our laboratory revealed translationally mediated adaptation that increased synthesis of many targets. Proteins (i.e.CD98hc) that paradoxically increase in production contribute to persistence of cells that survive treatment. By contrast, transcriptional responses to rocaglates remain minimally studied. Here we sought to fill this gap through unbiased transcriptomics.
Method: RNA sequencing (RNA-seq) was performed on zotatifin treated DLBCL cells (SU-DHL10) vs DMSO controls. Genes with a false discovery rate p-value (FDR) ≤0.05, logarithm of counts per million reads (logCPM) ≥ 0 and P value ≤0.05 were considered differentially expressed. Log2 fold change (FC) ≥ +/-2-fold for a specific gene was considered significantly differentially expressed between the two groups. Pathway analysis was performed using Gene Set Enrichment Analysis (GSEA).
Results: We found 4450 differentially expressed genes, 12 significantly upregulated, and 42 significantly downregulated in response to zotatifin (FC ≥ 2). Further pathways analyses showed 4/25 gene sets significantly upregulated, and 3/22 gene sets significantly downregulated (FDR <0.25).

We found significantly upregulated genes related to mechanisms stress and survival pathways including NF-kB induction by TNF signaling (normalized enriched score (NES)=2.28; p-value <0.0001), genes induced in response to hypoxia translational stress responses (NES=1.85; nominal p-value=0.008).
Conclusions: These results implicate induction of specific survival pathways that induce transcriptionally mediated adaptation to the stress of rocaglate therapy, but it is unclear if these responses can result in altered protein production in the context of eIF4A inhibition. Parallel assessment of the translatome currently under analysis will provide a more complete picture of overall adaptation and provide rational combination targets for rocaglates in lymphoma as clinical development progresses.

#4879
Inhibition of amino acid transporters as a novel mechanism of action of the repurposed anti-cancer agent tranexamic acid
Brian K. Law, Mary E. Law, Amanda F. Ghilardi, Elham Yaaghubi, Brad J. Davis, Zaafir M. Dulloo, Mengxiong Wang, Olga A. Guryanova, Coy D. Heldermon, Stephan C. Jahn, Ronald K. Castellano. *University of Florida, Gainesville, FL*

Tranexamic Acid (TA) is an anti-fibrinolytic agent that inhibits Plasminogen activation and is used to control bleeding. Past studies have suggested that the ability of TA to block Plasminogen activation may be useful for ablating the growth or invasion of cancer. Based on the similarity of TA to the amino acid Lysine we hypothesize that TA might exhibit novel mechanisms of action independent of blocking Plasminogen activation. Analysis of a series of signaling pathways indicated that TA inhibits phosphorylation of S6K1 and STAT3 on sites required for their activation and reduces expression of the MYC oncogene in a concentration-dependent manner. Interestingly, MYC transformed MCF10A human mammary epithelial cells exhibited enhanced sensitivity to TA-mediated reduction of cell viability, suggesting that TA may exhibit selectivity for MYC overexpressing breast cancers. Treatment of breast tumor bearing mice with TA strongly blocked tumor growth and was associated with extensive cancer cell death compared with control tumors. Analysis of extracts from TA or vehicle treated tumors showed that TA blocked S6K1

phosphorylation in vivo in a statistically significant manner. Since S6K1 phosphorylation is regulated by amino acid levels, we hypothesized that due to the structural similarity between TA and Lysine and Arginine, TA may block Lysine or Arginine uptake by blocking cationic amino acid transporters (CATs). Molecular docking simulations utilizing the structure of the bacterial CAT predicted that TA binds to CAT with affinity similar to that of Lysine. Amino acid uptake experiments performed with radiolabeled Arginine and Lysine showed that TA blocked both Arginine and Lysine absorption by cancer cells in a concentration-dependent manner. Together, these results indicate a novel mechanism by which TA inhibits uptake of Arginine and Lysine, triggering loss of S6K1 activity in parallel with tumor growth inhibition. Initial studies suggest the feasibility of designing TA analogs with significantly improved potency for amino acid transporters, and with corresponding increases in selective toxicity to breast cancer cells. Based on these novel mechanisms of TA action, we expect TA to exhibit anti-cancer activity against a broad range of human malignancies.

#4880

Anti-membrane IgM monoclonal antibody, WBMP-4, induces apoptosis in B-cell malignancies by modulation of kinase expression and phosphorylation

Rachel S. Welt[1], Jonathan A. Welt[2], Virginia Raymond[3], David Kostyal[4], Sydney Welt[1]. *[1]Welt Bio-Molecular Pharmaceutical, Briarcliff Manor, NY,[2]University of California, Irvine, Irvine, CA,[3]Biogent Consultants, LLC, Armonk, NY,[4]ARDL, Akron, OH*

The concept that the B-cell Receptor Complex (BCRC) initiates the dominant driver pathway in leukemia-lymphoma is clinically validated. However, the BCRC has been overlooked as a therapeutic target due to homology between the BCRC's membrane Ig (mIg) subunit and circulating serum Ig. Previously, we reported the generation of a first-in-class antibody, WBMP-4, to a neo-epitope specific to the mIgM-BCRC, which inhibits cell growth and induces apoptosis (Welt et al. 2016).
Here we evaluate kinase activity in Burkitt lymphoma (CA46) cells treated with WBMP-4 (at 5 and 20 ug/mL, and at 6 and 24 hours) via the Pamgene phosphotyrosine kinase assay. This assay measures kinase activity in cell lysates using a microarray chip containing peptide sequences that serve as

substrate for phophsotyrosine sites on well-characterized signaling proteins. We measure kinase activity at 189 phosphosites using this array, as well as protein expression and phosphorylation of key targets downstream of the BCRC using ELISA, flow cytometry, western blot, and immunohistochemistry, in WBMP-4-treated and untreated IgM-expressing B-cells.

Our Pamgene analysis reveals widespread kinase modulation following WBMP-4 treatment, with >180 of 189 phosphosites showing a significant change in phosphorylation signal intensity (with >153 showing a significant decrease) upon treatment. Western blot analyses of downstream BCRC kinases similarly show changes in phosphorylation at analyzed phosphosites (ZAP70, mTOR, AKT, and MEK) with WBMP-4 treatment. However, we also find changes in protein expression levels of CD79b, ZAP70, BTK, MEK, Myc (all decreased), and LCK (increased) following WBMP-4 treatment.

We show that the kinase activity of proteins in multiple signaling pathways is altered upon WBMP-4 binding to the BCRC's mIgM, with the vast majority exhibiting a downregulation of phosphorylation. We also find that protein expression is impacted in several kinases directly under the control of the BCRC. We hypothesize that WBMP-4's impact on protein expression contributes to BCRC signal disruption and the cytotoxic effect achieved by WBMP-4. For example, WBMP-4 induces a profound reduction in CD79b expression (undetectable by western blot following WBMP-4 treatment), which is consistent with the reduction in CD79a kinase activity found via Pamgene assay. These data support the concept that WBMP-4 binds an epitope on mIgM that is critical to its signal transduction to CD79a/b.Due to WBMP-4's specific targeting of IgM-expressing B-cells, we expect that the toxicities associated with approved therapies upon their interaction with non-lymphatic tissue (e.g. bleeding, infection, cytopenia, arrhythmia, secondary malignancies) will be avoided. With potent anti-tumor activity and expected reduced toxicities, WBMP-4 is a compelling candidate for clinical development.

#4881

Anti-cancer efficacy of a novel phenothiazine derivative is independent of dopamine and serotonin receptor inhibition

Marion Vanneste[1], Anita Venzke[1], Soumitra Guin[2], Damian Krysan[3], Marvin Meyers[2], Michael Henry[1]. *[1]Department of Molecular Physiology and Biophysics, Carver College of Medicine, University of Iowa, Iowa City, IA,[2]Department of Chemistry, St. Louis University, Saint-Louis, MO,[3]Department of Microbiology and Immunology, Carver College of Medicine, University of Iowa, Iowa City, IA*

Introducti**on:** An attractive, yet unrealized, goal in cancer therapy is repurposing psychiatric drugs that can readily penetrate the blood-brain barrier for the treatment of deadly primary brain tumors and brain metastasis. The phenothiazine (PTZ) class of anti-psychotic agents were originally developed to inhibit dopamine- and serotonin-receptors (DR/5-HTRs). PTZs have demonstrated anti-cancer properties in numerous studies through a variety of proposed mechanisms, including on-target (DR/5-HTR) and off-target (e.g. calmodulin (CaM) inhibition) effects. PTZs inhibit DR/5-HTRs in the low- to mid-nanomolar range whereas anti-cancer effects tend to be observed only at a higher (low micromolar) dose range. Thus, clinical efficacy of existing PTZs may be limited by toxicity of on-target effects (sedation) of these drugs as DR/5-HTR antagonists. However, it has been unclear whether anti-cancer effects of PTZs are entirely separate from their activity as DR/5-HTR antagonists. Here we evaluate the *in vitro* anti-cancer efficacy of a novel PTZ analog (CWHM-974, a *N*-benzyl-linked fluphenazine (FLU) derivative), originally developed to treat brain-resident fungal infections, that is a 100-1000-fold less potent DR/5-HTR antagonist than FLU.

Experimental procedures: To evaluate the anti-cancer efficacy of FLU and CWHM-974, we assessed cytotoxicity following 72h exposure against a broad panel of cancer cell lines. To investigate CaM as a target for CWHM-974, we evaluated the correlation between the sensitivity to CMW-974 and sensitivity to the CaM inhibitor W-7 as well as CaM gene expression levels in a panel of cancer cell lines. We also tested the anti-cancer efficacy of a sulfoxide analog of CWHM-974 (SLU-0010894) which lacks CaM binding activity.

Results: We confirmed the anti-cancer efficacy of FLU and demonstrated that CWHM-974 is consistently 2-10-fold more potent than FLU in a broad panel of cancer cell lines. Among the most sensitve cancer cell lines are melanoma, which is a cancer that frequently metastasizes to the brain.

Consistent with the hypothesis that CaM is a relevant target for CWHM-974, we found that: 1) CaM mRNA (CALM1) levels are correlated with sensitivity to CWHM-974 ; 2) the activities of CWHM-974 and W7 are correlated, and 3) most importantly, SLU-0010894 does not exhibit anti-cancer activity.
Conclusions: The anti-cancer efficacy of the PTZ derivative CWHM-974 is seperable from DR/5-HTR antagonism. Our data suggests that further optimization of this compound may preserve the desirable pharmacologic properties for targeting brain cancers while reducing toxicity due to DR/5-HTR antagonism. Moreover, we provide a variety of evidence suggesting that anti-cancer efficacy of CWHM-974 is associated with CaM binding. Ongoing efforts will characterize the activity of CWHM-974 in mouse models of brain metastasis.

#4882
Multi-omics analysis of mechanisms underlying sensitivity of Merkel cell carcinoma to pyrvinium pamoate
Jiawen Yang[1], James T. Lim[2], Paul Victor[3], Rick G. Schnellmann[3], James A. DeCaprio[4], Megha Padi[2]. *[1]University of Arizona Cancer Center, Tucson, AZ,[2]Department of Molecular and Cellular Biology, University of Arizona, Tucson, AZ,[3]Department of Pharmacology and Toxicology, The University of Arizona R. Ken Coit College of Pharmacy, Tucson, AZ,[4]Department of Medical Oncology, Dana-Farber Cancer Institute, Boston, MA*

Background: Merkel Cell Carcinoma (MCC) is a highly aggressive neuroendocrine cutaneous malignancy arising from either Ultraviolet-induced mutagenesis or Merkel cell polyomavirus (MCPyV) integration. Pyrvinium Pamoate (PP), an FDA-approved anthelminthic drug, has been reported to exhibit anti-tumor abilities in multiple cancers. By integrating transcriptomic, network, and molecular analyses, we discovered that PP is broadly effective against Merkel cell carcinoma cell lines, and that PP targets multiple proposed MCC tumorigenesis pathways.
Methods: We performed time-series RNA-seq profiling on a MCPyV inducible cell model and on PP-treated MCC cell lines, and inferred gene regulatory networks associated with PP response. We then integrated the network models with publicly available MCC tumor profiles and the LINCS L1000 database to explore the targets of PP in MCC. In addition,

we performed protein, RNA, growth rate, metabolic, and apoptosis assays on multiple MCC cell lines exposed to PP.
Results: Analyzing the effect of PP in the L1000 cancer cell line panel suggested that PP could inhibit key drivers of MCC tumorigenesis. We therefore tested the anti-proliferation and pro-apoptosis effects of PP in MCC cell lines. PP effectively inhibits proliferation of MCC at concentrations as low as 100 nM and in a dose and time-dependent manner. RNA-seq analysis of PP treated MCC cells suggested that PP triggers the p53-mediated intrinsic apoptotic signaling pathway, impairs the mitochondria's oxidative phosphorylation function and induces endoplasmic reticulum (ER) stress. Immunoblotting intrinsic apoptotic pathway protein markers and measuring the IC_{50} of PP and the MDM2 inhibitor Nutlin-3a in $p53^{WT}$ and $p53^{mut}$ or $p53^{-/-}$ MCC cell lines, we found that PP does not induce cell apoptosis only through p53 activation, but also through other mechanisms such as increasing Unfolded Protein Response (UPR) stress and decreasing expression of the anti-apoptotic protein survivin (BIRC5). Extracellular flux analysis revealed decreased oxidative phosphorylation rate in PP treated MCC cells. Western blot analysis suggests that PP directly inhibits mitochondria complexes genes ATP5A, MTCO1 and NDUF58 and induces UPR-ER stress. PP has also been reported to inhibit the canonical Wnt pathway. We found that WNT5B, the ligand for the non-canonical Wnt pathway, was significantly decreased in MCC tumors and in our MCPyV inducible cell model, and that PP can upregulate WNT5B significantly. MCC cells treated with WNT5B recombinant protein showed a retarded MCC phenotype.
Conclusion: Our results suggest that PP exerts anti-tumor activity through both non-specific growth inhibition - via the modulation of mitochondrial function, ER stress, and apoptotic signaling - and more specifically by perturbing the non-canonical Wnt pathway.

#4883

Pan cancer transcriptomic response to tumor treating fields (TTFields)

Kerem Wainer-Katsir[1], Gitit Lavy-Shahaf[1], Hila Fishman[1], Hila Ena[1], Roni Frechtel-Gerzi[1], Antonia Martinez-Conde[1], Eyal Dor-On[1], Shiri Davidi[1], Sara Jacobovitch[1], Itai Tzchori[1], Yaara Porat[1], Lianghao Ding[2], Michael Story[2], Renfei Du[3], Ulf Kahlert[3], Laura Mannarino[4], Federica Mirimao[5],

Monica Lupi[6], Maurizio D'Incalci[4], Adi Haber[1], Moshe Giladi[1], Uri Weinberg[1], Yoram Palti[1]. *[1]Novocure Ltd, Haifa, Israel,[2]Department of Radiation Oncology, University of Texas Southwestern Medical Center, Dallas, TX,[3]Molecular and Experimental Surgery, University Clinic for General-, Visceral-, Vascular- and Transplantation Surgery, Medical Faculty and University Hospital Magdeburg, Otto-von Guericke University, Magdeburg, Germany,[4]1) Laboratory of Cancer Pharmacology, 2) Department of Biomedical Sciences, IRCCS Humanitas Research Hospital, Rozzano and Humanitas University, Pieve Emanuele, Milan, Italy,[5]Department of Oncology, Istituto di Ricerche Farmacologiche Mario Negri IRCCS, Milan, Italy,[6]Laboratory of Cancer Pharmacology, IRCCS Humanitas Research Hospital, Rozzano, Milan, Italy*

Introduction: Tumor Treating Fields (TTFields) are electric fields that disrupt cellular processes critical for cancer cell viability and tumor progression, ultimately leading to cell death. TTFields therapy is versatile with multiple mechanisms of action, including: anti-mitotic effects, downregulation of DNA double strand break repair, generation of replication stress, upregulation of autophagy, and induction of immunogenic cell death. In this research we were interested in identifying common responses to TTFields across cancer types. We addressed this by integrating whole transcriptome analyses of cancers from various origins.
Methods: Control and TTFields-treated samples examined included gastric, ovarian, pancreatic, non-small cell lung carcinoma, and glioblastoma cell lines, pleural mesothelioma patient-derived cell lines, and a hepatocellular carcinoma animal model. A list of differentially expressed genes (DEGs) was generated from transcriptomics analysis. Gene Set Enrichment Analysis (GSEA) was conducted with the MSigDB, and additional pathway databases. Significantly overlapping pathways were identified using ActivePathways package, and an enrichment map was created according to the number of datasets supporting each pathway.
Results: The response to TTFields showed a positive correlation of expression across different cell lines and indications, including in an animal model. Downregulation was seen in cell cycle related pathways - E2F targets, Myc targets, G2M checkpoint, and mitotic spindle - indicative of cell cycle arrest, which was mediated by increased expression of tumor suppressors. Several DNA repair pathways were downregulated, including

nucleotide excision repair, base excision repair, and the Fanconi Anemia-BRCA pathway. Downregulation was also evident in nuclear envelope, DNA and RNA synthesis, metabolism of amino acids, translation, organelle organization, and splicing. Upregulation was observed in genes associated with the cytoskeleton, adhesion, extracellular proteins and transporters. In the majority of comparisons, an upregulation in the immune response was also observed.
Conclusions: Transcriptomic analysis of datasets from different tumor types revealed common expression patterns and pathways involved in the responses to TTFields. Some of the identified pathways corroborate previously described mechanisms, whereas some reveal new potential mechanisms that require further investigation.

#4884

Targeted investigational oncology agents (IOA) in the NCI60: a phenotypic systems-based resource

Joel Morris[1], Mark W. Kunkel[1], Stephen L. White[1], Donn G. Wishka[2], Omar D. Lopez[2], Lori Bowles[2], Penny Sellers[2], Patricia Ramsey[2], Julie Grams[2], Tiffany Rohrer[2], Karen Martin[2], Thomas Dexheimer[2], Dmitriy Sonkin[1], John D. Williams[2], Jerry M. Collins[1], James H. Doroshow[1], Beverly A. Teicher[1]. *[1]National Cancer Institute, Rockville, MD,[2]National Cancer Institute, Frederick, MD*

The NCI60 human tumor cell line panel is a useful tool in the discovery and development of new anticancer agents. The publicly available cell-line characterization and compound screening data from the NCI60 screen have contributed to identifying cellular mechanisms of potential new anticancer agents. Mean-graph sensitivity/resistance patterns in the NCI60 screen serve as a fingerprint for molecular target identification and mechanism of action (MOA). A new NCI60 resource was developed based on screening of 175 FDA-approved oncology drugs (AOD) plus >825 investigational oncology agents (IOA), representing >250 therapeutic targets and MOAs. Compounds targeting different components in a biochemical pathway tend to show high correlations in their GI_{50} patterns through COMPARE analysis forming clusters with similar NCI60 mean-graph patterns. COMPARE evaluation of compounds that target components in the

PI3K/AKT/mTOR pathway form correlation clusters linked by both target and pathway. Only 3 of 15 AKT inhibitors in the IOA set are not found in the connected cluster with a COMPARE correlation of 0.7 including the multi-kinase inhibitors perifosine and AT-13148. The AKT cluster includes both allosteric (MK-2206) and competitive inhibitors highlighting the NCI60 is a functional cell assay. More than 75% of PI3K inhibitors (32/42 agents), including the selective PI3K alpha and PI3K beta inhibitors, form a highly connected cluster at a 0.7 COMPARE correlation. The heat map view showed that >50% of the non-connected PI3K outliers were inactive in the NCI60 assay. The mTOR inhibitors (12/20) form a connected cluster at 0.7 COMPARE correlation, with half of the non-connected mTOR singletons representative of the rapamycin class of inhibitors. The BRAF/MEK/ERK pathway compounds (37) form a highly connected correlation cluster (13/15 BRAF, 14/15 MEK, 8/9 ERK inhibitors) at a 0.75 COMPARE correlation. The NCI60 heat maps for BRAF inhibitors show a consistent pattern of the melanoma cell lines and 2 of the colon cancer lines (COLO 205, HT29). The ERK inhibitors display sensitivity patterns similar to the BRAF agents with additional activity observed against a leukemia (HL-60), ovarian (OVCAR-5) and renal (A498) cell line and 3 other colon cell lines (HCC-298, HCT-116, SW-620). This data analysis resource will be available to the public (https://ioa.cancer.gov). NCI60 compound suppliers can incorporate their test compound(s) data to use the interactive visualization tools with AOD and IOA agents. This project was funded in part with federal funds from the NCI, NIH, under Contract # 75N91019D00024/75N91020F00003.

#4885

APR-246 cytotoxic effects are TP53 independent in endometrial cancer cell lines

Camilla Yu, Aaron Petty, Roberto Vargas. *Cleveland Clinic, Cleveland, OH*

Background**:** The majority (80%) of endometrial cancer (EC) related mortality is due to high-grade tumor histology, which harbor high rates of TP53 mutations. APR-246 is a small-molecule drug designed to restore WT p53 signaling in TP53-mutant cancers and has yet to be explored in EC. We aimed to test the cytotoxic potential for APR-246 in EC and its downstream impact.

Methods: Using 3 parental EC cell lines with differing TP53 statuses, JHUEM2 (WT), Hec108 (hetero P151H), and Hec1B (R248Q), we generated dose-response curves for APR-246. Cells were treated for 24 hours and viability assessed with CellTiter-Glo after 9 days. To assess for mutation specific effect, we generated dose-response curves using a WT non-targeting control (NTC), CRISPR/Cas9 KO of TP53, and five KO cell lines complemented with 5 common TP53 mutations (R248Q, R248W, R273C, R273H, Y220C). Western blot analysis was performed to assess for p53, p21, PUMA, GADD45, and NOXA using whole-cell lysates, after treatment with 20μM of APR-246 for 24 hours. To further evaluate for a time-dependent effect, 2 representative variants (R248Q and R273C) after 6 and 24 hours of incubation with 50μM APR-246 and 10μM of Nutlin-3.
Results: APR-246 demonstrated a negative, dose-dependent effect on cell viability in all EC cell lines. IC50s for JHUEM2, Hec108, and Hec1B were 2.5μM, 4.3μM, and 4.5μM respectively. For NTC, the IC50 was (1.7μM), while TP53-KO (7.5μM) demonstrated similar IC50 values to the variants (6.5-11.9μM). Two variants (Y220C and R248W), had significantly (<0.001 and <0.01 respectively) higher IC50 values (11.9 and 9.1 μM respectively). In Western blot analysis, no p53 downstream signaling via p21, GADD45, PUMA, and NOXA was observed for any variants.
Conclusions: Our results demonstrate that APR-246's cytotoxic effects in EC seem to be p53-independent. Potential mechanisms for the anti-neoplastic effects of APR-246 include activity targeting antioxidant pathways demonstrated in other solid tumors and provides an area for further investigation in TP53mut EC.

#4886

PARP-1 and γ-GCS inhibitors enhance platinum sensitivity in ovarian cancer

Luxmi Devi[1], Ashok Sharma[2], Lalit Kumar[1]. *[1]Medical Oncology, All India Institute of Medical Sciences (AIIMS), New Delhi, India,[2]Biochemistry, All India Institute of Medical Sciences (AIIMS), New Delhi, India*

Background: Ovarian cancer is the most important cause of gynaecological cancer-related mortality globally. Approximately 80% of patients are diagnosed with advanced stage (FIGO stage III-IV) of ovarian cancer. The standard treatment approach for advanced EOC is primary debulking

surgery followed by adjuvant chemotherapy using taxanes plus platinum. Resistance to platinum based chemo remains a key reason for treatment failure in advanced epithelial ovarian cancer (EOC). Therapeutic efficacy of Poly [ADP-ribose] polymerase 1 (PARP1) and Gamma-glutamyl cysteine Synthetase (γ-GCS)inhibitors in ovarian cancer remains undefined, either as a single agent or in combination with cisplatin.
Material and Methods: We determined the combined effect of PJ34 (PARP1 inhibitor) and BSO (Buthionine-sulfoximine- (γ-GCS inhibitor) with cisplatin in ovarian cancer cell lines (OVSAHO, KURAMOCHI, and IGROV1) by MTT assay. PARP1 and GCS levels were analyzed by western blotting. We employed flow cytometry for cell cycle analysis as well as for apoptosis studies. Analysis was done using Graph Pad Prism-6. Results were considered to be statistically significant when p value was < 0.05.
Results and Conclusion: Combination of cisplatin with PJ34 and BSO augmented cisplatin toxicity in vitro by decreasing cell proliferation and enhancing cell cycle block and cell death when compared with either single agent. A significant cell death ($p= <0.05$) was observed with the combination of cisplatin, BSO and PJ34.
Conclusion: In conclusion, our study provide experimental evidence on the combined effect of PARP-1 and GCS inhibition on CDDP-induced cytotoxicity in epithelial ovarian cancer cells. We propose that PARP-1and BSO inhibitors can be combined with cytotoxic chemotherapeutic agents such as CDDP to enhance the cytotoxicity of chemotherapeutic agents and inhibit key signalling pathways involved in cell proliferation and apoptosis. Future comprehensive studies are needed to demonstrate further validation of above combination.
Keywords: Ovarian Cancer, cisplatin, PARP-1, PJ34, γ -GCS, β-actin, Glutathione.
Abbreviations: Epithelial Ovarian Cancer (EOC), cisplatin (CDDP), Glutathione (GSH), Gamma Glutamyl Cysteine Synthetase (γ-GCS), Poly (ADP ribosyl) polymerase-1 (PARP1), Nucleotide excision repair (NER),homologous repair (HR), Enzyme-linked immunosorbent assay (ELISA), Buthionine Sulfoximine (BSO), Quantitative Polymerase Chain Reaction (qPCR), Peripheral Blood (PB). Propidium Iodide(PI).

Anticancer Approaches: Antibody-Drug Conjugates, Epigenetics, and Tumor Environment

#4890

A novel topoisomerase I inhibitor antibody-drug conjugate targeting CEACAM5 has potent anti-tumor activity in colorectal cancer models

Yves Baudat[1], Haley Neff-LaFord[2], Celine Nicolazzi[1], Dave Meyer[2], Johann Petur Sigurjonsson[2], Ryan Lyski[2], Valeria Fantin[3], Marie-Priscille Brun[1], Marielle Chiron[1], Stephanie Decary[1]. *[1]Sanofi R&D, Vitry-Sur-Seine, France,[2]Seagen, Bothell, WA,[3]Sanofi R&D, Cambridge, MA*

Carcinoembryonic antigen cell adhesion molecule 5, CEACAM5, is a glycosylphosphatidylinositol-anchored glycoprotein highly expressed on the cell surface of several epithelial tumors. CEACAM5 is expressed in virtually all colorectal cancer, ~90% of which to high levels while normal tissue expression is limited. The high prevalence of CEACAM5 expression in colorectal tumor cells prompted us to develop an investigational anti-CEACAM5 antibody-drug conjugate (ADC) for the potential treatment of CRC patients. We developed a novel ADC, by conjugating an anti-CEACAM5 antibody with a drug linker to a topoisomerase I inhibitor payload. The anti-CEACAM5 antibody was chosen based on its high selectivity for CEACAM5 and its potential to direct cytotoxic payloads to tumor. The topoisomerase I payload was optimized for potency, reduced PGP efflux and enhanced bystander activity. The novel anti-CEACAM5 topoisomerase I inhibitor ADC binds to CEACAM5 at nanomolar (nM) concentrations and kills CEACAM5-positive colon tumor cells with varying levels of CEACAM5 at sub-nM concentrations with no or very low cytotoxicity towards CEACAM5-negative cells. Mechanistically, the potent anti-tumor activity of the ADC is both mediated by direct internalization, processing, and release of the cytotoxic payload within the CEACAM5-expressing tumor cells, and by a bystander effect mediated by diffusion of the payload to the neighboring CEACAM5-negative tumor cells. The novel anti-CEACAM5 topoisomerase I inhibitor ADC is well tolerated in rats after repeated administration of 30 and 50 mg/kg/day, Q1W x 4. *In vivo* efficacy of this ADC at 1, 3 and 10 mg/kg (single administration) was evaluated in four CRC patient-derived xenografts (PDXs) models. The conjugate elicits potent and specific and dose dependent antitumor activity with complete regression (CR) at 10 mg/kg in the 4 models. This robust anti-tumor activity was further confirmed in a Single Mouse Trial of 16

CRC PDX models, consisting in the use of one animal per PDX model per treatment arm and for which the evaluation of efficacy was based on the criteria RECIST (Response Evaluation Criteria In Solid Tumors) used in clinic. In these criteria, the overall response rate includes complete response (CR) and partial response (PR) and the a disease control rate includes CR , PR and stable disease (SD). The ADC induces a disease control rate of 95% and an overall response rate of 50% following a single dose of 10 mg/kg. The outstanding anti-tumor activity across CRC PDX models and its favorable safety profile in rats support further evaluation of this investigational novel topoisomerase I ADC in CRC patients.

#4891

Ifinatamab deruxtecan (I-DXd), a novel B7-H3-targeting antibody-drug conjugate, demonstrates efficient payload delivery into tumor through target-dependent internalization

Len Katsumata[1], Tsuneo Deguchi[1], Jun Hasegawa[1], Michiko Yamato[1], Yumi Nishiya[1], Akiko Watanabe[1], Tomoyo Honda[1], Megumi Minami[2], Naomi Kasanuki[2], Takanori Maejima[1], Sumie Muramatsu[1], Monika Herrmann[3], Nina Schulte[3], Gernot Polier[3], Xuya Wang[4], Takanori Yoshida[2], Nanae Izumi[4], Xiaozhong Qian[4], Toshinori Agatsuma[1], Kenji Nakamaru[1].
[1]Daiichi Sankyo Co., Ltd., Tokyo, Japan,[2]Daiichi Sankyo RD Novare Co., Ltd., Tokyo, Japan,[3]Daiichi Sankyo Europe GmbH, Munich, Germany,[4]Daiichi Sankyo Inc., Basking Ridge, NJ

Ifinatamab deruxtecan (I-DXd; DS-7300) is a novel ADC which consists of an anti-B7-H3 antibody linked with a DNA topoisomerase I inhibiting anti-tumor agent, DXd. I-DXd has demonstrated potent anti-tumor activity in B7-H3-positive preclinical cancer models and showed early signs of promising clinical efficacy in patients with heavily pretreated, advanced solid tumors. ADCs are postulated to exert cytotoxicity specifically in tumors that express the target antigen via target-specific uptake of the compound. Accordingly, effective action of an ADC depends on multiple dynamic steps including antigen-specific binding, internalization, trafficking to lysosomes, linker cleavage and payload release, as well as payload potency. The goal of this research was to characterize I-DXd molecular dynamics in preclinical tumor cell models by investigating the

relationship among target expression and dynamics, its translocation to lysosomes, lysosomal enzyme-mediated linker cleavage, and payload release after I-DXd treatment. As a result, I-DXd demonstrated target dependent internalization, efficient trafficking to lysosomes, and subsequent payload release in the studied tumor cell lines. Payload release levels generally correlated with target expression in vitro using a panel of cell lines with varying levels of B7-H3 expression. Also, in cell-line derived xenograft models, tumor tissue payload concentration corresponded to I-DXd binding at the cell membrane. These results suggest the importance of cell surface B7-H3 expression and ADC dynamics that lead to payload release in target expressing tumors to exert anti-tumor activity in non-clinical model. In addition to target-dependent uptake in tumor cells, it was observed in viable human lung tumor slices that B7-H3 was also expressed in several non-tumor cells including cancer-associated fibroblasts, endothelial cells, and macrophages in the tumor microenvironment and I-DXd was shown to be internalized in these B7-H3-expressing non-tumor cells. In summary, this pre-clinical study characterizes the relationship between B7-H3 expression in the tumor microenvironment and I-DXd molecular dynamics. Our results support developing I-DXd as a targeted therapy against advanced solid tumors known to overexpress B7-H3.

#4892

MMAE drives immunomodulatory changes in a preclinical xenograft model that are distinct from other clinical-stage ADC payloads

Michelle Ulrich, Kerry Klussman, John J. Gosink, Sean Allred, Kelly Hensley, Piper M. Treuting, Nikhil J. Parekh, Elizabeth E. Gray, Shyra J. Gardai. *Seagen, Bothell, WA*

Monomethyl auristatin E (MMAE), the payload delivered by vedotin ADCs, exerts its cytotoxic effects via microtubule disruption and induction of ER stress, leading to apoptosis and tumor cell death. In addition, MMAE also has the ability to induce immunogenic cell death (ICD) and immune modulation in the tumor microenvironment (TME) (Liu, 2020; Gray, 2020). Other clinical-stage and approved ADCs incorporate payloads that also cause microtubule disruption (DM1, DM4), or that drive DNA damage through topoisomerase I inhibition (exatecan) as the primary mechanism of action (MOA). While ADCs with different linker payloads produce clinical

benefit, their long-term impact on survival and how they pair with PD(L)1 agents may differ based on their ability to elicit immune modulation. In this study we have investigated how these payloads compare to MMAE in their ability to drive immune changes in the TME and describe how these changes could support anti-tumor immunity and improve outcomes in the clinic.Building upon an initial in vitro assessment in which we observed superior induction of ICD markers and underlying ER stress with an MMAE ADC, we utilized a B7H4-expressing MDA-MB-468 xenograft model of triple-negative breast cancer to further characterize the ICD properties of ADC payloads. Tumor-bearing mice were treated with a single dose of B7H4-targeted antibody conjugated to either MMAE, DM1, DM4 or exatecan. Tumors were harvested seven days after treatment and processed for immunohistochemistry (IHC) to assess changes in immune cell infiltration and analyzed by RNA-seq to determine alterations in gene expression. Payload-driven anti-tumor activity was observed with all ADC treatments, each leading to a similar reduction in tumor volume compared to vehicle or unconjugated antibody. IHC staining of tumor sections for F4/80, a mouse macrophage marker, revealed that of the microtubule-disrupting agents, only MMAE significantly increased F4/80+ macrophage infiltration in both the tumor nests and stroma. Increased F4/80+ macrophages in tumor nests and stroma was also observed as a result of B7H4-exatecan ADC treatment. RNA-seq analysis revealed a unique profile for the MMAE conjugate, with an increase in human transcripts encoding cytokine and type I interferon response genes. In summary, the anti-tumor activity of the B7H4-MMAE ADC resulted in recruitment of mouse innate immune cells to the xenograft tumors. Importantly, immune response genes related to ICD were increased following B7H4-MMAE treatment compared to DM1, DM4, and exatecan conjugates. Together, these data suggest that treatment with vedotin ADCs results in robust immunomodulatory changes in vivo that are distinct from other clinical ADC payloads.

#4893

Evaluation of bystander antitumor effect of Dato-DXd in TROP2 (+) and TROP2 (-) lung cell lines admixed tumor xenograft mouse models

Satoru Yasuda[1], Takanori Maejima[1], Tadashi Toki[1], Tsuyoshi Karibe[1], Daisuke Okajima[1], Penny Phillips[2]. *[1]Daiichi Sankyo Co., Ltd., Tokyo,*

Japan,[2]Daiichi Sankyo, Inc., Basking Ridge, NJ

Background: Datopotamab deruxtecan (Dato-DXd) is an antibody-drug conjugate (ADC) consisting of a humanized anti-TROP2 IgG1 monoclonal antibody covalently linked to a highly potent topoisomerase I inhibitor payload (DXd) via a stable, tumor-selective, tetrapeptide-based cleavable linker (Nakada T. et al. Bioorg Med Chem Lett., 2016). Dato-DXd demonstrated encouraging efficacy in clinical studies in TROP2 expressing tumors, including NSCLC and TNBC (NCT03401385). Clinical efficacy of Dato-DXd in heterogeneous tumors is hypothesized to be derived not only via effective selective delivery of DXd to TROP2 (+) tumor cells but also DXd diffusion from TROP2 (+) tumor cells to nearby TROP2 (-) tumor cells due to high membrane permeability of the DXd payload, an effect called the bystander antitumor effect. In this preclinical study, the bystander antitumor effect was tested by establishing tumor xenograft mouse models containing admixed TROP2 (+) and TROP2 (-) lung cell lines. The antitumor activity of Dato-DXd was tested in these models to demonstrate the bystander antitumor effect of Dato-DXd.
Materials and Methods: EBC-1 cells and NCI-H526 cells or Calu-6 cells were used as models of TROP2 (+) cells and TROP2 (-) cells, respectively. TROP2 (+) cells and TROP2 (-) cells were mixed in various ratios and inoculated subcutaneously in mice to establish heterogeneous xenograft tumor models with various levels of TROP2 expression. Tumor growth inhibition in each model was evaluated by tumor volume after Dato-DXd or control-ADC administration. Immunohistochemistry (IHC) of DXd and TROP2 were performed in Dato-DXd treated tumors to analyze distribution in TROP2 (+) and (-) tumor cells. Tumor cells that responded to Dato-DXd treatment were identified by IHC assay of γH2AX (an indicator of DNA damage).
Results: TROP2 expression analysis showed that various TROP2 positivity tumor models were established by inoculating various ratios of admixed EBC-1 cells with NCI-H526 cells or Calu-6 cells. Dato-DXd did not inhibit growth of tumors consisting of only TROP2 (-) cells, as expected. In contrast, Dato-DXd showed strong tumor growth inhibition effect on all tumors in which TROP2 (+) cells were inoculated in various levels with TROP2 (-) cells. DXd-IHC analysis showed that Dato-DXd distributed to only TROP2 (+) tumor cells in admixed tumors, however, an increase of

γH2AX was observed not only in TROP2 (+) tumor cells but also TROP2 (-) tumor cells, suggesting TROP2 (-) tumor cells responded to DXd generated and distributed from Dato-DXd bound to TROP2 (+) tumor cells. Conclusion: Dato-DXd is effective not only in TROP2 (+) tumor cells but also TROP2 (-) tumor cells adjacent to TROP2 (+) tumor cells, thereby demonstrating the bystander antitumor effect of Dato-DXd. This property suggests Dato-DXd should be active in the clinical setting even given potential heterogeneity of TROP2 expression.

#4894

The anti-ROR1 ADC STRO-003 demonstrates immune-modulating properties that may enhance checkpoint blockade

Alice Yam, Helena Kiefel, Andrew McGeehan, Robert Yuan, Sihong Zhou, Dayson Moreira, Indrani Dutta, Xiaofan Li, Cuong Tran, Gang Yin, Kristin Bedard, Trevor Hallam. *Sutro Biopharma, Inc., South San Francisco, CA*

There is growing evidence that tumor-targeted cytotoxins can also enhance anti-tumor immunity by inducing immunogenic cell death (ICD) in tumor cells and promoting recruitment of immune effector cells. We sought to investigate the immune stimulating potential of STRO-003, an antibody drug conjugate (ADC) composed of an anti-Receptor Orphan Receptor Kinase 1 (ROR1) antibody conjugated to a topoisomerase I targeted exatecan warhead via a cleavable linker. ROR1 is an oncofetal transmembrane receptor with restricted expression in normal tissues. Its overexpression in several cancer indications has been described, including in ovarian, non-small cell lung carcinoma (NSCLC), triple negative breast cancer (TNBC), and hematological malignancies, thus making it an ideal ADC target. We have previously demonstrated potent in vivo activity of STRO-003 in a panel of ROR1-expressing lung cancer patient-derived xenograft (PDX) models. Here we show that the exatecan warhead, SC3386, and STRO-003 ADC induced ICD in vitro as evidenced by presentation of cell-surface calreticulin and release of HMGB1. Consistent with this finding, STRO-003-treated cells elicited monocyte activation in a PBMC co-culture assay. To determine if these immunogenic properties could improve therapeutic efficacy, we evaluated STRO-003 in combination with an immune checkpoint inhibitor in a mouse syngeneic model expressing ROR1. We have demonstrated that STRO-003 in

combination with checkpoint inhibition significantly enhances efficacy in a syngeneic mouse model and supports durable anti-tumor immunity. Follow-up vaccination studies were performed to further explore the significance of STRO-003-induced ICD and protective immunity *in vivo*. These results demonstrate that tumor cells pre-treated with STRO-003 or SC3386 undergo potent immunogenic cell damage which can, in turn, mount protective immunity *in vivo*.

#4895

Introduction of a platform for preclinical profiling of drug conjugates: a case study with sacituzumab govitecan

Vincent Vuaroqueaux[1], Nadine Obier[2], Anne-Lise Peille[1], Daniel Feger[2], Katharina Schaich[2], Thomas Metz[1], Sebastian Dempe[2], Heinz-Herbert Fiebig[1], Jan Erik Ehlert[2]. *[1]4HF Biotec GmbH, Freiburg, Germany,[2]Reaction Biology Europe GmbH, Freiburg, Germany*

Drug-conjugates are an emerging class of anticancer agents combining the cytotoxic activity of highly potent chemotherapeutic agents with the target specificity of an antibody, a small molecule or a peptide ligand directed against a cancer-associated protein. With nearly half a century of development, profound advancements have been made in the development of these therapeutics. The most advanced are antibody-drug conjugates (ADCs) with currently >100 in development and 11 approved by the FDA. To facilitate preclinical evaluation of novel drug conjugates, Reaction Biology and 4HF Biotec have developed a dedicated platform allowing specific *in vitro* and *in silico* analyses for this class of therapeutics. The platform is intended to provide information on the potency of the drug conjugate over the corresponding stand-alone cytotoxin, the cancer entities to be treated, the target engagement and the determinant(s) of cancer cell sensitivity. Here, we present our platform to refine antitumor potential of Sacituzumab govitecan (ScG), a recently approved TROP-2 targeted ADC used for the treatment of triple-negative breast cancer. First, we used the ProLiFiler™ (Reaction Biology), a cell proliferation and survival assay with 140 human cancer cell lines, to establish the antitumor profile of ScG, its payload SN-38 and three other cytotoxins (camptothecin, MMAE and mertansine) to validate the results of our assay. The IC50 obtained for the cytotoxins were next validated using the MoAFinder (4HF Biotec), a tool

derived from the NIH COMPARE algorithm that ranks drugs based on the similarity of their growth inhibitory profiles. The analysis confirmed that SN-38 and camptothecin antitumor profiles, as established with the ProLiFiler, correlated best with other topoisomerase-1 inhibitors from our database of more than 1,000 compounds. Mertansine and MMAE correlated best with tubulin inhibitors and were more potent than camptothecin and SN-38. Overall, the response to these cytotoxins was stronger in cell lines from hyperproliferative cancers such as hematological malignancies than in those from solid cancers. Next, by using OMICS data (internal and publicly available), qPCR and flow cytometry connected to drug sensitivity profiles, we will present a differential biomarker screen of ScG vs. SN-38 to identify molecular determinants of sensitivity toward the ADC and its cytotoxin. We will address the expression level of TROP2 and its predictivity for tumor cell sensitivity, screen for predictors of SN-38 response and investigate possible off-target effects in cell lines sensitive to ScG but lacking TROP2 expression. Overall, the study demonstrates the potential of our platform to investigate drug conjugates. The comparative profiling of ScG and its payload allows to identify candidate cancer entities for ScG treatment and to improve patient enrollment into clinical trials using biomarkers.

#4896

NF1 (neurofibromatosis 1) controls microtubule dynamics and dictates sensitivity to maytansinoids

Bruno A. Duso, Eleonora Messuti, Emanuele Bonetti, Giulia Tini, Alessia Castiglioni, Giuseppe Ciossani, Silvia Monzani, Chiara Soriani, Simona Rodighiero, Luigi Scietti, Costantino Jemos, Luca Mazzarella. *IEO - European Institute of Oncology, Milan, Italy*

The tumor suppressor NF1 is classically considered a negative RAS regulator, but sparse evidence suggests additional RAS-independent roles. Early studies suggested an interaction with tubulin, which remains poorly characterized to date but may be of particular therapeutic interest as NF1 is somatically mutated across multiple tumor types. We showed that multiple CRISPR-Cas9-engineeerd NF1 KO HER2+ breast cancer cells (BT-474, SK-BR3, HCC1954) become exquisitely sensitive to the Antibody-Drug Conjugate (ADC) Trastuzumab emtansine (T-DM1); we here investigate the underlying mechanism.TDM1 hypersensitivy was specific to the maytansin

microtubule-targeting payload, since it was i) replicated by the naked payload but not the naked antibody; ii) absent with other ADCs (T-DxD); iii) not accompanied by increased TDM1 uptake; iv) associated with increased tubulin-maytansin binding in KO cells, as per Cellular Thermal Shift Assay. The mechanism is likely RAS-independent, as KRAS G12V-overexpression did not alter TDM1 sensitivity. RNAseq revealed that KO cells deregulated genes associated with microtubular dynamics and G2-M transition more strongly upon TDM1-treatement. Multiple KO cells investigated by static and live imaging exhibited marked signs of altered mitosis, with longer G2/M, supernumerary centrosomes, chromosome misalignment and frequent aneuploidy, which could also be inferred in multiple public sequencing datasets (TCGA, MSK IMPACT, AACR GENIE). Based on this, we explored NF1 role on microtubule dynamics. We found several lines of evidence for a direct and mitosis-selective interaction between NF1 and tubulin: i) in Immunofluorescence (IF), NF1 was upregulated in mitosis and colocalized with the mitotic spindle; ii) NF1 co-Immunoprecipitated with tubulin in mitosis-enriched but not asynchronous cells; iii) purified NF1 co-eluted with tubulin in size-selection chromatography; iv) in silico modeling with AlphaFold2 predicted an interaction between NF1 central domains and the alpha-beta tubulin dimer. Crucially, KO cells exhibited severe microtubule hypodynamism in cold-induced depolymerization-repolymerization assays, replicated in multiple cell types and accompanied by imbalanced levels of plus/minus-end microtubule-associated proteins. By IF on cocultured WT/KO live cells, KO cells showed significantly higher GTP-tubulin, known to cause microtubular hyperstability, suggesting the intriguing possibility that NF1 may directly regulate tubulin intrinsic GTP-hydrolyzing activity, similar to its role on RAS. In conclusion, we provide extensive mechanistic evidence for a direct and previously underappreciated role of NF1 in microtubular dynamics, which reshapes our understanding of its tumor-suppressive activity and provides a rationale for pharmacological targeting of NF1-mutated tumors.

#4897

PRT543, a methyl transferase inhibitor, has potent anti-tumor activity against adenoid cystic carcinoma of salivary glands

Vasudha Mishra[1], Alka Singh[1], Xiangying Chen[1], Michael Korzinkin[2], Claudia Wing[1], Viktoria Sarkisova[2], Alexandra Ozerova[2], Oksana Glushchenko[2], Venkat Thodima[3], Koichi Ito[3], Peggy Scherle[3], Mark Lingen[4], Rifat Hasina[5], Alexander Pearson[1], Ari Rosenberg[1], Alex Zhavoronkov[2], Bruce Ruggeri[3], Nishant Agrawal[5], Evgeny Izumchenko[1].
[1]Medicine, Section of Hematology and Oncology, University of Chicago, Chicago, IL,[2]Insilico Medicine, Hong Kong, China,[3]Prelude Therapeutics, Wilmington, DE,[4]Pathology, University of Chicago, Chicago, IL,[5]Surgery, Section of Otolaryngology-Head and Neck Surgery, University of Chicago, Chicago, IL

Adenoid Cystic Carcinoma (ACC) is a rare but aggressive malignancy of salivary gland, associated with protracted clinical course and fatal outcome. Treatment modalities are restricted to surgery and/or adjuvant radiotherapy and patients develop recurrence and distant metastasis over time. The absence of effective systematic therapy makes it incurable in advanced stage. ACC display an overall low mutation frequency, therefore very few actionable genetic alterations critical to the ACC development have been recognized. *MYB* fusion/overexpression is the most frequently found genetic alteration in ACC and is present in ~70% patients. This is followed by activating *NOTCH* mutations, reported in ~20% patients. Despite the presence of few targetable genetic alterations, recent studies revealed substantial transcriptomic heterogeneity amongst ACC tumors suggesting the role of epigenetic alterations in ACC oncogenesis. Symmetric dimethylation is an important epigenetic mechanism that regulates mRNA splicing, transcription, translation, cell cycle and oncogenic signaling pathways. Protein Arginine Methyl Transferase 5 (PRMT5) is a predominant enzyme for symmetric dimethylation among a family of 9 methyl transferases. In was suggested that PRMT5 plays a role in regulating tumor progression via modulation of MYC signaling, cancer stemness, and a wide array of additional cellular and transcriptional pro-oncogenic processes. While inhibition of PRMTs showed anti-oncogenic response in several preclinical tumor models and a subset of patients with advanced solid malignancies (including ACC), preclinical studies investigating the effect of PRMT5 blockade in ACC remain inadequate. In part, due to the scarcity of ACC specimens and limited availability of the experimental

models. PRT543 is a selective and potent small molecule PRMT5 inhibitor that specifically targets PRMT5 among 37 methyl transferases. In the present study, we have investigated the effect this novel agent using a unique collection of ACC cell lines, organoids, and patient derived xenograft mouse models. To our knowledge, this is the first study investigating the therapeutic effect of PRT543 in several preclinical models of ACC. Specifically, we found that PRT543 has potent antitumor activity in in-vitro and in-vivo models with MYB expression and activating NOTCH mutations. Further, based on these observations, we have sequenced a collection of 50 ACC tumor samples to identify the subset of patients who may potentially benefit from PRT543 treatment based on their underlying genetic signatures. This study provides evidence underscoring the role of PRMT5 signaling in ACC and supports the clinical development of PRMT5 inhibitors for this indication.

#4898

Imipridones and EZH2 inhibitors induce similar changes in cytokines and regulated genes in GBM and DMG while vorinostat potentiates anti-tumor efficacy despite variability in cytokine profiles

Yiqun Zhang, Kelsey Huntington, Wafik S. El-Deiry. *Legorreta Cancer Center, Brown University, Providence, RI*

TIC10/ONC201 and ONC206 are small molecule imipridones with anti-cancer activity. ONC201, EZH2i and HDACi can modulate tumor microenvironment (TME) and antitumor immunity. We studied the impact of these drugs or their combinations on the TME or tumor immunity by investigating cytokine profiles. We treated U251 GBM and HCT116 CRC cells with vorinostat and found upregulation of CXCL11, CXCL14, INF-γ and TRAIL, and downregulation of prolactin, CXCL9, VEGF and CCL2 in U251. CXCL11 promotes anti-tumor immunity by increasing activated CD8+ T cells in tumors but was associated with metastasis of GBM. CXCL13 induces tertiary lymphoid structures and enhances infiltration of CD8+ T cells in tumors. INF-γ enhances antigen presentation and promotes activation of NK cells. Vorinostat upregulated the secretion of pro-immune cytokines and TRAIL which induces tumor apoptosis. Downregulated cytokines in U251 were prolactin, CXCL9 involved in tumor growth and metastasis, VEGF, and CCL2 involved in immunosuppression in GBM.

Cytokines upregulated in HCT116 included IL-8 contributing to CRC progression, and CXCL13, and CXCL11 which correlates with anti-tumor immunity in colon cancer. Downregulated cytokines in HCT116 were soluble TRAIL R2 functioning as a decoy receptor for TRAIL, VEGF, and prolactin. We treated DMG, GBM and HCC cells with imipridones, EHZ2i tazemetostat or HDACi panobinostat alone or combination of imipridones plus tazemetostat or panobinostat or the triple combination of imipridone plus tazemetostat and panobinostat. We observed that cytokines impairing immunity were downregulated and cytokines promoting immunity were upregulated by individual drugs or combinations. Hep3B HCC cells showed the most robust changes among the mentioned tumors with respect to the changes of cytokine profile following the treatments. Imipridone or EZH2i treated cells showed similar cytokine profile changes in tumor cells. Imipridones downregulated EZH1 and EZH2 proteins in tumor cells. We RNA-seq to investigate gene expression profiles following treatment with ONC201 or tazemetostat. In GBM and DMG, ONC201 and tazemetostat shared similar top regulated genes. GO enrichment analysis showed overlap of top regulated pathways between ONC201 and EZH2i treated cells. Shared regulated pathways in U251 included cell cycle arrest, cell adhesion, nervous system development, cell proliferation, negative regulation of proliferation, PERK-mediated unfolded protein response, extracellular matrix organization, regulation of transcription from RNA polymerase II promoter, and cellular response to hypoxia pathways. We conclude that imipridones ONC201, ONC206, and ONC212 which reduce EZH1 and EZH2 proteins share similar cytokine alterations, gene expression targets and actions with EZH2 inhibitors.

#4899

Inhibition of murine tumor growth by decitabine is correlated with enhanced expression of the mouse mammary tumor virus

Jieyu Zhang[1], Savannah Higgins[1], Riley Smith[1], Tania Reginald[1], Andrew Qi[2], Jiayi Li[1], Anna King[1], Yingguang Liu[1]. *[1]Liberty University, Lynchburg, VA,[2]Case Western Reserve University, Cleveland, OH*

The purpose of this study is to clarify the mechanisms of the antineoplastic effect of decitabine (DAC), a DNA methyltransferase inhibitor. We previously reported that DAC inhibited the proliferation of the 4T1

mammary cancer cell line *in vitro* while inhibiting MMTV *env* and *pol* expression in the same cells. Here we present findings *in vivo* using two murine tumor models. We inoculated 4T1 cells into BALB/c mice from which the cell line was derived. In addition, we inoculated the murine colon carcinoma cell line, MC38, into C57BL/6 mice, the mouse strain of its origin. We treated the mice with DAC when tumors became palpable. DAC inhibited tumor growth in both tumor models and inhibited metastasis of 4T1 cells into the lungs. Quantitative PCR detected elevated expression of MMTV genes in the tumor tissues of DAC-treated mice in both models. The levels of MMTV *env* RNA in tumor tissues were negatively correlated with tumor mass in both models, so were the levels of the MMTV Env protein in 4T1 tumors. DAC also significantly mitigated tumor-induced splenomegaly. Hepatotoxicity of DAC was observed in C57BL/6 mice. Our data suggest the possibility that decitabine inhibits tumor growth *in vivo* and *in vitro* via different mechanisms. The findings also support the current understanding of decitabine upregulating endogenous retroviruses (ERVs) which subsequently activate an interferon response. The negative correlation between tumor mass and MMTV Env protein expression suggests a possible role of ERV proteins serving as tumor-associated antigens and decitabine enhancing adaptive immunity against cancer by stimulating ERV expression on tumor cells. Further studies of the interaction between decitabine and MMTV using immunodeficient mice may help us understand the possible involvement of adaptive immunity in the pharmacodynamics of decitabine as well as the role of ERVs in tumor development.

#4900

Preclinical efficacy of targeting epigenetic mechanisms in AML with 3q26 lesions and EVI1 overexpression

Christine E. Birdwell, Warren C. Fiskus, Tapan M. Kadia, Christopher P. Mill, John A. Davis, Kaberi Das, Stephen Horrigan, Kapil N. Bhalla. *UT MD Anderson Cancer Center, Houston, TX*

EVI1 gene is located at 3q26.2 in the MECOM locus and encodes for a zinc-finger transcription factor. Chromosome translocation t(3;3) or inv(3) at 3q26 repositions the enhancer (E) of the tumor suppressor GATA2 to induce EVI1 over-expression, while concomitantly repressing GATA2.

EVI1 over-expression promotes self-renewal and blocks differentiation of leukemia stem-progenitor cells (LSCs) and causes therapy refractoriness and inferior overall survival in AML. Previous reports highlighted that targeting BRD4 with BET inhibitor (BETi) is active against AML cells with inv(3)/t(3;3). BETi treatment also represses EVI1 and its targets c-Myc and Bcl-xL. We recently reported that tegavivint (TV) (BC-2059), a disruptor of the nuclear TBL1/R1-β-catenin-TCF7L2 complex represses c-Myc, cyclin D1 and Survivin and inhibits growth and survival of AML LSCs. In present studies, a CRISPR screen in UCSD-AML1 cells (with 3q26 lesion and EVI1 overexpression) with gRNAs targeting epigenetic regulators highlighted BRD4 and p300 as dependencies. Treatment with BETi, e.g., OTX015, dose-dependently induced apoptosis of AML cell lines and patient-derived (PD) AML cells (AML191 and AML194) with inv(3) or t(3;3). OTX015 treatment repressed c-Myc, c-Myb, CDK4, MECOM, and MCL1, while inducing HEXIM1 and cleaved PARP levels. TV treatment also dose-dependently induced apoptosis in AML cell lines and PD AML cells with 3q26.2 lesions, associated with depletion of nuclear β-catenin, EVI1, TCF7L2, c-Myc, c-Myb, RUNX1, CEBPα, c-KIT, BCL2, Bcl-xL and MCL1, but increase in p21, CD11b, BIM and cleaved PARP levels. Hi-ChIP with H3K27Ac antibody demonstrated that TV treatment abolished chromatin loops between MYC and its Es within the super-E. RNA-Seq analysis showed negative enrichment (log2-fold) of gene sets of MYC, E2F and WNT targets, DNA replication/repair and reduction of the 17-gene stemness score. Confocal microscopy showed that TV treatment disrupted co-localization of EVI1 and β-catenin with TBL1, also confirmed by the Proximity Ligation Assay. CyTOF analysis confirmed that TV treatment reduced EVI1, c-Myc, RUNX1, β-catenin, Bcl-xL, BCL2, MCL1 and Ki67 but increased cleaved PARP levels in the phenotypically characterized LSCs (with high expression of CLEC12A, CD123, CD244 and CD99) harboring inv(3) with EVI1 overexpression. Co-treatment with OTX015 and TV or the p300 inhibitor GNE-049 synergistically induced *in vitro* apoptosis in the AML cell lines and the PD AML cells with 3q26.2 lesions. Notably, in the flank-implanted PDX of AML191 or tail-vein infused PDX of AML242 models in NSG mice, treatment with OTX015 and TV, compared to vehicle control or each drug alone, significantly reduced AML growth and improved survival, without any host toxicity. These findings highlight the promising pre-clinical efficacy of novel BETi-based

combinations against AML models harboring 3q26 lesions and EVI1 overexpression.

#4901

The role of protein disulfide isomerase and copper in the paraptotic cell death of clinically investigated anticancer thiosemicarbazones

Sonja Hager[1], Walter Berger[2], Christian R. Kowol[3], Eva A. Enyedy[4], Petra Heffeter[2]. *[1]Department of Food Chemistry and Toxicology/Center for Cancer Research, University of Vienna/Medical University Vienna, Vienna, Austria,[2]Center for Cancer Research, Medical University Vienna, Vienna, Austria,[3]Department of Inorganic Chemistry, Faculty of Chemistry, University of Vienna, Vienna, Austria,[4]Department of Inorganic and Analytical Chemistry, Interdisciplinary Excellence Centre, University of Szeged, Szeged, Hungary*

α-*N*-Heterocyclic thiosemicarbazones (TSCs) have long been investigated as anticancer compounds. Triapine is one of the best-known TSCs for anticancer therapy and is currently tested in a clinical phase III trial. To further improve the anticancer activity of TSCs, novel derivatives (such as DpC and COTI-2) have been developed and clinically investigated for their activity against solid tumors. These novel TSCs belong to a subclass (incl. the tetra-methylated Triapine derivative, Me_2NNMe_2) that are terminally disubstituted and demonstrated enhanced anticancer activity *in vitro* and *in vivo*. The improved activity of these TSCs correlated with their ability to form stable copper complexes as well as induce paraptosis, a form of programmed but caspase-independent cell death, that is characterized by the formation of vesicles originating from the endoplasmic reticulum (ER). However, the molecular events behind paraptosis induction are still not fully elucidated. Consequently, the aim of this study was to investigate the molecular signaling behind paraptosis as well as the reasons behind the induction of this quite unknown form of cell death by TSCs.
A whole-genome gene expression analysis of cells treated with a terminally disubstituted TSC revealed an upregulation of thiol homeostasis-related genes, copper metabolism, and metallothionein genes as well as ER stress response genes. In addition, we found an upregulation of the copper-sensitive and thiol-containing protein disulfide isomerase (PDI), which was

confirmed on protein level. In cell-free activity studies, PDI was indeed inhibited by terminally disubstituted TSCs, although only in form of their copper complexes. In agreement, removal of copper ions by specific chelators greatly reduced their anticancer activity as well as paraptotic potential in cell culture. This inhibition was hypothesized to be induced by a general disruption of the thiol redox homeostasis affecting also other responsive proteins and resulting in a more oxidative environment, especially in the ER. In confirmation, thiol-containing small molecules could reduce the compound's anticancer activity in viability assays. Furthermore, glutathione as well as PDI were detected predominantly in their oxidized form in cells treated with terminally disubstituted TSCs. Consequently, terminally disubstituted TSCs, which are characterized by higher anticancer activity, induce paraptosis due to their high copper complex stability. The formation of the complex results in the interaction with thiol-containing proteins and subsequently in the disruption of the thiol-redox homeostasis, which leads to paraptotic cell death. Overall this work shed light on the paraptotic cell death and will be of interest for future clinical development of anticancer TSCs, as paraptosis is hypothesized to overcome apoptosis-resistance of cancer cells.

#4902

Mitochondrial and cytosolic folylpolyglutamate synthetase in one-carbon metabolism and anti-tumor efficacy of mitochondrial-targeted antifolates

Carrie O'Connor[1], Jade Katinas[2], Mathew Schneider[1], Md. Junayed Nayeen[3], Xun Bao[1], Jing Li[1], Charles Dann[2], Aleem Gangjee[3], Larry H. Matherly[1], Zhanjun Hou[1]. *[1]Oncology, Barbara Ann Karmanos Cancer Institute, Detroit, MI,[2]Department of Chemistry, Indiana University, Bloomington, IN,[3]Division of Medicinal Chemistry, Duquesne University, Pittsburgh, PA*

Folates mediate one-carbon (C1) transfers, which are essential for cellular homeostasis and survival. C1 metabolism encompasses distinct cytosol (Cyto) and mitochondria (Mito) pathways connected by an interchange between serine, glycine and formate. Mito C1 metabolism provides cellular glycine and C1 units (as formate) for *de novo* synthesis of thymidylate and purine nucleotides in the Cyto. Polyglutamyl folates are the predominant

folate forms in cells and are generally preferred for C1 transfers. Thus, folate polyglutamylation is essential for cellular homeostasis. Folate polyglutamylation is catalyzed by folypolyglutamate synthetase (FPGS), including Cyto (cFPGS) and Mito (mFPGS) isoforms. C1 metabolism is critical for tumor growth and thus offers a plethora of therapeutic targets for cancer. Of particular interest are Mito C1 inhibitors including "non-classical" pyrazolopyran compounds SHIN1 and SHIN2, and "classical" pyrrolo[3,2-*d*]pyrimidine antifolate compounds typified by AGF347, all targeting serine hydroxymethyltransferase 2 (SHMT2). Both SHIN1 and AGF347 effected *in vitro* anti-tumor efficacy, and SHIN2 and AGF347 showed *in vivo* efficacy toward tumor xenografts. We systematically explored the roles of cFPGS and mFPGS levels as critical determinants of C1 inhibitor target engagement and net Cyto versus Mito C1 flux, resulting in anti-tumor efficacy. We found that FPGS transcript levels significantly correlated with the effects of AGF347 toward a panel of human pancreatic cancer cell lines including MIA PaCa-2. We engineered MIA PaCa-2 cells with FPGS gene knockout to stably express inducible mFPGS or cFPGS form. FPGS in mFPGS-transfected cells (mFPGS#32) was expressed mainly in Mito over Cyto, whereas FPGS in cFPGS-transfected cells (cFPGS#3) was expressed exclusively in Cyto. Accumulation of radiolabeled folate and AGF347 increased with increasing FPGS in both Cyto and Mito for mFPGS#32, but only in Cyto for cFPGS#3. Metabolomics with [2,3,3-^{2}H]serine in cFPGS#3 and mFPGS#32 established FPGS levels in Mito versus Cyto as important determinants of C1 fluxes. Increased FPGS levels in mFPGS#32 enhanced C1 flux in Mito far greater than in Cyto, and greater than for the increased FPGS in cFPGS#3. As a result, Cyto-targeted antifolates pemetrexed and AGF94 were only modestly impacted by increasing FPGS levels in both mFPGS#32 and cFPGS#3 (~3x). In contrast, increasing FPGS levels dramatically enhanced the inhibitory effects of Mito-targeted antifolates such as AGF347 in mFPGS#32 (~8-25x), and to a greater extent than in cFPGS#3 (~6-8x). Conversely, increasing FPGS levels substantially attenuated the cytotoxic effect of SHIN1 in mFPGS#32 (~19x). In summary, FPGS levels are an important determinant of C1 fluxes, particularly in Mito where they contribute to cytotoxic potencies of Mito-targeted C1 inhibitors at SHMT2.

#4903

Levels of folate transporters impact the compartmentalization of one-carbon metabolism in the mitochondria vs cytosol providing a unique vulnerability to SHMT inhibition

Mathew Joseph Schneider[1], Carrie O'connor[1], Xun Bao[1], Md. Junayed Nayeen[2], Zhanjun Hou[1], Jing Li[1], Aleem Gangjee[2], Larry H. Matherly[1].
[1]Oncology, Wayne State University School of Medicine, Detroit, MI,[2]Division of Medicinal Chemistry, Duquesne University, Pittsburgh, PA

These studies characterize the critical role of the Reduced Folate Carrier (RFC) and the Proton Coupled Folate Transporter (PCFT) as determinants of cancer cell reliance on mitochondrial vs cytosolic one carbon (C1) metabolism, to identify a unique susceptibility towards SHMT1 and SHMT2 inhibition in cancer cells. C1 metabolism is frequently reprogrammed in cancer cells to provide nucleotides, amino acids, and glutathione, and to maintain redox homeostasis for proliferation. The mitochondrial C1 converting enzymes serine hydroxymethyltransferase (SHMT) 2 and methylene tetrahydrofolate (THF) dehydrogenase 2 (MTHFD2) are among the top overexpressed metabolic enzymes in human cancers, suggesting these are important cancer-specific targets. We previously discovered novel 5-substituted pyrrolo[3,2-*d*]pyrimidine antifolates (with AGF347 being the lead) that potently inhibit mitochondrial SHMT2, as well as SHMT1. Folates are essential cofactors for C1 converting reactions; folates and antifolates primarily rely on the major facilitative folate transporters RFC and PCFT for internalization by tumor cells. In these studies, we explore the effects of folate transporter expression on the compartmentalization of C1 metabolism in the mitochondria and cytosol and the potential impact on SHMT1 and SHMT2 inhibition. We used a tetracycline inducible system for RFC expression in RFC/PCFT-null HeLa cells, with and without constitutive PCFT, and characterized the impact on transport and accumulation of folates and AGF347 in response to folate transporter expression. Increased accumulation of folates was observed with increasing RFC in the absence of PCFT. In the presence of PCFT, baseline folate accumulation was substantial and independent of RFC expression, indicating a major role of PCFT as a facilitative folate transporter. SHMT2 catalyzes the conversion of serine and THF to glycine and 5, 10-methylene THF in the mitochondria, while SHMT1 catalyzes the

reverse reaction in the cytosol, producing THF and serine. To determine how folate transporter expression affects the C1 flux through SHMT1 vs SHMT2, [2,3,3-^{2}H]serine tracer experiments were performed; increased mitochondrial C1 flux through SHMT2 was observed with increasing RFC in the absence of PCFT, whereas the mitochondrial flux through SHMT2 predominated in the presence of PCFT. By cell proliferation assays it was discovered that cells with lower RFC expression exhibit a hypersensitive phenotype towards AGF347 in the absence of PCFT, indicating a unique therapeutic opportunity for targeting SHMT forms in cancer cells with low folate transport activity. Here we identify RFC and PCFT as key determinants for the compartmentalization of C1 flux in the mitochondria vs the cytosol, in turn affecting the sensitivity of cancer cells towards SHMT inhibition.

#4904

Glutamine antagonist DRP-104 enhances anti-tumor responses in *KEAP1* mutant lung cancer

Ray Pillai[1], Sarah LeBoeuf[1], Ali Rashidfarrokhi[1], Shih Ming Huang[1], Triantafyllia Karakousi[1], Anastasia-Maria Zavitsanou[1], Warren Wu[1], Volkan Sayin[2], Robert Wild[3], Sergei Koralov[1], Thales Papagiannakopoulos[1]. *[1]NYU Grossman School of Medicine, New York, NY,[2]University of Gothenburg, Gothenburg, Sweden,[3]Dracen Pharmaceuticals Inc., San Diego, CA*

KEAP1 is mutated in approximately 20% of non-small cell lung cancer (NSCLC) and is associated with poor response rates to checkpoint blockade. Given the therapeutic challenge presented by *KEAP1* mutant tumors and the great potential held by immunotherapeutic approaches, there is an urgent need to identify the mechanisms that mediate immune evasion in patients with *KEAP1* mutant lung adenocarcinoma.
We previously demonstrated that metabolic rewiring in *KEAP1* mutant tumors leads to increased dependency on glutamine as a substrate for multiple anabolic pathways. DRP-104 (Sirpiglenastat) is a novel glutamine antagonist which inhibits all glutamine consuming reactions. Using pre-clinical mouse models and patient derived xenograft models we demonstrate that DRP-104 robustly impairs the growth of *KEAP1* mutant tumors. Furthermore, using an immunocompetent orthotopic lung

adenocarcinoma mouse model we find that treatment with DRP-104 increases survival of *Keap1* mutant tumor bearing mice treated with anti-PD1 therapy.
We have dissected the mechanism by which DRP-104 impacts *KEAP1* mutant tumors and the surrounding immune microenvironment. Notably, DRP-104 impairs nucleotide synthesis in *KEAP1* mutant tumors and thereby inhibits cancer cell growth. In addition, DRP-104 reduces exhausted T cell and T regulatory populations within the tumor microenvironment as well as increases effector T cell function. Overall, we find that DRP-104 impairs the growth of *KEAP1* mutant tumors through both targeting of tumor intrinsic metabolic vulnerabilities and through tumor extrinsic immunostimulatory mechanisms such as promoting the expansion of functional anti-tumor T cell populations. This data provides additional rationale for the ongoing phase I/II clinical trial (NCT04471415) using DRP-104 in NSCLC with mutations in *KEAP1* as well as for combining DRP-104 with checkpoint blockade.

#4905

Anticancer activity and paraptosis induction of novel bipyridine-silver(I) compounds against resistant colorectal and ovarian cancer cell lines

Alessia Stefanelli[1], Ricardo G. Teixeira[2], Adhan Pilon[2], Rebecca Warmers[3], Ingo Ott[4], Christian R. Kowol[5], Anamaria Brozovic[6], Ana Isabel Tomaz[2], Andreia Valente[2], Petra Heffeter[1]. *[1]Center for Cancer Research and Comprehensive Cancer Center, Medical University of Vienna, Vienna, Austria,[2]Centro de Química Estrutural, Institute of Molecular Sciences, Departamento de Química e Bioquímica, Universidade de Lisboa, Lisboa, Portugal,[3]Universität Konstanz, Konstanz, Germany,[4]Technische Universität Braunschweig, Braunschweig, Germany,[5]Institute of Inorganic Chemistry, Faculty of Chemistry, University of Vienna, Vienna, Austria,[6]Division of Molecular Biology, Ruđer Bošković Institute, Zagreb, Croatia*

Background: Platinum-based anticancer drugs (e.g. Carboplatin and Oxaliplatin) are frequently applied in chemotherapy regimens against several types of cancer including ovarian carcinoma (OC) and colorectal

carcinoma (CRC). However, intrinsic or acquired tumor resistance severely limit their clinical application. Here, we investigated the anticancer activity of several novel silver(I) 2,2'-bipyridine derivatives, containing either triphenylphosphane (PPh_3) or 1,2-bis(diphenylphosphino)ethane (dppe) ligands and tested their potential to overcome platinum resistance.
Methods: Cytotoxicity and cross resistance profiles of the newly synthesized compounds were tested against two OC models (SKOV-3 and MES-OV), a CRC model (HCT-116) and their corresponding sublines resistant to carboplatin or oxaliplatin, as well as non-malignant fibroblasts (F331) via an MTT-based cell viability assay after 72 h continuous drug exposure. Moreover, the intracellular levels of silver were measured via ICP-MS. In addition, thioredoxin reductase (TrxR) inhibition properties, impact on cell cycle distribution and apoptosis induction potential were investigated via multiple molecular biological methods. Morphological changes induced by the silver compounds were characterized via spinning disk confocal microscopy.
Results: All tested compounds displayed pronounced anticancer activity and cancer cell selectivity. Moreover, cell intrinsic resistance to carboplatin or oxaliplatin was not impacting on the cytotoxic activity of the compounds. Noteworthy, MES-OV and HCT-116 cells showed exceptional sensitivity to several silver(I) 2,2'-bipyridine derivatives with a 1,2-bis(diphenylphosphino)ethane (dppe) (AP-compounds). This sensitivity was not based on enhanced drug uptake, pronounced TrxR inhibition nor apoptosis induction or cell cycle arrest. In contrast, hypersensitive cells displayed pronounced endoplasmic reticulum (ER)-derived vesicles together with multiple others hallmarks of paraptotic cell death.
Conclusion: Our findings did not only demonstrate that the new silver compounds were unaffected by cancer cell intrinsic resistance mechanisms to platinum-based chemotherapy, but also indicated a high vulnerability of tumor (sub)types towards these bipyridine silver complexes. This hypersensitivity is based on the induction of paraptosis, a novel form of programmed cell death. To summarize, these silver compounds represent a new class of promising anticancer drugs, which demand further preclinical development.

#4907

Atovaquone-induced increase in reactive oxygen species leads to impaired glycolytic functions in ovarian cancer cells

Nicha Boonpattrawong, Sejal Sharma, Rob Schultz, Mayra A. Betancourt Ponce, Lisa M. Barroilhet, Manish Patankar. *University of Wisconsin-Madison, Madison, WI*

Atovaquone (ATO) is an FDA-approved anti-malarial drug, which has also shown potent anti-cancer effects. We have previously demonstrated ATO as an effective chemotherapy against high-grade serous ovarian cancer in cell lines and mouse model. In the present study, we aim to determine if ATO is asserting its anti-cancer properties by altering cellular metabolism. Glycolysis and oxidative phosphorylation (OXPHOS) are the two major sources of intracellular energy. ATO reduces OXPHOS energy production by inhibiting mitochondrial complex III. We first determined whether there is a shift in energy production when OXPHOS is inhibited by assessing glycolytic function in various human (OVCAR3 and OVCAR5) and mouse (ID8) ovarian cancer cell lines. Mitochondrial oxygen consumption rate (OCR) and extracellular acidification rate (ECAR) were assessed by the Seahorse XF Analyzer. First, we pretreated cells with ATO at IC70 concentrations for 1 hour prior to metabolic analysis. As expected, pretreatment with ATO reduces OCR in all cell lines. However, ATO treatment increased basal glycolysis but decreased glycolytic capacity and glycolytic reserve. This suggests that ATO-treated cells have an impaired ability to shift energy production towards glycolysis when there is an increase in energy demand. One of the initial events that occur in ATO-treated cells is a surge in reactive oxygen species (ROS) as measured by H2DCFDA ROS assay. In the human cell lines, we found that ATO significantly increased ROS by approximately 100-fold (MFI). Whereas, in the mouse cell line, the ATO-induced increase in ROS were comparatively attenuated. We hypothesized that the increase in ROS leads to inhibition of glycolysis. We tested this by pre-treating cells with 2mM N-acetylcysteine (NAC), an oxygen radical scavenger, for 1 hour before measuring the metabolic responses to ATO. We found that NAC attenuated the inhibition of glycolytic processes in human cell lines but not in the mouse cell line. Our lab has previously shown that ATO induced activation and increased expression of p53. Studies have shown that ROS activate p53, which in turn upregulates the TP53 induced glycolysis and apoptosis regulatory phosphatase (TIGAR), inhibiting the conversion of F6P to F-2,6-BP and ultimately leads to inhibition of glycolysis. Increases in ROS also shuttle

G6P towards the phosphate pentose pathways through G6P dehydrogenase for antioxidant production. We found that long-term ATO treatment for 24 hours also resulted in increases in both TIGAR and G6PD mRNA expression. Taken together, these results suggest that ATO decreased plasticity of metabolic capacity in ovarian cancer cells through ROS and ROS associated glycolytic pathways. Further, this study provides mechanistic insights into ATO's potential as a chemotherapeutic agent.

#4908

Study on Ca $^{2+}$-mediated regulation mechanisms on chemotherapy-induced peripheral neuropathy in multiple myeloma and non-Hodgkin lymphoma

Jinny Park[1], Jong-Suk Kim[2], Kwang-Hyun Park[3]. *[1]Hematology division /Internal medicine, Gil Medical Center, Gacheon University, Incheon, Korea, Republic of,[2]Department of Biochemistry, Institute for Medical Sciences, Chonbuk National University Medical School, Jeonju, Korea, Republic of,[3]Department of Emergency Medical Rescue, Nambu University, Gwangju, Korea, Republic of*

In general, when treating cancer patients, various anticancer drugs are used in combination to enhance the anticancer effect. However, most drugs exhibit side effects. Neurotoxicity, one of the side effects commonly accompanied, greatly affects the quality of life and also reduces compliance with treatment. Calcium signal transduction, which occupies a key position in cell signal transduction, has been found to be involved in various mechanisms including proliferation, differentiation, and death of cells, beyond the existing research direction that focuses on channels. To identify the mechanisms of calcium signal regulation that can reduce chemotherapy induced peripheral neuropathy (CIPN) while maintaining anticancer functions of drugs, we study with the two drugs frequently used in non-Hodgkin lymphoma and multiple myeloma, borteozomib (BTZ) and vincristine (VIN), whose main side effects are neurotoxicity. We used the human neuroblastoma cell line, SH-SY5Y cells, and performed MTT assay after treating them with N-Acetylcysteine (NAC), an antioxidant, to determine whether the reduction in cell viability by BTZ and VIN was due to the increase in ROS. When BTZ and VIN were treated with NAC, cytotoxicity by BTZ was significantly reduced and cell viability decreased

by VIN was significantly increased. From these results, we found that ROS are involved in BTZ and VIN -induced apoptosis. In addition, we performed MTT assay using calcium inhibitors to investigate whether intracellular calcium signaling is involved in BTZ and VIN-induced apoptosis, and 8-Br-cADPR, Ned-19, Xestospongin C, and Heparin were used as calcium inhibitors. To confirm that the cell viability reduced by BTZ and VIN is recovered by calcium inhibitors, BTZ and VIN were treated together with calcium inhibitors, respectively. Cell viability was found to increase significantly. These results suggest that intracellular calcium signaling is involved in cell death induced by BTZ and VIN. The increase in [ca^{2+}]i in the cytoplasm when treated with BTZ and VIN was measured using a fluorescence spectrophotometer. It was shown that the treatment with BTZ and VIN increased the calcium concentration in the cytoplasm within 1 minute. To confirm that the concentration of intracellular calcium was reduced by the calcium inhibitor, BTZ and calcium inhibitor were treated together, and it was confirmed that the intracellular calcium concentration increased by BTZ was decreased in a concentration-dependent manner at 2uM and 3uM of the calcium inhibitor. In conclusion, this experiment suggests that intracellular calcium signaling is involved in the BTZ and VIN's reduction of neuronal cell viability (CIPN) in multiple myeloma and non-Hodgkin lymphoma. *This research was supported by NRF 2021R1A2C1091322 (J.-S.Kim) and 2021R1F1A1064120 (J. Park).*

#4909

Molecular analysis of small cell lung cancer provides insights into mechanism of action underlying the novel drug combination of lurbinectedin and TIC10/ONC201

Ashley Sanchez Sevilla Uruchurtu[1], Nicholas Liguori[2], Leiqing Zhang[3], Kelsey Huntington[1], Lanlan Zhou[3], Young Lee[4], Abbas E. Abbas[5], Christopher G. Azzoli[6], Wafik S. El-Deiry[3]. *[1]Department of Pathology and Laboratory Medicine, Brown University, Providence, RI,[2]Lewis Katz School of Medicine, Temple University, Philadelphia, PA,[3]Legorreta Cancer Center at Brown University, Providence, RI,[4]Brown University, Providence, RI,[5]Warren Alpert Medical School, Brown University, Providence,*

RI,[6]Department of Medicine, Haematology/Oncology Division, Lifespan Health System and Brown University, Providence, RI

We previously explored the combination of novel imipridone TIC10/ONC201 and small molecule RNA polymerase inhibitor lurbinectedin as a potentially effective treatment regimen for small cell lung cancer (SCLC). Data from cell viability experiments demonstrated synergistic killing of SCLC cells with minimal death of healthy control cells. Analysis of intracellular proteins via Western blot indicated that combinatorial treatment induces the integrated stress response, DNA damage/cell cycle checkpoint responses, and increased apoptosis of tumor cells. We have utilized the Luminex 200 platform to perform analyses of cytokine levels in SCLC cell lines with various genetic alterations before and after ONC201 and lurbinectedin treatment. Our results revealed significant changes in cytokine levels following treatment indicating potential immunomodulatory and angioregulatory effects of ONC201 and lurbinectedin. CCL3, known to recruit and activate granulocytes, was found to be elevated by treatment with lurbinectedin, ONC201 and combination versus control. Angiopoietin 1, which contributes to blood vessel maturation, and angiopoietin 2, which promotes neovascularisation, were elevated by all drug treatments in H1882 SCLC cells. Our ongoing studies are further analysing the importance of specific cytokines in tumor vascularity and in recruitment and killing of SCLC cells by immune cells. Results from these experiments are helping to elucidate the molecular mechanisms underlying SCLC, its immune landscape, and treatment response.

#4910

Human tumor primary culture analyses for the prediction of response to chemotherapy, targeted agents, drug combinations and metabolic inhibitors: The role of *ex vivo* analysis of programmed cell death in cancer therapy

Adam J. Nagourney[1], Steven S. Evans[1], Paulo D'Amora[1], Nise Yamaguchi[2], Paula Bernard[1], Federico Francisco[1], Joshua B. Gipoor[1], Robert Alan Nagourney[1]. *[1]Rational Therapeutics, Inc., Long Beach, CA,[2]Instituto Avancos em Medicina, Sao Paulo, Brazil*

There is growing interest in the use of human tumor primary cultures for the prediction of response to drugs and drug combinations in cancer medicine. While the field has witnessed numerous attempts to apply human tissue for the prediction of response, fundamental errors in methodologic approaches severely limited the predictive validity and clinical applicability of these important technologies. The first error was a focus upon drug induced cell growth inhibition. This lead to the failure of the clonogenic (human tumor stem cell) and H3*Thymidine incorporation platforms in the 1970's and 1980's. As the concept of apoptosis arose following landmark observations in 1972, cell death endpoints became predominant including mitochondrial function (MTT, XTT), ATP content (luciferase) and delayed loss of membrane integrity (DISC, EVA/PCD) among others. These improvements led to more biologically relevant measures. However, a second hurdle arose as investigators chose to amplify subculture and propagate tumors into what are now referred to as human tumor organoids. While these 3-D cultures are more reflective of tumor cell-cell interactions found in cancers, they cannot recreate the cell-vasculature, cell-stroma, inflammatory environment nor cancer associated fibroblast interactions with human cancer cells required for accurate response prediction. To address these shortcomings we developed the ex vivo analysis of programmed cell death (EVA/PCD) platform that applies native state tumor explants directly from surgical specimens to select drugs and combinations. To date we have reported 11,680 individual analyses. Positive prospective results have been reported in breast cancer (TTP $p < 0.03$); ovarian cancer (TTP $p = 0.05$), lung cancer (2-fold improvement in ORR; TTP $p = 0.035$) and recently ovarian and uterine cancer (DFS $p = 0.038$) with two meta-analyses confirming the predictive validity in hematologic and solid tumors. With over 20 years of CLIA-approved laboratory experience in the study of human tumor primary culture explants, the EVA/PCD platform provides improved response and time to progression and offers the opportunity to streamline drug development, curtail costs and avoid futile care in patients with advanced and refractory malignancies.

#4911

A novel C-terminal of HSP90 inhibitor NCT-547 eliminates cancer stem-like subpopulation in triple-negative breast cancer

Eunsun Jung, Seojin Jang, Daeil Sung, Soeun Park, Minsu Park, Dongmi Ko, Seongjae Kim, Juyeon Seo, Kee Dal Nam, Yoon-Jae Kim, Ji Young Kim, Jae Hong Seo, Yong koo Kang, So Ra Seock, Jung Min Park. *Korea University Guro Hospital, Seoul, Korea, Republic of*

Triple-negative breast cancer (TNBC) harbors a higher cancer stem cell (CSC)-like population and exhibits a more aggressive metastatic phenotype. Due to the limitations of currently available targeted therapies, there remains a significant unmet need for the development of new targeted therapies for TNBC. Molecular chaperone heat shock protein 90 (HSP90) is attracting attention as an ideal therapeutic target due to it regulates essential biological functions such as cell proliferation, angiogenesis and metastasis. Although N-terminal HSP90 inhibitors have had little clinical success to date, C-terminal HSP90 inhibitors have received relatively little attention. We sought to investigate the effects of a new rationally designed NCT-547 on apoptosis, breast cancer stem cell (BCSC)-like properties, migration ability and heat shock response (HSR) *in vitro* and tumor growth and metastasis in CSC-enriched allograft model *in vivo*. NCT-547 inhibits TNBC cell proliferation by simultaneously inactivating several survival factors including AKT, MEK, and STAT3. In addition, NCT-547 effectively targets BCSC-like properties with impairment of ALDH1 activity, CD44+/CD24- phenotype, and 3D mammosphere-forming ability. The expression of HSF-1 target genes such as Hsp90, Hsp70, Hsp27, Hsp40 and Hsp65 is highly overexpressed in TNBC patients. The mRNA abundances of target genes were significantly decreased after NCT-547 challenge. NCT-547 effectively targets both the proliferating TNBC tumor cells and CSCs, markedly reducing tumor growth, coinciding with decreased Ki-67 proliferation index and enhanced apoptosis. Anti-tumor effect of NCT-457 was independent of heat shock response as evidenced by significant downregulation of HSF1 phosphorylation and expression of downstream targets HSPs members. It is noteworthy that NCT-547 did not affect markers of hepatic and renal acute toxicity and was not cytotoxic in non-malignant cells. NCT-547 may therefore have potential to address current limitations in the treatment of TNBC.

#4912

Anticancer activity of Hsp90 inhibitor AUY922 in nasopharyngeal carcinoma and non-small cell lung cancer cells

William C. S. Cho, Chi F. Wong. *Department of Clinical Oncology, Queen Elizabeth Hospital, Hong Kong SAR, China*

Introduction: Nasopharyngeal carcinoma (NPC) and non-small cell lung cancer (NSCLC) are two of the most prevalent cancers in Southern China. Although cisplatin therapy may be initially successful, its effectiveness is often significantly reduced in patients with relapsed disease. There is an urgent need to overcome cisplatin resistance in the treatment of NPC and NSCLC. Luminespib (AUY922) is an experimental drug candidate for the treatment of cancer. It is an inhibitor of heat shock protein 90 (Hsp90), a chaperone protein that plays a role in modifying a variety of proteins involved in tumorigenesis. Hsp90 inhibitors have demonstrated potent activity in preclinical testing and clinical trials against various cancer types. We sought to investigate the preclinical efficacy of AUY922 and evaluate its anticancer effect in cisplatin-resistant NPC and NSCLC cells.
Materials and Methods: Two NPC cells (HK1 and Hone1), four NSCLC cells (A549, SW900, NCI-H1975, and HCC4006), one normal lung cells (CCD11Lu), two cisplatin-resistant NPC cells (HK1-R and Hone1-R), and one cisplatin-resistant NSCLC cells (A549-R) were cultured and treated with 100 nM AUY922 for 48 hours. A cell proliferation assay was performed in triplicate to determine the antiproliferative effects of AUY922 on cancer cells. Flow cytometry was used for cell cycle analysis. The apoptotic cells were evaluated by Annexin V and Western blot analysis. Nude mice were used to test the effects of intraperitoneal injection of AUY922 on tumor growth.
Results: We found that AUY922 significantly inhibited *in vitro* growth in all the two NPC (44% and 40%) and four NSCLC (53%, 77%, 50%, and 62%) cells in comparison to the normal lung cells (4%). The two cisplatin-resistant NPC cells (63% and 37%) also showed significant inhibition of viability after treatment with AUY922. However, there was only a slightly reduced viability in the cisplatin-resistant NSCLC cells (14%). Flow cytometry revealed that AUY922 induced G2/M and S phase arrest in HK1 and HK1-R cells. On the other hand, AUY922 also induced pro-apoptotic peaks in A549, A549-R, Hone1, and Hone1-R cells. Interestingly, Annexin V and Western blot analysis showed that cell death was not caused by

apoptosis. *In vivo*, both AUY922 alone and the combination of AUY922 with cisplatin treatments inhibited NPC and NSCLC tumor growth without significant weight loss. In addition, the administration of AUY922 significantly reduced NPC and NSCLC tumor growth in the cisplatin-resistant mouse models.
Conclusion: AUY922 exhibits potent anticancer activities *in vitro* and *in vivo*. These findings provide evidence that AUY922 could be useful for the treatment of NPC and NSCLC as a single agent or in combination with cisplatin. Most importantly, our results provide a preclinical proof of concept for the efficacy of AUY922 in cisplatin-resistant NPC and NSCLC treatment.

#4913
Enhancer RNA profiles predict sensitivity to a novel GPX4 inhibitor
Timothy Read, David Simpson, Jenna Rimel, Christy Rhine, Casey Pham, Cole Liechty, Eric Martin, Joey Azofeifa. *Arpeggio Biosciences, Boulder, CO*

Inhibition of the GPX4 enzyme leads to the rapid accumulation of toxic lipid peroxides and cell death through a process known as ferroptosis. This mechanism has recently garnered significant attention in the field of oncology because many difficult-to-treat tumor types are particularly susceptible to this non-canonical form of cell death. However, robust biomarkers that predict sensitivity to ferroptosis are needed to help select well-defined tumor subtypes and patient segments that are likely to respond to GPX4-targeting. Our nascent RNA platform measures the active transcription of not only protein-coding transcripts, but also transcripts initiating from enhancer regions (enhancer RNAs) critical for defining cell type. We reasoned that these data could afford the unique opportunity to identify non-coding transcripts that could serve as novel biomarkers of sensitivity to ferroptosis. We recently discovered a potent and selective GPX4 inhibitor and profiled the compound for its ability to induce ferroptosis across a diverse group of cancer cell types. We chose several of the most sensitive and resistant cell lines for further examination using our nascent RNA platform and identified novel relationships between sensitivity to ferroptosis and cell-specific enhancer RNA profiles. Importantly, enhancer RNA profiles were more effective at stratifying

sensitive and resistant cell lines than protein-coding gene expression. Using enhancer RNA expression profiles as biomarkers of drug sensitivity represents a novel strategy that could ultimately improve our ability to select patient cohorts more likely to benefit from emerging drug candidates and established therapeutics.

#4914

Role of ClpP in the anti-cancer effects of imipridone ONC201 and ONC206

Andrew Lee, Cristina Maranto, Scott Foster, Sara Morrow, Joshua E. Allen, Randall Lanier, Phiroze Sethna, Varun V. Prabhu. *Chimerix, Inc., Durham, NC*

ONC201 is the first bitopic dopamine receptor D2 (DRD2) antagonist and allosteric mitochondrial protease ClpP agonist. Downstream of target engagement, ONC201 activates the integrated stress response pathway resulting in selective tumor cell death. ONC201 is well tolerated and induces durable tumor regressions in H3 K27M-mutant glioma patients. ONC206, a derivative of ONC201 currently in Phase I trials for adult and pediatric brain tumors, is also a bitopic DRD2 antagonist and ClpP agonist with nanomolar potency. We further evaluated in vitro efficacy and mechanism of action specific to ClpP for ONC206 and investigated acquired resistance to ONC201 and ONC206. FITC-casein and peptide degradation assays confirmed that ONC206 acts as an agonist of human ClpP with enhanced potency relative to ONC201. Broad efficacy in the nanomolar range for ONC206 (GI50 <78-889nM, 72h) was observed in 1,088 Genomics of Drug Sensitivity in Cancer (GDSC) cancer cell lines with increased sensitivity in cell lines exhibiting high ClpP mRNA expression. Among solid tumors, nervous system-related cell lines were particularly sensitive. Gene Expression Profiling Interactive Analysis (GEPIA) database analysis showed ClpP mRNA was overexpressed in glioblastoma cells relative to normal cells. GDSC observations were confirmed in glioblastoma (GBM) (T98G, A172, U87MG), H3.3 K27M mutant diffuse intrinsic pontine glioma (DIPG) (SF8628, SF7761) and astrocytoma (H4, U118MG) cell lines. ONC206 was more potent than ONC201 in cell viability assays for all glioma lines tested. SF8628 cells with a CRISPR-mediated ClpP knockout were shown to demonstrate

resistance to both ONC201 and ONC206. Polyclonal resistant cell lines were generated through prolonged passaging in increasing concentrations of ONC201 or ONC206 (SF8628 and T98G cells). Cells with acquired resistance to ONC201 (ONC201Res) or ONC206 (ONC206Res) showed cross resistance to both imipridones. Time-stability of resistance was confirmed by removing drug for 2 to 4 weeks and retesting. RNAseq analysis revealed upregulation of the integrated stress response with imipridone treatment in T98G parental cells but not resistant clones. Whole genome sequencing revealed ClpP mutations in both ONC201Res and ONC206Res cells. Our results confirm the role of ClpP in the mechanism of action of ONC201 and ONC206 in tumor cells.

#4915

Sensitivity to NAMPT inhibition: *In vitro* and *in vivo* characterization in ovarian cancer

Jenny J. Hong, Martina S. J. McDermott, Neil A. O'Brien, Enrique Guandique, Tong Luo, Dennis J. Slamon. *UCLA David Geffen School of Medicine, Los Angeles, CA*

Previous *in vitro* work on determining the unique sensitivities of various cancers to nicotinamide phosphoribosyltransferase inhibitors (NAMPTis) has demonstrated promising effects of treating cancer cells with NAMPTis such as FK866 and KPT9274. These inhibitors act by disrupting cellular energy metabolism and reducing intracellular NAD^+ levels. NAMPT inhibition thereby suppresses the proliferation of cancer cells which depend more heavily on the NAMPT enzyme to produce NAD^+ than noncancerous cells. Using pan-cancer in vitro screens in a large panel of molecularly characterized cell lines (n = 496) we identified a subset of ovarian cancer, a cancer with a high unmet need due to lack of diverse targeted therapies, as being extremely sensitive to NAMPT inhibition. Subsequent *in vivo* work using CD-1 nude mice demonstrate that NAMPT inhibitors can successfully reduce the ovarian tumor burden and may be an effective treatment option of some ovarian cancers.

Moreover, NAD^+'s function as a substrate to the poly ADP-ribose polymerase (PARP) enzyme makes NAMPTis rational candidates for including in combination therapies with PARP inhibitors, several of which are approved for maintenance therapy for ovarian cancer. By using

NAMPTis to disrupt the cellular metabolic process while simultaneously inhibiting PARP activity, an essential DNA damage repair enzyme, it is possible to exploit the dependence of ovarian cancer cells on functional PARP activity. This is particularly important in homologous recombination deficient subtypes. In addition to a synergistic growth inhibitory response in ovarian cancer cells, preclinical combination studies of NAMPTis with olaparib, an approved PARP inhibitor, exhibited higher levels of DNA damage accumulation than with single drug treatments. Our *in vitro* and *in vivo* characterizations of NAMPT inhibition suggest that NAMPTis as either single agents or in combination treatments with PARP inhibitors should be investigated further as potential treatment options for ovarian cancer patient populations.

#4916

Spatial analysis of local drug induced changes in tumor microenvironment predicts effective treatment combinations in breast cancer

Zuzana Tatarova[1], Dylan C. Blumberg[2], Gordon B. Mills[2], Lisa M. Coussens[2], Oliver Jonas[1], Joe W. Gray[2]. *[1]Brigham and Women's Hospital, Boston, MA,[2]Oregon Health & Science University, Portland, OR*

Anticancer therapeutics primarily designed to target tumor intrinsic mechanisms may also affect components of tumor microenvironment (TME) - immune cells and non-immune stroma. Recent literature reenforces the concept that complex interactions between drugs, neoplastic cells and cells of TME determine the efficacy of anticancer therapies. Systems understanding of these interactions can serve to predict effective treatment combinations simultaneously attacking tumor cell vulnerabilities, enhancing immune surveillance, and mitigating stromal mediators of resistance. The key challenge is to find such TME-modulating combinations in a fast and more informative way. We have developed an integrated analytical platform termed Multiplex Implantable Microdevice Assay (MIMA) to rapidly decompose cancer complexity in drug response and find biomarkers with predictive value for combination therapy efficacy including immunotherapy efficacy. The system deploys a (i) miniaturized implantable microdevice for localized intratumoral drug delivery and (ii) multiplex immunostaining to measure 30+ proteins in single cells at each

drug well. Computational analyses of local drug-induced changes provide information about the composition, functional state and spatial cell organization of the tumor and associated TME ultimately bringing new insights into drug mechanisms of action. We used MIMA in genetically engineered mouse models of breast cancer to evaluate effects of five targeted anticancer agents (olaparib, palbociclib, venetoclax, panobinostat, lenvatinib) and two chemotherapies (doxorubicin, paclitaxel) and predicted synergistic antitumor effects with anti-PD-1, anti-CD40, anti-CSF1R immunotherapies and vasculature modulating agents. Some of the most effective combinations were not reported before. A pan-HDAC inhibitor, panobinostat, that synergized with anti-PD-1, induced immunogenic cell death and infiltration of antigen presenting neutrophils. Further longitudinal spatial analyses revealed that mechanisms of resistance co-emerged with these response phenotypes and became prominent over time. We measured fibroblast, protumorigenic macrophage and cytotoxic B cell recruitment associated with heavy deposition of collagen VI, increased immune suppression and emergence of invasive and cancer stem cells. Combination with stroma modulating agent, losartan, improved the efficacy of panobinostat/anti-PD-1 in systemic studies implying that normalization of non-immune stroma might favorably alter aspects of TME for immune and targeted therapy efficacy. All in all, MIMA may represent a new approach to predict effective combination regimens for individual cancer patients. Extended MIMA use and computational modeling of the spatial cell patterns could provide actionable information for development of effective drug doses and schedules.

#4917

High-frequency irreversible electroporation ablation of glioma alters extracellular vesicles and disrupts the blood-brain barrier endothelium

Kelsey Murphy[1], Kenneth Aycock[2], Spencer Marsh[3], Alayna Hay[4], Christine Chang[5], Shay Bracha[6], Robert Gourdie[3], Rafael Davalos[2], John H. Rossmeisl[4], Nikolaos Dervisis[4]. *[1]Biomedical and Veterinary Sciences, Virginia-Maryland College of Veterinary Medicine, Blacksburg, VA,[2]Biomedical Engineering and Mechanics, Virginia Polytechnic and State Institute, Blacksburg, VA,[3]Fralin Biomedical Research Institute, Roanoke, VA,[4]Small Animal Clinical Sciences, Virginia-Maryland College*

of Veterinary Medicine, Blacksburg, VA,[5]Veterinary Small Animal Clinical Sciences, Texas A&M University College of Veterinary Medicine, College Station, TX,[6]The Ohio State University College of Veterinary Medicine, Columbus, OH

High-frequency irreversible electroporation (H-FIRE) is a nonthermal tumor ablation technology that kills cancer cells via pulsed electric fields. H-FIRE has been shown to precisely and nonthermally ablate brain tumors while transiently disrupting the peritumoral blood-brain barrier (BBB). The enhanced BBB permeability post-tumor ablation can be exploited to enhance therapeutic delivery to invasive tumor margins, but the mechanisms of H-FIRE-induced BBB disruption remain incompletely characterized. We hypothesize that bystander effects of H-FIRE tumor cell ablation, specifically the release of tumor-derived extracellular vesicles (TDEVs), mediate peritumoral BBB endothelium disruption. F98 glioma and bEnd.3 cerebral endothelial cell lines modelled primary brain cancer and the BBB endothelium, respectively. F98 glioma cells were treated *in vitro* with sham treatment, a sub-ablative (1,500 V/cm), or an ablative (3,000 V/cm) electric field dose of H-FIRE, and TDEVs were isolated from the supernatants via filtration and ultracentrifugation. Post-H-FIRE TDEVs were characterized via nanoparticle tracking analysis and transmission electron microscopy, with ablative doses of H-FIRE resulting in decreased release of TDEVs compared to sub-ablative H-FIRE and sham treatment. Post-H-FIRE TDEVs were then applied to Transwell models of the BBB endothelium to evaluate the effect of H-FIRE-induced TDEVs on BBB endothelium permeability. TDEVs released after the ablative H-FIRE dose (3,000 V/cm) significantly increased permeability of the BBB endothelium *in vitro* compared to TDEVs released after sub-ablative and sham H-FIRE treatment. TDEVs were then fluorescently labelled with CFSE, and confocal microscopy was used to characterize internalization of post-H-FIRE TDEVs by cerebral endothelial cells. The TDEVs released after ablative doses of H-FIRE were significantly internalized by bEnd.3 cerebral endothelial cells, while TDEVs released after sub-ablative and sham treatment were not internalized. The proteomic payloads of the post-H-FIRE TDEVs were characterized using mass spectrometry, and clustering analysis demonstrated that the *in vitro* BBB-modulatory TDEVs released after 3,000 V/cm H-FIRE had distinct proteomic payloads compared to the

non-BBB-modulatory TDEV populations released after sham and 1,500 V/cm H-FIRE treatment. Proteins associated with proteasomal degradation, cellular adhesion, and modulation of junctional integrity were increased in the BBB-modulatory group of TDEVs. Taken together, our results suggest that H-FIRE ablation of glioma significantly alters the proteomic cargo of TDEVs to increase internalization of TDEVs by cerebral endothelial cells and increase permeability of the BBB endothelium.

#4918

Natural compounds ursolic acid and digoxin exhibit anti-cancer effects through nuclear receptor RORγ-dependent and -independent mechanisms

Hongye Zou, Yatian Yang, Demin Cai, Hong-Wu Chen. *Department of Biochemistry and Molecular Medicine, UC Davis, Sacramento, CA*

Natural compounds such as ursolic acid (UA) and digoxin isolated from fruits and other plants display potent anti-cancer effects in preclinical studies. UA and digoxin have also been at several clinical trials for treatment of different cancers including prostate cancer, pancreatic cancer and breast cancer. However, they displayed limited benefit to patients. Currently, a poor understanding of their direct targets and mechanisms of action (MOA) in tumor cells severely hinders their further development. We previously identified nuclear receptor RORγ as a novel therapeutic target in castration-resistant prostate cancer (CRPC) and triple-negative breast cancer (TNBC). Previous studies implicated UA and digoxin as potential RORγ antagonists in modulating the functions of immune cells such as Th17 cells. Here we showed that UA displays a strong activity in inhibition of RORγ-dependent transactivation function, while digoxin exhibits no effect at clinically relevant concentrations. In prostate cancer cells, UA down-regulates RORγ-stimulated AR expression and AR signaling, whereas digoxin up-regulates AR signaling pathway. UA also showed potent anti-growth effects in AR-positive prostate cancer cells compared to AR-negative prostate cancer cells. In TNBC cells, UA but not digoxin alters RORγ-regulated cell proliferation and apoptosis gene programs. Together, our study shows for the first-time that UA, but not digoxin, acts as a natural antagonist of RORγ in prostate cancer and TNBC cells. Our finding that

RORγ is a direct target of UA in specific type of cancer will help select patients with tumors that likely respond to UA treatment.

#4919

Estrogen regulates the immune microenvironment and immunotherapy response of colorectal liver metastases

Yasmine Benslimane[1], Sarah Lapin[1], Julien Chambon[2], Stephanie Perrino[2], Pnina Brodt[1]. *[1]McGill University, Montreal, QC, Canada,[2]Research Institute of the McGill University Health Centre, Montreal, QC, Canada*

Liver metastases (LM) remain a major cause of cancer-related death and many cancers preferably metastasize to the liver due to its unique anatomical location, rich blood supply and immune-tolerant microenvironment. Up to 50% of colorectal carcinoma patients develop LM during their disease and this is associated with a poor prognosis. Our laboratory previously identified a sexual dimorphism in the regulation of the immune microenvironment (IME) of LM and showed that estrogen could promote the accumulation of myeloid-derived suppressor cells (MDSCs) and Tregs in the liver in response to invading cancer cells. The objective of this study was to elucidate the role of estrogen in the recruitment and polarization of other immune cells and to determine the therapeutic potential of Selective Estrogen Receptor Degrader (SERD) therapy in CRCLM bearing female mice, and evaluate if SERD would improve anti PD-1 immunotherapy efficacy. In estrogen-competent female mice bearing CRCLM, we found increased gene and protein expression of the immunosuppressive cytokine TGF-β, and inversely a decrease in the pro-inflammatory cytokine TNF-alpha. Furthermore, we identified a significant decrease of immunosuppressive CD68+CD163+ M2 macrophages, and an increase of the pro-inflammatory CD68+TNF-alpha+ M1 macrophages in estrogen-depleted (ovariectomized) mice as compared to estrogen-competent mice. This observation was reversed upon estradiol supplementation. Moreover, treatment of female mice with the SERD Fulvestrant, markedly reduced the number of CRCLM compared to vehicle-treated mice, reduced the cell frequencies and counts of M2 macrophages, significantly increased NK cells recruitment in the liver. The addition of SERD to immunotherapy has a better therapeutic effect than both therapies alone, and increased CD8+ T-cells, NK cells, and M1/M2 macrophages

ratio. Taken together, our results identify estrogen as a critical regulator of an immunosuppressive TME in the liver and a potential therapeutic target to enhance immunotherapy efficacy.

Drug Resistance in Molecular Targeted Therapies 3

#3851

Targeting RET solvent-front mutants with an alkynyl nicotinamide-based inhibitor

Ujjwol Khatri[1], Neetu Dayal[2], Xueqing Hu[1], Elizabeth Larocque[2], Nimishetti Naganna[2], Tao Shen[1], Xuan Liu[1], Frederick W. Holtsberg[3], M. Javad Aman[3], Herman O. Sintim[2], Jie Wu[1]. *[1]University of Oklahoma Health Sciences Center, Oklahoma City, OK,[2]Purdue University, West Lafayette, IN,[3]KinaRx, Rockville, MD*

Selpercatinib (LOXO-292, LY3527723) and pralsetinib (BLU-667) are first-in-class RET-targeted cancer therapy drugs. However, secondary RET mutations that confer selpercatinib/pralsetinib resistance have been identified, necessitating development of next-generation RET Tyrosine kinase inhibitors (TKIs). While the G810C/R/S/V mutations located at the RET kinase solvent-front site were detected in selpercatinib-treated patients, it was unclear whether all of these and other potential G810 mutants are resistant to selpercatinib and pralsetinib. We profiled selpercatinib and pralsetinib on all six possible G810 mutants derived from single nucleotide substitution. Surprisingly, the G810V mutant found in a clinical study was not resistant to selpercatinib or pralsetinib. Besides G810C/R/S, G810D also conferred selpercatinib/pralsetinib resistance. We found that alkynyl nicotinamide compounds such as HSN608 have better drug-like properties than alkynyl benzamides. HSN608 inhibited RET and RET V804M gatekeeper mutant, and all six G810 mutants with low nanomolar IC_{50}s in the BaF3/KIF5B-RET mutant cell model. In cell derived xenograft (CDX) tumors driven by KIF5B-RET(G810C), HSN608 caused regression of the selpercatinib-resistant tumors. This study clarifies the sensitivities of different RET solvent-front mutants to selpercatinib and pralsetinib, and identifies an alkylnyl nicotinamide-based RET TKI for inhibiting selpercatinib/pralsetinib-resistant G810 mutants.

#3852

IK-930, a paralog-selective novel TEAD-inhibitor, effectively attenuates drug-tolerant persister cell proliferation

Daniel Hidalgo, Marta Sanchez-Martin, Mihir Rajurkar, George Punkosdy, Jeffrey Ecsedy, Lan Xu. *Ikena Oncology, Boston, MA*

The Hippo pathway is commonly mutated or altered in human cancers. In addition to the primary genetic driving mutations, the downstream effectors of the Hippo pathway comprising the transcriptional coactivators YAP1 and TAZ and the TEAD transcription factors can be activated upon prolonged inhibition of other oncogenic pathways such as EGFR and MAPK. We showed that combining the novel, paralog selective TEAD inhibitor, IK-930, with osimertinib or trametinib in EGFR or KRAS mutated tumors, led to enhanced apoptosis *in vitro* and beneficial antitumor activity *in vivo*. Experimental models demonstrated that upon inhibition of EGFR with osimertinib, a subpopulation of drug tolerant cells defined as ‘persisters’ can survive treatment allowing for the accumulation of additional genetic and epigenetic alterations. These alterations in the persister cells can give rise to resistant tumors and cancer relapse. Previous studies have implicated YAP/TEAD signaling in the emergence and survival of the persister cells. To investigate the role of YAP/TEAD signaling in persister cell emergence, EGFR and KRAS mutant NSCLC cell lines were engineered to express a TEAD luciferase reporter. Treatment with EGFR or MEK inhibitors, at concentrations that do not elicit significant cell death, induced TEAD-mediated transcription after several days of treatment, indicative of an adaptive response to chronic target inhibition. Concurrent treatment with the TEAD inhibitor, IK-930, abolished TEAD-mediated transcription. Using time lapse microscopy, the cell cycle and proliferation of EGFR mutant cultured cells, engineered to express a fluorescence-based cell-cycle indicator (FUCCI), were quantified when treated with osimertinib alone or combined with IK-930. Treatment with osimertinib led to a rapid induction of cell death. However, after several days, a drug tolerant population emerged and reentered the cell cycle even with chronic osimertinib treatment. Interestingly, the emergence of these persister cells coincided with maximum TEAD activity. Concurrent addition of IK-930, as well as addition of IK-930 after the emergence of the osimertinib-tolerant persister

cells, attenuated cell proliferation and expansion, demonstrating the potential for IK-930 to prevent resistance to EGFR inhibitors and even reverse the effect when given after resistance has already emerged. Current efforts are focused on the characterization of the persister population and on evaluating the role of YAP/TEAD signaling in resistance to other targeted therapies.

#3853

The TWIST1-p27 signaling pathway is a critical determinant of MET TKI cell cycle arrest and resistance in *MET* altered non-small cell lung cancer

Vinod Kumar[1], Zachary A. Yochum[1], Princey Devadassan[1], Eric Huang[1], Ethan Miller[1], Vasavi Ayyala[1], Purva H. Rumde[1], Roja Baruwal[1], James O'Brien[1], Laura P. Stabile[2], Timothy F. Burns[3]. *[1]University of Pittsburgh School of Medicine, Pittsburgh, PA,[2]Pharmacology and Chemical Biology, University of Pittsburgh School of Medicine, Pittsburgh, PA,[3]Hematology-Oncology, University of Pittsburgh School of Medicine, Pittsburgh, PA*

Advancement in classifying NSCLC into molecularly defined subgroup that respond to specific therapies have shifted the treatment paradigm towards personalized targeted therapy approach. A major obstacle for the treatment of oncogene driven non-small cell lung cancer (NSCLC) patients is both *de novo* and acquired resistance to targeted therapies. Approximately 4-6% of NSCLC patients harbor *MET* amplifications/mutations which are important targetable oncogenic drivers in the clinic. In addition, *MET* amplification has also emerged as a common mechanism of acquired resistance to EGFR TKIs as well as other targeted therapies. Crizotinib, tepotinib and capmatinib are FDA approved MET TKIs for *MET* exon 14 skipping mutant NSCLC and have shown activity against *MET* amplified NSCLC as well. Despite high response rates with these newer TKIs, the majority of patients with targetable *MET* alterations fail to respond and acquired resistance is inevitable. Multiple molecular mechanisms of MET TKIs resistance encompassing both on-target (HGF overexpression) and bypass have been identified. Furthermore, at the time of resistance, an epithelial-to-mesenchymal (EMT) phenotype is often observed. We have found that HGF/MET pathway is a major regulator of the TWIST1, TWIST1 is required for *MET* altered NSCLC and cooperatives with HGF *in vivo* during

tumorigenesis. Here, we reported that EMT transcription factor TWIST1 mediates a bypass of a MET TKI-mediated p27-dependent growth arrest. To study the mechanism of TKI resistance in *MET* altered NSCLC, we used multiple *MET* dysregulated human cell lines (H1437, H596, H1993, and H1648), a novel acquired resistance model of MET TKI resistance (H1993-CR cells), two syngeneic tobacco carcinogen induced mouse lung cell lines (FVBW-17 and FVBCH-17), and three different animal models (mouse xenografts, PDXs, transgenic animals). We found that TWIST1 overexpression led to MET TKI resistance *in vitro* and *in vivo* in *MET* altered cell lines by overcoming cell cycle arrest. This was accompanied by a failure to induce p27 in the presence of TWIST1 overexpression. Similarly, loss of p27 induction and G1 arrest was also observed in our model of acquired MET TKI resistance. Conversely, TWIST1 inhibition restore sensitivity to TKIs *in vitro* and *in vivo* and lead to induction of p27. p27 appears to be require for MET TKI induced cell cycle arrest and sensitivity as silencing p27 lead to MET TKI resistance. Our findings suggest that targeting TWIST1 may be an effective therapeutic strategy to overcome HGF-MET-driven resistance in *MET*-driven NSCLC.

#3854

TNIK inhibition as a novel therapeutic in cMyc high/TTF1 low SCLC

Azusa Tanimoto[1], Robert J. Cardnell[1], Benjamin B. Morris[1], Kavya Ramkumar[1], Shen Li[2], Qi Wang[2], Allison C. Stewart[1], Carl Michael Gay[1], Jing Wang[2], Lauren Averett Byers[1]. *[1]Center Department of Thoracic/Head & Neck Medical Oncology, The University of Texas MD Anderson Cancer Center, Houston, TX,[2]Department of Bioinformatics & Computational Biology, The University of Texas MD Anderson Cancer Center, Houston, TX*

Background**:** Small cell lung cancer (SCLC) is a highly lethal malignancy, with rapidly acquired chemotherapy resistance. Some studies have reported that Wnt signaling pathway activation promoted cell proliferation and was correlated with chemo-resistance in SCLC. None of the therapies targeting Wnt pathway components of the transmembrane and the cytoplasm have been successful in a clinical application due to toxicity and insufficient efficacy. However, targeting Wnt signaling inside the nucleus has been drawing increasing attention as cancer therapeutics. TRAF2 and NCK-interacting protein kinase (TNIK), which interacts with downstream

effectors, TCF4/β-catenin transcriptional complex, is an essential activator of Wnt target genes. TNIK is highly expressed in several cancers for cell proliferation, thus TNIK is expected as a novel druggable target. On the other hand, the question remains whether TNIK is a critical target in SCLC. We hypothesize that a TNIK inhibitor has potent anti-tumor effects in SCLC and its promising biomarkers exist.
Methods: We used 29 SCLC cell lines including all four subtypes defined by differential expression of transcription factors ASCL1, NEUROD1, POU2F3, and inflamed gene signature (SCLC-A, N, P, and I, respectively) to evaluate the effect of a TNIK inhibitor, NCB-0846 in vitro. We correlated NCB-0846 IC50 values with proteomic profiling (Reverse Phase Protein Array, RPPA) data. Protein expression was examined by western blotting.
Results: NCB-0846 markedly reduced cell proliferation in SCLC-N and P cell lines. There was a strong positive correlation between cMyc and the efficacy of NCB-0846 ($r=-0.484$, $P<0.01$), while a negative correlation between TTF1 and the efficacy ($r=0.569$, $P<0.01$). Additionally, NCB0846 decreased the expression of cMyc in cMyc-high/TTF-1 low SCLC cells.
Conclusions: These findings indicate that TNIK inhibitors may be a new personalized molecular-targeted therapy in cMyc-high/TTF-1-low SCLC.

#3855
Establishment and characterization of a panel of breast XPDX models representing innate or acquired resistance to trastuzumab deruxtecan (T-DXd)
Maci DeBoer[1], Albert Paez[1], Johnnie Flores[1], Robyn Baeza[1], Alyssa Simonson[1], Jim Lund[1], Kyriakos Papadopoulos[2], Thomas Gribbin[3], Amy Lang[4], Gladys Rodriguez[4], Lorena Mozas[1], Lorena Gonzalez[1], Manish Sharma[5], Emiliano Calvo[6], Tatiana Hernandez[7], Michael J. Wick[1].
[1]XenoSTART, San Antonio, TX,[2]START San Antonio, San Antonio, TX,[3]CHCWM, Grand Rapids, MI,[4]START Center, San Antonio, TX,[5]START Midwest, Grand Rapids, MI,[6]START Madrid, Madrid, Spain,[7]START Barcelona, Barcelona, Spain

Background: Trastuzumab deruxtecan (T-DXd) is an ADC consisting of an anti-HER2 antibody linked to a novel topoisomerase I inhibitor payload approved for T-DM1-refractory, HER2+ breast cancer (BC) and metastatic,

recurrent HER2-low BC. While this therapy is effective in some patients, resistance often develops. To aid in developing new therapies for T-DXd-resistant BC and better understand potential resistance mechanisms, we established a panel of six breast XPDX models representing innate or acquired resistance to T-DXd. These models, designated ST4565C, ST4565D, STM148B, STM148C, STM148D, and ST4480B/EHR were developed and characterized for receptor expression, genomics, and drug sensitivities toward chemotherapies and targeted agents including T-DXd, T-DM1, and margetuximab.

Methods: ST4565C/D was established from a patient with ER+/HER2+, metastatic BC who was T-DXd treatment naïve. ST4565C was collected post chemo- and HER2-targeted therapies; ST4565D was collected following eribulin/margetuximab. STM148B/C/D were established from a patient with ER-/HER2+ metastatic BC following trastuzumab, T-DM1, and eleven months of T-DXd. ST4480B/EHR was established by chronic in vivo T-DXd dosing to the parent ST4480B ER+/HER2+ model until resistance developed. Resulting models were passaged and receptor expression confirmed by IHC and genomic analyses, including WES and RNA_{seq}, were performed to further characterize models. In vivo, models were tested with agents including: trastuzumab, T-DM1, and T-DXd; endpoints included tumor volume (TV) and time from treatment initiation (TTI) with %T/C values and tumor regression reported at study completion; a %T/C of ≤ 20 versus control was considered sensitive. Tumor regression (%T/C=<0) versus Day 0 TV was also reported.

Results: Models retained receptor expression and similar histology comparable with archival clinical or model samples. In vivo, all ST4565 and STM148 models were refractory to trastuzumab, T-DM1, and T-DXd up to 10 mg/kg weekly with an average %T/C of 75%. ST4480B/EHR showed similar resistance to trastuzumab and T-DM1 at 10 mg/kg, and T-DXd at 3 mg/kg; T-DXd tested at 3 mg/kg in the ST4480B parent model resulted in tumor regressions. Sequencing of ST4565C/D identified a novel fusion, MTAP/CDKN2A/B deletions and elevated expression of FGFR1 and CCND1. In STM148 models an AKAP8L-NOTCH3 fusion and PIK3CA and CCNE1 mutations were reported. ST4480B/EHR reported $PIK3CA^{E545K}$ and an ESR1-CCDC170 fusion identical to the parent model, but differential expression was noted in several genes in the RICTOR/TORC2 pathway.

Conclusion: We established and characterized six breast XPDX models representing innate or acquired resistance to T-DXd. These models are valuable tools in understanding resistance mechanisms and in developing novel therapies for T-DXd-resistant patients.

#3856

Evaluation of replication protein A inhibitor, NERx329 in combination with EGFR mutant targeted therapy

Reshma Bhowmick[1], John J. Turchi[1], Shadia I. Jalal[2]. *[1]Indiana University School of Medicine, Indianapolis, IN,[2]Hematology Oncology, Indiana University School of Medicine, Indianapolis, IN*

Lung cancer is the leading cause of cancer related deaths worldwide with the majority (~80%) of patients diagnosed with non-small lung cancer (NSCLC). Targeted therapies directed against tumor initiating growth factor receptors are effective treatment options for driver mutation positive NSCLC. Osimertinib is a third-generation EGFR-Tyrosine Kinase inhibitor (TKI) that has activity against EGFR exon 19, exon 21, and T790M mutations. Unfortunately, Osimertinib treated patients acquire resistance and median progression free survival is 18 months. Moreover, Osimertinib does not cure stage IV EGFR mutant NSCLC. The acquisition of secondary mutations leading to activation of bypass pathways, MET amplification, EMT, compensatory pathway activation and histological transformation to small cell phenotype are major causes of acquiring resistance to EGFR TKIs. Proliferating cancer cells regularly experience a low level of replication stress. Additionally, receptor tyrosine kinases such as EGFR are known to interact with DNA repair proteins and impact DNA damage repair following chemotherapy, radiation therapy, and EGFR TKI treatment. However, the role of DNA repair pathways in EGFR-TKI resistance is unknown and the interaction between EGFR pathway, DNA damage, and repair pathways has not been fully elucidated. At low-level replicative stress promotes genomic instability but at a high level through mitotic catastrophe it causes cell death. Replication protein A is a critical sensor of the DNA damage response detecting replication stress. The small molecule inhibitor of RPA, NERx 329, sequesters active RPA and induces replication catastrophe and cell death. Here we demonstrate that NERx329 in combination with Osimertinib enhanced Osimertinib mediated cell death.

CCk-8 assays performed after 48h of NERx329 and Osimertinib combination treatment result in a robust decrease in IC_{50} compared to single agent therapy. Dissection of signaling pathways leading to this death-promoting effect of NERx329 showed a combination of bypass pathway marker (AXL) and compensatory pathway marker (STAT) inhibition in AXL-high expressing EGFR mutant lung cancer cells. Whereas inhibition of STAT pathway was responsible for the death-promoting effect of NERx329 in AXL-low expressing EGFR mutant lung cancer cells. AXL and STAT inhibition are associated with induced DNA damage and impaired DNA repair. From these data, we infer that DNA damage repair pathways could be involved in TKI resistance and NERx329 could be a promising drug candidate for combination targeted therapy.

#3857

Exploring mechanisms of resistance to elraglusib in pancreatic cancer PDX models

Taylor Weiskittel[1], Ding Li[1], Lingling Han[1], Joseph McDermott[2], Benedito Caneiro[3], Hu Li[1], Daniel Billadeau[1], Andrew Mazar[4]. *[1]Mayo Clinic, Rochester, MN,[2]Latern Pharma Inc., Dallas, TX,[3]Brown University, Providence, RI,[4]Actuate Therapeutics Inc., Forth Worth, TX*

Metastatic pancreatic cancer patients who previously progressed on nab-paclitaxel/gemcitabine (average of 3 previous lines if treatment) were treated with elraglusib in combination with a rechallenge of this combination. The majority of patients demonstrated a prolonged progression free survival. While this early clinical evidence is highly encouraging, the biological determinants of elraglusib response are unknown. *In vitro* screens of elraglusib on pancreatic PDX cell lines showed that some tumor cells possess modest intrinsic resistance to elraglusib as measured by LD50 which ranged from 316.9 nM to 1080 nM in a screen of 10 cell lines. To explore this phenomena further, we induced resistance in three cell line models by growing cells in the presence of increasing concentrations of elraglusib. We then sequenced the transcriptome of the parental and resistant lines to identify potential mechanisms of elraglusib resistance. Comparison of RNA sequencing profiles identified upregulation of the Aldo-keto reductase (AKR) family of genes. This upregulation was confirmed by qRT-PCR and by immunoblot

demonstrating that AKRs were upregulated at both the transcriptomic and protein level. We further quantified the AKR levels in the remainder of the 10 cell lines and found that many of the more resistant lines had high expression of AKR1C2. However, not all of the resistant lines had high expression which could be because they have a separate mechanism of resistance to elraglusib. A large body of literature has found that AKR genes provide resistance to many other small molecule inhibitors either by direct metabolism or by indirectly relieving oxidative stress. Given these results, we identify aldo-keto reductases as potentially associated with elraglusib resistance, but further investigation is warranted to establish a causal link between AKR and the resistant phenotype.

#3858

Exploring Exportin-1 as a therapeutic vulnerability in squamous cell carcinoma

Vidushi Durani[1], Rebecca Caeser[2], Charles M. Rudin[3], Alvaro Quintanal-Villalonga[2], Harsha Sridhar[2], Parvathy Manoj[2], Sam E. Tischfield[2], Marina Asher[2], Umeshkumar Bhanot[2], Jacklynn V. Egger[2], Nicholas D. Socci D. Socci[2], Nisargbhai S S. Shah[2], Elisa de Stanchina[2], Natasha Rekhtman[2].
[1]Weill Cornell Grad. School of Medical Sci., New York, NY,[2]Memorial Sloan Kettering, New York, NY,[3]Memorial Sloan Kettering Cancer Center, New York, NY

Introducti**on:** Squamous cell carcinomas (LUSCs) account for 25-30% cases of non-small cell lung cancers, making them the second most common histology of lung cancer after adenocarcinomas. For the latter, molecular characterization has defined tumor subsets with discrete driver alterations sensitive to targeted inhibitors, leading to significant improvement in patient survival. However, for LUSCs, to date no specific drivers have been described that are amenable for pharmacological targeting and no targeted therapies are approved for use in this setting. Despite decades of research, LUSCs are still treated with cytotoxic chemotherapy, and now concomitant immunotherapy, which does not achieve durable responses in most patients. Thus, identification of targetable vulnerabilities in this setting remains a critical unmet clinical need. Preliminary data from our lab has identified the nuclear exporter exportin 1 as a therapeutic vulnerability in small cell lung carcinomas.

Exportin 1 (XPO1) inhibition with Selinexor, a drug approved for clinical use in the setting of hematological malignancies, induces significant sensitivity in combination with cisplatin and irinotecan. Here, we explored the role of XPO1 as a therapeutic target in LUSC.
Methods: We performed a comprehensive multi-omic molecular characterization of a library of LUSC patient-derived xenografts (PDXs) (N=28, with 17 clinical samples being matched pairs). IHC, RNA-seq and NGS via MSK-IMPACT were performed on 27 samples. To examine the potential of XPO1 inhibition as sensitizer to chemotherapy in LUSC, we performed genetic and pharmacological inhibition experiments in LUSC cell lines exhibiting high XPO1 expression.
Results: Of the 28 models, 19 samples (68%) were from primary tumors and 9 samples (32%) from metastasis. The sample set were roughly split in half with regard to treatment status; 15 samples (54%) were treatment naïve and 13 sample were treated (46%).XPO1 is highly expressed in LUSCs clinical specimens compared to other tumor types, and its knockdown reduces tumorigenic features of LUSC cell lines with high XPO1 expression, including proliferation and anchorage-independent growth. Targeted XPO1 inhibition with selinexor induces chemotherapy sensitization to carboplatin and paclitaxel, drugs currently used in the treatment of LUSC, as depicted by high cytotoxic synergy scores of selinexor with either drug.
Conclusion: Our data suggest that XPO1 expression may exert pro-oncogenic effects in LUSC, consistent with its upregulation in this tumor setting, and that its inhibition with selinexor may strongly sensitize to chemotherapy. Assessment of efficacy of combination therapies with selinexor *in vivo* will assess the potential of these combinations as a therapeutic approach for LUSC tumors. The clinical availability of selinexor would allow immediate clinical translation of the results generated in this project.

#3859
Alterations in hormone receptors regulome following response to kinase inhibitors in lethal prostate cancer
Remi M. Adelaiye-Ogala[1], Surendra Gulla[1], Jonathan E. Bard[2], David J. VanderWeele[3], Kathleen Kelly[4]. *[1]Medicine/ Division of Hematology and Oncology, University at Buffalo, Buffalo, NY,[2]Genomics and Bioinformatics*

Core, New York State Center of Excellence for Bioinformatics and Life Sc, University at Buffalo, Buffalo, NY,[3]Hematology and Oncology, Northwestern University, Chicago, IL,[4]Laboratory of Genitourinary Cancer Pathogenesis, NCI/NIH, Bethesda, MD

The androgen receptor (AR) signaling axis is critical for prostate cancer (PCa) pathogenesis and all subsequent phases of disease progression. Although initial success with androgen deprivation therapy and AR-targeted agents such as enzalutamide or abiraterone, most patients inevitably relapse due to therapeutic resistance. Previous studies have shown that genomic AR is unchanged despite resistance to AR antagonists, and its gene expression is unaltered. Therapeutic resistance is broadly classified into two categories; restoration of AR activity and tumor progression despite AR blockade. Indeed, others have noted an extensive reprogramming of the AR cistrome in clinical and preclinical specimens, where a shift in canonical to non-canonical AR cistrome is associated with an increase in Gleason grade. In previous studies, we observed increases in known AR target genes following exposure to kinase inhibitors which was marked by a decrease in tumor growth. We hypothesized that restoration of canonical AR cistrome can be mediated through kinase inhibition and is associated with re-sensitization to AR-targeted therapy. In addition, we treated cell lines and patient-derived xenograft models of advanced prostate cancer with kinase signaling pathway inhibitors, AR signaling inhibitors, or a combination of both for 24 hours (in vitro) or five days (in vivo). In addition, samples were collected and processed for RNA-seq and ChIP-seq. Our transcriptomic analysis showed enrichment of previously published non-canonical AR target genes in cells resistant to AR-targeted agents. When resistant cells were exposed to kinase inhibitors, we observed an enrichment of canonical AR target genes. In addition, we identified unique AR-enriched peaks at active sites associated with resistance. Through GSEA of gene annotated peaks, we found unique regulatory transcription factor targets, some of which are associated with cell proliferation and differentiation and may play a functional role in AR cistrome adaptation to resistance and survival. Overall, our data suggest that AR transcription adapts to the therapeutic resistance of AR antagonists via the enrichment of non-canonical AR cistrome. Furthermore, restoration of canonical AR cistrome is achieved

following kinase signaling pathway inhibition and is associated with re-sensitization to AR-targeted therapy.

#3860

ERK1/2 inhibition overcomes resistance to venetoclax in AML by altering mitochondrial metabolism

Priyanka Sharma[1], Lauren Ostermann[1], Sujan Piya[1], Natalia Baran[1], Anudishi Tyagi[1], Christopher Hindley[2], Kim-Hien Dao[3], Martin Sims[2], V. Lokesh Battula[1], Michael Andreeff[1], Gautam Borthakur[1]. *[1]Departments of Leukemia, UT MD Anderson Cancer Center, Houston, TX,[2]Astex Pharmaceuticals, Cambridge, United Kingdom,[3]Astex Pharmaceuticals, Inc., Pleasanton, CA*

Background: Primary or secondary resistance to venetoclax is pervasively associated with mutational/non-mutational activation of RAS/RAF/ERK pathway which confers metabolic alterations as a compensatory adaptation. Preclinical models of venetoclax resistance and primary patient samples (n=8) were used to assess the synergy of concomitant Bcl2 and ERK1/2 inhibition followed by RNAseq analysis to identify molecular mechanisms responsible for overcoming resistance to venetoclax.
Results: ERK1/2 inhibition using Compound 27 (ERKi, Heightman et al., J Med Chem. 2018), an analog of ASTX029, was highly synergistic with venetoclax at inducing apoptosis in AML. NRAS-mutant OCI-AML3 and THP1 cells, that are inherently resistant to venetoclax, were sensitized to venetoclax when combined with ERKi with ~90% apoptosis compared to 20% by venetoclax alone (Combination Index = 0.008). Synergy was also confirmed using isogenic OCI-AML2 cells with lab-generated acquired resistance to venetoclax, resulting in 75% apoptosis versus 22% by venetoclax (CI=0.6). Leukemia progenitor cells in primary AML samples were also depleted by the ven+ERKi combination (CI:0.03-0.23). In line with our in-vitro findings, treatment with ASTX029 as a single agent or in combination with venetoclax significantly inhibited leukemia burden and increased survival in an OCIAML3 xenograft model ($p<0.05$). Single agent ERKi and combination treatment using an NRAS-mutant PDX resulted in significantly impaired clonogenic potential and decreased expression of cMyc and CD44 in CD34+CD38- population as demonstrated by CyTOF, indicating depletion of progenitors. Transcriptomic profiling of OCIAML3

cells revealed upregulation of 6 pathways in response to venetoclax including oxidative phosphorylation (OXPHOS), electron transport chain, Myc targets, E2F targets, epithelial mesenchymal transition and KRAS signaling. Interestingly, these pathways were downregulated after ERKi+venetoclax treatment along with decrease in glycolysis and fatty acid metabolism (FDR<0.05). Since, venetoclax treatment significantly enriched for OXPHOS, we examined the metabolic effect of ERKi to overcome venetoclax resistance. Seahorse analysis showed increased basal and maximal respiration, and ATP production in OCIAML2 venetoclax resistant versus parental cells. Combining ERKi with venetoclax reduced OCR and ATP production in OCIAML3 and OCIAML2-venetoclax resistant cells. This was accompanied by an increase in membrane depolarization ($p=0.001$) as well as enhanced mitochondrial ROS ($p<0.001$).
Conclusion: The inhibition of ERK1/2 alters mitochondrial metabolism and functional integrity to overcome resistance to venetoclax by causing apoptosis in venetoclax resistant AML cells. These data provide a strong rationale for the combination of ERK1/2 and Bcl-2 inhibitors in treatment of AML and warrant further investigation in the clinic.

#3861
c-MYC mediated resistance to trametinib plus hydroxychloroquine in pancreatic cancer is overcome by CDK4/6 and lysosomal inhibition
Mark Silvis, Dilru Silva, Rohweder Riley, Sophia Schuman, Swapna Gudipaty, Amanda Truong, Jeffery Yap, Kajsa Affolter, Martin McMahon, Conan Kinsey. *University of Utah Huntsman Cancer Institute, Salt Lake City, UT*

Pharmacological inhibition of KRAS>RAF>MEK>ERK signaling has provided no clinical benefit to patients with pancreatic ductal adenocarcinoma (PDA). Interestingly, combined inhibition of MEK1/2 (with trametinib, T) plus autophagy (with chloroquine, CQ, or hydroxychloroquine, HCQ) demonstrated striking anti-tumor effects in preclinical models and in a patient (Patient 1). However, not all patients respond to the T/HCQ regimen, and Patient 1 eventually developed resistant disease. Here we report that primary or acquired resistance is associated with focal DNA copy number gains encompassing *c-MYC*. Furthermore, ectopic expression of c-MYC in PDA cell lines rendered them T/HCQ

resistant. Interestingly, a CDK4/6 inhibitor, palbociclib (P), also induced autophagy and overrode c-MYC-mediated T/HCQ resistance, such that P/HCQ promoted regression of T/HCQ resistant PDA tumors with elevated c-MYC expression. Finally, P/HCQ treatment of Patient 1 resulted in a biochemical disease response. These data suggest that elevated c-MYC expression is both a marker and a mediator of T/HCQ resistance, which may be overcome by the use of palbociclib plus hydroxychloroquine.

#3862

IGFBP3 promotes resistance to olaparib via modulating EGFR signaling in advanced prostate cancer

Amy R. Leslie, Shu Ning, Leandro S. D'Abronzo, Cameron Armstrong, Masuda Sharifi, Zachary A. Schaaf, Wei Lou, Christopher P. Evans, Hong-Wu Chen, Alan Lombard, Allen C. Gao. *Urologic Surgery, UC Davis, Sacramento, CA*

Background: Castration-resistant prostate cancer (CRPC) is an incurable disease and a leading cause of cancer death in men worldwide. Olaparib (Lynparza) was among the first PARP inhibitors (PARPi) approved for the treatment of CRPC tumors harboring DNA repair defects. However, clinical resistance to PARPi's has been documented. The mechanisms underlying resistance to PARPi's remain elusive. To study acquired resistance, we developed olaparib-resistant LN-OlapR and 2B-OlapR cell lines generated through chronic olaparib treatment of the olaparib-sensitive cell lines LNCaP and C4-2B, respectively. RNA-seq revealed IGFBP3 is overexpressed in both OlapR cell lines. IGFBP3 overexpression is correlated with poor clinical outcome and is thought to participate in DNA repair pathways. IGFBP3 plays a key role in nonhomologous end joining (NHEJ) repair through a ternary complex with EGFR and DNA-PKcs. The IGFBP3/EGFR signaling axis is thought to modulate NHEJ repair and could have implications for PARPi sensitivity. We hypothesize that increased IGFBP3 expression promotes PARPi resistance by enhancing DNA repair capacity.
Methods: RNA-sequencing and gene set enrichment analysis were used to determine the expression profile changes in resistant cells compared to parental cells. Real time PCR and western blots confirmed the expression of DNA damage repair genes such as γH2AX, EGFR, and DNA-PKcs. ELISA

was used to determine IGFBP3 secretion. RNAi was used to inhibit IGFBP3 and EGFR expression. Gefitinib was used to inhibit EGFR activity. Cell viability assays were used to assess cell growth.
Results: Transcriptomic profiling revealed that IGFBP3 is highly expressed in resistant models. We verified increased levels of IGFBP3 RNA and protein in both OlapR models. We found that RNAi inhibition of IGFBP3 increases γH2AX and cleaved-PARP protein levels in the resistant models, which suggests accumulation of DNA double strand breaks (DSBs) leading to genomic instability and cell death. We discovered increased phosphorylation of EGFR and DNA-PKcs in the resistant cells. Furthermore, silencing/inhibiting IGFBP3 and EGFR reduces OlapR cell viability and resensitizes resistant cells to treatment.
Conclusions: Our findings demonstrated that inhibiting IGFBP3 and EGFR aids in PARPi sensitivity in the resistant setting. Future work will utilize OlapR models to study how the IGFBP3/EGFR/DNA-PKcs protein complex promotes the development of resistance. Understanding the role of IGFBP3 in PARPi resistance will enhance our ability to re-sensitize resistant CRPC to PARPi therapeutics.

#3863
Aminoflavone confers activity against aromatase inhibitor-resistant breast cancer cells in part via miR125b2-3p restoration
Eileen J. Brantley, Nicole Mavingire, Salma Khan, Gayathri Nagaraj, Shawnee Angeloni, Charles Wang, Ubaldo Soto. *Loma Linda Univ. School of Medicine, Loma Linda, CA*

Aromatase inhibitor therapy is the most crucial adjuvant treatment option for postmenopausal women with hormone receptor-positive (HR+) non-metastatic breast cancer. However, up to 30% of these patients will experience relapse due in part to aromatase inhibitor resistance. We recently identified miR125b2-3p as a putative tumor suppressor in HR+ breast cancer. We also found that small molecule Aminoflavone (AF) induces miR125b2-3p expression in HR+ breast cancer cells. In the current study, we hypothesized that AF confers anticancer actions in breast cancer cells resistant to aromatase inhibitors via miR125b2-3p reactivation. Using the Alamar Blue and colony forming assays, we discovered that AF demonstrated anticancer activity in estrogen-deprived resistant (EDR) cells

designed to mimic aromatase inhibitor resistance. AntagomiR125b2-3p enhanced, while miR125b2-3p mimics diminished colony formation of EDR cells. AF-mediated suppression of colony formation in EDR cells was attenuated during co-treatment with antagomiR125b2-3p and was enhanced during co-treatment with miR125b2-3p mimics. Both miR125b2-3p mimics and AF suppressed EDR cell migration. AntagomiR125b2-3p counteracted AF-mediated suppression of cell migration. Our in silico profiling studies identified the alpha6-integrin, a mediator of breast cancer stem cell activity and metastasis, as one miR-125b2-3p target. Immunohistochemistry of patient tumor samples revealed that alpha 6-integrin protein expression intensified following relapse on the aromatase inhibitor anastrozole. MCF-7 cells transfected to overexpress the alpha 6-integrin were less responsive to anastrozole than those transfected with empty vector. These data suggest that AF restores the tumor suppressor function of miR125b2-3p to inhibit the alpha 6-integrin and confer activity against aromatase inhibitor-resistant breast cancer.

#3864

Targeting IL-6/STAT3 signaling in EGFR-mutant drug tolerant persister cells

Sonia A. Patel, Monique Nilsson, Yan Yang, Li Shen, Jing Wang, Alissa Poteete, Xiaoxing Yu, Xiaoyang Ren, Xiuning Le, John Heymach. *The University of Texas MD Anderson Cancer Center, Houston, TX*

While the majority of epidermal growth factor receptor (EGFR) mutant non-small cell lung cancer (NSCLC) patients initially respond to treatment with an EGFR tyrosine kinase inhibitor (TKI), most will eventually develop acquired resistance to these agents. The evolution of tumor cells with acquired resistance to targeted agents initially involves the persistence of a drug-tolerant subpopulation of tumor cells which display a transient and flexible resistant state. These persister cells can remain quiescent for prolonged periods of time, but eventually give rise to fully drug resistant tumor cells that resume growth and metastatic spread. The signaling pathways that allow persister cells to remain viable or to re-activate expansive growth are poorly understood. We and others have reported that EGFR TKI resistance that occurs independent of secondary EGFR mutations or MET amplification is associated with an epithelial to

mesenchymal transition (EMT). Our analysis of tumor cells that had undergone EMT-mediated resistance to the EGFR TKI osimertinib revealed that interleukin-6 (IL-6) was highly upregulated in resistant cells as compared to parental cells. We find that in the setting of EGFR mutant NSCLC, IL-6 suppresses the anti-tumor cell activity of T cells and NK cells. To assess the role of IL-6 in the early events of EGFR TKI resistance, we generated drug-tolerant persister cells by treating EGFR mutant HCC4006 and HCC827 NSCLC cells with the EGFR TKI osimertinib for 10 days and then assessed IL-6 expression. We observed that IL-6 was upregulated at both the RNA and protein levels in EGFR-TKI persister cells as compared to parental cells. While the cell surface expression of IL6R was not significantly increased in EGFR-TKI persister cells as compared to parental cells, we observed increased secretion of soluble IL6R in persister cells by ELISA assay. We next assessed changes in protein expression and activation in drug tolerant persister cells by reverse phase protein array (RPPA) and observed that p-STAT3, a key component of the IL-6 signaling pathway, was significantly elevated in persister cells as compared parental cells or cells treated with osimertinib for 24 hours. Using genetically engineered mouse models (GEMM) of $EGFR^{L858R}$ mutant lung cancer, we also observed a similar upregulation of both IL-6 and p-STAT3 expression at the RNA and protein levels in EGFR-mutant tumors treated with osimertinib for 2 or 4 weeks. Additionally, circulating levels of IL-6 also are elevated in $EGFR^{L858R}$ GEMMs treated with osimertinib for 2 or 4 weeks. Collectively, our data indicates that upregulation of IL-6 is an early event in the evolution of drug resistance. Given the role of IL-6 in promoting EGFR TKI resistance, further studies investigating whether targeting of IL-6 signaling may impair the survival or outgrowth of persister populations are warranted.

#3865

Multiple cancer types rapidly escape from multiple MAPK inhibitors to generate mutagenesis-prone subpopulations

Timothy E. Hoffman, Chen Yang, Varuna Nangia, Christopher Ryland Ill, Sabrina L. Spencer. *Biochemistry, University of Colorado, Boulder, CO*

Many cancers harbor pro-proliferative mutations of the mitogen-activated protein kinase (MAPK) pathway and many targeted inhibitors now exist for

clinical use, but drug resistance remains a major issue. We previously showed that BRAF-driven melanoma cells treated with BRAF inhibitors can non-genetically adapt to drug within 3-4 days to escape quiescence and resume slow proliferation. Here we show that this phenomenon is not unique to melanomas treated with BRAF inhibitors but rather is widespread across many clinical MAPK inhibitors and cancer types driven by EGFR, KRAS, and BRAF mutations. In all treatment contexts examined, a subset of cells can escape drug-induced quiescence within four days to resume proliferation. These escapee cells broadly experience aberrant DNA replication, accumulate DNA lesions, spend longer in G2-M cell cycle phases, and mount an ATR-dependent stress response. We further identify the Fanconi anemia (FA) DNA repair pathway as critical for successful mitotic completion in escapees. Long-term cultures, patient samples, and clinical data demonstrate a broad dependency on ATR- and FA-mediated stress tolerance. Together, these results highlight the pervasiveness with which MAPK-mutant cancers are able to rapidly escape drug and the importance of suppressing early stress tolerance pathways to potentially achieve more durable clinical responses to targeted MAPK pathway inhibitors.

#3866

Targeting AXL can effectively inhibit c-Met-induced therapeutic resistance in renal cancer

Akash Sabarwal[1], Laxminarayan Rawat[1], Johannes Wedel[1], Yuzuru Sasamoto[1], Sabina Signoretti[2], Toni K. Choueiri[3], Murugabaskar Balan[1], Soumitro Pal[1]. *[1]Nephrology, Boston Children's Hospital, Boston, MA,[2]Pathology, Brigham and Women's Hospital, Boston, MA,[3]Medicine, Dana-Farber Cancer Institute, Boston, MA*

Advanced stage renal cell carcinoma (RCC) often becomes resistant to the currently available therapeutic options. Receptor Tyrosine Kinase (RTK), c-Met, is overexpressed and hyperactivated in renal cancer; and it promotes tumor-promoting pathways following binding with its ligand, Hepatocyte Growth Factor (HGF). Cabozantinib (Cabo), an inhibitor of c-Met/few other RTKs (like, AXL and KDR), is being used for the treatment of RCC. However, acquired therapeutic resistance is a major hurdle in its clinical use. Mechanism(s) of drug resistance against c-Met inhibition is largely

unknown. Although Cabo (XL184) can effectively inhibit c-Met/RTK phosphorylation, very interestingly, we found that, prolonged treatment of Cabozantinib (24 hours, *in vitro*) increased the expression of total c-Met and AXL in renal cancer cells in a dose-dependent manner. AXL is also overexpressed in RCC and has a novel cross-talk with c-Met. We found that silencing AXL (either by gene knock-down approach or using a specific inhibitor (TP-0903)) markedly down-regulates Cabo-mediated total c-Met expression and enhances apoptosis of human RCC cells. We have also utilized murine model(s) of renal cancer growth (both xenograft and syngeneic), and found that Cabo treatment increases the levels of c-Met and AXL in tumor tissues, and the inhibition of AXL using TP-0903 can markedly inhibit the expression levels of total c-Met and AXL. We observed that HGF-mediated c-Met phosphorylation is short-lived when AXL is silenced. We also found that a lower concentration of Cabo can mediate cancer cell survival; and either the knock-down of AXL or using AXL inhibitor in combination with Cabo can reverse these effects. We have studied the downstream signaling pathways (Akt, ERK1/2 and STAT3) of c-Met, and found that AXL inhibition is crucial to down-regulate c-Met-induced signaling molecules following Cabo treatment. Our observations indicate that Cabo-mediated increase in total c-Met in RCC cells is not regulated at the transcriptional level; however, Cabo can interfere with the receptor degradation pathway leading to increased accumulation of c-Met. We have also studied the levels of c-Met and AXL in renal tumor tissues (archived specimens) from renal cancer patients before and after Cabozantinib treatment. Interestingly, we found increased levels of total c-Met and AXL in tumor tissues following Cabo treatment. Together our data suggest that AXL plays a critical role in mediating therapeutic resistance against c-Met inhibitor; and a combination of Cabo and an AXL/other RTK inhibitor can effectively block the resistance.

#3867

Chromatin modification driving sub-clonal resistance to KRAS G12C combination therapies in KRAS mutant non-small cell lung cancer

Chendi Li[1], Qian Qin[1], Mohammed Usman Syed[1], Anahita Nimbalkar[1], Barbara Karakyriakou[1], Sarah E. Clark[1], Anne Y. Saiki[2], Paul E. Hughes[2], Chris Ott[1], Luca Pinello[1], Aaron N. Hata[1]. [1]*Massachusetts General*

Hospital, Charlestown, MA,[2]Amgen Research, Amgen Inc., Thousand Oaks, CA

The FDA approval of the KRAS G12C inhibitor (G12Ci) sotorasib and the advancement of similar drugs into clinical trials marks a major milestone in treating KRAS G12C non-small cell lung cancer (NSCLC). However, not all patients respond (sotorasib - ORR = 37.1%, adagrasib - 43%, JDQ443 - 35%), motivating preclinical and clinical investigation into mechanisms of intrinsic and acquired resistance. For instance, clinical studies have reported on-target KRAS mutations and preclinical studies have demonstrated mitogen-activated protein kinase (MAPK) feedback reactivation including EGFP, SHP2, and WT RAS signaling. In response to targeted therapies, sub-populations of cells can enter quiescence or specific epigenetic-driven states that confer drug tolerance. However, epigenetic states defining drug-tolerant persister populations and contributing to adaptive resistance to KRAS G12Ci have not been reported. Using a lineage tracing barcoded system, we identify distinct and reversible subpopulations defined by specific chromatin and transcriptional states in KRAS NSCLC cell lines that contribute to KRAS G12Ci resistance *in vitro*, even prior to drug treatment. We observed that specific states, including activation of histone demethylation and SWI/SNF complex, may contribute to MAPK reactivation-driven resistance. These results suggest potential epigenetic vulnerabilities that can be exploited to improve the response to KRAS G12Ci. Moreover, we observed distinct persister subpopulations with resistance to KRAS G12Ci combination co-targeting orthogonal pathways (SHP2, CDK4/6, PI3K, and MCL-1), raising the possibility that distinct epigenetic-transcriptional states contribute to differential drug response and clonal evolution of persisters. Collectively, these results suggest that more complete tumor regression may be achieved by orthogonal strategies that target different resistant populations within the same tumor.

#3868

Aurora kinase A inhibition overcome adaptive resistance to KRAS G12C inhibitor by G1-checkpoint induced apoptosis in KRAS non-small cell lung cancer

Chendi Li[1], Jeremy Chang[2], Mohammed U. Syed[1], Anahita Nimbalkar[1], Yi Shen[1], Steve Altschuler[2], Lani Wu[2], Xueqian Gong[3], Aaron Hata[1].

[1]Massachusetts General Hospital, Charlestown, MA,[2]University of California San Francisco, San Francisco, CA,[3]Eli Lilly and Company, Indianapolis, IN

Cancer cells gain drug-tolerant states and evade therapy. In response to KRAS G12C inhibitor (G12Ci), KRAS mutant non-small cell lung cancer (NSCLC) cells maintain a drug-tolerant state by aurora kinase A (AURKA). AURKA can phosphorylate c-Raf to maintain new KRAS signaling, however, how AURKA becomes activated to cause KRAS G12Ci resistance is unclear. We show here that KRAS G12C + AURKA inhibition cause synthetic lethality in KRAS G12C NSCLC cells. LY3499446 (KRAS G12Ci) and LSN3321213 (aurora kinase A inhibitor) induced apoptosis that is independent of inhibited MAPK reactivation. Using high-content imaging that tracks single-cell fate during treatment, we observed that single-agent KRAS G12Ci induces G1 arrest in a sub-population of cells. Upon co-treatment with G12C + AURKAi, cells that are halted in G1 phase undergo early apoptosis, while those that initially evade G1 arrest and proceed through G2/M undergo apoptosis in subsequent G1. These data suggest the hypothesis that AURKA inhibition may increase the probability of G1 checkpoint-induced apoptosis by facilitating chromosomal misalignment and genomic instability. In summary, we provide clinical rationale for clinical testing of KRAS G12C + AURKA inhibitors. We also suggest a novel mechanism explaining the dependency of KRAS G12C resistant subpopulations on AURKA, leading to the opportunity to investigate the role of genomic instability in conferring KRAS G12Ci adaptive resistance.

#3869

Short or long-term treatment with CDK4/6 inhibitors in patients with ER+ breast cancer: characterization and comparative analysis of resistance in seventeen XPDX models

Alyssa Simonson[1], Johnnie Flores[1], Morgan Lynch[1], Emily Carpenter[1], Justine Hruzek[1], Jim Lund[1], Natalia Baños Herraiz[1], Kyriakos Papadopoulos[2], Amy Vander Woude[3], Gladys Rodriguez[2], Sreenivasa Chandana[4], Thomas Gribbin[3], Nehal Lakhani[4], Tatiana Hernandez[5], Maria Jose de Miguel[6], Amy Lang[2], Michael J. Wick[1]. *[1]XenoSTART, San Antonio, TX,[2]START Center, San Antonio, TX,[3]CHCWM, Grand Rapids, MI,[4]START*

Center, Grand Rapids, MI,[5]START Center, Barcelona, Spain,[6]START Center, Madrid, Spain

Background: Mechanisms of resistance to CDK4/6 inhibitors (CDK4/6i) have been well studied and several alterations identified including RB loss and altered expression of related genes including CCNE1, E2F4 and CDK6. However, whether duration of clinical treatment might elicit specific mechanism(s) of CDK4/6i resistance is unclear. To better understand if duration of clinical treatment correlates with unique resistance mechanisms, we established, characterized, and compared a panel of ER+ breast XPDX models from patients who benefitted then progressed on a CDK4/6i. Patients were separated into two groups by time to progression (TTP): those who responded up to twelve months (RES12) and patients with clinical response greater than one year (RES13+).
Methods: Seventeen breast cancer XPDX models were analyzed, including eight previously described (7xRES12; 1xRES13+: SABCS2021: T Hernandez et al). Nine new models were established from seven patients: six from fluid samples with three designated as ductal (ST3105B, ST3105C, STM001B) and three lobular carcinoma (STM182, STM229, STM229B); two from lymph node biopsies (ST5676, STM127) and one from a liver core biopsy (ST4887B), all reported as ductal carcinoma. STM182 was classified as RES12 and the remaining eight as RES13+. These models were passaged and challenged with CDK4/6i to confirm resistance. Receptor expression was determined by IHC and genomic analyses including WES and RNA_{seq}, were performed to identify mechanisms of resistance. For in vivo studies, CDK4/6i were dosed PO once daily at 50 mg/kg; endpoints included tumor volume (TV) and time from treatment initiation (TTI) with %T/C values and tumor regression reported at study completion; a %T/C of ≤20 versus control was considered sensitive. Tumor regression (%T/C<0) versus Day 0 TV was also reported.
Results: Clinical TTP for RES12 (n=8) was four to twelve months and RES13+ (n=9) from thirteen to forty-two months. All models retained ER expression in evaluated passages with similar histology compared with archival clinical samples. Sequencing identified several variants including RB1 truncations or deletions and increased gene expression in CCND1, CCNE1 and the PIK3CA/AKT pathway. Interestingly, 5/8 RES12 models reported ESR1 mutations or fusions versus 1/9 RES13+ and PIK3CA

mutations were reported in 1/8 RES12 versus 5/9 RES13+. Several RES13+ models also reported variants and increased amplification in the RICTOR/TORC2 pathway versus RES12.
Conclusion: We have established, characterized, and compared a panel of seventeen breast XPDX models from fourteen female patients representing early or late acquired resistance to CDK4/6i therapy and identified potential differences in each set. These models and resulting data are useful in developing novel therapies for CDK4/6i-resistant patients.

#3870
TNF-MK2 signaling drives protective autophagy following MAPK pathway inhibition in pancreatic cancer
Iftikhar Ali Khawar, Qing Wei, Timothy Hung-Po Chen, Lin Lin, Patrick M. Grierson, Kian-Huat Lim. *Washington University School of Medicine in St. Louis, St. Louis, MO*

Targeting the oncogenic KRAS-RAF-MEK-ERK (MAPK) pathway has remain unsuccessful in the clinic for patients with pancreatic ductal adenocarcinoma (PDAC), a highly lethal cancer with few effective treatment options. To identify novel, effective therapeutic strategies, we investigated the impact of MEK and ERK inhibitors on production of inflammatory cytokines in PDAC cells. We found that both MEK and ERK inhibitors dramatically upregulated production of TNF, leading to activation of multiple TNF signaling pathways which include the pro-death and pro-survival NF-kB and p38.MK2 cascades. Silencing of TNF receptor 1 (TNFR1) abrogated the pro-apoptotic effect of MAPK inhibitors, suggesting that pro-death effect driven by TNF signaling is required for the therapeutic effect of MAPK inhibitors. However, targeting the NF-kB and MK2 pathways greatly augment the suppressive effect of MAPK inhibitors. Notably, the mechanisms via which MK2 promotes PDAC cell survival are mediated through phospho-activation of Heat shock protein 27 (Hsp27) and Beclin1, a critical mediator of autophagy. Intriguingly, silencing of TNFR1 abrogated induction of proactive autophagy following MAPK inhibition, strongly suggesting autocrine signaling as the inciting event of autophagy. Mechanistically, we showed that TNF signaling upregulate unfolded protein response (UPR) in PDAC cells, which is required for autophagy induction. Targeting MK2 abrogated transcription of key UPR genes and blocks

subsequent autophagy. The combination of MK2 inhibitor ATI-450 and ERK inhibitor ulixertinib was more effective in curbing the growth of PDAC patient-derived xenograft in vivo and prolonged the survival of autochthonous PDAC mice (KPC model). Overall, our study provided novel insights on the mechanisms that drive protective autophagy following MAPK pathway inhibition and a rationale and feasible therapeutic combination that can be tested in clinical trials for PDAC patients.

#3871

KRAS G12C **mutant allele amplification drives resistance to sotorasib in vitro**

Deanna Mohn[1], Anne Y. Saiki[1], Pragathi Achanta[1], Andres Plata Stapper[2], J. Russell Lipford[1], Rati Verma[1]. *[1]Amgen Research, Amgen Inc., Thousand Oaks, CA,[2]Amgen Research, Amgen Inc., South San Francisco, CA*

Sotorasib is an approved $KRAS^{G12C}$-selective inhibitor for the treatment of *KRAS* p.G12C-mutant advanced and previously treated non-small cell lung cancers (NSCLC). Acquired resistance due to genomic alterations following sotorasib treatment has been observed in 28% of lung cancer patients (CodeBreaK100, ASCO 2022) and can include bypass signaling, inactivation of negative feedback loops, or compensatory mutations in $KRAS^{G12C}$ including amplification of *KRAS*.
Preclinical studies on the mechanisms of acquired resistance are critical for understanding these resistance patterns and can reveal new therapeutic or combination strategies in the clinic. For that reason, we developed an NCI-H358 lung cancer model of acquired resistance to $KRAS^{G12C}$ inhibition in vitro. NCI-H358 cells were continuously cultured in the presence of elevated concentrations of sotorasib (IC90) until resistance to $KRAS^{G12C}$ inhibitor was achieved. Expression analyses of the resistant cells by ddPCR and immunoblotting showed increases in both KRAS gene and protein levels, resulting in enhanced MAPK signaling. siRNA knockdown of *KRAS G12C* expression re-sensitized the resistant cells to an analog of sotorasib. Further characterization of this cell line by whole exome sequencing (WES) and fluorescence in situ hybridization (FISH) showed that resistance was not due to genetic co-alterations but amplification of the mutant allele specifically. In comparison to DMSO-treated and parental controls, the

sotorasib-resistant NCI-H358 cells contained an approximately 50-fold increase in *KRAS G12C* mutant allele copy numbers.
Preclinical data generated using a $KRAS^{G12C}$ inhibitor-resistant lung cancer cell line is consistent with clinical observations of acquired *KRAS* amplification following $KRAS^{G12C}$ inhibitor treatment as a mechanism of resistance. This model further provides an opportunity to study acquired *KRAS* amplification and investigate combination treatment options in vitro.

#3872

Targeting of YAP overcomes trastuzumab-resistance and promotes immune responses in HER2-positive cancers

Ah Rong Nam[1], Jeesun Yoon[2], Kyoung-Seok Oh[1], Jae-Min Kim[3], Ju-Hee Bang[1], Yoojin Jeong[1], Sea Young Choo[1], Hyo Jung Kim[1], Su In Lee[1], Tae-Yong Kim[1], Do-Youn Oh[2]. *[1]SNU Medicine, Cancer Research Institute, Seoul, Korea, Republic of,[2]Department of Internal Medicine, SNU Medicine, Seoul, Korea, Republic of,[3]SNU Medicine, Integrated Major in Innovative Medical Science, Seoul, Korea, Republic of*

Background: HER2 (Human epithelial growth factor receptor 2)-targeting therapies have been approved for patients with HER2-positive breast and gastric cancer and use have been attempted in various solid tumor types, including biliary tract cancer. However, resistance mechanism remains as a major challenge of HER2-targeting therapies. YAP (Yes-associated protein) is a major downstream effector of Hippo pathway, and it plays an essential role in cancer cell proliferation, survival and differentiation. Moreover, YAP is emerging as a key player of resistance mechanism of cytotoxic and targeted drugs. Yap is also an important immunosuppressive molecule as it works as a negative regulator of T cell tumor infiltration. In this study, we intend to elucidate the role of YAP in mechanism of trastuzumab resistance and T cell immune response in HER2-positive cancer cells.
Methods: We established four trastuzumab-resistant (HR) cell lines (N87HR, SNU216HR, SNU2670HR and SNU2773HR) from HER2-postive gastric and biliary tract cancer cell lines. To inhibit the function of YAP, siRNA and Verteporfin (YAP-TEAD inhibitor) were used. MTT assay, cell cycle analysis, western blot and migration assay were performed to analyze the antitumor effects through YAP downregulation. In order to

evaluate immune-modulation by YAP, human PBMC co-culture was used and immune markers were analyzed by RT-PCR and flow cytometry. Mouse xenograft models were established using SNU2773 and SNU2773HR cells. Results: We confirmed that the expressions of pYAP and YAP were elevated in HR cells (SNU216HR, SNU2670HR and SNU2773HR) compared to parental cells. Reducing the expressed YAP in HR cells inhibited tumor cell growth and migration and induced apoptosis. Immune suppression markers such as PD-L1, CD155, and galectin-9 were effectively decreased, while CD80, a stimulation marker, was increased by verteporfin treatment. Also, when YAP was decreased, CCL5 and CXCL10, well known $CD8^+$ T cell recruitment cytokines, were increased. In HR cells treated with siYAP and verteporfin, there was a trend of increasing $CD4^+$ and $CD8^+$ T cells when co-culture with PBMC. In vivo experiment data showed greater tumor growth inhibition effects with SNU2773HR than SNU2773 xenograft models when treated with verteporfin.
Conclusion: The expression of YAP is elevated in trastuzumab-resistant (HR) cells and inhibition of YAP shows anti-tumor effects and activation of T cell responses. Collectively, our data suggests that the inhibition of YAP is one of many promising strategies to overcome trastuzumab resistance and T cell regulatory mechanisms in HER2-positive cancers.

#3873

Candidate drug screening for TP53-mutated AML

Daehyeon Gwak[1], Dong Chan Kim[1], Heejun Jang[1], Jun Liu[1], Ja Min Byun[2], Junshik Hong[2], Dong Yeop Shin[2], Sung-Soo Yoon[2]. *[1]Seoul National University, Seoul, Korea, Republic of,[2]Seoul National University Hospital, Seoul, Korea, Republic of*

Acute myeloid leukemia (AML) is a clonal blood malignancy characterized by arrested maturation and abnormal proliferation of hematopoietic precursor cells. This paralysis of normal bone marrow function leads to severe decreased immune function and bleeding tendency, and if not treated, it is an acute disease that dies within a few months due to rapid progression of AML. *TP53* mutations occur in 5% to 10% of patients with de-novo acute myeloid leukemia (AML), with higher frequency in patients with relapsed/refractory AML. The treatment approach for many years has used combination chemotherapy, with usually an anthracycline and

cytarabine as the foundation. These induction therapy's complete response is achieved in 60 to 85% of adults who are 60 years of age or younger. In patients who are older than 60 years of age, complete response rates are inferior 40 to 60%. *TP53* mutated acute myeloid leukemia (AML) responds poorly to the conventional induction therapy and has a short overall survival rate with a median of 5-9 months. Poor outcomes in *TP53* mutated AML following chemotherapy have been observed and treatment options remain limited. Therefore, this study attempted to explore the drug candidates for effective treatment of *TP53* mutated AML. To study the cellular response to *TP53*-targeted therapy, we used the human AML cell line Kasumi-1, which harbors a homozygous *TP53* mutation. We treated Kasumi-1 cells with cytarabine and Idarubicin combi-treatment. And we produced Drug Tolerant Persisters (DTPs) which is a minor population of cancer cells may evade cell death from chemotherapy and targeted therapy by entering a reversible slow proliferation state. Similar to a previously described DTP phenotype the DTPs that survive cytarabine and Idarubicin combi-treatment displayed cell-cycle arrest and resistance to further cytarabine and Idarubicin combi-treatment. And we selected 125 drug candidates that would be effective for *TP53* mutated AML through in silico analysis and therapy strategies targeting p53. The drug candidates are composed of Compounds with the ability to reactivate mutant p53, Compounds directly target mutant p53, Synthetic lethal partners with mutant p53, and Compounds with the ability to anti-Leukemic Stem Cell and antineoplastic. We single out 46 of the 125 compounds for functional validation in DTPs. We chose these compounds because many of them are similar subtypes, suggesting they may have a common effect and mechanism. Using in vitro Cytotoxicity assay, we screened 46 candidate compounds at multiple doses and confirmed several drugs that effectively eliminate DTPs. Collectively, our study indicates that the combination of conventional drug and validated drug has the potential to eliminate DTPs and therefore prevent minimal residual disease, mutational drug resistance, and relapse in *TP53*-mutant AML.

#3874

Genomic mechanisms of resistance to tyrosine kinase inhibitors (TKIs) in HER2+ metastatic breast cancer (HER2+ MBC)

Heather A. Parsons[1], Conor Messer[2], Katheryn Santos[1], Brian P. Danysh[2], Melissa E. Hughes[1], Ashka Patel[1], Raquel A. Jacobs[2], Kara Slowik[2], Julian Hess[2], Chip Stewart[2], Kristy Schlueter-Kuck[2], Kahn Rhrissorrakrai[3], Filippo Utro[3], Chaya Levovitz[3], Nikhil Wagle[1], Jose Pablo Leone[1], Rachel Freedman[1], Laxmi Parida[4], Ian E. Krop[5], Gad Getz[2], Nancy U. Lin[1].
[1]Medical Oncology, Dana-Farber Cancer Institute, Boston, MA,[2]Broad Institute of MIT and Harvard, Cambridge, MA,[3]IBM Research, Yorktown Heights, NY,[4]IBM Research, Cambridge, NY,[5]Yale University, New Haven, CT

Background**.** Despite substantial progress in the treatment of HER2+ MBC, most patients (pts) still experience disease progression and cancer-related death. HER2-directed TKIs are highly effective therapies for pts with HER2+ MBC; however, an understanding of resistance mechanisms is needed. Pts receiving HER2-directed TKIs with cell-free DNA (cfDNA) sampling across the treatment spectrum present a unique opportunity to examine genomic alterations.
Methods. Pts with biopsy-proven HER2+ MBC were selected from DF/HCC approved protocols for ultra-low pass whole genome sequencing if ≥1 cfDNA and/or tissue sample had been collected prior to and after at least six weeks of TKI treatment. Only pts with ≥ 1 sample with tumor fraction (TFx) ≥ 9.5% and ≥ 1 additional sample with TFx ≥ 4.5% were analyzed. Whole exome sequencing (WES) was performed on 19 tumor biopsies and 64 cfDNA samples from 25 pts. WES samples were analyzed, variants called and annotated, copy number profiles inferred, and TFx estimated. *PhylogicNDT* was used to detect the phylogenetic architecture, and clones were identified as growing, stable, shrinking, or truncal; mutational signatures were called using *SignatureAnalyzer*. After filtering likely benign variants, mutations were labeled likely resistance mechanisms if there was known evidence of resistance to anti-HER2 therapy in a human breast cancer cell line, breast cancer mouse models, or in vivo. Findings were correlated with pt clinicopathologic data.
Results. In 4/8 pts with acquired resistance (TKI treatment ≥ 180 days), we identified alterations in previously characterized pathways and genes that could explain treatment resistance (e.g. *PIK3CA, ERBB2, FGFR2).* Mutations in growing subclones identified potential novel mechanisms of

resistance and included inactivating mutations in *CDK12*, *KMT2D*, *KMT2C*, *CHEK2*, *BRCA2*, and *FAT1* genes. In 7/17 pts with intrinsic resistance, we identified mutations in overlapping pathways and genes such as *ERBB2* and *PIK3CA,* which were present in both growing subclonal and truncal clones. Four pts with hormone receptor positive disease - two of whom had not received prior aromatase inhibitors - had an activating *ESR1* hotspot mutation (D538G). This raises the possibility that activating *ESR1* mutations may be involved in resistance in these cases. Mutational signature analysis revealed a subset of samples with widespread APOBEC activation (with and without hyper mutation), subclonal HR/MMR-related signature, and capecitabine-related 5FU signature.
Conclusions. Genomic analysis of paired samples from pts with HER2+ MBC identifies candidate resistance mechanisms to anti-HER2 TKIs and clonal evolution over time in the context of heterogeneity in treatment and sample timing. Additional studies will determine the functional role and clinical utility of assessing these alterations to overcome resistance.

#3875
Evaluation of resistance mechanisms to ARV471, an ER-targeted PROTAC
Delia Margaret Friel[1], Zachary Sandusky[1], Yijia Jiang[2], Xintao Qiu[2], Rong Li[2], Henry Long[1], Rinath Jeselsohn[1], Myles Brown[1]. *[1]Medical Oncology, DFCI/Harvard Medical School, Boston, MA,[2]Center for Functional Cancer Epigenetics, DFCI/Harvard Medical School, Boston, MA*

Estrogen receptor alpha (ER) is a ligand activated transcription factor and a driver of ER+ breast cancer. The discovery of activating mutations in ER (gene name ESR1), in patients with advanced endocrine-resistant ER+ breast cancer, has ignited a large pharmaceutical effort to develop next-generation ER antagonists that also target the mutant protein. Here, we profiled the potency and selectivity of many next-generation ER antagonists currently in clinical trials, including ER-targeted proteolysis-targeting chimeras (PROTACs), selective ER modulators (SERMs), and selective ER degraders (SERDs). To contextualize these antagonists, we evaluated their activity against the only FDA-approved SERD, Fulvestrant, at the level of chromatin, transcriptome, proteome, and cell viability, using cells expressing wild-type ER as well as activating mutant ER (ER^{Y537S} and

ER^{D538G}). Overall, we find that many of the novel oral SERDs are potent ER antagonists, including against mutant ER. To anticipate resistance mechanisms to these next-generation ER antagonists, we developed a strategy initially focused on ARV471 (the most clinically advanced ER PROTAC), with two approaches. First, we performed whole-genome CRISPR/Cas9-knockout screening in ER+ breast cancer cell lines treated with ARV471. Among the enriched gRNAs were PTEN, NF2, and CRBN. Loss of PTEN and NF2 results in activation of the PI3K and MAPK pathways, respectively, and CRBN is the ubiquitin E3 ligase required for ER protein degradation by ARV471. PTEN and NF2 are known mechanisms of endocrine resistance but it is not yet known if CRBN loss in response to PROTACs is a predominant clinical resistance mechanism. Therefore, in a second approach we generated ARV471 resistant breast cancer cell lines through long term exposure (LTE-ARV471). These cells developed an ER-independent resistance mechanism, with decreased ER expression and increased expression of pathways associated with Ras/MAPK and EMT. Therefore, as more potent ER degraders enter the clinic, such as PROTACs and oral SERDs, it may be important to monitor resistance mechanisms that involve loss of ER. Currently, we are following up our findings with LTE-ARV471 cells and performing CRISPR screening to identify targetable dependencies and combination therapies for endocrine resistant breast cancer.

#3876

Kinetics of RTK activation determine ERK signaling dynamics and resistance to BRAF and MEK inhibitors

Sungsoo Kim, Richard Carvajal, Minah Kim, Hee Won Yang. *Columbia University Irving Medical Center, New York, NY*

Combination treatment of BRAF inhibitor (BRAFi) and MEK inhibitor (MEKi) produces remarkable response rates and is expected to prevent ERK activation in *BRAF*-mutant melanoma. However, sporadic ERK reactivation occurs in melanoma models, and efficacy is severely limited by the emergence of drug resistance. The underlying molecular mechanisms that drive ERK reactivation and adaptation to BRAFi/MEKi remain elusive. Here, using single-cell imaging and optogenetic approaches, we show that the strength and duration of receptor tyrosine kinase (RTK) activation

determines ERK reactivation and the development of BRAFi/MEKi-resistant cells. Single-cell data reveal that despite global RTK activation by the same external stimuli, only small subsets of melanoma cells induce effective RTK and ERK activation to develop BRAFi/MEKi resistance. Furthermore, by directly controlling RTK activity, we demonstrate that the kinetics of RTK activation determine ERK signaling dynamics and the percentage of drug-resistant cells. While these drug-resistant cells are rare during early stages of drug treatment, they eventually become the dominant population through sustained RTK-mediated ERK activation that drives cell proliferation. Thus, RTK activation in established drug-resistant cells causes effective ERK activation and cell proliferation. Importantly, limiting RTK signaling activation reverses the BRAFi/MEKi-resistant state. We show that targeting SHP2, a mediator of RTK signaling, effectively suppresses RTK-mediated ERK activation and cell proliferation in BRAFi/MEKi-resistant cells. Our results provide mechanistic insights into the contribution of heterogeneity in RTK activation kinetics to ERK reactivation and BRAFi/MEKi resistance, also highlighting SHP2 activity as a promising target to overcome drug resistance in *BRAF*-mutant melanoma.

#3877

Systematic functional and phenotypic characterization of HER2 missense mutants and their impact in ER+ metastatic breast cancer

Nelson Vicente Guevara[1], Zirui Zhu[1], Esha Jain[2], Jennifer Kavran[1], Selime Arslan[1], Nikhil Wagle[2], Utthara Nayar[1]. *[1]Biochemistry and Molecular Biology, Johns Hopkins University, Baltimore, MD,[2]Broad Institute of MIT and Harvard, Cambridge, MA*

The estrogen receptor-positive (ER+) subtype accounts for 70% of breast cancer, and endocrine therapies that target ER are effective in the early-stage clinical setting. However, endocrine resistance is ubiquitous in late-stage metastatic breast cancer (MBC). The chief mechanism is the acquisition of ER mutations (ERmuts) in 25% of endocrine-resistant tumors; ERmuts are strongly resistant to aromatase inhibitor (AI) endocrine therapy. We previously identified four novel acquired activating mutations in human epidermal growth factor receptor 2 (HER2) by whole exome sequencing (WES) of paired ER+ MBC in a clinical cohort. These HER2

mutations (HER2muts) were enriched in multiple resistant tumors, and like ERmuts, were resistant to AIs. In contrast to ERmuts, these HER2muts also conferred complete resistance to all other classes of endocrine therapy, as well as cross-resistance to combination therapy with cyclin-dependent kinase 4/6 (CDK4/6) inhibitors; the latter is standard-of-care in the refractory setting in ER+ MBC. At the same time, these HER2muts had variable responses to HER2-targeting therapies used in HER2+ breast cancer. Thus, HER2muts represent only the second validated mechanism of clinical endocrine resistance in ER+ MBC, accounting for ~8% of cases, and that is therapeutically intractable. Systematic phenotypic characterization of HER2muts in ER+ MBC is a prerequisite for effective targeting of this class of resistance. We used cBioPortal to identify >20 novel HER2 variants of unknown significance (VUS) that were frequent pan-cancer, in ER+ breast tumors, or annotated in a domain-restricted HER2 saturation mutagenesis screen, and that had not been previously characterized in ER+ MBC. We also identified a novel HER2 VUS by WES in an ER+/HER2+ tumor with resistance to HER2 therapy, from a clinical cohort of breast cancer patients. We phenotypically characterized all VUS through clinically comprehensive targeted therapy viability assays, and downstream activation assays. In sum, we identified seven novel activating HER2muts, spanning domains, with clinically important phenotypes in ER+ MBC. We found these HER2muts also conferred complete resistance to all classes of endocrine therapies, and cross-resistance to CDK4/6 inhibition. While novel HER2muts had variable responses to HER2-targeting therapies, they could be endocrine re-sensitized by combination with an irreversible tyrosine kinase inhibitor. Lastly, we report that constitutive HER2 homodimerization via reduction-sensitive disulfide bridges that occur as a consequence of mutations in the extracellular and juxtamembrane domains is a more common mechanism of HER2 hyperactivation than previously appreciated. This finding has unique functional consequences, and provides important structure-function insight into HER2 biology, beyond its immediate clinical ramifications in ER+ MBC.

#3878

Targeting Hippo-YAP, BRD4 and RAS-MAPK interplay in lung cancer to forestall drug resistance

Nilanjana Chatterjee[1], Victor Olivas[1], Wei Wu[1], Ben Powell[2], Trever Bivona[1]. *[1]UCSF - University of California San Francisco, San Francisco, CA,[2]Kinnate Biopharma, San Francisco, CA*

Introduction: Identifying parallel survival pathways or compensatory mechanisms that limit the response to targeted therapy is critical to discover effective combinatorial strategies for the treatment of lung cancer and to prevent emergence of drug resistance
Results: Using combination drug screening in a panel of cell line models of non-small cell lung cancer (NSCLC), we identified the tumor suppressor STK11 (aka LKB1) as a molecular biomarker of sensitivity to BET and RAS-MAPK pathway inhibitors combination in NSCLC. We found a small molecule inhibitor of BET (bromodomain and extra terminal) family proteins (BRD4, 3, 2), PLX51107, suppressed BRAF and KRAS mutant NSCLC cell proliferation and in combination with RAS (KRAS G12C), RAF or MEK inhibitor led to pronounced loss in cell viability with potent MYC downregulation and synergistic apoptosis induction *in vitro* and potent tumor regression or stasis *in vivo* in several KRAS mutant CDX and PDX mouse models of NSCLC. However, BRAF and KRAS mutant NSCLC cells with co-occurring mutations in STK11 were resistant to BET and RAS, RAF or MEK co-inhibition. To unravel the underlying mechanism of resistance to BET and RAS-MAPK inhibitors upon STK11 loss we modeled STK11 deficiency in BRAF and KRAS mutant NSCLC cells and tumors. We found that STK11 loss creates an unprecedented dependence on YAP/TEAD TFs. STK11 silencing in BRAF and KRAS mutant NSCLC cells resulted in nuclear transfer/ activation of the HIPPO pathway effector, YAP, upregulation of the YAP target BIRC5 (aka Survivin) and rescued the synthetic lethality due to BET and RAS, RAF or MEK co-inhibition. Phenocopying STK11 loss, constitutively active YAP (YAP5SA), but not transcriptionally inactive YAP (YAPS94A), mitigated the deleterious effects of BET and RAS, RAF or MEK co-suppression in BRAF and KRAS mutant NSCLC cells with potent upregulation of the pro-survival factor BIRC5. Conversely, we found that co-silencing YAP or TEADs with BETs re-sensitized BRAF and KRAS mutant NSCLC cells with co-occurring mutations in STK11 to BET and RAS-MAPK inhibitors combination and caused synthetic lethality.

Conclusion: This study uncovered a functional interaction between BET proteins, STK11, HIPPO-YAP and RAS-MAPK signaling pathways in lung cancer. These results will help identify combinatorial strategies for treating aberrant RAS-MAPK pathway driven lung cancer more effectively and forestall drug resistance.

#3879

SETD2 is a novel and druggable dependency in IMiD/CELMoD resistant multiple myeloma models

Sarah Anne Bird[1], Marco Licciardello[1], Yakinthi Chrisochoidou[1], James Smith[1], Amy Barber[1], Jack Cheung[1], Yura Grabovska[1], Shannon Martin[1], Fernando Sialana[1], Harvey Che[1], Habib Bouguenina[1], Benjamin Bellenie[1], Brian Walker[2], Paul Clarke[1], Charlotte Pawlyn[1]. *[1]Institute of Cancer Research, Sutton, United Kingdom,[2]Indiana University School of Medicine, Indianapolis, IN*

Immunomodulatory agents (IMiDs) and cereblon E3 ligase modulators (CELMoDs) are a cornerstone of Multiple Myeloma (MM) treatment. They bind to the cereblon (CRBN) component of the CRL4 E3 ubiquitin ligase complex and designate a new set of substrates for proteasomal degradation. Most patients initially respond well to IMiD/CELMoD therapy but over time will become resistant. Understanding resistance mechanisms will enable the development of new targeted treatment strategies to overcome this pressing clinical challenge.
Acquired IMiD/CELMoD resistant human MM cell lines were generated by treating IMiD/CELMoD sensitive MM1s and H929 cells with lenalidomide (Len), pomalidomide (Pom) or iberdomide (Iber) at ~10x GI50 concentration for ~12 weeks until resistance was achieved. Cell lines were characterized by whole exome sequencing, RNA-Seq and proteomics. All resistant lines had reduced CRBN expression and some had *CRBN* mutations, reflecting patient data.

A genome-wide loss-of-function CRISPR screen (Brunello library) was carried out in Iber-resistant MM1s. Gene effect scores were calculated with the Chronos algorithm and compared to parental MM1s using data from the Broad Institute DepMap portal. Potential new dependencies in the resistant setting (defined as gene effect score <-1 in resistant cells and >-0.5 in parental cells) were identified in 47 genes including SETD2, a histone 3 lysine 36 methyltransferase (H3K36me2 -> H3K36me3).
The specific SETD2 inhibitor EPZ-719 reduced viability to a greater extent in the IMiD/CELMoD resistant lines compared to their controls in a 14-day trypan blue exclusion assay. This was most pronounced in the Pom- and Iber-resistant H929 lines. For example in Iber-resistant H929 compared to its control line the viability with EPZ-719 was 13% vs 66% at 1μM, 5% vs 46% at 5μM and 2% vs 45% at 10μM, $p<0.0001$ (% viability compared to DMSO control at day 14).
To investigate whether this novel dependency was related to reduced CRBN expression a *CRBN* knockout MM1s cell line was generated using CRISPR/Cas9. These cells showed a markedly greater reduction in viability with EPZ-719 compared to control MM1s (viability 20% vs 32% at 1μM, 8% vs 25% at 5μM and 2% vs 18% at 10μM, $p<0.001$).
A reduction in H3K36me3 was seen on immunoblotting after EPZ-719 incubation across all cell lines suggesting an on-target effect. ChIP-Seq and RNA-Seq experiments are underway to identify downstream mechanisms.
In conclusion, SETD2 inhibition is more active in IMiD/CELMoD-resistant cell lines compared to sensitive counterparts. Rapid clinical translation of these findings would be possible as a SETD2 inhibitor is currently in a phase 1 trial which includes MM patients. Previous pre-clinical data suggests the t(4;14) MM subgroup may be more sensitive to SETD2 inhibition but our data highlights a novel vulnerability in the IMiD/CELMoD resistant setting that should be explored further.

Drug Resistance in Molecular Targeted Therapies 4 / Regulation of Gene Expression in Drug Resistance

#3882
tumor adaptations to PI3K inhibition increases and its reversibility decreases as a function of time in drug

Radha Mukherjee[1], Kiran Gireesan Vanaja[2], Malvika Sharma[1], Yangjingyi Ruan Ruan[1], Hilla Solomon[1], Elisa deStanchina[1], Sarat Chandarlapaty[1], Neal Rosen[1]. *[1]Memorial Sloan Kettering Cancer Center, New York, NY,[2]Northeastern University, Boston, MA*

The PI3K pathway is a key regulator of metabolism, cell proliferation and migration and some of its components (e.g. PIK3CA, HER2 and PTEN) are frequently altered in cancer by genetic events that deregulate its output. However, inhibitors of components of the pathway have only modest antitumor effects and, in some instances, have resulted in “tumor flares” in patients upon cessation of therapy. Low efficacy has been attributed to toxicity and to adaptive resistance due to relief of feedback. Inhibition of the PI3K pathway has been associated with increased receptor expression and decreased expression of the PTEN phosphatase, a major negative regulator of the pathway. Now we show that changes in expressions of RTKs, PTEN, anti-apoptosis proteins like Mcl1, and transcription factors known to drive oncogenic and survival programs in tumors like c-Myc, c-Jun, FOXOs are induced upon continuous long-term PI3K inhibition (2 weeks and longer). These changes increase as a function of duration of inhibition and become less reversible with time in drug. Unbiased clustering of RNA seq data of cells treated with PI3K inhibitors revealed clusters of gene expression changes based upon short or long-term inhibition. Correspondingly the mRNA of the RTKs and transcription factors change with similar kinetics as that of the proteins and become less reversible with duration of inhibition. Moreover, the persister cells treated with PI3K inhibitors for 2 weeks or longer grow faster than the treatment naive cells upon drug removal both *in vitro* and *in vivo* and the degree of reversibility of the increased proliferation rate is inversely proportional to the duration of inhibition. Persister cells treated with PI3K inhibitors for more than two weeks have higher levels of expression of a oncogenic transcription factors, RTKs, Mcl1, and of pAKT after one week of drug wash-out and are less sensitive to re-inhibition of PI3K. However, combined and staggered inhibition of PI3K with Mcl1/Bcl2 inhibitors lead to greater reduction of cell survival and increased cell death selectively in the models that upregulate Mcl1 in response to PI3K inhibitors. The data suggests that induction of adaptive resistance is in part responsible for the continued persistence of tumor masses after the initial response to targeted therapy but

also selectively sensitizes them towards Mcl1/Bcl2 inhibitors due to the upregulation of an anti-apoptotic program. Therefore, pulsatile targeted inhibition of PI3K in combination with anti-apoptotic BH3 domain protein inhibitors in a subset of breast cancer patients may provide a wide therapeutic window and can circumvent chronic adaptation induced resistance and drive potent cell death thereby improving therapeutic outcomes.

#3883

Overcoming tamoxifen resistance by re-activating cAMP-Ca^{2+}-ROS-ferroptosis axis in ER+ breast cancer

Rashedul Alam[1], Ozge Saatci[1], Meral Bugadyci Uner[2], Kim-Tuyen Huynh-Dam[3], Metin Cetin[1], Mustafa Emre Gedik[1], Nevin Belder[4], Hilal Bal[4], Unal Metin Tokat[4], Elisabetta Marangoni[5], Sercan Aksoy[6], Aysegul Uner[6], Aytekin Akyol[6], Ozgur Sahin[7]. *[1]The Medical University of South Carolina (MUSC), Charleston, SC,[2]Department of Pathology, Hacettepe University Medical Faculty, Ankara, Turkey,[3]Department of Drug Discovery and Biomedical Sciences, University of South Carolina, Columbia, SC,[4]Department of Molecular Biology and Genetics, Bilkent University, Ankara, Turkey,[5]Translational Research Department, Institut Curie, PSL Research University, Paris, France,[6]Department of Medical Oncology, Hacettepe University Cancer Institute, Ankara, Turkey,[7]Department of Biochemistry and Molecular Biology, The Medical University of South Carolina (MUSC), Charleston, SC*

Estrogen receptor (ER) positive breast cancer accounts for about 75% of all breast cancer cases. Tamoxifen has been the mainstay therapy for over 40 years that is used to treat early, locally advanced, and metastatic ER-positive breast cancers. Despite the initial clinical success, approximately 20-30% of high-risk, advanced ER-positive breast cancer patients are resistant to tamoxifen or develop resistance over time which significantly decreases survival. Long-noncoding RNAs (lncRNAs) are a class of non-coding RNAs that are more than 200 nucleotides in length and are involved in tumorigenesis via carrying out diverse functions by interacting with DNA, RNA or proteins. Here, we identified a lncRNA (LINC00152) that is upregulated in tamoxifen resistant (TamR) cell lines by RNA sequencing,

and we validated its upregulation in endocrine resistant, ER-positive patient-derived xenografts (PDXs) as well as in tamoxifen-treated ER-positive breast cancer patient tumors. We performed in-situ hybridization of the LINC00152 in our own cohort of tamoxifen-treated ER+ breast cancer patients and demonstrated a significant association of high LINC00152 expression with worse disease-free survival and treatment response. Inhibiting LINC00152 using either siRNAs or anti-sense oligonucleotides or shRNAs restored tamoxifen sensitivity in TamR cells. Mechanistically, we demonstrated that LINC00152 knockdown in combination with tamoxifen increases the expression of TRPC1, a calcium channel located on the plasma membrane, and thereby causes the cytoplasmic accumulation of excessive amounts of Ca^{2+}, which ultimately leads to the generation of reactive oxygen species (ROS), lipid peroxidation and cell death by ferroptosis. Notably, we identified a cyclic AMP (cAMP)-specific phosphodiesterase, PDE4D as a novel interactor of LINC00152. We showed that PDE4D mRNA is stabilized by LINC00152 and reduces cAMP levels which then decreases the intracellular Ca^{2+} and blocks ROS generation, lipid peroxidation, and ferroptosis, ultimately leading to tamoxifen resistance. Therefore, targeting the LINC00152-PDE4D-cAMP-Ca^{2+} axis may represent a promising therapeutic approach to tackle tamoxifen resistance and improve clinical outcome in refractory ER-positive breast cancer.

#3884

Targeting the ARID1A mutations overcomes primary resistance to ALK inhibitors in EML4-ALK posistive NSCLC

Seung Yeon Oh, You Won Lee, Eun Ji Lee, Ju Young Kim, Sewon Park, Ju Yeon Park, Su-Jin Choi, Mi Ra Yu, Jii Bum Lee, Jiyun Lee, Chang Gon Kim, Sun Min Lim, Min Hee Hong, Mi Ran Yun, Byoung Chul Cho. *Yonsei University College of Medicine, Seoul, Korea, Republic of*

Introducti**on:** Anaplastic lymphoma kinase (ALK)-tyrosine kinase inhibitors (TKIs) have improved an initial clinical response of non-small-cell lung cancer (NSCLC) patients with ALK-rearrangements. However, a subset of patients shows a poor response to ALK-TKIs. Here, we aimed to identify novel mechanism of primary resistance in preclinical model from a

patient who presented an impressive resistance to sequential treatment with ALK TKIs.

Experimental design: The PDC YU-1076 cells were established from pleural effusion of the patient at the time he was receiving chemotherapy and radiotherapy after failure of ALK-TKI treatment. Sanger sequencing confirmed ML4-ALK variant 1 detected at the initial diagnosis. No resistance mutations in the ALK kinase domain were detected. To investigate co-occurring genetic alterations, we performed whole exome sequencing (WES) on YU-1076 cells and the matched blood sample. We further investigated the molecular profile of YU-1076 cells using RNA-sequencing analysis.

Results: YU-1076 cells exhibited cross-resistance to clinically available ALK-TKIs including crizotinib, ceritinib, alectinib, and lorlatinib. However, immunoblot analysis of YU-1076 cells treated with incremental doses of TKIs unexpectedly revealed an effective reduction of ALK activity and downstream signals. We noticed that YU-1076 cells gradually changed from a small, round shape to a fibroblast-like shape following the treatment of ALK-TKIs. Transcriptome analysis confirmed enrichment for gene signatures related epithelial-to-mesenchymal transition (EMT) in ALK TKI-treated YU-1076 cells, suggesting that ALK-TKIs treatment promotes YU-1076 cells toward a more mesenchymal phenotype. WES analysis identified a major chromatin remodeling complex subunit, AT-rich interacting domain 1A (ARID1A), as well as MYC amplification, CDKN2A loss, and TP53 mutations. We focused on a synthetic lethal strategies using the SFK inhibitor dasatinib and the EZH2 inhibitor GSK126 in ARID1A mutant cancers. The combination of dasatinib with ALK-TKIs restored the sensitivity to the ALK TKIs in YU-1076 cells, accompanied by suppression of EMT marker genes VIM and CDH2 and increase of apoptotic markers BIM, PARP, and CAS3. Congruently, dasatinib significantly impaired tumor growth in YU-1076-xenografts. GSK126 also induced synergistic inhibition of cell growth with upregulation of apoptosis marker genes in YU-1076 cells, but did not affect the expression of EMT marker genes.

Conclusion: Our data indicate that ARID1A could be potentially used as a predictive biomarker for unfavorable ALK-TKI response. In this context, a combination strategy of ALK TKI with dasatinib may be effective in overcoming primary resistance.

#3885

A secondary Gαq mutation confers resistance to Gαq inhibitors in uveal melanoma

Jiafang Ma[1], Meng Wang[1], Aashish Manglik[2], Boris C. Bastian[1], Xu Chen[1].
[1]Department of Dermatology, UCSF Helen Diller Family Comprehensive Cancer Ctr., San Francisco, CA,[2]UCSF School of Pharmacy, San Francisco, CA

Uveal melanoma (UM) is a rare subtype of melanoma that originates from melanocytes of the choroidal plexus, ciliary body and iris. Despite successful treatment of the primary by radiation or surgery, 50% of UM patients develop metastases, mostly in the liver, as an invariably lethal complication. Over 90% of UM harbor activating mutations in the closely related GNAQ or GNA11 genes, mainly at codons Q209, compromising the GTPase activity. Mutant GNAQ and GNA11 can be successfully targeted by the cyclic depsipeptide YM-254890. To anticipate mechanisms of resistance that might arise under treatment with this novel class of Gαq inhibitors, we generated UM cell lines resistant to YM-254890 using an in-vitro cell culture system. Upon chronic growth suppression of a $GNA11^{Q209L}$ mutant UM cell line, we established 12 YM-254890 resistance clones. We identified a secondary $GNA11^{F75Y}$ mutation in one clone and $GNA11^{Y192H}$ mutations in the other 11 clones. The secondary mutations were present *in cis* with the original $GNA11^{Q209L}$ mutations. To validate the functional role of these secondary mutations in conveying resistance, we engineered two double mutants, $GNA11^{Q209L/F75Y}$ and $GNA11^{Q209L/Y192H}$, and introduced them into 293FT cells respectively and confirmed that both F75Y and Y192H convey resistance to YM-254890 treatment. The proliferation of YM-254890-resistant cell lines was still dependent on GNA11 and downstream PKC/MAPK signaling. Combined inhibition of PKC and MEK synergistically reduced cell viability in YM-254890 resistant UM cells. Analysis of the crystal structure of YM-2548890 in complex with GNAQ predicts both F75Y and Y192H mutations directly affect the binding of YM-254890 to Gαq. Our data suggest that direct targeting mutant GNAQ/11 is promising but will select for secondary mutations within GNAQ /11 that will result in resistance. Combinatorial

targeting of other components in the Gαq signaling pathway will increase clinical efficacy.

#3886

Analysis of concomitant genetic alterations in advanced EGFR-mutated lung adenocarcinoma by targeted NGS : A multicenter prospective and real world study

In Ae Kim[1], Seung Joon Kim[2], Sung Yong Lee[3], Chang Min Choi[4], Jae Cheol Lee[5], Tae Won Jang[6], Seung Hun Jang[7], Chan Kwon Park[8], Wan Seop Kim[9], Jae Young Hur[9], Hee Joung Kim[10], Young Whan Kim[1], Key Young Lee[11]. *[1]Precision Medicine Lung Cancer Center, Konkuk Universtity Medical Center, Seoul, Korea, Republic of,[2]Division of Pulmonology, Department of Internal Medicine, Seoul St. Mary's Hospital, College of Medicine, The Catholic University of Korea, Seoul, Korea, Republic of,[3]Department of Internal Medicine, Korea University Guro Hospital, Seoul, Seoul, Korea, Republic of,[4]Department of Pulmonology and Critical Care Medicine & Oncology, Asan Medical Center, University of Ulsan, College of Medicine, Seoul, Korea, Republic of,[5]Department of Oncology, Asan Medical Center, University of Ulsan, College of Medicine, Seoul, Korea, Republic of,[6]Pulmonary division, Dept of Internal Medicine, Kosin University Gospel Hospital, Seoul, Korea, Republic of,[7]Division of Pulmonary, Allergy, and Critical Care Medicine, Department of Medicine, Hallym University Sacred Heart Hospital, Hallym University College of Medicine, Seoul, Korea, Republic of,[8]Precision Medicine Lung Cancer Center, Yeouido St. Mary's Hospital, College of Medicine, The Catholic University of Korea, Seoul, Korea, Republic of,[9]Department of Pathology, Konkuk Universtity Medical Center, Seoul, Korea, Republic of,[10]Precision Medicine Lung Cancer Center,3Department of Pulmonary Medicine, Konkuk Universtity Medical Center, Seoul, Korea, Republic of,[11]Precision Medicine Lung Cancer Center,Department of Pulmonary medicine, Konkuk Universtity Medical Center, Seoul, Korea, Republic of*

Background**:**The response of 1st-line EGFR-TKI treatment in advanced EGFR-mutated lung adenocarcinoma patients are highly effective, but its sustainability and clinical course are quite variable from patient to patient. In this study, we investigated the clinical impact of concomitant genetic

mutations analyzed by targeted NGS on PFS and acquired resistance in advanced EGFR-mutated lung adenocarcinoma patients.
Methods: Eighty-five advanced NSCLC patients harboring *EGFR* mutations were enrolled prospectively in multi-centers from 2019 to 2022 (NCT04122833). We performed the targeted next generation sequencing on 324 cancer-related genes by Foundation One CDx with pre-treated tumor samples. First- or second-generation *EGFR*-TKIs(gefitinib, afatinib, or erlotinib) were administered in 1st-line setting. After the progression, tissue re-biopsy or plasma liquid biopsy (FoundationOne Liquid CDx) for NGS if tissue biopsy is difficult or risk was performed.
Results: Of the 85 patients (70.6% of female, 65.8% of nonsmoker, 56.4% of E19del and 38.8% of E21 L858R mutation), 50 patients experienced a disease progression in November, 2022. The median PFS was 20 months (95 %CI: 15.2-24.8). The most frequent co-mutations were *TP53* (47.1%), *CDKN2A/B* loss (34.1%), *MTAP* loss (20%), *NKX2-1amp(15.3%), MDM2amp (14.1%), RMB10, CCNE/CCND1 amp, NFKB1 amp (11.8%)* and *CDK4/6* amp (10.6%). Patients with *TP53, CDK4/6* amp and *MYC* amp were independently associated with shorter PFS. In a multivariate analysis, tumors with copy number alterations such as *CDK4/6* amp or Myc amp were also independently associated with shorter PFS. However, the CDKN2A/2B loss, MTAP loss, and MDM amp were not related with the PFS. In the number of co-mutations, patients harboring ≥5 co-mutations identified by NGS had shorter median PFS than patients with 0-1 or 2-4 co-mutations. (mPFS 0-1 : 2-4: ≥5 co-mutations=35: 18 : 9.3 months, $p<0.001$). At progression, 22 patients harbored an acquired T790M mutation (25.8%). Before TKI treatment, patients with *CDKN2A/B* loss, *MTP* loss or *CCND/CCNE1* amp in pretreatment tumor have more acquired T790M mutation after progression significantly ($p<0.05$)
Conclusion: We have demonstrated that concomitant mutations detected by targeted NGS analysis provide significant impact on the drug response and clinical course of advanced EGFR-mutated adenocarcinoma patients treated by 1st-line EGFR-TKIs. It is suggested that targeted NGS along with PCR-based detection will be necessary for precision medicine-based individualized practice of 1st-line EGFR-TKI-based combination treatment.

#3887

ATP-binding pocket substitutions as secondary or tertiary in-cis mutations are major on-target ripretinib resistance mechanisms in gastrointestinal stromal tumor

Thomas Mühlenberg[1], Johanna Falkenhorst[1], Tom Schulz[2], Benjamin S. Fletcher[1], Alina Teuber[2], Dawid Krzeciesa[1], Isabella Klooster[3], Jonas Lategahn[2], Wen-Bin Ou[3], Meijun Lundberg[3], Margaret von Mehren[4], Susanne Grunewald[1], Alicia I. Tüns[5], Mehdi Brahmi[6], Michael C. Heinrich[7], Cesar Serrano[8], Hans-Ulrich Schildhaus[9], Sonja Sievers[10], Jürgen Treckmann[11], Lydia Wilson[3], Chandrajit P. Raut[12], Adrian Marino-Enriquez[3], Suzanne George[13], Daniel Rauh[2], Jonathan A. Fletcher[3], Sebastian Bauer[1]. *[1]Internal Medicine (Tumor Research), Essen University Hospital, Essen, Germany,[2]Chemistry and Chemical Biology, Technical University Dortmund, Dortmund, Germany,[3]Pathology, Brigham and Women's Hospital, Boston, MA,[4]Hematology/Oncology, Fox Chase Cancer Center, Temple Health System, Philadelphia, PA,[5]Medical Oncology, Essen University Hospital, Essen, Germany,[6]Medical Oncology, Centre Leon Berard, Lyon, France,[7]Portland VA Health Care System and OHSU Knight Cancer Institute, Portland, OR,[8]Sarcoma Translational Research Laboratory, Vall d'Hebron Institute of Oncology, Barcelona, Spain,[9]Institute of Pathology, Essen University Hospital, Essen, Germany,[10]Compound Management and Screening Center, Max Planck Institute of Molecular Physiology, Dortmund, Germany,[11]Visceral and Transplantation Surgery, University of Duisburg-Essen Medical School, Essen, Germany,[12]Surgery, Brigham and Women's Hospital, Boston, MA,[13]Medical Oncology, Dana-Farber Cancer Institute, Boston, MA*

Introduction: Ripretinib (Rip) is a kinase inhibitor with broad preclinical activity against mutant KIT. Based on the INVICTUS trial, Rip was approved for patients with Gastrointestinal Stromal Tumors (GIST) after treatment with 3 or more kinase inhibitors. Most patients in this ≥4th-line setting progress on Rip within one year. Here, we characterized Rip-progressing GIST samples to identify resistance mechanisms.
Methods: Progressing lesions in 25 patients were analyzed by NGS after Rip failure. KIT mutations (muts) were recapitulated by gene editing. Activities of Rip, sunitinib (SU), and novel TKIs were characterized by cell

viability assays and immunoblot. Mutagenesis experiments were performed using ENU. SU- and Rip-resistant cell lines were pooled and treated with various regimens, with clonal composition deconvoluted by cDNA-based amplicon sequencing.
Results: 19/25 Rip-progressing GISTs displayed muts in the ATP-binding pocket (ATP-BP; e13/14). Four of these had pre-existing muts in the activation loop (AL; e17/18), which were confirmed to be in-cis with the primary and ATP-BP muts (triple in cis; TIC). Mutagenesis screens using a double KIT-mutant GIST line (e11 + AL) as a starting point confirmed that TIC-muts are a predominant escape mechanism when treated with Rip. A GIST subline (T1-triple) with TIC-muts in e11, e18 (A829P), and e13 (V654A) was highly resistant to Rip (GR50 > 2μM). Structural analyses of ATP-BP muts suggest steric interference and loss of van der Waals interactions that impede Rip binding and thereby confer Rip resistance. Another 3/25 Rip-progressing GISTs harbored pathogenic *KIT* muts in e9 only. A novel GIST cell line with primary *KIT* e9 mut (T1-e9) was 14-fold less sensitive to Rip than isogenic e11-driven cells (GR50 = 115 vs 8nM). Notably, adding a typical AL mut to T1-e9 (T1-e9-N822K) sensitized the cells to Rip (GR50 = 20nM). Immunoblots showed >95% inhibition of phospho-KIT in AL-mutant cell lines at Rip 100nM, whereas inhibition was weaker in T1-e9 (77%) and T1-V654A (46%), and absent in T1-triple. A compound screen of FDA-approved kinase inhibitors identified Nintedanib (NIN) as the most active compound against T1-triple. Clonal outgrowth assays of mixed cultures revealed SU (93% inhibition), and a weekly switch between Rip and either SU (96%) or NIN (79%) as the most effective inhibitors of pooled cell growth.
Conclusions: *KIT* e9 primary muts and e13/14 (ATP-BP) secondary muts are enriched in post-progression biopsies following Rip treatment. *KIT* TIC-muts are novel frequent events driving GIST clinical progression and confer a high degree of resistance. Strategies to overcome resistance may include combinations or sequences of approved drugs, and novel drugs that more efficiently inhibit TIC-mutant KIT.

#3888
N-glycosylation-defective IL6 activates the SRC-YAP-SOX2 signaling to potentiate metastasis and TKI resistance in NSCLC

Chun Hua Hung[1], Shang-Yin Wu Wu[1], Hsuan-Heng Yeh Yeh[2], Chien-Chung Lin[3], Wu-Chou Su[1]. *[1]Department of Oncology, National Cheng Kung Univ. Medical College, Tainan, Taiwan,[2]Center of Applied Nanomedicine, National Cheng Kung University, Tainan, Taiwan,[3]Department of Internal Medicine, National Cheng Kung Univ. Medical College, Tainan, Taiwan*

The IL6-GP130-STAT3 signaling pathway facilitates lung cancer progression and resistance to tyrosine kinase inhibitors. Although glycosylation alters the stability of GP130 receptor, its effect on the ligand IL6 remains unclear. In this study, we found that N-glycosylated IL6 primarily triggers JAK-STAT3 signaling and prolongs STAT3 phosphorylation, whereas N-glycosylation-defective IL6 (DeNG-IL6) induces shortened STAT3 activation and changes the downstream signaling preference for the SRC-YAP-SOX2 axis. This signaling shift promoted epithelial plasticity *in vitro* and metastasis *in vivo*, which were suppressed by specific inhibitors and shRNAs targeting SRC, YAP, and SOX2. EGFR TKI-resistant lung cancer cells secrete high levels of DeNG-IL6 via reduced N-glycosyltransferase gene expression and showed SRC-YAP activation. DeNG-IL6 contributes to drug resistance, as confirmed by *in silico* analysis of cellular and clinical transcriptomes, and signal expression in patient specimens. In summary, cell behaviors can be altered by modifying the N-glycosylation of IL6, and the glycosylation status of circulating IL6 might be a promising biomarker for monitoring the dynamics of lung cancer evolution.

#3889

The role of CXCL1 in crosstalk between breast cancer cells with ESR1 mutations and lymphatic endothelial cells

Daniel Galke, Kideok Jin. *Albany College of Pharmacy & Health Sciences, Albany, NY*

Various endocrine therapies have been developed such as selective estrogen receptor modulation (SERM), selective estrogen receptor downregulator (SERD) and ligand deprivation using aromatase inhibitors (AI). Tamoxifen, fulvestrant, and AIs are the most used adjuvant treatment for pre- and postmenopausal women with early-stage estrogen receptor positive breast

cancer. Tamoxifen and AIs have widespread anti-neoplastic and chemopreventive effects, yet despite this, many breast cancers that are initially receptive ultimately become resistant and recur. There are many known underlying molecular processes that result in resistance, but no overarching pattern has yet been identified. Our previous research demonstrates that the crucial molecular and cellular players secreted from a crosstalk between stromal cells and breast cancer cells can control the development of the tumor and the metastatic process in breast cancer. Breast cancer metastasis involves lymphatic dissemination in addition to hematogenous spreading. Although stromal lymphatic vessels (LVs) serve as initial metastatic routes, roles of organ-residing LVs are underinvestigated. In this report, we demonstrated that crosstalk between ESR1 mutant cells (Y537S and D538G), and lymphatic endothelial cells (LECs), a component of lymphatic vessels, promoted ESR mutant cell growth and migration. To identify a critical secreted factor in this crosstalk, we performed the cytokine array in secretome of crosstalk between ESR1 mutant cells and LECs, and found that CXCL1 is highly secreted from LECs. Knockdown of CXCR2 in ESR1 mutant cells attenuated ESR1 cell migration in the conditioned media of LECs crosstalked with ESR1 mutant cells. To investigate a potential impact given the current clinical landscape of endocrine resistant breast cancer with ESR1 mutations, we performed a cell viability assay and migration assay using reparixin, CXCR1/2 inhibitor in co-culture with ESR1 mutant cells and LECs. Significantly, reparixin decreased ESR1 mutant cell viability and migration compared to vehicle. We found that the combination treatment of reparixin and Palbociclib and ribociclib significantly inhibited ESR1 mutant cell growth and migration compared the single treatment. These findings implicate CXCL1-CXCR1/2 signaling as a critical event in the growth of breast cancer with ESR1 mutation and metastasis. Therefore, we have provided evidence that supports the hypothesis that functional inhibition of the CXCL1 and CDK4/6 signaling pathway has the potential to circumvent endocrine resistant tumor growth and metastasis.

#3890

TMPRSS2 serin protease is a novel biomarker for ER+ breast cancer patient prognosis and survival and mediates resistance to anti-estrogen treatment in ER+ breast cancer

Rumeysa Ozyurt, Nermin Kahraman, Pinar Atalay Dundar, Bulent Ozpolat.
Nanomedicine, Houston Methodist Research Institute, Houston, TX

Breast cancer (BC) is the most commonly diagnosed cancer in women and the second leading cause of cancer related deaths in the US. About 70-80% of patients have ER+ BC and initially respond to anti-estrogen (ie, Tamoxifen) or endocrine/homonal treatments. However, about 60% of the patients inevitably develops resistance to anti-estrogen therapies (due to intrinsic (15-20%) and acquire resistance (30-40%), representing a major clinical problem, resulting in relapses and metastasis, leading to significant patient mortality. Therefore, understanding the underlying mechanisms causing resitance to hormonal or anti-estrogen treatments is needed the for developing highly effective threapies and improving patient survival. Cell surface proteases, including serine proteases, are proteolytic modifiers of particular targets, including growth factors and protease-activated receptors, which are critical for the activation of oncogenic signaling pathways. TMPRSS2, a member of type II transmembrane serine protease (TTSP) family, has been shown to be highly expressed in prostate cancer cells and its role in carcinogenesis. We found that TMPRSS2 is highly upregulated well established tamoxifene resistant cell lines derivative of MCF7 (LCC2 and LCC9) compared to MCF7 cells. Performing Kaplan-Meier survival analyses in TCGA-BC database we also found that TMPRSS2 expression is associated with poor prognosis and significantly shorter patient survival in ER+ BC patients ($p=0.015$, $n=221$ patients). In addition, we found that TMPRSS2 is regulated by Estrogen/ Estrogen Receptor-alpha (ERα) signaling as in vitro inhibition of estrogen/ ERα signaling by ERα siRNA, tamoxifen or faslodex reduced TMPRSS2 protein expression ER+ MCF7 BC cells. Moreover, we found that inhibition of TMPRSS2 by 3 different siRNA molecules suppressed cell proliferation of MCF7 cells and reduced expression critical proteins for cell cycle and proliferation, including cyclin D1, c-Myc and pERK/MAPK signaling, suggesting that TMPRSS2 promotes the oncogenic signaling pathways in ER+ BC cells. Currently, we are targeting TMPRSS2 in in vitro and in vivo Tamox-resistant LCC2 and LCC9 models in mice by siRNA alone and in combination with Tamoxifen or faslodex to demostrate inhibition of TMPRSS2 sensitize tumors to anti-estrogen treatments. In conclusion, TMPRSS2 is a potential biomarker for poor patient survival and anti-estrogen resistance, and targeting TMPRSS2

alone as a monothreapy and in combination with anti- Tamoxifen or faslodex may be a promising approach for overcoming resistance to estrogen thereapies in ER+ BC patients.

#3891

Epigenetic rewiring promotes antiandrogen resistance and metastasis via heterogenous oncogenic drivers in prostate cancer

Xiaoling Li, Su Deng, Julisa Gonzalez, Carla Rodriguez Tirado, Choushi Wang, Nickolas A. Johnson, Lauren Metang, Ping Mu. *Molecular Biology, UT Southwestern Medical Center, Dallas, TX*

Prostate cancer (PCa) is the most diagnosed cancer among American men, which has traditionally been treated through hormone therapy. However, after hormone therapy many patients with PCa still develop a more aggressive stage of PCa, called metastasis castration resistant prostate cancer (mCRPC). The second- generation antiandrogens, such as enzalutamide or apalutamide, are used to competitively inhibit the androgen receptor (AR) signaling and achieved great clinical success. However, most of the mCRPC patients would develop resistance to the targeted therapy drugs within 6 months to 2 years after initial administration. Consequently, understanding the molecular mechanism of antiandrogen resistance, has become a critical endeavor to provide a greater benefit to patients. mCRPC is characterized by extensive heterogeneity of genomic copy number alterations, which may lead to antiandrogen resistance. TP53 and RB1 alterations have been reported to be dramatically enriched in mCRPC neuroendocrine cancer and we have previously found that inactivation of both TP53 and RB1 confers resistance to antiandrogen through lineage plasticity, where cancer cells can transdifferentiate from a luminal lineage to a mixture of basal and neuroendocrine lineages, which is no longer dependent on AR signaling. Despite these exciting discoveries, only 10% of patients have TP53 and RB1 loss and it is estimated that approximately 40% of patients develop antiandrogen resistance through an undiscovered mechanism.To identify more genomic alterations which confer antiandrogen resistance, we performed an *in vivo* library screening and identified some of the frequently depleted genes as top candidates mediating antiandrogen response, including the chromatin helicase DNA-binding factor (CHD1). Strikingly, the loss of CHD1 establishes an altered

chromatin landscape and enables the activation of heterogenous resistant subclones to emerge, including clones with ectopic NR3C1/GR, POU3F2/BRN2, TBX2, and NR2F1. This work provided an innovative model to explain the dramatically increased tumor heterogeneity in therapy resistant prostate cancer and suggested potential druggable targets to overcome resistance. Building on those exciting results, we are now examining the underlying mechanism how the epigenetic rewiring in resistant tumor clones confer resistance and monitoring the evolution of those heterogenous resistant subclones. Furthermore, we are revealing the collaborative function of those four resistant driver genes in promoting metastasis to various distal organs through multidisplinary approaches including single cell transcriptomics and 3D organoid modeling. The completion of this study will not only add clarity to the mechanism of antiandrogen resistance but may also lead to the development of novel biomarker and therapeutic approaches to overcome resistance.

#3892

EZH2 mediated kinome reprogramming drives AR phosphorylation and activation in receptor tyrosine kinase inhibitors resistant renal carcinoma models

Christopher Rupert[1], Stephanie Metcalf[2], Saranya Rajendran[2], Sean Colligan[1], Peter Hollenhorst[2], Roberto Pili[3]. *[1]University at Buffalo, Buffalo, NY,[2]Indiana University, Bloomington, IN,[3]Medicine, University at Buffalo, Buffalo, NY*

Systemic treatment of recurrent/metastatic renal cell carcinoma (RCC) largely uses receptor tyrosine kinase inhibitors (RTKI), as single agents or in combination with immune checkpoint inhibitors. Unfortunately, patients commonly develop resistance to RTKI's, leaving few options for further treatment. Therefore, understanding the mechanisms responsible for drug resistance is critical to improve the clinical outcome in this disease. Our previous studies of acquired resistance to the RTKI sunitinib identified two major regulators, EZH2 and androgen receptor (AR). Inhibition of EZH2 or AR in combination with sunitinib re-sensitizes cells to sunitinib both *in vitro* and *in vivo*. To further explore the link between EZH2 and AR in drug resistance, 786-0 RCC cells with acquired resistance to sunitinib (786-0^{RS}) was compared to drug naive 786-0 cells with exogenous AR (786-0^{AR}).

Chromatin immunoprecipitation sequencing (ChIP-seq) showed that AR and EZH2 bind the same genomic locations, but only in the resistant strain. Interestingly, treatment of 786-0^{AR} cells with sunitinib caused AR to translocate to the nucleus observed by the presence of AR at EZH2 bound sites. Additionally, mass spec of AR purified from 786-0^{RS} cells and 786-0^{AR} cells found high phosphorylation of S81 and S213, two markers associated with ligand independent activation, in 786-0^{RS} cells, but not in 786-0^{AR} cells. Previously, our lab has reported that 786-0^{RS} cells display a reprogramming of the tyrosine kinome which is dependent on EZH2 likely *via* a non-canonical mechanism. Consistent with this, EZH2 with a phosphomimetic mutation in Serine 21 (S21D) could promote sunitinib resistance when over-expressed with AR, whereas wild-type and phosphonull (S21A) EZH2 could not. We have also expanded the serine/threonine phosphoproteomic analysis and found extensive rewiring of these signaling networks in 786-0^{RS} cells with an enrichment of EGFR mediated MAPK and AKT signaling when compared to 786-0 cells. Finally, our lab has generated 786-0 strains resistant to other RTKI including pazopanib and lenvatinib, and found that AR is expressed in these resistant models, solidifying AR activation as a conserved feature of RTKI resistance. Overall, our results suggest that AR activation is driven by phosphorylation induced by EZH2 dependent kinome reprogramming. Untangling the cross talk between AR and EZH2 in RTKI resistant RCC will provide the rationale for novel therapeutic strategies to improve the clinical outcome in patients with this disease.

#3893
KRAS G12C colon cancer resistance to vertical MAPK inhibition converges on FOS-JUN signaling through orthogonal mechanisms
Mohamad Karim Koleilat, Lawrence Kwong. *UT MD Anderson Cancer Center, Houston, TX*

KRAS G12C mutations in cancer can be targeted by G12C-specific inhibitors, but resistance develops rapidly. Preclinical studies suggested multiple drug combinations to improve efficacy, including CDK4/6, MEK, ERK, EGFR, and SHP2 inhibitors, collectively called vertical MAPK inhibition (“vMAPKi”). To identify mechanisms of resistance to vMAPKi, we treated the G12C-mutant colon cancer cell line SW837 with different

vMAPKi triple combinations incorporating G12C, MEK, ERK, EGFR, SHP2, and/or S6K1 inhibitors until resistance developed. Notably, we identified two modes of resistance: fast growing colonies and slow growing or quiescent persisters. Unlike other fast growing resistant models that have pre-existing resistance mutations (e.g. EGFR-T790M for EGFR inhibitors), we did not identify any obvious resistance mutations by targeted exome sequencing in 6 separate colonies, each derived from a different vMAPKi combination. Instead, Reverse-Phase Protein Array revealed robust JNK pathway activation across all colonies, regardless of initial drug combination. Indeed, all colonies showed cross-resistance to all vMAPKi combinations, and sequence analysis revealed shared non-oncogenic mutations across colonies, suggesting that they pre-existed in the parental population. These data suggest that such pre-existing clones are fated for dominance, regardless of the vMAPKi combination used – implying that vertical pathway inhibition has intrinsic limitations. However, all colonies also gained exquisite sensitivity to single-agent JNK inhibition ("JNKi") compared to parental controls (with identical results in a second cell line, SW480), suggesting a gained vulnerability. Indeed, brief high-dose JNKi treatment completely eliminated colonies, as they did not grow back when JNKi was switched back to vMAPKi. By contrast, JNKi had no effect on quiescent persisters. To understand the differences between colonies and persisters, we conducted RNA-seq on the isolated populations. Although persisters showed no evidence of upstream JNK activation, they showed high expression of FOS, FOSB, and FOSL1, the binding partners of JUN. Indeed, expression of any FOS paralog was sufficient to confer vMAPKi resistance. Thus, both colonies and persisters converge on FOS-JUN signaling, one through upstream JNK activation and the other through transcriptional upregulation of FOS family members. Interestingly, pre-treatment of parental SW837 with high-dose JNKi has no effect on later resistance development, contrasted to the elimination of colonies if JNKi is given after resistance developed. This implies that colonies must undergo a reprogramming step to gain sensitivity to JNKi. We are currently conducting longitudinal single cell and barcoding sequencing assays to understand how such reprogramming occurs and whether this can reveal earlier therapeutic vulnerabilities.

#3894

The role of ELF3 in acquired resistance to endocrine therapy in ER-positive breast cancer

Na Zhang[1], Rongbin Zheng[2], Myles Brown[1]. *[1]Dana-Farber Cancer Institute, Brookline, MA,[2]Boston Children's Hospital, Boston, MA*

Endocrine therapies targeting the estrogen receptor (ER) are the major treatments of ER+ breast cancer, however acquired resistance to endocrine therapy is almost unavoidable and is the main cause of death with breast cancer. The only FDA-approved selective estrogen receptor degrader (SERD) fulvestrant has been used in the second line treatment to overcome aromatase inhibitor- or tamoxifen-resistance. However, fulvestrant has poor pharmacokinetic properties, which has inspired the development of a new generation of oral SERDs including amcenestrant and giredestrant. To understand the mechanisms of acquired resistance to SERDs in ER+ breast cancer, we established ER+ breast cancer cell lines (MCF7 and T47D) resistant to fulvestrant, amcenestrant or giredestrant. We found that all of our MCF7 and T47D SERD-resistant cell lines showed cross-resistance to each of the three SERDs. We then performed multiple genome-wide profiling assays including CRISPR-KO screen, whole exome sequencing (WES), RNA-seq, ATAC-seq and H3K27ac ChIP-seq on the parental and SERD resistant cell lines. Our findings from the CRISPR-KO screens suggest that ETS transcription factor ELF3 is a potential driver of resistance to SERDs. ELF3 expression is negatively regulated by estrogen signaling. Cells that developed acquired resistance to different SERDs consistently show depletion of ER expression but also a dramatic increase of ELF3 expression, while knockdown of ELF3 in the resistant cells leads to cell growth inhibition, suggesting that ELF3 can drive cell survival in the SERD resistant cells. When comparing the open chromatin regions and active enhancer regions between SERD resistant and parental cells via ATAC-seq and H3K27ac ChIP-seq respectively, ELF3 DNA binding motif was found significantly enriched in SERD resistant cells versus parental cells further indicating that ELF3 may play an important role in the SERD resistant cells. ELF3 ChIP-seq was also performed to identify genes enriched with ELF3 binding sites in SERD resistant and parental cells. Pathway analysis of ELF3-targeted genes reveals that ELF3 may regulate cell metabolism specifically in SERD resistant cells but not in parental cells. Our study

suggests that ELF3 may be a novel driver of acquired resistance to SERDs in ER+ breast cancer.

#3895

New potential mechanism of mnx1-as1 in the regulation of the carboplatin chemoresistant phenotype in ovarian cancer cell lines

Tamara Alejandra Viscarra Alvarez[1], Kurt Leopoldo Buchegger Mena[2], Daniela Inés León Garrido[1], Carmen Gloria Ili Gangas[1], Jorge Sapunar Zenteno[1], Marcela Berrios Flores[3], Ramón Silva Pezoa[4], Sindy Paola Cabarca Barreto[1], Priscilla Brebi Mieville[1]. *[1]Universidad de La Frontera, Temuco, Chile,[2]Ciencias Básicas, Universidad de La Frontera, Temuco, Chile,[3]Fundación Arturo López Pérez, Santiago, Chile,[4]Universidad Autónoma de Chile, Temuco, Chile*

Introduction: Ovarian cancer (OC) is one of the most lethal diseases in the female population worldwide, being considered by 2020 the eighth most common type of cancer and the eighth cause of cancer death in that population. The most widely used chemotherapy treatment is based on the application of platinum based drugs, carboplatin (CBDCA) being one of the most common, in combination with taxanes and cisplatin. Unfortunately, a high percentage of the population relapses shortly after chemotherapy treatment, presenting a drug resistant phenotype. This phenotype reduces overall survival in patients with OC. In this context, various mechanisms have been investigated to understand and study these chemoresistant phenotypes. In the last decade, lncRNAs have been identified in multiple biological processes, including the development of drug-resistant phenotypes in malignant tumors, however, little is known about their role in carboplatin resistance in OC. This study seeks to characterize the effect of lncRNA expression on the chemoresistant phenotype and its potential molecular mechanism involved.
Materials and Methods: Ovarian cancer cell lines corresponding to: A2780-R-CBDCA, A2780-P, UCI-101, OVCAR3 and SKOV3 were used. Drug susceptibility assays were performed using MTT. Relative expression was performed via RTqPCR. RNAseq was performed on a CBDCA resistance model in vitro using the Illumina HiSeq 4000 platform. Gene Ontology (GO) was analyzed using ClueGO. Gene set enrichment analysis (GSEA) was performed to define enriched biological pathways. Triplexator was

used to predict the triplex forming oligonucleotides (TFO) and triplex target sites (TTS) that may be involved in the formation of RNA-DNA triplexes. Results: RNAseq analysis showed 156 differentially expressed protein coding genes (DEGs). The most enriched and deregulated signaling pathway was Wnt/β-catenin. In this context, several regulators of this pathway were found to be altered, including sFRP1, sFRP4, PCDHB6, CTNNA2, DACT1, PCDHB6, WNT3A, and CER1. In addition, 17 lncRNAs involved in CDBCA resistance were found to be deregulated. In this sense, MNX1-AS1 showed high levels of expression in CBDCA resistant cell lines. Interestingly, it has been shown that MNX1-AS1 has the ability to form a triplex with the PCDHB6 gene, which is a tumor suppressor gene and whose expression was found to be decreased in CBDCA resistant cell lines.
Conclusions: Our results indicate that MNX1-AS1 expression could contribute to the modulation of platinum drug resistance through regulation of PCDHB6 expression via triplexes formation in OC. This finding could explain a new mechanism in CBDCA resistance in OC.

#3896

Alteration of malignancy and histone-H3 lysine-methylation status in osteosarcoma cells which acquire methotrexate resistance *in vitro*

Yusuke Aoki[1], Yasunori Tome[1], Hiromichi Oshiro[1], Ryo Katsuki[1], Kohei Mizuta[1], Kotaro Nishida[1], Robert M. Hoffman[2]. *[1]Department of Orthopedic Surgery, Graduate School of Medicine, University of the Ryukyus, Nishihara, Japan,[2]Department of Surgery, University of California, San Diego, La Jolla, CA*

Since methotrexate (MTX) resistance of osteosarcoma is a frequent cause of poor prognosis, new treatment strategies are needed to overcome this recalcitrant problem. The present study investigated if MTX resistance increased malignancy of osteosarcoma cells and its possible mechanism, via histone-H3 lysine-methylation status. We also propose a new therapeutic strategy for MTX resistant osteosarcoma. MTX resistant 143B osteosarcoma cells (143B-MTXR) were established from 143B parental osteosarcoma cells (143B-P) by culturing the cells with increasing concentrations of MTX stepwise (0.04 μM to 100 μM) for 12 months. The degree of malignancy of the isogenic pair of 143B-MTXR and 143B-P cells

was compared by testing clonogenic capacity in cell culture, on both plastic and soft agar. Malignancy was also compared by tumor growth in orthotopic xenograft mouse models by implantation of 2.5×10^5 cells in the tibia of nude mice. Histone-H3 lysine-methylation status was determined by Western immunoblotting. 143B-MTXR and 143B-P cells were also tested for methionine addiction by sensitivity to recombinant methioninase (rMETase). Welch's t-test was performed to statistically evaluate results and a probability value ≤ 0.05 was defined as statistically-significant difference. The mouse studies were approved by Institutional Animal Care and Use Committee of AntiCancer Inc. After 12 months selection in increasing concentrations of MTX, we isolated 143B-MTXR cells, which had an MTX IC_{50} of 384 μM compared to 143B-P cells, which had an IC_{50} of 0.27 μM, demonstrating that the 143B-MTXR cells acquired a 1422-fold resistance to MTX. In cell culture, 143B-MTXR cells had reduced clonogenic capacity on plastic and in soft agar ($P < 0.01$), indicating reduction in malignancy. In orthotopic xenograft nude-mouse studies, 143B-MTXR cells formed much smaller tumors than 143B-P cells ($P < 0.01$), further indicating that 143B-MTXR cells lost malignancy. 143B-MTXR cells showed an increase of histone H3K9me3 ($P = 0.01$), H3K27me3 ($P < 0.01$), and H3K79me3 ($P < 0.01$) methylation, which may account in part for their decreased malignancy. However, there was no difference in methylation of H3K4me3 ($P = 0.12$) or H3K36me3 ($P = 0.29$). The 143B-MTXR cells had an IC_{50} of 0.358 U/ml for rMETase, similar to an IC_{50} of 0.38 U/ml for 143B-P cells, indicating the 143B-MTXR cells did not lose their methionine addiction. The increase in histone H3K9me3, H3K27me3, and H3K79me3 shown in the present study in 143B-MTXR cells suggested potential biomarkers of methotrexate-resistance. MTX resistant osteosarcoma may be treated by methionine restriction with rMETase, as the MTX-resistant osteosarcoma cells are highly methionine addicted.

#3897

MNX1-AS1 expression is positively correlates with expression of drug efflux pumps in ovarian cancer

Kurt Buchegger Mena[1], Tamara Viscarra Alvarez[2], Daniela León Garrido[2], Ramón Silva Pezoa[3], Carmen Ili Gangas[2], Sindy Cabarca Barreto[2], Marcela Berrios Flores[4], Jorge Sapunar Zenteno[2], Priscilla Brebi Mieville[2].

[1]Ciencias Básicas, Universidad de La Frontera, Temuco, Chile,[2]Universidad de La Frontera, Temuco, Chile,[3]Universidad Autónoma de Chile, Temuco, Chile,[4]Fundación Arturo López Pérez, Santiago, Chile

Introduction: Ovarian cancer is one of the most lethal diseases in the female population worldwide. Indeed, the survival rate of ovarian cancer is very low when diagnosed lately and the success rate of current chemotherapy regimens is not very efficient. One of the main chemotherapy treatment regimens is the use of platinum drugs, specifically carboplatin (CBDCA). Nevertheless, one of the main reasons for this low success rate is the acquired chemoresistance of these cancers during their progression. The mechanisms responsible for this chemoresistance are numerous, including efflux pumps, repair mechanisms, survival pathways and tumor suppressors. In the last decade, lncRNAs have been identified as a new element responsible in the regulation of chemoresistant phenotype since they have been linked to multiple biological processes and acting in combination with other mechanism involved in chemoresistant. However, little is known about their role in carboplatin resistance in OC. This study seeks to characterize the effect of lncRNA expression on the chemoresistant phenotype and its correlation with the hyperactivation of drug efflux pumps.
Materials and Methods: Ovarian cancer cell lines A2780-R-CBDCA, A2780-P, UCI-101, OVCAR3 and SKOV3 were used in this study. Chemosensitivity to carboplatin was measured by MTT Assay in 96-well plates after 24, 48 and 72h treatment for determinating IC50 values. Relative expression of MNX1-AS1 associated with CBDCA-resistant phenotype and efflux pumps were evaluated by qRT-PCR.
Results: It was observed that A2780-R-CBDCA, SKOV3 and OVCAR3 cell lines presented the highest resistance indices in contrast to UCI-101 and A2780-P, which turned out to be highly sensitive to treatment with CBDCA. The relative expression of MNX1-AS1 was found elevated in those lines that presented higher levels of resistance to the drug, while in those more sensitive to treatment, the expression of MNX1-AS1 was found to be decreased. On the other hand, the expression levels of the ABCB1 and ABCC1 efflux pumps showed contradictory results in relation to their expression compared to the resistance index shown in each cell line. Mainly, it could be observed that ABCB1 presented a decreased expression

in A2780-R-CBDCA, while ABCC1 was found to be increased in the same line.
Conclusion: Our results indicate that the expression of MNX1-AS1 could contribute to the development or maintenance of a chemoresistant phenotype to platinum drugs. Meanwhile, the effect of the expression of MNX1-AS1 on the efflux pumps is not yet possible to relate as a modulator of its hyperactivation. However, their potential participation in this mechanism is not ruled out and new analyzes are necessary to rule out this possible relationship.

#3898

Synergistic combination of the iron chelator deferasirox with cisplatin and doxorubicin chemotherapies against nonsmall cell lung carcinoma

Natalia I. Ortiz Alvelo[1], Grace Torres[1], Sthephanie Estrada[2], Daraishka Pérez[3], Yancy Ferrer[3], Yamixa Delgado[1]. *[1]San Juan Bautista School of Medicine, Caguas, Puerto Rico,[2]University of Puerto Rico Cayey, Cayey, Puerto Rico,[3]Universidad Central del Caribe, Bayamon, Puerto Rico*

Lung cancer is the second most common and leading cause of cancer-related deaths worldwide with 85% of these cases being non-small cell lung carcinoma (NSCLC). Unfortunately, despite improvements in NSCLC outcomes, many of these tumors develop resistance against principal chemotherapies (e.g., cisplatin (CisPt) and doxorubicin (Doxo)), inducing abysmally low survival prognosis. Deferasirox (Def), an FDA-approved iron chelation therapy, is a drug under study for cancer therapy due to iron plays a key role in cell growth and energy production. Herein, we determined the effect of Def alone and in combination with CisPt and Doxo on NSCLC A549 cells. Viability assays results showed that Def has synergistic cytotoxic effects in combination with CisPt and Doxo at low uM concentrations after 24 h of incubation using the Chou Talalay method. In addition, qPCR gene expression studies showed that Def induced a significant downregulation of EGFR, VEGF, MMP9, MMP2, CHD4 genes related to resistance and metastatic process. In addition, we determined the overexpression of NDRG1 gene mediated by Def confirming the chelation of iron and disruption of iron metabolism. Overall, this work will set the basis for adjuvant therapies against chemoresistance and metastasis processes using an iron chelator.

#3899

CHST11 mediated SEMA7A expression contributes to TKI resistant in lung cancer

Chien-Hsiu Chris Li[1], Ming-Hsien Chan[1], Yu-Chan Chang[2], Michael Hsiao[1]. *[1]Academia Sinica - Genomics Research Center, Taipei, Taiwan,[2]Department of Biomedical Imaging and Radiological Sciences, National Yang Ming Chiao Tung University, Taipei, Taiwan*

An extracellular matrix has been demonstrated to be one of the substances that promote tumor cells to become driven by external stimuli to change their biology or malignancy. The main component of extracellular matrix, chondroitin sulfate, has been confirmed as a factor in the progression of tumors. Nevertheless, a great deal remains unknown regarding the precise mechanisms that drive Chondroitin sulfate production and how these details are communicated to cancer cells. According to our previous studies, the main enzyme responsible for Chondroitin sulfate synthesis, carbohydrate sulfotransferase 11 (CHST11), plays a crucial role in lung cancer cell metastatic spread. Nevertheless, the relationship between CHST11 expression and regulatory mechanism in response to lung cancer treatment is unclear, especially for tyrosine kinase inhibitor (TKI). A clinical correlation analysis was used in this study to identify molecules which were highly correlated with the overexpression of CHST11 and identified GPI-anchored protein semaphorin 7A (SEMA7A) as a candidate. According to the TCGA database, expression of upregulated SEMA7A is correlated with poor prognosis and cellular malignancy in lung cancer patients. A SEMA7A-based gene correlation analysis finds that the affected gene ontology is highly similar to CHST11, particularly integrin signaling, which may contribute to Gefitinib resistance. A GSEA analysis reveals a significant effect of CHST11 overexpression on mitotic spindle processes, some of which molecules are clinically relevant to CHST11 or SEMA7A. These molecules have been reported to be involved in TKI resistance events such as MARCKS, MYO1E, and PDLIM5. Based on the TCGA database, these molecules and integrins also display significant clinical relevance in lung cancer patients. A CHST11-mediated increase in SEMA7A in the mitotic spindle process of cells may serve as one of the possible means of reducing TKI-induced mitotic cell death, and thereby promoting the ability

of lung cancer cells to become resistant to TKIs. Hence, targeting the CHST11-SEMA7A axis may offer a therapeutic strategy option that could be used to target drug resistance in lung cancers. [Keywords: CHST11, SEMA7A, Integrin, Drug resistant, Lung cancer] (Reference: https://pubmed.ncbi.nlm.nih.gov/35985204/ ; https://pubmed.ncbi.nlm.nih.gov/36181245/)

#3900

***In vivo* inhibition of metastatic HER2 positive trastuzumab resistant breast cancer using engineered destabilized 3UTR ARE of HER2 improves survival outcomes**

Chidiebere U. Awah, Joo Sun Mun, Baris Boylu, Alooka Paragodaarachchi, Chika Ochu, Hiroshi Matsui, Olorunseun O. Ogunwobi. *The City University of New York, New York, NY*

Breast cancer is the most common form of cancer in women with mortality of about 58% in developing countries. HER2+ breast cancers are treated with trastuzumab in various forms in combination with chemotherapy and has been successful in targeting HER2 overexpression in HER2+ breast cancer and improving survival as a standard first line therapy for more than a decade. However, about 25% of early and 75% of late stage HER2 driven breast cancers are resistant to trastuzumab. For these patients, the clinical outcomes are grim. We report the destabilization of HER2 3‘UTR ARE which degraded oncogene HER2 transcript, protein expression, HER2 dependent kinases and interactome. *In vitro*, we transfected the engineered destabilizing HER2 constructs into BT474 clone 5 trastuzumab resistant breast cancer and within days, we inhibited cancer cell growth and degraded HER2 transcript and protein. The degradation of HER2 leads to loss of many kinases especially YES1 and WNK1 that are known causes of chemoresistance in HER2 positive trastuzumab resistant breast cancer. *In vivo*, we administered the destabilizing constructs as naked constructs or as complexed with nanocages to mice bearing tumors of BT474 clone 5 trastuzumab resistant cells. We found that our constructs, both the naked and nanocage-delivered, conferred significant survival (p values: 0.0178 and 0.00492) to about 60% of the exceptionally surviving mice compared to the controls. Taken together, we have developed a new therapy to target

trastuzumab resistant HER2+ metastatic breast cancers with increased survival outcomes.

#3901
Identification of genomic pathways associated with resistance of NSCLC to immunotherapies containing granzyme B
Ana Alvarez-Cienfuegos, Lawrence H. Cheung, Khalid A. Mohamedali, Ganiraju C. Manyam, Jing Wang, John V. Heymach, Michael G. Rosenblum. *UT MD Anderson Cancer Center, Houston, TX*

Immuno-oncologic (IO) approaches have completely transformed lung cancer treatment. Unfortunately, most patients with NSCLC develop primary resistance during IO and less than 20% achieve partial or complete response. Understanding the pathways to resistance is a significant challenge that requires a focused approach combining both clinical and basic research. Because resistance to IO is complex and likely multimodal, it is vital to find alternative strategies to overcome these challenges. IO generally employs cellular-mediated delivery of granzyme (GrB) as the final toxic payload and fusion proteins containing GrB serve as a targeted therapeutic with an identical mechanism of cytotoxic action. Subsequent development of resistance to GrB-based fusions may provide a look into the intrinsic mechanism of resistance related to cell signaling and gene expression for IO agents. The human fusion protein GrB-Fc-IT4 contains a single chain variable fragment targeting the Fn14 (fibroblast growth factor-inducible 14) receptor for TWEAK that is overexpressed in several tumor types, including NSCLC. GrB-Fc-IT4 exhibits high affinity and selective cytotoxicity within the nanomolar range when tested against a large panel of Fn14+ human cancer cell lines including NSCLC. We generated 3 resistant clones from a NSCLC GrB-sensitive cell line (A549) by exposing the cells to increasing concentrations of GrB-Fc-IT4. We then conducted a comprehensive genomic characterization of the GrB-sensitive A549 and compared to the GrB-Fc-IT4 resistant clones (A549R-F5, A549R-F7 and A549R-F8) to identify significant differentially expressed genes (DEGs) and pathways involved in GrB-resistance mechanisms. By mapping gene expression changes we have established that clones A549R-F5 and A549R-F7 have a very similar genomic profile, while the clone A549R-F8 displays a distinctive genomic profile. These results suggest that clones A549R-F5

and A549R-F7 shared a similar mechanism of resistance whereas clone A549R-F8 mechanism of resistance might be different. Comparison of the GrB-resistant clones with 7 NSCLC cell lines sensitive to GrB-Fc-IT4 revealed 43 significant DEGs (padj<0.05), suggesting these genes could be involved in the GrB response. From these DEGs, 34 genes had a higher basal expression in the GrB-resistant clonal cell lines while 9 DEGs were downregulated. Significantly, sensitivity of GrB-resistant cell lines to the chemotherapy agent cisplatin showed that the GrB-resistant clones were 6-fold more resistant than the parental cell line. We found that 13 DEGs of the 43 DEGS have also been described to be involved with cisplatin- or damage-response. These novel candidates for GrB resistance could prove to be important prognostic markers or targets for tailored combined therapy in the future. Research conducted, in part, by the Clayton Foundation for Research and Lung Spore (P50CA070907).

#3902

Glutathione as a potential marker of tamoxifen resistance in breast cancer

Yazan I. Hamadneh[1], Mohammad AlWahsh[2], Jawad Alrawabdeh[1], Roland Hergenröder[3], Lina A. Dahabiyeh[4], Lama Hamadneh[2]. *[1]School of Medicine, University of Jordan, Amman, Jordan,[2]Department of Pharmacy, Al-Zaytoonah University of Jordan, Amman, Jordan,[3]Leibniz-Institut für Analytische Wissenschaften - ISAS - e.V., Dortmund, Germany,[4]Faculty of Pharmacy, University of Jordan, Amman, Jordan*

Glutathione (GSH) is an antioxidant with an important protective intracellular role against reactive oxygen species. Increased glutathione level is associated with higher rates of metastases and a more aggressive behavior in breast cancer. This study aims to study the molecular and metabolic changes in glutathione synthesis in tamoxifen resistant (TAM-R) MCF-7 breast cancer cell lines.Methods: Three tamoxifen resistant MCF-7 cell lines were produced by using two methods. The first was achieved by treating the cells with tamoxifen and gradually increasing the amount until reaching a predetermined concentration of tamoxifen. The second was achieved by giving multiple fixed concentrations of tamoxifen, the third model was produced from the second by treating the cells with continuous 1μM of tamoxifen. mRNA and metabolites were extracted from the cell

lines. cDNA was synthesized from the extracted mRNA, and gene expression of glutathione synthetase (*GSS*) was measured using real-time PCR. Nuclear Magnetic Resonance technique with PABO probe was used for metabolic profiling of extracted metabolites from the resistant and sensitive MCF-7cells and Chenomix software for quantification. Additionally, Kaplan Meier plotter (https://kmplot.com/) was used to predict the significance of GSS gene expression to overall survival of breast cancer patients. Results: A significant increase in glutathione accompanied with significant decrease in cysteine levels were found in TAM-R cells compared to control TAM sensitive cells. However, there was a 2 times reduction in the expression of *GSS* in TAM-R cells. Correlation of *GSS* gene expression among ER +ve, PR +ve patients who received tamoxifen in their therapy showed that its down regulation is significantly linked to poor overall survival (*p-value* 0.022 and HR of 0.7). Conclusion: The significant increase of glutathione in TAM-R cells may contribute to their increased resistance to oxidative stress and exhibition of a more aggressive behavior. Moreover, the decrease in *GSS* expression is a strong indicator of decreased glutathione synthesis in TAM-R cells as a result of cysteine depletion in the cells that was correlated to poor overall survival among BC patients. However, high glutathione levels in TAM-R cells could be due to increased glutathione regeneration in TAM-R cell lines compared to control.

#3903

Role of the miR-301a/Fra-2/GLIPR1 axis in lung cancer cisplatin resistance

Francesca Lovat[1], Gian Luca Rampioni Vinciguerra[1], Marina Capece[1], Rosario Distefano[1], Giovanni Nigita[1], Andrea Vecchione[2], Carlo M. Croce[1]. *[1]The Ohio State University, Columbus, OH,[2]University of Rome 'Sapienza', Rome, Italy*

Lung cancer is the leading cause of cancer-related mortality in both men and women worldwide. Despite the administration of platinum compounds represents the main treatment, the majority of tumors remains intrinsically resistant. In lung cancer, miR-301a exerts a main role by modulating the activity of transcription factors like NF-kB and Stat3. Here, we dissected the contribution of miR-301a in the regulation of its new identified target Fos-related antigen-2 (Fra-2), a transcription factor that belongs to the

Fos/AP-1 family. By microarray analysis, we discovered that Fra-2 overexpression increased glioma pathogenesis-related protein 1 (GLIPR1) levels, a mediator of cisplatin resistance in lung cancer. Its mechanism of regulation is still unclear. We demonstrated that GLIPR1 is also a miR-301a target. In vitro, modulation of miR-301a reduced Fra-2 and GLIPR1 levels; conversely, Fra-2 overexpression significantly increased GLIPR1 and miR-301a. Then, by chromatin immunoprecipitation assay, we confirmed that Fra-2 interacts with the promoter regions of both GLIPR1 and MIR301A genes, supporting that miR-301a/Fra-2/GLIPR1 axis could be autoregulated by feedback loop in which Fra-2 promotes the transcription of MIR301A gene. Investigating the effect of this new axis on the response to cisplatin, we observed that both Fra-2/GLIPR1 overexpression and miR-301a silencing induced cisplatin resistance in lung cancer cells. By contrast, silencing of GLIPR1 and combined administration of low doses of Fos/AP-1 inhibitor restored the cisplatin sensitivity in Fra-2 overexpressing cells. In the lung adenocarcinoma samples from the TCGA dataset, miR-301a overexpression inversely correlated with Fra-2 and GLIPR1 expression. Consistently, the overexpression of miR-301a identified a fraction of tumors with low expression of Fra-2 and GLIPR1 in an internal cohort of lung cancer samples. Altogether, our findings identify the miR-301a/Fra-2/GLIPR1 axis that contributes to cisplatin resistance in lung cancer cells and could serve as biomarker to stratify patients who may benefit from cisplatin administration, alone or in combination with Fos/AP-1 inhibitors.

#3904

Simvastatin intensifies anti-androgen efficacy against treatment-resistant prostate cancer cells

Aino Siltari, Olga Korhonen, Paavo Raittinen, Merja Bläuer, Heimo Syvälä, Teuvo L. Tammela, Teemu J. Murtola. *Prostate Cancer Research Center, Tampere University, Tampere, Finland*

Androgen receptor (AR) signaling inhibitors (ARSIs) bicalutamide (Bic) and enzalutamide (Enza) are used in the treatment of castration resistant prostate cancer (CRPC). Prostate cancer (PCa) cells eventually develop treatment resistance against these drugs causing clinical challenges. The mechanisms behind treatment resistance are complex and only partially known. Androgen signaling is linked to lipid and cholesterol metabolism,

and they likely play a role in the development of treatment resistance. Cholesterol producing mevalonate pathway can be inhibited by statins, but it is unknown whether statin treatment could enhance effects of ARSIs. We studied combined effects of simvastatin (Sim) with or without Bic or Enza in VCaP originated PCa cell lines resistant to these ARSIs. Unique treatment resistant cell lines were created with long-term cultures of VCaP cells. The cells were kept under anti-androgen influence until the cells were growing normally despite the ARSIs. We analyzed changes in cell growth, RNA expression, and relevant AR signaling and cholesterol metabolism protein expression. Prostate-specific antigen (PSA) secretion was measured as a marker of AR signaling activity. In Bic or Enza resistant cell lines, combination of 2.5 or 5 μM simvastatin + 10 μM Bic/Enza decreased cell growth more than Sim alone, i.e., ARSIs demonstrated efficacy in combination therapy against ARSI resistant cells. In Bic and Enza resistant cells, combination treatment increased the expression of 60 and 26 and decreased the expression of 33 and 48 genes, respectively, compared with simvastatin alone. Altogether, 16 genes expression changed similarly in both cell lines in response to combination therapy. In both cell lines, over 70% of all gene changes were seen on AR-regulated genes. In Bic resistant cells, Sim decreased PSA levels with or without Bic. On the contrary, in Enza resistant cells PSA levels were increased with combination of Sim and Enza. We showed that combined treatment with ARSI and Sim inhibited cell growth more than Sim alone in ARSI resistant cell lines. This suggests that inhibition of the mevalonate pathway could enhance androgen signaling inhibition and potentially circumvent ARSI resistance mechanisms. This phenomenon is supported by epidemiological studies as patients treated with anti-androgens responded better during simultaneous statin treatment. Gene expression differed in combination treatment compared to Sim alone. Future studies are needed on whether interventions on lipid and cholesterol metabolism could enhance treatment of CRPC. Knowledge about the precise mechanisms behind the treatment responses and resistance might lead to new therapeutic applications.

#3905

Epigenetic primming reveals the central role of epigenetic state in the anti-tumor activity of vitamin D in pancreatic ductal adenocarcinoma

Bo He, Lauren Stoffel, Clifford Jiajun He, Albert Mao Li, Haowen Jiang, Kumsun Cho, Brittany M. Flowers, Sofia Ferreira, Laura D. Attardi, Jiangbin Ye. *Department of Radiation Oncology, Stanford University School of Medicine, Stanford, CA*

Pancreatic ductal adenocarcinoma (PDAC) has a dismal prognosis, which is largely due to the intrinsic resistance to a broad spectrum of therapies. Vitamin D (VD) has been extensively studied as a potential preventive or therapeutic agent for PDAC treatment. Although accumulating evidence supports that VD has beneficial effects on PDAC treatment, controversies still exist. The major reason for this inconsistency is that VD resistance widely occurs in PDAC. However, the underlying mechanism by which the VD resistance occurs remains largely unknown. Here, we report that epigenetic primming by glyceryl triacetate (GTA) and 5-azacytidine (5-Aza) overcomes VD resistance in PDAC. Mechanistically, increasing global H3K27 acetylation with GTA and reducing global DNA methylation with 5-Aza not only elevate the VDR expression but also reprogram the VD responsive genes. Consistently, combination treatment with VD analogue calcipotriol (CPT) and epigenetic primming overcomes the VD resistance to inhibit cell proliferation and migration through activating genes involved in negative regulation of cell proliferation and cell migration, while CPT treatment alone has the opposite effects. Intriguingly, further studies in mouse PDAC cells suggest that VDR expression does not always corelate with VD responsiveness. Using the gain and loss of function experiments, we demonstrate that VDR is necessary but not sufficient to trigger the anti-tumor activity of VD, highlighting that epigenetic state is the key determinant of VD responsiveness in PDAC. Collectively, these data reveal a previously undefined mechanism for VD resistance in PDAC and has the potential to guide VD clinical trials in the future.

#3906

The mRNA translational plasticity of small cell lung carcinoma is associated with its phenotypic transdifferentiation

Haoning Peng[1], Mengyao Wang[1], Lu Li[2], Lunxu Liu[3], Shensi Shen[1]. *[1]Institute of Thoracic Oncology, West China Hospital, Sichuan University, Chengdu City, China,[2]Lung Cancer Center, West China Hospital, Sichuan*

University, Chengdu City, China,[3]Department of Thoracic Surgery, West China Hospital, Sichuan University, Chengdu City, China

Small cell lung carcinoma(SCLC), classified as a recalcitrant cancer type, accounts for 13-15% of all lung cancers with a median overall survival less than 10 months in patients with extensive stage SCLC. SCLC was once considered as molecularly homogeneous due to nearly universal loss of TP53 and RB1, whereas subsets of MYC-driven, non-neuroendocrine (non-NE) SCLC variants, possess chemoresistance, suggesting its high plasticity and intertumoral heterogeneity related to rapid refractory to first-line chemotherapies. Current pathognomonic classification stratifies SCLC into two NE subtypes (ASCL1+, NEUROD1+) and two non-NE subtypes (POU2F3+ and triple negative), associated with different expression patterns of MYC family proteins. MYC is a master regulator of mRNA translation, whether translational regulation actively tunes SCLC plasticity and the associated chemosensitivity remains an enigma. Here, we delineate the translation landscape of NE and non-NE SCLC cells by using paired human NE SCLC cell line and constitutive or induced non-NE SCLC cells. As expected, non-NE SCLC cells are more resistant to the clinically relevant first-line chemotherapy than NE SCLC cells. With polysome profiling in combination with polysome RNA-seq, we showed differential expression at both transcription- and translation-level. However, transcription-level changes minimally overlapped with the translational changes between NE and non-NE SCLC cells, with a global reduction of translation activity observed in non-NE SCLC cells. Through analyzing the polysome profiles, we observed a striking accumulation of 60S monosomes and diminishment of 80S ribosomes derived from non-NE SCLC cells compared to those from NE SCLC cells. This unique translational pattern in non-NE SCLC cells was correlated with an increased expression of eIF6, a ‘sitting on the bench’ member of eukaryotic initiation factor (eIF) family. The eIF6 couples 60S monosome maturation and recycling, enrolling a quintessential role in functional 80S ribosome formation. Positive correlation between eIF6 expression and non-NE SCLC tumors was observed in 81 tumor samples derived from patients with limited stage SCLC and CCLE cell consortium, in which c-MYC expression was also positively correlated with eIF6 level. By using both ultracentrifugation and fraction analysis from polysome profiling, we found that less association of

eIF6 with 60S may mitigate 80S ribosome assembly in non-NE SCLC cells. In addition, in vivo xenograft models showed that eIF6 expression was higher in residual tumors upon chemotherapy.
Taken together, these data revealed an eIF6-dependent translational regulation in non-NE transdifferentiation of SCLC subtypes, suggesting an underappreciated function of translational regulation of SCLC plasticity and the potential therapeutic value of eIF6 for overcoming SCLC resistance to chemotherapy.

#3907
Targeting adaptive resistance to EGFR and KRAS G12C inhibitors by TT125-802, a novel and specific CBP/p300 bromodomain inhibitor
Thomas Bohnacker, Dorothea Gruber, Sara Laudato, Martin Schwill, Charles-Henry Fabritius, Raquel Herrador, Katrin Westritschnig, Thushara Pattupara, Vikram Ayinampudi, Stefanie Flückiger-Mangual. *TOLREMO therapeutics AG, Muttenz, Switzerland*

Resistance to targeted therapies is a major challenge in oncology. Disease progression is caused by multiple resistance mechanisms. Besides pre-existing and acquired genetic alternations, adaptive non-mutational reprogramming as well as modulation of phenotypic plasticity have emerged as drivers of disease progression. For example, in epidermal growth factor receptor (EGFR)-mutated non-small cell lung cancer (NSCLC) patients who were treated with osimertinib, ~50% of progressive disease could not be attributed to genetic mutations (Leonetti et al., *BJC* 2019). Similarly, in ~ 40% of patients suffering from KRAS G12C-mutated NSCLC and colorectal cancer (CRC), disease progressed under sotorasib treatment without identifiable acquired mutations (Zhao et al., *Nature* 2021). Thus, targeting non-genetic adaptive resistance mechanism such as drug-induced transcriptional reprogramming might be of great therapeutic benefit. Here we identified small molecules, that interfere with cancer drug-induced transcriptional escape mechanisms using a phenotypic screen based on an SRY-Box Transcription Factor 2 (SOX2) reporter system. The screen led to the development of TT125-802, a highly specific and potent, orally available small molecule inhibitor of the bromodomain of the transcriptional and epigenetic regulator CBP [cyclic adenosine monophosphate response element binding protein (CREB) binding protein]

and its paralogue p300. TT125-802 dose-dependently prevented osimertinib resistance development in EGFR-mutated NSCLC cell lines HCC827 and HCC4006, as well as sotorasib resistance development in KRAS G12C-mutated NCI-H358 (NSCLC), SW837 and SNU-1411 (CRCs) as assessed by label-free long-term live microscopy assays. Data generated in mouse xenograft studies confirmed the ability of TT125-802 increasing response rates and prolonging the duration of response to osimertinib and sotorasib *in vivo*. In cells and tumours which were already resistant to osimertinib or sotorasib, TT125-802 could still delay cell or tumor growth. Complementary and longitudinal analysis of transcriptional changes using RNA sequencing *in vitro* and *in vivo* identified several early adaptive and late acquired resistance signatures that were reversed by TT125-802. A first-in-human study of TT125-802 in cancer patients is on track to start in 2023.

#3908

M^{6}A RNA modifications regulate expression of transcripts that promote transition to cisplatin resistance in bladder cancer

Emmanuelle Hodara, Aubree Mades, Tong Xu, Amir Goldkorn, Suhn Rhie.
Keck School of Medicine of USC, Los Angeles, CA

BACKGROUND**:** Chemotherapy resistance is recognized to occur not only through selection of pre-existing genetically resistant clones, but also through rapid phenotypic plasticity mechanisms. We previously reported that bladder cancer cells can rapidly transition to and from a chemo-resistant phenotype. Recently, N6-methyladenosine (m^{6}A) RNA modifications were shown to dynamically and reversibly regulate mRNA processing, differentiation, and cell fate. Here, we tested the hypothesis that m^{6}A modifications regulate phenotypic plasticity and transition to cisplatin resistance in bladder cancer (BC).
METHODS: We utilized methyl-RNA-immunoprecipitation followed by sequencing (MeRIP-seq) and by RNA-seq to identify transcripts that were both differentially methylated and differentially expressed between cisplatin-sensitive and cisplatin-resistant BC cell lines. Candidate transcripts were annotated using Gene Ontology (GO) enrichment analysis and Gene Set Enrichment Analysis (GSEA). Clinical relevance was evaluated using databases such as The Cancer Genome Atlas (TCGA) and

the Oncology Research Information Network (ORIEN) avatar. Cancer-relevant genes were then validated in vitro by targeted immunoprecipitation and PCR (MeRIP-PCR) and qPCR. Candidate genes were then functionally validated in cell lines and in patient derived organoids (PDOs) by siRNA-mediated knockdown and cisplatin treatment, as well as by m6A measurement after short-term cisplatin treatment.
RESULTS: MeRIP-seq and RNA-seq revealed that cisplatin-sensitive and cisplatin-resistant BC cells have distinct m^6A profiles, with 130 transcripts that were both differentially methylated and differentially expressed. Using clinical and functional database tools, we filtered this list to 37 transcripts and ranked them based on clinical relevance in BC. Of the top 15 candidates, eight were successfully validated in vitro via repeat qPCR and MeRIP-PCR. In cisplatin-resistant cells, one candidate, SLC7A11, was found to have decreased m6A level, which was associated with increased RNA stability and elevated transcript and protein levels. Consistent with this, 48 hr cisplatin treatment of cisplatin-sensitive cells led to SLC7A11 hypomethylation, increased RNA stability, and elevated transcript and protein levels. Furthermore, depletion of SLC7A11 by siRNA-knockdown re-sensitized BC cell lines and PDOs to cisplatin.
CONCLUSIONS: Using unbiased transcriptome-wide m^6A profiling followed by targeted validation, we demonstrated that m^6A modifications regulate expression of clinically relevant gene transcripts in BC, and that a subset of these modifications may promote resistance to chemotherapy. Collectively, these results implicate epitranscriptomic plasticity as a driver in potentiating cisplatin resistance in bladder cancer.

#3909
THY1 regulates therapy resistance in glioblastoma recurrence
Sunita Shankar, Visweswaran Ravikumar, Hanxiao Wang, Sunjong Ji, Zainab Hasan, Ziad Fehmi, Yacoub Haydin, Daniel R. Wahl, Arvind Rao, Alnawaz Rehemtulla, Wajd Al-Holou. *University of Michigan, Ann Arbor, MI*

Glioblastoma (GBM), is the most common primary brain tumor. It is a lethal disease with a median survival of 15 months characterized by treatment resistance, aggressive brain invasion, and inevitable recurrence. Less than 10 percent of patients survive beyond 5 years. Here, we

developed an intracranial longitudinal *in vivo* recurrence model using HF2303, a patient derived explant, to produce paired specimens (pre- and post-recurrence) following temozolomide(TMZ) and radiation(IR) treatment. Mouse brain tissues from the two groups were compared to identify genes and pathways driving treatment resistance. This analysis showed an elevated THY1 expression in recurrent HF2303 tumors compared to naïve tumors. Increased Thy1 expression was also associated with a more mesenchymal phenotype. THY1 expressing cells from naïve HF2303 were also resistant to TMZ/IR treatment in an intracranial model. In U87 neurospheres, overexpression of THY1 increased resistance to TMZ/IR. Interestingly, stable knockdown of Thy1 in GBM cells and human derived GBM organoids (GBOs) expressing high THY1 levels led to reduced cell proliferation. Yet, an inducible knockout of THY1 using CRISPR/Cas9 in human GBOs showed increased sensitivity to TMZ/IR. This suggests a clear link between THY1 expression and TMZ/IR resistance.Single cell RNA sequencing of over 25 primary GBM and 4 recurrent tumors (spanning over 120,000 cells) shows that cells expressing high levels of THY1 are associated with two distinct populations; neuronal precursor-like (NPC-like) and mesenchymal-like (MES-like). Furthermore spatial transcriptomics from 3 primary GBMs suggests that high THY1 expressing cells are colocalized with macrophages within the perivascular niche contributing to the mesenchymal phenotype. We will present these studies and our more recent work analyzing spatial recurrent GBM samples. Particularly, we will address how THY1 expression in these spatially distinct NPC-like and MES-like differ and how each of these states may contribute towards TMZ/IR resistance.

Identification of Molecular Targets 1

#3913
Genomic loss of UQCR11 creates therapeutic vulnerability in triple-negative breast cancer

Samantha Sharma[1], Tao Yu[1], Abhinav Achreja[2], Xinna Zhang[1], Deepak Nagrath[2], Xiongbin Lu[1]. *[1]Department of Medical and Molecular Genetics, Indiana University School of Medicine, Indianapolis, IN,[2]Department of Biomedical Engineering, University of Michigan, Ann Arbor, MI*

Recurrent loss-of-function deletions are prevalent genomic alterations in tumors; nonetheless, these deletions occasionally create conditional therapeutic vulnerabilities in tumors. Our previous study used The Cancer Genome Atlas High-Grade Serous Ovarian Carcinoma (TCGA-HGSOC) dataset to identify the 19p13.3 locus as the most pervasive deletion in the high-grade serous ovarian carcinoma (HGSOC). Subsequently, the machine learning integrated-precision oncology platform identified that the loss of UQCR11, a gene located within the chromosome 19p13.3 locus, created a therapeutic collateral target, the MTHFD2. Furthermore, pharmacological inhibition of MTHFD2 in the UQCR11-deleted cells led to complete tumor remission in our in vivo mouse model (Nature metabolism, 2022). Encouraged by the promising anti-tumor effect of the MTHFD2 inhibitor, we extended our research to other tumor types. By analyzing the TGCA datasets, we found that UQCR11 deletion was a common occurrence among humans' most prevalent solid tumors, especially in pan breast and lung cancer. Within the pan breast cancer dataset, we found that over 50% of patients with triple-negative breast cancer (TNBC), the most difficult-to-treat breast cancer subtype in women, displayed either heterozygous or homozygous deletions in the UQCR11 gene. Moreover, the TGCA-TNBC dataset analysis revealed that the genomic copy loss of UQCR11 positively correlates with the deceased mRNA expression of the gene, bringing our interest to validate the collateral lethal targets in this breast cancer subtype. We first analyzed The Cancer Cell Line Encyclopedia (CCLE) database and further explored the correlation between the copy number alteration and mRNA expression of UQCR11 in several breast cancer cell lines. Then, we selected seven human TNBC cells with copy number neutral or deletion UQCR11 and validated the copy number and gene expression of UQCR11 and MTHFD2 using qPCR and western blot. We next treated these cells with a selective MTHFD2 inhibitor, DS18561882, and found that UQCR11-deleted cells showed a more favorable response than the UQCR11-intact cells. Finally, to test the therapeutic potential of targeting MTHFD2-null tumors in vivo, we generated isogenic mouse breast cancer cell lines using shRNA-mediated UQCR11 knockdown. Consistent with our previous findings, the MTHFD2 expression level was upregulated upon UQCR11 knockdown, suggesting a compensation function of MTHFD2 in UQCR11-deleted cells. Furthermore, the UQCR11 knocked-down cells showed better responses to MTHFD2 inhibitor treatment than the parental control cells. In

summary, our study provides evidence that targeting MTHFD2 holds strong therapeutic potential in over 50% of the TNBC patients with UQCR11 deletion and highlights the broad efficacy of targeting MTHFD2 for individualized therapeutic strategy in different tumor types co-occurring with UQCR11 deletion.

#3914

BTK and MALT1 are critical for cell adhesion and dissemination in mantle cell lymphoma

Vivian Changying Jiang, Yang Liu, qingsong Cai, Joseph M. McIntosh, Yijing Li, Zhihong Chen, Heng-Huan Lee, Wei Wang, Yixin Yao, Lei Nie, Michael Wang. *UT MD Anderson Cancer Center, Houston, TX*

Bruton's tyrosine kinase (BTK) is a great target in mantle cell lymphoma (MCL). This is evident by multiple FDA approvals of covalent BTK inhibitors (BTKi, e.g. ibrutinib, acalabrutinib and zanubrutinib) and recent exciting clinical data on non-covalent BTKi pirtobrutinib. However, resistance to BTKi is a major clinical challenge and the resistance mechanism is not yet fully understood. To address this, we generated JeKo BTK KD cells via *BTK* knockdown (KD) through by CRISPR Cas9 in BTKi-sensitive JeKo-1 cells, which resulted in superior resistance to BTKi and cell growth defects in vitro. Interestingly, JeKo BTK KD cells demonstrated early tumor cell engraftment and growth in subcutaneous xenograft models, while parental JeKo-1 cells showed much later engraftment but with much faster growth kinetics. To understand this and the BTKi-resistance mechanism, we first performed bulk RNA sequencing analysis and identified *MALT1*, but not its well-known binding partners *CARD11* and *BCL10*, as one of the top overexpressed genes in BTKi-resistant MCL cells, including JeKo BTK KD cells. Genetic knockout (KO) of *MALT1* or *CARD11* by CRISPR Cas9 in JeKo-1 resulted in defects in cell growth in vitro and delayed tumor engraftment and growth in vivo. In contrast, *MALT1* KO, but not *CARD11* KO, in JeKo BTK KD cells remarkably suppressed cell growth in vitro, and tumor engraftment and growth in vivo. These data demonstrate that MALT1 overexpression can drive ibrutinib resistance via bypassing BTK-CARD11 signaling. BTKi-resistant cells including JeKo BTK KD cells showed much higher potency in adhesion to extracellular matrix or stromal cells compared to BTKi-

sensitive cells. BTK inhibition or MALT1 inhibition significantly suppressed cell adhesion and migration to extracellular matrix or stromal cells. Furthermore, *BTK* KD and *MALT1* KO but not *CARD11* KO in JeKo-1 cells remarkably suppressed tumor cell dissemination and growth in spleen, liver, bone marrow and peripheral blood. *MALT1* KO in JeKo BTK KD cells further suppressed tumor cell dissemination. Consistent with this, MALT1 inhibition greatly suppressed tumor cell dissemination and growth in spleen, bone marrow and peripheral blood of an ibrutinib-resistant patient-derived xenograft model. Therefore, both BTK and MALT1 are critical for tumor cell adhesion and dissemination in vivo in a CARD11-independent manner. Furthermore, co-targeting MALT1 with safimaltib and BTK with pirtobrutinib induced potent anti-MCL activity in BTKi-resistant MCL cell lines and patient-derived xenografts. Therefore, we conclude that (1) BTK and MALT1 are key molecules that control MCL cell growth and dissemination, (2) MALT1 overexpression drives resistance to BTKi in MCL, (3) targeting MALT1 is a promising therapeutic strategy to overcome BTKi resistance, and (4) co-targeting of BTK and MALT1 improves efficacy and durability beyond single agents.

#3915

RNAseq analysis reveals differentiation gene drivers as potential therapeutic targets in anaplastic thyroid cancer

Kaci Kopec[1], Tara Jarboe[1], Michael Guo[1], Nicole R. DeSouza[1], Sarnath Singh[1], Augustine Moscatello[2], Humayun K. Islam[1], Jan Geliebter[1], Raj K. Tiwari[1]. *[1]New York Medical College, Valhalla, NY,[2]Westchester Medical Center, Valhalla, NY*

Papillary thyroid cancer (PTC) is a well-differentiated and highly treatable cancer with a 5-year survival rate of almost 99%. In contrast, anaplastic thyroid cancer (ATC) lacks differentiation and loses its thyroid-like functions, including lack of response to radioiodine therapy. Due to ATC's aggressive metastatic phenotype, it is always diagnosed as stage IV with a 5 year survival rate of less than 3%. ATC lacks targetable genetic lesions making it a difficult cancer to treat, therefore RNAseq analysis was performed in an effort to investigate the differentially expressed genes between ATC to PTC. Exploration of differential gene expression between ATC and PTC was undertaken to further elucidate the differences in

expression that drive the aggressive nature of ATC phenotype. RNA was isolated from human thyroid cancer cell lines T238 (ATC) and K1 (PTC) and RNA sequencing was conducted by Azenta Life Sciences. Our analysis resulted in 4,931 significant differentially expressed genes between ATC and PTC. Looking at the gene ontology analysis, pathways involving cell differentiation, proliferation, and migration revealed 90, 70, and 47 genes differentially expressed in ATC vs PTC respectively. These pathways putatively give rise to ATC's aggressive phenotype when compared to PTC, therefore, we narrowed down the focus from 4,931 genes to 207. Through RNAseq analysis, Homeobox D4 (HOXD4) was observed to significantly increase in ATC (7.69 log2 fold change) compared to PTC. HOXD4 is a transcription factor that plays a crucial role in cell differentiation and has been associated with a worse prognosis in cancers such as ovarian serous carcinoma. As loss of differentiation is essential to ATC's refractory nature and therapeutic resistance, targeting pathways involved in differentiation can be crucial in making ATC amenable to therapy. Other differentiation regulatory genes identified include BLK and LAMA5. BLK (3.95 log2 fold change) is a Src family tyrosine kinase proto-oncogene that is not only involved in cell proliferation but also differentiation. LAMA5 (4.76 log2 fold change) is an extracellular glycoprotein that has been linked to differentiation, migration and metastasis. Validation of the RNAseq results was completed via western blot analysis of multiple ATC and PTC cells lines. We found that HOXD4 expression was higher in ATC cell lines T238, 8505C, and SW1736 than PTC cell lines K1, TPC1, and BCPAP. Further validation was carried out by immunohistochemistry of human thyroid tissue. Preliminary IHC on ATC, PTC, and normal thyroid patient samples showed ATC has significantly increased HOXD4 expression (27.5%) compared to PTC (8.7%) and normal thyroid tissue (2.3%). Ongoing studies in the laboratory to identify novel genetic drivers of cell differentiation and proliferation so as to discover a therapeutic target to fulfill an unmet clinical need is underway.

#3916

role of her3 v104l mutation on tumor growth and her3 stabilization

Rosalin Mishra[1], Mary Kate Kilroy[1], Wasim Feroz[1], Hima Patel[2], Samar Alanazi[1], Joan T. Garrett[1]. *[1]James L.Winkle College of Pharmacy,*

University of Cincinnati, Cincinnati, OH,[2]UTSW Simmons Comprehensive Cancer Center, Dallas, TX

We aimed to determine if naturally occurring HER3 mutations could drive oncogenic activity of HER2+ HCC1569 cells in which endogenous HER3 was knocked out using CRISPR-Cas9 technology. A series of HER3 mutations found in breast cancer patients (F94L, V104L, G284R, D297Y, T355I, and E928G) were introduced via lentiviral transduction and stable cell lines were generated in HER3 knock out (KO) HCC1569 cells and were maintained in 0.5 mg/mL puromycin. Our data indicated that cells stably transduced with HER3V104L mutation had significantly higher cell growth with higher p-HER3 expression versus wild-type (wt) and empty-vector (EV) HER3. We found that HCC1569HER3KO cells with WT and V104L were sensitive to increasing concentration of neratinib (0.1-0.5 μM) as indicated by crystal violet assay. Next we examined if V104L mutation rendered resistance to another FDA- approved irreversible HER2 tyrosine kinase inhibitor, tucatinib. Our results showed that V104L cells were sensitive to higher concentration of tucatinib compared to neratinib. In other experiments, we used COS7 cells to examine the signaling pathways of HER3V104L mutation. Our western blot data demonstrated that transient transfection of COS7 cells with HER3V104L mutant significantly upregulated p-HER3 and p-HER2 expression versus WT HER3 in a NRG-dependent manner. In addition, we found that the V104L mutation stabilizes HER3 protein expression independent of ligand stimulation. Our western blot data showed that V104L induced HER3 stabilization is independent on HER3 binding partners HER1, HER2 and HER4. Our cycloheximide chase data indicated that V104L mutation stabilizes HER3 expression in COS7 cells as well as low HER3 expressing colon cancer cell line, SNUC5. Our western blot data indicates that V104L mutation activates ERK signaling in NRG dependent manner over AKT pathway in COS7 cells. In addition, we are using various PDXs with different HER3 mutations (V104M and E928D) to determine the role of these driver HER3 mutations in cancer and how this can be targeted in the clinic using HER targeted therapy.

#3918
Kinase domain duplications of *FGFR1* and *MET* are potential therapeutic targets

Chaelin Lee[1], Sungyoung Lee[2], Hongseok Yun[2], Jeonghwan Youk[3], Tae Min Kim[3], Soyeon Kim[4], Bhumsuk Keam[3], Miso Kim[3], Dong-Wan Kim[3].
[1]Cancer Research Institute, Seoul National University, Seoul, Korea, Republic of,[2]Department of Genomic Medicine, Center for Precision Medicine, Seoul National University College of Medicine and Seoul National University Hospital, Seoul, Korea, Republic of,[3]Department of Internal Medicine, Seoul National University College of Medicine and Seoul National University Hospital, Seoul, Korea, Republic of,[4]Integrated Major in Innovative Medical Science, Seoul National University, Seoul, Korea, Republic of

Background: Kinase domain duplication (KDD) is recently recognized as an oncogenic driver. Therapeutic potential has been established in *EGFR*-KDDs in non-small cell lung cancer, and our group recently showed resistance mechanism in lung cancers harboring *EGFR*-KDDs treated with EGFR tyrosine kinase inhibitors (TKIs). However, the frequency and oncogenic role of KDDs in other receptor tyrosine kinases has been elusive.
Methods: To investigate the frequency of KDDs in advanced cancer patients, we developed in-house algorithm to detect KDDs in high-depth panel sequencing dataset and evaluated its performance using large-scale panel sequencing data from Seoul National University Hospital (SNUH). In short, the algorithm collects reads with soft clips from a modified GATK best practice pipeline for clinical NGS data processing. The collected reads are then grouped according to their matched position and insert size, and evidences of each group (number of splitting and spanning reads) are collected to yield a set of initial candidates. Finally, the initial candidates were manually inspected after quality control by removing false-positive candidates, such as non-target genes or consistent findings. Then, we established cell lines transfected with KDDs of *FGFR1* and *MET* to validate oncogenic role of identified KDDs in the cohort. Using these transformed cell lines, we investigated carcinogenicity with cell viability assay, immunoblot assay and colony formation assay. FGFR TKIs and MET TKIs were used to uncover the possibility of therapeutic targets in the KDDs.
Results: Using the in-house algorithm, we identified *FGFR1*-KDDs from brain tumors (n=4), *EGFR*-KDDs from lung (n=1) and brain (n=2) tumors, and *MET*-KDD from a lung tumor (n=1) in a total of 3,932 cancer samples, with 0.2% frequency. All three kinds of KDDs contained full-length of

kinase domains of each gene. Ba/F3 cells transfected with the *FGFR1*-KDD constructs proliferated well without IL-3 (1239- and 1019-fold higer than wild-type *FGFR1*), while wild-type *FGFR1* Ba/F3 cells did not. This growth potential was diminished by FGFR TKIs BGJ398 (IC50, 0.063 ± 0.065nM), PD173074 (IC50, 1.498 ± 1.021nM), and ponatinib (IC50, 5.69 ± 3.05nM). Reduced expressions of downstream pathway proteins including phospho-FGFR1, phospho-Akt, and phospho-Erk were confirmed by immunoblot assays. NIH-3T3 cells transfected with *MET*-KDD construct also showed growth advantage compared to wild-type *MET* NIH-3T3 cells. Capmatinib, a MET TKI, inhibited colony formation of *MET*-KDD NIH-3T3 cells with reduced phospho-MET expression.
Conclusion: In this study, we validated newly developed KDD-detection computational methods using targeted DNA sequencing data. Using this algorithm, we found 0.2% of KDDs in 3,932 cancer samples, including *EGFR*, *FGFR1*, and *MET*. In addition to *EGFR*-KDDs, our study reveals that both *FGFR1*- and *MET-KDD* can be oncogenic and therapeutic targets in brain and lung cancer patients.

#3919

SHP2-DDX3X complexes contribute to translational control of CD274 mRNA in KRAS-active non-small cell lung cancer

Palapoom Wongsaengpiboon. *University of Kentucky, Lexington, KY*

Background: Immune checkpoint inhibitors (ICIs) have shifted the landscape in management for non-small cell lung cancer (NSCLC) and improve treatment outcomes. However, the 5-year overall survival rate of 23.2% for treatment-naïve patients with late-stage NSCLC on Pembrolizumab therapy can likely be improved. Clinical benefit is correlated with tumoral expression of PD-L1 and mutation burden. Many groups seek to identify other therapeutic targets that could improve response and overall survival. Ongoing work from our group demonstrated that SHP2, a tyrosine phosphatase, can negatively regulate PD-L1 expression in KRAS-active NSCLC, and we seek to understand the mechanism by which this occurs. SHP2 was ectopically expressed in H460 cells, immunoprecipitated and identification of interacting proteins was achieved by mass spectrometry. DDX3X, an RNA helicase, and eukaryotic translation initiation factor 1a (eIF-1a) were identified as high-ranking,

potential partners of SHP2. We hypothesized that SHP2 complexes with DDX3X and eIF-1a on newly transcribed CD274 mRNA to negatively regulate PD-L1 expression.
Materials and Methods: To confirm SHP2 interactions with DDX3X and eIF-1a, two pull-down assays were performed: 1. bacterially-expressed, his-tagged and immobilized proteins was used as bait for proteins contained in A549 and H460 extracts, and 2. immunoprecipitation of each endogenous protein in A549 and H460 cell extracts. Western blot analysis was performed to evaluate interacting proteins. To determine whether phosphatase activity of SHP2 is required for these interactions, immunoprecipitation was also carried out in the presence of allosteric inhibitors of SHP2 (SHP-099 and RMC-0455). SHP2 ablation was carried out with CRISPR and siRNA to examine PD-L1 expression, also determined by western blot assay.
Results: His-tagged DDX3X from bacterial expression systems was able to capture SHP2 protein from both A549 cells and H460 cells, and vice versa with his-tagged SHP2. Immunoprecipitation of endogenous SHP2 was able to co-precipitate DDX3X and vice versa. Phosphatase activity of SHP2 was not required for complex formation nor does it change PD-L1 expression in A549 or H460 cells. Ablation of SHP2 leads to increased PD-L1 expression.
Conclusion: A complex containing SHP2 and DDX3X may regulate the translation of CD274 in concert with eukaryotic initiation factors. Other groups have previously reported the control of translation of CD274 mRNA carried out at the 3' UTR, and we believe this is novel evidence of a translation initiation complex monitoring the expression of CD274. Ribosome footprint and RNA immunoprecipitations are underway to address these questions.

#3920

Functional analysis of the role of RAP1GDS1 and RhoA in KRAS-driven lung adenocarcinoma

Marta Roman Moreno[1], Kaja Kostyrko[1], Kari Herrington[2], Michael Bassik[3], Peter Jackson[4], Alejandro Sweet-Cordero[1]. *[1]Pediatrics, UCSF - University of California San Francisco, San Francisco, CA,[2]Biochemistry and Biophysics Center for Advanced Light Microscopy, UCSF - University of California San Francisco, San Francisco, CA,[3]Genetics, Stanford*

University, Stanford, CA,[4]Baxter Laboratory for Stem Cell Biology, Stanford University, Stanford, CA

While KRAS is among the most frequently mutated oncogenes, our understanding of the mechanisms of KRAS-driven oncogenesis remains limited. A significant remaining gap is a lack of understanding of tissue-specific effectors of Ras activation and the role of specific KRAS mutations in determining downstream vulnerabilities. Previously, we used a combination of proteomics and CRISPR/Cas9 screens in human lung adenocarcinoma (LUAD) cells to identify a KRAS-specific vulnerability induced by the combined loss of RHOA and the long isoform of RAP1GDS1, suggesting a potentially novel approach for targeting KRAS-driven cancer. Here we use biochemical, proteomic, and genetic approaches to dissect the isoform-specific roles of RAP1GDS1 to elucidate its synthetic lethal interaction with RHOA in KRAS-driven LUAD.
We performed AP/MS in KRAS-mutant A549 cells using both the long (RAP1GDS1-607) and the short (RAP1GDS1-558) isoforms of RAP1GDS1 as bait to identify overlapping and isoform-specific RAP1GDS1 interactors. We enriched this analysis with orthologous datasets from DepMap, published protein-protein interaction (PPI) data and RAP1GDS1-specific prenylome. This comprehensive analysis identified a cluster of RAB GTPases, proteins involved in vesicular transport and lysosomal function, as specific interactors of RAP1GDS1-607. We subsequently used the proximity ligation assay (PLA) to confirm the direct interaction between RAP1GDS1-607 and two of the strongest interactors - RAB7A and RAB22A – according to the PPI data. We also depleted either or both RAP1GDS1 isoforms in cells expressing GFP-tagged RAB7A, RAB22A or KRAS and used live cell imaging to determine how loss of RAP1GDS1 changes their subcellular localization. We found that depletion of both RAP1GDS1 isoforms and, to a lesser extent, single loss of RAP1GDS1-607, significantly decreased KRAS localization at the plasma membrane. We also used PLA to confirm that RAP1GDS1-607 has a stronger interaction with KRAS compared to the short isoform. Moreover, we demonstrated that loss of the long RAP1GDS1 isoform significantly decreased the membrane localization levels of GTP-bound KRAS, compared to the control or RAP1GDS1-558 knock-down. Finally, to identify the molecular mechanism of R1G1/RhoA synthetic lethality with

KRAS, we performed a Genome Wide-CRISPR screen in R1G1-607 and RhoA knock-out cells. We identified the strongest hits and designed a focused CRISPR library of approximately 400 genes to screen a larger panel of KRAS-mutant LUAD cell lines (H23, A549 and H358). The aim is to identify other genes that are synthetic lethal in combination with RhoA or R1G1-607 loss and genes that could mediate the lethal effect of their combined loss.
In conclusion, these data demonstrate a specific role of the long RAP1GDS1 isoform in the membrane-localization and activation of KRAS, which supports its role as a potential therapeutic target for KRAS mutant tumors.

#3921

Malic enzyme 2 identified as metabolic target in triple-negative breast cancers with increased serine biosynthesis

Mark D. Slayton[1], Jin Heon Jeon[2], Abhinav Achreja[2], Zackariah A. Farah[1], Brisilda Nilaj[1], Yi-Hsien Eu[1], Alisa Lui[1], Mason Collard[1], Liwei Bao[1], Celina Kleer[3], Deepak Nagrath[2], Sofia D. Merajver[1]. *[1]Internal Medicine, University of Michigan, Ann Arbor, MI,[2]Engineering, University of Michigan, Ann Arbor, MI,[3]Pathology, University of Michigan, Ann Arbor, MI*

Background **& Hypothesis:** Triple-negative breast cancer (TNBC) is a difficult to treat and deadly form of breast cancer. Pyruvate is an essential intermediate component of cellular metabolism which cancerous cells, including breast cancer cells, rely upon. Importantly, pyruvate and phosphoenolpyruvate are important nodes in the glycolytic pathway that support serine synthesis, lactate production and the TCA cycle. As a result of this, inhibition of the metabolic enzymes which regulate pyruvate production is currently used for cancer therapy. Apart from the glycolytic pathway, malic enzyme 2 (ME2) contributes to pyruvate and NADPH production through the oxidation of malate. Therefore, ME2 is a critical pathway supporting multiple metabolic needs of TNBC. Here, we investigate TNBC cell lines and assess their reliance on ME2 to drive accelerated growth, and thus potentially making ME2 a therapeutic target in TNBC.

Methods: We investigated four TNBC lines (HCC1806, Hs578T, BT20, MDAMB468) with distinct serine synthesis activity assessed via western blotting of serine metabolism enzymes. To knockdown ME2 in TNBC cell lines, we used siRNA transient transfection and shRNA-encoding lentiviral vectors. The growth rates of TNBC cells were determined by cell counting in the BioTek BioSpa 8. Lastly, we used immunohistology to analyze the expression of ME2 and serine metabolic genes in a TNBC tumor microarray.
Results: Modulation of the serine synthesis pathway revealed an unexpected synergy between serine metabolism and ME2. Knockdown of ME2 reduced the expression of serine metabolism genes but did not affect the expression of ME1 or ME3. The proliferative rate of cells with elevated serine synthesis, BT20 and MDAMB468 - was significantly reduced under ME2 knockdown, while Hs578T and HCC1806 experienced a modest reduction. Immunohistologic staining of TNBC tumors corroborated the link between ME2 and serine metabolism.
Conclusions: We observed that TNBC cell lines with elevated, but not reduced, expression of serine synthesis genes were growth-inhibited in the absence of ME2. Our results indicate that ME2 is required for optimal growth in some forms of TNBC and may serve as a therapeutic target for the treatment of cancers with elevated serine biosynthesis. Ongoing studies are aimed at discerning additional biomarkers of sensitivity to ME2 inhibition in TNBC and other aggressive cancers.

#3922

Assessing clonal evolution of myeloid neoplasms by flow cytometry guided, cell-enriched next generation sequencing

Sarah Johnson, Keegan Vaughan, Alexis Kurmis, Zeni Alfonso, Nathan Riccitelli. *Navigate BioPharma Services, Carlsbad, CA*

Introduct**ion:** Genetic information is highly relevant to the classification and risk assessment of myeloid neoplasms, especially myelodysplastic syndrome (MDS) and acute myeloid leukemia (AML). Next generation sequencing (NGS) is increasingly used to track mutations and monitor measurable residual disease, but with the increased data comes a need to distinguish driver mutations from potentially unrelated variants caused by age-related clonal hematopoiesis (ARCH) or clonal hematopoiesis of

indeterminant potential (CHIP). Herein, we evaluate a combined flow cytometry and NGS approach to identify oncogenic driver mutations within specific cell populations and increase variant accessibility by NGS.
Methods: Proof of cell enrichment methodology was performed with a cell line expressing CD34 (hallmark of myeloid blasts). The cell line was spiked into healthy donor PBMCs at defined levels to create samples with varied tumor percentage. Purchased AML patient samples were also analyzed. CD34 expression of samples was confirmed by flow cytometry prior to- and following enrichment by anti-CD34 magnetic cell sorting technology. Sequencing libraries were prepared using the Archer VariantPlex Core Myeloid kit and sequenced on Illumina MiSeqs. Mutations were characterized using Archer software. The association between NGS and flow cytometry data was assessed through mapping the VAF data to the tumor population determined by flow cytometry.
Results: Identified mutations in tested samples included known oncogenic mutations as well as mutations associated with ARCH/CHIP events. In a subset of samples, at least one mutation was identified at a VAF correlating to the tumor percentage determined by flow cytometry analysis; these mutations were enriched in the CD34+ cell fraction following magnetic cell sorting. Sequencing the enriched tumor fraction increased the VAF of these mutations, and simultaneously revealed additional tumor-associated mutations that were previously below the detection limit of the assay. Conversely, potential ARCH/CHIP mutations were present in both CD34+ and CD34- cell populations.
Conclusion: Using a combination of flow cytometry, magnetic cell sorting, and NGS, variants specific to the tumor fraction of samples were identified. For patient specimens, the presence of ARCH/CHIP mutations in both enriched and residual cell populations indicate these variants evolved prior to the emergence of true leukemic progenitor cells; the identification of the flow-matched mutations only in the enriched population indicates the key role of these changes in the disease progression. Together, flow cytometry and cell-enriched NGS have the potential to enhance detection of disease-driving mutations earlier, thus, could be used as novel approaches to identify and treat myeloid neoplasms early with existing therapies and/or support development of new investigational agents.

#3923

Identification of membrane-expressed CAPRIN-1 as a novel and universal cancer target and generation of a therapeutic anti-CAPRIN-1 antibody TRK-950

Fumiyoshi Okano[1], Takanori Saito[1], Yoshitaka Minamida[1], Shinichi Kobayashi[1], Takayoshi Ido[1], Yasushi Miyauchi[2], Ukei Wasai[1], Jiang Ke[3], Alexandra Aicher[4], Christopher Heeschen[5], Tetsu Yonehara[1]. *[1]New Frontiers Research Laboratories, Toray Industries, Inc., Kamakura, Japan,[2]Kamakura Techno–Science, Inc., Kamakura, Japan,[3]Center for Single-Cell Omics and Key Laboratory of Oncogenes and Related Genes, Shanghai Jiao Tong University School of Medicine, Shanghai, China,[4]Graduate Institute for Biomedical Sciences Precision Immunotherapy Group, China Medical University, Taichung City, Taiwan,[5]Pancreatic Cancer Heterogeneity, Candiolo Cancer Institute - FPO - IRCCS, Candiolo, Italy*

Specific targets for cancer treatment are highly desirable, but still remain to be discovered. While previous reports suggested that CAPRIN-1 localizes in the cytoplasm, here we now show that part of this molecule is strongly expressed on the cell membrane surface in most solid cancers, but not normal tissues. Notably, the membrane expression of CAPRIN-1 extended to the subset of highly tumorigenic cancer stem cells and EMT induced metastatic cancer cells. In addition, we revealed that cancer cells with particularly high CAPRIN-1 surface expression exhibited enhanced tumorigenicity. We generated a therapeutic humanized anti-CAPRIN-1 antibody (TRK-950), which strongly and specifically binds to various cancer cells and shows anti-tumor effects via engagement of immune cells. TRK-950 was further developed as a new cancer drug and a series of pre-clinical studies demonstrates its therapeutic potency in a tumor bearing mouse model and safety in a relevant cynomolgus monkey model. Together our data demonstrate that CAPRIN-1 is a novel and universal target for cancer therapies. A phase I clinical study of TRK-950 (NCT02990481) has been completed and a phase Ib study (combination with approved drugs) is currently underway (NCT03872947).

#3924

Cooperation between mutant IL7R and TLX3 generates mixed myeloid lymphoid leukemia from thymocyte progenitors

Gisele Rodrigues. *National Cancer Institute, Frederick, MD*

Acute lymphoblastic leukemia (ALL) is the most common cancer in children. Despite the current pediatric treatment protocols have resulted in 5-year overall survival rates of up to 90%, treatments have substantial side effects. Therefore, it is important to identify more specific therapeutic targets and develop more effective and less toxic drugs and drug combinations. We have shown that overexpression of TLX3 in association with mutant IL7R (mutIL7R) is sufficient to generate aggressive leukemia from transduced CD4-CD8- (DN) thymocyte progenitors. To better understand mutIL7R/TLX3-mouse leukemia, we combined single cell RNA sequencing (scRNAseq), Cellular Indexing of Transcriptomes and Epitopes by Sequencing (CITE-seq), DNA Next Generation Sequencing (NGS) Chromatin Immunoprecipitation Sequencing (ChIP-Seq) and flow cytometry to explore the cooperation of mutIL7R and TLX3 in orchestrating leukemogenesis. We found that mutIL-7R+TLX3 induced murine mixed T/myeloid leukemia. Myeloid cell clones (CD11b+) expressed identical TCR rearrangements as the T cell clones (CD8+), indicating that mutant IL-7R+TLX3 generated mixed leukemia from T cell progenitors. Moreover, the passaged leukemia lost the T-cell phenotype and acquired a pro-B-like phenotype, suggesting preferential expansion of pro-B cells (CD19+, B220+ IgM-), which were not detected in the founder leukemia presumably due to its low frequency. We next sought to determine whether the oncogene combination is sufficient to drive a similar immunophenotype profile *in vitro*. We showed that ectopic expression of mutIL7R and TLX3 in DN primary thymocytes growing on OP9-DL4 pushed the cells to myeloid (CD11b+, Gr1+) and B-cell (B220) phenotype over a time course of 4, 8 and 20 days, while T-cell development was blocked, suggesting that TLX3 expression prevented differentiation into CD4+/CD8+ T-cells. To better understand the genes regulated by TLX3 on driving a mixed phenotype leukemia we performed ChiP-seq of D1 cell line ectopically expressing mutIL7R and TLX3. We identified RUNX as a possible key mediator of the mixed-phenotype-leukemia induced by TLX3 in combination with mutIL7R. Additionally, scRNAseq showed upregulation of PU.1 in mice leukemia, suggesting PU.1 as a potential therapeutic target. To assess whether targeted therapy could successfully treat mutIL7R/TLX3-mouse leukemia, we treated mice that had been

injected with the thymocytes transduced with mutIL-7R+TLX3 genes. We found that PU.1 inhibition reduced spleen weights, indicating decreasing of leukemia engraftment. Taken together, we generated a high-resolution dataset with detailed information about the transcriptional landscape and immunophenotype of leukemia generated by mutIL-7R+TLX3, a combination that is observed in patient samples, and suggests new therapeutic drug strategies.

#3925

JunB regulates expression of HPV genes in head and neck cancer

Hina Rehmani, Travis P. Schrank, Natalia Issaeva, Wendell G. Yarbrough.
Otolaryngology, University of North Carolina at Chapel Hill, Chapel Hill, NC

The incidence of HPV-positive head and neck squamous cell carcinoma (HNSCC) is now being considered an epidemic in the US and Western Europe as rates have surpassed those for cervical cancer. For approximately 14,400 patients per year in the US, initial therapy is aggressive and often results in adverse lifelong side effects such as difficulty swallowing and speaking. Despite having a higher cure rate than HPV-negative HNSCC, the recurrence rate is still approximately 30%. Therefore, new treatment options need to be available for these relapsed patients. Our lab was prompted to explore demethylation as a therapeutic option as HPV-positive HNSCC have a more hypermethylated genome than HPV-negative cancers. 5-azacytidine (5-aza) is a synthetic cytidine analog that causes DNA demethylation by trapping methyltransferases to chromatin; it is FDA-approved for the treatment of myelodysplasia and acute myeloid leukemia. Our lab found that low doses of 5-aza delayed HPV-positive xenograft tumor growth and that HPV-positive tumor samples from patients treated with 5-aza in a window trial had increased apoptosis. They also observed a marked downregulation of HPV gene expression after 5-aza. Decreased HPV E6 expression, followed by reactivation of tumor suppressor p53, induced p53-dependent apoptosis in HPV-positive HNSCC. To further explore the mechanism of this sensitivity to 5-Aza, we first determined that 5-aza regulates the transcription of HPV genes, but not the stability of HPV transcripts. We found that the transcriptional regulation of HPV genes after 5-aza depends on the proto-oncogene JunB, a component of the

transcription factor Activator Protein 1 (AP-1). Additionally, silencing of JunB abolished the expression of HPV E6/E7 genes and reactivated tumor suppressor p53 in HPV-positive HNSCC. Furthermore, we revealed that clonogenic survival of HPV-positive head and neck cancer cells is dependent on JunB expression. Our study exposes an important component of 5-Aza-associated sensitivity and toxicity in HPV-positive HNSCC and identifies a novel dependency on JunB, potentially providing a new rational targeted therapy.

#3926

Activating missense mutations in ROS1 receptor harbor oncogenic potential and are sensitive to tyrosine kinase inhibition

Sudarshan R. Iyer[1], Kevin Nusser[1], Kristen Jones[1], Pushkar Shinde[2], Catherine Z. Beach[1], Clare Keddy[1], Erin Aguero[1], Jeremy Force[3], Ujwal Shinde[2], Monika A. Davare[1]. *[1]Pediatrics, Oregon Health and Science University, Portland, OR,[2]Chemical Physiology, Oregon Health and Science University, Portland, OR,[3]Duke University, Durham, NC*

ROS1 encodes the largest receptor tyrosine kinase (RTK) in the human genome. Chromosomal rearrangements of the *ROS1* gene generate oncogenic ROS1 fusion proteins that have been successfully targeted with tyrosine kinase inhibitors (TKIs), most notably in lung cancer. To date, ROS1 fusions are the only known biomarkers for therapeutic implementation of ROS1 TKIs. However, unlike known oncogenic mutations in EGFR and ALK RTKs, the functional impact of point mutations within the full-length ROS1 RTK is unknown. Here we queried the AACR Genie database, which consists of pan-cancer clinical genomic sequencing data from thousands of patient samples, for ROS1 aberrations and nominated thirty-four missense mutations residing in the ROS1 tyrosine kinase domain for functional interrogation. Immunoblotting revealed distinct impact of the mutations on kinase function, ranging from complete loss to significant increase in catalytic activity. Notably, Asp and Gly substitutions at the D2113 position within the ROS1 kinase domain dramatically increased autophosphorylation and activation of downstream signaling pathways. ROS1$^{D2113N/G}$ were found to be ROS1 TKI-sensitive transformative oncogenes in independent cell-based models. Molecular

dynamic simulations of ROS1^{D2113N} kinase revealed dramatic alterations in the activation loop of the mutant kinase as compared to wildtype. Global proteomics and phosphoproteomics showed that ROS1^{D2113N} upregulates signaling via phosphorylation of known effectors (SHP2 and STAT3) similar to ROS1 fusions, but also upregulates other pathways, including mTORC2, JNK1/2, AP-1 and TGFB1. *In vivo,* ROS1^{D2113N} drove tumor formation that was inhibited with ROS1 TKIs. Taken together, these data demonstrate for the first time that select point mutations within ROS1 drive tumorigenesis and can be therapeutically targetable with existing FDA-approved ROS1-TKIs.

#3927

Genome-wide screening and validation of molecular targets and biomarkers for lung cancer

Yataro Daigo, Atsushi Takano, Yusuke Nakamura. *Institute of Medical Science, The University of Tokyo, Tokyo, Japan*

The number of lung cancer patients who respond well to currently available standard therapies is still small, new molecular targeted therapies with companion diagnostics are eagerly needed. We have been developing new molecular therapies targeting oncoproteins with their cancer biomarkers as follows, i) To identify strongly expressed genes in 120 lung cancers by genome-wide gene expression profile analysis, ii) To verify the candidate genes for their scarce expression in 23 normal organs, iii) To validate the clinicopathological significance of their protein expression by tissue microarray covering about 400 lung cancers (non-small cell lung cancers (NSCLCs) and SCLCs), iv) To examine their importance in the growth and/or invasion of cancer cells by siRNA, small molecule inhibitor, cell permeable peptides targeting their function and/or antibody assays, and v) To analyze the oncogenic function of the target molecules. By this system, we identified 50 oncoproteins and selected a LSERT (lung cancer-specific receptor tyrosine kinase) as a candidate. Immunocytochemical and immunohistochemical analyses confirmed that LSERT protein was expressed in cytoplasm and cytoplasmic membrane of lung cancer cells, but it was hardly expressed in normal lung cells. Strong LSERT expression was associated with poorer prognosis for surgically-treated NSCLC patients, and it was an independent prognostic factor. Exogenous expression of

LSERT increased the cell growth and invasion probably through its elevated kinase activity and subsequent phosphorylation of downstream proteins. Inhibition of LSERT expression by siRNAs or treatment with anti-LSERT antibody suppressed the growth of lung cancer cells. Our genome-wide screening might be a useful approach to identify target molecules for developing new therapeutics and diagnostics. LSERT could be a candidate cancer biomarker and therapeutic target for lung cancer.

#3928

Therapeutic targeting of NOTCH1 and neddylation pathway in T cell acute lymphoblastic leukemia

Carla Bertulfo, Pablo Perez-Duran, Teresa Palomero, Adolfo Ferrando.
Columbia University Irving Medical Center, New York, NY

T-cell Acute Lymphoblastic Leukemia (T-ALL) is hematologic tumor characterized by the diffuse infiltration of the bone marrow by malignant hematopoietic cells expressing immature T cell markers. Although T-ALL currently has better cure rates primarily due to multiagent or intensified chemotherapy, the prognosis for patients who are resistant or develop relapse to therapy remains very poor. Aberrant Notch homolog-1 (NOTCH1) signaling is a major driver of T-ALL pathogenesis as more than 60% of T-ALL cases harbor activating mutations in the NOTCH1 gene. Gamma Secretase Inhibitors (GSIs) which effectively block the activation of oncogenic protein NOTCH1 are potential candidates for the treatment of T-ALL. However, the clinical application of GSIs is hampered by severe gastrointestinal toxicity due to the inhibition of NOTCH1 signaling in the gut. Here we demonstrate that combination therapy of GSIs and a small molecule inhibitor of the neddylation pathway circumvents the GSI-induced gut toxicity in vitro and in vivo. Genome-wide CRISPR loss-of-function screen in LS174T adenocarcinoma cells revealed neddylation pathway as a main regulator of massive goblet cell differentiation upon NOTCH1 inhibition. Genetic and pharmacologic inhibition of the neddylation pathway in LS174T cells rescued GSI-induced differentiation and cell death. Mechanistically, neddylation inhibition increases the protein stability of Hairy and enhancer of split-1 (HES1), a known regulator of absorptive and secretory cell fate decisions. Combination treatment of GSI and neddylation inhibitor in C57/BL6 mice showed a profound decrease in the

number of goblet cells and maintained HES1 protein levels in the intestinal epithelium compared to GSI treatment alone. Remarkably, combined treatment of GSI and neddylation inhibitor in NOTCH1-induced T-ALL mice showed leukemia regression and improved overall survival without any associated gut toxicity. Overall, these results substantiate the potential of targeting NOTCH1 and neddylation pathway in the treatment of NOTCH1-induced T-ALL.

#3929

MDMX overexpression in cancer cells confers significant resistance to MDMX inhibitor XI-006 and may modulate chemosensitivity through suppressing p53 activation of pro-apoptotic factors

Andrew George[1], Arielle De La Cruz[1], Shengliang Zhang[1], Ilyas Sahin[2], Praveen Srinivasan[1], Maximilian Schwermann[1], Morgan Turcotte[1], Taylor Arnoff[1], Wafik S. El-Deiry[1]. *[1]Legorreta Cancer Center, Brown University, Providence, RI,[2]Division of Hematology/Oncology, University of Florida, Gainesville, FL*

MDM2 inhibition has gained popularity in recent years as a therapeutic strategy in targeting both solid tumors and hematological malignancies, and several small molecule inhibitors of the p53-MDM2 binding interface have progressed into clinical trials in recent years. Alongside direct stabilization of p53, MDM2 has further been identified to have immune implications in terms of CD8+ T-cell mediated anti-tumor immunity and checkpoint-blockade therapies. However, little work has been done to explore the therapeutic targeting potential of related protein MDMX (MDM4). Pan-cancer analyses conducted by our lab (in part presented at the ASCO 2022 Annual Meeting) identify an important role of MDMX in several tumor types. Particularly, MDMX amplification is associated with a higher risk of brain and liver metastasis, and MDMX amplification itself also presents with significant frequency (10%) in glioblastoma multiforme (GBM). Notably, MDMX amplification also served as a better predictor of reduced overall survival in NSCLC following checkpoint-blockade. We have also previously reported on associations between MDMX amplification and CDKN2A deep deletions in melanoma, a predictor of favorable response to checkpoint blockade. Such findings establish the need for further exploration to be done and the role of MDMX both in cell phenotype and

potential immune regulation to be better characterized. Preliminary data acquired from transient overexpression experiments using lipofection of MDMX cDNA and MDMX inhibitor XI-006 (NSC207895) alone and in combination with chemotherapy further supports the viability of MDMX-inhibition as a therapeutic strategy in several cell lines. Overexpression of MDMX in HCT116 $p53^{WT}$ cells demonstrably confers remarkable resistance to MDMX inhibitor XI-006 at a 72-hour timepoint (IC50 of 104.75 uM in overexpressing cells versus 29.03 uM in WT), and treatment with oxaliplatin reveals both reduced basal and post-treatment expression of p53-upregulated modulator of apoptosis (PUMA). Further mechanistic workup of this phenomenon is underway, particularly with an emphasis on immuno-oncological therapeutic translations. Altogether, initial findings ultimately establish the need for further investigation into the mechanistic basis of MDMX-correlated clinical outcomes and the therapeutic potential of MDMX inhibition.

#3930

MCT1 as a potential target in the progression of oral premalignant dysplasia to invasive squamous cell carcinoma

Ethan J. Wong[1], Ali Khammanivong[1], Ravi Maisuria[2], Erin B. Dickerson[3], Raj Gopalakrishnan[2]. *[1]Veterinary Clinical Sciences, University of Minnesota, Saint Paul, MN,[2]Division of Oral and Maxillofacial Pathology, University of Minnesota, Minneapolis, MN,[3]University of Minnesota, Saint Paul, MN*

Introducti**on:** Most oral squamous cell carcinomas (OSCC) progress through clinically identifiable stages, starting from premalignant epithelial dysplasia to early invasive OSCC. How cells transform from premalignant dysplasia to early invasive OSCC is unknown. High monocarboxylate transporter 1 (MCT1; *SLC16A1*) expression is correlated with poor outcomes in OSCC patients, where it is thought to promote tumor growth by supporting metabolic coupling between cancer cells and tumor stroma. Because expression of MCT1 is markedly increased in OSCC patients, we sought to determine if MCT1 played a role in the progression of oral dysplasia in early invasive OSCC.

Methods: Immunohistochemistry (IHC) was used to evaluate changes in the levels of MCT1 expression across adjacent normal, dysplasia, and

OSCC tissues to identify expression patterns during cancer progression. Genetic knockout (KO) of *SLC16A1* via CRISPR/Cas9 and pharmacological blockade by the MCT1 inhibitor AZD3965 were used on OSCC (TR146) and dysplastic (DOK) cell lines. KO was confirmed by qRT-PCR and immunoblotting. MCT1-KO and AZD3965-treated cells were assayed for changes in cell invasion using Matrigel-coated transwell assays. Correlative changes in gene expression based on MCT1 staining and disease progression were also observed in adjacent normal, dysplasia, and OSCC regions in each tissue section using Nanostring GeoMx Digital Spatial Profiler.
Results: Expression of MCT1 was directly correlated to the progression of disease from dysplasia to early superficially invasive OSCC relative to normal adjacent epithelium. KO of MCT1 significantly decreased the invasion of dysplastic and OSCC cell lines compared to the wild-type (parental) controls. AZD3965 also decreased invasion in the parental dysplastic and OSCC lines. To identify progressive changes in gene expression across normal, dysplasia, and early invasive OSCC, transcripts for cancer-related genes were quantified in the epithelial and stromal compartments from patient samples. Compared to the normal epithelium, upregulation in gene expression, including *SLC16A1*, was observed in the cell cycle and metabolic pathways in OSCC tissues.
Conclusions: Our data suggest that MCT1 plays a key role in breaching of the basement membrane and facilitating tumor cell migration and invasion. Targeting MCT1 in oral dysplasia may prevent progression to OSCC in oral cancer patients.

#3931
BRD4, BRD3, NSD3, and ZNF532 fusions in histologies beyond NUT carcinomas: Investigation of a large pan-cancer cohort
Ian R. Nykaza[1], Christopher A. Febres-Aldana[2], Sabrina T. Lin[3], Ryma Benayed[2], Kerry Mullaney[3], Emiliano Cocco[4], Alexia Iasonos[3], Marc Ladanyi[5], Alexander E. Drilon[6], Yonina R. Murciano-Goroff[6]. *[1]Weill Cornell Medical College, New York, NY,[2]Department of Pathology, Memorial Sloan Kettering Cancer Center, New York, NY,[3]Department of Epidemiology & Biostatistics, Memorial Sloan Kettering Cancer Center, New York, NY,[4]University of Miami Miller School of Medicine and Sylvester Comprehensive Cancer Center, University of Miami Miller School of*

Medicine, Miami, FL,[5]Department of Pathology, Human Oncology and Pathogenesis Program, Memorial Sloan Kettering Cancer Center, New York, NY,[6]Weill Cornell Medical College and Memorial Sloan Kettering Cancer Center, New York, NY

Background**:** *NUT* rearrangements drive NUT carcinomas (NCs), which are rare, poorly differentiated tumors with a survival from diagnosis of ~6-7 months. Common NUT fusion partners (NCFPs) include *BRD4*, *BRD3*, *NSD3*, and *ZNF532*, which are associated with epigenetic changes leading to tumor growth. Recent clinical trials have aimed to address NCs, but little is known about fusions involving NCFPs in other histologies. We characterized NCFPs in a large, pan-cancer cohort.
Methods: The MSK-IMPACT (DNA sequencing; n=71,423) and MSK-Fusion (RNA sequencing; n=10,897) clinical cohorts were mined to identify patients (pts) with all forms of structural variants (SVs) involving NCFPs, detected between April, 2015 and June, 2022. The targeted NGS panels included *BRD4* and *NSD3* only; detection of *BRD3* and *ZNF532* SVs was possible for fusions with a partner present on either panel. SVs were manually reviewed to identify in-frame fusions with oncogenic potential if critical domains present in NC fusions were conserved. Pts were followed through July 2022 and manual chart review enabled assessment of treatment history and clinical outcomes.
Results: SVs involving NCFP genes were detected in 182 (*BRD4*=110, *NSD3*=61, *BRD3*=8 and *ZNF532*=3) pts (0.002%). Putative NCFP fusions not involving any of the NUT gene family members comprised a total of 20 fusions with likely oncogenic potential including 11 with *BRD4* (55%), 5 with *NSD3* (25%), 3 with *ZNF532* (15%), and 1 with *BRD3* (5%). *BRD4::NOTCH3* and *ZNF532::MALT1* were the most enriched fusions, present in 3 samples each. The most common histologies were breast (3 ductal; 1 lobular), lung (2 squamous cell carcinoma, 1 adenocarcinoma and 1 mixed histology), and colon and esophageal adenocarcinoma (2 samples each). Median age at diagnosis was 62. 11 (55%) pts were female and 9 (45%) were male. 13 (65%) pts ultimately were diagnosed with stage IV disease and had a median overall survival from stage IV diagnosis of 2.5 years (95% CI: 1.41, NR). DNA sequencing in 19/20 tumors revealed a mean tumor mutational burden (TMB) of 5.0 mut/Mb including 15 with low TMB (<10) and 3 with high TMB (>10). No tumor showed

microsatellite instability (MSI-high). *TP53* mutations were the most common co-alteration, found in 11 (58%) cases. 18/20 pts received systemic therapy; 18 (90%) received cytotoxic chemotherapy and/or mAb therapy, including 13 (65%) who received a platinum. 8 pts (40%) received immunotherapy (IO), and 4 (20%) received small molecule inhibitors. No pts received BET inhibitors. Among pts who received IO, median time to treatment discontinuation was 64 days (95% CI: 20, NR).
Conclusion: Tumor sequencing from a large cohort reveals potential oncogenic fusions involving *BRD4*, *BRD3*, *NSD3*, and *ZNF532* across multiple histologies. Further biological characterization of their oncogenicity and potential targetability is warranted.

#3932
Targeting cyclin K in pancreatic cancer
Yi Xiao, Jixin Dong, Yuanhong Chen. *University of Nebraska Medical Center, Omaha, NE*

This study focuses on investigating the role of Cyclin K in pancreatic cancer growth and chemotherapeutic sensitivity, aiming to provide pre-clinical evidence for Cyclin K-targeted therapy in pancreatic cancer. Unlike other well-known cyclins, Cyclin K is largely understudied in cancers. Data extracted from the TCGA database indicated that Cyclin K was overexpressed in pancreatic ductal adenocarcinoma (PDAC) and associated with reduced overall survival. Consistently, western blotting showed that Cyclin K was abundantly expressed in human and mouse PDAC cell lines. By using a Tet-On inducible system, we established Cyclin K-depleted and Cyclin K-overexpressed cell lines to evaluate the function of Cyclin K in pancreatic cancer. The proliferation assay showed that Cyclin K depletion led to retarded PDAC cell proliferation, whereas Cyclin K overexpression boosted cell growth. We further confirmed that Cyclin K was required for pancreatic cancer growth *in vivo*. In addition, cell cycle analysis showed that Cyclin K deficiency resulted in G1-S arrest, while Cyclin K overexpression promoted G1-S progression. By using an RT2 cell cycler array, we identified CDC20 as an important target of Cyclin K that mediated Cyclin K-induced PDAC cell proliferation. To investigate the influence of Cyclin K on chemo-sensitivity, we treated the PDAC cell lines with two newly synthesized Cyclin K molecular glue degraders (HQ461

and NCT02). We found that these degraders specifically ablated Cyclin K and its cognate kinase CDK12 in a very efficient manner. Importantly, we demonstrated that Cyclin K abrogation, either by Cyclin K degrader or Cyclin K knockdown, rendered PDAC cells more sensitive to GemTaxol (gemcitabine plus Taxol) treatment and PARP inhibitors (olaparib or niraparib), as indicated by increased cleavage of PARP or caspase 3. Together, our current results suggest: 1. Cyclin K promotes cell proliferation and G1-S transition in pancreatic cancer; 2. CDC20 mediates the function of Cyclin K on pancreatic cancer cell proliferation; 3. Cyclin K depletion synergizes with GemTaxol or PARP inhibitor in pancreatic cancer treatment. Our study revealed for the first time that Cyclin K plays an essential role in pancreatic cancer growth and chemo-sensitivity, and targeting Cyclin K may offer a great therapeutic avenue for pancreatic cancer patients.

#3933

RRM2 inhibition by COH29 is a potential therapeutic strategy for atypical teratoid rhabdoid tumors

Le Hien Giang, Tai-Tong Wong, Che-Chang Chang. *Taipei Medical University, Taipei, Taiwan*

Introduction: Atypical teratoid rhabdoid tumors (ATRT) are a rare but aggressive malignancy in central nervous system, commonly occurring in early childhood. ATRT patients face a dismal prognosis despite aggressive therapy. Development of both effective and protective targeted therapy is an emerging necessity. It has been reported that RRM2 is a master driver of aggressiveness and a poor prognosis biomarker in several cancers. However, little is known about RRM2 function in ATRT. The aim of this study is to assess the roles of RRM2 in ATRT and elucidate the therapeutic potential of RRM2 to cure the ATRT.
Methods: Expression of RRM2 was evaluated by molecular profiling analysis and was confirmed by IHC in both ATRT patients and PDX tissues. Follow-up *in vitro* studies used 3 different cell lines to elucidate the oncogenic role of RRM2 in ATRT cells. The efficacy of COH29, an RRM2 inhibitor, was assessed *in vitro*. ATRT model of SCID mice orthotopically injected with ATRT cells were used to test the efficiency of COH29 for *in*

vivo. Western blot and RNA-sequencing were used to determine the mechanisms of RRM2 transcriptional activation in ATRT.
Results: Molecular profiling results revealed that RRM2 was relatively highly expressed in ATRT tissues and cell lines. Clinical relevance analysis results showed that the RRM2 expression level was associated with poor prognosis among ATRT patients. Knockdown of RRM2 by shRNAs significantly reduced ATRT cells colonies formation, proliferation and migration. A similar but more pronounced inhibitory effect was observed when COH29 was used to target RMM2. Inhibition of RRM2 by shRNAs or COH29 significantly induced cell death via DNA damage and/or apoptosis pathways. *In vivo* results demonstrated that COH29 could suppressed ATRT tumor growth and extend mice overall survival.
Conclusion: Our study identified RRM2 as a potential mediator of oncogenic cellular functions in ATRT cell lines. We propose that highly expressed RRM2 is associated with poor patient outcomes, and inhibition of RRM2 by COH29 may present a significant therapeutic value in ATRT.

#3934

PRMT5 is an actionable target in CDK4/6 inhibitor-resistant ER+/Rb-deficient breast cancer

Chang-Ching Lin[1], Tsung-Cheng Chang[2], Yunguan Wang[3], Yanfeng Zhang[3], Andrew Lemoff[4], Yisheng V. Fang[5], He Zhang[3], Dan Ye[1], Isabel Soria-Bretones[6], Alberto Servetto[7], Kyung-min Lee[8], Xuemei Luo[4], Joseph J. Otto[4], Hiroaki Akamatsu[9], David W. Cescon[10], Lin Xu[3], Yang Xie[3], Joshua T. Mendell[2], Ariella B. Hanker[1], Carlos L. Arteaga[1]. *[1]Harold C. Simmons Comprehensive Cancer Center, UT Southwestern Medical Center, Dallas, TX,[2]Department of Molecular Biology, UT Southwestern Medical Center, Dallas, TX,[3]Department of Population & Data Sciences, UT Southwestern Medical Center, Dallas, TX,[4]Department of Biochemistry, UT Southwestern Medical Center, Dallas, TX,[5]Department of Pathology, UT Southwestern Medical Center, Dallas, TX,[6]Repare Therapeutics, Montreal, QC, Canada,[7]Department of Clinical Medicine and Surgery, University of Naples Federico II, Naples, Italy,[8]Department of Life Science, Hanyang University, Seoul, Korea, Republic of,[9]Third Department of Internal Medicine, Wakayama Medical University, Wakayama, Japan,[10]Princess Margaret Cancer Centre, University of Toronto, Toronto, ON, Canada*

RB1 loss-of-function genomic alterations confer resistance to CDK4/6 inhibitors (CDK4/6i) and are enriched post treatment of CDK4/6i in estrogen receptor-positive (ER+) metastatic breast cancer. ER+/Rb-deficient breast cancer is a rising patient population in need of novel therapeutic strategies. Herein, we used a genome-wide CRISPR screen and identified protein arginine methyltransferase 5 (PRMT5) as a molecular vulnerability in this refractory breast cancer subtype. sgRNA-induced depletion of *PRMT5* arrested growth of MCF-7 and T47D *RB1* knockout (RBKO) cells. PRMT5 catalyzes symmetric dimethylation of arginine (SDMA). In RBKO cells carrying doxycycline-inducible shRNA targeting the 3'UTR of *PRMT5*, rescue with wild-type but not an enzymatically dead mutant of PRMT5 restored cell growth, supporting that PRMT5 methyltrasferase activity is essential for growth of these cells. Gene set enrichment analysis (GSEA) of RNA-seq data revealed significant downregulation of cell cycle-related Hallmark gene signatures in RBKO cells treated with *PRMT5* siRNA versus control siRNA. Both gene silencing and pharmacological blockade of PRMT5 with the small molecule inhibitor pemrametostat impeded G1-to-S cell cycle progression in MCF-7 and T47D RBKO cells and in lung, prostate, and triple-negative breast cancer cells with natural *RB1* mutations or deletions, suggesting that PRMT5 inhibition can block the G1-to-S transition even in the absence of Rb. To identify the protein interactome of PRMT5 and the mechanism by which it promotes cell cycle progression in Rb-deficient cells, we performed proteomics analysis of Co-IP mass spectrometry and an SDMA post-translational modification scan and pinpointed FUS (fused in sarcoma) as a putative downstream effector of PRMT5. FUS is known to regulate RNA polymerase II (Pol II)-mediated transcription. Inhibition of PRMT5 with pemrametostat significantly reduced SDMA levels on FUS and dissociated FUS from Pol II as evidenced by FUS Co-IP and immunoblot analysis. ChIP-seq analysis revealed that treatment of RBKO cells with pemrametostat derepressed phosphorylation of Ser2 in the C-terminus of Pol II at transcription start sites (*TSS*) of genes involved in cell cycle progression. In accordance with the abnormal accumulation of pSer2 Pol II at *TSS*, pemrametostat treatment also resulted in an increased Pol II pausing index and an enrichment of intron retention splicing variants. Finally, therapeutic inhibition of PRMT5 with pemrametostat synergized with fulvestrant (a selective ER degrader)

against growth of ER+/Rb-deficient breast cancer cell line- and patient-derived xenografts in mice, suggesting this combination as a novel therapeutic strategy for ER+/Rb-deficient metastatic breast cancers.

#3935

CRISPR/Cas9 screens to identify proliferation and resistance mechanisms in uveal melanoma

Richard L. Bennett[1], Darby Monagle[1], Katelyn R. Raburn Smith[1], Amin Sobh[1], Keiran S. M. Smalley[2], J. William Harbour[3], Jonathan D. Licht[1].
[1]University of Florida Health Cancer Center, Gainesville, FL,[2]Department of Tumor Biology, Moffitt Cancer Center and Research Institute, Tampa, FL,[3]Department of Ophthalmology, UT Southwestern Medical Center, Dallas, TX

Purpose: Uveal (ocular) melanoma (UM) is a highly aggressive and frequently fatal cancer of the eye. While only 2-4% of patients have metastases at diagnosis, up to 50% of develop metastatic disease, overwhelmingly to the liver. Almost all UM harbor an initiating mutation in the Gαq signaling pathway, most commonly in GNAQ. Most UM also contain secondary mutations that drive tumor progression, the most common being BAP1 loss. Targeted therapies such as MEK inhibitors have been utilized in UM, but tumors rapidly become refractory. The aims of this study were to identify novel mechanisms specifically activated in UM cells that drive proliferation and escape from MEK inhibitor therapy.
Procedures: We performed CRISPR-Cas9 mediated gene disruption screening of UM cell lines 92.1, Mel202 and Mel270 using the Brunello sgRNA library targeting the whole genome. Cells were transduced at 0.3 MOI and 500X coverage then split into two groups to compare treatment with the MEK inhibitor (MEKi) trametinib (6nM) vs. untreated control cells. Cell pellets were collected at day 2 (baseline) and after every 3 cell divisions for 21 cell divisions (treated and control). In addition, we generated 92.1 and Mel270 cell lines stably expressing Cas9 and transduced cells at 1000x coverage with a sgRNA library targeting either 192 epigenetic regulators or 482 kinases. At least two replicates for each screen were performed. sgRNA representation between samples was compared using MAGeCK. Genes specifically essential in UM cell lines were distinguished from commonly essential genes using the Broad institute

dependency map (DepMap). These hits were validated by individual sgRNAs and pharmacological inhibition.
Results: Whole genome screens revealed a set of 84 genetic dependencies unique for UM cells that were required for proliferation. Among these genes were those required for the lipoic acid biosynthesis pathway: MCAT, MECR, LIPT2, LIAS as well as genes encoding the MITF-SOX10-TFAP2 transcription factors, the H3K9 methyltransferase SETDB1, and members of the MLL3/4 complex. Screening of UM cell lines with a focused guide RNA library targeting epigenetic regulators revealed that BRD2, TRIM28, KMT2D, SETD1B and HDAC1 were specifically required for UM survival. Screens with a sgRNA library targeting the kinome revealed CDK2, CDK4 and TRRAP were required for UM survival. After 1 week of treatment with MEKi trametinib, we identified 112 genes whose disruption increased the anti-proliferative effects of trametinib in Mel202 and Mel270 cells and 10 of these genes were essential only in UM. These genes included metabolic enzymes critical for fatty and lipoic acid synthesis such as MECR, MCAT and TAZ. By contrast disruption of TP53, NF1, or PTEN led to MEKi resistance.
Conclusions: These results identify novel mechanisms of proliferation and therapy resistance specifically required in GNAQ mutant UM cells that may represent new therapeutic targets.

#3936
ALK fusion oncogene driven *SERPINB4* expression enhances tumor survival in NSCLC
Tzu-Po Chuang[1], Wei-Yun Lai[1], Jonatan L. Gabre[1], Dan E. Lind[1], Ganesh Umapathy[1], Abdulmalik A. Bokhari[1], Bengt Bergman[2], Linnea Kristenson[1], Fredrik B. Thorén[1], Anh Le[3], Robert Doebele[3], Jimmy V. D. Eynden[4], Ruth H. Palmer[1], Bengt Hallberg[1]. *[1]University of Gothenburg, Gothenburg, Sweden,[2]Sahlgrenska University Hospital, Gothenburg, Sweden,[3]University of Colorado School of Medicine, Aurora, CO,[4]Ghent University, Ghent, Belgium*

Anaplastic lymphoma kinase (ALK) fusion variants in non-small-cell-lung cancer (NSCLC) consist of numerous dimerising fusion partners, with the most common being EML4. Clinical data suggests that the degree of treatment benefit in response to ALK tyrosine kinase inhibitors (TKIs)

differs among the variant present in the patient tumor. Therefore, a better understanding the oncogenic signaling networks driven by different ALK-fusion variants is important. Here, we developed highly controlled doxycycline-inducible cell models bearing four different ALK fusion proteins, namely EML4-ALK-V1, EML4-ALK-V3, KIF5B-ALK, and TFG-ALK, in the context of non-tumorigenic NL20 human bronchial epithelial cells. These were complimented by patient-derived NSCLC cell lines harboring either EML4-ALK-V1 or EML4-ALK-V3 fusions. RNA-seq and phosphoproteomics analysis were employed to identify dysregulated genes and hyper/hypo-phosphorylated proteins associated with ALK fusion expression. Among ALK fusion induced responses, we noted a robust inflammatory signature that included up-regulation of the Serpin B4 serine protease inhibitor in both NL20-inducible cell models and ALK-positive NSCLC patient-derived cell lines. We show that STAT3 is a major transcriptional regulator of SERPINB4 downstream of ALK fusions, along with NF-kB and AP1. The upregulation of SERPINB4 promotes survival of ALK fusion expressing cells and inhibits natural killer (NK) cell-mediated cytotoxicity. In conclusion, our study reveals a novel ALK downstream survival axis that regulates Serpin B4 expression and identifies a molecular target that has potential for therapeutic impact targeting the immune response together with ALK TKIs in NSCLC.

#3937

An intracellular variant of zona pellucida glycoprotein 3 is expressed in cancer

Iman J. Schultz[1], Yvette Zimmerman[1], Cathy B. Moelans[2], Marcin Chrusciel[3], Jan Krijgh[1], Paul J. van Diest[2], Ilpo T. Huhtaniemi[4], Herjan J. T. Coelingh Bennink[1]. *[1]Pantarhei Bioscience B.V., Zeist, Netherlands,[2]University Medical Center Utrecht, Utrecht, Netherlands,[3]University of Turku, Turku, Finland,[4]Imperial College London, London, United Kingdom*

This study describes the expression of an intracellular variant of the Zona Pellucida glycoprotein 3 (ZP3) that is predominantly expressed in cancer. ZP3 is an important constituent of the Zona Pellucida (ZP), the extracellular layer surrounding oocytes. It is highly expressed in maturing oocytes, but not in other adult human tissues. As ZP3 protein has also been detected in

cancer, it may serve as an interesting diagnostic and therapeutic target. Here, we extend the cancer-related ZP3 expression data using immunohistochemistry (IHC) of tumor biopsies, interrogating publicly available RNA-sequencing (RNA-seq) data of cancer cell lines (CCLs) and tumor and normal tissues, as well as computational analysis and real-time quantitative PCR (qPCR) of CCLs. IHC data for several cancer types shows abundant ZP3 protein expression, which is confined to the cytoplasm, contradicting the extracellular ZP3 localization in oocytes. An alternative *ZP3* mRNA variant, which we term 'ZP3-Cancer', is annotated in the NCBI and Ensembl databases, and lacks the genetic information encoding the N-terminal signal peptide that governs extracellular secretion. Analysis of publicly available RNA-seq data of 1339 CCLs indicates that ZP3-Cancer is the dominant variant as compared to ZP3-Oocyte, which was validated by independent computational analysis. Expression of ZP3-Cancer in CCLs was confirmed by qPCR. Publicly available RNAseq data of tumor and normal tissues confirms strongly enhanced expression of ZP3-Cancer in cancer cells. In addition, ZP3-Cancer expression is upregulated in advanced stages and shows a relationship with patient survival in a number of cancer types. The folliculogenesis specific transcription factor FIGLA, which activates transcription of ZP3-Oocyte in maturing oocytes, appears absent in cancer as inferred from publicly available transcriptome data, indicating alternative ZP3-Cancer transcriptional activation mechanisms in this disease. The cancer restricted expression of this *ZP3* transcript variant renders it an attractive tumor specific antigen for the development of a therapeutic cancer vaccine, particularly using mRNA technology.

#3938

In vivo genome-wide CRISPR screen in pancreatic ductal adenocarcinoma defines HSPE1 as a potential oncogene by acting through G_2/M cell cycle arrest

Julien Boudreault, Ni Wang, Gang Yan, Meiou Dai, Sophie Poulet, Girija Daliah, Jean-Jacques Lebrun. *McGill University Health Centre Research Institute, Montreal, QC, Canada*

Superior knowledge of cancer biology has enabled unprecedented innovations in therapies targeting mutated driver genes. Despite the attempt of targeting cancer-inducing genes such as KRAS, the life expectancy of

patients diagnosed with pancreatic ductal adenocarcinoma (PDAC) has poorly improved. We performed an unbiased genome wide *in-vivo* loss-of-function CRISPR screen to discover novel oncogenes and identified heat-shock protein HSPE1, whose function is still unknown in PDAC. By decreasing HSPE1 expression with shRNA and CRISPR technology, we detected a slowdown in cell growth of PDAC cancer cells. HSPE1 knock-out cells injected in mice displayed a drastic reduction in tumor volume. We exploited this vulnerability by disrupting HSPE1 function by using KHS101, a validated HSPD1-HSPE1 complex inhibitor. Several PDAC cell lines cultured *in vitro* were sensitive upon KHS101 treatment and *in vivo* administration of KHS101 reduced tumorigenesis. Compiling the negative fitness scores from DepMap database revealed a co-dependency between HSPE1 and PLK1, a protein involved in regulating G_2/M checkpoint. Indeed, we detected a protein-level decrease of PLK1 in our experimental model of PDAC cells having either a drug-induced HSPE1 deficiency by KHS101 exposure or a HSPE1 gene-expression reduction by shRNA. We found that the cell cycle was disrupted through G_2/M arrest in PDAC cells treated with KHS101. Our findings highlight a new role underlying PDAC tumorigenesis for HSPE1 and could unlock a new area of research towards precision medicine.

#3939

Inhibition of USP7 upregulates USP22 through desuppression of transcriptional activity of Sp1 in human cancer cells

Keqiang Zhang, Ting Sun, Wendong Li, Jun Wu, Dan Raz. *City of Hope National Medical Center, Duarte, CA*

Deubiquitinases (DUBs) play important roles in various human cancers and targeting DUBs is considered as a novel anticancer therapeutic strategy. Overexpression of ubiquitin specific protease 7 and 22 (USP7 and USP22) are associated with malignancy, therapy resistance, and poor prognosis in many cancers. Although both DUBs are involved in the regulation of similar genes and signaling pathways, such as histone H2B monoubiquitination (H2Bub1), c-Myc, FOXP3, and P53, the interdependence of USP22 and USP7 expression has never been described. In the study, we found targeting USP7 via either siRNA-mediated knockdown or pharmaceutical inhibitors dramatically upregulates USP22 in

cancer cells. Mechanistically, the elevated USP22 occurs through a transcriptional pathway, possibly due to desuppression of the transcriptional activity of SP1 via promoting its degradation upon USP7 inhibition. Importantly, the elevated USP22 leads to significant activation of downstream signal pathways including H2Bub1 and c-Myc, which may potentially enhance cancer malignancy and counteract the anticancer efficacy of USP7 inhibition. Importantly, targeting USP7 further suppresses the *in vitro* proliferation of USP22-knockout (USP22-Ko) A549 and H1299 lung cancer cells and induces a stronger activation of P53 tumor suppressor signaling pathway. In addition, USP22-Ko cancer cells are more sensitive to a combination of cisplatin and USP7. USP7 inhibitor treatment further suppresses the *in vivo* angiogenesis and growth and induced more apoptosis in USP22-Ko cancer xenografts. Taken together, our findings demonstrate that USP7 inhibition can dramatically upregulate USP22 in cancer cells; and targeting USP7 and USP22 may represent a more effective approach for targeted cancer therapy, which warrants further study.

#3940

Validation of *TFX1*, a first-in-class target for cancer metastasis

Arnab Roy Chowdhury[1], Manoj Pandre[1], Chinmaya Amarkanth[1], Debabani Roy Chowdhury[1], John Ellingboe[2]. *[1]Mestastop Solutions, Bangalore, India,[2]Mestastop Inc., Marlton, NJ*

Most of the drugs approved for metastatic epithelial carcinomas treat the proliferation of the tumor and not the biology of metastasis. To date, all clinical trials around metastasis that focused on proteases, kinases, or integrins have failed in clinics. As a result, metastasis biology-focused drug discovery has been deprioritized.We asked the question as to what the rate-limiting steps of metastasis were. To answer it, we created a cell-based functional assay platform, METAssay™, that dissected all metastasis biology steps into thirty cellular assays and characterization steps. The platform identified the functional differences between metastatic and proliferating cells. This platform was normalized with patient tumor cells, and a machine learning algorithm, METSCAN™, was subsequently applied to identify the weighted steps that contributed towards successful metastasis. This led to the identification of four first-in-class targets; two transcription factors, one cytokine receptor and one nuclear hormone

receptor.We then validated the relevance of the first target, *TFX1,* by overexpressing it in both colorectal and triple-negative breast cancer cell lines. Interestingly, apart from the expected increase in migration and invasion, all cell lines showed an increase in ROS, Autophagy, PDL-1, CD-73, quiescence, exosome uptake and a decrease in apoptosis, mitosis, and exosome secretion. Conversely, the downregulation of *TFX1* showed the opposite effect. *TFX1* was purified, and a biochemical isothermal calorimetry (ITC) assay was standardized with a tool compound with a K_D of 107 nM. The compound effectively reduced metastatic properties in the cell lines and in multiple patient samples, as analyzed by the METAssay™ platform. Colorectal cancer cell lines overexpressing *TFX1* also showed increased platelet binding, which was reduced by the tool compound, but not triple-negative cancer cell lines. Also, the effect of overexpression in non-metastatic cells was more profound than in metastatic cells, suggesting a saturating effect. Further characterization of the tool compound is currently ongoing to help establish a baseline for a novel discovery programme.The ideal drug to delay metastasis should be given to primary tumor patients with no evidence of clinical metastasis, irrespective of their pathological grading. Therefore, it should have a high bar for safety. Our goal is to collaborate on a discovery journey to identify candidates and create a companion diagnostic that will identify primary tumor patients at high risk of metastasis, thereby selecting the right patient cohort for clinical trials.

#3941

Enzymatic nitration in oncology

Arun Kashyap, Sami Hussein, Sahar Mazar, Kate Markham, Anthony Mastracci, Ritu Sharma, Sheerin K. Shahidi-Latham, Irene Griswold-Prenner. *Nitrase Therapeutics, Inc., Brisbane, CA*

Background: We have discovered a new class of enzymes, that we name the nitrases, that catalyze the post-translation nitration of specific tyrosine residues of key proteins, several of which regulate important oncogenic pathways and are negatively prognostic in multiple cancer types.
Materials And Methods: To identify protein substrates for 31 candidate nitrases, we incubated each nitrase with a 23,000 protein chip in a nitrase assay containing peroxynitrite and using anti-nitrotyrosine antibodies to

detect the proteins that were nitrated. We then confirmed this nitration in separate biochemical assays and determined the specific site of nitration by LC-MS. Further, nitrases were evaluated in silico against TCGA gene expression and GISTIC copy number databases for specific cancer associations.
Results: We have discovered that several proteins known to regulate tumor cell survival and/or evasion of immune surveillance are specifically nitrated by different nitrases and that their biochemical activities are regulated by this nitration. Pak4, a protein that has been implicated as an oncogenic driver, as well as in immune evasion is specifically nitrated by Nitrase #3 and increases its kinase activity. Interestingly, Nitrase #3 also nitrates Pak5, but not any of the other Pak family members, demonstrating high enzymatic specificity. Targeted inhibition or degradation of nitrated Pak4 or inhibition of Nitrase #3 may have therapeutic potential in oncology. Similarly, RhoA, a protein implicated in the oncogenic state of tumors is nitrated by Nitrase #12. This nitration activates RhoA biochemically and in cells. Bax is a specific substrate for Nitrase #11. Nitration of Bax reduces the cytochrome C release from the mitochondria induced by Bax. For each of these enzymes, we will develop specific inhibitors to determine their therapeutic potential in tumorigenesis.
We further performed in silico analysis of nitrases for overall survival association in 17 cancer types. Utilizing TCGA RNA expression data and The Human Protein Atlas, nitrases were screened for association with overall survival in relation to nitrase RNA expression. Nitrases showing higher overall survival with low nitrase RNA expression and p. value <0.001 were identified as negatively prognostic. 10 nitrases showed negative prognostic association, suggesting that they could be favorable therapeutic targets. Three nitrases, N11, N12, N18, were negatively prognostic in renal clear cell carcinoma and nitrases N1 and N13 were negatively prognostic in liver cancer.
Conclusions: A new class of enzymes we discovered offers multiple opportunities for development of effective chemotherapeutic agents against a variety of oncogenic targets and in specific cancers that show negative association of high nitrase expression.

#3942

Differential expression of a novel transport receptor, SORT1 (sortilin), in cancer versus healthy tissues that can be utilized for targeted delivery of anti-cancer drugs

Guylaine Roy[1], Pratik Kadekar[1], Lynn Marie Douglas[1], Maude Frappier[1], Jean-Christophe Currie[1], Jess Dhillon[2], Gregory Cesarone[2], Richard Siderits[2], Karen Kirchner[2], Michel Demeule[1], Christian Marsolais[1].
[1]Theratechnologies Inc., Montreal, QC, Canada,[2]Discovery Life Sciences LLC, Newton, PA

Sortilin (SORT1), or neurotensin receptor-3, is a scavenging receptor in the Vacuolar Protein Sorting 10 protein (Vps10p) family. SORT1 is involved in the internalization and trafficking of its ligands through an endocytic process and is associated with cancer cell survival and progression, making SORT1 a candidate for novel drug delivery. We recently reported on the pattern and prevalence of SORT1 expression in endometrial, breast, ovarian, colorectal, pancreas cancers, and skin melanoma. To better understand SORT1 expression, we screened tissues from different cancer types using the same immunohistochemistry (IHC) method. A total of 19 cancer tissue microarrays (TMAs) with 1394 evaluable cancer cores were screened. Each cancer core was scored using an H-score ranging from 0 to 300, where 0 corresponds to no cell stained for SORT1, while 300 corresponds to strong SORT1 staining in all cells. The table below summarizes the % of cores with moderate to high SORT1 expression (defined as H-score ≥100) as well as the average H-Score for each cancer type evaluated. Sub-analyses of SORT1 expression by tumor histological sub-type, stage and grade are also being performed.

Cancer Type	**No. evaluable cores**	**% of indication with H-score ≥ 100**	**Average H-Score**
Endometrial	94	90	197
Thyroid	108	92	188
Melanoma	155	83	184
Lung	152	58	112
SCLC	*44*	*95*	*183*
NSCLC	*108*	*43*	*82*
Bladder	118	81	156

Testis	40	100	116
Small intestine	54	63	102
Eye	26	46	83
Cervix	376	38	75
Prostate	150	39	71
Liver	121	23	52

A total of 234 healthy or normal adjacent tissues cores were also assessed. Weak or null staining was observed in these tissues. Moderate staining was observed in specific cell types in kidney tubules and glomeruli, colonic mucosa, splenic sinusoidal spaces in red pulp, blood vessels in smooth muscle of spleen and colon, dendritic and axonal extensions of pyramidal-type neurons in brain, and testicular seminiferous tubules. SORT1 is currently being studied as a cancer target in a first-in-human (FIH) study of a peptide-drug conjugate (clinicaltrial.gov: NCT04706962). These results suggest that SORT1 is highly expressed in multiple tumors and is a promising target for the delivery and internalization of cancer therapeutic agents.

Identification of Molecular Targets 2 / New Nonclinical Models for Targets

#3946

Radiolabeled αvβ3 analog ^{177}Lu-EB-RGD is an effective therapeutic agent in thyroid cancer xenograft mouse model

Sonam Kumari[1], Zhantong Wang[1], Shilpa Thakur[1], Laura Abaandou[1], Oksana Gavrilova[1], Huiyan Lu[1], Lixin Lang[1], Dale Kiesewetter[1], Vasyl Vasko[2], Joanna Klubo-Gwiezdzinska[1]. *[1]National Institutes of Health, Bethesda, MD,[2]Uniformed Services University of the Health Sciences, Bethesda, MD*

Background: Integrins are cell adhesion receptors consisting of 18α and 8β subunits. A subset of integrins (αvβ3) recognizes Arg-Gly-Asp (RGD) peptide motifs which are involved in the neovascularization and progression

of various cancers. The aim of the study was to investigate if αvβ3 can serve as a molecular target for the treatment of thyroid cancer (TC) with a novel radiolabeled RGD analog ^{177}Lu-EB-RGD.
Methods: Integrin αvβ3 mRNA and/or protein expression was evaluated in 496 TC included in The Cancer Genome Atlas, tissue microarray including 70 TC and 10 normal thyroid samples, and 14 TC cell lines. *BRAF*-like or *RAS*-like expression profile was determined through standard BRS scores ranging from -1 to 0 for *BRAF*-like and 0 to 1 for *RAS*-like TC. The association between BRS and the αvβ3 expression was tested by the Spearman correlation (r). Nude mice xenografts developing αvβ3 expressing TC after subcutaneous injection of 5*10^6 TC cells were subjected to monotherapy with 0.5 mCi ^{177}Lu-EB-RGD (^{177}Lu) or in combination with Lenvatinib (^{177}Lu+L). The therapeutic efficacy of ^{177}Lu-EB-RGD was compared with standard-of-care Lenvatinib alone (L) and placebo (P). The continuous data were presented as medians with [25-75% interquartile ranges] and compared using Kruskal-Wallis test. The mixed-effects models were used for longitudinal data analysis with adjusted $p \leq 0.05$ considered statistically significant.
Results: We found a moderate negative correlation between BRS and αv ($r=-0.5$, $p<0.001$), and β3 ($r=-0.27$, $p<0.001$), revealing that *BRAF*-like tumors have a higher mRNA expression of αvβ3 integrins. Consistently, the highest αvβ3 mRNA and/or protein expression was found in the *BRAF*-like TC cell lines OCUT2 (BRS=-0.56), TPC1 (BRS=-0.4), K1 (BRS=-0.29), and Hurthle TC cell line XTC1 (BRS=-0.46). The immunostaining revealed a higher αvβ3 expression in papillary TC compared with follicular TC ($p=0.002$), and in normal thyroid ($p<0.001$). Poorly differentiated TC had a similar αvβ3 expression to papillary TC ($p=0.14$). In the thyroid cancer xenograft mouse model, all treatment modalities were more effective than the placebo in decreasing tumor size as early as 5 days after therapy initiation. A significant difference in growth curve and tumor volume was maintained at the study endpoint (L 0.584 cm^3 [0.196-0.984] vs P 0.911 cm^3 [0.183-1.68], $p=0.001$; ^{177}Lu 0.259 cm^3 [0.103-0.376] vs P, $p<0.001$; and ^{177}Lu+L 0.274 cm^3 [0.108-0.406] vs P, $p<0.001$). The combination therapy (^{177}Lu+L) resulted in decreased tumor volume as compared with monotherapy with Lenvatinib ($p=0.05$) but had a similar effect as compared with ^{177}Lu-EB-RGD monotherapy ($p=0.99$).

Conclusions: The radiolabeled αvβ3 analog ^{177}Lu-EB-RGD has potent growth inhibitory effects in TC characterized by a high integrins expression. The αvβ3 integrin could potentially serve as a molecular target for therapy with radiolabeled RGD analogs in TC.

#3947

S100A8/A9-RAGE pathway and chronic airway inflammation in cigarette smoke-induced lung carcinogenesis

Hye Seon Kang[1], In Kyoung Kim[2], Chang Dong Yeo[3], Jin Woo Kim[4], Sang Haak Lee[3]. *[1]Bucheon St. Mary's Hospital, The Catholic University of Korea, Bucheon, Korea, Republic of,[2]Cancer Research Institute, College of Medicine, The Catholic University of Korea, Seoul, Korea, Republic of,[3]Eunpyeong St. Mary's Hospital, The Catholic University of Korea, Seoul, Korea, Republic of,[4]Uijeongbu St. Mary's Hospital, The Catholic University of Korea, Uijeongbu, Korea, Republic of*

Background**:** Cigarette smoke-induced chronic airway inflammation increases the risk of lung cancer, and plays a multifaceted role in lung cancer initiation and progression, and RAGE-ligand axis (HMGB1, S100A8/A9) contributes Cigarette smoke-induced persistent and progressive inflammation. The aim of the present study was to determine the inflammatory effect on S100A8/A9-RAGE pathway in smoke-induced carcinogenesis in lung cancer.
Methods: Human alveolar adenocarcinoma cells (A549) and normal bronchial epithelial cells (BEAS-2B) were co-cultured for 24 h with the PBMC and then, cells were incubated in the presence or absence of 1.5% cigarette smoke extract (CSE) for 24 h. The cells transfected with siRNA targeting S100A8/9 or RAGE. The cell viability, colony-forming ability, migration, invasion, metastasis and morphological changes were assessed. Female A/J mice were given a benzo(a)pyrene (100mg/kg) in 0.1 ml corn oil via oral gavage at once a week for 3 weeks, and administrated CSE (1.25 ul/g) via intratracheal (IT) at twice a week for 4 weeks. Tumor load was determined by averaging the total tumor volume in each group. BAL differential cells were counted to analyze inflammatory cells.
Results: Cellular growth and colony-forming were promoted by exposure to CSE, and significantly inhibited by S100A8/9 and RAGE-siRNA transfection, especially in A549 cells than BEAS-2B. Cell migration,

invasion, MMP-2/9 activities, and the mRNA and protein expression of TLR4, NF-κB, RAGE, S100A8/9 and HMBG1 were higher in CSE exposed A549 cells. S100A8/9 and RAGE-siRNA transfection attenuated those expression, significantly. B(a)P induced an average tumor volume 7.28 mm^3 per mouse, and CSE significantly increased tumor volume (8.10 mm^3) compared to the B(a)P group. The total cell number and lymphocytes in BAL fluids tended to increase after CSE administration in lung cancer mouse group. Moreover, CSE significantly induced the levels of S100A8/9 and RAGE, p38 and p-ERK, and decreased JNK in serum and tumors with adjacent lung tissues ($p < 0.05$).
Conclusions: We identified cigarette smoke-induced S100A8/A9-RAGE pathway promoted airway inflammation and lung carcinogenesis *in vitro* and *in vivo*. Although S100A8/A9 protein contributes to many types of disease, this study will help us gain a better understanding of the complexities of cancer progression. Further studies are needed for therapeutic target of cigarette smoke-induced inflammation and immunosuppression in tumor microenviornment.

#3948
DDX5 helicase resolves G-quadruplex and transactivates MYC expression
Guanhui Wu, Zheng Xing, Luying Chen, Elizabeth J. Tran, Danzhou Yang.
Department of Medicinal Chemistry and Molecular Pharmacology, Purdue University, West Lafayette, IN

DDX5 (DEAD-box protein 5) plays an important role in cell proliferation, differentiation, and tumorigenesis. DDX5 is a founding member of the DEAD-box RNA helicase family and known as a non-processive RNA helicase. It acts as a transcriptional co-activator of many cancer-associated genes, such as *MYC,* however, the underlying molecular mechanism is unknown. *MYC* is one of the most critical oncogenes and has a DNA G-quadruplex in its proximal promoter region (MycG4) that functions as transcriptional silencer. Guanine-rich DNA and RNA sequences can form G-quadruplex, a non-canonical secondary structure. However, MycG4 is highly stable and its regulatory role in transcription requires active unfolding. Here, we report that DDX5 unfolds MycG4 with extreme efficiency, and thereby transactivates *MYC* expression. To understand the

effects of DDX5 on MycG4, we characterized the unfolding of MycG4-DNA within the DDX5-MycG4 complex using DNA footprinting, FRET and CD spectroscopy. While DDX5 is known as a dsRNA helicase, our results showed that DDX5 is a highly active DNA G4-resolvase. Strikingly, MycG4 unfolding requires neither ATP hydrolysis nor extended loading of single-stranded flanking. Our protein-binding-ELISA experiments revealed specific and high-affinity binding of DDX5 to G4 structures regardless of whether the substrate is DNA or RNA. To elucidate the cellular functions of DDX5, we analyzed publicly available DDX5 ChIP-seq data and identified G-rich sequences in cancer cells as chromatin binding sites of DDX5. Moreover, our ChIP and Western Blot results showed that DDX5 is enriched at the *MYC* promoter and activates *MYC* transcription. Importantly, G-quadruplex interactive small molecules can inhibit the DDX5 interaction with the promoter MycG4 and DDX5-mediated transcriptional activation of the *MYC* gene. In addition, knock-down of DDX5 expression with DDX5-specific siRNA in cancer cells resulted in downregulation of *MYC* expression and sensitization to G4-interactive small molecules. In summary, we identified resolving DNA and RNA G-quadruplexes as novel function of DDX5. Our results establish that the *MYC*-transactivation by DDX5 is mediated through unfolding of the *MYC* promoter quadruplex and thereby establish a new molecular target to suppress *MYC* for cancer intervention.

#3949

CYR61, a member of the CCN protein family, regulates IGF-1 in metastatic prostate cancer

Greisha L. Ortiz-Hernandez[1], Mya Walker[2], Leanne Woods-Burnham[3], Rick A. Kittles[4], Carlos A. Casiano[5], Susan L. Neuhausen[1]. *[1]Population Sciences, City of Hope National Medical Center, Duarte, CA,[2]Diabetes and Cancer Metabolism, City of Hope National Medical Center, Duarte, CA,[3]Physiology, Morehouse School of Medicine, Atlanta, GA,[4]Community Health and Preventive Medicine, Morehouse School of Medicine, Atlanta, GA,[5]Center for Health Disparities and Molecular Medicine, Loma Linda University School of Medicine, Loma Linda, CA*

The cysteine-rich angiogenic inducer 61 (CYR61) is a member of the cellular communication network (CCN) protein family that can be induced

by growth factors. CYR61-specific functions are dependent on cellular context. In prostate cancer (PCa), CYR61 contributes to cell growth and survival through its interactions with extracellular ligands, such as integrins avb3 and a6b4, in the extracellular matrix space. Interestingly, CYR61 contains an insulin-like growth factor-binding protein domain suggesting that it may interact with insulin-like growth factor-I (IGF-1). High serum levels of IGF-1 are directly linked to PCa development and recently have been studied as a predictor of metastatic disease. Given the important roles that IGF-1 and CYR61 play in PCa and their potential interaction, it is critical to investigate their molecular interplay. This study is designated to specifically determine and characterize the molecular interaction between CYR61 and IGF-1 in metastatic PCa and to determine if this interaction contributes to aggressive tumor properties (e.g., proliferation, tumorsphere formation). Using immunoblotting, we demonstrated that CYR61 is upregulated in the metastatic cell line PC3 and downregulated in the docetaxel-resistant cell line PC3-DR. Furthermore, optimized knockdown of CYR61 using siRNA significantly reduced PC3 cell proliferation, viability, and prostasphere formation. To examine the underlying mechanisms associated with IGF-1 signaling, we assessed the activation of either the PI3/Akt and MAPK pathways in PC3 cells with CYR61 silencing. CYR61 siRNA-mediated knockdown decreased activation of the PI3/Akt pathway but did not affect the MAPK pathway. We also initiated studies to determine the co-localization of CYR61 and IGF-1 using immunofluorescence microscopy (IF). Based on the initial IF observations, we will proceed to examine if their interaction is primarily intra- or extra-cellular. For intracellular interactions, we will co-immunoprecipitate CYR61 with IGF-1 and for extracellular interactions, we will use the AVidity-based EXtracellular Interaction Screen (AVEXIS) system. Our goal is to establish the contribution of CYR61-IGF1 protein-protein interaction to PCa cell proliferation. Specifically, the correlation between PCa aggressiveness and circulating levels of CYR61 and IGF-1 is poorly studied. Their combined role may explain a proportion of aggressive PCa.

#3950

Sensitizing oncogenic mutant p53-expressing non-small cell lung cancer to proteasome inhibitors

Kranthi Kumar Chougoni[1], Victoria L. Neely[2], Boxiao Ding[1], Eziafa Oduah[2], Khanh Nguyen[2], Bin Hu[2], Jennifer Koblinski[2], Bradford Windle[2], Hisashi Harada[2], Steven Grossman[1]. *[1]University of Southern California, Los Angeles, CA,[2]Virginia Commonwealth University, Richmond, VA*

Background: Lung cancer is the leading cause of cancer deaths worldwide, with non-small cell lung cancer (NSCLC) accounting for ~80% of all lung cancers. Up to 69% of NSCLC are mutated for the tumor suppressor gene *TP53,* and of these, 84% are missense mutations, where wild-type (WT) *TP53* tumor suppressor function is lost and in most cases, emergent cancer-promoting oncogenic activities are acquired. Due to the poor draggability of mutated p53 protein, the focus of therapeutics targeting NSCLC tumors with oncogenic missense mutant p53 has been on vulnerabilities that are not present in normal cells expressing WT p53. One such vulnerability involves oncogenic mutant p53-dependent attenuation of the oxidative stress response. The ability of cancer cells to survive oxidative stress depends on the regulated synthesis and activity of cellular antioxidants, including glutathione (GSH). Proteasome inhibitors (PIs) are known to induce cellular stress at multiple levels, including proteotoxic, autophagic, and oxidative stress, but the clinical utility of PIs has been limited by lack of efficacy in patients with solid tumors, including unselected lung cancer patients. Methods and Results: We now show bortezomib (BTZ) and other PIs are preferentially cytotoxic in oncogenic mutant p53-expressing lung cancer cells in culture. Furthermore, BTZ-treated oncogenic mutant p53-expressing cells display elevated levels of reactive oxygen species and BTZ's cytotoxic effects were rescued by antioxidants such as N-acetyl cysteine, indicating that oxidative stress is the critical driver of BTZ cytotoxicity. Upon BTZ treatment of oncogenic mutant p53-expressing NSCLC cells, but not in WT p53 expressing NSCLC cells, we also observed the transcriptional induction of pro-apoptotic BH3-only BCL-2 family protein NOXA, consistent with an apoptotic mechanism of BTZ-induced cell death. Furthermore, in combination with BTZ, the use of BH3-mimetics such as venetoclax (ABT-199) or navitoclax (ABT-263) to inhibit the function of pro-survival proteins BCL-2/BCL-X_L synergistically enhanced BTZ cytotoxicity, but only in oncogenic mutant p53-expressing NSCLC cells. *In vivo* mouse xenograft studies demonstrated that combination treatments of BTZ + venetoclax or BTZ + carboplatin (a

standard of care chemotherapy for NSCLC) significantly attenuated oncogenic mutant p53-expressing tumor growth.
Conclusions: Our data suggest that the preferential cytotoxicity of BTZ, and potentially other PIs, in oncogenic mutant p53-expressing NSCLC cells depends on the induction of toxic oxidative stress leading to NOXA-dependent apoptosis. Thus, combining PIs with drugs that limit antioxidant responses and/or sensitize cells to NOXA-induced apoptosis (e.g., BH3-mimetics) should synergistically and selectively kill NSCLC cells expressing oncogenic mutant p53 and open novel therapeutic avenues for the treatment of NSCLC.

#3951

Unprecedented forward genetic screens reveal mechanisms of action, drug resistances, and hidden efficacies at amino acid resolution: combination of 5-ALA and Artesunate as a treatment option for glioblastoma multiforme

Michael Orthofer[1], Jasmin Taubenschmid-Stowers[2], Marianna Rozsova[1], Anna Laemmerer[3], Daniela Loetsch[3], Johannes Gojo[3], Andreas Peyrl[3], Walter Berger[3], Ullrich Elling[4], Moritz Horn[1], Josef M. Penninger[5]. *[1]JLP Health GmbH, Vienna, Austria,[2]Altos Labs Cambridge Institute, Cambridge, United Kingdom,[3]Medical University Vienna, Vienna, Austria,[4]Institute of Molecular Biotechnology, Vienna, Austria,[5]Life Sciences Institute, UBC, Vancouver, BC, Canada*

Forward genetic screens have revolutionized the field of target discovery, target deconvolution, and target validation, particularly in the cancer field. However, most approaches are limited to the interrogation of non-essential factors and identify gene networks rather than direct target structures. Inspired from work in the nematode *C. elegans,* we perform forward genetic screens based on chemical mutagenesis. This approach randomly introduces single nucleotide variants into the entire genome resulting in cell populations which carry substitutions in statistically more than 90% of all amino acids. Challenging such mutagenized cell populations with a drug candidate of interest, followed by next generation sequencing and analysis, reveals drug resistance mechanism, direct drug target interactions, and potential concealed efficacies. The alteration of single amino acids thereby allows interrogation of non-essential as well as most essential factors and

increases screening resolution to the amino acid level. From such screens we inferred and tested a novel treatment option for glioblastoma multiforme. The natural compound Artemisinin and its derivative Artesunate are widely used anti-malarial drugs. Based on theircytotoxic activity, they are also tested as anti-cancer therapies, while the definite mechanism of action and critical host cell targets have remained largely elusive. Using forward genetic screening approaches, we demonstrate that porphyrin biosynthesis governs Artemisinin's cytotoxicity. Genetic or pharmacological modulation of porphyrin production is sufficient to alter Artemisinin cytotoxicity in multiple eukaryotic cells, including human cancer cells. Combining Artesunate with 5-ALA treatment we translated the screening results to clinically relevant model systems of brain tumor development, such as glioblastomas in engineered cerebral organoids, patient-derived brain tumor spheroids, and orthotopic xenograft models. 5-ALA is a clinically approved photodynamic porphyrin enhancer and surgical fluorescence marker, which specifically marks tumorigenic brain areas. With this additional level of selectivity, we demonstrate a strong antineoplastic effect of the 5-ALA-Artesunatecombination in all tested model systems. These findings extend to the triple combination with temozolomide and urgently await further testing in clinical setups.

#3952

Preclinical anti-tumor effects of MDM4/MDMX inhibitor XI-006 in breast cancer and prostate cancer cell lines mediated through reduced tumor cell migration

Arielle De La Cruz[1], Andrew George[1], Payton De La Cruz[1], Maximilian P. Pinho-Schwermann[1], Kimberly S. Meza[1], Taylor Arnoff[1], Ilyas Sahin[2], Stephanie L. Graff[1], Benedito A. Carneiro[1], Wafik S. El-Deiry[1]. *[1]Brown University, Providence, RI,[2]University of Florida, Gainesville, FL*

MDM2 and MDM4/MDMX have emerged as potential mediators of tumor progression, organ-specific metastasis, and hyper-progression after immune checkpoint blockade therapy. While there are currently a number of MDM2 inhibitors in clinical trials, we found no pure MDM4/MDMX inhibitors under clinical investigation. Because hormone-resistant cancers pose a significant challenge for clinical intervention, the identification of translatable novel therapeutic targets remains an important goal. Analysis of

triple-negative breast cancer (TNBC) and castration-resistant prostate cancer (CRPC) reveals overexpression of p53 negative regulator MDM4/MDMX as a frequent alteration in these cancers. There is an urgent need to study and target MDM4/MDMX in cancer therapy and this may ultimately include dual MDM2 and MDM4/MDMX inhibitors. However, it is clear that MDM4/MDMX is a primary oncogenic driver that requires specific therapeutic targeting. As metastasis is often observed clinically in patients diagnosed with breast and prostate cancer, we sought to expand our understanding of the metastasis reduction potential of a previously described preclinical MDM4/MDMX inhibitor, a 4-nitrobenzofuroxan derivative, XI-006 (NSC207895). In a scratch assay using breast and prostate cancer cell lines, increasing doses of XI-006 decreased tumor cell migration in a time and dose-dependent manner, demonstrating the benefit of MDMX inhibition in preventing the induction of tumor cell migration. The exact mechanism of this result remains unclear, and further investigation is needed to elucidate the impact of XI-006 on TNBC and CRPC cell proliferation and migration. Our future directions include identifying the synergistic potential of combining MDM4/MDMX inhibitor XI-006 with other cancer therapies, assessing the impact of XI-006 on immune responses in co-culture studies, and testing therapeutic efficacy *in vivo*.

#3954

Evaluation of long mononucleotide repeat markers for detection of microsatellite instability

Suping Chen[1], John H. Lin[1], Aparna Pallavajjala[1], Tamara L. Lotan[1], Jeffery W. Bacher[2], James R. Eshleman[1]. *[1]Johns Hopkins University School of Medicine, Baltimore, MD,[2]Promega Corporation, Madison, WI*

Microsatellite instability (MSI) and mismatch repair immunohistochemistry are biomarkers of defective MMR (dMMR) that predict response to immune checkpoint inhibitor therapy in solid tumors. The microsatellites in the Promega MSI Analysis System Version 1.2 may not be ideal to detect MSI in certain cancer types. Long mononucleotide repeat (LMR) markers may improve detection of microsatellite instability in early colorectal lesions and non-colorectal cancers.In this study, we compared the performance of the current gold standard, MSI Analysis System Version 1.2

(Promega), which consists of 5 mononucleotide repeat markers (21-27 bases), with a new LMR kit (Promega), which consists of 4 markers from the MSI V1.2 panel and 4 LMR loci (52-60 bases). We studied five cohorts including 24 MMR proficient (pMMR) and 24 dMMR colorectal cancer (CRC) samples, 24 pMMR and 42 dMMR endometrial cancer (EC) samples, 12 dMMR prostate cancer (PC) samples, 22 MSI-high (MSI-H) samples of other cancer types, and 12 MSI-low (MSI-L) samples, where MMR status was confirmed by immunohistochemical (IHC) staining and/or MSI Analysis System Version 1.2.The specificity and sensitivity of the LMR MSI panel for dMMR detection were both 100% in CRC. The specificity of the MSI V1.2 and LMR MSI panels in EC was both 100%, and the sensitivity was 88% versus 98%, respectively. The 22 MSI-high (MSI-H) samples of other cancer types, these include cholangiocarcinoma, appendix, duodenal, pancreatic and gastric cancer, which were previously classified as MSI-H by using the MSI V1.2 panel were also classified as MSI-H by using the LMR MSI panel. Among 12 samples that were previously classified as MSI-L by the MSI V1.2 panel, 9 of the samples were classified as MSI-L, and 3 of the samples were diagnosed as MSI-H using the MSI LMR panel. The LMR panel has performed well on 80 samples over the past 6 months.The LMR MSI panel is highly concordant with the MSI V1.2 panel for dMMR detection in colorectal cancer and showed increased sensitivity in endometrial cancer. The LMR MSI panel showed improved dMMR detection in non-colorectal cancers.

#3955

Functional evaluation of pancreatic cancer prognostic marker, LXN, utilizing multiomics analysis based on patient-derived cancer model

Chan Hee Park, Hee Seung Lee, Jin Su Kim, Yoo Keung Tae, Jin Young Lee, Seungmin Bang. *Yonsei University College of Medicine, Seoul, Korea, Republic of*

Background: Pancreatic cancer is the most dreadful malignant tumor and expected becoming the second cause of death in 2030. Despites of vigorous studies, there were no definitive prognostic biomoleculars marker for pancreatic cancer. Herein, we already established primary pancreatic cancer cell lines from the real patients of pancreatic cancer, using conditionally reprogrammed cell culture (CRC). We tried to find novel prognostic

biomarkers with multi-omics analysis of our primary pancreatic cancer cell lines.
Methods: In this study, we selected pancreatic cancer prognostic markers using established CRCs and FFPE samples and validated the molecular mechanism of LXN. As the first step, we performed both transcriptome and proteome analysis using RNA sequencing and liquid chromatography-tandem mass spectrometry (LC/MS-MS) with 6 primary pancreatic cancer cell lines established by CRC. After analysis, we mined several candidate markers of prognosis including latexin (LXN) and sialic acid acetylesterease (SIAE). And we validated these markers clinicopathologically using immunohistochemical (IHC) staining of 136 tissues from a different set of pancreatic cancer patients. And we confirmed the knock-down effect of LXN using siLXN in pancreatic cancer cells.
Results: We selected 2 highly prognostic markers with LXN and SIAE after transcriptome and proteome analysis. In these genes, high LXN expression group showed longer median overall survival (OS) than low expression group, respectively (14.8 vs. 10.4 months, *P*-value=0.28), respectively. For the evaluation of IHC, we established 3D organoid model using CRCs and confirmed the correlation between mRNA expression and protein expression with western blotting and IHC. The expression of Akt/mTOR was decreased after siLXN treatment compared to control groups. In order to validation as a prognostic marker, we stained formalin-fixed, paraffin-embedded (FFPE) slide from 136 pancreatic cancer patients. After IHC analysis, LXN high group (H-score > 12) showed significantly longer OS than low LXN group (52 vs. 28 months, *P*-value = 0.043).
Conclusion: In this study, we found LXN as a prognostic marker with inhibition of proliferation utilizing patient-derived cancer model and FFPE samples.

#3956
Identifying PIKfyve as potential target in clear cell renal cell carcinoma with a loss of the von Hippel-Lindau tumor suppressor gene
Nadia Bouhamdani, Sandra Turcotte. *Université de Moncton, Moncton, NB, Canada*

Background**.** Clear cell renal cell carcinoma (ccRCC) is the most frequent type of cancer in the kidney. These tumors are highly vascular and correlate

with poor prognosis. Biallelic inactivation of the von Hippel-Lindau (VHL) tumor suppressor gene is a truncal event of ccRCC carcinogenesis, which yields new insights for targeted therapy. Our studies identified a small molecule, STF-62247, that is toxic to cells lacking VHL compared to RCC with a functional gene. We reported that STF-62247 blocks late stages of autophagy by targeting lysosome dynamics. Moreover, we identified lysosomal vulnerability in VHL-mutated ccRCCs, which could lead cells to death.
Goal. This study aims to recognize and characterize STF-62247 potential targets.
Results. Using biochemical approaches, our results indicated that STF-62247 cytotoxicity is driven by PIKfyve inhibition. Binding affinity between PIKfyve and STF-62247 is around 5 nM. Intracytoplasmic vacuoles and enlargement of endolysosomes were observed, which was prevented by adding exogenous $PI(3,5)P_2$. Moreover, PIKfyve inhibitors such as apilimod, YM201636, Vacuolin-1, APY0201 sensitize ccRCC with a loss of VHL. Finally, genetic knockdown of PIKfyve was achieved by CRISPR/Cas9 leading VHL-inactivated cells to death.
Conclusion. Altogether, our studies identified, for the first time, PIKfyve as potential target for kidney cancer cells with a loss of VHL.

#3957
Anticancer effect of novel 1,4-benzodiazepine derivatives through tubulin polymerization inhibition
Alzbeta Srovnalova[1], Jiri Rehulka[1], Sona Gurska[1], Pavel Polyshchuk[1], Sergey Bachinsky[2], Petr Dzubak[1], Marian Hajduch[1]. *[1]Palacky Univ. Faculty of Medicine, Olomouc, Czech Republic,[2]A.V. Bogatsky Physico-Chemical Institute of NAS of Ukraine, Odessa, Ukraine*

Benzodiazepines are well known as a key scaffold in medicinal chemistry, providing bioactive compounds for a wide variety of biological targets. Among their primary use as anxiolytics and sedatives, the 1,4-benzodiazepine derivatives and their metabolites play a role as antitumor, antithrombotic, antiviral and antimalarial agents. Recent studies revealed the influence of the benzodiazepine derivatives on microtubule assembly or stability with subsequent mitotic failure. These microtubule-targeting effects were evaluated in novel benzodiazepine derivatives. The

antiproliferative activities of novel derivatives were tested against a panel of 10 cancer cell lines and 2 non-cancer cell lines. The compounds with IC50<10 μM were further analyzed for the cell cycle. Flow cytometry and fluorescent cell cycle indicator (FUCCI) assays were performed to evaluate the effects of derivatives on the cell cycle phases. The immunofluorescence alpha-tubulin assay and tubulin polymerization assay were accomplished to detect the changes in the mitosis. Implementation of molecular docking revealed the specific binding site of the derivatives. All tested derivatives reveal the G2/M block in the cell cycle and 3 of them were identified as M-phase blockers. The immunofluorescence alpha-tubulin assay detected the disruption of the cellular microtubule network, and the tubulin polymerization assay uncovered the potential of the tested compounds to inhibit tubulin polymerization. Molecular docking confirms that benzodiazepine derivatives fit the colchicine site best and are partially overlaid with the native colchicine binding pose. This suggests that these compounds may adapt to the tubulin binding site in a conformation induced by colchicine The inhibition of tubulin polymerization by novel derivatives is one of their possible mechanisms of action on antiproliferative effect on cancer cell lines. More rigorous studies will be performed further to establish pose stability and explain structure-activity relationships. This work was supported by European Union - Programme EXCELES, ID Project No. LX22NPO5102, the Czech Ministry of Education, Youth and Sports (CZ-OPENSCREEN - LM2018130, EATRIS-CZ - LM2018133), and by the internal grant of Palacky University Olomouc (IGA_LF_2022_033) and European Regional Development Fund - Project ENOCH (No. CZ.02.1.01/0.0/0.0/16_019/0000868).

#3958

Transcriptome analysis of Small Cell Osteosarcoma reveals an embryonic stem cell-like phenotype

Maria Antonella Laginestra[1], Alessandro Parra[1], Elisa Simonetti[1], Laura Formentini[1], Michela Pasello[1], Alberto Righi[2], Davide Maria Donati[3], Cristina Ferrari[1], Laura Pazzaglia[1], Katia Scotlandi[1]. *[1]Experimental Oncology Laboratory, IRCCS Istituto Ortopedico Rizzoli, Bologna, Italy,[2]Department of Pathology, IRCCS Istituto Ortopedico Rizzoli, Bologna, Italy,[3]Third Orthopaedic Clinic and Traumatology, IRCCS Istituto Ortopedico Rizzoli, Bologna, Italy*

Introducti**on:** Small round cell osteosarcoma (SCOS) is a very rare type of osteosarcoma, composed by small cells producing bone matrix, with limited studies that mainly focus on histological features. In this study we employed RNA sequencing to discover the transcriptional profile of SCOS in order to find a specific gene signatures useful to find new potential therapeutic targets. To date, the tumor is treated according to the osteosarcoma protocols.

Material and Methods: We studied 15 primary tumor including 6 SCOS and 9 high grade Osteosarcoma (OS) by RNASeq . Pair-end libraries were synthesized using TruSeq RNA Library Prep Kit for Enrichment and loaded on NextSeq 500 platform (Illumina). After FastqQC quality control, fastq data were aligned to Homo_sapiens GRCh38 with STAR algorithm and counted by featureCounts. In Addition we randomly selected 30 muscle-skeletal normal tissues from 800 available samples from Genotype-Tissue Expression repository (GTEX). Using surrogate variables to remove batch effects and other unwanted variations, we performed differentially expression analysis employing DESeq2 (R package). We considered as differentially expressed genes those BH adj p-value <0.01 and absolute $|\log_2 FC|=2$. We then performed preranked Gene set Enrichment analysis (GSEA) for biological function assessment

Results: To elucidate the transcriptome landscape of SCOS we first performed differential gene expression analysis between SCOS and normal tissue identifying 5061 deregulated genes (2516 up-regulated and 2545 down-regulated in SCOS). Then, from this signature we filtered out the signature differentially expressed between OS and normal tissue, obtaining a specific SCOS signature of 1371 genes (1013 up-regulated and 358 down-regulated). To study the biological function behind SCOS we performed GSEA and we found that SCOS gene signature resulted enriched in epigenetics mechanisms as well as in embryonic stem cell (ES) gene sets. In particular, we found the overexpression of *EZH2, ASXL1, HDAC9, MYCN, MYB* genes involved in Polycomb group complex. This on one side confirms the highly undifferentiated nature of this tumor that could explain the more aggressive behaviour of SCOS in comparison to OS; on the other side, offers in epigenetic drugs a new therapeutic perspective. Validation studies are in progress.

Conclusions: This work firstly profiled the transcriptome of SCOS and identifies new pathways that can be of interest for diagnostic and/or therapeutic purposes.
This work was supported by Ministry of Health 5x1000, Anno 2020 Redditi 2019, contributions to the IRCCS, Istituto Ortopedico Rizzoli.

#3959
Novel spliced isoform of the proteasome subunit ADRM1/Rpn13 promotes hepatocellular carcinoma (HCC) development through selective degradation of tumor suppressor p53
Yanmei Sun, Mingjing Xu, Ho Lee Wan, Alissa M. Wong, Kelvin K. C. Ng, Nathalie Wong. *Faculty of Medicine, Department of Surgery, Sir Y.K. Pao Centre for Cancer, Prince of Wales Hospital, The Chinese University of Hong Kong, Shatin, NT, Hong Kong*

The Ubiquitin-Proteasome System (UPS) is the major pathway in eukaryotic cells that regulates intracellular protein degradation and turnover. Cumulative evidence has suggested that defects in the UPS machinery are involved in the pathogenesis of human diseases, including cancer. The proteasome-associated polyubiquitin receptor ADRM1 (also known as Rpn13) orchestrates the process of substrate recruitment with deubiquitination in the proteasome through its N-terminal ubiquitin-binding domain and C-terminal activation of deubiquitinating enzyme. Using long-read SMRT-seq to profile the RNA splicing landscape in hepatocellular carcinoma (HCC), we previously reported on an unannotated alternative spliced variant of ADRM1 in human hepatocellular carcinoma (HCC) (*Hepatology 2019*). This novel isoform exhibits an exon 9 skipping (ADRM1-ΔEx9) that resulted in an altered C-terminus of the protein. In this study, we undertook further investigations to characterize the detailed functional effects of ADRM1-ΔEx9 in HCC biology and the underlying mechanism. Initial study by junction-specific Taqman PCR assay showed that ADRM1-ΔEx9 is more frequently upregulated in HCC tumors than the canonical full-length counterpart (ADRM1-FL). There is an interchange between the two isoforms as tumor develops which underscores an isoform-switch in favor of HCC development. Indeed, our result showed that ADRM1-ΔEx9, but not ADRM1-FL, correlated significantly with inferior patient survival. Functionally, ADRM1-ΔEx9 knockdown profoundly

suppressed proliferation by inducing spontaneous apoptosis in HCC cell lines and patient-derived HCC organoids. The corresponding effects were less apparent from ADRM1-FL knockdown. Consistently, overexpression of ADRM1-ΔEx9 in normal human liver organoids promoted pre-malignant features alongside increased in-vitro propagation time. Ubiquitin Proteome profiling revealed that ADRM1-ΔEx9 led to a reduced expression of the pivotal tumor suppressor p53. A parallel transcriptome also substantiated that ADRM1-ΔEx9 modulated genes involved in the p53 and apoptosis pathways. Collectively, our study demonstrated that the non-canonical spliced isoform ADRM1-ΔEx9 confers growth and pro-survival advantages in HCC through mediating selective degradation of tumor suppressor p53 protein.

#3960

Therapeutic targeting of HIF-1 alpha induced CD73 expression in experimental esophageal adenocarcinoma

Md Sazzad Hassan[1], Aktar Ali[2], Saisantosh Ponna[3], Dimitri Scofield[4], Niranjan Awasthi[1], Mark Jantz[5], Urs von Holzen[1]. *[1]Department of Surgery, Indiana University School of Medicine - South Bend, South Bend, IN,[2]Warren Family Center for Drug Discovery, University of Notre Dame, South Bend, IN,[3]Department of Chemistry, University of Notre Dame, South Bend, IN,[4]Indiana University (South Bend, IN), South Bend, IN,[5]Department of Biology, University of Notre Dame, South Bend, IN*

Introduction: Esophageal adenocarcinoma (EAC) is one of the most aggressive human cancers with poor prognosis, and the overall 5-year survival rate is less than 20 percent. Prognosis for EAC remains poor even with modern combination therapies due to high resistance to chemotherapy. Therefore, new therapeutic approaches for EAC treatment improvements are urgently needed. Hypoxia or insufficient tissue oxygenation contributes to cancer aggressiveness and poor clinical prognosis. Overexpression of hypoxia-inducible factor 1-alpha (HIF-1 alpha) and immunosuppressive CD73, an ecto-5'-nucleotidase enzyme in cancer can give rise to tumor progression with drug resistance. CD73 has never been proposed as a therapeutic target in EAC and its relationship with hypoxia or HIF-1 alpha has not also been investigated in EAC. In this study, we therefore

investigated the therapeutic targeting of HIF-1 alpha and CD73 by acriflavine in experimental EAC.
Methods: Hypoxia in EAC cells were induced by 3D culture and hypoxic exposure. NanoCulture® plates and dishes were used for 3D cultures. For hypoxic exposure, cells were placed in a sealed modular incubator chamber flushed with a gas mixture containing 1% O2, 5% CO2 and 94% N2. Hypoxic status was detected by adding hypoxia probe LOX-1 and fluorescent microscopy. Nanoparticle albumin-bound paclitaxel (NPT) was used as chemotherapeutic agent, whereas acriflavine was used as hypoxia-targeting agent. In vitro cell growth was detected by WST-1 and Cell Titer-Glo (CTG) luminescent assays, in vivo tumor growth was detected by measuring subcutaneous xenografts, apoptosis was detected by cleaved caspase 3/PARP expressions and hypoxia-targeting was detected by HIF-1 alpha/CD73 expressions.
Results: We observed overexpression of both HIF-1 alpha and CD73 in 3D culture and hypoxic exposure of EAC cells. Interestingly acriflavine treatment drastically inhibited both HIF-1 alpha and CD73 expression in EAC 3D culture and hypoxic exposure. 3D culture was more resistant to antiproliferative effect of chemotherapeutic agent NPT over 2D monolayer culture. Contrary to that, hypoxia-targeting agent acriflavine showed stronger antiproliferative effects in 3D culture than in 2D culture. We also observed hypoxia inside the 3D culture spheroids. In addition, acriflavine showed significant in vivo antitumor efficacy both as monotherapy and in combination with NPT. In subcutaneous xenografts using OE19 EAC cells, acriflavine monotherapy exhibited a significant decrease in relative tumor volume to 55.02% compared to control ($p=0.04$) and addition of NPT with acriflavine also showed a significant enhancement effect of tumor regression as tumor size decreased to 32.70% compared to control ($p=0.002$).
Conclusion: These results support the potential of acriflavine as HIF-1 alpha and CD73 targeting and its combination with chemotherapy NPT as an effective option for EAC therapy.

#3961

Identification of lncRNAs as potential novel therapeutic targets in triple negative breast cancer

Megan O'Malley[1], Zohaib Rana[2], Debina Sarkar[1], Jolyn Chia[1], Sarah Diermeier[1]. *[1]Department of Biochemistry, University of Otago, Dunedin, New Zealand,[2]University of Otago, Dunedin, New Zealand*

Triple negative breast cancer (TNBC) lacks targeted therapies. Recently, our laboratory and other groups described long non-coding RNAs (lncRNAs) as new drivers of TNBC progression, which represent an exciting new avenue for targeted treatments. LncRNAs are the most versatile and diverse class of non-coding RNAs with roles in the progression of TNBC development, including cell proliferation, differentiation, apoptosis, metastasis and drug resistance. LncRNAs have greater tissue-specific expression compared to proteins and can be targeted using nucleotide sequence-specific RNA therapeutics, leading to reduced systemic toxicities when used as a cancer target. Using a combined approach of computational analysis of patient data and CRISPR functional screening, we identified hundreds of lncRNAs as novel drivers of TNBC. We prioritized one lncRNA target (*lncTNBC3*) with high translational potential. *LncTNBC3* knockdown lead to reduced TNBC cell proliferation in two different loss-of-function models. To gain initial insights into the mechanism via which *lncTNBC3* functions, RNA sequencing was carried out on knockdown cells, revealing that *lncTNBC3* impacts cell cycle and DNA repair pathways. Cell cycle analysis confirmed an increase in G2/M cell cycle arrest upon *lncTNBC3* knockdown. In conclusion, we have identified a promising novel lncRNA target with a role in TNBC growth.

#3962

Development of selection-free HER4-mutated CRISPR/Cas9 knock-ins in cutaneous melanoma cell lines

Marta Valenti[1], Yonglun Luo[2], Neil T. Conlon[1], Lisa D. Eli[3], Alvin Wong[3], John Crown[4], Denis M. Collins[1]. *[1]National Institute of Cellular Biotechnology, Dublin City University, Dublin, Ireland,[2]Department of Biomedicine, Aarhus University, Aarhus, Denmark,[3]Puma Biotechnology, Los Angeles, CA,[4]St. Vincent's University Hospital, Dublin, Ireland*

Background: Cutaneous melanoma showed the highest HER4 genomic alteration frequency (17.34%) across 33 different cancer types (cBioPortal). HER4 is a tyrosine kinase receptor belonging to the human epidermal growth factor receptor (HER/ErbB) family. The role of HER4 in cancer has not been fully studied, potentially due to its complex biology (four isoforms, different stability/tissue-specific expression patterns, and oncogenic/tumor suppressor roles). Using computational analysis, we identified two potentially oncogenic HER4 mutations in melanoma (HER4 R106C and R711C). We then developed CRISPR/Cas9-modified selection-free melanoma cell lines for interrogating the role of these mutations as biomarkers of response to the oral, irreversible pan-HER (EGFR, HER2, HER4) tyrosine kinase inhibitor (TKI) neratinib (NER).
Methods: Two melanoma cell lines (WM115, SKMEL24) were genome-edited by using a selection-free CRISPR/Cas9 approach. Single guide RNAs (sgRNAs) were designed by using the CRISPRon (v1.0) web tool, and Homology Directed Repair (HDR) single-stranded OligoDeoxyriboNucleotides (ssODNs), containing the HER4 mutations, were designed with the SnapGene Software (v6.1.1). The RNP complex (Cas9 and sgRNAs) and the HDR_ssODNs, for each HER4 mutation, were delivered into the melanoma cells through electroporation. Upon validation of the CRISPR/Cas9-efficiency via PCR and Sanger Sequencing, the CRISPR/Cas9-modified cells were single-cell sorted via FACS, by using two singlets gating (FSC-A/FSC-H and SSC-A/SSC-H) and a live/dead (propidium iodide) gating, to perform single-cell cloning. Colonies were then amplified and screened via PCR and Sanger sequencing to isolate pure selection-free HER4 CRISPR/Cas9 knock-ins clones of melanoma cells.
Results: The WM115 and SKMEL24 melanoma cell lines were found to be wild-type for the HER4 receptor in the Depmap Portal (mutation 22Q2, 2022 data release 2). R106C and R711C CRISPR/Cas9 knock-ins were created in the melanoma cell lines three days after the electroporation of the CRISPR/Cas9 complex. The efficiency of the HER4 R106C CRISPR/Cas9 knock-in was 22% and 7% in the SKMEL24 and WM115 melanoma cells, respectively, with a respective total indel percentage of 76% (SKMEL24) and 55% (WM115). The HER4 R711C CRISPR/Cas9 knock-in efficiency was 15% in the SKMEL24 (with 26% total indels) and 1% in the WM115 (with 33% total indels). Single-cell colonies of the HER4 CRISPR/Cas9-

mediated knock-ins (HER4 R106C and R711C), were formed at four days (SKMEL24) and at one week (WM115) after single-cell sorting.
Conclusions: CRISPR/Cas9 technology can be utilised to introduce single-point mutations in HER4 to melanoma cell lines. *In vitro* functional characterisation of the isolated HER4 CRISPR/Cas9-edited melanoma cell lines will be performed in order to understand the activating potential of HER4 R106C and R711C and their sensitivity to NER.

#3963

Mass spectrometry reveals a downregulation of calreticulin after neoadjuvant chemotherapy in pancreatic cancer

Michael C. Stoffel, Elisabeth BH Dingendorf, Dahlia L. Kittel, Glen Kristiansen, Tristan Lerbs. *Institute of Pathology, University of Bonn, Bonn, Germany*

Introduction: Pancreatic ductal adenocarcinomas are one of the deadliest cancer types with limited response to current therapies. Thus, this study examined changes in the proteome of epithelial cells in pancreatic cancer after neoadjuvant chemotherapy with gemcitabine, to identify new therapeutic targets.
Methods: Upon receiving patient consent, fresh pancreatic cancer tissue was received from surgical tumor resections at the University Hospital of Bonn. We mechanically and enzymatically digested and purified the tissue to create single-cell suspensions. After staining the cells against CD45 und CD326, we purified epithelial cells, blood cells, and stroma through FACS. To analyze their proteome, the sorted cells were lysed in TEAB buffer and the protein lysates were measured by the mass spectrometry core facility at the University of Bonn. We then analyzed the data using DAVID and Shiny GO.
Results: Gene enrichment analyses showed a significantly reduced expression of calreticulin after neoadjuvant chemotherapy in epithelial cells. A direct comparison between untreated and treated epithelium cancer cells using a heat map showed a decreased expression of actin and enzymes of glycolysis in treated cancer cells. Moreover, untreated epithelial cells showed an increase of proteins related to MHC class Ib protein complex assembly and antigen processing and presentation of endogenous peptide antigen via MHC class. In contrast, treated cells showed a higher presence

of proteins for nutrient supply from the blood. Furthermore, untreated stroma cells exhibited an increased number of proteins responsible for mesenchymal migration and for actin filament fragmentation.
Conclusion: This study shows that neoadjuvant chemotherapy with gemcitabine leads to distinct changes in the proteome of tumor cells in pancreatic cancers. In particular, a decreased expression of the “eat-me-signal” calreticulin impairs macrophage-mediated cancer cell phagocytosis, thereby indicating a mechanism by which cancer cells protect themselves after chemotherapy.

#3964

APE1 protects SMAD3 against ROC1 ubiquitin mediated degradation in esophageal adenocarcinoma cells

Farah Ballout, Heng Lu, Dunfa Peng, Wael El-Rifai. *University of Miami Miller School of Medicine, Miami, FL*

Background: The incidence of esophageal adenocarcinoma (EAC) has increased more than six-fold over the past three decades and continues to rise in the Western world. The 5-year survival rate for EAC patients is less than 20% which underscores the need to better understand the underlying mechanisms to identify new therapeutic approaches. This study aimed at investigating the potential role of APE1 in regulating SMAD3 and promoting EAC progression.
Methods and Results: Western blot data showed that APE1 and SMAD3 were highly expressed in EAC cell lines. APE1 silencing reduced SMAD3 nuclear expression and downregulated its downstream targets SERPINE1 and c-myc. These results were confirmed by immunofluorescence staining showing loss of nuclear accumulation of SMAD3 after APE1 knockdown. Mechanistically, immunoprecipitation and proximity ligation assays revealed a direct binding between APE1 and SMAD3 in the nucleus. Further investigation showed that APE1 binds to the C-terminal MH2 domain of SMAD3, and this binding protects SMAD3 from ubiquitin mediated proteasomal degradation by blocking its interaction with the RING finger protein, ROC1. Interestingly, APE1-redox-specific inhibition (APX2009) downregulated SMAD3 expression and the APE1 redox-deficient mutant (C65A) disrupted APE1-SMAD3 binding indicating that this regulation depends on APE1 redox activity.

Conclusion: Our findings establish a role of APE1 in regulating SMAD3 in EAC. These findings provide a potential therapeutic approach for the treatment of EAC by the pharmacological inhibition of APE1.

#3965

KIFC1 is a therapeutic target in lung cancers with extra centrosomes

Christopher Z. Zhang[1], Benson Z. Wu[1], Yin Fang Wu[1], Caterina di Ciano-Oliveira[1], Ju-Yoon Yoon[1], Tak W. Mak[2], David W. Cescon[2], Kelsie L. Thu[1]. *[1]Keenan Research Centre, St. Michael's Hospital, Toronto, ON, Canada,[2]University Health Network, Toronto, ON, Canada*

Introducti**on:** Lung cancer is a deadly malignancy and new treatments targeting mechanisms promoting its growth and progression are needed. Genomic instability (GIN) is a recurrent feature of lung tumours that promotes drug resistance and other cancer hallmarks. One mechanism that enables tumour-promoting GIN is centrosome amplification (CA). Centrosomes are organelles involved in chromosome segregation during cell division and two centrosomes in a bipolar arrangement normally ensure equal division of the genome during mitosis. CA, an abnormal increase in centrosome number, is frequently observed in lung and other cancers despite the fact that it can cause lethal multipolar mitotic spindles that potentiate aneuploidy. To mitigate detrimental consequences of CA, cancer cells can cluster extra centrosomes into pseudo-bipolar mitotic spindles. This process is facilitated by a protein called KIFC1 which is upregulated in a large proportion of lung cancers. However, KIFC1's potential as a therapeutic target in lung cancers with CA has not been explored. Here we investigate the hypothesis that lung cancers with CA are dependent on KIFC1 and sensitive to its inhibition.

Methods: Western blotting for KIFC1 and immunofluorescence (IF) for the centrosomal protein, CEP192, were used to measure basal expression and CA, respectively, across a panel of 21 lung adenocarcinoma (LUAD) and 3 non-malignant (NM) cell lines. KIFC1 loss-of-function (LOF) in H1299 and PC9 (LUAD), and BEAS-2B (NM) was achieved using CRISPR/Cas9 and siRNA. *In vitro* competition assays were done to assess the relative fitness of mCherry-tagged wild-type and GFP-tagged KIFC1-LOF cells in mixed populations over 3-4 cell passages using flow cytometry. CA was potentiated in cells using low doses of the compound, CFI-400945.

Clonogenic survival and IF experiments were also done to determine the consequences of KIFC1 LOF.
Results: Our findings suggests that basal KIFC1 expression and CA across 21 LUAD cell lines and 3 NM controls are variable. However, we observed a positive correlation ($R^2 = 0.52$, $p = 0.01$) between KIFC1 expression and CA in LUAD lines. Competition assays revealed that KIFC1 LOF sensitizes LUAD cells with high KIFC1 expression, but not LUAD with low KIFC1 expression or NM cells, to pharmacologically-induced CA. Complementary siRNA experiments confirmed that KIFC1 LOF impairs the survival of cells with CA. Finally, we found that KIFC1 LOF was associated with an increase in multi-polar spindles.
Conclusion: These findings support our hypothesis that LUAD with CA are dependent on KIFC1. We suspect its role in centrosome clustering explains this phenotype. Ongoing work is focused on validating these observations in additional models and clinical tumours to confirm its therapeutic potential in LUAD with CA, since combining KIFC1 inhibition with standard of care therapies that induce CA (eg. cisplatin, radiation) could represent an effective therapeutic strategy.

#3966

Targeting S100A10, a SOX9 binding protein, for the treatment of triple negative breast cancer

Yanxia Ma[1], Jing Qian[1], Cassandra Moyer[1], Amanda Lanier[2], Jamal Hill[1], Darian Coleman[1], David H. Hawke[3], Abhijit Mazumdar[1], Powel H. Brown[4]. *[1]Department of Clinical Cancer Prevention, UT MD Anderson Cancer Center, Houston, TX,[2]University of Texas Health Science Center Medical School, Houston, TX,[3]Department of Systems Biology, UT MD Anderson Cancer Center, Houston, TX,[4]Department of Clinical Cancer Prevention, Department of Breast Medical Oncology, UT MD Anderson Cancer Center, Houston, TX*

Background: Triple-negative breast cancers (TNBCs) are the most aggressive breast cancers and have a very poor prognosis. Since TNBCs lack the expression of the estrogen receptor (ER), human epidermal growth factor receptor 2 (HER2), and progesterone receptor (PR), development of new TNBC treatment strategies is an urgent clinical need. Our previous

studies have demonstrated that high expression and activity of SOX9 transcription factor positively related to TNBC cell growth and tumor metastasis *in vivo*. It may be possible to target the SOX9 transcription factor by targeting upstream SOX9-activating proteins.
Hypothesis: SOX9-binding protein, S100A10, regulates SOX9 activity and control TNBC growth.
Material and Methods: Immunoprecipitation (IP) in combination with mass spectrometry (IP-MS) analysis was used to identify SOX9 binding proteins, with support from MD Anderson's proteomics core. The Mascot Score is a statistical score used as a measure of the reliability of identifying a specific protein by IP-MS. The data was summarized based on the Mascot Score. IP-Western Blotting analysis was used to confirm that S100A10 bound SOX9 in TNBC cells. We then treated TNBC cells with or without siRNAs of S100A10 to evaluate its effect on TNBC growth. Cell growth was measured using an automated cell counting assay. Protein and mRNA levels were examined by western blotting and qRT-PCR assays. SOX9 activity on regulating β-catenin pathway was measured using TOP/FOP luciferase activity analysis. Data are presented as mean values ± SD. Statistical significance was calculated using the Student's *t*-test unless otherwise indicated.
Results: Using immunoprecipitation combined with mass spectrometry (IP-MS), we identified multiple SOX9-binding proteins. One of the identified SOX9-binding proteins was S100A10 (S100A10). Knockdown of S100A10 decreased TNBC cell growth *in vitro*. Using TOP/FOP luciferase activity analysis, we demonstrated that S100A10 regulates the β-catenin pathway. Thus, S100A10 is a potential activator of SOX9 that can be targeted to inhibit SOX9 downstream signaling and TNBC growth.
Conclusion: Our results demonstrate that S100A10 is a SOX9-binding protein, that regulates SOX9 downstream signaling and controls TNBC cell growth.
Implications: Inhibition of S100A10 represents a novel strategy to treat TNBCs. S100A10 inhibitors should be developed as promising new drugs to treat these aggressive breast cancers.
Grant Support: These studies were supported by a Breast Cancer Research Foundation (BCRF) grant (PB). The Proteomics and Metabolomics Facility was supported in part by Cancer Prevention Research Institute of Texas

(CPRIT) grant number RP130397 and NIH grant numbers 1S10OD012304-01 and P30CA016672.

#3967

CRISPR/Cas9 screening identified novel membrane targets sensitizing hepatocellular carcinoma cells to natural killer cell-mediated cytotoxicity

Shuo Li, Lin Han, Siyao Zhang, Guangfeng Geng, Lei Huo, Dawei Huang, Zhaoren He, Shuoran Li, Zhaoshi Jiang, James X. Rong. *BioMap, Beijing, China*

Natural killer cells (NK) play a central role in cancer immune surveillance by directly killing cancer cells and producing pro-inflammatory cytokines to stimulate and recruit other immune cells to elaborate long-lasting anti-tumor responses. However, little is known about the immune escape mechanisms and regulatory proteins, particularly those for NK, involved in hepatocellular carcinoma (HCC), one of the most common and lethal cancers. To identify the determinants of NK killing function, we performed an HCC cell line-based CRISPR/Cas9 loss-of-function genetic screen, using a human whole membrane protein library containing ~7000 genes curated from 3 public membrane protein datasets. The human SNU449 was chosen as a representative HCC cell line for CRISPR/Cas9 editing based on the genetic profile analysis, representing one HCC patient subpopulation (> 30%) in the TCGA cohort. The cell line was incubated with NK92 cells at ratios of 2:1, 1:1, and 0.5:1. Bioinformatics methods for prioritizing genes (e.g., MAGeCK) were applied on 3 tested groups with different ratios. Single guide RNAs targeting genes in the antigen presentation machinery were depleted, including HLA-C, B2M, and TAP1/2, whereas components of the tumor-immune synapse, such as NCR3LG1 and ICAM1, were enriched, confirming the validity of the screen. SLC33A1 (an endosomal acetylCoA transporter) and SLC31A1 (the major copper influx transporter) were also depleted, previously unknown as NK regulators. The effects of SLC33A1 and SLC31A1 were validated in individual gene knockout cells generated respectively by lentiviral sgRNA expression. Furthermore, knockout of either transporter in SNU449 cells increased IFNγ secretion, confirming NK92 activation. Our results revealed that CRISPR/Cas9-based functional genomics screens in HCC cell lines could identify novel targets

modulating NK-mediated killing. Further analysis of mechanisms of action, and particularly functional validation in *in vivo* systems, will potentially provide novel targets for the treatment of HCC.

#3968

Conophylline-target ARL6ip1 regulates Ran-mediated cellular migration and invasion in human colorectal cancer cells

Yinzhi Lin[1], Sivasundaram Karnan[2], Hideaki Ito[3], Kazuo Umezawa[4].
[1]Department of Microbiology and Immunology, Aichi Medical Univ., Nagakute, Japan,[2]Department of Biochemistry, Aichi Medical Univ., Nagakute, Japan,[3]Department of Pathology, Aichi Medical Univ., Nagakute, Japan,[4]Department of Molecular Target Medicine, Aichi Medical Univ., Nagakute, Japan

Introduction: Conophylline is an alkaloid isolated from the leaves of *Ervatamia microphylla*. We isolated conophylline as an inhibitor of K-Ras functions. It is known to ameliorate various disease models in animals, including cancer, diabetes mellitus, NASH, and hepatic cirrhosis. On the other hand, its molecular target was determined to be ADP-ribosylation factor-like 6-interacting protein 1 (ARL6ip1) using a conophylline-biotin conjugate. ARL6ip1 is located in the endoplasmic reticulum (ER) membrane, and the conophylline-binding domain was determined by deletion mutation analysis. Known functions of ARL6ip1 include inhibition of apoptosis, inhibition of glutamate transporter, and modulation of the ER structure. However, whether ARL6ip1 is involved in the mechanisms of various biological activities of conophylline has not been proven, since knockdown of ARL6ip1 has often failed to change the cellular phenotypes. Therefore, in the present research, we knocked out ARL6ip1 in human colon carcinoma cells by CRISPR-Cas9 and studied the involvement and mechanism of ARL6ip1 in the anticancer activity of conophylline. Ran activity was measured by a pull-down assay with Ran-GTP antibody.
Materials and Methods: Conophylline was isolated from the leaves of *Ervatamia microphylla*. We employed HCT116 and DLD1 cells as human colorectal cancer cells. Tumorigenicity was measured by soft agar colony formation. Cellular migration was measured by a wound healing assay and cell tracking analysis. Cellular invasion was measured by a Matrigel chamber assay.

Results: Conophylline inhibited soft agar colony formation in HCT116 and DLD1 cells. It inhibited migration and invasion in HCT116 and DLD1 cells at nontoxic concentrations. Knockout of ARL6ip1 also decreased tumorigenicity, migration, and invasion in HCT116 and DLD1 cells. The mechanistic study was carried out with HCT116 cells. ARL6 and Ran are both G-proteins and are reported to interact with ARL6ip1. Although knockdown of ARL6 did not change the cell migratory activity, knockdown of Ran inhibited the migration. Conophylline inhibited the interaction of ARL6ip1 to Ran in the proximity ligation assay. Moreover, conophylline inhibited the Ran activity.
Conclusion: CRISPR-Cas9 knockout of ARL6ip1 showed a similar anticancer activity as treatment with conophylline. It is likely that the anticancer activity of conophylline would be mediated by the ARL6ip1-Ran system. Thus, ARL6ip1 would be a useful molecular target for the treatment of cancer.

#3969
Screening of kinase inhibitors as bioenergetic metabolism modulator using the XF Real-Time ATP Rate Assay
Yoonseok Kam, Lisa Winer, Natalia Romero. *Agilent Technologies, Inc., Lexington, MA*

Cancer cells are metabolically reprogrammed through tumor initiation and progression, and there are increasing developments in cancer therapies exploiting the potential metabolic vulnerability. A better understanding of cancer cell metabolic regulation can also contribute to modulating the harsh tumor microenvironment, which strongly affects the efficacy of emerging anti-cancer immunotherapies. As one of the critical contributors to cancer therapy design, there is increasing demand for time-efficient and reliable analytic tools when searching for drugs and genes modulating cancer cell metabolism. The XF Real-Time ATP Rate Assay measures ATP production from glycolysis and mitochondrial respiration simultaneously and provides a quantitative overview of the bioenergetic phenotype of the cells. By using ATP production rate as a universal unit of bioenergetic metabolism, this assay quickly detects metabolic modulations induced by chemical stimuli or genetic modifications. It allows the identification of potential targets for therapy design. In this study, we used the Seahorse XF Pro Analyzer

combined with the XF ATP Rate assay to screen 80 kinase inhibitors for the suppressive effects on energy metabolism and/or inducing a metabolic phenotype shift in THP-1 cells, a monocytic leukemia cell line, using PBMC as the control. We identified four mitochondrial and two glycolytic suppressors using the screening and dose-response views available in Seahorse Analytics, a cloud-based data analysis tool for Seahorse XF assays. These compounds showed moderate or no effects on the net ATP production rates but induced a significant shift in the metabolic phenotype of THP-1 cells. Among the selected kinase inhibitors, AG-879 (ErbB2 inhibitor), SU-1498 (VEGFR inhibitor), and U-0126 (MEK1/2 inhibitor) showed the most potent inhibitory effect on mitochondrial energy production in THP-1 cells. Dose-response studies indicated that SU-1498 and U-0126 have higher potency in THP-1 than PBMC, and thus they can be considered good cancer-cell targets for mitochondrial suppressors. In contrast, AG-879 showed a similar or higher inhibitory effect on PBMC even though it is the most potent mitochondrial suppressor among the selected compounds. These results demonstrate that the XF Real-Time ATP Rate Assay can be used as a primary assay for screening and validating drug candidate(s) targeting the bioenergetic metabolism of cancer cells.

#3970

NCG-hIL15 humanized mice: an ideal model for human immune reconstitution of NK cells

Xing Liu[1], Meirong Wu[1], Huiyi Wang[1], Weiwei Yu[1], Jianming Xu[1], Hongyan Sun[1], Cunxiang Ju[1], Hongyu Wang[1], Santi Suryani Chen[2], Zhiying Li[2], Mark Wade Moore[2], Jing Zhao[1], Xiang Gao[1].
[1]Gempharmatech Co., Ltd., Nanjing, China,[2]GemPharmatech LLC., La Jolla, CA

Introduction: IL-15 is a four α-helix bundle cytokine which is produced by dendritic cells, monocytes, and epithelial cells. IL-15 is necessary for the development, survival, and activation of natural killer (NK) cells. NK cells are unable to persist in immunodeficient NCG mice reconsituted with human NK cells, but after knocking in human *IL-15* (*hIL-15*), NCG-hIL15 mice can support the reconstitution and survival of human NK cells. Results: Compared with NCG mice, the level of hIL-15 was significantly increased in NCG-hIL15 mice. After transplanting human PBMC

(huPBMC) or NK (huNK) cells into NCG-hIL15 mice, the peripheral blood level of NK cells in huNK-NCG-hIL15 mice was much higher than in huPBMC-NCG-hIL15 mice. The expression of perforin in peripheral blood of huNK-NCG-hIL15 mice was significantly higher than that in huPBMC-NCG-hIL15 mice. Considering the obvious ADCC of rituximab acting on Raji cells *in vitro*, we evaluated the efficacy of rituximab in huNK-NCG-hIL15 mice subcutaneously engrafted with Raji cells. Rituximab significantly inhibited the tumor growth in huNK-NCG-hIL15 mice. Conclusion: NCG-hIL15 is a great mouse model to evaluate the anti-tumor efficacy of drugs targeting human NK cells without the interference of T cells.

#3971

Developing cancer cell based *in vitro* and *in vivo* models with CRISPR-mediated knock-in technology for anti-tumor drug discovery

Nengwei Xu, Reifeng Wang, Jian Xiang, Qingyang Gu, Xiangnan Qiang.
WuXi AppTec, Suzhou, China

Human cancer cell lines have long been applied for anti-tumor drug discovery considering their acquired genomic diversity of different carcinomas. Genetic engineering based on cancer cell lines is no doubt a useful and promising approach in induction of new therapeutic targets/elements while maintaining intrinsic characteristics of original cell in parallel. Recently, the emergence of CRISPR knock-in technology has accelerated precise editing across whole genome, from gene depletion, small fragment insertions to site-direct mutations, thereby prompting our understanding of the influence of a specific oncotarget in given tumor genetic background. Herein, by employing CRISPR/Cas9 system, two human cancer cell line-based, inheritable drug resistance models were established where the mutation site C481S of BTK in REC-1 conferred resistance to Ibrutinib and the mutation site R537S/D538G of ESR1 exerted resistance to Fulvestrant in MCF-7. In addition, the engineered cell models also enable the mechanism characterization and development of viable therapeutic agents targeting those oncogenic-driver mutations in a subtype of cancers. The murine colon cancer cell line CT26, which harbors $KRAS^{G12D}$ mutation, was genetically modified to express $KRAS^{G12C}$ protein to allow for an expandable pocket providing opportunities for

compound recruitment. The resultant $KRAS^{G12C}$ CT26 cell line showed pronounced inhibitory effect after treatment with AMG510. More interestingly, the therapeutic combination involving both AMG510 and anti-PD1 antibodies demonstrated more effective anti-tumor activities when compared to monotherapy. Moreover, CRIPSR-mediated engineered knock-in cells with a traceable tag linked to endogenous oncotarget also exhibit capability in new therapeutic modality discovery. Based on HiBiT protein tagging technology, we generated a series of HiBiT knock-in cell lines for real-time cell-based protein degradation analysis on various compelling targets, such as ESR1, KRAS, and BRD4, *et al*. Thereby, the construction of these *in vitro* and *in vivo* models with the ease of CRISPR KI technology is indispensable in new generation of therapeutic drug exploration.

#3972

Novel renal cell carcinoma therapy targeting glutaminolysis

Yoshinari Muto[1], Akihito Takeuchi[1], Kenji Zennami[2], Eiji Sugihara[3], Ryoichi Shiroki[2], Hideyuki Saya[3], Makoto Sumitomo[1]. *[1]Fujita Cancer Center and Department of Urology School of Medicine, Fujita Health University, Toyoake, Japan,[2]Department of Urology School of Medicine, Fujita Health University, Toyoake, Japan,[3]Fujita Cancer Center, Fujita Health University, Toyoake, Japan*

Objective: Metabolic reprogramming of cancer cells contributes to tumor development and provides a target for cancer therapy ASCT2 is a glutamine transporter on the plasma membrane. Glutamine is converted into the cell to glutamate by glutaminase (GLS) and utilized by the TCA cycle. This glutaminolysis has been implicated in tumor progression in various malignancies, including renal cell carcinoma. In the present study, we investigated whether the unique strategy that effectively targets glutamine addiction would be effective as a treatment for RCC.
Methods: Tumor tissue (T) and normal renal tissue (N) from surgical specimens of 66 patients with RCC were collected, and metabolomic analysis using liquid chromatography-mass spectrometry (LC/MS) to calculate the T/N ratio of Gln and Glu, respectively, were performed. In addition, immunohistological (IHC) staining of paraffin-embedded sections of 106 metastatic RCC cases was used to compare GLS and ASCT2 expression in tumor and normal tissue. In vitro, cell viability of the human

RCC cell lines 786-O and 769-P was assessed by WST-8 assays. The protein expression was detected by Western blotting. Intracellular concentrations of glutamine and glutamate were analyzed using LC/MS. V9302 was used as the specific ASCT2 inhibitor, and CB839 as the specific GLS inhibitor. As the xenograft model in vivo, athymic nude mice were injected subcutaneously with 786-O cells and given various doses of V9302 and CB839 intraperitoneally.
Results: LC/MS assays using surgical specimens showed a notable increase in glutamine concentration in tumor tissue. IHC assays confirmed high expression of ASCT2 in tumor tissue, and patients with high expression of ASCT2 had a poorer prognosis than those with low expression. Treatment of V9302 with 786-O and 769-P resulted in a limited decrease in cell viability. LC/MS analysis confirmed that V9302 treatment reduced glutathione metabolites. V9302 administration was shown to increase intracellular glutamine levels, presumably by compensatory mechanisms, whereas the combination of V9302 and CB839 significantly decreased glutamine levels in 786-O cells. Western blot analysis showed that the expression levels of ASCT2 and GLS1 decreased after the combination therapy. The xenograft study confirmed that the combination of V9302 and CB839 significantly inhibited 786-O tumor growth compared with controls within three weeks after treatment ($p < 0.001$).
Conclusion: It has been shown that ASCT2 expression is a marker of poor prognosis in RCC and that suppression of ASCT2 has an antitumor effect by affecting glutathione metabolism. On the other hand, the administration of V9302 raised the issue that a compensatory mechanism increases intracellular glutamine levels. Our results suggest that a novel combination strategy using CB839 in addition to V9302 could overcome the tolerance for the monotherapy and effectively target glutamine addiction in RCC.

#3973

Precision RNAi using synthetic shRNAmir target sites

Ralph Neumüller[1], Thomas Hoffmann[2], Alexandra Hörmann[1], Maja Corcokovic[1], Johannes Zuber[2]. *[1]Boehringer Ingelheim RCV GmbH & Co. KG, Vienna, Austria,[2]Institute of Molecular Pathology (IMP), Vienna, Austria*

Genetic loss-of-function methods including short-hairpin RNAs (shRNAs) and CRISPR are key methods for target gene validation across a variety of different disease areas. While these methods have revolutionized target gene discovery and characterization, both methods suffer from limitations in the context of *in vivo* target validation due to off-target effects and insufficient knock-down for shRNAs and resistant clones for CRISPR. In this study, we describe a method, artificial RNA interference (ARTi) that overcomes these limitations by fundamentally changing the basic experimental strategy of RNAi-based loss-of-function studies. Instead of newly designing gene-specific shRNA for individual target genes, ARTi utilizes ultra-effective and selective artificial miRNA-based shRNAs that do not match any transcribed gene in the target genome. In addition, these sequences are optimized for ultra-efficient miRNA processing and knockdown of synthetic target genes, and are deeply characterized to not trigger major off-target effects, enabling highly stringent target validation in vivo with unprecedented temporal control, selectivity and potency. We validate the approach by studying the *in vitro* and *in vivo* phenotypes of EGFR, KRAS and STAG1, genes relevant to cancer biology. This loss-of-function strategy will enable novel experimental strategies in therapeutic target validation and will be instrumental in guiding the lead optimization process by establishing genetic benchmark phenotypes.

#3974

Discovery and validation of therapeutic targets in immune cells by mass spectrometry-based proteomics

Yu-Wah Au[1], David Satijn[1], Martin Mehnert[2], Amaury Lachaud[2], Yuehan Feng[2], Jakob Vowinckel[2], Hélène Bon[1]. *[1]Genmab A/S, Utrecht, Netherlands,[2]Biognosys AG, Schlieren, Switzerland*

Immuno-oncology (IO) has substantially improved the survival of cancer patients over the past several years encouraging the discovery of novel IO targets which are typically proteins expressed on the surface of immune cells. Sensitive quantification of proteins in complex biological samples is routinely achieved by immunoassays that use antibodies specific to target proteins. Such approaches can be a limitation in IO drug discovery and development as de novo development of antibodies is associated with long lead times, high costs, and high failure rates.

Protein quantification using mass spectrometry (MS) is agnostic to species and matrices and removes the barriers of availability or specificity of antibody-based assay. Further, MS proteomics workflows can support both large scale discovery studies but also represent an attractive alternative to targeted quantitative studies.
The main purpose of this work is to assess the performance of the TrueDiscovery™ and TrueSignature™ MS-proteomics platforms for the deep proteome and surfaceome profiling of human primary and immortalized immune cells compared to flow cytometry solutions. We assess the number of quantified proteins and specifically the coverage of immune cell marker proteins in primary human immune cells across cell count groups from 2 million down to 2500 immune cells. In addition, we compared the quantification of a multiplexed surface antigens panel using TrueSignature™ and QIFI® flow cytometry platforms.
We found that the applied MS-based proteomics workflows achieve high sensitivity and robustness in detection and quantification of immune cell markers down to 2500 primary immune cells. Additionally, we observed a strong correlation of the quantitative data derived from our MS-based proteomics workflows with flow cytometry supporting the substitution of immunoassays by MS-based proteomics workflows in target discovery and validation.

Molecular Targets

#5725
The USP1 inhibitor I-138 kills BRCA1-deficient tumor cells and overcomes PARP inhibitor resistance

Alexandre Andre B. A. Da Costa, Arindam Bose, David Martignetti, Cecilia Ayala-Zambrano, Ramya Ravindranathan, Golbahar Sadatrezaei, Yuqing Jiao, Bose Kochupurakkal, Huy Nguyen, Jean-Bernard Lazaro, Kalindi Parmar, Geoffrey I. Shapiro, Alan D. D'Andrea. *DFCI/Harvard Medical School, Cambridge, MA*

Targeting BRCA-deficient tumors with PARP inhibitors has improved the progression-free survival of ovarian and breast cancer patients in the clinic. However, the majority of patients develop acquired resistance. PARP inhibitor (PARPi) resistance in tumors can occur by restoration of

homologous recombination (HR) or replication fork stability and/or by suppression of single-stranded DNA (ssDNA) gaps at replication forks. USP1 is a ubiquitin specific protease which deubiquitinates PCNA and FANCD2. We have previously shown that USP1 deficiency causes replication fork instability and is synthetic lethal with BRCA1 deficiency, suggesting USP1 as a potential therapeutic target for overcoming PARPi resistance (Lim et al, Mol Cell, 2018). Accordingly, USP1 inhibitors are now undergoing preclinical and clinical development. Here, we evaluated the activity of the novel USP1 inhibitors such as I-138 (Simoneau et al, Mol Cancer Ther, 2022) and TNG-6132 in preclinical models of BRCA1-deficient tumors. I-138 preferentially killed BRCA1-deficient ovarian and breast cancer cells and increased the cellular level of ubiquitinated PCNA. An aniPOND analysis demonstrated an accumulation of ubiquitinated PCNA specifically at the replication fork in I-138-treated cells. Consistent with our previous study (Lim et al, Mol Cell, 2018), I-138 treatment led to replication fork instability and DNA damage in BRCA1-deficient cancer cells. I-138 exposure also resulted in the accumulation of ssDNA gaps, as detected by an S1 nuclease assay. Interestingly, the induction of ssDNA gaps was detected in I-138-sensitive but not in I-138-resistant BRCA1-deficient cells, suggesting a mechanism of cytotoxicity by USP1 inhibition. Persistent monoubiquitinated PCNA accumulation was the cause of cell killing after USP1 inhibition. Knockdown of RAD18, the E3 ubiquitin ligase known to ubiquitinate PCNA, in BRCA1-deficient ovarian cancer cells resulted in reduced PCNA-Ub levels, resistance to I-138, and suppression of ssDNA gaps. Notably, I-138 exhibited monotherapy activity in ovarian and breast cancer cell lines with acquired PARPi resistance and re-sensitized the cells to PARP inhibition. Similarly, PARPi-resistant *BRCA1*-mutated organoids, derived from patient-derived xenograft (PDX)-derived models of ovarian cancer, were also sensitized by USP1 inhibition by TNG-6132. Interestingly, the ssDNA gap accumulation induced by I-138 strongly correlated with the drug sensitivity of both PARPi-sensitive and PARPi-resistant cells. In conclusion, I-138 exhibits monotherapy activity in both PARPi-sensitive and -resistant preclinical models of BRCA1-deficient cancer, induces ssDNA gaps and overcomes PARP inhibitor resistance. Taken together, these data support use of a USP1 inhibitor, with or without a PARP inhibitor, as a therapeutic strategy for a subset of PARP-inhibitor-resistant BRCA1-deficient tumors.

#5726

Pan-cancer proteogenomics expands the landscape of therapeutic targets

Jonathan T. Lei[1], Sara R. Savage[1], Xinpei Yi[1], Bo Wen[1], Hongwei Zhao[2], Lauren K. Somes[1], Paul W. Shafer[1], Yongchao Dou[1], Qiang Gao[2], Valentina Hoyos[1], Bing Zhang[1]. *[1]Baylor College of Medicine, Houston, TX,[2]Fudan University, Zhongshan Hospital, Shanghai, China*

Background: Molecularly targeted therapies are critical for improving cancer treatment. Since proteins are the targets of these therapies and functional effectors of genomic aberrations, proteogenomics data from the Clinical Proteomics Tumor Analysis Consortium (CPTAC) provides an unprecedented opportunity to characterize existing and future therapeutic targets for cancer treatment.
Approach: CPTAC proteogenomics data from >1000 cancer patients spanning 10 cancer types was used to evaluate current and potential therapeutic targets curated from four databases. Cell line data from DepMap was further integrated to distinguish causations from associations. Computational pipelines were deployed to identify synthetic lethality for targeting tumor suppressor loss and to prioritize tumor associated antigens as immunotherapy targets.
Results: We systematically collected 3050 druggable proteins and classified them into 5 tiers to facilitate different applications such as companion diagnostics, drug repurposing, and new therapy development. Many druggable proteins showed poor mRNA-protein correlation, including secreted proteins and proteins whose abundance was correlated with their interaction partners instead of cognate mRNA, highlighting the necessity of direct proteomic quantification of drug targets. 618 druggable proteins showed both overexpression in tumors compared to normal and significant dependency in CRISPR-Cas9 screens of cell lines of the same lineage. Notably, PAK1, a kinase targeted by investigational drugs, demonstrated both overexpression and dependency in all cancer types. A similar analysis of phosphoproteomics data focusing on known activating sites of druggable proteins further revealed targetable dependencies driven by protein hyperactivation. The phosphosite pS50 on PTPN1, a phosphatase targeted by experimental drugs, was increased in 7 cancer types and PTPN1

demonstrated dependency in related cancer cell lines. Based on tumor proteogenomic data and cell line CRISPR-Cas9 screen data, we identified synthetic lethality for difficult to target tumor suppressor losses, revealing TP53 mutations as a candidate biomarker to select breast cancer patients for CHEK1 inhibition, and endometrial cancer patients for treatment with doxorubicin. We identified 140 proteins whose expression was restricted in normal tissues but abnormal in tumors. Experimental analysis of peptides predicted to have high binding affinity to the most common allotype HLA-A02 for 7 prioritized proteins identified 21 peptides from 5 proteins with both strong binding affinity and immunogenicity which could be further investigated as immunotherapy targets.
Conclusion: We generate a comprehensive resource of protein and peptide targets that covers multiple therapeutic modalities. This unique resource will pave the way for repurposing of currently available drugs and developing new drugs for cancer treatment.

#5727

Identification of synthetic lethal vulnerabilities in cancers with loss of function mutations in NOTCH

Deli Hong[1], Matthew A. Booker[2], Sidrah Anjum[2], Yixiang Li[1], Tran C. Thai[1], Michelle Y. Wang[3], David A. Barbie[1], Michael Y. Tolstorukov[2], Jun Qi[3], Matthew G. Oser[1]. *[1]Medical Oncology, Dana-Farber Cancer Institute, Boston, MA,[2]Informatics, Dana-Farber Cancer Institute, Boston, MA,[3]Cancer Biology, Dana-Farber Cancer Institute, Boston, MA*

Loss of Function (LOF) mutations in the *NOTCH* receptors are found in several different cancers most notably in small cell lung cancer (SCLC) and squamous cell carcinomas (SCC). We previously developed genetically engineered mouse models (GEMM) of SCLC using CRISPR/Cas9 engineered to be *NOTCH1*-Mutant, *NOTCH2*-Mutant, and *NOTCH*-WT. Synthetic lethality provides a paradigm for targeting cancers with LOF mutations in tumor suppressor genes. In applying this paradigm, one looks for specific vulnerabilities that are created upon loss of the gene of interest. Using 6 cell lines developed from these CRISPR-based SCLC GEMMs which are isogenic to *NOTCH*, we performed CRISPR/Cas9 LOF negative selection screens (using an sgRNA library enriched in druggable enzymes) to identify synthetic lethal interactors with LOF *NOTCH* mutations. Our

CRISPR/Cas9 screen identified TRIM28 (Tripartite Motif Containing 28, or KAP1) as a highly significant synthetic lethal interactor with NOTCH1 or NOTCH2. We validated the synthetic lethal interaction between NOTCH1/2 and TRIM28 using both human and mouse NOTCH-isogenic cell lines. Interestingly, RNA-sequencing of *NOTCH2*-Mutant or *NOTCH*-WT SCLC cell lines after TRIM28 CRISPR inactivation showed robust increases in endogenous retroviral (ERV) expression and the MDA5/RIG-I/MAVS RNA-sensing machinery leading to hyperactivation of the TBK1/IRF3/7 innate immune signaling pathway and the pro-inflammatory cytokine CXCL10 selectively in cells with NOTCH inactivated. Notably, inactivation of TBK1 activity or JAK-STAT activity using specific small molecule inhibitors of TBK1 or JAK completely reversed the synthetic lethality between NOTCH and TRIM28 suggesting that the synthetic lethality phenotype is a consequence of hyperactivation of innate immune signaling, which is known to be cytotoxic. Together our findings uncover a novel vulnerability in SCLCs with LOF *NOTCH* mutations and perhaps other cancers with LOF NOTCH mutations and suggest a strategy that could also potentiate anti-tumor immunity by increasing innate immune signaling in tumor cells.

#5728

Inhibition of TACC3 blocks the growth of highly aggressive breast cancers with centrosome amplification

Ozge Saatci[1], Ozge Akbulut[2], Metin Cetin[1], Vitali Sikirzhytski[2], Ozgur Sahin[1]. *[1]The Medical University of South Carolina (MUSC), Charleston, SC,[2]University of South Carolina, Columbia, SC*

Centrosome amplification (CA) is a hallmark of cancer that is strongly associated with highly aggressive disease and worse clinical outcome. Clustering extra centrosomes into opposite spindle poles during mitosis is critical for preventing multipolar cell division and apoptosis in cancer cells with CA. However, the underlying molecular mechanisms have largely been unexplored. Here, we identified Transforming Acidic Coiled-Coil Containing Protein 3 (TACC3) as a novel CA-directed dependency, driving highly aggressive cell growth by forming distinct functional interactomes during cell cycle progression. We demonstrated, for the first time, that TACC3 interacts with the Kinesin Family Member C1 (KIFC1) via its

TACC domain in mitotic cells with CA to promote centrosome clustering (CC) and facilitate mitotic progression. On the other hand, TACC3 interacts with the members of the nucleosome remodeling and deacetylase (NuRD) complex (HDAC2 and MBD2) in the nucleus of interphase cells with CA, thereby suppressing the transcription of key tumor suppressors to facilitate G1/S progression and cell survival. Inhibiting TACC3 in mitotic cells blocks the formation of TACC3/KIFC1 complex, leading to formation of multipolar spindles and activation of spindle assembly checkpoint (SAC)/CDK1/p-Bcl2 axis that ultimately results in mitotic cell death; whereas TACC3 inhibition in interphase cells blocks TACC3/HDAC2/MBD2 complex, leading to enhanced transcription of cyclin-dependent kinase inhibitors (e.g., p21 and p16) and apoptosis regulators (e.g., APAF1), ultimately causing p53-independent G1 arrest and strong apoptosis. Notably, inducing CA by chemical (cytochalasin D) or genomic (PLK4 overexpression or p53 loss) modulations renders cancer cells highly sensitive to TACC3 inhibition, showing the dependency of cells with CA to TACC3. Targeting TACC3 by small molecule inhibitors or CrispR-CAS9-mediated knock-out significantly reduces colony formation ability, inhibits the growth of organoids of patient-derived xenografts (PDXs) with CA, and strongly inhibits tumor growth in breast cancer cell line xenografts and PDXs with CA via induction of mitotic arrest and inhibition of G1/S progression. Notably, we demonstrated that high CA tumors express much higher levels of TACC3, and high TACC3 expression leads to drastically worse clinical outcome in cancer patients with CA. Altogether, our results show, for the first time, that TACC3 is a multifunctional driver of the growth of the highly aggressive breast tumors with CA and that targeting TACC3 is a promising approach to tackle this aggressive disease.

#5729

Imiqualines for pancreatic cancer: first-in-class potent and synergistic inhibitors of microtubule polymerisation

Kevin Bigot[1], Véronique Garambois[1], Nadia Vie[1], Marine Bruciamacchie[1], Pierre-Emmanuel Colombo[2], Diego Tosi[2], Cindy Patinote[3], Yann Maggipinto[1], Pierre-Antoine Bonnet[3], Céline Gongora[1], Carine Deleuze-Masquefa[3], Christel Larbouret[1]. *[1]Team Drug Resistance and New Cancer Therapy, IRCM INSERM U1194, Montpellier, France,[2]Institut du Cancer de*

Montpellier, Montpellier, France,[3]équipe F16, IBMM, Univ Montpellier, CNRS, ENSCM, Montpellier, France

Background : The survival rate for patients with Pancreatic Ductal Adenocarcinoma (PDAC) is dramatically poor with a five-year survival rate less than 10%. The research of new treatments, which could complement the current therapeutic arsenal constituted by Gemcitabine, FOLFIRINOX (fluorouracile, leucovorin, irinotecan, oxaliplatin) and nab-paclitaxel, is a major challenge. Imiqualines are new original small heterocyclic chemical molecules based on the quinoxalinic moiety. Among these first in class compounds, the lead EAPB02303 (1) displays outstanding nanomolar activities comparable to those of the current best anticancer agents on a panel of human cancer cell lines, notably on poorly sensitive cancer like PDAC and melanoma. We tested here if EAPB02303 could be an attractive first in class molecule in PDAC and we conducted in-deep molecular characterization and bioinformatics studies to decipher its mechanism of action.
Methods: We characterized EAPB02303 effect on tumor growth *in-vitro* by conducting sulforhodamine B assay on a panel of PDAC cells including cells derived from PDX (Patient Derived Xenograft) and 3D models with Cancer Associated Fibroblasts. We assessed in-vivo activity on subcutaneous PDAC xenografts mouse models. We then studied EAPB02303 effect on cell cycle, apoptosis and microtubule polymerisation by flow cytometry and immunofluorescence. We analyzed mRNAseq and Reverse Phase Protein Assay (RPPA) data of PDAC cell lines treated with EAPB02303 at multiple time points and concentrations to identify signaling pathways and key proteins implicated in EAPB02303 effect. We performed differential gene expression and gene set enrichment analysis by using EdgeR, Deseq2 and fgsea packages. We also used PharmacoGx package to seek for similar transcriptomic profiles among the CMAP perturbational database.
Results : We showed that EAPB02303 exerts activity at low nanomolar concentrations *in-vitro* in PDAC cell lines and 3D models, and is able to reduce tumor growth in our xenografts *in-vivo* mouse models. We also found a potent synergy with Paclitaxel at lower concentrations of both compounds. Furthermore, we found that EAPB02303 induces mitosis arrest and impairment of spindle assembly after 24h treatment. Cells also

underwent apoptosis after 48h treatment. mRNAseq and RPPA data showed activation of several signaling pathways including MAPK kinases. CMAP database mining revealed a high connectivity score of transcriptomic signatures between EAPB02303 and inhibitors of microtubule polymerization.
All these data suggest that EAPB02303 is a new microtubule-disrupting agent with *in-vivo* activity in PDAC and *in-vitro* synergy with Paclitaxel, showing potential for future clinical investigations.
(1) Imidazo[1,2a]quinoxalines and derivatives thereof for treating cancers. WO 2009 043934A1. Deleuze-Masqeufa C. et al.

#5730
Targeting intrinsically disordered protein βII-spectrin prevents metabolic syndrome and hepatocellular carcinoma on a sex-based bias
Xiaochun Yang, Krishanu Bhowmick, Xiyan Xiang, Kazufumi Ohshiro, Anil Vegesna, Lopa Mishra. *Institute for Bioelectronic Medicine, Department of Medicine, Div of Gastroenterology and Hepatology, The Feinstein Institutes for Medical Research, & Cold Spring Harbor Laboratory, Northwell Health, New York, NY*

Background**:** Hepatocellular carcinoma (HCC) is a lethal cancer that affects males 2-4 times more than females. HCC incidence is rising in parallel with risk factors such as non-alcoholic steatohepatitis (NASH) and alcohol induced cirrhosis. A major enzyme in alcohol metabolism, aldehyde dehydrogenase 2 (ALDH2) deficiency affects ~560 million people globally. In males, different ALDH2 genotypes exhibit significant metabolic differences from females. Yet the mechanism for the sex differences remains unclear. We have found that targeting an intrinsically disordered protein and TGF-β signaling Smad3/4 adaptor, βII-spectrin (Sptbn1) blocks NASH and HCC in a liver-specific knockout (LSKO) mice and siRNA to human NASH microfluidic cultures (*Sci Transl Med. 2021. 13(624): eabk2267*). In mouse mutants of Smad3/Sptbn1 with HCC, stem cell proteins are markedly altered. Here, we sought to examine this further by intercrossing Sptbn1 deficient mice with ALDH2 deficient mice.
Methods: Global heterozygous knockout of *Sptbn1* mice were intercrossed with *Aldh2* knockout mice (ASKO) to explore the role of βII-spectrin in aldehyde-related liver injury. LSKO mice were intercrossed with ALDH2

deficient mice (ALSKO) and siRNA treatment to explore the therapeutic effects of targeting *Sptbn1* during the progression of metabolic syndrome (MetS) or HCC induced by Western diet (WD)/chemical (DEN) in the context of ALDH2 deficiency in both male and female mice. We performed phenotypic analyses of metabolic state, liver pathology, intestinal pathology, and gut microbiomes.
Results: LSKO displayed obvious therapeutic effects against liver steatosis in male mice, whereas female mice did not. ASKO mice developed NASH spontaneously and showed impaired glucose handling, disordered lipids metabolism, with increased intestinal permeability and pro-inflammatory species of *Bacteroidetes* and *Firmicutes*. ALDH2 deficiency exacerbated toxic reactive aldehydes accumulation. LSKO mice were protected from WD induced MetS and NASH, including decreased body weight and fat weight, decreased serum triglyceride and AST/ALT, downregulated expression of proinflammatory genes and profibrotic genes and improved NAS Score. LSKO mice were also protected from WD/DEN-induced HCC: mice had less tumor number, smaller tumor size and less proliferation. siRNA targeting *Sptbn1* also showed similar therapeutic effects as LSKO. Further, LSKO and siRNA targeting *Sptbn1* also improved NASH phenotypes resembling MetS in $Aldh2^{-/-}$ mice: decreased liver fat accumulation, improved glucose handling and reduced inflammatory cell infiltration.
Conclusions: Our data suggest that βII-spectrin, an intrinsically disordered protein, is a potential therapeutic target for diet/chemical-induced Mets/NASH and preventing HCC development and could provide new insight into sex-based differences in HCC.

#5731

Apoptosis Inducing Agent 1 enhances cancer therapy-induced apoptosis by direct interaction with BAX and BAK

Xingping Qin[1], Cameron Fraser[1], Adam Presser[1], Johan KE Spetz[1], Stacey J. Yu[1], Gary A. Bradshaw[2], Marian Kalocsay[2], Bo R. Rueda[3], Tudor Moldoveanu[4], Kristopher A. Sarosiek[1]. *[1]Harvard T.H. Chan School of Public Health, Boston, MA,[2]Harvard Medical School, Boston, MA,[3]Department of Obstetrics and Gynecology, Vincent Center for Reproductive Biology, Massachusetts General Hospital, Boston,*

MA,[4]Department of Biochemistry and Molecular Biology, University of Arkansas for Medical Sciences, Little Roeck, AR

Many of the most effective anti-cancer therapies induce apoptosis in cancer cells by damaging DNA. Even when effective at eradicating primary cancers, DNA-damaging anti-cancer agents cause mutations that can lead to the development of secondary cancers. Furthermore, DNA damage responses are dependent on wild-type p53, which is mutated in over 50% of cancers and causes resistance to therapies. Fortunately, many p53 mutant cancers continue to express high levels of the pro-apoptotic, pore-forming proteins BAX and BAK and are consequently "primed for apoptosis." Primed cells are highly sensitive to pro-apoptotic signals and this vulnerability can be exploited using inhibitors of pro-survival BCL-2 family proteins such as the BCL-2 inhibitor ABT-199, which has been successful as therapy for chronic lymphocytic and acute myeloid leukemias (AML). Furthermore, most irreplaceable cells within healthy tissues are apoptosis resistant and express low levels of BAX and BAK. We therefore hypothesized that direct activators of BAX or BAK could be effective single-agent therapies for primed cancers and chemo-/radio-sensitizers for unprimed cancers. Using WT versus BAX -/- BAK -/- HeLa cells, we performed a high-throughput screen of nearly 100,000 compounds to identify small molecules that could directly activate BAX or BAK. 196 compounds were identified as hits and multiple orthogonal validation studies identified Apoptosis Inducing Agent 1 (AIA1) as the most specific and potent putative activator of BAX and BAK. Further validation studies demonstrated that AIA1 directly induces cytochrome c release from mitochondria in a BAX/BAK dependent manner and strongly enhances BIM-mediated activation of BAX and BAK and permeabilization of liposomes. Single-agent AIA treatment triggers apoptotic cell death in a broad panel of cancer cell lines and also sensitizes cancer cells to chemotherapeutic agents and especially BH3 mimetics targeting pro-survival BCL-2 family proteins. Importantly, AIA1 sensitizes ovarian cancer cells to BCL-X_L inhibitors and AML cells to BCL-2 inhibitors regardless of p53 status. In vivo, AIA1 suppresses tumor growth and prolongs overall survival in both ovarian cancer and AML xenograft models without causing weight loss, thrombocytopenia or leukopenia. Notably, unprimed cancer cells that don't immediately undergo apoptosis in

response to single-agent AIA1 treatment upregulate expression of BAX and BAK, pro-survival proteins (BCL-$X_{L,}$ BCL-2, MCL-1) and pro-apoptotic proteins (BIM, BID, PUMA, Noxa) to produce a more highly primed apoptosis pathway and setting the stage for increased sensitivity to BH3 mimetics. Based on these findings, AIA1 may exploit and induce apoptotic vulnerabilities in cancers in a p53-independent manner and represent a safer strategy to target primed cancer cells while eliminating the potential for secondary malignancies and p53-mediated resistance.

New Tricks for Known Targets: Novel Approaches to Inhibit Oncogenic Signaling

#5733
Combining KRAS^{G12C}(ON) inhibition with SHP2 and immune checkpoint blockade to enhance anti-tumor immunity and overcome development of resistance in lung cancer

Panayiotis Anastasiou, Mona Tomaschko, Jesse Boumelha, Sareena Rana, Christopher Moore, Miriam Molina-Arcas, Julian Downward. *The Francis Crick Institute, London, United Kingdom*

The recent approval of KRAS^{G12C} mutant-specific inhibitors has transformed the clinical practice of lung cancer patients harboring KRAS^{G12C} mutations. However, clinical data show that resistance develops rapidly after initial responses, suggesting that combination therapies will be needed. Ideally, these combinations should not only overcome adaptive or acquired resistance but also maintain or even enhance the positive immunomodulatory effects that KRAS^{G12C} inhibitors (G12Ci) have in the tumor microenvironment (TME). Most of the G12Ci being tested in clinical trials target GDP-bound KRAS (OFF state), which makes them vulnerable to upstream pathway reactivation. In this study we use a covalent tri-complex KRAS^{G12C}(ON) inhibitor, RM-029, which targets KRAS^{G12C} in the active state. Treatment with RM-029 still resulted in some degree of adaptive RAS pathway reactivation, which can be blocked using the SHP2 inhibitor RMC-4550. In vivo, this combination enhanced tumor regressions and improved overall survival in two different KRAS^{G12C} lung cancer models. In an immunogenic KRAS^{G12C} lung cancer model both

$KRAS^{G12C}$(ON) and SHP2 inhibitors remodel the TME and are able to drive durable responses, which are enhanced when both compounds are combined. However, in this anti-PD1 sensitive model the combination of RM-029 with anti-PD1 generated more complete responses than the combination of RM-029 and RMC-4550. In an immune-excluded anti-PD1 resistant model, $KRAS^{G12C}$(ON) and SHP2 inhibitors also promoted a profound remodelling of the TME, with increased infiltration and activation of T cells accompanied by a reduction of tumor-promoting myeloid cells. Importantly, only the combination of both $KRAS^{G12C}$(ON) and SHP2 inhibitors sensitized these immune-excluded tumors to anti-PD1 blockade, resulting in durable responses and immune memory. Our preclinical results show that RM-029 as single agent or in combination with RMC-4550 and/or anti-PD1 can induce anti-tumor immunity and generate complete responses, especially in immunogenic models. To study if this immunological response could also target G12Ci-resistant subpopulations within the tumor, we used our immunogenic cell line (KPAR) to generate reporter-traced G12Ci sensitive ($KPAR^{G12C}$) and resistant ($KPAR^{G12D}$) cells that can be monitored over time via in vivo luciferase imaging and end point flow cytometry. We find evidence of bystander immune mediated killing of G12Ci-resistant cells in response to the different treatment combinations. Overall, our preclinical results demonstrate the potential of the combination of $KRAS^{G12C}$(ON) inhibitors with SHP2 and/or immune checkpoint blockade not only by targeting KRAS-driven proliferation in tumor cells but by stimulating anti-tumor immunity to target both G12Ci sensitive and resistant cells.

#5734

Designing RAF and MEK inhibitor combinations based on their biochemical properties to effectively target MAPK-driven cancers

Ana Orive-Ramos[1], Christos Adamopoulos[1], Beau Baars[1], Jason Lam[1], Ankita Punetha[2], Jason Huang[1], Vasileios I. Petrou[2], Stuart A. Aaronson[1], Poulikos I. Poulikakos[1]. *[1]Oncological Sciences, The Tisch Cancer Institute, Icahn School of Medicine at Mount Sinai, New York, NY,[2]Microbiology, Biochemistry, and Molecular Genetics, New Jersey Medical School, Rutgers Biomedical Health Sciences, Newark, NJ*

Oncogenic alterations of the RAS/RAF/MEK/ERK signaling pathway drives growth of over 40% of human tumors, frequently due to activating mutations of components of the pathway, such as RAS or BRAF. Targeting the pathway using BRAF inhibitors (BRAFi) in combination with MEK inhibitors (MEKi) is now the standard of care for metastatic melanoma patients harboring the BRAF(V600E) mutation. However, effective targeted therapies are lacking for most cancers driven by other pathway alterations, including those with RAS activating mutations. The effectiveness of current clinical BRAFi relies on the fact that they bind selectively and inhibit the mutationally activated monomeric form of the BRAF(V600E) kinase in tumors but not wild-type BRAF in normal tissue where BRAF signals in its dimeric form. Yet, the development of adaptive resistance, frequently due to RAF dimerization, limits BRAFi therapeutic effectiveness. Another class of BRAFi equipotent for both monomeric and dimeric BRAF have been developed, but are predicted to have lower therapeutic index due to inhibition of dimeric wild-type BRAF in normal tissues as well. Recently, we identified and characterized a novel class of BRAFi that preferentially binds and inhibits dimeric BRAF over monomeric BRAF(V600E) (i.e. RAF dimer-selective inhibitors). Furthermore, we rationally designed a combinatorial approach utilizing a BRAF monomer-selective plus a BRAF dimer-selective inhibitor plus a MEK inhibitor, that potently disrupts the BRAF/MEK complex, to maximally inhibit BRAF(V600E) signaling in tumors while retaining a broad therapeutic index. This triple combination potently suppressed tumor growth of multiple BRAF(V600E) colorectal cancer and melanoma models resistant to the current clinical BRAFi and MEKi combinations both *in vitro* and *in vivo*. To design effective therapeutic approaches for RAS-mutated tumors, we also assessed the effectiveness of RAF and MEK inhibitors belonging to diverse biochemical and structural classes, either alone or in combination in RAS-mutant tumor models and normal cells with wild-type RAS signaling. We found that RAF dimer-selective inhibitors potently antagonized MAPK signaling and growth in various RAS mutant cancer models as compared to normal cells. We found further that RAF and MEK inhibitor combinations belonging to certain biochemical classes resulted in more potent MAPK suppression in RAS-mutant tumor as compared to wild-type RAS normal cells (“therapeutic synergy”) and should be prioritized for clinical testing. In contrast, those combinations which are more potent in normal over tumor

cells (“adverse synergy”) are unlikely to be clinically successful. Thus, rationally designed combinations of selected RAFi and MEKi, based on their distinct biochemical properties, can uncover new therapeutic opportunities tailored for more effective targeting of BRAF or RAS mutant tumors.

#5735

Novel KRAS G12D degrader ASP3082 demonstrates in vivo, dose-dependent KRAS degradation, KRAS pathway inhibition, and antitumor efficacy in multiple KRAS G12D-mutated cancer models

Takeyuki Nagashima, Tomohiro Yoshinari, Yoshihiro Nishizono, Mamoru Tasaki, Kohei Inamura, Hiroki Ishioka, Atsushi Suzuki, Fumio Osaki, Yosuke Yamanaka, Masahiko Hayakawa. *Astellas Pharma, Inc., Tsukuba-shi, Japan*

KRAS is one of the most frequently mutated oncogenes in various cancers. Among KRAS mutations, KRAS G12D is the most frequent driver mutation and is found in approximately 34% of patients with pancreatic ductal adenocarcinoma (PDAC), 12% of patients with colorectal cancer (CRC), 4% of patients with lung adenocarcinoma, and in a subset of patients with other solid tumors. We have identified ASP3082 as a novel KRAS G12D degrader with high potency and selectivity. Here, we have evaluated in vivo antitumor activities and pharmacodynamic properties of ASP3082 in various KRAS G12D-mutated xenograft models. ASP3082 was intravenously administered to KRAS G12D-mutated cancer-xenograft-bearing mice, and plasma and tumors were collected at defined time points. The drug concentration and KRAS-related signal transduction were measured in the xenograft model. The in vivo efficacy of ASP3082 monotherapy was confirmed in multiple xenograft mouse models following intravenous administration. Once-weekly intravenous administration of ASP3082 induced dose-dependent and significant growth inhibition of KRAS G12D PDAC tumors, resulting in profound tumor regression without body weight loss. ASP3082 showed sustained concentrations in the xenograft tumors after a single intravenous administration and decreased KRAS G12D-mutated-protein levels according to the duration of the sustained ASP3082 concentrations. ASP3082 also demonstrated marked inhibition of extracellular signal-

regulated kinase phosphorylation and its downstream genes, and potently induced cleavage of caspase 3. In addition, ASP3082 exhibited potent antitumor activities in not only PDAC but also CRC and non-small cell lung cancer KRAS G12D-mutated mouse models. These studies demonstrated that ASP3082 induced degradation of KRAS G12D protein, inhibition of KRAS downstream molecules, and an apoptotic response to show dose-dependent antitumor activity in multiple KRAS G12D-mutated cancer models. ASP3082 is a potential therapeutic agent for patients with tumors harboring the KRAS G12D mutation. Currently, a phase 1 clinical trial is underway in patients with previously treated, locally advanced or metastatic solid tumors with KRAS G12D mutation (NCT05382559).

#5736

AZD9592: An EGFR-cMET bispecific antibody-drug conjugate (ADC) targeting key oncogenic drivers in non-small-cell lung cancer (NSCLC) and beyond

Frank Comer[1], Yariv Mazor[1], Elaine Hurt[1], Chunning Yang[1], Ryan Fleming[1], Harini Shandilya[1], Balakumar Vijayakrishnan[2], Meghan Sterba[1], Ruoyan Chen[1], Edward Rosfjord[1], Nicolas Floch[3], Anton I. Rosenbaum[4], Yue Huang[4], Jiaqi Yuan[4], Kevin Beaumont[5], Lisa Godfrey[6], Lara McGrath[7], Fernanda Arnaldez[1], Puja Sapra[1]. *[1]AstraZeneca, Gaithersburg, MD,[2]AstraZeneca, London, United Kingdom,[3]AstraZeneca, Cambridge, United Kingdom,[4]AstraZeneca, South San Francisco, CA,[5]AstraZeneca, Chesterford, United Kingdom,[6]AstraZeneca, Melbourn Science Park, United Kingdom,[7]AstraZeneca, Waltham, MA*

De novo and acquired drug resistance can limit the long-term efficacy of targeted cancer therapies such as tyrosine kinase inhibitors targeting key oncogenic drivers like EGFR and cMET. Mechanisms of resistance include secondary mutations of EGFR and cMET and other downstream oncogenic pathways such as KRAS and amplification of alternate growth factor receptors. MET amplification or protein overexpression has been established as the most common mechanism of clinical resistance to EGFR inhibitors such as osimertinib. AZD9592 is a first-in-class bispecific ADC designed to target EGFR and cMET, while overcoming pathway-mediated resistance mechanisms that limit other targeted agents. Here we describe the

generation, characterization and preclinical evaluation of AZD9592. The ADC was constructed on the backbone of the clinically validated DuetMab monovalent bispecific IgG platform and was engineered with higher affinity for cMET compared to EGFR (>15 fold), with the aim of reducing EGFR-driven toxicity in normal tissues. The antibody is conjugated via a cleavable linker to a proprietary topoisomerase 1 inhibitor (TOP1i) payload (AZ14170132). The internalization and *in vitro* cytotoxicity (IC_{50} in the low nM range) of AZD9592 were found to be optimal when both EGFR and cMET were engaged. When EGFR alone was engaged, cytotoxicity was significantly reduced, consistent with the lower affinity for EGFR. Treatment of cells with AZD9592 induced multiple DNA damage response pathway markers (like ATM, ATR, γH2AX), consistent with the proposed primary mechanism of action (MOA) of direct tumor-cell killing caused by double strand DNA breaks. AZD9592 monotherapy showed activity *in vivo* in patient-derived xenograft (PDX) models representing multiple EGFR and cMET expressing tumor types, including both EGFR mutant (m) and wild-type NSCLC and head and neck squamous cell carcinoma. Responses (≥30% regression from baseline tumor volume) were observed across a wide range of clinically relevant dose levels, including a 41% response rate in EGFRm NSCLC tumors treated at the lowest tested dose of 2 mg/kg. AZD9592 combined with osimertinib also showed benefit in PDX models derived from patients who progressed on osimertinib alone, as well as models representing primary resistance (EGFR ex20ins). AZD9592 was well tolerated in cynomolgus monkeys over a 6-week period (dosing every 3 weeks). The key safety findings were limited hematological effects, consistent with the MOA of the TOP1i payload. Plasma pharmacokinetics in cynomolgus monkeys showed an acceptable profile at tolerated doses, in line with other EGFR and cMET directed antibodies. These results demonstrate that AZD9592 has a promising efficacy and safety profile in preclinical models representing diverse opportunities in multiple clinical settings.

#5737

Evaluation of the relationship between target expression and *in vivo* anti-tumor efficacy of AZD9592, an EGFR/c-MET targeted bispecific antibody drug conjugate

Lara McGrath[1], Ying Zheng[2], Simon Christ[3], Christian C. Sachs[3], Sihem Khelifa[3], Claudia Windmüller[3], Steve Sweet[2], Yeoun Jin Kim[2], Daniel Sutton[4], Michal Sulikowski[4], Arthur Lewis[4], Ivan Inigo[2], Nicolas Floch[4], Edward Rosfjord[2], Fernanda Arnaldez[2], Frank Comer[2]. *[1]AstraZeneca, Waltham, MA,[2]AstraZeneca, Gaithersburg, MD,[3]AstraZeneca Computational Pathology GmbH, Munich, Germany,[4]AstraZeneca, Cambridge, United Kingdom*

AZD9592 is a bispecific antibody drug conjugate (ADC) designed to deliver a topoisomerase 1 inhibitor (TOP1i) cytotoxic payload (AZ14170133) to tumor cells. AZD9592 selectively binds to epidermal growth factor receptor (EGFR) and c-MET, two cell surface receptors highly expressed in solid tumors including non-small-cell lung cancer (NSCLC) and head and neck squamous cell carcinoma (HNSCC). Here we evaluate the pharmacodynamic activity of the TOP1i payload delivery by AZD9592 in an NSCLC-derived xenograft model using immunohistochemistry (IHC) approaches. Treatment-induced DNA double-strand breaks (DSB) and apoptotic cell death were measured using γH2AX, phospho-RAD-50 (pRAD50), and cleaved-caspase-3 (CC3) across increasing exposure to AZD9592. Furthermore, we report *in vivo* antitumor efficacy of AZD9592 in a panel of NSCLC and HNSCC patient-derived xenograft (PDX) models that were characterized for somatic tumor alterations, including oncogenic driver mutations in EGFR, tumor cell expression of EGFR and c-MET by IHC and deep-learning based image analysis, and targeted proteomics by mass spectrometry. Results demonstrate dose-dependent increases in pRAD50 and γH2AX upon treatment with AZD9592, signifying induction of DNA damage. Increased CC3 and reduced tumor volume (TV) in all treatment groups compared with control groups supports that AZD9592 induces tumor cell death due to formation of DNA DSB. In PDX experiments, tumor growth inhibition (TGI), defined as ≥30% reduction in TV from baseline after a single dose of AZD9592 8 mg/kg, was observed in 73% (16/22) of EGFR mutant NSCLC models. The models evaluated included tumors with or without prior exposure to EGFR tyrosine kinase inhibitors, and harboring diverse mutational profiles and heterogeneous expression levels of EGFR and c-MET. In EGFR wildtype NSCLC and HNSCC PDX, TGI was observed in 60% (12/20) and 44% (4/9) of models, respectively. IHC demonstrated an

association of target expression and response to treatment, suggesting a potential predictive feature of response in tumors with elevated antigen expression. Targeted proteomics demonstrated an association between the expression of SLFN11, a known TOP1i sensitivity marker, and treatment response. Collectively, these results support the hypothesized mechanism of action of AZD9592: TOP1i induced tumor cell death due to formation of DNA DSB, and suggest opportunities in the treatment of tumors with a range of molecular features. AZD9592 is currently in a Phase 1 clinical trial in advanced solid malignancies.

#5738

A pan-ras mRNA vaccine elicits specific immune responses and inhibits tumor growth in the mouse model of colon cancer

Renxiang Chen[1], Wei Liu[2], David M. Brown[1], Yong-Sik Bong[1], Jiaxi He[1], Dong Shen[1], Cun Yu Wang[2]. *[1]RNAimmune, Inc., Germantown, MD,[2]Jonsson Comprehensive Cancer Center and School of Dentistry, UCLA, Los Angeles, CA*

KRAS mutations are present in about 25% of tumors, making them one of the most common mutated oncogenes among human cancers. Specifically, KRAS G12 mutation (89%) is the most common in tumors, followed by G13 (9%) and Q61 (1%). These mutations were once considered "undruggable" for many years until appearance of sotorasib . However, it was developed only for G12C mutation.

We designed a Pan-Ras neoantigen mRNA vaccine (mRNA-1521), which covers all prevalent RAS mutations to achieve broad-spectrum cancer therapy. We synthesized a multiepitope neoantigen KRAS mRNA vaccine (mRNA-1521) and examined its immune response and anti-tumor efficacy in the colon cancer of Balb/c mice . Two groups (A, B) of mice were immunized with mRNA-1521 on days 0, 21, and 49, while PBS was given to two other groups (C, D) as the control on the same days. All mice were inoculated with CT26 cells (colon carcinoma cell line harboring G12D mutation) on day 56. Afterward, anti-PD1 antibodies were administered to groups A and C every two days. Tumor sizes were measured every 3 days after inoculation until anyone exceeded 1500mm^3 in the control group. The serum IgG titer and T cell response of mice were explored using ELISA and splenocyte ELISpot assay after euthanasia. Tumor tissues were harvested

and embedded in paraffin for the immunohistochemistry (IHC) test. Next-generation sequencing (NGS) was also applied to investigate the whole transcriptome analysis.
Tumor growth rates in all treatment groups were slower than in the control group. Among them, the mean tumor size and weight in the combination group of mRNA-1521 and anti-PD1 (372mm^3, 0.48g) were only 25% of the PBS group (1488mm^3, 2g). On average, the anti-PD1 and vaccine groups had moderate tumor size and weight (1100mm^3/1.5g and 886mm^3/1.26g, respectively). The splenocytes from the mice in each group were collected. The IFN-γ secreting splenocytes in the combination group were 50% higher than the mRNA-1521 group. Furthermore, the total IgG titer of vaccine-immunized mice (OD450nm>2) was 3 and 4 times higher than the anti-PD1 and control groups. The IHC showed that the tumor tissues in the vaccine groups had more CD8+ and granzyme B+ CD8+ T cell infiltrations than in the control group. Whole transcriptome analysis showed that RAS downstream gene expressions were significantly lower in the vaccine group, indicating that the RAS vaccine was effective in inhibiting signaling pathways accounting for tumor proliferation, progression, and migration. In conclusion, prophylactic immunization of mRNA-1521 inhibited tumor growth in the mouse model of colon cancer. Its inhibitory effects on tumor growth were more remarkable in the combination of anti-PD1 antibodies. Moreover, the vaccine could elicit specific T and B cell responses, which are crucial in anti-cancer immunotherapy.

#5739

Targeting WEE1 to improve the therapy of KRAS G12C mutant non-small cell lung cancer

Gaku Yamamoto, Kosuke Tanaka, Ryo Kamata, Shunta Mori, Jie Liu, Toyohiro Yamauchi, Yuta Sakae, Akihiro Ohashi, Susumu S. Kobayashi.
National Cancer Center Japan, Kashiwa, Chiba, Japan

Background: While sotorasib is the first clinically approved small-molecule inhibitor of KRAS G12C in non-small-cell lung cancer (NSCLC), efficacy of sotorasib alone is limited, presumably due to adaptive resistance mechanisms in cancer cells. To expand therapeutic potential of sotorasib, combination strategies need to be developed. In this study, we conducted a large-scale screening to identify novel combination candidates with

sotorasib. In addition, molecular mechanisms of synergistic effects were investigated in multiple preclinical models.
Methods: To identify novel combination partners of sotorasib, we conducted high-throughput screening using a kinase inhibitor library containing 1,400 chemical compounds. Anti-proliferative and apoptotic effects in vitro were assessed by ATP-based cell viability assay and/or clonogenic assay, and caspase 3/7 assay and/or Annexin V assay, respectively. Synergistic effects were evaluated by calculating the BLISS index and visualized by SynergyFinder Plus. Immunoblotting was performed using antibodies against pCDK1 (Tyr15), pERK, pAkt, MCL1, BIM, PUMA, BCL2, or BCL-xL. In vivo efficacy studies were performed using a KRAS G12C mutant H358 xenograft nude mouse model.
Results: Through the large-scale unbiased combination screening of -1,400 kinase inhibitors, we identified a WEE1 inhibitor (AZD1775), a G2/M checkpoint abrogator in clinical-stage development, as a promising combination partner of sotorasib in KRAS G12C mutant NSCLC. The synergistic effects in vitro were broadly observed in multiple KRAS G12C mutant NSCLC cell lines, regardless of single-agent sensitivity to sotrasib or co-occurring oncogenic mutation profiles. The combination treatment upregulated pro-apoptotic protein BIM, leading to apoptosis. In vivo efficacy studies in H358-xenografted models also demonstrated remarkable tumor regression and durable response in mice treated with sotorasib and AZD1775 compared to ones with a single agent alone.
Conclusion: We identify AZD1775, a WEE1 inhibitor, as a novel combination candidate, which enhanced the anti-tumor activity of sotorasib both in vitro and in vivo preclinical models. These findings can lead to a novel therapeutic strategy for KRAS G12C mutant NSCLC.

Novel Antitumor Agents, PI3K/AKT Inhibitors, Proteasome Inhibitors, and Topoisomerases

#4923

Prostaglandin E2 receptor EP2: A novel target for high-risk neuroblastoma

Ruida Hou[1], Ying Yu[2], Jun Yang[3], Jianxiong Jiang[2]. *[1]University of Tennessee Health Science Center, Memphis, TN,[2]Pharmaceutical Sciences,*

University of Tennessee Health Science Center, Memphis, TN,[3]Surgery, St. Jude Children`s Research Hospital, Memphis, TN

Neuroblastoma (NB) is the most common pediatric extracranial solid tumor. Based on tumor stage and histological features, 50% of NBs are classified as high-risk diseases, a subtype characterized by a quite unsatisfactory long-term survival even with the striking advances in NB management that have been achieved in the past decades. Cyclooxygenase-2/prostaglandin E2 (COX-2/PGE_2) cascade has been reported to foster a proinflammatory tumor-nourishing microenvironment in NB. However, the specific downstream PGE2 receptor (EP) subtype which directly mediates this tumor promoting effect remains elusive. Therefore, in our research, we aim to 1) elucidate the culprit EP receptor that is directly involved in NB development; 2) evaluate the feasibility of inhibiting the PGE_2 receptor subtype as a novel treatment strategy for high-risk NB. To start with, we analyzed the gene expression profiles of the COX2/PGE_2/EP pathway from four major NB datasets (Versteeg, Kocak, SEQC, and NRC) on R2 platform. It indicates that the COX-2/PGE_2/EP2 signaling axis is highly associated with the expression of high-risk NB markers, as well as an abysmal overall survival rate. Moreover, a time resolved fluorescence resonance energy transfer (TR-FRET) method was adopted to reveal that EP2 receptor is the key Gαs-coupled receptor that mediates PGE2-initiated cAMP signaling in high-risk NB cell lines. Genetic interference of EP2 receptor expression by CRISPR/Cas9-mediated genome editing and doxycycline induced conditional knockdown significantly inhibited high-risk NB development and progression both in neuro-sphere formation assay and in nude mice xenograft models. Finally, we tested the anti-NB efficacy of our recently developed selective and bioavailable small-molecule EP2 antagonists. With a consecutive treatment of three weeks, decreased tumor size and weight have been observed in both high-risk NB xenograft model and immunocompetent allograft model, simultaneously with decreased inflammation, angiogenesis, and enhanced apoptosis. Collectively, our results suggest that the PGE2/EP2 pathway contributes to the growth and malignant potential of high-risk NB; pharmacological inhibition on EP2 receptor by our drug-like compounds might provide a novel therapeutic strategy for this deadly pediatric cancer.

#4924

Alternative lengthening of telomeres is associated with hypersensitivity to topoisomerase 1 inhibition in glioblastoma xenograft models

Stephen T. Keir, Heng Liu, Justin T. Low, Christopher J. Pirozzi, Nathan Reynolds, Eric S. Lipp, Annick Desjardins, Henry S. Friedman, Mustafa Khasraw, Darell D. Bigner, David M. Ashley, Matthew S. Waitkus. *Duke University School of Medicine, Durham, NC*

Glioblastoma (GBM), the most common primary malignant brain tumor in adults, is an incurable disease that has an inevitable tendency to recur following standard of care surgery, radiotherapy, and temozolomide chemotherapy. There is an urgent need for improved medical therapies. The topoisomerase I inhibitor irinotecan has been investigated and used in the treatment of GBM for over 20 years. Clinical trials investigating irinotecan as monotherapy and in combination with temozolomide and bevacizumab have failed to show an overall survival benefit for newly diagnosed and recurrent GBM. Consequently, irinotecan is not commonly recommended for GBM treatment. However, these trials were conducted prior to the advent of molecularly-guided GBM subtyping, which is now a cornerstone of glioma diagnostics according to the updated WHO 2021 classification. To understand the extent to which molecularly-defined glioma subgroups differentially respond to clinically relevant therapies, we investigated the sensitivity of GBM patient-derived xenografts (PDXs) against a panel of chemotherapeutic agents, including temozolomide, bevacizumab, and irinotecan. All GBM PDXs (n=9) were responsive to irinotecan when grown as subcutaneous tumors. Two PDX lines exhibited hypersensitivity to irinotecan, which was marked by treatment-induced regression of subcutaneous tumors and increased median survival of 61 and 90+ days. Molecular analyses revealed that these hypersensitive lines were both ATRX-deficient tumors that displayed the alternative lengthening of telomeres (ALT) phenotype, while the less sensitive lines were all ATRX-intact and demonstrated *TERT* activation. One of the hypersensitive lines was $IDH1^{R132H/WT}$ while the other was $IDH1^{R132H/-}$ (historically termed secondary GBM; grade 4 astrocytoma per 2021 WHO classification). Cell-based studies showed that irinotecan sensitivity did not correlate with D-2HG producing capacity of the cells and was not impacted by inhibition of

the mutant IDH1 enzyme. Irinotecan treatment significantly prolonged survival of orthotopic ALT+ PDXs relative to a vehicle control (64 days versus 41.5 days median survival). These results suggest that ALT+ gliomas may be particularly sensitive to topoisomerase inhibitor therapy. Our study highlights the need to interpret glioma clinical trial results in light of key molecular biomarkers, including indicators of ALT activity (e.g. ATRX deficiency, ultrabright telomeric foci, and C-circles). In addition, our results suggest that ALT-related biomarkers may be useful for identifying glioma patients who may benefit from topoisomerase inhibitor therapy.

#4925

Cannabidiol and *Cannabis Sativa* as a potential treatment in vitro prostate cancer cells silenced with RBBp6 and PC3 xenograft

Lesetja Raymond Motadi, Zodwa E. Jantjies. *University of Johannesburg, Johannesburg, South Africa*

Background: Prostate cancer is the second most frequently occurring carcinoma in males worldwide and one of the leading causes of death in men around the world. Recent studies estimate that over 1.4 million males are diagnosed with prostate cancer on an annual basis, with approximately 375 000 succumbing to the disease annually. With current treatments continuing to show severe side effects, there is a need for new treatments. In this study we looked at the effect of *cannabis sativa* extract, cannabidiol and cisplatin on prostate cancer cells, PC3.
Methods: In addressing the above questions, we employed the MTT assay to measure the antiproliferative effect on PC3 cells following treatment with varying concentrations of *Cannabis sativa* extract, cisplatin and cannabidiol. xCELLigence was also used to confirm the IC50 activity in which cells were grown in a 16 well plate coated with gold and monitor cell attachment. Caspase 3/7 activity was also measured using 96 well-plate following treatment. Western-blot and qRT-PCR was also used to measure the gene expression of tumor suppressor genes, p53, Bax and Bcl2. Animal studies were employed to measure the growth of PC3-mouse derived cancer to evaluate the effect of compounds *in vivo* .
Results: From the treatment with varying concentrations of *Cannabis sativa* extract, cannabidiol and cisplatin, we have observed that the three compounds induced antiproliferation of PC3 cancer cell lines through the

activation of caspase 3/7 activity. We also observed induction of apoptosis in these cells following silencing of retinoblastoma binding protein 6 (RBBP6), with upregulation of p53 and bax mRNA expression, and a reduction in Bcl2 gene expression. The growth of tumors in the mouse models were reduced following treatment with cisplatin and cannabidiol. Conclusion: We demonstrated that cannabidiol is a viable therapy to treat prostate cancer cells, in combination with silencing of RBBP6. This suggests that cannabidiol rather *Cannabis sativa* extract may play an important role in reducing cancer progression.

#4926

Alpelisib in combination with trastuzumab and pertuzumab as maintenance therapy in patients with HER2+, *PIK3CA*-mutant advanced breast cancer: EPIK-B2 Study Part 1 safety and efficacy results

Sara A. Hurvitz[1], François-Clement Bidard[2], Wei Li[3], Xichun Hu[4], Sonia Pernas[5], Joseph Thaddeus Beck[6], Mario Campone[7], Kevin Punie[8], Michelle Miller[9], Mathilde Kaper[9], Yu Han[9], Farhat Ghaznawi[9], Guy Jerusalem[10].
[1]Department of Medicine, UCLA David Geffen School of Medicine, Jonsson Comprehensive Cancer Center, Los Angeles, CA,[2]Department of Medical Oncology, Institut Curie, UVSQ/Université Paris-Saclay, Saint-Cloud, France,[3]Cancer Center, The First Hospital of Jilin University, Changchun, China,[4]Department of Medical Oncology, Fudan University Shanghai Cancer Center, Shanghai, China,[5]Department of Medical Oncology, Institut Català d'Oncologia, L'Hospitalet, Barcelona, Spain,[6]Highlands Oncology, Springdale, AR,[7]Institut de Cancérologie de l'Ouest, Saint Herblain, France,[8]Department of General Medical Oncology and Multidisciplinary Breast Centre, Leuven Cancer Institute, University Hospitals Leuven, Leuven, Belgium,[9]Novartis Pharmaceuticals Corporation, East Hanover, NJ,[10]CHU Sart Tilman Liège and Liège University, Liege, Belgium

Introduction: Current standard first-line (1L) treatment (tx) for patients (pts) with human epidermal growth factor receptor 2 (HER2)-positive advanced breast cancer (ABC) includes taxanes plus trastuzumab (T) and pertuzumab (P). Mutations (mut) in phosphatidylinositol-4,5-bisphosphate 3-kinase catalytic subunit alpha (*PIK3CA*) gene encoding PI3Kα have been reported

in 12%-39% of HER2+ BCs and associated with worse prognoses and lower pathological complete response to anti-HER2 tx in the neoadjuvant setting. Alpelisib (ALP) is an oral, α-specific PI3K inhibitor approved at 300 mg per day (QD) in combination with fulvestrant in hormone receptor (HR)-positive, HER2−, *PIK3CA*-mut ABC following progression on/after endocrine therapy. EPIK-B2 is a 2-part Phase 3 study to evaluate ALP plus T+P as 1L maintenance tx in pts with HER2+, *PIK3CA*-mut ABC, without progressive disease at study entry. Here, we report results of Part 1, the safety run-in of EPIK-B2.

Methods: Part 1 of EPIK-B2 was open label and assessed safety of ALP plus T+P in pts with HER2+ ABC and confirmed the recommended Phase 3 dose of ALP for the randomized Part 2. Pts with HER2+ ABC, with or without a *PIK3CA* mut, who had completed induction taxane chemotherapy plus T+P were eligible for Part 1. Part 2, currently enrolling, allows only *PIK3CA*-mut pts. Pts in Part 1 received 300 mg (Cohort A) or 250 mg (Cohort B) ALP QD plus 6 mg/kg T and 420 mg P, on Day 1 of each 21-day cycle. The primary endpoint of Part 1 was incidence of dose-limiting toxicities (DLTs) in the first 6 wk of tx; secondary endpoints included safety/tolerability and ALP exposure by dose level. Preliminary confirmed overall response rate (ORR; best overall response [BOR] of CR/PR) and clinical benefit rate (CBR; BOR of CR/PR/SD lasting ≥24 wk) were evaluated per RECIST v1.1 during the on-treatment period.

Results: Three pts in Cohort A and 12 in Cohort B received 300 mg and 250 mg ALP, respectively. DLTs, 1 event each of hyperglycemia and dermatitis acneiform, were seen in Cohort A, none were reported in Cohort B pts given 250 mg ALP; however, Part 2 of EPIK-B2 will be initiated with 200 mg ALP with the option of intrapatient dose escalation to 250 mg QD, the maximum tolerated dose, per FDA feedback to consider a lower toxicity threshold in 1L maintenance setting. No unexpected AEs were reported; most common AEs were diarrhea, decreased appetite, and hyperglycemia. Six of 15 pts (40%; 2 in Cohort A, 4 in Cohort B) had *PIK3CA*-mut disease. Among these, ORR was 50% (n/N=3/6) and CBR was 100% (n/N=6/6). Tumor response was maintained in 5 of 6 pts with *PIK3CA* mutations (83%) after ≥21 cycles of tx (range, 21-31).

Conclusions: ALP plus T+P combination is safe; reported AEs align with those in previous ALP studies. Preliminary efficacy data suggest promising

clinical benefit with ALP plus T+P for pts with HER2+ *PIK3CA*-mut disease.

#4927

Exarafenib (KIN-2787) is a potent, selective pan-RAF inhibitor with activity in preclinical models of BRAF class II/III mutant and NRAS mutant melanoma

Tim S. Wang[1], Catherine Lee[1], Paul Severson[2], Robert J. Pelham[2], Richard Williams[2], Nichol L. G. Miller[1]. *[1]Kinnate Biopharma, San Diego, CA,[2]Kinnate Biopharma, San Francisco, CA*

Background: MAPK activating mutations are common in melanoma, with 40% of cases attributed to oncogenic BRAF mutations and 20-25% NRAS mutations. Secondary MAPK activation is a known resistance mechanism to approved BRAF inhibitors in BRAFV600 melanoma. While BRAF inhibitors are approved for Class I BRAFV600 melanomas, patients with dimer-driven BRAF Class II/III and RAF1-dependent NRAS activated melanomas lack approved targeted therapy. Development of next-gen pan-RAF inhibitors targeting all RAF proteins and mutant dimers remains a priority. Emerging clinical data from pan-RAF inhibitors combined with MEK inhibitors suggests increased benefit for MAPK-altered melanoma patients. Exarafenib (KIN-2787) is a clinical stage, novel, highly selective pan-RAF inhibitor designed to be effective in RAF-dependent cancers.Methods: KIN-2787 was evaluated using enzyme assays across the human kinome and activity against oncogenic RAF alterations were validated in BaF3 cells. MAPK pathway suppression and cell growth inhibition were assessed across a panel of human tumor cell lines. Combination dose matrices were performed with KIN-2787 and binimetinib (bini) to evaluate synergistic cell growth inhibition. Extended cell growth studies were performed by Incucyte. In vivo KIN-2787 efficacy was evaluated in cell line-derived xenograft (CDX) and patient-derived xenograft (PDX) models of human BRAF and NRAS mutant cancer.Results: Exarafenib demonstrated exceptional kinome selectivity with minimal off-target kinases significantly inhibited relative to BRAF. Exarafenib potently inhibited a broad panel of oncogenic BRAF mutations in biochemical and BaF3 cell assays. Functional MAPK signaling and viability studies in human tumor cell lines highlighted exarafenib activity in

BRAF and NRAS mutant melanoma with minimal activity in normal (BRAF WT) cells. Synergy with the MEK inhibitor bini was determined and the exarafenib + bini combination durably inhibited growth in NRAS mutant melanoma cell lines. In line with cellular studies, treatment with exarafenib demonstrated significant tumor growth inhibition at 30 mg/kg BID in CDX and PDX models of human NRAS mutant melanoma. 10 mg/kg BID exarafenib combined with a clinically relevant dose of bini resulted in combination benefit and durable suppression of the MAPK pathway, relative to either agent alone.Conclusions: The superior kinome selectivity of exarafenib and its activity across multiple RAF-dependent melanoma models position it as a potentially class-leading pan-RAF inhibitor. In addition to efficacy in BRAF mutant tumors, these data support use of exarafenib in combination therapy with MEK inhibitors in NRAS mutant melanoma. A Ph I dose escalation clinical trial evaluating the safety and efficacy of exarafenib in monotherapy and in combination with binimetinib is ongoing (NCT04913285).

#4928

Gedatolisib, a well-tolerated pan-PI3K/mTOR inhibitor, exhibits potent therapeutic effects on gynecological cancer models regardless of their PI3K pathway mutational status

Stefano Rossetti, Aaron Broege, Ian MacNeil, Ben Rich, Jhomary Molden, Brian Sullivan, Lance Laing. *Celcuity, Minneapolis, MN*

Background: The PI3K, AKT, and mTOR (PAM) pathway is one of the most commonly activated oncogenic pathways in gynecological cancers. Loss of PTEN function and PIK3CA activating mutations are especially frequent in endometrial cancer (EC). Targeting the PAM pathway, in combination with other cooperative oncogenic pathways (e.g., the estrogen pathway), is a promising EC treatment strategy. Currently, everolimus, an mTORC1 inhibitor, in combination with letrozole, an aromatase inhibitor, is one of the available hormonal therapy options for patients with advanced endometrioid EC. Most PAM inhibitors (PAM-i) selectively spare (or weakly inhibit) one or more key PAM pathway components, which can lead to drug resistance. To minimize drug resistance, a more comprehensive inhibition of the PI3K isoforms and downstream mTOR complexes may be required. We hypothesized that gedatolisib, which potently inhibits all Class

I PI3K isoforms, mTORC1, and mTORC2, can potentially be an effective and well tolerated therapy for patients with EC.
Methods: A panel of endometrial, ovarian and cervical cancer cell lines with different PI3K pathway mutational status were assayed for their sensitivity to gedatolisib and other PAM inhibitors (PI3K-α: alpelisib, pan-PI3K: copanlisib; AKT: capivasertib; mTORC1: everolimus; pan-PI3K/mTOR: gedatolisib). Cell viability, cell proliferation, and flow cytometry analytical assays were conducted. Xenograft studies evaluating gedatolisib in EC cell lines were also performed.
Results: Gedatolisib strongly inhibited PAM pathway activation, and reduced cell cycle progression and cell viability in the endometrial, ovarian, and cervical cancer cell lines. Compared to the other PAM-i, Gedatolisib exhibited superior anti-proliferative potency and efficacy in almost all the cell lines tested, regardless of the PI3K pathway mutational status or cancer type. In EC xenografts, gedatolisib substantively inhibited tumor growth irrespective of the cell line models' PI3K pathway mutational status.
Conclusions: We demonstrated that, gedatolisib induces superior anti-proliferative activity compared to the other PAM pathway inhibitors, regardless of the PI3K pathway mutational status of the cancer cell lines evaluated. Gedatolisib as a single agent and in combination with other therapies has previously reported promising preliminary clinical efficacy and safety in various solid tumor types, including EC. In summary, nonclinical and preliminary clinical data supports the development of gedatolisib in combination with hormonal therapy for treatment of patients with EC.

#4929
ICX-101, a novel MYC inhibitor, shows antitumor activity in patient-derived cells of advanced lung cancer with high MYC expression
Wonyoung Choi, Kyung-Chae Jeong, Seog-Yun Park, Sunshin Kim, Eun Hye Kang, Mihwa Hwang, Ji-Youn Han. *National Cancer Center, Goyang, Korea, Republic of*

Background: MYC is an attractive therapeutic target in lung cancer. ICX-101 is a novel potent, selective small molecule that directly inhibits the binding of MYC/MAX dimers to the DNA binding sequence E-box. Here, we show that ICX-101 shows antitumor activity in patient-derived cells

(PDC) of advanced lung cancer and that the drug responses are correlated with the MYC expression levels.
Methods: PDCs of lung cancer were treated with ICX-101, and the area under the dose-response curve (AUC) was measured as the readout for antitumor efficacy. MYC expression level of each PDC was measured with the fold expression of mRNA compared to the normal lung tissue. The patient's clinical data and survival outcomes were analyzed to correlate with the drug responses of PDCs.
Results: We collected 100 PDCs from 82 lung cancer patients. The histologic types included adenocarcinoma (N = 82), squamous cell carcinoma (N = 10), non-small cell lung cancer (NSCLC) not otherwise specified (NOS) (N = 4), and small cell lung cancer (SCLC, N = 4). PDCs derived from SCLC showed higher MYC expression levels than NSCLC ($P = 0.004$). MYC was a prognostic factor, as the patient groups with the top and bottom 25 percentiles of MYC mRNA expression had an overall survival of 932.5 and 256 days, respectively ($P = 0.029$). However, MYC expression was predictive for the response to ICX-101, as the PDCs with the top 25 percentiles of MYC levels showed markedly lower AUC values than those with the bottom 25 percentile ($P < 0.001$). Additionally, the MYC mRNA levels and AUC values were inversely correlated with statistical significance ($R = -0.46$, $P < 0.001$).
Conclusion: ICX-101 is a potent MYC inhibitor that shows antitumor activity in lung cancer PDCs. Our results suggest the potential of ICX-101 as a possible therapeutic option in advanced lung cancer with high MYC expressions.

#4930
Foldamers mimicking the B-DNA surface as a new class of DNA topoisomerase I inhibitors
Aurélie Garcin[1], Valentina Corvaglia[2], Madeleine Bossaert[3], Marie-Jeanne Pillaire[3], Ivan Huc[2], Sébastien Britton[3], Vincent Parissi[4], Philippe Pourquier[1]. *[1]INSERM U1194 - IRCM (Montpellier), Montpellier, France,[2]Department of Pharmacy and Center for Integrated Protein Science, Ludwig-Maximilians-Universität, Munich, Germany,[3]Institut de Pharmacologie et Biologie Structurale, IPBS - CNRS, Toulouse, France,[4]Laboratoire de Microbiologie Fondamentale et Pathogénicité (MFP) UMR 5234 CNRS, Bordeaux, France*

DNA mimicry has been the subject of intensive research and resulted in the development of DNA analogues such as PNAs and LNAs. There are also examples of proteins with structural and/or charge distribution analogies with respect to the DNA double helix which allow them to interfere with other DNA-binding proteins and modulate the biological processes in which they are involved. We previously characterized a new class of DNA-surface mimic molecules constituted by repetitions of dimeric units of 8-amino-2-quinolinecarboxylic acid (Q) and 8-aminomethyl-2-quinolinecarboxylic acid (mQ). The helical folding of these entities can mimic a B-DNA molecule, displaying a minor and a major groove that can be modulated depending on the dimers and of the nature of their side chains. In vitro, these DNA mimics could inhibit, in a relative selective manner, the catalytic activity of DNA topoisomerase I (Top1), whereas they had no effect on the activity of DNA polymerases or DNAses. Inhibition of Top1-mediated relaxation of supercoiled DNA plasmid increased with the length of the DNA mimics. Here, we further characterized the mechanism of Top1 inhibition by these DNA mimics. We found that, conversely to camptothecin (CPT) and its derivatives that poison Top1 via the inhibition or the re-ligation step of the reaction, DNA mimics inhibited Top1-mediated DNA cleavage *in vitro* by preventing the binding of the enzyme to its substrate, a mechanism of Top1 competitive inhibition that was formerly referred to as catalytic inhibition. We also found that co-incubation of DNA mimics with CPT had an additive effect on the inhibition of Top1-mediated relaxation of supercoiled DNA, further suggesting a mechanism that is different from CPT. Because transfection of DNA mimics could inhibit the growth of various cancer cell lines, we further investigated whether Top1 could play a role in this cytotoxicity. We found that Top1 knock-down in OVCAR4 ovarian cancer cells resulted in decreased sensitivity to the (mQQ4)8 DNA mimic as compared to OVCAR4 control cells, suggesting that Top1 is a target of DNA mimics in cells and is involved in their cytotoxic effects. Conversely to CPT, transfection of HCT116 cells with the (mQQ4)8 DNA mimic was not associated with an increase in γH2AX, suggesting that DNA mimics do not induce DNA breakage. We are currently analyzing whether the (mQQ4)8 can have an impact on CPT-induced Top1-DNA complexes formation. Interestingly, we also showed that several SN38-resistant HCT116 cell clones characterized by specific

Top1 mutations were still sensitive to the (mQQ4)8 DNA mimic. Together our results demonstrate that DNA mimics can be considered as a new class of competitive inhibitors of Top1. Further studies are ongoing to identify the structural features that are essential for Top1 inhibition in order to generate more potent derivatives that could be used to counteract resistance to CPT derivatives used in the clinic.

#4931

Novel cancer suppressing role of REIC/DKK3 protein through a downregulation of cell surface PD-L1 in breast cancer cells

Yuma Gohara, Nahoko Tomonobu, Rie Kinoshata, Lena Audebert, Youyi Chen, Ni Luh Gede Yoni Komalasari, Fan Jiang, Chikako Yoshizawa, Hitoshi Murata, Ken-ichi Yamamoto, Masakiyo Sakaguchi. *Okayama University Graduate School of Medicine, Dentistry and Pharmaceutical Sciences, Okayama, Japan*

Adenovirus vector carrying REIC gene (Ad-REIC) is currently in clinical evaluation. The anti-cancer effect of Ad-REIC is mainly caused by two ways, cancer specific apoptosis via endoplasmic reticulum stress with an abundant REIC protein and indirect immune effects by the secreted REIC protein. The former had been well studied that gave us general comprehension of its mechanisms, however latter has still not been fully elucidated. To clear this, we have aimed to identify putative receptor(s) to the extracellularly secreted REIC protein, and have fortunately succeeded to identify five candidates. Surprisingly, the identified receptors all worked to bind with PD-L1 and hold it to stabilize on the plasma membrane, and the REIC binding to the receptors induced liberation of PD-L1 from the receptors' lock, resulting in an accelerated degradation of PD-L1. This novel insight may lead to the elucidation in important part of the REIC-mediated indirect anti-cancer role.

#4932

The role of KB-S in treating pancreatic cancer

Sadia Noosrat Boshra, Kirpal Bisht, Mildred Acevedo-Duncan. *Chemistry, University of South Florida, Tampa, FL*

Pancreatic cancer remains one of the most lethal malignant cancers because the symptoms of this cancer do not exhibit until the disease progresses to an advanced stage. Late diagnosis may result in metastasis. When metastasis occurs, cancer can no longer be removed with surgery and therefore, requires treatment with FDA approved chemotherapeutic drugs or radiotherapy and they often fail to treat the disease. KB-S is a synthetic thymidine nucleoside analogue which is broadly used for the treatment of Human Immunodeficiency Virus (HIV). In this work, we explored the therapeutic potential of KB-S as an anticancer drug, with focused against pancreatic cancer. Our aim is to establish a connection between cellular kinase of KB-S and atypical protein kinase C (aPKC) to decipher signaling pathways. Pancreatic adenocarcinoma, ASPC-1 cell line was used for the study. Hemocytometer was used for cell counting for the dose response curve after treating with KB-S. Immunoprecipitation study was conducted using anti-PKC-iota beads. Western blot assay was performed using primary antibody PKC-zeta and a secondary antibody. Our results showed that KB-S decreases cell proliferation significantly on AsPC-1 cells over increasing the concentrations. KB-S decreased the proliferation by 20% for 0.5 μM ($P \leq 0.09$), 37% for 5 μM ($P \leq 0.02$), 44% for 10 μM ($P \leq 0.01$), 48% for 20 μM ($P \leq 0.002$) and 54% for 50 μM ($P \leq 0.001$) in AsPC-1 cells. We used the lowest concentration of 10 μM with significant inhibition for further experiments. We immunoprecipitated for PKC-ι and immunoblotted for PKC-ζ and the immunoblots showed that there is no association between PKC-ι and PKC-ζ in pancreatic cancer cell line (AsPC-1). But when we performed reverse immunoprecipitation, we found that there is an association between PKC-ι and PKC-ζ. Again, we immunoprecipitated for thymidine kinase and immunoblotted for PKC-ι and immunoblots showed that there is an association between thymidine kinase and PKC-ι. But when we did the reverse immunoprecipitation, we did not find any association between thymidine kinase and PKC-ι in pancreatic cancer cell line. Based on our preliminary studies, we report the anti-cancer effect of KB-S in treating a pancreatic cancer cell line leading to further future investigations. To the best of our knowledge, this is the first demonstration of therapeutic efficacy of KB-S against a cancer. Given that, KB-S is already approved by FDA for the treatment of HIV, it carries the potential to be repurposed for difficult to cure cancerous diseases such as pancreatic cancer.

#4933

Duvelisib eliminates CLL B Cells, impairs CLL-supporting cells, and overcomes ibrutinib resistance in a patient-derived xenograft model

Shih-Shih Chen[1], Jacqueline C. Barrientos[1], Gerardo Ferrer[1], Priyadarshini Ravichandran[1], Michael Ibrahim[1], Yasmine Kieso[1], Jeffery L. Kutok[2], Marisa Peluso[2], Sujata Sharma[2], David T. Weaver[3], Jonathan A. Pachter[3], Kanti R. Rai[1], Nicholas Chiorazzi[1]. *[1]The Feinstein Institutes for Medical Research, Manhasset, NY,[2]Infinity, Cambridge, MA,[3]Verastem Oncology, Needham, MA*

Duvelisib (IPI-145), a first-in-class, oral, dual PI3K-δ,γ inhibitor, has been approved by the FDA for the treatment of patients with chronic lymphocytic leukemia (CLL), small lymphocytic and follicular lymphoma. Duvelisib potently inhibits PI3K-δ and PI3K-γ, thereby offering a novel therapeutic approach. Here we aimed to understand how duvelisib targets CLL cells and the tumor microenvironment (TME) and hence how it affects CLL, even with BTK-resistant disease.

We first assessed the distinct contributions of PI3K-δ and PI3K-γ on CLL cell survival, proliferation, and migration *in vitro* by using PI3K-δ (PI3K-δi) or PI3K-γ (PI3K-γi) specific inhibitors in addition to duvelisib. We found a significant reduction in viable CLL cells after exposure to PI3K-δi and duvelisib. By measuring Ki67 and p-AKT levels, we found duvelisib and PI3K-δi more potently block CLL cell proliferation than PI3K-γi. PI3K-δi and duvelisib also significantly reduced the migration of CLL B cells into the spleen relative to control. In contrast, PI3K-γi inhibited T cell not B cell homing in vitro and in vivo.

We then investigated the impact of single versus dual inhibitory agents on myeloid cells. Tumor-associated macrophages (TAMs) of the "M2 phenotype" contribute to a pro-tumor TME by preventing the induction of T cell mediated anti-tumor immunity. We expanded murine bone marrow derived monocytes and then polarized them to M2 macrophages, in the absence or presence of PI3Ki. At 100nM, PI3K-γi, but not PI3K-δi, significantly inhibited M2 polarization. Duvelisib significantly reduced *Arg1* expression at doses equal to or above 10nM. While co-culturing leukemic B cells with M2-polarized murine macrophages increased CLL-cell survival, addition of duvelisib to such co-cultures significantly reduced

CLL cell survival. Altogether, duvelisib sensitizes primary CLL cells to apoptosis and abrogates M2 cell-mediated CLL-cell survival.
Finally, in a patient-derived xenograft mouse model (PDX), we demonstrated the essential roles of PI3K-δ and PI3K-γ in the CLL TME. Specifically, we found a more efficacious inhibition in CLL cell burden by dual inhibition of PI3K-δ,γ. Also, samples from patients whose disease progressed on ibrutinib were responsive to duvelisib therapy in PDX, irrespective of *BTK* mutations. In support of this, we identified an ibrutinib resistant CLL patient, with a clone exhibiting *BTK* and *PLCγ2* mutations who responded immediately to single agent duvelisib with redistribution lymphocytosis followed by a partial clinical remission associated with subsequent modulation of T and myeloid cells.
In conclusion, our data define the mechanism of action whereby dual inhibition of PI3K-δ,γ affects CLL B cell numbers and T and myeloid cell pro-leukemia functions, supporting the use of duvelisib as a potentially valuable therapeutic intervention, including for patients refractory to BTKi.

#4934

CAPAC: a modular platform that can improve the safety and efficacy of existing cancer therapies

George Coricor, Jesse M. McFarland, Masa Aleckovic, Sangeetha Srinivasan, John Lee, Leslie Priddy, Matthew Tso, Tri-Hung Nguyen, Jose M. Mejia Oneto. *Shasqi Inc, San Francisco, CA*

Click chemistry is a Nobel Prize winning technology that has been widely used in research across the life sciences. Shasqi's Click Activated Protodrugs Against Cancer (CAPAC^{TM}) platform is pioneering the therapeutic application of click chemistry reactions in humans. The 1st gen CAPAC technology enables activation of potent anti-cancer agents at the tumor site while reducing systemic exposure and is comprised of a tetrazine-modified biopolymer (tumor targeting agent) injected intratumorally and a systemically administered trans-cyclooctene-modified payload, named a protodrug. Our lead clinical candidate SQ3370 (SQL70 biopolymer + SQP33, doxorubicin protodrug), is being evaluated in a Phase 2a study in solid tumors (NCT04106492). CAPAC platform is highly modular and can be applied to multiple cancer drugs especially those with narrow therapeutic index(s) due to toxicity. Because the tumor targeting

agent (i.e., biopolymer) is separate from the protodrug, it enables the flexibility of interchanging different protodrugs with different mechanism of actions such as tubulin inhibitors (e.g., paclitaxel), topoisomerase inhibitors (e.g., exatecan), immune activators (e.g., TLR agonists), and others. This benefit can be translated in the clinic with tailored combinations for individual patients. Here we will present data on protodrugs of paclitaxel, exatecan, and TLR7/8a agonist. These therapeutics have shown considerable safety concerns either alone or in combination with other therapies in the clinic and may benefit from the precise activation at the tumor site that can be achieved by the CAPAC platform. *In vitro* cytotoxicity assays showed ≥20 fold-attenuation of both paclitaxel and exatecan protodrugs in various cancer lines. In a proliferation assay using mouse splenocytes we observed ≥100-fold attenuation of a TLR7/8a protodrug. These results suggest that the protodrugs may exhibit higher therapeutic indeces with enhanced safety profile. We tested the anti-tumor efficacy of paclitaxel protodrug in combination with SQL70 biopolymer in NCI-N87 gastric cancer xenograft tumor model. The doses of paclitaxel protodrug were 4x or 10x molar equivalent to the MTD of conventional paclitaxel. We observed significant reduction of tumor growth compared to vehicle ($p<0.0001$) and minimal body weight loss suggesting enhanced safety profile. *In vivo* studies to determine the safety and efficacy of these protodrugs are ongoing and will be presented. The data presented illustrates how the CAPAC platform is modular and expands the therapeutic window of different cancer therapies to achieve greater effect. This modularity enables the rapid access of therapeutic combinations. Moreover, as the click chemistry activation is independent of biological characteristics of tumors, CAPAC payloads are highly translatable across species and accelerate the path to the clinic.

#4935

Cannabidiol and cannabis extract protect cells against platinum-based chemotherapy via cellular uptake

Tereza Buchtová, Lucie Beresova, Katarina Chroma, Martin Mistrik.
Faculty of Medicine and Dentistry, Institute of Molecular and Translational Medicine, Palacky University, Olomouc, Czech Republic

Cannabinoids including cannabidiol belong between constituents of cannabis sp. (marijuana plant). Purified or as a part of cannabis products, the compounds are frequently used by cancer patients to attenuate chemotherapy-induced side effects such as pain, nausea, and vomiting. The presence of cannabis products on the public market expands each year while the illegality status weakens in an increasing number of countries. U.S. Food and Drug Administration has approved several cannabis-based drugs for seizures induced by Lennox-Gastaut syndrome, Dravet syndrome, or tuberous sclerosis complex, also for the lost appetite of AIDS patients, and chemotherapy-induced nausea and vomiting. Oncological patients are further and strongly motivated to take the drugs in combination with chemotherapy by numerous reports demonstrating the anticancer effects of cannabinoids. Nevertheless, here we present unsettling data that cannabis extract together with CBD negatively interferes with worldwide approved platinum-based drugs cisplatin, carboplatin, and oxaliplatin. The phenomenon is proven across three cellular models including primary cells. Even low concentrations of cannabidiol or cannabis extract reduced the toxicity of platinum-based drugs using long-term colony forming assay and/or short-term crystal violet assay. Increased resistance of cells was also accompanied by decreased cellular stress as evaluated by quantitative immunofluorescence microscopy and immunoblotting. Most importantly, concomitant cannabidiol and cisplatin exposure results in the decreased presence of cisplatin-modified DNA. Following the information, we determined platinum content in cells by ICP-MS. The experiment uncovered significantly decreased intracellular platinum content indicating an effect on cellular transport. Furthermore, the mechanism is translational independent as shown by the experiment with cycloheximide. This study offers crucial information that patients and physicians should take into account regarding possible interactions between platinum-based drugs and cannabis-based products. Furthermore, the study on the contradictory effects of cannabis products in cancer treatment may be motivated by this project.

#4936

Activity of carfilzomib in head and neck cancer cell lines in vitro

Abdullah S. Eldaly[1], Douglas B. Stairs[2], Mitchell Machtay[1]. *[1]Radiation Oncology, Penn State Hershey Cancer Institute, Hershey, PA,[2]Pathology*

and Laboratory Medicine, Penn State Hershey Cancer Institute, Hershey, PA

Background: Carfilzomib (CF) is a 2nd generation proteasome inhibitor with activity in hematologic cancer, but its study in solid tumors like squamous cell carcinoma of the head and neck (SCCHN) is limited. We investigated its antitumor activity in three SCCHN cell lines.
Methods: Cells: We studied two human tongue cell lines (CAL27; SCC-25) and one pharynx line (FaDu); all HPV-negative and p53-mutant. MTT assays: We utilized MTT assays to evaluate cytotoxicity of CF, cisplatin, and their combination. The IC_{50} of CF and Combination Index (CI) of varying concentrations of combined CF and cisplatin were calculated. Clonogenic assays: Cells were seeded at low density and after 24 hours, cells were treated with varying concentrations of CF. Plates were incubated for 10 days. The cells were fixed and stained with crystal violet dye and colonies counted. Wound Healing assays: After cells reached 100% confluence, a scratch was created using a 200 µL micropipette. Cells were treated with CF and images were acquired at 0, 24, 48, and 72 hours post-scratch.
Results: MTT assays: IC_{50} values as a function of exposure lengths are shown in Table 1. CAL27 was the most sensitive while SCC-25 was the most resistant. In all cell lines, the results of combined CF and cisplatin were complex: at lower doses there was evidence of antagonism, while at higher doses there was synergy. Clonogenic assays: CF significantly inhibited clonogenicity compared to DMSO control ($P \leq 0.05$). The surviving fraction for CF 2.5, 5, and 10 nM were 0.411. 0.151, 0.051, and 0.5, 0.339, 0.102 in CAL27 and SCC-25 cell lines, respectively. Wound Healing assays: Wound closure % after treatment with CF5 was significantly different from DMSO control ($P \leq 0.05$). Wound closure % for CF5 were 30.97, 56.75, and 28.03% compared to 94.65, 75.88, and 42.05% for control in CAL27, FaDu, and SCC-25 cell lines, respectively.
Conclusion: CF exhibits antitumor effects in SCCHN in vitro. Our findings support further investigation of CF in combination with conventional agents in vitro and in vivo.

IC50 values for carfilzomib in head and neck cancer cell lines

Cell line	24 hours	48 hours	72 hours

CAL27	18.02 (11.76- 28.22)	9.364 (7.189- 12.45)	6.401 (5.579- 7.373)
FaDu	57.34 (41.98-84.90)	16.22 (13.438- 19.446)	8.237 (7.260- 9.365)
SCC25	77.78 (67.18- 91.30)	12.87 (11.36- 14.64)	11.49 (10.51- 12.58)

#4937

Immunoproteasome inhibitors for the treatment of t(4;11)-driven ALL

Alexei F. Kisselev[1], Tyler W. Jenkins[2], Elise Fitzerald[2], Andrey V. Maksimenko[3], Peter Panizzi[2], Jennifer L. Fields[4], Steven N. Fiering[4], Amit K. Mitra[2]. *[1]Auburn University Harrison College of Pharmacy, Auburn, AL,[2]Drug Discovery and Development, Auburn University Harrison College of Pharmacy, Auburn, AL,[3]Drug Discovery and Developmentpment, Auburn University Harrison College of Pharmacy, Auburn, AL,[4]Norris Cotton Cancer Center, Geisel School of Medicine at Dartmouth College, Lebanon, NH*

The t(4;11)(q21;q23) chromosomal translocation that creates the MLL-AF4 fusion protein, confers a poor prognosis in infant acute lymphoblastic leukemia (ALL). This translocation also sensitizes cells to proteasome inhibitors bortezomib and carfilzomib, which are approved by the FDA for the treatment of multiple myeloma. Clinical activity of bortezomib in combination with standard chemotherapy has been documented in several clinical trials of ALL patients, and a case of a single-agent activity against relapsed leukemia driven by the MLL-AF4 translocation has been described. However, toxicities of bortezomib and carfilzomib may be unacceptable to pediatric patients. We found that the overwhelming majority of proteasomes in this subtype of ALL are lymphoid tissue specific immunoproteasomes. Cells with MLL-AF4 translocations were sensitive to pharmacologically relevant concentrations of specific immunoproteasome inhibitors ONX-0914 and M3258. Furthermore, both compounds dramatically delayed growth of orthotopic xenograft tumors in mice. Thus, immunoproteasomes are therapeutic targets in ALL and replacing bortezomib and carfilzomib with immunoproteasome inhibitors in ALL should reduce toxicities associated with inhibition of the proteasomes in non-lymphoid tissues.

#4938

DP-9024, an investigational small molecule modulator of the integrated stress response kinase GCN2, synergizes with asparaginase therapy in leukemic tumors

Gada Al-Ani, Kristin M. Elliott, Qi Groer, Aaron J. Rudeen, Patrick C. Kearney, Jeffery D. Zwicker, Yu Mi Ahn, Stacie L. Bulfer, Cale L. Heiniger, Molly M. Hood, Salim Javed, Joshua W. Large, Max D. Petty, Kristen L. Stoltz, Bertrand Le Bourdonnec, Bryan D. Smith, Daniel L. Flynn. *Deciphera Pharmaceuticals, LLC, Lawrence, KS*

Background: The integrated stress response (ISR) is a major adaptive pathway stress response pathway and plays an important role in cell fate determination in response to stress. Oncogene addicted tumors are under high levels of stress, both extrinsic as well as intrinsic, and are dependent on a well-balanced ISR to cope with the high metabolic demands for accelerated growth. The ISR is a double edge sword of survival and cell death, and depending on context, activation of the ISR kinase GCN2 can have either cytoprotective or cytotoxic effects. Activation of GCN2 was identified as a resistance mechanism to asparaginase (ASNase) in asparagine synthetase (ASNS)-low leukemic cells and MAPK-driven solid tumors.[1-3] The inhibition of GCN2 in the context of ASNase-resistant leukemic cells can be pharmacologically leveraged to induce anti-tumoral effects.

Methods: Modulation of ISR kinases was characterized using enzymatic assays. Kinome selectivity profiling was determined using enzymatic and cellular assays. ISR pathway modulation was assessed using cellular assays of phospho-GCN2 and ATF4 by Western blot or ELISA under basal, ASNase-treated, or amino acid starvation conditions. Re-sensitization of leukemic cells to ASNase was tested in cell proliferation assays *in vitro*. *In vivo* compound-mediated reversal of ASNase-induced upregulation of tumoral ATF4 was determined in a leukemia PK/PD xenograft model. Inhibition of tumor growth was determined in leukemia xenograft models *in vivo*.

Results: DP-9024 was designed as a selective and potent modulator of PERK and GCN2. DP-9024 was found to reverse ASNase-mediated upregulation of ISR readouts (phospho-GCN2 and ATF4) in leukemic cells *in vitro*. Additionally, DP-9024-mediated inhibition of GCN2 was found to

re-sensitize leukemic cells to ASNase *in vitro*. *In vivo* asparagine depletion by Leunase (L-asparaginase) led to upregulation of ATF4 in leukemia tumors in a PK/PD xenograft model and oral dosing of DP-9024 reversed Leunase-mediated upregulation of tumoral ATF4 down to basal levels. Importantly, we found that DP-9024-mediated inhibition of GCN2 strongly synergized with ASNase *in vivo*, leading to potent inhibition of tumor growth in leukemic xenografts and causing a reversal of ASNase resistance in leukemic tumors *in vivo*.
Conclusions: The ISR kinase GCN2 was identified as a resistance mechanism to ASNase in ASNS-low leukemic cells. Inhibition of the ISR pathway through the potent and selective small molecule modulator of GCN2, DP-9024, synergized with ASNase and re-sensitized leukemic cells to amino acid withdrawal *in vitro* as well as in leukemic xenograft models *in vivo*.
References:
Nakamura et al. 2018. PNAS 115(33):E7776-E7785
Apfel et al. 2021. ACS Pharamacology and Trans Sci 4(1):327-337
Gwin et al. 2018. Cancer Cell 33(1):91-107

#4939
Combinatorial approach using covalent menin inhibitor, BMF-219, and/or covalent FLT3 inhibitor, BMF-500, with MEK or BCL2 blockade potentiates therapeutic use in AML
Brian Law. *Biomea Fusion, Inc., Redwood City, CA*

Introduct**ion:**
Acute myeloid leukemia (AML) is a clinically and genetically heterogeneous disease characterized by a highly diverse genomic landscape. Despite recent advances in therapies, treatment outcome remains variable and largely defined by genomic abnormalities such as gene fusions, copy number alterations and point mutations. Mutations in epigenic modifiers, nucleophosmin (NPM1c), signaling and kinase pathway such as KMT2A-re-arrangements (KMT2A-r), internal tandem duplication (ITD) insertions in FLT3, and NRAS mutations are amongst the highest alterations in AML patients with a propensity towards poor response to treatment and overall disease outcome. Such limitations impact the ability to achieve long-lasting response to treatment and result in therapy-induced resistance eventually

leading to relapse. Combinatorial strategies are required to combat resistance and maximize duration of antitumor activity.
BCL2 and MEK blockade in combination with menin and/or FLT3 inhibitors potentiates an improved therapeutic strategy to achieve increased antitumor activity and overcome AML resistance. Here we explored the use of our clinical-stage covalent menin inhibitor, BMF-219, and BMF-500, a covalent FLT3 inhibitor, in combination with each other and in combination with BCL2 and MEK inhibitors in MV-4-11 and MOLM-13 cell lines for 4-days, then viability was measured using CellTiter Glo.
Results:
BMF-219 and BMF-500 as single agents induce effective antitumor activity on MOLM-13 and MV-4-11 cells lines. When dosed in combination, BMF-219 and BMF-500 show beneficial effects affording higher cell killing at lower concentrations. Repeated experiments revealed patterns of increased cell killing is achieved when trametinib, MEK inhibitor, and venetoclax, BCL2 inhibitor, are combined with BMF-219 treatment.
Conclusions:
Collectively, our studies demonstrate the utility of combination strategies to achieve higher antileukemic cell killing with reduced concentrations of menin and FLT3 covalent inhibitors. Additionally, we show benefit of combinatorial approaches of menin and FLT3 covalent inhibitors with MEK and BCL2 blockade. These data provide initial pre-clinical evidence for combining pathway specific inhibitors as a promising therapeutic strategy for further investigation in acute leukemia.

#4940
Proteasome and survivin inhibitors synergize to inhibit the growth of oral cancer organoids
Muhammad Furqan[1], Iffat Aleem[2], Muhammad Tahseen[3], Raza Hussain[3], Asif Loya[3], Muhammad Tariq Mahmood[3], Philippe Gautier[4], Kevin Myant[4], Saira Saleem[3], Amir Faisal[1]. *[1]Life Sciences, Lahore University of Management Sciences, Lahore, Pakistan,[2]Basic Sciences, Shaukat Khanum Memorial Cancer Hospital and Research Centre, Lahore, Pakistan,[3]Pathology, Shaukat Khanum Memorial Cancer Hospital and Research Centre, Lahore, Pakistan,[4]Department of Pathology, Institute of Genetics and Cancer, University of Edinburgh, Edinburgh, United Kingdom*

Oral squamous cell carcinoma (OSCC) is the most prevalent subtype of head and neck cancers that has a disproportionately high incidence and mortality in developing countries in South-Central Asia, including Pakistan. The standard treatment for OSCC generally consists of surgery combined with radiotherapy or chemotherapy; however, the overall survival rates have not improved, and only ~50% of patients survive the disease. Therefore, identifying and validating new drug targets can provide new therapeutic options for improved treatment and better prognosis for OSCC patients. The present study aimed to develop an organoid model from patient-isolated primary tumour cells and determine their drug sensitivity profile coupled with mutational analysis. New combinations of targeted drugs with synergistic activity in oral cancer cells were identified through high-throughput screening followed by validation of their activity in oral cancer cells in 2D monolayer and 3D organoid cultures. Results indicate a synergistic activity of proteasome (PR-171) and survivin (YM155) inhibitors in all tested patient-derived tumour cells and four oral cancer cell lines. Moreover, chitosan-based nanocapsules harboring these drugs showed therapeutic efficacy comparable to free drug combinations, indicating a potential for efficient and targeted delivery. Next-generation sequencing data identified missense mutations in eleven cancer-related genes that encode BRAF, EGFR, KRAS, NRAS, HRAS, MEK1, PIK3CA, PTEN, NOTCH1, TP53 and TERT. The ongoing research aims to correlate the drug sensitivity data with the mutational profile of patient-derived tumour cells to find novel targets. In conclusion, we have developed 3D organoids from patient-derived primary tumours and utilized them to validate the synergistic combination between screen-identified proteasome and survivin inhibitors. Our preclinical study provides a rationale for further evaluation of the novel drug combination in vivo and in clinical settings.

#4941

Development of small molecule RPN13 inhibitors for treatment of glioblastoma

Yung-Nien Chang[1], Ravi K. Anchoori[1], Alex Shimura Yamashita[2], Marina da Costa Rosa[2]. *[1]Up Therapeutics LLC, Frederick, MD,[2]Neurosurgery, Johns Hopkins University, Baltimore, MD*

Glioblastoma (GBM) is an aggressive and deadly brain cancer with a one-year median survival due to the lack of effective targeted treatments. Our goal is to develop a small molecule inhibitor targeting RPN13 protein in the 19S proteasome complex as a new drug for GBM. RPN13 is a proteasome ubiquitin receptor that recognizes ubiquitin-conjugated proteins that are thus tagged for degradation via the 20S proteasome enzymatic complex. GBM is highly sensitive to proteasome inhibition due to its aggressive growth and accumulation of misfolded polyubiquitinated proteins that is insufficiently managed despite increased proteasome levels and enhanced proteasome activity (i.e. proteotoxic stress). Up Therapeutics judiciously designed drug-like RPN13 inhibitors to overcome limitations in the prototype RPN13 inhibitor RA190 identified at Johns Hopkins University. We selected Up284 as lead compound based upon our preliminary studies showing drug-like characteristics, specificity (binding to Cys88 of RPN13), and proteasome inhibition that produces a cytotoxic accumulation of polyUb proteins, ER stress, and reactive oxygen species. Up284 treatment selectively triggers apoptosis in solid tumor types including GBM cell lines and oncospheres. A suitable Up284 formulation was selected by measuring aqueous solubility, stability and on-target activity in mice imaged using a proteasome-dependent in vivo reporter. Up284 can be administered i.v. or orally, and it penetrates through the BBB. As a proof of concept for treatment of GBM, Up284 demonstrated on-target activity in intracranial syngeneic GL261 tumor model by inhibiting proteasome function in tumor tissues. Up284 also well tolerated and regressed tumors in syngeneic, xenograft and spontaneous models of ovarian and breast cancers with acceptable safety profile. Up284 also synergize with current frontline chemotherapeutics and can be used as a single agent or in combination for the treatment of wide range of cancers.

#4942

Heme targeting and its mechanistic role in triple-negative breast cancer suppression

Eranda Berisha, Maria del Carmen Chacon Castro, Adnin Ashrafi, Narges Salamat, Parinaz Sadat Alemi, Li Zhang. *UT Dallas, Richardson, TX*

Breast cancer is the second leading cause of cancer-related deaths and comprises of approximately 30% of all cancer cases affecting women in the

United States. There are three subtypes of breast cancer based on receptor profiles, with the third subtype being triple-negative breast cancer. TNBC accounts for about 10-15% of all breast cancers. The TNBC subtype lacks estrogen, progesterone, and HER2 receptors; it is associated with BRCA1 and BRCA2 mutations. This type of cancer has poor prognosis, tends to be more aggressive, and has limited treatment options compared to the other two subtypes. Heme is an essential molecule in the oxidative phosphorylation pathway and in the generation of reactive oxygen species (ROS). ROS generation causes oxidative stress and induces DNA damage in breast cancer. Therefore, targeting its activity potentially suppresses TNBC tumors. Heme-sequestering protein 2 (HeSP2) binds and sequesters heme. It has been shown that HeSP2 treatment of MDA-MB-231 cells inhibited cell proliferation and colony formation. Moreover, HeSP2 suppresses tumor growth in subcutaneously implanted TNBC MDA-MB-231 xenografts in NOD/SCID mice. Furthermore, in vitro studies using murine TNBC cell models 4T1-fluc Neo and EMT6-fluc Puro cells have also shown that cell proliferation and colony formation were inhibited after HeSP2 treatments of increasing concentrations. Thus, these results encourage the potential use of HeSP2 for breast tumor suppression. To further explore the effects of heme targeting and sequestration, we will determine heme flux in TNBC cell models by measuring the levels of heme uptake, export, synthesis, and degradation. Moreover, we will examine mitochondrial markers for OXPHOS complexes in HeSP2 treated TNBC xenografts using immunohistochemical analysis. Further studies are still underway to understand the role of heme in breast cancer, with preliminary results indicating that heme targeting, and sequestration effectively suppress triple-negative breast cancer and its progression.

#4943

SP-1-39 as a novel tubulin inhibitor overcomes taxane resistance in castration-resistant prostate cancer model

Rui Wang, Kelli L. Hartman, Satyanarayana Pochampally, Duane D. Miller, Wei Li. *University of Tennessee Health Science Center, Memphis, TN*

Colchicine binding site inhibitors have proven to have potent anti-cancer efficacy in many cancer types. Inhibition of tubulin polymerization, a popular mechanism of action for anti-cancer activities, will be activated

once the inhibitor interacts with the colchicine binding site. We have previously developed and reported a potent tubulin inhibitor (SB-216). One of its derivatives, the compound SP-1-39, a pyrimidine dihydroquinoxalinone derivative, has been recently designed to further improve the potency and therapeutic properties. Here, we examined the impact of SP-1-39 on preclinical prostate cancer models in vitro and in vivo. EBI competition assay confirmed that SP-1-39 binds to colchicine-binding site and inhibits the formation of EBI:β-tubulin adduct. The anti-proliferation abilities of SP-1-39 was tested against melanoma, breast cancer, pancreatic cancer, prostate cancer, and paclitaxel-resistant prostate cancer cell lines by MTS assay, and defined IC50 values of 0.2-4 nmol/L. Other in vitro results showed SP-1-39 disrupted microtubule network, induced cell cycle arrest at G2/M phase, and caused apoptosis in paclitaxel-resistant human prostate cancer cells (PC-3/TxR). For in vivo study, 2.5mg/kg SP-1-39 significantly attenuated tumor growth in PC-3/TxR xenograft mouse model, inhibited angiogenesis, and overcame taxane resistance. Our findings demonstrate the preclinical therapeutic efficacy and safety of SP-1-39, and provide support for further exploration of novel tubulin inhibitors as anti-cancer agent for cancer therapy.

#4944

Evaluating the efficacy of spermine analogue ivospemin (SBP-101) in combination with chemotherapy in ovarian cancer

Cassandra E. Holbert[1], Jackson R. Foley[1], Tracy Murray Stewart[1], Michael J. Walker[2], Elizabeth M. Bruckheimer[2], Jennifer K. Simpson[2], Robert A. Casero[1]. *[1]Johns Hopkins University School of Medicine, Baltimore, MD,[2]Panbela Therapeutics, Waconia, MN*

Polyamines are small cationic alkylamines that play critical roles in essential cellular processes governing growth and proliferation. As such, cancers are fully reliant on increased polyamine pools maintained through dysregulation of polyamine metabolism. Pharmaceutical modulation of polyamine metabolism is a promising avenue in cancer therapeutics and has been attempted with enzyme inhibitors, including DFMO (difluoromethylornithine), and polyamine analogues. Ivospemin is a spermine analogue that has shown efficacy in slowing pancreatic and ovarian tumor progression both *in vitro* and *in vivo* and demonstrated

encouraging results in pancreatic cancer clinical trials. We have shown that ivospemin decreases polyamine content through depression of the activity of the polyamine biosynthetic enzyme ornithine decarboxylase (ODC) in a variety of cancer cell lines. Treatment of the VDID8$^+$ murine ovarian cancer model with ivospemin resulted in a marked increase in survival. Here we examine the potential of combining ivospemin and chemotherapeutic agents that are used to treat cisplatin-resistant ovarian cancer. Treatment with gemcitabine, topotecan, and doxorubicin increased the *in vitro* toxicity of ivospemin, while paclitaxel and docetaxel did not have any added benefit over ivospemin alone. Using the VDID8$^+$ model, we further evaluated the efficacy of ivospemin in combination with gemcitabine, topotecan, and doxorubicin *in vivo*. Ascites fluid was used as a marker of tumor burden and evaluated for polyamine content. Addition of ivospemin improved the survival of mice treated with any of the three chemotherapeutics. The ivospemin and doxorubicin combination mice had the greatest median survival time; this combination is being further evaluated in mechanistic studies and additional murine studies. Ovarian cancers have extremely immunosuppressive tumor microenvironments (TME) and metabolic reprogramming of the TME to reduce immunosuppressive phenotypes is a promising approach for treatment. Sustained elevation of polyamine levels supports an immunosuppressive TME, and evidence suggests that pharmacologic depletion of polyamines may reduce immunosuppressive phenotypes. DFMO treatment in the immunosuppressive VDID8$^+$ model influences the immune cells of the TME, and we therefore are investigating the combination of ivospemin and DFMO in ovarian cancer. In addition to the cooperativity of ivospemin and chemotherapeutic agents, we have observed a cooperative antiproliferative response in ovarian cancer cells following DFMO and ivospemin cotreatment. Together, these studies suggest the potential of polyamine modulation by ivospemin and DFMO in combination with standard of care chemotherapy. Future studies will determine influences on the immune microenvironment and will evaluate cooperativity between ivospemin, DFMO, and chemotherapy.

#4945

Inhibition of wild-type PI3Kα signaling is required for durable efficacy in PI3Kα mutant cancer cells due to robust re-activation of wild-type

PI3Kα signaling

John R. MacDougall, Mengqi Zhong, Hanne Merritt, Joselyn S. Del Cid, John Bradley, Raymond Mak, Neil Dhawan, Wei Chen. *Totus Medicines Inc., Emeryville, CA*

PI3Kα is the most mutated oncogene with a high mutation rate in breast, lung, colorectal, gastric, bladder, and other tumor types. However, current inhibitors have had little efficacy in the clinic due to their inability to achieve maximal PI3Kα target engagement in a highly specific and durable manner. Contributing to this is that most PI3Kα mutant cancer cells are prone to robust pathway feedback and re-activation of remaining wild type PI3Kα signaling upon initial inhibition. We have analyzed pathway feedback in a variety of PI3Kα mutant cancer cell lines across multiple diverse indications and found this to be a common trait among PI3Kα mutant cancer cells. Additionally, when the mutant PI3Kα protein alone is targeted in these cells using mutant-specific inhibitors, we observed robust pathway re-activation and tumor cell proliferation. In contrast, TOS-358, a highly selective first-in-class covalent PI3Kα inhibitor, achieved complete inhibition of both PI3Kα mutant and wild type signaling and this correlated with the induction of cell cycle arrest and cell death across a wide variety of PI3Kα mutant tumor types. Furthermore, stimulation of PI3Kα signaling with serum rapidly re-activated the PI3K-AKT pathway in the presence of reversible and mutant specific inhibitors. Covalent molecules (namely TOS-358) achieved complete inhibition of pathway signaling in this format. Overall, this reveals the need to achieve sustained inhibition of both PI3Kα mutant and wild type signaling to achieve durable efficacy in PI3Kα mutant tumors.

#4946

TOS-358, a first-in-class covalent PI3Kα inhibitor, demonstrates superior efficacy and does not induce significant hyperglycemia at efficacious doses in multiple animal models

John R. MacDougall, John Bradley, Raymond Mak, Neil Dhawan, Wei Chen. *Totus Medicines Inc., Emeryville, CA*

PI3Kα is frequently mutated in a variety of cancer types, and the PI3K-AKT signaling axis also plays a role in insulin signaling and glucose

homeostasis. TOS-358 is a highly selective first-in-class covalent inhibitor of PI3Kα and is currently in clinical development in multiple solid malignancies. Interestingly, TOS-358 potently and specifically inhibits PI3Kα deeply and durably, but does not induce significant hyperglycemia in a variety of animal models. TOS-358 has consistently demonstrated superior efficacy comparing to reversible PI3Kα inhibitors (ATP-competitive and Allosteric) across 30+ different PDX and CDX mutant PI3Kα dependent cancer models. Detailed metabolic studies also revealed TOS-358 does not induce significant hyperglycemia effects in mice, rats and dogs at efficacious doses, which mirrors previous finding that show that PI3Kα knockout does not induce significant hyperglycemia. Furthermore, we elucidate that previous reversible PI3Kα inhibitors lead to dramatic hyperglycemia due to their potent inhibition of multiple PI3K isoforms at effective concentrations of the molecules in a cellular setting. This data reveals that highly specific and potent covalent inhibition of PI3Kα leads to dramatically superior efficacy and an improved safety profile.

#4947

Exploration of Annamycin Organotropism to Target Primary and Metastatic Liver Cancers

Rafal J. Zielinski, Krzysztof Grela, Shaohua Peng, Edd Felix, Roberto Cardenas-Zuniga, Damian Grybowski, Stanislaw Skora, Izabela Fokt, Waldemar Priebe. *UT MD Anderson Cancer Center, Houston, TX*

Background. Hepatocellular carcinoma (HCC) is the most common type of primary liver cancer and is responsible for more than 12,000 deaths per year in the US. In addition to primary tumors, the liver is a common site for metastases of many types of cancer, including colorectal, and pancreatic cancer. The life expectancy and outlook for people with liver metastases are typically poor.Annamycin (ANN) is a novel anthracycline of our design that is clinically evaluated as a liposome formulated drug product, L-ANN. ANN and L-ANN display unique organotropism that differs from doxorubicin (DOX). In addition, ANN was shown to have increased potency against multidrug resistant cancer cell lines, and, importantly, L-ANN appeared to be non-cardiotoxic. Objective. The objective of this study was to analyze the pharmacokinetics of two formulations of ANN in the liver in comparison with DOX and to determine its tumoricidal potential in

an HCC model in situ and in an experimental model of liver metastasis. Methods. The pharmacokinetics and tissue-organ distribution studies of L-ANN, free ANN, or DOX were performed in mice and rats. The levels of ANN and DOX in plasma and tissue homogenates were assessed using LC/MS. The antitumor efficacy of L-ANN was studied using HEPA 1-6 hepatocellular carcinoma models (subcutaneous, orthotopic, and experimental liver metastatic models) and compared with CT26 colon cancer liver metastasis experiments.Results. ANN exhibited dramatically higher accumulation in the liver parenchyma when compared to DOX (6-fold higher AUC values). We found that the increased liver uptake of the drug had a direct effect on activity of the drug in vivo. First, we observed clear, dose-dependent inhibition of the subcutaneous tumor growth after systemic (IV) administration of L-ANN. Next, remarkable activity of L-ANN was observed in orthotopic models. For instance, significant inhibition of the tumor growth and extension of the survival of L-ANN treated mice vs. vehicle-receiving animals was observed in HEPA 1-6 models (median survival 29.5 vs 50 days ($p<0.0001$) and 28 vs 59 days ($p<0.0001$), respectively). The significant delay in tumor progression was similar to that recorded in the CT26 experimental metastatic models, and L-ANN treatment strongly correlated with survival in this model as well (median survival 32 vs 53 days in L-ANN and vehicle groups, respectively, $p<0.0001$).Conclusions. Annamycin is a potent, non-cardiotoxic anthracycline with proven in vivo activity against different types of tumors. It showed increased penetration and accumulation in the liver, which correlated with high antitumor activity in HEPA 1-6 hepatocellular carcinoma and CT26 colon cancer liver metastasis models. Expanded studies to assess L-ANN activity in different tumor liver metastasis models as well as HCC models are being planned. It should be noted that L-ANN is currently undergoing clinical trials in patients with pulmonary metastasis soft tissue sarcoma and acute myeloid leukemia.

#4948

The role of zafirlukast and isoquercetin in thiol isomerase inhibition in relation to cancer and its complications

Justine A. Gelzinis, Daniel R. Kennedy. *Western New England University, Springfield, MA*

High levels of thiol isomerases in cancer patients have been correlated with increased tumor growth and an increased risk of cancer-induced thrombosis. Inhibition of major extracellular thiol isomerases, which include the enzymes PDI, ERp57, ERp72 and ERp5 in both cancer and thrombosis, have strong therapeutic potential to treat cancer while also inhibiting cancer-induced thrombosis. In this study, we explored the effects of two thiol isomerase inhibitors, isoquercetin (IsoQ) and zafirlukast (Zafi) against OVCAR8 ovarian cancer cells and a xenograft mouse model created from those cells. To explore the potential of these drugs to inhibit tumor growth and cancer-induced thrombosis, multiple *in vitro* and *in vivo* experiments were performed. Alterations of cellular OVCAR8 thiol isomerase activity were measured using a DI-E-GSSG assay where, after drug treatment separately with both drugs, DTT and the PDI specific fluorescent probe were added to OVCAR8 cells and then monitored kinetically at $520_{nm}/550_{nm}$. Further, the ability of the drugs to inhibit the coagulative potential of OVCAR8 cells was measured by monitoring Factor Xa generation as a marker for tissue factor release. Cells were seeded at a concentration of 100,000 cells, then monitored for Factor Xa generation after addition of a fluorescent probe that is a Factor Xa substrate, Factor VIIa, calcium and Factor X. To explore the effects of IsoQ and Zafi *in vivo,* an OVCAR8 xenograft mouse model was created. Tumors were allowed to grow to an average of $30mm^2$ and mice were then treated with 10 mg/kg IsoQ, 30 mg/kg IsoQ or 30 mg/kg Zafi for 46 days via oral gavage. Blood was collected on Day 46, plasma was isolated and examined for alterations in p-selectin expression via ELISA and alterations in thiol isomerase activity by the DI-E-GSSG assay. Cell surface thiol isomerase activity on OVCAR8 cells was inhibited by 32% after with Zafi and by 35% after treatment with IsoQ. OVCAR8 cell induced Factor Xa generation was significantly reduced by 79% after Zafi treatment and by 35% after IsoQ treatment. In the xenografts, 10mg/kg of IsoQ, 30 mg/kg of IsoQ, and 30 mg/kg of Zafi were all separately able to suppress tumor growth by approximately 85% compared to controls. P-selectin expression decreased by approximately 50% and thiol isomerase activity was decreased by approximately 40% under all 3 treatment conditions. These results demonstrate the potential of thiol isomerase inhibitors to not only treat cancer-induced thrombosis but also the cancer itself, as cancer induced

thrombosis markers and tumor size were both significantly reduced in these experiments.

#4949

Identification of novel regulators of response to PI3Ka inhibition in PIK3CA mutant gastric cancer

Lyla Stanland[1], Hazel Ang[2], Jacob Hoj[3], Yunqiang Chu[4], Patrick Tan[4], Kris Wood[3], Micah Luftig[1]. *[1]Molecular Genetics and Microbiology, Duke University School of Medicine, Durham, NC,[2]Pharmacology and Cancer Biology, Duke University School of Medicine, Durham, NC,[3]Duke University School of Medicine, Durham, NC,[4]Duke National University Singapore, Singapore, Singapore*

PIK3CA, encoding the active alpha isoform of PI3K, is the second most commonly mutated gene in cancer leading to aberrant PI3K/AKT/mTOR signaling and increased protein translation, glucose metabolism, cellular proliferation, survival and migration. Some 4-25% of gastric cancers (GC) display activating *PIK3CA* mutations including 80% of the EBV-associated GC subset. Small molecules including pan-PI3K, dual PI3K/mTOR, and pan-AKT inhibitors have shown only moderate clinical success, primarily due to high toxicity and off target effects. Even isoform specific PI3K inhibitors, such as PI3Kα inhibitors, have displayed similar clinical problems. Importantly, PI3Kα mutation-selective inhibitors are on the horizon and will be key for treatment of *PIK3CA* mutant tumors. However, single agent drug resistance is still an anticipated clinical problem and both intrinsic and acquired resistance will affect success of new drugs. There has been a concerted effort to define mechanisms of resistance as well as identify synergistic drug combinations. In this study we aimed to identify mechanisms of sensitivity and resistance to the PI3Kα-specific inhibitor, BYL719, in *PIK3CA* mutant gastric cancers by using a CRISPR/Cas9-based screening approach. We found that loss of either NEDD9 or BCL-XL was synergistic with BYL719 and led to increased cell cycle arrest and apoptosis, respectively. In addition to identifying these sensitizer genes, the screening approach allowed us to model intrinsic resistance, and we discovered that knockout of the translation and transcription factor, CBFB, conferred resistance to BYL719. To model acquired resistance, we cultured cells in increasing concentrations of BYL719 over three months and

generated clones that were resistant when compared to parental cells. We found that in the clones with acquired resistance, CBFB was significantly down-regulated at the protein and RNA level suggesting a conserved mechanism of drug resistance. We found that CBFB loss led to up-regulation of the serine/threonine protein kinase PIM1, which can phosphorylate and activate several of the same downstream substrates as AKT thereby maintaining pathway activity in the presence of PI3Kα inhibition. Furthermore, a pan-PIM inhibitor re-sensitized both *CBFB* knockout and acquired resistant cells to BYL719. In the TCGA clinical dataset, we found that CBFB is over-expressed in gastric tumors, specifically in the EBV-associated subset, compared to normal tissue and is significantly over-expressed in *PIK3CA* mutant compared to wild type tumors. Consistently, we found that PIM1 expression displays the inverse phenotype. These data suggest that while *CBFB* loss is a key step in the development of PI3Kα inhibitor resistance, *PIK3CA* mutant gastric tumors may be good candidates for clinical success with BYL719 alone and resistance could be prevented with combination with a PIM kinase inhibitor.

#4950

Discovery of potent and selective CK1α molecular degrader with a favorable safety profile for acute myeloid leukemia and solid tumors

Jinuk Kong[1], Jisu Park[1], Heekyu Lee[1], Hyunseok Kang[2], Deokjae Lee[1], Hyunsun Jo[1]. *[1]Pin Therapeutics, South San Francisco, CA,[2]Hematology and Oncology, UCSF School of Medicine, San Francisco, CA*

CK1α, an isoform of casein kinase 1 (CK1), promotes tumor growth by enhancing negative effects of MDM2 and MDMX on p53. Unlike other cancer types, the frequency of *TP53* mutations is relatively low (< 20%) in acute myeloid leukemia (AML). Therefore, promoting apoptosis by activation of p53 pathway has been a promising strategy for treatment of AML with wild-type (WT) *TP53*. However, preclinical activities of p53 activators have not been fully translated into clinic, partly due to their on-target hematological toxicities. We hypothesized that inhibition of CK1α can be an alternative strategy. To develop a small molecule targeting CK1α, we identified a novel CK1α-selective molecular glue degrader (MGD), PIN-A1 through screening of compounds hijacking cereblon (CRBN) E3 ligase. Here, we report its robust pharmacological activities in various

preclinical AML models as a single agent or in combination with other targeted therapies along with its superior safety profile to MDM2 inhibitors. First, we demonstrated PIN-A1 can form a ternary complex with CK1α and CRBN using TR-FRET assay. Selective degradation of CK1α by PIN-A1 was also confirmed by global proteomics analysis. PIN-A1 induced rapid degradation of CK1α in human AML MV-4-11 cells harboring WT *TP53*, followed by increasing the level of p53 protein and its downstream target genes, ultimately leading to apoptotic cell death. Consistent with these results, preferential sensitivity of AML cells with WT *TP53* to the CK1α degrader was demonstrated in screening assay of broad panel of liquid cancer cell lines. When combined with other targeted therapies agents used for AML, PIN-A1 displayed strong synergistic effects in cell killing. To evaluate its pharmacological activity *in vivo*, PIN-A1 was tested in a xenograft model engrafted with MV-4-11 and a dissemination model of MOLM-14, respectively. Systemic administration of PIN-A1 alone resulted in robust antitumor activity consistent with > 90% CK1α degradation in tumor tissues, comparably achieved at a much lower dose in combo treatments. Importantly, animals remained tumor-free (5/8) in the MV-4-11 model or prolonged survival in the disseminated model even after they were no longer on the combination treatment of PIN-A1 with a targeted agent X. Lastly, while PIN-A1 had negligible effects on the viability of human PBMC with minimal activation of the p53 pathway at an efficacious dose range for MV-4-11 (Therapeutic index= 8,333), agent X induced p53 pathway and enhanced anti-leukemic activity to a similar extent in two cell types (Therapeutic index=4). Also, we found that the combination treatment of PIN-A1 with agent X had a substantial effect on several solid tumors driven by enhancing the stability and activity of p53. In summary, these results suggest that a CK1α MGD with its favorable safety profile has a potential to become an effective treatment option for advanced AML and solid tumors.

#4951

Proteasome inhibitor carfilzomib induces apoptosis via downregulation of AKT pathway in HPV negative HNSCC

Woo-Jin Jeong[1], Jiyeong Kim[2], Hye-yeon Lee[2], Zhiyong Wang[3], Walt Amornphimoltham[4], Silvio Gutkind[3]. *[1]Seoul National University Bundang Hospital, Seongnam-si, Korea, Republic of,[2]Seoul National University*

Bundang Hospital, Seoul, Korea, Republic of,[3]University of California San Diego, San Diego, CA,[4]Walailak University, Bangkok, Thailand

Background Head and neck squamous cell carcinoma (HNSCC) presents in heterogenous sites, varied etiology and risk factors, and has diverse genetic background which confer dissimilar response to treatments, including chemotherapy. Here we tested the hypothesis that investigation of HPV presence in a HNSCC cell line would identify pathway contributing to oncogenesis of other HNSCC. We sought to identify pathways that differentially affect HNSCC according to the genetic background, therefore identifying targets and suitable candidate for treatment. We used genetic and pharmacological approaches to inhibit AKT pathway in HNSCC cell lines.
Materials & methods Chemical genetic library screening against 6 HNSCC cell lines were performed. The high throughput combinatorial small molecule screening for cell viability and apoptosis was carried out. Candidate agents were validated in both CAL-27 (HPV-negative) and UM-SCC-47 (HPV-positive) cell lines. Identified pathways and representative targeted agents were validated *in vitro*. Expression of related protein were confirmed by western blot assay.
Results EGFR, PIK3CA, mTOR, CDK1, HSP90AB1, HDAC1, and PSMD1 pathways were identified to be susceptible pathways in HNSCC using high throughput chemical genetic library screening. *In vitro* validation of carfilzomib showed IC50 of 7.07nM in CAL-27 cells and IC50 of 26.3nM in UM-SCC-47 cells. Knockdown of PSMD1 transcripts by transfected siRNAs reduced CAL-27 cells viability. Carfilzomib regulates the AKT pathway by decreasing t-AKT, p-AKT, p-ERK, p-S6 proteins and increasing p21 in CAL-27.
Conclusion Inhibition of AKT pathway treatment with proteasome inhibitor carfilzomib is effective in HPV-negative HNSCC cells. Taken together, our findings reveal carfilzomib induced the apoptotic pathway and suggest that carfilzomib, the representative of a new class of chemotherapeutic drug, may be utilized for overcoming cisplatin-resistance in human SCC.

Novel Targets and Pathways

#4955

Kurarinone, a natural notch signaling inhibitor and modulator of breast cancer stemness

Prem Prakash Kushwaha[1], Mohd Shuaib[2], Kumari Sunita Prajapati[2], Atul Kumar Singh[2], Mahesh Kulharia[3], Shashank Kumar[2], Sanjay Gupta[1].
[1]Urology, Case Western Reserve University School of Medicine, Cleveland, OH,[2]Biochemistry, Central University of Punjab, Bathinda, India,[3]Central University of Himachal Pradesh, Kangra, India

Aberrant activation of Notch signaling pathway plays an important role in breast cancer development, progression, and stem cell renewal. Activation of Notch signaling is triggered by the interaction of Notch receptors with different ligands expressed on neighboring cells that bind and induce a second cleavage by a membrane-tethered metalloprotease. The remaining membrane-bound fragment is cleaved by γ-secretase (GS) releasing the Notch Intracellular Domain (NICD), which translocate to the nucleus to activate the expression of Notch target genes. Current indirect approaches to inhibit Notch signaling are based on agents that bind to GS substrates. In the search of novel Notch signaling inhibitor(s), we screened a number of plant flavonoids for their binding potential to GS substrate. Our *in-silico* study identified kurarinone (KU), a lavandulyl flavanone, having ability to bind to GS complex. The KU-GS complex was structurally and energetically stable during the molecular dynamics simulation period. Interestingly, dose and time dependent toxicity of KU was observed in T47D and MDA-MB-231 breast cancer cells at 1-25μM concentration. KU treatment of cells led to inhibition in cyclin D1 expression, arrest of cells in the G1 phase of the cell cycle and subsequently undergoes apoptosis. KU-mediated apoptosis was a result of altered mitochondria membrane potential and increased ROS production. In dual-luciferase Notch promoter assay, KU inhibited GS-mediated NICD production in transfected HEK293 cells. Furthermore, KU treatment decreased the mammosphere formation potential of MCF-7 cells through altered gene expression involved in self-renewal and stemness. KU treated MDA-MB-231 cells and MCF-7 derived mammosphere showed downregulation of Notch signaling through alteration in the expression of downstream genes such as Hey1, Hes1, and E-cadherin at both transcript and protein levels. Taken together, the present study identified KU as a novel natural Notch signaling inhibitor that could

provide a novel and safer approach for the treatment of breast cancer through reduction in stemness and self-renewal properties.

#4956

Discovering novel targetable pathways by combining functional and multi-omic data from primary ovarian cancer samples

Irene Gutierrez-Perez[1], Bekir Ergüner[1], Pisanu Buphamalai[1], Joost Van Ham[1], Paul Heinz[1], Valentin Aranha[1], Rin Okumura[1], Elisabeth Waltenberger[1], Isabella Alt[1], Claudia Baumgaertler[2], Maja Stulic[2], Edgar Petru[3], Christoph Minichsdorfer[4], Judith Lafleur[5], Lukas Hefler[5], Laudia Hadjari[5], Lucia Dzurillova[6], Jozef Sufliarsky[6], Nikolaus Krall[7], Thorsten Füreder[4], Gregory Ian Vladimer[1], Bojan Vilagos[1], Robert Sehlke[1].
[1]Translational Research, Exscientia, Vienna, Austria,[2]Clinical Operations, Exscientia, Vienna, Austria,[3]Department of Obstetrics and Gynecology, Medical University of Graz, Graz, Austria,[4]Internal Medicine I, Medical University of Vienna, Vienna, Austria,[5]Ordenslinikum Linz - Barmherzige Schwestern, Linz, Austria,[6]National Oncology Institute of Slovakia, Brataslava, Slovakia,[7]Precision Medicine, Exscientia, Vienna, Austria

Background: There is a critical necessity to reveal novel and tractable targets for anti-cancer treatments in indications with high unmet medical need, such as high grade serous ovarian cancer (HGSOC). However, standard process for target discovery using models such as outgrown cell lines and well-averaged readouts has yielded a less than 5% approval rate for drugs entering trials (Thomas *et al.* 2016 Bio.org).
Here, we describe patient-centric target discovery through the use of disease relevant primary OC samples and single cell functional characterization using a platform with proven hemonc translatability (Kornauth *et al.* 2021, Snijder *et al.* 2017). We integrate data from our functional drug testing platform under multiple drug perturbations with matching genomic and transcriptomic data to reveal associations with novel downstream regulators of sensitivity.
Methods: Sensitivity of the cancer cell compartment in primary malignant ascites samples (n = 20; 75% HGSOC) to 85 small molecule drugs, was evaluated using a proprietary and translatable deep learning-driven single cell imaging platform (Vladimer *et al.* 2017). Cancer cell sensitivity from

the drugs was combined with WES, bulk-RNAseq and drug induced changes in phosphoproteome, and single cell RNAseq transcriptome to identify perturbed targets and pathways.
Results: Here we describe a family of TKIs including ALKi that induce cytotoxicity of cancer cells in primary samples, not previously captured in publicly available cell line drug sensitivity screening data (Iorio *et al.* 2016). We report novel sensitivity of OC driven by non-canonical targets of ceritinib such as FAK1 or IGF1R, mediated by the downstream signaling hub YBX1 (Kuenzi *et al.* 2017), involved in NFB pathway regulation (Motolani *et al.* 2021). Indeed, transcriptomic scRNA analysis upon ceritinib treatment of primary OC cells revealed rapid perturbation of numerous NFB pathway members, alongside YBX1 inactivation.
Conclusions: Combining functional endpoints and single cell-based differential expression analysis of primary OC samples, we have identified the NFB pathway and the regulator YBX1 as a promising novel sensitivity for HGSOC treatment development. These and several other important targetable nodes identified, sit outside the recently suggested JAK/STAT pathway (Izar *et al.* 2020), thereby demonstrating a pipeline towards novel drug target and pathway discovery driven by patient-centric, disease relevant models of high-need indications.

#4957

The targeting drug conjugate Tye1001 displayed its potent anti-tumor efficacy in lymphoma

Lichun Sun[1], Mengli Yang[2], Haihua Xiao[1], Yuan Tian[2], Natalya Vasilevich[2], Joseph Fuselier[1], David Coy[1]. *[1]Tulane Univ. Health Sciences Ctr., New Orleans, LA,[2]Tyercan Bio-Pharm Company, Shenzhen, China*

Multiple drug-targeting strategies have been applied to drug development in order to reduce the toxic side effects of the traditional chemotherapy while enhancing its anti-tumor efficacy. Various peptides, proteins and antibodies are usually used to conjugate cytotoxic agents via acting as drug delivery vehicles. In our previous studies, we identified that peptides displayed their efficacious functions to deliver small molecules or oligo DNA to the target sites through ligand-receptor interactions and quick internalization. In our present study, we attempt to synthesize serial drug conjugates via coupling these compounds to peptide or protein vehicles. Tye1001, one of these

conjugates, displayed similar potent anti-proliferation activities in lymphoma cells and many other cancer cells compared to the small molecule itself. In particular, this conjugate significantly enhanced its potent anti-tumor efficacy in xenografts. Meanwhile, this conjugate has much less toxic side effects. In our in vivo assays, the similar results were also observed in multiple other tumors such as gastric cancer and leukemia. Our findings provide a more potential druggable opportunity in the clinical applications of cancer patients and the treatment of different types of cancers.

#4959

TIC10/ONC201 activates ClpP to degrade ALAS1 while PG3 does not degrade ALAS1 in pathway to HRI, ATF4 and CHOP activation leading to tumor cell death

Xiaobing Tian, Wafik S. El-Deiry. *Brown University, Providence, RI*

TRAIL-inducing compound TIC10/ONC201 binds and activates mitochondrial protease ClpP leading to integrated stress response (ISR) and ATF4 transcription factor activation. Our lab previously reported that ONC201 activates HRI (heme-regulated inhibitor) kinase but does not signal eIF2-alpha phosphorylation through PERK or GCN2. However, the connection between ClpP activation of HRI remains unknown. PG3, a prodigiosin analog that bypasses a defective p53 pathway potently induces ATF4 and pro-apoptotic PUMA. Our data indicate that PG3 activates ATF4 through ISR via HRI as knockdown of HRI but not PKR blocked upregulation of ATF4 and CHOP in several tumor cell lines. We have been exploring how ClpP activation leads to HRI and ISR activation, and the mechanism by which PG3 leads to HRI activation. We find that activation of HRI by PG3 or ONC201 is not through the OMA1/DELE1HRI activation pathway. Moreover, ROS and NO are not responsible for ONC201- or PG3-induced HRI activation. ALAS1 (5'-aminolevulinate synthase 1) catalyzes the first rate-limiting step in heme (Iron-protoporphyrin) biosynthesis. ONC201 treatment leads to potent downregulation and inhibition of ALAS1, indicating that ONC201 inhibits heme biosynthesis. It is well known that reduced heme results in activation of the HRI kinase. We show that an inhibitor of heme biosynthesis or knockdown of ALAS1 results in HRI activation, while knockdown of HRI

blocks upregulation of ATF4 by ONC201. Knockdown of ClpP rescues ONC201-induced downregulation of ALAS1 which blocks ONC201-induced upregulation of CHOP. Our studies identify a novel link between ClpP activation induced by ONC201 treatment and ATF4 upregulation, via the ClpP/ALAS1HRIATF4/CHOP pathway. However, PG3 does not inhibit ALAS1, reduce its expression or therefore signal through ClpP. PG3 treatment did not lead to degradation of ALAS1, indicating that PG3 does not activate ClpP as ALAS1 is a known ClpP direct substrate. We are further investigating the signaling pathway that leads to PG3-induced activation of HRI. Our results suggest that different small molecule inducers of the ISR such as ONC201 and PG3 can achieve an anti-tumor effect through different pathways involving kinase HRI ultimately leading to ATF4/CHOP activation and tumor cell death.

#4960

Fascin inhibitor decreases gynecological cancer cell growth through cell cycle regulation

Wanyi Chen[1], Yufeng Wang[1], Liangliang Ji[2], Ming O. Li[2], Xin-Yun Huang[3]. *[1]Weill Cornell Medical College, Cornell University, New York, NY,[2]Memorial Sloan Kettering Cancer Center, New York, NY,[3]Weill Cornell Medical College, New York, NY*

The actin cytoskeleton is essential for maintaining cell morphology and architecture. Actin-bundling proteins such as fascin cross-link actin filaments into bundles and play critical roles in regulating cell protrusion and motility. Fascin protein expression is low or absent in normal human epithelial cells but high in cancer cells. Elevated fascin levels are correlated with aggressive clinical progression, poor prognosis, and shorter survival outcomes. It is regarded as a cancer progression biomarker and a therapeutic target. We have developed a small molecule fascin inhibitor and shown its efficacy in blocking tumor cell migration, invasion, and metastasis, as well as prolonging the overall survival of mice bearing different types of cancers. Our recent data reveals a new mechanism of this fascin inhibitor in cell cycle regulation of gynecological cancer cells. It blocks the G2/M progression and decreases the mitotic index. Fascin inhibitor treatment also results in aneuploidy, which is a well-known factor for triggering downstream apoptosis. Our data suggests that fascin is

involved in maintaining the fidelity of chromosome segregation and cell division. This will advance our understanding of the interplay between actin and microtubule cytoskeleton during cell mitosis.

#4961

Novel biased PAR2 inhibitors with best-in-class properties reduce resistance to both chemotherapy and immunotherapy in oncology models

Thibaut Brugat[1], Francesco Bergami[1], Baptiste Rugeri[1], Aurélie Janvier[1], Edith Steinberg[1], Luc Baron[1], Mandy Recolet[1], Xavier Wirth[1], Meriem Semache[2], Antoine Mousson[1], Camille Dietsch[1], Quentin Ruet[1], Orphée Blanchard[1], Célia Jacoberger-Foissac[3], Isabelle Cousineau[3], Maleck Kadiri[3], Anne-Laure Blayo[1], Christel Franchet[1], Stanislas Mayer[1], John Stagg[3], Nathalie Lenne[1], Stephan Schann[1]. *[1]Domain Therapeutics, Illkirch, France,[2]Domain Therapeutics NA, St-Laurent, QC, Canada,[3]Centre hospitalier de l'Université de Montréal (CHUM), Montréal, QC, Canada*

A large-scale meta-analysis has recently identified Protease-activated receptor 2 (PAR2) gene expression to be significantly associated with resistance to immune checkpoint blockade (ICB) in cancer patients and preclinical models. PAR2 and its ligands (proteases) are indeed upregulated in different cancer types and are expressed by various cells in the tumor microenvironment. In cancer cells, the PAR2 receptor controls cell migration, proliferation, survival, and expression of inflammatory cytokines. In immune cells, it influences the infiltration and phenotype of macrophages and T cells. Therefore, PAR2 represents a promising therapeutic target in oncology and immuno-oncology. A novel series of potent and selective PAR2 inhibitors has been developed at Domain Therapeutics. *In vitro* experiments demonstrated unique properties of our PAR2 small molecule antagonists when compared to those of competitors. The antagonists inhibit pathogenic signaling pathways (i.e. Gz, G13, Gq, G14 and G15 protein activation as well as intracellular calcium) but not βarrestin2 recruitment, potentially reducing the risks of drug resistance. Furthermore, they maintain high potency and insurmountability in conditions that mimic the tumor microenvironment (high concentration of proteases and acidic pH). Finally, their pharmacokinetic properties are

compatible with a once-a-day oral administration and demonstrate no signs of *in vivo* toxicity except at high doses (>500 mg/kg). Proof-of-concept experiments showed that PAR2 antagonists prevented PAR2-mediated resistance to Gefitinib *in vitro* and increased the potency of anti-PD1 therapy *in vivo* in pre-clinical syngeneic mouse models. Immunohistochemistry analyses from cancer patient biopsies confirmed that high expression levels of PAR2 in cancer and stromal cells within the tumor microenvironment significantly associates with the patient overall survival. In conclusion, new potent and selective negative allosteric modulators of PAR2 have been developed, they demonstrate strong potency by alleviating the resistance to both chemo- and immunotherapy in cancer models. These findings confirm the high value of PAR2 as a therapeutic target and demonstrates the relevance of small molecule inhibitors targeting this receptor to treat cancer.

#4962

Discovery of cancer-specific E3 ligase ligands for targeted protein degradation

Zhaofu Wang, Lynette Zhang, Zhen Chang, Mengxi Zhao, Guobin Li, Fang Qin, Shichao Ma, Yunfeng Li, Zhongguo Zhang, Xinghao Wang, Ying Kong, Shidi Lou, Sheng Chen, Lanzhen Liu, Shuaijie Xu, Hailong Zhang.
Blueray Biopharma, Shanghai, Shanghai, China

F-box/WD repeat-containing protein 7 (FBXW7) is the substrate recognition component of SCF (SKP1-CUL1-F-box protein) E3 ubiquitin-protein ligase complex which mediates the ubiquitination and subsequent proteasomal degradation of target proteins. FBXW7 recognizes and binds phosphor-degrons within target proteins and capture them to SCF complex for ubiquitination. Know FBXW7 substrates include cyclin-E, DISC1, JUN, MYC, NFE2L1, NOTCH2, MCL1, RICTOR, and NOTCH1 released notch intracellular domain (NICD). FBXW7 is frequently mutated in cancer, results in loss of substrate recognition and binding. R465C is a one of the major FBXW7 mutations and is found in over 70,000 cancer patients worldwide. From a high-throughput screen, we discovered compounds that selectively bind to FBXW7 R465C mutant. PROTACs against various protein targets have been made with these mutant specific ligands. Some of these PROTACs could induce targeted protein degradation in cells carrying

FBXW7 R465C mutant but not wild-type FBXW7. Targeted protein degradation with these PROTACs could represent a novel therapeutic approach against FBXW7 R465C mutant cancer.

#4963

Heme Sequestration as an effective strategy for the suppression of tumor growth and progression of SCLC

Adnin Ashrafi, Narges Salamat, Eranda Berisha, Parinaz Sadat Alemi, Maria Del Carmen Chacon Castro, Zakia Akter, Li Zhang. *UT Dallas, Richardson, TX*

Small-cell lung cancer (SCLC) accounts for 15% of all lung cancers with exceptionally high proliferative rate, early metastasis, and poor prognosis. Chemotherapy has provided SCLC patients considerable survival benefits over the past three decades. Etoposide-platinum (EP) is the preferred first-line regimen. SCLC is initially highly responsive to cisplatin and etoposide chemotherapy, but in almost every case becomes rapidly chemo resistant. Despite attempts to improve outcomes utilizing multiple different strategies, drug resistance remains a major obstacle in clinical consequences of patients with SCLC. Recent research aims to elucidate mechanisms of resistance to improve drug response and treatment outcomes. Our lab has shown that limiting heme via inhibition of heme uptake using heme sequestering peptide (HeSP2) can delay growth and progression of NSCLC tumors. This HeSP2 can also effectively inhibit angiogenesis, normalize tumor vasculature, and alleviate tumor hypoxia in NSCLC tumors and thereby inhibit lung tumor advancement. Here we aim to determine if HeSP2 can be used to enhance the therapeutic efficacy of traditional chemotherapy in the treatment of SCLC. Our preliminary results show that HeSP2 can effectively reduce cell proliferation of SCLC cells like H889 and H720. To understand the mechanism by which the heme sequestering protein limit tumor development, we generated human SCLC H889 xenograft lung tumor model in NOD/SCID mice subcutaneously. Mice were treated with saline (control), HeSP2 alone, cisplatin-etoposide, and HeSP2-cisplatin-etoposide in combination. Tumor growth was monitored using caliper measurements. Tumors tissues were harvested, processed and paraffin embedded for immunohistochemistry (IHC) and histology experiments. The results imply that heme sequestration can be a potential

strategy for suppressing small cell lung cancer tumor progression and improve survival outcome of patients.

#4964

SW-682: A novel TEAD inhibitor for the treatment of cancers bearing mutations in the Hippo signaling pathway

Lei Chen[1], Paula Milani de Marval[1], Kendall Powell[1], Mark Johnson[1], Greg Falls[1], Brian Lawhorn[1], Aurélie Candi[2], Amuri Kilonda[2], Bart Vanderhoydonck[2], Arnaud Marchand[2], Matthias Versele[2], Georg Halder[3], Stephen L. Gwaltney[1], Adeela Kamal[1]. *[1]SpringWorks Therapeutics, Stamford, CT,[2]Cistim Leuven vzw & Centre for Drug Design and Discovery (CD3), Leuven, Belgium,[3]VIB Center for Cancer Biology and Department of Oncology, University of Leuven, Leuven, Belgium*

Many cancers harbor mutations in the Hippo pathway that lead to constitutive activation of the transcriptional co-activators YAP/TAZ that then bind the transcription factor TEAD and drive aberrant transcription of target genes involved in cell proliferation and tumor progression. Hyperactivation of YAP/TAZ has also been associated with resistance to targeted therapies, including MAPK pathway inhibitors. To target cancers that bear mutations in the Hippo pathway or are resistant to therapies due to YAP/TAZ activation, we developed SW-682, a pan-TEAD small molecule inhibitor that blocks TEAD-dependent transcription by binding to the palmitoylation pocket of all TEAD isoforms. *In vitro*, SW-682 inhibited the proliferation of human Hippo-mutant mesothelioma cells with nanomolar potency, with little to no effect on Hippo wild-type tumor cells. SW-682 down-regulated TEAD-dependent reporter gene expression in a dose-dependent manner, while having no effect on reporters monitoring other pathways. *In vivo,* daily oral administration of SW-682 to adult mice resulted in tumor regression in Hippo-mutant mesothelioma models and caused down-regulation of expression of the TEAD-dependent genes CCN1 and CCN2 and a YAP gene signature, as measured by qPCR or RNA-seq analysis. SW-682 has a favorable PK profile with good oral bioavailability in the mouse and was well tolerated with no signs of body weight loss. To test the hypothesis that TEAD inhibition can overcome YAP-driven resistance mechanisms, we explored SW-682 in combination with MEK inhibitors in several *in vitro* and *ex vivo* patient-derived tumor models

including BRAF and NRAS mutated melanoma. Moreover, to identify new indications that may benefit from TEAD inhibition, we screened patient-derived 3D organoid tumor cells and matching patient-derived xenograft models that have been molecularly profiled. In summary, SW-682 is a potent and selective investigational TEAD inhibitor which demonstrated anti-tumor effects in models harboring aberrant expression of the Hippo pathway, suggesting therapeutic potential in multiple Hippo-mutant solid tumors.

#4965

Targeting the mitotic kinesin, KIF18A, in chromosomally unstable cancers

James D. Joseph[1], Katherine Schutt[2], Kira Fisher[2], Katelyn Queen[2], Olivia Budington[2], Weifeng Mao[3], Wei Liu[3], Zhengqing Zhu[3], Xiangping Zhang[3], Yisong Xiao[4], Kunmin Lai[4], Xiaohui Gu[4], Jason Stumpff[2], Fred Aswad[5].
[1]Biology, Apeiron Therapeutics, Durham, NC,[2]Department of Molecular Physiology and Biophysics, University of Vermont, Burlington, VT,[3]Biology, Apeiron Therapeutics, Shanghai, China,[4]Chemistry, Apeiron Therapeutics, Shanghai, China,[5]Biology, Apeiron Therapeutics, San Francisco, CA

Background**:** Chromosome instability (CIN), characterized by frequent and ongoing loss or gain of chromosome number, is commonly observed in tumor cells. Although long recognized as a vulnerability of cancer cells, potential CIN-selective therapeutic targets have only recently been discovered. Genetic studies from multiple groups have identified the mitotic kinesin, KIF18A, as selectively essential for the proliferation of CIN and aneuploid cells. By targeting KIF18A genetically and with novel small molecule inhibitors here we present data supporting KIF18A as therapeutic target in CIN tumors.
Methods and Materials: To explore the therapeutic potential of KIF18A, we evaluated the effects of KIF18A genetic depletion and small molecule inhibition in both CIN-positive and CIN-negative cell lines. Biochemical, cell proliferation and phenotypic assays were used to characterize the potency and cellular activity of reference and novel KIF18A small molecule inhibitors. Anti-tumor activity of KIF18A inhibitors was assessed in CIN-positive cell line xenograft models.

Results: In triple negative breast and colorectal CIN positive cancer cell lines siRNA mediated *KIF18A* knockdown and small molecule inhibition of the KIF18A ATPase activity both lead to a reduction in proliferation associated with an increase in mitotic index and multi-polar spindles. Consistent with *KIF18A* knockdown, KIF18A inhibition results in increased spindle length and chromosome alignment defects. Importantly, these effects are not observed with *KIF18A* knockdown or KIF18A inhibition in non-transformed, near diploid cells. In vivo, treatment of CIN-positive xenograft tumors with potent, novel KIF18A inhibitors results in robust anti-tumor activity with minimal impact on body weight.
Conclusions: Collectively our data support KIF18A as a therapeutic target and provide rationale for the continued development of potent selective small molecule KIF18A inhibitors for the treatment of CIN positive cancers.

#4966

Targeting LIF/LIFR autocrine loops with EC359 in ovarian cancer: A novel LIFR targeted therapy

Behnam Ebrahimi[1], Suryavathi Viswanadhapalli[1], Uday P. Pratap[1], Rahul Gopalam[1], Xue Yang[1], Bindhu Santhamma[2], Swapna Konda[2], Xiaonan Li[1], Hui Yan[3], Gangadhara R. Sareddy[3], Zhenming Xu[3], Edward R. Kost[3], Rajeshwar R. Tekmal[3], Hareesh B. Nair[4], Ratna K. Vadlamudi[5]. *[1]ObGyn, UT Health Science Center at San Antonio, San Antonio, TX,[2]Evestra Inc, San Antonio, TX,[3]UT Health Science Center at San Antonio, San Antonio, TX,[4]Evestra, San Antonio, TX,[5]UT Health Science Center at San Antonio, Helotes, TX*

Background**:** Of all gynecologic cancers, ovarian cancer (OCa) has the highest mortality rates. Nearly 90% of patients who receive standard surgical and cytotoxic treatment experience disease recurrence. Leukemia inhibitory factor (LIF) and its receptor LIFR are implicated in the progression of several cancers. A knowledge gap exists on whether LIF/LIFR plays a role in the evolution of OCa. We recently developed EC359, a first-in-class LIFR inhibitor. Here, we examined whether autocrine loops of LIF/LIFR contribute to OCa progression and tested the utility of EC359 as a potential targeted therapy.

Methods: Eighteen different OCa model cells, both established and primary, were used to profile the expression of LIF and LIFR. Cell viability, colony formation, apoptosis, and reporter assays were used to assess EC359 impact on OCa cells. Mechanistic studies were carried out using RNA-seq and RT-qPCR analysis. Using cell-based xenografts, syngeneic xenografts, patient derived organoids (PDO), and patient derived xenograft (PDX) models, the effectiveness of LIFR inhibitor EC359 as a targeted therapy was examined.
Results: Kaplan-Meier survival analysis (KMplot) revealed increased expression of LIF and LIFR was linked to poor progression-free survival in OCa patients. The levels of LIF and LIFR were considerably greater in OCa chemotherapy non-responders than responders. We validated the existence of LIF/LIFR autocrine signaling using 18 distinct OCa cells. Treatment with the LIFR inhibitor EC359 dramatically decreased OCa cell viability, cell survival and increased apoptosis, with an IC50 of 5 to 50 nM. The activation of STAT3, mTOR, AKT, and p42/44 MAPKs as well as other downstream LIFR signaling was markedly decreased by EC359 treatment. Treatment with EC359 also decreased the stemness of OCa cells, slowed PDO development, and sensitized chemotherapy-resistant OCa cells to chemotherapy. One of the significant pathways elevated by EC359, according to RNA-seq data, is the regulation of apoptosis. In six different cell-based xenografts and PDX tumors, we demonstrated that the EC359 at 5mg/kg dose significantly reduced the OCa xenograft growth. In comparison to the vehicle control, the tumor volume was significantly reduced by EC359 treatment of murine ID8 xenografts in C57BL6 mice. Our findings indicated that EC359 had both intrinsic and extrinsic effects on tumors. Tumor-associated macrophages (TAMs) with a significant M1 polarity (CD11b+Gr1-CD68^{high} /phosphoSTAT1+/cMAF-) and robust tumor infiltration by (CD45+) leukocytes were enhanced with EC359 therapy of ID8 xenograft tumors. Importantly, normal T, B, and other immune cells in the blood demonstrated that EC359 had no effect on immune cell homeostasis.
Conclusions: Together, our findings support the existence of LIF/LIFR autocrine loops, and EC359 is a viable treatment option for OCa.

#4967

Investigating the therapeutic efficacy of EO3001 in clear cell carcinoma of the ovary

Amal M. EL-Naggar[1], Yuchen Ding[1], Lucy Li[2], Forouh Kalantari[1], Jeffrey Bacha[3], Dennis Brown[3], David Huntsman[1]. *[1]Department of Molecular Oncology, BC Cancer Research Institute, Vancouver, BC, Canada,[2]Department of Molecular Oncology, University of British Columbia, Vancouver, BC, Canada,[3]Edison Oncology Holding Corp., Menlo Park, CA*

Introducti**on** Clear cell ovarian cancer (CCC) accounts for 5-11% of ovarian cancers in North America with a higher frequency reported in cohorts from Japan. CCC usually arises directly from endometriosis, which is associated with oxidative stress. The latter plays a critical role in the pathogenesis of both endometriosis and CCC. CCC is inherently resistant to standard chemotherapies, and the outcomes for patients with advanced stage CCC have not changed in several decades. Therefore, there is an urgent need for new treatment options for advanced CCC. CCC possess a distinct genetic profile; >50% harbour ARID1A mutations typically resulting in loss of protein function and often with co-occurrence of PIK3CA mutation or gene amplification leading to PI3K/AKT pathway hyper-activation. ARID1A mutations leads to accumulation of ROS, decrease in GSH due to downregulation of SLC7A11 and related reduction in the GSH precursor cystine thereby rendering cancer cells highly dependent on oxidative phosphorylation. EO3001 is a small molecule drug candidate with selective activity against ARID1A-deficient cell lines *in vitro*. It has been shown that EO3001 directly binds and inhibits FDX-1 function to block iron-sulfur cluster formation in complex I, a critical component of the mitochondrial electron transport chain. Iron-sulfur clusters play a critical role in the oxidation-reduction reactions of electron transport in mitochondria relied on by cancer cells that have made an adaptive shift from glycolysis to high mitochondrial dependence. Complex I plays a role in redox control and the biosynthesis of macromolecules and nucleic acids necessary for cell proliferation. It is suggested that these complex I-dependent events contribute to tumor formation, resistance to cell death, and metastasis of cancer cells in part by causing an increase in ROS levels

Methods We generated isogenic ovarian cancer cell lines (RMG-1 and OVCA438, -/+ ARID1A loss) using CRISPR/Cas9. We will assess

therapeutic effects of EO3001 on cells' tumorigenic potential *in vitro* -under ambient and stress conditions, notably endometriotic cyst content which derives malignant transformation, and in vivo on cell viability, cell proliferation, ROS levels, migration, invasion, and metastasis. We will use the organoids modeling system -using primary endometrial cells harboring ARID1A mutations- to assess the impact of EO3001 on organoid growth and response to stress conditions and evaluate the effect of EO3001 on cancer metastesis by the ex vivo pulmonary metastasis assay (PuMA). **Conclusions** Exploiting the vulnerability in reliance on OXPHOS in ARID1A-deficient CCC using EO3001 might represent a promising strategy for the treatment of these patients as well as patients harboring other ARID1A-deficient malignancies.

#4968

Characterization of the clinical development candidate TNG348 as a potent and selective inhibitor of USP1 for the treatment of BRCA1/2mut cancers

Antoine Simoneau, Hsin-Jung Wu, Madhavi Bandi, Katherine Lazarides, Sining Sun, Shangtao Liu, Samuel Meier, Ashley Choi, Hongxiang Zhang, Binzhang Shen, Douglas Whittington, Sirimas Sudsakorn, Wenhai Zhang, Yi Yu, Yong Liu, Colin Liang, Michael Palmieri, Yingnan Chen, Brian Haines, Alice Tsai, Minjie Zhang, Alan Huang, Jannik Andersen, Tianshu Feng, Scott Throner, John Maxwell. *Tango Therapeutics, Boston, MA*

TNG348 is a selective and potent inhibitor of the deubiquitinating enzyme USP1 specifically designed to target BRCA1/2mut vulnerabilities in breast and ovarian tumors. Here we present the biochemical, mechanistic, and in vitro and in vivo characterization of TNG348, an oral, allosteric and highly potent inhibitor of USP1. Upon treatment, TNG348 causes loss of viability in a panel of breast and ovarian BRCA1/2mut cancer cell lines and displays dose-dependent tumor growth inhibition in BRCA1/2mut xenograft models. Furthermore, TNG348 activity extends beyond BRCA1/2mut models with PARP inhibitor (PARPi) sensitivity and oncogene-induced replication stress being additional features correlating with USP1 inhibitor sensitivity based on cell line panel and CRISPR screening results. We show that TNG348 induces cell death through a pathway that is distinct from PARPi and TNG348 demonstrates robust synergy when combined with first- or second-

generation PARPi. The clinical development plan intends to evaluate TNG348 in patients with BRCA1/2 mutations as single agent and in combination with PARP1i in patients naïve to PARPi and with prior PARPi treatment history.

#4969

Enhancing the efficacy of small molecule inhibitor of TRIP13 in prostate cancer using thymoquinone

Santosh K. Singh[1], Manoj K. Mishra[2], Sooryanarayana Varambally[3], Rajesh Singh[1]. *[1]Morehouse School of Medicine, Atlanta, GA,[2]Alabama State University, Montgomery, AL,[3]The University of Alabama at Birmingham, Birmingham, AL*

Prostate cancer (PCa) is one of the leading causes of cancer-related death in men worldwide. Chemotherapy is effective in the early management of PCa; long-term use activates drug efflux pumps, resulting in resistance and recurrence. In this context, finding the genetic changes causing PCa development could significantly alter therapeutic results. The approach has been to search for specific molecular targets for the selective elimination of cancer cells. Small molecule inhibitor drugs have successfully targeted cancer cell growth and metastasis promotion. Still, small molecule inhibitors bind to multiple molecular targets, including cell surface receptors and other intracellular proteins, thus increasing the risk of toxicity and having a short life span. Therefore, it is crucial to identify new anti-cancer agents that work with small molecule inhibitors to target cancer cells while preventing normal cells. It has been reported that overexpression of the Thyroid hormone receptor interactor 13 (TRIP13) gene, a critical mitosis regulator, plays a role in many cancers. Our analysis using **UALCAN** (ualcan.path.uab.edu) showed overexpression of TRIP13 in PCa and it plays a role in PCa biology. When TRIP13 is overexpressed, it phosphorylates EGFR and activates a downstream pathway, making cancer cells more aggressive. Recently, DCZ0415, a small molecule TRIP13 inhibitor, was reported to prevent cell proliferation and invasion in several malignancies. Nevertheless, the therapeutic targeting of TRIP13 driving PCa is not well understood. In this study, we demonstrated Thymoquinone (TQ), a natural compound with multifaceted chemo-preventive potential and anti-cancer agent, could reinforce the effect of DCZ0415 in PCa cell

lines (DU145 and PC3). PCa cells were treated with TQ or DCZ0415 alone or combined, followed by cell viability (MTT assay) to determine the optimal IC_{50} values. In a western blot, RT-qPCR analysis, and flow cytometry assays, the combined drug treatment was most effective in blocking TRIP13, inhibiting cell proliferation, and inducing apoptosis. Furthermore, this study determines the combination can upregulate the expression of cell cycle inhibitor (p21WAF1/CIP1), which, in turn, inhibits the expression of CDK4/ Cyclin D1 complex, resulting the cell cycle arrest. In addition, TQ, in combination, downregulates the activation of EGFR-dependent PI3K/Akt-1/ ERK1/2 and epithelial-mesenchymal transition (EMT) pathways in both cell lines. In conclusion, these findings show thymoquinone's potential to improve DCZ0415 effectiveness and suggest a new promising anti-cancer strategy for treating patients with prostate cancer.

#4970

TNG462 is a potential best-in-class MTA-cooperative PRMT5 inhibitor for the treatment of MTAP-deleted solid tumors

Kimberly J. Briggs, Alice Tsai, Minjie Zhang, Matthew R. Tonini, Brian Haines, Alan Huang, Kevin M. Cottrell. *Tango Therapeutics, Cambridge, MA*

MTAP deletions occur in 10-15% of all human cancers, which provides one of the largest precision oncology patient populations. MTA-cooperative PRMT5 inhibitors leverage the well-characterized synthetic lethal relationship between PRMT5 inhibition and MTAP deletion. TNG908 is a clinical stage MTA-cooperative PRMT5 inhibitor for the treatment of MTAP-deleted solid tumors. TNG462 is an investigational stage MTA-cooperative PRMT5 inhibitor with significantly enhanced potency, selectivity, and extended target coverage designed to be a best-in-class treatment for patients with MTAP-deleted cancer. In vitro, TNG462 is 45X selective for MTAP-deleted cancer cell lines over isogenic MTAP WT cell lines and has marked selectivity for MTAP-deleted cancer cell lines independent of lineage in a large, diverse cell line panel. Oral administration of TNG462 drives dose-dependent antitumor activity including durable tumor regressions and complete responses in cell line- and patient-derived xenograft models representative of clinically relevant

histologies. Preclinical data suggest a low risk for drug-drug interactions, supporting clinical combination strategies. With enhanced potency and selectivity for MTAP-deleted cancer cells and improved pharmacokinetic properties to extend target coverage, TNG462 has the potential for broader and deeper clinical activity in MTAP-deleted solid tumors than the MTA-cooperative PRMT5 currently being evaluated in clinical trials.

#4971

Identification of statins as a potential treatment for ovarian cancer

Brendan M. Reilly, Sarah J. Miseirvitch, Sarah R. Walker. *University of New Hampshire, Durham, NH*

Late-stage diagnoses make ovarian cancer extremely hard to treat. This leads to ovarian cancer accounting for 5% of female cancer deaths and 2.5% of female cancer incidence. Since there are few options for early detection of ovarian cancer, targeted therapies could lead to better outcomes. One target that has been implicated in ovarian cancer, is the transcription factor Signal Transducer and Activator of Transcription 3 (STAT3). STAT3 function is associated with tumor growth, metastasis, drug resistance, angiogenesis, and resistance to apoptosis. These many STAT3 controlled, cancer-associated cellular functions, make it an ideal and versatile target for cancer therapy. Using the Broad institute's online C.L.U.E. tool and a STAT3 gene signature, we identified statin drugs as potential inhibitors of STAT3 activity. To assess the ability of statins to inhibit STAT3, we treated ovarian cancer spheroids with statins and analyzed STAT3 activity. We have found that statins do not induce a change in the phosphorylation of STAT3 on either tyrosine 705 or serine 727 residues, the two major sites of phosphorylation on STAT3. However, there are other poorly understood post-translational modifications of STAT3, that have previously shown effects on STAT3 function, that may be involved. Importantly, we have observed that statin treatment reduces the viability of Ovcar8 and Heya8 ovarian cancer cell spheroids. We also found that statin treatment induced apoptosis of ovarian spheroids by measuring Annexin V staining. A major problem for ovarian cancer patients is metastasis. Our preliminary evidence suggests that statins reduce the ability of ovarian cancer spheroids to clear a mesothelial monolayer of cells, an early step in ovarian cancer metastasis. There are several membrane-associated signaling

proteins, including RAF and RAS, that affect STAT3 activity. Both Ovcar8 and Heya8 spheroids showed a decrease in cell viability with statin treatment, which is partially rescued by geranylgeranyl pyrophosphate (GGPP), a downstream metabolite in the mevalonate pathway. The partial recovery by GGPP indicates a mechanism involving the prenylation of membrane associated proteins. This data shows statins may provide effective treatments for ovarian cancer and defining the mechanisms behind the effects of statins may lead to better therapies and outcomes for ovarian cancer patients.

#4972

Anti-tumor activity of Helicon inhibitors of B-catenin-TCF interaction in patient-derived xenograft models

YaGuang Si[1], Minjung Choi[1], Xinwei Han[1], Brian White[1], Ziyang Wu[1], Erica Visness[1], Pieter Beerepoot[1], Elizabeth Jaensch[1], Jessica Ramirez[1], Charles Ponthier[1], Xiaogang Han[1], Paula Ortet[1], Peicheng Du[1], Sorabh Agarwal[1], Mirek Lech[1], Aaron Fulgham[1], Sarah Cappucci[2], Zhi Li[3], John McGee[4], Lihua Yu[4], Martin Tremblay[4], Keith Orford[4], Gregory Verdine[4], Jonathan Hurov[1]. *[1]FogPharma, Inc., Cambridge, MA,[2]Prime Medicine, Inc, Tyngsborough, MA,[3]Georgetown University, Washington, DC,[4]Fog Pharmaceuticals, Cambridge, MA*

Genetic and epigenetic alterations in the Wnt signaling pathway leading to constitutive activation of the driver oncogene B-catenin occur in at least 20% of all human cancers. We have developed conformationally hyperstabilized α-helical peptides (Helicons) that bind directly to B-catenin with picomolar affinity and block its interaction with TCF transcription factors. We describe here the characterization of anti-tumor efficacy, pharmacodynamic biomarkers and mechanism of action using multiple in vivo patient-derived xenograft (PDX) models treated with Helicons. Helicon treatment leads to dose-dependent anti-tumor effects and durable regressions in PDX models from multiple indications with Wnt pathway activating mutations. Anti-tumor responses are seen in the presence of additional driver mutations, including KRAS and PIK3CA. RNA-sequencing and Gene Set Enrichment Analysis confirm Helicon treatment inhibits both Wnt/B-catenin and MYC-regulated gene sets. Inhibiting B-

catenin-TCF interaction with Helicons represents a first-in-class therapeutic approach for the treatment of cancers resulting from aberrant transcriptional signaling via B-catenin.

#4973

Investigating the role of non-canonical NF-kappaB signaling in tumor cells and macrophages in ovarian cancer

Andrew J. Wilson[1], Dominique Parker[2], Robert Cheng[2], Todd Giorgio[2], Marta Crispens[1], Fiona Yull[2]. *[1]Vanderbilt University Medical Center, Nashville, TN,[2]Vanderbilt University, Nashville, TN*

Background**:** Ovarian cancer is the most lethal gynecologic malignancy, with a 5-year survival rate of less than 50%. To have a major impact on improving clinical outcomes, a better understanding of the progression of disease and identification of truly novel treatment strategies is critical. Canonical nuclear factor-kappaB (NF-κB) signaling has been extensively studied in preclinical ovarian cancer models; however, systemic NF-κB inhibitors have had disappointing results in early clinical trials. Whether the alternative, non-canonical NF-κB signaling pathway (nc-NF-κB) represents a distinct and improved target for therapy in ovarian cancer is unknown. Here, we aim to investigate the role played by nc-NF-κB signaling both in malignant epithelial cells and in macrophages, a key immune cell component in the tumor microenvironment. Repolarizing tumor-associated macrophages (TAMs) away from pro-tumor M2-like functions towards an anti-tumor M1-like phenotype is a critical priority in macrophage-directed therapies.

Methods: In ovarian cancer cell lines, mouse ovarian TAMs cultured *ex vivo*, and immortalized bone marrow-derived macrophages (BMDMs), nuclear levels of p52 were measured by western blot as a read-out of active nc-NF-κB signaling. Effects of macrophage polarization on nc-NF-κB signaling were determined in unpolarized (M0), M1 polarized (LPS/IFNγ treated) or M2 polarized (IL-4 treated) BMDMs. Finally, effects of inhibiting nc-NF-κB using a specific peptide inhibitor of p52 nuclear import (SN52) on cancer cell growth and macrophage phenotype were determined in sulforhodamine B growth assays and by western blot analysis of PCNA (proliferation marker) and arginase-1 (M2 macrophage marker).

Results: We observed high levels of p52 expression in the majority of ovarian cancer cell lines, and in our cultured macrophage models. The functional relevance of these observations was confirmed by experiments showing reduced growth in ovarian cancer cells treated with SN52 and reduced expression of arginase-1 in SN52-treated macrophages. We saw similar results in breast cancer cells and mouse mammary TAMs, showing that nc-NF-κB signaling may also have pro-tumor effects in other cancer types. Complementary studies showed that M2 polarized macrophages expressed markedly higher levels of nuclear p52 than observed in M0 or M1 cells. Based on these promising results, experiments (i) using transgenic mice to allow targeted, inducible activation of nc-NF-κB in macrophages during ovarian cancer progression and (ii) testing the therapeutic effects of SN52 in these cancer models are underway.

Conclusions: Although further studies are required to establish the translational relevance of our findings, we hope to identify non-canonical NF-κB signaling as a new therapeutic target in malignant epithelium and macrophages in ovarian cancer and potentially other cancer types.

#4974

Development of novel pyrimido-pyrazolo-quinolone derivative, IND-2 as multi-targeted inhibitor for the treatment of prostate cancer

Swapnaa Balaji[1], Rabin Neupane[1], Chandrabose Karthikeyan[2], Jayachandra Babu Ramapuram[3], Amit K. Tiwari[1]. *[1]The University of Toledo, Toledo, OH,[2]Indira Gandhi National Tribal University, Lalpur, India,[3]Auburn University, Auburn, AL*

Prostate cancer (PC) is the most commonly diagnosed cancer in men. In PC, multiple molecular signaling networks are perturbed, so monotherapies are less effective, creating an urgent need to discover chemotherapeutic agents that target multiple tumor-promoting proteins simultaneously. Drug discovery research is increasingly embracing poly-pharmacology, in which one drug targets multiple oncogenic targets concurrently. We have identified a novel quinoline derivative, IND-2 (4-chloro-2-methylpyrimido[1″,2″:1,5]pyrazolo[3,4-b]quinolone), that has been shown to significantly inhibit the expression of several oncogenic and epigenetic targets in PC cells. It was observed that IND-2 significantly inhibited the proliferation of PC-3 and DU-145 with IC_{50} values of 3 μM and 3.5 μM, respectively. Furthermore, 5 and 10 μM of IND-2 produced morphological changes in PC-3 cells characteristic of apoptosis. The levels of reactive oxygen species (ROS) increased significantly after IND-2 was added to PC cells. Additionally, 5 and 10 μM of IND-2 reduced mitochondrial membrane potential in PC-3 cells. Furthermore, IND-2 increased the expression of cleaved caspase-3, cleaved caspase-7, and cleaved poly (ADP-ribose) polymerase (PARP). The PC-3 cells incubated with 5 μM of IND-2 showed a significant reduction in expression of B-cell lymphoma 2 (Bcl-2). These data convincingly show that IND-2 inhibits PC cells through apoptosis induction. It is interesting to note that IND-2 (2.5, 5 and 10 μM) also induces mitotic catastrophe in PC-3 cells. Wound healing assay and expression of several EMT (epithelial to mesenchymal) markers indicated significant anti-metastatic activity of IND-2. Target identification studies

have demonstrated that IND-2 mimics etoposide (VP-16) and binds more specifically to Topoisomerase IIβ. In our preliminary studies, we found that IND-2 inhibits several oncogenic and epigenetic targets including Topoisomerase II-Hsp90 complex and LSD1/HDAC1 of the transcriptional corepressor CoREST complex. However, these targets need to be validated to understand IND-2's mechanism. Overall, IND-2 may lead to the development of more effective poly-targeted compounds for PC treatment.

#4975

Anti-cancer effect of a probiotic bacteria-derived compound, 1,4-Dihydroxy-2-naphthoic acid in prostate cancer

Shreeja Srinivas Bitla, Gnanasekar Munirathinam. *Biomedical Sciences, University of Illinois College of Medicine (Rockford), Rockford, IL*

Cancer incidence has been increasing globally and the major cause for mortality associated with this disease is due to metastasis development. Followed by skin and lung cancer, prostate cancer (PCa) is one of the most common cancers prevailing among older men in the United States. Although androgen deprivation therapy (ADT) is the mainstay treatment for PCa, most patients undergoing ADT eventually develop metastatic PCa. Moreover, other treatment options, such as chemotherapy and radiotherapy, have toxic side effects and are ineffective in controlling advanced PCa. Hence, there arises a need for identifying alternative agents with possibly fewer side effects. The gut biome plays a significant role in regulating many bodily functions like digestion, immunity, and including cancer prevention. Probiotics, commonly known as 'good bacteria,' are living microorganisms that provide health promoting benefits. A probiotic metabolite, 1,4-Dihydroxy-2-naphthoic acid (DHNA), is an anti-inflammatory aryl hydrocarbon receptor (Ahr) agonist which is yet to be explored for its anticancer activity. Inhibiting the inflammatory signaling axis and activating Ahr by DHNA could be a promising strategy to counteract metastatic PCa. Cell viability assays revealed that 1,4-DHNA is highly toxic in metastatic prostate cancer cell lines such as DU145 and PC3 compared to normal prostate epithelial cells like RWPE-1 and human prostate stromal myofibroblast cell line, WPMY-1, with an approximate IC50 value of 5 μM in DU145 and PC3 and about 20 μM and 75 μM in WPMY-1 and RWPE-1 respectively. DHNA reduced the colony forming

abilities of BPH-Cd, PC3, and DU145 in clonogenic assay and suppressed the BPH-Cd spheroid growth in spheroid formation assay, revealing its anti-tumorigenic potential. Trans-well migration assay using BPH-Cd, PC3, and DU145 showed a decrease in cell migration, hinting at the drug's anti-metastatic ability. G2/M phase arrest in cell cycle analysis and dose-dependent increase in apoptosis of DHNA-treated DU145, PC3, and LNCaP cell lines reiterated its anti-cancer potential. Western blot results in PC3 and DU145 showed significant dose-dependent inhibition of protooncogene β-catenin expression. Downregulation of cell cycle proteins like cyclin D1 and increased expression of effector caspase, cleaved caspase 7 support cell death promoting effects of DHNA via an intrinsic apoptotic pathway. Our pre-clinical data suggest that DHNA can be a potential drug for inhibiting both prostate tumor growth and metastasis. Further research is warranted to ascertain the anti-metastatic and underlying anti-cancer mechanisms to help translate the findings to clinical use.

#4976

Preclinical characterization of BGI-9004, a covalent TEAD inhibitor with exceptional anti-cancer activity and combination potential

Shirley Guo, Shashank Shrishrimal, Jason Cui, Guoqing Wang, Vivian Zhang, Ning Deng, Iris Dong, Anna Chen, Steve Luo, David Sperandio, Ping Cao, Wolf R. Wiedemeyer. *BridGene Biosciences, Inc., San Jose, CA*

Pharmacological inhibitors of TEAD transcription factors have emerged as a promising novel class of anti-cancer agents. TEAD inhibitors disrupt oncogenic YAP/TAZ signaling, resulting in cell cycle arrest and cell death in susceptible cancers. In preclinical models, cancer cell lines with alterations in the Hippo signaling pathway, such as mutations or loss of NF2 or LATS, are particularly sensitive to inhibition of TEAD signaling. In addition, YAP/TAZ-TEAD signaling is thought to play a role in resistance to several targeted therapies, such as EGFR inhibitors and MEK inhibitors. BGI-9004 is a covalent inhibitor of TEAD1-4 with low nanomolar potency in a TEAD reporter cell line and anti-cancer activity *in vitro* and *in vivo*. In the NF2-deficient NCI-H226 and the NF2-wildtype, LATS-mutant MST-O211H mesothelioma xenograft models, BGI-9004 treatment resulted in sustained tumor regressions over a 28d treatment course. Anti-cancer activity was accompanied by significant inhibition of TEAD-mediated

transcription in BGI-9004-treated tumors, and no adverse effects on the body weight of treated mice were observed. Moreover, proteome-wide protein binding of BGI-9004 was assessed by Isobaric Mass Tagged Affinity Characterization (IMTAC^{TM}), which confirmed its high selectivity for TEAD. In line with this, BGI-9004 had a clean profile in a panel of protein targets that present potential safety liabilities (CEREP safety panel). These findings prompted us to explore the combination potential of BGI-9004 with other targeted therapies, including inhibitors of EGFR, MEK and mutant KRAS^{G12C}. Here, we found that BGI-9004 potentiated the effect of other targeted therapies. In particular, we generated dose response matrices for BGI-9004 and inhibitors of KRAS^{G12C} and KRAS^{G12D} in several KRAS-mutant cell lines, including three lung cancer cell lines, and demonstrated synergy for the combination. These results suggest that inhibition of YAP/TAZ-TEAD signaling may improve the efficacy of KRAS-targeted therapy. Taken together, the covalent TEAD inhibitor BGI-9004 has demonstrated promising activity both as a single agent and in combination with other targeted agents, a favorable pharmacokinetic profile and high target selectivity in preclinical models, supporting its evaluation as a novel anti-cancer agent in clinical trials.

#4977

Development of small molecule inhibitors of protein interaction with glycosaminoglycans

Tahir N. Sheikh, Elgilda Musi, Alex J. Rai, Gary K. Schwartz. *Columbia University Irving Medical Center, New York, NY*

Glycosaminoglycans (GAGs), such as heparan sulfate and chondroitin sulfate, are an important component of the tumor microenvironment (TME). These carbohydrates are attached to proteoglycans at the surface of tumor cells and play a vital role in malignant transformation. Heparan sulfate (HS) glycosaminoglycans have been demonstrated to play a pleiotropic role in regulating the activity of important cellular receptors and downstream signaling pathways, and are implicated in cancer cell proliferation, angiogenesis, invasion, and metastasis. Heparinase, an endoglycosidase that specifically cleaves heparan sulfate side chains of heparan sulfate proteoglycans is expressed in several sarcoma subtypes. We measured heparinase activity in several cell lines and found that A673, CHP100,

CHLA9 and RD-ES Ewing's sarcoma cell lines have significantly higher levels of heparinase activity compared to the heparinase-deficient CHO-K1 psgD-677 cell line. Interference with heparinase or heparin sulfate function(s) may represent a therapeutic approach in sarcoma. To this end, we tested these cell lines by measuring cell growth using a cell viability assay, in the presence or absence of GTC3300P, a small molecule inhibitor of protein interaction with glycosaminoglycan. We demonstrate that the Ewing's sarcoma cell lines exhibit potent and significant inhibition in cell growth *in vitro*, in the presence of drug. Western blot analysis shows induction of cleaved Poly-ADP Ribose Polymerase (PARP), yH2AX, as well as cleaved caspase-3, known markers of apoptosis and down regulation of mTORC1 targets such as phospho-S6 (p-S6), in Ewing's sarcoma. Apoptosis was confirmed by the induction of sub-G1 population in Ewing's sarcoma by cell cycle analysis. Previous reports have indicated that heparinase activity is strongly implicated in cell migration and invasion and is associated with tumor metastasis, angiogenesis and inflammation. This was confirmed by LC-MS/MS proteomics and bioinformatics (gene ontology and gene set enrichment) analysis of these multiple cell lines, which identified alterations in numerous biomarkers in these pathways, including multiple ribosomal protein subunits, spliceosomes components, and complement coagulation cascade. We further conducted a cell migration assay and demonstrate that GTC3300 significantly inhibits cell migration in Ewing's sarcoma cell lines, but not in heparinase-deficient psg677 cells. Taken together our data strongly suggests that targeting protein interaction with glycosaminoglycans including heparan sulfate in Ewing's sarcoma represents a novel approach and merits further investigation

#4978

Combination of a clinical stage-hedgehog inhibitor, GT1708, improves Venetoclax-induced apoptosis by down-regulating MCL-1 proteins in AML cells

Liandong Ma, Qianxiang Zhou, Honghua Yan, Min Dong, Xiahe Han, Jiangwie Li, Jie Qu, Weidong Qian, Youzhi Tong. *Suzhou Kintor Pharmaceuticals, Inc, Suzhou, China*

Acute Myeloid Leukemia (AML) is the third hematological malignancies with the worst relative overall 5-year survival rate (11.7%) in hematological malignancies. AML is a heterogeneous disease with a broad spectrum of genomic changes and molecular mutations that lead to a poor prognosis and clinical outcome. Leukemic stem cells progress to myoblasts that continue to proliferate without differentiating, namely, immature blasts in AML. The hedgehog (HH)/glioma-associated oncogene homolog (GLI) signaling pathway is essential for embryonic and stem cell developments. This pathway has been one of the most promising targets for drug discovery and developments for AML. Although HH inhibitor Glasdegib in combo with low-dose cytarabine achieved FDA approval for AML, Venetoclax (BCL-2 inhibitor/ABT-199) plus a hypomethylating agent (HMA) have been dominating the regimens in AML recently. Here we reported GT1708, a HH inhibitor, improves ABT-199 (venetoclax)-induced apoptosis by down-regulating MCL-1 proteins in AML cells. GT1708 is a potent HH inhibitor (IC50=0.11 nM in HH pathway-driven cellular assay) and inhibited GLI expression with doses of 1, 3 and 10 mpk in a HH-dependent medulloblastoma animal models. In Molm-13 (AML) cells, GT1708 was shown to down-regulate the expression of MCL-1 proteins (anti-apoptotic proteins). In contrast, ABT-199 increased the expression of MCL-1. Furthermore, ABT+Aza (Azacidine/HMA drug) induced more MCL-1 expression than ABT-199. Importantly, GT1708 was shown to induce the expression of cleaved-PARP (c-PARP/apoptotic marker) and to increase c-PARP expression when combined with ABT-199. Due to ABT+Aza induced MCL-1 overexpression, the combination of both agents failed to induce c-PARP, suggesting MCL-1 overexpression conferring resistance to ABT+Aza therapy in Molm-13 cells. GT1708 was further evaluated in flow cytometry-based apoptotic assays. GT1708, ABT-199 and Aza were demonstrated to induce an early apoptosis by 9.98%, 47.5%, and 8.64%, respectively. In comparation, ABT+GT1708 were revealed to induce a 61% of apoptosis superior to 47% or 48.5% of apoptosis induced by either ABT or ABT+Aza in Molm-13 cells. These results confirm the role of MCL-1 overexpression in conferring resistance to ABT+Aza therapy, which can be overcome by ABT+GT1708 combo. GT1708/ABT combo were also shown a marginable superior antitumor activity than ABT along in Molm-13 animal models. GT1708 has been testing in a phase I study in AML patients with previous multiple lines of regimens. GT1708 has been shown to

reduce blast counts in three of 13 AML patients treated with higher doses and demonstrated favorite PK and safety profiles. In brief, these results support the clinical development of GT1708 in combination with ABT-199 in AML patients.

#4979

Evaluation of heme inhibitory therapy in combination with radiation of lung cancer

Narges Salamat[1], Tianyuan Wang[2], Eranda Berisha[1], Maria Del Carmen Chacon Castro[1], Adnin Ashrafi[1], Debabrata Saha[2], Ralph P. Mason[2], Li Liu[2], Li Zhang[1]. *[1]UT Dallas, Richardson, TX,[2]Radiology, UT Southwestern Medical Center, Dallas, TX*

Lung cancer is the leading cause of cancer-related death in the United States, with a 5-year survival rate of less than 25%. While most lung cancer patients receive radiation therapy, radioresistance severely impacts treatment outcomes. Thus, development of therapeutics to potentiate durable response to radiation therapy may be key to improving treatment outcomes. Research in our lab has previously implicated heme, a central biosynthetic molecule with important functions in diverse molecular and cellular processes, in lung cancer development and progression. To target heme, we designed heme-sequestering protein 2 (HeSP2) which displays potent anti-tumor activity in mouse tumor models. By decreasing tumor metabolic demand through heme sequestration, HeSP2 can significantly alleviate tumor hypoxia, a dominant radioresistance mechanism. Tumor hypoxia correlates with poor clinical outcomes by acting via multiple mechanisms such as inhibiting radiation-induced DNA damage and inducing the HIF-1 pathway that leads to antioxidant generation. Here, our preliminary data show that HeSP2 potentiates the antitumor efficacy of ionizing radiation. To see the effect of HeSP2 in combination with radiotherapy, in summary we subcutaneously implanted A549-luc, NSCLC cell lines with mutation in Kras and KLB1 in SCID mice. After 1-2 weeks mice were treated with saline (Control), HeSP2(25 mg/kg, i.v, twice a week), radiation (5 Gray, once per week at week 2 and 3), and HeSP2 combined with radiation (25 mg/kg, i.v, twice a week plus 5 Gray, once per week at week 2 and 3. Tumor tissues were harvested, processed and paraffin embedded for immunohistochemistry (IHC). Preliminary results

indicate HeSP2 in combination with radiation reduce the levels of multiple angiogenic markers and vascular markers as well as microvessel density. These results indicate that heme sequestration in combination with radiation can be an effective strategy for suppressing lung tumors.

#4980

Design and functional characterization of a first-in-class irreversible inhibitor of HOIL-1-interacting protein (HOIP) with selective antitumor activity against B-cell non-Hodgkin lymphoma

Ana Maria Montagut[1], Marc Antoni Armengol Cubillos[2], Gema Gorjón-de-Pablo[1], Judith Farrés[3], Laia Huguet Garcia[2], Núria Profitós-Pelejà[2], Juliana Carvalho Santos[2], Marcelo Lima Ribeiro[2], Miranda Fernández-Serrano[2], Roger Estrada Tejedor[1], José I. Borrell[1], Gaël Roué[2]. *[1]Group of Pharmaceutical Chemistry, IQS School of Engineering, Barcelona, Spain,[2]Lymphoma translational group, Josep Carreras Leukaemia Research Institute, Badalona, Spain,[3]Anaxomics Biotech SL, Barcelona, Spain*

Activating single-nucleotide polymorphisms of HOIL-1-interacting protein (HOIP), the catalytic subunit of the linear ubiquitin chain assembly complex (LUBAC), have recently been shown to promote myeloid differentiation primary response 88 (MYD88)-mediated B-cell lymphomagenesis. To assess the relevance of targeting HOIP in the activated B-cell-like (ABC) subtype of diffuse large B-cell lymphoma (DLBCL) with *MYD88* mutation, we used systems biology to build a mathematical model aimed at evaluating the impact of HOIP depletion on DLBCL. From this model, an AI-mediated query demonstrated that HOIP blockade was associated with the suppression of three main pathophysiological motifs in malignant B cells, i.e., cell growth and proliferation, apoptosis evasion and deregulated metabolism. We then undertook a computational study that consisted of a combinatorial substitution of several α-β unsaturated moieties to be used as covalent binding warheads to the catalytic cysteine residue of HOIP. The resulting chemical library was used on subsequent molecular docking to assess the best HOIP binding candidates. Out of the four candidates synthesized from this library, we isolated compound A (Cpd A), a covalent irreversible inhibitor of HOIP with a pyrido[2,3-*d*]pyrimidine core, which exerted

selective antitumor activity in a panel of ABCL-DLBCL cell lines (mean IC_{50} at 48hours: 90.7± 13.09 μM) while sparing normal B cells. Immunoprecipitation studies demonstrated that Cpd A was able to modulate the interaction between HOIP and the LUBAC component, SHARPIN, leading to the blockade of NF-κB signaling and to the downregulation of several downstream effectors, including CCL3, IL6 and IRF4. Specificity of Cpd A towards HOIP was confirmed by a drug affinity responsive target stability (DARTS) assay based on the immuno-detection of persistent HOIP peptides after Cpd A-mediated blockade of enzymatic proteolysis, and thereafter in a CRISPR-engineered HOIP-knockout ABC-DLBCL model. Finally, efficacy of the compound was confirmed *in vivo* in a chicken embryo chorioallantoic membrane (CAM)-derived model of ABCL-DLBCL subjected to a twice weekly dosing with Cpd A, in which the compound achieved a 25% tumor growth inhibition, associated with a 60.5% and 89% reduction in brain and bone marrow infiltration by lymphoma cells, respectively. Altogether, our results confirm that HOIP represents a promising therapeutic target for ABC-DLBCL with activating MYD88 mutation, and that a pyrido[2,3-*d*]pyrimidine derivative can successfully and specifically block HOIP, resulting in NF-κB disruption and selective antitumor activity in this aggressive subtype of B-cell lymphoma.

#4981

The potent quadruplex-binding compound QN-302 down-regulates the S100P gene in *in vitro* and *in vivo* models of pancreatic cancer: a potential therapeutic target and biomarker for PDAC

Nicole Williams[1], Jenny Worthington[1], Ahmed Ahmed[2], Tariq Arshad[3], Stephen Neidle[2]. *[1]Axis Bioservices, Coleraine, United Kingdom,[2]School of Pharmacy, University College London (UCL), London, United Kingdom,[3]Qualigen Therapeutics Inc, San Diego, CA*

The compound QN-302, a tetra-substituted naphthalene diimide (ND) derivative has been designed to have high affinity for G-quadruplex (G4) nucleic acids. It has single-digit nM anti-proliferative activity in a panel of human pancreatic cancer cell lines (Ahmed et al., ACS Med Chem Lett, 2020, 11, 1634-1644) and anti-tumor activity in xenograft, orthotopic and genetic (KPC) models for pancreatic cancer (PDAC). Its mode of action involves the targeting of G4-forming sites in promoter regions of cancer-

associated genes, where their prevalence is over-represented compared to other genes. Transcriptome analyses of QN-302 in MIA-PACA2 cells have confirmed genes involved in cancer-associated pathways and carry G4 motifs in their promoters as targets. We have found that expression of the S100P gene, a well-authenticated indicator of PDAC disease and progression, is highly down-regulated in QN-302 treated cells. The S100P gene contains at least five putative G4 motifs, including a classic G4 promoter site just upstream of the transcription start site. We have observed that transcriptome analyses on tumor material from human PDAC patients, and those from poorly differentiated as well as more highly differentiated tumors, have shown that the S100P gene is highly over-expressed (especially in poorly differentiated tumors). We now report on gene expression analysis of S100P using control and treated tumor tissues from a therapeutic study in PDAC MIA-PACA2 xenografts in mice, by means of RT-qPCR and Western blot analyses. The data shows statistically significant dose-dependent decreases in expression of S100P at both the mRNA (to ca 25% of control values) and protein levels (to ca 22% of control values), giving added confidence to the concept that the S100P gene is a therapeutic target in PDAC and may also be useful as a marker of QN-302 response in future clinical use. QN-302 is bio-available at therapeutic doses and is well tolerated at these levels in the animal models. It is being developed for clinical evaluation by Qualigen Therapeutics Inc and is currently at the pre-IND stage.

#4982

The somatic mutation signature detected in gynecological mucosal melanoma

Zhongwu Li[1], Lianyi Shen[1], Siyao Liu[2]. *[1]Peking University Cancer Hospital, Beijing, China,[2]ChosenMed Technology Co. Ltd, Beijing, China*

Background: Gynecological Mucosal Melanoma(GMM) is aggressive disease with a poor prognosis, where few studies focusing on its target drug and mutation signatures. Cancer as outcome of DNA mutagenesis process and can be inferred from somatic mutations signature by analyzing the genome sequence. Due to the rapid development of next-generation sequencing (NGS) and molecularly driven targeted therapy, discovering

different mutation signature in cancer plays an important role in precision medicine.
Methods: The study was conducted at a high-volume melanoma center, the Peking University Cancer Hospital. We enrolled female patients with melanoma (n = 22) from 2017 to 2021. Subsequently, whole-exome sequencing performed on the Formalin-fixed paraffin-embedded (FFPE) specimens from 22 GMM patients and match normal tissues of patients. Tumor mutational burden (TMB) was measured as the number of nonsynonymous somatic mutations of whole-exome sequence coding region. Mutation signature detection base pair of six substitution subtypes: C>A, C>G, C>T, T>A, T>C, and T>G. NMF can be used to decompose matrix A into two nonnegative matrices.
Results: In all mutations of 22 GMM patients, we screen two mutation signatures. Signature 1 showed a strong correlation [0.77;cosine similarity value (CSV)] to the signature 3 from the COSMIC database, which represents failure of DNA double-strand break-repair by homologous recombination, which predominated in 55%(12/22) GMM patients. Signature 2 showed a strong correlation to Cosmic signature 1 (CSV = 0.791), which is has been found in all cancer types correlated with age cancer diagnosis. Patient-18 did not any treatment in our hospital, follow-up was lost. Kaplan-Meier revealed that Signature 2 was associated with longer overall survival in GMM patients and later recurrence or progression.
Conclusions: This study aimed to identify prognostic markers and the development of targeted therapy for the treatment of GMM.

#4983
Anaplastic thyroid cancer cells upregulate mitochondrial one-carbon metabolism to meet purine demand, eliciting a targetable vulnerability
Adam J. Sugarman, Luong Do Huynh, Antonio Di Cristofano. *Albert Einstein College of Medicine, Bronx, NY*

Anaplastic thyroid cancer (ATC) is one of the most aggressive and lethal tumor types, characterized by loss of differentiation, epithelial-to-mesenchymal transition, extremely high proliferation rate, and generalized resistance to therapy. To identify novel relevant, targetable molecular alterations, we have analyzed gene expression profiles from a genetically

engineered ATC mouse model and from two human patient datasets, and have found consistent and coordinated upregulation of several genes encoding enzymes involved in the one-carbon metabolic pathway, which uses serine and folates to generate nucleotides, glutathione and glycine. We have used a combination of cell line and in vivo approaches to assess the role of this pathway in the progression and maintenance of ATC and the effect of its inhibition on tumor behavior. Genetic and pharmacological inhibition of both *MTHFD2* and *SHMT2*, key enzymes of the mitochondrial arm of the one-carbon pathway, rendered mouse and human ATC cells auxotroph for glycine and led to significant inhibition of tumor cell proliferation and colony forming ability, which was primarily caused by depletion of the purine pool leading to arrest in S phase. Notably, these growth-suppressive effects were significantly amplified when cells were grown in the presence of physiological types and levels of folates. Genetic blockage of the one-carbon pathway dramatically impaired tumor growth in vivo, both in immunocompetent allograft models and in immunocompromised xenograft models of ATC. Together, these data establish the upregulation of the one-carbon metabolic pathway as a novel and targetable vulnerability of ATC cells, which can be exploited for therapeutic purposes.

#4984

Integrated platform enables KRAS-targeted drugs discovery

Beibei Liu, Lian Li, Xiangyang Zuo, Jie Yang, Ruifeng Wang, Feifei Fan, Wenting Shi, Qingyang Gu. *WuXi App Tec, Suzhou, China*

The Kirsten rat sarcoma viral oncogene homolog (KRAS) is mutated in approximately 25% of all human cancers and is known to be a major player promoting and maintaining tumorigenesis through the RAS-MAPK pathway. Activating mutations in KRAS increase the ability for GTP-loading, making it difficult to displace, thus constitutively activate downstream MAPK pathway and promote cancer formation. Fortunately, a revolutionary strategy to use covalent allosteric inhibitors that target a shallow pocket on the KRAS surface has provided new impetus for KRAS inhibitor development efforts. These inhibitors, such as AMG510 and MRTX849, show promising results in patients with tumors harboring KRAS G12C mutation. While the approval of AMG510 was a major

breakthrough for those patients harboring KRAS G12C mutations, G12C only accounts for a fraction of those with KRAS mutations and eventual resistance to G12C inhibitors is unavoidable. Therefore, develop new drugs direct various KRAS mutants and combination strategies that target resistance mechanisms have become vital in the war against KRAS-mutant tumors.
To enable the discovery of novel KRAS inhibitors, we established a one-stop service platform, covering affinity detection of compounds to KRAS mutants, KRAS upstream and downstream protein-protein interaction detection, pathway activation detection, cell proliferation assay (2D/3D culture system), and *in vivo* efficacy evaluation in KRAS mutant xenograft models. Our platform provides assays on nearly all the current mainstream mutants of KRAS, such as G12C/G12D/G12R/G12S/G13D, and engineered Ba/F3 cell lines that harboring single or double KRAS mutation. In addition, we developed a panel of resistant models to KRAS G12C inhibitor that bringing a better understanding of the biological basis of drug resistance, and will serve as a new tool to optimize KRAS-G12C inhibitor regimens and combinatorial strategies. The comprehensive KRAS-targeted drug discovery platform is empowering new drug research and development.

Oncogenes and Tumor Suppressor Genes as Targets for Therapy 3

#3978
The growth inhibitory effect of MDV3100 on hormone receptor-positive, HER2-negative breast cancer cell lines with low DYRK2 expression
Yoshimi Imawari[1], Rei Mimoto[2], Kiyotsugu Yoshida[2]. *[1]Univ. of Tokyo Inst. of Medical Science, Tokyo, Japan,[2]Jikei Univ. Sch. Med., Tokyo, Japan*

Introduction: Tumor progression is the main cause of death in patients with breast cancer. Accumulating evidence suggests that dual-specificity tyrosine-regulated kinase 2 (DYRK2) functions as a tumor suppressor by regulating cell survival, differentiation, proliferation and apoptosis. Recently, we reported for the first time that DYRK2 inhibits breast cancer stem cells and tumor cell proliferation through transcriptional downregulation of KLF4 and CDK14, respectively.Our previous study

showed that Androgen receptor (AR) was a DYRK2-dependent transcriptional activator. In this context, we hypothesized that MDV3100, an inhibitor of AR, may be effective for breast cancer with low DYRK2 expression.
Methods: We established stable DYRK2-depleted cells. MCF-7 cells, hormone receptor-positive, HER2-negative breast cancer cell line, were transfected with pSuper-puro vector (pSuper control) or pSuper-puro DYRK2 shRNAs (shDYRK2) along with puromycin to isolate stable cell lines.These manipulated cells were compared with the control cells by various assays. We analyzed the activity of AR by Androgen receptor reporter assay. MTS assays were used to assess growth inhibition after treatment with MDV3100.
Results: Androgen receptor reporter assay showed that knocking down DYRK2 induced AR transcription activity in MCF-7 cells.In MCF-7 DYRK2-depleted cells, MTS assays revealed that the treatment by MDV3100 was more effective than that in MCF-7 control cells.
Conclusion: These findings demonstrate that reduced DYRK2 expression in hormone receptor-positive, HER2-negative breast cancer increases the activity of AR and significantly inhibits the growth by treatment with MDV3100.

#3979

Tandem peptides targeting HER2 for delivery of CD44 siRNA into HER2+ breast cancer cells *in vitro*

James W. Kalogeros, Audreanna Miserendino, Angela Alexander-Bryant, Brian Booth. *Bioengineering, Clemson University, Clemson, SC*

Introduction: This research aims to characterize and evaluate the potential of two novel tandem peptides for their ability to mediate the delivery of CD44 siRNA into HER2+ breast cancer cell lines. HER2+ cancer accounts for 20%-25% of invasive breast cancers and shows overexpression of HER2 protein. The tandem peptides examined consist of P51 or P25 targeting peptide sequences that bind to the HER2 protein, and DIV3W, a fusogenic peptide that allows for siRNA protection, cellular internalization, and endosomal escape. We hypothesize that delivery of tandem peptide will result in the observation of mRNA knockdown of CD44, a reduction of

CD44 protein expression, and a decrease in metastatic properties of breast cancer cells.
Methods: Western blot analysis was used to determine the basal expression of CD44 in HER2+ breast cancer cell lines, SKBR3 and BT474, and breast epithelial cell line MCF10A. Tandem targeting/fusogenic peptides termed P51-DIV3W and P25-DIV3W were electrostatically complexed with non-targeting siRNA (siNT) at increasing N:P ratios to determine the minimum ratios needed to complex free siRNA. Various ratios of peptide-siRNA complexes were also treated with FBS and RNase A to determine whether the peptides protected siRNA from degradation. MTS assays were performed in SKBR3, BT474, and MCF10A cells to determine cytotoxicity using increasing peptide concentrations. Dynamic light scattering was performed using a Zetasizer to determine the size of the peptide-siRNA nanocomplexes.
Results: Western Blot data of the three cell lines showed that CD44 protein was present in cancerous and normal cells, whereas HER2 protein was only present in SKBR3 and BT474 cells. Peptide-siRNA complexes for both P51-DIV3W and P25-DIV3W formed at a minimum N:P ratio of 20:1. Both peptide complexes protected siRNA from degradation in FBS and RNase A at N:P ratios ranging from 20:1 to 60:1. DLS results showed that P25-DIV3W-siRNA complexes had an average diameter of 200.23 nm and a zeta-potential of 24.7 mV.
Conclusions: The data collected shows that the tandem peptides successfully complex with siNT and protect siNT from degradation. The peptide complexes formulate at a size that serves as an effective carrier for siRNA to breast cancer cells. Future work will focus on evaluating the ability of the tandem peptides to target HER2 and effectively silence CD44 in HER2+ breast cancer cells.
Acknowledgements: This research was supported in part by the Dabo Swinney All In Foundation and Materials Assembly and Design Excellence in South Carolina (MADE in SC) under the National Science Foundation EPSCoR Program under NSF Award # OIA-1655740. We also thank SC BioCRAFT, NIH award P30 GM131959, for the use of core equipment and facilities.

#3982

Anti-Stanniocalcin 1 antibody as a potential therapeutic strategy for liver fibrosis and hepatocellular carcinoma

Alfred Long-Hin Suen[1], Kristy Kwan-Shuen Chan[1], Regina Cheuk-Lam Lo[2]. *[1]Department of Pathology, The University of Hong Kong, Hong Kong, Hong Kong,[2]State Key Laboratory of Liver Research, The University of Hong Kong, Hong Kong, Hong Kong*

Introduction: Hepatocellular carcinoma (HCC) is the sixth most frequently diagnosed cancer and the third leading cause of cancer deaths. Liver fibrosis (LF) is a progressive disease and cirrhosis, the advanced stage of LF, is *per se* a risk factor for HCC. Moreover, LF persists after the development of HCC. Stanniocalcin 1 (STC1), as a serum biomarker of both HCC and LF as we previously reported, was found to be secreted from HCC cells and hepatic stellate cells (HSCs). STC1 promoted cell migration and invasion of HCC and activation of HSCs, suggesting that STC1 could be an actionable target of both diseases. As a secretory protein, STC1 could potentially be targeted by an antibody approach.
Objectives: This study aims to investigate the therapeutic values of targeting secretory STC1 in HCC and LF models using antibody approach, including in the interplay between HSCs and HCC cells.
Methods: Human anti-STC1 antibody was harvested and purified from a hybridoma cell line of a designed epitope. *In vitro* transwell migration and invasion assays were performed on human HCC cell lines. Co-culture assays were set up with HCC cells cultured in conditioned medium (CM) collected from LX2, a human HSC cell line. Expression of fibrogenic markers were measured by western blotting, qPCR and ELISA.
Results: Enforcement of STC1, either by viral transfection of STC1-overexpressing vector or by the treatment of recombinant STC1 protein, increased the migration and invasion of HCC cells. The effects were abrogated by the co-treatment of anti-STC1 antibody. The enhanced migratory and invasive abilities of HCC cells induced by activated HSC CM were abolished by anti-STC1 antibody. In addition, anti-STC1 antibody suppressed the secretion of type I collagen (COL1) and the intracellular expression of fibrogenic markers alpha-smooth muscle actin (αSMA) and TIMP metallopeptidase inhibitor 1 (TIMP1) in TGFβ1-activated HSCs.
Conclusion: Anti-STC1 antibody displays therapeutic effects on HCC *in vitro*. It is also shown to suppress the expression of fibrogenic markers in

activated HSCs. Anti-STC1 antibody is a potential therapeutic strategy for both HCC and LF.

#3983

Defining the role of FANCA in breast cancer development and cell cycle progression

Liang Luo[1], Wenjun Liu[2], Anna Palovcak[1], Fenghua Yuan[1], Fang Li[1], Daniel Calkins[1], Yan Li[1], Karoline Briegel[1], Daniel Bilbao[1], Evan Roberts[1], Christian Mason[1], Zhao-Jun Liu[1], Sylvia Daunert[1], Yanbin Zhang[1].
[1]University of Miami Miller School of Medicine, Miami, FL,[2]Zhejiang University School of Medicine, Hangzhou, China

FANCA is one of the 22 known Fanconi anemia (FA) pathway genes and is indispensable for interstrand crosslink (ICL) repair. It is reported that FANCA is responsible for about 64% of FA cases and one important clinical characterization of FA patients is predisposition to cancer. However, analysis of TCGA database reveals that FANCA level is elevated in breast cancer patients, especially in ER- breast cancer, which is associated with the methylation status at the S-shore of CpG island ahead of FANCA gene. Moreover, the FANCA level is negatively correlated with the survival rate of breast cancer patients. To understand the implication of FANCA in breast cancer development, we have targeted FANCA by either CRISPR mediated knock-out (KO) or shRNA mediated knockdown (KD) in MDA-MB-231 breast cancer cells. Our data suggest that depletion of FANCA protein inhibits breast cancer growth both in vitro and in vivo. On the other hand, overexpressing FANCA in low-FANCA breast cancer cell line MDA-MB-468 promotes cancer cell proliferation. Cell cycle profiling reveals an inefficiency of MDA-MB-231 FANCA KO cells in G1 to S transition due to p21 and p27 upregulation in FANCA KO cells. In addition, the proliferation inefficiency in MDA-MB-231 FANCA KO cells is caused by Rb hypophosphorylation. Therefore, we conclude that FANCA contributes to the breast cancer development by promoting cell cycle progression through Rb/E2F signaling pathway. Our immunoprecipitation (IP) results indicate that in MDA-MB-231, FANCA is interacting with HES1, which is a transcription suppressor that binds to the promoter region of CDKN1A and CDKN1B to promote cell cycle progression, explaining how FANCA participates in cell cycle progression in breast cancer.

#3984

NB compound FOXM1 inhibitors have potent anti-cancer activity in high-grade serous ovarian carcinoma

Makenzie Vorderbruggen[1], Cassie Liu[1], Catalina Muñoz Trujillo[1], Sung Hoon Kim[2], John A. Katzenellenbogen[2], Benita S. Katzenellenbogen[2], Adam R. Karpf[1]. *[1]University of Nebraska Medical Center, Omaha, NE,[2]University of Illinois Urbana-Champaign, Champaign, IL*

Introduction: High-grade serous ovarian carcinoma (HGSC) is characterized by frequent overexpression and activation of the Forkhead Box M1 (FOXM1) transcription factor, suggesting it as a therapeutic target. This study focused on characterizing the activity of 1,1-diarylethylene FOXM1 inhibitors (NB compounds) against HGSC models.
Methods: We assessed the effects of three NB compounds (NB-55, NB-73, and NB-115) on FOXM1, transcriptionally active p-FOXM1-T600, FOXM1 targets, and other FOX family members using western blotting. We used RT-qPCR to assess the effect of NB compounds on mRNA expression of *FOXM1* and its canonical targets. We used CyQuant, colony formation, and apoptosis assays to determine the effects of NB compounds on cell viability. We compared the effects of NB compounds and other FOXM1 inhibitors on HGSC cells vs. non-transformed fallopian tube epithelial (FTE) cells. We determined the relationship between FOXM1 degradation and apoptosis and conducted drug washout to determine the length of FOXM1 reduction following NB compound treatment. We used Compusyn to determine whether NB compounds synergize with carboplatin.
Results: NB compounds caused a dose- and time-dependent decrease in FOXM1 and p-FOXM1 and reduced expression of FOXM1 targets with effects on FOXM1 maintained up to 72 hours post-washout in HGSC cells. In contrast, other FOX family members, including FOXA1 and FOXO3A, were minimally affected. RT-qPCR confirmed decreased mRNA levels of *FOXM1* and its target genes, including CCNB1, SKP2, and CDC25B, in HGSC cells treated with NB compounds. As determined by CyQuant, NB compounds were potent in HGSC cells, with nanomolar IC50 values, and impaired both 2D and 3D HGSC cell colony formation. Compared to other FOXM1 inhibitors, e.g., thiostrepton and FDI-6, NB compounds were more potent in HGSC cells with reduced effects in non-transformed FTE cells

(FT282). NB compounds promoted HGSC cell apoptosis, while FT282 cells were unaffected at similar concentrations. Additionally, ectopic FOXM1 expression sensitized FT282 cells to NB compound mediated reduced cell viability. Co-treatment with the pan-caspase inhibitor Q-VD-OPh abrogated apoptosis but not FOXM1 degradation in HGSC cells. NB compounds synergized with carboplatin following simultaneous treatment, and to a greater extent when HGSC cells were treated with NB compounds prior to carboplatin. *In vivo* toxicity studies using C57/BL6 mice indicate that NB compounds are tolerable when administered intraperitoneally. Ongoing studies are assessing the *in vivo* activity of NB compounds using the ID8, p53-/- syngeneic mouse HGSC model.
Conclusions: NB compounds target FOXM1 and the FOXM1 pathway, are potent inhibitors of HGSC cell viability, have a favorable therapeutic index *in vitro,* and are tolerable in mice *in vivo*. These data support NB compound FOXM1 inhibitors as a novel therapeutic approach for HGSC.

#3985
S100A10 promotes HCC development and progression via transfer in extracellular vesicles and regulating their protein cargos
Lu TIAN, Xia WANG, Jingyi LU, HongYang Huang, Goofy Yu-Man Tsui, Karen Man-Fong Sze, Tan-To Cheung, Irene Oi-Lin NG. *The University of Hong Kong, Hong Kong, Hong Kong*

Growing evidence indicates that tumor cells exhibit characteristics similar to their lineage progenitor cells. We found that S100 calcium binding protein A10 (S100A10) exhibited an expression pattern similar to that of liver progenitor genes. However, the role of S100A10 in hepatocellular carcinoma (HCC) progression is unclear. Furthermore, extracellular vesicles (EVs) or exosomes are critical mediator of tumorigenesis and metastasis, but the extracellular functions of S100A10, particularly those related to EVs (EV-S100A10), are unknown. In this study, we observed that S100A10 was upregulated at mRNA level in patients' HCC tumors as compared to the corresponding non-tumorous livers, associated with a copy-number gain. Overexpression of S100A10 was correlated with more aggressive tumor features and poor prognosis. Furthermore, functional assays demonstrated it promoted HCC initiation and progression, including increased sphere forming ability in vitro, enhanced chemoresistance, upregulated liver cancer

stemness markers and activated AKT and ERK pathways. In addition, in orthotopic injection mouse model, S100A10 enhanced both the intrahepatic and pulmonary metastasis of HCC xenografts, with upregulated epithelial-mesenchymal transition (EMT) changes. Of significance, we found that S100A10 was present in EVs secreted by HCC cells. Functionally, the EVs secreted by HCC cells promoted the migratory and invasive abilities of recipient HCC cells. Consistent with the oncogenic role of S100A10 in HCC, EVs from S100A10-overexpressing HCC cells enhanced the tumor promoting effects, while the S100A10-depleted HCC cells abrogated the effects, as compared to the vector control group. To further consolidate the tumor promoting role of S100A10-EV, we blocked the effects using neutralizing antibody (NA) by pretreating HCC cells with S100A10 NA together with EV. Indeed, the NA significantly abrogated the stemness and metastatic properties induced by S100A10-EVs both in vitro and in vivo. In addition, the EMT changes and activation of AKT and ERK were also validated in the recipient HCC cells with the S100A10-EV treatment, while they were abolished with the NA treatment. Moreover, we found that S100A10 governed the protein cargos in EVs and mediated the binding of MMP2, fibronectin and EGF to EV membranes through physical binding with integrin αV to promote the motility of recipient cells. Of note, we observed a simultaneous change of p-EGFR, indicating potential activation of AKT and ERK induced by EGFR. On the other hand, we found the plasma EV-S100A10 level was relatively higher in HCC patients than healthy donors. Collectively, the data showed that S100A10 could be transferred among cells through EVs and activated signaling pathways to facilitate metastasis. Targeting S100A10 may be a potential therapeutic strategy for HCC.

#3986

Novel LIPA targeted therapy for treating ovarian cancer

Alexia B. Collier[1], Suryavathi Viswanadhapalli[1], Tae-Kyung Lee[2], Kara Kassees[2], Karla Parra[3], Gaurav Sharma[3], Tanner Reese[3], Michael Hsieh[3], Xihui Liu[3], Xue Yang[1], Behnam Ebrahimi[1], Uday P. Pratap[1], Rahul Gopalam[1], Chia Yuan Chen[2], Scott Terry Elmore[2], Gangadhara Reddy Sareddy[1], Edward R. Kost[1], Jung-Mo Ahn[2], Ganesh V. Raj[3], Ratna K. Vadlamudi[1]. *[1]UT Health Science Center at San Antonio, San Antonio,*

TX,[2]UT Dallas, Richardson, TX,[3]UT Southwestern Medical Center, Dallas, TX

BACKGROUND**:** Ovarian cancer (OCa) is the deadliest of all gynecologic cancers in the United States. Currently approved therapies have improved OCa survival for clinically localized disease, however, the majority (~90%) of patients with high-grade serous OCa (HGSOC) experience relapse with incurable metastases. There is a dire need for new therapeutic approaches. We hypothesized that the high basal endoplasmic reticulum stress (ERS) in OCa represents a critical and targetable vulnerability and may overcome the tumor heterogeneity. The objective of this project is to exploit increased ERS in ovarian cancer cells by engaging the novel target LIPA using the unique compound ERX-41.
METHODS: The utility of ERX-41 as a new therapy was evaluated using MTT and CellTiter-Glo Cell Viability Assays. We used multiple established and patient derived OCa cell lines. The effect of ERX-41 on the Cell viability of patient-derived organoids (PDO) was measured using CellTiter-Glo 3D Assay. Long term effects of ERX-41 on cell survival were measured using colony formation assays. Apoptosis was measured using Annexin V and Caspase-Glo® 3/7 Assays. Cell cycle analysis was analyzed by Flow Cytometry. Mechanistic studies were done using LIPA knockout (KO) cells, RT-qPCR, and western blotting. Status of LIPA in OCa was determined using TNMplot database. *In vivo* efficacy of ERX-41 was tested using both cell line derived (CDX) and patient derived (PDXs) xenografts.
RESULTS: TNM plot results showed that LIPA is highly expressed in OCa tumors compared to normal tissues and LIPA expression correlated with clinical grade. Kaplan-Meier plotter analyses of TCGA data revealed that LIPA expression is negatively correlated with overall survival in OCa patients. MTT and CellTitre-Glo assay results showed that ERX-41 significantly reduced the cell viability of both established and primary OCa cells, and PDO's with an IC_{50} of ~500nM. ERX-41 treatment also significantly reduced the cell survival, increased S-phase arrest, and promoted apoptosis of OCa cells. A time course study revealed a robust and consistent induction of ERS markers (CHOP and sXBP1) in OCa cells by ERX-41 within 4h. Western blotting analyses also confirmed increased expression of ERS markers including CHOP, elF2α, PERK, and ATF4 upon ERX-41 treatment confirming that ERX-41 induces ERS. In xenograft

studies, ERX-41 treatment resulted in ~66% reduction of tumor volume measured by Xenogen-IVIS. Further, in studies using PDX tumors, treatment with ERX-41 resulted in a significant reduction (~60%) of tumor volume and tumor weight.
CONCLUSION: Collectively, our results suggest that ERX-41 is a novel therapeutic agent that targets the LIPA with a unique mechanism of action and implicate ERX-41 binding to LIPA induces ER stress, and apoptosis of OCa cells. Further molecular characterization of how ERX-41 binding to LIPA induces ER stress in OCa cells is ongoing.

#3987
Targeting nucleotide synthesizing enzyme dUTPase (DUT) represents a metabolic weakness and therapeutic opportunity in liver cancer
Yue Liu, Mingjing Xu, Ho Lee Wan, Alissa M. Wong, Xiaofan Ding, Kelvin K. C. Ng, Nathalie Wong. *Surgery, Sir Y.K. Pao Centre for Cancer, Prince of Wales Hospital, The Chinese University of Hong Kong, Shatin, NT, Hong Kong*

Hepatocellular carcinoma (HCC), the most common type of primary liver cancer, has an overall 5-year survival rate of around 20%, making it the third leading cause of cancer-related death worldwide. Upregulated nucleotide metabolism is frequently identified in HCC and represents a metabolic weakness of tumor cells. The enzyme dUTPase (DUT) catalyzes the synthesis of nucleotide precursor and prevents undesired uracil misincorporation into DNA, and thus plays an important role in the maintenance of DNA integrity and cell viability. Although common upregulation of DUT has been reported in cancers, its role in HCC remains largely unknown. In this study, we investigated the mechanism underlying DUT biology in HCC and tumor susceptibility to drug targeting dUTPase. Overexpression of DUT was found in 42% of HCC cases and significantly correlated with advanced stage tumors. CRISPR-Cas9 mediated knockout of DUT resulted in growth retardation, cell cycle arrest and a spontaneous induction of DNA damage in multiple HCC cell lines. A protective effect from oxidative stress was also demonstrated in both knockout and overexpression DUT assays. Metabolomics analysis showed altered DUT expression in HCC cells resulted in profound impact on pyrimidine and purine metabolism. In addition, levels of DUT protein strongly correlate

with cellular level of dUTP and dTDP, which suggested its critical role in dNTP homeostasis. Interestingly, hepatic organoids overexpressing DUT showed drug resistance to tyrosine kinase inhibitor (TKI) Sorafenib. Both *in vitro* and *in vivo* assays confirmed that targeting dUTPase activity with TAS-114 synergized the effect of Sorafenib in suppressing HCC growth. In conclusion, our study showed that upregulated DUT conferred growth advantage to HCC cells by reducing uracil misincorporation and favoring nucleotide synthesis. Targeting DUT with its first-in-class inhibitor TAS-114 in combination with Sorafenib represents an effective treatment regime for HCC.

#3988

The role of HER3 mutations in the progression of colon cancer and modulation of drug sensitivity and resistance

Mary K. Kilroy, Rosalin Mishra, Anastasia Stupecki, Wasim Feroz, Samar Alanazi, Joan T. Garrett. *Pharmaceutical Sciences, University of Cincinnati, Cincinnati, OH*

Colorectal cancer is a disease of the colon and rectum that will claim about 52,580 American lives in2022. The most common treatment of colorectal cancer is surgery plus chemotherapy, although thereare some FDA approved targeted therapies such as regorafenib (targeting VEGF) or cetuximab (targetingEGFR). EGFR, along with HER2, HER3, and HER4 are members of the HER family of receptor tyrosinekinases that upon homo- or heterodimerization activate downstream signaling, growth, and survivalpathways. In recent years, more attention has been paid to HER2 and HER3's roles in colorectal cancers,as they may cause resistance to targeted therapies. OWe are investigating naturally occurring mutantHER3's role in colorectal cancer, as about 6% of all colorectal cancers contain a HER3 mutation. We arecurrently investigating how HER3 mutations may affect sensitivity to current therapies through HERfamily receptor dimerization and be involved in tumor metastasis. We are assessing the degree to whichmutant and wild-type HER3 have the ability to dimerize with EGFR, HER2, MET, and IGF1R the resultingeffects in colon cancer, as these receptor tyrosine kinases are HER3 binding partners. As HER3 bindingpartners are diverse, it may be that the pathway HER3 and its binding partner activate may influencetreatment strategy. It has been noted

that mutant HER2 and HER3 could confer sensitivity to HER familyinhibitors, i.e. afatinib, in bladder cancer, and we have seen a difference in IC50 values of afatinibbetween cell lines containing wild-type or mutant HER3. If mutant HER3 is involved in therapeuticresistance or sensitivity and tumor progression, our findings may present a new biomarker for targetedtreatments in colorectal cancer with the eventual goal of increased overall patient survival.

#3989

EVI1 oncogenic role in non-canonical AR driven lethal prostate cancer

Surendra Gulla[1], Jonathan E. Bard[2], David J. VanderWeele[3], Kathleen Kelly[4], Remi Adelaiye-Ogala[1]. *[1]Department of Medicine/Division of Hematology and Oncology, University at Buffalo, Buffalo, NY,[2]Genomics and Bioinformatics Core, University at Buffalo, Buffalo, NY,[3]Hematology and Oncology, Northwestern University Feinberg School of Medicine, Chicago, IL,[4]Center for Cancer Research, National Cancer Institute, Bethesda, MD*

Background**:** Androgen receptor (AR) remains active in castration-resistant prostate cancer (CRPC), and AR cistrome can become extensively reprogrammed with disease progression. Recent findings from our group and others have shown an association with non-canonical AR signature with resistance to enzalutamide. However, the complete mechanism is not fully revealed. EVI1 belongs to the zinc-finger transcription factor family, and overexpression of EVI1 is associated with poor patient outcomes. However, its role in the context of resistance to AR-targeted therapy remains unclear. Our preliminary data from ChIP-seq and GSEA analysis shows a significant enrichment of EVI1 target gene-set captured from annotated enzalutamide-resistant AR binding sites.
Hypothesis: EVI1 cooperates in regulating the non-canonical AR activity associated with resistance to AR targeted therapy and blocking EVI1 may overcome resistance to target therapy.
Methods: Using a PDX model of advanced enzalutamide-resistant CRPC, we performed single-cell ATAC-seq + gene expression multi-omic assay. Next, we determined the enrichment of canonical vs. non-canonical AR signatures across cell populations. Using motif analysis and transcription

factor foot printing, we determine EVI1 (MECOM) motif z score and enrichment.
Results: Our findings demonstrate enrichment of non-canonical AR signatures in distinct population of cells following exposure to enzalutamide. In addition, the subpopulation of cells enriched for non-canonical AR cistrome also exhibited high EVI1 (MECOM) motif z-scores.
Conclusion: Our data suggests a potential link between EVI1 and non-canonical AR signaling. Ongoing mechanistic studies will provide insight mechanism by which EVI1 controls non canonical AR activity and its vulnerabilities.

#3990
Imaging molecular alterations during tucatinib response in preclinical models of HER2+ breast cancer
Patrick Song, Ameer Mansur, Anna Sorace. *University of Alabama at Birmingham, Birmingham, AL*

Introduction**:** Human epidermal growth factor receptor 2 (HER2) is overexpressed in 25% of breast cancers. Tucatinib, a small molecule HER2 inhibitor, was FDA approved for inoperable or metastatic HER2+ breast cancer. As many of these patients have inoperable tumors, there is a need to identify imaging metrics that can characterize response to tucatinib. Positron emission tomography (PET) imaging can quantify changes in the tumor microenvironment that precede changes in tumor size through imaging with radiopharmaceuticals that target proliferation (fluorothymidine, [^{18}F]-FLT), hypoxia (fluoromisonidazole, [^{18}F]-FMISO) and HER2 expression ([^{89}Zr]-Pertuzumab). The goal of this study is to use advanced PET imaging to non-invasively monitor response to tucatinib in HER2+ primary breast cancer and quantify the subsequent tumor microenvironment modulation.
Methods: HER2+ cell line (BT474) and patient derived xenograft (BCM 3472) tumor models were engrafted and developed to 270 ± 166.4 mm^3 before being enrolled into experiments. Mice were treated with 50 mg/kg tucatinib via PO and were imaged with [^{18}F]-FLT PET (N = 8) on days 0, 3 and 7, [^{18}F]-FMISO PET (N = 6) on days 0, 3 and 7, or [^{89}Zr]-Pertuzumab PET (N = 5) on days 0 and 14. Intratumoral proliferation, hypoxia and HER2 expression were quantified with standardized uptake value (SUV).

Following the final imaging timepoint, tumors were excised for immunohistochemistry against Ki-67 (proliferation), pimonidazole (hypoxia), and HER2. A non-parametric T-test was used to assess for significance.

Results: Tucatinib treated BT474 and BCM3472 tumors had a 2.07 and 2.63 fold decrease in tumor volume, respectively ($p<0.01$). Tucatinib treated BT474 and BCM3472 tumors had significantly decreased hypoxia and proliferation, relative to control tumors ($p<0.05$). Tucatinib treated BT474 tumors had significantly decreased HER2 expression ($p<0.05$); however, no significant change in HER2 expression was observed in tucatinib treated BCM3472 tumors.

Conclusion: Tucatinib significantly decreases tumor volume and decreases intratumoral proliferation and hypoxia in both cell-line and patient-derived xenograft models of HER2+ breast cancer. Our data suggests molecular imaging may drive understanding of and predict response to tucatinib therapy.

Acknowledgements: Tucatinib was provided by Seagen Inc. Bothell, Washington, USA.

#3991

NOS inhibition enhances docetaxel-mediated anti-tumor effect in obese mice with triple negative breast cancer

Ivonne Uzair, Kai Sun, Ann Anselme, Wei Qian, Jianying Zhou, Roberto Rosato, Jenny Chang. *Houston Methodist Research Institute, Houston, TX*

Purpose of **the study:** To evaluate the role of obesity in tumor progression and tumor microenvironment (TME) dynamic after the inhibition of nitric oxide synthase (NOS) in syngeneic murine models engrafted with triple negative breast cancer (TNBC) tumors. For this study, we wanted to deepen the results of our recently completed phase I/II clinical trial, where treatment with NG-methyl-L-arginine (L-NMMA, a pan-NOS inhibitor) increased the response rate to chemotherapy (docetaxel) in obese metastatic TNBC (ER-/PR-/HER2-) patients to 86% vs. 60% in normal weight individuals. TME analysis from responders revealed a neutrophil phenotype shift from protumor N2 to antitumor N1. We thus hypothesize that combined treatment with L-NMMA and docetaxel enhances antitumor effect by modulating TME in obese mice with TNBC.

Experimental procedures: 3-week old female C57BL/6 mice were fed for 10 weeks either with high fat diet (HFD) or normal diet (ND). At week 13, TNBC mouse E0771 tumor cells were injected into the mice mammary fat pad. Once tumors reached 100 mm^3, the animals were randomized to four groups: vehicle; docetaxel; L-NMMA; and docetaxel plus L-NMMA treatment. Tumor volume was measured throughout the experiment and growth rate was compared between groups at the end of treatment. Blood, tumor and perigonadal white adipose tissue (pgWAT) were collected. Cytokines and nitrite/nitrate levels (NO2-/NO3-, a NO indicator) were measured from blood and conditioned media (CM) from pgWAT using appropriate kits. Tumor immune cell infiltration was evaluated by immunohistochemistry. GraphPad software was used for statistical analysis and P-values <0.05 were considered to describe statistically significant differences between groups.
Results: Tumor growth rate was significantly higher in HFD mice compared to ND mice. Treatment with the docetaxel/L-NMMA combination significantly slowed tumor growth in HFD mice (p=0.015), and showed a similar trend in ND mice (p=0.92) vs. the corresponding vehicle-treated groups. The reduction of tumor growth was significantly higher in HFD mice vs. ND mice (median of differences -2.0, p=0.031). HFD mice presented higher levels of pro-inflammatory cytokines, [IL-1b (p=0.011), IL-6 (p<0.0001) and TNFa (p<0.0001)] vs ND mice in pgWAT CM, as well as increased levels of NO2-/NO3- and expression of iNOS in tumors and in perigonadal adipose tissue.
Conclusion: HFD mice had a pro-inflammatory profile with a significantly faster tumor growth and higher expression of iNOS in tumor and adipose tissues. Treatment with the docetaxel/L-NMMA combination resulted in a more significant anti-tumor effect in HFD mice, likely through remodeling of TME. Spatial analysis, including CODEX and immunophenotyping are being conducted to determine the TME influence in obesity associated TNBC and the effect of NOS inhibition.

#3992
Elucidating reciprocal interactions between bone marrow stromal cells and a novel γδ CAR T cell therapy in the context of bone metastatic prostate cancer

Jeremy S. Frieling[1], Xiomar Bustos[2], Ryan T. Bishop[1], Leticia Tordesillas[2], Daniel Abate-Daga[2], Conor C. Lynch[1]. *[1]Tumor Biology, Moffitt Cancer Center, Tampa, FL,[2]Immunology, Moffitt Cancer Center, Tampa, FL*

Bone metastatic castrate resistant prostate cancer (CRPC) generates tumors hallmarked by extensive bone formation due to enhanced mesenchymal stem cell (MSC)-osteoblast differentiation. These lesions are at present incurable and substantially diminish patient quality of life, but exciting preclinical studies by our group have shown that these metastases are highly sensitive to gamma delta (γδ) T cell-based CAR-T therapies. However, the impacts of CAR-T cell therapies on the bone microenvironment are presently unknown. Because MSCs are an important stromal component of the cancer-bone microenvironment with emerging immunoregulatory activities, we have recently focused on characterizing the interactions between γδ CAR-T cells and the MSC compartment and their implications for bone metastatic CRPC. Our data show that: 1) γδ CAR-T cells or conditioned media (CM) did not significantly alter MSC viability, 2) MSCs were robustly chemotactic to CM derived from tumor-activated γδ CAR-T cells, 3) MSCs treated with tumor-activated γδ CAR-T CM showed a significant induction of ICAM-1 (9.12-fold, P=0.00640) compared to controls, 4) ICAM-1 silencing significantly reduced γδ CAR-T educated MSC migratory ability, 5) tumor-activated γδ CAR-T CM differentially regulated key genes involved in MSC-osteoblast differentiation, a finding supported by Alizarin red S staining and alkaline phosphatase functional assays, and 6) tri-cultures of MSCs, CRPC cells, and γδ CAR-T cells demonstrate that MSCs significantly enhanced γδ CAR-T mediated CRPC killing. Taken together, we have shown that γδ CAR-T cells promote MSC recruitment in an ICAM-1 dependent manner, and MSCs enhance γδ CAR-T targeted CRPC killing. Reciprocally, γδ CAR-T can promote MSC commitment to osteoblast lineage without impacting their viability. These data are the first to interrogate how bone stromal components regulate γδ CAR-T mediated killing in the context of bone metastatic CRPC. We are currently investigating the mechanisms underpinning the bi-directional interplay between these cell populations.

#3993

In vivo efficacy of an anti-human IL11RA antibody in B-hIL11RA mice with APAP-induced liver damage

Fang He[1], Rufeng Zhang[1], Mari Kuraguchi[2], Lei Zhao[1], Zhaoxue Yu[2].
[1]Biocytogen Pharmaceuticals (Beijing) Co., Ltd., Beijing, China,[2]Biocytogen Boston Corp, Wakefield, MA

Acetaminophen (*N*-acetyl-*p*-aminophenol; APAP) overdose is a common cause of drug-induced acute liver injury, thereby making APAP administration a frequently used experimental model due to its highly reproducible and dose-dependent hepatoxicity. APAP-induced liver injury (AILI) mouse models exhibited upregulated IL11 expression, indicating that targeting IL11 or its cognate receptor, IL11RA, could have therapeutic potential. To evaluate the *in vivo* efficacy of anti-human IL11RA antibodies in AILI mouse models, we first generated a human IL11RA knock-in mouse model (B-hIL11RA), in which human *IL11RA* replaced murine *Il11ra, in situ*. Human IL11RA mRNA and protein levels were detected in B-hIL11RA mice. We next examined whether therapeutic inhibition of IL11 signaling was effective in reducing AILI following administration of an anti-human IL11RA antibody. *In vivo* efficacy data showed that anti-human IL11RA antibody inhibited all aspects of AILI, including hepatocyte death (ALT, AST and TUNEL) and centrilobular necrosis. These data suggest that B-hIL11RA mice are an effective tool for preclinical *in vivo* efficacy evaluation of therapeutic anti-human IL11RA antibodies.

#3994

Differential regulation of hormone receptors and Ki67 in luminal breast carcinomas and tumor-adjacent mammary glands by mifepristone treatment

Leo Saldain[1], Silvia Vanzulli[1], Paula Martinez Vazquez[2], Javier Burruchaga[2], Eunice Spengler[3], Claudia Lanari[1], Paola Rojas[1]. *[1]IBYME-CONICET (Institute of Biology and Experimental Medicine), Buenos Aires, Argentina,[2]Breast and Gynecological Surgery, Magdalena V. Martinez Hospital, General Pacheco, Argentina,[3]Pathology, Magdalena V. Martinez Hospital, General Pacheco, Argentina*

Since antiprogestins inhibit the growth of preclinical mammary tumor models expressing higher levels of progesterone receptor (PR) isoform A (PRA) than isoform B (PRB), we designed a window-of-opportunity trial (MIPRA; NCT02651844) to study the benefits of mifepristone (MFP) in luminal breast carcinomas from postmenopausal patients selected by their PR+ expression (>50%) and their PR isoform ratio (PRA/PRB>1.5; PRA-H). A decrease in the cell proliferation marker Ki67 was registered after treatment in 14 out of the 20 tumors evaluated. This inhibition was associated with a decrease in PR, estrogen receptor (ER) and pSer118ER evaluated by immunohistochemistry while no changes in pSer167ER expression were observed (PMID: 36269797). In selected tissues from these samples we observed that the staining intensity in trapped glands within the MFP-treated tumors did not follow a similar trend as that of tumor cells. Thus, the aim of this study was to evaluate the expression of hormone receptors and Ki67 in non-neoplastic human mammary glands (nnMG) adjacent to the PRA-H tumor tissue of postmenopausal patients, treated (n=8) or not (n=9) with MFP. No differences in PR, ER and pSer118ER expression were observed between MFP-treated nnMG and those from untreated patients. Notably, contrarily to what occurred in tumors, there was a significant decrease of pSer167ER expression (p=0.008) in the MFP-treated nnMG compared to the untreated glands, suggesting a selective modulation in the AKT-mediated activation of ER. Regarding the proliferative state of the nnMGs, there was a slight but significant increase (p=0.02) in Ki67 expression in MFP-treated *vs.* non-treated nnMG. Data regarding the effect of antiprogestins in normal mammary glands is limited and points, in premenopausal women, to a decrease in the Ki67 index after treatment. The basal quiescent status of nnMG in postmenopausal women may explain this slight stimulatory effect. In conclusion, our results show that MFP exerts a specific regulatory effect in PRA-H tumors that is not observed in the nnMG, probably due to the fact that nnMG have presumably equimolar levels of PRA and PRB. In addition, to counteract the possible stimulatory effect that MFP may induce on nnMG, the combination of MFP and tamoxifen treatment is suggested.

#3995

Trastuzumab deruxtecan, antibody-drug conjugate targeting HER2, effectively inhibits growth of patient-derived xenograft model with

CIC-rearranged sarcoma

Yuki Kojima[1], Shigehiro Yagishita[2], Kazuki Sudo[1], Tatsunori Shimoi[1], Shintaro Iwata[1], Shun-ichi Watanabe[1], Chitose Ogawa[1], Akihiko Yoshida[1], Yasushi Yatabe[1], Kan Yonemori[1], Akinobu Hamada[1]. *[1]National Cancer Center Hospital, Tokyo, Japan,[2]National Cancer Center Research Institute, Tokyo, Japan*

Background: Capicua-double homeobox 4 (CIC-DUX4)-rearranged sarcomas (CDS) are extremely rare and highly aggressive sarcomas. There is no standard therapy for the patients with advanced CDS, and therapeutic development is needed. We evaluated preclinical efficacy of trastuzumab deruxtecan (T-DXd), a humanized monoclonal HER2-targeting antibody conjugated to a topoisomerase 1 inhibitor, DXd, in patient-derived xenograft (PDX) models with CDS.
Methods: Patient-derived tumor tissue was transplanted into subcutaneous around the flank of female NOG mice, which were treated with vehicle or T-DXd (3 mg/kg, intravenous, Day0) when the mean tumor volume reached 200 mm^3. Tumor volume was assessed twice weekly for 3 weeks to assess the efficacy of T-DXd.
Results: This study included 3 CDS-derived PDXs. HER2 expression was low in one PDX and not expressed in two PDXs. One PDX was established from a specimen at initial diagnosis, two were established from specimens after prior-chemotherapy. T-DXd demonstrated significant tumor growth delay compared to vehicle in all PDX models investigated. One PDX with no efficacy was HER2-negative and had a treatment history of topoisomerase I inhibitor. In contrast, PDX of HER2-negative topoisomerase I inhibitor-resistant Ewing sarcoma was also administered T-DXd under the same conditions and was found to be refractory.
Conclusion: The present study showed that a therapeutic potential of T-DXd in CDS patients, including HER2-negative.

#3996

The impact of HER3 dynamics on the efficacy of HER3-DXd, a novel HER3 directed antibody-drug conjugate

Nagiho Komatsu, Saori Sato, Sumie Muramatsu, Ryuichi Nakamura, Kumiko Koyama. *Daiichi Sankyo Co., Ltd., Tokyo, Japan*

Background**:** HER3 is broadly expressed in various solid tumor types, and its expression can be upregulated by treatment with receptor tyrosine kinase inhibitors (RTKi) such as EGFR TKIs used to treat *EGFR*-mutated NSCLC. HER3-DXd, a novel antibody-drug conjugate (ADC) composed of a human anti-HER3 IgG1 monoclonal antibody (patritumab) covalently linked to a topoisomerase I inhibitor payload (DXd), is currently being studied in clinical trials for breast cancer and NSCLC. As previously reported, HER3-DXd treatment transiently decreases HER3 expression levels in tumors and EGFR TKIs increase HER3 membrane expression. However, the impact of HER3 dynamics on payload delivery has not been clarified yet. In this study, we investigated HER3 dynamics including HER3 receptor turnover and payload delivery in cancer cells using HER3-DXd both as a single agent and in combination with RTKi including osimertinib, which is in clinical trials in combination with HER3-DXd.
Methods: HER3/ADC internalization was evaluated by using confocal imaging in MDA-MB-453 cells treated with HER3-DXd. Internalization and payload release were quantitatively measured in 3 cancer cell lines treated with HER3-DXd. HER3 turnover on the cell surface was also evaluated upon wash-out of HER3-DXd. In xenograft models, mice were administered two doses of HER3-DXd at different doses and dosing intervals, and membrane HER3 expression and tumor payload concentration were examined over time. NSCLC cell lines harboring *EGFR* activating mutations, *ROS1* fusions, or *ALK* fusions were used to evaluate the effect of osimertinib, lorlatinib, or ceritinib on cell surface HER3 expression and payload release (osimertinib only).
Results: HER3-DXd was rapidly transferred to early endosomes after binding to HER3. HER3 dynamics varied among the cell lines tested in vitro, and payload release reflected cell surface HER3 expression levels, HER3 internalization speed and turnover rates. In xenograft models, a higher dosage of HER3-DXd resulted in a larger decrease in membrane HER3 expression. Dosing interval also affected membrane HER3 expression levels; the degree of tumor payload concentration increase after the second dose was dependent on the recovery of HER3 expression after the first dose. Furthermore, we confirmed that RTKi increased the cell surface HER3 expression in NSCLC cell lines with targetable driver genomic alterations and that osimertinib increased payload delivery in PC-9 cells through the upregulation of cell surface HER3 expression.

Conclusion: HER3 expression was dynamically changed by HER3-DXd dosing regimen and by RTKi treatment, resulting in a substantial impact on payload release. These findings support our strategy of clinical studies using HER3-DXd after drugs that increase HER3 expression including EGFR TKI and indicate that HER3 dynamics may play a key role in achieving optimal efficacy of HER3-DXd.

#3997

Preclinical characterization of ARX517, a next-generation anti-PSMA antibody drug conjugate for the treatment of metastatic castration-resistant prostate cancer

Lillian Skidmore, David Mills, Ji Young Kim, Prathap Shastri, Nick A. Knudsen, Jeff Steen, Jay Nelson, Ying Buechler, Feng Tian, Shawn Zhang.
Ambrx Biopharma Inc., La Jolla, CA

Prostate cancer is the most common cancer, and the second leading cause of cancer death, among men in the United States. Metastatic castration-resistant prostate cancer (mCRPC) is an advanced stage of disease in which patients ultimately fail androgen-deprivation therapies and exhibit a poor survival rate. Recently, prostate-specific membrane antigen (PSMA) has been validated as a prostate cancer tumor antigen with its over-expression in prostate tumors and low level of expression in select normal tissues. Using an expanded genetic code to create Engineered Precision Biologics (EPBs), Ambrx has developed ARX517, an anti-PSMA targeted next-generation antibody drug conjugate (ADC), for treatment of mCRPC patients. ARX517 is composed of a humanized anti-PSMA antibody site-specifically conjugated to drug linker AS269 (a potent tubulin inhibitor), yielding a drug-to-antibody ratio of 2. After binding to PSMA expressed on the surface of tumor cells, ARX517 is internalized and delivers a cytotoxic payload which inhibits tubulin polymerization and induces cellular apoptosis. In vitro testing of ARX517 in prostate cancer cell lines with variable PSMA expression demonstrated highly specific and potent sub-nanomolar activity in cells with high PSMA expression. To minimize premature payload release, ARX517 employs a non-cleavable PEG linker and stable oxime conjugation chemistry to enhance stability in circulation. ARX517 exhibited a long terminal half-life and high serum exposure in mice. The serum stability of ARX517 should effectively deliver more

payload to target tumor cells, and in multiple CDX and PDX prostate cancer models, ARX517 showed dose-dependent anti-tumor activity in both enzalutamide-sensitive and enzalutamide-resistant models. Repeat dose toxicokinetic studies in non-human primates demonstrated ARX517 was tolerated at exposures well above therapeutic exposures in mouse pharmacology studies, indicating a wide therapeutic index. In summary, ARX517 elicited highly specific, potent cell killing in cell lines with high PSMA expression, inhibited tumor growth in enzalutamide-sensitive and enzalutamide-resistant CDX and PDX models, demonstrated a tolerable safety profile in cynomolgus monkeys, and has a clear therapeutic index based on preclinical serum exposure data. The strong preclinical data and recent clinical validation of PSMA as a mCRPC target provide rationale for evaluation of ARX517 as a potential prostate cancer treatment. ARX517 is currently in a Phase 1 dose escalation trial (ARX517-2011 [NCT04662580]) in the United States.

#3998

Metronomic gemcitabine plus neratinib effectively inhibits the growth of human Her-2 positive breast cancer cells intracranially implanted into immunodeficient mice

Serina Batson[1], Alejandro Sanchez[1], Hector M. Padilla[1], Diana L. Prospero[1], Brenda Lugo[1], Valeria V. Lopez[1], Daniella E. Estrada[1], Nydia De Avila[1], Saeedeh Darvishi[1], Arlene Levario[1], Shan Man[2], Ping Xu[2], Robert S. Kerbel[2], Guido Bocci[3], Giulio Francia[1]. *[1]The University of Texas at El Paso, El Paso, TX,[2]The University of Toronto, Toronto, ON, Canada,[3]The University of Pisa, Pisa, Italy*

Metastatic breast cancer is a major cause of death for women in the US, and breast cancers that metastasize to the brain have a particularly poor prognosis. To treat brain metastases of Her-2 positive breast cancers a number of Her-2 targeting drugs are now clinically available, including lapatinib, neratinib and tucatinib, among others. However, in part as a consequence of poor penetration of many drugs into the brain, combinations of standard chemotherapy plus targeted agent have only modest impact on progression free survival for such patients. We have developed preclinical models of human Her-2 positive breast cancer brain metastases to help address these issues. We selected human MDA-MD-361 and BT474 breast

cancer cells lines by in vivo passaging in SCID mice, followed by molecular tagging of the derived variants (MDA361R and BT474R respectively), and then the stereotactic implantation of such cells into the brain of female SCID mice. Using luciferase-tagged BT474R we implanted 75,000 cells into the brains of the mice, and thereafter confirmed by luminescence the growth of the cells, which allowed for randomization of the mice to receive control saline (n=7), metronomic gemcitabine (100mg/kg/3days; i.p.; n=8), neratinib (40mg/kg/3 days; p.o.; n=7), or the combination of gemcitabine plus neratinib (n=8), which continued for 5 months largely in the absence of overt toxicity. The gemcitabine plus neratinib combination prolonged survival over the controls (150 days vs 65 days, $p<0.5$), although eventually all mice succumbed to disease. Tumors cells have been isolated from these therapy-administered mice for further characterization. Neratinib alone did not result in an increase in survival compared to controls, whereas metronomic gemcitabine improved survival but was inferior to the combination. We confirmed these findings using MDA361R tagged with human chorionic gonadotropin (hCG), which allows for the growth of cells to be monitored by assessment of hCG in the mouse urine, and these cells were implanted intracranially into female SCID mice. After urine hCG levels confirmed the presence of growing cells in the brain, the mice were randomized to the above 4 therapies (n=4/group), which showed an increase in survival of the combination compared to controls. These results point to intriguing effects of chemotherapy when used at continuous low (metronomic) doses, that in these studies involved gemcitabine administration every 3 days, and which in these models can be effectively combined with neratinib to suppress the growth of Her-2 positive breast cancer cells implanted into the mouse brain. These results highlight promising combination that could be used to suppress Her-2 positive breast cancer brain metastatic growth, and the developed models should facilitate the study of this subset of breast cancers.

#3999

Combination of T-DXd with the irreversible pan-HER TKI afatinib drives combination benefit in HER2-low gastric and lung tumors

Deepa Bhavsar[1], Laura Kazlauskas[2], Flavia Michelini[3], Matt Griffin[4], Matt Wilson[5], Fabiola Cecchi[6], Liz Croydon[7], Kim Maratea[8], Elisa de

Stanchina[9], Yelena Y. Janjigian[10], Maurizio Scaltriti[11], Theresa Proia[12], Jerome Mettetal[13]. *[1]Research and Early Development Oncology Bioscience, Senior Scientist, Oncology R&D, AstraZeneca, Waltham, MA,[2]Research and Early Development Oncology Bioscience, Senior Scientist, Oncology R&D, AstraZeneca, Waltham, MA,[3]Translational Medicine, Translational Medicine Lead, Oncology R&D, AstraZeneca, Waltham, MA,[4]Research and Early Development Bioscience, Senior Scientist, Oncology R&D, AstraZeneca, Waltham, MA,[5]Research and Early Development Oncology Bioscience, Scientist, Oncology R&D, AstraZeneca, Cambridge, United Kingdom,[6]Translational Medicine, Senior Director, Oncology R&D, AstraZeneca, Gaithersburg, MD,[7]Clinical Development, Senior Global Development Medical Director, Oncology R&D, AstraZeneca, Central Cambridge, United Kingdom,[8]Clinical Pharmacology and Safety Science, Senior Director, Oncology Safety Pathology, BioPharmaceuticals R&D, AstraZeneca, Waltham, MA,[9]Antitumor Assessment Core Facility Molecular Pharmacology Program, Memorial Sloan Kettering Cancer Center, New York, NY,[10]Memorial Sloan Kettering Cancer Center, New York, NY,[11]Translational Medicine, VP Translational Medicine TDE, Oncology R&D, AstraZeneca, Waltham, MA,[12]Research and Early Development Oncology Bioscience, Director, Oncology R&D, AstraZeneca, Waltham, MA,[13]Research and Early Development Oncology Bioscience, Senior Director, Oncology R&D, AstraZeneca, Waltham, MA*

Background: Trastuzumab deruxtecan (T-DXd) has been approved for advanced or metastatic breast, gastric and lung cancers. It has been postulated that irreversible tyrosine kinase inhibitors (TKIs) increase HER2 internalization, thus enhancing T-DXd efficacy. Here we report studies evaluating the combination of TKIs with T-DXd in preclinical models of HER2-low disease.
Methods: Surface HER2 was measured with flow cytometry quantifying fluorescently labelled trastuzumab on the surface of HER2-low cell lines HCC38 and HCC1171 treated with afatinib, neratinib, lapatinib or tucatinib for 12 h. HER2 receptor dynamics on cell surface was also measured in NCI-N87 (HER2 IHC 3+) and HCC38 at 24, 48, 72 and 96 h post-treatment with afatinib, and recovery was measured up to 72 h after drug washout. *In vivo* efficacy was established with T-DXd alone and in combination with

afatinib or tucatinib in two gastric patient-derived xenograft (PDX) models, HD-2 (HER2 IHC 1+) and FU (HER2 IHC 2+), and one lung PDX model, MEDI-NSCLC-04 (HER2 IHC 1+).
Results: In both HER2-low cell lines, treatment with irreversible inhibitors neratinib or afatinib led to enhanced internalization with a greater than 50% surface HER2 reduction, while treatment with the reversible inhibitors lapatinib or tucatinib led to 13-35% higher surface HER2 levels. Washout experiments indicated that receptor recovery at the plasma membrane begins between 4-12h post-washout of afatinib, with complete recovery at about 72h. Tumor shrinkage was significant in HER2-low gastric PDXs when T-DXd was combined with afatinib, but not with tucatinib. In HD-2, T-DXd 10mg/kg with afatinib 20mg/kg, and T-DXd 3mg/kg with tucatinib 25mg/kg combinations resulted in 74% and -3% (with respect to T-DXd) tumor growth inhibition (TGI), respectively. In FU, T-DXd 3mg/kg with afatinib 20mg/kg, and T-DXd 3mg/kg with tucatinib 25mg/kg combinations resulted in 80.3% and 24.7% TGI, respectively. Similarly, in MEDI-NSCLC-04 PDX model, benefit was observed in 5mg/kg T-DXd combination with 20mg/kg QD afatinib (95.3% TGI with respect to monotherapy T-DXd), but not with tucatinib (0.37% TGI). Intermittent schedules (QW, MWF) were also tested for afatinib in combination with T-DXd, with the MWF showing 49.2% TGI and QW showing 33.0 %TGI. In tissue samples from MEDI-NSCLC-04 efficacy study, γH2AX was detected by IHC in T-DXd and T-DXd+afatinib combination. In western blots, a decrease in HER2 as well as pHER2 was observed in response to T-DXd and 20mg/kg afatinib treatment, but not with tucatinib.
Conclusions: In HER2 low gastric and lung preclinical models, T-DXd combined with irreversible pan-HER inhibitor induced superior antitumor effects compared to single agents or the combination of T-DXd with reversible inhibitors. These data support the rationale to test combination of T-DXd and pan-HER irreversible inhibitors in the clinical setting.

#4000
A novel pegylated bispecific antibody-drug conjugate (P-BsADC) targeting Her2+ cancers with improved efficacy and therapeutic window
Yu (Yvonne) Wen, Shuqiang Yin, Weidong Lyu, Yang Lei, Qiudong Zhuo, Zibin Wu, Bin Sun, Shuangyu Tan, Lidong Jiang, Teng Zhang, Bo Gao, Rui

Xu, Yong Li, Liling Zheng, Shumin Liu, David (Dechun) Wu. *Shenzhen Enduring Biotech, Ltd., Shenzhen, China*

Despite the fact that ADCs improve the efficacy and target selectivity comparing to the non-specific small molecule cytotoxicity drugs in cancer treatment, traditional ADCs still suffer from many issues which include low tumor penetration and accumulation, inefficient internalization, undesired efflux of ADC from tumor cells, significant on-target off-tumor toxicity, Fc mediated uptake that results in off-target toxicity, limited extravasation across capillary walls due to big molecular size, poor diffusion into the tumor masses due to increased tumor interstitial fluid pressure, and the binding-site-barrier. To address these issues, we previously reported that the compound JY201, a Polyethylene Glycol (PEG)-based bispecific ADC (P-BsADC) targeting two epitopes of Her2, demonstrated advantages in tumor penetration, internalization efficiency, lysosome trafficking effectiveness, no Fc related toxicity, and better efficacy in tumor inhibition than transtuzumab deruxtecan (Ds-8201). Continuing from our previous study, here we further reveal that JY201 can penetrate the tumor deeply and distribute more homogeneously in entire tumor masses while Ds-8201 limits its diffusion to the regions very close to the blood vessels in the tumor. Furthermore, JY201 shows better efficacy than Ds-8201 in inhibiting tumors with low expression of Her2 in pdx (patient derived xenograft) and cdx models. In addition, JY201 can effectively inhibit tumors resistant to Ds-8201. In an in-vitro plasma stability test, JY201 demonstrated high stability in cynomolgus monkey and human serums. JY201 also has a biodistribution profile advocating better safety than Ds-8201 in tumor bearing mice. In the repeated-dosing toxicological study in Her2 transgenic mice, JY201 with the dose of 50mg/kg was well tolerated and did not induce any tissue/organ damage to the animals. Due to much shorter half-life (5 times shorter) in mice for PEGylated proteins than in primates, we expect JY201 will have much higher tolerated dose than the 50mg/kg in primates. In summary, the findings from this study provide solid preclinical evidence for JY201 to be developed further as an efficacious and safe clinical treatment for patients with Her2 positive cancers.

Targeting Protein Kinases and Phosphatases for Therapy 1

#4988

A tailored platform enables BRAF-targeted drug discovery and precision medicine

Hui Qi, Fuyang Wang, Bingrui Han, Xiaomin Wang, Xiangnan Qiang, Zhixiang Zhang, Qingyang Gu. *WuXi AppTec, Shanghai, China*

Mutant BRAF, one of the most frequently mutated serine/threonine kinase, drives tumorigenesis via activating MAPK signaling across various tumor types. Expanded genomic and mechanistic studies over the past two decades have revealed the heterogeneity regarding BRAF mutation status and characterized a classification system for BRAF mutations based on their mode of action. Class I (V600 mutants) and class II (K601 mutants, G469A/V/R, etc) BRAF mutants function as RAS-independent active monomers or dimers to amplify MAPK signaling, whereas class III (G466 mutants, D594 mutants, G469E, etc) mutants, which are kinase impaired or dead, promote MAPK signaling via enhanced RAS binding and subsequent CRAF activation. To date, combination therapies of BRAF and MEK inhibitors have been approved for treatment of patients harboring class I BRAF mutations, while viable therapeutic options for those with class II and III BRAF mutations are still ambiguous. Therefore, developing new drugs and personalized therapeutic strategies directing different classes of BRAF mutations, especially class II and III subtypes, have become vital in the war against BRAF-mutant tumors. To enable BRAF-targeted drug discovery and precision medicine, we developed a tailored platform based on the classification of BRAF mutations, which integrates whole exome sequencing (WES) for identification of mutant BRAF subtypes with *in vivo* efficacy evaluation in patient-derived tumor xenograft (PDX) models. Our platform covers all three classes of BRAF mutants, such as V600E/G469A/D594N/G469E. Moreover, this platform faithfully recapitulate the responses of multiple targeted therapies, such as BRAF, MEK and EGFR inhibitors, reported for treating BRAF-mutant tumors in preclinical and clinical studies, highlighting the potential translation values. Taken together, the platform reported in this study empowers the discovery of novel BRAF inhibitors that can be translated into clinical trials and provides personalized therapeutic options for patients who have poorly responded to standard clinical therapies.

#4989

Discovery and evaluation of ISM6466A, a novel covalent CDK12 inhibitor for the treatment of cancer

Lihua Min[1], Hongfu Lu[1], Yihong Zhang[1], Jianping Wu[1], Xin Cai[1], Min Zheng[1], Hui Cui[1], Junwen Qiao[1], Xiao Ding[1], Sujata Rao[2], Feng Ren[1], Alex Zhavoronkov[1]. *[1]Insilico Medicine, Shanghai, China,[2]Insilico Medicine, New York, NY*

Cyclin-dependent kinase 12 (CDK12) belongs to the cyclin-dependent kinase (CDK) family of serine/threonine protein kinases. The CDK12/cyclin K complex regulates the elongation step of RNA transcription by phosphorylating Ser2 on the carboxy-terminal domain (CTD) of the largest subunit of RNA polymerase II, and selectively affects the expression of genes, such as BRCA1 and BRCA2, involved in DNA Damage Response (DDR). CDK12 mutations as well as overexpression have been reported in different types of malignancies, making it an attractive cancer target. In this study, a series of covalent CDK12 inhibitors were designed and profiled in biochemical and cellular assays. ISM6466A was identified as a lead compound, demonstrating good *in vitro* efficacy, ADME properties, safety pharmacology profile (e.g., CYP, hERG), and a reasonable *in vivo* PK profile. Biochemically, ISM6466A exhibited reasonable selectivity over other CDKs, and inhibited cell proliferation in a panel of tumor cell lines with IC_{50} values in the nanomolar range (e.g., IC_{50} of ~100nM in the TNBC and AML cell lines, SUM149PT and MV4-11, respectively). Cell-based assays showed that ISM6466A has a selective inhibitory action for the phosphorylation of Ser2 on the CTD, but not for that of Ser5 or Ser7. Notably, ISM6466A demonstrated excellent *in vivo* anti-tumor efficacy in the SUM149PT breast cancer CDX model (Tumor Growth Inhibition, TGI, of 114% at 60 mg/kg QD) and in the MV4-11 AML CDX model (TGI of 95% at 30 mg/kg QD), without body weight loss. Data from an endpoint PKPD study in the MV4-11 CDX model revealed that ISM6466A inhibited phosphorylation of Ser2 on the CTD, and also inhibited DDR genes such as BRCA1 and ATR. Results from a 28-day rat DRF study revealed that the compound did not show evident signs of toxicity at the tested doses, suggesting a reasonable safety window for ISM6466A.In summary, the novel, covalent, small-molecule CDK12 inhibitor, ISM6466A, demonstrated excellent preclinical efficacy along

with favorable drug-like properties. Our results underscore the therapeutic potential of ISM6466A for the treatment of cancer.

#4990

Dual inhibitor of ACVR1 and MEK 1/2 E6201 and PI3K/mTOR inhibitor paxalisib synergistically inhibit cell growth in DMG

Hyuk Jean Kwon[1], Abigail Tindall[1], Charles Eberhart[2], Jeffrey Rubens[1], Eric Raabe[1]. *[1]Pediatric Oncology, Johns Hopkins University School of Medicine, Baltimore, MD,[2]Neuropathology, Johns Hopkins University School of Medicine, Baltimore, MD*

Diffuse midline glioma (DMG) is an aggressive pediatric glioma with no curative treatment options. Mutation in MAPK pathway is common in many DMG tumors, however, has not been largely explored before. E6201 is a dual inhibitor of ACVR1 and MEK 1/2. It is currently in a phase 1 clinical trial for BRAF/MEK mutant melanoma. E6201 achieves higher levels in brain compared to other MEK inhibitors, suggesting it might be a promising therapeutic option for DMG. Previously, E6201 was effective in DMG cell lines with ACVR1 mutation, such as HSJD007. We have evaluated the effect of E6201 in two MAP kinase pathway activated, novel DMG cell lines, DIPG2JA and JHH-DIPG17. DIPG2JA has a *KRAS* mutation, leading to upregulation of MAPK pathway, and JHH-DIPG17 has two *NF1* alterations predicted to disrupt this tumor suppressor, resulting in activation of MAPK pathway. Treatment of DIPG2JA with E6201 identified an IC50 of 44 nM, which is comparable to an IC50 of 71nM in the ACVR1 mutant DMG HSJD007. E6201 suppressed phospho—ERK and induced apoptosis as measured by cPARP western blot in DMG cells. Evaluation of cell viability by CellTiterBlue viability assay demonstrated that E6201 suppressed DMG growth between 0.05uM to 1uM concentrations. (DIPG2JA $p=0.0004$, JHH-DIPG17 $p<0.0001$ by *t-test* compared to control). Compensatory upregulation of mTOR pathway is often associated with downregulation of MAPK pathway, and we hypothesized that E6201 will synergize with a PI3K/mTOR inhibitor to induce DMG cell death. We selected the brain-penetrant PI3K/mTOR inhibitor paxalisib, because this drug is currently being tested in early phase clinical trials for DMG. Through CellTiterBlue cell viability assay, we showed that E6201 synergizes with paxalisib to inhibit cell growth. The ZIP

synergy scores were 13.1 for HSJD007 and 12.7 for DIPG2JA according to the SynergyFinder program, suggesting synergistic interaction between E6201 and paxalisib. In *vitro* experiments for further evaluation of the combination treatment of E6201 and paxalisib are underway and in vivo studies are pending. From our data, E6201 as a single agent is a promising therapeutic option for DMG. With further evaluation of combination of E6201 and paxalisib, we believe that combination therapy will be an even more effective treatment option for DMG.

#4991

Phosphorylation of MERTK is required for nuclear localization in non-small cell lung cancer (NSCLC)

K.M. Tanim[1], Deborah DeRyckere[2], Douglas K. Graham[2]. *[1]Emory University, Atlanta, GA,[2]Department of Pediatrics, Emory University, Atlanta, GA*

MERTK is a transmembrane receptor that belongs to the TAM (TYRO3, AXL, MERTK) family of receptor tyrosine kinases. The role of MERTK in cancer progression and resistance to therapies are reported in many cancer types, including non-small cell lung cancer (NSCLC). In canonical signaling, MERTK is localized at the cell membrane and mediates intracellular signal transduction pathways. Non-canonical signaling of receptor tyrosine kinases (RTKs) has been reported, including signaling which occurs when RTKs translocate to the nucleus. Our group previously reported nuclear localization of MERTK in leukemia cells and we now extend these findings to non-small cell lung cancer. We found exogenous MERTK localized to the nucleus in cells transfected with a plasmid expressing wild-type MERTK. Additionally, endogenous nuclear MERTK was phosphorylated, suggesting that MERTK may have a functional role in the nucleus. MERTK kinase inhibitor MRX-2843 modulates its nuclear translocation. Introducing point mutations to MERTK autophosphorylation sites diminished nuclear translocation in comparison to cells transfected with wild-type MERTK. Our analysis of proteins that may interact with MERTK to regulate nuclear localization and function demonstrated co-immunoprecipitation of nuclear MERTK and STAT1. Current studies are underway to further explore nuclear MERTK functions and how these roles may be modulated upon interaction with STAT1.

#4992

Taxol-elevated PLK1 overcomes BETi-resistant in prostate cancer via triggering phosphorylation-dependent degradation of BRD4

Yanquan Zhang, Ka Will Fong, Fengyi Mao, Ruixin Wang, Yifan Kong, Chaohao Li, Jinghui Liu, Zhiguo Li, Derek B. Allison, Dana Napier, Daheng Li, Jinpeng Liu, Chi Wang, Yeqing Zhang, Guangbing Li, Xiaoqi Liu. *University of Kentucky, Lexington, KY*

Background: Bromodomain-containing protein 4 (BRD4) has been widely studied as an attractive therapeutic target of prostate cancer (PCa). Currently, a number of BRD4 inhibitors or degraders have been discovered. However, recent studies revealed that *SPOP* mutant of prostate cancer patients leads to BRD4 stabilization and resulted in JQ1-resistant. Therefore, to reveal the mechanism underlying BRD4 stability may improve the clinical response rate and efficacy of BRD4-targeted therapy in PCa patients.

Methods: To evaluate the level of BRD4 during the mitosis phase, we applied a Confocal microscope and WB. *In vitro* kinase assay and Mass spectrometry were applied to test the phosphorylation of BRD4 by PLK1. A homemade phosphorylation-specific antibody was used to verify p-BRD4 in PCa cells and a tissue micro-array. A PDX-tumor model was used to evaluate the combination efficacy of Taxol to overcome JQ1-resistant.

Result: We found that the level of BRD4 obviously decreased during the mitosis phase of PCa cells. Upon releasing from M-phase arrest, BRD4 level increased along with PLK1 decreasing in PCa cell lines, suggesting PLK1 might be involved in the degradation of BRD4 in the M-phase. We found that PBD domain of PLK1 was responsible for interacting with CTD of BRD4. Enforced overexpression of PLK1 promoted BRD4 dramatically reduced. Reversely, tet-induced depletion or inhibition of PLK1 led to BRD4 stabilization. Furthermore, applying gain or loss of function assay, we found that PLK1 directly phosphorylated BRD4 and triggered its phosphorylation-dependent degradation in M-phase, which was confirmed in clinical samples that high level of PLK1 was negatively correlated with BRD4. Accordingly, we found that overexpression of PLK1 lowered the stabilized BRD4 caused by *SPOP* mutant in PCa cells and consequently made cells sensitive to JQ1. Intriguingly, upon treated with Taxol, a

commonly used medicine for PCa patients, PLK1 level was dramatically elevated as well as p-BRD4 status but total BRD4 downregulated in PCa cells. Moreover, sequential treatment of Taxol and JQ1 resulted in significant inhibition of proliferation, colony formation, and PDX tumor carrying *SPOP* mutant, indicating application of Taxol overcame JQ-1 resistant.
Conclusion: Collectively, our results suggested that PLK1 phosphorylates BRD4 and consequently triggers its phosphorylation-dependent degradation in PCa cells. Sequential treatment of Taxol and JQ1 overcomes *SPOP* mutant-related BETi-resistant in prostate cancer.

#4993

Development of abbapolin inhibitors of the PLK1 PBD as potential therapeutics for prostate and other challenging cancers

Jessy Stafford, Danda Chapagai, George Merhej, Justin Pressley, Chintada Nageswara-Rao, Michael Wyatt, Campbell Mcinnes. *University of South Carolina, College of Pharmacy, Columbia, SC*

Polo-like kinase 1 (PLK1) has a plethora of roles within the cell of which mitotic regulation is the best characterized. This kinase is overexpressed and upregulated in cancer cells, making it an attractive target for therapeutics. Drug discovery efforts have mainly focused on the ATP binding site however have met with little clinical success to date. Targeting substrate recognition and subcellular localization through the Polo-Box domain represents an attractive alternative to generating PLK1 specific compounds and to avoid the tumor suppressor functions of PLK3. REplacement with Partial Ligand Alternatives through Computational Enrichment, REPLACE, is validated strategy used to convert peptide inhibitors of protein-protein interactions into more drug like compounds. Through the use of this methodology, we have discovered promising non-ATP competitive inhibitors based on a 2-(4-AlkylBenzamido) Benzoic Acid (ABBA) pharmacophore which bind to the polo-box domain of PLK1. These compounds, designated as abbapolins, engage PLK1 as evidenced by their ability to block phosphorylation of TCTP, a key substrate of PLK1, induce PLK1 degradation and are potently anti-proliferative in prostate cancer cell lines. Based on these observations, lead compounds were investigated further for their pharmacokinetic properties and *in vivo*

efficacy and key compounds showed development potential based upon preliminary results. To further investigate their potential in other tumors, selected abbapolins were tested against the NCI-60 tumor cell panel and other cancers with poor prognosis. Results indicate that neuroblastoma, lung, colorectal and certain leukemias are the most sensitive cell lines and thus provide impetus to investigate the abbapolins for difficult to treat and resistant tumors. We present the further optimization of the abbapolins to determine their structure-activity relationship and identify compounds with novel structures and improved drug-like properties. This includes their ability to engage PLK1 and anti-proliferative activities against selected cell lines that represent therapeutically challenging cancers. Furthermore, these compounds serve as chemical biology probes to elucidate roles of the PBD in conformationally regulating PLK1 activity, through *in vitro* experiments and specifically in the abbapolin sensitive cell lines.

#4994

Crizotinib enhances the efficacy of BX-795 identified by high-throughput screening of pan-active drugs in colorectal cancer cells

Susmita Ghosh[1], Fan Fan[1], Jason Roszik[2], Reid Powell[3], Yong Park[3], Clifford Stephan[3], Lee M. Ellis[4], Rajat Bhattacharya[1]. *[1]Surgical Oncology, UT MD Anderson Cancer Center, Houston, TX,[2]Melanoma Medical Oncology, UT MD Anderson Cancer Center, Houston, TX,[3]Department of Translational Medical Sciences, Texas A&M College of Medicine, Houston, TX,[4]Surgical Oncology, Molecular and Cellular Oncology, UT MD Anderson Cancer Center, Houston, TX*

Background: Colorectal cancer (CRC) is a heterogeneous disease with various driver genetic mutations. Recent improvements in targeted therapies have shown some benefit in patients with BRAF mutated metastatic CRC (mCRC), while several efforts focusing on $KRAS^{G12C}$ inhibitors (alone or in combination) are being examined with outcomes pending. Immunotherapies have shown efficacy in only ~5% of patients with mCRC having MSI-H. Hence, it is important to utilize unbiased approaches in order to identify novel therapies that have the potential to improve the outcomes in a large proportion of patients with mCRC.
Aim: We aimed to perform high-throughput screening (HTS) using “pan-active” drugs to identify novel effective therapeutic combinations for

patients with KRAS/BRAF mutated mCRC.
Methods: We performed unbiased HTS with a set of 250 drugs that were either approved by the FDA or are currently in clinical trials. The effect of these drugs on cell growth inhibition were determined as single agents in 2D and 3D cultures using KRAS or BRAF mutated CRC cell lines. Drugs that decreased cell proliferation in both 2D and 3D cultures and effective in both HCT116 (KRAS mutated) and HT29 (BRAF mutated) cell lines, were termed as "pan-active" drugs. 57 "pan active" drugs were identified that primarily fall into 9 classes based on targets/pathways they inhibit. Next, the efficacy of the top three candidate drugs from each class of "pan-active" drugs were determined by pairing with drugs of other classes to identify combinations that are most effective in inducing cell death in CRC cells. Using the Bliss model of synergy, BX-795 was identified to be synergistic with Crizotinib. Effects of combining BX-795 with Crizotinib were further validated *in vitro* by 1) cell growth assays, and 2) measuring changes in cell signaling pathways and apoptotic mediators by western blotting and flow cytometry.
Results: Pairwise HTS studies using "pan-active" drugs demonstrated that combining BX-795 with Crizotinib was synergistic in multiple CRC cell lines. This combination was further validated *in vitro* by MTT and colony formation assays. Analyses of markers for apoptosis by western blotting demonstrated that the drug combination increased cell death in multiple CRC cell lines as compared to single agents. Flow cytometry results using FITC Annexin V and PI confirmed that the combination increased apoptotic cell death in multiple CRC cell lines when compared to the monotherapies.
Conclusions: Our unbiased HTS along with *in vitro* validation studies demonstrated that the combination of BX-795 with Crizotinib can serve as a possible novel effective therapeutic combination in patients with mCRC. Our preclinical *in vitro* studies serve as the basis for *in vivo* efficacy studies and future clinical studies in order to determine the efficacy of this drug combination in patients with mCRC.

#4995

Targeting PLK1 effectively suppresses growth of small cell lung cancer

John C. Schmitz[1], Guojing Zhang[1], Andrey A. Ivanov[2], Abbe Pannucci[1], Maya Ridinger[3], Taofeek K. Owonikoko[1]. *[1]Medicine, Univ. of Pittsburgh,*

Pittsburgh, PA,[2]Pharmacology and Chemical Biology, Emory University School of Medicine, Atlanta, GA,[3]Cardiff Oncology, San Diego, CA

Small cell lung cancer (SCLC) is an aggressive neuroendocrine tumor characterized by rapid disease progression and poor patient survival. Key transcription factors implicated as drivers of unique biological phenotypes of SCLC include ASCL1, NEUROD1, YAP1, and POU2F3. Strategies to exploit these phenotypes for innovative precision medicine approaches will be impactful. Using an unbiased agnostic preclinical drug screen to uncover therapeutic opportunities in SCLC, we identified a strong signal with PLK1 inhibitors (PLK1i) with low nanomolar IC50. We extended the *in vitro* findings by testing the efficacy of PLK1i *in vivo* using traditional xenograft of SCLC H526 cell line and patient derived xenografts (PDX). Volasertib achieved significant tumor growth inhibition relative to control in H526 xenografts. Also, onvansertib significantly inhibited growth of platinum-resistant and platinum-sensitive PDXs. The combination of PLK1i with standard chemotherapeutic agents identified promising synergy of the combination of onvansertib and paclitaxel. We further interrogated for predictive biomarkers of PLK1i sensitivity using gene expression profile comparing highly sensitive to less sensitive cell lines. High expression of *C-MYC* but not *PLK1*, *TP53* or *RB* was associated with resistance to PLK1i. Conversely, while *TP53* expression level did not correlate, TP53 gene mutation status (inactivating disruptive mutations) correlated with cell sensitivity to PLK1i. We queried the publicly available CCLE and the Cancer Therapeutics Response Portal to evaluate whether any of the SCLC subtypes have therapeutic vulnerability to PLK1i. In general, high expression of YAP1 in SCLC cell lines correlated with greater sensitivity to PLK1i. A YAP1 positive cell line, SW1271, with strong TP53 expression was particularly resistant to PLK1i. CRISPR knockout of YAP1 in this cell line enhanced SW1271 sensitivity to PLK1i suggesting that YAP1 expression as a marker of vulnerability to PLK1i could be context dependent especially when co-occurring with TP53 mutations. The mechanism of this interaction will be discussed.

#4996

Axl inhibition sensitizes cholangiocarcinoma cells to cytotoxic chemotherapy

Shohei Takaichi[1], Dong-Gi Mun[2], Jennifer L. Tomlinson[1], Amro M. Abdelrahman[1], Danielle M. Carlson[1], Alaa Abou Daher[1], Nathan W. Werneburg[1], Xinyan Wu[2], Akhilesh Pandey[2], Gregory J. Gores[3], Rory L. Smoot[1]. *[1]Division of Surgery, Division of Surgery, Mayo Clinic, Rochester, MN,[2]Division of Laboratory Medicine and Pathology, Division of Laboratory Medicine and Pathology, Mayo Clinic, Rochester, MN,[3]Division of Gastroenterology and Hepatology, Division of Gastroenterology and Hepatology, Mayo Clinic, Rochester, MN*

Background: Cholangiocarcinoma (CCA) is a lethal disease with limited therapeutic options. We have previously discovered LCK driving signaling through AXL, a TAM receptor tyrosine kinase (RTK), by phosphoproteomic analysis of CCA (*J Hepatol* 2022). AXL mediates acquired drug resistance in solid cancers. However, the exact role of AXL in CCA still remains to be elucidated. Here, we investigated the significance of AXL expression as a potential therapeutic target in CCA and the role of phosphorylated AXL Y866.
Methods: We first evaluated the expression levels of AXL in CCA and its associations with patient outcomes using The Cancer Genome Atlas (TCGA) database. Next, to evaluate whether AXL inhibition sensitizes CCA cells to gemcitabine and cisplatin (GemCis) therapy, AXL downregulation was achieved via the siRNA approach and the selective inhibitor bemcentinib. We examined the 50% inhibitory concentration (IC_{50}) value of HuCCT1, a well-characterized CCA cell line, on GemCis therapy with or without AXL knockdown using cell viability assay. Then we assessed the efficacy of the combinatorial therapy of GemCis and bemcentinib utilizing Calcusyn software. Apoptosis was evaluated by Annexin V assay. I*n vivo* efficacy was assessed using an SB-1 (murine CCA cell line) and a syngeneic murine model of CCA treated with vehicle, GemCis, bemcentinib, and the combination of GemCis and bemcentinib. Finally, to investigate the role of AXL Y866 in CCA, we performed BioID to identify and compare the interactomes of AXL WT and AXL Y866F in HuCCT1 cells.
Results: In the TCGA cohorts, AXL is significantly expressed in CCA ($P < 0.01$), and disease-free survival and overall survival in the low AXL expression group are significantly longer than those in the high AXL

expression group (P = 0.04, 0.01). In *in vitro* study, the IC_{50} value of GemCis was decreased from 685nM to 129nM after AXL knockdown. A synergistic effect was observed with CI = 0.17 and Fa = 0.50 in the combinatorial therapy. The combinatorial therapy caused significantly increased apoptosis compared to GemCis or bemcentinib alone (P < 0.01, P < 0.01). In *in vivo* study, the combinatorial therapy significantly suppressed the tumor growth compared to GemCis or bemcentinib alone (P = 0.04, 0.01), and the expression levels of Ki67 and the phosphorylation levels of PEAK1 decreased in the combinatorial therapy group compared to other groups in immunostaining examination. In BioID experiments, among the 222 proteins detected in both AXL WT and AXL Y866F interactomes, PEAK1 kinase, which localizes to actin cytoskeleton and focal adhesions, was the kinase most affected by AXL Y866. In gene ontology analysis to characterize the interactome of AXL Y866, cell-cell adhesion and focal adhesion-related proteins were enriched.
Conclusions: AXL inhibition sensitizes CCA cells to cytotoxic chemotherapy in the preclinical model. AXL Y866-PEAK1 signaling axis is a potential target for the treatment of CCA.

#4997

PLK1 promotes the metastasis and drug resistance in melanoma

Fengyi Mao, Yifan Kong, Chaohao Li, Yanquan Zhang, Xiongjian Rao, Qiongsi Zhang, Xinyi Wang, Zhiguo Li, Xiaoqi Liu. *Toxicology and Cancer Biology, University of Kentucky, Lexington, KY*

Melanoma is one of the most frequently diagnosed cancers in the caucasian population of both genders. The survival rate of advanced melanoma patients will be exceedingly poor, as low as 27.3%. BRAF-V600E is the most common mutation found clinically, resulting in the constitutive activation of the MAPK signaling pathway. Vemurafenib, a specific inhibitor of mutant BRAF, has shown an impressive response in phase 3 clinical trials and was approved by FDA in 2011. However, due to the rapid development of resistance, the duration of response under a single treatment is frequently short, highlighting the urgent requirement for novel therapy in melanoma treatment. Polo-like kinase 1 (PLK1), a crucial cell cycle regulator, participates in multiple mitotic processes, including centrosome maturation, mitotic entry, spindle assembly, sister chromatid segregation,

mitotic exit, and cytokinesis. Compared to normal tissues, the expression level of PLK1 significantly upregulates in multiple cancers. More importantly, the expression level of PLK1 negatively correlates with the melanoma patients' survival rate based on the TCGA database. Besides, PLK1 is identified as an oncogene to promote proliferation, motility, and resistance to various drugs. In the present study, we found that overexpression of PLK1 promotes tumor growth, metastasis, metabolic reprogramming, and vemurafenib resistance in the $Braf^{CA}/Pten^{loxp}$ mouse melanoma model. Through phosphorylation, overexpressed PLK1 stabilizes BACH1, a critical transcriptional factor of multiple metastatic and metabolic genes, and protects it from degradation. Subsequently, a higher level of BACH1 leads to increasing metastasis, upregulation of glycolysis, and suppression of OXPHOs. Besides, we have validated the strong synergy between PLK1 inhibitor volasertib and vemurafenib in treating melanoma carrying BRAF-V600E. Our in vitro and in vivo experiments have shown an improved efficacy of this combined therapy on inhibition of cell proliferation, induction of cell death, and suppression of cell metastasis compared to mono-treatment. In short, our data has indicated PLK1 as a potent and promising target in cancer treatment.

#4998

Selective PLK4 inhibition demonstrates synthetic lethality in TRIM37 amplified neuroblastoma and breast cancer models while less selective inhibitors do not

Siobhan K. McRee, Chelsea Chen, Christophe Colas, Wie Fang, Wayne Kong, Fang Liu, Jason Long, Jared Moore, Alex Pankov, Dan Shore, Joanne Tan, Robert Warne, Rakesh Vekariya, Amy Young, Anneleen Daemen, Anthony Romero, Melissa R. Junttila, Lori S. Friedman, Kyle A. Edgar. *ORIC Pharmaceuticals, South San Francisco, CA*

Amplification and copy number gains of the 17q23 amplicon are common in breast cancer and neuroblastoma and have been associated with early relapse and poor prognosis (Ganesan et al 2012; Takita et al. 2017). A synthetic lethal interaction of PLK4 with 17q23 amplicon-driven overexpression of TRIM37 was discovered in these tumor types (Meitinger et al. 2020; Yeow et al. 2020). High levels of TRIM37 prevented acentrosomal spindle assembly and rendered cells mitotically vulnerable to

inhibition of polo-like kinase 4 (PLK4), a serine/threonine protein kinase that controls centriole duplication. We have discovered that exquisitely selective small molecule inhibitors of PLK4, which are highly selective against the kinome including against the closely related aurora kinases and PLK1-3, display this synthetic lethal interaction with TRIM37, while less selective inhibitors do not. PLK4 protein levels are regulated through proteasomal degradation induced by PLK4 trans-autophosphorylation of the phosphodegron. PLK4 inhibition results in blocked trans-autophosphorylation leading to stabilization of PLK4, thus directly demonstrating target engagement in cells. Importantly, PLK4 protein stabilization correlated with cell viability for selective PLK4 inhibitors but not for less selective compounds, providing a quantifiable pharmacodynamic (PD) association with antitumor activity. Cell viability assessment in cancer cell lines revealed that highly selective PLK4 inhibitors showed greater potency in TRIM37 high cancer cell lines as compared to TRIM37 low cell lines. In contrast, less selective compounds, including from the clinical literature, did not display differential potency in TRIM37 high versus low cancer cell lines. Additionally, selective PLK4 inhibition induced significantly greater apoptosis in TRIM37 high versus low cancer cell lines as measured with a caspase 3/7 assay. We confirmed that only selective PLK4 inhibitors are synthetic lethal with TRIM37 amplification using an engineered cell line system of PLK4 G95L, in which the Leucine mutation blocks compound binding but allows the PLK4 enzyme to function. In cell viability assays, selective PLK4 inhibitors were potent in the parental G95 cells and lost activity in L95 cells, unlike less selective inhibitors whose potency did not depend on PLK4. Oral dosing of a selective PLK4 inhibitor resulted in tumor growth inhibition in TRIM37 high xenograft tumors with no body weight loss.
In summary, we have discovered that highly selective small molecule inhibitors of PLK4 confirm the potential of the synthetic lethal impact in treating tumors with high levels of TRIM37.

#4999
Preclinical evaluation of MCLA-129, a bispecific antibody targeting EGFR and c-MET on solid tumor cells, in comparison with amivantamab

David J.J. de Gorter[1], Alexandre Deshiere[1], Arjen Kramer[1], Martijn van Rosmalen[1], Franziska Mortensen[1], Cecile Geuijen[2]. *[1]Merus N.V., Utrecht, Netherlands,[2]Merus US Inc., Utrecht, Netherlands*

The HGF/c-MET pathway is frequently upregulated in tumors that are resistant to EGFR tyrosine kinase inhibitors. MCLA-129 is an antibody-dependent cellular cytotoxicity (ADCC) enhanced Biclonics® that targets epidermal growth factor receptor (EGFR) and c-MET in non-small cell lung cancer (NSCLC) and other solid tumors. MCLA-129 is a potent inhibitor of tumor growth applying various mechanisms of action (MOA), including inhibition of c-MET and EGFR signaling, antibody-dependent cellular phagocytosis (ADCP) and ADCC. Here we compared the MOA of MCLA-129 with the MOA of the EGFR-c-MET bispecific antibody amivantamab. The binding of MCLA-129 to tumor cells expressing different levels of EGFR and c-MET was quantified using radiolabeled antibodies. Scatchard plot analysis showed that the affinity of MCLA-129 for both c-MET and EGFR is in the low nanomolar range. In FACS, MCLA-129 and amivantamab show similar binding to tumor cells harboring *EGFR* or *c-MET* exon14-skipping mutations. Crossblock experiments with the c-MET binding antibody onartuzumab analog showed that MCLA-129 competes for the same HGF-binding region of c-MET, which is distinct from the binding site of amivantamab according to Neijssen et al, 2021 (PMC8113745). MCLA-129 and amivantamab did not downmodulate EGFR or c-MET. ADCP was also comparable for MCLA-129 and amivantamab, as measured with monocyte-derived macrophages incubated with pHrodo-labeled target cells with readout of tumor cell phagocytosis on the Incucyte® system. In contrast, MCLA-129 displayed ADCC activity similar to or more potently than amivantamab in an ADCC reporter assay with either high affinity FcγRIII 158V-variant or low affinity 158F-variant effector cells in absence or presence of soluble EGFR and soluble c-MET. MCLA-129-induced ADCC appears to be less affected than amivantimab by the presence of soluble EGFR and soluble c-MET. In conclusion, MCLA-129 is a Biclonics® common light chain bispecific antibody with multiple MOA including inhibition of c-MET and EGFR ligand binding, ADCP and ADCC comparable or more potent than amivantamab. A phase 1/2 clinical trial of MCLA-129 in solid tumors is ongoing. These data

support the further clinical development of MCLA-129 in patients with NSCLC and other solid tumors.

#5000

MYTX-011: A novel cMET-targeting antibody drug conjugate (ADC) engineered to increase on-target uptake in and efficacy against cMET expressing tumors

Nimish Gera, Kyle Fitzgerald, Vijay Ramesh, Purvi Patel, Lena Kien, Deepak Kanojia, Simon Aoyama, Federico Colombo, Amit Deshpande, William Comb, Thomas Chittenden, Brian Fiske. *Mythic Therapeutics, Waltham, MA*

MET alterations can act as an oncogenic driver in non-small cell lung cancer (NSCLC) and elevated cMET expression occurs in many cancers. Antibody drug conjugates targeting cMET (cMET-ADCs) have been developed as a strategy to treat cMET+ tumors irrespective of dependency on cMET signaling. cMET- ADCs have shown promising clinical activity, but largely in a subset of NSCLC patients having the highest cMET levels, indicating tumor cMET levels may be limiting for efficacy. We sought to create an ADC with the potential to benefit a broader population of patients including those expressing moderate cMET levels. Here, we describe MYTX-011, an ADC incorporating the clinically validated vcMMAE linker-payload conjugated to a novel, pH-dependent anti-cMET antibody. We hypothesized that engineering the antibody to rapidly lose affinity at acidic endosomal pH would boost ADC uptake and efficacy in cMET+ tumor cells by avoiding non-productive ADC recycling. We conducted mutagenesis of anti-cMET antibodies, screening for variants that selectively lost binding under acidic conditions, and, in parallel, assessed antibody internalization in cell-based assays. The resulting lead humanized IgG1 antibody was conjugated to vcMMAE at engineered cysteine residues (DAR=2) to create MYTX-011, which exhibited rapid dissociation from cMET at pH5.4 but retained high affinity binding at pH7.4 and 6.4. MYTX-011 showed markedly higher (>3 fold) internalization in cMET+ tumor cells and broader, more potent cytotoxicity across a large panel of cMET+ cancer cell lines *in vitro* compared to a matched ADC based on the unmodified parent antibody lacking pH-dependent binding, or an in-house version of a clinical stage cMET ADC. These findings translated *in vivo*

where MYTX-011 showed superior efficacy (>3 fold based on dose titration) in NSCLC xenograft models with high (EBC-1) or only moderate cMET expression levels (H1373, H1975) compared to the matched parent ADC or an in-house version of a clinical stage cMET ADC. PK and toxicity studies in cynomolgus monkeys revealed that MYTX-011 exhibited favorable PK characteristics, and a toxicity profile similar to previously described MMAE-based ADCs. Together, these findings highlight the potential of MYTX-011 as a therapeutic candidate for treating a broader range of cMET+ malignancies than other cMET-ADCs.

#5003

Repurposing passenger amplifications for specific therapeutic targeting of solid cancers

Sonia Jiménez Vázquez[1], Christos Patsis[2], Luise Butthof[1], Joan Crous Masó[2], Hendrik Wiethoff[3], Matthias Gaida[4], Thomas Longerich[3], Rosella Pellegrino[3], Ilse Hofmann[2], Judith Feucht[5], Darjus Felix Tschaharganeh[1].
[1]Cell Plasticity and Epigenetic Remodeling, German Cancer Research Center, Heidelberg, Germany,[2]German Cancer Research Center, Heidelberg, Germany,[3]University Hospital Heidelberg, Heidelberg, Germany,[4]University Medical Center Mainz, Mainz, Germany,[5]Cellular Therapies, University Hospital Tübingen, Tübingen, Germany

Current cancer therapies focus on targeting driver alterations responsible for tumorigenesis - either oncogenic point mutations or oncogenic driver events within large somatic copy number alterations (SCNAs). However, these alterations are often not actionable or are only present in a small subset of patients. Thus, new therapeutic targets are urgently needed. Apart from oncogenic drivers, SCNAs usually also comprise neutral bystander genes without an active role in neoplastic transformation. We hypothesized that passenger events, specifically in amplified regions, could be therapeutically exploited by providing actionable molecules on the cell surface. Using publicly available multi-omics data, we screened cell surface protein-coding genes for their genomic status and expression levels in liver cancer. This screen identified *MPZL1* (*Myelin protein zero-like 1*), a gene amplified in 75% of hepatocellular carcinomas, accompanied by high mRNA expression in tumors compared to normal livers. *MPZL1* is located on chromosome 1q,

one of the most commonly amplified regions across several solid cancer types, and codes for a glycosylated cell surface receptor. We further validated MPZL1 protein expression in a wide range of human cancer entities (n=2038 samples) and normal tissues (n=163 samples) by immunohistochemistry and assigned expression scores analogous to the clinically implemented HER2-score. A high percentage of tumors showed scores 2 or 3 (e.g. 48% of HCCs or 89% of TNBCs), whereas healthy tissues were mostly negative or just faintly positive (scores 0 or 1). Moreover, in order to target MPZL1-expressing cells, we generated a highly specific monoclonal antibody directed to the extracellular domain of human MPZL1 protein and thoroughly characterized its binding capacity. Next, the scFv sequence of this antibody was used to generate a CAR (chimeric antigen receptor) construct targeting MPZL1. Luciferase-based cytotoxic assays showed that T cells transduced with this construct can kill various MPZL1-high human cancer cell lines *in vitro* (liver, breast and lung malignant cell lines, among others), whereas they fail to kill respective isogenic cell lines harboring knockout of *MPZL1*. Upon antigen-specific exposure, MPZL1-28ζ CAR-T cells underwent antigen-dependent proliferation and showed increased cytokine production (IFNγ, TNFα, IL-2, GZMB), further confirming their specificity. In summary, our findings reveal MPZL1 as a new target for treatment of 1q-amplified cancers and implement a novel immunotherapeutic strategy based on MPZL1-28ζ CAR-T cells. Furthermore, our work provides a proof of concept that passenger events within large chromosomal amplifications can serve as potent therapeutic targets and thus opens a new avenue for innovative approaches in anti-cancer drug development.

#5004

DDR-targeting small molecule inhibitor as a novel therapeutic for treating pancreatic ductal adenocarcinoma

Trong Phat Do[1], Sajid Khan[1], Daohong Zhou[1], Matthew Hart[2], Stanton McHardy[3], Manjeet Rao[1]. *[1]UT Health Science Center at San Antonio, San Antonio, TX,[2]The University of Oklahoma Health Science Center, Oklahoma City, OK,[3]UT San Antonio, San Antonio, TX*

Background: Pancreatic ductal adenocarcinoma (PDAC) is the second most significant cause of cancer-related mortality, with a 5-year survival rate of

just 11%. PDACs are one of the most difficult to treat cancers, mainly because of the desmoplastic tumor microenvironment enriched with tumor-supportive extracellular matrix (ECM) and stromal cells. Unfortunately, the efficacies of current pancreatic cancer therapies are limited partly by stroma-mediated drug resistance. We reason that Discoidin Domain Receptors, which belong to the receptor tyrosine kinase family and bind to fibrillar collagens present in the ECM, may be a critical promoter of PDAC growth and progression. Though several drugs targeting DDR proteins have been developed, no inhibitors specific to DDR proteins have been developed. Moreover, those drugs have not been approved for treating PDACs.
Methods. A high throughput screen using small molecule inhibitors was performed to identify bonafide inhibitors of DDR proteins. Structural and reported-based essays were done to determine the specificity. Functional assays were performed to test the potency of the candidate inhibitors. Mechanistic studies were done using RNA-seq, real-time PCR, and western blot.
Results: Using an unbiased screening approach, we identified inhibitors that specifically target DDR proteins. Our studies revealed that small molecule inhibitors blocked the short and long-term viability as well as migration/invasion of PDAC cells. In addition, they induced apoptosis and halted the cell cycle at the G1-S checkpoint. Mechanistic studies revealed that the pro-growth signaling cascade was significantly inhibited.
Conclusions: Our results showing specific DDR inhibitors blocking the growth and progression of PDAC cells without affecting the viability of normal cells suggest that these inhibitors may serve as a safe and potent regimen for treating pancreatic cancers.

#5005
Targeted down regulation of FGFR1 through G-quadruplex stabilization in metastatic breast cancer
Muhammad Hassan Safdar, Hang Lin, Sarah Dagher, Jonathan Dickerhoff, Danzhou Yang, Michael K. Wendt. *Medicinal Chemistry and Molecular Pharmacology, Purdue University, West Lafayette, IN*

Metastatic breast cancer (MBC) is the most advanced stage of breast cancer. Our understanding of the molecular mechanisms which drive MBC remain

incomplete. Epithelial to mesenchymal transition (EMT) and mesenchymal to epithelial transition (MET) promote drug resistance and metastasis. It has been reported that fibroblast growth factor receptor 1 (FGFR1) plays a key role during the EMT:MET cycle. Furthermore, FGFR1 is amplified in 13% of primary and 20% of metastatic breast cancer patients. Therefore, optimizing inhibition of FGFR1 is crucial for the therapeutic targeting of the late stage breast cancer. First, we examined the efficacies of FGFR kinase inhibitors in the murine based dormant 4T07 tumor model. Inhibition of FGFR kinase activity leads to tumor growth inhibition but fail to eradicate dormant breast cancer cells. Therefore, we explored broader approaches to inhibit FGFR1 expression in addition to blockade of its kinase activity. G-quadruplex (G4) structures are secondary DNA structures commonly found upstream of transcriptional start sites (TSS) of oncogenes restricting their expression. Consequently, pharmacological stabilization of G4 structures within the promoters of cancer-related genes via use of small molecules has emerged as a promising therapeutic approach in cancer. Results herein demonstrate that the proximal promoter of FGFR1 contains sequences that form G4. Circular dichroism was used to verify formation of G4 in the FGFR1 proximal promoter. Importantly, use of the G4-binding compound CX-5461 stabilized the FGFR1 G4 structure, blocked the transcriptional activity of the FGFR1 proximal promoter and decreased FGFR1 expression. Therefore, we implemented the G4 stabilizers in FGFR1 expressing and metastatic drug-resistant cell lines. This approach results in dramatic downregulation of FGFR1 in the protein level after treatment with the G4 stabilizer. G4 stabilizing agents also interfere with constitutive FGFR1 and EMT-driven FGFR1 expression. Importantly, use of the G4-targeting compound CX5461 effectively blocked FGFR1 expression and inhibited FGFR1 downstream signaling, resulting in eradication of dormant breast cancer cells using a 3D culture model system. Finally, *in vivo* application of CX5461 reduced pulmonary tumor growth and prolonged animal survival in an FGFR1-driven model of metastasis. In conclusion, our evaluation of FGFR kinase inhibitors validates clinically observed resistance to this approach in MBC. Moreover, our findings suggest that G4 stabilization may be a potential therapeutic strategy for FGFR1 expressing MBC.

#5006

Discovery of novel heterobifunctional degraders of mutant EGFR proteins for NSCLCs harboring various EGFR mutations

Dong Hyuk Ki[1], Min Sung Joo[1], Joonwoo Nam[1], Hunmi Choi[1], Kyoungwan Seo[1], Eun-Jung Kim[1], Jiyeon Kim[2], Chulwon Kim[2], Jimmy Taiguang Jin[3], Wooseok Han[1]. *[1]Cyrus Therapeutics, Seoul, Korea, Republic of,[2]Bridge Biotherapeutics, Seongnam, Korea, Republic of,[3]Bridge Biotherapeutics, Cambridge, MA*

Abnormal expression and activation of Epidermal Growth Factor Receptor (EGFR) contribute to malignancy development, especially in non-small cell lung cancers (NSCLCs). Although the first- to third-generation EGFR small molecule inhibitors have made significant progress in the treatment of EGFR mutant NSCLC patients, acquired mutations have been developed rapidly, resulting in drug resistance. Targeted protein degradation (TPD) technologies including PROteolysis Targeting Chimeras (PROTACs) have recently emerged as a promising alternative modality to address the confronting issues of small molecule inhibitors such as drug resistance. Recently, we have developed a series of heterobifunctional degraders of EGFR mutant proteins, which showed strong degradation ability against a variety of mutant EGFRs including triple mutants with C797S. DC_{50} (half-maximal degradation concentrations) values of the degraders were obtained using HiBiT assay in NCI-H1975 (EGFR $^{L858R/T790M}$), HCC827 (EGFR ^{Del19}), and H1299 (EGFR ^{WT}) cells. Our lead compounds demonstrated excellent EGFR degradation potency with high selectivity against EGFR wild type. Moreover, C-09045, C-09066, and C-13951 strongly inhibited the cell growth of Ba/F3 cells harboring one of the EGFR mutations including L858R/C797S, Del19/C797S, L858R/T790M/C797S, Del19/T790M/C797S, and Exon20 NPH insertion. By contrast, these compounds showed much weaker potency in normal lung fibroblast (HFL-1) and Ba/F3 cells harboring EGFR wild-type. In PK analysis, C-09066 showed good oral bioavailability in mice (F%=41.4) with desirable pharmacokinetic parameters and robust tumor growth inhibition efficacy in the NCI-H1975 EGFR $^{L858R/T790M/C797S}$ xenograft and the Ba/F3 $^{Del19/C797S}$ allograft mouse models. In summary, we have identified selective, potent, and orally bioavailable degraders of various EGFR mutant proteins with broad spectrum anti-tumor efficacy both *in vitro* and *in vivo*.

Targeting Protein Kinases and Phosphatases for Therapy 2

#5009
Inhibition of TGFBR2 signaling re-sensitizes TMZ-resistant glioblastoma cells to therapy

Maya K. Johnson, Jack Korleski, Amanda Johnson, Sophie Sall, John Laterra, Hernando Lopez-Bertoni. *Neurology, Neuroscience, Oncology, Kennedy Krieger Research Institute, Baltimore, MD*

Glioblastoma (GBM), the most aggressive and lethal form of brain tumors, recurs in 90% of cases and the standard protocol of care—temozolomide (TMZ)—is an ineffective method to combat chemo-resistant GBM. It is therefore imperative that we identify, develop, and design novel therapeutics to effectively combat recurrent GBM (rGBM). Multi-potent stem-like cell subpopulations within GBM (also referred to as glioma stem cells or GSCs) play important roles in tumor propagation, therapeutic resistance, and recurrence following treatment. Understanding the molecular mechanisms that drive resistance in GSCs can lead to novel therapeutic approaches for rGBM. Bioinformatics analyses of transcriptome data sets from rGBM clinical specimens identified transforming growth factor-beta receptor type 2 (TGFBR2) as a putative driver of resistance and recurrence in GBM. We show that TMZ-resistant cells become more stem-like concurrent with higher expression of TGFBR2 protein and mRNA. Importantly, shRNA-mediated inhibition of TGFBR2 decreases proliferation of TMZ-resistant cells and enhances the effects of TMZ. We hypothesize that by developing targeted therapeutics to reduce TGFBR2 expression we will inhibit the growth capacity and/or re-sensitize rGBM cells to ionizing radiation (IR) or TMZ treatment by simultaneously targeting multiple putative oncogenes implicated in the induction of stem-like resistant GBM cell subsets. Future directions include inhibiting TGFBR2 signaling in clinical specimens derived from rGBM patients using two translatable approaches: (1) ITD1, a small molecule TGFBR2 inhibitor predicted to cross the blood-brain-barrier and (2) microRNAs to target multiple TGFBR2 target genes up-regulated in rGBM.

#5010

Inhibition of discoidin domain receptor 1 (DDR1) as a new therapeutic strategy for osteosarcoma

Jinglu Wang, Robert Walker, Francis Hornicek, Zhenfeng Duan. *University of Miami, Miami, FL*

Osteosarcoma is the most common type of bone cancer. Current management for osteosarcoma includes neoadjuvant chemotherapy and surgery. Unfortunately, some patients eventually develop recurrent or metastatic diseases and treatment options are extremely limited. Discoidin domain receptor 1 (DDR1) is a unique collagen-activated tyrosine kinase that participates in various human diseases, including cancer. DDR1 promotes the adhesion, proliferation, differentiation, migration, and metastasis of cancer cells. However, the expression and function of DDR1 remain unknown in osteosarcoma. The purpose of this study is to assess the expression, clinical prognostic relationship, and functional roles of DDR1 in osteosarcoma. The correlation between DDR1 expression in tumor tissues and clinicopathological features and prognosis was assessed via immunohistochemical staining of a unique tissue microarray (TMA) constructed from osteosarcoma specimens. Furthermore, DDR1 expression in osteosarcoma cell lines was determined by Western blot. DDR1-specific siRNA and a highly selective DDR1 inhibitor, 7rh, were applied to determine the impact of DDR1 expression on osteosarcoma cell growth and proliferation. In addition, the effect of DDR1 inhibition on clonogenicity was evaluated using a clonogenic assay, and a 3D cell culture model was used to mimic DDR1 effects in an *in vivo* environment. The results demonstrate that higher DDR1 expression significantly correlates with recurrence, metastasis, and shorter overall survival in osteosarcoma patients. The expression of DDR1 is also inversely correlated to the response to neoadjuvant chemotherapy. Therapeutically, DDR1 knockdown with siRNA or selective inhibition with 7rh decreases the proliferation and growth of osteosarcoma cells. In conclusion, our study supports DDR1 expression as an independent predictor of poor prognosis and a promising therapeutic target for osteosarcoma.

#5011

Targeting kinome reprogramming in ESR1 fusion-driven breast cancer

Xuxu Gou[1], Beom-Jun Kim[1], Meenakshi Anurag[1], Jonathan T. Lei[1], Meggie N. Young[1], Matthew V. Holt[1], Diana Fandino[1], Craig T. Vollert[1], Purba Singh[1], Mohammad A. Alzubi[1], Anna Malovannaya[1], Lacey E. Dobrolecki[1], Michael T. Lewis[1], Shunqiang Li[2], Matthew J. Ellis[3], Charles E. Foulds[1]. *[1]Baylor College of Medicine, Houston, TX,[2]Washington University, Saint Louis, MO,[3]AstraZeneca, Gaithersburg, MD*

Background: Transcriptionally active ESR1 gene fusions (ESR1-TAF) are a potent cause of estrogen receptor alpha-positive (ERα+) breast cancer endocrine therapy (ET) resistance. These ESR1-TAF are gain-of-function mutations, exhibiting estrogen-independent cell growth, motility and ET resistance. They are not directly druggable because the ERα C-terminal ligand binding domain (LBD) encoding sequence is replaced with a translocated in-frame partner gene sequence. Herein we utilized proteomic approaches to develop novel targeted therapies against ESR1-TAF driven tumorigenesis.

Methods: *ESR1* fusion cDNA constructs were expressed in ERα+ breast cancer cell lines (T47D and MCF7). Cell growth was assayed by an Alamar blue assay. A mass spectrometry (MS)-based Kinase Inhibitor Pulldown Assay (KIPA) was employed to identify druggable kinases that are commonly upregulated by diverse ESR1-TAFs. A panel of 22 ERα+ patient-derived xenograft (PDX) models were profiled using proteomics and phosphoproteomics to identify models with sensitivity to RET kinase inhibition.

Results: KIPA detected an increased abundance of a receptor tyrosine kinase, RET, in T47D cells expressing ESR1-TAFs in an estrogen-independent manner, compared to stable cell lines expressing transcriptionally inactive fusions as well as wild-type ERα protein. Interestingly, RET was also increased when constitutive activating ERα LBD point mutants, Y537S and D538G, were expressed in breast cancer cells. Inhibition of the RET kinase *in vitro* by repurposing pralsetinib, an FDA-approved RET inhibitor for advanced thyroid and non-small-cell lung cancers, demonstrated a significant reduction in the growth of cells expressing ESR1-TAFs and ERα LBD mutants. These data nominate RET kinase as a common therapeutic vulnerability for ESR1-TAF expressing breast cancers. Proteomic profiling of 22 biologically heterogenous ERα+ PDX tumors defined targetable pathways and predicted tumor subsets that

were responsive to RET inhibition therapy. Organoids and xenografts from the pan-ET resistant WHIM18 PDX (that expresses the ESR1-YAP1 TAF) were inhibited by pralsetinib to a similar extent as the CDK4/6 inhibitor palbociclib. These data provide key preclinical rationale for the consideration of RET inhibition for the treatment of ESR1-TAF-driven ET-resistant breast cancer. Interestingly, the growth of WHIM37 PDX (that expresses ERα D538G) that had low level of RET and high level of GFRα-1, the co-receptor of RET, was also suppressed by pralsetinib. This data suggests that either RET or GFRα-1 is a predictive biomarker for RET inhibitor efficacy.
Conclusions: Kinome analysis of *ESR1* translocated breast tumors using KIPA followed by drug sensitivity studies nominated RET as a new therapeutic target for ET-resistant ERα+ breast cancer.

#5012

Characterizing the functional significance of PDGFRA^{K385I} and PDGFRA^{K385L} extracellular domain mutations in the newly defined myxoid glioneuronal tumor

Catherine Z. Beach[1], Romel Somwar[2], Matthew D. Wood[3], Monika A. Davare[4]. *[1]Oregon Health & Science University, Portland, OR,[2]Human Oncology and Pathogenesis Program, Memorial Sloan Kettering Cancer Center, New York, NY,[3]Pathology, Oregon Health & Science University, Portland, OR,[4]Pediatrics, Oregon Health & Science University, Portland, OR*

In 2021, the World Health Organization (WHO) approved new diagnostic guidelines that stratify central nervous system (CNS) tumors based on molecular, transcriptomic, and epigenetic analysis instead of relying solely on phenotypic characterization and added twenty-two new CNS tumor entities based on these guidelines. Our focus is on one of these newly defined entities—myxoid glioneuronal tumors—a slow growing, mucinous glial tumor defined by a pathognomonic dinucleotide substitution in the extracellular domain of PDGFRA p.K385I/L. PDGFRA p.K385I/L remains a variant of unknown significance, however, constitutive activation of PDGFRA is well established as a pharmacologically actionable, oncogenic driver present in a variety of tumor types. Here we report the functional

characterization of PDGFRA^{K385I} and PDGFRA^{K385L} by assessing transforming potential using Ba/F3 cells and immortalized human astrocytes. Our results demonstrate that both p.K385I and K385L substitutions are oncogenic, driving cytokine-independent Ba/F3 cell growth and anchorage-independent colony formation. Western blot analysis of downstream cellular signaling pathways in the absence of PDGF-ligand further confirm the activating nature of these mutations, showing robust phosphorylation of PDGFRA and constitutive phosphorylation of downstream signaling effectors ERK1/2, SHP2, and STAT3. To assess whether PDGFRA^{K385I} and PDGFRA^{K385L} are pharmacologically actionable, we tested multiple tyrosine kinase inhibitors with known activity against PDGFRA aberrant cancers using our mutant-transformed PDGFRA Ba/F3 cells. We found that the PDGFRA^{K385I} and PDGFRA^{K385L} mutants were sensitive to inhibitors axitinib, AZD-3229, and avapritinib at therapeutically relevant concentrations. Further, these mutants showed resistance to imatinib, nilotinib, and crenolanib underscoring the importance of pharmacogenomic investigation. No appreciable difference in sensitivity or resistance profiles was observed between the two mutants. In summary, our findings indicate that these previously uncharacterized p.K385I/L extracellular domain mutations in PDGFRA are oncogenic and represent a pharmacologically actionable target that could be harnessed to increase therapeutic options in the setting of myxoid glioneuronal tumors.

#5013

Effects of PP2A-activating drugs on FLT3 inhibitor resistance mediated by diverse mechanisms in acute myeloid leukemia with FLT3-ITD

Moaath Mustafa Ali, Aditi Chatterjee, Jonelle K. Lee, Mario Scarpa, Maria R. Baer. *Department of Medicine, University of Maryland Greenebaum Comprehensive Cancer Center, Baltimore, MD*

Internal tandem duplication (ITD) of the *fms*-like tyrosine kinase 3 (FLT3) receptor tyrosine kinase is present in AML cells in 25% of patients, causing constitutive activation and aberrant signaling. *FLT3*-ITD+ AML patients have a high relapse rate following chemotherapy and short disease-free and overall survival. Incorporation of FLT3 inhibitors (FLT3is) into therapy for *FLT3*-ITD+ AML has improved outcomes, but FLT3i efficacy is limited by

onset of resistance, which occurs by diverse mechanisms. The tumor suppressor protein phosphatase 2A (PP2A) is inactivated in *FLT3*-ITD+ AML, and we previously showed that PP2A-activating drugs (PADs), including DT-061 and FTY720, enhance FLT3i efficacy through enhanced proteasomal degradation of c-Myc and Pim-1, mediated by activation of the serine/threonine kinase GSK-3β (Mol Cancer Ther 20:676, 2021). Here we sought to determine whether concurrent treatment with PADs overcomes resistance to FLT3is. We studied MOLM-14 human AML cells, with heterozygous *FLT3*-ITD, and FLT3i-resistant MOLM-14 cells with D835Y tyrosine kinase domain and F691L gatekeeper *FLT*3 mutations and M14(R)701 MOLM-14 cells (from Dr. Donald Small, Johns Hopkins) with a G12D *NRAS* activating mutation. IC_{50}s, determined by WST-1 cytotoxicity assays, of Type 1 FLT3i gilteritinib in MOLM-14, D835Y, F691L and M14(R)701 cells were 9.2, 18.6, 56 and 57.5 nM, and the Type II FLT3i quizartinib, 2.8, 211, 659 and >4,000 nM. Both DT-061 and FTY720 sensitized MOLM-14 D835Y cells to quizartinib (IC_{50}s <10 nM) but not to gilteritinib in cytotoxicity assays and showed synergy with quizartinib (combination indexes 0.6, 0.5), but not with gilteritinib in drug combination studies using Chou-Talalay analysis. In contrast, DT-061 and FTY720 did not sensitize to or synergize with quizartinib or gilteritinib in MOLM-14 F691L cells. Finally, FTY720 markedly sensitized M14(R)701 cells to both quizartinib and gilteritinib and showed substantial synergy (combination indexes <0.1), while DT-061 did not. In mechanistic studies, quizartinib alone did not decrease phospho-FLT3 expression by western blot analysis in MOLM-14 D835Y cells, but DT-061 or FTY720 and quizartinib co-treatment markedly decreased phospho-FLT3, but not FLT3, expression. Thus PADs resensitize cells with D835Y to quizartinib by inactivating FLT3-ITD, thereby enabling the binding of quizartinib to FLT3-ITD. Additionally, while FTY720, but not DT-061, markedly sensitized M14(R)701 cells to quizartinib and gilteritinib, FTY720 and DT-061 increased phosphatase activity similarly in a PP2A immunoprecipitation phosphatase assay, indicating that sensitization by FTY720 likely occurs by a mechanism other than PP2A activation. Potential induction of ceramide accumulation by FTY720, a sphingolipid analog, in M14(R)701 cells is being studied.

#5014

HPK1 gene knockout reporter cell line: an efficient drug screening system

Yunpeng Zhai, Lidan Li, Jianyu Hao, Yuqing Hu, Jinying Ning, Feng Hao.
Kyinno Biotechnology Co., Ltd, Beijing, China

Immunotherapy is the stimulation of the immune system, improving on the ability of immune system to treat cancer. It is expected to be the most effective therapy for patients with tumor metastasis. Checkpoint inhibitor (CPI) therapy is a form of cancer immunotherapy which can block inhibitory checkpoints, restoring immune system function. Tumor cells could recruit immunomodulatory cells and induce inhibitory signals, resulting in losing immunomodulatory. Therefore, there is an urgent need to develop new therapeutic agents that work in concert with CPI. HPK1, also known as MAP4K1, can act as a negative regulator of activation signals generated by T cell receptor (TCR). The development and screening of HPK1 inhibitors have great potential in the cancer immunotherapy. Herein, we constructed a HPK1 knockout reporter cell line Jurkat-NFAT-Luc2-HPK1-Knockout-Cell-Line by CRISPR/Cas9 which can be used in high-throughput HPK1 inhibitors screening. Wild type cells were incubated with HPK1 inhibitors and luciferase signals were compared in HPK1-knockout cells. Our HPK1 knockout reporter cell line has high sensitivity and specificity. The reporter system can achieve high-throughput compound library screening. After selected the compound with selective inhibitory activity, further validation and optimization would be performed. Moreover, we constructed a Jurkat-HPK1-HiBiT reporter cell line by CRISPR/Cas9. It can be used in the screening of HPK1 degradants. We believe that HPK1 gene editing cell lines play an important role in the high-throughput screening of drugs. It could facilitate the development of drugs in tumor immunotherapy.

#5015

Wee1 inhibition and its synthetic lethal combination with Chk1 inhibition in mouse model of neuroendocrine prostate cancer

Yapeng Chao, Yuzhou Chen, Yu Liu, Jaclyn A. Connelly, Hong Wang, Qiming Jane Wang. *University of Pittsburgh, Pittsburgh, PA*

The mitotic regulator Wee1 is a critical regulator of G2/M cell cycle checkpoint and DNA damage response pathways. Wee1-targeted agents are under active clinical investigation in multiple cancer types. However, Wee1 and its inhibitors have not been well studied in prostate cancer, particularly neuroendocrine prostate cancer (NEPC). In this study, we investigated the therapeutic potential of Wee1 inhibitor AZD1775 and its synthetic lethal combination with Chk1 inhibitor in the context of NEPC. Our data demonstrated increased Wee1 expression in NEPC cells and tumors. Treatment of NEPC cells with AZD1775 inhibited NEPC tumor cell survival with greater potency as compared to other prostate cancer cells, demonstrating increased vulnerability of NEPC cells to Wee1 inhibition. We further identified synthetic lethality between the inhibition of Wee1 and several protein kinases, particularly Chk1, another key G2/M checkpoint kinase. Using an autochthonous adenocarcinoma mouse prostate (TRAMP) model that gives rise to NEPC tumors, we assessed the efficacy of AZD1775 and a highly selective Chk1 inhibitor SRA737 as single agents and in combination on the progression, survival, and metastatic spread of NEPC tumors *in vivo*. AZD1775 and SRA737 when used as single agents significantly suppressed tumor growth, improved overall survival, and incidence of distant metastases of mice with NEPC tumors. The combination of AZD1775 and SRA737 on a sequential 2-wk treatment schedule was more efficacious in suppressing tumor growth and metastasis than each drug alone in castrated TRAMP NEPC tumors. Mechanistically, the combination of Chk1 and Wee1 inhibitors synergized to reduce the inhibitory phosphorylation of CDK1 at Y15 and Cdc25c at S216, resulting in enhanced activation of CDK1/cyclin B complex, abrogation of G2/M checkpoint, and consequent premature mitotic entry, which ultimately led to mitotic catastrophe and apoptosis. Our findings provide promising preclinical evidence supporting the therapeutic values of Wee1 and Chk1 inhibitors as single agents and in combination for the treatment of NEPC.

#5016
IL-6 influences PIM1 expression in renal cell carcinoma
Kimberly S. Meza, Sheldon L. Holder. *Brown University, Providence, RI*

Renal cell carcinoma (RCC) is the most common kidney neoplasm, accounting for over 430,000 new cases worldwide and 179,000 deaths

annually. The overexpression of the proviral integration site for moloney murine leukemia virus 1 (PIM1) kinase is associated with poor clinical outcomes in patients with RCC. PIM1 is a constitutively active effector serine/threonine kinase with roles in tumor progression including cell proliferation, apoptosis, invasion, and migration. Yet, the mechanisms underlying PIM1 expression and its function in RCC are not fully delineated. IL-6 is a pleiotropic cytokine involved in the activation of the JAK/STAT signaling cascade. High serum IL-6 levels are implicated in the poor prognosis of RCC patients and are hypothesized to contribute to RCC invasion and metastasis. PIM1 is shown to be transcriptionally regulated downstream of JAK/STAT signaling and an IL-6/STAT3/PIM1 axis exists in pancreatic cancer. We thus hypothesize that this pathway also regulates expression of PIM1 in RCC. Here, we explore the levels of PIM1 in RCC and identify potential signaling pathways influencing PIM1 expression. Our results show five RCC cell lines, 769-P, 786-O, ACHN, CAKI-1, and RCC-4 cells overexpress PIM1 relative to normal renal proximal tubule epithelial cells. In RCC cell lines, IL-6 secretion correlates with PIM1 protein levels. Treatment with ruxolitinib, a JAK1/2 inhibitor, leads to a dose and concentration dependent decrease in PIM1 levels. We then tested whether incubation with an IL-6 neutralizing antibody is sufficient to regulate PIM1 protein levels. Indeed, use of an IL-6 antibody resulted in decreased pJAK2 protein and PIM1 protein. Our initial studies suggest that differential expression of PIM1 among RCC cell lines may be linked to autocrine IL-6 signaling. Interestingly, 769-P cells demonstrate increased PIM1 levels but do not secrete IL-6 and neither ruxolitinib treatment nor incubation with an IL-6 neutralizing antibody appear to affect PIM1 levels. Therefore, an IL-6/JAK-independent pathway resulting in increased PIM1 protein levels likely exists in 769-P cells. Further investigation is required to elucidate the contexts of PIM1 regulatory pathways in order to develop novel targeted anti-cancer strategies in RCC.

#5017

Simultaneous targeting of EphA3 on glioblastoma and tumor microenvironment to overcome resistance to CART cell therapy in brain cancer

Ekene J. N. Ogbodo[1], Michael W. Ruff[2], Reona L. Sakemura[1], Claudia ManriquezRoman[3], Truc Huynh[1], James H. Girsch[4], Olivia L. Sirpilla[1],

Kun Yun[3], Carli M. Stewart[3], Ismail Can[3], Lionel K. Fonkoua[3], Mehrdad Hefazi[3], Elizabeth L. Siegler[3], Saad S. Kenderian[3]. *[1]Department of Immunology, Mayo Clinic, Rochester, MN,[2]Department of Neurology, Mayo Clinic, Rochester, MN,[3]Department of Hematology, Mayo Clinic, Rochester, MN,[4]Division of Hematology, Mayo Clinic, Rochester, MN*

Glioblastoma multiforme (GBM) is the most aggressive and common form of brain tumor, and it is characterized by an immunosuppressive tumor microenvironment (TME) that supports tumor growth and pathology. An integral part of the GBM stroma is the mesenchymal stem cells (MSC), which promote GBM growth. Receptor tyrosine kinase EphA3, a member of the Eph family, is overexpressed in GBM tumors and in MSCs within TME, making it an attractive target for Chimeric antigen receptor T-cell (CART) therapy. CART has proven incredible promise in certain hematological malignancies therapy but remained short in solid tumors, particularly GBM. We hypothesize that concurrent targeting of cancers and TME by EphA3-CART can be a potential therapeutic option in GBM. We first showed the expression of the EphA3 receptor by Immunohistochemistry and western blot on GBM patient-derived xenograft (PDX), as well as on the SNB-19 and U87 human GBM cell lines and adipose-derived MSCs using flow cytometry. We then generated EphA3-CAR construct derived from a clinically validated anti-EphA3 scFv cloned in a lentiviral vector containing CD28 and CD3ζ, and generated EphA3 CART cells with over 90% efficiency. EphA3 CART cells demonstrated potent antigen specific effector functions. To demonstrate the antitumor activity *in vivo*, we subcutaneously grafted 1 x 10^6 GBM cells per NOD-SCID-γ-/- mice and at ~150-300 mm^3 tumor volume, mice were then treated with 5 x 10^6 EphA3-CART or un-transduced (UTD) T cells control. Tumors were monitored by bioluminescence imaging (BLI) and caliper measurements, and mice were followed for survival. Mice treated with EphA3 CART cells exhibited a significant reduction in tumor volume ($p<0.005$), and prolonged overall survival ($p=0.0015$). Finally, we tested the ability of EphA3-CART cells to overcome MSC induced CART cell suppression by co-culturing EphA3-CART cells with MSC and $EphA3^+$ GBM target cells while using the $CD19^+$ mantle cell lymphoma cell line JeKo-1 and CART19 as control. MSC conditioned coculture of GBM and

CART showed significant suppression of CAR19 in the CART19 - JeKo-1 system (p=000.3), but no significant suppression of EphA3-CART cells. In summary, our results indicate that EphA3 CART cells exhibited potent and specific antitumor activity in vitro and in vivo and ameliorated MSC induced inhibition of CART cell functions, representing a potentially promising therapeutic option in GBM.

#5018

PROTAC degraders of CDK8/CDK19 Mediator kinases potently suppress multiple myeloma proliferation

Li Zhang[1], Jing Li[1], Charles E. Dowling[1], Eugenia V. Broude[1], Igor B. Roninson[1], Campbell McInnes[1], Mengqian Chen[2]. *[1]Drug Discovery and Biomedical Sciences, University of South Carolina, Columbia, SC,[2]Senex Biotechnology, Columbia, SC*

CDK8 and CDK19 are kinase components of the CDK module that comprises CDK8 or CDK19 together with their binding partner cyclin C (CCNC) and two other proteins; the CDK module is associated with transcriptional Mediator complex. CDK8/19 Mediator kinases potentiate transcription induced by different signals, regulate protein levels of Mediator complex components and protect CCNC from proteolytic degradation; the latter activity is exerted in a kinase-independent manner. CDK8/19 kinase inhibitors have entered clinical trials for solid tumors and leukemias. To extend the effects of CDK8/19 inhibition and to suppress their kinase-independent activities, we have developed three series of PROteolysis TArgeting Chimeras (PROTACs) based on different selective inhibitors of CDK8/19 kinases, connected via different linkers to a moiety binding cereblon (CRBN) E3 ligase. The most potent PROTACs degraded both CDK8 and CDK19 in different cell types with DC50s of 10-20 nM. RNA-Seq analysis of 293 cells treated with a CDK8/19 kinase inhibitor or PROTAC showed that the bulk of the PROTAC's transcriptomic effects matched the effects of the kinase inhibitor. In contrast to the kinase inhibitors, CDK8/19-degrading PROTACs also induced CCNC degradation. Cancer Dependency Map (DepMap) analysis revealed that multiple myelomas (MM), where CRBN is an established therapeutic target, show greater dependency on CCNC than most of the tumor cell lines. We have tested two strongly CCNC-dependent MM cell lines and one CCNC-

independent MM line for sensitivity to different CDK8/19 kinase inhibitors and PROTACs. Kinase inhibitors showed low to moderate anti-proliferative activity in all three MM lines, whereas CDK8/19 PROTACs were an order of magnitude more potent than the kinase inhibitors in the two CCNC-dependent MM lines (IC50s of 20-30 nM) but not in the CCNC-independent line. The effects of CDK8/19-degrading PROTACs were stronger than those of the CRBN-targeting drug pomalidomide (approved for MM), a CRBN-binding PROTAC acting on androgen receptor or a CDK8 degradation-inactive PROTAC analog containing CDK8/19- and CRBN-binding moieties. These results suggest the potential of CDK8/CDK19-degrading PROTACs for the treatment of MM.

#5019

Next-generation DYRK1A inhibitors as a new therapeutic approach for the treatment of hematological malignancies

Matthew C. Jarvis, Gopi Mittapalli, Emily Creger, Chelsea Nora, Maureen Ibanez, Deepti Bhat, Brian Hofilena, Josh Stewart, Elizabeth A. McMillan, Hadi Falahatpisheh, Chi-Ching Mak, Michael White, John S. Hill, Carine Bossard. *Biosplice Therapeutics, Inc., San Diego, CA*

Background: The dual-specificity tyrosine-regulated kinase 1A (DYRK1A) can phosphorylate multiple targets involved in key cellular processes that have been associated with the hallmarks of cancer, including proliferation, survival, cell cycle regulation and the DNA damage response[1]. In addition, compounds that inhibit DYRK1A have demonstrated anti-tumor activity both in vitro and in vivo. However, until recently, there was a paucity of potent, specific, and bioavailable DYRK1A inhibitors that did not target the related cdc2-like kinases (CLKs) and glycogen synthase kinase 3β. In this study, we describe a set of next-generation DYRK1A inhibitors and used them to evaluate the specific contribution of DYRK1A activity to tumor biology and evaluate the therapeutic potential of DYRK1A inhibition in cancer.

Methods: *DYRK1A* expression was analyzed in The Cancer Genome Atlas and Cancer Cell Line Encyclopedia databases. Cancer cell growth dependencies were evaluated by DepMap analysis. Cell-based target engagement (TE) was assessed by NanoBRET™. Cell viability was assayed with CellTiter-Glo® following 4-day treatment with DYRK1A

inhibitors. Synergy was calculated using Chalice software. Pharmacokinetics (PK) were evaluated in rodents and Tumor Growth Inhibition (TGI) in nude mice. Preliminary toxicology was assessed in a 14 day rat study.
Results: *DYRK1A* expression and a systematic DYRK dependencies analysis in human cancers revealed that hematological malignancies, Small Cell Lung and Ovarian cancers rely on *DYRK1A* expression for their proliferation. A series of potent (biochemical IC_{50}s 3nM to 10nM, TE 19 nM to 134 nM) and highly selective ATP-competitive DYRK1A inhibitors were designed with minimal inhibition of the rest of the kinome (1%-2.3% of kinases inhibited $\geq$ 90%) Cancer cell lines (n=160) were treated with DYRK1A inhibitors and those belonging to hematological lineages were among the most sensitive ($P<0.01$). In vitro combination of DYRK1A inhibitors with the anti-leukemia agent venetoclax revealed high synergy in 3 out of the 5 AML cell lines tested (synergy score >20). Compounds that showed good oral bioavailability and plasma exposures in rodents were selected for further characterization in vivo. In the MV-4-11 xenograft model, mice treated daily with 25mg/kg, or 50mg/kg of 2 different DYRK1A showed 72-99% TGI compared to vehicle. Preclinical toxicity profile in rats showed next generation DYRK1A inhibitors were well tolerated.
Concluding Remarks: these studies support further evaluation of DYRK1A inhibitors as a therapeutic strategy for some cancers, especially hematological malignancies including AML.
[1] Boni, J.; Rubio-Perez, C.; López-Bigas, N.; Fillat, C.; de la Luna, S. The DYRK Family of Kinases in Cancer: Molecular Functions and Therapeutic Opportunities. *Cancers* 2020, *12*, 2106. https://doi.org/10.3390/cancers12082106

#5020

IRAK1 is a critical mediator of hyaluronic acid induced stemness

David Standing[1], Prasad Dandawate[1], Jaimie Johnson[1], Sumedha Gunewardena[1], Michele T. Pritchard[1], Harsh Pathak[1], Dineo Khabele[2], Katherine Roby[1], Andrew Godwin[1], Roy Jensen[1], Scott Weir[1], Shrikant Anant[1]. *[1]University of Kansas Medical Center, Kansas City, KS,[2]Washington University in St. Louis, St. Louis, MO*

Ovarian cancer (OvCa) is the leading cause of gynecologic cancer-related deaths, due in part to late-stage diagnoses. While the overall response rate to first line therapy is encouraging (~80%), the majority of women develop recurrent disease, characterized by resistance to standard chemotherapy. There is convincing evidence that cancer stem cells (CSCs) have implications in resistance and recurrence of OvCa. To understand the pathways involved in enhancing this stem-like phenotype, we performed RNA sequencing and identified TLR-ILR1 (TIR) pathways as highly activated in cisplatin resistant OvCa and stem-cell populations. Subsequently, using a tumor microarray, we observed that interleukin receptor-associated kinase 1 (IRAK1), a critical mediator of TIR signaling, is upregulated in OvCa patient tissues compared to normal. This expression further correlated with younger diagnosis age and shorter overall survival, suggesting a role in OvCa tumorigenesis. Knockdown of IRAK1 by specific shRNA in OvCa cells, significantly impaired CSC enriched spheroid growth and orthotopic tumor growth in mouse models replicating advanced peritoneal OvCa. RNA sequencing of IRAK1 knocked down cells identified downregulation of CSC related genes including STAT3, MYC, NOTCH1, and NOTCH3. In addition, there was a reduction in the cisplatin efflux transporter ABCC1 and stemness marker gene CD44. Advanced OvCa is often associated (~90% in stage III and IV) with the development of malignant ascites. We demonstrate for the first time that significant amounts of low molecular weight hyaluronic acid fragments (LMW HA) are present in ascites. LMW HA induced IRAK1 dependent activation of non-canonical signaling through PKC-β leading to induction of STAT3 phosphorylation and MYC. This was further accompanied by increased spheroid formation, demonstrating a critical role for IRAK1 in HA-induced stemness. We have further identified a selective IRAK1 inhibitor, TCS2210 (1,2-Dihydro-N-hydroxy-2-oxo-3-(3-phenylpropyl)-6-quinoxalinecarboxamide). TCS2210 abrogated LMW HA induced activation of IRAK1 and expression of stemness genes MYC, NOTCH1, and NOTCH3. Lastly, we found that TCS2210 effectively suppresses OvCa cell growth *in vitro* and *in vivo*, synergizing with standard-of-care cisplatin. Our data suggests a role of IRAK1 in OvCa, by enhancing cancer cell growth and stemness. It further suggests that IRAK1 is a putative target for advanced OvCa.

#5021

Preclinical evaluation of immunomodulatory effects of aurora kinase inhibition in HPV+ cancers

Pragya Sinha, Soma Ghosh, Faye M. Johnson, Jagannadha K. Sastry.
Thoracic Head and Neck Medical Oncology, The University of Texas MD Anderson Cancer Center, Houston, TX

Human papillomavirus (HPV) is the causative agent of cervical cancer and some cancers of the penis, vulva, vagina, anus, and oropharynx. In an earlier study, we identified Aurora Kinase (AK) inhibitors from a large-scale drug screening as a unique class of reagents to induce selective apoptosis in HPV+ human tumor cells in vitro and in vivo (using HPV+ PDX mouse models). We tested the in vivo efficacy of alisertib, an Aurora Kinase A inhibitor, in an immunocompetent mouse model (mEER) for HPV+ oropharyngeal cancers. In preparation for this, we first tested 300 nM alisertib on 3 HPV+ murine cancer cell lines: TC-1, C3.43, and mEER for 48h. We observed that when compared to the vehicle (DMSO) control group, the level of phospho Aurora Kinase A was completely inhibited. Furthermore, in multiple HPV+ murine tumor cell lines we observed significant apoptosis as measured by annexin V 7-AAD staining along with higher cell surface expression of calreticulin (CRT), and high mobility group box 1 protein (HMGB1) which are markers for immunogenic cell death (ICD). Both CRT and HMGB1 serve as “eat me” signals that in turn trigger APC-mediated dead-cell antigen uptake, a crucial event for priming the responses from the innate immune system. In support of this, we observed that in a co-culture setting, the conditioned medium from alisertib-treated tumor cells increased the frequencies of CD8+ cells expressing GnzB as well as a significant decrease in the population of T regulatory cells (Tregs) (CD4+ FoxP3+). Additionally, we observed an increase in the innate immune natural killer cell subset. Future studies will explore the in vivo efficacy of Aurora Kinase inhibition along with immune checkpoint blockade and/or therapeutic vaccination. Our proposed research will have a positive impact because we will gain insight into the immune responses underlying the co-dependency of HPV+ cancers on Aurora kinase. Our research may lead to an increase in the rates of long-term, durable clinical responses or may allow for therapy de-escalation.

#5022

Atypical protein kinase C inhibitors abrogate malignant breast cancer

Nuzhat Nowshin Oishee, Khandker Mohammad Khalid, Dr. Mildred Acevedo-Duncan. *Chemistry, University of South Florida, Tampa, FL*

Breast cancer is the most common cancer type with expected cases of approximately 284,200 according to the National Cancer Institute. Atypical Protein Kinase C (aPKC) plays a significant role in many cancer types. A positive correlation between elevated PKC levels and both the invasive and chemotactic potential of human breast cancer cell lines has been suggested in *in-vitro* studies. In addition, the atypical protein kinase C isoforms (aPKC), PKC- and PKC- are involved in the increased proliferation of several cancer types, including breast cancer and ovarian cancer. Hence, this project focused on utilizing aPKC inhibitors, ICA-1S (5-amino-1-((1R,2S,3S,4R)-2,3-dihydroxy-4-methylcyclopentyl)-1H-imidazole-4-carboxamide and - Stat (8-hydroxy-1,3,6- naphthalenetrisulfonic acid), on two malignant breast cancer cell lines (T47D and BT549) to observe the effect on cell proliferation. To observe the effects of the aPKC inhibitors on the malignant breast cancer cells, cell proliferation assays were conducted, where cells were treated with ICA-1S, and - Stat for 72 hours (about 3 days). Furthermore, to observe if ICA-1S induces apoptosis in the malignant breast cancer cells, both the cell lines were treated with ICA-1S for 120 hours (about 5 days), and western blotting techniques were utilized. The results indicated that in T47D cell line, treatment with ICA-1S (50uM) and - Stat (10uM) caused 52% and 75% reduction in cell proliferation, respectively. Moreover, with BT549 cell line, treatment with - Stat (1uM) decreased the cell proliferation by 40%. Additionally, it was observed by western blotting that ICA-1S induces apoptosis in BT549 cell line. This was shown by an increase in the cleavage of caspase 3 and PARP, along with a decrease in survivin, and phospho-BAD. However, ICA-1S did not induce apoptosis in T47D cell line. Further investigation will be conducted on determining the effect of aPKC inhibitors on the proliferation, invasion, and migration of the malignant breast cancer cell lines. In addition, siRNA treatment will be applied to knockdown PKC- and PKC- and subsequent effect will be observed. In conclusion, PKC- and PKC- plays a significant role on breast cancer, and further investigation will be conducted to analyze these roles, which will lead to the determination of a signaling

pathway via which atypical protein Kinase C functions in breast cancer.

#5023

PFKP contributes to ovarian cancer metastasis, stemness and anchorage-independent growth via α5 integrin and ERK/MMP9 signaling

Ruiqian Zhang[1], Michelle K.Y. Siu[1], Xuetang Mo[1], Mingo M.H. Yung[1], Jingjing Wang[1], Yuxin Jiang[1], Annie N.Y. Cheung[2], Hextan Y.S. Ngan[1], Karen K.L. Chan[1]. *[1]Departments of Obstetrics and Gynaecology, Li Ka Shing Faculty of Medicine, The University of Hong Kong, Pok Fu Lam, Hong Kong,[2]Departments of pathology, Li Ka Shing Faculty of Medicine, The University of Hong Kong, Pok Fu Lam, Hong Kong*

Background: Ovarian cancer is one of the most aggressive malignancies threatening women's health worldwide. Its high mortality rate is largely due to symptoms not appearing until late in the disease, usually after the cancer has metastasized. Despite current state-of-the-art treatments, the prognosis for patients remains poor. New effective treatments are urgently needed to improve patient survival. High lactate production and low glucose oxidation, independent of oxygen availability, is known as the Warburg effect and is common in cancer. Phosphofructokinase 1 (PFK-1) irreversibly converts fructose 6-phosphate to fructose 1,6-bisphosphate, the first step in the Warburg effect. The platelet isoform of PFK (PFKP) regulates glycolysis and plays roles in tumorigenesis in other human cancers, the precise mechanisms has yet to be defined. Moreover, PFKP in ovarian cancer remain unknown. We hypothesize that PFKP modulates metastasis and stemness in ovarian cancer.
Methods: Expression of PFKP in clinical samples, ascites-derived tumor cells, normal ovarian epithelial cells (HOSEs) and ovarian cancer cell lines was determined by immunohistochemistry/immunofluorescence and qPCR/immunoblotting, respectively. The correlation between PFKP and clinicopathological parameters was analyzed. Ectopic expression or knockdown of PFKP followed by migration, invasion, sphere formation and soft agar assays were performed in ascites-derived tumor cells and ovarian cancer cell lines to investigate the effects on metastasis, stemness and malignant transformation respectively. Additionally, the related signaling pathway was explored by qPCR and immuoblotting.

Results: Up-regulation of PFKP in clinical samples, ascites-derived tumor cells and ovarian cancer cell lines was found when compared to HOSEs. Higher PFKP was correlated to shorter overall and disease-free survival. Functionally, knockdown of PFKP by siRNA/shRNA approaches in ascites-derived tumor cells, ES-2 and HeyA8 cells decreased migration, invasion, sphere formation and colony formation in soft agar, which was accompanied by decreased expression α5 integrin, pERK and MMP9. Ectopic expression of PFKP in SKOV-3 cells showed opposite effects. Intriguingly, we found that MEK-1 inhibitor (U0126) or an anti-MMP9 neutralizing antibody could block PFKP-mediated migration/sphere formation abilities.
Conclusion: PFKP was overexpressed in ovarian cancer and regulates metastasis, stemness and anchorage-independent growth. α5 integrin and ERK/MMP9 signaling were involved in such functional effects. PFKP could be a potential prognostic marker and therapeutic target for ovarian cancer.

#5024

Role of protein kinase C ζ and ι inhibitors on ovarian cancer cell lines in combination with cisplatin

Mahfuza Marzan, Nuzhat Nowshin Oishee, Khandker Mohammad Khalid, Mildred Acevedo-Duncan. *Chemistry, University of South Florida, Tampa, FL*

Ovarian cancer causes more death than any other cancers of the female reproductive system. Current treatment strategies are surgical removal of cancerous parts and chemotherapy with platinum drugs (e.g. cisplatin, carboplatin) or taxols. However, recurrence of cancer with drug resistance is frequent. Previously two inhibitors; ICA-1S (5-amino-1-((1R,2S,3S,4R)-2,3-dihydroxy-4-methylcyclopentyl)-1H-imidazole-4-carboxamide and ζ-stat (8-hydroxy-1,3,6- naphthalenetrisulfonic acid) specific for two atypical protein kinases, PKC-ι and PKC-ζ respectively have been reported. These inhibitors have an anticancer effect in different cancers, including clear-cell ovarian cancer. Our aim was to find if cisplatin has any synergistic effect with ICA-1S and ζ-stat on ovarian cancer cell proliferation, migration, and apoptosis. Ovarian cancer cell line ES-2, which has mutation in p53 gene was used in this study. After 72 hours of

treatment with ICA-1S (10 μM) and ζ-stat (10 μM), proliferation of ES-2 cell line was inhibited by 42.5% and 23.5% respectively compared to control. When combined with cisplatin (0.5 μM), the inhibition of cell proliferation increased to 67% for ζ-stat and 65.8% for ICA-1S (N=3 trials) which is synergistic. Wound healing assay with ES-2 cells showed that ICA-1S and cisplatin inhibited the migration of ES-2 cells separately as well as in combination. SDS-PAGE and subsequent western blotting showed that ICA-1S monotherapy and combination with cisplatin reduced the expression mutant p53, PI3K, AKT, Bcl2, and phopho-BAD. IP with PKC ζ beads showed the association of PKC ζ with PKC-ι and p53 in ES-2 cell line. As mutation in p53 is quite frequent in ovarian cancer with gain of function, ICA-1S may have an advantageous role in inhibiting mutated p53 regulated pathway. Inhibition of ES-2 cell line with ICA-1S and ζ-stat also suggested that PKC-ι and PKC ζ play important roles in ovarian cancer and may augment traditional chemotherapy. Further study on the pathway affected by aPKC inhibitors combined with cisplatin would be investigated through WST, western blotting and immunoprecipitation assay.

#5025

Reduced level of protein kinase C iota renders human glioblastoma less invasive and induces apoptosis via modulating Tak1/NF-κB pathway

Khandker Mohammad Khalid, Wishrawana S. Ratnayake, Avijit Dey, Nuzhat N. Oishee, Mahfuza Marzan, Mildred Acevedo-Duncan. *University of South Florida, Tampa, FL*

Glioblastoma (GBM) is characterized by poor therapeutic response and overall survival. It is the most aggressive form of primary brain tumor with a tendency to invade surrounding healthy brain tissues, rendering them largely incurable. In this study, small-interference RNA was used to knock down the expression of protein kinase C PKC-ι. The reduced PKC-ι expression impaired the phosphorylation of LIM kinase 1/2 (LIMK), which is a critical step in cofilin recycling and actin polymerization. Additionally, there was a down-regulation of matrix metalloprotease-9 expression in LN-229 and U87G cells, which coincided with decreased invasion. Therefore, PKC-ι regulates both cytoskeleton rearrangement and cell adhesion, which contributed to cell migration. Silencing of PKC-ι also dampened Transforming growth factor-β (TGF-β)-activated kinase 1 (Tak1) level.

TAK1 is an essential component in genotoxic stresses-induced NF-κB-activation and mitogen-activated protein kinase (MAPK)-pathways in GBM. TAK1, when activated, forms a complex with TAB1-3 (Tak1 binding proteins). Our data reveal, reduced Tak1 level after silencing PKC-ι interferes with complex formation and reduces NF-κB-activation. Diminished PKC-ι level also reduces activation of Tak1/JNK axis. This deactivation exerts an anti-oncogenic effect on glioblastoma via suppression of Akt1, c-Myc, and STAT3. This implies PKC-ι may have a crucial role in the activation of Tak1. Reduced migration and invasion in glioblastoma cells upon inhibition of PKC-ι was further confirmed by Scratch assay and Boyden assay. These results indicate that PKC-ι is involved in the control of glioblastoma cell migration and invasion. PKC-ι is a central component of multiple converging and bifurcating pathways and is a potential therapeutic target against GBM survival and infiltration.

#5026

Protein tyrosine phosphatase Ptpn1 knockout in mouse models drives B-cell hematological malignancies

Toshihiro Matsukawa[1], Nupur Nigam[1], Ryan Bertoli[1], Michel L. Tremblay[2], Mianmian Yin[1], Peter D. Aplan[1]. *[1]NIH-NCI, Bethesda, MD,[2]McGill University, Montreal, QC, Canada*

Background: Ptpn1 is a member of Protein Tyrosine Phosphatase family that dephosphorylates tyrosine residues. We previously reported that an Mcm2 hypomorphic mouse (designated Mcm Cre/Cre) develops T cell acute lymphoblastic leukemia (T-ALL), due to acquisition of 100-1000 kb interstitial deletions involving tumor suppressor genes. When crossed to mice that express a NUP98-HOXD13 (NHD13) fusion gene, NHD13+;Mcm2Cre/Cre mice develop B-cell precursor ALL (BCP-ALL). Sparse whole genome sequencing revealed somatic copy number variants (CNV) involving Pax5 and Ptpn1. The role of Pax5 in B-cell development, differentiation, and leukemia has been widely studied. However, little is known about deletions of Ptpn1 and its role in BCP-ALL.
Objective: The principal objective is to investigate how deletion of Ptpn1 impacts BCP-ALL development in mouse models.
Methods: Mice expressing NHD13 fusion (NHD13+) were crossed with Ptpn1 knockout mice. The F2 cross generated 6 genotypes that were

positive or negative for NHD13 and wild type/heterozygous/homozygous for Ptpn1. Mice were studied for incidence of BCP-ALL, which was characterized by whole-exome sequencing, molecular pathway analysis and transcriptome-sequencing.
Results: NHD13+;Ptpn1-/- mice developed BCP-ALL, characterized by hyperleukocytosis, variable anemia and thrombocytopenia, expression of B220 and/or CD19, and invasion of non-hematopoietic tissues (liver, kidney, lung). In addition, NHD13+;Ptpn1+/- mice that developed BCP-ALL lost the wild-type (WT) Ptpn1 allele in the leukemic cells. Similar to human BCP-ALL, NHD13+;Ptpn1-/- mice that developed BCP-ALL showed presence of clonal TCR-delta rearrangements as well as IGH rearrangements in the leukemic cells. Whole exome sequencing showed presence of acquired mutations in genes known to be involved in B-cell differentiation, such as Pax5 or Bcor, as well as genes involved in B cell signaling pathways, such as Jak3, Jak1 and Flt3 and Western blots demonstrated accumulation of phosphorylated STAT3 protein.
Conclusion: This study demonstrates that Ptpn1 loss along with expression of an NHD13 fusion gene leads to a highly penetrant BCP ALL in mice, suggesting a role for Ptpn1 in preventing malignant transformation. Taken together, these findings are consistent with a collaborative model for BCP ALL in which the NHD13 transgene leads to increased stem cell self-renewal, somatic Bcor or Pax5 mutations block normal B cell differentiation, and somatic signaling mutations (Jak1/3, Flt3) lead to hyperproliferation, which is potentiated by Ptpn1 deficiency.

#5027

Targeting *ARAF* p.S214C mutation with sorafenib in non-small cell lung cancer

Carol Lee, Sze Man Chan, Sai Fung Yeung, Stephen Kwok-Wing Tsui.
School of Biomedical Sciences, The Chinese University of Hong Kong, Hong Kong, Hong Kong

Sorafenib is an FDA-approved multi-kinase inhibitor for the treatment of several cancer types, but is still under investigation for non-small cell lung cancer (NSCLC). Although sorafenib has not shown significant survival benefit in clinical trials for NSCLC patients, one study identified a patient with advanced lung adenocarcinoma harboring *ARAF* p.S214C mutation as

an exceptional sorafenib responder. As NSCLC lacks clinically validated predictive biomarkers for drug responses, we aim to evaluate the potential of *ARAF* p.S214C mutation as a biomarker for sorafenib sensitivity and its mechanism of action. Constructs with *ARAF* p.S214C mutation, *ARAF*-wild type (WT) and EGFR-vector control were ectopically expressed in a lung adenocarcinoma cell line, H2023, by retroviral transduction. Western blot confirmed stable overexpression of ARAF proteins over time. MTT assay showed that sorafenib inhibited growth of cells expressing *ARAF* p.S214C more pronouncedly than cells expressing *ARAF*-WT or vector control. In addition, spheroids formed by cells expressing *ARAF* p.S214C were more sensitive to sorafenib inhibition, indicating sorafenib sensitivity of *ARAF* p.S214C in NSCLC *in vitro*. To evaluate whether such sorafenib sensitivity is dependent on the kinase activity of ARAF, phospho-MEK and MAPK levels in mutant cells will be determined. As ARAF belongs to the Raf protein family which also includes BRAF and RAF1, knockdown studies and co-immunoprecipitation will be performed to determine whether BRAF and RAF1 are essential for *ARAF* p.S214C activity. The *in vivo* sorafenib sensitivity of *ARAF* p.S214C will be validated in tumor xenografts established from cells expressing the above constructs upon sorafenib treatment. Tumor volume will be assessed and expression of the tumor marker cytokeratin will be evaluated by immunohistochemistry. This study may reveal *ARAF* p.S214C as a potential biomarker for sorafenib sensitivity and a new target for precision medicine in NSCLC.

#5028

The regulation of inflammatory signaling in cancer via A20 phosphorylation

Tania Lopez Palacios, Tsz-Yin Chan, Christina Egbert, Jacob Truman, Spencer Ashworth, Alec Vaughan, Joshua L. Andersen. *Chemistry and Biochemistry, Fritz B. Burns Cancer Research Laboratory at Brigham Young University, Provo, UT*

A20 is an anti-inflammatory protein with a dual ubiquitin-editing activity. Through its N-terminal ovarian tumor (OTU) domain, A20 negatively regulates NF-κB by removing the K63-linked ubiquitin chains on RIP1 that act as platforms for NF-κB activation downstream of tumor necrosis factor alpha (TNFα). On the other hand, A20 also catalyzes the addition of K48-

linked ubiquitin chains on RIP1 via its C-terminal zinc finger domain 4 (ZnF4) to promote its proteasomal degradation. Through both mechanisms, A20 is a means of negative feedback on TNFα-induced NF-κB activity. Importantly, inactivation of A20 is frequently found in B-cell lymphomas, where loss-of-function A20 truncations promote cell proliferation and upregulation of NF-κB signaling. Among the post-translational modifications (PTMs) reported in A20, there are several phosphorylation events in its C-terminus, including within the ZnF4 domain. Besides its known E3 ubiquitin ligase activity, previous reports show that the C-terminal region of A20 is important for ubiquitin binding, having preference for K63-linked poly-ubiquitin. However, a little is known about the effects of phosphorylation at this region on A20 activity as well as its consequences in downstream signaling. Our current work suggests that phosphorylation in the C-terminus of A20 inhibits its E3 ubiquitin ligase activity and disrupts its interaction with ubiquitin, which may also affect its deubiquitinase activity by preventing its recruitment to ubiquitinated proteins in the TNFα receptor (TNFR) complex. We also propose that the C-terminal region is important for the formation of the A20 ubiquitin-editing complex, necessary to downregulate NF-κB-activated inflammatory signals. Based on these observations, we hypothesize that not only gene-inactivating mutations, but also post-translational mechanisms, such as phosphorylation, inhibit A20 to promote cancer development. Our research is now focused on understanding the upstream signaling that regulates A20 phosphorylation.

#5029

Determining the biological function of TNK1

Emmalee Kohler, Tania Lopez-Palacios, Tsz-Yin Chan, Christina Egbert, Jacob Truman, Spencer Ashworth, Alec Vaughan, Joshua Andersen, D. Madhusanka. *Chemistry and Biochemistry, Fritz B. Burns Cancer Research Laboratory at Brigham Young University, Provo, UT*

Thirty-eight-negative kinase 1 (TNK1) is a poorly characterized member of the ACK family of non-receptor tyrosine kinases, which we recently identified as a driver of cell survival in a subset of primary hematological malignancies. However, the biological function of TNK1 is not well understood. We also found that TNK1 is unusual among kinases for the

presence of a functional ubiquitin association (UBA) domain on its C-terminus. We discovered that the TNK1 UBA domain binds to poly-ubiquitin with high affinity and has no apparent preference for ubiquitin chain length or linkage type. Interestingly, the UBA domain is important for TNK1 function, given that deletion of the UBA domain (TNK1 ΔUBA) alters its localization and phospho-substrate network, while also weakening the oncogenic activity of TNK1 in cell transformation assays. Based on these data, we hypothesized that the UBA domain tethers TNK1 to its substrates. To test this hypothesis, we performed quantitative phospho-tyrosine proteomics using murine pro-B cells transformed with either TNK1 full length or TNK1 ΔUBA and identified TANK-binding kinase 1 (TBK1) as a putative UBA-dependent TNK1 substrate. TBK1 is a serine/threonine kinase involved in the regulation of inflammation, autophagy, and NF-κB signaling. During the selective autophagic degradation of misfolded proteins (aggrephagy), TBK1 phosphorylates p62 at S403 to increase its affinity to ubiquitin, and thereby increases p62-mediated recruitment of misfolded proteins into the condensate. Unchecked growth of ubiquitin condensates can overwhelm the size capacity of autophagosomes, potentially causing misfolded proteins to become proteotoxic aggregates. Our preliminary data suggest a model in which active TNK1 accumulates at ubiquitin condensates to phosphorylate and inhibit TBK1. Based on these data, we propose that TNK1 acts as a kinase sensor of poly-ubiquitin to control the TBK1-mediated growth of ubiquitin condensates.

#5030

Treatment of aromatase inhibitor-resistant cells with polyisoprenylated cysteinyl amide inhibitors stimulates the mitogen-activated protein kinase pathway enzymes, impedes cell proliferation and causes cell death

Jassy Mary S. Lazarte, Syreeta L. Tilghman, Nazarius S. Lamango. *Florida A&M University College of Pharmacy & Pharmaceutical Sciences, Tallahassee, FL*

Overexpression and hyperactivity of the estrogen receptor drives 67-80% and 90% of breast cancer in women and men, respectively. Resistance to aromatase inhibitor (AI) therapies necessitates the continuous search for novel therapies. Previous studies demonstrate AI-resistance is associated

with hormone-independence, enhanced motility, and increased growth factor signaling. Here, long-term letrozole-treated (LTLT-Ca) breast cancer cells were used to evaluate polyisoprenylated cysteinyl amide inhibitors (PCAIs) as potential alternative therapies for the treatment of aromatase inhibitor-resistant breast cancer. We determined the potency of PCAIs as anticancer agents by evaluating their effects on cell viability, phosphorylation of MAPK pathway enzymes, G-proteins levels, cell migration and apoptosis. Among the PCAIs tested, NSL-YHJ-2-27 showed significant potency against cell viability with an EC_{50} of 3.6 μM. MEK (p-MEK1/2), ERK (p-ERK1/2), and p90RSK (p-p90RSK) phosphorylation were significantly increased by 178, 119 and 125%, respectively, over controls. In addition, of the seven G-proteins evaluated, only KRAS and NRAS showed significant increases of 49% and 97%, respectively. Cell proliferation and colony formation were impeded by 82% and 74%, respectively, after PCAIs treatment. Migration of the LTLT-Ca cells was inhibited by 80% following treatment with 5 μM of NSL-YHJ-2-27. Lastly, the PCAIs also caused the degeneration of the spheroids after 10 μM PCAIs treatment, dead cells were very apparent after AO/EB staining. Our findings suggest that the PCAIs' suppression of cell viability and activation of the MAPK pathway causes apoptosis possibly through the activation of the proapoptotic p-p90RSK isoforms. The results reveal the ability of the PCAIs to effectively cause a negative impact on several cancer hallmarks suggesting their potency as anticancer agents. These findings also support a potential role for PCAIs' use in treating breast cancers that have become resistant to aromatase inhibitor therapies.

Theranostics and Radionuclides / Pharmacologic Approaches

#5034
Targeting CXCR4 and thioredoxin reductase in high grade neuroendocrine tumors and neuroendocrine carcinomas

Melissa A. Fath, Dijie Liu, Claudia Robles-Planells, Jordan T. Ewald, Keegan A. Christensen, Spenser S. Johnson, Stephen A. Graves, Douglas R. Spitz, Yusuf Menda, M. Sue O'Dorisio. *University of Iowa, Iowa City, IA*

Introduction/Background: Atypical lung carcinoids and lung neuroendocrine carcinomas (NECs) are currently incurable. Most of these

cancers express the C-X-C chemokine receptor 4 (CXCR4), making CXCR4 an attractive target for cancer diagnosis and treatment using radioligand therapy (RLT) with nuclides such as alpha emitter Pb^{212} conjugated to Pentixather (Pent). Alpha particles produce dense ionization tracks and damage cytosolic structures such as mitochondria, leading to the generation of reactive oxygen species such as superoxide ($O_2^{\bullet -}$) and hydroperoxides (H_2O_2 and ROOH) in targeted cancer cells. The FDA approved thioredoxin reductase inhibitor, auranofin (Aur), inhibits peroxiredoxin-mediated hydroperoxide metabolism increasing cell killing in targeted cancer cells.
Hypothesis: Inhibition of hydroperoxide metabolism using Aur can enhance therapeutic efficacy of alpha particle emitting ^{212}Pb-Pent in preclinical models of lung carcinoids and NECs.
Results: Clinically, IHC revealed greater than 75% of atypical carcinoids and NECs tested had moderate to high CXCR4. qRT-PCR, flow cytometry and immunohistochemistry performed on different lung carcinoid and NEC lung cell lines, determined that the majority moderately or highly express CXCR4. The minimal non-toxic dose of Aur that inhibits 50-70% of thioredoxin reductase activity was 4 mg/kg (intraperitoneal once a day) in DMS273 (small cell lung cancer) xenografts. ^{212}Pb-Pent given IV (1 and 3 μCu/g) was effective at increasing the survival of mice with DMS273 xenografts. Mice were then treated with 1.5, 3 or 6 μCu/g ^{212}Pb-Pent w/wo Aur 4 mg/kg/day. A trend test showed that both increasing dose of ^{212}Pb-Pent and the addition of Aur, caused a significant ($p<0.01$) delay in tumor growth. There were no significant changes in body weights, complete blood counts, and serum alanine aminotransferase indicating the combination treatments were well tolerated. Radiation dosimetry estimates using quantitative SPECT/CT imaging with Pb^{203}-Pent demonstrated average absorbed doses of 0.133 Gy/μCi (liver), 0.098 Gy/μCi (kidneys), 0.013 Gy/μCi (H292 xenografts), 0.028 Gy/μCi (DMS53 xenografts), 0.057 Gy/μCi (DMS273 xenografts), and 0.096 Gy/μCi (H69AR xenografts). Xenograft absorbed dose levels were positively correlated with CXCR4 expression.
Conclusion: The use of ^{212}Pb-Pent therapy to target CXCR4 on NECs showed pre-clinical efficacy in a dose dependent manner that was enhanced by Aur without significant normal tissue toxicity supporting the hypothesis

that CXCR4 can be successfully targeted with the radionuclide theragnostic pair, Pb^{212}/Pb^{203}-pentixather.

#5035

Preclinical development of a ^{89}Zr-labeled human antibody as a novel immuno-PET agent for noninvasive cancer detection and monitoring response to treatment

Abhay Kumar Singh, Calvin D. Lewis, Cristian AWV Boas, Philipp Diebolder, Prashant N. Jethva, Aaron Rhee, Jong Hee Song, Young Ah Goo, Shunqiang Li, Yongjian Liu, Buck Rogers, Vaishali Kapoor, Dennis E. Hallahan. *Washington University School of Medicine in St. Louis, Saint Louis, MO*

Lung cancer is the leading cause of cancer death worldwide. There is an unmet need for therapies to improve lung cancer outcomes without causing additional toxicities. Tax-interacting protein 1 (TIP1) is a radiation-inducible antigen that plays a role in lung cancer progression and resistance to therapy. TIP1 is a targetable cell surface protein. We developed human antibodies (Ab) that bind specifically to lung cancer. This study aimed to evaluate our lead anti-TIP1 human antibody targeting lung cancer *in vitro* and *in vivo*. Anti-TIP1 IgG1 Ab was developed by biopanning phage display human antibody library. The purified Ab was characterized by size-exclusion chromatography-HPLC (SEC-HPLC), mass spectrometry, ELISA, BIAcore and flow cytometry. Ab was labeled with ^{89}Zr using desferrioxamine chelator. The surface binding of ^{89}Zr-Ab was evaluated in the A549 and H460 lung cancer cells. Stability of the ^{89}Zr-Ab was assessed in human serum. Mice bearing 3 patient-derived xenografts (PDX) lung tumors or A549 tumors were injected with 50 μCi of ^{89}Zr-Ab. Small animal PET imaging and biodistribution were conducted over 7 days. Specific tumor uptake was evaluated in biodistribution studies on day 5 by injecting cold Ab before ^{89}Zr-Ab. We obtained 95% pure anti-TIP1 Ab by SEC-HPLC. Mass spectrometry confirmed the intact mass and glycosylation pattern of the anti-TIP1 IgG1. The Ab is bound to recombinant TIP1 protein and cancer cell surface with high affinity. The radiochemical purity of the ^{89}Zr-Ab was 99.9%, and the molar activity was 11.54 MBq/nmol with a radiolabeling yield of 91.4%. Both A549 and H460 cell lines demonstrated

specific binding as >70% inhibition was observed when the cold Ab was added. The ratio of SUV tumor to SUV muscle increased from 5.8 at 2 days to 6.3 at 7 days in PDX. In biodistribution studies, we found significantly higher ($p<0.05$) tumor uptake of the anti-TIP1 Ab (9.15±3.13 %ID/gm) vs. isotype control (5.72±1.02 %ID/gm). Cold anti-TIP1 Ab significantly blocked ($p<0.0001$) binding of the ^{89}Zr-Ab in A549 tumors. The anti-TIP1 Ab targets lung cancer cells *in vitro* and *in vivo*. The Ab retained antigen-binding potential following labeling with ^{89}Zr. This Ab can detect TIP1 positive tumors for therapy when conjugated with therapeutic radionuclides. IND enabling studies with the lead anti-TIP1 Ab are underway.

#5036

Single dose treatment with a novel Yttrium-90-labeled high affinity anti-B7-H3 antibody selective for the 4Ig-B7-H3 isoform provides long term survivors for established radioresistant colorectal carcinoma

Sarah Glazer, Margie Sutton, Ping Yang, Federica Pisaneschi, Seth Gammon, David Piwnica-Worms. *UT MD Anderson Cancer Center, Houston, TX*

The immune checkpoint antigen B7-H3 (CD276), expressed on cell surfaces of a variety of epithelial solid tumors, is a type 1 transmembrane protein consisting of an extracellular domain of repeating immunoglobulin constant and immunoglobulin variable domains (IgV, IgC, IgV, IgC), known as the 4Ig-B7-H3 isoform. 4Ig-B7-H3 is the dominant isoform in human cancers and is expressed at much lower levels on normal tissues. Humans also express a sheddable 2Ig-B7-H3 isoform containing only one immunoglobulin variable and constant extracellular domain (IgV, IgC) that is found in circulation (soluble 2Ig-B7-H3) and presents a challenge for systemic targeting of solid tumors. To develop an antibody suitable for fulfilling the promise of B7-H3 as a systemic therapeutic target, herein we report a murine antibody (MIL33B) that demonstrates mid-picomolar affinity to human 4Ig-B7-H3 (Kd, 72 pM) with 8-fold selectivity over 2Ig-B7-H3 (Kd, 580 pM) extracellular domains. Furthermore, MIL33B maintains high affinity to porcine 4Ig-B7-H3 (Kd, 102 pM), selectivity over murine 2Ig-B7-H3 (Kd, 41 nM), facilitating pre-clinical testing, and low cross-reactivity to other B7 family members (Kd, >1 μM). MIL33B-AF495 conjugates showed selective binding by live cell fluorescence microscopy

to HeLa and HCT116 cells with high endogenous 4Ig-B7-H3 expression and 4T1, B16F10 and CT26 cells induced to express human 4Ig-B7-H3 compared to HeLa 4Ig-B7-H3 KO cells or murine cell lines with endogenous 2Ig-B7-H3 expression. Compared to uptake in respective KO or vector control tumors, quantitative analysis *in vivo* with ^{89}Zr-DFO-MIL33B and PET imaging of tumor models demonstrated significantly higher normalized tumor-specific uptake in tumors with high endogenous expression of 4Ig-B7-H3 (HeLa) (3.25 ± 0.65 vs. 0.79 ± 0.13 SUV ratio, * $p = 0.02$) or those induced to express human 4Ig-B7-H3 (B16F10 and CT26) (3.16 ± 0.30 vs. 1.20 ± 0.69 SUV ratio, ** $p = 0.0032$; and 3.62 ± 1.62 vs. 1.89 ± 0.85 SUV ratio, *** $p < 0.0001$, respectively). As a first radio-theranostic treatment application, MIL33B labeled with yttrium-90 (^{90}Y-DOTA-MIL33B), a therapeutic beta-emitter, administered as a single dose I.V. (100 mCi, 3700 kBq), induced complete tumor regression and long-term survival of > 50% of mice harboring established syngeneic radioresistant colorectal CT26 tumors expressing human 4Ig-B7-H3 compared to vector control tumors (* $p = 0.0376$, log-rank test). ^{90}Y-DOTA-MIL33B-responsive mice developed immunologic memory and depletion assays *in vivo* demonstrated that CD8b+ cells contributed to the therapeutic efficacy of ^{90}Y-DOTA-MIL33B. These results point to the promise of ^{90}Y-DOTA-MIL33B as a selectively-targeted immune priming agent for radioligand therapy of 4Ig-B7-H3-expressing solid tumors.

#5037

DARPins as powerful targeting agents for radioligand therapeutics

Andreas Bosshart[1], Stephan Wullschleger[1], Martin Behe[2], Alain Blanc[2], Stefan Imobersteg[2], Alexandra Neculcea[1], Jacqueline Blunschi[1], Liridon Abduli[1], Sarah Schütz[1], Julia Wolter[1], Christian Reichen[1], Amelie Croset[1], Alessandra Villa[1], Christian Lizak[1], Anne Goubier[1], Roger Schibli[2], Daniel Steiner[1]. *[1]Molecular Partners AG, Schlieren, Switzerland,[2]Paul Scherrer Institute, Villigen, Switzerland*

The development of effective radioligand therapeutics (RLTs) is frequently hampered by the lack of high-quality targeting agents that selectively deliver radioactive payloads to the site of disease while sparing healthy tissues. Antibodies can have high affinity and specificity to tumor targets,

but their large size results in limited tumor penetration and long systemic half-life is frequently causing haematological toxicities. Alternatively, targeting agents with low molecular weight such as small molecules and peptides often suffer from limited affinity and specificity to the tumor target, resulting in off-target effects and limited tumor retention. DARPins (Designed Ankyrin Repeat Proteins) developed by Molecular Partners combine small size (15 kDa) and ideal binding properties. Due to their rigid-body target binding mode DARPins combine very high affinity and specificity and unless engineered accordingly, DARPins have very short systemic half-lives. Thanks to a simple and robust architecture, DARPins can be efficiently coupled with radioactive payloads, even at elevated temperatures; and they can tolerate sequence-engineering approaches, which are not compatible with other protein scaffolds. To establish the DARPin platform for RLT, we have used DARPin candidates against different tumor targets. We have previously shown that increasing affinity to the tumor target correlates with elevated tumor uptake and long tumor residence in preclinical mouse models. We now also show that DARPins exhibit a homogeneous and deep tumor penetration *in vivo* that is highly superior to antibody benchmarks. Globular proteins below 60 kDa in size are typically cleared from the bloodstream via the renal pathway. This generally results in a strong kidney accumulation of small sized, protein-based targeting agents and their coupled residualizing radionuclides, leading to dose-limiting kidney toxicities. To overcome this limitation, we have undertaken an extensive engineering approach of the DARPin scaffold. Our results show that sequence engineering strongly reduces kidney uptake of DARPins without affecting their tumor uptake. This effect was confirmed with independent DARPin candidates suggesting a general applicability of the approach. Combined with other orthogonal strategies, we are able obtain favourable tumor to kidney ratios in preclinical mouse models. These results show that our proprietary optimized DARPin platform offers an attractive solution to the limitations of protein-based targeting agents for RLT applications. Together with the fact that high-affinity DARPins can be generated against a large variety of tumor targets, we conclude that our platform provides a powerful basis for the development of next-generation RLTs. Several DARPin-RLT programs in indications with high unmet medical need are currently in development.

#5038

Evaluation of anti-tumor immunity in response to [^{177}Lu]Lu-PSMA in a mouse model of prostate cancer

Gemma Dias, Sarah Able, Irini Skaripa-Koukelli, Rachel Anderson, Gracie Wilson, Katherine A. Vallis. *Oncology, University of Oxford, Oxford, United Kingdom*

[^{177}Lu]Lu-PSMA improves progression-free and overall survival in metastatic castration resistant prostate cancer. However, the role of immune stimulation by molecularly targeted radionuclide therapy (MRT) is poorly understood. The aim of this study was to evaluate the anti-tumor immune response induced by [^{177}Lu]Lu-PSMA. The markers of immunogenic cell death (ICD), translocation of calreticulin (CRT) to the cell membrane, HMGB1 release and ATP release, were evaluated in the RM1 cell line (PSMA-negative murine prostate carcinoma) and its derivative, RM1-PGLS (stably transduced with human PSMA and SFG-EGFp/Luc), using flow cytometry, ELISA and a luminescence detection assay respectively. The *in vivo* biodistribution of [^{177}Lu]Lu-PSMA in RM1-PGLS tumor-bearing C57BL/6 mice was investigated using microSPECT-CT imaging, and the *in vivo* efficacy of [^{177}Lu]Lu-PSMA was tested in RM1-PGLS tumor growth inhibition studies. Vaccination/rechallenge experiments were performed to elucidate whether [^{177}Lu]Lu-PSMA elicits ICD *in vivo*. The Nanostring Pan Cancer Immune Profiling Platform was used to assess changes in the tumor immune microenvironment (TIME) in response to [^{177}Lu]Lu-PSMA. External radiation (EBRT; ^{137}Cs γ-radiation; 6-10 Gy) was used as a comparator treatment in most experiments. We observed a dose-dependent increase in cell surface CRT following [^{177}Lu]Lu-PSMA and EBRT at 24 and 72 h and of HMGB1 release in response to [^{177}Lu]Lu-PSMA and EBRT at 96 and 144 h. At 24 h following [^{177}Lu]Lu-PSMA (60 MBq) there was a significant increase in ATP release compared to untreated samples. Collectively these data indicate [^{177}Lu]Lu-PSMA causes ICD. A high RM1-PGLS tumor:muscle uptake ratio (210 ± 59) was noted in biodistribution experiments confirming highly specific tumor accumulation of [^{177}Lu]Lu-PSMA. In tumor growth inhibition studies the time for tumors to reach a volume of 400 mm^3 was delayed in mice treated with [^{177}Lu]Lu-PSMA (60 MBq) compared to no treatment (30 versus 21 days; $P<0.01$).

We showed that a subcutaneous inoculum of [^{177}Lu]Lu-PSMA (60 MBq)-treated RM1-PGLS cells prevents tumor growth in approximately 50% of cases on rechallenge with viable RM1-PGLS cells one week later. This indicates that [^{177}Lu]Lu-PSMA induces ICD *in vivo*. We observed a significant reduction in most tumor infiltrating lymphocyte (TIL) types at 2 days after *in vivo* exposure to [^{177}Lu]Lu-PSMA (80 MBq), followed by an increase in TILs by Day 7. The observed pattern is similar to that after EBRT (6 Gy). There was overlap in the top 10 differentially expressed genes (treatment versus no treatment) for the [^{177}Lu]Lu-PSMA and EBRT groups. The gene showing the greatest level of upregulation at day 7 in [^{177}Lu]Lu-PSMA-treated tumors, IDO1, is known to be involved in immune tolerance and radioresistance. In conclusion, [^{177}Lu]Lu-PSMA induces ICD *in vitro* and *in vivo* and modulates the TIME.

#5039

Development of a prostate cancer PDX model radioresistant to PSMA targeted radionuclide therapy

Maria Thaysen[1], Esben Christensen[1], Rikke N. Nielsen[1], Michael Wick[2], Mette M. Wessel[1], Lotte K. Kristensen[1], Sebastian Gnosa[1], Carsten H. Nielsen[1]. *[1]Minerva Imaging, Oelstykke, Denmark,[2]XenoSTART, San Antonio, TX*

Prostate cancer is the second most common cancer diagnosis worldwide and the fifth leading cause of cancer related death among men. Lutetium Lu 177 vivivotide tetraxetetan was recently approved by the FDA for treatment of prostate-specific membrane antigen (PSMA)-positive metastatic castration-resistant prostate cancer. However, not all patients respond to treatment and combination therapies may improve outcomes. One approach is to combine targeted radionuclide therapy with inhibitors targeting DNA damage response pathways such as ATM/ATR inhibitors to enhance the radiosensitivity of the cancer cells. Currently, models used to study radioresistance in prostate cancer are based on cancer cell lines or cell-line derived xenograft models, but these models do not account for the heterogenous and complex biology of the disease.
To overcome this issue, we aimed at developing a radioresistant PSMA positive prostate cancer patient-derived xenograft (PDX) model based on

the ST1273 model (XenoSTART). ST1273 originates from a sixty-five-year-old Hispanic male that did not receive treatment prior to sampling. The model is characterized by overexpression of androgen receptor and PSMA. Tumors were implanted in nude mice and radioresistance was induced by external beam radiation therapy (3x2Gy per cycle) until tumor growth was unresponsive to the treatment. Flow cytometry were applied to evaluate if altered proliferation rate or changes in the tumor microenvironment (TME) convers the resistance.
Out of five initially treated tumors, one tumor re-occurred after 19 days. Repeating the treatment led to an initial decrease in tumor volume but the growth delay was reduced to 12 days. A third treatment rendered the tumor resistant as tumor growth was unaffected. Current evidence confirms that radioresistance was maintained when passaging, and PSMA expression was unaffected. Next, we tested whether the tumor would also withstand targeted radionuclide therapy. Animals implanted with parental or radioresistant ST1273 tumors were treated with Lu177-PSMA-617 (5MBq, QW x2). The treatment reduced tumor size in both tumor types, but significantly less in the resistant model. Moreover, parental tumors had a significantly slower recurrence of 45 days compared to the resistant tumors that relapsed 24 days after the first dosing. Flow cytometry analysis of control and treated tumors (parental and radioresistant) showed that the radioresistance might be attributed to alterations in the cell cycle control. Altogether, we developed a PDX prostate cancer model that is resistance to external beam radiation and PSMA targeted radionuclide therapy. This model will allow us to further characterize radioresistance and evaluate combinatorial therapy in a clinically relevant model.

#5040

Novel HER3 targeting antibody radioconjugates, ^{225}Ac-HER3 ARC and ^{177}Lu-HER3 ARC, exhibit potent antitumor efficacy in HER3-positive solid tumors

Denis Beckford-Vera, Megan McCloskey, Jason Li, Caroline Jennings, Le-Cun Xu, Debbie Lewis, Patrik Brodin, Amanda Chin, Monideepa Roy, Mary Chen, Helen Kotanides. *Actinium Pharmaceutical, Inc., New York, NY*

Background: HER3 is a unique member of the EGFR family that collaborates with other EGFR receptors to induce tumorigenesis and drug resistance. Moreover, HER3 expression is linked to poor survival for patients with solid tumors. Despite HER3 being a rational cancer therapeutic target, no HER3-directed therapies have been approved for clinical use. However, new therapeutic strategies such as antibody drug conjugates (ADCs) are being investigated. Targeted radiotherapy, including radiolabeled antibodies (ARCs), is unique mechanistically by inducing cell death independent of biologic pathway inhibition, and can be efficacious with less toxicity relative to other therapeutic modalities. Therefore, we hypothesized that the cytotoxic effects of alpha (^{225}Ac) or beta (^{177}Lu) emitting radionuclides combined with the specificity of anti-HER3 antibody targeting is a compelling therapeutic approach for HER3-expressing tumors. Here we evaluated the antitumor effects of ^{225}Ac or ^{177}Lu armed HER3 ARCs across multiple HER3-expressing cancer models such as ovarian, colorectal, prostate, and renal cancer.
Methods: ARCs were prepared by radiolabeling AT-02, an anti-HER3 antibody, with ^{225}Ac or ^{177}Lu using *p*-SCN-Bn-DOTA to yield ^{225}Ac or ^{177}Lu-HER3 ARC. The binding activity and tumor cell cytotoxicity of HER3 ARCs were assessed by ELISA using human recombinant HER3, flow cytometry on HER3-expressing cells, and colony forming assays. To evaluate the antitumor growth effects of ^{225}Ac-HER3 and ^{177}Lu-HER3 ARCs in vivo, preclinical human tumor xenograft models were developed. Mice bearing HER3-positive tumors were dosed with ^{225}Ac-HER3 ARC (0.2 or 0.4 μCi), or ^{177}Lu-HER3 ARC (200 or 400 μCi) and tumor growth and body weight was monitored.
Results: The pharmacological binding properties of HER3 antibody radiolabeled with ^{225}Ac or ^{177}Lu were similar to that of unmodified antibody as demonstrated by HER3 binding ELISA and flow cytometry. HER3 ARCs induced cytotoxicity and inhibited colony formation of HER3-positive tumor cell lines. Significant in vivo human tumor xenograft growth inhibition was observed in response to ^{225}Ac or ^{177}Lu HER3 ARCs compared to control groups (unmodified AT02 or IgG ARCs) in the models studied. No significant loss of body weight was observed in mice treated with HER3 ARCs suggesting that all treatments were well tolerated.

Conclusions: In this study, both ^{225}Ac-HER3 ARC and ^{177}Lu-HER3 ARC demonstrated significant antitumor activity against HER3-expressing tumors in a dose-dependent manner. The HER3 targeted radiotherapy approach that we have undertaken could potentially overcome the limitations of current solid tumor therapies in resistance settings and warrants further evaluation in patients with HER3-expressing tumors.

#5041

TEM-1 targeted alpha therapeutic [Ac-225]-FPI-1848 induces regression in pre-clinical sarcoma xenograft models

Sean Collens, Nicole Robinson, Matt Moran, Ryan Simms, Yarina Storozhuk, Meiduo Hu, Natalie Grinshtein, John Forbes, Christopher P. Leamon, John Valliant. *Fusion Pharmaceuticals Inc. (Canada), Hamilton, ON, Canada*

Background**:** Tumor endothelial marker 1 (TEM-1 or CD248) is a cell surface receptor belonging to a family of C-type lectin transmembrane proteins. Identified as a fetal antigen, expression peaks during embryogenesis but is minimally detected in adulthood. In pathological conditions TEM-1 has been shown to be overexpressed in cancer and fibrosis. In sarcomas, expression occurs throughout the tumor environment in malignant cells, stromal cells and perivascular cells. The first line of treatment for sarcomas is surgical removal; however, many sarcomas arise in inoperable sites prompting a need for novel therapies. Herein, we describe the development of a novel TEM-1 targeting radiotherapeutic, [^{225}Ac]-FPI-1848, in mouse xenograft models of sarcoma.
Methods: [^{225}Ac]-FPI-1848 is a radioimmunoconjugate consisting of a humanized anti-TEM-1 monoclonal antibody conjugated to a proprietary DOTA-based chelate (FPI-1397) and radiolabeled with actinium-225 **[**^{225}Ac]. [^{177}Lu]-FPI-1835 is the lutetium-177 radiolabeled analogue. The biodistribution and therapeutic efficacy of these radioimmunoconjugates were evaluated in human sarcoma xenograft models using *nu/nu* mice of Balb/c background. For biodistribution studies, approximately 37 MBq/kg of [^{177}Lu]-FPI-1835 was injected intravenously into mice and tumor/organ radioactivity was quantified *ex vivo* at timepoints between 4 and 196 h. For therapeutic studies, a single intravenous dose of [^{225}Ac]-FPI-1848 was

administered over a dose range of 18.5 to 740 kBq/kg. Tumor size and body weight were monitored for 28 days.
Results: Biodistribution studies with [^{177}Lu]-FPI-1835 confirmed robust tumor uptake with minimal normal tissue uptake in three sarcoma models expressing high (SJSA-1), moderate (SK-N-AS) or low (A673) levels of TEM-1. Furthermore, the degree of uptake trended with TEM-1 expression levels across these models (SJSA1> SK-N-AS> A673). In corresponding therapeutic studies, [^{225}Ac]-FPI-1848 demonstrated dose-dependent efficacy consistent with tumor uptake. In the SJSA-1 model, tumor regression was observed at doses of 92.5 kBq/kg or greater. Tumor regression was observed at doses of 185 kBq/kg or greater in the SK-N-AS model. In the low TEM-1 expressing A673 model, significant tumor regression was only observed at the highest radionuclide dose level (740 kBq/kg). Overall, therapy was well tolerated with no significant loss of body weight or clinical signs of poor health.
Conclusions: [^{177}Lu]-FPI-1835 demonstrated target-dependent uptake consistent with the degree of TEM-1 expression in human sarcoma xenograft models. In turn, corresponding efficacy studies with [^{225}Ac]-FPI-1848 demonstrated strong dose-dependent, and target level-dependent efficacy with no apparent toxicity. These results suggest [^{225}Ac]-FPI-1848 could be a promising therapy for TEM-1 expressing sarcomas.

#5042
Anti-tumor activity of RYZ101 (Ac-225 DOTATATE) in somatostatin receptor-expressing preclinical models of small-cell lung cancer
Guangzhou Han, Eunmi Hwang, Fanching Lin, Renee Clift, Daniel Kim, Eric Bischoff, Susan Moran, Gary Li. *RayzeBio, Inc, San Diego, CA*

Introduction: Overexpression of somatostatin receptors (SSTRs), particularly SSTR2, is found in gastroenteropancreatic neuroendocrine tumors (GEP-NETs), and subsets of other solid tumors such as small-cell lung cancer (SCLC). β-emitting radiopharmaceutical therapy Lu-177 DOTATATE has been approved for SSTR-expressing (SSTR+) GEP-NETs, but the relatively low objective response rate and frequent post-treatment progression represent an unmet medical need. Based on preliminary clinical anti-tumor efficacy, RYZ101 (Ac-225 DOTATATE) is being developed for inoperable SSTR+ well-differentiated GEP-NETs with disease progression following Lu-177-somatostatin analogue (SSA) therapy (ACTION-1, NCT05477576). SCLC accounts for approx. 13% of lung cancer and lacks effective therapeutic options. Immunohistochemistry analysis indicates that ~50% of SCLC tumors are SSTR2+, with a substantial subset showing high and homogenous expression. The goal of this study was to provide preclinical support for RYZ101, as a single-agent or in combination with carboplatin and etoposide, for SSTR+ SCLC.
Methods: RYZ101 is comprised of the α-emitting radioisotope actinium-225, chemical chelator DOTA, and SSA octreotate (TATE). Binding affinity to human SSTR1-5 was determined using a competitive radioligand binding assay in engineered cell lines expressing individual SSTR. Internalization was measured by PathHunter SSTR2 Activated GPCR Internalization Assay. The preclinical biodistribution of RYZ101 was carried out in non-tumor-bearing BALB/c mice of both sexes. The efficacy studies were performed in cell line-derived and patient-derived xenograft (PDX) models of SCLC.
Results: In preclinical studies where Lanthanum (La^{3+}) was used as a surrogate for Ac-225, RAYZ-10001-La (La-DOTATATE) had high binding affinity (K_i=0.057nM) to human SSTR2 (>600-fold more potent than other SSTR subtypes) and exhibited efficient internalization. In a preclinical biodistribution study, RYZ101 performed similarly to Lu-177 DOTATATE. In multiple SCLC xenograft models, RYZ101 significantly inhibited tumor growth and prolonged survival, with deeper responses, including sustained regression, observed in the models with higher SSTR2 level. The anti-tumor effect was further enhanced when combining RYZ101 with carboplatin and etoposide at clinically relevant doses.

Conclusions: In summary, RYZ101 is a first-in-class, highly potent, α-emitting radiopharmaceutical therapy being developed for the treatment of SSTR+ solid tumors. Preclinical data demonstrate the potential of RYZ101 for the treatment of patients with SSTR+ SCLC.

#5043

Radium-223 demonstrates increased antitumor activity in combination with ^{177}Lu-PSMA-617 in the intratibial LNCaP xenograft model of bone metastatic prostate cancer

Arne Scholz[1], Matias Knuuttila[2], Justyna Zdrojewska[3], Mari I. Suominen[3], Esa Alhoniemi[4], Christoph A. Schatz[1], Sabine Zitzmann-Kolbe[1], Sanna-Maria Käkönen[2], Urs B. Hagemann[1]. *[1]Research & Development, Pharmaceuticals, Bayer AG, Berlin, Germany,[2]Aurexel Life Sciences Ltd., Askainen, Finland,[3]Pharmatest Ltd., Turku, Finland,[4]Inoi Oy, Turku, Finland*

Radium-223, a bone-specific alpha particle therapy, increased survival of patients with metastatic castration-resistant prostate cancer (mCRPC) and bone metastases (Parker *et al.,* NEJM 2013). ^{177}Lu-PSMA-617 is a small molecule radioligand that delivers beta-particle radiation to cancer cells expressing prostate-specific membrane antigen (PSMA). Despite improving overall survival of patients with heavily pretreated mCRPC (Sator *et al.,* NEJM 2021), responses to ^{177}Lu-PSMA-617 are often not durable and many patients develop progressive disease presumably due to microscopic osseous lesions. Compared to beta-particle radiation, alpha particles have a shorter range and higher linear energy transfer, making them more suitable for treating microscopic lesions. In this study, we evaluated preclinical antitumor efficacy and potential beneficial combination effects of radium-223 combined with ^{177}Lu-PSMA-617 in the intratibial LNCaP xenograft model mimicking progressive prostate cancer micrometastases in bone. LNCaP prostate cancer cells were inoculated into the right tibiae of male NOD.scid mice. Six weeks after inoculation, the mice were randomized to treatment groups based on serum prostate-specific antigen (PSA) and treated with two injections (Q4Wx2, i.v.) of vehicle, radium-223 (330 kBq/kg), ^{177}Lu-PSMA-617 (10 MBq) or their combination. ^{177}Lu-PSMA-617 was given 24 hours after radium-223. PSA and bone formation marker

procollagen type I intact N-terminal propeptide (PINP) were measured from blood samples and tumor-induced abnormal bone growth was determined by radiography. Terminal blood samples were analyzed for hematologic status at sacrifice.
The combination treatment of radium-223 and ^{177}Lu-PSMA-617 demonstrated robust antitumor efficacy, as indicated by lower serum PSA (mean change relative to pretreatment levels: 63.9 % vs 631 % (vehicle control), $p=0.026$), decreased tumor-induced abnormal bone area in tumor-bearing tibiae ($p<0.001$) and suppression of abnormal bone metabolic activity as evidenced by a reduced level of the bone formation marker PINP ($p<0.001$), compared with vehicle. Tolerability of the combination treatment was evidenced by the lack of significant body weight loss and the absence of cumulative hematological toxicity.
In conclusion, these preclinical results show that the combination of radium-223 and ^{177}Lu-PSMA-617 is well-tolerated and efficacious in inhibiting osseous tumor growth and improving response. The combination of radium-223 and ^{177}Lu-PSMA-I&T is currently being investigated in patients with mCRPC in a phase 1/2 trial (AlphaBet, NCT05383079).

#5044

Antitumor activity comparison of two somatostatin receptor ligands radiolabeled with Lutetium-177 (SSO110 and DOTA-TATE) alone or combined with chemotherapy in mice bearing AR42J SST2-positive tumors

Olivier Raguin[1], Marcel Krüger[2], Peggy Provent[1], Funda Cay[2], Elodie Marie dit chatel[1], Marie Lux[1], Stéphane Lezmi[3], Florence Meyer-Losic[3], Pascale Plas[3], Ben Pais[4], Cyril Berthet[1]. *[1]Oncodesign Services, Dijon Cedex, France,[2]Werner Siemens Imaging Center, Tübingen, France,[3]IPSEN, Les Ulis, France,[4]Ariceum Therapeutics, Berlin, Netherlands*

Only a limited number of studies have compared the therapeutic effects of repetitive cycles of radiolabeled somatostatin (SST) analogues or assessed potential synergy of these analogues with chemotherapy agents.
Hence, a comparison was conducted in an in vivo AR42J tumor model with an SST2 antagonist, [^{177}Lu]Lu-satoreotide tetraxetan ([^{177}Lu]LuSSO110),

and a SST2 agonist, [^{177}Lu]Lu-DOTA-TATE. The efficacy of treatment combining [^{177}Lu]Lu-satoreotide tetraxetan with capecitabine plus temozolomide was also assessed.
Swiss Nude mice were xenografted with AR42J tumor cells. For the evaluation of the tumor response to radiation therapy, animals received one weekly dose of [^{177}Lu]LuSSO110 or [^{177}Lu]Lu-DOTA-TATE for four consecutive weeks. For combined treatments, animals received one weekly dose of [^{177}Lu]LuSSO110 at 20 MBq for four consecutive weeks in association with daily doses of capecitabine and temozolomide (CAPTEM). Weekly treatment for four consecutive weeks with [^{177}Lu]LuSSO110 at 15 MBq revealed a significantly reduced tumor growth, with 68 days to reach a tumor volume of 850 mm^3, compared to [^{177}Lu]Lu-DOTA-TATE at 15 MBq or 30 MBq, with, respectively, 43 days and 48 days. This was associated with a 3.5 fold higher tumor uptake of [^{177}Lu]LuSSO110 (15 MBq) compared to [^{177}Lu]Lu-DOTA-TATE, with no or mild effects on body weight, hematological toxicity, or renal toxicity.
In AR42J tumor-bearing mice treated once a week for four consecutive weeks, [^{177}Lu]LuSSO110 (15 MBq) associated with CAPTEM regimen did not significantly increase the median time to reach a tumor volume of 1000 mm^3 as compared to treatment with [^{177}Lu]Lu-satoreotide alone: 50.7 vs 42.2 days, respectively. The association of the two treatments only led to mild weight losses.
Repeated administrations of [^{177}Lu]LuSSO110 were able to potentiate peptide receptor radionuclide therapy with a higher tumor uptake and longer median survival compared to [^{177}Lu]Lu-DOTA-TATE. The The combination of [^{177}Lu]Lu-satoreotide with capecitabine and temozolomide did not show any synergy, but no antagonism was observed either.

#5045
NTSR1-targeted alpha therapeutic [Ac-225]-FPI-2059 induces growth inhibition in a preclinical colorectal tumor model
Saleemulla Mahammad, Jaline Broqueza, Brigitte L. Theriault, John Forbes, Christopher P. Leamon, John Valliant. *Fusion Pharmaceuticals Inc. (Canada), Hamilton, ON, Canada*

Background: Neurotensin receptor 1 (NTSR1) is overexpressed in multiple cancer indications that include pancreatic, colorectal and prostate cancers, all of which have limited therapeutic treatment options and unmet medical need. Fusion is developing novel targeted alpha therapeutics (TATs) that enable the specific delivery of high energy alpha particles (actinium-225; [^{225}Ac]) to tumor cells while sparing surrounding normal tissues. The alpha radiation released by TATs causes cell damage through the induction of multiple double-stranded DNA breaks leading to tumor cell death. Here, we describe the therapeutic efficacy of an [^{225}Ac]-conjugated, NTSR1 targeting small molecule in a colorectal cancer tumor model.
Materials and Methods: CT26 colorectal cancer cells overexpressing murine NTSR1 (mNTSR1) were generated by lentiviral transduction. Selected cells were evaluated for stable mNTSR1 expression by an *in vitro* radioligand binding assay and subsequently implanted subcutaneously into Balb/c mice for *in vivo* evaluations. FPI-2056 (parent compound) was radiolabeled with either lutetium-177 ([^{177}Lu]-FPI-2057) or actinium-225 ([^{225}Ac]-FPI-2059). Biodistribution assessment studies were conducted in mice bearing CT26-mNTSR1 tumors dosed intravenously with [^{177}Lu]-FPI-2057. Therapeutic efficacy studies were conducted by intravenous administration of single doses of 0.185 - 5.55 MBq/kg of [^{225}Ac]-FPI-2059 (0.1-3 μCi) to animals bearing CT26-mNTSR1 tumors, followed by tumor growth monitoring for 50 days. Study endpoints included tumor volume measurements and impact on animal health status.
Results: Evaluation of [^{177}Lu]-FPI-2057 biodistribution and excretion revealed rapid renal clearance via urine with a clearance from the blood by 24 h. Uptake of [^{177}Lu]-FPI-2057 was detected in the CT26-mNTSR1 tumors with a maximum concentration of 7.0 %ID/g at 6 h post-injection, dropping to 4.6 and 2.8 %ID/g at 24 and 48 h post-injection, with 20-fold higher uptake in the tumor vs. blood levels at both 24 and 48h time points. Therapeutic administration of a single dose of [^{225}Ac]-FPI-2059 resulted in dose-dependent tumor growth inhibition at doses above 1.85 MBq/kg of [^{225}Ac]-FPI-2059 (1 μCi), which translated into increased survival compared to control animals.
Conclusion: These results demonstrate that targeted delivery of [^{225}Ac]-FPI-2059 to NTSR1 expressing tumors results in significant growth

inhibition and enhanced survival, thereby providing promising preclinical evidence to support the clinical development of [^{225}Ac]-FPI-2059.

#5046

Cerenkov luminescence imaging of interscapular brown adipose tissue using TSPO-targeting probe to overcome off-target effect of [^{18}F]FDG

Seok-Yong Lee[1], Ho Rim Oh[1], Young-Hwa Kim[2], Sung-Hwan Bae[2], Yongseok Lee[3], Yun-Sang Lee[4], Byung Chul Lee[5], Gi Jeong Cheon[6], Keon Wook Kang[7], Hyewon Youn[3]. *[1]Seoul National University College of Medicine, Seoul National University of Graduate School, Cancer Research Institute, Seoul, Korea, Republic of,[2]Seoul National University College of Medicine, Cancer Research Institute, Seoul, Korea, Republic of,[3]Seoul National University Hospital, Seoul, Korea, Republic of,[4]Seoul National University College of Medicine, Seoul National University of Graduate School, Seoul, Korea, Republic of,[5]Seoul National University Bundang Hospital, Seoul National University, Seongnam, Korea, Republic of,[6]Seoul National University College of Medicine, Seoul National University Hospital, Seoul, Korea, Republic of,[7]Seoul National University College of Medicine, Seoul National University of Graduate School, Seoul National University Hospital, Seoul, Korea, Republic of*

Aim/Introd**uction**: [^{18}F]fluorodeoxyglucose-positron emission tomography ([^{18}F]FDG-PET) has been used as an imaging methods for measuring interscapular brown adipose tissue (iBAT) activity. However, [^{18}F]FDG-PET has limitations for obtaining iBAT-specific images due to off-target effects with high uptake in skeletal muscle, tumors, and inflamed tissue. Uncoupling protein 1 (UCP1), a well-known biomarker for BAT, located in mitochondria also has been suggested as BAT imaging marker. Recently, UCP1 ThermoMouse was established as a reporter mouse for monitoring UCP1 expression. Translocator protein-18 kDa (TSPO) located in the mitochondria outer membrane along with UCP1 is overexpressed in BAT. TSPO targeting probe has been proposed as a potential imaging marker for iBAT imaging. To date, there have been no studies for BAT imaging using TSPO-targeting probe in UCP1 ThermoMouse reflecting UCP1 expression. Moreover, Cerenkov luminescence imaging (CLI) which captures Cerenkov radiation emitted from PET probes has been suggested as an alternative

option for PET. In this study, we aim to evaluate [^{18}F]fm-PBR28-d_2 as a TSPO-targeting probe for iBAT imaging using PET and CLI in the UCP1 ThermoMouse.
Materials and Methods: UCP1 ThermoMouse with insertion of a Luc2-T2A-tdTomato cassette into the initiation of codon of the Ucp1-coding sequence exon 1 were used to monitor UCP1 expression. UCP1 ThermoMouse were characterized with Western blotting and immunohistochemistry to measure the levels of UCP1 expression. PET images were acquired with SimPET, and optical images such as bioluminescence imaging (BLI), fluorescence imaging (FLI) and Cerenkov luminescence imaging (CLI) were acquired with IVIS 100.
Results: BLI or FLI reflecting UCP1 expression were clearly showed iBAT in UCP1 ThermoMouse. Also, UCP1 and TSPO expression were correlated in iBAT. TSPO-targeting PET probe with [^{18}F]fm-PBR28-d_2 showed iBAT-specific signals without off-target effect in brain or heart. In addition, [^{18}F]fm-PBR28-d_2 better reflected individual variation in different UCP1 expression than [^{18}F]FDG. In particular, higher molar activity of [^{18}F]fm-PBR28-d_2 was required to obtain better imaging quality of CLI as well as PET. In physiological changes such as cold stimulation and isoflurane exposure, we observed increased imaging signals with cold exposure and decreased imaging signals with prolonged isoflurane exposure.
Conclusions: We showed that the TSPO-targeting probe is superior to [^{18}F]FDG as a reliable imaging probe reflecting UCP1 expression in iBAT imaging. Probes with higher molar activity provide better images and are required for quantitative analysis of TSPO-CLI and PET. Our data suggest that CLI with TSPO-targeting probe could be an alternative option for PET.

#5047

PSMA-targeted actinium-225 conjugate (^{225}Ac-pelgifatamab) potentiates the antitumor efficacy of darolutamide in androgen-dependent and -independent prostate cancer models

Christoph A. Schatz[1], Bernard Haendler[1], Sabine Zitzmann-Kolbe[1], Aasmund Larsen[2], Hartwig Hennekes[1], Carsten H. Nielsen[3], Maria Z. Alfsen[3], Alan Cuthbertson[2], Stefanie Hammer[1], Arne Scholz[1], Urs B. Hagemann[1]. [1]*Research & Development, Pharmaceuticals, Bayer AG,*

Berlin, Germany,[2]Bayer AS, Oslo, Norway,[3]Minerva Imaging, Copenhagen, Denmark

Patients with advanced prostate cancer have few treatment options. While androgen receptor (AR) inhibitors are the standard of care for the systemic treatment, patients often develop resistance despite an initial response. Thus, novel therapeutic approaches are required. Prostate-specific membrane antigen (PSMA; *FOLH1*) is highly expressed in prostate cancer with limited expression in normal tissues. Therefore, PSMA presents an attractive target for radionuclide therapy and PSMA-targeted therapies have already shown efficacy in the clinical setting. Here, we evaluated the efficacy of ^{225}Ac-pelgifatamab, a PSMA-targeted actinium-225 conjugate, in combination with the AR inhibitor darolutamide in androgen-dependent and -independent prostate cancer models. AR inhibitors are known to upregulate PSMA expression, therefore providing a rationale for combining ^{225}Ac-pelgifatamab with darolutamide and potentially resulting in an enhanced treatment effect.

In vitro, darolutamide induced the expression of PSMA in androgen-dependent VCaP and androgen-independent 22Rv1 cells by more than 10-fold and 2-fold, respectively. The efficacy of darolutamide in combination with ^{225}Ac-pelgifatamab was synergistic in these cells with combination indexes of 0.12 and 0.47, respectively. In the androgen-dependent, patient-derived ST1273 model, a single i.v. injection of ^{225}Ac-pelgifatamab at 75 kBq/kg resulted in a treatment/control (T/C) ratio of 0.22 on day 30, while twice daily (BID) oral (p.o.) treatment with 100 mg/kg darolutamide showed a T/C ratio of 0.29. However, the combination of darolutamide and ^{225}Ac-pelgifatamab resulted in enhanced antitumor efficacy with a T/C ratio of 0.008. Furthermore, 5/10 mice remained tumor-free 86 days after the ^{225}Ac-pelgifatamab injection. In the androgen-independent cell line-derived 22Rv1 model, darolutamide (100 mg/kg, p.o., BID) monotherapy was not efficacious with a T/C of 0.84 on day 16 but a single i.v. dose of ^{225}Ac-pelgifatamab at 150 kBq/kg resulted in a T/C ratio of 0.69. Remarkably, the combination of darolutamide and ^{225}Ac-pelgifatamab resulted in further enhanced efficacy with a T/C ratio of 0.34. Flow cytometric analysis of isolated 22Rv1 tumors showed a 50-fold increase in PSMA expression upon darolutamide treatment compared with vehicle. Taken together, these

results suggest that upregulation of PSMA expression contributes to the higher efficacy observed when darolutamide is combined with ^{225}Ac-pelgifatamab.
In conclusion, our results provide a proof of concept for investigating the combination of ^{225}Ac-pelgifatamab with darolutamide in the clinical setting.

#5048
Combatting pancreatic cancer stem cells by novel titanium peroxides nanoparticles combined with X-ray radiation
Mohammed Salah[1], Hiroki Kawaguchi[2], Hiroaki Akasaka[3], Yasuyuki Shimizu[3], Kenta Morita[4], Yuya Nishimura[5], Hikaru Kubota[3], Tomomi Sogawa[3], Naritoshi Mukumoto[3], Chiaki Ogino[6], Ryohei Sasaki[3]. *[1]South Valley University, Qena, Egypt,[2]Division of Radiation oncology, Kobe University Graduate School of Medicine, Kobe City, Japan,[3]Division of Radiation Oncology, Kobe University Graduate School of Medicine, Kobe City, Japan,[4]Graduate School of Engineering, Kobe University Graduate School of Engineering,, Kobe City, Japan,[5]Kobe University Graduate School of Science, Technology and Innovation,, Kobe City, Japan,[6]Graduate School of Engineering, Kobe University Graduate School of Engineering, Kobe City, Japan*

Background: Radiotherapy is widely used as the main treatment for multiple malignancies. However, several types of cancers, including pancreatic cancer, show resistance to radiation therapy. The presence of cancer stem cells (CSCs) are the major cause of radiation resistance in pancreatic cancer. Whereas, titanium peroxides nanoparticles (TiOxNPs) which are a modified form of titanium oxide nanoparticles promote enhanced remarkable efficacy of radiation therapy. Therefore, we examined the efficacy of TiOxNPs as radiosensitizers to eradicate pancreatic cancer stem cells.
Methods and materials: In vitro, Sphere-forming assay, survival assay, migration, and invasion assay were evaluated after using TiOxNPs prior to radiation exposure to pancreatic cancer cell line. In vivo, tumor-bearing nude mice were injected by TiOxNPs either intratumoral or intravenous one hour prior to radiation treatment, and the tumor volume, body weight, and

mice survival was calculated. In addition, proteins-related stemness were measured in vitro and in vivo to evaluate the usage of TiOxNPs as radiosensitizers to pancreatic CSCs. Moreover, we planned to evaluate the mechanism beyond the efficacy of TiOxNPs as radiosensitizers to CSCs by detecting reactive oxygen species (ROS) production, mitochondrial function, and the phosphorylation of some signaling proteins. We found that TiOxNPs combined with ionizing radiation showed anti-cancer effects on radioresistant CSCs both in vitro and in vivo.
Results: In vitro, a marked reduction in growth was detected after exposing the TiOxNPs-treated cells to radiation therapy, specifically with a 5Gy dose compared with 2Gy dose. TiOxNPs exhibited a synergistic effect with radiation on pancreatic CSC-enriched spheres by downregulating self-renewal regulatory factors and CSC surface markers. In vivo, we first established an aggressive xenograft by injecting MIA PaCa-2 sphere cells into the flank region of BALB/c nude mice, and found that animals treated with combined TiOxNPs and irradiation showed a dramatic reduction in tumor volume and weight compared to the untreated group. Moreover, combined treatment suppressed epithelial-mesenchymal transition, migration, and invasion properties in primary and aggressive pancreatic cancer cells by reducing the expression of proteins relevant to these processes. Radiosensitizing TiOxNPs suppressed pancreatic xenograft outgrowth after primary or dissociating sphere MIA PaCa-2 cell implantation. It is assumed that synergy is created by inactivating the AKT signaling pathway and producing unbearable amounts of ROS.
Conclusion: Our findings showed that using TiOxNPs in combination with radiation might be a favorable therapeutic approach to eradicate pancreatic CSCs.

#5049

Pb-203 image guided Pb-212 receptor targeted alpha particle therapy for cancer - a powerful emerging paradigm

Michael King Schultz[1], Yusuf Menda[2], Dijie Liu[3], Mengshi Li[3], Frances Johnson[3], Brianna Cagle[3], Nicholas Baumhover[3], Ivy Vance[3]. *[1]University of Iowa, Hills, IA,[2]University of Iowa, Iowa City, IA,[3]Viewpoint Molecular Targeting, Inc., Coralville, IA*

Objective: Pb-203 and Pb-212 have emerged as a promising elementally-matched theranostic pair for imaging-guided alpha-particle radiotherapy for cancer. A somatostatin receptor 2 (SSTR2)-targeted peptide coupled with novel Pb specific chelator (PSC) has been developed (PSC-PEG2-TOC). Here, preclinical *in vitro* and *in vivo* evaluation of ^{203}Pb/^{212}Pb-labeled PSC-PEG2-TOC was conducted including head to head therapy of SSTR2+ tumors in mice vs standard of care beta particle therapy and first in humans clinical imaging of SSTR2+ tumors.
Method: [^{203}Pb]PSC-PEG2-TOC and [^{212}Pb]PSC-PEG2-TOC was prepared by published methods. Radiochemical stability of [^{203}Pb]PSC-PEG2-TOC, [^{212}Pb]PSC-PEG2-TOC and [^{212}Bi]PSC-PEG2-TOC in human serum was determined. Binding affinity of [^{203}Pb]PSC-PEG2-TOC was determined by binding assays in AR42J cells. *In vivo* SSTR2-mediated tumor targeting of [^{203}Pb]PSC-PEG2-TOC was determined by SPECT imaging in athymic nude mice bearing AR42J xenografts. *In vivo* biodistribution of [^{212}Pb]PSC-PEG2-TOC in normal organs and potential redistribution of ^{212}Bi daughter were determined in CD-1 Elite mice. Clinical imaging was conducted under appropriate regulations to determine the biodistribution of the agent in patients bearing SSTR2+ tumors as determined by gold standard 68Ga-DOTATOC PET imaging.
Results: Rapid incorporation of ^{203}Pb and ^{212}Pb in PSC-PEG2-TOC was observed after reactions at temperatures as low as 4ºC within 15 min. Greater than 95% radiochemical stability was observed for both [^{203}Pb]PSC-PEG2-TOC and [^{212}Pb]PSC-PEG2-TOC after incubation in human serum for up to 55 hours. Stable decay product [^{212}Bi]PSC-PEG2-TOC with minimal free ^{212}Bi was observed. Agents demonstrated superior binding affinity to SSTR2 with K_d=0.59 nM. In *in vivo* studies, rapid tumor uptake and renal clearance of [^{203}Pb]PSC-PEG2-TOC were observed in athymic nude mice bearing AR42J xenografts. In the biodistribution study, nearly identical biodistribution profiles of [^{212}Pb]PSC-PEG2-TOC and progeny [^{212}Bi]PSC-PEG2-TOC were found. No redistribution of ^{212}Bi activity was identified, indicating that ^{212}Bi remained co-localized with parent [^{212}Pb]PSC-PEG2-TOC *in vivo*. Therapeutic studies in this same mouse model resulted in 100% complete responses for both a single dose 4.4 MBq administration of [^{212}Pb]PSC-PEG2-TOC or a fractionated

regimen of 4 x 1.1 MBq. First in humans clinical imaging showed PK properties that included rapid tumor accumulation and retention at over 20 h post administration, coupled with fast renal clearance of residual agent. Conclusion: [^{203}Pb]PSC-PEG2-TOC and [^{212}Pb]PSC-PEG2-TOC have promising potential for image-guide alpha-particle therapy for SSTR2 positive tumors. Agents have received a Fastrack designation by the US FDA and a safe to proceed for a Phase 1 trial.

#5050

Case report: A 17-year-old patient developed glioblastoma secondary to intracranial germ cell tumor and was stabilized with chemoradiotherapy combined with Tumor Treating Fields

Shaoqun Li, Mingyao Lai, Hainan Li, Juan Li, Jiangfen Zhou, Qingjun Hu, Minting Ye, Ruyu Ai, Junqiao Zhu, Lijun Huang, Linbo Cai. *Guangdong Sanjiu Brain Hospital, Guangzhou, China*

Background: Germ Cell Tumor (GCT) is a rare intracranial tumor occurring in children and young adults. Some patients with GCT are curable with radiotherapy and chemotherapy. Due to long-term survival, the tumor secondary to radiotherapy is of concern. The treatment of the secondary tumor is less elaborated and worth exploring.
Case Presentation: Here we report a patient with GCT who developed radiotherapy-induced glioblastoma. He was diagnosed as pineal gland GCT at the age of 12. Afterwards, he underwent a set of treatments, including chemotherapy, radiotherapy, and surgery. Unfortunately, after 5 years of tumor-free survival, he developed an intracranial mass involved the right thalamus and brainstem, around pineal region. The GCT recurrence was firstly considered, however, the failure of 7 cycles of chemotherapy drew attention. Then brain biopsy underwent by ROSA robot showed high-grade glioma. Next Generation Sequencing showed *IDH*-wildtype, *MGMT* methylation, *CDKN2A/B* homozygous deletion, *EGFR* amplification, the +7/−10 signature, which supported the diagnosis of glioblastoma. Resection operation is not applicable for this patient as the involvement of thalamus and brainstem. Considering the difficulty of treatment and poor prognosis of glioblastoma, re-radiotherapy is a feasible choice. Chemoradiotherapy with Tumor Treating Fields (TTFields) is a innovative try for secondary glioblastoma in a 17-year-old patient. After the combination therapy, the

intracranial mass went regression and the patient has lived for more than 1 years.
Conclusions: For the patients with brain tumor who anticipate long-term survival, the secondary tumor after radiotherapy is of concern. Secondary Glioblastoma is rare and difficult to treat. Chemoradiotherapy with TTFields is a feasible and safe treatment option for some patients, but we need more evidence to support.

#5051
Assessment of boron delivery peptides with angiopep-2 for boron neutron capture therapy
Qi Liu, Jing Xiang, Lin Ma, Qiushi Ren. *Shenzhen Bay Laboratory, Shenzhen, China*

Boron neutron capture therapy (BNCT) induces intracellular nuclear reactions that release heavy charged particles to destroy cancer cells during thermal neutron radiation. In order to selectively eliminate cancer cells but avoid harmful effects to normal tissues, targeted delivery of boron-10 in cancer cells is required, whereas the conventional boron delivery agent phenylalanine (BPA) is unsatisfactory. Angiopep-2 is a cell-penetrating peptide that can trigger transcytosis and traverse the blood-brain barrier by recognizing low density lipoprotein-related protein 1. In this study, we developed angiopep-2 for boron delivery in BNCT. Angiopep-2 was labeled with boron-10 using solid-phase peptide synthesis with 4-carboxyphenylboronic acid and fluorenylmethyloxycarbonyl (Fmoc)-protected amino acids, namely ANG-B. Molecular mass of the synthesized ANG-B were validated by mass spectrometry. In a cell proliferation assay, little toxicity of ANG-B was detected. Boron concentrations in 6 cell lines from different cancer types and an intracranial glioblastoma mouse model after treatment with ANG-B or BPA were analyzed by ICP-AES. The in vivo distribution of ANG-B showed that the ratio of boron content of tumor tissue to that of blood (T/B ratio) was 9.42±2.47 at 4h post treatment, while the ratio of boron content of tumor tissue to that of normal brain tissue (T/N ratio) was 5.61±1.0, demonstrated an optimal tumor targeting ability of ANG-B. We further measured the effects of ANG-B in BNCT by clonogenic cell survival assay in vitro or by PET/CT imaging on a glioblastoma mouse model in vivo. Radiation for BNCT was given with

neutron flux at $3.0\pm0.4\times10^{11}$ n/cm^2. BNCT with 5 mM ANG-B resulted in 86.5%±5.3% clonogenic cell death, while the number was 72.9%±5.1% for BPA. The effect of ANG-B based BNCT in vivo was also better than BPA. The glioblastoma tumors in ANG-B treated group at 31 days after BNCT were shrank by 62.9% in average, while the BPA treated tumors shrank by only 23.0% ($P<0.05$). Therefore, we concluded that ANG-B is an efficient boron delivery agent, which may improve BNCT performance in clinical trials.

#5052

IB-DNQ enhances radiation induced ferroptosis in NQO1-positive cancer cells

Xiumei Huang[1], Xiaolin Su[1], Matthew W. Boudreau[2], Paul J. Hergenrother[2]. *[1]Indiana University School of Medicine, Indianapolis, IN,[2]University of Illinois at Urbana-Champaign, Urbana, IL*

Cancer is the second leading cause of death worldwide. Current treatments for solid cancers are associated with inherent resistance mechanisms and are ineffective against non-cycling cancer cells. Thus, there is a critical need to develop novel tumor-selective combination therapies to overcome resistance while optimally spare normal tissues. In this study, we investigate the mechanistic basis for tumor-selective potentiation of ionizing radiation (IR) in combination with IB-DNQ, a novel NQO1-bioactivatable agent. We found that combination of a low dose of ionizing radiation (IR, 2 Gy) with a sublethal dose of IB-DNQ dramatically increased Fe^{2+} leakage and induced elevated lipid peroxidation and ferroptosis in NQO1-positive cancer cells via upregulating the expression of ACSL4, a lipid metabolism enzyme required for ferroptosis. Knockdown of endogenous ACSL4 significantly inhibited lipid peroxidation via downregulating the expression of PTGS2 and dramatically inhibited the cell death that induced by IR or IB-DNQ alone or combination treatment. We further found that this combination treatment significantly decreased IR or IB-DNQ alone mediated upregulation of the expression of GPX4 that led to the accumulation of lipid peroxides, which suggests that IR or IB-DNQ-induced expression of GPX4 may function as a negative feedback loop to restore cell survival upon a sublethal dose of IR or IB-DNQ treatment. Finally, we demonstrated that this combination therapy synergistically suppressed tumor growth and

dramatically extended mouse lifespan in orthotopic pancreatic and non-small-cell lung cancer xenograft models. Together, our study provides novel preclinical evidence for new combination therapy in NQO1-positive solid tumors that may overcome IR-induced resistance.

#5053

A critical role for copper in enhanced radioirdide uptake in thyroid cancer cells

Katie Brookes[1], Ling Zha[1], Jana Kim[2], Vinodh Kannappans[3], Weiguang Wang[3], Kavitha Sunassee[2], Philip J. Blower[2], Vicki E. Smith[1], Martin L. Read[1], Christopher J. McCabe[1]. *[1]Institute of Metabolism & Systems Research, University of Birmingham (UK), Birmingham, United Kingdom,[2]School of Biomedical Engineering & Imaging Sciences, King's College London, London, United Kingdom,[3]Research Institute in Healthcare Science, University of Wolverhampton, Wolverhampton, United Kingdom*

New drug approaches are urgently required to improve radioiodide (RAI) uptake for efficient ablation of thyroid cancer cells in RAI-refractory disease. Employing high-throughput screening of FDA-approved compounds we recently identified drugs capable of robust induction of sodium iodide symporter (NIS) activity to promote RAI uptake[1]. In particular, a leading drug candidate - the well-established anti-alcoholism drug disulfiram (DSF) - had not been previously implicated in regulating NIS. Here, we demonstrate that the ability of DSF to increase RAI-uptake in thyroid TPC-1 (3.1-fold; $p<0.01$) and 8505C (4.9-fold; $p<0.001$) cells can be significantly potentiated by combination with Cu^{2+} to 5.1-fold and 18.9-fold increases respectively. Despite promising data, DSF is known to have poor bioavailability *in vivo* due to its rapid metabolism to diethyldithiocarbamate (DDC) within the stomach and circulation with subsequent methylation in the liver. Whilst methylated-DDC did not have any effect on NIS function, DDC chelated to divalent copper ions [$Cu(DDC)_2$] was highly effective at increasing RAI uptake (up to 8-fold; $P<0.001$) in multiple thyroid cell types and induced significant NIS protein expression (up to 36.2-fold; 250nM; $P<0.001$). Importantly, $Cu(DDC)_2$ retained the ability to enhance NIS function in thyroid cells ablated for

expression of either VCP or its co-factor NPL4, indicating its effect on NIS was via VCP-independent pathways. Instead, a transcriptional effect of $Cu(DDC)_2$ was revealed by significant induction of NIS mRNA levels in TPC-1 (8.5-fold; $P<0.001$) and 8505C (104.8-fold; $P<0.001$) cells. In wild-type Balb/c mice the intraperitoneal administration of albumin nano-encapsulated $Cu(DDC)_2$ significantly induced thyroidal uptake of technetium-99m (^{99m}Tc) after 30 min (~40% increase; n=11 per group; 3 mg/kg dose; $P<0.001$). Thus, our study demonstrates a promising drug strategy utilizing copper to significantly enhance NIS function with clinical potential to improve treatment effectiveness in RAI-refractory thyroid cancer patients.

[1]Read ML, Brookes K, Thornton CEM, Fletcher A, Nieto HR, Alshahrani M, Khan R, Borges de Souza P, Zha L, Webster JRM, Alderwick LJ, Campbell MJ, Boelaert K, Smith VE, McCabe CJ (2022) Targeting non-canonical pathways as a strategy to modulate the sodium iodide symporter. Cell Chem Biol. 29(3):502-516.e7.

#5054

The study of synergy mechanism between surufatinib and vinorelbine in the treatment of non-small cell lung cancer

Xiaoran wu[1], Yanfang Zheng[1], Lingyu qin[1], Ying li[1], Zhongjian yu[1], Xiongjie zhu[1], Rui cai[1], Feiyu niu[1], Yan yuan[1], Peng jiang[1], Shaoshi wen[2], Xing lv[2], Jiancai zhou[2]. *[1]The First Affiliated Hospital of Guangzhou Medical University, Guangzhou, China,[2]Hutchison MediPharma Ltd, Shanghai, China*

Background: The incidence and mortality rate of lung cancer ranks first among malignant tumors. Non-small cell lung cancer (NSCLC) is the most common pathological type of lung cancer. Combined use of targeted therapy can enhance the efficacy of chemotherapy drugs while reduce the related side effects in clinical practice. Surufatinib is a potent, small-molecule tyrosine kinase inhibitor (TKI), selectively targeting VEGF receptors (VEGFR) 1, 2, and 3, Fibroblast growth factor receptor 1 (FGFR1), and CSF-1R, which simultaneously prevents tumor angiogenesis and tumor immune evasion. Our clinical study (NCT04922658) has showed the promising effect and safety of surufatinib plus vinorelbine in NSCLC

patients, but the potential mechanism is still to be revealed. Herein, tumor-bearing models and cancer cell culture platform would be established for further studying, which may shed light on the synergy mechanism between surufatinib and vinorelbine, and guide the clinical treatment ultimately. Methods: Subcutaneous tumorigenesis in nude mice were successfully established, and then treated with related experimental drugs. The tumor size was observed and CD31 expression of tumor tissue was measured using immunohistochemical analysis. In vitro study, the A549 and PC9 cell multiplication capacities were measured by CCK8 assay and plate cloning assay. The abilities of cancer cell migration and apoptosis were detected using cell scratch assay and flow cytometry kit, respectively. Results: Monotherapy with surufatinib or vinorelbine showed a moderate tumor suppression, whereas the combination therapy of surufatinib and vinorelbine showed the remarkable inhibition of tumor growth in vivo. Surufatinib and the combination therapy obviously decreased the expression of CD31 in tumor issue which might cause the anti-angiogenesis. Monotherapy with surufatinib or vinorelbine significantly inhibited the proliferation of lung cancer cells (A549 cells and PC9 cells) in a concentration-dependent manner, and surufatinib could memorably promote the anti-proliferation activity of vinorelbine. As a result, combination therapy of surufatinib and vinorelbine distinctly inhibited lung cancer cell proliferation when compared with monotherapy with vinorelbine. Consistently, the synergistic effects of surufatinib plus vinorelbine were also observed in cell migration and apoptosis analysis. Conclusions: Synergistic effect of surufatinib and vinorelbine resulted in a conspicuous tumor regression, which is consistent with the clinical observation. In a depth data analysis, surufatinib enhanced the antitumor activity of vinorelbine probably by inhibiting tumor cell proliferation and migration, suppressing tumor angiogenesis and promoting tumor apoptosis in NSCLC patients.

#5055

Targeting $BRAF^{V600E}$/$NRAS^{Q61K}$-melanoma brain metastases by pharmacological intervention modulating ER/redox stress and EMT

Jana Jandova, Sophia L. Park, Jeremy A. Snell, Georg T. Wondrak.
Pharmacology and Toxicology, R Ken Coit College of Pharmacy and UA Cancer Center, The University of Arizona, Tucson, AZ

Intracranial melanoma metastases originating from peripheral malignancy remain a frequent clinical condition with unsatisfactory pharmacological options. After screening a focused library of clinical artemisinin-combination therapeutic (ACT) antimalarials with established brain availability, we report here that an oral antimalarial regimen {(*R*,*S*)/(*S*,*R*)-[2,8-bis(trifluoromethyl)quinolin-4-yl]-piperidin-2-ylmethanol; BQPM} blocks (*i*) melanoma cell invasiveness and EMT-related gene expression and (*ii*) tumor growth in a bioluminescent murine model of BRAFi-resistant intracranial melanoma. First, we examined apoptotic elimination of cultured malignant melanoma cell lines, also examining feasibility of overcoming BRAFi-resistance comparing isogenic melanoma cells that differ only by NRAS mutational status (BRAFi-sensitive A375-$BRAF^{V600E}$/$NRAS^{Q61}$ versus BRAFi-resistant A375-$BRAF^{V600E}$/$NRAS^{Q61K}$). Among ACT antimalarials tested, BQPM was the only apoptogenic agent causing melanoma cell death at low micromolar concentrations. Comparative gene expression-array analysis (A375-$BRAF^{V600E}$/$NRAS^{Q61}$ versus A375-$BRAF^{V600E}$/$NRAS^{Q61K}$) revealed that BQPM is a dual inducer of endoplasmic reticulum (ER) and redox stress responses that precede BQPM-induced loss of viability. Moreover, we observed that BQPM treatment blocked EMT-related gene expression and phenotypic invasiveness in both BRAFi-sensitive and -resistant human cell lines, observable also in murine CNS-tropic Ret-melanoma cells. These data (combined with clinical evidence that documents brain availability of BQPM) suggest that blockade of brain metastasis and inhibition of intracranial tumor growth, even if BRAFi-resistant, can be achieved using BQPM as a repurposed ACT-antimalarial.

#5056

ABN401 demonstrates robust anti-tumor efficacy in orthotopic PDX models of MET-driven NSCLC brain metastases in a pre-clinical study

Nirmal Rajasekaran[1], Kyung Eui Park[1], Saehyung Lee[1], Na Young Kim[1], Suk-Jae Chung[2], Young Kee Shin[3], Jun Young Choi[1]. *[1]ABION INC., Seoul, Korea, Republic of,[2]Seoul National University, Seoul, Korea, Republic of,[3]Graduate School of Convergence Science and Technology, Seoul National University, Seoul, Korea, Republic of*

Background Brain metastases (BM) are manifested in approximately 30-50% of patients with non-small cell lung cancer (NSCLC) and are associated with catastrophic implications on prognosis and survival. The development of blood-brain barrier-penetrant therapies for brain metastases of NSCLC is imperative and is a major clinical hurdle. ABN401, a highly potent and selective c-MET inhibitor, shows promising anti-tumor activity without significant safety concerns in patients with advanced NSCLC. Here, we report that ABN401 exhibits potent anti-tumor efficacy in pre-clinical orthotopic patient-derived xenografts (PDXs) derived from MET-driven NSCLC brain metastases.
Methods Anti-tumor efficacy of ABN401 was assessed in two lung cancer PDXs (LU5349 and LU5406) from BM models harboring high-level MET amplification grown in NOD/SCID mice. Subcutaneous PDXs (n=14/group) were treated with ABN401 (60 mg/kg QD, 125 mg/kg QD, and 165 mg/kg QD) or control groups. Established PDXs were orthotopically implanted into the brain (n=14/group) and were treated with ABN401 (125mg/kg QD), or control groups. The tumor volume of orthotopic model was monitored using magnetic resonance imaging (MRI). Brain, plasma, and tumor samples were collected for pharmacokinetics (PK) and pharmacodynamics (PD) correlation analysis.
Results The efficacy of ABN401(125 mg/kg QD) was confirmed in the subcutaneous PDX models (LU5349 and LU5406). Treatment with ABN401 showed up to 95% and 99% tumor growth inhibition in the LU5349 and LU5406 models, respectively. ABN401 (125 mg/kg QD) treatment induced complete or near-complete tumor growth regressions in the orthotopic tumor model. ABN401 also showed a desirable PK and safety profile with no significant changes in body weight.
Conclusions ABN401 treatment showed robust anti-tumor efficacy in PDX models of MET-driven NSCLC brain metastases. Our findings suggest that ABN401 has excellent potential for treating NSCLC patients with BM and supports its ongoing clinical development.

#5058

Impact of dexamethasone on chemotherapy response in ovarian cancer

Annapoorna Venkatachalam[1], Cristina Correia[1], Cordelia D. Mcgehee[2], Sarah Finstuen-Magro[3], Jamison VanBlaricom[3], Paula A. Schneider[4],

Kevin L. Peterson[4], Ethan P. Heinzen[5], Melissa C. Larson[6], Xiaonon Hou[3], Ann L. Oberg[7], Saravut John Weroha[8], Scott H. Kaufmann[9]. *[1]Molecular Pharmacology and Experimental Therapeutics, Division of Oncology Research, Mayo Clinic, Rochester, MN,[2]Molecular Pharmacology and Experimental Therapeutics, Mayo Clinic, Rochester, MN,[3]Oncology Research, Mayo Clinic, Rochester, MN,[4]oncology Research, Mayo Clinic, Rochester, MN,[5]4Division of Computational Biology, Department of Quantitative Health Sciences, Mayo Clinic, Rochester, MN,[6]Division of Computational Biology, Department of Quantitative Health Sciences, Mayo Clinic, Rochester, MN,[7]4Division of Computational Biology, Department of Quantitative Health Sciences, Research, Mayo Clinic, Rochester, MN,[8]Medical Oncology, Mayo Clinic, Rochester, MN,[9]Department of Molecular Pharmacology and Experimental Therapeutics; Oncology Research;Hematology, Mayo Clinic, Rochester, MN*

Background: Ovarian cancer ranks fifth in cancer deaths among women. The gold standard of care for advanced disease includes cytoreductive surgery along with adjuvant or neoadjuvant platinum/taxane-based chemotherapy. Although response to this treatment is high, chemotherapy-induced nausea and vomiting due to platinum agents and allergic reactions due to both agents are common. For nearly half a century, the glucocorticoid (GC) dexamethasone (DEX) has been administered as part of supportive care. However, there have periodically been questions about the possible deleterious effects of DEX on chemotherapy response, especially in solid tumors.
Methods: Platinum-sensitive, glucocorticoid receptor (GRα) expressing ovarian cancer cells were exposed to DEX prior to chemotherapy and clonogenic survival was assessed. The effects of DEX on cell cycle and apoptosis were assessed by flow cytometry. Changes in the tumor cell transcriptome after acute DEX treatment were determined by RNA sequencing. Mice bearing orthotopic ovarian cancer patient-derived xenografts (PDXs) were treated with chemotherapy ± DEX to assess changes in chemotherapy response *in vivo.*
Findings: DEX pre-treatment decreased platinum cytotoxicity in ovarian cancer cell lines *in vitro* and diminished platinum response in some PDXs analyzed for chemotherapy response *ex vivo*. RNA-seq analysis revealed

changes in transcripts encoding proteins involved in platinum detoxification and TNFα pro-survival signaling. In ovarian cancer PDXs, DEX decreased platinum response in one model and had limited impact on both platinum and platinum/taxane chemotherapy in three distinct studies.
Interpretation: DEX appears to modulate chemotherapy response in some settings *in vitro* and *ex-vivo*. The impact of DEX on chemotherapy response *in vivo* appears to be limited. However, further investigation of this question *in vivo* in non-immunosuppressed murine models appears warranted.

#5059
High-throughput monitoring of proteoforms and pathways through multiplexed and customizable mass spectrometry assay panels
Sebastian Müller, Véronique Laforte, Simonas Savickas, Maik Müller, Yuehan Feng, Lukas Reiter. *Biognosys AG, Schlieren, Switzerland*

Proteins represent a key class of analytes in pharmacodynamic (PD) analysis, an essential component in preclinical and clinical studies which inform about a biological system's response to drug treatment. Pharmacodynamic signatures typically comprise target engagement marker and downstream pathway markers. With recent development in targeted therapies and novel therapeutic modalities such as protein degraders, the scope of PD has widened to cover predictive and stratification biomarkers which can inform patient selection and contribute to further understanding of potential drug resistance.
Using peptides as surrogate for proteins of interest, mass spectrometry (MS)-based approach alleviates the barriers of reagent specificity of antibody-based methods which can be affected by species and matrices used in preclinical drug development. Moreover, the use of stable-isotope labeled standard (SIS) reference peptides grants targeted MS assays unraveled specificity and the ability to determine absolute quantity of a given analyte. Harnessing the power of targeted MS, we present an oncology-focused assay repository which contains 804 peptides corresponding to 582 proteins. All 804 peptide surrogates were chosen under strict selection criteria such as uniqueness/proteotypicity and stability. Off-the-shelf availability (PQ500 kit) of SIS reference peptides for all 582 proteins facilitates the deployment of any of these assays in a plug-and-play manner. The collection of 582 protein targets cover > 180 cellular pathways

(Reactome pathways e.g. cytokine signaling, cell-cell communication, activation of matrix metalloproteinases) together with 49 FDA-approved drug targets. To further evaluate the performance of these assays, we carried out a case control study comprising plasma samples from 5 patient groups (lung, colorectal, pancreatic, breast and prostate cancer) and age and gender-matched healthy subjects. In total, we measured absolute quantities of 582 proteins across 180 plasma samples while validating the expression profiles of well-characterized biomarkers in patient plasma.
To conclude, we've demonstrated the application of targeted MS approach for the routine analysis of pharmacodynamic biomarkers. Its multiplexing capability, together with the adaptability to various species allow this method to maneuver through preclinical and clinical scenarios.

#5060

Tucatinib does not alter oxaliplatin PK or associated renal function: An OCT2 and MATE transport inhibition study

Ariel R. Topletz-Erickson[1], Anthony Lee[2], Vineet Kumar[2], Michelle Ubowski[3], JoAl G. Mayor[3], Layth I. Abdulrasool[3], Clark M. Henderson[2], Joseph A. Ware[4], Christopher J. Endres[1]. *[1]Clinical Pharmacology and Pharmacometrics, Seagen, Bothell, WA,[2]Translational ADME and PKPD, Seagen, Bothell, WA,[3]Clinical Development, Seagen, Bothell, WA,[4]Clinical Pharmacology and Pharmacometrics, Seagen, South San Francisco, CA*

Background**:** Oxaliplatin (OX)-containing regimens are frequently utilized to treat gastrointestinal (GI) cancers. OX is eliminated predominately via urinary excretion (GFR and active tubular secretion). The contribution of active transport via OCT2 and MATE1/2-K to OX clearance is not fully understood. Tyrosine kinase inhibitors (TKIs) are frequently found to interact with OCT2/MATE transporters; however, a gap in knowledge remains between their clinical potential to impact OX pharmacokinetics (PK) and in turn, impact renal function. Tucatinib (TUC) is a highly selective human epidermal growth factor receptor 2 (HER2)-directed TKI approved in multiple regions in combination with trastuzumab and capecitabine for adult patients with metastatic HER2+ breast cancer and is currently being investigated in other HER2+ tumors. TUC inhibits OCT2/MATE-mediated transport of metformin and creatinine in vitro and

in vivo. In this study, we investigated the impact of TUC on OX plasma PK, OX renal clearance (Clr), and renal function.
Methods: In vitro inhibition of OCT2/MATE-mediated transport of OX by TUC was assessed in OCT2, MATE1, or MATE2-K-expressing MDCK-II cells. SGNTUC-024 (NCT04430738) is a Ph1b/2 clinical study in patients with HER2+ GI cancers evaluating the impact of TUC on the safety and PK of OX. Patients received TUC 150 mg (Cohort 1A) or 300 mg (Cohort 1B) BID starting on C1D8 of a 2-week cycle in combination with modified FOLFOX6/7. Intensive PK was collected in plasma and urine for OX alone (C1D1) or with steady-state TUC (C2D1). Total plasma platinum (Pt, analyzed as a surrogate for OX and catabolites), plasma Pt ultrafiltrate (PUF, unbound), and urine Pt were quantitatively analyzed via ICP-MS. Serum Cystatin C (CysC) was measured as a pharmacodynamic (PD) renal function marker in Cohorts 1A and 1B.
Results: TUC inhibited in vitro OX transport by MATE1 (IC_{50} = 0.0639 μM), MATE2-K (IC_{50} = 0.0382 μM), and OCT2 (IC_{50} = 0.491 μM). In 11 patients, total Pt and PUF $AUC_{0\text{-}8h}$ geometric mean ratio (GMR) and 90% confidence intervals (CI) between patients who received OX alone compared to in combination were 1.1 (0.98, 1.3) and 1.0 (0.78, 1.4) in Cohort 1A (n=4) and 1.1 (0.96, 1.2) and 1.0 (0.98, 1.1) in Cohort 1B (n=7), respectively. OX GM (%CV) renal clearance ($Cl_{r,0\text{-}8h}$ in mL/min) and fraction excreted 24h post-dose ($f_{e,0\text{-}24h}$) were similar with and without TUC in both Cohort 1A (C1D1 $Cl_{r0\text{-}8h}$ = 277 (33), $f_{e,0\text{-}24h}$ = 22% (17); C2D1 $Cl_{r0\text{-}8h}$ = 249 (78), $f_{e,0\text{-}24h}$ = 21% (15)) and Cohort 1B (C1D1 $Cl_{r0\text{-}8h}$ = 189 (37), $f_{e,0\text{-}24h}$ = 17.7% (16); C2D1 $Cl_{r0\text{-}8h}$ = 177 (40), $f_{e,0\text{-}24h}$ = 16.6% (35)). Reversible slight increases in CysC (normalized to baseline) on day 3 of each cycle, irrespective of tucatinib, were observed.
Conclusions: This investigation of in vitro and in vivo determinants of OX PK demonstrates that TUC does not alter the renal clearance of oxaliplatin nor renal function when OX is administered in combination with TUC.

#5061
Toxicological characterization and comparison of ATR inhibitors in mice
Joshua J. Deppas[1], Brian F. Kiesel[1], Jianxia Guo[2], Lora H. Rigatti[3], Joseph Latoche[4], Anthony Green[5], Paul Knizner[5], Christopher J. Bakkenist[6], Jan

H. Beumer[1]. *[1]Pharmaceutical Sciences, University of Pittsburgh, Pittsburgh, PA,[2]Cancer Therapeutics Program, UPMC Hillman Cancer Center, Pittsburgh, PA,[3]Division of Laboratory Animal Resources, University of Pittsburgh, Pittsburgh, PA,[4]Medicine, University of Pittsburgh, Pittsburgh, PA,[5]Biospecimen Core Research Histology, University of Pittsburgh, Pittsburgh, PA,[6]Radiation Oncology, University of Pittsburgh, Pittsburgh, PA*

Cancer is often treated with DNA-damaging cytotoxic and ionizing radiation (IR) therapies. However, anticancer efficacy is limited by activation of DNA damage response (DDR) pathways that support DNA repair resulting in cancer cell survival. Disruption of DDR pathways may enhance cancer cell sensitivity to DNA-damaging therapies. Ataxia telangiectasia and Rad3 related (ATR) protein kinase, an apical initiator of DDR, is highly relied on by tumor cells and is critical for survival. Pharmacological ATR inhibitors (ATRi) can sensitize cancer cells to DNA damaging therapies. Although combining radiation therapies with ATRi may enhance anticancer efficacy, the resultant toxicity to normal organs is largely unknown. The ATRi furthest in development are the orally administered AZD6738 (ceralasertib), BAY-1895344 (elimusertib) and the intravenously administered M6620 (berzosertib, VX-970). We aimed to characterize and compare the preclinical toxicity of ATRi with and without total body irradiation (TBI) by pathology and complete blood counts (CBC). To determine the appropriate TBI dose for combination with ATRi, female balb/c mice (n=6) were grouped to receive 2, 4, 6 or 8 Gy. Within these cohorts, mice (n=2) were subdivided for euthanization times of 48, 72 and 96 h post TBI. Next, mice (N=5) were treated with a single dose of ATRi, 6 Gy TBI, the combination (TBI within 30 min of ATRi), or control. Mice were euthanized 48 h post treatment and blood was collected for analysis of CBC. Changes to body weight were documented and tissues with known sensitivities to radiation-related toxicity were collected for histopathology. Statistical analyses were performed using ANOVA with Tukey's multiple comparisons test. A 6 Gy TBI dose and 48 h euthanasia time point were selected for investigation in combination studies with ATRi. TBI alone resulted in ~5% decreased body weight compared to vehicle controls. The addition of any ATRi appeared to ameliorate this loss,

but not to a significant extent. TBI caused leukocytopenia and lymphocytopenia, which was not exacerbated by the addition of any ATRi. Neutrophilia was observed after ATRi alone and abolished by addition of TBI. TBI caused moderate toxicity in spleen, small intestine and bone marrow, and the addition of ATRi did not exacerbate these findings. AZD6738 caused moderate pericarditis and myocarditis, which was abrogated by the addition of IR. Collectively, ATRi administered alone are associated with neutrophilia at 48 h. AZD6738 appeared to be associated with cardiac toxicity, consistent with clinical observations of related CHK1 inhibitors. M6620 alone is associated with a significant decrease in lymphocytes compared to vehicle control, however in the setting of TBI, M6620 appears to ameliorate TBI-induced lymphocytopenia. This study demonstrated that the addition of ATRi did not increase toxicity associated with TBI in mice.

#5062

Small molecule superoxide dismutase mimetic avasopasem manganese for the mitigation of cisplatin induced ototoxicity

Keegan A. Christensen[1], Osama Tarabichi[1], Sei Sho[1], Hidaly Hernández[2], Bryce Hunger[1], Melissa A. Fath[1], Jeffery Keene[3], Robert Beardsley[3], Marlan Hansen[1], Douglas R. Spitz[1]. *[1]Carver College of Medicine, University of Iowa, Iowa City, IA,[2]Wartburg College, Waverly, IA,[3]Galera Therapeutics, Malvern, PA*

Introducti**on**: Avasopasem manganese (GC4419) is a selective superoxide dismutase mimetic which has recently completed a Phase 3 clinical trial (NCT03689712) demonstrating a significant reduction in the severity of oral mucositis in patients receiving standard cisplatin and radiotherapy for head and neck squamous cell carcinoma (HNSCC). Up to 66% of HNSCC patients experience ototoxicity from platinum-based chemotherapy, resulting in tinnitus and hearing loss. The analysis of clinical trial data also revealed that patients treated with GC4419 in addition to cisplatin (cis) and radiotherapy reported less tinnitus than those treated with standard therapy alone. The generation of reactive oxygen species has long been recognized as an important contributor to cis-induced hearing loss; therefore, we hypothesize that administration of GC4419 with cisplatin can prevent ototoxicity by scavenging superoxide.

Results: Organotypic cultures using postnatal day 2 or 3 mouse cochlea were treated with cis 4 μM and 0.5, 2, or 4 μM GC4419 for 24 hours. The explants were then stained for anti-myosin-VIIa. Hair cells were counted, and it was determined that 4 μM cis was sufficient to cause a decrease in hair cell numbers and GC4419 dose as low as 2 μM protected against this biological endpoint. To assess the effects of GC4419 on hearing loss *in vivo*, CBA/CaJ mice were treated as follows: 5 mice (1 female, 4 males) received 3 mg/kg cis IP, 4 mice (2 males and 2 females) received vehicle, 3 mice (2 females, 1 males) received 10 mg/kg IP GC4419, and 5 mice (2 females, 3 males) were treated with GC4419 10 minutes prior to cisplatin injection. Cis and GC4419 were administered for four consecutive days followed by two days of GC4419. The animals were allowed 8 recovery days, with Normosol SQ and high calorie food administered, prior to a second repetition of the treatment cycle. This protocol for cis dosing was found to be lethal in three mice in the cisplatin only group. Auditory brainstem response testing was performed before and after treatment, revealing elevated hearing thresholds in cis treated mice but not in mice treated with GC4419 and cis. Additionally, the cis treatment group experienced greater weight loss than the mice treated with GC4419 and cis Separately, in an H1299 tumor xenograft model in nu/nu mice, GC4419 5 mg/kg IP BID over 14 days was shown not to interfere with, and in fact somewhat increased, the tumor growth delay with cis 5 mg/kg IP QW x 3. **Conclusion**: These results support the hypothesis that treatment with the SOD mimetic GC4419 can reduce cis induced ototoxicity by scavenging superoxide and justify further studies to determine if this mechanism based approach can be implemented in cancer therapy. (Supported by a sponsored research agreement between the University of Iowa and Galera Therapeutics, Inc.)

#5063

Optimizing benefit/risk in oncology: Review of post marketing dose optimization

Pooneh Soltantabar, Hoi-Kei Lon, Kourosh Parivar, Diane Wang, Mohamed Elmeliegy. *Pfizer, Inc., San Diego, CA*

Introducti**on:** Molecularly targeted (MTAs) and immune-oncology (IO) agents are more selective with wider therapeutic window than cytotoxic

agents resulting in maximal activity at doses < MTD. However, these agents commonly selected the MTD (or highest tested dose) which is assessed using dose-limiting toxicities in escalating doses in limited number of patients/dose. This led to several post-marketing requirement (PMR) studies to evaluate alternative dosing regimens to optimize the benefit-risk.
Methods: Post-marketing dose optimization studies (required by FDA or sponsor initiated) for oncology MTAs/IO agents were reviewed. These studies/analyses were classified in to attempts to improve efficacy, safety, or 'life cycle management' (ie, fixed vs body size-based dosing, favorable route of administration, or extending the dosing interval). Approvals 1999-April/2022 were evaluated using FDA review documents and published literature. PMR studies for organ impairment, DDI, or food effect were excluded.
Results: Overall, 27 (16 MTAs and 9 IO) out 126 FDA oncology approvals reviewed were identified to have conducted post-approval dose optimization studies (27/126, 21.4%). Dose optimization studies were either efficacy-driven (n = 4), safety-driven (n = 13), or to improve method of administration (ie, IV to SC route; body-weight to fixed dosing; less dosing frequency) (N = 14). Efficacy-driven PMRs evaluated a higher dose either for the overall population (1/4) or for a subgroup with lower exposure (3/4); the latter cases showed no clear benefit in this subgroup vs case-matched subgroup from the control arm. No changes of label dosing recommendations resulted from efficacy-driven PMRs. All safety-driven PMRs which evaluated lower doses were for drugs with a positive exposure-safety relationship and most had a flat exposure-efficacy relationship (9/13, 69%) suggesting that a lower dose might improve safety without compromising efficacy. Completed safety-driven PMR studies resulted in changing the approved dose in 2/7 cases (29%). Lower doses were commonly associated with better safety profiles, however, establishing efficacy non-inferiority vs approved doses was typically not successful except in 1 case where non-inferiority was met for the primary endpoint of overall survival; this did not lead to label change as secondary endpoints, eg, PFS, favored the higher dose.Attempts to improve method of administration tended to be feasible and resulted in a successful change of the label dose for drugs with relatively flat exposure-efficacy and safety profiles and with adequate efficacy/safety data at multiple dose levels.

Conclusion: Our results suggest that safety or efficacy-driven post-marketing dose optimization studies were rarely successful in changing the label dose. Dose optimization could be more important for drugs with a steep exposure-safety relationship and a flat exposure-efficacy relationship.

Tyrosine Kinase and Phosphatase Inhibitors 1

#4004
Targeting drug-resistant acute myeloid leukemia (AML) cells using novel casein kinase II (CK2) inhibitor

Koby Duke[1], Katherine Mercer[2], Rajesh Rajaiah[1], Muhammad Daniyal[1], Yi Qiu[1], Ashok Purandare[3], Yasin Uzun[1], Lijun Zhang[4], Morgann Klink[4], Chandrika Gowda[1]. *[1]Pediatrics, Penn State Hershey - College of Medicine, Hershey, PA,[2]Penn State Health Milton S. Hershey Medical Center, Hershey, PA,[3]Bristol-Myers Squibb, Princeton, NJ,[4]Penn State Hershey - College of Medicine, Hershey, PA*

Introduction: Protein Kinase CK2 level and activity are high in Acute Myeloid Leukemia (AML) stem cells. Genetic inhibition of CK2 promotes apoptosis and shows synergistic cytotoxic activity with cytotoxic therapy. Here we report the anti-leukemia efficacy of a novel and potent small molecule inhibitor of CK2, BMS-135, in AML mouse models.
Methods: AML cell lines (n=8) and primary AML cells (n=3) representing various AML genetic subtypes (MLL rearranged, FLT3-ITD, TP53 mutation) were tested in vitro. Cells were treated with serial dilution of BMS-135 for 24 to 48hrs, and cell viability was measured using calorimetric cell viability (WST) assay. Similarly, treated cells were analyzed for cell cycle distribution, apoptosis, and colony formation. We measured the mRNA and protein levels of known CK2 targets. RNA sequencing and gene expression analysis was done to evaluate gene expression changes following treatment with BMS-135. Cell line-derived xenograft and patient-derived xenograft of AML were treated with BMS-135 at a dose of 7.5mg/kg oral gavage twice daily for 21 days or vehicle.
Results: Combined *in vitro* and *in vivo* experiments establish the efficacy of BMS-135. Cytotoxicity at inhibitory concentrations of 30-800nM, G0-G1 cell cycle arrest, increased apoptosis, and poor colony formation following treatment were noted consistently in all cells. Single-drug treatment with

BMS-135 achieved 50-80% leukemia inhibition and significantly prolonged survival in treated mice after 3 weeks of therapy. Following in vivo treatment with BMS-135, we confirmed the inhibition of known CK2 targets (AKT, PI3K, Bcl-xL) in the bone marrow and spleen AML cells. No significant myelosuppression or organ toxicity was noted in tumor-bearing mice following 3 weeks of treatment when compared to vehicle-treated mice. BMS-135 shows synergistic cytotoxic activity with daunorubicin and cytarabine.
Conclusions: Selective inhibitor of CK2 is well tolerated and shows superior in vivo efficacy and target inhibition in a series of AML cells and xenografts. BMS-135 works synergistically with cytotoxic agents like daunorubicin and cytarabine. These results support further pre-clinical characterization and clinical development of BMS-135 for treating AML in combination with cytotoxic therapy.

#4005

PH009-1, a highly potent and selective fourth-generation EGFR-TKI overcoming EGFR common mutations and T790M/C797S-mediated resistance in NSCLC

Feng Gao[1], Bin Liu[1], YongYong Wu[1], Liandong Jing[1], Pengzhi Zhang[1], Jing Wang[1], Shuai Yuan[1], Hui Zhao[1], Yu Gao[1], Zhizhong Li[2], Xiaofan Wang[3], Yongqi Guo[1]. *[1]Puhe Biopharma, Beijing, China,[2]Shiyu Children Foundation, Beijing, China,[3]Duke University Medical Center, Durham, NC*

Background: Epidermal growth factor receptor (EGFR) activating mutations have been reported in 10-50% of patients with non-small cell lung cancer (NSCLC). The common mutations, ex19del (D) and L858R (L) substitution, are sensitive to first- and second-generation EGFR-TKIs. However, acquired on-target resistance, especially T790M (T) mutation, comprises the anti-tumor effects of these inhibitors. Though the third-generation EGFR-TKI Osimertinib potently inhibits both EGFR common mutations and T790M mutation, 10-24% of patients acquire C797S (C) resistant mutation. Here, we report a highly potent and selective fourth-generation EGFR-TKI, PH009-1, designed to overcome both EGFR common mutations and T790M/C797S-mediated resistance in NSCLC.
Methods: Kinase selectivity of Ph009-1 was assessed by KINOMEscan against 468 human kinases. A functional safety panel including 47 targets

contributing to clinical adverse drug reactions was used to evaluate pharmacological profiling of PH009-1. Biochemical enzyme activities were detected with kinase assays and anti-proliferative activities were measured in various tumor and engineered Ba/F3 cell lines. The *in vivo* anti-tumor efficacy was tested in four cell derived xenograft (CDX) mouse cancer models with tumor harboring single, double or triple mutant EGFR. The *in vitro* and *in vivo* pharmacokinetic (microsome metabolic stability, hepatocyte metabolic stability, plasma protein binding, drug-drug interaction, oral absorption, et al) and safety properties (hERG potassium channel assay, Ames assay, repeated dosing study, et al) of PH009-1 were assessed in various species with corresponding assay methods.
Results: High kinase selectivity and very low off-target effects were observed in KINOMEscan and safety panel assays, respectively. PH009-1 inhibited kinase activity of all tested EGFR mutants with IC_{50}<4 nM. Furthermore, PH009-1 displayed potent anti-proliferation activity against Ba/F3 (EGFR L, D, LC, DC, DT, LTC, DTC) with IC_{50} of 3.6, 3.1, 1.6, 1.7, 0.3, 3.9, 3.1 nM, respectively. Excellent selectivity of PH009-1 was observed when compared the above values to IC_{50} against Ba/F3 (WT, 93.3 nM), A431 (WT, 2415 nM), LoVo (WT, 3700 nM) and NCI-H23 (WT, 2359 nM). In all four CDX cancer models including HCC827 (D), Ba/F3 (DC), Ba/F3 (LC) and Ba/F3 (DTC), PH009-1 at a dose of 40 mg/kg BID induced tumor regression or eradication without significant effect on mouse body weight. Favorable pharmacokinetic and safety profiles were suggested in *in vitro* and *in vivo* pharmacokinetic and safety evaluations.
Conclusion: The present data suggest that PH009-1 is a promising and highly selective fourth-generation EGFR TKI with potent *in vitro* and *in vivo* activity against single, double and triple EGFR mutations including T790M and C797S.

#4006

TRX-221, a novel 4th-generation EGFR inhibitor for overcoming C797S mutation-mediated acquired resistance in NSCLC

Sumin Lim[1], Seulgi Choi[1], Ju-Kyung Lee[1], Eunhyun Choi[1], Sungwon Lee[1], Kwangwoo Chun[1], Myoungki Baek[1], Jiyeon Park[1], Jihyun Kim[1], Areum Kang[1], Younghoon Kim[2], Namkyoung Kim[2], Byoungchul Cho[3], Taebo Sim[2], Koo Lee[1]. *[1]Therapex Co., Ltd, Seoul, Korea, Republic of,[2]Sevrance*

Biomedical Science Institute, Yonsei University College of Medicine, Seoul, Korea, Republic of,[3]Division of Medical Oncology, Yonsei Cancer Center, Yonsei University College of Medicine, Seoul, Korea, Republic of

Targeting mutated EGFR is a clinically validated approach for tackling non-small cell lung cancer (NSCLC). Approximately 20% of patients with advanced NSCLC harbor an EGFR mutation. Osimertinib is a 3rd-generation oral EGFR-TKI targeting the EGFR sensitizing mutations Del19 and L858R, as well as an acquired mutation, T790M. Despite osimertinib's efficacy in NSCLC, resistance develops and the mechanisms of resistance to osimertinib are complex. Development of another mutation, C797S is the most common mechanism of acquired resistance following osimertinib treatment. This mutation occurs with about 12% frequency after a 1L therapy of osimertinib, and with approximately 17% frequency after a 2L therapy. Here, we report TRX-221 as a novel 4th-generation EGFR-TKI that can overcome C797S-mediated acquired resistance in NSCLC models in vitro and in vivo. TRX-221 exhibited potent inhibitory activity against multiple EGFR mutant kinases, including Del19/T790M/C797S, L858R/T790M/C797S, Del19/C797S, L858R/C797S, Del19/T790M, L858R/T790M, Del19, and L858R. Likewise, TRX-221 potently inhibited the proliferation of Ba/F3 cells stably overexpressing these eight EGFR mutants. TRX-221 however showed sparing activity against EGFR wild-type kinase and cell lines. TRX-221 also demonstrated marked anti-proliferative activity against osimertinib-resistant patient-derived cancer cell lines (PDCs). With favorable DMPK profiles, once-daily oral dosing of TRX-221 induced strong anti-tumor effects in a dose-dependent manner in a variety of osimertinib-resistant CDX and PDX models. As a reversible, selective, and broad-spectrum 4th-generation EGFR-TKI, TRX-221 is currently undergoing IND-enabling studies and shows strong potential as a therapeutic solution to treat advanced NSCLC patients harboring EGFR mutations.

#4007

Efficacy of vepafestinib in preclinical models of *RET* fusion-driven sarcoma models

Igor Odintsov[1], Ryan C. Cheng[2], Allan J. W. Lui[3], Tom Zhang[4], Yue C. Lu[4], Renate I. Kurth[4], Morana Vojnic[5], Inna Khodos[4], Qing Chang[4], Kevin

Chen[4], Claudio Giuliano[6], Annalisa Bonifacio[6], Isao Miyazaki[7], Elisa de Stanchina[4], Emanuela Lovati[6], Marc Ladanyi[4], Romel Somwar[4].
[1]Pathology, Brigham and Women's Hospital, Boston, MA,[2]Pathology, Memorial Sloan Kettering Cancer Center, New York, NY,[3]Cancer Research UK, Cambridge, United Kingdom,[4]Memorial Sloan Kettering Cancer Center, New York, NY,[5]Northwell Health, New York, NY,[6]Helsinn Healthcare, Lugano, Switzerland,[7]Taiho Pharmaceutical Co. Ltd, Ibaraki, Japan

Background: Vepafestinib (TAS0953/HM06, Vepa) is a 2nd generation RET-selective inhibitor that effectively penetrates the brain, and inhibits the wildtype RET kinase domain (KD) and RET KD mutants (G810, V804, Y806, L730) (presented at AACR-NCI-EROTC 2021 meeting). *RET* rearrangements are found in an increasing number of soft tissue sarcomas, including infantile fibrosarcoma (IFS). Here we investigated the efficacy of Vepa in comparison to other RET-selective inhibitors in preclinical models of pediatric sarcomas harboring *RET* fusions.
Methods: Multiple preclinical models of *SPECC1L::RET*-driven sarcomas were established: 1) Paired patient-derived xenograft (PDX) and cell line models from a brain metastasis (BM) of an IFS tumor (SR-Sarc-0001); 2) A human mesenchymal stem cell line with RET fusion introduced with CRISPR-Cas9 (HMSC-RET); 3) A murine BM model produced by injection of luciferase-expressing HMSC-RET into the cerebellum. CNS penetration of Vepa was assessed by pharmacokinetic profiling in the prefrontal cortex (PFC), cerebrospinal fluid (CSF), and plasma in freely-moving male Han Wistar rats after oral administration of 3, 10, or 50 mg/kg single doses.
Results: Exposure of SR-Sarc-0001 and HMSC-RET cells to Vepa resulted in dose- and time-dependent decreases in phosphorylation of RET, ERK1/2, AKT, STAT3 and S6, expression changes in cell cycle regulators (p27 up, cyclin D1 down), induction of pro-apoptosis proteins (c-PARP, BIM), and loss of MYC expression. Growth of SR-Sarc-0001 (IC_{50}: 0.09 μM, 95% CI: 0.03-0.2) and HMSC-RET cells (IC_{50}: 0.2 μM, 95% CI: 0.09-0.5), but not parental HMSC cells (IC_{50} > 1 μM), was suppressed by Vepa, with concomitant elevation of caspase 3/7 activity. Vepa was more effective than vandetanib and similar to the FDA-approved RET inhibitors, selpercatinib

(Selp) and pralsetinib (Pral), in all *in vitro* assays. Significant regression of SR-Sarc-0001 PDX tumors was seen after Vepa treatment (64.8 ± 0.5%). Notably, no regrowth was observed up to 46 days after cessation of Vepa treatment, whereas 25 days after stopping Selp (10 mg/kg BID) and Pral (15 mg/kg BID) treatment, 1/5 and 3/5 tumors started to regrow, respectively. Similar efficacy was observed in the HMSC-RET xenograft model. Vepa was more effective than Selp at blocking HMSC-RET brain xenograft tumor growth (p=0.001) and increasing survival (p=0.0001). CNS penetration of Vepa was excellent, with near-equivalent concentrations detected in the PFC, CSF, and plasma-free fraction after equilibration between body fluid compartments.
Conclusions: Our preclinical results suggest that vepafestinib has the potential to more effectively manage CNS metastasis compared to selpercatinib, representing a promising new therapeutic option for patients with RET-driven sarcomas. Vepafestinib is currently in a phase 1/2 trial for adult patients with advanced solid tumors harboring *RET* alterations (margaRET, NCT04683250).

#4008

TAS2940, a novel brain-penetrable pan-ERBB inhibitor, exhibits tumor regression and prolongs survival in intracranial models bearing ERBB aberrations

Kei Oguchi, Hikari Araki, Shingo Tsuji, Masayuki Nakamura, Akihiro Miura, Kaoru Funabashi, Akiko Osada, Sakiho Tanaka, Takamasa Suzuki, Shinji Mizuarai. *Discovery and Preclinical Research Division, Taiho Pharmaceutical Co., Ltd, Tsukuba, Japan*

Background: Primary and metastatic brain tumors have significant unmet medical needs as few drugs can penetrate the blood-brain barrier (BBB). Brain metastasis is more common in non-small cell lung cancer (NSCLC) and breast cancer than in other cancers. Genetic alterations in *ERBB* family genes are frequently observed in those cancers, with about half of *HER2/EGFR* aberrations metastasizing in the brain. *EGFR* aberrations have been also observed in glioblastoma. Several pan-ERBB inhibitors are clinically available or under clinical development, such as afatinib, neratinib, and poziotinib. However, none are highly brain-penetrable as they are pumped out via the BBB. Here, we report TAS2940 as a novel potent

pan-ERBB inhibitor that elicits brain penetrability and anti-tumor effects in brain metastasis models.
Methods: The kinase selectivity of TAS2940 was evaluated in a panel of 257 kinases. Autophosphorylation of wild-type and mutant ERBB in stably expressing cell lines was evaluated using a quantitative immunofluorescence assay. The growth inhibitory effect on cell lines expressing HER2/EGFR aberrations was evaluated based on quantitation of the cellular ATP concentration. Cell lines were transplanted subcutaneously or intracranially in BALB/cAJcl-nu/nu mice. HER2 tyrosine kinase inhibitors, including TAS2940, were then orally administered once daily followed by evaluation of tumor volume and body weight.
Results: TAS2940 showed potent and selective inhibition against ERBB family proteins over more than 250 kinases on enzymatic assay. TAS2940 also showed preferential cytotoxicity in cells harboring *HER2/EGFR* genetic alterations *in vitro*, while sparing cells without *ERBB* genetic aberrations. TAS2940 showed potent anti-proliferative activity in cells containing *HER2* genetic alterations or *EGFR* exon 20 insertions, commonly found in NSCLC or breast cancer, as well as EGFRvIII alterations, frequently observed in glioblastoma. *In vivo* xenograft tumor models with various *EGFR* genetic alterations showed that TAS2940 exerted anti-tumor effects, such as growth retardation or regression. We further examined brain penetration by assessing the brain to blood concentration of TAS2940 in mice with intact BBBs, showing higher brain penetrability compared to other ERBB inhibitors. Evaluation of TAS2940 in intracranial brain metastasis mouse models resulted in tumor regression and prolonged survival.
Conclusion: TAS2940 is a novel potent and selective pan-ERBB inhibitor with high brain penetrability *in vivo*. These results support the clinical development of TAS2940 in primary and metastatic brain tumors driven by *ERBB* genetic aberrations.

#4009

Discovery of PLM-102, a highly potent 3rd generation FLT3 inhibitor, in drug-resistant FLT3-ITD-TKD mutated acute myeloid leukemia

Jin-Hee Park[1], Jae-Seon Lee[1], Su-jin Oh[1], So-Deok Lee[1], Yong June Choi[2], Keon Wook Kang[2], Miran Moon[1], Soo Yeon Jang[1], Myung Jin Kim[1], Yong-

Chul Kim[1]. *[1]PeLeMed, Seoul, Korea, Republic of,[2]Seoul National University, Seoul, Korea, Republic of*

Mutations of the FMS-like tyrosine kinase 3 (FLT3) gene occur in approximately 25 ~ 30% of all acute myeloid leukemia (AML) cases and FLT3-ITD mutations are associated with a particularly unfavorable prognosis, with an increased risk of relapse and shorter overall survival (OS) compared with AML patients without the mutation. Even though multiple FLT3 inhibitors are in various stages of clinical evaluation, resistance to FLT3 inhibitors resulting from acquired point mutations in tyrosine kinase domain (TKD) have limited the sustained efficacy of treatments. Among them, a “gatekeeper” mutation (F691L) is resistant to most available FLT3 inhibitors. Here, we show the efficacy and mechanism of PLM-102, developed an orally available and highly selective small molecule, in overcoming drug-resistant FLT3-ITD-TKD mutations as a strong candidate of the 3rd generation of FLT3 inhibitor.

PLM-102 displays extraordinary potency of enzyme inhibitory activities of all FLT3 WT/mutants including F691L with IC_{50} values of <1 nM. In FLT3-ITD-positive cell lines (MV4-11, MOLM-13, MOLM-14, Ba/F3-ITD-D835Y, Ba/F3-ITD-F691L), PLM-102 shows about 18~25-fold higher anti-proliferative activities than Gilteritinib. Also, PLM-102 potently inhibited the phosphorylation of FLT3 and its downstream signaling pathways, and induced apoptosis as evidenced by PARP-cleavage and caspase-3 activation.

Moreover, in AML-related xenograft mouse models (MV4-11, MOLM-14, Ba/F3-ITD-D835Y, Ba/F3-ITD-F691L), once-daily oral dose of PLM-102 significantly suppressed the tumor growth and achieved complete tumor regression. In addition, the outstanding efficacy of our compound has been confirmed in large tumor xenograft models. These results are very encouraging because large tumors have a limited blood supply and high interstitial fluid pressure, leading to a poor absorption of anticancer drugs. Pharmacokinetics of PLM-102 displayed higher bone-marrow exposure indicating better target engagement and benefits in the clinical translation in AML.

In conclusion, PLM-102 is a promising therapeutic candidate for the FLT3-ITD-mutated AML as well as the acquired resistance to current FLT3 inhibitors.

#4010

Inhibition of PERK by HC-5404 sensitizes clear cell renal cell carcinoma tumor models to anti-angiogenic tyrosine kinase inhibitors

Michael E. Stokes, Veronica Calvo, Crissy Dudgeon, Sho Fujisawa, Sharon Huang, Leyi Shen, Nupur Ballal, Joe McGinley, David Liu, Mark J. Mulvihill, Alan C. Rigby, Nandita Bose, Eric S. Lightcap, David Surguladze. *HiberCell, New York City, NY*

Anti-angiogenic agents form the backbone of standard of care for advanced clear cell renal cell carcinoma (ccRCC), but their clinical impact is limited by primary and secondary resistance mechanisms that remain a critical problem. Furthermore, the approvals for VEGFR-targeting receptor tyrosine kinase inhibitors (VEGFR-TKIs), cabozantinib in second-line, and tivozanib in third-line RCC patients were based on modest objective response rates and median progression-free survival. There is an urgent need for novel mechanisms that target adaptive tumor responses that drive resistance to these agents, as well as combination drug partners that improve outcomes for patients.

As part of their mechanism, VEGFR-TKIs induce oxygen- and nutrient-deprivation that drives ER stress. Tumors can evade deleterious ER stress by activating PERK branch of the integrated stress response, which arrests global translation and restores homeostasis. We hypothesized that inhibiting PERK would enhance the anti-tumor activity of VEGFR-TKIs *in vivo* and tested this using HC-5404, a potent and selective PERK inhibitor currently in Ph1 clinical testing (NCT04834778). Here, we present preclinical evidence that supports combining HC-5404 with VEGFR-TKIs in ccRCC. We demonstrate that axitinib, cabozantinib, lenvatinib, and sunitinib all activate PERK in 786-O ccRCC xenografts in a dose-responsive manner. The addition of HC-5404 significantly enhanced the tumor growth inhibition (TGI) of VEGFR-TKIs across multiple ccRCC tumor models, resulting in tumor stasis or regression in combination groups. Expression profiling and IHC analysis of tumor sections revealed that HC-5404 enhanced the anti-angiogenic effects of axitinib and lenvatinib in 786-O tumors, highlighting the protective role of PERK in response to anti-angiogenics.

To evaluate whether the combination treatments could benefit a diverse patient population, sensitivity to HC-5404 and axitinib was evaluated across a panel of patient-derived xenograft (PDX) models. This experiment confirmed widespread responsiveness to the combination treatment that in some cases achieved ≥50% tumor regression. As tumor progression on VEGFR-TKIs limits the success of these agents in the clinic, we evaluated the effect of adding HC-5404 to tumors that have previously progressed on axitinib. In this study, 786-O xenografts were treated with axitinib for 2-weeks and non-responders were rerandomized into groups of either single agent or combination of HC-5404 and axitinib. The combination treatment significantly improved TGI relative to either monotherapy, resulting in tumor regression of ~20%. Taken together, these findings highlight that by disrupting an adaptive stress response evoked by VEGFR-TKIs, HC-5404 presents a clinical opportunity to enhance the anti-tumor effects of well-established standard of care therapies in ccRCC.

#4011

Preferential cytotoxicity of ESK981 in neuroendocrine prostate cancer

Yang Zheng[1], Kyle J. Garcia-Rogers[2], Yi Bao[1], Rahul Mannan[1], Tongchen He[1], Sarah N. Yee[2], Caleb Cheng[1], Xia Jiang[1], Isabella E. Taylor[2], Xuhong Cao[1], Yuzhuo Wang[3], Yuanyuan Qiao[4], Arul M. Chinnaiyan[4]. *[1]Michigan Center for Translation Pathology; Department of Pathology, University of Michigan, Ann Arbor, MI,[2]Michigan Center for Translation Pathology, University of Michigan, Ann Arbor, MI,[3]Vancouver General Hospital and Department of Urologic Sciences; The Vancouver Prostate Centre, University of British Columbia, Vancouver, BC, Canada,[4]Michigan Center for Translation Pathology; Department of Pathology; Rogel Cancer Center, University of Michigan, Ann Arbor, MI*

Introduction: Despite advances in the understanding of neuroendocrine prostate cancer (NEPC) development, effective therapeutic options remain limited. We previously reported that ESK981, a phase I-cleared multi-tyrosine kinase inhibitor (MTKI), exhibited tumor growth inhibitory abilities in multiple preclinical castration resistant prostate cancer (CRPC) and androgen-negative models by blocking the PIKfyve activity and disrupting autophagy. The results suggested that AR-negative prostate

cancer have better response to ESK981 induced tumor inhibition than AR+ prostate cancer (Qiao et al, *Nature Cancer* 2022).
Methods: In order to examine the tumor growth efficacy of ESK981 in NEPC, we assessed the efficacy of ESK981 monotherapy in six NEPC (LTL-352, LTL-331R, LTL-545, and LTL-610 patient-derived xenografts (PDXs); and NCI-H660 cell line-derived xenograft) *in vivo* models. PDXs were maintained in CB17 SCID male mice and passaged by subcutaneous implantation. When the tumors reached ~100mm^3, mice were randomized and treated with either vehicle (Ora-plus) or 30mg/kg ESK981 administered by oral gavage once a day in a five-day per week schedule. Mouse body weight and tumor volume was monitored throughout the treatment schedule. Subcutaneous tumors were collected post five days of treatment for early assessment and long-term treatment for efficacy evaluation, respectively. H&E staining, TUNEL *in situ* cell death assay, and western blotting were performed to determine the morphology changes and apoptosis after ESK981 treatment. Single cells were isolated from tumors and stained with Zombie live/dead dye, CD45, CD11b and Ly6G fluorescently conjugated antibodies to assess neutrophil population by flow cytometry.
Conclusions: We demonstrated that ESK981 monotherapy is well tolerated in all *in vivo* models and ESK981 exerted greater cytotoxicity in NEPC than previous evaluated prostate adenocarcinoma by percent tumor growth inhibition. ESK981 also induced dramatic cell deaths in NEPC preclinical models, determined by H&E staining, TUNEL-positive apoptotic tumor cells, and increased protein level of PARP cleavage via western blotting. Moreover, flow cytometry analysis revealed a dramatic increase in the intratumoral neutrophil infiltration after ESK981 treatment in the NEPC preclinical models in a time-dependent manner. NEPC tumors are sensitive to ESK981 monotherapy *in vivo*, suggesting NEPC patients may be the right population to target with ESK981. Together, ESK981 monotherapy is safe and effective therapy in NEPC preclinical models, and these results will warrant the clinical trial of ESK981 on NEPC patients.

#4012
Preclinical development of SHP2 allosteric inhibitor ICP-189
Ruixia Liang, Yingxiang Gao, Fangfang Yang, Yingrui Han, Zuopeng Wang, Richard Liu, Charles Ying Wang, Jason Bin Zhang, Xiangyang

Chen, Davy Xuesong Ouyang. *InnoCare Pharma Tech co. Ltd, Beijing, China*

Background: SHP2 is a non-receptor protein tyrosine phosphatase which functions as a convergent signaling node downstream of multiple receptor tyrosine kinases (RTKs), and upstream of RAS to promote oncogenic signaling and tumor growth. SHP2 also mediates PD-1 immune blockade of T cells by binding to the immune receptor tyrosine-based inhibitory motif (ITIM) and immune receptor tyrosine-based switch motif (ITSM) of PD-1. SHP2 has long been considered as a plausible oncology drug target not only as an oncoprotein, but also as an important immune modulator. However, for decades, SHP2 was thought to be "undruggable" due to difficulties in targeting its catalytic site. Recent discovery of allosteric site of SHP2 has inspired a novel approach for SHP2 targeting. Here we report the development of ICP-189, which is a potent, highly selective, and orally bioavailable allosteric inhibitor of SHP2, demonstrated robust efficacies in various *in vitro* and *in vivo* RAS/MAPK pathway-driven models as mono-therapeutic agent or in combination with other anti-cancer drugs.
Results: ICP-189 inhibits phosphatase activity of SHP2 with IC_{50} values < 5 nM. In a phosphatase profiling assay, ICP-189 efficiently inhibits the catalytic activity of SHP2, with no significant effects on 21 other tested tyrosine and serine/threonine phosphatases, indicating its high selectivity for SHP2. ICP-189 has demonstrated robust *in vitro* efficacies in a panel of tumor cell lines bearing activated RTK, RAS, NF1 loss-of-function, or BRAF class III mutations. It has also exhibited synergistic tumor killing effects in combination with EGFR, $KRAS^{G12C}$, MEK and CDK4/6 inhibitors. In a series of *in vivo* efficacy studies, ICP-189 treatment results in robust tumor growth control of MIA-PaCa-2, KYSE-520 and NCI-H358 xenografts. ICP-189 has also shown strong synergies in tumor killing when combined with MEK inhibitor trametinib, $KRAS^{G12C}$ inhibitor sotorasib, EGFR inhibitor osimertinib in xenograft models; and when combined with anti-PD-1 antibody in EMT6 syngeneic tumors. The *in vivo* efficacy of ICP-189 is well accompanied by pharmacodynamic modulations, where ICP-189 exposure levels correlate with the inhibition of p-ERK and *DUSP6* mRNA level in tumors. The pharmacokinetic parameters of ICP-189 are overall favorable, with high oral bioavailability. Nonclinical safety

evaluations also exhibit acceptable drug tolerability in SD rats and Beagle dogs.
Conclusions: ICP-189 is a novel allosteric inhibitor of SHP2 with broad-spectrum anti-tumor activities as a single agent or in combination with other targeted or immune modulating anti-cancer therapeutics. ICP-189 is now in phase I clinical trial in China and United States.

#4013

Combination of BTK inhibitor orelabrutinib, anti-CD19 antibody tafasitamab, and IMiD lenalidomide for the treatment of B cell malignancies

Hongjuan Zhang, Ruixia Liang, Haipeng Xu, Xiaorong Li, Renbin Zhao, Jason Bin Zhang, Davy Xuesong Ouyang. *InnoCare Pharma Tech co. Ltd, Beijing, China*

Background: R-CHOP has been widely recognized as effective first-line treatment for DLBCL. However, 30-50% of the patients are either refractory or eventually develop relapsed diseases (r/r DLBCL). The CD19-targeted cytolytic antibody tafasitamab, in combination with immunomodulating drug (IMiD) lenalidomide, has been approved as one of the very few treatment options for transplant-ineligible patients with r/r DLBCL. Tafasitamab is a Fc-enhanced anti-CD19 monoclonal antibody, mediating B cell tumor lysis through ADCC/ADCP activities and direct cytotoxicity. Bruton's tyrosine kinase (BTK) is a key oncogenic driver in many B cell malignancies. Orelabrutinib is a highly selective BTK inhibitor approved for r/r CLL/SLL and r/r MCL in China. In addition, multiple clinical trials of orelabrutinib are being carried out for the treatment of other B cell lymphomas including the MCD subtype of DLBCL. In this study, we have investigated the potential benefit of combining orelabrutinib with tafasitamab and lenalidomide in pre-clinical B cell tumor models.
Results: ADCC activity of tafasitamab alone or in combination with lenalidomide and orelabrutinib/ ibrutinib was measured by co-culturing $CD19^+$ B cell tumor cells TMD8 or RS4;11 with Jurkat-CD16a(V158)-NFAT reporter cells or PBMC. In both assays, orelabrutinib slightly enhances, or well retains the ADCC activity of tafasitamab, while ibrutinib consistently suppresses the ADCC function of tafasitamab. Mechanistically, our data indicate that ibrutinib has an off-target effect on ITK, a key kinase

regulating FcR signaling in NK cells, which in turn may lead to compromised ADCC activity of tafasitamab. In contrast, orelabrutinib is a highly selective BTK inhibitor with no effect on ITK, which confers its ability to enhance or retain the ADCC activity of tafasitamab. Combination of orelabrutinib with tafasitamab and/or lenalidomide also leads to synergistic tumor lysis activity, with or without the presence of immune effector cells. *In vivo* efficacy study of REC-1 xenografts has further demonstrated much improved tumor growth inhibition with combinatory treatment of orelabrutinib, tafasitamab and lenalidomide compared to single agents.
Conclusions: The highly selective BTK inhibitor orelabrutinib offers an alternative to ibrutinib as a combinatory partner with antibody therapeutics whose mechanism of action is highly dependent on ADCC. Confirmation of the synergistic effects of orelabrutinib with tafasitamab and lenalidomide in various preclinical models has provided scientific rationales for testing the combinatory treatment in clinical studies. An open-label, single-arm, multi-cohort phase I study to evaluate the safety and efficacy of orelabrutinib, tafasitamab and lenalidomide combinations in patients with relapsed/refractory non-Hodgkin's lymphoma (NHL) is ongoing.

#4014

Comparative biochemical kinase activity analysis identifies rivoceranib as the most selective VEGFR-2 inhibitor compared with other TKIs with known activity against VEGFR-2

Seong Jang[1], Bill Strickland[1], Lynda Finis[1], Jeffrey J. Koojiman[2], Janneke J. T. Melis[2], Guido J. R. Zaman[2], Jan V. Tornout[1]. *[1]Elevar Therapeutics, Salt Lake City, UT,[2]Oncolines B.V., Oss, Netherlands*

Introduction: Vascular endothelial growth factor receptor 2 (VEGFR-2) is a key regulator of tumor angiogenesis that is highly expressed in several tumor types and is a known target for anti-cancer therapy. Yet the clinical use of VEGFR-2 inhibitors has been challenged by limited efficacy and various side effects, potentially due to the low selectivity of these TKIs for VEGFR-2. Thus, potent VEGFR-2 inhibitors with improved selectivity are needed. Rivoceranib is an oral tyrosine kinase inhibitor (TKI) that potently and selectively inhibits VEGFR-2. A comparison of the potency and

selectivity of VEGFR-2 inhibitors can provide a rationale for selecting a specific TKI for anticancer therapy in the clinic.
Methods: Binding of rivoceranib to VEGFR-2 was determined on a Biacore T200. The affinity constant (K_D) was derived from the association and dissociation rate constants. Inhibitory potency of rivoceranib and 10 FDA-approved reference inhibitors on kinase enzyme activity was determined using mobility shift assays (MSA) or immobilized metal ion affinity particle (IMAP) assays. The half-maximum inhibitory activity (IC_{50}) of the 11 inhibitors on VEGFR-2 was determined in 10-point dose-response curves. The selectivity of the inhibitors was determined on 270 wild-type kinases at a fixed concentration of each inhibitor. Rivoceranib was tested at 10- and 100-times IC_{50} (160 nmol/L and 1.6 μmol/L). Reference inhibitors were tested at 1 μmol/L (35 to 1056-times IC_{50}).
Results: Rivoceranib had a K_D of 3 nmol/L on VEGFR-2. In enzyme activity assays, rivoceranib had intermediate potency compared with the 10 reference inhibitors, with a VEGFR-2 kinase inhibition IC_{50} value of 16 nmol/L. Analysis of the residual activity of the panel of 270 kinases in the presence of rivoceranib or the reference inhibitors showed wide variation in selectivity for VEGFR-2, with rivoceranib identified as the most selective inhibitor (activity of 16 additional kinases inhibited by >50% at 1.6 μmol/L). Tivozanib, the most potent VEGFR-2 inhibitor, displayed greater than 50% inhibitory activity against more than 70 additional kinases. Sunitinib was identified as the least selective inhibitor included in this study, inhibiting 125 additional kinases by >50%.
Conclusion: Variations in selectivity among TKIs with similar anti-VEGFR-2 potency can help explain differences in their clinical toxicity profiles, which may be partially due to variant inhibitory effects against TKIs other than VEGFR-2. This comparative biochemical analysis highlights the potential for rivoceranib to address clinical limitations associated with the poor selectivity of currently available VEGFR-2 inhibitors. Rivoceranib is under ongoing investigation as monotherapy and in combination with chemotherapy in various tumor types.

#4015
EGFR activation via c-Jun axis promotes adaptive resistance to third generation ALK-TKI lorlatinib in ALK-rearranged non-small cell lung

cancer cells

Yuki Katayama[1], Tadaaki Yamada[1], Kenji Morimoto[1], Hiroaki Ozasa[2], Shinsaku Tokuda[1], Koichi Takayama[1]. *[1]Kyoto Prefectural University of Medicine, Kyoto, Japan,[2]Kyoto University, Kyoto, Japan*

Anaplastic lymphoma kinase-tyrosine kinase inhibitors (ALK-TKIs), including lorlatinib have shown dramatic efficacy in patients with ALK-rearranged lung cancer; however, complete response in these patients is rare, as a small population of tumor cells survives due to adaptive resistance. In this preclinical study, we investigated the adaptive resistant mechanisms to lorlatinib and its therapeutic strategies to overcome, using in vitro and in vivo experiments. We have identified EGFR as an adaptive resistance mechanism of lorlatinib using phospho-RTK array and siRNA library. Cell line-based assay showed that exposure of lorlatinib accelerated EGFR signal activation as an adaptive response via activation of JNK cascade in ALK-rearranged lung cancer cells. Knockdown for EGFR suppressed the survival signal of ALK lung cancer cells when treated with lorlatinib. The combination of lorlatinib and erlotinib, a first-generation EGFR-TKI, was shown to enhance cell growth inhibition by inducing cell apoptosis via suppressing the anti-apoptotic factor Bcl-xl compared with lorlatinib monotherapy. Moreover, cell line-derived xenograft model indicated that the combination of lorlatinib plus erlotinib enhanced anti-tumor effects compared with lorlatinib monotherapy. Taken together, our results displayed that EGFR activation plays an important role in the initial adaptive resistance to lorlatinib for ALK-rearranged lung cancer. The combination of lorlatinib and erlotinib is expected as the promising strategy for those tumors.

#4016

Discovery of a small-molecule EGFR inhibitor that can potently target various EGFR mutants, including C797S mutant, in vitro and in vivo

Yeejin Jeon, Kiram Lee, Anna Jang, Miyeon Kim, Kyeong Jin Yoon, Yeri Lee, Dongsu Kim, Donggeon Kim, Dohyun Park, Sang Kyun Lim, Sung Pil Choi. *Kanaph Therapeutics Inc, Seoul, Korea, Republic of*

EGFR is one of receptor tyrosine kinases (RTKs) and, upon ligand binding, turns on the downstream signals that include oncogenic RAS/MEK/ERK,

PI3K/AKT/mTOR, and JAK/STAT pathways. EGFR gene mutations, such as Exon 19 deletion (Del19) and L858R mutations, induce abnormal activation of the EGFR protein even in the absence of the ligand leading to various cancers. EGFR mutations are found in non-small cell lung cancer (NSCLC) patients with 10-15% frequency (approximately 50% in Asian patients).
Starting from Del19 and L8585R mutations, additional mutations in the EGFR gene occur during the treatment with 1st/2nd/3rd generation EGFR inhibitors, resulting in Del19/T790M, L858R/T790M, Del19/T790M/C797S, L858R/T790M/C797S, Del19/C797S, and L858R/C797S mutations. While double mutations that include the T790M mutation have been efficaciously treated with Osimertinib, there are currently no approved therapies that can effectively target the C797S-containing mutants.
Here we present preclinical data showing a small-molecule inhibitor that effectively disables EGFR mutants, including Del19/T790M/C797S, L858R/T790M/C797S, Del19/C797S, and L858R/C797S mutants. High potency and selectivity were confirmed by in vitro kinase assays and cellular assays. Outstanding anti-cancer activity was observed in mouse xenograft models with various EGFR mutations and, importantly, it was inactive in the EGFR wild-type model. With confirmed brain penetrance through in vivo studies, our potent EGFR inhibitor may provide a great therapeutic potential for patients with EGFR mutation-driven NSCLC.

#4017

TAS2940 inhibits intracranial tumor growth and prolongs survival in HER2-aberrant and EGFR-amplified patient-derived xenograft models

Jing Han[1], Mikhila Mahendra[1], Poojabahen Gandhi[1], Joseph R. Daniele[1], Caroline C. Carrillo[1], Benjamin J. Bivona[1], Ningping Feng[1], John V. Heymach[2], Funda Meric-Bernstam[3], Kei Oguchi[4], Shinji Mizuarai[4], Timothy P. Heffernan[1], Christopher P. Vellano[1], Joseph R. Marszalek[1].
[1]TRACTION Platform, Therapeutics Discovery Division, UT MD Anderson Cancer Center, Houston, TX,[2]Department of Thoracic, Head and Neck Medical Oncology, UT MD Anderson Cancer Center, Houston, TX,[3]Department of Investigational Cancer Therapeutics, UT MD Anderson

Cancer Center, Houston, TX,[4]Discovery and Preclinical Research Division, Taiho Pharmaceutical Co, Tsukuba, Japan

Patients with brain tumors and metastases have poor prognosis and overall survival rates despite the advancements in neurosurgery, radiotherapy, and chemotherapy. Genomic alterations in HER2 are present in brain metastases of breast cancer (BC; ~20%) and non-small cell lung cancer (NSCLC; 13-20%), and EGFR alterations occur frequently in glioblastoma multiforme (GBM; >50%). Despite the advancements in standard of care options, optimal treatment management for these patients remains an unmet medical need. Recent evidence suggests activity of systemic therapy for immune and targeted therapies in the brain, including agents targeting HER2/EGFR. HER2-targeted tyrosine kinase inhibitors lapatinib, neratinib, and tucatinib and the HER2-targeted antibodies trastuzumab and pertuzumab, in combination with chemotherapy, have been shown to improve survival of patients with HER2 overexpressing BC in the presence of brain metastases. The limited penetration of these compounds into the CNS, however, limits their efficacy. TAS2940 is an irreversible pan-ErbB inhibitor with greater brain-penetrability than poziotinib, tucatinib, and neratinib. Here, we demonstrate that TAS2940 induces downregulation of phosphorylated HER2/EGFR, reduces tumor burden, and promotes a significant increase in survival in intracranial xenograft mouse models with HER2-amplification (BC), HER2-Exon20 insertion mutation (NSCLC), and EGFR-amplification (GBM). These promising preclinical data highlight potential novel therapeutic strategies for patients with EGFR-aberrant GBM and brain metastases harboring HER2/EGFR alterations, and may help support the advancement of the ongoing first-in-human clinical trial (NCT04982926) for TAS2940 in solid tumors with EGFR and/or HER2 alterations.

#4018

BBT-207 is a broad-spectrum, highly potent, 4th generation EGFR TKI with enhanced activity to both sensitizing and treatment-emergent EGFR mutations including T790M and C797S

Chulwon Kim[1], Youn Hee Jung[1], Naeun Jeon[1], Yong-Hee Lee[2], Sang-Yoon Lee[3], Jimmy Taiguang Jin[2]. *[1]Research Center, Bridge Biotherapeutics, INC., Seongnam-si, Korea, Republic of,[2]Bridge Biotherapeutics, INC.,*

Cambridge, MA,[3]Bridge Biotherapeutics, INC., Seongnam-si, Korea, Republic of

Background: *EGFR* mutation in non-small cell lung cancer (NSCLC) presents a viable therapeutic target for which tyrosine kinase inhibitor (TKI) therapy has shown impressive clinical benefit over the past 20 years. Unfortunately, most patients inevitably progress on earlier-generation EGFR TKIs due to various mechanisms after a period of therapy. The most commonly acquired on-target resistance mutations are T790M and C797S, often appearing after progression on 1st-, 2nd-generation, and 3rd-generation EGFR TKIs, respectively. To prevent the emergence of drug-resistant subclones, a next-generation EGFR TKI must have activity against both treatment-emergent and drug-naïve mutants. Further preclinical studies were conducted to evaluate the activity of BBT-207 in delaying tumor regrowth or prolonging survival in NSCLC tumor models driven by the *EGFR* T790M and C797S mutation.
Method: We evaluated the inhibitory potency of BBT-207 against wild-type (WT) and mutated EGFR proteins. In vivo anti-tumor activity was evaluated in Ba/F3 *EGFR* ex19del/T790M (DT), L858R/T790M (LT), ex19del/C797S (DC), L858R/C797S (LC), ex19del/T790M/C797S (DTC) or L858R/T790M/C797S (LTC), H1975 *EGFR* LTC cell line-derived xenograft (CDX), and *EGFR* DTC-patient-derived xenograft (PDX) models. In vivo inhibition of brain metastases (BM) was evaluated in a luciferase-expressing PC-9 *EGFR* DTC BM model through direct intracranial implantation.
Results: BBT-207 is broadly active against activating and acquired resistance *EGFR* mutants and displayed potent anti-proliferation activity against Ba/F3 *EGFR* DT, LT, DC, LC, DTC, LTC with 4, 4, 1, 16, 5 and 8nM, respectively while being highly selective against Ba/F3 *EGFR* WT (184 nM). BBT-207 also showed IC_{50} values <5 nM against Osimertinib-resistant *EGFR* L792H triple mutants, DTL and LTL in cell-free *in vitro* kinase assay. QD administration as a single agent resulted in significant tumor regression in the Ba/F3 *EGFR* DT, LT, DC, LC, DTC, LTC CDX models and *EGFR* DTC PDX model. Indeed, BBT-207 showed sustained anti-tumor efficacy in Ba/F3 *EGFR* DC CDX model. Furthermore, BBT-207 exerted dose-dependent intracranial anti-tumor activity and enhanced

survival rate of mice in the PC-9/*EGFR* DTC_Luc BM model. PK studies revealed CNS penetration with good B/P ratios in animals.
Conclusion: BBT-207 is a reversible, mutant-specific, broad-spectrum TKI, active to clinically observed mutations of *EGFR* and is expected to be compatible with monotherapy of QD schedule in humans. BBT-207 is well-positioned to augment the treatment of *EGFR* mutated NSCLC, either for acquired drug resistance or in earlier line, with potential to treat or prevent CNS metastasis. PK/TK evaluation justify exploration in humans. First-in-human study in patients harboring *EGFRm* and previously treated with EGFR TKI, is to begin enrollment in USA 1H 2023.

#4019

Preclinical Activity of ELVN-002: A Potent, Selective, Irreversible and CNS Penetrant HER2 and pan-HER2 Mutant Small-Molecule Inhibitor for the Treatment of HER2-Driven Malignancies

Monette Aujay, Amanda J. Broad, Stefan D. Gross, Li Ren, Joseph P. Lyssikatos, Samuel Kintz, Qi Wang, Helen Collins. *Enliven Therapeutics, Boulder, CO*

Mutation or amplification of the human epidermal growth factor receptor 2 (HER2) gene has been identified in numerous solid tumor types, including non-small cell lung cancer (NSCLC), breast, and colorectal cancer. These genetic alterations are believed to confer elevated HER2 activity resulting in oncogenic transformation. In NSCLC, an estimated 3% of patients harbor activating mutations in the HER2 gene. Enhertu (T-DXd), a HER2-specific antibody-drug conjugate was recently approved as an important therapy for this patient population. However, for patients who are not candidates for T-DXd or have discontinued treatment due to an adverse event or disease progression, there exist few therapeutic options. Accordingly, HER2 inhibitors have the potential to provide meaningful therapeutic benefit to these patients. Due to significant structural homology between EGFR and HER2, most investigational small molecule HER2 kinase inhibitors are dual EGFR/HER2 inhibitors and are substantially dose-limited by EGFR-related toxicities in patients. These toxicities likely limit their clinical activity. Currently, tucatinib is the only HER2-selective small molecule inhibitor approved for metastatic breast cancer in combination with trastuzumab and capecitabine. However, it lacks sufficient potency against several of the key

clinically relevant mutations, including HER2 YVMA, the most common exon 20 insertion mutation, prevalent in HER2 mutant NSCLC. ELVN-002 is a potent, irreversible inhibitor of HER2 with a >100-fold selectivity over EGFR. ELVN-002 potently inhibits the phosphorylation of HER2 in cell lines endogenously expressing HER2 or in those engineered to express specific clinically relevant HER2 mutants. This activity readily translates into marked anti-proliferative activity against cell lines dependent upon HER2 for their growth and survival. In addition, ELVN-002 is highly selective for HER2 and HER2 mutants versus wild-type EGFR as demonstrated via assessment of both EGFR-driven proliferation and EGFR phosphorylation in cells. Furthermore, ELVN-002 is highly active in mouse models of HER2-driven cancers, including subcutaneous models driven by wild type or mutant HER2. ELVN-002 is also active in an NCI-N87 wild-type HER2 intracranial model. In all models tested, ELVN-002 treatment is well tolerated and resulted in tumor regressions at exposures believed to be clinically achievable. Due to its selectivity and breadth of activity versus the clinically relevant HER2 mutants, ELVN-002 has the potential to be an effective treatment for HER2 mutant NSCLC as well as other HER2 mutant amplified solid tumors, including metastatic HER2 positive breast cancer. Additionally, ELVN-002 could provide a meaningful therapeutic option for patients with CNS metastases. ELVN-002 has been selected for clinical development.

#4020

HMPL-760 is a highly potent and selective reversible BTK inhibitor, targeting BTK and BTK^{C481S} in B-cell malignancies

Linfang Wang, Junqing Liang, Zhihu Gao, Jia Hu, Weigang He, Xianwen Yang, Fangfang Mao, Wei Zhang, Ying Yu, Qihang Zhang, Na Yang, Chun Zhang, Jian Wang, Yu Cai, Xiong Li, Weiguo Qing, Guangxiu Dai, Yongxin Ren, Michael Shi, Weiguo Su. *HUTCHMED Limited, Shanghai, China*

Introduction: Bruton's tyrosine kinase (BTK), a member of the Tec family, plays a crucial role in signaling through B-cell receptor (BCR). BTK inhibition blocks BCR signals and prevents B-cell activation and growth. First-generation BTK inhibitors such as ibrutinib covalently binds to a cysteine residue (C481) of BTK. Their most frequent acquired resistance is the development of a serine mutation in the binding site (C481S). Next

generation BTK inhibitors such as LOXO-305 and ARQ 531 are being developed to overcome this resistance to first-generation inhibitors.
Methods: HMPL-760 was tested in biochemical assays using recombinant human wild type (WT) and C481S mutant BTKs. Its selectivity was carried out using Eurofins Cerep KinaseProfiler^{TM} panel. Cellular activity of HMPL-760 was evaluated in HEK293 cells stably transfected with BTK^{WT} or BTK^{C481S}, and other tumor cell lines, which are either human diffuse large B cell lymphoma (DLBCL) or mantle cell lymphoma (MCL) cell lines. The in vivo antitumor activity and PKPD correlation of HMPL-760 was studied in HBL-1 xenograft mouse models bearing BTK^{WT} or BTK^{C481S} respectively.
Results: In biochemical assays, HMPL-760 strongly inhibits BTK kinase activities towards wild-type BTK (BTK^{WT}) and C481S mutant (BTK^{C481S}), and binds to BTK in a reversible way. HMPL-760 demonstrates high selectivity in a panel containing 413 kinases. In cellular assays, HMPL-760 displays strong anti-proliferative activities in B-cell lymphoma cells (TMD-8, OCI-LY10, REC-1, HBL-1 and HBL-1-BTK^{C481S}) harboring either BTK^{WT} or BTK^{C481S} (GI_{50}: 0.0015-0.046 μM). In human whole blood assay, HMPL-760 inhibits activation of B-cells at nanomolar concentrations measured by inhibition of immunoglobulin-induced CD69 expression in $CD19^{+}$cells. HMPL-760 shows ≥ 10-fold inhibitory potency than ARQ 531 in both BTK^{WT} and BTK^{C481S} cells, and ~3-fold higher inhibitory potency than that of LOXO-305 in BTK^{C481S} cells. In cellular assay by detecting p-BTK after compound washout, HMPL-760 maintains a longer duration of target inhibition than LOXO-305 in both BTK wild type (HBL-1) and BTK mutant (HBL-1-BTK^{C481S}) cell lines. HMPL-760 displays dose-dependent antitumor efficacy in multiple human B cell lymphoma xenograft models in mice when orally administered at 3~50 mg/kg once daily. Complete tumor regression occurs in most of the tested models at the high dose levels. HMPL-760 shows much stronger antitumor efficacy than LOXO-305 and ARQ 531 at similar dose level, which may be associated with HMPL-760's higher drug exposures and more sustainable inhibition on BTK phosphorylation in the tumor tissues.
Conclusion: HMPL-760 is a reversible, selective, highly potent, BTK inhibitor targeting both BTK^{WT} and BTK^{C481S}. The first-in-human Phase 1

clinical trials of HMPL-760 are under way in patients with r/r B-NHL (NCT05190068, NCT05176691).

#4021

CTS2016, a novel AXL/FLT3 inhibitor for targeting AML/MDS and solid tumors

Hui Shi, Meng Wang, Jiaxin Huang, Qiugeng Ouyang, Jiannan Guo, Youzhen Wang, Yuan Mi, Haiping Wu. *CytosinLab Therapeutics Co., Ltd., Shanghai, China*

We identified CTS2016 as a novel, selective, orally bioavailable small molecule inhibitor with single-digit nanomolar enzymatic activity to AXL and FLT3. Overexpression of AXL is associated with metastasis, drug resistance, and poor prognosis of various hematological and solid tumors, which are all broadly modulated with epigenetic regulation. In addition, inhibition of AXL phosphorylation may overcome drug resistance to current FLT3 inhibitors in *FLT3-ITD*+ Acute Myeloid Leukemia (AML) (Park *et al*., 2015). We tested CTS2016 as a single agent or in combination with either venetoclax, a Bcl-2 inhibitor, or azacitidine, a hypomethylating agent (HMA) and an epigenetic modulation drug, in a series of *in vitro* and *in vivo* studies using various AML models. CTS2016 resulted in a potent growth inhibitory effect with strong induction of cell death in a spectrum of AML cell lines carrying *FLT3* mutations (*FLT3-ITD* and/or *FLT3-TKD*). CTS2016 orally administered once daily, demonstrated potent and dose-dependent antitumor responses in a variety of AML xenograft mouse models. The anti-tumor activity was correlated with the inhibition of receptor tyrosine kinase signaling, as measured by decreased phosphorylation of key downstream signaling targets of FLT3. In a tail vein injection of mouse LLC-Luciferase model, CTS2016 treatment could significantly reduce tumor metastasis. A combination of CTS2016 with venetoclax or azacitidine provides a therapeutic benefit over monotherapy and supports a rationale for testing these combination therapies in patients with relapsed or refractory (R/R) AML and myelodysplastic syndromes (MDS). In addition, CTS2016 significantly reduced the tumor burden of a leukemia model harboring *FLT3-ITD-F691L*, a drug-resistant mutation of *FLT3*. Notably, the selectivity of CTS2016 over other kinases (such as c-KIT) mitigates the off-target toxicity effects on normal hematological

differentiation which is common in clinics for other FLT3 inhibitors. These data demonstrate that CTS2016 could be a promising therapy for treating patients diagnosed with AML and MDS harboring *FLT3* mutations and solid tumors such as NSCLC and TNBC with high-expression of AXL. More proof-of-concept data would come from the ongoing clinical trial.

#4022

Preclinical intracranial activity of NVL-655 in an alectinib-resistant patient-derived model harboring EML4-ALK fusion with G1202R mutation

Jii Bum Lee[1], Mi Ra Yu[1], Mi Ran Yun[1], You Won Lee[1], Seung Yeon Oh[1], Eun Ji Lee[1], Anupong Tangpeerachaikul[2], Henry E. Pelish[2], Byoung Chul Cho[1]. *[1]Yonsei University College of Medicine, Seoul, Korea, Republic of,[2]Nuvalent Inc, Cambridge, MA*

Introduction: NVL-655 is a brain-penetrant, ALK-selective tyrosine kinase inhibitor (TKI) designed to maintain activity against ALK and ALK mutations that confer resistance to currently approved therapies, and to avoid neurological adverse events and dose-limiting toxicities associated with TRK inhibition. Brain metastases are common in ALK-positive non-small cell lung cancer (NSCLC), with an incidence of ~40% at diagnosis and ~60% after progressive disease on the first-generation ALK TKI (crizotinib) due to its limited brain penetration. Second- (ceritinib, alectinib, brigatinib, and ensartinib) and third-generation (lorlatinib) ALK TKIs have higher intracranial responses than crizotinib but are still limited by emergence of resistance mutations, most commonly G1202R-containing single and compound mutations. We previously reported that NVL-655 has intracranial activity in a preclinical model of Ba/F3 EML4-ALK v1 G1202R/L1196M. Here we further demonstrate the intracranial activity of NVL-655 in a preclinical patient-derived model harboring EML4-ALK v3 G1202R.

Methods: The YU-1077 cell line was established from a patient with ALK-positive NSCLC after relapse on alectinib and was confirmed to harbor EML4-ALK v3 G1202R alteration. ALK TKIs (crizotinib, ceritinib, alectinib, brigatinib, ensartinib, lorlatinib, and NVL-655) were profiled against YU-1077 cells in 3-day viability assays and signaling assays. YU-1077 cells were intracranially implanted in Balb/c nude mice and treated

with NVL-655 orally twice daily. Brain tumor burden was monitored weekly using magnetic resonance imaging (MRI).
Results: NVL-655 suppressed the viability of YU-1077 cells bearing EML4-ALK v3 G1202R (IC_{50} < 1 nM) with potency >10-fold that of lorlatinib. NVL-655 at ≤10 nM fully inhibited ALK signaling as measured by ALK, ERK, and S6 phosphorylation, compared to ≥100 nM of lorlatinib required to achieve similar inhibition. Other ALK TKIs tested had limited activity against YU-1077 cells in viability and signaling assays, consistent with the G1202R mutation conferring resistance to first- and second-generation ALK TKIs. In mice intracranially implanted with YU-1077 cells, MRI scans confirmed rapid tumor regression upon treatment with 0.5 and 1.5 mg/kg NVL-655.
Conclusion: Patient-derived models are widely viewed as among the most disease-relevant models for evaluating new therapies and drug resistance. Using a xenograft model derived from an alectinib-relapsed patient, we showed that NVL-655 had high intracranial activity against brain tumors bearing the ALK G1202R mutation that confers resistance to multiple ALK TKIs. NVL-655 is being evaluated in a Phase 1/2 clinical trial for patients with advanced NSCLC and other solid tumors harboring ALK rearrangement or activating ALK mutation (ALKOVE-1): NCT05384626.
[J. Lee and M. Yu contributed equally.]

#4023
Inhibiting GRP78 in non-small cell lung cancer with acquired resistance to EGFR-TKI
Jaewoo Park, Baskaran Purushothaman, Sera Hong, Munkyung Choi, Joon Myong Song, Keon Wook Kang. *Seoul National University College of Pharmacy, Seoul, Korea, Republic of*

Epidermal growth factor receptor tyrosine kinase inhibitors (EGFR-TKIs) have improved the survival of non small cell lung cancer (NSCLC) patients with active mutation of EGFR. However, some of the patients who received EGFR-TKIs showed the acquired resistance, and eventually relapsed within several months. In the TCGA data sets, gene expression of glucose-related protein 78 (GRP78), an ER chaperone, was upregulated in NSCLC tissues. We also confirmed that protein level of GRP78 was increased in HCC827-GR, H1993-GR and H1993-ER NSCLC cell lines with acquired resistance

to EGFR-TKIs. Since GRP78 modulates ER stress level which induces ROS and apoptosis, Ru(II) complex 1 and HA15, both the known GRP78 inhibitors induced higher ER stress and ROS generation accompanying more remarkable anti-proliferative and apoptotic effects in EGFR-TKI-resistant NSCLC cell lines. GRP78 level was also found to be higher in H1975, EGFR-TKI-resistant T790M-mutant cell line than other NSCLC cell lines. Blockade of GRP78 also led to apoptosis in H1975, which is consistent with the results found in the acquired EGFR-TKI-resistant cell lines. In summary, we suggest GRP78 targeting as a potential therapeutic strategy for the acquired EGFR-TKI-resistant NSCLC patients.

#4024

Overcoming ALK resistance with covalent cysteine-reactive inhibitors in lung cancer

Diane Yang[1], Stefan Harry[2], Edwin Zhang[1], Zavontae Oppong-Holmes[1], Alexander Daniel Carlin[1], Wenxin Yang[1], Abigail Smith[1], Maristela Onozato[1], Liron Bar-Peled[1], Anthony J. Iafrate[1]. *[1]Massachusetts General Hospital, Boston, MA,[2]Massachusetts General Hospital/Harvard University, Boston, MA*

The EML4-ALK fusion gene is the main oncogenic driver in 5% of non-small cell lung cancer and has been effectively targeted using ALK-specific tyrosine kinase inhibitors. While survival rates have improved steadily with each new generation of ALK TKI, resistance generally develops, including second site ALK kinase mutations as well as by-pass track activation. Since almost all anti-ALK approaches have focused on kinase domain inhibition, we sought to develop novel inhibitors with alternative mechanisms of action against ALK to overcome current drug resistance. Cysteine-reactive small molecule drugs may enable new mechanisms of target inhibition, and clinically successful examples of recent FDA-approved drugs in NSCLC include afatinib, osimertinib, sotorasib, and adagrasib.We aimed to explore and uncover novel cysteine-reactive covalent inhibitors of EML4-ALK. Using cysteine druggability mapping (CDM), a proteome-wide mass spectrometry target engagement assay, we first determined the landscape of reactive cysteines in ALK-positive cell lines and identified various targetable cysteines within the MAPK pathway and within the EML4-ALK fusion protein itself. To identify small molecules that modulate ALK

activation, degradation, and downstream signaling, we conducted a high-content phosphorylated protein screen by testing 4,400 reactive cysteine compounds and found 20 potential hits that impacted ALK phosphorylation or expression. Using proteomic analysis, we have determined the comparative specificity of these compounds, and have ranked them based on p-ALK reduction efficiency and on their off-target binding patterns. We have initiated hit-to-lead development on a compound that binds to the EML4 portion of the fusion and we are performing a detailed analysis of its mechanism of action. To further optimize the potency of the compound, we designed, synthesized, and are testing several hundred analog compounds. By applying the hit compounds from the screen in ALK TKI-resistant models, we will be able to evaluate the ability of these compounds to overcome ALK resistance. To our knowledge, we have identified the first EML4-ALK covalent binder targeting the EML4 domain. Using the unique mechanism of action of the current ALK kinase inhibitor, we have uncovered a potential compound to overcome ALK resistance.

Tyrosine Kinase and Phosphatase Inhibitors 2

#4027
TSN084, a multi-kinase inhibitor, overcomes acquired drug-resistant mutations of cMet, Trks, and Flt3, and displays broad activities against kinase oncotargets Axl, DDRs, and CDK8/19
Boyu Zhong, Tony Zhang, Chunlan Dong, Shengtang Mark Ma, Ziyang Jia, Guangming Chen, Renjuan Zheng, Jing Cindy Li, Han Fu. *Tyligand Bioscience (Shanghai), Ltd., Shanghai, China*

Background: Up to date, over 80 small molecule kinase inhibitors have been approved for the treatment of cancers worldwide. This class of targeted therapy benefits millions of patients by improving their disease management and quality of life. However, acquired drug resistance can develop quickly after treatment in most of the patients. Herein, we disclose TSN084, a unique small molecule multi-kinase inhibitor, which can overcome many common acquired drug-resistant mutations of cMet, Trks, and Flt3, etc. It also inhibits other oncotargets including Axl, DDRs, and CDK8/19.

Method: The primary screen of TSN084 against 468 kinases at a single concentration was carried out by Eurofins DiscoverX Corporation. Its inhibitory activity on interested kinases and relevant cellular proliferation were determined separately. A series of cell-derived xenograft (CDX) models were used to evaluate its *in vivo* antitumor effect. Both *in vitro* and *in vivo* PK study was performed in mouse, rat, dog, and monkey. An *in vitro* safety panel and *in vivo* GLP animal studies were carried out to assess its preliminary toxicity profile in preparation for human clinical trials.
Results: Kinase activity profiling assay revealed that TSN084 is a multi-kinase inhibitor. Among the 468 kinases tested, 33 showed >50% inhibition at 0.1 uM, including many oncotargets and their mutants such as Met, Met-Y1235D, Met-M1250T, Flt3, Flt3-N841I, Flt3-ITD, Flt3-K663Q, Flt3-D835Y, Flt3-D835V, Axl, TrkA, DDR1, and CDK8/19. It demonstrated potent anti-proliferation activity against many tumor cell lines, e.g. KM12, MKN45, MV-4-11, and HS746T. It also effectively inhibited tumor growth in several CDX drug-resistant models like NTRK-G667C and NTRK3-G696C and showed outstanding survival advantage. TSN084 is an orally bioavailable small molecule agent in mouse, rat, dog, and monkey. It is clean in a safety panel assessment of 44 concerning targets and considered safe enough to advance into clinical study.
Conclusion: TSN084 targets several oncogenic kinases and their drug-resistant mutants. It demonstrated potent antitumor effects in both *in vitro* and *in vivo* studies. It showed excellent PK properties and acceptable preclinical safety profile. A phase I clinical trial of TSN084 in patients with advanced or metastatic malignancies is currently ongoing (NCT05300438). As of Oct 30, 2022, 6 patients have been enrolled into the trial, and no DLTs or treatment-related AEs were observed. It is a promising agent for the potential treatment of resistant cancers in the clinic.

#4028

High-dose short-exposure of osimertinib robustly inhibits growth of patient-derived metastatic colorectal cancer organoids

Kirti K. Iyer, Dennis Poel, Anne Miggelenbrink, Wouter Kerkhof, Erik van den Hombergh, Loek A. W. de Jong, Nielka P. van Erp, Daniele V. F. Tauriello, Henk M. W. Verheul. *Radboudumc, Nijmegen, Netherlands*

Despite major interest in tyrosine kinase inhibitors (TKIs) as a treatment option for metastatic colorectal cancer (mCRC), almost all TKIs tested for mCRC fail in early-phase clinical trials. Although showing specific target inhibition at low concentrations, TKIs have a much broader kinase inhibitory potency at higher concentrations. Alternative high dose regimens have been proposed to explore if efficacy can be improved with acceptable toxicity. We used 3D matrix-embedded tumor organoids as a preclinical platform to determine optimal drug exposure, i.e. *preclinical pharmacology*, and to dissect the mechanisms of action to potentially convert the dismal translational success rate of TKIs for mCRC. We established patient-derived tumor organoids (PDTOs) from mCRC biopsies and, based on favorable physicochemical and pharmacokinetic properties, selected 3 TKIs (sunitinib, cediranib and osimertinib). Following standard IC50 assessment using continuous dosing with a concentration range, we investigated the cytotoxic antitumor effect of high-dose, short-exposure (HDSE) treatment. Five PDTOs were exposed to 20 μM TKI for 1-24h, washed and given normal medium, and PDTO-outgrowth was determined 1 week later. At exposures of 1, 3 and 6h, we measured intra-tumoroid TKI concentrations using a clinically validated LC/MS-MS method. PDTO cell death was observed using live-cell microscopy, and quantified by both caspase 3/7 enzyme activity assay and cleaved caspase-3 immunofluorescent staining. While PDTOs could be categorized for their sensitivity across tested TKIs, all were highly sensitive for osimertinib (IC50 values 0.40-3.8 μM). Lower sensitivity was observed for sunitinib (2.0-10.5 μM) and cediranib (2.5-7.1 μM). Only for osimertinib exposure to 20 μM for 3h was sufficient to block proliferation in all PDTOs. Interestingly, peak intra-tumoroid TKI concentration measurements across PDTOs revealed marked cellular accumulation, indicating an expanded potential for target inhibition. The concentrations correlated with sensitivity: for sunitinib from 1.5 mM for the most sensitive PDTO to 0.72 mM for the least sensitive PDTO. Likewise, the corresponding cediranib concentrations were 0.15 mM *vs* 0.062 mM. All PDTOs had high intra-tumoroid osimertinib concentrations (0.90-1.6 mM). Lastly, we detected a significant increase in apoptosis after 3h of HDSE with osimertinib. Whereas our HDSE regimen shows promising results for all 3 TKIs, very short exposure with high-dose osimertinib effectively reduces proliferation and induces cell death in all mCRC PDTOs. While this is likely due to high intra-tumoroid concentrations

reached by osimertinib—the mechanism of action at these concentrations remains unknown and is subject to further studies. In parallel, we propose that a HDSE osimertinib regimen warrants clinical exploration as a potential new treatment option for mCRC.

#4029

JIN-A04, highly effective tyrosine kinase inhibitor targeting HER2 exon 20 insertion mutations in NSCLC

Mi Ra Yu[1], Mi Ran Yun[1], Jii Bum Lee[2], Ji Yun Lee[3], So Won Aum[4], Su Jin Choi[4], Ju Yeon Park[4], Seung Yeon Oh[5], Eun Ji Lee[5], Krishna Babu Duggirala[6], Kwangho Lee[6], Min Hee Hong[7], Sun Min Lim[7], Anna Jo[8], Ethan Seah[8], Choonok Kim[8], Byoung Chul Cho[2]. *[1]Yonsei New Il Han Institute for Integrative Lung Cancer Research, Yonsei University College of Medicine, Seoul, Korea, Republic of,[2]Division of Medical Oncology, Yonsei Cancer Center, Yonsei University College of Medicine, Seoul, Korea, Republic of,[3]Lung Cancer Center, Yonsei Cancer Center, Yonsei University College of Medicine, Seoul, Korea, Republic of,[4]Yonsei Biomedical Research Institute, Yonsei University College of Medicine, Seoul, Korea, Republic of,[5]Department of Medical Science, Graduate School of Medical Science, Brain Korea 21 Project, Yonsei University College of Medicine, Seoul, Korea, Republic of,[6]Bio & Drug Discovery Division, Korea Research Institute of Chemical Technology, Daejeon, Korea, Republic of,[7]Division of Medical Oncology, Department of Internal Medicine, Yonsei University College of Medicine, Seoul, Korea, Republic of,[8]J INTS BIO, Seoul, Korea, Republic of*

Introduction: Non-small cell lung cancer (NSCLC) is the most common type of lung cancer, accounting for about 85% of lung cancer patients. 2% - 4% of patients with NSCLC harbor human epidermal growth factor receptor 2 gene (HER2) mutations, being the 90 % of them exon 20 insertions. The most common HER2 mutations in NSCLC are exon 20 mutation A775_G776insYVMA (YVMA) mutation in the kinase domain. Currently, treatment options for this subset of patients are limited. JIN-A04 is an orally available tyrosine kinase inhibitor (TKI) targeting HER2 exon20 insertion mutations and has the potential to be a best-in-class drug candidate to address this unmet clinical need.

Method: The inhibitory activity of JIN-A04 was evaluated by cell viability assay in both Ba/F3 cell lines expressed HER2 YVMA and HER2 P780_Y781insGSP (GSP) mutations. Also, Ba/F3 HER2 wild-type (WT) and normal cell lines for HUVEC (endothelial cells) and BEAS-2B (human bronchial epithelial cells) were used to assess cellular activity. In addition, to confirm mechanism action, western blotting analysis was performed on Ba/F3 YVMA and Ba/F3 GSP cell lines.
Results: In cell viability assay, JIN-A04 strongly inhibited cellular activity against Ba/F3 cell lines engineering to express the mutants HER2 YVMA (IC_{50} = 11.1 nM) and GSP (IC_{50} = 1.4 nM). It was superior to Mobocertinib (IC_{50} = 27.1 nM for YVMA and IC_{50} = 3.3 nM for GSP) and comparable with Poziotinib (IC_{50} = 3.4 nM for YVMA and IC_{50} = 0.4 nM for GSP). In normal cell lines, JIN-A04 did not inhibit the activity of HUVEC (IC_{50} = > 1000 nM) and BEAS-2B (IC_{50} = > 1000 nM) cell lines, largely sparing HER2 WT activity (IC_{50} = > 1000 nM). In protein expression analysis, JIN-A04 was effectively inhibited in all signaling pathway of p-EGFR, p-AKT, p-ERK1/2, and p-S6 on Ba/F3 YVMA and Ba/F3 GSP cell lines at a low dose level.
Conclusion: JIN-A04 is highly potent against HER2 exon 20 insertion mutations including YVMA and GSP, while largely sparing HER2 WT activity. Also, JIN-A04 demonstrated effective HER2 pathway inhibition. Based on these robust activities for HER2 exon 20 insertion, JIN-A04 is expected to provide a potent therapeutic opportunity for NSCLC patients with HER2 exon20 insertion mutations.

#4030

Generation of profound anti-tumor immunity by AUR-109, a spectrum-selective tyrosine kinase inhibitor, either as a single agent or in combination with immune checkpoint inhibitors

Girish Daginakatte, Saravanan Thiyagarajan, Kiran Aithal, Mamon Dey, Reshma Reghu, Monalisha Mandal, Kavitha Nellore, Susanta Samajdar, Murali Ramachandra. *Aurigene Discovery Technologies Limited, Bengaluru, India*

AUR-109 is an orally bioavailable clinical stage receptor tyrosine kinase inhibitor (RTK) that inhibits the activity of proangiogenic and oncogenic

pathway-related RTKs including DDR1, FGFR, VEGFR, PDGFR, and RET. DDR1 instigates immune exclusion by promoting collagen fiber alignment thereby altering extracellular matrix (ECM) components in tumor immune microenvironment (TIME). DDR1 expression inversely correlated with reduced immune cell infiltration in TIME leading to exhaustion of tumor-fighting immune cells, tumor escape, EMT and metastasis. FGFRs induce the expression the PD-L1 and VEGFRs promote the proliferation of regulatory T cells (Treg), inhibit T-cell development and maturation of dendritic cells. These findings suggest that the spectrum-selective inhibition of these RTKs by AUR-109 has the potential to strongly modulate the anti-tumor immune response. Clinically successful immune checkpoint inhibitors (ICI) (anti-PD1, anti-PD-L1, and anti-CTLA4 antibodies) block the pathways that inhibit immune cell activation thus stimulating immune responses against the tumor cells. Although ICIs show improved survival in patients with many types of cancers, they suffer from the lack of response in majority of patients along with the development of resistance to therapy. To overcome the resistance and improve the efficacy, a number of combinations of PD-1 blockade with other anticancer therapies are being evaluated. We have undertaken a detailed characterization of the anti-tumor immune response by AUR-109 either as a single agent or in combination with anti-PD1 antibodies. The effect of AUR-109 on CD4 T cells and Treg cells was evaluated in the Renca subcutaneous tumor model. Immune cell population in the blood and tumor microenvironment were analyzed by FACS. Anti-tumor efficacy was analyzed in both subcutaneous and orthotopic Renca syngeneic tumor models. AUR-109 treatment resulted in an increase of total and CD4 T cells. Higher ratio of total T cells to regulatory T cells was observed indicating that there is an increase in effector T cells. In the TILs, there was decrease in the expression of PD-1 and PD-L1 with a concomitant increase in IFN-γ expression on CD8 T cells and NK cells indicating a profound immune activation caused by AUR-109 within the tumor. These results demonstrate the therapeutic potential of AUR-109 in combination with PD-1 blockade in preclinical models and the results from the ongoing combination studies will be presented.

#4031

***In vivo* studies demonstrate differences in target inhibition and anticancer efficacy between NXP900 and dasatinib in ovarian clear cell**

carcinoma model

Saúl Navarro-Marchal[1], Carolin Temps[1], Iñigo Lanzagorta-Calvillo[1], John C. Dawson[1], Enrique Poradosu[2], Neil O. Carragher[1], Valerie G. Brunton[1], Asier Unciti-Broceta[1]. *[1]Edinburgh Cancer Research, University of Edinburgh, Edinburgh, United Kingdom,[2]Nuvectis Pharma, Fort Lee, NJ*

Background: NXP900 (formerly known as eCF506) is a novel SRC/YES1 family kinase (SFK) inhibitor that locks SRC into its native closed conformation (= type 1.5), thereby inhibiting both kinase activity and complex formation with protein partners including FAK (Temps et al. Cancer Res. 2021, 81, 5438-5450). This mode of inhibition differentiates it from dasatinib, which blocks SRC into an open conformation (type 1) that promotes SRC-FAK interactions and increases FAK autophosphorylation. According to Watanabe and coworkers (Higuchi et al. Cell Rep 2021, 34, 108876), the enhancement of SRC-protein complex formation makes type 1 SFK inhibitors allosteric facilitators of conformational protein activation. Although dasatinib is a potent inhibitor of kinase activity, because of its allosteric effects, an in vivo decrease in tumor drug exposure below the active threshold could lead to fast activation of SFK-mediated signaling, temporarily promoting cancer growth until the next dose is administered. In contrast, the capacity of NXP900 to inhibit SRC in its inactive conformation should result in a more durable blockade of SFK-induced signaling; a critical advantage to prolong on-target inhibition and improve antitumor efficacy.
Materials and Methods: Mice strain: CD1 Nude. Cell line: TOV-21G. Xenograft: bilateral SC implantation of 0.1M cells with matrigel.
Groups: Vehicle PO QD; dasatinib 30 mpk PO QD; NXP900 20 mpk PO QD; NXP900 40 mpk PO QD; NXP900 80 mpk PO QD. PD study (n=3): 3 d treatment, tumors retrieved 3 and 24 h after last dose. H&E, IHC. Efficacy (n=5): 28 d treatment.
Results: An ovarian clear cell carcinoma (OCCC) cell model, TOV-21G, was implanted subcutaneously in mice to study SRC and FAK phosphorylation (Y419 and Y397, respectively) after oral administration of NXP900 and dasatinib. Tumors were excised 3 and 24 h post-treatment and analyzed by IHC. NXP900 showed lower phosphorylated SRC levels compared to the vehicle control for all doses. Dose response correlation was clearly observed for NXP900 in tumors analyzed 24 h after the last dose,

with complete inhibition achieved at 40 mg/Kg. Importantly, comparison between vehicle and dasatinib groups showed that the tumors from the dasatinib-treated group exhibited higher levels of phospho-SRC 24 h after the last dose, evidence of the paradoxical activation of SRC proposed by Watanabe as a consequence of blocking SRC in an open conformation. Analysis of tumor growth showed that treatment with NXP900 resulted in higher anticancer effect than that of dasatinib.
Conclusions: NXP900 induces superior target inhibition and anticancer activity than dasatinib in an OCCC xenograft model. The PD study suggests that the conformation selective mode of inhibition of NXP900 is more favorable for clinical development against SFK-driven cancers.

#4032

Discovery of a potent, selective, and orally available SHP2 inhibitor that can penetrate blood-brain barrier

Miyeon Kim[1], Dongsu Kim[1], Kyeong Jin Yoon[1], Yeejin Jeon[1], Dohyun Park[1], Mijung Lee[2], Dahye Jeon[2], Soyeon Jang[2], Jinhwan Kim[2], Eunji Kim[2], Jihoon Park[3], Victor Hong[3], Sang Kyun Lim[1], Sungpil Choi[1].
[1]Kanaph Therapeutics, Seoul, Korea, Republic of,[2]Yungjin Pharm, Suwon, Korea, Republic of,[3]Keimyung University, Daegu, Korea, Republic of

Src homology region 2-containing protein tyrosine phosphatase 2 (SHP2/PTPN11) is one of the key signaling proteins in many oncogenic receptor tyrosine kinase (RTK) pathways. It mediates RAS-driven downstream signaling and activates gene expression for tumorigenesis. Importantly, a critical role of SHP2 has been found during the process of temporal adaptation and ERK re-activation after the treatment of RAS/RAF/MEK/ERK inhibitors, which means that SHP2 could be a promising therapeutic target to shut down the oncogenic RAS pathway, especially in combination with RAS/RAF/MEK/ERK inhibitors. Here we present preclinical data of an allosteric small-molecule SHP2 inhibitor that is highly potent, selective, and brain-permeable. In vitro biochemical and cellular assays showed excellent potency against SHP2 protein. In addition, we confirmed exceptional in vivo activity in mouse xenograft models, and demonstrated combination effects with a KRAS G12C inhibitor. Most importantly, the BBB penetration and anti-tumor activity in brain was confirmed both in vitro and in vivo, supporting the great potential in

treating brain-metastasized tumors. In summary, we have successfully discovered and developed a potent and blood-brain barrier permeable SHP2 inhibitor that provides a novel therapeutic option for diverse cancers associated in the RAS pathway.

#4033

Pan-exon mutant KIT inhibitor DCC-3009 demonstrates tumor regressions in preclinical gastrointestinal stromal tumor models

Bryan D. Smith, Subha Vogeti, Timothy M. Caldwell, Hanumaiah Telikepalli, Yu Mi Ahn, Gada Al-Ani, Stacie L. Bulfer, Andrew Greenwood, Cale L. Heiniger, Joshua W. Large, Cynthia B. Leary, Wei-Ping Lu, Kylie Luther, William C. Patt, Max D. Petty, Yeni K. Romero, Forrest A. Stanley, Kristen L. Stoltz, Daniel C. Tanner, Sihyung Yang, Yu Zhan, Bertrand Le Bourdonnec, Daniel L. Flynn. *Deciphera Pharmaceuticals, LLC, Lawrence, KS*

Introduction: Gastrointestinal stromal tumors (GISTs) are typically driven by primary mutations in KIT exons 9 or 11. Heterogeneous drug-resistant secondary mutations arise in patients treated with FDA approved KIT inhibitors, including imatinib and sunitinib. Drug resistant secondary mutations are found at multiple regions in the ATP pocket (encoded by exons 13 and 14) or activation switch (encoded by exons 17 and 18) of KIT kinase. In addition, multiple drug-resistant clones can arise within a tumor or in metastatic tumor sites. An inhibitor that can broadly and potently inhibit the spectrum of KIT mutations is highly sought. Ripretinib has been FDA approved as a 4^{th} line treatment for GIST and has broad activity against KIT mutations, including clinical potency in patients with mutations in KIT exons 11, 17, or 18. DCC-3009 was designed as a next generation KIT inhibitor that broadly and potently inhibits primary KIT mutations in exons 9 and 11 and secondary drug-resistant mutations across exons 13, 14, 17, and 18. DCC-3009 is a potent and selective inhibitor in enzyme and cell-based assays, and has demonstrated efficacy in xenograft models driven by drug resistant KIT mutations.

Methods: DCC-3009 was tested for inhibition of KIT mutants using standard enzyme and cell-based assays. Levels of phosphorylated KIT were determined by Western blot or ELISA. Proliferation was measured using the fluorescent dye resazurin. KIT mutant xenograft or patient-derived

xenograft models were performed at Crown Biosciences or Labcorp, AAALAC accredited facilities, with the approval of Animal Care and Use Committees.
Results: In BaF3 cells transfected with KIT mutants, DCC-3009 was shown to potently inhibit the spectrum of known primary and secondary drug-resistant mutations in GIST. The pan-mutant KIT profile of DCC-3009 was shown *in vitro* to be superior to 2nd and 3rd line standard of care therapies sunitinib and regorafenib. DCC-3009 was selective for KIT when screened against a large panel of kinases. DCC-3009 has optimized pharmaceutical properties for oral administration. In pharmacokinetic/pharmacodynamic studies DCC-3009 achieved sufficient free drug levels to significantly inhibit drug-resistant KIT mutants for 12 hr post dose. In xenograft studies, treatment with DCC-3009 twice daily led to tumor regression in drug-resistant models with KIT exon 9/13, 11/13 or 11/17 mutations.
Conclusions: DCC-3009 is a pan-exon mutant KIT inhibitor exhibiting high potency in KIT mutants in pre-clinical models spanning exons 9, 11, 13, 14, 17 and 18. *In vivo,* DCC-3009 exhibited efficacy in drug-resistant models with KIT exon 9/13, 11/13 or 11/17 mutations. Based on this profile, DCC-3009 has entered formal preclinical development.

#4034

A potent and highly selective irreversible HER2 inhibitor for treating HER2-driven cancers

Chunmei Zhao, Lana Kulyk, Iriny Botrous, Kelly Chen, Chang Zhao, Afsheen Banisadr, Mary L. Anderson, Fred Manby, Tom Miller, Chao Zhang, Laurent Gomez, Zhongdong Huang. *Entos, Inc, La Jolla, CA*

HER2 amplification and mutations occur frequently in multiple human cancers, including breast, ovarian, gastric and lung cancers. Despite HER2 being one of the earliest oncogenic drivers discovered, HER2 inhibitors have had limited clinical success compared to inhibitors of other kinase oncogenes. This has been attributed to a compensatory mechanism present in HER2-driven cancers that significantly raises the exposure threshold for durable pharmacological inactivation of HER2 signaling in vivo. This requires a therapeutic index far exceeding that of available pan-ERBB and HER2 inhibitors, all of which are hampered by dose-limiting side effects from collateral or residual EGFR inhibition.To address this critical unmet

need, we present a novel irreversible HER2 inhibitor, ENT-H1, discovered via artificial intelligence-enabled chemistry. ENT-H1 potently inhibits wild-type and mutated HER2, including the recalcitrant exon 20 insertion mutations, while sparing wild-type EGFR. In a panel of Ba/F3 cells whose growth is driven by HER2 or EGFR expression, ENT-H1 displayed low nanomolar potency across 23 representative HER2 mutations, while showing minimum effect on the growth of Ba/F3 EGFR cells. This exquisite selectivity was confirmed by comparing the sensitivity of cancer cell lines that over-express HER2 (e.g. BT-474 and Calu-3) and EGFR (e.g. A431), and translated into a high in vitro therapeutic index when ENT-H1 was evaluated in a gastrointestinal toxicity assay. In vivo, ENT-H1 demonstrated strong efficacy and better tolerability than benchmark HER2 inhibitors in multiple HER2-amplified or -mutated tumor models, including those bearing HER2 exon 20 insertion mutations (e.g. A775G776insYVMA and G776VC). Treatment with ENT-H1 led to significant tumor regression without causing body-weight loss. In these models, ENT-H1 showed robust and rapid pharmacodynamic effect in reducing phosphorylated HER2 and downstream phosphorylated AKT and ERK levels, confirming that the antitumor effect was a result of targeted inhibition of HER2 oncogenic signaling. Further analysis showed that ENT-H1 concentrations were significantly higher in xenograft tumors than in plasma; this distribution profile has the potential to maximize target engagement in the tumor while minimizing untoward systemic side effects. These data establish that ENT-H1 is a safe and effective HER2 small-molecule inhibitor. With 100-fold selectivity against the highly homologous EGFR and a desirable pharmacokinetic profile, ENT-H1 represents a promising drug candidate to realize the full therapeutic potential of a HER2-targeting agent while avoiding side effects associated with EGFR inhibition.

#4035

Preclinical activity of BAY 2927088 in HER2 mutant non-small cell lung cancer

Franziska Siegel[1], Gizem Karsli-Uzunbas[2], Kristyna Kotynkova[2], Quinn McVeigh[2], Stephan Siegel[3], Daniel Korr[4], Volker Schulze[3], Markus Berger[3], Georg Beckmann[5], Andrew Cherniack[2], Matthew Meyerson[6], Heidi Greulich[2]. *[1]Research & Early Development Oncology, Bayer AG, Berlin, Germany,[2]Broad Institute of MIT and Harvard, Cambridge,*

MA,[3]Synthetic Modalities, Bayer AG, Research & Development, Pharmaceuticals, Berlin, Germany,[4]Therapeutic Compound Research, Nuvisan ICB GmbH, Berlin, Germany,[5]Biomedical Data Science, Bayer AG, Research & Development, Pharmaceuticals, Berlin, Germany,[6]Dana-Farber Cancer Institute, Boston, MA

HER2 mutations are potent oncogenic drivers in various cancer indications. In NSCLC, about 2% of patients carry either a HER2 exon20 insertion mutation or a HER2 point mutation. With the recent approval of fam-trastuzumab deruxtecan-nxki, the first targeted treatment option became available for HER2 mutant NSCLC patients. However, there remains a high unmet need for more effective and better tolerated therapies with the potential to improve response rates and response durability.
BAY 2927088 is a reversible small molecule inhibitor that is currently being evaluated in a first-in-human, phase I clinical trial in patients with EGFR mutant NSCLC (NCT05099172).
Here, we present the preclinical activity profile of BAY 2927088 in HER2 mutant NSCLC. BAY 2927088 shows strong antiproliferative activity in an isogenic Ba/F3 cell line panel of HER2 exon20 insertion mutations as well as HER2 point mutations. BAY 2927088 is highly potent on the most frequent HER2 exon20 insertion mutations A775insYVMA and G776del insVC, as well as in the HER2 point mutations S310F, S335C, and L755S, among others. In addition, the compound was active in a subset of endogenously HER2 mutant cancer cell lines. The *in vitro* activity of BAY 2927088 was validated *in vivo* in a patient-derived xenograft model carrying the HER2 exon20 insertion mutation A775insYVMA.
The strong preclinical activity of BAY 2927088 in HER2 mutant NSCLC supports clinical evaluation in this indication and might offer a novel targeted therapy option for NSCLC patients that carry HER2 mutations.

#4036

NMS-0963 is a novel potent, selective and orally available Syk inhibitor with promising preclinical activity in diffuse large B-cell lymphoma

Grazia Saturno, Michele Modugno, Paolo Orsini, Giovanni Cervi, Laura Buffa, Ilaria Motto, Nilla Avanzi, Marisa Montemartini, Fabio Gasparri, Gemma Texido, Arturo Galvani, Antonella Isacchi. *Nerviano Medical Sciences, Nerviano, Italy*

The B-cell receptor (BCR) is a key survival molecule for normal B cells and for most B-cell malignancies, such as Chronic Lymphocytic Leukaemia (CLL) and Non-Hodgkin's Lymphomas (NHL) including Diffuse Large B-cell Lymphomas (DLBCL). Small molecule inhibitors of key signaling kinases involved in the BCR pathway, such as the Btk inhibitor ibrutinib and the PI3Kdelta inhibitor idelalisib, have already demonstrated significant clinical activity. Spleen tyrosine kinase (Syk) is a non-receptor cytoplasmic tyrosine kinase that plays a fundamental role in BCR signaling initiation thus representing an additional potential therapeutic target for the inhibition of the BCR pathway. Here, we report the discovery and characterization of NMS-0963, a novel potent, selective and orally available Syk inhibitor, identified through an integrated medicinal chemistry and rational design approach. NMS-0963 showed potent inhibitory effect on Syk in an in vitro biochemical assay and displayed a good selectivity profile on a broad panel of kinases. On-target potency was confirmed in a cell-based assay using BaF3 cells engineered to express constitutively activated Syk, showing potent inhibition of Syk activity resulting in antiproliferative effect with IC50s in the low nanomolar range. Effective inhibition of BCR-mediated signaling pathway was observed in DLBCL-derived cell lines. NMS-0963 showed favourable ADME profile and good in vivo pharmacokinetic profiles after oral administration in mouse, rat and dog. Furthermore, NMS-963 demonstrated striking in vivo efficacy in tumor models of CD79/Myd88 mutated DLBCL, superior to competitors. Together with a permissive preclinical safety profile, these results support a rational for clinical development of NMS-0963 in DLBCL.

#4037

Doxazosin exerts anti-metastatic potential in triple-negative breast cancer via impairment of cancer stem-like features

Seongjae Kim, Dongmi Ko, Juyeon Seo, Soeun Park, Minsu Park, Kee Dal Nam, Yong koo Kang, So Ra Seock, Jaeyoun Park, Eunhye Oh, Eunsun Jung, Yoon-Jae Kim, Ji Young Kim, Jae Hong Seo. *Korea University Guro Hospital, Seoul, Korea, Republic of*

Background **and Purpose:** Triple-negative breast cancer (TNBC) tumors typically harbor a high cancer stem-like population leading to chemo-

resistance, recurrence, and metastasis. Tumor metastasis is associated with 90% of cancer-related deaths, highlighting the urgent clinical unmet need. Doxazosin is known to inhibit cell migration and invasion in several cancer cell types; however, the precise mechanisms underlying doxazosin's anticancer effects in TNBC have not been fully elucidated. In the present study, we sought to investigate the mechanism of action of doxazosin responsible for its effects on apoptosis, cancer stem cell (CSC)-like properties, cell migration, and metastasis in TNBC.
Experimental designs: Doxazosin on TNBC cell lines [MDA-MB-231, BT549, and 4T1] in vitro was evaluated in cell viability, apoptosis, cell migration, CD44/CD24 staining, ALDH1 activity, and mammosphere formation. The effect of doxazosin on tumor growth, angiogenesis, and metastasis was evaluated in an orthotopic allograft mice model with CSC-enriched population.
Results: Doxazosin significantly reduced cell viability and induced apoptosis in MDA-MB-231 and BT549 cells via activation of caspase-3/-7 and cleavage of PARP. Doxazosin significantly suppressed cell migratory capability, concomitant with disrupting cytoskeletal proteins, including vimentin and F-actin expression in TNBC cells. An impairment of BCSC-like properties was associated with reduction of ALDH1 activity and the CD44+/CD24- population, concomitant with suppression of mammosphere-forming ability. Doxazosin administration reduced tumor growth and lung metastasis, as evidenced by a sharp decline in bioluminescence signal intensity. Inhibitory effect of tumor growth was accompanied by a significant decrease of Ki-67 and enhancement of apoptosis with DNA fragmentation and increased cleaved-caspase-3 expression. The latter phenomenon was associated with the impediment of JAK2/STAT3 signaling pathway and CSC-like properties. Furthermore, no toxic effects of doxazosin were found in liver and kidney function in animals.
Conclusion: Taken together, our findings highlight doxazosin as a promising candidate for drug repurposing in suppressing metastatic TNBC.

#4038
Discovery of potent and selective inhibitors of the protein tyrosine phosphatases PTPN2 and PTPN1 to trigger anti-tumor immunity through sensitization of tumor cells and activation of immune cells

Kalliopi Pervolaraki[1], Egle Katkeviciute[2], Dominique Lambin[1], Sandro Boland[1], Amuri Kilonda[1], Vincent Pericolle[1], Marnik Nijs[1], Wanda Haeck[1], Kristine Metzger[1], Hugo Klaassen[1], Arnaud Marchand[1], Patrick Chaltin[1], Matthias Versele[1], Marianne Spalinger[2], Michael Scharl[2]. *[1]CD3 (Centre for Drug Design and Discovery), Leuven, Belgium,[2]Department of Gastroenterology and Hepatology, University of Zurich, Zurich, Switzerland*

Protein tyrosine phosphatase nonreceptor type 2 (PTPN2) has emerged as a promising cancer immunotherapy target. Previously, we reported on the functional role of PTPN2 in the pathogenesis of colorectal carcinoma (CRC). We demonstrated increased PTPN2 phosphatase activity correlates with disease progression and decreased immune responses in tumor tissues, while loss of PTPN2 in T-cells or in dendritic cells (DCs) reduces tumor burden in several CRC models and potentiates anti-PD1 efficacy (Katkeviciute et al., 2021). Others reported that loss of PTPN2 in tumor cells sensitizes to immune-mediated tumor killing (Manguso et al., 2017; Goh et al., 2022). Thus, PTPN2 was proposed as a critical node to modulate anti-tumor immunity, and PTPN2 inhibition is expected to enhance anti-tumor immunity by sensitizing tumor cells and by activating immune cells. Recently, also the closely related phosphatase PTPN1 (PTP1B) was demonstrated to restrain T-cell mediated tumor killing (Wiede et al., 2022). Inhibition of Protein Tyrosine Phosphatases has historically been a demanding area for drug discovery. However, both allosteric PTP inhibitors (*eg* targeting SHP2/PTPN11) and catalytic-site inhibitors (targeting PTPN2/N1) have recently progressed to clinical studies. We now identified a chemical series of novel dual PTPN2/N1 inhibitors. These inhibitors bind to the catalytic site of PTPN2, as confirmed by crystallography. The best molecules of the series are low nM inhibitors of PTPN2 and PTPN1 enzymes with excellent selectivity across other phosphatases. As an immediate consequence of PTPN2/N1 inhibition, these compounds augment phosphorylation of STAT1 and/or STAT5 isoforms in myeloid and T-cell lines, and in primary T-cells, macrophages and DCs. This results in immune-cell activation as evidenced by increased production of effector cytokines (e.g. IFNγ), immune-activation, levels of cytotoxicity markers in T-cells (e.g. granzyme B) as well as upregulation of antigen presentation and co-stimulatory markers in macrophages and DCs. Furthermore,

inhibition of PTPN2/N1 sensitizes murine and human cancer cell lines to IFNγ, and enhances immune-mediated tumor killing in co-culture assays *in vitro*. *In vivo* evaluation of selected examples is in progress and results will be presented at the conference. Our data indicate that inhibition of PTPN2/N1 phosphatase activity is a powerful pharmacologic strategy to promote anti-tumor immunity, with strong potential to be exploited for cancer immunotherapy both as a single agent treatment in anti-PD1 refractory cancers, and in combination with anti-PD1 therapy.

#4039

RET overexpression is frequent in lung neuroendocrine tumors (NET) and associates with response to RET tyrosine kinase inhibitors (RET TKIs) in NET cell lines

Jaume Roca-Arias[1], Jordi Bertran-Alamillo[1], Ruth Román[1], Cristina Aguado[1], Laura López[2], Leticia Ferro-Leal[3], Beatriz Garcia-Pelaez[1], Rodrigo de Oliveira Cavagna[3], Silvia Teixeira[3], Rafael Rosell[4], Rui Manuel Reis[3], Miguel A. Molina-Vila[1], Ivana Sullivan[5]. *[1]Laboratory of Oncology, Pangaea Oncology, Dexeus University Hospital, Barcelona, Spain,[2]Pathology Department, Hospital de la Santa Creu i Sant Pau, Barcelona, Spain,[3]Molecular Oncology Research Center, Hospital de Amor, Barretos, Brazil,[4]Hospital Dexeus, Barcelona, Spain,[5]Medical Oncology Department, Hospital de la Santa Creu i Sant Pau, Barcelona, Spain*

Background**:** *RET* (rearranged during transfection) is a proto-oncogene encoding for a tyrosine kinase membrane receptor that promotes protein synthesis and cell proliferation. A small percentage of human tumors harbor *RET* fusions or mutations as oncogenic drivers and RET-TKIs have been developed. Two of them, selpercatinib and pralsetinib, have recently been approved. However, their effect on tumors overexpressing wild-type RET (wt-RET) has not been investigated. A large-scale mRNA analysis performed by our group revealed that ~2% of lung tumors present high expression of wt-RET in absence of fusions. Interestingly, ~60% of high wt-RET tumors presented neuroendocrine characteristics.

Methods: Twenty large cell neuroendocrine (LCNEC) and 19 small cell (SCLC) lung carcinomas from two additional institutions were analyzed by nCounter® to validate the previous results. For *in vitro* experiments, a panel

of cell lines derived from lung NETs (DMS-53, NCI-H82, NCI-H727) was used, together with a lung adenocarcinoma cell line (LC2/ad, a positive control harboring the *CDCC6-RET* translocation). *RET* fusions and mRNA expression were analyzed by nCounter®, RET protein expression by Western blotting and immunohistochemistry (IHC) and *RET* mutations by next generation sequencing. The inhibitory effects of selpercatinib and pralsetinib were analyzed *in vitro* by MTT in 2D and spheroid/3D cultures. Finally, *in vivo* experiments implanting tumor cells into athymic nude mice are ongoing.
Results: Among the 20 LCNECs and 19 SCLCs analyzed, 3 (15%) and 3 (15%) presented very high levels of wt-RET mRNA by nCounter, respectively. Fusions were absent in all cases. The NCI-H82 and NCI-H727 NET cell lines showed very low RET mRNA and protein expression by nCounter, Western blotting and IHC. In contrast, DMS-53 cells presented levels of RET mRNA and protein higher than the observed in the *RET*-fusion positive LC2/ad. In 2D models, the three NET cell lines tested showed moderate resistance to pralsetinib and selpercatinib, with IC50s of 1.5 - 9.7 μM for pralsetinib and 4.6 - 6.1 μM for selpercatinib; while the RET-fusion positive LC2/ad cells showed an IC50 in the nM range, as expected. In 3D cultures, DMS-53 was found to be sensitive to RET TKIs, with IC50s of and 0.3 μM for praseltinib and 2.5 μM for selpercatinib. In contrast, spheroids of the two RET low cell lines showed complete resistance to both drugs (IC50>10 μM). Experiments in animal models are currently ongoing, final results will be presented at the meeting.
Conclusions: Overexpression of RET is frequent in lung tumors with neuroendocrine features (LCNEC, SCLC). Selpercatinib and Pralsetinib show antitumor activity in lung NETs cells expressing high levels of wt-RET.

#4040
Asciminib activates erythroid differentiation in K562 cell line
Hammad Hassan, Sarah Yousuf, Syed Muhammad Areeb Ahmed, Karim Ruknuddin, Hadiqa Raees, Sadia Habib, Fizza Iftikhar, Afsar Ali Mian, Elnasir Lalani. *Centre for Regenerative Medicine and Stem Cell Research, Aga Khan University, Aga Khan University, Pakistan*

Background**:** Asciminib an allosteric tyrosine kinase inhibitor (TKI) was recently approved by the FDA for managing Philadelphia positive chronic myeloid leukemia (CML) patients in chronic phase who had failed to respond to previous TKIs. In this study, we used human erythroleukemic K562 cell line to investigate the role of asciminib as an inducer of erythroid differentiation. Additionally, imatinib, which has previously been reported as a potential inducer of erythroid differentiation, was also tested on these cells, both independently as well as in combination, in order to investigate the degree of erythroid differentiation in a K562 cell line.
Methodology: In this study, we investigated the effect of asciminib (5-20nM) with and without imatinib (50-200nM) in differentiating the erythroleukemic cell line K562 towards erythroid lineage. K562 cells were cultured over a 12-day period in basic (IMDM) media and an EPO-based differentiation media to select optimal medium conditions. In addition, an *in-vitro* drug cytotoxicity experiment (XTT) was used to determine the preliminary toxicity of asciminib with IMDM media and EPO-based differentiation media. CD235a and CD71 surface marker expressions were analyzed by flow cytometry at all time-points to determine the degree of differentiation achieved by each of the conditions. Moreover, to analyze and identify hemoglobin producing cells ensuing differentiation, benzidine staining was performed at indicated time points.
Results: Our results suggest that asciminib, imatinib or a combination of both drugs in EPO-based differentiation media results in efficient erythroid differentiation with high levels of GPA expression (approx. 90%) and significant upregulation of globin genes (p value = 0.0001). These results were further confirmed by benzidine staining, where drug addition and dose escalation significantly increased benzidine-positive cells. Our results also demonstrated that asciminib was able to achieve maximum differentiation at a much earlier time point as compared to imatinib. Moreover, asciminib, when combined with another TKI such as imatinib, can also aid in lowering the drug concentrations being used, hence resulting in lessening the toxicity of the drug when used alone required at high doses.
Conclusion: The results from this study highlighted the novel role of asciminib in erythroid differentiation using an *in-vitro* K562 model that can give high-levels of surface markers and globin expression. Potential clinical application of asciminib in hematological diseases that are associated

specifically with a failure in the expression of globin genes should be evaluated.
Keywords:K562, erythroid differentiation, asciminib, imatinib, glycophorin A, transferrin receptor, hemoglobin

#4041

The EML4-ALK fusion protein mediates reduced sensitivity to the combination of neratinib and dasatinib

Myra E. Castel[1], Neil T. Conlon[1], Lisa D. Eli[2], Alvin Wong[2], John Crown[3], Denis M. Collins[1]. *[1]NICB, Dublin City University, Dublin 9, Ireland,[2]PUMA Biotechnology, Inc, Los Angeles, CA,[3]St. Vincent's University Hospital, Dublin, Ireland*

Introducti**on:** The anaplastic lymphoma kinase (ALK) gene encodes a receptor tyrosine kinase involved in cellular proliferation, differentiation, and cell death. ALK becomes oncogenic when it forms a fusion gene. The EML4-ALK fusion gene has been identified mainly in non-small cell lung cancer (NSCLC). It is unknown whether neratinib, an irreversible pan-HER tyrosine kinase inhibitor (TKI) targeting EGFR, HER2 and HER4, is effective in cancers harboring EML4-ALK gene fusion. The objective of this study was to assess *in vitro* efficacy of neratinib in combination with dasatinib (Src/Abl TKI) or crizotinib (ALK TKI) in EML4-ALK+ NSCLC.
Methods: The antiproliferative effects of neratinib, dasatinib and crizotinib were assessed in the CRISPR/Cas9-modified EML4-ALK fusion-A549 (EML4-ALK+) and parental A459 (A549-Par) NSCLC cell lines by 5-day acid phosphatase assay. IC_{50} values were calculated using CalcuSyn software. To assess the synergy between neratinib and dasatinib, and neratinib and crizotinib, matrix assays were performed and analyzed using Combenefit software. To further assess the efficacy of the TKIs, changes in signaling pathways were assessed by Western blotting, and apoptosis induction and cell migration were measured with the Incucyte® S3 imaging system.
Results: Neratinib, crizotinib, and dasatinib displayed nanomolar IC_{50} values in both cell lines. As expected, EML4-ALK+ cells were more sensitive to crizotinib than A549-Par cells (IC_{50} = 595 nM vs 1 μM, $p \leq 0.05$). EML4-ALK expression led to numerical increases in neratinib IC_{50}

value (326.37 ± 44.34 nM in EML4-ALK+ vs 247 ± 32.65 nM in A549-Par) and dasatinib IC_{50} value (39.95 ± 5.67 nM in EML4-ALK+ vs 27.75 ± 18.53 nM in A549-Par) but these changes were not statistically significant. Matrix assays showed that neratinib-crizotinib (NC) was more effective than crizotinib alone in both cell lines, with more potent sensitivity in EML4-ALK+ cells. The neratinib-dasatinib (ND) combination was synergistic in the A549-Par cell line but only additive in the EML4-ALK+ cell line, suggesting a reduced sensitivity to the ND combination. EML4-ALK+ cells had sustained pERK1/2 levels after treatment with all TKIs, except NC, compared to A549-Par cells. Neratinib alone was significantly less effective at inhibiting pAkt (99.2 ± 5.3 % in EML4-ALK+ vs 64.9 ± 19.0 %, $p \leq 0.05$) and pERK1/2 (91.3 ± 4.6 % in EML4-ALK+ vs 54.9 ± 15.9 %, $p \leq 0.01$) in EML4-ALK+ cells than in A549-Par cells at 24h. In A549-Par cells, ND caused the highest apoptotic induction, followed by NC. Apoptosis levels induced by ND in EML4-ALK+ cells were 4-fold lower at 72hr than in A549-Par cells ($p \leq 0.0001$). Dasatinib and ND were more effective than crizotinib or NC at preventing cell migration in both cell lines.

Conclusion: EML4-ALK potentially decreases sensitivity to the neratinib-dasatinib combination. This warrants further investigation in other EML4-ALK+ models.

#4042

Role of individual HER family members and pan-HER targeting treatment strategy in NRG1 fusion positive cancer

Hibiki Udagawa, Monique Nilsson, Junqin He, Alissa Poteete, John Victor Heymach. *Department of Thoracic Head and Neck Medical Oncology, The University of Texas MD Anderson Cancer Center, Huston, TX*

NRG1 gene fusions are rare, clinically actionable somatic alterations identified in 0.1% of all tumors. Previous studies have demonstrated that NRG1 fusions signal through *ERBB*/HER family members and that HER2 inhibition has anti-tumor activity in *NRG1* fusion-driven cancers. However, NRG1 can also bind to HER4 in addition to HER3, and the contribution of individual HER family members in tumor cells with NRG1 fusions has not been fully elucidated. To determine the role of individual HER family members in NRG1 fusion positive cancer cells, we engineered Ba/F3 cells

to express various HER family members along with NRG1 fusions. Expression of NRG1 fusions in combination with EGFR/HER3, HER2/HER4 or HER4 induced cellular transformation as measured by IL-3 independent growth. These results indicated that in addition to HER2/HER3 signaling, EGFR/HER3, HER4, and to a greater extent, HER2/HER4 signaling, may activate key oncogenic signaling pathways in cells expressing NRG1 fusions. We next assessed whether targeted inhibition of HER family members could inhibit the growth of NRG1 fusion positive cancer cells using our panel of engineered Ba/F3 cells, human tumor cell lines, and xenograft models. Our data indicated that pan-HER tyrosine kinase inhibitors (TKIs), such as poziotinib, were more effective at blocking HER2/HER3, EGFR/HER3 and HER4 signaling in NRG1-fusion expressing cells as compared to TKIs with greater relative specificity for EGFR (erlotinib, lapatinib), HER2 (pyrotinib), EGFR/HER2 (afatinib, dacomitinib, neratinib) or HER2/HER4 (TAS0728,tucatinib). In NRG1 fusion-positive cancer cell lines, poziotinib showed potent anti-tumor cell activity with IC_{50} values of 0.2 - 0.4 nM. The IC_{50} values of EGFR/HER2 TKIs were 0.3 - 23 nM, and HER2/HER4 TKIs showed modest activity with IC_{50} values of 11 - 560 nM. Next, we assessed whether inhibition of HER family dimerization also had activity against tumor cells harboring NRG1 fusions. We observed that pertuzumab, a HER2 antibody which inhibits HER2 dimerization with other HER family members, had improved single agent activity as compared to trastuzumab, a HER2 antibody that inhibits HER2 activation, suggesting crosstalk between HER family members. Moreover, an additive effect was observed when tumor cells were treated with trastuzumab in combination with pertuzumab. Treatment with cetuximab, an antibody that targets EGFR, in combination with trastuzumab and pertuzumab yielded a synergistic effect on tumor cell killing. These data indicate that HER4 and EGFR can play a role in NRG1 fusion-driven signaling through crosstalk with HER2/HER3 and thus, pan-HER/EGFR inhibitors are more effective than EGFR/HER2 or HER2/HER4-selective inhibitors, highlighting the therapeutic potential of targeting multiple members of the HER family in NRG1 fusion driven cancers.

#4043

Stimulation of the mapk and pi3k/akt pathways in pancreatic cancer cells by polyisoprenylated cysteinyl amide inhibitors

Kweku Ofosu-Asante, Jassy M. Lazarte, Amarendar G. Burra, Nazarius S. Lamango. *Florida A&M University College of Pharmacy & Pharmaceutical Sciences, Tallahassee, FL*

Pancreatic cancer is the third deadliest cancer with a 5-year survival rate of less than 10%. Over 90% of reported cases are driven by *KRAS* mutations. KRAS signals through the MAPK and PI3K pathways. Targeting mutant KRAS has been a decades-long challenge until recently whereby drugs that react with specific mutant proteins have been developed. Polyisoprenylated cysteinyl amide inhibitors (PCAIs) are potential anticancer agents with an alternative design strategy targeting polyisoprenylation-dependent processes of hyperactive mutant or overexpressed G-proteins. The effect of PCAIs on the viability and downstream mediators of KRAS signaling was determined on PANC-1 and MIAPaCa-2 cells. Of the 16 different analogs tested, NSL-YHJ-2-45 and NSL-YHJ-2-27 were the most potent with EC_{50} values of 3.6 and 3.8 against PANC-1 cells, respectively. For MIAPaCa-2 cells, NSL-YHJ-2-27 was the most potent with an EC_{50} value of 2.2. Western blotting analysis of PCAIs-treated PANC-1 cells revealed that phosphorylated BRAF, MEK 1/2, ERK 1/2 and p90RSK increased by 64, 129, 152 and 79%, respectively, while phosphorylated CRAF levels decreased by 27%. Moreover, monomeric G-proteins, CDC42, RHOA and RAC 1/2/3 protein levels decreased by 20, 58 and 13%, respectively. NSL-YHJ-2-27 (5 μM) also increased the levels of pAKT (Ser 473) and pAKT (Thr 308) by 72 and 192%, respectively. When MIAPaCa-2 cells were treated with 0-5 μM NSL-YHJ-2-27, MEK 1/2, ERK 1/2 and p90RSK phosphorylation increased by 78, 270 and 260%, respectively. However, at 5 μM NSL-YHJ-2-27, there were no significant changes in protein levels of the monomeric G proteins RAC 1/2/3 and RHOA, but protein levels of CDC42 increased by 132%. NSL-YHJ-2-27 (5 μM) increased the levels of pAKT (Ser 473) and pAKT (Thr 308) of MIAPaCa-2 cells by 97 and 82%, respectively. The results indicate the effect of PCAIs on the phosphorylation of important kinases involved in MAPK and AKT pathways. These effects on these signaling pathways strongly indicate the potential of the PCAIs against RAS-driven cancers.

#4044

Development of UCT-01-097, a novel orally available ERK1/2 inhibitor for the treatment of ERK1/2 dependent cancers

Neil A. O'Brien[1], Martina S. J. McDermott[1], Brendan M. O'Boyle[2], Corey M. Reeves[2], Michael Bartberger[2], Oliver Loson[2], Kevin Chau[1], Jenny J. Hong[1], Weiping Jia[1], Naeimeh Kamranpour[1], Tong Luo[1], Raul Ayala[1], Athena M. Madrid[1], John A. Glaspy[1], Brian M. Stoltz[3], Dennis J. Slamon[1].
[1]UCLA - University of California Los Angeles, Los Angeles, CA,[2]1200 Pharma, Culver City, CA,[3]Division of Chemistry and Chemical Engineering, California Institute of Technology, Pasadena, CA

The MAPK signaling pathway is the most commonly mutated and/or dysregulated pathway in cancer. Strategies to target it have yielded some success with inhibitors against $KRAS^{G12C}$ and BRAF, and to a lesser extent, MEK1/2. However, the impact of these molecules is often limited by toxicity and rapid and diverse mechanisms of resistance; both adaptive and/or acquired. For example, treatment with MAPK pathway targeting agents results in compensatory activation of the downstream mediator ERK1/2 and enables tumors to subvert the targeted therapy. Thus, targeting ERK1/2 provides promising potential advantages in overcoming and/or preventing adaptive and acquired resistance. We evaluated multiple preclinical and clinically staged ERK1/2 inhibitors—including ERAS-007 and BVD-523—in a 500+ cell line screening platform and identified cancers with subpopulations that are sensitive to this class of inhibitor. KiNativ analyses helped to inform the differences in sensitivity/selectivity that we observed between each ERK1/2 inhibitor. Comprehensive molecular profiling of the cell lines at baseline allowed us to screen for potential molecular markers of sensitivity/resistance to these compounds. Using this platform, we have developed a novel, potent ERK1/2 small molecule inhibitor, UCT-01-097, with improved selectivity over other clinically staged inhibitors. These data, coupled with the broad spectrum of in vitro responses, suggests an improved therapeutic index with this molecule. UCT-01-097 shows kinase selectivity in both cell free and in-cell assays and robust efficacy in panel of pancreatic PDX models. Inhibition of xenograft tumor growth was achieved using both daily dosing and intermittent dosing schedules. We have successfully submitted a regulatory

IND and are currently enrolling a Phase 1 clinical trial in advanced solid tumors for treatment with UCT-01-097 (NCT04761601).

#4045

DCC-3084, a RAF dimer inhibitor, broadly inhibits BRAF class I, II, III, BRAF fusions, and RAS-driven solid tumors leading to tumor regression in preclinical models

Stacie L. Bulfer, Bertrand Le Bourdonnec, Jeffery D. Zwicker, Yu Mi Ahn, Gada Al-Ani, Hikmat Al-Hashimi, Chase K. Crawley, Kristin M. Elliott, Saqib Faisal, Andrew M. Harned, Cale L. Heiniger, Molly M. Hood, Salim Javed, Michael Kennedy, Joshua W. Large, Cynthia B. Leary, Wei-Ping Lu, Kylie Luther, Max D. Petty, Hunter R. Picard, Justin T. Proto, Yeni K. Romero, Forrest A. Stanley, Kristen L. Stoltz, Daniel C. Tanner, Hanumaiah Telikepalli, Mary J. Timson, Lakshminarayana Vogeti, Subha Vogeti, Sihyung Yang, Lexy H. Zhong, Bryan D. Smith, Daniel L. Flynn.
Deciphera Pharmaceuticals, LLC, Waltham, MA

Background**:** Mutations in the RAS/MAPK pathway are a frequent driver of cancer, with oncogenic RAS or RAF mutations occurring in >30% of all cancers. First generation BRAF inhibitors are approved for use for tumors with Class I BRAF mutations (V600X). However, these drugs are not efficacious in RAF dimer mutant and RAS mutant cancers due to paradoxical activation of RAF dimers. Herein, we describe DCC-3084, a potent and selective investigational Switch Control inhibitor of BRAF and CRAF kinase dimers that targets Class I, II and III BRAF mutations, BRAF fusions, and BRAF/CRAF heterodimers. DCC-3084 combines with inhibitors of additional nodes in the MAPK pathway to potentially target a large unmet medical need in RAS and RAF mutant cancers.
Methods: Inhibition of RAF kinases, including off-rate analysis, was measured using recombinant enzymes. X-ray crystallography was used for structure-based drug design. Cellular proliferation was measured using resazurin to monitor cell viability. Synergy in cells was measured using BLISS scores and curve shift analysis. Inhibition of ERK or RSK phosphorylation was measured by AlphaLISA or ELISA. Pharmacokinetics (PK) in the plasma, brain and CSF compartments were measured following oral dosing in Wistar rats. RAF and RAS mutant mouse xenograft models were used to assess PK, pharmacodynamics (PD), and efficacy.

Results: DCC-3084 is a potent and selective Switch Control inhibitor of RAF dimers that was designed to target Class I, II, III BRAF mutants, BRAF fusions, and BRAF/CRAF heterodimers. DCC-3084 inhibits BRAF and CRAF, exhibiting slow off-rates ($t_{1/2}$ >20 hr). Potent single-agent inhibition of MAPK pathway signaling and cellular proliferation was observed in a wide range of Class I, II, III BRAF and BRAF fusion altered cell lines. Synergy was observed in combination with inhibitors of other nodes in the RAS/MAPK pathway in RAS mutant cell lines. DCC-3084 was demonstrated to be CNS penetrable and exhibited dose dependent oral exposure with robust inhibition of the RAS/MAPK pathway in PK/PD models. DCC-3084 accumulated in tumor tissue relative to plasma, further demonstrating a favorable pharmaceutical profile. Oral treatment of DCC-3084 as a single agent resulted in tumor regression in BRAF mutant and KRAS Q61K mutant mouse xenograft models and tumor growth inhibition in KRAS G12C/D mutant models. Additionally, DCC-3084 in combination with a MEKi resulted in tumor regression in KRAS mutant models.
Conclusions: The Switch Control inhibitor DCC-3084 broadly inhibits Class I, II and III BRAF mutations, BRAF fusions, and BRAF/CRAF heterodimers leading to tumor regression in preclinical models. The overall preclinical profile of DCC-3084 supports IND-enabling activities towards clinical development in a key area of unmet medical need in RAS and RAF mutant cancers.

IMMUNOLOGY

Adoptive Cell and Natural Killer Cell Therapy

#4049

TIDAL-01: A selected TIL process that enriches for neoantigen reactive TIL in solid tumors

Larissa A. Pikor[1], Antoine Bernard[2], Nathalie Brassard[2], Anna Fritzsche[1], Anna Kluew[1], Zachary K. Jilesen[1], Jake Nikota[3], Rohan Bareja[4], Christian Laing[4], David F. Stojdl[1], TJ Langer[4], Stewart Abbot[4], Barbara Sennino[4], Simon Turcotte[2]. *[1]Turnstone Biologics, Ottawa, ON, Canada,[2]CHUM, Montreal, QC, Canada,[3]Turnstone Biologics, Hamilton, ON, Canada,[4]Turnstone Biologics, San Diego, CA*

Background**:** Tumor infiltrating lymphocyte (TIL) therapy is capable of mediating durable complete responses in melanoma. While solid tumors such as colorectal cancer (CRC), non-small cell lung cancer (NSCLC), ovarian and breast have been shown to contain neoantigen reactive TIL, the success of bulk TIL therapy in these tumors has been limited. Enhancing tumor reactivity through the selective expansion of neoantigen-reactive subpopulations, has demonstrated success in cancers outside of melanoma underscoring the potential of a neoantigen selected TIL approach in indications with lower tumor mutational burdens. Here we demonstrate that the TIDAL-01 process, which utilizes tumor-specific mutation containing peptides to select neoantigen reactive TIL produces TIL products significantly enriched in neoantigen reactivity.
Methods: Fresh tumors were cut into fragments or dissociated and cultured in a primary expansion (preREP). Antigen presenting cells (APCs) were isolated and expanded from patient matched blood. Whole exome and RNA sequencing was performed on tumor tissue and autologous PBMCs and used to predict and prioritize neoantigen mutations. Peptides encoding the mutations were synthesized, loaded onto APCs and co-cultured with autologous TIL. Neoantigen reactive TIL were selected by fluorescence activated cell sorting (FACS), based on the upregulation of the activation markers CD134 and CD137 and expanded with a rapid expansion protocol (REP). Bulk and unselected TIL were expanded alongside for comparison. Neoantigen reactivity was quantified and deconvoluted by cytokine secretion, degranulation, upregulation of CD134/CD137 by flow and when practical, killing of autologous tumor cell lines or organoids.
Results: Successful TIL expansion was achieved in 31/34 (91%) tumors (14/17 CRC, 10/10 NSCLC, 3/3 ovarian and 3/3 melanoma) using both tumor fragments and dissociated tumors. CRC tumors accounted for half of the samples (17/34), and the tumor mutational burden within these samples varied substantially, ranging from 229 to 5436 mutations. Upregulation of CD134 and CD137 and increased IFN-γ production was observed in all samples upon co-culture with peptide loaded APCs. Peptide restimulation and deconvolution revealed that the TIDAL-01 process is capable of enriching for both CD4 and CD8 reactivities. Selected TIL products produced up to 50x more IFN-γ, TNF-α and Granzyme B than bulk TIL and

at least 2x higher levels of degranulation, indicative of greater killing potential.
Conclusions: TIL from metastatic CRC, melanoma, NSCLC and ovarian tumors were successfully expanded from the majority of patients. Co-culture of TIL and peptide loaded APCs followed by FACS significantly enriched for neoantigen reactivity compared to bulk TIL, demonstrating the potential of the TIDAL-01 process to produce selected TIL products for the treatment of non-melanoma tumors.

#4051

Microfluidic incubation of patient derived tumor and immune cells boosts lymphocyte cytotoxic phenotype

Damian C. Hutchins[1], Cecilia R. Schaaf[1], Nicholas P. Edenhoffer[1], Mitra Kooshki[2], Robyn Greissenger[3], Steven D. Forsythe[1], Adam R. Hall[4], Lance D. Miller[5], Shay Soker[6], Pierre L. Triozzi[7], Konstantinos Votanopoulos[8].
[1]Wake Forest Organoid Research Center (WFORCE), Wake Forest University School of Medicine, Winston Salem, NC,[2]Hematology and Oncology, Wake Forest University School of Medicine, Winston Salem, NC,[3]Wake Forest Organoid Research Center (WFORCE), Virginia Tech-Wake Forest School of Biomedical Engineering and Sciences, Winston Salem, NC,[4]Biomedical Engineering, Virginia Tech-Wake Forest School of Biomedical Engineering and Sciences, Winston Salem, NC,[5]Cancer Biology, Wake Forest University School of Medicine, Winston Salem, NC,[6]Wake Forest Institute of Regenerative Medicine, Wake Forest University School of Medicine, Winston Salem, NC,[7]Division of Medical Oncology, Wake Forest University School of Medicine, Winston Salem, NC,[8]Division of Surgical Oncology, Department of Surgery, Wake Forest University School of Medicine, Winston Salem, NC

Introducti**on:** Tumor infiltrating lymphocytes (TILs), hold promise in advancing adoptive cell therapy for patients with otherwise limited treatment options. However, many tumors do not attract TILs, or the TILs themselves are exhausted which limits treatment availability and efficacy. Consequently, there is a need for alternative sources of tumor reactive T cells. Here, we address this need through the *ex vivo* 3D cell culture biofabrication of immune competent patient tumor organoids (iPTOs).

These constructs, composed of patient-matched cancer cells, antigen presenting cells (APCs), and stromal cells encapsulated in extracellular matrix (ECM)-like hydrogel, closely mimic the *in vivo* tumor microenvironment. We demonstrate that constant circulation of peripheral blood mononuclear cells (PBMCs) through a microfluidic device housing iPTOs can emulate lymph node activation of immune cells to the tumor, yielding organoid interacting lymphocytes (OILs) that possess increased markers of activation, cytotoxicity, proliferation, homing markers, and inflammatory cytokine production relative to uncirculated PBMCs.
Methods: Tumor tissue, APCs (from lymph nodes or spleen), and peripheral blood were collected from 8 patients with mesothelioma (3), melanoma (2), and appendiceal cancer (3). Chips were built from a glass slide and laser cut Polymethyl methacrylate. IPTOs were made such that a concentration of 3 APCs for every 1 tumor cell were added to a collagen and hyaluronic acid mixture that was then photocrosslinked in the chip chamber. PBMCs were circulated through chips housing the photocrosslinked iPTOs for 7 days and then expanded. Following expansion, a subpopulation of these cells were cocultured with tumor only organoids for a 7 day period. Single and secondary tumor exposure populations of effector, memory, and reactive T cells were analyzed via flow cytometry, immunohistochemistry, and cell culture medium proteomic analysis, and compared with both uncirculated PBMCs and patient TILs.
Results: Data collected from patients with appendiceal, melanoma, and mesothelioma tumors shows generation of OILS with increase in cytotoxic T lymphocyte, effector memory, and central memory phenotypes when compared to uncirculated PBMCs, greater than or comparable to TILs and with similar effector cytokine and enzyme expression. OILs were also found to express less immunosuppressive signals (i.e., Tim3, PD1, and IL 10). Critically, chip-based T cell activation resulted in 10x more viable OILs than were typically observed with TILs following parallel growth period of 14 days.
Conclusions: This data suggests that microfluidic incubation of lymphocytes with lymph node and tumor cells can generate large amounts of viable tumor-specific T cells on-demand with characteristics similar to TILs but with increased viability, cell expansion propensity, and cytotoxic responsiveness.

#4052

Direct selection of PD1$^+$ CD39$^+$ tumor infiltrating lymphocytes (TIL) from tumor dissociates enrich for functional tumor-reactive cells

Christophe Pedros[1], Larissa Pikor[2], Anna Fritzsche[2], Zachary K. Jilesen[2], Bethany Macleod[2], Niloufar Khojandi[1], Bryant Thompson[1], Matthew Thayer[1], Nikolas Bryan[1], Emily Carron[1], Sowbarnika S Ratliff[1], April Fraley[1], Jake Nikota[2], Robert Fisher[2], Sebastien Delpeut[2], Anna Kluew[2], Madysson Scott[2], Christian Laing[1], Leo He[1], Antoine Bernard[3], Nathalie Brassard[3], Simon Turcotte[3], Timothy J Langer[1], David Stojdl[2], Stewart Abbot[1], Barbara Sennino[1]. *[1]Turnstone Biologics, San Diego, CA,[2]Turnstone Biologics, Ottawa, ON, Canada,[3]Centre Hospitalier de l'Universite de Montreal (CHUM), Montreal, QC, Canada*

Background**:** The autologous cell therapy field has investigated numerous novel strategies and processes to improve response rates and expand the use of adoptive cell therapies (ACT) to patient suffering from a broad range of cancers. Tumor infiltrating lymphocytes (TIL) can be harvested from tumors, expanded *in vitro,* and infused to patients leading to substantial clinical benefits in some patient populations. Tumor reactivity of TIL can vary greatly, representing a key limiting factor of bulk TIL therapies. The ability to generate an autologous cell product enriched in tumor reactive cells while limiting the presence of potentially detrimental and/or competitive non-reactive cells is highly desirable for next generation TIL products. Here we demonstrate that direct selection of antigen experienced TIL from tumor dissociates is feasible and allows to obtain functional cells enriched for tumor reactivity from various tumor indications.

Methods: Patient-derived tumor material from various indications, including ovarian, kidney, colorectal cancer and lung tumors were first processed into single cell suspensions, maximizing TIL recovery and viability. Antigen experienced TIL were immediately selected based on the co-expression of PD-1 and CD39, using fluorescence-activated single cell sorting (FACS). The sorted cells or the unselected counterparts were expanded in a rapid expansion protocol (REP), then analyzed for phenotypic and functional characteristics and reactivity against autologous tumor cells.

Results: The PD-1$^+$ CD39$^+$ selection strategy consistently allowed sorting of a population of viable TIL that was amenable to *in vitro* culture from tumors of various cancer indications. The selected TIL successfully expanded in a rapid expansion protocol. TCR sequencing analysis revealed that the PD-1$^+$ CD39$^+$ sorted populations were enriched in unique clones compared to the unselected populations. Expanded PD-1$^+$ CD39$^+$ selected cells demonstrated the ability to produce key effector cytokines upon restimulation in polyclonal assays. Importantly, the PD-1$^+$ CD39$^+$ expanded TIL were enriched for tumor reactive T cells and showed improved cytotoxic activity against autologous tumors.
Conclusions: PD-1$^+$ CD39$^+$ selected TIL can be successfully isolated and expanded *in vitro*, generating a TIL product of superior reactivity in multiple cancer indications. PD-1$^+$ CD39$^+$ selected TIL showed increased cytokine secretion and cytotoxic activity against autologous material, indicating that this selection strategy enriches for functional tumor-reactive lymphocytes, which is likely to be a key feature of successful ACT.

#4053

A mesothelin targeting chimeric antigen receptor macrophage (CAR-M) for solid tumor immunotherapy: pre-clinical development of CT-1119

Nicholas R. Anderson, Brinda Shah, Alison Worth, Rashid Gabbasov, Brett Menchel, Kerri Ciccaglione, Daniel Blumenthal, Stefano Pierini, Sabrina Ceeraz DeLong, Sascha Abramson, Thomas Condamine, Michael Klichinsky. *Carisma Therapeutics, Philadelphia, PA*

While adoptive cell therapies have seen significant success in the treatment of hematological malignancies, solid tumors remain challenging for the field. A significant obstacle is the exclusion of T cells from the tumor microenvironment (TME). In contrast, monocytes/macrophages are naturally recruited to the TME. These cells then have the potential to phagocytose tumor cells, activate the TME, and prime a broad anti-tumor adaptive immune response via T cell recruitment and activation. We have previously developed CT-0508, a chimeric antigen receptor macrophage (CAR-M) targeting HER2 which showed efficacy in a variety of pre-clinical models and is currently in a Phase I clinical trial for patients with HER2+ solid tumors. Mesothelin is overexpressed in a variety of solid

tumors, including mesothelioma, lung, pancreatic, and ovarian cancers. To leverage tumor biology with myeloid cells, we engineered primary human macrophages using the chimeric adenoviral vector Ad5f35 to express a CAR containing a human scFv against human mesothelin. We used both *in vitro* cell based assays and *in vivo* xenograft models to assess the activity of CT-1119. CAR-M engineered with an Ad5f35 vector demonstrated high CAR expression, high viability, upregulated M1 (anti-tumor) macrophage markers, and downregulated M2 (pro-tumor) macrophage markers. CT-1119 specifically phagocytosed multiple mesothelin expressing tumor cell lines in a CAR-dependent and antigen-dependent manner. CT-1119 demonstrated robust *in vitro* killing of the relevant tumor cell lines A549 and MES-OV expressing mesothelin. CAR engagement also induced the release of pro-inflammatory cytokines such as TNFα following stimulation with mesothelin in both cell-free and cell-based contexts in a dose-dependent manner. *In vivo*, CT-1119 significantly reduced tumor burden in a murine xenograft model of lung cancer. Similarly, human monocytes targeting mesothelin were successfully generated using the same Ad5f35 vector and demonstrated specific activity against mesothelin positive tumor cells. The presented results demonstrate that CT-1119, an autologous human anti-mesothelin CAR-M, can cause phagocytosis, tumor cell killing, and pro-inflammatory cytokine release in response to stimulation with mesothelin. These results show that CAR-M is a feasible approach for the treatment of mesothelin expressing sold tumors via the potential for induction of a systemic anti-tumor response.

#4054

Macrophages engineered with cytokine switch receptors: Development of a modular platform for rebalancing inflammation in microenvironments

Chris Sloas, Yuhao Huangfu, Rehman Qureshi, Michael Ball, Thomas Condamine, Michael Klichinsky, Yumi Ohtani. *Carisma Therapeutics, Philadelphia, PA*

Motivation: Cytokines in tissue microenvironments regulate the balance between pro- and anti-inflammatory signals. Dysregulated cytokines cause deleterious immunosuppression or inflammation, which underpins the pathophysiology of solid tumors, chronic kidney disease, and more.

Rebalancing inflammation/immunosuppression by rectifying cytokine signals offers a generalizable approach for treating numerous diseases. While doing so through cytokine blockade carries risks due to systemic administration, cellular immunotherapies offer a localized approach that could detect pathogenic cytokines then proportionately rebalance inflammation as needed. Specifically, macrophages are homeostatic regulators responsible for initiating and resolving inflammation. Here, we leveraged macrophages' ability to regulate inflammation by equipping them with synthetic cytokine switch receptors (SR) that convert immunosuppressive M2 signals into pro-inflammatory M1 responses for solid tumor microenvironment conversion, or *vice versa* for inflammatory disease. We termed this platform "Engineered Microenvironment Converters" (EM-C) and evaluated its modular ability to target disease-associated cytokines.

Methods: EM-Cs targeting IL10, TGFβ, IFNγ and IL17A were generated by expressing SR in primary human macrophages. M2-to-M1 SR were designed to convert IL10 or TGF-β into pro-inflammatory stimuli, and M1-to-M2 SR were designed to IFNγ or IL17A into immunosuppressive signals. The *in vitro* response of EM-Cs to their target cytokine was monitored using phenotypic characterization of surface molecules, measurement of cytokine production, mRNA sequencing, and biochemical analysis of downstream signaling. Co-culture assays with bystander cells were used to assess the ability of EM-Cs to alter their microenvironment.

Results: Pro-inflammatory EM-Cs converted IL10 and TGFβ, two prevalent immunosuppressive cytokines in the TME, into pro-inflammatory signals. Unlike wildtype macrophages, these EM-Cs responded to IL10 or TGFβ with upregulated M1 markers and cytokines in a dose-dependent manner. Furthermore, EM-Cs repolarized bystander M2 macrophages towards a pro-inflammatory phenotype following co-culture. Similarly, anti-inflammatory EM-Cs responded IFNγ and IL17A, two cytokines canonically overexpressed in inflammatory disease, by upregulating M2 markers and inducing an anti-inflammatory environment.

Conclusion: We present for the first time a novel immunotherapy platform that harnesses macrophages as "living converters" to locally regulate inflammation for oncology and inflammatory applications. By demonstrating EM-Cs in the M2-to-M1 and M1-to-M2 direction, this

platform offers modularity in controlling the inflammatory status of tissue microenvironments without systemic cytokine antagonism.

#4055

CD40L stimulates melanoma infiltrating B cells and enhances *ex vivo* TIL expansion

Renata Ariza Marques Rossetti[1], Leticia Tordesillas[1], Matthew Beatty[1], Dongliang Du[2], Yian Ann Chen[2], Amod Sarnaik[3], Shari Pilon-Thomas[1], Daniel Abate-Daga[1]. *[1]Immunology, H. Lee Moffitt Cancer Center, Tampa, FL,[2]Biostatistics and Bioinformatics, H. Lee Moffitt Cancer Center, Tampa, FL,[3]Cutaneous Oncology, H. Lee Moffitt Cancer Center, Tampa, FL*

Adoptive transfer of tumor infiltrating lymphocytes (TIL) is a feasible and effective therapy for melanoma and lung cancer[1,2]. Multiple factors may determine the quality of the TIL product including components of the tumor microenvironment. In this work, we analyzed the role of melanoma infiltrating B cells in the context of TIL expansion based on their documented association with response to other types of immunotherapies[3]. We stimulated melanoma infiltrating B cells using human recombinant CD40L on the first day of *ex-vivo* TIL expansion. Samples were expanded from cryopreserved melanoma tumor single cell suspensions, in high dose IL-2 alone (standard protocol), or in high dose IL-2 plus CD40L. After 48h, analysis of activation markers on the CD40-expressing cells by flow cytometry was performed. For further investigation of the changes induced by CD40L stimulation, TIL expansion cultures (+/- CD40L) were analyzed using scRNA-seq (10X Genomics Chromium NextGEM Single Cell 5' v2 and V(D)J Reagent kits; Illumina NovaSeq 6000 instrument with S4 sequencing flow cell) at 48h of culture (n=7 patients). The TIL expansion success rate was 68% with the CD40L treatment condition compared to 36% with the standard protocol. TILs cultured in the presence of CD40L expanded to on average three times more than with the standard protocol ($P \leq 0.01$). Treatment with CD40L increased the percentage of CD39- CD69- T cells ($P \leq 0.05$). Within the tumor digests, a higher percentage of B cells, including switched memory B cells ($CD27^+$ IgD^-), was associated with successful TIL expansion (P=0.04). scRNA-seq analysis demonstrated different clustering patterns within the B cell compartment based on culture

conditions. No clear partition was observed for other cell types, including the myeloid compartment. B cells displayed 126 DEGs associated to CD40L addition, CCL22, CD83, EBI3 and CD58 were among the upregulated genes in the CD40L-treated B cells. Other cell types experienced minimal to no change in transcriptomic profiles. B cell clusters were sub-classified based on CD27 and IgD expression[4], showing a predominance of naïve and switched memory B cells. Our results show that higher presence of B cells within tumors is associated with better TIL expansion, suggesting an interplay between T and B cells, and providing rationale for the design of improved TIL expansion protocols based on B cell stimulation with CD40L. This work has been supported in part by the Flow Cytometry, Genomics and Biostatistics and Bioinformatics Core Facilities at Moffitt Cancer Center, an NCI designated Comprehensive Cancer Center (P30-CA076292). We acknowledge Moffitt's Melanoma Center of Excellence and the Mark Foundation for the financial support. [1] Sarnaik, A.A. et al. JCO 39, 2656-2666 (2021). [2] Creelan, B. et al. Nat Med 27, 1410-1418 (2021). [3] Cabrita, R. et al. Nature 577, 561-565 (2020). [4] Sanz, I. et al. Front Immunol 10, 2458 (2019).

#4056

Intratumoral delivery of autologous tumor antigen specific CD4 Th1 cells combined with dendritic cells eradicates HER2 mammary carcinoma

Ganesan Ramamoorthi, Amy Aldrich, Colin Snyder, Brian Czerniecki.
Clinical Science & Immunology Program, Moffitt Cancer Center, Tampa, FL

Human epidermal growth factor receptor 2 (HER2) overexpression accounts for 30% of invasive breast cancer (BC) and is critically associated with aggressive disease, recurrence and metastasis. Adoptive cell therapy approaches using cytotoxic CD8 T cells and natural killer cells have been shown to trigger anti-tumor immunity in BC. However, the immunosuppressive tumor microenvironment (TME) can inhibit response to these therapies and diminish the presence and function of tumor-infiltrating lymphocytes. Recently, we have shown a critical role for anti-tumor CD4 Th1 cells in dendritic cells (DC) intratumoral (i.t.) delivery in combination with anti-HER2 therapy. This combination therapy enhanced

systemic and local anti-tumor immunity and eradicated tumors in HER2 positive BC with a requirement for CD4 Th1 cells. Here we investigated the efficacy of i.t. delivery of both autologous anti-tumor CD4 Th1 cells and tumor antigen pulsed type 1 polarized dendritic cells (HER2-DC1) in a HER2 mammary carcinoma model. CD4 T cells were isolated from BALB/c mice that had completely regressed (pCR) from orthotopic TUBO tumors following HER2-DC1 i.t. or combination therapy with anti-HER2 antibody. CD4 Th1 cells were then expanded by co-culturing with HER2-DC1 in the presence of interleukin (IL)-2 and IL-7 cytokines. BALB/c mice bearing orthotopic TUBO tumors were treated weekly for six weeks with anti-tumor CD4 Th1 cells i.t., non-specific CD4 Th1 cells i.t., HER2-DC1 i.t. or combination therapy. The i.t. delivery of anti-tumor CD4 Th1 cells combined with HER2-DC1 induced a strong anti-tumor response with survival benefit and complete tumor eradication in 50% of treated mice. Importantly, the i.t. delivery of anti-tumor CD4 Th1 cells were critical for providing priming signals to HER2-DC1 within the TME via CD40/CD40L engagement (licensing). This was supported by a strong anti-tumor response and complete tumor regression in 60% of orthotopic TUBO tumor bearing mice treated with CD40/CD40L licensed HER2-DC1 i.t. therapy compared to un-licensed HER2-DC1 i.t. therapy. Additionally, enhanced survival and functionality of human and mouse HER2-DC1 was observed following activation of CD40/CD40L signaling using anti-CD40 agonistic antibody *in vitro*. Collectively, these results suggest a new promising therapeutic strategy using DC1-anti-tumor CD4 Th1 adoptive cell therapy intratumoral delivery to induce DC1 priming and create robust anti-tumor immunity within the TME in BC.

#4057

T cells co-expressing a highly potent NY-ESO-1-specific TCR and a chimeric PD1-41BB co-stimulatory switch receptor show a favorable polyfunctional profile for the treatment of solid tumors

Andrea Coluccio[1], Stefanie Tippmer[1], Petra Prinz[1], Maja Buerdek[1], Kathrin Mutze[1], Barbara Loesch[1], Kathrin Davari[1], Giulia Longinotti[1], Dolores J. Schendel[2]. *[1]Medigene Immunotherapies GmbH, Munich, Germany,[2]Medigene AG, Munich, Germany*

T cell receptor (TCR)-based immunotherapies have shown great potential for the safe and efficacious treatment of patients suffering from various solid malignancies. However, novel strategies are needed to overcome the immunosuppressive tumor microenvironment (TME) and to enhance the efficacy of TCR-T cell (TCR-T) therapies in solid tumors. NY-ESO-1 is a cancer/testis antigen that is highly expressed in various solid tumor indications while its expression in healthy tissues is restricted to male germ cells. Our HLA-A2-restricted, NY-ESO-1-specific TCR used here was selected from a non-tolerized T cell repertoire of a healthy donor using Medigene's proprietary Allo-HLA TCR priming technology and high-throughput TCR isolation and characterization processes. To prevent inhibition of TCR-T cell function via the PD1-PDL1 axis within the TME, the NY-ESO-1-TCR was co-expressed with a chimeric PD1-41BB co-stimulatory switch receptor, consisting of the extracellular domain of PD1 and the intracellular domain of the 41BB co-stimulatory receptor. Thereby, an inhibitory signal from the PD1-PD-L1 axis is turned into a co-stimulatory one, which results in a dual mechanistic benefit, and superior TCR-T cells with respect to tumor cell killing, cell proliferation and poly-cytokine secretion. Co-expression of PD1-41BB on NY-ESO-1 TCR-T cells led to a 3-fold increase in IFN-γ release and a higher proliferation index (~1.5 fold) (after antigen encounter. Under conditions of repeated antigen exposure *in vitro* using HLA-A2/NY-ESO-1/PDL1-positive tumor spheroids, TCR-T cells co-expressing PD1-41BB showed enhanced functional activities compared to TCR-T cells carrying the TCR alone. *In vitro* single-cell secretome analyses demonstrated up to a 5-fold increase in polyfunctional T cells and a higher polyfunctional strength index (PSI) for NY-ESO-1 TCR-T cells expressing PD1-41BB compared to "naked" NY-ESO-1 TCR-T cells lacking PD1-41BB. Typical Th1 cytokines/proteins like IFN-γ, TNF-α and Granzyme B mainly contributed to the superior PSI of NY-ESO-1-TCR-T cells co-expressing PD1-41BB. Importantly, our data indicate that transgenic PD1-41BB has the capacity to provide a co-stimulatory signal despite the presence of endogenous PD1 which is upregulated in stimulated "naked" NY-ESO-1 TCR-T cells. In summary, we find that co-expression of a chimeric PD1-41BB co-stimulatory switch receptor significantly enhances *in vitro* NY-ESO-1 TCR-T cell proliferation, functionality and anti-tumor activity. Analyses of single-cell T cell cytokine polyfunctionality helped us to unravel the mode of action of

NY-ESO-1 TCR-T cells co-expressing PD1-41BB and point to their complex display of effector, stimulatory and chemoattractant cytokines as a potential driver for superior recognition of tumor cells.

#4058

In vitro binding, efficacy and safety studies to support engineered T cell therapies

Sophie Vermond[1], Benita Quist[1], Monique Hazenoot[1], Rene McLaughlin[1], David Cobeta Lopez[1], Namrata Jayanth[1], Folkert Verkaar[1], Omar Aziz[2], Maria LH Vlaming[1], Sabrina de Munnik[1], Gemma Moiset[1]. *[1]Charles River Laboratories, Inc., Leiden, Netherlands,[2]Charles River Laboratories, Inc., Portishead, United Kingdom*

Engineered T cell therapies such as Chimeric Antigen Receptor (CAR) T cells and T cell receptor (TCR)-engineered T cells have emerged as a promising cancer therapy. To date, four anti-CD19 CAR-T and two anti-BCMA CAR-T products have been approved by the FDA for the treatment of hematological malignancies. Many more T cell therapy products are currently being explored, directed towards both liquid and solid tumors as well as for other clinical indications. High-quality and robust *in vitro* and *in vivo* assays are essential for the discovery and characterization of lead T cell therapy products. Furthermore, despite demonstrating therapeutically successful, the further development of T cell immunotherapies has been hindered by safety concerns. Selected target antigens might be expressed in healthy tissues or engineered T cells may non-specifically bind to antigens in healthy tissues, potentially resulting in severe side effects. In addition, the random integration of the CAR- or TCR-encoding DNA cassettes in the host cell genome has the potential risk of causing insertional mutagenesis and may contribute to oncogenic transformation of the T cells. The aim of this study was to develop several *in vitro* assays for the assessment of target cell binding, efficacy and safety of T cell therapies using CAR-T cells targeting the Human Epidermal growth factor Receptor 2 (HER2) as a model system. The z-Movi cell avidity analyzer was used to study the binding strength between the CAR-T cells and target tumor cells. Cytotoxicity co-culture assays were developed using increasing effector:target cells ratios and an impedance-based readout to quantify the viability of HER2-positive and -negative cancer cell lines in real-time, to

confirm the activity and selectivity of the HER2-CAR-T cells. Furthermore, co-culture assays were also developed for a variety of primary or iPSC-derived healthy human cells (representing various tissues) to assess potential off-tumor effects of the HER2-CAR-T cells against healthy cells. In addition, an oncogenicity assay was developed to quantify the survival and proliferation of the HER2-CAR-T cells in the absence and presence of cytokines by flow cytometry, to determine whether the genomic editing of the T cells affected their cytokine-dependency. In conclusion, Charles River Laboratories developed several *in vitro* assays for the preclinical assessment of T cell therapy binding, efficacy, potency, specificity and safety to aid early-stage lead discovery, optimization and development, and to support Investigational New Drug (IND) applications. Charles River has the capabilities to support a full CAR/TCR program from inception to IND filing.

#4059

Developing an allogeneic iPSC derived macrophage cell therapy for oncology

Huafeng Wang[1], May Sumi[1], Christine Huh[1], Fereshteh Parviz[1], Jessica Mastroianni[1], Jane Healy[1], Nicole Stevens[1], Leah Mitchell[1], Susanne Lang[1], Dan Kaufman[2], Robert Hollingsworth[1], David T. Rodgers[1].
[1]Shoreline Biosciences, Inc., San Diego, CA,[2]UCSD, San Diego, CA

The full potential of cell therapy has yet to be realized in solid tumor indications and new approaches are urgently required. Macrophages are innate immune cells that can kill tumor cells and orchestrate the anti-tumor immune response. Macrophage cell therapy is an exciting new approach to treat cancer with the aim to harness the powerful activity of macrophages to reignite the immune system. Patient derived macrophages, however, are difficult to genetically engineer and do not proliferate, which makes generating high-quality cells at clinically relevant scales challenging. To address this, we have developed an induced pluripotent stem cell (iPSC) approach to macrophage cell therapy. These cells can be genetically engineered at the iPSC stage and then differentiated into billions of highly functional iPSC derived macrophages (iMACs). This allogenic cell therapy product can then be cryopreserved and stored for immediate use in the clinic when the patient is ready.

Here we show that iMACs function like normal macrophages. They migrate towards tumor cells, respond to challenges through innate immune receptors, and produce immune recruiting and activating cytokines and chemokines. iMACs also express high levels of antibody receptors and we show that these cells can be directed to kill tumors *in vitro* and *in vivo* via antibody dependent cellular phagocytosis. Furthermore, we have conducted a robust screen to develop a novel CAR that is optimized for use in iMACs. These receptors can be engineered into iMACs at the iPSC stage and trigger robust tumor cell killing. In summary, these data highlight the therapeutic potential of iMACs in oncology and support the further development of this technology for clinical use.

#4060

Selective Neoantigens Peptide TILs (snapTILs): A next generation tumor infiltrating lymphocytes (TIL) therapy platform

Tithi Ghosh Halder[1], Shelby Rheinschmidt[1], Sydney Adamson[1], Anna Larson[2], Taylor Bargenquast[2], Ryan Rodriguez del Villar[1], Serina Ng[1], Kate Gutowsky[1], Alexis Weston[1], Trason Thode[1], Mohan Kaadige[1], Erin Kelley[1], Jorge Soria-Bustos[1], Jorge Giron[1], John Altin[1], Raffaella Soldi[1], Sunil Sharma[1]. *[1]TGen (The Translational Genomics Research Institute), Phoenix, AZ,[2]HonorHealth Clinical Research Institute, Scottsdale, AZ*

Background**:** Immunotherapies using autologous tumor infiltrating lymphocytes (TILs) have become effective treatment modalities for several patients with solid tumors, yielding a response rate of around 49% in patients with metastatic melanoma. Most clinical centers utilize bulk, randomly isolated TILs from the tumor tissue for *ex vivo* expansion and infusion. Only a minor fraction of these administered TILs recognize tumor antigens and most are non-mutated public antigens. Moreover, expression of these antigens on normal cells can trigger central and peripheral tolerance mechanisms. Against this background, cancer neoantigens derived from private mutations represent an ideal class of cancer antigens to target because they are highly tumor specific by nature, therefore reducing the potential induction of central and peripheral tolerance. We recently developed a new technology to enrich TILs with predefined neoantigen specificities, which we termed Selective Neo Antigens Peptides TILs (snapTILs). Here we describe the efficacy studies of a melanoma and

pancreatic cancer patient's snapTILs done in autologous settings both *ex vivo* and *in vivo*.

Methods: Our workflow consisted of a multistep process performed on a patient-specific basis. Briefly, mutations were called by whole-exome sequencing of tumor vs. normal DNA to generate a peptide library. The peptides were further filtered using an in-silico prediction algorithm and our proprietary peptide-MHC binding assay. Selected peptides were then incubated with TILs isolated from the patient's tumor biopsy, resulting in TIL population enriched of T cells that recognize the neopeptides (snapTILs). After rapid expansion, snapTIL efficacy was tested by checking their ability to infiltrate in patient-derived tumor organoids, their activation status (IFNγ), cytotoxicity (Granzyme B), and T-cell exhaustion markers. Lastly, snapTILs *in vivo* efficacy was tested in human melanoma and pancreatic cancer xenograft models using hIL-2 transgenic mice.

Results: Our initial data showed that the levels of infiltration of snapTILs into tumor organoids was significantly higher compared to IL2-stimulated TILs in both cancer models. Also, snapTILs recognized tumors with great specificity as they showed significantly less infiltration in organoids generated from generally uninvolved tissues from the same patients. Moreover, snapTILs were found to be more cytotoxic in nature than the IL2-stimulated TILs in terms of IFNγ and Granzyme B secretion after coculture with autologous tumor cells. Our *in vivo* data confirmed these observations by showing 70% tumor growth inhibition in highly immunogenic melanoma and 50% tumor growth restriction in a poorly immunogenic pancreatic tumor model. In conclusion, our approach proves the potential for personally tailored immunotherapies to yield more effective and safer cancer treatments using snapTILs.

#4061

Systemic autologous lymphocyte transfer can enhance tumor-infiltrating lymphocyte infiltration in glioblastoma and license co-stimulatory immunotherapy

Kirit Singh, Kelly M. Hotchkiss, Eliese Moelker, Gary E. Archer, John H. Sampson, Mustafa Khasraw. *Duke Brain Tumor Immunotherapy Program, Duke University Medical Center, Durham, NC*

Glioblastoma is an immunologically 'cold' malignancy where few tumor infiltrating lymphocytes (TILs) are present. We sought to overcome this by 'seeding' the tumor with TILs via administration of autologous lymphocytes (ALT). We hypothesized that prior administration of ALT will enhance subsequent immunomodulatory therapies (e.g. immune checkpoint blockade (ICB) or co-stimulation). To evaluate this, we initially generated a pro-infiltrative TIL phenotype. CD45.1 splenocytes (C57/Bl6 background) were co-cultured with either IL2 and Concanavalin A (Con A) or IL7 and Con A for 5 days. Flow cytometric analysis found that both conditions resulted in similar CD4:CD8 ratios (20:80%) but IL7 co-culture upregulated expression of VLA-4, a pro migratory integrin. We then compared the entry of TILs into tumor bearing CNS when co-cultured with either IL2 or IL7. 8–10-week-old C57/Bl6 mice (n=5-6 per group) were implanted orthotopically with 30,000 CT2AvIII cells (syngeneic glioma) which established for 14 days. Mice received (1) CD45.1 lymphocytes activated with IL-7 and Con A (single intravenous (IV) injection, 1 x 10^7 cells) or (2) CD45.1 lymphocytes activated with IL2 and serial Con-A stimulation. Mice were sacrificed 3- and 48-hours following ALT and brains analysed for CD45.1+CD3+ populations. Groups were compared using a Mann-Whitney U test. Mice in Group 1 demonstrated significantly enhanced entry of CD8+ effector and memory T cells into tumor bearing hemispheres at both time points following administration compared to Group 2 ($p = 0.005$, $p = 0.0159$ respectively). By 48 hours post ALT, IL7 co-culture resulted in an average 810.1% expansion of CD8 T cell numbers in tumor bearing CNS compared to counts at Day 0. We then evaluated if mice with a TIL enriched CNS might be more responsive to ICB or co-stimulatory therapy. 8–10-week-old C57/Bl6 mice (n=5-7 per group) were implanted with 30,000 CT2AvIII cells that established over 10 days. On day 10, mice

received IV ALT of either IL7 T cells only, or IL-7 and treatment courses of IP ICB (anti-PD1, anti-CTLA 4 or anti-41BB). Mice given ICB following IL7 ALT demonstrated a median survival (aPD1: 27 days, aCTLA-4: 25 days) similar to mice given IL7 ALT alone (25 days). However, 4/7 mice who received IL7 ALT and anti-41BB were still alive 45 days post tumor implantation (p=0.0004). Taken together, we demonstrated that certain *ex vivo* autologous lymphocyte co-culture conditions can generate a T cell population which infiltrates tumor bearing CNS in significant numbers. Further, we found that seeding a tumor with TILs prior to stimulatory therapy yields long term survival *in vivo*. Future work will focus on optimizing *ex vivo* culturing approaches for ALT and determine whether therapeutic efficacy is due to expansion of resident TILs at the tumor site, or ongoing recruitment of endogenous T cells from the periphery.

#4062

The discovery and development of a CRISPR/Cas9-engineered tumor-infiltrating lymphocytes product (GT316) as a next-generation TIL therapy

Yarong Liu, Jingwei Sun, Yao Sheng, Jingman Wang, Jiahui Jin, Fei Li, Lingyun Chen, Di Zhou, Yongchao Tan, Quanwei Wang, Zhao Xu, Haibao Li, Pin Wang, Jun Cui. *Grit Biotechnology, Shanghai, China*

Adoptive cell therapy by tumor-infiltrating lymphocytes (TILs) has demonstrated promising therapeutic effects in multiple types of solid tumors and significantly prolonged the survival of late-stage patients. However, the “prone-to-exhaustion” phenotype of the final TIL product after rapid expansion during manufacture and the presence of various immunosuppressive mechanisms in tumor microenvironment (TME) compromises the persistence and anti-tumor efficacy of TIL post infusion. To discover potential immunoregulatory targets that could maximize the function of TIL, we established a genome-wide CRISPR/Cas9 screening platform, ImmuT Finder®, to unbiasedly identify functional gene targets in primary T cells. Notably, this platform employed T cells bearing a tumor-antigen specific TCR-T that were repeatedly stimulated by tumor cells with cognate tumor antigen and demonstrated similar exhaustion profile as TIL. We selected top 30 targets after several rounds of screening and quickly validated their function in a 96-well array. Then, the top targets that showed

significantly enhancement in proliferation and function of TCR-T were further selected, and their combinational effects on TIL were tested both in vitro and in vivo. Finally, double KO of GT304 and GT312 (GT316) stands out as the most potent combination, which significantly improves TIL proliferation and cytokine release, eradicates tumor growth in both CDX and PDX mouse models and promotes long-term in vivo persistence with low-dependence on IL-2. Specific and potent sgRNAs targeting both targets have been selected, and manufacturing process of GT316 TIL product has been developed (KOReTIL®). In summary, these data demonstrated that our ImmuT Finder® platform enables unbiased discovery of potent and novel targets for the development of T cell therapy and support the clinical assessment of GT316 as a next-generation TIL therapy. Currently, an investigator-initiated trial of GT316 is ongoing in China.

#4063

Adoptive transfer of NF-kB p50 knockout immature myeloid cells shows a trend towards slower glioblastoma tumor growth in an orthotopic mouse model

Patrick J. Beck[1], Theresa Barberi[2], Alan D. Friedman[2]. *[1]Virginia Tech Carilion School of Medicine, Roanoke, VA,[2]Division of Pediatric Oncology, Johns Hopkins University, Baltimore, MD*

Background: Glioblastoma (GBM) is a universally fatal brain tumor. Tumor-associated macrophages (TAMs) comprise up to 40% of GBM tumors and predominantly demonstrate an M2 phenotype, favoring tumor growth while suppressing host immune response. Previously, we showed that in p50-/- mice lacking the repressive NF-κB subunit, GBM TAMs are biased toward the pro-inflammatory M1 phenotype, limiting GBM tumor growth by increasing activated tumor T cells. The present study aims to determine whether adoptively transferred immature myeloid cells lacking p50 (p50-IMC) localize to mouse GBM tumors and slow tumor growth. Methods: Lineage-negative bone marrow (BM) cells were isolated from C57BL/6 (B6) p50-/- mice, expanded, and treated with Macrophage-Colony Stimulating Factor (M-CSF) for 24h to produce p50-IMC. BM-derived myeloid cells from both wild-type (WT) and p50-/- mice were subjected to analysis of M1 (TNFα, IL-12b) and M2 (Fizz1, Mannose Receptor) markers via quantitative PCR after exposure to M-CSF for 24h or after M2-

polarization via five days in M-CSF and then two days in IL-4. B6-derived GL261-Luc GBM cells were inoculated intracranially into wild-type B6 mice, and four days post-implantation, mice were given 5-fluorouracil to deplete endogenous leukocytes. Mice then received either no additional treatment or three doses of ten million p50-IMCs 9-, 11-, and 14-days post-implantation, and tumor growth was monitored via bioluminescence, measured following luciferin injection using the Spectrum in vivo imaging system. The number of p50-IMCs localizing to the GBM-containing brain was determined by CFSE-dye-labeling of IMC followed by flow cytometry analysis 24h after injection.
Results: Both TNFα and IL-12b were increased in p50-/- cells after 5 days M-CSF, and increased IL-12b expression was maintained even after M2-polarization with IL-4. Of the 10 million injected p50-IMCs, 0.07% of those cells were found in the brain. Despite such a small number of p50-IMCs localizing to the tissue of interest, inhibition of GBM growth was observed. Mice receiving the p50-IMC treatments (n = 4) demonstrated a 2.3- and 2.4-fold reduction in tumor growth at 15 ($p = 0.13$) and 18 ($p = 0.14$) days post-implantation, respectively, compared to control mice (n = 5). At 21 days post-implantation, tumor size was effectively equivalent between the two groups ($p=0.76$). p50-IMC treatment did not correlate with improved survival.
Conclusion: Loss of p50 skews myeloid cells toward a proinflammatory phenotype, even under M2-polarizing conditions. Adoptive transfer of p50-IMC transiently impairs GBM growth in an orthotopic mouse model. Although statistical significance was not attained, this may be due to the small number of animals used in this experiment. Further investigation is needed to evaluate the full potential of p50-IMC as an immunotherapy option for GBM patients.

#4064

PD-1 blockade therapy enhances the antitumor effects of lymphodepletion and adoptive T cell transfer

Satoshi Watanabe[1], Miho Takahashi[2], Ryo Suzuki[1], Masashi Arita[1], Ko Sato[3], Toshiya Fujisaki[4], Aya Ohtsubo[1], Satoshi Shoji[1], Kunihiro Shono[1], Takaaki Masuda[1], Tomoki Sekiya[1], Koichiro Nozaki[1], Tomohiro Tanaka[1], Rie Kondo[1], Yu Saida[1], Satoshi Hokari[1], Toshiyuki Koya[1], Toshiaki Kikuchi[1]. *[1]Niigata University Medical & Dental Hospital, Niigata,*

Japan,[2]Saiseikai Niigata Hospital, Niigata, Japan,[3]Joetsu General Hospital, Joetsu, Japan,[4]Tachikawa Medical Center, Nagaoka, Japan

Background: Lymphodepleting cytotoxic regimens, such as chemotherapy and radiotherapy, have shown the ability to enhance antitumor immunity. Although the mechanisms of antitumor effects augmentation in tumor-bearing hosts after lymphodepletion and T cell transfer have been intensively investigated, the influence of lymphodepletion followed by T cell transfer on immune checkpoint molecules (ICMs) expressed on tumor cells and immune cells remains to be elucidated. In the current study, we evaluated the effects of lymphodepletion and adoptive T cell transfer on ICMs in the tumor microenvironment. In addition, we investigated whether lymphodepletion and adoptive transfer of T cells augments antitumor effects of anti-PD-1 blockade therapy.
Methods: B6 mice were inoculated subcutaneously with the MCA205 murine fibrosarcoma. On day 7, mice were lymphodepleted by sublethal irradiation with 500 cGy and were reconstituted intravenously with spleen cells from normal mice as a source of naïve T cells. These mice were injected intraperitoneally with anti-PD-1 mAb on days 7 and 14. On day 21, tumor tissues were harvested, and single cell suspensions were labeled with fluorophore-conjugated antibodies for FACS analyses.
Results: The expressions of ICMs, including PD-L1, PD-1, TIGIT, TIM-3 and LAG-3, were upregulated on recipient $CD4^+$ and $CD8^+$ T cells in the tumor microenvironment. In contrast, these ICMs were significantly reduced in transferred donor T cells. Administration of anti-PD-1 antibodies after lymphodepletion and adoptive transfer of T cells significantly inhibited tumor progression. Furthermore, transfer of both donor $CD4^+$ and $CD8^+$ T cells was responsible for this augmentation of antitumor effects.
Conclusions: Our observations suggest that a possible mechanism of the antitumor effect augmentation mediated by lymphodepletion followed by T cell transfer is the prevention of donor T cell exhaustion and dysfunction. Blockade of PD-1 significantly enhanced the antitumor effects of lymphodepletion and T cell transfer.

#4065

Modulation of Trastuzumab antitumoral activity by co-culture with different T cell subtypes in 2D and 3D T cell killing assays targeting

HER2+ breast cancer

Ina Rohleff, Matthias Bleisch, Kanstantsin Lashuk, Julia Schueler. *Charles River Laboratories, Inc., Freiburg, Germany*

Breast cancer is one of the leading causes of death in women worldwide. Hence, it is important to develop and improve (immuno)therapies for breast cancer patients. Adoptive T-cell therapy with autologous $CD8^+$T cells is a promising method that has already succeeded in melanoma patients. A possible combination with antibody-dependent cell-mediated cytotoxicity dependent (ADCC) antibodies such as Trastuzumab might be beneficial for relapsed late-stage patients. We developed an in vitro protocol to generate antigen-specific $CD8^+$T cells by priming on the HER2+ breast cancer cell line JIMT-1. Subsequently, these primed $CD8^+$T cells were tested in a 2D and a 3D immune cell killing assay in a life cell imaging device in combination with an endpoint viability assay. The activity was compared with unspecific $CD8^+$T cells activated by phytohemagglutinin (PHA) or αCD2/αCD3/αCD28 beads. All T cells were tested as monotherapy and in combination with trastuzumab in JIMT-1 and SKBR-3. The antigen specific CD8+T cells displayed a significantly improved killing potential of JIMT-1 cells compared to unspecific activated or non-activated CD8+T cells. Along these lines, those cells showed the highest TNF-alpha secretion and expression of CD69 (determined by flow cytometry) among all T cell lines. Antigen-specific CD8+T cells from different settings displayed a significantly improved killing potential towards JIMT-1 than non-antigen-specific activated or non-activated CD8+T cells. The use of peripheral blood monocytes (PBMC) instead of isolated CD8+T cells did not influence the activity against JIMT-1 significantly. Interestingly, antigen-specific CD8+T cells activated as PBMC increased the activity of Trastuzumab significantly as compared to unspecific activated CD8+T cells. Testing of different donors revealed a donor dependent degree of killing, however in all donors the activity pattern was the same with antigen specific CD8+T cells being the most active. A direct comparison of fresh vs frozen immune cells from the same donors indicated no significant differences in the killing activity of unspecific activated CD8+T cells. Yet, there were substantial differences in antigen-specific immune cells: the killing potential of the freshly isolated immune cells was significantly higher than of the frozen. In summary, we have developed a protocol to produce antigen-specific tumor-

infiltrating $CD8^+$T cells primed to the heterologous JIMT-1 breast cancer cell line. The antigen-specific $CD8^+$T cells showed an increased killing potential over non-specific $CD8^+$T cells. In addition, they were able to increase ADCC-mediated antitumoral activity of trastuzumab. The 2D as well as the 3D immune cell killing assay proved to be robust and amendable for mid throughput screening. The impact of donor variability and fresh vs frozen immune cells must be further evaluated.

#4066

Lipid nanoparticle library towards development next generation genomic medicines

Nikita Jain, Sedigheh Nazaripour, Rehan Higgins, Zhengyu Chen, Suraj Abraham, Leanna Yee, Srinivas Abbina, Gayatri Mehar Namala, Helena Son, Sams Sadat, Sijo Chemmannur, Malathi Anantha, Ruchi Sharma, Kobe Tickner, Eve Boyer, Shannon Tsai, Seetalakshmi Thambatti, Vinay Mayya, Emily Soon, Jay Paquette, Samuel Clarke, Anitha Thomas.
Precision NanoSystems ULC, Vancouver, BC, Canada

Ionizable amino lipids are a major constituent of the lipid nanoparticles for delivering nucleic acid therapeutics (e.g., DLin-MC3-DMA in ONPATTRO®, ALC-0315 in Comirnaty®, SM-102 in Spikevax®). Scarcity of lipids that are suitable for cell therapy, vaccination, and gene therapies continue to be a problem in advancing many potential diagnostic/therapeutic/vaccine candidates to the clinic.
Herein, we describe the development of novel ionizable lipids to be used as functional excipients for designing vehicles for nucleic acid therapeutics/vaccines in vivo or ex vivo use in cell therapy applications. We first studied the transfection efficiency (TE) of LNP-based mRNA formulations of these ionizable lipid candidates in primary human T cells and established a workflow for engineering of primary immune T cells. We then adapted this workflow towards bioengineering of CAR constructs to T cells towards non-viral CAR T therapy. Lipids were also tested in rodents for vaccine applications using self-amplifying RNA (saRNA) encoding various antigens. We have then evaluated various ionizable lipid candidates and their biodistribution along with the mRNA/DNA translation exploration using various LNP compositions. Further, using ionizable lipids from the library, we have shown gene editing of various targets in rodents.

We believe that these studies will pave the path to the advancement in nucleic acid based therapeutics and vaccines, or cell & gene therapy agents for early diagnosis and detection of cancer, and for targeted genomic medicines towards cancer treatment and diagnosis.

#4067

RNA primed SMAR-T^{TM}cells against multiple driver mutations, all HLA's, designed for first line therapy

Benjamin A. Schwarz, Farzonai Muzaffar, Ryan G. Campbell, David Ryan, Walter Barry, Abenezer Abera, Alfred E. Slanetz. *Geneius Biotechnology, Inc., Natick, MA*

Immune checkpoint inhibitors, such as anti-PD1 antibodies, have revolutionized cancer immunotherapy. Their success demonstrates that a patient's own T cells recognize and treat cancer. However, anti-PD1 therapy is most effective in the treatment of cancers with high mutational burden, ~5% of all malignancies. Therefore, an alternative strategy is necessary to target cancer with lower mutational burden (the other ~95%). Importantly, the efficacy of PD-1 blockade is associated with the recruitment of new T cells from the blood rather than the activation of pre-existing tumor infiltrating lymphocytes (Yost K.E., *et al*. Nat. Med. 2019). Our approach is to use RNA to prime and expand T cells from the blood to cancer-specific mutations *ex vivo*. We can generate T cell populations reactive to as few as 8 and as many as 40 cancer-specific mutant proteins in a single production run. *In vitro*, these T cells have mutation-specific cytotoxicity and do not kill the normal cells. These T cells express homing receptors that allow them to infiltrate the tumor and express high levels of TNFα and IFNγ, both of which are associated with effective tumor cytotoxicity and pro-inflammatory modification of the tumor microenvironment (TME). The predominant immunophenotype of these cells is consistent with central and effector memory, CD4+ and CD8+ T cells, with almost no regulatory or exhausted T cells. We believe these T cells can be used as a cellular therapy in conjunction with, or as an alternative to, immune checkpoint inhibitors to treat lower mutational burden cancers that comprise most patients' tumors.

#4068

Ganglioside SSEA4 in Ewing sarcoma: A marker of tumor cells with highly aggressive features and a potential immune target

Silke Jamitzky[1], Bianca Altvater[1], Carolin Krekeler[1], Laura Hoen[1], Caroline Brandes[1], Lisa Richter[1], Julia Ebbinghaus[1], Laurin Ochs[1], Nicole Farwick[1], Katja Urban[1], Dennis Görlich[2], Ian Johnston[3], Rita Pfeifer[3], Claudia Rossig[1], Wolfgang Hartmann[4], Sareetha Kailayangiri[1]. *[1]University Children's Hospital Münster, Muenster, Germany,[2]Institute of Biostatistics and Clinical Research, University Hospital Muenster, Muenster, Germany,[3]Miltenyi Biotec B.V. & Co. KG, Bergisch Gladbach, Germany,[4]Division of Translational Pathology Gerhard-Domagk-Institute of Pathology, University of Muenster, Muenster, Germany*

Cancers can aberrantly express carbohydrate antigens restricted to immature cells during prenatal human development, and these may be exploited for selective immune targeting. We studied expression and functional associations of the globo-series ganglioside stage-specific embryonic antigen 4 (SSEA4), a cell surface marker of human embryonic stem cells, in Ewing sarcoma (EwS). Flow cytometry revealed SSEA4 expression on the cell surface of each of 13 EwS cell lines, with moderate to high expression densities in 6 of 13 (46%) cell lines. Of 31 primary EwS tumor biopsies, 21 (68%) were SSEA4 positive by immunofluorescence staining. No associations of SSEA4 positivity with molecular or clinical disease parameters were found. Comparisons of paired tumor cell subpopulations with high and low/negative SSEA4 expression selected by cell sorting from 8 EwS cell lines revealed increased cell proliferation and colony formation of SSEA4^{high} tumor cells, along with higher doxocrubicin chemoresistance and a higher propensity to migrate in transwell assays. SSEA4 negative cells selected from bulk populations of EwS cells regained SSEA4 expression during continued *in vitro* culture as well as after in vivo xenografting into immunodeficient mice. SSEA4^{high} expression in EwS cells was not dependent on expression levels of the EWSR1-FLI1 fusion transcript or its direct targets, nor associated with markers of epithelial/mesenchymal plasticity. To retarget human T cells to SSEA4, we generated a second-generation, 41BBζ CAR using the antigen-binding domains of a murine anti-SSEA4 monoclonal antibody. SSEA4-specific CAR T cells specifically interacted with SSEA4 positive EwS cells in a

strictly antigen-dependent manner, resulting in effective tumor cell lysis in vitro. We conclude that targeting of SSEA4 with CAR T cells or alternative immune therapeutics could be an attractive strategy to eliminate tumor cell subsets with high propensity to drive disease progression in EwS and therefore deserves further evaluation towards clinical translation.

#4070

Engineering TRAIL-expressing immune cells to target GI malignancies

Praveen R. Srinivasan, Shengliang Zhang, Wafik S. El-Deiry. *Pathology and Laboratory Medicine, Legorreta Cancer Center at Brown University, Providence, RI*

While adoptive cell therapies, such as chimeric antigen receptor (CAR) T cells, have had promising results in hematologic malignancies, their translation to solid tumors has been mostly unsuccessful. A significant limitation to use of adoptive cell therapy in solid tumors has been life-threatening off-target toxicities, including acute respiratory toxicity and cytokine release syndrome. The native T cell program releases a diverse range of toxic proteins upon activation, including interferons, interleukins, perforins, and granzymes. Rather than activate the native T-cell program, selective expression of tumor-targeting agents may be advantageous. TNF-related apoptosis-inducing ligand (TRAIL) is known to selectively target tumor cells with minimal toxicity to normal tissues. We therefore engineered Jurkat (a human CD4+ T cell leukemia cell line) and THP-1 (a human monocytic leukemia cell line) cells to constitutively express wild-type TRAIL using a third-generation lentivirus system. These cells killed multiple cell lines across colorectal and pancreatic cancer, thus representing a possible therapeutic strategy to target GI malignancies. Furthermore, the addition of the ferroptosis induced erastin enhanced cytotoxicity of TRAIL-engineered cells, suggesting that targeting ferroptosis in addition to apoptosis is a promising strategy for enhancing immune killing. Future work will focus on overcoming TRAIL resistance, tumor trafficking, and alteration of the tumor microenvironment.

#4071

Identification of myeloma-specific T cell receptors by functional single cell interaction analyses

Tim R. Wagner[1], Eren Boğa[2], Patrick Schmidt[2], Wolfram Osen[1], Michael Platten[3], Hartmut Goldschmidt[4], Marc S. Raab[4], Mirco J. Friedrich[4], Stefan B. Eichmüller[1]. *[1]Research Group GMP & T Cell Therapy, German Cancer Research Center, Heidelberg, Germany,[2]Medical Oncology, National Center for Tumor Diseases, Heidelberg, Germany,[3]Clinical Cooperation Unit Neuroimmunology and Brain Tumor Immunology, German Cancer Research Center, Heidelberg, Germany,[4]Internal Medicine V, University Hospital Heidelberg, Heidelberg, Germany*

Innovative immunotherapy approaches such as adoptive transfer of chimeric antigen receptor (CAR) T cells or tumor infiltrating lymphocytes (TILs) have shown great success in the treatment of solid tumors and hematological malignancies. Although treatment of multiple myeloma with CAR T cells can induce deep responses, relapses frequently occur due to antigen escape and limited CAR T cell persistence. TCR-engineered T cells may mediate sustained antitumor effects upon recognition of intracellular targets, thereby significantly increasing the range of relevant target antigens. In our project, we propose to identify T cell receptors (TCRs) specifically targeting autologous myeloma cells. Tumor-reactive T cells were identified using the Berkeley Lights Lightning platform, allowing simultaneous functional analysis of up to 1500 individual T cell/target cell interactions per run. Reactive T cells have been identified upon detection of secreted chemokines (IFNγ, TNFα, IL-2) and by measurement of CD137 surface expression. Tumor-reactive T cells showing various cytokine secretion patterns and CD137 expression profiles could be detected in each myeloma patient (7 to 26 of approx.1200 cells tested per patient). Individual tumor reactive T cells have been isolated for TCR sequencing. Recovered TCR genes will be cloned and overexpressed in autologous T cells for functional validation and analysis of tumor derived neoepitope specificity. In summary, we present a pipeline allowing identification of myeloma-recognizing T cells and recovery of bona fide tumor-reactive TCRs eligible for patient-individualized T cell therapy.

#4072

Class I HLA-independent lysis of immunotherapy-resistant melanoma by CD8 T cells

Hongyan Xie[1], Aiping Jiang[2], Anne Jenney[3], Yi Sun[1], Tatyana Sharova[1], Moshe Sade-Feldman[1], Or-yam Revach[1], Angelina Cicerchia[1], Martin Q. Rasmussen[1], Nir Hacohen[1], Robert T. Manguso[2], Russell W. Jenkins[1].
[1]Massachusetts General Hospital Cancer Center, Harvard Medical School, Boston, MA,[2]Broad Institute of MIT and Harvard, Cambridge, MA,[3]Laboratory of Systems Pharmacology, Harvard Program in Therapeutic Sciences, Harvard Medical School, Boston, MA

Cancer immunotherapy with immune checkpoint blockade (ICB) has transformed the treatment of melanoma, although intrinsic or acquired resistance develops in nearly half of patients. Tumor-infiltrating CD8+ T lymphocytes (TILs) are key determinants of anti-tumor immunity in melanoma and other cancers, and single-cell RNA-sequencing has identified T cell states associated with improved clinical response to ICB, as well as adoptive T cell therapy (ACT). Despite these advances, strategies to identify and analyze tumor-reactive TILs in ICB-resistant patients remain limited. Here, we demonstrate that TILs from ICB-resistant melanoma patients can recognize and eliminate autologous tumor cells independent of class I HLA-TCR interactions. TILs eliminated matched melanoma cells in a time and dose-dependent fashion associated with secretion of effector cytokines. Strikingly, the deletion of B2M (resulting in loss of class I HLA surface expression) did not alter the activity of these TILs. Immunophenotyping studies confirmed that TILs are largely (>95%) effector memory (Tem) CD8 T cells (CD45RA-CD45RO+CCR7-) and give rise to terminal effector cells after co-culture with matched melanoma cells. Further, the elimination of melanoma cells by TILs required intact JAK1/2 signaling, although interferon-gamma (IFNγ) was neither necessary nor sufficient for tumor cell elimination. Together, these findings demonstrate that expanded TILs from ICB-resistant melanoma patients are capable of eliminating melanoma cells via a novel, class I MHC-independent mechanism.

#4073

Tunable STAT activation by synthetic pathway activators (SPAs) increases engineered T-cell potency and persistence

Thomas J. Gardner, Beatriz Millare, Anzhi Yao, Ashley Cass, Suchismita Mohanty, Jeremy Chen, Alma Gomez, David DeTomaso, Manching Ku,

Lionel Berthoin, Meng Lim, Azalea Ong, Vince Thomas, Nicholas Quant, Brian Hsu, Amy-Jo Casbon, Natalie Bezman, Aaron Cooper, Levi Gray-Rupp, Angela C. Boroughs, W. Nicholas Haining. *Arsenal Biosciences, South San Francisco, CA*

Clinically effective adoptive T cell therapy for the treatment of solid tumors will require robust T cell expansion, persistence, and potency. The Janus-kinase signal transducer and activator of transcription (JAK-STAT) pathway governs T cell activation and differentiation, and can thereby serve as a critical regulator of these properties. To take advantage of the benefits of STAT signaling in programming an antitumor T-cell response, we used synthetic biology to create a library of proteins, termed Synthetic Pathway Activators (SPAs) which constitutively drive STAT signaling without the need for external cytokine input. SPAs can be designed to engage activity of multiple STAT family transcription factors at variable levels through rational design. We have developed several classes of SPAs, including but not limited to Class I SPAs, which primarily increase pSTAT3 activity, and Class II SPAs, which increase pSTAT5 activity. When constitutively expressed in ArsenalBio Integrated Circuit T (ICT) cells, SPAs result in significant enhancements in T-cell potency and expansion. Repetitive stimulation assays, wherein T cells are challenged with tumor cells every 2 days, reveal that Class I SPAs result in 6-log or higher improved tumor cell clearance over a 2-week assay period. Across various mouse xenograft models, SPA-expressing ICTs reach at least 6-fold improved tumor growth inhibition. RNAseq and ATACseq analysis indicate dramatic changes to gene expression profiles in T cells expressing Class I SPAs, with maintenance of T cell stem-like phenotypes, and restricted accessibility of various exhaustion marker genes. Importantly, despite significantly increased levels of expansion, ICTs equipped with SPAs are not immortalized, showing no signs of cytokine-independent outgrowth. In addition, SPA-expressing ICT cells rapidly contract following tumor clearance in-vivo. The SPA platform represents a novel, tunable, and T cell intrinsic approach for engineering cell fates that result in potent anti-tumor properties.

#4074

Cellular immunotherapy targeting kappa myeloma antigen for the treatment of multiple myeloma

Jessica Li[1], Nicole Haynes[1], Katherine Cummins[1], Kavitha Gowrishankar[2], Kenneth Micklewaithe[2], Halley Hilton[3], Rosanne Dunn[3], Jane Oliaro[1], Simon Harrison[1]. *[1]Peter MacCallum Cancer Centre, Melbourne, Australia,[2]University of Sydney, Sydney, Australia,[3]Haemalogix, Sydney, Australia*

Multiple myeloma (MM), the second most common blood cancer, is characterized by the accumulation of malignant plasma cells in the bone marrow. Chimeric Antigen Receptor (CAR)-T cell therapy has recently entered the standard of care for relapsed and refractory MM, following the recent FDA-approval of two CAR-T cell products, ide-cel® and cilta-cel®, which target the B cell maturation antigen (BCMA). However, despite impressive response rates, most patients relapse within 1-3 years. Kappa (κ) myeloma antigen (KMA) is a tumour specific membrane associated protein expressed on malignant plasma cells in patients with kappa light-chain restricted (κ-type) MM. KMA is absent on normal plasma cells and haematopoietic stem cells, making it an attractive and alternative target antigen for CAR-T cell therapy for MM. The monoclonal antibody, KappaMab (MDX-1097), binds to a conformational epitope on KMA, and has been assessed in phase I, IIa and IIb clinical trials in relapse refractory myeloma patients (1). Here, we have engineered a lentiviral vector encoding a second-generation CAR expressing a scFv from MDX-1097, fused to a 4-1BB co-stimulatory domain and CD3 zeta chain. We successfully generated human anti-KMA CAR-T cells with high and stable CAR expression and a predominately memory T cell phenotype. The CAR-T cells selectively killed KMA-expressing tumour lines, secreted interferon-gamma upon target recognition, and demonstrated potent anti-tumour activity in a xenograft model. Anti-KMA CAR-T cell therapy therefore represents a novel and potent treatment ready to enter a phase I clinical trial for patients with myeloma. (1) Spencer et al. Blood Cancer Journal (2019) 9:58

#4075

A modified FcγRI expressing-T cell, SolidT, enables antibody-mediated cytotoxicity to overcome the limitations of CAR-T cell therapy against

solid tumors

Diana Rasoulouniriana[1], Nadine Santana-Magal[2], Amit Gutwillig[2], Leen Farhat-Younis[2], Hana Shpilt[1], Shahar Dotan[1], Noam Pilpel[1], Peleg Rider[1], Yaron Carmi[2]. *[1]Gilboa Therapeutics Inc., Rehovot, Israel,[2]Department of Pathology, Sackler School of Medicine, Tel Aviv University, Tel Aviv, Israel*

The pioneering design of chimeric antigen receptor T-cell (CAR-T) therapy demonstrated the potential of reprogramming the immune system. Nonetheless, T-cell exhaustion, toxicity, and suppressive microenvironment limit their efficacy in solid tumors. Recently, we characterized a novel subset of tumor-infiltrating $CD4^+$ T-cells expressing the FcγRI receptor (Rasoulouniriana et al, 2019). Herein we detail the engineering of a novel receptor, based on the FcγRI structure, which is retrovirally transduced into PBMCs (both CD4 and CD8 T-cells). These cells, named SolidT cells, can target tumor cells using antibody intermediates. They show effective and specific cytotoxicity only when an appropriate antibody is added. Only target-bound antibodies activate these cells, while free antibodies are internalized without activation. Their cytotoxic activity is correlated to target protein density, therefore targeting tumor cells with high antigen density while sparing normal cells with low or no expression. This activation mechanism prevents premature exhaustion. Furthermore, during ADCC these cells secrete attenuated cytokine levels compared to CAR-T, thereby enhancing their safety profile. These cells eradicate established melanoma tumors, infiltrate the tumor microenvironment and facilitate host immune cell recruitment in immunocompetent mice. In NSG mice, they infiltrate, persist, and eradicate tumors. As opposed to CAR therapies, which require changing the receptor across different types of cancer, our engineered T-cells remain the same throughout tumor types, while only the injected antibody changes. As such, can be adapted to treat a wide range of solid cancers without changing the manufacturing program. Overall, SolidT cells are capable of binding tumor cells with high affinity, while preserving the cytotoxic specificity only to cells expressing a high density of tumor-associated antigens.

#4076

4-1bb selection augments DC/AML fusion vaccine-educated T cells for adoptive cell therapy

Kathrine S. Rallis*[1], Jessica Liegel*[1], Giulia Cheloni[1], Dina Stroopinsky[1], Poorva Bindal[1], Kenel Dufort[1], Daniela Torres[1], Isabella Saldarriaga[1], Samuel Herzlinger[1], Abigael Morin[1], Raphael Kesselman[1], Jeremy Rosenbaum[1], Georges Chedid[1], Sophia Adamia[1], Donald Kufe[2], Jacalyn Rosenblatt[1], David Avigan[1]. *[1]Hematology-Oncology, Beth Israel Deaconess Medical Center, Harvard Medical School, Boston, MA,[2]Dana Farber Cancer Institute, Harvard Medical School, Boston, MA*

Introducti**on:** Our group has pioneered a novel vaccine by fusion of patient-derived tumor with autologous dendritic cells (DCs) that presents an array of tumor antigens generating a polyclonal immune response. DC/AML vaccination led to expansion of leukemia-specific T cells with survival benefit in a phase II clinical trial. We postulated that ex vivo generation of vaccine-educated T cells would provide a powerful platform for adoptive immunotherapy with opportunity to augment T-cell functional potency prior to infusion. We report on an ex vivo system in which vaccine-educated T cells are further enriched for activated antigen-specific effector cells via an agonistic 4-1bb antibody. We report phenotypic and functional characteristics of 4-1bb-enriched vaccine-educated T cells.
Methods: DC/AML fusion vaccines were generated from C57BL/6J mice DCs and syngeneic C1498 mCh/luc$^+$ AML cells. Splenic T cells were co-cultured with autologous irradiated DC/AML fusions in presence of IL-2/7/15. Selection with biotinylated agonistic 4-1bb (3H3) was performed on vaccine-educated T cells followed by expansion with anti-CD3/CD28 activation beads. T cells were phenotyped for activation (CD25/CD69), immune checkpoints (PD1/LAG3/TIM3), memory (CD44+CD62L-) and enrichment (anti-rat H&L). Cytotoxicity was evaluated by luminescence. Mice were inoculated with C1498 and injected with T cells 7 days later. BLI imaging was performed and 100-day survival measured.
Results: Vaccine-educated T cells demonstrated evidence of immune activation and memory phenotype compared to unstimulated naïve T-cell controls (TN) (7.24-fold, CD4+CD25+CD69+; 1.7-fold, CD3+CD44+CD62L-). Vaccine-educated T cells selected based on 4-1bb expression showed enhanced markers of activation (15.3-fold, CD4+CD25+CD69+) and memory phenotype (5-fold, CD3+CD44+CD62L-) compared to TN. Selection enriched for 4-1bb$^+$

vaccine-educated T cells resulting in enhanced antigen-specific recognition as measured by tumor lysate induction of IFNg expression. Tumor specificity and activation was maintained following CD3/CD28-mediated expansion. The 4-1bb+ vaccine-educated T cells showed enhanced cytotoxicity (1.9-fold increase/TN at 10:1 E/T, $P<0.0001$). Phenotypic and functional analysis support 3-5 days as the optimal duration of time for T-cell vaccine education. In vivo, 60% of mice treated with 4-1bb^{+} vaccine-educated cells were alive at 60 days vs. 20% treated with unselected vaccine-educated cells.

Conclusion: We demonstrate that vaccine-educated T cells subject to selection via an agonist 4-1bb antibody confer enhanced tumor selectivity and potency. Optimal duration for T-cell education was 3-5 days. T-cell stimulation and enrichment by agonistic 4-1bb selection enhanced cytotoxicity and memory phenotype. Thus, 4-1bb selection is a novel approach for antigen-specific T-cell enrichment for superior adoptive immunotherapy in AML.

#4077

Dual-targeted CAR-NK cell therapy: optimized CAR design to prevent antigen escape and elicit a deep and durable response in multiple myeloma

Cuiqing Yang[1], Yifang Wang[1], Tingting Liu[1], Chao Wang[1], Huanyu Wang[1], Qingyang Wang[1], Qin Wang[1], Gang Ye[1], Renhong Tang[2], Zhuoxiao Cao[1].
[1]Shanghai Simnova Biotechnology Co., Ltd., Shanghai, China,[2]Jiangsu Simcere Pharmaceuticals Co. Ltd, Shanghai, China

Introduction: Multiple myeloma (MM) is an incurable hematologic malignancy and new strategies that offer a chance of obtaining long-term progression free survival are urgently needed. MM is associated with profound immune alterations and dysfunction of natural killer (NK) cells have been demonstrated to be crucial factors in MM progression. Myeloma cells are susceptible to killing by natural killer (NK) cells but acquire the ability to elude NK cell surveillance by avoiding recognition and suppressing NK cell function. Given the role of NK cells in the pathogenesis of MM, interest in harnessing NK cells to treat the cancer has been energized by the remarkable success of other adoptive cell therapies such as chimeric antigen receptor (CAR)-T cells. However, relapses

associated with residual low-to-negative BCMA-expressing MM cells have been reported, necessitating the identification of additional targets. GPRC5D, expressed on MM cells from primary marrow samples with a distribution independent of BCMA.
Methods: To prevent BCMA-antigen escape and elicit a deeper and more durable response in MM, we developed a new multiplexed edited NK cell configuration to restore anti-myeloma NK cell immunity, consisting of anti-BCMA VHH and anti-GPRC5D VHH antibodies, NKG2D and 2B4 co-stimulation signaling domains, and IL-15.
Results: Dual targeting BCMA/GPRC5D CAR-NK showed potent in vitro killing of both BCMA+ and GPRC5D+ myeloma cells. Utilizing a repeated rounds of cancer cell clearance assay, BCMA/GPRC5D CAR NK cells showed remarkable persistence and antigen-mediated expansion of CAR-NK cells after more than 4 rounds of tumor cell re-challenges. Moreover, in comparison with single targeted BCMA CAR-NK cells, Dual targeting BCMA/GPRC5D CAR-NK cells effectively lysed BCMA negative target cells. In addition, in BCMA-antigenic escape model, it achieved more sustained tumor control than single targeting BCMA CAR-NK cells. PD-1/PD-L1 axis inhibition has been reported to enhance NK cell activity against MM cells by augmenting NK cell trafficking, immune complex formation, and cytotoxicity against PD-L1-expressing MM cells. We also demonstrated that combination of BCMA/GPRC5D CAR-NK with anti-PDL1-IL15 also showed more persistent tumor control.
Conclusions: Our studies demonstrate the development of dual targeting BCMA/GPRC5D CAR NK cells may represent a highly effective off-the-shelf therapeutic product as a monotherapy or in combinations with other immune-regulating agents.

#4078

Optimized chimeric antigen receptors (CARs) for CAR-NK cell therapies

Cuiqing Yang[1], Yifang Wang[1], Tingting Liu[1], Fuwei Jiang[1], Qingyang Wang[1], Qin Wang[1], Gang Ye[1], Renhong Tang[2], Zhouxiao Cao[1]. *[1]Shanghai Simnova Biotechnology Co., Ltd., Shanghai, China,[2]Jiangsu Simcere Pharmaceuticals Co. Ltd, Nanjing, China*

Introduction: CAR-T-cell therapy has shown great success in treating hematopoietic malignancies. Allogenic NK cell-based therapies have also been shown to mount potent responses against hematopoietic malignancies. Unlike T-cell therapies, allogeneic NK cells do not cause toxicities such as serious cytokine release syndrome, neurotoxicity, or graft-vs-host-disease. Several groups have demonstrated the clinical efficacy of allogeneic CAR-expressing NK cells that utilize CARs developed for T-cells. However, activating receptor signaling in NK cells is different from T cells. NK cell-mediated cytotoxicity is regulated by a repertoire of activating and inhibitory receptors. Activating receptors include natural cytotoxic receptors (NCRs) such as NKG2D, CD16, LFA-1, CD244 (2B4), and CD137 (4-1BB) and so on. These activating cell surface receptors have the capacity to trigger cytolytic programs as well as cytokine and chemokine secretion via intra-cytoplasmic immunoreceptor tyrosine-based activation motifs (ITAMs) such as in 2B4 and 4-1BB and/or via other transmembrane signaling adaptors. Recent studies using NK cell-based activating receptor signaling modules such as NKG2D and 2B4 as CAR co-stimulatory domains proved increased anti-tumor activity compared to T-cell CARs.
Methods: The goal of this study is to develop next-generation NK cell-optimized CARs to improve targeting and potency of NK cell treatment. To achieve this, we constructed a library of CARs containing signaling modules from diverse T cell signaling receptors and NK cell specific signaling receptors, and then screened for CAR activity using short-term and long-term NK cell cytotoxicity assays. In comparison with T cell signaling receptors, CAR-NK cells with NK cell signaling receptors showed more potent cytotoxicity. Using a repeated rounds of cancer cell clearance assay, serial re-stimulation by fresh cancer target cells was tested. CAR-NK cells with NK cell signaling receptors showed remarkable persistence and antigen-mediated expansion of CAR-NK cells compared with T cell signaling receptors.
Results: We identified a NK cell-CAR containing two NK cell co-stimulatory domain and CD3z signaling domain,showing better persistence than T-cell CAR (CD28-CD28-zeta) and 2 previously described NK cell-CARs (NKG2D-2B4-zeta and 2B4).
Conclusions: We have successfully identified an optimized CAR suitable for NK cells that enable increased potency of NK cells compared to other CAR designs. The most potent CARs identified in our screen are being

engineered into a highly effective dual targeting BCMA-GPRC5D CAR-NK cell product as a next-generation “off-shelf” cell therapy.

CAR T-cell Therapy 2

#4082
Impact of immunosuppressive monocytes on CART19 cell effector functions and outcomes

Kun Yun[1], Reona Leo Sakemura[1], Michelle J. Cox[1], Truc Huynh[1], Claudia Manriquez-Roman[1], Olivia Sirpilla[1], Carli M. Stewart[1], James H. Girsch[1], Ekene J. Ogbodo[1], Ismail Can[1], Brooke Kimball[1], Lionel A. Kankeu Fonkoua[1], Mehrdad Hefazi[1], Michael W. Ruff[1], Elizabeth L. Siegler[1], Mike Mattie[2], Sao-Mai Nguyen-Mau[2], Simone Filosto[2], Saad S. Kenderian[1].
[1]Mayo Clinic, Rochester, MN,[2]Kite, a Gilead company, Santa Monica, CA

CD19 directed chimeric antigen receptor T (CART19) cell therapy has resulted in remarkable outcomes in B cell malignancies and was FDA approved in multiple indications. However, durable remissions are limited to 40% of treated patients. Inhibitory myeloid cells in tumor microenvironment have been found to suppress T cell expansion and contribute to failure of CART19 cell therapy. In this study, we aimed to unravel the interactions between monocytes, CART19 cells and tumor cells to understand how monocytes-CART19 cell interactions impact CART19 cell effector functions and clinical outcomes. Two sets of experiments were conducted, 1) use of healthy CART19 cells, CD19+ tumor cells, and healthy monocytes; 2) use of brexu-cel products from ZUMA-2 clinical trial treating mantle cell lymphoma (MCL), patient-matched monocytes and circulating MCL tumor cells (n = 11; 6 durable responders, 2 relapsed after initial response and 3 non-responders).
CD28 costimulated CART19 (CART19-28ζ) cells generated in the lab from healthy donors were co-cultured with donor freshly isolated monocytes in the presence of Jeko-1 cells (a CD19+ MCL cell line). CART19 antigen specific proliferation was not inhibited by freshly isolated monocytes . When monocytes were co-cultured with CART19 and tumor cells, higher levels of eotaxin, GRO, MCP-3 and IL-7 were detected. When CART19 cells were co-cultured with the CD19+ JeKo-1 cells in the presence of ex vivo M2 polarized macrophages, CART19 antigen specific proliferation

was inhibited (p=0.0045). Transwell experiments demonstrate that M2-induced CART19 inhibition is not contact dependent. Cytokine profile analysis indicated increased level of IL-1ra, IP-10 and MCP-1 and decreased level of IL-17A, sCD40L, IL-9 and MIP-1α when M2 macrophages were co-cultured with CART19 and tumor cells compared to co-cultures of tumor cells and CART19.
Then we conducted ex vivo co-cultures of brexu-cel products, autologous monocytes and circulating MCL tumor cells from MCL patients (ZUMA-2) collected prior to CART19 cell infusion. Here we observed trends of elevation of IL-13 and IL-5 and reduction of GRO, MCP-3, MIP-1β and IL-8 in non-responders, compared to responders (durable responses or relapsed patients).
Our results support that monocyte- and macrophage-dependent cytokine release could modulate CART19 effector and trafficking functions, and thus CART19 clinical outcomes. This warrants further investigation around strategies to improve durable responses to CART cell therapy.

#4083

In vivo efficacy of LGR5-targeting CAR-T cell therapies developed for the treatment of colorectal cancer

Dylan McPeake[1], Timona Tyllis[1], Caitlin Abbott[1], Jade Foeng[1], Veronika Bandara[2], Batjargal Gundsambuu[2], Elaheh Rohani-Rad[1], Silvana Napoli[2], Timothy Sadlon[3], Simon Barry[4], Shaun McColl[1]. *[1]Department of Molecular & Biomedical Science, The University of Adelaide, Adelaide, Australia,[2]The Robinson Research Institute, Adelaide, Australia,[3]The Robinson Research Institute/Women and Childrens' Health Network, Adelaide, Australia,[4]The Robinson Research Institute/Women and Childrens' Health Netwok, Adelaide, Australia*

While CAR-T cells have demonstrated significant efficacy in the treatment of haematological malignancies, there are many challenges to overcome in developing CAR-T cell therapies against solid tumours. In particular, the scarcity of recognised effective target antigens in solid tumours remains a significant hurdle. Leucine-rich repeat-containing G-protein coupled receptor (LGR5) is a cancer stem cell marker, which mediates important roles in tumor initiation and metastasis. Upregulated LGR5 expression in malignant cell contexts highlights this surface receptor as a promising target

for CAR-T cell therapy. In this study, we evaluated the efficacy of LGR5-targeting CAR-T cells against a range of human cancers. We demonstrate that LGR5 is expressed, both *in vitro* and *in vivo*, by numerous human cancers, including colorectal, ovarian, hepatic, brain, and pancreatic cancer. LGR5-targeting CAR-T cells effectively kill LGR5-expressing cancer cells in *in vitro* cytotoxicity assays and display significant anti-tumor activity *in vivo* when administered at 1, 2 or 3 weeks post-tumor inoculation in a subcutaneous human colorectal cancer xenograft mouse model. Furthermore, LGR5-targeting CAR-T cells that induce primary tumor rejection confer complete protection against a secondary tumor challenge 5 weeks post-T cell transfer. *In vivo* spatiotemporal distribution and repeated dosing studies demonstrate that LGR5-targeting CAR-T cells accumulate at the tumor site until tumor elimination, do not persist in off-target organs by d28 post-tumor inoculation and are safe and well-tolerated under the conditions tested. Together, these results provide the foundation for furthering the development of LGR5-targeting CAR-T cells for use in the clinic against colorectal cancers and other solid tumours.

#4085

Development and *in vitro* validation of an LGR-5 targeting CAR-T against colorectal cancer

Veronika Bandara[1], Batjargal Gundsambuu[2], Silvana Napoli[2], Stuart Mills[3], Emma Thompson[4], Lih Tan[4], Jade Foeng[5], Dylan McPeake[5], Timona Tylis[5], Caitlin Abbott[5], Allison Cowin[3], Claudine Bonder[6], Timothy Sadlon[7], Shaun McColl[8], Simon C. Barry[9]. *[1]Molecular Immunology, Robinson Research Institute, Adelaide, Australia,[2]Robinson Research Institute, Adelaide, Australia,[3]Future Industries Institute, University of South Australia, Adelaide, Australia,[4]Centre for Cancer Biology, Adelaide, Australia,[5]Chemokine Biology, University of Adelaide, Adelaide, Australia,[6]Centre for Cancer Biology, University of South Australia, Adelaide, Australia,[7]Molecular immunology, Robinson Research Institute, Adelaide, Australia,[8]Chemokine Biology, Carina Biotech Pty and University of Adelaide, Adelaide, Australia,[9]Robinson Research Institute and Carina Biotech Pty Ltd, Adelaide, Australia*

Chimeric antigen receptor (CAR) T cells have demonstrated robust clinical efficacy against B-cell malignancies, and rapid translation to approval for use in man has inspired the search for CAR-T cells against solid tumours. Cancer stem cells are a small population of cells within a tumour that have the capacity to self-renew, differentiate, and initiate new tumours. Cancer stem cells are known to be resistant to chemotherapy and radiotherapy and are enriched in residual disease, which allows relapse. Targeting cancer stem cells is desirable as it will reduce a tumours' ability to generate new cells, resulting in tumour remission. Leucine-rich G protein-coupled receptor 5 (LGR5) expression is restricted to stem cell populations in several tissues in adults. In addition, LGR5 is a marker of cancer stem cells and $LGR5^{+}$ cancer cells are implicated in tumour progression and metastasis. We have designed and tested a CAR targeting the extracellular domain of LGR5, and optimised gene delivery to purified human CD3+ T cells showed robust CAR expression. Having confirmed on target specificity and cytotoxicity we show antigen-specific IFNγ release against colorectal cancer (CRC) and neuroblastoma cell lines *in vitro.* We confirmed the specificity and safety of the LGR5 targeting CAR-T cells by testing against normal human tissues from colon, liver, kidney, lung and heart. Using optimised gene delivery and CAR-T manufacturing protocols, we generated clinical scale batches to evaluate their potency in a preclinical CRC xenograft mouse model. A protocol for clinical scale manufacture of LGR5-targeting CAR-T cells has been developed using CD3+ T cells from healthy donors and now we have successfully tested this protocol using CRC patient-derived CD3+ T cells. This protocol is GMP ready and has been tested in a GMP manufacturing facility. Using T cells from healthy donors and CRC patients we were able to generate optimal cell numbers (80-fold expansion) with high CAR expression. These CAR-T cells showed high *in vitro* cytotoxicity and IFNγ release when co-cultured with LGR5 expressing CRC cell line. Post expansion, CAR-T cell products expressed markers of self-renewing naïve-like and central memory phenotype and showed very low percentage of cells that were triple-positive for PD1, TIM3 and LAG3. These results suggest a CAR-T targeting LGR5 may provide long-term protection against tumour growth. Our data positions LGR5-targeting CAR-T therapy as a viable therapeutic for human metastatic colorectal cancer types with minimal off-target effects, which we now aim to test in human clinical trials.

#4084

Globo H-targeted CAR T cell cancer immunotherapy

Jiann-Shiun Lai, Shiou-Ling Jian, Woan-Eng Chan, Ming-Tain Lai. *OBI Pharma, Inc, Taipei, Taiwan*

Background: Globo H (GH), a Globo-series glycosphingolipid (GSL), is highly expressed in epithelial tumors, such as colon, endometrial, gastric, pancreatic, lung, prostate, and breast cancers. Aberrant expression of Globo H has been reported to be associated with the metastatic potential and poor prognosis of these cancers. However, in normal tissues, GH expression is limited to the secretory borders of apical epithelial cells, making it difficult to access by the immune system. GH is therefore a promising target for anticancer therapeutics. Clinical studies with the Globo H vaccines (OBI-822 and OBI-833) and the humanized anti-Globo H antibody (OBI-888) demonstrating an excellent safety profile. In recent years, cell therapy using chimeric antigen receptor T (CAR T) cells have shown impressive clinical outcomes. As a result, development of CAR T targeting GH may offer a novel anticancer therapeutic agent.

Aim: The aim of this study was to develop a CAR T cell therapy targeted against Globo H (obi-R007) using lentivirus-mediated genetic engineering with a proprietary Globo H-specific antibody. Methods: We conducted *in vitro* and *in vivo* studies to determine the characteristics of GH CAR T obi-R007.

Results: *Ex vivo* expansion of obi-R007 from healthy donors ranged from 40- to 200-fold post-activation for 10 days. Previous studies have suggested that less differentiation and fewer exhaustion markers of CAR T cells are beneficial for therapeutic persistence. In our study, there was less differentiation in the $CD62L^+$ population (T_{SCM} and T_{CM}) in greater than 80% of obi-R007 cells, and no significant exhaustion markers (PD-1, LAG-3, etc.) were detected. obi-R007 showed specific cytotoxicity against Globo H-positive tumor cells with an E/T ratio of 0.5:1~2:1 and exhibited Globo H-specific activation through the expression of CD69, CD25, and Granzyme B as well as the release of Interferon γ and IL-2. Moreover, the activation and proliferation of obi-R007 were dependent on the presence of target cells. All the *in vitro* results indicate the specific targeting of obi-R007 to Globo H resulting in cytotoxic T cell responses. In the *in vivo*

study, the efficacy of obi-R007 was demonstrated by adoptive cell transfer in several xenograft models and obi-R007 was shown to be persistent under multiple tumor challenges in the NCI-N87 gastric cancer model. Luminance labelling of CAR T cells showed that the distribution of CAR T cells in mice was specific to the tumor site and lymphoid organs suggesting a homing activity of the CAR T cells. Furthermore, no obviously physiological toxicity was observed *in vivo*.
Conclusion: In conclusion, our *in vitro* and *in vivo* pharmacology and preliminary toxicology studies support clinical development of Globo H CAR T immunotherapy for patients with cancer.

#4086
Mitigating the CD5 CAR-CD5 interaction enhances the functionality of CD5 CAR-T cells by alleviating the T-cell fratricide
Lee Young Ho, Seung Rok Yu, Jeong Hoon Jeong, Hyeong Ji Lee, Hyeon Jeong Cho, Hyung Cheol Kim. *Curocell Inc., Daejeon, Korea, Republic of*

Chimeric antigen receptor (CAR) T-cell therapy has been used with unprecedented clinical responses in relapsed/refractory B-ALL or B-NHL, MM patients. However, CAR-T therapy has not yet been proven effective in other hematological malignancies, such as T cell lymphoma and leukemia (T-NHL/T-ALL) and acute myeloid leukemia (AML). Developing CAR-T cells for patients with T-cell malignancies remains challenging as most CARs targeting T-lineage antigens, such as CD5, CD7, and CD3, target themselves, potentially resulting in fratricide of CAR-T cells. Thus, there is a need for technical approaches to alleviate the fratricide of CAR-T to treat T-cell malignancies successfully. As part of the approach, we studied whether the affinity of CAR and cognate antigen expression of CAR-T cells influence the intensity of CAR-T`s fratricide and hypothesized that if a single chain Fragment variable (scFv) with a low intensity of fratricide is applied to T-lineage antigen-downregulated CAR-T cells, the effector function of CAR-T cell targeting T cell antigen can be maximized. For this, we screened full human scFvs targeting CD5, a pan T-cell marker, tested the affinity of scFvs for CD5 antigen, and generated anti-CD5 CAR-T cells (CAR5). We evaluated the intensity of *in vitro* fratricide in CAR5 based on cell expansion and cytokine secretion *in vitro* and tested their anti-tumor activity in a CD5+ T-ALL xenograft model (Jurkat). In addition, to

minimize CAR recognition to a cognate antigen expressed in CAR-T cells, we also generated CD5-downregulated CAR5s (CD5-KD CAR5) using a short hairpin RNA cassette integrated into an anti-CD5 CAR vector to test if the downregulation of CD5 in CAR5s can reduce the fratricide. We found that a CAR5 clone (C7CAR5) with the lowest level of fratricide in vitro, showed superior anti-tumor activity compared to other CAR5s *in vivo* and that CD5-downregulated C7 CAR5 (CD5-KD C7CAR5) further reduced the fratricide, maximizing the anti-tumor activity. In conclusion, we demonstrate that high-affinity CAR may not always show superior functionality in T cell malignancy CAR-T therapy, explaining one or more strategies to alleviate the fratricide are required. These studies provide the foundation for developing CD5 CART products to treat relapsed T-cell malignancies.

#4087

Co-expression of membrane bound IL-15 enhanced anti-tumor response of CAR-T

Cuiqing Yang[1], Fuwei Jiang[1], Yifang Wang[1], Tingting Liu[1], Chao Wang[1], Qingyang Wang[1], Qin Wang[1], Gang Ye[1], Renhong Tang[2], Zhuoxiao Cao[1].
[1]Shanghai Simnova Biotechnology Co., Ltd., Shanghai, China,[2]Jiangsu Simcere Pharmaceuticals Co. Ltd, Nanjing, China

Introduction: Chimeric antigen receptors (CARs) T cells have been used successfully to treat patients with hematologic malignancies, but showed less effective in solid tumors. We investigated multiple approaches to engineer and enhance CAR-T activity in solid tumors. It has been previously reported that improvement in the quality of CAR-T cells, through CAR design or manufacturing optimization, could enhance the therapeutic potential of CAR-T cells. One parameter influencing the effectiveness of CAR-T cell therapy is the differentiation status of the final product: CAR-T cells that are less-differentiated and less exhausted are more therapeutically potent. It is well known that IL-2 is the main cytokine used to culture cells for adoptive cell therapy, as it plays an important role in the proliferation and functional effect of T cells. However, it has been noted T cells cultured with IL-2 are phenotypically heterogeneous, being predominantly composed of effector memory cells. In comparison with IL2, IL-15 can induce a memory stem-like T cell phenotype, which is less

differentiated and with a superior capacity for cell expansion and survival. Several groups reported that compared with cells cultured with IL-2, CAR-T cells expanded with IL-15 preserve a less-differentiated stem cell memory (Tscm) phenotype and exhibited reduced expression of exhaustion markers, higher antiapoptotic properties, increased proliferative capacity upon antigen challenge, and promoted superior anti-tumor responses in vivo.
Method: To provide localized IL-15 mediated signaling to T cells, we constructed a version of IL-15 as a membrane-bound molecule (mIL-15) designed to stimulate T cells in cis and in trans, and mIL-15 is tethered to the cell surface and functions locally to enhance the functionality of the CAR-T cell without systemic delivery of IL-15.
Result: Expression of mbIL-15 is shown to enhance T cell expansion, preserve a less-differentiated Tscm phenotype and prevent CAR-T cell exhaustion, leading to longer persistence and an enduring anti-tumor response over the conventional CAR-T cells.
Conclusion: We demonstrate that CAR-T activity and persistence can be enhanced by simultaneous expression of mIL-15, which preserves the CAR-T cell Tscm phenotype and improves their metabolic fitness, resulting in superior antitumor activity. These preclinical data support the notion that CAR-T cells are designed and optimized to persist in the hostile tumor microenvironment and potentially improve efficacy against solid tumors.

#4088

A neovasculature-inducible CA9 CAR resistant to FASL and TGFb mediated suppression for the treatment of ccRCC

Angela C. Boroughs, Irene Scarfo, Nickolas Attanasio, Thomas Gardner, Jenessa B. Smith, Jennifer McDevitt, Laura Lim, Nishant Mehta, Suchismita Mohanty, James Zhang, Eric Cui, Vibhavari Sail, Amanda Fearon, Samuel Williams, Stephen Santoro, W. Nicholas Haining, Levi Gray-Rupp. *Arsenal Biosciences, South San Fransisco, CA*

Clinically effective CAR-T cell therapy for solid tumors, such as clear cell renal cell carcinoma (ccRCC), will require substantial T cell engineering to increase their specificity and potency. We have developed an Integrated Circuit T cell (ICT) that encodes multiple synthetic “modules” in order to overcome diverse barriers to efficacy in ccRCC; ICT cells are generated via CRISPR-mediated, targeted knock-in of a single large transgene into the

novel GS94 safe-harbor locus. Both primary and metastatic sites of ccRCC are highly vascularized, with the majority of tumor cells expressing elevated levels of carbonic anhydrase IX (CA9), suggesting CA9 may be an excellent CAR target. However, CA9 is also expressed in healthy bile ducts and stomach tissue which has led to on-target, off-tumor toxicities in patients treated with constitutive CA9 CAR T cells. To improve the therapeutic index of CA9 CAR T cells, we developed an "AND" logic gated ICT cell that requires the presence of two antigens to trigger tumor cell killing, thereby enhancing tumor specificity. Induction of the CA9 CAR is gated on the expression of PSMA found on the tumor neovasculature of ccRCC. Importantly, PSMA and CA9 are not co-expressed in normal tissues. When the anti-PSMA priming receptor (PrimeR^{TM}) binds PSMA, PrimeR^{TM} engagement triggers proteolytic release of a chimeric, fully human transcription factor that induces expression of a CA9 CAR. We confirmed the feasibility of vascular priming using a transwell assay where ICTs were primed by a PSMA expressing endothelial cell line and then migrated across the transwell membrane to kill CA9 expressing RCC cells. In addition, a dual flank xenograft model was used to show logic gated circuits selectively kill tumors that express both CA9 and PSMA, and not tumors that express CA9 alone.
Transforming growth factor beta (TGFb) is an immunosuppressive cytokine known to be highly expressed in ccRCC. To further increase the potency and persistence of the ICT cells an shRNA cassette was developed targeting both FAS and TGFBR2, a receptor required for TGFB signaling in T cells. Addition of FAS/TGFBR2 shRNA enhanced antitumor activity of PSMAxCA9 logic gate expressing T cells during in vitro chronic stimulation assays conducted in the presence of exogenous TGFb. Furthermore, FAS/TGFBR shRNA containing ICTs demonstrated enhanced antitumor activity in multiple xenograft RCC models. Collectively, these results demonstrate that PSMAxCA9 ICT cells can (i) selectively target antigens that cannot be safely targeted by conventional CARs and (ii) overcome multiple suppressive mechanisms in the tumor microenvironment.

#4089
PanCAR-specific antibody-cytokine fusion proteins

John T. Keane, Avery D. Posey. *Perelman School of Med. Univ. of Pennsylvania, Philadelphia, PA*

CAR-T cells are a potent immunotherapy that redirect T cell specificity towards cell surface tumor-associated antigens. While this therapy has been effective in hematological malignancies, therapies against solid tumors not achieved the same efficacy due to a multitude of additional challenges, including a lack of tumor specific antigens and an immunosuppressive tumor microenvironment. One strategy to increase T cell potency is to use fourth generation CAR-T cells that also secrete an immunostimulatory factor, such as a cytokine. We have created CAR-T cells targeting Tn-MUC1 utilizing a scFv from the 5E5 antibody that also secrete interleukin-12 (IL-12), interleukin-18 (IL-18), and interleukin-23 (IL-23). These cytokine-secreting CAR-T cells have shown an increase in efficacy against multiple epithelial based tumors in impedance-based killing assays. In a xenograft model of human breast cancer, CAR-T cells secreting IL-12 and IL-23 were able to significantly delay tumor growth compared to non-transduced T cells, CAR-T cells alone, and CAR-T cells secreting IL-18. While these cells showed good efficacy *in vivo*, clinical translation is difficult due to concerns over cytokine storm due to the constitutive secretion of cytokines. To overcome this, we created a fusion protein utilizing an antibody specific to an invariant region found in majority of CAR molecules, including those utilized commercially available therapies and under pre-clinical development, fused to the three immunostimulatory cytokines. In impedance-based killing assays, antibody-cytokine fusions stimulated non-cytokine secreting CAR-T cells to completely clear the tumor at an E:T ratio in which the CAR-T cells incubated with only the antibody alone were unable to control the tumor growth. Interestingly, combination therapy of CAR-T cells and antibody-cytokine fusions outperformed CAR-T cells constitutively secreting the same cytokines in *in vitro* assays. This work highlights the use of a single reagent capable of increasing the efficacy of the majority of CAR-T cell therapies and may be an important contribution towards treating solid tumor malignancies with CAR-T cell therapies.

#4090

Regional administration of IL-12 endowed CAR T cells effectively targets systemic disease

Hee Jun Lee[1], Yuki Yamaguchi[1], Jackson Gibson[1], Cody Cullen[1], John P. Murad[1], Anthony K. Park[1], Isabel Monroy[1], Cari Young[2], Lea Christian[1], Lauren Adkins[1], Lawrence Stern[1], Wen-Chung Chang[1], Catalina Martinez[1], Stephen J. Forman[1], Saul J. Priceman[1]. *[1]City of Hope National Medical Center, Duarte, CA,[2]Irell and Manella Graduate School of Biological Sciences, City of Hope, Duarte, CA*

While chimeric antigen receptor (CAR) T cells have received FDA approvals in treating hematological malignancies, clinical responses of CAR T cells for solid tumors have been underwhelming. Intense investigation is underway to improve CAR T cells trafficking, persistence and efficacy. Interleukin-12 (IL-12) is a potent inflammatory cytokine that recruits and activates various endogenous and adoptively transferred immune cells, but development of its clinical applications is hindered by toxicity of systemic IL-12 signaling. In this study, we engineered and expressed membrane-bound IL-12 (mbIL12) in CAR T cells to overcome current limitations in CAR T cell and IL-12 therapies.

We evaluated CAR T cell function using co-culture assays and preclinical murine models bearing human tumor xenografts. We modeled systemic metastasis of ovarian and breast cancer and assessed the impact of mbIL12 in CAR T cells on targeting regional and systemic diseases. Syngeneic mouse models were used to evaluate toxicity induced by mbIL12 in CAR T cells.

We observed a greater number of CAR T cells in the peripheral blood of mice receiving locoregionally delivered CAR T cells engineered with mbIL12, suggesting that mbIL12 improves CAR T cell trafficking and persistence. Furthermore, mice bearing regional and systemic diseases experienced more potent and durable anti-tumor activity when treated with mbIL12 endowed CAR T cells. These results were mirrored in vitro where mbIL12 improved CAR T cells activation, proliferation and IFNg secretion when co-cultured with tumor cells, recapitulating our findings in vivo. Toxicities observed in immune-competent mice receiving systemic IL-12 delivery were not detected in those administered CAR T cells with mbIL12. We demonstrated that mbIL12 enhances anti-tumor function of CAR T cells for treatment of solid tumors. This study also showed that mbIL12 is safe,

providing a translatable engineering strategy to improve CAR T cell therapy. IL-12 signaling is well known to modulate function of various immune cells, but the impact of CAR T cells with mbIL12 on immune tumor microenvironments remains to be elucidated. We are currently investigating changes in the immune landscape that CAR T cells with mbIL12 induce.

#4091

Engineered hypoimmune CAR T cells provide lasting tumor control in immunocompetent allogeneic humanized mice even with re-challenge

Xiaomeng Hu, Pascal Beauchesne, Karl Manner, Corie Gattis, Priscilla Ngo, Rowena De Jesus, Ramya Ankala, Chi Young, Frank Wells, Lindong Weng, Kathy White, William E. Dowdle, Aaron Foster, Terry J. Fry, Sonja Schrepfer. *Sana Biotechnology, South San Francisco, CA*

Off-the-shelf CAR T cells potentially offer advantages over autologous strategies such as ease of manufacturing, quality control, off-the-shelf availability, and lack of T cell dysfunction, as well as the ability to generate a more consistent CAR T product from healthy T cells. However, the vigorous host-versus-graft immune response against histoincompatible T cells prevents expansion and persistence of allogeneic CAR T cells and mitigates the efficacy of this approach. A major challenge is that, while HLA deletion can result in adaptive immune evasion, innate reactivity is enhanced with this approach. CD47 overexpression can block both NK cell and macrophage killing (J Exp Med 2021;218(3):e20200839), and we hypothesized that T cells would lose their immunogenicity when human leukocyte antigen (HLA) class I and II genes are disrupted and CD47 is over-expressed. We describe here the engineering of human immune evasive CAR T cells building on our previously described hypoimmune technology (Nat Biotechnol 2019;37(3):252-258 and Proc Natl Acad Sci U S A 2021;118(28):e2022091118).Human T cells from healthy donors were obtained by leukapheresis. CRISPR/Cas12b technology was used to disrupt the B2M, CIITA, and TCR genes, and lentiviral transduction was used to overexpress CD47 and to express a CD19 CAR to generate hypoimmune (HIP) CD19 CAR T cells. Control T cells were unmanipulated except for overexpression of the CD19 CAR (unmodified).For 3 months persistence studies, allogeneic SGM3 humanized mice were injected with 1×10^6 Luc^+

Nalm6 cells and received 7×10^6 control CD19 CAR T cells or HIP CD19 CAR T cells.In the mice treated with either unmodified CD19 CAR T cells and HIP CD19 CAR T cells, tumor control was initially rapidly achieved. However, unmodified CD19 CAR T cells were eventually rejected by the host and the loss of these cells resulted in re-growth of tumor. By contrast, in HIP CD19 CAR T injected mice, tumor control was maintained throughout the study, including following a rechallenge at day 83 with NALM6 cells without further administration of HIP CD19 CAR T cell. Flow cytometry at endpoint from bone marrow and spleen confirmed persistence of HIP CD19 CAR T cells.These findings show that HIP CD19 CAR T cells are immune evasive in allogeneic recipients and data suggest that HIP CD19 CAR T cells are able to persist and maintain efficacy without immunosuppression.

#4092

Development of nucleotide metabolic reprogrammed CAR T cell therapy suitable for solid tumors

Yue Hu[1], Abhijit Sarkar[1], Kevin Song[1], Magnus Hook[1], Andras Heczey[2], Xiaotong Song[1]. *[1]Texas A&M University, Houston, TX,[2]Baylor College of Medicine, Houston, TX*

CAR T cell therapy has represented an exciting breakthrough in the treatment of patients with hematologic malignancies. In contrast, the antitumor activity of CAR T cell therapy in solid tumors has been modest so far in clinical studies. The suboptimal clinical efficacy is a result of multiple factors including limited T cell trafficking, persistence, and the immunosuppressive tumor microenvironment (TME). While current strategies utilize costimulatory molecules and cytokines to activate CAR T cells, a key but largely overlooked problem of CAR T cell therapy is nutrient competition between tumor cells and T cells in the nutrient-poor TME. In our previous studies, a metabolic screen identified inosine as an alternative fuel for T cells which can support T cell growth and function in the absence of glucose. T cells could metabolize inosine into hypoxanthine and phosphorylated ribose by purine nucleoside phosphorylase. Moreover, we demonstrated that T cells have advantage over cancer cells in utilizing inosine, and supplementation with inosine enhances the antitumor efficacy of PD-1 mAb and adoptive T cell transfer in mouse models. In this study,

we therefore engineered CAR T cells to express CD26 on the cell surface and a secreted adenosine deaminase (ADA) fused with an anchor. These metabolic reprogrammed CAR (designated as $_{MR}$CAR) T cells exerts their activities through different mechanisms. ADA irreversibly converts adenosine to inosine, overcoming adenosine-mediated immunosuppression and providing inosine for CAR T cell growth, while CD26 induces a rich chemokine receptor profile enabling CAR T cells to traffic to solid tumors. We demonstrated that CD26-overexpressed CAR T cells displayed superior migration capacity and resisted TGF-beta suppression, while the CD26 expression on unmodified CAR T cells was significantly down-regulated by TGF-beta. We further proved that ADA is conditionally secreted in stress condition (i.e., low pH, lack of nutrient and oxygen) based on ADA's biological characteristics, suggesting that ADA activates CAR T cells as a trans-signaling to the CAR construct in a tumor specific manner. Remarkably, we observed that the $_{MR}$CAR T cells inhibit tumor growth more effectively than unmodified CAR T cells in both Huh7 human hepatocellular carcinoma (GPC3-$_{MR}$CAR) and A549 human non-small cell lung cancer (HER2-$_{MR}$CAR) mouse models. Thus, MR-CAR T cell therapy represents a promising approach to improve CAR T cell therapy against solid tumors.

#4093

Dual targeted CAR immunotherapy for neuroblastoma using γδ T cells

Hunter C. Jonus, Jasmine Y. Lee, Jordan A. Silva, H. Trent Spencer, Kelly C. Goldsmith. *Emory University, Atlanta, GA*

Cellular immunotherapy for aggressive pediatric solid tumors like neuroblastoma (NB) has focused on autologous products of αβ T cells, that so far, have been uniformly unsuccessful. γδ T cells offer a potentially superior, off-the-shelf therapy that is directly cytotoxic towards tumors without alloreactivity. Furthermore, γδ T cell infiltration of the hostile, solid tumor microenvironment is a prognostic marker of favorable disease outcome. Our team recently opened a first-in-child evaluation of unengineered allogeneic γδ T cells in combination with dinutuximab, an anti-GD2 antibody, and chemotherapy (NCT05400603). Our focus now is to optimize a second-generation γδ T-cell therapy by engineering the

expression of tumor targeting chimeric antigen receptors (CAR). We hypothesize that CAR-targeting will further enhance γδ T-cell homing and antitumor potency. While anti-GD2 antibodies have been clinically successful immunotherapies for NB, GD2-targeted cell therapies need improvement. Our team recently validated a novel immunotherapy target for NB, protein tyrosine kinase 7 (PTK7), an inactive tyrosine kinase expressed highly amongst all NBs with low to no normal pediatric tissue expression.

We designed a dual-targeting platform directed against both GD2 *and* PTK7 using γδ T cells, where CARs are separately encoded and dually expressed. Previously optimized transgenes containing GD2 or PTK7 scFv targeting domains followed by a CD8 hinge region, CD28 co-stim/trans-membrane domain, and CD3ζ signalling domain were inserted under the T7 promoter for mRNA production. Purified mRNA was electroporated into γδ T cells following their thaw from cryopreservation. Electroporation titrations were performed to optimize CAR expression to be detected up to 72 hours post-modification, which is compatible with the approximate *in vivo* lifespan γδ T cells in mice. Simultaneous expression of both CARs appears highest 24 h after electroporation, with ~70% of the target γδ T cell population modified. Anti-GD2/PTK7 γδ T cells are potent against the NB cell line IMR5 (GD2+PTK7+) in a 4 h cytotoxicity assay at effector:target ratios as low as 0.5:1. Importantly, specificity is also shown against NB cell lines genetically engineered to represent the clinical heterogeneity of GD2 and PTK7 expression that may be observed, where the dual CAR therapy is effective against $GD2^{+}PTK7^{+}$, $GD2^{+}PTK7^{-}$, and $GD2^{-}PTK7^{+}$, but not $GD2^{-}PTK7^{-}$ NBs.

In conclusion, we developed a dual CAR-based cellular therapy for NB using γδ T cells as an effector population in place of classical αβ T cells. Early studies demonstrate feasibility for innovative dual CAR expression and show promise for strong anti-NB potency. Future work will optimize CAR signaling domains for maximal efficacy in solid tumors, as well as confirm efficacy and safety *in vivo* with results rapidly translatable into our established γδ T cell clinical trial pipeline.

#4094

Enhanced CRISPR-Cas9 edited CAR-T cells through simultaneous inactivation of multiple T cell exhaustion pathways

Oksana Sergeeva, Amber Fearnley, Shu Shien Chin, Xingyue An, Nana Adjoa Pels, Kristen Metzler, Kyla Joinville, Lizet Aquino Calderon, Abudukadier Abulizi, Hayden Karp, Julio Rodriguez, Louis Matis, Jay Fine, Jeremy Myers. *EvolveImmune Therapeutics, Inc, Branford, CT*

T cell exhaustion is a hallmark of tumor-infiltrating T cells and a major therapeutic challenge for immunotherapy which is not sufficiently understood. To identify T cell exhaustion promoting genes which may be targeted by new therapies, we combined highly efficient CRISPR/Cas9 gene knockouts in primary human T cells with functional assessment of effector function under exhaustion-inducing chronic T cell activation conditions. We conducted an initial CRISPR/Cas9 T cell exhaustion screen focused on previously identified genes reported as enhancers of anti-tumor T cell response in mouse tumor models, published exhaustion genes, and genes associated with CD8 T cell activation. Based on these results, we constructed gene networks from these screen hits and performed a secondary CRISPR-Cas9-based screen. We found that eight genes, when efficiently knocked out, limited T cell exhaustion, as measured by increased proliferation under chronic activation, reduced expression of T cell exhaustion markers, and improved tumor cell killing in CD3-bispecific antibody-mediated tumor/T cell co-culture assays. Prioritized T cell exhaustion gene hits were also evaluated in assays assessing anti-CD19 CAR-T cell function. The CRISPR-mediated ablation of five T cell exhaustion gene hits resulted in significantly more effective CD19-positive human tumor cell killing, compared to the non-targeting control CAR-T cells. These five genes included a transcriptional regulator, a member of a CD28-independent costimulatory pathway, and a series of ligand/receptor pairs that have been previously associated with T cell exhaustion and dysfunction. Interestingly, knockdown of combinations of the top three T cell exhaustion gene hits resulted in CAR-T cells that were more effective in tumor killing than any of the single gene knockouts, suggesting a non-redundant role for each gene, most likely comprising independent pathways. Furthermore, enhanced tumor cell killing was observed when each T cell exhaustion gene hit was ablated in combination with PDCD1 (PD-1) in double knockout CAR-T cells, suggesting that the T cell exhaustion pathways we identified were complementary to the PD1-PDL1 immune checkpoint pathway in regulating effector T cell function. By using

a multidimensional, functional CRISPR-Cas9-based T cell exhaustion screen, we have uncovered genes that are involved in T cell exhaustion. These gene knockouts can be universally applied individually or in combination to create CAR-T cells with more durable effector activity, with the potential to achieve superior patient outcomes in a variety of tumor indications.

#4095

Preclinical characterization of switchable allogeneic chimeric antigen receptor T cells to support first in human clinical study in CD123-positive hematologic and lymphatic malignancies

Armin Ehninger[1], Johannes Spehr[1], Simon Loff[1], Anika Langer[1], Julia Riewaldt[1], Julia Reinhardt[1], Jan-Erik Meyer[1], Josephine Dietrich[1], Gabriel Jurado[1], Reynald Lescarbeau[2], Marc Cartellieri[1]. *[1]AvenCell Europe GmbH, Dresden, Germany,[2]AvenCell Therapeutics, Inc., Cambridge, MA*

Approximately 80% of AML patients express CD123 on their leukemic blasts and CD123 is frequently expressed on other hematologic and lymphatic malignancies. Chimeric antigen receptor (CAR) T-cell therapy has demonstrated significant efficacy in B cell malignancies. Breakthrough of conventional CAR-T technology in AML has been hampered by expression of suitable target antigens on normal hematopoietic progenitor cells posing a risk for continued aplasia. Thus, innovative approaches putting the power of CAR-T technology under the control of reliable and fast-acting on/off switches to avoid and/or abrogate acute and long-term side effects are required. We have recently reported clinical proof-of-concept for autologous switchable CAR-T cell therapy in AML (Wermke et al. *Blood* 2021). However, manufacturing of autologous products is very costly and rrAML patients are often in urgent need for a product and multiple prior lines of treatment may be detrimental for product quality. While current clinical allogeneic approaches successfully prevent graft-versus-host disease, observed persistence has been limited due to rejection of the grafted T cells by host immune cells. Here, we report preclinical development of a donor-derived allogeneic switchable CAR-T therapy for CD123-positive hematologic and lymphatic malignancies (AVC-201). The reverse universal chimeric antigen receptor platform (RevCAR) is a 2-component CAR-T platform. The first component is a universal CAR-T

cell. Its binding domain is a short, non-immunogenic peptide that by itself does not recognize any human cell surface antigen but is specifically bound by an scFv included in the second component, a soluble adaptor called targeting module (TM). To target CD123, a TM with a short half-life was selected (R-TM123), enabling a rapid switch-off of the RevCAR system by TM withdrawal to avoid acute and long-term toxicity usually associated with continuous activation of CAR-T cells. The allogeneic cells are generated by three edits with CRISPR-Cas9, which is meant to fully overcome graft-versus-host disease as well as graft rejection by host T and NK cells. Therefore, we expect a persistent T cell product that can be re-expanded with additional TM cycles. A summary of preclinical characterization of AVC-201 will be presented at the meeting including *in vitro* and *in vivo* pharmacology and toxicology experiments. Activation of Allo-RevCAR-T cells is strictly dependent on the presence of CD123-positive target cells and R-TM123. Allo-RevCAR-T cells redirected by R-TM123 efficiently lyse CD123-positive AML cells *in vitro* and *in vivo,* and *in vitro* EC_{50} values are in the low picomolar range of R-TM123 concentrations. In conclusion, preclinical data support the clinical exploration of AVC-201 in a first in human study.

#4096

Assessing individual variability in efficacy and toxicity of autologous and allogeneic chimeric antigen receptor T-cell immunotherapy using a PBMC-humanized mouse model

Won Lee[1], Destanie Rose[1], Katelyn Burleigh[2], Blair Armstrong[2], Heather Gustafson[2], Rebecca Gardner[3], James G. Keck[1], Jiwon Yang[1]. *[1]Innovation & Product Development, The Jackson Laboratory, Sacramento, CA,[2]Ben Towne Center for Childhood Cancer Research, Seattle, WA,[3]Division of Hematology-Oncology, Seattle Children's Hospital, Seattle, WA*

Chimeric antigen receptor T-cell (CAR-T) therapy has emerged as a revolutionary therapeutic to fight cancer. However, side effects such as cytokine-release syndrome and neurotoxicity often accompany and remain unpredictable. While autologous CAR-Ts are FDA-approved, allogeneic CAR-Ts are in active development in pursuit of “off-the-shelf” availability and reduced manufacturing costs. However, the same concern for adverse events applies. Importantly, how the immune characteristics of the patient

may predispose towards toxicity is not well modeled. Further, it is unclear how autologous versus allogeneic products interact with the patient immune system. Toxicity does not correlate with in vitro characterization of the CAR-Ts, adding unpredictability to the toxicity and efficacy. These highlight the need for in vivo mouse models to explore biological variation, predictive biomarkers, and therapeutic intervention. Therefore, we developed a humanized mouse model using NSG™-MHC Class I/II double knock-out (DKO) mice engrafted with human PBMCs to access individual variability in CAR-T-induced toxicity and efficacy. DKO mice are optimal for assessing human cytokine induction from CAR-Ts as they show delayed onset of GvHD and low baseline cytokine levels. To test donor variation in autologous CAR-T toxicity, we humanized mice and treated with autologous CD19 CAR-Ts containing the CD28 costimulatory domain and CD3z chain from two human PBMC donors (Donor A and B). CAR-T successfully eliminated human B cells from both PBMC donors in vivo. We observed drastic body weight loss and 83% of Donor A mice (engrafted with 17M PBMCs) reached the humane endpoint. In contrast, Donor B mice did not experience body weight loss. CAR-T induced human cytokines such as IFN-γ, IL-2, IL-4, IL-6, IL-10, TNFα, MIG, MIP-1a, and IP-10, recapturing clinical data. To test donor variation in allogeneic CAR-T toxicity, we engrafted mice with 10M PBMCs from 6 healthy donors and treated with allogeneic CAR-Ts from Donor A or B. Allogenic efficacy was greater in Donor B CAR- than Donor A CAR-Ts. Donor-specific variability was observed; mice humanized with one of the six donors, experienced significant body weight loss only from the Donor B CAR-Ts but not from Donor A CAR-Ts. Principal component analysis of cytokine data revealed that Donor B CAR-Ts induced more distinguished cytokine responses than Donor A CAR-Ts, driven by IFN-γ and IL-10. Lastly, the data indicates that the CAR-T cells show poor expansion in allogeneic treatment, corresponding to the current literature. PBMC-humanized mice provide an in vivo platform to assess the toxicity and efficacy of autologous and allogeneic CAR-T treatment. This platform can be used to preclinically assess cytokine induction from the interaction between the patient immune system and allogeneic CAR-Ts from healthy donors.

#4097

Functional and translatable efficacy of CAR-T cells targeting B cell lymphomas

Lauren Kelsey[1], Karin Latta[2], Joey Kolb[2], Bincy John[2], Ilona Aylott[1], Daniel Rocca[1], Alexandru Bacita[1], Christopher Kirkham[1], Patrick Walters[1], Charlotte Humphery[1], Lorena Sueiro Ballesteros[1], Jezrom Self-Fordham[1], Louise Brackenbury[1], Chassidy Hall[2], Harris David[2], Julia Schueler[3], Robert Nunan[1]. *[1]Charles River Laboratories, Inc., Bristol, United Kingdom,[2]Charles River Laboratories, Inc., Morrisville, NC,[3]Charles River Laboratories, Inc., Freiburg, Germany*

Chimeric Antigen Receptor (CAR)-T cell therapy has achieved great success in treating a variety of liquid tumors, in particular CD19+ lymphomas. CAR technology is advancing rapidly, with notable improvements in efficacy, safety and complexity as human ingenuity seeks solid tumor applicability. Here we describe how to efficiently generate, expand and validate *in-vitro* and *in-vivo* efficacy of a clinically tested CD19-specific CAR. HLA-A*02:01+ CD3+ T-cells were transduced to express a CD19-CAR to >80% efficiency (in 5 donors) and reproducibly expanded to >68 fold over a 19 day period. *In-vitro* studies were used to assess tumor killing ability, utilizing a HLA-A*02:01+ patient derived xenograft (PDX) CD19+ cell line, alongside human cancer cell lines RAJI (CD19+) and K562 (CD19-). Analysis revealed the potent ability of CD19-CAR-T cells to specifically target CD19+ cells in a dose dependent manner. Supernatant analysis showed highly elevated IFNγ concentrations, identifying enhanced activation of CAR-T cells in the presence of CD19+ target cells only. *In-vivo* survival studies were completed to identify translatability & efficacy in both systems. Mice were inoculated with CD19+ cells to produce multiple tumor burdened models (RAJI, JEKO-1 & PDX4009). This demonstrated high efficacy of CAR-T at targeting both tumor cell line RAJI or PDX *in vivo*, with almost complete tumor regression seen in both models. JEKO-1 tumors saw progression slowed in comparison to non-transduced or no treatment controls however due to the nature of this cell line (highly tumorigenic) the level of tumor regression was not matched to the other models. Cell bio-distribution was assessed with CAR-T cells tracking successfully to the tumors as well as the highly vascularized tissues, which was expected and consistent with previous data. These assays can be translated to any CAR construct aimed at targeting

either solid or hematological tumors and demonstrates an integrated platform for translating CAR research that can be utilized end to end.

#4098

Chimeric antigen receptor (CAR) T cells overexpressing Bcl-xL increase proliferation and antitumor activity alone and in combination with BH3 mimetics

Felix Korell[1], Michael Olson[2], Diego Salas-Benito[1], Mark B. Leick[1], Rebecca C. Larson[1], Harrison Silva[1], Alessandro Gasparetto[1], Trisha R. Berger[1], Amanda Bouffard[1], Michael C. Kann[1], Markus Mergen[1], Tamina Kienka[1], Marc Wehrli[1], Stefanie R. Bailey[1], Anthony Letai[2], Marcela V. Maus[1]. *[1]Cellular Immunotherapy Program, Massachusetts General Hospital Cancer Center, Harvard Medical School, Boston, MA,[2]Department of Medical Oncology, Dana-Farber Cancer Institute, Boston, MA*

Background**:** Chimeric antigen receptor (CAR) T cells have become a well-established treatment option for patients, with six products approved for different hematologic diseases and new approvals allowing for their therapeutic use as early as second line. However, relapse rates of around 50% have been observed in all patient subsets, with one major mechanism associated with CAR T failure being cancer cell resistance to apoptosis. A form of cancer therapeutic named BH3-mimetics has been designed to inhibit members of the anti-apoptotic B cell lymphoma-2 (Bcl-2) family and, therefore, directly activate the apoptotic machinery in malignant cells. We hypothesized that integration of these anti-apoptotic molecules into CAR T cells would induce resistance towards the BH3 mimetics and allow combinational therapeutic approaches.

Methods: 4-1BB and CD28 CAR constructs were designed to overexpress one of four anti-apoptotic proteins: wildtype Bcl-2, a Venetoclax-resistant Bcl-2 variant (G101V), B cell extra-large (Bcl-xL), or myeloid cell leukemia-1 (Mcl-1). CAR T cells made from these constructs were tested against leukemia (Nalm6) and lymphoma (JeKo-1) cell lines in combination with three different BH-3 mimetics: Venetoclax (ABT-199, an FDA-approved Bcl-2 inhibitor), Navitoclax (ABT-263, a Bcl-2/Bcl-xL inhibitor), and AZD5991 (an Mcl-1 inhibitor).

Results: CAR T cells with a 4-1BB costimulatory domain tended to have increased killing over CARs with CD28 and were less susceptible to

apoptosis; therefore, 4-1BB CARs were used for all further testing. Integration of Bcl-2 family proteins into CAR T cells didn't impair or even increase tumor cell clearance *in vitro*; however, in combination with Venetoclax, Navitoclax, or AZD5991, killing capacity significantly increased compared to control CAR T cells. Even without combination with drugs, CAR T cells overexpressing Bcl-xL and Bcl-2 (both wildtype and mutant) provided higher anti-tumor activity and prolonged survival against JeKo-1 cells *in vivo*, whereas only Bcl-xL overexpression showed increased tumor control compared to regular 4-1BB CARs against Nalm6 cells. **Conclusion:** Of the tested antiapoptotic proteins, Bcl-xL overexpressing CAR T cells proved superior, having higher proliferation and increased anti-tumor activity in combination with or without BH3 mimetics, providing a new strategy to optimize CAR T cell function for the treatment of leukemia and lymphoma.

#4099

Dual targeting of tumor cells and cancer associated fibroblasts enhances CAR T efficacy in solid tumors

Bo Huang[1], Suilan Zheng[1], Haiyan Chu[2], Ramesh Mukkamala[1], Suresh K. Bowroju[1], Yashapal Singh[1], Sudarsan R. Kasireddy[1], Md Sazzadul Bari[1], Madduri Srinivasarao[1], Laurie Beitz[2], Byoung Ryu[2], Michael Jensen[3], Andrew M. Scharenberg[2], Philip S. Low[1]. *[1]Purdue University, West Lafayette, IN,[2]Umoja Biopharma, Seattle, WA,[3]Seattle Children's Hospital, Seattle, WA*

CAR T cell therapies have demonstrated considerable potency in treating hematologic cancers, but only limited efficacy in eliminating solid tumors. One reason for this discrepancy may derive from the immunologic and physical barriers created by infiltration of cancer associated fibroblasts (CAFs) into solid tumors. These CAFs, which can comprise 15-85% of the stromal cells in a tumor mass, are correlated with poor patient survival and can reduce CAR T cell efficacies by secreting immunosuppressive cytokines, stimulating tumor cell proliferation, and depositing fibrotic barriers to CAR T cell penetration. Here, we are pursuing a method to suppress or eliminate CAF activities in the tumor microenvironment (TME).

A potential CAR T cell target that is uniquely expressed on CAF surfaces is fibroblast activation protein (FAP). In this study, we have employed a novel, highly specific FAP targeting small molecule to direct our universal CAR T cells to CAFs. For this purpose, we have designed a CAR that contains an otherwise classical CAR except the extracellular scFv specifically binds fluorescein. Upon addition of a bispecific adaptor comprised of fluorescein linked via a short spacer to our FAP ligand, a bridge is formed between the anti-fluorescein CAR on the T cell and FAP on the CAF, resulting in formation of an immunologic synapse between the CAR T cell and CAF that triggers CAF destruction and CAR T cell proliferation. Importantly, this CAR T cell design also permits simultaneous administration of a second bispecific adaptor (i.e. fluorescein linked via a short spacer to a cancer-specific ligand) that can enable the same CAR T cell to concurrently kill adjacent cancer cells.
To test whether this universal CAR T cell can eliminate both cancer cells and CAFs, we have implanted KB cells (i.e. a cell line that creates an immunologically “cold” folate receptor (FR) expressing solid tumor) into NSG mice and quantitated the CAR T cell’s toxicity in the presence of one or both bispecific adapters. While administration of the universal CAR T cells followed by intravenous injection of an FR-targeting bispecific adaptor achieved significant anti-tumor efficacy, co-injection of a FAP-targeted bispecific adaptor enhanced this efficacy without apparent toxicity. Analyses of tumor masses from the therapy further revealed that co-administration of the FAP-targeted bispecific adaptor not only promoted CAF elimination but also enhanced CAR T infiltration and activation. Importantly, a similar improvement in anti-tumor efficacy could be readily demonstrated in a second immunologically “cold” PSMA-expressing solid tumor model. Taken together, we conclude that the bispecific adaptor/universal CAR T approach offers a unique opportunity to concurrently eradicate cancer cells and tumor-supporting CAFs in a manner that can improve the overall performance of the CAR T cells in solid tumors.

#4100
Co-stimulatory signaling boosts CAR T cell efficacy against chronic lymphocytic leukemia

Ziran Zhao[1], McKensie Collins[2], Clare Sun[3], Adrian Wiestner[3], J. Joseph Melenhorst[1]. *[1]Center for ImmunoTherapy & PrecisionImmuno-Oncology, Lerner Research Institute, Cleveland Clinic, Cleveland, OH,[2]Department of Pathology and Laboratory Medicine, University of Pennsylvania, Philadelphia, PA,[3]Hematology Branch, National Heart, Lung, and Blood Institute, National Institutes of Health, Bethesda, MD*

Chimeric antigen receptor (CAR) T cell therapy has been promising in chronic lymphocytic leukemia (CLL) treatment showing durable remission. However, only a third of CLL patients can achieve complete remission with persistent effect featured by early memory T cells. This disparity is attributed to T cell-intrinsic defects or tumor-mediated immunosuppression. The mechanism how CLL cells impact CAR T cell potency still remains poorly understood. Here we used second-generation CD19- and ROR1-directed CAR T cells with a 4-1BB intracellular signaling domain. To recapitulate CLL-derived T cell defects, we developed an *in vitro* model of chronic antigen stimulation using CAR T cells recursively exposed to primary CLL cells. Upon each round of CLL stimulation, both types of CAR T cells were lack of proliferation and differentiation, accompanied with cytokine production failure in IL-2, suggesting hypofunction of CAR T cell induced by CLL. We next found that this lack of CAR T cell response is not permanent but can be rescued by strong antigen stimulus or IL-2 administration. On the other hand, IL-2 affects phenotype of CLL cells by enhancing expression of co-stimulatory molecules CD80 and CD86, suggesting that IL-2 supplementation or auxiliary co-stimulation via CD80/CD86 can rescue CAR T cell reactivity against these tumor cells. To test this hypothesis, we employed the immunomodulatory drugs (IMiDs) lenalidomide and pomalidomide that have previously been demonstrated to upregulate co-stimulatory molecules on CLL and restore T-cell function via IL-2 upregulation. We sought to test if IMiDs can improve CAR T cell response to CLL. CAR T cells repeatedly exposed to primary CLL cells were co-treated with IMiDs at each round, showing significantly increased proliferation compared to the group without drug treatment. Furthermore, IMiDs can enhance the functions of these CLL stimulated CAR T cells, including differentiation (higher frequency of effector memory T cells), activation (HLA-DR, CTLA-4), proliferation (Ki67), and effector function (Granzyme B). In addition, IMiDs can increase cytotoxic efficacy of CD8+

CAR19 T cells on CLL cells. Overall, our study unveiled that in CLL, activation defect of 4-1BB, CD3-signaling anti-CD19 CAR T cells was attributable to low levels of co-stimulatory molecules on CLL cells and can be effectively overcome via upregulation of co-stimulation. Our data suggested that CLL resistance to CAR T cell can be successfully rescued by concurrent treatment with IMiDs. This study provides a potential translational approach to overcome the bottleneck of CLL treatment by CAR T cells.

#4101

Control of orthotopic melanoma and breast tumor growth and metastases is achieved by alpha$_v$ beta$_3$ CAR T cells and is augmented via PD-1 blockade

Dustin A. Cobb, Philip Mollica, Lixia Liu, Barbara Dziegielewska, Daniel W. Lee. *Pediatrics, University of Virginia, Charlottesville, VA*

Purpose: The purpose of this study was to determine the efficacy of $\alpha_v\beta_3$ CAR T cells deployed against melanoma and triple-negative breast cancer tumors, two malignancies recognized for harnessing the $\alpha_v\beta_3$ pathway for angiogenic and invasion purposes.

Procedures: CAR T cells expressing an anti-$\alpha_v\beta_3$ scFv containing either a CD28 or 4-1BB co-stimulatory domain and CD3zeta were generated by retroviral transduction. *In vitro* cytotoxicity of $\alpha_v\beta_3$ CAR T cells was assessed by co-culture with melanoma or breast tumor cells and evaluated by impedance-based real-time cell analysis and effector cytokine production by ELISA. Xenograft studies, including melanoma and orthotopic breast tumors, were carried out in NSG mice to evaluate *in vivo* efficacy of systemically administered $\alpha_v\beta_3$ CAR T cells. Immunohistochemistry was performed to evaluate T cell infiltration of tumors and changes in the microenvironment. NSG mice implanted with orthotopic tumors were monitored for disease progression and development of metastases using bioluminescent imaging.

Results: $\alpha_v\beta_3$ CAR T cells exert rapid cytotoxicity and prominent cytokine production against all melanoma and triple-negative breast tumor lines tested. Systemic administration of $\alpha_v\beta_3$ CAR T cells potently inhibited growth of SK-MEL-28 melanoma xenografts as demonstrated by

significant differences in tumor volume relative to control CARs. In orthotopic MD-AMB-231 breast tumors, $\alpha_v\beta_3$ CAR T cells were able to control tumor growth, prevent the formation of spontaneous lung metastases from the primary tumor, and resulted in improved survival. $\alpha_v\beta_3$ CAR T cells also mediated control and clearance of established lung metastases established via intravenous injection of breast tumor cells. Histological analysis of tumors at endpoint revealed striking infiltration of residual tumors by T cells in mice administered $\alpha_v\beta_3$.28z CARs, but to a lesser extent in $\alpha_v\beta_3$.BBz CAR-treated xenografts. Infiltration was accompanied by tumors up-regulating PD-L1 expression in response to treatment. Coadministration of $\alpha_v\beta_3$ CAR T cells with anti-PD-1 treatment led to augmentation of the therapeutic response against melanoma tumors. **Conclusions:** These studies highlight a renewed potential for targeting integrins, specifically $\alpha_v\beta_3$, for the treatment of solid tumors. These data suggest that $\alpha_v\beta_3$ CAR T cell therapy for melanoma can be further improved by combination therapy with checkpoint inhibition. Together with our prior work demonstrating robust efficacy of $\alpha_v\beta_3$ CAR T cells to treat orthotopic glioblastoma and DIPG, these results highlight the broad applicability of utilizing CAR T cells targeting $\alpha_v\beta_3$ for treatment of multiple cancer types with reduced risk of on-target, off-tumor toxicity due to the restricted expression of $\alpha_v\beta_3$ in normal tissues. Results of these studies warrant further development of $\alpha_v\beta_3$ CAR T cells for clinical use.

#4102

attIL12-T cell therapy destructs cancer-associated fibroblasts and extracellular matrix in heterogenous osteosarcoma xenograft models

Jiemiao Hu, Alexander Lazar, Davis Ingram, Wei-Lien Wang, Wendong Zhang, Zhiliang Jia, Dristhi Ragoonanan, Jian Wang, Xueqing Xia, Kris Mahadeo, Richard Gorlick, Shulin Li. *UT MD Anderson Cancer Center, Houston, TX*

The extracellular matrix (ECM) and cancer-associated fibroblasts (CAFs) play major roles in tumor progression, metastasis, and the poor response of many solid tumors to immunotherapy. CAF-targeted CAR-T cell therapy does not impair ECM components such as collagen. In this study, we

investigated whether the recently invented attIL12-T cells could destroy CAFs to disrupt the ECM and uncovered the underlying mechanism by which attIL12-T cells penetrate stroma-enriched osteosarcoma tumors. RNA sequencing demonstrated that attIL12-T cell treatment altered ECM-related gene expression. Immunohistochemistry staining revealed disruption or elimination of high-density CAFs and ECM in osteosarcoma xenograft tumors following attIL12-T cell treatment and that CAF/ECM density was inversely correlated with T-cell infiltration. Other IL12-armed T cells, such as wild-type IL12-T or ttIL12-T cells, did not disrupt the ECM because this effect depended on the engagement between cell-surface vimentin (CSV) on the tumor cell surface and its ligand on the attIL12 -T cells. Mechanistic studies found that attIL12-T cell treatment elevated IFNγ production upon interacting with CSV^+ tumor cells to suppress TGFβ secretion and in turn upregulate FAS-mediated CAF apoptosis. CAF destruction reshaped the tumor stroma to favor T cell infiltration and tumor destruction. Thus, this study unveiled a novel therapy—attIL12-T cells—for targeting CAFs/ECM. These findings are highly relevant to humans because CAFs are abundant in human osteosarcoma.

#4103

The IgG4 hinge with CD28 transmembrane domain improves V_HH-based CAR T cells targeting a membrane-distal epitope of GPC1 in pancreatic cancer

Nan Li[1], Alex Quan[1], Dan Li[1], Hua Ren[1], Weiming Ni[2], Jing Zhou[2], Raul Cachau[1], Mitchell Ho[1]. *[1]National Insts. of Health, Bethesda, MD,[2]Isoplexis, Branford, CT*

Heterogeneous antigen expression is a key barrier influencing the activity of chimeric antigen receptor (CAR) T cells in solid tumors. Here, we developed CAR T cells targeting glypican-1 (GPC1), an oncofetal antigen expressed in pancreatic cancer. We report the generation of dromedary camel V_HH nanobody (D4) based-CAR T cells targeting GPC1 and the optimization of the hinge (H) and transmembrane domain (TM) to improve activity. We found that a structurally rigid IgG4H and CD28TM domain making the two D4 fragments in proximity drove CAR dimerization, which led to enhanced T cell signaling and tumor regression in orthotopic

pancreatic cancer models with low antigen density. Furthermore, single-cell-based proteomic and transcriptomic analysis of D4-IgG4H-CD28TM CAR-T cells revealed specific genes (e.g., *ID1*) associated with high T cell polyfunctionality. This study demonstrates the potential of V_HH-based CAR-T for pancreatic cancer therapy and provides an engineering strategy for developing potent CAR T cells targeting membrane-distal epitopes.

#4104

Development of adoptive T-cell therapies to target heterogeneity of mCRPC

Lupita S. Lopez[1], Nathanael Bangayan[2], Owen Witte[2], Saul J. Priceman[1].
[1]Beckman Research Institute of The City of Hope, Duarte, CA,[2]University of California, Los Angeles, Los Angeles, CA

Metastatic castration resistant prostate cancer (mCRPC) remains a significant challenge with limited durable therapeutic responses, and innovative and effective treatment strategies are needed. Advanced mCRPC often comprises a heterogeneous population of prostate adenocarcinoma (PrAd) and neuroendocrine prostate cancer (NEPC), and current targeted therapies often result in transient anti-tumor responses. Chimeric antigen receptor (CAR) T-cell therapies are being actively investigated to target mCRPC, including CARs targeting antigens that are overexpressed in PrAd. Our group has developed a CAR T cell targeting the PrAd antigen, prostate stem cell antigen (PSCA), and have an ongoing phase 1 trial at City of Hope in patients with mCRPC. However, we anticipate that targeting NEPC in addition to PrAd will be required to achieve durable anti-tumor responses in patients. Here, we have developed novel dual-targeting approaches for the simultaneous treatment of both PrAd and NEPC. Our first approach optimizes a tandem CAR T-cell approach capable of targeting distinct antigens found on both PrAd and NEPC. Additionally, we are actively developing combinations of PSCA-CAR T-cells with secretable T-cell bispecific antibodies to target NEPC antigens. Our studies encompass the *in vitro* and *in vivo* safety and efficacy of CAR T-cells engineered to co-target PrAd and NEPC for the treatment of heterogeneous mCRPC.

#4105

Improvement of CD133-specific chimeric antigen receptor T cells by secreting anti-PD-L1 single-chain variable fragment against cholangiocarcinoma

Thanich Sangsuwannukul, Kamonlapat Supimon, Thaweesak Chieochansin, Kornkan Choomee, Jatuporn Sujjitjoon, Mutita Junking, Pathai Yenchitsomanus. *Division of Molecular Medicine, Research Department, Siriraj Center of Research Excellence for Cancer Immunotherapy (SiCORE-CIT), Faculty of Medicine Siriraj Hospital, Mahidol University, Bangkok, Thailand*

Cholangiocarcinoma (CCA) is rare but hard-to-treat solid cancer affecting people worldwide. Cancer stem cells (CSCs) in CCA contribute to tumor heterogeneity and resistance to conventional therapies. Thus, CSCs are notable targets for cancer immunotherapy. CD133 is a potential CSC surface marker overexpressed in various cancers. T cell-based immunotherapy, namely chimeric antigen receptor (CAR) T-cell targeting CD133 has shown potential in eradication of some solid tumors including CCA. Nevertheless, anti-tumor function of CAR T cell could be decreased under immunosuppressive tumor microenvironment (TME). Thus, to improve its function under TME, the next-generation of CD133-specific CAR T-cell is required. We therefore constructed two lentiviral vectors containing: (i) anti-CD133 single-chain variable fragment (scFv), 4-1BB costimulatory molecule, and CD3ζ (133CAR), and (ii) anti-CD133 scFv, 4-1BB, and CD3ζ in tandem with anti-PD-L1 scFv (133CARsL). The lentiviruses were transduced to generate CD133-specific CAR T cells expressing the second-generation (133CART) or anti-CD133 CAR with self-secreting anti-PD-L1 scFv (133CARTsL). The latter was able to simultaneously target CD133 and PD-L1 molecules on CCA cells. CCA cells endogenously expressing CD133 and PD-L1 were cocultured with either 133CART or 133CARTsL. In short-term coculture, the antitumor effects of 133CARTsL were not different from that of 133CART. However, in long-term coculture and after tumor re-challenge, 133CARTsL showed lower expression of programmed cell death protein (PD-1) and better cytotoxic function against high CD133 and PD-L1 CCA cells. The higher potential of 133CARTsL with reduced exhaustion profile would offer great promise for application of CD133-targeting CAR T cells in solid tumors.

#4106
Non-autonomous enhancement of gPDL1 CAR-T annihilates TNBC development

Chia-Wei Li[1], Shih-Han Wang[1], Yun-Ju Lai[2], Jyun Wang[3], Chun-Tse Kuo[1], Shih-Duo Hsu Hung[1], Shou-Hou Liu[1]. *[1]Academia Sinica - Institute of Biomedical Sciences (IBMS), Taipei, Taiwan,[2]Solomont School of Nursing,, University of Massachusetts Lowell, Lowell, MA,[3]Topmunnity Therapeutics, Taipei, Taiwan*

Triple-negative breast cancer (TNBC) is the most aggressive and challenging breast cancer subtype, which does not respond to traditional endocrine and anti-HER2-targeted therapies. PD-L1 is highly enriched in TNBC and has been considered a therapeutic target. Despite the excellent anti-cancer activity, the atezolizumab-based chimeric antigen receptor (CAR) T cells showed a robust off-target effect. In addition, the treatment of solid tumors with CAR-T is limited by abnormal glycosylation in malignant tumors. Targeting glycosylated PD-L1 (gPD-L1) provided tissue specificity against TNBC, implying it can prevent antigen escape and off-target effect. In this study, we generated gPD-L1 CAR-T cells using lentiviral vectors expressing the scFv regions of the anti-gPD-L1 antibody. The gPD-L1 CAR-T cells exhibited antigen-specific activation, cytokine production, and cytolytic activity against TNBCs *in vitro* and in the xenograft tumors model. CyTOF and single-cell RNA sequencing (scRNA-seq) showed distinct IFNγ-positive cell types. Mechanistically, IFNγ crosstalked with EGFR signaling through Src activation and, in turn, triggered B3GNT3-mediated PD-L1 glycosylation. Inhibition of Src resulted in reduced gPD-L1 expression in TNBC. CRISPR/Cas9 knockout of B3GNT3 in TNBC cells impaired gPD-L1 CAR-T response. As a result of nonautonomous gPDL1 amplification in TNBCs, gPD-L1 CAR-T cells continued to annihilate TNBCs. Additionally, since gPD-L1 CAR-T cells provided higher specificity on TNBC, they had lower normal tissue toxicity. Overall, gPD-L1 CAR-T exhibits excellent anti-tumor activity against TNBCs, and it could be a promising immunotherapy tool to treat TNBCs in clinic. Furthermore, targeting glycosylation moiety on the tumor antigen is a novel approach to lessen CAR-T toxicity in patients.

#4107

Cytotoxic T cells armed with IL-4 receptor-targeting and PD-L1-blocking peptides inhibits lung tumor growth

Dong Gyun Jo, Gunassekaran Gowri Rangaswamy, Poongkavithai Vadevoo Sri Murugan, Byungheon Lee. *Kyungpook National Univ. School of Med, Daegu, Korea, Republic of*

Tumor homing of adoptively transferred cytotoxic T cells (CTLs) to solid tumors is still inefficient. In addition, CTLs that arrive at tumor tissues meet the immune-suppressive tumor microenvironment. To reduce these limitations in adoptive T-cell therapy against solid tumors, we here exploited CTLs dual-labeled with IL-4 receptor (IL4R)-targeting peptide and programmed cell death-ligand 1 (PD-L1)-blocking peptide. IL4R is commonly upregulated in many solid tumors including lung tumor. PD-L1, an immune checkpoint, is frequently upregulated in tumor cells and contributes to the suppression of CTLs in the tumor microenvironment. CTLs were isolated from the splenocytes of LLC lung tumor-bearing mice and non-genetically labeled with IL4RPep-1, an IL4R-targeting peptide, and PD-L1Pep2, a PD-L1-blocking peptide, using a sulfhydryl-reactive cross linker. Compared to unlabeled CTLs, IL4R-targeted, PD-L1-blocking CTLs showed more robust cytokine secretion and tumor cell lysis during co-culture with LLC tumor cells. The CTLs armed with the dual-acting peptides exerted higher levels of tumor homing and anti-tumor growth activity in LLC lung tumor-bearing mice, which was accompanied by decrease of immune-suppressive cells in the tumor tissues. These results suggest that the IL4R-targeted, PD-L1-blocking CTLs can be a promising strategy in adoptive T-cell therapy against solid tumors.
Key words: Adoptive T-cell therapy, CTLs, IL-4 receptor, lung tumor, PD-L1

#4108

Transient epigenetic reprogramming enhances T-cell proliferation and tumor clearance

Alec McQuiston, Junbao Yang, Jason Romero, Naveen Bojjireddy, Travis McQuiston, Vittorio Sebastiano, Mustafa Turkoz. *Immunology, Turn Biotechnologies, Inc., Mountain View, CA*

Manufacturing-induced differentiation and accelerated T-cell exhaustion prevent CAR-T therapies from reaching their full therapeutic potential and broader application in the treatment of cancer. To combat these inherent

challenges, Turn Biotechnologies is developing its novel and proprietary mRNA-based technology, Epigenetic Reprogramming of Aging (ERA^{TM}), to i) preserve a less differentiated status; ii) diminish (or even eliminate) exhaustion; and iii) improve the cytotoxicity and efficacy of CAR-T cell cells. Prolonged CAR-T cell manufacturing process leads to a more differentiated and effector-like phenotype, which is susceptible to accelerated exhaustion *in vivo*. Unfortunately, clinical evidence suggests that less differentiated and stem-cell like CAR-T products have increased proliferative capacity, reduced exhaustion, and greater efficacy. Additionally, aging is known to compromise T-cell function, reducing chances of CAR-T therapy candidacy for older patients. These compounded effects of manufacturing and aging severely limit CAR-T cell functionality in terms of proliferation, perdurance, and cytotoxic capacity, as well as precluding wider patient access. Leveraging our previous work with other aged human cells, we hypothesized that the transient expression of ERA^{TM} factors could impact manufacturing of CAR-T cells by mitigating their differentiation, promoting T stem cell memory (Tscm) phenotype, reducing/eliminating exhaustion, and resetting the epigenetic clock in CAR-T cells. Here, we present preclinical data showing that ERA^{TM} treatment of T cells delivered using our proprietary eTurna^{TM} platform can restore youthful functionality, reducing exhaustion and effects of aging, improving their ability to fight cancer while safely maintaining cellular identity. ERA^{TM} -treated T cells have higher proliferation capacity and cytotoxicity upon tumor cell engagement *in vitro* compared to control cells. Treatment of ERA^{TM} -treated T-cells also increases the production of beneficial cytokines to support their survival and cytotoxic activity. Importantly, ERA^{TM} treatment preserves T-cell identity and T-cell repertoire, while avoiding unwanted hyperproliferation or clonal expansion. In murine models of hematological cancers, these effects of ERA^{TM} treatment on T-cells results in superior cancer cell killing and clearance. These benefits of ERA^{TM} technology to current CAR-T manufacturing processes have the potential to translate into the clinic as improved patient outcomes and survival with reduced side effects, thereby expanding patient access and enabling immunotherapies to serve as a first-in-line lifesaving solution.

Combination Immunotherapies 1

#5067

Inhibition of CD47-SIRPα axis to enhance immunity against different molecular subtypes of breast cancer

Xingru Ma, Zachary Hartman, Li-Chung Tsao, Tao Wang, Cong-Xiao Liu, Xiao Yang, Gangjun Lei, Junping Wei. *Duke University, Durham, NC*

Background: The CD47-SIRPα axis is an innate immune checkpoint that primarily regulates myeloid cells. In the context of cancer, tumor cells upregulate CD47 to engage SIRPα inhibitory signaling to block phagocytosis. Thus, inhibition of this axis may enhance myeloid cell phagocytosis and adaptive immune responses against cancer. While our previous studies identified that CD47 mAbs enhance HER2-specific mAb therapy (Tsao et al., 2019), clinical trials have revealed that CD47-targeting mAbs are associated with severe side effects of anemia and thrombocytopenia in patients. We thus hypothesized that targeting SIRPα, which is more restrictively expressed on myeloid cells, may achieve similar but less toxic treatment effects.

Methods: To ascertain the impact of SIRPα inhibition against different molecular subtypes of breast cancer, we utilized and validated a novel SIRPα KO mouse, along with SIRPα mAbs in our previously utilized models of Triple-Negative Breast Cancer (TNBC) and HER2+ Breast Cancer (Crosby et al., 2018; Tsao et al., 2019). Using both in vitro and in vivo tumor models, we tested the therapeutic impact of SIRPα inhibition/blockade combined with immunogenic chemotherapy (doxorubicin) in TNBC or combined with HER2-specific mAbs in HER2+ Breast Cancer (HER2+ BC).

Results: After validating the loss of SIRPα in KO mice, we found that E0771 TNBC cells had reduced rates of engraftment in SIRPα KO mice compared to controls, but comparable rates of growth once tumors were established. We then treated E0771 engrafted SIRPα KO and wildtype mice with doxorubicin. This treatment elicited tumor rejection in the majority of SIRPα KO mice (70% of injected tumors), compared to only 10% rejection in SIRPα WT mice. To study tumor antigen-specific immunity, we expressed different forms of OVA (secreted, cytoplasmic, membrane) in tumor cells. We found that membrane expressed OVA led to universal tumor rejection (10/10 mice) with high levels of OVA-specific Abs, in

contrast to non-membrane expressed forms of OVA. This suggested the importance of tumor-specific Abs in eliciting tumor rejection. To specifically test the antitumor effect of tumor-specific antibodies in the context of SIRPα blockade, we evaluated the impact of a HER2 mAb (Trastuzumab) on HER2+ BC cells. We found enhanced phagocytosis and antitumor effects by SIRPα KO macrophages in comparison to wild-type macrophages, suggesting the potential of targeting SIRPα along with the use of standard-of-care mAb.
Conclusion: Our study demonstrates that SIRPα loss can prevent tumor engraftment but may not have a strong effect against established tumors without secondary immune stimulation. However, addition of immunogenic cell death-eliciting chemotherapy or tumor-specific Abs promote tumor phagocytosis and stimulate anti-tumor immunity. These results support further investigation of SIRPα-targeting combination therapies for cancer.

#5068

Nintedanib enhances antitumor effects of anti-PD-1 therapies through inhibition of immunosuppressive cells in tumor microenvironment

Ryo Suzuki[1], Satoshi Watanabe[1], Kunihiro Shono[1], Takaaki Masuda[1], Tomoki Sekiya[1], Yuka Goto[1], Toshiya Fujisaki[1], Masashi Arita[1], Aya Ohtsubo[1], Satoshi Shoji[1], Tomohiro Tanaka[1], Koichiro Nozaki[1], Rie Kondo[1], Yu Saida[1], Satoshi Hokari[1], Riuko Ohashi[2], Kenjiro Shima[1], Yosuke Kimura[1], Nobumasa Aoki[1], Yasuyoshi Ohshima[1], Toshiyuki Koya[1], Toshiaki Kikuchi[1]. *[1]Department of Respiratory Medicine and Infectious Diseases, Niigata University Graduate School of Medical and Dental Sciences, Niigata, Japan,[2]Division of Molecular and Diagnostic Pathology, Niigata University Graduate School of Medical and Dental Sciences, Niigata, Japan*

Background: Although programmed cell death-1 (PD-1) inhibitors have achieved promising and durable responses in patients with several types of cancer, many patients show intrinsic resistance to PD-1 inhibitors. Extensive studies have demonstrated that immunosuppressive cells are induced in tumor microenvironment and inhibit antitumor effects of PD-1 inhibitors. The aim of current study is to investigate whether nintedanib, which targets multi-tyrosine kinase including vascular endothelial growth

factor, fibroblast growth factor, and platelet-derived growth factor, reduced immunosuppressive cells in tumor microenvironment and augments antitumor effects of PD-1 inhibitors.
Method: Mice were inoculated subcutaneously with CT26 murine colon carcinoma or MC38 murine colon carcinoma and were treated with nintedanib (50 mg/kg), αPD-1mAbs (10 mg/kg) or nintedanib plus αPD-1mAbs. The tumor size was measured in 2 perpendicular dimensions 3 times per week. Types of cells infiltrating into tumors and immune status of tumor-draining lymph nodes were assessed using flow cytometry and immunohistochemistry (IHC).
Results: RNA sequencing data revealed that nintedanib decreased gene expression related to endothelial mesenchymal transition, angiogenesis and coagulation. Flow cytometry showed that nintedanib significantly decreased the percentage of myeloid-derived suppressor cells and cancer-associated fibroblast in tumor tissues. Both of flow cytometry and IHC analysis showed that nintedanib significantly increased IFN-$\Upsilon^{+}CD4^{+}$ and $CD8^{+}$ T cells infiltrating in tumors. In addition, nintedanib plus αPD-1mAbs significantly retarded tumor progression.
Conclusion: Nintedanib decreased immunosuppressive cells, increased effector T cells, and enhanced anti-tumor effects of αPD-1mAbs. Based on these findings, there are possibility that nintedanib improves clinical outcomes of cancer patients treated with PD-1 inhibitors.

#5069

Cancer immunotherapy based on the RNAi-based PD-L1 inhibitor, MN-siPDL1, demonstrates efficacy in preclinical pancreatic adenocarcinoma

Byunghee Yoo[1], Mozhdeh Sojoodi[1], Veronica Clavijo Jordan[2], Pamela Pantazopoulos[1], Subrata Ghosh[3], Peter Caravan[1], Zdravka Medarova[3].
[1]Harvard Medical School, Boston, MA,[2]Athinoula A. Martinos Center for Biomedical Imaging, Massachusetts General Hospital, Harvard Medical School, Lexington, MA,[3]TransCode Therapeutics Inc, Boston, MA

The recent past has seen impressive progress in the treatment of various malignancies using immunotherapy. One of the most promising approaches involves immune checkpoint inhibition, mainly relying on monoclonal antibodies or small molecules. With specific relevance to pancreatic cancer,

however, checkpoint inhibitors are largely ineffective, in part because of poor T cell infiltration, low tumor mutational burden, an immunosuppressive tumor microenvironment, and the presence of a dense desmoplastic stroma. To overcome these challenges, here we describe the preclinical testing of a new checkpoint inhibitor named MN-siPDL1 in combination with gemcitabine in an aggressive model of PDAC. MN-siPDL1 utilizes the RNA interference mechanism (siRNA) to block the synthesis of the critical immune checkpoint mediator, PD-L1 by tumor cells. The siRNA is delivered by a nanoparticle carrier (MN) that is optimized for oligonucleotide delivery to solid tumors. The efficacy and preliminary safety of MN-siPDL1 were tested in an orthotopic syngeneic model of pancreatic ductal adenocarcinoma generated by implanting Hy15549 murine PDAC cells into the pancreas of C57BL/6J mice. Our studies demonstrated that MN-siPDL1 was successfully delivered and effective even in the highly desmoplastic and hypovascular Hy15549 murine model of PDAC, which has been deemed nonresponsive to antibody-based immune checkpoint blockade. Anatomic MRI showed that in the animals treated with MN-siPDL1 plus gemcitabine, tumor growth rates were lower than in the vehicle control. After two weekly treatments with MN-siPDL1 plus gemcitabine, tumor volumes were four times smaller than in untreated animals. Importantly, animal survival was improved dramatically in animals treated with MN-siPDL1 plus gemcitabine compared to all other groups. Among the animals treated with MN-siPDL1 plus gemcitabine, the hazard ratio for overall survival (OS) relative to PBS was 0.08. Interestingly, even in the absence of gemcitabine, MN-siPDL1 as monotherapy improved survival more dramatically than gemcitabine (HR, 0.24 for MN-siPDL1 vs. 0.42 for gemcitabine). Immunohistology on the tumor tissues post-necropsy indicated that the treatment inhibited PD-L1 and induced a cytotoxic immune response. Finally, as an initial measurement of tissue damage due to the treatment, we analyzed major organs by histopathology and saw no differences from the vehicle-treated controls. Considering the aggressive and fibrous nature of the Hy15549 model and its resistance to traditional checkpoint inhibitors, the described RNAi-based therapeutic approach could be promising against PDAC and could make an impact on one of the most intractable cancers which has long evaded the power of modern medicine to deliver long-term survival.

#5070

Anti-tumor activity of HPN328, a DLL3-targeting tri-specific, half-life extended T cell engager, is enhanced by combining with an anti-PD-L1 antibody in an immunocompetent mouse model

Laura B. Valenzuela[1], Chi-Heng Wu[2], Wade Aaron[2], Raphalea R. Banzon[1], Mabel Bush[1], S. Jack Lin[1], Sony S. Rocha[1], Subramanian Thothathri[1], Holger Wesche[1], Mary Ellen Molloy[2], Banmeet S. Anand[2]. *[1]Translational Medicine, Harpoon Therapeutics, Inc., South San Francisco, CA,[2]Harpoon Therapeutics, Inc., South San Francisco, CA*

TriTAC® is a T cell engager platform comprised of three binding domains: a target binder for tumor cell engagement, an albumin binder for half-life extension, and a CD3 binder for T cell engagement. HPN328 is a Delta-like ligand 3 (DLL3)-targeting TriTAC currently being evaluated in a Phase 1/2 clinical trial enrolling patients with advanced cancers associated with DLL3 expression, including small cell lung cancer (SCLC) and other neuroendocrine malignancies (NCT04471727). While HPN328 has demonstrated single agent clinical activity in relapsed/refractory SCLC patients, combinations with other immunotherapeutic agents could further potentiate HPN328 anti-tumor activity and enable the testing of HPN328 in earlier lines of therapy. To test this hypothesis, we developed a human CD3ε (hCD3ε) immunocompetent mouse model that has the epitope of human CD3ε, as recognized by TriTAC molecules, specifically knocked-in (KI) to the mouse CD3ε gene. hCD3ε KI mice have comparable immune cell repertoire as wild-type mice. However, unlike wild-type mice, TriTAC molecules bind to the T cells in hCD3ε KI mice. In a MC38 tumor model, an EGFR-targeting TriTAC was able to exert the expected anti-tumor activity and EGFR-dependent toxicity, thereby confirming TriTACs can engage and activate endogenous T cells in this immunocompetent hCD3ε KI mouse model. Next, we tested HPN328 in hCD3ε KI mice with MC38 tumors that have been engineered to express human DLL3. As expected, HPN328 inhibited tumor growth in a dose-dependent manner. HPN328 also resulted in a notable upregulation of PD-L1 in these tumors, suggesting that HPN328 in combination with an anti-PD-L1 antibody could potentially drive deeper anti-tumor responses. Indeed, sub-therapeutic doses of HPN328 in combination with an anti-PD-L1 antibody enhanced the anti-tumor activity of HPN328 when compared to either treatment alone.

Atezolizumab and durvalumab, anti-PD-L1 antibodies, are approved in combination with platinum-doublet chemotherapy as part of front-line therapy for extensive-stage SCLC. These results demonstrate the utility of combining anti-PD-L1 antibodies to enhance the anti-tumor activity of HPN328 and further supports investigation of this combinatorial approach in patients. Clinical studies of HPN328 in combination with atezolizumab are planned.

#5071

Olverembatinib (HQP1351) enhances antitumor effects of immunotherapy in renal cell carcinoma (RCC)

Guangfeng Wang[1], Eric Liang[2], Ping Min[1], Huidan Yu[3], Bingxing Wu[3], Dajun Yang[3], Yifan Zhai[2]. *[1]Ascentage Pharma Co., Ltd., Shanghai, China,[2]Ascentage Pharma Group Inc., Rockville, MD,[3]Ascentage Pharma Co., Ltd., Suzhou, Jiangsu Province, China*

In solid tumors, resistance to checkpoint inhibitors (CPIs) is frequently observed, partially due to upregulation of vascular endothelial growth factor A (VEGFA) and programmed death-ligand 1 (PD-L1). This culminates in an immunosuppressive tumor microenvironment and immune escape. Inhibitors against VEGF and the VEGF receptor (VEGFR) foster tumor vessel normalization and immunostimulatory reprogramming, in turn promoting treatment effects of immunotherapies. In recent years, TKIs, including axitinib, lenvatinib, and cabozantinib, plus immunotherapy have been approved to treat advanced RCC. Currently under clinical development for relapsed or refractory chronic myeloid leukemia and gastrointestinal tumor, olverembatinib (HQP1351) is a new-generation multikinase inhibitor with targets including VEGFR, fibroblast growth factor receptor (FGFR), SRC, BCR-ABL1, c-KIT, and platelet-derived growth factor receptor. The aim of this study was to assess whether olverembatinib combined with immunotherapy can promote inhibitory effects on RCC. In cell-free kinase assays, olverembatinib inhibited VEGFR1, -2, and -3 with IC_{50} values of 4.2, 6.1, and 4.1 nM, respectively. Compared to lenvatinib, olverembatinib had more potent antiproliferative effects on human umbilical vein endothelial cells. Olverembatinib also had antiproliferative activity in murine RCC lines RANCA and RAG, with IC_{50}

values of 141 and 53 nM, respectively. When olverembatinib was coadministered with an anti-PD-1 antibody in a RANCA-derived syngeneic model, both agents exerted synergistic effects, with tumor growth inhibition rates reaching 60.6%. Mechanistically, olverembatinib influenced cancer cell proliferation directly by inhibiting phosphorylation of FGFR and downstream proteins. Increased cleavage of caspase-3 and poly (ADP-ribose) polymerase 1 were observed, suggesting induction of apoptosis. Olverembatinib also influenced proliferation of vascular endothelial cells by inhibiting phosphorylation of VEGFR, SRC, and downstream proteins Akt and extracellular signal-regulated kinases. Olverembatinib also reduced expression of PD-L1 in RCC cells. In tumor-infiltrating lymphocyte assays, olverembatinib increased numbers of cytotoxic T cells (CTL, $CD8^+$) and natural-killer cells (NK, $CD3^-/CD49B^+$) in RANCA tumor tissues. Combined with an anti-PD-1 antibody, olverembatinib increased CTLs, NK cells, dendritic cells (DCs, $MHC\text{-}II^+/CD11C^+$), and M1 macrophages ($F4/80^+/CD11B^+/CD86^+$) in RANCA tumor tissues, indicating an immunoregulatory effect of olverembatinib. Taken together, these data suggest that combining olverembatinib with a CPI confers synergistic antitumor effects in an RCC cancer mouse model by targeting tumor growth, angiogenesis, and immune regulation. This novel combination may provide an alternative approach to enhance treatment effects with CPIs in renal cancers.

#5072

"Armed" oncolytic herpes simplex virus enables CD19 CAR-T for solid tumor cell treatment as a combination therapy

Yanxin Zheng[1], Yuanyuan Liu[1], Tianyi Deng[1], Yue Huang[1], Ziwen Liu[1], Borui Zhan[1], Xusha Zhou[1], Runbin Yan[1], Jiangtao Ren[2], Yun Xing[2], Guixing Wu[2], Yonghong Liu[1], Jing Zhao[1], Xiaoqing Chen[1], Grace Zhou[1].
[1]ImmVira Co., Limited, Shenzhen, China,[2]Nanjing Bioheng Biotech Co., Ltd., Nanjing, China

Background: Chimeric antigen receptor (CAR) T cell therapy has achieved unprecedented success in treating hematologic malignancies but still struggles in the context of solid tumors. The challenges of effective CAR-T cell therapy for solid tumors are multifaceted including 1) physical barriers

that limit T cell infiltration; 2) tumor heterogeneity and antigen escape leading to resistance to therapy; 3) immunosuppressive tumor microenvironment (TME) dampening T cell function. As a novel modality for cancer therapy, oncolytic virus (OV) can be engineered to overcome the limitations of CAR-T therapy in solid tumor. Here we developed a new-generation of oncolytic herpes simplex virus (oHSV) to enable clinically approved CD19 CAR-T for solid tumor therapy.
Methods: oHSV MVR-T7011 (T7011) was genetically engineered to drive ectopic expression of the extracellular domain of CD19, the blood tumor antigen, on solid tumor cell surface upon viral infection. In addition, multiple payloads, CCL5, IL-12, and anti-PD-1 antibody were introduced into T7011 to modulate the TME. Payload expression was detected both *in vitro* and *in vivo*. Co-culture studies were performed to test the cell-killing activity of CD19 CAR-T combined with T7011. Antitumor activities of T7011 administrated via intratumoral (IT) or intraperitoneal (IP) in combination with CD19 CAR-T cells were assessed in immunodeficient and immunocompetent mice.
Results: The *in vitro* studies indicated that the expression of CD19 on tumor cell surface was detected as early as 4 hours post infection (hpi) and retained for at least 96 hours in the T7011-infected cells. In mouse study showed that the CD19 expression on tumor cells was detected as early as 8 hpi and lasted for 20 days when T7011 was injected via IT in immunodeficient mice. The payload of CCL5, IL-12, and anti-PD-1 antibody showed a similar expression pattern as CD19. Co-culture studies showed that T7011 infection enhanced cell-killing activity of CD19 CAR-T but the virus had no effect on viability and proliferation of CAR-T cell itself, which concludes that T7011 does not dampen the CAR-T function as its combination treatment. The *in vivo* efficacy studies demonstrated that IT and IP administration of T7011, rather than MVR-T3011 virus which lacks CD19, specifically promoted CD19 CAR-T anti-solid tumor activities in both immunodeficient and immunocompetent mice.
Conclusions: The new-generation of HSV oncolytic virus T7011 expressing the targetable CD19 antigen on tumor surface enables the CD19 CAR-T for solid tumor cell treatment as a combination therapy. In addition, T7011 also carries multi-immunomodulators further to enhance antitumor efficacy by reinvigorating the infiltrated CAR-T cells and reversing the immunosuppressive TME. T7011 is expected to be a promising

combinational therapy with CD19-specific CAR-T cells enabling effective cell therapy against multiple solid tumors.

#5073

NT219 induces tumor PD-L1 expression and potentiates anti-PD-1 efficacy

Ricardo Alexandre de Azevedo[1], Hadas Reuveni[2], Menashe Bar-Eli[3], Michael Curran[1]. *[1]Department of Immunology, The University of Texas MD Anderson Cancer Center, Houston, TX,[2]Purple Biotech, Rehovot, Israel,[3]Department of Cancer Biology, The University of Texas MD Anderson Cancer Center, Houston, TX*

While the advent of immune checkpoint blockade (ICB) has dramatically improved the prognosis of many immune-infiltrated cancers, for others, unfortunately, these benefits have yet to be realized. The major challenge before the field, then, is to identify combination therapies that act both to combat evolved resistance. NT219 is a novel dual inhibitor of insulin receptor substrates 1 and 2 (IRS) and STAT3. NT219 demonstrated antitumor effects against both in situ and metastatic human melanoma models in mice as a stand-alone treatment and in combination with mutated BRAF and MEK inhibitors. The potential of NT219 to overcome resistance and increase efficacy was demonstrated in PDX models with multiple drug classes. Collectively, these findings provided preclinical proof-of-concept NT219 as a promising novel cancer therapy. Given this data, the goal of our study was to assess the efficacy of combining NT219 with anti-PD-1 and anti-CTLA-4 ICB, and test capacity of the combination to overcome immune resistance. To that end, we have examined PD-L1 expression levels in vitro following NT219 treatment in two different strains of melanoma cells, B16-tdTomato (TMT) and B16 3I-F4, ICB sensitive and ICB resistant derivative lines, respectively. In addition, to evaluate the combination effect of NT219 with ICB therapy in ICB-resistant PDX model, we used a humanized PDX model of pembrolizumab-resistant gastroesophageal tumor (GEJ). These mice were injected with PBMCs from the same patient. Using multiple syngeneic immunocompetent models of melanoma (TMT and 3I-F4 cells) and the humanized PDX model, we investigated the potential of each ICB with NT219. Our findings showed that NT219 increased PD-L1 expression levels on both melanoma cell lines in vitro, however, the PD-L1

expression levels were much more elevated 3I-F4 than TMT cells. Interestingly, the levels of both IRS and activated pSTAT3, the targets of NT219, which consist well known resistance mechanisms, were higher in the resistant cells as compared to the sensitive line. In accordance we found that NT219 was able to restore anti-PD-1 sensitivity in 3I-F4 model (TGI = 58%) in the syngeneic model, promoting tumor rejection and increasing survival rates. The combined approach between NT219 and anti-CTLA-4 displayed a moderate effect (TGI = 37%). In the TMT, NT219 combined with anti-PD-1 showed greater efficacy compared to anti-PD-1 alone (TGI = 63% and TGI = 47%, respectively). These results were confirmed using the humanized ICB-resistant PDX model, where impressive synergy between NT219 and the anti-PD-1 (TGI = 98%) was demonstrated. To summarize, we found a significant synergistic effect of NT219 combined with anti-PD-1 therapy, supported by a mechanism of PDL-1 induction making ICB resistant tumors amenable to ICB treatment. Collectively, these findings demonstrated that NT219 has the potential to reverse ICB resistance in both human PDX and murine syngeneic tumor model systems

#5074

Addition of MAPK inhibitors to prime and sensitize poorly differentiated thyroid cancers as a strategy to improve TSHR-CART cell therapy antitumor activity

Claudia Manriquez Roman[1], Kendall J. Schick[2], Justyna J. Gleba[3], Truc N. Huynh[4], Elizabeth L. Siegler[4], James L. Miller[3], Aylin Alasonyalilar Demirer[3], Matthew L. Pawlush[3], Ahmet Biligili[3], Long K. Mai[4], Erin Tapper[4], Leo R. Sakemura[4], Michelle J. Cox[4], Carli M. Stewart[4], Ismail Can[4], Ekene J. Ogbodo[4], Gaofeng Cui[5], Georges Mer[5], Gloria R. Olivier[6], Yushi Qiu[7], Robert C. Smallridge[8], Zubair C. Abba[8], Han W. Tun[9], John A. Copland[10], Saad S. Kenderian[4]. *[1]Mayo Clinic, Rochester, MN,[2]Molecular Pharmacology and Experimental Therapeuthics, Mayo Clinic, Rochester, MN,[3]Cancer Biology Departmetn, Mayo Clinic, Jacksonville, FL,[4]T cell Engineering, Mayo Clinic, Rochester, MN,[5]Biochemistry and Molecular Biology, Mayo Clinic, Rochester, MN,[6]Business Development, Mayo Clinic, Rochester, MN,[7]Cancer Biology Department, Mayo Clinic, Jacksonville, FL,[8]Endocrine Division, Internal Medicine Department, Mayo Clinic,*

Jacksonville, FL,[9]Internal Medicine Department, Mayo Clinic, Jacksonville, FL,[10]Cancer Biology, Mayo Clinic, Jacksonville, FL

Thyroid cancer is the most common endocrine cancer in the US, and its incidence is rising. Most thyroid cancer deaths are attributed to treatment-refractory, metastatic tumors. Thyroid stimulating hormone receptor (TSRH) expression is largely limited to the thyroid gland and is abundantly expressed on thyroid tumor cells, making TSRH a compelling target for advanced thyroid cancer diagnostics and therapeutics. Therefore, we developed a novel TSHR-targeted chimeric antigen receptor (CAR) T cell therapy to treat aggressive thyroid cancers. TSHR-CAR constructs were cloned into a lentiviral CAR construct containing 4-1BB and CD3ζ. First, we demonstrated potent TSHR-CART antigen-specific anti-tumor activity in vitro. Then, NOD-SCID-γ-/- (NSG) mice were inoculated subcutaneously with TSHR+ tumor cells and randomized by tumor volume to treatment with TSHR-CART cells or control Untransduced T cells (UTD). Treatment with TSHR-CART cells resulted in dose-dependent antitumor activity and prolonged survival. De-differentiated anaplastic thyroid cancers (ATC) downregulate TSHR. Our TSHR immunohistochemistry results corroborated these findings and displayed minimal TSHR protein expression, precluding successful TSHR-CART treatment. We therefore sought to sensitize these tumors with MAPK inhibitors, as a strategy to upregulate TSHR expression in patients with metastatic thyroid cancer. TSHR expression was upregulated in patient-derived xenograft (PDX) ATC models after one week of daily administration of the MAPK inhibitors ($p=0.0024$). After confirming that MAPK inhibition does not dampen TSHR-CART effector functions, we tested sequential and combination therapy of TSHR-CART with MEK and BRAF inhibition in vivo. NSG mice were engrafted with ATC BRAF-mutant PDX tumors and randomized by tumor volume to daily oral treatment with placebo or trametinib (MEK inhibitor) plus dabrafenib (BRAF inhibitor). One week later, mice received either UTD or TSHR-CART. Mice conditioned with trametinib plus dabrafenib ($p=0.0018$) and subsequently treated with TSHR-CART showed superior antitumor activity. However, the improved antitumor activity in this setting was transient. We therefore tested the durability of TSHR upregulation following MEK/BRAF inhibition and demonstrated that TSHR upregulation lasts less than 48-72

hours after discontinuation. Finally, we tested the combination of TSHR CART cells with MEK/BRAF inhibitors in ATC BRAF-mutant PDX tumors. Here, combining TSHR-CART cells with MEK/BRAF inhibitors result in durable control of the tumors. Collectively, our findings indicate that MEK/BRAF inhibition of de-differentiated thyroid cancers upregulated TSHR expression and enhanced TSHR-CART antitumor activity. This work represents a viable strategy to improve outcomes of patients with aggressive, metastatic thyroid cancers.

#5075

Antitumor activity of liposomal formulation of eribulin combined with anti-human PD-1 antibody using hPBMC-humanized mouse models

Yuki Niwa, Taro Semba. *Molecular Profiling Department, Discovery Concept Validation Function, Eisai Co., Ltd., Tsukuba-shi, Japan*

Eribulin (ERI) has been reported a microtubule dynamics inhibitor with unique tumor microenvironment modulations such as vascular remodeling and reversal of epithelial-mesenchymal transition activities. In the previous meeting (AACR2022), we reported that ERI and liposomal formulation of ERI (ERI-LF) have immunomodulatory activity that induces CD8+ T cells via its vascular remodeling activity and ERI-LF has greater immunomodulatory activity than ERI. Furthermore, we also reported that these immunomodulatory activities contribute combination antitumor activity of ERI and ERI-LF with anti-PD-1 antibody (Ab) using a P-glycoprotein-knockout 4T1 mouse breast cancer syngeneic model; however, evaluation of antitumor activity of immune-checkpoint inhibitor (ICI) using mouse cancer syngeneic model has limitation because numbers and cancer types of mouse cancer cell lines are limited. In this study, we developed humanized mouse model bearing both human cancer cell lines and human peripheral blood mononuclear cells (hPBMC) to evaluate antitumor activity of ICI for various cancer types. Furthermore, we also evaluated combination antitumor activity of ERI-LF with anti-human PD-1 Ab using this hPBMC-humanized mouse models to verify generality of this combination. We first isolated hPBMC from healthy volunteers and the obtained hPBMC was intravenously injected into NOG mice. To confirm transplantation of hPBMC in the mice, we performed flow cytometric analysis of peripheral blood of mice in a time course manner. In the

peripheral blood of humanized mice, chimera ratio of hCD45+ cells gradually increased until 5 weeks after hPBMC-injection and then decreased after 6 weeks after hPBMC-injection. Because tumor growth of some cancer cell lines was rejected by hPBMC transplantation, we evaluated some human cancer cell lines that are able to grow in hPBMC-humanized condition and selected MKN45 and NCI-H526 cell lines for human gastric cancer and small cell lung cancer models, respectively. Finally, we verified combination antitumor activity of ERI-LF with anti-human PD-1 Ab in hPBMC-humanized MKN45 and NCI-H526 models. In both models, combination of ERI-LF with anti-human PD-1 Ab showed significantly stronger antitumor activity compared with each monotherapy. In summary, we demonstrated that combination of ERI-LF with anti-PD-1 Ab is effective for gastric and small cell lung cancers, suggesting that this combination therapy is effective for various cancer types. Currently, Phase 1b/2 clinical trial of ERI-LF plus nivolumab in patients with selected solid cancers including gastric and small cell lung cancers (NCT04078295) is underway.

#5076

Combination PancVAX neo-epitope vaccine with anti-CTLA-4 and anti-PD-1 antibodies enhances infiltration of cytotoxic T cells and mitigates T cell exhaustion in a murine model of pancreatic ductal adenocarcinoma

Jacob T. Mitchell, Amanda Huff, Emily Davis-Marcisak, Fangluo Chen, Todd D. Armstrong, Luciane T. Kagohara, James Leatherman, Rulin Wang, Srinivasan Yegnasubramanian, Elizabeth M. Jaffee, Elana J. Fertig, Neeha Zaidi. *Oncology, Johns Hopkins University School of Medicine, Baltimore, MD*

Pancreatic ductal adenocarcinoma (PDAC) is a deadly cancer with a low tumor mutational burden and therefore few neoantigen targets that can be recognized by cytotoxic T cells. Most PDACs are thus insensitive to either single or dual immune checkpoint inhibitor (ICI) therapy. Personalized neoantigen vaccines can expand the number and repertoire of anti-tumor T cells that infiltrate the tumor and mediate cytotoxicity. To model a personalized neoantigen vaccine treatment strategy in PDAC, we previously developed PancVAX, a peptide-based vaccine targeting 12 neoantigens

expressed in the murine pancreatic cell line Panc02 (Kinkead et al, *JCI Insight* 2018). Although we observed increased T cell infiltration present in the tumor post-vaccination, these cells expressed high levels of exhaustion markers. We therefore hypothesized that sequential administration of anti-CTLA-4 and anti-PD-1 would enhance the pool of T cells primed by the neoantigen vaccine and maintain activation of antigen-experienced T cells, respectively, to yield optimal and durable neoantigen-specific anti-tumor immunity in PDAC. To address this, mice bearing subcutaneous Panc02 tumors were vaccinated with two rounds of the PancVAX neoantigen vaccine followed by anti-CTLA-4 and anti-PD-1 3 days later. Anti-PD-1 maintenance was given twice weekly beginning at the first vaccine dose. Twelve days after the last peptide vaccine dose, tumors were harvested and dissociated into single-cell suspensions for paired single-cell RNA-sequencing and TCR-sequencing. Mice that were untreated or given ICIs without PancVAX had the highest proportions of CD8+ T cells expressing exhaustion markers. PancVAX-treated mice had more intratumoral cycling CD8 T cells and effector CD8+ T cells with high cytotoxic gene expression. Among mice treated with PancVAX, tumors from mice treated with PancVAX + anti-PD1 or PancVAX + anti-PD1 + anti-CTLA-4 had the highest proportions of effector CD8+ T cells. Ongoing analyses include differential gene expression and pathway analysis between treatment conditions in the T cell compartment in mice treated with combination ICI and PancVAX. Additionally, we will assess changes in T cell clonality and diversity within the tumors when mice are treated with single or combination therapy. These results will define a transcriptional signature associated with the generation of a productive anti-tumor immune response when neoantigen vaccines and ICI are used in combination. This work demonstrates how the addition of ICIs to personalized neo-epitope vaccines for PDAC can further enhance the quality of vaccine-induced T cell effector function in an otherwise immunologically cold tumor type and supports their inclusion in neoantigen vaccination strategies for patients with PDAC.

#5077

Engineering dendritic cell-derived exosomes forbrain metastases immunotherapy

Hao-Nien Chen[1], Xiangliang Yuan[1], Yimin Duan[1], Yi Xiao[1], Shao-Ping Yang[1], DIhua Yu[2]. *[1]Department of Molecular and Cellular Oncology, UT*

MD Anderson Cancer Center, Houston, TX,[2]Department of Molecular and Cellular Oncology, DIhua Yu, Houston, TX

Brain metastases (BrMs) represent an unmet challenge for the therapy of most aggressive cancers owing to the extremely poor survival and the limited efficacy of available therapies. Currently, NO curative therapy for breast cancer BrM (BCBrM) is available and we urgently need to develop new and effective therapies. Immune checkpoint therapies (ICT) have revolutionized cancer treatment, but are generally unsuccessful in treating BrMs, including BCBrM. A crucial reason for this is the unique brain immune microenvironment with low antigen exposure/presentation in BrMs and fewer antigen-specific T cells in the brain parenchyma. The priming and activation of antigen-specific T cells require professional antigen-presenting dendritic cells (DCs) for effective antigen presentation through multifaceted communication between DCs and T cells by direct intercellular contact and indirect distant communication via exosomes and other means. DC-derived exosomes (DCEXs) carry functional MHC-I/peptide complexes (pMHC-I) and costimulatory molecules, hence facilitating systemic T cell immune responses. DCEXs have been developed as immunotherapies which exhibit advantages over DC-based immunotherapies. However, DCEXs in ongoing clinical trials showed limited efficacy. We found that increased non-receptor protein tyrosine phosphatase SHP1, a DC-intrinsic inhibitory checkpoint, in monocyte-derived DCs (MoDCs) ex vivo led to DC exhaustion that limits DCEXs function resulting in poor systemic T cells stimulation in vivo. To improve DCEXs functions, we developed next-generation DCEXs by genetic knockout of SHP1 in DCs from which DCEXs (iSHP1-DCEXs) were isolated. Remarkably, the modified iSHP1-DCEXs exhibited significantly increased pMHC-I expression and more effectively improved T cell proliferation compared to control DCEXs, indicating a greater capacity of antigen presentation of engineered iSHP1-DCEXs. In the EO771-OVA mammary tumor cells-bearing mouse model, iSHP1-DCEXs treatment greatly increased tumor infiltration of OVA antigen-specific CD8+ T (OT-1) cells resulting in tumor inhibition and prolonged mouse survival, indicating that iSHP1-DCEXs elicited an effective and specific antitumor immunity in vivo. Moreover, combining iSHP1-DCEXs with anti-PD1 Ab yielded a strong syngenetic therapeutic response in mice bearing the anti-PD1-

resistant EO771 tumors, as indicated by delayed tumor growth and prolonged survival. importantly, iSHP1-DCEXs also significantly increased tumor-infiltrating antigen-specific T cells and synergized with PD-1 Ab leading to tumors clearance in mice bearing the B16-GMCSF melanoma. To further test the iSHP1-DCEXs effect in BCBrM, we co-injected EO771-OVA and iSHP1-DCEXs into mice and found that iSHP1-DCEXs inhibited BrM. Together, the engineered iSHP1-DCEXs offer a promising option to generate a potent antigen-specific T cell immune response for BCBrM inhibition.

#5078

Immune response markers following combination treatment with oncolytic adenovirus AMUN-003 and immune checkpoint inhibitors in a murine model of triple negative breast cancer

Soon Cheon Shin[1], Beniamin Filimon[1], Yuefeng Yang[2], Zebin Hu[3], Vijayakrishna K Gadi[4], Weidong Xu[1]. *[1]NorthShore University HealthSystem, Evanston, IL,[2]Department of Experimental Medical Science, Key Laboratory of Diagnosis and Treatment of Digestive System Tumors of Zhejiang Province, Ningbo, China,[3]National Institutes for Food and Drug Control, Beijing, China,[4]Translational Oncology Program, University of Illinois Cancer Center, Chicago, IL*

Background: Accounting for about 10-15% of all breast cancer diagnoses, triple negative breast cancer (TNBC) has the highest mortality rate partly attributable to few effective treatment options. We evaluated a novel oncolytic adenovirus (rAd.sT.GM; named as AMUN-003 by AmunBio, Inc) encoding sTGFβRIIFc (a TGF-β protein decoy) and GM-CSF transgenes in combination with ICI treatments in the mouse TNBC 4T1 subcutaneous model. We previously reported that infection of target cancer cells with AMUN-003 and co-treatment with ICI led to potent inhibition of tumor progression and lung metastasis without off-target organ or systemic toxicity. Here, we provide details on the specific immune markers associated with responses.
Methods: Immune competent BALB/C mice harboring 4T1 tumors were treated with combinations of anti-PD1 antibody, anti-CTLA antibody, AMUN-003 or sham injections. We measured inflammatory serum

cytokines/chemokine levels by Meso Scale immunoassays and immune modulator gene expression in lung, spleen and tumor by qRT-PCR.
Results: The "Triplet" combination of AMUN-003, anti-PD1 and anti-CTLA-4 antibodies was associated with decrease of poor prognosis biomarkers in serum: **TGF-β1**: Triplet $p< 0.001$, ICIs $p<0.01$, AMUN-003 $p< 0.05$; **IL-27p28/IL-30**: Triplet and ICIs $p< 0.05$; **IL-1β**: Triplet, AMUN-003, ICIs, and AMUN-003+anti-CTLA-4 $p< 0.05$; **TNF-α**: Triplet $p< 0.01$, ICIs $p<0.05$, and increase of immune stimulatory IFN-γ: Triplet $p<0.01$ (all compared to the buffer). In lung tissue, no significant changes in cytokine/chemokine expression were detected, however **Granzyme B** levels were significantly increased in Triplet: $p< 0.05$. In spleen, we detected increased cytokine expression (**IL-2**: Triplet, anti-CTLA-4, AMUN-003+anti-PD-1 $p< 0.05$; **IL-4**: Triplet $p< 0.001$, AMUN-003+anti-PD-1, AMUN-003+anti-CTLA-4: $p< 0.01$). In tumor, expression of TGF-β1 was significantly decreased by triplet and ICIs treatments (both $p<0.05$), but increases in IFN-γ, **IL-4**, **CXCR4**, and **Perforin** were observed in several treatment groups.
Conclusions and Summary: Our data support the interpretation that the most potent intratumoral and systemic anti-tumor response took place with triplet therapy. Specifically, triplet therapy led to reduction of markers of systemic pathogenic inflammation but activation of anti-tumor cellular immunity (e.g., IFN-γ). In lung (site of 4T1 metastases), Granzyme B expression indicated activated NK cell and cytotoxic T cell infiltration was greatest in Triplet. Tumor expression data for IFN-γ, IL-4, CXCR4, and Perforin have limited interpretability because several animals had complete remissions at the primary tumor. Collectively, quantitative protein and expression immune response data presented here further support advancement of combination testing of AMUN-003 and ICIs in human clinical trials.

#5079

Intratumoral CD40 agonist enhances the antitumor effect of anti-PD1 immunotherapy by activation of antigen-presenting cells and selective expansion of effector CD8+ T cells

Barbara Pazdrak, Heather M. Sonnemann, Salah-Eddine Bentebibel, Barbara M. Nassif, Greg Lizee, Adi Diab. *UT MD Anderson Cancer Center, Houston, TX*

Agonistic CD40 antibodies have shown promise when used in combination with checkpoint inhibitors in clinical trials for the treatment of malignancies. However, the mechanisms driving antitumor immune responses in patients are not well understood. The aim of this study was to use a preclinical melanoma model to evaluate the impact of intratumoral anti-CD40 administration on treatment efficacy and the tumor immune landscape in the context of systemic anti-PD1 therapy. Mice bearing 8-day established B16 melanoma tumors were injected with CD40 agonist intratumorally, either alone or in combination with anti-PD1 Ab, every 3 days for a total 4 doses. All mice treated with the combination therapy exhibited tumor growth arrest while progressive tumor growth was observed in control mice and mice treated with anti-PD1 alone. At day 15, tumor weights were 7- and 3-fold reduced in mice treated with the combination therapy as compared to control IgG or PD1 monotherapy, respectively. CyTOF analysis showed a 4-fold increase in the frequency of tumor-infiltrating immune cells in mice treated with either CD40 agonist alone or the combination therapy. Interestingly, CD40 agonistic Ab selectively expanded CD8+ T cells and the combination therapy exhibited a more pronounced effect compared to treatment with anti-PD1 Ab alone. Moreover, CD39+ CD8 T cells, representing tumor antigen-specific cytotoxic T cells, were 14- and 3-fold higher in tumors from mice treated with the combination therapy as compared to control or PD1-treated mice, respectively. This effect correlated with increases in the frequency of antigen-presenting cells, including cDC1 (6-fold) and B cells expressing CD40 (3-fold) in response to the combination therapy. In addition, the combination therapy significantly decreased myeloid cell population resulting in an 8-fold reduction in the ratio of myeloid cells to T cells. Amongst myeloid cells, the density of the monocytic population was diminished, with a selective 10-fold reduction of CD206+ M2-macrophages in tumors from mice treated with both Abs. Our findings provide evidence that combining systemic anti-PD1 therapy with intratumoral CD40 agonist enhanced antitumor immune responses by selectively expanding tumor antigen-specific effector CD8+ T cells, which was associated with increased infiltration of antigen-presenting cells and attenuation of immunosuppressive myeloid cells.

#5080

TU2218, a novel ALK5/VEGFR2 dual inhibitor, overcomes tumor endothelial cell anergy and enhances anti-PD1 immunotherapy efficacy

Jihyun Lee, Nam-hoon Kim, Hun-Taek Kim. *Discovery2, TiumBio, Seongnam-si, Korea, Republic of*

Immune tolerance by TGF-β and VEGF is inextricably related with poor outcomes of approved anti-PD-(L)1 therapy. Accordingly, a dual target for ALK5 and VEGFR2 via single or combination treatments can be an unequivocal tactic to tune tumor-microenvironment (TME) favorable to ICI, and to essentially overcome immune evasion against TGF-β- and VEGF-enriched tumors. Specifically, several reports from clinical data suggest that VEGF-induced endothelial cell anergy (ECA) acts as a vascular immune checkpoint in TME immune response, and the activation of ECA is associated with worse outcomes. Herein, we demonstrate that TU2218, a *first-in-class*, orally available inhibitor against ALK5 and VEGFR2 can recover the downregulated endothelial adhesion molecules, i.e., ICAM-1 and VCAM-1, and suppress ECA. In this work, TU2218 completely recovered the expression of ICAM-1 and VCAM-1 on VEGF-induced ECA in HUVECs. The restored level of ICAM-1 and VCAM-1 at 1 μM TU2218 was equivalent to the activity of combined treatment of 1 μM Vactosertib (ALK5 inhibitor) and 25 μg/ml Ramucirumab (VEGFR2 inhibitor). 1 μM of Vactosertib alone, however, did not show such restoration. These results indicate that VEGF-induced ECA is mediated by both VEGFR2 and TGF-β signal, thereby validating the superiority of dual target strategy for ALK5 and VEGFR2 over a single target in overcoming ECA. We further tested if TU2218 could restore VEGF-induced decrease of Jurkat adhesion to HUVECs, considering the close relationship between the expression of adhesion-molecules of endothelial cell surface and the adhesion of lymphocytes to endothelium. TU2218 recovered the number of Jurkat adhering to VEGF-elicited HUVEC monolayer in a dose-dependent manner, but Vactosertib did not. Furthermore, the activity of TU2218 on Jurkat adhesion was reversed by VCAM-1 neutralizing antibody. Therefore, our results demonstrate that TU2218 improves Jurkat adhesion by restoring VCAM-1 expression. Finally, the *in vivo* translatability of TU2218 in overcoming ECA was confirmed with B16F10-bearing mice, a well-defined immune desert model, after treatments of anti-PD1 antibody, TU2218, or

combined regimen for 15 days. TU2218 combined with an anti-PD1 antibody significantly suppressed tumor growth by c.a. 74 % compared to vehicle, thus being superior to a single treatment (e.g., tumor growth inhibition (TGI) 44% for TU2218, TGI 45% for anti-PD1). In this combination, TU2218 increased the number of both $CD31^{+}VCAM\text{-}1^{+}$ and $IFN\gamma^{+}CD8^{+}$ T cells in the tumor. We conclude that TU2218 leads not only to the enhancement of T cell-traffic toward TME, but also to the conversion of immune balance favorable to anti-PD1 therapy. The Phase 1b trial of TU2218 combined with pembrolizumab is underway for advanced solid cancers (NCT05204862).

#5081

Anti-tumor activity of HPN217, a BCMA-targeting tri-specific T cell engager, is enhanced by γ-secretase inhibitors in preclinical models

Payton C. Laurie, Mary Ellen Molloy, Patrick P. Ng, Banmeet S. Anand.
Translational Medicine, Harpoon Therapeutics, Inc., South San Francisco, CA

HPN217 is a Tri-specific T Cell-Activating Construct (TriTAC) currently being evaluated in a phase 1 clinical trial for relapsed or refractory multiple myeloma (MM) (NCT04184050). It consists of a single domain antibody (sdAb) specific for B-cell maturation antigen (BCMA), a serum albumin-specific sdAb for half-life extension, and a single chain Fv (scFv) specific for the CD3ε subunit of the T cell receptor (TCR) complex for T cell engagement. BCMA is a cell surface receptor highly expressed on malignant plasma cells in MM patients and plays an important role in B-cell proliferation and survival. Soluble BCMA (sBCMA) is produced when the extracellular domain of BCMA is cleaved by γ-secretase and enters circulation. sBCMA may act as a sink for BCMA targeted therapies, potentially decreasing anti-tumor efficacy. Previous studies have shown γ-secretase inhibitors (GSIs) can increase membrane bound BCMA expression on MM cells and decrease sBCMA concentrations, providing a rationale for combining GSIs with HPN217. Here we describe preclinical studies evaluating that combination *in vitro* and *in vivo*. To evaluate the effects of GSIs on BCMA expression, MM cell lines MOLP8, KMS-12-BM, and MM.1S were incubated with GSIs LY3039478, PF03084014, or RO4929097overnight. GSI treatment led to a 3-7-fold increase in BCMA

expression on MM cell surface. To determine the effects of increased BCMA expression mediated by GSIs on the activity of HPN217, an *in vitro* T cell dependent cell cytotoxicity assay (TDCC) was conducted. GSIs enhanced the activity of HPN217, in some cases leading to a 3.5-fold increase in potency compared to HPN217 alone. Next, the impact of the combination was tested *in vivo* using a disseminated MOLP-8 xenograft model engrafted with T cells from a healthy human donor. Vehicle treated mice succumbed to disease burden with a median survival of 23 days as assessed by body weight loss and clinical observations. A suboptimal dose of 4 ug/kg HPN217 protected mice from disease burden for an additional 3 days. By contrast, the combination of HPN217 and LY3039478 led to a significant increase in survival compared to vehicle or either monotherapy, with a median survival of 43 days. Taken together these results demonstrate the potential utility of GSIs to enhance the anti-tumor activity of HPN217 and supports further investigation of this combinatorial approach in patients.

#5082

Heterodimeric IL-15 (hetIL-15) immunotherapy synergizes with Fatty Acid Metabolism Modulator (FAMM) to eradicate TNBC EO771 murine tumors

Sevasti Karaliota[1], Dimitris Stellas[2], Vasiliki Stravokefalou[2], Breana Myers[1], Barbara K. Felber[2], George N. Pavlakis[2]. *[1]Frederick National Laboratory for Cancer Research, Leidos Biomedical Research, Frederick, MD,[2]National Cancer Institute at Frederick, Frederick, MD*

Introducti**on:** Metabolic fitness and T cell survival are crucial in anti-tumor responses because nutrients are often scarce and other regulatory molecules may be unfavorable in the tumor microenvironment leading to T cell dysfunction, stress, and apoptosis. Tumor-infiltrating cytotoxic $CD8^+$T cells frequently acquire an altered state of differentiation referred to as "exhaustion" and, as a result, they fail to control tumor outgrowth. IL-15 cytokine stimulates the generation, proliferation and cytotoxic function of tumor specific $CD8^+$ T cells and NK cells. The objective of this study was to assess the effects of hetIL-15 immunotherapy in triple negative breast cancer tumors (TNBC), to evaluate the metabolic profile of the tumor-

infiltrating T cells and to study any potential synergy using a Fatty Acid Metabolism Modulator (FAMM) to enhance T cell metabolism.
Study design and methods: We used the murine EO771 orthotopic breast cancer model to study the efficacy of locoregional administration of hetIL-15 immunotherapy in combination with a FAMM. We monitored the effect of treatment on number, metabolism and mitochondrial function of the tumor-infiltrating immune cells by flow cytometry, Seahorse flux analysis and Mitotracker, 2-NBDG and/or Bodipy staining.
Results: hetIL-15 locoregional administration, as as single agent, resulted in complete regression in 40% of the treated animals and increased survival. Tumor-infiltrating cytotoxic $CD8^+$T and NK cells increased in hetIL-15 treated tumors and showed enhanced activation and proliferation. Metabolic flux analysis of the tumor-infiltrating cytotoxic $CD8^+$T cells from hetIL-15-treated mice confirmed a rise in oxygen consumption rate (OCR) with substantial increase of spare respiratory capacity, which supports an activated/non exhausted phenotype of these hetIL-15 treated effector cells. Since, further promoting fatty acid (FA) catabolism improves the tumor-infiltrated $CD8^+$T cells's ability to slow tumor progression, we combined hetIL-15 immunotherapy with a FAMM. Combination therapy resulted in increased mitochondrial function, FA uptake and OCR, revealing a more metabolically active phenotype compared to the tumor-infiltrating $CD8^+$T cells from hetIL-15 monotherapy group. In addition, combined treatment of IL-15 immunotherapy and FAMM resulted in statistically significant EO771 tumor growth delay and complete eradication of the tumors in 85% of mice.
Conclusions: Our results indicate that hetIL-15 synergizes with metabolic reprogramming of T cells to achieve superior antitumor efficacy and complete cures. We suggest that metabolic reprogramming of tumor-specific $CD8^+$Tcells might represent a strategy to promote survival in the metabolically hostile TME as part of an approach to enhance the clinical efficacy of immunotherapy.

#5083
Investigating the development and therapeutic potential of intra-tumoral $CXCR6^+$ effector/effector memory T cells ($T_{EFF/EM}$) in triple-negative breast cancer

Bryan Jian Wei Lim[1], Xiao-Fan Wang[2], Qi-Jing Li[3]. *[1]Duke University, Durham, NC,[2]Pharmacology and Cancer Biology, Duke University, Durham, NC,[3]Institute of Molecular and Cell Biology, Agency of Science and Technology (A*STAR), Singapore, Singapore*

Triple-negative breast cancer (TNBC) is an aggressive subtype that makes up 10-20% of all breast cancer cases. Because of the higher risk of metastasis and recurrence post-treatment, there is a need to develop novel therapeutics to address these challenges. In previously published work, we demonstrated that CXCL16 traps $CXCR6^{+}PD\text{-}1^{+}$ effector/effector memory ($T_{EFF/EM}$) within the primary tumor and that these T cells have anti-metastatic function that can be harnessed when released into peripheral sites with intra-tumoral administration of anti-CXCL16 prior to surgical resection. However, whether CXCL16 blockade can be used in combination with conventional checkpoint targets and the developmental route of this $CXCR6^{+}$ $T_{EFF/EM}$ is not known. To develop a novel neoadjuvant therapy, we use the spontaneously metastasizing murine TNBC model, 4T1. Here, we report that anti-4-1BB, and not anti-PD-1, when used in combination with blockade of CXCL16 can prolong survival post-surgical resection. Using anti-4-1BB in combination with CRISPR-generated *Cxcl16*-KO 4T1 model, we show that both deficiency of CXCL16 within the tumor microenvironment (TME) and anti-4-1BB contribute synergistically to survival advantage. To study the development of this population of T cells, we use the Py8119 murine TNBC model. We definitively show that $CXCR6^{+}PD\text{-}1^{+}$ $T_{EFF/EM}$ is uniquely generated within the primary tumor. Co-expression of CXCR6 and PD-1 indicates that T cell receptor (TCR) signaling is a potential regulator of the development of this $T_{EFF/EM}$ sub-population. Analyses of our previously published scRNA-seq dataset reveals *Lat2* to be the top gene involved in TCR signaling. Tumors growing on *Lat2*-KO animals show a significant increase in tumor size accompanied by significant reduction of $CD44^{high/mid}$ $CXCR6^{+}PD\text{-}1^{+}$ $T_{EFF/EM}$. However, competitive transfer of naïve WT and *Lat2*-KO T cells into *Tcra*-KO recipients led to comparable levels of $CXCR6^{+}$ $T_{EFF/EM}$. Surprisingly, transferred *Lat2*-KO T cells failed to engraft within the primary tumor relative to WT T cells. Future work will address if this engraftment defect is

due to expansion/survival defects. Therefore, regulation of TCR signaling within the TME via LAT2 potentially represents a mechanism in which primary tumors trap T cells, promoting their exhaustion. Importantly, this can be harnessed through combinatorial activation and blockade of 4-1BB and CXCL16 respectively.

#5084

Targeted delivery of low-dose radiation alleviates tumor resistance to CAR-T cell therapy

Yanping Yang[1], Yago Alcaina[1], Yogindra Vedvyas[1], Maria Cristina Riascos[1], Edward K. Fung[2], Brett Vaughn[1], Sarah M. Cheal[1], Irene M. Min[1], Claire Vanpouille-Box[2], Moonsoo M. Jin[1]. *[1]Radiology, Weill Cornell Medicine, New York, NY,[2]Weill Cornell Medicine, New York, NY*

Purpose: Current understanding of resistance to CAR-T cell therapy in solid tumors implicates inadequate CAR-T cell potency in the immunosuppressive tumor microenvironment (TME). We have previously developed a platform using somatostatin receptor 2 (SSTR2) as a positron emission tomography (PET) reporter to detect CAR-T cell expansion and trafficking. The current study aimed to leverage SSTR2 for low-dose targeted radionuclide therapy (^{177}Lu-DOTATATE, Lutathera), which under dosimetry guidance might enhance antitumor immunity by reprograming the TME and promoting T-cell reinvigoration.
Methods: Using intercellular adhesion molecule 1 (ICAM-1) as a model antigen, we evaluated the immunomodulatory effects of low-dose radiation in a gastric cancer animal model. NSG mice were inoculated subcutaneously with firefly luciferase-expressing Hs 746T cells (0.1×10^6 per mouse) and treated 5 days later with 10×10^6 SSTR2-expressing ICAM-1 CAR-T cells. CAR-T cell expansion was monitored weekly by PET scan using ^{18}F-NOTA-Octreotide, a radiotracer targeting SSTR2. Three weeks post-T cell infusion, a cohort of mice were injected with 7.4 MBq of ^{177}Lu-DOTATATE via the tail vein. SPECT imaging was performed for dosimetry analysis. Tumor growth was monitored by bioluminescence imaging and tumor size measurement. Serum cytokines were analyzed.

Results: Single dose ^{177}Lu-DOTATATE treatment (delivering 1-6 Gy to tumor) improved response of established gastric cancer tumor (>1,000 mm^3) that was not responsive to CAR-T cell treatment alone and significantly prolonged survival. All mice receiving CAR-T cells plus ^{177}Lu-DOTATATE displayed rapid tumor shrinkage, with 83% of mice achieving complete remission within 3 weeks of ^{177}Lu-DOTATATE treatment. SPECT imaging confirmed specific delivery of ^{177}Lu-DOTATATE by tumor-infiltrating CAR-T cells, with tumor uptake of 0.43 ± 0.24 and 0.19 ± 0.08 MBq/g at 24 and 144 hours post ^{177}Lu-DOTATATE injection, respectively. Most radioactivity reduction over time (73%) is explained by physical decay of ^{177}Lu, indicating persistent tumor retention of ^{177}Lu-DOTATATE. In contrast, rapid clearance of ^{177}Lu-DOTATATE was observed in liver and kidneys. Importantly, longitudinal CAR-T cell imaging using ^{18}F-NOTA-Octreotide revealed increased CAR-T cell expansion induced by low-dose radiation. Furthermore, we detected high levels of IFN-γ and perforin in serum after ^{177}Lu-DOTATATE treatment, which were >10 folds higher than that in control mice receiving CAR-T cell only, indicating activation of T cells by low-dose radiation.
Conclusions: We developed a translatable radioimmunotherapy platform that incorporates a FDA-approved theranostic endoradiotherapy (Lutathera) to improve tumor response to CAR-T cell therapy. The next steps would be to explore the immunomodulatory effects of low-dose radiation systematically and elucidate the mechanism of action.

#5085
Blockade of tumor derived CSF1 promotes an immune-permissive tumor microenvironment
Maria Del Mar Maldonado, Duane H. Hamilton, Jeffrey Schlom. *Center for Immuno-Oncology, NIH-NCI, Bethesda, MD*

The macrophage colony stimulating factor 1 (CSF1) is a chemokine essential for the survival, proliferation, and differentiation of especially mononuclear phagocytes, such as macrophages and monocytes. However, within the tumor microenvironment (TME), CSF1 regulates the production, survival, and recruitment of tumor associated macrophages (TAMs), further promoting a protumorigenic and immunosuppressive M2-like phenotype.

Overexpression of CSF1 in breast, prostate, and ovarian cancers has been shown to promote tumorgenicity, invasiveness, and accelerate tumor metastasis. In this study, we demonstrate for the first time, that treating established murine MC38 colon and 4T1 breast carcinoma tumors with a CSF1R blocking antibody promotes the expansion of neoepitope-specific T cells. To assess the role of tumor derived CSF1 in these model systems, we generated and characterized CSF1 CRISPR-Cas9 knockouts. In both models, elimination of tumor-derived CSF1 results in a decreased tumor growth in both syngeneic and immune-compromised mice as compared to the parental cell lines. Inhibition of CSF1/CSF1R signaling axis generated enhanced immunity against 4T1 and MC38 tumor neoepitopes, potentially promoting an immune permissive TME in tumor bearing mice. Combination of a neoepitope targeting cancer vaccine with anti-PDL1 in the MC38 CSF1-/- tumor model significantly decreased tumor growth *in vivo*. Furthermore, combining CSF1R blockade with adeno-TWIST1 vaccine decreased tumor volume, lung metastasis, and synergistically increased in CD8 T cell infiltration in 4T1 mammary tumors. Analysis of the tumor microenvironment demonstrated increased infiltration in CD8 T cells accompanied by a reduction in tumor associated macrophages following CSF1R inhibition in both tumor models. Our findings confirm the therapeutic potential of combining CSF1 targeting agents with vaccine agents to further modulate anti-tumor immune responses in the tumor microenvironment.

#5086

Transcriptomic analysis in a renal cancer PDX model enables the deconvolution of additive and synergistic effects of six different standard of care compounds with anti-PD-1 treatment

Kanstantsin Lashuk[1], Eva Oswald[1], Oliver Jonas[2], Julia Schueler[1]. *[1]Charles River Laboratories, Inc., Freiburg, Germany,[2]Kibur Medical Inc, Boston, MA*

Identifying how to optimally combine immunotherapies with other available anti-cancer therapies is a major challenge in oncology. We have utilized an implantable microdevice performing cassette (IMD) microdosing that measures intratumor drug responses and anti-tumor immunity for six agents in parallel. This approach was combined with the

systemic administration of anti-PD1 treatment to examine whether immunogenic cell death (ICD) induced by a given drug potentiates the immunotherapy's anti-tumor effect. Local tumor response was measured by multiplex immunohistochemistry (IHC) and transcriptomic analyses. The study was performed in a humanized mouse model of a clear cell renal cancer, patient derived xenograft (PDX) RXF488. RXF488 was implanted subcutaneously in 30 NSG mice. Animals were stratified into 6 groups with n= 4-6. Humanization was performed by the intravenous injection of 5x10e6 human peripheral blood mononuclear cells prior to the first treatment. Systemic aPD1 treatment was applied in the presence and absence of the microdevice loaded with six different drugs. Control groups received the empty IMD in the presence or absence of PBMC. Several agents showed a significant increase in apoptosis induction when aPD1 was added: The largest increase was observed for the panRAF inhibitor LXH254, Sorafenib, Oxaliplatin and Doxorubicin. The increased efficacy from immunotherapy administration has a strong positive correlation with increased induction of ICD in the tumor microenvironment determined by CD11b, ICAM-1 and MHC-II expression: drugs that showed the highest increase in apoptosis when combined with aPD-1 showed an increased likelihood for markers associated with ICD, namely Oxaliplatin and LXH254. A transcriptomic analysis on the tumor tissue revealed nine different clusters. The implantation of the empty device modulated the expression data in a way that these samples clustered together and separate from the untreated tumor samples. Other clusters were defined by presence of absence of aPD1 and the different local treatments. A more focused analysis using a subset of 19 genes described to be predictive for ICD in solid cancer confirmed the activity of LXH254 but identified Sunitinib in combination with anti PD1 as another potential inducer of ICD. An induction of ICD by Oxaliplatin as indicated by the IHC results could not be confirmed by the expression data. Overall treatment arms the systemic treatment with anti-PD1 led to an increased expression of the above mentioned 19 genes. Our results demonstrate that local tumor response signatures of ICD can be used to systemically identify synergistic combinations of a range of drugs with immunotherapy on a tumor specific basis. A deeper dive into the transcriptomic data will help to identify other predictive biomarker for efficacy beyond ICD.

#5087

Combination therapy of immune checkpoint inhibitor and HIF1α/c-MET peptide vaccine suppresses metastasis by modulating tumor microenvironment in triple-negative breast cancer

JinHwa Hong, Jimin Lee, Soon Young Lim, Ju Won Kim, Ah Reum Lim, Kyong Hwa Park. *Korea University, Seoul, Korea, Republic of*

Triple-negative breast cancer (TNBC) accounts for 20% of all breast cancer and has limited therapeutic option except for immunotherapy because ER, PR, and HER2 targeted for treatment are absent. It also tends to be more aggressive meaning more likely to metastasize faster to other organs such as lungs, liver, and bone, and its recurrence rate is high which leads to a poor prognosis. Immunotherapy is an option to treat TNBC such as programmed death ligand 1 (PD-L1) antibody. However, tumor cells use various immune evasion mechanisms in addition to PD-1/PD-L1 pathway to interrupt the effect of immunotherapy. Moreover, tumor microenvironment (TME) is one of the important factors for the effective anti-tumor immune responses from immunotherapy. Hypoxia is a typical event in TNBC. Hypoxia inducible factor 1-alpha (HIF1α) is a transcription factor that regulates angiogenesis by expressing VEGF, and in addition, upregulates the c-MET which increases the proliferation, migration, and survival of tumor cells. Moreover, HIF1α directly regulates the expression of CD47. CD47 is a transmembrane protein that binds to SIRPα of macrophages to inhibit the phagocytosis of macrophages. Therefore, the efficacy of immune checkpoint inhibitors decreases even if there is a higher degree of tumor-infiltrating lymphocytes (TILs). Combination therapy with immune checkpoint and tumor associated antigens (TAAs) derived peptide vaccine could inhibit metastasis. In present study, we found that HIF1α/c-MET peptide vaccination delayed metastasis in C3(1)Tag mouse. We also investigated whether combination therapy with immune checkpoint inhibitors and peptide vaccine inhibited metastasis. Next, we observed that combination strategy of HIF1α/c-MET peptide vaccine and treated anti-PD-L1 antibody or/and anti-CD47 antibody was more effective in systemically inoculated M6 cells growth in C3(1)Tag mice. Immunohistochemical analysis of the tumors showed that the protein expression of CD47, HIF1α, and c-MET were significantly decreased. On the other hand, $CD4^+$ T cells, $CD8^+$ T cells and M1 macrophages increased, but M2 macrophages

decreased, resulting in delayed metastasis in combination therapy group compared to single therapy and control group. In addition, IFNγ ELISPOT showed that peptide vaccination significantly increased the HIF1α/c-MET specific IFNγ-secreting T cell response in splenocytes. We also assessed osteoclastogenesis in bones, which showed reduction of osteoclast in combination therapy group compared to single therapy and control group.Taken together, combination therapy with immune checkpoint inhibitor targeting PD-L1 and CD47 and peptide vaccine appears to be a promising strategy that inhibit metastasis by modulating tumor microenvironment in triple negative breast cancer.

#5088

MDSC-targeted TFF2-MSA synergizes with PD-1 blockade therapy in diffuse-type gastric cancer

Jin Qian[1], Sandra Ryeom[1], Bruce Daugherty[2], Seth Lederman[2], Timothy C. Wang[1]. *[1]Columbia University Irving Medical Center, New York, NY,[2]Tonix Pharmaceuticals, Inc., New York, NY*

Aims: Recent studies revealed myeloid-derived suppressor cell (MDSC) in the tumor microenvironment as an appealing therapeutic target to sensitize intestinal-type gastric cancer (GC) to PD-1 blockade therapy. However, whether MDSC inhibition can improve survival in the more aggressive diffuse-type GC is unknown. Trefoil factor family 2 (TFF2), a secreted anti-inflammatory peptide, suppresses MDSC expansion partly via CXCR4 receptor. Here, we developed a novel MDSC-targeted peptide TFF2-MSA and investigated whether it can synergize with anti-PD1 to prolong survival in syngeneic diffuse GC mouse models.
Methods: Murine serum albumin (MSA) was appended to the murine TFF2 to generate TFF2-MSA peptide with an extended serum half-life. ACKP (Atp4b-Cre; Cdh1-/-; LSL-KrasG12D; Trp53-/-) GC cells developed from a highly malignant diffuse GC mouse model were grafted subcutaneously into HDC-GFP transgenic mice in which the more immunosuppressive histidine decarboxylase (HDC)-expressing myeloid cells were traced with GFP. These recipient mice subsequently received either TFF2-MSA or anti-PD-1 antibody or both. Further, to assess treatment efficacy in inhibiting spontaneous lung metastasis, subcutaneous flank tumors were resected in ACKP cell-grafted mice once tumors reached 500 mm^3, and mice then

received treatment with TFF2-MSA or anti-PD-1 or the combination. At the endpoint, flow cytometry and histopathological analyses were performed to examine immune profiles and tumor metastasis. In another model, ACKP-luc cells were implanted orthotopically to stomach submucosa, and recipient mice received the same treatments started from 1 week later to assess their efficacy.
Results: While either TFF2-MSA or PD-1 antibody showed little benefit as a single agent (TGI 15% and 25% respectively, $p>0.05$), their combination dramatically suppressed ACKP s.c. tumor growth (TGI 78%, $p<0.0001$) and markedly prolonged median survival (64 days vs. 32.5 days in control) of host mice in a synergistic manner. The combination therapy efficiently reduced HDC-GFP$^+$ MDSCs (by 67% vs. control, $p<0.01$), and profoundly increased tumor-infiltrating cytotoxic CD8$^+$ T cells (by 18 fold, $p<0.001$). Further, while standard chemotherapy (5-fluorouracil and oxaliplatin) showed limited efficacy in this model, addition of chemotherapy to the TFF2-MSA/PD-1 antibody combination further improved treatment efficacy (TGI 91%) and extended median survival to 73 days. In addition, combination of TFF2-MSA/PD-1 antibody significantly reduced 80% lung metastasis (vs. control, $p<0.0001$), in contrast to minimal inhibition observed with either monotherapy ($p>0.05$). Finally, in the orthotopic model, the combo regimen eradicated GC in 50% mice compared to 0% in either monotherapy treatment.
Conclusion: Targeting MDSCs using TFF2-MSA synergizes with PD-1 blockade therapy in advanced and metastatic syngeneic mouse models of diffuse-type GC.

#5089
Small molecule Bax activator enhances immunotherapy against lung cancer
Abu Syed Md Anisuzzaman, Muhammad Waliul Talukdar, Xingming Deng.
Emory University, Atlanta, GA

Induction of apoptosis is a critical mechanism underlying the durable efficacy of cancer treatment agents. Bax is a major proapoptotic protein whose activation is required for apoptotic cell death. We have recently discovered that small molecule Bax activator CYD-2-11 targets the S184 structural pocket in the c-terminal tail of Bax, directly activates its

proapoptotic activity via conformational change and formation of Bax homo-oligomers in mitochondrial membranes. CYD-2-11 has potent anti-tumor activity against lung cancer in various animal models. Here we found that CYD-2-11 in combination with radiation, cisplatin or BH3 mimetic Bcl2 inhibitor venetoclax (ABT-199) synergistically suppressed tumor growth in non-small cell lung cancer (NSCLC) xenograft models. It is known that LKB1 mutations or deficiency are associated with therapeutic resistance to PD-1/PD-L1 checkpoint blockade immunotherapy. To test whether Bax activator CYD-2-11 reverses resistance to immunotherapy in immunologically "cold" genetically engineered LSL-KRAS^{G12D} LKB1 $^{fl/fl}$ (KL) mouse model, KL mice were treated with CYD-2-11, PD-L1 antibody or in combination. Results indicate that PD-L1 antibody alone has no significant anti-tumor effect in KL mice. CYD-2-11 alone can reduce tumor burden, but combination of CYD-2-11 with PD-L1 antibody has very strong synergistic effect and produces maximum efficacy in tumor burden reduction and significantly prolongs survival of KL mice. Mechanistically, combined treatment with CYD-2-11 and PD-L1 antibody enhances T cell infiltration in tumor tissues. These findings provide preclinical evidence for pharmacologic combinations of small molecule Bax activator with chemoradiotherapy, Bcl-2 inhibitor or PD-L1 antibody as novel strategies to treat lung cancer more effectively.

#5090

TU2218, a dual inhibitor against ALK5/VEGFR2, increases anti-CTLA4 antitumor efficacy in syngeneic tumor models

Nam-Hoon Kim, Jihyun Lee, Hun-Taek Kim. *TiumBio, Seongnam-si, Korea, Republic of*

The combination of pembrolizumab with low-dose ipilimumab shows substantial antitumor activity and manageable profile of toxicity in anti-PD-(L)1 antibody failure-setting (NCT02743819). This suggests a breakthrough for the absence of treatment option after relapsed/refractory anti-PD-(L)1 therapy. Accordingly, the anti-CTLA4 drug-based combination can be considered as a promising strategy for beneficial outcomes against resistance acquired from immunotherapy. Herein, we demonstrate that TU2218, a *first-in-class*, orally available inhibitor against ALK5 and VEGFR2, showed synergistic antitumor efficacy when combined with an

anti-CTLA4 antibody in preclinical tumor models which is being accompanied by increasing ratio of CD8 T cell to regulatory T cell and enhanced immunological memory. In this work, antitumor efficacy of TU2218 combination with an anti-CTLA4 antibody was assessed with CT26-, 4T1-, B16F10- and WEHI-164-bearing mice. In the CT26 model, the combination of TU2218 with an anti-CTLA4 antibody significantly inhibited tumor growth up to 92% compared to vehicle, thus being superior to single treatments (e.g., tumor growth inhibition (TGI) 46% for TU2218, TGI 74% for anti-CTLA4). In this combination group, the complete regression (CR) rate was 75 % (i.e., six cases among eight mice), while single treatments showed lower CR rates (e.g., CR 10% (1/10) for TU2218, CR 30% (3/10) for anti-CTLA4). Meanwhile, the role of CD8+ T cell in antitumor activity was elucidated by *in vivo* depleting CD8+ T cell in mice treated with combination therapy. The depletion of CD8+ T cells reduced the antitumor response, which suggests the indispensable role of CD8+ T cells in the antitumor efficacy of TU2218 and anti-CTLA-4 antibody combination. In addition, the long-term immune-memory was evaluated by re-implanting tumor cells into both mice cured by combination therapy and age-matched tumor-naïve mice. In this case, 6 mice cured of original implantation with CT26 tumors showed complete resistance to the re-implantation of CT26 cells during an untreated period for 21 days, whereas all age-matched tumor-naïve mice have developed tumors after 10 days from cell-transplants. Importantly, we could confirm the positive correlation between the immunological memory-response of combination therapy and the increasing rate of effector memory CD4+ and CD8+ T cells in spleens compared to those of age-matched group. In 4T1-, B16F10- and WEHI-164-bearing mice, combination of TU2218 with an anti-CTLA4 antibody led to higher CR rate as well as enhanced inhibition of tumor growth. Overall, our findings showed that TU2218 plays multifaceted roles in inducing immune activation under combination with an anti-CTLA4 antibody, which may be attributed to the increased ratio of cytotoxic CD8 T cell to regulatory T cell and improvement of adaptive immunity with long-term immunological memory.

#5091

Potentiating immunogenicity of PD1 blockage with metronomic Oral CAPOX for local and liver metastasized colorectal cancer

Seong Jin Park, Seho Kweon, Moyo Knowledge Mudhibadhi, Ha Rin Kim, Youngro Byun. *Seoul National University College of Pharmacy, Seoul, Korea, Republic of*

Since the appearance of oxaliplatin, FOLFOX therapy is positioned as the standard of care for colorectal cancer (CRC). And after the advent of capecitabine, an oral prodrug of 5-FU, both FOLFOX and CAPOX remain the first-line treatment for local and advanced CRC. Even though oral 5-FU prodrug has approved more than two decades ago, orally available oxaliplatin has not been developed yet. Oral chemotherapy has garnered attention in the era of cancer immunotherapy because oral form of the therapy makes metronomic therapy feasible. In this regard, we invented orally absorbable oxaliplatin exploiting complexation with bile acid moiety. The invention encouraged to expand the dosing of combination treatment of 5-FU and oxaliplatin, the most established chemotherapy combination of CRC, into metronomic scheduling. Oral CAPOX therapy is developed to administrate 5-FU and oxaliplatin combination (FOX) metronomically for chemo-immunotherapy. Metronomic dosage successfully induced immunogenic cancer cell death in colorectal cancer xenograft mouse model not exerting toxicity to other organs abolishing immune suppressive effect of chemotherapy. Oral CAPOX boosted tumor immunity translating immune microenvironment. Immune cell population and activation was analyzed using flow cytometry. Suppressive immune cell population decreased after Oral CAPOX treatment. Especially, immune-suppressive macrophage population diminished. Macrophages became immunogenic and presented antigen more frequently. Improved tumor microenvironment combined with anti-PD1 treatment activated and proliferated T cells locally and systemically. Oral CAPOX and anti-PD1 combination therapy activated cytotoxic T cell in tumor tissue and tumor draining lymph node. This therapy also activated NK cells systemically. Oral CAPOX and anti-PD1 combination treatment regressed established tumor completely in more than 90% of the mouse showing its capacity for clinical usage. Liver is the region which makes CRC least immunogenic among metastatic site and the organ CRC is metastasized most abundantly. Immuno-suppresive macrophage in liver is known for the factor discriminating liver metastasized CRC from other organs metastasized one suppressing T cells. Because Oral CAPOX therapy converts macrophage more immunogenic,

Oral CAPOX therapy could reverse immunosuppressive tumor microenvironment of liver metastasized colorectal cancer. Oral CAPOX and anti-PD1 combination is treated liver metastasized CRC model and showed standing out antitumor efficacy, and T cell activation.

#5092

Non-IL-2 blocking Treg-depleting anti-human CD25 mAb primes potent anti-tumor immunity and synergizes anti-tumor effects of anti-PD-1 in a novel hIL-2RA knockin model

Daniel He. *Shanghai Model Organisms Center, Inc., Shanghai, China*

The therapeutic effects for cancer immunotherapy are largely hampered by intratumoral $CD4^+CD25^+$ regulatory T cells (Tregs) which leads to poor outcome in many cancer patients upon treatment of immune checkpoint inhibitors. Moreover, the balance between effector T (Teff) cells and Treg cells in the tumor microenvironment (TME) impacts on tumor progression and anti-tumor immunity. Depleting tumor-infiltrating Tregs by selectively targeting CD25 to reduce the ratios of regulatory to effector T cells (Treg/Teff) without disturbing IL-2 signalling is a promising strategy to advance anti-tumor immunity. Hence, we evaluated the in vivo anti-tumor effects of Non-IL-2 blocking Treg-depleting anti-hCD25 mAb versus IL-2-blocking anti-hCD25 mAb (Basiliximab) in an engineered hCD25 (IL-2RA) knockin mouse model.Firstly, we developed the genetically engineered CD25 (IL-2RA) humanized mouse model by ES cell targeting, in which mouse Cd25 exons 2-6 are replaced by human counterparts corresponding to the extracellular domain leaving the intracellular regions intact. Then, we performed flow cytometry analysis to confirm the surface expression of hCD25 on naive Treg cell from peripheral blood and spleen in homozygous hCD25 knockin mice. In addition, we found the hCD25 expression is upregulated on activated Treg cell derived from splenocytes for both heterozygous and homozygous hCD25 knockin mice. Furthermore, the female homozygous hCD25 knockin mice subcutaneously engrafted with MC38 syngeneic tumors received two different therapeutic anti-CD25 mAb treatment in parallel and we found the Non-IL-2 blocking Treg-depleting anti-human CD25 mAb (anti-$hCD25^{NB}$) displayed more potent anti-tumor response compared to IL-2-blocking Treg-depleting anti-human CD25 mAb (anti-$hCD25^{BL}$), supporting that keeping IL-2 signaling on

effector T cells are required to enhance effector activation and anti-tumor immunity. Notably, the study groups treated with anti-hCD25^{NB} plus anti-mPD-1 showed synergistic therapeutic effects as expected. As a matter of fact, both CD4$^+$CD25$^+$ T cells and CD4$^+$CD25$^+$FoxP3$^+$ Treg cells reduced significantly upon treatment of anti-hCD25^{NB} and anti-hCD25^{BL} in spleen and tumors, but no big change in the number of CD4$^+$FoxP3$^+$ Treg cells.Likewise, anti-hCD25^{NB} in combination with anti-mPD-1 leads to more significant CD4$^+$CD25$^+$ Treg depletion in spleen and tumors along with increased CD8$^+$Granzyme B$^+$ cytotoxic T cells.Collectively, our CD25 (IL-2RA) humanized mouse provides a powerful model to assess the in vivo preclinical therapeutic effects of CD25$^+$ Treg-depleting antibodies for cancer immunotherapy.

#5093

Chemically inducible splice-neoantigens for cancer immunotherapy

Shingo Matsushima[1], Masahiko Ajiro[1], Kei Iida[2], Kenji Chamoto[1], Tasuku Honjo[1], Masatoshi Hagiwara[1]. *[1]Kyoto Univ. Graduate School of Medicine, Kyoto, Japan,[2]Kindai Univ. Faculty of Science and Engineering, Osaka, Japan*

Although immune checkpoint blockade therapies have dramatically improved the survival rate of patients with cancer compared with other treatment approaches, a substantial number of patients show poor response or resistance to these therapies. Meta-analyses for programmed cell death 1 (PD-1) blockade responses highlight the importance of neoantigens, derived from non-synonymous mutations in cancer cells, for antitumor immune responses. Intriguingly, recent transcriptome and genomics studies predict the presence of putative neoantigens as a result of an irregular pre-mRNA splicing regulation in cancer cells, indicating that alterations in RNA splicing in cancer cells might induce antitumor immune responses. Here, we report that induction of serine/arginine-rich splicing factor (SRSF)-dependent splicing boosts the production of splicing-associated neoantigens (splice-neoantigens) and potentiates the response to PD-1 blockade. Administration of a synthetic SRSF activator RECTAS suppressed tumor growth in a host CD8$^+$ T cell- and tumor major histocompatibility complex class I-dependent manner and promoted the antitumor effect of anti-PD-L1

antibody without detectable autoimmunity. Subsequent transcriptome analysis and validation for immunogenicity identified six splice-neoantigen candidates whose expression was induced by RECTAS treatment. Importantly, vaccination of the identified neoepitopes elicited T cell responses capable of killing cancer cells in vitro, in addition to suppression of tumor growth in vivo upon sensitization with RECTAS. Collectively, these results provide support for the further development of splice variant-inducing treatments for cancer immunotherapy.

Combination Immunotherapies 2

#5098

B7-H3 blockade in combination with natural killer cell activity enhancers including NKTR-255 and venetoclax synergistically induces cytotoxicity in B7-H3+ AML cells

Anudishi Tyagi[1], A. Mario Marcondes[2], Willem Overwijk[2], Venkata Lokesh Battula[3]. *[1]Department of Leukemia, UT MD Anderson Cancer Center, Houston, TX,[2]Nektar Therapeutics, San Francisco, CA,[3]UT MD Anderson Cancer Center, Houston, TX*

Background: Acute myeloid leukemia (AML) is characterized by clonal proliferation of malignant myeloid blasts in the bone marrow. We have recently reported that blocking B7-H3 using a novel monoclonal antibody (mAB), T-1A5 enhances natural killer (NK) cell mediated cytotoxicity against AML cells. IL-15 is an essential component for NK cell activity. Recombinant human IL-15 (rIL-15), however, degrades rapidly and therefore may provide a suboptimal stimulus to NK cells. Studies have shown that BCL2 inhibitor, venetoclax (ABT-199), enhances NK cell induced antibody dependent cellular cytotoxicity (ADCC) against cancer cells. However, the combined effect of B7-H3 blocking and BCL2 inhibition remains unexplored in AML. We hypothesized that blocking B7-H3 using T-1A5 in the presence of novel investigational polymer-engineered IL-15 receptor agonist, NKTR-255, and the BCL2 inhibitor synergistically induces NK cell mediated ADCC in AML cells.
Methods: CD16 and NKG2D activation markers measured by flow cytometry in AML patient and healthy donor derived NK cells. The NKTR-255 was used to generate NK cells, and their cytotoxicity was compared to

that of NK cells generated with rIL-15 using IncuCyte. To investigate these NK cells' cytotoxic activity against AML cells, we treated B7-H3$^+$ AML cell lines (OCI-AML3 and MV4-11) with anti-B7-H3 chimeric mAb ChT-1A5 in the presence and absence of NK cells generated using NKTR-255 or rIL-15. To assess the potential synergy of BCL2 and B7-H3 in NK cell mediated anti-leukemic activity against AML cells, we treated B7-H3$^+$ cells with T-1A5 with or without ABT-199in the presence or absence of NK cells.
Results: The expression of NK cell activation markers were significantly lower in NK cells derived from AML patients than healthy donors. To assess the effect of NKTR-255 on NK cell activity, we generated NK cells using NKTR-255 and compared them with NK cells generated using rIL-15 using the standard 14-day culture protocol. We observed similar proliferation and NK cell numbers between NKTR-255 and rIL-15. However, NK cells stimulated with NKTR-255 showed significantly enhanced (more than 2-fold) cytolytic activity against B7-H3$^+$ AML cell lines compared with NK cells stimulated with rIL-15. Moreover, when combined with ChT-1A5, NKTR-255 significantly enhanced NK cell mediated ADCC activity in B7-H3$^+$ AML cells compared to rIL-15. Interestingly, we observed that the combination of T-1A5 and venetoclax synergistically induced an anti-leukemic effect in B7-H3$^+$ AML cell lines when compared with either drug alone or isotype IgG1 in a dose-dependent manner.
Conclusion: Our data demonstrate that blockade of the immune checkpoint protein, B7-H3 with the IL-15 receptor agonist, NKTR-255, or the BCL2 inhibitor, ABT-199, synergistically induces NK cell mediated cytotoxicity against B7-H3$^+$ AML cells.

#5099

Anti-tumor effect of DA-4505, a novel AhR antagonist as an immunotherapy in the tumor microenvironment

Daewon Cha, Dajeong Kim, Jongho Cho, Chaelim Ryu, Hyeon Uk Jeong, Dae Young Lee, Kyu-Hwan Kim, Sunghwa Kim, Jee-Heun Kim, Taedong Han, Hyounmie Doh. *Dong-A ST, Yongin-si, Korea, Republic of*

Aryl hydrocarbon receptor(AhR) is a ligand-dependent transcription factor that regulates the activity of innate and adaptive immune cells subsequent to

binding of numerous endogenous and exogenous ligands. Recently, kynurenine (Kyn), a tryptophan metabolite, has been identified as the most prominent endogenous ligand of AhR, which is constantly secreted into the tumor microenvironment by cancer cells via IDO1 and TDO2. As this secretion is known to cause a broad immunosuppression, AhR is considered to be a central mediator of suppressing immune responses, thereof, a novel target for cancer immunotherapy. In this study, we have discovered a novel small molecule AhR antagonist, DA-4505, and investigated whether it can pursue the restoration of functionally suppressed immune cells in the tumor microenvironment, then, achieve a consequent anti-tumor effect specifically via altering various aspects of tumor microenvironment. DA-4505, AhR antagonist, exhibited high potency (IC50=3 nM) and showed comparable antagonism to Compound B (an AhR antagonist drug candidate being studied in the clinical phase) in both human and mouse hepatocytes. Furthermore, DA-4505 showed superior alleviating activity on benzo[a]pyrene and 2,3,7,8-tetrachlordibenzodioxin (TCDD, an AhR ligand) induced CYP1A1 mRNA level compared to Compound B in mouse livers. Similarly, DA-4505 treatment presented comparable or even better recovery effect on TNF production under Kyn-induced immunosuppressive condition in monocytes of mouse and human compared to Compound B. DA-4505 dose-dependently enhanced activation of human CD8+ T cells comparable to Compound B and rescued IL-2 and IFNγ production under Kyn treated condition. Moreover, DA-4505 specifically polarized macrophages towards inflammatory macrophage phenotype (M1).Oral administration of DA-4505 induced a significant tumor growth inhibition in several murine syngeneic mouse models and was synergistic in combination with anti-PD1 antibody. DA-4505 enhanced the infiltration of M1-macrophage and CD8+ T cells while suppressed the infiltration of M2-macrophage and Treg, thus, presenting anti-tumor effect. Specifically, we confirmed that the anti-tumor effect of DA-4505 is CD8+ T cell-dependent by CD8+ T cell depleted MC38 mouse model. Taken together, our result showed that DA-4505, AhR antagonist, presented its anti-tumor effects in two distinctive but cooperative way into some extent. Firstly, DA-4505 activated stimulatory immune cells such as monocytes, dendritic cells (DC) and effector T cells. Secondly, DA-4505 reduced the immunosuppressive mechanisms by regulating Treg and M2-macrophage. Thus, our data demonstrate the potential of AhR as a promising therapeutic target for

cancer immunotherapy as well as proposing DA-4505 as a novel therapeutic agent for both mono and aPD-1 combinatory therapeutic scheme.

#5100

Combination of κλ bispecific antibodies targeting innate (CEAxCD47, NILK-2401) and adaptive immunity (CEAxCD3, NILK-2301 and CEAxCD28, NILK-3301) for next generation immunotherapy of CEA-expressing cancers

Anja Seckinger[1], Lise Nouveau[2], Sara Majocchi[2], Valéry Moine[2], Vanessa Buatois[2], Bruno Daubeuf[2], Franck Gueneau[2], Ulla Ravn[2], Krzysztof Masternak[2], Yves Poitevin[2], Emeline Rousset[2], Giovanni Magistrelli[2], Pauline Malinge[2], Limin Shang[2], Nicolas Fischer[2], Klaus Strein[1], Walter Ferlin[2], Dirk Hose[1]. *[1]LamKap Bio Group, Pfäffikon, Switzerland,[2]Light Chain Bioscience - Novimmune SA, Geneva, Switzerland*

Background: The CEAxCD3 bispecific antibody (bsAb) NILK-2301 couples CEA (CEACAM5) on cancer cells and CD3 on T-cells inducing T-cell activation (signal 1) and tumor cell killing (TDCC). T-cell activation can be boosted by CEA-targeted CD28-costimulation (NILK-3301; signal 2). NILK-2401, carrying a fully effective IgG1 Fc, induces antibody-dependent phagocytosis (ADCP) and antibody-dependent cytotoxicity (ADCC) of tumor cells by co-targeting CEA and the innate immune checkpoint CD47 (“don’t eat me” signal). We present here next generation immunotherapy to overcome limited single class activity in CEA-expressing solid cancers.

Methods: BsAbs were generated using LCB’s fully human κλ body platform. TDCC, ADCP, and ADCC with human PBMC or monocyte-derived macrophages were assessed using CEA+ colorectal (n=3), lung (n=2), and gastric (n=2) cancer lines. Combination activity of NILK-2401 + NILK-2301 (± NILK-3301) was assessed by flow cytometry. In vivo activity was tested in xenograft NOG or NSG/human PMBC-, HIS-, and hSIRPα/hCD47/hCD3/hCD28 transgenic mice. Safety data include binding to other CEACAMs, cytokine release in whole blood, erythrophagocytosis, platelet activation, exclusion of superagonism (NILK-3301), as well as PK- and tolerability in cynomolgus monkeys and Tg32-mice.

Results: NILK-2301 induced dose-dependent killing of all tested cell lines, which was also visualized by live cell imaging. Combination of NILK-2301 (1 nM) + NILK-3301 vs. NILK-2301 alone (10 nM) increased TDCC (3-8-fold), T-cell activation (CD25, CD69, HLA-DR), cytokine secretion (interferon-γ, granzyme B, perforin), and CD4+/CD8+ T-cell proliferation. NILK-2401 blocked CD47-SIRPα interaction and induced ADCP/ADCC-mediated elimination of all cell lines. NILK-2301 + NILK-2401 treatment increased maximum activity (Emax) and reduced necessary dose of the T-cell bsAb to reach Emax. E.g., Emax of 30% killing (NILK-2301 alone) was increased in combination with NILK-2401 at 0.1/1/10 µg/mL to 40%, 80%, and 80%. *In vivo,* NILK-2301 (10 mg/kg IV, BIW) decreased tumor progression. NILK-2301/-3301 combination induced tumor regression in 8/8 mice. NILK-2401 delayed tumor growth vs. mean of control in 100% (15/15) of mice and prevented establishment of detectable tumors (>50mm^3) in 53% (8/15). Results of double and quadruple transgenic mice, including triple bsAb combinations, will be presented at the meeting. No relevant safety signals were detected.
Conclusions: NILK-2301 and NILK-2401 are active as single agents. Addition of NILK-2401 or NILK-3301 to NILK-2301 significantly increases activity, already at 10 -100x lower CEAxCD3 doses. GMP drug substance has been produced for NILK-2301 and NILK-2401. Generation of the clonal cell line for NILK-3301 clinical material production is ongoing.

#5101
Inhibition of Notch reverses immunosuppression in basal-like breast cancer
Qiang Shen, Kiichi Murakami, Pamela Ohashi, Michael Reedijk. *UHN Princess Margaret Cancer Centre, Toronto, ON, Canada*

Aberrant Notch activation is a defining feature of basal-like breast cancer (BLBC), which has poor prognosis compared to other breast cancer molecular subtypes. Despite the clinical success of immune checkpoint blockade (ICB) in many malignancies including melanoma and small cell lung cancer, ICB has failed to demonstrate similar response in BLBCs, where most cases are highly infiltrated by tumor-associated macrophages (TAMs). There is increasing evidence that Notch is decisive in regulating

intercellular communication in the tumor immune microenvironment (TIME). This includes the recruitment of TAMs which contribute to an immunosuppressive TIME, illuminating the potential of Notch-inhibition as adjuvant immunotherapy in BLBC. To examine the immune phenotype and therapeutic response of BLBC to combined Notch-inhibition and ICB, we employed an *in vivo* tumorgraft model using murine basal-like mammary tumor 4T1 cells. Briefly, tumor cells were orthotopically injected into the mammary fat pads of BALB/c mice. Using a crossover design, mice were randomly allocated to treatment with either Notch inhibitor (γ-secretase inhibitor, LY411575), anti-PD1 (RMP1-14), or control treatment for 12-days (stage-1), followed by randomization to a second 12-day period (stage 2) with the same, or one of the other treatments. Results: Despite the low response rate of BLBC to ICB alone, Notch inhibition reduced TAMs and induced responsiveness to sequential ICB. This response was characterized by increased cytotoxic T lymphocytes (GrB+, CTL) infiltration of the primary tumor. Similar results were observed when Notch-regulated cytokines (IL-1β and CCL2), crucial to TAM recruitment, were inhibited. Moreover, a more impressive therapeutic effect of sequential treatment was observed in lung metastasis, whereby TAM depletion and increased CTL infiltration were accompanied with near-complete abolition of metastases. Mechanistically, tumor cell Notch signaling upregulates a group of circulating cytokines including IL-1β and CCL2, which prime the lung for metastases. Additionally, compared to primary tumor cells, PD ligand 1 is up-regulated in lung metastases, rendering them profoundly sensitive to sequential ICB treatment. These findings highlight the potential of sequential Notch inhibition and ICB as a novel immunotherapeutic strategy in BLBC.

#5102

Developing CYNK-001-derived exosomes to deliver TGF-β siRNA for GBM immunotherapy enhancement

Marina Gergues, Veronica Farag, Alex Hariri, Qian Ye, Yuechao Zhao, Lin Kang, Robert Hariri, Shawn He. *Celularity Inc., Florham Park, NJ*

Introduction: Glioblastoma Multiforme (GBM) is the most aggressive brain malignancy in adults, where the 5-year survival rate is less than 10%. Celularity Inc. has developed an allogenic, off-the-shelf and cryopreserved

human placental $CD34^+$ derived natural killer (CYNK-001) cell therapy as potential treatment for GBM. NK cell-derived exosomes are notable for their anti-tumor activity. Exosomes have been demonstrated their ability to pass through blood-brain barrier in vivo. We hypothesized that engineering exosomes to deliver TGF-β short interfering RNA (siRNA) would reduce TFG-β expression, thus enhance the anti-tumor activity of CYNK-001 against GBM cells. This study aims to investigate if (i) CYNK-001-derived exosomes (CYNK-Exo) have anti-tumor effects against GBM, (ii) CYNK-Exo loaded with TGF-β siRNA (siCYNK-Exo) can effectively knockdown TGF-β expression in tumor cells, and (iii) siCYNK-Exo and CYNK-001 have a synergistic effect against GBM cells.
Methods: CYNK-Exo were isolated from CYNK-001 conditioned media by one-step sucrose cushion ultracentrifugation and characterized by nano-tracking analysis (NTA) and on-bead flow cytometry. Cytotoxicity of CYNK-Exo against tumor cells was measured by real-time impedance-based xCELLigence assay. To measure uptake of siRNA, Cy3-tagged siRNA was loaded into CYNK-Exo and quantified by flow cytometry. Knockdown of TGF-β was measured by RT-qPCR and ELISA.
Results: CYNK-Exo showed a median size of 117.4 nm by NTA and expressed the exosomal-characteristic CD9 and CD81, as well as NK cell-characteristic CD56, CD226 and CD11a biomarkers. CYNK-Exo displayed cytotoxicity against GBM cell line U251 in a time- and dose- dependent manner. U251 cells treated with siCYNK-Exo showed efficient uptake with 97.7% $Cy3^+$ cells. RT-qPCR results demonstrated 78.6% reduction in TGF-β mRNA expression and ELISA results demonstrated 71.8% reduction in TGF-β secretion. Similar findings were demonstrated on LN-229 GBM cell line. To test if knocking down TGF-β could reduce tumor immunosuppression, U251 cells were treated with siCYNK-Exo followed by CYNK-001. Enhanced cytotoxicity against U251 was demonstrated with combination treatment when compared to that with CYNK-001 alone: 73.9% vs. 36.5% respectively. Compared to CYNK-001 alone, combination siCYNK-Exo and CYNK-001 treatment not only increased the secretion of the proinflammatory cytokines GM-CSF, IFN-γ, and TNF-α by CYNK-001 cells, but also enhanced the production of perforin, granzyme A and granzyme B, which are typically inhibited in NK cells by TGF-β.
Conclusion: Our results demonstrated anti-tumor activity of CYNK-Exo against GBM cells; efficient TGF-β knockdown in GBM cells by siCYNK-

Exo; and synergistic anti-tumor activity of
TGF-β siCYNK-Exo in combination with CYNK-001 against GBM cells. Our data support a potential combination therapy using CYNK-001 and TGF-β siCYNK-Exo for GBM treatment.

#5104

Targeting IL-1B synergizes with PD-1 blockade for enhanced T and B cell immune responses and inhibition of early lung cancer development

Warapen Treekitkarnmongkol[1], Guangchun Han[1], Zahraa Rahal[1], Jiping Feng[1], Ansam Sinjab[1], Tina Cascone[1], Christopher S. Stevenson[2], Cheryl Sweeney[2], Matt Edwards[2], Avrum Spira[2], Junya Fujimoto[1], Seyed Javad Moghaddam[1], Linghua Wang[1], Humam Kadara[1]. *[1]UT MD Anderson Cancer Center, Houston, TX,[2]Lung Cancer Initiative at Johnson and Johnson, Boston, MA*

Early immunotherapy with inhibitors of immune checkpoints such as PD-1 has revolutionized lung adenocarcinoma (LUAD) treatment. Still, many patients do not respond or relapse following PD-1 blockade. Tumor-promoting inflammation, such as that mediated by the pleiotropic cytokine interleukin 1 beta (IL-1B), fosters immunosuppression in the tumor immune microenvironment (TIME). Our group and others showed that IL-1B blockade inhibits lung cancer development. We thus hypothesized that addition of IL-1B blockade to anti-PD-1 treatment may enhance outcomes against LUAD. Using a human-relevant, tobacco-associated, mouse model of LUAD development, we compared the effects of combined PD-1 and IL-1B blockade relative to treatment with single-agents (anti-IL-1B or anti-PD-1) and control antibody on early lung tumor development and the TIME. Drugs (anti-PD-1 + anti-IL-1B, anti-PD-1, anti-IL-1B, control IgG) were administered at end of exposure to the tobacco-specific carcinogen NNK, to evaluate effects on formation of early lesions (preventive), or at 3 months post-NNK (prophylactic) to interrogate LUAD development (8 groups). Comprehensive interrogation of the lung ecosystem and the TIME was performed using deep single-cell RNA-sequencing (scRNA-seq) analysis in a subset of the mice (n = 3 to 4) from each of the 8 groups (n = 31 total; 143,897 cells after stringent quality control). Mice treated with combined PD-1 and IL-1B blockade displayed reduced development of lung tumors when compared to animals treated with anti-IL-1B, anti-PD-1, or control

antibodies. Fractions of cytotoxic *Cd8*+ T cells were conspicuously higher and those of tumor cells and exhausted *Cd8*+ T cells evidently lower in lungs of mice treated with combined PD-1 and IL-1B blockade relative to monotherapy- or control antibody-treated animals. *Igha*+ plasma cells were strikingly highest in lungs of mice treated with combined PD-1 and IL-1B blockade and nearly absent in monotherapy- and control-treated groups. Lungs of mice treated with combined PD-1 and IL-1B blockade showed higher fractions of *Cd80+/Cd86*+ memory B cells and, consistently, T follicular helper T cells, while exhibiting reduced fractions of naïve B and *Cd24a+/Tgfb1*+ B cells suggestive of enhanced activation of B cell responses by the combinatorial treatment. These effects were, overall, present, or much more pronounced, in animals that were prophylactically treated. Flow cytometry analysis of lung tissues and immune profiling of bronchioalveolar lavage fluid overall confirmed augmented immune cell responses by combined PD-1 and IL-1B blockade. Our findings show that blocking IL-1B synergizes with anti-PD-1 in regression of early tumor cells and reversal of immunosuppression. Combined blockade of PD-1 and IL-1B may be a promising strategy for early treatment of lung cancer that warrants further clinical studies.

#5105

TIMP1 mediates astrocyte-dependent local immunosuppression in brain metastasis

Neibla Priego[1], Pedro García-Gómez[1], Ana de Pablos-Aragoneses[1], María Perea-García[1], Laura Álvaro-Espinosa[1], Carolina Hernández-Oliver[1], Elena Martínez-Saez[2], Ángel Pérez-Núñez[3], Aurelio Hernández-Laín[3], Rebeca Sanz-Pamplona[4], Marc Schmitz[5], Stephen J. Crocker[6], Diego Serrano[7], Asís Palazón[8], RENACER Red Nacional de Metástasis Cerebral[1], Manuel Valiente[1]. *[1]Spanish National Cancer Research Ctr. (CNIO), Madrid, Spain,[2]Vall d´Hebron Hospital, Barcelona, Spain,[3]Hospital Universitario 12 de Octubre Research Institute, Madrid, Spain,[4]Aragon Health Research Institute (IISA), Zaragoza, Spain,[5]Faculty of Medicine Carl Gustav Carus, TU Dresden, Dresden, Germany,[6]University of Connecticut School of Medicine, Farmington, CT,[7]Applied Clinical Research (CIMA)-Navarra University, Navarra, Spain,[8]Cooperative Research in Biosciences (CIC BioGUNE) and Ikerbasque Basque Foundation for Science, Bilbao, Spain*

Brain metastasis is an unmet clinical need, affecting between 10-30% of cancer patients with 200000 to 400000 newly diagnosis per annum in the US. Recently, several clinical trials have reported benefits using immunotherapy to treat brain metastasis. However, variability of the responses is broad and high benefit is found mainly in asymptomatic brain metastasis, while the benefit is dramatically reduced in the clinically relevant stage. Thus, it is currently unknown how to effectively target symptomatic brain metastases with immunotherapy. We previously reported a clinically relevant protumoral program driven by STAT3 activation in a subpopulation of reactive astrocytes in these advanced stages of the disease. Our current study further exploited the heterogeneity within the metastasis-associated microenvironment as a resource to identify novel therapeutic vulnerabilities to improve the benefits of immunotherapies based on immune checkpoint blocking antibodies (ICB) in symptomatic brain metastasis.

Our results demonstrate that reactive astrocytes are strong immunomodulatory cells in brain tumors. We have identified the molecular profile of disease-associated glial cells and defined its connection to modulatory activities on specific lymphocyte populations in experimental brain metastasis as well as human-derived samples. scRNASeq and high content multiplex immunofluorescence allowed us to report a novel local immunomodulatory axis dependent on TIMP1 (astrocytes)/CD63 (CD8 T cells), which is present in brain metastasis patients with high immunoscore and would imply an additional immunosuppressive signal for potential ICB responders in brain metastasis.

Genetic and pharmacologic approaches targeting this STAT3-dependent local immunomodulatory axis have allowed us to define the rationale to combine immune checkpoint blockade with a STAT3 inhibitor, which we previously used in patients. We proved that such combined immunotherapy boost the systemic activation of T cells while also preventing the local blockade. Additionally, our comprehensive strategy includes the possibility to stratify patients that are best qualified to benefit from this therapy by measuring TIMP1 in liquid biopsies from CSF. Even more, our data using Patient Derived Organotypic Cultures (PDOC) from fresh brain metastasis neurosurgeries confirms that our therapeutic strategy might benefit brain metastases generated from any primary source.

In conclusion, we describe an immunosuppressive mechanism in the brain microenvironment that could explain the lack of response to ICB in patients with advanced brain metastasis. Our finding provides the rationale to implement complementary approaches targeting local immunosuppression to increase the benefit of immunotherapy in symptomatic brain metastasis.

#5106

The addition of radiation therapy to simultaneous targeting of PD-1 and IL2Rβγ enhances antigen-specific CD8 T cell anti-tumor immunity in pancreatic cancer models

Maureen Hoen[1], Miles Piper[1], Laurel B. Darragh[1], Diemmy Nugyen[1], Jacob Gadwa[1], Maria Amann[2], Greta Durini[2], Michael Knitz[1], Benjamin Van Court[1], Tiffany Pham[1], Ross Kedl[1], Pablo Umana[2], Laura Codarri-Deak[2], Christian Klein[2], Angelo D'Alessandro[1], Sana D. Karam[1].
[1]University of Colorado Anschutz Medical Campus, Aurora, CO,[2]Roche Innovation Center Zurich, Schlieren, Switzerland

Although IL-2 has been shown to critically mediate NK and T cell effector functions, when used in clinical trials this cytokine has failed due to toxicity and severe side effects of the systemic treatment. Our lab has investigated the use of a next-generation IL-2 compound, murine PD1-IL2v, which consists of an anti-PD-1 antibody fused to a IL2-variant with abolished binding to IL2Rα. Previous work shows this molecule results in tumor-antigen specific T cell expansion and differentiation towards immune effectors. Here, we report for the first time that radiation therapy amplifies the anti-tumor effect observed with PD1-IL2v treatment of murine orthotopic models of local tumor growth and metastasis. This anti-tumor effect is correlated with increases in proliferative and polyfunctional CD8 T cells across tumor, lymph node, and blood compartments. Furthermore, using an OVA-antigen specific orthotopic model, we found that radiation in combination with PD1-IL2v treatment enhances infiltration and activation of antigen-specific CD8 T cells, which have been shown to be critical for immunotherapy clinical success. A portion of tumor-bearing mice treated with radiation and PD1-IL2v fully eradicated their primary tumors and tumor rechallenges, which we show correlates with increased markers of memory in CD8 T cells of these mice. To demonstrate the clinical relevance of these preclinical findings, we performed RNA sequencing on paired

pancreatic adenocarcinoma (PDAC) patient tumor tissue samples prior to and following radiation. We observed enhanced IL2Rβ and IL2Rγ expression as well as IL2R signaling in PDAC-patient responders to radiation therapy compared to non-responders. In conclusion, the antigen-specific, lasting memory response to preclinical PDAC models demonstrated here provides rationale for the treatment of PDAC with a radiation and PD1-IL2v combination.

#5107

A novel AhR inhibitor 'DA-4505' improved the anti-cancer efficacy of surgical and chemotherapy via synergistic anti-tumor effects of aPD-1

DongKwon Kim[1], Sujeong Baek[2], Seung Min Yang[2], Yu Jin Han[2], Seong-san Kang[3], Chun-Bong Synn[1], Mi Hyun Kim[2], Heekyung Han[2], Kwangmin Na[2], Young Taek Kim[2], Sungwoo Lee[3], Taedong Han[4], Hyounmie Doh[4], Jongho Cho[4], Dajeong Kim[4], Daewon Cha[4], Jae Hwan Kim[2], Youngseon Byeon[2], Young Seob Kim[2], Mi Ran Yun[5], Ji Yun Lee[6], Jii Bum Lee[6], Chang Gon Kim[6], Min Hee Hong[6], Sun Min Lim[6], Byoung Chul Cho[6], Kyoung-Ho Pyo[5]. *[1]Brain Korea 21 PLUS Project for Medical Science, Yonsei University College of Medicinei University Inst. for Cancer Research, Seoul, Korea, Republic of,[2]Severance Biomedical Science Institute, Yonsei University College of Medicine, Seoul, Korea, Republic of,[3]JEUK Institute for Cancer Research, JEUK Co., Ltd, Gumi, Korea, Republic of,[4]Dong-A ST Research Institute, Yongin, Korea, Republic of,[5]Yonsei New Il Han Institute for Integrative Lung Cancer Research, Yonsei University College of Medicine, Seoul, Korea, Republic of,[6]Division of Medical Oncology, Department of Internal Medicine, Yonsei Cancer Center, Severance Hospital, Yonsei University College of Medicine, Seoul, Korea, Republic of*

Background: The Aryl hydrocarbon receptor (AhR) is one of the most predominant regulators of cancer metabolism. The AhR exerts important immunosuppressive functions by activating Treg cells and myeloid-derived suppressor cells and repressing $CD8^+$ effector T cells. Here, we propose that a best-in-class AhR inhibitor, DA-4505, improves anti-tumor efficacy via modulation of tumor immune surveillance compared to BAY2416964, an AHR antagonist drug candidate being studied in the clinical phase.

Methods: To evaluate anti-tumor effects of DA-4505 and BAY2416964, the two AhR inhibitors were dosed at 10 mg/kg once daily alone or in combination with aPD-1 (10 mg/kg) in surgical and chemotherapy models, and a PDX model (YHIM2004). Tumor volume, relapse, and survival were evaluated, and immune profiles were analyzed with IHC, flow cytometry, and scRNAseq.
Results: A significant tumor reduction appeared in the CT26 and 4T1 tumor models after the DA-4505 treatment compared to vehicle group ($P<0.05$). In contrast, DA-4505 treatment did not induce significant tumor regression compared to vehicle group in tumor-bearing NOG mice, suggesting that anti-tumor effects of DA-4505 were driven by immunologic mechanisms. To evaluate the role of DA-4505 in conjunction with surgery, DA-4505 alone or in combination with anti-PD-1 was given prior to and following resection of the tumors in 4T1 tumor-bearing mice. Survival of mice treated with DA-4505 alone or DA-4505 combined with anti-PD-1 was significantly prolonged after resection compared to aPD-1 treatment group ($P<0.05$). In addition, there were four mice that did not have a relapse by treating DA-4505 with or without aPD-1 after surgery (4/5). A tumor regression also appeared in the YHIM2004-engrafted humanized mouse study. A tumor reduction was shown by treating DA-4505 alone or in combination with pembrolizumab compared to vehicle group ($P<0.05$). Next, we co-administered an AhR inhibitor and aPD-1 as a partner to improve the antitumor effects of chemotherapy. The DA-4505 add-on group showed tumor regression when compared with the combination therapy group treated with aPD-1 and chemotherapy ($P<0.0001$). In addition, a significant increase in survival rate was shown in the group treated with a DA-4505 add-on compared to vehicle group ($P<0.001$). Analysis of scRNAseq showed that M1 macrophage expressing CCL7 and CCL8 were increased in DA-4505 treated group compared to the vehicle and aPD-1 groups. This suggests that immune modulatory effect of DA-4505 may be due to enhanced recruitment of immune cells into the tumor site by macrophages with high chemotactic activity.
Conclusion: The AhR inhibitor DA-4505 demonstrated an improvement in anti-tumor efficacy. In addition, it has shown a synergistic effect when combined with aPD-1. Discoveries from this study provide a preclinical rationale for future clinical implications in solid tumor.

#5108

Overcoming roadblocks of immunotherapy in non-small cell lung cancer

Tanmoy Saha, Shiladitya Sengupta. *Harvard Medical School, Brigham and Women's Hoapital, Cambridge, MA*

Non-small cell lung cancer (NSCLC) is one of the major causes of cancer-related death worldwide. Immunotherapy has helped to increase the survival of NSCLC patients, but the therapeutic response is limited to 23-26% of patients. While many factors impact immunotherapy failure, we have focused on a few, (**a**) heterogeneous expression of immune checkpoints (ICs) limiting the use of single immune checkpoint inhibitor (ICI) for everyone, (**b**) additional ICs responsible for blocking innate immune system and lack of antigen presentation to the T cells, and (**c**) lack of rationally designed combination therapies.Commonly used immunotherapies for NSCLC block PD1-PDL1 interaction, but the majority of the NSCLC patient does not have high PDL1 expression indicating PD1-PDL1 as a subsidiary mode of immune evasion. So, it is necessary to include additional ICIs in order to achieve adequate objective response in all NSCLC patients. In order to investigate the immune checkpoint expression, we screened several NSCLC patient-derived tumor tissues, and only 33% of them showed high expression of PDL1, whereas 64.6% of patients had high CD47 expression. CD47, an innate immune regulator, is overexpressed in lung cancer cells and delivers an "*eat-me-not*" signal by binding to signal regulatory protein alpha (SIRPα) in macrophage resulting in diminishing phagocytosis and antigen presentation to the T cells.Combining anticancer drugs with immunotherapy agents has become a popular approach to achieve a less toxic and long-acting objective therapeutic response. Here, we introduce antibody conjugated drug loaded nanotherapeutics (ADNs) consisting of a targeted therapy drug, phosphatidylinositol 3-kinase (PI3K) inhibitor PI103, and decorated with two ICIs for CD47 and PDL1. The ADN particles have been designed based on classical liposomal supramolecular nanoparticles followed by surface functionalization by the specific antibody. The anti-CD47-PDL1-ADN has shown increased cellular internalization and delivery of PI103 than IgG-ADN and anti-PDL1-ADN. The anti-CD47-PDL1-ADN showed low hematotoxicity and higher cell-killing potency for the cancer cells. The bispecific anti-CD47-PDL1-ADNs can block PD1-PDL1 and SIRPα-CD47 immune checkpoint interaction, activating both the innate (macrophage) and adaptive (T cells) immune responses. Reduced tumor growth and higher survival probability have been observed in the syngeneic LLC tumor model for anti-CD47-PDL1-ADN than monotherapy and traditional immunotherapy.*In summary,* we have introduced a lung cancer treatment

strategy that can be an effective therapy for NSCLC patients, irrespective of the PDL1 expression level. The strategy combining bispecific immunotherapy and targeted therapy for activating the innate and adaptive immune systems and delivering targeted therapy drugs can emerge as a significant advance in the treatment of NSCLC patients.

#5109

The anti-PD1+anti-LAG3 and anti-CTLA4+anti-PD1 combinations have non-overlapping mechanisms of action in melanoma cranial and extra cranial metastases

Manali S. Phadke, Jiannong Li, Jessica Mandula, Ann Chen, Paulo C. Rodriguez, Keiran S. M. Smalley. *Moffitt Cancer Center, Tampa, FL*

Around 40-60% of patients with advanced melanoma develop brain metastases. Recent clinical studies have demonstrated that the efficacy of anti-PD1+anti-LAG3 may be equivalent to anti-PD1+anti-CTLA4. The goal of our project is to understand the mechanisms of action and resistance to anti-PD1+anti-LAG3 in mouse model of melanoma brain metastases. We used orthotopic syngeneic mouse model in which SM1 and B16100kVII2 cells are injected stereotactically into the brain and into the flank. The mice were treated with anti-PD1+anti-LAG3 and anti-PD1+anti-CTLA4 every 5 days. Single cell RNA-seq platform was used to determine the impact of both the combination therapies upon each individual cell type. Flow cytometry experiments were carried out to assess the percentage of immune cells recruitment. The *in vivo* studies demonstrated that the anti-PD1+anti-CTLA4 had similar efficacy to anti-PD1+anti-LAG3 at both cranial and extracranial sites over a period of 80 days in the SM1 model. In the less responsive B16100kVII2 model, anti-PD1+anti-LAG3 was initially less effective, but similar numbers of mice failed both each combination. scRNA-seq and IHC analysis of responding tumors showed that the anti-PD1+anti-LAG3 led to a greater accumulation of B cells, DCs, CD4+ T cells and different subsets of CD8+ T cells. Of note, the anti-PD1+anti-CTLA4 was associated with infiltration of Tregs, whereas the anti-PD1+anti-LAG3 was associated with CD4+ Th1 helper cells. Depletion of CD4+ T cells decreased responses to anti-PD1+anti-LAG3 in both the cranial and extracranial tumors, with no change in the magnitude of response to the anti-PD1+ anti-CTLA4. By contrast, depletion of CD8+ T

cells suppressed responses to both combinations. Depletion of CD4+ T cells decreased activated CD8+ T cells by 30% in anti-PD1+anti-LAG3 treated tumors and conversely increased numbers of activated CD8+ T cells by 40 % in anti-PD1+anti-CTLA4 tumors. In anti-PD1+ anti-LAG3 treated tumors, T helper function was directed towards CD8+ T cells and not B cells, with B cell depletion impacting responses to both combination immunotherapies in a similar manner. Analysis of relapsing brain tumors from both anti-PD1+anti-LAG3 treated mice showed an increased association of MDSCs and loss of tumor reactive CD8+ T cells. The anti-PD1+anti-LAG3+anti-CTLA4 triplet had a good efficacy and suppressed the growth of both flank and brain tumors over a period of 35 days, an effect associated with increased CD8+ T cell infiltration and reduced numbers of MDSCs and Tregs.We show that anti-PD1+anti-LAG3 can drive CD4+ Th1 T helper cell responses hence increasing the accumulation of effector CD8+ T cells and B cells in melanoma and melanoma brain metastases, improving the durability of response. The triplet combination maximizes the efficacy and duration of response in treatment of melanoma brain metastases.

#5110

Locally administered Interleukin-15 combined with cancer cell-targeted near-infrared photoimmunotherapy in a syngeneic mouse cancer model

Hiroshi Fukushima, Aki Furusawa, Takuya Kato, Seiichiro Takao, Shuhei Okuyama, Peter L. Choyke, Hisataka Kobayashi. *Molecular Imaging Branch, Center for Cancer Research, National Cancer Institute, National Institutes of Health (NIH), Bethesda, MD*

Near-infrared photoimmunotherapy (NIR-PIT) is a new anti-cancer treatment by NIR light-induced photochemical reactions within antibody-IRdye700DX conjugates, leading to significant immunogenic cell death. The efficacy of NIR-PIT is synergistically enhanced by combining immune activating agents including immune checkpoint inhibitors and cytokines. However, there are still needs for improving the efficacy of NIR-PIT. A recent study showed that cytokines could exert strong anti-cancer effects when administered locally. Interleukin-15 (IL-15) elicits immune responses that include the generation and persistence of cytotoxic T cells and natural

killer (NK) cells. Based on these findings, we hypothesized that local IL-15 administration combined with cancer cell-targeted NIR-PIT could be a highly effective therapy. The efficacy of IL-15 was evaluated by intratumorally or intraperitoneally injecting 5 μg of human IL-15 in C57BL/6 mice inoculated s.c. with murine colon cancer MC38 cells. Human IL-15-secreting MC38 (hIL-15-MC38) was constructed by introducing human IL-15-coding plasmids into MC38 cells and the efficacy of CD44-targeted NIR-PIT was compared in vitro and in vivo. The efficacy of intratumoral IL-15 injection combined with CD44-targeted NIR-PIT was also evaluated in MC38 tumor models. Moreover, bilateral tumor models were used to analyze whether local IL-15 administration combined with CD44-targeted NIT-PIT could induce abscopal effects in untreated tumors. Intratumoral IL-15 injection significantly suppressed tumor growth and induced immune activities compared with intraperitoneal injection. Both hIL-15-MC38 and parental MC38 cells had high CD44 expression on their cell surface and in vitro NIR-PIT induced rapid cell death in both two cell lines. When hIL-15-MC38 or MC38 tumor-bearing mice were treated with or without NIR-PIT, hIL-15-MC38 tumor-bearing mice treated with NIR-PIT showed the best tumor growth inhibition and survival. The hIL-15-MC38 tumors treated with NIR-PIT showed significant increases in the cell number/g tumor of CD8+ T cells, NK cells, and natural killer T cells, and significantly higher Granzyme B expression in these cells compared with the control MC38 tumors. Similar results were observed in vivo by intratumoral IL-15 injection combined with NIR-PIT. Moreover, in bilateral tumor models with right hIL-15-MC38 and left MC38 tumors, NIR-PIT against right hIL-15-MC38 tumors significantly suppressed the growth of left untreated MC38 tumors. In conclusion, local IL-15 administration combined with CD44-targeted NIR-PIT promoted anti-cancer immune responses, resulting in the inhibition of growth of treated tumors, longer survival of mice, and abscopal effects in untreated tumors. Thus, locally administered IL-15 is a promising anti-cancer therapy in combination with cancer cell-targeted NIR-PIT.

#5111

VentX-modulated tumor associated macrophages revert immune suppression in tumor microenvironment and promote efficacy of gemcitabine against pancreatic cancer

Joanna Le[1], Hong Gao[2], Yi Le[3], William Richards[4], Scott Radig[5], Ronald Bleday[4], Thomas Clancy[4], Zhenglun Zhu[3]. *[1]Obstetrics and Gynecology, University of Massachusetts Medical Center, Worcester, MA,[2]Medicine, Tufts Medical Center, Boston, MA,[3]Medicine, Brigham and Women's Hospital, Boston, MA,[4]Surgery, Brigham and Women's Hospital, Boston, MA,[5]Pathology, Brigham and Women's Hospital, Boston, MA*

Pancreatic ductal adenocarcinoma (PDA) is a lethal malignancy with median survival of less than one year and overall 5-year survival less than 5%. Gemcitabine has been the cornerstone in PDA treatment, yet its efficacy remains limited. Over the past decades, extensive investigations suggested a role of tumor microenvironment (TME) in rendering PDA resistance to gemcitabine, however, its underlying mechanism remained largely unknown. Cellular profiling has revealed the macrophages as a major immune cell component of PDA-TME. Our recent study showed that the expression of the homeobox protein VentX, a master regulator of macrophage plasticity, is significantly down-regulated in tumor associated macrophages (TAMs) of PDA. We demonstrated that restoration of VentX expression in PDA-TAMs polarizes the TAMs from a pro-tumor M2-like phenotype to an anti-tumor M1-like phenotype. We showed further that VentX-regulated-TAMs (VentX-TAMs) revert immune suppression of PDA-TME by inhibiting CD4 Treg differentiation and by promoting CD8 proliferation and activation. Using a newly developed tumor immune microenvironment-enabling model system (TIME-EMS), we showed that VentX-TAMs drastically promote efficacy of gemcitabine against PDA for about 4-fold but not cytotoxicity on normal pancreatic tissue. As such, our data suggested a function of VentX-TAMs to promote chemosensitivity of gemcitabine and to improve PDA prognosis.

#5112

Immune biomarkers of clinical response after NSAID treatment in combination with vaccination targeting EGFR-COX2-CDC25B in the APC(Min/+) mouse model

Denise L. Cecil, Ying Liu, Lauren Corulli, Mary L. Disis. *University of Washington, Seattle, WA*

Studies from our group have shown that administration of NSAIDs in mouse models of Familial Adenomatous Polyposis (FAP) results in a decrease in the development in small intestinal polyps with a significant increase in CD8 tumor infiltrating lymphocytes (TIL) and downregulation of PD-L1 on tumors. Furthermore, we have demonstrated that NSAIDs could be used in combination with vaccination to even further reduce the development of intestinal polyps. We questioned what tissue specific biomarkers could define the efficacy of response with the combination treatment. APC(Min/+) male and female mice (4-6 weeks old) were immunized with a multi-antigen (EGFR, COX2, CDC25B) peptide vaccine with CFA/IFA as an adjuvant. Control mice received immune adjuvant alone. Regular chow or chow containing 400 ppm naproxen was provided intermittently (3 weeks on, 3 weeks off for 3 cycles) or continuously (18 weeks on) at the initiation of the vaccine regimen. Animals were euthanized at 22 weeks and tumors quantified. TIL were evaluated by flow cytometry. Since intermittent naproxen treatment was just as effective at inhibiting tumor development as continuous naproxen treatment, with or without vaccine, we did not differentiate between NSAID regimens. We observed an increase in CD8+ (83%; $p<0.0001$), Tbet+CD4+ (94%; $p<0.001$), effector memory (EM) CD4+ (76%; $p<0.0001$) and EM CD8+ (94%; $p<0.0001$) TIL in the tumors that did develop in the mice treated with the combination NSAID and vaccination as compared to control. There was increased CD8+ (Pearson correlation coefficient: −0.506, $p<0001$), Tbet+CD4+ (Pearson correlation coefficient: -0.6222, $p<0.001$), EM CD4+ (Pearson correlation coefficient: 0.-6074, $p<0.001$) and EM CD8+ (Pearson correlation coefficient: -0.7155, $p<0.001$) in mice with greater tumor inhibition than those with less protection. Receiver operator curves revealed that CD8+ (AUC: 0.7623; $p=0.002$), Tbet+CD4+ (AUC 0.7273; $p=0.008$), EM CD4+ (AUC 0.6782; $p=0.04$) and EM CD8 (AUC 0.7897; $p<0.001$) TIL can differentiate mice receiving the combination of NSAID and vaccination as compared to either monotherapy alone. These data define potential biomarkers of response that can guide human clinical trials of NSAIDs +/- vaccination in patients with FAP.

#5113

INTASYL self-delivering RNAi therapeutic dual targeting PD-1 and CTLA-4 provides synergistic antitumor efficacy in the treatment of

murine colon cancer *in vivo*

Benjamin G. Cuiffo, Andrew Boone, Dingxue Yan, Melissa Maxwell, Brianna Rivest, James Cardia, Simon P. Fricker. *Phio Pharmaceuticals, Marlborough, MA*

Combination immune checkpoint inhibition (ICI) with antibodies targeting PD-1 and CTLA-4 provides superior outcomes compared to either monotherapy alone. This combination has been approved for advanced melanoma, metastatic colon cancer and others. However, combination therapy with anti-PD-1/CTLA-4 antibodies results in serious immune related adverse events (irAEs), presenting an obstacle for effective treatment with combination systemic anti-PD-1/CTLA-4. Intratumoral (IT) immunotherapy is a strategy to enhance local activity while decreasing systemic irAEs. While clinical testing of IT antibodies is underway, antibodies' high molecular weight may limit their local diffusion and retention time within tumors. RNAi is an emerging therapeutic modality well-suited for local clinical application of ICI. We have demonstrated that self-delivering RNAi therapeutics built on proprietary INTASYL™ technology specifically silence their targets in tissues without need for specialized formulations or delivery systems, and convey robust antitumor efficacy in vivo. Furthermore, multiple INTASYL compounds can be easily co-formulated into a multi-targeting therapeutic, providing specific silencing of multiple therapeutic targets in a single injection. Here, we present proof-of-concept (POC) in vivo data demonstrating synergistic efficacy of a novel INTASYL dual-targeting murine PD-1 (mPH-762) and CTLA-4 (27790) coformulation in PBS in a syngeneic CT26 model of murine colon cancer. Dual on-target silencing was first validated in murine T cells in vitro. In vivo, CT26 cells were implanted subcutaneously into female BALB/c mice. Vehicle (PBS) or INTASYL IT treatment commenced when tumors reached a mean threshold volume (150 mm^3; Day 1) with doses given on Days 1, 4, 7, 10, and 13. Mice received a total 1 mg/dose with the dual-targeting INTASYL, comprised of 0.5 mg of each compound. Another group received the dual-targeting INTASYL at 2 mg/dose. Tumor volumes and body weights were recorded longitudinally and analyzed by area under the curve (AUC). Tumors were isolated on Day 15 and mechanistic immunomodulation of the tumor microenvironment (TME) was assessed by flow cytometry. IT INTASYL dual-targeting PD-1

and CTLA-4 elicited robust dose-associated antitumor efficacy that was superior to the identical total dose of either single-targeting INTASYL, when comparing mean tumor volume AUC, demonstrating antitumor synergy by the dual-targeting coformulation. On-target mechanistic immunomodulatory effects were observed in the TME. These data demonstrate POC synergistic efficacy of IT INTASYL dual-targeting CTLA-4/PD-1 in vivo, supporting further development to maximize efficacy and minimize irAEs. PH-762 is currently under clinical investigation in a Phase 1b study for advanced melanoma.

#5114

Development of personalized RNA-based immunotherapeutics for glioblastom

Vrunda Trivedi, Changlin Yang, Oleg Yegorov, Kelena Klippel, Graeme Fenton, Christina von Roemeling, Lan Hoang-Minh, Elizabeth Ogando-Rivas, Paul Castillo, Kyle Dyson, Ginger Moore, Duane Mitchell.
Neurological Surgery, University of Florida, Gainesville, FL

Background: The development of successful immunotherapy targeting antigens in glioblastoma multiforme (GBM) remains a challenge owing to antigen heterogeneity and the low mutation burden in GBM. Cancer immunogenomics represents a complementary approach to the application of genomics in developing novel immunotherapies for GBM. Our goal is to develop a personalized RNA-based therapeutic vaccine that simultaneously targets a selected pool of tumor rejection antigens including all neoantigens and tumor-associated antigens (TAAs) as identified using cancer immunogenomics. We evaluated the treatment efficacy of these RNA therapeutics in combination with adoptive cellular therapy and checkpoint inhibitors.
Methods: We identified immunogenic neoantigens and TAAs that are aberrantly overexpressed in KR158-luc and GL261 murine GBM tumors using our cancer immunogenomics pipeline called the Open Reading Frame Antigen Network (O.R.A.N.). A tumor antigen-specific RNA library was created for each tumor using a novel gene enrichment strategy and validated by RNAseq. Tumor-bearing animals were treated with adoptively transferred ex vivo expanded lymphocytes and dendritic cells loaded with the tumor antigen-specific RNA as vaccines. Additionally, we treated

animals with the tumor antigen-specific RNA vaccines in combination with anti-PD-1 checkpoint-blockade therapy. Tumor progression and survival outcomes were analyzed to evaluate the treatment efficacies. We determined the peripheral and tumor-infiltrating lymphocyte responses using flow cytometry, TCR sequencing, and single cell RNAseq.
Results: The tumor antigen-specific RNA vaccines were significantly effective in slowing the progression of murine GBM tumors in combination with both the adoptive cellular therapy and the checkpoint blockade therapy and improved the outcome of these therapies as compared to monotherapy alone. Additionally, we identified antigen-specific T cells targeting several of our predicted antigens and an increase in tumor-infiltrating lymphocytes and memory T cells in the treated animals.
Conclusion: Here, we developed an RNA-based immunotherapy that simultaneously targets numerous tumor-specific antigens and demonstrated its therapeutic efficacy in preclinical models of GBM.

#5115

Novel humanized anti-GD2 antibody inhibits GD2-mediated immunosuppression by targeting GD2+ breast cancer stem-like cells

Vivek Anand[1], Venkatesh Hegde[1], Maryam Siddiqui[1], Anudishi Tyagi[1], Bolutyfe Oderinde[1], Mario Marcondes[2], Willem Overwijk[2], Venkata Lokesh Battula[3]. *[1]Department of Leukemia, UT MD Anderson Cancer Center, Houston, TX,[2]Nektar Therapeutics, San Francisco, CA,[3]UT MD Anderson Cancer Center, Houston, TX*

Background: Breast cancer stem-like cells (BCSCs) are reported to be a major contributing factor for tumor growth and chemotherapy resistance in triple-negative breast cancer (TNBC). We reported that the disialoganglioside GD2 is highly expressed on BCSCs and that targeting GD2 with dinutuximab (chimeric anti-GD2 antibody) in combination with NK cells synergistically reduced tumor volumes in TNBC animal models. Here, we hypothesize that naxitamab targets $GD2^+$ BCSCs and inhibits breast cancer (BC) growth by enhancing macrophage mediated phagocytosis and T cell mediated cytotoxicity. In addition, we explore whether addition of an investigational polymer-engineered IL-15 receptor-agonist, NKTR-255 treated NK cells, can further enhance this anti-GD2 mediated anti-cancer activity.

Methods: Naxitamab is a US FDA approved fully humanized anti-GD2 (hu3F8) monoclonal antibody for the treatment of pediatric neuroblastoma. We evaluated the effects of naxitamab treatment on macrophage mediated phagocytosis of BC cells using the live cell imaging system, IncuCyte®. Next, we compared the effects of NKTR-255 treated NK cells with recombinant human IL-15 (rIL-15) treated NK cells in naxitamab induced ADCC in $GD2^+$ BC cells. We also performed immunohistochemistry (IHC) to examine GD2 expression and correlate it with T cell infiltration in primary TNBC patient samples with high and low GD2 levels. The effect of naxitamab treatment on T cell mediated cytotoxicity in BC cells was also observed.
Results: When compared to control, naxitamab treatment promoted macrophage mediated phagocytosis of Hs578T and HCC1395 cells in a dose dependent manner *($p < 0.001$)*. Additionally, when co-cultured with healthy donor derived macrophages, we found a significant reduction in Hs578T spheroids treated with naxitamab in comparison to IgG control *($p<0.001$)*. Furthermore, we observed a significantly higher rate of apoptosis in $GD2^+$ Hs578T and HCC1395 breast cancer cells treated with naxitamab and NK cells generated using NKTR-255, compared to rIL-15 treated NK cells (*$p<0.0001$*). Interestingly, IHC analysis showed that TNBC patients with high GD2 expression have significantly lower $CD3^+$ T cell infiltration than patients with low GD2 expression *($p<0.05$)*. We also observed increased T cell mediated killing of BT549 and T47D cells treated with naxitamab in comparison to IgG control *($p<0.001$)*.
Conclusion: TNBC with high GD2 expression inhibits immune cell infiltration and naxitamab can inhibit BCSC growth by targeting GD2. Combination of naxitamab with macrophages induced macrophage mediated phagocytosis TNBC cells. NK cells were more stable and cytotoxic when generated with NKTR-255 vs. native IL-15, and naxitamab further enhanced NK cell mediated ADCC of $GD2^+$ BCSCs. The increased T cell mediated killing of breast cancer cells treated with naxitamab further supports the immunomodulatory role of GD2.

#5116

Inflammasome unleashing during anti-PD-1 therapy modulates $CD8^+$ T cell exhaustion through Th17 cells

Sofia Russo, Mateo Malcuori, David Charbonnier, Mercedes Segovia, Marcelo Hill. *Institut Pasteur De Montevideo, Montevideo, Uruguay*

PD-1/PD-L1 blockade has greatly improved overall and progression free survival in a variety of cancers. However, only a minority of patients with advanced disease benefit from this approach. We have recently showed that inflammasome unleashing by inhibition of the intracellular cation channel TMEM176B with Boritinib (BayK8644) augments anti-PD-1 efficacy. However, the mechanisms involved were not completely understood. We hypothesized that inflammasome activation triggered by Boritinib may recruit Th17 cells to modulate $CD8^+$ T cell exhaustion. To test this hypothesis, we have analyzed Th17 cells and subsets of exhausted $CD8^+$ T cells in the tumor microenvironment of WT mice treated with anti-PD1 ± Boritinib. Combining Boritinib with anti-PD-1 led to an increased frequency of Th17 cells in the tumor microenvironment compared to anti-PD-1 alone. Furthermore, CD73 expression was down-regulated whereas IFN-γ was up-regulated in Th17 cells in the tumor microenvironment of Boritinib + anti-PD-1 treated mice, suggesting an effector phenotype of these cells. In addition, combination of anti-PD-1 with Boritinib results in an increased frequency of progenitor exhausted $CD8^+$ T cells ($CD44^+PD\text{-}1^+TCF1^+TOX^+$) and transitory exhausted $CD8^+$ T cells ($CD44^+PD\text{-}1^+TCF1^-TOX^-CX3CR1^+$) in the tumor microenvironment compared to anti-PD-1 alone. Similar results were obtained using *Tmem176b*$^{-/-}$ mice treated with anti-PD-1, suggesting an on-target effect of Boritinib. To assess a potential role of Th17 cells in the anti-tumor immunity triggered by Boritinib + anti-PD-1, we treated WT and *Il17a*$^{-/-}$ mice. We found that *Il17* is necessary for the anti-tumor effect of Boritinib + anti-PD-1, since *Il17a*$^{-/-}$ mice showed a reduced overall survival compared to WT mice. Under this combined therapy, IL-17 may impact on exhausted $CD8^+$ T cells subsets since we found that transitory and terminally exhausted $CD8^+$ T cells in the tumor microenvironment of *Il17a*$^{-/-}$ mice had less granzyme B than in WT mice. To directly show the role of Th17 cells in the anti-PD-1 anti-tumor immunity we adoptively transferred *in vitro* differentiated effector Th17 cells. Adoptive transfer of effector Th17 cells into tumor-bearing mice treated with anti-PD-1 resulted in better survival than mice treated with anti-PD-1 alone. To characterize the downstream mechanisms, we

performed an *in vivo* cytotoxicity assay. We found that mice adoptively transferred with effector Th17 cells exhibited greater cytotoxicity by $CD8^+$ T cells than mice treated with anti-PD-1 alone. Furthermore, this could be explained by an increased frequency in progenitor exhausted $CD8^+$ T cells. Thus, effector Th17 cells potentiate $CD8^+$ T cells on anti-PD-1 treatment. In conclusion, combination of anti-PD-1 with Boritinib augments the efficacy of the former by unleashing the inflammasome which results in an increased frequency of Th17 cells leading to modulation of exhausted $CD8^+$ T cells.

#5117

Combined treatment with the epigenetic drug CM272 and an anti-BCL-XL proapoptotic drug sensitizes solid tumors to immune checkpoint blockade

Yaiza Senent[1], Vicente Fresquet[1], Victoria Jimenez[1], Karmele Valencia[1], Ana Remirez[1], Francisco Exposito[2], Marisol Gonzalez-Huarriz[1], Borja Ruiz-Fernandez de Cordoba[1], Haritz Moreno[1], Daniel Ajona[1], Marta M Alonso[1], Fernando Lecanda[1], Antonio Pineda-Lucena[1], Felipe Prosper[1], Alfonso Calvo[1], Jose Angel Martinez-Climent[1], Ruben Pio[1]. *[1]Center for Applied Medical Research (CIMA)-University of Navarra, Pamplona, Spain,[2]Yale School of Medicine, Yale Cancer Center, New Haven, CT*

Epigenetic modulators in combination with proapoptotic drugs have become a standard of treatment for acute myeloid leukemia. However, the clinical efficacy of these combinations in solid tumors has shown to be negligible. Our group has demonstrated that the epigenetic drug CM272, which targets DNMT and G9a, induces synergistic responses in combination with proapoptotic drugs in hematological malignancies (Cancer Discovery 2021). We have also reported that CM272 induces an immunogenic cell death that sensitizes tumor cells to immune checkpoint blockade (ICB) (Nature Medicine 2020). Here, we hypothesized that CM272 in combination with proapoptotic drugs may sensitize tumor cells to ICB, resulting in profound anti-tumor responses. To test this hypothesis, we evaluated *in vitro* the sensitivity of cancer cells to different combinations of epigenetic and proapoptotic drugs. The most efficient combination was tested in various immunocompetent mouse models,

followed by an immunophenotypic characterization of the tumor microenvironment. We found that CM272 in combination with inhibitors of BCL-XL, BCL2 or MCL1, yielded synergistic *in vitro* responses in a large collection of human and mouse cell lines derived from solid tumors. Mechanistically, the treatments induced the expression of endogenous retroelements/retroviruses, which led to the activation of RIG-1 and MDA5 viral sensors, ATP hydrolysis and tumor cell death. Remarkably, we found that CM272 in combination with BCL-XL inhibition had more potent anti-tumor effects than that found with BCL2 or MCL1 inhibitors. *In vivo*, the triple combination CM272, A1331852 (BCL-XL inhibitor) and an anti-PD-1 moAb significantly reduced tumor growth and increased overall survival in three subcutaneous lung cancer models (LLC, 393P, Lacun-3) in comparison to double treatments. Moreover, this triple combination also induced significant anti-tumor responses in subcutaneous mouse models of colon cancer (MC38) and melanoma (B16), as well as in orthotopic models of lung cancer (LLC), glioblastoma (CT-2A) and breast cancer (ANV5), leading to prolonged survival and cure in a fraction of animals. The triple therapy was associated with a significant increase in the ratio of CD8 T versus immunosuppressive Treg cells, and M1 versus M2 macrophages. In conclusion, we report a novel regimen combining a dual epigenetic inhibitor, an anti-BCL-XL, and an anti-PD-1 moAb that results in potent responses in multiple pre-clinical models of solid tumors. The mechanisms underneath the antitumor responses include the modulation of the energy metabolism in tumor cells, leading to cell death boosted by an anti-BCL-XL pro-apoptotic drug, along with fostering the immune system to generate an efficient anti-tumor response assisted by ICB. This study reveals the potential of epigenetic therapeutics to treat and cure patients with solid tumors.

#5118

STING agonist and TLR7/8 agonist overcome anti-PD-1 resistance mediated by loss of β2M

Li Hua, Chenpan Nie, Jie Lin, Annie Xiaoyu An, Ludovic Bourre, Jingjing Wang. *Crown Bioscience, Inc., San Diego, CA*

Introduction: PD-1 blockade has achieved great success in the clinic. However, only a small subset of patients benefits from the treatment and

most responders develop acquired resistance thereafter. One of the resistance mechanisms is beta-2-microglobulin (β2M) mutation mediated dysfunction of MHC-I antigen presentation, which contributes to attenuation of cellular cytotoxicity triggered by adaptive $CD8^+$ T cells. Activating innate immunity, such as natural killer (NK) cells, can be used as a strategy to circumvent the attenuation. Immune-stimulating agents like Stimulator of interferon genes (STING) agonists and Toll-like receptor (TLR) 7/8 agonists can elicit NK cell-mediated tumor rejection in preclinical tumor models, independent of $CD8^+$ T cells. Thus, to evaluate novel therapeutic strategies overcoming anti-PD-1 resistance, we established a MC38-OVA-β2M KO tumor model.
Methods: We knocked out β2M genes in a murine MC38-OVA colorectal cancer cell line using CRISPR/Cas9 to generate MC38-OVA-β2M KO cells. β2M knockout was verified by western blot and flow cytometry. For *in vitro* testing, both MC38-OVA and MC38-OVA-β2M KO cells were treated with IFN-α, IFN-β and IFN-γ for 24h, and then MHC-I and OVA peptide SIINFEKL expression were analyzed by flow cytometry. For *in vivo* testing, 1×10^6 MC38-OVA cells and MC38-OVA-β2M KO cells were subcutaneously injected into C57BL/6 mice and the models were treated with anti-PD-1. Finally, the MC38-OVA-β2M KO tumor model was treated with anti-PD-1, cyclic nucleotides (CDN), R-848 and anti-PD-1 combined with either CDN or R-848. At the endpoint, the composition of immune cells in spleens were analyzed by flow cytometry.
Results: Following confirmation of β2M knockout, MHC-I expression and MHC-I-OVA peptide presentation were also diminished on MC38-OVA-β2M KO cells, even after treatment of IFN- α, IFN-β, or IFN-γ. *In vivo*, anti-tumor efficacy of PD-1 blockade was significantly diminished in MC38-OVA-β2M KO model (TGI=31%, $p<0.001$), compared to MC38-OVA model (TGI=91%). To overcome the resistance, CDN, a STING agonist or R-848, a TLR7/8 agonist was administered alone or combined with anti-PD-1 in the MC38-OVA-β2M KO model. Single treatment of either CDN (TGI=73%) or R-848 (TGI=89%) markedly impeded tumor growth, and combination with anti-PD1 greatly enhanced their anti-tumor effects (TGI of 98% and 99%, respectively). Additionally, flow cytometry analysis showed a decrease of Myeloid-derived suppressor cells (MDSCs) and an increase of NK cells in spleens of the mice treated with CDN and

anti-PD-1. In parallel, a decrease of MDSCs was also observed in the mice with combined treatment of R-848 and anti-PD-1.
Conclusion: The successfully established MC38-OVA-β2M KO model is a useful tool for investigating therapeutic strategies to overcome MHC-I down-regulation mediated immunotherapy resistance. Moreover, STING agonists and TLR7/8 agonists may be potential candidates.

#5119

Nano-immunotherapy targeting PD-L1, PLK1, and TLR9 for treatment of non-small cell lung cancer

Moataz Reda[1], Worapol Ngamcherdtrakul[1], Ruijie Wang[2], Noah Crumrine[1], Cole Baker[1], Alyssa Wallstrum[1], Jeremy Saito[1], Natalie White[1], Wassana Yantasee[2]. *[1]Pdx Pharmaceuticals, Inc., Portland, OR,[2]Oregon Health & Science University, Portland, OR*

Given the complexity of cancer, it is becoming apparent that combination therapy - in which complementary biological pathways are simultaneously targeted - is required to achieve clinically meaningful responses. To that end, PDX Pharma, in collaboration with Oregon Health & Science University, has developed a proprietary nanoparticle platform (Pdx-NP™) that can effectively co-deliver a plethora of therapeutic modalities while maintaining a small size in saline (100 nm), suitable for infusion and tumor accumulation. This enables the targeting of complementary cancer and immune pathways, leading to synergistic clinical benefits. Herein, we report on the second generation ARAC-02 (Antigen Release Agent and Checkpoint Inhibitor) which is designed to improve the efficacy of immune checkpoint inhibitors (ICIs) in non-small cell lung cancer (NSCLC). While ICIs have improved survival in a subset of patients with advanced NSCLC, only a minority of patients respond to ICIs, highlighting the need for combination immunotherapy. ARAC-02 co-delivers a polo-like kinase 1 (PLK1)-targeted therapy (volasertib), a PD-L1 antibody, and the immune-stimulant CpG. These three agents were carefully selected based on their roles in cancer and immune pathways. Volasertib 1) selectively kills cancer cells, 2) modulates the immune-suppressive tumor microenvironment, and 3) upregulates PD-L1 expression in cancer cells, providing opportunity for targeted delivery with PD-L1 antibody on the nanoparticles. CpG is a TLR9 agonist that enhances antigen presentation to generate tumor-specific T

cells. PD-L1 antibodies serve as tumor targeting agent for nanoparticle delivery as well as an ICI (i.e., PD-L1 degradation upon internalization with the nanoparticles), releasing the brakes and allowing T cells to attack the cancer. We found that the optimized ARAC-02 is preferentially internalized in PD-L1 expressing NSCLC cells, demonstrating a 10-fold greater uptake to PD-L1(high) NSCLC cells than PD-L1(low) normal cells. ARAC-02 effectively kills NSCLC cells regardless of their mutational status, while sparing normal cells. In a metastatic lung tumor model, ARAC-02 treatments reduced the tumor burden by 30-fold vs. saline control and 8-fold vs. the first generation ARAC (not containing CpG), whose effect was mainly mediated by CD8+ T cells. ARAC-02 was found to be safe to mice as assessed by body weight, serum biomarkers, and histology. Importantly, intravenous infusions of the platform was also found to be safe in a preliminary toxicology study in non-human primates. Due to its unique ability to catalyze various steps of the adaptive immune response, ARAC-02 is anticipated to provide superior outcomes in NSCLC and a broad range of tumor types regardless of baseline PD-L1 expression.

#5120

NPRL2 gene therapy induces effective antitumor immunity in KRAS/STK11 mutant anti-PD1 resistant metastatic human NSCLC in a humanized mouse model

Ismail M. Meraz[1], Mourad Majidi[1], Renduo Song[1], Feng Meng[1], Gao Lihui[1], Qi Wang[2], Jing Wang[2], Elizabeth Shpall[3], Jack A. Roth[1]. *[1]Thoracic and Cardiovascular Surgery, UT MD Anderson Cancer Center, Houston, TX,[2]Bioinformatics and Computational Biology, UT MD Anderson Cancer Center, Houston, TX,[3]Stem Cell Transplantation, UT MD Anderson Cancer Center, Houston, TX*

NPRL2/TUSC4 is a potent tumor suppressor gene whose expression is reduced in many cancers including NSCLC. Restoration of NPRL2 expression in cancer cells induces DNA damages which leads to cell cycle arrest and apoptosis. We investigated the antitumor immune responses to NPRL2 gene therapy on anti-PD1 resistant KRAS/STK11 mutant NSCLC in a humanized mouse model. H1299 cells transfected with NPRL2 showed significant inhibition of colony formation after NPRL2 transfection. Humanized mice were generated by transplanting fresh human cord blood

derived CD34 stem cells into sub-lethally irradiated NSG mice. The level of engraftment of human CD45, CD3 T, CD19 B, NK cells was verified before tumor implantation. Mice harboring > 25% human CD45 cells were considered humanized. KRAS/STK11 mutant anti-PD1 resistant A549 NSCLC cells were injected intravenously into humanized NSG mice and developed lung metastasis. Metastases were treated with intravenous injection of NPRL2 gene loaded cationic lipid nanoparticles with or without pembrolizumab (anti-PD1). A dramatic antitumor effect was mediated by NPRL2 treatment, whereas pembrolizumab was ineffective. A significant antitumor effect was also found in non-humanized NSG mice, although the effect was greater in humanized mice suggesting that the possible role of antitumor immunity. The antitumor effect of NPRL2 was associated with increased infiltration of human CD45, CD3 T, cytotoxic T, NK cells, and a decreased number of human regulatory T cells (Treg) in tumors. PD1 expressing exhausted CD8 T cells were downregulated in both the NPRL2 and pembrolizumab groups. The number of activated T cells ($CD69^+CD8^+T$), effector (EM) and central memory (CM) CD8 T cells were significantly increased by NPRL2 treatment. NPRL2 induced antigen presenting HLA-DR^+ dendritic cells. When NPRL2 was combined with pembrolizumab, no synergistic antitumor effect was found in the KRAS/STK11 mutant anti-PD1 insensitive tumors. However, a robust and synergistic antitumor effect was observed in the KRAS wild type, anti-PD1 sensitive H1299 tumors grown in humanized mice treated with NPRL2 + pembrolizumab. Cytotoxic T cells, NK cells, and HLA-DR^+ DC were associated with the antitumor effect. DOTAP-NPRL2 was tested in a syngeneic mouse model with LLC2 tumors that are KRAS mutant and anti-PD1 resistant. Consistent with the A549 humanized mouse model, NPRL2 showed a significantly strong antitumor effect whereas anti-PD1 was not effective in this model. The antitumor effect of NPRL2 was again correlated with the upregulation of HLA-DR^+ DC, CD11c DC, TILs, NK and downregulation of Treg and myeloid cells in the tumor microenvironment. Taken together, these data suggest that NPRL2 gene therapy induces antitumor activity on KRAS/STK11 mutant anti-PD1 resistant tumors through DC mediated antigen presentation and cytotoxic immune cell activation.

#5121

TriTCE Co-stim, next generation costimulatory trispecific T cell engagers for the treatment of solid tumors

Lisa Newhook, Purva P. Bhojane, Peter W. Repenning, Diego Perez Escanda, Nichole K. Escalante, Patricia Zwierzchowski, Alec Robinson, Lauren Clifford, Harsh Pratap, David N. Douda, Chayne L. Piscitelli, Nicole J. Afacan, Thomas Spreter von Kreudenstein, Nina E. Weisser.
Zymeworks Inc., Vancouver, BC, Canada

Bispecific T cell engager (TCE) therapies have exhibited clinical utility against hematological cancers, but limited success in solid tumors. Treatment of solid tumors has additional challenges - including immunosuppressive environments and low T cell infiltration - limiting the antitumor activity of CD3-bispecific TCEs. Conventional T cell activation and sustained proliferation requires signaling via CD3 (signal 1) and costimulatory molecules (signal 2), such as CD28. The balance between signals 1 and 2 is critical for optimal T cell activation – signal 1 in the absence of signal 2 results in T cell anergy, while overactivation via signals 1 and 2 can lead to T cell dysfunction and cytokine release, as observed with toxicities associated with αCD28 superagonist antibodies (Abs). Optimal signal 2 costimulation via CD28 results in improved T cell fitness, activation and proliferation. To improve T cell responses in solid tumors, we developed costimulatory trispecific TCEs (TriTCE Co-stim) that engage CD3, CD28 and a tumor-associated antigen (TAA).

Our novel TriTCE Co-stim Abs were generated using the Azymetric^{TM} and EFECT^{TM} platforms to facilitate heterodimeric TriTCE Co-stim assembly and to knockout Fc gamma receptor interactions, respectively. To limit potential CD28-mediated toxicities, we evaluated a conventional αCD28 agonist paratope and generated a paratope library with varying affinities for CD28. TriTCE Co-stim Abs were engineered with various formats, geometries, paratope affinities, and TAA specificities. To understand the impact of TriTCE Co-stim Abs on T cell activation, we assessed *in vitro* cytotoxicity, cytokine production and proliferation of primary human CD3 T cells in co-culture with TAA-expressing cancer cell lines. A human PBMC-engrafted xenograft model was used to assess *in vivo* antitumor activity in a TAA^{high} tumor model.

TriTCE Co-stim Abs exhibited a range of cytotoxic potency, with several formats exhibiting greater potency than bispecific TCEs, and induced

greater cytotoxicity of tumor cells in long term co-cultures at low effector to target ratios. TriTCE Co-stim Abs exhibited TAA-dependent cytokine release and T cell proliferation, with enhanced IL-2 production and proliferation compared to that induced by bispecific TCEs. Tumor growth regression was observed *in vivo* following treatment with different TriTCE Co-stim Ab formats. In summary, we identified TriTCE Co-stim Ab formats that exhibit improved proliferation and antitumor activity against multiple TAA targets compared to bispecific TCE, which may translate to improved and more durable antitumor responses in solid tumors with low T cell infiltration. The evaluation of multiple formats, geometries and paratope affinities allowed optimization of activity and selectivity to promote maximal therapeutic index and efficacy, key factors that may contribute to improved clinical outcomes.

#5122

Electrochemotherapy and IL-12 gene electrotransfer in treatment of mast cell tumors in companion dogs

Maja Cemazar[1], Ursa Lampreht Tratar[1], Nina Milevoj[2], Katarina Znidar[1], Katja Ursic Valentinuzzi[1], Andreja Brozic[1], Gregor Sersa[1], Natasa Tozon[2].
[1]Institute of Oncology Ljubljana, Ljubljana, Slovenia,[2]Veterinary faculty, University of Ljubljana, Ljubljana, Slovenia

When cells or tissues are exposed to an electric field, structural changes can be induced in the cell membrane, allowing molecules to flow into the cells. This condition is useful for delivering cytotoxic drugs whose transport into cells is impeded, such as bleomycin and cisplatin. This is referred to as electrochemotherapy (ECT). When DNA or RNA molecules are transported into cells, the approach is called gene electrotransfer (GET). ECT is an effective local treatment for tumors, but it lacks the systemic component of treatment that is essential for fighting metastatic disease. Cancer progression and metastasis are closely related to an inadequate antitumor immune response. Therefore, the antitumor efficacy of interleukin 12 (IL -12), a cytokine that stimulates the innate and adaptive immune response, has been tested in preclinical studies using plasmid DNA encoding IL -12 delivered into the tumor by gene electrotransfer (IL -12 GET). In addition, the combined treatment of ECT and IL -12 GET has already been shown to be effective in the treatment of mouse tumors and has been used in clinical

trials in companion dogs to treat various histological types of spontaneous tumors. The results of these studies showed that the treatment is safe and effective. However, in these clinical trials, IL -12 GET was administered by different routes, either intratumorally (i.t.) or peritumorally (peri.t.). Therefore, the aim of this study was to compare the two IL -12 GET routes of administration in combination with ECT and to determine their contribution to the enhanced response to ECT. In the clinical trial, 59 dogs with spontaneous mast cell tumors (MCT) were divided into two groups: one group was treated with the combination of ECT and GET peri.t. (29 dogs) and the other with the combination of ECT + GET i.t. (30 dogs). The efficacy of the treatment was compared with the group of 18 dogs treated with ECT alone. In addition, immunohistochemical studies of tumor samples before treatment and flow cytometric studies of PMBC before and after treatment were performed to determine immunological aspects of the treatment. The results of this study showed that local tumor control was significantly better in the ECT + GET i.t. group ($p < 0.05$) than in the ECT + GET peri.t. and ECT groups. In addition, the disease-free interval (DFI) and progression-free survival (PFS) were significantly longer in the ECT + GET i.t. group than in the other two groups ($p < 0.05$). The data on local tumor response, DFI and PFS were consistent with immunological studies, as we detected increased infiltration of antitumor immune cells after treatment in the ECT + GET i.t. group, also suggesting a systemic effect.

#5123

The anti-tumor and anti-angiogenic effects of a lipid nanoparticle suspension of an AKT-1 anti-sense oligonucleotide

Fengyang Xie[1], Jia Wei[2], Lan Deng[2], Chao Wang[2], Ben Zhao[1], Robert J. Lee[1], Yuxin Angela Men[2]. *[1]Zhejiang Haichang Biotechnology Co., Ltd., Hangzhou, China,[2]The WhiteOak Group, Inc., Rockville, MD*

Background: AKT-1 is known to play a critical role in cancer progression by stimulating cell proliferation and inhibiting apoptosis. AKT inhibition has been shown to inhibit tumor growth as well as tumor angiogenesis. Archexin is a fully phosphorothioated 20-mer antisense oligonucleotide, which can specifically bind to AKT-1 mRNA resulting in RNase H-based AKT-1 downregulation. WGI-0301 is a proprietary lipid nanoparticle (LNP) formulation of Archexin designed for enhanced delivery. A phase I

clinical study has recently been initiated for WGI-0301 in patients with advanced solid tumors.
Methods: Anti-tumor efficacy of WGI-0301 was studied *in vivo* in a Hepa1-6 syngeneic murine tumor model for hepatocellular carcinoma (HCC). The mice were injected i.v. with vehicle control or WGI-0301 at 8 mg/kg once weekly for 4 doses (n=8). Tumor size and body weight changes were monitored. In addition, the anti-angiogenesis activity of WGI-0301 was investigated *in vitro* using human umbilical vein endothelial cells (HUVEC). In the study, combination of WGI-0301 with Lenvatinib or Sorafenib were investigated to determine possible synergism. Three experimental groups were set up, including WGI-0301(0, 0.2, 2 and 20 μM), WGI-0301+ 2 μM Sorafenib, and WGI-0301+ 5 μM Lenvatinib. The cells were plated at 1.5×10^4 per well. The cells were treated with 50% Matrigel and then cultured in the 24 well plate in triplicates and were incubated for an additional 6 hours.
Results: The *in vivo* study demonstrated anti-tumor efficacy of WGI-0301 in the Hepa1-6 model. The tumor growth inhibition % (TGI) for WGI-0301 was 46.16%, and the medium survival time (MST) of the treatment group was 55 days, which was significantly different from that of the control group (37 days). There was no severe adverse event observed during the study. In the *in vitro* anti-angiogenesis study, WGI-0301 alone or in combination with 2 μM Sorafenib and 5 μM Lenvatinib exhibited dose-dependent inhibition of angiogenesis. Compared with the control group, 20 μM WGI-0301 either alone or in combination with 2 μM Sorafenib and 5 μM Lenvatinib showed significantly inhibitory effect on angiogenesis. The 2 μM WGI-0301 in combination with 5 μM Lenvatinib also showed a significant inhibition effect on angiogenesis.
Conclusion: Data obtained demonstrated anti-tumor and anti-angiogenesis efficacy of WGI-0301. In addition, combining WGI-0301 with Sorafenib or Lenvatinib resulted in increased anti-angiogenetic activity relative to monotherapy. WGI-0301 warrants further investigation as a selective AKT-1 inhibitor.

#5124
The effect of lenvatinib in combination with chemotherapy plus immune checkpoint inhibitors on tumor microenvironments in the mouse syngeneic tumor model

Yu Kato[1], Yoichi Ozawa[1], Keito Adachi[1], Masahiko Kume[1], Yusuke Adachi[1], Yudai Narita[1], Megumi Kuronishi[1], Junji Matsui[2], Akira Yokoi[1], Yasuhiro Funahashi[2]. *[1]Eisai Co., Ltd., Tsukuba, Japan,[2]Eisai Inc., Nutley, NJ*

Introducti**on:** Lenvatinib (LEN) is an oral, multiple-receptor, tyrosine kinase inhibitor that mainly targets vascular endothelial growth factor and fibroblast growth factor receptors. Combination therapy with LEN and everolimus is approved for people with advanced renal cell carcinoma (RCC). Combination therapy with LEN and pembrolizumab, an anti human-programmed-cell-death-1 (PD-1) antibody, is also approved for the treatment of people with advanced endometrial cancer and advanced RCC. In this study, we investigated the antitumor activity of LEN in combination with chemotherapy and immune checkpoint inhibitors (ICIs), and explored the mechanism of action underlying these effects, in the mouse lung cancer syngeneic model.
Methods: In the LL/2 mouse Lewis lung carcinoma model, LEN was dosed at either 3 or 10 mg/kg (orally; once daily for 2 weeks) with or without cisplatin 4 mg/kg (intravenously; 3 or 4 times, twice weekly) and with or without anti-PD-1 200 ug/head + anti cytotoxic T-lymphocyte antigen 4 (CTLA4) antibodies 10mg/kg (intraperitoneally; twice weekly). Functional blood vessels were evaluated in tumor microenvironments by injections of Hoechst 33342 (Hoechst) into the tail veins of mice. The Hoechst-stained area and expressions of angiogenesis/immune-cell-related molecules were analyzed by immunohistochemistry (IHC) analysis.
Results: In this model, the combination treatment of LEN 3 mg/kg + cisplatin showed significant tumor growth inhibitory activity compared with each single agent without any marked body-weight loss. LEN 10 mg/kg + cisplatin did not show enhanced antitumor activity vs LEN 10 mg/kg as a single agent. IHC analysis using anti-CD31 antibody showed that LEN 3 mg/kg daily decreased microvessel density in tumors after 4 days. In addition, LEN 3 mg/kg daily for 4 days showed a trend toward an increase of the number of functional blood vessels stained with Hoechst in the tumor microenvironment compared with untreated controls. The combination of LEN 3 mg/kg + cisplatin + ICIs (anti-PD-1+anti-CTLA4) significantly inhibited tumor growth compared with combinations of cisplatin + ICIs.

Conclusion: Our findings show that LEN 3 mg/kg enhances the antitumor activity of cisplatin in the LL/2 mouse Lewis lung carcinoma tumor model; and LEN 3 mg/kg + cisplatin + ICIs shows greater antitumor activity compared with cisplatin + ICIs. The results of the IHC analysis suggest that LEN 3 mg/kg inhibits angiogenesis. Conversely, LEN 3 mg/kg increases functional vessels in tumor microenvironments. This situation could enhance combination antitumor activity of chemotherapy, and also chemotherapy + ICIs combination treatment. Further analysis of the mechanism of action of LEN 3 mg/kg in combination with chemotherapy + ICIs is warranted.

#5125

Depletion of CCR8+ tumor Treg cells with SRF114 or anti-CCR8 therapy promotes robust antitumor activity and reshapes the tumor microenvironment toward a more pro-inflammatory milieu

Marisella Panduro, Yue Ren, Ricard Masia, Yu Yang, Andrew C. Lake, Vito J. Palombella, Jonathan A. Hill, James F. Mohan. *Surface Oncology, Inc., Cambridge, MA*

$FOXP3^+$ regulatory T (Treg) cells play a crucial role in orchestrating immune responses across several tissues, including the tumor microenvironment (TME). The dominant immune regulatory activity of Treg cells is evidenced, both clinically and preclinically, by the profound inflammatory dysregulation that arises in their absence. Leveraging controlled depletion of Treg cells in tumor tissue while sparing Treg cells in healthy tissue may be achieved through antibody-mediated targeting of the C-C chemokine receptor 8 (CCR8). CCR8 is a seven transmembrane G-coupled chemokine receptor protein whose expression is predominantly upregulated on Treg cells in several types of tumors compared with peripheral blood. Importantly, depletion of CCR8-expressing Treg cells in tumors provides a novel pathway to immunotherapy that is mechanistically independent of checkpoint inhibition (CPI).
Using single-cell transcriptome and flow cytometry analyses, we evaluated the pharmacodynamic changes after treatment with anti-CCR8 antibodies to elucidate the effect of tumor Treg cell-targeting therapies on the downstream mechanisms of antitumor immunity within the TME.

SRF114, a highly selective human anti-CCR8 afucosylated antibody, and an anti-mouse CCR8 antibody were utilized to preferentially deplete $CCR8^+$ Treg cells in human CCR8 knock-in (hCCR8KI) or wild-type mice, respectively. Treatment with SRF114 or anti-mouse CCR8 antibody resulted in robust monotherapy activity in models susceptible to CPI. Moreover, pronounced monotherapy activity was also seen in checkpoint-resistant model(s), highlighting a mechanistically CPI-independent role for intratumoral Treg cell depletion to elicit potent antitumor activity. Treatment of tumor-bearing mice with anti-CCR8 antibodies resulted in a significant reduction of tumor-associated Treg cells, while peripheral Treg cells remained unchanged. Analysis of bulk tumor lysates showed that anti-CCR8 therapy elevated levels of pro-inflammatory cytokines and pro-angiogenic and chemoattracting factors. Evaluation of effector T cells demonstrated that anti-CCR8 therapy drives proliferation of $CD8^+$ T cells and an increase in intracellular cytokine production of IFNγ, TNFα, and granzyme A. Additionally, the tumor myeloid compartment was strongly affected by anti-CCR8 therapy. Multiple myeloid cell subsets had increased levels of co-stimulatory molecules and expression of PD-L1. Altogether, selective depletion of intratumoral $CCR8^+$ Treg cells results in robust antitumor activity by reshaping the TME toward a more pro-inflammatory milieu, providing an orthogonal approach to CPI for eliciting antitumor immunity and a strong rationale for evaluating SRF114 as a therapeutic agent for the treatment of cancer. SRF114 is currently in Phase 1 clinical studies.

Determinants of Immunotherapeutic Effectiveness

#4112
Evaluating the survival outcomes of an anti-isoaspELAVL4 response in a small cell lung cancer mouse model

Diego A. Velarde, Sarah A. Elmalh, Hannah Lee, Joseph Valdes, Matthew Gladstone, Ryan E. Dinigle, Martin Kast, Ite A. Offringa. *USC Norris Comprehensive Cancer Center, Los Angeles, CA*

Small cell lung cancer (SCLC) has a 95% mortality rate and a 5-year survival of 8%, resulting in the death of over 20,000 Americans each year. There has been marginal improvement in therapy over the past 30 years,

with the recent addition of immune checkpoint inhibition therapy modestly increasing overall SCLC patient survival from 10.3 to 12.3 months [PMID 30280641]. This highlights the need for additional SCLC therapies. Previous studies have identified a subset of SCLC patients (10-20%) exhibiting a naturally occurring immune response called 'anti-HuD'. It is associated with improved response to therapy and improved survival [PMID 9256130; 26606748]. Previous work identified the anti-HuD antigen to be ELAVL4. The Offringa lab and collaborators determined that the antigenic epitope consists of isoaspartylated ELAVL4 (isoAspELAVL4) [PMID 27725125]; the protein carries isoaspartylated residues in the N-terminal region (amino acids 1-36). All tested Anti-Hu-positive SCLC patient serum samples reacted with isoAspELAVL4, and all examined SCLC tissue samples stained positive for isoAspELAVL4 [PMID 27725125]. Here we used the Trp53fl/fl; Rb1fl/fl inducible SCLC mouse model [PMID 14522252] to examine 1) whether immunization with isoAspELAVL4 prior to SCLC induction is protective, and 2) whether immunization with isoAspELAVL4 following completion of 3 rounds of cisplatin+etoposide therapy increases survival. In both cases, mice were immunized with recombinant N-terminal fragment of ELAVL4 (amino acids 1-117) generated in *Clear Coli* and emulsified in incomplete Freund's adjuvant (IFA) or control (phosphate-buffered saline in IFA). The trajectories of mice have been monitored with a detailed body metric score and blood has been drawn every 2 weeks to monitor the anti-ELAVL4 antibody response. Kaplan-Meier analysis will be used to assess survival differences between the immunized and control groups and will be presented. The study will provide insight into interplay between SCLC and the immune response to isoAspELAVL4.

#4113

Classification of patient-specific sensitivity to immunotherapies by *ex vivo* tumor testing

Lieke Johanna Ceton[1], Marta Garcia Montero[1], Fanny Grillet[1], Dieudonné J. van der Meer[1], Willemijn Vader[1], Anne van Altena[2], Cor D. de Kroon[3], Nelleke Ottevanger[4], Judith Kroep[5]. *[1]VitroScan B.V., Leiden, Netherlands,[2]Gynecology, Radboud University Medical Centre (Radboudumc), Nijmegen, Netherlands,[3]Gynecology, Leiden University Medical Centre (LUMC), Leiden, Netherlands,[4]Radboud University*

Medical Centre (Radboudumc), Nijmegen, Netherlands,[5]Leiden University Medical Centre (LUMC), Leiden, Netherlands

Background: Immunotherapy has brought great progress with durable responses for cancers that were difficult to treat. However, it remains challenging to select sensitive patients upfront. PD-L1 expression, TMB and MSI/MSS status, do not optimally differentiate between the potential sensitivity to the individual immunotherapies.
Purpose: We aim to improve stratification of patients for immunotherapy through classification of patient-specific tumor sensitivity based on 3D ex vivo drug measurement.
Material: Our study includes 108 Patients with predominantly ovarian carcinoma (81/108). Tumor tissue was collected in ongoing clinical trials from biopsies, ascites or pleural fluid. Five immune checkpoint inhibitors and a STING pathway activator were tested.
Method: Fresh tumor clusters were seeded into 384 well plates and exposed to different immunotherapies, while preserving the TME. Tumor killing and immune cell proliferation were measured using 3D image analysis. Ex vivo tumor sensitivity was classified as no response (<10%), weak (10-20%), strong (20-50%), and very strong (>50%), based on percentage tumor killing and statistical significance (p-value: * < 0.05, ** < 3.33e-4).
Results: Differential patient response profiles were observed (Table 1). For the current cohort, we measured a highly significant immunotherapy response for ~30% of the samples. The assay has a technical success rate of 89%.
Conclusion: This study reports the development of a robust ex vivo tumor testing platform that classified patient-specific sensitivity to 6 immunotherapies for over 100 patients, demonstrating the potential of ex vivo tumor testing to optimize patient stratification for immunotherapy.
Discussion: The platform enables improved efficiency in clinical development of novel treatments and supports treatment decisions in the clinic. Clinical trials are ongoing to establish the correlation of our testing with patients' response to immunotherapy in lung cancer.

Overview of ex vivo immunotherapy response per category

Therapy	**# Samples tested**	**% Response**	**No response**	**Weak**	**Strong**	**Very strong**
SEA (control)	*108*	*43%*	*62*	*5*	*19*	*22*

		*(30%**)*				
CD3/CD28 Dynabeads (control)	*18*	*33% (17%**)*	*12*	*1*	*5*	*0*
Pembrolizumab	89	16% (8%**)	75	6	5	3
Nivolumab	72	10% (4%**)	65	1	5	1
Ipilimumab	97	20% (11%**)	78	4	10	5
Atezolizumab	62	15% (11%**)	53	1	4	4
Durvalumab	52	2% (0%**)	51	1	0	0
ADU-S100	60	37% (27%**)	38	5	9	8

#4114

Can exosomal cargoes predict checkpoint inhibitor response in melanoma, and can we overcome drug resistance?

Pablo Eduardo Puente[1], Dan Nguyen[1], Niramol Savaraj[1], Chunjing Wu[1], Medhi Wangpaichitr[1], Stephane Roche[2], Guangkuan Zhao[2], Alexis Richaud[2], Jose Lutzky[3], Leonel Hernandez Aya[3], Mecker Moller[3], Jessica Crystal[3], Neha Goel[3], Lynn Feun[3]. *[1]Miami VA Healthcare System, Miami, FL,[2]Florida Atlantic University Department of Chemistry and Biochemistry, Boca Raton, FL,[3]University of Miami Miller School of Medicine, Miami, FL*

Immune check point inhibitor(s) have become a main stay of treatment for melanoma regardless of its mutational status. However, not all patients respond to treatment. In fact, only 40-60% respond to treatment. Currently, only PD-L1/PD-1 expression and mutational burden can predict response to treatment. Published data have shown that exosomal PD-L1 is an important factor contributing to response/failure to checkpoint inhibitor treatment. Exosome is known to carry several types of cargoes and is one of the

important delivery systems in the body. We have begun to examine the role of exosomal PD-L1, PD-1 in predicting response, and as well as how to overcome drug resistance. We initiated an institutional study in metastatic melanoma patients who underwent immunotherapy treatment (anti-PD-1 + anti-CTLA 4 drugs). Blood samples were obtained at baseline and at subsequent treatment. Both serum and plasma exosomes were isolated. Eighteen patients were entered in the study. We have found that 1) Patients with PD-L1 negative tumor can have high exosomal PD-L1 expression, 2) all patients had exosomal PD-L1, and 3) all patients with decreased exosomal PD-L1 expression after treatment showed antitumor response [partial response (PR) or complete response (CR)]. In contrast, patients who had consistently high exosomal PD-L1 expression post-treatment showed no response, and this can be seen after the third cycle of treatment. Patients who achieved CR showed low exosomal PD-L1 and no exosomal PD-1 post-treatment. Importantly, we have also found that exosomes carry antiapoptotic protein and proapoptotic protein, as well as ATG family protein, which is related to autophagy. Whether these proteins also play a role in determining the cell fate in the metastatic sites is not known and will need future investigation. Interestingly, the two patients who showed no response also had high p-AKT. Since traditional anti PD-1 and anti-PD-L1 drugs do not have effect on exosomal PD-L1 and PD-1, we formed a collaboration with Dr. Stephane Roche at Florida Atlantic University, who has designed novel peptides by exploiting the innate plasticity of the PD-1 receptor (pembrolizumab H3 loop mimics). Thus far, we have screened many compounds and have selected 2 compounds for further testing. Together, we have also designed new PD-L1 peptides that can inhibit both PD-L1 and PI3K/AKT pathways simultaneously. Hence one can overcome checkpoint inhibitor resistance due to exosomal PD-L1/PD-1. Supported by grant from Sylvester Comprehensive Cancer Center and R21GM132754.

#4115

KLRG1 marks tumor-infiltrating CD4 T cell subsets associated with immune escape and immunotherapy response

Casey Ager, Matthew Chaimowitz, Shruti Bansal, Meri Rogava, Johannes Melms, Catherine Spina, Cory Abate-Shen, Charles G. Drake, Matthew Dallos, Benjamin Izar. *Columbia University, New York, NY*

Current methods for biomarker discovery and target identification in immuno-oncology rely on static snapshots of tumor immunity. To better capture the dynamic and compartmentalized nature of antitumor immune responses, we generated longitudinal “temporal atlases” of productive versus non-productive antitumor immune responses in murine tumor models. We utilized a 34-parameter full spectrum flow cytometry panel to comprehensively profile immune composition within tumors, draining and non-draining lymph nodes, and blood in and around key inflection points of tumor regression or progression. We leveraged two distinct preclinical models for this; the NPK-C1 ectopic prostate cancer model to map dynamics of spontaneous cancer immunoediting, and anti-PD-1 treated MC38 tumors to study response or non-response to immune checkpoint blockade (ICB). We utilized UMAP and FlowSOM algorithms for iterative dimensionality reduction and clustering, respectively, to reveal novel phenotypes associated with productive versus non-productive immunity across model systems, tissues, and time points. We discovered expression of KLRG1 within the intratumoral CD4 T cell compartment was highly associated with tumor progression and response to ICB. Specifically, both FoxP3+ Tregs and FoxP3- Tconv cells within tumors accumulated KLRG1 expression through disease progression, but this was not observed in CD4 T cell or other immune subsets residing in lymph nodes or circulating in blood. Among all intratumoral clusters, KLRG1+ Tconv were the only subset significantly correlated with tumor burden at each time point tested and across both models. KLRG1+ Tconv were significantly enriched in NPK-C1 tumors undergoing progression to escape versus those under immune-mediated equilibrium ($p=0.0004$) and were lost in animals undergoing curative responses to ICB ($p=0.003$). In the Treg compartment, unsupervised clustering revealed a KLRG1+Helios- tumor Treg subset that was positively correlated with transition from equilibrium to escape in the NPK-C1 model ($p=0.005$). Also indicating a potential functional significance, this phenotype was absent in tumors undergoing curative responses to ICB ($p=0.0002$). Systematic investigation of the functional characteristics, transcriptional programming, and translational significance of intratumoral KLRG1+ CD4 T cell subsets is ongoing. Together, these findings identify KLRG1+ CD4 T cell populations as subsets for further investigation in cancer and demonstrate the utility of longitudinal full

spectrum flow cytometry profiling as an engine of dynamic biomarker and/or target discovery in immuno-oncology.

#4116

Modulating gut microbiota to improve intrahepatic immunity against hepatocellular cancer

Xiaogiang Qi, Ming Yang, Lixin Ma, Jonathan Mitchem, Jussuf Kaifi, Shiyou Chen, Aaron Ericsson, Eric Kimchi, Kevin Staveley-O'Carroll, Guangfu Li. *University of Missouri - Columbia, Columbia, MO*

Gut microbiota plays a pivotal role in the pathogenesis of hepatocellular cancer (HCC), significantly affecting the HCC treatment. It has been reported that the HCC patients' response to the immunotherapy of PD-1/PD-L1 blockade was associated with their gut microbiota profiles. However, the impact of gut microbiota on anti-HCC immunity and its underlying mechanism are poorly understood. Treating HCC-bearing mice with a specific and non-hepatotoxic antibiotic cocktail caused the increased relative abundance of specific commensal bacteria such as *Bacteroides*, resulting in suppression of HCC growth and development which was involved in the activation of intrahepatic antitumor immune responses. Gut microbiota recolonization of *Bacteroides thetaiotaomicron (B. th)* in gut-sterilized HCC-bearing mice significantly improved the therapeutic efficacy of anti-PD-1 antibody (αPD-1 Ab) against HCC. Fecal microbiota transplantation (FMT) from HCC patients who received and responded to αPD-1 Ab treatment improved the efficacy of αPD-1 Ab treatment against HCC in mice model. Mechanistic studies demonstrated that the modulation of Krüppel-like factor 2 (KLF2) / Toll-like receptor 9 (TLR9) signaling and the accumulation of CpG-enriched genomic DNAs of *B. th* in livers/tumors activated the tumor antigen-specific $CD8^+$ T cells through the dendritic cell in a TLR9-dependent manner. In conclusion, gut microbiota as a causative factor can be targeted to improve anti-HCC immunotherapy.

#4117

Molecular insights into resistance mechanisms to therapy with T cell bispecific antibodies

Johannes Sam[1], Llucia Alberti Servera[1], Sina Nassiri[1], Atul Sethi[1], Alison Ribeiro[1], Gabrielle Leclercq-Cohen[1], Petra Schwalie[2], Tamara Hüsser[1],

Emilio Yangueez[1], Sylvia Herter[1], Christian Klein[1], Pablo Umana[1], Marina Bacac[1]. *[1]Roche Glycart AG, Schlieren, Switzerland,[2]Roche Innovation Center Basel, Basel, Switzerland*

T Cell Bispecific Antibodies (TCBs) are potent molecules that induce durable complete remissions with a favorable safety profile in Relapsed Refractory Non Hodgkin Lymphoma patients. Despite the promising clinical efficacy, a proportion of patients escape under treatment due to the occurrence of primary and acquired resistance mechanisms that may involve the modulation of target antigen expression, cancer cell intrinsic mechanisms, T cell functionality or treatment-induced changes in the tumor microenvironment (TME). Therefore, a better understanding of TCB-induced resistance mechanisms is of great importance to enable the design of novel therapeutic approaches and/or combination strategies to overcome resistance. We present the results of exploratory preclinical analysis using an aggressive lymphoma model in humanized mice and a syngeneic melanoma model in immunocompetent mice, focusing on the assessment of T cell functionality, TME reprogramming, and cancer cell intrinsic changes upon longitudinal TCB treatments, encompassing tumor regression and escape. Flow cytometry, IHC, scRNAseq and ex vivo functional analysis of T cell cytotoxicity and cytokine release demonstrate that intra-tumor T cell functionality is preserved over serial TCB treatments, including tumor escape. On the other hand, TCB treatment induced a reprogramming of the TME consisting of rapid myeloid cell infiltration, followed by the expansion of intra-tumor T cells at a later time point (favoring higher CD8:CD4 ratio). Cumulative evidence from in vitro and in vivo scRNAseq experiments provided insights into macrophage reaction to TCB-mediated T cell inflammation, consisting of a rapid (as early as 2 h) activation and upregulation of several pro-inflammatory molecules (IL-1b, CXCL8, CXCL9, CXCL10, CXCL1, CCL2, CCL3, CCL4, CCL5, IFN-g-induced genes: GBP2 -8 and BATF2). This was followed by a shift towards a more suppressive phenotype at later time points (20-96 h) as evidenced by the expression of PD-L1, INHBA, IDO, FLT1 genes. The analysis of cancer cells showed upregulation of Wnt/beta catenin, p53 and Hedgehog signaling pathways at tumor escape. In contrast, proliferation signatures including MYC, E2F target genes, MTORC signaling, and G2M checkpoint, along with metabolic pathways of oxidative phosphorylation

and glycolysis were enriched in cancer cells at regression. Taken together, our data show that T cell cytotoxicity and functional states are preserved during tumor regression and tumor escape phases, suggesting that T cell dysfunctionality is unlikely to be the sole cause of TCB resistance. TME reprogramming, consisting of a rapid myeloid cell infiltration and their acquisition of a suppressive phenotype over time, along with a selection of cancer cell clones that escape the TCB-mediated cytotoxicity and upregulate Wnt, p53 and Hedgehog pathways could contribute to TCB-mediated resistance, leading to tumor escape.

#4118

The role of microRNAs in the tumor immune microenvironment

Catherine T. Cronister, Robert S. Seitz, Brian Z. Ring, Douglas T. Ross, Brock Schweitzer. *Oncocyte Inc., Nashville, TN*

Background: miRNA have been shown to be central communicators between the immune system and cancer. They are attractive as candidate blood-based cancer detection targets because they are secreted in high copy number from cancer cells, are bound to circulating proteins and have secondary structures that prolong their half-life in blood. miRNAs that are thought to communicate between cancer associated fibroblasts and immune cells are of special interest for their potential involvement in transitions in the TIME from "hot" - an inflammatory state with a greater likelihood of sensitivity to immune checkpoint inhibitors - to "cold" - tumors with an immunosuppressive state or immune inert state or vice versa. We have previously described a gene expression signature that distinguishes immunomodulatory (IM, inflammatory cells), mesenchymal (M, EMT differentiated cells), and mesenchymal stem-like (MSL, cancer associated fibroblasts) features of the TIME, and when converted to a binary classifier, has been shown to be correlated with response to immune checkpoint inhibitors (ICI). Here we use TCGA microRNA data to identify a microRNA correlate of this classifier.
Methods: miRNA and RNA expression were collected from TCGA across five tissue types. Each tumor case was assigned a TIME phenotype as previously described [1]. Lung, breast, colon, and bladder data were used to identify miRNA’s whose expression pattern significantly correlated with at least one of three immune phenotypes identified by the previously defined

algorithm. Data from the IntAct database were used to identify putative gene targets of the candidate miRNA.
Results: Of the 151 miRNAs of interest, 147 known interactions were found in the IntAct database. Of these 147 interactions, 107 were between miRNA and genes of different TIME (or immune) phenotypes while 89 were interactions between miRNAs and genes implicated in regulating immune hot and cold phenotypes.
Conclusions: We identified miRNA whose expression patterns correlates with a classifier of the TIME that has been shown to identify likely responders to immune checkpoint inhibitors. This candidate gene list was significantly enriched for both miRNA targets of known immune mediators and or targets implicated in modulating the TIME. Next steps are to further narrow the list to those detectable in blood in cancer, and to train a blood-based diagnostic that might be able to predict response to ICI therapy for those patients where tissue is not available.
References: [1] Seitz, R.S., Hurwitz, M.E., Nielsen, T.J. et al. Translation of the 27-gene immuno-oncology test (IO score) to predict outcomes in immune checkpoint inhibitor treated metastatic urothelial cancer patients. J Transl Med 20, 370 (2022). https://doi.org/10.1186/s12967-022-03563-9

#4119

Anti-KRAS antibody aggregates KRAS in the cytoplasm of live *ex vivo* cultured human colorectal adenocarcinoma cells and prevents its trafficking to the plasma membrane

Peh Yean Cheah[1], Kuen Kuen Lam[1], Yee Syuen Low[1], Michelle Lo[1], Michelle Wong[1], Choong Leong Tang[1], Emile Tan[1], Aik Yong Chok[1], Issac Seow En[1], Siew Heng Wong[2]. *[1]Singapore General Hospital, Singapore, Singapore,[2]JW Bioscience, Singapore, Singapore*

Worldwide, colorectal cancer (CRC) is the third highest incidence cancer and a leading cause of cancer mortality. Metastasis to distal organ is the major cause of cancer mortality. However, chemotherapeutic treatment of metastatic CRC has a dismayed success rate of less than 30%. Patients who are resistant to chemotherapy and who are *KRAS* wildtype are sometimes offered anti-EGFR as a second line therapy. Nevertheless, only about ½ of these patients respond and those who do inevitably develop resistance within months due to selection for downstream *KRAS* mutations. Moreover,

most (80%) sporadic CRCs are microsatellite-stable and are refractory to immune checkpoint blockade therapy. Hence, there is an unmet need to identify novel therapeutics for CRC. KRAS is a gatekeeper gene in colorectal tumorigenesis but is 'undruggable' due to its structure not being easily amenable to inhibitor docking. Focus has been diverted to develop small molecule inhibitors for its downstream effectors such as ERK/MAPK and AKT. Despite intense research efforts for the past few decades, however, no small molecule inhibitor has been in clinical use for CRC. Recently developed Sotorasib inhibitor specific for *KRAS* G12C mutations (rare in CRC) is not effective for CRC. Antibodies have high affinity to their target proteins without having to bind to specific pocket and are fully human in nature and hence less toxic. Antibody targeting KRAS itself is thus an attractive alternative. We developed a transient *ex vivo* patient-derived matched mucosa-tumor primary culture to assess whether anti-KRAS antibody can be internalized to bind and inactivate KRAS. We showed that anti-KRAS antibody can enter live matched mucosa-tumor cells and specifically aggregate KRAS in the cytoplasm, thus hindering its trafficking to the inner plasma membrane. The mis-localization of KRAS reduces KRAS dwelling time at the site where it tethers to activate downstream effectors. We previously showed that expression of SOX9 was *KRAS*-mutation-dependent and possibly a better effector than ERK in CRC. In the present study, we showed that anti-KRAS antibody treated tumor cells have less intense SOX9 cytoplasmic and nuclear staining compared to untreated cells suggesting down-regulation of *KRAS* signaling. Our results demonstrated that anti-KRAS antibody can be internalized and specifically inhibits KRAS function in live tumor cells. With an efficient intracellular antibody delivery system, this can be further developed as combinatorial therapeutics for CRC and other KRAS-driven cancers.

#4120

Depletion of tissue-resident B cells by a CD20xCD3 IgM bispecific T cell engager in cynomolgus monkeys demonstrates effective tissue penetration and potent target cell killing

Miho Oyasu, Angus M. Sinclair, Haben Ghermazien, Genevive Hernandez, Thomas Manley, Maya K. Leabman, Stephen F. Carroll, Bruce A. Keyt, Maya F. Kotturi. *IGM Biosciences, Inc., Mountain View, CA*

Imvotamab (IGM-2323) is an engineered high-affinity, high-avidity bispecific anti-CD20 IgM antibody T cell engager (TCE) that is currently being studied as monotherapy in a Phase 1/2 clinical trial for relapsed/refractory non-Hodgkin's lymphoma (NHL) (NCT04082936). Imvotamab offers a novel treatment strategy in NHL by depleting CD20-expressing tumor cells through multiple mechanisms, including the recruitment of T cells to kill tumor cells through T cell dependent cellular cytotoxicity, complement-dependent cytotoxicity, and enhanced immune modulation via IFNγ-dominant cytokine stimulation. We evaluated the activity of a surrogate cynomolgus monkey cross-reactive CD20xCD3 IgM bispecific TCE, IGM-2324, in depleting CD20-expressing B cells in peripheral blood and lymphoid tissues of cynomolgus monkeys in vivo. We hypothesized that the high affinity and valency of IGM-2324 would enable potent B cell killing in blood and tissues even when B cells express low levels of CD20. Cynomolgus monkeys were administered vehicle or IGM-2324 at 5 mg/kg or 25 mg/kg through intravenous infusion twice weekly for a total of four doses on days 1, 4, 7, and 10. B cell depletion in peripheral blood was assessed by measuring the frequency of CD19+ B cells through flow cytometry. Administration of IGM-2324 at 5 and 25 mg/kg resulted in a nearly complete depletion in peripheral CD19+ B cells at 8 hours post the 1st dose through 24 hours post the last dose on day 11. Depletion of tissue-resident B cells was evaluated in the spleen, mesenteric lymph node (MLN) and bone marrow (BM) of monkeys at 24 hours post the last dose of vehicle or IGM-2324 on day 11. Immunohistochemistry studies were conducted on the formalin-fixed paraffin-embedded lymphoid tissues by staining for CD19 and CD20 expression. The number and intensity of CD19 or CD20 positive B cells were determined by quantitative imaging analysis. Compared to vehicle-treated animals, significant dose-dependent reductions in both CD19 and CD20-expressing B cells were observed in spleen, MLN and BM following treatment with 5 and 25 mg/kg of IGM-2324. Most importantly, IGM-2324 treatment led to the depletion of not only high and moderate tissue-resident CD20-expressing B cells, but also B cells that expressed low levels of CD20. Our preclinical data indicate that a CD20xCD3 IgM bispecific TCE can penetrate tissues and mediate direct killing of CD20-expressing target cells. B cell depletion in the periphery and tumors of relapsed/refractory NHL patients is currently being evaluated

as biomarker of pharmacodynamic activity and/or efficacy for imvotamab in a Phase 1/2 clinical study.

#4121

Heterogenous cellular responses to GITR and TIGIT immunotherapy in the human gastrointestinal tumor microenvironment

Anuja Sathe[1], Carlos Ayala[2], Xiangqi Bai[1], Sue M. Grimes[1], Andrew Shelton[2], Byrne Lee[2], Cindy Kin[2], George Poultsides[2], Hanlee P. Ji[1].
[1]Stanford University School of Medicine, Stanford, CA,[2]Department of Surgery, Stanford University, Stanford, CA

Many new immunotherapy agents fail in clinical trials. Major gaps remain in our understanding of their precise mechanism of action, with findings from preclinical studies that do not translate into the clinic. We identified the cellular and molecular responses to co-stimulatory GITR and co-inhibitory TIGIT immunotherapy by using an experimental approach that overcomes these challenges. We investigated these responses in a patient-derived *ex vivo* system that maintains the original tumor microenvironment (TME) in its near-native state. Using single-cell RNA sequencing (scRNA-seq) and paired single-cell TCR sequencing (scTCR-seq), we identified treatment induced transcriptional reprogramming in different cell lineages in the TME. We established *ex vivo* slice cultures from ten surgical resections of colorectal or gastric cancer. These cultures maintained all epithelial, stromal, and immune cell types and transcriptional cell states found in the original tissue sample. All tumors responded with activation of CD8, CD4 and T regulatory (Treg) cells following PMA/Ionomycin treatment, confirming the viable and functional status of the model system. GITR agonist led to a modest increase in cytotoxic gene expression in CD8 T cells in four out of nine patients. Transcriptional non-responders had significantly increased dysfunctional phenotype at baseline compared to responders. *Ex vivo* analysis confirmed that only cells with an effector non-exhausted cell state responded to GITR agonist, while exhausted cells did not. GITR agonist did not induce significant changes in expression in regulatory T (Treg) or T follicular helper-like (TFh-like) cells. TIGIT antagonist increased TCR signaling and activation in all five patients. These responses were observed in both effector and exhausted cells. A reduced transcriptional response to TIGIT in CD8 T cells correlated with the

increased expression of *GZMK*, *TXNIP* and *RGS1* together with reduced expression of metallothionine family genes. TIGIT antagonist also increased activation specifically in expanded TCR clonotypes, which are indicative of tumor antigen reactive cells. TIGIT antagonist further increased activation of TFh-like cells together with increased expression of B cell attracting chemokine *CXCL13*. Tregs responded with a reduced expression of *CTLA4* and *TNFRSF4* (OX40), indicative of modulation of immunosuppressive cell state.Our approach successfully identified heterogenous cellular and patient responses to GITR stimulation and TIGIT inhibition in gastrointestinal cancers. TIGIT antagonist led to a wider reprogramming of the TME compared to the limited effects of GITR agonist. Our strategy identified mechanisms of action of immunotherapy and factors associated with response or resistance, which can aid in prioritization of targets and their clinical translation.

#4122

TIL-containing patient-derived explant cultures reveal role of metformin on antigen presenting cell activation

Rita J. K. Turpin[1], Ruixian Liu[1], Pauliina Munne[1], Aino Peura[1], Jenna Rannikko[2], Gino Philips[3], Natasha Salmelin[1], Elina Hurskainen[1], Ilida Suleymanova[1], Minna Mutka[4], Tuomo Meretoja[5], Johanna Mattson[6], Satu Mustjoki[7], Päivi Saavalainen[8], Diether Lambrechts[3], Jeroen Pouwels[1], Maija Hollmén[2], Juha Klefström[9]. *[1]University of Helsinki, Helsinki, Finland,[2]Medicity Research Laboratories, University of Turku, Turku, Finland,[3]Human Genetics, VIB - KU Leuven Center for Cancer Biology, KU Leuven, Belgium,[4]Department of Pathology, HUSLAB and Haartman Institute, Helsinki, Finland,[5]Breast Surgery Unit, Helsinki University Central Hospital, Helsinki, Finland,[6]Department of Oncology, University of Helsinki & Helsinki University Hospital, Helsinki, Finland,[7]Clinical Chemistry and Hematology, University of Helsinki, Helsinki, Finland,[8]and Folkhälsan Research Center, University of Helsinki, Helsinki, Finland,[9]and FICAN Cancer Institute, and FICAN South Helsinki University Hospital, University of Helsinki, Helsinki, Finland*

Globally, breast cancer is among the most diagnosed cancer types for women. Current and upcoming breast cancer therapies are being

investigated in combination with compounds that stimulate an immune response, but whether the therapeutic agents themselves have unexpected immunomodulatory effects is often overlooked. Here, we have developed a method to grow 3D cultures of intact fragments of patient-derived tissue (Patient-Derived Explant Cultures; PDECs) to assess the preclinical potential of studying human tumor cells and immune cells simultaneously *ex vivo.* Single cell sequencing, flow cytometry, gene expression profiling and cytokine profiling data show that the tumor immunocontexture is conserved in PDECs and that these resident immune cells respond to distinct immune stimulus. We performed gene expression profiling, flow cytometry, and cytokine profiling of drug-treated human explants and found that metformin has antitumor potential through the activation of antigen presenting cells. We further validated *in vitr*o that metformin-mediated APC activation is largely through mitochondrial respiration inhibition irrespective of the presence of tumor cells. Our PDEC platform highlights the preclinical potential of *ex vivo* explants by simultaneously offering information of tumor and immune cell toxicity and mechanism.

#4123

Rhus verniciflua Stokes (RVS) inhibits PD-1 expression and induces anticancer effects via enhancing T-cell function

Seoyoung Kim[1], Young-Kwan Lee[1], Hyoun Jong Moon[1], Sunki Lim[1], Yujeong Gho[1], Wang Jun Lee[2], Sanghun Lee[3], Excelsisbio Inc.. *[1]New Horizon Cancer Institute, Myongji Hospital, Goyang-Si, Korea, Republic of,[2]Myongji Hospital, Goyang-Si, Korea, Republic of,[3]Dankook Univ. Hospital, Goyang-Si, Korea, Republic of*

Rhus verniciflua Stokes (RVS) has traditionally been used for centuries as a therapeutic herb and food supplement in East Asian countries. Over the last decade, the anticancer effects of RVS have been demonstrated in various preclinical and clinical studies. RVS contains major flavonoids such as fustin, fisetin, and sulfuretin, which were known to have apoptotic or anti-proliferative activities in various cancer cell lines. In clinical retrospective studies, RVS administration exclusively suggested more favorable outcomes with prolonged overall survival in solid cancer patients. However, the effect of RVS on immuno-oncology, especially the functional properties

of T cells and their phenotypes remain unclear. Dried RVS grown in Wonju (Korea) was extracted with sterile distilled water after removing the allergen (urushiol). Peripheral blood mononuclear cells (PBMCs) from breast cancer patients with HLA-A*02:01 were isolated using a vacutainer tube and cultured for T cell expansion in the presence of interleukin (IL)-2 for 14 days. Cells were enriched above 90% $CD3^+$ T cells after 14 days of expansion. Red fluorescent protein (RFP)-expressing HLA-A*02:01-matched breast cancer cell lines (MCF7 and MDA-MB-231), were used to determine the anticancer activity of T cells in the presence or absence of RVS. For *in vitro* killing assays, MCF7 and MDA-MB-231 cell lines expressing RFP were co-cultured with T cells with or without RVS treatment for 48 h, and cell viability was measured by the MTT assay. The phenotypic characteristics of the T cells were profiled by staining with various T cell surface markers, including CD3, CD4, CD8, PD-1, and CTLA4. RVS toxicity in the target cells (MCF7 and MDA-MB-231) was not observed at RVS concentrations up to 250 ug/mL. The anticancer activity of T cells against breast cancer cells was significantly increased by adding both 10 ug/mL and 100ug/mL of RVS. T cells co-cultured with MCF7 and MDA-MB-231 cells in the presence of 100 ug/mL of RVS showed 20.6% increases in cytotoxicity in MCF7 cells and 36.2% in MDA-MB-231 cells compared to no RVS treatment. Interestingly, relative reductions in programmed death-1 (PD-1) were found in T cells co-cultured with target cells by adding RVS, even though there was no significant difference in the other markers observed. Our findings showed that RVS could improve the function of T cells against cancer cells in the tumor microenvironment, as interpreted by reduced PD-1 expression in T cells after RVS treatment. Therefore, the components of RVS are candidates for restoring T cells exhausted against cancer. Active compounds should be identified for clinical efficacy, and further studies are necessary for combination strategies with conventional cancer treatments, such as chemotherapy and radiotherapy.

#4124

Targeting the clock pathway to modulate immune response in MSI-high colorectal cancer (CRC): evidence from a preclinical *in vivo* model

Shivani Soni[1], Francesca Battaglin[1], Sofi Castanon[1], Jae Ho Lo[1], Goar Smbatyan[1], Priscilla Chan[2], Meng Qu[2], Priya Jayachandran[1], Hiroyuki

Arai[1], Natsuko Kawanishi[1], Wu Zhang[1], Steve A. Kay[2], Heinz Josef Lenz[1], Evanthia T. Roussos Torres[1]. *[1]Medical Oncology, USC Norris Comprehensive Cancer Center, Los Angeles, CA,[2]Department of Neurology, University of Southern California, Los Angeles, CA*

Background**.** Immune checkpoint inhibitors have substantial clinical success in MSI-H/dMMR metastatic CRC. However, only a subset of patients exhibits durable responses, emphasizing the importance of identifying mechanism of innate and acquired resistance. The relation between the circadian clock and the immune system is well established. We used a syngeneic mouse model of MSI-H CRC to investigate whether a targeted enhancement of clock repressor proteins cryptochrome 1/2 (CRY 1/2) may affect tumor growth and response to anti-PD1 (aPD1).
Methods. $1X10^6$ MC38 cells were subcutaneously implanted into the right flank of 8 weeks old C57BL/6 mice. Mice were randomized into 1 control and 3 treatment arms (10 mice/group): A. CRY stabilizer SHP656(10 mg/kg PO, 5 days/week); B. aPD1 (100 μg/mouse IP, twice/week administered for 2 weeks); C**.** combination SHP656 + aPD1. Tumors from 4 mice/group were processed for tumor infiltration studies. Remaining 6 mice/group were kept for 3 weeks on maintenance aPD1 (twice/week) for survival studies. Treatment response was measured by tumor growth and survival. Treatment effects on immune cell infiltration in the tumor microenvironment (TME), functional myeloid derived suppressor cells (MDSCs) and T cells markers were investigated via flow cytometry.
Results. Single agent SHP656 significantly improved survival when compared with vehicle treated mice. Similarly, combination treatment with SHP656 + aPD1 improved survival, however no additional benefit was observed over treatment with aPD1 alone. All treatment groups had a response rate of 67% (4/6 mice/treatment group showed 2-fold decrease in tumor volume 24 days after tumor challenge vs vehicle). In responders, SHP656 as a single agent or in combination with aPD1 were more effective in suppressing tumor growth as compared to aPD1 alone. Flow cytometry of 14 tumor samples demonstrated that monocytic-MDSC infiltration was significantly decreased in the combination therapy and aPD1 alone treatment arms ($p = .016$) as compared to vehicle suggestive of a less suppressive TME. T cell analysis suggested a decrease in intratumoral exhausted $CD8^+$ T cells ($TIM3^-PD\text{-}1^+$, $p = .02$) in SHP656 + aPD1 vs

vehicle, while infiltration of $CD4^+$ T cells and T regulatory cells were not significantly affected by any treatment. Nanostring profiling on treated tumors also confirmed immune activation in responders.
Conclusions. Our results show for the first time that targeting the clock pathway through modulation of CRY affects TME and tumor progression in *in vivo* models of MSI-H CRC. A decrease in infiltration of mMDSCs and exhausted $CD8^+$ T cells seems to play a critical role in combination treatment efficacy but needs to be studied further. These results, suggests that pharmacological targeting of the circadian machinery holds great potential and could significantly impact the efficacy of immunotherapy in metastatic CRC.

#4125
Rencofilstat exerts a dominant role in synergistic anti-PD1-combination effects in a fatty liver model of hepatocellular carcinoma
Daren Ure[1], Jack Leslie[2], Lacey Haddon[1], Claude Fu[1], Jelena Mann[3], Derek Mann[4]. *[1]Hepion Pharmaceuticals, Edison, NJ,[2]Newcastle University, Newcastle, United Kingdom,[3]Fibrofind Ltd, Newcastle, United Kingdom,[4]Newcastle University and Fibrofind Ltd, Newcastle, United Kingdom*

Rencofilstat is a clinical-phase drug candidate that inhibits multiple cyclophilin isomerases and affects many cellular processes. The objectives of this study were to characterize rencofilstat's anti-tumor effects alone and in combination with anti-PD1 in a murine model of fatty liver-associated hepatocellular carcinoma (HCC). Murine Hep53.4 HCC cells were orthotopically implanted into livers of C57BL/6 mice fed either a normal diet or western diet. Treatments included rencofilstat and anti-PD1 IgG, alone or in combination, from Weeks 2-4 post-implantation. End-of-study analyses included tumor growth, survival, and tumor gene expression by bulk RNA sequencing. Hep53.4 tumors in fatty livers ("fatty tumors") were more resistant to treatments compared to tumors in nonfatty livers ("nonfatty tumors"). On the normal liver background, rencofilstat and anti-PD1 IgG as monotherapies or in combination decreased tumor volumes by 76-83%. In contrast, only combination treatment consistently decreased tumor volumes (84%) in fatty livers. Rencofilstat plus anti-PD1 IgG also extended mouse survival in the fatty liver model. Tumor transcriptomic

analyses revealed marked differences between treatments and tumor types. Rencofilstat altered the expression of 3-times more genes than anti-PD1 in fatty tumors (differentially expressed genes; DEGs), whereas the two treatments affected similar number of genes in nonfatty tumors. The same was true when analysis was restricted to only those genes whose expression correlated with tumor volume. The identities of the DEGs were very different between rencofilstat and anti-PD1 treatments in nonfatty tumors. In contrast, in fatty tumors, 40% of the anti-PD1 DEGs also occurred in rencofilstat-treated tumors, suggesting that rencofilstat can moderately mimic anti-PD1 in fatty tumors. Rencofilstat DEGs also overlapped significantly with combination-treatment DEGs (46%) in fatty tumors, whereas only 7% of the anti-PD1 DEGs were represented in the combination treatment tumors. DEG pathway mapping revealed that the biological pathways predicted to be affected by rencofilstat and anti-PD1 were highly dependent on the type of tumor. In nonfatty tumors both drug treatments predominantly affected cellular biology processes such as protein processing and metabolism, but in fatty tumors both drug treatments overwhelmingly affected immune-related processes such as T cell differentiation, natural killer cells, checkpoint pathways, and cytokine-chemokine signaling. These results highlight major differences in phenotype and treatment response of tumors in fatty livers compared to nonfatty livers. Furthermore, they suggest that a combination of a checkpoint inhibitor with rencofilstat may be especially efficacious for HCC in individuals with NAFLD or NASH, due in part to rencofilstat's multi-pathway targeting.

#4126

Anti-tumor immunity of M9657, a conditional CD137 immune agonist, is correlated with mesothelin expression on tumor cells

Chunxiao Xu[1], Xueyuan Zhou[1], Sireesha Yalavarthi[1], Rene Schweickhardt[1], Andree Blaukat[2], Laura Helming[1]. *[1]EMD Serono, Billerica, MA,[2]Merck KGaA, Darmstadt, Germany*

Background: In clinical trials, systemic administration of first-generation CD137 agonist monotherapies was suspended due to either low anti-tumor efficacy or hepatotoxicity mediated by the epitope recognized on CD137 and Fc gamma receptor (FcγR) ligand-dependent clustering. M9657 is a

bispecific conditional agonist that has been developed to bind simultaneously to mesothelin (MSLN) and CD137 to stimulate an anti-tumor immune response in the tumor microenvironment. M9657 was engineered in a tetravalent bispecific antibody (mAb^{2}™) format with a human IgG1 backbone with LALA mutations, which abrogates binding to FcγRs but retains FcRn binding for IgG-like pharmacokinetics. M9657 is expected to have enhanced anti-tumor efficacy while avoiding systemic immune activation.
Methods: MSLN surface copy number was quantified in a series of cancer cell lines with a broad range of MSLN expression. $CD8^+$ T cell-mediated tumor cell cytotoxicity and cytokine release from $CD8^+$ T cells were investigated in a series of in vitro functional assays. The receptor occupancy (RO) of MSLN on the tumor cell surface and of CD137 on $CD8^+$ T cells was determined by flow cytometry. MSLN in EMT-6 cells was knocked out using CRISPR and confirmed by immunohistochemistry. The anti-tumor efficacy of FS122m, a murine-reactive surrogate of M9657, was investigated in EMT-6 parental and MSLN knockout syngeneic tumor models.
Results: M9657 displayed MSLN-dependent cytokine release and tumor cell cytotoxicity. IFNγ release by $CD8^+$ T cells correlated with MSLN copy number on tumor cells. MSLN copy number of 3000 was found to be the minimum required to trigger CD137 agonism. CD137 RO by M9657 on activated human $CD8^+$ T cells and MSLN RO by M9657 on tumor cells increased with increasing concentrations of M9657. M9657 caused full agonism (EC_{100}) when CD137 RO on activated human $CD8^+$ T cells was approximately 30-38%. The mouse surrogate FS122m demonstrated potent dose-dependent anti-tumor efficacy in the EMT-6 tumor model, while no anti-tumor efficacy was observed in MSLN knockout tumors, which further confirmed that MSLN expression is required for M9657 anti-tumor immunity.
Conclusion: M9657 exhibits promising and potent MSLN-dependent conditional immune agonism, supporting its clinical investigation.

#4127
ANV600 is a potent, C*is*-signaling, non-alpha IL-2 agonist which efficiently expands intratumoral stem-like CD8 T cells

Patrizia Murer, Ulisse Salazar, Nicole Egli, Laetitia Petersen, Pia Neubert, Kirsten Richter, Christian Stocker, Alexander Rau, Andreas Katopodis, Christoph Huber. *Anaveon AG, Basel, Switzerland*

Non-alpha IL-2-based therapeutic modalities with preferential signaling through the IL-2 beta(CD122)/gamma(CD132) receptor are in clinical development and have the potential to substantially increase the therapeutic index of recombinant IL-2 (aldesleukin) for cancer therapy. ANV600 is a novel bispecific compound, which features an anti-IL-2 antibody/IL-2 fusion protein and a proprietary hPD-1 binding moiety for specific delivery of the non-alpha IL-2 to tumor antigen experienced PD-1+ T cells. Compared to the untargeted control, ANV600 has increased potency to induce STAT5 phosphorylation in human PD-1+CD8 T cells *in vitro*. At the same time, stimulation with ANV600 results in markedly reduced STAT5 phosphorylation on Treg cells compared to aldesleukin. In activated human PBMCs, ANV600 induces PD-1 co-internalization with the CD122-CD132 complex, reducing detectable PD-1 on CD8 and CD4 T-cells. Surface PD-1 levels decrease is not observed on cells incubated with untargeted bispecific compound. In transgenic human PD-1 mice ANV600 treatment leads to marked tumor growth retardation in the B16F10 and MC38 subcutaneous tumor models compared to untargeted compound and vehicle. Immunophenotyping of the tumor infiltrating lymphocytes revealed a dose-dependent increase of intratumoral stem-like PD-1+T cells and cytotoxic GrzB+PD-1+T cells in mice treated with ANV600. ANV600 has potent and selective effects on antigen-experienced CD8 T cells both in human PBMCs and mouse syngeneic tumor models. This agent may be a promising anti-tumor therapeutic against poorly immunogenic tumors and warrants further pharmaceutical development.

#4128

AJ17 potentiates agonist CD40 antibody efficacy and attenuates agonist CD40 induced PD-L1 expression and associated toxicity in murine tumor models

Vidit Gaur[1], Anjali Barnwal[1], Bushra Ateeq[2], Jayanta Bhattacharyya[1]. *[1]Center for Biomedical Engineering, Indian Institute of Technology Delhi (IIT Delhi), New Delhi, India,[2]Department of Biological Sciences and*

Bioengineering, Indian Institute of Technology Kanpur (IITK), Kanpur, India

Agonist CD40 antibody (αCD40) has shown excellent anti-tumor efficacy in both pre and early clinical studies. However, in clinics, αCD40 has failed to prove its potential as αCD40 is associated with dose-limiting toxicity due to cytokine release syndrome (CRS), grade 3 to 4 hematological and liver toxicities. In addition, αCD40 induces immune checkpoint proteins (PD-L1, CTLA-4) which makes the tumor microenvironment (TME) immunosuppressive. In this context, this study investigates the therapeutic efficacy of a novel combination of αCD40 and AJ17, a small molecule inhibitor of receptor tyrosine kinase. Combination treatment showed a significant delay in the tumor growth and improved overall survival in mice bearing B16-F10 melanoma and 4T1 orthotopic tumor by increasing the population of $CD8^+$ T cells and lowering the expression of PD-L1, $Foxp3^+$, and arginase in both tumor and spleen. Most interestingly, AJ17 lowered the *in vivo* toxicity associated with αCD40 monotherapy by lowering the levels of alanine aminotransferase (ALT), aspartate aminotransferase (AST), and IL-6 in serum. In conclusion, this combination can be further explored in clinics to improve the *in vivo* anti-tumor efficacy of αCD40 while lowering the associated toxicity.

#4129

Preclinical assessment of GlycoConnect™ ADCs with potency-modulated derivatives of PNU-159,682

Floris L. van Delft, Remon van Geel. *Synaffix, Nijmegen, Netherlands*

PNU-159,682 is an oxidized secondary metabolite of nemorubicin (MMDX), and substantially more potent (2100-6400-fold) than the commonly used chemotherapeutic anthracycline doxorubicin/adriamycin, but without the dose-limiting cardiotoxicity. Based on these beneficial features, PNU-159,682 is currently being clinically evaluated (phase 1) for solid tumor indications as a payload in various antibody-drug conjugates (NBE-002, SO-N102). It must be noted, however, that the HNSTD of current PNU-based ADCs in non-human primates (~1 mg/kg) may end up in a clinical dose that is sub-optimal to achieve high tumor uptake, due to putative target-mediated drug disposition in healthy tissue.

We embarked on a program to develop a set of 2nd-generation PNU-159,682 analogues with attenuated potency, to enable the generation of ADCs with a potentially improved pharmacokinetic profile. Moreover, we reasoned that the adaptation of the new PNU analogues to our proprietary best-in-class ADC technology (GlycoConnect™)[1], in combination with our polar spacer technology (HydraSpace™)[2] might enable PNU-based ADCs with significantly expanded therapeutic index (TI).
We here exhibit the chemical synthesis of a panel of PNU-analogues with attenuated potency and enhanced tolerability, based on specific tailoring of the aminosugar morpholino group. Homogeneous and stable GlycoConnect™/HydraSpace™ ADCs were subsequently generated and evaluated *in vitro* and *in vivo* to assess efficacy and tolerability. These studies demonstrate the potential of attenuated PNU derivatives for application in stable and site-specific ADCs with anticipated higher clinic dose and potentially improved therapeutic index.

[1] Wijdeven et al., Enzymatic glycan remodeling-metal free click (GlycoConnect™) provides homogenous antibody-drug conjugates with improved stability and therapeutic index without sequence engineering. *mAbs* **2022**, 14.
[2] Verkade *et al*. A Polar Sulfamide Spacer Significantly Enhances the Manufacturability, Stability, and Therapeutic Index of Antibody-Drug Conjugates. *Antibodies* **2018**, *7*, 12, doi:10.3390/antib7010012.

#4130

Genetically modified hematopoietic stem cells for improvement of immunotherapies against solid malignancies

Laura Falceto Font, Dan Jin, Connor P. Francis, Bayli DiVita Dean, John W. Figg, Brianna McDonald, Catherine Flores. *Neurosurgery, University of Florida, Gainesville, FL*

Hematopoietic stem cells (HSCs) are routinely used in the clinic to treat several diseases and their side effects, including cancers. Our group has previously shown that the combination of HSCs with two different immunotherapies improves survival in brain tumors, but it is still not curative. In this study, we wanted to explore whether modifying HSCs can drive them into a dendritic cell phenotype or suppress them from becoming immunosuppressive myeloid cells at the tumor microenvironment to

increase survival when combined with immunotherapy in a glioma model. HSCs have been historically challenging to grow *in vitro* for long-term culture due to the short periods of time they remain undifferentiated, which creates an extra challenge for the genetic modification of HSCs. Here, we test different *in vitro* conditions for expansion and modification of murine and human HSCs by employing the following methods for modulation of HSCs: shRNA lentiviral delivery, overexpression constructs, RNA electroporation, CRISPR, and AAV. This study describes the efficacy of each method as well as the observed limitations of each technique on HSCs. Furthermore, preliminary data shows IL6R downregulation as a candidate for driving HSCs into the dendritic cell lineage. Ultimately, these genetically modified cells will be used as an adjuvant therapy to improve the efficacy of various immunotherapeutic strategies against solid malignancies.

#4131

Long-term anti-tumor immunity induced by of HPN328, a DLL3-targeting trispecific, half-life extended T cell engager, in a preclinical immunocompetent mouse model

Mary Ellen Molloy[1], Laura B. Valenzuela[1], Chi-Heng Wu[1], Holger Wesche[1], Banmeet S. Anand[2]. *[1]Translational Medicine, Harpoon Therapeutics, Inc., South San Francisco, CA,[2]Harpoon Therapeutics, Inc., South San Francisco, CA*

Tri-specific T Cell-Activating Constructs (TriTACs) are T-cell engagers that have been developed to redirect T cells to kill tumor cells. HPN328 is a Delta-like ligand 3 (DLL3)-targeting TriTAC currently being evaluated in a Phase 1/2 clinical trial enrolling patients with advanced cancers associated with DLL3 expression, including small cell lung cancer (SCLC) and other neuroendocrine malignancies (NCT04471727). HPN328 consists of three binding domains: a CD3 binder for T cell engagement, an albumin binder for half-life extension, and a DLL3 binder for tumor cell engagement. We have previously reported that HPN328 induces potent dose-dependent killing of DLL3 expressing SCLC cell lines together with dose-dependent T cell activation and cytokine release in T cell co-cultures *in vitro*. Based on these data and the proposed mechanism of TriTAC induced tumor cell killing we hypothesized that HPN328 could induce epitope spreading and

long-term immunogenic effects. To test this hypothesis, we generated an immunocompetent mouse model in which six amino acid residues corresponding to the portion of human CD3ε which TriTAC molecules bind were added to the N terminus of the mouse CD3ε subunit. Homozygous knock-in mice (hCD3ε) were implanted subcutaneously with MC38 murine colon cancer cell line expressing human DLL3 and treated with HPN328 following tumor establishment. HPN328 treatment led to eradication of established tumors in mice. In addition, tumor infiltrating lymphocyte (TIL) analysis was performed on tumors harvested on day 4 post HPN328 treatment. Activation markers CD69 and CD25 were induced on both CD4+ and CD8+ TILs in this model. To evaluate if HPN328 can induce long-term immunity, mice whose tumors were cured by HPN328 were rechallenged on the opposite flank. As expected, tumors grew in treatment naïve mice, but no tumors were detected in mice previously treated with HPN328, demonstrating sustained and durable anti-tumor immunity induced by HPN328 treatment. Anti-tumor immunity is an indicator of T cell memory against tumor antigens. Concomitant with anti-tumor immune response, we detected increases in memory T cells in the spleens of mice previously treated with HPN328. Together these results indicate that HPN328 can induce epitope spreading and prolonged anti-tumor immunity, suggest a novel mechanism for its activity and efficacy *in vivo*.

#4132

Effect of mechanical cues on T cell killing of cancer cells

Hannah Dada[1], Kun Do[2], Alexander Cartagena-Rivera[2], Grégoire Altan-Bonnet[1]. *[1]NIH-NCI, Bethesda, MD,[2]NIH-NIBIB, Bethesda, MD*

Cancer immunotherapies have focused on strategies to strengthen immune cell activation and effector function. These treatment strategies enhance the effector function of immune cells, particularly cytotoxic T cells (CTL), driving tumor eradication. Methods to improve the killing mechanisms of CTLs are not well studied and largely focused on assessing/strengthening the antigenic responses of T cells. We hypothesize that the mechanical landscape of CTL-tumor interactions can also drastically impact CTL cytotoxicity. By altering the physical context for T cell recognition of tumors, we measured cytotoxicity changes and subsequently used these changes in killing capacities to train and generate a quantitative

parametrization of T cell killing. CTLs utilize cytokine expression to kill and shape the inflammatory milieu. Taking advantage of a robotic platform that enables the automatic collection of cytokines, we assembled datasets of T cell attacks of tumor cells grown on substrates with varying stiffness levels. The stiffness levels were altered using polyacrylamide (PAA) gels and ranged from 0.2kPa to approximately 113 kPa. Preliminary results from two different models (i.e., mouse and human TCR-transgenic T cells) suggest that there exists an optimal stiffness value for maximal response by T cells. These results suggest that CTLs utilize biophysical cues in addition to molecular cues (antigen) to properly elicit an immune response—modeling and fine-tuning these mechanical cues can be a novel and effective approach to improving cancer immunotherapies.

#4133

OncoTAM, a comprehensive preclinical platform to explore macrophages as key drivers of cancer progression and develop new therapies against tumor-associated-macrophages

Caroline Mignard, Damien France, Francis Bichat, Nicolas Legrand, Olivier Duchamp. *Oncodesign Services, Dijon Cedex, France*

Tumor-Associated Macrophages (TAMs) play an important role in the development of tumors, modulation of neoangiogenesis, immune suppression, and metastasis. A high infiltration of macrophages in the tumor is also correlated with a poor prognosis in several cancer types. Therefore, they became an attractive target for cancer immunotherapies. Several macrophage-targeting approaches in anticancer therapy are under development, including TAM depletion, inhibition of new TAM differentiation, or re-education of TAM activation for cancer cell phagocytosis. In this presentation, we will share different examples of in vitro assays and in vivo models we are implementing to support preclinical development of novel TAM-targeting strategies. Antibody-dependent cellular phagocytosis (ADCP) has been used to demonstrate one crucial mechanism of action of different antibody (Ab) therapies targeting macrophages. Some of these Ab (including anti-CSF1) have then been tested in syngeneic in vivo tumor models. To reach this goal, we demonstrated that the tumor implantation site in mice (subcutaneous vs orthotopic) could impact the polarization of macrophages (M1 vs M2).

Differences in the ratio of M1 and M2 subtypes infiltrating the PAN-02 pancreatic murine tumors were observed, and anti-CSF1 antibodies increased the survival of mice bearing orthotopic Renca murine kidney tumor by eliminating TAMs. Additionally, in xenograft models of human breast tumors in NOD-SCID mice, the eradication of TAMs by anti-CSF1R clearly demonstrated the importance of macrophages in the tumor progression and in the anti-tumor efficacy of Abs mediated by macrophages. By using an orthotopic Hepa1-6 murine liver cancer model, we showed high antitumor efficacy of compounds targeting the STAT6 pathway by reprogramming immunosuppressive TAMs into an M1 phenotype that promotes the induction of a cytotoxic immune response. For compounds displaying no cross-reactivity with murine target, we developed models and characterized the TAMs in breast, colon, melanoma and head & neck PDX and CDX tumors in different huCD34-engrafted mouse models. Altogether, the panel of in vitro assays and in vivo tumor models in OncoTAM should be useful to provide insights on the mechanism of action and antitumor efficacy of novel immune-oncology strategies targeting macrophages.

#4134

Boosting anti-tumor immunity by promoting high endothelial venule and tertiary lymphoid structure formation in solid tumors via LTBR agonism

Disi An, Guoying Chen, Wei Wang, Katja Mohrs, David DiLillo, Christopher Daly, Gavin Thurston, John Lin, Namita Gupta, Mickey Atwal, Frank Kuhnert. *Regeneron Pharmaceuticals, Inc., Tarrytown, NY*

High endothelial venules (HEV) are specialized blood vessels that mediate lymphocyte trafficking to lymph nodes. Tertiary lymphoid structures (TLS) are ectopic lymphoid formations that develop in inflamed, infected or tumoral tissues. TLS contain HEV and B cell follicles surrounded by a T-cell zone and are characterized by abundant chemokine expression. The presence of TLS and HEV in solid tumors is positively correlated with patient survival in many cancer types, and may even be predictive of better response to immune-checkpoint blockade. However, the molecular mechanisms underlying the intratumoral HEV and TLS formation remain unclear. Using murine syngeneic tumor models, we found that systemic

activation of lymphotoxin beta receptor (LTBR) with an agonistic antibody induced tumor-specific HEV formation, increased dendritic cell (DC) and T cell infiltration, and enhanced T cell activation in the tumor. *In vitro* assays revealed that LTBR agonism directly upregulated activation and maturation markers in bone marrow-derived DCs and promoted DC-mediated CD4 and CD8 T cell activation. Single agent LTBR agonist treatment attenuated Colon26 tumor growth in a CD8 T cell-dependent manner. In combination treatment studies, LTBR agonism further augmented anti-tumor efficacy of anti-PD1 and of CAR-T therapy. Notably, LTBR agonist mAb treatment upregulated the expression of TLS-related chemokines and induced TLS-like structures in approximately 20% of treated tumors. To enhance TLS induction, we generated syngeneic tumor models engineered to express several cytokines/chemokines and performed an *in vivo* screen for tumor-associated TLS formation. We identified some factors that in combination with LTBR agonism induced B cell enrichment and immature TLS formation, while others promoted robust TLS induction and anti-tumor effect. TLS formation induced by combined LTBR agonism and cytokine expression is associated with augmented anti-tumor responses to anti-CTLA-4 treatment. By studying anti-tumor mechanisms of LTBR agonism-mediated HEV and TLS formation, this work informs the future therapeutic strategies to boost T cell infiltration and activation in solid tumors.

#4135

A novel plasma cell-based mechanism of action of adenosine immunomodulation and A2AR antagonism

Chiara Martinoli[1], Paola Tieppo[1], Marjorie Mercier[1], Hussein Shehade[1], Noemie Wald[1], Anais Vezzu[1], Annelise Hermant[1], Boris Pirlot[1], Stephanie Ma[2], Maurizio Ceppi[1], Yvonne McGrath[1], Maura Rossetti[1]. *[1]iTeos Therapeutics, Charleroi, Belgium,[2]A4P Consulting Ltd, Sandwich, United Kingdom*

High levels of extracellular adenosine, often found in the tumor microenvironment (TME), promote immune suppression mainly through the A_{2A} receptor ($A_{2A}R$) expressed by tumor-infiltrating immune cells. Inupadenant (formerly known as EOS100850) is an oral, non-brain penetrant, potent and highly selective small molecule antagonist of $A_{2A}R$.

In a Phase I/Ib clinical trial (NCT03873883), inupadenant as monotherapy showed initial evidence of clinical benefit in subjects with advanced solid tumors. In this study, tumor biopsies with a high number of $A_{2A}R$-expressing immune cells at baseline were associated with response or stable disease.We now report that infiltration of $A_{2A}R^{+}$ cells was strongly correlated with the expression of B- and, more specifically, antibody-secreting cell (ASC)-related genes, as assessed by gene expression (Nanostring) and immunohistochemistry (IHC), hinting at a potential novel role for $A_{2A}R$ in B cell biology. Therefore, we explored the expression and function of $A_{2A}R$ in human B cells. Immunocytochemistry staining of $A_{2A}R$ on sorted tonsillar B cell subsets showed that $A_{2A}R$ was predominantly expressed on ASCs, including plasma cells and plasma blasts versus naïve or memory B cells. The preferential expression of $A_{2A}R$ by ASCs was confirmed on NSCLC tissues by multiplex immunofluorescence. In addition to $A_{2A}R$, ASCs expressed other adenosine pathway markers such as CD39, suggesting that the adenosine pathway is a key mechanism through which ASC functions may be modulated. Using B cells derived from peripheral blood, the $A_{2A}R$ agonist CGS-21680 was shown to inhibit the maturation of B cells into plasma cells, and that maturation could be fully restored by inupadenant. CGS-21680 did not affect B cell or plasma cell viability, indicating that the effect of $A_{2A}R$ signaling on plasma cell differentiation is not due to preferential plasma cell death in culture. Importantly, baseline expression of B cell- and ASC-related markers measured by Nanostring and IHC was associated with response or stable disease to inupadenant monotherapy, supporting the notion that these cells may be a novel target of inupadenant. This is in line with recent reports showing that B cells, plasma cells and tertiary lymphoid structures are associated with favorable responses to cancer immunotherapy. Interestingly, four out of the five non-progressors treated with inupadenant as monotherapy and with available biomarker data showed a reduction in ASC infiltration after inupadenant treatment, suggesting that inupadenant may promote terminal plasma cell differentiation and migration out of the tumor tissue and to the bone marrow.Altogether, these data support a novel plasma cell-centric

mechanism of action of inupadenant, which may complement its reported T cell-mediated anti-tumor activity.

Developments in Anticancer Immunotherapy

#4139
Functional human myeloid cells in BRGSF-HIS humanized mice enables myeloid-directed therapy assessment
Florence Renart-Depontieu[1], Gaëlle Martin[1], Valery Moine[2], Coline Burnet-Merlin[2], Florent Creusat[1], Alexis Gonon[1], Perrine Martin-Jeantet[1], Fabiane Sônego[1], Lise Nouveau[2], Yacine Cherifi[1], Kader Thiam[1].
[1]genOway, Lyon, France,[2]Light Chain Bioscience, Plan-Les-Ouates Genève, Switzerland

Translational preclinical assessment of myeloid-targeting therapies is considered challenging due to the reduced availability of humanized mouse models expressing both lymphoid and myeloid compartments. Most of the humanized models harboring myeloid compartment overexpress human cytokines, leading to body weight loss, anemia and a short life span. Recent report described the BRGSF-HIS as an alternative model displaying all major human hematopoietic cell subsets, such as B, T, natural killer (NK), dendritic cells (DCs), plasmacytoid cells (pDCs) and monocytes/macrophages. Human myeloid cells developed in the BRGSF-HIS mice without side effects and human immune system engraftment is stable for over a year (Labarthe et al., 2019), favoring long terms studies with agents requiring a wide therapeutic window. Here we report that myeloid compartment developed in BRGSF-HIS mice is recruited in the tumor microenvironment of tumor bearing mice, and are also capable of triggering effector mechanisms such as ADCP and ADCC. Myeloid cells developed in the BRGSF-HIS mice are functional as, *ex vivo* stimulation with TLR and STING agonists induce CD83 expression and pro-inflammatory cytokine secretion (TNF-α, IL-1β, CCL2, ⋯) by monocytes and bone marrow derived macrophages (BMDM). *In vivo*, myeloid cells are activated through LPS challenge, leading to increased CD83-expressing cDCs frequency and CD83 and CD86 expression levels. Furthermore, BMDM are efficiently skewed toward M1 and M2-like profiles in response to LPS and IL-4, respectively. Analyses of TME from MDA-MB-231, show

the recruitment of human immune cells, including T cells, NK cells, cDC and activated M2 macrophages (expressing both CD86 and CD206). Expression of FcγR, essential for antibody dependent cellular cytotoxicity (ADCC) and antibody dependent cellular phagocytosis (ADCP) activities, is found on human peritoneal macrophages and BMDM from BRGSF-HIS. ADCP activity mediated by macrophages was established as tumor cells are specifically phagocyted *ex vivo* in presence of a bispecific antibody (anti-human CD47 x tumor-associated antigen). Such findings were corroborated by B cell depletion *in vivo* induced by Rituximab (anti-CD20 mAb - hIgG1), which has been described to trigger CDC, ADCC and ADCP via FcγR (Teige *et al*., 2019). Finally, OKT3 induces cytokine release syndrome in these mice, evidenced by cytokine release, body weight and temperature drop. Treatment with Infliximab reduced these symptoms, suggesting that BRGSF-HIS mice enable assessment of safety and its clinical management. In summary, BRGSF-HIS mice develop myeloid cells without side effects and has a wide therapeutic window, enabling the assessment of effector mechanisms such as ADCP and ADCC, triggered by of myeloid-targeted therapies.

#4140

Oncogenic KRAS inhibition with ADT-007 primes T cell responses in pancreatic ductal adenocarcinoma

Jeremy B. Foote[1], Tyler E. Mattox[2], Adam B. Keeton[3], Ganji N. Purnachandra[1], Yulia Maxuitenko[3], Xi Chen[4], Jacob Valiyaveettil[3], Donald J. Buchsbaum[1], Gary A. Piazza[3], Bassel F. El-Rayes[1]. *[1]University of Alabama at Birmingham, Birmingham, AL,[2]University of South Alabama, Mobile, AL,[3]Auburn University, Auburn, AL,[4]Auburn Univeristy, Auburn, AL*

Background**:** Pancreatic ductal adenocarcinoma (PDAC) has low (<11%) 5-year survival due to the presence of advanced disease at diagnosis. Currently standard of care provides a median survival of 1 year in the majority of patients presenting with advanced disease. Targeting oncogenic KRAS, which is mutated in >90% of human PDAC tumors, provides an opportunity to inhibit a critical pathway and significantly impact standard of care in patients diagnosed with PDAC. Furthermore, evidence indicates that inhibiting-oncogenic KRAS signaling modulates anti-tumor immune

responses and demonstrates synergy with immune checkpoint blockade in pre-clinical models. The purpose of this study is to evaluate efficacy and impact on anti-tumor immunity of a novel inhibitor, ADT-007 that demonstrates pan-RAS inhibitory activity.
Methods: Female C57BL/6J, C57BL/6J. Ifng/Thy1.1 KI;Cg-Tg-IL2$^{tm1/eGFP/Weav}$ (IFNg-Thy1.1/IL-2-GFP reporter mice), or immune deficient (T/B cells) Rag 1 $^{-/-}$ mice (n=5-10/group) were implanted SQ with 10^6 mouse derived PDAC cell lines (7160c2 and 2838c3) bearing KRAS^{G12D} mutation, and then randomized (day 7), into vehicle (5% DMSO/5% Kolliphor/90% H_2O) or ADT-007 treatment, which was administered SQ (peritumoral), BID at 5 mg/kg for 2 - 3 weeks. Tumor growth *in vitro* (IC_{50}), KRAS-MAPK/AKT signaling, *in vivo* tumor volumes (tv = L x W^2/2), and tumor immune responses were assessed by CellTiter Glo, phosphoflow/western blotting, bi-weekly caliper measurements, and multi-parameter flow cytometry, respectively.
Results: ADT-007 inhibited KRAS-MAPK/AKT signaling in human and mouse PDAC cell lines inducing G2-M phase arrest and apoptosis at low nanomolar concentrations. Peritumoral administration of ADT-007 inhibited tumor cell growth *in vivo*, modulating T cells in the tumor microenvironment (TME), specifically, an increase in tumor infiltrating, $CD44^+$ $CD62L^-$ $CD4^+$ and $CD8^+$ T cells and increases in production of TNFα, IFN-γ, IL-2, and granzyme B upon stimulation with PMA/ionomycin.
Conclusion: The small molecule inhibitor, ADT-007 blocks oncogenic KRAS signaling and modulates T cell activation and function in the TiME of immune competent, syngeneic mouse models of PDAC. More broadly, these findings indicate that a pan-RAS inhibitor is capable of modulating anti-tumor immune responses extending previous observations that targeted inhibition of oncogenic KRAS^{G12C} modulates tumor immunity in animal models of colon and lung cancer.

#4141
Effects of exercise on tumorigenesis, immune system, and the gut microbiome in a bladder carcinogen mouse model
Joseph P. LaMorte, Brittany Tian, Rashida Ginwala, Laura Bukavina, Philip Abbosh. *Fox Chase Cancer Center, Philadelphia, PA*

Recent studies have begun to demonstrate the therapeutic capacity of physical exercise on cancer treatment outcomes. While this research suggests exercise may improve health in cancer patients, the specific mechanisms by which exercise influences tumor progression remain largely unknown. We hypothesized that exercise alters the gut microbiome and promotes immune cell activation in relevant immune sites. Therefore, we utilized BBN (N-butyl-N-(4-hydroxybutyl)-nitrosamine), a carcinogen that mimics human muscle invasive bladder cancer conditions, and voluntary exercise wheels to determine the effect of exercise on bladder carcinogenesis, gut microbiome, and the immune system. Ultrasound imaging revealed that the average tumor volume of female exercising mice was 11.9% of the total bladder volume at time of sacrifice, while the tumor volume of their non-exercising counterparts was 56.4%, a difference determined to be significant using a two-tailed t-test with p-value of 0.05. A similar trend was seen in male mice, though the difference between groups was not significant. Immune cell analysis did not show significant variation in cytotoxic T cell, helper T cell, macrophage, or dendritic cell populations between exercising and non-exercising mice in spleen, colon, or bladder tissues as measured by FACS. Standardization of the amount exercised, as evaluated by expression of myosin and actin levels in the tibialis anterior muscle, and sequencing of the gut microbiome are in progress and could better indicate the mechanism of exercise-induced tumor suppression.

#4142

CD4 T cell-driven response to immunotherapy against mouse melanoma tumors

Amy K. Erbe, Arika S. Feils, Alina Hampton, Dan Spiegelman, Noah Tsarovsky, Anna Hoefges, Peter M. Carlson, Alex Pieper, Callie Haertle, Mackenzie Heck, Sabrina VandenHeuvel, Lizzie Frankel, Lauren Zebertavage, Alexa Heaton, Zachary S. Morris, Ravi Patel, Alexander Rakhmilevich, Paul M. Sondel. *University of Wisconsin-Madison, Madison, WI*

Using an *in situ* vaccine (ISV) regimen that includes a combination therapy of radiation (given at D0) with hu14.18-IL2 immunocytokine [anti-GD2 linked to IL2, (Anyxis Immuno-Oncology GmbH (Austria)); given at D5-

D9], we can cure mice of large B78 melanoma tumors (B78s). GD2 is expressed on many solid tumors, including most melanomas, and is not often expressed on immune cells. Mice cured with ISV of B78 tumors demonstrate long-term immune memory, with mice rejecting tumor rechallenge >180 days post initial cure of tumor. Traditionally, immune effector memory is thought to be mediated via CD8 T cells, which require antigen presentation via MHC Class I (MHCI). However, B78s express little to no MHCI, but do express MHCII when stimulated with IFNγ. Expressed on 50-70% of melanomas in humans, the role of MHCII on response is unclear. We explored implications of MHCII and MHCI expression on response (initial response to ISV and memory response). Mice bearing B78s depleted of NK cells or CD8 T cells during ISV respond to therapy, but mice depleted of CD4 T cells fail to respond to ISV. Likewise, B78-cured mice depleted of NK and CD8 T cells during rechallenge are able to reject the B78 tumor rechallenge, whereas those depleted of CD4 T cells failed to reject their B78 rechallenge. Together these data suggest that CD4 T cells are required for the initial antitumor response to ISV as well as for immune memory formation and function. Tumors and tumor draining lymph nodes were harvested during ISV treatment in B78-bearing mice at D8 and assessed by scRNAseq, flow cytometry, IncuCyte and ImageStream (live-cell imaging assays), and IsoPlexis (cytokine profile). Though not required for initial or memory response, both CD8 and NK cells are activated and exhibit cytotoxic phenotypes in the tumor microenvironment (TME). Furthermore, a population of cells co-expressing both GD2 and CD45 was observed in the TME following ISV that was not observed in untreated mice. These GD2+/CD45+ cells were predominantly CD4+ T cells incorporate patchy GD2 expression on their surface via trogocytosis. We hypothesize that the interaction between MHCII on tumor cells and CD4 T cell receptors mediates the trogocytosis, activating CD4 T cells to function as helper T cells, initiating a cascade of antitumor immunity, as well as causing direct CD4 T cell-mediated cytotoxicity.

MHCII is expressed on some melanoma tumors, and its expression has been correlated with a positive response to immunotherapies. MHCII expression on tumors can directly engage CD4 cytotoxic T cells, suggesting an important role in the response to immunotherapy for CD4 T cells in melanoma tumors that express MHCII. Understanding the cellular and

molecular mechanisms involved in the ISV-induced immune recognition and destruction of B78 may guide future improvements of this clinically-relevant immunotherapy regimen.

#4143

Enhancing adaptive immune responses with telomerase-mediated telomere targeting therapeutics in hepatocellular carcinoma

Ann Marie Flusche[1], Jerry Shay[1], Ilgen Mender Ogunrinde[2]. *[1]UT Southwestern Medical Center, Dallas, TX,[2]MAIA Biotechnology, Chicago, IL*

Hepatocellular carcinoma (HCC) is the most common primary malignant tumor of the liver and is the third leading cause of cancer-related deaths. In recent years, immune checkpoint inhibitors (ICIs) have improved treatment of solid tumors including HCC. However, due to low response rates with current standard of care immunotherapy and angiogenic inhibitors, there is an urgent need to develop new therapeutic strategies to improve the efficacy of immunotherapy against HCC. Our lab has shown that 6-thio-2' deoxyguanosine (6-thio-dG), a telomerase-mediated telomere targeting agent, is incorporated into newly synthesized telomeres by telomerase and causes rapid telomere uncapping, thereby inducing telomere-associated DNA damage in cancer cells. These damaged DNA fragments can then lead to enhanced adaptive immune responses. In this study, we evaluated the therapeutic effects of 6-thio-dG *in vitro* and *in vivo* together with ICIs in liver tumors to determine whether combining immunotherapy with a telomere-targeting agent could serve as an effective strategy for HCC. To explore whether 6-thio-dG is effective in killing liver cancer cells, we ran cell viability and telomere dysfunction induced foci (TIF) assays to assess DNA damage on telomeres *in vitro* and compared tumor volumes of mice following 6-thio-dG monotherapy, immunotherapy, and sequential treatment of 6-thio-dG and immunotherapy in syngeneic mouse models. We observed that 6-thio-dG reduced cell viability and induced telomere dysfunction in a panel of human and mouse liver cancer cells. In addition, 6-thio-dG enhanced the therapeutic effect of immunotherapies in liver syngeneic mouse models. Overall, our findings show that the telomere-targeting anticancer agent 6-thio-dG inhibits HCC as a single monotherapy and/or sequential therapy together with immunotherapies. These results

provide an experimental rationale for a potentially new immunochemotherapy strategy based on the administration of a telomere-targeting agent.

#4144

Characterization of immune cell phenotypes in patient derived malignant pleural effusion treated with thiostrepton

Terri Messier[1], Roxana Del Rio Guerra[1], George Naumov[2], Brian Cunniff[1].
[1]Larner College of Medicine at The University of Vermont, Burlington, VT,[2]RS Oncology, LLC, Cambridge, MA

Tumor cells generate elevated levels of reactive oxygen species (ROS) and therefore exhibit increased expression, activity, and reliance on critical ROS scavenging pathways, including the mitochondrial peroxiredoxin 3 (PRX3) system. PRX3 is a critical reactive oxygen species (ROS) scavenging enzyme localized to the mitochondrial matrix. Our group has characterized the mechanism of action of the PRX3 inhibitor and pro-oxidant therapeutic thiostrepton (TS). TS covalently crosslinks the peroxidatic and resolving cysteines of PRX3, leading to increased levels of mitochondrial ROS, resulting in tumor cell death. We have characterized the cellular and chemical composition of malignant pleural effusion (MPE) from patients with advanced cancer and evaluated cellular responses to TS. TS targets PRX3 in both adherent tumor cells and in non-adherent immune cell populations in a dose-dependent manner. We further characterized MPE-infiltrated immune cells and cytokines released following TS-treatment. Together, these data provide the first evidence for the activity of TS in MPE and resulting changes to immune cell profiles. TS is the active pharmaceutical ingredient of RSO-021, a new covalent inhibitor of PRX3 currently being tested in the MITOPE phase 1/2 clinical trial in patients with malignant pleural effusion (MPE) due to advanced solid tumors or malignant mesothelioma (NCT05278975).

#4145

Frizzled-4 expression enhances hepatocellular carcinoma progression, sorafenib resistance and suppresses anti-tumor CD8 T cell immunity

Jie Luo, Lanqi Gong, Yuma Yang, Qin Liu, Jiao Huang, Xiaona Fang, Xin-Yuan Guan. *The University of Hong Kong, Pokfulam, Hong Kong*

Background**:** Hepatocellular carcinoma (HCC) is one of the most common and deadliest cancers. Sorafenib remains the globally accepted systemic first-line treatment for advanced HCC although acquired drug-resistance is becoming increasingly common. Hopefully, immune-checkpoint inhibitor therapy has recently revolutionized the treatment for advanced HCC that have poor response to sorafenib, but the durable response rate remains low in most patients for unknown reasons. This fuels a wave of research into the molecular mechanisms of tumor-intrinsic resistance to both chemotherapy and immune checkpoint blockade (ICB), which may provide potential systemic treatment options for advanced HCC patients.
Methods and Results: RNA sequencing of sorafenib-resistant HCC cell lines was performed to identify Frizzled-4 (FZD4) as a critical gene for drug resistance that was further validated in animal models. Clinical implication of FZD4 overexpression was studied in HCC patients. Using genetic and pharmacological approaches, we found that FZD4 was sufficient to increase clonogenicity, migration and invasion, and prevent sorafenib-induced apoptosis. In addition, FZD4 could reduce secretion of tumor necrosis factor-alpha (TNF-α) and interferon-gamma (IFN-γ), as well as intracellular levels of cytotoxic granzyme A and perforin in $CD8^+$ T cells, indicating significant suppression of $CD8^+$ T cell-mediated antitumor immunity in HCC tumors. *In vivo* studies also revealed that FZD4 expression promoted tumorigenesis and accelerated HCC cell metastatic lung colonization. Combination therapy of FZD4 inhibitor FzM1 with sorafenib in HCC of *MYC*/sg*p53*-induced model showed a tendency to significantly impede tumor growth and improve mice survival. Moreover, gene set enrichment analysis (GSEA) identified the cholesterol homeostasis and fatty acid metabolism signaling signatures as the top activated pathways in FZD4-high HCC cells. This evidence suggests a crucial role of FZD4-involved lipid metabolism linked to the development of therapeutic resistance.
Conclusion: Our study demonstrates that FZD4 expression plays a pivotal role in HCC progression and holds the potential for expanding the scope of targeted/ICB therapies to tumors that are currently unresponsive, especially in advanced HCC. The resistance mechanisms will be addressed in further work.

#4146

Unlocking IO drug potential by high content imaging of immune cell co-cultures with cancer organoids from diverse cancer indications

Saskia de Man, Chiara Foini, Tomas Veenendaal, Michelle Kop, Christos Santaris, Sergei Chavez Abiega, Nataliia Beztsinna, Daniel Okkes, Ashgard Weterings, Leo Price, Gera Goverse. *Crown Bioscience Netherlands B.V., Leiden, Netherlands*

Introduction

Immuno-oncology (IO) drugs have shown great results for specific cancer indications in the clinic, most notably for hematological cancers, as well as some solid cancers such as melanoma. However, the potential of many IO drugs as well as mechanisms of resistance in different indications remain to be uncovered. With the development of organoid technology, it is now possible to grow tumor objects in 3D scaffolds with a high resemblance to the original patient tumor in terms of genetics, transcriptomics and morphology. This technology is highly suited for pre-clinical screens and of great translational value. Here we present a high throughput platform using this organoid technology to study IO drug candidates in different indications.

Material and methods

Patient-derived organoids (PDOs) from different origins, including colorectal, lung, breast, melanoma and ovarian cancers, were cultured in protein hydrogels. Allogenic PBMCs were isolated from two healthy donors and were activated with superantigens or CD3/CD28 beads. PDOs and PBMCs were then co-cultured together in presence of IO drugs, such as monoclonal and bispecific antibodies, and analyzed for immune cell migration, infiltration and PDO killing. This was assessed by 3D high content imaging (HCI) and quantified with an automated image segmentation pipeline, which segments tumor objects and immune cells in the 3D reconstituted stack.

Results and discussion

Image-based analysis on PBMC numbers, migration and infiltration, and PDO volumes was performed. Data analysis showed that the activation status of the PBMCs induced different levels of infiltration and killing, as measured by the number of infiltrated immune cells and PDO volumes

respectively. In addition, different PDOs showed different sensitivities for immune cell-mediated killing and compound effects.
Conclusion
Our PDO - immune cell co-culture system in combination with HCI allows the detection and quantification of migration towards, infiltration into and killing effects of immune cells on PDOs in a single assay. This 3D assay allows the identification of IO drug mode of action, specificity, resistance and sensitivity and immune cell activation. Here, we observed a broad spectrum of responses based on the specific characteristics (e.g. morphology and gene expression) of different PDOs and differential activation of PBMCs. The broad range of PDOs available from our biobanks empowers IO drug developers to explore their candidates in multiple cancer indications or in multiple models of a single indication with a range of different genetics, target expression and morphology. Ultimately this allows for the testing of IO drugs, such as engineered T Cells, tumor targeting antibodies, bispecific T Cell engagers, and immune cell modulators in clinically relevant models, bringing the promise of IO therapies to more indications and patients.

#4147

Activated pyroptosis prior to treatment marks a potential response to immunotherapy in cancers

Yumo Xie, Xiaolin Wang, Meijin Huang, Yanxin Luo, Huichuan Yu. *The Sixth Affiliated Hospital of Sun Yat-sen University, Guangzhou, China*

Purpose: Immune checkpoint inhibitors (ICIs) have achieved remarkable survival improvement in multiple cancers by exerting anti-tumor effects through augmenting adaptive immunity. However, 60%-70% of patients showed primary resistance to ICIs, and the underlying mechanisms remained unclear. Pyroptosis is a programmed cell death accompanied by a robust inflammatory response with the secretion of pro-inflammatory molecules, and thus it has the potential to be a promising biomarker for immunotherapy.
Methods: A dataset with the clinical and transcriptomic profiles was derived from 16 randomized controlled trials and studies on ICIs treatment in multiple solid tumors, including melanoma, urothelial cancer, non-small cell lung cancer, renal cell cancer, breast cancer, and esophageal cancer. The

responder was defined as patients achieving complete or partial response, while the non-responder was defined as patients with stable or progressive disease. According to previous studies, we generated a cytotoxic pyroptosis-related gene set, including *CASP1, CASP3, CASP4, CASP5, CASP8, GSDMB, GSMDC, GSDMD, GSDME, GZMA, GZMB,* to explore the association of cytotoxic pyroptosis with response to ICIs. In addition, the previously defined gene set from the Gene Ontology working group that contains a pyroptosis-related gene set was also included to represent the level of total pyroptosis. Single sample Gene Set Enrichment Analysis (ssGSEA) was performed, and the fold-changes and p-values of gene sets were merged with the R package "MetaVolcanoR". Patients in each subset were split by the median of the ssGSEA score of pyroptosis-related genes and identified as with relatively activated and inhibited pyroptosis, respectively. A P-value < 0.05 was considered significant.
Results: A total of 1,407 patients were analyzed, including 475 responders and 932 non-responders. The ssGSEA revealed that both the pyroptosis and the cytotoxic pyroptosis gene sets were enriched in responders, while the cytotoxic pyroptosis-related gene set was one of the top five ones among the 545 enriched in responders. Moreover, the survival analysis showed that in urothelial and non-small cell lung cancer, patients with activated pyroptosis prior to treatment had better progression-free survival and overall survival after ICIs therapies. These results suggested that an activated status of pyroptosis, especially the pyroptotic process related to cytotoxic events, is a marker for better response to ICIs.
Conclusions: The transcriptomic analysis of universal immunotherapy biomarkers identifies an pre-existing activated status of pyroptosis within the tumor microenvironment was associated with a better ICIs response across different cancer types, and thus these pyroptosis-related genes may serve as valuable immunotherapy markers and in silico fundamental tool for exploring pyroptosis in tumor immunity.

#4148

Immunophenotyping of responses to immunotherapy in syngeneic tumor models using multiplex immunofluorescence compared to multiparametric flow cytometry

Philipp Metzger, Carla Castro, Cynthia Obodozie, Holger Weber. *Reaction Biology Europe GmbH, Freiburg, Germany*

In the last decades, several major breakthroughs in cancer treatment were achieved through a better understanding and therapeutic targeting of the immune system. Multiparametric flow cytometry is a robust and powerful tool to evaluate the frequency and activation status of a large variety of immune cells. However, for flow cytometric analysis tumor, tissue must be digested into a single cell suspension, and thereby the information on the tumor architecture as well as the spatial distribution of immune cells is lost. The distribution of immune cells in the tumor microenvironment is often heterogeneous and a favorable immune cell distribution is crucial for an efficacious anti-tumor immunotherapy. The recent advances in multiplex immunofluorescence (mIF) allows the analysis of multiple parameters simultaneously so that the frequency as well as the spatial distribution of multiple immune cells can be analyzed.
In this study, immunotherapy-responsive tumor cell lines (colon carcinoma cell lines MC38-CEA and CT26wt as well as melanoma cell line Clone M3) were implanted in the mammary fat pad (subQperiorTM), which leads to reduce ulceration rate and homogenous tumor growth compared to subcutaneous implantation. Anti-PD-1 immunotherapy reduced the tumor growth in all three tumor models significantly. Formalin-fixed paraffin-embedded tumor samples were collected from control and anti-PD-1 treated animals. Murine specific InSituPlex® (ISP) technology (Ultivue) was used to perform multiplex immune profiling of the markers CD3, CD4, CD8 and FOXP3 on mouse whole slide FFPE tumor serial sections. Slides were then imaged for high quality images of the four targets and downstream analysis performed. The evaluated T cell frequency and spatial distribution was compared to flow cytometric data of anti-PD-1 treatment in these models. In summary, flow cytometry and multiplex immunofluorescence (mIF) are valuable tools in the evaluation of immune responses in pre-clinical tumor models. Both technologies enable an improved understanding of treatment responses and facilitate the development of novel treatment modalities as well as the identification of potential predictive biomarkers.

#4149
Anti-CTLA-4 generates memory T-cells with greater expansion and functionality than anti-PD-1

Stephen Mok, Nana-Ama A.S. Anang, James J. Mancuso, James P. Allison.
UT MD Anderson Cancer Center, Houston, TX

Blocking either cytotoxic T-lymphocyte antigen-4 (CTLA-4) or programmed cell death-1 (PD-1) pathway relieves the negative regulation of T-cells resulting in durable tumor rejection in patients with cancer and improved survival rate. However, it remains unclear how these immunotherapies affect memory T-cell response. Here we address whether anti-CTLA-4 and anti-PD-1 have different effects on memory T-cells. We used anti-CTLA-4 or anti-PD-1 therapy in combination with irradiated cancer vaccine in mice. After re-challenge, we observed that in murine tumor models, anti-CTLA-4 generates a more robust memory antitumor response than anti-PD-1 as demonstrated by smaller tumor volumes at all time points. We have traced and profiled antigen-specific CD8 T-cells throughout priming, memory phase, and re-challenge. We observed the memory responses generated by anti-CTLA-4 and anti-PD-1 diverge at priming; where anti-CTLA-4 generates more TCF-1+ memory-like T-cells than anti-PD-1, and remains apparent throughout activation and expansion as anti-PD-1 results in a higher percentage of TOX1+ terminally-differentiated T cells. During re-challenge, the memory T-cells generated by anti-CTLA-4 1) expand in greater frequency, 2) have greater cytokine production and antitumor activity, and 3) more frequently differentiate into the population of KLRG1+ effector CD8 T-cells than those generated with anti-PD-1. We found each of these traits correlated with a more effective memory response.

#4150

Novel preclinical model for the evaluation of cytokine release syndrome in response to CD19xCD3 bispecific antibody in humanized mice

Deep S. Shah[1], Catalina Simion[2], Shuang Hu[2], Rhonda Chronis[2], Tre McClellan[2], Jae Hwang[2], Ryan Yang[2], Heather Baker[2], Danying Cai[2], James Keck[2], Lindsay Shopland[2]. *[1]The Jackson Laboratory, Sacramento, CA,[2]In Vivo, The Jackson Laboratory, Sacramento, CA*

Cytokine Release Syndrome (CRS) is a systemic inflammatory response that is caused by the large, rapid release of cytokines in the blood by immune cells affected by infection or immunotherapy and remains a

prominent challenge for T cell-based therapeutics. Bispecific T cell engagers (BiTEs) are fusion proteins that are generated by linking the targeting region of two antibodies: one arm binds to the tumor-associated antigen, and the other arm binds to T cells to promote T cell-mediated cytotoxicity in an MHC-independent manner. A CD19xCD3 BiTE has been approved by the FDA for the treatment of CD19-positive B-cell lymphoma. Despite having great clinical efficacy, CRS remains a major concern for BiTE therapy. This necessitates the development of a translational model that could predict CRS toxicity more accurately. Various *in-vitro* models proposed to assess BiTE-related CRS have several shortcomings as they do not provide details about the systemic immune response, off-target effects, neurotoxicity, tissue damage, and organ failure. Here we propose an *in-vivo* approach to concomitantly assess the efficacy and CRS toxicity of CD19xCD3 BiTE either alone or in combination with Rituximab (monoclonal antibody targeting CD20) in the Raji luciferase xenograft model of Burkitt's lymphoma in PBMC humanized NSG-MHC Class I/II knockout mice. Five days post human PBMC engraftment (Study Day- SD 5), the mice were injected with Raji-luciferase cells. On SD 6, the mice were treated with BiTE, Rituximab, or the combination of BiTE and Rituximab. Additional control groups included OKT3 and Anti-CD28, the anti-T cell antibodies that failed clinically due to severe CRS. Efficacy was assessed through in-vivo imaging on SD5, SD8, and SD11. We observed tumor growth inhibition with BiTE, Rituximab, and the combination treatment. Clinical observations were recorded daily post treatment. Following cytokines were measured 6 hours after dosing and at study termination - IL-2, IL-4, IL-6, IL-10, TNF-α, and IFN-γ. Elevated cytokine levels were observed in the BiTE/combination group 6 hours post dosing but not in the Rituximab alone group. Together, the data suggest that the model could be used to assess the preclinical efficacy and CRS toxicity of BiTE.

#4151

Anti-CEACAM5 immune stimulant TLR7/8 agonist antibody drug conjugate is a potent myeloid cell activator for the treatment of CEACAM5-expressing tumors

Stephanie Decary, Lydia Blot, Charlotte Lahoute, Sandrine Benoist, Anne Caron, Francesca Graziano, Marc Trombe, Loreley Calvet, Alexandra

Ferrier, Marc Frederic, Sukhvinder Sidhu, Marie-Priscille Brun, Marielle Chiron. *Oncology, Sanofi, Vitry-sur-Seine, France*

Toll Like Receptor 7 and 8 (TLR7/8) agonists are a promising approach to treat tumors by harnessing the innate immune system to trigger anti-tumor innate and adaptive immunity. One of the main obstacles to the use of this class of low molecular weight molecules in cancer treatment is the toxicity associated with systemic immune activation after intravenous administration. We developed a novel immune stimulant ADC by conjugating the anti-CEACAM5 (carcinoembryonic antigen related cell adhesion molecule 5) tusamitamab antibody with a resiquimod (R848) TLR7/8 agonist payload. This tumor-targeted compound administered systemically and locally active, is expected to eradicate CEACAM5-positive (+) tumors by recruiting and activating immune cells in tumor microenvironment to promote anti-tumor immune response. Tusamitamab R848 ADC, evaluated *in vitro*, binds to CEACAM5+ tumor cells via its Fab moiety, and to myeloid cells via its Fc part at nanomolar (nM) concentrations. TLR7/8 pathway activation was evaluated on myeloid THP1 reporter cells. The conjugate elicits a potent and FcyR-dependent activity at low nM concentration. In co-culture of human blood cells and human CEACAM5+ gastric cancer cells, it was shown to induce phagocytosis activity, associated with increased activation/maturation of both monocytes and dendritic cells. Tusamitamab R848 ADC evaluated *in vivo* in CEACAM5+ pancreatic human tumor model, HPAFII, leads to robust antitumor activity with complete regressions (CR) after single administration at 5 mg/kg. In a pharmacodynamic study using lung tumor patient-derived xenograft mouse model, this ADC triggers murine cytokine inductions, innate immune cell enrollment at tumor site, and tumor necrosis in a dose-dependent manner. Based on preclinical *in vitro* and *in vivo* data, the tusamitamab R848 ADC is an innovative ADC approach with the potential to eradicate CEACAM5+ tumors in patients.

#4152

Longitudinal local and peripheral immunologic changes associated with PD-L1 response in a murine breast cancer model

Ann Hanna[1], Xiaopeng Sun[2], Emily Tran[2], Quanhu Sheng[1], Brandie C. Taylor[2], Susan R. Opalenik[1], Justin M. Balko[1]. [1]*Vanderbilt University*

Medical Center, Nashville, TN,[2]Vanderbilt University, Nashville, TN

Immune checkpoint inhibitors (ICI) have significantly enhanced patient survival in many cancers but yield limited success in breast cancer. ICIs activate anti-tumor immunity by overriding the inhibition of tumor infiltrating lymphocytes (TILs). Clinical trials in triple negative breast cancer (TNBC) patients, who harbor TILs within tumor stroma, have demonstrated increased survival (IMpassion130) and pathologic complete response (KEYNOTE-522) to ICI leading to FDA-approval of ICI and chemotherapy combinations in metastatic TNBC. However, ICI benefit is heterogeneous among patients. We sought to model ICI response in vivo to evaluate therapeutic resistance and response heterogeneity and to ascertain predictive biomarkers for favorable ICI outcomes. An immunocompetent EMT6 orthotopic mammary tumor model was used to investigate the efficacy of anti-PD-L1. Matched longitudinal samples of the tumor microenvironment (TME) (collected by fine-needle aspiration) and peripheral blood (PBMC) from mice were profiled by bulk RNA and T-cell receptor sequencing.

Anti-PD-L1 robustly suppressed primary tumor growth and extended survival beyond the control group. The addition of chemotherapy demonstrated moderate therapeutic efficacy but failed to enhance ICI benefit. Phenotypic profiling of the TME revealed increased T cells, DCs, and NK cells in anti-PD-L1 only and chemotherapy combination groups. Despite using a genetically identical tumor model and host, PD-L1 blockade induced heterogeneous responses, like clinical outcomes in TNBC patients, ranging from complete response (CR) to intrinsic resistance (IR). The primary TME showed upregulated signatures of cytotoxic T cell response and activation, specifically inflammatory interferon signaling (both prior to and post ICI administration) that corresponded to favorable outcomes to anti-PD-L1 in individual mice. Longitudinal analysis of the peripheral blood identified modest changes among mice at baseline that progressively deviated by response type (IR-vs-CR). Mice harbored enriched myeloid signatures and clonal T cell expansion during therapy corresponding to ICI resistance and response, respectively. Further investigations of matched peripheral blood and the primary TME signatures may identify systemic biomarkers and tumor antigen-specific T cell clones

to accurately predict ICI response in patients and uncover mechanisms for sensitizing tumors refractory to ICI.
Thus, we identify an in vivo model that emulates TNBC patient heterogeneous outcomes to ICI combinatorial approaches. We describe host-specific signatures, specifically from myeloid cells, that correlate with differential responses to ICI, which may serve as a basis for peripheral blood tracking of breast cancer patient responses.

#4153

SETD2 loss and ATR inhibition synergistically promote cGAS signaling and immunotherapy response in renal cell carcinoma

Xiande Liu[1], Yanting Zhang[1], Xuesong Zhang[1], Daniel McGrail[2], Truong Lam[1], Anh Hoang[1], Elshad Hasanov[1], Ganiraju Manyam[1], Christine B. Peterson[1], Haifeng Zhu[1], Shwetha V. Kumar[1], Rehan Akbani[1], Nizar M. Tannir[1], Guang Peng[1], Eric Jonasch[1]. *[1]UT MD Anderson Cancer Center, Houston, TX,[2]Center for Immunotherapy and Precision Immuno-Oncology, Cleveland, OH*

Rationale: Immune checkpoint blockade (ICB) demonstrates durable clinical benefit only in a minority of renal cell carcinoma (RCC) patients. Identifying molecular features that determine response and developing approaches to enhance the response remain an urgent clinical need. Targeting S phase DNA damage repair (S-DDR) network has been reported to activate cGAS signaling and convert a non-immunogenic tumor microenvironment to an immunogenic tumor microenvironment, thus improving immunotherapy response in breast cancer and small cell lung cancer. SETD2 has been known to be required for ATM-mediated DNA damage response, and we hypothesize that *SETD2* loss confers greater dependence on ATR activity and provides vulnerability to ATR inhibitors, which may further potentiate the response to immunotherapy.
Methods: Applying molecular, cellular, and bioinformatic approaches, we comprehensively investigated the effects of *SEDT2*/*Setd2* loss on the cytosolic DNA damage response pathway, the cGAS-mediated cytosolic DNA sensing pathway, the tumor immune microenvironment, and immunotherapy response in RCC cell lines, in the Renca-BALB/c immune competent murine model, and in RCC patients cohorts with or without ICB therapy.

Results: We found that, in multiple RCC cell lines, pharmacological inhibition of the ATR-CHK1 axis activated the cGAS-IRF3-dependent cytosolic DNA sensing pathway, resulting in inflammatory cytokine expression. *SETD2* mutated RCC cell lines or tumor samples were associated with preferential ATR-CHK1 activation over ATM-CHK2 activation. *SETD2* knockdown promoted the cytosolic DNA sensing pathway and conferred greater sensitivity to ATR inhibition. In murine Renca tumors, *Setd2* knockdown and the ATR inhibitor VE822 synergistically activated the cytosolic DNA sensing pathway, immune cell infiltration, and immune checkpoint protein expression. *Setd2* deficient Renca tumors demonstrated greater vulnerability to ICB monotherapy or in combination with ATRi than *Setd2* proficient tumors. *SETD2* mutations were associated with a higher response rate and prolonged overall survival in ICB-treated RCC patients, but not in non-ICB-treated RCC patients. Conclusion: This study reveals that *SETD2*/*Setd2* loss and ATR inhibitor synergize to enhance cGAS signaling and RCC tumor immune responsiveness, and provides mechanism-based guidance to develop more personalized combination therapy regimens for RCC patients with *SETD2* mutations.

#4154
mRNA-based immunotherapies to treat women's cancers
Dan Tse. *Geneleap, Woburn, MA*

With its ability to potentially code for any given protein, peptide and fragments, synthetic mRNA has landed itself a broad range of cancer immunotherapy applications, including costimulatory receptors, therapeutic antibodies, vaccines, and cytokines able to change the tumor microenvironment.We have been able to leverage our mRNA platform to generate a vaccine for HPV-associated cervical cancer (CC), as well as an immune-stimulatory cytokine for triple negative breast cancer (TNBC), both diseases that disproportionately affects minorities who do not participate in routine medical screenings and contribute to disparity in mortality beyond individual risk factors.IL-12 is a potent pro-inflammatory type 1 cytokine with potential to enter the clinical practice as immunotherapy for cancer. Its use in the form of recombinant protein and/or DNA plasmid has been hampered by issues with systemic toxicity or

protein bioavailability within the tumor. To overcome these roadblocks, we developed a novel secreted single chain IL-12p70 mRNA. Intra-tumoral dosing of this mRNA induced tumor regression in a syngeneic and orthotopic mouse model of TNBC. Almost all cervical cancers are HPV (human papilloma virus) associated. We have developed a therapeutic vaccine, based on a single mRNA coding for two de-risked antigens, that is able to induce a T cell response against the oncogenic proteins E6 and E7 of the most common serotype (HPV16). When injected intramuscularly in mice bearing C3.43 masses, this vaccine suppressed tumor growth and generated immunological memory.Currently, these women's cancers do not have a cure or an effective standard of care. With an efficacy that relies on a few injections and non-invasive routes of administration, we believe our innovative RNA-based pharmaceuticals might close some treatment gaps.

#4155

The RAF/MEK clamp avutometinib (VS-6766) induces an immunogenic tumor microenvironment and potentiates the efficacy of anti-PD-1

Silvia Coma[1], Miriam Molina Arcas[2], Julian Downward[2], Jonathan A. Pachter[1]. *[1]Verastem Oncology, Needham, MA,[2]The Francis Crick Institute, London, United Kingdom*

The RAS/RAF/MEK/ERK (MAPK) pathway is one of the most commonly mutated oncogenic pathways in human cancers. Although RAS, RAF and MEK have been validated as anticancer targets with approval of KRAS G12C, BRAF and MEK inhibitors, combination strategies with chemotherapy, targeted therapies and/or immune checkpoint inhibitors may be optimal for deep and durable response. Avutometinib (avuto, VS-6766) is a unique RAF/MEK clamp that potently inhibits MEK kinase activity and induces a dominant negative RAF/MEK complex preventing phosphorylation of MEK by ARAF, BRAF and CRAF. Preclinically, avuto has shown strong anti-proliferative potency across tumor cell lines carrying various MAPK pathway alterations. Clinically, avuto monotherapy has shown responses in gynecological cancers and KRAS mutant non-small cell lung cancer. Here, we tested the immune modulatory effects of avuto on tumor cells and tumor-infiltrating immune cells and assessed anti-tumor efficacy in mice treated with avuto in combination with an anti-PD1

antibody. In a panel of KRAS and BRAF mutant human tumor cell lines, avuto treatment increased the expression of MHC-I complex genes, including B2M, HLA-A and TAP1. In the CT26 KRAS G12D syngeneic colorectal cancer model, upregulation of B2M and TAP1 by avuto was confirmed in vivo, suggesting that avuto may increase antigen presentation. Furthermore, avuto upregulated the expression of markers of T cells (CD8, PDCD1), NK cell activation (NCR1) and interferon response (IFNG, IRF7, IL12) in the CT26 model. Interestingly, all these pro-immune changes observed with avuto were stronger than those observed with an equivalent dose level of the MEK-only inhibitor trametinib. Avuto also increased expression of B2M, CD8A, PDCD1, NCR1 and IRF7 in a KPARG12C orthotopic lung cancer model. Flow cytometry analysis showed that avuto also significantly increased MHC-II expression by tumor cells and the numbers of CD8 T cells and M1 macrophages, and significantly decreased monocytic and granulocytic MDSCs. These immune changes indicate that avuto induces an immunogenic tumor microenvironment that may potentiate the efficacy of immuno-oncology agents such as anti-PD-1. Accordingly, in the CT26 model, whereas avuto and anti-PD-1 each delayed tumor growth, combination of avuto with anti-PD-1 increased antitumor efficacy and prolonged survival. Furthermore, all complete responders in the avuto + anti-PD-1 group were able to reject a re-challenge with CT26 tumor cells and showed increased CD8 and CD4 effector memory T cells relative to untreated naïve control mice, indicating that avuto + anti-PD-1 treatment induces durable immune memory. These results support clinical evaluation of avutometinib in combination with an anti-PD-1 antibody for treatment of patients with solid tumors harboring MAPK pathway alterations such as KRAS or BRAF mutations.

#4156

Site specific tumor response to combination chemotherapy and immune checkpoint inhibitor in the syngeneic Pan02 pancreatic ductal adenocarcinoma model

Andrew Wong, Patrick Fadden, Cara Clouse, Patrick Wood, Marianna Brown-Augustine, Fei Zhao, Elliot Ser, Joseph Kolb, Chassidy Hall, Elizabeth Rainbolt. *Charles River Laboratories, Inc., Durham, NC*

Syngeneic tumor models provide a platform to assess novel immune-oncology therapeutics in fully immuno-competent mice. A subcutaneous flank tumor implant provides a convenient and accessible location to monitor the tumor growth and response to therapy. However, the tumor microenvironment, and therefore, the responsiveness to immuno-oncology therapies, is greatly impacted by the location in which the tumor develops (Ho 2021, Oliver 2018). Given the potential of different immuno-suppressive features driven by the specific tumor location, we wanted to compare the tumor infiltrating leukocyte populations in the subcutaneous flank and orthotopic pancreatic Pan02 syngeneic models, as well as the response to standard of care therapies. Pan02 cells were either implanted orthotopically in the pancreas or subcutaneously in the flank and allowed to establish before dosing with either vehicle, oxaliplatin, anti-CTLA-4 or the combination of therapies. Established tumors from untreated orthotopic and flank models were sampled for flow cytometry to assess infiltration by a broad range of immune cell populations. Response to therapy was clearly dependent on tumor location with flank tumors being resistant to both monotherapy and combination therapy, while the orthotopic tumors responded modestly to monotherapy but displayed synergy with the combination therapy. The results suggest that for a given syngeneic tumor cell line with identical mutational load and antigenicity, we can generate unique tumor microenvironments dependent on implant location leading to different outcomes when testing novel immune-oncology therapies. These types of models can help define the context in which novel immune-oncology therapeutics can be expected to drive an effective immune response.

#4157

Tumor context dictates reliance on TCF1 for response to immunotherapy

Giulia Escobar[1], Katherine Tooley[1], Joan Pages Oliveras[1], Linglin Huang[1], Hanning Cheng[1], Chang Xue[1], Davide Mangani[1], Natanael Hazel[1], Carola Rutigliani[1], Luca Biasco[2], Ana C. Anderson[1]. *[1]Harvard Medical School/Brigham and Women's Hospital, Boston, MA,[2]Great Ormond Street Institute of Child Health, University College London, London, United Kingdom*

Stem-like CD8 T cells are regulated by the transcription factor TCF1 and are key players in the response to immune checkpoint blockade (ICB). However, recent findings indicate that the dependance on $TCF1^+$ stem-like T cells for ICB efficacy may not be equal across patients or in different tumor contexts. Here we leveraged TCF1 conditional knock-out (TCF1 cKO) mice to investigate how TCF1 instructs the early fate and functions of CD8 T cells upon ICB therapy in tumors that differ for immunogenicity and levels of tumor antigen expression. Strikingly, we discovered that TCF1 expression in CD8 T cells is required for ICB efficacy in poorly immunogenic B16OVA melanomas but is dispensable in highly immunogenic MC38OVA colorectal tumors. Single-cell RNA sequencing and immunophenotyping in the tumor draining lymph node (TDLN) revealed defective priming and expansion of tumor-specific TCF1 cKO T cells in B16OVA- but not MC38OVA-bearing mice treated with ICB. Conversely, ICB therapy efficiently expanded tumor-specific TCF1 WT T cells in the TDLN of both tumor models. In vitro, we found defective proliferation, reduced PD1 and CD28 up-regulation and reduced phosphorylation of key molecules downstream the T cell receptor pathway in TCF1 cKO T cells stimulated with low but not high TCR signals. These data indicate that TCF1 poises T cells for optimal responsiveness in suboptimal priming conditions such as those found in low antigen expressing tumors. Furthermore, in the absence of TCF1 we found the accumulation in the TDLN of a subset of tumor-specific naïve T cells poised to give rise to short-lived effectors, which are less suited to sustain anti-tumor responses in poorly immunogenic tumors where expansion of T cells retaining memory potential is required for durable responses. Single-cell RNA sequencing and immunophenotyping within the tumor microenvironment showed that in MC38OVA tumors both WT and TCF1 cKO mice expanded a CD8 subset sharing a signature with transitory effectors, which were shown to mediate ICB efficacy in chronic viral infection models. Expansion of cytotoxic CD8 T cells likely accounted for the strong anti-tumor response observed in both WT and TCF1 cKO mice. Conversely, B16OVA tumors failed to expand transitory effectors and accumulated Tox^+ dysfunctional CD8 T cells. Importantly, in the absence of TCF1 dysfunctional T cells became destabilized, failed to persist and shared features with CD8 T cells found in patients that fail ICB. Altogether, the reduced priming of stem-like T cells in the TDLN combined with a

destabilized dysfunctional T cell state in the tumor contributed to the failure of TCF1 cKO mice to sustain effective ICB responses in poorly immunogenic tumors. Our study highlights a role for TCF1 during the priming and early stages of the anti-tumor CD8 T cell response with important implications for guiding optimal therapeutic interventions in cancers with low frequency of $TCF1^+$ CD8 T cells and low neoantigen expression.

#4158

Selective targeting of CD122 combined with radiotherapy triggers CD8 and NK mediated immunity, abrogating metastasis in head and neck squamous cell carcinoma

Jacob Gadwa[1], Maria Amann[2], Thomas E. Bickett[1], Michael W. Knitz[1], Laurel B. Darragh[1], Miles Piper[1], Benjamin Van Court[1], Sanjana Bukkapatanam[1], Tiffany T. Pham[1], Xiao-Jing Wang[3], Laura Codarri Deak[2], Christian Klein[2], Pablo Umana[2], Angelo D'Alessandro[4], Sana D. Karam[1].
[1]Radiation Oncology, University of Colorado, Aurora, CO,[2]Roche Innovation Center Zurich, Zurich, Switzerland,[3]Pathology, University of Colorado, Aurora, CO,[4]Biochemistry and Molecular Genetics, University of Colorado, Aurora, CO

The implementation of cancer immunotherapies, while revolutionary in certain cancer types, has seen limited clinical success in head and neck squamous cell carcinomas (HNSCC). This revelation has prompted investigation in alternative targets to invigorate anti-tumor immunity. IL-2 signaling governs the survival and functionality of lymphocytes, thus making IL-2 receptor signaling an attractive target for new immunotherapies. However, therapies to enhance IL-2 signaling are often limited in their efficacy by modulating the activation of regulatory T cells (Tregs), which preferentially binds IL-2 via the high affinity receptor IL-2Rα (CD25). Selectively targeting IL2Rβ (CD122), the intermediate affinity receptor, can be leveraged to induce anti-tumor immune responses in effector T cells and natural killer (NK) cells while limiting negative regulation conferred by Tregs. The novel bispecific immunocytokine PD1-IL2v preferentially activates IL-2 signaling through CD122 on PD-1 expressing cells, activating immune effectors, and preventing immune

exhaustion by blockade of PD-1. However, PD-1 blockade can amplify immunosuppression by Tregs, necessitating their depletion using αCD25. Here, we observe that radiation therapy and combination of PD1-IL2v with an Fc-optimized αCD25 antibody induces systemic activation of effector CD4 and CD8 T cells, reducing overall tumor burden. Concordant with improved local tumor control, we also observed a decrease in metastatic spread using a newly developed Kras/smad4/p53 mutated metastatic tumor model. NK cells, which are known to play a central role in the control of tumor
cell dissemination though direct cytotoxicity, displayed a phenotypic shift towards an activated state upon treatment with PD1-IL2v, highlighted by enhanced cytotoxicity, NK receptor diversity, and metabolic activity. Although relatively uncommon in comparison to other cancer types, those patients who present with metastases display a substantially poorer outcome, demonstrating the need for therapies which target this axis of cancer disease progression. In summary, we find that radiation therapy and PD1-IL2v imparts potent anti-tumor immunity, reducing local tumor growth and distant tumor spread, which taken together contribute to increased overall survival.

#4159

The COX-2/PGE2 pathway as a mediator of resistance to anti-PD-1 therapy

Shuming Chen[1], Seoho Lee[2], Tracee L. McMiller[2], Isaac Morales[2], Preethi Sankaran[2], Brian Francica[3], Robert D. Leone[4], Tom W. Dubensky[3], Suzanne L. Topalian[2]. *[1]Surgery, Johns Hopkins University School of Medicine, The Sidney Kimmel Comprehensive Cancer Center, and The Bloomberg~Kimmel Institute for Cancer Immunotherapy, Baltimore, MD,[2]Surgery, Johns Hopkins University School of Medicine, Baltimore, MD,[3]Tempest Therapeutics, South San Francisco, CA,[4]Oncology, Johns Hopkins University School of Medicine, Baltimore, MD*

Background: We previously found upregulation of the cyclooxygenase-2/prostaglandin E2 (COX-2/PGE2) pathway in the tumor microenvironment (TME) of cancer types that respond poorly to anti-PD-1 therapy, and showed that TME-resident cytokines such as IL-1B induce COX-2 expression in human tumor and myeloid cells. To investigate a potential

role for COX-2/PGE2 in anti-PD-1 resistance, we studied PGE2-mediated effects on human myeloid and T cells and their dependence on prostaglandin (EP) receptor signaling.
Methods: Monocytes (Monos) and T cells were enriched from normal donor peripheral blood by negative selection. PGE2 effects were tested on Monos activated with IFN-g (PD-L1 expression; FACS) or LPS (cytokine secretion; ELISA). PGE2 effects on monocytic dendritic cells (DCs) generated with GM-CSF+IL-4 and matured with CD40L were assessed by phenotyping for costimulatory molecules (CD80, CD86) and subpopulation markers (CD14, CD16, CD83). T cells activated with anti-CD3/CD28 +/- PGE2 for 2-6 days were assessed for expression of CD25, CD69, CD107a, CD137, OX40, GITR, LAG-3, PD-1, PD-1, PD-L1 and TIM3 (FACS); proliferation markers (Ki67, CFSE; FACS); cytokine secretion (IFN-g, IL-2, IL-10, TGF-b; ELISA); and metabolic function (Seahorse assay). In some experiments, cells were pre-incubated with inhibitors of EP2 (PF-04418948), EP4 (ONO-AE3-208), or the dual inhibitor TPST-1495 (Tempest Therapeutics).
Results: Myeloid cell functions were suppressed by PGE2, which reduced IFNg-induced PD-L1 expression and modulated LPS-induced cytokine secretion. Furthermore, PGE2 inhibited DC maturation, evidenced by persistent CD14 and CD16 expression and a decreased CD83+ subset. In CD4 and CD8 T cells activated with anti-CD3/CD28, PGE2 reduced expression of CD25 and CD69 (early activation markers), CD107a (cytolytic potential), Ki67 (cell proliferation), co-stimulatory molecules (CD137, OX40, GITR) and checkpoint molecules (LAG-3, PD-1, PD-L1, TIM3) in a dose-dependent manner. PGE2 also reduced the CFSE-low (proliferating) population in activated CD4, CD8 and Treg cells. Secretion of proinflammatory cytokines IFN-g and IL-2, and inhibitory cytokines IL-10 and TGF-b from activated T cells was also suppressed by PGE2. These effects were specifically reversed by chemical inhibitors of EP2 and/or EP4. PGE2 exposure at the time of T cell activation was associated with depressed mitochondrial oxidation and cellular glycolysis, suggesting global effects on T cell metabolism.
Conclusion: Understanding and preventing anti-PD-1 resistance is a critical goal in oncology. Our results suggest that the COX-2/PGE2 pathway exerts immunosuppressive effects on myeloid and T cells via the EP2 and EP4 receptors. COX-2 and PD-L1 are distinct immune checkpoints, providing a

rationale to test anti-PD-1 in conjunction with COX-2 pathway inhibitors such as IL-1B antagonists and highly specific EP2 and EP4 inhibitors in patients with cancer.

#4160

Characterization of cytotoxic resilient T cells in patients with advanced cancers in response to salvage radiation therapy or chemotherapy

Joanina K. Gicobi[1], Yiyi Yan[2], Hu Zeng[1], Sean Park[1], Haidong Dong[1].
[1]Mayo Clinic College of Medicine and Science, Rochester, MN,[2]Mayo Clinic College of Medicine and Science, Jacksonville, MN

Although cancer burden in patients with advanced diseases results in T cell exhaustion and failed prior therapies, some of them achieved durable clinical responses to salvage therapy (chemotherapy or radiation therapy) implying a presence of tumor-reactive resilient T cells in them. However, the phenotype and functional features of resilient T cells have not been clearly defined. We found that $CX3CR1^+$ $CD8^+$ T cells with low mitochondrial membrane potential demonstrated features of resilient T cells: (a) their cytotoxic T cell function (degranulation/CD107a expression) recovered quickly after tumor burden has been reduced by radiation therapy or chemotherapy; (b) they maintain a low profile of glycolysis but produce optimal levels of ATP; (c) they express lower levels of PD-1 and TOX; (4) they share a feature of stem-like T cells ($TCF1^+PD\text{-}1^+$) that can be responsive to immunotherapy; (5) they avoid accumulation of a harmful level of cytosolic reactive oxygen species (ROS) that may cause T cell exhaustion; (6) they upregulate malic enzyme 1 (ME1) to balance glycolysis and ROS, and to expand cytotoxic effector T cells. These unique features of resilient T cells may not only be used as T cell biomarker to design rational combination therapy to control advanced cancers but can also be used to convey a resilient functional state to T cells in patients who lack them.

#4162

T-cell metabolic profiling with bioluminescent assays

Maggie Bach, Natasha Karassina, Julia Gilden, Donna Leippe, Mike Valley, Kayla Sylvester, Jolanta Vidugiriene. *Promega, Fitchburg, WI*

Cellular energy metabolism is crucial for cell survival and the balance of metabolic pathways determines the health of the cell. Determining and understanding metabolic profiles of cells can aid in overall insight of cell health and improvement of cell therapeutics, especially for immune interventions. T-cells actively regulate their metabolic profile from quiescent to a highly metabolically active state after activation. Activation rewires the cell to drive glycolysis and oxidative phosphorylation for production of reducing power and ATP for cell growth and proliferation. A small population of these cells then transition to a more quiescent state and persist as memory cells to aid in secondary responses. Although the trend of T-cell metabolism after activation has been studied, the method of investigation is cumbersome and lacks depth of information of overall cell health. To address this, we developed a bioluminescence NAD(P)H core technology and applied it to build a set of cell-based assays covering diverse metabolic pathways including glucose, glycogen, and amino acid metabolism, and the TCA cycle. Here we utilize those assays to investigate changes in metabolic profiles of naïve, effector, and memory T-cells as they transition from a state of oxidative phosphorylation to increased glycolytic rates, dependence on different fuel consumption and storage, including an increase in fatty acid oxidation and glycogen accumulation. We demonstrate flexibility of the assays for detecting multiple metabolites from the same sample and monitoring metabolite changes over time by assaying multiple samples. We show that the assays are amenable to various volumes (96-,384-well plates) and low cell numbers. For example, activity of dehydrogenases involved in glycolysis, pentose phosphate and TCA cycles can be detected with less than 400 cells/well. In conclusion, understanding the processes governing dynamic metabolic changes of T-cells during their transition from naïve to activated to memory phenotypes is required for next-generation cell therapy development. The developed bioluminescence cell-based assays provide the sensitivity, throughput and robustness required for rapid evaluation of such changes.

#4163

Enhanced immune response according to different radiation fractionations in colorectal cancer cell lines

Sang Jun Byun[1], Shin Kim[2], Incheol Seo[3], Hye Won Lee[4], Sung Uk Bae[5], Seong Kyu Baek[5], Woon Kyung Jeong[5], Seung Gyu Park[1], Euncheol Choi[1].

[1]Department of Radiation Oncology, Keimyung University School of Medicine, Daegu, Korea, Republic of,[2]Department of Immunology, Keimyung University School of Medicine, Daegu, Korea, Republic of,[3]Department of Immunology, Kyungpook National University School of Medicine, Daegu, Korea, Republic of,[4]Department of Pathology, Keimyung University School of Medicine, Daegu, Korea, Republic of,[5]Department of Surgery, Keimyung University School of Medicine, Daegu, Korea, Republic of

Background: Concurrent chemoradiation therapy is standard treatment in locally advanced rectal cancer. 5-FU is a commonly used chemotherapeutic agent, and radiotherapy is delivered with conventional or short-course fractionations. Immunotherapy is a new strategy with systemic effect, and several combinations with other treatments including surgery, chemotherapy, or radiotherapy in various sequences are evaluated. After irradiation, there is immunogenic changes in the tumor microenvironment, which is expected to improve the response of the added immunotherapy. The purpose of this study is to investigate the difference in immune response according to the radiation fractionation schedules after irradiation in various colon cancer cell lines.
Materials and Methods: The human colorectal cancer cell lines, DLD-1 and HCT116, were cultured and irradiated with total 1.8 Gy of X-rays in 10 fractions and 5 Gy of X-rays in 3 fractions using linear accelerator for 10 and 3 consecutive days. The mRNA expression levels of immune related genes including *CD274*, *TREX1*, *CD74*, *IFNG*, *CALR*, *HMGB1*, *TGFB1* were evaluated using real-time PCR in 0, 3, and 7 days after irradiation.
Result: The mRNA expression levels of *CD74*, *HMGB1* and *CD274* were increased in both DLD-1 and HCT116 cell lines, and *IFNG* increased only in DLD-1. However, there was a difference in the increasing patterns over time between the two radiation fractionations. According to the radiation fractionation, increasement of the mRNA expression levels was more prominent in 1.8 Gy in 10 fractions than 5 Gy in 3 fractions. In addition, the radiation-resistant DLD-1 cell line showed a more marked increase in the levels of CD274 mRNA as well as other genes associated with CD274 than the radiation-sensitive HCT116 cells. Moreover, DLD-1 cell line, which is more resistant to radiation, showed more prominent elevation in *CD274* mRNA level than HCT-116.

Conclusions: We could find that more fractionated irradiation schedule with smaller dose per fraction further increases the immune response. Even in radio-resistant tumor cells, better immune response could be expected after irradiation than radio-sensitive cells. It would be needed to verify the results in real tumor conditions, such as the tumor microenvironment containing immune cells and cancer-associate fibroblasts. It is also thought that studies on the appropriate time to use immunotherapeutic agent are needed.

#4164

Relieving immune suppressive pathways in breast cancer to improve outcomes

Amanda Poissonnier[1], Eivind Valen Egeland[2], Rossin Erbe[3], Wesley Horton[4], Ana Howells-Ferreira[4], Shamilene Sivagnanam[5], Nell Kirchberger[1], Dhaarini Murugan[1], Andrew Fields[6], Peter Ordentlich[7], Andrew C. Adey[8], Elana J. Fertig[9], Lisa M. Coussens[1]. *[1]Cell, Developmental and Cancer Biology, OHSU Knight Cancer Institute, Portland, OR,[2]Dept of Tumor Biology, Institute for Cancer Research, Oslo University Hospital, Norway,[3]Div. of Quantitative Sciences, Sidney Kimmel Comprehensive Cancer Center / Johns Hopkins University, Baltimore, MD,[4]Cell, Developmental and Cancer Biology / Computational Biology, OHSU Knight Cancer Institute, Portland, OR,[5]Cell, Developmental and Cancer Biology/ Computational biology, OHSU Knight Cancer Institute, Portland, OR,[6]Molecular and Medical Genetics, OHSU Knight Cancer Institute, Portland, OR,[7]Syndax Pharmaceuticals, Waltham, MA,[8]Molecular and Medical Genetics / CEDAR, OHSU Knight Cancer Institute, Portland, OR,[9]Div. of Quantitative Sciences, Sidney Kimmel Comprehensive Cancer Center / Johns Hopkins Univ, Baltimore, MD*

Triple negative breast cancer (TNBC)represents the most aggressive subset of breast cancer with limited treatment options leading to high mortality. While treatment of metastatic cancers with immune checkpoint inhibitors (ICIs) offers promise for many, early results from clinical trials evaluating ICIs in TNBC showed benefit for only a subset of patients. Preclinical data indicate that infiltrating macrophages foster tumor progression by limiting $CD8^+$ T cell infiltration, activation and cytotoxicity in tumor microenvironments. We hypothesized that response to ICI therapy could be

enhanced by sequentially combining a microtubule poison (paclitaxel; PTX) that enhances tumor immunogenicity, with a macrophage-depleting/reprograming agent, e.g. colony-stimulating factor 1 receptor blocking antibody (aCSF1R), in addition to an ICI targeting the PD-1/PD-L1 axis. Immune-competent mammary tumor-bearing MMTV-PyMT transgenic mice were randomized at day 80, and enrolled into experimental groups evaluating PTX, aCSF1R mAb, αPD-1 mAb, as monotherapy and in combinations. Cohorts were analyzed at distinct time points for primary and metastatic tumor burden, in addition to immunophenotyping (flow cytometry), transcriptional (RNA-Seq), epigenetic (sciATAC-Seq), and T cell receptor (TCR) changes correlating with outcomes. These studies revealed tumor regression and improved outcome for 60% of mice receiving PTX/aCSF1R/aPD-1, associated with localized $CD8^+$ T effector and resident memory cell expansion, increased antigen-specific clonal expansion at the primary tumor site. To address epigenetic plasticity as a limiting factor for long-term T cell memory, a class 1 benzamide histone deacetylase (HDAC) inhibitor (e.g., entinostat) was sequentially added to PTX/aCSF1R/aPD-1 triple therapy resulting in primary tumor stasis in 100% of mice, and significantly enhanced overall survival. Improved outcome and tumor stasis were associated with an increased presence of long-lived central and stem-like memory $CD8^+$ T cell infiltration, associated with increased intra-tumoral B memory cell and $CD4^+$ T follicular helper cell infiltration. Improved outcomes were $CD8^+$ T cell-dependent; depletion of $CD19^+/CD20^+$ B cells resulted in complete loss of granzyme B $^+$ $CD8^+$ T cell infiltration into primary tumors, and rapid tumor expansion. These preclinical studies indicate that therapies targeting myeloid-mediated T cell suppression can be leveraged to improve anti-tumor T cell memory, and that durable long-term T cell memory can be instated upon addition of an epigenetic modulator.

#4165

A systemically administered killed bacteria-based multiple immune receptor agonist for pulsed anti-tumor immunotherapy

Michael J. Newman. *Indaptus Therapeutics, San Diego, CA*

Systemic activation of multiple immune receptors, such as Toll-like (TLR), NOD-like (NLR) and Stimulator of Interferon Genes (STING) is essential

for efficient innate and adaptive immune responses. Attempts to use single receptor agonists for advanced cancers have not produced approved products. Limitations include insufficient immune activation and dose-limiting toxicities associated with continuous exposure. Gram-negative bacteria (G-NB) contain multiple TLR, NOD and STING agonists. Potential utility of G-NB for cancer immunotherapy is supported by observation of tumor regression in the setting of infection and Coley's Toxins. Coley reported that i.v. administration was likely most effective but produced toxicity. The discovery of TLRs, particularly the broad/potent activities of the TLR4 agonist lipopolysaccharide (LPS) suggest that it may be both a critical active ingredient and a dose-limiting feature of i.v. G-NB. Non-pathogenic *E. coli* were treated with polymyxin to achieve ~90% reduction of LPS activity without lysis and were then killed and stabilized with glutaraldehyde. The resulting product, Decoy10, was shown to contain multiple TLR, NOD and STING agonists and exhibited reduced i.v. toxicity (mice, rabbits) relative to unprocessed cells. Surprisingly, despite reduction in LPS activity and toxicity, Decoy10 induced secretion of similar or higher levels of most cytokines/chemokines by peripheral blood mononuclear cells, compared to unprocessed bacteria. Higher cytokine/chemokine induction was also observed compared to monospecific TLR agonists. Administration of 4 to 8 weekly or twice a week i.v. doses of Decoy10 to mice with established s.c., orthotopic or metastatic syngeneic breast, colorectal, hepatocellular, pancreatic carcinomas or syngeneic or human non-Hodgkin's lymphoma was well-tolerated and produced single agent anti-tumor activity and/or combination-mediated durable tumor regressions, with induction of immunological memory. Regressions were observed, without significantly increased toxicity, when Decoy10 was combined with chemotherapy, a non-steroidal anti-inflammatory drug, anti-PD-1 therapy or rituximab. Tumor regressions were associated with activation of innate and adaptive immune pathways in tumors after one dose of Decoy10 and were mediated by NK, $CD4^+$ and $CD8^+$ T cells.

Published studies have demonstrated that systemic bacteria are engulfed by and activate immune cells in the liver and spleen, with rapid clearance in mice, rabbits, and humans. Systemic bacteria have also been shown to accumulate in or around tumors. We have taken advantage of these phenomena to produce a detoxified but potent multiple immune agonist that induces systemic innate and adaptive anti-tumor immune activation without

requirement for continuous systemic exposure. A Decoy product has been cleared by the US FDA for a Phase 1 oncology trial.

#4166

Effects of cyproheptadine in eliciting natural killer cell-mediated immune response in bladder cancer

Himani Kumari[1], Guan-Ling Lin[1], Chih-Chieh Yeh[1], Ciao-Ni Chen[1], Yu-Ming Chuang[1], Wan-Hong Huang[1], Wen-Long Huang[1], Steven Lin[2], Michael W. Y. Chan[1]. *[1]Biomedical Science, National Chung Cheng Univ., Chiayi, Taiwan,[2]Institute of Biological Chemistry, Academia Sinica, Taipei, Taiwan*

Bladder cancer is one of the most common occurring cancers in urothelial carcinoma. The previous study suggested that cancer cells undergo immunoevasion due to epigenetic silencing of NKG2DL, in which NKG2D-NKG2DL interaction induced natural killer (NK) cell-mediated cytotoxicity. We hypothesized that NK-mediated cytotoxicity can be reactivated by restoring the expression of NKG2DL on tumor cells. Our previous studies demonstrated that cyproheptadine (CPH) is a novel HDAC inhibitor exhibiting antitumor activity by cell cycle arrest and apoptosis. To understand the mechanism behind, RNA-seq showed an upregulation of ULBP2, a NKG2DL, in bladder cancer cells treated with CPH. Interestingly, upregulation of ULBP2, was accompanied with the enrichment of H3K27Ac and H3K4me3 at ULBP2 promoter, was observed in cells treated with CPH. Increased NK-specific lysis was observed in CPH-treated cells co-cultured with NK-92 cells. More importantly, treatment of CPH enhanced the efficacy of immune checkpoint inhibitor in a syngeneic mice bladder cancer model. In conclusion, our results suggested that CPH may be a novel HDAC inhibitor which may elicit immune response in NK-cell dependent manner.

#4167

Translational control of T cell exhaustion in melanoma, perspectives in therapeutics

Samad Muhammadnejad[1], Biswendu Biswas[1], Ramdane Guemiri[1], Naima Benannoune[2], Jérémy Lavigne[1], Virginie Quidville[1], Jean-Yves Scoazec[3],

Stephan Vagner[4], Caroline Robert[5]. *[1]INSERM U981, Gustave Roussy, Villejuif, France,[2]INSERM U981 & Department of Cancer Medicine, Gustave Roussy, Villejuif, France,[3]INSERM U981, Gustave Roussy & University Paris Saclay, Villejuif, France,[4]CNRS UMR3348 & INSERM U1278, Curie Institute, Orsay, France,[5]INSERM U981 & Department of Cancer Medicine, Gustave Roussy & Paris Saclay University, Villejuif, France*

Background: Eukaryotic initiation factor 4F (eIF4F) complex plays a pivotal role in the selective translational control of protein expression in cancer. We previously showed that the inhibition of eIF4F had both a direct antitumor effect that could overcome resistance to BRAF inhibition in *BRAFV600* melanoma and an indirect immune-mediated antitumor effect via PD-L1 down regulation resulting from STAT1 decreased translation. We now explore further the translational control of immune checkpoints (ICs) on T cell and its link with lymphocyte exhaustion.
Methods: We performed polysome profiling (PP) on peripheral blood-derived activated and resting T lymphocytes as well as tumor-infiltrating lymphocytes (TILs) isolated from melanoma specimens in the presence or absence of silvestrol as an eIF4A (the helicase component of eIF4F) inhibitor. We studied the expression of ICs and exhaustion-associated transcription factors on lymphocytes at the various stages of exhaustion. The tumor cell lysing capacity of PBMC was evaluated with and without silvestrol. We also assessed the effect of silvestrol on tumor microenvironment in the BP syngeneic melanoma tumor model.
Results: Silvestrol decreased the translation of multiple ICs in activated CD4+ and CD8+ T cells, including TOX, NFAT1, NFAT2, LAG3, and TIM3 (the two latter being also transcriptionally regulated). FACS analysis confirmed the dose-dependent decrease of protein expression of exhaustion-associated transcription factors TOX, NFATc1, TCF1 and T-bet in activated lymphocytes. This effect was more prominent in more exhausted T cells. Silvestrol decreased T cell proliferation but, in co-culture experiments, it increased immune cell killing of melanoma cells by T-lymphocytes. In the BP murine model, the antitumor effect of silvestrol was associated with denser T cell infiltration and less exhausted TILs than control tumors.
Conclusion : Our findings demonstrate the role of eIF4F in the orchestrated regulation of functionally related proteins involved in T cell exhaustion.

They highlight the drugability of eIF4A for the cancer treatment and suggest that eIF4A inhibitors could be useful with IC inhibitors in combination or sequentially.

#4168

BALB/c-CD3EDG HuGEMM^{TM} mouse model for evaluation of CD3-targeted tumor immunotherapy

Demi Xiaojuan Liu, Kaixia Lian, Xuefei Yan, Jie Lin, Lei Zheng, Annie Xiaoyu An, Xiaoxi Xu, Ludovic Bourre, Jingjing Wang. *Crown Bioscience, Inc., San Diego, CA*

Introducti**on:** T cell immune response plays critical roles in cancer immunotherapy. CD3 complex, composed of CD3ε, CD3δ and CD3γ chains, is an essential component of TCR-CD3 complex mediating TCR signaling. Targeting CD3 complex has therefore become a popular strategy for manipulation of T cell function. Clinically relevant animal models for proper evaluation of human CD3 antibodies is in great demand in the field. Currently, adoptive transfer of human CD3+ T cells or transplantation of human hematopoietic stem/precursor cells to immunodeficient mice are usually employed. However, these mouse models are not fully immunocompetent. In this study we have evaluated in vitro CD3 EDG functionality and in vivo therapeutic efficacy, in BALB/c-hCD3EDG knock-in mouse in which all the three components of the CD3 complex — Cd3ε, Cd3δ, and Cd3γ— are replaced by their human counterparts, CD3E, CD3D, and CD3G.

Methods: A humanized CD3EDG mouse model (Hu**GEMM**) on BALB/c background was generated by replacing the entire mouse CD3EDG with its human counterpart through ES cell-based gene targeting. The cell surface expression of CD3E and intracellular expression of CD3D and CD3G were confirmed by FACS. Naïve CD3+ T cells were isolated from the splenocytes of homozygous CD3EDG Hu**GEMM** and activated by anti-hCD3 antibody. T cell proliferation was demonstrated by CFSE dilution assay. To validate the TCR functionality of humanized CD3EDG *in vivo*, we evaluated bispecific antibody anti-hCD3/hEpCAM5 in BALB/c-CD3EDG Hu**GEMM** bearing CT26-hEpCAM5.
Results: The expression of human CD3E, CD3D and CD3G were confirmed by flow cytometry. hEpCAM5 antigen expression was confirmed in CT26 cell line in vitro and tumor in vivo by flow cytometry. The TCR functionality was detected by *in vitro* T cell activation assays using anti-hCD3 antibody. *In vivo* efficacy was demonstrated using a bispecific antibody that simultaneously binds to human CD3 and human tumor associated antigen EpCAM5 in human *CD3 EDG* knock-in mice engrafted with CT26-hEpCAM5 tumor. The therapeutic efficacy of the bispecific antibody showed 32% tumor growth inhibition compared to control treatment. No significant body weight loss was recorded in any of the animals.
Conclusion: This study showed the successful establishment of humanized CD3 knock-in BALB/c mouse models providing a full immunocompetent model for human CD3-targeted tumor immunotherapies evaluation.

Inflammation and Immunity in the Tumor Microenvironment

#5129
Neutrophil extracellular traps induced by surgical stress regulate cancer metabolism leading to tumor growth

Tony Haykal, Ruiqi Yang, Celine Tohme, Ronghua Wang, David Geller, Christof Kaltenmeier, Hamza Yazdani, Samer Tohme. *University of Pittsburgh, Pittsburgh, PA*

Introducti**on:**
Surgery is a crucial intervention to cure malignancies. However, evidence shows that the surgical insult and its accompanying immune response can

enhance tumor growth and metastasis. Neutrophil Extracellular Traps (NETs) released systemically during surgical stress were previously shown to contribute to this process. In fact, to generate increased energy demands required for growth and metastasis, cancer cells in a stressful microenvironment need an adaptive mechanism where metabolic reprogramming to fatty acid (FA) oxidation has been emerging as an important process. Here, we aim to explore the direct effects of surgical NETs in regulating cancer cell metabolism leading to tumor growth and metastasis.

Methods:

For the indolent tumor model, C57BL/6 mice were injected with a small number of LLC-1 (Lewis Lung Cancer-1) cells subcutaneously (SQ) and a group was subjected to laparotomy for 30 mins, with or without intraperitoneal DNAse (NET inhibitor) injection perioperatively. Tumor growth was then followed for 4 weeks. For the tumor metastasis model, LLC-1 cells were injected SQ and allowed to grow for 3 weeks before resection with or without perioperative DNAse. Tumor metastasis to the lungs was assessed after 3 weeks. In vitro experiments on LLC-1 and MC-38 (murine colon adenocarcinoma) cancer cells were performed using NETs released from neutrophils freshly isolated from mice bone marrow and stimulated with Phorbol myristate acetate (PMA).

Results:

For the indolent tumor model, injection of cancer cells did not lead to any significant tumor growth after 4 weeks unless mice underwent surgical stress via laparotomy. Treatment with DNAse significantly reversed their growth. For the tumor metastasis model, tumor resection alone led to significant lung metastasis, but DNAse treatment during resection or resection in PAD-4 KO mice (unable to form NETs) led to significantly less metastatic burden. Furthermore, in vitro treatment of cancer cells with NETs lead to significant cell proliferation, relatively more under hypoxic and serum conditions. This was paralleled with a significant increase in fluorescently labeled FA uptake into cancer cells as detected by flow cytometry, as well as a significant upregulation of gene expression of FA transport proteins and oxidation enzymes.

Conclusion:

Surgical stress can promote tumor growth and metastasis through cancer cell metabolic reprogramming induced by systemically released NETs. We

hope that elucidating the molecular mechanism behind this process can help in finding therapeutics to prevent the protumorigenic effects of surgical stress.

#5130

Multi-plex cytokine profiling for mice on Bleomycin induced systemic sclerosis model

Yanping Yuan, Cheng Qian, Chuanzhi Yangmeng, Li Fang, Ruiqing Yan.
WuXi AppTec, Shanghai, China

Systemic sclerosis (SSc) is recognized as an autoimmune disorder characterized by immune dysregulation, obliterative vasculopathy, excessive accumulation of extracellular matrix, and fibrosis of the skin and other organs. It also ranks on the highest position of disease-related mortality and morbidity with an impaired quality of life among the rheumatologic illnesses. However, the immunological mechanism related to SSc remains to be elucidated systemically, which may lay for the novel therapeutic methodology. In the present study, we combined the MSD methodology and flow cytometry to landscape the chemokine or cytokine network, immunology response and signaling axis in mice on Blomycin induced SSc model. Our results provide the reference and path for the future direction of novel therapeutic reagents discovery.

#5131

Pulmonary influenza infection promotes the awakening of dormant metastatic breast cancer cells

Shi Biao Chia[1], Bryan Johnson[1], Julio A. Aguirre-Ghiso[2], Mercedes Rincon[3], James DeGregori[1]. *[1]Biochemistry and Molecular Genetics, University of Colorado Anschutz Medical Campus, Aurora, CO,[2]Cell Biology, Albert Einstein College of Medicine, New York, NY,[3]Immunology and Microbiology, University of Colorado Anschutz Medical Campus, Aurora, CO*

Breast cancer is the most common form of cancer and the second cancer-causing death in females. Although remission rates are high if detected early, survival rates drop substantially when breast cancer becomes metastatic. The most common sites of metastatic breast cancer are bone,

liver and lung. Respiratory viral infections inflict illnesses on countless people. The latest pandemic caused by the respiratory virus, SARS-CoV-2, has infected more than 600 million worldwide, with documented COVID-related death upward of 1 million in the United States alone. Respiratory viral infections result in increased inflammation with immune cell influx and expansion to facilitate viral clearance. Prior studies have shown that inflammation, including through neutrophils, can contribute to dormant cancer cells reawakening and outgrowth. Moreover, inhibition of IL6 has been shown to decrease breast cancer lung metastasis in mouse models. However, how respiratory viral infections contribute to breast cancer lung metastasis remains to be unraveled. Using MMTV/PyMT and MMTV/NEU mouse models of breast cancer lung metastasis and influenza A virus as a model respiratory virus, we demonstrated that acute influenza infection and the accompanying inflammation and immune cell influx awakens and dramatically increased proliferation and expansion of dormant disseminated cancer cells (DCC) in the lungs. Acute influenza infection leads to immune influx and expansion, including neutrophils and macrophages, with increased proportion of $MHCII^+$ macrophages in early time points, and a sustained decrease in $CD206^+$ macrophages starting 6 days post-infection until 28 days after the initial infection. Additionally, we observed a sustained accumulation of $CD4^+$ T cells around expanding tumor cells for as long as 28 days after the infection. Notably, neutrophil depletion or IL6 knockout reversed the flu-induced dormant cell expansion in the lung. Finally, awakened DCC exhibited downregulation of vimentin immunoreactivity, suggesting a role for phenotypic plasticity in DCC outgrowth following viral infection. In conclusion, we show that respiratory viral infections awaken and increase proliferation of dormant breast cancer cells in the lung, and that depletion of neutrophils or blocking IL6 reverses influenza-induced dormant cell awakening and proliferation.

#5132

The immunomodulatory role of paracrine signaling factor VSIG4 in peritoneal cancers

Yik Yan Chong[1], Sasinthiran Thiagarajan[1], Qiu Xuan Tan[1], Hui Jun Lim[1], Joey Wee-Shan Tan[1], Josephine Hendrikson[1], Gillian Ng[1], Ying Liu[1], Clara Yieh Lin Chong[1], Chin Jin Seo[2], Jolene Si Min Wong[2], Claramae Shulyn

Chia[2], Nicholas Brian Shannon[1], Chin-Ann Johnny Ong[1]. *[1]Laboratory of Applied Human Genetics, National Cancer Centre Singapore, Singapore, Singapore,[2]Department of Sarcoma, Peritoneal and Rare Tumours (SPRinT), National Cancer Centre Singapore, Singapore, Singapore*

Introduction: Colorectal cancer (CRC) is one of the most common cancers worldwide, often presenting with regional spread to the peritoneum. Peritoneal carcinomatosis (PC) has a significantly poorer prognosis compared to metastasis to the other regions of the body. Immunotherapy makes use of the memory and specificity of the adaptive immune system to achieve long lasting effective anti-tumor response. Tumor associated macrophages (TAMs) in the tumor microenvironment have been implicated in tumorigenesis by creating an anti-inflammatory environment suitable for the growth of cancer cells. Thus, our group sought to identify factors associated with immunomodulation in colorectal PC.
Methods: We interrogated publicly available colorectal cancer single cell database (n=5) to identify putative immune markers associated with macrophage activation in cancers. Validation was performed using V-set and immunoglobulin containing domain 4 (VSIG4) immunohistochemistry (IHC) staining on tumor microarrays (TMAs) of colorectal primary tumors (n=210). VSIG4 protein expression was assessed in cell-free ascites (n=39) derived from PC.
Results: Using publicly available single cell database, we shortlisted the top 100 genes from the expression data of CD136-positive TAMs cluster. Among these macrophage-associated genes, two putative markers, VSIG4 and NR1H3, were involved in the regulation of macrophage activation. NR1H3, also known as liver X receptor-alpha (LXR-α), is particularly associated with cholesterol metabolism and thus was excluded from our exploration of TAMs activity. Interestingly, our target of choice, VSIG4, is a membrane protein expressed by M2 macrophages, which is associated with the activation of anti-inflammatory macrophage subtype and the downregulation of pro-inflammatory macrophages. IHC staining of CRC TMA demonstrated that low VSIG4 expression in stroma of primary CRC is associated with poor prognosis (p=0.018). Moreover, enzyme-linked immunosorbent assay (ELISA) of the ascites from colorectal PC patients showed varying amounts of VSIG4, suggesting a possible biological role of VSIG4 amongst patients with upregulated VSIG4 levels in ascites. Taken

together, our studies suggest that VSIG4 plays a possible immunomodulatory role in colorectal PC and warrants further studies to assess its potential role as a therapeutic target in PC.
Conclusion: In view of its potential as a target for immunotherapy, further studies should be conducted to understand the role of VSIG4 in the progression of colorectal PC.

#5133

Oxazolone induced atopic dermatitis mouse model using hIL-4/hIL-4Ra double knock-in mice, a preclinical mouse model for evaluating Dupilumab biosimilars

Tao Yang[1], Rongfei Lu[1], Xiaofei Xu[1], Likun Zhang[1], Dawei Wang[1], Xinhe Feng[1], Xiaoyu An[1], Jessie (Jingjing) Wang[1], Xianfei He[2], Carl K. Edwards[1]. *[1]Crown Bioscience, Inc., San Diego, CA,[2]Shanghai Model Organisms Center, Inc, Shanghai, China*

Background. Th2 cytokines (e.g. IL-4, IL-5, IL13) drive defined allergic reactions and various autoimmune and inflammatory diseases including atopic dermatitis (AD), asthma and rhinitis. IL-4Ra is a receptor shared by both IL-4 and IL-13, thus blocking of IL-4Ra could prevent both IL-4 or IL-13 mediated Th2 inflammatory response. Dupilumab (Dupixent) is a humanized anti-IL-4Ra monoclonal antibody which binds to human IL-4Ra and attenuates IL-4/IL-13 mediated Th2 inflammation. It has been approved for treating moderate to severe AD and asthma. However, since Dupilumab isn't cross-reacting to mouse IL-4Ra, there is an unmet need for a robust mouse model to evaluate Dupilumab biosimilars at preclinical stages. In this study, we described an oxazolone induced AD model in hIL-4/hIL-4Ra double knock-in mice and its application to evaluate Dupilumab and its biosimilars.
Methods. The oxazolone induce AD mouse model was established in hIL-4/hIL-4Ra double knock-in mice by repeated topical applications of Oxazolone on ears. Oxazolone-induced mice received subcutaneous injection of Dupilumab at 25 mg/kg or 50 mg/kg. Dermatitis activity was assessed by measuring ear thickness, ear skin erosion, redness and scaling every other day. Serum were collected at the study end and IgE levels were measured by ELISA. In addition, spleens were also collected and their

weights were compared. Ear were collected at study end and proceeded with cytokine analysis and pathology evaluation.
Results. Repeated topical application of oxazolone on mouse ears induced AD-like phenotypes including ear skin swelling, erythema and scaling, drastic elevation of IgE in serum, excessive production of human IL-4 cytokine as well as excessive inflammatory cell infiltration in ear skin, which suggests oxazolone is able to induce AD in this hIL-4/hIL-4Ra double knock-in mice. Subcutaneous injection of Dupilumab at two different doses levels, 25 mg/kg and 50 mg/kg successfully ameliorated ear skin swelling, erythema and scaling at the study end. In addition, Dupilumab at both dose levels significantly reduced the IgE level in serum and mitigated the inflammatory cell infiltration, e.g. eosinophil infiltration, in mouse ear. Furthermore, Dupilumab treatment significantly reduced mouse IL-6 and mouse KC/GRO levels in mouse ear. However, Dupilumab at both dose levels did not change the serum levels of human IL-4 as well as some other Th1 cytokines such as IFN-γ, IL-1β, TNF-α, etc. in mouse ear.
Conclusion. In summary, repeated challenge with Oxazolone in hIL-4/hIL-4Ra double knock-in mice resulted in the development of AD with a Th2-like hypersensitivity, mimicking the key features and pathology of the human disease, which responded to standard of care treatment Dupilumab. This provides a valuable translational model for the evaluation of future biosimilars of Dupilumab.

#5134
PD-1/PD-L1 signalling axis, “a double-edged sword” in DSS induced colitis mouse model
Tao Yang, Rongfei Lu, kaixia lian, Likun Zhang, Dawei Wang, Xinhe Feng, Xiaoyu An, Jessie (Jingjing) Wang, Carl K. Edwards. *Crown Bioscience, Inc., San Diego, CA*

Background. Immune checkpoint molecules are essential for modulating immune responses and maintaining self-tolerance. While immune checkpoint inhibitors have improved the treatment of a broad spectrum of cancers, many of them are also believed to play a critical role in the induction of immune related adverse events (irAEs) such as autoimmune and inflammatory diseases. For example, patients receiving anti-PD-1 based therapy frequently develop colitis. In addition, dysfunctional PD-1

signalling has also been linked to increasing susceptibility to autoimmune and inflammatory diseases. Therefore, immune checkpoint molecule agonist which could, like their natural ligands, confer a great potential in suppressing excessively activated immune response observed in autoimmune and inflammatory diseases.
Methods. In the first part, the proinflammation effects of a Pembrolizumab analogue was evaluated in a MC38-OVA colorectal tumor bearing mice treated with or without DSS. In the second part, an anti-hPD-1 agonistic antibody at 10 mg/kg was evaluated in acute DSS IBD model.
Results. In the MC38-OVA colorectal cancer model, mice treated with Pembrolizumab analogue only or Pembrolizumab analogue plus 1.5% DSS showed significant tumor growth inhibition (100% TGI and 92.01% TGI, respectively at Day 27) compared to their respective control group, which suggests this Pembrolizumab analogue induced robust anti-tumor immunity against MC38-OVA tumors. Notably, 8/8 mice treated with Pembrolizumab analogue only showed complete tumor regression, while only 5/8 mice treated with Pembrolizumab analogue plus DSS showed complete tumor regression. Taken together, these results suggest DSS treatment leading to a proinflammatory context could compromise anti-hPD-1 anti-tumor efficacy. Moreover, mice treated with Pembrolizumab analogue plus DSS also showed 3.59% more Body Weight Loss (BWL) in comparison to 1.5% DSS only group, suggesting that Pembrolizumab analogue could exacerbate DSS induced colitis. In the acute DSS IBD model, mice treated with an agonistic anti-hPD-1 antibody showed significantly lower disease score (DAI 5.3 vs DAI 2.4) and less BWL (BWL 13.44% vs BWL 3.31%) in comparison to isotype control group. In addition, pathology results showed that mice treated with agonistic anti-hPD-1 exhibits significantly less inflammatory cell infiltration and colonic lesions when compared to isotype control group.
Conclusion. In summary, we reported in this study that blocking of PD-L1/PD-1 signalling axis by a PD-1 antagonist activated T cell function which at the same time aggravated DSS induced colitis in mouse. In contrast, activation of PD-L1/PD-1 signalling pathway by a PD-1 agonist alleviated DSS induced colitis.

#5135

Standardized off-the-shelf engineered NK cell therapy with improved ADCC properties to treat malignancies

Yanan Lin[1], Shengbang Zhang[1], Jie Ran[1], Can Song[1], Shengcang Zhu[1], Hui Shi[1], Ping Guo[1], Shengjiang Tan[2], Yuchun Gu[1], Lida Wu[1]. *[1]Allife Medical Science and Technology Co., Ltd., Beijing, China,[2]Cambridge Institute for Medical Research, Cambridge Stem Cell Institute, University of Cambridge, Cambridge, United Kingdom*

In the treatment of solid tumors, chimeric antigen receptor(CAR)-engineered NK (CAR-NK) cells have distinct advantages over CAR-T cells, such as a lack graft-versus-host disease in allogenic setting to make “off the shelf” medicine; much safer because they are less likely to cause cytokine storms; and NK cells have their own activated receptors that recognize tumor surface antigens and thus have a natural ability to kill a wide range of tumors. In addition, NK cells are the main performers of antibody-dependent cell-mediated cytotoxicity (ADCC), which binds to the Fc-terminus of antibodies through their surface Fc receptor CD16A, thereby killing antibody-targeted tumor cells. Enhancing the ADCC action of NK cells themselves enhances the therapeutic efficacy of monoclonal antibodies targeting tumor surface antigens and is therefore of great importance in the treatment of tumors, especially solid tumors. We screened two optimal structures among nine different Fc chimeric receptors, and NK cells overexpressing these two receptors killed K562 and Daudi six times more intensely than normal NK cells when combined with rituximab, while the killing ability was comparable to that of normal NK without rituximab, indicating that NK cells expressing chimeric Fc receptors have stronger ADCC effects. Moreover, these NK cells can kill target cells in multiple rounds. In vivo experiments in mice demonstrated that NK cells expressing chimeric Fc receptors in combination with EGFR monoclonal antibodies had a stronger inhibitory effect on tumor growth than monoclonal antibodies or NK cells alone. Here we provide a novel broad “off the shelf” NK cells that can significantly enhance the killing ability of hematological and solid tumors in combination with different monoclonal antibodies.

#5136

Surgical stress promotes long-lasting protumorigenic changes in bone marrow derived progenitor cells

Hamza O. Yazdani, Tony Haykal, Ruiqi Yang, Celine Tohme, David A. Geller, Samer Tohme. *University of Pittsburgh, Pittsburgh, PA*

Introducti**on:** Surgery is a crucial intervention for cancer patients. However, the perioperative period is characterized by an increased risk for accelerated growth of metastatic disease. Our recent work shows that the protumorigenic systemic inflammatory changes and the formation of neutrophil extracellular traps (NETs) persist months after surgery in both mice and humans, and parallel micrometastatic tumor growth and recurrence. Here we hypothesized that surgery may induce long-term sustained epigenetic and transcriptomic changes in bone marrow derived granulocytes-monocytes progenitor cells (GMPs) leading to functional reprogramming of mature neutrophils and persistent systemic release of these protumorigenic NET-forming neutrophils.
Methods: Eight-week-old mice were subjected to non-lethal surgical stress (laparotomy) for 30 mins. Seven days after, mice were inoculated with 1x106 MC38 (murine colorectal cancer cells) subcutaneously. For bone marrow (BM) transplant model, a group of B6 congenic (CD45.1) mice were subjected to laparotomy. BM derived cells were harvested 7 days after the procedure and orthotopically transplanted into B6 CD45.2 irradiated (1000 rads) mice. After the establishment of hematopoiesis (6 weeks), MC38 cancer cells were implanted into the recipient mice.
Results: Mice that underwent laparotomy had significantly increased tumor volume at 3 weeks compared to control mice, that only underwent anesthesia (Laparotomy vs control **$p<0.01$). While the intratumoral flowcytometry analysis showed no difference in the frequency of infiltrating immune cells, quantitative (q) PCR analysis revealed significant plasticity in the tumor infiltrating neutrophils (TANs) observed by an increase in the expression of genes (MCP1, Arg1) associated with pro-inflammatory (N2) type neutrophils compared to control. A persistent increased level of NETs was also observed within the tumors and circulation of mice several weeks after laparotomy. ATAC-seq and Bulk-RNA-seq analysis further revealed major epigenetic and transcriptomic changes in TANs, circulating neutrophils and GMPs. To substantiate long-lasting surgical effects, tumor burden was assessed in the BM recipient mice and showed to be significantly increased in mice that had received BM cells from laparotomy mice versus BM cells from sham group.

Conclusion: Surgery promotes long-term rewiring of the bone marrow derived cells resulting in increased tumor growth. Understanding the underlying molecular mechanism may help with therapeutic interventions to prevent protumorigenic surgical effects and improve patient outcomes.

#5138

Systemic agonist anti-CD40 treatment delivers precise melanoma immunotherapy within established autoimmune landscapes

Julio C. Valencia, Michael Sanford, Howard A. Young. *National Cancer Institute at Frederick, Frederick, MD*

The overlapping signatures of type 1 interferons (IFN) and IFN-gamma (IFNg) has proven challenging in human autoimmunity and cancer immunotherapy, particularly for resistance to anti-programmed death 1 (anti-PD1) monotherapy. By contrast, agonist abs targeting of CD40 (anti-CD40) antibodies (abs) has clinically elicit anti-tumor immunity with limited autoimmune complications. Here, we explore the relationships between anti-PD1 or agonist CD40 responses in melanoma tumors from type 1 IFN alpha receptor (IFNAR)-sufficient and type 1 IFNAR-deficient lupus-prone mice that overexpress IFNg. To address this, RNA-sequencing (RNA-seq) data on tumors treated with either anti-PD1 or agonist anti-CD40 was evaluated for tumor objective responses compared to untreated controls. Cellular and canonical pathway identification from RNA-seq data were interrogated from the IPA library for significantly differential expressed genes (DEG). Variance patterns of the anti-PD1 and anti-CD40 monotherapies identified known resistance and response pathways highly concordant with IFN co-expression patterns in the RNA-sequencing data, respectively. IPA biomarker analysis for uniquely regulated genes showed that anti-PD1 induced only 59 DEG; while anti-CD40 induced 494 DEG including Il-27, and PR/SET Domain 1 (PRDM1), a transcription factor regulated by IL-27. Specifically, signatures of MDSC development (irf8, il10); and adaptive resistance (pdcd1, pdcd1lg2, and TNFRSF5/CD40)) were negatively associated with response to anti-P1 monotherapy. By contrast, signatures of IFN activation (stat1, Ifng, and Ifngr1), chemotaxis (Cxcl10, Il12b and Il-27), attractants (Sema3g and Sema4a), and antigen presentation MHC II (h2-Aa, h2-Ab1, and ciita) were associated positively with response to agonist anti-CD40 monotherapy. Importantly, anti-CD40

alone delivered anti-tumor immune responses in type 1 IFN receptor-deficient lupus-prone mice that overexpress IFNg (Ifnar-/-ARE-/-) mice suggesting synergy with therapies blocking type 1 IFN signaling. Thus, these findings indicate that the rational use of CD40 agonists abs provide a better therapeutic platform to deliver precise anti-melanoma responses in complex autoimmune landscapes.

#5139

Chemerin suppresses prostate tumor growth by modulating the recruitment of NK and CD8+ T-cells to tumor microenvironment

Muhammad A. Saeed, Kevin Kim, Russell K. Pachynski. *School of Medicine, Washington University in St. Louis, St. Louis, MO*

Infiltration of immune cells into the tumor microenvironment (TME) can regulate growth and survival of malignant cells, thereby affecting tumorigenesis and tumor progression. While immune checkpoint inhibitors and agonism of costimulatory molecules can act to stimulate leukocytes, the lack of adequate recruitment of effector cells into TME often results in suboptimal immune responses. Chemerin (retinoic acid receptor responder 2, RARRES2) is an endogenous chemoattractant that is widely expressed by many tissues and recruits innate leukocytes through its receptor, CMKLR1 which is expressed on NK cells, some dendritic cells, and macrophages. Previous studies show that RARRES2 is downregulated across multiple tumor types including prostate cancer. Here, using a syngeneic transgenic adenocarcinoma mouse prostate (TRAMP-C1) model, we show that forced overexpression of RARRES2 by tumor cells results in significant tumor suppression and recruitment of NK and CD8+ T-cells within the TME. Male C57/BL/6 mice were inoculated with either RARRES2-overexpressing, vector control (VC) or mixed (50:50; VC: RARRES2) TRAMP-C1 cells. Chemerin overexpression in TRAMP-C1 cells did not alter their phenotypic behavior *in vitro*, but significantly suppressed tumor growth *in vivo* in mice. Furthermore, we observed a significantly higher influx of NK (CD3-CD19-NK1.1+) and CD8+ T-cells (CD3+CD8+) in tumor-infiltrating leukocytes (TILs) from mice with mixed tumors compared with VC tumors. Depletion of NK cells, CD4+, or CD8+ T cells showed that NK cells and CD8+ T-cells, but not CD4+ T-cells, were required for chemerin-dependent suppression of TRAMP-C1 tumor growth.

We found significant increases in splenic NK and CD8 T cells, and a concomitant significant decrease in splenic G-MDSC in mice with chemerin-expressing tumors compared to controls, suggesting chemerin expression within the TME has an effect on systemic immune responses. Treatment of control tumors with anti-PD1 checkpoint inhibition did not result in significant tumor suppression, while anti-PD1 treatment of chemerin-expressing tumors significantly reduced tumor growth, doubling the complete response rate in these unresponsive tumors. Thus, for the first time we have demonstrated that increasing chemerin expression within the prostate TME can suppress growth by augmenting recruitment of NK and CD8+ T-cells and has the potential to be combined with checkpoint inhibitors in order to improve response rates in non-responsive tumors. Overall, these data suggest that a tumor-targeted chemerin therapeutic may have potential to treat human prostate cancers.

#5140

Combined administration of poly(I:C) and resiquimod triggers effective antitumoral response in mouse models of pancreatic adenocarcinoma

Aldo Ummarino[1], Clément Anfray[2], Andrea Mariancini[1], Domenico Supino[2], Cecilia Garlanda[2], Fernando Torres Andòn[3], Alberto Mantovani[2], Paola Allavena[2]. *[1]Humanitas University, Milan, Italy,[2]Department of Inflammation and Immunology, IRCCS Humanitas Research Hospital, Milan, Italy,[3]Center for Research in Molecular Medicine and Chronic Diseases, Santiago de Compostela, Spain*

Pancreatic ductal adenocarcinoma (PDAC) represents one of the deadliest malignancies worldwide. The lack of clinical symptoms in the early stages of the disease and the poor immunogenicity of PDAC are two major causes of late diagnosis and inefficient therapies. The tumor microenvironment of PDAC is rich in stromal cells inducing desmoplasia, complicating the arrival of medical compounds, as well as in immune cells, that are suppressed by several mediators produced by cancer cells. In this setting, it has been shown that some medications can restore the antitumoral activity of innate immune cells that, in turn, re-activate also adaptive immune cells. In this study, we present the combination of the TLR agonists poly(I:C) (pIC - TLR3) and resiquimod (R848 - TLR7/8) as an immunotherapeutic

tool in PDAC. In a subcutaneous model of PDAC (K8484 cells, isolated from KPC mice that spontaneously develop PDAC and recapitulate the features of human pancreatic cancer), the intratumoral administration of pIC+R848 for 5 times every 2-3 days led to the complete regression of the tumor in 100% of the treated mice. Moreover, all mice were protected from a second and a third rechallenge with the same cell line, performed months after the first treatments. Mechanistic studies performed on the tumors with flow cytometry demonstrated an increase of MHC-II positive cells in the monocytic (Ly6C+) compartment, as well as an increase in the number of mature CD8+ T cells and NK cells. Similar findings were demonstrated also in another heterotopic model obtained injecting Panc02 cells, another cell line with a sarcomatous phenotype. Consistently with the flow cytometry data, the depletion of CD4+ and CD8+ T cells abolished the antitumoral efficacy of pIC+R848, while the depletion of NK cells and CSF-1R+ cells was not sufficient to abolish the antitumoral response, suggesting a strong involvement of the adaptive immunity. In line with these findings, the intratumoral administration of pIC+R848 in mice unable to produce IFN-γ failed to reduce the tumor growth. In conclusion, our work clearly demonstrates that pIC+R848 are an effective treatment for PDAC when injected intratumorally and that this activity strongly relies on IFN-γ and adaptive immunity. Further investigations are ongoing to assess their potential in orthotopic models using different routes of administration, in a setting closer to the real clinical situation.

#5141

Macrophage transcriptomic signature validation in scRNA seq and overall survival differences in urothelial carcinoma

Laura Bukavina[1], Spencer Bell[1], Daniel Geynisman[1], Ilaha Isali[2], Daniel Ranti[3], John Sfakianos[3], Henkel Valentine[1], Adam Calaway[2], Alexander Kutikov[1], Andres Correa[1], Robert Uzzo[1], Lee Ponsky[4], Philip Abbosh[1].
[1]Fox Chase Cancer Center, Philadelphia, PA,[2]Case Western Reserve School of Medicine, Cleveland, OH,[3]Mount Sinai, New York, NY,[4]University Hospitals Cleveland Medical Center, Cleveland, OH

Introduction: While the prognostic value of immune system biomarkers has been well explored, role of cancer associated macrophages in bladder

cancer(BC) is unclear due to lack of consistent results, coupled with tissue *nonspecific* transcriptomic signature.
Methodology: Data acquisition from 3,936 patients of The Cancer Genome Atlas (TCGA) in addition to Gene Expression Omninus (GEO) data sets GSE13507, GSE16945, GSE48277, GSE32894, GSE149582, as well as European Genotype Phenotype EGAS000001004507 was obtained. Tumor associated macrophages M1 and M2 were defined utilizing 188 and 159 gene expression profiles via xCell computational algorithm. To obtain bladder tissue residence macrophage signatures, scRNA seq was performed on tissue collected from surgical resection of 5 HG bladder cancer patients and 2 healthy controls. CellRanger software package with default parameters was utilized giving a total of 8,068 cells. FindAllMarkers was utilized for integration of DEG genes (cancer vs control) among the cluster and identification of BC macrophage specific markers. Endpoint of OS were measured in months from the time of cystectomy to follow up.
Results: Surprisingly, presence of M1 infiltration was found to be associated with improved OS in two out of eight cohorts only (GSE32894, GSE70691, $p<0.001$), while the remainder detected no significant difference. Similarly, no association with OS was detected among all 8 cohorts with M2 infiltration. To improve our understanding of tissue specific markers of macrophage population in bladder, we then analyzed macrophage clusters detected within scRNAseq of BC patients compared to healthy. Gene ontology enrichment analysis of functions within tumor specific macrophages demonstrated an exaggerated expression of *mTORC1* signaling, *PI3K/AKT/mTOR* signaling, *TGF beta* and *EGF* receptor pathways compared to non-cancer controls. Reanalysis of 22 tissue specific markers for M1/M2 infiltration showed no difference in any of the 8 cohorts with M1 high vs low infiltration. Similarly, addition of M2 infiltration as predictive marker yielded no further associations with OS in all but one cohort (GSE32894, $p=0.00041$), where high M2 tumor presence was associated with improved OS.
Conclusion: Our study represents the largest TAMs evaluation of BC across 8 cohorts with additional scRNA seq exploration of tissue specific signatures, demonstrating no association with OS in bladder cancer.

#5142

50-parameter flow cytometry by CyTOF empowers comprehensive single-cell immune profiling of pulmonary immunosenescence in aged mice

Wenxi Xu, Stephen Li, Alexandre Bouzekri, Lauren Tracey, Christina Loh.
Standard BioTools, Markham, ON, Canada

High-parameter flow cytometry is essential for human and mouse studies to discover novel immunological mechanisms of cancer, infections, and immunosenescence. It plays an increasingly important role in cancer research to ensure clinical therapeutic success but is limited by the large amount of cell samples needed for staining controls. CyTOF® technology has transformed flow cytometry by enabling 50-plus-marker analysis per tube of sample, with easy panel design and no need for single-stained or autofluorescence controls. Flow cytometry by CyTOF provides an efficient and unbiased approach to discovering novel subsets and unique functional states of immune cells, maximizing insights from precious samples.
Immunosenescence perturbs lung cancer onset and development, yet the mechanisms remain largely unknown. To study the pulmonary immune populations in aged (75 weeks old) and young adult (6-8 weeks old) mice, we built a 50-parameter panel (2 for single live-cell identification, 6 for live-cell sample barcoding, and 42 for immune profiling). A core panel of 32 antibodies was selected from Standard BioTools™ catalogs to detect key cell lineage and functional surface markers. A complementary panel with 10 Maxpar® antibodies was added to further study functional cell states. Maxpar Pathsetter™ software was used to create an automated analytical model for high-dimensional analysis.
The 50-parameter panel successfully identified over 30 lymphoid and myeloid cell subsets including but not limited to T cells, B cells, NK cells, alveolar macrophages (AMs), dendritic cells, and neutrophils. The panel enabled high-fidelity detection of over 15 functional markers mediating proliferation, activation, inhibition, migration, tissue residence, and cellular metabolism. Automated in-depth analysis by Maxpar Pathsetter efficiently identified many aging-associated alterations in cell frequencies and functional states such as the enrichment of PD-1+ T cells and CD27- γδ T cells that could potentially perturb anti-tumor immunity. Moreover, CyTOF technology is uniquely advanced in characterizing autofluorescent cells

such as AMs. A pro-inflammatory state (higher expression of MHC-II, CD80, and PD-L1) was specifically defined for AMs in aged lungs.
This study demonstrates comprehensive single-cell immune profiling of mouse tissues with the products and solutions provided by Standard BioTools. Both the 50-parameter panel and Maxpar Pathsetter analytical model can be customized for deep characterization of specific immune populations according to the requirements of various cancer studies in mice. By utilizing end-to-end solutions offered by Standard BioTools, flow cytometry by CyTOF can significantly facilitate the mechanistic studies of mouse models to expand the understanding of human cancers and accelerate therapeutic development.

#5144

Spatial T-cell atlas in more than 100 different tumor entities using BLEACH&STAIN

Zhihao Huang, Elena Bady, Jan H. Müller, Tim Mandelkow, Magalie C. J. Lurati, Ronald Simon, Christian Bernreuther, Frank Jacobsen, Guido Sauter, Katharina Möller, Andreas Luebke, Andrea Hinsch, Till S. Clauditz, Eike Burandt, Niclas C. Blessin. *University Medical Center Hamburg-Eppendorf, Hamburg, Germany*

Background: The composition and functional state of T-cell subpopulations can highly impact patient's outcome and response to immune checkpoint therapy. However, only little is known about the spatial interplay of most rare T-cell subpopulations.
Design: To assess the density, composition, degree of immune checkpoint expression, and spatial interplay of T-cell subpopulations in 5989 tumor samples from more than 100 tumor entities, two different types of tissue microarrays (0.6 mm and 4 mm in diameter) were stained with antibodies directed against CD3, CD4, CD8, FOXP3, T-bet, GATA3, RORyT, BCL6, FOXP3, CD56, CD45RA, CD45RO, TIM3, PD-1, CTLA-4 Granzym B, and Ki67 using our BLEACH&STAIN multiplex fluorescence immunohistochemistry approach. A deep learning-based framework comprising two different convolutional neuronal networks (U-Net and DeepLabv3+) was used for image analysis.
Results: For identification and definition of immune cell subpopulations unsupervised X-shift clustering and 2D/ 3D t-distributed stochastic

neighbor embedding (t-SNE) using the "Rtsne" package (Rtsne (RRID:SCR_016342)) were applied and revealed 102 T-cell subpopulations at certain functional state. Within these subpopulations, the well-characterized expression profiles were visually matched with single T-cell expression profiles and documented as digital images. This process resulted in 12 main T-cell subsets that were further subclassified according to their functional state (proliferation, immune checkpoint expression) and studied according to their spatial orchestration. Interestingly, the vast majority of T-cell subsets were found in all analyzed tumor entities. However, their spatial orchestration, immune checkpoint expression profile was highly variable between different tumor entities.
Conclusion: This study provides a comprehensive overview of rare T-cells subpopulations and its spatial orchestration in more than 100 different tumor entities.

#5145

Targeting TREX1 induces innate immune response in chemoresistant small cell lung cancer

Takahiko Murayama[1], Navin R. Mahadevan[2], Tetsuo Tani[2], Xueying Ma[1], Hideo Watanabe[3], David A. Barbie[2], Israel Cañadas[1]. *[1]Blood Cell Development and Function Program, Fox Chase Cancer Center, Philadelphia, PA,[2]Department of Medical Oncology, Dana-Farber Cancer Institute, Boston, MA,[3]Department of Medicine, Division of Pulmonary, Critical Care and Sleep Medicine, Icahn School of Medicine at Mount Sinai, New York, NY*

Small cell lung cancer (SCLC) is the most lethal type of lung cancer. The uniqueness of this tumor consists of an initial exquisite response to chemotherapy. However, at relapse, which occurs nearly in all patients, the tumor is resistant to all available therapies, causing a premature death of the patient. Despite the addition of immune checkpoint blockade (ICB) therapy to standard chemotherapy, response rates are modest and only a very small fraction of SCLC patients responds to these therapies. The mechanistic basis for acquired chemoresistance and impaired immunogenicity in SCLC remains to be elucidated. Here, we report that the expression of three prime repair exonuclease 1 (TREX1) is strongly induced in chemoresistant SCLCs. ATAC-seq and ChIP-seq analyses revealed a significant increase in

chromatin accessibility of TREX1 gene locus in drug resistant SCLC cells. Depletion of TREX1 in SCLC cells caused the activation of cyclic GMP-AMP synthase (cGAS)-stimulator of interferon genes (STING) pathway due to the cytoplasmic accumulation of DNA damage-associated double-stranded DNA (dsDNA) and micronuclei. Furthermore, targeting TREX1 induced an innate immune response and re-sensitized chemoresistant SCLC cells to chemotherapy. These findings suggest that TREX1 upregulation may be an important mediator of cGAS/STING pathway inactivation in cancer, contributing to the survival of resistant cells, and its inhibition may represent a promising therapeutic strategy to potentiate the efficacy of chemotherapy and immunotherapy in chemoresistant and immunologically 'cold' tumors, such as SCLC.

#5146

***In vitro* neutrophil assays to support immuno-oncology drug development**

Alanah Pieters, Martijn Vlaming, Jezabel Lefevere, Sofie Pattyn.
ImmunXperts, a Q2 Solutions Company, Gosselies, Belgium

Neutrophils have shown a lot of plasticity with important consequences on cancer disease progression and have been associated with multiple functions such as killing antibody-opsonized cancer cells, directly kill tumor cells through the release of reactive oxygen and nitrogen species and a controversial role in the tumor micro-environment with both pro- and anti-tumor roles. Studying neutrophil function in vitro can be done using the Incucyte® live imaging system to monitor antibody-dependent cell-mediated cytotoxicity (ADCC). Optimised in vitro assays using fresh human neutrophils and fluorescent-labeled tumor cells can be used to screen the potency of candidate therapeutics. Additionally, neutrophil chemotaxis can be monitored using transwell plates and live imaging via Incucyte®. Finally, multiplex cytokine and chemokine analysis after activation and stimulation of neutrophils can be evaluated using Luminex technology. When studying neutrophil activity in vitro, important factors such as access to fresh blood and optimized protocols for purifying untouched neutrophils are key for reproducible and reliable results.

#5147

Mice with T cells deficient in the Cytosolic Branched Chain Aminotransferase reduce the tumor burden of low and high immunogenic strains of Lymphoma

Lucas D. Figueroa, Tanner Wetzel, Leighton Wheeler, Christie Adam, Michael Boyer, Elitsa Ananieva. *Des Moines University, Des Moines, IA*

Current immunotherapies rely on modulating host immunity to induce an anti-tumor immune response. The efficacy of such a response depends on the immunogenicity of the tumor, which varies greatly between different cancers or the same cancer in different individuals. While most lymphomas are immunogenic, non-malignant T cells that infiltrate the lymphoma microenvironment are subjected to immunosuppressive signals and areas of nutrient depletion, which leads to T cell exhaustion and inhibition of T cell function. Metabolic enzymes, such as the cytosolic branched chain aminotransferase, BCATc, exert immunosuppressive effects limiting T cells ability to function. Previous research described BCATc as a negative regulator of T cell activation, thus identifying BCATc as a potential target for immunotherapeutic modulation in the tumor microenvironment (TME). In the current study we exploit a low (EL4) and high (EL4-OVA) immunogenic murine lymphoma strains to explore how a loss of BCATc in T cells impacts their ability to produce anti-lymphoma immunity in mice. We used 12 week old male mice with BCATc deleted from T cells (T-BCATc^{KO}) and control T-BCATc$^{fl/fl}$ mice that express the transgenic floxed version of BCATc. Mice were injected with 2.5x10^5 cells belonging to the low (EL4) or high (EL4-OVA) immunogenic strains and tumor growth, body weight, and food intake were monitored for up to 15 days followed by collection of tumor tissues and organs. Tumors were then lysed, and the protein profile of each tumor was determined by monitoring changes in expression of protein markers of T cell exhaustion (TOX, CD39), apoptosis (BAX, PUMA), or signaling proteins, such as the ribosomal S6 protein, the protein kinase B (AKT), and the energy sensor the AMP-activated protein kinase (AMPK).

T-BCATc^{KO} mice showed significant reduction in tumor growth compared to control mice regardless of the lymphoma strain being tested. The mouse cohort with the biggest number of tumor free mice was the T-BCATc^{KO} cohort injected with EL4 cells (13% of the mice were tumor free on day 9). However, EL4-OVA cells grew into smaller tumors across all cohorts. Mice

had comparable food intake but T-BCATc^{KO} mice, injected with EL4 cells, had a significantly lower body weight. In T-BCATc^{KO} mice, the reduced EL4 tumor mass correlated with upregulated AMPK and AKT along with higher expression of PUMA. The reduced EL4-OVA tumor masses correlated with downregulated S6 and decreased TOX expression, but high expression of BAX compared to the corresponding tumors isolated from T-BCATc$^{fl/fl}$ mice. These findings suggest that T cells deficient in BCATc can reduce lymphoma growth regardless of the immunogenicity of the lymphoma stain likely by establishing catabolic state and inducing apoptosis. Thus, BCATc may play an immunosuppressive role in the lymphoma TME and the absence of BCATc from T cells may help T cells combat lymphoma.

#5148

Interrogating immuno-oncological interactions in the tumor microenvironment

Ben Patterson, Cheng-Yi Chen, Nicolas Fernandez, Leiam Colbert, Jiang He*. Vizgen, Cambridge, MA*

Single-cell RNA sequencing is a powerful and innovative tool for assessing individual cancer prognoses and outcomes; however, the process of generating this data typically destroys the spatial complexity of the tumor microenvironment. Understanding the spatial complexities within cancer provides crucial information for evaluating individual tumor development and progression. Vizgen's MERSCOPE^{TM} Platform, built on Multiplexed Error-Robust Fluorescence in situ Hybridization (MERFISH) technology, enables the direct profiling of the spatial organization of intact tissue with subcellular resolution. Here, we present a Pan-Cancer approach to demonstrate the MERSCOPE's ability to characterize breast, colon, prostate, ovarian, lung, and skin cancers from human clinical samples. Specifically, using a 500-gene panel to assess the canonical signaling pathways of cancer, cancer type-specific genes, select immune genes, proto-oncogenes, and tumor-suppressor genes, we show that the MERSCOPE was able to spatially profile gene expression across multiple tumor types. We utilized the Vizgen Cell Boundary Stain kit to generate a molecular and cellular atlas of individual patient tumors by clustering cells based on gene expression and mapping their spatial organization. To gather insight into

immuno-oncological interactions and their effect on gene expression across these tumor types, we performed a neighborhood analysis to determine how proximity to immune cells altered gene expression in tumor cells, and vice versa. We found significant gene expression changes in MHC activation and downstream pathways in immune cells located nearest to tumor cells; in tumor cells nearest to immune cells, we identified increased expression of genes related to immune response mediation and inflammation. Furthermore, we compared the annotated immune cell populations across the various cancer types to observe differences in gene expression. Here, we used publicly available single-cell RNA-sequencing data to impute gene expression for these immune cell populations. This analysis demonstrated the transcriptional variation possible in identical immune cell types that are acting in different tissue contexts. Notably, we were able to map and catalogue different patterns of gene expression relating to inflammation, immune signaling, and immune cell exhaustion. These findings demonstrate how the MERSCOPE platform can provide deep insights into the complex heterogeneity observed between different tumor types and tissues.

#5149

Age-associated remodeling of anti-tumor T cell immunity and metabolism

SeongJun Han[1], Peter Georgiev[1], Alison Ringel[2], Arlene Sharpe[1], Marcia Haigis[1]. *[1]Harvard University, Boston, MA,[2]MIT, Boston, MA*

Aging results in remodeling of T cell immunity and is associated with poor clinical outcome in age-related diseases such as cancer. Amongst the hallmarks of aging, changes in host and cellular metabolism are critically involved in the development, maintenance, and functional responses of T cells. Although metabolic perturbations impact anti-tumor T cell responses, the link between age-associated metabolic dysfunction and anti-tumor immunity remains unclear. First, we utilized B16, MC38 and E0771 tumor-bearing young (2-4 months) and aged (18-24 months) C57BL/6 mice to examine the effects of aging on tumor growth. Aged mice exhibited accelerated tumor growth in B16, MC38 and E0771 tumor models. Flow cytometric analyses of tumor infiltrating lymphocytes (TILs) revealed distinct changes in $CD8^+$ T cell population, decreased activation status and tumor-specificity in aged mice. Consistent with these findings, $CD8^+$ T

cells functionally played a limited role in controlling tumor growth in aged mice. Here, we will explore the mechanisms of age-associated metabolic dysfunction in T cells and its implications in anti-tumor immunity. As the average life expectancy continues to increase, understanding the interplay between age-related metabolic reprogramming and maladaptive T cell immunity will be instrumental in the development of novel therapeutic strategies for older patients.

#5150

Improvement of hematopoiesis in primary low risk MDS with the TGFBR1 investigational inhibitor TP-6379

Erika A. Eksioglu[1], Gabriela M. Wright[1], Jason M. Foulks[2], Matthew Lalonde[2], Steven L. Warner[2], Kenneth L. Wright[1]. *[1]Immunology, Moffitt Cancer Center, Tampa, FL,[2]Sumitomo Pharma Oncology, Inc., Lehi, UT*

Background: The inflammaging modulator, S100A9, mediates immunosuppression and plays a key role in the pathogenesis of low-risk myelodysplastic syndrome (MDS). Specifically, S100A9's feedforward activation in the bone marrow (BM) induces pyroptotic cell death of hematopoietic stem and progenitor cells (HSPC) and the activation and accumulation of myeloid-derived suppressor cells (MDSC). This process creates a suppressive microenvironment including the secretion of transforming growth factor β (TGFβ) that signals through the TGFβ receptor 1 (TGFBR1) to induce inhibitory processes that contribute to this phenotype. We hypothesize that targeting with an investigational TGFBR1 inhibitor, TP-6379, reduces immune suppression and restores hematopoiesis in MDS.

Methods: Primary low risk MDS BM mononuclear cells (BMMNC) were obtained from the Moffitt Total Cancer Care Protocol and cultured in vitro with TP-6379. Healthy BMMNC were purchased, treated with or without recombinant S100A9 and TP-6379.

Results: Treatment of primary MDS BMMNC (n=15) and S100A9-treated healthy BMMNC (n=5) with TP-6379 for 48 hours was observed to significantly improve proliferation of hematopoietic progenitor cells as measured by colony forming capacity. Total colonies, and BFU-E specific colonies, showed significant increase. This expansion of progenitors with treatment was validated by flow cytometric analysis of Lineage$^-$HLA-DR$^-$

$CD34^+$ HSPC and showed a reduction in genomic instability, measured by γH2AX. In addition, TP-6379 was observed to reduce the numbers of suppressive mediators; MDSC, T regs and senescent lymphocytes and increase the number of cytotoxic cells, including NK cells. Our analysis revealed that BMMNC with spliceosomal mutations, including SF3B1, have elevated sensitivity to TP-6379 treatment. Therefore, we tested wild type and SF3B1 K700E CRISPR knock-in K562 cells in the presence of TP-6379 for 48 hours. K562 is a well-established cell line model for study of MDS. The SF3B1 mutant expressing cells have significantly reduced BFU-E colony forming capacity, compared to wild type cells, concordant with higher pyroptosis activation and consistent with the BMMNC results. Hence, we measured phospho-SMAD activity, as a direct measure of TGFBR1 inhibition. SF3B1 mutant expressing cells were shown to be highly sensitive to TP-6379, with a significant loss of SMAD activation. Expression analysis of primary MDS, S100A9-treated healthy BMMNC cells and K562 SF3B1 mutant cells revealed elevated expression of SERPINE1 which was rescued by TP-6379 treatment.
Conclusions: TP-6379 restores healthy hematopoiesis in low-risk MDS, which may translate into a strong therapeutic option in a disease with few clinical options. Importantly, our work also suggests a specific role for spliceosome dysfunction in bone marrow failure and a novel role for SERPINE1 in MDS and S100A9-induced suppression.

#5151

Enzalutamide resistance results in immunosuppressive alterations in prostate tumor immune microenvironment

Pengfei Xu, Joy C. Yang, Bo Chen, Christopher Nip, Jonathan E. Van Dyke, Christopher P. Evans, William J. Murphy, Chengfei Liu. *UC Davis, Sacramento, CA*

Background: Emerging data suggested that enzalutamide-treated prostate cancer patients with increased programmed death-ligand 1 (PD-L1) expression may benefit from anti-PD-L1 treatment. Unfortunately, the Phase III IMbassador250 trial revealed that the combination of atezolizumab (PD-L1 inhibitor) and enzalutamide failed to extend overall survival in patients with castration-resistant prostate cancer (CRPC). The mechanisms underlying treatment failure remain unknown. In this study, we

investigated the regulation of immunosuppressive signaling in enzalutamide resistant prostate cancer and characterized the immune infiltrating cells in murine prostate tumors.
Methods: The expression of interferon gamma-related genes was determined using qRT-PCR and/or western blotting. Androgen receptor (AR) and AR-V7 levels were downregulated using specific siRNA. Myc-CaP cells were chronically exposed to increasing concentrations of enzalutamide (5-50 μM) for >12 months, and the cells resistant to enzalutamide were referred to as Myc-CaP MDVR. The gene-regulating mechanisms in drug-resistant prostate cancer cells were determined by RNA sequencing analyses. Myc-CaP and Myc-CaP MDVR xenograft tumors were established in FVB mice, and tumor-infiltrating lymphocytes were isolated using Ficoll. The stained immune cells were determined by flow cytometry, and the data were analyzed using Flowjo.
Results: Immune-related signaling pathways (interferon alpha/gamma response, T cell activation, and cell chemotaxis pathways) were suppressed in C4-2B MDVR cells. However, PD-L1 expression was highly upregulated and negatively regulated by AR in C4-2B MDVR cells. Enzalutamide treatment decreased $CD8^+$ T cell but increased monocytic myeloid-derived suppressor cell (M-MDSC) population and PD-L1 expression in murine Myc-CaP tumors. Consistently, chemotaxis and immune response-regulating signaling pathways were suppressed, and PD-L1 expression was increased in enzalutamide-resistant Myc-CaP MDVR cells. Notably, MDSC populations were significantly increased in Myc-CaP MDVR orthotopic tumors compared with those in Myc-CaP parental tumors. Co-culturing bone marrow cells with Myc-CaP MDVR cells significantly promoted MDSC differentiation and polarized macrophages from the M1 to M2 phase.
Conclusions: Immunosuppressive signaling is activated in enzalutamide resistant prostate cancer cells. The activated immune-related signatures involved in T cells, MDSC, and macrophages may reduce the efficacy of immune checkpoint inhibitors in enzalutamide-resistant prostate cancer.
Grant Support: This work was supported in part by grants NIH/NCI R37CA249108 (C, Liu) and R01CA251253 (C, Liu).

#5152

Photodynamic therapy promotes immune infiltration and control of malignant pleural mesothelioma through NF-kB mediated upregulation of E-Selectin in the tumor vasculature

Louis-Emmanuel Chriqui[1], Yameng Hao[2], Damien Marie[1], Michel Gonzalez[1], Thorsten Krueger[1], Etienne Meylan[3], Johanna Joyce[4], Sabrina Cavin[1], Jean-Yannis Perentes[1]. *[1]Lausanne University Hospital, Lausanne, Switzerland,[2]Ecole Polytechnique Fédérale de Lausanne, EPFL, Lausanne, Switzerland,[3]Free University of Brussels, Brussels, Belgium,[4]University of Lausanne, Lausanne, Switzerland*

Introducti**on**: Malignant pleural mesothelioma (MPM) is an aggressive cancer with limited treatment options. The application of photodynamic therapy (PDT) was shown to significantly improve patient survival. Previously, we found that low dose PDT (L-PDT) enhanced the immune infiltration of MPM and increased the impact of immune checkpoint inhibitors on tumor control. However, the mechanisms behind these observations are unknown. Here, in an orthotopic murine model of MPM, we show that L-PDT upregulates tumor vascular E-Selectin expression via NF-kB. This upregulation favors enhanced leukocyte trafficking and immune mediated MPM regression.

Methods: We analyzed adhesion molecules (E-Selectin, ICAM-1, VCAM-1) and canonical NF-kB activation (phosphorylated IκBα) protein levels in endothelial (ECRF-24) cells treated by L-PDT in the presence or absence of a NEMO/IKKγ siRNA in vitro. For in vivo validation, AB12-Luc MPM cells were grown in the pleural cavity of syngeneic BALB/c mice and treated with L-PDT (verteporfin 400 μg/kg, fluence 10 J/cm^2, fluence rate 50 mW/cm^2) alone or in presence of NF-kB or E-Selectin inhibitors (NEMO Binding Domain (NBD) peptide and E-Selectin blocking antibody respectively). For each treatment group, we determined the expression of endothelial adhesion molecules (E-Selectin, ICAM-1, VCAM-1) and the tumor immune infiltrate by immunohistochemistry and flow cytometry. In parallel, the impact of L-PDT on MPM growth and mouse survival were assessed in the presence of E-Selectin inhibition.

Results: L-PDT increased the levels of endothelial adhesion molecules E-Selectin, ICAM-1 and VCAM-1 9 to 24 hours after L-PDT treatment in vitro. This was preceded by an increase of IκBα phosphorylation. In the

presence of NEMO siRNAs, the expression of NEMO/ IKKγ was reduced and led to E-Selectin repression. In orthotopic MPM bearing mice, the treatment of MPM by L-PDT enhanced adhesion molecules expression in tumor vasculature at 24 hours. This correlated with increased infiltration of $CD4^+$ and $CD8^+$ granzyme B^+ T-cells and improved tumor control and mouse survival. NF-kB inhibition impaired tumor vascular adhesion molecules upregulation and the recruitment of tumor infiltrating lymphocytes in MPM. The targeted inhibition of E-Selectin abrogated the immune infiltration and tumor regression of MPM following L-PDT, which ultimately decreased animal survival in our MPM model.
Conclusion: Low dose PDT relieves MPM tumor vascular anergy via NF-kB mediated adhesion molecules expression. Endothelial E-Selectin has been identified, in our MPM model, as a major determinant for L-PDT enhanced lymphocyte trafficking, tumor control and animal survival.

#5153
The role of CCL22-specific CD4 T cells in modulating the immunosuppressive tumor microenvironment in ovarian cancer
Ines Lecoq, Evelina Martinenaite, Marie C. W. Westergaard, Inge Marie Svane, Mads H. Andersen. *National Center for Cancer Immune Therapy (CCIT-DK), Copenhagen, Denmark*

Background: CCL22, a macrophage-derived chemokine, is overexpressed in ovarian cancer and exerts immunosuppressive functions by the recruitment of regulatory T cells (Tregs) to the tumor microenvironment (TME). Our research group described naturally occurring T cells specific for an MHC class I epitope derived from CCL22. CD8+ CCL22-specific T cells isolated from cancer patients could recognize CCL22-expressing cells and decrease the levels of CCL22 in ovarian ascites *in vitro*. Expansion of CCL22-specific CD8+ T cells in animal models of cancer by peptide vaccination led to a therapeutic anti-tumor effect by reducing Treg recruitment into the TME. In this study we aimed at characterizing CD4+ CCL22-specific T cells and their potential for modulating the tumor microenvironment in ovarian cancer.
Methods: CCL22-responses were screened with a library of overlapping 20mer peptides covering the entire sequence of CCL22 in PBMCs from healthy donors and ovarian cancer patients. CCL22-specific T cells were

isolated from PBMCs and ovarian ascites for functional characterization through IFNγ ELISpot and ICS against peptides and CCL22-expressing target cells. Cytokine secretion was measured with protein multiplex immunoassays. Vaccination and therapeutic efficacy were evaluated in BALB/c CT26 and 4T1 syngeneic models.
Results: We identified an immunogenic region in the CCL22 protein sequence and detected CD4 T-cell responses against CCL22-derived peptides in healthy donors and ovarian cancer patients through IFNγ ELISpot. CCL22-specific CD4+ cells have also been identified *ex vivo* in the ascites fluid from patients with ovarian cancer. We isolated and expanded CCL22-specific CD4+ T-cell clones from the ovarian ascites and demonstrated their reactivity against CCL22-producing cell lines. Furthermore, the stimulation of CCL22-specific CD4+ T cells in the PBMC culture and ascites samples was associated with a modulation of the cytokine environments. Additionally, vaccination with surrogate murine 20mer and MHC-II restricted CCL22-derived peptides lead to successful induction of specific T-cell responses in the spleens and draining lymph nodes of vaccinated animals. Activation of such CCL22-specific CD4 T cell responses was associated with a therapeutic effect seen as reduction of the tumor growth in different models of cancer.
Conclusion: This study provides evidence for the ability of pro-inflammatory CD4+ CCL22-specific T cells to modulate the tumor microenvironment, particularly in ovarian cancer. Altogether we provide the rationale for the development of a CCL22-based immune modulatory vaccination for ovarian cancer.

#5154
The cytosolic branched chain aminotransferase is an important metabolic checkpoint of T cell function in the lymphoma microenvironment
Tanner J. Wetzel, Lucas Figueroa, Leighton Wheeler, Alexander Martin, Christie Adam, Michael Boyer, Elitsa Ananieva. *Des Moines University, Des Moines, IA*

Rapidly growing lymphoma cells deplete the tumor microenvironment (TME) of nutrients needed to maintain anti-tumor T cell immunity. This metabolic disadvantage leads to diminished T cell function and reduced

clearance of tumor cells. The branched chain amino acids (BCAAs) are required for growth of tumor and immune cells. In the TME, BCAAs are preferentially taken up by tumor cells for protein synthesis or energy production. The first step in BCAA degradation is reversible transamination catalyzed by the cytosolic branched chain aminotransferase, BCATc. Recent investigations suggest that BCATc is immunosuppressive in the TME. We found BCATc is induced upon T cell activation, during which time, BCATc negatively regulates T cell metabolism. We hypothesized that a loss of BCATc from T cells restores effector T cell function in the TME. Tumor studies were conducted using mice with BCATc deleted from $CD4^+$ and $CD8^+$ T cells (T-$BCATc^{KO}$ mice) and corresponding controls expressing the floxed transgene of BCATc in T cells (T-$BCATc^{fl/fl}$ mice). Mice were subcutaneously injected with $2.5x10^5$ murine EL-4 lymphoma cells [tumor-injected mice, n=8-9/group] or phosphate-buffered saline [vehicle-injected mice, n=4-6/group]. Tumor growth, body weight, and food intake were monitored for 15 days followed by collection of tumors and organs. Splenocytes were used to isolate $CD4^+$ and $CD8^+$ T cells that were activated with anti-CD3 and anti-CD28, and, after initial expansion with cytokine IL-2, reactivated to hypotolerant or fully activated $CD4^+$ Th1 cells, or expanded to effector $CD8^+$T cells for 96h, in the presence or the absence of the leucine antagonist, N-acetyl-leucine amide (NALA). Supernates were tested for secretion of IFNγ ($CD4^+$T cells) or perforin and granzyme B ($CD8^+$T cells). T-$BCATc^{KO}$ mice demonstrated significant delay in lymphoma appearance and a 50% reduction in tumor volumes when compared to control mice. The removal of BCATc from T cells did not cause systemic overactivation of the immune system, with no changes in size or appearance of the spleen, liver, or intestines. Hypotolerant and fully activated T-$BCATc^{KO}$ $CD4^+$ T cells released significantly more IFNγ when compared to T-$BCATc^{fl/fl}$ T cells. The addition of NALA reduced the IFNγ levels to those found in control cells. $CD8^+$ T cells from T-$BCATc^{KO}$ mice released significantly more granzyme B and perforin compared to T-$BCATc^{fl/fl}$ T cells. These findings demonstrate that BCATc-deficient T cells provide better systemic response to lymphoma likely due to improved Th1 and effector $CD8^+$ T cell with diminished Treg function. Thus, BCATc may act as an important metabolic checkpoint of the lymphoma TME

#5155

Targeting tumor infiltrating myeloid cells in prostate cancer

Marco A. De Velasco[1], Yurie Kura[1], Naomi Ando[1], Noriko Sako[1], Kazutoshi Fujita[1], Kazuko Sakai[1], Alwin G. Schuller[2], Kris F. Sachsenmeier[2], Masahiro Nozawa[1], Eri Banno[1], Kazuhiro Yoshimura[1], Kazuto Nishio[1], Hirotsugu Uemura[1]. *[1]Kindai University School of Medicine, Osaka-Sayama, Japan,[2]AstraZeneca, Waltham, MA*

The tumor microenvironment (TME) is a dynamic milieu comprised of various cell types and molecular complexes that eventually evolves to promote cancer cell proliferation, metastasis, and immune evasion. Myeloid cells are a key component of the TME and play key roles in initiating antitumor responses and coordinating with cells of the adaptive immune system. However, these cells are eventually hijacked by tumors and provoke local inflammation that results in chronic cancer-associated inflammation and immune escape. Extracellular adenosine (ecADO) is an immunosuppressive metabolite that is produced in tumors that binds the adenosine 2a receptor (A2aR) which is widely expressed in immune cells. Studies have shown that blocking A2aR signaling has the potential to enhance antitumor immunity by boosting T and NK cell immune responses. However, the relationship between ecADO and tumor-associated myeloid cells is less characterized. We previously reported on the antitumor activity of A2aR and CD73 blockade in preclinical models of *Pten*-null prostate cancer and their impact on T cell mediated responses. Here, we examine tumor-associated myeloid cell infiltration in models of castration-naïve (CNPC) and castration-resistant prostate cancer (CRPC) the impact of A2aR and CD73 blockade. Transcriptomic, flow cytometric, and immunohistochemical (IHC) profiling studies of CNPC and CRPC from conditional *Pten*-knockout (KO) and *Pten/Trp53*-double knockout (DKO) showed that tumor-infiltrating myeloid cells constituted a significant proportion of the prostate tumor microenvironment. CD11b+/Ly6G+ cells representing tumor associated neutrophils (TANs) and myeloid derived suppressor cells (MDSCs) were the most abundant immune cell type comprising 14.9% and 32.1% of the total population, and 46.5% and 69.7% of infiltrating leukocytes in in CNPC and CRPC, respectively. Furthermore, CD11b+/Ly6G+ expressed high levels of CD73. Pte-null prostate tumors were characterized with enriched adenosine signaling signatures which

were greater in CRPC compared to CNPC. Treatments with the A2aR inhibitor AZD4635 alone and in combination with CD73 antibody blockade reduced adenosinergic genes as well as genes associated with TAN/MDSC immunosuppressive functions. Additionally, tumors from treated mice exhibited improved T cell mediated cytotoxicity. Together, our findings indicate that tumor associated myeloid cells are an additional source of ecADO contributing to immune suppression which can be targeted with A2aR and CD73 inhibitors.

#5156

The mutagenic effects of APOBEC3A and APOBEC3B in urothelial carcinoma

Michael S. Sturdivant[1], Andrew S. Truong[1], Mi Zhou[2], Jeffrey S. Damrauer[2], William Y. Kim[3]. *[1]Pharmacology, UNC Chapel Hill, Chapel Hill, NC,[2]UNC Lineberger Comprehensive Cancer Center, Chapel Hill, NC,[3]Genetics, Pharmacology, UNC Lineberger Comprehensive Cancer Center, Chapel Hill, NC*

APOBEC3A (A3A) and APOBEC3B (A3B) are members of a family of cytidine deaminase enzymes that catalyze the removal of an amino group from cytosine nucleotides generating an uracil in its place that serve as a source of mutations. The resulting C->U transition has been linked to various oncogenic mutations, most predominately in bladder cancer. While both A3A and A3B activity can account for widespread changes to the genomic landscape, prior studies have shown tumor specific effects. In hepatocellular carcinoma, A3A has been shown to be the only APOBEC3 family member capable of driving tumor formation in the presence of p53 downregulation, while studies in breast cancer have suggested A3B as a driver of tamoxifen resistance. Currently, it is unclear if both A3A and A3B drive APOBEC-induced mutagenesis in bladder cancer, or if one enzyme plays a larger mutagenic role than the other. In urothelial carcinoma, there has not been a direct comparison of A3A and A3B mutagenic activity, highlighting the need to determine the effects of each respective enzyme. To explore the effects of A3A and A3B enzymes, we accessed publicly available single cell RNA (scRNA seq) data of tumor samples from 8 bladder cancer patients. Analysis from scRNA seq data revealed an enrichment of A3A expression in both monocyte and urothelial cell

populations, while A3B expression is primarily restricted to urothelial cells, suggesting a cell type specific functional difference between A3A and A3B in bladder cancer. Immunogenomic analysis of TCGA bladder cancer tumors stratified by APOBEC mutational load (High, Low, No) showed that tumors with APOBEC high mutational load had high levels of interferon gamma response, lymphocyte infiltration signature score, M1 macrophages, intratumor heterogeneity, and stromal fraction compared to tumors with low APOBEC mutational load. In addition, increases in features of genomic instability was observed in tumors with high APOBEC mutational load. Interestingly, we saw unique correlations of A3A and A3B in TCGA bladder tumors. A3A expression correlated with characteristics of an inflamed tumor microenvironment while A3B expression correlated with features of genomic instability. To elucidate the divergent effects of A3A and A3B independently, we have generated isogenic mouse bladder cancer cell lines that overexpress HA tagged A3A and A3B, to directly compare their mutagenic effects through *in-vitro* and *in-vivo* experiments. We have validated through deamination assays, the functionality of A3B in these cell lines. *In silico* data has shown differential roles for A3A and A3B as it relates to the tumor/immune environment; we hypothesize that this might result in subunit specific response and resistance to anti-PD-1 immunotherapy. Elucidation of the A3 specific driver of APOBEC mutagenesis in urothelial carcinoma will help identity a predictive and/or prognostic biomarker to anti-PD-1 checkpoint immune inhibition.

#5157

ATRA treatment induces an interferon response to reprogram the immunosuppressive tumor microenvironment and overcomes resistance to immune checkpoint inhibition in murine models of LKB1 deficient non small cell lung cancer

William P. Crosson[1], Rui Li[2], Ramin Salehi-Rad[3], Raymond J. Lim[3], Jensen Abascal[2], Bitta P. Kahangi[2], Edgar Perez Reyes[2], Michael Oh[2], Camelia Dumitras[2], Nico Edgar[2], Ryan Chew[2], Rashel Jacobo[2], Zhe Jing[2], Kostyantyn Krysan[2], Linh M. Tran[2], Steven Dubinett[3], Bin Liu[2].
[1]Molecular and Medical Pharmacology, UCLA - University of California Los Angeles, Los Angeles, CA,[2]UCLA - University of California Los

Angeles, Los Angeles, CA,[3]Department of Medicine, UCLA - University of California Los Angeles, Los Angeles, CA

Lung cancer remains the deadliest form of cancer, claiming the lives of 1.8 million individuals worldwide in 2020. While treatment options have improved with the advent of immune checkpoint inhibitors (ICI), many patients do not respond to immunotherapy or develop resistance following initial response. A significant subset of non-small cell lung cancer (NSCLC) patients harbor somatic co-mutations in *Kirsten rat sarcoma virus (KRAS)* and *Liver kinase 1 [LKB1,* also known as *serine/threonine kinase 11 (STK11*)] genes, whose tumors are characterized by a predominance of neutrophils and an immune suppressive tumor microenvironment (TME) that are resistant to ICI. Our studies revealed that *all-trans* retinoic acid (ATRA), a metabolite derived from vitamin A, sensitized a murine model of NSCLC (*Kras* ^{G12D} *P53*$^{-/-}$*Lkb1*$^{-/-}$; KPL) to PD-1 blockade. The ATRA and anti-PD-1 combination therapy improved local and systemic T cell activation and generated systemic tumor-specific immunity. We further observed that ATRA augmented anti-PD-1 efficacy in additional murine NSCLC models with or without LKB1 loss. To understand ATRA-mediated anti-tumor effects, we performed single cell RNA sequencing (scRNA-seq) of KPL murine tumors with or without 6 daily ATRA treatments. scRNA-seq analysis indicated a reduction of neutrophils as well as an enrichment in T cell and natural killer (NK) cell populations in the TME. Furthermore, scRNA-seq analysis revealed elevated expression of interferon (IFN) downstream genes in multiple immune subpopulations in the TME. Preliminary *ex vivo* studies indicated that ATRA increases NOX2 levels, intracellular reactive oxygen species (ROS), and IFN signaling in the myeloid-derived suppressor cells (MDSC) of KPL tumors. Our findings suggest that ATRA may reshape the TME by activating IFN signaling in multiple cell subtypes to sensitize resistant tumors to ICI immunotherapy.

Modifiers of the Tumor Microenvironment

#5161
Molecular mechanisms of early-stage lung adenocarcinoma initiation

Alice Rodriguez-Fuguet[1], Luis Silva[1], John Asara[2], Xiaoman Li[3], Susumu Kobayashi[2], Wen Cai Zhang[1]. *[1]Burnett School of Biomedical Sciences,*

Division of Cancer Research, University of Central Florida, Orlando, FL,[2]Department of Medicine, Division of Signal Transduction, Beth Israel Deaconess Medical Center, Harvard University, Boston, MA,[3]Department of Computer Science, University of Central Florida, Orlando, FL

Lung cancer initiation and progression driven by epidermal growth factor receptor (EGFR) mutation has been extensively studied in the past decade. Though many leaps have been made in the field in terms of treatment, early diagnosis screening is not widely available or well established. Meanwhile, EGFR mutation is a significant driver of tumorigenesis and drug resistance. This receptor is related to many downstream pathways that influence cancer metabolism and the ability of tumor cells to adapt to changes in the tumor microenvironment. Our study finds that cancer metabolism plays a prominent role in the progression of tumorigenesis in early-stage lung cancer. Kynurenine, a metabolite from the tryptophan pathway, was highly upregulated in early-stage, EGFR-mutation driven lung cancer by metabolomic analysis. The connection between EGFR mutation and the upregulation of kynurenine remains largely unknown. We hypothesize that kynurenine, based on our preliminary data and as a ligand of the aryl hydrocarbon receptor, may have a dual role in early tumorigenesis. We propose that kynurenine may be used by tumor cells to modulate their response to stress by triggering anti-apoptotic pathways. Additionally, kynurenine may be used as a signaling molecule in the tumor microenvironment to allow the early tumor cells to evade immune detection through the transformation of macrophages from M1 to M2. Currently, our data show that indoleamine 2,3- dioxygenase 1 (IDO1), the rate-limiting enzyme of the tryptophan-kynurenine pathway, is significantly upregulated in early-stage, EGFR-driven lung cancer murine models by RNA-seq analysis. This supports our idea that IDO1 could help to modulate the response to cellular stress and to regulate the immune response to favor tumor development. We hope that IDO1 could be a potential clinical target and a potential biomarker for the dysregulation of this pathway.

#5162

Discovery of INCB098377: a potent inhibitor of phosphoinositide 3-kinase gamma (PI3Kγ)

Diana A. Arias, Stephen Douglass, Lisa Truong, Qian Wang, Kathy H. Wang, Gengjie Yang, Michael Hansbury, Sybil O'Connor, Kevin Bowman, Robert Collins, Matthew Stubbs, Leslie Hall, Christina Stevens, Christopher Maddage, Brent Douty, Maryanne Covington, Lynn Leffet, Eddy Yue, Andrew Combs, Sunkyu Kim, Niu Shin, Holly Koblish, Rodrigo Hess. *Incyte Research Institute, Wilmington, DE*

Immune checkpoint blockade has shown impressive efficacy in patients with inflamed tumors, although minimal activity has been observed in tumors lacking T cells. Myeloid cells are one of the most abundant cell types in both inflamed and non-inflamed tumors, and may contribute to immune checkpoint blockade resistance. The plasticity of macrophages enables them to directly and indirectly modulate T cell responses, and directly kill tumor cells via phagocytosis. This suggests that targeting myeloid cells could be an effective therapeutic approach. Class I PI3Ks are a family of dual specificity lipid and protein kinases. Unlike other class I PI3Ks, PI3Kγ is predominantly expressed in myeloid cells. PI3Kγ has been shown to be a key mediator that drives the immunosuppressive macrophage program by stimulating AKT/mTOR signaling and promote C/EBPβ expression while inhibiting NF-κB activity (Keneda MM. *Nature*. 2016;17:437-442). Here, we present the discovery and characterization of INCB098377, a potent and selective PI3Kγ inhibitor. Specific inhibition of PI3Kγ with INCB098377 may induce anti-tumor activity by reshaping the tumor immune microenvironment. In cell-based assays, INCB098377 has an IC_{50} of 1.4 nM and is greater than 100-fold selective over other PI3K isoforms. It also shows a favorable PK profile in several animal species. Treatment of M2 polarized macrophages with INCB098377 resulted in changes towards a more pro-inflammatory phenotype. CD163 and CD206 were decreased, whereas HLA-DR and co-stimulatory CD80/86 molecules were increased. MHC-I expression was unchanged, suggesting a role for these macrophages in MHC-II-mediated antigen presentation. Furthermore, INCB098377 treatment reduced macrophage-mediated immunosuppression and restored T cell proliferation in M2 polarized macrophages co-cultured with allogeneic human T cells. In vivo, significant tumor growth inhibition was observed with once-daily dosing of 10 mg/kg INCB098377 in both syngeneic and humanized mouse tumor models without toxicity. Moreover, efficacy was observed in inflamed and non-inflamed tumor models.

Consistent with the proposed mechanism of action, INCB098377 inhibited phospho-AKT levels in vivo and in human PBMCs. Treatment with INCB098377 induced pro-inflammatory responses without macrophage depletion suggests that robust tumor microenvironment changes are responsible for observed anti-tumor efficacy. In addition, INCB098377 inhibited neutrophil migration in the Carrageenan-induced paw inflammation model. INCB098377, a potent and selective inhibitor of PI3Kγ, shows effective anti-tumor activity in a variety of mouse and humanized cancer models through the inhibition of immunosuppressive cells trafficking into the tumor, modulation of myeloid cell function, and enhancement of T cell proliferation.
Acknowledgments: Diana Alvarez Arias and Stephen Douglass contributed equally to this study.

#5163

Local delivery of mRNA immunotherapy encoding HPV16 antigen, IL-12, and LIGHT/TNFSF14 results in superior immunogenicity and tumor clearance in a murine model of HPV16-driven cancer

Weiqun Liu[1], Diane M. Da Silva[2], Edward E. Lemmens[1], Colin J. McKinlay[1], Sangeeta Nath[1], Meredith L. Leong[1], Samuel Deutsch[1], W. Martin Kast[2], Ole Audun W. Haabeth[1]. *[1]Nutcracker Therapeutics, Inc., Emeryville, CA,[2]Norris Comprehensive Cancer Center, University of Southern California, Los Angeles, CA*

While intramuscular vaccination with HPV16 antigens has been shown to induce robust tumor-specific immune responses in the periphery, this has led to limited efficacy in the clinic. One potential explanation is the lack of sufficient infiltration of antigen-specific T cells into the tumor. The few T cells that make their way into the tumor are met with a plethora of negative signals that suppress their activity and abrogate local T cell expansion. To overcome this limitation of intramuscular cancer vaccines, we have developed an approach using in situ vaccination with a combination of immune modulators and tumor antigens, all encoded by mRNAs and delivered using nanoparticles. In this study, we show the superior efficacy and immunogenicity of a locally delivered mRNA cancer vaccine over that of an intramuscular HPV16 cancer vaccine. Both routes of administration result in robust induction of antigen-specific T cells, but local

administration of mRNA-encoded antigens and immune modulators also resulted in enhanced infiltration of immune cells into the tumor, local Th1/M1 cytokine induction, and more-complete tumor clearance. Specifically, we found that the inclusion of the immunomodulators IL-12 and TNFSF14/LIGHT enabled tumor clearance in a murine tumor model. While tumors treated with mRNA-encoded HPV16 antigen alone induced robust systemic antigen-specific responses, minimal levels of local T cell expansion and infiltration, proinflammatory cytokine induction, and tumor control were observed. By contrast, tumors treated with mRNA-encoded HPV16 antigen, IL-12p70, and TNFSF14 completely cleared large established HPV16 expressing tumors with long-lasting recurrence free survival and immune memory. This observation was replicated in in a second murine tumor model, confirming the superior potency of locally delivered mRNA cancer vaccines in combination with immunomodulators. Consequently, we are developing a locally administrated mRNA therapy for the treatment of patients with cervical intraepithelial neoplasia (CIN).

#5164

Liposomal Delivery of an Immunostimulatory CpG Induces Robust Antitumor Immunity and Long-Term Immune Memory by Reprogramming Tumor-Associated Macrophages

Yujin Kim[1], Sangyong Jon[2]. *[1]Life Science Research Institute, Korea Advanced Institute of Science and Technology, Daejeon, Korea, Republic of,[2]Biological Sciences, Korea Advanced Institute of Science and Technology, Daejeon, Korea, Republic of*

Background: The efficacy of current T cell-based immunotherapy is known to be limited by various factors that induce immune suppression in the tumor microenvironment (TME). Tumor-associated macrophages (TAMs) are representative TME-comprising immune suppressive cells and influence tumor growth and progression. TAMs are considered as an attractive target for cancer immunotherapy. However, current TAMs-targeting strategies are not sufficient to induce continuous antitumor responses. Here, we suggest a new strategy that can reprogram TAMs and further bridge innate-to-adaptive immunity by utilizing immunostimulatory CpG oligodeoxynucleotides (ODNs). In this study, we investigated the new role of TLR9 agonist CpG ODN as an immunotherapeutic agent and tested

whether liposomal delivery of CpG could modulate the function of TAMs and lead to remodeling of the TME.
Methods: A liposome-based nanomaterial encapsulating CpG ODN was constructed. A small lipid nanoparticle (SLNP) used as the CpG delivery platform in this study was made of a cationic cholesterol derivative and two biocompatible phospholipids. The CpG-encapsulating SLNP (SLNP@CpG) was prepared by a thin-film formation and rehydration method. *In vitro* studies were conducted to assess whether SLNP@CpG could reprogram macrophages. To assess antitumor therapeutic efficacy of the SLNP@CpG, two subcutaneous tumor models were established in mice and tumor growth and survival rates of mice were monitored. For tumor rechallenge experiment, mice showing complete tumor regression were rechallenged with same cancer cells and their splenocytes were analyzed to confirm the development of immune memory. To elucidate the immunological mechanism of SLNP@CpG-mediated antitumor efficacy, changes of immune cell subpopulations in treated tumors were analyzed by flow cytometry.
Results: SLNP@CpG enhanced macrophage-mediated phagocytosis of cancer cells and tumor antigen cross-presentation, and skewed the polarization state of macrophages *in vitro*. Intratumorally injected SLNP@CpG exerted its therapeutic efficacy in an established E.G7-OVA tumor via uptake by TAMs. SLNP@CpG treatment significantly suppressed the E.G7 tumor growth and also considerably prolonged the survival of mice, with 83.3% of mice becoming tumor-free. Local administration of SLNP@CpG resisted E.G7 tumor rechallenge by inducing immunological memory and long-term antitumor immunity. Local administration of SLNP@CpG even exerted its antitumor efficacy in an aggressive B16-F10 melanoma by remodeling TME towards immune stimulation and tumor elimination.
Conclusion: Liposomal delivery of CpG via local treatment reprogrammed TAMs by enhancing phagocytic activity and repolarizing M2 to M1 phenotype and also reshaped immunosuppressive TME, leading to antitumor immunity and long-term memory responses.

#5165
In vivo therapeutic validation of NRT-YHD_001, a novel macrophage checkpoint inhibitor, in liver cancer

Suk Woo Nam, Sangyean Kim, Min Jeong Na, Eunbi Shin, Jin Woong Ha, Soyoung Jeon, Jeong Hwan Yoon. *Dept of Pathology, Catholic University of Korea, College of Medicine, Seoul, Korea, Republic of*

Previously, we demonstrated that recovery of Histone deacetylase 6 (HDAC6) elicited let-7i-5p suppression to de-repress the thrombospondin-1 (TSP1) expression, and thereby it occupied CD47 receptor to block CD47-SIRPα mediated anti-phagocytosis of macrophage in liver cancer. NRT-YHD_001 is a modified antisense miRNA of let-7i-5p for liver cancer treatment. NRT-YHD_001 was substituted with O-methoxyethyl and phosphothioate for stability, and N-acetylgalactosamine was attached for specific delivery to the liver. In *in vitro* phagocytosis assay, NRT-YHD_001 showed macrophage phagocytosis activity with similar or better results compared to non-modified antisense let-7i-5p (AS_let-7i-5p). In addition, it was confirmed that NRT-YHD_001 inhibited endogenous let-7i-5p of liver cancer cells and activated macrophage phagocytosis at 4°C or 25°C for up to 2 weeks. When NRT-YHD_001 activity was investigated *in vivo* after 1 week, 2 weeks, and 4 weeks after administration of single dose NRT-YHD_001 to the tail vein of a mouse, NRT-YHD_001 was not degraded, and let-7i-5p was inhibited while maintaining activity in liver tissue for 2 weeks after injection. To investigate the *in vivo* therapeutic effect, a mouse spontaneous (Ras-transgenic) liver cancer model was used and compared with the sorafenib-administered group. After administration of NRT-YHD_001 and sorafenib each week at the time when liver mass was detected, the tumor size and growth rate were compared. As a result, the NRT-YHD_001 administration group showed significant therapeutic effect compared to sorafenib. These results showed that NRT-YHD_001 had a strong anticancer effect by converting the macrophage of don't eat me into eat me signal in the tumor microenvironment of liver cancer, thereby removing or inhibiting liver cancer cells.
Keywords: let-7i-5p, macrophage, phagocytosis, liver cancer, NRT-YHD_001

#5166

Intratumoral delivery of mRNA encoding USP6 activates multiple immuno-stimulatory pathways simultaneously and inhibits local and distal tumor growth in murine models

Ian Henrich[1], Margaret Billingsley[2], Kanika Jain[2], Laura Quick[3], Rob Young[3], Margaret Chou[2], Michael Mitchell[2]. *[1]Blumberg Institute and Merlin Biotech, Philadelphia, PA,[2]University of Pennsylvania, Philadelphia, PA,[3]Children's Hospital of Philadelphia, Philadelphia, PA*

Advances in immunotherapy have revolutionized cancer treatment, with patients with otherwise incurable disease having long-lasting responses. Unfortunately, deep remissions only occur in a select subset of patients. Cancer progression is common as many current immunotherapies only target one or two pathways, which can quickly lead to tumor resistance. Novel approaches that target several pathways concurrently are therefore needed to promote stronger responses in a wider patient population.
Our group has recently discovered that the protein Ubiquitin-specific protease 6 (USP6) upregulates multiple, distinct immunostimulatory pathways. Tumor cell-specific expression of USP6 significantly increases CXCL9, CXCL10, and CCL5 chemokine production that enhances cytotoxic immune cell recruitment. Simultaneously, USP6 also upregulates several ligands and receptors that promote immune cell activation and killing of tumor cells such as CD112, MICA/B, ICAM1, and MHC Class I. In addition, USP6 increases the tumor cell's sensitivity to immune-derived factors such as Type I and Type II interferons and TRAIL by raising the surface expression of their respective receptors. USP6 is hominid-specific and therefore requires xenografting human tumor cells into athymic, T-cell deficient nude mice. Despite the immunocompromised model, USP6 expression was found to increase immune cell recruitment to the tumor while repolarizing the immune microenvironment toward a more activated, tumor-suppressive state. Strikingly, immune cells in the peripheral blood were also affected with an increase in natural killer cell (NK) activation and a skewing of the myeloid population away from an immunosuppressive phenotype. Our group subsequently demonstrated that a $USP6^{+}$ tumor was able to inhibit the growth of a $USP6^{-}$ distal tumor, with a concordant increase in NK, macrophage, and dendritic cell activation in the distal $USP6^{-}$ tumor.
Given our data, we sought to translate USP6 into a novel immunotherapy. Delivery of mRNA encoding the USP6 protein recapitulates the immunostimulatory effects of USP6 *in vitro*. Intratumoral (I.T) injection of

a lipid nanoparticle (LNP) encapsulating USP6 mRNA significantly inhibited Ewing sarcoma and acute myeloid leukemia growth in athymic mice, despite the model lacking a fully functional immune system. Moreover, I.T injection of USP6 mRNA LNPs inhibited the growth of a non-injected, distal tumor. Altogether, these data support that USP6 is a potentially powerful target and continued development of I.T USP6 mRNA LNPs as a novel immunotherapy.

#5167

Entinostat's modulation of myeloid derived suppressor cells through the STAT3-NFκB-AP-1 axis decreases suppressive signaling

Aaron G. Baugh[1], Edgar Gonzalez[1], Valerie H. Narumi[1], Sofi Castanon[1], Jesse Kreger[2], James Leatherman[3], Won Jin Ho[3], Ashley Cimino-Mathews[3], Vered Stearns[3], Roisin M. Connolly[4], Elizabeth M. Jaffee[3], Adam L. MacLean[2], Evanthia T. Roussos Torres[1]. *[1]Keck School of Medicine of USC, Los Angeles, CA,[2]University of Southern California, Los Angeles, CA,[3]Johns Hopkins University, Baltimore, MD,[4]University College Cork, Cork, Ireland*

Metastatic breast cancer remains one of the leading causes of global cancer incidence in women, despite the benefit of immune checkpoint inhibitors (ICIs) in managing various cancers and improving patient quality of life. Metastatic breast cancer is characterized by extensive infiltration of the tumor microenvironment (TME) with immunosuppressive cells, such as myeloid derived suppressor cells (MDSCs), that inhibit anti-tumoral immune cells and prevent effective activation of the adaptive immune system by ICIs. Previously, our group has shown in the breast TME that epigenetic reprogramming of MDSCs by entinostat, a histone deacetylase inhibitor, decreases MDSC immunosuppressive function and enhances response to ICIs, in part mediated by altered signaling within the Signal transducer and activator of transcription 3 (STAT3) and Nuclear factor kappa B (NFκB) axis. Next, we sought to examine the effects of entinostat on MDSC reprogramming in a distant metastatic TME. Using the syngeneic NT2.5LM NeuN mouse model of metastatic breast cancer, we established spontaneous lung metastases and treated with either vehicle or entinostat (5 mg/kg by oral gavage, 5x /week) for 3 weeks. Single cell RNA sequencing (scRNAseq) of macro-dissected lung metastases revealed a large MDSC

population, and unsupervised pathways analysis of the MDSC cluster showed differential regulation of the IL6-JAK-STAT3 and TNFα-signaling-via-NFκB pathways upon entinostat treatment. In line with reports of crosstalk among STAT3, NFκB, and AP-1 pathways regulating inflammation in breast cancer, we also found through scRNAseq differential expression of AP-1 subunits JunB and FOSL1 upon entinostat treatment. At the protein level, western blot analysis of isolated intratumoral MDSCs from lung metastases revealed decreased STAT3 phosphorylation upon entinostat treatment. Using J774M cells, an MDSC-like cell line, we found decreased JunB phosphorylation and decreased FOSL1 protein upon entinostat treatment. Furthermore, preliminary evaluation of imaging mass cytometry (IMC) from tumor biopsies in selected patients with metastatic breast cancer treated with entinostat during the clinical trial NCI-9844 confirmed decreased STAT3 phosphorylation in MDSCs. Taken together, we provide new evidence in the metastatic lung TME that implicates a STAT3-NFκB-AP-1 mediated mechanism leading to decreased MDSC suppression. Evaluating this mechanism in MDSCs taken directly from treated lung metastases represents the most biologically relevant mechanistic study to date, and preliminary translation of findings in patients suggests that planned studies will lead to identification of the mechanism driving response.

#5168

In vitro suppressive Treg bioassays for screening of candidate therapeutics

Martijn Vlaming, Alanah Pieters, Jezabel Lefevere, Sofie Pattyn.
ImmunXperts, a Q2 Solutions Company, Gosselies, Belgium

The increasing interest in the tumor microenvironment leads to a focus on new bioassays to represent all the players of the cancer immune response. Some of these players like regulatory T cells play an important role by downregulating the anti-tumor response. Their regulation mechanisms constitute an important target for new therapeutics. In order to study these mechanisms in a human model, suppressive Treg bioassays mimicking the suppressive action of these cells were developed and optimized. In vitro suppressive assays come with many technical challenges, therefore protocols for the purification and in vitro culture of regulatory T cells were

optimized and fine-tuned to result in an optimal assay window e and allow screening of multiple candidates. Donor-to-donor variation is controlled by pre-evaluation of multiple donors and standardized methods are used for isolation and in vitro culture of responding and suppressive cells. Access to a large and broad panel of healthy donors is required for the evaluation of therapeutic agents targeting the regulatory T cell pathway.

#5169

Aurora-A kinase promotes anti-tumor immunity in high lymphocyte-infiltrated colorectal cancer

Shiang-Jie Yang[1], Ming-Derg Lai[1], Liang-Yi Hung[2]. *[1]The Institute of Basic Medical Sciences, National Cheng Kung University, Tainan, Taiwan,[2]Department of Biotechnology and Bioindustry Sciences, College of Bioscience and Biotechnology, National Cheng Kung University, Tainan, Taiwan*

Introduction: The tumor microenvironment (TME) is composed of different cell types and is involved in tumor progression. Several immunosuppressive signaling pathways can promote tumor growth by inhibiting anti-tumor immunity in TEM. Therefore, targeting the immunosuppressive signaling pathways is a potential cancer treatment. Recent studies reported that inhibition of oncoproteins could lead to reduced anti-tumor immunity in several cancers; therefore, it's critical to identify the potential oncoproteins which can lead to enhanced anti-tumor immunity. Aurora-A is a serine/threonine kinase that plays an important role in the centrosome, cell mitosis, and chromosome stability. Previous studies indicated that cancer patients with poor prognoses are associated with a high Aurora-A level in tumor cells. Inhibition of Aurora-A is considered as a promising strategy for cancer treatment. However, Aurora-A inhibitors have not had a breakthrough in phase II or phase III clinical trials. The role of Aurora-A in tumor immunity is still unclear. Here, we investigated the role of Aurora-A in tumor immunity.
Materials and Methods: shRNA was used to knock down Aurora-A, and Alisertib was added to inhibit Aurora-A. RT-qPCR and western blot were performed to determine the IL-16 expression. The secretion of cytokines was measured by cytokine array and ELISA. BALB/c and NOD/SCID mice were subcutaneously injected with CT26 and then administered daily with

Alisertib or treated with anti-IL-16 antibody. The tumor-infiltrating immune populations were analyzed by flow cytometry. IHC and H/E stain were performed to analyze Aurora-A expression and lymphocyte infiltration in human CRC specimens.
Results: CRC patients with lower lymphocyte infiltration and higher Aurora-A are associated with poor prognosis and vice versa. Knockdown of Aurora-A in CT26 promotes tumor growth in immunocompetent mice by inhibiting the infiltration and cytotoxic activity of $CD8^+$ T cells. Aurora-A negatively regulates IL-16 expression in a kinase-dependent manner in CRC cells. Blockade of IL-16 by anti-IL-16 antibody can reverse the tumor growth and $CD8^+$ T cell cytotoxic activity in Aurora-A knocked-down CT26 tumors. Alisertib can inhibit CT26 tumor growth and promote IL-16 secretion in TME in mice. A combination of Alisertib and IL-16 antibody can promote the therapeutic effect of Alisertib in CT26 tumors.
Conclusion: Tumor-intrinsic Aurora-A plays a diverse role in tumor progression depending on the status of lymphocyte infiltration in TME. Aurora-A can promote anti-tumor immunity via negatively regulating IL-16 in a kinase activity-dependent manner in hot CRC tumors. In tumors with high lymphocyte infiltration, Aurora-A inhibition can suppress cancer cell growth and reduce anti-tumor immunity; the combination of Aurora-A inhibitors and IL-16 antibodies may provide a novel and effective strategy for cancer therapy in hot tumors.

#5170
STING inflames NF1 malignancies for immunotherapy
Nipunika Somatilaka[1], Laasya Madana[2], Ali Sadek[3], Renee M. McKay[1], Lu Q. Le[1]. *[1]Dermatology Department, UT Southwestern Medical Center, Dallas, TX,[2]University of Texas at Dallas, Dallas, TX,[3]Duke University, Durham, NC*

Introduction: Neurofibromatosis Type 1 (NF1) is caused by mutations in the NF1 gene that encodes neurofibromin, a RAS GTPase-Activating Protein. Inactivating NF1 mutations result in hyperactivation of RAS-mediated signaling. NF1 patients develop benign tumors on the skin and along nerves in the spinal cord and brain, and ~10% of these progress to Malignant Peripheral Nerve Sheath Tumors (MPNST). Attempts to inhibit RAS-signaling to treat MPNST have not worked in clinical trials. Surgical

removal is the only cure for MPNST, which is challenging due to large tumor size and/or proximity to nerves. MPNSTs often recur, metastasize, and respond poorly to chemo- and radiotherapy. As a result, MPNSTs are the leading cause of death in NF1 patients. Immune Checkpoint Blockade (ICB) is an approach to treat inoperable, undruggable cancers. Immune checkpoint proteins (ICPs) terminate normal immune responses to prevent collateral tissue damage. Cancer cells hijack this mechanism and express ICPs to avoid immune detection. ICB disrupts this process, enhancing antitumor immunity. Monoclonal antibodies (mABs) that disrupt the interaction between Programmed Cell Death Receptor 1 (PD-1) and its ligand Programmed Cell Death Ligand 1 (PD-L1) are a widely used ICB therapy. Having a T cell-enriched hot tumor microenvironment (TME) is required for successful ICB. However, MPNSTs lack a T cell-inflamed TME and respond poorly to ICB therapy. Activation of the protein "stimulator of interferon genes" (STING) enhances anti-tumor immunity via induction of pro-inflammatory cytokines, thus increasing T cell infiltration into the TME. We hypothesized that reprogramming the MPNST TME by STING pathway activation would turn cold MPNSTs into hot tumors amenable to ICB.
Methods: We treated mouse MPNSTs with STING agonist or STING agonist + anti-PD-1/anti-PD-L1 mAb. Tumor size was measured throughout treatment. The mice were sacrificed and tumor tissue was analyzed for STING pathway activation, T cell infiltration, cell proliferation, and apoptosis. MPNST allograft tumors in athymic mice were controls.
Results: STING pathway activation and increased T cell presence was observed in STING agonist-treated MPNSTs compared to vehicle-treated. MPNSTs treated with STING agonist alone or STING agonist + PD-1/PD-L1 mAbs showed less tumor growth relative to vehicle. Importantly, STING agonist + PD-1/PD-L1 mAb-treated tumors showed significant cell death increase while cell proliferation remained unchanged. Interestingly, tumors in athymic mice continued to grow despite treatment suggesting the antitumor effects seen in immunocompetent mice were mediated by T cells.
Conclusions: Our data show that MPNSTs can become T cell-rich tumors by activating STING signaling. Reprogramming the TME made MPNSTs susceptible to immune destruction by ICB therapy. Our studies support this novel treatment strategy for MPNST, an aggressive, deadly tumor for which no molecular therapy currently exists.

#5171

TP-6379, an investigational TGFBR1 inhibitor, shown to remodel the tumor microenvironment and enhance anti-tumorigenic immunological responses in syngeneic mouse models of cancer

David A. Kircher, Tetyana V. Forostyan, Richard E. Heinz, Curtis A. Allred, Sal Sommakia, Yuta Matsumura, Adam Siddiqui, Jason M. Foulks, Steven L. Warner. *Sumitomo Pharma Oncology, Lehi, UT*

Transforming growth factor-β (TGF-β) receptors regulate SMAD signal transduction and a wide-range of biological processes including, wound healing, angiogenesis, immune modulation, epithelial-mesenchymal transition, cell differentiation, apoptosis, growth, and motility. In transformed cells, TGF-β signaling is frequently exploited to reshape the architecture of the tumor microenvironment (TME) and establish a fibrotic barrier that insulates the tumor from surrounding normal tissue. As a result, immunological threats to the tumor are restricted, as is the anti-tumorigenic potential of immunotherapeutic interventions. Clinically, TGF-β hyperactivity is associated with immunotherapy resistance and poor outcome in a variety of malignancies. We hypothesize that TP-6379, an investigational small molecule inhibitor of TGFBR1, may remodel the TME to expand the access of tumor-seeking lymphocytes to tumor tissue. Herein we describe several anti-tumorigenic effects of TP-6379 observed in multiple mouse models of cancer both as a single agent, and in combination with immunotherapy. In an EMT6 syngeneic mouse model of triple-negative breast cancer (TNBC), we observed that tumor phospho-SMAD2/3 (pSMAD2/3) levels quickly declined post-TP-6379-treatment and were suppressed by 74% after 8 hours. Preclinical data showed TP-6379 plasma levels inversely correlated with pSMAD2/3 suppression. TP-6379 alone was observed to inhibit tumor growth in EMT6 and 4T1 TNBC models, an activity that was enhanced when augmented by immunotherapy. In a Cloudman S91 syngeneic melanoma mouse model, there was a clear subset of mice that responded to combination treatment. Histological analyses of TNBCs and responsive melanomas showed that TP-6379 treatment conferred a loss of induration of tumors, increased vascularization, and increased infiltration of CD45+ leukocytes (including CD8+ T cells), particularly when combined with immunotherapy. High-throughput

analyses of tumors uncovered an array of MHC class I and II factors that were observed elevated subject to TP-6379 treatment, an activity that was oftentimes enhanced when combined with immunotherapy. Collectively, these data suggest that TP-6379 may improve immune cell access to tumor tissue via TME remodeling and normalization of vascular networks. Thus, TP-6379 treatment may present a unique and multifactorial anti-tumor strategy, 1) as a single agent to improve anti-tumorigenic immunological responses, and 2) as a combination treatment to boost immunotherapeutic activity.

#5172

Tumor-immune microenvironmental profiling during chemo- and targeted therapy for head and neck squamous cell carcinoma

Alisa Kimura[1], Takahiro Tsujikawa[1], Junichi Mitsuda[1], Aya Miyagawa-Hayashino[2], Hiroki Morimoto[1], Sumiyo Saburi[1], Kanako Yoshimura[1], Gaku Ohmura[1], Sigeyuki Mukudai[1], Hikaru Nagao[1], Yoichiro Sugiyama[1], Hiroshi Ogi[3], Saya Shibata[4], Eiichi Konishi[2], Kyoko Itoh[3], Shigeru Hirano[1]. *[1]Departments of Otolaryngology-Head and Neck Surgery, Kyoto Prefectual University of Medicine, Kyoto, Japan,[2]Departments of Surgical Pathology, Kyoto Prefectual University of Medicine, Kyoto, Japan,[3]Departments of Pathology and Applied Neurobiology, Kyoto Prefectual University of Medicine, Kyoto, Japan,[4]SCREEN Holdings Co., Ltd., Kyoto, Japan*

Understanding longitudinal changes of tumor-immune microenvironment during chemo/targeted therapies contributes to the development of optimized combinations of immunotherapy with chemotherapy and targeted therapy for patients with head and neck squamous cell carcinoma (HNSCC). We previously reported a chromogenic sequential immunohistochemical (IHC) platform enabling quantitative and spatial assessment of 29+ biomarkers in a single tissue section (Tsujikawa T et al. Cell Reports 2017, Banik G et al. Methods Enzymology 2020). Using this platform, densities, phenotypes, and distributions of tumor and immune cells were evaluated, comparing baseline and post-treatment specimens from the same individual treated by paclitaxel, carboplatin, and cetuximab (PCE) for advanced HNSCC (N = 30). Immune cell density analyses based

on $CD8^+$ T cells, helper T cells, regulatory T cells, B cells, natural killer cells, macrophages, dendritic cells, mast cells, granulocytes revealed the presence of differential immune cell compositions, where immune profiles were divided into hypo-, lymphoid-, and myeloid-inflamed groups according to the same criteria as in our previous report (Tsujikawa et al. Cell Reports 2017). Lymphoid and hypo-inflamed groups exhibited significant tumor volume reduction, increased $CD45^+$ immune cell densities and elevated combined positive scores of PD-L1 at the post-treatment status, suggesting the potential involvement of immunogenic mechanisms related to therapeutic response. On the other hand, the myeloid group exhibited no significant tumor volume reduction, together with higher expression of HIF1α and ZEB2 on tumor cells which are potentially associated with hypoxia and epithelial-mesenchymal transition. In conclusion, longitudinal tissue-based monitoring revealed the presence of differential tumor-immune complexity profiles related to therapeutic efficacy and resistance. Hypo-inflamed profiles might require upfront chemo/targeted therapy before immunotherapy, and myeloid-inflamed profiles might require myeloid cell-targeted therapies, mandating the establishment of rapid clinical assessment of tumor-immune microenvironment.

#5173

BET inhibition reprograms pancreatic cancer associated fibroblasts to promote anti-tumor immunity

Trisha Minocha, Alison Thomas, Brian M. Olson. *Hematology/Oncology, Winship Cancer Institute of Emory University, Atlanta, GA*

BACKGROUND**:** Pancreatic ductal adenocarcinoma (PDAC) is the most malignant neoplasm of the pancreas, and is refractory to most therapeutic strategies, including immunotherapy. We have previously demonstrated that loss of CDKN2A in PDAC tumor cells promotes an immunologically-cold tumor microenvironment, which can be counteracted through the use of bromodomain and extraterminal domain inhibitors (BETi). The immunosuppressive PDAC tumor microenvironment is also characterized by a dense desmoplastic stroma, rich in cancer associated fibroblasts (CAFs). These CAFs are a highly plastic population of cells, comprised of myofibroblastic, inflammatory, and antigen-presenting CAFs (myCAFs,

iCAFs, and apCAFs, respectively). Previously research has suggested BETi can alter the function of CAFs, suggesting this therapeutic strategy may be effective at targeting both the tumor and stromal compartments of PDAC. Here we hypothesize that BETi enhances anti-tumor immunity in CDKN2A-deficient PDAC by modulating the phenotype and function of PDAC CAFs.
METHODS: Isogenic wild-type and CDKN2A-deficient KPCluc pancreatic cancer cell lines were used in conjunction with KPCluc-derived murine CAF cells. CAF spheroids were used to evaluate the effects of BETi on CAF phenotype (as measured by flow cytometry) and function (as measured by NanoString analysis, checkpoint ligand expression by flow cytometry, and T cell migration assays). Additionally, the impact of BETi-induced modulation of CAF phenotype and function on wild-type and CDKN2A-deficient tumor cell spheroids was measured by flow cytometry.
RESULTS: Treatment of pancreatic CAFs with BETi induced expression of genes associated with DNA damage responses and type I IFN expression. Additionally, while CAF supernatants suppressed T cell migration *in vitro*, treatment with BETi restored T cell migration across a transwell. This was due in part to DNA damage/STING/NF-κB signaling induced in PDAC CAF following BETi. Supernatants from BETi-treated PDAC CAFs were found to modulate PD-L1 expression on PDAC tumor cells. Direct treatment of CAFs with BETi induced a dramatic dose- and time-dependent polarization of CAF spheroids towards a myCAF phenotype. However, while BETi induced DNA damage/STING/NF-κB signaling in CAF cells, this signaling did not contribute towards this myCAF polarization, as treatment of CAF spheroids with BETi and STING or NF-κB inhibitors did not impact myCAF polarization. Additional mechanisms of polarization are currently being evaluated and will be updated at presentation.
CONCLUSIONS: BET inhibition modulates CAF cell phenotype and function to promote anti-tumor immune responses. Taken together with the impact of BET inhibition on CDKN2A-deficient PDAC tumor cells, these data suggest BETi is a rational treatment approach to promote anti-tumor immunity in this genetically defined immunotherapy resistant patient population.

#5174

PEGylated liposomal doxorubicin improves oral cancer response to radio-immunotherapy

Laxman Devkota[1], Rohan Bhavane[2], Andrew Badachhape[1], Ratna Veeramachaneni[3], Renuka Menon[1], Prajwal Bhandari[1], Sofia Cortes[3], Fabio Henrique Brasil Da Costa[3], Ketan Ghaghada[2], Simon Young[4], Andrew G. Sikora[3], Ananth V. Annapragada[2]. *[1]Radiology, Baylor College of Medicine, Houston, TX,[2]Radiology, Texas Children's Hospital, Houston, TX,[3]Head and Neck Surgery, MD Anderson Cancer Center, Houston, TX,[4]Department of Oral & Maxillofacial Surgery, The University of Texas Health Science Center at School of Dentistry, Houston, TX*

Introduction: The immunosuppressive tumor microenvironment (TME) in oral cancer inhibits response to conventional treatment (surgery +/- chemoradiotherapy) and check-point inhibitor (αPD1) immunotherapy. The chemotherapeutic agent doxorubicin and its PEGylated liposomal nanoparticle formulation (PLD) have been shown to target myeloid derived suppressor cells (MDSCs) in the TME. In this preclinical work, we investigated whether PLD improves response to radio-immunotherapy in a highly aggressive and immunologically 'cold' oral cancer model.
Experimental Procedure: Studies were performed in the MOC2 syngeneic mouse model of oral cancer. Mice were randomized to one of seven treatment groups: αPD1, Radiation (XRT), αPD1+XRT, PLD, PLD+αPD1, PLD+XRT, PLD+αPD1+XRT. High-resolution nanoparticle contrast-enhanced computed tomography (nCECT) imaging was performed, and whole-body T2-weighted magnetic resonance imaging (MRI) used to monitor primary tumor response and development of metastases. Response evaluation criteria in solid tumors (RECIST) were used to evaluate treatment outcomes.
Results: Tumors in all non-PLD groups were treatment resistant and grew progressively, consistent with the immunologically 'cold' MOC2 model. In contrast, all PLD groups showed tumor regression with 25-38% complete responders (CR) and 12-88% partial responders (PR) while all animals in non-PLD groups showed progressive disease (PD). MR imaging identified a high incidence of regional and distant metastases in the non-PLD groups while the PLD groups showed decreased regional and no distant metastases (Table1). Presence of metastases was confirmed by nCECT imaging and histopathological analysis.

Conclusion: PLD improved response to radio-immunotherapy in a highly aggressive immunologically 'cold' mouse model of oral cancer while simultaneously preventing disease progression and metastasis.

#5175

DX-002, a dual EP2 and EP4 antagonist, alters the tumor microenvironment to enhance tumor immunogenicity and responses to immune checkpoint inhibitors

Lintong Li, Guorui Yao, Wei Zheng, Yongshuai Chai, Zhongying Huang, Guojian Ma, Linlin Nie, Dengfeng Xu, Jiuquan Yang, Nanxin Li.
GuangDong NewOpp Biopharmaceuticals Co., Ltd, Guangzhou, China

Prostaglandin E2 (PGE2) generated by the cyclooxygenase (COX) pathways regulates both inflammation and tumor microenvironment (TME). Among the four E-type prostanoid receptors EP1-4, it has been demonstrated that PGE2 exhibits its immune suppression and tumorigenic function through engagement with EP2 and EP4. Mechanistically, tumor-derived PGE2 acts on EP2 and EP4 in immune cells (e.g., NK cells and dendritic cells) and elicits immunosuppression in TME[1,2]. Importantly, the deletion of both EP2 and EP4, but not deletion of either receptor, is required to reverse PGE2-mediated immune evasion. Furthermore, high levels of PGE2-EP2/EP4 associated inflammatory signature have been shown in multiple human cancer types to correlate with poor prognosis and worse response to immune checkpoint blockade in the clinic[1]. Therefore, PGE2-EP2/EP4 signaling likely acts as a key regulatory node linking inflammation and immunosuppression in TME, and its inhibition may lead to a less immunosuppressive TME and enhance the response to immune checkpoint inhibitors. COX inhibitors have been used to block PGE2 synthesis but cause cardiovascular and gastrointestinal risks due to the inhibition of all prostanoids synthesis[3]. Thus, therapeutically targeting both EP2 and EP4 is an effective and more selective approach to limit the immunosuppressive functions of PGE2 while avoiding potential side effects associated with COX inhibition.
Here we describe the discovery of a potent and selective EP2/EP4 dual antagonist DX-002. At 10 nM concentration, it displayed >90% inhibition of PGE2 binding to EP2 or EP4, whereas no significant inhibition was seen towards PGE2 binding to EP1 or EP3. In human NK cells DX-002 reversed

PGE2-mediated inhibition of IFN-γ production more potently than selective EP2 or EP4 antagonist. DX-002 has excellent pharmacokinetics profiles across all animal species. In the mouse tumor model, treatment of DX-002 produced superior tumor regression as a monotherapy over selective EP2 or EP4 antagonists. In addition, DX-002 also provided significant synergistical effect for tumor regression in combination with anti-PD1 in both immune checkpoint inhibitor insensitive and sensitive models, in association with increased tumor infiltration of CD8+ T cells. Based on its in vitro and in vivo profiles along with other properties, DX-002 is being profiled as a development candidate as a potential cancer immunotherapeutic agent.

#5176

CDDO-methyl ester redirects macrophage polarization and reduces lung tumor burden in a Nrf2-dependent manner

Jess Ann Moerland, Karen T. Liby. *Michigan State University, East Lansing, MI*

The cytoprotective Nrf2 pathway impacts immune cell function and has been proposed as a target for many inflammation-related diseases, but the effects of Nrf2 activation on immune cells in the cancer context are not well characterized. With Nrf2 activators under development and in clinical trials, it is critical to understand the influence of these drugs on cancer progression. While the anti-inflammatory nature of Nrf2 activation protects healthy cells from malignant transformation, cancer cells can utilize the pathway to promote resistance to anti-cancer drugs and increase tumor cell survival. Up to 30% of human lung adenocarcinomas acquire mutations in the Nrf2 pathway which result in constitutive activation. However, triterpenoids, including CDDO-methyl ester (CDDO-Me, also known as bardoxolone methyl), are potent pharmacological Nrf2 activators with demonstrated anti-cancer activity in preclinical models. Lung cancer is the leading cause of cancer-related mortality worldwide, and macrophages are the most common immune cell type in the lung tumor microenvironment. To investigate Nrf2 activation in macrophages in the context of lung cancer, bone marrow-derived macrophages (BMDMs) were isolated from wild type (WT) and Nrf2 knock out (KO) mice and cultured in conditioned media from lung cancer cells to produce a tumor-educated phenotype. The triterpenoid CDDO-Me had anti-inflammatory effects in BMDMs

stimulated with the conventional cytokines IFN-γ and LPS. Conversely, CDDO-Me increased ($p < 0.05$) the M1 macrophage markers TNFα, IL-6, and MHC-II and decreased the M2 macrophage markers VEGF, CCL2, and CD206 in tumor-educated BMDMs in a Nrf2-dependent manner. The phenotypic changes were observed on transcription, protein, and surface marker levels. This context-dependent reversal of BMDM polarization suggests that Nrf2 activation has different outcomes in different environments. To test CDDO-Me *in vivo*, lung tumors were initiated with vinyl carbamate in A/J WT and Nrf2 KO mice, and animals were fed either control diet or CDDO-Me (12.5-50 mg/kg of diet) for 16 weeks. CDDO-Me significantly ($p < 0.05$) decreased tumor number, size, and overall burden and reduced the histopathological severity of tumors in a Nrf2- and dose-dependent manner. Additionally, CDDO-Me increased the infiltration of CD64+ macrophages but decreased CD206+ expression in macrophages in the lungs of WT tumor-bearing mice. Interestingly, CD206 expression was higher on macrophages in the spleen of WT mice treated with CDDO-Me, suggesting a cancer context dependency. Future studies will evaluate the dependency of Nrf2 activation in macrophages for the anti-tumor activity of CDDO-Me.

#5177

Nilotinib suppresses the myofibroblastic cancer-associated fibroblast phenotype

Katherine Anne Johnson, Yousef Gadalla, Cheri A. Pasch, Dustin A. Deming. *Univ. of Wisconsin Madison Sch. of Med. & Public Health, Madison, WI*

Background: Cancer-associated fibroblasts (CAFs) modulate the tumor immune microenvironment and are an exciting target for improving response to immunotherapy. Major roles of CAFs in the immune microenvironment include deposition of extracellular matrix (ECM) to prevent immune cell infiltration, a function associated with myofibroblastic CAFs (myCAFs), and production of cytokines to alter the immune milieu, associated with inflammatory CAFs (iCAFs). Recently we have demonstrated the potential for tyrosine kinase inhibitors (TKIs) to alter CAF phenotypes. Here we investigate the ability of dasatinib and nilotinib to alter the immune regulatory functions of CAFs.

Methods: Bulk RNA sequencing comparing the effects of nilotinib and dasatinib on primary-derived patient CAFs was performed. CAFs from two rectal cancer patient tumors were isolated, cultured, and treated for 96 hours with 2.5μM nilotinib, 100nM dasatinib, or control feeding media. RNA isolation, library preparation, sequencing, data processing, and differential expression analysis was done through the University of Wisconsin - Madison Gene Expression Center, Biotechnology Center, and Bioinformatics Resource. Gene set enrichment analyses were done using GSEA 4.2.3 (Broad Institute) and all other analyses done in R.
Results: The primary variance in samples is between CAF lines (RC1 and RC2), followed by treatments. RNA expression markers for myCAFs significantly associate with the Gene Ontology molecular function ECM structural constituent ($q < 0.001$). Nilotinib decreased expression of this gene set in RC1 ($q < 0.001$), while dasatinib treatment increased these genes in RC2, though not significantly ($q = 0.2$). Both dasatinib and nilotinib downregulated immune-related hallmark gene sets including IL6/JAK/STAT3 signaling (RC2 dasatinib $q < 0.05$, $q < 0.001$ for others) and TNFα signaling through NFκB (RC1 dasatinib $q < 0.001$, RC2 niltoinib $q < 0.05$, others $q = 0.001$,). Additionally, dasatinib induced increased expression of genes involved in myogenesis in both CAF lines (RC1 $q = 0.001$, RC2 $q < 0.001$), while nilotinib significantly decreased these genes in RC1 ($q = 0.001$). MYOCD is a transcription factor involved in myogenesis that regulates important myCAF genes such as *ACTA2* and *TAGLN*. Nilotinib treatment decreased expression of *MYOCD* (RC1 log2FC -1.3 $q < 0.001$, RC2 -0.75 $q < 0.05$) and its target genes in both lines, whereas dasatinib did not significantly alter expression.
Conclusions: CAFs derived from different cancers harbor different transcriptional profiles and have different responses to TKIs. Dasatinib treatment led to an increase in expression of ECM genes associated with the myCAF phenotype, while nilotinib decreased this phenotype, potentially by inhibiting *MYOCD* expression. Further investigation into the mechanisms by which nilotinib treatment decreases expression of ECM genes and whether these trends continue *in vivo* are warranted.

#5178
Humanized OX40/OX40L mice as a tool for evaluating novel therapeutics

Chonghui Liu[1], Jiawei Yao[1], Xiaofei Zhou[1], James Jin[2], Zan Zhang[1]. *[1]Biocytogen Pharmaceuticals (Beijing) Co., Ltd., Beijing, China,[2]Biocytogen Boston Corp, Wakefield, MA*

The use of immune-competent mouse models that express target human genes provide a promising preclinical platform aimed at developing novel immunotherapies. Emerging immunotherapies include targeting OX40 and OX40 ligand (OX40L), which can lead to enhanced T cell activation, proliferation, and effector function. Blocking the OX40/OX40L pathway improves autoantigen-specific T cell responses and decreases immunocompetence across several autoimmune diseases. To explore the potential of OX40 and OX40L antibody efficacy studies, we developed double humanized B-hOX40/hOX40L mice by replacing the extracellular domain sequences of murine *Ox40* and *Ox40l* with the corresponding human sequences. We validated human *OX40L* gene expression by RT-PCR and OX40/OX40L protein expression by flow cytometry in B-hOX40/hOX40L mice. Additionally, percentages of splenic, blood, and lymph node immune cells were similar between B-hOX40/hOX40L and wild-type C57BL/6 mice. Altogether, this data demonstrates that B-hOX40/hOX40L mice are suitable for *in vivo* efficacy studies using anti-human OX40 and OX40L antibodies.

#5180

T cell receptor repertoire analysis revealed tissue tropism of tumor-reactive T-cell clones in cell cycle reporter mice

Mikiya Tsunoda[1], Hiroyasu Aoki[1], Munetomo Takahashi[2], Haruka Shimizu[1], Haru Ogiwara[1], Shigeyuki Shichino[1], Kouji Matsushima[1], Satoshi Ueha[1]. *[1]Research Institute for Biomedical Sciences, Tokyo University of Science, Noda-shi, Japan,[2]Faculty of Medicine, The University of Tokyo, Bunkyo-ku, Japan*

Tumor-reactive T cells are composed of clones with various TCRs, and each clone has different in vivo kinetics. By analyzing TCR repertoire of tumor and tumor-draining lymph node (dLN), we have demonstrated that Tumor-reactive CD8+ T cells can be classified into “dLN Major”, “Tumor Major”, and “Double Major” clones, which exhibited high frequency in the

dLN, tumor, or both tissues. To investigate whether this classification was related to the tissue tropism in the proliferation of each clone, we here employed tumor-bearing Fucci transgenic mice expressing a fluorescent cell-cycle indicator to identify the proliferation of T-cell clones in each tissue. We purified proliferating- and resting-CD8+ T cells from the tumors and dLN and analyzed their TCR repertoire in an LLC subcutaneous tumor model. All Tumor Major clones were proliferated in the tumor, while nearly 0% for dLN Major, indicated their different proliferative capacity in the tumor. The percentage of proliferating clones in the dLN was 20% for Tumor Major and 15% for dLN Major, indicating that these clones had equivalent proliferative capacity in the dLN. These proliferating dLN major clones overlapped more with the tumor than the non-proliferating dLN major clones, suggesting that proliferating dLN Major clones had higher tumor migration capacity. Furthermore, these proliferating dLN major clones were more proliferative in the tumor. These results suggested that dLN Major responded to antigen presentation in the dLN but not in the tumor, whereas Tumor Major responded to those in the dLN and tumor. In addition, there are two types of dLN major, “clones that are proliferating in dLN” and “clones that are not proliferating in dLN” indicating that the former may contribute to the anti-tumor response. Immune checkpoint inhibitor (ICI) treatment not only reactivates clones in the tumor but also activates tumor-reactive clones in the dLN. In conformity with these previous studies, the percentage of proliferating clones among dLN Major increased to about 50% and 80% in the dLN in mice with anti-PD-L1 and anti-CD4 treatment, respectively. This result suggests ICI treatment enhances anti-tumor responses mainly by promoting the activation and proliferation of dLN Major clones. This study shows new findings that tumor-reactive T cells differ in the tissue tropism of their proliferation of each clone. In the future, a quantitative understanding of the contribution of each class of clones to the anti-tumor response will hopefully lead to the development of new combined immunotherapies that optimize the anti-tumor T-cell response.

#5181

The role of Neuropilin-1 signaling in CD4 conventional T cell immune function in non-small cell lung cancer

Bitta P. Kahangi[1], Raymond J. Lim[2], Jensen Abascal[2], William P. Crosson[2], Edgar Perez Reyes[2], Camelia Dumitras[2], Linh M. Tran[2], Kostyantyn Krysan[2], Ramin Salehi-Rad[2], Steven M. Dubinett[2], Bin Liu[2]. *[1]Medicine - Pulmonary and Critical Care, UCLA - University of California Los Angeles, Los Angeles, CA,[2]UCLA - University of California Los Angeles, Los Angeles, CA*

Despite advances in therapy, lung cancer remains the leading cause of cancer related deaths. In non-small cell lung cancer (NSCLC), a subset of tumor-infiltrating CD4 T cells express Neuropilin-1 (NRP1), a transmembrane protein that binds to multiple ligands with diverse functions in tumor and immune cells. Recent studies reveal that NRP1 can be induced upon T cell receptor stimulation and that NRP1 signaling promotes increased stabilization and function of CD4+ FoxP3+ regulatory T cells (Tregs), while signaling on CD8 T cells results in inhibition of CD8 T cell migration and cytotoxicity; therefore, NRP1 is implicated as a newly defined immune checkpoint protein. The functional role of NRP1 in CD4+ FoxP3- T conventional cells (CD4 Tconv) and the ligands involved are largely unexplored. We have found that human lung cancer malignant pleural effusions (MPE) from a subset of metastatic lung cancer patients contain both NRP1+ and NRP1- CD4 Tconv cells, providing a relevant clinical setting to study the function of NRP1 in human T cells. Our preliminary studies reveal that MPE-derived NRP1+ CD4 Tconv cells have altered expression of CD25, suggestive of a more activated state as compared to that of NRP1- CD4 Tconv cells. Additionally, we have observed disproportionate cell death of NRP1+ CD4 Tconv cells that can be partially rescued with anti-NRP1 monoclonal antibodies (mAbs). Surviving NRP1+ cells are more likely to express PD-1 and secrete effector cytokines. In our murine NSCLC model carrying key driver mutations $Kras^{G12D}$ $P53^{-/-}$ $Lkb1^{-/-}$ and higher tumor mutational burden (KPL-3M), analysis of tumor-infiltrating CD4 Tconv cells confirm that NRP1+ CD4 T cells are preferentially found within tumors and with higher PD-1 expression as compared to NRP1- cells. Furthermore, treatment with anti-NRP1 mAbs confers anti-tumor efficacy in this model, indicating that NRP1 is a functionally important inhibitor of host anti-tumor immune responses. These data suggest that CD4 Tconv cells expressing NRP1 are activated but

prone to cell death, warranting further investigation into its potential as a therapeutic target for NSCLC.

#5182

CD47 is a promising therapeutic target in non-small cell lung cancer

Asa P. Y. Lau[1], Shawn P. Kubli[2], Andrew Wakeham[3], Tak W. Mak[3], Kelsie L. Thu[1]. *[1]Keenan Research Centre, St. Michael's Hospital, Toronto, ON, Canada,[2]Treadwell Therapeutics, Toronto, ON, Canada,[3]University Health Network, Toronto, ON, Canada*

Introducti**on:** Immune checkpoint inhibitors can elicit remarkable tumor regressions in non-small cell lung cancer (NSCLC), but not all patients are eligible for these drugs and only a small fraction of those who are respond. Thus, additional immunotherapies (IO) for NSCLC patients are needed. CD47 is an immunosuppressive protein frequently overexpressed in NSCLC. When bound to its receptor, SIRPα, the phagocytic function of antigen presenting cells (APCs) is impaired which dampens the innate immune response and anti-tumor immunity. CD47-SIRPα-targeted IOs are under investigation in clinical trials but little efficacy has been seen in solid tumours, suggesting further preclinical knowledge is needed to guide effective use in NSCLC. To address this need, we aim to decipher immune-mediated and cell-intrinsic mechanisms governing NSCLC response to CD47 inhibition.

Methods: CRISPR/Cas9 was used to generate mixed and clonal *Cd47* knockout (KO) populations in two murine, syngeneic NSCLC models (LLC and CMT167). The effect of *Cd47* inactivation on tumor cell fitness was assessed by multicolour competition assays conducted *in vitro* and in orthotopic tumors grown in immunocompetent C57BL/6 mice. Survival studies were also done in immune competent (C57BL/6) and deficient (NCG) mice to provide insights into cell-intrinsic versus immune-mediated effects of *Cd47* KO on tumor growth. Immunophenotyping of tumours grown in syngeneic hosts was done using flow cytometry to compare immune cell infiltration in wildtype (WT) versus *Cd47* KO tumors.

Results: Multicolour competition assays revealed that *Cd47* LOF reduced the fitness of LLC and CMT167 cells grown in mice but not in cells grown *in vitro*, suggesting *Cd47* KO does not compromise cell proliferation. Consistent with these results, survival studies conducted in immune

competent hosts showed prolonged survival of mice with *Cd47* KO compared to WT tumors in both models. An increase in activated Cd8+ cytotoxic T cells and M1-polarized macrophages was observed in *Cd47* KO tumors relative to WT controls. Interestingly, the same survival studies conducted in immune compromised mice also showed a significant survival benefit for mice with *Cd47* KO tumors, suggesting immune- and proliferation-independent, cell-intrinsic functions of *Cd47* may also regulate NSCLC growth and progression.
Conclusions: Our results confirm the therapeutic potential of Cd47-targeted IO in NSCLC. The increased infiltration of anti-tumor lymphocytes and myeloid cells in *Cd47* KO tumours supports a role for the immune system in mediating enhanced survival. However, because immune deficient mice with *Cd47* KO tumors also exhibited a survival benefit, additional studies are required to deduce how *Cd47*-regulated cell-intrinsic mechanisms promote NSCLC biology. Our findings warrant further preclinical research to define effective anti-CD47 strategies for NSCLC.

#5183
Development of an aerosol-based immunotherapy for lung cancer
Yongren Li[1], Zhen Zhao[2], John Fetse[3], Reaid Hasan[3], Umar-Farouk Mamani[1], Yuhan Guo[3], Kun Cheng[3]. *[1]University of Missouri - Kansas City, Kansas City, MO,[2]School of Health Science & Biomedical Engineering, Hebei University of Technology, Hebei, China,[3]School of Pharmacy, University of Missouri - Kansas City, Kansas City, MO*

Lung cancer is one of the leading causes of cancer death and the second most cancer in the world. Compared to systematic administration, local delivery of therapeutic agents to the lung increases their accumulation in lung cancer cells and reduces the toxicity in other organs. We previously discovered an anti-PD-L1 peptide that can be potentially uses for lung cancer therapy. This project aims to develop an aerosolized formulation of the anti-PD-L1 peptide for the treatment of lung cancer. We hypothesize that the aerosolized peptide has higher accumulation in the lung compared to systematic formulations, leading to high therapeutic index with less side effects. We developed a spray freeze-drying procedure and optimized the formulation to prepare the peptide dry powders. The median mass aerodynamic diameter (MMAD) and geometric standard deviation (GSD)

of the aerosols were determined by an 8-stage Andersen Cascade Impactor. The morphology of the aerosols was studied using a scanning electron microscope (SEM). The stability of the aerosols in lung fluid was evaluated. Blocking assay suggested that the aerosolized formulation maintains the blocking efficiency of the peptide. Intratracheal administration of the peptide dry powder shows a high accumulation of the peptide in the lung.

#5184

Anti-HVEM mAb therapy improves antitumoral immunity both *in vitro* and *in vivo*, in a novel transgenic mouse model expressing human HVEM and BTLA molecules challenged with HVEM expressing tumors

Laurent GORVEL[1], Clemence Demerle[1], Marielle Mello[2], Sonia Pastor[1], Clara Degos[1], Ana Zarubica[2], Fabien Angelis[2], Frederic Fiore[2], Jacques Nunes[1], Bernard Malissen[2], Laurent Greillier[3], Geoffrey Guittard[1], Herve Luche[2], Fabrice Barlesi[4], Daniel Olive[1]. *[1]Centre de Recherche en Cancérologie de Marseille (CRCM), Marseille, France,[2]Centre d'Immunophénomique - CIPHE (PHENOMIN), Marseille, France,[3]Aix Marseille University, APHM, INSERM, CNRS, CRCM, Hôpital Nord,, Marseille, France,[4]Multidisciplinary Oncology and Therapeutic Innovations, Aix Marseille University, CNRS, INSERM; Gustave Roussy Cancer Campus, Marseille, France*

TNFRF-14/HVEM is the ligand for BTLA and CD160 negative immune co-signaling molecules as well as viral proteins. Its expression is dysregulated with an overexpression in tumors and a connection with tumors of adverse prognosis. We developed C57BL/6 mouse models co-expressing human huBTLA and huHVEM as well as antagonistic monoclonal antibodies (mAbs) that completely prevent the interactions of HVEM with its ligands. Here, we show that the anti-HVEM18-10 mAb increases primary human αβ-T cells activity alone (CIS-activity) or in the presence of HVEM-expressing lung or colorectal cancer cells *in vitro* (TRANS-activity). Anti-HVEM18-10 synergizes with anti-PD-L1 mAb to activate T cells in the presence of PDL-1 positive tumors, but is sufficient to trigger T cell activation in the presence of PD-L1 negative cells. In order to better understand HVEM18-10 effect *in vivo* and especially disentangle its

CIS and TRANS effects, we developed a knock-in (KI) mouse model expressing human BTLA (huBTLA$^{+/+}$) and a KI mouse model expressing both human BTLA and human HVEM (huBTLA$^{+/+}$ /huHVEM$^{+/+}$ (DKI)). *In vivo* pre-clinical experiments performed in both mouse models showed that HVEM18-10 treatment was efficient to decrease human HVEM+ tumor growth. In the DKI model, anti-HVEM 18-10 treatment induces a decrease of exhausted CD8^{+} T cells and regulatory T cells and an increase of Effector memory CD4^{+} T cells within the tumor. Interestingly, mice which completely rejected tumors (± 20%) did not develop tumors upon re-challenge in both settings, therefore showing a marked T cell-memory phenotype effect. Altogether, our preclinical models validate anti-HVEM18-10 as a promising therapeutic antibody to use in clinics as a monotherapy or in combination with existing immunotherapies (anti-PD1/anti-PDL-1/anti-CTLA-4).

#5185

Intratumoral *Escherichia* is associated with response to single-agent immune checkpoint inhibition in patients with advanced non-small cell lung cancer

Arielle Elkrief, Anita S. Bowman, Ayyuce Begum Bektas, Wenfei Kang, Katia Manova-Todorova, Jacklynn V. Egger, Hira Rizvi, Daniel Kelly, Eric Chan, Eric Rosiek, Fan Ning, Gregory J. Riely, Álvaro Quintanal Villalonga, Snjezana Dogan, Umesh Bhanot, Mithat Gonen, Matthew D. Hellmann, Adam J. Schoenfeld, Charles M. Rudin, Marc Ladanyi, Chad M. Vanderbilt. *Memorial Sloan Kettering Cancer Center, New York, NY*

The impact of the intratumoral microbiome on immune checkpoint inhibitor (ICI) efficacy in patients (pts) with non-small cell lung cancer (NSCLC) is unknown. In preclinical studies, the presence of lung intratumoral *Escherichia* was associated with a proinflammatory tumor microenvironment and decreased metastases within lung tissue. We sought to detect intratumoral bacteria in pts with advanced NSCLC using hybrid capture-based, next generation sequencing (NGS). We studied 849 pts treated with ICI-based therapy who underwent NGS at our center. We extracted unmapped reads from BAM files, and these were queried for bacteria (blastn alignment using the NCBI database). Putative environmental contaminants were subtracted from the analysis using “no

template" controls (n=2,539) to exclude possible artifactual false positives. A custom *E.Coli* fluorescence in situ hybridization (FISH) probe was used to visualize *Escherichia* within the tumors after co-registration with H&E. In 849 pts, a median of 30 bacterial reads was detected per sample (inter-quartile range (18-85)). Among 68 pts with paired primary/metastatic samples, the bacterial spectra were similar in both sites, suggesting that tumor resident bacteria might travel with cancer cells to distant sites. Antibiotic use within 30 days of tumor sampling was associated with decreased intratumoral bacterial diversity (p=0.023 by Inverse Simpson, p=0.038 by Shannon). Intratumoral *Escherichia* was associated with better PFS (HR 0.78, 95% CI 0.62-0.98, p=0.036), and OS (HR 0.74, 95% CI 0.58-0.95, p=0.017) in pts treated with single-agent ICI, but not combination Chemo/ICI. In a multivariable model adjusting for prognostic features in NSCLC including PD-L1 tumor proportion score, the presence of intratumoral *Escherichia* was associated with better PFS (p=0.040) and OS (p=0.045) upon single-agent ICI therapy. *Escherichia* appeared to be intracellular based on co-registration of FISH staining and serial H&E sections. These findings warrant further investigation of the possible inter-relationships between intratumoral *Escherichia*, tumor immune micro-environment, and ICI therapeutic outcomes.

New Opportunities for Combinatorial Immunotherapies

#5741

Harnessing macrophages, while protecting T cells, enhances anti-tumor efficacy

Sean A. Yamada-Hunter[1], Johanna Theruvath[1], Molly T. Radosevich[1], Brianna J. McIntosh[2], Katherine A. Freitas[1], Naiara Martinez-Velez[1], Elena Sotillo[1], Amaury Leruste[1], Peng Xu[1], Moksha H. Desai[1], Bita Sahaf[1], Allison Banuelos[3], Savannah L. Wasserman[1], Irving L. Weissman[3], Jennifer R. Cochran[4], Crystal L. Mackall[1]. *[1]Center for Cancer Cell Therapy, Stanford University School of Medicine, Stanford, CA,[2]Cancer Biology Program, Stanford University School of Medicine, Stanford, CA,[3]Institute for Stem Cell Biology and Regenerative Medicine, Stanford University School of Medicine, Stanford, CA,[4]Department of Bioengineering, Stanford University, Stanford, CA*

Chimeric antigen receptor T (CAR T) cells are synthetically engineered to target specific tumor antigens. CD47 is a ubiquitous receptor that serves as a “don’t eat me” signal by binding to SIRPα on macrophages and is often over-expressed by cancer cells. Despite individual promise of CAR T and anti-CD47 therapies, neither has demonstrated clear efficacy in treating solid tumors in the clinic and there is thus an urgent need to develop novel approaches that enhance the potency of these therapies. We interrogated the potential pairing of CAR T with anti-CD47 therapy to overcome tumor resistance mechanisms inherent to each therapy alone, by engaging non-redundant properties of two arms of the immune system. However, upon coadministration of anti-CD47 therapy and CAR T cells across multiple tumor models *in vivo*, we observed potent and consistent macrophage-mediated clearance of CAR-T cells via on-target, off-tumor binding of anti-CD47 therapies to CAR T cells. This anti-CD47 mediated CAR T cell depletion blunts the therapeutic benefits of treatment and renders the pairing of the current versions of the two agents impractical.To overcome this challenge, we used directed evolution and yeast surface display to engineer a novel variant of CD47 (eCD47) with selective binding, identifying mutations that resulted in loss of binding to the anti-CD47 antibody B6H12, while maintaining the CD47 “don’t eat me” function through binding to SIRPα, which is essential for T cell persistence *in vivo*. T cells engineered to express eCD47, but not native, wild-type CD47, were resistant to targeting by multiple anti-CD47 antibodies but maintained binding to SIRPα. These T cells were no longer susceptible to anti-CD47 mediated macrophage phagocytosis *in vitro,* nor were they depleted *in vivo* after B6H12 administration. We demonstrated a striking improvement in therapeutic efficacy upon treatment of multiple solid tumor models when anti-CD47 therapy was combined with CAR T cells expressing eCD47, compared to combination with CAR T cells expressing wild-type CD47. We interrogated a mechanistic basis for this improved efficacy in an osteosarcoma model through single-cell RNA-sequencing of isolated tumors. We discovered that CAR T treatment led to a large influx of unique populations of macrophages into the tumor, which were lost upon CAR T depletion after anti-CD47 treatment. These T cell recruited-macrophages were maintained after anti-CD47 treatment in the presence of CAR T cells expressing eCD47, harnessing macrophage mediated anti-tumor activity

after combination treatment. Thus, for the first time, eCD47 allows for effective pairing of CAR T therapy and anti-CD47 therapy for cancer treatment, by sparing T cells from macrophage mediated depletion, and revealing impressive synergy when adoptive T cell therapy is combined with macrophage activation.

#5742

Pharmacologic modulation of RNA splicing enhances anti-tumor immunity

James D. Thomas[1], Sydney X. Lu[2], Emma De Neef[1], Erich Sabio[3], Benoit Rousseau[3], Mathieu Gigoux[3], David A. Knorr[3], Benjamin Greenbaum[3], Yuval Elhanati[3], Simon J. Hogg[3], Andrew Chow[3], Arnab Ghosh[3], Abigail Xie[3], Dmitriy Zamarin[3], Daniel Cui[3], Caroline Erickson[3], Michael Singer[3], Hana Cho[3], Eric Wang[3], Bin Lu[3], Benjamin H. Durham[3], Harshal Shah[3], Diego Chowell[4], Austin M. Gabel[1], Yudao Shen[5], Jing Liu[5], Jian Jin[5], Matthew C. Rhodes[6], Richard E. Taylor[7], Henrik Molina[8], Jedd D. Wolchok[3], Taha Merghoub[3], Luis A. Diaz Jr[3], Omar Abdel-Wahab[3], Robert K. Bradley[1]. *[1]Fred Hutchinson Cancer Center, Seattle, WA,[2]Stanford Medical School, Stanford, CA,[3]Memorial Sloan Kettering Cancer Center, New York, NY,[4]Cleveland Clinic, Cleveland, OH,[5]Icahn School of Medicine at Mount Sinai, New York, NY,[6]University of Notre Dame, Notre Dame, IN,[7]Department of Chemistry & Biochemistry, Notre Dame, IN,[8]The Rockefeller University, New York, NY*

Immune checkpoint blockade therapy has revolutionized cancer care, including the treatment of advanced metastatic disease. However, most patients derive little or no clinical benefit from these therapies and many cancer types are notoriously non-responsive. Motivated by (1) the correlation between tumor neoantigen abundance and anti-tumor immunity and (2) that most cancers are characterized by widespread dysregulation of RNA processing, we reasoned that pharmacologic modulation of RNA splicing might increase cancer cell immunogenicity via the generation of splicing-derived neoantigens. We demonstrated that two compounds which modulate RNA splicing via distinct mechanisms, inhibited tumor growth and enhanced response to immune checkpoint blockade in a manner dependent on host T cells and peptides presented on tumor MHC class I.

Critical for their clinical translatability, therapeutic doses of splicing inhibitors were non-toxic, tolerated by the host immune system, and did not affect T cell activation, proliferation, and anti-cancer killing activities. Mechanistically, splicing modulation induced stereotyped, dose-dependent "splicing failure" — dramatic intron retention, alternative exon skipping, etc. — that was consistent across multiple mouse and human tumor types. By combining RNA-seq-based peptide predictions and mass spectrometry of the MHC I-bound immunopeptidome, we identified drug-induced, splicing-derived peptides that promote the expansion of antigen-specific CD8+ T cells and trigger anti-tumor T cell responses in vivo. These data definitively identify splicing modulation as an untapped source of immunogenic peptides and provide a means to enhance response to checkpoint blockade that is readily translatable to the clinic.

#5743

Reprogramming myeloid cells by JAK inhibition to enhance checkpoint blockade immunotherapy

Jaroslav Zak[1], Isaraphorn Pratumchai[1], Brett S. Marro[1], Kristi L. Marquardt[1], Michael B. A. Oldstone[1], Judith A. Varner[2], Veronika Bachanova[3], John R. Teijaro[1]. *[1]The Scripps Research Institute, La Jolla, CA,[2]Moores Cancer Center, University of California, San Diego, La Jolla, CA,[3]Division of Hematology, Oncology and Transplantation, University of Minnesota, Minneapolis, MN*

Background: Checkpoint inhibitors have achieved a wide adoption for treatment of advanced cancer, but the majority of patients fail to respond. Among the underlying causes are redundant mechanisms driving cytotoxic lymphocyte dysfunction. Motivated by the discovery of JAK inhibitors as hit compounds in a screen for the reversal of T cell exhaustion, this study investigates the hypothesis that JAK inhibition could enhance the efficacy of checkpoint inhibitors.
Methods: Murine immunocompetent models of cancer were utilized (A20, EL4, LLC1, MC38). The combination therapy of systemic treatment with the JAK inhibitor ruxolitinib with anti-PD1 + anti-CTLA4 was evaluated for efficacy and biomarkers compared to checkpoint inhibitors (ICI) alone. Tumor-infiltrating, blood and lymphoid organ immune cells were phenotyped using single-cell transcriptomics, functional assays and flow

cytometry. The combination therapy was clinically tested in an investigator-initiated Phase I/II clinical trial of ruxolitinib with nivolumab in relapsed or refractory Hodgkin lymphoma (NCT03681561). Patients who previously failed to respond to ICI received ruxolitinib for 1 week then nivolumab every 4 weeks concurrent with ruxolitinib twice daily. Peripheral blood was collected at baseline, 1 week after ruxolitinib and 4 weeks after 1st nivolumab dose. Hematologic and transcriptomic analyses were performed on peripheral blood samples.
Results: The ruxolitinib + ICI combination was superior to ICI in 3/4 of the tumor models examined in controlling tumor growth. Tumor sizes were reduced by >50% in the MC38 (mean volume 123.1 vs 283.2 mm^3, ICI + rux vs ICI, respectively, n=9 per group, ANOVA p=0.0094), LLC1 and A20 models (survival hazard ratio 0.24, ICI + rux vs ICI, n=8 per group, p=0.048). Remarkably, we observed a broad shift of tumor monocytes and granulocytes from a suppressive into an immunostimulatory state characterized by the expression of MHC molecules and the ability to stimulate T cell proliferation. Hodgkin lymphoma patients in the ruxolitinib with nivolumab trial exhibited an interim disease control rate of 76% (13/17). Ruxolitinib treatment in these patients did not impair T cell cytokine production but significantly reduced the neutrophil-to-lymphocyte ratio (NLR, mean difference -0.82, n=14, p=0.0023) and the expression of myeloid derived suppressor cell markers in monocytes (normalized enrichment score -1.74, n=14, q<0.001) compared to pre-treatment. The reduction in NLR was significantly greater in complete responders than in progressive disease patients (mean -2.6 vs -0.58, respectively, p=0.023).
Conclusions: The combination of ruxolitinib with ICI was effective in preclinical models of cancer and in a Phase I/II Hodgkin lymphoma clinical trial. Unexpectedly, JAK inhibitor-mediated reprogramming of myeloid cells and the associated enhanced T cell activity may be important for the observed efficacy.

#5744

Decreasing toxicity of immunocytokines by transient and selective inhibition of their intracellular signaling activation

Giulia Rotta[1], Ettore Gilardoni[2], Domenico Ravazza[2], Jacqueline Mock[3], Samuele Cazzamalli[4], Roberto De Luca[1], Emanuele Puca[3], Dario Neri[3], Sheila Dakhel Plaza[1]. [1]*Therapeutic Antibodies, Philochem AG, Otelfingen,*

Switzerland,[2]Bio-MS, Philochem AG, Otelfingen, Switzerland,[3]Philochem AG, Otelfingen, Switzerland,[4]Chemistry, Philochem AG, Otelfingen, Switzerland

The use of cytokine-based therapeutics has traditionally been limited by systemic toxicity, but it is now becoming evident that it may be possible to circumvent this problem in a number of ways. Tumor-targeting antibody-cytokine fusion proteins (also called “immunocytokines”) typically allow dose escalation to therapeutically active regimens as a result of their selective localization at the site of disease (Neri 2019; Helguera, Morrison, and Penichet 2002). Despite the enhancement of the therapeutic index, when the concentration of the payload in blood exceeds a certain threshold, patients may experience dose-limiting immune-related adverse events (irAEs). In most cases, irAEs disappear when the immunocytokine is cleared from circulation (Ko et al. 2004; Spitaleri et al. 2013; Rudman et al. 2011). Here, we describe an innovative approach to mask off-target activity of immunocytokines by transient inhibition of their intracellular signaling cascade. Small molecules are particularly attractive for this application since their serum half-life matches the clearance rate of the immunocytokine from circulation. L19-TNF and L19-IL12 are two clinical-stage antibody-cytokine fusion proteins that display potent activity by triggering the receptor-interacting serine/threonine-protein kinase 1 (RIPK1) and Janus Kinase 2 (JAK2) signaling pathways, respectively (Amin et al. 2018; Hu et al. 2021). In a first study, GSK’963, a potent small molecule inhibitor of RIPK1, was tested in tumor-bearing mice with the aim to reduce acute systemic toxicity associated with TNF signaling. Transient inhibition of RIPK1 allowed the administration of L19-murTNF doses which would otherwise be lethal. The combination with GSK’963 did not affect the selective localization of the immunocytokine to tumors. Moreover, L19-murTNF was still able to induce tumor necrosis and to exert potent anti-cancer activity. In a second study, tumor-bearing mice receiving L19-murIL12 were pretreated with Ruxolitinib, a commercially available JAK2 inhibitor. The addition of Ruxolitinib could significantly improve the tolerability profile of L19-murIL12 without affecting the anti-cancer properties of the immunocytokine. In clinical trials, it has been observed that IL12 treatment can induce cytokine release syndrome and liver damage (Atkins et al. 1997). Our data demonstrate that the pre-treatment with

Ruxolitinib restricted the pro-inflammatory effects of L19-murIL12 to the tumor site, protecting the mice from body weight loss as well as reducing blood cytokine levels and hepatotoxicity. Overall, this preclinical work is of clinical relevance, as patients treated with targeted cytokines could potentially benefit from judicious combinations treatments using small molecule inhibitors.

#5745

Proposing the best MET inhibitor to improve anti-PD-1 efficacy in HCC

Ricardo A. de Azevedo, Broderick Turner, Priyamvada Jayaprakash, Krithikaa Rajkumar Bhanu, Anupallavi Srinivasamani, Brittany Morrow, Michelle Winkler, Shweta Mahendra Hedge, Arthur Liu, Ravaen Slay, Michael A. Curran. *Department of Immunology, The University of Texas MD Anderson Cancer Center, Houston, TX*

Despite recently approved immunotherapy combinations, Hepatocellular carcinoma (HCC) remains among the most therapeutically intractable cancers with a 5-year survival rate of only 18%. Underlying chronic liver disease due to hepatitis B/C infection, alcohol abuse, hemochromatosis, or nonalcoholic steatohepatitis promotes HCC development. Current therapeutic strategies include surgery, radiotherapy and multikinase inhibitors alone or with immune-checkpoint blockade (ICB). In particular, the receptor tyrosine kinase MET and its ligand hepatocyte growth factor (HGF) are known drivers of HCC through promotion of tumor growth, survival, tissue invasion, and angiogenesis. Previously, our collaborators showed that the limited clinical benefit of MET kinase inhibition was partially a result of induced upregulation PD-L1 leading to local T cell suppression. We hypothesized that combining MET inhibition with blockade of the PD-1 immune checkpoint would overcome the limitations of each individual approach and act synergistically to promote HCC tumor regression. We first validated that both MET selective (Capmatinib and Tivantinib) and non-selective (Cabozantinib) inhibitors all induced PD-L1 on HCC cell lines in vitro. Next, we compared Capmatinib and Cabozantinib alone and with PD-1 ICB in vivo in the ICB-sensitive Hepa1-6 and HCA-1 models of HCC. In HCA-1, statistically significant benefit of the MET inhibitor and αPD-1 combination was evident in limitation of

tumor growth and extension of survival. In each case, the Capmatinib combination trended toward better outcomes with PD-1 blockade. Mechanistically, the Capmatinib and αPD-1 combination decreased tumor Treg cells while promoting increased accumulation of activated, non-exhausted, proliferating CD8 T cells. Central memory CD8 T cell frequencies were increased by the combination during the effector phase, and combination treated animals were better protected against subsequent rechallenge than those cured by αPD-1 alone. In the myeloid compartment, M1 macrophage frequencies were increased while PMN-MDSC both decreased in frequency and in Arginase 1 levels. Finally, we studied a serially-passaged, αPD-1 refractory DEN HCC model. Despite lack of efficacy of either component therapy, the MET inhibitor and αPD-1 combination significantly extended survival and inhibited tumor growth. As in the αPD-1 sensitive setting, Capmatinib appeared to offer the most therapeutic benefit with αPD-1. Ongoing studies are focused on characterizing changes mediated by the combination therapy which confer aPD-1 sensitivity to the otherwise refractory DEN HCC tumor microenvironment. Molecular studies are focused on understanding the superior ICB potentiating capacity of Type I MET inhibitors versus the other classes. Given the clinical availability of numerous MET and PDL-1 inhibitors, we hope to inform near-term optimization of MET and αPD-1 clinical trial design for HCC.

#5746

Flexible tumor-specific cytokine and antigen delivery through the T-SIGn vector platform enables effective CAR-T cell therapy against solid tumors

Maria Stella Sasso, Rachel Bergin, Rochelle Lear, Darren Plumb, Manuela Zonca, Eva Vainiute, Meg Snowden, Tae Hyun Jang, Alice Muntzer, Carla C. Cerqueira, Katy West, Samantha Bucktrout, Brian R. Champion.
PsiOxus Therapeutics Ltd, Abingdon, United Kingdom

Efficacy of Chimeric Antigen Receptor (CAR) T cell therapy against solid tumors is hampered by multiple barriers, including tumor-associated immunosuppression, poor CAR-T cell trafficking into solid tumor masses and shortage of highly expressed cancer-specific target antigens. The T-SIGn (Tumor Specific ImmunoGene) platform generates viral vectors that

can produce combinations of transgenes selectively within the tumor microenvironment (TME). T-SIGn is clinically validated for intravenous (i.v.) delivery, enabling vectors to reach primary and metastatic sites to produce their therapeutic payloads specifically in malignant epithelial cells. Using an A549 human tumor xenograft and metastasis model, we previously demonstrated that i.v. administration of a T-SIGn vector encoding IFNα, MIP1α and CD80 results into potentiated CAR-T cell activation and therapy efficacy (Sonzogni et al. 2022). Here, we further evaluated the potential of T-SIGn combination with Cell Therapy by investigating the impact on CAR-T cell activity of vectors encoding different arrays of cytokines and chemokines. Using an *in vivo* A549 model and anti-HER2 CAR-T cells in NSG mice, we demonstrated that T-SIGn vectors can enable effective CAR-T cell therapy against solid tumors by providing diverse localized cytokine/chemokine-mediated T cell boosting, with IL-12-encoding vectors resulting in complete and durable tumor clearance. Furthermore, we explored the use of the T-SIGn platform to encode secreted bispecific "adaptor" molecules able to simultaneously bind to a tumor surface antigen and to a CAR specific for an antigen not naturally expressed by the tumor, allowing the redirection of CAR-T cells against desired tumor types. We designed a vector (NG-1125) encoding an anti-HER2 ScFv_CD19 bispecific construct as a model "adaptor" molecule, together with IFNα and CXCL9, and we showed that this construct can effectively redirect anti-CD19 CAR-T cell against $HER2^{+}CD19^{-}$ tumor cells. *In vitro* X-CELLigence-based cytotoxicity assays demonstrated killing of both $HER2^{+}CD19^{-}$ A549 and SKOV3 cells by anti-CD19 CAR-T cells in presence of vector-derived anti-HER2 ScFv_CD19. Following i.v. NG-1125 dosing of A549 tumor-bearing mice, *ex vivo* flow cytometry analysis of tumor masses revealed binding of the encoded adaptor molecule to both vector-infected and uninfected tumor cells. Furthermore, *in vivo* NG-1125 administration together with anti-CD19 CAR-T cells resulted into increased intra-tumoral densities of transferred T cells. Collectively, these data show the potential of T-SIGn vectors in overcoming solid tumor resistance mechanisms to CAR-T and pave the way for the development of other immunotherapeutics to be expressed within the TME via T-SIGn vectors in combination with CAR or TCR-based therapies.

#5747

A novel combination therapy of arenavirus vectors and PD1-IL2v strongly potentiates tumor specific T cell responses resulting in synergistic anti-tumor efficacy

Judith Strauss[1], Diana Reckendorfer[1], Kimberly Pojar[1], Laura Codarri Deak[2], Valeria Nicolini[2], Roger Sutmuller[2], Christian Klein[2], Pablo Umaña[2], Klaus K. Orlinger[1], Henning Lauterbach[1]. *[1]HOOKIPA Pharma Inc, New York, NY,[2]Roche Innovation Center Zurich, Schlieren, Switzerland*

It is undisputed that CD8 T cells play a critical role in controlling tumor growth and killing tumor cells, and that tumor specific T cells are essential for clinical responses to immune checkpoint inhibitors. Yet, the induction and maintenance of functional tumor antigen specific T cell responses represent still one of the greatest challenges in cancer immunotherapy. Therapeutic cancer vaccines based on engineered arenavirus vectors have been shown preclinically to overcome self-tolerance to tumor associated antigens (TAA) and mount unprecedented T cell responses, both, in preclinical tumor models as well as HPV16+ cancer patients in an ongoing Phase 1/2 trial. The novel PD-1 targeted IL-2 variant (PD1-IL2v) was created to maximize the potency of IL-2R activation of effector T cells while overcoming the toxicities of wildtype IL-2. *Cis* binding of PD1-IL2v to PD-1 and IL-2Rβγ on the same cell was recently shown to promote differentiation of stem-like CD8 T cells into better effectors and was therefore identified as an ideal compound for combination therapies with arenavirus vectors. Combination of vectors encoding tumor associated foreign or self-antigens with PD1-IL2v lead to a massive, up to 60-fold, increase of peripheral tumor specific CD8 T cell numbers compared to vector treatment alone. Notably, frequency of peripheral regulatory T cells was not enhanced by this combination. The massive increase of TAA specific CD8 T cells was associated with synergistic anti-tumor efficacy in two independent tumor models, resulting in longer survival times and up to 60% complete responders. Complete tumor clearance resulted in a stable memory T cell population and protection against tumor re-challenge. Ongoing studies will address modifications of the tumor microenvironment and further characterization of tumor infiltrating T cells upon combination therapy.

These preclinical data establish the combination of arenavirus vectors and PD1-IL2v as a promising next generation cancer immunotherapy.

Novel Preclinical Models for Cancer Immunotherapy

#5188

Interrogating the role of the immune microenvironment in the response of brain metastases to immunotherapy using new preclinical melanoma models

Amélie Lopès[1], Jessica Rappaport[1], Eva Pérez Guijarro[2], Quanyi Chen[3], Emily Wu[2], Isabella Church[2], April Huang[4], Jessica Bridge[5], Sung Chin[5], Cari Smith[5], Charli Gruen[2], Khiem C. Lam[1], Romina E. Araya[1], Antonella Sassano[2], Chi-Ping Day[2], Glenn Merlino[2], Romina S. Goldszmid[1].
[1]Inflammatory Cell Dynamics Section, Laboratory of Integrative Cancer Immunology, CCR, Inflammatory Cell Dynamics Section, Laboratory of Integrative Cancer Immunology, Center for Cancer Research, National Cancer Institute, Bethesda, MD,[2]Laboratory of Cancer Biology and Genetics, CCR, Laboratory of Cancer Biology and Genetics, Center for Cancer Research, National Cancer Institute, Bethesda, MD,[3]Inflammatory Cell Dynamics Section, Laboratory of Integrative Cancer Immunology, CCR, Inflammatory Cell Dynamics Section, Laboratory of Integrative Cancer Immunology, Center for Cancer Research, National Cancer Institute and Kelly Government Solutions, Bethesda, MD,[4]Inflammatory Cell Dynamics Section, Laboratory of Integrative Cancer Immunology, CCR, Inflammatory Cell Dynamics Section, Laboratory of Integrative Cancer Immunology, Center for Cancer Research, National Cancer Institute and Leidos biomedical research, Bethesda, MD,[5]Frederick National Laboratory for Cancer Research, National Cancer Institute, Frederick, MD

Brain metastases (BrM) remain an intractable, deadly complication for advanced melanoma patients and efficient therapeutic strategies are desperately needed. The tumor microenvironment (TME) plays an important role in response to therapy. However, studies addressing the contribution of the TME to therapy efficacy for BrM are lacking, mostly due to limited access to human samples and scarcity of appropriate preclinical models. Here, we describe two novel isogenic immunocompetent BrM models generated by intracardiac injection of UV-

induced mouse melanoma cell lines, representative of mutant-RAS human melanoma subtypes. We used these models to test immune checkpoint blockade (ICB) therapy and to interrogate the role of the TME in therapeutic efficacy. To evaluate response, we developed and applied a new machine-learning method to quantify metastatic burden. We investigated the TME by high-parametric flow cytometry and single-cell RNA sequencing (scRNA-seq). We showed that the models have distinct metastatic behaviors, with BR1 being mostly brain tropic and BR3 displaying widespread metastases. Notably, BR1 BrM were sensitive to ICB with a better response to anti-PD-L1/anti-CTLA-4 combination therapy as compared to monotherapies. In contrast, BR3 BrM were resistant to both mono- and combination therapies. Interestingly, we found that ICB efficacy on extracranial BR3 metastases is organ-dependent. Characterization of the BrM immune microenvironment before and after treatment revealed dramatic differences between the models. Untreated BR1 BrM showed significant recruitment of T cells, dendritic cells, and natural killer cells, while neutrophils were enriched in untreated ICB-resistant BR3 BrM. Moreover, we uncovered phenotypically distinct microglia populations exclusively present in ICB-sensitive BR1 BrM that positively correlated with T cell infiltration. Consistent with this finding, scRNA-seq showed upregulation of genes encoding for T cell-attracting chemokines and antigen presentation uniquely in the BR1-associated microglia. Post-treatment analysis of the brain TME highlighted beneficial changes induced by ICB in the responsive BR1 model, including increased recruitment of CD8 T cells with an activated phenotype, while a mild recruitment of exhausted T cells was observed in the resistant BR3 model. Altogether, our data emphasize the importance of interrogating the BrM TME to understand therapeutic response. Our unique BrM models, mirroring the diversity of ICB response observed in patients, provide a robust platform for the much-needed mechanistic studies to optimize BrM therapy. Deciphering the contribution of the newly identified BR1 BrM-associated microglia to ICB efficacy will be crucial to the identification of novel therapeutic targets.

#5189

Comparisons of Rituximab and CD19xCD3 BiTE antitumor response across multiple humanized NSG strains engrafted with human hematopoietic stem cells

Won Yeong Kang, Guoxiang Yang, Ilian Radichev, Li-Chin Yao, Mingshan Cheng, James G. Keck. *Innovation and Product Development, The Jackson Laboratory Sacramento, Sacramento, CA*

Humanized NSG mice engrafted with hematopoietic stem cells (HSCs) is a well-known in vivo platform for reconstitution of human immune system in a mouse host. In this study we tried to dissect the role of various human cytokines in the generation of the human immune system, expansion of human B cell lymphoma cells, and drug response to two anti-cancer therapies - Rituximab and CD19XCD3 BiTE (Bispecific T-cell Engager). To exclude donor variabilities, we first humanized five NSG-based, human cytokine-transgenic mouse strains (NSG, NSG-IL15, NSG-SGM3, NSG-SGM3-IL15, and NSG-FLT3L) with HSCs from one donor (0084). We found that tumor growth was enhanced in NSG-SGM3 mice when compared to NSG mice. In contrast, IL15 expression suppressed tumor growth in NSG-IL15 and NSG-SGM3-IL15 mice. Furthermore, NK cell frequencies in blood are higher in NSG-IL15 and NSG-SGM3-IL15 than in other strains. suggesting that NK cell-mediated cytotoxicity is involved in suppression of tumor cell growth in the strains expressing human IL-15. Rituximab treatment resulted in tumor growth inhibition and significant B cell depletions across NSG-IL15, NSG-SGM3, and NSG-SGM3-IL15 mice engrafted with 0084 PBMC. We also observed a donor variability of tumor growth rates in NSG-SGM3-IL15 mice engrafted with donors 0084, 0662A, and 0733. The tumor growth in NSG-SGM3-IL15 mice engrafted with 0084 PBMC was significantly slower than the one in mice engrafted with the other two donors (0084 vs. 0662A, P=0.002; 0084 vs. 0733, P=0.004 on day 21); interestingly, this strain of mice exhibited higher frequencies of $CD8^+$ T cells and lower frequencies of NK cells. Next, we tested CD19XCD3 BiTE treatment in multiple NSG strains engrafted with HSCs from different donors. The BiTE administration inhibited Raji tumor growth and significantly depleted B cells in all tested strains as NSG-SGM3-IL15 showed highest frequencies of NK cells and $CD8^+$ T cells. The combination of Rituximab and BiTE showed even better tumor inhibition efficacy. In conclusion, regardless of the donor and strain variations in tumor growth and human immune cell subset development, the administrations of rituximab or BiTE significantly and consistently inhibited tumor growth and depleted peripheral B cells across all mouse strains. These results

indicate that utilizing a comprehensive humanized mouse platform could drive more impactful conclusions in terms of evaluating the anti-tumor efficacy of immune therapies.

#5190

Systematic immune-profiling of immune-deficient mouse models: A rational to select ideal host for tumor implantation

Hervé Luche[1], Lillia Hadjem[1], Marielle Mello[1], Priscilla Canavese[1], Fabien Angelis[1], Anais Joachim[2], Sylvie Bouilly[3], Frederic Guinut[3], Frederic Fiore[1], Bernard Malissen[2], Ana Zarubica[1], Erwan Corcuff[3]. *[1]Immuno-Phenotyping Module, CIPHE, Marseille, France,[2]Immunomics, JC Discovery, Marseille, France,[3]Janvier labs, Laval, France*

Preclinical tumor oncology research relies historically on the analysis of mouse or human tumor cell lines implanted onto severely immune-deficient mouse models carrying nude, SCID or Rag mutations on different genetical background (C57Bl/6N, BalbC, NMRI, CB17 or NOD). These lines harbor defects in several leukocyte lineages among which Tc, Bc and NKc might be affected. Humanized mice are emerging models that have been transplanted with human cells or tissues (and/or equipped with human transgenes). Currently, the most advanced strains are the nonobese diabetic, severe combined immunodeficiency (NOD-SCID) mouse with complete disruptions in the interleukin-2 (IL-2) common γ-chain (IL2R γ null) receptor (NSG) and BALB/c $Rag2^{-/-}$ IL2R γ null $Sirpa^{NOD}$ mice (BRGS).[1] Juvenile chimera NSG or BRGS are reconstituted with hematopoietic progenitor cell (HPCs) from human cord blood yielding robust engraftment of a human immune system (HIS).. Recent work showing the binding of human IgG4 to mouse FcgR receptor reducing clinical efficacy of therapeutic antibodies highlights the need to characterize extensively the residual immune system present in these models prior humanization in order to precisely evaluate immunotherapies. In other to fulfill this task, we genetically modified the mouse genome introducing mutations involved in Tc, Bc and NKc development. We then immuno-phenotyped over 20 lines of mouse mutants produced from the same animal house to minimize the impact of microbiota on innate immune cell populations. High content cytometry analysis of BM, spleen, thymus and peripheral blood was performed in a standardized manner. The resource obtained of these

immunotypes was used to highlight similarities and differences among these lines across several genetical background. This work has shown instrumental in selecting the most appropriate model to use for humanization followed before tumor implantation.

#5191

Modeling age-related changes in the tumor microenvironment in an orthotopic immunocompetent murine pancreatic cancer model - a novel approach

Morgan M. Green, Tara Fujimoto, Cullen Taniguchi, Natalie Fowlkes. *UT MD Anderson Cancer Center, Houston, TX*

Pancreatic cancer is the third leading cause of cancer-related deaths in the U.S. and is most frequently diagnosed between the ages of 65-74 years. Only 11.5% of patients are expected to survive 5 years after diagnosis. There is extensive evidence that tumor microenvironment (TME) plays a critical role in cancer progression and metastasis. Despite the fact that most patients are diagnosed over the age of 60, most preclinical murine tumor models utilize young, healthy, adolescent mice, failing to account for structural and/or functional changes in stroma and immune cells that occur in tissues over time and contribute to tumor progression. Marked differences in lifespan between mice and humans preclude natural development of many age-related physiologic changes in mice that occur in humans over the course of decades. We performed a pilot study to test our hypothesis that KPC pancreatic tumors grown orthotopically in the pancreas of genetically engineered, C57BL/6-Tg (LMNA*G608G) HClns/J mice, a model of Hutchinson-Gilford progeria syndrome with features of accelerated aging, would have altered tumor growth in comparison to tumors in age-matched wild type controls. We found that tumor growth in LMNA mice outpaced that of WT mice. Quantitative digital image analysis showed significantly reduced intratumoral infiltration of CD45+ leukocytes in LMNA mice in comparison to WT ($p=0.0098$). There was a significant reduction in tumor-infiltrating CD3+ T cells ($p=0.038$) and F4/80+ macrophages ($p=0.0102$). Our data supports the hypothesis that functional, age-related, immune and/or stromal changes in the TME impact pancreatic tumor growth and progression. Innovative strategies that better model age-

related changes in the TME may better recapitulate the aggressive course of pancreatic cancer in aged patients.

#5192

NCG-MHC-dKO mice: an excellent model for PBMC reconstitution and pharmacodynamic evaluation in the absence of GvHD

Huiyi Wang[1], Jun Xing[1], Jialu Fan[1], Huanhuan Hou[1], Santi Suryani Chen[2], Zhiying Li[2], Mark Wade Moore[2], Jing Zhao[1], Xiang Gao[1], Cunxiang Ju[1].
[1]GemPharmatech Co., Ltd., Nanjing, China,[2]GemPharmatech LLC., La Jolla, CA

Human immune cell reconstitution (PBMC or $CD34^+$ hematopoietic stem cell; HSC) is commonly performed in immunodeficient mouse strains such as NCG, NSG, or NOG. The use of PBMC is preferred for multiple reasons, including faster engraftment, lower cost, and the presence of mature immune cell populations. Although there are donor-to-donor variations in GvHD occurrence, and specific donors can be screened, the symptoms of GvHD typically occur within 4 weeks. GvHD significantly limits the study window required to evaluate the efficacy of therapeutic agents, such as cancer immunotherapies.

GvHD is an immune reaction triggered mainly by donor T cells identifying the mouse MHC class I and class II as foreign and attacking the host cells and organs. Deletion of β2m (NCG- β2m-KO) reduces the occurrence of GvHD; however, β2m is not only in the MHC class I subunit but also in the FcRn subunit, of which deletion shortens the half-life of IgG, making it unsuitable for IgG antibody agent evaluation. In addition, the deletion of MHC class I or class II alone results in an imbalanced CD4/CD8 ratio. To solve these problems, we developed the NCG-MHC-dKO mouse model by knocking out the *H2K1, H2D1,* and *H2Ab1* genes. Compared with the existing NCG- β2m-KO or other β2m null mouse models, the NCG-MHC-dKO significantly prolonged survival, reduced GvHD occurrence, and did not affect the CD4/CD8 ratio when reconstituted with PBMC. Furthermore, treatment with anti-PD-L1 antibodies significantly inhibited MDA-MB-231 tumor cell growth in PBMC-reconstituted NCG-MHC-dKO mice, similar to NCG mice. Based on our preliminary data, the NCG-MHC-dKO mouse is a promising model for antibody and cell therapy agent evaluation, assessing

treatment-related cytokine release syndrome, and evaluating long-term toxicities of cell therapies.

#5193

Assessing the efficacy of immune checkpoint blockade as part of a combination therapy in a zebrafish model of rhabdomyosarcoma

Madeline Fritzke, Andrea Largent, Eleanor Chen. *Univ. of Washington School of Medicine, Seattle, WA*

Rhabdomyosarcoma (RMS) is a rare and devastating pediatric soft tissue cancer. There is urgent need to identify more effective therapy options for children suffering from RMS. Immune checkpoint blockade (ICB) has shown promise in several sarcoma types including RMS. In some cancer types, ICB shows enhanced efficacy in combination with a chemotherapeutic agent or an inhibitor against the epigenetic modifiers. Selective chemotherapeutic agents and epigenetic inhibitors (e.g. histone deacetylase inhibitors) have also been shown to increase tumor immunogenicity and sensitize tumor cell response to immune checkpoint inhibitors. However, it remains to be further investigated in RMS how chemotherapy and epigenetic inhibitors modulate immune cell landscape and function and whether the efficacy of ICB combined with either a chemotherapeutic agent or an epigenetic inhibitor is enhanced compared to ICB monotherapy. There is currently no tractable mammalian model for assessing the efficacy of immunotherapy in RMS. Taking advantage of the conserved immune and cancer biology, short tumor onset, high-throughput capability of the zebrafish RMS model, our ongoing research is assessing 1) the efficacy of ICB combined with either a chemotherapeutic agent or an epigenetic inhibitor (histone deacetylases [HDACs] or DNA methyltransferases [DNMTs]) compared to ICB monotherapy on inhibiting RMS tumor growth; 2) effects of chemotherapy and epigenetic inhibition on the make-up and function of tumor-infiltrating immune cells. Our preliminary data so far showed that treatment of zebrafish RMS tumors with the combination of the standard-of-care chemotherapeutic agent, temozolomide, and the immune checkpoint inhibitor, nivolumab, showed increased T cell infiltration. By expression profiling, both temozolomide and nivolumab decreased expression levels of markers for immune checkpoint (pdl1, havcr2) and regulatory T cells (foxp3a) and increased

expression levels of markers for inflammatory response (tnfa and infg1). By developing an immune-competent animal model for large-scale testing of important immunotherapy targets and characterizing the immune cell types in the tumor microenvironment of RMS in response to therapy, our research will establish the zebrafish model as a pre-clinical screening tool for testing promising immunotherapeutic agents *in vivo*, which will facilitate the process of prioritizing promising immunotherapy targets for testing in pre-clinical models and clinical trials and in turn provide therapeutic benefits to children with RMS.

#5194

Humanized PD-1 knock-in mice as a model system for combination therapies with human specific PD-1 therapeutics

Philipp Metzger[1], Fabiane Sônega[2], Hervé Berthomme[2], Cynthia Obodozie[1], Holger Weber[1]. *[1]Reaction Biology Europe GmbH, Freiburg, Germany,[2]genOway, Lyon, France*

Checkpoint inhibitor treatment has become a common therapy for various cancer types. As an escape mechanism, tumor cells express PD-L1 on their surface, as a ligand for PD-1 with players of the immune system (such as T cells), aimed at preventing the immune system from exerting its anti-tumour activities. Antibodies blocking the PD-L1/PD-1 interaction have emerged as front-line treatments for various oncological indications. Several anti-PD-L1 and anti-PD-1 therapeutics are already approved and in clinical use. For preclinical testing of such human specific antibodies, syngeneic tumour models are of limited use due to the limited cross-specificity of such antibodies, giving rise to the development of humanized mouse models in which combination therapies testing new drugs with already clinically approved human checkpoint inhibitors addressing human specific targets can be evaluated.
The anti-tumor efficacies of pembrolizumab (Keytruda) a human specific anti-hPD-1 checkpoint inhibitor and the mouse specific anti-mPD-1 counterpart (clone RPMI1-14) were tested in C57BL/6 wildtype and humanized hPD-1 C57BL/6 mice engrafted with syngeneic MC38-CEA colorectal carcinoma cells. The MC38-CEA tumor cells were implanted into the mammary fat pad (subQperiorTM), a procedure that prevents tumor ulceration and leads to a more homogenous tumor growth compared to

subcutaneous implantation. Treatment with pembrolizumab extended the survival of tumor-bearing human PD-1 C57BL/6 mice significantly, whereas no effect in C57BL/6 wildtype mice was observed, in line with the reported specificity of Keytruda towards the human version of PD-1. Further supporting this finding, the application of the anti-mPD-1 antibody led to a prolonged survival of C57BL/6 mice with no life extension of hPD-1 C57BL/6 mice.
The validation of the humanized subQperior™ platform was further complemented by conducting flow cytometry analysis of intra-tumoral immune populations present in tumor tissues at 7 days post-treatment. Two staining panels were executed: a well-established and validated 17 marker staining allowing to quantify the frequency of all major immune cell populations and a staining panel addressing the activity of T and NK cells after ex vivo stimulation with PMA/Ionomycin. An increased activity of CD8+ T cells and NK cells was observed as major players in the response to treatment with these anti-PD-1 antibodies.
In summary, the humanized subQperior™ platform using hPD-1 C57BL/6 mice is a suitable tool to evaluate novel cancer therapies in combination with human specific anti-PD-1 therapeutics and tumor ulceration was completely prevented by subQperior implantation of the tumor cells.

#5195
BNDG B2m KO plus mouse model is a powerful tool for immunotherapy
Hongmei Jiang, Jianqiu Xiao, Travis Rothrock. *Inotiv/Envigo, St. Louis, MO*

The B-NDG (*B*iocyotgen; *N*OD; *D*NAPK null; IL2r*g* knockout) mouse model was developed to be an ideal testing platform for anti-tumor therapies in Cell-Line and Patient Derived Xenograft Models (CDX and PDX respectively). B-NDG mice exhibit several notable advantages over classical NOD-*scid* mice, including increased life span, NK cell deletion, and significantly improved xenograft efficiency. However, like the NOD-*scid* mice, the utility of B-NDG mice in long-term studies is severely limited by a high incidence of severe and early-onset GvHD (*G*raft *v*ersus *H*ost *D*isease) - limiting experimental durations to as little as 30 days. To reduce the incidence and severity of GvHD in B-NDG mice, Biocytogen

developed the B-NDG *B2m* KO plus mice. B-NDG B2m KO plus mice was generated using Cas9 approach. Specifically, endogenous mouse *B2m* was deleted, while *B2m* cDNA was fused with *Fcgrt* . MHC Class I and Class II expressions, and immune markers were verified by flow cytometry. Concentration of i.v. administered human IgG was quantified by ELISA. CDX models were generated, and antitumor therapies were administered using established protocols described below. Compared with NOD-*scid* and B-NDG mice, B-NDG B2m KO plus mice showed undetectable MHC Class I expression in all tested tissues, without compromising MHC Class II expression. Moreover, no significant change in immune profiles or IgG turnover was detected, demonstrating highly targeted disruption of MHC Class I expression in B-NDG B2m KO plus mice. In the human PBMC-induced GvHD model, B-NDG B2m KO plus mice showed significantly improved survival, delayed onset and reduced clinical severity throughout the course of the model. Compared with B-NDG mice, B-NDG B2m KO plus mice exhibits significantly prolonged usefulness, demonstrating utility for up to 50 days after engraftment. To demonstrate the advantages of our B-NDG B2m KO plus mouse model, we conducted two proof-of concept studies that are often limited by GvHD. In the first study, B-NDG B2m KO plus mice were engrafted with human PBMCs and tumorigenic RKO cells on Day 0 and 14 respectively, treated with either vehicle or pembrolizumab and ipilimumab on Day 20, and observed until Day 48. Pembro/ipi treatment significantly inhibited tumor growth. In the second study, B-NDG B2m KO plus mice were engrafted with tumorigenic human NCI-H226 cells on Day 0, treated with either vehicle or CAR-T cells (5E5) once tumor size reached ~150 mm^3 (around Day 20), and observed until Day 56. CAR-T treatment significantly suppressed tumor growth. Together, these studies demonstrated that the B-NDG B2m KO plus mouse model is a powerful tool for extended term anti-tumor studies, especially for studies involving immuno- and CAR-T therapies.

#5196

Novel humanized CD36 mouse model for therapeutic studies

Linlin Wang[1], Chang Liu[1], Rebecca Soto[2], Chengzhang Shang[1], Qingcong Lin[2]. *[1]Biocytogen Pharmaceuticals (Beijing) Co., Ltd., Beijing, China,[2]Biocytogen Boston Corp, Wakefield, MA*

Activation of oncogenic signaling pathways can be mediated by various transporters on tumor cells that facilitate trafficking of lipids. CD36 has been identified as a fatty acid transporter and participates in tumor growth and drug resistance. To explore potential therapeutic strategies targeting CD36, we generated a human *CD36* knockout/knock-in *in situ* (B-hCD36) mouse model to evaluate the efficacy of anti-human CD36 antibodies. We first confirmed human CD36 gene and protein expression in B-hCD36 mice by RT-PCR and flow cytometry, respectively. We next observed that the overall development, differentiation, and distribution of splenic, blood and lymph node immune cells were similar between wild-type C57BL/6 and B-hCD36 mice. Lastly, *in vivo* efficacy studies using anti-human CD36 antibodies alone or in combination with anti-mouse PD-1 antibodies, were effective in controlling MC38 tumor growth in B-hCD36 mice. Our data demonstrates that B-hCD36 mice are a powerful preclinical model for *in vivo* efficacy evaluation of anti-human CD36 antibodies.

#5197

NCG-hIL2 mice: a novel model to support the development of T regulatory and NK cells

Xinxin Zhang[1], Meirong Wu[1], Huiyi Wang[1], Weiwei Yu[1], Fang Zhu[1], Jianming Xu[1], Hongyan Sun[1], Hongyu Wang[1], Cunxiang Ju[1], Santi Suryani Chen[2], Zhiying Li[2], Mark Wade Moore[2], Jing Zhao[1], Xiang Gao[1].
[1]Gempharmatech Co., Ltd., Nanjing, China,[2]GemPharmatech LLC., La Jolla, CA

Interleukin 2 is a key molecule that promotes the expansion and activation of lymphocytes, including T regulatory cells (Tregs) and natural killer (NK) cells. Tregs are specialized subpopulation of T cells that suppress the immune response by inhibiting T cell proliferation and cytokine production. NK cells are the predominant innate immune subset that mediates anti-tumor and anti-viral responses. Both Tregs and NK cells are two critical immune cells that play an important role in cancer immunotherapy, however, there is a lack of models that supports the in vivo status of these two immune subsets. To address this, we developed a severe immunodeficient mouse model, NOD/ShiLtJGpt-Prkdc^{em26Cd52}Il2rg^{em26Cd22}/Gpt (NCG-hIL2), by knocking in the human IL-2 gene on the NCG background. The ability of this model to support Treg

and NK cells was then compared to NCG and tested with the reconstitution of human peripheral blood mononuclear cells (PBMC) and human hematopoietic stem cells (HSC).
In the PBMC engrafted mice, the presence of IL-2 supported the development of T cells, especially the Tregs, with 53.74% in Tregs in NCG-IL2 compared to 4.81% in NCG mice (test at 2 weeks of reconstruction). Similarly, the NK cells are also supported with those cohort engrafted with human HSC (91.63% in NK cells in NCG-IL2 compared to 0.53% in NCG mice, test at 10 weeks of reconstruction). Notably, reconstituted NK cells expressed various NK receptors such as NKp30, NKp44, NKp46, NKG2D, and CD94 in NCG-IL2 mice. They produced comparable levels of granzyme when compared with human peripheral blood-derived NK cells, and a considerable amount of perforin protein was detected in the plasma of huHSC-NCG-hIL2 mice.
In conclusion, compared with NCG mice, humanized NCG-hIL2 mice can reconstruct more abundant immune cells and have a wider application in anti-tumor research. It is an ideal model for the preclinical study of anti-tumor therapeutics.

#5199

B7-H3 & PD-L1 double-humanized BALB/c mouse: a novel animal model for preclinical studies of human B7-H3 antibodies or bispecific antibodies

Shiying Guo[1], Lingyu Song[1], Xin Qin[1], Jianming Xu[1], Hongyan Sun[1], Cunxiang Ju[1], Hongyu Wang[1], Santi Suryani Chen[2], Zhiying Li[2], Mark Wade Moore[2], Jing Zhao[1], Xiang Gao[1]. *[1]Gempharmatech Co., Ltd., Nanjing, China,[2]GemPharmatech LLC., La Jolla, CA*

Immune checkpoint molecule B7-H3, also known as CD276, is a member of the B7-CD28 family of immunomodulatory proteins. It is a type I membrane protein with sequence similarities to the extracellular domain of programmed death-ligand 1 (PD-L1).
B7-H3 is highly expressed in most human cancers, but has limited distribution in normal tissues, remaining elusive of its receptor. Due to its promising safety as a dominant tumor target, various strategies have been developed to modulate the effect of B7-H3 via monoclonal antibodies, bispecific antibodies, ADC, or CAR-T. To study the effect of these

therapies in an immunocompetent mouse model, we established a double humanized B7-H3 and PD-L1 mouse model on BALB/c background (BALB/c-hB7-H3/hPD-L1). In this model, the extracellular domain of murine fragments was replaced by the human counterparts while the trans-membrane and cytoplasmic domain were kept intact. When engrafted with CT26 colon cancer cells, which stably overexpress human B7-H3 and PD-L1 while endogenous murine counterparts were knocked out, the tumor growth was inhibited certain degree by anti-B7-H3 antibody (8H9 Biosimilar, 20mpk, TGI=18.56%) treatment while inhibited significantly after the monotherapy of anti-PD-L1 (Tecentriq, 3 mpk, TGI=55.89%, $p<0.001$). The same dosage combination of anti-B7-H3 and anti-PD-L1 had a significant inhibition on tumor growth (TGI=76.85%, $p<0.001$), and had a synergistic effect (CDI<0.7) compared with the monotherapy. Analysis of tumor-infiltrating lymphocytes (TILs) at the end of the efficacy study showed that the proportion of CD45+ immune cells was significantly increased in all of the treated groups. The NK cells were significantly increased and the Treg cells were significantly decreased especially in the combined treatment group.
Based on the above, the B7-H3 and PD-L1 double humanized mouse model is suitable for the pre-clinical evaluation of mono or combined immune checkpoint blockade with anti-human B7-H3 and PD-L1 therapy.

#5200

Novel Immuno-Oncology drugs evaluation by humanised immune cells and cancer co-inoculated models

Bin Xie[1], Xin Hou[1], Hanglu Chen[1], Pengfei Yang[1], Yanbin Zhou[1], Danyi Wen[2]. *[1]R&D, Shanghai LIDE Biotech Co., Ltd., Shanghai, China,[2]Shanghai LIDE Biotech Co., Ltd., Shanghai, China*

Currently more and more immunotherapeutic drugs and engineered cells have been developed to use human immune system against cancer. While humanized peripheral blood mononuclear cell reconstitution in immune deficient mice is a forward-straight model for evaluating therapeutic antibodies, this conventional model has several drawbacks to hinder its widespread use, including the graft-versus-host-disease happened after one month of reconstitution, insufficient immune cell infiltration from reconstituted circulatory system and hardly retention of functional innate

immune cells, such as macrophages and nature killer cells. To overcome this, LIDE has developed a specific human immune cell and cancer cell co-inoculation model. Cancer-priming PBMC and/or its derivates were well mixed with the fresh cancer cells in MatriGel, co-transferring into NCG mice to form a relatively "hot tumor" tissue for immunotherapy, including drugs targeting T cells, dendritic cells and macrophages. Additionally, we also take advantage of human IL15 transgenic mice to study the function of ex vivo expanded NK cells. This novel method has successfully helped evaluate biological function of immune checkpoint blockers and immune agonists in multiple cancers, such as melanoma, breast cancer, lung cancer, hepatocellular carcinoma and ovarian cancer.

#5201

TNFR2 humanized mice: an ideal model for studying anti-TNFR2 antibodies

Huiyi Wang[1], Ying Li[1], Mingkun Zhang[1], Xu Su[1], Santi Suryani Chen[2], Zhiying Li[2], Mark Wade Moore[2], Jing Zhao[1], Xiang Gao[1], Cunxiang Ju[1].
[1]GemPharmatech Co., Ltd., Nanjing, China,[2]GemPharmatech LLC., La Jolla, CA

Tumor necrosis factor (TNF) receptor 2 (TNFR2) is mainly expressed on the surface of regulatory T cells (Tregs) and CD8+ T cells, which can stimulate the proliferation of these cells through NF-kB activation. TNFR2 is also highly expressed on the surface of various human tumors, such as colorectal cancer and lung cancer. Therefore, a TNFR2 antagonist blocking the binding of TNFR2 to its ligand that targets TNFR2+ tumor-infiltrating Tregs can directly enhance the killing ability of effector T cells (Teff) against TNFR2-expressing tumors. Many pharmaceutical and biotech companies have lined up TNFR2-targeting drugs, and most TNFR2 antibodies related research is in the early preclinical/clinical stage.
We established a humanized TNFR2 (hTNFR2) genetically engineered mouse model on the BALB/c background, in which the extracellular domain of the mouse TNFR2 was replaced with its human counterpart, and the murine transmembrane and cytoplasmic domain kept intact. The hTNFR2 chimeric protein is mainly expressed on Teff and Treg cells in BALB/c-hTNFR2 and BALB/c-hPD1/hPDL1/hTNFR2 mice, which is similar to mouse TNFR2 protein expression profiles in wild-type mice. Our

data showed that anti-TNFR2 antibodies could significantly inhibit tumor growth in BALB/c-hTNFR2 mice bearing CT26 tumor cells or BALB/c-hTNFR2 mice bearing CT26-hTNFR2 tumors. Furthermore, within the tumor-infiltrating lymphocytes, there was a reduction in Tregs cells and an increase in cytotoxic CD8 T cells, which accurately mimics the mechanism of action of anti-TNFR2 antibodies.
In conclusion, BALB/c-hTNFR2 and BALB/c-hPD1/hPDL1/hTNFR2 mice are ideal models for studying the efficacy and pharmacodynamics of anti-TNFR2 antibodies as a single agent or in combination with anti-PD-1/PD-L1 therapies.

#5202

NCG-M humanized mice: an excellent model for human immune reconstitution of myeloid lineages

Huiyi Wang[1], Jialu Fan[1], Shiying Guo[1], Mingkun Zhang[1], Shuai Li[1], Santi Suryani Chen[2], Zhiying Li[2], Mark Wade Moore[2], Jing Zhao[1], Xiang Gao[1], Cunxiang Ju[1]. *[1]GemPharmatech Co., Ltd., Nanjing, China,[2]GemPharmatech LLC., La Jolla, CA*

Severe immunodeficient mice engrafted with human hematopoietic stem cells (HSC) have been extensively used in immuno-oncology related studies to evaluate the efficacy of cancer therapies. However, because of species differences, murine cytokines provide limited support to human immune cells, thus immunodeficient mice have limited engraftment of human immune cells. Increasing evidence has shown that myeloid cells, especially macrophages and dendritic cells, are critical for the induction of anti-tumor immunity. We developed a mouse model, NCG-M, that can support human T, B, NK and myeloid cells such that in vivo evaluation of agents that require the interplay between these immune cells can be examined. This model was genetically engineered on the severe immunodeficient strain NCG and can produce human granulocyte/macrophage colony stimulating factor 2 (GM-CSF, also known as CSF2), interleukin-3 (IL-3) and stem cell factor (SCF, also known as KITLG). Upon human $CD34^+$ HSC cell engraftment, increased myeloid lineage cells, such as granulocytes, monocytes, neutrophils, macrophages, and dendritic cells, were observed in the NCG-M cohort compared to NCG mice. The NCG-M mouse also supports the development of human T cells, and preliminary data showed

increased B and NK cells. The NCG-M is an appropriate mouse model for studying the efficacy of therapeutic agents that require human T cells and myeloid cells.

#5203

Naturally occurring colorectal cancer in rhesus macaques as model for human cancer immunotherapy: a first report on pembrolizumab ± radiotherapy

Simon Deycmar[1], George W. Schaaf[1], Brendan J. Johnson[1], J. Daniel Bourland[2], James D. Ververs[2], Christopher T. Whitlow[3], J. Mark Cline[1].
[1]Department of Pathology, Wake Forest University School of Medicine, Winston-Salem, NC,[2]Department of Radiation Oncology, Wake Forest University School of Medicine, Winston-Salem, NC,[3]Department of Radiology, Wake Forest University School of Medicine, Winston-Salem, NC

Introduction: Rhesus macaques share extensive similarities with humans including immune cell populations, regulatory mechanisms, and targets for cancer immunotherapy but also naturally develop cancers at similar life stages. Hence, treating rhesus macaques with spontaneous tumors bears enormous potential as model for human cancer immunotherapy.
Material and Methods: We identified 2 female rhesus macaques, 23.6y (CRC_1) and 20.3y (CRC_2) old with naturally occurring colorectal cancer by imaging and clinical assessments. We collected a pre-treatment tumor biopsy in CRC_1 prior to treatment with 8 Gy intensity-modulated radiotherapy (IMRT) to the proximal portion of the tumor and 2 mg/kg i.v. pembrolizumab. The second candidate (CRC_2) was not tumor biopsy-eligible due to anemia and was treated with pembrolizumab alone. We collected blood and peripheral lymph nodes (LNs) pre- and on-treatment and complete tissue collection was performed at the 3w time point including tumor-adjacent mesenteric LNs. Follow-up assessments include IHC (e.g. CD3, CD20, IBA1), flow cytometry, cytokine assessment in plasma, and transcriptomics of LN and tumor samples.
Results and Discussions: Imaging revealed focal thickening of the proximal colonic wall with disrupted architecture in CRC_1 and focal colonic thickening and an enlarged adjacent LN in CRC_2. Both tumors displayed mismatch repair-deficiency (MLH1 & PMS2 loss) and a drastic reduction in infiltrating CD3 cells in neoplastic areas compared to adjacent healthy

colon. On treatment, tumor-associated LNs demonstrated a mild increase in CD20+ cells in the medullary sinuses of both patients and increased follicle numbers with normal follicular architecture in reference to peripheral LNs. In both patients there was an increased number of tertiary lymphoid structures (TLS) surrounding the tumors, predominately populated with CD20+ cells and with Ki67+ germinal centers, profoundly so in CRC_2. Moreover, IBA1+ cells abundantly infiltrated both tumors but showed a higher aggregation within the stromal elements of the neoplasms. A gradient of histologic differentiation was evident in CRC_1 and coincided with a reduction of TLS, IBA1+ cell abundance, and CD3+ cell infiltration in those areas which were poorly differentiated. Within the irradiated tumor of CRC_1, there were abundant apoptotic cells which stained positively with cleaved caspase 3 at the 3w time point. Circulating blood counts as preliminary peripheral read-out revealed a reduction in circulating lymphocytes in both patients beginning at 3d (CRC_1) resp. 6d (CRC_2) and a sharp increase in monocytes at 3d in unirradiated patient CRC_2. Conclusion: The immunological and tumoral response to pembrolizumab and radiotherapy matches the clinical response in humans and enables an unprecedented examination of the peripheral and local lymph node response.

#5204

Preclinical models for translational immuno-oncology research: Rare patient-derived xenografts on humanized mice

Maria Stecklum[1], Annika Wulf-Goldenberg[1], Bernadette Brzezicha[1], Wolfgang Walther[2], Jens Hoffmann[1]. *[1]EPO GmbH, Berlin, Germany,[2]Charité Universitätsmedizin, Berlin, Germany*

Background

The preclinical evaluation of novel immune checkpoint modulators is dependent on models with functional human immune cells. In previous experiments, we have demonstrated, that we can use either peripheral blood mononuclear cells (PBMC), subset of immune cells like NK cells or hematopoietic stem cells (HSC) to establish a humanized immune system on highly immunodeficient 1st and 2nd generation NOG mice with functional T-, B-, and NK cells, as well as monocytes and dendritic cells. Furthermore, we determined PD-L1 expression as a predictive marker and

target for immunotherapy on different patient-derived xenografts (PDX). By co-transplantation of rare PDX, like leukemia or Nuclear-protein-in-testis (NUT) carcinoma , we successfully generated a fully human tumor-immune-cell model in mice. Finally, we evaluated the functionality of the model by the treatment with checkpoint inhibitors like Ipilimumab (Ipi), Nivolumab (Nivo) or Pembrolizumab (Pembro). In parallel, we investigated the functionality of the human immune cells and evaluated concepts for combination therapies i.e. with chemotherapy or radiation.

Methods

HSC-humanized mice were generated by i.v. HSC transplantation and engraftment of immune cells was monitored by FACS analysis. For PBMC-humanized mice, immune cells were implanted i.v.. PDX models from different entities (leukemia or NUT carcinoma) were transplanted on HSC-humanized (HIS) mice and treated with Ipi, Nivo and Pembro alone or in combination with radiation. Blood and tumor samples were analysed by FACS for immune cell infiltration and activation.

Results

The transplanted HSC showed engraftment in mice with proliferation and differentiation. 14 weeks after HSC inoculation up to 20% of the human immune cells in the blood were T-cells, characterized by a high PD-1 expression. We have transplanted PDX from different tumor entities on HSC-humanized mice. Most of the investigated PDX (>70%) successfully engrafted on humanized mice and showed no significant difference in tumor growth compared to growth on non-humanized mice. However, for some PDX we observed a delayed tumor growth or a complete rejection. Engraftment delay seems to correlate with the PD-L1 expression of PDX (the higher PD-L1, then the higher growth delay). Furthermore, our results demonstrate the functionality of the engrafted human immune cells against some PDX. Treatment with Ipi, Nivo or Pembro led to a minor tumor growth delay. Response to checkpoint inhibitors showed a correlation to innate immune response and PD-L1 expression of PDX and could further be increased by combination with radiotherapy.

Conclusions

Our humanized immune-PDX models enable appropriate preclinical translational research on tumor immune biology and the evaluation of new therapies and combinations, as well as the identification and validation of biomarkers for immune therapy, especially in rare PDX models.

#5205

B6-*Kras*$^{LSL-G12C}$ mouse model for assessing the occurrence and development of lung and pancreatic cancer tumors

Xiaoliu Yang[1], Yunlong Jiang[1], Xue Wu[1], Mingkun Zhang[1], Jing Zhao[1], Santi Suryani Chen[2], Zhiying Li[2], Erica Trujillo[2], Mark Wade Moore[2], Xiang Gao[1], Cunxiang Ju[1]. *[1]GemPharmatech Co., Ltd., Nanjing, China,[2]GemPharmatech LLC., La Jolla, CA*

In May 2021, the FDA approved sotorasib (Lumakras™) as the first treatment for adult patients with non-small cell lung cancer (NSCLC) harboring the *KRAS*^{G12C} genetic mutation. To study the relationship between the mutational activation of KRAS and tumorigenesis, and promote the development of KRAS-G12C inhibitors, we established the B6-Loxp-Stop-Loxp Kras G12C (B6-*Kras*$^{LSL-G12C}$) strain. Upon induction of Cre recombinase, floxed Stop sequences will be deleted in the mouse genome, and the oncogenic KRAS-G12C protein will be expressed at endogenous levels allowing for control of the timing and location of tumor initiation. The C57BL/6-*Kras*$^{LSL-G12C}$ mice were crossed with the Lyz2-cre mice to develop a spontaneous lung cancer model. KRAS G12C mutant could be detected in type II alveolar epithelial cells (ATII). Furthermore, these mice develop lung cancer at 8-10 weeks of age. In addition, when B6-*Kras*$^{LSL-G12C}$ mice were crossed with the B6-*P53*$^{LSL-R172H}$ and Ptf1/p48-Cre mice, the offspring developed pancreatic cancer after 10-12 weeks of tamoxifen treatment.

In conclusion, B6-*Kras*$^{LSL-G12C}$ mice can be used to study the occurrence and development of pancreatic and lung cancer, as well as the potential applications of cancer therapies.

#5206

A novel mouse model for preclinical efficacy evaluation of anti-CD3/GPRC5D bispecific antibodies

Xiaoliu Yang[1], Xinyuan Liang[1], Mingkun Zhang[1], Santi Suryani Chen[2], Zhiying Li[2], Erica Trujillo[2], Mark Wade Moore[2], Jing Zhao[1], Xiang Gao[1], Cunxiang Ju[1]. *[1]GemPharmatech Co., Ltd., Nanjing, China,[2]GemPharmatech LLC., La Jolla, CA*

The FDA has granted Breakthrough Therapy Designation (BTD) for talquetamab, which targets both GPRC5D on multiple myeloma cells and CD3 on T-cells, for treating adult patients with relapsed or refractory multiple myeloma. Results showed that patients who received talquetamab experienced adverse events, including cytokine release syndrome (CRS), neutropenia, skin-related adverse events and dysgeusia. To allow preclinical in vivo evaluation of anti-human CD3/GPRC5D bispecific antibodies, we developed a BALB/c-hCD3EDG mouse model and a human GPRC5D-expressing A20 murine lymphoma cell line. The BALB/c-hCD3EDG cohort (6-8 weeks old) was subcutaneously inoculated with A20-hGPRC5D cells and then treated with anti-CD3/GPRC5D bispecific antibodies. As expected, anti-CD3/GPRC5D bispecific antibody treatment strongly inhibited the growth of A20-hGPRC5D tumors in BALB/c-hCD3EDG mice.

To allow a comprehensive safety evaluation of anti-CD3/GPRC5D candidates, including the possibility of CRS and target organ toxicity, we engineered BALB/c-hCD3EDG mice that express hGPRC5D, denoted BALB/c-hCD3EDG/hGPRC5D. Human GPRC5D was detected in the liver, lung, thymus, adipose tissue, and thyroid. In vivo evaluation of anti-CD3/GPRC5D therapy in this mice is currently underway.

In conclusion, BALB/c-hCD3EDG/hGPRC5D and BALB/c-hCD3EDG mice bearing A20-hGPRC5D tumors are suitable models for preclinical studies testing anti-CD3/GPRC5D bispecific antibodies.

#5207

Development of MHC I/II knock-out immunodeficient mouse strains for alleviating GvHD induced by human PBMC reconstitution

Qiang Liu[1], Chengzhang Shang[1], Xiaofei Zhou[1], Jenna Frame[2], Zhiyuan Shen[1], Zhaoxue Yu[2]. *[1]Biocytogen Pharmaceuticals (Beijing) Co., Ltd, Beijing, China,[2]Biocytogen Boston Corp, Wakefield, MA*

Severely immunodeficient mouse strains, such as B-NDG mice, lack B, T, and NK cells, and have been widely used as an in vivo model to evaluate human immune responses, including applications in immuno-oncology in recent years. However, when human peripheral blood mononuclear cells (PBMCs) are engrafted in these mice, severe acute xenogeneic graft-versus-host disease (GvHD) arises due to engagement of human T cell receptors (TCRs) with major histocompatibility complex (MHC) proteins I and II on the surface of murine immune cells. GvHD shortens the animal life span such that there is only a brief window of evaluation of human immune cell functions in these mouse models. Consequently, efforts have been undertaken to reduce human PBMC-induced GvHD and to subsequently extend the window of human immunity assessment in immunodeficient mouse strains by eliminating mouse MHC I and MHC II. We previously engineered a novel *B2m* gene knock-out strain on the B-NDG background (NOD.CB17-*Prkdc*^{scid}*Il2rg*^{tm1}/Bcgen), which is deficient in MHC I expression, but expresses the *B2m* gene fused into the *FcRn* gene to retain FcRn-mediated antibody metabolism. In order to eliminate MHC II expression, we also engineered an *H2-Ab1* gene knock-out strain on the same B-NDG background and cross-bred the two strains together to obtain an MHC I/II double KO mouse model, termed B-NDG MHC I/II DKO mice plus. Splenocytes collected from the engineered strains were analyzed by flow cytometry. As expected, mouse H-2K^{b}/H-2D^{b} was not detectable in B-NDG B2m KO plus mice or B-NDG MHC I/II DKO mice plus. While mouse I-Ak was detected in B-NDG mice and B-NDG B2m KO plus mice, it was not detected in B-NDG MHC I/II DKO mice plus. Pharmacokinetic assessments demonstrate that B-NDG mice and B-NDG B2m KO mice plus groups were able to recycle human IgG, with no differences when compared with wild-type C57BL/6 mice, indicating normal FcRn function. Finally, the three strains of mice were irradiated and engrafted with human PBMC from three donors to evaluate GvHD incidence. As expected, the reconstitution levels of CD45+ leukocytes, T cells, CD4+ T cells, CD8+ T cells, Tregs and NK cells were similar among the three strains. However, lack of MHC I/II in B-NDG MHC I/II DKO mice plus can significantly extend the life span and reduce GvHD induced by human PBMC engraftment compared to B-NDG mice and B-NDG B2m KO mice plus. These results indicate that B-NDG MHC I/II DKO mice plus provides a useful mouse model for reducing GvHD after human PBMC reconstitution

in immunodeficient mice. This model may be a powerful preclinical tool for future *in vivo* evaluation of cell therapies and antibodies.

#5208

Development of immunodeficient mice expressing human IL3, GM-CSF, CSF1 and THPO for improved human myeloid and lymphoid cell reconstitution

Ruili Lv[1], Yanhui Nie[1], Jing Zhang[1], Jenna Frame[2], Qiang Liu[1], James Jin[2].
[1]Biocytogen Pharmaceuticals (Beijing) Co., Ltd, Beijing, China,[2]Biocytogen Boston Corp, Wakefield, MA

Mice reconstituted with human immune cells are essential tools to study human immune reactions *in vivo*, including those involving cancer immunotherapies. A major limitation of these models is the poor development of human myeloid cells to mediate effective human immune cell-tumor interactions. This is because hematopoietic cells are highly dependent on several human cytokines for efficient differentiation, maturation, and survival. THPO (thrombopoietin) can enhance the maintenance of functional human hematopoietic stem cells, and stimulates the production and differentiation of megakaryocytes, which produce large numbers of platelets in the bone marrow. IL3 (interleukin 3), GM-CSF (granulocyte-macrophage colony-stimulating factor, CSF2) and CSF1 (macrophage colony-stimulating factor, M-CSF) are cytokines that promote the proliferation and differentiation of a variety of myeloid cells, including monocytes, macrophages, granulocytes, dendritic cells, and platelets. Because these cytokines lack sufficient cross-reactivity between human and mice, it is difficult to reconstitute human immune cells of these lineages in immunodeficient mice. Therefore, we predict that genetic humanization of these four cytokines will improve the reconstitution of human myeloid cells in immunodeficient mice. We engineered an M-CSF, GM-CSF, THPO, and IL3 humanized strain in the background of B-NDG mice (NOD.CB17-*Prkdc*^{scid}*Il2rg*^{tm1}/Bcgen), termed B-NDG MGMT3 mice. The full sequences of mouse *Il3*, *Csf2, Csf1* and *Thpo* genes (except the UTRs) were respectively replaced with the coding sequences (CDS) of human *IL3, CSF2, CSF1* and *THPO* genes. Human GM-CSF, CSF1 and THPO proteins were confirmed to be expressed by ELISA in B-NDG MGMT3 mice. Human CD34^{+} HSCs (3E4) were intravenously engrafted into wild-type B-

NDG mice and homozygous B-NDG MGMT3 male and female newborn mice via the temporal vein. B-NDG mice were treated with 1.0 Gy irradiation, while B-NDG MGMT3 mice were not irradiated. The survival rate of B-NDG MGMT3 mice was similar to B-NDG mice until 16 weeks post-$CD34^+$ engraftment. However, the body weight of B-NDG MGMT3 mice was significantly higher than that of B-NDG mice. Analysis of peripheral blood lymphocytes showed that the proportion of $hCD45^+$ cells in B-NDG MGMT3 mice reached 25% starting from 12 weeks after engraftment and continued to rise; levels were significantly higher than that observed in B-NDG mice. The proportions and cell number of T cells, NK cells, monocytes, MDSCs, DCs and Tregs engrafted in B-NDG MGMT3 mice were higher than B-NDG mice. The results indicate that B-NDG MGMT3 mice are a novel humanized model for human myeloid and lymphocytic cell reconstitution that does not require preconditioning.

#5209

Generation of humanized TREM2 mice for preclinical evaluation of therapeutics targeting tumor-associated macrophages

Ruili Lv[1], Jia Yu[1], Zhiyuan Shen[1], James Jin[2]. *[1]Biocytogen Pharmaceuticals (Beijing) Co., Ltd., Beijing, China,[2]Biocytogen Boston Corp, Wakefield, MA*

In recent years, immune checkpoint inhibitors (ICIs) have improved treatment for several types of cancer. However, the overall response rates remain low, and drug resistance can occur in patients after initial responses. This resistance is thought to be due in part to tumor-associated macrophages (TAMs), which can deploy a number of mechanisms to suppress anti-tumor immunity, resulting in tumor immune escape. Triggering receptor expressed on myeloid cells-2 (TREM2), a transmembrane receptor that is part of the immunoglobulin superfamily, is highly expressed on the surface of TAMs. Moreover, the expression level of TREM2 is reported to be higher in cancerous tissues vs normal tissues, with higher expression associated with poorer patient outcomes across multiple solid tumor types. Conversely, mice that lack Trem2 experience slower tumor cell expansion and are more responsive to anti-PD-1 immunotherapy, suggesting that TREM2 may be a promising therapeutic target for improving responses to ICI immunotherapies. To better assist the efficacy

evaluation of anti TREM2 antibodies, Biocytogen has generated a humanized TREM2 mouse model. In these mice, exons 1-5 and the 3'UTR of mouse Trem2 gene, which encodes the full-length protein, were replaced by its human counterpart. In homozygous mice, human TREM2 protein expression is detected. The distribution of basal leukocyte subpopulations of blood, spleen, and lymph nodes in humanized B-hTREM2 mice were similar and comparable to those in wild-type C57BL/6 mice. Using the MC38 tumor model, we showed modest efficacy of an anti-human TREM2 antibody in inhibiting tumor growth in vivo. In summary, TREM2 humanized mice provide a powerful preclinical model for in vivo evaluation of anti-human TREM2 antibodies for cancer treatment.

#5210

Ablation of an immunogenic human endogenous retrovirus in renal cell carcinoma cells through dual-guide CRISPR-Cas9 genome editing

Long Chen[1], Elena Cherkasova[1], Stephanie Pierre[2], Savannah England[3], Muna Igboko[1], Joseph Clara[1], Stefan Barisic[1], Angie Parrizzi[1], Rosa Rios Nadal[1], David Allan[1], Mala Chakraborty[1], Robert Reger[1], Richard Childs[1].
[1]NIH National Heart, Lung & Blood Institute, Bethesda, MD,[2]Memorial Sloan Kettering Cancer Center, New York, NY,[3]Saint Louis University School of Medicine, St. Louis, MO

Human endogenous retroviruses (HERVs) comprise 8% of the human genome and can be abnormally expressed in different tumor cells. Our lab discovered a unique and highly immunogenic HERV-E, CT-RCC HERV-E, that is selectively expressed in most clear cell renal cell carcinoma (ccRCC) cells. Although the function of select HERVs in some tumors has been defined, the role of CT-RCC HERV-E in ccRCC remains unclear. To characterize the impact of HERV-E expression on tumor oncogenesis in ccRCC, we developed a highly efficient strategy to ablate CT-RCC HERV-E through dual-guide CRISPR-Cas9. For isolation of edited cells, we knocked in a truncated CD19 (tCD19) into the same gene edited locus using adeno-associated virus (AAV) as donor templates. In order to ablate the entire 8.8 kb HERV-E region, we designed three single guide RNAs (sgRNAs) flanking the CT-RCC HERV-E genomic locus: one at the upstream site, sgRNA HERV-E Upst(1), and two downstream, sgRNA HERV-E Dwst(3) and sgRNA HERV-E Dwst(4). A single sgRNA targeting

β2M was used as a negative control. HERV-E knockout was verified via real-time PCR, and the combination of sgRNAs Upst1-Dwst3 were chosen as the guides for all experiments, due to their higher knockout efficiency. We tested the MOIs of 2, 4, and 10 x 10^5 for AAV transduction following CRISPR knockout. Expression of CD19 was the highest at the MOI of 10 x 10^5, which was used for all experiments. Two RCC cell lines, RCC-TIU and RCC-UOK220, were used to validate this methodology. Edited ccRCC cells were enriched by CD19 magnetic microbeads, resulting in CD19 expression of over 96%. Genomic DNAs isolated from the two RCC cell lines confirmed simultaneous knockout of HERV-E and knock-in of tCD19. To isolate a population of cells that had homogenous HERV-E knockout, we single-cell sorted and then expanded $CD19^+$ ccRCC cells in vitro. 252 and 145 clones were harvested from RCC-TIU and RCC-UOK220 respectively. PCR analysis of genomic DNA from 48 selected clones of each of the aforementioned cell lines unveiled both monoallelic and biallelic knockout of HERV-E. Eight biallelic knockout clones were harvested and further expanded, which gave rise to four clones from RCC-TIU and three clones from RCC-UOK220. Additional PCR screening confirmed that RCC-TIU A7, A9, and RCC-UOK220 D3 were biallelic knockout clones. Finally, we used digital PCR to examine the expression of two CT-RCC HERV-E transcripts, Env and RCC-8; No expression of these transcripts was found in the aforementioned clones. In summary, we established a highly efficient method to reliably ablate a human endogenous retrovirus in human tumor cells. The dual-guide CRISPR-Cas9 genome editing method utilized here allowed for the successful isolation of tumor cells that had a biallelic knockout of the CT-RCC HERV-E. These knockout cell lines will be utilized to explore the oncogenic impact of CT-RCC HERV-E expression in ccRCC cells.

MOLECULAR/CELLULAR BIOLOGY AND GENETICS

Cancer and Metabolism 1

#3671
Targeting SLC2A1 and SLC38A2-mediated metabolic shift in SMARCA4/A2-dual deficient cancer

Xianbing Zhu[1], Zheng Fu[1], Shary Chen[2], Dionzie Ong[2], Giulio Aceto[1], Rebecca Ho[2], Jutta Steinberger[1], Eunice Li[2], David Huntsman[2], William Foulkes[3], Sidong Huang[1], Yemin Wang[4]. *[1]Department of Biochemistry, McGill University, Montreal, QC, Canada,[2]University of British Columbia, Vancouver, BC, Canada,[3]Departments of Medicine, Oncology and Human Genetics, McGill University, Montreal, QC, Canada,[4]Pathology and Laboratory Medicine, University of British Columbia, Vancouver, BC, Canada*

SMARCA4 (BRG1) and SMARCA2 (BRM) are the two paralogous ATPases of the SWI/SNF chromatin remodelling complexes. These two ATPases are frequently inactivated in cancers and cancer cells deficient in either of them have been shown to depend on the remaining counterpart for survival. Contrary to this paralog synthetic lethality, concomitant loss of SMARCA4 and SMARCA2 occurs in a subset of cancers that are often associated with very poor patient outcomes. Here, we uncover that dual loss of SMARCA4/A2 represses the expression of SLC2A1, encoding the glucose transporter GLUT1, which results in reduced glucose uptake and glycolysis accompanied with increased dependency on oxidative phosphorylation (OXPHOS); adapting to this, these SMARCA4/A2-dual deficient cells rely on elevated SLC38A2, an amino acid transporter, to increase glutamine import for fueling OXPHOS. Consequently, SMARCA4/A2-dual deficient cells and tumours are highly sensitive to inhibitors targeting OXPHOS or glutamine metabolism. Furthermore, supplementation of alanine, also imported by SLC38A2, restricts glutamine uptake through competition and selectively induces death in SMARCA4/2-dual deficient cancer cells. At a clinically relevant dose, alanine supplementation synergizes with OXPHOS inhibition or conventional chemotherapy eliciting marked antitumor activities in SMARCA4/A2-dual deficient cancer cell lines and patient-derived xenografts. Our findings reveal multiple druggable vulnerabilities of SMARCA4/A2-dual loss exploiting a GLUT1/SLC38A2-mediated metabolic shift. Particularly, unlike dietary deprivation approaches, alanine supplementation can be readily applied to current regimens for better treatment of these aggressive cancers. * Authors contributed equally# Co-corresponding

#3672

RNA epigenetic regulation of cholesterol metabolism in neuroblastoma
Mohit Bansal, Anamika Gupta, Han-Fei Ding. *University of Alabama at Birmingham, Birmingham, AL*

Pseudouridylation (conversion of uridine to pseudouridine) is a common epigenetic modification of RNA which increases its structural stability. RNA pseudouridylation is catalyzed by the family of pseudouridine synthases (PUS). The functional significance and biological relevance of mRNA pseudouridylation are poorly understood. Here we report that the oncogene MYCN, which drives the development of high-risk neuroblastoma, transcriptionally upregulates the PUS1 gene. Further, examination of gene expression profiling data from neuroblastoma patients (the SEQC dataset) reveals that higher PUS1 expression is associated with poor prognosis. The transcriptional upregulation of PUS1 expression in MYCN amplified cell lines is of functional significance, as our studies reveals that knockdown of PUS1 expression in neuroblastoma cell lines suppresses cell survival and proliferation. Our RNA-seq analysis reveals that a key downstream target of PUS1 is cholesterol metabolism. PUS1 knockdown reduces the expression of key enzymes in the mevalonate pathway for cholesterol synthesis. Mechanistically, PUS1 may targets SREBP2, a master regulator of cholesterol metabolism responsible for transcriptional upregulation of enzymes for cholesterol biosynthesis. We showed that PUS1 expression is essential for maintaining SREBP2 expression in MYCN-amplified neuroblastoma cells and for statin-induced feedback activation of the mevalonate pathway, a commonly used system for assessing the transcriptional activity of SREBP2. These findings suggest that a function of PUS1 in sustaining the proliferation of neuroblastoma cells is to promote cholesterol metabolism, which could be exploited as a therapeutic strategy against high-risk neuroblastoma.

#3673
Plk1 phosphorylation of PHGDH to regulate serine metabolism
Xiongjian Rao, Derek B. Allison, Robert M. Flight, Yuanyuan Wu, Timothy Scott, Daheng He, RuiXing Wang, Zhiguo Li, Chaohao Li, Yifan Kong, Fengyi Mao, Chi Wang, Richard M. Higashi, Andrew N. Lane, Hunter NB Moseley, Xiaoqi Liu. *University of Kentucky, Lexington, KY*

Polo-like kinase 1 (Plk1) has been reported to be highly expressed in most tumors, especially in advanced tumors, while how Plk1 elevation benefits tumor growth remains elusive. Metabolic reprogramming is one of the hallmarks of cancer, but how the tumors fully take advantage of deregulated metabolism is an enigma. Here, we found that Plk1 could divert serine metabolism from de novo synthesis to exogenous uptake by regulating PHGDH (phosphoglycerate dehydrogenase), the first rate-limiting enzyme of de novo serine biosynthesis. We show that PHGDH is phosphorylated by Plk1 at a cluster site (S512, S513, S517) and that Plk1-associated phosphorylation of PHGDH results in its protein degradation, thus reduced de novo serine biosynthesis. As a compensatory response, cells with an elevated level of Plk1 significantly increase the uptake of serine to produce more sphingosines, which are pivotal metabolites for the growth of cancer cells. Our finding may provide guidance on how to target de novo biosynthesis of serine, serine uptake or sphingosine metabolism to treat advanced prostate cancer.

#3674

The polyamine acetylation enzyme SAT1 drives mesenchymal features and therapeutic resistance in glioblastoma

Ayush B. Rana, Timothy M. Horton, Vijay S. Thakur, Scott M. Welford.
Radiation Oncology, University of Miami Miller School of Medicine, Miami, FL

Background**:**
Glioblastoma multiforme (GBM) is the most common and lethal brain tumor in adults. Characterization of GBM heterogeneity has identified four molecular subtypes based on transcriptomic profile: classical, neural, proneural and mesenchymal. Tumors harboring the mesenchymal gene signature are considered the most aggressive, invasive, and multitherapy-resistant. We identify the polyamine acetylation enzyme, SAT1 (spermidine/spermine N1-acetyltransferase 1) as a component of the mesenchymal gene signature and mesenchymal-associated gene sets including (1) Hallmark EMT and (2) Hallmark TNFa signaling via NF-κB.
Design/Methods:
To validate the role of SAT1 in driving mesenchymal features *in vivo*, we utilized a genetically flexible, CRISPR-based model of GBM. Tumor

bearing mice were generated through *in utero* electroporation, resulting in ablation of PTEN, P53 and NF1 in developing cortical cells. SAT1 knockout was achieved through cloning of additional guide RNA's against SAT1 into the tumor initiating plasmid.

Results:

In our model, we found increased levels of both SAT1 and acetylated polyamines in tumors compared to normal brain. Ablation of SAT1 was insufficient to prolong overall survival in mice but rendered the otherwise treatment resistant tumors highly sensitive to chemoRT. Bulk RNA sequencing of murine tumors revealed that SAT1 knockout resulted in reduced expression of the mesenchymal gene signature as well as genes implicated in EMT and TNFa/NFKb signaling.

Conclusions:

Collectively, these results reveal that SAT1 not only identifies mesenchymal GBM but also drives expression of the mesenchymal gene signature and mesenchymal features including multi-therapy resistance.

#3675

Targeting the mevalonate pathway, a novel anti-ferroptosis pathway, in hepatocellular carcinoma (HCC) treatment

Yiling Chen, Derek Lee, Misty Shuo Zhang, Jacinth Wing-Sum Cheu, Carmen Chak-Lui Wong. *Department of Pathology, University of Hong Kong, Li Ka Shing Faculty of Medicine, Hong Kong, China*

Ferroptosis is a novel immunogenic and regulated cell death caused by iron-dependent lipid peroxidation. Glutathione peroxidase 4(GPX4)/glutathione and ferroptosis suppressor protein 1(FSP1)/Coenzyme Q10(CoQ10) are two major anti-ferroptosis systems that prevent lipid ROS-induced cell death. Our current study unprecedentedly uncovered that the Mevalonate pathway (MVA) protects HCC from ferroptosis by two parallel mechanisms: 1) by providing the lipophilic antioxidant CoQ10 for FSP1; 2) by generating isopentenyl pyrophosphate (IPP), a substrate for Selenocysteine (Sec)-tRNA modification for selenoprotein GPX4 translation. Selenoproteins are a class of proteins composed of selenocysteine, the 21st amino acid not found in the codon table. Selenocysteine is recoded by the stop codon UGA and synthesized on its tRNA. The Sec-tRNA incorporates Sec into selenoproteins such as GPX4. We showed that perturbation of the MVA

pathway by genetic knockdown or pharmacologic inhibition repressed CoQ10 synthesis and the translation of selenoproteins, thereby leading to lipid-derived ROS and ferroptotic cell death. Furthermore, we showed that Mevalonate diphosphate decarboxylase (MVD), a MVA enzyme, was a transcriptional target of Nuclear Factor Erythroid 2- related factor 2 (NRF2), a master regulator of oxidative stress response. High expression of MVD was associated with poor prognosis in HCC. Strikingly, MVD inhibitor treatment profoundly suppressed HCC. Reduced tumor size and increased tumor-infiltrated effector T cells and macrophages were found *in vivo*. To conclude, our study has provided novel mechanistic insight about how NRF2/MVA pathway promotes HCC and suggested that MVD might be a good prognostic indicator and therapeutic target in human HCC.
Funding Support: RGC Postdoctoral Fellowship Scheme 2021/22 (Project #102010048)

#3676

De novo lipogenesis and cholesterol synthesis pathways can be simultaneously targeted to induce metabolic synthetic lethality in prostate cancer

Caroline Fidalgo Ribeiro[1], Silvia Daniele Rodrigues[1], Guilherme Tamarindo[2], Hubert Pakula[1], Massimo Loda[1]. *[1]Pathology and Laboratory Medicine, Weill Cornell Medicine, New York, NY,[2]Institute of Biology, University of Campinas, Campinas, Brazil*

Aberrant activation of fatty acid synthase (FASN) and *de novo* lipogenesis (DNL) is a major metabolic event in prostate cancer (PCa). Targeting lipid synthesis through FASN blockade can inhibit prostate tumor growth. Another metabolic pathway commonly altered in PCa is the mevalonate pathway, responsible for the synthesis of cholesterol from acetyl-CoA. The rate-limiting enzyme of the mevalonate pathway, 3-hydroxy-3-methylglutaryl coenzyme A reductase (HMGCR), can be targeted with statins, drugs commonly prescribed for the management of hypercholesterolemia. Following FASN inhibition with IPI-9119, genes involved in the mevalonate pathway and cholesterol synthesis are transcriptionally upregulated. Metabolomics data confirmed an increase in intracellular levels of cholesterol after FASN inhibition, suggesting a compensatory mechanism to support PCa cell survival in the absence of *de*

novo synthesized lipids. Interestingly, we also observed an increase in mRNA levels of Acyl-CoA Synthetase Short Chain Family Member 2 (ACSS2), the enzyme that converts acetate into acetyl-CoA. Next, we evaluated how FASN blockade affected acetate utilization by PCa cells and observed that acetate uptake increases with DNL inhibition. Metabolic analysis confirmed that ^{14}C-acetate incorporation into lipids was increased after IPI-9119 treatment. The concomitant inhibition of FASN and HMGCR reduced acetate lipid incorporation, suggesting that acetate is fueling cholesterol synthesis. To better understand this effect, we analyzed the cell membrane after FASN inhibition, and an increase in fluidity was seen, which could be rescued by palmitate. Lipidomics analysis showed an increase in polyunsaturated fatty acids (PUFA) esterified to phospholipids, as well as overall increase in fatty acyl chain length, events that can affect membrane structure and fluidity. Due to the important role of lipids as energy reservoir, we also analyzed the effect of FASN blockade in neutral lipids. IPI-9119 treatment caused depletion of triacylglycerides, while levels of cholesterol esters (CE) and Acetyl-CoA Acetyltransferase 2 (ACAT2), an enzyme involved in CE synthesis, are upregulated. Acyl chain length and unsaturation are also increased in CE fatty acids, indicating further utilization of PUFAs in the absence of FASN activity. As expected, the combination of FASN and HMGCR inhibitors significantly potentiates cell death, observed by stronger reduction in cell growth than either of the single agents, both in androgen-sensitive and castration-resistant models of PCa. Altogether, our data suggests that cholesterol synthesis is a survival mechanism of PCa induced by DNL inhibition, likely to correct for membrane fluidity and energy supply. Finally, statin therapy can be combined with FASN inhibition to suppress PCa growth more efficiently than monotherapy.

#3677

DNA damage signaling activates *de novo* GTP synthesis to promote chemoradiation resistance in glioblastoma

Andrew J. Scott[1], Alexandra M. O'Brien[1], Weihua Zhou[1], Vidhi Pareek[2], Zhou Sha[2], Sravya Palavalasa[1], Ayesha U. Kothari[1], Kari Wilder-Romans[1], Li Zhang[3], Anthony C. Andren[3], Sriram Chandrasekaran[4], Jason Heth[5], Yoshie Umemura[6], Nathan Qi[3], John Woulfe[7], Sriram Venneti[8], Meredith A. Morgan[1], Theodore S. Lawrence[1], Wajd N. Al-Holou[5], Costas A.

Lyssiotis[3], Daniel R. Wahl[1]. *[1]Radiation Oncology, University of Michigan Medical School, Ann Arbor, MI,[2]Chemistry, The Pennsylvania State University, University Park, PA,[3]Molecular & Integrative Physiology, University of Michigan Medical School, Ann Arbor, MI,[4]Biomedical Engineering, University of Michigan Medical School, Ann Arbor, MI,[5]Neurosurgery, University of Michigan Medical School, Ann Arbor, MI,[6]Neurology, University of Michigan Medical School, Ann Arbor, MI,[7]The Ottawa Hospital Research Institute, Ottawa, ON, Canada,[8]Pathology, University of Michigan Medical School, Ann Arbor, MI*

Glioblastoma (GBM) is uniformly fatal due to inherent radiation (RT) and chemotherapy resistance. We have found this therapeutic resistance is mediated by alterations in tumor cellular metabolic activity. Our group and others have found that metabolites can regulate DNA repair and RT resistance in brain tumors, but little is known about how DNA damage regulates metabolic pathway activity in cancer. Here, we show that DNA damage acutely increases guanine-containing purine metabolites in multiple *in vitro* and intracranial GBM models. By interrogating metabolic fluxes *in vitro* using a variety of stable isotope tracers, we confirmed RT-induced elevation in guanylates was due to increased *de novo* purine synthesis (DNPS) rather than activation of purine salvage. By developing and using novel stable isotope tracing methods to directly measure DNPS in awake, unrestrained mice, we confirmed that orthotopic GBMs have higher DNPS rates than adjacent cortical tissue that further increase after treatment with RT. Neither salvage synthesis of purines nor pyrimidine synthesis were impacted by RT in any intracranial tissues. With these findings, we opened a clinical study to directly measure purine synthesis in patients, and we found that human GBMs have similarly high purine synthesis rates compared to normal brain tissue. Because DNA damage activated DNPS without affecting purine salvage or pyrimidine synthesis, we reasoned that active signaling may be involved. Indeed, therapy-induced DNPS increases are lost *in vitro* and *in vivo* upon pharmacological or genomic inhibition of the DNA-damage sensing kinase DNA-PK. Moreover, RT and DNA-PK have direct influence over the spatial organization of DNPS enzymes, including IMPDH, the rate-limiting step in guanylate synthesis. Because purines can promote DNA repair, these findings suggest that DNA-PK

signaling helps promote DNA repair in part by causing the spatial reorganization of DNPS enzymes, thereby activating purine synthesis. To determine if disrupting this regulation can augment GBM treatment efficacy, we combined an FDA-approved inhibitor of purine synthesis with chemoradiation in a variety of mouse models of GBM. Critically, targeting GTP synthesis improved the efficacy of both RT alone and chemoradiation in multiple patient-derived and syngeneic intracranial models, suggesting a potential therapeutic targeting opportunity in patients. In this study, we have developed novel methodology to directly measure purine synthesis in brain tumors in mice and humans. With these tools, we discovered that after DNA damage, DNA-PK mediates a novel pathway controlling the spatial reorganization of purine synthesis enzymes and subsequent DNPS increases. The resulting elevation of GTP levels promotes therapy resistance in tumors, and we are now directly measuring and inhibiting this molecular activity in patients with GBM in an effort to improve standard therapy.

#3678

Rewiring of amino acid metabolism in neurofibromatosis type 1-related tumors

Martina La Spina. *University of Padova, Padova, Italy*

Neurofibromatosis type 1 (NF1) is a tumor-predisposing genetic disorder caused by heterozygous mutations in the *NF1* gene encoding for the tumor suppressor Neurofibromin. Biallelic *NF1* inactivation in Schwann cells leads to the onset of neurofibromas, benign neoplasms that can cause severe medical complications and give rise to malignant peripheral nerve sheath tumors (MPNSTs), for which no treatment exists. Neurofibroma cells undergo bioenergetic changes required to sustain their malignant transformation. Our group has shown that inhibition of the mitochondrial chaperone TRAP1, a master metabolic regulator, hampers MPNST cell tumorigenicity. A growing number of evidence indicates that urea cycle (UC) dysregulation can redirect metabolic substrates to specific biosynthetic routes in many tumor cell types. We have found that a complete UC is absent in MPNST cell models, as they lack ornithine transcarbamylase (OTC), a key UC enzyme that converts ornithine into citrulline. In the absence of TRAP1, MPNST cells strongly reduce arginine

levels and accumulate ornithine through the activity of the mitochondrial enzymes arginase 2 (ARG2) and ornithine aminotransferase (OAT). These changes can reverberate on glutamine and proline levels ultimately affecting extracellular matrix deposition, motility and ROS homeostasis, as well as on ornithine-dependent polyamine biosynthesis that can regulate cell growth and proliferation. Surprisingly, in the absence of TRAP1 MPNST cells also accumulate citrulline, even though they do not express either OTC or any nitric oxide synthase (NOS) isoform that converts arginine into citrulline. We ascribe citrulline production to the activity of dimethylarginine dimethylaminohydrolase (DDAH) enzymes, involved in the catabolism of asymmetric dimethylarginines. Induction of DDAHs indicates an elevated protein catabolism that could contribute to tune MPNST cell tumorigenicity. A thorough comprehension of the amino acid metabolism rewiring in NF1-related tumors may unveil new targetable liabilities of cancer cells to be exploited for the design of new effective therapeutic approaches.

#3679

DNAJB1-PRKACA fusion in fibrolamellar hepatocellular carcinoma induces glutamine addiction and an immunosuppressive tumor microenvironment

Zeal Kamdar[1], Tamara Lopez-Vidal[1], Kathryn Howe[1], Kabeer Munjal[1], Ali Saeed[1], Daniel Zabransky[1], Daniel Shu[1], Gabriella Longway[1], Emma Kartalia[1], James Leatherman[1], Aditya Mohan[2], Pratik Khare[1], Cissy Zhang[1], Anne Le[3], Erika Pearce[1], Mark Furth[4], Marina Baretti[1], Robert Leone[1], Elizabeth Jaffee[1], Mark Yarchoan[1]. *[1]Johns Hopkins University School of Medicine, Baltimore, MD,[2]Duke University, Durham, NC,[3]Gigantest, Baltimore, MD,[4]Fibrolamellar Cancer Foundation, Greenwich, CT*

Fibrolamellar hepatocellular carcinoma (FLC) is a rare and often lethal form of liver cancer that primarily affects children and young adults. A fusion between DNAJB1, a heat shock chaperone protein, and PRKACA, the catalytic domain of protein kinase A (PKA) has been identified as a signature genomic event in FLC, but the effect of this fusion on the tumor immune microenvironment is not understood. We created an orthotopic,

syngeneic model of FLC (TIBx-FLC) by inducing the DNAJB1-PRKACA fusion in a murine hepatoblastoma-derived cell line (TIBx). CD8 T cells isolated from TIBx-FLC tumors demonstrated markedly impaired activation as compared to CD8 T cells isolated from control TIBx tumors. We investigated metabolic programming as a potential mechanism for DNAJB1-PRKACA immunosuppression in FLC. Labeled glucose metabolomics performed on TIBx-FLC and TIBx tumor cells demonstrated a metabolic shift away from aerobic metabolism to an increased glucose contribution towards the hexosamine biosynthetic pathway and purine synthesis, which requires glutamine as a nitrogen source. As compared to the parental TIBx cell line, the TIBx-FLC cell line demonstrated high sensitivity to glutamine antagonism *in vitro*, consistent with glutamine addiction. Systemic treatment of BALB/c mice bearing TIBx-FLC tumors with JHU-083, a glutamine antagonist, in combination with immune checkpoint inhibitor therapy enhanced survival as compared to vehicle or monotherapy. These data identify altered glutamine metabolism as a target in FLC, and may provide an explanation for immune suppression seen in the FLC tumor microenvironment.

#3680

Multiomics analysis of triple negative breast cancer identifies potential metabolic vulnerability for overcoming the resistance of neoadjuvant therapy

Zuen Ren[1], Kiran Kurmi[2], Robert Morris[1], Shakchhi Joshi[2], Eric Zaniewski[1], Johannes Kreuzer[1], Gabrielle Elena Gioia[1], Wilhelm Haas[1], Marcia C. Haigis[2], Leif W. Ellisen[1]. *[1]Harvard Medical School/Massachusetts General Hospital, Boston, MA,[2]The Department of Cell Biology, Harvard Medical School, Boston, MA*

Triple-negative breast cancer (TNBC) is a heterogeneous disease that remains currently medically incurable. We comprehensively analyzed clinical, proteomic, and metabolomic data of a cohort of 12 highly selected primary TNBCs. Among them, 7 patients after neoadjuvant chemotherapy had residual disease and micro- or macro-metastases that were non-pathologically complete response (non-pCR); 5 patients had pathologically complete response (pCR). Interestingly, both proteomic and metabolic profiling results revealed dramatically different molecular signatures in

non-pCR relative to pCR. Non-pCR were enriched in metabolites involving aspartic acid, fumarate, nicotinamide, and adenosine that are critical intermediates for nitrogen recycling and tricarboxylic acid (TCA) cycle, which are essential fuels for tumor biomass. Moreover, non-pCR were enriched in urea cycle, oxidative phosphorylation, glycolysis, sirtuin signaling, nucleotide *De Novo* biosynthesis, which are resistance-associated. Putative therapeutic targets were identified in non-pCR patients. Collectively, our multiomics analysis demonstrated the heterogeneity of TNBCs at multi-levels and enabled the development of personalized therapies targeting unique tumor metabolic profiles.

#3681

c-MAF-driven metabolic reprogramming mediates H3K27 hyperacetylation to regulate super enhancer-associated genes

Phyllis SY Chong[1], Sze Lynn Julia Lim[2], Jianbiao Zhou[2], Aaron Chung Yong Leow[2], Wee Joo Chng[3]. *[1]National University of Singapore (NUS), Singapore, Singapore,[2]Cancer Science Institute Singapore, Singapore, Singapore,[3]National University Cancer Institute, Singapore (NCIS), Singapore, Singapore*

Overexpression of transcription factor c-MAF is found in about 50% of multiple myeloma cases, and associated with the prognostically unfavorable t(14;16) translocation subtype. Genetic alterations can modify the epigenome through metabolite availability that act as substrates in histone modifications, but how this translates into specificities in gene regulation is unclear. Here, we report a novel involvement of c-MAF in metabolically-driven histone acetylation, including the superenhancer mark H3K27ac, through altering acetyl-CoA metabolism. To sustain high levels of acetylation, c-MAF acquired the metabolic flexibility to utilize glutamine in addition to glucose, feeding into the tricarboxylic acid (TCA) cycle as acetyl-CoA sources. Loss-of-function studies indicated that c-MAF is important for citrate-derived acetyl-CoA and H3K27ac levels through metabolic enzymes citrate synthase (CS) and ATP-citrate lyase (ACLY). Furthermore, blocking citrate export from mitochondrial via CRISPR/Cas9 targeting of SLC25A1 reproduced the reductions in H3K27ac. Silencing of c-MAF also displayed defective mitochondrial oxidative phosphorylation attributed to reduced metabolic flux through TCA cycle and downregulation

of electron transport chain complex I/II expression, without affecting mitochondrial DNA content. To identify c-MAF-regulated superenhancer genes, we overlapped our previously published H3K27ac ChIP-seq dataset on t(14;16) MM cell lines with c-MAF RNA-seq data. We found signal enrichment of H3K27ac at ZC3H3 locus responsible for its transcriptional upregulation, and knockdown of ZC3H3 inhibited cell growth specifically in the t(14;16) subtype. Altogether, we demonstrated a non-canonical c-MAF role in epigenetics that is connected to its altered metabolic state, and suggest metabolic disruptions as a new therapeutic direction in t(14;16) myeloma.

#3682

Glutamine addiction of c-MAF overexpressing cells drives dysregulation of purine metabolism

Julia Sze Lynn Lim[1], Phyllis Shu Yun Chong[2], Wee-Joo Chng[3]. *[1]Cancer Science Institute of Singapore, NUS, Singapore, Singapore,[2]Medicine, Yong Loo Lin School of Medicine, National University of Singapore, Singapore, Singapore,[3]Department of Hematology-Oncology, National University Cancer Institute of Singapore, National University Health System, Singapore, Singapore*

c-MAF, a bZIP transcription factor, is overexpressed as a consequence of t(14;16) translocation and represents a driver oncogene in this subtype. Clinically, patients with t(14;16) translocation constitute a high-risk group with adverse survival outcomes. Since transcription factors are not classical targets for the development of small molecule inhibitors, elucidating pathways downstream of c-MAF could present as potential therapeutic targets. Critically, gene expression profiling studies of c-MAF showed a class of recurrently deregulated metabolic genes. Hence, this warrants further studies into the underexplored role of metabolism and the deregulated metabolic pathways mediated by c-MAF. First, we confirmed that t(14;16) cells were dependent on c-MAF expression for cell viability. Abrogation of c-MAF deregulated sensitivity to glycolytic inhibitors and influenced metabolite readouts. Importantly, analysis of quantitative metabolic profile of c-MAF driven myeloma using metabolomics identified 41% (48/116) of metabolites to vary significantly. Classification of differential metabolites into metabolic pathways was performed using the

software MetaboAnalyst 5.0 to elucidate a role of c-MAF in de novo purine metabolism. Despite an increased source of PRPP derived from the pentose phosphate pathway, we observed significant decrease in output of IMP (fold change=0.6, p=0.028). We postulate that this might result from lowered levels of some non-essential amino acids substrates needed by enzymes in the de novo purine biosynthesis pathway such as glutamine (fold change=0.08, p=0.155) and aspartate (fold change=0.3, p=0.022). Furthermore, GSEA from RNA-seq data performed by c-MAF loss-of-function studies identified *ADCY1, ADCY5* and *GALR3*, suggesting a direct regulation of purine metabolic genes by c-MAF. Notably, to validate whether c-MAF displayed metabolic dependency on glutamine to drive purine biosynthesis, we performed nutrient starvation studies which showed glutamine dependency in c-MAF overexpressed cells. We also systematically knockdown glucose transporters (GLUT8 and GLUT4) or glutamine transporters (ASCT2 and SNAT1) and saw a greater dependency on glutamine transporters for cell viability. As a proof of concept, c-MAF overexpressed cells were more sensitive to purine depletion by LTX suggesting its dependency on purine metabolism. The downstream identification of biological association of c-MAF with cancer metabolism may emerge as a new therapeutic strategy for MM patients. Taken together, our study suggests that metabolic perturbations present as a likely key Achilles heel in MM, and could potentially shift the current treatment paradigm.

#3683

Activation of purine anabolism creates a therapeutic vulnerability in hepatocellular carcinoma via m6A-mediated epitranscriptomic regulation

Man-Hsin Hung[1], Ching Wen Chang[1], Kathy Cheng Wang[1], Jittiporn Chaisaingmongkol[2], Mathuros Ruchirawat[2], Tim F. Greten[1], Xin Wei Wang[1]. *[1]National Cancer Institute, Bethesda, MD,[2]Laboratory of Chemical Carcinogenesis, Chulabhorn Research Institute, Bangkok, Thailand*

Introduction Purines are building blocks for genomics and the abundance of purine nucleotides is controlled by purine synthesis and purine degradation. Imbalance of purine nucleotide pool in tumors has been shown, but how synthesis and degradation of purine integrates in tumors has not been well

characterized. Hepatocellular carcinoma (HCC) is the most common liver cancer with a high mortality rate and limited treatments. Aberrant purine metabolism was observed in HCC, but the functional status of global purine metabolism in HCC and how that drive HCC fitness and therapeutic response remain unclear. Method HCC-specific purine metabolic changes were identified from the transcriptomic and metabolic data of tumor and paired non-tumor liver tissues obtained from 62 HCC patients from Thailand (discovery cohort) and validated in an additional 672 HCC with different race/ethnicities and etiologies. Correlation analysis of purine metabolic alteration and tumor-associated genomic, transcriptome and metabolome were conducted. The impacts of purine metabolism on HCC survival and therapeutic vulnerability were investigated. Biological functions of purine metabolic alterations were assessed *in vitro* and *in vivo* on multiple HCC cell lines. Results Using multi-omics integrative analyses, we found a tumor-specific activation of purine anabolism, induced by upregulation of purine de novo biosynthesis and inhibition of purine degradation, in HCC. A high purine anabolic status was associated with dysregulation of the DNA damage repairing (DDR) machinery in HCC, accompanied by unique somatic mutational signatures linked to patient prognosis. By examining drug responses to 180 molecular targeted agents in HCC cells, we found that increasing purine anabolism induced a therapeutic vulnerability of HCC to DDR targeting agents. Mechanistically, we found that excessive purine metabolites induced N6-methyladenosine (m6A) modification on DTL, a DDB1 cullin4 associated factor, thereby delaying the degradation of DTL mRNA transcriptomic remodeling of the DDR machinery and tumor fitness. Experimentally, we demonstrated that suppressing purine anabolism or exposing to DDR targeting agent, such as berzosertib, inhibited the growth of HCCs with high purine anabolism *in vitro* and *in vivo*. Conclusion Our study suggests that targeting purine anabolism or DDR may represent as attractive strategies in patients with high purine anabolic HCCs, and purine anabolic status could be a valuable biomarker to allocate systemic treatments for patients with advanced HCC.

#3685

Targeting a novel cell surface serine protease TMPRSS11B for lung cancer therapy

Hari Shankar Sunil[1], Barrett Updegraff[2], Jingfei Zhu[3], Bret M. Evers[3], John D. Minna[3], Ralph J. Deberardinis[3], Trudy G. Oliver[4], Kathryn A. O'Donnell[1]. *[1]Molecular Biology, University of Texas Southwestern Medical Center, Dallas, TX,[2]Seagen, Bothell, WA,[3]University of Texas Southwestern Medical Center, Dallas, TX,[4]Duke University, Durham, NC*

Lung cancer is the leading cause of cancer-related deaths worldwide. Patients have few therapeutic options, and disease progression is inevitable. Anti-PD-1/PD-L1 antibodies can induce potent anti-tumor immunity and have been approved as a first-line therapy for non-small cell lung cancer (NSCLC). However, only ~20% of all NSCLCs benefit from checkpoint blockade, underscoring the critical need for the development of new and innovative approaches to identify actionable therapeutic targets to treat NSCLC. We identified the Transmembrane Serine Protease *TMPRSS11B* as a novel gene that promotes the transformation of human bronchial epithelial cells *in vitro* and induces tumorigenesis *in vivo* (Updegraff et al., *Cell Reports*, 2018). Our data show that TMPRSS11B promotes solubilization of Basigin, an obligate chaperone of the lactate monocarboxylate transporters MCT1 and MCT4, and that TMPRSS11B interacts and co-localizes with Basigin and MCT4. Moreover, Basigin release mediated by TMPRSS11B enhances lactate export and glycolytic metabolism, thereby promoting tumorigenesis. This is of significant interest because *TMPRSS11B* is frequently overexpressed in human lung squamous cell cancers (LSCC) and high expression is associated with poor survival of NSCLC patients. Moreover, as a cell surface protein and enzyme, TMPRSS11B represents an exciting putative target for therapeutic intervention. Our new studies demonstrate that the catalytic activity of TMPRSS11B may be important for the interaction with Basigin and enhanced lactate export. We also evaluated the effect of *Tmprss11b* depletion in the KLN205 syngeneic LSCC mouse model. CRISPR/Cas9 knockout of *Tmprss11b* in KLN205 LSCC cells significantly reduced tumor burden in immunocompetent DBA/2 WT mice. Moreover, mass spectrometry analysis revealed TMPRSS11B-interacting proteins that may represent novel substrates of this enzyme. Current studies are focused on elucidating the molecular mechanisms through which TMPRSS11B promotes tumorigenesis and investigating the efficacy of TMPRSS11B inhibition in syngeneic and autochthonous mouse models of LSCC, where the effects on immune cell function will be assessed.

#3686

Blocking fatty acid oxidation suggests a potential new therapeutic approach for pancreatic cancer

Sang M. Woo, Sung-Sik Han, Ho Lee, Soo-Youl Kim. *National Cancer Center - Korea, Goyang-si, Gyeonggi-do, Korea, Republic of*

Background: Glycolysis is known as the main pathway for ATP production in cancer cells. However, in pancreatic ductal adenocarcinoma (PDAC) cells, glucose deprivation for 24 h did not reduce ATP levels, whereas it suppressed lactate production. We found that ATP production in PDAC cells critically depended on fatty acid oxidation (FAO) while normal cells showed no dependency on fatty acid. Therefore, FAO inhibition significantly decrease oxygen consumption rate as well as ATP production only in cancer cells.
Methods: To test whether cancer depends on fatty acid for energy metabolism, high- or low-fat diet was tested in spontaneous PDAC cancer model (KPC mouse: Kras(G12D)/p53(R172H)/Pdx1-Cre model). To test whether FAO is absolute requirement for ATP production in cancer, overall survival (OS) was monitored in KPC mice by crossbreeding with FAO gene knock out mice.
Results: First, the effects of calorie balanced high- or low-fat diets were tested to determine whether cancer growth is modulated by fatty acid instead of calories. A low-fat diet caused a 70 % decrease in pancreatic preneoplastic lesions accompanying decrease of body weight 20% compared with the control, whereas high-fat diet caused a 2-fold increase in preneoplastic lesions accompanied with 25% increase of body mass index in Kras(G12D)/p53(R172H)/Pdx1-Cre model (KPC model; spontaneous PDAC model). Second, the effect of FAO gene knock down was tested to determine whether OS is increased in KPC model. The crossbreeding of FAO gene knockout (+/-) and KPC mice resulted in 2-fold increase of OS.
Conclusions: The two results suggest that controlling obesity by diet as well as targeting FAO can enhance anti-cancer effect of cancer therapeutics including conventional anti-cancer drug or immune-oncology drug.
Clinical Trial Identification: IND for PDAC therapy with drugs targeting FAO will be submitted in 2022.

Legal Entity Responsible for the Study: This study is legally under review by IRB in National Cancer Center, Korea, and sponsored by National Research Foundation of Korea (NRF) and NCC-Bio Co.
Funding: Funding source: Basic Science Research Program through the National Research Foundation of Korea (NRF) funded by the Ministry of Science and ICT (NRF-2019M3A9G1104345)

#3687

Disruption of nucleotide homeostasis confers cancer cell susceptibility to oxidative phosphorylation inhibition independently of energy depletion

Xiaohong Zhao[1], Yuan Yuan Zhang[1], Liang Xu[1], Ting La[1], Yu Chen Feng[1], Hai Jie Tang[1], Ran Xu[1], Vinod K. Narayana[2], David P. De Souza[2], Lake-Ee Quek[3], Jeff Holst[4], Rick F. Thorne[1], Mark Baker[1], Tao Liu[5], Lei Jin[1], Xu Dong Zhang[1]. *[1]The University of Newcastle, Callaghan, Australia,[2]Metabolomics Australia, University of Melbourne, Melbourne, Australia,[3]The University of Sydney, Sydney, Australia,[4]The University of New South Wales, Sydney, Australia,[5]Children's Cancer Institute Australia for Medical Research, Randwick, Australia*

Cancer metabolism is highly heterogenous and flexible with the Warburg effect or oxidative phosphorylation (OXPHOS) prevailing in a cancer type- and context-dependent manner. Past studies have demonstrated that targeting OXPHOS robustly inhibits glycolysis-deficient cancer cell viability and tumorigenicity. However, the therapeutic potential of OXPHOS inhibition in metabolically flexible glycolysis-competent cancers is unclear. Furthermore, whether the depletion of OXPHOS-derived ATP or the abolition of OXPHOS-supported biosynthesis is the major determinant of cancer cell susceptibility remains obscure. To address these questions, we exposed a panel of metabolically flexible glycolysis-competent cancer cell lines to OXPHOS inhibitors and tested cell survival and proliferation. We monitored metabolic phenotypes and changes in metabolites using seahorse metabolic flux assays and targeted metabolomics, respectively. Stable isotope-tracing was carried out with uniformly labelled [^{15}N]-/[^{13}C]-aspartate. Patient-derived xenograft (PDX) models of colorectal cancer in NSG mice were used for *in vivo* validation. Here we provide evidence that

OXPHOS inhibition potently diminishes metabolically flexible glycolysis-competent cancer cell proliferation and tumorigenicity without causing devastating energy stress. The inhibition of cell proliferation by OXPHOS inhibitors is associated with S-phase cell cycle arrest and the enrichment of the G2/M DNA-damage check point regulation pathway, suggestive of replication stress. Indeed, IACS treatment significantly reduces the purine/pyrimidine nucleotide pools, which is primarily caused by aspartate deficiency resulting from a shortage in the electron acceptor NAD^+. The supplementation of exogenous nucleosides, aspartate, or pyruvate that can accept electron generating NAD^+, into the culture medium rescues cells from IACS-induced cell cycle arrest. Instructively, inhibition of GOT1, which catalyzes cytosolic aspartate biosynthesis when mitochondrial aspartate production is dampened, renders cancer cells grown in two- and three-dimensional cultures more susceptible to OXPHOS inhibition. Collectively, these results indicate that 1) disruption of nucleotide homeostasis is a major determinant of cancer cell susceptibility to OXPHOS inhibition; 2) OXPHOS inhibition is a promising avenue for the treatment of cancers that are metabolic flexible and glycolysis competent; and 3) GOT1 targeting is potentially a useful approach to improve the therapeutic efficacy of OXPHOS inhibition for cancer treatment.

#3688

Exploring metabolic vulnerabilities of metastatic prostate cancer to bone

Federica Mossa[1], Daniele Robesti[2], Christopher Vellano[1], Mark Titus[1], Joe Marszalek[1], Daniel Frigo[1], Christopher Logothetis[1], Taranjit Gujral[3], Eleonora Dondossola[1]. *[1]UT MD Anderson Cancer Center, Houston, TX,[2]San Raffaele Hospital, Milan, Italy,[3]Fred Hutchinson Cancer Center, Seattle, WA*

Currently, limited knowledge is available on subtype-specific metabolic features and their implications for treatment. Here, we investigated the metabolic determinants of the two major subtypes of castration-resistant prostate cancer (androgen receptor-expressing prostate cancer, ARPC; and aggressive variant prostate cancer, AVPC). Transcriptomic analyses revealed enrichment of gene sets involved in oxidative phosphorylation in ARPC tumor samples compared to AVPC. Unbiased screening of metabolic

signaling pathways in PDX models by proteomic analyses further supported an enrichment of oxidative phosphorylation in ARPC compared to AVPC, and a skewing toward glycolysis by AVPC. Metabolic in vitro analyses showed that C4-2B cells depended on aerobic respiration, while PC3 cells relied more heavily on glycolysis, as further confirmed by pharmacological interference using IACS-010759, a clinical grade inhibitor of oxidative phosphorylation tested in patients. In vivo studies confirmed a significant reduction by IACS-010759 in C4-2B tumors implanted subcutaneously or in bone, and no effect in subcutaneous PC3 tumors. Unexpectedly, PC3 tumors in bone responded to IACS-010759, indicating a microenvironment-induced metabolic reprogramming. These results suggest that castration-resistant ARPC and AVPC exhibit different metabolic dependencies with aerobic respiration being a major driver of ARPC, while AVPC depends on glycolysis, but can undergo metabolic reprogramming in bone. Such metabolic vulnerabilities may be exploited to either introduce further lines of treatments or in combination with the existing therapies. These findings also underscore the important role that the tumor microenvironment can play in reprogramming prostate cancer metabolism and thus, influence the efficacy of metabolically targeted therapies.

#3689

Uncovering the metabolic vulnerabilities in activated B cell diffuse large B cell lymphoma

Satishkumar Singh, Fouad Choueiry, Anuvrat Sircar, Narendranath Epperla, Jiangjiang Zhu, Lalit Sehgal. *The Ohio State University Wexner Medical Ctr., Columbus, OH*

DLBCL is the most common B cell malignancy in adults accounting for 30-40% of non-Hodgkin lymphoma. Only 60% of these cases are curable, with activated B cell DLBCL (ABC-DLBCL) having inferior outcomes than the germinal center (GCB) DLBCL. The use of ibrutinib to treat non-responsive/relapsed ABC-DLBCL cases has significantly improved the treatment of this disease. However, in more than 40% of ABC-DLBCL cases, the disease progresses or develops resistance to ibrutinib. Thus, there is an urgent unmet need to understand the molecular basis of resistance mechanisms and identify novel therapeutic regimens to treat IR DLBCL. Utilizing high throughput metabolomics, we identified cysteine-methionine

metabolism and alanine, aspartate, and glutamate metabolism to be deregulated in IR cells. We further identified interleukin four induced 1 (IL4I1), an L-amino acid oxidase that partakes in cysteine and methionine metabolism by contributing to the methionine salvage pathway. The amino acid cysteine contributes to cancer metabolic remodeling by a), in its free form, in redox control, as a component of the antioxidant glutathione or its involvement in protein s-cysteinylation, b), as a substrate for the production of hydrogen sulfide (H2S), which feeds the mitochondrial electron transfer chain and mediates persulphidation of ATPase and glycolytic enzymes, thereby stimulating cellular bioenergetics; and, c), as a carbon source for epigenetic regulation, biomass production, and energy production. Consistent with this, we show that loss of IL4I1 expression induced aberrant cysteine and methionine metabolism accompanied by metabolic reprogramming to OXPHOS, which collectively enabled increased drug tolerance of DLBCL. This adaptive metabolic mechanism exhibited increased cysteine and cystathionine intracellular levels in IR-DLBCL lacking IL4I1 expression. As cysteine and glutathione are scavengers of free radicals (mainly reactive oxygen species (ROS)), they can nullify the effects of the majority of oxidative or alkylating drugs used in cancer therapy, affording a vital resistance mechanism and disruption of cysteine homeostasis appears to be promising strategy for induction of cancer cell death and provide therapeutic approaches to treat Ibrutinib-resistant-ABC-DLBCL for improved patient care.

Cancer and Metabolism 2

#3693
Single-cell flux estimation analysis reveals the metabolic states of tumor-specific CD4$^+$ T cells

Mercy Kehinde-Ige[1], Ogacheko Okoko[2], Zhi-Chun Ding[2], Gang Zhou[2], Huidong Shi[2]. *[1]Department of Biochemistry and Molecular Biology, Georgia Cancer Center, Medical College of Georgia at Augusta University, Augusta, GA,[2]Georgia Cancer Center, Medical College of Georgia at Augusta University, Augusta, GA*

Adoptive Cell Therapy (ACT) holds great promise to transform cancer treatments. However, applying ACT to a broad patient population still faces

major challenges. The significant barriers to the success of ACT have been attributed to multiple factors, including functional exhaustion, poor persistence, and the inability of T cells to efficiently compete against tumor cells for metabolic resources in the tumor microenvironment (TME). These functional deficiencies highlight the importance of targeting T cell metabolism to improve ACT treatment outcomes. In the TME, tumor cells preferentially utilize glycolysis to rapidly generate ATP, converting pyruvate into lactate and creating a hypoxic environment that is inconducive for effector T cells due to a lack of access to the metabolites needed for sustenance, leading to T cell exhaustion, and declined proliferation. Consequently, T cells lose their function and are unable to persist against tumor cells. The expression of Constitutively Active Signal Transducer and Activator of Transcription 5A (CASTAT5) on tumor-specific $CD4^+$ T cells has been shown to improve their persistence, polyfunctionality, and anti-tumor effects. Our hypothesis is that the improved polyfunctionality and persistence of CASTAT5-$CD4^+$ T cells are partly due to the reprogramming of their metabolic landscape by CASTAT5, resulting in improved metabolic fitness. Single-cell metabolic pathway enrichment analysis of the identified polyfunctional CASTAT5-$CD4^+$ T cells revealed increased capacity for glycolysis, electron transport chain, oxidative phosphorylation, and amino acid metabolism. Single-cell Flux Estimation Analysis (scFEA) further revealed increased metabolic fluxes in amino acid uptake and synthesis, glycolysis, tricarboxylic acid (TCA) cycle, and polyamine synthesis. Interestingly, CASTAT5-$CD4^+$ T cells showed increased polyamine (spermine and spermidine) synthesis, with the upregulation of the metabolic fluxes from putrescine to spermine, catalyzed by spermidine synthase (Srm) and spermine synthase (Srs), both of which are also upregulated in the polyfunctional $CD4^+$ T cell populations. Spermidine and spermine have been shown to enhance mitochondrial metabolism in T cells, increasing their proliferation and survival. Here, we show that there is increased synthesis of spermine in CASTAT5-$CD4^+$ T cells, which may contribute to their increased capacity for oxidative phosphorylation and TCA cycle, leading to the observed improvements in their persistence and anti-tumor function. These findings suggest a role for the polyamine synthesis pathway in the improvement of T cell function. Further studies modulating targets within the polyamine synthesis pathway will help provide an improved understanding of the underlying mechanisms

affecting T cell function, thus, unveiling potential metabolic targets to improve the efficacy of tumor-specific T cells.

#3694

Metabolic response in human cervical cancer cells to modifications in bioavailable ATP

Parth K. Jayaswal, Taha Muhammad, Ashley Brown, Jeffrey Norris, Shaleen B. Korch. *Midwestern University - Glendale Campus, Glendale, AZ*

Introduction: Cancer cells utilize a markedly reduced oxidative phosphorylation (OXPHOS) when experiencing conditions of high oxygen stress (Warburg Effect/aerobic glycolysis), a phenomenon first studied by Otto Warburg. While there have been many discoveries associated with metabolic differences across cancer cells, one of the most common alterations is the primary means of generating ATP. The importance of deciphering these cellular decisions will enable an understanding of the multifaceted role ATP has in cancer proliferation, senescence, and chemotherapeutic resistance. The use of synthetic protein DX, a man-made ATP chelator with high specificity and affinity, is a proposed method of investigating the metabolic response in cancer cells. Hypothesis: Following DX expression, HeLa cells respond to energy stress (reduced intracellular ATP) via metabolic adaptations, specifically inducing the spare respiratory capacity.
Methods: The impact of DX on cell viability was determined using a tetrazolium-based colorimetric cell viability assay and a caspase 3/7 assay. To correlate phenotypic/viability change with DX activity, bioavailable ATP levels were measured at specific time points following DX expression. Additionally, the relative contribution of glycolysis and OXPHOS to the total ATP production rate was measured using the label-free XF Real Time ATP Rate Assay and XF Cell Mito Stress Test (XFe96 Seahorse, Agilent Technologies) over time post DX expression. To determine the impact of ATP stress on mitochondrial and nuclear content, both were quantified following DX-expression.
Results: In a time- and dose- dependent manner, DX negatively impacted cell growth and induced cell death via apoptosis, at a time concomitant with a decrease in bioavailable ATP. In response to DX over time, the total ATP

production rates in HeLa cells significantly decreased. Importantly, this reduction in the rate of ATP production was associated with a significant downregulation in both OXPHOS and glycolysis.
Conclusion: Advances in synthetic biology have allowed for the intentional design of artificial proteins that maintain function in vivo. These proteins can be developed into powerful investigative tools to study biological questions, such as cellular decisions involved in cancer cell metabolism. In response to DX-potentiated ATP stress, the significant reduction in both glycolysis and oxidative phosphorylation suggests metabolic downregulation is required to maintain HeLa cell viability.

#3695
Mitochondrial uncoupling reverses reductive carboxylation in cancer
Haowen Jiang, Clifford Jiajun He, Albert M. Li, Bo He, Yang Li, Jiangbin Ye. *Stanford University School of Medicine, Stanford, CA*

When electron transport chain (ETC) activity is inhibited upon hypoxia or when cultured in suspension, reductive carboxylation plays an essential role in supporting tumor growth through converting α-ketoglutarate (α-KG) to citrate, which is converted to acetyl-coenzyme A (acetyl-CoA) for lipogenesis. However, there is no effective way to target reductive carboxylation for tumor therapy. In this study, we use the mitochondrial uncoupler niclosamide ethanolamine (NEN) and BAM15 to reverse reductive carboxylation in cancer cells. Uncoupler treatment activates ETC and increases the cellular NAD^+/NADH ratio. Using U-^{13}C-glutamine and 1-^{13}C-glutamine tracers, we discovered that uncoupler treatment accelerates the oxidative TCA cycle and blocks reductive carboxylation, particularly under hypoxia and spheroid culture condition. Uncoupler treatment significantly reduces tumor cell proliferation, survival and sphere formation. In addition, the intracellular acetyl-CoA levels are significantly decreased by NEN treatment. Furthermore, lipidomics analysis showed that NEN treatment reduced fatty acid abundance and altered the lipid composition under both normoxia and hypoxia. Together, these data demonstrate mitochondrial uncoupling redirects the α-KG flux from reductive carboxylation back to the oxidative TCA cycle, highlighting that the ETC activity and NAD^+/NADH ratio is the key switch that determines

the metabolic fate of α-KG. Reversing reductive carboxylation could be one key mechanism that mitochondrial uncoupler inhibits tumor growth.

#3696

L-arginine depletion causes different proliferation responses in breast cancer subtypes - Relation to gene expression profiles of L-arginine metabolic pathways

Juliane Hannemann, Fiona Franke, Mariola Kastner, Rainer Böger. *Institute of Clinical Pharmacology and Toxicology, University Medical Center Hamburg-Eppendorf, Hamburg, Germany*

Metabolic fingerprinting provides insight into cancer biology, improving personalized therapeutic strategies. We sought to unravel responses of the molecular subtypes of breast cancer to L-arginine depletion in vitro. Availability of the semi-essential amino acid L-arginine limits protein synthesis and cell proliferation. L-Arginine is the substrate for nitric oxide synthases (NOS) and arginases (ARG), enzymes also involved in the regulation of cell proliferation. Clinical studies have provided contrasting results regarding the role of L-arginine in breast cancer.We studied the response of different breast cancer cell lines to L-arginine depletion and the molecular mechanisms underlying this effect. MCF-7, SK-BR-3, BT-474, MDA-MB-231, and MDA-MB-468 cells were cultured under standard conditions and compared to MCF-12A normal breast epithelial cells. Cells were maintained in culture media with 200 mg/L (control) or 0 mg/L of L-arginine (depletion) for up to 240 h. Cell proliferation was analyzed and intracellular concentrations of L-arginine, L-ornithine, and L-citrulline were measured by UPLC-MS/MS every 24 h. mRNA expression of genes involved in L-arginine metabolism was quantified by qRT-PCR.
MCF-12A control cells did not proliferate in the absence of extracellular L-arginine. Their intracellular L-arginine content dropped sharply, whilst L-ornithine and L-citrulline were only slightly reduced. By contrast, proliferation of BT-474, SK-BR-3, and MDA-MB-468 cells was unaffected by L-arginine depletion ($p<0.05$), whilst MCF-7 and MDA-MB-231 cells showed significantly higher proliferation rates in the absence of L-arginine ($p<0.05$). L-arginine concentration dropped sharply within 24 h in MCF-7 cells, but only by 25-50% in the other cell lines ($p<0.01$). L-ornithine dropped to almost zero within 24 h in both estrogen receptor positive cell

lines (MCF-7 and BT-474), whilst being only slightly reduced in SK-BR-3 cells ($p<0.01$). L-ornithine was not significantly reduced in MDA-MB-231, but strongly reduced in MDA-MB-468 cells ($p<0.05$). L-citrulline showed no significant change in any of the cell lines. mRNA expression of NOS, ARG, and the L-arginine salvage pathway (ASS1 and ASL) was differentially expressed amongst the cell lines. SK-BR-3 showed high expression of the L-arginine salvage pathway; BT-474 had the highest expression levels of NOS and ARG2, and MDA-MB had high ARG2 but very low NOS expression. Gene expression patterns of MCF-12A and MCF-7 were very similar.
In conclusion, metabolic fingerprinting reveals complex and differential regulation of L-arginine pathways in breast cancer cell lines. These analyses may help to understand differences in proliferation during L-arginine depletion, thus offering a perspective to further personalize treatment options within classical molecular breast cancer subtypes.

#3697

Modulation of Nicotinamide N-Methyl Transferase (NNMT) expression in TNBC is associated with altered cell membrane cholesterol levels

Woei-Yaw Chee[1], Deniz Nesli Dolcen[2], Lynda Bennett[1], Suzanne D. Conzen[1]. *[1]Internal Medicine, UT Southwestern Children's Medical Center Research Institute, Dallas, TX,[2]Internal Medicine, Stanford University, San Francisco, CA*

Introducti**on:** Cancer cells often develop a program of metabolic adaptability and epigenetic remodelling to promote gene expression changes causing cancerous cell proliferation and invasion. The metabolic-epigenetic axis as a an underlying mechanism of carcinogenesis could lead to new approaches to cancer treatment. Nicotinamide N-Methyl Transferase (NNMT) is a metabolic enzyme that catalyzes the transfer of a methyl group from S-Adenosyl methionine (SAM) to nicotinamide, thereby decreasing the overall methyl pools for RNA, histone and DNA methylation. High NNMT expression has been previously associated with a poor outcome in TNBC.
Hypothesis: We hypothesized that high versus low NNMT activity and resulting oncogenic gene expression in TNBC may alter histone methylation is association with altered metabolic pathway activation.

Methods: We used two TNBC cell lines models, MDA-MB 231 and SUM159, to study the association between high versus low NNMT activity and metabolic pathway activation. Surprisingly, we identified gene expression pathways suggestive of increased free cholesterol biosynthesis gene expression with low NNMT, and then used biochemical assays and filipin to measure free cholesterol in both total high and low NNMT TNBC cell lysates and relative cholesterol expression in the High vs Low NNMT cell membranes.
Results: *In vitro*, NNMT knockdown resulted in increased cholesterol synthetic pathway enzyme expression in both TNBC cell lines. I*n vivo* studies also showed that protein expression of cholesterol synthesis enzymes was also increased in NNMT-depleted MDA-MB 231 xenografted tumors. Interestingly, the increased cholesterol level upon NNMT depletion was mainly localized at the plasma membrane via Filipin III staining, suggesting a possible association with less cellular membrane fluidity and a decreased oncogenic phenotype. In ongoing experiments, we are evaluating whether changes in histone methylation in high vs low NNMT cells are associated with differential expression of cholesterol biosynthetic genes, and free cholesterol production. We hypothesize that NNMT might epigenetically decrease the methylation of histones regulating cholesterol production in TNBC.

#3698

Epigenetic modification induced reprogramming of PUFAs-associated metabolism during trastuzumab resistance formation of HER2-positive breast cancer

Yongmei Yin[1], Ningjun Duan[1], Yijia Hua[1], Shuang Hu[2]. *[1]Oncology, The First Affiliated Hospital of Nanjing Medical University, Nanjing, China,[2]Nanjing Maternity and Child Health Care Hospital, Nanjing, China*

Background: Secondary trastuzumab resistance seriously affects the treatment of HER2-positive breast cancer. Although studies have demonstrated several potential reasons that cause trastuzumab resistance, we still have poor knowledge about the changes in cell itself as well as its interaction with tumor microenvironment (TME) components during resistance formation. Here we suggested that altered histone modification reprograms polyunsaturated fatty acids (PUFAs) metabolism, which reduces

cellular PUFAs and stimulates prostaglandin E2 (PGE2) production. Excessive PGE2 may further affect both cancer cells as well as immune cells in TME.
Materials and Methods: Secondary trastuzumab-resistant cell line SKBR3_HR was generated from sensitive SKBR3 cells by raising trastuzumab concentration gently from 1ug/ml to 20ug/ml in 30 weeks. Cell viabilities were measured by CCK8 test. CUT&Tag with anti-H3K4me3 and anti-H3K27me3 antibodies were applied to make sequencing libraries. Total RNA and protein were collected for transcriptome and proteome analysis. Activity scores of metabolism processes were defined and calculated as the relative gene expression value averaged over all genes in this pathway in certain cell types. Oxidized PUFAs and PGE2 were assessed by flow cytometry with BODIPY-C11 and ELISA, respectively.
Results: SKBR3_HR cells showed similar viability as primary resistant JIMT1 cells and were significantly higher than original SKBR3 cells. Pathway analysis indicated reduced PUFAs synthesis and activated arachidonic acid metabolism. As a consequence, oxidized PUFAs decreased while PGE2 accumulated heavily in SKBR3_HR cells, which may promote tumor and vascular endothelial cell proliferation but interrupt immune cell activity in TME. Transcriptional activity of two critical PUFAs synthesis-related genes, FASN and SCD, were reduced in resistant cells, while two key genes in arachidonic acid metabolism, PTGS1 and PTGES, were activated. H3K4me3 and H3K27me3 play opposite but critical rules in transcriptional regulation. During resistance formation, changes happened on 3256 H3K27me3 peaks as well as 316 H3K4me3 peaks. In detail, although little H3K27me3 changes were found at the promoter regions of four genes (FASN, SCD, PTGS1 and PTGES), reduced H3K4me3 levels may inhibit FASN and SCD expression while raised levels could stimulate PTGS1 and PTGES transcription.
Conclusions: Combining the transcriptome and histone modification data, we have a deeper understanding of the cellular adaptions to trastuzumab. Altered trimethylation of H3K4 but not H3K27 remodels the expressions of FASN, SCD, PTGS1 and PTGES, drives the reprogramming of PUFAs-associated metabolism, and finally reduces cellular PUFAs while stimulates PGE2 production. High PGE2 level may affect the activities of tumor and TME-related cells.

#3699

Involvement of p53 and KRAS in the regulation of SLC38A5 in colon cancer

Nhi Thi Phuong Nguyen, Sathish Sivaprakasam, Vadivel Ganapathy. *Cell Biology and Biochemistry, Texas Tech University Health Sciences Center, Lubbock, TX*

Cancer-associated upregulation has been demonstrated for selective glucose transporters and amino acid transporters. The amino acid transporter SN2 (SLC38A5) represents the latest addition to this list. Transcriptomic analysis of tumor tissues has shown SLC38A5 is upregulated in breast and colon cancer. SLC38A5 is an amino acid-dependent Na^+/H^+ exchanger, induced in cancer, which not only supplies amino acids to cancer cells but also maintains an alkaline intracellular pH. The substrates for SLC38A5 include glutamine, asparagine, histidine, methionine, glycine, and serine, highlighting the role of SLC38A5 in glutamine addiction and one-carbon metabolism, both pathways being essential for cancer cells. In addition, SLC38A5 activates macropinocytosis, a process involved in cellular uptake of proteins in the extracellular fluid to meet amino acid demands in cancer cells. Since the transporter is upregulated in colon cancer, we hypothesized that the multiple functions of SLC38A5 fuel the growth, proliferation, and survival in colon cancer cells and that its induction involves oncogenic mutations in p53 and KRAS that are common mediators of carcinogenesis in colon. Firstly, we used a panel of colon cancer cells and analyzed SLC38A5 expression and its functional characteristics. Next, we compared SLC38A5 expression and function between two isogenic cell lines: SW48 with and without the oncogenic mutation (G12D) in KRAS and HCT116 with and without the tumor suppressor p53. Among the colon cancer cells examined, KM12L4 showed highest expression of SLC38A5; therefore, we characterized the function of the transporter in detail in this cell line. Our studies showed that KM12L4 cells were able to take up serine, one of the substrates for SLC38A5, in a Na^+-dependent manner in the presence of 5 mM tryptophan, which is not a substrate for SLC38A5 but is known to block LAT1 transporter, which also transports serine. SLC38A5 exhibited an active serine-uptake when Na^+ was replaced with Li^+ at a higher pH. Li^+ tolerance and a higher activity at an alkaline pH are two unique features of SLC38A5. The oncogenic mutation G12D in KRAS increased SLC38A5

activity in SW48 cells. In contrast, loss of p53 decreased SLC38A5 activity in HCT116 cells. These data demonstrate that SLC38A5 is induced in colon cancer cells and its activity is increased in the presence of oncogenic KRAS mutations and suppressed when p53 is inactivated, thus providing a valuable insight into the molecular mechanisms for the upregulation of the transporter in colon cancer. We conclude that SLC38A5, an amino acids transporter, is upregulated in colon cancer and its functions are uniquely suited to promote cell proliferation and tumor growth. We also conclude that KRAS and p53 functional status play a critical role in the increased SLC38A5 expression and activity in colon cancer. These data suggest that SLC38A5 could be exploited as a drug target for cancer therapy.

#3700

Isocitrate dehydrogenase 1 sustains a hybrid cytoplasmic-mitochondrial tricarboxylic acid cycle in prostate cancer

Kevin Gonthier[1], Cindy Weidmann[2], Line Berthiaume[2], Cynthia Jobin[1], Aurélie Lacouture[1], Camille Lafront[1], Mario Harvey[2], Bertrand Neveu[3], Jérémy Loehr[2], Alain Bergeron[3], Yves Fradet[1], Louis Lacombe[1], Julie Riopel[3], Éva Latulippe[3], Chantal Atallah[3], Michael Shum[1], Jean-Philippe Lambert[1], Frédéric Pouliot[1], Martin Pelletier[1], Étienne Audet-Walsh[1].
[1]Université Laval, Québec, QC, Canada,[2]CRCHU de Québec-Université Laval, Québec, QC, Canada,[3]CRCHU de Québec, Québec, QC, Canada

Background: The androgen receptor (AR) is an established orchestrator of cell metabolism in prostate cancer (PCa), notably by inducing an oxidative mitochondrial program. Intriguingly, AR regulates cytoplasmic isocitrate dehydrogenase 1 (IDH1) but not its mitochondrial counterparts IDH2 and IDH3. Here, we aimed to understand the functional role of IDH1 in PCa.
Methods: Mouse models, *in vitro* human PCa cell lines, and human prostate organoids were used to study the expression and activity of IDH enzymes in the normal prostate and PCa. Genetic and pharmacological inhibition of IDH1 was then combined with extracellular flux analysis and gas chromatography-mass spectrometry for metabolomic analyses and cancer cell proliferation *in vitro* and *in vivo*.
Results: In PCa cells, more than 90% of the total IDH activity is mediated through IDH1 rather than its mitochondrial counterparts. This profile seems

to originate from the specialized prostate metabolic program, as observed using mouse prostate and human patient-derived organoids.
Pharmacological and genetic inhibition of IDH1 impaired mitochondrial respiration, suggesting that this cytoplasmic enzyme contributes to the mitochondrial tricarboxylic acid cycle (TCA) in PCa. Mass spectrometry-based metabolomics confirmed this hypothesis, showing that inhibition of IDH1 impairs carbon flux into the TCA cycle. Consequently, inhibition of IDH1 decreased PCa cell proliferation *in vitro* and *in vivo*.
Conclusions: These results demonstrate that PCa cells have a hybrid cytoplasmic-mitochondrial TCA cycle that depends on IDH1. This metabolic enzyme represents a metabolic vulnerability of PCa cells and a potential new therapeutic target.

#3701
Targeting wild-type IDH1 enhances chemosensitivity in pancreatic cancer
Mehrdad Zarei[1], Omid Hajihassani[1], Jonathan J. Hue[2], Hallie J. Graor[1], Arian Hajihassani[3], Alexander W. Loftus[2], Luke D. Rothermel[2], Jordan M. Winter[2]. *[1]Case Western Reserve University School of Medicine, Cleveland, OH,[2]University Hospitals, Cleveland, OH,[3]University of Pittsburgh Medical Center, Pittsburgh, PA*

Introduction: Pancreatic ductal adenocarcinoma (PDAC) is a leading cause of cancer mortality in the United States. The poor prognosis is in part due to development of chemotherapy resistance, despite improvements in multiagent regimens. Our previous work demonstrated that oxidative stress plays an important role in drug resistance. Wild-type isocitrate dehydrogenase 1 (IDH1) is an important enzyme that generates cytosolic NADPH to maintain redox homeostasis and protect cancer cells from oxidative damage. Additionally, we demonstrated that ivosidenib (AG-120), an FDA-approved mutant IDH1 inhibitor, is actually a potent inhibitor of wild-type IDH1, under low magnesium and nutrient levels that are present in the tumor microenvironment.
Methods: We evaluated IDH1 expression in PDAC using The Cancer Genome Atlas (TCGA). Cell viability was assessed by Trypan blue and PicoGreen in drug combination assays. Cellular reactive oxygen species (ROS) levels were determined by the DCFDA method. To further assess the

therapeutic potential of AG-120 in combination with chemotherapy, tumor volume analyses were performed using patient-derived xenografts (PDX) in athymic nude mice, and survival studies were performed in C57BL/6J mice transplanted with orthotopic murine pancreatic cancer.
Results: Analysis of TCGA data indicated that IDH1 is overexpressed in pancreatic cancer tumors. Treatment of MiaPaca2 and Panc1 cancer cells with 5- fluorouracil (5-FU) induced expression of wild-type IDH1 in vitro. Short-term cell viability data demonstrated that targeting IDH1 with AG-120 when combined with DNA-damaging agents (5-FU, oxaliplatin) had a synergistic effect with a positive synergy score and Bliss score greater than 1. Additionally, we assessed long-term cell survival using colony formation assays, which yielded a dramatic reduction in cell survival for both Panc1 and MiaPaCa-2 cells when 5-FU was combined with AG-120, as compared to single-agent controls. Inhibiting IDH1 impairs the ability of pancreatic cancer cells to scavenge ROS levels, enhances chemotherapy-induced apoptosis in pancreatic cancer cells via ROS-mediated damage in vitro. Both PDX tumor volume studies and overall survival analyses revealed that the combination of these AG-120 and chemotherapy synergistically enhanced anti-tumor activity and doubled the survival benefits as compared to single-agent alone.
Conclusion: IDH1 plays a critical role in tumorigenesis and chemoresistance in pancreatic cancer. Our data demonstrate that IDH1 inhibition with AG-120 may enhance chemotherapy efficacy and represents an important area for future investigation in the form of clinical trials.

#3702

Serine promotes aggressive phenotype in renal cancer

Suman Karki[1], Anirban Kundu[1], Garret Brinkley[2], Hyeyoung Nam[3], Kayla Goliwas[4], Jessy Deshane[5], Sunil Sudarshan[1]. *[1]Department of Urology, University of Alabama at Birmingham, Birmingham, AL,[2]Department of Urology, Tulane University, New Orleans, LA,[3]University of Alabama at Birmingham, Birmingham, AL,[4]Division of Pulmonary, Allergy, and Critical Care, University of Alabama at Birmingham, Birmingham, AL,[5]Department of Medicine, University of Alabama at Birmingham, Birmingham, AL*

Tumor cells are known to have increased demand for nutrients to support proliferation. Among the most highly utilized nutrients by tumor cells are nonessential amino acids (NEAAs). While the role of NEAAs in supporting tumor growth is well-established, their role in supporting aggressive phenotypes such as migration and invasion is poorly understood. Yet, the major cause of morbidity from malignancies such as renal cell carcinoma (RCC) is metastasis. Through an unbiased approach, we assayed the role of NEAAs in promoting the migration of RCC cells. We demonstrate that exogenous serine and glutamine are essential and sufficient to support aggressive phenotypes in RCC. Moreover, the availability of both NEAAs is critical for the expression of the proinvasive transcription factor SNAIL. Our data converge on the role of these two NEAAs in supporting the translation of this factor. Perturbations that limit the availability and/or synthesis of either result in translational reprogramming through the integrated stress response (ISR) that leads to loss of SNAIL1 expression and attenuates aggressive phenotypes. Our findings associate nutrient status to the ISR including ER stress. Collectively, our study highlights new insights for NEAA metabolism in supporting aggressive tumor phenotypes and could reveal novel approaches to mitigate metastasis by targeting NEAA availability and/or utilization.

#3703

Multimodal metabolic imaging and proteomics of radiation resistance in head and neck squamous cell carcinoma

Jesse D. Ivers, Sina Dadgar, Narasimhan Rajaram. *Biomedical Engineering, University of Arkansas System, Farmington, AR*

Radiation resistance can halt a well-curated treatment plan in its tracks, but it may take weeks to realize this lack of efficacy resulting in lost time and unnecessary side effects. In this study, we sought to elucidate novel biomarkers of radiation resistance to predict treatment response in head and neck squamous cell carcinoma (HNSCC) at much earlier timepoints. We grew tumor xenografts from radiation-resistant UM-SCC-47 (n=25) and -sensitive UM-SCC-22B (n=37) cells in nude athymic mice. Each group was randomly divided into treatment and control groups, which were further subdivided into four timepoints for tumor excision: pre-treatment baseline, 1-, 24-, and 48-hours post-treatment. Prior to excision, we injected

pimonidazole to quantify tumor hypoxia. We determined the two-photon excited fluorescence intensity and lifetime of NADH and FAD and quantified the optical redox ratio, ratio of free to bound NADH, and mean NADH lifetime of frozen sections of each tumor. We observed spatial and temporal heterogeneity in these high-resolution optical maps that indicated different metabolic programs in radiation-resistant and -sensitive tumors. A histogram-based heterogeneity analysis revealed time dependent shifts toward glycolysis in the radiation-resistant UM-SCC-47 treatment group, while the sensitive UM-SCC-22B treatment group showed the opposite trend. Proteomics performed on both cell lines identified multiple dysregulated proteins that are often implicated in HNSCC and associated with metabolic reprogramming — specifically, EGFR and SMAD4. We also found elevated levels of hypoxia and HIF-1 in the UM-SCC-47 tumors compared with the UM-SCC-22B tumors prior to and post-radiation. Using spatially co-registered optical imaging and immunohistochemical maps of the same field of view, we will present correlations between our optical markers and EGFR, SMAD4, and HIF-1. These studies will provide evidence of how protein dysregulation causes changes to optical metabolic imaging markers.

#3704

The essential role of an alternate mRNA translation initiation in the regulation of breast cancer cell metabolism

Hanna Rosenstock[1], Erna Mitaishvili[2], Columba de la Parra[3]. *[1]Chemistry, Herbert H. Lehman College, City University of New York, New York, NY,[2]Biology Ph.D. Program, The Graduate Center, City University of New York, New York, NY,[3]Chemistry, Herbert H. Lehman College, City University of New York & The Graduate Center, New York, NY*

Translational control and metabolic reprogramming are hallmarks of advanced cancers. Important genes involved in cancer progression express mRNAs that are selectively translated, including regulators of cancer cell metabolism.

Cancer cells acquire an altered metabolism, switching from oxidative phosphorylation (OXPHOS) to a glycolytic phenotype (Warburg effect), to increase reliance on alternate metabolic pathways to support growth, proliferation, and metastasis. Triple-negative breast cancer (TNBC), one of

the most aggressive and highly metastatic subtypes with the poorest outcome, is characterized by elevated glycolysis and low OXPHOS. Still, the exact mechanism for this metabolic switch is largely unknown. Using a TNBC cell model it has been shown an alternate mechanism of cap-dependent but mTORC1/eIF4Eindependent mRNA translation by the eIF4G homolog, DAP5, which directly binds the cap-binding protein eIF3d. Our research indicates that this alternate translation initiation is essential in regulating several mRNAs involved in breast cancer metabolism. DAVID analysis from genome-wide transcriptomic and translatomic studies, metabolomic assays including Glycolysis Assay [Extracellular Acidification], Oxidative Phosphorylation, and Mitotracker Assay, as well as RT-PCR and western blot analysis was performed from well-characterized triple-negative aggressive breast cancer cell lines,4T1 and MDA-231, Non-silencing (Nsi) control and silencing DAP5 (shDAP5) samples.
Several mRNAs related to glucose metabolism decreased after silencing DAP5 and on the opposite, critical mRNAs associated with OXPHOS increased, independent of their steady-state mRNA abundance. Silencing DAP5 increased Oxidative Phosphorylation activity and decrease the glycolytic rate in TNBC breast cancer cells. Proteins correlated with aberrant glycolytic metabolism including the E-cadherin transcriptional repressors Snail (SNAI1) were reduced after silencing of DAP5. Our data indicates that the alternate mRNA translation initiation mechanism by DAP5 of specific mRNAs correlated to glycolysis and OXPHOS could play an essential role in the mechanism by which TNBC breast cancer cells orchestrate a metabolic switch required for malignant progression and metastasis.

#3705

L-2HG, oncometabolite-driven epigenetic and epitranscriptomic reprogramming creates metabolic vulnerability in renal cancer

Anirban Kundu[1], Garrett J. Brinkley[1], Hyeyoung Nam[1], Suman Karki[1], Richard Kirkman[1], Hayley Widden[2], Michelle Johnson[3], Juan Liu[4], Yasaman Heidarian[5], Nader Mahmoudzadeh[1], Devin Absher[6], Han-Fei Ding[7], David Crosman[2], William J. Placzek[2], Jason Locasale[4], Dinesh Rakheja[8], Victor Darley-Usmar[2], Jason Tennessen[5], Sunil Sudarshan[1].
[1]Urology, University of Alabama at Birmingham, Birmingham,

AL,[2]University of Alabama at Birmingham, Birmingham, AL,[3]Molecular and Cellular Pathology, University of Alabama at Birmingham, Birmingham, AL,[4]Pharmacology and Cancer Biology, Duke University, Durham, NC,[5]Biology, Indiana University, Bloomington, IN,[6]HudsonAlpha Institute for Biotechnology, Huntsville, AL,[7]Pathology, University of Alabama at Birmingham, Birmingham, AL,[8]Pathology, UT Southwestern, Dallas, TX

The oncometabolite, L-2-hydroxyglutarate (L-2HG) is elevated in the most common form of renal cell carcinoma-RCC (clear cell histology) and promotes tumor progression. L-2HG is structurally similar to α-ketoglutarate (α-KG). Therefore, L-2HG can competitively inhibit enzymes that utilize α-KG as a cofactor including α-KG-dependent dioxygenases that can profoundly impact gene expression via effects on the epigenome and epitranscriptome. RCC cell lines lack the L-2HG dehydrogenase enzyme (L2HGDH), resulting in their high L-2HG level. RNA-seq of control (high L-2GH) and an L2HGDH reconstituted (low L-2HG) RCC cell line has revealed that L-2HG suppresses the expression of serine biosynthesis genes, *PHGDH* and *PSAT1*. The findings were consistent in the patient samples where high L-2HG renal tumors had lower levels of *PHGDH* and *PSAT1* expressions than that of the low L-2HG renal tumors and the patient-matched normal kidneys. Consistently, ^{13}C-metabolomics labeling studies demonstrate that raised L-2HG suppresses *de novo* serine biosynthesis. Moreover, LC-MS analysis of the metabolites isolated from the kidneys of L2HGDH KO and wild-type (WT) mice revealed less serine content in the absence of L2HGDH, further confirming that high L-2HG suppresses serine biosynthesis *in vivo*. We found that L-2HG-mediated inhibition of the α-KG-dependent histone demethylase KDM4C silences ATF4 transcription. ATF4 is a master regulator of amino acid biosynthetic genes including *PHGDH* and *PSAT1*. Using ATF4 gain of function analysis, we confirmed that high L-2HG causes the suppression of PHGDH and PSAT1 in an ATF4-dependent manner. In addition, we demonstrate that L-2HG promotes the accumulation of the epitranscriptomic mark N^6-methyladenosine (m6A) via inhibiting α-KG-dependent RNA demethylases ALKBH5 and FTO. In the setting of high L-2HG, m6A is enriched in the 3'-UTR region of transcripts including *PSAT1*. Using mutational analysis, we demonstrate that L-2HG promotes m6A accumulation at a specific site within the 3'UTR

of *PSAT1* that silences its translation. In accord with these data, found that high L-2HG RCC cells require exogenous serine for *in vitro* proliferation and *in vivo* tumor growth. Furthermore, this serine liability can be rescued upon lowering cellular L-2HG levels. Metabolomics analyses demonstrate that exogenous serine is required to maintain cellular pools of glutathione in high L-2HG RCC which supports both proliferation and resistance to oxidative stress. The data indicate that the L-2HG elevation in RCC reconfigures tumor metabolism through a bimodal mechanism via remodeling of both the epigenome and epitranscriptome. This results in a serine liability in the setting of raised L-2HG. Collectively, our data unmask a metabolic vulnerability that can be harnessed for precision-based approaches to kidney cancer.

#3706

The significance of cholesteryl ester profiles in hepatocellular carcinoma

Nazar Rahmanov[1], Zhirong Liu[2], Jinghe Mao[3], Patrick Kyle[1], Xinchun Zhou[1]. *[1]Pathology, University of Mississippi Medical Center, Jackson, MS,[2]Biochemistry, Shanxi Medical University, Taiyuan, China,[3]Biology, Tougaloo College, Tougaloo, MS*

Introduction: The association between cholesteryl ester (CE) profiles in the liver and oncogenesis, gender, and age disparities in hepatocellular carcinoma (HCC) has not been studied to date. This study aims to compare CE profiles between benign liver tissue (BLT) and HCC, and to correlate these findings with oncogenesis and disparities in patients with HCC.
Methods: Paired BLT and HCC samples obtained from 32 patients with the diagnosis of HCC were used for lipid extraction. Electrospray ionized mass spectrometry (ESI-MS) was used to determine CE profiles, including 22 individual CE species and the total levels of CE. The CE profiles in BLT and HCC were compared and stratified between subgroups based on the gender and age of the patients. The student T-test was used for statistical analysis and the significant p-value was set at 0.05.
Results: Total CE levels were higher in HCC than in BLT, but not statistically significant (1.8-fold, p=0.16). Interestingly, 5 saturated CE individual species and 2 mono-unsaturated individual CE species (C14:0, C16:0, C16:1, C18:0, C18:1, C19:0, and C20:0) were significantly higher in

HCC than in BLT (2.4 to 14-fold higher). None of the individual poly-unsaturated CE species showed a statistical difference between HCC and BLT. In males, the levels of 3 saturated individual CE species (C16.0, 16:0, and C20:0) were significantly higher in HCC than in BLT (1.9 to 21.3-fold higher levels). In contrast, CE 16:1 was significantly lower in HCC than in BLT (0.9-fold, p=0.02) in males. In females, none of the CE profiles showed a significant difference between HCC and BLT. Total CE levels were 2.1-fold higher in males with HCC than in females with HCC (18.6nM vs. 8.92nM). In young patients (<66-year-old), individual CE species C14:0 was significantly higher in HCC than in BLT (19.1-fold, p=0.038). In old patients (≥66-year old), individual CE species C20:0 was significantly higher in HCC than in BLT. Total CE levels were 2.1-fold higher in young HCC patients than in old HCC patients (13.68nM vs. 6.45nM).
Conclusion: This study reveals that an increase in hepatic total CE levels and individual CE species are associated with the oncogenesis of HCC and show gender and age disparities. These findings could be helpful in prevention, treatment, exploring biomarkers, and understanding disparities in HCC.

#3707
UXS1 is a synthetic lethal target in cancer
Michelle Patricia Cicchini[1], Shuzhen Wu[2], Yang Peng[1], Yanhua Rao[1].
[1]GlaxoSmithKline, Collegeville, PA,[2]GlaxoSmithKline, Boston, MA

Studies presented here were conducted to validate UXS1 as a synthetic lethal target in UGDHhigh expressing cancer. *In vitro* and *in vivo* knockout studies were used to investigate the role of UXS1 in UGDH-high cancers. UXS1 has been validated as a synthetic lethal target in cancer cell lines highly expressing UGDH *in vitro* by CRISPR-mediated knockout of UXS1 in a panel of lung cancer cell lines. In addition to UGDH expression predicting UXS1 dependency, we have shown UGDH overexpression functional drives UXS1 dependency, such that knockout of UGDH rescues cellular growth defects seen with UXS1-knockout alone. Furthermore, catalytic activity of UXS1 was shown to be required, as wildtype but not catalytic deficient UXS1 was able to rescue cellular growth defects seen with endogenous UXS1 knockout in UGDH-high cancer cell lines. Together

this data suggests that dysregulation of some metabolite(s) is driven by high expression of UGDH when knockout of UXS1 prevents normal pathway flux of UDP-Glucuronic Acid (UDP-GA) to be converted to UDP-Xylose (UDP-X), leading to the synthetic lethal effect observed as impaired cellular growth. To validate UXS1 as a target *in vivo*, an inducible genetic knockout system to knockout UXS1 showed impaired tumor growth, but no tumor regression. Sanger sequencing of UXS1 knockout efficiency at different time course suggested a slow and incomplete dropout of the UXS1-KO cells *in vivo.* Although *in vitro* efforts have shown UXS1 to a synthetic lethal target, the failure to induce a robust *in vivo* effect of UXS1 knockout have casted doubts on the promise of UXS1 being an effective target for the proposed indication.

#3708

Platelet-derived microparticles modulate breast cancer malignant processes

Vanessa Veilleux, Nicolas Pichaud, Luc H. Boudreau, Gilles A. Robichaud.
Université de Moncton, Moncton, NB, Canada

Breast cancer is one of the leading causes of morbidity and mortality among women, where metastasis accounts for the majority of deaths associated with this disease. Thus, the potential to effectively target tumor malignancy offers hope to mitigate disease progression and improve patient outcomes. It is well established that platelets promote multiple processes of metastasis cascade. Recently, platelets have received new attention for their impact in cancer through the production of platelet-derived microparticles (PMPs). Interestingly, PMPs allow intercellular exchange and trafficking of bioactive material through the internalization of these vesicles into recipient cells. As a result, the delivery of the intravesicular cargo can modulate signaling and activation processes of recipient cells. We recently identified a new subpopulation of these vesicles (termed mitoMPs) containing functional mitochondria. Given the predominant role of mitochondria in cancer malignancy, we believe that mitoMPs provide an important source of foreign mitochondria to support recipient breast cancer cells in malignancy and disease progression. We therefore set out to study the impact of mitoMPs on breast cancer metabolic and phenotypic processes involved in metastasis. Technically, PMPs were generated and purified from human

blood platelets and co-incubated with various breast cell models (MB231, MCF7 and MCF10A). The physiological significance of mitoMPs in breast cancer disease was then assessed using various cellular and molecular assays. We demonstrate that the level of PMP internalization is highly dependent upon the type of breast cancer recipient cells. Furthermore, we show that the cargo of mitoMPs (notably mitochondria) is biologically active where recipient breast cancer cells acquired mitochondria-dependent functions, such as increased oxygen consumption rates and intracellular ATP production. Finally, we observe that mitoMPs promote malignant features such as cancer cell migration and invasion. Overall, we demonstrate that PMPs can modulate cancer cell activation and behaviour. These findings provide a better understanding of the extracellular tumor environment and the contribution of mitoMPs in supporting breast cancer cells through the metastatic landscape. The knowledge gained will further provide new avenues for therapeutic strategies in breast cancer patients.

#3709

Hyperglycemia induces metabolic reprogramming and promotes epithelial-mesenchymal transitions in pancreatic cancer: an in vitro and in vivo experiment

Zhao Liu, Hiromitsu Hayashi, Kazuki Matsumura, Yoko Ogata, Hiroki Sato, Yuta Shiraishi, Norio Uemura, Tatsunori Miyata, Takaaki Higashi, Shigeki Nakagawa, Kosuke Mima, Katsunori Imai, Hideo Baba. *Kumamoto Univ Graduate School of Medical Sci, Kumamoto, Japan*

Background: Pancreatic cancer is a serious life-threatening disease due to its highly invasive and metastatic potential. Hyperglycemia is a well-known initial symptom in patients with pancreatic ductal adenocarcinoma (PDAC). Metabolic reprogramming in cancer, described as the Warburg effect, can induce epithelial-mesenchymal transition (EMT). In this study, we elucidate the biological and clinical impact of hyperglycemia in PDAC progression.
Methods: Biological impact of hyperglycemia on malignant behavior in PDAC was examined by *in vitro* and *in vivo*experiment.
Results: Hyperglycemia promoted EMT by inducing metabolic reprogramming into a glycolytic phenotype via yes-associated protein (YAP)/PDZ-binding motif (TAZ) overexpression, accompanied by GLUT1 overexpression and enhanced phosphorylation Akt in PDAC. In addition,

hyperglycemia enhanced chemoresistance by upregulating ABCB1 expression, and triggered PDAC switch into pure-basal-like subtype with activated Hedgehog pathway (GLI1 high, GATA6 low expression) through YAP/TAZ overexpression. PDAC is characterized by abundant stroma that harbors tumor-promoting properties and chemoresistance. Hyperglycemia promotes production of collagen fiber-related proteins (fibronectin, fibroblast activation protein, COL1A1, and COL11A1) by stimulating YAP/TAZ expression in cancer-associated fibroblasts (CAFs). Knockdown of *YAP* and/or *TAZ* or treatment with YAP/TAZ inhibitor (K975) abolished EMT, chemoresistance, and a favorable tumor microenvironment even under hyperglycemic conditions *in vitro* and *in vivo*. Indeed, YAP/TAZ overexpression was significantly associated with worse prognostic outcomes in human PDAC patients.
Conclusion: Hyperglycemia induce metabolic reprogramming into a glycolytic phenotype and promote EMT via the YAP/TAZ-Hedgehog signaling axis in PDAC. Hyperglycemia as an initial symptom may be the cause of highly invasive and metastatic potential by inducing YAP/TAZ overexpression, while YAP/TAZ could be a novel therapeutic target in PDAC patients.

#3710

Serum tryptophan metabolites mediate constitutive AHR activity in head and neck squamous cell carcinoma cells

Dhwani Patel, Ethan W. Morgan, Fangcong Dong, Iain A. Murray, Gary H. Perdew. *Penn State University, State College, PA*

The aryl hydrocarbon receptor (AHR) is transcription factor, that is activated upon binding to various exogenous and endogenous ligands. AHR activation leads to induction of target gene expression, including the members of cytochrome P450 enzyme family that metabolize many xenobiotics. Numerous studies have shown that the AHR is involved in multiple regulatory pathways important during carcinogenesis. High level of AHR protein and activation was observed in head and neck squamous cell carcinoma (HNSCC) and has been correlated with aggressive tumor phenotypes and migratory potential. Endogenous compounds derived from host tryptophan metabolism such as kynurenine, as well as the derivatives of indole derived from bacterial tryptophan metabolism such as indole-3-

propionic acid are known to activate AHR. A fundamental question not previously addressed is whether these circulating tryptophan (Tryp) metabolites can mediate persistent AHR activation within tumor tissues and its effect on tumorigenesis. The focus of our research is to determine whether the continuous exposure of Tryp metabolites at relevant concentrations leads to sustained AHR activation in HNSCC cells and its subsequent effect on tumor cell phenotypes. Here, we present data demonstrating sustained AHR activation by Tryp metabolites in two HNSCC cell lines. A total of 6 tryptophan (Tryp) metabolites present at significant levels in serum with known AHR agonist activity were identified and quantified from 40 healthy individuals on a controlled diet by LC/MS/MS. HN30 and OSC19 cells were treated with a representative pool of 6 Tryp metabolites in a cell culture system to achieve continuous exposure to the Tryp metabolites, thus mimicking blood circulation in vivo. Treated cells were collected at six different time points and AHR activation within cells was determined by measuring mRNA and protein expression of AHR target genes. The effect of Tryp pool on HN30 and OSC19 cell viability was determined. The presence of Tryp metabolites within the cells and media was quantitated by LC/MS/MS at six time points over the course of 24 h. Continuous exposure of Tryp metabolites resulted in sustained AHR activation in HN30 and OSC19 cells, confirmed by induced mRNA expression of target genes and subsequent protein levels. The LC/MS data revealed the presence of all six Tryp metabolites in media collected at all time points, suggesting no spontaneous degradation of metabolites. Tryp metabolites were detected inside the cells starting from 2 h post-treatment to the last time point 24 h. Viability assays indicated no cytotoxic effects of Tryp metabolites on cells. Overall, our work has demonstrated a pattern of sustained AHR activation in HNSCC cells resulting from continuous exposure of Tryp metabolites, supporting the concept that endogenous Tryp metabolites in HNSCC patients would impact tumor progression, metastasis, and treatment outcomes.

#3711

Molecular and cancer-related roles of ATP-citrate lyase exon 14

Julianna G. Supplee, Hayley C. Affronti, Richard Duan, Rebekah C. Brooks, Phuong Nguyen, Kollin Schultz, Ronen Marmorstein, Kathryn E. Wellen. *University of Pennsylvania, Philadelphia, PA*

Introduction: ATP-citrate lyase (ACLY) links carbohydrate and lipid metabolism as well as provides acetyl-CoA necessary for histone acetylation, linking cell nutrient status and epigenetic regulation. Several studies have shown that ACLY is upregulated in multiple cancer types. ACLY has two major splice isoforms: the full-length canonical “long” isoform and an uncharacterized “short” isoform where exon 14 is spliced out. RNAseq data from The Cancer Genome Atlas (TCGA) shows that the Percent Spliced In (PSI) of exon 14, i.e., the proportion of long isoform, is increased in several cancers compared to normal tissues. We therefore hypothesize that ACLY exon 14 inclusion can support tumor growth.
Experimental Procedures: Extensive statistical analysis was performed on TCGA data to explore the connection between ACLY PSI and clinical parameters including tumor type, stage, and survival. We also noted a serine within exon 14 that is dynamically phosphorylated according to multiple phosphoproteomics studies. We used an in vitro activity assay and differential scanning fluorimetry to biochemically characterize purified ACLY isoforms and phosphomutants. We also expressed these isoforms and mutants in cells lacking endogenous ACLY to evaluated rescue of known ACLY functions including proliferation, de novo lipogenesis, and histone acetylation. Since exon 14 is located near a putative nuclear localization sequence, we also used confocal microscopy to study subcellular localization of these constructs. Ultimately, we developed a new C57BL6/J mouse model with ACLY exon 14 deleted by CRISPR to study the role of exon 14 in metabolic physiology and tumor growth in vivo.
Results: In vitro assays showed no differences in activity and stability between ACLY isoforms and phosphomutants. Similarly, both isoforms and mutants were able to rescue known ACLY functions in cells, and deletion of exon 14 in mice does not impact normal metabolic physiology. Analysis of TCGA data offers compelling evidence that the long ACLY isoform is upregulated early in tumorigenesis and is associated with deadlier tumors and certain immune cell signatures, suggesting that exon 14 is particularly relevant in this disease context. Our mouse model was cross-bred to ApcMin/+ mice, a genetic model of colon cancer, and studies are underway to determine the impact of exon 14 on colon tumors and immune infiltration.

Conclusions: ACLY exon 14 does not have obvious roles in enzymatic activity and known ACLY functions. However, alternative splicing could impact pathophysiological phenotypes such as cancer or other yet undescribed functions of ACLY.

Chromatin Structure and Function in Cancer

#4716

Characterization of 3D genome in nasopharyngeal carcinoma (NPC)

Dittman Lai-Shun Chung, Larry Ka-Yue Chow, Wei Dai. *Department of Clinical Oncology, University of Hong Kong, The - Li Ka Shing Faculty of Medicine, Hong Kong, Hong Kong*

Background: Epstein-Barr virus (EBV) can be detected in more than 90% of NPC patients in Hong Kong. It has been shown that EBV infection could hijack the human epigenome in B cell lymphoma and EBV+ gastric cancer, however, the role of EBV in epigenetic dysregulation remains largely unknown in NPC. Recently, our epigenomic landscape study demonstrated EBV was associated with changes of chromatin accessibility in NPC, which were largely involved in the binding sites of CTCF, a master regulator of chromosome organization. Therefore, we aim to further characterize the 3D chromatin structure in NPC.
Methods: We used the Hi-C (Omni-C Seq) to profile the chromatin interactions in the EBV-positive (EBV+) NPC, EBV-negative (EBV-) NPC, and normal immortalized epithelial (NPE) cell lines. The Omni-C Seq data were integrated with the ATAC-Seq, RNA-Seq, and CUT&RUN-Seq data. The histone markers including H3K4me3, H3K27ac, and H3K27me3, were applied to classify the active and inactive status of the chromatins. The chromatin looping and topologically associated domains (TADs) were defined by the CTCF binding sites.
Results: We observed a much larger compartmentalization size in EBV+ NPC with a consistent increase of active to inactive (A to B) compartments, compared to NPE and EBV- NPC. Pathway enrichment analysis showed that these changes potentially influenced immune response, cell differentiation and development, metabolism, ERBB pathway, and calcium signaling transduction. In addition to the changes in compartmentalization, we observed a reduction of CTCF binding signals at the TADs boundaries

and the loss of chromatin looping at the 10kb resolution. Consistently, the aggregate peak analysis has shown a significant reduction of the CTCF anchor, indicating the abandonment of architectural CTCF in EBV+ NPC. More importantly, we found EBV tethering to the host chromatins. In the EBV genome, the tethering sites were often located at the regions associated with OriP, EBNA1, and BARTs. In the human genome, the tethering sites were dramatically enriched in the inactive to active (B to A) compartments, which were highly associated with the enhancer regions with H3K27ac. We identified a specific target gene *CD74* with EBV tethering at the nearby super-enhancer region. Our results suggest the upregulation of *CD74* could be controlled via remodulating the host 3D genome in EBV+ NPC. The spatial transcriptome analysis indicated that the expression of CD74 was highly correlated with HLA-DRA. The spatial analysis further showed that the NPC patients with upregulated HLA-DRA often had *de novo* distant metastasis after treatment (p=0.007). Conclusions: The EBV tethering to the host genome has a significant impact on host 3D genome organization, affecting chromatin accessibility and gene regulation, providing survival
advantages of cancer cell growth and potentially contributing to immune suppression and metastasis.

#4718

Analyses of epigenetic marks and mechanisms in disease: Your guide to a successful CUT&RUN assay

Angela H. Guo, Christopher R. Comeau, Fang Chen, Christopher J. Fry.
Cell Signaling Technology, Inc., Danvers, MA

Like the chromatin immunoprecipitation (ChIP) assay, Cleavage Under Targets & Release Using Nuclease (CUT&RUN) is a powerful and versatile technique used for probing protein-DNA interactions within the natural chromatin context of the cell. The CUT&RUN assay can be combined with downstream qPCR or NG-seq to analyze histone modifications and binding of transcription factors, DNA replication factors, or DNA repair proteins at specific target genes or across the entire genome. CUT&RUN provides a rapid, robust, and true low cell number assay for detection of protein-DNA interactions in the cell. Unlike the ChIP assay, CUT&RUN is free from formaldehyde cross-linking, chromatin fragmentation, and

immunoprecipitation. Previously, we have shown that, compared to ChIP, CUT&RUN requires fewer starting cells (100K), has a much faster protocol (one day from cells to DNA), generates lower background signal (requires less sequencing depth), and offers spike-in control DNA for effective normalization of signal between samples and between experiments. We recently updated the CST CUT&RUN Assay Kit for use with 5,000-20,000 cells and added protocols for fixed cells and tissue. I will discuss the basics of the CUT&RUN assay and important factors to consider when setting up your experiment. In addition, I will provide data showing the versatility of this assay for mapping various histone modifications, transcription factor, and transcription cofactor binding across multiple sample types. Finally, I will discuss how the general protocol is optimized for greater signal to noise ratio, reduced number of starting cells, and provide an alternative digestion method to prepare the input DNA as a critical control of the CUT&RUN experiment.

#4719

Alterations of chromatin structure and TGF-β signaling in ARID1A-mutated colon cancer cells

Jiwon Kim[1], Giyong Jang[2], Soo-Jin Lee[1], Sang Eun Lee[1], Sung-Yup Cho[3].
[1]Department of Biomedical Sciences, Seoul National University College of Medicine, Seoul, Korea, Republic of,[2]Medical Research Center, Genomic Medicine Institute, Seoul National University College of Medicine, Seoul, Korea, Republic of,[3]Seoul National University College of Medicine, Seoul, Korea, Republic of

ARID1A, a subunit of the SWI/SNF complex which regulates gene expression by remodeling chromatin structure, is often mutated in various cancer and is known as a tumor suppressor gene. Many studies revealed the loss of ARID1A promotes tumor progression by activating PI3K-Akt signaling, but other pathways have not yet been fully elucidated. By analyzing RNA sequencing data and ATAC-seq data with ARID1A wild-type cell lines HCT116 and isogenic ARID1A Q456*/Q456* which has truncation mutations for ARID1A, we investigated the alterations of epigenomic and transcriptomic characteristics according to the loss of ARID1A. The overall openness of chromatin decreased in ARID1A Q456*/Q456* cells. Since SWI/SNF complex regulates chromatin structure

and gene expression accordingly, we analyzed genes whose change of RNA expression and openness of chromatin in the same direction. The results showed 109 upregulated genes and 715 downregulated genes compared to wild type cell line with $P_{adj} < 0.05$, $|log2FC| > 0.58$ from both RNA sequencing and ATAC-seq. To determine which gene sets are activated in the ARID1A-deficient cell line, the differentially expressed genes with consistent chromatin openness were subjected to Gene Ontology analysis. The upregulated genes in the ARID1A-deficient cell line were enriched in 'Cell proliferation' and 'TGF-β signaling'. In addition, the expression of representative genes associated with TGF-β signaling increased in ARID1A-deficient cells. Our data suggests that loss-of-mutation in ARID1A significantly changes the chromatin structure, resulting in alterations of gene expression associated with cell proliferation and TGF-β signaling.

#4720

Chromatin conformation alterations in prostate cancer progression and formation of castration resistance

Tuomo Virtanen, Ebrahim Afyounian, Riikka Nurminen, Teuvo Tammela, Tapio Visakorpi, Juha Kesseli, Kirsi Rautajoki, Matti Nykter. *Tampere University, Faculty of Medicine and Health Technology, Tampere, Finland*

Introduction: Prostate cancer (PC) is the most common cancer in men and second in cancer related deaths. Aggressive prostate cancer is typically treated with androgen depletion therapy which often results in the formation of castration resistant prostate cancer (CRPC). Androgen receptor (AR) is a transcription factor that regulates hundreds of target genes and is responsible for the differentiation and function of normal prostate epithelial cells. In addition to AR, multiple other TFs that bind to distal enhancers have been implicated in PC, such as FOXA1, MYC and HOXB13. Understanding the role of these distal regulators is paramount in PC.
Methods: To study the changes in chromatin conformation in prostate cancer progression, we have sequenced clinical benign prostatic hyperplasia (BPH), PC and CRPC samples using Hi-C sequencing. From each group 6 samples were sequenced with a total of 18 samples in the cohort. In addition, we have combined a multi omics cohort consisting of chromatin accessibility, transcriptome and methylome sequencing data from matching

samples. Together these data types allow us to map out the regulatory networks in PC and CRPC by probing the distal active regulatory sites and their interactions. To account for artifacts caused by genomic aberrations in cancer samples we have established a pipeline for normalizing these effects in HiC-data.
Results: Overall topologically associated domains (TADs) and A/B-compartments remain stable between the groups. However, local changes of compartments in loci of key genes, such as AKR1C3 and FOXA1 correlate with their gene expression. We detect differential loops between sample groups and these changes are associated with gene expression alterations in PCs. Distal enhancers of PC up-regulated genes are enriched for FOXA1 and HOXB13. Interestingly, up-regulated loops in CRPC are enriched for FOXA1 and HOXB13, while no systematic effect on gene expression is seen on a genome wide scale, apart from genes such as AR and CENPE whose expression correlates strongly with their association to distal enhancers. We also detect enhancer hijacking events in driver genes. One example is the recurrent ETV1-MIPOL1 fusion, where promoter of ETV1 forms contacts with FOXA1 enhancer regions.
Conclusions: Alterations in loop structures are strongly associated with regulatory programs that have been previously implicated in PC, including regulation by FOXA1, HOXB13 and other transcription factors. This highlights the importance of chromatin conformation in facilitating the effects of regulatory programs that rely on distal enhancers in PC. These changes appear more systematic in untreated PCs, whilst CRPCs exhibit more heterogeneity in chromatin conformation across the samples.

#4721

Yin Yang 1-induced long non-coding RNA DUXAP9 drives oral squamous cell carcinoma by blocking CDK1-mediated EZH2 degradation

Wei Cao, Wenkai Zhou. *Department of Oral and Maxillofacial& Head and Neck Oncology, Shanghai Ninth People's Hospital, Shanghai Jiao Tong University School of Medicine, Shanghai, China*

Background: lncRNAs play a critical role in oral squamous cell carcinoma (OSCC) progression and metastasis. However, the detailed molecular mechanism is not fully understood.

Methods: Differential-expressed lncRNAs between OSCCs and paired adjacent tissues were identified by microarray. The expression of lncRNADUXAP9 (DUXAP9) was detected by RNAscope and quantitative real-time PCR (qRT-PCR). The gain-of-function and loss-of-function of DUXAP9 were evaluated *in vitro* and *in vivo* assays. Chromatin immunoprecipitation (ChIP)and luciferase assays were performed to analyze the transcriptional regulation of DUXAP9. RNA pull-down assays, LS-MS/MS analysis, RNA immunoprecipitation assays, and Co-immunoprecipitation (Co-IP) were performed to address the molecular mechanism through which DUXAP9promotes OSCC progression. Results: By analyzing lncRNA microarray data, we identified a novel nuclear-localized DUXAP9, which is upregulated in OSCC. The high level of DUXAP9is positively associated with lymph-node metastasis, poor pathological differentiation, advanced clinical stage, worse overall survival, and worse disease-specific survival in OSCC patients. DUXAP9 significantly promotes cell proliferation, migration/invasion, and metastasis *in vitro* and *in vivo* through an EZH2-dependent manner. Yin Yang 1(YY1) was found to activate the transcriptional expression of DUXAP9 in OSCC. Furthermore, DUXAP9was proven to physically interact with EZH2 and inhibit EZH2 degradation via the suppression of the phosphorylation of EZH2, thereby blocking EZH2nucleus to cytoplasm translocation. Conclusions: Here we demonstrated a novel mechanism mediated by lncRNA DUXAP9 at the posttranslational level, which contributes to OSCC progression, thus providing a promising target for OSCC therapy.
Keywords: LncRNA DUXAP9, YY1, EZH2, Ubiquitination, Oral squamous cell carcinoma

#4722

Chronic upregulation of glucocorticoid hormones triggers chromatin remodeling in NSCLC through dynamic regulation of histone H3 chaperones

Benito M. Traversa, Devesh Raizada, Eva Kragelj, Julia Spegel, Didem Ilter, Ana P. Gomes. *H. Lee Moffitt Cancer Center, Tampa, FL*

Lung cancer is the most common cause of cancer death worldwide, with a five-year survival rate of only 18.6%. Aging is a well-established risk factor for lung cancer development. However, our understanding of how the aging

process affects lung cancer remains cripplingly small. In this study, we aim to bridge this gap by evaluating the effects of glucocorticoid hormones (e.g. cortisol), which become chronically upregulated during the aging process, in lung cancer cells. Phenotypically, our studies revealed that chronic exposure to age-related levels of cortisol trigger a mesenchymal-like senescent state in lung cancer cells that favors motility and invasiveness. Acquisition of pro-aggressive features are generally recognized to be driven by epigenetic regulation. Epigenetic regulation occurs at several levels, but perhaps one of the most fundamental levels is nucleosome remodeling via histone variants and their cognate chaperones. Histone H3 variants are critical regulators of nucleosome stability and have a highly specialized histone chaperone network when compared to other histones. Strikingly, we observed that chronic exposure of lung cancer cells to cortisol leads to a pronounced decline in canonical histone levels, which was accompanied by a 40% increase in chromatin accessibility genome-wide. Chromatin accessibility by transcriptional machinery is heavily influenced by histone variants, thus, we hypothesized that cortisol also regulates deposition of histone H3 variants into chromatin. The CAF-1 complex deposits the canonical H3 variants (H3.1/H3.2) onto DNA in a cell-cycle-dependent manner while other histone chaperones, HIRA at genic and DAXX at telomeric regions, deposit the H3.3 variant independently of cell cycle. In accordance with the decline in canonical histone levels, treatment with cortisol suppressed the expression of the CAF-1 complex. Reduced canonical histone abundance is known to trigger “gap filling” of naked DNA with the H3.3 variant to maintain integrity. In support of the idea that H3.3 becomes enriched in chromatin upon chronic exposure of lung cancer cells to cortisol, our results showed that the proportion of H3.3 increases upon cortisol exposure, and concomitantly H3.3 chaperone HIRA is induced upon treatment with cortisol. These data support a model in which chronic exposure to glucocorticoids, as it occurs with aging or through treatment with synthetic glucocorticoids (e.g. dexamethasone), regulates nucleosome abundance and composition in lung cancer cells through dynamic regulation of histone H3 chaperone systems. Together, we propose that this glucocorticoid-induced nucleosome remodeling establishes a chromatin environment that enables the transition to a mesenchymal-like senescent state in lung cancer cells that favors aggressiveness and poor prognosis.

#4723

DNA G-quadruplex facilitates MYC enhancer-promotor interaction

Dieila Giomo De Lima, Gustavo Narvaes Guimarães, Bianca Caroline Figueiredo Bianco, Ana Paula De Souza, Aline Cristiane Planello.
Histology and Embriology, State University of Campinas, Piracicaba, Brazil

Background: G-quadruplexes (G4) are nucleic acid secondary structures formed in guanine-rich regions of DNA or RNA. The biological significance of G4 has been attributed to the regulation of gene expression, and more recently, to the stabilization and generation of enhancer-promotor interaction. Since G4 are enriched in the promoter region of the proto-oncogene MYC, we sought to investigate the role of G4 in stabilizing the enhancer-promoter loop using the locus 8q24 (hg38) 127,700,000-128,500,000 that contains the MYC gene as a model.
Methods: Two different cell lines were used, the spontaneously immortalized, non-oncogenic human epidermal keratinocyte (HaCaT), in which the enrichment of G4 in the MYC promoter was demonstrated, and the primary normal human epidermal keratinocyte (nHEK) that is depleted of G4 in MYC promoter. Both cell lines were exposed to the G4 selective stabilizer 360-A drug and the half-maximal inhibitory concentration (IC50) could be calculated. Gene expression was accessed by RT-qPCR and DNA methylation by Methylation-Sensitive High Resolution Melting (MS-HRM). Chromatin Conformation Capture (3C-qPCR) technique was performed interrogating the MYC gene (chr8:127,733,798-127,744,729) and the putative enhancer in the lncRNA PVT1 gene (chr8:127,914,509-127,922,393) to compare the frequency of promoter-enhancer interaction between the two cell lines.
Results: The HaCaT cells showed interaction between the MYC promoter and the distal region. The nHEK cells that are not enriched for G4 showed no promoter interaction with the distal region. The use of 360-A in IC50 did not change the results. The gene expression analysis of the MYC showed higher expression in HaCaT cells compared to nHEK. There was no difference in DNA methylation in the MYC promoter between the two cell lines.

Conclusions: The data suggest an important role of G4 for the interaction of the MYC promoter and downstream enhancer. Additional analyzes of other genomic regions enriched for G4 should be performed to confirm the mechanism.

#4724

Single cell multiomic profiling of high-grade serous carcinoma

Leticia Assad Maia Sandoval[1], Wazim Mohammed Ismail[1], Amelia Mazzone[1], Amik Munankarmy[1], Jagneet Kaur[2], Tsering Tashi[3], Xiaonan Hou[1], Nagarajan Kannan[1], Ann Oberg[1], Scott H. Kaufmann[1], Saravut John Weroha[1], Alexandre Gaspar-Maia[1]. *[1]Mayo Clinic, Rochester, MN,[2]St. George's University, True Blue, Grenada,[3]Wartburg Collage, Waverly, IA*

Ovarian cancer is one of the most common gynecologic malignancies, with high-grade serous carcinoma (HGSC) as the most frequent and deadliest type of ovarian cancer (OC). With the recent advances in cancer epigenomic profiling, it has become clear that intra-tumor heterogeneity driven by genetic and epigenetic factors may be the basis of resistance, where current treatments could efficiently target sub-populations of cells while a sub-group may be resistant, or prone to develop resistance. With epigenomic profiling and single cell sequencing technology, we aim to characterize cell signatures that translate as prognostic markers and novel drug targets. We have mapped the epigenomic landscape of HGSC in 12 patient-derived xenografts (PDX), and their metastatic counterparts (circulating tumor cells and ascites present in the PDX models) using an assay for transposase-accessible chromatin (or ATAC-seq) and compared it with normal fallopian tube organoids to identify tumor and metastatic-specific regulatory elements. We also performed RNA-seq to validate potential transcriptional dependencies associated with resistance to chemotherapy. In order to identify potentially chemotherapy-resistant subpopulations and further validate the activity of some of the transcription factors that can be driving resistance, we performed single cell multiomic profiling using the 10x Multiome sequencing platform (scRNA+scATAC from the same nuclei) in HGSC patient samples and PDX. Finally, we performed immunohistochemistry of patient tissue slides for target markers and correlated it with overall survival in OC patients. As previously suggested, a subset of cancer clonal cells can drive treatment resistance and

metastasis and result in poor patient outcomes. Data derived from PDX ATAC-seq showed a cancer stem cell signature driven by SOX2 in metastatic samples compared to the paired PDX primary tumor, suggesting a role for SOX2 in disease progression. Interestingly, SOX2 expression in epithelial cells in the Multiome analysis is more patient-specific than other stem cell markers, like CD133. We also observed that SOX2 expression negatively correlated with prognosis. These data, taken together, point out the promising role of SOX2 as a prognostic and targetable marker for HGSC.

#4725

The epigenetic determinants of BTKi efficacy in chronic lymphocytic leukemia

Zhiquan Wang[1], Huihuang Yan[1], Justin C. Boysen[1], Esteban Braggio[2], Sameer A. Parikh[1], Neil E. Kay[1]. *[1]Mayo clinic, Rochester, MN,[2]Mayo clinic, Scottsdale, AZ*

Introduction: The introduction of Bruton's tyrosine kinase (BTK) inhibitors (BTKi) to target B cell receptor (BCR) pathways in chronic lymphocytic leukemia (CLL) has significantly improved clinical responses. However, the effectiveness of BTKi is limited by the development of adaptive drug resistance. Therefore, there is an urgent need to identify critical biologic features that determine BTKi efficacy in order to develop more effective therapies. Epigenetic aberrations play an important role in tumor initiation, progression, and drug resistance. However, it is currently unknown if BCR signaling is also dependent on epigenetic mechanisms to support oncogenic gene expression and survival in CLL B cells.
Methods and Results: To gain new insights into the role of epigenetic regulation of BTKi treatment in CLL B cells, we analyzed the genome wide chromatin accessibility (ATAC-seq) and histone modification (H3K4me1, H3K4me3, H3K27ac, H3K27me3) profiles (CUT&Tag) of leukemic cells from 4 CLL patients on ibrutinib treatment in a sequential fashion (i.e., baseline, on ibrutinib treatment, and at relapse). We also performed the same analysis in other cohorts at two stages of ibrutinib treatment (baseline and while on treatment, n=20). Our studies show that suppressing BCR signaling by BTKi treatment leads to an alteration of a pro-survival epigenetic signature (defined by histone modifications and chromatin

accessibility landscapes) in CLL and that the genes regulated by these chromatin changes are enriched in pathways associated with malignant B cell survival (i.e., BCR signaling and apoptosis pathways). Importantly, disruption of this pro-survival epigenetic signature is necessary for effective BTKi treatment. We further find that the transcription factor (TF) Nuclear factor of activated T-cells, cytoplasmic 1 (NFATc1) couples the BCR signaling to control this pro-survival epigenetic program that supports CLL B cell survival. In specific, we show that nuclear depletion of NFATc1 is required for BTKi induced epigenetic alteration and effective BTKi treatment. Depletion of NFATc1 disrupts the pro-survival epigenetic signature and inhibits CLL B cells survival, which improves the efficacy of BTKi treatment in CLL.
Conclusion: Here using leukemic cells from CLL patients with BTKi treatment, we demonstrate that epigenetic regulators are exploited by the oncogenic signaling pathway to support malignant cell survival. Specifically, NFATc1 is utilized by the BCR signaling pathway to control an epigenetic signature that supports CLL cell survival. This BCR regulated epigenetic machinery can be targeted to maintain and enhance BTKi treatment efficacy in CLL.

#4726
KMT5C-dependent regulation of mesenchymal-related genes and identification of KMT5C interactome using BioID
Jihye Son, Alejandra Agredo, Ally Glaws, Andrea L. Kasinski. *Purdue University, West Lafayette, IN*

Epigenetic dysregulation has recently been recognized as a new hallmark of cancer. Dysregulation of chromatin remodelers is estimated to affect 10-20% of cancer. Thus, understanding how epigenetic-based mechanisms contribute to cancer initiation and progression is critical. KMT5C is a histone methyltransferase that catalyzes histone H4 lysine 20 trimethylation (H4K20me3), which has historically been associated with formation and maintenance of constitutive heterochromatin regions. Albeit recent evidence from our lab also suggests regulation of gene-rich euchromatin regions. In this previous body of work we discovered that loss of KMT5C promotes development of resistance to tyrosine kinase inhibitors (TKI) in EGFR-mutant non-small cell lung cancer (NSCLC) cells (PC9 and

HCC827). Patient data further supports that the KMT5C transcript level is downregulated following resistance to osimertinib, a third-generation TKI. Our data suggests that KMT5C is involved in non-canonical regulation of genes outside of heterochromatic regions through its methyltransferase activity. Analysis of data deposited into the Cell Miner database and publicly available RNA-sequencing and ChIP-sequencing data revealed that the KMT5C-H4K20me3 axis has significant negative correlations with several genes involved in epithelial-to-mesenchymal transition (EMT). Our validation studies support this observation. However the mechanisms involved in KMT5C facilitating this change at EMT-related genes is unknown. KMT5C is well understood to be recruited to heterochromatin regions through its interaction with HP1, yet the mechanism for recruitment of KMT5C to gene-rich euchromatin regions remains to be elucidated. We hypothesize that KMT5C is recruited to its target genes in euchromatin in an HP1-independent mechanism. In this study, we aim to identify the interactome of KMT5C using an unbiased proximity labeling BioID approach. This study is expected to uncover a novel epigenetic mechanism that contributes to development of resistance to TKIs and may inform of strategies to target KMT5C-downregulated TKI-resistant cancers.

#4727

RAS and PP2A activities converge on phosphoregulation of epigenetic complexes in cancer

Mukund Sharma[1], Anna Aakula[1], Francesco Tabaro[2], Henrik Honkanen[1], Jesse Kamila[1], Matthieu Schapira[3], Cheryl Arrowsmith[3], Matti Nykter[2], Jukka K. Westermarck[1]. *[1]University of Turku, Turku, Finland,[2]Tampere University, Tampere, Finland,[3]University of Toronto, Toronto, ON, Canada*

RAS-mediated human cell transformation requires inhibition of the tumor suppressor Protein Phosphatase 2A (PP2A). Both RAS and PP2A mediate their effects by phosphoregulation, but phosphoprotein targets in which RAS and PP2A activities converge in human cancers have not been systematically analyzed. Here, based on mass spectrometry phosphoproteome data, we discover that phosphosites co-regulated by RAS and PP2A are enriched on proteins involved in epigenetic gene regulation. As examples, RAS and PP2A co-regulate the same phosphorylation sites on HDAC1/2, KDM1A, MTA1/2, RNF168 and TP53BP1. Mechanistically, we

validate co-regulation of NuRD chromatin repressor complex by RAS and PP2A. Consistent with their known synergistic effects in cancer, RAS activation and PP2A inhibition resulted in epigenetic reporter de-repression and activation of oncogenic transcription. Notably, transcriptional de-repression by PP2A inhibition was associated with increased euchromatin and decrease in global DNA methylation. In RAS-driven cancers, PP2A activity is inhibited by nuclear PP2A inhibitor proteins PME-1 and SET. We further demonstrate that these PP2A inhibitors drive oncogenic transcription, but that their transcriptional targets are highly diversified. Whereas PME-1 controls RAS and MYC-driven transcription, SET controls TP53 targets and G2/M checkpoint genes. We further provide evidence that these nuclear PP2A inhibitors significantly differ in their roles in regulating DNA methylation. Collectively the results indicate that epigenetic protein complexes involved in oncogenic gene expression constitute a significant point of convergence for RAS hyperactivity and PP2A inhibition in cancer. Further, the results provide a rich source for future understanding of phosphorylation as a previously unappreciated layer of regulation of epigenetic gene regulation in cancer, and in other RAS/PP2A-regulated cellular processes.

#4728

Biochemical and genomic approaches for high throughput drug discovery in chromatin remodeling research

Lu Sun[1], Hannah Willis[1], Matthew R. Marunde[1], Vishnu U. S. Kumary[1], Matthew J. Meiners[1], Saarang Gopinath[1], Jonathan M. Burg[1], Bryan J. Venters[1], Allison Hickman[1], Zu-Wen Sun[1], Martis W. Cowles[1], Pierre Esteve[2], Hang Gyeong Chin[2], Chaithanya Ponnaluri[2], Sriharsa Pradhan[2], Michael-Christopher Keogh[1]. *[1]Epicypher, Durham, NC,[2]New England Biolabs, Ipwich, MA*

Chromatin remodeling is mediated by ATP-dependent enzymes that play key roles regulating gene expression and genome replication / repair. Aberrant nucleosome organization from dysregulated chromatin remodeling can severely alter chromatin accessibility and disrupt these important processes, thereby driving various cancers. Remarkably, nearly 20% of all human cancers contain mutations in subunits from the SWI/SNF family of chromatin remodeling complexes, making them of great interest to basic

research and therapeutic intervention. *In vitro* studies on the remodeling enzymes (and their multi-subunit complexes) are challenging, partially due to the strong preference for nucleosome-based substrates (the physiological target of these enzymes). We have created the EpiDyne® nucleosome portfolio to examine chromatin remodeler activity in biochemical assays, and here present the development of novel readouts (-PicoGreen™ and -TR-FRET). These nonradioactive plate-based assays are automation adaptable, ready for high-throughput inhibitor screening, and can be customized for various remodeling enzymes that exhibit preferences in nucleosome composition (*e.g.* histone type or DNA linker length).For parallel *in vivo* studies we note that genome-wide remodeler localization and open chromatin mapping are fundamental for understanding the function / activity of these enzymes in cancer development and inhibitor response. However, traditional genomic approaches have significant issues: *e.g. ChIP-seq* is unable to effectively map ATPases without heavily modified high-noise protocols; while *ATAC-seq* to map open regions cannot deal with cross-linking that could stabilize transient states on interest. To this end, we have optimized the CUTANA™ CUT&RUN approach to efficiently capture the localization of all major classes of chromatin remodelers with high signal to background. We have also adopted NicE-seq for chromatin accessibility profiling in cross-linked material. As complementary tools to the EpiDyne platform, CUT&RUN and NicE-seq facilitate epigenomic research on chromatin remodelers in cancer therapeutic intervention. Keywords: Chromatin Remodeling, EpiDyne, Nucleosome repositioning, high-throughput screening (HTS), CUTANA™ CUT&RUN, NicE-seq

#4729

LSD1 activates oncogenic super-enhancers in castration-resistant prostate cancer by forming nuclear condensates with BRD4

Mingyu Liu[1], Muqing Li[1], Dong Han[1], Zifeng Wang[1], Wanting Han[2], Housheng Hansen He[3], Shuai Gao[4], Changmeng Cai[1]. *[1]University of Massachusetts - Boston, Boston, MA,[2]Fred Hutchinson Cancer Center, Seattle, WA,[3]University of Toronto, Toronto, ON, Canada,[4]New York Medical College, Valhalla, NY*

Lysine-specific demethylase (LSD1) was initially identified as a transcriptional repressor through demethylation of mono/di-methylated histone 3 lysine 4 (H3K4me1/2). Subsequent work suggests that LSD1 may trigger gene activation via demethylating H3K9me1/2 in the context of steroid receptors. Our previous studies have confirmed that LSD1 functions broadly as a coactivator of androgen receptor (AR)-regulated enhancers but retains its H3K4 demethylation function at these sites. Importantly, our recent work revealed that LSD1 regulates the accessibility of active enhancers through the interaction with FOXA1, which functions as a pioneer transcription factor by facilitating AR access to chromatin. LSD1 inhibition disrupts the global binding of FOXA1 by blocking the demethylation of K270 of FOXA1, leading to inhibition of AR binding and transcriptional activity. However, in addition to AR signaling, it remains largely unknown whether LSD1 regulates other critical oncogenic programs during prostate cancer (PCa) progression. In this study, we aimed to fully understand the functional targets of LSD1 in castration-resistant PCa (CRPC) models.

We performed a large transcriptomic profiling of CRPC patient-derived xenograft (PDX) models that are sensitive to LSD1 inhibitors. Our analyses indicated that LSD1 inhibition targeted multiples oncogenic programs, including previously known pathways such as AR, FOXA1, and E2F, and a previously undefined pathway, MYC signaling. Through single-cell RNA-seq analysis in a CRPC PDX model, we confirmed that MYC signaling was decreased in the responsive tumor cells and identified a previously unknown molecular subtype, $AR^{+}/FOXA1^{+}/LSD1^{low}/RB1^{-}$, which was resistant to LSD1 inhibition. It is well known that *MYC* is driven by super-enhancers (SEs), which are regulated by BRD4 (bromodomain and extraterminal (BET) protein). We further evaluated LSD1, FOXA1 and BRD4 ChIP-seq and defined SEs by using H3K27ac ChIP-seq followed by ROSE analysis. We found that LSD1, FOXA1, and BRD4 co-occupied at MYC SEs and BRD4 was recruited by unmethylated FOXA1 but not K270-methylated FOXA1. In addition, we observed the puncta-like formation of LSD1/BRD4 marked nuclear condensates under confocal immunofluorescence microscopy. By examining the public datasets of H3K27ac ChIP-seq of samples with different stages of PCa development, we identified a subset of SEs which were distinctly activated in CRPC. Using multiple CRPC PDXs, we revealed that combining LSD1 inhibitors

with BET inhibitors exhibited strong synergy possibly via disrupting the CRPC-specific SEs.
In summary, this study reveals a novel oncogenic function of LSD1 in driving PCa progression by activating SE-driven oncogenic programs, such as MYC signaling. These results provide a strong therapeutic potential of combining inhibitors of LSD1 and BRD4 in treating CRPC.

#4730

ASCL1 activates neuronal stem cell-like lineage programming through the remodeling of the chromatin landscape in prostate cancer

Shaghayegh Nouruzi[1], Dwaipayan Ganguli[1], Nakisa Tabrizian[2], Maxim Kobelev[2], Olena Sivak[1], Takeshi Namekawa[1], Alastair Davies[1], Amina Zoubeidi[1]. *[1]Vancouver Prostate Center, Vancouver, BC, Canada,[2]Experimental Medicine, University of British Columbia, Vancouver, BC, Canada*

Introduction: Second-generation AR pathway inhibitors such as Enzalutamide (ENZ) are highly effective in treating castration-resistant prostate cancer (CRPC). However, they play an important role in the emergence of AR-independent phenotypes, including treatment-induced neuroendocrine prostate cancer (tNEPC). Few genetic differences are observed between CRPC and tNEPC, suggesting an epigenetic dysregulation underlining this conversion.
Method: To capture the evolution of CRPC to tNEPC, we measured changes in chromatin accessibility of CRPC cells upon exposure to ENZ and in tNEPC cell lines via ATACseq. We performed RNAseq from matched cell lines. We conducted ASCL1, H3K27me3 and EZH2 ChIPseq. Multi-omic analysis were performed integrating RNAseq, ATACseq, ChIPseq, RNA and protein expression.
Result: We identified the motif of the transcription factor ASCL1 becoming accessible as early as 3 days, with continued enrichment at 10 days post ENZ-treatment and in NEPC cell-lines. ASCL1 expression and activity are significantly upregulated in NEPC cell lines and patient tumors. Using our unique model of tNEPC, we showed that knockdown of ASCL1 causes extensive chromatin reorganization leading to reduced expression of neuronal and plasticity markers and overall abolishment of the NEPC program. Loss of ASCL1 dysregulated Polycomb repressor complex 2

activity (loss of H3K27 methylation) via di-association of complex due to phosphorylation of EZH2 at T311 resulting in loss of EZH2 binding to the chromatin and likely cause of the H3K27 demethylation. Cell fractionation and confocal microscopy combined with ChIPseq data confirmed loss of EZH2 binding to the chromatin. We identified that loss of ASCL1, phenocopying EZH2 inhibition, reactivated luminal programming and potentially re-sensitizing tNEPC cells to further AR targeted therapies. Altogether, suggests that ASCL1 may drive early transcriptional and epigenetic reprogramming through the PRC2, facilitating the emergence and maintenance of tNEPC.
Conclusion: Our research provides the centrality of epigenetic reprogramming in driving the uprising of a plastic phenotype in response to AR pathway inhibition and provides insight into the role of ASCL1 in early drug-induced epigenomic plasticity that supports this reprogramming toward androgen independence. We report that ASCL1 modulates the chromatin dynamics to support a plastic lineage by influencing neuronal stem cell-like regulatory networks. In the treatment-resistant, high plasticity state, inhibition of ASCL1 reverses the lineage to an epithelial-luminal state, providing potential for targeting these highly aggressive tumors. This work provides much-needed insight into ASCL1 function and dependency that together nominates ASCL1 as a bona fide clinical target.

#4731

Novel epigenetics technology for high-throughput processing of limited samples to study cancer using cavitation-based pixelated ultrasound and tagmentation-indexing ChIP-Seq

Rwik Sen, Ngoc Tran, Sarah Traynor, Eric Maina, Jason Poole. *Active Motif, Carlsbad, CA*

Epigenetics has shown great potential in translational, clinical, and precision medicine research, but with inadequate implementation. This is due to major problems with sample availability, and processing which is laborious, costly, slow, inconsistent, and leads to sample loss. Epigenetics studies need samples with certain minimum concentrations and volumes to address all necessary questions. The samples often need to be in single cell or nuclear suspensions. For chromatin immunoprecipitation (ChIP), a consistent size of approximately 300 base pairs of DNA is essential but

difficult to achieve. To address the above problems, we present novel cutting-edge epigenetics methodologies. Homogenization of various tissue types from diverse patients with different disease states is the first crucial step in sample processing. Hence, we present new protocols which are compatible with high-throughput cavitation-based pixelated ultrasound sonication. It processes limited quantities of samples in a 96-well plate where cells can be grown and antibody can be coated for ChIP. Further, 1 to 12 columns of the 96-well plate can be flexibly regulated to extract lysates. Our results show how this rapid and simple technology integrates with ChIP-sequencing (seq) and RNA-seq workflows, yielding very consistent output from limited tissue samples. Bioinformatics analysis of the ChIP-seq shows the corresponding biological significance. Certain limitations of ChIP has led to the evolution of other methods but they are mostly unsuccessful in mapping transcription factors. Hence, we next present a modified ChIP-seq combined with tagmentation, indexing and pooling, coupled to pixelated ultrasound based-cavitation. Here, individual samples are placed in each well of a 96-well plate containing unique indexing adapters fused to Tn5 transposase. Hence, each sample undergoes tagmentation - a process where DNA gets fragmented and simultaneously inserted with index adapters. Next, pixelated ultrasound helps to rapidly extract the complex of protein-tagmented DNA from 96 samples which are pooled into a single tube because they are uniquely indexed, then split up for immunoprecipitation by different antibodies. Bioinformatics analysis shows that the results are robust, consistent, and match ENCODE datasets. Hence, our methods can help to process high-throughput samples for AACR Project GENIE. Overall, we present novel technology to process limited human samples for enabling epigenetics research at the clinical interface from bench to bedside. The simple and less expensive methods yield high quality samples to enable high-throughput analysis of epigenetics including transcription factors which are important in cancer. They help us to understand targeted epigenetic regulations of genes for therapeutic developments and treating cancer.

#4733

Effect of KDM6A mutation in bladder cancer

Ninh B. Le[1], Hong Qiu[2], Emily E. Fink[3], Surbhi Sona[3], Angela H. Ting[3], Byron H. Lee[2]. *[1]Department of Epigenetics and Molecular Carcinogenesis,*

University of Texas MD Anderson Cancer Center, Houston, TX,[2]Cardiovascular & Metabolic Sciences, Cleveland Clinic Lerner Research Institute, Cleveland, OH,[3]Genomic Medicine Institute, Cleveland Clinic Lerner Research Institute, Cleveland, OH

As of 2020, bladder cancer is the tenth most common cancer in the world, with a heavier toll exerted on males. Its higher tumor recurrence and progression rates cause major treatment challenges. One of the most frequent mutations in bladder cancer is in lysine-specific demethylase 6A (KDM6A). This gene encodes for ubiquitously transcribed tetratricopeptide repeat on chromosome X (UTX), which catalyzes the demethylation of di- and tri- methylated histones H3 lysine 27 and works as part of "COMPASS-LIKE" protein complexes to coordinate many transcriptional processes. The molecular basis for how KDM6A mutations promote carcinogenesis is still under investigation. In this study, we use single-cell RNA sequencing data from bladder cancers with and without KDM6A mutations in both human and mice to examine the effects of KDM6A mutations on the cellular composition and gene expression of tumor and normal bladders. In mice without tumors, KDM6A mutations seem to correlate with enrichment of macrophages in the bladder tissue microenvironment. The opposite is true, however, in the presence of tumors, as there were not only more macrophages but also more dendritic cells in wildtype mice. This pattern was also observed in human, suggesting differences in immune infiltrates in the tumor microenvironment are part of the phenotype of KDM6A mutation. Lastly, KDM6A mutations may also impact urothelial cell states at baseline, as KDM6A KO mouse bladders contain higher proportions of intermediate cell populations compared with their wildtype counterparts. Together, these observations contribute to a better understanding of the role KDM6A plays in bladder cancer.

#4734

BRD8-driven EP400 complex hijacks H2AZ to maintain proliferation in glioblastoma

Sherine Xueqin Sun, Olaf Klingbeil, Christopher Vakoc, Alea Mills. *Cold Spring Harbor Laboratory, Cold Spring Harbor, NY*

Glioblastoma (GBM) is the most notorious primary brain tumor. The median survival of GBM patients is only about one year and about 95% patients succumb after five years. This gloomy picture has not been improved for decades, even with extensive treatments including surgery, radiotherapy, and chemotherapy. Hence, a better understanding of the mechanisms underlying GBM development may provide new therapeutic opportunities. Primary GBM generally harbors a low mutational load when compared to other human cancers. Even P53—the guardian of the genome that is essentially disabled in nearly all human cancers, remains unmutated in about 71% of GBM cases. Moreover, these P53 wildtype GBM cases are as aggressive as those with P53 mutations. To explore the mechanism by which P53 wildtype GBM thrive in the presence of intact P53, we performed CRISPR screens in a panel of human cancer cell lines using an sgRNA library specifically targeting the functional domains of ~200 chromatin regulators. We discovered that BRD8's bromodomain—a druggable domain as shown by the tremendous success in preclinical and clinical trial in diverse cancers—is a vulnerability specifically in P53 wildtype GBM cases. Our mechanistic studies demonstrate that BRD8 functions through the EP400 chromatin remodeling complex and hijacks the histone variant H2AZ at P53 target loci, enforcing a compact chromatin state that blocks P53's accessibility to its targets. We show that targeting the BRD8 bromodomain releases H2AZ, opens up chromatin, engages P53-mediated transactivation, and triggers growth arrest. Consistent with these findings, BRD8 is highly expressed with H2AZ in patient-derived proliferating GBM cells, and is inversely correlated with the expression of P53 targets. Our work solves a long-standing mystery in P53 wildtype GBM, and presents a promising therapeutic target for the majority of GBM patients.

Epigenetic Mechanisms as Drivers of Tumorigenesis

#4738
Dysregulated miR-371b-5p/CSDE1/RAC1 axis is involved in pathogenesis of triple-negative breast cancer
Yesol Kim, Je Yeong Ko, Soo-Been Lee, Jaehee Jun, Yejin Ahn, Jinui Min, Chaewon Oh, Jong Hoon Park. *Sookmyung Women's University, Seoul, Korea, Republic of*

Triple-negative breast cancer (TNBC) is the most aggressive subtype of breast cancer; however, pathogenesis of TNBC has not yet been fully understood. Here, we identified dysregulated microRNAs (miRNAs) by analyzing miRNA microarray of TNBC patients. MiR-371b-5p expression was reduced, and ectopic expression of miR-371b-5p significantly inhibited TNBC progression *in vitro* and *in vivo*. In addition, we found that expression of cold shock domain-containing protein E1 (CSDE1), a direct target gene of miR-371b-5p, was upregulated in TNBC cells, and inhibition of CSDE1 alleviated TNBC cell growth by decreasing RAC1 known as pro-metastatic gene. Mechanistically, CSDE1, phosphorylated C-terminal domain (p-CTD) of RNA polymerase II (RNAPII), and CDK7 form a complex, and downregulation of CSDE1 results in weak interaction between RNAPII p-CTD and CDK7, which leads to a decrease in RNAPII p-CTD expression to reduce RAC1 transcript levels in CSDE1-deficient TNBC cells. Our data revealed the oncogenic function of miR-371b/CSDE1 involved in Rac1 transcription regulation, thus providing a basis for the pathological mechanism of TNBC along with potential biomarkers for TNBC.

#4740

Molecular effects of histone deacetylase inhibitor Quisinostat on diffuse midline glioma of the pons

Danyelle Paine[1], Nanyun Tang[1], Yue Hao[1], Matt Biery[2], Carrie Meyers[3], Alyssa Noll[3], Nicholas Vitanza[3], Michael Berens[1]. *[1]TGen (The Translational Genomics Research Institute), Phoenix, AZ,[2]Seattle Childrens Hospital, Seattle, WA,[3]Seattle Children's Hospital, Seattle, WA*

Diffuse Midline Glioma of the pons (DMG) is a lethal, aggressive heterogeneous brain stem tumor. Median overall survival is less than a year, with radiation as the only standard treatment. Recently, mutations in DMGs have arisen as potential therapeutic targets, specifically a mutation in one of the histone H3 genes, resulting in methionine substituted for lysine at site 27 (H3K27M). H3K27M induces a marked reduction in global acetylation of histone tails, altering chromatin structure and causing aberrant gene expression. Histone deacetylase inhibitors, HDACis, are epigenetic drugs that show anticancer activity. In our studies, Quisinostat (Quis) is used to

preserve histone acetylation. Using two H3K27M-DMG treatment-naive preclinical models (PBT22 and PBT29) we detected a 100-fold differential response to the histone deacetylase inhibitor, Quisinostat. PBT-22 harbors mutations in *H3F3A*, *TP53*, and *ASXL2*, while PBT-29 has mutations in *H3F*3A, *TP53*, *PIK3CA* and *FGFR1*. Following Quis treatment (48 hrs) in both preclinical models, total H3K27ac protein abundance increased 3-fold, suggesting HDACi stabilizes or impedes turnover of K27 acetylated H3 histone. We are pursuing studies to test whether sensitivity to HDACi in DMGs is determined by a shift in relative or total abundance of respective H3wt- and H3K27M- histones. We posit that changes in H3K27ac manifest as shifts in nucleosome integration with genes responsible for cell survival/death. This project will profile differentially expressed genes (DEGs) from Quis-treated PBT22 and PBT29. Additionally, total and relative abundance of H3 proteins (wt and mt, me, me2, me3, and ac) from treated cells will be determined. Gene ontology analysis will focus on pathways accounting for chromatin remodeling, cell death, and growth arrest. RNA (qRT-PCR) and proteins (western blot) from analytes from a larger panel of DMG cell lines and neural stem cells treated with Quis will be used to validate the findings. Overall, the data depicts DMG preclinical models with large differential sensitivity to Quis, which may be partially due to different oncoprints between the models. The markedly different sensitivity of these models enables mechanistic study of the consequences of elevated abundance of histone 3 acetylation. The long term goal is to discover a molecular profile of DMGs indicative of the vulnerability to HDACi.

#4741

NUDT21 regulates PIGN through APA mechanism to affect the progression of MDS and AML

Jeffrey J. Pu[1], Fanggang Ren[2], Na Zhang[2], Shuo Li[3], Lan Zhang[4], Eric Miller[2], Guirong Wang[2], Hongwei Wang[5]. *[1]University of Arizona Cancer Center, Tucson, AZ,[2]State University of New York Upstate Medical University, Syracuse, NY,[3]The Second Hospital of ShanxiMedical University, Shanxi, China, Shanxi, China,[4]State University of New York Upstate Medical university, Syracuse, NY,[5]The Second Hospital of Shanxi Medical University, Shanxi, China*

Introducti**on:** *PIGN* gene is crucial in regulating mitotic integrity to maintain chromosomal stability and prevent MDS leukemic transformation and progression. Alternative Polyadenylation (APA) regulation and 3' RNA cleavage are 2 known vital processes in cellular DNA damage response to maintain genomic stability. *NUDT21* gene encodes protein that is one subunit of the cleavage factor Im complex required for 3' RNA cleavage and APA processing. Although *PIGN* gene has six potential polyadenylation sites, the exact role of *NUDT21* product on *PIGN* expression regulation has not been illustrated before.

Methods: At first, we analyzed *NUDT21* gene expression profile in AML, MDS, and normal control specimens and to plot the relationship between *NUDT21* gene expression status and patient survival length from 5 datasets. We also used correlation regression analysis method to predict the gene expression correlations between *NUDT21* gene and *PIGN* gene. Then, we used Caspas9 technology and vector overexpression technology to knockout or overexpress *PIGN* in HEK293 cells; RNA interference to knockdown the *NUDT21* gene in HEK293, HL60, K562, THP-1,SKM-1 and MUTZ-1 cells. MTT and CCK8 methods were used to evaluate cell proliferation. Meanwhile, cell cycle, apoptosis, Reactive Oxygen Species (ROS) and GPI-anchored proteins (CD55, CD59, and CD235) expression profiles were evaluated by flowcytometry; Immunofluorescence experiment, RT-PCR were used to evaluate the impact of *NUDT21* gene knockdown on *PIGN* expression. *in vivo* mice siRNA interference tests were conducted to verify the impact of *NUDT21* knockdown on *PIGN* gene expression. RNA-Seq & Dapars analyses were conducted on mRNAs from 3 cell lines with various *PIGN* gene expression status to observe the effects of *NUDT21* knockdown on PIGN 3'UTR processing.

Results: *NUDT21* expression increases in AML and high-risk MDS. *NUDT21* expression level is negatively correlated with overall survival. *NUDT21* knockdown decreases cell proliferation but increases cell differentiation via prolonging G1 phase, decreasing S phase, and increasing apoptosis. *NUDT21* knockdown increases cell membrane GPI-anchoring proteins (CD55, CD59, and CD235) expressions; increases ROS and Caspas3 expressions but decreases CyclinD1 expression. *NUDT21* knockout can increase *PIGN* expression, but *PIGN* expression status has no impact on *NUDT21* expression. RT-PCR and WB results showed that

NUDT21 knockdown can increase *TP53* expression but decrease *p21* expression. *in vivo* mice siRNA interference tests confirmed that *NUDT21* knockdown increases *PIGN* gene expression. The RNA-Seq/Dapars analyses results showed that 3'UTR of *PIGN* transcript was significantly shortened and *PIGN* expression increased after *NUDT21* knockdown.
Conclusion: *NUDT21* modulates *PIGN* gene expression through APA mechanism. *PIGN* polyadenylation may regulate cell proliferation status via modulating cell cycle and apoptosis.

#4742
Familial adenomatous polyposis epigenetic landscape as a precancer model of colorectal cancer
Hayan Lee[1], Gat Krieger[2], Tyson Clark[2], Yizhou Zhu[3], Aziz Khan[3], Casey R. Hanson[3], Aaron Horning[3], Edward D. Esplin[3], Mohan Badu[3], Kristina Paul[3], Roxanne Chiu[3], Bahareh Bahmani[3], Stephanie Nevins[3], Annika K. Weimer[3], Ariel Jaimovich[2], Christina Curtis[3], William Greenleaf[3], James M. Ford[3], Doron Lipson[2], Zohar Shipony[2], Michael P. Snyder[3]. *[1]Fox Chase Cancer Center, Philadelphia, PA,[2]Ultima Genomics, Newark, CA,[3]Stanford University, Stanford, CA*

Aberrant shifts in DNA methylation have long been regarded as an early biomarker for cancer onset and progression. However, it is unclear when methylation aberrance starts and how it interacts with other epigenomic modifications. To address how epigenomic changes occur and interact during the transformation from normal healthy colon tissue to malignant colorectal cancer (CRC), we collected 51 samples from 15 familial adenomatous polyposis (FAP) and non-FAP colorectal cancer patients. We generated 30-70x of whole-genome enzymatic methylation sequencing (WGEM-seq) data via the novel Ultima Genomics ultra high-throughput sequencing platform. We observed hypermethylation and hypomethylation emerge early in the malignant transformation process in gene promoters and distal regulatory elements. We performed multifaceted analysis on methylation alterations with whole-genome sequencing (WGS), transposase accessibility (ATAC-seq), high-resolution chromatin accessibility (Tri-C), and gene expression (RNA-seq) data. Our multidimensional analysis demonstrates how collectively epigenomic alterations have affected gene

expression throughout normal colon mucosa, benign and dysplasia polyps to adenocarcinoma. Epigenomic changes start as early as benign polyps, followed by other epigenomic shifts, including bivalent domains. Various epigenomic aberrances are associated with concomitant gene expression level changes. Our integrative analysis of multi-epigenomics data implicates collective and cumulative epigenomic instability in the early onset of colon carcinogenesis.

#4743

Wnt/beta-catenin mediated epigenetic modifications drive age-dependent oral squamous cell carcinoma evolution

Emily R. Fisher[1], Anthony Spinella[2], Nina C. Hardy[3], Xaralabos Varelas[4], Manish Bais[3], Maria A. Kukuruzinska[3]. *[1]Department of Biomolecular Pharmacology, Boston University, Boston, MA,[2]Department of Stem Cell and Regenerative Biology, Boston University, Boston, MA,[3]Department of Translational Dental Medicine, Boston University, Boston, MA,[4]Department of Biochemistry, Boston University, Boston, MA*

Oral Squamous Cell Carcinoma (OSCC) is a devastating disease associated with high morbidity, poor survival, and few therapeutic options. This malignancy is driven, in part, by epigenetic reprogramming of the chromatin landscape directed by β-catenin in complex with CREB-binding protein (CBP) and mixed lineage leukemia methyltransferase 1 (MLL1). The β-catenin/CBP/MLL1 complex promotes an open chromatin structure by enabling transcription of genes associated with cell plasticity, including cancer stem cells and cells with partial EMT (p-EMT) phenotypes. Growing evidence indicates that cell plasticity and cellular senescence are integral processes shared by cancer and aging. Given that the median age of OSCC diagnosis is 66 years, it is likely that aging promotes OSCC evolution to advanced disease.

To examine the effects of aging on OSCC evolution, we adapted a syngeneic mouse model of tobacco-associated oral carcinogenesis. This model utilizes a mouse cell line, 4MOSC1, derived from 4-nitroquinoline-1 oxide- (4NQO)-induced tongue tumor which, when implanted into mouse tongues, generates tumors that recapitulate human OSCC mutanome. The growth of 4MOSC1 derived orthotopic tumors was studied in 6- and 80-week-old mice. Tumors were allowed to develop for 18 days, after which

they were harvested and processed for single cell RNA sequencing, histopathology and immunofluorescence (IF) analyses.
Results showed that tumors grew at a faster rate and to a greater overall size in old mice compared to their young cohorts. OSCC harvested from the old mice displayed statistically significant reduction in membranous E-cadherin concomitant with increased Cbp and H3K4me3 abundance, suggesting an age-associated upregulation of β-catenin/Cbp/Mll1 epigenetic activity. Increased expression of Bmi1, keratin 14, and podoplanin supported increased cell plasticity in OSCC from aged mice. Further, these tumors exhibited augmented cellular senescence, as judged by the disruption of lamin B1-associated nuclear membrane integrity, and by an increased cell population with markers of senescence from single cell sequencing analyses.
These data suggest that aging is associated with increased β-catenin/Cbp/Mll1 epigenetic signaling, cell plasticity and cellular senescence, which collectively contribute to the evolution of OSCC.

#4744

Epigenetic reprogramming induced by lipids fosters mammary cell plasticity in non-transformed breast epithelial cells

Mariana Bustamante Eduardo[1], Gannon Cottone[1], Shiyu Liu[2], Seema Khan[1], Susan Clare[1]. *[1]Northwestern Univ. Feinberg School of Medicine, Chicago, IL,[2]Department of Pharmacology and Cancer Biology, Duke University, Durham, Durham, NC*

Introducti**on**. Lipid exposure of non-transformed breast epithelial cells results in increased flux modifications, and profound changes in gene expression. The upregulated genes are involved in stemness, neural development, and neural crest pathways. Neural genes are highly expressed in an estrogen receptor negative breast cancer (ERnegBC): the triple negative subtype. We aim to identify mechanisms that link lipids and epigenetic reprogramming to the genesis of ERnegBC.
Methods. Non-transformed MCF-10A cells exposed to octanoic acid (OA) were utilized for U13C-glucose tracing. S-adenosylmethionine (SAM), 2-HG and other metabolites were analyzed following treatment with OA ± PHGDH inhibitor. CUT&RUN for H3K4me3 and H3K27me3 was performed, and genes affected by OA (PMID: 28263391) were compared

with OA-responsive peaks. OA-induced genes with CUT&RUN peaks were measured in breast organoids derived from reduction mammoplasty samples exposed to OA. The Aldefluour assay was used to identify stem-like (ALDH+) cells.
Results. U13C-glucose tracing in presence of OA showed decreased glucose uptake, glycolysis and pentose phosphate pathway flux, with little effect on the TCA cycle. One-carbon (1C)-THF was redirected to the methionine cycle increasing flux to methylation. The methyl donor SAM and the demethylase inhibitor 2-HG increased after 15- and 30-min OA exposure, respectively; PHGDH inhibitor blocked these increases likely via effects on 1C metabolism. H3K4me3 CUT&RUN revealed 661 differential peaks (FDR < 0.05) comparing OA to control. The genes associated with these peaks are involved in neuron differentiation, neural crest, EMT and neural genes expressed in ERnegBC. 73% of H3K4me3 OA-associated peaks were in regulatory regions of OA-induced genes (FDR < 0.01), including NGFR (log2FC = 11.7), NGF (log2FC = 8), NTRK1 (log2FC = 2.1). OA-induced genes with enriched H3K4me3 peaks were also upregulated in breast organoids exposed to OA, such as NGFR (FC = 2.2), NGF (FC = 4.7), NTRK1 (FC = 6.6). Motif analysis revealed an overrepresentation of transcription factors ($p < 0.05$) associated with EMT (Zeb1, Slug), neural functions (E2A, AP1, JunB), neuronal-injury (Atf3) and stress response (Chop, Atf4). Twelve H3K27me3 peaks were enriched in control (FDR < 0.05) and associated with increased gene expression in OA, among them were LGR6 (log2FC = 1.9), a gene associated with ERnegBC and PLAG1 (log2FC = 2.8) a stem cell marker. ALDH+ cells' percentage increased by at least 10% after OA exposure.
Conclusions. Lipid exposure affects the production of SAM and 2-HG, which results in epigenetic fostered plasticity, leading to reprogramming/selecting cells with a multi-potential embryonic or stem-like state and/or differentiation to a neural/neural crest-like state which may facilitate ERnegBC genesis.

#4745
Prostatic fluid-based cfDNA methylation profiling distinguish benign hyperplasia from prostate cancer
Hang Dong, Haoran Tang, Yue Zhang, Shidong Jia. *Huidu (Shanghai) Medical Sciences, Ltd., Fengxian District, Shanghai, China*

Introducti**on:** A challenge in the early diagnosis of prostate cancer (PC) is to distinguish between malignant tumor and benign prostatic hyperplasia (BPH) because of the similar symptoms. Methylation profiles provide a way for discriminating BPH from PC, which could prevent overdiagnosis and overtreatment. Applying methylation biomarkers to liquid biopsy specimens provides higher sensitivity to detect tumors.
Methods: Prostatic fluid samples were prospectively collected from 40 patients following digital rectal exam and isolated cell-free DNA to perform whole genome methylation sequencing using PredicineEPIC platform. Combing differentially methylated regions (DMR) with methylation signature identified from massive public data, a panel of methylation patterns was developed. The difference of methylation signal in profiled region were implemented by machine learning to robustly distinguish BPH from prostate cancer.
Results: We identified 324 biomarkers from prostatic fluid samples and collected 46 methylation biomarkers reported from previous research. Regions with extreme difference between benign prostatic hyperplasia and prostate cancer were identified as candidate biomarkers. A diagnostic model trained on these 55 biomarkers could distinguish BPH from PC in 10-fold cross-validation (AUC = 0.92). And this model could be applied for discriminating normal tissue from prostate tumor tissue with highly performance (AUC > 0.95). Using this set of regions, we developed an NGS-based panel for detecting methylation alteration of cfDNA from prostate liquid, which inherited the ability of differentiation.
Conclusion: These methylation patterns could be developed as the novel biomarkers to support the development of prostatic fluid-based non-invasive diagnostic test and reduce unnecessary biopsies. This panel could be applied for differential diagnosis of benign hyperplasia and prostate cancer.

#4746

Amelioration of hemoglobinopathies by targeted deletion of zinc finger domain within *BCL11A* gene using CRISPR-Cas9 technology

Irfan Hussain, Kainaat Mumtaz, Hammad Hassan, Afsar Ali Mian. *Centre for Regenerative Medicine and Stem Cell Research, Aga Khan University, Karachi, Pakistan*

Background**:** In humans, the β-like globin genes are encoded from a single locus comprising five globin genes (ε-, Gγ-, Aγ-, δ-, and β-globin in sequence) and their expression is under developmental control. The γ-globin genes (Gγ- and Aγ-) are expressed during fetal life and replaced by adult β-globin after birth. Mutations in the β-globin gene cause β-hemoglobinopathies such as sickle cell disease (SCD) and β-thalassemia. The clinical severity of SCD and β-thalassemia can be mitigated by elevated fetal hemoglobin (HbF) levels, which have been found in individuals with the benign hereditary persistence of fetal hemoglobin (HPFH) syndrome. Thus, reactivating the expression of γ-globin genes is an attractive treatment strategy for β-hemoglobinopathies. Reactivation of γ-globin expression by disrupting the binding of the *BCL11A* transcriptional repressor complex to the γ-globin gene promoter, provides a novel approach for inducing fetal hemoglobin.
Methodology: The *BCL11A* binds a 5′-TGACCA-3′ element (spanning nucleotides −118 to −113) of globin genes using its three C-terminal Zinc fingers (*Znf*). The binding efficiency of Znf4, Znf5, and Znf6 was predicted by using *in silico* tools (SIFT, SNAP, PolyPhen-2, PANTHER, I-Mutant, PROVEAN, SNPs&GO, mCSM, and PhD-SNP), molecular dynamic simulation and homology modelling. K562 cells were electroporated with CRISPR-Cas9 targeting the *BCL11A* Znf4.
Results: The binding energy scores illustrate that deleting Znf5 and Znf6 decreased the binding affinity by ~3.7-fold, whereas deleting Znf4 decreased the affinity by > 70-fold. Using CRISPR-Cas9 genome-editing strategy, we deleted Znf4 (260bp genomic region) within the *BCL11A* in K562 cell lines. Znf4 deletion resulted in a readily detectable γ-globin increase with a preferential increase in G-gamma.
Conclusion: Altogether, our findings highlight the valuable insights for improving gene editing therapy strategies by either deleting Znf4 of *BCL11A* or the TTGACCA motif to disrupt the interaction between *BCL11A* and other interacting partners and the γ-globin gene promoter. Complete failure in the protein-protein interactions with functional partners and to the γ-globin gene promoter revealed that Znf4 is a suitable target for disrupting BCL11A-mediated hemoglobin switching.

#4747

NSD2 mutation drives oncogenic programming in mantle cell lymphoma

Jianping Li[1], Marta Kulis[2], Alberto Riva[1], Heidi Casellas Román[1], Daphne Dupere-Richer[1], Amin Sobh[1], Charlotte Leonie Kaestner[1], Richard L. Bennett[1], Inaki Martin[2], Jonathan D. Licht[1]. *[1]University of Florida, Gainesville, FL,[2]Fundació Clínic per a la Recerca Biomèdica, Barcelona, Spain*

Background**:** NSD2, a histone methyltransferase, is an oncoprotein first characterized by its overexpression in multiple myeloma (MM). *NSD2* mutations within the catalytic SET domain are found in acute lymphoblastic leukemia (ALL) and mantle cell lymphoma (MCL). We previously demonstrated that *NSD2* p.E1099K mutation caused an imbalance of H3K36me2/H3K27me3 and drove glucocorticoid resistance in ALL. *NSD2* mutations, especially p.E1099K and p.T1150A, were identified in 10-15% of cases of MCL and are enriched in patients who relapse from targeted therapies such as ibrutinib. However, the activity of *NSD2* mutations in MCL remains unexplored.

Aim: To demonstrate the role of *NSD2* mutations in MCL progression due to aberrant chromatin modification.

Methods: We created isogenic MCL cell lines by knock-in *NSD2* p.E1099K mutation into Z138 and Jeko-1 cell lines using CRISPR/Cas9 gene editing. We then determined the effect of the mutation on H3K36me2/H3K27me3 levels and biological activities including cell growth (IncuCyte), apoptosis (Annexin V/PI Staining), and cell cycle (BrdU incorporation). We determined transcriptome (RNA-Seq) and histone modification profiles (ChIP-Seq) in isogenic Z138 cell lines. Finally, we integrated analysis of RNA-Seq of human patients and our human MCL cell lines to comprehensively disclose the epigenetic landscape in MCL with *NSD2* mutation.

Results: We successfully created isogenic Z138 cell lines with heterozygous and homozygous *NSD2* p.E1099K mutation and a Jeko-1 cell line with heterozygous *NSD2* p.E1099K mutation. Insertion of *NSD2* p.E1099K by CRISPR/Cas9 gene editing led to a striking increase of H3K36me2 and concomitant decrease of H3K27me3 in both Z138 and Jeko-1 cell lines. *NSD2* mutation significantly increased cellular growth with enhanced S phase entry, decreased number of cells in G0/G1 phase and

decreased spontaneous apoptosis. RNA-Seq analysis demonstrated striking changes in gene expression with 1794 genes upregulated and 1492 genes downregulated in *NSD2* mutant MCL cells. Among them, anti-apoptotic genes *BCL2* and *BCL2L2* were upregulated while pro-apoptotic genes *BAX*, *BID*, and *BIK* were downregulated in *NSD2* mutant cells, which was consistent with the biological phenotypes. Surprisingly, *CCND1*, *CCNE1*, *CCNE2*, *TP53*, and *CDKN2C* (*p21)* were downregulated while *CDKN2D*, *CDKL3*, and *CDKL5* were upregulated in *NSD2* mutant cells. Altered gene expression in isogenic Z138 cells were compared with patient expression profiles, with gene ontology revealing significant overlap and enrichment of cell adhesion, neural pathways, and evidence of activated signaling. Aberrant histone modification H3K27ac contributed to many of differentially expressed genes pattern.
Conclusions: The *NSD2* mutation led to increased tumor cell growth but decreased apoptosis due to the dysregulation of epigenetic landscape and transcriptome, suggesting an oncogenic reprogramming driven by an activated *NSD2* mutation in MCL.

#4749

Effects of *miR-34a-5p* and *miR-181b-5p* silencing and induction on their potential targets in uterine leiomyosarcoma cells

Bruna C. de Almeida[1], Laura G. dos Anjos[1], Katia C. Carvalho[2].
[1]Obstetrics and Gynecology, University of São Paulo, Faculty of Medicine, São Paulo, Brazil,[2]University of São Paulo, Faculty of Medicine, São Paulo, Brazil

Background: Leiomyosarcoma (LMS) is a malignant tumor of the uterine body that represents 40-60% of all gynecological sarcomas. Up to now, there is no specific treatment or diagnostic biomarkers for this tumor. The identification and characterization of miRNAs signature could help to its management. In addition, miRNAs represent targets for therapies due to their ability to modulate various signaling pathways simultaneously. Thus, the present study aimed to evaluate the effects of genetic manipulation of *miR-34a* and *miR-181b* on their predicted target genes in LMS cells.
Methods: SK-UT-1 cells from uterine LMS were transfected with synthetic miRNA mimics and inhibitors (siRNA) of *miR-34a* and *miR-181b*. The efficacy of transfection was assessed by miRNA expression (qRT-PCR)

assays. In order to identify potential genetic interactions network of *miR-34a* and *181b*, predicted target genes were selected by in silico analysis (miRTargetLink 2.0 and miRDB). After SK-UT-1 cells transfection, the expression of target genes was evaluated by qRT-PCR.
Results: SK-UT-1 cells showed greater efficiency of mimics and siRNA transfections after 48h treatment for both *miR-34a* and *181b*. *MDM4, TP53, BCL2, KMT2D, NOTCH2,* and *CCND1* were identified as predicted target genes of *miR-34a*; and the *TIMP3, FGFR1, BCL2, NOTCH2, ATM*, and *IRS1* target genes for *miR-181b*. Expression profile of selected target genes was assessed after each treatment. The *miR-34a* mimic significantly increased the expression of *MDM4* after 96h of treatment, while the *BCL2* and *TP53* showed an increase in expression with siRNA after 48h of treatment. *CCND1* showed a greater expression in both treatments at 48h. An increase in *KMT2D* and *NOTCH2* expression was also observed after treatment, even though without statistically significant. Treatment with *miR-181b* mimic led to increased *FGFR1* expression within 72h. Although some expression alterations were observed in *TIMP3, BCL2, NOTCH2, ATM,* and *IRS1* genes after mimic and siRNA treatments, there was no statistical significance.
Conclusion: The effect of *miR*-34a upregulation leads to induction *MDM4* and *CCND1* expression, the first being a *TP53* inhibitor and the second, responsible for cell cycle maintenance. The *miR-34a* downregulation had an inductor effect on expression of *MDM4*, *BCL2* (apoptosis regulator), *TP53* (tumor suppressor), and *CCND1*. The *miR-181b* upregulation induced the expression of fibroblast growth factor receptor, *FGFR1*. In uterine LMS cells, *miR-34a* seems to exert an important role in regulating the expression of cell cycle and apoptosis-related genes.

#4750
TWIST2 mediated chromatin remodeling promotes fusion-negative rhabdomyosarcoma
Akansha M. Shah, Lei Guo, Maria Gabriella Morales, Priscilla Jaichander, Kenian Chen, Huocong Huang, Karla Cano Hernandez, Lin Xu, Rhonda Bassel-Duby, Eric N. Olson, Ning Liu. *UT Southwestern Medical Center, Dallas, TX*

Rhabdomyosarcoma (RMS) is a common soft tissue sarcoma in children that resembles the developing skeletal muscle. Unlike normal muscle cells, RMS cells fail to differentiate despite expression of the myogenic determination protein MYOD. The TWIST2 transcription factor is frequently overexpressed in fusion-negative RMS (FN-RMS). TWIST2 blocks differentiation by inhibiting MYOD activity in myoblasts, but its role in FN-RMS pathogenesis is incompletely understood. Here, we show that knockdown of TWIST2 enables FN-RMS cells to exit the cell cycle and undergo terminal myogenesis. TWIST2 knockdown also substantially reduces tumor growth in a xenograft model of FN-RMS. Mechanistically, TWIST2 controls H3K27 acetylation at distal enhancers by interacting with the chromatin remodelers SMARCA4 and CHD3 to activate growth-related and repress myogenesis-related target genes, respectively. These findings provide novel insights into the role of TWIST2 in maintaining an undifferentiated and tumorigenic state of FN-RMS and highlight the potential of suppressing TWIST2-regulated pathways to treat FN-RMS.

#4751

The function of bromodomain containing protein 4 (BRD44) in hematopoiesis

Francine Nihozeko. *Cells System and Anatomy (Cancer Biology), UT Health Science Center at San Antonio, San Antonio, TX*

Bromodomain containing protein 4 (BRD4) is an epigenetic transcription regulator that reads acetylated chromatin and is involved in the recruitment of transcriptional factors to initiate gene transcription. BRD4 is functionally versatile and has extensively been studied for its role in cell cycle progression, gene transcription regulation, chromatin organization and remodeling, as well as DNA replication and repair . In addition, BRD4 has been implicated in many solid and liquid tumors, and its inhibition shows promising preclinical activity, especially in hematopoietic malignancies. BRD4 is overexpressed in Leukemia and has been reported to play a role in hematopoietic stem cell expansion and progenitor development. However, the mechanisms of BRD4 in hematopoietic stem cell functions and disease development remain poorly understood. Using BRD44 knockout (BRD44 Δ/Δ , driven by Mx1 Cre to delete BRD44 in hematopoietic system) mouse model, we found that BRD4 is required for HSCs self-renewal and the loss

of BRD44 impaired erythroid differentiation and skewed myeloid differentiation. BRD44 Δ/Δ HSPCs showed G0/G1 arrest, decreased S-phase, and increased senescence compared to wild type (WT) HSPCs. Our study demonstrates that BRD4 is essential for normal hematopoiesis. To further investigate the role of BRD4 in hematopoiesis, we generated BRD44 transgenic mice (driven by Vav1 promoter, to assure all BRD44 transgene expression is instructed in the hematopoietic system). Ongoing studies focus on determining the impact of BRD4 overexpression on hematopoietic stem cell functions.

#4752

Loss of the methyltransferase KMT5C drives resistance to tyrosine kinase inhibitors via H4K20me3 regulation in non-small cell lung cancer

Alejandra Agredo[1], Arpita Pal[2], Jihye Son[2], Nadia A. Lanman[2], Andrea L. Kasinski[1]. *[1]Purdue University Center for Cancer Research, West Lafayette, IN,[2]Purdue University, West Lafayette, IN*

Lung cancer is still the leading cause of cancer-related deaths, and although important therapy advancements have been achieved, ~1.6 million people die from lung cancer annually. Non-small cell lung cancer (NSCLC), which makes up ~85% of lung cancer cases, is mainly treated with radiotherapy, chemotherapies, and targeted agents. Targeted agents are selected based on the mutation spectrum of the tumor. In NSCLC the epidermal growth factor receptor (EGFR) is commonly mutated and, leads to increased proliferation and cell survival. The standard-of-care treatment for patients with activating mutations in EGFR is treatment with tyrosine kinase inhibitors (TKI), such as erlotinib. While tumors initially respond to TKIs, most patients develop resistance after 1-2 years. In ~60% of TKI resistant tumors, resistance is the result of a secondary mutation in EGFR, whereas, in the remaining 20%, tumors turn on bypass track-signals to overcome inhibition of the EGFR pathway. In the remaining 15-20% of the cases the mechanisms underlying resistance are unknown. Most studies focus on the gain of function of oncogenes as mediators of resistance; however, little is known about the role that tumor suppressors play in TKI resistance. Hence, we performed a genome-wide CRISPR Cas9 knock-out screen to identify genes that when knocked-out would drive erlotinib resistance. Fold enrichment analysis of

sgRNAs, identified KMT5C as a top candidate. KMT5C is a histone methyltransferase that trimethylates H4K20 (H4K20me3), enabling the establishment of constitutive and facultative heterochromatin. The process by which KMT5C is reduced in tumors is unknown, yet data from human samples suggests that the *KMT5C* transcript is globally downregulated in NSCLC and in tumor samples resistant to the third-generation TKI osimertinib. Additionally, loss of the modification made by KMT5C (H4K20me3), influences the prognosis of NSCLC, indicating that loss of KMT5C function is a crucial mechanism in carcinogenesis. We recently described how loss of KMT5C leads to increased transcription of the oncogene MET, due to a loss in H4K20me3-mediated repression of a long non-coding RNA transcription (LINC01510) upstream of MET. This mechanism was found to be responsible for driving TKI resistance in EGFR mutant cells. Historically, KMT5C has been associated with generation of constitutive heterochromatin (cHC); however, recent reports, including our own, indicate that KMT5C also regulates transcription in regions outside of cHC. Our preliminary evidence suggests that deposition of H42K0me3 via KMT5C in regions outside of cHC, is less stable than in cHC regions. This novel finding led us to hypothesize that regulation of KMT5C and H42K0me3 at different regions of heterochromatin is a dynamic process, and future work will aim at understanding this process and its relevance in cancer progression and TKI resistance.

#4753

LSD1–mediated FOXA2/AP1 transcription program drives lineage plasticity in prostate cancer

Zifeng Wang[1], Mingyu Liu[1], Songqi Zhang[1], Muqing Li[1], Susan Patalano[1], Jill A. Macoska[1], Dong Han[1], Shuai Gao[2], Hansen He[3], Changmeng Cai[1].
[1]University of Massachusetts, Boston, MA,[2]New York Medical College, Valhalla, NY,[3]Princess Margaret Cancer Centre, Toronto, ON, Canada

Background: While castration-resistant PCa (CRPC) can be further treated with second-generation androgen deprivation therapies (ADTs), the tumor can quickly generate resistance through multiple mechanisms. One critical mechanism is that tumor cells can progress to AR-indifferent stem cell-like (SCL-PCa or SCLPC) or neuroendocrine-like CRPC (NE-PCa or NEPC) through lineage plasticity. However, the underlying molecular basis remains

to be determined, and clinical treatment options for these aggressive CRPC subtypes are currently limited. FOXA1 and FOXA2, which are members of the FOXA (Forkhead Box A) protein family, are pioneer transcription factors. While FOXA1 is well known for its function as a critical pioneer factor of AR and pivotal for maintaining AR signaling, the molecular function of FOXA2 in PCa cells is poorly understood despite that FOXA2 is known to be overexpressed in NEPC. Moreover, since FOXA2, like FOXA1, is currently undruggable in the clinic, there is an urgent need to decipher the molecular basis for the chromatin binding of FOXA2 and identify druggable targets that regulate FOXA2 binding and activity in the aggressive FOXA2-positive CRPC.

Methods: In the current study, we first examined the role of FOXA2 in tumorigenesis and metastasis by using various *in vitro* and *in vivo* assays including mouse subcutaneous injection and zebrafish embryo injection approaches. We then conducted integrated whole genomic transcriptome and cistrome analyses in SCLPC and NEPC cell line models to characterize the activity of FOXA2 on chromatin and to identify its collaborating transcription factors that may play specific functions in promoting SCLPC or NEPC using a series of biochemical and bioinformatic approaches.

Results: We found that FOXA2 silencing decreased the growth and metastasis of SCLPC and NEPC cells. Importantly, we discovered that FOXA2 chromatin binding is tightly associated with binding of JUN family proteins (primarily c-Jun) and FOXA2 silencing dramatically interrupted the global chromatin binding of c-Jun and FOSL1. The transcription targets of FOXA2/AP-1 are highly enriched for neuroendocrine and plasticity associated genes and associated with poor clinical outcomes. Furthermore, we also found that FOXA2 chromatin binding is globally enhanced by an epigenetic factor LSD1, and LSD1 inhibition can repress FOXA2/AP-1 activity in multiple CRPC models.

Conclusion: Overall, our data indicate that FOXA2 functions to maintain tumor growth and metastasis in SCLPC and NEPC models. Mechanistically, FOXA2 can act as a pioneer factor of AP-1 (c-Jun/FOSL1) and reprogram AP-1 transcription activity. This FOXA2/AP-1 axis is regulated by LSD1 via demethylating FOXA2 protein and LSD1 inhibition represses FOXA2-dependent CRPC tumor progression. These findings provide novel mechanistic insights into the molecular mechanisms for PCa lineage plasticity and treatment resistance.

#4754

Investigating the impact of hotspot mutations in a chromatin reader on leukemogenesis

Yiman Liu, Qinglan Li, Sylvia Tang, Chujie Gong, Liling Wan. *University of Pennsylvania, Philadelphia, PA*

Acute myeloid leukemia (AML) is one of the most aggressive forms of hematological malignancies with a low overall 5-year survival rate (< 26%). The mainstay of treatment for AML includes chemotherapy, but the response of a subset of patients to current treatment options remains poor. Thus, new therapeutic approaches are desperately needed. AML often arises from somatic mutations in chromatin regulators that result in uncontrolled proliferation and a block of differentiation in myeloid progenitor cells. As such, investigation of the role and molecular mechanism of chromatin regulator in AML is being actively pursued. Previously, we discovered the eleven-nineteen-leukemia (ENL) protein, a chromatin "reader" and transcription co-activator, as an unrecognized requirement for the survival of AML. We developed a potent and orally bioavailable small-molecule inhibitor of ENL, which displaces ENL from chromatin and blocks AML progression. Hotspot mutations have been found in ENL YEATS domains, both in Wilms tumor and in leukemia, and these mutations confer a gain of condensation property, leading to aberrant gene activation. However, the impact of ENL mutation on tumorigenesis is largely unknown. The over-arching goal of this project is to explore the impact of the hyper-activated ENL pathway (ENL mutation) in AML. Results from this project will elucidate how newly discovered chromatin reader mutations drive tumorigenesis and offer new biology insights that will facilitate both basic mechanistic studies and clinical studies.

#4755

Screening non-small cell lung cancer organoids with epigenetic probes

Khadija Jafarova[1], Panagiotis Prinos[2], Nikolina Radulovich[3], Takamasa Koga[3], Cheryl Arrowsmith[2], Geoffrey Liu[3], Ming Sound Tsao[3]. *[1]Medical Biophysics, University of Toronto, Toronto, ON, Canada,[2]Structural Genomics Consortium, University of Toronto, Toronto, ON, Canada,[3]Princess Margaret Cancer Centre, Toronto, ON, Canada*

Introduction: NSCLC is associated with high cancer-related mortality worldwide. Epigenetic modifications at the chromatin level have widely been linked to carcinogenesis. Epigenetic regulation not only contributes to the development of cancer, but it may also confer resistance to therapies by promoting the survival of clones that can overcome treatment-induced stress or give rise to complex tumor heterogeneity in response to cancer therapy. Investigating susceptibility resulting from epigenetic aberrations in tumor cells may reveal novel markers of therapies that target epigenetic aberrations. In this study, we treated NSCLC organoid models with a library of 41 epigenetic probes to identify epigenetic targets that affect tumor cell survival.
Methods: Epigenetic screen. NSCLC organoid models were established from resected patient tumors or patient-derived xenografts. Organoids were dissociated into single cells and plated in matrigel-coated 384-well plate. Each model was treated with a library of epigenetic probes (1uM) and a DMSO control over a period of 8 days. Library was provided by Structural Genomics Consortium (www.thesgc.org) and contained compounds targeting a variety of protein domains some of which had activity on acetylation, methylation, histone de-methylation etc. CellTiter-Glo assay was performed to measure cell survival.
Results: Among the epigenetic probe compounds tested on 26 models, LLY 283 (PRMT5 inhibitor) showed the most significant effect on inhibition of cell growth in 69% of organoid models
(18/26) with suppression of >=40% as compared to the DMSO control. To assess differential responses to treatment with LLY 283, four organoid models were treated with 21 different concentrations of PRMT5 inhibitor. Growth curves of a sensitive (XDO181) and a less sensitive (XDO4056) models were compared. For XDO181 and XDO4056, IC50 values were calculated to be 4.7 nM and 31.8 nM respectively, indicating that a less sensitive model is associated with a 7-fold increase in IC50 value compared to the sensitive model.
Conclusion: A screen using epigenetic compounds on NSCLC patient-derived organoids revealed sensitivity to PRMT5 inhibitor in 69% of the organoid models tested. Further investigation will explore the mechanisms that are associated with sensitivity to PRMT5 inhibition.

#4756

NSD1/2 histone methyltransferases regulate cell growth in HPV-negative head and neck squamous cell carcinoma (HNSCC)

Iuliia Topchu[1], Igor Bychkov[1], Petr Makhov[2], Evgeny Izumchenko[3], John Karanicolas[2], Jindan Yu[1], Jochen Lorch[1], Yanis Boumber[1]. *[1]Robert H. Lurie Comp. Cancer Ctr. of Northwestern Univ., Chicago, IL,[2]Fox Chase Cancer Center, Philadelphia, PA,[3]University of Chicago, Chicago, IL*

Members of the NSD protein family (NSD1, NSD2, and NSD3) are histone methyltransferases (HMTs) that catalyze lysine 36 dimethylation (K36me2) at histone H3. H3K36 modifications play an important role in regulating the function and structure of chromatin, affecting transcription, replication, and repair. Abnormal H3K36 methylation is often detected during tumor development and progression. Inactivating NSD1 mutations are frequent in head and neck squamous cell carcinoma (HNSCC). They commonly occur in HPV-negative oropharyngeal (OP) and laryngeal (LC) carcinomas, and define a prognostic subtype in LC, associated with significantly improved overall and progression-free survival. Notably, the SCC4 cell line, carrying a damaging mutation in the *NSD1* gene demonstrated reduced dimethylation level of H3K36 compared to NSD1 wild-type HNSCC counterparts. To explore the biological impact of the NSD1/NSD2 loss of function in HNSCC, we established cell lines with doxycycline-inducible shRNA knockdown of NSD1 and NSD2 in the set of HNSCC cell lines originating from different sites (JHU011, JHU022, Cal27, and FaDu cell lines). The depletion of NSD1 and NSD2 led to reduction of K36me2, significant decrease in cell growth as measured by cell titer blue (CTB) and clonogenic assays. NSD1/NSD2 depletion in these HNSCC cells also caused a significant increase in apoptosis. Gene Set Enrichment Analysis (GSEA) of RNA-seq for NSD1 wt versus knockdown cells indicates that NSD1 knockdown reduced expression of E2F target genes. Among the E2F transcription factor family, E2F2 gene expression was significantly decreased in all NSD1 knockdown cell lines. NSD1 knockdown also activated gene pathways related to autophagy and response to starvation. NSD1 knockdown reduced the levels of autophagy initiation gene ULK1 at both mRNA and protein levels. We also probed for protein signaling in HNSCC cells following NSD1 depletion using a reverse protein phase array (RPPA) approach, and validated Phosphatidylinositol-5-Phosphate 4-Kinase

Type 2 Beta (PIP4K2B), but not other members of this family (PIP4K2A and PIP4K2C), as NSD1-regulated. PIP4K2B was regulated at the mRNA level by NSD1 as well. The CHIP-qPCR assay demonstrated the loss of H3K36me2 at the promoter of the PIP4K2B gene in NSD1 knockdown cells, suggesting direct regulation by NSD1. Moreover, PIP4K2B siRNA depletion has also led to a significant decrease in HNSCC proliferation, which suggests that the NSD1 may regulate proliferative activity through PIP4K2B. Taken together, while this data supports the suggestion that NSD histone methyltransferases have multiple downstream targets, the underlying mechanism remain to be investigated in more detail. Further, NSD proteins are attractive targets for drug development for improving treatment strategies for HNSCC.

#4757

Loss of KDM5A supports KRAS-driven pancreatic cancer

Jasper R. Chen[1], Jincheng Han[2], Cullen M. Taniguchi[1], Ronald A. DePinho[2]. *[1]Radiation Oncology, UT MD Anderson Cancer Center, Houston, TX,[2]Cancer Biology, UT MD Anderson Cancer Center, Houston, TX*

Objective: Mutant KRAS is a primary driver of pancreatic ductal adenocarcinoma (PDAC), which exhibits marked hypoxia. Despite the strong association of hypoxia and PDAC, the relationship between KRAS and hypoxia is still poorly understood. The oxygen-sensitive histone lysine demethylase, KDM5A, was recently reported to mediate epigenetic responses to hypoxia independent of the hypoxia-inducible factors. KDM5A epigenetically represses transcription via two mechanisms: by its demethylase activity on activating H3K4me3 marks, and through its interaction with deacetylase complexes containing HDAC1/2, which deacetylates activating H3K9ac and H4K16ac histone marks. Under hypoxic conditions, KDM5A loses its activity, leading to restoration of these H3K4me3 marks, thereby activating KDM5A target genes. The purpose of this study is to understand how KDM5A loss of function contributes to pathogenesis of mutant KRAS-driven pancreatic cancer. Methods: Cell lines derived from mice with pancreas-specific p53 deletion and doxycycline-inducible expression of $Kras^{G12D}$ (iKPC). Protein lysates were prepared using RIPA buffer. Histones were purified by acid extraction.

Immunoblotting was used to probe for protein levels of Kdm5a, H3K4me3, H3K9ac, and H4K16ac. Genetic ablation of $Kras^{G12D}$ was performed by culturing iKPCs in tetracycline-free medium. Kras was induced by adding doxycycline to the culture medium. Pharmaceutical inhibition of MEK, proteasome, and Kdm5a were performed by treating iKPCs with mirdametinib, MG-132, and CPI-455, respectively. Knockdown of β-TrCP and FBXW7 were performed by stable expression of shRNA in iKPCs. Protein motif scanning was performed using the Eukaryotic Linear Motif (ELM) Prediction online software.
Results: We discovered that Kdm5a protein levels were abrogated by induction of $Kras^{G12D}$ and stabilized by genetic ablation of Kras. Pharmaceutical inhibition of MEK or proteasome function stabilized Kdm5a, indicating that Kras induces Kdm5a proteasomal degradation through the MEK/ERK pathway. H3K4me3, H3K9ac, and H4K16ac histone marks were increased in Kras-on iKPC compared to Kras-off iKPC, consistent the expected effect of Kras-induced Kdm5a degradation. Pharmaceutical inhibition Kdm5a in the Kras-off setting restored H3K4me3, suggesting that Kdm5a contributes to demethylation of H3K4me3 in iKPC. We identified two phosphodegron sites corresponding to β-TrCP and FBXW7 of the ubiquitin ligase complex within the Kdm5a protein sequence. Knockdown of either β-TrCP or FBXW7 in iKPC both stabilized Kdm5a despite induction of Kras.
Conclusion: We conclude that Kdm5a plays a tumor suppressor role in pancreatic cancer by epigenetically repressing transcriptional programs necessary for KRAS-driven oncogenesis.

#4758

***SETD4* transcription levels correlates with leukemic burden and *SMYD2* transcription in acute lymphoblastic leukemia**

Luis Augusto Muniz Telles, Luis Henrique Toshihiro Sakamoto, Alan Jhones Barbosa de Assis, Doralina de Amaral Ramos Rabello, Andrea Barretto Motoyama, Fabio Pittella-Silva. *Faculty of Health Sciences and Medicine, University of Brasilia, Brasilia, Brazil*

Acute lymphoblastic leukemia (ALL) is the most common childhood malignancy worldwide. It has a history of great rates of success in treatment, but adults and infants still share a dismal prognosis. This

condition makes the development of new prognostic markers linked to effective therapeutic strategies a matter of pressing concern. While cancer has traditionally been viewed as a genetic disease derived from alterations in oncogenes and tumor suppressors, it is well known nowadays that epigenetic changes also play a fundamental role in tumorigenesis. The SET family of lysine methyltransferases (KMT) has been implicated in a number of cancers, and *SETD4* is a member that is still poorly characterized. In the present study we used qPCR to analyze the expression pattern of *SETD4* among 83 pediatric ALL patients and non-neoplastic bone marrow (BM) samples and investigated the correlation between *SETD4* transcription changes with the leukemic burden in ALL patients during chemotherapy. We found that *SETD4* transcription levels are significantly upregulated in BM samples derived from ALL patients compared to non-neoplastic BM (8,5-fold higher, $p < 0{,}001$) and its expression correlated with leukemic burden. Importantly, levels of *SETD4* decreased in patients that responded to chemotherapy treatment. We further investigated whether *SETD4* transcription levels associates with that of *SMYD2*, another KMT previously identified as a prognostic marker in ALL. Transcription levels of *SETD4* and *SMYD2* were examined on day 15^{th} and 29^{th} of chemotherapy. Surprisingly, a high level of correlation (Spearman $r = 0.925$, $p < 0.01$) between both genes was observed in both treatment time points. Finally, survival outcomes were worst in ALL patients with high levels of *SETD4* transcription (log-rank test, $p < 0{,}05$), evidencing its dysregulated expression is associated with an unfavorable disease prognosis. Together, these results point to *SETD4* as a useful prognostic marker, a possible tool to assess response to therapy and an attractive target for drug development.

#4759

Dissecting EP300 and CBP function in prostate cancer models

Kiran Mirpuri, Alok K. Tewari, Myles A. Brown. *Dana-Farber Cancer Institute, Boston, MA*

Prostate adenocarcincoma is dependent on androgen and its cellular receptor the androgen receptor (AR) for most of the natural history of the disease including progression to the advanced and lethal state. Many prostate cancer therapeutics target the androgen signaling pathway, although tumors invariably become resistant to these treatments. EP300 and

CBP are protein paralogs that are co-regulators of AR-mediated gene transcription and are mutated at low frequency in prostate cancers. Expression of CBP and EP300 has been found to correlate with AR expression in advanced disease, and their inhibition can impact AR-mediated transcription in model systems. However, both proteins are not equally essential in prostate cancer cell lines. As drugs inhibiting the bromodomains of these proteins are in early clinical trials, a greater understanding of the common and unique functions of EP300 and CBP may inform the clinical application of these therapeutics. Using chemical inhibition or degradation of either each paralog or both, in combination with genetic depletion, we identify converging and diverging epigenomic and transcriptional programs regulated by each paralog both in the presence and absence of androgens. If validated in tumor samples from patients, these results may nominate biomarkers of response to EP300/CBP inhibitors.

#4760

KDM4A promotes NEPC progression through regulation of MYC expression

Celia Sze Ling Mak[1], Ming Zhu[1], Xin Liang[1], Feng Wang[2], Anh G. Hoang[1], Xinzhi Song[2], Peter Shepherd[2], Derek Liang[2], Jessica Suh[2], Jiwon Park[2], Miao Zhang[2], Eric Metzger[3], Roland Schule[3], Abhinav K. Jain[2], Ellen Karasik[4], Barbara A. Foster[4], Min Gyu Lee[2], Paul Corn[2], Christopher J. Logothetis[2], Ana Aparicio[2], Nora Navone[2], Patricia Troncoso[2], Jianhua Zhang[2], Sue-Hwa Lin[2], Guocan Wang[1]. *[1]Department of Genitourinary Medical Oncology, UT MD Anderson Cancer Center, Houston, TX,[2]UT MD Anderson Cancer Center, Houston, TX,[3]Klinikum der Albert-Ludwigs-Universitat Freiburg, Freiburg, Germany,[4]Roswell Park Comprehensive Cancer Center, Buffalo, NY*

Despite advancements in treatment, prostate cancer (PCa) remains the second leading cause of death among men. Neuroendocrine prostate cancer (NEPC) represents one of the most lethal forms of PCa and lacks life-prolonging treatment. Here we identified histone lysine demethylase KDM4A as a driver in NEPC progression and an effective therapeutic target. KDM4A mRNA and protein are overexpressed in human and mouse NEPC compared to adenocarcinoma. Knockdown or knockout of KDM4A in NEPC cell lines suppressed cancer cell growth *in vitro* and *in vivo*. Importantly, the inactivation of *Kdm4a* in a genetically engineered mouse model of prostate cancer reduces tumor burden, reduces the incidence of NEPC, and prolongs overall survival. Mechanistically, KDM4A directly regulates the transcription of MYC, which is hyper-activated in human and mouse NEPC. Furthermore, a potent pan-KDM4 inhibitor QC6352 significantly reduces NEPC cell growth *in vitro* and *in vivo*. Taken together, we demonstrate that KDM4A promotes NEPC progression through regulation of MYC expression and targeting KDM4A can be an effective therapeutic strategy for NEPC.

#4761

Identifying molecular targets to overcome CNS infiltration in acute lymphoblastic leukemia associated with an activating mutation of the

NSD2 histone methyltransferase

Charlotte L. Kaestner, Amin Sobh, Jianping Li, Katelyn Raburn, Alberto Riva, Jason O. Brant, Richard L. Bennett, Jonathan D. Licht. *University of Florida, Gainesville, FL*

Background**:** One of the major clinical challenges in acute lymphoblastic leukemia (ALL) is the treatment of central nervous system (CNS) involvement. CNS-directed therapy is currently limited to agents associated with substantial neurotoxicity and the lack of mechanistic understanding of how ALL cells infiltrate the CNS is preventing novel therapy development. Our laboratory has previously shown in murine xenografts that ALL cells with a point mutation (E1099K) in the histone methyltransferase NSD2 aggressively infiltrate not only the leptomeninges of the brain, but also the brain parenchyma. Accordingly, we also showed that NSD2-E1099K cells have an enhanced ability to migrate through a Boyden chamber and adhere to endothelial cells of the blood brain barrier (BBB cells). Furthermore, RNA-seq data on four NSD2-E1099K cell lines revealed genes that may play a role in ALL brain infiltration. However, it remains unknown which of the genes upregulated by NSD2 could be potential therapeutic targets against CNS leukemia.

Aim: This study aims to identify therapeutically targetable genes that are important for (1) migration of ALL cells through a Boyden chamber, (2) adhesion of ALL cells to BBB cells, and (3) intercellular signaling between ALL and BBB cells.

Methods: We used a focused CRISPR-gene-knockout library targeting 500 genes upregulated in NSD2-E1099K cells to ascertain genes important for migration in the RCHACV cell line. Next, we used the genome-wide Brunello library to identify genes critical for ALL cell adhesion to BBB cells. To study intercellular communication between ALL and BBB cells, we co-cultured SEM-WT or SEM-NSD2-E1099K cells with BBB cells for 48h. ALL cells were then isolated from BBB cells using CD19+ magnetic beads and all groups were further processed for RNA-seq.

Results: Our CRISPR screen studies identified genes whose knockout led to enhancement of migration or adhesion, as well as genes whose knockout resulted in inhibition of migration or adhesion. One of the top candidate genes identified in the migration screen was PTPRG. Validation studies with shRNA and CRISPRa constructs confirmed that PTPRG is a

modulator of migration and adhesion in NSD2-E1099K ALL cells. In addition, RNA-seq studies identified important differences in how SEM-WT (low-CNS infiltrating) and SEM-NSD2-E1099K (high-CNS infiltrating) cells communicate with BBB cells. Specifically, our analysis predicted that IL1B secretion of SEM-NSD2-E1099K cells, but not SEM-WT cells, leads to increased IL1B target gene expression in BBB cells, potentially contributing to CNS infiltration.
Conclusion: Our findings implicate PTPRG and the IL1B pathway as important modulators of migration and adhesion or intercellular signaling, respectively. These genes may have the potential to be novel therapeutic target for preventing ALL brain infiltration.

#4762
Oncogenic over-expression of MED12 is epigenetically fostered in the core-binding factor subgroups of acute myeloid leukemia
Samrat Roy Choudhury[1], Arkajyoti Bhattacharya[2]. *[1]University of Arkansas for Medical Sciences, Little Rock, AR,[2]University Medical Center Groningen, Groningen, Netherlands*

Mediator (MED) proteins typically assemble and recruit distal coactivators at binding sites of RNA polymerase II to help regulate a gene's transcriptional output. The MED-kinase module consists of four subunits, MED12/12L, MED13/13L, CDK8/19 and Cyclin C, and reversibly interacts with the MED-core complex to function as a lineage-specific transcriptional activator. In particular, MED12 has been reported to recruit BRD4, FLI/ERG, CBP/p300, and GATA2 transcription factors on H3K27ac-enriched super-enhancer (SE) loci in hematopoietic stem and acute myeloid leukemia (AML) cells to maintain cell fate determination or leukemic growth respectively. Given the regulatory role MED12 in AML, there is a sustained interest in identifying targeted inhibitors against this MED-protein. Herein, we aimed to investigate if the oncogenic over-expression of MED12 is epigenetically regulated in AML. We analyzed the MED12 transcriptomic data in AML patients, belongs to 6 cytogenetic subgroups having chromosomal aberrations such as inv(16) (n=28), t(15;17) (n=37), t(8;21) (n=40), MLL-rearranged (n=38), AML-complex (n=48), and normal karyotype (n=351), compared to normal bone marrow (NBM) mononuclear cells (n=73), from the Microarray Innovations in Leukemia (MILE) study

(Stage I). MED12 was found significantly ($p<0.01$) upregulated in AML subgroups, except for the AML-complex subgroup along 3 probe sets (211342_x_at, 203506_s_at, and 216071_x_at). The highest upregulation of MED12 was observed in the inv(16) subgroup having the mean differential expression of 0.78, followed by 0.57 in t(8;21) and 0.5 in t(15;17) subgroup, compared to NBM. Considering the fact that inv(16) and t(8;21) subgroups showed highest expression of the gene, and are categorized as the core-binding factor (CBF) AML-subgroups, we examined DNA-methylation and chromatin modifications of MED12 in patients [n=3 for inv(16) and n=1 for t(8;21)], based on the whole-genome bisulfite sequencing and chromatin immunoprecipitation sequencing data, as available at the BLUEPRINT epigenome, and DNAse sequencing (K562 cells) data at ENCODE. We observed DNAse hypersensitive peaks at the exon-26 and a region (229 bp) spanning the transcription start site (TSS) and upstream promoter of the gene, indication an open chromatin conformation. The TSS and upstream promoter also contained a broad H3K4me3 domain [1.7 kb in inv(16) and 1.2 kb in t(8;21)], with an overlapping hypomethylated CpG-island. Collectively, our findings suggest that MED12 oncogenic over-expression in CBF AML-subgroups are fostered by an epigenetically active promoter. Future studies will be aimed at understanding the impact of targeted perturbation of MED12 in the enhancer mechanism and sustenance of leukemic growth in CBF AML-subgroups.

#4763

Two epigenetically distinct cellular states in osteosarcoma are regulated by a state-specific set of transcription factors driving differential drug response

Eunice Lopez Fuentes[1], Andrew Clugston[1], Leanne Sayles[1], Maria Pons Ventura[1], Alex Lee[1], Vijay Ramani[2], E. Alejandro Sweet-Cordero[1].
[1]Pediatrics, UCSF - University of California San Francisco, San Francisco, CA,[2]Biochemistry & Biophysics UCSF, Gladstone Institute for Data Science & Biotechnology, San Francisco, CA

Osteosarcoma is a highly aggressive cancer seen mostly in children and young adults which is characterized by aneuploidy and dramatic structural rearrangements associated with large copy number gain and widespread

chromosomal loss. Osteosarcoma therapy has not change in over forty years, highlighting the need for deeper molecular understanding of this disease which could in turn identify new therapeutic opportunities. While DNA-level heterogeneity between tumors has been well-described, not much is known regarding epigenetic heterogeneity within osteosarcoma and how this may impact critical phenotypes such as therapy response and metastasis. To characterize the osteosarcoma epigenome, we integrated ATAC-seq and RNA-seq across a unique set of patient samples, PDXs and PDX-derived cell lines obtained across the disease continuum including biopsies, resections, and metastases. ATAC-seq analysis revealed the presence of at least two distinct epigenetic cell states, epigenetic cluster 1 (EC1) and epigenetic cluster 2 (EC2). We used the GREAT algorithm to identify enriched pathways for the genes linked to these differential open regions (~2000 unique peaks per EC). EC1 is defined by genes related to mesenchymal cell proliferation and osteoblast differentiation, whereas EC2 is enriched in genes related to extracellular matrix organization and regulation of kinase activity. Accessible chromatin peaks in EC1 showed transcription factor binding motifs related to development including RUNX2/3, MEOX2, HOXA2/5 and DLX; whereas members of the AP1 complex including FOSL1/2, c-FOS, JUN were enriched in open regions in EC2. This is correlated with high protein expression of these transcription factors in a cluster-specific manner and differential binding to chromatin. We defined a gene-signature of 343 genes by integrating differential open chromatin with differential gene expression of EC1 and EC2. This gene-signature is able to separate gene expression data of patient samples into 2 clusters, suggesting these epigenetic cell states are found in patient samples. We assigned the patient samples to one EC and performed a survival analysis using only primary patient samples. EC1 shows a lower survival probability than EC2. To identify possible therapeutic implications of these EC, we evaluated a drug response dataset generated with ~40 targeted agents for the same panel of PDX-cell lines. Whereas EC1 cell lines were highly sensitive to a selective inhibitor of Aurora B, cell lines in EC2 were inhibited by a MEK inhibitor. PDX-cell lines injected in a subcutaneous model recapitulated the differential drug response in vivo. In summary, we have identified two epigenetically cell states regulated by a state-specific set of transcription factors defining a gene signature that could help to define osteosarcoma subclasses and predict drug response.

#4764

The therapeutic potential of *lnc-HLX-2-7* in group 3 medulloblastomas in children

Keisuke Katsushima[1], Bongyong Lee[1], Menglang Yuan[1], Stacie Stapleton[2], George Jallo[2], Sudipta Seal[3], Charles G. Eberhart[1], Ranjan J. Perera[1].
[1]Department of Oncology, Sidney Kimmel Comprehensive Cancer Center, Johns Hopkins University, Baltimore, MD,[2]Johns Hopkins All Children's Hospital, St. Petersburg, FL,[3]University of Central Florida, Orlando, FL

Medulloblastoma (MB) is an aggressive brain tumor that predominantly affects children. Recent high-throughput sequencing studies suggest that the non-coding RNA genome, in particular long non-coding RNAs (lncRNAs), contributes to MB formation and tumor progression. Here we report the identification of a novel lncRNA, *lnc-HLX-2-7*, as a potential therapeutic target in group 3 MBs. In this study, we report that *lnc-HLX-2-7* RNA specifically accumulates in the *HLX* (host gene of *lnc-HLX-2-7)* promoter region and activates HLX expression by recruiting multiple factors including enhancer elements. RNA sequencing and chromatin immunoprecipitation revealed that HLX directly binds to the promoters of several tumor-promoting genes, including *MYC*, and activates their expression. Furthermore, intravenous treatment with antisense oligonucleotides targeting *lnc-HLX-2-7* coated with cerium-oxide nanoparticle (CNP-*lnc-HLX-2-7*) reduced tumor growth (40-50%) in intracranial MB xenograft mouse model (n=10, $p<0.01$, *t-test*). We found that the combinatorial therapy of CNP-*lnc-HLX-2-7* and cisplatin further inhibits tumor growth and significantly prolongs mouse survival compared to CNP-*lnc-HLX-2-7* monotherapy (n=10, $p<0.01$, *t-test*) only. We report here the importance of the *lnc-HLX-2-7-HLX-MYC* axis in regulating group 3 MB progression and provide a strong rationale for using *lnc-HLX-2-7* as a specific and potent therapeutic target for the group 3 MBs in children.

#4766

Hypoxia increases the methylated histones to prevent histone clipping during Raf-induced senescence

Hyunsung Park, Soojeong Chang. *Dept. of Life Science, University of Seoul, Seoul, Korea, Republic of*

Hypoxia increases methylated histones by inhibiting O_2- and α-ketoglutarate-dependent histone lysine demethylases (KDMs). This study is the first to demonstrate how the hypoxic increment of methylated histones cross-talks with other epigenetic changes, such as histone clipping and heterochromatin redistribution, named senescence-associated heterochromatin foci (SAHF), which are found during oncogene-induced senescence (OIS). Raf-activation in primary human fibroblasts IMR90 increases mature cathepsin L (CTSL)-mediated clipping of histone H3, H2B and H4. Hypoxia protects histones from CTSL by increasing histone methylation without reducing the amount and activity of CTSL. Forced enhancement of methylated histones protected histones from clipping during OIS, even under normoxia, but failed to block SAHFs. Altogether, these results suggest that maintenance of methylated histones is sufficient to protect histones from CTSL, not sufficient but necessary for inhibiting SAHFs, suggesting that besides inhibiting KDMs, hypoxia adopts other mechanisms to inhibit SAHFs**.** Hypoxia protects histones and chromatin from dramatic epigenetic changes by increasing methylated histones.

Gene Regulation and Transcription Factors in Cancer

#5749

Core transcriptional regulatory circuitry in AML

Taku Harada[1], Monika Perez[1], Jeremie Kalfon[1], Kenneth Eagle[2], Flora Dievenich Braes[3], Rashad Batley[3], Kimberly Stegmaier[2], Stuart Orkin[2], Maxim Pimkin[2]. *[1]DFCI/BCH, Boston, MA,[2]DFCI/Harvard Medical School, Boston, MA,[3]BCH, Boston, MA*

Cell states are established by small sets of lineage-restricted transcription factors (TFs). A generally accepted model posits that core regulatory TFs positively regulate their own and each other's genes, forming a network of interconnected feed-forward loops termed core regulatory circuitry (CRC). Here, we sought to test the CRC concept by defining the direct gene-regulatory programs of the critical oncogenic TFs in acute myeloid leukemia (AML) . We employed a targeted protein degradation (dTag) strategy with a homozygous knock-in of the $FKBP12^{F36V}$-coding DNA

sequence into the endogenous TF-coding loci of 7 core myeloid TFs and 1 cofactor (MYB, PU.1/SPI1, GFI1, RUNX1, RUNX2, MEF2D, IRF8, IRF2BP2), all of which represent selective AML dependencies and display the canonical pattern of feed-forward CRC binding. Following complete degradation of TFs for 1-2 hours, we measured the genome-wide rates of nascent mRNA synthesis by SLAM-seq. Genes whose transcription rates change significantly and immediately after a TF's degradation represent its direct transcriptional targets. Strikingly, each TF directly regulates only between 100-450 target genes. Furthermore, rather than forming a core regulatory circuit with fully interconnected feed-forward loops, the core TFs form a very sparsely interconnected hierarchy with a cascading regulatory structure. Each evaluated TF is capable of both direct gene activation and repression. For instance, MYB directly inhibits 135 genes, most of which are associated with myeloid differentiation and inflammation. Feed-forward loops appear to be much less common than previously anticipated. Indeed, we detected only 336 feed-forward loops formed by any combination of the 8 TFs genome-wide. GFI1 and IRF2BP2 negatively regulate their own expression, and the rest of the TFs show no evidence of direct self-regulation. The entire regulatory network converges on MYC and immune signaling. A time-course SLAM-seq experiment after MYB degradation highlighted the secondary nature of eventual global transcriptional collapse and revealed bi-phasic kinetic behavior of feed-forward loops that MYB forms with GFI1 and IRF2BP2. A pseudo-steady state of cellular transcription, ensuing 8-12 hours after MYB degradation, accurately predicts MYB-dependent gene expression patterns in human AML samples. Indeed, a much higher expression of inflammatory mediators and cytokines is observed in patients with low MYB expression, consistent with the observation that MYB directly regulates inflammatory pathways and potentially explaining the known survival benefit of high MYB expression in human AML. Accordingly, MYB degradation results in immediate release of the pro-inflammatory cytokines TNF and CCL2. Our data represent the first example of systematic elucidation of direct regulatory functions of multiple core regulatory TFs in a single cellular context and support a new model of core regulatory circuitry organization in human cells.

#5750

The mutational landscape of ultraconserved elements in human cancers

Recep Bayraktar[1], Yitao Tang[2], Mihnea P. Dragomir[1], Linda Fabris[1], Giulio F. Draetta[3], Han Liang[2], George A. Calin[1]. *[1]Department of Translational Molecular Pathology, UT MD Anderson Cancer Center, Houston, TX,[2]Department of Bioinformatics and Computational Biology, UT MD Anderson Cancer Center, Houston, TX,[3]Department of Genomic Medicine, UT MD Anderson Cancer Center, Houston, TX*

Background: Ultraconserved regions or elements (UCEs) are greater than 100-base pairs in length and are perfectly (100%) conserved across large evolutionary distances in the genomes of at least 3 of 5 placental mammals: human, cow, dog, rat, and mouse. Most UCEs are located in non-coding regions of the genome; however, some UCEs overlap with coding exons. In addition, some UCEs have been found to be transcriptionally active as long non-coding RNAs and are involved in a variety of cellular processes such as cellular proliferation. Although a few UCE sequence variations were reported to be associated with human diseases, the molecular functions of somatic mutations in UCEs remain largely unexplained in human cancers. In this study, we characterized the distribution of somatic UCE mutations throughout a spectrum of cancers and investigated the biological functions of cancer associated UCEs.

Methods: We examined somatic UCE mutations in 2,449 cases of 22 cancer types using the PCAWG and ICGC platforms. To validate these mutation patterns, UCE sequencing was performed on the Illumina NovaSeq 6000 platform for MD Anderson patient cohorts. A custom AsCpf1 guide library was built to identify potential regulatory UCE functions in colorectal cancer models, and 3 guides were designed to target 2,247 UCEs. The proliferation ratio of knockout UCEs was analyzed. We then generated stable mutated UCE clones using the CRISPR AsCpf1 technology in colorectal cancer cells. We conducted RNA sequencing (RNA-seq) of mutated UCE cells. The expression of target proteins and genes were analyzed by qRT-PCR and western blotting. To address the effects of the mutated UCE_11311 tumor growth, DLD1 cells were injected in athymic nude mice.

Results: We analyzed the WGS data on 2,449 cases of 22 cancer types and identified 24,039 somatic mutations in 10,090 (73.46%) UCEs. These were mostly located in non-coding DNAs, mainly in introns.Based on the RNA-

seq data, one of the strongest impacts of mutated UCEs was on ARID1B. We confirmed that specific mutated UCE decreased ARID1B mRNA and protein levels. Our *in vivo* results demonstrated that UCE mutations enhanced the tumorigenicity of DLD1 xenograft tumors. As a summary, UCE_11311 has a transcriptional enhancer activity on the ARID1B gene and UCE_11311 mutations are actively participating in the tumorigenesis at least in part through regulating ARID1B expression.
Discussion: We identified hundreds of unexplored tumorigenic UCEs that need to be further characterized functionally and clinically, and proved one of them to be a transcriptional enhancer of the tumor suppressor ARID1B. Collectively, these data support the concept that certain somatic UCE mutations are frequent and functional in cancer evolution, acting as driver mutations that can be used as new therapeutic targets; other somatic UCE mutations are cancer specific or patient specific, are markers of aggressiveness, and can be used to personalized therapy.

#5751
Single-cell epigenomic analysis reveals an important role of the receptor kinase Ror2 in the erosion of cellular identity during pancreatic carcinogenesis
Simone Benitz[1], Ian Loveless[2], Malak Nasser[1], Hui-Ju Wen[1], Daniel Long[1], Erick Davis[1], Jacee Moore[1], Ivonne Regel[3], Filip Bednar[4], Howard Crawford[1]. *[1]Surgery, Henry Ford Health System, Detroit, MI,[2]Public Health Sciences, Henry Ford Health System, Detroit, MI,[3]Department of Medicine II, Ludwig Maximilian University of Munich, Munich, Germany,[4]Surgery, University of Michigan, Ann Arbor, MI*

Background The major genetic driver for pancreatic ductal adenocarcinoma (PDAC) is oncogenic KRAS. However, adult acinar cells, a probable origin of PDAC, are largely refractory to $Kras^{G12D}$-mediated oncogenic transformation in mouse models. With the concomitant loss of transcription factors that regulate acinar cell differentiation, such as Pdx1 (Pancreatic and Duodenal Homeobox 1), acinar cells undergo a rapid cell identity switch, known as acinar-to-ductal metaplasia (ADM). Consequently, $Kras^{G12D}$;$Pdx1^{f/f}$ (Pdx1 knockout) mice present with massively accelerated

tumor formation. How loss of cell identity cooperates with oncogenic Kras to induce pancreatic transformation is largely unclear.
Methods To elucidate mechanisms responsible for the cellular reprogramming in $Kras^{G12D}$;$Pdx1^{f/f}$ animals, single-cell ATAC-seq from pancreatic bulk tissue was performed. Chromatin accessibility states were captured at early stages of carcinogenesis and correlated to RNA-seq data. Expression of differentially regulated genes was validated by RNAscope and immunohistochemistry staining. The role of identified target genes was studied in pancreatic cancer cell lines.
Results Single-cell ATAC-seq proved as a powerful tool for defining cell-type identity, cellular reprogramming and target genes in early metaplastic transformation of pancreatic tissue. While sole expression of oncogenic Kras lead to reduced accessibility of acinar differentiation genes in acinar cells, these changes were much more prominent in $Kras^{G12D}$;$Pdx1^{f/f}$ mice, promoting metaplastic conversion. Notably, acinar cells of $Kras^{G12D}$;$Pdx1^{f/f}$ animals as well as a proportion of metaplastic lesions in both, $Kras^{G12D}$ and $Kras^{G12D}$;$Pdx1^{f/f}$ mice, showed elevated accessibility and expression of the *Ror2* gene. As a receptor protein tyrosine kinase, Ror2 controls essential signaling pathways, such as Ras-MAPK signaling. By analyzing Ror2 knockout mice, we found that the receptor kinase regulates the identity of metaplastic epithelia. Immunostaining of pancreatic cancer tissues from $Kras^{G12D}$;$p53^{mut}$ (KPC) mice and human PDAC specimens also revealed ROR2 expression in a subset of cancer cells. Knockdown of ROR2 in pancreatic cancer cell lines significantly decreased cell proliferation, while overexpression induced a profound increase in proliferation and in epithelial-to-mesenchymal transition based on the downregulation of multiple epithelial markers and an upregulation of an array of mesenchymal genes.
Conclusions Our in-depth sequencing data revealed that expression of $Kras^{G12D}$ with the concomitant loss of Pdx1 leads to vast alterations of acinar cell identity and significantly accelerated transformation. We identified induced expression of the receptor kinase Ror2, which regulates pancreatic cancer initiation and drives pancreatic cancer cell aggressiveness.

#5752

Enhancer amplification defines lineage addiction in human lung adenocarcinoma

John Louis Pulice[1], Matthew Meyerson[2]. *[1]Harvard Medical School, Boston, MA,[2]Medical Oncology, Dana-Farber Cancer Institute, Boston, MA*

Lung cancer is the most common cause of death from cancer worldwide, and lung adenocarcinoma (LUAD) is the most common type of lung cancer. NKX2-1 (also known as TTF-1, TITF-1) is a lineage defining transcription factor for normal lung development. In LUAD, NKX2-1 is a highly specific and sensitive marker for both primary and metastatic LUADs, with 85-90% expressing NKX2-1. We and others identified that NKX2-1 as the most significantly amplified gene in LUAD, with 22.5% of primary LUADs exhibiting copy number gains. NKX2-1 is amplified as the earliest stages of LUAD development, and NKX2-1 amplification is a truncal event in multi-region LUAD evolution. Despite strong evidence for an oncogenic role for NKX2-1, little is known about the mechanisms of NKX2-1 activation, or how its oncogenic regulation drives LUAD.

Here, we identify recurrent focal amplification targeting a super-enhancer (SE) of NKX2-1 as a driving event in LUAD. Using epigenomic data from LUAD cell lines and tumors, we identify this region as a alveolar lineage super-enhancer (NKX2-1 SE) that is specifically active in NKX2-1(+) LUAD cell lines and primary tumors. Notably, this region is co-amplified with NKX2-1 in 96-100% of NKX2-1-amplified samples, suggesting this region a critical component of the NKX2-1 amplicon. Using endogenous ChIP-seq and exogenous luciferase assays, we show the enhancer activity of the NKX2-1 SE is comprised of three constituent enhancers, and demonstrate that the key enhancer elements can activate transcription of the NKX2-1 promoter. Using CRISPR inhibition (CRISPRi) and CRISPR activation (CRISPRa) in LUAD cell lines expressing high or low levels of NKX2-1, we show that activity of the NKX2-1 SE defines endogenous NKX2-1 expression.

Using RNA-seq, ChIP-seq, and ATAC-seq, we find that NKX2-1 controls the transcriptional and epigenomic landscape of lung adenocarcinoma. NKX2-1 knockdown activates an epithelial-mesenchymal transition (EMT) gene signature and downregulates an alveolar differentiation signature, including critical markers of LUAD differentiation, such as NAPSA, SFTPA1/2, and HOPX, at which NKX2-1 mediates lineage enhancer

accessibility to regulate target gene expression. Global clustering of LUAD cell lines by RNA-seq or H3K27ac ChIP-seq identifies a distinct NKX2-1(+) cluster, and we find that NKX2-1 directly regulates the genes (57/97) and enhancers that distinguish this subpopulation. Using genome-wide shRNA and CRISPR screens, we identify a NKX2-1 dependency in NKX2-1(+) LUAD cell lines, and find that the majority of NKX2-1(+) LUAD cell lines (11/14) assayed are dependent on NKX2-1.
Our data demonstrates that enhancer amplification is a hallmark of oncogenic NKX2-1 activation in LUAD, through which NKX2-1 drives a lineage addicted state and oncogenic cell proliferation. This suggests that NKX2-1 is a critical defining oncogene for LUAD, and that targeting of NKX2-1 or its enhancer may suppress LUAD.

#5753

RUNX3 disrupts MYC/MAX complex and promotes MYC degradation

Yoshiaki Ito[1], Vincent Oei[1], Linda Chuang[1], Junichi Matsuo[1], Supriya Srivastava[2], Ming Teh[3]. *[1]Cancer Science Institute of Singapore, Singapore, Singapore,[2]Department of Medicine, National University of Singapore, Singapore, Singapore,[3]Department of Pathology, National University of Singapore, Singapore, Singapore*

We reported earlier that heterozygous deletion of RUNX3 in the mouse induces adenoma in small intestine, mammary gland (1) and lung (2) and a precancerous stomach epithelium that is highly sensitive to a chemical carcinogen (3). We therefore propose that RUNX3 is a gatekeeper of cancer development (1).
In our recent study on how RUNX3 inhibits early-stage cancer development in multiple tissues, we uncovered a previously unknown mode of MYC destabilization by RUNX3. From RNA sequencing, knockdown experiments, tumorigenic assays, protein interaction and ubiquitination studies, we show that the strong inhibitory effects of RUNX3 on proliferation and tumor growth may, in part, be attributed to its ability to promote MYC degradation. The evolutionarily conserved Runt domain of RUNX3 interacts directly with the basic helix-loop-helix leucine zipper of MYC, resulting in the disruption of MYC/MAX interaction, enhanced GSK3β-mediated phosphorylation of MYC protein at threonine-58 and its subsequent degradation via the ubiquitin-proteasomal pathway (4). MYC

inhibitor Omomyc, a short peptide comprising the b HLH LZ domain of MYC with 4 amino acid substitutions, is extremely effective in disrupting MYC/MAX interaction (5). RUNX3 appears to function similarly to Omomyc: is RUNX3 a Nature-designed Omomyc?
References:(1) Ito K et al, Cancer Cell 14;226-237, 2008; (2) Lee YS et al, Cancer Cell 24: 603-616, 2013; (3) Ito K et al, Gastroenterol 140:1536-1546, 2011; (4) Oei V, Chuang LSH, et al, Submitted; (5) Soucek et al, Nature 455:679-683, 2008

#5754

Determining the regulatory logic of breast cancer cells using single-cell multi-omics

Matthew J. Regner[1], Aatish Thennavan[2], Susana Garcia-Recio[3], Kamila Wisniewska[4], Philip M. Spanheimer[4], Joel S. Parker[2], Charles M. Perou[2], Hector L. Franco[2]. *[1]Bioinformatics and Computational Biology, University of North Carolina at Chapel Hill, Chapel Hill, NC,[2]Bioinformatics and Computational Biology, Dept of Genetics, University of North Carolina at Chapel Hill, Chapel Hill, NC,[3]Dept of Genetics, University of North Carolina at Chapel Hill, Chapel Hill, NC,[4]Lineberger Comprehensive Cancer Center, University of North Carolina at Chapel Hill, Chapel Hill, NC*

Cancer cells rewire regulatory elements scattered throughout the genome (such as enhancers) to drive aberrant gene expression. Thus, deconvoluting the regulatory mechanisms that contribute to oncogenic gene expression in cancer cells is key to understanding tumor biology. To this end, we have charted the transcriptional and epigenetic landscape of breast cancer at single-cell resolution to quantitatively link variation in chromatin accessibility to gene expression across malignant and non-malignant cell types. Our comprehensive dataset profiles the chromatin landscape (scATAC-seq) in concert with the transcriptional profiles (scRNA-seq) of 4 breast cancer cell lines, 12 primary breast tumors, and 4 normal mammary reduction tissue specimens collected and processed immediately after surgical resection. This dataset, encompassing over 250,000 individual cells, allowed us to define the regulatory logic of cancer cells by 1) revealing how the epigenome underlies cellular heterogeneity of these tumors in comparison to normal mammary tissue, 2) defining how

malignant cells hijack enhancer elements to drive key transcriptional programs in a subtype-specific manner, and 3) annotating which cancer-specific enhancer-to-gene connections portend a worse outcome in patients. Notably, we discovered that cancer cells acquire *de novo* non-coding enhancer elements to modulate hallmark cancer pathways that were previously hidden using bulk genomics approaches. This highlights the potential for cancer-specific enhancers to serve as markers with diagnostic and prognostic potential, or even serve as tractable targets for therapeutic intervention. Together these data enable the annotation of the cellular composition, transcriptional, and epigenetic landscape of breast tumors to help pinpoint clinically relevant mechanisms of tumorigenesis.

#5755

TP63 fusions drive enhancer rewiring, lymphomagenesis, and dependence on EZH2

Gongwei Wu[1], Noriaki Yoshida[1], Jihe Liu[2], Xiaoyang Zhang[3], Yuan Xiong[1], Tayla Heavican-Foral[1], Huiyun Liu[1], Geoffrey Nelson[4], Lu Yang[5], Renee Chen[5], Katherine Donovan[1], Marcus Jones[1], Mikhail Roshal[6], Yanming Zhang[6], Ran Xu[1], Ajit Nirmal[1], Salvia Jain[7], Catharine Leahy[1], Kristen Jones[1], Kristen Stevenson[1], Natasha Galasso[8], Nivetha Ganesan[8], Tiffany Chang[8], Wen-Chao Wu[1], Abner Louissaint[7], Lydie Debaize[1], Hojong Yoon[1], Paola Dal Cin[9], Wing Chan Chan[10], Shannan Ho Sui Ho Sui[2], Samuel Ng[1], Andrew Feldman[11], Steven M. Horwitz[8], Mathew Meyerson[1], Karen Adelman[4], Eric Fischer[1], Chun-Wei Chen[5], David Weinstock[1], Myles Brown[1]. *[1]Dana-Farber Cancer Institute, Boston, MA,[2]Harvard T.H. Chan School of Public Health, Boston, MA,[3]Huntsman Cancer Institute, Salt Lake, UT,[4]Harvard Medical School, Boston, MA,[5]City of Hope Comprehensive Cancer Center, Monrovia, CA,[6]Memorial Sloan Kettering Cancer Center, New York, NY,[7]Massachusetts General Hospital, Boston, MA,[8]Memorial Sloan Kettering Cancer Center, New York, MA,[9]Brigham and Women's Hospital, Boston, MA,[10]City of Hope Medical Center, Boston, MA,[11]Mayo Clinic, Rochester, MN*

Recurrent chromosomal rearrangements are a hallmark of hematologic malignancies and play critical roles in pathogenesis. The *TP53* analog *TP63* is rearranged in 5-10% of diverse subtypes of both aggressive T- and B-cell

lymphomas. Patients with *TP63*-rearranged lymphomas have dismal outcomes, with 5-year overall survival rates between 0-17%, depending on cohorts. The function and mechanisms of *TP63* rearrangements and TP63 fusion proteins in tumorigenesis are poorly understood. As a result, attempts to treat these patients to date have been largely empiric. Thus, there is an urgent need to understand how TP63 fusions contribute to tumorigenesis and to translate the findings into novel therapeutic options for these patients.

Here, we demonstrated that TP63 fusions are essential for the propagation of T-cell lymphomas (TCLs). Knockdown of TP63 fusions with specific shRNAs in TCL cell lines harboring TP63 fusions suppressed both cell growth *in vitro* and tumor growth *in vivo*. Retroviral expression of TBL1XR1-TP63, the most common TP63 fusion, conferred cytokine independence in Ba/F3 cells, consistent with its role as an oncogene. To investigate the role of TP63 fusions in T- and B-cell lymphomagenesis, we engineered a CAG-Loxp-Stop-Loxp-*TBL1XR1-TP63* conditional knock-in mouse model and crossed with h*CD2*-Cre mice. This results in expression beginning during early lymphoid development. As observed in patients, transgenic mice developed multiple subtypes of both T- and B-cell lymphoma. To define the effects and mechanisms of TP63 fusions within T cells, we performed CRISPR scanning, transcriptomic, epigenomic, and proteomic analyses. Our data showed that domains within both the N-terminal TBL1XR1 and C-terminal TP63 portions contribute to the function of this fusion. We found that the N-terminal component of TP63 fusions interacts with components of the NCOR/SMRT complex. At the same time, the C-terminal portion of TP63 (which recapitulates the deltaN-p63 isoform expressed in some carcinomas) interacts with the enhancer modifier KMT2D and its complex members. TBL1XR1-TP63 binds to a novel distal enhancer to drive *MYC* expression, and thus upregulates the expression of the histone H3K27 methylase *EZH2*. Finally, we assessed whether EZH2 is a vulnerability of *TP63*-rearranged lymphomas. We found that knockdown of EZH2 in *TP63*-rearranged lines significantly impaired cell growth, as did treatment with the EZH2 and 1 dual inhibitor valemetostat. Valemetostat, which is now being tested in patients with lymphoma, counteracted the oncogenic effects of TP63 fusions in multiple preclinical models *in vivo*. Together, our results identify the TP63 fusion as a highly unique oncogenic

driver in lymphomagenesis capable of recruiting multiple epigenetic modifier complexes and inducing a targetable dependence on EZH2.

Gene Regulation in Cancer

#3715

Pharmacological targeting of circadian clock genes reveals regulatory mechanisms of E-box regulated genes in cancer

Yuanzhong Pan[1], Heinz-Josef Lenz[2], Evanthia Roussos Torres[2], Steve A. Kay[3]. *[1]Department of Neurology, Keck School of Medicine, University of Southern California, Los Angeles, CA,[2]Division of Medical Oncology, Norris Comprehensive Cancer Center, Keck School of Medicine, University of Southern California, Los Angeles, CA,[3]Department of Neurology; Norris Comprehensive Cancer Center, Keck School of Medicine, University of Southern California, Los Angeles, CA*

Transcription factors (TFs) are key regulators of homeostasis and cancer. Recent advances in pharmacological targeting of TFs makes them valuable targets in various diseases, but systems-level understanding of the function and regulation of TFs from different families in cancers remains lacking. Our lab and collaborators have been developing new small molecules to modulate the functions of key regulators of the circadian clock BMAL1 and CLOCK, which are bHLH family TFs that activate gene expression by binding to a DNA motif called E-box, with a consensus sequence of CANNTG. E-boxes are ubiquitous in the genome and broadly regulate essential physiological processes of the cell, but their molecular biology in cancer is largely unknown. In the current work we tested the ability of small molecules to regulate the expression of BMAL1 and CLOCK target genes. Across different cell lines of various cancer types, we found that stabilization of one of the negative regulators of CLOCK, CRY2, by our novel compound called SHP1705, is the most consistent to suppress canonical BMAL1 target genes. GO and GSEA analysis of RNA-seq data shows that SHP1705 also significantly changed most core regulators of circadian rhythms as well as other E-box-binding proteins. However, SHP1705 has IC50 values above 10μM in most tested cells, creating a challenge for efficacy in a clinical setting. Because BMAL1 requires the proteasome to sustain the turnover of a transcription burst, we hypothesized

proteasome inhibitors (PI) MG132 and carfilzomib may synergize with SHP1705. Consequently, we found strong synergy with both PIs. Analysis of TF-target genes in combination-treated cells reveals significant changes in expression profiles, suggesting that these genes are regulated by E-box, and other related/alternative promoter elements: CCAAT-box, CG-rich motifs, and ATGGC. Co-enrichment of these elements revealed the components of E-box containing promoters and showed potential properties of E-box-regulated gene expression. Co-existence of these motifs in the same proximal promoter also potentially allows RNAPII multiple choices of alternative promoters and could promote expression of variants in cancer cells. Our results support the necessity of inhibiting the whole promoter and provide an example of how to approach designer pharmacological strategies to achieve this purpose.

#3716

RNA N^6-methyladenosine binding protein, YTHDF1 regulates DNA repair and cancer immunity in protein synthesis levels

Dongjun Jang, Hae Rim Jung, Jaeik Oh, Sung-Yup Cho. *Seoul National University, Seoul, Korea, Republic of*

N^6-methyladenosine RNA methylation is one of the most abundant post transcriptional modifications in eukaryotic messenger RNAs and plays crucial roles in cancer development and progression. YTHDF1 is an m6A reader protein and has been reported to increase the translation of mRNAs in cooperation with YTHDF3. In gastric cancer, YTHDF1 was reported to be overexpressed in cancer tissues, but detailed effects of YTHDF1 in cancer immunity have not been fully elucidated. In RNA sequencing data from a TGCA gastric cancer cohort, the expression of YTHDF1 was inversely correlated with the cytotoxic T cell markers, such as CD8A, GZMA, and GZMB. To investigate the effect of YTHDF1 overexpression on gene expression regulation in protein levels, we performed the proteomic analysis for newly synthesized proteins using non-canonical amino acid azidohomoalanine and click chemistry tagging reaction in the presence of interferon-γ (IFN-γ). Protein synthesis of genes in ‘DNA damage response’ and ‘DNA repair’ gene sets increased in YTHDF1-overexpressed samples. On the contrary, protein synthesis of genes in ‘Allograph rejection’, ‘NK cell mediated cytotoxicity’, and ‘NF-κB signaling’ gene sets decreased in

YTHDF1-overexpressed samples. Especially, YTHDF1 reduced basal expression of DNA damage marker, γH2AX, suggesting that DNA damage repair was enhanced by YTHDF1 overexpression. Our study suggests that YTHDF1 plays pervasive roles in DNA repair and cancer immunity by regulating gene expression in protein levels.

#3717

Defining the mechanism of ER receptor transcription complex activity and its effect on epigenetic modulations using super resolution microscopy

Tara Akhshi, Myles Brown. *Dana-Farber Cancer Institute/Harvard Medical School, Boston, MA*

Estrogen Receptor α (ERα) is expressed in ER^+ breast cancers, one of the leading causes of death among women. Despite effectiveness of endocrine therapy, a significant number of patients experience resistance to these treatments. One of the major hurdles is lack of comprehensive information about ERα transcriptional complex activity. While biochemical assays have improved our knowledge significantly, it is critical to imply techniques that allow direct visualization of ERα activity and gain spatiotemporal information. We used super resolution microscopy to examine the mechanism of ERα transcriptional activity. We showed that ERα interactions with its co-activators (P300, SRC-3), is influenced upon administration of Tamoxifen and Fulvestrant, an effect that is lost in cells carrying multination in ERα ligand binding site. Additionally mutant cells are no longer able to recruit ERα co-inhibitor (NCORI). Using STORM microscopy, we showed estrogen treatment caused an “open” chromatin (H3K27ac) structure which may represent active areas of gene expression, while Tamoxifen and Fulvestrant treatments caused chromatin to form “closed” structures which likely represent close and inactive phase of chromatin.

#3718

FOXM1 switches protein conformations upon C-terminal domain-mediated-autoregulation dictating its transcriptional activity in cancer cell proliferation

Chia-Chan Hsu, Xiang Yao, I-Ching Wang. *Institute of Biotechnology, National Tsing Hua University, Hsinchu, Taiwan*

Transcription factor Forkhead box M1 (FOXM1) participates in tumor initiation, tumor development and tumor metastasis through regulating transcriptional network of its target genes. Activated FOXM1 promotes G1/S and G2/M transition via manipulating Cdc25B, Cyclin B1, TOPOIIa, Aurora and Polo-like kinases, as well as cancer cell survival and invasion through upregulating Survivin, SNAIL and MMP-9. The depletion of Foxm1 repressed the oncogenic Kras (G12D) driven mice lung cancer, Rb/Trp53/Myc triple knockout mice small cell lung cancer and carcinogen induced mice hepatocellular carcinoma. Given the roles of FOXM1 in tumorigenesis and its relevance to clinical outcomes, deciphering the mechanism underlying the regulation of FOXM1 activity might provide new therapeutic target for cancer study. It is known that FOXM1 activity drops when the C-terminal transcription activation domain (TAD) is blocked by the N-terminal repression domain (NRD), which is called autorepression. Furthermore, the NRD-deleted FOXM1 displays extraordinarily high transactivity. Compared to the NRD, the TAD is relatively longer and consists of around 420 amino acid with most of them being intrinsically disordered region (IDR). Previous studies showed that the NRD binds to a relatively ordered small region on the TAD. However, it is poorly understood about whether the IDR of TAD partakes in the FOXM1 self-regulated activity and how FOXM1 protein structure switches in living cells. Our co-immunoprecipitation (co-IP) and dual-luciferase reporter assay (DLR) suggested that FOXM1 TAD self-interacts via its IDR and the C-terminal αβα motif, which promotes FOXM1 transactivation. The IDR-driven FOXM1 autoactivation was mimicked by the chemically-induced dimerization system (CID) that forces IDR-αβα proximity intermolecularly. Using fluorescence resonance energy transfer (FRET) microscopy, we observed that the IDR-αβα interaction was elevated when cell cycle progression from G1/S to G2/M in living cells. The IDR-αβα interaction and FOXM1 activity were both suppressed by PLK1 inhibition. Furthermore, the characteristics of IDR-αβα interaction did not resemble NRD-TAD interaction as revealed by FRET data where we showed the NRD-TAD interaction dropped after G1/S. The NRD-TAD interaction underlying FOXM1 autorepression was recapitulated by CID. Through co-

IP and yeast-two hybrid assays (Y2H), we further identified the minimal yet biological functional unit ββαβ on NRD that suppressed FOXM1 activity and lung adenocarcinoma A549 cells *in vitro* and *in vivo*. Collectively, our work suggested that FOXM1 might be switched from the NRD-TAD mediated autorepression toward the IDR-αβα mediated activation by Plk1 during S-G2 phase. And ββαβ peptide treatment might be applied to lung cancer as a potential therapeutic strategy.

#3719

Targeting the eIF6 and 60S ribosomal subunit interaction interface in cancers

Kavya Meena Harish, Aparna Biswas, Poonam Roshan, Sofia Origanti.
Saint Louis University, St. Louis, MO

Translational control is integral to cancer initiation and progression. A subset of translation initiation factors are deregulated in cancers to facilitate their rampant growth and proliferation. Eukaryotic translation initiation factor 6 (eIF6) is one such factor that is over expressed in many cancers including lung, colon, ovarian and breast cancers, and deregulation of eIF6 is correlated with a poor cancer prognosis. Association of eIF6 with 60S is critical for 60S assembly. However, eIF6 must be released from 60S prior to translation to permit inter subunit interactions between 60S and 40S and to facilitate the formation of translationally proficient 80S complex. Release of eIF6 is deregulated in the ribosomopathy- Shwachman Diamond Syndrome that is predisposed to leukemias. Also, loss of eIF6 markedly delays tumorigenesis without affecting normal growth, which presents eIF6 as a viable therapeutic target. A potential therapeutic strategy is to target the eIF6 and 60S ribosomal interaction interface. Through extensive biophysical analyses, we had identified residues that are critical for the interaction between eIF6 and 60S ribosomal subunit. We show that targeting these key residues in the eIF6-60S interaction interface markedly delays colonic cancer growth and inhibits protein synthesis. Interestingly, targeting eIF6 leads to an upregulation of p53 independent of the DNA damage response, suggesting that ribosomal stress contributes to the stabilization of p53. Future studies will determine the mRNA targets that are translationally deregulated by inactivation of eIF6. We will also

determine the effect of targeting eIF6 function in inhibiting tumor growth and progression *in vivo*.

#3720

Cysteine palmitoylation of astrocyte elevated gene-1/Metadherin (AEG-1/MTDH) regulates its biological and immunological activity

Maria Del Carmen Camarena[1], Garrison Komaniecki[2], Debashri Manna[1], Rachel Mendoza[1], Mark A. Subler[1], Jolene J. Windle[1], Mikhail G. Dozmorov[1], Hening Lin[1], Devanand Sarkar[1]. *[1]Virginia Commonwealth University - VCU, Richmond, VA,[2]Cornell University, Ithaca, NY*

Non-alcoholic steatohepatitis (NASH) is a major risk factor for hepatocellular carcinoma (HCC). Astrocyte elevated gene-1/Metadherin (AEG-1/MTDH) augments steatosis, inflammation, and tumorigenesis, thereby promoting the whole spectrum of this disease process. Targeting AEG-1 is a potential interventional strategy for NASH and HCC. Thus, proper understanding of the regulation of this molecule is essential. We found that AEG-1 is palmitoylated at residue Cysteine75 (Cys75). Mutation of Cys75 to Serine (Ser) completely abolished AEG-1 palmitoylation.Systematic knockdown studies identified zinc finger DHHC-type palmitoyltransferase 6 (ZDHHC6) as the palmitoyltransferase catalyzing the process. To obtain insight into how palmitoylation regulates AEG-1 function, we generated a knock-in mouse by CRISPR/Cas9 in which Cys75 of AEG-1 was mutated to Ser (AEG-1-C75S). No developmental or anatomical abnormality was observed between AEG-1-wild type (AEG-1-WT) and AEG-1-C75S littermates. However, global gene expression analysis by RNA-sequencing unraveled that signaling pathways and upstream regulators, which contribute to cell proliferation, motility, inflammation,angiogenesis, and lipid accumulation, are activated in AEG-1-C75S hepatocytes compared toAEG-1-WT. Feeding these mice with high fat/high sugar diet for 20 weeks showed accumulation of T-regulatory cells and exhausted CD8 T-cells in the livers of AEG-1-C75S mice vs AEG-1-WT, and only in females, suggesting that inhibition of AEG-1 palmitoylation creates an immunosuppressive milieu favoring tumorigenesis. Collectively, these findings suggest that AEG-1-C75S functions as dominant positive, and palmitoylation restricts oncogenic and NASH-promoting functions of AEG-1. Studies are ongoing to unravel the

mechanism by which palmitoylation restricts AEG-1 function, and to understand the sex-specific immune-modulatory role of AEG-1 palmitoylation in hepatocarcinogenesis.

#3721

The C1 domain of capicua has functional importance in human CIC-DUX4

Cuyler Luck[1], Kyle A. Jacobs[2], Ross A. Okimoto[1]. *[1]Medicine, UCSF - University of California San Francisco, San Francisco, CA,[2]Cell and Tissue Biology, UCSF - University of California San Francisco, San Francisco, CA*

Genomic rearrangements between the HMG-box family transcriptional repressor capicua (CIC) and multiple partner genes result in fusion oncoproteins that activate transcription to drive sarcoma growth and progression. In the case of CIC-DUX4, the most common CIC-rearranged fusion oncoprotein, the fusion often retains over 90% of the wild type CIC protein structure including the HMG box and C-terminal C1 domain. Structure-function studies in *Drosophila* have suggested that the C1 domain of CIC, a non-HMG box DNA binding domain, is important for the transactivating capacity of a synthetic fly-human CIC-DUX4. Consistent with these findings, we performed a retrospective analysis of over 70 breakpoints described from CIC-DUX4 human derived tumors, which revealed that the C1 domain is structurally conserved within the context of the CIC-DUX4 fusion. To further understand the functional role of the C1 domain in human CIC-DUX4 we generated human CIC-DUX4 C1 domain and HMG-box deletion (alone or in combination) mutant constructs and performed a series of studies to test the functional impact on CIC-DUX4 protein levels, subcellular localization, and transcriptional activity. Through these analyses we have found that deletion of the C1 domain does not impact CIC-DUX4 oncoprotein expression or localization but does dramatically reduce target gene expression. In ongoing *in vivo* studies, we aim to evaluate the significance of the C1 domain in inducing CIC-DUX4 driven tumorigenesis. Collectively, our findings validate the functional importance of the C1 domain in human CIC-DUX4 and to our knowledge provide the first harmonized analysis of breakpoint locations in CIC-rearranged sarcoma.

#3722

Exploring the role of eIF4E in cancer cells with targeted protein degradation

Swee Y. Sharp[1], Marianna Martella[1], Christopher I. Milton[1], George Ward[2], Caroline Richardson[2], Andrew Woodhead[2], Paul A. Clarke[1]. *[1]Cancer Research UK Cancer Therapeutics Unit, The Institute of Cancer Research, London, United Kingdom,[2]Astex Pharmaceuticals, Cambridge, United Kingdom*

Initiation of translation is considered the main rate-limiting step of protein synthesis and requires the recognition of 5' m^7G-cap on mature mRNAs and the formation of eukaryotic translation initiation factor 4F (eIF4F) multi-protein mRNA cap-binding complex. Formation of this complex requires the interaction of eIF4E and the scaffold protein eIF4G, and RNA helicase eIF4A. This eIF4F complex along with eIF3 mediate the recruitment of the 40S ribosomal particle to the 5′ cap of mRNA. Activation of eIF4E is a regulatory hub of many major oncogenic pathways, thus, targeting eIF4E has emerged as a potential therapeutic strategy in cancer. Here we have used a targeted protein degradation approach coupled with genetic rescue to explore the molecular and cellular dependency of cancer cells on eIF4E. Stable H1299 human NSCLC clones expressing $FKBP12^{F36V}$-tagged eIF4E but lacking endogenous eIF4E were established. Treatment of multiple N- or C-tagged-eIF4E clones with dTAGv-1, an $FKBP12^{F36V}$ selective heterobifunctional molecule that recruits VHL, induced rapid degradation of eIF4E to undetectable levels by 6hr exposure. This also resulted in reduced expression of MCL1, a previously reported biomarker of eIF4E activity. Longer exposures to dTAGv-1 resulted in a cytostasis that was not associated with cell death. A diastereomer negative control of dTAGv-1 that cannot recruit VHL did not elicit loss of eIF4E or the downstream events associated with its loss. Global analysis of protein synthesis initiation by RIBOseq and proteome profiling following dTAGv-1 treatment out to 32hr exposure demonstrated surprisingly few alterations in protein expression despite the significant effect on cancer cell growth. We also expressed wild-type or eIF4E mutants predicted to disrupt key functions and determined their ability to rescue molecular or cellular phenotype associate with eIF4E-loss following dTAGv-1 treatment.

Expression of wild-type eIF4E completely rescued cell growth and MCL1 expression. A W56A mutant predicted to disrupt mRNA-cap binding was unable to rescue eIF4E loss. In contrast, expression of W73F or S290A mutants (predicted to disrupt eIF4G binding or exhibit reduced eIF4E activity, respectively) were able to rescue the loss of eIF4E.
In summary, our rescue experiments show that mRNA-cap binding by eIF4E is required and that eIF4E:eIF4G interaction in cells may be more complex than predicted. This may also explain the challenges associated with developing selective and cellularly potent inhibitors of the eIF4E:eIF4G interaction and that targeting mRNA-cap binding may be a more effective strategy. We predicted that removing eIF4E would impact on the global synthesis of many proteins. However, our data demonstrate that targeting eIF4E leads to limited effects on protein synthesis that remain sufficient to inhibit cancer cell growth. Further experiments are underway to understand which proteins drive this dependency on eIF4E.

#3723

Identification and functional characterization of long noncoding RNAs that regulate TGF-β-Smad pathway as Smad co-factors

Masatoshi Kitagawa, Kosuke Ota, Tatsuya Ohhata, Satoshi Sakai.
Hamamatsu University School of Medicine, Hamamatsu, Japan

TGF-β-Smad pathway participates in various biological processes such as development, differentiation, growth regulation, and cancer progression including epithelial-mesenchymal transition (EMT). Long non-coding RNAs (lncRNAs) also involved in carcinogenesis and cancer malignancies. To identify lncRNAs regulating TGF-β-Smad pathway, we comprehensively identified lncRNAs induced by TGF-β and found and reported a lncRNA *ELIT-1* (EMT-associated lncRNA induced by TGF-β-1) which was induced by TGF-β and promoted EMT by facilitating TGF-β-Smad signaling. *ELIT-1* bound to Smad and participated in expression of TGF-β target genes including *Snail.* Prognosis of lung adenocarcinoma and gastric cancer patients with high expression of *ELIT-1* was poor suggesting that *ELIT-1* may be useful as a novel prognostic and therapeutic target. Recently, we found that *lincNMR* (long intergenic noncoding RNA-nucleotide metabolism regulation) was induced via TGF-β-Smad pathway in various cell lines. Moreover, RNA-seq analysis using *lincNMRs*-depleted

cells indicated that *lincNMRs* was involved in expression of *APOBEC3B*, a cytidine deaminase, promoting C to U mutation and highly expressed in various human cancers. Although, regulatory mechanisms of *APOBEC3B* expression have not been fully elucidated, we proved that *lincNMRs* bound to Smad and promoted the activity of *APOBEC3B* promoter. These data suggest that *lincNMRs* participate in APOBEC3B expression by collaborating with TGF-β-Smad pathway. Additionally, high expression of *lincNMRs* was positively correlated with high expression of APOBEC3B in various cancer cell lines. The high expression of APOBEC3B as well as *lincNMR* was significantly associated with their poor prognosis in liver and lung cancer patients, suggesting that *lincNMR* may contribute to tumor malignancy by enhanced expression of APOBEC3B via TGF-β-Smad pathway.

#3724

RAI2 controls polycomb-mediated repression of *CDKN1A* by its interaction with CtBP1

Sarah Greimeier[1], Bettina Steinbach[1], Simon Sander[1], Lina Merkens[1], Nishit Goradia[2], Matthias Wilmanns[2], Eric Metzger[3], Klaus Pantel[1], Stefan Werner[1]. *[1]Institute of Tumor Biology, University Medical Center Hamburg-Eppendorf, Hamburg, Germany,[2]European Molecular Biology Laboratory, Hamburg, Germany,[3]Department of Urology and Center for Clinical Research, University of Freiburg Medical Center, Freiburg, Germany*

RAI2 has initially been identified as a metastasis-associated gene in breast cancer. Recently, we found that increased RAI2 protein in primary tumors predicts early biochemical relapse of prostate cancer patients. On the molecular level, RAI2 interacts with CtBP1 as transcriptional co-repressors via a non-consensus tandem ALDLS-motif in hormone-dependent cancer cells. In this study, we aim to investigate the cell-biological relevance of this molecular interaction in prostate cancer cells using the *CDKN1A* gene as an example of a transcriptional target of CtBP-mediated gene regulation. To analyze a molecular relation between the RAI2/CtBP1 interaction and repressor of the *CDKN1A* gene, we first applied a transactivation assay in 293T cells, transiently transfected with CtBP1 and different RAI2 protein variants. Next, we depleted the RAI2 protein in VCaP prostate cancer cells. We used this cell line model to analyze gene expression and protein

concertation of RAI2, CtBPs and p21 under different conditions. We studied the subcellular localization and chromatin binding of the proteins of interest by confocal laser-scanning microscopy and ChIP analysis.
The gene reporter assay revealed that combined overexpression of RAI2 and CtBP1 reliefs the repression of the proximal *CDKN1A*-promotor and that RAI2 with an intact ALDLS tandem motif is required for this process. RAI2 depletion in VCaP cells resulted in a significant reduction of both CtBP1 and CtBP2 and almost complete abolishment of p21 protein levels, which is accompanied by reduced interaction of RAI2 with CtBP1 in nuclei. In parental VCaP cells, genotoxic stress significantly induced *CDKNA1* gene expression and p21 protein concentration. In contrast, in RAI2-depleted VCaP cells we did not observe any of these effects, demonstrating the requirement of RAI2 to cause the relief of *CDKNA1* repression. RAI2 together with CtBP1 appeared as definite foci in the nuclei of VCaP cells that are co-localized with key factors of polycomb 1 and 2. The ChIP analysis revealed that RAI2-depletion significantly induced binding of CtBPs to the *CDKN1A* promoter. In contrast, the binding of the polycomb protein LCoR to chromatin is significantly reduced in RAI2-depleted cells. Irrespective of the RAI2 status, the EZH2 binding to the chromatin remained unaltered, whereas a significant increase in H3K27me3 in RAI2-depleted cells was observed.
In summary, we found that interruption of the interaction of RAI2 with CtBP1 is leading to increased chromatin binding of CtBP1 and trimethylation of H3K27 of the *CDKN1A* promotor, which is associated with repression of *CDKN1A* gene expression. We conclude that the molecular interaction of RAI2 with CtBP1 is a new molecular mechanism of corepression by modulating the histone-modifications of the target gene.

#3725

ABI1 regulates STAT3 transcription through a DNA binding activity

Xiang Li[1], Neeru Arya[2], Baylee A. Porter[1], Allysa P. Kemraj[3], Xuesen Dong[4], Dominique Frueh[2], Alaji Bah[3], Leszek Kotula[1]. *[1]Department of Urology and Department of Biochemistry and Molecular Biology, SUNY Upstate Medical University, Syracuse, NY,[2]Department of Biophysics and Biophysical Chemistry, John Hopkins University, School of Medicine, Baltimore, MD,[3]Department of Biochemistry and Molecular Biology, SUNY*

Upstate Medical University, Syracuse, NY,[4]Vancouver Prostate Centre, Vancouver, BC, Canada

Prostate cancer (PCa) is characterized by the complexity of oncogenic signaling and heterogeneity of transcriptional landscapes. Adaptor protein ABI1 is a tumor suppressor in PCa, as evidenced by its loss or downregulation in high-grade and metastatic tumors. STAT3 activation is a hallmark of high-risk prostate tumors. ABI1 loss is associated with STAT3 activation leading to transcriptional reprogramming and epithelial-mesenchymal-transition (EMT) of prostate cancer cells (Nath, Li et al. *Cell Commun Signal.* 2019). EMT changes involve several homeobox transcription factors. The fact that ABI1 contains a homeobox homology region (HHR) suggests the possibility that it plays a role in EMT by directly regulating transcriptional activity by DNA binding. To examine this hypothesis, we set out to analyze ABI1-DNA binding. Structural NMR studies and in-vitro protein-DNA binding assays confirmed ABI1 binding to DNA regulated by alternative spliced ABI1 Exon 4 region located on the C-terminus of ABI1 HHR. RNA-sequencing data and PCa cell lines qPCR assays reveal the alternative ABI1 Exon 4 spliced-in is enriched in high Gleason-scored PCa samples. ABI1 and STAT3 co-regulate their nuclear vs. cytoplasm localization, and the subsequent functional studies using PCa lines expressing wild type or HHR Exon 4 deletion mutant of ABI1 demonstrated that HHR regulates the STAT3 DNA binding patterns, STAT3 mediated chromatin structure programming as well as its transcription activities. We propose that ABI1 is a critical regulator of STAT3 activity during prostate cancer progression.

#3726

Histone acetylation axis in the control of RNA Pol2 clusters

Berkley E. Gryder, Diana Chin, Hyunmin Kim, Issra Osman. *Case Western Reserve University School of Medicine, Cleveland, OH*

Core regulatory transcription factors (CR TFs) orchestrate the placement of super enhancers (SEs) to activate transcription of cell-identity specifying gene networks and are critical in promoting cancer. We defined the core regulatory circuitry of fusion positive rhabdomyosarcoma (FP-RMS, a cancer of childhood) in primary tumors and cell lines, which includes

PAX3-FOXO1 (P3F), MYOD1, SOX8, MYCN and others. To find chemical probes able to selectively inhibit CR TF transcription, we screened the Structural Genomics Consortium epigenetic probe set by RNA-seq. We found that chemical probes along the acetylation-axis, and not the methylation-axis, are able to cause selective disruption of CR TF transcription. Inhibitors of HDACs (acetylation erasers), BRD4 (acetylation readers) and CBP/p300 (acetylation writers) were all able to selectively halt CR TF transcription. For HDACs, this raised a conundrum: why would too much histone acetylation, an active chromatin mark, stop transcription at CR TFs? ChIP-seq showed that CR TFs build SEs that have the largest quantities of histone acetylation and the enzymes that write acetylation (i.e., p300), yet paradoxically also harbor the highest amounts of the opposing histone deacetylases (HDACs). To investigate the architectural effects of disabling HDACs and causing hyper acetylation, we developed Absolute Quantification of Architecture (AQuA) HiChIP, revealing erosion of native SE contacts at CR TFs, and extensive aberrant contacts. This did not cause an elongation defect, but rather removed RNA Pol2 from core regulatory genetic elements and eliminated RNA-Pol2 phase condensates in 20 minutes. We further dissected the contribution of HDAC isoforms using a set of HDAC selective inhibitors, finding HDAC1/2/3 are co-essential to CR transcription. Using HAT inhibitors/degraders, we discovered a profound dependence on CBP/p300 for clustering of Pol2 loops that connect P3F to its target genes. In the absence of CBP/p300, Pol2 long range enhancer loops collapse, Pol2 accumulates in CpG islands and fails to exit the gene body. These results reveal a potential novel axis for therapeutic interference with P3F in FP-RMS and clarify the molecular relationship of P3F and CBP/p300 in sustaining active Pol2 clusters essential for oncogenic transcription. Overall, our data reveals a SE-specific need for balancing histone acetylation states to maintain SE architecture, Pol2 clustering in 3D, and CR TF transcription.

#3727

Development of a new All-In-One inducible lentiviral shRNA/gRNA Vector

Lipeng Wu, Hua Su, Justin Fellows, Mao Fu, Julian Heller, Brian Park, Dezhong Yin. *OriGene Technologies, Inc., Rockville, MD*

Tet-On is a powerful inducible system and a classical tool to regulate gene expression in mammalian cells. It has also been applied to regulate Pol III-driven transcription, such as shRNA or gRNA driven by a U6 or H1 promoter. However, all of the current versions of Tet-On shRNA vectors are based on H1-2O2 or U6-2O2 promoters, which are only compatible with first-generation tetracycline repressor TetR. In addition, these promoters have the problem of driving downstream transcription without the binding of the Tet regulatory protein. Here, we developed a new system that is built upon tetracycline activator protein, Tet-On 3G, combined with a new structure of Tet responsive promoter H1-4O4, which tightly regulates the downstream transcription of gRNA or shRNA. The responsiveness of our system to Doxycycline regulation is dramatically improved compared with the current versions. The new Tet-On system is further optimized into a compact structure to be compatible with the lentivirus package (All-In-One Lenti-Tet-On system), which still keeps the leaky expression at an undetectable level. Combined with all these features, the new generation of the Tet-On system offers broad applications in gene knocking down and genomic editing.

#3728

A novel, simplified, streamlined workflow for high-throughput whole transcriptome RNA-seq library preparation for a variety of sample types

Chelsea Pinegar, Dora Posfai, Gautam Naishadham, Bradley W. Langhorst, Keerthana Krishnan. *NEBNext, New England Biolabs, Inc., Ipswich, MA*

RNA sequencing (RNA-seq) has become an invaluable tool in the study of biology, but often requires multiple days to process samples from total RNA to final libraries that can be loaded on to a sequencer. Researchers use RNA-seq to gain insight into whole tumor gene expression, and in combination with other omics data make treatment decisions. In cancer research, time taken to yield sequencing results can be critical for clinical samples. Within oncology research, libraries are often prepared from RNA sourced from formalin-fixed, paraffin-embedded (FFPE) tissues which can be particularly challenging and is not compatible with all library preparation methods.

Here, we present a new protocol that allows users to easily generate robust RNA-seq libraries from a variety of sample types in a single day from 25-250 ng of total RNA. Compatible with poly(A) enrichment or ribosomal RNA depletion, this new workflow has reduced preparation time by about 40% compared to current library prep kits without sacrificing quality of libraries or any sequencing metrics, including 5'-3' coverage, GC bias. Our new method provides equivalent transcript expression in FFPE samples when compared with existing protocols. In addition to master mixed components and reduced incubation times, the reduction in bead cleanup steps significantly reduces hands-on time for library preparation, simplifying and streamlining the process.
This new library preparation method is also ideal for processing samples of various inputs with a single condition at every step throughout the protocol, without modifying cycling conditions or dilutions based on input amount. This workflow provides a great advantage in efficiently generating RNA-seq libraries while simultaneously maintaining high quality sequencing results and compatibility with both high- and low-quality RNA such as FFPE.

#3729

Targeting the writers of enhancers as a new therapeutic strategy in pediatric AML

Joanna S. Yi[1], Kevin Duong[1], Abiola Obawemimo[1], Tingjian Wang[2], Faith Joseph[3], Nicolas L. Young[3], Stephen Mack[4], Jun Qi[2], Adam Durbin[5].
[1]Pediatrics, Baylor College of Medicine/Texas Children's Hospital, Houston, TX,[2]Cancer Biology, Dana-Farber Cancer Institute, Boston, MA,[3]Biochemistry, Baylor College of Medicine, Houston, TX,[4]Neurobiology, St. Jude Children's Research Hospital, Memphis, TN,[5]Oncology, St. Jude Children's Research Hospital, Memphis, TN

Introduction: Children with acute myeloid leukemia (AML) urgently need new targeted therapeutics to improve their outcomes. Super-enhancers (SEs) are extensive chromatin regions denoted by abundant histone 3 lysine 27 acetylation (H3K27ac), which are associated with high-level expression of cell-identity genes, including oncogenes. SE-regulated genes have unique sensitivity to transcriptional inhibitors, allowing for cancer type-

specific approaches. Thus, targeting CBP/EP300 (the highly homologous enzymes responsible for catalyzing H3K27 acetylation) may be a specific strategy to target lineage-specifying oncogenes in AML. However, to date, the high degree of homology between EP300 and CBP has limited chemical strategies to tissue-specific disruption. Gene editing studies have shown that CBP, and not EP300, is essential for maintaining normal hematopoiesis, while EP300 regulates AML growth and myeloid differentiation. We hypothesized that selectively targeting EP300 would suppress AML growth while sparing effects on normal myeloid differentiation.
Methods: We studied publicly available expression and CRISPR screening databases for EP300 and CBP data in AML. We treated pediatric AML (pAML) cell lines and patient samples with the EP300/CBP HAT inhibitor A485 and the EP300-selective PROTAC [PROteolysis TArgeting Chimera]) JQAD1, and measured effects on cell growth by CellTiter-Glo, and apoptosis, differentiation, and cell cycle changes by flow cytometry. We treated pAML cells with compounds for 2 hours and performed mass spectrometry on HPLC-purified H3 proteins.
Results: pAML patient samples have higher EP300 expression than normal bone marrow samples in the TARGET dataset, and AML cell lines have enhanced dependency on EP300 over CBP by CRISPR knockout analysis. Treatment of pAML cell lines with A485 slowed proliferation and induced apoptosis, cell cycle arrest, and differentiation. In contrast, equimolar concentrations of JQAD1 had more marked antileukemic effects in both pAML cell lines and primary samples. Immunoblotting analysis demonstrated reduced H3K27ac in pAML cells treated with both JQAD1 and A485, but EP300 degradation only with treatment with JQAD1, consistent with findings in other cancer models. Studies on the effects of EP300 degradation versus combined EP300/CBP inhibition on global and SE-regulated gene expression are ongoing. Middle-down mass spectrometry recapitulates decreased H3K27 acetylation with both agents. JQAD1 combined with the BCL2 inhibitor Venetoclax has a synergistic effect on cell line and patient sample growth, with coordinate induction of apoptosis and differentiation. A four-arm study of this combination in a pAML patient-derived xenograft model is ongoing.
Conclusion: Selective degradation of EP300 using the PROTAC JQAD1 is a new strategy that demonstrates preclinical efficacy in pAML as a single agent and in combination with BCL2 inhibitors.

#3730

A new type of transcriptional reprogramming by an IRF4 mutation in lymphoma

Pierre Cauchy. *German Cancer Research Center, Freiburg im Breisgau, Germany*

Disease-causing mutations in genes encoding transcription factors (TFs) are a recurrent finding in hematopoietic malignancies and might involve key regulators of lineage adherence and cellular differentiation1-3. Such mutations can affect TF-interactions with their cognate DNA-binding motifs4,5. Whether and how TF-mutations impact upon the nature of binding to TF composite elements (CE) and influence their interaction with other TFs is unclear. Here, we report a new mechanism of TF alteration in human lymphomas with perturbed B cell identity. It is caused by a recurrent somatic missense mutation c.295T>C (p.Cys99Arg; p.C99R) targeting the center of the DNA-binding domain of Interferon Regulatory Factor 4 (IRF4), a key TF in immune cell-differentiation and -activation6,7. IRF4-C99R fundamentally alters IRF4 DNA-binding, with loss-of-binding to canonical IRF motifs and neomorphic gain-of-binding to canonical and non-canonical IRF composite elements (CEs). Furthermore, IRF4-C99R thoroughly modifies IRF4 function, by blocking IRF4-dependent plasma cell induction, and up-regulating disease-specific genes in a non-canonical Activator Protein-1 (AP-1)-IRF-CE (AICE)-dependent manner. Our data explain how a single arginine mutation creates a complex switch of TF specificity and gene regulation. These data open the possibility of designing specific inhibitors to block the neomorphic, disease-causing DNA-binding activities of a mutant transcription factor.

#3731

The polyamine-hypusine circuit controls an oncogenic translational program essential for malignant transformation in MYC-driven lymphoma

Shima Nakanishi[1], Jiannong Li[2], Anders E. Berglund[2], Youngchul Kim[2], Yonghong Zhang[2], Ling Zhang[3], Chunying Yang[1], Raghavendra G. Mirmira[4], John L. Cleveland[1]. *[1]Tumor Biology, Moffitt Cancer Center, Tampa, FL,[2]Bioinformatics and Biostatistics, Moffitt Cancer Center, Tampa,*

FL,[3]Pathology and Laboratory Medicine, Moffitt Cancer Center, Tampa, FL,[4]Department of Medicine, The University of Chicago, Chicago, IL

The *MYC* oncoprotein is activated in a broad spectrum of human malignancies and transcriptionally reprograms the genome to drive cancer cell growth. Given these functions, it is unclear if targeting a single effector of MYC will have therapeutic benefit. MYC activates the polyamine-hypusine circuit, which post-translationally modifies a single lysine residue (Lys-50) of eukaryotic translation initiation factor eIF5A in a process coined hypusination via two enzymes,deoxyhypusine synthase (DHPS) and deoxyhypusine hydroxylase (DOHH). The roles of this circuit in cancer are unclear. Here we report essential intrinsic roles for hypusinated eIF5A in the development and maintenance of MYC-driven lymphoma, where loss of eIF5A hypusination completely abolishes malignant transformation of MYC-overexpressing B cells in transgenic mice predestined to develop lymphoma. Mechanistically, integrating RNA-seq, Ribo-seq and proteomic analyses revealed that efficient translation of select targets is dependent upon eIF5A hypusination, including regulators of G1-to-S phase cell cycle progression and DNA replication. Thus, this circuit controls MYC's proliferative response at several levels and is activated in many tumor types. These findings suggest the hypusine circuit as a therapeutic target for a broad spectrum of malignancies.

#3733

Disconnect between APOBEC3 expressions and mutations across cancers

Azad Khosh[1], Hamid Hamidi[2], Hamzeh Rahimi[3], Diako Ebrahimi[3].
[1]Zeelamo Academy, San Diego, CA,[2]University of Calgari, Calgari, AB, Canada,[3]Texas Biomedical Research Institute, San Antonio, TX

DNA of many tumors is barraged by C-to-T/G mutations within TCW (W:T,A). These mutations are attributed to the aberrant expression and activity of APOBEC3 enzymes. They have been shown to account for many driver mutations in genes such as PIK3CA, ERBB2, and PPP2R1A, however their precise source and also their roles in tumor development, evolution, and patient survival are debated. Currently, quantification of APOBEC3 expression changes in tumor cells is confounded by the

ubiquitous expression of these enzymes in infiltrating immune cells. In this study, we used quantitative biology approaches to separate the expression profiles of APOBEC3 enzymes in tumor and tumor microenvironment cells and determine their associations with tumor mutational signatures. For this purpose, we analyzed diverse datasets including TCGA tumor/matched normal RNAseqs, tumor somatic mutations, cell line RNAseqs and mutations, estimates of tumor purities and immune cell compositions, and expression of purified cell populations to precisely determine how APOBEC3 enzymes are dysregulated across tumors and whether their dysregulations are proportional to tumor mutational signatures. Unexpectedly, we found that dysregulation of APOBEC3 enzymes is independent of tumor C-to-T/G mutational burden. Importantly, our data suggest that this disconnect is likely not due to the episodic bursts of APOBEC3-induced mutations in cancer.

#3734

Neuroendocrine differentiation (ND) in sensitivity of neuroendocrine tumor (NET) cells to ONC201/TIC10 cancer therapeutic

Elizabeth C. Ding, Wafik S. El-Deiry. *Pathology and Laboratory Medicine, Brown University, Providence, RI*

Neuroendocrine tumors (NETs) harbor neuroendocrine differentiation (ND) with specific markers including protein gene product 9.5 (PGP9.5) and Chromogranin A (CgA). In prostate cancers (PC), ND is induced by BRN2/SOX2 transcription factors. NET-like cells with low or absent androgen receptor (AR) signaling cause hormone therapy resistance and poor prognosis in PC. Small cell lung carcinoma (SCLC), a high-grade NET, presents with metastasis early and has poor survival. ONC201/TIC10 is a small molecule inducer of TRAIL signaling in clinical trials. ONC201 antagonizes dopamine D2 or D3 receptors (DRD2/DRD3) and is an agonist of mitochondrial caseinolytic protease P (ClpP) resulting in activation of DR5/TRAIL-dependent apoptosis involving the integrated stress response (ISR). ONC201 is active in various malignancies including H3K27M-mutated glioma and NETs expressing high levels of DRD2. We hypothesized that altered BRN2/SOX2 may impact NET apoptosis by ONC201 through the ISR and TRAIL/DR5. We analyzed the expression of neuroendocrine markers PGP9.5, CgA, SOX2, and BRN2, as well as

markers of TRAIL signaling pathway markers ATF4, DR5, ClpP, ClpX, and DRD2/DRD3 in PC and SCLC cell lines (N=6) ± treatment with ONC201. Specifically, we compared pre-treatment protein expression levels with the IC50. Our results reveal that DU145 (IC50=3.11μM), PC3 (IC50=3.02μM), and LNCaP (IC50=1.33μM) are ONC201 sensitive. H1417 SCLC expresses CgA, unlike PC3 and DU145. PGP9.5 is expressed in these lines. PGP9.5 is expressed in PC3, DU145, H1417, and H1048 but not in LNCaP and 22RV1. BRN2 is expressed in PC3, H1417, and H1048 but not DU145, LNCaP, or 22RV1. ClpX is expressed in all 6 lines but at lower levels in SCLC. ClpP is expressed in the 6 lines. DR5 is expressed at higher levels in PC3, DU145, LNCaP, and 22RV1 PC versus H1417 and H1048 SCLC. SOX2 is expressed at high levels in H1417 cells. These results are establishing the landscape of ND in PC and SCLC lines for further experimentation and testing of our hypothesis. To characterize the association of BRN2 dysregulation with ONC201 sensitivity, we are performing BRN2/SOX2 knockdown experiments using siRNA and evaluating effects towards ONC201 sensitivity. Our results provide insights into molecular mechanisms of ND in PC and SCLC sensitivity to ONC201. We are also currently working to overexpress BRN2 and SOX2 in cell lines to analyze the impact on neuroendocrine differentiation and ONC201 sensitivity.

#3735

N-terminal and C-terminal elephant-to-human p53 variants and truncations alter p53 transactivation

William H. Yang, Wei-Hsiung Yang. *Biomedical Sciences, Mercer University School of Medicine, Savannah, GA*

Cancer is one of the most dreaded diseases of the 21st century for humans. Currently, the human cancer mortality rate is approximately 11-25%. However, for some animals, such as elephants, the cancer mortality rate is lower than 5%. p53 is a significant cellular regulator in human cancers, and its important role in response to DNA damage has been highlighted by the discovery of p53 retrogene found in elephants (19 copies) but not humans (0 copies). Therefore, the main question is whether (1) more copies of p53 are better at combating cancer development or (2) is elephant p53 is better than human p53 in p53-mediated function? Herein, we demonstrate for the

first time that N-terminal and C-terminal elephant-to-human p53 variants and truncations alter p53 transactivation. First, we created elephant-to-human p53 variants (such as T387R, L383P, LSTEL, etc.) and truncations at the N-terminus and C-terminus of human p53. Secondly, R175H and R273H p53 mutants (conformational and contact mutants, respectively) were used as negative control. Using a p53 (14X) response element LUC and several natural p53 downstream gene promoters, we demonstrated that several N-terminal and C-terminal p53 variants and truncations increases p53 transactivation compared to WT p53. Moreover, we found that deletion of the region between aa374 and aa382 is integral for p53 transactivation. Taken together, our preliminary results demonstrate that several N-terminal and C-terminal elephant-to-human p53 variants enhance p53 transactivation and possible stability. This data is the first step to support the notion that elephant p53 is better than human p53 in p53-mediated function.

#3736

ZBTB46/FOXA2/HIF1A transcription activator complex promotes MCTP1-regulated neuroendocrine differentiation and epithelial-to-mesenchymal transition

Vu Thuy Dung Phan[1], Yu-Ching Wen[2], Wei-Yu Chen[3], Wei-Hao Chen[1], Kuo-Ching Jiang[1], Han-Ru Li[1], Van Thi Ngoc Tram[4], Zi-Qing Chen[5], Wan-Hsin Wang[5], Yen-Nien Liu[1]. *[1]Graduate Institute of Cancer Biology and Drug Discovery, Taipei Medical University, Taipei, Taiwan,[2]Department of Urology, Taipei Medical University, Taipei, Taiwan,[3]Department of Pathology, Taipei Medical University, Taipei, Taiwan,[4]International Ph.D Program in Medicine, Taipei Medical University, Taipei, Taiwan,[5]Division of Clinical Pharmacy, Taipei Medical University, Taipei, Taiwan*

Androgen deprivation therapy (ADT)-induced neuroendocrine differentiation (NED) is a well-known lethal subtype of prostate cancer (PCa) with a median survival rate of less than one year. Despite the increasing research attention on this variant of PCa, the underlying mechanism orchestrating therapy-related neuroendocrine prostate cancer (NEPC) remains elusive. We found that ADT-induced hypoxia-associated ZBTB46/FOXA2/HIF1A signaling enhances the multiple C2 domain transmembrane protein 1 (MCTP1), which promotes NED and epithelial-to-

mesenchymal transition (EMT) of PCa. Mechanistically, ZBTB46 physically interacts with the HIF1A/FOXA2 complex, in which ZBTB46 may be a co-activator of the hypoxia-related FOXA2 transcription factor. Interestingly, this ZBTB46/FOXA2/HIF1A complex accumulates after hypoxia and functions as a transcriptional activator of MCTP1. Hypoxia-upregulated MCTP1 subsequently leads to NED and the increase in EMT, whereas the opposite is true for the knockdown of MCTP1 in PCa cells. Consistent with previous results, MCTP1 is highly expressed in high-grade castration-resistance prostate cancer (CRPC) and small-cell PCa (SCPC) tissues and is associated with NE markers and ZBTB46/FOXA2/HIF1A abundance. In this study, we explored the direct interaction of ZBTB46 protein with hypoxia-related FOXA2/HIF1A complex in PCa cells under hypoxic conditions, which promote MCTP1-driven EMT and NED. Our finding suggests that MCTP1 could be used as a biomarker for diagnosing NEPC and as a therapeutic target in clinical applications.

#3737

A novel mechanism of NF-κB activation by genotoxic chemotherapy

Jaganathan Venkatesh[1], Magesh Muthu[1], Arun K. Rishi[2]. *[1]Oncology, Barbara Ann Karmanos Cancer Institute, Wayne State University School of Medicine, Detroit, MI,[2]Oncology, John D. Dingell VA Medical Center, Barbara Ann Karmanos Cancer Institute, Wayne State University School of Medicine, Detroit, MI*

CARP-1, a perinuclear phospho-protein, is a biphasic regulator of cell survival and apoptosis signaling. Genotoxic drugs induce apoptosis in part by elevating CARP-1 levels while also promote cell survival in part by activating NF-κB that involves CARP-1 interaction with NF-κB kinase subunit γ (aka, NEMO). We previously noted interaction of CARP-1 with RIPK1, and since RIPK1 is known to regulate NF-κB signaling, we investigated whether RIPK1-CARP-1 interaction is involved in genotoxic chemotherapy-dependent apoptosis or NF-κB-activated survival signaling. Mutagenesis and co-IP-WB analyses revealed that a 40-amino acid epitope within the amino-terminal catalytic domain of RIPK1 interacted with CARP-1 (611-640) peptide. Overexpression of this CARP-1/CCAR1-binding (CB) epitope peptide or RIPK1 mutant that has in-frame deletion of CB-epitope resulted in moderate but significant reduction in viabilities of

cells treated with Adriamycin or Cisplatin relative to the viability loss noted in cells expressing RIPK1 (WT). However, no significant differences in loss of cell viabilities were noted in cells expressing various substitution mutants of RIPK1 (aspartate (D) 138 to asparagine (N), serine (S) 109 and threonine (T) 110 to alanines (A), lysine (K) 87 to arginine (R), K97 to R, K105 to R, or K115 to R) relative to their RIPK1 (WT) expressing counterparts when treated with genotoxic drugs. Interestingly, CB-epitope mutant, but not RIPK1 (WT), failed to translocate to cytoplasm in Adriamycin-treated cells. Genotoxic drugs activated p65/RelA in cells expressing RIPK1 (WT), while expression of RIPK1 CB-epitope mutant resulted in abrogation of p65/RelA activation by Adriamycin or Cisplatin but not by TNFα. Collectively our data demonstrate that CARP-1 interaction with RIPK1 promotes nuclear export of RIPK1 and consequent NF-κB activation in cells exposed to genotoxic drugs.

#3738

A novel mechanism of STAT3 activation by genotoxic chemotherapy

Jaganathan Venkatesh[1], Magesh Muthu[1], Nuwan C. P.N Acharige[2], Mary K. H. Pflum[2], Arun K. Rishi[3]. *[1]Barbara Ann Karmanos Cancer Institute, Detroit, MI,[2]Chemistry, Wayne State University, Detroit, MI,[3]Oncology, John D. Dingell VA Medical Center, Barbara Ann Karmanos Cancer Institute, Wayne State University School of Medicine, Detroit, MI*

CARP-1, a perinuclear phospho-protein, is a biphasic regulator of cell survival and apoptosis signaling induced by genotoxic drugs. We have previously found that apoptosis induced by genotoxic drugs involved elevated levels of CARP-1. Exposure to genotoxic drugs also induced CARP-1 interaction with NF-κB kinase subunit γ (aka, NEMO) to promote NF-κB activation and cell survival. To further elucidate chemotherapy-activated, CARP-1-dependent cell survival mechanisms, we UV cross-linked protein extracts from Adriamycin-treated HeLa cervical cancer cells with a CARP-1 (614-638) peptide, and conducted liquid chromatography-tandem mass spectrometry (LC-MS/MS) analyses of the peptide-bound protein complexes. This experiment revealed STAT3 interaction with CARP-1 (614-638) peptide. Our mutagenesis and co-IP-WB experiments revealed CARP-1 (550-650) directly interacts with a 40 amino acid peptide located in the STAT3 DNA binding domain. Overexpression of mutant

STAT3 with in-frame-deletion of CARP-1/CCAR1-binding epitope (CE) peptide (Gst-STAT3 (ΔCE) mutant), but not Gst-STAT3 (WT), failed to translocate to nucleus in Adriamycin-treated cells. Disruption of STAT3-CARP-1 interaction or expression of STAT3 (ΔCE) mutant abolished Adriamycin-induced STAT3 Y705 and S727 phosphorylation. Collectively our data demonstrate that CARP-1 interaction with STAT3 regulates genotoxic chemotherapy-activated STAT3 and its nuclear translocation to promote cancer cell survival and growth.

#3739
MAFG promotes melanomagenesis through the transcriptional regulation of hypoxic and immune responses
Olga Vera, Michael Martinez, Florian A. Karreth. *Moffitt Cancer Center, Tampa, FL*

The small MAF family of transcription factors, consisting of MAFG, MAFF, and MAFK, dimerize with CNC/BACH proteins to regulate diverse transcriptional programs. Previously, we have shown that miRNA-29 suppresses melanoma development, at least in part, by repressing MAFG expression. Moreover, analysis of the TCGA revealed frequent copy number gains and/or overexpression of MAFG in melanoma. However, whether MAFG has oncogenic effects in and is critical for melanoma is unknown. We found that silencing of MAFG, but not MAFF or MAFK, abrogates growth of melanoma cells in vitro, while melanocyte cell lines are less reliant on MAFG. Conversely, MAFG overexpression promoted proliferation and focus formation of human melanocyte and melanoma cell lines. Using a high-throughput melanoma mouse modeling (ESC-GEMM) platform, we found that in vivo overexpression of MAFG in $BRAF^{V600E}$; $PTEN^{+/-}$ mice potently accelerated melanoma development. RNA-sequencing revealed that MAFG regulates transcriptional programs associated with hypoxic and immune responses. Accordingly, MAFG overexpressing cells exhibited better ability to survive under hypoxic conditions, probably through the regulation of HIF1A. Moreover, MAFG overexpressing cells showed increased expression of cytokines of the of the C-C chemokine family, CCL3 and CCL5. MAFG overexpressing tumors from ESC-GEMM mice and MAFG-High melanomas from TCGA had features of immune-cold milieus, characterized by reduced infiltration of

$CD45^+$ immune cells and $CD8^+$ T cells. Altogether, we demonstrate that MAFG promotes melanomagenesis, in part, by regulating the response to hypoxic conditions and chemokine expression, which may rewire the tumor immune microenvironment.

Non-coding RNAs in Brain, Melanoma, Lung, and Head/Neck

#3743
circPMS1 is a pro-metastatic circular RNA in melanoma
Nicol Mecozzi, Olga Vera, Florian Karreth. *Moffitt Cancer Center, Tampa, FL*

Deregulated gene expression is a major driver of melanoma metastasis, a process that results in the majority of melanoma-related deaths. Importantly, these alterations are not limited to protein-coding mRNAs, but also include noncoding RNAs. Despite many recent studies implicating circular RNAs (circRNAs) in cancer development, it is unknown if their deregulation contributes to melanoma metastasis. To identify circRNAs with putative roles in melanomagenesis, we performed RNA sequencing on a panel of melanoma and melanocyte cell lines. 21 differentially expressed circRNAs were validated by qPCR and Sanger sequencing of the backsplice junction. Further analyses of the ratio of the circular and cognate linear RNA transcripts and expression in a larger panel of cell lines identified *circPMS1* as a circRNA that is upregulated in melanoma through enhanced backsplicing of the linear *PMS1* mRNA. Using transposon-mediated delivery, we examined the effects of stable *circPMS1* overexpression on melanoma cells. While proliferation and focus formation were not impacted, migration and invasion were enhanced by *circPMS1*. Moreover, tail vein injection of *circPMS1* overexpressing melanoma cells increased lung metastasis. In addition to this transplant model, we generated the first genetically engineered mouse model of melanoma overexpressing a pro-tumorigenic circRNA. These mice are currently being analyzed. Mechanistically, we find that circularization is required for the pro-migratory effects of the *circPMS1* overexpression construct. Additionally, *circPMS1* harbors the canonical *PMS1* start codon, a predicted ORF spanning over the backsplice junction, and a predicted IRES sequence. Indeed, inserting a flag-tag in the overexpression construct revealed

circPMS1 to be translated into a truncated 25kD PMS1 protein as well as a 20kD protein likely arising from an in-frame downstream start codon. Importantly, these truncated circPMS1 proteins are endogenously expressed and increased in melanoma compared to melanocytes while the full-length PMS1 protein is evenly expressed. These findings suggest that *circPMS1* promotes melanoma metastasis, at least in part, by coding for truncated circPMS1 proteins. Further work will establish the functions of the *circPMS1*-encoded proteins and their roles in driving melanoma progression and metastasis.

#3744

A circulating microRNA panel predicts recurrence and survival in early-stage lung adenocarcinoma

Mei-Chee Tai[1], Leonidas E. Bantis[2], Gargy Parhy[1], Taketo Kato[3], Ichidai Tanaka[3], Chi-Wan Chow[1], Junya Fujimoto[1], Carmen Behrens[1], Tetsunari Hase[3], Koji Kawaguchi[4], Johannes F. Fahrmann[1], Edwin Ostrin[1], Kohei Yokoi[3], Toyofumi F. Chen-Yoshikawa[3], Yoshinori Hasegawa[5], Samir M. Hanash[1], Ignacio I. Wistuba[1], Ayumu Taguchi[6]. *[1]The University of Texas MD Anderson Cancer Center, Houston, TX,[2]University of Kansas Medical Center, Kansas City, KS,[3]Nagoya University Graduate School of Medicine, Nagoya, Japan,[4]Mie University Graduate School of Medicine, Tsu, Japan,[5]National Hospital Organization Nagoya Medical Center, Nagoya, Japan,[6]Aichi Cancer Center, Nagoya, Japan*

Background: Early-stage lung adenocarcinoma (LUAD) patients have substantial risk for recurrence and disease-related death. Cisplatin-based adjuvant chemotherapy remains the standard for care of LUAD patients who have undergone surgical resection with a high risk of recurrence. However, adjuvant chemotherapy is associated with increased risk of toxicity including chemotherapy-related death, with only a modest survival benefit. Therefore, there is an unmet need of biomarkers for assessment and identification of those in an early stage who would likely benefit from adjuvant chemotherapy. Circulating miRNAs are stably present in blood and potentially reflect different expressions in cancerous and non-cancerous tissues, making them attractive biomarkers. The purpose of this study was

to identify circulating miRNAs useful for predicting recurrence in early-stage LUAD.
Materials and Methods: miRNA microarray analysis was performed with pooled pretreatment plasma samples from stage I LUAD patients who developed recurrence within two years after curative surgery or remained recurrence free over a six-year follow-up period, as well as from healthy controls. miRNA biomarker candidates were assayed in two independent plasma sample sets from 85 stage I LUAD (validation set) and from 57 stage I and II LUAD (test set) patients.
Results: Based on miRNA microarray data and previous reports, predictive performance of miR-23a-3p, miR-23b-3p, miR-191-5p, miR-185-5p, miR-151a-3p, miR-320c, miR-21-5p, miR-125b-5p, miR-30d-5p, and miR-197-3p was evaluated in the validation set. Plasma levels of miR-23a-3p, miR-185-5p, miR-320c, miR-21-5p, miR-125b-5p, miR-30d-5p, and miR-197-3p were significantly higher in those with recurrence as compared to those without. A miRNA panel comprised of miR-23a-3p, miR-320c, and miR-125b-5p was developed based on a logistic regression, with yielding an AUC of 0.776 (95% confidence interval [CI] = 0.660 to 0.893). The three-miRNA panel with fixed coefficients yielded an AUC of 0.804 (95% CI = 0.688 to 0.920) with a sensitivity of 45.8% at 95% specificity in the test set. The miRNA panel score was a significant and independent factor for predicting disease-free survival (DFS; $P < 0.001$, HR = 1.64, 95% CI = 1.51-4.22) and overall survival (OS; $P = 0.001$, HR = 1.51, 95% CI = 1.17-1.94).
Conclusion: This circulating miRNA panel may serve as a noninvasive blood test for predicting DFS and OS in early-stage LUAD patients. Our findings provide rationale for further investigation to stratify early-stage LUAD patients using blood-based biomarkers to increase the ability to provide more personalized care.

#3745
GRAS1 long non-coding RNA binds and stabilizes NF-kB activating protein to protect lung cancer cells from DNA damage
Tong Su, Bobby Kong, Jonathan Zhu, Colleen A. McHugh. *UC San Diego, La Jolla, CA*

Long non-coding RNAs (lncRNAs) control numerous biological processes, including epigenetic regulation, gene expression, proliferation and metabolism. However, the detailed biological mechanisms by which lncRNAs regulate cellular processes are still poorly understood. We identified a set of growth regulator non-coding RNAs based on data mining of CRISPR/Cas9 screens and high-throughput sequencing studies from patient normal and tumor cells. We hypothesized that growth regulator lncRNAs play a role in cancer development by recruiting effector proteins to regulate gene expression. In our screen, the Growth Regulator Antisense 1 RNA (GRAS1) was identified as a key factor controlling growth in non-small cell lung cancer cells. Loss of GRAS1 resulted in altered expression of genes involved in DNA repair, cell cycle progression, and p53 and NF-KB signaling pathways. Extensive DNA damage occurred within 48 hours after GRAS1 knockdown, with a significant increase in the number of γH2AX loci visualized by immunofluorescence assay. We used RNA antisense purification combined with mass spectrometry to identify the NF-KB activating protein (NKAP) as the top directly interacting partner of GRAS1 lncRNA. NKAP stability decreased after GRAS1 knockdown, and this phenotype could be reversed with proteasome inhibition. Further, RelA levels were decreased in GRAS1 knockdown cells. We found that GRAS1 lncRNA binds and stabilizes NKAP to enable survival and protect against DNA damage in lung cancer cells.

#3746

Dynamic characterization of small RNAs in non small cell lung cancer exosomes under immune-checkpoint inhibitor treatments

Maria Garrido-Barros, Javier Oliver, Juan Luis Onieva, Beatriz Martinez-Galvez, Jaime Duddelman, Antonio Rueda, Elisabeth Perez, Emilio Alba, Inmaculada Ramos, Juan Zafra, Manuel Cobo, Isabel Barragán. *UGCI, Inst of Biomedical Investigation, Malaga, Spain*

Immunotherapy based on Immune Checkpoint blockade (ICB) has become a significant therapeutic option for advanced Non Small Cell Lung Cancer (NSCLC) patients. However, there is an urgent need to find novel biomarkers that to reliably stratify good responders to immunotherapy. Currently, the available biomarkers are not specific enough. Exosomes are small membrane vesicles with sizes of 30-100 nm secreted by most cell

types including cancer cells. Exosomes operate as an intercellular communication system by sending proteins, mRNA and miRNAs among other relevant RNA molecules. Exosomes enriched with miRNAS are involved in proliferation, differentiation, maduration and immune cell activation. Moreover, in cancer cells miRNA and other small RNA molecule expressions are dysregulated. Exosomes produced from cancer patient's plasma have been shown to be accurate diagnostic tools for the disease. In this study we profiled miRNAs and other small RNA cargo by exosome of plasma samples from 77 Non Small Cell Lung Cancer (NSCLC) metastatic patients before and after the first cycle of immunotherapy to evaluate the potentiality of predicting response to immunotherapy. We perform exosomes together with RNA isolation and small RNAseq sequencing from plasma samples before and after the first ICB cycle. Two independent softwares were used to identify small RNAs (RNAtoolbox and mirMaster). Prior ICB treatment we did not find differentially expressed miRNAs or other small RNA between good and bad responders. Interestingly we identified 12 exosomal miRNA differentially expressed between good and bad responders after the first cycle of ICB. Intriguingly, levels of miR-134-5p, miR-142-3p, miR-143-3p among others previously associated with NSCLC were found to be considerably higher in the good responder group than the bad responder group. Regarding other smallRNA molecules we observed a great variety and variability of piRNA, rRNA, scaRNA, lncRNA, snoRNA, snRNA, miscRNA and circRNA. To address the function of miRNA and other differentially expressed RNA molecules, we consulted KEGG, GO and Reactome for gene regulatory networks. Interestingly, KEGG results show pathways in cancer as top hit and Reactome highlight Immune System and cancer hits. In conclusion, we observed that patients that have favorable response to ICB have distinctive plasma exosomal miRNA patterns that could be used as possible biomarkers for predicting the effectiveness of immunotherapy in advanced NSCLC patients

#3747

Transcribed ultra-conserved regions (TUCRs): A first computational and molecular characterization of an understudied class of molecules in gliomas

Myron K. Gibert, Bilhan Chagari, Christian Roig-Laboy, Aditya Sarkar, Roger Abounader. *Department of Microbiology, Immunology, and Cancer Biology, University of Virginia, Charlottesville, VA*

Gliomas are the most common malignant primary brain tumors. Particularly, glioblastoma (GBM) is the most common and deadliest malignant brain tumor. Most glioma research has focused on protein-coding genes and much less on the non-coding transcripts that make up 98% of cellular RNA. Transcribed Ultra-Conserved Regions (TUCRs) represent an understudied class of molecules that are found highly conserved across multiple species, including 100% conservation in mouse and rat genomes. These 481 transcripts are highly resistant to variation and are commonly deregulated in cancer, which suggests regulatory and functional importance when considered along with their high degree of conservation. We performed the first-ever characterization of TUCRs in gliomas *in silico.* Using an elaborate workflow, we annotated and identified TUCRs that are deregulated in GBM and low-grade glioma (LGG), associated with patient outcomes, and predicted their function in glioma initiation and progression. Most TUCRs were long non-coding RNAs. Of these, we investigated the most highly upregulated intergenic TUCR, uc.110, *in vitro* and *in vivo* in glioma cell lines. Knockdown of uc.110 expression via siRNA resulted in reduced glioma cell accumulation, viability, and invasion *in vitro* while reducing tumor volume and increasing overall survival *in vivo*. Concurrent lentiviral overexpression of uc.110 partially rescued wild-type expression, accumulation, viability, and invasion *in vitro*. Therefore, it is likely that this TUCR is functioning as an oncogene within the context of GBM. Our study represents the first comprehensive characterization of TUCRs in gliomas and can serve as a foundation and framework for similar studies in gliomas and other cancers.

#3748

Epstein-Barr virus BART lncRNAs induce *IKZF3*/Aiolos to maintain EBV latency and promote tumorigenicity in nasopharyngeal carcinoma

Songtao He, Jiayan Liu, Bobo Wing-Yee Mok, Sai Wah Tsao, Honglin Chen. *The University of Hong Kong, Hong Kong, Hong Kong*

Epstein-Barr virus (EBV) maintains latency in its associated tumors, including nasopharyngeal carcinoma (NPC), expressing very few viral proteins but abundant levels of noncoding RNAs (mainly EBERs and BARTs) in NPC cells. We found that *IKZF3*/Aiolos is a downstream target of BART lncRNAs in NPC cells. The functions of BART lncRNAs and *IKZF3* in EBV latency and pathogenesis of NPC remain elusive. In this study, meta-analysis of eight EBV-associated studies showed that *IKZF3*/Aiolos was consistently upregulated in EBV-infected NPC cells. Our study further showed that transcription of *IKZF3*/Aiolos is highly upregulated in EBV-infected NPC cells and clinical tissue samples due to the action of EBV encoded BART lncRNAs, with *IKZF3*/Aiolos was expressed at higher levels in late stage (stage III & IV) NPC patients than in early stage (stage I & II) disease. Secondly, we found that *IKZF3*/Aiolos was upregulated in BART-activated NPC cells but downregulated in BART-knockdown NPC cells. In addition, this study further demonstrated that I*KZF3*/Aiolos modulates transcription of EBV BZLF1 and the cellular gene, *LRIG1*, to maintain EBV latency and promote NPC tumorigenesis *in vitro* and *in vivo*. Our results showed that the EBV lytic reactivator BZLF1 was upregulated in *IKZF3*/Aiolos knockout or Aiolos inhibitor-treated NPC cells. ChIP-qPCR, immunoprecipitation and immunofluorescence analyses further revealed that *IKZF3*/Aiolos induces H3K27 deacetylation to silence expression of BZLF1 and maintain EBV latency in NPC cells. Moreover, functional analyses and western blotting showed that *IKZF3*/Aiolos inhibited the tumor suppressor, LRIG1, to upregulate expression and phosphorylation of the cellular proto-oncogene Erb-B2 for NPC pathogenesis. Sphere- and colony-formation assays demonstrated that *IKZF3*/Aiolos enhances growth of NPC cells *in vitro*, and *in vivo* experiments further showed that *IKZF3*/Aiolos promotes tumorigenicity of NPC cells in NOD mice. Mechanically, we found that the expression of EBV lytic reactivator BZLF1 and cellular LRIG1 were negatively regulated by BART lncRNA/*IKZF3*/Aiolos regulatory machinery in NPC cells, while Erb-B2 was positively regulated, which indicated that *IKZF3*/Aiolos is a new biomarker for NPC and may lead to the development of novel diagnostic tests and treatments for NPC.

#3749

Oncogenic role of Epstein-Barr virus lnc-BARTs in EBV associated tumors

LIU JIAYAN, Bobo Wing-Yee Mok, Songtao He, Honglin Chen.
Microbiology, The University of Hong Kong, Hong Kong, China

While majority of humans infected with Epstein-Barr virus (EBV) is asymptomatic for whole life, EBV is found to associate with several human cancers, including Burkitt's lymphoma, Hodgkin's diseases, post-transplant lymphoproliferative disorder (PTLD), nasopharyngeal carcinoma (NPC) and gastric carcinoma. Among these EBV associated tumors, EBV genome is found in 100% of NPC tumor cells. EBV establishes a latent infection in NPC cells, expressing few viral proteins, but elevated levels of non-coding RNAs transcribed from the *BamHI*-A region of the EBV genome, designated *BamHI*-A rightward transcripts (BARTs). The family of EBV BART RNAs comprises BART-microRNAs (miRNAs) and long non-coding RNAs (lnc-BARTs). While versatile functions of BART miRNAs have been revealed, little is known about the role of EBV lnc-BARTs. Here, we provided evidence to show that BARTs mRNA which derived from multiple exons of BART function as regulatory long non-coding RNA, namely *lnc-BARTs*, in modulating the core network for maintaining EBV latency and promoting NPC oncogenesis through epigenetic mechanisms. Our results showed that the apoptosis rate of NPC cell lines with knockdown of EBV *lnc-BARTs* was significantly increased, suggesting that *lnc-BARTs* have an anti-apoptotic effect in EBV associated tumors. MS analysis was performed to identify host factors which interact with EBV *lnc-BARTs* in NPC cells. *Lnc-BARTs* were shown to directly interact with several transcriptional regulators, including BRD4 and SC35. Notably, RNA-FISH assays demonstrated that lnc-*BARTs* co-localize with BRD4 and SC35 complexes in nuclear speckles, with these complexes being disrupted by treatment with JQ1, a BRD4 competitive inhibitor. RNA immunoprecipitation and RNA pulldown assays confirmed that *lnc-BARTs* bind to BRD4. ATAC sequencing analysis and transcriptome analysis further demonstrated that knockdown of BARTs in the EBV-harboring NPC cell line, C666-1, resulted in globally reduced chromatin accessibility downregulation of oncogenes like MYC and BCL2. In addition, ChIP sequencing analysis revealed that *lnc-BARTs* interfere PolII phosphorylation on promoters of genes. Our findings suggest that EBV *lnc-BARTs* are

involved in epigenetic modulation of host gene expression through functional interaction with elongation regulatory machinery to maintain EBV latency and drive tumorigenesis in NPC.

#3750

miR-590-3p inhibits multiple oncogenic nodes within the TGFBR2:SMAD2/3 pathway in recurrent GBM cells

Sophie Sall[1], Jack Korleski[2], Amanda Johnson[2], Maya Johnson[1], Hernando Lopez-Bertoni[2]. *[1]Kennedy Krieger Research Institute, Baltimore, MD,[2]Neurology, Johns Hopkins University School of Medicine, Baltimore, MD*

Glioblastoma (GBM) is the most lethal and aggressive primary brain malignancy with high recurrence rates and virtually no long-term survival. Despite our expanding knowledge regarding GBM at the genomic/molecular level, we still don't fully comprehend the molecular mechanisms responsible for GBM recurrence. Current knowledge implicates tumor-propagating Glioma Stem Cells (GSCs) in the evolution of treatment resistance and tumor recurrence. Understanding these cellular/molecular events will inform strategies for preventing and/or treating recurrent GBM (rGBM). Gene set enrichment analysis (GSEA) of RNA sequencing datasets obtained from GSCs and clinical rGBM specimens identified TGFBR2 signaling as a high frequency and potentially targetable pathway in rGBM. We show that SMAD2/3 signaling, a downstream effector of TGFBR2, is enriched in rGBM and that patients with elevated TGFBR2 have statistically shorter long-term survival outlooks. The functional relevance of these findings was supported using ITD1, a selective TGFBR2 inhibitor, which decreased the GSC phenotype and cell viability of cells derived from clinical rGBM (rGBM cells), while simultaneously re-sensitizing them to temozolomide (TMZ) in-vitro. Since GBM is known to efficiently develop resistance to receptor-targeting monotherapies, we sought to simultaneously target multiple putative oncogenic drivers downstream of TGFBR2. To achieve this, we applied an unbiased miRNA-based network analysis that identified miR-590-3p as an inhibitor of SMAD2/3 signaling at multiple nodes and thus a potential tumor suppressor in rGBM. Transgenic miR-590-3p robustly decreased the expression of >30 putative oncogenes, reduced the GSC phenotype and cell

viability, as well as re-sensitized rGBM cells to TMZ. These results predict that blocking TGFBR2 signaling will negatively impact the tumor phenotype of rGBM as well as its GSC capacity. Ongoing directions for this research include comparing the efficacy of ITD1 monotherapy with miR-590-3p therapy in rGBM models in-vivo. These results identify a significant role of TGFBR2 signaling in both TMZ resistance and the GSC phenotype in rGBM and provide a miRNA-based strategy for simultaneously targeting multiple oncogenic nodes within the TGFBR2 and potentially other oncogenic signaling pathways.

#3751

Characterizing the role of the y chromosome-expressed long non-coding RNA linc-SPRY3 family in lung cancer radiation resistance

Emily S. Westemeier-Rice. *Mary Babb Randolph Cancer Center at West Virginia University, Morgantown, WV*

Lung cancer is the leading cause of cancer-related deaths worldwide. A major issue for clinicians and patients alike is inherent resistance to radiation therapy. Recently, certain long non-coding RNAs (lnc-RNAs) have been shown to regulate pathways involved in resistances to lung cancer treatments. Our group recently published that a group of long non-coding RNAs, named the linc-SPRY3 family, play an important role in radiation therapy sensitivity. Originating from the Y-Chromosome, these long non-coding RNAs have been shown in vitro and in vivo to decrease the tumor burden after radiation. Interestingly, certain male Non-Small Cell Lung Cancer (NSCLC) cell lines have been shown to have complete loss of the Y-chromosome (LOY), showing a radiation resistant phenotype. To test this, the DYZ1 region of the Y-chromosome, where the linc-SPRY3 family is expressed, was artificially introduced into radiation resistant male NSCLC cell lines with LOY. Remarkably, by adding the DYZ1 region of the Y-chromosome into these cells, they became more sensitive to radiation and had increased apoptosis. Based on this preliminary data, we hypothesize the linc-SPRY3 family interacts with important pathways in the cell to increase sensitivity to DNA double strand breaks. Through RNA-Sequencing and other preliminary experiments, we found that the linc-SPRY3 family regulates the expression of Cell Division Cycle 6 (CDC6) and Cell Division Cycle 25A (CDC25A) genes. Preliminary data suggests

these interactions play a role in influencing NSCLC ability to invade and metastasize. We are currently characterizing this family of linc-RNAs by flow cytometry, in vivo metastasis models, and fluorescent in situ hybridization. We will characterize the mechanism of the linc-SPRY3 family in radiation resistance through genetic modifications and further downstream analysis via the over-expression and knockdown of these linc-RNAs. The characterization of these linc-RNAs will be critical for the development of potential diagnostic or therapeutic therapies.

#3752

The role of miR-200 in anaplastic thyroid cancer aggressiveness

Hugo Huth, César Fuziwara, Edna Kimura. *Department of Cell and Developmental Biology, Institute of Biomedical Sciences (ICB), University of São Paulo, São Paulo, Brazil*

Anaplastic Thyroid Cancer (ATC) is the most aggressive and lethal of all thyroid cancer histotypes, characterized by undifferentiated, highly proliferative and invasive cells, which are intrinsically resistant to conventional treatment. Deregulation of microRNAs (miRNAs), a group of small non-coding RNAs that post-transcriptionally regulates protein expression, has been linked with cancer development. Specifically, the miR-200 family has been postulated to control the balance between epithelial and mesenchymal cell states through Epithelial-Mesenchymal Transition (EMT), a critical process for tumor metastasis. Previous results showed that miR-200c, a member of miR-200 family, is downregulated in ATC, but the biological effect of its deregulation remains unclear. Therefore, this study aims to evaluate the antitumor effect of miR-200c on ATC cell aggressiveness. Using plasmid overexpression, we induced miR-200c upregulation in KTC2 (KTC2-200c) and SW1736 (SW-200c) cells to analyze its role in cell differentiation, proliferation, migration, and EMT markers expression. Light microscope images showed that KTC-200c and SW-200c cells presented an epithelial morphology in contrast with the control group which displayed mesenchymal morphology. Analysis by qPCR and western blot of KTC-200c and SW-200c cells showed that upregulation of miR-200c expression enhanced mRNA and protein expressions of the epithelial marker E-cadherin, while diminished the mRNAs and protein levels of the mesenchymal markers N-cadherin and

ZEB1/2. Additionally, KTC2-200c and SW-200c presented reduced cell colony formation and cell proliferation, and reduced cell migration visualized by wound healing assay and transwell assay. In conclusion, this study evidences the tumor suppressor role of miR-200 in controlling ATC cell aggressiveness. Grants from FAPESP (2021/12284-0, 2019/17282-5, 2019/25116-8) and CNPq (311210/2021-0).

#3753

miR-567 modulates the progression of melanoma cells and functions of macrophages

Mai-Huong Thi Nguyen[1], Chen-Huan Lin[1], Yu-Chi Huang[1], Mu-Shiun Tsai[2], Ming-Hong Chen[3], Azusa Miyashita[4], Satoshi Fukushima[4], Nianhan Ma[1]. *[1]National Central University, Taoyuan, Taiwan,[2]Landseed Hospital, Taoyuan, Taiwan,[3]Saint Paul's Hospital, Taoyuan, Taiwan,[4]Kumamoto University, Kumamoto, Japan*

Purpose: Target therapy and immunotherapy are advancements in the treatment of melanoma; unfortunately, a subset of patients does not benefit or produces drug resistance. Therefore, an alternative strategy should be investigated to further improve clinical benefits. Macrophages are the abundant immune cells related to the progression of melanoma and resistance to drugs. In this study, we explored the novel roles of miR-567 in the progression of melanoma and effects of macrophages.
Methods: miR-567 expression in nevus and melanoma tissues was analyzed by in situ hybridization. miR-567 was transfected into melanoma cells to investigate its biological effects through functional assays such as proliferation, colony formation, soft agar, and migration assays. In addition, miR-567-related signal transduction pathways in the melanoma cells were studied by western blot and next-generation sequencing analyses. Different phenotypes of macrophages polarized from THP-1 monocyte cells were used as *in vitro* model to investigate the effects of miR-567 on macrophages.
Results: Our results showed that miR-567 expression levels were decreased in melanoma cells compared to melanocyte cells. Consistently, expression of miR-567 was 0.403-fold lower in melanoma tissues (n=118) as compared to nevus tissues (n=40). In addition, the receiver operating characteristic presented that the area under the curve value of miR-567 is 0.9495.

Importantly, higher expression of miR-567 enhanced the overall survival of melanoma patients. Overexpression of miR-567 significantly reduced proliferation, survival, anchorage-independent growth, migratory, and invasive abilities of melanoma cells and BRAF-inhibitor resistant cells. Furthermore, our results demonstrated that IGF1R, E2F1, and Cyclin B2 are direct targets of miR-567 and knockdown of these genes attenuated proliferation and survival of melanoma cells. Interestingly, introduction of miR-567 downregulated MAPK/ERK and PI3K/AKT pathways in melanoma cells and regulated multiple pathways related to immune response. Of note, overexpression of miR-567 reduced the promoting melanoma growth induced by M2 or melanoma-associated macrophages, indicating the involvement of miR-567 in regulation of macrophages. Conclusion: miR-567 could be served not only as biomarkers but also as potential molecular target for prevention of melanoma progression.

#3754

The cell- and non-cell autonomous actions of UCA1 dysregulation in hypopharyngeal cancer

Li-Wha Wu. *Institute of Molecular Medicine, National Cheng Kung University, Tainan, Taiwan*

Long non-coding RNAs (lncRNAs), encoding noncoding transcripts greater than 200 nucleotides, are multifunctional regulator of gene expression and play vital roles in various biological processes. Urothelial cancer-associated 1 (UCA1) is one such molecule and found to be dysregulated in the development of several cancer types, including those in bladder, colon, stomach, lung and breast. One previous study showed that an upregulation of UCA1 expression profile in hypopharyngeal cancer tissues relative to their adjacent normal counterparts significantly negated overall survival among these cancer patients. However, the molecular mechanism whereby UCA1 played any role in HPC, a subtype of head and neck cancer and often detected in advanced stages, remains elusive. In this report, we showed that ectopic UCA1 expression promoted cell migration and invasion while reducing cell proliferation. The increase of migration and invasion was accompanied by partial epithelial mesenchymal transition. By contrast, UCA1 depletion had the opposite effect. In addition to the presence of UCA1 in the culture medium (CM) and a stimulatory effect of CM derived

from UCA1-OE cells on cell migration and invasion, we found a predominant nuclear localization of UCA1 in HPC cells. PTBP3, a RNA-binding protein, was identified as a novel interacting partner of UCA1 by RNA pulldown and mass spectrometry. PTBP3 silencing significantly reduced UCA1 mRNA expression, suggesting a regulatory role in UCA1 stability. While mapping the interacting domains between UCA1 and PTBP3, we are also in the process of identifying the involvement of UCA1-PTBP3 axis in hypopharyngeal carcinogenesis. We hope to validate if UCA1 can serve as a novel therapeutic target against or diagnostic marker for hypopharyngeal cancer.

#3755

***Dlx4os*: a lncRNA associated with malignant melanocyte transformation**

Ana Luísa P. Ayub[1], Hatylas Azevedo[2], Diogo Pessoa[3], Leinal Sejour[4], Ioannis Vlachos[4], Eduardo M. R. Reis[3], Frank J. Slack[4], Miriam G. Jasiulionis[1]. *[1]Pharmacology, Federal University of São Paulo (UNIFESP), São Paulo, Brazil,[2]Surgery, Federal University of São Paulo (UNIFESP), São Paulo, Brazil,[3]Biochemistry, University of São Paulo (USP), São Paulo, Brazil,[4]Pathology, Harvard Medical School Initiative for RNA Medicine, Boston, MA*

It is estimated that more than 90% of the human genome is transcribed into non-coding RNAs (ncRNA). It has been demonstrated that ncRNAs have an important role in biological processes such as proliferation, differentiation, and cell migration. Changes in their expression have been associated with several diseases, including cancer. Melanoma is one of the most aggressive types of cancer, with high probability of metastasis and an unfavorable response to therapies. Our lab has developed an *in vitro* melanoma progression model, which was established by exposing nontumorigenic melanocytes (melan-a) to sustained stress conditions (cycles of adhesion blockage), sequentially generating different cell lines (i.e., 4C, premalignant melanocytes; 4C11-, non-metastatic melanoma cells; and 4C11+, metastatic melanoma cells), in which each cell line represents a distinct stage of tumor progression. Previous RNA sequencing data comparing these 4 cell lines identified a total of 3404 long non-coding transcripts which displayed differential expression (DE) levels when comparing two or more cell lines.

We have clustered 531 of them into three distinct signatures: malignancy, epithelial-to-mesenchymal transition (EMT), or metastasis, according to their expression profiles. We also analyzed the neighboring genes of those lncRNAs, as it is known that lncRNAs might regulate gene expression in *cis*. We identified the lncRNA *Dlx4os*, highly expressed in undifferentiated and mesenchymal-like 4C and 4C11- cells, and 6 neighboring genes whose expression correlate to the EMT signature and overall survival in human melanoma patients. Among these genes we found *Dlx4*, which shares the same promoter site with *Dlx4os* and whose expression correlates to a poor prognosis. We silenced *Dlx4os* in the 4C11- cells through interference RNA technology. The downregulation of *Dlx4os* led to expression changes in EMT-related genes, such as *Snail1*, *Sox10* and *Mitf*, indicating that it might play a role in EMT. *Dlx4os* downregulation also inhibited cell migration *in vitro* and tumorigenesis *in vivo*. These results overall indicate a role of *Dlx4os* in melanocyte malignant transformation.

#3756

miR-145 and its gene targets as therapeutic target and prognostic biomarkers for non-small cell lung cancer

William C. S. Cho, Chi F. Wong, Leo K. P. Li, Alvin H. W. Fong.
Department of Clinical Oncology, Queen Elizabeth Hospital, Hong Kong SAR, China

Introduction: Our previous study found that miR-145 was downregulated in non-small cell lung cancer (NSCLC) tissues and it could inhibit cell proliferation in transfected NSCLC cells. This study aimed to investigate the potential anticancer effect and tumor suppressive function of miR-145, to identify its gene targets, as well as to assess the role of its gene targets as prognostic biomarkers for NSCLC patients.
Materials and Methods: Cell proliferation, transwell migration, and invasion assays were performed on three miR-145 mimics transfected NSCLC cells. The effect of miR-145 in the cell cycle *in vitro* was assessed by flow cytometry analysis. *In vivo* transfection of miR-145 was performed to examine the cancer growth in eight BALB/c nude mice. Luciferase reporter assay was used to identify the gene targets. To reveal the role of the identified gene targets in patient survival, the clinical data of 500 lung

adenocarcinoma patients from The Cancer Genome Atlas (TCGA) database was used for Kaplan-Meier survival analysis.
Results: Upregulation of miR-145 significantly inhibited proliferation, migration, and invasion in NSCLC cells *in vitro*. Flow cytometry analysis revealed that the transfection of miR-145 into NSCLC cells did not show any effect in the cell cycle. After 37 days, transfection of miR-145 showed a reduction in tumor size (49% smaller) and tumor weight (57% lighter) than mimic negative *in vivo*. MicroRNA target prediction database miRTarBase and luciferase reporter assays identified GOLM1 and RTKN as the direct targets of miR-145. TCGA survival analysis found that the high expressions of GOLM1 ($p < 0.0001$) and RTKN ($p < 0.0045$) were significantly correlated with poor overall survival in lung adenocarcinoma patients.
Conclusion: Our results revealed that miR-145 inhibited proliferation, migration, and invasion, but did not affect cell cycle regulation in NSCLC. It also caused a reduction in tumor growth and weight. Most importantly, we identified two direct targets (GOLM1 and RTKN) of miR-145, in which RTKN was first identified as a miR-145 target in NSCLC. Moreover, both GOLM1 and RTKN play an imperative role in patients' overall survival. Taken together, our findings suggest that miR-145 may serve as a molecular therapeutic target for NSCLC, and its gene targets GOLM1 and RTKN may serve as prognostic biomarkers. Their potential clinical applications warrant further investigation.

#3757
miR-200 inhibits the activation of cancer-associated fibroblasts in lung tumor microenvironment
Inyoung Cheon, Sieun Lee. *Ewha Womans University School of Medicine, Seoul, Korea, Republic of*

Cancer-associated fibroblasts (CAFs) are key components of the tumor microenvironment and promote cancer progression and metastasis. CAFs are regulated by diverse processes including regulation by miRNAs. To identify miRNAs involved in the regulation of CAF activation, we profiled miRNA expression within mouse lung normal fibroblasts (LFs) and CAFs using the NanoString nCounter method. Among numerous miRNAs differentially expressed between CAFs and LFs, miR-200 was selected for

further investigation, which is more highly downregulated in CAFs. Overexpression of miR-200 in CAFs suppressed the migration and invasion of lung cancer cells in co-culture systems and inhibited metastasis in a mouse model. In addition, we verified that lung cancer patients with high miR-200 levels showed a good prognosis than those with low miR-200 levels. Next, we tried to identify novel miR-200 targets based on RNA sequencing data, lung adenocarcinoma TCGA, and TargetScan. NRP2 was confirmed to be a target of miR-200 by 3′-UTR assay. NRP2 knockdown by siRNAs in CAFs suppressed cancer cell invasion, and NRP2 addback in CAF-200 restored cancer cell invasion inhibited by miR-200. NRP2 functions as a co-receptor with VEGFR, thus, CAF-200 was less responsive to VEGF than control CAFs. Collectively, this study suggests that downregulation of miR-200 in CAFs promotes lung cancer progression in tumor microenvironment; therefore, miR-200 will be a good therapeutic target or a biomarker in lung adenocarcinoma.

#3758

Tumor tissue and cerebrospinal fluid microRNA profiles enable the classification of brain metastasis accordingly to their origin

Dagmar Al Tukmachi[1], Michaela Ruckova[1], Marek Vecera[1], Tana Machackova[1], Petra Pokorna[1], Marketa Hermanova[2], Michal Hendrych[2], Leos Kren[3], Ivana Roskova[4], Vaclav Vybihal[4], Hana Valekova[5], Radim Jancalek[5], Jiri Sana[6], Martin Smrcka[4], Ondrej Slaby[7]. *[1]The Central European Institute of Technology, Masaryk University, Brno, Czech Republic,[2]First Department of Pathology, St. Anne's Unversity Hospital, Brno, Czech Republic,[3]Department of Pathology, University Hospital Brno, Brno, Czech Republic,[4]Department of Neurosurgery, University Hospital Brno, Brno, Czech Republic,[5]Department of Neurosurgery, St. Anne's University Hospital Brno, Brno, Czech Republic,[6]Comprehensive Cancer Care Department, Masaryk Memorial Cancer Institute, Brno, Czech Republic,[7]Department of Biology, Faculty of Medicine MU, Brno, Czech Republic*

Brain metastases (BMs) comprise a heterogeneous group of the most frequent intracranial tumors in adults, most originating in lung, breast, renal cell, and colorectal carcinomas and melanomas. Despite the recent

improvements in imaging methodology resulting in earlier BM identification and advancements in treatment strategies, BMs are still a significant cause of patient morbidity. Furthermore, BMs frequency increases due to more prolonged survival of cancer patients and population aging. Since the most widely used prognostic scoring systems for BMs require prior knowledge of the primary origin and up to 14% of BMs are classified as BMs of unknown primary, there is an urgent unmet need for accurate biomarkers for identification of BM origin. MiRNAs are non-coding RNAs with an approximate length of 22 nucleotides, functioning as post-transcriptional regulators of gene expression. Dysregulated miRNA expression profile has been observed in many pathological processes, including the complex and not fully understood metastatic cascade. These molecules are very stable and present not only in tissues but also in human body fluids, including blood plasma and cerebrospinal fluid (CSF). Based on these facts, both tissue and circulating miRNAs are extensively studied as potential diagnostic biomarkers. Specific miRNA signatures of BMs were obtained using high-throughput miRNA profiling (Illumina small RNA sequencing) on 3 types of samples (metastatic tissue, blood plasma, CSF) from a cohort of 30 patients with BMs originating in the 5 tumor types – lung, breast, renal cell and colorectal carcinomas and melanomas (6 patients per group, 87 samples in total, only 3 CSF samples from RCC patients available). We identified significantly differentially expressed miRNAs in BM tissues with the ability to differentiate between primary origins. Tissue miRNAs could identify BMs originating from breast, colorectal and renal cell carcinomas and melanomas with high specificity and sensitivity. Interestingly, the heterogeneity of lung carcinomas was also characteristic for the corresponding BMs, making it challenging to distinguish accurately from other BMs. Even though the tissue-specific miRNA signature was the most precise, our results suggest a significant diagnostic potential of circulating miRNAs from CSF for BM patients. Therefore, these short and stable molecules could potentially help identify the origin of BMs of unknown primary. The research is supported by project National Institute for Cancer Research (Programme EXCELES, ID Project No. LX22NPO5102) - Funded by the European Union - Next Generation EU.

#3759

Impact of individual and combined deregulation of miR-143 and miR-506 on cytokinetic and morphometric parameters in A549 lung cancer cells

Archana Shrestha[1], Behnaz Lahooti[2], Mahboubeh Madadi[3], Constantinos M. Mikelis[4], George Mattheolabakis[1]. *[1]Pharmaceutical and Toxicological Sciences, University of Louisiana at Monroe, Monroe, LA,[2]Department of Pharmaceutical Sciences, Texas Tech University Health Sciences Center, Amarillo, TX,[3]Department of Marketing and Business Analytics, Lucas College and Graduate School of Business, San Jose State University, San Jose, CA,[4]Department of Pharmacy, University of Patras, Patras, Greece*

Lung cancer (LC) is among the leading causes of death from malignancies worldwide. miRNAs (miRs), small noncoding RNAs capable of regulating gene expression through the cell's RNAi mechanism, have emerged as promising molecules for cancer treatment. In our previous work, we identified two miRs, miR-143 and miR-506, whose transient transfection induced apoptosis, cell cycle inhibition, and cyclin-dependent kinase (CDK) 1, 4, and 6 downregulations. Here, we developed stable deregulations of the miRs' expressions in A549 cells, individually or in combination, to evaluate their effect on LC cell behavior. To establish homogeneous populations of deregulated cells, A549 cells with stable up and downregulated miR-143 and miR-506, alone or in combination, were sorted according to marker expression using fluorescence-activated cell sorting (FACS). miR deregulations were confirmed with quantitative real-time polymerase chain reaction (qRT -PCR) analysis, and the cells were analyzed for changes in cell proliferation through cell cycle analysis using flow cytometry and cell doubling time using Quantitative Phase Imaging (QPI). With the same method, morphometric characteristics were quantified. Finally, we evaluated the motility of the cells using a scratch assay and determined the gene expression of CDKs. Taqman qPCR analysis indicated a >5-fold increase of the respective miR's basal expression due to the stable transfections. The cell cycle analysis indicated a complex behavior for the individual miRs, while, in contrast, the combined upregulation of the two miRs indicated a G2 inhibition, representing a well-defined behavior in comparison to both the control and downregulation groups. Furthermore, the combined miR upregulation increased the cell doubling time compared to the control and respective downregulations.

Similarly, using QPI microscopy, we observed that the miR combination upregulation had higher cellular sphericity, perimeter, and area compared to the control group. The wound healing assay did not indicate statistically significant differences among the different groups, with miR-506 upregulation demonstrating the slowest closure rate, followed by miR -143. In contrast, the differences between the miR-combination and control group were small, although the anti-miR-combination indicated an accelerated closure. In conclusion, the combined upregulation of both miRs inhibited cell proliferation through a G2 arrest, while the deregulation of the individual miRs demonstrated a complex behavior. Thus, the miR-combination's consistent, promising behavior would indicate potential benefits using the two miRs against LC that merits further evaluation.

#3760

MicroRNA-1 run down the growth and metastasis of small cell lung cancer

Parvez Khan[1], Jawed A. Siddiqui[1], Shailendra Kumar Maurya[1], Tamara Mirzapoiazova[2], Prakash G. Kshirsagar[1], Ramakanth Chirravuri Venkata[1], Sanjib Chaudhary[1], Ranjana Kanchan[1], Naveenkumar Perumal[1], Mahek Fatima[1], Md Arafat Khan[1], Asad Ur Rehman[1], Imayavaramban Lakshmanan[1], Sidharth Mahapatra[1], Prakash Kulkarni[2], Apar Kishor Ganti[1], Maneesh Jain[1], Ravi Salgia[2], Surinder Kumar Batra[1], Mohd Wasim Nasser[1]. *[1]University of Nebraska Medical Center, Omaha, NE,[2]City of Hope's Comprehensive Cancer Center, Duarte, CA*

Small cell lung cancer (SCLC) is a highly aggressive and metastatic lung cancer subtype with universal relapse and poor prognosis. The lack of potential drug targets limits targeted therapies for SCLC patients. To track down the potential therapeutic molecules in SCLC, we performed micro-RNA sequencing from the serum samples of SCLC patients and compared with the bulk RNA-sequencing data from SCLC tumor tissues. A consistent downregulation of microRNA-1 (miR-1) was observed in the SCLC patient serum samples, cell lines, and tumor tissues compared to their matched normal control. Overexpression of miR-1 in SCLC cell lines decreased cell growth and oncogenic signaling. Metastatic studies using the intracardiac injection model of SCLC cell lines showed that miR-1 overexpression

decreases distant organ metastasis. Interestingly, the loss of function studies using miR-1Zip/sponging showed increased tumorigenesis and metastasis in SCLC subcutaneous and intracardiac xenografts. Mechanistic investigations revealed the CXCR4/FOXM1/RRM2 axis as a unique downstream target of miR-1 in SCLC. We found that FOXM1 transcriptionally regulates the RRM2 expression by directly binding to its promoter site, and miR-1 modulates these interactions through CXCR4. The results of the present study provided a strong preclinical rationale that miR-1 has a high potential for developing innovative SCLC therapies.

#3761

Mediators of RNA sorting and export in non-small cell lung cancer derived extracellular vesicles

Humna Hasan[1], Nadia A. Lanman[2], Sagar Utturkar[1], Jeremiah J. Jauch[1], Ikjot S. Sohal[1], Zulaida Soto-Vargas[1], Andrea L. Kasinski[1]. *[1]Department of Biological Sciences, Purdue University, West Lafayette, IN,[2]Department of comparative pathobiology, Purdue University, West Lafayette, IN*

Extracellular vesicle (EV) mediated transfer of biologically functional molecules between cancer cells and the surrounding environment significantly impacts cancer progression. Our previous study established that non-small cell lung cancer (NSCLC) cell-derived EV-RNA is an important mediator of this communication, since it significantly augments the invasive potential of recipient non-tumorigenic cells (BEAS2Bs). This led us to determine the EV-RNA cargo that is specific to NSCLC EVs. Our RNA sequencing analysis revealed preferential enrichment of specific repertoires of RNA in NSCLC EVs amongst which miR-10b, miR-100 and miR-155 show synergistic effects with regard to an invasive phenotype elicited in recipient BEAS2B cells. Interestingly, our RNA sequencing analysis also revealed a global decrease in specific subsets of microRNAs (miRNAs) in NSCLC (H358 and Calu6) cells in comparison to non-tumorigenic BEAS2B cells. In contrast, the dysregulated miRNAs were found to be exclusively abundant in the respective NSCLC cell derived EVs. This suggests a precise and active mechanism of RNA sorting and loading into EVs. A cohort of dysregulated miRNAs was shortlisted, and their cellular and EV expression was validated using RT-qPCR and flow cytometry analysis by conjugating each one of the candidates to a

fluorophore. After confirming that inclusion of a fluorophore to the RNA does not disrupt RNA sorting into the EVs, we transfected the cohort of shortlisted miRNAs including miR-122, miR-451a, miR-486, miR-150, miR-200b, and miR-142 each conjugated with a separate fluorophore and evaluated the dynamics of export. As a control, one cell-retained miRNA was also transfected with the pool of candidate miRNAs and the fluorescence of transfected cells was monitored at different times. Our results indicate that of all miRNAs, the fluorescence specific to miR-122 and miR-150 diminishes in less than 72 hours while others are retained longer, indicating that all miRNAs are not sorted or exported similarly. EV-RNA release was validated by treating the cells with an inhibitor of EV biogenesis i.e., nSMase inhibitor Gw4869. The inhibitor caused the cells to retain the candidate fluorescence corresponding to the respective EV-RNAs. To investigate sequence similarities between the miRNAs exclusively enriched in EVs of NSCLC cells, multiple sequence alignment analysis (*STREME*) was conducted, and specific motif sequences overrepresented in EVs and lost in the cells were shortlisted. Multiple lines of evidence indicate that dysregulated RNA subsets are not only causal agents of cancer progression but also contribute to poor patient outcome. Hence, there is a *critical need* to evaluate EV export of these RNAs as a potential mechanism of RNA dysregulation in cancer. Resulting data from this study is expected to not only reveal mechanistic details of EV-RNA export but will also inform future therapeutic targets.

#3762

A novel lncRNA, *GTF2A1-AS1*, is required for cell cycle progression and cell proliferation

Yael Goldstein, Tali Nizri-Megnaji, Doron Ginsberg. *Bar Ilan University, Ramat Gan, Israel*

Long noncoding RNAs (lncRNAs) are major regulators of many cellular processes including cell cycle progression, cell proliferation and tumorigenesis. In this study, we identify a novel lncRNA, GTF2A1-AS1, and reveal its effects on cell cycle progression and cancer growth. Inhibition of GTF2A1-AS1 expression alters cell cycle distribution, leading to a decrease in the number of G1 cells and a concomitant increase in all other stages of the cell cycle, and in particular S phase, suggesting its

involvement in the regulation of G1/S transition. Accordingly, knock down of GTF2A1-AS1 enhances G1 phase exit upon release from a late G1 block. In agreement with its suggested role in G1/S transition, prolonged silencing of GTF2A1-AS1 enhances proliferation of human cancer cells. GTF2A1-AS1 RNA is mostly nuclear and its gene is localized upstream to the protein-coding gene GTF2A1. GTF2A1-AS1 functions in trans to repress the expression of EIF5A2 and HOXA13. Knockdown of either EIF5A2 or HOXA13 rescues the effects of GTF2A1-AS1 silencing on cell proliferation, indicating that it functions mainly by modulating the levels of these two proteins. In agreement with the effect of GTF2A1-AS1 silencing on cell cycle progression and cell proliferation, low levels of GTF2A1-AS1 are associated with reduced survival in brain cancer patients. In conclusions**,** our data identify GTF2A1-AS1 as a novel lncRNA that regulates cell-cycle progression and cell proliferation and has a potential role in human cancer.

#3763

microRNAs associated with metastatic potential in salivary gland mucoepidermoid carcinoma

Maria Eduarda S. Trevizani[1], Katia K. Oliveira[1], Fabio A. Marchi[2], Daniela Bizinelli[1], Fernanda V. Mariano[3], Cibele P. Nagano[4], Felipe A. Costa[1], Clóvis A. L. Pinto[1], Luiz P. Kowalski[1], Silvia V. Lourenço[2], Cláudia M. Coutinho-Camillo[1]. *[1]A.C. Camargo Cancer Center - Brazil, São Paulo, Brazil,[2]Universidade de São Paulo, São Paulo, Brazil,[3]Unicamp, São Paulo, Brazil,[4]Universitè Paris-Diderot, Paris, France*

Mucoepidermoid carcinoma (MEC) is the most common malignant tumor of the salivary glands. Metastatic spread occurs in up to 80% of high-grade tumors and it is a strong predictor of poor outcome, however, the mechanisms underlying this process are largely unknown. Large-scale microRNA expression profiling studies of human cancers have demonstrated that dysregulation of miRNA is frequently associated with many cancer types. The aim of this study was to investigate the microRNA profile in metastatic versus non-metastatic MECs. Using Real Time RT-PCR (qPCR) we have analyzed the expression of 384 miRNAs and controls in 4 non-metastatic MECs, 3 MECs with lymph node metastasis, 3 MECs with distant metastasis, and 2 non-neoplastic human salivary gland samples.

The microRNA profile was able to discriminate between non-neoplastic and tumor samples and between metastatic and non-metastatic tumors. Considering non-neoplastic samples and non-metastatic MECs, 12 microRNAs were differentially expressed. The non-neoplastic versus lymph node metastasis MEC analysis demonstrated that 10 microRNAs were differentially expressed. Considering non-neoplastic versus distant metastasis MECs, 3 microRNAs were differentially expressed: 1 down-regulated and 2 up-regulated. Comparing non-metastatic MECs versus lymph node metastasis MECs we observed 17 up-regulated microRNAs. Considering non-metastatic MECs versus distant metastasis MECs, 2 microRNAs were up-regulated. One microRNA is differentially expressed between lymph node metastasis MECs and distant metastasis MECs. Our results suggest that microRNA profiles could discriminate the metastatic potential of salivary MECs and might be helpful in diagnostic and prognostic evaluation of patients.

#3764

Expression patterns of microRNAs and associated target genes in ulcerated primary cutaneous melanoma

Emily Schwarz[1], Mallory J. DiVincenzo[1], Casey Ren[1], Zoe Barricklow[1], Maribelle Moufawad[1], Lianbo Yu[1], Paolo Fadda[1], Colin Angell[1], Sara Zelinskas[1], Steven Sun[1], John H. Howard[1], Catherine Chung[1], Craig Slingluff[2], Alejandro A. Gru[2], Kari Kendra[1], William E. Carson[1]. *[1]The Ohio State University, Columbus, OH,[2]University of Virginia, Charlottesville, VA*

Tumor ulceration in cutaneous melanoma represents one of the top prognostic indicators for clinical outcome, associated with reduced progression free and overall survival. Despite this influence, the underlying biology driving tumor ulceration remains largely unexplored. One of the potential mediators of ulceration are microRNAs (miRNAs). These short, non-coding RNAs are frequently dysregulated in cancer and can impact tumor biology via mediation of gene expression. Distinct miRNA expression patterns have been identified in melanoma that can function as predictive biomarkers of disease progression and metastasis. However, the presence of a unique miRNA profile in ulcerated melanoma has not yet been assessed.

miRNA and mRNA expression was assessed in 35 ulcerated and non-ulcerated cutaneous melanomas using the NanoString Human miRNA and Tumor Signaling 360 mRNA assays and validated in an independent cohort. Linear models and moderated *t*-tests were used to detect differential expression between ulcerated and non-ulcerated tumors. Pathway enrichment and functional annotations were determined using public databases. Pearson correlations were employed to predict miRNA-mRNA binding pairs. Differentially expressed mRNAs were identified as miRNA targets using Ingenuity Pathway Analysis.
Comparison between groups revealed significant upregulation of 13 miRNAs in ulcerated relative to non-ulcerated tumors ($p < 0.03$). 4 of these miRNAs were also significantly upregulated in the validation cohort (miR-363-3p, miR-196b-5p, miR-135b-5p and miR-223-3p, $p < 0.02$). Conversely, 11 miRNAs were significantly downregulated in ulcerated relative to non-ulcerated tumors ($p < 0.05$), of which, miR-376c-5p was also significantly downregulated in the validation cohort ($p=0.009$). 21 mRNAs were differentially expressed in ulcerated relative to non-ulcerated tumors, with 3 being significant in the validation cohort as well (FPR, IL-11, and ADM, $p < 0.05$). 9 of these 21 mRNAs were then identified as predicted targets of multiple differentially expressed miRNAs in ulcerated tumors. 2 of the differentially expressed mRNAs had an inverse correlation in expression with regulatory miRNAs in our tumor samples (SOCS3 and miR-218-5p, and IL7R and miR-376c-5p). Each of the mRNAs significantly upregulated in both the original and validation cohorts have been previously associated with angiogenesis, migration or pro-metastatic cell survival in the context of cancer and pathway analysis identified significant enrichment for “granulocyte adhesion and diapedesis” ($p=0.02$) in ulcerated tumors.
This study demonstrates that a unique subset of miRNAs and mRNAs are differentially expressed in ulcerated melanoma when compared to non-ulcerated. These findings also provide novel insight regarding how increased angiogenesis and metastasis may contribute to melanoma tumor ulceration.

#3765
Long non-coding RNAs are dysregulated in glioblastoma and LINC00634 may affect the diffuse growth of U251-derived tumors *in*

vivo

Marek Vecera[1], Lenka Radova[1], Radim Lipina[2], Stefan Reguli[2], Martin Smrcka[3], Radim Jancalek[4], Michal Filip[5], Marketa Hermanova[6], Leos Kren[7], Dagmar Al Tukmachi[1], Tana Machackova[1], Petra Pokorna[1], Jiri Sana[8], Ondrej Slaby[9]. *[1]Central European Institute of Technology (CEITEC), Masaryk University, Brno, Czech Republic,[2]Department of Neurosurgery, University Hospital Ostrava, Ostrava, Czech Republic,[3]Department of Neurosurgery, University Hospital Brno and Faculty of Medicine of Masaryk University, Brno, Czech Republic,[4]Department of Neurosurgery, St. Anne's University Hospital and Faculty of Medicine of Masaryk University, Brno, Czech Republic,[5]Department of Neurosurgery, Tomas Bata Regional Hospital, Zlin, Czech Republic,[6]First Department of Pathological Anatomy, St. Anne's University Hospital and Faculty of Medicine of Masaryk University, Brno, Czech Republic,[7]Department of Pathology, University Hospital Brno and Faculty of Medicine of Masaryk University, Brno, Czech Republic,[8]Central European Institute of Technology (CEITEC), Masaryk University & Department of Pathology, University Hospital Brno & Department of Comprehensive Cancer Care, Masaryk Memorial Cancer Institute, Brno, Czech Republic,[9]Central European Institute of Technology (CEITEC), Masaryk University & Department of Biology, Faculty of Medicine, Masaryk University, Brno, Czech Republic*

Introduction: Glioblastoma (GBM) is the most frequent primary astrocytoma characterized by an aggressive and diffuse growth and a poor prognosis. The median survival of patients with GBM is only 12 to 16 months from diagnosis despite conventional therapy. It is, therefore, important to identify new therapeutic targets, which would allow a more effective treatment. In our present study, we focus on long non-coding RNAs (lncRNAs), the regulators of gene expression in both physiological conditions and GBM pathology, and their potential as targets for future therapy.

Material and Methods: Our study included 219 GBM patients and 29 intractable epilepsy patients as controls who signed an informed consent prior to treatment. Previously, cDNA libraries were prepared from 77 rRNA-depleted RNA samples and sequenced, and the expression of 11

significantly dysregulated lncRNAs was validated in 188 specimens by RT-qPCR. Results were newly validated in an independent TCGA-GBM cohort. Moreover, LINC00634 expression was upregulated in U251 and T98G cells. Cells transfected with an empty vector served as negative controls (NCs). The effect of upregulated LINC00634 expression on viability, migration, and clonogenicity was studied in vitro, and, in the case of U251-derived cell line, in vivo in immunodeficient mice with the focus on GBM growth and diffuse character.
Results: Out of the 538 significantly dysregulated lncRNAs ($P < 0.001$) identified by transcriptome sequencing, a panel of 10 downregulated lncRNAs (SNAI3-AS1, LINC00882, RFPL1S, MIR137HG, TTLL7-IT1, PWAR6, LINC00634, LINC00632, DGCR5, LINC00982; $logFC \leq -2$; $P < 0.001$) and 1 upregulated lncRNA (BTN2A3P; $logFC \geq 2$; $P < 0.001$) in GBM was validated previously by qPCR in another cohort ($P < 0.0001$ for all lncRNAs) and newly in an independent TCGA-GBM dataset. The upregulated LINC00634 expression in U251 and T98G cells was confirmed by qPCR to be approximately 11,000-fold and 600-fold, respectively, compared to the expression in NCs. Although no significant effect on viability, migration and clonogenicity was observed in vivo, a less diffuse growth pattern was observed in U251-derived GBMs with upregulated expression of LINC00634 in vivo compared with NCs.
Conclusion: A significant dysregulation of lncRNAs was previously observed in GBM compared to non-tumor controls using both transcriptome sequencing and RT-qPCR and was newly confirmed also by analyzing the TCGA-GBM dataset. We also showed possible effect of LINC00634 upregulation on the growth pattern of U251-derived GBM tumors in vivo. Our study shows that lncRNAs are dysregulated in GBM and could, therefore, serve as promising diagnostic biomarkers in GBM as well as potential therapeutic targets. The research was supported by the project National Institute for Cancer Research (Programme EXCELES, ID Project No. LX22NPO5102, funded by the European Union - Next Generation EU).

Non-coding RNAs in Breast and Gynecological/Urinary Tract Cancers and New Techniques/Technologies

#3769

Intracellular miR-1290 promotes breast cancer stemness in HER2-enriched and triple-negative breast cancer

Grace L. Wong, Mariana Najjar, Yoshua Esquenazi, Nitin Tandon, Angelina T. Regua, Hui-Wen Lo. *Vivian L. Smith Department of Neurosurgery, McGovern Medical School, The University of Texas Health Science Center at Houston, Houston, TX*

HER2-enriched breast cancer and triple-negative breast cancer (TNBC) have the highest propensity to metastasize to the brain; patients with breast cancer brain metastasis (BCBM) survive only 6-18 months after diagnosis. Mechanisms that drive brain metastasis remain unclear, contributing to limited effective treatments and poor prognoses for HER2-enriched breast cancer and TNBC patients. Our lab recently reported that breast cancer with truncated glioma-associated oncogene homolog 1, a BCBM-promoting transcription factor, secretes high levels of extracellular vesicle (EV)-derived miR-1290 (Cancer Letters 540:215726, 2022). EV-miR-1290 activates astrocytes in the brain microenvironment. Using mammosphere assays, which enrich breast cancer stem cells (BCSCs), we found conditioned media from miR-1290-activated astrocytes promotes mammosphere formation of breast cancer cells. Furthermore, miR-1290-activated astrocytes secrete high levels of ciliary neurotrophic factor (CNTF) to promote the progression of brain metastases through the novel EV-miR-1290-FOXA2-CNTF signaling axis. However, it remains unknown whether intratumoral miR-1290 promotes BCSCs and BCBM. To help fill this knowledge gap, we first examined whether a miR-1290 mimic enhanced expression of known BCSC markers in SKBR3, HER2-enriched breast cancer, and CN34, TNBC, cells. Our results showed that overexpression of miR-1290 significantly increased the expression of stemness genes, CD44, Nanog, and OCT4, in both cell lines. Furthermore, we determined whether miR-1290 promotes formation of mammospheres that are enriched with BCSCs, and the results indicated that ectopic miR-1290 expression significantly enriched BCSCs in SKBR3 and CN34 cells. Conversely, inhibition of miR-1290 suppressed mammosphere-forming ability of SKBRM and CN34-BRM cells, two brain metastatic breast cancer cell lines derived from SKBR3 and CN34 cells, respectively. We further observed that miR-1290 overexpression in SKBR3 cells significantly increased the percentage of $CD44^{+}/CD24^{-}$ cells, indicative of the BCSCs.

Analysis of Gene Expression Omnibus breast cancer patient datasets revealed that miR-1290 expression is significantly increased in HER2-positive and basal subtypes of breast cancer patient tumors. Using the publicly available miR-1290 gene signature, we performed Gene Set Enrichment Analysis and found that high miR-1290 gene activation signature is positively enriched with multiple pathway gene signatures that are known to be upregulated in breast cancer, such as EGFR, MAPK, PI3K, and STAT3 pathways. Furthermore, the miR-1290 gene signature is upregulated in HER2-positive breast cancer and TNBC tumors, and is correlated with worse metastasis-free survival (MFS) and brain-MFS in breast cancer patients. In summary, our study suggests an important role for intratumoral miR-1290 in BCSCs and BCBM.

#3770

Hypoxia-induced circular RNA*circSFMBT2* inhibits tumor malignancy in breast cancer cells

Chia-Ming Liu, Yi-Chun Ke, Liang-Chuan Lai. *National Taiwan University, Taipei, Taiwan*

Breast cancer is the most prevalent cancer among women, and the second major cause of cancer-related deaths in women worldwide. The hypoxic microenvironment of solid tumors is formed in the progress of carcinogenesis, which leads to more malignant and treatment resistance. Recently, circular RNAs (circRNA), a kind of noncoding RNA, were discovered to influence the progress of tumorigenesis, and were induced under hypoxia. However, the regulation and functions of hypoxia-induced circRNA in breast cancer remain unclear. Therefore, the purpose of this study is to identify the regulatory mechanism and its function of a hypoxia-induced circRNAs, *circSFMBT2*, in breast cancer cells. Firstly, hypoxia-responsive circRNA candidates in breast cancer MCF-7 cells under different oxygen concentrations were identified by RNA-sequencing. Among the differentially expressed circRNAs, *circSFMBT2* was chosen for further experiments. The up-regulation of *circSFMBT2* under hypoxia was validated by quantitative RT-PCR. The functional assays showed that overexpression of *circSFMBT2* inhibited cell proliferation, migration, invasion, and epithelial-mesenchymal transition. Next, in order to investigate the regulatory mechanisms of *circSFMBT2*, nuclear and

cytoplasm fractionation was performed. The results showed *circSFMBT2* predominantly localized in the cytoplasm, indicating that the regulatory mechanism of *circSFMBT2* might be via interaction with microRNA or RNA-binding proteins (RBP). In order to identify the RBPs, bioinformatic tools, RBPDB, ATtRACT, and RBPmap, were first used to predict the candidate RBPs and validated by RNA pulldown assays. The RNA-binding protein PABPC1 was proved to bind with *circSFMBT2*. On the other hand, the potential sponging microRNAs were predicted by ENCORI and miRDB, followed by qRT-PCR. No miRNAs were shown to bind with *circSFMBT2*. Lastly, the functions of *circSFMBT2* were explored by identifying its downstream genes using Affymetrix microarrays. The top 10 differentially expressed genes were chosen for validation by quantitative RT-PCR. However, no genes showed significant changes in cells overexpressing *circSFMBT2*, implying the regulation of *circSFMBT2* might not be at the transcriptional level. In summary, *circSFMBT2* was able to inhibit the cellular function of breast cancer and bind to PABPC1. With a deeper understanding of the regulatory mechanisms of *circSFMBT2*, we hope to develop a novel treatment regime for breast cancer.

#3771

PiR-hsa-4447944 promotes the progression of prostate cancer through NEFH and induces androgen-independent growth

Qiang Peng, Jingkai Sun, Peter Ka-Fung Chiu, Tingting Xie, Jeremy Yuen-Chun Teoh, Chi-Fai Ng. *Surgery, The Chinese University of Hong Kong, Hong Kong, Hong Kong*

Introduction and Objective: Non-coding RNAs (ncRNAs) represent a diverse family of regulatory transcripts that drive tumorigenesis of prostate cancer (PCa) and various other types of cancers by their hyperactivity or diminished function. PIWI-interacting RNAs (piRNAs) are a class of small ncRNAs mechanistically similar to but much less studied than microRNAs. As the most diversified small ncRNAs, piRNAs are widely involved in the pathogenesis of different types of cancers. Our study aimed to investigate the role of piRNAs in the development of castration-resistant prostate cancer (CRPC).
Methods: Small RNA sequencing was used to explore the CRPC associated piRNAs on a basis of 10 benign prostate tissues, 10 paired hormone-

sensitive PCa tissues and CRPC tissues from the same patients. The top 12 upregulated piRNAs were validated through qRT-PCR in a bigger cohort. piR-hsa-4447944 was selected and investigated its biological function by gain of function in vitro. To study its loss of function role, an androgen-independent PCa cell (LNCaP-AI) was established. For mechanistic investigation, high-throughput RNA sequencing was conducted to identify dysregulated genes in PCa cells with control or piR-hsa-4447944 overexpression. Then, potential downstream targets were further predicted by miRanda program and validated by qRT-PCR, western-blot and dual-luciferase reporter assay.
Results: piR-hsa-4447944 demonstrated a relatively higher expression level in both CRPC tissues and CRPC cell lines when compared with PCa tissues and cells. Functionally, overexpression of piR-hsa-4447944 could confer resistance to androgen deprivation and anti-androgen in PCa cells in vitro, whereas anti-sense RNA against the piR-hsa-4447944 could potentiate the sensitivity to androgen deprivation in LNCaP-AI cell. In addition, piR-hsa-4447944 showed the ability in promoting migration and invasion of PCa cells. Mechanistically, mRNA sequencing results identified a panel of downstream target-genes. Among them, neurofilament heavy chain (NEFH) was predicted and validated to have a direct binding relationship with piR-hsa-4447944, and was successfully verified to be negatively regulated by piR-hsa-4447944 in PCa cells.
Conclusions: Our study showed, for the first time, that piR-hsa-4447944 can contribute to androgen insensitivity in CRPC. This sheds a new insight into the regulation of CRPC by a small ncRNA piRNA, which may form the basis of a novel target in the treatment of CRPC.

#3772

The association of androgen receptor with microRNA expression in triple-negative breast cancer

Bayan O. Abu Alragheb[1], Hassan Abushukair[2], Maysa Al-Husseini[3], Randa Bawadi[4], Mamoun Ahram[4]. *[1]School of Medicine, The University of Jordan, Amman, Jordan,[2]School of Medicine, Jordan University of Science and Technology, Irbid, Jordan,[3]Department of Pathology and Laboratory Medicine, King Hussein Cancer Center, Amman, Jordan,[4]Department of Physiology and Biochemistry, School of Medicine, The University of Jordan, Amman, Jordan*

Introduction: Triple-negative breast cancer (TNBC) is an aggressive type that lacks targeted therapies posing a challenge in its management. This necessitates identifying novel targets that may play a role in the regulation and progression of TNBC. There is renewed interest in targeting the androgen receptor (AR) since it is expressed in TNBC and plays an important role in its biology. Studies have shown that AR can influence the behavior of TNBC via affecting the of expression microRNA molecules (miRNAs), which can modulate the expression of cancer-regulatory proteins. We aimed to profile the expression of miRNAs in human TNBC tissue samples in relation to the expression of AR and investigate their prognostic value.
Methods: The expression of 84 miRNAs in 24 TNBC tissue samples (12 AR-positive and 12 AR-negative) was examined using PCR array technology. Several bioinformatics tools were then utilized on the differentially expressed miRNAs (DE-miRNA) to determine the potentially affected protein targets and signaling pathways. Potential target genes (DEGs) for each miRNA were identified by miRWalk2.0. Gene Ontology (GO) and Kyoto Encyclopedia of Genes and Genomes (KEGG) pathway enrichment analyses were conducted for the target genes using the DAVID 6.8 bioinformatics tool. String and Cytoscape were used for establishing a PPI network and identifying the hub genes. Jamovi2.2 was used for the statistical analysis.
Results: A total of 7 DE-miRNAs were found to be significantly expressed in the tissue samples relative to AR expression. Good and poor survival outcomes, respectively, were found to be linked to miR-328-3p and miR-489-3p. Interestingly, these two miRNAs were found to be up-regulated in AR-positive tumors. The association of miR-328-3p with AR corroborates our previous findings that this miRNA is up-regulated upon AR activation in TNBC cells. Two other miRNAs, miR-17-5p and iR-193b-3p, were found to be significantly associated with high T3 and low N2 status, respectively. Gene Ontology (GO) analysis for the 7 DE-miRNAs indicated a role in the regulation of the cell cycle in various cellular components (CC) such as the “nucleus”, “centrosome”, and “transcription factor complex”. GO analysis also showed enrichment in kinase and transcription factor activities. Kyoto Encyclopedia of Genes and Genomes (KEGG) pathway enrichment analyses retrieved numerous relevant signaling pathways such

as that of the TGF-beta, MAPK, Th17 cell differentiation, and endocrine resistance.
Conclusion: This study offers an understanding of the molecular etiology of TNBC and further implicates miRNAs in mediating the effect of AR on TNBC. We also provide an integrative analysis of the AR-miRNA-TNBC gene network that can help in identifying potential therapeutic targets.
Keywords: Breast Cancer, TNBC, Bioinformatics, miRNA, Androgen Receptor

#3773
DeMixMir: deconvolution of microRNA sequencing data from heterogeneous tumor samples
Matthew Montierth[1], Kinga Nemeth[2], Xinghua Tao[3], George Calin[2], Wenyi Wang[4]. *[1]Baylor College of Medicine, Houston, TX,[2]Translational Molecular Pathology, The University of Texas MD Anderson Cancer Center, Houston, TX,[3]The University of Texas MD Anderson Cancer Center, Houston, TX,[4]Bioinformatics and Computational Biology, The University of Texas MD Anderson Cancer Center, Houston, TX*

Measuring tumor heterogeneity is a key issue in modern clinical oncology, with relevance to understanding cancer progression, resistance to therapy, and recurrence. Studies of the transcriptomic landscape in cancer have rapidly advanced in scale, enabled by novel methods and advancing technologies. One such novel method is TmS, a computational estimate of tumor-specific total messenger RNA content from heterogeneous tumor samples, which is calculated by combining genomic and transcriptomic deconvolutions. We have previously shown TmS as a promising pan-cancer biomarker for patient prognosis. Given the fruitful study of tumor cell total messenger RNA content, a logical extension is to investigate the utility of estimating tumor cell content of other RNA species. MicroRNAs (miRNAs) are small noncoding RNAs that regulate mRNA expression, and their dysregulation is a hallmark feature observed across cancers. A computational method to derive tumor cell total miRNA content from bulk sequencing data is especially needed since miRNAs cannot yet be reliably profiled at single cell resolution. Here we develop and benchmark DeMixMir, a new expansion of our reference-free transcriptomic deconvolutional model DeMixT, in order to recover tumor-specific miRNA

proportions from mixed samples. For benchmarking, we generated an artificially mixed dataset of small RNA sequencing consisting of a total of 30 samples that were made by mixing HS-5 fibroblast cells with either wildtype or Dicer1 knockout HCT116 colorectal cancer cells. The tumor and fibroblast cell lines were mixed at 5 different proportions, to simulate a broad spectrum of tumor/nontumor cell mixing scenarios, with three independent replicates generated at each mixing ratio. DeMixMir demonstrated high accuracy in estimating the tumor-specific miRNA proportions in both the wildtype and the Dicer1 knockout mixtures. We further calculated tumor cell total miRNA content using DeMixMir output. Our proof-of-concept study suggests estimating tumor cell total miRNA content across tumor tissues at scale is feasible and likely valuable for advancing understanding of the complex roles miRNAs play in the cancer ecosystem.

#3774

MiR-34b promotes cellular senescence and ROS generation in human cervical cancer cells

K J Sindhu, Devarajan Karunagaran. *Indian Institute of Technology Madras (IIT Madras), Chennai, India*

Background: Cervical cancer is one of the most common cancers in women worldwide, particularly in low- and middle-income countries. Due to low surveillance and late detection, it is one of the major health issues leading to high mortality rates. MicroRNA-34 family (miR-34a, b, c) is thought to be tumor suppressive in several cancers but the mechanistic basis is not clear. Methods: Stable cell lines were generated with inducible hsa-miR-34b lentiviral vector from Dharmacon and maximal time and dose for induction of miR-34b with doxycycline were determined. Cell viability studies on HeLa, SiHa and C33A were investigated by MTT assay. Acridine orange/Ethidium bromide (AO/EB), senescence associated β-galactosidase (SA- β gal) assays for apoptosis and senescence and assessment of DNA damage (γH2AX) were performed. Total reactive oxygen species (ROS), superoxide, hydroxyl and peroxynitrite and H2O2 radicals were quantitated by DCFDA, DHE, HPF dyes and pHyper-dMito plasmid, respectively. Results: Overexpression of miR-34b reduced cell viability in cervical cancer cell lines except SiHa. Further investigation by AO/EB staining

revealed no significant increase in the proportion of apoptotic cells on overexpression of miR-34b. Analysis of SA- β gal on overexpression of miR-34b revealed an increase in the proportion of senescent population in all 3 cell lines. Increased DNA damage is also observed in agreement with an increase in cellular senescence. In addition, an increase in oxidative stress was observed in miR-34b overexpressing cell lines as total ROS was elevated in all 3 cell lines with increased superoxide, hydroxyl and peroxynitrite and H2O2 radicals in HeLa and C33A while SiHa showed increased levels of H2O2 radicals with no significant change in other radicals.
Conclusions: Overexpression of miR-34b can promote an increase in cellular senescence and oxidative stress in cervical cancer. The differential action in different cell lines may be due to the difference in expression of miR-34b in these cell lines. Our results highlight the potential of miR-34b to be used for therapeutic intervention in cervical cancer.

#3775

Multi-omic spatial analysis with simultaneous detection of small RNAs, mRNAs and proteins using the novel RNAscope™ Plus technology

Anushka Dikshit, Sayantani Basak, Sonali Deshpande, Manvir Sambhi, Li-Chong Wang, Maithreyan Srinivasan. *Bio-Techne Corporation, Newark, CA*

Regulatory RNA molecules such as microRNAs (miRNA) and long non-coding RNAs play critical roles in regulating translation of mRNA to protein. Several miRNAs have been implicated in disease initiation and progression, especially in cancer. The regulatory mechanisms of miRNAs and other small RNAs such as antisense oligos (ASOs) and silencing RNAs (siRNA) have been exploited to develop oligonucleotide therapies for 1. undruggable targets, 2. achieving longer-term effects 3. rapid production of therapeutics and 4. lower drug development costs. These therapeutics have the promise to treat debilitating neurodegenerative diseases, rare and inherited disorders. RNA therapies are typically delivered as a part of nanoparticles or a viral vector. Regardless of the delivery mechanism, methods to understand the biodistribution of the vector, transgene expression and cell type identification in a spatial context is crucial to study the safety and efficacy of these therapies. Built on the flagship RNAscope technology, the RNAscope Plus assay can detect 1 small RNA and 3 mRNA

targets using TSA-based fluorescent readouts and is compatible with the new fluorescent Vivid™ dyes . Fixed, fresh frozen samples and formalin fixed paraffin embedded (FFPE) tissues are supported by manual and automated workflows using the Leica Bond Rx system. We have leveraged this technology to investigate spatial expression profile of miRNA and associated RNA targets across different tissue types and applications. We can also combine protein detection using a target antibody to visualize cell-type specific markers. This assay was used to demonstrate expression of miRNAs and target genes implicated in tumor initiation, progression, and angiogenesis. Expression of miR-205 , associated tumor target genes such as *PanCK*, *PTEN* and tumor suppressor *TP53* was visualized in head and neck cancer tumors. Downregulation of tumor-suppressor, *TP53* resulted in upregulation of miR-205 which downregulates *PTEN* expression. *Pan-CK* stained the tumor region in the tissue. Similarly, miR-155 expression was observed in niche areas within breast cancer, head and neck cancer and cervical cancer tumors. Expression of miR-155 demonstrated correlation with high *VEGF* expression suggesting its role in angiogenesis. This novel platform will enable researchers to visualize regulatory RNA simultaneously with target RNAs, cell-type and morphology markers in intact cells/tissues with single cell resolution. This technology can provide meaningful insights into disease pathology driven by miRNAs as well as assess biodistribution and efficacy of oligonucleotide therapeutics.

#3776

Identification of hypoxia regulated long noncoding RNA, MARVEL in kidney cancer

Ranju Nair[1], Joseph Samuel[2], Philip Marsden[3]. *[1]Laboratory Medicine and Pathobiology, University of Toronto and St. Michael's Hospital, Toronto, ON, Canada,[2]Laboratory Medicine and Pathobiology, University of Toronto, Toronto, ON, Canada,[3]Laboratory Medicine and Pathobiology, and Department of Nephrology, University of Toronto and St. Michael's Hospital, Toronto, ON, Canada*

Background: The kidney is a highly vascular organ, receiving about 1/4th of the total cardiac output. Not surprisingly, kidney cancer is a highly vascular malignancy. According to WHO, worldwide, there are over 400,000 new cases and over 170,000 deaths yearly due to kidney cancer. The aggressive

subtype of kidney cancer, clear cell renal carcinoma (ccRCC), represents 80% of all cases. The Von Hippel Lindau (VHL) gene, a tumor suppressor, is functionally inactive in 90% of ccRCC, which activates the oxygen-sensing machinery responsible for inducing angiogenesis. Long noncoding RNAs (lncRNAs) are RNA molecules of 200 nucleotides and longer in size. LncRNAs can be highly tissue-specific, defining tumor growth and metastasis, hence potential biomarkers for clinical staging, disease progression, and unique therapeutic targets. We hypothesize that the functional inactivation of VHL induces robust changes in the lncRNA transcription during ccRCC tumorigenesis and vascularization.
Methodology: To understand the pro-angiogenic RNA signals in ccRCC induced by functional VHL inactivation, human 786-O and RCC4 cell lines were used. Microarray analysis comparing the reconstituted functional and non-functional VHL in these tumor cells then defined mRNA and lncRNAs that are VHL- and HIF-dependent. These lncRNAs were further validated in ccRCC patients. 5' RACE (Rapid Amplification of cDNA ends), RT-qPCR, and cellular compartmentalization were used to characterize the most abundant lncRNA in ccRCC.
Results: Microarray-based transcriptomic ccRCC from VHL-deficient cell lines and patients divulged a novel lncRNA- "MARVEL" (Mortality Associated in RCC, VHL-deficient Expressed Long Noncoding RNA). Analysis in The Atlas of Noncoding RNAs in Cancer (TANRIC) database for ccRCC patients with 447 tumor cases and 67 normal kidney tissues revealed MARVEL predicts overall patient survival by log-rank regression analysis with Cox $p < 0.005$ and correlated with a higher stage of the disease by the decision tree analysis. MARVEL is VHL-, hypoxia-, and HIF- dependent. ReMap, ChIP-seq data on HIF1 and HIF2 confirmed binding within 1 Kb upstream of the start site of MARVEL. 5' RACE characterized three transcriptional start sites and three spliced variants. The most abundant transcript of MARVEL has seven exons with six introns that follow the GT-AG rule of splicing. Further, CRISPRi and CRISPRa led loss- and gain-of-function studies on MARVEL are ongoing both *in vitro* and *in vivo* to characterize its role in tumorigenicity and angiogenesis.
Significance: This study defines tumor property of hypoxia and a functional outcome of survival in patients to define the lncRNAs. We identified a novel lncRNA- MARVEL that can be a potential biomarker to predict advanced tumor stage and overall survival in renal cell carcinoma. The

functional characterization of MARVEL can reveal its therapeutic potential in ccRCC.

#3777

MicroRNA-inducible CRISPR/Cas9 for cell type-specific genome regulation in cancer

Seung Ja Oh[1], Cheol-Hee Shin[2], Ji Min Lee[3], Juyong Lee[4], Su Chan Park[3]. *[1]Kyung Hee University, Yongin-si, Korea, Republic of,[2]Korea Institute of Science and Technology, Seoul, Korea, Republic of,[3]Korea Advanced Institute of Science and Technology, Daejeon, Korea, Republic of,[4]Seoul National University, Seoul, Korea, Republic of*

MicroRNA-dependent mRNA decay plays an important role in gene silencing by facilitating posttranscriptional and translational repression. Inspired by this intrinsic nature of microRNA-mediated mRNA cleavage, here, we describe a microRNA-targeting mRNA as a switch platform called mRNA bridge mimetics to regulate the translocation of proteins. We applied the mRNA bridge mimetics platform to Cas9 protein to confer it the ability to translocate into the nucleus via cleavage of the nuclear export signal called CRISPR Self Check-In. This system performed programmed gene editing in vitro and in vivo. Combinatorial treatment with cisplatin and miR-21-EZH2 axis-targeting CRISPR Self Check-In improved sensitivity to chemotherapeutic drugs in vivo. Using the endogenous microRNA mediated mRNA decay mechanism, our platform is able to remodel a cell's natural biology to allow the entry of precise drugs into the nucleus, devoid of non-specific translocation. The mRNA bridge mimetics strategy is promising for applications in which the reaction must be controlled via intracellular stimuli and modulates Cas9 proteins to ensure safe genome modification in diseased conditions.

#3778

Genome-Scale CRISPRa and CRISPRi screening for lncRNA drivers of prostate cancer progression

Simone Weiss[1], Allegra Lord[2], Bernhard Schmierer[2], Anne B. Rovsing[3], Emil A. Thomsen[3], Jacob G. Mikkelsen[3], Benedicte Ulhøi[4], Jakob S. Pedersen[1], Michael Borre[5], Karina D. Sørensen[1]. *[1]Department of Molecular*

Medicine, Aarhus University Hospital, Aarhus, Denmark,[2]CRISPR Functional Genomics, SciLifeLab and Department of Medical Biochemistry and Biophysics, Karolinska Institutet, Stockholm, Sweden,[3]Department of Biomedicine, Aarhus University, Aarhus, Denmark,[4]Department of Pathology, Aarhus University Hospital, Aarhus, Denmark,[5]Department of Urology, Aarhus University Hospital, Aarhus, Denmark

Background: Overtreatment of indolent prostate cancer (PC) and delayed treatment of aggressive PC is common due to suboptimal risk stratification tools, thus warranting identification of novel prognostic biomarkers. Although a few long non-coding RNAs (lncRNAs) with biomarker potential in PC are known, the majority of lncRNAs remain uncharacterized. Here, we aimed to identify novel lncRNA biomarker candidates. We hypothesized that strong candidates would have a functional role in driving PC progression in addition to their expression being linked to PC prognosis, and we therefore combined functional CRISPR screening with lncRNA expression profiling of PC patients.
Methods: Total RNA sequencing (RNAseq) data was generated from 31 adjacent normal (AN) and 125 tumor samples from 141 clinically localized PC patients, along with 17 primary tumor samples from metastatic PC patients. Raw reads were mapped to the hg38 reference genome and kallisto was used for quantification. CRISPR activating (CRISPRa) and CRISPR interference (CRISPRi) screens were performed in the LNCaP PC cell line stably expressing either dCas9-VP64 or dCas9-KRAB, respectively. Cells were transduced in duplicate with custom single guide RNA (sgRNA) libraries targeting 20,306 and 20,474 lncRNA transcripts of interest using 72,281 and 72,360 sgRNAs (CRISPRa and CRISPRi, respectively). Cells were harvested and DNA extracted from an early (day 4 post-transduction) and a late (day 17-21) timepoint and next-generation sequenced. MAGeCK was used for data analysis.
Results: To identify lncRNAs with biomarker potential in PC, we analyzed lncRNA expression in total RNAseq data from 158 PC patients. Using differential expression analysis and cox regression analysis with biochemical recurrence as endpoint, we identified 6,928 lncRNAs with biomarker potential. To investigate if any of these had a functional role in driving PC progression, we performed CRISPRa and CRISPRi screens to assess how lncRNA activation/inhibition affected PC cell proliferation.

Based on the screens, lncRNA candidates with the most prominent phenotypes (normalized read count difference >200 and log-fold change >33% between the early and late timepoint for ≥3 sgRNAs in both replicates) were selected for individual validation. This identified 7 (CRISPRa) and 8 (CRISPRi) negative hits (decreased cell proliferation) along with 5 (CRISPRa) and 2 (CRISPRi) positive hits (increased cell proliferation). Individually activated/inhibited LNCaP cell lines have been established for the 22 candidate lncRNAs and proliferation assays are performed to validate their functional role in PC progression.
Conclusion: We identified numerous lncRNAs with biomarker potential and a possible driver role in PC progression.

#3779

Evaluation of anti-cancer efficacy of lipid nanoparticles containing siRNA against HPV16 E6 and E7 combined with cisplatin in xenograft model of cervical cancer

Sung Wan Kang[1], Shin-Wha Lee[2], Ji-young Lee[1], Ok Ju Kang[2], Hyejeong Kim[3], Yisak Kim[4], Yong-Man Kim[2]. *[1]Asan Institute for Life Science, Seoul, Korea, Republic of,[2]Obstetrics and Gynecology, Asan Medical Center, University of Ulsan College of Medicine, Seoul, Korea, Republic of,[3]EnhancedBio Inc., Seoul, Korea, Republic of,[4]Enhancedbio Inc., Seoul, Korea, Republic of*

Background**:** High-risk human papillomavirus (HPV) type 16 is the major etiological agent found in more than 60% of patients with cervical cancer and associated with cancer development and progression. Persistent expression HPV E6 and E7 oncoproteins are essential for the initiation and maintenance of cervical cancer. The therapeutic approaches targeting HPV E6 and E7 have been proved to be highly efficient in killing malignant cells. The suppression of HPV 16 E6/E7 expression by the short interfering RNA (siRNA) was more effective in combination therapy with cisplatin (CDDP) for cervical cancer. ENB101-LNP is an ionizable lipid nanoparticles (LNPs) encapsulating siRNA against E6/E7 of HPV 16 for delivery to the tumor cells.
Methods: To investigate the anticancer efficacy and mechanism of ENB101-LNP combined with cisplatin in cervical cancer; the xenograft model was generated by the injection of CaSki cells subcutaneously into

BALB/c nude mice. Mice were randomly divided into six groups: 1) blank control; 2) 1mg/kg ENB101-LNP; 3) 3mg/kg ENB101-LNP; 4) CDDP; 5) 1mg/kg ENB101-LNP-CDDP; 6) 3mg/kg ENB101-LNP-CDDP. ENB101-LNP was treated with intravenous injection three times weekly for 3 weeks and CDDP was treated with IP injection once a week for 3 weeks. Tumor growth curves were plotted to calculate the tumor inhibition rate. Mice were sacrificed one week after the last treatment and the tumor tissues were investigated using histopathology, immunohistochemical staining and western blotting.
Results: Compared with the control and the other treatment groups, the tumor growth was significantly inhibited ($P < 0.05$). The tumor inhibition rate was 29.7% in 1mg/kg ENB101-LNP group, 29.6% in 3mg/kg ENB101-LNP group, 34.0% in CDDP group, 47.0% in 1mg/kg ENB101-LNP-CDDP group. At the dose of 3mg ENB101-LNP/kg combined with CDDP exhibited superior antitumor efficacy, the tumor inhibition rate was 68.8%. The successful ENB101-LNP mediated knockdown (with up to 80%) of HPV16 E6/E7 in tumors of both 1mg/kg and 3mg/kg groups was confirmed by RT-PCR. The ENB101-LNP increased p53 and p21 expression in tumors compared to control and CDDP alone groups and combination treatment with CDDP showed decreased expression of PD-L1 expression compared to CDDP alone group. The treatment of ENB101-LNP and combination with CDDP showed significant increase in apoptotic cells compared to control and single-agent groups respectively.
Conclusions: The ENB101-LNP inhibiting E6 and E7 of HPV 16 in combination with CDDP showed promising anticancer activity in the cervical cancer cells xenograft mouse model.

#3780
Reciprocal regulation between DNA methyl transferase 3A and 3B and microRNAs 299-3p and -30e are the causal factors for down regulation of microRNAs targeting androgen receptors in prostate cancer
Kavya Ganapathy[1], Christian Harrs[1], Samuel Harris[1], Ayman Khatib[1], Jong Park[2], Ratna Chakrabarti[1]. *[1]University of Central Florida, Orlando, FL,[2]Moffitt Cancer Center, Tampa, FL*

Promoter hypermethylation is one of the events that downregulate microRNAs (miRNA), resulting in differential expression of genes and

progression of cancer. Previously we showed down-regulation of two miRNAs, miR-299-3p and -30e that target androgen receptor (AR) in advanced prostate cancer (PCa), and their function as tumor suppressors. In this study, we examined the contributing events for the loss of expression of these miRNAs and if the expression varies in PCa tissues and cells from racially disparate group of patients. To test whether promoter hypermethylation is one of the reasons, we examined the effect of treatment of DNA methyl transferase (DNMT) inhibitor 5-Aza-2'-deoxycytidine (Aza-C) on expression of these miRNAs in PCa cells. We noted that the expression of miRs-299-3p, -30e and -34c, another AR-targeting miRNA can be restored in PCa cells upon Aza-C treatment, which suggests that promoter hypermethylation is possibly responsible for down regulation of these miRNAs. We noted that miR- miR-299-3p, -34c and -30e are differentially expressed in PCa tissues and cells from African American (AA) and European American (CA) patients. Through bisulfite sequencing, we showed differential promoter methylation of *mir-34c and -299-3p* genes in PCa cell lines from AA and CA origins, which can be reversed through treatment with Aza-C. Differential expression and activities of DNMT3A and DNMT3B were also noted in PCa cells. Analysis of miRNA target prediction databases suggested that both miRs-299-3p and -30e have one or more binding sites at the 3'UTRs of DNMT3A and DNMT3B, which was confirmed by luciferase reporter assays. Interaction of these DNMTs with miR-299-3p was further established by Argonaut (Ago)-2-based RNAIP using induced C4-2B PCa cells overexpressing miR-299-3p. Interaction of miR-30e with these DNMTs was also confirmed by transfection of biotinylated miRNA mimic and streptavidin-based RNA pulldown assays. Overexpression of miRs-299-3p and -30e in PCa cells downregulated expression of mRNAs and proteins, and the activity of DNMTs. Ectopic expression of miR-299-3p restored expression of miR-34c and -30e in PCa cells. Similarly, overexpression of miR-30e restored expression of miR-34c and -299-3p. These observations confirmed that the increased expression of miRs-30e or -299-3p overcomes the loss of expression of miRNAs including miRs-299-3p and -34c, which is potentially mediated by DNMT induced promoter hypermethylation. This study established a reciprocal regulatory loop of AR targeting miRNAs and DNMTs in PCa cells and provides a mechanistic insight into the aberrant expression of AR in

advanced PCa as a result of down regulation of miRs-299-3p, -34c and -30e and stabilization of expression and activities of DNMTs.

#3781

NF-κB classical and alternative signaling differentially regulate miRNA expression in ovarian cancer

Rahul D. Kamdar[1], Brittney S. Harrington[1], Soumya Korrapati[1], Emma Attar[2], Nathan Wong[1], Carrie D. House[3], Christina M. Annunziata[1].
[1]National Cancer Institute, Bethesda, MD,[2]Colgate University, Hamilton, NY,[3]Department of Biology, San Diego State University, San Diego, CA

The NF-κB signaling pathway has been shown to contribute to epithelial ovarian cancer (EOC) through its classical and alternative pathways, characterized by the RelA and RelB transcription factors respectively. Previous studies have highlighted the role of RelA in sustaining the proliferative cancer cell population, while RelB aids in promoting the survival of chemoresistant, stem-like tumor-initiating cells (TICs) that promote disease relapse. In further characterizing the downstream effects of NF-κB signaling on EOC, we hypothesize NF-κB signaling differentially regulates the expression of several microRNAs (miRNAs) to promote TIC survival and proliferation through its classical and alternative pathways. miRNAs comprise a subset of small, noncoding RNAs that regulate gene expression, making them amenable for therapeutic targeting. Inducible shRNA stably expressed in OV90 EOC cells to knockdown RelA or RelB were analyzed by miR-seq to identify the differential expression of miRNAs in cells grown in TIC vs adherent (adh) conditions. Several miRNAs were differentially expressed in these conditions with RelA or RelB knockdown; we identified and validated the expression of two candidate miRNAs: hsa-miR-452-5p and hsa-miR-335-5p. We observed the decreased expression of hsa-miR-452-5p when either RelA or RelB is knocked down, while also observing the increased expression of hsa-miR-335-5p when RelA is knocked down. By inhibiting miR-452-5p in conjunction with disrupting NF-κB activity, we found changes in cell viability, sphere formation, and expression of the stem cell marker ALDH. Understanding the role of miRNA signaling in the context of NF-κB will better define the transcriptional roles of RelA and RelB in EOC. Ongoing

work will further characterize the downstream targets of these miRNAs as potential therapeutic targets.

#3782

Targeting cancer cells using folate conjugated to a fully modified version of miR-34a (FolamiR-34a) to produce enhanced and sustained anti-tumor activity

Shreyas Ganesan Iyer[1], Ahmed M. Abdelaal[1], Ikjot Singh Sohal[1], Sudarsan R. Kasireddy[2], Andrea L. Kasinski[1]. *[1]Department of Biological Sciences, Purdue University, West Lafayette, IN,[2]Purdue University, West Lafayette, IN*

Due to the pleiotropic nature of miR-34a, including its ability to downregulate multiple genes that drive resistance to currently used anti-cancer therapies, we hypothesize that the best use of miR-34a in a clinical setting would be in combination with standard-of-care treatments. For *in vivo* use, such a molecule would necessitate the following: i) a stabilized version of miR-34a that can withstand the harsh environment in circulation and intracellular nucleases, and ii) a robust, specific, and safe delivery vehicle. With regard to stability, we successfully generated the first fully modified version of miR-34a. This new chemically modified molecule is over 400-fold more stable than the previously used partially modified version and induces enhanced and sustained target gene repression. To assess *in vivo* activity of fully modified miR-34a requires a suitable delivery vehicle. Indeed, while various approaches have been used to restore miR-34a in tumors, clinically relevant mechanisms for delivery of miR-34a have been a challenge due to poor tumor uptake, unfavorable bioavailability, and unwanted toxicity. Previously, we determined that a partially modified version of miR-34a can be delivered specifically and robustly to cancer cells in a targeted, vehicle-free manner through direct conjugation to folate, a ligand of the high-affinity folate receptors. Thus, we conjugated our fully modified miR-34a (FM-miR-34a) to folate generating FM-FolamiR-34a. Following *in vivo* delivery of FM-FolamiR-34a to mice with breast cancer xenografts we observed enhanced and sustained target gene repression, in comparison to our first-generation partially modified folate-miR-34a conjugate (FolamiR). Critical miR-34a target genes involved in promoting resistance, including MET, AXL, and CD44 were downregulated over 90%

for at least 120 hours following a single 1.5 nmol dose of FM-FolamiR-34a. Our final objective is to evaluate FM-FolamiR-34a in combination with standard-of-care agents *in vivo*.

#3783

Role of microRNA 28-3p in prostate cancer progression

Amritha Sreekumar, Sharanjot Saini. *Augusta University, Augusta, GA*

Prostate cancer (PCa) is a leading cause of cancer incidence and mortality among men. Prostate cancer is driven by androgens acting via androgen receptor (AR). Therefore, this cancer is treated with androgen deprivation therapy (ADT) initially. However, the cancer rapidly evolves to be resistant to ADT and progresses to a more invasive stage referred to as 'Castration Resistant prostate cancer' (CRPC). CRPC is treated with second generation of AR pathway inhibitors such as Enzalutamide and Abiraterone. These treatments are effective initially. However, drug resistance develops in a significant fraction of patients and the cancer undergoes 'neuroendocrine trans-differentiation (NED) to a lethal variant called 'neuroendocrine prostate cancer' (NEPC). As a result of NED, PCa cells express neuronal markers such as synaptophysin, chromogranin A and enolase. The molecular basis of NED is not yet fully defined. With a focus on identifying the role of microRNAs (miRNAs) in NEPC, we performed small RNA sequencing in CRPC tumors with and without NED. This sequencing identified miR-28-3p to be significantly downregulated in CRPC-NE samples as compared to CRPC-adenocarcinomas (CRPC-Adeno). In view of this, we examined the role of this miRNA in NEPC. Analyses of TCGA data of prostate adenocarcinomas suggest that miR 28-3p has an oncogenic role in primary prostate tumors. However, its expression declines in tumors with increasing Gleason score. We profiled the expression of miR-28-3p in patient-derived xenograft models and clinical CRPC-NE and CRPC-Adeno tissues by real time PCR. Our profiling showed a trend towards downregulation with increased NED. Basal expression of miR 28-3p in various prostate cancer cell lines showed an elevated level in androgen dependent cell lines whereas significantly less expression in NEPC cell lines, LASCPC-01 and NCI-H660. In this study, we generated PC3 cell line that stably expresses miR-28 for understanding its functional role in regulating PCa. Preliminary functional assays including cell viability assay,

cell cycle studies and invasion and migration assay suggest a tumor suppressor role of miR-28-3p in advanced prostate cancer. In conclusion, our data shows that miR 28-3p potentially has a biphasic role in PCa, where it is oncogenic in early stages and acts as a tumor suppressor in late stage PCa.

#3784

miR-489 induces apoptosis and immunogenic cell death through targeting FOXM1 in triple negative breast cancer cells

Gourab Gupta, Ryan Titus, Yogin Patel, Shakthika Sarvanan, Hexin Chen.
Biological Science, University of South Carolina, Columbia, SC

It has been well established that microRNAs (miRNAs) have an important role in cancer sustenance and progression. Our previous studies have established the role of miR-489 as a tumor suppressor miRNA in breast cancer. However, the multiple targets of this miRNA have diversified its mechanism from preventing tumor cell proliferation to promoting cell death pathways. In this study we have aimed to establish the role of miR-489 in cell cycle inhibition, leading to Endoplasmic Reticulum stress (ER stress) and ultimately immunogenic cell death (ICD). Firstly, we found that overexpression of miR-489 in triple negative breast cancer (TNBC) cell lines including MDA-MB-231, BT 549, drastically reduced cell proliferation using colony formation assay and real-time cell analysis. Furthermore, studies like GO analysis, sequence analysis and cell cycle analysis demonstrated that miR-489 induces cell cycle arrest and apoptosis in TNBC by directly targeting FOXM1 and regulating other kinases like CDK1. It was also shown for the first time that miR-489 overexpression induces ER stress and the release of damage associated molecular patterns (DAMPs), consistent with hallmarks of ICD like Calreticulin exposure on cellular surface and ATP release, triggering phagocytosis. It was also established that miR-489-induced apoptosis lead to the elevation of cleaved caspase 3, which was responsible for the activation of PANX1 and the consequent release of ATP. In conclusion, we tried to mechanistically understand the role of miR-489 in cell cycle arrest leading to cellular stress. Stress induced apoptosis and consequent ICD was also a possible outcome and it turned out miR-489 overexpression without any other ICD inducer

was good enough to trigger the release of DAMPs and elucidate an immunogenic response.

#3785

Telomerase RNA component lncRNA regulates hsa-miR-320 family and promotes prostate cancer metastasis

Mandisa Mbeje[1], Jeyalakshmi Kandhavelu[2], Clement Penny[3], Zodwa Dlamini[1], Rahaba Marima[1]. *[1]University of Pretoria, Pretoria, South Africa,[2]Georgetown University Medical Center, Washington, DC, WA,[3]University of the Witwatersrand, Johannesburg, South Africa*

Telomerase RNA component (TERC) is a long non-coding (lncRNA) associated with prostate cancer progression and has novel prognostic biomarker potential. Differential methylation patterns of lncRNAs affect their expression levels, leading to cancer. This study aimed to profile and elucidate differential lncRNA expression patterns in prostate cancer (PCa). A 384-well plate of PCa associated lncRNA gene array panel was used in castration resistant PC-3 PCa cells vs androgen-sensitive PCa LNCaP cells. Annotation and enrichment analysis of lncRNA differential gene expression was performed using a human lncRNA sets database, LncSEA. Furthermore, digital droplet PCR (ddPCR) was used to verify the PCR array results. Up or down-regulation of ±2 and $p < 0.05$ were considered significant. Decreased hsa-miR-320 gene family expression has been reported in various tumors including PCa. However, the precise mechanisms of hsa-miR-320 gene family in PCa remain to be elucidated. Thirty six of 84 lncRNAs were shown to be upregulated, while 14% of the lncRNA genes were downregulated. Notably, TERC lncRNA was upregulated in high metastatic PC-3 cells. Hypermethylation patterns of this lncRNA in high metastatic PC-3 cells was also shown by enrichment analysis. Furthermore, TERC lncRNA was demonstrated to regulate the hsa-miR-320 family, suggesting a correlation between TERC hypermethylation and downregulation of hsa-miR-320 gene family expression in PCa, as revealed by bioinformatics analysis. TERC lncRNA promotes PCa cell proliferation, migration, invasion and metastasis by sponging hsa-miR-320 family. This TERC/hsa-miR-320 interaction holds potential to understanding PCa prognostic mechanisms by lncRNAs and may also be targeted for novel therapeutics.

#3786

In vivo miR-449b mimic-based nanotherapy suppresses growth and progression of triple-negative breast cancer

Goknur Kara, Bulent Ozpolat. *Houston Methodist Research Institute, Houston, TX*

Triple-negative breast cancer (TNBC) comprises 15-20% of breast cancers and is associated with an aggressive course and the highest mortality rate in all breast cancer subtypes owing to high rates of early metastasis recurrence, and a low response to adjuvant chemotherapy. Currently, there is no effective targeted therapy strategy for TNBC due to significant genetic heterogeneity and a lack of defined molecular targets. Recent evidence from our and other laboratories revealed that non-coding RNAs such as tumor suppressor microRNAs (miRNAs) are dysregulated in cancer cells by regulating the expression of target genes (mRNAs) that are involved in critical cellular processes such as cell cycle, proliferation, differentiation, and migration/invasion, drug resistance, and tumor growth. Analyzing the TCGA-patient database, we recently found that reduced miR-449b expression was associated with significantly shorter survival in TNBC patients (n=56 patients with high expression, n=41 patients with low expression, p=0.0011). Our studies revealed that miR449b expression is reduced in TNBC cell lines and its ectopic expression using commercially available transfection reagent inhibited TNBC cell proliferation, migration, and invasion. Since in vivo delivery of miRNA therapeutics has been challenging, we developed magnetic nanoparticles for miR-449b delivery which inhibited in vitro cell proliferation, invasion, and migration. To elucidate molecular mechanisms underlying miR-449b-induced tumor suppressive effects, we investigated potential targets of miR449b using several target prediction algorithms and found that miR-449b has binding sites in the 3'-UTR of the proto-oncogene, eukaryotic elongation factor-2 kinase (eEF2K) gene. We demonstrated eEF2K expression is highly upregulated in TNBC cell lines and eEF2K expression correlates with shorter overall survival in patients with TNBC. More importantly, eEF2K expression was markedly inhibited after ectopic expression of miR-449b in TNBC cells. TNBC cells were also treated with siRNAs specific for eEF2K which led to reduced cell growth and invasion/migration, recapitulating the

effects of miR-449b expression Furthermore, in vivo administration of miR-449b-loaded magnetic nanoparticles (0.6 mg/kg once a week in TNBC orthotopic xenograft models (MDA-MB-231) in mice resulted in significant inhibition of eEF2K and tumor growth. Additionally, magnetic nanoparticles-miR-449b treatment in mice did not cause detectable side effects. These findings suggest that miR-449b functions as a tumor suppressor by targeting eEF2K-mediated oncogenic signaling leading to the tumor growth and progression of TNBC. Taken together, our study suggests that the miR-449 nanotherapy using magnetic nanoparticles may be a promising therapeutic strategy that provides a safe and effective antitumor efficacy against TNBC.

#3787

miR 2355-5p regulates tumor growth and angiogenesis in VHL-inactivated clear cell renal cell carcinoma

Patric Page[1], Sandra Turcotte[1], Mykella Martin[1], Patrick Richard[2], Tamiko Nishimura[3], Yasser Riazalhosseini[3]. *[1]Chemistry and Biochemistry, Université de Moncton, Moncton, NB, Canada,[2]Université de Sherbrooke, Sherbrooke, QC, Canada,[3]McGill University, Montreal, QC, Canada*

Background: Clear Cell Renal Cell Carcinoma (ccRCC) constitutes more than 75% of kidney cancer diagnostics. Inactivation of the tumor suppressor gene termed von Hippel-Lindau (VHL) is considered the major truncal event and occurs in more than 85% of patients. The most notable role of VHL is its ability to negatively regulate the Hypoxia-Induced Factors (HIFα), which in turn, stimulate the transcription of multiple oncogenes, including microRNAs (miRNAs). MiRNAs are small non-coding RNAs that negatively regulate gene expression through complementary base pairing. Using ccRCC cell models, we observed an overexpression of the miR 2355-5p following the loss of VHL in a HIF2α dependent manner. Hypothesis: We hypothesize that the miR 2355-5p overexpression is involved in the tumorigenesis of VHL-inactivated ccRCC. Our specific aims are to i) quantify the expression of miR 2355-5p in ccRCC clinical samples, ii) characterize the functional impact of miR 2355-5p in ccRCC development, and iii) identify miR 2355-5p targeted genes in ccRCC tumors.

Methods: Clinical samples (tissues and plasma) from consented patients with ccRCC were recruited through the Université de Sherbrooke. Normal adjacent tissue and plasma from healthy individuals were used as controls. miR 2355-5p expression was quantified through RT-qPCR with Taqman probes. Then, 786-0 and A498 VHL-deficient ccRCC cell lines were used. miR 2355-5p knockout models (KO) were generated using CRISPR/cas9 technology or stably overexpressed using miRNA precursor plasmid (786-0++2355). The impact on cell survival and proliferation was assessed with clonogenic assay and daily cell counts, respectively. Furthermore, cell models were injected into immunodeficient mice. Angiogenesis was evaluated by tube formation assay and angiogenesis proteome profiler kit. Finally, miRNA pulldown was performed to identify miR 2355-5p potential targets.
Results: Our findings showed a significant increase in miR 2355-5p expression in tumor tissue compared to normal adjacent tissue as well as in plasma samples compared to healthy individuals. Inhibition of miR 2355-5p significantly reduced cell survival and cell proliferation *in vitro* and *in vivo*. Altered expression of the miRNA also disturbed the expression of multiple angiogenic factors and reduced the ability of cells to stimulate tube formation. MiRNA pulldown identified over 267 potential targets, where 161 were mRNA coding for functioning proteins. Close to 80% of identified proteins were direct targets of miR 2355-5p according to prediction software. Further analysis showed an inverse correlation between the tumor suppressor gene SPRY4 and miR 2355-5p, uncovering a potential link between the two.
Discussion: Our results demonstrate an important role of miR 2355-5p on angiogenesis and ccRCC tumor growth. Further research on the interaction between miR-2355-5p, BTG2, SLIT2, and CMTM4 could unlock new potential avenues for targeted therapies.

#3788

Profiling of microRNAs in androgen independent prostate cancer cells

Shashwat Sharad, Hua Li. *Murtha Cancer Center, Department of Surgery, USUHS, Center for Prostate Disease Research (CDPR), Bethesda, MD*

Introducti**on:** Short noncoding microRNAs (miRNAs) function as tumor suppressors or oncogenes playing important roles in tumorigenesis and

metastasis. In prostate cancer, the studies had indicated the potential roles of miRNA as biomarkers for earlier detection, diagnosis, prognosis evaluation and therapy targets. The castration resistance and metastasis remain the major challenges for the administration of prostate cancer patients, and the underlying biology is still not fully understood. Here, we reported the comparative profiling of miRNAs in hormone dependent and independent prostate cancer cells, aiming to identify novel miRNAs for monitoring aggressive disease progression and therapy targets.

Methods: The hormone sensitive LNCaP cells, and androgen independent C42B and PC3 cells were used to miRNA sequencing. The miRNA sequencing libraries were prepared with NanoDrop ND-1000. The DNA fragments were denatured to generate single-stranded DNA molecules and amplified in situ with TruSeq Rapid SR Cluster kit. Sequencing was performed using the Illumina NextSeq 500. Raw sequencing data passing the Illumina chastity filter were used for further analysis. Trimmed reads were aligned to reference genome with bowtie software. The expression levels of miRNAs were calculated using mirdeep2. Differentially expressed miRNAs analysis were performed with R package edgeR. miRNA target prediction was filtered based on miRNA Target databases. The analysis of Gene Oncology (GO) enrichment and Kyoto Encyclopedia of Genes and Genomes (KEGG) pathway were further conducted for miRNA biological function assessments.

Results: Among 777 known miRNAs, high expression (CPM>30) of 356, 325 and 358 miRNAs were detected in LNCaP, C42B and PC3 cells, respectively. No expression (CPM=0) of 93, 114 and 75 miRNAs were detected in LNCaP, C42B and PC3 cells, respectively. Only miR-1247-3p was detected with high expression in LNCaP cells but no expression in C42B cells. Furthermore, there were 19 miRNAs with high expression in PC3 cells, and 20 miRNAs with high expression in PC3 cells but no expression in C42B cells including miR-125b-1-3p, miR-181a-3p, miR-31-3p, miR-1247-3p and miR-873-5p. In contrast, only 5 miRNAs with high expression in LNCaP cells and 7 miRNAs with high expression in C42B cells but not detectable in PC3 cells such as miR-141-5p. Pathway analysis further revealed that the miRNA regulated pathway of TGF-β, Hippo and Wnt were activated and the pathway of FoxO, P53, MAPK and Hedgehog were suppressed in C42B cells compared to LNCaP cells. Similarly, the

pathway of HIF-1 was activated and the pathways of PI3K-Akt, ErbB and GnRH were inhibited in PC3 cells.
Conclusion: The sequencing of miRNA of hormone dependent and independent prostate cancer cells generated the distinct miRNA signatures which granted further validation in human prostate cancer samples and underlying biology study in aggressive disease progression.

#3789
Circular RNA expression is enriched in breast cancer extracellular vesicles and is associated with chemotherapy resistance
Harrison Ngue[1], Jitendra Shrestha[2], Hyejin Kim[2], Shobha Vasudevan[2].
[1]Harvard University, Cambridge, MA,[2]Massachusetts General Hospital Cancer Center, Harvard Medical School, Boston, MA

Up to 90% of failures in chemotherapy treatment are associated with metastatic-related drug resistance. Extracellular vesicles (EVs) are believed to play a role in the spread of chemotherapy resistance through the horizontal transfer of oncoproteins and noncoding RNA species, but the underlying mechanisms for this are not fully understood. Here, we study EV biogenesis, release, and uptake in the context of breast cancer chemoresistance. Specifically, we characterized the bioactive cargoes in EVs secreted by chemoresistant triple negative breast cancer cells and chemoresistant estrogen receptor-positive breast cancer cell lines. Preliminary data show that these EVs contain unusually high levels of circular RNAs, small RNA species formed covalently through backsplicing and are typically noncoding. When chemosensitive cells absorb these circRNA-enriched EVs, they experience a significant increase in resistance phenotypes. Moreover, knockdown of the circRNAs via antisense oligonucleotides results in decreased chemoresistance, suggesting a role of circRNAs in the development of chemotherapy resistance. Previous studies have shown that tumor-derived exosomal circRNAs may confer resistance by sponging microRNAs. We are exploring what the circRNAs do mechanistically to promote tumor survival, and clarifying these mechanisms as a whole will serve to potentially provide therapeutic targets against chemotherapy resistance and cancer recurrence.

Non-coding RNAs in Gastrointestinal, Blood, and Bone Marrow Cancers

#3793

Regulation of miR-124 expression by promoter methylation in CRC and its relationship with KITENIN expression

So-Yeon Park, Rui Zhou, Chathurika D. B. Gamage, Sultan Pulat, Mücahit Varlı, Hangun Kim. *Sunchon National University, College of Pharmacy and Research Institute of Life and Pharmaceutical Sciences, Sunchon, Korea, Republic of*

The mechanisms that regulate microRNA expression in cancer are not fully understood. However, recently reported data show that the epigenetic mechanism plays an important role in the regulation of microRNA expression. In in this study, we investigated the relationship between miR-124 promoter methylation and target genes in CRC. The expression of miR-124 was increased by Aza treatment and the expression of KITENIN was decreased in CRC cells. First, we examined the methylation status of miR-124 promoter in two normal cell lines and seven CRC cell lines using pyrosequencing assay. As a result, miR-124 promoter was hypermethylated in CRC cells and low in normal cells. Next, we evaluated the DNA methylation status for a miR-124 promoter in paired colorectal normal tissues and colorectal cancer tissues specimens from 10 patients. Overall, methylation of the miR-124 promoter was high in cancer among clinical tissues, and the expression of miR-124 was low in cancer tissues. The expression of the KITENIN was also higher in cancer tissues than in normal tissues. These results prove that DNA hypermethylation contributes to the transcriptional down-regulation of miR-124 in colon cancer, and that the epigenetic silencing of miR-124 in cancer cells modulate the activity of KITENIN. Our findings provide basic data that can be useful for clinical treatment of CRC patients through the mechanism of miR-124 regulation identified as a regulator of KITENIN.

#3794

Sensitive detection of microRNA biomarkers of pancreatic cancer using one-pot endonucleolytically exponentiated rolling circle amplification by CRISPR-Cas12a

He Yan, Song Han, Steven Hughes, Yong Zeng. *University of Florida, Gainesville, FL*

While miRNAs offer a promising source for developing diagnostic cancer biomarkers, the progress towards clinical utilities remains largely limited, due in part to the long-standing challenge in sensitive, specific, and robust detection of miRNAs in human biofluids. Emerging next-generation molecular technologies, such as the CRISPR-based methods, promise to transform nucleic acid testing. The prevailing strategy used in existing CRISPR-based methods is to orthogonally hyphenate two separate reactions for pre-amplification, e.g., rolling circle amplification (RCA), and amplicon detection by Cas12a/13a trans-cleavage in tandem. Thus, existing CRISPR-based miRNA assays require multiple manual steps and lack the analytical performance of the gold standard, RT-qPCR. Radically deviating from the existing strategies, we developed a one-step, one-pot isothermal miRNA assay termed "Endonucleolytically eXponenTiated Rolling circle Amplification with the dual-functional CRISPR-Cas12a" (EXTRA-CRISPR) for miRNA detection with RT-qPCR-like analytical performance, including high sensitivity with a single-digit fM detection limit, single-nucleotide specificity, and rapid and flexible turnaround (from 20 min to 3 h for the entire analysis depending on targets and samples). We adapted the EXTRA-CRISPR assay to quantifying miRNA biomarkers in extracellular vesicles (EVs), a major carrier of miRNAs in human biofluids, for liquid biopsy diagnosis of pancreatic ductal adenocarcinoma (PDAC). Using the EXTRA-CRISPR, we demonstrated highly sensitive and specific profiling of a panel of four miRNA markers (miR-21, miR-196a, miR-451a, and miR-1246) in plasma EVs (PDAC patients (n = 20) and healthy donors (n = 15)). Based on the individual EV-miRNA tests (AUC values ranging from 0.677 for miR-196a to 0.793 for miR-451a), an EV signature (EV-Sig) combining miR-21, miR-451a and miR-1246 was devised with a machine learning method to improve the diagnostic performance for PDAC (AUC = 0.853). The diagnostic performance of the EXTRA-CRSPR tests were

rigorously validated by parallel RT-qPCR analysis of the same clinical samples, and the RT-qPCR signature combining the three markers confers a similar AUC of 0.874 for PDAC detection. Overall, the analytical and diagnostic performance of our method were shown to be comparable with that of the commercial RT-qPCR assays, while greatly simplifying the analysis workflow. Therefore, we envision that our technology provides a promising tool to advance miRNA analysis and clinical marker development for liquid biopsy-based cancer diagnosis and prognosis. Moreover, this simple and robust assay permitted direct coupling with a 3D printed smartphone-based portable device and the lateral flow assay for signal readout, demonstrating its potential adaptability to low-cost point-of-care diagnostics.

#3795

Deciphering the *in vivo* roles of a novel long non-coding RNA in chronic lymphocytic leukemia and Richter syndrome

Swati Mohapatra[1], Erik Knutsen[2], Mihai Iurascu Gagea[3], Linda Fabris[1], George Adrian Calin[1]. *[1]Translational Molecular Pathology, The University of Texas MD Anderson Cancer Center, Houston, TX,[2]Department of Medical Biology, UiT The Arctic University of Norway, Tromsø, Norway,[3]The University of Texas MD Anderson Cancer Center, Houston, TX*

The ultraconserved regions (UCRs) are the genomic segments manifesting perfect conservation between the orthologous genomes of humans, rats, and mice that get transcribed into mono-exonic long non-coding RNAs (lncRNAs) known as transcribed ultraconserved regions (T-UCRs). Increasing evidence demonstrates the importance of T-UCRs in human cancers, however, their involvement in the pathogenesis of Chronic Lymphocytic Leukemia (CLL) is poorly understood. Our lab has recently identified a lncRNA transcribed from a UCR and named it TRUC-16 (Translational Regulatory UltraConserved gene affecting p16), which is overexpressed in CLL and correlates with treatment-free survival. We have developed a transgenic C57BL6 mouse model to overexpress TRUC-16 in B cells. We monitored the number and development of B cell subsets over time in peripheral blood and lymphoid organs (lymph nodes, spleen, and bone marrow), and performed immunophenotyping to assess clonality and

proportion of the cells considered to be the origin for CLL (i.e. B1 cells and IgM memory B cells that are CD5+). We followed mice survival (n=10 for each gender) and performed necropsy with histopathologic and immunophenotypic analysis. If blood sampling suggests developing a CLL-like state, we will monitor for evolution to Richter Syndrome by flow cytometry analysis and biochemistry markers. We have validated the TRUC-16 overexpression specific to the B-cell compartment in the mice cohorts and have observed lymphoma in several organs. Interestingly, TRUC-16 overexpressing mice showed significantly higher splenic weights compared to controls. The mice were found to develop adulthood lymphoma that we are now analyzing molecularly and phenotypically. We are planning to further characterize the subtype of lymphoma by utilizing specific diagnostic markers through immunohistochemistry and flow cytometry. This is the first-ever transgenic mice modeling overexpression of UCR in the context of cancer. Validation of the functional correlation between the TRUC-16 phenotype and CLL patients' clinical data will provide a valuable resource to pursue a multitude of preclinical studies to find targets that might help better understand the disease pathophysiology.

#3796

Exosomes enhance the radiation sensitivity via miR-6823-5p and modulate metastases in pancreatic cancer model

Ai Nakaoka[1], Makiko Nakahana[1], Sachiko Inubushi[2], Yasuyuki Shimizu[1], Kazuma Iwashita[1], Naritoshi Mukumoto[1], Kana Kobayashi[1], Takeaki Ishihara[1], Daisuke Miyawaki[1], Ryohei Sasaki[1]. *[1]Division of Radiation Oncology, Kobe University Graduate School of Medicine, Kobe, Japan,[2]Division of Breast Surgery, Kobe University Graduate School of Medicine, Kobe, Japan*

Introduction: Pancreatic cancer (PC) is believed to be a difficult disease because of its radio-resistance and metastases. Radiotherapy reported to modify tumor microenvironment (TME) and to affect PC progression. Exosomes containing such as microRNAs (miRNAs), messenger RNAs (mRNAs), and proteins of cells, play essential roles in cell-to-cell communications. However, characteristics and mechanisms for radiation responsive exosomes remain unclear. Here, we first report mechanisms of

exosomes-mediated radiation response and regulation in PC metastasis with focusing on intra/intercellular communications via miRNA.
Methods: MIAPaCa-2 cells, human pancreatic carcinoma, was used. To isolate exosomes, cell culture media was ultracentrifuged at 100,000 x g for 90 min at 4℃. Exosomes derived from non-irradiated culture media was named ‘0 Gy-Exo’ and those from irradiated with 5 Gy culture media is called ‘5 Gy-Exo’. Exosome sizes and features were evaluated by transmission electron microscopy (TEM). Intracellular reactive oxygen species (ROS) levels induced by exosomes and by X-ray irradiation were evaluated by the C-H_2DCF dye staining. To detect DNA damage, cells were fixed and stained by γ-H2AX antibody. The expression of superoxide dismutase 1 (SOD1) was evaluated by using immunoblots. Total RNA was extracted from 0 Gy-Exo and 5 Gy-Exo, and then comprehensive miRNA expression analysis was performed to analyze 2,565 human miRNA sequences. The Gene Expression Omnibus database (GSE163133) and the TargetScan were used for specific miRNAs identification. Living MIAPaCa-2 cells in the presence or absence of those exosomes were injected in the spleen of Balb/c nude mice to establish liver metastatic models. Eight weeks after the injection, mice were sacrificed, and then the spleen and the liver were harvested as a whole organ. H-E staining and immunohisitochemical analyses using S100A4 and SMAD4 antibodies were performed to detect liver metastases.
Results: Isolated exosomes were shaped in the form of closed, round vesicles with a diameter of 10~100 nm. Intracellular ROS levels and the numbers of γ-H2AX foci in the cells with 5 Gy-Exo were significantly increased compared to those the control (without adding exosomes, $p<0.01$). Intracellular SOD1 expression in the cells with the 5 Gy-Exo was decreased compared with that in the control. The miR-6823-5p was identified to have a complementary base sequence to SOD1. The average occupied proportions with MIAPaCa-2 cells in the liver was modulated according to those exosomes. The SMAD4 expression was highly observed in the liver and the spleen suggesting that the SMAD4 could be a useful marker of liver metastases.
Conclusion: Exosomes increased radiation sensitivity through increase of intracellular ROS levels via exosomal miRNAs and also could affect liver metastases in pancreatic cancer models.

#3797

Fecal miRNA profiles and gut metagenome composition in Lynch syndrome: results from a mouse model study and human subjects

Giulia Francescato[1], Giulio Ferrero[2], Marc Beltrà[2], Sonia Tarallo[1], Giulia Piaggeschi[1], Carla Di Battista[1], Antonio Francavilla[1], Carlijn Bruggeling[3], Fabio Penna[2], Barbara Pardini[1], Paola Costelli[2], Annemarie Boleij[4], Alessio Naccarati[1]. *[1]Italian Institute for Genomic Medicine (IIGM), Candiolo, Italy,[2]Department of Clinical and Biological Sciences, University of Turin, Turin, Italy,[3]Radboud Institute for Molecular Life Sciences (RIMLS), Radboud University Medical Center, Nijmegen, Netherlands,[4]Department of Pathology, Radboud Institute for Molecular Life Sciences (RIMLS), Radboud University Medical Center, Nijmegen, Netherlands*

Bsacground: Lynch Syndrome (LS) is an inherited cancer syndrome associated with an increased lifetime risk of colorectal cancer (CRC) and characterised by germline mutations in DNA mismatch repair (MMR) genes. Abnormalities in the function of MMR genes lead to errors during DNA replication, including microsatellite instability. Despite regular colonoscopies, up to 15% of LS patients still develop CRC. Gut microbiome, bowel inflammation, the environment and host genetic and epigenetic factors are involved in CRC development. In this sense, the concomitant analysis of stool host microRNA (miRNA) profiles and gut microbiome composition may arise to the identification of specific fecal markers in LS explaining the molecular basis for the development of cancer in these patients. PURPOSE: In the present study, the fecal miRNome and microbiome were characterized in a time progression in an *in vivo* model using a mismatch repair deficient mice model that recapitulates human LS. The main aim was to evaluate the changes and crosstalk of miRNAs released in the stool by the host and the microbial population residing in the gut during the carcinogenesis process induced in animals. Findings in mice were compared and correlated to data obtained from a cohort of human subjects affected by LS.

Methods: We used an *in vivo* model for LS based on a conditional knockout mouse with the tissue-specific inactivation of Msh2 ($Msh2^{LoxP}$) in the intestinal mucosa, combining $Msh2^{LoxP}$ allele with the Villin-Cre transgene ($VCMsh2^{LoxP}$). Stool from mice were collected at different time points (6, 9

and 12 months of age). Small RNA-sequencing (sRNA-seq) and shotgun metagenomics analyses were performed in stool from all samples. In concomitance, we collected 78 stool samples of clinically diagnosed LS subjects, at different follow up time. At the sampling, 36 resulted negative for colorectal adenomas/lesions, 12 were negative but with a previous history of lesions, 23 presented a neoplasia and 6 developed a lesion in the follow-up. Twenty-two stool samples from healthy subjects were used as controls.
Results: In mice, preliminary results from sRNA-seq and metagenomics analyses showed several dysregulated miRNAs and differential microbial relative abundances, either between *VCMsh2*^{loxP} and controls or at different time points. In humans, we identified 41 and 17 miRNAs respectively up- and downregulated in LS subjects who presented a lesion compared to those not having any lesion at follow-up. In the same comparison the metagenomic data showed significantly different microbial abundances, including those of *Eubacterium ramulus*.
Conclusions: This is the first study characterizing the concomitant alterations in microbial composition and host miRNome overtime in relation to the onset of cancerous/precancerous lesions due to LS.

#3798
lncRNA LIMp27 promotes p53-defective cancer pathogenesis
Ting La[1], Song Chen[2], Xiao Hong Zhao[1], Yuan Yuan Zhang[1], Yu Chen Feng[1], Xu Dong Zhang[1], Lei Jin[1]. *[1]University of Newcastle, Australia, Callaghan, Australia,[2]Zhengzhou University, Zhengzhou, China*

Inactivation of p53 occurs in approximately 50% of human cancers, where p53-mediated p21 activation is devoid and p27 becomes essential for the establishment of the G1/S checkpoint upon DNA damage. Here, we show that the E2F1-responsive lncRNA LIMp27 selectively represses p27 expression and promotes proliferation, tumorigenicity, and treatment resistance in p53-defective colon adenocarcinoma (COAD) cells. LIMp27 competes with p27 mRNA for binding to cytoplasmically localized hnRNA0, which otherwise stabilizes p27 mRNA, leading to cell cycle arrest at the G0/G1 phase. In response to DNA damage, LIMp27 is upregulated in both wild-type and p53-mutant COAD cells, whereas cytoplasmic hnRNPA0 is only increased in p53-mutant COAD cells due to

translocation from the nucleus. Moreover, high LIMp27 expression is associated with poor survival of p53-mutant but not wild-type p53 COAD patients. These results uncover a lncRNA mechanism that promotes p53-defective cancer pathogenesis and suggest that LIMp27 may constitute a target for the treatment of such cancers.

#3799

Regulation of p16-E2F1-CDK4/6 signaling by TRUC-16 ultraconserved long non-coding RNA

Linda Fabris[1], Erik Knutsen[2], Maria Teresa S. Bertilaccio[1], Steliana Calin[1], Recep Bayraktar[1], George T. Eisenhoffer[1], Leonard Girnita[3], George A. Calin[1]. *[1]UT MD Anderson Cancer Center, Houston, TX,[2]The Arctic University of Norway, Tromsø, Norway,[3]Karolinska Institutet, Stockholm, Sweden*

High phylogenetic conservation of genomic loci is a potential marker of essential biological functionality. Ultraconserved elements (UCEs) are DNA sequences entirely conserved through millions of years of evolution, but their functions are not well understood. Several long non-coding RNAs (lncRNAs) are transcribed from UCEs and play active roles in cancer development. Using a combination of *in vitro* and *in vivo* experiments with two animal models and 4 patient cohorts, we discovered several remarkable aspects of ultraconservation. Using a multi-step genetically defined carcinogenesis model, we identified one UCE, uc.206, and its associated overexpressed lncRNA *TRUC-16* as a regulator of cell proliferation in chronic lymphocytic leukemia (CLL). High levels of *TRUC-16* inhibit $p16^{INK4A}$ translation, causing increased proliferation through an E2F1-mediated mechanism in CLL patients, as well as in zebrafish and murine models. uc.206/*TRUC-16* function is extremely conserved throughout evolution. We found cell cycle-related effects of *TRUC-16* in both mice and zebrafish, in which we observed increased proliferation of blood cells after overexpression of the human *TRUC-16*. High levels of CDK4/6 consequent to *TRUC-16* overexpression and p16 decrease can be specifically targeted in both CLL and Richter's Transformation (RT), a rare but deadly consequence of CLL. Inhibition of CDK6 is a therapeutic option never tested in CLL, but in use for another type of B cell malignancy, such as the mantle cell lymphoma. Our results highlight the multifaceted contribution

of a UCE to human tumorigenesis and open new possibilities for the use of long-noncoding RNAs in cancer therapies.

#3800

The disruption of miR-125b-SLC1A5 cascade defines the oncogenicity and differential immune profile in oral carcinoma

Ying-Chieh Liu, So-Yu Liu, Yu-Cheng Lin, Chung-Ji Liu, Kuo-Wei Chang, Shu-Chun Lin. *National Yang Ming Chiao Tung University, Taipei, Taiwan*

Head and neck squamous carcinoma (HNSCC) including oral SCC (OSCC) is a worldwide malignancy that requires vigorous efforts for interception. The metabolic reprogramming sustains malignant tumor cells to overcome stressful microenvironments. As the glutamine is the one of the essential components which helps cells to erase reactive oxygen species and energy production, the increased uptake of glutamine is a common metabolic hallmark in cancers. Bioinformatic analysis of TCGA HNSCC datasets and RNAseq results in our cohort indicated that solute carrier family 1 member 5 (SLC1A5) is the most eminently dysregulated transporter member among the seven glutamate or neutral amino acid transporters in SLC1A family. This work identified that the knockdown of SLC1A5 expression decreased *in vitro* oncogenicity, xenografic tumorigenesis and glutamine uptake; increased oxidative stress, cell cycle arrest, and sensitivity to cisplatin and ferroptosis inducer in OSCC cells. By way of contrast, the upregulation of endogenous SLC1A5 expression mediated by CRISPR/dCas9 activation system drove the OSCC oncogenesis. The reporter assay and functional analysis demonstrated that suppressor miRNA miR-125b targeted and attenuated SLC1A5, while NEAT1 lncRNA sponged and ablated miR-125b-SLC1A5 axis. The analysis of TCGA and GEO datasets confirmed the concordant upregulation of NEAT1 and downregulation of miR-125b along with the SLC1A5 upregulation in tumors. Besides, SLC1A5 upregulation defined the worse HNSCC patient survival. In our tumor cohort, OSCC harboring higher SLC1A5 expression had lower CD4+ immune score, and higher scores in M0 and M1 macrophage. GSEA algorithm further deciphered that tumors having higher SLC1A5 expression manifested the repression in glycolysis, apoptosis and p53 signaling. This study concludes that the frequent disruption of NEAT1-miR-125b-SLC1A5

cascade modulates the pluripotent oncogenic activities, the treatment efficacy and the immune landscape in oral carcinoma.

#3801

Identification of circular RNAs associated with the ferroptosis of pancreatic cancer cells

Jessica Jazmin Pena Paladines, Shao Weng Wang, Chi Hin Wong, Yang Chao Chen. *The Chinese University of Hong Kong, Hong Kong, Hong Kong*

The five-year survival rate for pancreatic cancer patients is significantly low which is predominately due to the lack of early-detection biomarkers, and poor response to currently available treatments that include drug resistance development. Recent studies suggest cancer cells can be highly sensitive to a newly defined type of cell death, ferroptosis, which is related to the development of resistance to standard chemotherapy drugs for pancreatic cancer such as gemcitabine and 5-Fluorouracil. However, the role of circular RNAs (circRNAs) in ferroptosis remains largely unexplored. Hence, this project aims to identify circRNAs in ferroptosis to uncover further components and mechanisms, and potentially provide specific effective targets for anticancer therapies. To achieve this, different ferroptosis inducers were tested, where the cystine-depletion method demonstrated higher efficiency based on cell viability and ferroptosis markers such as iron and lipid peroxidation levels. This method was used to induce ferroptosis for 24 hours in pancreatic cancer cells for subsequent circRNA sequencing, and to establish a ferroptosis-resistant cell line. From the sequencing data, 31 differentially expressed (DE) circRNAs were obtained, and eight were selected for further validation. Three circRNAs; circPPP2R2B, circNDUFAB1, and circNLN, showed consistent differential expression in ferroptosis non-resistant (downregulated) and resistant (upregulated) cells after cystine-depletion treatment. The knockdown of these circRNAs decreased the viability, invasion, migration, and colony formation ability of PDAC cells. Simultaneously, lipid peroxidation and intracellular iron levels, which are ferroptosis markers, were increased. Additionally, bioinformatic analysis of these circRNAs demonstrated their possible interaction with proteins and miRNAs with reported ferroptosis-related functions. In summary, these findings suggest that circPPP2R2B,

circNDUFAB1, and circNLN may be critically involved in PDAC progression and the evasion of ferroptosis which supports the further investigation of their oncogenic and ferroptosis-related action mechanism to propose a potential target for anticancer therapies.

#3802

miR-199a and miR-199b stimulate the progression of diffuse gastric cancer through direct targeting of Frizzled-6

Jihye Park[1], Sieun Lee[1], Soon Auck Hong[2], Yoon Ho Ko[3], Young-Ho Ahn[1].
[1]Department of Molecular Medicine, Ewha Womans University College of Medicine, Seoul, Korea, Republic of,[2]Department of Pathology, Chung-Ang University College of Medicine, Seoul, Korea, Republic of,[3]Division of Oncology, The Catholic University of Korea, Seoul, Korea, Republic of

There is no pathological difference between early and advanced diffuse gastric cancer (DGC), particularly in the gastric mucosa. In this study, we tried to identify microRNAs (miRNAs) as diagnostic biomarkers that can differentiate between early and advanced DGC. miRNA expression profiling was performed by NanoString nCounter method in human DGC tumors. miR-199a and miR-199b (miR-199a/b) were particularly up-regulated in advanced DGC compared with early DGC. Ectopic expression of miR-199a/b accelerated growth, viability, and motility of SNU601, human GC cells, and expedited tumor development in a mouse xenograft model. miR-199a/b also inhibited cell adhesion. Through 3'-UTR luciferase assay, Frizzled-6 (FZD6) was confirmed as a direct target of miR-199a/b. siRNA-mediated depletion of FZD6 increased cell growth and motility and addback of FZD6 restored cell growth, motility, and adhesion. To explore their clinicopathological roles in patients, miR-199a/b levels were measured by in situ hybridization in human DGC tumor sections. High miR-199a/b was correlated with advanced lymphovascular invasion, advanced T stages, and lymph node metastasis. Collectively, miR-199a/b promote the progression of DGC via targeting FZD6. These results imply that miR-199a/b can be used as diagnostic and prognostic biomarkers of DGC.

#3803

The landscape of circular RNAs in metastatic colorectal cancer

Sidi Zhao, Amy Ly, Jacqueline L. Mudd, Emily B. Rozycki, Ghofran Othoum, Jingqin Luo, Ha X. Dang, Ryan C. Fields, Christopher A. Maher.
Washington University in St. Louis, St. Louis, MO

Colorectal cancer (CRC) is the most common gastrointestinal malignancy and a leading cause of cancer death in the U.S.. Approximately 50% of patients with CRC develop metastatic disease (mCRC) with an average 5-year survival rate of 13%. Circular RNAs (circRNAs), covalently closed RNA molecules produced from pre-mRNAs through backsplicing, have recently emerged as an important class of non-coding RNAs regulating CRC tumorigenesis and progression. In this study we established a comprehensive catalog of circRNAs in mCRC. To evaluate circRNAs in mCRC progression, total RNA-Seq was performed on 30 matched normal, primary, and distant metastatic samples from 14 mCRC patients. Additionally, the transcriptome of five CRC cell lines were sequenced to evaluate circRNAs expressed in cell lines. CircRNAs were identified and quantified using the number of backspliced reads, normalized against the total number of mapped reads. Differential expression (DE) analysis was performed to identify circRNAs deregulated between normal, primary, and metastatic tissues. Our analysis identified approximately 62,000 expressed circRNAs in mCRC including approximately 32,000 expressed in patients and 48,000 expressed in cell lines, originating from approximately 9200 linear genes. Approximately 42,000 circRNAs (67%) were unannotated when compared with the circRNA consortium MiOncoCirc annotation. DE analysis identified 376 circRNAs deregulated in CRC progression from normal to primary, and metastasis. A higher proportion of DE circRNAs (82%) was downregulated in primary or metastasis, consistent with earlier reports of lower circRNA concentration in tumor due to rapid cell cycles. Among DE circRNAs were the downregulation of circRNAs that have been known to suppress tumor proliferation, migration, and invasion in mCRC such as circSMARCA5, circFBXW7, and circSETD3, and the upregulation of circFIRRE, a circRNA known to promote tumor progression in osteosarcoma. A significant portion (37%) of deregulated circRNAs also had their parental linear genes found to be deregulated, suggesting parental gene regulation contributed to circRNA regulation. Interestingly, a large portion of circRNAs (63%) were found to be deregulated while their parental linear gene expression was unchanged, suggesting alternative

mechanisms of circRNA deregulation. Gene set enrichment analysis showed that linear genes co-deregulated with circRNAs were enriched in signatures of tumor progression including proliferation, epithelial mesenchymal transition, and metastasis, suggesting potential involvement of deregulated circRNAs in tumor progression. Through RNA sequencing of both patients and cell lines, we established a comprehensive compendium of circRNAs and identified those deregulated in mCRC. This provides a valuable resource for further experimental characterization of circRNAs function in mCRC progression.

#3804

Linear *PVT1* isoforms and circPVT1 regulate DNA damage response and immunological pathways in acute myeloid leukemia and have a potential role in the crosstalk between leukemic cells and the tumor microenvironment

Martina Ghetti[1], Lorenzo Ledda[1], Ivan Vannini[1], Eugenio Fonzi[1], Maria Teresa Bochicchio[1], Tristan Cardon[2], Andrea Ghelli Luserna di Rorà[3], Matteo Paganelli[1], Chiara Servili[1], Francesco Fabbri[1], Sabina Marianini[4], Giovanni Marconi[1], Michela Rondoni[5], Roberta Chicchi[6], Rino Biguzzi[7], Francesco Lanza[5], Michel Salzet[8], Giovanni Martinelli[1], Giorgia Simonetti[1]. *[1]Istituto Scientifico Romagnolo per lo Studio e la Cura dei Tumori "Dino Amadori" (I.R.S.T.), Meldola, Italy,[2]Univ. Lille, Inserm, U1192—Proteomique Reponse Inflammatoire Spectrometrie de Masse (PRISM), Lille, France,[3]Fondazione Pisana per la Scienza, San Giuliano Terme, Pisa, Italy,[4]University of Bologna, Bologna, Italy,[5]UOC di Ematologia dell'Ospedale Santa Maria delle Croci, AUSL Romagna, Ravenna, Italy,[6]U.O. Medicina Trasfusionale e Officina Trasfusionale della Romagna, AUSL Romagna, Forlì-Cesena, Italy,[7]Direttore U.O. Medicina Trasfusionale e Officina Trasfusionale della Romagna, AUSL Romagna, Forlì-Cesena, Italy,[8]Univ. Lille, Inserm, U1192—Proteomique Reponse Inflammatoire Spectrometrie de Masse (PRISM), France, Italy*

The human *Plasmacytoma Variant Translocation 1* (*PVT1*) gene encodes for 176 linear (*PVT1*, lncipedia.org) and 29 circular isoforms (circPVT1, www.circbase.org). The most common isoform of circPVT1 is 410bp and is a product of back-splicing containing the whole exon 2 of *PVT1* in a closed

loop-like structure (*hsa_circ_0001821)*. *PVT1* and circPVT1 have oncogenic roles in several tumor types and can contribute to the suppression of anti-tumor immune responses. Our study aims to investigate whether and how *PVT1* isoforms and circPVT1 promote an aggressive phenotype in acute myeloid leukemia (AML) and are involved in the crosstalk between leukemic and immune cells. Six out of the 14 *PVT1* isoforms expressed by white blood cells and lymphnodes (noncode.org) were detected in a panel of AML cell lines along with circPVT1. Downregulation (KD) of groups of linear isoforms (based on sequence homology) or of circPVT1 by antisense-oligonucleotides (ASOs) in the t(8;21) KASUMI-1 and the *NPM1*-mut OCI-AML3 cells induced an impairment of leukemia cell growth especially when all the 6 linear isoforms were silenced by ASO combination , in both cell lines, under normoxia and hypoxia mimicking the bone-marrow microenvironment. Interestingly circPVT1-KD induced apoptosis in OCI-AML3 cells. Moreover, MYC protein expression decreased by ASO combination or circPVT1_KD in OCI-AML3 under normoxia and in KASUMI-1 under hypoxia. To further investigate the biological consequences of *PVT1*/circPVT1-KD, we performed RNAseq. Analysis on AML cell lines revealed that downregulation of *PVT1* and, especially circPVT1, altered the expression of genes involved in RNA transport and degradation, as expected for a long non-coding genes, but also in DNA damage response (DDR) and immunological pathways, as also confirmed by transcriptomic data of primary AML cases and proteomic analysis of both cell lines. Based on these novel findings, we tested the downregulation of *PVT1*/circPVT1 in combination with inhibition of ATM or ATR, key DDR transducers. Interestingly, circPVT1-KD sensitized OCI-AML3 to ATM (71% *vs* 95% live cells) or ATR (75% *vs* 90% live cells) inhibitors. *PVT1* and circPVT1 expression was also detected at the level of cell-free RNA in primary AML samples, the latter showing higher levels. We then analyzed extracellular vesicles (EVs) from AML peripheral blood and healthy subjects. EVs from patients were larger, increased in number and expressed higher levels of myeloid lineage markers. Finally AML EVs had more circPVT1 cargo. In conclusion, we uncovered novel potential roles of *PVT1* isoforms and circPVT1 in the DDR and in the tumor microenvironment that pave the way for novel therapeutic combinations.

#3805

Revealing the role of microRNAs in the emergence of cancer stem cell heterogeneity during colorectal cancer progression

Molly Lausten[1], Victoria Stark[2], Caroline Facey[3], Lynn Opdenaker[3], Bruce M. Boman[1]. *[1]Biological Sciences, University of Delaware, Newark, DE,[2]University of Delaware, Newark, DE,[3]Cawley Center for Translational Cancer Research, Newark, DE*

Our goal is to identify microRNAs (miRNAs) that target mRNAs involved in stem cell (SC) signaling pathways involved in colorectal cancer (CRC) tumorigenesis. SC overpopulation drives CRC progression but exact mechanism is unclear. *Hypothesis*: specific miRNAs target SC genes, which leads to the emergence of multiple cancer SC (CSC) sub-populations and tumor heterogeneity. We used flow cytometry to identify CSC sub-populations based on expression of SC markers including ALDH1, LGR5 and others in the HT-29 CRC cell line. CSC sub-populations were isolated and measured using FACS and expression of miRNAs in each CSC sub-population was quantified using NanoString profiling. The level of miRNA upregulation in each CSC sub-population was ranked based on differential expression of the miRNAs between different CSC sub-populations. We chose to further analyze the LGR5 and ALDH SC sub-populations because they showed: *i*) the largest difference between CSC sub-population sizes, *ii*) the smallest size (<1%) of the co-positive (LGR5+/ALDH+) cell sub-population, *iii*) the highest numbers of differentially expressed miRNAs. Note that WNT signaling mainly occurs via LGR5+ CSC and retinoic acid (RA) signaling mainly occurs via ALDH+ CSCs. We report herein miRNAs that are differentially expressed between ALDH+/LGR5- compared to ALDH-/LGR5- subpopulation and LGR5+/ALDH- versus ALDH-/LGR5-. The mRNAs expressed in CSC subpopulations identified from Nanostring profiling were analyzed using bioinformatics for their predicted binding by upregulated miRNAs. Our findings show that: *1*) multiple CSC subpopulations exist in the HT-29 cell population; *2*) each CSC subpopulation has a unique miRNA signature. Notably, *RXRA* mRNA is significantly upregulated in the ALDH+/LGR5- CSC sub-population but not in the LGR5+/ALDH- CSC subpopulation. We identified 5 miRs upregulated in the LGR5+/ALDH- CSC subpopulation that are predicted to target the 3'UTR of *RXRA* mRNA. One of these miRs, miR-660-3p, is specifically upregulated in the LGR5+/ALDH- CSC subpopulation and

binding of miR-660-3p to *RXRA* mRNA was validated using luciferase assay in HT-29 cells. We previously reported that RXRA is selectively expressed in ALDH + CSC sub-populations. Also, RXRA is known to bind with β-catenin leading to its degradation and suppression of WNT-based transcriptional activity. Taken together, these results indicate that expression of miR-660-3p, by inhibiting *RXRA* expression, increases WNT signaling and decreases RA signaling in LGR5+/ALDH- CSCs. Thus, upregulated miR-660-3p targets a key gene in the RA signaling pathway (*RXRA*) which could contribute to the emergence of SC sub-populations during CRC development.

#3806

Investigating the role of miRNA-34a in the resistance of esophageal adenocarcinoma to neoadjuvant chemoradiation therapy

Christina Cahill[1], Stephen G. Maher[1], Rebecca O'Brien[1], Wei-Lin Winnie Wang[2], John V. Reynolds[1], Jacintha O'Sullivan[1], Niamh Lynam-Lennon[1].
[1]Department of Surgery, Trinity St. James's Cancer Institute, Dublin, Ireland,[2]miR Scientific LLC, Rensselaer, NY

Background**:** The current standard of care for locally advanced esophageal adenocarcinoma (EAC) involves neo-adjuvant chemoradiation therapy (neo-CRT) followed by surgery. However, response to neo-CRT is poor and resistance remains a significant barrier to effective treatment. There are currently no clinical biomarkers to predict treatment response in EAC. Evidence supports a role for microRNA-34a (miR-34a) as a tumor suppressor in cancer, however, the role of miR-34a in the tumor response to therapy in EAC is largely unknown.
Methods: Irradiation of EAC cell lines was performed using an Xstrahl RS225 X-ray irradiator at a clinically-relevant dose of 2 Gy. Radiosensitivity of EAC cell lines (OE33 P, OE33 R, OE33, OE19, Flo-1^{Par} and Flo-1^{LM}) was assessed by the gold standard clonogenic assay. miR-34a expression was assessed by qPCR. EAC tumor biopsies were obtained from consenting patients undergoing diagnostic endoscopy. Pathological response of the resected tumor was assigned by a pathologist using the Mandard Tumor Regression scale. miRTarBase and KEGG pathway analysis were used to identify predicted target genes and pathways of miR-34a.

Results: miR-34a was demonstrated to be expressed in a panel of EAC cell lines (OE33 P, OE33 R, OE19, Flo-1^{Par} and Flo-1^{LM} cells). Interestingly, miR-34a expression was significantly decreased in EAC cell line models of both acquired radioresistance (OE33 R) and inherent radioresistance (OE19). miR-34a was also significantly decreased in a model of radioresistant metastatic EAC (Flo-1^{LM}). Supporting *in vitro* data, in pre-treatment tumor biopsies from EAC patients (n=18), miR-34a was significantly decreased in patients having a subsequent poor pathological response to neo-CRT, when compared to patients having a good pathological response to neo-CRT. Target and pathway analysis demonstrated miR-34a-mediated regulation of genes and pathways associated with treatment resistance, including the complement system, cellular metabolism and p53 signaling, among others.
Conclusion: Decreased miR-34a expression is associated with radioresistance across a panel of *in vitro* EAC models and in pre-treatment tumor biopsies from EAC patients having a poor pathological response to neo-CRT. This highlights a potential role for miR-34a as a novel biomarker predicting response to neo-CRT in EAC. Analysis of validated and predicted gene targets of miR-34a identified a number of pathways associated with treatment resistance. We are currently investigating the functional role of miR-34a in modulating tumor response to radiation *in vitro* to determine its potential as a novel therapeutic target to boost treatment response in EAC.

#3807

MicroRNA-29a synergizes with PD-1 therapy to regulate anti-tumor immunity

Xuebing Leng, Svetlana Ristin, Christine Rafie, Lance Buchness, Alejandro Villarino, Erietta Stelekati. *University of Miami Miller School of Medicine, Miami, FL*

CD8 T cells initiate potent anti-tumor immune responses. However, tumor cells employ PD-1 ligand, (PD-L1) to obstruct CD8 T cell responses and drive exhausted T cells (T_{EX}) differentiation. T_{EX} are characterized by sub-optimal functionality and inability to efficiently eliminate tumor cells. Checkpoint inhibitor therapy such as anti-PD-1 can partially restore the effector functions of T_{EX}, but the stable epigenetic programs of T_{EX} lead to

the loss of reinvigoration and tumor relapse, providing a challenge for the efficacy of checkpoint blockade therapy. We recently demonstrated that miR-29a acts as a key regulator of T_{EX} differentiation, promotes memory-like differentiation and attenuates exhaustion during chronic infection. Importantly, miR-29a favors the expansion of a progenitor T_{EX} subset expressing the transcription factor TCF-1 that responds to immunotherapy. Therefore, we hypothesized that miR-29a can substantially alter T_{EX} differentiation and synergize with checkpoint blockade to enhance anti-tumor immune responses. A well-established mouse model of chronic infection (LCMV clone-13) was used to induce T_{EX} differentiation, with transcriptional and epigenetic profiles similar to T_{EX} from human tumors. We found that combination of miR-29a overexpression and anti-PD-L1 treatment enhanced CD8 T cell expansion > 20 fold, whereas anti-PD-L1 alone marginally increased the number of CD8 T cells, suggesting that miR-29a synergizes with anti-PD-L1 to enhance CD8 T cell responses. Immune reinvigoration induced by anti-PD-L1 therapy is characterized by a partial reduction of inhibitory receptors and increase in effector responses. Instead, miR-29a overexpression combined with anti-PD-L1 promoted memory-like differentiation and long-term persistence of CD8 T cells, without compromising effector functions. Mechanistically, miR-29a synergized with anti-PD-L1 by inducing expression of a key memory-associated transcription factor, TCF-1, and antagonizing the master epigenetic regulator of exhaustion, TOX. To further understand whether miR-29a promotes only expansion of a progenitor $TCF1^+$ subset or fundamentally alters T_{EX} subset differentiation, equal numbers of miR-29a overexpressing and control $TCF1^+$ CD8 T cells were isolated and adoptively transferred to secondary host mice followed by PD-L1 blockade. $TCF1^+$ CD8 T cells with enforced miR-29a expression responded to PD-L1 blockade more efficiently than control TCF^+ CD8 T cells. These results suggest that miR-29a fundamentally alters T_{EX} differentiation by regulating key exhaustion-related transcriptional and epigenetic circuits. Therefore, we suggest that miR29a has the potential to be used as a novel therapeutic inducing robust and durable immune responses upon PD-1 therapy.

#3808

MicroRNA-206 drives antitumor immunity by disrupting the communication between Kupffer cells and Tregs

Guisheng Song, Ningning Liu. *Medicine, University of Minnesota Medical School, Minneapolis, MN*

Kupffer cells (KCs) account for 15% of the total liver cells. However, their roles in hepatocellular carcinoma (HCC) is poorly described. Clec4fCre-tdTomato knock-in mice expressing Cre recombinase and tdTomato-NLS under the KC-specific Clec4f promoter were hydrodynamically injected with oncogenic AKT and Nras (AKT/Ras) to induce HCC. A LoxP-stop-LoxP (LSL) system was used to express miR-206 in KCs of mice. AKT activation was observed in hepatocytes and KCs of HCC patients. Hydrodynamic injection (HDI) of AKT/Ras led to activation of AKT signaling in KCs and hepatocytes. AKT/Ras mice developed lethal HCC within 6-8 weeks post injection. Activation of AKT signaling led to M2 polarization of KCs, increased hepatic Tregs and exhaustion of CTLs. MicroRNA (miR) profiling revealed that AKT/Ras impaired miR-206 biogenesis in KCs by driving translation of Yin Yang 1 (YY1), a transcription repressor of miR-206. HDI of miR-206 into AKT/Ras mice fully prevented HCC, while all control mice died of HCC 6-8 weeks post injection. However, HDI of miR-206 only transfected ~ 20% of hepatocytes, indicating that it is unreasonable to conclude that the full prevention of HCC in AKT/Ras/miR-206 mice is caused by inhibited proliferation of HCC cells. We, therefore, posited that miR-206-mediated recovery of immune surveillance, at least in part, accounted for the full prevention of HCC in AKT/Ras/miR-206 mice. We next used the LSL system to overexpress miR-206 in KCs of Clec4fCretdTomato mice injected with AKT/Ras. KC-specific expression of miR-206 fully prevented HCC in AKT/Ras mice, while 100% control mice died of HCC. Mechanistically, AKT signaling in KCs drove CCL22 (C-C motif chemokine ligand 22) production by phosphorylating β-catenin that activates transcription of *Ccl22*. In contrast, miR-206 disrupted β-catenin signaling by targeting LEF1 (lymphoid enhancer-binding factor 1), an "architectural" transcription factor of β-catenin. CCL22 recruits Tregs. Indeed, KC-specific expression of miR-206 led to elevated CCL22, M2 to M1 transition of KCs, reduced hepatic Tregs, and elevated CTLs. Depletion

of CTLs in AKT/Ras mice fully offset the ability of miR-206 to prevent HCC.
Conclusions: AKT-educated KCs initiate Treg recruitment via a regulatory loop consisting of YY1, β-catenin/LEF1, miR-206, and CCL22; once this loop is activated, AKT activates β-catenin axis, which drives CCL22 production, Treg recruitment and HCC growth; while KC-specific expression of miR-206 reversed this process by blocking β-catenin axis in KCs. miR-206 represents a novel immunotherapy against HCC.

#3809
Differential regulation of novel long non coding RNAs and their mechanism of action in p73 dependent manner
Chanchal Bareja, Apoorva Uboveja, Daman Saluja. *University of Delhi, New Delhi, India*

The p53 tumor suppressor family is classically activated after DNA damage and plays a central role in cell fate decisions. Although, the p53 family activates many of the same genes in response to DNA damage, p73 plays distinct biological functions in development and metastasis. It is likely that p73 activates a unique transcriptional network which is critical for its anti-metastatic and anti-invasive action. Long non-coding RNAs (lncRNAs) are a class of mRNA- like transcripts longer than 200 nucleotides. They lack protein-coding ability and are believed to be involved in various kinds of biological processes. Increasing evidence suggests that lncRNA are frequently aberrantly expressed in cancers. Therefore, the roles of dysregulated functional lncRNA in human malignant tumors have attracted considerable scientific interest. The objective of our study is to find out novel long non-coding RNAs that can act as transcriptional targets of p73 and to delineate their role in p73-mediated anti-metastatic response. For this purpose, we performed transcriptome sequencing in HCT116p73wt and HCT116p73KD cells and screened the data for modulation of expression of lncRNAs in differential manner. Quantitative Real Time PCR was further carried out to validate the data obtained after screening RNA seq Data. Promoter analysis was carried out for the identification of p73 binding sites in the selected upregulated or downregulated lncRNAs which was further confirmed by Luciferase reporter, ChIP and site directed mutagenesis assays. About six lncRNAs were observed to be significantly upregulated

while four were down-regulated upon knockdown of p73. The promoters of selected lncRNAs were analysed *in silico* using TF Bind and JASPAR software for p73 binding sites and luciferase reporter assays suggested regulation of lncRNAs by p73. Chromatin immunoprecipitation showed promoter enrichment of the selected lncRNAs. Together, our study provides insights into the differential regulation of long non- coding RNAs in p73 dependent manner which further will provide the mechanism of their action at the genome level.

#3810

MicroRNA-483-5p inhibits cell steatosis and fibrosis by targeting PPARa, TIMP2 and HCC cell proliferation by modulating notch signaling

Suryakant Niture[1], Sashi Gadi[1], Qi Qi[1], Maxwell Gyamfi[2], Leslimar Rios-Colon[1], Rency Varghese[3], Habtom Ressom[3], Deepak Kumar[1]. *[1]BBRI, North Carolina Central University, Durham, NC,[2]Department of Pharmaceutical Sciences, College of Pharmacy, The University of Tennessee Health Science Center, Memphis, TN,[3]Lombardi Comprehensive Cancer Center, Georgetown University Medical Center, Washington, DC*

MicroRNAs (miRNAs) are small non-coding RNA molecules that bind with 3' untranslated regions (UTRs) of genes and regulate expression. Downregulation of miR-483-5p (miR-483), is associated with the progression of hepatocellular carcinoma (HCC). However, the molecular and mechanistic role of miR-483 in nonalcoholic fatty liver disease (NAFLD), alcoholic fatty liver diseases (AFLD), and HCC remain elusive. In the current study, we investigated the biological significance of miR-483-5p in NAFLD, AFLD, and HCC *in vitro* and *in vivo*. Our data show that the expression of miR-483 was downregulated in tumor samples from HCC patients. Overexpression of miR-483 in HCC cells dysregulated Notch signaling, inhibited cell proliferation/migration, induced apoptosis, and increased sensitivity towards sorafenib/regorafenib; anti-HCC drugs. Interestingly, miR-483 overexpression downregulated cell steatosis and fibrogenic signaling in HCC cells. Mechanistically, miR-483 targets peroxisome proliferator-activated receptor α (PPARα) and tissue inhibitor of metalloproteinases 2 (TIMP2) gene expression by binding to 3'-UTR and suppress cell steatosis and fibrosis. Down-regulation of miR-483 was

observed in mice fed with a high-fat diet (HFD) or alcohol which lead to increased hepatic steatosis/fibrosis. Our data suggest that miR-483 inhibits cell steatosis and fibrogenic signaling, and functions as a tumor suppressor in HCC. Therefore, miR-483 may be used as a novel therapeutic target for NAFLD/AFLD/HCC management in patients with fatty live diseases/ HCC.

#3811

Micro-RNA induced inactivation of inflammatory cytokine signaling pathways in Waldenstrom macroglobulinemia compared to IgM-MGUS

Karan Chohan[1], Jonas Paludo[2], Surendra Dasari[2], Jithma P. Abeykoon[2], Prashant Kapoor[2], Esteban Braggio[3], Michelle K. Manske[2], Aneel Paulus[4], Craig B. Reeder[3], Sikander Ailawadhi[4], Asher A. Chanan-Khan[4], Robert A. Kyle[2], Morie A. Gertz[2], Anne J. Novak[2], Stephen M. Ansell[2]. *[1]Medicine, Mayo Clinic, Rochester, MN,[2]Mayo Clinic, Rochester, MN,[3]Mayo Clinic, Scottsdale, AZ,[4]Mayo Clinic, Jacksonville, FL*

Introducti**on:** Cytokines are protein factors that regulate diverse cellular processes. The malignant progression of immunoglobulin M monoclonal gammopathy of undetermined significance (IgM-MGUS) to Waldenstrom macroglobulinemia (WM) is in part cytokine mediated, and we have previously shown IL-6 mediates IgM secretion in WM via the JAK/STAT pathway. Cytokine signaling can be epigenetically modulated by micro-RNAs (miRs). We aimed to identify the role of miRs in the regulation of inflammatory cytokine pathways between these diseases.
Methods: Bone marrow samples of patients with IgM-MGUS (n=7) and WM (n=25) were prospectively collected and sorted for CD19+ and/or CD138+ malignant cells. Total RNA extraction and sequencing were performed, miR and mRNA profiling was conducted, and differential expression was calculated between WM and IgM-MGUS using a log2 fold change (FC)>0.5 and <-0.5, false discovery rate<0.05. Experimental differentially expressed miR-mRNA pairing was performed, and pairs were filtered for correlated expression (i.e., upregulated miR/downregulated mRNA, and vice-versa). Filtered pairs were analyzed using the Ingenuity Pathway Analysis to identify pathways between WM and IgM-MGUS with absolute activation Z-score ≥1.

Results: We identified 34 differentially expressed miRs experimentally targeting 1132 mRNAs. Pathway analysis showed overall miR-based inactivation of inflammatory cytokine signaling pathways in WM compared to IgM-MGUS, especially of the interleukin (IL) family: IL-2, IL-6, IL-8, IL-9, IL-15, and IL-17. Underlying multiple pathways was upregulation of miRs-146a, 150, 194, all targets of Signal Transducer and Activator of Transcription 1 (*STAT1)*, observed to be downregulated. Of relevance, miR-146a has been previously shown to be an inhibitor of inflammatory cytokines, including IL-6. Next, we observed upregulation of miR-142 which targets phosphoinositide-3-kinase regulatory subunit 6 (*PIK3R6*), observed to be downregulated. Both the STAT and PIK3 families are important cytokine signal transducers, and we have previously shown the PI3k-AKT-IkB-p65 pathway induces expression of IL-6 via a GLI2-mediated mechanism. We additionally observed granulocyte-macrophage colony-stimulating factor (GM-CSF) signaling to be inactivated in WM. Here, miR-19b and miR-30e were upregulated, both target CSF 2 receptor subunit beta (*CSF2RB)*, found to be downregulated. CSF2RB is the common receptor subunit of GM-CSF, IL-3, and IL-5.
Conclusion: Our study identifies multiple cytokines pathways involved in inflammation and the tumor microenvironment to be potentially inactivated by differentially expressed miRs in WM compared to IgM-MGUS. Downregulation of these pathways and targeting of the STAT and PIK3 family indicates a possible miR-based negative feedback loop to down-modulate inflammatory cytokine signaling in WM.

#3812

Circular RNAs from the PAX5 oncogene are overexpressed in B-cell malignancies and modulate cancer processes

Danick M. Martin[1], Brandon Hannay[2], Alexis Martin[1], Vanessa Veilleux[1], Nicholas Finn[3], Gilles A. Robichaud[1]. *[1]Chemistry and biochemistry, Université de Moncton, Moncton, NB, Canada,[2]Atlantic Cancer Research Institute, Moncton, NB, Canada,[3]Dr. Georges-L.-Dumont University Hospital Centre, Moncton, NB, Canada*

Circular RNAs (circRNAs) represent a new class of gene products involved in many biological processes. Due to their ability to bind and modulate co-interacting proteins and microRNAs (miRs), circRNAs represent new

signaling mediators in cell biology and cancer processes. Recently, we identified circRNAs from the *PAX5* oncogene (circPAX5) in B-cells. Given that *PAX5* gene products are well established as potent oncogenic regulators of B-cell cancer lesions, we hypothesized that circPAX5 may also be potentially involved in pathogenic processes of B-cell malignancies. In this study, we wanted to understand the role of circPAX5 in B-cell cancer processes and elucidate new potential targets for diagnostic and therapeutic avenues. Using a series of B-cell cancer models and clinical samples, we sequenced, mapped, and profiled circPAX5 expression profiles and found that circPAX5 products are indeed overexpressed in various cancer cell types where the predominant expressed isoform consisted of exons 2 to 5 (circPAX5_2-5) of the *PAX5* locus. In addition, we isolated circPAX5 complexes from cancer cells and identified co-interacting small non-coding RNAs, notably microARNs (miRs) by deep sequencing. To further elucidate the functional role of circPAX5 and miR co-interactions, selected miRs from the list were then conditionally overexpressed in B-cells followed by cellular phenotypic assays. Altogether, our results characterize new signaling products and pathways in B-cells. Our data also suggests that circPAX5 products are involved in B-cell cancer processes and could potentially represent new cancer pathways targeted for strategic therapeutic and/or diagnostic strategies in B-cell cancer lesions

#3813

Role of CDKN2B antisense RNA 1 in Epstein-Barr virus associated gastric carcinoma

Keila Torres[1], Wilda Olivares[1], Gonzalo Carrasco[2], Andres Rodriguez[1], Alejandro H. Corvalan[3]. *[1]Pontificia Universidad Catolica de Chile, Santiago, Chile,[2]Hospital Clinico Universidad de Chile, Santiago, Chile,[3]Advanced Center for Chronic Diseases (ACCDiS), Pontificia Universidad Catolica de Chile, Santiago, Chile*

Background: Epstein-Barr Virus (EBV)-associated gastric carcinoma (GC) (EBVaGC) is a subtype of GC which represents approximately 10% of this tumor. CDKN2B antisense RNA 1 (CDKN2B-AS1) is a long non-coding RNA associated with chronic diseases like cardiovascular disease and cancer. This study aimed to evaluate if the loss of CDKN2B-AS1 shifted the balance of the competing endogenous RNA (ceRNA) networks favoring

an apoptosis resistant phenotype through ebv-miR-BART4-5p/BID in EBVaGC.
Material and Methods: Seven gastric cancer cell lines were used to determine the expression of CDKN2B-AS1. Specific cell lines were used for CDKN2B-AS1 inhibition assays, the transfection of ebv-miR-BART4-5p and the binding between CDKN2B-AS1 and ebv-miR-BART4-5p. The detection of BID protein was determined by Western Blot. To validate the *in vitro* results, we detected CDKN2B-AS1, BID, and ebv-miR-BART4-5p expression levels by RT-qPCR in four EBVaGC positive and five negative cases. Apoptosis was detected by in situ hybridization (ISH).
Results and Discussion: CDKN2B-AS1 is expressed at higher levels in NCI-N87 and SNU-1 cell lines and at lower levels in AGS and KATO-III. A significant decrease in BID protein expression was observed after co-transfection with ebv-miR-BART4-5p and CDKN2B-AS1 inhibitor. However, these results were not significant at mRNA level. The luciferase assay validated the predicted binding between ebv-miR-BART4-5p and CDKN2B-AS1. In EBVaGC samples, a significant decrease in BID expression and cleaved caspase-3 in the presence of miR-BART4-5p was observed. Our results show that decreasing CDKN2B-AS1 expression favors viral miR binding on BID mRNAs through ceRNA networks. Also, these results could explain why positive EBVaGCs have lower apoptosis rate than EBVaGC negative cases.
Grant support: ANID/FONDECYT/POSTDOCTORADO/3201028, CONICYT-FONDAP-15130011, FONDECYT-1191928

#3814

In CLL the U1 snRNA driver mutation alters splicing in multiple genes and pathways

Andrea Senff-Ribeiro[1], Fatemeh Almodaresi[1], Quang Trinh[1], Shimin Shuai[2], David Spaner[3], Xose S. Puente[4], Elias Campo[4], Lincoln D. Stein[1].
[1]Ontario Institute for Cancer Research, Toronto, ON, Canada,[2]Southern University of Science and Technology (SUSTech), Shenzhen, China,[3]Sunnybrook Health Sciences Centre, Toronto, ON, Canada,[4]Centro de Investigación Biomédica en Red de Cáncer (CIBERONC), Madrid, Spain

5-10% of patients with the IGHV wild type form of chronic lymphocytic leukemia (CLL) carry a g.3A>C driver mutation in the U1 small nuclear RNA (snRNA). We investigatedthe patterns of mis-splicing and their pathway consequences in three U1-mutant CLL cellline models using long read sequencing in order to better understand the mechanisms ofoncogenicity in tumors carrying this mutation. CLL cell lines (HG3, JVM3 and MEC1) expressing the U1 mutation and their wild-type counterparts were submitted to Oxford Nanopore sequencing to generate full-length RNA transcripts. This transcriptomic datawas evaluated, together with previously obtained short-read data. The g.3A>C mutation occurs at a specific location of the U1 snRNA, a core component of the eukaryotic spliceosome, and acts by altering the 5' splice site (5'SS) recognition sequence to cause consistent patterns of mis-splicing. Long read analysis identified multiple instances of intron retention and suppression of exon skipping, and in silico translation of these mis-splicing events predicted stop-gain and other loss of function mutations in several expressed genes, as well as widespread changes in gene expression levels. We performed a pathway overrepresentation analysis of the altered gene expression patterns in the mutant cells using the Reactome knowledgebase and identified an enrichment in the processes of translation, non-sense mediated decay (NMD) and immune signaling, including interferon signaling. In particular, there was a marked down-regulation of genes related to ribosomal assembly and the translational machinery. A more comprehensiveanalysis of the U1 mutation phenotype in CLL may accelerate the development of better therapeutic and diagnostic approaches in patients.

Oxidative Stress, Metabolism, and Cell Senescence

#4771

Prevention of doxorubicin-induced cardiotoxicity by benfotiamine

Justin R. Taylor, Kyra Harames. *Biomedical Sciences, Noorda College of Osteopathic Medicine, Provo, UT*

Anthracyclines such as daunorubicin and doxorubicin (DOX) are currently used as chemotherapeutic agents in the prevention of various cancers including breast cancer, lung cancer, leukemia, and lymphoma. Although,

anthracyclines are successful in controlling various cancers growth, the major drawback is the unwanted cardiotoxicity. Specifically, high doses of DOX used for the therapy of advanced cancers could cause life threating conditions. Therefore, specific interventions are required to decrease the cardiac toxicity associated with the DOX. Benfotiamine, a lipid soluble vitamin B1 derivative has shown be a potent anti-oxidant and anti-inflammatory agent. However, the efficacy of benfotiamine in the prevention of cardiotoxicity associated with the anthracyclines is not known. In this study, we examined the effect of benfotiamine in the prevention of DOX-induced cytotoxicity in the human umbilical vascular endothelial cells (HUVECs). Treatment of HUVECs with DOX caused significant endothelial cells death and benfotiamine in a concentration-dependent manner prevented the dox-induced endothelial cell death. Further, benfotiamine prevents the DOX-induced apoptosis in endothelial cells by preventing the activation of caspase-3. Benfotiamine also prevents DOX-induced reactive oxygen species generation. Our results also indicate that benfotiamine regulates DOX-induced expression of pro-apoptotic mediators such as BAD, phosphor-P53, and pro-caspase-3, and anti-apoptotic mediators such as BCL-2, BCL-x, IAPs, and HSP and others such as FADD, DR5, and SMAC/diablo. We plan to further explore how benfotiamine prevents DOX-induced cardiotoxicity using human cardiac myocytes and mouse models. Thus, based on our cell culture studies, benfotiamine through its potent anti-oxidative property could prevent endothelial cytotoxicity and suggests that it could be further developed as adjuvant therapy in controlling cardiotoxicity associated with the anthracycline chemotherapy.

#4772

β3-adrenoceptor minimize doxorubicin effect in Ewing sarcoma by UCP2 activation

Claudia Masi[1], Amada Pasha[1], Francesco Carrozzo[1], Martina Rosati[1], Alessandro Pini[2], Maura Calvani[1], Claudio Favre[1]. *[1]Meyer Children's Hospital, Firenze, Italy,[2]University of Florence, Firenze, Italy*

The phenomenon of “Oxygen Paradox” arises when reactive oxygen species (ROS) overcome the cellular anti-oxidant defense system through either an escalation in ROS levels or a reduced capability of the cells to

increase an antioxidant response. The deregulated redox signaling that stimulate an uncontrolled ROS increase, could induce both tumor initiation and progression, and cell death after chemotherapy treatment. In recent decades, the therapeutic choice for Ewing Sarcomas (ES) consisting of a multi-drug chemotherapy regimen combined with radiotherapy and surgery, has significantly improved the survival up to 70% in localized diseases. ES patients, often show resistance to multi chemotherapeutic agents since ES cells exhibit a high sensitivity to rapid changes in intracellular redox environment. In this context, an antioxidant-inhibiting strategy was evaluated *in vitro* to test chemotherapeutic efficacy used in the standard treatment of ES such as the anthracycline doxorubicin (DOX) that increases ROS generation and oxidative stress (OS) in mitochondria. DOX is a strong exogenous ROS generator but lacks target specificity thereby it also affects normal cells resulting in several side-effects. Literature shows that DOX ability to reduce tumor progression is due to a DOX-induced ROS overproduction that occurs in mitochondria, known to be the main site of constant ROS production, and this effect is mediated by the mitochondrial NADPH oxidase (NADPHox) activity. To investigate why DOX causes resistance in ES patients, experiments *in vitro* were conducted with A673 ES cell line. A673 cells express a high level of the β3-adrenergic receptor (β3-AR) and are high susceptible to OS. Recently, β3-AR has become highly attractive in cancer biology for its ability to reduce tumor growth, metastasis, and its antioxidant properties as main regulator of the cellular response to OS. β3-AR working as ROS sensor control the redox state of the cells, driving them to life or death through mitochondria bioenergetics function. In our experimental setting DOX induced β3-AR expression which influenced the uncoupling protein 2 (UCP2) expression. β3-AR/UCP2 axis strongly decreased the mitochondrial activity by reducing ATP synthesis and mitochondrial ROS content and this effect was reverted by β3-AR antagonist, SR59230A. In summary, the DOX chemotherapy promotes β3-AR expression that decreases ROS levels through β3-AR/UCP2 axis. Decreased ROS levels allow ES cells to survive chemotherapy.

#4773
DEAD Box 1 (DDX1) protects its RNA targets in cells exposed to oxidative stress

Mansi Garg, Roseline Godbout. *University of Alberta, Edmonton, AB, Canada*

DEAD box 1 (DDX1) belongs to the family of RNA helicases involved in all aspects of RNA metabolism, from transcription to transport, expression, and decay. DDX1 is overexpressed in a subset of retinoblastoma, neuroblastoma, and breast cancers. In breast cancer, the overexpression and cytoplasmic localization of DDX1 is correlated with poor prognosis. Cancer cells often exhibit high metabolic rates which can lead to genomic instability, oxidative stress, and endoplasmic stress. DDX1 is known to play a role in resolving genotoxic stress by participating in DNA double-strand break (DSB) repair. We propose that DDX1 also plays a key role as a stress response regulator in cells undergoing oxidative stress. When cells are exposed to oxidative stress, DDX1 is recruited to cytoplasmic stress granules (SGs). Although the exact function of SGs remains elusive, it is generally believed that tightly controlled SG assembly and disassembly are important for cell survival under stress. We found that while DDX1 is dispensable for SG assembly, depletion of DDX1 leads to impaired SG disassembly and hence, delayed stress recovery. Thus, DDX1 may play a role in stress resolution after the removal of stress conditions. To further understand the role of DDX1 in stress resolution, we performed RNA-immunoprecipitation followed by next-generation sequencing and identified DDX1-bound RNAs under normal and oxidative stress conditions. We found enhanced binding of DDX1 to its RNA targets in the presence of oxidative stress. Furthermore, we observed that DDX1 protects its target RNAs from degradation in the cytoplasm of cells undergoing oxidative stress. This RNA protection after stress exposure was more prominent in DDX1-overexpressing neuroblastoma cells, possibly explaining the faster stress recovery observed in these cells. Taken together, our results suggest that DDX1 plays a role in protecting cells from oxidative stress. This study may shed light on our understanding of cancer cell resistance to anticancer therapies.

#4774

Adaptation to chronic oxidative stress promotes metabolic rewiring to maintain redox balance in HER2+ breast tumors

Caitlynn Nicole Mirabelli[1], Rachel La Selva[1], Matthew Annis[1], Ouafa Najyb[2], Steven Hébert[2], Claudia Kleinman[3], Julie St-Pierre[4], Peter Siegel[1], Josie Ursini-Siegel[5]. *[1]Medicine, McGill University, Montreal, QC, Canada,[2]Lady Davis Institute for Medical Research, Montreal, QC, Canada,[3]Human Genetics, Lady Davis Institute for Medical Research, Montreal, QC, Canada,[4]Biochemistry, Microbiology and Immunology, University of Ottawa, Ottawa, ON, Canada,[5]Oncology, Lady Davis Institute for Medical Research, Montreal, QC, Canada*

Breast cancer is the most commonly diagnosed malignancy in women worldwide. Breast tumors possess a high degree of intra- and inter-tumoral heterogeneity, enabling the emergence of aggressive, therapy-resistant tumors. One contributor to breast tumor heterogeneity is reactive oxygen species (ROS), which are unstable oxygen-containing molecules that modify proteins, lipids, and DNA. Our lab has developed unique models of HER2+ breast cancer that evolved in vivo under conditions of low (ROS^{LOW}) and high (ROS^{HIGH}) chronic oxidative stress to acquire more aggressive properties. As such, we became interested in understanding the underlying mechanisms by which breast cancer cells capitalize on sustained oxidative stress to acquire more aggressive properties. We show that, relative to their parental and ROS^{LOW} counterparts, ROS^{HIGH}-evolved tumors are better able to maintain redox balance by coping with ROS-induced damage in vivo and following H_2O_2 treatment in vitro. Moreover, ROS^{HIGH}-evolved breast cancer cells lose their aggressive phenotype in vitro, implying a necessary microenvironmental contribution. RNAseq analysis of parental and aggressive breast cancers further identified glycolytic and hypoxic transcriptional signatures that were preferentially induced in breast cancers that adapted to chronic oxidative stress. Therefore, we hypothesized that breast cancer cells conditioned to cope with chronic oxidative stress may re-wire their glucose metabolism to support ROS buffering, which may be facilitated by a hypoxic tumor microenvironment. Notably, ROS^{HIGH}-evolved tumors are insensitive to inhibition of glycolysis using 2-deoxyglucose (2-DG); however, we show that they are specifically sensitized to inhibition of glutathione synthesis, and this sensitivity is exacerbated when treated in combination with 2-DG. As well, we show through glucose tracing that ROS^{HIGH}-evolved tumors

exhibit increased incorporation of glucose-derived carbons into glutathione. This data confirms that breast tumor adaptation to chronic oxidative stress promotes metabolic re-wiring to support ROS scavenging. To begin interrogating the role hypoxia plays in this phenotype, we assessed cell proliferation and levels of hypoxia-responsive genes following hypoxia exposure in our breast cancer models in vitro. Relative to their parental counterparts, breast cancer cells that adapted to chronic oxidative stress exhibit enhanced proliferation in hypoxia and are better able to upregulate hypoxia-responsive genes, even in response to modest changes in oxygen levels. Overall, our study shows that tumor adaptation under chronic oxidative stress promotes metabolic rewiring which may be facilitated by a hypoxic microenvironment.

#4775

Knockout of *Sod2* accelerates *Kras^{G12D}*-driven formation of pancreatic cancerous lesions

Alicia K. Fleming Martinez[1], Brandy H. Edenfield[1], Irene Esposito[2], Peter Storz[1]. *[1]Department of Cancer Biology, Mayo Clinic, Jacksonville, FL,[2]Institute of Pathology, Heinrich-Heine-University and University Hospital Duesseldorf, Düsseldorf, Germany*

Recent studies demonstrate that mitochondrially-generated reactive oxygen species (ROS) downstream of oncogenic KRAS drive acinar-to-ductal metaplasia (ADM), a key first step in the pancreatic ductal adenocarcinoma (PDA) progression model. MnSOD/*SOD2* is a mitochondrial enzyme that converts superoxide into hydrogen peroxide. Previous studies have shown that *SOD2* is biologically relevant to the study of pancreatic cancer. Some patients with a *SOD2* polymorphism resulting in less active MnSOD at the mitochondrial matrix are at increased risk of developing pancreatic cancer. Additionally, MnSOD is lost in high-grade human PanIN, further suggesting a role in tumor development. To elucidate the role of MnSOD in pancreatic cancer initiation and progression, we crossed *Sod2$^{lox/lox}$* mice into the *p48^{Cre};LSL-Kras^{G12D}* (KC) mouse model. We found increased ROS, abundantly more abnormal tissue development and presence of flat lesions indicating accelerated early progression. However, Kaplan Meyer survival analysis of KC and KC;*Sod2$^{-/-}$* mice did not indicate faster

progression to cancer, suggesting that for later steps additional signaling is needed. In summary, we identify MnSOD as a key antioxidant molecule preventing initiation of PDA.

#4776

NRF2 is overexpressed in esophageal adenocarcinoma and its targeting sensitizes tumor cells to cisplatin through induction of ferroptosis and apoptosis

Farah Ballout, Heng Lu, Zheng Chen, Tianling Hu, Lei Chen, Wael El-Rifai, Dunfa Peng. *University of Miami, Miami, FL*

Background: Esophageal adenocarcinoma (EAC) is the predominant type of esophageal cancer in the United States, with the 5-year survival rate is below 20%. EAC develops through Barrett's esophagus (BE)-dysplasia-carcinoma cascade. Gastroesophageal reflux disease (GERD), where acidic bile salts refluxate into the esophagus, is the main risk factor for the development of BE and its progression to EAC. The NFE2-related factor 2 (NRF2) is the master cellular antioxidant regulator, involving in many cancer hallmarks.
Methods and Results: Using western blotting and immunohistochemistry technologies, we detected high NRF2 protein levels in EAC cell lines and primary EAC tissues, as compared with normal esophagus and non-neoplastic Barrett's esophagus samples. The knockdown of NRF2 using NRF2 specific siRNAs significantly increased oxidative stress in response to cellular stress stimuli by bile salts or cisplatin. This was associated with an increase in DNA damage and inhibition of EAC cell growth. Brusatol, a NRF2 inhibitor, significantly inhibited NRF2 transcriptional activity and downregulated NRF2 target genes. We discovered that in addition to inducing apoptosis, Brusatol alone or in combination with CDDP induced significant lipid peroxidation and ferroptosis as evidenced by reduced xCT and GPX4 expression, two known ferroptosis markers. Moreover, the combination of Brusatol and CDDP significantly inhibited EAC tumor xenografts growth in vivo. We confirmed the in vitro data showing ferroptosis as an important mechanism in the xenografted tumors treated with Brusatol or Brusatol and CDDP combination using IHC staining.
Conclusion: Our data support the role of NRF2 in protecting against stress-induced apoptosis and ferroptosis in EACs. Targeting NRF2 in combination

with platinum therapy can be an effective strategy for eliminating cancer cells in EAC.

#4777

Exploring ferroptosis pathway for the development of therapeutic strategy in liposarcoma

Chueh-Chuan Yen[1], San-Chi Chen[2], Chih-Hsueh Chen[3], Jir-You Wang[4], Chao-Ming Chen[4], Po-Kuei Wu[4], Muh-Hwa Yang[2]. *[1]Department of Medical Research, Taipei Veterans General Hospital, Taipei, Taiwan,[2]Department of Oncology, Taipei Veterans General Hospital, Taipei, Taiwan,[3]Department of Pathology and Laboratory Medicine, Taipei Veterans General Hospital, Taipei, Taiwan,[4]Department of Orthopedics, Taipei Veterans General Hospital, Taipei, Taiwan*

Background: Liposarcoma (LPS) is one of the most common soft tissue sarcoma (STS) subtypes. Both well-differentiated LPS (WDLPS) and dedifferentiated LPS (DDLPS) have 12q13-15 amplification. Mouse double minute 2 homolog (MDM2) is one of the most important oncogenes within this region. Ferroptosis is a unique type of necrotic cell death featured accumulation of lipid-based reactive oxygen species (ROS) derived from the oxidative modification of phospholipid membranes. Cysteine metabolism is the critical part of ferroptosis regulation. Cystine-glutamate antiporter (system xc-; xCT), encoded by two subcomponents, the solute carrier family 7 member 11 (SLC7A11) and SLC3A2, is responsible for cystine supply from extra-cellular environment. Imported cystine is then reduced to cysteine, a key component of tripeptide glutathione (GSH). Glutathione peroxidase 4 (GPX4) requires GSH to repair lipid peroxidation and prevent ferroptosis. Inactivation of GPX4, either through cystine deprivation due to xCT inhibitor erastin, or by GPX4 inhibitor Ras-selective lethal small molecule 3 (RSL3), will lead to accumulation of lipid-based ROS, and eventually ferroptosis cell death. The tumor suppressor p53 (TP53) could suppress the expression of SLC7A11 and induce ferroptosis. TP53 could also indirectly suppress 3-hydroxy-3-methyl-glutaryl (HMG)-coenzyme A (CoA) reductase (HMGCR) activity, a key pathway for generation of biomolecules with anti-ferroptosis property. MDM2, the key oncogene in DDLPS, and homolog MDM4 could facilitate ferroptotic death in TP53-dependent or -independent mechanisms.

Methods: We explored public domain database to identify possible aberrations of ferroptosis-related genes in DDLPS. We then examined the sensitivity of DDLPS cell lines to possible ferroptosis-inducing agents. Furthermore, we used nutlin-3, a MDM2 inhibitor, to modulate the MDM2 expression in DDLPS cell line, and explored the potential synergistic effect of nutlin-3 with ferroptosis-inducing agents. Finally, we used immunoblotting study to reveal the potential mechanism responsible to possible synergistic effect.
Results: Expression level of GPX4 is significantly lower in DDLPS than adipose tissue and WDLPS, and DPP4 was general higher in LPS than adipose tissue. HMGCR, SLC7A11 and SLC3A2 were mostly up-regulated in LPS in comparison with benign counterpart. Both DDLPS cell lines showed sensitivity to erastin and RSL3. In addition, nutlin-3 could exert synergistic ferroptosis-inducing effect and cytotoxicity with erastin and RSL3 in sequential manner. Furthermore, nultin-3 treatment could upregulate SLC3A2 with altered cystine/glutamate exchange in DDLPS cell lines, indicating possible mechanism responsible for nultin-3 resistance and the synergistic effect of nultin-3 with erastin or RSL3.
Conclusion: Our study showed that modulation of ferroptosis is a potential treatment strategy in DDLPS.

#4778

Novel bioluminescence approaches for measuring fatty acid β-oxidation and production of reactive oxygen and nitrogen species

Kim Haupt[1], Matt Larsen[2], Hui Wang[2], Natasha Karassina[1], Mike Valley[1], Wenhui Zhou[2], Jolanta Vidugiriene[1]. *[1]Promega, Madison, WI,[2]Promega, San Luis Obispo, CA*

Energy uptake and utilization in eukaryotic cells is a dynamic process regulated by a series of interacting metabolic networks. Interrogation of this complex network relies on rapid, sensitive approaches that do not require extensive sample handling and are easily adaptable to 96- and 384-well plates. Previously, using the Ultra-Glo luciferase reaction we developed a panel of bioluminescent assays that can be used to monitor numerous aspects of cellular metabolism and mitochondrial function including ATP production, glucose and amino acid metabolism, and the TCA cycle. Here, we extend the use of the luciferase reaction and report on the development

of novel bioluminescence probes for studying two important metabolic cellular responses: fatty acid β-oxidation (FAO) and production of reactive oxygen and nitrogen species. For studying FAO, we developed a cell permeable probe with caged-luciferin attached to a fatty acid chain. The probe enters the cells and following FAO cycling, free luciferin is released and detected using Luciferin Detection Reagent. We validated the approach using known FAO activators and inhibitors and used it to monitor the changes in FAO during T-cell activation. For measuring reactive oxygen and nitrogen species, highly selective bioluminescence probes were developed. Upon reaction of the probes with their corresponding ROS target, they form the stable D-luciferin reporter molecule, causing luciferin to accumulate. Upon treatment with luciferase in the detection step, the generated light allows for quantification of the superoxide or nitric oxide formed. Both probes are suitable for in vitro and cell-based detection of ROS in an "add and read" format, providing for a simple workflow amenable to high throughput experimentation.

#4779

MnSOD mimetic mitoquinone mesylate (MitoQ) increases DCLK1^{+}pancreatic cancer stem cells

Jeffrey Mario Perera, Alicia K. Fleming Martinez, Peter Storz. *Department of Cancer Biology, Mayo Clinic Florida, Jacksonville, FL*

Mitochondrially-generated reactive oxygen species (mROS) have been shown to induce acinar-to-ductal metaplasia (ADM). ADM, in presence of an oncogenic KRAS mutation, is an initiating step for progression to pancreatic intraepithelial neoplasia (PanIN) and eventually pancreatic ductal adenocarcinoma (PDA). Here, we utilize primary murine cells as well as the *p48^{Cre};LSL-Kras^{G12D}* (KC) mouse model to explore the use of the mitochondria-targeted mimetic of manganese superoxide dismutase MitoQ for targeting PDA initiation and progression. Previously published data by our laboratory has shown that treatment with MitoQ decreases the abundance of pancreatic low-grade lesions in KC mice. However, we here demonstrate that superoxide depletion by MitoQ at the same time increases formation of DCLK1^{+} cancer stem cells in such lesions. We here evaluate if the detoxification of mitochondrial superoxide results in a build-up of hydrogen peroxide, which is a major driver of the DCLK1^{+} cell type. We

determine how altered expression of ROS detoxifying enzymes in different cell types contribute to PDA stem cell formation and PDA development. Eventually we test if the increase in DCLK1^{+} cancer stem cells can contribute to changes in the microenvironment and accelerated progression of abnormal tissue.

#4780

Comparison of safety and efficacy outcomes with nonthermal plasma and tirapazamine in porcine skin and mouse melanoma models

Matthew Yehl[1], Dominik Kucharski[2], Michelle Eubank[2], Xavier Ramadan[1], Ahmad Dianat[2], Bianca Pham[1], Timothy C. Hutcherson[1], Sandra Sexton[3], Shoshanna N. Zucker[1]. *[1]D'Youville College School of Pharmacy, Buffalo, NY,[2]University at Buffalo, Buffalo, NY,[3]Roswell Park Comprehensive Cancer Center, Buffalo, NY*

A novel preclinical experimental therapy for various cancer types including melanoma is the combination of nonthermal plasma (NTP) and tirapazamine (TPZ) delivered *in situ*. This patented combination therapy delivers reactive oxygen species (ROS) and reactive nitrogen species (RNS) from the atmosphere that are activated and ionized with helium gas to create the state of matter known as plasma. The combination with the prodrug, TPZ, that only activates to become a ROS in hypoxic environments, shows synergistic targeting of cancer cells. In this study, we assayed the effects of the dual therapy on porcine skin, which is the closest model to represent human skin and is commonly used for testing drug therapy. The results demonstrated that porcine skin showed no significant cell killing with the therapy. We also compared the combination therapy in normal skin keratinocytes and 1205Lu cells derived from a melanoma metastasis to the lung. The cells were treated with NTP and TPZ and maintained in a hypoxic chamber. Four days following therapy the keratinocytes continued to grow in culture, whereas the melanoma cells expressing endogenous gap junctions, or overexpressed Cx43 gap junctions showed decreased viability. However, the melanoma cells with a dominant negative Cx43 mutant did not show this loss in viability. This confirms our previous report that gap junctions mediate the passage of derivatives of ROS to increase the extent of cell death. To determine the effects of NTP on

regulating the lethal dose of TPZ, we performed IC_{50} curves for TPZ in the presence or absence of NTP in B16-F10 murine metastatic melanoma cells. We demonstrated a decrease in the IC_{50} from 28 μM without NTP to 17.4 μM with NTP. In further analysis, the effects of treating with NTP in the presence or absence of tissue culture media were compared. The results showed a highly significant increased efficacy of NTP in the absence of media. The combination therapy was more effective than each independent treatment. To further confirm the experimental analysis, we induced tumor formation with the B16-F10 cells in a syngeneic C57BL/6 mouse model. The tumors from mice that were untreated or treated with NTP or TPZ alone, showed a significant increase in tumor volume as compared to the tumors from mice receiving the combination treatment *in situ*. In comparison of the tumor growth rates, the control, NTP-, or TPZ-treated tumors had increased by approximately 350% by day 10, whereas the tumors in the mice that received the dual therapy only increased by an average of 70%. The results from these studies collectively implicate the combination of NTP and TPZ as a potential synergistic treatment for *in situ* melanomas that offer selectivity as compared to normal tissue.

#4781

New generation of fluorescent probes for cell-based measurements of caspase activation and mitochondrial superoxide

Bhaskar S. Mandavilli, Daniel Beacham, Yi Zhen Hu, Jongtae Yang, Aimei Chen. *Thermo Fisher Scientific, Eugene, OR*

Cell health and stress readouts are critical indicators of altered or impaired function in normal and diseased states of cells, and work has been underway to develop improved small molecule sensor dyes compatible with traditional imaging and High Content Analysis (HCA) interrogation of apoptotic and mitochondrial stress pathways.
The CellEvent™ Caspase Green dye effectively reports caspase activation, but suffers complications in assay configuration when attempting to multiplex with the Green Fluorescent Protein (GFP), calcein, or other 488 laser line tools in fluorescence microscopy. Here, we describe the testing and functional characterization of a new candidate molecule for measuring apoptosis in living cells. Our sensor is comprised of a fluorogenic reporter dye that is liberated from a DEVD peptide substrate by caspase activation,

but operates in the Texas Red, 590nm excitation band, with an emission peak near 610 nm, permitting easy multiplex with GFP or calcein stained neurons in both traditional and HCA microscopy configurations. Similarly, mitochondrial superoxide accompanying cell stress is probed in microscopy with the MitoSOX™ Red Mitochondrial Superoxide Indicator dye, which localizes to mitochondria and reports superoxide generation, ignoring other Reactive Oxygen Species (ROS) and Reactive Nitrogen Species (RNS). This dye has an unusually long Stokes' shift, requiring specialized microscopy and HCA filters that excite at 405nm, and capture emission at 610nm for specific superoxide detection. This unconventional spectroscopic profile prevents the dye's use on many imaging platforms and promotes phototoxicity. To this end, our team has produced a dye with the same level of specificity for superoxide that will operate in one of the traditional fluorescence microscopy channels. Our candidate dye, here named MitoSOX™ Green Mitochondrial Superoxide Indicator also localizes to mitochondria of live cells and selectively reports superoxide generation, while ignoring other ROS and RNS species in ex vivo testing. With an Excitation/Emission profile in the GFP/FITC microscopy channel, a series of comparative studies in immortalized and neural cells are shown, highlighting photostability, specificity and signal amplitude from the dye. These reagents are research use only, not for diagnostic purposes

#4782

A biflavonoid TY1 induced mitochondrial oxidative stress in 5-fluorouracil-resistant colorectal cancer cells to suppress tumor progression

Ting-Yan Jian[1], Shian-Ying Sung[2], Yu-Ling Lin[1]. *[1]Agricultural Biotechnology Research Center, Academia Sinica, Taipei, Taiwan,[2]International Ph.D. Program for Translational Science, Taipei Medical University, Taipei, Taiwan*

The high metastasis and drug resistance of colorectal cancer (CRC) cause high mortality and rank third among the top ten cancer deaths. TY1 is a biflavonoid isolated from *Taxus* x *media* cv. Hicksii. We have previously reported that TY1 inhibits metastatic behavior by inhibiting F-actin polymerization. However, the biological activities of TY1 to overcome drug resistance remain unclear. In this study, we investigated the

pharmacological mechanism of TY1 for inhibiting 5-fluorouracil (5-FU)-resistant CRC cells and its therapeutic effect. The 5-FU sensitive (COLO205) and 5-FU resistant (HT-29) CRC cells were used to determine the antitumor activity of TY1. Bioinformatic analysis was conducted to explore the antitumor effects of TY1 in 5-FU resistant HT-29 cells. The effects of TY1 on 5-FU-resistant CRC cells were determined by cell-based analyses, including MTT assay, cellular and mitochondrial ROS-superoxide detection, and confocal images. Finally, the therapeutic effects of TY1 were evaluated in HT-29 xenograft CRC mice. We found TY1 inhibited cell proliferation but did not affect the cell cycle. TEM images showed that TY1 induced vacuole production. Transcriptome data indicated that interferon-related genes specifically mitochondrial interferon alpha-inducible protein (IFIP) were significantly decreased after TY1 treatment. TY1 increased oxidative stress generated by reactive oxygen species (ROS) and superoxide. When IFIP was overexpressed, TY1-induced oxidative stress was reduced. In xenograft CRC mouse, TY1 effectively inhibited tumor growth. The anticancer activity of TY1 is attributed to TY1-induced ROS and superoxide by downregulating mitochondrial IFIP expression. Therefore, these data suggest that TY1 may be a promising new compound in the treatment of 5-FU-resistant CRC.

#4783

ADO is essential for redox homeostasis in liver cancer

Sandy C-E S. Lee[1], Andrea H. A. Pyo[1], Helia Mohammadi[1], Ji Zhang[1], Anna Dvorkin-Gheva[1], Lucie Malbeteau[1], Stephen Chung[1], Shahbaz Khan[1], Thomas Kislinger[1], Julie A. Reisz[2], Courtney Jones[1], Marianne Koritzinsky[1]. *[1]UHN Princess Margaret Cancer Centre, Toronto, ON, Canada,[2]University of Colorado, Aurora, CO*

2-Aminoethanethiol dioxygenase (ADO) is a thiol dioxygenase that plays a direct role in both metabolism and protein stability. Oxidation of the metabolite cysteamine produces hypotaurine, while oxidation of N-terminal cysteines targets protein substrates for N-degron pathway-mediated degradation. Despite these known functions, the (patho)physiological roles of ADO remain obscure. By analyzing TCGA datasets we discovered that high ADO expression is associated with poor outcome for patients with hepatocellular carcinoma (HCC) (HR 1.2, $p<0.001$). HCC is linked to viral

hepatitis, alcohol, metabolic syndrome, non-alcoholic fatty liver disease and chronic inflammation. It is the third leading cause of cancer-related deaths worldwide and is significantly more common in males than females. With poor outcomes, there is a need to better understand HCC biology and vulnerabilities. To assess the functional roles of ADO, we created ADO knockout mice as well as two liver cancer cell line models where ADO was depleted by siRNA, doxycycline-inducible shRNA, or CRISPR/Cas9. While male ADO knockout mice were viable, fertile and healthy, depletion of ADO in liver cancer models significantly reduced cancer cell proliferation and colony formation. ADO was also essential for supporting xenograft growth when implanted subcutaneously in immune-compromised mice. Taken together, this suggested that ADO depletion represents a cancer-specific vulnerability. Comprehensive metabolomic, transcriptomic and proteomic characterization of HCC cells isogenic for ADO demonstrated that loss of ADO resulted in dysregulation of glutathione, ascorbate, polyamine and proline metabolism. Consistent with this, ADO depleted cells had high levels of reactive oxygen species (ROS) measured by CellROX flowcytometry, and an increased ratio of oxidized to reduced glutathione, indicative of oxidative stress. Since mitochondria represent a substantial source of ROS, we assessed mitochondrial mass and function using Mitotracker^{TM} flow cytometry and Seahorse stress tests, respectively. ADO depleted cancer cells had higher mitochondrial mass and higher maximal respiration rates compared to control cells. Finally, exogenously supplied antioxidants could rescue the survival of HCC cells with ADO depletion, demonstrating that the observed loss of viability is due to oxidative stress. This work shows that ADO is essential for redox homeostasis in liver cancer models and suggests that interfering with ADO function may represent a novel targeting strategy for HCC.

#4784

Multiomic landscape of evolution of Warburg effect identifies drivers of breast cancer

Rafael Renatino Canevarolo[1], Praneeth Reddy Sudalagunta[1], Joon-Hyun Song[2], Erez Persi[3], Mehdi Damaghi[2], Ariosto Siqueira Silva[1]. *[1]Cancer Physiology, H. Lee Moffitt Cancer Center, Tampa, FL,[2]Pathology, Stony Brook University, New York, NY,[3]NCBI/NIH, Bethesda, MD*

Early breast carcinogenesis is characterized by an intermittently hypoxic, acidic and nutrient-deprived microenvironment, eventually selecting for the invasive, aerobically glycolytic phenotype known as Warburg Effect (WE), a universal cancer hallmark. We have reproduced the emergence of WE *in vitro*, by subjecting the nontumorigenic breast epithelial cell line MCF10A to multiple intermittent cycles of media starvation followed by recovery in growth media. Clonal expansion of surviving cells demonstrated increased lactate production in aerobic conditions (WE). A comprehensive molecular characterization, through WES and single cell multiomics, was performed to study the relationship between mutations, CNA, cytogenetic abnormalities, transcriptional dysregulation, and epigenetic modifications. Mutational analysis of 6 WE clones identified 249 shared mutations, including *HRAS*(G12V), *BRAF*(P523L) and *ALK*(Q180X). COSMIC mutational signature 18 (ROS-induced) was identified as the main DNA lesion across all WE clones, suggesting oxidative stress as a main source of mutagenesis associated with WE development. Non-synonymous mutations in *FUS*, *HDAC3*, *EZH2*, *MAZ*, *KMTD2*, *MET*, and other oncogenes were found in the clones, consisting in secondary events in the WE transformation. Geneset enrichment analysis identified over-expression of MYC/E2F targets, MTORC1 signaling, glycolysis and cell cycle pathways, as well as under-expression of EMT/cell adhesion pathways, in WE clones. CNA, based on a consensus from WES, scRNAseq (inferCNV) and scATACseq (epiAneufinder), confirmed amplification of MYC, E2F1 and MYBL2, as well as Gain(19q) and Gain(20) in all WE clones, as well as loss of *TP63* in 5 out of 6 WE clones. Integrative single cell transcriptome/chromatin accessibility analysis (ArchR) identified decreased accessibility and expression of EMT-related genes, as a consequence of differential expression of *pioneer* transcription factors (i.e. reduced expression of *TP63*, due to deletion, led to silencing of TP53/63/73 targeted genes), as well as well-established EMT regulators (ZEB1, SNAI1/2, NFKB1), among others. We propose that the WE phenotype emerges after intermittent nutrient-derived oxidative stress induces increased expression of *HRAS*-regulated genes, acutely increasing mutation rate and transcriptionally inducing an EMT-like state. Once *HRAS*(G12V), MYC/E2F1 amplification and *TP53* deletions are fixed in the population, the clones will maintain the ROS production and EMT-like state, even in optimum growth media conditions, completing the transition from an acute

response to a chronic-inheritable phenotype known as WE. These findings reinforce the importance of microenvironmental stress driving early carcinogenesis, bridges the gap between environment and genomic-driven causes of malignant transformation and provides testable hypotheses of causal events in connection with WE.

#4785

S-nitrosylation of p53 in melanoma alters p53-DNA binding and downstream gene expression

Jordan Winfield[1], Mariana Grigoruta[1], Yiliang Li[2], Fancui Meng[2], Yong Qin[1], Elizabeth Grimm[3], Leyuan Chen[2], Kevin Rosenblatt[4], Li Li[5]. *[1]The University of Texas at El Paso, El Paso, TX,[2]Tianjin Key Laboratory of Radiation Medicine and Molecular Nuclear Medicine, Tianjin, China,[3]MD Anderson Cancer Center the University of Texas, Houston, TX,[4]The University of Texas Health Science Center at Houston, Houston, Houston, TX,[5]The University of Texas Health Science Center at Houston, Houston, TX*

Aberrant expression of inducible nitric oxide synthase (iNOS) and chronic nitrosative stress is correlated with growth, metastasis, resistance to therapy, and poor patient survival of metastatic melanoma. One physiological influence of nitric oxide (NO) is exerted directly through the post-translational modification of many proteins, including the unique S-nitrosylation (SNO). To date, the role of SNO in melanoma development has not been fully characterized. Herein, we focus on the mechanism of how nitrosative stress regulates the tumor suppressor p53 in melanoma cells. We first examined the effects of different levels of NO donors, S-nitrosoglutathione (GSNO) and diethylenetriamine (DETA) NONOate, on the growth of melanoma cells by the MTT assay. Low levels of nitrosative stress (NO donors ≤ 20 μM) did not suppress the growth of human melanoma A375 and SB2 cells, but high levels of nitrosative stress (NO donors ≥ 50 μM) inhibited melanoma cell growth. Our biotin switch assays (BSA) showed that the treatment of NO donors significantly increased total S-nitrosylated proteins in A375 and SB2 cells. Markedly, p53 is confirmed to be one of the S-nitrosylated proteins derived from BSA. Our mass spectrometry analysis of SNO proteins in melanoma cells confirms that p53 is S-nitrosylated in A375 cells under nitrosative stress. Further proteomic

characterization identifies Cys242, Cys275, and Cys277 as the SNO sites of p53. We conducted a molecular dynamics (MD) simulation of p53-DNA binding under SNO modification. The structural analysis shows that the SNO of Cys277 reduces the hydrogen bonds between p53 and the targeted DNA, interfering with the recognition and binding of p53 to DNA. Moreover, the chelating ability of Cys242 for Zn2+ is weakened after SNO, indicating the SNO of p53 reduces p53 binding to Zn^{2+} and affects its active form. The electrophoretic mobility shift assay also confirmed that the treatment of 100 μM of DETA NONOate, significantly decreased the nuclear p53 of A375 and SB2 cells binding to the consensus p53-binding DNA. The induction of nitrosative stress by NO donors also significantly increased mouse double minute 2 homolog (MDM2), p21, and p53 expression but decreased p53 upregulated modulator of apoptosis (PUMA) expression.This study confirms that the crucial tumor suppressor, p53, is S-nitrosylated in melanoma cells under nitrosative stress. Notably, for the first time, the SNO sites of p53 and the effects of SNO on p53 functions were characterized. Our results describe an important mechanism of how nitrosative stress modifies crucial cysteines of p53, alters p53 DNA-binding activities, and regulates downstream gene expression through SNO. Our study provides much-needed insights into identifying novel NO-driven SNO proteins in melanoma as new biomarkers and targets for drug development.

#4786

Imipridones induce lipid peroxidation and oxidative stress in gastrointestinal malignancies

Arielle De La Cruz[1], Praveen R. Srinivasan[1], Andrew George[1], Varun V. Prabhu[2], Maximilian P. Pinho-Schwermann[1], Wafik S. El-Deiry[1]. *[1]Brown University, Providence, RI,[2]Chimerix Inc., Durham, NC*

Colorectal and pancreatic cancer collectively comprise 20% of all cancer-related deaths in the United States. Despite therapeutic advancements, the current standard of care often results in significant toxicity. Therefore, there is an urgent need to develop more efficacious novel therapies. The imipridones, ONC201/TIC10, ONC206, and ONC212, are novel small-molecules that bind mitochondrial ClpP and induce activation of the integrated stress response (ISR), tumor necrosis factor-related apoptosis-

inducing ligand (TRAIL) signaling, and oxidative stress. Each has previously demonstrated antitumor effects in a variety of preclinical *in vitro* and *in vivo* cancer subtypes, including colorectal cancer, with limited toxicity. Reactive oxidation species (ROS) are natural biproducts of cellular oxidative metabolism and play important roles in the modulation of cell death pathways, differentiation, and immune response. Using varying doses of ONC201, ONC206, and ONC212, we observed increased lipid peroxidation in several colorectal and pancreatic cancer cell lines using the C-11 BODIPY assay which measures lipid-specific peroxides. Lipid peroxidation was reversed by the ferroptosis inhibitor liproxstatin-1, suggesting that in addition to inducing apoptosis, imipridones may be involved in ferroptosis induction. Future directions include mechanistic work, investigation of the effect of imipridone-induced lipid peroxidation on immune cell cytotoxicity, and understanding the relative importance of lipid peroxidation in the clinical efficacy of imipridones.

#4787

The cancer targeting synergy of tertbutylhydroquinone and a manganese porphyrin

Joseph P. LaMorte, Sandra Tamarin, Margueritte Lalo, David J. Sokoloski, Jared J. Paul, Aimee L. Eggler. *Villanova University, Villanova, PA*

Cancer cells utilize high basal levels of reactive oxygen species (ROS) to create conditions that facilitate rapid cell proliferation. This creates an Achilles heel, making cancer cells more susceptible than normal cells to cell death caused by a bolus dose of ROS. The common food preservative, tert-butylhydroquinone (tBHQ), generates ROS intracellularly via redox cycling. Herein, we tested the effect of combining tBHQ with a manganese porphyrin, compounds originally designed as super oxide dismutase mimetics which can also generate ROS intracellularly in cancer cells and have radioprotective effects under clinical investigation. We find that the combination treatment of tBHQ and the commercially available Mn(III) tetrakis(1-methyl-4-pyridyl)porphyrin pentachloride (MnTMPyP) is much more toxic to leukemic Jurkat lymphocytes than either compound alone, e.g., lowering the LC50 of tBHQ by two orders of magnitude to 1.0 μM. MnTMPyP acts as a catalyst to oxidize tBHQ, shown by UV-Vis spectroscopy. Flow cytometry analysis revealed that while 5 μM tBHQ

decreases cell viability by less than 10% in 4 hours, the combination of 5 μM tBHQ and 12 μM MnTMPyP decreases viability by 60%, primarily by apoptosis. A clinically tested manganese porphyrin, Mn(III) *meso*-tetrakis(N-n-butoxyethylpyridinium-2-yl)porphyrin (Mn2BuOE), was as effective and more potent than MnTMPyP. We evaluated the cancer-targeting effect of tBHQ and Mn2BuOE in both Jurkats and a matched primary CD4 T cell line. The combination treatment induced significantly more cell death in cancerous Jurkats than in the normal CD4 cells. With the promise Mn2BuOE shows in pre-clinical studies and early clinical trials as adjunctive to radiotherapy, and the wide use of tBHQ in prepared food, the results shown here in CD4 cells suggest their combination may be an effective therapy to target cancer cells.

#4788

Oxidative stress promotes colorectal cancer aggressiveness through transmembrane chloride intracellular channel 1 (tmCLIC1) antioxidant activity

Francesca Cianci[1], Ivan Verduci[1], Carlotta Tacconi[1], Gaetano Cannavale[1], Matteo Ranucci[1], Giulia Bertolini[2], Paolo Malatesta[3], Federica Barbieri[3], Alessandro Fantin[1], Luca Roz[2], Tullio Florio[3], Michele Mazzanti[1].
[1]University of Milan, Milan, Italy,[2]IRCCS Istituto dei tumori, Milan, Italy,[3]University of Genova, Genova, Italy

In developed countries, colorectal cancer is the third leading cause of mortality. Despite significant advances in therapeutic approaches, metastases remain the primary concern in the treatment of colorectal cancer. Ion channels have an important role in the development of aggressive behavior, but the majority of them are involved in regular physiological activities. Chloride Intracellular Channel 1 (CLIC1) is a promising contender among the new possible biomarkers. CLIC1 is expressed as a cytosolic monomer by all cell types during physiological homeostasis. The main characteristic of this protein is that it can exist in both cytosolic and transmembrane forms (tmCLIC1), with the latter being involved in a variety of clinical conditions, including cancer. CLIC1 mRNA overexpression in colorectal cancer cells has been linked to a poor prognosis. The primary goal of this study is to understand the role of tmCLIC1 in the carcinogenesis, invasion, and migratory potential of colorectal cancer. We

initially investigated the level of CLIC1 protein expression and the activity of its transmembrane form as an ion channel in numerous colorectal cancer cells at various stages of development. Our results show that tmCLIC1 protein expression and activity are related to cell aggressiveness, and that its role in cellular proliferation, migration, and invasion is critical. The role of tmCLIC1 activity in colorectal cancer was confirmed also in *in vivo* models. Experiments in zebrafish and mouse models have shown that silencing CLIC1 impairs primary tumor development and significantly reduces the generation of distal metastases. Furthermore, when the CLIC1 protein is missing, many distinct metastatic genes are downregulated, particularly those associated to oxidative stress, typical of cancer cells. As a matter of fact, CLIC1's peculiar activity and its interaction with glutathione make this protein critical for the redox equilibrium of colorectal cancer cells. Overall, the findings could be considered as a beginning point for elucidating a mechanism of action that could constitute a new milestone in anticancer research.

#4789

Spin oscillating magnetic field sOMF of oncomagnetic device selectively kills glioma cancer cells by inducing oxidative stress and DNA damage

Shashank Hambarde[1], Arvind Pandey[1], David S. Baskin[2], Santosh A. Helekar[2]. *[1]Houston Methodist Research Institute, Houston, TX,[2]Neurosurgery, Houston Methodist Research Institute, Houston, TX*

A new noninvasive therapeutic device developed in our laboratory called the Oncomagnetic device provides a novel approach to glioblastoma (GBM) treatment. It involves repeated stimulation with oscillating magnetic fields (sOMF) produced by spinning permanent magnets. It is technologically and mechanistically distinct from the Optune® device approved by the FDA for the treatment of newly diagnosed and recurrent GBM. Use of this device in end-stage GBM patients reversed the progression of their recurrent tumor causing >30% reduction in its contrast-enhanced volume within 4-6 weeks of treatment. Mice with implanted mouse glioma cells in their brains also showed marked reduction in tumor size, increased survival ($p< 0.05$, $n = 10$) and higher DNA damage (γ-H2AX foci) after sOMF treatment with a whole-body stimulation method developed by us. Normal mice exposed to sOMF for 4 months had no

adverse effects on the brain and other organs. *In-vitro*, sOMF markedly increased reactive oxygen species (ROS) levels in cancer cells leading to the selective death of these cells, while sparing normal neurons and astrocytes. Detection of γ-H2AX and 53BP1 foci showed that sOMF caused significant DNA damage in GBM cells and diffuse intrinsic pontine glioma (DIPG) cells but not in normal astroglial SVGp12 cells. Furthermore, sOMF exposure for just 2 h resulted in >40% loss of surviving GBM and DIPG cell colonies detected by clonogenic cell survival assay, similar to that produced by 2 Gy radiation dose. This loss was rescued by the antioxidant Trolox. These results indicate that sOMF stimulation has high anticancer potency comparable to low dose radiation therapy at the cellular level with an underlying mechanism of action that is substantially different from that proposed for Optune® TTF.

#4790

Oxidation in the nucleotide pool as a novel targetable vulnerability in pancreatic ductal adenocarcinoma

Beatriz Mateo-Victoriano[1], Ling Zhang[2], Govindi J. Samaranayake[1], Cassie Due[3], Clara Troccoli[1], Julia Zaias[4], Nagaraj Nagathihalli[5], Michael VanSaun[6], Michael G. Mohsen[7], Eric T. Kool[7], Priyamvada Rai[2]. *[1]Sheila and David Fuente Graduate Program in Cancer Biology, University of Miami Miller School of Medicine, Miami, FL,[2]Radiation Oncology, University of Miami Miller School of Medicine, Miami, FL,[3]School of Nursing and Health Studies, University of Miami Miller School of Medicine, Miami, FL,[4]Department of Pathology and Laboratory Medicin, University of Miami Miller School of Medicine, Miami, FL,[5]Department of Surgical Oncology, University of Miami Miller School of Medicine, Miami, FL,[6]Sylvester Comprehensive Cancer Center, University of Miami Miller School of Medicine, Miami, FL,[7]Department of Chemistry, Stanford University, Stanford, CA*

Oncogenic RAS signaling is mediated by reactive oxygen species (ROS) signaling. However, oncogenic ROS also evoke tumor suppressive damage, necessitating adaptive redox protective mechanisms. We previously reported that MTH1, the main mammalian 8-oxodGTPase, comprises one such critical adaptation. High MTH1 expression significantly correlates

with poor disease-free survival in several KRAS-driven tumors. We have shown in RAS-driven xenograft cancer models that MTH1 is critical for the maintenance of ROS-driven signaling and prevention of DNA damage-induced senescence. However, how MTH1 loss affects KRAS-driven spontaneous tumor formation is unknown. We focused on pancreatic ductal adenocarcinoma (PDAC) due to the high prevalence of driving oncogenic KRASG12D mutations, and the lack of MTH1 studies. Therefore, we depleted MTH1 via shRNA in MIA PacCa-2 and SU.86.86 cell lines and generated novel MTH1-null Pdx1^{Cre}; LSL-Kras$^{G12D/+}$; LSL-Trp53$^{R172H/+}$ (KPC), Ptf1a$^{cre/+}$;LSL-Kras$^{G12D/+}$;Tgfbr2$^{flox/flox}$ (PKT) and corresponding MTH1-wildtype strains. We found MTH1 knockdown significantly reduced growth of KRAS-driven PDAC cells, and that germline MTH1 deficiency reduced tumor burden in the short latency PKT but not the long latency KPC animals. The PKT tumors exhibited higher overall 8-oxodGTPase activity and reduced total 8-oxo-dGTPase activity in the MTH1-deficient background, unlike KPC tumors. This finding suggests that in aggressive KRAS-driven tumors, redundant 8-oxodGTPase activity cannot compensate for MTH1 loss to prevent oncogenic stress-induced tumor suppression. Additionally, both MTH1-depleted PDAC cell lines and the smaller MTH1-null PKT tumors had decreased EGFR expression, suggesting MTH1 loss compromises this ROS-driven pathway. RNA-seq analysis revealed MTH1 deficiency altered MDSC gene expression in the PKT model, suggesting better anti-tumor response through improved immune infiltration in a typically immunologically cold tumor. Our results indicate MTH1 targeting could benefit aggressive PDAC stages. We further show PDAC tumors possess redundancy in MTH1 8-oxodGTPase function, which needs to be better understood in order to therapeutically leverage current MTH1 inhibitors, which do not target this redundancy.

#4792

Characterizing cellular senescence response to senolytic compounds using cell culture media analysis

Evelyn Wang[1], Stephen Kurzyniec[1], Ethan Hain[1], Yoshiyuki Okamura[1], Yang Yang[2], Dongwen Lv[2]. *[1]Shimadzu Scientific Instruments Incorporated, Columbia, MD,[2]University of Texas Health Science Center, San Antonio, TX*

Cellular senescence is an emerging hallmark of cancer. Senescent cells can lead to tumor development and chronic inflammation that stimulate age-related diseases. The secretion of senescent cells also generates an inflammatory environment that promotes tumor growth. Senolytics are pharmaceutical agents that selectively eliminate senescent cells through various mechanisms. Identifying the mechanism is crucial for the further development of senolytic drugs. ABT263 (also named navitoclax), a Bcl-2 and Bcl-xl dual inhibitor, is a well-known senolytic agent. Recently the first Bcl-2 and Bcl-xl dual-targeting proteolysis-targeting chimera (PROTAC), 753b, was developed, which has increased potency against senescent cells but minimized platelet toxicity. EF24 is another senolytic agent but the direct target is still unclear. Comprehensive analysis and comparison of the media environments from young cells, senescent cells, and senescent cells dosed with different senolytics can contribute toward solving senolytic mechanisms and make the drug discovery process more efficient and effective. WI38 cell culture media was used to grow young, senescence, and senolytic (753b or EF24)-dosed senescent cells for 72 hours. Cell culture media was collected at 10 different growth time points, subjected to protein crash using acetonitrile, and diluted with water prior to analysis. A 17-minute liquid chromatography triple quadrupole mass spectrometry method was developed for senescent cell and senolytic-added senescent cell culture media analysis. One hundred and forty-five cell culture related compounds including amino acids, nucleic acids, metabolites, sugars, and vitamins were simultaneously analyzed. A relative concentration trend graph was generated as the result for each of the cell growth related analytes. Thirteen compounds exhibited trends that distinguished at least one experimental group from the others in the 72 hours growth period. These compounds were asparagine, 5’-Methylthioadenosin, saccharopine, serotonin, alanyl-glutamine, urocanic acid, o-phosphoethanolamine, hypoxanthine, xanthosine, uracil, pyridoxal, nicotinic acid, and pyruvic acid. The differences observed in the cell environment reflect the differences of the activated pathways and mechanisms between the young, senescent, and senolytics-dosed senescent cells. This rapid and multicomponent cell culture analysis method enables scientists to analyze the environment as senescent cell and senolytic-dosed senescent cells grow. Comparing the chemical profile in the cell environments can be a potential strategy in understanding the mechanisms of the senolytic drugs. This information may

also be valuable in predicting the toxicity and side effects of the new senolytic drugs.

#4793

A role for fibroblast derived SASP factors in the activation of non-apoptotic cell death in normal mammary epithelial cells

Lisa M. Hom[1], Seunghoon Sun[2], Jamie Campbell[2], Ireland Murphy[2], Shannon Culbert[2]. *[1]University of Notre Dame, Notre Dame, IN,[2]Biological Sciences, University of Notre Dame, Notre Dame, IN*

In normal tissue homeostasis, bidirectional communication between different cell types can shape numerous, biological outcomes. Fibroblasts are one cell type in constant communication with neighboring epithelial cells, and as a result, can alter various cellular parameters. Additionally, fibroblasts are prone to undergo senescence, exemplified by an irreversible cell cycle arrest, in response to a variety of stimuli. Senescent cells exhibit alterations in gene expression and are characterized by substantial changes in their secretome; termed the senescence associated secretory phenotype (SASP). The role of fibroblast derived SASP factors on normal epithelial cells is an area that remains poorly understood. Our studies have found that treatment of normal mammary epithelial cells with conditioned media from senescent fibroblasts (SASP CM) results in a robust programmed cell death. The capacity of SASP CM to cause cell death is maintained across multiple senescence-inducing stimuli. Interestingly, our data suggest that the cell death caused by SASP CM is dependent on caspase activation, but independent of canonical extrinsic or intrinsic apoptotic pathways. shRNA-mediated reduction of caspase 1 or GSDMD in normal mammary epithelial cells ameliorates the ability of the SASP CM to induce cell death, suggesting that these cells are dying by pyroptosis. Interestingly, breast cancer cells and normal mammary epithelial cells engineered to express oncogenic signals are not susceptible to this SASP CM induced cell death, suggesting that cancer cells have evolved a mechanism to evade SASP CM-mediated pyroptosis.. Taken together, our data reveal a novel relationship between the activation of senescence in stromal cells and the induction of non-apoptotic cell death in normal mammary epithelial cells.

#4794

Deciphering tumor recurrence post-therapy: Interactions between the tumor microenvironment and therapy-induced senescent glioblastoma

Valerie DeLuca, Priya Digumarti, Michael E. Berens. *TGen (The Translational Genomics Research Institute), Phoenix, AZ*

Glioblastoma (GBM) remains one of the most lethal forms of cancer due, in part, to the capacity of tumor cells to persist during therapy and then recover. Understanding how these residual tumor cells survive is therefore imperative to developing more effective treatment strategies. We have demonstrated that GBM cells, including those from patient-derived xenografts, undergo a state of therapy-induced senescence (TIS) rather than cell death following temozolomide (TMZ) and radiation (IR). Both TMZ and IR treatment at physiologically relevant doses result in elevated senescence-associated-β-galactosidase, altered morphology, p21 induction, and increased expression of the senescence-associated-heterochromatic-foci marker H3K9Me3. Further, despite TIS-induction in a majority of the residual cells post-treatment, GBM viable cell number increases after a prolonged stasis, indicating that populations are capable of reentering a proliferative state. However, our current understanding of how the tumor microenvironment influences this growth arrest and subsequent proliferative recovery is underdeveloped. We aim to bridge that gap by investigating the paracrine communications between astrocytes and GBM cells undergoing IR-induced senescence in order to identify how these interactions foster disease progression. Current studies are focused on evaluating the effect of astrocytes on the induction and durability of TIS in GBM cells. Proteomic studies will be pursued to characterize the secretome of astrocyte-GBM co-cultures and identify factors that drive GBM senescent response to IR. Finally, based on preliminary data demonstrating that normal astrocytes are also damaged by IR, we will undertake mechanistic studies to understand how cell-intrinsic events within the astrocyte population drive extrinsic-influence on GBM cells. We anticipate that these identified signaling events may serve as potential therapeutic targets.

#4795

Conditionally active biologics eliminates senescence cells in cancer and aging

Jian Chen[1], Christina Wheeler[1], Jing Wang[1], Matt Lucas[1], Haizhen Liu[1], Kyrie Johnson[1], Kathryn Woodard[1], Solmarie Joyner[1], Cathy Chang[1], William J. Boyle[2], Jay M. Short[2]. *[1]R&D, BioAtla, Inc., San Diego, CA,[2]BioAtla, Inc., San Diego, CA*

The aberrant accumulation of senescent cells in aged and cancerous tissue triggers inflammatory signaling through a senescence-associated secretory phenotype (SASP), promoting aging and tumor progression. Pharmacologically, clearing senescent cells has been shown to have promising effects against cancer and age-related pathologies in preclinical models as well as early human clinical trials. However, current senescent cell elimination strategies are focused on targets that do not distinguish between hyper-inflamed or SASP senescent cells versus relatively non-inflamed senescent cells. In addition, current senescence targets are predominately intracellular with important functions in normal cell population. Therefore, the use of senolytics in the clinic is still limited due to their cytotoxicity to either normal cells or potentially beneficial senescent cells. A more effective senescence cell targeted approach is needed to reduce side effects and increase the efficiency of senescence cell removal or reduction. Conditionally Active Biologics (CAB) technology is a proprietary platform that is unique in its ability to selectively activate in the context of diseased tissues, but not normal tissues, taking advantage of the acidic pH conditions in the inflammatory tumor/aged tissue microenvironment. Senescent cells, similar to tumor cells, are dependent on glycolysis to support molecule synthesis, for hyperinflammation in the case of senescent cells, and thus generate a glycolytic microenvironment (GME), resembling that of the tumor microenvironment. Since our CAB technology is already being deployed in cancer therapy by targeting cell surface markers such as AXL, ROR2, and CTLA4 in clinical studies, we explored whether CAB technology allows selective removal of senescent cells in SASP-associated microenvironments. To identify senescence-specific surface antigens that are broadly and specifically upregulated in senescent cells, we screened our CAB cell surface antigen library in different senescence *in vitro* models, *in vivo* aging mouse tissues and a chronic kidney disease mouse model. We have identified several novel senescence markers. Furthermore, *in vitro* binding assays demonstrated that CAB antibodies targeting these senescence markers have no or very low binding

to the target antigen on senescence cells in physiological, alkaline conditions, but have strong binding in glycolytic, acidic SASP conditions. Moreover, we performed antibody-dependent cell-mediated cytotoxicity assays and demonstrated that CAB antibodies were more potent against senescent cells compared to proliferating cells and displayed high selectivity for the glycolytic, acidic microenvironment condition. In conclusion, CAB technology provides a new generation of biologics with an increased safety margin and therapeutic index targeting SASP, acidic senescence cells in cancer and age-related diseases.

#4796

Chemotherapy induced senescence drives peripheral neuropathy

Taylor Malachowski, Ganesh Raut, Satarupa Mullick Bagchi, Shelia Stewart. *Washington University in St. Louis, St. Louis, MO*

Chemotherapy is a mainstay of cancer therapy. Unfortunately, while chemotherapy can profoundly impact disease free survival, it's often accompanied with devastating side effects, including peripheral neuropathy. Indeed, 30-40% of patients treated with neurotoxic chemotherapy develop long-term and often debilitating chemotherapy-induced peripheral neuropathy (CIPN). Unfortunately, there are currently no preventative measures for CIPN and while it is transitory in some patients, for others the side effects can persist for months or even years after the cessation of chemotherapy. Recent work suggests that cellular senescence, which is robustly induced by chemotherapy, contributes to CIPN. Senescent cells are typically characterized by increased CDKn2a (i.e., p16) expression, increased SA-β-gal hydrolyzation, and expression of the senescence-associated secretory phenotype (SASP) that can influence multiple cell types in the microenvironment. Through utilization of a mouse model that employs paclitaxel (PTX), we find that PTX robustly induces senescence in the hindpaws and dorsal root ganglia (DRG) of mice that display loss of peripheral axons and decreased response to mechanical stimuli. To address the role of senescence in CIPN, we utilized the INKATTAC mouse that allows for inducible elimination senescent cells. Using this model, we find that the elimination of senescent cells rescues CIPN. Further, the use of senolytics, drugs that kill senescent cells, also rescues CIPN, raising the possibility that we can treat patients with CIPN. To address the mechanism

behind CIPN we have carried out single cell RNA-Seq to identify the population of senescent cells senescing in response to chemotherapy. These analyses will allow us to understand the mechanisms that drive CIPN and may lead to new treatments for patients suffering from CIPN.

#4797

β3-AR blockade induces differentiation of malignant leukemia T cells in mature T lymphocytes

Francesco Carrozzo, Gennaro Bruno, Claudia Masi, Alessia Boaretto, Claudio Favre, Maura Calvani. *AOU Meyer, Firenze, Italy*

Acute lymphoblastic leukemia (ALL) is a genetically heterogeneous cancer that arises from diverse genetic alterations during early lymphocyte development. About 10-15% of T-cell acute lymphoblastic leukemia (T-ALL) cases occur in childhood; despite having an event-free survival (EFS) rate of 85%, relapse is the main problem of this type of cancer. Mitochondria metabolic reprogramming plays a crucial role in the development of lymphocytes both in physiological and pathological processes such as differentiation and neoplastic transformation respectively. Mitochondria are the main actors of cellular homeostasis. They use glycolysis products exploiting them in the Krebs cycle and in oxidative phosphorylation to produce energy and plays key roles in reactive oxygen species (ROS) generation, Ca2+ signaling, cell death induction, and cellular differentiation. In particular, the increase of ROS is important to reduce tumor cell viability and at the same time is involved in induction of hematopoiesis. β3-adrenoreceptors (β3-Ars) is a class of receptors associated with pro-tumoral signaling in different tumors. In this study, we first have observed the expression of β3-Ars in leukemia T cells and then we studied how the modulation of this receptors affected tumor-related pathways. The treatment with an antagonist of β3-Ars (SR59230A) induced an increase of ROS leading to lymphoblastic cells differentiation, decrease of proliferation and enhanced induction of apoptosis signaling. Overall, these results suggest that β3-Ars could be a possible target for treatment of T-ALL.

Responses to Hypoxic, Proteotoxic, and Other Novel Forms of Cell Stress

#4801

Laurine acid enhances GEM-chemosensitivity targeting hypoxia-induced mitochondrial disfunction and stemness in pancreatic ductal adenocarcinoma

Tadataka Takagi[1], Hiroki Kuniyasu[2], Masayuki Sho[3], Rina Tani[2], Shiori Mori[2], Shingo Kishi[2], Yukiko Nishiguchi[2], Yudai Hojo[2]. *[1]Department of Molecular Pathology, Department of Surgery, Nara Medical University, Kashihara, Japan,[2]Department of Molecular Pathology, Nara Medical University, Kashihara, Japan,[3]Department of Surgery, Nara Medical University, Kashihara, Japan*

Hypoxia is a feature of the pancreatic ductal adenocarcinoma (PDA). Although gemcitabine (GEM) is widely used in chemotherapy for PDA, drug resistance restricts its clinical effectiveness. We have found that hypoxia contributes to chemoresistance, however the mechanism is still unclear. The aim of this study is to clarify the mechanism and to develop a new therapeutic strategy. First, we examined the effect of hypoxia to GEM sensitivity, stemness and energy metabolism in three human pancreatic ductal carcinoma cell lines. The inhibition rate by GEM was lower under CoCl2-induced chemical hypoxia than normoxia. Reactive oxygen species (ROS) after GEM was increased under normoxia but not under hypoxia. Flux analysis showed that both oxidative phosphorylation (OXPHOS) and glycolysis were suppressed under hypoxia, indicating a quiescent state. Next, we investigated the relationship between hypoxia and stemness. Hypoxia increased stem cell markers mRNA (C-Myc, Oct-3/4, CD24, CD44, CD133) expression and tumorsphere formation efficiency (TFE). In addition, hypoxia and GEM administration reduced sphere size but increased the number of spheres and TFE. This indicated that hypoxia and GEM suppressed proliferation, however promoted stemness. Second, to examine the mechanism of GEM resistance, we established two GEM-resistant cell lines from human PDA cells by continuous treatment with GEM and CoCl2-induced chemical hypoxia. One resistant cell line possessed reduced OXPHOS and decreased mitochondrial ROS levels, while the other resistant cell line possessed increased stemness. In both cell lines, ethidium bromide-stained mitochondrial DNA levels decreased, suggesting mitochondrial DNA damage. In addition, tetramethylrhodamine-

stained mitochondrial membrane potential levels decreased, suggesting mitochondrial impairment. This indicated that long hypoxia and treatment with GEM induced mitochondrial impairment and acquisition of stemness, causing chemoresistance. We further investigated the effect of lauric acid (LAA), a medium-chain fatty acid, on GEM resistance. We have previously reported that LAA causes reprogramming of energy metabolism and induces cell death in cancer cells. Treatment with LAA restored GEM sensitivity in both GEM-resistant cell lines. Flux analysis showed that both OXPHOS and glycolysis were promoted, indicating displacement from quiescent state by LAA. These results suggest that decreased energy production, decreased mitochondrial ROS levels, and increased stemness associated with mitochondrial damage caused by GEM lead to GEM resistance, and that hypoxia may promote this process. Furthermore, forced activation of OXPHOS by LAA could be a tool to overcome GEM resistance.

#4802

Identification of critical hypoxia induced factors in castrate resistant prostate cancer

Oloruntoba I. Osagie, Jordann Smakk, Deborah E. Citrin, Travis H. Stracker. *NIH-NCI, Maryland, MD*

Background**:** Prostate cancer (PCa) is the second most diagnosed cancer in men and the second cause of cancer-related death amongst men worldwide. PCa is a heterogeneous disease, and the outcome is worse for patients when the disease progresses from localized PCa to a castrate-resistant disease. Androgen receptor (AR) signaling is crucial for PCa development and has been a major therapeutic target for decades. Despite the success made with hormone therapy to block AR signaling, castration resistant disease can arise through mutations and amplifications of the androgen receptor (AR) and AR splice variants (AR-Vs). Amongst them, AR-V7 and AR-V12 can promote AR signaling independent of androgen. Furthermore, prostate tumors are highly hypoxic due to abnormal tumor vasculature. Hypoxia influences the efficacy of local and systemic treatment strategies, such as radiotherapy, hormone therapy, and chemotherapy, resulting in poorer clinical outcomes for PCa patients. Therefore, a complete understanding of

AR and AR variant function, as well as how they are modulated by hypoxia and therapy is warranted for developing new strategies to treat PCa.
Methods: To identify the transcriptional apparatus associated with the AR and its variants under normal and hypoxic conditions, we carried out Bio-ID proximity labeling mass spectrometry (BioID-MS). We generated stable androgen-independent human prostate cancer cell lines, PC-3 and DU145, expressing AR and the AR-V7 and AR-V12 variants fused to a MiniTurboID (MTID) enzyme. To delineate the AR proximal interaction network, we treated cells with androgen or vehicle for 3 hours and affinity-purified biotinylated proteins after the addition of biotin for the final 2 hours. Cells were grown in normoxia (20% O_2) or treated with hypoxia (95% N2,5% CO_2 and 0.5% O_2) for 24 h. Nonspecific interactions were filtered using controls and statistical methods to identify high-confidence interactomes.
Results: BioID proximity labeling in PC3 cells identified several AR-associated proteins, including many knowninteractors, validating the approach. Hypoxic conditions led to a striking alteration in proximal interactions and many metabolic proteins were highly enriched with AR upon exposure of cells to hypoxia for 24h. Among these, phosphoglycerate kinase 1 (PGK1) was a top hit. PGK1 has been reported to interact with AR to mediate the expression of genes that regulates cell proliferation and apoptosis. Additionally, PGK1 has an essential role in metabolic reprogramming induced by c-MYC and HIF-1α, leading to enhanced tumorigenesis.
Conclusion: Bio-ID mass spectrometry was used to map the proximal interactome of AR and its variants, identifying novel interactions partners for further analysis. We found that hypoxia strongly alters interactors with the AR, and we identified PGK1 as a hypoxia induced AR interaction in PCA. Current work to functionally validate this interaction will be presented.

#4803
BMAL2 is a KRAS-dependent master regulator of hypoxic response in pancreatic ductal adenocarcinoma
Alvaro Curiel Garcia[1], Carlo H. Maurer[2], Kate Hollinshead[3], Pasquale Laise[4], Anthony Andren[5], Stephen A. Sastra[1], Carmine F. Palermo[1], Irina

R. Sagalovskiy[6], Li Zhang[5], Sam Holmstrom[7], Kristen Johnson[8], Gulam A. Manji[1], Alina Luga[9], Costas A. Lyssiotis[5], Andrea Califano[1], Alec Kimmelman[3], Kenneth P. Olive[1]. *[1]Columbia University Irving Medical Center, New York, NY,[2]Technische Universität München, Munich, Germany,[3]NYU Grossman School of Medicine, New York, NY,[4]DarwinHealth Inc, New York, NY,[5]University of Michigan, Ann Arbor, MI,[6]Private Health Management, Inc., Los Angeles, CA,[7]UT Southwestern Medical Center, Dallas, TX,[8]University of New Hampsire, Manchester, NH,[9]University of North Carolina, Chapel Hill, NC*

To identify novel drivers of PDA malignancy, we employed a regulatory network analysis, which accurately infers the activity of transcription factors and other regulatory proteins based on the integrated expression of their positive and negative target genes. This highly validated approach enables the identification of the most hyper-activated and hyper-repressed regulatory proteins (i.e. the “master regulators (MRs)”) that drive phenotypic distinctions. We applied this technique to a set of 200 laser capture microdissected human PDA samples as well as 45 low-grade precursors for which we had matched histopathological, clinical, and epidemiological annotation. We identified the MRs associated with four malignancy phenotypes: precursors vs. PDA (initiation), low-grade vs. high grade histopathology (progression), survival post resection, and association with KRAS activity. Integrating across these phenotypes, the top MR of PDA malignancy was found to be BMAL2, a member of the PAS family of bHLH transcription factors. Although the canonical function of BMAL2 is linked to the circadian rhythm protein CLOCK, gene set enrichment analysis highlighted a potential role in hypoxia response. We previously demonstrated that PDA in humans and in the genetically engineered “KPC” mouse model is hypovascularized, hypoperfused, and profoundly hypoxic, with a partial oxygen pressure <1mmHg. Given the close homology of BMAL2 to HIF1B (ARNT) and its potential to heterodimerize with HIF1A, we investigated whether BMAL2 plays a role in the hypoxic response of PDA. Indeed, BMAL2 activity was induced in response to hypoxia and inhibited following treatment with multiple RAF, MEK, and ERK inhibitors, validating its computationally-inferred association with RAS activity. Strikingly, knockout or knockdown of BMAL2 in human PDAC

cells led to defects in viability and invasion in the setting of hypoxia. BMAL2 knockout cells lost the ability to induce glycolysis upon exposure to severe hypoxia and this was associated with a loss of expression of the glycolysis enzyme LDHA. A large-scale CRISPR screen found that LDHA was the single most critical gene necessary for viability of PDA cells in the setting of hypoxia. Moreover, the set of inferred transcriptional targets of BMAL2 were highly enriched in hypoxia-responsive proteins, including GLUT1, the second top hit in our hypoxia survival CRISPR screen. Strikingly, knockout of BMAL2 led to a complete loss of HIF1A stabilization in response to hypoxia, consistent with the stabilizing role of HIF1A heterodimerization partners such as HIF1B. By contrast, HIF2A was further upregulated under hypoxia in the setting BMAL2 loss. We conclude that BMAL2 is a key master regulator of hypoxia responses in PDA that serves as a molecular switch between the disparate metabolic roles of HIF1A- and HIF2A-dependent hypoxia responses. This will be further validated in ongoing metabolomic studies

#4804

p38 MAPK-dependent regulation of HIF-1 and expression of the hypoxia-inducible gene *IGFBP-3* in leiomyosarcoma cells

Nuha Haque, Eric Shelden. *School of Molecular Biosciences, Washington State University, Pullman, WA*

Hypoxia is a common feature of tumor microenvironments and stimulates a variety of responses in a cell. Tumor hypoxia is also associated with poor prognosis in soft tissue sarcomas (STS), including leiomyosarcomas. Genes upregulated under hypoxia contribute to the adaptation of tumor cells and promote tumor progression. Using transcriptome-wide gene expression analysis, we identified *IGFBP-3* as one of the most highly upregulated genes in SK-LMS-1 leiomyosarcoma cells in hypoxic conditions. IGFBP-3 has been studied in several tumor types, including STS, and is associated with their altered pathogenesis. Mechanisms responsible for the hypoxia-induced expression of *IGFBP-3* in STS have not been previously well defined. Hypoxia results in the stabilization of the hypoxia-inducible transcription factor, HIF-1, and production of reactive oxygen species (ROS) in other cell types. Here, we examined HIF-1 and ROS-dependent mechanisms to determine their roles in the hypoxia-induced expression of

IGFBP-3 and other genes in SK-LMS-1 cells. Our data indicate that both ROS production and HIF-1 activation are required for the enhanced *IGFBP-3* mRNA expression in hypoxic SK-LMS-1 cells. We also tested the roles of the stress activated protein kinase p38 and the tumor suppressor p53 for their potential to contribute to the regulation of *IGFBP-3* expression in these cells. Inhibition of p53 tumor suppressor activity only partially reduced *IGFBP-3* expression. We also determined that neither hypoxia nor inhibition of p53 affected the expression of the p53 target gene, *CDKN1A* (p21), in these cells. In contrast, inhibition of p38 MAPK completely prevented the hypoxia-induced increase in *IGFBP-3* expression. Additionally, we found that p38 MAPK inhibition reduced HIF-1 protein accumulation and activity but had no effect on its mRNA expression under hypoxic conditions. Together these results suggest that ROS-dependent activation of p38 MAPK stabilizes HIF-1 and promotes the downstream expression of *IGFBP-3*. In contrast, p53 appears to have a limited effect on the expression of *IGFBP-3* in SK-LMS-1 cells. Our results clarify the signaling pathway involved in the response of soft tissue sarcoma cells to hypoxia and may provide new avenues for intervention in cancer progression.

#4806

Spry1 as a potential new hypoxia modulator in cutaneous melanoma

Barbara Montico[1], Giorgio Giurato[2], Roberto Guerrieri[1], Annamaria Salvati[2], Francesca Colizzi[1], Lorena Baboci[1], Luca Sigalotti[1], Alessia Covre[3], Michele Maio[3], Agostino Steffan[1], Tuula A. Nyman[4], Alessandro Weisz[2], Maurizio Mongiat[1], Eva Andreuzzi[1], Elisabetta Fratta[1]. *[1]Centro di Riferimento Oncologico IRCCS, Aviano, Italy,[2]'Scuola Medica Salernitana', University of Salerno, Salerno, Italy,[3]Center for Immuno-Oncology, University Hospital of Siena, Siena, Italy,[4]Institute of Clinical Medicine, University of Oslo, Oslo, Norway*

Introducti**on:** At present, the precise role of Spry proteins in tumor progression is still debated. Our previous study showed that Spry1 knockdown ($Spry1^{KO}$) in $BRAF^{V600}$-mutant cutaneous melanoma (CM) promoted cell cycle arrest and apoptosis, repressed cell proliferation *in vitro*, and reduced tumor growth *in vivo*. Furthermore, we observed that

Spry1 loss impaired angiogenesis *in vivo*. Hypoxia has been recognized as one of the crucial features of CM. Hypoxia results in the activation of the transcription factor hypoxia-inducible factor 1α (HIF-1α), which represents a master regulator of angiogenesis. Hence, the present study was designed to explore a possible role of Spry1 in modulating angiogenesis and hypoxia in CM.

Material and method: SPRY1 gene was knocked-out using the CRISPR-strategy in the BRAF wild-type (wt) Mel 313 and in the BRAF-mutant Mel 593 cell lines. Angiogenic potential was assessed through *in vivo* CD31 staining and *in vitro* tube formation assays. By using *in vitro* and *in vivo* models, the effects of $Spry1^{KO}$ on hypoxia-related genes were investigated through RNA-sequencing (RNA-seq), quantitative real-time PCR, western blot, and immunofluorescence analyses. To gain insight into Spry1 interactome, immunoprecipitation coupled to mass-spectrometry (IP-MS) was employed.

Results and discussion: Consistent with our previous data, tumors arising from Mel 313 and Mel 593 $Spry1^{KO}$ clones were significantly smaller than those from their corresponding parental cells. Tumor growth inhibition was accompanied by a substantial reduction of angiogenesis, as assessed by the immunofluorescence staining of CD31 *in vivo* and the tube formation assay *in vitro*. Accordingly, RNA-seq analysis indicated that the vascular endothelial growth factor A was significantly down-regulated following Spry1 silencing. Notably, Ingenuity Pathway Analysis identified "HIF-1α Signaling" as the most significant molecular and cellular function affected *in vivo* by Spry1 silencing regardless of the BRAF mutational status. Analyses of tumor tissues confirmed that $Spry1^{KO}$ significantly reduced HIF1-α protein abundance. Interestingly, HIF-1α mRNA levels were minimally affected, thus suggesting that $Spry1^{KO}$ might impact on HIF-1α expression post-translationally. IP-MS identified about 50 Spry1 protein partners, and most of them were mitochondrial. Importantly, western blot analysis of cytosolic and mitochondrial proteins revealed that Spry1 was largely expressed in CM cell lines irrespective of BRAF mutation.

Conclusions: Altogether, these data lead us to speculate that Spry1 might play a role in mitochondria homeostasis, thus impacting on hypoxia and angiogenesis in CM.

#4807

BACH1 proline hydroxylation regulates the hypoxia response and metastasis in triple negative breast cancer

Long Chi Nguyen[1], Christopher Dann[1], Dongbo Yang[1], Emily Shi[1], Thomas Li[1], Joseph Wynne[2], Letícia Stock[1], Madeline Henn[1], Zeyu Qiao[3], Andrea Valdespino[1], Raven Watson[4], Wenchao Liu[1], Lydia Robinson-Mailman[1], Galina Khramtsova[5], Mitsuyo Matsumoto[6], Raymond Moellering[3], Olufunmilayo I. Olopade[5], Kazuhiko Igarashi[6], Marsha R. Rosner[1]. *[1]Ben May Department for Cancer Research, University of Chicago, Chicago, IL,[2]Ben May Department for Cancer Research, Food and Drug Administration, Washington, DC,[3]Department of Chemistry, University of Chicago, Chicago, IL,[4]Department of Pathology, University of Chicago, Chicago, IL,[5]Section of Hematology and Oncology, Department of Medicine, University of Chicago, Chicago, IL,[6]Department of Biochemistry, Tohoku University Graduate School of Medicine, Sendai, Japan*

Hypoxia is an important hallmark of aggressive solid tumors. Here we show that the pro-metastatic BTB and CNC homology 1 (BACH1) transcription factor is prolyl-hydroxylated by the HIF Prolyl Hydroxylase 1 (PHD1) in an oxygen-dependent manner. Using mass spectrometry, we identified two major prolyl hydroxylation sites in BACH1 and demonstrate that prolyl hydroxylation increased protein turnover in normoxia. Notably, a clinically relevant BACH1 mutant ($BACH1^{M}$) resistant to hydroxylation displays enhanced BACH1 DNA binding capacity. Triple-negative breast cancer (TNBC) cells expressing $BACH1^{M}$ showed higher invasion in vitro and increased metastasis in vivo. Loss of BACH1 reduced the cellular transcriptional hypoxic response. Under hypoxia, BACH1 increases chromatin accessibility and gene expression through chromatin remodeling involving direct BACH1 binding and indirect epigenetic regulation. These results indicate that hypoxia stabilizes and enhances the pro-metastatic transcriptional activity of BACH1 through loss of prolyl hydoxylation in TNBC. Our findings identify BACH1 as an oxygen sensitive effector of the hypoxia response and a clinically relevant target for attenuating hypoxia induced, pro-metastatic signaling and therapeutic resistance in cancers.

#4808

Hypoxic HIF-1α stabilization dependent on β3-adrenoceptor localization in Ewing sarcoma

Amada Pasha[1], Claudia Masi[1], Francesco Carrozzo[1], Martina Rosati[1], Alessia Boaretto[1], Alessandro Pini[2], Claudio Favre[1], Maura Calvani[1].
[1]Meyer Children's Hospital, Firenze, Italy,[2]University of Florence, Firenze, Italy

Hypoxia is a condition of oxygen deficiency which occurs in most growing solid tumors and stimulates a cascade of cell signals through a family of transcription factors named as hypoxia inducible factors (HIFs) that transactivate several regulatory genes involved in tumor proliferation. β3-adrenoceptors (β3-ARs) are involved in several hypoxic scenarios and in pathological conditions where hypoxia leads to important steps for cancer progression. Studies showed that β-AR blockade of mice suppressed hypoxia induction of renal HIF-1α accumulation, erythropoietin production, and erythropoiesis *in vivo*. In this work we assumed that β3-AR mediates hypoxia sensing and that it was necessary for HIF-1α stabilization thus we investigated a putative correlation between β3-AR/HIF-1α. Data showed a similar outcome of β3-ARs and HIF-1α at short time of hypoxia, and that β3-AR antagonist, SR59230A reduced HIF-1α protein expression under hypoxia. β3-AR silencing under hypoxia revealed an evident reduction of HIF-1α protein expression that confirmed the β3-AR modulation of HIF-1α expression. SR59230A treatment strongly reduced the HIF-1α target genes as *GLUT1, HK-2* and *HIF-1α* expression at long time treatment confirming the β3-AR modulation of HIF-1α transcriptional activity. Conversely, the HIF-1α-transcriptional inhibitor Topotecan did not affect β3-AR expression confirming that is β3-AR that mediates HIF-1α activation. Immunofluorescence analysis showed that β3-AR co-localized with the nucleus under hypoxia more than normoxia. These results were confirmed by nuclear-cytoplasmic fragmentation that showed the presence of both β3-AR and HIF-1α proteins in the nucleus under hypoxia. Co-immunoprecipitation of β3-AR/HIF-1α revealed that under hypoxia, HIF-1α dissociates from β3-AR binding, but this process was abrogated by SR59230A. HIF-1α, released under hypoxia from the link with β3-AR, can play its transcriptional activity in the nucleus, while the binding with β3-AR blocks its transcriptional activity. Moreover, β3-AR regulation on HIF-1α was exerted through PHD2 activity at short time as SR59230A treatment

under hypoxia increased the PHD2 protein expression but not at long time treatment, thus showing a different regulation of HIF-1α at different time points. In conclusion, the β3-AR upstream of the signaling β3-AR/HIF-1α axis exerts its role by PHD2 activity.

#4809

A novel microfluidic platform for PDAC organoid culture and drug screening

Marlene Geyer[1], Daniel Schreyer[2], Lisa-Marie Gaul[1], Désiréé Goubert[1], Susanne Pfeffer[1], Christian Pilarsky[3], Karla S. Queiroz[1]. *[1]MIMETAS, Oegstgeest, Netherlands,[2]University of Glasgow, Glasgoow, United Kingdom,[3]Universitätsklinikum Erlangen, Erlangen, Netherlands*

Pancreatic Ductal Adenocarcinoma (PDAC), the most common pancreatic cancer type, will become the second leading cause of cancer-related deaths by 2030 with mortality rates of up to 93%. Current standard-of-care for patients with PDAC includes chemotherapeutic regimens and pancreatic cancer surgery. However, only 20% of the patients are eligible for surgery due to late diagnosis. Although chemotherapeutic regimens are the leading treatment to PDAC patients, these are still very limited and the development of resistance to treatment is often observed. PDAC tumors are characterized by high-density stroma and hypovascularization, therefore these present high interstitial pressure and hypoxia. These features potentially interfere with the efficiency of chemotherapeutic drugs and highlight the urgent need for novel PDAC screening platforms. Here, we describe the establishment of PDAC organoid cultures in the MIMETAS OrganoPlate®. The aim of this project was to determine the treatment response of PDAC organoids in mono-, and co-culture with pancreatic stellate cells (PSCs) under hypoxic and normoxic conditions. To recapitulate in-vivo like conditions, the 2-lane OrganoPlate® from MIMETAS was used to study organoid growth and sensitivity to treatment. Several standard of care (chemo-)therapeutics were tested on PDAC organoids embedded within an extracellular matrix in the Organoplate® 2-lane. These were exposed to chemotherapeutic treatments for 72h. PDAC organoids showed an overall better survival when grown in co-culture with PSCs. Interestingly, organoids grown in co-culture showed a higher survival rate under hypoxic conditions. In contrast, when grown in monoculture cell

viability was higher or similar under normoxic conditions than in hypoxia for the different chemotherapeutics. The OrganoPlate® 2-lane provides an excellent platform for (co-) cultivation and high-throughput phenotypic drug screening of PDAC organoids, thereby potentially enabling the development of novel *in-vivo* like model systems for efficient patient stratification and drug discovery.

#4810

HIF1α is involved in radiation-induced DNA damage repair and anti-apoptotic pathways in pancreatic ductal adenocarcinoma

Kevin J. Tu[1], Sanjit K. Roy[2], Amit Sawant[2], Hem D. Shukla[2]. *[1]Cell Biology and Molecular Genetics, University of Maryland, College Park, MD,[2]Radiation Oncology, University of Maryland School of Medicine, Baltimore, MD*

Purpose/Objective(s): Pancreatic ductal adenocarcinoma (PDAC) is characterized by an unusually high degree of hypoxia in the tumor microenvironment, which activates hypoxic signaling pathways orchestrated by hypoxia-inducible factor 1α (HIF1α). It has been shown previously that HIF1α significantly increases PDAC radioresistance and growth, though its mechanism of action is unknown. Here, we test the hypothesis that HIF1α confers these traits in PDAC through involvement in DNA damage repair and KRAS signaling *in vitro*.

Materials/Methods: We performed studies with the KPC cell line ($Kras^{LSL\text{-}G12D/+}$;$TP53^{LSL\text{-}R172H/+}$). We used CRISPR-Cas9, a genome editing tool, to generate a HIF1α knockout (KO) cell line. Hypoxic microenvironments were induced using 100uM of the oxygen scavenger $CoCl_2$. Radioresistance and double-strand DNA damage was evaluated and compared between wild-type (WT) and KO cells after treatment with increasing doses of ionizing radiation using neutral comet assays. Tumor signaling pathways were mapped and analyzed using western blot and co-immunoprecipitation. The $KRAS^{G12D}$ inhibitor, BI-2852, was obtained from Boehringer-Ingelheim. Cancer cells were evaluated for growth and migration using cell proliferation assays and scratch wound assays following treatment with 50 uM BI-2852. Bioinformatic analysis was conducted using TCGA (The

Cancer Genome Atlas) data; high and low expression were defined as samples with mRNA expression z-scores ≥ 1 and ≤ -1, respectively,
Results: HIF1α KO cells demonstrated significantly increased radioresistance compared to WT cells following 8 and 10 Gy of radiation in hypoxic conditions (t-test, $P<0.05$). The olive moment of KO cells treated with the IC_{50} radiation dose (4 Gy) was significantly higher than that of WT cells (t-test, $P<0.0001$), suggesting that the DNA damage repair was upregulated by HIF1α. In addition, WT cells demonstrated higher tumor proliferation (t-test, $P<0.01$) and migration (t-test, $P<0.05$) compared to KO cells under hypoxia, suggesting HIF1α promoted tumor growth. WT cells treated with BI-2852 demonstrated significantly lower levels of TP53; using coimmunoprecipitation, we show that TP53 was likely degraded through Mdm2. HIF1α KO was necessary to induce high levels of apoptosis in cells treated with BI-2852. Our results suggest that HIF1α may act synergistically with KRAS to promote tumor survival through anti-apoptotic pathways that target TP53 for degradation. TCGA data also suggest that tumors with high expression of HIF1α is are associated with significantly poorer prognosis coimpared to tumors with low expression of HIF1α (Logrank test, $P=0.003$).
Conclusion: Overall, this study demonstrates that HIF1α promotes DNA damage repair in PDAC and reveals a HIF1α/KRAS/p53 signaling axis. Future studies will test anti-HIF1α and anti-KRAS combination therapies in PDAC mouse models.

#4811

Oxygen tension - dependent differences in cancer cell kinome

Adedeji K. Adebayo[1], Brijesh Kumar[2], Christopher Davis[3], Steven P. Angus[3], Harikrishna Nakshatri[2]. *[1]Department of Biochemistry and Molecular Biology, Indiana University School of Medicine, Indianapolis, IN,[2]Department of Surgery, Indiana University School of Medicine, Indianapolis, IN,[3]Department of Pediatrics, Indiana University School of Medicine, Indianapolis, IN*

Current approaches to preclinical cancer research often fail to consider the impact of ambient oxygen (O_2; ~21%) on cancer cells. This is also true for hypoxia studies that typically involves cancer cells previously grown in

ambient O_2 before subsequent transfer to hypoxia. However, the tumor microenvironment is characterized by significantly lower O_2 levels. We have previously demonstrated the impact of ambient O_2 on stem cell populations, signaling pathways and resistance to therapy. We developed an experimental approach that allows us to collect and process tumor tissues from transgenic mammary tumor mouse models and ovarian cancer patients under physioxia (3% O_2), such that they are never exposed to ambient O_2. In this study, our goal was to explore oxygen-dependent signaling pathway alterations and to determine how these pathways are influenced by targeted drugs in the context of physioxia or ambient air (AA). Our studies revealed increased basal phosphorylation levels of EGFR (Y1068) in the tumor cells in AA, relative to physioxia. However, downstream signaling effectors AKT and ERK showed higher phosphorylation levels under physioxia, compared to AA, suggesting that their activation is independent of EGFR signaling. These findings correlate with the decreased sensitivity of the tumor cells under physioxia to target drugs lapatinib and alpelisib. We then sought to examine basal and target drug induced kinome changes in tumor cells under physioxia and AA via Multiplexed Inhibitor Beads (MIBs) kinome assay. This assay revealed significant differences in the kinome of the tumor cells under physioxia compared to AA. Although direct comparison between vehicle and lapatinib treated cells in physioxia and ambient air showed very minimal changes, pairwise comparison between lapatinib treated physioxia cells and vehicle treated AA cells revealed an increase in the activity of PDGFRB in lapatinib treated physioxia cells. Similarly, a receptor tyrosine kinase (RTK) array and western blotting showed increased basal and lapatinib induced phosphorylation of PDGFRB (Y751) under physioxia. Next, we determined the potential role of PDGFRB in downstream signaling pathway activation of AKT and ERK and resistance to lapatinib. We found that sunitinib, a multitarget RTK inhibitor with high affinity for PDGFR effectively decreased PGDFRB activity under physioxia, with a concurrent decrease in the phosphorylation of AKT. Moreover, tumor cells under physioxia were more sensitive to sunitinib treatment, relative to ambient air. Furthermore, a combination of lapatinib and sunitinib rendered tumor cells under physioxia more sensitive to treatment than with lapatinib alone. These findings suggest that ambient and physioxic oxygen tensions differentially impact cancer relevant

signaling pathways. Therefore, it may be necessary to carry out preclinical cancer studies in the context of physiologically relevant oxygen tensions to aid translatability.

#4812

Inhibition of Smurf2 E3 ubiquitin ligase by heclin and its analogues enhances HIF-1α expression and transcriptional activity in normoxia or hypoxia

Shuai Zhao, Wafik S. El-Deiry. *Brown University, Providence, RI*

Hypoxia-inducible factors (HIFs) act as transcription factors and play an essential role in cellular and systemic responses to low oxygen environments. HIF-1α expression is induced in acute hypoxia typically through failure of its ubiquitination and degradation mediated by Von Hippel-Lindau (VHL). Previously we discovered a non-canonical mechanism where the SMAD specific E3 ubiquitin protein ligase 2 (Smurf2) promotes the ubiquitination of HIF-1α and reduces HIF-1α level in HCT116 colorectal cancer cells. Smurf2 is a HECT-type ubiquitin ligase known to interact with Smad proteins, leading to their ubiquitination and proteasomal degradation. Overexpression of Smurf2 decreased HIF-1α expression in HCT116 and SW480 colorectal cancer cells under hypoxia as well as in RCC4 VHL-deficient kidney renal clear cell carcinoma cells under normoxia. Treatment with MG132 at least partially rescued the expression of HIF-1α following Smurf2 overexpression, indicating involvement of proteasome-dependent degradation in Smurf2-mediated HIF-1α destabilization. Knockdown of *SMURF2* increased HIF-1α expression under normoxia in HCT116 and RCC4 cells. To investigate the effect of Smurf2 inhibition, we tested a selective reversible inhibitor of HECT E3 ubiquitin ligases, heclin, along with its analogues, PYR-41, C646 and 4E1RCat. Treatment with heclin increased HIF-1α expression in HCT116 under hypoxia as well as in SW480 and RCC4 cells under normoxia in a dose-dependent manner. PYR-41 elevated the level of HIF-1α level in HCT116 cells under hypoxia, in RCC4 cells under normoxia and in SW480 cells under both normoxia and hypoxia. To examine the effect on HIF transcriptional activity, we performed luciferase reporter assay using plasmids containing the hypoxia response element (HRE) from the *PGK1* promoter and the *VEGF* promoter, respectively. PYR-41 induced

transcriptional activity on *PGK1*-HRE in both HCT116 and SW480 cells. 4E1RCat robustly activated transcription on both *VEGF*-HRE and *PGK1*-HRE in HCT116 and SW480 cells. In summary, Smurf2 targets HIF-1α for ubiquitination and degradation independently of oxygen concentration and inhibition of Smurf2 to stimulate HIF activity under normoxia or hypoxia may be beneficial in pathological circumstances featuring anemia and hypoxemia.

#4813

ERX-208 as a novel therapeutic for treating ovarian cancer by enhancing endoplasmic reticulum stress

Suryavathi Viswanadhapalli[1], Tae-Kyung Lee[2], Kara Kassees[2], Gaurav Sharma[3], Rahul Gopalam[1], Karla Parra[3], Tanner Reese[3], Michael Hsieh[3], Uday P. Pratap[1], Xue Yang[1], Behnam Ebrahimi[1], Chia Yuan Chen[2], Scott Terry Elmore[2], Christian Cervantes[1], Zhenming Xu[1], Edward Kost[1], Gangadhara Reddy Sareddy[1], Rajeshwar Rao Tekmal[1], Jung-Mo Ann[2], Ganesh V. Raj[3], Ratna K. Vadlamudi[1]. *[1]UT Health Science Center at San Antonio, San Antonio, TX,[2]UT Dallas, Richardson, TX,[3]UT Southwestern Medical Center, Dallas, TX*

Background: Ovarian cancer (OCa) is the deadliest of all gynecologic cancers in the United States. Despite initial response to chemotherapy, most OCa patients become chemo resistant and progress to metastatic disease. Here, we tested the hypothesis that the high basal level of endoplasmic reticulum stress (ERS) in OCa represents a critical vulnerability and drugs that further aggravate this already engaged system in OCa may exhaust its protective features and contribute to apoptosis induction. The objective of this proposal is to identify a hit compound that enhances ERS in OCa and to conduct mechanistic studies.
Methods: We synthesized a small library of >200 chemically distinct oligobenzamide analogs with maintenance of the chemical backbone but altered R groups of ERX-11. We performed the primary screening of this library to evaluate the induction of mRNA levels of two canonical ERS/UPR (unfolded protein response) genes- sXBP1 and CHOP. Biological activity of ERX-208 was validated using multiple OCa cells. Mechanistic studies were conducted using CRISPR/Cas9 KO, Western blotting, reporter

gene assays, IHC and RNA-seq analysis. PK (pharmacokinetics) and toxicity studies were done using C57BL/6 mice. Cell line-derived xenografts (CDXs), patient-derived xenografts (PDXs), patient-derived explants (PDEs), and patient-derived organoids (PDO) were used for preclinical evaluation.
Results: From a screen of a curated ERX-11 derived oligobenzamide library, we identified a hit compound, ERX-208 that potently (IC_{50}~100nM) induces ERS/UPR and apoptosis in multiple OCa cells *in vitro.* CRISPR KO screen identified the lysosomal acid lipase A (LIPA) protein as the critical target of ERX-208. LIPA KO abrogates response to ERX-208, while reconstitution of LIPA restores ERX-208 response. The time course studies showed a robust and consistent induction (>15-fold CHOP, and >10-fold sXBP1) by ERX-208 treatment within 24h. We confirmed induction of classic UPR components peIF2α, CHOP and LC3B using Western blotting in multiple OCa cells. Functionally, ERX-208 causes growth inhibition of OCa cells, as noted by MTT cell viability assays using 15 OCa cells with an IC_{50} of ~50-100nM. The activity of ERX-208 is distinct among oligobenzamides as ERX-11 has limited/no activity against OCa cells. RNA-seq analysis confirmed that ERX-208 induces significant ERS, UPR, and apoptosis. Further, ERX-208 reduced the growth of OCa PDO's *in vitro*, PDEs *ex vivo* and CDXs and PDXs *in vivo.* ERX-208 treatment did not show any signs of toxicity and body weight of mice was not affected. IHC analyses showed increased activation of ERS/UPR markers such as GRP78, p-PERK and decreased proliferation measured by Ki67.
Conclusions: Collectively, our results demonstrated the utility of ERX-208 and will establish a novel therapeutic paradigm in OCa that overcomes tumor heterogeneity by targeting LIPA and enhancing ERS leading to apoptosis.

#4814

Compensatory interplay of p97 segregase and HSP70 chaperone protect cancer cells from heat-induced proteotoxicity

Zdenek Skrott[1], Katarina Chroma[1], Petr Muller[2], Ales Panacek[3], Jiri Bartek[4], Martin Mistrik[1]. *[1]Insitute of Molecular and Translational Medicine, Faculty of Medicine and Dentistry, Palacký University in Olomouc, Olomouc, Czech Republic,[2]Regional Centre for Applied*

Molecular Oncology, Masaryk Memorial Cancer Institute, Brno, Czech Republic,[3]Department of Physical Chemistry, Regional Centre of Advanced Technologies and Materials, Faculty of Science, Palacký University in Olomouc, Olomouc, Czech Republic,[4]Danish Cancer Society Research Center, Copenhagen, Denmark

Due to malignant transformation, cancer cells are characterized by elevated levels of genotoxic, replication or proteotoxic stresses, which makes them vulnerable to various external conditions, including increased temperature. Thus, hyperthermia represents a very effective therapeutic modality usually combined with standard chemotherapy or radiation. Moreover, the elevated temperature is often used in experimental studies related to protein aggregation, cellular heat shock response and other proteostasis mechanisms relevant to cancer progression and treatment. Recently, we developed a single-cell method to inflict defined, subcellular thermal damage, adopting the plasmon resonance principle. Dose-defined heat causes protein damage in subcellular compartments, rapid heat-shock chaperone recruitment, and ensuing engagement of the ubiquitin-proteasome system, providing unprecedented insights into spatiotemporal response to protein damage relevant to cancer. Using this versatile method, we discovered so-far unsuspected compensatory interplay of p97 translocase, the ubiquitin-proteasome system and heat shock protein chaperones in the processing of heat-damaged proteins. As both, p97 and heat shock proteins, represent potential cancer-relevant drug targets, these results can contribute to the development and better implementation of related therapies in cancer treatment.

#4815

TMEM9 decreases ER stress-induced misfolded proteins via lysosomal protein degradation

Dong-Han Wi[1], Su-Rin Jung[1], Seong-Ju Lee[1], Ye-seul Jeon[1], Youn-Sang Jung[1], Jae-Il Park[2]. *[1]Life Science, Chung-Ang University, Seoul, Korea, Republic of,[2]Experimental Radiation Oncology, The University of Texas MD Anderson Cancer Center, Houston, TX*

The endoplasmic reticulum (ER) contributes to various protein modifications such as protein folding. Also, the ER-associated degradation

(ERAD) complex removes defective proteins, which prevents the accumulation of misfolded proteins to avoid abnormality of physiological activity. Several physiological and pathological stimuli, such as hypoxia and nutrient starvation lead to unfolded protein responses (UPRs). Given that hyper-proliferation causes hypoxia and glucose shortening, cancer cells might induce UPRs resulting in misfolded protein accumulation and aggregation. Although the ERAD complex removes defective proteins, the capacity of the proteasomal degradation pathway is not enough to completely clear defective proteins in hyper-proliferative cancer cells. Thus, it is likely that cancer cells require additional misfolded protein degradation systems. Transmembrane protein 9 (TMEM9) has been identified as a vesicular acidification amplifier, which is upregulated in cancer cells for Wnt/β-catenin signaling activation via lysosomal protein degradation. In this study, TMEM9 downregulated ER stress-induced misfolded proteins that decrease cancer cell proliferation and viability. ERAD inhibitor declined cancer cell proliferation, reverted by TMEM9. Intriguingly, TMEM9 decreased ERAD-induced apoptosis instead of promoted autophagic cell death under glucose shorten conditions. Here we suggest that lysosomal protein degradation is an additional protein degradation system for the removal of defective proteins and contributes to stable cancer cell proliferation via the clearing of garbage proteins.

#4816

Targeting GCN2 regulation of amino acid homeostasis sensitizes prostate cancer cells to senolytic therapies

Noah R. Sommers[1], Ricardo A. Cordova[1], Angela J. Klunk[1], Roberto Pili[2], Ronald C. Wek[1], Kirk A. Staschke[1]. *[1]Biochemistry and Molecular Biology, Indiana University School of Medicine, Indianapolis, IN,[2]Medicine, University at Buffalo, Buffalo, NY*

The integrated stress response (ISR) features a family of eIF2 kinases that sense cellular stress, triggering translational and transcriptional modes of gene expression that enhance cell adaptation to the underlying stress. Previously we reported (Cordova et al., 2022 *eLife*) that prostate cancer (PCa) cells rely on one of these eIF2 kinases, GCN2, for maintenance of amino acid homeostasis and sustained proliferation. GCN2 functions to enhance expression of amino acid transporters and subsequent import of

essential amino acids (EAAs) that are necessary to sustain PCa growth. Genetic loss or pharmacological inhibition of GCN2 results in decreased expression of amino acid transporters, severe depletion of intracellular EAAs, and decreased proliferation of PCa cells in culture and mouse xenograft models. Although loss of GCN2 in PCa cells reduces proliferation, depletion of this eIF2 kinase is suggested to lead to cell stasis and modest cell death. We hypothesize that the static phenotype by GCN2 inhibition in PCa cells renders these cells vulnerable to senolytic treatment and is a potential therapeutic target in combination therapies. To address this idea, we utilized models of androgen-sensitive and castration-resistant PCa and non-tumorigenic prostate epithelial cells. GCN2 inhibition induced a static phenotype in PCa cell lines, but not non-tumorigenic prostate epithelial cells, and this was accompanied by increased expression of the senescent markers p53, p21, p27, and MCL-1. Furthermore, induction of senescent markers following GCN2 inhibition in PCa cells was reversed by supplementation with EAAs, suggesting that limitation of EAAs is critical to the induction of cell stasis. Of importance, treatment of PCa cells with Navitoclax, a senolytic agent that targets Bcl-2 family of anti-apoptotic proteins, in combination with GCN2 inhibition resulted in enhanced cell death and apoptosis compared to each single treatment alone. Our results suggest that GCN2 inhibition in PCa cells leads to depletion of EAAs and induction of a static phenotype, rendering these cells vulnerable to targeting the Bcl-2 family of proteins to expedite cell death. As such, therapies integrating GCN2 inhibition and senolytic agents are proposed to be effective strategies for treatment of PCa.

#4817

Protein aggregation promotes HSF1 activity enhancing cell survival during metastatic breast cancer colonization

Natasha Hockaden, Gabi Leriger, John Wang, Haimanti Ray, Richard Carpenter. *Indiana University School of Medicine, Bloomington, IN*

Breast cancer is the most commonly diagnosed cancer in women and is the second leading cause of cancer-related deaths in women. Approximately 20-30% of patients will develop metastases and metastasis is responsible for greater than 90% of breast cancer deaths. Metastasis is a complex process in which the cells combat many forces to survive and spread to

different areas of the body. Metastatic colonization is the rate-limiting step of metastasis and is an inefficient process in which most cells die and only a small fraction of those that survive can form metastases. We have previously shown that heat shock factor 1 (HSF1) promoted epithelial-to-mesenchymal transition (EMT) and the breast cancer stem-like population, potentially linking HSF1 to metastasis. Utilizing an HSF1 gene expression signature that assesses HSF1 transcriptional activity, we further found that patients with high HSF1 activity have significantly worse metastasis-free survival. The physiological function of HSF1 is the master regulator of the heat shock response wherein it upregulates chaperone proteins under stress conditions. Because of these functions and the fact that the process of metastatic colonization is known to involve the stem cell population and incur external stressors, we hypothesized that HSF1 may function in metastatic colonization. To test this, we subjected human breast cancer MDA- MB-231 cells with or without HSF1 knockdown to intracardiac injections in nude mice. This model injects cells directly into the circulation allowing for assessment of metastatic tumor formation in which the major barrier will be metastatic colonization. Mice receiving cells with knockdown of HSF1 had a significantly reduced metastatic burden, indicating HSF1 is necessary for the completion of metastasis and colonization. Consistent with these findings, bone metastatic tumor specimens from patients show increased HSF1 activation compared to their matched primary breast tumors. The mechanism by which HSF1 enables metastatic colonization is unknown. Metastatic colonization likely requires at least two stages that include tumor initiation (or early colonization) characterized by the seeding of a tumor followed by tumor expansion (or late colonization) characterized by rapid proliferation and an increase in tumor size. We observed increased protein amyloid aggregates that correlate with an increase in HSF1 activity during mammosphere formation, suggesting that colonization induces aggregation leading to HSF1 activation that promotes a cell survival response. Overall, my results indicate that HSF1 activity increased during breast cancer metastasis and HSF1 is necessary for colonization. Going forward, I want to understand what controls HSF1 activation during metastasis, which I hypothesize that protein aggregation is increased leading to HSF1 activation.

#4818

GCN2 eIF2 kinase and p53 coordinate amino acid homeostasis and metabolism in prostate cancer

Ricardo A. Cordova[1], Noah R. Sommers[1], Angela J. Klunk[1], Haroon M. Mohiuddin[1], Roberto Pili[2], Ronald C. Wek[1], Kirk A. Staschke[1].
[1]Biochemistry and Molecular Biology, Indiana University School of Medicine, Indianapolis, IN,[2]Department of Medicine, University at Bufallo, Bufallo, NY

Activation of the integrated stress response (ISR) contributes to the progression of many cancers, including prostate cancer (PCa). The ISR features a family of protein kinases that phosphorylate the eukaryotic translation initiation factor 2 (eIF2) during different stress conditions, resulting in repression of global protein synthesis. In parallel, eIF2 phosphorylation also enhances the translation of select gene transcripts, such as ATF4, which directs the transcription of ISR-target genes that are critical for cancer stress adaptation. We recently reported (Cordova et al., 2022 *eLife*) that the eIF2 kinase GCN2 is a driver of the ISR in PCa and is critical for the maintenance of essential amino acid (EAA) homeostasis. GCN2 is activated in PCa due to EAA limitations, resulting in increased expression of key amino acid transporters which provide for nutrient import to facilitate protein synthesis and metabolism that drive PCa proliferation. Genetic loss or pharmacological inhibition of GCN2 results in lowered expression of amino acid transporters, leading to severe depletion of intracellular essential amino acids and reduced proliferation in PCa cell lines and xenograft models. These results support the therapeutic potential of targeting GCN2 in PCa.We recently determined that loss of GCN2 in PCa triggers a G1 nutrient-sensitive cell cycle checkpoint that is dependent on p53 and its target gene CDKN1A, encoding p21 inhibitor of cell cycle. Induced G1 arrest and p53/p21 signaling by GCN2 inhibition is reversed by supplementation with EAAs, suggesting amino acid limitation is critical for activation of p53. Metabolic stresses, such as amino acid starvation, have been suggested to activate p53 in different cancers and p53 regulates metabolic pathways that are critical for cancer cells adaptation to stresses. We also showed that depletion of specific amino acids activates GCN2 and p53 in cultured PCa cells. Using transcriptomic and metabolomic analyses, we determined that loss of GCN2 or p53 in PCa cells impacted multiple metabolic pathways, specifically those involved in amino acid and

nucleotide metabolism, supporting the importance of GCN2 and p53 in metabolic homeostasis. In addition, deletion of p53 in PCa cells exacerbates the activation of GCN2 and the ISR, suggesting that loss of p53 results in amino acid imbalances that further activate GCN2. Importantly, inhibition of GCN2 in combination with loss of p53 resulted in increased cell death and apoptosis in PCa. Our study suggests that GCN2 and p53 can be activated in parallel in PCa and these stress response pathways are crucial for PCa cells to maintain homeostasis and adapt to metabolic stress. We propose that GCN2 and p53 function to coordinate PCa growth and progression by regulating metabolism and cell cycle control. Targeting these stress pathways in combination may provide enhanced efficacy for the treatment of PCa.

#4819

Mechanism of disturbance of nuclear size homeostasis in cancer cells

Changgon Kim, Joon Kim. *Korea Advanced Institute of Science and Technology, Daejeon, Korea, Republic of*

Abnormal increase in nuclear size is one of the criteria for distinguishing cancer cells. The main causes and functional consequences of nuclear size increase in cancer cells are not well known. In this study, we analyzed genome-wide RNAi library screen data to discover genes involved in the maintenance of nuclear size homeostasis. Importantly, many of the screen hits mapped to the functional categories of replication stress and DNA damage repair. We confirmed that depletion of genes required to prevent replication fork collapse causes a significant increase in nuclear size. Excessive replication stress and defects in the DNA repair system are common in many cancers. Therefore, disturbances of nuclear size homeostasis may be due to excessive replication stress and enhanced DNA damage response. To identify effectors that link replication stress and nuclear size change, we investigated candidates such as cell cycle progression, the mTOR pathway, and the cytoskeleton. As previously known, cell cycle arrest at G2 phase increased nuclear size, but replication fork collapse increased nuclear size even more excessively, suggesting the existence of other mechanisms. Inhibition of the mTOR pathway did not block replication stress-induced nuclear enlargement. Interestingly, we found that actin polymerization inside the nucleus plays a role in

determining nuclear size in replication stress condition. Inhibition of nuclear actin polymerization reversed nuclear enlargement due to replication fork collapses. The Increase in nuclear size appeared to reduce the invasive ability of cancer cells. In addition, the enlarged nuclei resisted mechanical stress-mediated nuclear envelope rupture. We also observed a change in the abundance of the tri-methylation of lysine 27 on histone H3. These results suggest that nuclear size homeostasis is perturbed as a result of excessive replication stress, and changes in nuclear size affect the invasive capacity and gene expression of cancer cells. However, it is not clear whether nuclear enlargement act as a strong barrier to metastasis, as nuclear size can readily change through changes in nuclear actin dynamics. Further studies are needed to understand the impact of nuclear size changes on cancer initiation and progression.

#4820

The disassembly of amyloid-bodies

Chloe Kirk, Michael Bokros, Alex Grunfeld, Stephen Lee. *University of Miami Miller School of Medicine, Miami, FL*

The ability of cells to adapt to a wide variety of stress conditions plays a critical role in various physiological and pathological settings, including development, cancer and neurological disorders. We recently reported the discovery of stress-induced low complexity noncoding RNA derived from stimuli-specific loci of the ribosomal intergenic spacer (rIGSRNA); an enigmatic region of the human genome historically dismissed as “junk” DNA. We showed that low complexity rIGSRNA activate a physiological amyloidogenic program that converts the nucleolus into Amyloid-bodies: a molecular prison of immobilized proteins in an amyloid-like state. This conserved post-translational regulatory pathway enables cells to rapidly and reversibly store an array of endogenous proteins in Amyloid-bodies and enter a dormant-like phenotype in response to severe environmental insults. While many membrane-less compartments have been described as liquid-like (e.g., stress granules, P-bodies, germ cell granules), our discovery of Amyloid-bodies provided evidence of an amyloidogenic process that can physiologically transition biological matter to a solid-like state. The ability of mammalian cells to efficiently dissemble Amyloid-bodies raises a fundamental question: Are mammalian cell disaggregases involved in

Amyloid-body disassembly? Here, we show that Amyloid-bodies undergo a solid-to-liquid-phase transition to release sequestered proteins and restore nucleolar functions. An RNAi screened identified key Heat Shock Proteins (Hsps) that remodel Amyloid-bodies back to the liquid nucleoli on stress termination. The composition of mammalian disaggregases differs considerably from non-metazoans and those involved in disassembly of pathological amyloids in vitro. Activation of mammalian disaggregases and Amyloid-body disassembly is dependent on ATP concentration. Conceptually, this work identifies metazoan disaggregases challenging the widely accepted paradigm that the amyloid state is irreversible in mammalian cells. The data also provides alternative insights into pathogenic amyloids by examining their disassembly in cellular systems.

#4821

Exploring the role of a solid-like condensate in breast and prostate cancer

Alexander Grunfeld, Michael Bokros, Chloe Kirk, Stephen Lee.
Biochemistry and Molecular Biology, University of Miami Miller School of Medicine, Miami, FL

Cancer cells are exposed to harsh environmental conditions, which they adapt to by engaging various stress response pathways. A common cellular response to these stressors is the assembly of membraneless compartments known as biomolecular condensates. Our lab discovered one such pathway where exposure to environmental stressors reversibly converts nucleoli into solid-like condensates known as Amyloid bodies (A-bodies). A-bodies induce a state of cellular dormancy by sequestering in an amyloid-like state key proteins involved in processes such as DNA replication and cell cycle progression. *In vitro* experiments showed that suppressing A-body formation in cancer cell lines accelerates tumorigenesis, suggesting that system-wide amyloidogenesis is a mechanism of tumor suppression. The goal of this project was to investigate how A-bodies correlate with tumorigenesis in the context of human tissues. Using formalin-fixed paraffin embedded (FFPE) sections of breast invasive ductal carcinoma and prostate adenocarcinoma, we first confirmed the presence of A-bodies in tumors by staining with the amyloidophilic dye Amylo-glo. In agreement with *in vitro* data in breast and prostate cancer cell lines,

immunohistochemical staining further showed these condensates contain known A-body constituent proteins. Co-staining tissues with Amylo-glo and the proliferation marker Ki67 revealed a negative correlation between A-bodies and cell proliferation, supporting the hypothesis that A-bodies suppress cell growth. Finally, tissue staining comparing primary tumors with distant metastases suggests that A-body biogenesis is reduced in the progression to metastatic disease. Together, our preliminary data presents a biomolecular condensate which can be visualized in human tissues and inversely correlates with cell proliferation. Future directions include examining additional tumor types for the presence of A-bodies and testing the correlation between A-bodies and other markers of proliferation, cell cycle arrest, and environmental stress.

#4822

Signaling pathways associated with stress factors in gastrointestinal cancers

Amayrani Sanchez, Kyle D. Doxtater, Samantha Lopez, Sophia Leslie, Elias George, Vijian Dhevan, Meena Jaggi, Subhash Chauhan, Manish K. Tripathi. *Immunology and Microbiology, University of Texas Rio Grande Valley, McAllen, TX*

Gastrointestinal (GI) cancer affects various significant organs along the gastrointestinal tract, which contains several of the leading cancer-related deaths in the United States. According to the American Cancer Society, colorectal and liver cancers are among the top ten leading deaths due to cancer, ranking third and sixth, respectively. In the Rio Grande Valley region with a majority Hispanic population, colorectal cancer and liver have a higher occurrence than in the entire state of Texas. However, for many, a cancer diagnosis can worsen with stress, which is also a common occurrence within the Rio Grande Valley region due to 30% of its population living in poverty. Stress can cause changes to the immune system's functionality and the inflammatory response that could lead to insufficient surveillance for any potential oncogenicity. When the Hypothalamic-Pituitary-Adrenal (HPA) axis becomes activated by stress, it will release several stress hormones, such as leptin and cortisol, in response that can play a role in the progression and growth of cancer tumors. To further explore this relationship, hepatocellular carcinoma (HCC) cells and

colorectal cancer (CRC) cells were treated with cortisol and leptin at various time points to create models mimicking acute and chronic stress exposure. Afterward, the mRNA mean fold change levels were obtained utilizing the RT-PCR method to determine the levels of each gene in various liver and colorectal cancer cell lines.Additionally, a kinase assay will provide further insight and evidence into the signaling pathway based on the results of the RT-PCR. The current results have shown an upregulation of lncRNA MALAT1, ZNF384, and YB-1 genes at varying degrees depending on the cell line, stress hormone, and duration of treatment. Consequently, these findings have shown an upregulation of oncogenic long non-coding RNA and transcription factors, presenting a signaling oncogenic pathway model by stress factors in HCC and CRC cell lines. Therefore, understanding the role of stress-factors in the oncogenicity and progression of cancer can aid in creating therapeutics for a population where stress can play a role in cancer disparity.

#4823

The novel miR-15a/Fra-2/IGF1R axis drives response to starvation-induced cell stress in pancreatic ductal adenocarcinoma

Gian Luca Rampioni Vinciguerra[1], Marina Capece[1], Luca Reggiani Bonetti[2], Paolo Magistri[3], Federica Calore[1], Giovanni Nigita[1], Rosario Distefano[1], Roberto Ballarin[4], Fabrizio Di Benedetto[3], Andrea Vecchione[5], Barbara Belletti[6], Gustavo Baldassarre[6], Francesca Lovat[1], Carlo M. Croce[1]. *[1]The Ohio State University, Columbus, OH,[2]Department of Diagnostic, Clinic and Public Health Medicine, University of Modena and Reggio Emilia, Modena, Italy,[3]Hepato-pancreato-biliary Surgery and Liver Transplantation Unit, University of Modena and Reggio Emilia, Modena, Italy,[4]3Hepato-pancreato-biliary Surgery and Liver Transplantation Unit, University of Modena and Reggio Emilia, Modena, Italy,[5]4Department of Clinical and Molecular Medicine, Faculty of Medicine and Psychology, University of Rome "Sapienza", Rome, Italy,[6]5Division of Molecular Oncology, Centro di Riferimento Oncologico di Aviano (CRO), Aviano, Italy*

Pancreatic ductal adenocarcinoma (PDAC) is a relatively uncommon malignancy; however, its incidence is rising worldwide, and it is expected

to become the second-leading cause of cancer-related death by 2030. From a histological point of view, PDAC is characterized by a prominent desmoplastic reaction that compresses blood vessels, limiting oxygen and nutrient availability in the tumor microenvironment. Despite that, PDAC cells are capable to adapt dynamically to these stress conditions, adopting different strategies that includes the strict regulation of the autophagic flux. Thus, studying these adaptive mechanisms is crucial to understand PDAC progression and to establish new therapeutic modalities to tackle it. Here, we explore the role of the tumor suppressor miR-15a in the regulation of its putative target Fra-2, a transcription factor, commonly activated by cell stress. By employing IPA on PDAC tumors from TCGA dataset, we found that both miR-15a and its target Fra-2 are predicted to regulate the IGF-1 signaling pathway. In an independent cohort of 44 PDAC samples, miR-15a levels inversely correlated with both Fra-2 and IGF1R expression; conversely, Fra-2 significantly correlated with IGF1R. By chromatin immunoprecipitation and luciferase assay, we assessed that miR-15a directly targeted Fra-2 and IGF1R that, in turn, is transcriptionally regulated by Fra-2 activity. Then, we investigated the role of miR-15a/Fra-2 regulation of IGF1R in the response to starvation-induced cell stress. In starved PDAC cell lines, Fra-2 transcriptional activity triggered IGF1R promoter, causing IGF1R overexpression in control cells but not in miR-15a-overexpressing cells. Consistently, the IGF1 release after starvation induced phosphorylation of IGF1R and activation of the downstream mTOR pathway in control cells but not in miR-15a-overexpressing cells. Therefore, TEM and western blot analysis demonstrated that activation of mTOR *via* IGF1 release reduced the autophagic flux of PDAC control cell lines compared to miR-15a overexpressing cells under starvation. To assess our results in vivo, we injected PDAC cells wild type or Fra-2 knockout into the flank of nude mice. At tumor onset, mice were randomly divided in two groups and fed with control or hypoproteic diet for three weeks. Hypoproteic diet did not interfere with the growth of wild-type tumors, by contrast, significantly impaired Fra-2^{KO} tumors growth rate. Tumor analysis revealed that hypoproteic diet potently induced IGF1R overexpression and mTOR pathway activation in wild-type tumors but not in Fra-2^{KO} tumors. Our findings demonstrate that IGF1R expression is regulated by miR-15a directly and indirectly *via* Fra-2 in PDAC. This novel miR-15a/Fra-2/IGF1R axis, triggered by starvation, regulates the autophagic flux and

growth of PDAC cells in stress condition, and could be targeted by specific small inhibitors.

#4824

Intracellular ferritin expression levels regulate growth and resistance to ferroptosis in pancreatic cancer cell lines

Masataka Maruno[1], Yo-hei Kanamori[2], Takashi Matsumoto[1], Yuta Shiraishi[1], Toru Takematsu[1], Tatsunori Miyata[1], Kosuke Mima[1], Shigeki Nakagawa[1], Hidetoshi Nitta[1], Hiromitsu Hayashi[1], Toshiro Moroishi[2], Hideo Baba[1]. *[1]Gastroenterological Surgery, Kumamoto Univ Graduate School of Medical Sci, Kumamoto City, Japan,[2]Department of Cell Signaling and Metabolic Medicine, Kumamoto Univ Graduate School of Medical Sci, Kumamoto City, Japan*

Background: Pancreatic cancer is one of the cancers with the highest mortality rate, and it is important to develop effective treatments and elucidate prognostic factors. It has been reported that elevated serum ferritin is associated with the prognosis of pancreatic cancer. However, there are few reports on how ferritin in pancreatic cancer tissue acts in pancreatic cancer. Ferritin heavy chain (FTH) is a major component of ferritin, which stores iron and plays a role in suppressing iron-induced generation of reactive oxygen species. In this study, we aimed to examine the expression level of FTH in pancreatic cancer cells and its prognostic and cell biological roles.
Methods: We performed immunostaining of FTH in pancreatic cancer tissue specimens operated on at our hospital and classified the expression level of FTH by scoring the immunostaining intensity and staining rate. The expression levels and prognosis were then evaluated. The overexpression and knockout strains of FTH were generated using a human pancreatic cancer cell line (MIAPaCa-2), and their proliferative and stress tolerance abilities were compared with those of the control group.
Results: Immunostaining of 149 pancreatic cancer surgical specimens showed that the group with high FTH had a significantly shorter overall survival rate than the group with low FTH (5-year survival rate; 16.8% vs. 36.9%, p = 0.018). In multivariate analysis, high FTH expression was also a prognostic factor: in vitro, cell lines overexpressing FTH had enhanced proliferative potential compared to controls, while knockout lines were

suppressed. In addition, the knockout lines showed decreased resistance to RSL-3, an inducer of ferroptosis. Additional studies are currently underway to examine resistance to other drugs and the production of reactive oxygen species in the cells.
Conclusion: In pancreatic cancer, high ferritin expression is associated with worse prognosis and may enhance cell proliferation and stress tolerance, and might be a new treatment or biomarker.

Role of Mitochondria and Signaling Pathways in Cancer

#4828
Therapeutic targeting of P2X4 receptor and mitochondrial membrane potential in renal cell carcinoma
Christopher Rupert[1], Roberto Pili[1], Filomena DeNigris[2]. *[1]University at Buffalo, Buffalo, NY,[2]Universita di Napoli, Luigi Vanvitelli, Naples, Italy*

Clear cell renal cell carcinoma (ccRCC) is the most common lethal subtype of kidney cancer. Large-scale metabolomics data have associated metabolic alterations with the pathogenesis and progression of renal cell carcinoma and have correlated mitochondrial activity with poor patient survival. Our group has recently reported that the lysosome purinergic receptor P2X4 (P2X4R) regulates neoangiogenesis. As ccRCC is characterized by increased angiogenesis we hypothesized that P2X4R may play a role in this disease. Interestingly, TCGA data suggest that P2X4R over-expression correlates with poor overall ccRCC patient survival. Our preliminary results also suggest that oxophosphorylation is the main source of tumor-derived ATP, which exerts a critical impact on tumor energy metabolism and mitochondrial activity in ccRCC. P2X4 receptor expression appears to contribute to the homeostasis of intracellular calcium and integrity of mitochondrial membrane potential in different ccRCC models. Seahorse experiments showed that P2X4R inhibition by 5BDBD, a potent and selective antagonist, caused a rapid dose-dependent reduction of mitochondrial activity. Moreover, prolonged mitochondrial failure induced by 5BDBD was associated with increased radical oxygen species, changes in mitochondrial permeability (i.e. opening of the transition pore complex, dissipation of membrane potential and calcium overload), and cell death *via* both necrosis and apoptosis. P2X4R inhibition by 5BDBD was associated

with a significant anti-tumor effect both *in vitro* and *in vivo* by utilizing several ccRCC cell lines and patient-derived organoids. Interestingly, higher mitochondrial activity was associated with greater sensitivity to 5BDBD. Overall, our results suggest that the perturbed balance between lysosomal integrity and mitochondrial activity induced by P2X4R inhibition may be a therapeutic strategy for a subset of renal carcinoma patients

#4829

Monitoring metabolic plasticity in the tumor microenvironment *in vivo*

Marissa Ashton Howard. *George Mason University, Manassas, VA*

Tumor metabolic reprogramming is a hallmark of cancer progression, survival, and therapeutic resistance. A targetable class of cancer metabolic adaptation exploits mitophagy, a specialized autophagy pathway known to be linked to the cancer phenotype. Mitophagy selectively eliminates dysfunctional mitochondria by targeting them, via autophagosome shuttling, to the lysosome for degradation. Cancer cell mitophagy is triggered by elevated oxidative stress and mitochondria DNA damage caused by hypoxia, radiotherapy, molecular therapy, and immunotherapy. A high mitophagy demand can overwhelm the lysosome capacity resulting in the accumulation of damaged mitochondria that is harmful to the cell, and can suppress biogenesis of healthy mitochondria. We hypothesize that the newly discovered process of secretory mitophagy exports damaged mitochondrial fission-released segments to reduce the overload pressure on the lysosomal system, and thereby sustains cancer cell survival in the face of therapeutic mitochondrial stress. We have discovered a form of secretory mitophagy occurring *in vivo* in a growing solid tumor. Our molecular analysis of the full repertoire of extracellular vesicles (EV) shed into the resident tumor interstitial fluid (IF) *in vivo* yielded a rich set of information about the functional state of mitochondria within the tumor cells, and the host cells. A set of proteins required for sequential steps of fission-induced mitophagy preferentially populated the CD81+/PD-L1+ IF EVs; including PINK1 and ARIH1 E3 ubiquitin ligase (required for Parkin-independent mitophagy), DRP1 and FIS1 (mitochondrial pinching), VDAC-1 (ubiquitination state triggers mitophagy away from apoptosis), and VPS35, SEC22b, and Rab33b (vacuolar sorting). Comparing *in vivo* IF EVs to *in vitro* EVs revealed 40% concordance, with an elevation of mitophagy

proteins in the CD81+ EVs for both murine and human cell lines subjected to metabolic stress. The export of cellular mitochondria proteins to CD81+ EVs was confirmed by density gradient isolation from the bulk EV isolate followed by anti-CD81 immunoprecipitation, MitoTracker export into CD81+ EVs, and ultrastructural characterization. Further, we stimulated mitochondrial oxidative stress and blocked the fusion of the mitophagosome with the lysosome, which markedly stimulated the export of the secretory mitophagy unit. We also found that mitophagy inducer PINK1 cleavage status (full length versus cleaved), is prominently reflected in the set of mitochondrial proteins exported within IF EVs, and may constitute a new quantitative measurement tool to monitor the real-time state of tumor intracellular mitophagy. The outcome is new understanding of the importance of secretory mitophagy that can constitute an important therapeutic target, and a new clinically relevant means of monitoring the in vivo state of mitophagic flux within the tumor microenvironment.

#4830

Uncoupling protein 2 (UCP2) loss of function mediates PDAC tumor suppression by mitochondrial fusion

Ariana Carolina Acevedo-Diaz[1], Emily G. Caggiano[2], Meifang Yu[1], Cullen Taniguchi[1]. *[1]Department of Experimental Radiation Oncology, The University of Texas MD Anderson Cancer Center, Houston, TX,[2]The University of Texas MD Anderson Cancer Center UT Health Graduate School of Biomedical Sciences, The University of Texas MD Anderson Cancer Center, Houston, TX*

Background: Pancreatic ductal adenocarcinoma (PDAC) is a lethal cancer with a dependence on highly active mitochondria to grow and metastasize. We previously found that mitochondrial fusion suppressed PDAC growth and metastasis, leading to improved survival in a preclinical model. The tumor suppressive mechanisms of mitochondrial fusion remain unclear, and thus we explored the role of redox homeostasis through uncoupling protein 2 (UCP2).
Methods/Results: Murine pancreatic cancer cells (KPC) with enhanced mitochondrial fusion (sgDrp1) exhibited higher levels of mitochondrial ROS compared to controls targeting GFP (sgGFP), suggesting altered redox homeostasis. We performed RNAseq on these two cell lines and found that

sgDRP1 cells exhibited reduced levels of UCP2. The UCP2 protein is known to have indirect antioxidant effects by reducing mitochondrial reactive oxygen species via uncoupling of ATP production from the electron transport chain. We found that abrogating UCP2 in KPC cells reduced its capacity for OXPHOS. Moreover, rescue of UCP2 in sgDrp1 cells restored their mitochondrial activity.
Conclusions: Mitochondrial fusion may suppress tumor growth and induce mitophagy by altering redox homeostasis. UCP2 may be a mediator of the tumor suppressive phenotype induced by mitochondrial fusion**,** thus linking mitochondrial dynamics and PDAC antioxidant strategies.
Future Work: These results will be explored for their translation *in vivo* and the effects of pharmacological inhibition of UCP2, both *in vitro* and *in vivo*, via the specific inhibitor Genipin, will be explored.

#4831
Mitochondrial plasticity enables metabolic reprogramming and metastatic latency
Pravat Kumar Parida[1], Srinivas Malladi[2]. *[1]UT Southwestern Medical Center, Dallas, TX,[2]Pathology, UT Southwestern Medical Center, Dallas, TX*

Introduction: Metastatic relapses are common in epidermal growth factor receptor 2 (HER2) amplified breast cancer patients considered disease-free after primary diagnosis and treatment. Stem-like disseminated tumor cells with specialized metastatic traits adapt and survive as latent metastases in distal organs by overcoming oxidative stress, nutrient limitation, microenvironmental and immune defenses. These latent subclinical metastatic cells are responsible for late recurrences. Understanding the traits and vulnerabilities of these cells is critical for developing strategies to prevent metastatic relapse.
Method: Here, we employed mouse models and patient samples along with RNA sequencing, Steady-state metabolite analysis, Lipid profiling, C^{13}-isotope tracing, C12-BODIPY pulse chase, Lentiviral shRNA Knockdown, Transmission electron microscopy etc. to investigate how disseminated latent metastatic cells meet their cellular energetic demands and initiate overt metastasis in the lipid-rich brain microenvironment.

Result: The ability to utilize available nutrients in distal organs and rewire metabolism is critical for survival of disseminated tumor cells. We report that latent metastatic cells in the brain uptake, store, and utilize fatty acids secreted by tumor-associated reactive astrocytes to meet their cellular energetic needs. Fatty acid oxidation (FAO) and dynamin-related protein 1(DRP1) driven punctate mitochondria enabled utilization of fatty acids and promote survival of latent cells by maintaining cellular bioenergetics and redox homeostasis. Attenuating fatty acid oxidation by genetic and pharmacological inhibition disrupted mitochondrial dynamics and limits metastatic incidence. Likewise, depleting DRP1 altered mitochondrial dynamics that results in reduced FAO, increased reactive oxygen species and attenuated metastatic latency and relapse in HER2+ breast cancer brain metastatic models. Furthermore, comparison with patient-matched primary tumor and brain metastasis identified increased pDRP1 expression in brain metastatic lesions. Moreover, pharmacological inhibition of DRP1 reduced brain metastatic burden in these preclinical models.
Conclusion: Despite significant advances in targeted therapies, HER2+ breast cancer patients often develop brain metastasis and their prevention and management remain an unmet need. Our findings in latent HER2+ breast cancer brain metastatic models demonstrate mitochondrial plasticity and altered fatty acid metabolism are key determinants of metastatic adaptation to the brain and establish DRP1 as a promising therapeutic target for treating brain metastasis.
Key Words: Breast Cancer Brain Metastasis, Mitochondrial Plasticity, DRP1, Metastatic Latency, Redox Homeostasis.

#4832

Copy number amplification of OXPHOS genes drives tumor hypoxia in NSCLC

Martin Benej, Katarina Benejova, McKenzie Kreamer, Jinghai Wu, Syed Ashraf, Caroline Wheeler, Rebecca Hoyd, Daniel Spakowicz, Nicholas C. Denko. *The Ohio State University Wexner Medical Ctr., Columbus, OH*

Non-small cell lung cancer (NSCLC) is a highly aggressive disease with a dismal prognosis associated with high rates of treatment resistance and disease recurrence. High-dose stereotactic body radiation therapy (SBRT) is the standard of care for locally advanced non-resectable NSCLC. However,

as discovered more than six decades ago, tumor hypoxia is a significant barrier to effective radiation therapy. In the last decade, immunotherapy targeting immune checkpoints such as programmed cell death 1 (PD-1) has been introduced as first-line NSCLC treatment, yet long-term disease control occurs in less than 25% of patients. Therefore, understanding the mechanisms of the treatment resistance is essential to address the need for novel synergistic therapies to sensitize refractory NSCLC tumors to anti-cancer treatment. Tumor hypoxia has been associated with treatment resistance for decades, yet its role in the clinical management of NSCLC remains largely unexplored. The basis of tumor hypoxia has traditionally been attributed to the oxygen supply deficit as malformed tumor vasculature fails to meet the high demand of the rapidly proliferating tumor mass. However, our preliminary analysis of NSCLC patient datasets in the Cancer Genome Atlas (TCGA) revealed a significant correlation between high-level expression of nuclear genes encoding mitochondrial subunits essential for oxidative phosphorylation (OXPHOS) and the expression of validated hypoxia-regulated genes (Buffa hypoxia score). The oxygen-consumption expression signature was implemented in software that enables the calculation of numerous tumor microenvironment expression signatures, called tmesig. Furthermore, we have observed a direct positive correlation between the hypoxia expression signatures levels in NSCLC patient samples and the copy number amplification (CNA) of essential OXPHOS genes. Because mitochondrial function consumes up to 90% of available cellular oxygen, its activity may indirectly regulate oxygen availability in the tumor microenvironment by rapidly consuming oxygen upon its delivery to the tumor. Mechanistically, this leads to the hypothesis that OXPHOS gene amplification drives mitochondrial function, which may, in turn, promote tumor hypoxia and treatment resistance in NSCLC.

#4833

Inhibiting the mitochondrial RNA degradosome complex SUV3 and PNPase increases dsRNA in the cytoplasm, triggers a viral mimicry response and kills AML cells and progenitors

Geethu Emily Thomas[1], Kazem Nouri[1], Jong Bok Lee[2], Rose Hurren[1], Yongran Yan[1], Neil MacLean[1], Yulia Jitkova[1], Li Ma[1], Xiao Ming Wang[1], Chaitra Sarathy[1], Andrea Arruda[1], Mark D. Minden[1], Li Zhang[2], Vito Spadavecchio[3], Aaron Schimmer[1]. *[1]UHN Princess Margaret Cancer*

Centre, Toronto, ON, Canada,[2]Toronto General Hospital Research Institute, Toronto, ON, Canada,[3]Interlinked Therapeutics LLC, Portland, OR

Eukaryotic cells have two separate genomes; nuclear chromosomal DNA and circular mitochondrial DNA. Mitochondrial DNA lacks introns, and encodes 2 rRNAs, 22 t-RNAs and 13 of the 90 proteins that constitute the mitochondrial respiratory chain. To maintain homeostasis, mitochondrial RNA degradation machinery regulates RNA turnover. ATP-dependent helicase, SUV3 (gene SUPV3L1), and exonuclease PNPase (gene PNPT1) function as a complex to degrade mitochondrial dsRNA. By immunoblotting, PNPase and SUV3 proteins were increased in 7/7 AML patient samples and 13/13 of AML cell lines, compared to the normal hematopoietic cells. Analysis of the TARGET AML dataset revealed AML patients with increased expression of SUPV3L1 ($p = 0.051$, $p= 0.045$) and PNPT1 ($p = 0.0013$, $p = 0.018$) had decreased overall and event free survival. Genetic knockdown or knockout using shRNA or sgRNA against PNPT1 or SUPV3L1 decreased growth and viability of OCI-AML2, TEX, K562, U937, NB4 and OCI-AML 8227 cells. Furthermore, SUPV3L1 & PNPT1 ranked in the top 5.2% and 7.4% of essential genes in 26 leukemia cell lines in CRISPR screens and 2.7% and 4.9% in RNAi screens (depmap.org). Knockdown of PNPT1 & SUPV3L1 also reduced the clonogenic growth of OCI-AML2, TEX and U937 cells and significantly reduced engraftment of TEX cells into the marrow of immune deficient mice, demonstrating the functional importance on leukemia initiating cells in vivo. SUPV3L1 knockdown in primary AML cells reduced engraftment in marrow of immune deficient mice. Bioinformatics analysis to detect processes associated with PNPT1 and SUPV3L1, we identified associations with Response to exogenous dsRNA, Response to virus, and RNA catabolic process ontologies. Consistent with this, we observed knockdown of PNPT1 or SUPV3L1 increased expression of genes (INFgR1, ICAM, IRF7 & JAK/STAT) suggesting an interferon response. As PNPT1 and SUPV3L1 degrade mitochondrial dsRNA, we measured levels of dsRNA after knockdown of these genes. Knockdown of PNPT1 and SUPV3L1 in OCI-AML2 cells increased levels of cytoplasmic/mitochondrial dsRNA 3-4 fold compared to control. Knockdown of PNPT1 and SUPV3L1 also increased dsRNA in 143B cells, but not Rho (0) 143B cells that lack mitochondrial DNA. Upregulation of inflammatory genes leads to viral mimicry and can

increase sensitivity to immune mediated killing. We observed enhanced sensitivity to Double Negative T (DNT) cells mediated killing in PNPT1 and SUPV3L1 knockdown OCI-AML2 cells compared to control cells. In summary, RNA degradosome complex proteins SUPV3L1 and PNPT1 are overexpressed in AML, and are essential for the survival of AML cells and AML stem/progenitors. These enzymes regulate levels of mitochondrial dsRNA, and their inhibition leads to increased cytoplasmic dsRNA triggering a viral mimicry response and enhanced sensitivity to immune-mediated killing.

#4834

Mitochondrial ClpXP degrades serine phosphorylated protein aggregates

Yue Feng, Yulia Jitkova, Alexander Keszei, Jonathan St-Germain, Yongran Yan, Brian Raught, Mohammad Mazhab-Jafari, Aaron Schimmer. *UHN Princess Margaret Cancer Centre, Toronto, ON, Canada*

ClpXP is a serine protease localized to the mitochondrial matrix and maintains mitochondrial proteostasis by degrading damaged/aggregated respiratory chain complex proteins. Both inhibition and hyperactivation of ClpP lead to impaired OXPHOS function and kill leukemic cells *in vitro* and *in vivo*. Yet, the marks that tag proteins for degradation by ClpXP remain unknown.

The bacterial homologue of ClpXP degrades damaged proteins with arginine phosphorylation. Therefore, we assessed how phosphorylation affects ClpXP protease activity. Recombinant ClpXP was incubated with its unnatural substrate, FITC-tagged casein, in the presence of increasing concentrations of phospho-serine (pSer), phospho-threonine (pThr), phospho-arginine (pArg), or phospho-tyrosine (pTyr). In a dose-dependent manner, pSer and pThr free amino acids and short peptides inhibited casein degradation by ClpXP. In contrast, free Ser, Thr, phosphate, pArg and pTyr did not inhibit ClpXP protease activity. In addition, we characterized ClpP peptidase activity and ClpX ATPase activity using the Ac-Trp-Leu-Ala-AMC (Ac-WLA-AMC) peptidase activity assay and the Malachite Green ATPase assay. Neither pSer nor pThr inhibited ClpX ATPase activity or ClpP peptidase activity. Thus, pSer and pThr only blocked ClpXP from

degrading full-length protein without altering the enzymatic activity of the complex.
Next, we characterized pSer and pThr binding to ClpXP by thermal shift binding assay. pSer and pThr free amino acids and short peptides bound to ClpX but not ClpP. All the dephosphorylated counterparts did not bind to ClpX. Therefore, pSer and pThr interact with ClpX outside the ATPase site. cyroEM studies of ClpX and pSer peptides indicated a putative pSer docking site in the central pore of ClpX.
Previously, we identified OXPHOS complex II subunit SDHA as a potential ClpXP endogenous substrate. Therefore, we used SDHA as a model to assess whether serine phosphorylation influenced ClpXP protein degradation in intact cells. Using pSer immunoprecipitation, we observed increased serine phosphorylated SDHA in AML cells after ClpP and ClpX knockdown. The increased serine phosphorylated SDHA was specifically found in the insoluble fraction of the mitochondrial proteins. Supporting that serine phosphorylated SDHA represents aggregated protein, treatment of cells with ROS-inducing antimycin or 42°C heat shock also increased levels of serine phosphorylated SDHA in the fraction of insoluble mitochondrial proteins. Finally, adding recombinant ClpXP to mitochondrial lysates specifically degraded SDHA with serine phosphorylation.
In summary, mitochondrial ClpXP degrades aggregated mitochondrial proteins marked by serine phosphorylated. Thus, this work identifies new degradation machinery for mitochondrial protease, advances the function of mitochondrial ClpXP, and highlights a new therapeutic strategy to target this protease.

#4835

EP4 increases the mitochondrial respiration and promotes cell migration in oral cancer

Rina Nakakaji[1], Masanari Umemura[1], Kohei Osawa[1], Soichiro Ishikawa[1], Kenji Mitsudo[2], Yoshihiro Ishikawa[1]. *[1]Cardiovascular Research Institute, Yokohama City University Graduate School of Medicine, Yokohama, Japan,[2]Department of Oral and Maxillofacial Surgery, Yokohama City University Graduate School of Medicine, Yokohama, Japan*

Introduction: EP4 is one of the prostaglandin E_2 (PGE_2) receptors. We previously reported that EP4 promoted cell migration via Ca^{2+} signaling, however the underlying mechanism has remained unclear. In Ca^{2+} signaling, Store-operated Ca^{2+}entry (SOCE) is a major mechanism of Ca^{2+} import from the extracellular to the intracellular space. Orai1, one of the selective Ca^{2+} channels, plays an important role in SOCE. We focused on the correlation with EP4 and Orai1. Additionally, we found that EP4 promoted the phosphorylation of calcium/calmodulin-dependent protein kinase kinase 2 (CaMKK2) and AMP-activated protein kinase (AMPK) located downstream of CaMKK2, *i.e.*, cell energy regulators. AMPK activation can control positively or negatively the cellular adenosine triphosphate (ATP) supply. Therefore, we investigated how EP4 regulated the mitochondrial function via Ca^{2+} and promoted the cell migration in oral cancer cells.
Materials and Methods: HSC-3, human tongue squamous cell carcinoma cell line was used. ONO-AE1-437 was used as EP4 agonist. HSC-3 cells were transduced with Orai1 shRNA, and control shRNA using lentivirus. The migration ability was evaluated by scratch assay. Measurement of intracellular Ca^{2+} concentration was measured using Fura-2. Immunoprecipitation was performed to evaluate the interaction between EP4 and Orai1. XF Cell Mito Stress Test and XF Real-Time ATP Rate Assay were performed to evaluate the mitochondrial aspiration and the ATP production using Extracellular Flux Analyzer.
Results: Scratch assay showed EP4 promoted cell migration in oral cancer cells (n=4, $p<0.05$). In contrast, Orai1 knockdown negated EP4-induced cell migration. EP4 rapidly increased the intracellular Ca^{2+} concentration, while Orai1 knockdown negated EP4-indued Ca^{2+} increase (n=4, $p<0.05$). Immunoprecipitation showed that EP4 was colocalized and formed complexes with Orai1 (n=4, $p<0.05$). These results indicated that EP4 promoted the cell migration via Ca^{2+} signaling through Orai1. EP4 increased the maximal respiration 3h after the stimulation (n=6, $p<0.05$). ATP production rate shifted mitoATP dominant. These data indicated that EP4 increased the mitochondrial function and the respiratory capacity, potentially regulating its energy supply. These results demonstrated that EP4 promoted mitochondria respiration and then increased the energy production from mitochondria in oral cancer cells.

Conclusion: We concluded that EP4 regulated the mitochondrial function via Ca^{2+} through Orai1 and promoted the cell migration in oral cancer cells.

#4836

Fasting induces greater expression of mitochondrial proteins associated with fatty acid metabolism and non-shivering thermogenesis in brown adipose tissue of knock-in ACSS1K635Q mice

Aishani Sivasai Gargapati[1], Mahboubeh Varmazyad[2], David Gius[2]. *[1]Rice University, Houston, TX,[2]Department of Radiation Oncology, The University of Texas Health San Antonio, San Antonio, TX*

Introduction: Acyl-CoA Synthetase Short Chain Family Member 1 (ACSS1) is an important mitochondrial enzyme for the production of ATP from short chain fatty acids under energetic stress. ACSS1 is highly expressed in brown adipose tissue, heart, and skeletal muscle. ACSS1 is regulated in part by a post-translational modification of ACSS1, whereby the side chain of Lysine-635 is acetylated. The activity of ACSS1 is downregulated by the acetylation of Lysine-635. The downregulation of ACSS1 activity has been shown to impose changes on fatty acid metabolism and body temperature. Our lab observed that homozygous knock-in ACSS1 mice that fasted for 48 hours were hypothermic with a temperature of 30 °C. Here, we utilized mutant mice to simulate acetylated ACSS1, to investigate the role of ACSS1K635Q in mitochondrial fatty acid metabolism and maintenance of body temperature under fasting conditions. Methods: A knock-in ACSS1 mouse model with a mutation of ACSS1K635Q was designed to model the downregulation of ACSS1. Wild Type mice and Homozygous Knock-in ACSS1K635Q mice were either fasted for 48 hours (F48) or fed with a normal diet (ND). Four experimental groups - Wild Type ND and F48 mice and Homozygous Knock-in ACSS1K635Q ND and F48 mice - were examined. Protein was extracted from 10 samples each containing 20 mg of brown adipose tissue. Tissue samples were lysed and immunoblotted with primary and secondary antibodies. Western Blot Western Blot was performed on the proteins Uncoupling Protein 1 (UCP1), UCP2, ACC, and AMPK. Membranes were imaged using the FluorChem M system, and chemiluminescence was quantified using the NIH ImageJ software. ANOVA and t-test were used to conduct statistical analysis ($P < 0.05$).

Results: Homozygous Ki-ACSS1K635Q F48 mice expressed higher levels of UCP1 and UCP2 in BAT than Homozygous Ki-ACSS1K635Q ND mice. We observed a greater difference in UCP1 expression between Homozygous Ki-CSS1K635Q ND and F48 mice compared to the difference in UCP1 expression between Wild Type ND and F48 mice. In Wild Type and Homozygous Ki-ACSS1K635Q mice, UCP1 expression was lower than UCP2 expression. Fasting for 48 hours significantly upregulated p-AMPK in Wild Type mice.
Conclusions: Under fasting conditions, metabolic processes may shift towards a greater proportion of non-shivering thermogenesis due to ACSS1 inactivity. UCP1 likely contributes more to non-shivering thermogenesis than UCP2. Understanding the impact of acetylating ACSS1 provides avenues towards developing personalized treatments that effectively respond to metabolic stressors.

#4837

Inhibition of mitochondrial fission activates glycogen storage to support cell survival in colon cancer

Sumati Hasani[1], Lyndsay E. A. Young[1], Moumita Banerjee[2], Dylan Rivas[2], Jinhwan Kim[2], Ramon Sun[3], Matthew Gentry[3], Xiaopeng Xiong[2], Tianyan Gao[2]. *[1]Molecular and Cellular Biochemistry, University of Kentucky, Lexington, KY,[2]Markey Cancer Center, University of Kentucky, Lexington, KY,[3]Biochemistry and Molecular Biology, University of Florida, Gainesville, FL*

Metabolic reprogramming has been increasingly recognized as one of the major mechanisms that fuels tumorigenesis and disease progression. Our previous studies have shown that in response to fatty acid uptake, colon cancer cells activate mitochondrial fission to support fatty acid oxidation and downstream Wnt signaling. Given the potential benefit of inhibiting mitochondrial fission, Dynamin-Related Protein 1 (Drp1), a pro-fission factor, has become an attractive target for developing anticancer agents. Here we investigated the role of Drp1 in promoting metabolic adaptation in colon cancer. We found that knockdown of Drp1 decreased mitochondrial respiration which resulted in increased glucose uptake and lactate production. In addition, downregulation of Drp1 increased AMP-activated protein kinase (AMPK) activity which coincided with glycogen

accumulation. Consistently, results from GC/MS analysis of cellular metabolites revealed that the levels of glucose-6-phosphate, a precursor for glycogenesis, were significantly elevated in Drp1 knockdown cells whereas pyruvate and other TCA cycle metabolites remained unchanged. Mechanistically, AMPK transcriptionally activates the expression of glycogen synthase 1 (GYS1) and hexokinase 2 (HK2) genes and silencing GYS1 abolished the glycogen accumulation phenotype in Drp1 knockdown cells. Using APC-derived 3D organoids, we demonstrated that the glycogen levels were elevated in $Apc^{f/f}$ $Drp1^{f/f}$ tumor organoids upon deletion of Drp1. Similarly, increased GYS1 expression and glycogen levels were detected in xenograft tumors derived from Drp1 knockdown colon cancer cells compared to control. Functionally, increased glycogen storage allowed Drp1 knockdown cells to survive glucose starvation conditions suggesting an enhanced survival capacity compared to control cells. Taken together, our findings indicate that Drp1 inhibition by itself is unlikely to be sufficient to eradicate cancer cells as adaptive metabolic mechanisms are activated to promote cell survival. However, combining Drp1 inhibition may enhance the efficacy of chemotherapeutic agents for colon cancer treatment.

#4838

Exploiting mitochondrial metabolism to enhance the response to standard of care treatments in ovarian cancer

Laura Formenti, Alessandra Decio, Valentina Dematteis, Giulia Dellavedova, Maria Rosa Bani, Raffaella Giavazzi, Carmen Ghilardi.
Oncology, Istituto di Ricerche Farmacologiche Mario Negri IRCCS, Milano, Italy

Ovarian cancer best practice consists of debulking surgery followed by platinum/taxane based chemotherapy combined with the angiogenesis inhibitor bevacizumab, and the PARP inhibitor olaparib for HRD positive tumors. However, despite significant improvements in its treatment, the 5-year survival rate remains low due to disease recurrence and resistance to therapy. Emerging evidence suggests that the metabolic requirements of cancer cells change after exposure to chemotherapy or targeted therapies, generating a potential Achilles' heel. Here, we focused on exploiting the intrinsic or therapy-induced metabolic vulnerabilities of ovarian cancer to

improve its response to the standard medical care. To this aim, ovarian cancer patient-derived xenografts (OC-PDX), injected orthotopically in nude mice, were used to assess i) the association between the metabolic profile of OC-PDXs and their responsiveness to treatments (i.e. cisplatin, bevacizumab, olaparib), ii) the metabolic changes induced by the treatments and iii) the therapeutic benefit of combining an OXPHOS inhibitor with the above-stated therapies. The effect on tumor progression was evaluated as increase of survival of OC-PDX bearing mice. First, we characterized the metabolic profile of OC-PDXs and divided them into high- and low-OXPHOS according to their dependence on mitochondrial metabolism. Then, we evaluated their response to the standard of care treatments and found that 75% of high-OXPHOS OC-PDXs were sensitive to cisplatin and olaparib, while 100% of low-OXPHOS OC-PDXs were poorly responsive. Response to bevacizumab varied in the two OC-PDX subsets. Further, we demonstrated that cisplatin or bevacizumab treatment induced the emergence of a sub-population of cells from malignant ascites with higher mitochondrial content and tricarboxylic acid cycle (TCA) intermediates and reduced expression of glycolysis-related genes, thus suggesting a shift toward oxidative metabolism in the residual cancer cells after treatment. Targeting these OXPHOS-dependent cells with the respiratory chain complex I inhibitor IACS-010759 improved the survival of mice. These results indicate that the metabolic profile of ovarian cancer cells is associated with the response to cisplatin and olaparib and lay the ground for the rational combination with OXPHOS inhibition to prolong therapies efficacy and eventually delay the development of recurrent disease.
Supported by AIRC IG2019 ID 23520 to RG.

#4839

Chemotherapy alters mitochondrial metabolism in melanoma

Alexander W. Loftus[1], Mehrdad Zarei[2], Omid Hajihassani[2], Johnathan J. Hue[3], Hallie J. Graor[2], Ali Vaziri-Gohar[2], Jordan M. Winter[4], Luke D. Rothermel[4]. *[1]University Hospitals Cleveland Medical Center, Cleveland, OH,[2]Case Comprehensive Cancer Center, Case Western Reserve University, Cleveland, OH,[3]Surgery, University Hospitals Cleveland Medical Center, Cleveland, OH,[4]Department of Surgical Oncology, University Hospitals Cleveland Medical Center, Cleveland, OH*

Background: Advanced and metastatic melanoma carries significant mortality despite recent advances. Metabolic plasticity is a hallmark of cancer and an important resistance mechanism in the face of anti-neoplastic therapies. We sought to understand the effect of chemotherapy, Temozolomide (TMZ), on OXPHOS and TCA cycle metabolism in melanoma cell lines. By understanding these metabolic adaptations to chemotherapy, we hope to identify novel combination therapies.
Methods: A375 and SK-MEL-28 cell lines were used for all experiments. Cell viability assays were performed with 1500 cells per well, treated with TMZ and oligomycin or phenformin, and viability was assessed using PicoGreen dsDNA assay. Western blot was used with primary antibodies against TOM20 and B-actin. LCMS metabolites were assessed by QTRAP triple quadrupole mass spectrometry coupled to a Prominence UFLC HPLC system. This assessed approximately 299 metabolites. Seahorse XFp miniextracellular analyzer was used to obtain OCR with and without TMZ exposure, and after sequential injections of oligomycin, FCCP, and rotenone with antimycin A. Mitochondrial assays included TMRE staining (membrane potential) and Mitotracker Green (mitochondrial mass).
Results: Metabolic profiles of melanoma cell lines change with exposure to chemotherapy. After melanoma cells are exposed to IC30 dose of TMZ, LCMS metabolomics revealed statistically significant increase in TCA cycle metabolites such as succinate, succinyl CoA, malate, oxaloacetate, isocitrate, alpha-ketoglutarate, and fumarate. Melanoma increases OXPHOS in the presence of chemotherapy. Mitochondrial mass, measured by Mitotracker, increased in response to TMZ exposure. We also found increased mitochondrial membrane potential and increased TOM20 expression after cells were treated with TMZ. Seahorse XF Cell Mito Stress Assay demonstrated increased oxygen consumption rate after exposure to TMZ. We then combined TMZ and two mitochondrial inhibitors, phenformin (complex I) and oligomycin (complex V). Combination of phenformin and TMZ was synergistic in cell viability assays as determined by Bliss equation. Oligomycin sensitized both cell lines to TMZ.
Discussion: We have shown that melanoma cells rely on mitochondrial function when exposed to TMZ by increasing levels of TCA cycle intermediates, increasing mitochondrial tropism, and increased expression of mitochondrial enzymes. This demonstrates a metabolic resistance mechanism in response to chemotherapy to promote melanoma cell

survival. Finally, we exploit this adaptation by pharmacologic inhibition of mitochondrial electron transport chain (ETC) with phenformin and oligomycin A. This treatment was synergistic with conventional chemotherapy. Our findings point out that the ETC compartment of mitochondria could be a novel and readily available combination treatment strategy for patients with advanced and refractory melanoma.

#4840

Dysregulation of mitochondrial function by PLK1-mediated PDHA1 phosphorylation promotes Cr(VI)-associated lung cancer progression

Qiongsi Zhang[1], Zhiguo Li[1], Xiongjian Rao[1], Derek B. Allison[2], Qi Qiao[3], Zhuangzhuang Zhang[1], Yifan Kong[1], Ruixin Wang[1], Teresa W. M. Fan[1], Richard M. Higashi[1], Andrew N. Lane[1], Xiaoqi Liu[1]. *[1]Department of Toxicology and Cancer Biology, University of Kentucky, Lexington, KY,[2]Department of Pathology and Laboratory Medicine, University of Kentucky, Lexington, KY,[3]Department of Chemical and Materials Engineering, University of Kentucky, Lexington, KY*

Hexavalent chromium (Cr(VI)), an class I environmental carcinogen, not only induces lung epithelial cell transformation but also promotes lung cancer progression by alterations of the cell cycle and cellular energy metabolism. Using Cr(VI)-transformed (CrT) bronchial epithelial cells (BEAS-2B) and parental BEAS-2B cells, we demonstrate that the level of polo-like kinase 1 (PLK1) is highly upregulated in CrT cells, which blocks mitochondrial function, and further promotes cell proliferation both in vitro and in vivo. Cells expressing a high level of PLK1 exhibited repressed mitochondrial activity due to defective modulation of pyruvate dehydrogenase E1 subunit alpha 1 (PDHA1), which facilitates the carbon influx to TCA cycle via catalyzing pyruvate/ Acetyl-CoA conversion. Mechanistically, we show that PDHA1 can be directly phosphorylated by PLK1 at T57, which triggers collapse of E1 and PDHA1 degradation via activation of mitophagy. These defects resulted in the inhibition of oxidative phosphorylation and reduction of mitochondrial reactive oxygen species (ROS) generation, eventually inhibiting mitochondrial-mediated apoptotic response. Defining the role of PLK1 in metabolic reprogramming in Cr(VI)-associated cancer progression may give us a new perspective and a target to inhibit Cr(VI)-induced cancer development. In addition, PLK1

inhibitors may be used to increase the chemo-sensitivity of cancer cells by restoring the normal function of mitochondria, thus alleviating the drug resistance caused by dysfunction and hyperpolarization of mitochondria.

#4841

SLC25A46 as a novel mitochondrial regulator and biomarker in breast cancer

Heather K. Beasley[1], Ky'Era V. Actkins[2], Tyne Miller-Flemming[2], Nancy J. Cox[2], Rachel Martini[3], Melissa B. Davis[4], Timothy Chu[5], Nicolas Robine[5], Bret C. Mobley[2], Antentor O. Hinton[1]. *[1]Vanderbilt University, Nashville, TN,[2]Vanderbilt University Medical Center, Nashville, TN,[3]Weill Cornell Medical College, NY, NY,[4]Weill Cornell Medical College, Nashville, TN,[5]New York Genome Center, New York, NY*

Triple-negative breast cancer (TNBC) is an aggressive, highly malignant breast cancer (BC) subtype further characterized by poor prognosis and chemoresistance. TNBC disproportionately affects African American and Latina women, where the differences in treatment efficacy cannot only be explained by social determinants of health. A better understanding of treatment outcomes requires a deep analysis of the ancestral-related underpinnings that affects treatment. Accounting for the role of ancestry in BC prognosis and progression, we hypothesize that ancestry has significant influences on BC etiology. Metabolic reprogramming of TNBC cells is shown to influence response to treatments. These distinct metabolic adaptations require the proper function of the mitochondrion, a highly dynamic organelle that coordinates and maintains the energetic demands of the cell. To this end, we sought to investigate novel proteins important in mitochondria function yet are understudied in BC phenotypes. *SLC25A46* plays a significant role in regulating mitochondrial dynamics, cristae maintenance, and respiratory function. Although SLC25A46 poorly characterized, it has been demonstrated to interact with mitochondrial proteins, such as MFN-2 and OPA1, and the MICOS complex, making it an attractive pharmacological target. We were therefore interested if *SLC25A46* has any potential as a target or biomarker in BC. First, we applied PrediXcan, a gene-based statistical algorithm, to calculate genetically predicted gene expression for *SLC25A46* in 70,349 patients of European descent and 14,462 patients of African descent in BioVU, the

Vanderbilt University Medical Center (VUMC) biorepository linked to de-identified electronic health records (EHRs). Models were built using RNA-seq data from the publicly available GTEX version 8 dataset. After fitting a multivariable logistic regression model to test *SLC25A46* predicted expression against 1,704 phenotypes for each tissue, we observed that patients with high predicted expression were more likely to receive diagnosis of 'abnormal findings in mammograms' (P=2.76E-06, OR=2.26) or 'lump or mass in breast' (P=8.9E-06, OR=2.61) in the European descent group, which is well powered; however, we are not powered to replicate this finding in the African descent group. Therefore, we investigated *SLC25A46* expression in an international RNAseq cohort enriched with women of African ancestry, including African Americans (AA), West and East Africans with TNBC (n=26). Interestingly, *SLC25A46* shows significantly higher expression among self-reported AA than Ghanaian or Ethiopian women with TNBC (P=0.003). Thus, we postulated that these differences in *SLC25A46* for patients of African ancestry might serve as a novel biomarker for cancer outcomes. Together, these data suggest that *SLC25A46* has implications in BC as a novel target in cancer development, specifically in patients with admixed ancestry.

#4842

Stress-induced mitochondrial adaptations in the polyaneuploid cancer cell state

Melvin Li, Laurie G. Kostecka, Sarah R. Amend, Kenneth J. Pienta. *Cancer Ecology Center, The Brady Urological Institute, Johns Hopkins University School of Medicine, Baltimore, MD*

Metastatic cancer is responsible for 90% of cancer deaths and is incurable due to resistance to all systemic anticancer therapies. While the classic model of therapy resistance is described by the presence of pre-existing resistant clones from tumor cell heterogeneity, our lab proposes the polyaneuploid cancer cell (PACC) state as a survival mechanism that cancer cells access when exposed to environmental stress such as hypoxia and chemotherapy. Our preliminary data has shown that cells that enter the PACC state exhibit repeated whole genome doubling, an increase in cell size, and proliferative arrest. In addition, we observed that a subpopulation of PACCs can give rise to non-polyploid, proliferative progeny after release from chemotherapy, modeling cancer recurrence. We hypothesize that the PACC state drives therapeutic resistance and elimination of this adaptive state is key in tackling the incurability of cancer. Mitochondria are essential organelles that have multifaceted roles in the cellular stress response and drug resistance. They integrate metabolic pathways for ATP generation and macromolecule biosynthesis, regulate apoptotic cell death, and activate stress response mechanisms in presence of drug treatment. We found that cells in the PACC state increase mitochondrial biogenesis and live cell imaging with MitoTraker dyes indicate that they also have higher activity per mitochondria when compared to parental cells. Cells that accessed the PACC state also had higher levels of TCA cycle metabolites including citrate, isocitrate, alpha-ketoglutarate, succinate, fumarate, and malate, suggesting increased mitochondrial function. Future work includes analysis of mitochondrial morphology via live cell confocal microscopy and of mitochondrial function via metabolic flux analysis on glucose and glutamine metabolism of cells in the PACC state. Our eventual goal is to characterize how cells in the PACC state alter their mitochondrial structure and function to survive therapy. Identifying vulnerabilities of the PACC phenotype will enable new therapeutic approaches to overcome therapy resistance in cancer.

#4843

Characterization of T-cell metabolic defects in chronic lymphocytic leukemia preclinical model

Wael Gamal[1], Melanie Mediavilla-Varela[2], Kamira Maharaj[2], Angimar Uriepero[2], Vishaal Kunta[2], Eva Sahakian[2], Javier Pinilla-Ibarz[2].
[1]Department of Molecular Medicine, Morsani College of Medicine, University of South Florida, Tampa, FL,[2]Department of Immunology, H. Lee Moffitt Cancer Center & Research Institute, Tampa, FL

Chronic lymphocytic leukemia (CLL) is the most predominant leukemia affecting elderly population in western countries. T-cell dysfunction is a CLL hallmark contributing to the low success rates of adoptive cell therapy in patients. Generally, exhausted states of tumor infiltrating lymphocytes are associated with defects in metabolic and mitochondrial adaptation, preventing normal cytotoxic functions. A handful of recent reports have demonstrated metabolic defects in CLL patients' T-cells. Nevertheless, the field is still lacking sufficient studies to validate these metabolic changes in the preclinical Eμ-TCL1 murine model which is the most established model for CLL. Our aim is to uncover T-cell mitochondrial and metabolic defects in the Eμ-TCL1 splenic microenvironment. In this study, CLL was induced in mice via the adoptive transfer of leukemic splenocytes from transgenic Eμ-TCL1 mice into wild type (WT) recipients. Multiparameter flow cytometry was used to investigate mitochondrial properties and cellular glucose uptake of splenic CLL $CD8^+$ T-cells. Moreover, we measured the expression levels of PGC-1α, a master regulator of mitochondrial function, and exhaustion-related markers in $CD8^+$ T-cells. T-cell mitochondrial function was measured using mitochondrial stress test following *in vitro* CD3/CD28 stimulation for 72 hours. Nanostring gene expression analysis was done to compare metabolic gene expression profiles of $CD8^+$ T-cells from either WT or Eμ-TCL1 mice. Probing Eμ-TCL1 splenocytes with mitotracker green and tetramethylrhodamine methyl ester revealed accumulation of depolarized mitochondria in $CD8^+$ T-cells compared to WT counterparts. Our results also showed significant changes in mitochondrial and cellular reactive oxygen species levels as indicated by mitosox and H_2DCFDA staining, respectively. Additionally, marked reduction of

glucose uptake by Eμ-TCL1 $CD8^+$ T-cells was noted following incubation with 2-NBDG glucose analog. Observed mitochondrial abnormalities in the Eμ-TCL1 $CD8^+$ T-cells were associated with a significant downregulation of PGC-1α expression. Flow cytometry analysis demonstrated a significant increase in the expression of exhaustion markers in Eμ-TCL1 $CD8^+$ T-cells and reduction in self-renewal marker, TCF-1. Interestingly, the abnormal mitochondrial properties were directly correlated with PD-1 expression in Eμ-TCL1 T-cells. Nanostring significance score analysis of Eμ-TCL1 versus WT $CD8^+$ T-cell RNA revealed upregulation of glycolysis, mitochondrial respiration, T-cell receptor and costimulatory pathways. On the other hand, there was a downregulation in autophagy, AMPK and amino acid transporter pathways. In conclusion, our work characterizes for the first time the metabolic and mitochondrial defects of $CD8^+$ T-cells from Eμ-TCL1 murine model and outlines the correlation of these defects with T-cell exhaustion in CLL.

#4844

Development of an oxygen consumption rate assay for a standard plate reader

Ian Marozas, Zhiyang Zeng, Mike Valley, Jolanta Vidugiriene, James Cali, Wenhui Zhou. *Promega, San Luis Obispo, CA*

Cells generate ATP by two metabolic pathways, oxidative phosphorylation (OXPHOS) and glycolysis. Together, the amount of ATP generated by both OXPHOS and glycolysis define a cell's metabolic phenotype and fitness. Researchers are interested in methods to characterize cellular metabolic fitness, which can be a powerful a selection criterion for cell-based therapies such as CAR-T cell therapy. Researchers are also interested in measuring the effects of drug treatment on metabolic fitness, to identify metabolic targets for cancer therapeutics and to determine mitochondrial toxicity of novel therapeutics. Here, we have developed a low-cost strategy for a standard plate reader to monitor the rate change of oxygen concentration, or the oxygen consumption rate (OCR), which is a measure of OXPHOS activity. In our assay, oxygen quenches a phosphorescent porphyrin dye in a concentration dependent manner, allowing one to calculate the oxygen concentration of the culture system with the Stern-Volmer relationship. The porphyrin dye is embedded within nanobeads that

are suspended above the cell monolayer and the phosphorescence of the beads is measured from the bottom of the well with a standard plate reader. We found that the OCR increased with cell seeding density in three separate cell lines: HEP-G2, HCT-116, and K-562 suspension cells. We showed that inhibitors of the electron transport chain (ETC) decreased OCR, whereas an uncoupler of the electron transport chain, FCCP, increased OCR in a dose dependent manner. Lastly, mitochondrial fitness (e.g., spare respiratory capacity) was determined by sequentially dosing the mitochondria with poisons specific to the different ETC complexes.

#4845

Ultra-deep sequencing of mitochondrial genome to explore the dynamic mutational changes associated with oral cavity squamous cell carcinoma progression

Alka Singh[1], Ashwin Lakshman Koppayi[1], Ping Wu[2], Mark Lingen[3], Vasudha Mishra[1], Alexander Pearson[1], Ari Rosenberg[1], Nishant Agrawal[4], Karthik Suresh[5], Evgeny Izumchenko[1]. *[1]Medicine, Section of Hematology and Oncology, University of Chicago, Chicago, IL,[2]Otorhinolaryngology Head and Neck Surgery, Central South University, Changsha, China,[3]Pathology, University of Chicago, University of Chicago, IL,[4]Surgery, Section of Otolaryngology-Head and Neck Surgery, University of Chicago, Chicago, IL,[5]Pulmonary Critical Care Medicine, Johns Hopkins University, Baltimore, MD*

Oral cavity squamous cell carcinoma (OCSCC) is a devastating disease, causing substantial morbidity and mortality. While many OCSCCs arise from an existing dysplastic lesion, not all oral premalignant lesions progress to OCSCC. Current methods for oral premalignancy and OCSCC diagnosis (visual and tactile exam followed by tissue biopsy and histologic evaluation) cannot discriminate between benign inflammatory changes and high-risk premalignant lesions that require interventions, underscoring the need for molecular-based biomarkers. The multi-step cancer progression from normal epithelium to premalignant lesion and invasive SCC is driven by the accumulation of genetic alterations, including changes in mitochondrial DNA (mtDNA). Due to the lack of protective histones and limited repair mechanisms, mtDNA is susceptible to damage by

environmental carcinogens and reactive oxygen species, a byproduct of the oxidative phosphorylation system. As a result, mutation rate in mtDNA is ~10 times higher than in nuclear DNA, and may greatly facilitate the risk of mitochondrial dysfunction. Previous studies underscore that acquisition of somatic mtDNA mutations directly involved in tumorigenesis, and not merely epiphenomena. However, the impact of these studies is limited by an incomplete understanding of mitochondrial genomic alterations in the transition of preneoplastic lesions to invasive disease. In this study we used a unique cohort of 27 patients with matched longitudinally collected samples (histologically normal mucosa, dysplastic lesion, and SCC) coupled with novel ultra-deep mitochondrial sequencing (mtDNA-Seq) method to assess the mtDNA mutational landscape throughout the continuum of OCSCC progression. Using a custom bioinformatics workflow, somatic mutations were detected in a subset of the premalignant lesions, with overall higher mutational load observed in OCSCC specimens. While sequencing revealed a large degree of inter-patient heterogeneity, a panel of non-synonymous aberrations were present in both premalignant and invasive neoplasms. The majority of shared mutations showed an increase in fractional abundance in tumors, compared to the precursor lesions (suggesting a spatial expansion of these clones as they progressed histologically), and were enriched for coding mutations in complex-I subunits (critical region for ATP production), which is associated with an oncogenic phenotype. Additionally, mtDNA content increased in OCSCC tumor in a subset of patients, suggesting a cell compensation for defective oxidative phosphorylation and lower ATP production per mitochondria. Here we report the first comprehensive characterization of mitochondrial mutational landscape in dysplastic and invasive SCC lesions, and reveal key molecular events associated with the transition from non-invasive to invasive state.

#4846

Mitochondria packaged from platelet-derived microvesicles modulate the metabolism and mitochondrial dynamics of breast cancer cells

Vanessa L. Gauvin, Vanessa Veilleux, Nicolas Pichaud, Gilles A. Robichaud, Luc H. Boudreau. *Université de Moncton, Moncton, NB, Canada*

The incidence of breast cancer among women far exceeds those of other cancers where metastasis accounts for the majority of deaths associated with the disease. It is well established that platelets play a prominent role in breast cancer malignancy and disease progression. Recently, activated platelets have been characterized to release platelet-derived microparticles (PMPs), which can also package functional mitochondria of platelet origin (termed mitoMPs). We recently demonstrated that mitoMPs can interact with breast cancer cells where they transfer their cargo (i.e., mitochondria) to recipient cancer cells upon their internalization. Given that metabolic reprogramming through mitochondrial dynamics represents a hallmark trait of cancer progression, the intercellular trafficking of foreign mitochondria provided by mitoMPs represent a new mechanistic avenue for cancer cell metabolic plasticity and disease progression.Therefore, the aim of this study was to evaluate the impact of mitoMP-packaged mitochondria on recipient breast cancer cell mitochondrial dynamics upon internalization. Technically, a series of breast cancer cell models (MB231, MCF7 and MCF10A) were co-cultured with mitoMPs and profiled for mitochondrial dynamics and function using complementing experimental approaches, such as flow cytometry, confocal microscopy, and RT-qPCR. We show that mitoMPs and their mitochondria cargo internalize primarily into the malignant MB231 cell model. To investigate the impact of mitoMP uptake by cancer cells on the mitochondrial dynamics, RT-qPCR and Western blot analyses were performed to profile the expression levels of several fusion and fission proteins, including OPA1, MFF, DRP1, MitoFusin 1 and MitoFusin 2. Finally, using fluorescent-based assays, we confirmed that mitoMPs modulated ATP production in MB231 breast cancer cells through upregulation of the OXPHOS pathway. Our research provides a new mechanism by which extracellular vesicles (mitoMPs) play an important role in cancer cell mitochondrial dynamics and function to support metabolic plasticity during the metastatic journey of cancer cells. The knowledge gained from these studies will further provide new avenues for strategic intervention to mitigate the morbidity and mortality associated with breast cancer disease.

#4847

Investigating the transcriptional regulation by estrogen-related receptor alpha (ERRα) under different metabolic conditions

Brittney A. Hua, Chien-yu Chen, Yang Li, Lina He, Bangyan Stiles, Ielyzaveta Slarve. *Pharmacology and Pharmaceutical Sciences, University of Southern California, Los Angeles, CA*

Estrogen-related receptors (ERRs) are orphan nuclear receptors identified based on their high sequence similarity to estrogen receptors (ERs), but ERRs do not have a known endogenous ligand. ERRs play a primary role in regulating the transcription of genes involved in mitochondrial and lipid metabolism and are abundantly expressed across tissues. Because of ERR's role in metabolism, it is suggested that they may also play a role in tumor metabolism, where dysfunction in lipid metabolism promotes tumor cell growth. The ERR subfamily is comprised of three isoforms: ERRα, ERRβ, and ERRγ. Studies targeting the ERR isoforms found that the absence of ERRα presents obesity and insulin resistance with an increase in bone mass, deletion of ERRβ causes placental abnormalities and embryonic lethality, and deletion of ERRγ leads to mitochondrial dysfunction. Together, these studies strongly suggest that ERRs, particularly ERR α and γ, function primarily as metabolic regulators, with ERRα being the predominant isoform expressed in the liver. In addition, the mechanisms leading to lipid accumulation vary under different feeding conditions. Previous studies from our lab showed that PTEN and PI3K/AKT signaling regulates ERRa expression and its function. Furthermore, we demonstrated that inhibiting ERRα blocks liver steatosis and steatohepatitis developed in a mouse model where loss of tumor suppressor PTEN drives both steatosis and cancer development. In addition, we found that ERR-PA, a small molecule inhibitor for ERR, attenuated cancer cell growth and proliferation in both mouse hepatocytes and human cancer cell lines. Here, we report transcriptome network regulated by ERRα under different metabolic conditions and further explored its regulation by the PI3K/AKT pathway. A better understanding of the role ERRα plays in physiology will allow further development of ERR-PA as a potential therapy for liver steatohepatitis, which progresses to end stage cirrhosis and ultimately liver cancer.

#4848

Effects of cinnamon extracted under acidic conditions on proliferation of MCF7 cells

Madison Anderson, Amy Stockert. *Ohio Northern Univ., Ada, OH*

Recent evidence suggests that MCF7 cells utilize free fatty acids as a primary energy source by increasing lipase activity in neighboring adipocytes. Research in our lab suggests that lipase activity is increased by cinnamon extract in differentiated 3T3-L1 adipocytes. We hypothesized that since co-cultures between adipocytes and MCF7 cells demonstrated an increase in lipase activity and increased proliferation, cinnamon extract may increase proliferation of MCF7 cells, making cinnamon an important ingredient to avoid in patients with breast cancer. Cells were plated and treated with varying amounts of cinnamon and monitored for proliferation using the MTT assay. Cells consistently, albeit not significantly, showed an increase in proliferation when treated with cinnamon. Additional studies need to be completed in order to confirm these effects and look for significance, although the importance of this finding warrants rapid reporting. Our lab will examine the effects of cinnamon extract at varying concentrations on MCF7 cell proliferation under variable media conditions as well as monitoring the lipase activity in the MCF7 cells.

#4849

PPARγ and FoxO1 expression and activity in aqueous cinnamon extract treated cells

Sean Mild, Cole Swartz, Amy Aulthouse, Amy Stockert. *Ohio Northern Univ., Ada, OH*

Peroxisome-proliferator activated receptor (PPARγ) has been proven to have inhibitory effects on tumor angiogenesis. Research has demonstrated that natural PPARγ ligands are anti-tumorigenic due to growth inhibition and anti-proliferative effects. Cinnamon is one potential PPARγ ligand tested to explore its effects on PPARγ and FoxO1 expression and activity. Literature also suggests that breast cancer proliferation is increased with obesity and co-cultures of adipocytes with MCF-7 cells have suggested an increase in lipase activity. We therefore sought to explore the effects of cinnamon on these transcription factors and lipase activity in 3T3-L1 cells to determine if cinnamon is a plausible co-therapeutic for breast cancer patients. 3T3-L1 cells were cinnamon treated for 48-96 hours post differentiation. Nuclear protein was extracted for ELISA quantification of

PPARγ and FoxO1 binding potential. Cytosolic and nuclear protein extracts were analyzed via Western blot of FoxO1 and PPARγ. Copy DNA was produced from the total RNA and expression levels of PPARγ and FoxO1 were examined by TaqMan real-time PCR assays. A lipase activity assay was performed on freshly extracted protein from cultured cells. Western blot data demonstrates an increase in FoxO1 protein with cinnamon treatment at 96 hours post differentiation. PPARγ data shows no significant changes in protein quantity, however ELISA data suggests increases in binding potential PPARγ as well as FoxO1 transcription factors with cinnamon treatment. Preliminary expression analysis suggests changes in both PPARγ and FoxO1. Lipase activity data suggests a significant increase in cinnamon treated adipocytes. Data from the study suggests that cinnamon activates PPARγ and that it may play a role in decreasing tumorigenic activity. However, with particular concern in breast cancer cells, the activation of PPARγ in adipocytes appears to increase the lipase activity, thus producing more free fatty acids and potentially enhancing energy dependent proliferation.

#4850

High salt diet induced tumor initiating stem cells mediate breast cancer progression

Lisa Tucker[1], Sonya Reid[2], Jeffrey C. Rathmell[2], Venkataswarup Tiriveedhi[1]. *[1]Tennessee State University, Nashville, TN,[2]Vanderbilt University, Nashville, TN*

High-salt (sodium chloride) diets have been associated with several chronic inflammatory diseases. While the role of chronic inflammation in cancer is well established, the specific role of high salt diet in carcinogenesis is unknown. Previous studies with syngeneic murine breast cancer models, both in our laboratory and others, have shown that high salt (HS) diet induced tumor regression through inflammatory activation of anti-tumor adaptive immune responses. We tested this counter-intuitive and suspiciously beneficial role of HS diet by performing sequential passage studies in preclinical murine models. Six week old mice were placed on high salt diet for 2 weeks prior to injection with syngeneic 4T1 and Py230 triple negative breast cancer cells (into BALB/c and C57Bl/6J mice, respectively, referred to as passage-1). Tumors were harvested after four

weeks of injection. The cancer cells depleted of immune cells were collected from these harvested tumors and reinjected into new non-tumor bearing mice. This cycle was repeated three times. In passage-1 cohort, by day 28, HS diet induced reduced tumor progression in both 4T1-BALB/c (267 ± 59 mm^3) and Py230-C57Bl/6J (238 ± 54 mm^3) as compared to regular salt (RS) diet cohort (611 ± 94 mm^3 and 473 ± 69 mm^3, respectively; $p<0.05$ for both). However, in passage-4 cohort, by day 28, HS diet induced significantly higher tumor progression in both 4T1-BALB/c (806 ± 91 mm^3) and Py230-C57Bl/6J (743 ± 81 mm^3) models, as compared to regular salt (RS) diet cohort (577 ± 83 mm^3 and 462 ± 77 mm^3, respectively; $p<0.05$ for both). Cellular analysis by flow cytometry revealed that there was a 12-19 fold increase in tumor initiating stems cells (TISCs) in passage-4 HS diet cohort compared to RS diet cohort. Mechanistic studies have demonstrated that there was increased TGFβ expression on TISCs obtained from passage-4 HS diet cohort which correlated with enhanced exhaustion phenotype ($CTLA4^+$) of tumor infiltrating adaptive immune cells (CD4 and CD8 T cells) in this cohort. Co-treatment with anti-TGFβ and anti-CTLA4 monoclonal antibodies (mAb) in passage-4 HS diet cohort, significantly reduced tumor progression ($p<0.05$), as compared to treatment with either mAb alone. Taken together, these data demonstrated that chronic HS diet leads to expansion of TGFβ expressing TISCs leading to host immune exhaustion and tumorigenesis. Importantly, anti-TGFβ mAb exerted a favorable synergistic effect to enhance the anti-tumor efficacy of immune check-point inhibitors.

#4851

Improving the efficacy of dual ERK-MAPK and autophagy inhibition as a therapeutic strategy for pancreatic ductal adenocarcinoma

Jonathan M. DeLiberty, Clint A. Stalnecker, Kristina Drizyte-Miller, Elyse G. Schechter, Noah L. Pieper, Runying Yang, Channing J. Der, Adrienne D. Cox, Kirsten L. Bryant. *University of North Carolina at Chapel Hill, Chapel Hill, NC*

Pancreatic ductal adenocarcinoma (PDAC) is characterized by KRAS- and autophagy-dependent growth. We and others recently demonstrated that inhibition of the RAF-MEK-ERK pathway resulted in upregulated autophagy, and that dual treatment with the autophagy inhibitor

hydroxychloroquine (HCQ)/chloroquine (CQ) and MEK or ERK inhibitors (MEKi, ERKi) synergistically blocked PDAC growth. These findings provided rationale for our initiation of Phase I/II clinical trials evaluating the combination of MEKi (binimetinib; NCT04132505) or ERKi (LY3214996; NCT04386057) with HCQ in PDAC. However, HCQ/CQ are not specific or potent autophagy inhibitors. Thus, we sought to identify a more efficacious autophagy inhibition strategy. To this end, we performed a CRISPR-Cas9 mediated genetic loss-of-function screen with a library encompassing cancer signaling pathways in the presence or absence of CQ. In the absence of CQ, we identified PIKfyve, a lipid kinase critical for the recycling dynamics of lysosomes, as an essential autophagy-related gene in PDAC cells. PIKfyve inhibition, by the clinical candidate inhibitor apilimod, resulted in potent reduction of autophagic flux and growth. Additionally, PIKfyve inhibition resulted in robust intracellular vacuolization. Vacuoles stained positive for the lysosomal marker, LAMP1, and exhibited reduced acidity and impaired cargo degradation. Importantly, when we inhibited MEK, with the clinical stage MEKi mirdametinib, and PIKfyve (with apilimod) together, we observed decreased MEKi-induced autophagic flux and synergistic impairment of PDAC cell proliferation. Growth inhibition was due in part to an induction of apoptosis unique to combination treatment. Synergistic growth suppression was maintained in a panel of patient derived PDAC organoids, suggesting this may be an efficacious therapeutic strategy for PDAC treatment. In the presence of CQ, our CRISPR-Cas9 screen showed that loss of upstream autophagy-related genes sensitized PDAC cells to CQ treatment. Validation indicated that vertical inhibition (dual inhibition of distinct nodes of a linear pathway) of the autophagy pathway further reduced autophagic flux relative to inhibition of any single node and synergistically reduced PDAC cell growth. Furthermore, combining ERK-MAPK inhibition with vertical inhibition of autophagy improves the *in vitro* efficacy of this treatment strategy. Ongoing studies are aimed at delineating the mechanism underlying the synergy observed with anti-autophagy inhibitor combinations and further validation in more advanced preclinical models of PDAC.

#4852

Metabolomic rewiring in endocrine therapy resistant estrogen receptor positive breast cancer

Songyeon Ahn[1], Junhyoung Park[1], Sandra L. Grimm[1], Badrajee WB Piyarathna[1], Nagireddy Putluri[1], Gokul Das[2], Cristian Coarfa[1], Benny A. Kaipparettu[1]. *[1]Baylor College of Medicine, Houston, TX,[2]Roswell Park Comprehensive Cancer Center, Buffalo, NY*

Breast cancer (BC) is one of the most commonly diagnosed cancers worldwide and the most common in women in the United States. The majority of the BC are estrogen receptor alpha positive (ER+) and are likely to respond to endocrine therapy. Tamoxifen and fulvestrant are the most widely used hormonal treatments for ER+ BC. However, nearly half of patients receiving endocrine therapy suffer from the risk of recurrence due to either intrinsic or acquired resistance. Thus, it is vital to understand the mechanisms of resistance to endocrine therapy in ER+ BC. Metabolic reprogramming is one of the significant hallmarks of cancer and it is now known that many tumors utilize mitochondrial oxidative phosphorylation (OXPHOS) for their energy needs. Our lab previously reported that metastatic triple-negative breast cancer (TNBC), which does not express ER, has a high energy dependency on mitochondrial fatty acid beta-oxidation (FAO). In this project, we developed a gene signature by integrating the transcriptomic, metabolomic, and lipidomic data from FAO rate-limiting gene (CPT1) modulated TNBC cells. Our signature represented the FAO-regulated gene set relevant to metabolic or lipidomic changes. We discovered a significant reliance on this TNBC signature in endocrine-resistant ER+ BC. Clinical data suggests that our gene signature predicts the survival of endocrine-treated ER+ BC patients. Though increased fatty acid consumption is reported in tamoxifen-resistant cells, the role of FAO in endocrine treatment resistance is largely unclear. We then analyzed the metabolic reprogramming in ER+ BC cell lines after tamoxifen or fulvestrant therapy. Molecular, genetic, and metabolic analyses suggested that endocrine therapy-induce AMPK-FAO-OXPHOS signal activation in ER+ BC cells. Furthermore, the knockdown of CPT1, the rate-limiting enzyme of FAO, or treatment with FAO inhibitors significantly enhanced the response to endocrine therapies. We have also reported that FAO induces the autophosphorylation of the c-Src proto-oncogene in TNBC tumors. Thus, we analyzed this phenomenon in the

endocrine-resistant ER+ BC cells. As expected, endocrine therapy-induced FAO activated the Src pathway in ER+ BC also. Moreover, in vitro, and in vivo studies confirmed that endocrine-resistant ER+ BC cells have increased sensitivity to FAO, OXPHOS, and Src inhibitors. Finally, analysis of clinical data suggests that low expression of FAO rate-limiting genes in the ER+ primary tumors have better recurrence-free and distant metastasis-free survival after endocrine therapy. Overall, our findings suggest that the gene signature generated from FAO-modulated TNBC cells predicts response to endocrine therapy in ER+ BC. Moreover, metabolic reprogramming in endocrine-resistant ER+ tumors induce FAO, OXPHOS, and Src pathways, providing potential targets to overcome endocrine-resistance ER+ BC patients.

#4853

Evaluating the role of melatonin in thyroid cancer cell (MDA-T41) apoptosis and metabolism modulation

Angela Huang, Daniel Sanches. *Natural Sciences, South Florida State College, Sebring, FL*

Melatonin, a hormone produced by the pineal gland, is typically known for its modulation of a number of physiological functions, alongside its ability to synchronize the sleep-wake rhythms. In recent years, however, its interactions with cancerous cells and role in prevention and treatment have been increasingly studied. It has been demonstrated that melatonin can improve the efficacy of chemotherapeutic drugs and directly inhibit tumorigenesis in experimental models of neoplasia. In addition, while melatonin typically displays anti-apoptotic effects in normal cells, it holds pro-apoptotic effects in cancer cells. Despite this, the mechanisms by which melatonin affects cell death and metabolism remain unclear due to the seeming difference from cell to cell. We aim to better understand the role of melatonin in regulating thyroid cancer cell apoptosis and metabolism. The MDA-T41 thyroid cancer cell line was cultured with varying quantities of melatonin. Steady volumes of staurosporine (an inductor of apoptotic cell death) were applied to cultures, and cell death levels were subsequently measured using the Realtime-Glo Annexin V Apoptosis and Necrosis assay. Our results showed that melatonin provided anti-apoptotic effects to MDA-T41 cells treated with staurosporine. Both apoptosis and necrosis were

reduced by 50% in melatonin-treated cells 24 hours after staurosporine-induced cell death. Our next steps will be to evaluate the mechanisms and further signaling pathways involved in this apoptosis inhibition through Bcl-2 and p53 protein expression.

#4854

PKM2 Modulates hepatic macrophage regulation of NASH, ferroptosis and HCC through TGF-β signaling

Kazufumi Ohshiro[1], Krishanu Bhowmick[1], Xiaochun Yang[1], Addison Klebanov[1], Sahara John[1], Dillon Voss[2], Adrian Krainer[2], Lopa Mishra[1].
[1]The Institute for Bioelectronic Medicine, Dept of Medicine, Div. of Gastroenterology and Hepatology, The Feinstein Institutes for Medical Research, & Cold Spring Harbor Laboratory, Northwell Health, Manhasset, NY,[2]Cancer Center, Cold Spring Harbor Laboratory, Cold Spring Harbor, NY

Background**:** Non-alcoholic steatohepatitis (NASH) and cirrhosis are major risk factors for hepatocellular carcinoma (HCC), which affects men 2-4 times more than women. In tumors Pyruvate kinase M2 (PKM2), induces aerobic glycolysis (Warburg effect) and proinflammatory and non-apoptotic cell death, ferroptosis. Raised levels of hepatic macrophage PKM2 expression are associated with poor prognosis HCC. We previously found that liver specific TGF-β/SMAD4 knockout mice develop iron deposition and hemochromatosis due to a dramatic loss of hepcidin. Moreover, *Smad4*$^{+/-}$*Sptbn1*$^{+/-}$ mice develop gastrointestinal cancers but only in the presence of an altered microbiome. Recently, we found that liver-specific knockout of a TGF-β/SMAD3/4 adaptor protein, βII-spectrin (LSKO) blocks diet-induced NASH and HCC in mice, as well as in siRNA treated human NASH microfluidic cultures (*Sci Transl Med.* 2021;13(624): eabk2267). We hypothesized that βII-spectrin modulates PKM2 expression in NASH fatty liver, promoting proinflammatory cytokine release, inflammation and tumorigenesis. In addition, microbiome changes could alter hepcidin function and modulate ferroptosis. Our goal is to understand the molecular mechanism underlying PKM2 driven NASH and HCC.
Methods: For our NASH mouse model, we fed SPTBN1^{Flox} (control) and liver-specific βII-spectrin knockout (SPTBN1^{LSKO}) mice a Western diet

(WD). Body weight, total cholesterol, and triglyceride concentrations in serum were monitored, and PKM2 expression levels in the liver tissues was analyzed. SPTBN1^{Flox} and SPTBN1^{LSKO} mice were treated with both WD and Diethylnitrosamine (DEN) for HCC, and gut microbiome profiles were performed in these mice. To evaluate PKM2 expression in the NASH-associated HCC mouse model, immunohistochemical labeling was performed on liver tissues of these mice with PKM2-specific antibody. Inflammation, lipidosis and fibrosis were determined with H&E, Oil Red O and Sirius Red staining.
Results: We found upregulation of PKM2 expression in NASH and HCC Kupffer cells (WD SPTBN1^{Flox} mice). In contrast, PKM2 expression was markedly reduced in the liver in WD SPTBN1^{LSKO} that blocked NASH and HCC. Interestingly, microbiome profiles were altered and TGF-β/SMAD3-regulated fibrosis as well as expression of inflammatory genes were significantly reduced in LSKO mice, compared to the NASH mice.
Conclusions: Our findings suggest that the knockdown of the Smad3/4 adaptor βII-spectrin decreases PKM2 expression in Kupffer cells, thereby suppressing pro-inflammatory cytokine production, blocking NASH-associated HCC. Hepatic macrophages such as Kupffer cells and monocyte-derived macrophages could therefore play a critical role in the ferroptosis-mediated protumor immune microenvironment. In addition, our work provides new insight into potential mechanism for two disorders that affect males more than females, hemochromatosis and HCC.

MULTIDISCIPLINARY

AACR Project GENIE Use Cases

#4252
CCNE1 amplification in high-grade serous ovarian cancer: analysis of the GENIE database

Ashaar Al-Akhras, Shaden Tashtoush, Alina Ghazou. *Faculty of Medicine, Jordan University of Science and Technology, Irbid, Jordan*

Background: High-grade serous ovarian cancer (HGSOC) is the most common histological subtype of ovarian cancer as well as the most lethal. A primary oncogenic driver in a subset of HGSOC patients, CCNE1

amplification is associated with poorer outcomes and resistance to standard treatment. This study aims to investigate the copy number gain of CCNE1 and the genetic mutations associated with CCNE1 amplification using a large cohort of clinico-genomic data. Methods: We queried the American Association of Cancer Research-Genomics Evidence Neoplasia Information Exchange (GENIE) registry database v12.1 for patients with HGSOC. We studied CCNE1 amplification and the clinical, demographic, and genetic mutation associations. Results: A total of 3297 HGSOC samples were extracted from the registry. The mean age of patients at sequencing was 62 ± 10 years. Out of 2416 samples profiled for copy number alterations, CCNE1 amplification was found in 13.6%, being the most commonly amplified gene, followed by AGO2 (11.7%) and MYC (9.7%). Co-amplification between CCNE1 and AKT2 was demonstrated. Between the 397 samples with CCNE1 amplification and 2088 without, the genes that were more frequently mutated in the CCNE1 amplified group were AKT2 (20.4% vs 3.2%, $p<0.001$), KRAS (11.3% vs 4.3%, $p<0.001$), BRD4 (8.0% vs 4.4%, $p = 0.006$), and ERBB2 (7.9% vs 4.0%, $p = 0.003$). Other genes were less frequently mutated in the CCNE1 amplified cohort such as NF1 (7.6 % vs 12.9%, $p = 0.009$), BRCA1 (3.7% vs 10.0%, $p<0.001$), BRCA2 (2.7% vs 7.4%, $p = 0.003$), RB1 (2.7% vs 6.4%, $p = 0.013$), and PTEN (1.2% vs 4.0%, $p = 0.02$). Frequencies of MYC, PIK3CA, KMT2D, CDK12, and TSC2 mutations were similar between the two groups. TP53 was mutated in 100% of samples. There were no significant differences between the two groups in primary race or total mutation count, and mean age at sequencing was similar. Conclusion: Somatic sequencing is warranted to identify patients of this subset of HGSOC, and understanding the co-amplifications and co-mutations is essential so that they are targeted for optimal survival outcomes.

#4253

Pan-cancer analysis of *XPO1* R749Q mutations across 217,570 patients reveals association with high tumor mutational burden and therapy resistance

Tulasigeri M. Totiger[1], Yasmine Baca[2], Wannasiri Chiraphapphaiboon[3], Sana Chaudhry[1], Skye Montoya[1], Monika Chojnacka[1], Gabriel Gaidosh[1], Jumana Afaghani[1], Maurizio Affer[1], Christopher D. Armstrong[1], Ryan Notti[4], Jenna Zabroski[1], Jacob Jahn[1], Vindhya Nawaratne[1], Ramiro

Verdun[1], Hai Dang Nguyen[3], Chadi Nabhan[5], Thomas J. Herzog[6], Phil Walker[2], Andrew Elliott[2], Emil Lou[7], Wafik S. El-Deiry[8], Edith Mitchell[9], Jose Antonio Rodriguez[10], Justin Taylor[11]. *[1]Medicine/Hematology, University of Miami Sylvester Comprehensive Cancer Center, Miami, FL,[2]Caris Life Sciences, Phoenix, AZ,[3]Department of Pharmacology, Masonic Cancer Center, University of Minnesota, Minneapolis, MN,[4]Memorial Sloan Kettering Cancer Center, New York, NY,[5]Medicine/Hematology, Caris Life Sciences, Phoenix, AZ,[6]University of Cincinnati, Cincinnati, OH,[7]Hematology, Oncology and Transplantation, University of Minnesota, Minneapolis, MN,[8]Brown University, Providence, RI,[9]Medical Oncology, Thomas Jefferson University, Sidney Kimmel Cancer Center, Philadelphia, PA,[10]Genetics, Physical Anthropology and Animal Physiology, University of the Basque Country(UPV/EHU), Barrio Sarriena s/n, Leioa, Spain,[11]Translational and Clinical Oncology Program, University of Miami Sylvester Comprehensive Cancer Center, Miami, FL*

Background: XPO1 is a nuclear export receptor responsible for exporting >200 proteins out of the nucleus, including many cancer-related proteins. We previously reported recurrent hotspot mutations occurring in XPO1 in cancer and identified *XPO1* R749Q variant only in solid tumors. To determine the prevalence of XPO1 mutations across cancer types, we performed a large-scale genomic analysis of 217,570 patients with cancer to identify and characterize *XPO1* variants from real-world patient tumors.
Methods: Solid tumor samples representing 14 cancer types were submitted to Caris Life Sciences (Phoenix, AZ) for Next-generation sequencing of DNA (592 genes or WES). TMB-High (defined as $\geq$10 mt/MB) and dMMR/MSI-H was tested by IHC/NGS. We engineered CRISPR knock-in HCT116 and LS-174T colon cancer isogenic cell lines bearing XPO1 R749Q mutations and Stochastic Optical Reconstruction Microscopy (STORM) analysis was performed. Structural modeling was performed with published XPO1 structures by mapping XPO1 mutations from the MSKCC-IMPACT dataset.
Results: A total of 96 patients with *XPO1* R749Q mutations were identified (50% occurred in endometrial cancer and 23% occurred in colorectal cancer). TMB-H was observed in 92% of *XPO1* R749Q mt tumors (9% were dMMR/MSI-H), while 86% of *XPO1* R749Q mt tumors were *POLE*-

mutated within the endonuclease domain. Median variant allele frequency for *XPO1* R749Q mt and *POLE* mt were 25% and 29%, respectively. STORM imaging revealed that *XPO1* R749Q mutant cells had significant localization of *XPO1* in the cytoplasm compared to *XPO1* WT cells, especially at the outside edge of the nuclear pores. Structural modeling predicted that *XPO1* R749Q mt affected the regulatory H9-loop of XPO1 favoring increased shuttling and retention in the cytoplasm. Mass spectrometry analysis of nuclear and cytoplasmic fractionated proteomes confirmed that *XPO1* R749Q mt cells had increased export of proteins compared to *XPO1* WT cells. A library screen of >200 FDA-approved drugs revealed a strong therapeutic resistance of *XPO1* R749Q cells, especially to chemotherapies used in the treatment of colon cancer. XPO1 inhibition with selinexor synergized with chemotherapy in *XPO1* R749Q mt cells *in vitro* and overcame resistance to irinotecan *in vivo* in xenograft mice models.
Conclusion: This study sheds novel insights into the role of nuclear export in cancers. Specifically, *XPO1* R749Q mutations are enriched in TMB-H endometrial and colon cancers and increase nuclear export of key proteins that confer resistance to therapies using DNA-damaging agents. Our current work aims to identify novel therapies that can overcome resistance to DNA-damaging therapies seen in *XPO1* mutant cells, such as immune checkpoint inhibitor (ICI) therapy given the co-occurrence with *POLE* mutations and recent reports of high level of response to ICI therapy in TMB-H and *POLE* mt colorectal cancers.

#4254

The ratio of key metabolic transcripts is a predictive biomarker of breast cancer metastasis to the lung

Deepti Mathur[1], Chen Liao[1], Wendy Lin[1], Alessandro La Ferlita[2], Salvatore Alaimo[2], Alfredo Ferro[2], Yi Zhong[3], Christine Iacobuzio-Donahue[1], Joao Xavier[1]. *[1]Memorial Sloan Kettering Cancer Center, New York, NY,[2]University of Catania, Catania, Italy,[3]Hackensack Meridian Health Center for Discovery and Innovation, Hackensack, NJ*

Understanding the rewired metabolism of organ-specific metastasis in breast cancer is an under-appreciated problem, with implications for the treatment and prevention of metastatic disease. Here, we used a systems

biology approach and the MDA-MB 231 model to compare metabolic fluxes used by parental breast cancer cells and their brain- and lung-homing derivatives. We combined metabolomic profiling, flux measurements, spatial tissue mimetic systems, and mathematical modeling to dissect the cells' metabolic rewiring, and identified changes specific for lung metastatic selection. We validated our results in other cell lines as well as patient data from project GENIE and the MBCP. Our results produced five biological insights: First, levels of mRNA and metabolic intermediates may *anticorrelate* with flux. Second, different lineages evolved from the same line can have distinct heritable metabolic fluxes. Metastatic lineages in our model display higher glycolytic flux and bioenergetics than parental cells, with lung-homing cells exhibiting by far the greatest glucose uptake and lactate production. Importantly, this occurs despite low levels of glycolytic intermediates in lung-homing cells. Third, this apparent paradox can be reconciled if feedback inhibition of the glycolysis pathway is prevented, a finding we modeled with flux-balance analysis and confirmed by ^{13}C glucose tracing and measuring glycolytic enzymatic activities directly. Fourth, this distinct metabolic behavior in lung-homing cells is maintained by a high ratio of lactate dehydrogenase (LDH) to pyruvate dehydrogenase (PDH) gene expression, which also correlates with lung metastases in patients with breast cancer. Feature classification models trained on clinical characteristics alone were unable to predict tropism; however, the LDH/PDH ratio was a significant predictor for lung but not brain metastases, independent of other transcriptomic signatures, suggesting that this feature is a potential biomarker for lung metastasis. Fifth, this metabolic effect did not increase cellular growth rate, suggesting that lactate secretion may itself be a trait under selection in breast cancer lung metastasis. Follow up experiments and game theory-based models in a spatially structured tissue-mimetic system showed that lung-homing cells grow more favorably than brain-homing cells in nutrient-deprived gradients, demonstrating how divergent metabolisms of the lineages could lead to selection in different environments. Notably, lung metastases in a mouse model of pancreatic cancer had higher lactate production than other metastases, suggesting that this metabolic trait could be important for other cancer types. Together, our *in vitro*, *in silico*, and clinical data analyses highlight that metabolism—currency of all physiological processes—plays

an essential role in the connection from gene to phenotype in metastatic disease.

#4255

Concurrent KRAS and TP53 mutations in pancreatic cancer real-world data (RWD) highlight convergent tumor evolutionary patterns

Kaumudi Bhawe, Adrienne Nugent, Deb Christensen, Lauren Levine, Emma Shtivelman. *Cancer Commons, Mountain View, CA*

Pancreatic cancer is one of the most fatal of all cancers. Pancreatic adenocarcinomas have been historically difficult to treat, in part due to lack of early detection, and due to their resistance to conventional chemotherapy. There has recently been an improved understanding of the biologic processes driving pancreatic tumorigenesis, and an increase in clinical trial options available to patients, especially in the context of KRAS mutation positive pancreatic ductal adenocarcinoma (PDAC). KRAS is a known driver of pancreatic cancer initiation, with concurrent loss of TP53 in many cases. Among all mutated genes in pancreatic cancer, KRAS, TP53, CDKN2A, and SMAD4 are most frequently reported, followed by CDKN2B and ARID1A among others. Mutations in TP53 commonly found in pancreatic cancer are either missense or truncating. The specific type of mutation may be important to note since point mutations may produce dysfunctional proteins that acquire gain of functions that are tumor-promoting, although the most well-agreed upon effects of TP53 mutations stem from the absence or decrease of its normal physiologic functions including cell cycle arrest, apoptosis promotion, DNA damage response triggering, maintenance of cell polarity, and maintenance of genomic stability. Here we present an in-depth multi-dimensional analysis of 29 pancreatic adenocarcinoma patients, consisting of 11 patients with KRAS G12D mutations, 5 patients with KRAS G12V mutations, 3 patients with non-canonical KRAS mutations, and 10 patients with no KRAS mutations identified in their tumors. Individual TP53 mutations were highlighted in the context of associated KRAS mutations and tumor genomic landscape at the time of testing. Real-world data was collected with patient consent through community embedded Oncology Clinical Team (ceOCT) facilitated engagement. Tumor evolution prediction rules were constructed based on mutational landscapes of the 29 patients and evidence published in peer-

reviewed journals. Pancreatic cancer patient data from the AACR GENIE Cohort v12.0-public database and the cBioportal for Cancer Genomics public site was subsequently used for testing predicted tumor evolutionary trajectories. Here we describe multiple independent combinations of KRAS and TP53 mutations leading to convergent functional outcomes for tumor cells, in the context of patient-specific gene mutation landscapes. Recurrent patterns of paired mutations with common cellular function dysregulation outcomes highlight core underlying mechanisms of pancreatic tumor evolution.

#4256

cBioPortal for Cancer Genomics

Ino de Bruijn[1], Tali Mazor[2], Adam Abeshouse[1], Diana Baiceanu[3], Stephanie Carrero[1], Elena Garcia Lara[3], Benjamin Gross[1], David M. Higgins[4], Prasanna K. Jagannathan[5], Priti Kumari[6], Ritika Kundra[1], Bryan Lai[1], Xiang Li[1], James Lindsay[2], Aaron Lisman[1], Divya Madala[1], Ramyasree Madupuri[1], Angelica Ochoa[1], Yusuf Ziya Özgül[1], Oleguer Plantalech[3], Sander Rodenburg[3], Baby Anusha Satravada[1], Robert Sheridan[1], Lucas Sikina[2], Jessica Singh[3], S Onur Sumer[1], Yichao Sun[1], Pim van Nierop[3], Avery Wang[1], Manda Wilson[1], Hongxin Zhang[1], Gaofei Zhao[1], Sjoerd van Hagen[3], Ugur Dogrusoz[7], Allison Heath[4], Adam Resnick[4], Trevor J. Pugh[5], Chris Sander[8], Ethan Cerami[2], Jianjiong Gao[6], Nikolaus Schultz[1]. *[1]Memorial Sloan Kettering Cancer Center, New York, NY,[2]Dana-Farber Cancer Institute, Boston, MA,[3]The Hyve, Utrecht, Netherlands,[4]Children's Hospital of Philadelphia, Philadelphia, PA,[5]Princess Margaret Cancer Centre, Toronto, ON, Canada,[6]Caris Life Sciences, Irving, TX,[7]Bilkent University, Ankara, Turkey,[8]Harvard Medical School, Boston, MA*

cBioPortal for Cancer Genomics is an open-source platform for interactive, exploratory analysis of large-scale clinico-genomic data sets. cBioPortal provides a suite of user-friendly visualizations and analyses, including OncoPrints, mutation “lollipop” plots, variant interpretation, group comparison, survival analysis, expression correlation analysis, alteration enrichment analysis, cohort and patient-level visualization.

The public site (https://www.cbioportal.org) is accessed by >35,000 unique visitors each month and hosts data from >350 studies spanning individual labs and large consortia. In addition, at least 74 instances of cBioPortal are installed at academic institutions and companies worldwide. To better support all users, we unified our documentation (https://docs.cbioportal.org) and added a user guide and an ongoing series of 'how-to' videos to address common questions.

In 2022 we added 32 studies (>38,000 samples) to the public site. In addition, we added a nonsynonymous tumor mutation burden (TMB) value for all samples and enhanced the TCGA PanCancer Atlas studies with DNA methylation and treatment data. All data is available in the cBioPortal Datahub: https://github.com/cBioPortal/datahub.

We also host a dedicated instance for AACR Project GENIE, enabling access to the GENIE cohort of >165,000 clinically sequenced samples from 19 institutions (https://genie.cbioportal.org). The GENIE Biopharma Collaborative (BPC) enables the collection of comprehensive clinical annotations, including response, outcome, and treatment history. The first BPC cohorts are now available: ~2,000 non-small cell lung cancer samples and ~1,500 colorectal cancer samples.

Support for multimodal data analysis has been a major focus, including several new integrations with external tools. Single cell data is now available in the CPTAC GBM study and can be visualized throughout cBioPortal, and via integration with cellxgene. On the patient page, H&E and mIF images can be visualized via integration with Minerva, and the genomic overview now integrates IGV.

We continue to enhance existing features. In the study view, users can now add charts comparing categorical vs continuous data, and the plots tab includes a heatmap option. We replaced the existing fusion data type with a generalized structural variant data type that supports detailed information including breakpoints and orientation, to enable new visualizations and analyses. Pathway level analysis has been extended with a new integration with NDEx.

cBioPortal is fully open source (https://github.com/cBioPortal/). Development is a collaborative effort among groups at Memorial Sloan Kettering Cancer Center, Dana-Farber Cancer Institute, Children's Hospital of Philadelphia, Princess Margaret Cancer Centre, Caris Life Sciences,

Bilkent University and The Hyve. We welcome open source contributions from others in the cancer research community.

#4257

Using Multilevel Regression and Poststratification (MRP) to inform estimates of biomarker prevalence for target populations of interest using linked clinico-genomic databases

Jeremy W. Snider[1], Brennan Beal[1], Lilia Bouzit[1], Cheryl Cho-Phan[1], Leah Comment[2], Garrett Frampton[2], Tamara Snow[1]. *[1]Flatiron Health, New York, NY,[2]Foundation Medicine, Boston, MA*

Background

Contemporary evidence on the size of biomarker-defined cancer populations is crucial for clinical and economic healthcare decision makers. Estimates can be derived from real-world data (RWD), but may be affected by biases stemming from differences in observed populations vs. general populations of patients under the purview of decision makers. These differences may be driven by patient or clinical characteristics, as well as differences in assays used to assess biomarker status. This study demonstrates the applicability of an emerging method in survey science (Multilevel Regression and Poststratification (MRP)), which leverages common covariates across source data and larger, more representative set of observations to inform estimates of biomarker prevalence for target populations of interest.

Methods

In disease-agnostic cohorts of patients with solid-tumor cancers from two, large clinico-genomic cancer databases (AACR GENIE 12.0, and nationwide (US-based) de-identified Flatiron Health - Foundation Medicine Clinico-Genomic Database(CGDB)), we used covariate-adjusted regression (age, sex, race, stage at diagnosis (for CGDB patients), and cancer type) to predict the probability of a patient having an NTRK fusion and/or a BRAF V600E mutation detected in their sequenced cancer tissue. AACR Project GENIE (n = 118,649) is a cancer registry of real-world data assembled through data sharing between 19 international cancer centers. The de-identified data in the CGDB (n = 91,719) originated from approximately 280 US cancer clinics (~800 sites of care).We then implemented post-stratification adjustments (Gelman, 2006; Downes 2018) using the

Surveillance, Epidemiology, and End Results (SEER) 17 2022 cancer registry to estimate prevalence of the alterations in the large, population-based registry.
Results
Prevalence estimates were generally consistent between sources. Adjusted prevalence (%) estimates for NTRK Fusion (AACR: 0.25% (raw), adjusted to 0.21% (0.01%-0.48%) (MRP-adjusted mean % (95% quantile intervals)); CGDB: 0.29, adjusted to 0.26 (0.02-0.63), and for BRAF V600E (AACR: 2.19, adjusted to 1.72 (0.77-2.66); CGDB: 2.44, adjusted to 2.68 (1.50-3.89)) reflected differential patient characteristics (predominantly tumor type) in these sources compared to SEER. MRP also enabled creation, from posterior distributions, of tumor-level estimates, along with credible interval bounds.
Conclusion
While both clinico-genomic databases offered generally consistent estimates of biomarker prevalence, representativeness methods that are used in the survey literature may be suited for addressing biases in RWD sources to improve biomarker prevalence estimates of target populations of patients with cancer.

#4258
Racial and ethnic differences in the mutational landscape of low-grade serous ovarian cancer
Muhammad Danyal Ahsan, Emily M. Webster, Sarah R. Levi, Natalie T. Nguyen, Juan R. Cubillos-Ruiz, Evelyn Cantillo, Eloise Chapman-Davis, Melissa K. Frey, Kevin Holcomb. *Gynecologic Oncology, Weill Cornell Medicine, New York, NY*

Objective To characterize the mutational landscape of low grade serous ovarian cancer (LGSOC) with racial/ethnic stratification.
Methods The AACR Project GENIE database version 12.0 was queried via cBioPortal (http://genie.cbioportal.org) for low-grade serous ovarian cancer (LGSOC) samples. This is a publicly available, de-identified, multi-institutional database of next-generation sequencing genomic profiling results for tumor samples. Mutation frequencies for 9 homologous recombination deficiency (HRD) genes, 4 MAP-Kinase (MAP-K) pathway genes and 6 mismatch-repair (MMR) deficiency genes were reported and

compared between racial/ethnic groups using chi-squared or Fischer's exact tests. The threshold used for statistical significance was a two-sided alpha of 0.05.

Results Among 317 tumor samples of LGSOC, there were high rates of MAP-K pathway gene mutations but low rates of HRD, MMR and TP53 gene mutations (Table 1). Non-Hispanic Black patients had significantly higher rates of KRAS mutations compared to non-Hispanic White patients (6/7, 86% vs 48/178, 27%, $p<0.01$). There was no difference in KRAS mutation frequency among Asian (6/17, 35%), Hispanic (7/24, 29%) and Native American (2/2, 100%) patients when compared to non-Hispanic White patients. BRAF mutations were less common compared to KRAS mutations (32/317, 10%), with no racial/ethnic differences in mutation frequency.

Conclusion High rates of MAP-K pathway mutations in LGSOC support development and trials of drugs targeting this pathway, such as MEK protein inhibitors. Furthermore, prior literature has demonstrated the prognostic advantage of KRAS and BRAF mutations in LGSOC as well as the association of KRAS mutations with progression of serous borderline tumors to LGSOC. These racial/ethnic differences in frequencies of these mutations are thus hypothesis generating for clinical research to evaluate the impact of race/ethnicity on the development and prognosis of this rare ovarian cancer.

Mutation frequencies of HR, MAP-kinase, MMR and TP53 genes in low-grade serous ovarian cancer

Gene	No. of samples with ≥1 mutation	No. of samples profiled for mutation	Mutation frequency
BRCA1	3	287	1.05
BRCA2	7	287	2.44
BRIP1	5	271	1.85
CHEK2	2	278	0.72
BARD1	2	239	0.84
RAD51B	-	-	-
RAD51C	-	-	-
RAD51D	2	246	0.81
PALB2	2	279	0.72

KRAS	93	317	29.34
NRAS	29	317	9.15
BRAF	32	317	10.09
EIF1AX	14	144	9.72
MSH2	3	275	1.09
MSH3	1	113	0.88
MSH6	6	286	2.10
MLH1	1	317	0.32
MLH3	3	96	3.13
PMS2	1	270	0.37
TP53	12	317	3.79

#4259

Identification of anti-neoplastic therapy given before initial visit at a referral center using natural language processing applied to medical oncology initial consultation notes

Thinh N. Tran[1], Karl B. Pichotta[2], Si-Yang Liu[3], Christopher Fong[3], Anisha Luthra[3], Brooke Mastrogiacomo[3], Steven Maron[3], Deborah Schrag[3], Sohrab P. Shah[3], Pedram Razavi[3], Bob T. Li[1], Gregory J. Riely[3], Nikolaus Schultz[3], Justin Jee[3]. *[1]Gerstner Sloan Kettering Graduate School, Memorial Sloan Kettering Cancer Center, New York, NY,[2]Sloan Kettering Institute, Memorial Sloan Kettering Cancer Center, New York, NY,[3]Memorial Sloan Kettering Cancer Center, New York, NY*

Anticancer therapy changes tumor physiology and genomics, making it a key variable in cancer studies. Although antineoplastics given at a single institution may be available in research-ready format, treatment at external institutions prior to receiving care at academic medical centers, common among patients at these centers, is often only described in free-text clinical notes, necessitating manual curation for downstream analysis. To overcome this bottleneck, we trained and validated natural language processing (NLP) models using initial consult notes to identify whether patients had received treatment at external institutions and studied the impact of these putative treatments on tumor genomics.

Training data were derived from the AACR Project GENIE Biopharma Collaborative (BPC) for 2,663 patients at Memorial Sloan Kettering (MSK) across four cancer types. For each patient, we selected initial visits with medical and radiation oncologists based on an a priori note prioritization scheme and determined "ground-truth" prior external medications based on manually curated BPC administration records, whitelisting MSK-given medications. We trained logistic regression and clinical longformer models to identify external treatment receipt and evaluated model performance with 5-fold cross-validation. The clinical longformer model performed best across evaluation metrics, with an average area under the receiver operating characteristic curve of 0.972, macro-averaged precision/recall of 0.854/0.902 and macro-averaged F1 score of 0.876. Re-review of discrepant cases suggested that 75% of "false positives" may be due to curation error. We used our model to infer treatment status in a pan-cancer cohort with tumor genomic profiling using our institutional sequencing platform. Out of 48,447 patients, 11,900 were predicted to have received external treatment. Patients with putative external treatment had higher alteration frequencies in resistance-related genes than untreated patients and comparable to known pre-treated patients, including ESR1 in patients with breast cancer, AR in patients with prostate cancer, and EGFR T790M in patients with EGFR-mutated non-small cell lung cancer. Patients with putative external treatments, similar to known pre-treated patients, had shorter survival compared to treatment-naïve patients of the same cancer type.
NLP can abstract external treatment status from clinical notes. When applied at scale, our model could help mitigate confounding variables and identify relationships between clinicogenomic variables and anticancer therapy.

#4260

Understanding genomic and social determinants of cancer immunotherapy outcome across ancestry

Christopher J. Fong[1], Michele Waters[1], Karl Pichotta[1], Justin Jee[2], Devika R. Jutagir[3], David Ma[1], Tomin Perea-Chamblee[1], Susie Kim[4], Kanika Arora[5], Brooke Mastrogiacomo[1], Thinh Tran[4], Steven Maron[2], Mirella Altoe[1], Anisha Luthra[1], Joseph Kholodenko[1], Arfath Patha[1], Doori Rose[6], Michael F. Berger[5], Gregory J. Riely[2], Nikolaus Schultz[1], Sanna Goyert[7], Adam Schoenfeld[2], Francesca Gany[3], Jian Carrot-Zhang[1]. *[1]Computational*

Oncology Service, Memorial Sloan Kettering Cancer Center, New York, NY,[2]Department of Medicine, Memorial Sloan Kettering Cancer Center, New York, NY,[3]Immigrant Health and Cancer Disparities Service, Memorial Sloan Kettering Cancer Center, New York, NY,[4]Gerstner Sloan Kettering Graduate School of Biomedical Sciences, Memorial Sloan Kettering Cancer Center, New York, NY,[5]Human Oncology & Pathogenesis Program, Memorial Sloan Kettering Cancer Center, New York, NY,[6]Memorial Sloan Kettering Cancer Center, New York, NY,[7]CUNY School of Medicine, City University of New York, New York, NY

Compared with previous standards of care, the use of immune checkpoint inhibitors (ICI) has brought significant improvements in survival and quality of life for lung cancer patients. However, only a small proportion of these patients respond durably. People with different ancestries differ probabilistically in genetic factors, environmental exposures, and socio-economic conditions. Whether patients of different ancestry benefit equally from ICIs remains unclear.

We studied the impact of genomic ancestry, tumor genomics, and social determinants of health (SDH) factors and factors that are impacted from SDH including recorded race/ethnicity, inferred low-income status from patient zip codes, exposure to smoking, and BMI on ICI response, defined by cancer progression-free survival (PFS, minimum 6 months FU), for non-small cell lung cancer (NSCLC) patients with MSK-IMPACT targeted panel sequencing. This FDA approved assay includes matched tumor-white blood cell sequencing to distinguish germline from somatic variants and has been applied to 1,802 NSCLC patients who received ICI treatment, including 81 and 117 patients with at least 80% of African (AFR) and East Asian (EAS) ancestry, respectively. Moreover, 173 samples were derived from admixed patients with more than one major ancestry.

We first used a natural language processing (NLP) model to obtain PFS from free-text clinical notes. A multivariable cox proportional hazard model was then used to associate PFS with ancestry, race, smoking status, ICI drug regimen, PD-L1 status, disease stage, tumor mutational burden (TMB), inferred income, and BMI. Neither genetic ancestry nor self-reported race/ethnicity was associated with the PFS. Moreover, ICI drug regimen types, low-income status, and BMI were not associated with PFS in our cohort. TMB-high was associated with longer PFS across all ancestries,

although TMB was lower in patients with EAS ancestry (Median 7.9 vs. 5.3 mut/Mb, $p<0.001$).
These results suggest that the benefits of ICI extend across ancestry, race, and income lines in a single institution, arguing for more equitable patient access to these medications. We also show that TMB is a generalizable biomarker for ICI outcome across ancestries. However, more diverse patient populations are needed to understand whether there is ancestry-specificity in other ICI outcome biomarkers.

#4261

Genomic landscape of 2128 thyroid cancers from the aacr genie database: Implications for targeted therapies

Blessie Elizabeth Nelson[1], Mohammed Gouda[1], Jason Roszik[2], Mimi L. Hu[3], Maria Cabanillas[3], Vivek Subbiah[1]. *[1]Investigational Cancer Therapuetics, UT MD Anderson Cancer Center, Houston, TX,[2]Melanoma Medical Oncology, UT MD Anderson Cancer Center, Houston, TX,[3]Endocrine Neoplasia and Hormonal Disorders, UT MD Anderson Cancer Center, Houston, TX*

Background**:** Understanding molecular biology of thyroid cancer has revolutionized diagnosis, tumor classifications and identifying effective precision oncology therapies.
Methods: Using AACR GENIE database v.12, we cataloged genetic and co-occurring alterations in all thyroid cancers.
Results: We identified 2128 cases from 153,834 samples where tumor sub-histologies included Papillary Thyroid Cancer (PTC: 55%; 1162), Poorly Differentiated Thyroid Cancer (PDTC: 12%; 262); Medullary Thyroid Cancer (MTC: 12%; 244), Anaplastic Thyroid Cancer (ATC: 10%; 220); Follicular Thyroid Cancer (FTC: 5%; 111); Hurthle Cell Thyroid Cancer (HCTC: 5%; 95); and others (1; 34). Median age at sequencing was 59 years. Gender distribution was higher in female (54%; n=1104) compared to male (46%; n=933). Ethnicities included 73.2% (n=1,493) White, 8.9% (n=178) Asian, and others.Most frequent genomic mutational alterations overall were *BRAF* (40.8%; 868) [96% (n=845) V600E, 0.6% (n=5) G469A, 0.6% (n=5) V600_K601delinsE, 0.2% (n=2) K601E, 0.2% (n=2) A404Cfs*9, and 2.7% (n=24) others]; *TERT* (35%; 624); *NRAS* (11.6%;

247); *TP53* (11.6%; 247) and *RET* (9.3%; 197) genes. There was variability in genomic alterations between sub-histologies (Table 1).

Histology	Most frequent Alterations	%	n
PTC	BRAF	62.3%	724
	TERT	32.7%	332
PDTC	TERT	49%	117
	NRAS	28.2%	74
MTC	RET	71.3%	174
	HRAS	7.8%	19
ATC	TP53	58.2%	128
	TERT	56.7%	106
FTC	TERT	41%	27
	NRAS	26.1%	29
HCTC	TERT	41%	34
	TP53	17.9%	17

There was statistically significant co-occurrence between *BRAF and TERT, TERT* and *TP53*, *TERT* and *NRAS* alterations ($p<0.001$). Mutually exclusive alterations were *BRAF* and *NRAS, BRAF* and *RET, TERT* and *RET, NRAS* and *RET, TP53* and *RET,* and *BRAF* and *TP53 ($p<0.001$).*Copy number alterations (CNA) were observed in 497 samples and were most frequent in *CDKN2A, NKX2-1, CDKN2B, NF2,* and *CRKL* genes (16.5%, 16%, 15.5%, 13.1%, and 13%). 362 oncogenic fusions were noted predominantly in *CCDC6-RET, RET-NCOA4, ETV6-NTRK3, BRAF*-Intragenic (20%, 7.2%, 3%, 1.6%).

Conclusion: Genomic profiling identified full breadth of BRAF, RET and NRAS alterations and co-occurring oncogenic driver alterations. This approach may refine use of targeted therapy in thyroid cancer.

#4262

Genomic profiling of uveal melanoma patients using the GENIE database

Shaden Tashtoush, Ashaar Al-Akhras, Alina Ghazou, Sebawe Syaj. *Jordan University of Science & Technology, Irbid, Jordan*

Uveal melanoma (UM) is the most common primary adult intraocular tumor. Frequently mutated genes in UM include BAP1, EIF1AX, GNA11, GNAQ CHEK2, and SF3B1. This study aims to investigate the genomic characteristics of UM patients using a large cohort of clinicogenomic data. We assessed the frequency of genetic mutations in UM patients obtained from the AACR Project Genomics Evidence Neoplasia Information Exchange (GENIE) cohort v12.1. We excluded patients with samples from a local recurrence, not otherwise specified tumor samples, and data not collected for sampling localization from our cohort. A total of 296 UM patients were included in this study, 164 (55.4%) of which were male and 131 (44.6%) were female. The sample mean age was 59.5 (SD: 14.1), and most patients were of white ethnicity (83.8%). Of 243 patients with known vital status, 32.1% (n = 78) of them were alive, while 67.9% (n = 165) of them were deceased. Sequencing samples were collected from the primary tumor in 141 patients, and from a metastatic nodule in 146 patients. We found that GNAQ and GNA11 were mutated in 43.9% and 43.6% of patients, respectively. BAP1 was mutated in 35.1%, SF3B1 in 22.3%, and EIF1AX in 13.2% of patients. No patients had GNAQ and GNA11 mutations concurrently. All patients had a median mutation count of 3, with no differences between the two genders. No significant differences were found in the frequency of mutations in regard to gender. GNAQ and GNA11 mutations were identified to be the most frequent mutations among UM patients, with a mutual exclusivity relationship between the two genes. New therapeutic modalities should consider the comprehensive genomic profiling of UM patients to improve their overall survival rate and quality of life.

#4263

Anti-Siglec 7 antibody displays potent anti-tumor immunity and demonstrates improved tumor control in combination with anti-PD1 in ovarian cancer

Devivasha Bordoloi[1], Abhijeet J. Kulkarni[1], Opeyemi S. Adeniji[1], M. Betina Pampena[2], Pratik S. Bhojnagarwala[1], Shushu Zhao[1], Elizabeth M. Parzych[1], Rugang Zhang[3], Michael R. Betts[2], Mohamed Abdel-Mohsen[1], David B. Weiner[1]. *[1]Vaccine & Immunotherapy Center, The Wistar Institute, Philadelphia, PA,[2]Department of Microbiology, Perelman School of Medicine, University of Pennsylvania, Philadelphia, PA,[3]Department of*

Microbiology, Perelman School of Medicine, The Wistar Institute, Philadelphia, PA

High grade serous ovarian cancer (OC) and ovarian carcinosarcoma, referred as “Cold” tumors have restricted treatment choices and being associated with high mortality. Current immune checkpoint inhibitors (CPIs) have had modest impact for OC treatment; with anti PD-1/PD-L1 single therapies reported response rates of 4-15%. Accordingly, additional approaches are important for these patients. Natural killer (NK) cells represent an important subset of effector lymphocytes with strategic approaches for maximizing NK reactivity to target OC are likely important. Of interest, an inhibitory receptor and glyco immune checkpoint- Siglec 7 is expressed on 100% of peripheral blood and umbilical cord NK cells**.** We have generated antibodies against Siglec 7 through an optimized human Siglec 7 DNA/protein immunization approach in humanized next generation transgenic mice. By high throughput flow screening, we identified several Siglec 7 antibodies and down selected relevant clones. A unique clone DB7.2 was highly specific for Siglec 7. We demonstrated the ability of DB7.2 (human IgG1) to activate NK cells and induce OC cell killing using xCELLigence RTCA for in vivo OC challenge studies. DB7.2 (1μg/ml) bound to >90% of NK cells including both CD56dim and CD56bright subsets, evaluated in the PBMCs of multiple donors. It showed strong binding to recombinant Siglec 7 and Siglec 7 transduced HEK293T but not to wild type 293T cells supporting specificity. DB7.2 induced specific killing of multiple OC lines (OVCAR3&10,TOV21G, CaOV3, OVISE, PEO4) carrying different mutations; BRCA1&2, AKT, TP53, PIK3CA, BRAF etc. and resistant against a wide array of cancer drug targets; HSP90, HDAC, MTORC, DNA alkylating agents, EGFR, PARP, PI3K, and WEE1. Tumor killing was indicated to be mediated via enhanced secretion of soluble Fas, perforin, granulysin as well as granzyme A. Of note, OVISE (BRCA1mutated) and PEO4 (BRCA2 mutated, PARPi resistant) were susceptible to DB7.2 killing with EC50- 82.67 and 68.67 nM respectively. A single dose of in vivo expressed DB7.2 significantly reduced the tumor burden in an OVISE challenged humanized mice model enhancing median survival by 57 days. As OCs are highly diverse in nature and likely to require combinatorial approaches for simultaneous targeting of immune pathways; we combined DB7.2 with anti-PD1 for further

investigation. In xCELLigence assay, anti-PD1 demonstrated killing of PEO4 cells with EC50 680 nM. The combination of anti PD-1 with DB7.2 showed further enhancement of OC killing in the presence of human PBMCs. This is the first demonstration of the impact of Siglec 7 targeting mAb alone as well as in combination with anti-PD1 (NK and T cell CPIs) studied for targeting OC or any human tumor. These studies have important implications for tumor therapy and provide a novel non T cell CPI potential approach to augment current immune therapy strategies.

#4264

The genomic landscape of RET fusions in non-small cell lung cancer and the impact of co-occurring genomic alterations on the efficacy of selective RET inhibitors

Tuqa Al Khalaf[1], Simon Heeke[1], Lei Feng[1], Leylah M. Drusbosky[2], Jeff Lewis[1], Waree Rinsurongkawong[1], Vadeerat Rinsurongkawong[1], Jack Lee[1], Jianjun Zhang[1], Don Gibbons[1], Ara Vaporciyan[1], Vincent Lam[3], Vivek Subbiah[1], John Heymach[1], Yasir Elamin[1]. *[1]The University of Texas MD Anderson Cancer Center, Houston, TX,[2]Guardant Health, Inc., Redwood City, CA,[3]The Sidney Kimmel Comprehensive Cancer Center, Johns Hopkins University School of Medicine, Baltimore, MD*

Purpose: *RET* fusions drive oncogenesis in 1-2% of non-small cell lung cancer (NSCLC) and are sensitive to the selective RET inhibitors selpercatinib and pralsetinib. They have also emerged as mechanisms of acquired resistance to other targeted therapies. The genomic landscape of *RET* fusions and the impact of co-occurring genomic alterations on the efficacy of selective RET inhibitors is yet to be fully described.
Methods: A total of 678 *RET* fusion-positive samples were analyzed from three cohorts: Guardant360® circulating tumor DNA (ctDNA) (n=467), tissue and/or plasma from the American Association for Cancer Research Project Genomics Evidence Neoplasia Information Exchange (AACR Project GENIE) non-squamous NSCLC cohort (n=161), and the MD Anderson Cancer Center (MDACC) cohort of patients treated with selpercatinib or pralsetinib (n=50). Molecular characteristics were compared across all three cohorts and to the entire non-*RET* non-squamous NSCLC AACR Project GENIE cohort (n=17770). Fisher's exact test was used to evaluate the difference in response rate between patient groups, and

Cox proportional hazard models were used to calculate hazard ratios for time-to-event endpoints for patients in the MDACC clinical cohort (n=51, 50 patients with *RET* fusion, 1 patient with *RET* point mutation).
Results: The most common fusion partner in all cohorts was *KIF5B* (ctDNA: 73%; GENIE: 69%; MDACC: 71%), followed by *CCDC6* (19%; 17%; 18%) and *NCOA4* (5%; 1%; 7%). Across all cohorts, co-mutations in *TP53* were most common (60%; 34%; 40%) and *EGFR, CDKN2A/B*, *MET*, and *ATM* consistently co-occurred across all cohorts. *EGFR* co-occurred more frequently with non-*KIF5B* fusion partners (chi-square $p < 0.006$). *MYC* and *CCND1* amplifications were enriched in all three cohorts compared to the non-*RET* cohort. In the MDACC clinical cohort (n=51), the majority were female, never-smokers, with adenocarcinoma histology. The median follow-up time was 28.3 months (95% CI: 15.2 ~ 35 months). Overall response rate (ORR) was 74.4% (95% CI: 58.8 ~ 86.5%), where patients with *TP53* mutation had numerically lower ORR compared to patients without *TP53* mutation (58.5% vs. 87.5%; $p = 0.0632$). Median progression-free survival (PFS) time was 16.5 months (95% CI: 13.5 ~ 27.4 months) and *KIF5B* fusions trended towards worse PFS outcome compared to non-*KIF5B* fusions (HR: 2.24; 95% CI: 0.88 ~ 5.67; $p = 0.0896$). *TP53* alterations were associated with a significantly worse overall survival (OS) (HR: 2.93; 95% CI: 1.08 ~ 7.95; $p = 0.0346$).
Conclusion: In the largest *RET* fusion-positive NSCLC cohort to date, *RET* fusions frequently co-occurred with other genomic alterations, most commonly in *TP53*. *TP53* alterations are associated with a significant reduction in overall survival in patients treated with the selective *RET* inhibitors. Additional analysis is underway.

#4265

Humanized 3D tumor models that are mutationally aligned with AACR GENIE patients predict IMM-1-104 activity in RAS-addicted tumors

Praveen Nair[1], Sarah Kolitz[2], Jason Funt[1], Peter J. King[1], Kevin D. Fowler[1], Anna Travesa[1], Ian Rose[1], John Brothers[2], Amy Axel[1], Scott Barrett[3], Benjamin J. Zeskind[3], Brett M. Hall[1]. *[1]Immuneering Corporation, San Diego, CA,[2]Immuneering Corporation, Cambridge, MA,[3]Immuneering Corporation, New York, NY*

Introducti**on:** IMM-1-104, with pan-RAS activity through deep cyclic inhibition MEK, was evaluated in humanized 3D preclinical tumor models displaying diverse MAPK pathway activation events. Based on drug-response, sensitivity and resistance profiles, a biomarker signature for IMM-1-104 was developed in order to project potential therapeutic response of cancer patients found in the AACR Project GENIE (GENIE) database.

Experimental Procedures: Humanized 3D preclinical models better predict *in vivo* tumor responses versus 2D culture and more accurately replicate biology of human tumors. Therefore, the antitumor activity of IMM-1-104 was evaluated in over 130 tumor models spanning 12 distinct histologies in the humanized 3D tumor growth assay (3D-TGA). Cell-based whole exome sequencing readouts were combined with 3D-TGA results to build a pharmacogenomic response algorithm. When applied to the GENIE patient database, resultant tumor-specific response landscapes helped to inform an early pan-RAS clinical trial design for IMM-1-104.

Summary of New Data: A machine learning model was developed to predict IMM-1-104 sensitivity using response-associated genes and signaling networks that were identified using 3D-TGA pharmacogenomics data. This model was used to estimate GENIE patient IMM-1-104 response profiles across key solid tumor indications. In addition, mutation constellations from GENIE were compared with those observed in cell lines to identify preclinical models that best resemble real-world patients. This effort was designed to further enrich the translational fidelity of specific tumor models with the goal of translationally identifying patient populations most likely to benefit from IMM-1-104 treatment.

Conclusions: The depth of response to IMM-1-104 was evaluated across a panel of diverse 3D-TGA tumor models and led to identification of a biomarker signature for therapeutically addressable MAPK pathway addiction. To translate these findings into a relevant clinical application, a response algorithm was developed and applied to the GENIE database, which has cataloged the molecular profiles of over 100,000 cancer patients. Mutational landscapes of patients within GENIE helped identify preclinical models that better represent patient profiles likely to be encountered in the clinic. This approach could, as a general principle, be applied as a tool for improving biomarker discovery and clinical translation of oncology drugs.

#4266

Genomic landscape of prostate cancer: Bioinformatic analysis of TCGA PanCancer data by race and identification of key pathways and genes in PTEN mutation

Olumide Arigbede, Sarah G. Buxbaum, Sara Falzarano, Suhn K. Rhie.
Florida A&M University College of Pharmacy & Pharmaceutical Sciences, Tallahassee, FL

Issue: Prostate cancer (Pca) is still among the most frequently diagnosed cancers in adults. The most often mutated gene in PCa is PTEN (Phosphatase and Tensin Homolog), making it a possible biomarker for prospective customized therapy. The root causes of health inequalities in PCa have not received much attention. Numerous online databases, like The Cancer Genome Atlas (TCGA), provide gene expression data and other data, allowing researchers to further investigate new processes or therapy options. However, there hasn't been much study on tailored therapy up to this point since there may have been difficulties with access to genomic information and bioinformatic tools.
Methods: The PCa data in cBioPortal comprises 494 samples. We selected 154 samples comprising 7 Blacks and 147 Whites. We used the TCGA database to obtain the PCa gene expression and DNA methylation data for study. In order to examine the data by race/ethnicity, gene expression, DNA methylation, and genomic changes, we evaluated at the differentially expressed and methylated genes using online tools (cBioPortal). To evaluate gene methylation, expression, and alterations, log ratios of means in Blacks to means in Whites were computed across the data. Additionally, Kaplan-Meier survival analysis, protein interaction analysis, and multivariable data analysis were carried out.
Results: PCa data in the TCGA database showed PTEN mutation in 20% patients. The median age of participants was 63 years (range: 42-78). For every category of data assessed, there were significant differences by race/ethnicity ($q < 0.05$). In the survival analysis, SLC2A1, NUDT12, CUTALP, and other genes were associated with survival.
Conclusion: Genetic alteration, expression, and DNA methylation are each significantly different by the two race groups compared. According to our research, PTEN mutation in PCa may influence several genes and biological processes.

POPULATION SCIENCES

Cancer Screening and Health Equity

#4172

Serum PVT1 exon 9 copy number is a better predictor of positive prostate biopsy in Black and Hispanic men than serum prostate specific antigen

Emmanuel Owusu Asante-Asamani[1], Sobana Handi D. Sewwandi De Silva[1], Gargi Pal[2], Micheal Liss[3], Robin J. Leach[4], Olorunseun O. Ogunwobi[5]. *[1]Mathematics, Clarkson University, Potsdam, NY,[2]Biology, Hunter College, New York, NY,[3]UT Health San Antonio, San Antonio, TX,[4]Department of Cell Systems and Anatomy, University of Texas Health San Antonio, San Antonio, TX,[5]Biology, Hunter College of CUNY, New York, NY*

Background: Men of African ancestry (moAA) experience the highest incidence and mortality rates of prostate Cancer (PCa) in the United States, where 1 in 8 men are expected to be diagnosed with the disease in their lifetime. Yet, most biomarkers used in PCa screening today, which are based on prostate specific antigen (PSA), are developed and validated in predominantly White populations with weak or nonexistent validation in moAA, making moAA more likely to be subjected to unnecessary prostate biopsies. To reduce this disparity in PCa detection and management, there is a critical need for new biomarkers that target the unique genetic make-up of moAA. We recently showed that plasmacytoma variant translocation 1 (PVT1), exons 4A, 4B, and 9 are overexpressed in the prostate tissues and detected in higher copy numbers in serum of moAA with PCa. In this study, we investigated the predictive power of these potential biomarkers in detecting PCa across different racial populations.
Methodology: Forty serum samples from White, Hispanic, and Black men, 50 percent of whom had PCa, were analyzed to obtain copy numbers for PVT1 exons 4A, 4B, and 9. Seven logistic regression models were developed to predict PCa using single biomarkers, all pairwise combinations of biomarkers and all three biomarkers. The median area under the receiver operator characteristic curve (AUC) was used to measure

the predictive accuracy of each model after a repeated, stratified k-fold cross validation. Model accuracy was first evaluated using data from all races and then for just the Black or Hispanic subpopulation. Our best performing models were compared with PSA as a predictor of PCa. We also evaluated the predictive accuracy of composite models that combined our biomarkers with PSA.
Results: In predicting PCa for all races, our model with only PVT1 exon 9 achieved the highest median AUC of 0.71, which was better than the AUC of 0.63 obtained with just PSA. When PSA and PVT1 exon 9 were combined, the median AUC increased to 0.75. Combining all three biomarkers with PSA increased the median AUC to 0.813. For the Black or Hispanic subpopulation, PVT1 exon 9 achieved the highest AUC of 0.92 which was significantly higher than the median AUC of 0.63 achieved with PSA. No significant change in AUC was observed when the PVT1 biomarkers were combined with PSA. Conclusion: Our results show that PVT1 exon 9 is more accurate than PSA in predicting PCa, achieving near perfect accuracy within the Black or Hispanic subpopulation. Whereas combining PSA with PVT1 biomarkers improved the performance of PSA for all races, no significant improvement in PSA's performance was observed in Black or Hispanic subpopulation. Thus, PVT1 exon 9 may hold the key to reducing disparity in PCa detection among moAA while improving the predictive accuracy of PSA for the general population.

#4173

Lipidome of mammographic breast density in premenopausal women

Kayla R. Getz, Myung S. Jeon, Chongliang Luo, Jingqin Luo, Adetunji T. Toriola. *Department of Surgery, Division of Public Health Sciences, Washington University School of Medicine in St. Louis, St. Louis, MO*

Introducti**on:** High mammographic breast density (MBD) is a strong risk factor for breast cancer, but the biological mechanisms underlying high MBD are not well understood. We, therefore, comprehensively investigated for the first time the associations of lipid species with volumetric measures of MBD to elucidate potential biological mechanisms of high MBD in premenopausal women.
Methods: We performed lipidomic profiling on 705 premenopausal women recruited during their annual screening mammogram at Washington

University School of Medicine, St. Louis, MO. Lipidomic profiling for 982 lipid species was completed at Metabolon (Durham, NC®). Lipid species with greater than 300 missing values (N=125) were excluded from the analysis. Using nearest neighbor methods, we imputed the lipid species missing less than 300 values. We used Volpara 1.5 (Volpara Health®) to quantify volumetric measures of MBD - volumetric percent density (VPD), dense volume (DV), and non-dense volume (NDV). We investigated the associations of the lipid species with MBD measures using multivariable linear regression models adjusting for age, age at menarche, body shape at age 10, race/ethnicity, body fat %, family history of breast cancer, oral contraceptive use, parity/age at first birth, and alcohol use. MBD measures were $\log_{10}$-transformed, and lipid species were standardized. Linear coefficients were back-transformed to the original scale and considered significant if the Bonferroni corrected $p<0.05$.
Results: In multivariable linear regression models, 34 lipid species were inversely associated with VPD. The lipid species belong to the triacylglycerol (TAG, N=26), diacylglycerol (DAG, N=6), phosphatidylcholine (PC, N=1), and cholesterol ester (N=1) pathways. DAG(16:0/18:2) and TAG54:6-FA20:4 displayed the largest inverse associations with one standard deviation increase in DAG(16:0/18:2), and TAG54:6-FA20:4 corresponding to 9.9% (p=0.002), and 9.6% (p=0.007) decrease in VPD, respectively. Eleven lipid species were significantly associated with NDV, with 10 species (all TAG) having a positive association and 1 inverse association PC(18:1/18:1). The strongest positive association was observed with TAG54:6-FA20:4. One standard deviation increase in TAG54:6-FA20:4 was associated with a 9.8% increase in NDV (p=0.01). Several of the lipid species (N=8, 23.5%) that were associated with VPD were also associated with NDV, but in opposite directions. No lipid species were significantly associated with DV.
Conclusions: Our study identified many lipid species, especially in TAG and DAG pathways, that were associated with VPD and NDV and offer new insights into the biological mechanisms underlying high MBD in premenopausal women. Future studies are needed to validate our results and the translational potential.

#4174

Incorporating continuous mammographic density into the BOADICEA breast cancer risk prediction model

Lorenzo Ficorella[1], Mikael Eriksson[2], Kamila Czene[2], Goska Leslie[1], Xin Yang[1], Tim J. Carver[1], Douglas F. Easton[1], Per F. L. Hall[2], Antonis C. Antoniou[1]. *[1]Department of Public Health and Primary Care, University of Cambridge, Cambridge, United Kingdom,[2]Department of Medical Epidemiology and Biostatistics, Karolinska Institutet, Stockholm, Sweden*

BOADICEA, implemented in the CanRisk tool (www.canrisk.org) can be used to calculate future breast cancer risk using data on cancer family history, genetics (rare high- or moderate-risk pathogenic variants; polygenic scores (PGS)), questionnaire-based risk factors and mammographic density (MD) measured using the BI-RADS classification. The BI-RADS categorization requires manual reading which is not feasible at population level. Moreover, BI-RADS captures MD in 4 categories, whereas continuous measures are stronger risk predictors. Here, BOADICEA was extended to incorporate continuous breast density measured by the fully automated Volpara and STRATUS software, working on raw and processed images, respectively. We used data from the KARMA prospective screening cohort (60,276 participants; 1,167 incident breast cancers). The associations between Volpara or STRATUS density measurements and incident breast cancer risk were estimated in a randomly selected training subset consisting of two-thirds of the full dataset. For this, we calculated density residuals after regressing on participant's age at mammography. Hazard ratios (HR) for the normalized residuals were calculated using a Cox proportional hazards model, adjusting for family history, BMI and all risk factors included in BOADICEA. Multiple Imputation by Chained Equations (MICE) was used to impute missing data. The remaining one-third of the KARMA cohort was used to assess the performance of BOADICEA in predicting 5-year risks, after including the estimated Volpara and STRATUS associations.Under the best fitting multivariable model including PGS, the HRs per SD of residual STRATUS density were estimated to be 1.67 (95%CI: 1.44-1.93) and 1.38 (95%CI: 1.26-1.51) for pre- and post-menopausal women, respectively. The HR estimates per SD of residual Volpara density were 1.38 (95%CI: 1.19-1.59) and 1.39 (95%CI: 1.27-1.52) for pre- and post-menopausal women, respectively. After incorporating these associations in BOADICEA, there was a marked improvement in the

model discriminatory ability in the test dataset, compared to using the BI-RADS classification. The largest increase in AUC was observed for STRATUS residual density, with a 3% increase compared to using BI-RADS vs a 1.6% increase in AUC when using Volpara residual density. These increases were consistent across BOADICEA models considering different combinations of risk factors, including PGS.Including continuous breast density in BOADICEA can lead to improved breast cancer risk stratification and could allow for automated measures of MD to be more readily deployed in breast cancer risk prediction. Additional prospective studies are required to further validate the findings. The models will be implemented in the CanRisk tool.

#4175

Development of breast cancer risk assessment tool: The Korean decision aid for cancer screening (K-DACS) study

Wonyoung Jung[1], Yong-Moon Mark Park[2], Sang Hyun Park[3], Kyungdo Han[4], Junhee Park[5], Yohwan Yeo[6], Jung Kwon Lee[7], Dale P. Sandler[8], Dong Wook Shin[5]. *[1]Kangdong Sacred Heart Hospital, Seoul, Korea, Republic of,[2]Department of Epidemiology, University of Arkansas for Medical Sciences, Little Rock, AR,[3]Department of Biostatistics, The Catholic University of Korea, Seoul, Korea, Republic of,[4]Department of Statistics and Actuarial Science, Soongsil University, Seoul, Korea, Republic of,[5]Department of Family Medicine and Supportive Care Center, Samsung Medical Center, Seoul, Korea, Republic of,[6]Department of Family Medicine, Hallym University Dongtan Sacred Heart Hospital, Hwaseong, Korea, Republic of,[7]Department of Medicine, Sungkyunkwan University School of Medicine, Seoul, Korea, Republic of,[8]Epidemiology Branch, National Institute of Environmental Health Sciences, Research Triangle Park, NC*

Purpose: Widely used breast cancer risk prediction tools are based on data from Western countries, but risk factors may differ for Asian women. Hence, we aimed to develop a risk assessment tool for breast cancer in Asian women, using a nationwide, population-based cohort in Korea. Methods: Women aged ≥ 40 years who participated in both breast cancer screening and general health examination in 2009 were eligible for this

study. Age, body mass index (BMI), breast density, lifestyle and reproductive factors, and comorbidities were used to develop 5-year breast cancer risk prediction models in premenopausal (n=771,856) and postmenopausal (n=1,108,047) women at baseline. Backward stepwise selection in the Cox proportional hazards model was used to construct the best-fit risk prediction model, which was then converted into a risk score nomogram, representing an individual probability estimate of incident breast cancer. Model performance was evaluated by discrimination and calibration. Results: Among premenopausal women, high BMI, low parity, short breastfeeding period, early age at menarche, high breast density, history of benign breast mass, and family history of breast cancer contributed to breast cancer risk prediction. The appropriate predictors in postmenopausal women additionally included age, type 2 diabetes, dyslipidemia, late age at menopause, hormone replacement therapy use, except for number of parities. The concordant statistic of risk prediction model was 0.58 (95% confidence interval [CI] 0.57-0.59) for premenopausal women, and 0.64 (95% CI 0.63-0.65) for postmenopausal women. Our model correlated well in the calibration plot in both premenopausal and postmenopausal women.Conclusions: Our breast cancer risk prediction model showed good performance for postmenopausal women, providing the background for risk-based screening recommendations in Asian women.

#4176

Timing of pregnancy-related factors and breast cancer risk for women across a range of absolute risk

Jasmine A. McDonald[1], Yuyan Liao[1], Esther M. John[2], Allison W. Kurian[2], Jeanine M. Genkinger[1], Saundra S. Buys[3], John L. Hopper[4], kConFab Investigators, Mary Beth Terry[1]. *[1]Department of Epidemiology, Columbia University Irving Medical Center, New York, NY,[2]Department of Epidemiology & Population Health, Stanford University School of Medicine, Palo Alto, CA,[3]Department of Medicine, Huntsman Cancer Institute, Salt Lake City, UT,[4]Centre for Epidemiology and Biostatistics, Melbourne School of Population and Global Health, The University of Melbourne, Melbourne, Australia*

Background**:** Studies in women with pathogenic variants in *BRCA1* or *BRCA2* suggest that underlying breast cancer (BC) risk modifies the associations between pregnancy-related factors and BC risk. Less is known about whether the associations are modified across a range of predicted absolute BC risk based on age and the extent of BC family history.
Objective: Examine the association between pregnancy-related factors and BC risk and modification by predicted absolute BC risk in the Prospective Family Study Cohort (ProF-SC) with women enrolled between 1992-2011 and a median 10.0 years of follow-up time.
Methods: ProF-SC includes the six international sites of the Breast Cancer Family Registry [USA, Canada, and Australia] and the Kathleen Cuningham Foundation Consortium for Research into Familial Breast Cancer (kConFab). 17,274 women with 943 prospectively ascertained BC cases were eligible for the prospective analysis with 87% of cases self-identifying as non-Hispanic White. Questionnaires at study entry assessed self-reported pregnancy-related factors (parity, number of full-term pregnancies (FTP), age at first FTP, years since last FTP, breastfeeding, and age at menarche). We used Cox proportional hazards regression models with age as a time scale to estimate Hazard Ratios (HR) and the 95% Confidence Intervals (CI) for each reproductive variable (main effect) and examined modification by predicted absolute risk of BC, measured by a 1-year absolute risk score (continuous) estimated by the BOADICEA (interaction effect). We also examined associations stratified by estrogen receptor (ER) subtype.
Results: Women with a first FTP at age ≥30 vs. <20 years had an increased risk of BC (HR=1.49, 95% CI 1.10, 2.02); no other pregnancy-related factors were associated with BC risk. Compared to nulliparous women, the main effect for higher parity was associated with increased ER-negative BC (PARS*≥4 FTP HR 2.34, 95% CI 1.09, 5.01). In contrast, increasing absolute BC risk for women with higher parity was associated with reduced risk of ER-negative BC (PARS*≥4 FTP $HR_{interaction}$ 0.66, 95% CI 0.48, 0.90; $p_{interaction}$=0.01). Increasing absolute BC risk for nulliparous or first FTP at age ≥25 years had a >20% increased risk of ER-negative BC compared to first FTP at age <20 years ($p_{interaction}$=0.002); the main effects for nulliparity and first FTP at age ≥25 years and ER-negative BC were null (*p-values*=0.2-1.0). Compared to nulliparous women, increasing absolute risk for women who were within 5 years of their last FTP was positively

associated with ER-negative BC ($HR_{interaction}$=1.54, 95% CI 1.03, 2.31); main effects were null (HR=1.00, 95% CI 0.39, 2.54).
Conclusion: The association between pregnancy-related factors and BC risk are modified by predicted absolute BC risk, with stronger associations observed for ER-negative BC. Women at higher absolute BC risk may benefit from more frequent BC monitoring following childbirth.

#4177

Genetic testing for hereditary colorectal cancer syndromes in Algerian patients: A multicenter study

Farid Cherbal[1], Asma-Lamia Boumehdi[1], Feriel Khider[1], Karima Landelouci[1], Abdelwahab Zemam[1], Sarah Sabri[1], Adam.Walid Damache[1], Mohammed Oukkal[2], Hassen Mahfouf[3], Ferhat Zebboudj[4], Mustapha Maaoui[5]. *[1]Molecular Genetics Team, LMCB, Faculty of Biological Sciences,University of Science and Technology Houari Boumediene (USTHB), Algiers, Algeria,[2]Clinic of Medical Oncology Amine Zirout, University Hospital of Beni-Messous, School of Medicine, University of Algiers-1, Algiers, Algeria,[3]Mohamed El Kolli Public Hospital, Academic Medical Oncology Services, School of Medicine, University of Algiers-1, Rouiba, Algiers, Algeria,[4]Mohamed El Kolli Public Hospital, Academic General Surgery Services, School of Medicine, University of Algiers-1, Rouiba, Algiers, Algeria,[5]Bachir Mentouri Public Hospital, Academic General Surgery Services, School of Medicine, University of Algiers-1, Kouba, Algiers, Algeria*

Background To date, 5% to 6 % of all colorectal cancers (CRCs) are associated with germline pathogenic variants in cancer predisposition genes that confer inherited predisposition to CRC. The use of genetic testing to identify individuals at risk for hereditary CRC syndromes can help to prevent the development of cancer and in the clinical management of the colorectal patients in the areas of both prevention and treatment. We report here the experience of our research laboratory of genetic testing for hereditary polyposis syndromes and Lynch syndrome (LS), respectively, in 126 patients.
Methods Fifty four (54) severe familial adenomatous polyposis (FAP) patients and 72-suspected Lynch syndrome (LS) patients, respectively, were

selected from 2851 consecutive colorectal patients at five public hospitals during 2012-2019. Family histories of cancer were obtained from interviews, pedigrees and medical records of patients. Index cases and relatives diagnosed with FAP syndrome or Lynch syndrome have been tested for germline variants in *APC*, *MLH1*, *MSH2*, *MSH6* and *PMS2* genes, respectively, using PCR-Sanger Sequencing or by NGS using a cancer panel of 30 hereditary cancer genes (Color Genomics).
Results We detected 13 germline pathogenic variants in *APC* gene in 17 unrelated families, one germline pathogenic variant in *BMPRA1* gene in juvenile polyposis syndrome (JPS) patient; seven (7) germline pathogenic variants and 2 variants of uncertain clinical significance (VUS) in MMR genes. Interestingly, 4 novel germline pathogenic variants in *APC* gene and 3 novel germline pathogenic variants in MMR genes, respectively, have been detected in our study. The most occurring germline pathogenic variants in APC gene were c.3927_3931del and c.4728dup that were identified in four and two index cases in 6 unrelated FAP families, respectively. In Lynch syndrome patients, the rare germline pathogenic variant *MLH1* c.1546C>T has been found in 21 individuals from 9 LS families, 6 of them related, with two large kindreds. In addition, the recurrent germline pathogenic variant *MSH2* c.942+3A>T has been detected in five unrelated index cases with a strong family history of LS syndrome. Moreover, the rare germline VUS *PMS2* c.989-107_989-106insA has been detected in 14 unrelated LS patients and could be reclassified as likely benign. Interestingly, our NGS analysis detected the novel *BMPR1A* pathogenic variant c.1474-1G>C in young JPS patient that has been misdiagnosed as FAP. The *in-silico* analysis for this novel variant showed an alteration of the wild type acceptor site and an activation of a cryptic acceptor site, respectively, most probably affecting splicing.
Conclusions Our current study will contribute to the molecular genetics characterization of hereditary colorectal cancer syndromes in Algerian population that is relevant for clinical management in the areas of genetic testing, early diagnosis, treatment and prevention.

#4178
Lysosomal storage dysfunction as a risk factor in pancreatic cancer
Hyemin Kim[1], Youngil Koh[2], Joo Kyung Park[1]. *[1]Samsung Medical Center, Sungkyunkwan University, Seoul, Korea, Republic of,[2]Seoul National*

University Hospital, Seoul, Korea, Republic of

Background: Lysosome is closely linked to autophagy activity which has an important role in pancreatic adenocarcinoma (PDAC). We investigated whether lysosome storage dysfunction (LSD) contributes to PDAC development.
Materials and Methods: Comparison of germline putative pathogenic variants (PPV) in genes involved in lysosome functions was performed between PDAC patients (N=418) and healthy controls (N=745) using next generation sequencing. Using mouse pancreas organoid, consequences of GALC downregulation in PDAC development was evaluated. Transcriptome data analysis of human PDAC organoid according to PPV status was followed.
Results: PPV in LSD related genes were enriched in PDAC patients compared to healthy controls (Log2OR = 1.65, P = 3.08×10^{-3}). For limited stage PDAC patients, PPV carriers were diagnosed with PDAC in younger age compared to non-carriers (mean age 61.5 vs. 65.1 years, p=0.038). In mouse pancreas organoid, Ki-67 index significantly increased as GALC was downregulated. Altered autophagy activity with increased autophagy flux following GALC dysfunction was observed in both human cancer cell line and mouse organoid. mTOR downregulation was noted in mouse pancreas organoid. RNA sequencing analysis of human PDAC organoid revealed metabolism alteration related to LSD.
Conclusion: Genetically defined lysosome dysfunction is frequently observed in young age onset PDACs. Lysosome dysfunction might contribute to PDAC development via altered metabolism and autophagy activity.
Key words: lysosomal storage disease (LSD), germline, pancreatic ductal adenocarcinoma (PDAC)

#4179

Anal cancer risk factors and utilization of cancer preventive strategies in people living with HIV in Puerto Rico

Sandra I. Garcia-Camacho[1], Jeslie M. Ramos-Cartagena[1], Marievelisse Soto-Salgado[2], Vivian Colon-Lopez[2], Karen J. Ortiz-Ortiz[2], Ashish A. Deshmukh[3], Ana P. Ortiz[2]. *[1]Graduate School of Public Health, University of Puerto Rico, San Juan, PR,[2]University of Puerto Rico Comprehensive*

Cancer Center, San Juan, PR,[3]Medical University of South Carolina, Charleston, SC

Introducti**on:** Anal cancer (AC) risk is greatly elevated among persons living with HIV (PLWH), particularly men who have sex with men (MSM). The incidence of anal cancer among PLWH in Puerto Rico is 60.5 per 100,000 in MSM. Smoking and sexual behaviors may enhance anal cancer risk among PLWH. Therefore, we describe the prevalence of risk factors for AC, overall and by sexual risk group (MSM, women, and men who have sex with women [MSW]). We also evaluated receipt of cancer preventive strategies: HPV vaccination and AC screening, among a sample of PLWH in Puerto Rico.

Methods: A cross-sectional study was conducted (Sept 2020 - Dec 2021) among PLWH ≥26 aged in Puerto Rico (n=212). Participants answered a phone interview that collected information on relevant characteristics. AC risk factors evaluated were current smoking, age of sexual initiation (≤15 years), lifetime anal sex, 10 or more lifetime sexual partners, history of AIDS, genital warts, and HPV infection. HPV vaccination and AC screening status were also evaluated. The overall and sexual risk group specific prevalence of AC risk factors and preventive behaviors were described. In addition, the prevalence ratio (PR) of the variables of interest, comparing the sexual risk groups, was estimated with 95% confidence intervals using Poisson regression.

Results: Mean age of participants was 52.8 ± (SD=10.2); 44.1% were MSM, 23.2% were MSW, and 32.7% were women. Most PLWH had public health insurance (84.4%), an education level of high-school or less (45.7%), and 9.5% had a history of intravenous drug use. Regarding the prevalence of AC risk factors, 58.3% had 10 or more lifetime sex partners, 51% had their first sexual relationship at age ≤15 years, 29.3% were current smokers, and 75.8% of women had history of anal sex. In addition, 20.8% reported being diagnosed with AIDS, 16.5% had a history of genital warts, and 12.0% had HPV infection. Only 7.5% reported HPV vaccination and 52.2% reported ever having had an anal pap test. MSM had the highest prevalence of risky sexual behaviors, although no statistical difference was seen in the PRs. For preventive strategies, women (PR: 3.13, 95% CI 1.52-6.46) and MSM (PR: 3.42, 95% CI 1.70-6.90) had higher prevalence of anal pap uptake than MSW.

Conclusion: Persons living with HIV in Puerto Rico had high prevalence of current smoking use and risky sexual behavior. Despite their increased risk of AC, and only over half had been screened for AC. Continued education and awareness about AC risk factors, smoking cessation, and importance of prevention strategies are important among PLWH.

#4180

Knowledge and barriers to colorectal cancer screenings in people experiencing homelessness in Central Florida

Harini Sankar, Cassie L. Odahowski. *Health Sciences, University of Central Florida, Orlando, FL*

Purpose of the study: The purpose of this study is to assess how existing knowledge about colorectal cancer screenings and access to resources affect the ability to obtain colorectal cancer screening in people experiencing homelessness in Central Florida.
Procedures: A team of researchers from the University of Central Florida will survey subjects who do not have stable housing in two Central Florida locations: a local shelter for men, women, and children and a resource center for the unsheltered. The survey will take place in February 2023 with a sample size goal of 400. The survey will assess current understanding of CRC screenings and available/lacking resources necessary for completing CRC screening in this population. Our inclusion criteria include those who are undomiciled, age 45 and over who speak Spanish or English.
Preliminary Results: Anticipated results from previous work by our research team with this population indicate that we will have a large, diverse study sample. The results will include demographic data, frequency of insurance coverage, type of insurance coverage, knowledge of CRC screening recommendations, concerns related to CRC, rate of past completed screening, and perceived barriers to accessing CRC screening.
Conclusions: This study will be the first to examine this research topic in Florida. The results will identify the knowledge of CRC screening recommendations, barriers to CRC screening and identify resources needed for the unhoused population to achieve CRC screening in the future.
Key words: homelessness, colorectal cancer screenings, barriers to screening

#4181

Geospatial heterogeneity in colorectal cancer screening among Hispanic subgroups

Robert Blake Buchalter[1], Johnie Rose[2], Mariana C. Stern[3], Jane C. Figueiredo[4], Stephanie L. Schmit[5]. *[1]Quantitative Health Sciences, Cleveland Clinic Lerner Research Institute, Cleveland, OH,[2]Center for Community Health Integration, Case Western Reserve University, Cleveland, OH,[3]Keck School of Medicine, University of Southern California, Los Angeles, CA,[4]Samuel Oschin Comprehensive Cancer Center, Cedars-Sinai Medical Center, Los Angeles, CA,[5]Genomic Medicine Institute, Cleveland Clinic Lerner Research Institute, Cleveland, OH*

The U.S. Hispanic population has significantly lower colorectal cancer (CRC) screening rates than any other racial/ethnic group, resulting in unchanged incidence and mortality rates over recent decades. Recent studies have identified geographic variation in Hispanic CRC screening rates, but little is known about patterns among Hispanic subgroups. Here, we examine statistical and geographic relationships between broadly defined racial groups, Hispanic subgroups, and nationwide CRC screening rates. USPSTF guideline-adherent CRC screening rates for census tracts were obtained from 2018 CDC Places. Tract race/ethnicity %s, including non-Hispanic White (NHW), non-Hispanic Black (NHB), Asian, and Hispanic subgroups (Mexican, Cuban, Puerto Rican (PR), Dominican, Central/South American (CSAm), and other Hispanic), female %, and area deprivation index (ADI) were obtained from 2015-2019 American Community Survey 5-year estimates. Race/ethnicity %s were transformed using additive log ratios to account for the compositional nature of racial categories. A linear model and geographically weighted regression (GWR) were fit with CRC screening rate as the outcome. The mean CRC screening rate for 72,117 U.S. census tracts (99% of tracts) was 63.7% (SD=7.0). Linear modeling (R^2=0.68) showed significant positive linear associations between CRC screening and female % ($p<0.001$), NHW % ($p<0.001$), NHB % ($p<0.001$), and Asian % ($p=0.002$), and significant negative associations between screening and ADI ($p<0.001$) and all Hispanic subgroups ($p<0.001$). Mexican, Cuban, PR, Dominican, and CSAm subgroups had significant screening rate drops of -1.48%, -0.26%, -0.15%, -0.30%, and

-0.52%, respectively, per 1 unit increase in subgroup %. ADI had strong effects on all screening-race associations, with a flip in directionality for NHB% (negative to positive) and weakening of slopes for all other racial categories after adding ADI in the final adjusted model. GWR results (R^2=0.94) displayed spatial heterogeneity in local coefficients of all predictor variables, with distinct regional patterns in relationships between screening and ADI (strongly negative local coefficients in OH and OK), Mexican % (strongly negative in TX, AZ, NV, and CA), and NHB % (strongly negative in FL, GA, MS and WI; positive in SC and NC). This work suggests Mexican, CSAm, and Dominican subpopulations may be driving the low CRC screening rates among Hispanics overall. Local variability suggested the importance of where subpopulations live in determining guideline-concordant screening. ADI strongly altered screening-race relationships, with directionality changing for NHB %, further displaying the importance of area deprivation in CRC screening. Future work should explore micro-level drivers of spatial heterogeneity in screening rates across both broadly defined racial groups and Hispanic subgroups in the U.S.

#4182

Genetic associations with smoking relapse and proportion of follow-up in relapse throughout adulthood in pre- and post-menopausal women

Stephanie K. Jones[1], Anthony J. Alberg[2], Kristin Wallace[3], Brett Froeliger[4], Matthew J. Carpenter[3], Bethany J. Wolf[3]. *[1]Baylor University, Waco, TX,[2]University of South Carolina, Columbia, SC,[3]Medical University of South Carolina, Charleston, SC,[4]University of Missouri, Columbia, MO*

Cigarette smoking is a major contributor to the cancer burden, so identifying genetic variants associated with smoking cessation is important for cancer prevention. Prior genetic studies of smoking cessation have been limited by short-term follow-up and not accounting for quit attempts and relapse events experienced by most smokers. In this study, candidate SNPs previously found to be associated with smoking cessation were studied in relation to smoking relapse throughout adulthood. Participants were from two, all-female longitudinal cohort studies with repeated smoking behavior measurements collected every 2 years. The study included 12,060 ever-smokers of European ancestry with genotype data who quit smoking at ≥1

timepoint. Median follow-up after first quitting smoking was 32 years. Associations between selected single nucleotide polymorphisms (SNPs) and odds of smoking relapse and, conditional on relapse, SNP associations with the proportion of follow-up in relapse were modeled using zero-inflated beta regression. Genotype by menopausal status interactions were evaluated. Women with AA genotypes for *CHRNA5* SNP rs16969968 G>A or *CHRNA3* SNP rs1051730 G>A (p-value = 0.04 for both) had lower odds of relapse. Among women who relapsed, those with AA genotypes for *CHRNA5* SNPs rs588765 G>A or rs680244 G>A had 2.6% [95% CI 0.1 - 5.0%] and 2.4% [95% CI 0.2 - 4.9%] more follow-up in smoking relapse, respectively, compared to women with AG or GG genotypes. Women with AA or AG genotypes for *DRD2* SNP rs6277 G>A had 3.3% [95% CI 0.8 - 5.7%] more follow-up in relapse than women with GG genotypes. In contrast, women with AA genotypes for *COMT* SNP rs4680 G>A had 2.7% [95% CI 0.2 - 5.2%] lower proportion of follow-up in relapse than women with AG or GG genotypes. These associations with the proportion of follow-up in relapse were stronger among post-menopausal women. The association of SNPs rs588765, rs680244, and rs6277 with a higher proportion of follow-up in relapse was significantly stronger among women who quit smoking post-menopause [rs588765 difference in proportion follow-up in relapse = 9.5% (95% CI 3.8 -15.2%), rs680244 difference in proportion follow-up in relapse = 10.1% (95% CI 4.4% - 15.9%), rs6277 difference in proportion follow-up in relapse = 7.6% (95% CI 1.5 - 13.6%)]. No statistically significant difference in proportion follow-up in relapse by genotype was observed among women who quit smoking prior to menopause. Several SNPs were not associated with odds of smoking relapse but, conditional on relapse, were associated with the proportion of follow-up in relapse. The findings show selected genetic variants contribute to susceptibility to smoking relapse in the long term and that the genetic risk can differ by the stage of smoking cessation. For several SNPs stronger associations were observed among post-menopausal women, indicating the importance of menopausal status.

#4183

Employment status moderates the relationship between patient-provider communication and prostate cancer screening among Black men

Brian J. Carter[1], Tzuan A. Chen[2], Dalnim Cho[1], Lorna H. McNeill[1], Lorraine R. Reitzel[1]. *[1]Health Disparities Research, The University of Texas MD Anderson Cancer Center, Houston, TX,[2]Department of Psychological, Health, & Learning Sciences, University of Houston, Houston, TX*

Purpose: Black men have 76% higher prostate cancer incidence rate than White men, and 120% higher mortality rate. They are also less likely to be screened via prostate-specific antigen (PSA) testing. Potential harms of PSA testing include overdiagnosis and overtreatment, but recent research suggests that the harm-benefit trade-off may be uniquely favorable for Black men. Increasing Black men's PSA testing rates may therefore reduce prostate cancer disparities. Studies suggest that employment status and accompanying roles (e.g., family breadwinner or workplace leader) are often central to masculine identity and that employed men may thus anticipate prostate cancer diagnosis and work-disruptive treatment threatening their identity, engendering screening avoidance. Patient-provider communication (PPC), if ideal, may help to reframe PSA testing and overcome barriers unique to employed men. The current work explored this possibility.
Methods: A convenience sample of 246 Black men aged ≥45 (M_{age} = 56.94±7.88) was recruited from Houston, TX. Self-reported data included satisfaction with PPC (Consumer Assessment of Healthcare Providers and Systems; ideal vs not ideal), current employment status (employed for wages or self-employed vs none), and receipt of PSA test in the past 2 years (yes vs no). A logistic regression model examining the association between PPC and PSA testing assessed moderation using an interaction term, controlling for sociodemographic variables (e.g., age, income, insurance status), family/personal cancer history, cancer risk perceptions, spirituality, and social support.
Results: Overall, 67% of respondents were employed, 39% endorsed ideal PPC, and 73% had a PSA test in the past 2 years. Employed men comprised 68% of those screened. Moderation was significant; employed men reporting nonideal PPC were less likely to have had a PSA test than employed men reporting ideal PPC (OR: 0.262, $CI_{95\%}$ = 0.097-0.708). For unemployed men, there was no significant association between PPC and having had a PSA test in the past 2 years.

Conclusion: Ideal PPC may be important to effectively mitigate unique employment-related patient concerns and spur PSA testing for employed Black men. Ideal PPC may be developed by providers building trust with patients, asking them about concerns, verifying their understanding, and engaging them in shared decision-making that respects their values. Employee wellness programs, health insurance companies, cancer centers, cancer survivors, church leaders, and health ministries can work to improve PPC by encouraging patients to have open discussions about prostate cancer with their providers by sharing concerns and asking questions. PSA testing may be cost-prohibitive for unemployed men regardless of PPC; more work is needed to reach this group.

#4184

Congruent views among substance use treatment center leadership on organizational readiness to implement a tobacco-free workplace program is linked to provider uptake of non-cigarette tobacco use treatment

Brian J. Carter[1], Tzuan A. Chen[2], Maggie Britton[1], Isabel Martinez Leal[1], Virmarie Correa-Fernández[2], Anastasia Rogova[1], Bryce Kyburz[3], Teresa Williams[3], Kathleen Casey[3], Lorraine R. Reitzel[1]. *[1]Health Disparities Research, The University of Texas MD Anderson Cancer Center, Houston, TX,[2]Department of Psychological, Health, & Learning Sciences, University of Houston, Houston, TX,[3]Integral Care, Austin, TX*

Purpose: Tobacco use, linked to 17 cancers, is the leading cause of preventable death in the US. Despite elevated tobacco use among patients, substance use treatment centers (SUTCs) do not routinely address tobacco use. A tobacco-free workplace program (TFWP) implemented in SUTCs included tobacco-free policy guidance, provision of resources, and education for providers on evidence-based tobacco use treatment, which emphasized use of the 5As: Asking about tobacco use, Advising to quit, Assessing willingness to quit, Assisting with quitting, and Arranging follow-up. Congruent SUTC leadership views on readiness for TFWP implementation may forecast greater organizational support for implementation and thus enhanced provider uptake. Given the increasing use of non-cigarette tobacco products, this study examined associations between congruent views among SUTC leadership on readiness to

implement the TFWP and changes in providers' delivery of the 5As for non-cigarette tobacco-using patients (i.e., uptake) from pre- to post-program implementation.
Methods: Post-enrollment but before TFWP implementation, CEOs and Directors from each of 15 participating SUTCs (n=84) completed the Organizational Readiness for Implementing Change (ORIC), which has an overall readiness score and 5 subscale scores (resource availability, change efficacy, change valence, change commitment, and task knowledge). Center-level ORIC congruence was measured by calculating the difference between CEO-reported ORIC and mean Director-reported ORIC scores. Providers from each SUTC completed pre- and post-implementation surveys (pre n=259, post n=194) on their delivery of the 5As to non-cigarette tobacco-using patients during the prior month. Generalized linear regression analyses explored the effect of ORIC congruence on changes in the use of each of the 5As over time.
Results: Use of each of the 5As increased over time. Providers from SUTCs with more leadership congruence on (a) task knowledge and overall readiness had greater increases in Assisting with quitting and (b) resource availability, change efficacy, task knowledge, and overall readiness had larger increases in Arranging follow-up.
Conclusion: Reducing the research-to-practice translation gap in tobacco control through TFWP implementation in settings where users receive care is a critical cancer prevention strategy. TFWPs may facilitate greater provider uptake of evidence-based treatment and more effectively address patients' non-cigarette tobacco use in SUTCs by purposefully aligning leadership support for change. Strategies to align leadership support may include convening CEOs and Directors to identify multi-level organizational barriers and facilitators and engage in group problem-solving with respect to any barriers.

#4185
Inclusive basic and advanced translational laboratory research competencies for research in cancer biology and therapeutics
Wafik S. El-Deiry, Andrew George, Francesca Di Cristofano, Praveen Srinivasan, Lindsey Carlsen, Kelsey E. Huntington, Arielle De La Cruz, Leiqing Zhang, Marina Hahn, Shuai Zhao, Attila Seyhan, Bradley D. DeNardo, Aaron W. P. Maxwell, Dae Hee Kim, Alex Raufi, Hina Khan,

Stephanie L. Graff, Don S. Dizon, Christopher Azzoli, Abbas E. Abbas, Roxanne Wood, Rishi R. Lulla, Howard P. Safran, Benedito A. Carneiro, Arunasalam Navaraj, Xiaobing Tian, Shengliang Zhang, Lanlan Zhou.
Legorreta Cancer Center at Brown University, Providence, RI

Our Laboratory was established in 1994 at Univ. of Pennsylvania. Lab members demonstrated initial competencies by performing cell culture, western blots, immunofluorescence, and flow cytometry showing induction of p53/p21(WAF1) in cells treated with chemotherapy. Years later, our Laboratory of Translational Oncology & Experimental Cancer Therapeutics moved to Penn State Univ., Fox Chase Cancer Center/Temple Univ. and then Brown Univ. By 2020, with desire for inclusiveness (everyone succeeds), scientific rigor/reproducibility mandated by NIH, and as a training and mentoring activity (lab scientists/trainees/students mentoring others at High School level and beyond), we established a process for onboarding and training new cancer researchers. By Fall of 2022, there were 17 current Brown University undergraduate students (10 receiving research credit and 7 not receiving credit), HS students, 7 graduate students (PhD, masters, MD/PhD), and 6 medical students working with collaborating faculty at our laboratory at Brown's Legorreta Cancer Center. After completion of biosafety training, and required trainings such as by IACUC, new lab members complete basic competencies in cell culture, cell viability, and western blot analysis that include technical, presentation quality output, and quantitative/statistical rigor to satisfy current standards for journal publication. For cell culture this includes pathogen free conditions, authentication, attention to details of routine procedures, documentation of morphology, freezing, thawing, passaging, seeding density, and managing cell populations to not run out of cells. Cell viability assessment includes attention to culture conditions, synergy analysis, data robustness, and presentation, and for western blots attention to quality of blots, protein quantification, loading, labeling, antibody specificity and sensitivity controls, presentation at 2022 standards, conventions for splicing, and issues with reproducibility including biological replicates, and generalizability. Additional and advanced competencies include RT-PCR, long-term colony assays, 3-D cultures (spheroids, organoids), transfection (overexpression, knockdown, CRISPR), co-culture and triculture with immune cells and fibroblasts, cytokine profiling, in vivo studies, in vivo

imaging, immunohistochemistry, flow cytometric analysis, single cell techniques, viral infection, circulating tumor cell isolation, blood immune and cytokine analysis, and work with transgenic organoids and inducible cancer predisposing alleles. Modeling the tumor microenvironment, relevance to human cancer and translational directions are emphasized. Shared online lab resources, protocols, practices, videos, and manuscripts are available for lab members. The framework herein may be of interest to others involved in similar training programs.

#4186

Underrepresentation of low- and middle-income country affiliated authors in NCI-supported cancer research

Linsey Eldridge, Elise Garton, Kalina Duncan, Satish Gopal. *National Cancer Institute, Rockville, MD*

Introduction: We conducted a bibliometric analysis to assess authorship of recent publications involving collaborations in low- and middle-income countries (LMICs) supported by the National Cancer Institute (NCI) of the National Institutes of Health (NIH).
Methods: We identified active NCI grants awarded directly to LMIC institutions or to US institutions with a collaborator site or sites exclusively in LMICs between 2015-2019 in NIH Query View Report (QVR). Grants were linked to resulting publications using Dimensions for NIH. Because grants may have been active in 2015 while beginning in earlier years, we analyzed any linked publications from 2011 to 2020. Publications with missing author information were excluded. Author institutional affiliation was used to classify author country income level as defined by the World Bank. Authors with multiple institutional affiliations from a high-income country (HIC) and LMIC were classified as such. Relative citation ratio (RCR) and Altmetric data from Dimensions were used to compare citation impact measures using the Wilcoxon rank sum test.
Results: NCI funded 159 grants to US institutions exclusively with LMIC collaborators and five awards directly to institutions in LMICs from 2015 to 2019, resulting in 2,428 publications between 2011 and 2020, of which 49% had at least one author affiliated with an LMIC institution. Of all publications, 78% and 83% had a first and last author with high-income country (HIC) affiliation, respectively. Publications with HIC-affiliated last

authors had significantly higher median RCR and Altmetric attention scores than publications with LMIC-affiliated last authors (p=0.0134 and p=0.0004, respectively). Publications with HIC-affiliated first authors had significantly higher Altmetric scores than publications with LMIC-affiliated first authors (p=0.001).
Conclusion: LMIC-affiliated authors are represented on only approximately half of publications resulting from NCI grants awarded directly to LMIC institutions or to US institutions with LMIC collaborators, and rarely in the first or last author position. LMIC-affiliated authors also receive less bibliometric attention when represented. Increased scientific capacity and more equitable collaboration should be critical priorities for the cancer research community working in LMICs moving forward.

#4187

Development of a virtual platform to improve global access to oncology education & combat healthcare inequities

Yan Leyfman[1], William B. Wilkerson[2], Shubhadarshini G. Pawar[3], Muskan Joshi[4], Gayathri P. Menon[4], Pallavi Pai[4], Sean Jackewicz[5], Alexandra van de Kieft[6], Chandler Park[7]. *[1]Icahn School of Medicine at Mount Sinai South Nassau, Rockville Centre, NY,[2]Dickinson College, Carlisle, PA,[3]Shree Vighnaharta Superspecialty Hospital, Maharashtra, India,[4]Tbilisi State Medical University, Tbilisi, Georgia,[5]Mercer University School of Medicine, Macon, GA,[6]Cornell University, Ithaca, NY,[7]Norton Cancer Center, Louisville, KY*

Introduction: Social media has emerged as a formidable outlet for medical information through its vast global reach of individuals of all educational levels and socioeconomic statuses but especially those in resource limited regions. However, misinformation has presented a universal challenge and contributed to adverse medical outcomes. *MedNews Week*, a virtual education platform, was developed to combat medical misinformation, especially within hematology-oncology, and contribute to global health education by providing the mainstream public with free access to its weekly programming. Keynote Conference is a weekly show featuring live presentations from hematology-oncology's premier global leaders discussing the latest developments in their field before a global mainstream

audience. The goal of this study was to assess the global reach and impact of MedNews Week's programming.
Methods: From January to June 2022, *MedNews Week* hosted 22 global leaders (h-index = 60) as Keynote Speakers discussing the latest developments in oncology. Viewership, impressions, and outreach data was collected from *MedNews Week*'s and its respective members' social media accounts and with the help of Symplur, data was analyzed to provide insight on global reach and engagement. A mixed-method approach was used to analyze engagement.
Results: *MedNews Week* generated over 11.9K tweets, 5.7K retweets, and 41 million Twitter impressions over this six-month time period reaching over 54 countries. A network analysis of *MedNews Week's* main accounts demonstrated cross-community engagement on Twitter. Hashtags successfully showcased Keynote Conferences, expanded global audience viewership, and enhanced overall engagement. To estimate the level of incoming and outgoing communications between *MedNews Week* and our audience, we focused our analysis on the *MedNews Week* Twitter chat organizers (@yleyfman and @CParkMD) and supporting researcher (@ShimaghavimiMD). We identified these usernames on the network map. Not all other participants were identified. We have also noticed a steady increase in the number of attendees at Keynote Conference.
Conclusion: Given *MedNews Week'*s continued growth in global viewership and international reach, it has emerged as a viable platform to combat medical misinformation, especially in lower socioeconomic regions. Although internet access is one of the main barriers to high quality medical information, as technology involves and internet access becomes more widespread, the positive impact of medical education platforms like *MedNews Week* will continue to grow. The platform's ability to showcase global leaders to a mainstream audience for free offers a practical approach to combat educational inequity. *MedNews Week* has the potential to positively impact global hematology-oncology education.

#4188
Multifaceted approach to engaging basic cancer scientists in community-based research
Namoonga M. Mantina, Juan Contreras, Monica Yellowhair, Cynthia Miranti, Jennifer Hatcher. *University of Arizona Cancer Center, Tucson, AZ*

Background**:** The University of Arizona Cancer Center (UACC) is the only NCI-designated Comprehensive Cancer Center in Arizona, serving a 5-county catchment area that is approximately 40% Hispanic/Latinx. To ensure that UACC is conducting culturally relevant and meaningful research that is aligned with community priorities, we established the Research Outreach for Southern Arizona (ROSA) program. The ROSA program aims to facilitate bidirectional learning opportunities between scientists and the community, focusing on cancer biology and basic science. Multiple approaches were taken to engage cancer biology researchers with the communities in the catchment area with an ultimate aim of developing Basic science Community based participatory research projects.
Method: Through a partnership between the UACC's Office of Community Outreach and Engagement and the Cancer Biology Program, the ROSA program employed multiple strategies to educate and engage basic scientists on best practices to effectively engage community members, which included: collaborative working groups, meet the scientist learning opportunities, student and community ambassadors, and creation of the ROSA Café Series (community conversations with UACC basic scientist). These strategies facilitated avenues for scientists to educate, learn from, and engage with the community.
Results: The working group consisted of UACC basic scientists and community members that helped develop a ROSA survey that will be used to gain community input and learn more about community research priorities, knowledge base and culturally appropriate research. Additionally, ROSA community and student ambassadors were enrolled into a curriculum where they learned fundamentals of cancer biology via conversations with the basic scientists and provided opportunities for scientists to practice using lay language to express scientific ideas. Bidirectional learning opportunities were also presented within the structure of the ROSA Café's with the ultimate goal of having community members learn directly from the researchers about current and potential projects. These strategies have ultimately led to interactions between the basic science and lay community that serve as a basis for future basic science projects that are community inspired and have potential for high community input and impact.
Discussion: Helping basic scientists integrate their science more fully into communities has the potential for advancing science and promoting health

equity in minoritized communities. This partnership is predicated on preparing basic scientists to interact comfortably and effectively with community members, necessitating common language and fuller understanding of community ways of knowing. The strategies employed and explicated here provide a model for cancer centers to develop culturally and community relevant basic science programs.

#4189

Community cancer scientist program: A model for community member advocacy for cancer research

Brooke M. Hensel[1], Fern J. Webb[2], Eduardo Ibarra[3], Carolina Aristizabal[4], Rosa Barahona[5], Diana J. Wilkie[6], Sandra Suther[7], Lourdes Baezconde-Garbanati[3], Mariana C. Stern[3]. *[1]University of Florida, Orlando, FL,[2]University of Florida, Jacksonville, FL,[3]University of Southern California Norris Comprehensive Cancer Center, Los Angeles, CA,[4]University of Sothern California Norris Comprehensive Cancer Center, Los Angeles, CA,[5]University of California Norris Comprehensive Cancer Center, Los Angeles, CA,[6]University of Florida, Gainesville, FL,[7]Florida Agricultural and Mechanical University, Tallahassee, FL*

Community Cancer Scientist (CCS) programs are designed to educate community members on the importance and ethical conduct of clinical research that serves to connect researchers and the general population. This type of program allows research advocates to interact with their community, helping minoritized individuals to form trust with cancer researchers and in clinical trials.The purpose of our study was to develop and evaluate a novel bi-coastal and bilingual program to inform, educate and empower community members to become cancer research advocates in Florida (FL) and California (CA). Our program was tailored for African American (AA) and Hispanic/Latinx (H/L) adults. Primary objectives are to increase person power for cancer research advocacy and increase multi-directional communication between cancer advocates with cancer survivors, community members, academic scientists and policy makers. The CCS program is a 13-week program implemented 100% virtual by the FL-CA Cancer Research, Education and Engagement (CaRE^2) Health Equity Center, a bi-coastal partnership between the Florida A&M University,

University of Florida, and University of Southern California where participants learned about cancers that disproportionately impact AA and H/L adults. Participants completed surveys at program start, midway, and end to assess knowledge gained and satisfaction, and a mentored advocacy project for community implementation. Five months after program end, we surveyed participants on impact and to provide support for their research advocacy.To date, a total of 26 adults have graduated from our program. We present data from the 2022 CCS cohort (N = 20) that included participants from FL and CA, which are among the top five states in the U.S with the largest AA and H/L populations. Regarding race and ethnicity, 13 participants were AA, 6 H/L, and 1 White, with 80% female participants. This cohort had 90% program completion (N = 18) and 5 advocacy projects: 2 on breast cancer, 1 on lung cancer, 1 on pancreas cancer, and 1 on prostate cancer. More than 50% of participants showed increased knowledge regarding cancer incidence, mortality and standard screening practices while program satisfaction remained high at end of program. Participants also provided feedback and recommendations such as offering a hybrid model for participants to interact with cancer researchers, and desired visiting CaRE^2 scientific laboratories for hands-on engagement. In conclusion, we present findings from a novel virtual CCS bi-coastal and bilingual training program tailored for AA and H/L adults that can foster multi-directional communication between cancer research advocates with multiple stakeholders. We also discuss how these research advocacy cancer programs can be tailored to focus on specific initiatives important to eliminate cancer health disparities such as or examining cancer health disparities from a lifespan perspective.

#4190

Current educational needs in the management of patients with advanced NSCLC: Results of a US case-based survey

Emily Belcher, Gregory D. Salinas, Asa Renfroe. *CE Outcomes, LLC, Birmingham, AL*

According to the American Cancer Society, over 80% of lung cancers present in the form of non-small cell lung cancer (NSCLC). This study evaluated the current attitudes, practice patterns, and educational gaps of United States oncology clinicians to better understand clinician educational

needs in the treatment of advanced NSCLC. A case-based survey was developed in collaboration with an expert in NSCLC. The survey was then evaluated by practicing clinicians within the target audience with experience managing patients with advanced NSCLC. The survey was programmed on a Web-based platform and fielded in March 2022. Study inclusion criteria consisted of clinicians who see at least 1 patient with NSCLC per month and at least 1% of NSCLC patients having advanced disease.

Responses were gathered from oncologists (n = 135), oncology nurse practitioners/physician associates (NPs/PAs) (n = 43), and oncology nurses (n = 52) for analysis. The most important factors regarding treatment choice for a patient with advanced NSCLC were overall and progression-free survival associated with the treatment regimen, response rate, and treatment safety profile. 90% of clinicians reported referring to clinical practice guidelines when managing patients with NSCLC, most commonly NCCN. When managing patients with advanced NSCLC, clinicians reported being very comfortable monitoring for and managing the adverse effects of therapy as well as discussing the risks involved. Oncologists, but particularly NPs/PAs, were less comfortable determining optimal second and third-line treatment options. When presented with a second-line treatment patient case scenario, clinicians were split in their treatment approach—with 25% of oncologists, 30% of NPs/PAs, and 46% of nurses referring the patient for a clinical trial.

Oncologists' and NPs/PAs' top goal in managing and treating advanced NSCLC was to extend survival, whereas nurses prioritized maintaining quality of life. In terms of barriers to treatment, clinicians overall highlighted obtaining biomarker testing for diagnosis, adverse effects of available treatments, and managing adverse effects as most significant. Nurses considered lack of patient support systems, limitations to accessing care, and insurance status as the most significant barriers.Oncologists were most interested in future education covering appropriate sequencing of treatment and new/emerging therapies. NPs/PAs were most likely to choose education on new/emerging treatments and side effects. Nurses demonstrated the most interest in side effects and oncology genetics. Clinicians are requesting education on topics aligned with practice variation identified in this study. Once past initial management, there is little consensus on the most appropriate treatment to use. Expert opinion and

guidance on progression of therapy is important for future education initiatives.

#4191

Assessing performance of biomarker extraction from electronic health records: Data augmentation methods for a hierarchical self-attention network (HiSAN)

Shalini Priya, Alina Peluso, Mayanka Chandra Shekhar, Ioana Danciu, Jordan Miller, Heidi A. Hanson. *Oak Ridge National Laboratory, Oak Ridge, Tennessee, TN*

Background: Extraction of HER2 status from electronic health records (EHR) may expedite clinical trials matching and be used for survivorship research. Deep learning (DL) algorithms have potential to extract this data; however, inherent class imbalance leads to reduced model performance. We compare state of the art strategies to handle class imbalance in models trained to extract HER2 status. This comparative analysis may be used as a guideline for HER2 extraction.
Methods: 680,117 pathology reports collected from 2017-2021 by the National Cancer Institutes' Surveillance, Epidemiology, and End-Results (SEER) program were used for this study. Pathology reports are manually labelled by cancer registrars as HER2 -, HER2+, or Unknown (class ratio 65%, 11%, 24% respectively). We compare six data augmentation (DA) methods: balanced frequency weighting, ROS while up-sampling HER2+ by 595%, RUS while down-sampling HER2- by 83% , SMOTE, ADASYN, and SMOTE-Tomek. As a comparison we consider the HiSAN model i.e., a DL architecture currently used by SEER for automatic classification of reports.
Result: Applying DA strategies did not improve the performance of the HiSAN model (Table 1). Frequency based class-weighting (Acc=0.78), ROS (Acc=0.81), and RUS (Acc=0.80) perform worse than the baseline model, suggesting simple data augmentation methods do not boost performance for this task. Advanced oversampling with SMOTE (Acc=0.88) and ADASYN (Acc=0.88) perform better than simple approaches, but do not improve the predictive accuracy of the baseline HiSAN. Table 1

Method	Accuracy	Sensitivity	Specificity	Precision

	(Acc)			
HiSAN (Baseline)	0.8898	0.7583	0.8944	0.8507
Frequency class weighting	0.7826	0.8033	0.8932	0.7040
Random Over Sampling (ROS)	0.8057	0.7672	0.8883	0.7130
Random Under Sampling (RUS)	0.8042	0.7883	0.8930	0.6902
Synthetic Minority Oversampling Technique (SMOTE)	0.8796	0.7341	0.8827	0.8340
Adaptive Synthetic Sampling (ADASYN)	0.8764	0.7467	0.8863	0.8142
SMOTE-Tomek	0.8823	0.7620	0.8956	0.8200

Conclusion: Common DA methods do not improve the performance of the HiSAN biomaker method. While the overall accuracy of the baseline HiSAN model is quite high, other methods for improved accuracy should be explored.

#4192

***CervicalMethDx*: A precision DNA methylation test to identify advanced disease risk in cervical cancer screening algorithms**

Laura Palmieri[1], Fernando T. Zamuner[1], Dieila Giomo De Lima[1], Keerthana Gosala[1], Eli Winkler[1], Yash Prashar[1], Ana Purcell-Wiltz[2], Amanda García-Negrón[2], Ashley Ramos-Lopez[3], David Sidransky[1], Mariana Brait[1], Rafael Guerrero-Preston[4]. *[1]Oncology, Johns Hopkins University School of Medicine, Baltimore, MD,[2]LifeGene-Biomarks, Inc, San Juan, Puerto Rico,[3]LifeGene-Biomarks, Inc, San Juan, PR,[4]LifeGene-Biomarks, Inc, Baltimore, MD*

Cervical cancer is one of the most common cancers in women. Despite progress in prevention through Human Papilloma Virus [HPV] vaccination and success in early detection of cervical cancer through cytologic screening and HPV detection, there remains an unequal burden in low-resource settings in developed and developing countries. Applying novel

methylation-based detection methods, we validated a panel of three human methylated genes (*ZNF516*, *FKBP6* and *INTS1*) on discarded cervical liquid cytology samples from clinical laboratories in the United States during the development of the *CervicalMethDx* test. We hypothesized that the *CervicalMethDx* test can identify HPV positive women most likely to be diagnosed with Cervical Intraepithelial Neoplasia (CIN) grades 2 and 3 by anatomic pathologists, before they are referred to colposcopy-driven biopsies. We assessed DNA methylation by Quantitative Real Time Methylation Specific PCR (QMSP) analysis of sodium bisulfite-modified genomic DNA. Primers and probes were previously designed to specifically amplify the promoters of the 3 genes of interest and the promoter of a reference gene, *β-actin*, to assess DNA input. We performed blinded retrospective studies on well-characterized, discarded, HPV-positive clinical samples in PreservCyt sample transport media (Thin Prep, Hologic), comparing DNA methylation levels in samples from CIN2 and CIN3 cases (346), and 120 controls without evidence of Intraepithelial Lesions or Malignancy (NILM) as an endpoint. Our results showed that the *CervicalMethDx* test can correctly classify 96% of CIN2 (n=197) samples with 93% Sensitivity, 100% Specificity, and an AUC of 0.96 as well as 95% of CIN3 (n=149) samples with 91% Sensitivity, 100% Specificity, and an AUC of 0.96. Moreover, the assay correctly classified 94% of CIN2-CIN3 samples combined (n=346) with 92% Sensitivity, 100% Specificity, an AUC of 0.96, and a 100% positive predictive value (PPV), when compared to samples with NILM (n=120). The *CervicalMethDx* test high PPV supports the addition of this low-cost molecular test to cervical cancer screening algorithms worldwide. Our results suggest that the *CervicalMethDx* test is a new and valuable tool to stratify HPV positive women prior to colposcopy-driven biopsies in developed countries and ablative treatment in developing countries, most of which are unnecessary. These results warrant further evaluation of the *CervicalMethDX* test in prospective, population-based studies, assessing the use of precision DNA methylation algorithms to triage women before colposcopy-driven biopsies or ablative treatments worldwide.

#4193

N-NOSE technology based on *C. elegans* olfaction. Multi-cancer early detection with high sensitivity using urine. Pancreatic-cancer-specific early detection with high sensitivity using urine

Eric Di Luccio[1], Takaaki Hirotsu[2]. *[1]Hirotsu Bio Science INC., Fujisawa city, Japan,[2]Hirotsu Bio Science INC., Tokyo, Japan*

N-NOSE (Nematode Nose) is a cancer screening test based on the chemotactic characteristics of the nematode *C. elegans*. *C. elegans* shows avoidance of the urine of healthy individuals while displaying a chemotactic attraction toward the urine of patients with 15 types of cancer (stomach, colon-rectum, lung, breast, pancreas, liver, prostate, uterus, esophagus, gallbladder, bile duct, kidney, urinary bladder, ovary, oropharynx) rendering N-NOSE a primary multi-cancer screening test. N-NOSE has a high sensitivity of 87.5% and 90.2% specificity, on average, from early stage 0-I. N-NOSE is non-invasive because it relies on a urine sample and is affordable (JPY 13,800, ~USD 100).N-NOSE by Hirotsu Bio Science has been available in Japan since late 2020 and is a commercial hit with over 250,000 screenings performed, rapidly increasing. In this presentation, we outline the N-NOSE technology and business in Japan. We review N-NOSE clinical research and critical findings compared to competitors that highlight its excellent performance as a non-invasive primary cancer screening for early detection. N-NOSE is a multi-cancer early detection test. Next, we introduce an evolution of N-NOSE for identifying the cancer type. Pancreatic cancer is the 12th most common cancer worldwide but remains one the deadliest cancer with a 5-year relative survival rate at only 11%, all stages combined. An affordable, non-invasive, and highly sensitive early-stage pancreatic cancer screening test is sorely needed. As an evolution of N-NOSE we genetically engineered *C. elegans* by knocking out in AWC olfactory neurons a specific olfactory receptor (GPCR), triggering a chemotactic response particular to the only pancreatic cancer urine specimen at an early stage. In this study, we outline, for the first time, the critical discovery of *cr-4* GPCR in AWC, which is crucial for a specific chemotaxis response to the urine of patients with pancreatic cancer. Next, we briefly conclude by outlining the link between N-NOSE primary cancer screening followed by N-NOSE cancer type identification, effectively completing the whole cancer screening and identification process in a non-invasive way.

#4194

The FuSion Project of Pan-Cancer Early Screening in Chinese-- An integrative study by Fudan University and Singlera

Chen Suo[1], Renjia Zhao[1], Yanfeng Jiang[1], Yunzhi Zhang[2], Qiye He[2], Zhixi Su[2], Rui Liu[2], Li Jin[1], Xingdong Chen[1]. *[1]Fudan University, Shanghai, China,[2]Singlera Genomics (Shanghai) Ltd, Shanghai, China*

Background: Cancer is the leading cause of premature deaths. Screening in the population can effectively improve the prognosis by diagnosing cancer early. Previous studies have found that cancer biomarkers, for example, ctDNA methylation and protein biomarkers are clearly associated with the occurrence and development of cancer. To evaluate the performance of reported biomarkers for cancer early screening in real world, we launched an integrative study by Fudan University and SInglera for pan-cancer early detectiON (FuSion) project since 2021. Method: The FuSion Project (NCT05159544) is a prospective and multicenter cohort study of pan-cancer screening in Chinese population. We will construct a stepwise model of risk stratification for screening of multiple cancer types, including lung, esophagus, stomach, liver, pancreatic and colorectal cancers. A total of 50,137 individuals recruited in the Taizhou Longitudinal Study (TLS) between 2012 and 2021 are investigated. Eligible participants are aged 20-75 years and without

history of cancer. They have completed a questionnaire and provided blood samples for baseline tests, which measure a total of about 50 indicators in the routine blood work, blood biochemistry, and serum cancer biomarkers, such as carbohydrate antigen 19-9 and carcinoembryonic antigen. Informed consent is obtained from all participants. We build risk stratification models based on risk factors collected in the questionnaire and from baseline test results for each cancer type, respectively. Then, 10,000 high-risk- and 5,000 low-risk individuals of cancers are identified by the cancer-specific risk stratification model. They will be screened by the PanSeerX assay using cancer-related DNA methylation markers, and medically followed-up for at least two years. Sensitivity, specificity, positive- and negative-predictive values of the screening models will be determined based on the true cancer incidences. Finally, we will validate the cancer screening strategies using 10,000 average-risk participants recruited from multiple centers by regular checkups and from other large-scale cohort studies.

#4195

Spatially resolved single cell transcriptomic profiling in formalin-fixed paraffin-embedded (FFPE) tissues

Jiang He, Justin He, Timothy Wiggin, Rob Foreman, Renchao Chen, Nicolas Fernandez, George Emanuel. *Vizgen, Cambridge, MA*

Formalin-fixed paraffin-embedded (FFPE) tissues are the most widely used clinical sample types in histology and molecular diagnosis, but these samples are often challenging for single-cell transcriptomic analysis due to RNA degradation and protein crosslinking. A spatial transcriptomics technique with high detection efficiency and single molecule resolution is required in order to accurately profile the gene expression in FFPE samples in situ. Vizgen's MERSCOPE platform, built on multiplexed error robust in situ hybridization MERFISH technology, directly profiles intact tissue's transcriptome with subcellular spatial resolution. Here, we demonstrate the FFPE MERSCOPE workflow in tissues from 10 mouse and human samples, including archival clinical samples. In each sample, hundreds of thousands of cells were captured with >100 million transcript counts, generating detailed spatial transcriptomic data for the profiled genes in each sample. A comparison of FFPE and matched fresh frozen samples indicated that the FFPE workflow performs similarly in detection efficiency as compared to the fresh frozen protocol. We further demonstrated the MERSCOPE FFPE workflow is compatible with protein imaging by performing simultaneous protein-based cell boundary staining with MERFISH to accurately profile gene expression and map cell types in archival clinical human samples. Finally, we constructed a spatially resolved single cell atlas across eight major tumor types, mapped and cataloged different cell types within the tumor microenvironment and systematically characterized the gene expression among cells. This study demonstrates the potential for spatially resolved transcriptomic profiling of FFPE samples at single cell level to contribute to a wide range of biomedical research areas, including many applications to study human diseases.

Descriptive Epidemiology and Environmental Risk Factors

#4200

Association between reproductive factors with lung cancer incidence and mortality: A pooled analysis of over 308,000 females in the Asia Cohort Consortium

Xin Yin[1], Rie Kishida[1], Sarah Krull Abe[2], Md. Rashedul Islam[3], Md. Shafiur Rahman[4], Eiko Saito[5], Qing Lan[6], Batel Bletcher[6], Melissa Merritt[7], Ji-Yeob Choi[8], Aesun Shin[9], Ryoko Katagiri[10], Xiao-Ou Shu[11], Norie Sawada[12], Akiko Tamakoshi[13], Woon-Puay Koh[14], Ichiro

Tsuji[15], Chisato Nagata[16], Sue K. Park[17], Sun-Seog Kweon[18], Yu-Tang Gao[19], Shoichiro Tsugane[12], Takashi Kimura[13], Jian-Min Yuan[20], Yukai Lu[15], Seiki Kanemura[15], Yumi Sugawara[15], Keiko Wada[16], Min-Ho Shin[18], Habibul Ahsan[21], Paolo Boffetta[22], Kee Seng Chia[23], Keitaro Matsuo[24], You-Lin Qiao[25], Nathaniel Rothman[6], Wei Zheng[11], Manami Inoue[2], Daehee Kang[26], Wei Jie Seow[27]. *[1]National University of Singapore (NUS), Singapore, Singapore,[2]Division of Prevention, National Cancer Center Institute for Cancer Control, Tokyo, Japan,[3]1. Division of Prevention, 1. National Cancer Center Institute for Cancer Control 2. Hitotsubashi Institute for Advanced Study, Hitotsubashi University, Tokyo, Japan,[4]1. Division of Prevention, 1. National Cancer Center Institute for Cancer Control, 2. Research Center for Child Mental Development, Hamamatsu University School of Medicine, Tokyo, Japan,[5]Institute for Global Health Policy Research, National Center for Global Health and Medicine, Tokyo, Japan,[6]Division of Cancer Epidemiology and Genetics, Occupational and Environmental Epidemiology Branch, National Cancer Institute, Bethesda, MD,[7]The Daffodil Centre, The University of Sydney, a joint venture with Cancer Council NSW, Sydney, Australia,[8]Department of Biomedical Sciences, Seoul National University Graduate School, Seoul, Korea, Republic of,[9]Department of Preventive Medicine, 1. Cancer Research Institute, Seoul National University, 2. Seoul National University College of Medicine, Seoul, Korea, Republic of,[10]1. Division of Cohort Research, 1. National Cancer Center Institute for Cancer Control, 2. National Institute of Health and Nutrition, National Institutes of Biomedical Innovation, Health and Nutrition, Tokyo, Japan,[11]Division of Epidemiology, Vanderbilt-Ingram Cancer Center, Vanderbilt Epidemiology Center, Vanderbilt University Medical Center, Nashville, TN,[12]Division of Cohort Research, National Cancer Center Institute for Cancer Control, Toyko, Japan,[13]Department of Public Health, Hokkaido University Faculty of Medicine, Sapporo, Japan,[14]1. Healthy Longevity Translational Research Programme, Yong Loo Lin School of Medicine, National University of Singapore. 2. Singapore Institute for Clinical Sciences, Agency for Science Technology and Research (A*STAR), Singapore, Singapore,[15]Tohoku University Graduate School of Medicine, Sendai, Japan,[16]Department of Epidemiology and Preventive Medicine, Gifu University Graduate School of Medicine, Gifu, Japan,[17]Department of Preventive Medicine, Seoul National University College of Medicine, Seoul, Korea, Republic of,[18]Department of Preventive Medicine, Chonnam National University Medical School, Gwangju, Korea, Republic of,[19]Department of Epidemiology, Shanghai Cancer Institute, Shanghai, China,[20]1. Division of Cancer Control and Population Sciences, 2. Department of Epidemiology, 1. UPMC Hillman Cancer Center, University of Pittsburgh, 2. Graduate School of Public Health, University of Pittsburgh, Pittsburgh, PA,[21]Department of Public Health Sciences, University of Chicago, Chicago, IL,[22]2. Department of Medical and Surgical Sciences, 1. Stony Brook Cancer Center, Stony Brook University, 2. University of Bologna, Stony Brook, NY,[23]Saw Swee Hock School of Public Health, National University of Singapore, Singapore, Singapore,[24]1. Division Cancer Epidemiology and Prevention, 2. Department of Cancer Epidemiology, 1. Aichi Cancer Center Research Institute, 2. Nagoya University Graduate School of Medicine, Nagoya, Japan,[25]School of Population Medicine and Public Health, Chinese Academy of Medical Sciences and Peking Union Medical College, Beijing, China, Beijing, China,[26]Seoul National University College of Medicine, Seoul, Republic of Korea, Seoul, Korea, Republic of,[27]2. Department of Medicine, 1. Saw Swee Hock School of Public Health, National University of Singapore, 2. Yong Loo Lin School of Medicine, National University of Singapore and National University Health System, Singapore, Singapore*

Background: Previous studies have investigated the association between reproductive factors and lung cancer risk; however, findings have been inconsistent. This study aims to assess the association between reproductive factors with lung cancer incidence and mortality among Asian women.
Methods: A total of 308,949 female participants with a mean age of 55.13 from 11 prospective cohorts and four Asian countries (Japan, Korea, China, and Singapore) in the Asia Cohort Consortium (ACC) were included. Cox proportional hazards regression models were used to estimate the hazard ratios (HR) and 95% confidence intervals (CIs).
Results: A total of 3,119 primary lung cancer cases and 2,247 lung cancer deaths were identified with a mean follow-up of 16.4 years. Parous women had a lower risk of lung cancer incidence and mortality as compared with nulliparous women, with HRs of 0.82 (95% CI = 0.70 - 0.96) and 0.78 (95% CI = 0.65 - 0.94). Corresponding HRs were lowest among women with 1-2 children, with HRs of 0.78 (95% CI = 0.66 - 0.93) and 0.72 (95% CI = 0.59 - 0.87) for lung cancer incidence and mortality. The protective association of parity and lung cancer incidence was greater among ever-smokers (HR=0.66, 95% CI = 0.49 - 0.87) than in never-smokers (HR=0.90, 95% CI = 0.74 - 1.09) (*P*-interaction = 0.029). Compared with age at first delivery ≤20 years, older age at first delivery (≥26 years) was associated with a lower risk of lung cancer incidence and mortality. Compared with age at menopause <45 years, older age at menopause (≥55 years) was associated with a decreased risk of lung cancer mortality (HR=0.75, 95% CI = 0.58 - 0.96). Women who ever used hormone replacements had a higher likelihood of developing non-small cell lung cancer (HR = 1.30, 95% CI = 1.01 - 1.67), compared to those who never used hormone replacements.
Conclusions: Distinct from Western women, Asian parous women, especially those who have 1-2 children had a lower risk of lung cancer incidence and mortality compared with nulliparous women. Future studies are needed to assess the underlying mechanisms, the relationships within these female reproductive factors, and the potential changes in smoking habits over time.

#4201

Associations of pre-diagnostic serum liver enzymes levels with lung cancer risk: results from the Southern Community Cohort Study

Shuai Xu[1], Hui Cai[2], Jie Wu[2], Hyung-Suk Yoon[2], Regina Courtney[2], Xiao-Ou Shu[1], William J. Blot[2], Wei Zheng[1], Qiuyin Cai[1]. *[1]Vanderbilt University, Nashville, TN,[2]Vanderbilt University Medical Center, Nashville, TN*

Introduction: Lung cancer is the leading cause of cancer death in the United States (U.S.). Lung cancer disproportionately affects African Americans (AAs) more than other racial/ethnic groups. Previous studies have linked liver diseases to lung cancer risk; however, few studies have evaluated the associations of circulating liver enzyme levels with lung cancer risk. In this study, we evaluated the associations of the serum alanine transaminase (ALT) and alkaline phosphatase (ALP) levels with the risk of subsequently developing lung cancer.
Methods: We conducted a nested case-control study within the Southern Community Cohort Study, a well-conducted prospective cohort study in the southern U.S. mainly consisting of low-income AAs and European Americans (EAs). We included 552 incident lung cancer cases and 1,039 controls individually matched on age, sex, recruitment sites, and date of blood draw. Baseline serum levels of ALT and ALP were measured using the Beckman Coulter clinical chemistry analyzer. Conditional logistic regression and generalized estimating models were used to estimate odds ratios (ORs) and 95% confidence intervals (CIs) after adjusting for age, education, household income, body mass index (BMI), smoking status, pack-years, alcohol consumption, physical activity levels, history of chronic obstructive pulmonary disease, hypertension, and diabetes.

Results: Higher serum levels of ALT were associated with a lower overall risk of lung cancer. Compared with the lowest tertile, participants in the second and third tertiles had OR (95% CI) of 0.74 (0.48-1.14) and 0.47 (0.28-0.78) ($P_{trend} < 0.01$). The inverse association was observed in both AAs and EAs. However, the inverse associations between serum ALT levels and lung cancer risk were more evident among men [$OR_{T3\ vs\ T1} = 0.36$ (0.18-0.70)], current smokers [$OR_{T3\ vs\ T1}$ =0.65 (0.47-0.90)], participants with lower BMI [$OR_{T3\ vs\ T1}$=0.55 (0.38-0.79)], or lower physical activity [$OR_{T3\ vs\ T1} = 0.55$ (0.37-0.83)]. Stratified analyses by time interval between blood collection and lung cancer diagnosis showed that the inverse associations were observed in both those diagnosed within [$OR_{T3\ vs\ T1}$ =0.48 (0.23-1.00)] and after [$OR_{T3\ vs\ T1} = 0.36$ (0.19-0.69)] a median follow up time of 3 years. The serum ALT level was not associated with overall lung cancer; however, higher serum ALP levels were significantly associated with increased lung cancer risk among AA men [$OR_{T3\ vs\ T1} = 1.98$ (1.18-3.34)].
Conclusion: Our results indicate that in a predominantly low-income AA and EA population, serum ALT levels may be related to a lower risk of lung cancer. Further studies are warranted to confirm our findings and elucidate the potential underlying mechanisms of the associations.

#4202
Kidney function and risk of renal cell carcinoma
Karine Alcala[1], Nicolas Alcala[1], Richard Martin[2], Paul Brennan[1], David Muller[3], Hilary A. Robbins[1], Mattias Johansson[1]. *[1]Genomic Epidemiology Branch, International Agency for Research on Cancer, Lyon, France,[2]Bristol Medical School, University of Bristol, Bristol, United Kingdom,[3]Imperial College London, London, United Kingdom*

Background: The relationship between kidney function and risk of renal cell carcinoma (RCC) is not well understood. In this study, we evaluated the association between estimated glomerular filtration rate (eGFR) and risk of incident RCC, and assessed whether this association depends on time between eGFR measurement and RCC diagnosis. We also sought to evaluate if eGFR may be useful to predict RCC risk.
Methods: We conducted this study in the UK Biobank cohort based on 440,983 participants of whom 984 were diagnosed with RCC during 4,552,747 person-years of follow-up. The temporal relation between kidney function and RCC was evaluated with flexible parametric survival models for eGFR calculated from creatinine, cystatin C and both, adjusted for C-reactive protein (CRP) and common RCC risk factors. We also assessed the benefit of combining CRP and eGFR with a published RCC risk prediction model by estimating calibration and discrimination using a resampling algorithm as internal validation.
Results: We found that a lower eGFR - an indication of poor kidney function - was associated with higher RCC risk when measured up to five years prior to diagnosis. We estimated the RCC hazard ratio per standard deviation decrease in eGFR when measured one year before diagnosis at 1.22 (95% confidence interval [95% CI]: 1.11-1.34), and at 1.14 (95% CI: 1.05-1.19) when measured five years before diagnosis. The corresponding RCC HR for eGFR measured ten years before diagnosis was 1.03 (95% CI: 0.95-1.12). Adding eGFR to the RCC risk model provided a small improvement in risk discrimination 2 years before diagnosis with a C-index of 0.76 (95% CI: 0.71-0.81) compared to the published model (0.73, 95% CI: 0.68-0.79).
Conclusion: This study demonstrated that markers of kidney function are robustly associated with RCC risk when measured within the last five years leading up to diagnosis. However, kidney function markers do not seem to provide important improvements in RCC risk discrimination beyond established risk factors.

#4203

A prospective study of birth weight and prostate cancer risk: extended analysis in the Health Professionals Follow-up Study

Qinran Liu[1], Yiwen Zhang[2], Jane B. Vaselkiv[2], Lorelei A. Mucci[2], Edward L. Giovannucci[2], Elizabeth A. Platz[3], Siobhan Sutcliffe[4]. *[1]Department of Public Health Sciences, Miller School of Medicine, University of Miami, Miami, FL,[2]Department of Epidemiology, Harvard T.H. Chan School of Public Health, Boston, MA, Boston, MA,[3]Department of Epidemiology, Johns Hopkins Bloomberg School of Public Health, Baltimore, MD,[4]Department of Surgery, Washington University School of Medicine Division of Public Health Sciences, St. Louis, MO*

Introduction: Birth weight, a potential marker of the *in utero* hormonal and growth factor milieu, has been associated with an increased risk of prostate cancer (PCa) in some, but not all, previous studies. It was also associated with a non-significantly greater risk of advanced stage PCa (relative risk [RR] = 1.37, 95% confidence interval [CI]: 0.61-3.05 for ≥10 lbs compared to 7.0-8.4 lbs, *p*-trend = 0.087) in our previous analysis in the Health Professionals Follow-up Study (HPFS). However, these suggestive findings were based on a relatively small number of advanced stage cases and short follow-up. We have now updated our previous analysis of birthweight and PCa risk in the HPFS with an additional 14 years of follow-up.

Method: Birth weight was assessed by self-report on the 1994 follow-up questionnaire using pre-specified categories. PCa diagnoses were ascertained on each biennial follow-up questionnaire and confirmed by medical record review. Cox proportional hazards regression was used to evaluate the association between birth weight and PCa risk through 2016.

Result: Of the 17,949 eligible men who reported their birth weight in 1994, 3,167 were subsequently diagnosed with PCa. With the exception of a suggestive positive trend between increasing birth weight and high-grade PCa (RR_{adj} per pound: 1.06; 95% CI: 0.98-1.16; *p*-trend=0.15), no associations were observed between birth weight and risk of total, organ-confined, low-grade, advanced stage, lethal, or fatal PCa.

Conclusion: Overall, no association was observed between birth weight and PCa risk and mortality in this large prospective cohort study of US male health professionals.

Table 1. Associations between self-reported birth weight and prostate cancer in the Health Professionals Follow-up Study, 1994-2016

		Birth weight (lbs)					
		<5.5(<2,495 g)	5.5-6.9*(2,495-3,174 g)*	7.0-8.4*(3,175-3,855 g)*	8.5-9.9*(3,856-4,535 g)*	≥10.0*(≥4,536 g)*	Per 1 lb *(454g)* increase
Total prostate cancer	Cases/person-years	125/17,019	518/80,053	1,931/297,495	396/60,445	197/22,993	
	HR[a] (95% CI)	0.98 (0.81-1.18)	0.86 (0.78-0.95)	1.00	0.85 (0.76-0.95)	0.98 (0.84-1.13)	1.01 (0.96-1.05)
High-grade prostate cancer (Score	Cases/person-years	23/17,117	119/80,434	453/299,015	105/60,741	52/23,148	

4+3 and higher)							
	HR[a] (95% CI)	0.76 (0.50-1.16)	0.83 (0.68-1.03)	1.00	0.93 (0.75-1.16)	1.03 (0.76-1.39)	1.06 (0.98-1.16)
Advanced stage prostate cancer (T3b+) at diagnosis	Cases/person-years	4/17,135	29/80,516	109/299,370	25/60,811	12/23,195	
	HR[a] (95% CI)	0.53 (0.19-1.46)	0.91 (0.60-1.40)	1.00	0.98 (0.62-1.54)	1.02 (0.54-1.92)	1.08 (0.91-1.29)
Lethal prostate cancer	Cases/person-years	11/17,127	70/80,491	225/299,247	51/60,791	27/23,178	
	HR[a] (95% CI)	0.81 (0.43-1.50)	1.15 (0.86-1.52)	1.00	1.07 (0.78-1.47)	1.01 (0.66-1.54)	1.00 (0.89-1.13)
Fatal prostate cancer	Cases/person-years	10/17,551	59/82,316	197/307,363	43/62,246	23/23,996	
	HR[a] (95% CI)	0.88 (0.45-1.67)	1.17 (0.86-1.60)	1.00	1.11 (0.78-1.56)	1.03 (0.65-1.63)	1.00 (0.87-1.14)

RR=relative risk; CI = confidence interval. [a] Adjusted for age, calendar time, race, smoking status, family history of prostate cancer (yes or no), PSA testing in >50% of previous cycles (yes or no), physical activity, diabetes, diet (tomato sauce intake, coffee, and energy intake), alcohol intake, multivitamin use, vitamin E supplement use, and aspirin use.

#4204

Incidence of early-onset and average-onset colon cancer among Medicaid beneficiaries with and without HIV: a cohort study

Corinne Joshu[1], Keri Calkins[2], Jacqueline E. Rudolph[1], Xiaoqiang Xu[3], Eryka Wentz[1], Maneet Kaur[1], Filip Pirsl[1], Sally B. Coburn[1], Richard D. Moore[3], Bryan Lau[1]. *[1]Johns Hopkins Bloomberg School of Public Health, Baltimore, MD,[2]Mathematica, Ann Arbor, MI,[3]Johns Hopkins School of Medicine, Baltimore, MD*

Background: Colorectal cancer has increased among people living with HIV (PLWH). Studies have reported either no difference or lower risk of colorectal cancer incidence among PLWH as compared to the general population. We evaluated the incidence of colon cancer, both average-onset (diagnosed at 50 or older) and early-onset (diagnosed at less than 50), among a diverse population of people with and without HIV who have comparable sociodemographic factors and access to care.

Methods: We obtained Medicaid Analytic eXtract (MAX) data from 2001-2015 for 14 states. We included 42,244,679 unique individuals with at least 7 months of continuous eligibility. HIV and colon cancer diagnoses were identified from inpatient and other non-drug claims. We used Cox proportional hazards regression models to assess the incidence of colon cancer, controlling for age, sex, race/ethnicity, calendar year of enrollment, state of enrollment, and number of comorbidities. Analyses were also adjusted for or stratified by age, sex, and race/ethnicity.
Findings: We identified 191 colon cancer cases among 523,969 person-years among PLWH and 15,098 colon cancer cases among 63,579,078 person-years among beneficiaries without HIV. Colon cancer incidence increased with age among beneficiaries with and without HIV. Overall, HIV was modestly, inversely associated with colon cancer incidence (HR:0.84, 95%CI: 0.73, 0.98). PLWH 18-39 years old had increased hazard of colon cancer as compared to those without HIV (HR:1.67, 95%CI: 1.06, 2.65); this association was attenuated after adjustment for co-morbidities. HRs were null when early-onset colon cancer was assessed among all beneficiaries less than 50 years. PLWH had lower hazard of average-onset colon cancer compared to those without HIV (HR:0.81, 95%CI: 0.68, 0.96); this association was statistically significant among male, but not female, beneficiaries.
Interpretation: Compared to beneficiaries without HIV, PLWH had a lower risk of average-onset colon cancer. PLWH had higher incidence of early-onset colon cancer, but this difference was attenuated after adjustment for comorbid conditions.

#4205

Profiling symptom burden of RAS and BRAF mutations in patients with colorectal cancer: Results from the ColoCare Study

Gazelle Rouhani[1], Amanda M. Bloomer[2], Maria F. Gomez[2], Gillian K. Trujillo[2], Devon N. Conant[2], Seth I. Felder[2], Cornelia M. Ulrich[3], Christopher I. Li[4], Jane C. Figueiredo[5], Adetunji T. Toriola[6], Biljana Gigic[7], Martin Schneider[7], David Shibata[8], Erin M. Siegel[2]. *[1]University of Miami Miller School of Medicine, Miami, FL,[2]Moffitt Cancer Center, Tampa, FL,[3]Huntsman Cancer Institute, Salt Lake City, UT,[4]Fred Hutchinson Cancer Center, Seattle, WA,[5]Samuel Oschin Comprehensive Cancer Institute, Cedars-Sinai Medical Center, Los Angeles, CA,[6]Washington University School of Medicine, St. Louis, MO,[7]Heidelberg University Hospital, Heidelberg, Germany,[8]University of Tennessee Health Science Center, Memphis, TN*

Background**:** Colorectal cancer (CRC) is a complex and heterogeneous disease characterized by distinct molecular features such as RAS and BRAF mutations. Assessing these molecular aberrations provides clinical guidance for selecting and predicting response with therapeutic modalities. Few reports have suggested that patient symptom burden at diagnosis differs across molecular subtypes of CRC. However, the association of RAS and BRAF mutations and symptom burden post-diagnosis in CRC patients has yet to be examined in a prospective cohort.
Methods: We assessed CRC patients, stage I-IV, enrolled in the Moffitt ColoCare Study site with clinical molecular testing results and who completed a six-month questionnaire. Tumor mutation (MT) status (RAS/BRAF/Wildtype (WT)) was abstracted from the medical record. The MD Anderson Symptom Inventory (MDASI) was used to assess the severity of 13 cancer-related symptoms on a 1-to-10 scale. Mean scores in mutation subgroups were compared with one-way ANOVA. Linear regression analysis evaluated the association between symptom burden and mutation status. Multivariable regression models were adjusted for age, sex, stage at diagnosis, treatment, and microsatellite instability (MSI).
Results: Among the 158 patients, the mean age at diagnosis was 60.9 ± 11.58 years. The prevalence of RAS and BRAF mutations was 30.4% (N=48) and 6.3% (N=10), respectively.

Statistically significant mean differences between the mutation subgroups were distress (p=0.005), difficulty remembering (p=0.015), lack of appetite (p=0.042), and sadness (p=0.007). Patients with a BRAF-MT reported significantly more distress (p=0.001), difficulty remembering (p=0.029), and sadness (p=0.002) at six months compared to RAS-MT or RAS/BRAF-WT. Patients with a RAS-MT reported an increased lack of appetite (p=0.038) compared to BRAF-MT or RAS/BRAF-WT. Patients with a BRAF-MT reported higher severity of symptoms interfering with the enjoyment of life (p<0.001), work (p=0.005), and mood (p<0.001) compared to RAS-MT or RAS/BRAF-WT. In an adjusted multivariable model, patients with BRAF-MT tumors reported significantly greater distress compared with RAS/BRAF-WT patients [β = 3.18 per unit increase in severity, 95% CI (1.30 - 5.07), p=0.001)]. Overall symptom burden was associated with greater interference with daily activities for BRAF-MT patients when compared to RAS/BRAF-WT patients [β = 2.95, 95% CI (1.42 - 4.48), p<0.001)].
Conclusions: Tumors with BRAF-MT are molecularly classified into the serrated pathway, which has distinct clinical characteristics and risk factor profile. In this study, patients with tumors harboring BRAF-MT reported a higher symptom burden six months post-diagnosis than those with RAS-MT or RAS/BRAF-WT tumors. While the prevalence of BRAF-MT was low in this population, these findings warrant further investigation in a larger cohort.

#4206
The impact of two decades of multidisciplinary efforts to reduce the risk of recurrence from colorectal cancer - a Danish population-based registry-study
Jesper Nors[1], Kaare A. Gotschalck[2], Rune Erichsen[3], Lene H. Iversen[4], Claus L. Andersen[1].
[1]Department of Molecular Medicine, Aarhus University Hospital, Aarhus, Denmark,[2]Department of Surgery, Horsens Regional Hospital, Horsens, Denmark,[3]Department of Clinical Epidemiology, Aarhus University Hospital, Aarhus, Denmark,[4]Department of Surgery, Aarhus University Hospital, Aarhus, Denmark

Purpose: Over the last two decades, several initiatives have aimed at reducing risk of recurrence in patients operated for non-metastatic colorectal cancer (CRC). The focus has been on improving treatment in a multidisciplinary setting and implementing a population-based screening program. However, the combined impact of these initiatives on the risk of recurrence is not well described. Therefore, the primary aim of this study was to determine and compare recurrence rates for three calendar periods 2004-2008, 2009-2013, and 2014-2019 (after implementation of screening) in CRC. Material and Methods: Patients undergoing surgery for UICC TNM stage I-III CRC in the period 2004 to 2019 were included. All patients were identified using the nationwide clinical quality database DCCG, and hereafter linked with data from the Danish Cancer Registry, the Danish National Registry of Patients, and the Danish Pathology Registry. Recurrence status was determined using a validated algorithm defining recurrence based on diagnosis codes of local recurrence or metastases, the receipt of chemotherapy, or a pathological tissue assessment code of recurrence. The algorithm has shown a positive predictive value of 94% and a negative predictive value of 99%. Cumulative risk of recurrence and relapse-free survival (RFS) was reported by grouping the patients in calendar periods.
Results: Of 33,470 stage I-III patients, 7,002 developed recurrence within 5 years after primary surgery (incidence rate = 60.4 per 1,000 person years, 95% CI: 59-61.8) with highest incidence among rectal cancer patients. The 5-year cumulative incidence of recurrence decreased for both colon cancers (2004-2009: 26% (95% CI: 25-27%); 2009-2013: 21% (95% CI: 20-22%); 2014-2019: 15% (95% CI: 14-16%)) and rectal cancers (2004-2009: 30% (95% CI: 29-32%); 2009-2013: 25% (95% CI: 24-27%); 2014-2019: 19% (95% CI: 18-20%)). The same pattern was found

within each of stages I, II and III when stratifying by the three calendar periods. Screening-detected (SD) patients had lower risk of recurrence when compared to non-screening detected patients. The 5-year cumulative incidence of recurrence remained lower for 2014-2019 compared to previous calendar periods when excluding SD patients. Adjusted RFS improved significantly from 2004-2008 (reference) to 2014-2019 for colon cancer patients across all UICC stages; I) HR=0.49 (95%CI: 0.42-0.57), II) HR=0.56 (0.51-0.62) and III) HR=0.67 (0.62-0.73). The same pattern was seen for rectal cancer patients with HR=0.50 (0.42-0.60), HR=0.60 (0.52-0.69) and HR=0.67 (0.60-0.75) for stage I, II and III, respectively.
Conclusion: The national multidisciplinary initiatives to improve the outcome of CRC within the past two decades have borne fruit, as reflected by significant reductions in CRC recurrence risk and prolonged RFS observed for Danish stage I-III CRC patients.

#4207

Systematic review and meta-analysis of cancer incidence after blood transfusion in the general population

Youjin Oh[1], Soowon Lee[2], Sebin Bok[1], Chan Mi Jung[1], Ilene Hong[1], Liam Il-Young Chung[1], Jeeyeon Lee[3], Young Kwang Chae[1]. *[1]Northwestern Univ. Feinberg School of Medicine, Chicago, IL,[2]Baylor University, Waco, TX,[3]Kyungpook National University Chilgok Hospital, Daegu, Korea, Republic of*

Background: The impact of blood transfusion on cancer survival and mortality has been widely studied. However, few studies have investigated its relationship with cancer incidence. This is the first systematic review and meta-analysis evaluating the correlation between blood transfusion and cancer incidence.
Methods: Five studies were identified through Pubmed, Embase, and Cochrane library. Four cohort studies and one case-control study (N = 3,048,906) were included. Over seventy percent were female (N =2,167,580), and about thirty-one percent (N = 956,522) were transfused. Meta-analysis was conducted between blood transfusion and cancer incidence. Subgroup analyses were performed by cancer types, follow-up period, and units of transfused blood. We pooled available risk estimates, which were adjusted for confounding factors, including age and sex, were pooled.
Results: Overall cancer risk increased statistically significantly in people who received transfusion compared to the population that did not (1.70, 95% CI, 1.30 to 2.10). The result was consistent regardless of time intervals from transfusion or units of transfused blood. Cancer incidences in all solid tumors, except breast, thyroid, and uterine cancer, were higher in blood transfusion recipients (Table 1). The elevated risk of stomach, bladder, and kidney cancer was sustained for up to fifteen years. Furthermore, lung cancer, liver cancer, and non-Hodgkin lymphoma risk remained high among the blood transfusions group even after fifteen years. The three types of cancer with the highest incidence following transfusion were leukemia, stomach cancer, and liver cancer.
Conclusions: Blood transfusion increases the risk of cancer in transfusion recipients. The impact of blood transfusion on cancer development varies depending on the cancer type and the time from transfusion. Further prospective studies are warranted to validate the findings and investigate the underlying mechanism.

The pooled risk of cancer according to cancer types, units of transfusion, and time from transfusion

	Risk* (95% CI)			
	Total	< 5 yrs	5-15 yrs	≧ 15 yrs
All cancer types	1.70 (1.30 - 2.10)	1.89 (1.13 - 2.65)	1.18 (0.97 - 1.40)	1.10 (1.06 - 1.14)

Leukemia	2.79 (2.00 - 3.57)	4.07 (2.72 - 5.42)	1.15 (1.04 - 1.27)	0.91 (0.66 - 1.16)
Non Hodgkin lymphoma	1.94 (1.49 - 2.40)	2.66 (1.82 - 3.50)	1.43 (0.89 - 1.98)	1.23 (1.00 - 1.46)
Stomach	2.37 (1.70 - 3.04)	2.37 (1.70 - 3.04)	1.13 (1.03 - 1.23)	1.17 (0.91 - 1.43)
Liver	2.25 (1.67 - 2.84)	2.80 (1.80 - 3.80)	1.67 (1.48 - 1.86)	2.54 (1.85 - 3.23)
Colon	2.34 (1.62 - 3.05)	3.49 (1.90 - 5.08)	1.02 (0.96 - 1.08)	1.05 (0.90 - 1.20)
Pancreas	1.85 (1.36 - 2.34)	2.37 (1.50 - 3.24)	1.19 (0.72 - 1.66)	1.28 (0.97 - 1.59)
Rectum	1.40 (1.06 - 1.75)	1.71 (1.04 - 2.39)	0.98 (0.91 - 1.05)	1.00 (0.81 - 1.19)
Lung	1.49 (1.21 - 1.77)	1.71 (1.18 - 2.23)	1.24 (1.17 - 1.30)	1.27 (1.09 - 1.45)
Kidney	2.27 (1.63 - 2.90)	3.30 (1.89 - 4.17)	1.15 (1.03 - 1.27)	1.39 (0.70 - 2.08)
Bladder	1.40 (1.12 - 1.68)	1.56 (1.06 - 2.06)	1.19 (1.11 - 1.27)	1.35 (0.15 - 2.54)
Breast	0.96 (0.84 - 1.09)	1.06 (0.91 - 1.22)	0.95 (0.90 - 1.00)	1.12 (1.03 - 1.21)
Uterus	1.02 (0.84 - 1.19)	1.13 (0.85 - 1.25)	0.81 (0.46 - 1.16)	1.00 (0.78 - 1.22)
Thyroid	1.16 (0.91 - 1.41)	1.32 (0.87 - 1.77)	0.92 (0.70 - 1.14)	1.12 (0.64 - 1.78)
	1-2 units		≧ 3 units	
All cancer types	1.53 (1.15 - 1.90)		1.93 (1.39 - 2.48)	
*Risk is pooled from odds ratio, hazard ratio, relative risk, and standardized incidence ratio.Abbreviations: CI=Confidence Interval				

#4208

Incidence of papillary thyroid cancer: comparison of the military with the general population by race, gender, and tumor stage/size

Julie A. Bytnar[1], Lindsey Enewold[2], Craig D. Shriver[1], Kangmin Zhu[1]. *[1]Murtha Cancer Center Research Program, Uniformed Services University Walter Reed Surgery, Henry M. J, Bethesda, MD,[2]Division of Cancer Control & Population Science, National Cancer Institute, Rockville, MD*

Background: A previous study found that the incidence of papillary thyroid cancer was higher in the US military than in the general population and the difference was larger among Black than White patients for both men and women. This study compared the military to the general population in thyroid cancer incidence by not only race and gender but also tumor stage and size to assess possible factors related to the identified differences.
Methods: The study subjects were men and women aged 18-59 histologically diagnosed with papillary thyroid cancer from 1990-2013 in the military and the general population. The data were from the Department of Defense's Automated Central Tumor Registry (ACTUR) and the National Cancer Institute's Surveillance, Epidemiology, and End Results (SEER) program. Age adjusted rates and incidence rate ratios (IRR) and 95% confidence intervals (95% CI) comparing ACTUR to SEER were calculated. Comparisons were made by race (Black, White), gender, cancer stage (local, regional, distant), and tumor size (0-2 cm, >2 cm).
Results: Higher age-adjusted incidence rates in ACTUR than SEER were more obvious for Black (IRR=2.07, 95% CI=1.56-2.70) than White (IRR=1.17, 95% CI=1.07-1.26) men and for Black (IRR=2.30, 95% CI=1.91-2.71) than White (IRR=1.50, 95% CI=1.38-1.64) women, respectively. In further analysis by tumor stage, the difference between the two populations was observed only for localized tumors, which was larger for Blacks for both men and women. The analysis by tumor size showed that the difference between the populations existed in both 0-2 cm and >2 cm tumors, but only in Blacks among men and was larger for Blacks than Whites among women.

Conclusion: The observations that a higher incidence in the military than the general population primarily existed in localized tumors suggest that universal care in the military may lead to earlier detection of the cancer. The larger differences for Blacks than Whites suggest that such impact may be larger for Blacks, who are less likely to have timely care in the general population. Nevertheless, the observed differences between the populations for tumors larger than 2cm suggest that other factors may also play a role.
Disclaimer: The contents of this publication are the sole responsibility of the authors and do not necessarily reflect the views, opinions or policies of NCI, USUHS, HJF, the DoD or the Departments of the Army, Navy or Air Force. Mention of trade names, commercial products or organizations does not imply endorsement by the US Government.

#4209

Cancers of unknown primary: survival by histologic type, demographic features, and treatment in the US Military Health System

Julie A. Bytnar[1], Jie Lin[1], Joel T. Moncur[2], Craig D. Shriver[1], Kangmin Zhu[1]. *[1]Murtha Cancer Center Research Program, Uniformed Services University Walter Reed Surgery, Henry M. J, Bethesda, MD,[2]The Joint Pathology Center, Silver Springs, MD*

Background: Cancers of unknown primary (CUP), a group of heterogenous metastatic cancers lacking a known primary site, have poor prognosis. This study compared survival by histologic type, patient characteristics, and treatment in the U.S. Military Health System (MHS), which provides universal care to its members.
Methods: Patients diagnosed with CUP were identified from the U.S. Department of Defense's Automated Central Tumor Registry. Median survival with 95% confidence intervals was calculated for demographic and treatment variables by histologic type. A multivariable accelerated failure time model estimated time ratios and 95% confidence intervals.
Results: The study included 3,358 CUP patients. The most prevalent CUP in this study was well and moderately differentiated adenocarcinomas. Median survival varied by histologic type with squamous cell carcinoma having the longest at 25.1 months and poorly differentiated carcinomas having the shortest at 3.0 months. For each histologic type, survival was generally similar by sex and active-duty status. Younger patients tended to have longer survival than those aged 65 years or older. Women with well and moderately differentiated adenocarcinoma had longer survival than their male counterparts. Generally, there were no racial differences in survival except poorer survival for Blacks than Whites with other histologic types. Patents with chemotherapy and radiation treatment generally had improved survival whereas patients with squamous cell carcinoma who received chemotherapy had shorter survival than those without.
Conclusion: Survival generally did not differ between racial groups, which may be related to equal healthcare access despite racial background. Further studies are warranted to better understand how survival in the MHS compares with that in the general U.S. population.
Disclaimer: The contents of this publication are the sole responsibility of the authors and do not necessarily reflect the views, opinions or policies of USUHS, HJF, the DoD or the Departments of the Army, Navy or Air Force. Mention of trade names, commercial products or organizations does not imply endorsement by the US Government.

#4210

Over 10 years since HPV vaccine approval, awareness of the causal link between HPV and HPV-associated cancers remains low in the US

Eric Adjei Boakye[1], Mrudula Nair[1], Joel Fokom Domgue[2], Dina K. Abouelella[3], Heena Y. Khan[4], Nosayaba Osazuwa-Peters[3]. *[1]Henry Ford Health System, Detroit, MI,[2]The University of Texas MD Anderson Cancer Center, Houston, TX,[3]Duke University School of Medicine, Durham, NC,[4]Saint Louis University, Saint Louis, MO*

Background**:** Over 90% of Human papillomavirus (HPV)-associated cancers could be prevented with the HPV vaccination; yet vaccine uptake remains suboptimal. Awareness that HPV causes several cancers has been shown to improve HPV vaccination uptake. While several efforts to increase HPV-associated diseases awareness as a way to improve vaccine uptake have been made, it is unclear if these efforts have resulted in increased HPV-associated cancers awareness over the years. We examined the awareness of the link between HPV and HPV-associated cancers between 2014 and 2020 in the US.

Methods: We used the Health Information National Trends Survey (HINTS) data from 2014 (HINTS 4 cycle 4) to 2020 (HINTS 5 cycle 4). HINTS is a nationally representative survey of adults aged ≥18 in the civilian non-institutionalized US population. HPV-associated cancer awareness was assessed with the question "Do you think HPV can cause i) anal ii) cervical iii) oral and iv) penile cancers". Responses were "yes", "no" and "not sure". Weighted prevalence estimates and corresponding 95% CIs were calculated for all four HPV-associated cancer awareness questions at each timepoint.

Results: There were five timepoints included in the study: HINTS 4 cycle 4 (2014, n=2239), HINTS 5 cycle 1 (2017, n=2034), HINTS 5 cycle 2 (2018, n=2050), HINTS 5 cycle 3 (2019, n=2270), and HINTS 5 cycle 4 (2020, n=2340). Awareness of the link between HPV and cervical cancer was high (77.6% in 2014) but decreased by 7.4% between 2014 and 2020 (Table). However, awareness of the link between HPV and anal, oral, and penile cancers was low (around 30% for each cancer type) and remained stable between 2014 and 2020 (Table).

Conclusions: Awareness of the link between HPV and HPV-associated cancers has remained steady for anal, oral and penile cancers or declined slightly for cervical cancer over time. There is a need for implementing novel and target interventions to increase awareness and counteract HPV vaccine disinformation.

Awareness of the link between HPV and HPV-associated cancers

			Weighted percent (95% CI)		
	H4C4 (2014)	**H5C1 (2017)**	**H5C2 (2018)**	**H5C3 (2019)**	**H5C4 (2020)**
HPV cause anal cancer	27.9 (24.7, 31.1)	29.1 (25.7, 32.5)	24.4 (21.3, 27.5)	28.8 (25.5, 32.0)	27.4 (24.3, 30.6)
HPV cause oral cancer	31.2 (28.0, 34.4)	30.7 (27.6, 33.9)	27.0 (23.8, 30.1)	31.1 (27.8, 34.4)	29.5 (26.3, 32.8)
HPV cause penile cancer	30.3 (27.1, 33.6)	31.2 (28.1, 34.2)	29.2 (25.9, 32.5)	32.0 (28.7, 35.4)	28.4 (25.1, 31.6)
HPV cause cervical cancer	77.6 (74.9, 80.3)	81.5 (78.9, 84.2)	75.0 (72.0, 78.1)	73.9 (70.4, 77.3)	70.2 (67.0, 73.5)

#4211

Geospatial analyses identify hot spots of late-stage cervical cancer at diagnosis in Texas

Itunu O. Sokale, Aaron P. Thrift, Abiodun O. Oluyomi. *Medicine, Baylor College of Medicine, Houston, TX*

Background: Women with advanced cervical cancer at diagnosis have higher morbidity and mortality. Despite advancements in prevention and early detection, cervical cancer care disparities persist by race/ethnicity and geographical distribution. We aimed to identify spatial clusters of late-stage cervical cancer at diagnosis in Texas, a state with a higher than national cervical cancer rate, especially among racial/ethnic minority populations.**Methods**: Incident cervical cancer data were obtained from the Texas Cancer Registry for women aged 18 years or older diagnosed from 2000 to 2018. First, we conducted purely spatial scan analysis using the SaTScan Bernoulli model to identify geographic clusters (hot spots and cold spots) of late-stage cervical cancer (vs. early-stage) at diagnosis. Maximum cluster size was set at 50% of the at-risk population, and statistical significance at p <0.005 was explored by 999 Monte Carlo simulations. Finally, we used multivariable logistic regression models to investigate the characteristics of cases within each of the identified clusters.**Results**: SaTScan identified six clusters, three with significantly lower than expected number of late-stage cervical cancer cases (cold spots) and three with significantly higher than expected number of late-stage cervical cancers cases at diagnosis (hot spots). Hot spots were found around Public Health Regions 5/6 (Houston, a large metropolitan city with the highest rate of uninsured residents in Texas), Region 10 (El Paso, a border region) and Region 8 (San Antonio, the largest majority Hispanic population region). Compared to White women, Black women were less likely to be in cold spots (Cluster 1: odds ratio (OR) 0.44 (95% CI 0.33-0.57), Cluster 2: OR 0.42 (95% CI 0.28-0.64)), but more likely to be in hot spots (Cluster 3 OR 1.33 (1.15-1.54). Similarly, Hispanic women had greater odds of being in hot spots (Cluster 4: OR 5.26 (95% CI 4.15-6.68), Cluster 5: OR 12.43 (95% CI 8.82-17.52)) than non-Hispanic women. Likewise, compared to women living in census tracts with lower neighborhood-level poverty, those women living in census tracts with higher deprivation were more likely to be in the hot spots (Cluster 3: OR 1.28 (95% CI 1.10-1.49), Cluster 4: OR 55.07 (95% CI 17.63-172.00), Cluster 5: OR 8.24 (95% CI 4.87-13.95)). **Conclusions**: Considerable inequalities exist in late-stage cervical cancer diagnosis in Texas, in terms of place, race/ethnicity, and neighborhood disadvantages. Strategic and multicomponent population-based interventions are needed to address cancer care inequities.**Impact:** The study findings could be incorporated into designing effective multilevel interventions, including place-based and race-targeted strategies to improve cervical cancer outcomes.

#4212

Comparison of thirty-year population-based incidence rates of invasive lobular vs ductal vs mixed breast carcinoma in Ontario, Canada

David Wai Lim[1], Vasily Giannakeas[1], Steven Narod[1], Kelly A. Metcalfe[2]. *[1]Women's College Research Institute, Women's College Hospital, Toronto, ON, Canada,[2]Lawrence S. Bloomberg Faculty of Nursing, University of Toronto, Toronto, ON, Canada*

Purpose: We calculated crude, age-adjusted and age-specific incidence rates for invasive lobular, ductal and mixed ductal-lobular breast carcinoma from 1990 to 2020 in the province of Ontario, Canada. We further examined incidence relationships between clinical stage, age at diagnosis and time.

Methods: We used population-based administrative healthcare datasets from the Institute of Clinical Evaluative Sciences (ICES Ontario), including the Ontario Cancer Registry, to identify all women diagnosed with breast cancer between 1990 and 2020. We calculated crude, age-adjusted

and age-specific incidence rates for invasive lobular (ILC), ductal (IDC) and mixed ductal-lobular (IDC-ILC) breast carcinoma. Incidence rates were adjusted to the 2011 Canadian female standard population. We further examined the incidence relationships between clinical stage and age at diagnosis over time.
Results: From 1990 to 2020, the 5-year crude incidence rates of ILC increased from 53.1 to 73.4 per 100,000 (+38%), while IDC increased from 501 to 746.5 per 100,000 (+49%). The crude incidence of mixed IDC-ILC peaked at 45 per 100,000 between 2005 and 2009 and is currently 29 per 100,000. The age-adjusted 5-year incidence rate of ILC has slightly increased from 64 to 70 per 100,000 (+9%) while that of IDC has increased from 598 to 726 per 100,000 (+21%). The age-adjusted 5-year incidence of mixed IDC-ILC peaked at 47 per 100.000 between 2005 and 2009 and has declined to 29 per 100,000. Age-specific 5-year incidence rates for ILC has decreased over time in women < 40 years of age and increased in women over the age of 65. In contrast, age-specific 5-year incidence rates for IDC have remained stable in women over 75. For mixed IDC-ILC, age-specific 5-year incidence rates have increased over time in all age categories. Among women with ILC, there is a greater proportion of women under the age of 50 diagnosed with stage III disease (30%) compared with women diagnosed over the age of 50 (16%). Women between the ages of 50 and 74 have higher rates of being diagnosed at stage I (43%) compared with 35% and 31% for women diagnosed between the ages of 40-49 and over 75, respectively.
Conclusions: The incidence of invasive lobular breast carcinoma in increasing, particularly in women over the age 65. Consequently, the burden of lobular breast carcinoma is expected to increase, as the proportion of women over the age of 65 is expected to rise exponentially in the foreseeable future, highlighting a need for further study of this not uncommon breast cancer subtype. While representing a smaller proportion of breast cancer diagnoses, the incidence of mixed invasive ductal-lobular subtype is increasing in all age groups.

#4213

Comparison of benign breast disease subtypes and breast cancer risk among Hispanic and non-Hispanic white women in New Mexico

Kush Raj Lohani[1], Andrea M. Nibbe[2], Robert A. Vierkant[3], Laura M. Pacheco-Spann[4], Lisa R. Seymour[5], Celine M. Vachon[6], Mark E. Sherman[7], Amy C. Degnim[8], Deirdre Hill[9]. *[1]Division of Breast and Melanoma Surgical Oncology, Department of Surgery, Mayo Clinic, Rochester, MN,[2]Consultant, Department of Biostatistics, The University of New Mexico Health Sciences, Albuquerque, NM,[3]Consultant, Department of Biostatistics, Mayo Clinic, Rochester, MN,[4]Sr. Program Coordinator & Department Diversity Leader, Quantitative Health Sciences, Mayo Clinic, Jacksonville, FL,[5]Senior Research Protocol Specialist, Department of Surgery Research, Mayo Clinic, Rochester, MN,[6]Professor and Chair, Division of Epidemiology, Department of Quantitative Health Sciences, Mayo Clinic, Rochester, MN,[7]Professor, Division of Epidemiology, Department of Health Sciences Research, Mayo Clinic, Jacksonville, FL,[8]Professor, Division of Breast and Melanoma Surgical Oncology, Department of Surgery, Mayo Clinic, Rochester, MN,[9]Research Assistant Professor, Department of Internal Medicine, Division of Epidemiology, The University of New Mexico Health Sciences, Albuquerque, NM*

Introduction: Benign breast disease (BBD) is an important breast cancer (BC) risk factor, which may be classified as non-proliferative disease (NPD), proliferative disease without atypia (PDWA), or atypical hyperplasia (AH) for risk stratification. Data related to the frequency of specific types of BBD and their relationship to BC risk in the Hispanic American population are limited. To

address this knowledge gap, we compared BBD and associated BC risk among Hispanic white (HW) and non-Hispanic white (NHW) in New Mexico (NM).
Methodology: A retrospective IRB-approved study was performed of women 19 years or older residing in six counties in NM (Bernalillo, Sandoval, Sante Fe, Socorro, Torrance, Cibola/Valencia) between 1996 and mid-2007 to compare the frequency of BBD subtypes and BC risk among HW and NHW. We excluded women who had a history of BC prior to BBD diagnosis or who were diagnosed with BC within 6 months after BBD biopsy. Race and ethnicity were self-reported by women at the time of biopsy. BBD was categorized as NPD, PDWA, or AH based on medical records. Incident BC (in-situ or invasive) was ascertained via linkage to the NM Surveillance Epidemiology End Results (SEER) Registry and BC risk was assessed using standardized incidence ratios (SIRs), comparing the observed number of BC events to that expected based on the NM SEER six-county race- and ethnicity-specific incidence rates, accounting for age and calendar period.
Results: Our analysis included 3,870 HW and 6,996 NHW women with BBD. The HW were younger (47.1 vs. 51 years) compared to NHW. HW women had slightly more NPD (69.4% vs. 66.6%) but less PDWA (26.2% vs. 29.4%) and similar frequency of AH (4.3% vs. 3.9%) as compared to NHW. Over a median post-BBD follow-up period of 13 years (range 6 months-17 years), 644 BCs were observed (4.81% in HW and 6.55% in NHW). The observed BC risk among women with BBD was higher than population-based expected rates (SIR 1.98, 95% CI 1.82-2.13, $p<0.001$) and showed expected increases in risk with increasing degrees of BBD abnormality: SIR=1.90 for NPD, 2.00 for PDWA, and 3.01 for AH. Comparing BC risk by ethnic subgroups, HW women had an overall risk of BC after BBD that was statistically indistinguishable from NHW women (SIR=2.17, 95% CI 1.86-2.48 in HW women, and SIR=1.91, 95% CI 1.73-2.08 in NHW women). Within the major subgroups of the BBD findings, there were no significant differences in risk of BC after BBD for HW versus NHW women.
Conclusions: In this population-based study, benign breast disease subtypes and their associated breast cancer risk were similar among the Hispanic and non-Hispanic white women.

#4214

Exposure to air pollution during pregnancy and risk of premenopausal breast cancer: A Swedish nation-wide cohort study including more than 1 million women

Jessica Lena Edlund[1], Malin Gustafsson[2], Jenny Linden[2], Wendy Yi-Ying Wu[1], Anna Oudin[3], Sophia Harlid[1]. *[1]Radiation Sciences, Oncology, Umeå University, Umeå, Sweden,[2]Swedish Environmental Research Institute, Göteborg, Sweden,[3]Department of Laboratory Medicine, Lund University, Lund, Sweden*

Background: Air pollution has been linked to an increased risk of breast cancer, but most previous studies have not considered if the exposure occurred during windows of susceptibility, such as pregnancy. Pregnancy is a period of rapid changes to both the breast tissue and the surrounding microenvironment. Exposures during this sensitive time-period could therefore result in erosion of the protective effect of pregnancy and make women more susceptible to external breast cancer risk factors. Aim: The aim of this study was to identify associations between air pollution exposure, occurring specifically during pregnancy, and risk of premenopausal breast cancer.
Method: Using nation-wide data from Swedish registers we constructed a cohort consisting of all women in Sweden who gave birth to their first child between January 1st 1991 and December 31st 2015. Women with a cancer diagnosis prior to pregnancy were excluded. Data on air pollution (yearly averages of PM_{10}, $PM_{2.5}$ and NO_2), was collected from the residence of women during, and to some extent between, pregnancies. Associations between air pollution and premenopausal breast

cancer is evaluated using Cox proportional hazards regression to estimate hazard ratios (HR), using age as the time scale and including appropriate confounders such as socioeconomic variables, comorbidities and family history of breast or ovarian cancer.
Results: The full cohort included 1 074 925 unique women and 2 302 256 pregnancies (the mean number of pregnancies for each woman was 1.75). During the study period, 13 292 (1.2 %) were diagnosed with breast cancer before they turned 50 years.
Conclusion: Our working hypothesis is that women exposed to higher levels of air pollution during pregnancy will have a higher risk of breast cancer. This large-scale study will have enough statistical power to detect the effect of air pollution on breast cancer risk, taking into account exposure both during and between pregnancies.

#4215

Air pollution exposure during pregnancy and risk of premenopausal breast cancer among women with a family history of cancer

Anna Hettinger[1], Jessica Edlund[1], Malin Gustafsson[2], Jenny Lindén[2], Wendy Yi-Ying Wu[1], Anna Oudin[3], Sophia Harlid[1]. *[1]Radiation sciences, Oncology, Umeå University, Umea, Sweden,[2]Swedish Environmental Research Institute, Göteborg, Sweden,[3]Department of Public Health and Clinical Medicine, Division for Sustainable Health, Umeå University, Umea, Sweden*

Background: Having a family history of breast or ovarian cancer is an important risk factor for premenopausal breast cancer. One reason for this could be that women with an underlying genetic susceptibility are more sensitive to environmental exposures due to gene-environment interactions. This might be especially important if the exposure occur during windows of susceptibility, such as pregnancy. Aim: The aim of this project is to determine if exposure to air pollution during pregnancy is associated with premenopausal breast cancer in a population with a known family history of breast or ovarian cancer.
Methods: The project is based on nation-wide data from Sweden's national registers and utilizes a cohort study design. The original cohort consists of women who gave birth to their first child between 1992 and 2015 (n=1 074 925), from this cohort we will select women with at least one first degree relative with breast or ovarian cancer (confirmed through register linkage). The primary outcome is primary breast cancer diagnosed before 50 years of age, and the exposure is levels of air pollution (PM_{10}, $PM_{2.5}$ and NO_2) at the participant's home address during each pregnancy. Cox proportional hazards regression will be used to determine hazard ratios using age as the time-scale.
Results: The registry based linkage makes it possible to distinguish between both relational context (mother or sister), number of afflicted first degree relatives and type of cancer (breast or ovarian). All included women also have at least one recorded pregnancy (prior to any cancer diagnosis).
Conclusion: This large scale study will be able to provide important information about the impact of air pollution exposure during pregnancy on breast cancer risk in a population with a documented family history of breast or ovarian cancer.

#4216

Interactions of greenness with air pollution in relation to postmenopausal breast cancer risk in UK Biobank

Carmen Smotherman[1], Brian Sprague[2], Susmita Datta[3], Dejana Braithwaite[1], Huaizhen Qin[1], Lusine Yaghjyan[1]. *[1]Epidemiology, University of Florida, Gainesville, FL,[2]Surgery, University of Vermont, Burlington, VT,[3]Biostatistics, University of Florida, Gainesville, FL*

Purpose: The evidence of the association between natural vegetation, or greenness, and breast cancer (BCa) remains inconsistent, with some studies reporting possible interactions with air pollution. We previously found a positive association of particulate matter with diameters than are 10 micrometers or smaller (PM_{10}) with BCa risk among postmenopausal women in the UK Biobank. In this study, we investigated the associations of greenness with postmenopausal BCa risk, as well as whether association of PM_{10} with BCa differ by the level of greenness.
Methods: This study included 155,235 postmenopausal women (6,146 with BCa) from UK Biobank, a population-based prospective cohort. Cancer diagnoses were ascertained through the linkage to the UK National Health Service Central Registers. Greenness measures (Greenspace percentage [GP], Natural environment percentage [NEP], and the Normalized Difference Vegetation Index [NDVI]) were available at baseline assessment (2006 -2010). GP and NEP coverage were calculated at 300 m and 1000 m, respectively, around participant residence locations, while the mean NDVI was calculated within a 500 m residential buffer of each UK Biobank participant. Annual averages for PM_{10} were available from 2007 and 2010. Information on BCa risk factors was collected at baseline. We used Cox proportional hazards regression to evaluate associations between greenness (continuous as well as quartiles) and BCa risk, while adjusting for BCa risk factors. Next, we examined associations for year-specific and cumulative average PM_{10} exposure measures (per 5 $\mu g/m^3$) within each stratum of greenness measure. Interactions between PM_{10} and greenness measures were assessed by including an interaction term in the main models.
Results: BCa risk increased by 29% per one unit increase in NDVI (Hazard ratio [HR]=1.29, 95% CI 1.03, 1.61). Compared to women in the lowest NDVI quartile, women with higher levels of NDVI had higher risk of BCa (HR=1.10, 95% CI 1.01, 1.21 for 2nd quartile, HR=1.10, 95% CI 1.00, 1.20 for 3rd quartile, and HR=1.13, 95% CI 1.04, 1.24 for 4th quartile, p-trend=0.012). No significant associations were found for any other greenness measure in relation to BCa risk. We found a significant interaction between NDVI and cumulative average PM10 exposure ($p<0.0001$). The association of PM10 cumulative average with BCa risk was stronger at lower levels of NDVI (HR per 5 $\mu g/m^3$=1.12, 95% CI 1.07, 1.17 for 1st quartile) compared to higher levels of NDVI (HR=1.04, 95% CI 1.02, 1.07 for 4th quartile). We found no interactions with other greenness measures.
Conclusions: We found a positive association of NDVI with BCa risk and an interaction between cumulative average PM_{10} and NDVI, with stronger positive association of cumulative average PM_{10} exposure with postmenopausal BCa risk at lower compared to higher levels of greenness.

#4217

Cumulative environmental quality is associated with breast cancer incidence differentially by summary stage and urbanicity

Larisa M. Gearhart-Serna[1], Kate Hoffman[2], Hillary Hsu[3], Gayathri R. Devi[4]. *[1]Department of Surgery, Duke University Medical Center, Durham, NC,[2]Nicholas School of the Environment, Duke University, Durham, NC,[3]Trinity College of Arts and Sciences, Duke University, Durham, NC,[4]Department of Surgery; Cancer Risk, Detection, and Interception Program, Duke Cancer Institute, Department of Surgery, Duke University Medical Center; Cancer Risk, Detection, and Interception Program, Duke Cancer Institute, Durham, NC*

Individual environmental contaminants have been associated with breast cancer (BCa); however, simultaneous evaluations of multiple exposures are limited. The USEPA has constructed an

environmental quality index (EQI) that includes different exposures across air, water, land, sociodemographic, and built environments. As links between BCa and the EQI have so far been confined to total BCa incidence, herein we investigated if these multiple exposures in broad EQI domains were associated with BCa incidence stratified by stage of disease.
Incidence rates of total, in situ, localized, regional, and distant breast cancer were assessed by linking the EQI dataset to county-level age-standardized incidence rates obtained from the North Carolina Central Cancer Registry (2010-2014), which reports all cancer cases diagnosed in NC residents. Generalized linear models (SAS 9.3) were constructed to determine the associations between breast cancer incidence rates by summary stage and the EQI in total and by domain, compared across rural versus urban counties. Models were adjusted for percent African American (AA), percent smokers, and mammography screening rates in each county. Mann-Whitney rank tests and D'Agostino-Pearson normality tests were used to determine statistical significance.
Results showed that the EQI is variable across NC, akin to variability across the U.S. (interquartile range 25th-75th% for total EQI in NC: -0.187 to 0.734 vs in the U.S.: –0.606 to 0.706). In counties with poor total EQI scores, and thus poor overall environmental quality, total BCa incidence increased by 10.82 cases per 100,000 persons (95%CI: 2.04, 19.60, p=0.016). This association was most pronounced for localized BCa (β=5.59, 95%CI: 0.59, 10.58, p=0.029). Higher incidence of early-stage disease (carcinoma in situ β=5.25, 95%CI: 2.34, 8.16, p=0.001 and localized BCa β=6.98, 95%CI: 2.24, 11.73, p=0.004) and total breast cancer (β=11.44, 95%CI: 3.01, 19.87, p=0.008) also occurred in counties with poor land quality, especially urban counties. The county AA percentage was associated with increased incidence of regional (0.12 cases per % increase, 95% CI 0.01, 0.22, p=0.022) and distant BCa (0.06 per % increase, 95% CI 0.02, 0.10, p=0.003). Associations persisted and were strengthened in urban counties for regional BCa, and in rural counties for distant BCa.
In sum, we found that BCa is associated with environmental quality differentially by disease stage, environmental domain, and urbanicity. Although what drives poor EQI varies by region, our analyses are generalizable to other states and counties across the U.S. and suggest that cumulative environmental exposures should be assessed in the context of cancer stage. Funding: Duke Cancer Institute pilot (GRD, KPH) in P30 Cancer Ctr grant; NIEHS T32-ESO21432-05; NCI-3P20CA202925-04S2 Diversity Supplement (LGS).

#4218

Cancer prevalence among Ohio firefighters: data from the Ohio Cancer Incidence Surveillance System (OCISS) 1996-2019

Susan E. Olivo-Marston[1], Shashank Singh[2], Robert B. Hood[3], Olorunfemi Adetona[4]. *[1]Medical Microbiology, Immunology and Cell Biology, Simmons Cancer Institute at Southern Illinois University School of Medicine, Springfield, IL,[2]West Virginia School of Osteopathic Medicine, Lewisburg, WV,[3]Epidemiology, Rollins School of Public Health at Emory University, Atlanta, GA,[4]Environmental Health Sciences, The Ohio State University College of Public Health, Columbus, OH*

Firefighting is classified as a Group 1 carcinogen or “carcinogenic to humans” by the International Agency for Research on Cancer. Compared to the general population, firefighters have a 9% increased risk of cancer incidence and a 14% increased risk of cancer mortality. Although there have been previous studies of cancer incidence among firefighters in Florida and Massachusetts, there have been no studies examining cancer incidence among firefighters in the state of Ohio. Therefore, this is the first study to examine cancer prevalence among Ohio firefighters. The study utilized data from the Ohio Cancer Incidence Surveillance System (OCISS), the Ohio state cancer

registry. This study examined data from 1996-2019, including a total of 1,314,318 people. Occupation was classified as firefighter, police, or general population. The odds of being a firefighter versus a police officer or the general population was calculated for specific cancer types. In addition, this analysis was stratified by gender. Police were used as a comparison group because it is an occupation similar to firefighters with the exception of exposure. There was a total of 3,397 firefighters, 3,341 police, and 1,307,580 people in the general population. Among firefighters, they were mostly male (86.8%), White (92.7%), Non-Hispanic (3.4%), married (67.7%), and never used tobacco (19.8%). The mean age at cancer diagnosis among firefighters was 66 years and most of them were diagnosed between 2010 and 2014. A similar distribution was seen among police except the mean age at cancer diagnosis was 63 years and most of them were current tobacco users (18.5%). The distribution was similar among the general population except the majority of them were female (51.6%). Firefighters had increased odds of esophageal cancer, cancers of the soft tissue including the heart, skin, prostate, testis, bladder, and brain compared to the general population. Cancer of the oral cavity, pharynx, and kidney were also increased among firefighters; however, they did not reach statistical significance. Compared to police, firefighters had increased odds of breast, uterine, prostate, brain, and thyroid cancer. In addition, they had decreased odds of pancreatic and bladder cancer. When stratified by gender, among the 2,948 male firefighters, there were increased odds of cancer of the soft tissue including heart, prostate, brain, cranial nerves, and thyroid cancer compared to the general population. They also had decreased odds of cancer of the larynx, lung & bronchus, and bladder. Number of female firefighters was small generating unstable odds ratios. We observed increased prevalence of several types of cancer among Ohio firefighters, similar to previous studies. Although there were limitations present due to many people lacking data on occupation, the current study supports that Ohio firefighters have an increased risk of many different types of cancer.

#4219

Smoky coal exposure is associated with epigenetic accelerated aging

Batel Blechter[1], Andres Cardenas[2], Seraphina (Junming) Shi[3], Mohammad L. Rahman[1], Jason Y.Y. Wong[1], Wei Hu[1], George S. Downward[4], Lutzen Portengen[4], Richard Cawthon[5], H. Dean Hosgood[6], Jihua Li[7], Debra T. Silverman[1], Yunchao Huang[8], Roel Vermeulen[4], Nathaniel Rothman[1], Qing Lan[1]. *[1]Division of Cancer Epidemiology and Genetics, National Cancer Institute, Rockville, MD,[2]Department: Epidemiology and Population Health, Stanford University, Palo Alto, CA,[3]Department of Biostatistics, UC Berkeley School of Public Health, Berkeley, CA,[4]Division of Environmental Epidemiology, Utrecht University, Utrecht, Netherlands,[5]Department of Human Genetics, University of Utah School of Medicine, Salt Lake City, UT,[6]Division of Epidemiology, Albert Einstein College of Medicine, Bronx, NY,[7]Quijing Center for Diseases Control and Prevention, Quijing, China,[8]Department of Cardiothoracic Surgery, Third Affiliated Hospital of Kunming Medical University, Kunming, China*

Household air pollution (HAP) from indoor combustion of solid fuel is a global health burden that has been linked to lung cancer. A striking example occurs in Xuanwei, China where the lung cancer rate for never smoking women is among the highest in the world and largely attributed to high levels of various toxic constituents, including polycyclic aromatic hydrocarbons (PAHs), a combustion product of smoky (bituminous) coal used for cooking and heating. Several air pollution constituents have been associated with epigenetic accelerated aging (EAA) derived from DNA methylation (DNAm)-based biomarkers that are highly correlated with biological processes

underlying aging-related diseases. We aim to assess the association between HAP exposure and EAA in Xuanwei, China.
We analyzed 106 never smoking women in an exposure assessment study in Xuanwei, China with a repeat DNA sample from 23 subjects. Household fuel type used for cooking and heating (smoky vs. smokeless coal) was collected using a questionnaire, and exposure models were used to predict levels of 43 individual HAP constituents for current and childhood exposure. Leukocyte DNAm was measured using Illumina EPIC array. EAA was derived for five clocks using the Horvath calculator and defined as the residuals resulting from regressing each clock on chronological age. We used generalized estimating equations to assess the associations between fuel type, clusters derived from predicted levels of HAP exposure, and ambient 5-methylchrysene (5-MC), a carcinogenic PAH previously associated with lung cancer in Xuanwei and selected *a priori* for analyses, as independent variables and EAA clocks as dependent variables, while accounting for repeated-measurements.
We observed a significant increase in GrimAge EAA among smoky coal users compared to smokeless coal users for current (β=1.84 years (y), 95% confidence interval (CI): 0.59, 3.09, P-value=0.004) and childhood (β=4.14 y, 95% CI: 1.63, 6.64, P-value=0.001) exposures. We also observed a monotonic increase in GrimAge EAA for a cluster of 31 PAHs reflecting current exposure (β=0.77 y, 95% CI: 0.36, 1.19, P-value=$3x10^{-4}$) and for a cluster of 33 PAHs reflecting childhood exposure (β=0.92 y, 95% CI: 0.40, 1.45, P-value=0.001). Ambient 5-MC, one of the constituents within the PAH clusters, was found to have an increasing monotonic relationship with GrimAge EAA for current (β=0.15 y, 95% CI: 0.05, 0.25, P-value=0.003) and childhood (β=0.30 y, 95% CI: 0.13, 0.47, P-value=$4.7x10^{-4}$) exposures.
Our findings suggest that exposure to PAH from indoor smoky coal combustion is associated with EAA, particularly for the GrimAge clock, a strong biomarker of mortality. This finding is consistent with our recent observation linking accelerated GrimAge to increased risk of lung cancer in a prospective study of never smoking women in China. Additionally, our study provides further support for 5-MC as a prominent carcinogenic component of smoky coal emissions.

#4220

Occupational pesticide use and relative leukocyte telomere length in the biomarkers of exposure and effect in agriculture study

Patricia A. Erickson[1], Vicky C. Chang[1], Casey L. Dagnall[2], Kedest Teshome[2], Mitchell J. Machiela[3], Kathryn H. Barry[4], Shahinaz M. Gadalla[5], Laura E. Beane Freeman[1], Gabriella Andreotti[1], Jonathan N. Hofmann[1]. *[1]Occupational and Environmental Epidemiology Branch, National Cancer Inst. Div. of Cancer Epidemiology & Genetics, Rockville, MD,[2]Cancer Genomics Research Laboratory, Frederick National Laboratory for Cancer Research, Leidos Biomedical Research, Inc., Rockville, MD,[3]Integrative Tumor Epidemiology Branch, Clinical Genetics Branch, National Cancer Inst. Div. of Cancer Epidemiology & Genetics, Rockville, MD,[4]Dept. of Epidemiology & Public Health, Greenebaum Comprehensive Cancer Center, University of Maryland School of Medicine, Baltimore, MD,[5]Clinical Genetics Branch, National Cancer Inst. Div. of Cancer Epidemiology & Genetics, Rockville, MD*

Background: Previous epidemiologic studies have reported increased risks of certain cancers in relation to specific pesticide exposures, although the mechanisms underlying many of these associations remain poorly understood. Within the Biomarkers of Exposure and Effect in Agriculture (BEEA) study, a molecular epidemiologic investigation of pesticide applicators in Iowa and North Carolina, we examined whether occupational use of pesticides is associated with

alterations in leukocyte telomere length. Telomeres are essential in maintaining chromosomal stability and altered telomere length has been linked to various malignancies.
Methods: Relative telomere length (RTL) was measured using quantitative PCR in leukocytes from 1,539 male pesticide applicators ≥50 years of age. Using self-reported information on pesticide use, we characterized lifetime use of specific pesticides in terms of ever use and intensity-weighted lifetime days (IWLDs), a metric integrating total lifetime days of use and other factors influencing exposure. Multivariable linear regression models were used to estimate differences in geometric mean RTL (and corresponding 95% confidence intervals) by ever vs. never use of 48 pesticides and in exposure-response analyses for IWLDs of use of 46 pesticides, adjusting for age, state of residence, race/ethnicity, body mass index, and cigarette smoking status and pack-years.
Results: Among ever users of the insecticides lindane and aldicarb, mean RTL was significantly longer compared to never users (p=0.01 and 0.03, respectively); in exposure-response analyses, we also observed a suggestive but non-statistically significant trend between increasing IWLDs of lindane use and longer RTL (p-trend=0.07). Higher IWLDs of use of the insecticide diazinon was also associated with longer RTL (p-trend=0.03) while increasing IWLDs of the insecticide heptachlor and the herbicide 2,4,5-TP were associated with shorter RTL (p-trends=0.04 and 0.03, respectively).
Conclusions: This is, to our knowledge, the largest investigation of occupational pesticide use and RTL to date. Our findings provide novel evidence suggesting that use of certain pesticides could be associated with altered leukocyte telomere length. Notably, diazinon and lindane have previously been associated with increased risks of lung and lymphoid malignancies, respectively, and longer leukocyte telomere length has been implicated in the development of these cancers.

#4221

Aflatoxin exposure in a population-based representative sample of adults in Mexico in 2018

Adriana Monge[1], Katherine McGlynn[2], Luis Santiago-Ruiz[1], Jose Maria Remes-Troche[3], Karina Hernandez-Flores[3], Salvador Villapando-Hernandez[1], Martin Romero[1], John Groopman[4], Martin Lajous[1]. *[1]Instituto Nacional de Salud Pública, Ciudad de Mexico, Mexico,[2]National Cancer Institute, Rockville, MD,[3]Universidad Veracruzana, Veracruz, Mexico,[4]Johns Hopkins University, Baltimore, MD*

Importance: Southern Mexico and Guatemala, together represent the region with the highest liver cancer burden in the Americas. There is a higher burden of liver cancer in rural regions in eastern and southern Mexico and remarkably there is an equal number of cases in men and women. Reasons for this increased burden are not clear, but previous studies of food samples have found that contamination of maize with aflatoxin B1 (AFB1), a potent liver carcinogen, is common in the region while HBV and HCV seroprevalence is less than 0.5%. Few examinations of AFB1 levels in persons have been conducted.
Objective: To estimate the prevalence of exposure and circulating levels AFB1 in a representative sample of adults living in five regions across Mexico.
Study Design: We randomly selected a subsample of 955 adults ≥40 years who participated in Mexico's National Health and Nutrition Survey 2018 (ENSANUT). These residents were from five states in eastern and southern Mexico and all provided a venous blood sample. We assessed AFB1 levels as pg AFB1-lys/µL in serum using mass spectrometry. The limits of detection and quantification were both 0.010 pg/µL.
Results: The mean age of participants was 56 years (± SD 11.7) and 54% were female. The overall prevalence of AFB1-lys detection was 92% (95% confidence intervals; 95%CI 88, 94%). The region with the lowest prevalence, 88% (95%CI 78, 94%), was Chiapas and the region with the

highest prevalence was Veracruz 95% (95%CI 84, 98). Median AFB1 was 0.127 pg AFB1-lys/μL (interquartile range; IQR 0.054, 0.446) with a range from 0.066 (IQR, 0.033, 0.147) in Yucatán to 0.476 (IQR, 0.199, 1.355) in Veracruz. AFB1 exposure levels were higher in persons aged ≥60 years, men, and participants living in rural areas. We observed decreasing levels of AFB1 exposure with increasing socioeconomic status.
Conclusions: In a representative sample of adults in eastern and southern Mexico we observed a high prevalence of exposure to AFB1. For certain regions, AFB1 levels are comparable to those in Guatemala. These results suggest that AFB1 may be related to the increased burden of liver cancer in eastern and southern Mexico.

#4222

Glyphosate and AMPA exposure: Associations with dietary intake and other factors

Rachel McFarland Lucia[1], Xiyue Liao[2], Wei-Lin Huang[1], Danielle Forman[3], Alexis Kim[4], Argyrios Ziogas[1], Trina M. Norden-Krichmar[1], Deborah Goodman[1], Andrea Alvarez[1], Irene Masunaka[1], Khyatiben Pathak[5], Marissa McGilvrey[5], Victoria David-Dirgo[5], Apurva Hegde[5], Patrick Pirrotte[5], Hannah Lui Park[1]. *[1]University of California, Irvine, Irvine, CA,[2]California State University, Long Beach, CA,[3]University of California, Los Angeles, Los Angeles, CA,[4]Yale University, New Haven, CT,[5]Translational Genomics Research Institute, Phoenix, AZ*

Background: Animal and epidemiologic studies suggest that exposure to the weed killer, glyphosate, and its primary metabolite aminomethylphosphonic acid (AMPA), is associated with increased risk for cancer, including breast cancer and non-Hodgkin's lymphoma. The International Agency for Research on Cancer (IARC) has categorized glyphosate as a “probable carcinogen,” yet glyphosate is the most highly used pesticide in the world. Biomonitoring studies assessing levels of human glyphosate and AMPA exposure in the United States have been limited. Thus, we examined urinary levels of these chemicals in a cohort of postmenopausal women residing in Southern California and evaluated associations with demographics, dietary intake, and other behavioral factors.
Methods: 338 postmenopausal women provided two first-morning urine samples and at least one paired 24-hour dietary recall. Participants also reported on demographic and other factors. Urinary glyphosate and AMPA were measured using LC-MS/MS.
Results: Glyphosate was detected in nearly 90% of urine samples and AMPA in 67.2%. Urinary glyphosate and AMPA levels were lower in women who reported high levels of organic eating (p=0.04 and p=0.01, respectively). Urinary glyphosate was lower in women who reported higher levels of physical activity (p=0.03). Multivariate analysis showed that grain consumption, particularly refined grains, was significantly associated with higher urinary glyphosate levels (adjusted p=0.004). Alcohol consumption (adjusted p=0.001) and frequency of eating fast-food (adjusted p=0.006) were associated with higher urinary AMPA levels, while fruit (adjusted p=0.03) and corn (adjusted p=0.008) consumption were associated with lower AMPA.
Conclusions: In the largest study to date examining paired dietary recall data and measurements of urinary glyphosate and AMPA, the vast majority of women sampled had detectable levels. Consumption of certain foods, including grains and alcoholic beverages, were associated with higher urinary levels of glyphosate and AMPA.

#4223

A metabolomic investigation of serum perfluorooctane sulfonate and perfluorooctanoate

Jongeun Rhee[1], Steven C. Moore[2], Demetrius Albanes[2], Tracy M. Layne[3], Erikka Loftfield[2], Rachael Stolzenberg-Solomon[2], Linda M. Liao[2], Mary C. Playdon[4], Mark P. Purdue[1].

[1]Occupational and Environmental Epidemiology Branch, Division of Cancer Epidemiology and Genetics, National Cancer Institute, Rockville, MD,[2]Metabolic Epidemiology Branch, Division of Cancer Epidemiology and Genetics, National Cancer Institute, Rockville, MD,[3]Department of Population Health Science and Policy, Icahn School of Medicine at Mount Sinai, New York, NY,[4]Division of Cancer Population Sciences, Huntsman Cancer Institute, Salt Lake City, UT

Background: Per- and polyfluoroalkyl substances (PFAS) are environmentally persistent synthetic chemicals detectable in the blood of most Americans. Elevated exposures to perfluorooctane sulfonate (PFOS) and perfluorooctanoate (PFOA), the two most prevalent PFAS, have been associated with several health outcomes including metabolic outcomes and some cancers. To evaluate possible mechanisms related to the biological effects of these chemicals, we conducted a pooled metabolome-wide association study (MWAS) of circulating PFOS and PFOA among 3,647 participants included in one of eight nested case-control serum metabolomic profiling studies conducted in the Prostate, Lung, Colorectal, and Ovarian Cancer Screening Trial (PLCO) population.
Methods: All metabolomic profiling was conducted by Metabolon Inc, using liquid-phase or gas chromatography coupled with mass spectrometry. All metabolites including PFOS and PFOA were centered (mean=0, standard deviation=1) and log-transformed. We conducted multivariable linear regression analyses to estimate study-specific associations between metabolite levels and PFOS and PFOA, adjusted for age at specimen collection, race/ethnicity, body mass index, smoking, case-control status, study center, and year of specimen collection. Sex was additionally adjusted for studies including both men and women. We then conducted combined the study-specific findings through meta-analysis using random effects models.
Results: The meta-analysis results of 1,040 metabolites for PFOS and 1,103 for PFOA identified 83 and 67 metabolites, respectively, associated at Bonferroni-corrected significance thresholds ($P=4.81 \times 10^{-5}$ for PFOS; $P=4.53 \times 10^{-5}$ for PFOA). For both PFOS and PFOA, the strongest positive associations were observed for the xenobiotics 3,5-dichloro-2,6-dihydroxybenzoic acid [PFOS, summary beta coefficient =0.74, 95% confidence interval=0.67,0.80; PFOA, 0.48 (0.35,0.61)] and 3-bromo-5-chloro-2,6-dihydroxybenzoic acid [0.57 (0.43,0.72) and 0.39 (0.23,0.55)]. We also observed strong positive associations with PFOS and PFOA for metabolites related to the sphingomyelin (SM) pathway, such as hydroxypalmitoyl sphingomyelin (d18:1/16:0(OH)) [PFOS, 0.44 (0.24,0.64)] and SM (d18:1/18:0) [PFOS, 0.35 (0.24,0.46); PFOA, 0.25 (0.16,0.34)], and SM (d18:2/24:2) [PFOS, 0.32 (0.17,0.47)]. The PFOS metabolite associations remained after model adjustment for PFOA; however, the PFOA associations were greatly attenuated after controlling for PFOS.
Conclusions: In this MWAS of PFAS, to our knowledge the largest to date, we observed robust positive associations with serum PFOS for several xenobiotic compounds and for metabolites related to the sphingomyelin pathway. Further investigation of these metabolites may offer insight into PFOS-related biologic effects contributing to disease development.

#4224

University of Chicago Comprehensive Cancer Center catchment area informatics platform

Ahmed Fadiel Metwaly[1], Adam Thomas Koster[2], Mohammad Abbasi[2], Adekunle Odunsi[1].
[1]Comprehensive Cancer Center, University of Chicago, Chicago, IL,[2]Research and Development, Interactome Bio, Kalamazoo, MI

Every cancer center has a surrounding geolocation known as a catchment area (CA). Data about this CA can help cancer centers better understand the population and type of patients the center is

targeting. In addition, collecting, analyzing, and visualizing this data can help the cancer center better understand population needs and gain more insights to provide predictive care instead of reactive care. However, the multidimensionality and complexity of the CA data requires the build of a specialized platform that can handle this heterogenous data. Motivated by this need and to answer specific questions about the CA, the UCCCC developed a new informatics platform that provides access to analytical tools, data handling, and an exchange environment. The goal of this platform is also to support a collaborative community to study CA dynamics related to health disparity and cancer. Here we present a new Geoinformatics platform that offers capabilities for using and modifying spatial data. It facilitates interrogating, modifying, executing, and mapping data. Data includes imagery, features, and base maps linked to spreadsheets and tables. The data is kept in the RDBMS (Relational Database Management System). Other query software tools are needed to deal with the database system including a server to launch the GIS application with specific RAM, GPU, and good SSD to back up the database. The database could be saved on google firebase to handle real-time queries. Thus, the maps can be easily shared and embedded in apps and accessible by virtually everyone, everywhere. The datasets used were downloaded from conventional websites (listed in the appendix) and internal datasets. The goal is to answer basic questions including the count of patients in that area, socioeconomic status, distribution in terms of demography (race, age, gender), physical environment, and other factors. Furthermore, it will be able to find correlations across many variables given the response variable, such as type of disease (lung, ovarian, breast cancer). Solving Critical Problems in Cancer Control using Spatial Science as well as being able to select a geographic location/region/area and plot the data across different dimensions, possibly on a map or another type of view. Geographic information needs a way to integrate data from several sources with varying degrees of accuracy. The platform provides real-time changes in the CA, so it needs to be updated frequently to stay current. The tool will connect the dataset to maps, integrating location data (where things are) with all kinds of descriptive information (how things are). Thus, a unique method of retrieval and manipulation is required for a significant portion of the data stored in GIS for practical usage.

GWAS/Post-GWAS

#5214

Expanding the spectrum of germline-driven cancers by leveraging population-scale targeted tumor and normal sequencing

Miika Mehine, Rebecca Caeser, Yelena Kemel, Daniel Muldoon, Sebastià Franch-Expósito, A. Rose Brannon, Aijazuddin Syed, Ozge Ceyhan-Birsoy, Maksym Misyura, Panieh Terraf, David B. Solit, Marc Ladanyi, Kenneth Offit, Zsofia K. Stadler, Diana L. Mandelker, Yonina R. Murciano-Goroff, Charles M. Rudin, Michael F. Berger, Chaitanya Bandlamudi. *Memorial Sloan Kettering Cancer Center, New York City, NY*

Large case-control and familial studies have established clear cancer-specific risk profiles for several key cancer predisposition genes (CPGs). For example, germline pathogenic variants (PVs) in *BRCA1/2* (*gBRCA*) are associated with increased risk for developing breast, ovarian, pancreatic, and prostate cancers. However, the extent to which *gBRCA* mutations are involved in mediating the tumorigenesis of other cancer types remains challenging to characterize. We hypothesized that integrating orthogonal features such as selection for biallelic inactivation of the PVs and depletion of canonical somatic drivers among the carriers can enrich the signal for identifying novel gene and cancer type associations. We then extend this framework to identify novel CPGs as well as to understand how tumors arise in patients with PVs in oncogenes.

To study this, we leveraged the prospective MSK-IMPACT matched tumor-normal sequencing cohort of 49,291 patients across 77 major cancer types. We study 90 well-known CPGs as well as >300 cancer genes not previously associated with cancer predisposition.
Overall, 8% (N=3,964) of patients harbored a PV in high or moderate penetrance CPGs. We identified 90 gene and cancer type associations with enrichment for biallelic inactivation (q<0.05), including 19 novel findings among clinically actionable genes. For example, we find enrichment for biallelic inactivation of *BRCA1/2* in unexpected lineages such as hepatobiliary, endometrioid, and ampullary cancers. These tumors were also significantly depleted for somatic gain-of-function driver alterations. Hepatobiliary cancers with *gBRCA1* mutations were also enriched for somatic loss of *NF1*.
Among carriers of PVs in oncogenes, we observe two possible mechanisms of first somatic hit towards malignant transformation. We find enrichment for copy number gain or copy neutral loss of heterozygosity of the germline PV in thyroid cancers with a PV in *RET*. We also find that lung cancers with a germline PV in *EGFR* frequently developed additional somatic point mutations located *in cis* with the PV.
Investigating genes with no prior association with germline predisposition to cancer, we find evidence for *KEAP1* and *CIC* as likely novel CPGs. Lung (n=8) and thyroid (n=4) cancers with deleterious germline variants in *KEAP1* were characterized by loss of the wild-type allele, co-occurring somatic *STK11* mutations, and depletion of canonical drivers such as *EGFR*. We also found biallelic loss of *CIC* in two patients with Neuroblastoma, each carrying a different germline loss-of-function mutation in *CIC*. Both tumors were also negative for *MYCN* and *ALK* defects.
Collectively, our findings expand our understanding of cancer predisposition in cancer, shed new insights into how tumors arise in germline carriers, and provide a framework for identifying new CPGs using population scale tumor-normal paired clinical sequencing data.

#5215
Clinical features of Li-Fraumeni syndrome in Korea
Ran Song, Seeyoun Lee, Jai Hong Han, Jae Yeon Woo, Min Jung Lee, Han-Sung Kang, Sunhwa Park, Eun-Gyeong Lee, Sun Young Kong, So-Youn Jung. *National Cancer Center, Goyang, Korea, Republic of*

Purpose: Li-Fraumeni syndrome (LFS) is a rare autosomal dominant hereditary disorder caused by a germline mutation in the TP53 gene. Because of the rarity of the disease, there were limited data on the types of the mutation, clinical features and treatment outcomes. The aim of this study is to evaluate the clinical characteristics and prognosis in Korean patients with germline TP53 gene mutation.
Methods: Patients who underwent genetic counseling and confirmed with TP53 gene mutation in National Cancer Center in Korea between 2011 and 2022 were reviewed retrospectively. Data on family history with pedigree, types of mutation, clinical features and prognosis were collected.
Results: Fourteen patients with LFS were included in the study. Missense mutations were shown in 13 cases and nonsense mutation in 1 case. The repeated mutations were p.Arg273His (n=2), p.Ala138Val (n=2) and pPro190Leu (n=2). A sister with breast cancer had the same mutation of p.Ala138Val. The median age at diagnosis of first tumor in 14 LFS patients was 32 (1-67) years. Seven patients (50%) had multiple primary cancers. Breast cancer was most frequently observed (n=9) and other types of tumor included sarcoma (n=5), thyroid cancer (n=3), pancreatic cancer (n=2), ovarian cancer (n=1), endometrial cancer (n=1), colon cancer (n=1), brain tumor (n=1), adrenocortical carcinoma (n=1), vaginal cancer (n=1), skin cancer (n=1) and leukemia (n=1). The median follow-up period was 51.5 (6-188) months. There were two cases of local recurrence and

four cases of distant metastasis during the periods. Two patients died from leukemia and pancreatic cancer at three months and 23 months after diagnosis, respectively.
Conclusion: As known in other countries, many Korean patients with LFS also had an early onset and multiple primary tumors. And patients showed various types of mutation, clinical features and prognostic outcomes. Further large-scale studies are required for proper screening and management in Korean patients with LFS. Grant: This study was supported by National cancer center, Korea, Grant no. 2110181

#5216

The effect of polymorphisms in *DAT1* and *DRD4* on dietary intake during chemotherapy for childhood leukemia

Jing Wen[1], Arul Duggimpudi[2], Shengguo Li[3], Elena Ladas[4], Kara M. Kelly[5], Peter D. Cole[3].
[1]Goryeb Children's Hospital, Morristown Medical center, Morristown, NJ,[2]Rutgers, The State University of New Jersey, New Brunswick, NJ,[3]Division of Pediatric Hematology/Oncology, Rutgers Cancer Institute of New Jersey, Rutgers, The State University of New Jersey, New Brunswick, NJ,[4]Division of Pediatric Hematology/Oncology/Stem Cell Transplant, Columbia University Medical Center, New York, NY,[5]Department of Pediatric Oncology, Roswell Park Cancer Institute and University at Buffalo School of Medicine and Biomedical Sciences, Buffalo, NY

Outcomes of acute lymphoblastic leukemia (ALL) are associated with both host and environmental factors. We hypothesized that there is also an interaction between them, with genetic variants influencing dietary choices. The dopamine transporter 1 (*DAT1*) and D4 subtype of the dopamine receptor (*DRD4*) genes are polymorphic, with a variable number of nucleotide repeats (VNTR) that affect dopaminergic neurotransmission, and reward circuitry for food cravings. Specifically, the 9-tandem repeats (9R) allele of DAT1 and the 7-tandem repeats (7R) allele of DRD4 are risk factors for eating disorders or undereating behavior in children. The goal of this study was to determine whether these polymorphisms are associated with altered dietary intake during therapy for childhood ALL. DNA was isolated from peripheral blood mononuclear cells collected from 439 children being treated on Dana Farber Cancer Institute ALL Consortium Protocol 05-001 (NCT00400946). Target alleles in DAT1 and DRD4 were determined using PCR product length analysis. Each subject was classified as having either zero or at least one copy of the target alleles. Dietary intake was previously determined using food frequency questionnaires collected at three timepoints: time of diagnosis, end of induction, and continuation therapy. As previously published dietary composition in fat and carbohydrate differed significantly among three timepoints. There was no significant difference between those with or without the target alleles in DAT1 or DRD4 in percent from fat or percent from carbohydrate at any of the three timepoints. However, significant differences were observed when dietary intake was compared to the Dietary Reference Intake (DRI). Notably, a greater portion of male participants with DAT1 9R polymorphism had fat consumption below the DRI at the time of diagnosis. On the contrary, significantly decreased portion of females with DAT1 9R had fat consumption below the DRI during continuation therapy. When compared to normative values, a significantly increased number of children had total calorie consumption below DRI during induction therapy. The DRD4 7R polymorphism was associated with fat intake below DRI during induction therapy in males. However, neither DAT1 nor DRD4 polymorphisms were related to variation in carbohydrates consumption. In addition, a greater portion of participants that carry both DAT1 and DRD4 polymorphism exhibited a trend toward undereating behavior in fat intake compared to the controls. Our results are the first to indicate that DAT1 and DRD4 polymorphisms are associated with altered dietary intake during chemotherapy

for childhood ALL. Future study will further elucidate whether this modulation is associated with changes in their body weight, BMI, glucose level, and disease relapse.

#5217

Genome-wide interactions of processed and red meat intake on colorectal cancer risk

Joel Sanchez Mendez[1], Mariana C. Stern[1], Andre Kim[1], John Morrison[1], Juan P. Lewinger[1], Li Hsu[2], Eric Kawaguchi[1], Ulrike Peters[2], William J. Gauderman[1], on behalf of GECCO, CCFR and CORECT. *[1]Population and Public Health Sciences, University of Southern California, Los Angeles, CA,[2]Public Health Sciences Division, Fred Hutchinson Cancer Research Center, Seattle, WA*

Introduction: Colorectal cancer (CRC) is the third most common cancer, and second cause of cancer death worldwide. High red meat and/or processed meat consumption are established risk factors for CRC. Genome-wide association studies have identified over 200 genetic variants that explain ~20% of the variability in CRC risk. However, few large studies have evaluated genome-wide gene by environment (GxE) interactions with meat in CRC. Using the largest CRC pooled dataset available to date we conducted a genome-wide GxE analysis to identify possible interactions between common variants and red meat and/or processed meat intake and CRC risk.
Methods: A pooled sample of 29,912 CRC cases and 39,704 unaffected controls of European (EUR) ancestry from 27 studies was analyzed. Sex- and study-specific quartiles for red meat and processed meat intake were constructed from harmonized questionnaire data on meat consumption. Genotyping arrays were imputated to the Haplotype Reference Consortium. To identify novel CRC interaction loci we used the two-step EDGE method, standard GxE analyses and a 1-3 degrees of freedom (DF) test . We removed previously known GWAS hits and SNPs in high linkage disequilibrium with them.
Results: Our Meta-analyses confirmed a positive association between quartile consumption increase of red meat and processed meat with CRC risk (Red meat OR = 1.30; 95%CI = 1.21-1.41; Processed meat OR = 1.40; 95% CI = 1.20 -1.63). Greater magnitude in point estimates were observed for case-control studies compared to cohort studies, for processed meat consumption among men compared to women, and for red meat consumption and distal colon localization compared to proximal colon or rectum. Two DF GxE tests of red meat consumption revealed two SNPs in chromosome (Chr) 8 (rs4871179 & rs75212442) and a SNP in Chr10 (rs117674361) that map downstream HAS2, COLEC10 and downstream CCSER2. In addition, the two-step EDGE GxE method identified the rs35352860 SNP that maps to the SMAD7 gene in Chr18. Genotype-stratified analyses showed that the red meat and CRC risk association was restricted to homozygous carriers of major alleles for rs4871179, rs75212442 & rs117674361. Moreover, we observed dose-response increase in the red meat and CRC risk association with additional copies of the T allele of the SNP in Chr18, with homozygous carriers of the T allele having 46% higher chance of developing CRC associated with high red meat intake; this in contrast to homozygous carriers of the reference C allele, that had an 18% higher risk of developing CRC. No statistically significant GXE interactions with processed meat intake were found.
Conclusion: In this large-scale genome-wide GxE analysis we identified interactions between 4 SNPs and red meat consumption affecting CRC risk. The interaction with the SMAD7 rs35352860 SNP provides supportive evidence for a role of heme iron in the carcinogenic pathway of red meat intake in CRC development.

#5218

Genome-wide association study of African Americans reveals new susceptibility loci contributing to lung cancer and mechanisms of population-specific etiology

Jinyoung Byun[1], Younghun Han[1], Xiangjun Xiao[1], Christine Lusk[2], Hoda J. Badr[1], Rayjean Hung[3], Ann G. Schwartz[2], Christopher I. Amos[1], INTEGRAL Consortium. *[1]Baylor College of Medicine, Houston, TX,[2]Wayne State University School of Medicine, Detroit, MI,[3]University of Toronto, Toronto, ON, Canada*

Lung cancer incidence and mortality in the U.S. have substantial ethnic disparities. African Americans of both sexes have the high incidence rate at 56.8 and the highest death rate at 38.1 per 100,000 people from 2015 to 2019. Non-Hispanic black men have the highest incidence at 73.9 and the highest death rate at 56.3 per 100,000 people. While many genome-wide association studies (GWAS) of lung cancer have discovered ~45 putative risk loci, a large proportion of the heritability of lung cancer remains unexplained. To date, most single population-based GWAS have been performed in Europeans while there are a few Asian ancestry-specific genetic studies and two cross-ancestry studies. Non-European GWAS of lung cancer has been underrepresented. Although African Americans have higher lung cancer incidence and poorer lung cancer survival rate, and smoke fewer cigarettes per day compared to Europeans, few comprehensive GWAS of lung cancer in African Americans has been conducted. This study aims to decipher the genetic component of predisposition to lung cancer among African Americans. This study aims to decipher the genetic component of predisposition to lung cancer among African Americans. We conducted an African-ancestry GWAS comprising 2,280 lung cancer cases and 4,301 controls to comprehensively characterize common and low-frequency lung cancer genetic susceptibility loci using HRC imputed lung cancer data. The novel variants in or near VWF on 12p13.31 (OR=1.29, $P=6.93\times10^{-9}$) for overall lung cancer and GACAT3 on 2p24.3 (0.65, 1.24×10^{-9}), TRIP13 on 5p15.33 (3.49, 1.00×10^{-8}), ERC1 on 12p13.33 (4.64, 6.08×10^{-9}), LMAN1L (near CYP1A1) on 15q24.1 (4.25, 8.71×10^{-9}) for lung squamous cell cancer were identified at a genome-wide significance level. Our GWAS of lung cancer identified five novel genetic susceptibility associations and confirmed several variants on 15q25 and 19q13. Further works are required to elucidate the possible biological mechanisms underlying these associations among lung cancer and histological subtypes in African Americans.

#5219

Telomere length distribution, metabolic trait association, and genome-wide association study among Singaporean cohorts

Trang Nguyen[1], Penny Chan[2], Ives Lim[3], Brian Kennedy[4], Neerja Karnani[2], Rajkumar Dorajoo[5], Joanne Ngeow[1]. *[1]Nanyang Technological University Singapore, Singapore, Singapore,[2]Singapore Institute for Clinical Sciences, Singapore, Singapore,[3]Bioinformatics Institute, Singapore, Singapore,[4]National University of Singapore, Singapore, Singapore,[5]Genome Institute of Singapore, Singapore, Singapore*

Leukocyte telomere length (LTL) is known as a heritable marker of cellular aging and is a risk factor for several chronic diseases. LTL distribution and association studies are essential in providing insights into telomere homeostasis, its relationship with different metabolic traits, and age-related conditions. Such studies have been underperformed in Asian population groups. Here we estimated LTL using whole-genome sequencing data in 8,045 Singaporean samples across three major ethnic groups - Chinese, Indian, and Malay divided into six cohorts: GUSTO, HELIOS, MEC, PRISM, SEED, and TTSH. LTLs were measured using TelSeq, with normalized LTL as

phenotype in subsequent analyses. We demonstrated that average LTL was robustly longer in the childhood cohort (GUSTO) compared to the adult cohorts ($P<1.19\times10^{-195}$). We observed ethnicity differences in LTL where adult Singaporean Chinese samples had the longest LTL (5.08kb) as compared to Malay (4.87kb) and Indian (4.65kb) samples in our datasets ($P<4.98\times10^{-12}$). Our genetic association analyses replicated multiple variants previously reported to be associated with LTL (binomial $P<0.00001$) in Asian population groups, providing added confidence in the methodologies used. At the same time, we identified a novel East-Asian-specific novel variant beyond genome-wide association levels (meta $P=2.05\times10^{-08}$) at the *COL28A1/MIOS* gene loci to be associated with LTL in our study. Individual analysis of the GUSTO childhood dataset highlighted a second novel genome-wide hit at *RAD17* gene locus to be associated with LTL in our study and indicated that the previously reported variant at the *TINF2* locus may have significantly opposing effects (compared to adults) during early developmental stages. Gene-level burden analysis for rare variants (MAF <5%) in adult Chinese cohorts revealed potential cancer association with *RET* gene (SKAT, $P=5.22\times10^{-03}$) and *MLH1* gene (SKAT, P=0.037), as well as telomere biology condition association with *RECQL4* gene (CMC, P=0.0399, and VT, P=0.0379). Our findings have broadened the understanding of LTL distribution and the underlying associated genetic characteristics in both childhood and adult Singaporean populations.

#5220

Prediagnostic vitamin D status and colorectal cancer survival by vitamin D-binding protein isoforms in the US cohorts

Hanseul Kim[1], Chen Yuan[2], Long H. Nguyen[3], Kimmie Ng[2], Edward L. Giovannucci[4].
[1]Massachusetts General Hospital and Harvard Medical School, Boston, MA,[2]Dana-Farber Cancer Institute and Harvard Medical School, Boston, MA,[3]Division of Gastroenterology, Massachusetts General Hospital and Harvard Medical School, Boston, MA,[4]Department of Nutrition, Harvard T.H. Chan School of Public Health, Boston, MA

Background: Lower levels of 25-hydroxyvitamin D [25(OH)D], a major form of circulating vitamin D, have consistently been associated with higher mortality among colorectal cancer (CRC) patients, though the dose-response relation is not well characterized {Ng 2008; Fedirko 2012; Wesa 2015; Zgaga 2014}. A study showed a strong effect modification (*P* for interaction = 0.0002) {Gibbs 2020} by Gc2 (or, vitamin D-binding protein) isoform where patients with the isoform had significantly higher mortality if they had deficient vitamin D levels. However, it is unknown whether this association differs by Gc isoforms in other populations.
Methods: We examined the association between prediagnostic 25(OH)D levels and overall and CRC-specific mortality among CRC patients within the two ongoing prospective US cohorts: Nurses' Health Study and Health Professionals Follow-Up Study. Cox proportional hazards regression model was used to estimate the hazard ratios (HRs) and 95% confidence intervals (CIs). We evaluated potential nonlinear association using the restricted cubic splines and assessed effect modification by Gc2 isoform with stratified analyses. Individuals with the Gc rs4588 CC, CA and AA genotypes were classified as having Gc1-1, Gc1-2, and Gc2-2 isoforms, respectively. Participants with a minor allele at Gc rs4588 (rs4588*CA or rs4588*AA genotypes) were defined as having the Gc2 isoform.
Results: A total of 588 patients were observed until the date of death or last follow-up in 2018, whichever came first. Deficient versus sufficient 25(OH)D concentrations (<30 vs ≥50 nmol/L) were associated with higher overall mortality (HR, 2.06; 95% CI, 1.34-3.18) and suggestively with higher CRC-specific mortality (HR, 1.51; 95% CI, 0.75-3.07). Spline results showed that the potential beneficial role of vitamin D plateaued around 50 nmol/L (*P* for nonlinearity = 0.04). The

HRs for overall mortality comparing deficient versus sufficient concentrations were 2.43 (95% CI, 1.26-4.70) for patients with Gc1-1 isoform (rs4588 CC) and 1.63 (95% CI, 0.88-3.02) for patients with Gc1-2 or Gc2-2 (rs4588 CA or AA) isoforms (*P* for interaction = 0.54). The HRs for CRC-specific mortality were 1.18 (95% CI, 0.27-5.14) for patients with Gc1-1 isoform and 1.41 (95% CI, 0.62-3.24) for patients with Gc1-2 or Gc2-2 isoforms (*P* for interaction = 0.94).
Conclusions: We found that lower 25(OH)D levels up to 50 nmol/L were associated with higher overall mortality, but this association did not differ by Gc isoforms in the two US cohorts.

#5221

Identifying acute lymphoblastic leukemia risk loci in latino children via admixture mapping

Jalen Langie[1], Soyoung Jeon[1], Xiaomei Ma[2], Catherine Metayer[3], Adam J. de Smith[1], Joseph L. Wiemels[1], Charleston W. K. Chiang[1]. *[1]Department of Population and Public Health Sciences, University of Southern California, Los Angeles, CA,[2]Department of Chronic Disease Epidemiology, Yale University, New Haven, CT,[3]School of Public Health, University of California Berkeley, Berkeley, CA*

Acute lymphoblastic leukemia (ALL) is the most common childhood cancer and accounts for 25% of malignancies before the age of 20. Despite decades of inquiry into ALL causes, Latino children have up to 1.4 times the rate of ALL compared to their non-Latino White counterparts. The etiology of ALL is complex and this disparity in risk has not been fully explained by social factors alone, suggesting the role of genetic variants and ancestry. Previous literature has implicated variants in *IKZF1, ARID5B, GATA3*, *PIP42KA*, and *ERG* with greater risk allele frequencies or population-specific risk effects in Latinos. Indigenous American ancestry has also been previously associated with ALL risk, relapse, and poor prognosis. To elucidate the genetic and ancestral etiology of ALL, we conducted the first admixture mapping analysis of 1930 childhood ALL cases and 8520 controls of self-identified Latino ethnicity. We uncovered putative admixture associations on chromosomes 2, 7, 10, and 15 ($P = 3.21 \times 10^{-5}$ to 7.32×10^{-8} among top associations across the four loci). Two of the four loci, on chromosomes 2 and 15, were previously not known to be associated with ALL. Following imputation with the TOPMed reference panel, we fine-mapped each putative locus by testing the ALL risk association of each variant with a minor allele frequency greater than 1%. The top associated variants at each locus showed substantial frequency differences between ancestries from the gnomAD or 1000Genomes project. For example, the top associated variant on chromosome 2 has a risk allele frequency of 43% in Native Americans from the Human Genome Diversity Panel, but a frequency of 0.10% in Non-Finnish Europeans in gnomAD. Including these variants in the admixture mapping model greatly attenuated the admixture signals at each locus, suggesting that they are likely the causal SNPs or close proxies of the causal SNPs. The top associated variants from three out of the four loci passed regional multiple testing burden and mapped to genes MGAT5, *IKFZ1* and *ARID5B* on chromosomes 2, 7 and 10, respectively. The top two SNPs on chromosome 15, which narrowly missed the regional threshold, mapped to genes RAB11A and MEGF11. We are pursuing replication of putative novel loci on chromosomes 2 and 15 in additional Latino GWAS datasets. Our results suggest that ALL risk variants with higher frequencies in individuals with Native American ancestry may contribute to the observed increased risk of ALL in Latino children. Investigation of such risk loci can contribute to the identification of new target genes for ALL prediction and therapeutics and new insights for precision medicine, which will reduce the burden of ALL.

#5222

Genetic variants associated with progression from monoclonal B-cell lymphocytosis (MBL) to chronic lymphocytic leukemia (CLL)

Raphael Mwangi[1], Geffen Kleinstern[2], Sara J. Achenbach[1], Dennis Robinson[1], Aaron D. Norman[3], Kari G. Rabe[1], Janet E. Olson[3], Neil E. Kay[4], Rosalie G. Waller[5], Nicholas J. Boddicker[5], James R. Cerhan[3], Esteban Braggio[4], Sameer A. Parikh[4], Curtis A. Hanson[6], Celine M. Vachon[3], Tait Shanafelt[7], Susan L. Slager[5]. *[1]Division of Clinical Trials and Biostatistics, Mayo Clinic, Rochester, MN,[2]School of Public Health, University of Haifa, Haifa, Israel,[3]Division of Epidemiology, Mayo Clinic, Rochester, MN,[4]Division of Hematology, Mayo Clinic, Rochester, MN,[5]Division of Computational Biology, Mayo Clinic, Rochester, MN,[6]Department of Laboratory Medicine and Pathology, Mayo Clinic, Rochester, MN,[7]Department of Medicine, Division of Hematology, Stanford University, Stanford, CA*

Low count (LC) MBL is characterized by a circulating population of clonal B-cells and is a precursor state to CLL. Most individuals with LC MBL do not progress to CLL and never come to clinical attention. An active area of research is to identify factors that distinguish those individuals with MBL who progress from those who do not. Currently, 41 single nucleotide polymorphisms (SNPs) are known to be associated with CLL risk, and a portion of these SNPs have also been found to be associated with MBL risk. We hypothesize that these CLL-susceptibility SNPs associated with both MBL and CLL risk are SNPs associated with developing a B-cell clone; whereas the remaining SNPs found not to be associated with MBL risk are associated with progression of the B-cell clone (i.e., progression from MBL to CLL). To test this hypothesis, we evaluated the association of these 41 SNPs with risk of progression to CLL using a case-control study of 1,911 CLL cases and 1,579 individuals with MBL from Mayo Clinic.

Individuals with MBL were identified through screening using 8-color flow cytometry assay. Individuals with LC MBL (defined by having a clonal B-cell population with the percent clonal B-cells out of total B-cell count <85%) who had an immunophenotype consistent with CLL were included as controls. CLL cases were obtained through the Mayo Clinic hematology practice. DNA was genotyped from whole blood. We analyzed the 41 CLL susceptibility SNPs with risk of progression to CLL using logistic regression and estimated odds ratio (OR) and 95% confidence interval (CI), adjusting for sex and age. We evaluated the CLL polygenic risk score (CLL-PRS), comprised of a weighted average of the 41 SNPs, with risk of CLL.

Out of the 41 established CLL susceptibility SNPs, 15 were associated with CLL progression from MBL to CLL (all P<0.05). Nine of these 15 significant SNPs were not previously found to be associated with risk of MBL. The most significant SNPs were rs9880772 (OR=1.23, CI: 1.11-1.36, $P=6.1x10^{-5}$), rs888096 (OR=1.25, CI: 1.12-1.38, $P=3.0x10^{-5}$), and rs305065 (OR=1.28, CI: 1.14-1.43, $P=1.5x10^{-5}$). One SNP (rs77551289) had a suggestive association (OR=1.21, P=0.069). The remaining 25 SNPs had no evidence of association with progression (ORs ranging between 0.9-1.1 and all P>0.1). The CLL-PRS was also associated with CLL risk (continuous OR = 1.25, CI: 1.15 - 1.35, $P = 6.7 X 10^{-8}$).

In our study accounting for the presence of B-cell clonal population, we identified 15 out of 41 CLL-susceptibility SNPs to be significantly associated with progression from LC MBL to CLL. The remaining 25 non-significant CLL-SNPs were not associated with progression and may instead be associated with development or initiation of the B-cell clone. These findings suggest that the established CLL susceptibility SNPs may play differing role (i.e., development or progression of the clone) in the etiology of CLL.

#5223

Circulating lipoprotein lipids and colorectal cancer risk: A Mendelian randomization analysis from the GECCO consortium

Lili Liu[1], Wanqing Wen[1], Jirong Long[1], Themistocles L Assimes[2], Luis Bujanda[3], Stephen B Gruber[4], Sébastien Küry[5], Brigid Lynch[6], Conghui Qu[7], Minta Thomas[7], Emily White[7], Michael O. Woods[8], Ulrike Peters[7], Wei Zheng[1]. *[1]Vanderbilt University, Nashville, TN,[2]VA Palo Alto Health Care System, Palo Alto, CA,[3]Universidad del País Vasco, San Sebastian, Spain,[4]City of Hope National Medical Center, Duarte, CA,[5]Centre Hospitalier Universitaire (CHU) Nantes, Nantes, France,[6]Cancer Council Victoria, Melbourne, Australia,[7]Fred Hutchinson Cancer Research Center, Seattle, WA,[8]Memorial University of Newfoundland, St. John's, NH, Canada*

Background Conventional observational studies have reported conflicting results regarding the association between low density lipoprotein cholesterol (LDL-C) and risk of colorectal cancer (CRC). We conducted a Mendelian randomization analysis to address this association.
Methods Single-nucleotide polymorphisms (SNPs) associated with five blood lipids (total cholesterol, HDL-C, high-density lipoprotein cholesterol [HDL-C], non-HDL-C, and triglyceride) were obtained from a genome-wide association study (GWAS) meta-analysis of European ancestry in the Global Lipids Genetics Consortium (GLGC, N ≤ 1 319 982), and two lipids (apolipoprotein A1 and apolipoprotein B) from a GWAS in the UK Biobank (UKB, N ≤ 441 016). Summary statistics were obtained for these SNPs from a GWAS of CRC in the Genetics and Epidemiology of Colorectal Cancer Consortium (GECCO) including 34,869 cases and 29,051 controls. Associations with CRC risk per one standard deviation increase in the genetically predicted lipids level were generated using inverse-variance weighted random-effects models.
Results No overall association was observed between genetically predicted levels of blood lipids and CRC risk. However, increased risks were observed for all LDL-C related traits among women, including total cholesterol (OR = 1.10; 95%CI = 1.02, 1.18), LDL-C (1.07; 1.00, 1.14), non-HDL-C (1.09; 1.02, 1.16), and apolipoprotein B (1.11; 1.02, 1.21); whereas no significant association was found among men. Similar but ostensibly stronger associations of these traits were seen with distal colon cancer cases, with no significant association showing on proximal colon or rectum cancer cases. We also observed similar positive associations of LDL-C related traits among those having CRC before their 50 years. Of note, risk reduction was found for apolipoprotein A1, a major component of HDL-C, in these early-onset cases (0.87; 0.78, 0.98).
Conclusion Results from this study suggest that high circulating LDL-C levels may increase the risk of CRC, particularly cancer of the distal colon, and the association may differ by sex and age at CRC onset.
Key words: Blood lipids; colorectal cancer; Mendelian randomization.

#5224

Genome-wide interaction study of smoking and bladder cancer risk: results from the COBLAnCE cohort

Maryam Karimi[1], Sebastian Mendez-Pineda[2], Hélène Blanché[3], Anne Boland[4], Jean-François Deleuze[4], Xiang-Yu Meng[5], Karine Groussard[2], Thierry Lebret[6], Julia Bonastre[1], Yves Allory[7], François Radvanyi[8], Simone Benhamou[2], Stefan Michiels[1]. *[1]Bureau de Biostatistique et d'Epidémiologie (BBE), Gustave Roussy, Villejuif, France,[2]Oncostat U1018, INSERM, Villejuif, France,[3]Biological Resources Center, CEPH-Fondation Jean Dausset, Paris, France,[4]Centre National de Recherche en Génomique Humaine, Evry, France,[5]Curie Institute, Paris, France,[6]Urology, Foch Hospital, Suresnes, France,[7]Department of Pathology, Curie Institute, Saint-Cloud, France,[8]CNRS UMR444, Curie Institute, Paris, France*

Introduction: Bladder Cancer (BC) is the 6th most common cancer and the 9th leading cause of cancer death among men worldwide. Tobacco smoking is the main risk factor for BC. Accumulating evidence has found that genetic variants are also associated with the risk of BC. More insights into the biological mechanism of the disease have been gained through candidate gene-environment interaction studies, with the most known examples of the interactions between cigarette smoking and NAT2 and GSTM1 gene variants. Our objective was to perform a genome-wide association case-only study using the French national prospective COBLAnCE cohort (COhort to study BLAdder CancEr), while focusing on three important smoking behavior characteristics.
Materials and Methods: The COBLAnCE cohort comprises 1,800 BC patients included within 14 centers in France between 2012 and 2018. Peripheral blood samples and complete history of tobacco smoking were collected at enrollment and genotyping was performed using the Illumina Global Screening Array with a Multi-Disease drop-in panel. After the quality control and imputation, 9,719,614 Single Nucleotide Polymorphisms (SNPs) were investigated. Genotyping data of 1,674 , 1,283 and 1,342 patients were analyzed for smoking status, average tobacco consumption and age at smoking initiation, respectively. Genome-wide association study (GWAS) was conducted using logistic (for smoking status) and linear (for age at smoking initiation and average tobacco consumption, both log-transformed) regression models with each of the imputed SNPs as the independent variable adjusting for gender, age and first ten genetic principal components.
Results: For smoking status, none of the SNPs reached the GWAS significant threshold of 5e-08, but results are suggesting tentative loci at 1p31.3 (rs114073636: OR [95%CI] = 0.31 [0.20-0.47], p = 8.68e-08; rs116571608: OR = 0.31 [0.20-0.47], p = 8.87e-08) and 4q22.1 (rs542541627: OR = 1.69 [1.39-2.06], p = 1.81e-07; rs1533294: OR = 1.63 [1.34-1.98], p = 1.01e-06). Analyses of age at smoking initiation revealed three significant SNPs: rs531756449, rs77186197 and rs78947799 with positive interaction associations (β (SE) = 0.3 (0.05), p = 8.26e-09; β = 0.29 (0.05), p = 3.74e-09; β = 0.31 (0.06), p = 3.97e-08, respectively). Only one SNP at 11q24.1, reached the significant threshold for the average tobacco consumption analyses: rs2714069 (β = 0.63 (0.11), p = 1.35e-08). The locus 16p13.3 seems to have protective variants for the interaction with average tobacco consumption: rs113683380 (β = -0.66 (0.12), p = 6.44e-08) and rs113590624 (β = -0.64 (0.12), p = 2.74e-07).
Conclusion: Our study suggests new candidate loci interacting with smoking behavior for the risk of BC. Based on a case-only approach, our results need to be validated in a case-control or cohort study. A large-scale meta-analysis GWAS would be needed to identify SNPs with small Minor Allele Frequencies.

#5225

Expression- and splicing-based multi-tissue transcriptome-wide association studies identified multiple genes for estrogen receptor-negative breast cancer

James L. Li, Julian C. McClellan, Guimin Gao, Dezheng Huo. *University of Chicago, Chicago, IL*

Although several transcriptome-wide association studies (TWAS) have been performed to identify genes associated with overall breast cancer risk, few genes were found to be associated with estrogen receptor-negative (ER-) breast cancer. These studies were based on gene expression prediction models trained mainly in breast tissue, and they did not account for alternative splicing of genes. In this study, we utilized two approaches to perform multi-tissue TWASs of ER- breast cancer: 1) an expression-based TWAS that combined TWAS signals for each gene across multiple

tissues and 2) a splicing-based TWAS that combined TWAS signals of all excised introns for each gene across tissues. To perform these two TWASs, we first obtained gene expression prediction models that were trained in 11 tissues from the Genotype-Tissue Expression including breast, ovary, uterus, vagina, EBV-transformed lymphocytes, whole blood, spleen, liver, subcutaneous adipose, visceral adipose, and cell-cultured fibroblasts. Furthermore, we obtained GWAS summary statistics for ER- breast cancer by performing a meta-analysis of 21,468 ER- cases and 105,974 controls from the Breast Cancer Association Consortium and 9414 BRCA1 mutation carriers who were breast cancer cases and 9494 BRCA1 mutation carriers who did not have breast cancer from the Consortium of Investigators of Modifiers of BRCA1 and BRCA2. For our expression-based TWAS, we utilized the Aggregated Cauchy Association Test (ACAT) to collate TWAS signals across all 11 tissues for each gene using equal weights for each tissue, while for our splicing-based TWAS, we utilized ACAT to collate TWAS signals for all excised introns in all tissues for each gene. Overall, we identified 63 genes in 29 loci that were significantly associated with ER- breast cancer, including 23 genes that were identified using both approaches, 27 that were uniquely identified in the expression-based TWAS, and 13 that were uniquely identified in the splicing-based TWAS. Of the 63 genes, 50 genes have not been previously reported in TWAS studies of breast cancer. Using a weighted ACAT method, in which breast tissue was given a 5-fold higher weight, we obtained similar results. In summary, our joint, multi-tissue TWAS corroborated previous GWAS loci for both ER- and overall breast cancer while highlighting how incorporating TWAS signals from multiple tissues and alternative splicing allowed us to discover new susceptibility genes for ER- breast cancer.

#5226

Exome-wide association study identifies coding variant in IL17RA associated with survival in cancer patients treated with immunotherapy

Sam O. Kleeman, Michael Chan, Matthew Chvasta, Tobias Janowitz. *Cold Spring Harbor Laboratory, Cold Spring Harbor, NY*

Immune checkpoint inhibitors (ICI) targeting PD-1/PD-L1 and CTLA4 are effective treatments in multiple cancer types, but durable responses are seen only in a minority of patients. Resistance to ICI is likely to reflect a combination of tumor-intrinsic, such as tumor mutational burden, and tumor-extrinsic factors, such as systemic immune suppression and host genetics. With the advent of large-scale germline genotyping studies, there is emerging evidence that host-specific genetic factors can substantially modify both disease risk and responsiveness to therapy. There has been limited characterization to date of the interaction between host genetics and response to ICI. Here, we perform harmonized mutation calling in available normal exome sequencing from 668 metastatic cancer patients treated with ICI (derived from n=7 studies, spanning n=3 cancer types and PD-1/PD-L1/CTLA4-directed therapy) and performed exome-wide association studies in European ancestry patients. For each cancer type (melanoma, renal cell carcinoma, urothelial carcinoma), we conducted exome-wide Cox regression (with PC1-4 and sex as covariates) to identify coding single-nucleotide polymorphisms (SNPs) associated with overall survival (OS). On fixed-effect meta-analysis, we identified a single coding variant (rs140221307, C allele, MAF 0.5% in European populations) that met genome-wide significance ($p=1.11x10^{-15}$, HR=4.86, 95% CI 3.30-7.15). This SNP causes a substitution of Trp to Arg at amino acid 320 at the interface between the transmembrane and extracellular domains of interleukin 17 receptor A (IL17RA). While the secretion mechanism is uncharacterized, soluble IL17RA can be readily detected in plasma and the survival-reducing variant is associated with substantially elevated plasma IL17RA ($p=1.90x10^{-9}$, beta=1.01, Sun et al. 2018) as well as reduced monocyte counts in UK Biobank

($p=2.20x10^{-308}$, beta=-0.60). We have established a prime editing strategy to induce this variant in cultured human monocytes to investigate its biochemical and functional consequences, and are performing validation studies in independent patient cohorts. Soluble IL17RA would be expected to function as a decoy receptor to antagonize IL17/IL17RA signaling, and so these data suggest that activation of IL-17 receptor signaling might improve responsiveness to ICI therapy.

#5227

Cross-trait genome-wide association meta-analyses of clonal hematopoiesis and solid tumor risk

Victoria Gray[1], George Richenberg[1], Pedro Quirós[2], Matthew Freedman[3], Paul Pharoah[4], Simon Gayther[4], Michelle Jones[4], George Vassiliou[5], Kate Lawrenson[4], Siddhartha Kar[1]. *[1]University of Bristol, Bristol, United Kingdom,[2]Instituto de Investigación Sanitaria del Principado de Asturias, Oviedo, Spain,[3]Dana-Farber Cancer Institute, Boston, MA,[4]Cedars-Sinai Medical Center, Los Angeles, CA,[5]University of Cambridge, Cambridge, United Kingdom*

Clonal hematopoiesis (CH) is an age-related phenomenon where hematopoietic stem cells and their progeny acquire specific somatic mutations in a small, well-defined set of leukemogenic genes conferring them with fitness advantage leading to clonal proliferation. Mosaic chromosomal alterations (mCAs) are somatic structural variants that are manifestations of genomic instability and a sign of CH when they occur in blood. The recent availability of large-scale cohorts with blood exome sequence and genotype data has powered genome-wide association studies (GWAS) investigating the germline genetic contribution to CH and mCA risk. However, phenotypes of somatic mutation acquisition in driver genes, clonal selection and expansion, and chromosomal mosaicism are processes that are not confined to blood and contribute to neoplastic transformation across tissue types. GWAS of solid tumor susceptibility have so far identified hundreds of germline variants associated with cancer risk and it is likely that a subset of these variants contributes to solid tumor risk by affecting these somatic phenotypes in the corresponding tissues of origin and that some of the variants exert these somatic effects across tissues. We aimed to identify this subset of solid tumor risk variants by undertaking fixed effects inverse-variance weighted meta-analyses combining breast, prostate, ovarian, and endometrial cancer GWAS (total n = 237,483 cases/317,006 controls; no UK Biobank samples included) with UK Biobank-based CH (10,203 “cases”/173,918 controls) and mCA (66,011 “cases”/378,188 controls) risk GWAS in pairs where each pair involved one solid tumor type and one of either CH or mCA (for example, breast cancer and mCA constituted a pair). These analyses collectively identified 61 independent (r^2<0.05) lead variants at combined cross-trait genome-wide significance ($P<5x10^{-8}$) across 22 genomic loci where each lead variant was associated with each trait individually at $P<10^{-3}$, had the same direction of allelic effect across traits, and little evidence of heterogeneity in effect (I^2<40%). New loci (>1 Mb away from previously reported risk loci for a given trait) counts were: 14 new loci in the context of mCA risk, 6 new loci for CH risk, 2 for breast cancer risk, and one each for prostate, ovarian, and endometrial cancer risks. *In silico* functional annotation of these loci suggested lead variant-target genes that could be assigned to the discrete pathways of mitotic spindle assembly (*INCENP*, *CENPN*, *ZWILCH*, *MAD1L1*), p53 signaling (*TP53*, *MDM4*, *SPI1*), DNA damage repair (*ATM*, *RAD51C*, *CHEK2*, *USP28*, *PARP8*), and myeloid oncogenesis (*WT1*, *HOXA9*, *L3MBTL3*). Our novel approach combining the latest and largest blood somatic genomic trait GWAS with large-scale solid tumor risk GWAS thus yielded clear mechanistic insights into the shared inherited genetic basis of solid tumor risk and somatic genomic traits.

#5228

Genome-wide association study and LD score regression analysis for cholangiocarcinoma

Younghun Han[1], Katherine A. McGlynn[2], Jinyoung Byun[1], Matthew A. Cooley[3], Manal M. Hassan[4], Christopher I. Amos[1], Lewis R. Roberts[3], The International Consortium for the Genetics of Biliary Tract Cancers. *[1]Baylor College of Medicine, Houston, TX,[2]National Cancer Institute, Rockville, MD,[3]Mayo Clinic, Rochester, MN,[4]The University of Texas MD Anderson Cancer Center, Houston, TX*

Cholangiocarcinoma (CCA) is a rare and aggressive cancer of the bile ducts, with a poor prognosis and limited treatment options. CCA are classified as intrahepatic and extrahepatic based on anatomical location. CCA are often diagnosed at an advanced stage because there are no effective tools for early detection. Although genome-wide association studies (GWASs) have discovered many genome-wide significant contributing risk loci, the genetic underpinning of cholangiocarcinoma remains poorly understood. To date, there is no cholangiocarcinoma-specific GWAS. We conducted GWAS of cholangiocarcinoma in 9,648 individuals of European ancestry using TOPMed reference panel. The putative associations in or near THSD7A on chromosome 7 (OR=2.61, $P=7.13\times10^{-8}$), ZBTB16 on 11 (OR=0.16, $P=6.02\times10^{-8}$) for non-PSC-related CCA, PUM3 on 9 (OR=10.74, $P=6.12\times10^{-8}$), AGBL1 on 15 (OR=2.08, $P=5.67\times10^{-8}$) for PSC-related CCA, and LINC02506 on 4 (OR=0.16, $P=8.83\times10^{-9}$) for extrahepatic CCA. We also implemented linkage disequilibrium score regression (LDSR) analysis to quantify the genetic correlation between phenotypes using publicly available GWAS summary statistics. Our study aimed to identify possible clinical and epidemiological traits associated with CCA. We identified numerous biomarkers, medical conditions, environmental and behavioral traits, and physical measurements showing high heritability, which is the proportion of phenotypic variance explained by all SNPs included in the analysis, and pairwise genetic correlation with CCA and other CCA subtypes. Elevations of selected biomarkers such as alkaline phosphatase, cystatin C, HbA1c, monocyte count, and white blood cell count show a positive genetic association with CCA in European-ancestry population. Also, autoimmune-mediated conditions show a strong positive genetic association with CCA, non-PSC related CCA, and intrahepatic CCA. The GWAS of CCA and CCA subtypes revealed potential genetic susceptibility associations and will allow us to compare the genetic architecture underlying CCA and other diseases of the bile ducts such as primary sclerosing cholangitis and liver cancer. LDSR provided an improved understanding of the genetic architecture between CCA and potential comorbid conditions and biomarkers. Mendelian randomization analysis will be needed to elucidate the causal relationship between CCA and traits of interest.

#5229

Pathogenic germline mutations and risk of multiple myeloma

Michael T. Conry[1], Nicola Camp[2], Celine Vachon[3], Michelle Hildebrandt[4], Elizabeth E. Brown[5], Steven M. Lipkin[6], Judy Garber[7], Susan L. Slager[8], Samantha Stokes[7], Aaron D. Norman[9], Aalin Izhar[1], Sita Dandiker[1], Kylee Maclachlan[1], Kenneth Offit[1], Saad Usmani[1], Vijai Joseph[1]. *[1]Memorial Sloan Kettering Cancer Center, New York, NY,[2]Huntsman Cancer Institute, University of Utah, Salt Lake City, UT,[3]Department of Health Sciences Research, Mayo Clinic, Rochester, MN,[4]Department of Lymphoma/Myeloma, MD Anderson Cancer Center, Houston, TX,[5]Department of Pathology, Heersink School of Medicine, University of Alabama at Birmingham, Birmingham, AL,[6]Department of Medicine, Weill Cornell Medical College, New York, NY,[7]Department of Medical Oncology, Dana Farber Cancer Institute, Boston, MA,[8]Department of Quantitative Health Sciences, Mayo Clinic, Rochester, MN,[9]Mayo Clinic, Rochester, MN*

BACKGROUND: Multiple Myeloma (MM) is an incurable disease with no known germline high penetrant risk gene. The higher risk of MM among affected relatives suggests a genetic contribution to the etiology. To date, 24 common risk variants with low effect sizes were identified using genome-wide association studies, which account for 17% of heritability. However, a systematic analysis of the known rare alleles in cancer predisposition genes has not been undertaken so far in MM. We collaborated with six other academic centers across the United States to identify and select cases for analysis of germline predisposition of MM.
METHODS: We performed whole exome, next-generation sequencing of 2,387 familial or early onset germline MM cases from the myeloma sequencing consortium (MMSEQ). We called 1.5 million variants and performed standard quality control of the data. We also obtained exome data on 1,285 cases from UK Biobank (UKBB) and 344,513 non-cancer controls (total=3,672 cases). We analyzed the ultra-rare, coding variants in 90 clinically relevant or putative candidates for cancer predisposition. We then used the automated variant curator PathoMAN to annotate and assert pathogenicity of each variant. We contrasted our results with assertions of pathogenicity from ClinVar and tested for gene association with MM.
RESULTS: Overall, we observed several pathogenic or likely pathogenic variants, both singleton and recurrent founder mutations. In the MMSEQ, 8.7% of MM cases harbored a pathogenic variant in these known/putative cancer predisposition genes. Predominant group of pathogenic variants were observed within CHEK2 (19%), TP53 (8%), and ATM (5%). A case-control analysis revealed strong association with TP53 and weakly with ATM. In the familial/early onset MMSEQ cases, TP53 mutations were enriched 68 times more than in the UKBB controls. Our

preliminary results suggest that known genes of cancer susceptibility such as TP53 and ATM may also play a role in myeloma risk.
CONCLUSION: In a large study of multi-center MM cases, we identified a significant proportion of individuals who are carriers of known (solid) cancer predisposition genes. This study suggests that these known cancer predisposition genes may be relevant in a subset of MM cases.

#5230

Comprehensive genetic analysis using clinical specimens of gastric adenocarcinoma and proximal polyposis of stomach

Chihiro Matsumoto[1], Masaaki Iwatsuki[1], Koshi Mimori[2], Hideo Baba[1]. *[1]Department of Gastroenterological Surgery, Graduate School of Medical Sciences, Kumamoto University, Kumamoto, Japan,[2]Department of Surgery, Kyusyu University Beppu Hospital, Oita, Japan*

Background and Purpose: Gastric adenocarcinoma and proximal polyposis (GAPPS) is an autosomal dominant genetic disorder that causes gastric carcinoma from fundus gland polyposis. Although germline mutation of APC promoter 1B was reported as a pathogenic variant in 2016, there are still many unknowns about the carcinogenesis. In this study, we performed a comprehensive Next generation sequencing (NGS) analysis of GAPPS clinical specimens to investigate the molecular profile characteristic of carcinogenesis.
Patients and Methods: Seven cases from three GAPPS families experienced in our department were included in this study. In each case, tissues were collected from normal mucosa, polyps, and carcinoma,
and FFPE and fresh-frozen samples were prepared. After pathological diagnosis was performed on each sample, RNA and DNA were extracted and analyzed based on data obtained by next generation sequence (NGS).
Results: In the RNA sequence, gene expression analysis was performed on 45 pathologically diagnosed samples, which were classified into four clusters by K-means clustering. Gene Set Enrichment Analysis (GSEA) of the four clusters showed that cancer-related genes such as p53 and KRAS were significantly enriched in the cluster of cancer, and genes related to immune response were significantly enriched in the cluster of cancer compared to the and clusters of polyp and normal. Gene mutation analysis using whole-exome sequence (read depth/coverage>20) confirmed mutation of APC promoter 1B in all samples. On the other hand, in tumor samples (N=10), the percentage of mutation of genes previously suggested to be associated with GAPPS (TP53, FBXW7, GNAS, and KRAS) were 50%, 0%, 30%, and 60%, respectively.
Conclusion: Comprehensive gene expression analysis by RNA sequence and whole-exome sequence was performed using clinical samples of GAPPS. In the future, we plan to identify specific gene-pathways involved in carcinogenesis.
(2460/2600 characters)

#5231

Whole genome sequencing reveals significant genetic admixture in multiple myeloma patients, impacting assessment of etiology

Kylee H. Maclachlan[1], Patrick Blaney[2], Dylan Gagler[2], Eileen M. Boyle[2], Benjamin Diamond[3], Urvi A. Shah[1], Neha Korde[1], Sham Mailankody[1], Malin Hultcrantz[1], Hani Hassoun[1], Carlyn Tan[1], Faith E. Davies[2], Alexander M. Lesokhin[1], C. Ola Landgren[3], Saad Z. Usmani[1], Francesco Maura[3], Gareth J. Morgan[2]. *[1]Memorial Sloan Kettering Cancer Center, New York, NY,[2]New York University Langone Health, New York, NY,[3]Sylvester Comprehensive Cancer Center, Miami, FL*

Background: In the U.S. population, having African ancestry (AA) conveys a higher risk of multiple myeloma (MM) than white ancestry (WA), however, published whole genome sequencing (WGS) data is predominantly from WA populations. The Polyethnic-1000 (P1000) is a multi-institutional WGS initiative together with the New York Genome Center, investigating cancers having a higher prevalence in AA populations. We are extending on the P1000 in MM precursor disease; prospectively defining genomic, immune and microbiome factors driving progression, focused on the impact of racial origin.
Hypothesis: Self-described race, according to proscribed categories, is insufficient to delineate biological contribution to MM development. We propose that unique biological insights first require a comprehensive definition of genetic origin, considering heterogeneity within historical groups.
Methods: For collaborative large-scale analysis, we've developed a comprehensive cross-institutional bioinformatic pipeline (https://github.com/pblaney/mgp1000). We've included admixture; a composition profile

based on SNPs with genotypes corresponding to reference samples from 23 geographic populations. AA is divided into 5 populations (Esan, Luhya, Mende, Gambian and Yoruba), and 3 American populations are defined (Peruvian, Columbian and Puerto Rican). WGS was performed on blood mononuclear cells from 44 patients with MM or precursor disease, 29 self-identified as AA and 18 as Hispanic.
Results: Estimating directly from WGS data, complexity hidden by self-reported race was revealed by genetically determined admixture. Filtering to ≥1%, 43/44 patients had contribution from >1 of the 23 reference populations. Patients varied widely in their genetic diversity; 3 had ≥90% from a single population, 21 had ≥25% from at least 2 populations (consistent with grandparents) and 37 had ≥12.5% from different populations (consistent with great-grandparents). Within those 37, 18 patients had contributing populations within the same superfamily (i.e., all African), while 19 were across superfamily's (i.e., African + East Asian). Hierarchical clustering produced 5 main clusters, with samples in 2 clusters having predominantly Esan and Mende contribution, while differing in contribution from other AA / non-AA populations. All samples in one cluster contained American contribution >60%, another had predominantly European and American contribution, and the final cluster had AA <10%, and heterogenous population contributions.
Conclusion: Self-reported race does not consider the significant variability of genetic admixture demonstrated by this analysis, and likely has insufficient granularity regarding inherited risk. Ongoing studies will incorporate genetic admixture alongside somatic genomic assessment to accurately investigate progression risk from precursor disease to MM.

#5232
Differential expression of stress-survival pathway genes related to Hispanic colorectal cancer disparities
Urbashi Basnet[1], Aditi Kulkarni[1], Frances A. Rangel[1], Abhijeet R. Patil[1], Sourav Roy[2]. *[1]The University of Texas at El Paso, El Paso, TX,[2]Biological Sciences, The University of Texas at El Paso, El Paso, TX*

Colorectal cancer (CRC) is one of the most life-threatening gastrointestinal cancers, with around 1.9 million new cases and 935,000 deaths in the year 2020 worldwide. It accounts for 12% and 8% of all estimated new cases of cancer and 11% and 9% of all cancer deaths in Hispanic men and women, respectively. Long-term cumulative exposure to environmental factors such as reactive oxygen species (ROS) has been implicated to cause molecular damage and DNA modifications that are critical for CRC pathogenesis through stress-survival pathway genes. However, limited number of studies related to the role of these pathways have not been conducted for the Hispanic population. The identification and validation of new ethnicity-specific transcriptomic markers within the stress-survival pathways is important for improving treatment, prognosis, and detection strategies. In this study, we have explored the role of stress-survival pathway genes in Hispanic and Non-Hispanic White (NHW) CRC tissues. In one of the previously published studies from our lab we used microarray and RNA-seq datasets obtained from the gene expression omnibus (GEO), the cancer genome atlas (TCGA), and the oncomine databases to identify 28 genes associated with CRC. These genes were screened for transcript level expressions in six CRC cell lines and a normal colon cell line, and in cDNA arrays containing the tumor (n=40) from different CRC stages, and control (n=8) samples by qRT-PCR. The protein level expressions were evaluated by immunohistochemistry (IHC) in CRC tissue microarrays (TMAs) containing different stages of tumor (n = 108) and control (n = 12) tissues. All 28 genes were also analyzed for their transcript-level expressions in Hispanic (n=10) and NHW (n=10) tumors and corresponding non-tumor adjacent (NATs; n=3) tissues. The stress-survival pathway genes associated with cell cycle regulation such as *CHEK1, MCM10, PDCD2L, CCNB1, CDK1* and *CDK4*, and an oxidative stress marker *PRDX4* were upregulated at both transcript and protein levels when compared to its normal counterparts. Additionally, the genes *CHEK1*, *MCM10, BCL2L1, CSE1L, ESPL1, GLA, GPX2, RRM2B, SH3GLB1, TNFRSF12A, TRAF5 and TRIB3* were observed to be upregulated whereas *GPX1, NOXA, NQO1, SLC7A11, BCL2L12, CCNB1, CDK1, CDK4, FOXM1, PDCD2L* and *SOD2* were found to be downregulated in Hispanic tumor tissues when compared to NHWs. Only *CDK1, CHEK1, FOXM1* and *NQO1* were seen to be differentially expressed in the Hispanic and NHW NATs; however, their expression patterns were different from that observed in the respective tumor tissues. Overall, our current findings evaluate the expression of stress-survival pathway genes across different CRC cell lines, stages, and Hispanic and NHW tissues. The genes identified to be differentially expressed in Hispanic tissues may be used as potential biomarkers or as therapeutic targets specific to the Hispanic population in future.

#5233
Germline CHEK2 variants and risk of lymphoma

Nicholas J. Boddicker[1], Raphael Mwangi[1], Dennis P. Robinson[1], Allison C. Rosenthal[2], Thomas M. Habermann[1], Andrew L. Feldman[1], Lisa M. Rimsza[3], Rebecca L. King[1], Melissa C. Larson[1], Brianna J. Gysbers[1], Stephen M. Ansell[1], Jithma P. Abeykoon[1], Grzegorz S. Nowakowski[1], Thomas E. Witzig[1], Anne J. Novak[1], Susan L. Slager[1], James R. Cerhan[1]. *[1]Mayo Clinic, Rochester, MN,[2]Mayo Clinic, Phoenix, AZ,[3]Mayo Clinic, Scottsdale, AZ*

Lymphoma is the sixth most commonly diagnosed cancer in the US. Genome-wide association studies have identified common variants associated with risk of specific lymphoma subtypes, but less is known about the contribution of rare inherited variants in the genetic architecture of lymphoma risk. *CHEK2* is important to DNA repair and 2 small studies have found evidence of an association between *CHEK2* variants and risk of lymphoma. Here, we investigated loss of function (LoF) variants in *CHEK2* with risk of lymphoma (overall and subtypes). The study population included newly diagnosed lymphoma cases from Mayo who were enrolled in the Lymphoma SPORE Molecular Epidemiology Resource (MER). Controls were from the Mayo Clinic Biobank, from which we excluded a prior hematologic malignancy. Whole exome sequencing was performed by Regeneron on an Illumina NovaSeq panel (mean coverage of 48X). Variants were called using GATK v4 and variant annotation was performed using BioR. All LoF variants (nonsense, frameshift and consensus splice sites) in *CHEK2* with a minor allele frequency < 0.5% were included in the analyses. Logistic regression was used to estimate odds ratio (OR) and 95% confidence intervals (CI) for the association between *CHEK2*mutation status and risk of lymphoma overall, and by lymphoma subtypes that had more than 5 mutation carriers, which included diffuse large B-cell (DLBCL), follicular (FL), and T-cell lymphoma (TCL). All analyses were adjusted for age (at diagnosis for cases and at enrollment for controls) and sex. A total of 4,852 lymphoma cases and 49,724 controls were included in this analysis. Median age for both cases and controls was 62 years (range 18-99 years). Males accounted for 57.5% (n=2,789) of the cases and 40.6% (n=20,186) of the controls. The DLBCL (23.6% of cases) and FL (23.3% of cases) subtypes were the most common; 7.6% of cases had TCL. A total of 407 (0.7%) individuals had a LoF variant. The frequency of LoF variants was 1.2% in lymphoma cases and 0.7% in controls. LoF variants were associated with increased risk of lymphoma overall (OR=1.77; 95%CI: 1.32-2.33), DLBCL (OR=2.07; 95%CI: 1.20-3.13), and TCL (OR=2.78; 95%CI: 1.178-5.50), but not FL (OR=1.31; 95%CI: 0.65-2.34). CHEK2 c.1100delC was the most frequently mutated variant in this population, accounting for 76% of all LoF variants. Individuals with a c.1100delC variant had an increased risk of lymphoma overall (OR=1.90; 95%CI: 1.37-2.58), DLBCL (OR=2.06; 95%CI: 1.09-3.54), and TCL (OR=3.17; 95%CI:1.24-6.58), but not FL (OR=1.05; 95%CI: 0.41-2.15). When restricted to cases, there was no significant difference in age at diagnosis (P=0.62) or sex (P=0.53) between LoF variant carriers and non-carriers. In this large lymphoma case-control study, *CHEK2* LoF variants were associated with increased risk of lymphoma, demonstrating that rare inherited variants may play an important role in the etiology of lymphoma. Additional work is needed to investigate missense variants in *CHEK2* and risk of lymphoma.

#5234

Novel predictive biomarker SNPs and polygenic risk scores of immune-related genes for colorectal cancer survival in Korea

Dabin Yun[1], Nan Song[1], Jin-Ah Sim[2], Min Jung Kim[3], Ji Won Park[3], Seung Yong Jeong[3], Aesun Shin[4]. *[1]School of Pharmacy, Chungbuk National University, Cheongju, Korea, Republic of,[2]School of AI Convergence, Hallym University, Chuncheon, Korea, Republic of,[3]Department of Surgery, Seoul National University College of Medicine and Hospital, Seoul, Korea, Republic of,[4]Department of Preventive Medicine, Seoul National University College of Medicine, Seoul, Korea, Republic of*

Background: One of the major topics about colorectal cancer (CRC) is the core role of various immune cells against cancer cells. To comprehensively understand genetic basis of immune system underlying CRC progression, association of single-nucleotide polymorphisms (SNPs) and polygenic risk scores (PRS) of immune-related genes were investigated with colorectal cancer survival.
Methods: CRC patients enrolled in the Seoul National University Hospital with prospective follow-up were included in the study. From blood-derived DNA from CRC patients, genome-wide SNPs were genotyped by using the Korea Biobank Array (KoreanChip). 2,729 immune-related genes were selected from Ensembl, Gene Ontology (GO), and KEGG database and 37,398 mapped SNPs were extracted. SNP or PRS-based Cox proportional hazard models were fit for events of overall survival (OS) and progression-free survival (PFS) estimating effect sizes with hazard ratios (HRs). PRS was calculated as effect size weighted sum of risk alleles of individual patients and

categorized into tertiles. To investigate enriched pathways, protein-protein interaction networks analysis was conducted. Bonferroni-corrected *p*-value (1.3×10^{-6}) was used as statistically significance threshold.
Results: Among 960 CRC patients, 154 (16.0%) occurred events of death and 245 (25.5%) of progression during the follow-up (median=1,698 days, range=7-2,563 days). For OS, a statistically significant associations were mapped to *ACTR3B* , *ST6GAL1*, *COTL1*, *PRKCZ*, and *CAMK1D* genes with the strongest SNP rs14808985 (HR=3.07, P=1.87×10^{-7}). For PFS, marginal association was mapped to *MECOM* gene with the strongest SNP rs16854234 (HR=1.48, *P*=6.13×10^{-6}). In PRS analysis, the highest tertile group showed the prominently increased risk for OS (HR=25.0, *P*<2.0×10^{-16}) and PFS (HR=5.88, *P*<2.0×10^{-16}) compared with the lowest group for a reference. In protein-protein interaction networks analysis, the strongest enrichments were shown in Th17 cell differentiation pathway for OS and in adherences junction for PFS.
Conclusions: We identified novel predictive biomarker genetic variants in *ACTR3B* and *MECOM* genes associated with OS and PFS, respectively, among CRC patients. Additionally, we presented PRS as a useful biomarker for survival outcomes and suggested enriched biological pathways involved in CRC progression. These knowledges can promote the understanding of CRC survival and the development of immune-related therapeutic interventions for CRC patients in the future.

#5235

Transcriptome-wide study of tumor samples from Peruvian women identifies dysregulated pathways in luminal tumors typically associated with more aggressive disease

Chenghuiyun Xu[1], Valentina A. Zavala-Cordero[2], Xiaosong Huang[2], David M. Rocke[2], Sandro Casavilca-Zambrano[3], Jeannie M. Navarro-Vásquez[3], Carlos A. Castañeda[3], Guillermo Valencia[3], Zaida Morante[3], Monica Calderón[3], Julio E. Abugattas[3], Henry Gómez[3], Hugo A. Fuentes[3], Ruddy Liendo-Picoaga[3], Jose M. Cotrina[3], Silvia P. Neciosup[3], Katia Roque[3], Jule Vásquez[3], Luis Mas[3], Marco Gálvez-Nino[3], Jovanny Zabaleta[4], Tatiana Vidaurre[3], Laura Fejerman[2]. *[1]Graduate Group of Biostatistics, Univerisity of California, Davis, Davis, CA,[2]Department of Public Health Sciences, Univerisity of California, Davis, Davis, CA,[3]Instituto Nacional de Enfermedades Neoplásicas, Lima, Peru,[4]Department of Pediatrics and Stanley S. Scott Cancer Center LSUHSC, Louisiana State University Health Sciences Center, New Orleans, LA*

Purpose: Breast cancer incidence and outcomes differ by US census racial/ethnic category. Since large-scale genetic studies of human disease are predominately focused on populations of European ancestry, little is known about breast cancer molecular biology in Hispanic/Latinos which can widen cancer health disparities due to suboptimal translation of discoveries into clinical practice or public health policy. We aim to describe relevant pathways in breast cancer subtype differentiation in breast cancer patients from Peru.
Patients and Methods: Formalin fixed paraffin embedded tumor tissues samples were whole exome sequenced for a total of 271 patients, recruited by the Peruvian Breast Cancer Genomics Study (PEGEN-BC) from the Instituto Nacional de Enfermedades Neoplásicas (INEN) in Lima, Peru. Quality control was conducted to remove genes with low counts. Intrinsic tumor subtypes were classified using the PAM50 method using genefu package in R. Differential gene expression between subtypes was performed by DEseq2 R package and statistical significance was determined using FDR<0.05 for samples with at least log2 1.5-fold change. Pathway analyses were performed to explore differences among the subtypes using GSEA with fgsea package in R. Indigenous American ancestry proportions for participants were estimated using germline genome-wide genotypes and the program Admixture.
Results: The mean age of patients was 50 and the median Indigenous American ancestry was 79%. PAM50 classification of the sequenced samples defined 20.2% of tumors as LumA, 27.9% as LumB, 27.1% as HER2, 22.5% as Basal and 2.3% as Normal. Transcriptomic pathway analysis showed that most of the significantly changed pathways were similar to those previously described such as upregulation of high proliferation pathways in LumB, HER2E and Basal tumors, and a strong dependency on the estrogen pathway for LumA. Top 10 significantly changed pathways show some unique findings: the epithelial-mesenchymal-transition (EMT) pathway is downregulated in Basal, comparing to LumA and HER2 tumors, which is unexpected given that the EMT is associated with stem cell features and poor outcomes. The E2F-targets pathway is upregulated in LumA when comparing to HER2 tumors, but downregulated when compared to Basal tumors.
Conclusions: We identified novel pathways associated with breast cancer subtypes in individuals with high Indigenous American ancestry from Peru and are working on testing the robustness of these findings. If our findings are confirmed, results would suggest a more aggressive profile of Luminal subtypes in the studied samples from Peru, with implications for treatment and survival.

#5236

Functional analysis of variants of uncertain significance of the *MSH6* mismatch repair gene

Elizabeth Szabo[1], Emily Blackburn[1], Patrick Pagano[2], Abhijit Rath[1], Christopher Heinen[1]. *[1]University of Connecticut Health Center, Farmington, CT,[2]University of Connecticut, Storrs, CT*

Lynch syndrome (LS) is a hereditary condition that increases patients' lifetime risk of cancer, primarily colorectal cancer. LS is caused by germline mutations in mismatch repair (MMR) genes, *MLH1, MSH2, MSH6*, and *PMS2*. Identification of these mutations is important in LS diagnosis in order to guide treatment plans and preventative care for patients' and their families. However, the consequences of some variants in these genes are not immediately obvious, granting them classification as variants of uncertain significance (VUS). Half of known variants in the MMR gene *MSH6* are VUS and, thus, the goal of my project is to provide evidence to help better determine their pathogenic significance. Laboratory functional analysis to determine whether these variants disrupt MMR function in human cells can provide such evidence toward this goal. We have previously used CRISPR gene editing to recreate variants in the endogenous loci for the MMR genes *MSH2* and *MLH1* in human embryonic stem cells (hESC) in order to test their effects on MMR function in a cellular environment. We will now use test whether this approach can be used to study *MSH6* VUS. Using these edited hESC lines we are examining the impact of the variants on RNA and protein stability, repair of DNA microsatellites, which is a hallmark of normal MMR function, and induction of the MMR-dependent DNA damage response. Using a panel of known *MSH6* pathogenic and benign controls, we will calibrate these functional assays in order to associate functional performance with likelihood of pathogenicity. We will next test a separate panel of known controls to validate these assays. Finally, we will examine up to 35 VUS. With this compilation of data, we will convert the results into a quantitative Odds of Pathogenicity value. This Odds of Pathogenicity score can be used by expert variant interpretation committees to help readily reclassify these variants, and provide a clearer diagnosis for these suspected Lynch syndrome patients.

#5237

Regulation of genes located in 6q25 by an Indigenous American genetic variant in breast cancer patients from Peru

Valentina A. Zavala[1], Xiaosong Huang[1], Sandro Casavilca-Zambrano[2], Jeannie Navarro-Vásquez[2], Carlos A. Castañeda[2], Guillermo Valencia[2], Zaida Morante[2], Monica Calderon[2], Julio E. Abugattas[2], Henry Gómez[2], Hugo Fuentes[3], Ruddy Liendo-Picoaga[2], Jose M. Cotrina[2], Katia Roque[2], Jule Vásquez[2], Luis Mas[2], Marco Gálvez-Nino[2], Jovanny Zabaleta[4], Tatiana Vidaurre[2], Laura Fejerman[1]. *[1]UC Davis, Davis, CA,[2]Instituto Nacional de Enfermedades Neoplasicas, Lima, Peru,[3]UC Instituto Nacional de Enfermedades Neoplasicas, Lima, Peru,[4]LSUHSC, New Orleans, LA*

Genetic studies in women of Hispanic/Latina origin identified a single nucleotide polymorphism (SNP) in the 6q25 region, rs140068132, that correlates with Indigenous American (IA) ancestry and is protective against BC. The underrepresentation of Latin American populations in public databases has hindered the study of the mechanisms by which this SNP confers a protective effect. We aimed to identify IA germline variants associated with BC risk and to test their association with tumor gene expression in this region.

We performed a case-control fine-mapping analysis in the 6q25 region. BC patients part of the PEGEN-BC Study (N=1809) were included as cases and women from a pregnancy outcomes study in Peru as controls (N=3334). Genome-wide genotype data were available and missing genotypes were imputed using the TOPMED Imputation Server. Logistic regression was used to test the association between each SNP and BC risk. We exome-sequenced 247 breast tumors of PEGEN-BC patients. Tumor subtype was assigned by the pam50 method. We excluded patients diagnosed with stage IV disease, with tumors classified as normal-like or as uncertain, and carriers of the GG genotype for rs140068132, leaving 242 samples. Association between rs140068132 and gene expression of genes in the 6q25 region was tested adjusting by age at diagnosis and IA ancestry.

The strongest signal corresponded to rs140068132 (odds ratio (OR)=0.53, p=1.9e-21). The model adjusted by rs140068132 revealed three additional independent variants that correlate with Indigenous American ancestry: rs184135739 (OR=0.8, p=0.006), rs141057867 (OR=0.87, p=0.006) and rs140125124 (OR=1.23, p=0.015). Gene expression analysis stratified by subtype revealed that among HER2+ tumors (N=63), rs140068132 was associated with ARMT1 (fold change comparing AA to AG (FC)=1.6, p<0.01), CCDC170 (FC=1.8, p<0.01), MTHFD1L (FC=0.7, p<0.01) and RMND1 (FC=1.4, p=0.013). Among Luminal-B (N=68) tumors, there was an association with ARMT1 (FC= 1.9, p=0.001), ESR1 (FC=1.4, p=0.04) and MTHFD1L (FC= 0.8, p=0.02). Only ESR1 was

associated with the SNP (FC= 0.5, p= 0.03) among basal tumors (N=56). No association was identified among Luminal-A tumors (N=55). rs141057867 showed evidence of cis-association with CLDN20 (FC=1.4, p=0.014) among HER2+ subtypes and rs184135739 with ZC3H12D (FC=2.1, p=0.02) and SUMO4 (FC=1.8, p=0.023) among Lumina-A tumors.
Two of the three novel IA SNPs are protective against BC and show association with gene expression. The rs140068132-G variant regulates the expression of genes in the 6q25 region in a subtype-specific manner. A possible mechanism explaining the protective effect of the rs140068132 polymorphism might be linked to the lower expression of MTHFD1L among G-allele carriers in some subtypes. This gene is deregulated in cancer and its expression is negatively associated with cancer survival, including BC.

#5238

The functional role of promoter germline variants in breast cancer susceptibility genes

Nelly Arlene Arroyo[1], Lenin J. Godoy[2], Julie Dutil[1]. *[1]Ponce Health Sciences University, Ponce, PR,[2]Basic Sciences, Ponce Health Sciences University, Ponce, PR*

It is estimated that inherited deleterious or pathogenic germline variants in high- to moderate- penetrance breast cancer (BC) susceptibility genes such as *BRCA1*, *BRCA2*, *STK11, CDH1*, *ATM*, *PALB2*, and *CHEK2* may explain up to 27% of the BC cases. For the remaining cases, BC develops as a result of the complex interaction between environmental and lifestyle risk factors as well as inherited familial predisposition. While low penetrance genetic variants have limited impact on BC risk when taken individually, their combined effect on polygenic risk scores may provide a risk elevated enough to justify clinical actions. Most of the previous work in hereditary breast cancer research has focused on variants located in the coding region of the genes and as a result, there is an abundance of information on the functional interpretation of such variants, while information on regulatory variants remains limited. The goal of this study was to assess the functional impact of germline variants in the promoter region of BC susceptibility genes on gene expression level. Genes evaluated include *CDH1*, *STK11*, and bidirectional promoter genes *ATM*/*NPAT* and *PALB2*/*DCTN5*. A bioinformatics approach was developed to identify and prioritize variants based on conservation level and predicted binding of transcription regulatory proteins. Selected variants will be introduced into pGL3 constructs harboring the promoter of interest using site-directed mutagenesis followed by transfection into HEK293T cells. Dual-glo luciferase expression assays are used to measure levels of promoter activities. Expression levels from promoters containing genetic variants are compared with those from constructs containing the reference sequence. The reference constructs for *STK11* and *CDH1* containing the genes complete promoters demonstrated functional activity. For bidirectional promoters, forwards and reverse construct were tested. Forward *ATM*/*NPAT and PALB2*/*DCTN5* constructs showed luciferase expression under the influence of ATM and *DCTN5* respectively. Work is on the way to assess promoter activity of the reverse complement sequence of those promoters and determine the impact of 13 candidate variants on the strength of these promoters. At the clinical level, identifying germline variants that contribute to BC risk could help better define BC risk in women with negative hereditary cancer genetic test results.

#5239

Integrative analysis of 3D chromatin organization at GWAS loci identifies *RAPGEF1* as a melanoma susceptibility gene

Rohit Thakur[1], Mai Xu[1], Alexandra Thornock[2], Hayley Sowards[1], Epring Long[1], Thomas Rheling[1], Karen Funderburk[1], Jinhu Yin[1], Rebecca Hennessey[1], Raj Chari[3], Tongwu Zhang[1], Lea Jessop[1], Timothy Myers[1], Matthew E. Johnson[4], Andrew D. Wells[4], Alessandra Chesi[4], Struan F. A. Grant[4], Mark I. Iles[5], Maria T. Landi[1], Matthew Law[6], Melanoma Meta-Analysis Consortium, Mitchell Machiela[1], Jiyeon Choi[1], Leonard I. Zon[2], Kevin M. Brown[1]. *[1]Division of Cancer Epidemiology and Genetics, National Cancer Institute, Rockville, MD,[2]Harvard Medical School, Harvard Department of Stem Cell and Regenerative Biology, Boston, MA,[3]Frederick National Lab for Cancer Research, National Cancer Institute, Frederick, MD,[4]Divisions of Human Genetics and Endocrinology, University of Pennsylvania, Philadelphia, PA,[5]Leeds Institute for Data Analytics, University of Leeds, Leeds, United Kingdom,[6]Statistical Genetics, QIMR Berghofer Medical Research Institute, Brisbane, Australia*

Many GWAS loci occur in non-coding regions and often overlap with gene regulatory elements such as distant enhancers, making functional interpretation and target gene discovery challenging. The 3D chromatin organization brings enhancers in spatial proximity with a promoter to regulate target gene expression. Therefore, to map

chromatin interactions between GWAS variants and target gene promoters we performed region-focused chromatin conformation capture assay (Capture-C) in primary human melanocytes. We baited the entire region of association for all 68 independent signals from the recent melanoma GWAS, and Capture-C interactions were called using CHiCAGO tool. Integrative analysis of Capture-C interactions with melanocyte- and melanoma-specific ATAC-sequencing, massive-parallel reporter assay (MPRA), ROADMAP chromatin imputed state model, and gene expression datasets helped prioritize target genes for functional follow-up.
Capture-C assays identified physical chromatin interactions between fine-mapped risk variants and candidate causal gene (CCG) promoters at 90% of the GWAS loci; For 84% of the 68 loci, we observed at least one variant-to-gene promoter interaction longer than 100 kb, and for 20% of loci we found interactions beyond 1 Mb. For 76% of the 68 loci, the CCG-interacting variant was in annotated melanocyte or melanoma enhancer regions consistent with CCG regulation via an enhancer-promoter interaction. We observed at least one CCG-interacting variant in 63% and 51% of the 68 loci with distinct allele specific transcriptional activity in melanocyte and melanoma MPRA datasets respectively. A majority of the loci (60%) harbored CCG-linked risk variants in accessible chromatin regions in melanocytes and melanoma. Pathway enrichment analyses of Capture-C-nominated CCGs identified embryonic development, aryl hydrocarbon receptor signaling, and DNA repair pathways. Notably, we observed chromatin interactions between risk variants located near the 3' of Rap Guanine Nucleotide Exchange Factor 1 (*RAPGEF1*) to the *RAPGEF1* and *UCK1* promoter regions. The risk allele of the lead variant (rs3780269) at this locus was associated with higher *RAPGEF1* mRNA expression and was not associated with *UCK1* expression in melanocytes. We performed a CRISPR knockout proliferation screen in immortalized melanocytes and identified *RAPGEF1* as an essential gene for melanocyte growth or survival. Further, we validated the results of this screen by overexpressing *RAPGEF1* in immortalized melanocytes and found that it leads to increased cellular growth. We are now characterizing its function in melanoma tumor incidence and progression in a zebrafish model. In summary, mapping GWAS loci chromatin interactions to target gene promoters and integrative analysis using cell-type specific datasets identified *RAPGEF1* as a melanoma susceptibility gene.

#5240

Validation of research cohort based penetrance estimates for multiple cancer types and multiple primary cancers on clinically ascertained families

Nam H. Nguyen[1], Elissa B. Dodd-Eaton[1], Jessica L. Corredor[2], Jacynda Woodman-Ross[2], Nathaniel D. Hernandez[2], Angelica M. Gutierrez Barrera[3], Banu K. Arun[3], Wenyi Wang[1]. *[1]Department of Bioinformatics and Computational Biology, MD Anderson Cancer Center, Houston, TX,[2]Department of Clinical Cancer Genetics, MD Anderson Cancer Center, Houston, TX,[3]Department of Breast Medical Oncology, MD Anderson Cancer Center, Houston, TX*

Age-at-onset penetrance is the probability of developing disease by a certain age given a patient's characteristics. Accurate penetrance estimates are important for cancer screening and diagnosis, and for policy making in public health. We developed two Bayesian semi-parametric models: a model that estimates cancer-specific penetrances to the first primary (CS), and a model that estimates penetrances to the second primary without distinguishing between the cancer types (MPC). Model training requires a dataset that is enriched with enough MPC cases, as well as with competing risks from a variety of cancer types. Thus, we trained our models using data from families affected by the Li-Fraumeni Syndrome (LFS), a genetic disorder characterized by germline mutation in the gene *TP53*. This dataset consists of 189 families, all of which were ascertained via probands who were diagnosed with pediatric sarcoma at MD Anderson Cancer Center (MDACC) between 1944 and 1983. We have validated our penetrance estimates on independent LFS datasets with different ascertainment criteria, namely a patient cohort prospectively collected from high-risk clinics at MDACC, and another cohort from the National Cancer Institute (NCI). These datasets were meticulously collected for research purposes. However, clinical datasets, which resemble the data that genetic counselors encounter in counseling sessions, are severely impacted by missing data, most commonly missing ages at diagnosis and ages at last contact, and only represent a snapshot of family history without extended follow-up. To investigate the utility of our research-based risk prediction models in real-world clinics, we evaluated our penetrance estimates on clinically ascertained LFS families that were collected through the Clinical Cancer Genetics (CCG) program at MDACC in the past 10 years. The CCG dataset consists of 3,275 individuals across 124 families, of which 645 were diagnosed with at least one primary and 127 tested positive for *TP53* mutation. Our CS model showed good performance when making cancer-specific predictions of the first primary, with Areas Under the Curve (AUCs) of 0.76, 0.81, and 0.68 for breast cancer, sarcoma, and all other cancer types combined. Our MPC model showed an AUC of 0.7 when predicting patients with MPC versus those with a single primary. Both the CS and MPC models perform better than the Chompret criteria when predicting

TP53 mutation, with AUCs of 0.75 and 0.77 respectively. These results suggest that our models can be utilized for personalized risk predictions in clinical settings, despite being trained on a research-based dataset. Given that the Chompret criteria tends to predict *TP53* mutation more conservatively, the ability of our models to cast a wider net is especially meaningful in the identification of potential carriers, which assists efficient genetic testing and screening.

#5241

Association of polygenic risk scores with breast cancer risk among women with benign breast disease

Stacey J. Winham[1], Mark Sherman[2], Robert Vierkant[1], Bryan McCauley[1], Christopher Scott[1], Mia Gaudet[3], Melissa Troester[4], Sandhya Pruthi[1], Derek Radisky[2], Amy Degnim[1], Kristan Aronson[5], Rachel Murphy[6], Pascal Guenel[7], Therese Truong[8], Jenny Chang-Claude[9], Heiko Becher[10], Montserrat Garcia-Closas[11], Stephen Chanock[11], Thomas Ahearn[12], Xiaohong Yang[11], Doug Easton[13], Manjeet Bolla[13], Celine Vachon[1], Breast Cancer Association Consortium. *[1]Mayo Clinic, Rochester, MN,[2]Mayo Clinic, Jacksonville, FL,[3]National Cancer Institute, Bethesda, MD,[4]University of Norh Carolina, Chapel Hill, NC,[5]Queens University, Kingston, ON, Canada,[6]University of British Columbia, Vancouver, BC, Canada,[7]Research Center for Epidemiology and Population Health, Villejuif, France,[8]Center for Research on Epidemiology and Population Health, Villejuif, France,[9]German Cancer Research Center, Heidelberg, Germany,[10]University Medical Center, Hamburg, Germany,[11]National Institutes of Health, Bethesda, MD,[12]National Institute of Health, Bethesda, MD,[13]University of Cambridge, Cambridge, United Kingdom*

Over one million biopsies are performed annually in the U.S. to evaluate suspicious breast lesions. Most biopsies lead to a diagnosis of benign breast disease (BBD) and these women have a 1.5- to fourfold increase in subsequent breast cancer (BC) risk compared with the general population. A polygenic risk score (PRS) including 313 common variants was developed to predict BC risk in the general population and has improved performance when added to existing BC prediction models. However, the value of PRS in risk prediction models among women with BBD has not been evaluated.

To evaluate the role of the established PRS, BBD, and BC risk, we pooled data from 15,194 white women (6,706 BC cases and 8,488 controls) participating in five Breast Cancer Association Consortium case-control studies. BC risk associations were evaluated by self-reported BBD history and combinations of PRS expressed in tertiles using odds ratios (OR), considering the lowest category of PRS among women without BBD as the referent. Associations were also assessed in an independent case-cohort study (831 BC cases and 1,845 controls) using hazard ratios (HR).

Among the case-control studies, the PRS was strongly associated with BC risk (OR=2.50 per standard deviation increase), and associations were similar in women with (OR=2.60) and without a history of BBD (OR=2.44, p-interaction=0.23). Women with BBD have a higher risk of BC than those without BBD within each level of PRS. Compared to women without BBD and in the lowest PRS category, those with BBD and PRS in the highest tertile had 5-fold increased odds of BC (OR = 5.38; 95% CI 4.73-6.13). Associations were similar in an independent case-cohort study.

These findings indicate that BBD history and PRS are independent contributors to BC risk, and consideration of both simultaneously could improve breast cancer risk prediction. Future studies are needed to integrate PRS with other risk measures to refine absolute BC risk prediction among BBD patients.

Associations of BC risk with combinations of PRS (tertiles) and history of BBD in five case-control studies and a case-cohort study from the Breast Cancer Association Consortium.

		Case-control studies			Case-cohort study		
PRS score range	History of BBD	n BC cases	n controls	OR (95% CI)[1]	n BC cases	n controls	HR (95% CI)[2]
Tertile 1 (≤ -0.57)	No	1009	2692	1.00 (Ref)	117	584	1.00 (Ref)
	Yes	508	902	1.54 (1.35-1.76)	69	163	2.05 (1.45-2.89)
Tertile 2 (-0.58, -0.03)	No	1469	2001	1.97 (1.78-2.17)	181	475	1.93 (1.48-2.51)
	Yes	760	798	2.65 (2.34-3.01)	108	170	2.99 (2.18-4.09)

Tertile 3 (≥ -0.02)	No	1910	1551	3.32 (3.01-3.67)	214	336	3.28 (2.52-4.26)
	Yes	1050	544	5.38 (4.73-6.13)	142	117	4.83 4.25-8.02)
1.Logistic regression analysis, adjusted for study site/genomic platform and age at enrollment. OR, odds ratio; CI, confidence interval.2.Cox proportional hazards regression analysis, accounting for the case-cohort study design and adjusted for age at enrollment. HR, hazard ratio; CI, confidence interval.							

#5242

Do polygenic risk scores add to clinical data in predicting pancreatic cancer? a scoping review

Louise Wang[1], Alyssa Grimshaw[2], Catherine Mezzacappa[1], Navid Rahimi Larki[3], Yu-Xiao Yang[4], Amy Justice[5].
[1]Section of Digestive Diseases, Department of Internal Medicine, Yale School of Medicine, New Haven, CT,[2]Harvey Cushing/John Hay Whitney Medical Library, Yale School of Medicine, New Haven, CT,[3]VA Connecticut Healthcare System, West Haven, CT,[4]Division of Gastroenterology, Department of Internal Medicine, Perelman School of Medicine, University of Pennsylvania, Philadelphia, PA,[5]Section of General Medicine, Department of Internal Medicine, Yale School of Medicine, New Haven, CT

Background: Individual susceptibility to pancreatic ductal adenocarcinoma (PDAC) is determined by both genetic and clinical factors. Polygenic risk scores (PRS) represent a summation of an individual's risk associated alleles across their genome but it is unclear whether PRS improve prognostic assessments beyond available clinical data.
Specific Aims: To evaluate the characteristics of studies examining PRS discrimination for PDAC before and after accounting for clinical factors.
Methods: Following the PRISMA extension for scoping reviews (DOI: osf.io/97hxw), we performed a comprehensive literature search in conjunction with a professional librarian to identify preprint and published research studies evaluating PDAC PRS.
Results: Nineteen studies (of 392 reviewed citations) examined associations between a PDAC-specific PRS and PDAC. The majority were conducted among the UK Biobank (n= 8) and pancreatic cancer consortia (n=4). The rest were institutional biobanks or hospital-based studies. Thirteen studies used a case-control design, and 7 adjusted for clinical risk factors (Table). Only 3 studies (15.8%) evaluated the change in discrimination with the addition of PRS to clinical factors vs. clinical factors alone, and 2 of these reported small but statistically significant improvements in discrimination (ΔAUC: 0.030, 0.039). Source populations were younger/healthier (n=9) than those at risk for PDAC, exclusively European (n=14), or drew controls without relevant exposures such as pancreatic diseases (n=2).
Conclusions: Most PDAC-specific PRS studies do not account for well-established clinical factors or evaluate changes in discrimination with the addition of PRS to clinical factors. Of the 3 studies that did, only 2 showed a modest improvement in discrimination. For PRS to be clinically useful, they must demonstrate more substantial improvements in discrimination beyond established risk factors.

Studies containing PDAC-specific polygenic risk scores and clinical risk factors

First Author	Journal	Year	Study Design	Aim/Purpose	Population Description	Population Size	Ancestry	Definition Pancreatic Cancer
Byrne	medRxiv	2021	cohort	evaluate the effect of lifestyle and genetic risk on overall cancer risk for 13 separate cancers	UK Biobank	195,822 total individuals (451 cancers)	European genetic ancestry	ICD codes cancer regi
Galeotti	BMJ	2021	case/control	test	PANcreaticDisease	9409 total	European	confirmed

				association of pancreatic cancer specific PRS, with addition of ABO SNPs, smoking, and diabetes	ReseArch (PANDoRA) consortium: controls were without any pancreatic diseases	individuals (3619 cases, 5790 controls)	genetic ancestry	diagnosis c pancreatic cancer
Kachuri	Nature Communications	2020	cohort	evaluate additive predictive value of adding PRS for 16 separate cancers	UK Biobank	413,753 total individuals (493 cancers)	self reported European anestry	ICD codes cancer/mor registries a inpatient hospital encouters
Nakatochi	Plos One	2018	case/control	develop a risk model to identify individuals at high risk for pancreatic cancer development in the general Japanese population	two separate case-control datasets in Japan controls: matched age/sex, no diagnosis of cancer at time of recuritment from five Japanese hospitals and the epidemiology research program at Aichi Cancer Center	1,328 total individuals (664 cases, 664 controls)	genetically determined Japanese ancestry	clinical diagnosis c histologica diagnosed pancreatic cancer, including 1 endocrine tumors
Rothwell	CGH	2022	cohort	evaluate metabolic syndrome, additional clinical factors across levels of polygenic risk score	UK Biobank	366,016 total individuals (478 cancers)	mainly European genetic ancestry	ICD codes
Salvatore	Journal of Biomedical Informatics	2021	case/control	evaluate various phenotype risk scores	Michigan Genomics Initiative (MGI) and UK Biobank;	431,658 total individuals (1088	European ancestry	ICD codes

				(PheRS) and assess their discriminatory ability, calibration, and accuracy in combination with polygenic risk scores and clinical risk models	controls were matched on age, sex, and length of followup	cases, 430,570 controls)		
Sharma	Gastroenterology	2022	case/control	test the performance of PRS to discriminate between new onset diabetes and long standing diabetic patients with pancreatic cancer	UK Biobank	11,462 total (1042 cases, 10420 controls); age and sex matched cancer free controls	European ancestry	incident ca of PDAC a measured b ICD codes self reporte

#5243

Functional characterization of genetic loci in basal cell carcinoma

Mingyue Li[1], Constance Turman[2], Peter Kraft[3], Jiali Han[4]. *[1]Department of Epidemiology, Indiana University Richard M. Fairbanks School of Public Health, Indianapolis, IN,[2]Department of Epidemiology, Harvard T.H. Chan School of Public Health, Boston, MA,[3]Program in Genetic Epidemiology and Statistical Genetics, Department of Biostatistics, Harvard T.H. Chan School of Public Health, Boston, MA,[4]Indiana University Melvin and Bren Simon Comprehensive Cancer Center, Indianapolis, IN*

Background**:** Genome-wide association studies (GWAS) have identified over 30 loci associated with basal cell carcinoma (BCC) susceptibility. However, the causal variants and mechanisms at these loci remain unknown. We performed statistical fine mapping and functional enrichment to identify credible causal variants at 31 established BCC risk loci.

Methods: We performed statistical fine mapping by applying the sum of single effects (SuSiE) method to a previously published GWAS from 12,945 BCC cases and 274,252 controls. To identify genomic annotations enriched for BCC-associated variants, we compared high Posterior Inclusion Probability (PIP) variants from SuSIE to low PIP variants: we performed multivariable logistic regression of high-PIP status on 17 variant annotations from the Functional Annotation of Variants Online Resources (FAVOR) database, including sequence-contextual and functional annotations.

Results: We identified 6 variants with PIP>0.99: rs1126809 (*TYR*), rs1805007 (*MC1R*), rs78378222 (*TP53*), rs12203592 (*IRF4*), rs35407(*SLC45A2* a.k.a. *MATP*), rs12916300 (*HERC2*). Five of these six variants are in pigmentation genes; the sixth is in the tumor suppressor *TP53*. At a seventh region, the 95% credible set contained two variants in or upstream of *RALY*, which has previously been shown to be associated with pigmentation traits and multiple non-skin cancers. Another four regions had fewer than 10 variants in the credible set; the median size of the credible set was 11 (range: 1-76). After adjusting for sequence context (including location relative to exons, introns, UTRs; GC content; local mutation density, and nucleotide diversity) variants in active chromatin regions (as determined from multi-tissue methylation marks), variants in transcription factor binding sites, and skin eQTLs were significantly more likely to be high-PIP variants.

Conclusions: Our results identify candidate variants, genes, and mechanisms for further study in BCC carcinogenesis.

Survivorship and Biomarkers of Prognosis

#5757

Breast cancer diagnosis and treatment associated with acceleration of biological aging over time in a racially diverse cohort of women

Jacob K. Kresovich[1], Katie M. O'Brien[2], Zongli Xu[2], Clarice R. Weinberg[2], Dale P. Sandler[2], Jack A. Taylor[2]. *[1]H. Lee Moffitt Cancer Center, Tampa, FL,[2]National Institute of Environmental Health Sciences, Research Triangle Park, NC*

Leukocyte DNA methylation (DNAm) at individual sites across the genome can be used to construct measures of biological age. Positive age acceleration—when biological age is older than chronological age—is associated with higher risk of age-associated diseases. Recent adjuvant therapy is reported to increase age acceleration, but the longer-term effects of a breast cancer diagnosis and treatment on age acceleration remain unknown. Here, we use blood samples collected at two timepoints to examine changes in age acceleration over time comparing women who did and did not develop breast cancer. Paired whole blood samples were drawn an average of 8 years apart (range: 5-11 years) in a sample of non-Hispanic White and Black (Hispanic and non-Hispanic) women. DNAm was profiled using Infinium MethylationEPIC BeadChips. Approximately half the women were diagnosed and treated for breast cancer between blood draws (cases; n= 190, baseline mean age= 57) whereas the other half remained breast cancer-free (controls; n= 227, baseline mean age= 56). Longitudinal changes in three age acceleration metrics were compared to determine whether an intervening breast cancer diagnosis and treatment was associated with trajectories in biological aging. On average, the cases were diagnosed with breast cancer 3.5 years after the initial blood draw and 4 years before the second blood draw. Among the cases, 36% were treated with chemotherapy, 65% with radiation therapy, and 70% with hormonal therapies; 45% of the cases received two types of therapy, and 13% received all three. Compared to women who remained cancer-free, women diagnosed and treated for breast cancer had increases in age acceleration over time as measured by PhenoAgeAccel (adjusted standardized mean difference (β)= 0.13, 95% CI: 0.00, 0.26), GrimAgeAccel (β= 0.13, 95% CI: 0.03, 0.24), and DunedinPACE (β= 0.35, 95% CI: 0.23, 0.48). The associations did not vary by timing of diagnosis between the blood draws or race; however, women diagnosed with estrogen receptor (ER) negative tumors appeared to experience faster increases in age acceleration than women diagnosed with ER positive tumors (GrimAgeAccel; ER negative β= 0.27, 95% CI: 0.07, 0.47; ER positive β= 0.10, 95% CI: -0.01, 0.21; P-interaction= 0.14). To investigate the impact of different types of breast cancer therapies, associations were examined using a case-only design. In models that simultaneously included chemotherapy, radiation therapy and hormone therapy, radiation therapy had the strongest associations with accelerated biological aging as measured by PhenoAgeAccel (β= 0.38, 95% CI: 0.18, 0.58), GrimAgeAccel (β= 0.27, 95% CI: 0.09, 0.45), and DunedinPACE (β= 0.25, 95% CI: 0.03, 0.47). We find that years after the initial diagnosis, breast cancer survivors have significantly accelerated biological aging; treatment modalities may differentially influence these rates.

#5758

Regular aspirin use, breast tumor characteristics and long-term breast cancer survival

Cheng Peng[1], Michelle D. Holmes[1], Wendy Y. Chen[2], Tengteng Wang[1], Kristen D. Brantley[1], Yujing Jan Heng[3], Pepper J. Schedin[4], Bernard A. Rosner[1], Walter C. Willett[5], Meir J. Stampfer[1], Rulla M. Tamimi[6], A. Heather Eliassen[1]. *[1]Brigham and Women's Hospital, Boston, MA,[2]Dana-Farber Cancer Institute, Boston, MA,[3]Beth Israel Deaconess Medical Center, Boston, MA,[4]Oregon Health and Science University, Portland, OR,[5]Harvard T. H. Chan School of Public Health, Boston, MA,[6]Weill Cornell Medicine, NY, NY*

Compelling epidemiologic data, supported by experimental evidence, suggest aspirin may improve survival in breast cancer patients. However, recent clinical trials showed a lack of protective effect, though length of intervention (18 months to 4.7 years) and follow-up (20 months to 4.7 years) were limited. We sought to examine the association between post-diagnostic aspirin use (frequency, dose, and duration), timing and age of initiation on breast cancer-specific mortality. Our study included 10,493 women diagnosed with stage I, II, or III invasive breast cancer. Participants were enrolled in the large, prospective Nurses' Health Study (NHS) and NHSII in 1980 and 1989 prior to diagnosis and followed up through June 1, 2017. We collected information on frequency, dose and

duration of aspirin use. Regular aspirin use was defined as using aspirin (standard- and low-dose) ≥2 days per week, and non-regular aspirin users were those who reported use of aspirin <2 days per week. We used Cox proportional hazard models to calculate multivariable adjusted hazard ratios (HRs) for breast cancer-specific mortality. After a median follow-up of 10 years, there were 2,506 total deaths and 1,221 breast cancer-specific deaths among 10,493 stage I to III breast cancer patients over 32 years of follow-up. In multivariable models, regular use of aspirin (n=3,523; 34%) was associated with a 38% lower risk of death from breast cancer compared with non-regular users (including nonusers) (HR=0.62, 95% CI: 0.54-0.71). The association was independent of pre-diagnostic aspirin use. Associations between aspirin use and breast cancer-specific mortality were stronger with longer time since diagnosis (HRs for <5 years since diagnosis: 0.73 (95% CI: 0.59-0.90), 5-<10 years: 0.63 (95% CI: 0.49-0.80), and ≥10 years: 0.53 (95% CI: 0.41-0.69)). The relations between aspirin use and breast cancer survival were similar across categories of dose (compared to non-users, HRs for 0.5-5 tablets per week: 0.59 (95% CI: 0.51-0.68); ≥6 tablets per week: 0.60 (95% CI: 0.48-0.74)) and appeared stronger with longer duration (compared to non-users, HRs for <5 years: 0.80 (95% CI: 0.57, 1.10); ≥5 years: 0.61 (95% CI: 0.51, 0.72)). For women who initiated regular aspirin use after age 70, regular aspirin use was associated with worse survival (HR=1.74, 95% CI: 1.16-2.63); on the other hand, initiation of regular aspirin use at age ≤60 (HR=0.72, 95% CI: 0.54-0.95) or 60-≤70 (HR=0.69, 95% CI: 0.50-0.95) was associated with improved survival (p-interaction=0.02). Regular aspirin use after diagnosis of nonmetastatic breast cancer was associated with improved long-term survival over 32 years. Although the associations between post-diagnostic regular aspirin use and improved survival did not differ by BMI, smoking or tumor characteristics, women who initiated regular aspirin use >70 years of age had increased risk of death due to breast cancer.

#5759

Accelerated cardiac aging in adolescent and young adult cancer survivors previously treated with cardiotoxic therapy

Michelle A. T. Hildebrandt[1], Cole J. Bernstein[1], Sairah Ahmed[1], J. Andrew Livingston[1], Efstratios Koutroumpakis[1], Michael E. Roth[1], Jose Banchs[2]. *[1]UT MD Anderson Cancer Center, Houston, TX,[2]University of Colorado - Anschutz Medical Campus, Aurora, CO*

Cancer in adolescents and young adults (AYA) is defined as cancer occurring between the ages of 15-39 years. Although cancer is the most common disease-related cause of death in this age group world-wide, the highly favorable overall 5-year survival rate for AYA cancer patients is creating a large and growing segment of the cancer survivorship population. Young cancer survivors have rates of comorbidities, frailty, and other phenotypes that are in line with that of individuals decades older, suggesting that cancer and/or treatment exposures accelerate the aging process in these survivors. Cardiotoxicity due to anthracycline and/or radiation exposure is a major contributor to poor cardiovascular health in AYA cancer survivors, yet the presence and the potential impact of accelerated cardiac aging remains unclear. We hypothesized that hearts in AYA cancer patients exposed to cardiotoxic treatment modalities have a functional phenotype that mirrors heart function in non-treatment exposed individuals who are decades older. In this cross-sectional study, 424 echocardiograms from 127 AYA Hodgkin lymphoma (N=98) and sarcoma (N=29) survivors who were treated with anthracyclines and/or radiation were reviewed for eight functional measures (left ventricular ejection fraction, A-wave, E-wave, E/A ratio, E'-wave, posterior wall thickness, mitral deceleration time, and left ventricular end-diastolic dimension). The median anthracycline dose received for the population was 291.0 mg/m^2 (SD: 133.7) and 44.9% were exposed to radiation to the chest. At last follow-up, 8.3% were taking cardiac medications and 15.8% had been diagnosed with a cardiovascular disease during an average follow-up period of 5.6 years. Echocardiograms were obtained on average 1.3 years post-diagnosis (range: 0-14) and were grouped based at AYA survivor age at procedure (20-29 years, 30-39 years, and 40-49 years). Left ventricular ejection fraction (LVEF) and E'-wave were significantly lower than controls in all three age groups (P<0.001), with four other measures being significant in both of the two younger age groups (P<0.05). Strikingly, 90% of the population had more than one functional measure that was indicative of hearts at least two decades older than the patient at time of echocardiogram with AYA survivors having an average of 4.2 measures displaying evidence of accelerated cardiac aging. These results suggest that AYA cancer survivors exposed to cardiotoxic treatment modalities have a high burden of poor cardiac function and that accelerated cardiac aging may responsible.

#5760

Molecular, immune, and microbial profiles of early-onset, intermediate-onset, and later-onset CRCs

Tomotaka Ugai[1], Yasutoshi Takashima[1], Andressa Dias Costa[2], Daniel Buchanan[3], Jeroen Huyghe[4], Li Hsu[4], Conghui Qu[4], Claire Thomas[4], Steve Gallinger[5], Robert Grant[6], Ulrike Peters[4], Amanda I. Phipps[4], Jonathan Nowak[1], Shuji Ogino[1]. *[1]Brigham and Women's Hospital, Boston, MA,[2]Dana-Farber Cancer Institute, Boston, MA,[3]University of Melbourne, Melbourne, Australia,[4]Fred Hutchinson Cancer Center, Seattle, WA,[5]Ontario Institute for Cancer Research, Toronto, ON, Canada,[6]Princess Margaret Cancer Centre, Toronto, ON, Canada*

Background: Despite heightened interest in early-onset CRC, little is known about the tumor molecular, immune, and microbial characteristics of early-onset CRC. It is also unclear whether CRCs diagnosed at or shortly after age 50 are similar to early-onset CRC. We hypothesized that tumor molecular, immune, and microbial characteristics in CRC tissue might show differential heterogeneity patterns between three age groups (<50 "early-onset", 50-54 "intermediate-onset", ≥55 "later-onset").
Methods: We examined 3,395 CRC cases with available tissue data, including 660 early-onset and 243 intermediate-onset cases in the Nurses' Health Study, Health Professionals Follow-up Study, and Ontario Familial Colon Cancer Registry. We profiled the *in situ* T-cell landscape of 959 cases using digital imaging, machine learning, and a customized 9-plex multiplexed immunofluoresence panel with antibodies directed against CD3, CD4, CD8, CD45RA, CD45RO, FOXP3, and MKI67 (Ki-67). Using chi-squared test or Spearman's correlation test, we assessed differences in tumor characteristics including microsatellite instability, CpG island methylator phenotype (CIMP), *KRAS*, and *BRAF* mutations, LINE-1 methylation levels, *pks*$^+$ *E. coli* and *Fusobacterium nucleatum* positivity, histopathologic lymphocytic reaction, and T-cell densities between early-onset, intermediate-onset, and later-onset cases.
Results: Compared to later-onset CRC (21%), early-onset (4.8%) and intermediate-onset CRCs (5.1%) exhibited a lower prevalence of CIMP-high status (P<0.001). The mean tumor LINE-1 methylation level increased with increasing age [59 (SD, 12) in early-onset, 61 (SD, 10) in intermediate-onset, and 64 (SD, 9.8) in later-onset CRC (P<0.001)]. Early-onset CRC (4.1%) had fewer *BRAF* mutations than intermediate-onset (10.4%) and later-onset CRC (15%) (P<0.001). Compared to later-onset CRC, early-onset CRC tended to show lower levels of tumor-infiltrating lymphocytes (P=0.013), and intratumoral periglandular reaction (P=0.025). Compared to later-onset CRC, early-onset CRC had a lower density of memory (both CD4$^+$ and CD8$^+$) T-cells (median 21 vs. 48 cells/mm^2; P=0.002) and a higher density of MKI67$^+$ immune cells (median 50 vs. 19 cells/mm^2; P=0.003) in tumor epithelial areas but not in the surrounding stroma. No significant differences in other tested characteristics were identified.
Conclusions: Compared to later-onset CRC, early-onset and intermediate-onset CRCs tended to have aggressive tumor phenotypes such as LINE-1 hypomethylation, lower lymphocytic immune reaction, and a higher density of MKI67$^+$ immune cells. These findings highlight the importance of the tumor microenvironment in the etiology of early-onset and intermediate-onset CRCs.

#5761

Bayesian estimation of a semi-parametric recurrent event model with competing outcomes for personalized risk prediction among cancer survivors

Nam H. Nguyen[1], Elissa B. Dodd-Eaton[1], Seung Jun Shin[2], Jing Ning[3], Wenyi Wang[1]. *[1]Department of Bioinformatics and Computational Biology, MD Anderson Cancer Center, Houston, TX,[2]Department of Statistics, Korea University, Seoul, Korea, Republic of,[3]Department of Biostatistics, MD Anderson Cancer Center, Houston, TX*

Multiple primary cancer (MPC) is becoming more common in the general population, accounting for approximately 20% of incidence cases in the United States. Epidemiological studies indicate a strong dependence of the subsequent primary on the characteristics of the first primary. For example, there is evidence that individuals with a first primary breast cancer is more likely to develop a second primary lung cancer. These observations highlight the need to develop a statistical model that characterizes age-to-onset of cancers beyond the first primary, while accounting for the complex relationships between the cancer occurrences. Such a modeling framework was previously lacking. We hereby propose a Bayesian semiparametric framework, where the occurrences of each cancer type follow a non-homogeneous Poisson process. The time-varying intensity of this process is conditioned on genetic and demographic covariates, such as status of genetic mutation and sex, as well as on a patient's cancer history, such as type and timing of the first primary, thus allowing our model to capture the heterogeneity in cancer risks across individuals. Since our model requires a dataset that is enriched with MPC cases, we utilize data collected from families affected with Li-Fraumeni Syndrome (LFS), which is a genetic disorder characterized by

germline mutations in the tumor-suppressor gene *TP53*. People with LFS are at higher risks of certain cancer types, and many cancer survivors develop additional primary malignancy. We train and cross-validate our model on a patient cohort selected according to clinical LFS criteria at MD Anderson Cancer Center from year 2000 to 2015. The cohort consists of 11,186 individuals across 429 families, out of which 2,286 were diagnosed with at least one primary cancer and 335 were tested positive for germline mutations in *TP53*. Upon model training, we construct cancer-specific penetrance curves for the second primary cancer, which vary considerably among patients with different covariates and cancer history, thus highlighting the utility of our model for personalized risk prediction. Our penetrance estimates display good performance when being used to make cancer-specific predictions of the second primary among cancer survivors, achieving AUCs (Areas under the Receiver Operating Characteristic curves) of 0.91, 0.76 and 0.68 respectively for sarcoma, breast cancer, and all other cancers combined. While we apply our model to an LFS dataset, the statistical framework is general, and can be tailored to analyze any time-to-event datasets with suitably selected sets of covariates. Future applications include population-based characterization of specific cancer type combinations over time to impact public health policy making.

#5762

New perspective on racial disparities in prostate cancer: identification of new molecular subsets using whole-mount radical prostatectomy

Wei Zhao[1], Pin Li[1], Shannon Carskadon[1], Craig Rogers[1], James Peabody[1], Mani Menon[2], Dhananjay Chitale[1], Sean Williamson[3], Nilesh Gupta[1], Nallasivam Palanisamy[1]. *[1]Henry Ford Health System, Detroit, MI,[2]Mount Sinai Health System, New York City, NY,[3]Cleveland Clinic, Cleveland, OH*

Introduction: Prostate cancer is a heterogenous multifocal disease. We hypothesize that different tumor foci may harbor distinct driver molecular aberrations, making it a more complex disease and difficult to manage. To avoid overlooking smaller tumor foci with clinical and biological significance, we used an innovative approach to understand the genetic underpinnings of each tumor foci based on the molecular analysis of whole-mount radical prostatectomy specimens rather than a systematic sampling of dominant nodules alone. Our study aimed to identify distinct molecular subsets of prostate cancer, if any, and correlate them with clinical outcomes in Caucasians (CA) and African Americans (AA).

Method: We randomly selected 834 whole-mount radical prostatectomy tissues including 463 (56%) CA and 371 (44%) AA. We used combined dual immunohistochemistry (IHC) for ERG and SPINK1 and dual RNA in-situ hybridization (ISH) for ETV1 and ETV4. The racial disparity in aberrant oncogene expression was analyzed by the Chi-squared test. The recurrence-free survival (RFS) of patients with distinct molecular subsets of prostate cancer was examined by the Kaplan-Meier method and cox-ph models. The Gleason's grades of prostate biopsies were summarized by spaghetti plot and compared by linear mixed models.

Results: Patients with localized prostate cancer expressing none, one, two, and three of four oncogenes were 16.4%, 58.4%, 21.7%, and 3.5%, respectively. The expression of ERG and SPINK1 was negatively correlated (odds ratio (OR)=0.38, 95% CI 0.29-0.51, p<.001). Compared with CA, AA had a lower incidence of ERG (38.8% vs 60.3%), a higher incidence of SPINK1 (63.3% vs 35.6%), and similar incidences of ETV1 (9.4% vs 9.3%) and ETV4 (4.6% vs 3.9%). Importantly, ETV1 expression was associated with a worse RFS in CAs (hazard ratio (HR)=2.49, 95% CI 1.15-5.38, p=.02). ETV4 expression was associated with a worse RFS in AA (HR=3.11, 95% CI 1.32-8.04, p=.01). In addition, ETV4 expression was associated with lymph node metastasis in AA (OR=4.0, 95% CI 1.06-12.44, p=.02) but not in CA (OR=0.56, 95% CI 0.03-2.85, p=.57). For those who had multiple biopsies before radical prostatectomy, Gleason's grade increased with time in AA (0.23 per year, p<.001) but was unchanged in CA. ERG expression was associated with a lower Gleason grade (-0.20, p=.03). ETV4 was associated with a higher Gleason grade (0.50, p=.02).

Conclusion: Our findings showed the molecular heterogeneity between CA and AA who had localized prostate cancer, and supported ETV1 and ETV4 as prognostic markers that can be incorporated into clinical practice to better predict prostate cancer recurrence after radical prostatectomy in CA and AA, respectively.

#5763

Risk factors, trends, and disparities in HPV-associated subsequent malignant neoplasms among adolescent and young adult cancer survivors

Judy Y. Ou, Natalie Bennion, Kellee Parker, Douglas Fair, Heidi A. Hanson, Deanna Kepka, Echo L. Warner, Joemy M. Ramsay, Heydon K. Kaddas, Anne C. Kirchhoff. *Huntsman Cancer Institute at the University of Utah; Social & Scientific Systems, Inc., a DLH Holdings Company, Salt Lake City, UT*

Background: Subsequent malignant neoplasms (SMN) are a leading cause of premature mortality among adolescent and young adult (AYA) cancer survivors, who have unique health needs. Human Papillomavirus-related second cancers (HPV-SMN) are generally preventable through screenings and vaccination. We identified disparities in HPV-SMN among AYA survivors by demographics and first cancer therapy, and examined temporal trends in incidence of HPV-SMN.
Methods: We identified diagnoses of any HPV-SMN, oropharyngeal-SMN, and cervical-SMN among AYA survivors in the SEER 9 1976-2015 registries starting two months after the first cancer. Standardized incidence ratios (SIR) compared risk between AYA survivors and general population. We used Fine and Gray competing risk models to estimate hazard ratios (HR) of therapy on risk for HPV-SMN while controlling for cancer site and demographic confounders. Age-period-cohort (APC) models identified temporal trends in HPV-SMN incidence.
Results: Of 374,408 survivors diagnosed with a first primary cancer ages 15-44, a total of 1,369 had an HPV-SMN occurring on average five years after the first cancer. Compared to the general population, AYA survivors had increased risks of 70% for any HPV-SMN (95%CI=1.61-1.79) and 117% for oropharyngeal-SMN (95%CI=2.00-2.35). Cervical-SMN risk was generally lower in survivors (SIR=0.85, 95%=CI 0.76-0.95). Hispanic AYA survivors had a significant increase in cervical-SMN relative to the general population (SIR=1.46, 95%CI=1.01-2.06). AYAs who were uninsured or on Medicaid at diagnosis had significant increases in HPV-SMN risk relative to the general populations (Uninsured SIR=5.23, 95%CI=2.26-10.31; Medicaid SIR=5.95, 95%CI=4.07-8.40). AYAs first diagnosed with Kaposi sarcoma, leukemia, Hodgkin, and Non-Hodgkin lymphoma had increased risk for HPV-SMN relative to the general population. Among survivors with HPV-related first primary cancers, radiation was associated with increased risk for HPV-SMN (HR=1.35, 95%CI-1.03-1.77). Among survivors whose first primary cancer was not HPV-related, chemotherapy was associated with increased risk for HPV-SMN (HR=1.20, 95%CI=1.00-1.44) but the general effect of treatment was not significant (p=0.16). In APC models, incidence of oropharyngeal-SMN significantly declined over time.
Conclusion and Impact: While the overall risk is low, AYA survivors are at higher risk for HPV-SMNs than the general population, largely driven by oropharyngeal-SMN. Hispanic survivors are the only group at higher risk for cervical-SMN than the general population suggesting a need to improve their cervical cancer screening. Uninsured/Medicaid AYA survivors also face higher HPV-SMN risks. Improving access to screening and HPV vaccination is needed to reduce the burden of HPV-SMN in AYA survivors.

PREVENTION / EARLY DETECTION / INTERCEPTION

Behavioral and Biological Opportunities to Improve Cancer Prevention, Early Detection, and Disparities

#5765

Promoter DNA methylation patterns in oral, laryngeal, and oropharyngeal anatomical regions are associated with tumor differentiation, nodal involvement, and survival in Latinos

BIanca Rivera-Peña[1], Oluwasina Folawiyo[2], Nitesh Turaga[2], Rosa J. Rodríguez-Benítez[3], Marco E. Felici[4], Jaime A. Aponte-Ortiz[5], Francesca Pirini[6], Sebastián Rodríguez-Torres[7], Roger Vázquez[1], Ricardo López[1], David Sidransky[8], Rafael E. Guerrero-Preston[9], Adriana Báez[10]. *[1]Department of Biology, University of Puerto Rico, Río Piedras, Puerto Rico,[2]Department of Otolaryngology-Head and Neck Surgery, Johns Hopkins University School of Medicine, Baltimore, MD,[3]Department of General Social Sciences, University of Puerto Rico, Río Piedras, Puerto Rico,[4]Puerto Rico Department of Health, San Juan, Puerto Rico,[5]Department of General Surgery, University of Puerto Rico Medical Sciences Campus, San Juan, Puerto Rico,[6]IRCCS Instituto Romagnolo per lo Studio dei Tumori (IRST) "Dino Amadori", Meldola, Italy,[7]University of Pittsburgh School of Medicine, Pittsburgh, PA,[8]Department of Oncology, Johns Hopkins University School of Medicine, Baltimore, MD,[9]LifeGene BioMarks, Baltimore, MD,[10]Department of Otolaryngology-Head and Neck Surgery, University of Puerto Rico Medical Sciences Campus, San Juan, Puerto Rico*

Hispanics/Latinos, Black Americans, and poor Non-Latino Whites in the United States are at higher risk of developing head and neck squamous cell carcinoma (HNSCC). The incidence of HNSCC in Puerto Rico is 2.5 higher than for Hispanics/Latinos living in the United States. These health disparities are a serious public health concern due to HNSCC high mortality and morbidity rates, higher treatment costs, and significant quality of life burden. We hypothesized that the discovery of actionable targets for HNSCC early detection, diagnosis, prognostication. Differentially Methylated Regions (DMRs) can be used as HNSCC diagnostic, prognostic, and therapeutic targets in precision medicine workflows. DNA from 23 HNSCC samples and 10 healthy oral tissue

samples from patients in Puerto Rico were hybridized to a genome-wide tiling array to identify DMRs in a discovery cohort. Downstream analyses identified differences in promoter DNA methylation patterns in oral, laryngeal, and oropharyngeal anatomical regions associated with tumor differentiation, nodal involvement, and survival. Genome-wide DMR analysis showed 2,565 DMRs common to the three subsites. We identified 738 DMRs unique to laryngeal cancer (n=7), 889 DMRs unique to oral cavity cancer (n=10), and 363 DMRs unique to pharyngeal cancer (n=6). Based on the genome-wide analysis, and a gene ontology analysis, we selected 10 candidate genes to test for prognostic value and association with clinicopathological features. *TIMP3* was associated with tumor differentiation in oral cavity cancer (p =0.039), *DAPK1* was associated with nodal involvement in pharyngeal cancer (p = 0.017), and *PAX1* was associated with tumor differentiation in laryngeal cancer (p = 0.040). We selected 5 candidate genes, *DAPK1, CDH1, PAX1, CALCA,* and *TIMP3*, for a prevalence study in a larger validation cohort: 42 oral cavity; 25 pharyngeal; and 52 laryngeal cancer samples. *PAX1* hypermethylation differed across HNSCC anatomic sub-sites (p= 0.029), and predominantly detected in laryngeal cancer. Kaplan-Meier survival analysis (p=0.043) and Cox regression analysis of overall survival (p=0.001) showed that *DAPK1* methylation is associated with better prognosis in HNSCC. Our findings show that HNSCC sub-sites (oral cavity, pharynx, and larynx) display substantial differences in aberrant DNA methylation patterns among Hispanic/Latinos HNSCC patients in the US. These data suggest further research may lead to the development of diagnostic medical devices, prognostic biomarkers and novel therapeutic targets that may lead to a reduction in HNSCC disparities among Hispanic/Latinos in the US.

#5766

Prospective evaluation of cell-free DNA fragmentomes for lung cancer detection

Peter J. Mazzone[1], Kwok-Kin Wong[2], Jun-Chieh J. Tsay[2], Harvey I. Pass[2], Anil Vachani[3], Allison Ryan[4], Jacob Carey[4], Debbie Jakubowski[4], Tony Wu[4], Yuhua Zong[4], Carter Portwood[4], Keith Lumbard[4], Joseph Catallini[4], Nicholas C. Dracopoli[4], Tara Maddala[4], Peter B. Bach[4], Robert B. Scharpf[5], Victor E. Velculescu[5]. *[1]Cleveland Clinic, Cleveland, OH,[2]NYU Langone Health, New York, NY,[3]University of Pennsylvania School of Medicine, Philadelphia, PA,[4]Delfi Diagnostics, Baltimore, MD,[5]The Sidney Kimmel Comprehensive Cancer Center, Johns Hopkins University School of Medicine, Baltimore, MD*

Background: Less than 10% of eligible persons undergo annual lung cancer screening by low-dose computed tomography (LDCT). Greater uptake of LDCT is hampered in part by its cost, inaccessibility, and balance of benefit to risk. A blood-based, low-cost, widely available initial blood test could boost screening participation and improve the net benefit of screening, if it were sensitive for cancer detection and affordable. The DELFI (DNA evaluation of fragments for early interception) technology uses low-coverage, whole-genome sequencing and machine learning to identify patterns of circulating cell-free DNA (cfDNA) fragmentation indicative of cancer. We report initial results of the cfDNA analysis from DELFI-L101 (NCT04825834), a prospective, observational, national case-control study to train and test DELFI classifiers for lung cancer detection.
Methods: Eligible participants were adults ≥50 years old with current or previous smoking histories of ≥20 pack-years and recent or planned thoracic CT imaging. At enrollment, medical history was recorded and blood samples were collected for DELFI analysis. A classifier for lung cancer detection was developed using repeated 10-fold cross-validation. A split study approach for the purposes of independent validation of the classifier is forthcoming.
Results: The study cohort included 242 patients with lung cancer and 652 individuals without cancer. Study participants largely represented those of a lung cancer screening population, with 45% stage I/IA. Most participants were ≥65 years old with roughly equal proportions of men and women. There was broad representation across lung cancer risk factors among both cases and controls. The cross-validated area under the receiver operator characteristic curve (AUC) was 0.81 for lung cancer detection. AUCs for adenocarcinoma and squamous cell carcinoma were not significantly different, but the AUC for small cell lung cancer was significantly higher than that for adenocarcinoma (p<.001) and squamous cell carcinoma (p=.02). Clinically meaningful sensitivity to detect all stages of disease was achieved.
Conclusions: A classifier developed using samples collected prospectively distinguished between lung cancer cases and controls with robust cross-validated performance across all stages and lung cancer subtypes. A cfDNA DELFI fragmentome test could represent an affordable, high-performing blood test that may improve lung cancer screening.

#5767

Pan-viral response in African Americans and European Americans with hepatocellular carcinoma

Theressa Ewa, Whitney L. Do, Limin Wang, Marshonna Forgues, Xin W. Wang. *Laboratory of Human Carcinogenesis, National Cancer Institute, Bethesda, MD*

Hepatocellular carcinoma (HCC) is often diagnosed at late-stages, with African Americans (AA) being diagnosed at a later stage with worse prognosis and high mortality rates. The poor screening and diagnosis of HCC and differences between racial/ethnic groups show a disproportion in mortality rates. Examining an individual's viral exposure history might serve as a useful biomarker of early disease that could address and, potentially, alleviate this disparity. We aim to investigate whether viral features can be used to identify HCC and individuals at high risk (HR) of HCC. Additionally, we examine the racial/ethnic differences in viral exposures and whether viral exposure history accounts for epidemiological disparity described previously. Herein we use a technique called VirScan, which conjugates Phage Immunoprecipitation sequencing (PhIP-seq) and DNA sequencing, to profile an individual's epitope antibody repertoire upon viral exposure. We performed VirScan on serum and plasma samples from 199 AA (130 HR and 79 HCC) and 260 European Americans (EA) (210 HR and 50 HCC) participants from the NCI-UMD cohort (NCT00913757; clinicaltrials.gov). We used a machine-learning XGBoost model to classify viral features that can discriminate HCC or HR. A composite viral score was generated using the SHAP value of the most significant viral features from the model with a higher score more predictive of HCC. Secondary analyses using Wilcoxon-Rank sums tests and Cox proportional hazard analysis revealed that while race/ethnicity did not differentially predict HCC in this cohort, the viral score was significantly higher in AA compared to EA in the HR group ($p = 0.027$). XGBoost search identified 235 important viral features which distinguish HCC from HR. Out of the 235 viral features, 20 viruses were different between AA and EA (FDR < 0.05). We also found the viral score was positively associated with incident mortality in HCC group over the study period of 8 years ($p=0.03$). Thus, we demonstrate that the viral history of an individual might be useful in early detection of HCC. This approach could be used to account for the disparities we see in both incidence and mortality of HCC between AA and EA.

#5768

Genetic screening in a tertiary medical center identifies carriers of cancer predisposition diseases that would be missed by clinical guidelines

Emily Gay[1], Niloy Jewel Samadder[2], Michelle L. Bublitz[3], Melanie M. Peterson[3], Tammy A. Wilson[3], Lorelei A. Bandel[3], Sebastian M. Armasu[3], Robert A. Vierkant[3], Matthew J. Ferber[3], Eric W. Klee[3], Nicholas B. Larson[3], Teresa M. Kruisselbrink[3], Timothy B. Curry[3], Jan B. Egan[1], Jennifer L. Kemppainen[3], Jessa S. Bidwell[3], Jennifer L. Anderson[3], Tammy M. McAllister[3], T'Nita S. Walker[3], Katie L. Kunze[4], Vanda Lindpere[4], Michael A. Golafshar[4], Margaret Klint[1], Richard J. Presutti[5], William V. Bobo[6], Aleksander Sekulic[7], Jolene M. Summer Bolster[3], Cheryl L. Willman[8], Konstantinos N. Lazaridis[9]. *[1]Clinical Genomics, Mayo Clinic Arizona, Phoenix, AZ,[2]Cancer Center, Mayo Clinic Arizona, Phoenix, AZ,[3]Mayo Clinic Rochester, Rochester, MN,[4]Biostatistics, Mayo Clinic Arizona, Phoenix, AZ,[5]Family Medicine, Mayo Clinic Florida, Jacksonville, FL,[6]Psychiatry, Mayo Clinic Florida, Jacksonville, FL,[7]Dermatology, Mayo Clinic Arizona, Phoenix, AZ,[8]Cancer Center, Mayo Clinic, Rochester, MN,[9]Center for Individualized Medicine, Mayo Clinic, Rochester, MN*

Two inherited autosomal dominant cancer predisposition conditions - *BRCA* related hereditary breast and ovarian cancer (HBOC) and Lynch syndrome (LS) - are termed Centers for Disease Control and Prevention Tier 1 (CDCT1) genetic conditions, for which early identification and intervention have a positive impact on public health. Selection of individuals for genetic testing for these conditions is based on personal and family history. The goal of this study was to evaluate whether screening in a tertiary medical center using exome sequencing could efficiently identify carriers of HBOC and LS and to determine the frequency of incremental carriers identified outside of traditional clinical practice guidelines.

Participants from three geographically diverse Mayo Clinic practices in the USA (Rochester MN, Phoenix AZ, Jacksonville FL) consented to clinical "Exome+" sequencing (Helix, San Mateo, CA; Mayo GeneGuide, Rochester, MN) in the TAPESTRY study (NCT05212428), which links sequencing data with electronic health records and the return of CDCT1 genetic findings. For this study we focused on two inherited cancer predisposition conditions: BRCA-related HBOC *(BRCA1* and *BRCA2*) and LS (*MLH1, MSH2, MSH6, PMS2* and *EPCAM*). Detailed chart review to collect demographic information, personal and family history, and assessment of clinical practice guidelines for genetic evaluation (National Cancer Control Network 2021).

To date, 44,306 patients have enrolled and sequenced in TAPESTRY. Annotation and interpretation of all variants in 7 genes for HBOC and LS resulted in identification of 550 carriers (prevalence 1.24%) which included 387 with

HBOC (27.2% *BRCA1*, 42.8% *BRCA2*) and 163 with LS (12.3% *MSH6*, 8.8% *PMS2*, 4.5% *MLH1*, 3.8% *MSH2* and 0.2% *EPCAM*). Demographics of the cohort included: 62.7% female, mean age 55.2 years, non-white race 9.6% and 3.8% Hispanic/Latino ethnicity. A personal history of cancer was present in 46.4% of test positive patients, including 22.5% of HBOC patients with breast or ovarian cancer and 20.9% of LS patients with colorectal or uterine cancer. More than half of the patients (52.1%) were newly diagnosed with HBOC and LS based on the results of this study. Overall, 39.2% of HBOC/LS carriers identified through Exome+ sequencing did not satisfy NCCN criteria for genetic evaluation, this was higher for LS (56.2%) compared to HBOC (32%). Amongst those newly diagnosed with HBOC/LS (n=286), NCCN criteria were not satisfied in 60% of cases (78% for LS and 51% for HBOC). Of the pathogenic germline variant carriers who met NCCN guidelines for testing, 34.2% were not aware of their diagnosis prior to participation in this study.
Our results emphasize the need for wide genomic screening for CDCT1 cancer predisposition syndromes. Such screening could identify at-risk carriers of HBOC and LS, who would not otherwise be identified through clinical practice guidelines.

#5769

Disparities in uptake of levonorgestrel-releasing intrauterine system (LNG-IUS): implications for uterine cancer primary prevention

Paul G. Yeh[1], Iakovos Toumazis[2], Charlotte Sun[2], Karen Lu[2], Larissa A. Meyer[2]. *[1]University of Texas Health Science Center At Houston, Houston, TX,[2]University of Texas MD Anderson Cancer Center, Houston, TX*

Introduction: Levonorgestrel-releasing intrauterine system (LNG-IUS) is associated with ~50% risk reduction for uterine cancer incidence and can be an effective primary prevention strategy. We aimed to understand current patterns of LNG-IUS use and identify disparities that could inform implementation strategies for more effective and equitable uterine cancer primary prevention.
Methods: We analyzed LNG-IUS use among U.S. women aged 18-50 with the 2017-2019 National Survey of Family Growth. Statistical analysis was stratified by race, sociodemographic, and health factors. Predictors of LNG-IUS use were assessed through weighted multivariable logistic regression using the Wald chi-square test.
Results: Current LNG-IUS use was significantly lower in Hispanic women compared to White women (AOR 0.65, *P*=0.049). Compared to women with up to a high school education, LNG-IUS use was higher for women with a college degree or higher in the overall sample (AOR 1.86, *P*=0.009), White women (AOR 1.91, *P*=0.04), and Black women (AOR 4.54, *P*=0.007), but not for Hispanic women (AOR 0.79, *P*=0.64). All racial/ethnic subgroups had lower odds of LNG-IUS for non-parous women than parous women (all *P*<0.002). Although a known uterine cancer risk factor, obesity was not associated with LNG-IUS use.
Conclusions: Hispanic women, women with lower educational levels, and nulliparous women have disproportionately low LNG-IUS use despite being at increased uterine cancer risk. Community-based educational interventions for high-risk women and their providers on the benefits of LNG-IUS on uterine cancer prevention are needed to mitigate uterine cancer disparities.
Table 1: Logistic Regression on Predictors for LNG-IUS Use in U.S. Women Aged 18-50

	OVERALL (N=4107)	**WHITE (n=1948)**	**HISPANIC (n=1052)**	**BLACK (n=861)**
	AOR (95% CI)	AOR (95% CI)	AOR (95% CI)	AOR (95% CI)
Race		Ref	**0.65* (0.42-0.98)**	0.77 (0.46-1.27)
Age				
18-24	1.16 (0.55-2.46)	1.15 (0.45-2.94)	**13.13* (1.42-121.3)**	0.55 (0.11-2.83)
25-34	1.65 (0.88-3.10)	1.46 (0.69-3.13)	**31.75** (4.04-249.5)**	0.63 (0.18-2.14)
35-44	1.07 (0.55-2.10)	1.10 (0.49-2.47)	**13.28* (1.51-116.6)**	0.54 (0.14-2.02)
45-50	Ref	Ref	Ref	Ref
Education				
≤High School	Ref	Ref	Ref	Ref
Some College	**1.56* (1.02-2.51)**	1.56 (0.83-2.94)	1.05 (0.47-2.32)	**3.90* (1.39-10.96)**
≥Bachelor's	**1.86** (1.17-2.97)**	**1.91* (1.03-3.54)**	0.79 (0.30-2.12)	**4.54** (1.51-13.65)**
BMI				
Normal	Ref	Ref	Ref	Ref

Overweight	1.44 (0.93-3.22)	1.40 (0.81-2.41)	0.96 (0.35-2.62)	1.54 (0.56-4.22)
Obese	0.87 (0.57-1.31)	0.86 (0.52-1.43)	0.68 (0.28-1.63)	1.01 (0.35-2.89)
Parity				
Parous	**2.85*** (1.89-4.30)**	**2.21** (1.33-3.67)**	**7.30*** (2.61-20.38)**	**5.38*** (2.27-12.76)**
Nulliparous	Ref	Ref	Ref	Ref

Abbreviations: AOR, adjusted odds ratio; BMI, body mass index; CI, confidence interval; Ref, reference group. *P<0.05; ** P<0.01; *** P<0.001. [a]Early Menarche <12yo; Normal Menarche 12-14yo; Late Menarche >14yo.

#5770

Cardiorespiratory fitness and BMI in youth and five-year mortality after site-specific cancer in men: a population-based cohort study with register linkage

Aron Onerup[1], Kirsten Mehlig[2], Agnes af Geijerstam[2], Elin Ekblom-Bak[3], Hans-Georg Kuhn[2], Lauren Lissner[2], Mats Börjesson[2], Maria Åberg[2]. *[1]St. Jude Children's Research Hospital, Memphis, TN,[2]University of Gothenburg, Gothenburg, Sweden,[3]The Swedish School of Sport and Health Sciences, Stockholm, Sweden*

Aim: Our aim was to assess the associations between cardiorespiratory fitness (CRF) and body mass index (BMI) in youth and five-year mortality following the diagnosis of 18 site-specific cancers in men.
Methods: We collected data on all men who underwent military conscription at ages 16-25 from 1968 through 2005 in Sweden. CRF was assessed as maximal aerobic workload on a cycle ergometer test and was classified as low, moderate, or high. BMI (kg/m2) was classified as underweight (<18.5), normal weight (18.5-24.9), overweight (25-29.9), or obesity (>30). Data was cross-linked on individual level through the Swedish unique identification number with follow-up data from national registers with high validity containing information on cancer diagnosis and mortality. Follow-up started at diagnosis and continued until death, emigration, five years after diagnosis, or end of follow-up (2019-12-31), whichever happened earliest. Time-to-event multivariable Cox regression analyses included CRF and BMI as well as age, year, and site of conscription and age at diagnosis. For CRF, primary analyses tested linear trends with categorical comparisons for interpretation while categorical comparisons were primary analyses for BMI.
Results: 84,621 cancer cases were included in the main analyses. The mean age at diagnosis of any cancer was 53 years and follow-up data were available during a mean of 6.5 years. Lower CRF and higher BMI were independently associated with higher mortality for several cancer sites (table 1).
Conclusion: We report clinically relevant, dose-dependent associations between CRF and BMI in youth and 5-year mortality after diagnosis of 18 site-specific cancers in men. The associations with mortality may be due to both direct cancer inhibition and an improved tolerance to withstand cancer treatment. These results further strengthen the incentive for promoting a healthy lifestyle during the whole lifespan of the population.

Table 1. Five-year mortality by cardiorespiratory fitness (CRF) and body mass index (BMI).

		Cardiorespiratory fitness (ref = low)		**BMI (ref = normal weight),** *= p<0.05, **=p<0.01, ***=p<0.001		
Cancer site	**n cases (% mortality)**	**High**	**p for linear trend for CRF**	**Underweight**	**Overweight**	**Obesity**
		HRR (95% CI)		HRR (95% CI)	HRR (95% CI)	HRR (95% CI)
Any cancer	84,621(16%)	0.70 (0.67-0.73)	***	0.98 (0.93-1.04)	1.38*** (1.30-1.46)	1.92*** (1.70-2.17)
Malignant skin	28,359(4%)	0.80 (0.69-0.93)	***	0.96 (0.78-1.17)	1.53*** (1.26-1.86)	2.16*** (1.33-3.49)
Bronchi and lung	2,502 (68%)	0.82 (0.72-0.94)	***	0.92 (0.80-1.07)	1.06 (0.87-1.28)	1.17 (0.81-1.69)
Head & neck	3,549 (20%)	0.69 (0.57-0.84)	***	1.07 (0.84-1.37)	1.52** (1.19-1.94)	1.41 (0.75-2.64)
Esophagus	991 (71%)	0.92 (0.76-1.13)		1.00 (0.76-1.32)	1.11 (0.88-1.39)	1.15 (0.75-1.76)

Stomach	1,269 (62%)						

0.94 (0.78-1.13)		0.95 (0.73-1.23)	1.06 (0.85-1.32)	1.20 (0.78-1.86)		
Pancreas	1,809 (71%)	0.83 (0.72-0.96)	*	1.07 (0.89-1.30)	0.96 (0.80-1.15)	1.38 (0.89-2.16)
Liver, bile ducts and gallbladder	1,573 (68%)	0.88 (0.74-1.03)	*	1.11 (0.90-1.36)	1.00 (0.81-1.22)	1.14 (0.75-1.71)
Colon	4,265 (31%)	0.96 (0.83-1.10)		1.13 (0.94-1.36)	0.99 (0.82-1.20)	1.12 (0.78-1.61)
Rectum	3,123 (27%)	0.82 (0.68-0.98)	**	1.01 (0.79-1.28)	1.47** (1.17-1.85)	1.50 (0.93-2.44)
Kidney	2,288 (24%)	1.07 (0.86-1.33)		0.70 (0.48-1.02)	1.36* (1.07-1.73)	1.83** (1.20-2.79)
Bladder	3,078 (12%)	0.71 (0.55-0.93)	*	0.75 (0.51-1.09)	0.93 (0.63-1.39)	2.06* (1.09-3.09)
Prostate	19,686(5%)	0.83 (0.70-0.97)	**	0.83 (0.66-1.05)	1.30* (1.02-1.66)	2.43** (1.40-4.21)
Central nervous system	2,937 (1,566)	0.89 (0.78-1.02)		1.05 (0.88-1.27	1.03 (0.85-1.23)	0.94 (0.58-1.52)
Thyroid gland	848 (11%)	0.94 (0.55-1.62)		1.27 (0.60-2.69)	1.36 (0.69-2.68)	3.53** (1.41-8.83)
Leukemia	2,698 (24%)	0.98 (0.80--1.20)		1.46** (1.12-1.89)	0.96 (0.73-1.28)	1.34 (0.77-2.33
Myeloma	1,209 (21%)	1.19 (0.86-		1.66* (1.06-	1.40 (0.93-	0.71 (1.18-

		1.65)		2.58)	2.09)	2.88)
Hodgkin's lymphoma	1,112 (10%)	0.82 (0.49-1.36)		1.55 (0.85-2.84)	0.89 (0.47-1.69)	2.47 (0.98-6.21)
Non-Hodgkin's lymphoma	3,261 (16%)	0.77 (0.62-0.96)	**	0.81 (0.57-1.14)	1.14 (0.86-1.52)	1.26 (1.03-1.24)

#5771

The vaginal microbiome as a mediator in the relationship between Black/White race and high grade cervical intraepithelial neoplasia

Katherine Y. Tossas[1], Stephanie Sullivan[2], Myrna Serrano[3], Jerome Strauss[1], Robert A. Winn[4], Gregory Buck[3]. *[1]Health Behavior and Policy, Virginia Commonwealth University School of Medicine and Massey Cancer Ctr., Richmond, VA,[2]OB/Gyn, Virginia Commonwealth University School of Medicine, Richmond, VA,[3]Microbiology, Virginia Commonwealth University School of Medicine, Richmond, VA,[4]Massey Cancer Center, Virginia Commonwealth University School of Medicine, Richmond, VA*

The vaginal microbiome (VMB) is implicated in the development of high-grade squamous intraepithelial lesions (HSIL). The VMB is taxonomically diverse, immunomodulatory, and racially differentiated. The VMB of Black women exhibits increased microbial diversity (associated with HPV tumorigenesis) and lower prevalence of taxa such as *Lactobacillus* (inversely associated with severity of cervical abnormalities) compared to white counterparts. Black women also have more persistent HPV infections and higher incidence of HSILs than whites. Our prior publication suggests the relationship between the VMB and HSIL might be differential by self-reported race. Herein we explore the underlying mechanisms by which race may lead to risk of HSIL through the VMB. We used 16S-rRNA VMB taxonomic profiles of 1,168 consented women receiving their annual routine exam between 2009-2013. Of these, 74 (6%) developed HSIL after the VMB sample collection (followed through 10/2020). The VMB profiles were categorized into three subgroups, based on *a priori* knowledge, by taxonomic abundance as "*Lactobacillus crispatus"* (including *L. crispatus*,

L. gasseri and *L. jensenii*, all generally associated with gynecologic health), "*L. iners"* (considered a transitional state), and "Other" (including taxa, such as *Gardenerella vaginalis*, *Atopibium vaginae*, *Lachnocurva vaginae* and others often associated with adverse gynecologic outcomes). HPV status was obtained by sequencing a fragment of the L1 gene. We used self-reported health histories, confirmed by electronic health records where available, and other socio-demographic information. HIV-positive women were excluded. We used structural equations modeling, following a normal theory maximum likelihood approach with robust errors to estimate the proportion of the association between race and HSIL mediated by the VMB, using STATA version 13.1. The cohort was predominantly Black (72%), with VMB prevalence by subgroup of 18%, 29% and 52% for *L. crispatus*, *L. iners*, and Other, respectively. Blacks had a higher prevalence of the "Other" VMB subtype, compared to nL-whites (59% vs. 49%). Forty-five percent of the sample tested positive for HPV, with no significant difference by race (p=0.9). The incidence of HSIL was nearly double for Blacks compared to whites (7% to 4%). Women with HSIL exhibited a higher prevalence of the "Other" VMB (68% vs. 51%) and were more likely to be HPV positive (73%vs. 44%) than their healthy counterparts. In SEM, only the following path was statistically significant at $p<0.05$: raceàVMBàHSIL, with an estimated proportion mediated by this path of 36%. Findings suggest the VMB is a mediator that might explain some of the underlying mechanisms of the relationship between race and risk of HSIL. If confirmed, this might have potential prophylactic and therapeutic implications as the VMB is amenable to pre and probiotics.

Diet, Nutrition, Lifestyle, and Environment and Cancer Prevention

#4228

Replacing red and processed meat with legumes modulates gut microbiome and microbiota-related metabolites linked to gut health and cancer prevention in healthy working-aged men

Tuulia Pietilä[1], Isabell Schreck[1], Tiina Pellinen[1], Johanna Vauhkonen[1], Essi Päivärinta[1], Mikko Neuvonen[2], Mikko Niemi[2], Anne Salonen[3], Anne-Maria Pajari[1]. *[1]Department of Food and Nutrition, University of Helsinki, Helsinki, Finland,[2]Department of Clinical Pharmacology, University of*

Helsinki, Helsinki, Finland,[3]Human Microbiome Research Program, University of Helsinki, Helsinki, Finland

Background **and Aim:** Changing dietary habits have great potential for colorectal cancer (CRC) prevention. Regardless of the accumulated evidence on the relationship between dietary protein sources and CRC, the explaining mechanisms remain not well established. Diet-delivered microbial metabolites such as secondary bile acids (BA), N-nitroso compounds (NOC), trimethylamine N-oxide (TMAO), short-chain fatty acid (SCFA), and branched-chain fatty acids (BCFA) have been suggested to mediate the relationship. The aim of this study was to examine the effects of partial replacement of red and processed meat (RPM), associated with higher CRC risk, with legumes on the fecal microbiota composition and metabolite profiles in healthy men.

Methods: The study was a partly controlled 6-wk parallel design randomized clinical trial (n=102, age 37 y (range 21 - 61 y), BMI 25.5 ± 3.3 kg/m^2) with two groups following either a diet supplemented with RPM (meat group) or a diet supplemented with legumes and RPM (legume group). The amount of RPM (200 g/wk) in the legume group was based on the maximum amount recommended by the EAT-Lancet Commission whereas the amount in the meat group (760 g/wk) corresponded the average intake of Finnish men. Fecal SCFAs (μg/ml) and BCFAs (μg/ml) were analyzed with GS-MS, BAs (arbitrary, analyte/standard ratios) with UHPLC-MS/MS, and NOCs (pmol/mg) with selective de-nitrosation and chemiluminescence-based detection. Urine TMAO was quantified by NMR and fecal microbiota composition was analyzed using 16S rRNA amplicon sequencing techniques. Dietary intakes were analyzed with 4-day food records.

Results: At the baseline, no significant differences ($p > 0.05$) were reported in age, BMI, dietary intake of total fiber (g/d), protein (E%), fat (E%), or in the fecal metabolites. The legume group had more pronounced effects on the gut microbiota community level, indicating ecosystem level differences. Total NOCs ($p < 0.0001$) and heme-originated NOCs (FeNO; $p < 0.0001$) were smaller in the legume group than in the meat group. Significant differences between the groups were observed in intake of total fiber ($p < 0.001$), cholesterol (mg/d, $p < 0.001$), saturated ($p < 0.005$), and polyunsaturated fat ($p < 0.001$). Although not significant ($p > 0.05$), total,

secondary and unconjugated BAs, and total BCFA were higher in the meat group, whereas primary and conjugated BAs and total SCFAs were higher in the legume group. The concentration of total SCFA and individual SCFA decreased in both groups during the intervention period. Overall, a large sample-to-sample variation was observed.
Conclusions: The results indicate that partial replacement of RPM with legume products can potentially change microbiota activity and gut metabolites, suggesting a protective gut metabolic profile against colorectal cancer.

#4229
Differential impact of rice bran based dietary interventions during inflammation-associated colorectal cancer on distinct immune infiltrates and their spatial distribution signature
Robin Kumar[1], Akhilendra K. Maurya[2], Lakshmi S. P. Bugata[3], Md. I. Kabir[3], Munendra Tomar[2], Rajesh Agarwal[2], Elizabeth P. Ryan[4], Komal Raina[3]. *[1]Dept. of Pharmaceutical Sciences, South Dakota State Univ., Brookings, SD,[2]Univ. of Colorado Anschutz Medical Campus, Aurora, CO,[3]South Dakota State Univ., Brookings, SD,[4]Colorado State University, Fort Collins, CO*

Modulating the immune cell infiltrates in the colonic tissue *via* dietary intervention or modulation of the gut microbiota and its crosstalk with the components of the diet is now recognized as an effective strategy to protect against inflammation-associated colorectal cancer (CRC). In this regard, we recently reported, both gut microbiota-dependent and independent mechanisms for dietary rice bran (RB) meditated protective efficacy against inflammation-associated azoxymethane /dextran sodium sulfate (AOM/DSS)-induced CRC. We also reported that *ex vivo* fermentation of RB with beneficial microbe '*Bifidobacterium longum'* did not exhibit similar protective benefits as RB in damaged colonic tissues in the absence of gut microbiota [germ-free (gf) mice]. The role of rice bran (RB) constituents as prebiotics and in preserving gut barrier and a healthy gut microbiota led to in-depth investigation into the protective efficacy of RB against CRC. Accordingly, in the present study, we performed multiplex imaging (9 color panel) to assess immune sub-typing and spatial phenotypic signature of the colonic tissue/tumor microenvironment in the AOM/DSS^{gf}

mice [following RB and fermented RB (FRB) dietary intervention]. Briefly, we determined the presence of T cells [$CD3^+$], cytotoxic T cells [$CD3^+$ $CD8^+$], helper T cells [$CD3^+$ $CD8^-$], regulatory T (Treg) cells [$CD3^+CD8^-$ $FoxP3^+$), natural killer (NK) cells [$CD49b^+$], NKT cells [$CD3^+CD49b^+$], macrophage (MΦ) [F4/80 $^+$], M1 [$F4/80^+iNOS^+CD206^-$] and M2 [$F4/80^+CD206^+$] subtypes and B cells [$B220^+$]. Results indicated an overall high infiltration of immune cells in female AOM/DSS^{gf} mice on control diet compared to males, which was positively correlated with severe pathological changes observed in the female colon tissues. Notably, RB and FRB diets showed a differential impact on the sub-type of immune cells and their spatial localization. Protective efficacy of RB was associated with decrease in infiltration of T cells (including their subtypes). Interestingly, while cytotoxic T cells were lower in FRB (AOM/DSS^{gf}) female mice, there was a significant increase in pro-inflammatory M1 MΦ sub-types in colon tissue of mice marred by epithelial erosion which compromised FRB potential. Spatial distance analysis also indicated that immune cells were distantly spaced in RB intervention groups compared to FRB and AOM/DSS^{gf} controls. Though, M2 MΦ were relatively higher in number in AOM/DSS^{gf} controls, their presence did not have influence on protective efficacy or lack thereof. In general, it was inferenced that the protective efficacy of the RB diets in the absence of gut microbiota was positively correlated with modulation of T cell infiltration while inflammation-associated CRC and epithelial erosion in FRB diet groups were associated with skewed MΦ sub-types-with increased presence of M1MΦ.

#4230

Transcriptomic evaluation of exercise-induced suppression of prostate cancer aggressiveness

Darpan I. Patel, Paul Rivas, Yidong Chen, Zhao Lai, Robert L. Reddick, Yuji Ikeno, Rita Ghosh, A. Pratap Kumar. *The University of Texas Health Science Center at San Antonio, San Antonio, TX*

Previous studies from our laboratory have showed that aerobic exercise significantly reduced the number of aggressive poorly differentiated tumors in the transgenic adenocarcinoma of the mouse prostate (TRAMP) model. Despite these encouraging data the underlying mechanism of how exercise

reduces tumor aggressiveness remains undefined. We aimed to fill this scientific gap by utilizing a transcriptomics approach to identify potential mechanisms by which aerobic exercise suppresses prostate tumor aggressiveness.
Methods: Twelve TRAMP mice, 8-10 weeks of age, were equally randomized to exercise or control group. Mice in the exercise group were singularly housed in cages with running wheels for 12 weeks. Mice in the control group maintained normal group housing and activity conditions for 12 weeks. At euthanasia, prostate tumors were excised, weighed and processed for immunohistochemistry and transcriptome analysis. Two independent pathologists, blinded to the interventions, performed histological analysis of the genitourinary mass. Outputs of sequencing data were assessed for quality and accuracy. Counts for all known mRNA, differential expression, and heatmap were prepared. Differential expression was filtered to identify genes that had a ≥2-fold change with an adjusted $p<0.05$. Gene ontology and pathway analyses was performed to reveal selective pathways activated.
Results: No significant difference in genitourinary mass, body mass or tumor free body mass was found between groups. Pathology revealed majority of the tissue from the control group exhibited moderate to poorly differentiated tumors (3/6). On the other hand, none of the animals in the exercise intervention group showed such pathology. Four out of five showed well differentiated tumors including prostatic intraepithelial neoplasia (PIN) lesions in one animal. Transcriptomic analysis coupled with gene set enrichment identified pathways associated with triglyceride catabolic process, lipid homeostasis, lipid metabolic process, triglyceride metabolic process to be most impacted. Differentially expressed genes of interest include haptoglobin (HP) and hormone sensitive lipoprotein lipase (Lipe) were significantly lower in the exercise group.
Conclusion: Our preliminary findings provide novel evidence suggesting that exercise suppresses prostate tumor aggressiveness, in part, through transcriptomic modulation and altered cellular pathways associated with intratumoral energy metabolism. This project was supported by the National Center Institute designated Mays Cancer Center at UT Health San Antonio.

#4231

The anti-cancer effects of vitamin D are blocked postpartum due to suppression of vitamin D metabolism in the liver

Sarah M. Bernhardt, Pepper Schedin. *Oregon Health & Science University, Portland, OR*

Postpartum breast involution is a physiologic inflammatory process that associates with increased risk of postpartum breast cancer (PPBC). In rodents, involution promotes breast cancer progression, and treatment with anti-inflammatory agents is protective. These data provide rationale for targeting the pro-tumor window of involution with anti-inflammatory agents for PPBC prevention. Vitamin D is another anti-inflammatory agent with a good safety profile. In postpartum women, vitamin D deficiency is prevalent, suggesting vitamin D supplementation during involution may prevent development of PPBC.

To model vitamin D deficiency and supplementation, BALB/c mice were fed diets deficient or supplemented with vitamin D for 4 weeks. Blood was then collected from nulliparous (never-pregnant) and 2 days post-wean (involution) mice, and serum vitamin D (i.e. 25(OH)D) measured. As expected, nulliparous mice fed a vitamin D supplemented diet showed a >2-fold increase in serum 25(OH)D (67.4±8.1nmol/L) compared to mice fed a vitamin D deficient diet (28.7±11.7nmol/L, $p<0.01$). In contrast, involution mice fed a vitamin D supplemented diet did not show increased serum 25(OH)D (supplemented 46.6±8.7nmol/L vs deficient 33.7±8.5nmol/L, $p>0.05$).

Activation of dietary vitamin D requires hydroxylation in the liver, producing both circulating (25(OH)D) and active ($1,25(OH)_2D$) forms. Thus, reduced serum 25(OH)D in vitamin D supplemented involution mice could be due to impaired vitamin D hydroxylation in the post-wean liver. Analysis of livers collected from involution and nulliparous mice found reduced expression of genes involved in vitamin D hydroxylation (*Cyp2r1*, *Cyp27a1*) during involution. Further, liver concentrations of $1,25(OH)_2D$ were reduced 3-fold in involution mice (0.31±0.29ng/g) compared to nulliparous mice (0.90±0.37ng/g, $p=0.04$). Together, these findings suggest that impaired metabolism of vitamin D in the postpartum liver may reduce bioavailability of active vitamin D, and provide corroborative evidence for weaning-induced liver involution.

To understand how suppressed vitamin D metabolism in the postpartum liver affects the anti-cancer activity of dietary vitamin D, mammary cancer cells (D2A1, 2×10^4 cells, 20μL) were injected into mammary fatpad of involution or nulliparous BALB/c mice, and tumor growth tracked for 4 weeks. In nulliparous mice, vitamin D supplementation associated with a 3-fold reduction in tumor growth (p=0.03); whereas no anti-cancer effects were observed in involution mice. Together, these findings suggest the anti-cancer effects of vitamin D are blocked postpartum, likely due to suppression of vitamin D metabolism in the liver. Understanding how postpartum liver metabolism influences efficacy of preventative agents that require liver metabolism (such as vitamin D) is required to optimize cancer prevention strategies that target this window.

#4232

Dairy product consumption across the life course and breast cancer risk

Emily Riseberg[1], Wai Ching Lam[2], You Wu[3], A. Heather Eliassen[1], Molin Wang[4], Xuehong Zhang[1], Stephanie Smith-Warner[1], Walter C. Willett[1].
[1]Nutrition, Harvard T.H. Chan School of Public Health, Boston, MA,[2]Epidemiology, Harvard T.H. Chan School of Public Health, Boston, MA,[3]Institute for Hospital Management, School of Medicine, Tsinghua University, Beijing, China,[4]Biostatistics, Harvard T.H. Chan School of Public Health, Boston, MA

Previous literature on dairy products and risk of breast cancer is inconsistent, and the relationship may depend on the life period of the dietary assessment and menopausal status. We aimed to prospectively investigate dairy product consumption during adolescence, pre-menopause, post-menopause, and lifetime in relation to risk of breast cancer overall and by tumor subtypes. We analyzed data from 59,655 women in the Nurses' Health Study (NHS) collected from 1980 to 2016. Average intake of dairy products during adulthood was assessed by validated semi-quantitative food frequency questionnaires (FFQ) assessed every 2 to 4 years throughout follow-up. Participants reported recalled adolescent dietary intake in 1986. Premenopausal intake was calculated as the cumulative average intake from the 1980 FFQ to the last FFQ completed prior to premenopausal breast

cancer diagnosis or menopause. Postmenopausal intake was calculated as the intake from the first FFQ after menopause to postmenopausal breast cancer diagnosis or end of follow-up. Lifetime intake was calculated as the average of adolescent, premenopausal, and postmenopausal intake. Cox proportional hazards models were used to estimate hazard ratios (HRs) relating dairy product consumption to breast cancer risk overall and by subtype. Models were adjusted for age, race, height, body mass index, alcohol intake, energy intake, and other breast cancer risk factors and lifestyle factors. We documented 5,549 incident cases of invasive breast cancer during 30 years of follow-up (N=5,128 postmenopausal). Adolescent total dairy intake was modestly associated with higher breast cancer risk (HR for a 1 serving/d increment=1.03; 95% confidence interval [CI]=1.00, 1.07). Similar results were found for adolescent milk intake (HR=1.04; 95% CI=1.02, 1.08). In contrast, adolescent cheese intake was associated with a lower risk of breast cancer (HR=0.83; 95% CI=0.70, 0.98). All three associations were more apparent for postmenopausal compared to premenopausal breast cancer. For lifetime intake, only the association with cheese intake was maintained (HR=0.83; 95% CI=0.73, 0.93). Observed inverse associations between lifetime and adolescent cheese intake and breast cancer appeared stronger among estrogen receptor negative and luminal B (adolescent only) subtypes. These findings suggest that adolescent and lifetime cheese intake may be associated with reduced risk of breast cancer and adolescent milk intake may be associated with increased risk.

#4233

The anti-genotoxic function of *Lactobacillus* species in the context of bile-mediated DNA damage and inflammation in experimental models of GERD

Joshua Bernard, Divya Joshi, Claudia Andl. *College of Medicine, University of Central Florida, Orlando, FL*

Lactobacillus species are commensal organisms with probiotic characteristics found in the human oral cavity and gastrointestinal tract. It has been shown that gram-positive organisms, including lactobacilli, make up the majority of the microbiome in the healthy human esophagus. The general consensus is that the microbiome shifts from gram-positive to

gram-negative bacteria during gastroesophageal reflux disease (GERD). In patients suffering from GERD, the esophageal tissue is injured by the low pH and bile acids present in the refluxate, resulting in Barrett's esophagus if untreated. Interestingly, it has been reported that there is a proportional increase in gram-positive lactobacilli within the esophagus during the progression from GERD to Barrett's esophagus, and finally esophageal adenocarcinoma. To investigate how lactobacilli are able to colonize and survive in a bile-rich environment of the esophagus during GERD, we first exposed three *Lactobacillus* species (*L. acidophilus, L. plantarum, and L. fermentum*) to cholate/deoxycholate bile salts or ox-bile as a more physiological model for human reflux. All three species exhibited bile resistance, in addition to bile adaptation after pre-exposure to sub-lethal concentrations. When assessed for changes in bacterial cell surface hydrophobicity, an indicator for bacterial adhesion to various surfaces, both bile types led to an increase of hydrophobicity in *L. plantarum* and *L. fermentum*, while *L. acidophilus* remained high. This provides mechanistic insight into how *Lactobacillus* species' attachment and colonization remain during reflux-related diseases. Next, we assessed the host-microbe interactions between lactobacilli and esophageal cells and the role these probiotic organisms may have in disease prevention. Acidic bile salts can induce inflammation and DNA damage to esophageal tissue through ROS during GERD, yet we found that the presence of lactobacilli co-cultured with bile-treated esophageal epithelial cells aids in the repair of bile-induced DNA damage in addition to NFKB reductions. To further investigate the host-microbe interactions, we supplemented epithelial cells with lactobacilli postbiotic metabolites and assessed cell viability during 48 hours of growth. Our current preliminary data show that postbiotic supplementation increases cell viability, providing insight into why lactobacilli are present within the normal and diseased human esophagus. This study demonstrates how the colonization of the esophagus during GERD with lactobacilli is based on their adaptability and survival due to changes in hydrophobicity thereby sustaining attachment. Furthermore, the anti-genotoxic and anti-inflammatory effects these organisms exhibit make them of significant interest in the prevention of Barrett's esophagus and esophageal adenocarcinoma in patients with GERD.

#4234

Effects of age-diet interactions on colorectal cancer (CRC) progression in mice

Jae Ho Lo[1], Shivani Soni[1], Yan Yang[2], Goar Smbatyan[1], Junxiang Wan[3], Joshua Millstein[2], Kelvin Yen[3], Hemal H. Mehta[3], Brendan Miller[4], Francesca Battaglin[1], Pooja Mittal[1], Lesly Torres Gonzalez[1], Wu Zhang[1], Pinchas Cohen[3], Heinz Josef Lenz[1]. *[1]Medical Oncology, USC Norris Comprehensive Cancer Center, Los Angeles, CA,[2]Department of Population and Public Health Sciences, University of Southern California, Los Angeles, CA,[3]Leonard Davis School of Gerontology, University of Southern California, Los Angeles, CA,[4]Salk Institute for Biological Studies, La Jolla, CA*

Background**.** CRC is the third leading cause of cancer related deaths worldwide with age and diet are among the strongest risk factors. CRC characteristics appear to be distinct between younger and older patients. We evaluated the effects of age on CRC tumor biology using syngeneic mice models with a focus on a) specific differences in tumor growth patterns and the role of the tumor microenvironment (TME) in young versus old mice harboring CRC allografts; b) differential dietary effects in young versus old hosts.

Methods. $1X10^6$ MC38 cells were subcutaneously implanted into the right flank of young (6 weeks) or old (24 months) C57BL/6 male mice. Mice were randomized into 3 diet groups: A. Standard Chow (SC); B. Calorie Restriction (CR: 30% reduction in total calories); C**.** High Fat (HF). Parameters studied were daily food intake, body weight, tumor growth and survival. Once endpoint reached, tumors were isolated and processed for RNA sequencing. Cytokine analysis was done on plasma using multiplex immunoassays on the Meso Scale Discovery platform.

Results. Both old and young mice showed significant reduction in tumor growth while on the CR protocol when compared to other dietary groups. Young mice fed with HF diet had increased tumor growth as compared to old. Cytokine analysis showed that the pro tumorigenic IFNγ, TNF α, IL10, IL-12p70, and 1L6 were higher in old mice relative to young. Caloric restriction irrespective of age led to significant reductions in IFNγ, TNFα, and 1L6 compared to other diets. Irrespective of diet, IL10, known for its immunosuppressive role in CRC, was significantly lower in young versus

old mice. Proinflammatory IL-5 was significantly higher in young fed a HF diet compared to the other groups. RNA sequencing of the allograft tumors at the end of the study revealed that differentially expressed genes (DEGs) between young and old mice tumors were dramatically influenced by diet. The most affected gene expression pathways were antigen processing and presentation, MHC-II complex assembly and T cell activation. Diet affected the tumor expression of key oncogenes associated with immune escape, cell proliferation, invasion, metastasis, chemotaxis, ECM remodeling and chemosensitivity which were upregulated in old mice and HF diet. **Conclusion.** Based on transcriptomic profiles and comprehensive cytokine analysis, our data shows that age-diet interactions significantly influence the host TME leading to differential gene expression in the tumor. Our findings will advance current understanding of the mechanisms by which aging and diet impact CRC onset, progression, metastasis, and therapeutic response but warrants further investigation.

#4235

Obesity drives inflammation and metabolic reprogramming in an orthotopic mouse model of early colon cancer

Elaine M. Glenny[1], Babak Mirminachi[2], Tori L. McFarlane[3], Jatin Roper[4], Stephen D. Hursting[1]. *[1]University of North Carolina at Chapel Hill, Chapel Hill, NC,[2]Medicine, Duke University, Durham, NC,[3]Nutrition, University of North Carolina at Chapel Hill, Chapel Hill, NC,[4]Medicine and Pharmacology and Cancer Biology, Duke University, Durham, NC*

Obesity is strongly associated with colon cancer incidence and, in animal models, promotes colon cancer growth and progression. Mounting evidence indicates that circulating growth factors and chronic inflammation are procancer factors likely mediating this relationship. While obesity blunts antitumor immunity in many cancer types, how obesity-driven inflammation and reduced antitumor immunity may cooperate to promote colon cancer progression is not yet clear. Here we used a murine syngeneic orthotopic transplantation model of colon cancer to profile changes driven by diet-induced obesity (DIO) in the immune and cancer cell compartments of the tumor using digital spatial profiling and RNA sequencing. 7-9-week-old male and female C57BL/6 mice remained on either a 10 kcal% fat diet (control, n=34) or a 60 kcal% fat diet (DIO, n=27) for at least 19 weeks.

700 *Apc-null;KrasG12D/+;Trp53-null;Smad4-null;tdTomato* (i.e., AKPS) organoids were transplanted into the colonic wall of control and DIO mice via colonoscopy-guided injection. Tumors were excised after four weeks of growth, an early time point to assess changes between diet groups independent of tumor size differences or weight loss associated with tumor growth. RNA sequencing was performed on RNA extracted from tumoral CD45+ and EpCAM+ cell fractions isolated using Milltenyi MicroBeads. DIO mice weighed more than controls (males: controls 37.0 g ± 5.1 *vs.* DIO 47.4 g ± 4.3; females: controls 26.4 g ± 3.7 *vs.* DIO 45.9 g ± 9.7) and had more mesenteric fat surrounding the colon (males: controls 388 mg ± 217 *vs.* DIO 577 mg ± 185; females: controls 201 mg ± 143 *vs* 1176 mg ± 589). Leptin, resistin, and plasminogen activator inhibitor-1 were significantly elevated in the serum of DIO mice relative to control mice. Tumor weight did not differ between groups. Gene set enrichment analysis demonstrated that tumor cells from DIO mice were significantly enriched for pathways related to inflammation (INFLAMMATORY_RESPONSE, IL6_JAK_STAT3_SIGNALING), glucose and lipid metabolism (GLYCOLYSIS, FATTY_ACID_METABOLISM), and proliferation (E2F_TARGETS, G2M_CHECKPOINT). Within the CD45+ transcriptomic profiles, Tumor Immune Estimation Resource (TIMER2.0) indicated an increase in M0- and M1-like macrophages and B cells in tumors from DIO compared with control mice. Analysis of whole tumor sections from DIO mice showed significantly reduced CD3+ cells by immunofluorescence and more Ki67+ CD45+ immune cells by digital spatial profiling relative to tumors from control mice. Taken together, obesity drives an inflammatory profile in both the immune and epithelial cell populations of AKPS murine tumors, which is associated with increased markers of proliferation. Future studies will address whether inflammatory signals from the mesenteric fat adjacent to the colon tumors may contribute to obesity-driven tumor inflammation, and thereby to colon cancer progression.

#4236

Obesity-associated endometrial cancer: Identifying the contributions of TMEM205 expression to the pathogenesis of disease

Takahiko Sakaue[1], Roman Zingarelli[1], Wafa Khadraoui[1], Uksha Saini[1], John Wallbillich[1], Muralidharan Anbazhakan[2], Ross Warner[1], Kalpana

Deepa Priya Dorayappan[1], Deepika Kalaiyarasan[1], Molly Morton[1], Casey Cosgrove[1], Adrian Suarez[1], Larry J. Maxwell[3], David O'Malley[1], David E. Cohn[1], Karuppaiyah Selvendiran[1]. *[1]The Ohio State University Wexner Medical center, Columbus, OH,[2]Tulane University, New Orleans, LA,[3]Inova Schar Cancer Institute, Fairfax, VA*

Background & Objective: Endometrial cancer (EC) is the most common gynecologic malignancy in the US. EC is more strongly associated with obesity than any other cancer type, with 57% of cases linked to obesity. As rates of obesity increase, the incidence of EC is also rising with worsening prognosis. The objective of this study is to identify the molecular mechanisms of TMEM205 expression that regulate exosome secretion, and the oncogenic proteins that underlie this transformation. Our findings are critical to understanding the pathways of obesity mediated EC and essential for developing novel strategies for preventing and treating EC.
Methods: The exosomes were then quantified using nanoparticle tracking analyzer (NTA) and their size measured by Transmission electron microscopy (TEM). TMEM205, STAT5, FAS and PIAS3 expression was confirmed by IHC, WB and RT-PCR in patient and high fat diet treated mouse tissue. Endometrial hyperplasia was developed in immunocompetent mice using high fat diet (HFD; 45 kcal% fat diet) for 16 weeks.
Results: To examine the effect of a continuous HFD (45 kcal% fat diet) on adipose, uterine and endometrial tissue, we first investigated body weight and uterine morphology in mice after 24 weeks of treatment. As expected, mice fed a HFD had a significantly higher body weight and increased adipose tissue when compared to control. In addition, mice in the HFD group showed marked enlargement in uterine horn size (hyperplasia) and inflammation with increased cell proliferation in the endometrial layer. The HFD treated mice were associated with increased exosome secretion and expression of the oncogenic proteins TMEM205 and STAT5. Expression of the tumor suppressor gene PIAS3 wasdownregulated in adipose and uterine tissues. L-2265 is a small molecule inhibitor that selectively inhibits TMEM205 and exosome secretion in EC cancer cells. To examine the effect of L-2263 in the context of obesity, we fed mice a HFD and treatment with L-2263 (2mg/kg/) weekly for 3 doses. L-2263 treatment resulted in significantly decreased body weight (BW) and decreased accumulation of adipose tissue relative to control HFD treated mice. Mice in the HFD group

showed marked enlargement in uterine horn size (hyperplasia), whereas mice that received L-2263 treatment had normal uterine morphology of mouse age. L-2263 treated mice also demonstrated a significant decrease in the expression of proteins involved in exosome secretion (e.g., TMEM205 and STAT5) and those found in exosomes.
Conclusion: This study provides fundamental insight into the mechanism of obesity-mediated TMEM205 expression and exosome secretion and their contribution to the pathogenesis of EC. This study is also provides pre-clinical evidence for the development of the first in-human studies of exosome-targeted therapies to prevent obesity-mediated EC.

#4237

Social isolation induces gut dysbiosis, mitochondrial metabolic dysfunction, and infiltration of tumor immunosuppressive cells: Do they explain enhanced mammary tumorigenesis?

Fabia de Oliveira Andrade[1], Maddie McDermott[1], Lu Jin[1], Vivek Verma[1], Karla Andrade de Oliveira[1], Christopher Staley[2], Leena Hilakivi-Clarke[1].
[1]The Hormel Institute, University of Minnesota, Austin, MN,[2]University of Minnesota, Minneapolis, MN

Social isolation (SI), are associated with increased mortality from many diseases, including breast cancer. Up to 41% of breast cancer patients are estimated to feel socially isolated when assessed between 6 months and 2 years following their cancer diagnosis. Since socially isolated breast cancer survivors are at a 64% higher risk of breast cancer-specific mortality than socially integrated survivors, the biological mechanisms which mediate the effects of SI need to be identified to prevent increased mortality. In a preclinical model, we found that SI caused recurrence of mammary cancers which had been treated with hormone therapy and thus led cancer cells to emerge from dormancy. We further found that mammary glands of SI rats exhibited upregulation of IL6/JAK/STAT3 signaling pathway and impaired oxidative phosphorylation (OXPHOS), compared with group housed (GH) rats. We investigated if these changes could be mediated through the gut-brain-axis. Stress can affect the gut microbiota, and the gut microbiota is critical for regulating the host immunity. In four separate experiments, the effect of SI on the gut microbiota composition was assessed in C57BL/6 mice that were either group housed or housed singly in SI for 4 weeks. In

each study replicate, several differences in the gut microbiota composition were seen, but these differences were mostly unique to each experiment. Beta-diversity was increased in three of the four experiments in SI mice. Nevertheless, at the genus level, SI suppressed the abundance of *Akkermansia* in all four replicates and increased *Acetatifactor* in three of the four replicates. These two bacterial changes are expected to disrupt OXPHOS, perhaps by resulting a suppression in short-chain fatty acid production. Further, low *Akkermansia* and high *Acetatifactor* are expected to increase inflammation. Thus, it is possible that the changes in the composition of the gut microbiota of SI animals explain an increase in IL6 signaling and a suppression in OXPHOS in their mammary gland. We also have studied immune cells in the spleen in SI and GH mice. SI increased the frequency of pro-inflammatory CD4+RORy+ cells, and the immunosuppressive Treg cells (CD4+Foxp3+) and myeloid derived suppressor cells (PMN-MDSCs). SI also increased PD1 expression in Foxp3+ cells. In an on-going study, we found that fecal microbiota transplant (FMT) from SI mice increased E0771 mammary tumor growth in antibiotic treated GH recipient mice, compared with mice receiving FMT from GH mice. Whether the FMT also altered IL6 and OXPHOS signaling in the mammary glands and tumors of recipient mice is currently being investigated. Our findings suggest that social isolation may increase breast cancer through inducing gut dysbiosis.

#4238

Specific oral microbiome is closely associated with oral potentially malignant disorders and oral squamous cell carcinoma

Mitomu Kioi, Hiroshi Isono, Shintaro Nakajima. *Oral and Maxillofacial Surgery, Yokohama City Univ. Graduate School of Med., Yokohama, Japan*

Background: Bacterial and virus infection may cause pre-malignant and malignant disorder such as hepatocellular carcinoma and cervical cancer. Recent studies reported that oral bacterium is associated with gastric and colon cancer. However, it is not clear yet if the oral microbiome affects the development of pre-malignant disorder in oral cavity and oral cancer. Thus, this study aims to identify the periodontal pathogen candidates involved in the onset and progression of oral squamous cell carcinoma (OSCC).

Materials and Methods: Saliva was collected from 112 patients without oral mucosal diseases (OMDs) as control, 36 patients with oral potentially malignant disorders (OPMDs), and 104 patients with OSCC, and DNA was extracted in each sample. Periodontal examinations were performed on all patients. Endpoint-PCR was performed on seven species of oral pathogens using the extracted DNA. 16S ribosomal RNA (rRNA) was utilized for analysis of oral microbiome with 20 samples in each group. 4-nitroqquinoline-1-oxide (4-NQO)-induced tongue tumor model in mice was analyzed with or without endotoxin of one of the oral bacteria, *Porphyromonas gingivalis* (*P. gingivalis*).
Results: From the statistical analysis of the clinical parameters, periodontal disease tended to worsen in the OMPD and OSCC groups compared to the control group. The number of oral bacteria was significantly higher in the OSCC group than those in other groups. From PCR results, the detection rates of *P. gingivalis*, *Aggregatibacter actinomycetemcomitans*, and *Treponema denticola* were significantly higher in the OSCC group than those in the control group. From 16S rRNA analysis, the relative abundance of *Prevotella buccae* and *intermedia* was significantly higher in OSCC groups than in the control group. Furthermore, the relative abundance of *P. gingivalis* was higher in the OSCC group compared to other groups, regardless of age and the number of teeth. In mouse model, mice treated with *P. gingivalis*-derived endotoxin developed oral leukoplakia at earlier time points and tumors significantly higher lesions compared to control group.
Conclusion: These results suggest that specific periodontal pathogens are present in the oral cavity of OPMDs and OSCC patients and those changes in the bacterial flora due to their presence may contribute to the onset and progression of OMDs.

#4239

Alternate-day fasting enhances the activity of anti-androgen therapy in prostate cancer models

Ricardo Cordova[1], May Elbanna[1], Angela Klunk[1], Christopher Rupert[2], Li Shen[2], Yanqing Wang[3], David Goodrich[3], Ron Wek[1], Kirk Staschke[1], Luigi Fontana[4], Roberto Pili[5]. *[1]Indiana University, Indianapolis, IN,[2]University at Buffalo, Buffalo, NY,[3]Roswell Park Cancer Institute, Buffalo, NY,[4]Sydney*

Medical School, Sydney, Australia,[5]Medicine, University at Buffalo, Buffalo, NY

Prostate cancer (PCa) is the most common cancer diagnosed in men in the Western countries. Epidemiological studies have suggested that environmental factors such as the Western diet, characterized by the consumption of high caloric food containing large amounts of animal protein and fats, play a key role in the pathogenesis of PCa. We propose that dietary intervention, by reducing caloric or protein intake, may be beneficial for the treatment of PCa. Our previous data suggests that dietary protein restriction reduces tumor growth in a LuCaP23.1 patient-derived xenograft (PDX) model of PCa. Thus, we tested the hypothesis whether caloric restriction induced by alternate-day fasting has a similar effect. Interestingly, caloric restriction had antitumor activity in the LuCaP23.1 model but only alternate-day fasting reduced the expression of androgen receptor (AR), a major driver of PCa growth. Therapies targeting AR activity, termed androgen deprivation therapies including the AR antagonist enzalutamide (ENZ), are the current standard of care for PCa. To address the therapeutic potential of combining alternate-day fasting with anti-androgens, we utilized the syngeneic mouse PCa xenograft models MyC-CaP and PTEN$^{-/-}$ RB$^{-/-}$, and the human LuCaP23.1 PDX model. These AR-positive xenograft models harbor the oncogenic drivers most frequently found in PCa (i.e., MYC amplification and loss of the tumor suppressor PTEN). Here, we show that alternate-day fasting enhances the activity of ENZ in these PCa xenograft models. Interestingly, the combination of alternate-day fasting with ENZ treatment reduced AR expression and signaling, and decreased proliferation and tumor growth as compared to either single treatment alone. Consistent with these findings, the reduction of AR activity by the depletion of endogenous androgens following surgical castration was enhanced with alternate-day fasting. Conversely, dietary protein restriction had no effect in combination ENZ *in vivo*, suggesting that modulation of AR by alternate-day fasting enhances the effect of anti-androgens. Transcriptomic analysis of tumors from fasted mice confirmed decreased AR transcriptional activity and revealed that several nutrient sensitive pathways were reduced by this dietary regimen, including PI3K/AKT signaling, mTORC1 signaling, and glycolysis. Additionally, we observed that several known factors induced by fasting were upregulated in

tumors from fasted mice, including SIRT1 which has been suggested to modulate AR transcriptional activity. In conclusion, we demonstrate that alternate-day fasting reduces AR signaling and enhances the activity of ENZ in several PCa xenograft models. Overall, this study suggests that caloric restriction may improve the efficacy of anti-androgen therapy in PCa patients.

#4240

Tumor PD-L1 induction associated with dietary protein restriction is modulated by PERK activation

Ricardo Cordova[1], Sean Colligan[2], Chris Rupert[2], Ronald Wek[1], Kirk Staschke[1], Roberto Pili[2]. *[1]Indiana University, Indianapolis, IN,[2]University at Buffalo, Buffalo, NY*

Tumor cells rely on the Integrated Stress Response (ISR) to adapt to different environmental and physiological stresses. The ISR is comprised of four eIF2 kinases that sense different stresses and catalyze phosphorylation of the alpha subunit of eIF2. This results in inhibition of global translation initiation, but at the same time results in preferential translation of select mRNA transcripts in order to relieve stress. Recent work has suggested that programmed death-ligand 1 (PD-L1), a cell surface protein commonly upregulated by tumors to evade the immune system, may be translationally regulated by the ISR in cancer. PD-L1 interaction with immune-checkpoint receptor programmed death-1 (PD-1) leads to the negative regulation of T cell activation and inhibitors that block the PD-L1/PD-1 interaction are widely used to treat different cancers. The ISR may serve as a novel therapeutic target to modulate PD-L1 protein levels and treat immune-evasive cancers. Our group has previously reported that dietary protein restriction increases the anti-tumor effect of PD-1 inhibition in the RENCA kidney cancer mouse model. Here, we show that in the RENCA model, phospho-PERK and phospho-eIF2α protein levels correlate with PD-L1 induction associated with dietary protein restriction. This is supported by TCGA data that shows a correlation between PERK and PD-L1 mRNA levels in different genitourinary cancers. *In vitro*, activation of the eIF2 kinases PERK and GCN2 by ER stress and amino acid starvation, respectively, in both RENCA cells and prostate cancer cells, leads to induction of PD-L1 protein without changing mRNA levels, suggesting

preferential translation under stress conditions. Inhibiting PERK using selective inhibitors blocked ER stress-induced induction of PD-L1. These data support the notion that PD-L1 is induced by dietary protein restriction and is translationally regulated by the ISR. Modulating PD-L1 protein levels in immune-evasive tumors by targeting the ISR in the context of dietary protein restriction may enhance the anti-tumor response to immune checkpoint inhibitors.

#4241

Reducing your risk cancer-focused health events to meaningfully engage the medically underserved and diminish future cancer disparities

Melinda Butsch Kovacic[1], Susan Gertz[2], Lauren Bates[3], Susan Hershberger[2], We Engage 4 Health Community-Academic Partnership.
[1]University of Cincinnati, Cincinnati, OH,[2]Miami University, Oxford, OH,[3]Cincinnati Children's Hospital Medical Center, Cincinnati, OH

Lack of access to cancer prevention education, early screening, and timely treatment, particularly in low socioeconomic, underserved communities, are cited as substantial barriers to improving survivorship. Outreach educational efforts with on-site screenings offered in partnership with community groups are known to be valuable in encouraging community members' uptake of healthy behaviors and adherence to screening recommendation. To create more engaging events, a community-academic partnership, We Engage 4 Health (WE4H), co-created 11 unique 4-panel comic-style stories designed to be read aloud together as attendees visit each event table. These colorful stories are shared on boards that stand on each table and are offered in both English and Spanish at this time. Many tables also have an accompanying hands-on activity. Together, they lead to meaningful "low stakes" discussions which support understanding of seemingly complex health information. Story topics include the cause of cancer (Cells Gone Wrong), cancer risk factors (Reducing Your Risk), the role of primary care in cancer screening (Primary Care for Prevention), the purpose of research (short Research Ready) and details about specific cancer types (Combatting Colon Cancer, Blocking Breast Cancer, Looking for Lung Cancer, Silencing Skin Cancer, Hindering HPV, and Professional Prostate Protection) and COVID-19 (Take Your Best Shot FAQs). A health

passport is used to facilitate table visitation and survey collection at each table enables meaningful evaluation of the event as well as provides the community hosts and their partners baseline cancer data to inform future programing. In 2022, WE4H and the University of Cincinnati Cancer Center partnered with three different communities to co-host pilot events that served over 100 adult residents. Community, research interns and university students volunteered to work the tables at the event and received training prior. Post event surveys and discussions indicated that community partners appreciated the different take on a health fair event. Most volunteers indicated that they would enjoy volunteering again. Attendees indicated that they liked the graphic-style story format used and most preferred it to text and text with graphics approaches. Taken together, the data indicates that Reducing Your Risk events are useful in meaningfully engaging hard to reach, at risk attendees. Additional in-person and virtual events are being planned for 2023 as an approach to reach the medically underserved throughout our region.

#4242

High sugar food consumption and breast cancer risk in a prospective cohort study

Woo-Kyoung Shin, Dan Huang, Katherine De la Torre, Sukhong Min, Aesun Shin, Jong-koo Lee, Wonshik Han, Jung Eun Lee, Daehee Kang.
SNU Medicine, Seoul, Korea, Republic of

Background**:** The association between excessive sugar intake and the risk of breast cancer has been considered in epidemiologic studied, however, the results are unclear. This study examined to evaluated between high-sugar food intake and breast cancer in a prospective cohort study.
Methods: This prospective cohort study included a total of 71,266 women aged 40-69 years from the Health Examinees-Gem (HEXA-G) study between 2004 and 2013. Information on cancer diagnosis was retrieved from the Korea Central Cancer Registry until 31 December 2018. Multivariate hazard ratios (HRs) and 95% of confidence intervals (CIs) for the risk of gastric cancer according to the consumption of high-sugar food were estimated using Cox proportional hazards models with age as the time scale.

Results: A total of 713 incident cases of breast cancer occurred over an average follow-up period of 9.20 years. The top food contributing to total sugar intake was fruit (42.89%). We found that increased consumption of sugary cereal was associated with increased risk of breast cancer; HR for sugary cereal consumption of more than one servings/two months vs. almost never consumed was 1.34 (95% CI: 1.08, 1.65; p for trend = 0.01). Also, consumption of loaf bread (p for trend = 0.03), ice cream (HR for ice cream consumption of more than one servings/week vs. almost never consumed = 1.26; 95% CI: 1.00, 1.58; p for trend = 0.03), and added sugar food (HR for all sugary food groups consumption of more than two servings/week vs. less than one serving/month consumed =1.28; 95% CI: 1.02, 1.61; p for trend = 0.05) was associated with increased risk of breast cancer.
Conclusion: Our results suggest that a high-sugar food consumption was associated with an increased risk of breast cancer among Korean women.
Key words: Sugar, High-sugar foods, Breast cancer, the Health Examinees (HEXA) study, prospective cohort study.

#4243

Dietary flavonoids prevent colon tumor formation in $Apc^{Min/+}$ mice in a microbiome- and sex-dependent manner

Beckey DeLucia, Jan Claesen. *Cleveland Clinic Lerner Research Institute, Cleveland, OH*

Background: A diet rich in colorful fruits and vegetables is effective for the prevention of various inflammation-induced cancer types. Mechanistically, this effect has been attributed to the potent antioxidant properties of flavonoid molecules. However, contrary to observations in mice, the success of flavonoids in human dietary cancer prevention trials is often dampened due to large interpersonal variation. Antioxidant activity alone does not explain this variability, suggesting there is an additional important variable that has not been accounted for. Since flavonoids have a poor bioavailability and predominantly passage into the large intestine, we hypothesize that gut microbial metabolism is essential for flavonoid bioactivity in colon cancer prevention.
Goals and Objectives: The goal of this study was to evaluate the impact of microbiota composition on the efficacy of dietary flavonoids in preventing

intestinal tumorigenesis.
Methods: We used the adenomatous polyposis coli - multiple intestinal neoplasia ($Apc^{Min/+}$) mouse model, which is genetically predisposed to develop adenomas along its gastrointestinal tract. Development of these adenomas and eventual adenocarcinoma formation is further influenced by factors such as inflammation, dietary input and the gut microbiota. Animals were fed a control high fat diet (HFD) or prevention diets consisting of 1% berry extract, 1% purified flavonoid or 1% microbial catabolite, all on the HFD background. The contribution of the microbiota was modelled by including experimental groups that received an antibiotic cocktail in their drinking water throughout the course of the experiment. For these animals, microbiota community composition was determined by 16S rRNA sequencing, plasma was collected for histological profiling and metabolomics analysis and end-point measurements of intestinal tumor numbers and size were performed.
Results: Supplementation with berry extract significantly reduced colon tumor numbers and incidence in male, but not in female mice. This effect was negated in mice on antibiotic drinking water, implicating the involvement of the gut microbiota. Community analysis revealed a relative increase in *Erysipelotrichaceae*, *Clostridia* and *Akkermansia* in the berry supplemented versus HFD control mice. In addition, their systemic monocyte counts were reduced. Dietary supplementation with a major gut microbial flavonoid catabolite, did not reduce colon tumor formation, suggesting the functional involvement of different microbial metabolites.
Conclusions: Our study demonstrates the involvement of the mouse gut microbiota in dietary prevention of colon tumor formation. These effects impact circulating monocytes and are linked to changes in the plasma metabolome. We are currently elucidating the microbial actors and associated molecular pathways involved.

#4244
Black soybean seed coat extract suppress intestinal tumorigenesis in APCmin mice
Yasuyuki Shimizu[1], Shunta Hirano[1], Yoko Yamashita[2], Tsuyoshi Fukumoto[3], Naritoshi Mukumoto[1], Ai Nakaoka[1], Namiko Hoshi[4], Takeaki Ishihara[1], Daisuke Miyawaki[1], Ashida Hitoshi[2], Ryohei Sasaki[1]. *[1]Division of Radiation Oncology, Kobe University Graduate School of Medicine,*

Kobe, Japan,[2]Department of Agrobioscience, Kobe University Graduate School of Agricultural Science, Kobe, Japan,[3]Division of Dermatology, Kobe University Graduate School of Medicine, Kobe, Japan,[4]Division of Gastroenterology, Kobe University Graduate School of Medicine, Kobe, Japan

Background: Colorectal cancer (CRC) is a major cause of cancer-related deaths in Japan and worldwide. Since CRC has been reported to have close relationship with diet, it seems significant to identify dietary constituents that might suppress occurrence of CRC. Recently, an epidemiological investigation for cancer incidence in Japan revealed that consumptions of black soybeans seem to reduce incidence of several cancers, especially colorectal cancer. Black soybeans coat extract (BE) is known to contain rich procyanidins which have many beneficial physiological activities such as anticancer effects. Therefore, we hypothesized that BE may have inhibitory effects to intestinal tumorigenesis and investigated using $APC^{min/+}$ mice models.

Materials and Methods: $APC^{min/+}$ male mice in the C57BL/6 genetic background were obtained from Jackson Laboratories. $APC^{min/+}$ genotypes of each mouse were confirmed by polymerase chain reaction analysis (PCR) using DNA extracted from the tip of mouse tails. Mice were weighed weekly once and monitored regularly for any signs of weight loss. APC min/+ mice at 4 weeks of age were randomly divided into three groups with 5 mice, and fed by either AIN-76A diet, AIN-76A diet containing 0.05% or 0.05% BE for 8 weeks. At 12 weeks of age, intestines were removed from each mouse and then sliced longitudinally. The small intestine was cut into three equally parts: proximal, middle, and distal. Numbers and sizes of intestinal polyps in each portion were evaluated under Video-Zoom-microscope XV-440. Intestinal polyps were categorized by size into 1-2 mm, 2-3 mm and >3 mm. Other parts of the intestines were placed in 10% phosphate-buffered formalin for histopathology and immunohistochemical (PCNA, β-catenin, and MUC2) analyses.

Results: Numbers of polyps in mice fed with containing 0.05% or 0.5% BE diet were significantly smaller than in mice fed without BE ($P < 0.05$). As for size of polyps, the number of polyps of 1 to 3 mm in size was decreased in mice with BE, however, there were no significant difference for numbers of polyps more than 3 mm in size regarding diets with or without BE. With

0.05% BE diet, reduction rates for occurrence of polyps were 81% for proximal, 48% for middle, and 47% for distal positions, while in with 0.5% BE diet, those reduction rates were 71% for proximal, 59% for middle, and 58% for distal positions, respectively. From these results, the BE, either 0.05% or 0.05% concentration, showed inhibitory effects for tumorigeneses in the small intestine of APC min/+ mice. In histological analyses, the BE was induced higher expression of MUC2-positive cells in normal intestinal lesions and lower expression of β-catenin in tumor sites
Conclusions: The BE showed inhibitory effects in occurrence and growth of intestinal polyps in $APC^{min/+}$ mice models. With further evaluation of mechanisms, the BE could be a promising nutrition for prevention of CRC in human.

#4245

Effects of black raspberries extract on DNA repair capacity and metabolic activation/detoxification of the tobacco carcinogen dibenzo[*def,p*] in human oral cells

Yuan-Wan Sun[1], Kun-Ming Chen[2], Ana H. Sales[3], Nicholas Geacintov[3], Karam El-Bayoumy[2]. *[1]Biochemistry @ Molecular Biology, Penn State College of Medicine, Hershey, PA,[2]Penn State College of Medicine, Hershey, PA,[3]New York University, New York, NY*

We previously reported that black raspberries (BRB) powder inhibits dibenzo[*def,p*]chrysene (also known as dibenzo[*a,l*]pyrene; DBP)-induced DNA damage, mutagenesis and carcinogenesis in the mouse oral cavity. The effects of BRB on the capacity of DNA repair was investigated in an established *in vitro* system using HeLa cells to assess the DNA repair capacity. We found that pre-treatment of Hela cells with BRB extracts (BRBE) can enhance the nucleotide excision repair (NER) of a bulky DNA adduct derived from the tobacco oral carcinogen benzo[a]pyrene by ~24% and this effect is correlated with the enhanced expressions of NER factors XPA and XPB. The NER activity of guanidinohydantoin (Gh), an oxidatively-derived non-bulky DNA lesion, is also enhanced by ~24%, while its base excision repair activity is enhanced by only ~6%. Using human oral leukoplakia (MSK-Leuk1) and oral squamous cell carcinoma SCC1483, we demonstrated that BRBE can inhibit DNA damage induced by DBP through the induction of GSH synthesis and enhancing GSH

conjugates thereby inhibiting DNA damage. The effects of BRBE in MSK-Leuk1 and SCC1483 cells were further investigated on the DNA excision repair protein ERCC1 at 1, 6 and 24 h. ERCC1 forms the ERCC1-XPF enzyme complex that participates in several DNA repair pathways. Western blot analyses revealed that BRBE induced higher ERCC1 expression in SCC1483 than those observed in MSK-Leuk1 cells in a time-dependent manner. The results of our study demonstrate that BRBE is capable of inhibiting the metabolic activation, enhancing the detoxification pathway and DNA repair capacity which are consistent with its chemopreventive activity *in vivo*. Supported by NIH grant #CA173465.

#4246

Synergistic inhibition of prostate tumor growth and progression by the combination of curcumin and ursolic acid in HiMyc mice

Chelsea A. Friedman, Achinto Saha, John DiGiovanni. *Division of Pharmacology and Toxicology, UT Austin College of Pharmacy; Center for Molecular Carcinogenesis and Toxicology, Austin, TX*

Prostate cancer (PCa) is the second leading cause of cancer death among men in the United States. According to the World Health Organization, approximately one-third of all cancer deaths could be prevented through an increased consumption of natural compounds. Through the use of a two-tiered screening method in PCa cells (depletion of cellular ATP level followed by glutamine uptake) of a phytochemical library, curcumin and ursolic acid were selected for further investigation. Twenty-four hour treatment of LNCaP, 22Rv1 and HMVP2 cells with the combination resulted in significant decreases in expression of members of the miR-17-92 and miR-106b-25 clusters, which are upregulated in PCa and have been shown to be involved in tumorigenesis, cell survival, and metastasis. In the HiMyc mouse model, where mice spontaneously develop primary PCa, supplementing diets with the combination of curcumin (1%) and ursolic acid (0.2%) resulted in significant inhibition of tumor growth and progression compared to diets containing either compound alone. There were no differences in body weight or food consumption in any of the diet groups during the tumor experiment. The current data suggests that the combination of curcumin and ursolic acid synergistically inhibits PCa growth and progression in HiMyc mice, which may be in part due to their

effects on microRNA expression. Ongoing studies are further examining the role of specific miRNAs as well as oncogenic signaling pathways potentially involved in the mechanism of synergistic chemopreventive action of this combination. The current data suggest that this novel combination could be a valuable therapeutic option for prevention and/or treatment of PCa. Funding: This work was supported by NIH Grant CA228404.

#4247

Impact of 70% ethanol intraductal injections in MNU rat models for breast cancer prevention

Erin K. Zaluzec[1], Mohamed Ashry[1], Elizabeth Kenyon[1], Elizabeth G. Phelps[1], Legend Kenney[1], Katherine Powell[1], Maximilian Volk[1], Shatadru Chakravarty[2], Jeremy M.L. Hix[1], Matti Kiupel[1], Erik Shapiro[1], Lorenzo F. Sempere[1]. *[1]Michigan State University, East Lansing, MI,[2]TechInsights Inc., Nepean, ON, Canada*

Breast cancer (BC) is the leading cancer diagnosis in women. While many BC treatment options exist, only two methods are approved for prevention. Prophylactic mastectomy is an invasive surgery that removes the breast, thereby removing the targeted epithelial ductal tree cells, where most BC arises. Despite a 90% risk reduction, recovery time, risk of infection, pain management, and mental health toll on women deter them from this surgery. Hormonal preventatives, tamoxifen and raloxifene, reduce BC risk by up to 50%. However, increased risk of uterine cancer and intolerable sides effect deter women from this option. Therefore, new preventative methods are needed to maintain BC risk reduction while minimizing current BC prevention deterrents. Intraductal (ID) injection is a technique that can circumvent systemic toxicity by inserting a needle directly into the ductal tree opening. We study BC prevention using 70% ethanol (EtOH) as a cell killing, ablative solution for ID injections and have shown its effectiveness of ablation in an aggressive genetically engineered mouse model with minimum collateral tissue damage. EtOH is a safe, inexpensive reagent clinically used as a sclerosing and ablative agent. We introduced ethyl cellulose (EC), a gelling agent which further minimized damage outside the ductal tree. To confirm successful ductal tree filling without animal sacrifice, we introduced Tantalum Oxide (TaOx), a nanoparticle-based

contrast agent for real time and long-term visualization of ductal tree filling. TaOx showed remarkable local retention, without impeding 70% EtOH ablative effects or EC compared to other contrast agents. Despite our refined ablative solution, ID injection is a difficult technique to perform with limited ability to confirm success of a fully filled ductal tree. To elucidate any impact of partial ductal tree filling, we utilized a Methyl-N-Nitrosourea (MNU) rat model. Rat models improve scalability toward clinical trials and increase ductal tree filling volume and control to study the impact of partial ductal tree filling. Our MNU rat model provides a time frame between carcinogen exposure and tumor formation optimal for prevention studies. Two weeks after intraperitoneal MNU injections, rats received full or half volume (partial) injections, fat pad (partial), or no injection into individual mammary glands. Rats were monitored for tumor formation from 2 weeks post injection until reaching euthanasia criteria. Fully injected glands had the highest tumor latency increase by 1 month (130 days, $p < 0.0001$) compared to non-injected controls (95 days). Partial and fat pad tumor latency also improved compared to control (122 days, $p < 0.01$ and 110 days, $p < 0.05$ respectively). No iatrogenic effects of EtOH were observed. Here, we show that ID injection of 70% EtOH is a safe, effective, and scalable technique for BC prevention, which can be enhanced with TaOx and EC for visualization and retention.

#4248

Epithelial ovarian cancer causes cardiac dysfunction and myofilament dysregulation

Leslie M. Ogilvie[1], Madison Pereira[1], Kathy Matuszewska[1], Bridget Coyle-Asbil[1], Luca J. Delfinis[2], Shivam Gandhi[2], Keith R. Brunt[3], Christopher G. R. Perry[2], W. Glen Pyle[1], Jim Petrik[1], Jeremy A. Simpson[1]. *[1]University of Guelph, Guelph, ON, Canada,[2]York University, Toronto, ON, Canada,[3]Dalhousie Medicine New Brunswick, Saint John, NB, Canada*

Introduction: The intersections between cancer and cardiovascular disease (CVD) have become increasingly relevant in the care of both patient populations. To date, the cardio-oncology field has largely focused on how cancer treatment influences long-term cardiac health. Indeed, many cancer therapeutics show various toxic effects to the cardiovascular system. However, studies have also shown cardiac deficits in therapy-naïve cancer

patients. This suggests that these two disease states interact through similar signaling pathways, yet the mechanisms underlying cancer-induced cardiac dysfunction remain unknown. Thus, we investigated cardiac structure and function throughout the progression of epithelial ovarian cancer (EOC).
Methods: We used an orthotopic, syngeneic mouse model of ovarian cancer. Briefly, transformed murine ovarian surface epithelial cells from C57BL/6 mice (ID8; $1.0x10^6$), or saline for surgical controls, were injected under the ovarian bursa of syngeneic mice. In this model, 60 days after tumor induction, mice form large ovarian masses, numerous peritoneal lesions, and develop abdominal ascites - consistent with the clinical features of stage III (advanced) EOC. To determine whether cardiac abnormalities precede the presence of advanced disease, at 45 days post-tumor induction, mice were anesthetized, and left ventricular (LV) structure and function were assessed by echocardiography and invasive hemodynamics, respectively. Myofilament activity was measured with an actomyosin MgATPase assay and protein phosphorylation was determined by SDS-PAGE with Pro-Q Diamond phosphoprotein staining.
Results: EOC mice showed systolic (i.e., reduced contraction rate) and diastolic dysfunction (i.e., reduced relaxation rate, elevated diastolic filling pressure), with no evidence of hypertrophy or atrophy (i.e., no change in LV wall thickness or dimension). While there were no observed differences in myofilament ATPase activity, phosphorylation of regulatory myosin light chain 2 (MYL2) and cardiac myosin binding protein C (cMyBP-C) decreased, and tropomyosin (Tpm) phosphorylation increased in EOC mice.
Conclusion: Together, these data demonstrate that ovarian cancer impairs cardiac function and alters the regulation of myofilament proteins critical for contraction and relaxation. Interestingly, the observed dephosphorylation of MYL2 and cMyBP-C and hyperphosphorylation of Tpm are consistent with features of heart failure. The findings build upon our current understanding of the interactions between cancer and CVD and show that deficits in the heart precede the development of advanced malignancy. Future work further will investigate the tumor-heart axis to identify how tumor development disrupts normal cardiac physiology.

Dietary Derivatives and Repurposed and New Drugs for Cancer Prevention

#5247

The effect of aspirin on the transcriptional landscape of the colon

Jonathan M. Downie[1], Connor M. Geraghty[1], Thaddeus S. Stappenbeck[2], Ömer H. Yilmaz[3], David A. Drew[1], Andrew T. Chan[1]. *[1]Gastroenterology, Harvard Medical School/Massachusetts General Hospital, Boston, MA,[2]Inflammation and Immunity, Cleveland Clinic, Cleveland, OH,[3]Pathology, Harvard Medical School/Massachusetts General Hospital, Boston, MA*

Colorectal cancer (CRC) remains the second leading cause of cancer mortality in the United States. Aspirin is the most promising CRC prevention agent with significant data supporting long-term use with a reduction in the incidence of adenomatous polyps and colorectal cancer. The adoption of aspirin as a preventive agent has been limited by an incomplete understanding of aspirin's mode of action in humans. To elucidate the mechanism of aspirin prevention, we sought to identify aspirin-associated transcriptional changes within the colon. To accomplish this objective, we performed RNA sequencing of biopsy-derived colonic epithelial cells from participants enrolled (N=180) in our ongoing aspirin randomized placebo-control trial (RCT) program, "ASPirin Intervention for the REDuction of colorectal cancer risk" (ASPIRED). Individuals with a recent resection of an adenoma were eligible. Participants for whom epithelial cells from rectosigmoid mucosal biopsies were successfully obtained at both pre- and post-treatment timepoints (n=130) were included in this analysis. Participants were randomized to once-daily placebo (n=45), low-dose aspirin (81 mg) (n=46), or standard-dose aspirin (325 mg) (n=39) for 8-12 weeks. For each timepoint, we performed Illumina RNA 100-bp paired-end sequencing of 4,000 fluorescence-activated cell-sorted (FACS) colonic epithelial cells (CD45-; EpCAM+). Transcriptomic read alignment and read counts per gene were obtained using *STAR* and *Salmon*. Quality control measures removed 52 participants (20 placebo, 18 low-dose aspirin, and 14 standard-dose aspirin) from the analysis. No significant differences in age, gender, ethnicity, or BMI were observed between placebo and aspirin-treated participants. We then identified genes whose expression is modulated by aspirin exposure (low and standard dose aspirin) while controlling for baseline gene expression differences between placebo and aspirin-exposed patients and for intra-sample gene expression variability

using *Dream*. We found 57 genes were significantly differentially expressed in aspirin-treated participants at an FDR < 0.10. *AGR2*, which is a CRC oncogene that is upregulated by prostaglandin E2 (PGE2), was significantly downregulated by aspirin treatment suggesting aspirin modules the expression of PGE2 responsive genes in the colonic epithelium. Gene enrichment analysis found aspirin significantly downregulated scaffold proteins (e.g. *KRT8*, *KRT18*, and *ACTB*) and structural ribosomal RNA binding proteins. These pathways are critical processes in epithelial cell differentiation. This finding supports previous *in vitro* evidence that aspirin results in cell composition changes within the colonic epithelium favoring stem-like cell states, which may underlie its preventive effect.

#5248

The use of reverse phase protein array (RPPA) to identify new tumor vulnerability and actionable drug targets against human cancer cell lines

Andrew Howell[1], Julia Wulfkhule[2], Rosa Gallagher[2], Jonathan Baker[1], Ashleigh Hannah[1], Emanuel F. Petricoin[2], Amy H. Tang[1]. *[1]Eastern Virginia Medical School, Norfolk, VA,[2]George Mason University, Manassas, VA*

Introduction: The EGFR/K-RAS pathway is a major tumor driver whose hyperactivation is associated with malignant tumor growth, multidrug resistance, early tumor relapse, chemo-resistance, and metastasis. Despite more than 40 years of research, oncogenic K-RAS activation remains an undruggable target in clinical oncology. Seven-In-Absentia (SINA) homologues (SIAH) are conserved E3 ubiquitin ligases that play a critical gatekeeper role downstream of the EGFR/K-RAS pathway. Our prior studies have shown that tumor growth was abolished in human tumor cell lines following SIAH inhibition; however, the underpinning molecular mechanisms that give rise to this anti-EGFR/K-RAS and anticancer phenotype remain unclear.
Specific Objectives: to delineate the molecular mechanism(s) of why anti-SIAH2PD targeted therapy is so effective in impeding growth, we conducted reverse-phase protein array (RPPA)-based kinomic analysis to discover how major cancer signaling pathways and K-RAS-dependent signaling networks are remodeled in response to SIAH2 inhibition.

Ongoing studies aim to identify and validate dysregulated phospho-proteins identified by RPPA-based kinomic analysis.
Methods: 300 proteins/phosphoproteins were quantitatively measured by the RPPA platform to identify new tumor vulnerabilities, actionable targets, and compensatory signaling network alterations in response to anti-SIAH targeted therapies in five cancer cell lines in triplicate. Doxycycline (DOX)-inducible Tet-ON MiaPaCa, MDA-MB-231, MDA-MB-468, HeLa, and A459 cell lines were generated from a single cell, and DOX-induced SIAH2PD expression was confirmed. Reverse Phase Protein Array (RPPA) was conducted to quantify fold-changes of proteins whose expression was significantly ($p<0.05$) altered in response to SIAH inhibition. Ongoing Western Blot and Immunofluorescence (IF) studies are being used to validate our key RPPA findings.
Results: Supported by statistical analyses, we identified 6 unique proteins that were significantly up-or down-regulated in response to SIAH inhibition. These proteins play a role in controlling and regulating cell growth, cell death, NFκB signaling, stress response, DNA damage, immune function, and cell attachment pathways. Thus, our data provide additional evidence supporting our tumor eradication phenotype observed in these human cancer cell lines lacking functional SIAH. Western Blot and IF validation studies have yielded further supporting evidence to confirm our RPPA results.
Conclusion: Validation studies are being conducted to gain insight into pathway alterations and dynamic rewiring in order to uncover SIAH as a major tumor vulnerability in multiple malignant cancers. Our data supports the explanation as to why anti-SIAH targeted therapy works so effectively to shut down malignant tumor growth, as reported in the literature.

#5249

Polyphenon E effects *MXD1* and *RGS4* gene expression in PC-3 prostate cancer cells

L. Michael Carastro[1], Ethan J. Vallebuona[1], Ricardo Cordova[2], Ashley N. Gannon[1], Corrine M. Costello[1], Ricardo A. Declet-Bauzo[3], Seung Joon Kim[4], Nagi Kumar[5], Jong Y. Park[5]. *[1]Department of Chemistry, Biochemistry and Physics, The University of Tampa College of Natural and Health Sciences, Tampa, FL,[2]Department of Biochemistry and Molecular Biology, Indiana University School of Medicine, Indianapolis,*

IN,[3]Department of Radiology, Louisiana State University School of Medicine, New Orleans, LA,[4]The Catholic University of Korea, Seoul, Korea, Republic of,[5]Moffitt Cancer Center, Tampa, FL

Polyphenon E (Poly E) is a standardized, caffeine-free green tea extract with defined polyphenol content. Oral Poly E administration confers chemoprotective activity against prostate cancer (PCa) progression in the TRAMP model of human PCa. Poly E has limited activity against human PCa, but only in those previously diagnosed with atypical small acinar proliferation or high-grade prostate intraepithelial neoplasia. The molecular mechanisms underpinning Poly E chemopreventive activities against PCa are not fully understood. We hypothesized Poly E treatment of PCa cells induces gene expression changes, which could involve molecular mechanisms underpinning the limited Poly E chemoprevention activity against PCa. PC-3 cells were cultured in complete growth media supplemented with varied Poly E concentrations (0, 100, 200, or 300 mg/L) for 24 hr. RNA was isolated for comparative DNA microarray (0 vs. 200 mg/L Poly E) and subsequent qRT-PCR analyses for validation. Microarray data for 54,613 genes were filtered for > 2-fold expression level changes, with 8,319 increased and 6,176 genes decreased. Seven genes (*CASP8, CBLB, CCNB1, HDAC4, MXD1, RGCC, RGS4*) involved in key cellular signaling pathways and with > 2-fold expression level changes, as well as a control gene (*RB1*), were selected for qRT-PCR analyses. These eight genes are listed with corresponding fold-change gene expression values for each microarray probe set (Table 1). The qRT-PCR analyses identified two genes with significantly increased expression, *MXD1* (13.98-fold; p=0.0003) and *RGS4* (21.98-fold; p=0.0011), between poly E treatment levels. The significantly increased *MXD1* and *RGS4* gene expression in Poly E-treated PC-3 cells, and the Poly E-dose dependence of *MXD1* gene expression increases, could implicate *MXD1* and *RGS4* in the PCa chemopreventive activity of Poly E. Future experimental directions include cell cycle profile and Annexin V analyses, immunoblotting analyses, and including other established PCa cell lines in these studies.

Microarray Data from Poly E-treated PC-3 Cells

Affymetrix Probe ID	Gene symbol	Log_2-Fold Change
213373_s_at	*CASP8*	-2.23

1553306_at	*CASP8*	-3.20
208348_s_at	*CBLB*	19.01
209682_at	*CBLB*	3.83
214710_s_at	*CCNB1*	-2.77
228729_at	*CCNB1*	-3.47
1554322_a_at	*HDAC4*	-2.47
204225_at	*HDAC4*	-3.23
228813_at	*HDAC4*	-4.45
206877_at	*MXD1*	13.56
228846_at	*MXD1*	7.35
226275_at	*MXD1*	1.91
211540_s_at	*RB1*	1.85
203132_at	*RB1*	-1.43
218723_s_at	*RGCC*	23.12
239827_at	*RGCC*	1.22
204338_s_at	*RGS4*	20.54
204337_at	*RGS4*	6.12
204339_s_at	*RGS4*	3.69

#5250

Effect of the β-blocker carvedilol in preventing DMBA-induced mammary gland tumor growth

Pabitra Kumar Sardar[1], Steven Yeung[2], Ayaz Shahid[2], Bradley T. Andresen[2], Ying Huang[2]. *[1]Western University of Health Sciences, Pomona, CA,[2]Pharmaceutical Sciences, Western University of Health Sciences, Pomona, CA*

According to global cancer statistics, breast cancer has now become the most diagnosed cancer and has become the fifth leading cause of cancer-related deaths worldwide. A promising method of retarding cancer-related mortality is cancer chemoprevention. However, there is no drug available that can be used routinely as a breast cancer-preventative agent. As carvedilol (CAR), an FDA-approved beta-adrenergic receptor blocker,

reduces breast cancer mortality, we hypothesized that CAR might act as a breast cancer preventative agent. Three protocols were utilized to evaluate the ability of CAR to prevent 7,12-Dimethylbenz(a)anthracene (DMBA)-induced mammary tumors in rats. In protocol 1, two doses of CAR (2 and 10 mg/kg) were administered in drinking water as a 7-day pretreatment and throughout the study. In protocol 2, 10 mg/kg tamoxifen and 10 mg/kg carvedilol were provided as a 7-day pretreatment, and treatment was halted after six weeks. In protocol 3, CAR and the non-β-blocking enantiomer R-carvedilol (10 mg/kg) were given as a 7-day pretreatment and throughout the study. In all studies, animals were palpated weekly beginning at week 5 to detect the presence and location of mammary tumors. Tumors were measured using a caliper, and the experiments terminated at week 13. In protocol 1, only 10 mg/kg CAR was effective in delaying DMBA-mediated tumor occurrence ($p = 0.0002$); the first appearance of tumors and median tumor appearance in CAR-treated rats were separated from rats receiving DMBA alone by 2 and 4 weeks, respectively. However, tumors that did form grew at the same rate in all groups. In protocol 2, tamoxifen served as a control to prevent DMBA-mediated tumors; only one tamoxifen-treated rat developed a tumor at the end of the study. The tamoxifen-treated rats tumor formation was not statistically different than negative controls; however, the CAR group was not statistically different from the DMBA group. In protocol 3, CAR and R-CAR treatment showed delayed tumor formation and growth compared to the DMBA-only group, although not statistically significant. Combining all DMBA and 1-week pretreatment CAR data (n = 58 and 40, respectively), CAR effectively prevents DMBA-induced tumor incidence ($p = 0.001$), with a 3-week differential in the median tumor formation between the two groups. Therefore, continuous CAR treatment is essential to achieve the observed chemopreventive effects. As carvedilol is a clinically used beta-blocker, the results provide significant implications in breast cancer chemoprevention.

#5251

Skeletonema marinoi algae extract and carotenoid fucoxanthin are endowed with potential chemopreventive and angiopreventive properties for prostate cancer

Adriana Albini[1], Luana Calabrone[2], Douglas M. Noonan[3], Marco Festa[2], Cinzia Ferrario[2], Valentina Carlini[2], Debora Macis[1], Luigi Pistelli[4],

Christophe Brunet[4], Clementina Sansone[4]. *[1]Istituto Europeo di Oncologia (IEO), Milano, Italy,[2]IRCSS MultiMedica, Milano, Italy,[3]University of Insubria, Varese, Italy,[4]Stazione Zoologica Anton Dohrn, Napoli, Italy*

Background: Research and production of natural anti-oxidants is growing and is developed both in experimental laboratories and in nutraceuticals and pharmaceutical industries. Marine microorganisms represent underestimated sources of bioactive compounds endowed with anti-oxidant, anti-inflammatory, cardiovascular protective and anti-angiogenic properties, all beneficial effects on human health.
Methods: Chemopreventive and anti-angiogenic activities of extracts from the marine coastal diatom *Skeletonema marinoi* (*Sm*) and carotenoid fucoxanthin, that is present in *Sm*, were evaluated in prostate cancer (PCa) and endothelial cell lines in *in vitro*. Morphogenesis assay was carried out to evaluate effects on HUVEC ability to form capillary-like structure on Matrigel. Gene expression analysis was performed by qPCR, measuring different inflammation and angiogenesis gene expression in cells treated with *Sm* extract and fucoxanthin. Membrane antibodies arrays were used to see alterations at protein level of pro- or anti-angiogenic factors.
Results: *Sm* extract and fucoxanthin were able to decrease cell viability, in MTT and Crystal violet assays. Furthermore, we observed that fucoxanthin enhanced the effects of chemotherapeutic drugs, 5-Fluorouracil (5-FU) and cisplatin (Cis-Pt), two of the most commonly used anti-cancer drugs. *Sm* extract and fucoxanthin hindered vascular mimicry of PCa cells and also inhibited capillary structure formation in endothelial cells. Finally, *Sm* extract and fucoxanthin shown a down-regulation of inflammation and angiogenesis associated genes.
Conclusions: Our study suggests promising potential chemopreventive and angiopreventive activities of *Skeletonema marinoi* extract and fucoxanthin for prostate cancer. Microalgae derived drugs can be a potential and relevant source of novel nutraceutical and preventive compounds, which can be considered as dietary supplements or in combination treatments in cancer prevention approaches.

#5252
Salsolinol suppresses the STAT3-EMT axis in liver carcinogenesis

Hyeon Jeong Oh[1], Seah Park[1], Hong-Kyung Yang[1], Hoon Ryu[2], Young-Joon Surh[3], Dae-Yong Kim[4], Hye-Kyung Na[1]. *[1]Sungshin Women's Univ., Gangbuk-gu, Seoul, Korea, Republic of,[2]Brain Science Institute, Korea Institute of Science and Technology, Seoul, Korea, Republic of,[3]College of Pharmacy, Seoul National University, Seoul, Korea, Republic of,[4]College of Veterinary Medicine, Seoul National University, Seoul, Korea, Republic of*

Liver cancer is one of the most common malignancies and a leading cause of death worldwide. However, it is still very difficult to treat and prevent liver cancer. Salsolinol (SAL) is an endogenous catechol isoquinoline generated by the condensation of dopamine with acetaldehyde, a major metabolite of ethanol. In the present study, we found that SAL inhibited the phosphorylation, dimerization, and subsequent nuclear translocation of STAT3 in a concentration-dependent manner in SK-Hep1 cells, a hepatic carcinoma cell line. SAL suppressed the expression of Cdk 4 and Cyclin D1, the major target protein of STAT3, and induced the cell cycle arrest at Go/G1 phase. However, SAL induced the expression of STAT1 in SK-Hep1 cells. In addition, SAL enhanced the expression of the cell cycle regulators such as p53 and p21 in SK-Hep1 cells. Epithelial-mesenchymal transition (EMT) promotes tumor invasion and metastasis in malignancies through STAT3 activation. SAL induced the expression of E-cadherin while suppressing the expression of Snail, N-cadherin, and Slug, which are related to EMT. SAL inhibited the migration of SK-Hep1 cells by suppressing the expression of MMP-9 and MMP-2. Furthermore, intraperitoneal injection of SAL reduced the number of tumors in the diethylnitrosamine (DEN)-induced liver carcinogenesis model without affecting the body weight change. Proliferative markers PCNA and KI-67 and p-STAT3 were down-regulated in the SAL-injected mice liver cancer tissue. The plasma level of alpha-fetoprotein, a tumor marker in the blood, was also reduced in the SAL-injected mice. Interestingly, SAL injection significantly reduced the anxiety-like behavior without affecting the locomotive activities in the DEN-induced hepatocellular carcinoma mouse model. Moreover, SAL injection recovered tyrosine hydroxylase, a key enzyme for producing dopamine from tyrosine in the substantia nigra compacta of DEN-treated mice. Together, SAL inhibits STAT3 signaling, thereby suppressing the cell cycle progression and EMT in SK-Hep1 cells, which may account for its

anti-depressant and anti-carcinogenic activity in DEN-induced liver carcinogenesis.

#5254

Topical inhibition of UV-induced PD-L1 expression and inflammatory signaling by the small molecule inhibitor BMS-202

Prajakta Vaishampayan[1], Jana Jandova[2], Yuchen (Ella) Ai[1], Viktoria Kirschnerova[1], Clara Curiel-Lewandrowski[3], Georg T. Wondrak[2], Sally E. Dickinson[4]. *[1]University of Arizona Cancer Canter, University of Arizona, Tucson, AZ,[2]R. Ken Coit College of Pharmacy, Department of Pharmacology and Toxicology, University of Arizona, Tucson, AZ,[3]College of Medicine, Division of Dermatology, University of Arizona, Tucson, AZ,[4]Pharmacology, University of Arizona, Tucson, AZ*

Immune evasion is a molecular hallmark of cancer, and overexpression of the immune checkpoint protein PD-L1 (CD274) has been documented in several tumors including cutaneous squamous cell carcinoma (cSCC). Notably, while baseline levels of PD-L1 in normal human epidermis are low, acute solar-simulated light (SSL) exposure increases the expression of this protein in epidermal keratinocytes, an effect which can be replicated in cultured keratinocytes and in mouse models. While current immunotherapies targeting the PD-1/PD-L1 axis using monoclonal antibodies are providing therapeutic benefits in many cancers including cSCC, small molecule inhibitors are also being developed to target PD-L1 which may be amenable for topical formulation and therefore early intervention with reduced systemic exposure. We have recently tested one such molecule, BMS-202, *in vitro* and *in vivo*. BMS-202 application to keratinocytes in culture inhibits UV-induced PD-L1 RNA and protein expression. Notably, exposure to this inhibitor also reduced UV-induced stress signaling as measured by AP-1 luciferase assay in cultured keratinocytes. Topical application of BMS-202 to immunocompetent SKH-1 mouse skin resulted in significant inhibition of SSL-induced epidermal PD-L1 as determined by immunoblot analysis. NanoString nCounter Pathway™ transcriptomic analysis of full-thickness SKH-1 mouse skin shows strong inhibition of SSL-induced inflammatory responses, chemokine activity, innate immune response and NF-κB activation in BMS-202 treated samples compared to SSL-only controls. Our results indicate

that early intervention against PD-L1 expression/activity could be a viable target for skin cancer photochemoprevention. Topical application of small molecule PD-L1 inhibitors such as BMS-202 may provide novel treatment options for populations at high risk for cSCC.

#5255

Effect of STAT3 inhibitors, TTI-101 and SH5-07, against bladder cancer in preclinical 3D tumor models

Surya P. Singh[1], Gopal Pathuri[1], Adam Asch[2], Brian Cholewa[3], Robert Shoemaker[4], Chinthalapally V. Rao[1], Venkateshwar Madka[1]. *[1]Medicine, Center for Cancer Prevention and Drug Development, Stephenson Cancer Center, Hem-Onc Section, University of Oklahoma HSC, Oklahoma City, OK,[2]Medicine, Stephenson Cancer Center, Hem-Onc Section, Oklahoma City, OK,[3]Division of Cancer Prevention, Chemopreventive Agent Development Research Group, National Cancer Institute, Rockville, MD, OK,[4]Division of Cancer Prevention, Chemopreventive Agent Development Research Group, National Cancer Institute, Rockville, MD, MD*

Bladder cancer (BC) is a lethal genitourinary malignancy associated with frequent recurrence and poor survival due to metastatic potential. Identification of key cancer cell signaling networks and developing promising agents is critical for effectively inhibiting tumor growth and progression. In many cancers, including bladder cancer (BC), signal transducer and activator of transcription 3 (STAT3) has emerged as an important molecular pathway due to its role in promoting proliferation, invasion, and chemoresistance. Thus, developing STAT3 targeting, orally bioavailable small molecule inhibitors may be helpful for the prevention of BC progression and improving the survival rate of patients with muscle invasive BC. Monolayer culture has limitations for drug testing. Therefore, spheroid and organoid culture are used extensively as they may mimic in-vivo drug response more accurately. The aim of our study is to examine the preclinical anticancer efficacy of STAT3 inhibitors [TTI-101 (C188-9) and SH5-07] in 3D (spheroid and tumoroid) invitro models of BC. We optimized the spheroid growth using various BC cell lines [human (J82), rat (NBT-II), and mouse (MB49) BC cells]. Similarly, tumoroids from rat (BBN-induced bladder tumors) and transgenic mice (UPII-SV40T) bladder tumors were developed. These spheroids and tumoroids were treated with

various concentrations (0 - 50 μM range) of STAT3 inhibitors and evaluated for their viability [Calcein AM (CA) and EtBr staining], ATP production (CellTiter-Glo™ 3D), and ROS production (MitoSOX^{TM}). Effect of drug treatment on biomarkers of cell proliferation, apoptosis, stemness, STAT3 signaling, and immune modulation was determined using western blotting and immunofluorescence. Treatment with TTI-101 (0 - 50 μM or SH5-07 (0 - 50 μM) for 144 hrs resulted in significant reduction in the spheroids size (39-45% smaller Vs untreated; $p<0.0001$), along with decreased ATP levels (20%-40%, $p<0.05$). MitoSOX^{TM} staining suggested that STAT3 inhibitors treatment increased ROS production in BC cells. CA and EtBr staining revealed that TTI-101 and SH5-07 treatment resulted in increased cell death in BC spheroids compared to control. Decreased spheroids and organoids size also correlated with increased apoptotic marker (cleaved caspase-3) along with decreased cyclin D1, PCNA, and pSTAT3 protein expression. Drug treated BC spheroids/tumoroids also showed reduction in CD44 (BC stemness and invasion marker) and induction of cGAS-STING pathway (cGAS, STING, TBK1, and IRF3) in comparison to the control. These findings indicate that STAT3 inhibitors, TTI-101 and SH5-07, could inhibit bladder cancer by suppressing STAT3 pathway activation and therefore warrant further study in vivo. (Supported by P30 CA225520 and Kerley-Cade Endowed Chair)

#5256

Understanding HPV vaccine confidence and conspiracy beliefs across the US: Opportunities to increase cancer prevention through HPV vaccine education

Josheili Ymar Llavona-Ortiz, William A. Calo. *Public Health Sciences, Penn State College of Medicine, Hershey, PA*

Purpose: The purpose of this study was to compare HPV vaccination confidence and HPV vaccination conspiracy beliefs across the US. By characterizing vaccine confidence and conspiracy beliefs by HPV vaccine initiation status and sociodemographic variables, opportunities to develop HPV vaccine education as a cancer prevention measure can be identified. **Methods:** Four questions measuring vaccine confidence and seven questions measuring vaccine conspiracy beliefs were adapted from validated scales. All questions were assessed utilizing a Likert scale ranging

from 1 (strongly disagree) to 5 (strongly agree). Participants were a sample of US parents of adolescents ages 11-17 (n=1,109). Participants were recruited online through a market research panel maintained by Qualtrics. To define HPV vaccine initiation status, parents were asked about the number of HPV shots their child had received. Parents that reported their child receiving at least one HPV shot were categorized as initiators while parents that were unsure or reported no HPV shot were defined as non-initiators. Boxplots were created for each category (confidence and conspiracy beliefs) by child's vaccination status and parent age group, sex, and racial/ethnic identity utilizing Stata/BE. T-tests and ANOVA models were used to assess statistical significance of overall mean scores (MS).
Results: Vaccine safety MS was lower among parents that had not initiated the HPV vaccination series for their child compared to parents that had initiated the HPV vaccination series for their children (3.69 vs 4.12, respectively). Across individual vaccine conspiracy beliefs by vaccination status, differences were observed regarding the belief that vaccine-related data is fabricated or covered up. For racial/ethnic comparisons, overall MS for vaccine confidence statements was lowest among Non-Hispanic Black (NHB) parents (MS=3.81). Concurrently, the overall MS for vaccine conspiracy beliefs was highest among NHB parents (MS=3.31). ANOVA models were statistically significant for overall confidence and conspiracy beliefs' scores by vaccination status, parent age group, and parent racial/ethnic identity ($p<0.05$).
Conclusions: Although parents that have initiated HPV vaccination for their children are more confident about vaccines than those that have not, conspiracy beliefs are still common among both groups. Additionally, NHB parents had lower confidence surroundings vaccines and higher report of belief in vaccine conspiracies, while trends have shown that NHB have higher overall risk of dying due to HPV-related cancers. The need to address HPV vaccination education for both vaccinated and unvaccinated communities, additionally tailored by racial/ethnic group, is essential to empower communities with knowledge they can feel certain about and increase protection against HPV-related cancers.

#5257
Activation of NRF2-mediated oxidative stress response pathway by curcumin analog FLLL12: Implication for chemoprevention

Raji Lukmon, Adeoluwa A. Adeluola, A.R.M. Ruhul Amin.
Pharmaceutical Sciences, Marshall University, Huntington, OH

Purpose: Carcinogenesis is a multi-step complex process initiated with irreversible genetic mutation due to endogenously derived or carcinogen-induced oxidative stress. Activation of the antioxidant pathways ameliorates oxidative stress, protects cells from carcinogenic insults, and plays a pivotal role in chemoprevention. We have previously reported that FLLL12 is a potent curcumin analog, possesses in vitro and in vivo anticancer activity, and has better pharmacokinetic profiles than curcumin. The purpose of the current study is to identify novel pathways activated by FLLL12 using RNASeq analysis.
Methods: MDA686, a head and neck cancer cell line, were treated with 2 μM FLLL12 for 24h. Total RNA was isolated and used for RNASeq analysis. 2-fold differentially expressed genes were used for Ingenuity Pathway Analysis to identify the most significantly affected pathways. Real-time qPCR and western blotting were used to confirm the expression of the genes associated with the most significantly affected pathways and their protein products respectively in normal, premalignant, and malignant cell lines.
Results: Whole transcriptome analysis using RNASeq identified 641 genes that were either upregulated or downregulated by 2-folds after FLLL12 treatment. Enrichment of this gene set with Ingenuity Pathway Analysis identified the ferroptosis signaling pathway, the tumor microenvironment pathway, and the NRF2-mediated oxidative response pathway as the top three most significantly affected pathways by FLLL12. We confirmed the activation of HMOX-1, NQO1, SLC7A11, and GCLC mRNA and proteins in HOK (normal), MSK-LEUK1 (premalignant), and MDA686TU (malignant) cells. Although these genes are common for the ferroptosis signaling pathway and the NRF2-mediated oxidative response pathway, treatment of cells with ferroptosis inhibitors, ferrostatin 1, and deferoxamine, had no effect on FLLL12-induced cell death suggesting that these genes are associated with oxidative stress response pathway.
Conclusions: Our results strongly suggest that FLLL12 activates the oxidative stress response pathway in normal, premalignant, and malignant head and neck cancer cell lines and has strong promise for chemoprevention.

#5258

Preclinical testing of CD73 inhibitor AB680 for pancreatic cancer immunoprevention

Lincoln N. Strickland[1], Erika Y. Faraoni[1], Nicolette R. Mardik[1], Lana Vornik[2], Michelle I. Savage[2], Shizuko Sei[3], Mark S. Miller[3], Holger K. Eltzschig[1], Powel H. Brown[2], Florencia McAllister[2], Jennifer M. Bailey-Lundberg[1]. *[1]Anesthesiology, Critical Care and Pain Medicine, University of Texas Health Science Center At Houston, Houston, TX,[2]Clinical Cancer Prevention, University of Texas MD Anderson Cancer Center, Houston, TX,[3]Cancer Prevention, National Cancer Institute, Rockville, MD*

Introducti**on:** Pancreatic ductal adenocarcinoma (PDAC) is characterized by a profoundly immunosuppressive microenvironment. Innovative therapeutic strategies are urgently needed to stop the progression of precancerous lesions into aggressive PDAC, which remains a lethal malignancy. The goal of this research project is to test immunopreventive strategies by targeting the 5' ectonucleotidase enzyme, CD73, one of the gatekeeper enzymes responsible for conversion of adenosine monophosphate (AMP), to an immunosuppressive metabolite, adenosine, in the tumor microenvironment (TME). We hypothesize that inhibition of CD73 will prevent pancreatic intraepithelial neoplasia (PanIN) formation and progression to PDAC by reversing adenosine directed immunosuppression. This research explores immunopreventive strategies aimed to restore tumor immune surveillance to prevent cancer initiation or progression.

Materials and methods: We used two models: a syngeneic model of PDAC using cells derived from *Kras^{G12D};Trp53$^{R172H/+}$;PdxCre* (KPC) mice and a *Kras^{G12D};PdxCre* (*KC*) genetically engineered mouse model (GEM) of PDAC. Oral gavage of AB680 (small molecule CD73 inhibitor) was given three days/week at 10mg/kg starting the day after KPC injections and tumor sizes were measured weekly. In the GEM model, the same treatment regimen began when the mice were between 6 and 9 weeks old and were euthanized either between 15 and 20 weeks of age or around 27 weeks of age, and pancreas tissue was harvested. Histology was analyzed and 6 fields per mouse were quantified using ImageJ.

Results: As we have described (*Singh, et al, bioRxiv*), in the syngeneic model, there was a significant reduction in tumor growth and significant increase in activated CD8-positive T cells, dendritic cells, and macrophages from AB680 treated mice. The intratumoral adenosine levels were significantly decreased in AB680 treated mice compared to vehicle treated mice. In the *KC* GEM model, we quantified significantly fewer early PanIN lesions ($p=0.0328$), a trend in decreased advanced PanIN ($p=0.0641$), and significant decrease in PDAC ($p=0.0058$) in the AB680 treated mice when compared to the vehicle treated mice. We quantified abundance of collagen deposition as a marker of fibrosis and observed significantly decreased collagen ($p<0.0001$) in AB680 treated *KC* mice. In addition, we quantified abundance of CK19+ lesions and observed a significant decrease in CK19+ lesions in AB680 treated mice ($p=0.0061$) compared to vehicle treated mice.
Conclusion: Inhibiting CD73 restructures TME and reduces PanIN incidence and progression to PDAC. CD73 inhibition may be a candidate immunoprevention strategy in pancreatic cancer. [Supported by NCI 75N91019D00021/75N91020F00002]

#5259
Bazedoxifene plus conjugated estrogen improves metabolic health and reduces mammary gland epithelial proliferation in an ovary intact rat model of obesity and breast cancer risk
Ramsey M. Jenschke[1], Karen A. Corleto[1], Carol J. Fabian[2], Stephen D. Hursting[3], Bruce F. Kimler[4], Danilo Landrock[1], Tara N. Mahmood[1], Katherine L. Cook[5], Erin D. Giles[6]. *[1]Texas A&M University, College Station, TX,[2]Department of Medicine, University of Kansas Comprehensive Cancer Center, Kansas City, KS,[3]University of North Carolina at Chapel Hill, Chapel Hill, NC,[4]University of Kansas Comprehensive Cancer Center, Kansas City, KS,[5]Wake Forest University School of Medicine, Winston-Salem, NC,[6]University of Michigan School of Kinesiology and Rogel Cancer Center, Ann Arbor, MI*

Background**:** The majority of women risk eligible for primary breast cancer prevention with tamoxifen or aromatase inhibitors refuse uptake due to concerns about side effects, especially vasomotor symptoms. Tamoxifen

may also have detrimental metabolic effects in overweight/obese women. Duavee™, a complex of bazedoxifene (BZA) and conjugated estrogen (CE), is FDA approved for relief of hot-flashes and prevention of osteoporosis. Preclinical studies suggest favorable metabolic effects in ovariectomized animals and potential for breast cancer risk reduction. A single arm clinical trial found reduction in Ki-67 and mammographic density such that BZA+CE is being further evaluated in a Phase IIB trial of peri and early postmenopausal women with vasomotor symptoms who are at high risk for breast cancer. Here, in a companion study, we assessed the effect of BZA+ CE on metabolic health and cancer risk in a rat model of carcinogen induced ER+ tumors and high fat diet induced obesity.

Methods: Rats received 50 mg/kg N-methylnitrosourea at 7 weeks to increase mammary tumor risk and were fed a high fat diet (46% kcal fat) to promote obesity. At 16 weeks lean and obese rat were selected based on % body fat and were then randomized to 8 weeks of daily oral vehicle control or 3mg BZA + 0.07mg CE/kg body weight. Systemic metabolic variables were measured at 16 and 24 weeks, and RNA from mammary glands analyzed by gene expression microarray (Affymetrix).
Results: BZA+CE resulted in systemic as well as mammary changes indicative of improved metabolic health, including: reduction in total and visceral fat ($p<0.01$), glucose ($p<0.05$), cholesterol ($p<0.001$), and triglycerides($p=0.08$), as well as an increase in the adiponectin:leptin ratio ($p<0.01$). BZA+CE vs control increased the ratio of small (insulin sensitive) to large adipocytes in the mammary gland. Gene set enrichment analysis (GSEA) showed BZA+CE downregulated proliferation-associated pathways which had been upregulated in obese rats, consistent with anti-cancer effects. Obese rats treated with BZA+CE also had upregulation of metabolic pathways, including adipocyte differentiation, fatty acid metabolism, and inflammatory response pathways.
Conclusions: Unlike tamoxifen, BZA+CE improved whole body and mammary gland metabolic health, particularly in obese rats. Transcriptional profiling and GSEA demonstrated a blunting of cell cycle and proliferation and enrichment of metabolic and immune-related pathways. Together this supports BZA+CE (Duavee) as an agent to be explored for breast cancer risk reduction in obese individuals.

Funding: This work was supported in part by P30 CA168524, R00 CA169430, and R25 CA203650.

#5260

Chemopreventive efficacy of everolimus and naproxen combination against carcinogen induced bladder cancer in F344 rats

Venkateshwar Madka[1], Gopal Pathuri[1], Surya P. Singh[1], Anil Singh[1], Anh Bao[1], Nicole Stratton[1], Stanley Lightfoot[2], Clinton J. Grubbs[3], Jennifer Fox[4], John L. Clifford[5], Brian Cholewa[5], Shizuko Sei[5], CV Rao[1]. *[1]OU Health Stephenson Cancer Center, Oklahoma City, OK,[2]formerly VA medical Center, Oklahoma City, OK,[3]Formerly University of Alabama, Birmingham, AL,[4]National Institute of Aging, NIH, Bethesda, MD,[5]Division of Cancer Prevention, NCI, Rockville, MD*

Bladder Cancer (BC) is the second common genitourinary cancer with high recurrence and mortality rate due to metastatic muscle invasive BC (MIBC). Since majority of BCs are non-invasive at diagnosis, developing agents that effectively block BC progression may be beneficial for clinical translation. In this study, clinically approved agents, everolimus, mTOR inhibitor, [0.19mg/kg;7x/week (low dose, LD) or 1.33mg/kg;1x or 2X/week (high dose, HD)] at various dosing schedules alone or in combination with naproxen, an NSAID (30mg/kg body weight) intermittent dosing (3 Wks ON/OFF) were tested for efficacy in an N-butyl-N-(4-hydroxybutyl)nitrosamine (BBN)-induced BC rat model. Female F344 rats (8 weeks age; N=30) were gavaged 16 doses of BBN (150mg/dose). Either one-week (early intervention) or 12-weeks (late intervention) after BBN treatment, rats in each group received respective drug treatments by gavage. At 50 weeks age, rats were euthanized, and tissues were analyzed. Results suggest that BBN-exposed rats developed high number of Non-MIBC (NMIBC) and MIBC and had significantly large bladders (430±57mg, Mean±SEM; $p<0.0001$) compared to normal bladders in vehicle group (68.8±1.3mg). Importantly, there was significant reduction in tumor growth and progression of hyperplasia/papilloma with naproxen alone (3 weeks intermittent dosing) by 70% (129.7±7.7mg; $p<0.0001$) and 58% (180.8±27.6mg; $p<0.001$) at early and later interventions respectively compared to untreated BBN-exposed rats. Continuous LD or HD everolimus regimens during early intervention showed significant inhibitory

effect on papilloma progression, whereas its delayed administration had modest to insignificant inhibitory effect of papilloma progression to NMIBC/MIBC. Intermittent dosing of naproxen alone inhibited large tumors (>200mg) incidence by 90% ($p<0.0001$) and by 75% ($p<0.0001$) with early and late interventions respectively. Early treatment with combinations led to >72% reduction in tumor weight (120.8±7.8mg, 121.8±11.5mg, and 118.6±5.2mg; $p<0.0001$) while late intervention had 58%-65% tumor reductions (179.6±14.4mg, 150.6±12.6mg, and 172.5±15.6mg; $p<0.0005$) with the combination dosing regimens. Notably, all 3 regimens of naproxen plus everolimus combinations significantly inhibited large tumor incidence at both early intervention (90%-100%; $p<0.0001$) and late intervention (60%-70%; $p<0.0005$), with significant suppression of papilloma progression to NMIBC and MIBC, including squamous cell carcinoma (SCC). Protein biomarker analysis suggested decrease in markers of proliferation, inflammation and mTOR signaling with an increased apoptosis. In summary, our study indicated that naproxen and everolimus combination can prevent bladder cancer progression and warrants further evaluation. (Supported by NCI-PREVENT program 75N91019D00020-75N91020F00003)

#5261

Prostate specific sustained anti androgen delivery to delay early stage prostate cancer progression

Pujan Desai[1], Maithili Rairkar[2], Nela Pawlowska[1], Scott Thomas[1], Pamela N. Munster[1]. *[1]UCSF - University of California San Francisco, San Francisco, CA,[2]Alessa Therapeutics, San Carlos, CA*

Prostate cancer is the most common cancer in men. Commensurate with risk, current approaches to localized prostate cancer include prostatectomy, prostate radiation with or without radiation therapy or active surveillance. Recent data suggest that systemic anti-androgen therapy with enzalutamide reduced the risk of prostate cancer progression in men on active surveillance but was associated with considerable side effects. We developed a novel polymer-based drug delivery method to provide sustained localized drug administration of anti-androgens selectively to the prostate. In vitro and in vivo mouse and canine studies show that this drug eluting implant delivers sustained high prostate to plasma therapeutic anti-

androgen levels for an anticipated range of 2 years while preventing accumulation of anti-androgens in the liver, lungs, heart and brain. We performed a proof of concept study in a canine prostate model implanting an 15mm x 1mm bicalutamide eluting implant into each lobe of the prostate. Bicalutamide levels in the prostate measured near the implant at 6 months were 3250 ± 1622 ng/g, n = 3 compared to 3809 ± 638 ng/g, n = 3 to those achieved at steady-state oral administration. Plasma and other off target levels were over 1000-fold lower in the implant cohort compared to oral administration: Plasma: 5.9 ± 0.2 ng/ml, liver: 11.3 ±4.3 ng/g, and brain: 5.4 ±0.8 ng/g versus plasma: 18170 ± 3820 ng/ml, liver: 35407 ±8510 ng/g, and brain: 8870 ±1797 ng/g. The implants were well tolerated without local toxicity and imaged easily with ultrasound. The design characteristics of the implant facilitates minimally invasive surgical implantation under standard image guidance and withstands the concomitant use of prostate radiation. This novel technology warrants future clinical exploration of prostate specific anti-androgen therapy for (neo)adjuvant therapy or in active surveillance.

Tissue	**Bicalutamide oral (2m) (ng/g)**	**Bicalutamide implant (6m) (ng/g)**
Plasma	18,170 (3820)	5.9 (0.2)
Prostate	3,809 (638)	3,250 (1622)
Liver	35,407 (8510)	11.3 (4.3)
Cerebrum	8,870 (1797)	5.4 (0.8)
Cerebellum	8,737 (1550)	6.2 (1.3)
Spleen	7,727 (1288)	4.2 (0.9)
Lung	27,013 (2896)	11.3 (4.3)
Heart	11,737 (3491)	10.0 (1.9)
Kidneys	17,413 (6581)	8.5 (2.0)

#5262

Avasimibe abolishes the breast cancer preventative efficacy of statin in a spontaneous mouse model of breast cancer

Anjana Bhardwaj, Zhenlin Ju, Alexander Koh, Rhea Bhala, Jing Wang, Isabelle Bedrosian. *UT MD Anderson Cancer Center, Houston, TX*

Background**:** The cholesterol biosynthesis pathway plays a central role in the normal cellular development and carcinogenesis. Relevant to breast cancer prevention, the breast epithelium in women with atypical hyperplasia has been shown to have increased in cholesterol levels and oxidative products of cholesterol. Additionally, cholesterol pathway genes such as HMGCR and HMGCS1 are known to be upregulated during progression of breast cancer in patients. We have previously shown in SV40C3TAg mice that the cholesterol lowering drug-fluvastatin reduces breast tumor incidence and burden by 50% and have noted that the efficacy of statin is reduced due to the tight regulation of the cholesterol biosynthesis pathway through multiple restorative feedback loops, thus bypassing the effect of statin blockade.
Hypothesis: We hypothesize that fluvastatin efficacy can be improved by co-targeting the restorative feedback pathways that are involved in resistance to statins.
Methodology: RNA seq data from statin resistant MCF10.AT1-R cell clones was compared to the statin sensitive parental MCF10.AT1 cells in order to identify pathways and targets involved in statin resistance. Genes that were also found to be upregulated in the statin non-responders mice mammary tumors relative to responders mice were tested for dual targeting. Efficacy of avasimibe, an ACAT inhibitor, to sensitize MCF10.DCIS cells to statin therapy was studied by the colony formation assay. In vivo validation of the statin + avasimibe dual therapy was performed in SV40C3TAg mice that spontaneously develop triple negative breast cancer.
Results: We found ACAT1 and ACAT2 to be overexpressed in statin resistance cell clones and non-responder mouse breast tumors. ACATs are involved in cholesterol esterification that is required for storing cholesterol in lipid droplets. Cholesterol esterification in conjunction with cholesterol synthesis and export constitute key mechanisms involved in maintaining cholesterol homeostasis. Thus, we tested if avasimibe treatment potentiates the fluvastatin efficacy to inhibit colonizing ability. Avasimibe and fluvastatin combination completely abolished the ability of MCF10.DCIS cells to form colonies. Next, we tested the efficacy of combination treatment to prevent breast tumors in SV40C3TAg mice. The treatments started at the age of 6 weeks, prior to the onset of cancer and continued until 22 weeks of age. We found fluvastatin and avasimibe combination to

be completely ineffective and 90% mice developed tumors. In addition, tumor burden was not reduced with dual treatment.
Conclusions: We postulate that avasimibe enhanced metabolism of fluvastatin in mouse system and thus completely abolishing the chemopreventive effects of statin. Genomically derived rationale drug combinations may result in unanticipated interactions and/or ancillary effects that limit efficacy in vivo/ in patients.

#5263

Licochalcone A is a candidate for breast cancer prevention through its reprogramming of metabolic and antioxidant pathways

Atieh Hajirahimkhan[1], Elizabeth Bartom[1], sriram Chandrasekaran[2], xiaoling xuei[3], Susan Clare[1], Seema Khan[1]. *[1]Northwestern University, Chicago, IL,[2]University of Michigan, Ann Arbor, MI,[3]Indiana University, Indianapolis, IN*

Background: Increased adiposity is a risk factor for postmenopausal breast cancer. It is accompanied by protumorigenic effects: chronic low-grade inflammation and elevated levels of reactive oxygen species. Breast cancer risk reducing drugs with proven efficacy have adverse side effects, significantly minimizing their uptake and impact. Effective alternative strategies with lower toxicity are needed. We have shown that licochalcone A (LicA) suppresses aromatase expression and activity, enhances the activity of detoxifying enzymes, and reduces estrogen genotoxic metabolism in cell lines and animal models. However, no previous data exist on the breast tissue of women at substantial risk of breast cancer. We hypothesize that LicA creates a tumor preventive environment in the breast by modulating antioxidant/anti-inflammatory responses in the breast and adipogenesis leading to decreased proliferation.
Methods: We prepared microstructures from the fresh tissue of contralateral unaffected mastectomy specimens of 6 postmenopausal women with incident unilateral breast cancer. After exposing them to DMSO (control) and LicA (5 μM), we performed total RNA sequencing. Differentially expressed genes were identified, and analyzed by gene ontology and pathway membership. The RNA-seq data was utilized also to conduct metabolism flux analysis. Combined enrichment scores > 4 and FDR < 0.05 was considered significant. The NanoString metabolism panel was

employed in 6 additional subjects. We performed live cell imaging to monitor proliferation of pre-malignant DCIS.COM, DCIS.COM/ER+ PR+; and malignant MDA-MB-231 (ER- PR-), MCF-7 (ER+ PR+), MCF-7aro, and BRCA1 defective HCC-1937, and HCC3153 cells.
Results: We observed upregulation of antioxidant genes (up to 8-fold), consistent with upregulation of *NRF2* and the thioredoxin system, the major regulators of antioxidant pathways. This was accompanied with the significant downregulation of RELA- and NF-kB1-dependent inflammatory pathways. In addition, we observed decreased expression of the pro-adipogenic transcription factors *SREBF1* and *SREBF2*, which may explain the downregulation (4 to 32-fold) of cholesterol biosynthesis and transport, and lipid metabolism genes. Metabolism studies confirmed these data and demonstrated a robust increase in the pentose phosphate shunt and NAD(P)H generation without enhancing ribose 5 phosphate formation, suggesting an antioxidant and anti-proliferative environment. LicA also suppressed proliferation of pre-malignant and malignant cells, with sustained effects on aggressive cells at doses < 10 μM.
Conclusion: Our data suggest that LicA is a good candidate for breast cancer prevention through modulation of metabolic and antioxidant pathways leading to decreased proliferation. Our ongoing in vivo study will further demonstrate the efficacy of LicA for breast cancer prevention.

#5264

Cucurbitacin D modulates the Nrf2 signaling pathway and protects against benzo[a]pyrene-induced liver injury

Shabnam Malik[1], Anyssa Rodriguiez[1], Mohammed Sikander[1], Daniel Zubieta[1], Fathi T. Halaweish[2], Subhash C. Chauhan[1], Meena Jaggi[1].
[1]Immunology and Microbiology, University of Texas Rio Grande Valley, Edinburg, TX,[2]South Dakota State University, Brookings, SD

Background**:** Accumulating studies have shown strong correlation of HCC and co-morbidity factors including smoking. Tobacco smoke contains benzo[a]pyrene, which is extremely carcinogenic and contributes to liver damage. Cucurbitacin, a triterpene, has a wide range of biological activities, including antioxidant, anti-inflammatory, and anti-cancer properties. However, their hepatoprotective effects remain poorly understood. In the current study, we examined the hepatoprotective activity of cucurbitacin D,

a novel analog of cucurbitacin, against benzo[a]pyrene-induced liver injury in human HepG2 cells.
Method: To investigate the hepatoprotective effect of cucurbitacin D against benzo[a]pyrene-induced liver damage, proliferation, clonogenicity, migration, invasion, Western blotting, and qPCR analyses were performed. The DCFDA assay was performed to determine the level of intracellular reactive oxygen species (ROS) in liver cells.
Results: Functional assays showed that cucurbitacin D exhibited cytoprotective effects against dose-dependent growth inhibition by benzo[a]pyrene in human HepG2 cells. This protective effect was likely associated with antioxidant potential of cucurbitacin D, as evidenced by the attenuation of ROS observed by fluorimeter and fluorescence microscopy. Western blotting analysis demonstrated Cucurbitacin D targets Nrf-2 signaling pathway and associated effector proteins including HO-1 and LC3A in protecting liver cells against benzo[a]pyrene induce oxidative damage. Further studies are underway to understand the underlying molecular mechanism of action.
Conclusion: These findings demonstrate the hepatoprotective effects of cucurbitacin D against benzo[a]pyrene-induced liver damage, making it a promising ingredient for nutritional supplements.

#5265

Investigating the role of Desmocollin-3 and immune infiltrate in bladder cancer

Chandreshwar P. Shukla[1], Nayan K. Jain[2], Michael A. O'Donnell[3], Kapil J. Vachhani[4], Rashmi Patel[5], Aruna Vanikar[5], Rajiv I. Modi[4], Sanjay V. Malhotra[6], Bakulesh Khamar[4]. *[1]Cadila Pharmaceuticals Pvt Ltd, Dholka, Ahmedabad - Gujrat, India,[2]Department of Life science,, Gujarat University, Ahmedabad - 380009, Gujarat, India,[3]Department of Urology, Carver College of Medicine, University of Iowa, Iowa City, IA,[4]Cadila Pharmaceuticals Pvt Ltd, Dholka, Ahmedabad-Gujrat, India,[5]Civil Hospital Campus,, Institute of Kidney Diseases and Research Center, Institute of Transplantation Sciences, Asarwa, Ahmedabad - Gujrat, India,[6]Knight Cancer Institute, Oregon Health & Science University, Portland, OR*

Introducti**on:** Adhesion molecules are important for tissue integrity, its maintenance as well as communication (signaling). Desmocollin-3 (DSC3) one of the desmosomal adhesion (Desmoglein 1, 2, 3 and Desmocollin 1, 2, 3) proteins is a trans-membrane glycoprotein present in basal/suprabasal layer of normal stratified epithelium. It is a p53-responsive desmosomal cadherin protein. Cancer development and progression are associated with either additional cytoplasmic expression of DSC3 as seen with squamous non-small cell lung cancer and colorectal cancer or loss of DSC3 expression as seen in prostate and breast cancer To investigate the role of DSC3 in bladder cancer, we evaluated the expression levels of DSC3 in biopsy samples of patients with non-muscle invasive bladder carcinoma (NMIBC) and muscle-invasive bladder carcinoma (MIBC) and correlated it with the clinical staging and immune cell infiltration. Also, its relationship with immune signature genes and immune cell subsets is evaluated using TCGA dataset available on c-bioportal.

Materials and Method: DSC3 protein expression was evaluated by Immunohistochemistry. H&E stained slides were evaluated by light microscopy to identify immune cells as macrophages or lymphocytes and their location as intrastromal or intratumoral as previously described. It was correlated with the type, stage, and grade of the tumor. Spearman correlation between DSC3 and 207 immune signature genes available in TCGA data was calculated using RSEM and methylation values of each gene.

Results: The data suggests that NMIBC is more likely to be DSC3 positive than MIBC. DSC3-positive samples are more likely to have tumor-infiltrating immune cells (TIL) compared to DSC3-negative samples. *In silico* analysis of bladder cancer shows that DSC3 mRNA expression is inversely proportional to its methylation. We found that DSC3 expression is biased towards the Th1 subset of immune cells. DSC3 is not correlated with PD-1/PDL1 expression, and the macrophage subsets are negatively correlated with DSC3.

Conclusion: DSC3 expression is associated with the Basal/Squamous type of bladder cancer. Therefore, this study suggests the potential of DSC3 as a predictive biomarker for response to systemic immunotherapy and resistance/poor response to conventional therapy (chemotherapy; radiotherapy, and cystectomy) and underscores the need for studies evaluating the potential of DSC3 expression as a biomarker.

#5266

Metabolic rewiring and epigenetic reprogramming by the environmental carcinogen benzo[a]pyrene in a two-stage skin carcinogenesis mouse model and cancer interception by triterpenoid ursolic acid

Md. Shahid Sarwar[1], Christina N. Ramirez[1], Hsiao-Chen Dina Kuo[1], Pochung Chou[1], Renyi Wu[1], Davit Sargsyan[1], Ahmad Shannar[1], Rebecca Mary Peter[1], Ran Yin[1], Yujue Wang[2], Xiaoyang Su[2], Ah-Ng Kong[1].
[1]Department of Pharmaceutics, Rutgers, The State University of New Jersey, Piscataway, NJ,[2]Medicine, Rutgers-Robert Wood Johnson Medical School, New Brunswick, NJ

Nonmelanoma skin cancer (NMSC) is the most common skin cancer burden on the U.S. population. Environmental exposure to chemical carcinogens is one of the major causes of NMSC initiation, promotion, and progression. Ursolic acid (UA) is a naturally abundant pentacyclic triterpenoid showing anticancer potentials against diverse cancers. In the current study, we developed a two-stage skin carcinogenesis model in SKH1 hairless mice by administering cancer-initiating agent benzo[a]pyrene (B[a]P) and promoting agent 12-O-tetra-decanoylphorbol-13-acetate to study the epigenetic, transcriptomic, and metabolic changes at different stages (5, 20, and 26 weeks) during the development of NMSC, and investigated how UA regulates B[a]P-mediated alterations for NMSC interception. We found that UA protects against B[a]P-induced tumorigenesis at different phases of NMSC. Epigenetic CpG methyl-seq showed UA abrogated B[a]P-mediated alterations in differentially methylated regions (DMRs) profiles. Transcriptomic RNA-seq data exhibited UA reversed the differentially expressed genes (DEGs) of several inflammatory genes, such as chemokine ligand 8 (*Ccl8*) and interleukin 17F (*Il17f*), and epigenetic genes, such as DNA-methyltransferase 3-like (*Dnmt3l*) and protein-l-isoaspartate O-methyltransferase domain-containing protein 1 (*Pcmtd1*) during different stages of NMSC. Association study between DEGs and DMRs showed that B[a]P promoted transcription of kallikrein-related peptidase 13 (*Klk13*) by promoter demethylation, while UA suppressed *Klk13* expression through hypermethylation in the promoter during the initiation stage, indicating the early intervention of UA.

Ingenuity pathway analysis further showed significant upregulation of macrophage-stimulating protein-recepteur d'origine nantais (MSP-RON) signaling pathway by B[a]P during the initiation stage while suppressed by UA treatment. The metabolomic study revealed UA modulated cancer-associated changes in metabolisms, including the TCA cycle and pyruvate metabolism/metabolites during the promotion phase, indicating UA plays a critical role in regulating B[a]P-regulated metabolic changes and intercepting NMSC progression. In summary, UA protects against the environmental carcinogen B[a]P-driven epigenetic, transcriptomic, and metabolic changes during the initiation, promotion, and progression of NMSC, potentially contributing to the anticancer effects of UA. (Supported by NIH R01 CA200129 to A.N.K)

#5267

Effects of polyphenon E treatment on gene expression in DU145 prostate cancer cells

Ethan J. Vallebuona[1], Ashley N. Gannon[1], Corrine M. Costello[1], Ricardo Cordova[2], Ricardo A. Declet-Bauzo[3], Seung Joon Kim[4], Nagi Kumar[5], Jong Y. Park[5], L. Michael Carastro[1]. *[1]University of Tampa College of Natural and Health Sciences, Tampa, FL,[2]Department of Biochemistry and Molecular Biology, Indiana University School of Medicine, Indianapolis, IN,[3]Department of Radiology, Louisiana State University School of Medicine, New Orleans, LA,[4]Department of Internal Medicine, The Catholic University of Korea College of Medicine, Seoul, Korea, Republic of,[5]Moffitt Cancer Center, Tampa, FL*

One promising focus of prostate cancer (PCa) research is the chemopreventive effects of Polyphenon E (Poly E), a defined mixture of green tea polyphenols. A previous study utilizing the TRAMP model of human PCa, displayed chemopreventive activity as a result of Poly E oral administration in a dose-dependent pattern. Human clinical trials of Poly E treatment exhibited activity in PCa of those previously diagnosed with atypical small acinar proliferation or high-grade prostate intraepithelial neoplasia. The molecular mechanisms of these Poly E chemopreventive activities against PCa are not well established. Our hypothesis is that Poly E treatment influences expression of genes involved in key cellular signaling

pathways. DU145 prostate cancer cells were cultured in complete growth media supplemented with varied Poly E concentrations (100, 200, 300 mg/L) for 24 hrs. RNA was isolated for comparative microarray (0 vs. 200 mg/L Poly E) and qRT-PCR analyses. Microarray data for 54,613 genes were filtered for > 2-fold expression level changes, with 5,272 increased and 6,467 genes decreased. Nine genes, (*CASP8, CBLB, CCNB1, HDAC4, MXD1, RGCC, RGS4, TBC1D7, ZNF462*) involved in key signaling pathways with >2-fold gene expression changes were selected for subsequent qRT-PCR analyses. Microarray probe set IDs and fold change gene expression values for these nine genes analyzed are listed (Table 1). From qRT-PCR analyses, six of these genes had significant gene expression changes between Poly E treatment levels, *MXD1* (14.20-fold; $p = 0.0122$), *RGCC* (0.6748-fold; $p < 0.0001$), *TBC1D7*(0.2416-fold; $p = 0.0037$), *ZNF462* (0.7030-fold; $p = 0.0173$), *CASP8* (0.4856-fold; $p = 0.0136$), and *CBLB* (2.149-fold; $p = 0.0036$). We conclude that two thirds (6/9) of the genes selected from the microarray data for qRT-PCR analyses had significant Poly E induced gene expression changes. Future experimental directions include cell cycle profiling and annexin V apoptosis analysis, as well as inclusion of other established PCa cell lines.

Microarray Data from Poly E-treated DU145 Cells		
Affymetrix Probe ID	Gene Symbol	Log_2-Fold Changes
207686_s_at	*CASP8*	1.79
213373_s_at	*CASP8*	-1.13
1553306_at	*CASP8*	-2.02
208348_s_at	*CBLB*	7.79
209682_at	*CBLB*	2.27
227900_at	*CBLB*	-1.13
228729_at	*CCNB1*	-2.55
214710_s_at	*CCNB1*	-2.70
1554322_a_at	*HDAC4*	-2.06
228813_at	*HDAC4*	-4.74
204225_at	*HDAC4*	-5.43
206877_at	*MXD1*	17.87
228846_at	*MXD1*	8.04

226275_at	*MXD1*	3.80
218723_s_at	*RGCC*	2.54
239827_at	*RGCC*	-3.90
204339_s_at	*RGS4*	

7.74		
204338_s_at	*RGS4*	-1.33
204337_at	*RGS4*	-1.80
1563839_at	*TBC1D7*	47.08
223461_at	*TBC1D7*	1.17
232393_at	*ZNF462*	28.62
226575_at	*ZNF462*	-1.38
244007_at	*ZNF462*	-1.61

#5268

Drug screening of non-small cell lung cancer patient-derived organoids in a microwell platform

Qiyue Luan[1], Ines Pulido[2], Jian Zhou[1], Takeshi Shimamura[2], Ian Papautsky[1]. *[1]Biomedical engineering, University of Illinois Chicago, Chicago, IL,[2]University of Illinois Chicago, Chicago, IL*

Patient-derived organoids (PDOs) have been widely accepted as ideal 3D tumor models for drug response prediction. However, research involving non-small cell lung cancer (NSCLC) PDOs is hampered by the compromised sample size and the lack of appropriate platforms tailored for scarce samples. Although BME2 domes show promising results in PDO maintenance and drug testing, the need for relatively large sample and the long incubation time hinder their application in drug response studies. Here, we report an agarose microwell (AMW) platform requiring miniscule sample volume for PDO rapid drug screening.

The AMWs were formed by 3D-printed molds and attached to the bottom of 24-well plates. Each well has ~400 agarose microwells with 200μm diameter, 75μm depth and U-shaped bottom. Seeded cells migrate and form spheroids in each microwell. NSCLC spheroids of H358 (KRASG12C), A549 (KRASG12S) and PDOs CK7152 (KRASG12C, obtained from NCI PDMR) were cultured in arrays and treated by KRASG12C inhibitor adagrasib.

PDOs normally grow in a BME2 dome, however large PDO size variability and consumption complicate drug evaluation. The AMWs are

biocompatible and have a smooth surface that allows single cells or PDOs to migrate into microwells within 1d. The amount of PDOs in one dome is enough for 4 wells of 24-well plate. After 7d culture, PDOs formed in AMW exhibited high viability (89%±7% in AMW vs. 89%±11%, in dome) and better size uniformity (CV 29% in AMW vs. 44% in dome).
AMWs can easily be implemented to standardize cytotoxicity evaluation. Following the exposure to adagrasib for 72h, we found that H358 spheroids were sensitive to KRASG12C specific inhibitor adagrasib in dose-dependent manner with an IC50 of 88nM; whereas A549 spheroids - without the target mutation- was not responsive. CK7152 PDOs were also exquisitely sensitive to adagrasib (34% and 21% viability reductions viability in AMWs and dome).
Drug sensitivity can be affected by several factors that maintain proliferative signals active in tumor microenvironment. We have been able to simulate the effect of the tumor microenvironment, by culturing spheroids and PDOs with fibroblast supernatant in AMWs. The IC50 of adagrasib for H358 spheroids treated with WI-38 supernatant was about 3.5× higher than that in normal medium (310nM vs. 88nM). We replicated these results with CK7152 PDOs treated with CAF supernatant that significantly decreased viability from 24% to 51% ($p<0.001$) following 72h treatment of 500nM adagrasib.
Our AMW is a convenient 3D culture platform that generates uniform spheroids from a small sample volume for highly consistent drug screening results. The adagrasib drug response observed in AMW was comparable to that in conventional dome culture. Resistance due to tumor microenvironment can be readily assessed using fibroblast supernatant in AMW platform, promising for pre-clinical drug screening and personalized medicine.

#5269

RF-1302, a novel dual inhibitor of PIM1 and FLT3 in preclinical treatment of acute myeloid leukemia

Weiwei Qi[1], Yanjun Zhang[2], Lei Zhao[3], Ailian Zhang[3], Chunze Zhang[3], Xiaoming Zhang[3], Lijuan Li[1], Huaquan Wang[1], Zonghong Shao[1], Rong Fu[1]. *[1]Hematology, Tianjin Medical University General Hospital, Tianjin, China,[2]Chinese Academy of Medical Science, Hematology Institute, Tianjin, China,[3]Ruifu Therapeutics, Inc., Beijing, China*

It was reported that PIM (Proviral Insertion site in Moloney murine leukemia virus) proteins are family kinases (PIM1, PIM2, and PIM3), which are upregulated in several cancer types, especially PIM1 is highly expressed in hematopoietic malignancies. PIM kinase family are responsible for enhancement of cell cycle, inhibition of apoptosis, activation of transcription, and cell homing/migration. Fms-like tyrosine kinase 3 (FLT3) is part of a family of receptor tyrosine kinases (RTKs), and a molecular therapeutic target of acute myeloid leukemia (AML). There are three FTL3 inhibitors, midostaurin, gilteritinib, and quizartinib have been approved for clinical treatment of AML. We have developed a novel dual inhibitor of PIM1 and FLT3, RF-1302 and evaluated its inhibition of cell proliferation *in vitro* and antitumor activity *in vivo*. RF1302 was found to have a strong inhibitory activity against target enzymes (PIM1 IC_{50} at 1.0-2.3 nM and FLT3 IC_{50} at 0.8-2.2 nM), which were more potent than the tested positive control drugs gilteritinib, quizartinib, and midostaurin. RF-1302 showed to be highly cytotoxic to cultured human acute myeloid leukemia (AML) cells (MV4-11 and Molm-13) with IC_{50} at 5.7nM and 9.5 nM, respectively. The *in vivo* antitumor activity of RF-1302 was evaluated and compared with midostaurin and gilteritinib in the treatment of the two AML xenograft models. RF-1302 at 20 mg/kg/daily x 14, oral) significantly delayed tumor growth and resulted in a tumor growth inhibition (TGI) of 95% ($p<0.001$ compared with the control group) in the Molm-13 AML model, and cured all of the tumor-bearing mice in the MV4-11 AML model. The antitumor activity of RF-1302 was superior to gilteritinib (TGI=46-55%) and midostaurin (TGI=63-75%). The treatment with RF-1302 showed very little toxicity (only 2% body weight loss) which were well below the maximum tolerated dose. These preclinical results suggest that RF-1302 represents a novel dual inhibitor of PIM1 and FLT3, which may constitute a highly efficacious modality for the treatment of FLT3 mutant AML, and is worthy of further clinical evaluation.

#5270

Silibinin modulates migration and survival pathways in bone marrow mast cells via RAC2: Implications in its anti-cancer activity in basal cell carcinoma growth and progression

Neha Mishra, Sandeep Paudel, Chapla Agarwal, Rajesh Agarwal. *Skaggs School of Pharmacy and Pharmaceutical Sciences, University of Colorado Anschutz Medical Campus, Aurora, CO*

Most of the non-melanoma skin cancers are basal cell carcinoma (BCC); thus, extensive efforts to discover chemopreventive agents against BCC are ongoing. Recently, we showed that silibinin (SB) exerts strong efficacy against ultraviolet B radiation (UVB)-induced BCC growth/progression, and mast cells (MCs) are one of the targets of its efficacy. Notably, 30 days of UVB exposure in patched (Ptch)+/- mouse model of UVB-induced BCC formation increased MC numbers by ~50% that was completely inhibited by SB. Hence, understanding pathways associated with MC regulation by SB seems valuable for its efficacy against BCC and other cancers. We generated bone marrow MCs (BMMCs) in presence of interleukin (IL)-3 and stem cell factor from C57BL/6 mice (confirmed using flow cytometry dual staining: cKit/Fc€RI). They were treated with two concentrations of SB (25 μM; SB 25 and 100 μM; SB 100) or untreated (control), and proteomics was performed (liquid chromatography mass spectrometry on Fusion Lumos mass spectrometer). Total 3575 proteins were identified and 166 were found to be statistically significant (ANOVA, Fisher's posthoc analysis, $p<0.05$, FDR<0.01) amongst the three groups (n=4/group). Proteins with highest differential expression among the groups (greatest fold change expression; n=50), greatest contribution to the selection (variable importance; n=15), and common expression profiles in both SB 25 and SB 100 compared to control (n=21) were selected for further pathway analysis. Important nodes found for SB regulation of MCs were tumor necrosis factor, interferon-gamma, and IL-13; IL-13 also emerged as a key regulatory node in normal BMMCs. Furthermore, to determine the effect of SB in BCC associated MCs, a subset of proteins implicated with skin-associated MC activity (determined using IPA) was generated. Most important molecules implicated included IL-13 and Rac Family Small GTPase2 (RAC2; regulates all myeloid lineages). RAC2 was found to modulate the expression of mast cell protease4 (MCPT4), mast cell transcriptase1 (TPSAB1), and macrophage migration inhibition factor. RAC2 also activates MC proteases via JNK signaling cascade. Together, via the regulation of MCPT4, TPSAB1, and JNK signaling, RAC2 regulates inflammatory responses, and controls MC migration via actin cytoskeleton

reorganization and lamellipodia formation. Phagosome maturation was also an important pathway implicated in our analysis; MCs lyse engulfed pathogens/debris via phagosome maturation and fusion with lysosomes. In conclusion, our findings demonstrate that SB increases RAC2 expression in BMMCs, which can regulate MC migration into the tumors and effectively increase the MC protease gene expression. Thus, SB treatment shifts BMMCs towards anti-tumorigenic pathways and RAC2 can be a novel therapeutic target in BCC and other cancers as well.

#5271

Inhibition of ultraviolet B radiation-induced mast cell recruitment by silibinin in its efficacy against basal cell carcinoma in Ptch$^{+/-}$ mouse model

Sandeep Paudel[1], Neha Mishra[1], Komal Raina[2], Chapla Agarwal[1], Rajesh Agarwal[1]. *[1]Skaggs School of Pharmacy and Pharmaceutical Sciences, University of Colorado Anschutz Medical Campus, Aurora, CO,[2]College of Pharmacy and Allied Health Professions, South Dakota State University, Brookings, SD*

Recently, we have reported the chemopreventive and therapeutic efficacy of topical silibinin (SB, a natural flavonolignan from milk thistle seeds) application against ultraviolet B radiation (UVB)-induced basal cell carcinoma (BCC) growth and progression. During the histopathological analyses of the skin tissues in these studies, we observed a significant decrease in mast cell (MC) numbers in SB-treated UVB-exposed groups. Although, the MCs are primarily responsible for conferring protection against diseases and pathogens, the dynamics of BCC and MCs are complex, where MCs may also contribute to tumor transformation/progression; furthermore, their role in BCC is poorly understood. To address this gap, we first assessed the course of MC recruitment in wild-type (C57BL/6) mice vs. Ptch$^{+/-}$ mice as a function of time following either a single or thrice weekly UVB (240 mJ/cm^2) exposure. Results indicated that Ptch$^{+/-}$ mice had significantly higher infiltration of MCs compared to C57BL/6 mice. MC infiltration into the epidermis/dermis was initiated as early as 30 min post single UVB exposure in Ptch$^{+/-}$ mice, and the MCs remained in the epidermis/dermis for a longer

duration in the Ptch$^{+/-}$ mice compared to C57BL/6 mice. Next, the effect of SB treatment (topical-9 mg/200 µl acetone) on MC recruitment upon UVB exposure in these mice was assessed. Notably, SB treatment significantly decreased MC numbers in both pre- and post-UVB single exposure by ~48% and ~43%, respectively, and in multiple exposure by ~55% and ~41%, respectively. Furthermore, UVB exposure for 26 and/or 46 weeks caused an increase in MC numbers by ~2.3 fold in BCC tumors, which was also decreased by both pre- (~38-39%) and post- (~20-26%) SB treatments at 26 and 46 weeks, respectively. Notably, in preformed BCC tumors (UVB 26 weeks exposure), SB treatment for 20 weeks post UVB stoppage also decreased the number of MCs by ~25%. Thus, it was evident that anti-BCC efficacy of SB was associated with its potential to decrease MC numbers. To further understand the role of SB in MC regulation, assessment of cell viability and migration (towards BCC cell lines) in *in vitro* assays were performed with/without SB exposure in bone marrow derived mast cells (BMMCs from C57BL/6 mice), which indicated that non-toxic doses of SB (25 -100 µM) at the 48-72 h timepoint were able to inhibit BMMC migration towards BCC cell lines. Furthermore, a correlation of other immune cells (T cells, macrophages, etc.) with MC recruitment and anti-BCC effect was also determined. Taken together, our results suggest that SB effectively regulates MC numbers/function in its efficacy against BCC in Ptch$^{+/-}$ mouse model; thus, further in depth-studies, deciphering the associated molecular pathways, could yield novel preventive/ therapeutic avenues targeting MCs in BCC and other cancers.

#5272

3D cell-culture strategy for screening novel agents in Fanconi anemia chemoprevention

Gretchen M. Unger[1], Beverly R. Wuertz[2], Mary E. Brown[3], Sanjana Arji[2], Janeen H. Trembley[4], Frank G. Ondrey[2]. *[1]Genesegues, Inc., St. Paul, MN,[2]Otolaryngology, University of Minnesota, Minneapolis, MN,[3]Neuroscience, University of Minnesota, University Imaging Centers, Minneapolis, MN,[4]Research Service, Minneapolis VA Health Care System, Minneapolis, MN*

Fanconi anemia (FA) patients have DNA repair mutations predisposing them to oral cancers so treatment with non-DNA damaging agents is highly desired. As cancer experimental therapeutics advance towards study paradigms that more carefully mimic physiology, e.g. organoids and spheroids. Presently, we are using a 3D cell culture method emphasizing layers of extracellular matrix (ECM) as FA premalignant lesions retain epithelial architecture. We conducted 3D screening studies using 2 layered geometries: 1) nanofibers coated with 1 ng/mL 2:1 Collagen III/IV (C3C4) then 100 pg/mL 2.75:1 Tenascin C/Fibronectin (TNFN) and 2) polystyrene layered with 50 ug/mL C3C4 then 3.5 ug/mL TNFN. We developed these coatings to maximize lipid raft recovery, a drug transport feature lost in 2D culture. The ECM impact on FA cell drug transport was characterized by comparing effective nuclear delivery of a 20nm nanoencapsulated FITC-labeled RNAi compound (s50-TBG-RNAi3UTR), known to require lipid rafts, to the same oligo formulated with Dotap in a FA HNSCC cell line (FA1). Using confocal microscopy and IMARS software to segment delivery at maximal nuclear intensity into nuclear or endolysosomal compartments, we found, for FA1 cells on ECM, nuclear oligo signal colocalization with nuclear compartment ± coefficient of variation was 62 ± 2.2% for the capsule vs 9.8 ± 8.5% for Dotap oligo. On glass, nuclear delivery was 10 ± 52% for s50 capsule vs 25 ± 32% for Dotap. Endolysosomal compartment sequestration was respectively 28 ± 12, 62 ± 10, 44 ± 19 and 51 ± 15%. This illustrates a relevant decrease in variation in FA cell biology from ECM addition. Next, we studied metformin (Met) and pioglitazone (Pio)(agents in current oral cancer prevention studies) combined with G2/M blockade inhibitors, MK1775 (Wee1 kinase inhibitor) and GSK461364 (PLK inhibitor) in FA1s. Inhibiting G2/M blockade, already induced by FA-derived DNA damage, could promote inappropriate cell division, mitotic catastrophe (MOC) and death. In initial 2D FA1 growth studies, increased death was observed with Met plus MK1775. 3D studies, in contrast, showed increased cell death for FA1s treated with Pio plus either MK1775 or s50-TBG-RNAiCK2 (RNAiCK2). Confocal mechanistic studies in cells plated on ECM and treated for 18 hours, indicated Pio + MK1775 inhibited Survivin and ß-catenin upregulation and FA1 cells did proceed into MOC and death. For Pio (PPARg agonist) + RNAiCK2, RXRa was dephosphorylated at S260, enabling its escape from cytosolic sequestration to bind nuclear PPARg, initiating differentiation.

Differentiation was indicated by upregulation panKeratin and Transglutaminase-3. We conclude combination therapies with high interest agents in FA-associated oral cancer can be performed in 3D culture systems and might confirm drug mechanisms of action, thus augmenting other standard methods of cancer drug evaluation and screening (e.g. cell proliferation and clonogenicity).

#5273

The E3 ubiquitin ligase SIAH2 promotes clear cell renal cell carcinoma epithelial-mesenchymal transition via regulation of SETD2 stability

Mengxue Yu[1], Lingao Ju[1], Gang Wang[2]. *[1]Zhongnan Hospital of Wuhan University, Wuhan, China,[2]Department of Urology, Zhongnan Hospital of Wuhan University, Wuhan, China*

Introduction & Objective: SETD2, a major histone H3K36 trimethyltransferase, has been shown to play an important role in multiple biological processes. Mutations in *SETD2* have been evidenced in several types of cancer, including clear cell renal cell carcinoma (ccRCC). Previous studies reported the potential involvement of SETD2 in driving ccRCC tumorigenesis. However, the mechanism by which SETD2 causes cell metastasis remains poorly understood.
Methods: Genome-wide CRISPR-Cas9-based screens and immunoprecipitation-mass spectrometry were used to identify candidates for regulating SETD2 stability. Immunohistochemistry staining of the ccRCC tissue array and bioinformatics analysis of TCGA database were used to investigate the clinical relevance of SETD2 in ccRCC. The gene expression was detected by qRT-PCR, and the protein level was detected by western blotting. Wound healing and transwell migration assay were used to explore the cell migration ability. SIAH2 was deleted from ccRCC cell lines using CRISPR/Cas9-mediated gene editing. Furthermore, we used BALB/c-nude mice to construct xenograft mouse models and pulmonary metastasis models. Moreover, RNA-seq, H3K36me3 CUT&Tag and RNA N^6-methyladenosine-IP were performed to uncover the mechanism.
Results: SETD2 mutant or low expression was correlated with poor prognosis in patients with ccRCC based on TCGA data and tissue array. Through the CRISPR/Cas9 screening system and immunoprecipitation-mass spectrometry, we identified the E3 ubiquitin ligase SIAH2 that

regulates the stability of SETD2. Then, we verified that the protein stability of SETD2 was downregulated by SIAH2 in a dose-dependent manner and further confirmed that the SIAH2 promotes SETD2 degradation in a proteasome-dependent pathway. In addition, we constructed a dominant negative mutant of SIAH2 and proved the degradation dependent on its enzymatic activity. Moreover, we showed that SIAH2 knockout increased the protein level of SETD2. In SETD2 stable knockdown ccRCC cell lines, loss of *SETD2* enhanced the capability of cell migration, while knockdown of *SIAH2* resulted in the rescue of *SETD2* deficient effect. Moreover, *SETD2* ablation significantly decreases H3K36me3 peaks of E-cadherin, further reducing the m^6A signal and stability of *E-cadherin* mRNA. Conclusion: In this study, we firstly revealed the mechanism that E3 ubiquitin ligase SIAH2 interacted with SETD2 and promoted the ubiquitination degradation of SETD2. Moreover, *SETD2* ablation in ccRCC cells enhanced EMT through impaired epigenetic regulation of *E-cadherin*, suggesting SIAH2/SETD2/E-cadherin axis as a potential therapeutic target for ccRCC.

TUMOR BIOLOGY

3D and Tissue Recombinant Models

#4550

Assessing efficacy and immune-stimulatory effects of tumor-derived dendritic cell reprogramming using immuno-competent 3D tumor spheroid model

Irina Agarkova[1], Nadezhda Rotankova[1], Michal Rudnik[1], Silvan Strebel[1], Olga Zimmermannova[2], Andre Rosa[3], Fabio F. Rosa[3], Wolfgang Moritz[1], Carlos-Filipe Pereira[2], Christiana F. Pires[3]. *[1]InSphero AG, Schlieren, Switzerland,[2]Molecular Medicine and Gene Therapy, Lund Stem Cell Centre, Lund University, Lund, Sweden,[3]Asgard Therapeutics, Lund, Sweden*

Immunotherapy has brought hope for cancer treatment, but its clinical success remains limited. Recently, overexpression of the transcription factors PU.1, IRF8 and BATF3 (PIB) was shown to induce direct reprogramming of tumor cells into antigen-presenting type 1 conventional

dendritic cells (cDC1s), a rare subset of immune cells with pivotal role in anti-cancer immunity. This strategy might open avenues to enhance cancer cell recognition and elimination by the immune system. However, currently existing in-vitro and in-vivo testing platforms do not qualify to reproduce all complex cell interactions essential for the approbation of this hypothesis. Here, we report the development of the InSphero 3D InSight™ Oncology Platform for in-vitro assessment of efficacy and immune-stimulatory effects of this novel cancer immunotherapy approach. The feasibility of 3D spheroid formation for several GFP-expressing tumor cell lines was evaluated by varying seeding conditions in AKURA 96 well plate. We have measured the growth (ATP content) and GFP signal overtime and analyzed the morphology of the spheroids by IHC. With this, we have established spheroid models of T98G (glioblastoma), PK59 (pancreatic cancer), and A375 (melanoma) cell lines that are growing and viable for at least 10 days. In parallel, using 2D cultures, we have identified the optimal multiplicity of infection of a lentiviral vector encoding for PIB and mCherry to enable high transduction (mCherry+ cells), reprogramming efficiency (mCherry+CD45+HLA-DR+ cells), and cell viability, quantified by flow cytometry and IHC. Then, we have demonstrated that cDC1 reprogramming progresses in the context of 3D cancer spheroids and tumor cells acquire expression of CD45+ and HLA-DR+ cells using IHC and confocal microscopy analysis. We developed an algorithm enabling automated analysis of confocal images and quantification of cDC1 reprogramming efficiency from individual image stacks calculated as a ratio of mCherry+, CD45+ and HLA-DR+ cells versus the number of DAPI+ nuclei. Using the new algorithm we have evaluated the reprogramming efficacy of the different virus dosages in all three types of 3D tumor spheroids. Lastly, we have cocultured tumor spheroids transduced with PIB with naïve or activated HLA-matched PBMCs and evaluated cytokine secretion as a readout of immune cell activation. We observed that reprogramming induces activation of T cells and correlated it to the number of reprogrammed cells in the tumor spheroid, evaluated by the HC imaging. In summary, we developed the InSphero 3D InSight™ Oncology Platform that allowed us to demonstrate the effects of direct reprogramming of tumor cells into immunogenic dendritic cells. Combined with high-content imaging analysis, this platform offers a powerful solution for preclinical translational research.

#4551

Reconstructing the metastatic tumor microenvironment of high grade serous ovarian cancer: understanding the contribution of malignant cells

Beatrice Malacrida, Samar Elorbany, Eleni Maniati, Florian Laforets, Ranjit Manchanda, Frances R. Balkwill. *Barts Cancer Institute, London, United Kingdom*

Following a 'deconstruction' of the metastatic tumor microenvironment (TME) of high grade serous ovarian cancer (HGSOC), we developed 3-dimensional (3D) human multicellular in vitro models using patient-derived primary cells and HGSOC malignant cell lines. In this study, we used these 3D in vitro human models to study how malignant cells influence the surrounding TME. Using patient-derived primary adipocytes, fibroblasts and mesothelial cells isolated from macroscopically normal omentum (the primary site of metastasis in HGSOC) from women undergoing gynaeco-oncology surgery, we built multicellular models combining those cells with different high grade serous malignant cell lines and monocytes isolated from healthy individuals. We found that peripheral blood monocytes were able to differentiate and polarize to macrophages in our pentacultures (i.e., five different cell types) with phenotypes also found in HGSOC omental metastases. In addition, the cells in our pentaculture models self-rearranged in ways that were dependent on the HGSOC malignant cell lines used in the culture. Macrophage phenotype and cytokine secretion from the multicellular cultures was also influenced by the different malignant HGSOC cell lines used in the model. RNAseq analysis of the pentacultures showed that the cultures clustered according to the malignant cell line used. In addition, we were able to identify some gene expression clusters in the macrophages and fibroblasts of the pentacultures that matched those found by single cell RNAseq analysis of human HGSOC biopsies. These human 3D in vitro multicellular models allow us to define the contribution of each cell type to tumor growth and spread, and also provide us a semi-high throughput platform to investigate antibody or drug targets.

#4552

3D-EXplore platform of fresh patient tumoroids with intact TME allows assessment of the efficacy of drugs targeting the tumor stroma on *ex vivo* tumor immunotherapy

Seth Currlin, Brittney Ruedlinger, Sharon Camacho, Angie Rivera, Jasmin D'Andrea, Jared Ehrhart, Soner Altiok. *Nilogen Oncosystems, Tampa, FL*

Introducti**on:** Cancer associated fibroblasts (CAFs) are a major component of the tumormicroenvironment (TME) and exhibit diverse tumorigenic functions such as immunosuppressionand extracellular matrix (ECM) remodeling. Treatment of solid tumors is often hindered by acomplex TME, which persists despite effective tumor-cell directed therapies. Therefore,treatment of solid tumors in combination with stromal-targeting therapies is essential toovercome CAF-facilitated tumor growth, and immunosuppression. Herein we interrogate theimpact of tumor stroma targeting therapeutics, in combination with nivolumab, on the efficacy oftumor cell killing (TCK) in a 3D human tumoroid *ex vivo* culture model (3D-EXplore). Resultingdata suggests that impairing the recruitment and activation of CAFs within the TME leads toenhanced TCK when combined with immune checkpoint blockade therapy.

Materials and Methods: All patients tumor samples were collected with patient consent andrelevant IRB approval. 3D tumoroids measuring 150 microns in size were generated from freshpatient tumors including endometrial, ovarian, and colorectal cancer tissues. Tumoroids werethen treated with stromal targeting strategies for TGF-beta (galunisertib), the FGF pathway(Dovitinib), FAK inhibitors (defactinib), and cell adhesion modulators (plerixafor) alone or incombination with nivolumab for 72-hours *ex vivo*. Tumor responses to *ex vivo* treatments wereassessed using a proprietary tumor cell killing assay and 21-color flow cytometry analysis.

Results and Summary: Here we evaluated the impact of stromal targeting therapeutics onCAFs and associated tumor cell killing as well as overcoming immune evasion mechanismspreserved in the tumoroid models. Furthermore, we used a multicolor flow panel to analyzewhether combination of stromal targeting drugs enhances nivolumab's effect on the activation oftumor resident CD4, CD8 T-cells, NKT, and NK cell populations as well as on macrophagepolarization. Treatment-mediated changes in the tumor immune microenvironment was furthercorroborated by a multiplex cytokine release assay detecting GM-CSF, sCD137, IFNγ,

sFas,sFasL, Granzyme A, Granzyme B, IL-2, IL-4, IL-5, IL-6, IL-10, IL-13, MIP-1α, MIP-1β, TNF-α,Perforin in tumoroid culture media and correlated with clinicopathologic findings and PD-L1expression for individual tumnors. Further, this 3D-tumoroid platform provides unique insightinto the microenvironment of both treatment responsive and non-responsive tumors and can aidin the development of patient-centered therapeutic regimens.

#4553

How do shiitake and reishi mushrooms work on lung cancer? : A high throughput screening of 3D cell culture

Mihi Yang[1], Hee-Kyung Jang[2], Huiwon Kang[1]. *[1]Sookmyung Women's University, College of Pharmacy, Seoul, Korea, Republic of,[2]Natural Dream, Goesan, Korea, Republic of*

Shiitake (*Lentinula edodes*) and reishi mushrooms (*Ganoderma sichuanense*) have been noticed for desirable chemoprevention, such as improving immunity, overcoming anticancer drug resistance, etc. Particularly, beta-glucans have been mostly mentioned as the active component of the mushrooms. However, the right preparation and effective usage of the mushrooms for cancers are unclear, yet. Thus, we screened various extractions of the two mushrooms and combinations of the extracts, using a high throughput screening of 3D cell culture system on 384-pillar plates with various cancer cells and Cell Titer-Glo 3D cell viability assay kit (Promega). We also quantified the beta-glucans in all extractions with the Megazyme Mushroom and Yeast Beta-Glucan kit (K-YBGL) by excluding the alpha-glucans content from the total-glucans. As results, most of the extracts showed cytotoxicity on the lung cancer cells, A549 cells, rather than on the other cells, such as HepG2 (N=9 for each treatment). The extracts of reishi mushroom in 60% of methanol (dose range, 0.21-2.3 mg/ml) showed the strongest cytotoxicity on the lung cells, IC50=0.90 +/- 0.01 mg/ml, among the extracts of different methanol contents (10-60%) or different temperatures (50-90 °C) of hot water. However, the 60 % of methanol reishi extracts included relatively low levels of beta-glucans, compared to other extracts (18.57 +/- 0.31 vs. 22.42 +/- 5.56 % w/w). In addition, the levels of beta-glucans in all of reishi mushroom extracts were lower than those in all of the shiitake extracts (17.70 +/- 1.89 % vs. 27.05

+/- 4.21 % w/w: $p<0.01$). Moreover, there was no association between the levels of beta-glucans and IC50 in A549 cells. Interestingly, the combination (1:1) of the above 60% of methanol extracts of reishi mushroom and the 30% methanol extracts of shiitake (dose range, 0.30-3.26 mg/ml) showed synergic effects, i.e., 2-7 fold stronger effects (average of IC50=0.40 mg/ml) than every single treatment (average of IC50=0.90-2.63 mg/ml). Taken together, the reishi mushroom may have other strong chemopreventive materials rather than beta-glucans, while the shiitake may have a potentiation effect, when combined with the reishi mushroom. In conclusion, our 3D cell culture system showed high throughput performance to find the right preparation and effective usage of the two mushrooms and provided useful information for the next clinical studies for lung cancer.

#4554

Head and neck cancer HuBiogel-embedded microtumor assay system for therapeutic efficacy testing of patient tumor specimens

Christopher D. Willey[1], Yedeh P. Ying[2], Anthony B. Morlandt[2], Hope M. Amm[2], Patricia H. Hicks[1], Joshua C. Anderson[1], Andee M. Beierle[1], Carissa M. Thomas[3], Jason M. Warram[3], Jingsong Chen[4], Jeffrey A. Thomas[4], Katie Banko[4], Raj K. Singh[4]. *[1]Radiation Oncology, O'Neal Comprehensive Cancer Center at UAB, Birmingham, AL,[2]Oral & Maxillofacial Surgery, O'Neal Comprehensive Cancer Center at UAB, Birmingham, AL,[3]Otolaryngology, O'Neal Comprehensive Cancer Center at UAB, Birmingham, AL,[4]LifeNet Health, Virginia Beach, VA*

Head and neck (HN) cancer recurrence is common, and selecting effective salvage systemic therapy remains difficult, particularly for oral cavity cancers. Developing a rapid, robust and predictive therapeutic testing system could support clinical decision-making and improve patient outcomes. We developed a Patient Therapy Evaluation System (PTES) that employs a three-dimensional (3D) fully human microtumor drug testing assay using tissue specimens collected during surgery of HN cancers. Remnant fresh tumor tissue from patients is dissociated into single-cell suspension that is embedded using a novel HuBiogel-cell encapsulation technology (3D microtumors). This high-throughput assay platform allows

morphologic, functional, and molecular evaluations in parallel by real-time imaging, cell proliferation, and biomarker protocols. Microtumor viability, growth profiles, and drug screening data are captured at multiple time points up to 14 days. Our initial cohort included 57 patient specimens (53 squamous cell carcinomas, 1 verrucous carcinoma, 1 osteosarcoma, 1 ameloblastoma, and 1 non-cancerous lichenoid mucositis). HuBiogel-embedded tumor cells formed numerous multicellular colonies exhibiting distinct organization and growth patterns in 14-day microtumor cultures. Interestingly, epithelial, stromal and stem-cell like populations were preserved in HN microtumor models based on marker expression. Treatment with single (cisplatin, 5FU, docetaxel) drugs and their combinations resulted in tumor inhibitory responses (IC50) evaluated by CellTiter-Glo assay, and residual surviving cells were also recorded by Calcein-AM staining of 3D Microtumors. While patient-derived HN microtumors were produced with high success rates, factors associated with lower microtumor yield included smaller tumor specimens and low viability after dissociation. In conclusion, our new all human microtumor assay models replicating phenotypic, functional, and molecular properties ex vivo provide a potential theranostic tool for rapidly predicting drug sensitivity and improving treatment strategy for HN cancer patients.

#4555

Aryl-hydrocarbon receptor inhibitors in combination with anticancer agents, especially proteasome pathway inhibitors, in a complex spheroid screen using patient-derived cell lines can result in greater-than additive cytotoxicity

BEVERLY A. TEICHER[1], Jeffrey A. Moscow[1], Joel Morris[1], James H. Doroshow[1], Thomas S. Dexheimer[2], Nathan P. Coussens[2], Thomas Silvers[2], Rene Delosh[2], Zahra Davoudi[2], Russel Reinhart[2], Chad Ogle[2], Eric Jones[2].
[1]DCTD, National Cancer Institute, Bethesda, MD,[2]Applied and Developmental Research Directorate, Frederick National Laboratory for Cancer Research, Frederick, MD

Three aryl-hydrocarbon receptor (AhR) selective inhibitors, BAY-2416964, GNF351 and CH-223191, were assayed alone and in combination with 25 approved or investigational anticancer agents in complex spheroids including tumor cells, endothelial cells, and mesenchymal stem cells. The

tumor cell lines were from the National Cancer Institute's Patient-Derived Models Repository (PDMR) collection (https://pdmr.cancer.gov/models/database.htm). The AhR is a ligand-activated helix-loop-helix transcription factor of the bHLH-PAS family. It is involved in the regulation of responses to planar aromatic hydrocarbons by activating the transcription of xenobiotic-metabolizing enzymes such as cytochrome P450 or by acting as an E3 ligase. Thus, the AhR activates detoxification pathways that dispose of small molecule toxins and damaged proteins. In the absence of xenobiotics, the AhR is located within the cytoplasm in complex with two Hsp90 molecules and co-chaperones. Upon xenobiotic binding, the AhR translocates to the nucleus and binds to the AhR nuclear translocator protein to form an active transcription factor complex and promote gene transcription. As single agents, the three AhR inhibitors showed little cytotoxicity at concentrations up to 10 μM. Combinations of AhR inhibitors with anticancer agents including doxorubicin, cisplatin, SN38, venetoclax, selinexor, and etoposide (https://dtp.cancer.gov/organization/dscb/obtaining/default.htm) produced primarily additive cytotoxicity in complex spheroids after a 7-day exposure. However, unexpected greater-than-additive effects were observed with AhR inhibitors in combination with proteasome pathway inhibitors. Bortezomib, a direct inhibitor of the chymotrypsin-like protease of the 26S proteasome, and pevonedistat, a NEDD8-activating enzyme inhibitor, produced additive or greater-than-additive cytotoxicity in some complex spheroids. However, the combination of BAY-2416964 with TAK-243, a ubiquitin activating enzyme inhibitor, produced profound greater-than-additive cytotoxicity in more than half of the 28 PDMR cell lines tested as complex spheroids. The combination resulted in an increase of 1- to 3-logs of excess cytotoxicity in malignancies including bladder cancer, pancreatic cancer, colon cancer, NSCLC, SCLC and glioblastoma. In vivo studies are under discussion. This project was funded in part with federal funds from the NCI, NIH, under contract no. HHSN261201500003I.

#4556

Matrix properties regulate 3D tumor spheroid growth and cancer drug response

Jaxson R. Libby, Linqing Li, Sarah R. Walker. *University of New Hampshire, Durham, NH*

3D cancer spheroids are vital in vitro models for cancer drug discovery. The current cancer spheroid generation utilizes low-adhesion plates or forced aggregation of single cells. However, certain cancers do not form stable spheroids in these protocols, nor do pre-formed tumor spheroids recapitulate in vivo development and progression. This project aims to overcome this limitation with the use of a biomimetic hydrogel system to mimic in vivo cancer cell growth and tumor development and use it as an in vitro platform for 3D cancer drug screening. The biocompatible and tunable hydrogel permits independent control of key biochemical and biophysical cues such as matrix degradation, cell adhesion, and stiffness; leading to systematic investigation of matrix parameter contribution to regulating in vitro tumor growth and treatment response. We modified a homo-polysaccharide dextran with methacrylate groups and generated dextran macromers (Dex-MA) containing ample reactive methacrylates per polymer. Cell adhesion is mediated by thiol-terminated RGD peptide added to the methacrylates, followed by crosslinking with di-thiolated MMP-labile peptides through Michael-type addition reaction. Varying the sequence of the crosslinker furthermore gives access to a range of degradability, independent of matrix stiffness. Our experiments showed that Dex-MA supported robust growth of SK-BR-3 breast cancer cells from single cell to 3D tumor spheroids, whereas the cell line failed to form tumor aggregates in low-adhesion plates. Alteration of hydrogel stiffness further revealed stiffness dependence of tumor growth, invasion, and response to treatment, suggesting the importance of matrix properties on regulating cell behavior. This dextran-based tunable hydrogel system provides key insights into how engineered matrix properties control tumor growth, critical for screening novel therapy compounds, and may reveal mechanisms for 3D tumor development, invasion, metastasis, and drug resistance.

#4557

3D-EXpress platform utilizing tumoroids from patients with MSS and MSI-H tumors allows rapid assessment of anti-tumor activity of immune checkpoint inhibitors and development of clinically relevant biomarkers of treatment response

Brittney Ruedlinger, Seth Currlin, Sharon Camacho, Alliyah Humphrey, Jared Ehrhart, Soner Altiok. *Nilogen Oncosystems, Tampa, FL*

Introducti**on:** Recent studies showed that patients with deficient mismatch repair(dMMR)/microsatellite instability-high (MSI-H) tumors, have higher sensitivity to immune checkpointinhibitors (ICIs) compared to patients with microsatellite-stable (MSS)/microsatellite instability-low(MSI-L) tumors. However, the mechanisms of treatment responsiveness and resistance is not wellunderstood. Here, we used a novel 3D-EXpress *ex vivo* fresh patient tumoroid platform to assess theefficacy of nivolumab/ipilimumab combination therapy in tumors with known MSS/MSI-H status andperformed correlative studies.

Materials and Methods: All tumor samples were obtained with patient consent and relevant IRBapproval. Tumoroids measuring 150 μm in size retaining tumor cell heterogeneity, tumor-residentimmune cells, stromal components, and cell-extracellular matrix interaction were prepared frompatients with endometrial and colorectal tumors among others. Tumoroid aliquots were cryopreservedin Nilogen's tumoroid Biorepository for future studies. For the 3D-EXpress studies cryopreservedtumoroids were selected based on MSS/MSI-H status and treated *ex vivo* with nivolumab andipilimumab alone and in combinations for 72h. Tumor responses to treatments were evaluated by aproprietary tumor cell killing assay and changes in tumor immune microenvironment. Furthermore,tumor PD-L1 expression levels were analyzed on the associated TMA slides.

Results: Treatment-induced tumor cell killing activity in intact tumoroids was assessed by a 3D high-content confocal imaging technique using a proprietary algorithm for data analysis. The impact of *exvivo* treatment by nivolumab and/or ipilimumab on tumor resident immune cell populations wasmonitored by a multiplex cytokine release assay analyzing release of GM-CSF, sCD137, IFNγ, sFas, sFasL,Granzyme A, Granzyme B, IL-2, IL-4, IL-5, IL-6, IL-10, IL-13, MIP-1α, MIP-1β, TNF-α, and Perforin usingculture supernatants isolated from treated tumoroid samples. Based on the *ex vivo* responses tumorswere assigned to treatment sensitive and resistant groups and correlative analyses were performed withindividual tumors' innate and adaptive immune cell populations detected by a 21-color flow cytometrypanel, in addition to tumor MSS/MSI-H and p53 status, and detailed clinicopathologic data readilyavailable for the tumors cryopreserved in the Biorepository.

Conclusion: The 3D-Express platform, using cryopreserved 3D tumoroids with intact TME is an effectivetool for the assessment of rational combinations which may prove relevant in the treatment of solidtumors. Furthermore, we believe this platform is a useful tool for the pre-clinical assessment of specifictherapeutic regimens designed for individualized patient care.

#4558

High-throughput, high content Imaging assay for assessing solid tumor phagocytosis in 3D spheroid model

Michal Rudnik, Özlem Yavaş Grining, Nadezhda Rotankova, Silvan Strebel, Francesca Chiovaro, Olivier Frey, Irina Agarkova, Wolfgang Moritz. *InSphero AG, Schlieren, Switzerland*

Emerging studies have demonstrated that innate immune checkpoints, regulating Tumor-associated Macrophage (TAM) phagocytic activity, play a crucial role in immune escape and survival of cancer cells. CD47-SIRPα axis is the best studied example of the “don’t eat me” signal, frequently overexpressed on cancer cell. Targeting of CD47 protein has shown impressive results in clinical trials in hematologic malignancies but remained challenging for solid tumors therapy. Therefore, tools facilitating the development of novel innate immune checkpoint inhibitors are of great interest. To address that unmet need, we established a high-throughput, 384-well-format assay for efficacy assessment of compounds inducing macrophage phagocytosis. As a model of solid tumor, we employed 3D spheroids aggregated of human cancer cell lines (A375, HCT116, MCF7, SKOV3) expressing GFP or PDX material (LXFA1647 lung adenocarcinoma, MEXF2106 melanoma) and cancer associated fibroblasts, as well as Monocyte-Derived Macrophages (MDMs) which altogether were co-aggregated to form spheroids mimicking the tumor microenvironment and immune-competence. In parallel MDMs were co-cultured with matured spheroid to emulate tumor infiltration. Both models were cultured in automation and High Content imaging compatible Akura™ 384-well plate. To evaluate our system, we targeted CD47-SIRPα axis by treatment of 3D spheroid models with αCD47 antibody (H6D12) in combination with atezolizumab (αPD-L1 antibody). Tumor viability and growth were assessed by fluorescence measurements and ATP level. Phagocytosis of

fluorescently labeled tumor cells was imaged by confocal microscopy and quantified by inhouse developed analysis pipeline. Immune cell activation was evaluated by a cytokine bead array. The treatment of cell line-based 3D models with αCD47 antibody resulted in an increased number of phagocytic macrophages followed by a decrease of fluorescence and size of tumor spheroids in a dose-dependent manner. Moreover, we observed an induced secretion of TNFα, IL-6, IL-10 and IL-RA after 48h. Similarly, in PDX-based models, we observed decreased spheroid size and ATP level at day 7. Notably, αCD47 antibody-induced level of cytokines was further increased in combination with atezolizumab. To conclude, we have developed a human disease relevant, high-throughput assay for the evaluation of novel therapeutic modalities targeting phagocytosis. Due to compatibility with microscopy and most of the biochemical assays, it represents a powerful tool for clinical candidate development.

#4559

Evaluation of T cell cytotoxicity, PD-L1 expression and phenotypic features in novel automated 3D microfluidic breast cancer co-culture platform

Ekaterina Moroz Nikolov[1], Anthony Thai[1], Lila Cooper[1], Mahomi Suzuki[2], Arvonn Tully[3], Rashmi Rajendra[1], Evan F. Cromwell[1]. *[1]Protein Fluidics, Inc., Burlingame, CA,[2]Yokogawa Electric Corporation, Ishikawa, Japan,[3]Yokogawa Corporation of America, Sugar Land, CA*

Immunotherapy is now recognized as a powerful therapeutic approach to treat and cure cancer. However, the objective response rates for most solid tumors are low (below 30%). Accumulating evidence has shown that chemotherapy can increase the efficacy of immune checkpoint blockade and improve cancer outcomes. We have investigated if chemotherapy can modulate anti-PDL1 enhanced T cell cytotoxicity in breast cancer using novel *in vitro* 3D co-culture assay system. 3D co-culture of cancer and immune cells is a powerful platform for disease modeling and therapies testing because it can mimic the tumor micro-environment and complex cellular interactions. In this study we evaluated the immunomodulatory effect of chemotherapy on spheroid-T cells interactions in response to PD-L1 inhibition in triple-negative breast cancer. MCF7 and MDA231 cell lines with differential PD-L1 status were formed into spheroids and used as a

tumor model. T cells were activated from PBMCs using ImmunoCult CD3/CD28 T cell Activator. Co-culture assays were performed over 72 hr in a Pu·MA System. The Pu·MA System is an automated microfluidic platform that enables phenotypic and functional assays using physiologically relevant 3D cell models. Cancer spheroids and T cells were cultured, manipulated, and measured in a single well of a microfluidic flowchip. The platform integrates 1) 3D cell model with delivery of immune cells, 2) drug delivery, 3) imaging of phenotypic features and 4) functional profiling for cytokine secretion and viability. T cells-spheroid interaction, invasion and cell viability was assessed using high-content fluorescence imaging CellVoyager CQ1 system. IL2, IFN-γ and TNF-α secretion was measured in collected supernatants using Lumit immunoassays. After viability determination, co-cultures were fixed and stained for cancer and T cell markers (E-Cadherin, F-Actin, CD3, CD8) using automated IF staining protocol and then imaged. Image analysis revealed colocalization and infiltration of the T cells into the spheroids. Disintegration of spheroid, loss of circular shape, and increased number of dead cancer cells indicated T cell mediated cancer cell death. To evaluate the immunomodulatory effect of chemotherapy on spheroid-T cells interactions in response to PD-L1 inhibition, co-cultures were exposed to PD-L1 inhibitor Atezolizumab in the presence or absence of Cisplatin/Pemetrexed. We have analyzed a shift in T cell-mediated killing activity and function in the presence or absence of chemotherapeutics. The proposed co-culture platform can be further extended to a more complex patient-derived 3D models using different cell types. Our functional immune-oncology 3D platform allows to study the crosstalk between immune, cancer and other cell interactions, evaluate new drug candidates and assess individual therapeutic approaches to advance precision medicine.

#4560

Assay-ready tissue-engineered cancer microspheres for high-throughput screening

Yuan Tian[1], Yongwoon Kim[2], Wen J. Seeto[1], Shantanu Pradhan[3], Dmitriy Minond[4], Rock Pulak[2], Elizabeth A. Lipke[1]. *[1]Chemical Engineering, Auburn University, Auburn, AL,[2]Union Biometrica, Holliston, MA,[3]Department of Biotechnology, Indian Institute of Technology Madras,*

Chennai, India,[4]Department of Pharmaceutical Sciences, Nova Southeastern University, Ft. Lauderdale, FL

For drug discovery, new *in vitro* cancer models are needed to obtain more translatable study outcomes in a low-cost and high-throughput manner. For this purpose, 3D cancer spheroids have been established as more effective than 2D models. Current commercial techniques, however, rely heavily on self-aggregation of dissociated cells and cannot replicate key features of the native tumor microenvironment, particularly due to a lack of control over extracellular matrix components and heterogeneity in size and aggregate-forming tendencies. Also, current spheroidal techniques are typically limited to one spheroid per well, therefore providing a narrow range of cell numbers per well, disadvantageous for assay development in drug screening. Here, we overcome these challenges by coupling tissue engineering toolsets with microfluidic technologies to create engineered cancer microspheres and sorting desired numbers of microspheres into assay-ready well-plate format. To form the engineered cancer microspheres, MCF7 (non-metastatic) and MDA-MB-231 (metastatic) breast cancer cells were encapsulated within poly(ethylene glycol)-fibrinogen hydrogels using our previously developed microfluidic platform. Highly uniform cancer microspheres (intra and inter-batch coefficient of variation $\leq 5\%$) with high cell densities (over 20×10^6 cells/ml) were produced rapidly, which is critical for use in drug testing. The microspheres supported the 3D culture of both breast cancer cell lines over at least 14 days in culture. Encapsulated cells displayed cell type-specific differences in morphology, proliferation, metabolic activity, ultrastructure, and overall microsphere size distribution and bulk stiffness. To prepare assay-ready pre-plated microspheres, a COPAS FP flow cytometer was used for its ability to analyze and sort large sample particles such as tumor spheroids and hydrogel cancer microspheres generated in this study. When using a 96-well plate, the sorting rate varied from 2.5 - 6 microspheres per second, depending on the sample concentration. When sorting a desired number of microspheres per well, the accuracy was greater than 95% as verified visually by microscopy. Viability of sorted microspheres was verified 24 hours post-sort. Shipping conditions were established that maintained cell viability for remote use in drug testing. Methods for compound addition by pinning and imaging were tested and optimized. Using these approaches, the microsphere system was

shown to be compatible with an automated liquid handling system for administration of drug compounds; MDA-MB-231 microspheres were distributed in 384 well plates and treated with chemotherapeutic drugs. Expected responses were quantitated using CellTiter-Glo® 3D and detected using automated imaging. Overall, our results demonstrate initial applicability for the tissue-engineered cancer microspheres for drug screening.

#4561

3D Reconstructed Pancreas: A model capturing the unique tumor microenvironment and stromal architecture of pancreatic cancer

Arnat Balabyev[1], Justin D. Phillips[1], Michael Steffey[2], Eleanore J. Kirshner[1], Aayushi Ahlawat[1], Arlette H. Uihlein[1], Daniel Saims[2], Scott Wise[2], David Draper[2], Julia Kirshner[1]. *[1]Predictive Oncology Inc, Eagan, MN,[2]Labcorp, Drug Development, Ann Arbor, MI*

As it is rarely discovered early, the prognosis for people with pancreatic cancer is poor, with an average 5-year survival rate of 10% and only 3% for those with metastatic illness. Pancreatic cancer patients have few therapeutic options and innovative therapies are sorely needed to improve treatment of the disease. This is mainly due to the late diagnosis and partially due to the biology of the disease. Capturing the components of the tumor microenvironment, which serve as both a physical barrier and a source of stromal-driven resistance to therapeutics, is one of the issues faced by drug developers searching for agents to combat pancreatic cancer. We have created a 3D model of the pancreatic tumor microenvironment, the *Reconstructed Pancreas* (r-Pancreas), using Mia PaCa-2, PANC-1, and BxPC-3 pancreatic tumor cell lines embedded in an extracellular matrix (ECM) that was formulated to recapitulate the typical ECM of pancreatic tumors. We have shown that gemcitabine was effective against pancreatic tumor cells cultured in r-Pancreas (IC_{50}=0.4-0.8μM), while 5-fluorouracil was ineffective (IC_{50} not reached), mimicking clinical response. In nude mice, subcutaneous PANC-1 tumors exhibited similar responses to gemcitabine and 5-fluorocurcil. Treatment with gemcitabine resulted in a Day 63 median ΔT/ΔC of 37% while 5-fluorouracil resulted in a Day 63 median delta ΔT/ΔC of 102%. Incorporating a collagen-rich capsule

increases the physiological relevance of the r-Pancreas model because it has been shown that human pancreatic tumors have an outer layer of stiff ECM that functions as a physical barrier and prevents drugs from penetrating the tumor. Recently, we showed that, at least in the Mia PaCa-2 and BxPC-3 tumor cell lines, introducing such a collagen capsule dramatically reduced sensitivity to gemcitabine. Disrupting the collagen capsule with MMP-9 restored the sensitivity of the tumor cells to gemcitabine demonstrating that the capsule provides a physical barrier to drug entry. Additionally, creating a co-culture of primary activated pancreatic stromal cells and pancreatic tumor cell lines produces a more complete 3D model that permits the testing of potential therapeutic agents inside the pancreatic tumor microenvironment. Hence, we have created a 3D model where pancreatic tumor cells were co-cultured with human pancreatic fibroblasts. According to our results, the IC_{50} values for pancreatic tumor cell lines treated with gemcitabine increased by twofold when co-cultured with activated pancreatic fibroblasts compared to control sets of tumor cells alone (IC_{50}=1-3μM). Together, these data imply that, to be clinically relevant, *in vitro* models of pancreatic cancer must integrate tumor-specific components of the microenvironment, including the collagen capsule and activated fibroblasts.

#4563

Measuring immunotherapy responses *ex vivo* using novel 3D culture platform: E-slice

Thomas D. Gallup[1], Jose A. Maldonado[2], Corina Margain[1], Min P. Kim[2], David F. Gallup[1], Kyuson Yun[2]. *[1]EMPIRI, Inc, Houston, TX,[2]Houston Methodist Research Institute, Houston, TX*

Immunotherapies have provided dramatic and life-saving results in some patients; however, their effectiveness varies greatly in different tumors, even among patients with the same clinical diagnosis. Clearly, a better system to evaluate the personalized response to immunotherapies will greatly benefit the patients and reduce the cost of care. In addition, due to their theoretical and demonstrated benefits in providing durable responses, new immunotherapies are avidly sought after by most major pharmaceutical companies, numerous biotech companies, and academic laboratories. However, preclinical evaluation of new immunotherapy efficacy is

challenging and inaccurate using most experimental model systems.E-slice is a faithful model of an individual cancer patient's tumor. It is a proprietary 3D tissue slice culture platform, and E-slices are generated by making thin sections of intact, fresh tumor tissues from patients. As such, immune components and the TME in E-slices are native to each patient's tumor. E-slice overcomes many of the limitations of other experimental systems for multiple reasons. The E-slice platform: 1) uses chemically defined, serum-free medium; 2) measures viability changes upon treatment longitudinally, from the same tissue, which allows both absolute and relative responses for as short as 4 days or as long as over 4 weeks ex vivo; 3) can be generated from any solid tumor tested thus far (breast, lung, colorectal, pancreas, brain, head 7 neck, and others) from patient tumors directly or from PDX and genetically engineered mouse models; 4) retains the native TME and tissue architecture because E-slices are never dissociated or otherwise reconstituted; 5) is compatible with biopsies as well as surgical samples; 6) has been shown to accurately predict individual patient treatment responses to chemotherapies and targeted therapies in 4-12 days, paving the way for evidence-based personalized treatment selections in a clinically actionable time frame.Specifically for immunotherapy response measurements, key differentiators of the E-slice platform from other ex vivo systems for immunotherapy responses are: 1) E-slice is generated from fresh patient tumor tissues with tumor-trained and resident immune cells and not artificially introduced PBMCs used in most other systems; 2) serum-free, chemically defined medium and does not artificially activate or suppress the immune system; 3) E-slice has been validated by single-cell RNA-sequencing to maintain immune cells in their native state up to 8 days ex vivo; 4) E-slices can be used to detect secreted protein and metabolic biomarkers in the conditioned media pre- and post-treatment; 5) E-slice can measure immunotherapy responses ex vivo in 8 days. In summary, we present a novel ex vivo 3D human tumor tissue drug sensitivity platform that can enhance immunotherapy development pipelines and clinical deployment.

#4564

Liquid-phase-based cell culture platform that enables polymer surface stimuli-induced generation of patient-specific glioma stem cell-like tumor spheroids

Junhyuk Song[1], Yoonjung Choi[1], Yumi Lee[1], Hyo E. Moon[2], Changjin Seo[1], Hyung W. Park[2], Dohyeon Kim[1], Chang W. Song[3], Daeyoup Lee[1], Sun H. Paek[2], Sangyong Jon[4]. *[1]Department of Biological Sciences, Korea Advanced Institute of Science and Technology (KAIST), Daejeon, Korea, Republic of,[2]Department of Neurosurgery, Cancer Research Institute and Ischemic/Hypoxic Disease Institute, Seoul National University College of Medicine, Seoul, Korea, Republic of,[3]Department of Radiation Oncology, University of Minnesota Medical School, Minneapolis, MN,[4]Department of Biological Sciences, Graduate School of Medical Science and Engineering, Korea Advanced Institute of Science and Technology (KAIST), Daejeon, Korea, Republic of*

Despite the rapidly growing interest on cancer stem cells (CSCs) from cancer biologists, oncologists and the clinic because of their crucial role in recurrence and metastasis due to resistance in solid cancers, including GBM, there is still a lack of robust, effective *in vivo*-like 3D CSC models from cancer cells or patient-derived tumor tissues. In this sense, we developed a novel functional polymer thin film (Poly-X-PTF) via a streamlined liquid-phase synthesis, a more facile and advanced version than previous lab-made vapor-deposited poly(2,4,6,8-tetravinyl-2,4,6,8-tetramethyl cyclotetrasiloxane) called pV4D4-PTF. Emerging from a previous success with pV4D4, the new platform, Poly-X, could also simply stimulate surface stimuli-guided, rapid transformation of differentiated cancer cells to a number of ECM-enriched, similar-sized 3D CSC-like tumor spheroids from both commercialized cancer cell lines and patient-derived primary GBM cells. Varied GBM patient-derived cancer spheroids demonstrated a variety of phenotypes and transcriptomic profiles known about glioma stem cells (GSCs) in common. Notably, respective sensitivities of different patient-based 3D GSC spheroids to irradiation with or without temozolomide were retrospectively associated with the individual therapeutic outcome and overall survival, as a result of clinically relevant concurrent chemoradiation treatment (CCRT) regimens proposed in a fast Poly-X-spheroids-based 3D viability assay format. Ultimately, this versatile platform may serve to study fundamental CSC biology. Furthermore, it may translate into a powerful preclinical *ex vivo* tool in glioma medical settings both to aid in on-site prospective prediction of the patient-specific prognosis via CCRT viability responses within around 10

days and assess a patient-tailored, promising drug candidate or combination treatment.

#4565

Drug screening by layered 3D co-cultured tumor model including vascularized stromal tissue

Yuki Takahashi[1], Yumi Nomura[1], Yuma Yokokawa[1], Shiro Kitano[1], Satoshi Nagayama[2], Eiji Shinozaki[2], Ryohei Katayama[3], Naoya Fujita[3]. *[1]Toppan Inc., Saitama, Japan,[2]Cancer Institute Hospital of JFCR, Japanese Foundation for Cancer Research, Tokyo, Japan,[3]Cancer Chemotherapy Center, Japanese Foundation for Cancer Research, Tokyo, Japan*

Introduction: *In vivo*, tumor microenvironments consist of not only cancer cells but also extracellular matrix and stromal tissues, such as fibroblasts, blood vessels, and so on. The interactions between cancer cells and stromal tissue have been reported to affect the behavior of cancer cells. So that *ex vivo* model recapturing the tumor microenvironment is needed to evaluate the efficacy of drugs under the condition mimicking the patient tumor tissue. Here, we developed the unique tissue engineering technique, which easily enables the construction of cell - stacked three dimensional (3D) tissue, and co-culture of 3D stromal tissues and patient-derived cancer cells (PDCs). We investigated drug sensitivity in conventional 2D culture, our 3D co-cultured model and *in vivo* tumor.
Methods: Fibroblasts and vascular endothelial cells were suspended in a buffer solution containing heparin and collagen to support cell aggregation. The heparin/collagen-treated cells were seeded in culture-inserts in over-confluent manner, and 3D layered stromal tissue called were constructed. PDCs established from colorectal cancer (CRC) and non-small cell lung cancer (NSCLC) patients in the Cancer Institute Hospital of JFCR were co-cultured with the 3D stromal tissue. The 3D co-cultured model applied to drug screening, and the results were compared with those of 2D culture model. *In vivo* drug evaluations were performed with the compounds in which marked differences were observed between 2D and 3D models.
Results: In our 3D model, drug sensitivities to most of the tested compounds tended to be decreased in comparison with those in 2D culture condition. Interestingly, a part of drugs did not effective in 2D showed marked tumor growth inhibition in our 3D model. The compounds that

showed favorable efficacy in 3D rather than 2D in multiple PDCs were accounted for about 5% of tested compounds. At least half of these drugs showed significant tumor growth suppression or tumor regression *in vivo*. On the contrary, in the case of drug sensitivities were considerably fallen in our 3D model, most of the evaluated compounds represented almost no anti-tumor effect *in vivo*. Results from gene and protein expression analyses supported that cancer cells co-cultured in our 3D stromal tissue have some similar profiles to in vivo tumor rather than 2D culture condition. Conclusion: Our study proposed the unique 3D co-cultured tumor model. The model may enable more accurate drug screening reflecting the *in vivo* circumstances. Further studies are needed to confirm the model's predictability of clinical outcomes.

#4566

3D cancer cell-fibroblast heterospheroids forming tumor-like microenvironments are valuable tools to study immune cell infiltration and as pre-clinical drug testing models

Boye Schnack Nielsen, Natasha H. Madsen, Jesper Larsen, Hjalte M. Larsen, Monika Gad, Kim Holmstrom. *Cellular Engineering & Disease Modelling, Bioneer A/S, Hørsholm, Denmark*

3D cancer cell cultures have enabled new opportunities for replacing compound testing in experimental animals and provide a basis for high content work-flows for drug testing. Here we present data obtained from 3D multicellular tumor spheroids (MCTS) composed of cancer cell lines, fibroblasts and macrophages. We cultured HT29 and SW480 CRC cell lines (as well as others) with fibroblasts and obtained heterospheroids that could be evaluated in cell viability and apoptosis assays, by flow cytometry and high content imaging (HCI). In addition, mature MCTS were embedded in paraffin and used for traditional biomarker characterization using immunohistochemistry and in situ hybridization. The cancer cell x fibroblast interactions promoted a tumor-like microenvironment that recruited monocytes isolated from primary donors. FACS analysis indicated that the infiltrating monocytes polarized into CD163-positive M2 macrophages in HT29 MCTS, and in pancreatic MIA PaCa-2 MCTS, using Pexidartinib and anti-CSF1R mAb, we found that monocyte infiltration was strongly CSF1R dependent. Preliminary data suggest that also infiltration of

T cells into the heterospheroids is possible, thus making the models useful for the study of immune cell infiltration. Whole transcriptomic analysis of mono-cultures of SW480 cancer cells and fibroblast spheroids and co-cultures (MCTS) identified traditional cell-type-related transcripts as well as a group of *de novo* expressed genes induced by co-culturing, such as serpin peptidase inhibitor clade A1 (serpinA1) and inhibin-β A (INHBA). The NGS analysis as well as immunohistochemical staining also showed that SW480 expressed high levels of P-glycoprotein (P-Gp, MDR1) in contrast to the fibroblasts. On the other hand, the HT29 MCTS were negative for P-Gp. Histological analysis and the apoptosis assay showed that the fibroblasts were more sensitive to 5FU and cisplatin treatment than the cancer cells. We are currently testing if the P-Gp inhibitor, PSC-833, can re-sensitize the cancer cells to 5FU and cisplatin. In conclusion, we have developed 3D multicellular heterospheroids mimicking tumor-like microspheres that can be used for drug testing of traditional drug compounds, biologics and even immunotherapeutic agents.

#4567

Transcriptomic analysis of a 3D engineered cancer model recapitulating stage-dependent heterogeneity in colorectal PDX tumors

Yuan Tian[1], Iman Hassani[1], Benjamin Anbiah[1], Bulbul Ahmed[2], William Van Der Pol[3], Elliot J. Lefkowitz[4], Peyton C. Kuhlers[2], Nicole L. Habbit[1], Martin J. Heslin[5], Elizabeth A. Lipke[1], Michael W. Greene[2]. *[1]Chemical Engineering, Auburn University, Auburn, AL,[2]Nutritional Sciences, Auburn University, Auburn, AL,[3]Center for Clinical and Translational Science, University of Alabama at Birmingham, Birmingham, AL,[4]Department of Microbiology, University of Alabama at Birmingham, Birmingham, AL,[5]Mitchell Cancer Institute, University of South Alabama, Mobile, AL*

Colorectal cancer (CRC) is the third-most leading cause of cancer-related deaths in the United States. To advance the understanding of CRC tumor progression, models which mimic the tumor microenvironment (TME) and have translatable study outcomes are urgently needed. CRC patient-derived xenografts (PDXs) are promising tools for their ability to recapitulate tumor heterogeneity and key patient tumor characteristics, such as molecular characteristics. However, as in vivo models, CRC PDXs are costly and low-

throughput, which leads to a need for equivalent in vitro models. To address this need, we previously established an in vitro model using a tissue engineering toolset with CRC PDX cells. However, it is unclear whether tissue engineering has the capacity to maintain patient- and/or cancer stage-specific tumor heterogeneity. To address this gap, we employed three PDX tumor lines, originated from stage II, III-B, and IV CRC tumors, in the formation of 3D engineered CRC PDX (3D-eCRC-PDX) tissues and performed an in-depth comparison between the 3D-eCRC-PDX tissues and the original CRC-PDX tumors. To form the tissues, CRC-PDX tumors were expanded in vivo and dissociated. The isolated cells were encapsulated within poly(ethylene glycol)-fibrinogen hydrogels and remained viable and proliferative post encapsulation over the course of 29 days in culture. To gain molecular insight into the maintenance of PDX line stage heterogeneity, we performed a transcriptomic analysis using RNA seq to determine the extent to which there were similarities and differences between the CRC-PDX tumors and the 3D-eCRC-PDX tissues. We observed the greatest correspondence in overlapping differentially expressed human genes, gene ontology, and Hallmark gene set enrichment between the 3D-eCRC-PDX tissues and CRC-PDX tumors in the stage II PDX line, while the least correspondence was observed in the stage IV PDX line. The Hallmark gene set enrichment from murine mapped RNA seq transcripts was PDX line-specific which suggested that the stromal component of the 3D-eCRC-PDX tissues was maintained in a PDX line-dependent manner. Consistent with our transcriptomic analysis, we observed that tumor cell subpopulations, including human proliferative (B2M+Ki67+) and CK20+ cells, remained constant for up to 15 days in culture even though the number of cells in the 3D-eCRC-PDX tissues from all three CRC stages increased over time. Yet, tumor cell subpopulation differences in the stage IV 3D-eCRC-PDX tissues were observed starting at 22 days in culture. Overall, our results demonstrate a strong correlation between our in vitro 3D-eCRC-PDX models and the originating in vivo CRC-PDX tumors, providing evidence that these engineered tissues may be capable of mimicking patient- and/or cancer stage-specific heterogeneity.

#4568

Evaluating response of renal cell carcinoma to tyrosine kinase inhibitor and immune checkpoint inhibitor using a human histo-culture

platform

Satish Sankaran[1], Kowshik Jaganathan[1], Gowri Shankar K[1], Saurabh Bhargav[2], Ganesh MS[3], Amritha Prabha[3], Prakash BV[4], Syamkumar V[1], Biswajit Das[1], Vasanth K[1], Manimaran A[1], Chandan Bhowal[1], Rajashekar M[1], Oliyarasi M[1], Ritu Malhotra[1], Govindraj K[1], Nandini Pal Basak[1].
[1]Farcast Biosciences, Bangalore, India,[2]Mazumdar Shaw Medical Centre, Bangalore, India,[3]Vydehi Multi Specialty Hospital, Bangalore, India,[4]Sri Lakshmi Multi Specialty Hospital, Bangalore, India

Tyrosine Kinase Inhibitors (TKIs) and Immune checkpoint inhibitors (ICIs) are used in first line treatment of clear cell renal cell carcinoma (ccRCC). Identifying patients who truly benefit from these treatments remains a challenge. Developing newer and better therapy options that fail in the clinical phase is yet another unmet need. Both these limitations could be addressed by employing testing platforms that best capture the heterogeneity and complexity of the tumor within the patient. Farcast™ TruTumor is a near native human histo-culture platform which retains the tumor and stroma along with the intra-tumoral immune compartment post culture that holds promise to improve treatment outcomes in patients. In this study, we developed a ccRCC platform using surgical excess specimens from consented patients and compared its immune profile with the head and neck squamous cell carcinoma (HNSCC) platform. ccRCC samples (n=10) were processed to generate explants and cultured for 72h and interrogated for response to treatment with Sunitinib (TKI :27.7ng/ml) or Nivolumab (anti-PD1:132µg/ml). On comparison of immune profiles between HNSCC and ccRCC at baseline, we observed a significantly lower total immune content in ccRCC. ccRCC showed comparatively higher variation in myeloid (70%CV) and lymphoid compartments (30%CV) as compared to HNSCC. Live tumor and immune cell population was found to be well preserved post-culture in ccRCC. Presence of various T cell sub-populations, monocyte and macrophage population post culture were confirmed using flowcytometry. Sunitinib treatment significantly increased caspase-3 expression (8/10 samples, p value<0.01), along with decrease in tumor content in 4/10 samples (average drop 23%). Two samples which did not respond to Sunitinib treatment showed an increase in Interferon gamma (IFNg) ($Log_2FC \pm SD$, 2.7± 0.7) and Granzyme B ($Log_2FC \pm SD$, 1.05±

0.85) secretion, in response to Nivolumab treatment. Of these, in one sample we observed an increase in CD8+ Granzyme B, CD8+ Ki67 and decrease in CD4+ FoxP3 population, with concomitant decrease in Pan CK+ population by flowcytometry. In this sample, we observed a decrease in tumor content indicating anti-tumor response to Nivolumab treatment. In summary, the TruTumor platform potentially offers personalized treatment choices to patients improving their chances of recovery. In addition, this platform could provide powerful insights into the mechanisms of a wide range of therapy molecules in development to predict their efficacy better than other simplistic and non-human testing models.

#4570

Expanding the 3D ex vivo patient tissue platform toolbox for (immuno)-oncology drug testing

Nataliia Beztsinna[1], Sander Basten[1], Ezgi Kaya Aksoy[1], Niels Meesters[1], Stefanos Timiliotis[1], Donny van der Meer[2], Kuan Yan[1], Emma Spanjaard[1], Willemijn Vader[2], Leo S. Price[1]. *[1]Crown Bioscience Netherlands B.V., Leiden, Netherlands,[2]Vitro Scan B.V., Leiden, Netherlands*

Introduction: The fast-paced (immuno)-oncology drug development pipeline requires sophisticated and reliable in vitro models to accurately represent all players of complex human tumor microenvironment (TME). Our 3D *Ex Vivo* Patient Tissue (EVPT) platform is a short-term 3D ex vivo culture system utilizing ultra-fresh human tumor material processed to preserve the rich TME with high content image (HCI) analysis for higher throughput screening. The EVPT platform has previously been validated for standard of care (SoC) and immunological drug testing, including immune checkpoint inhibitors (ICI), in ovarian and non-small cell lung cancer (NSCLC) samples. Here, we present the expansion of the EVPT platform to other cancer indications, including resections from bladder, prostate, breast cancer, melanoma, glioblastoma (GBM) and hepatocellular carcinoma (HCC).

Methods: Tumor tissues from NSCLC, ovarian, bladder, prostate, breast cancer, melanoma, GBM and HCC patients were processed within 24 hours. Freshly isolated tumor clusters were embedded in a protein-rich hydrogel and exposed to panels of (immuno)-oncology treatments at various doses in a 384-well format for 5-7 days. Phenotypic effects of treatment on

morphological features, such as tumor cell killing, growth arrest, and immune cell proliferation, were measured using our proprietary automated HCI platform. Whole blood samples were also collected and PBMCs were isolated for autologous co-culture assays with selected cancer samples. Additionally, biomarkers analysis, including IHC, FACS and cytokine measurements, was performed.
Results: At least two patient samples per new indication were processed. The success rate of the assay (30-40%) was primarily dependent on the sample quality, and the absence of necrotic, healthy, or fibrotic tissue within the sample. Panels of SoC drugs, targeted therapies, immunotherapies, and control compounds established for each indication were profiled per patient sample. For example, prostate cancer samples responded to Paclitaxel and Crizotinib, and one of GBM samples showed sensitivity to Regorafenib and Bevacizumab. Overall, similarly to clinical findings, about 20% of NSCLC and bladder cancer samples responded to ICI treatment, while 60-70% of the samples have responded to immunostimulatory controls (SEA and CD3/CD28).Although TME composition varied between NSCLC samples, IHC and FACs analysis showed a rich representation of immune compartment - T Cells (CD3+CD4+, CD3+CD8+), NK cells (CD16+), myeloid cells (CD14+, CD68+) alongside with EpCAM+ tumor cells.
Conclusion: Despite tissue quality remaining a challenge for many primary ex vivo assays, the gentle processing and short-term 3D culturing in our EVPT platform preserves the rich TME in a wide range of tumors. This makes our EVPT platform an innovative and translational tool for complex (immuno)-oncology drug testing in multiple cancer indications.

#4571

A novel *ex vivo* platform, 3D-EXpress, to rapidly assess the efficacy of KRAS targeting drugs alone and in combination with nivolumab using a biorepository of fresh patient tumoroids with intact tumor microenvironment

Jared Ehrhart, Brittney Ruedlinger, Angie Rivera, Romanus Ezeoke, Sharon Camacho, Seth Currlin, Soner Altiok. *Nilogen Oncosystems, Tampa, FL*

Introduct**on:** 3D-EXpress is a novel *ex vivo* drug testing platform using a Biorepository of neverdissociated, propagated, or reassembled fresh patient tumoroids with intact tumor microenvironment.Tumoroids measuring 150

μm in size retain tumor cell heterogeneity, tumor-resident innate andadaptive immune cells, stromal components, and cell-extracellular matrix interaction allowing to rapidlytest the efficacy of drugs and drug combinations targeting various components of the TME includingtumor cells, stroma, and immune cell populations. Here we employed the 3D-EXpress platform tocompare the efficacy of different drugs and drug combinations targeting KRAS and PD-1/PD-L1 immunecheckpoint *ex vivo.*
Materials and Methods: All tumor samples were obtained with patient consent and relevant IRBapproval. Cryopreserved tumoroids with known KRAS mutation status, PD-L1 expression, detailedimmune profiles and clinicopathologic data were selected from Nilogen's tumoroid Biorepository for the*ex vivo* assays. 3D tumoroids were treated with vehicle only, a SOS1::KRAS inhibitor, BI 1701963, apotent, selective, and covalent KRASG12C inhibitor, MRTX849, and a KRAS G12C inhibitor, sotorasib,alone and in combination with nivolumab for 72h. Treatment-mediated changes in tumor cell killing andtumor immune microenvironment were analyzed.
Results: To quantify treatment-mediated tumor cell killing activity we employed 3D high-contentconfocal imaging using a proprietary algorithm for data analysis. To monitor how *ex vivo* drugtreatments affect the tumor immune microenvironment culture supernatants isolated from treatedtumoroid samples were used for multiplex cytokine detection including GM-CSF, sCD137, IFNγ, sFas,sFasL, Granzyme A, Granzyme B, IL-2, IL-4, IL-5, IL-6, IL-10, IL-13, MIP-1α, MIP-1β, TNF-α, and Perforin.We observed a significant difference in tumor responses among patient samples to *ex vivo* tested drugsand drug combinations, which were further correlated with tumor resident innate and adaptive immunecell populations detected by a 21-color flow cytometry panel in addition to tumor KRAS mutation status,patient smoking history, tumor characteristics as well as PD-L1 expression levels analyzed on theassociated TMA slides.
Conclusion: Our data demonstrate that the 3D-Express platform, using cryopreserved 3D tumoroidswith intact TME, is an effective tool to assess the efficacy of KRAS and immune checkpoint inhibitorstargeting drugs to identify rational combination therapies and to develop clinically relevant biomarkersfor individualized patients in the future.

#4572

3D-EXpress ex vivo platform using a biorepository of characterized fresh patient tumoroids allows development of rational combinations with drugs targeting DNA damage response and immune checkpoint blockade

Jared Ehrhart, Seth Currlin, Sharon Camacho, Samantha Hoffman, Angie Rivera, Soner Altiok. *Nilogen Oncosystems, Tampa, FL*

Introducti**on:** Nilogen Oncosystems' 3D-EXpress platform allows for the detailed characterization offreshly resected patient tumor tissue for inclusion in studies investigating rational combinations of IOtherapeutics. Incorporating data on immune cell composition, tumor cell target expression, mutationalstatus, and HPV infection within tumoroids generated from HNSCC tissues provides tremendous input toidentify candidate tissues for therapeutic testing. The 3D-EXpress platform employed here providesdetailed observations investigating tumor cell viability using confocal microscopy and immune cellactivation indicated by increases in cytokine release.

Materials and Methods: 3D tumoroids measuring 150 microns in size were generated from fresh patientHNSCC resection samples collected with proper patient consent and relevant IRB approval. Tumoroidswere never enzymatically dissociated, propagated, or reassembled to maintain the intact tumormicroenvironment (TME). The resulting tumoroids were cryopreserved in the Biorepository, where eachsample had associated patient demographic data, tumor grade, stage, mutational and HPV status inaddition to a detailed tumor immune profile and a FFPE representative sample in TMA format for targetselection. Pooled tumoroids for each patient tumor were treated ex vivo both singly with a selectiveWEE1 inhibitor, AZD1775 and an ATR blocker AZD6738 alone and in combination with a PD-1 immunecheckpoint inhibitor antibody nivolumab for 72h.

Results and Summary: To quantify treatment-mediated tumor cell killing we used 3D high-contentconfocal imaging and a proprietary algorithm for data analysis. Additionally, culture supernatantsisolated from treated tumoroids were used for multiplex cytokine detection to monitor changes in theTME upon *ex vivo* treatment. Responses to treatments were further correlated with the composition ofinnate and adaptive TIL populations within each tumor as assessed by 21-color flow cytometry inaddition to

tumor mutational status, HPV infection, smoking status, as well as EGFR and PD-L1expression levels analyzed by multiplex IF on associated TMA slides.
Conclusion: These results demonstrate that targeting DNA damage response and immune checkpointblockade may provide a potential combination strategy for the treatment of HNSCC. Furthermore, weshowed that our 3D-EXpress *ex vivo* tumoroid model provides a unique platform to rapidly assess theefficacy of drugs and drug combinations in fresh patient tumor samples with intact TME. Correlation of*ex vivo* drug responses with characteristics of each tumor's immune microenvironment and detailedclinicopathological data may allow to identify clinically relevant biomarkers to enable the most effectivetreatment strategies for individual patients in the clinic.

#4573
Evaluation of tumor treating fields (TTFields) effects at 200 kHz on a glioblastoma, an anaplastic ependymoma and an oligodendroglioma sample in a patient-derived *ex vivo* organoid model
Vera Nickl[1], Ellina Schulz[1], Ellaine Salvador[1], Laureen Trautmann[1], Leopold Diener[1], Almuth F. Kessler[1], Camelia M. Monoranu[2], Ralf-Ingo Ernestus[1], Mario Löhr[1], Carsten Hagemann[1]. *[1]Department of Neurosurgery, Section Experimental Neurosurgery, University Hospital Wuerzburg, Wuerzburg, Germany,[2]Institute of Pathology, Department of Neuropathology, University of Wuerzburg, Wuerzburg, Germany*

TTFields are alternating electric fields of low intensity (1-3 V/cm) and intermediate frequency (100-500 kHz), which are effective and approved for the treatment of glioblastoma (GBM) using 200 kHz frequency. However, there is a lack of *ex vivo* models to evaluate effects on patients' tumor biology or to screen patients for treatment efficacy. Therefore, we adapted patient-derived three-dimensional GBM tissue culture models to be compatible with TTFields application and recently published the feasibility of such an approach (Nickl, et al., 2022, doi: 10.3390/cancers14215177). Here, we applied one of those models, i.e. tumor-organoids cultured as microtumors on murine organotypic hippocampal slice cultures (OHSCs), to additional brain tumor entities, namely a sample of an anaplastic ependymoma (AE) patient and an oligodendroglioma patient. Organoids

were generated from fresh intra-operatively obtained tumor tissue and cultured for 2 weeks. OHSCs were prepared by slicing the brains of mice 5-8 days postpartum to sections with a thickness of 350 µm using a vibratome, and culturing them for 2 weeks as well. Subsequently, organoids were placed onto the OHSCs. The inovitro™ laboratory research system was used for TTFields administration at 200 kHz and 1.5 V/cm for 72 h. Microtumor growth was evaluated on fluorescence images. Viable organoids formed from the GBM, AE and oligodendroglioma sample and grew to microtumors when placed onto OHSCs. Application of TTFields at 200 kHz led to a significant decrease of microtumor size of the GBM and AE (both $p<0.0001$), but not the oligodendroglioma sample. This proof-of-principle investigation proved that the application of patient-derived organoids cultured on OHSCs is feasible to investigate the effects of TTFields on different kinds of brain tumors. To our knowledge, this is the first evaluation of TTFields efficacy on patient derived AE and oligodendroglioma tissue cultures. While TTFields at 200 kHz led to a decrease in the microtumor size of the AE sample, the non-responsiveness of the oligodendroglioma sample may be due to different inter-patient sensitivity to TTFields or a suboptimal TTFields frequency.

#4574

Long-term drug efficacy evaluation using stiffness-tunable scaffolds colonized by a three-dimensional tumor microenvironment

Elly De Vlieghere, Olivier De Wever. *Ghent University Hospital, Gent, Belgium*

Long-term drug evaluation heavily relies upon rodent models. Methods to reduce animal models in oncology may include three-dimensional cellular systems that take into account tumor microenvironment (TME) cell types and biomechanical properties. Innovative translational research is needed in low-grade serous ovarian cancer (LGSOC) in which the presence of oncogenic mutations in the RAS pathway likely suggest the opportunity to test targeted treatments. To address all these needs this study reports on an elastic polymer, to print a scaffold that mimics tissue relevant stiffness. Introduction of single cell suspensions from LGSOC patient-derived early passage cultures of cancer cells and cancer-associated fibroblast form heterocellular spheroids mimicking the growth ratio and spatial

organization of the LGSOC TME. The resulting scaffold allows long-term (>40 days) follow-up and targeted compound evaluation confirmed the durable response to a drug combination. The drug-response results from this long-term *in vitro* model are compared with drug responses in an orthotopic LGSOC xenograft mouse model. In conclusion, the stiffness-tunable scaffolds colonized by a three-dimensional LGSOC TME allow long-term drug evaluation and can be considered as a valid alternative to reduce, replace and refine animal models in drug discovery.

#4575

High-throughput method to analyze the cytotoxicity of CAR T cells in a 3D tumor spheroid model using image cytometry

Samir Patel[1], David Zurowski[2], Daniel Hui[2], Mignane Ka[2], Charles Hernandez[1], Andrea Love[1], Bo Lin[1], Andrea Moore[2], Leo Li-Ying Chan[1].
[1]Nexcelom Bioscience, Lawrence, MA,[2]Resilience, East Norriton, PA

Chimeric antigen receptor (CAR)-T cell therapy is an antigen-dependent cellular therapy that has gained considerable traction in the field of cancer immunotherapy. CAR-T cell therapy involves specifically engineering T cells to attack tumor cells by binding a tumor antigen and inducing T cell activation resulting in intracellular signaling and cytokine release. Currently, there are six FDA-approved CAR-T cell therapies, which all target the CD19 or BCMA antigens for hematologic B cell malignancies. In the recent years, a strong focus has been placed on CAR T cell therapy discovery for solid tumors, which may better recapitulate physiological conditions, thereby potentially improving the selection of CAR construct candidates. Immune cell trafficking and immunosuppressive factors within the tumor microenvironment increase the relative difficulty in developing a robust CAR-T cell therapy against solid tumors. Therefore, it is critical to develop novel methodologies for high-throughput phenotypic and functional assays using 3D tumor spheroid models to better assess CAR-T cell therapies against solid tumors. Recently, plate-based image cytometry has emerged as a method to investigate and characterize CAR T cell functions in a high-throughput manner. Image cytometry has demonstrated capabilities in
analyzing transduction efficiency, cell proliferation, and cytotoxicity for CAR T cell therapy. With the development of 3D spheroid models, image

cytometry may provide the necessary tools and applications for CAR T cell therapy discovery geared towards solid tumors. In this work, we discuss the use of CAR-T cells targeted towards PSMA, an antigen that is found on prostate cancer tumor cells, the second most common cause of cancer deaths among men worldwide. Herein, we demonstrate the use of high-throughput plate-based image cytometry to characterize PSMA CAR-T cell-mediated cytotoxic potency against 3D prostate tumor spheroids and simultaneously monitor location of the T cells *in vitro*. We were able to kinetically evaluate the efficacy and therapeutic value of PSMA CAR-T cells by analyzing the cytotoxicity against prostate tumor spheroids. Furthermore, the T cells are fluorescently labeled with a tracer dye to visually locate the cells on the tumor spheroids. The proposed image cytometry method can overcome limitations placed on traditional methodologies to effectively assess cell-mediated 3D tumor spheroid cytotoxicity and efficiently generate time- and dose-dependent results.

#4576

3D *in vitro* models uncover malignant cell intrinsic and extrinsic mechanisms of CAR-T cell resistance in high grade serous ovarian cancer

Joash Dominic Joy[1], Beatrice Malacrida[1], Florian Laforêts[1], Panoraia Kotantaki[1], Eleni Maniati[1], Sarah Hopkins[2], Ianire Garrobo-Calleja[2], Julien Gautrot[3], Frances Balkwill[1]. *[1]Barts Cancer Institute, London, United Kingdom,[2]GSK Medicines Research Centre, Stevenage, United Kingdom,[3]Institute of Bioengineering Queen Mary University, London, United Kingdom*

Chimeric antigen receptor (CAR)-T cell therapies have promising outcomes in hematologic malignancies but limited activity in solid tumors. We used 3-dimentional (3D) *in vitro* human cell models of increasing complexity to investigate resistance to CAR-T cell therapy in high grade serous ovarian cancer (HGSOC), a disease with poor response to immunotherapy. We identified mucin-1 (MUC1) and TnMUC1 as target antigens in HGSOC omental metastasis and the HGSOC cell lines, OvCAR3 and G164. We then generated CAR-T cells against these targets and tested them in spheroids, collagen gels and microfluidic models. In spheroids, OvCAR3 cells were killed by CAR-T cells whereas, G164 cells were resistant to CAR-T cell

cytotoxicity. RNA sequencing suggested that the impaired apoptotic signaling in G164 cells caused malignant cell-intrinsic resistance to CAR-T cell cytotoxicity. Treating G164 spheroids with birinapant, an antagonist of cellular inhibitor of apoptosis protein, induced CAR-T cell cytotoxicity. Moreover, when resistant cells were co-cultured as spheroids with primary omental fibroblasts from ovarian cancer patients, CAR-T cells were activated and cytotoxic. G164 spheroids cultured in fibroblast-conditioned medium also induced CAR-T cell cytotoxicity due to C-C motif chemokine ligand 2 (CCL2) produced by fibroblasts. CCL2 activated CCR2/4+ CAR-T cells to induce cytotoxicity in an antigen-dependent manner. We then investigated CAR-T cell migration and cytotoxicity in malignant cell/fibroblast co-culture collagen gels. CAR-T cell migrated into OvCAR3 gels and were cytotoxic against the malignant cells. However, a dense extracellular matrix (ECM) produced primarily by fibroblasts prevented CAR-T cell migration and cytotoxicity in G164 gels. Treating G164 gels with transforming growth factor beta (TGFβ) receptor inhibitor SB431542 reduced ECM content and altered ECM structure, thus stimulating CAR-T cell penetration and restoring cytotoxicity against G164 cells. We also developed an ovarian cancer-on-a-chip model which involved culturing cell-seeded collagen gels in vascularized tri-channel microfluidic devices. CAR-T cells successfully penetrated and killed malignant cells in co-culture collagen gels when delivered through vascularized microfluidic devices. To our knowledge, this is the first report to use microfluidic tumor models to successfully deliver CAR-T cells. Using these different human 3D *in vitro* models, we uncovered malignant cell-intrinsic factors and novel mechanisms involving fibroblasts which may influence CAR-T cell activity. Complex human cell models may accelerate preclinical research into CAR-T cell therapies in solid tumors.

#4577

An innovative platform to mimic the tumoral vascular microenvironment (TME) of patients with metastatic colorectal cancer (mCRC) using bioprinted hydrogel microfluidics

Nadia Saoudi González[1], Francesc Salvà Ballabrera[1], Ariadna García[1], Javier Gonzalo-Ruiz[1], Iosune Baraibar[1], Javier Ros[1], Marta Rodriguez[1], María García Díaz[2], Marta Falcó Fusté[2], Melika Parchehbaf Kashani[2], Carlos Honrado[3], Alar Ainla[3], Josep Tabernero[1], Lorena Diéguez[3], Elena

Martínez Fraiz[2], Elena Élez[1]. *[1]VHIO Vall D'Hebron Institute of Oncology, Barcelona, Spain,[2]Institute for Bioengineering of Catalonia (IBEC), Barcelona, Spain,[3]International Iberian Nanotechnology Laboratory (INL), Braga, Portugal*

Introduction: Metastasis involves a set of complex events that finally result in malignant cells from primary tumors invading distant tissues by the pass of circulant tumor cells (CTC) through the blood circulation. To authentically comprehend the complex chain of events and even enable new therapeutic approaches in mCRC patients, ex-vivo functional models are an unmet research need.
Experimental Plan: PROMISE project is combining bioengineering solutions such as bioprinting biomaterials and microfluidics to mimic the tumor microenvironment (TME) of metastatic sites in mCRC. In this project, we are developing a bioprinted hydrogel-based microfluidic device that recapitulates this TME. Then, CTCs are isolated from mCRC patients, cultured, and characterized by microdroplet technology. Those CTCs are then infused on the biodegradable polymer that mimics vascular channels and surrounding stromal cells, through microfluidic connection, in order to mimic CTC-endothelial interactions, study the procedures of extravasation (the invasiveness potential of extravasated patient-derived CTCs into TME) and intravasation (the process of CTCs-derived and biopsy-derived tumor spheroids from the TME to the vascular channel).
The photopolymerizable hydrogel mimics vascular structures, supporting the growth of HUVEC cells, and is printed in a cost-effective manner (30 minutes) using a semi-direct printing method with visible light. The CROSS chip is used for fast and efficient isolation of CTCs from unprocessed blood of mCRC patients. In parallel, multi-omics of mCRC are done in circulant tumor DNA (ctDNA) and tumor biopsy of mCRC, therefore correlating the phenotypic and genetic profile of the patient cohorts studied.
A first pilot test has been carried out successfully obtaining blood from mCRc refractory patients, and excellent coordination between the multidisciplinary consortium has been achieved to draw blood from the patient, isolate CTCs and infuse them into the hydrogel. Extravasation and intravasation studies are ongoing.
Conclusion: This multidisciplinary project, which brings together bioengineering, microfluidic, and oncology experts' teams, is developing a

successful ex-vivo, in vitro, and dynamic model that will permit a better study and understanding of the metastatic process in mCRC, from the process of intravasation to extravasation of CTCs, passing thought the better multi-omic characterization of CTCs and ctDNA.

#4578

Miniaturized and multiplexed evaluation of NK cell cytotoxicity and infiltration in patient-derived sarcoma spheroids using a novel multichambered microwell chip

Valentina Carannante[1], Niklas Sandström[1], Karl Olofsson[1], Shi Yong Neo[2], Patrick Albert Sandoz[1], Hanna Van Ooijen[1], Quentin Verron[1], Jacopo Fontana[1], Damien Toullec[1], Elisabeth Moussaud-Lamodière[2], Brinton Seashore-Ludlow[2], Thomas Frisk[1], Madoka Takai[1], Päivi Östling[2], Felix Haglund[2], Andreas Lundqvist[2], Martin Wiklund[1], Björn Önfelt[1]. *[1]KTH Royal Institute of Technology, Stockholm, Sweden,[2]Karolinska Institutet, Stockholm, Sweden*

Tumor diversity and rarity of patient tumor material negatively contribute to the development of new effective treatments for sarcomas. As a high proportion of sarcoma patients presents inherent or acquired chemo-resistance, immune checkpoint inhibitors could represent an alternative for these cases. However, only a small fraction of sarcoma patients seem to respond to immune checkpoint therapy, suggesting the existance of heterogenous immune-suppressive mechanisms across individuals and sarcoma subtypes. Therefore, new strategies to boost the immune system, together with tools predicting which patients could benefit from therapy, are needed for sarcoma patients. There is still a lack of methods that take advantage of benefits, such as low consumption of patient material or reagents, offered by miniaturized *in vitro* analysis systems. In this work, we used a novel multichambered microwell chip for testing personalized immunotherapy on patient-derived sarcoma spheroids. We derived multiple primary sarcoma spheroids from various sarcoma subtypes and grades, which were used to test NK cell cytotoxicity in combination with anti-TIGIT, anti-PD-L1, anti-EGFR treatment. Using this combinatorial strategy, we could boost NK-mediated killing significantly. We analyzed immune cell infiltration in the original tumor and found PD-1^{+} and TIGIT^{+} cytotoxic

lymphocytes in both peripheral and central tumor tissues, suggesting that anti-TIGIT and anti-PD-L1 therapy could be appropriate in some sarcoma patients. In addition, high levels of pro-inflammatory cytokines were found in plasma from sarcoma patients, together with high levels of soluble PVR. This work provides a better understanding of immune surveillance of sarcoma and shows an important implementation of patient-derived spheroids. The miniaturized format allowing long-term cell culture, efficient screening and high-quality imaging of small sample volumes makes this methodology promising for personalized immunotherapy.

#4579

A three-dimensional model of glioblastoma for discovery of novel therapeutics

Viktoriia Kriuchkovskaia[1], Brendan A. C. Harley[2], Rebecca B. Riggins[3].
[1]Chemical and Biomolecular Engineering and Institute for Genomic Biology, University of Illinois Urbana-Champaign, Champaign, IL,[2]Chemical and Biomolecular Engineering, University of Illinois Urbana-Champaign, Champaign, IL,[3]Georgetown University, Washington, DC

Statement of Purpose: Glioblastoma (GBM) is the most common and lethal form of brain cancer. Despite an aggressive treatment strategy, including surgical resection followed by radio- and chemotherapy, GBM has one of the highest mortality rates among all human tumors. The leading causes of this devastating prognosis are rapid recurrence and therapeutic resistance; current chemo- and immunotherapies fail to control tumor growth and progression. Temozolomide (TMZ) remains the gold standard for GBM treatment since its FDA approval for GBM in 2005. Subsequently, GBM treatment strategy has seen no significant advancement, despite TMZ providing only minimal benefit to most patients. Recent efforts to develop novel therapies for GBM have primarily involved *in vivo* animal models and conventional 2D cell cultures. However, animal models do not allow for elucidating specific interactions between cancer cells and tumor microenvironment (TME), while 2D models fail to depict the complex tumor architecture. *In vitro* biomaterial models offer an opportunity to evaluate aspects of cell-cell and cell-matrix driven responses within the complex TME. Here, we construct and validate a 3D hydrogel platform to

evaluate drug response in GBM and to examine the role of TME in drug response, resistance, and local invasion.
Results: Our model departs from most biomaterial platforms by assessing a wide range of TMZ concentrations and further validating drug response at low doses. Moreover, we use a set of GBM cell lines with defined shifts in TMZ response. These lines are an ideal candidate to model TMZ response & resistance—a unique set of isogenically matched GBM cells (8MGBA vs. 8MGBA-TMZres; 42MGBA vs. 42MBGA-TMZres). This set exhibits TMZ responsiveness or resistance along with disparate proliferative and invasive patterns. Here, we analyze these cell models in GelMA hydrogels to elucidate mechanisms underlying the acquired TMZ resistance in GBM tumors. We validate our platform by using physiologically relevant TMZ doses, showing the possibility to study TMZ response in 3D at low, physiologically relevant (< 100 μM) concentrations. We determine the growth-rate (GR) inhibition, GR50, IC50, and metabolic activity to benchmark detection limits for acquired TMZ resistance in the engineered GelMA GBM model. Subsequently, we use WT and TMZres variants of 42MGBA and 8MGBA lines to determine the upper and lower bounds of detectable TMZ response in 3D GelMA hydrogels. These quantified shifts in TMZ-induced GR inhibition are a key benchmark for studies of the efficacy of novel therapeutics in patient-derived GBM models. Furthermore, we assess the effect of acquired drug resistance on local invasion of GBM. Ongoing experiments aim to adapt our platform for phenotypic drug screening and target validation of novel small-molecule therapeutics.

Advances in Angiogenesis

#4583
An essential role for Cmtr2 in endothelial cell function and vascular development

Alena Yermalovich[1], Zarin Mohsenin[1], Bruno Giotti[2], Douglas Wheeler[1], Kelly Xu[1], Alexander Tsankov[2], Matthew Meyerson[3]. *[1]Dana-Farber Cancer Institute, Boston, MA,[2]Icahn School of Medicine at Mount Sinai, New York, NY,[3]Medical Oncology, Dana-Farber Cancer Institute, Boston, MA*

Cancer genome sequencing studies have identified multiple novel tumor suppressor genes, including the FTSJD1 or CMTR2 gene that is subject to statistically significant levels of both nonsense and frameshift mutations in lung adenocarcinoma. However, these analyses are insufficient to determine the importance and modes of action of the gene in the disease. Follow-up functional studies are essential to elucidate these gene functions. The protein product of CMTR2 has been described as an mRNA cap methyltransferase, which O-methylates the ribose of the second guanine residue of the 5' cap, likely serving to modify efficiency of transcript processing, translation and stability, but the details of how and why specific transcripts undergo methylation by the enzyme, as well as its role in oncogenesis, remain to be elucidated. In this study we report the first comprehensive analysis of the physiologic consequences of Cmtr2 deficiency in knockout (KO) mice and primary human cells. Constitutive deletion of Cmtr2 results in embryos that die in midgestation with defects in embryo size, placental malformation and yolk sac vascularization. Endothelial-specific deletion of Cmtr2 in mice also results in vascular defects and perinatal lethality, suggesting that vascular development is a key function of Cmtr2 in animals. In summary, our study reveals that Cmtr2 plays a critical role in vascular development, maturation and remodeling. Further studies of CMTR2 function may provide insight not only into lung cancer biology but also to its broader roles in ontogeny.

#4584

Genetic disruption of vascular endothelial profilin-1 impacts tumor microenvironment supressing tumorigenicity of renal cancer

David M. Gau[1], Abigail Allen[1], Andrew Daoud[1], Jessica Kunkel[1], Stefan Duensing[2], Partha Roy[1]. *[1]Bioengineering, University of Pittsburgh, Pittsburgh, PA,[2]Universitätsklinikum Heidelberg, Heidelberg, Germany*

Renal cell carcinoma (RCC) is estimated to result in 79,000 new cases and 13,920 deaths in 2022. Clear cell renal cell carcinoma (ccRCC) is the most common subtype of RCC and is characterized by a highly vascularized tumor microenvironment (TME). While current anti-angiogenic therapies targeting VEGF signaling are initially effective, almost all patients develop resistance to these therapies. Therefore, there is a need to identify clinically relevant alternative molecular targets to suppress tumor angiogenesis and

progression in ccRCC. We previously discovered transcriptional upregulation of actin-binding profilin1 (Pfn1) in tumor-associated vascular endothelial cells (EC) in ccRCC and higher expression of Pfn1 correlated with adverse clinical prognosis. The goal of the present work was to further explore whether genetic manipulation of Pfn1 specifically in EC has therapeutic benefit in kidney cancer. We found that triggering vascular endothelial Pfn1 gene deletion, either in a widespread manner or locally in a kidney-restricted manner, suppresses tumor initiation and/or growth progression of pre-established kidney tumors in syngeneic mouse models. Loss of endothelial Pfn1 dramatically impacts the TME characterized by prominent suppression of tumor angiogenesis with massive tumor cell death and reduction of tumor-infiltrating immune cells. By performing cytokine array and Luminex assays of tumor lysates, we further identified Pfn1-dependent downregulation of several pro-angiogenic cell-secreted factors and pro-inflammatory cytokines that are major drivers of tumor progression in RCC including VEGF, endothelin-1, Cyr61, Macrophage Inflammatory Protein, G-CSF and IL6 *in vivo*. As a clinical correlate for mouse model data, we performed multiplexed quantitative immunohistochemistry analyses of human ccRCC specimens constructed on tissue microarray which also showed a positive correlation between Pfn1 expression (either in endothelial cells or tumor cells) and tumor infiltration of predominantly macrophages. Furthermore, through small molecule screening, we identified a novel inhibitor of the Pfn1-actin interaction (Pfn1i) and showed its ability to inhibit tumor angiogenesis and growth aggressiveness of tumor cells resembling various genetic landscapes of human ccRCC. Collectively, these findings establish endothelial Pfn1 as a critical regulator of TME and tumor progression in RCC, and provide a proof-of-concept for targeting Pfn1 as a potentially novel therapeutic strategy in RCC.

#4585

Tumor lymphangiogenesis sensitizes melanomas to the immunological effects of radiotherapy but also disrupts the local lymphatic vasculature

Anish Mukherjee[1], Nikolaos Mitrousis[1], Mari Stella Sasso[1], Margo MacDonald[1], Ainhoa Arina[2], Phillip Ang[3], Ariana Baginski[1], J. Emiliano G. Medellin[1], Ralph R. Weichselbaum[3], Melody A. Swartz[1]. *[1]Pritzker School of Molecular Engineering, University of Chicago, Chicago,*

IL,[2]Department of Radiation and Cellular Oncology, University of Chicago, Chicago, IL,[3]Pritzker School of Medicine, University of Chicago, Chicago, IL

Tumor lymphangiogenesis is typically associated with cancer progression and metastasis. However, recent studies from our group have demonstrated that tumor lymphangiogenesis promotes intratumor T cell infiltration and potentiates the efficacy of a wide range of immunotherapies in melanoma-bearing mice as well as patients undergoing checkpoint blockade. Radiotherapy (RT) can also induce immunogenic tumor cell death, so we investigated whether lymphangiogenic tumors would yield more immunogenic responses to RT than non-lymphangiogenic tumors. Here, we compared effects of RT in mice bearing B16-F10 melanomas expressing either a control vector (B16-Ctrl) or overexpression the lymphangiogenic factor VEGF-C (B16-VC), where lymphatic vessels were significantly increased in number and size compared to B16-Ctrl tumors. First, we find that B16-VC regress faster than B16-CT after RT (either a single 20 Gy dose or two 15 Gy doses), and that this regression was correlated with enhanced CD8+ T cell activity. On the other hand, lymphatic endothelial cells (LECs) can be more sensitive to damage from RT if they are undergoing lymphangiogenesis. We found that irradiated B16-VC tumors showed higher levels of intra-lymphatic fibrin. Consistent with this, LECs in the irradiated B16-VC tumors expressed higher levels of tissue factor and caspase-3, which correlated with the degree of lymphatic clotting. Fibrin clotting was also observed in the subcapsular sinus of the draining lymph nodes of irradiated B16-VC tumors. These findings highlight the complex role of tumor lymphangiogenesis in radiotherapy responses, where they may potentiate acute anti-tumor immune responses but may also cause localized damage of the vasculature, potentially leading to increased metastasis. Further studies are needed to investigate therapeutic targets to inhibit lymphatic coagulation and look at its effects on cancer immunotherapy and metastasis.

#4586

To define how the uvel melanoma-liver environment crosstalk shapes metastasis growth and therapeutic response

Sathya Neelature Sriramareddy[1], Zhihua Chen[1], Jiannong Li[1], Ann Chen[1], Jonathan D. Licht[2], J William Harbour[3], Keiran Smalley[1]. *[1]Tumor Biology, H lee Moffitt Cancer Center and Research Institute, Tampa, FL,[2]Department of Medicine, University of Florida Health Cancer Center, University of Florida, Gainesville, FL,[3]Department of Ophthalmology, University of Texas Southwestern Medical Center, Dallas, TX*

BACKGROUND: Uveal melanoma (UM) is derived from melanocytes of the eye. Up to 50% of individuals with primary uveal melanoma will eventually develop liver metastases through mechanisms that remain poorly described. At this time there are no systemic therapies that are effective against the majority of UM liver metastases. The goal of this study is to better understand the role of tumor-host cell crosstalk in the progression and therapeutic response of UM liver metastases.
METHODS: We used UM liver metastatic mouse models to study bidirectional cell-cell communication. Mice were treated with MEKi (trametinib, daily),HDACi (panobinostat, 3 times a week), or the combination for the period of 21 days.The tumor progression was monitored using MRI. Single cell RNA-Seq (scRNA-seq) was performed to delineate the host-tumor crosstalk and mechanisms of therapy response. Similarly, scRNA seq was conducted *in vitro* with mono- and co-cultures of hepatic stellate cells (HSCs) and uveal melanoma cells. Human cytokine arrays were carried out between mono and co-culture to identify and confirm unbiased growth factors released between HSCs and UM. ELISA assays were conducted to quantify the cytokine IL8 in mono and coculture cell culture supernatant. A vascular tube formation assay was carried to study the angiogenesis in presence of IL-8 and GDF15.
RESULTS: Our scRNA-Seq analyses of UM liver mets revealed a large infiltration of HSCs, along with myeloid derived suppressor cells, macrophages, dendritic cells and hepatocytes. As HSCs were the major host cell type in UM liver mets we performed scRNA-Seq on UM monocultures and UM-HSC co-cultures to determine the patterns of cell-cell interaction upon co-culture and in response to drug. Singlecell SignalR analysis identified key interactions between UM-HSC mediated through FGFR2 and RPS27A associated with increased IL-6, FOS/JUN, STA3, & NFκB signaling in the UM cells. Further studies showed that Class 2 UM cells secreted GDF15 that activated the HSCs resulting in the secretion of

multiple growth factors, including MMPs, VEGFA, TGF-β1, IL8 and multiple ECM genes.As many of the identified growth factors were associated with angiogenesis, we performed co-culture assays with UM, HSC and endothelial cells and noted increased vascular network formation in the presence of activated HSCs. Addition of exogenous IL-8 was found to mimic the effects vascular network formation *in vitro*, suggesting this to be a potential mediated of HSC-driven angiogenic response in UM mets. Treatment of established UM liver mets with the MEKi+HDACi combination significantly decreased angiogenesis in UM liver mets, an effect associated with inhibition of IL-8 and GDF15 release.
CONCLUSION: Bidirectional communication between hepatic stellate and UM cells induces angiogenic pathways in UM both in *in vitro* and *in vivo*, leading to vascular network formation and tumor progression in the liver.

#4587

Vascular-derived signature imprinted by tumor microenvironment-dependent transcriptional memory predicts colon cancer prognosis

Elisabeth Naschberger, Maximilian Fuchs, Nicholas Dickel, Meik Kunz, Charles G. Anchang, Richard Demmler, Bernt Popp, Arif B. Ekici, Steffen Uebe, Carol I. Geppert, Claudia Günther, Susanne Merkel, Vera S. Schellerer, Michael Stürzl. *University Hospital of Erlangen, Erlangen, Germany*

Background: Antiangiogenic therapy is part of the guideline therapy of colorectal cancer (CRC). Surprisingly, the impact of the tumor microenvironment (TME) on tumor vessel endothelial cells (TECs) is largely unclear. The aim of this study was to investigate the presence of a TME-dependent transcriptional memory in TECs isolated from patients and to exploit it to retrieve signatures that characterize TECs in different intratumoral TMEs with impact on patient outcome.
Methods: ECs from tumor and normal colon tissues, PBMCs and tumor cells were isolated from CRC patients with different prognostic TMEs. Cells were analyzed by qPCR, immunocytochemistry and multi-omics (transcriptomics, EPICmethylation chips, exome sequencing). Integrative bioinformatics was used to identify TME-dependent memory genes predicting prognosis and scRNASeq to validate endothelial gene expression in CRC tissues.

Results: Ultrapure TECs were isolated from CRC with different prognostic TMEs (Th1 vs. non-Th1) and systematically compared by multi-omics. A transcriptional memory differentiating the respective TEC groups was identified. This *in vivo* imprinted transcriptional memory was preferentially regulated by epigenetic DNA methylation but not by genomic alterations and was different from an *in vitro* primed transcriptional memory to IFN-γ. Moreover, it was specific for TECs and not observed in CAFs. With integrative bioinformatics a TME-dependent memory signature was extracted and its expression in TECs in CRC tissues was confirmed by scRNASeq. Notably, the identified signature predicted the prognosis of CRC patients.
Conclusion: We identified a tumor vessel-derived TME-dependent transcriptional memory signature that was manifested by epigenetic mechanisms and allowed tumor vessel-based prediction of CRC patients prognosis.

#4588

Vascular regulation of T-cell exclusion in melanoma

Ha-Ram Park[1], Anahita Shiva[1], Portia Cummings[1], Richard Carvajal[1], Gavin Thurston[2], Joon-Yong An[3], Amanda W. Lund[4], Hee Won Yang[2], Minah Kim[1]. *[1]Columbia University Irving Medical Center, New York, NY,[2]Regeneron Pharmaceuticals, New York, NY,[3]Korea University, Seoul, Korea, Republic of,[4]NYU Langone Health, New York, NY*

T-cell position in the tumor microenvironment determines the probability of target encounter and tumor killing. $CD8^+$ T-cell exclusion from the tumor parenchyma is associated with poor response to immunotherapy and yet the biology that underpins this distinct pattern remains unclear. Here we show that the vascular destabilizing factor angiopoietin-2 (ANGPT2) causes compromised vascular integrity in the tumor periphery, leading to impaired T-cell infiltration within tumor. We analyzed the spatial regulation of ANGPT2 in whole tumor cross-sections and its impact on $CD8^+$ T-cell position, vascular integrity, and response to immunotherapy using syngeneic murine melanomas. We found that T-cell exclusion was associated with peritumoral expression of ANGPT2 and elevated vascular leakage in human and murine melanomas. Both pharmacological and

genetic blockade of ANGPT2 promoted $CD8^+$ T-cell infiltration to the tumor core, exerting antitumor effects. Importantly, the reversal of T-cell exclusion following ANGPT2 blockade not only enhanced response to anti-PD-1 therapy in immunogenic, therapy responsive mouse melanomas, but also rendered non-responsive tumors susceptible. Therapeutic response after ANGPT2 blockade, driven by improved $CD8^+$ T-cell infiltration, coincided with TIE2 signaling activation and increased vascular integrity in the tumor periphery, indicating that maintenance of vascular integrity within tumors is necessary for robust response to immunotherapy. These data highlight ANGPT2/TIE2 signaling as a key mediator of T-cell exclusion and a promising target to potentiate checkpoint inhibitor efficacy in melanoma.

#4589

Deciphering collagen-responsive mechanism in pancreatic tumor progression and immunology at single-cell resolution

Yang Chen. *Translational Molecular Pathology, UT MD Anderson Cancer Center, Houston, TX*

A hallmark feature of PDAC is its desmoplastic stroma. However, clinical trials of generic strategies targeting PDAC stromal components have mostly failed or, in some cases, even accelerated tumor progression. These findings prompt us to re-evaluate the functional heterogeneity and selective targeting of the tumor stroma. Tumor stroma involves the prominent accumulation of type I collagen (Col1), the most abundant protein in PDAC and the human body. However, the precise molecular and mechanistic contributions of Col1 to PDAC remain unknown, due to the lack of mouse models for precise knockout of Col1. I have established a variety of novel transgenic mouse models that allow specific genetic deletion of Col1 in various cell populations including fibroblasts or cancer cells of spontaneous PDAC (Chen et al., Cancer Cell, 2022; Chen et al., Cancer Cell, 2021; Chen et al., Nature Communications, 2021). In addition, my prior studies underscore the importance of deciphering the functional heterogeneity of tumor microenvironment with both tumor-restraining and tumor-promoting functions (McAndrew, Chen, Darpolor et al., Cancer Discovery, 2022; Chen et al., Nature Reviews Clinical Oncology, 2021; Chen et al., EMBO Molecular Medicine, 2018; Chen et al., PLoS Biology, 2018). Specifically,

my recent studies identified that Col1 deletion in fibroblasts significantly aggravates tumor progression and immune suppression, with enriched myeloid-derived suppressor cells (MDSCs) and inhibited T/B cells (Chen et al., Cancer Cell, 2021). On the contrary, Col1 deletion in cancer cells inhibited PDAC progression and immunosuppression, leading to beneficial intra-tumoral microbiome and enhanced efficacy of immunotherapy (Chen et al., Cancer Cell, 2022). In contrast to the normal Col1 heterotrimer (α1/α2/α1) produced by fibroblasts, pancreatic cancer cells produce abnormal oncogenic Col1 homotrimer (α1/α1/α1). Col1 homotrimers produced by cancer cells exhibits potent tumor-promoting functions, in contrast to the tumor-restraining functions of Col1 heterotrimers produced by fibroblasts. These findings, as validated in both transgenic mouse models and pancreatic tumor patient datasets, identify the distinct impact of various Col1 subtypes on tumor progression, immune landscape, and microbiome profile. Furthermore, my results underscore the need for new therapeutic strategy preferably targeting Col1 homotrimer-specific oncogenic effects in cancer cells via cancer-specific receptors, without disturbing Col1 heterotrimer-induced tumor-restraining functions. My current studies aim to dissect the cancer cell-intrinsic response and immune response to Col1 homotrimer versus Col1 heterotrimer, which may unravel the fundamental collagen-responsive mechanism by which cancer cells survive in the desmoplastic microenvironment, revealing potential vulnerabilities of PDAC.

#4590

Anti-angiogenic mAb, anti-human VEGFR2(Cyramza) retards tumor growth in KDR (VEGFR2) humanized mice engrafted with syngeneic vs. xenograft solid tumors

Daniel He. *Shanghai Model Organisms Center, Inc., Shanghai, China*

Blood vessels is required for the growth of solid tumors and cutting off the blood supply to tumor is a potential novel strategy to retard tumor growth, although which may consequently result in pan-hypoxia and metastasis paradoxically. VEGFA is identified as the major angiogenic factor and VEGFR2 binds to all VEGFA isoforms and VEGFR2 (KDR) is a dominant mediator in regulating the angiogenic and permeability-enhancing effects of VEGFA. Importantly, in numerous solid tumors, VEGFA and VEGFR2 are

overexpressed to promote intratumoral angiogenesis to support local tumor survival, tumor growth and distant metastasis. Given that VEGFA/VEGFR2 interaction plays a crucial role in promoting intratumoral angiogenesis and tumor growth, it is appealing to develop novel potent anti-angiogenic agents for cancer treatment by direct against VEGFA-VEGFR2 interaction. However, the preclinical assessment of anti-angiogenesis agents are limited due to lack of suitable preclinical models for human-specific therapeutic antibodies which usually don't cross-bind to mouse targets. To this end, we developed the KDR (VEGFR2) humanized mouse model (hKDR model), in which the extracellular regions of mouse VEGFR2 corresponding to exons 4-15 are replaced by human counterparts via ES cell-based homologous recombination. As a result, hKDR humanized mouse expresses a chimeric VEGFR2 receptor containing the human extracellular domain plus mouse trans-membrane and intracellular domains. Firstly, we characterized the chimeric h/m KDR expression on the endothelial cells as well as in intratumoral blood vessels derived from hKDR knockin mice. Subsequently, we investigated the anti-tumor responses of anti-human VEGFR2 antibody (Cyramza, Ramucirumab) in hKDR mice bearing B16-F1 and MC38 syngenic solid tumors and we observed that Cyramza inhibited the tumor growth in vivo remarkably in a dose-dependent way, indicating the binding of anti-human VEGFR2 antibody to the chimeric h/m KDR receptor. Notably, we further generated hKDR knockin model in Rag2 knockout background (hKDR/Rag2^{KO}) by crossbreeding which lack mature T cells and B cells. The female hKDR/Rag2^{KO} mice were subcutaneously inoculated with human hepatocellular carcinoma LI0612 PDX model and human gastric cancer GA2419 PDX model to assess the anti-tumor effects of anti-angiogenic agents in xenograft solid tumors. The data suggested that Cyramza displayed moderate tumor growth inhibition (TGI) in LI0612 model at 10 mg/kg and weak TGI in GA2419 model at 10 mg/kg, respectively. Our findings support the notion that normalization of tumor vasculature is critical for tumor inhibition based on anti-angiogenic therapy and may synergize the anti-tumor effects with the immune checkpoint blockade or promote the cancer immunotherapy of immunomodulators in the future trials.

#4591

Mechanisms of tumor-mediated endothelial cell proliferation independent of VEGF

Kevin L. Sheng, Jude Raj, Kris C. Wood. *Duke University, Durham, NC*

A hallmark of cancer is dysregulated angiogenesis and blood vessel co-option, which are often driven by vascular endothelial growth factor (VEGF). Despite the key role of VEGF signaling in promoting endothelial cell (EC) proliferation, survival, and migration, the clinical use of VEGF inhibitors has modest success and faces many challenges. In particular, patients demonstrate variable initial responses to anti-VEGF therapy, and many of those who respond to treatment subsequently develop resistance. These challenges suggest that there may be VEGF-independent mechanisms driving EC proliferation in the tumor microenvironment. To study these mechanisms, we established an *in vitro* model using a dual-reporter system in a co-culture model of ECs and tumor cells. Specifically, we used an immortalized endothelial cell line (SVEC4-10) expressing GFP and *Renilla* luciferase and a mouse renal carcinoma cell line (RENCA) expressing Tomato and Firefly luciferase. This model allowed us to independently evaluate the growth rates and cell viabilities of both ECs and tumor cells in direct co-culture. Our preliminary data revealed that ECs exhibit increased growth rates when directly co-cultured with tumor cells. Interestingly, this EC proliferation is VEGF-independent and not impacted by VEGF-A knockout in tumor cells or with treatment of a pan-VEGFR small molecule inhibitor (axitinib). To further characterize if our phenotype was due to other tumor secreted factors, we used a transwell setup to eliminate direct contact between ECs and tumor cells and found that EC growth rates were substantially mitigated. These results revealed that tumor cells induced EC proliferation through a physical cell-to-cell interaction that is independent of VEGF. Further characterizing this unknown mechanism may inform therapeutic interventions to overcome the clinical challenges of anti-VEGF therapies for cancer. To expand our understanding of this VEGF-independent EC proliferation, we aim to characterize the cell surface proteome from tumor-conditioned ECs using cell surface mass spectrometry. We will validate hits from this study using our *in vitro* model and translate these findings to *in vivo* mouse models. We expect that our current and future research will reveal new insights into tumor co-option of

the vascular system and identify novel targets for developing therapies to effectively treat cancer.

#4592

In vivo efficacy evaluation of anti-human VEGFR2 antibodies in humanized B-hVEGFR2 mice

Lei Zhao[1], Chengzhang Shang[1], Rebecca Soto[2], Chonghui Liu[1], Zhaoxue Yu[2]. *[1]Biocytogen Pharmaceuticals (Beijing) Co., Ltd., Beijing, China,[2]Biocytogen Boston Corp, Wakefield, MA*

Angiogenesis, vascular development, vascular permeability, and embryonic hematopoiesis is partly regulated by VEGF binding to VEGFR2, which forms receptor dimers and activates downstream signaling pathways. In addition to developmental cues, VEGFR2 is also associated with disease progression for psoriasis, rheumatoid arthritis, diabetic retinopathy, and more significantly, tumor growth and drug resistance. Given this, inhibition of VEGFR2 signaling is actively being studied, and multiple VEGFR2 inhibitors have entered various phases of clinical studies and have shown promising results. To evaluate *in vivo* efficacy of anti-human VEGFR2 antibodies, we generated a human *VEGFR2* knock-in (B-hVEGFR2) mouse model by replacing the murine *Vegfr2* extracellular domain sequence with the corresponding human sequence. We validated human VEGFR2 gene and protein expression in B-hVEGFR2 mice by RT-PCR and flow cytometry, respectively. Furthermore, we observed an anti-tumor effect with anti-human VEGFR2 antibodies in homozygous B-hVEGFR2 mice subcutaneously implanted with MC38 colon cancer cells. Taken together, we established a novel preclinical B-hVEGFR2 mouse model for evaluation of VEGFR2-targeted immunotherapy.

#4593

Glioblastoma tumors that respond poorly to bevacizumab therapy show upregulation of an angiogenesis gene set

Roshan Lodha, Gaelle Muller-Greven, Lydia Guo, Candece Gladson. *Cleveland Clinic Lerner Research Institute, Cleveland, OH*

Glioblastoma (GBM) is the most common primary brain tumor in adults with a 15-month median survival, despite surgical-resection and radio-

chemotherapy, and a recurrence rate of 90%. Despite improving survival in only a small percentage of patients, bevacizumab, a monoclonal antibody toward vascular endothelial growth factor-A, is frequently used to treat recurrent-GBM. To find predictors of poor-response to bevacizumab, we performed RNA-sequencing on multiple GBM patient-derived xenograft (PDX) tumors after orthotopic propagation in athymic nude mice. The study was repeated, and once PDX-tumors were established, mice were treated with bevacizumab and grouped based on survival. Bioinformatic-analysis of RNA-sequencing data demonstrated differential gene expression in tumors that were poor-responders to bevacizumab (no survival change) as compared to tumors that were good-responders (longer survival), along with upregulation of an angiogenesis gene set in poor-responders. Within this gene set, multiple genes known to be regulated by the early growth response 1 (*EGR1*) transcription factor were identified; *CHRNA7* (cholinergic-receptor-nicotinic-α7-subunit) was selected for further study based on the reported role in promoting cancer cell migration and proliferation. Results were validated at the protein level using immunohistochemical staining. Additionally, Sry-box transcription factor-10 (*SOX10*) showed upregulation in poor-responders, potentially driven by impaired proteosome degradation. *SOX10* is known to promote mural-cell coverage of neovasculature, cancer cell migration, and glioma development when cooperating with platelet-derived growth factor-B (*PDGFB*). In summary, GBM PDX-tumors with upregulated expression of an angiogenesis gene set and of two transcriptional regulators (*EGR1* and *SOX10*) demonstrated a poor response to bevacizumab; upregulation of these genes could be used to predict bevacizumab response.

#4595

STAT-3 chemical inhibition modulates decidual-like polarization in NK cells from PCa patients and restore their anti-tumor activities

Matteo Gallazzi[1], Maria Teresa Palano[1], Martina Cucchiara[2], Federico Dehò[3], Paolo Capogrosso[3], Francesca Franzi[4], Fausto Sessa[4], Angelo Naselli[1], Lorenzo Mortara[2], Antonino Bruno[2]. *[1]IRCCS MultiMedica, Milano, Italy,[2]University of Insubria, Varese, Italy,[3]ASST Settelaghi, Ospedale di Circolo e Fondazione Macchi, Varese, Italy,[4]ASST Sette-Laghi, University of Insubria, Varese, Italy*

Introducti**on.** Natural Killer (NK) cells are innate lymphoid cells involved in tumour recognition/elimination. NK cells are altered in their phenotype and functions in diverse tumors, including prostate cancer (PCa). We demonstrated that PCa circulating NK cells (TANKs) acquire the pro-angiogenic/decidual-like $CD56^{bright}CD9^{+}CD49a^{+}$ phenotype, release IL-8 and MMP-9, functionally support endothelial cell activation and secrete monocyte-recruiting/M2-like macrophage-polarizing factors.

Materials and methods. Here, we characterized the phenotype of tumour infiltrating NKs (TINKs) and tumour-associated (TANKs) in PCa patients and evaluated the contribution of STAT3, as possible driver of NK cell polarization. PCa TINKs and TANKs were characterized by multicolour flow cytometry (FC) for decidual-like surface markers (CD9, CD49a) and degranulation capabilities (CD107a). STAT3 activation, was investigated in circulating PCa NK cells, by FC. Using a drug-repurposing approach with the antipsychotic agent Pimozide (a chemical inhibitor of STAT3), we modulated STAT3 activation, *ex vivo*, in PCa TANKs and monitored their secretome changes, by commercially available protein membrane arrays together with their capability to degranulate and produce perforin/GranzymeB.

Results and discussion. We observed that PCa TINKs acquire the same $CD9^{+}CD49a^{+}$ decidual-like NK cell phenotype, as found in PCa TANKs. We detected the presence of $CD56^{bright}CD9^{+}CD49a^{+}$ decidual-like NK cell also in peripheral blood of subjects with benign prostatic hyperplasia (BPH), but in a lower frequency, compared to those from PCa TANKs. Sera from PCa patients were enriched in IL-4, IL-6, IL-8 and IL-10, all cytokines able to activate STAT3 signalling. We detected increased phosphorylation of STAT3 in PCa TANKs, compared to NK cells from healthy controls, that was reduced following 24 hours of stimulation by Pimozide. This treatment resulted in decreased capabilities of PCa TANKs to secrete pro-angiogenic factors (IL-8, IL-6), molecules involved in monocytes recruitment/M2-like macrophage polarization (CCL-2, CCL5, GM-CSF, IL-10), together with increased degranulation, augmented secretion of (IFN-γ and TNF-α) and increased production of Perforin and Granzyme.

Conclusions. Our results suggest that STAT3 inhibition can be envisaged as a potential strategy to limit the generation of pro-angiogenic/decidual-like NKs, while contributing to NK cell re-education in PCa.

#4596

BIOhabitats clinical study (NCT05375318): Histopathological analysis of vascular habitats in glioblastoma defined by perfusion MRI

María del Mar Álvarez-Torres[1], Rebeca Burgos-Panadero[1], Jaime Agustí Martínez[2], Carlos Irles Vidal[3], Jaime Font de Mora[4], Elies Fuster-Garcia[1], Juan Miguel García-Gómez[1]. *[1]Biomedical Data Science Laboratory, ITACA., Universitat Politècnica de València, Valencia, Spain,[2]Pathology Department, Hospital Clínico Universitario of Valencia, Valencia, Spain,[3]Neurosurgery Department, Hospital Clínico Universitario of Valencia., Valencia, Spain,[4]Laboratory of Cellular and Molecular Biology, Instituto de Investigación Sanitaria La Fe, Valencia, Spain*

Tumor heterogeneity is a key hallmark and a major cause of therapeutic resistance in glioblastoma (GBM) patients. To characterize this heterogeneity, the automatic method ONCOhabitats delineate four habitats within the lesion using artificial intelligence analysis of perfusion magnetic resonance imaging (MRI): high angiogenic tumor (HAT), low angiogenic tumor (LAT), infiltrated peripheral edema (IPE), and vasogenic peripheral edema (VPE).

BIOhabitats has been successfully implemented in two Spanish hospitals, with the purpose of describing the vascular habitats at histopathological level. To collect samples from each habitat during the standard surgeries, the habitats masks were included in the neuronavigators. Posterior histopathological analyses of each sample were performed.

In this preliminary study, we present data from 37 samples from 9 GBMs. Neoplasic cellularity and density of mitosis were evaluated using Mann-Whitney test. In addition, we analyzed the proportion of samples of each habitat from the entire cohort with the presence of necrosis, reactive gliosis, microvascular proliferation (MVP), and glomeruloid vessels.

Table 1 includes results analyzing differences among habitats. Our results underline that HAT and LAT are characterized by more proliferative and vascular profiles compared to the edema habitats. However, the IPE habitat presented the highest value of reactive gliosis, which is associated with inflammatory processes and can be related to tumor infiltration. Higher proportions of necrosis, MVP, and glomeruloid vessels were also found in this habitat compared to VPE.

Despite this is a preliminary study, we found significant differences among tumor and edema habitats. We highlight the particular histopathological profile of the IPE habitat, different from the active tumor habitats but also from the VPE. BIOabitats is currently in progress including more patients for characterizing the habitats in depth.

Table 1. Histopathological analysis among vascular habitats.A) Mann Whitney results of analyzing ne

Neoplasic cellularity		HAT	LAT	IPE	VPE
	HAT	1	0.7852	0.0062*	0.0038*
	LAT		1	0.0047*	0.0030*
	IPE			1	0.6889
	VPE				1
Density of mitosis		HAT	LAT	IPE	VPE
	HAT	1	0.6863	0.0839	0.0087*
	LAT		1	0.0580	0.0070*
	IPE			1	0.4667
	VPE				1
% of samples with presence		HAT	LAT	IPE	VPE
Reactive gliosis		46,2	50,0	12,5	0,0
Necrosis		15,4	25,0	100,0	87,5
MVP		84,6	87,5	37,5	12,5
Glomeruloid vessels		38,5	50,0	12,5	0,0

#4597

TIMP1 is a major contributor of the angiogenic priming of tumor associated fibroblasts in lung adenocarcinoma

Natalia Isabel Diaz Valdivia[1], Paula Duch[1], Rafael Ikemori[1], Eduard Monso[2], Noemi Reguart[3], Jordi Alcaraz[1]. *[1]Unit of Biophysics and Bioengineering, Universitat de Barcelona, Barcelona, Spain,[2]CIBERES, Hospital Parc Taulí de Sabadell, Sabadell, Spain,[3]Medical Oncology, Hospital Clinic, Barcelona, Barcelona, Spain*

Background**:** Lung adenocarcinoma (ADC) and squamous cell carcinoma (SCC) are the most common histologic subtypes in lung cancer. Intriguingly, ADC and SCC exhibit distinct responses to the multi-tyrosine kinase inhibitor nintedanib and other antiangiogenic drugs, suggesting that angiogenesis may depend on the histologic subtype in lung cancer. In addition, tumor-associated fibroblasts (TAFs) are known regulators of angiogenesis, and we have recently reported that TAFs exhibit enhanced fibrosis and response to nintedanib in ADC compared to SCC, owing to the stronger epigenetic repression of SMAD3 in SCC-TAFs caused by excessive exposure to cigarette smoke particles. However, how the histotype-dependent fibrotic phenotype in TAFs impacts their pro-angiogenic functions remains unknown.

Methods: A panel of angiogenesis markers was assessed in patient samples using publicly available databases. The pro-angiogenic function of the conditioned medium of TAFs from ADC and SCC patients pre-activated with TGF-β1 was analyzed *in vitro* using migration and network formation assays of endothelial cells. The secretion of pro-angiogenic factors in TGF-β1-activated TAFs was analyzed using an angiogenesis antibody blot array. Selected factors were functionally validated *in vitro* and *in vivo* using genetic models.

Results: All angiogenesis markers were consistently upregulated in ADC compared to SCC concomitantly with a lower necrosis in ADC, unveiling a larger angiogenesis in ADC. We also observed that the conditioned medium of TGF-β1-activated TAFs elicited a larger endothelial cell network formation and migration in ADC than SCC, revealing that ADC-TAFs exhibit enhanced angiogenesis. Our immunoblot array analysis identified a subset of pro-angiogenic factors that were selectively overexpressed in ADC-TAFs compared to SCC-TAFs, including TIMP-1. Notably, TIMP-1 overexpression in ADC-TAFs was SMAD3-dependent and knocking down

TIMP-1 by siRNA in ADC-TAFs impaired angiogenesis *in vitro* and in tumor xenografts *in vivo*.
Conclusions: Our results reveal a larger angiogenesis in ADC compared to SCC, and implicate the TGF-β1/SMAD3/TIMP-1 pathway in the enhanced angiogenesis of ADC-TAFs. Our findings identify a biological process underlying the poor response of SCC to antiangiogenic therapies like nintedanib, and provide a rationale for the earlier metastasis of ADC patients compared to SCC patients based on the enhanced pro-angiogenic role of ADC-TAFs.

#4598
Vitamin b1 derivative, benfotamine, prevents VEGF-induced angiogenesis
Kieran V. Allowitz, Trevor J. Plowman, Kota V. Ramana. *Noorda College of Osteopathic Medicine, LLC, Provo, UT*

Several studies have indicated that thiamine, and more specifically its lipid soluble derivative benfotiamine, exerts an anti-oxidative and anti-inflammatory effect on the body. However, its effect in preventing cancer cell proliferation, migration, invasion, and metastasis is not yet clearly understood. It is known that angiogenesis plays a significant role in the growth and spread of many cancers but the role of benfotiamine in neovascularization is not yet known. Therefore, in this study, we hypothesized that benfotiamine would prevent VEGF-induced angiogenesis in vitro and in vivo. To examine this, we have treated human umbilical vein endothelial cells (HUVECs) with VEGF (Vascular Endothelial Growth Factor; 10 ng/ml) in the absence and presence of benfotiamine (0-100 uM) in a time and dose-dependent manner. We then examined the cell viability by MTT assay and apoptosis by Annexin-V staining and found that benfotiamine alone had minimal effect on cell viability and it prevents VEGF-induced cell proliferation. In vitro angiogenesis assay indicates that benfotiamine prevented the VEGF -induced tube formation of HUVECs. Further, benfotiamine regulated the expression of VEGF-induced growth factors such as VEGF, PIGF, IGFBP-1, ECGF, FGF-1 and 2, anti-angiogenic enzymes such as Serpin E1, TIMP-1, MMP-8, TSP-1, PTX3 and uPA and cytokines such as IL-8, Prolactin, ET-1, Endostatin, and CCL3. We will next examine how benfotiamine prevents in vivo

angiogenesis by utilizing a rat Matrigel plug model of angiogenesis in rats. The Matrigel sections will be stained with CD36, vWF, and other angiogenic markers to visualize the effect of benfotiamine on VEGF-induced angiogenesis. In conclusion, our current results indicate that benfotiamine has anti-angiogenic potential via inhibition of various pro-angiogenic growth factors and promoting anti-angiogenic factors in vitro and in vivo. Thus, our studies demonstrate that benfotiamine could be further developed as a novel therapeutic agent to prevent cancer growth and metastasis.

#4599

Blood and lymphatic endothelial cell contractility-mediated vessel permeability regulates interstitial fluid pressure and T cell infiltration in the tumor microenvironment

Yansong Peng, Esak Lee. *Nancy E. and Peter C. Meinig School of Biomedical Engineering, Cornell University, Ithaca, NY*

Solid tumors such as breast and pancreatic cancer are characterized by poor prognostic outcomes with high interstitial fluid pressure (IFP), which promotes tumor progression by modulating angiogenesis, matrix metalloproteinase activity, and cancer cell motility and compromises immunotherapies by keeping immune cells (e.g., T cells) from infiltrating into the tumor. To reduce tumor IFP, researchers tried to decrease solid stress and normalize hyperpermeable blood vessels (BV) in tumors, but how lymphatic vessels (LV) are impaired in the tumor microenvironment is poorly understood. Several studies reported that vascular endothelial growth factor C (VEGFC) treatment defeated tumors by promoting lymphangiogenesis and boosting T cell recruitment, while it has also been recognized to promote lymph node metastasis. Given the controversial roles of VEGFC, the main goals of this study are to control LV permeability and promote drainage by identifying currently unappreciated roles of rho-associated protein kinase 1 and 2 (ROCK1/2) in regulating lymphatic endothelial cell (LEC) contractility, junctions, and drainage in tumors. We will have blood endothelial cells (BEC) as controls to understand how ROCK1/2 and cell contractility affect LEC/BEC junctions and permeability differently. Here, we created a three-dimensional (3D) bioengineered model of vascularized pancreatic and breast tumors to study vessel junctions,

permeability, and IFP formation. The device consisted of a LEC or BEC lined, perfusable channel and a tumor-filled ECM chamber. We observed impaired barrier function of tumor BV/LV with increased permeability and loss of tight junctions compared to healthy vessels. To quantify the contractility of LEC/BEC, we employed traction force microscopy (TFM) by creating a 2D biomimicry of the endothelial monolayers using micropatterned polyacrylamide gel substrates with tunable stiffness. Using TFM, we showed that the combination of tumor-secreted factors and elevated matrix stiffness increased the traction of LEC/BEC, resulting in their loss of tight junctions. Using Rho kinase blockade to inhibit ROCK1/2 reduced the contractility of endothelial cells, reconstructed vessel structural integrity and functionality, and reduced intratumoral IFP in animal models. We expect that a decrease in the tumor IFP due to the restoration of lymphatic drainage would increase T cell infiltration, suppress tumor growth, and improve the survival of tumor-bearing mice combined with the anti-PD-1 or anti-PD-L1 therapy in our future studies. Together, our study provides new insights into understanding the physical interaction of endothelial, tumor, and immune cells, evidence of rho-kinases as a target for cancer immunotherapy, as well as a promising way to increase the efficacy of immunotherapies in cancer patients.

#4600

Phenotypic & functional diversity of tumor associated neutrophils in murine breast tumor models

Hasan Korkaya, Elayne Benson, Fulya Koksalar Alkan, Justin Wilson, Tulshi Patel, Hilmi K. Alkan, Virginia McEvoy, Nika Shekastehband, Nate Francois, Huidong Shi, Catherine C. Hedrick. *Augusta University, Augusta, GA*

Despite the advances in early diagnostics and therapeutics, women with metastatic breast cancer have limited treatment options. Women with TNBC, who constitute 15-20% of breast cancer patients, are often diagnosed with aggressive/metastatic disease. Advanced studies implicated immunosuppressive tumor microenvironment (TME) in aggressive/metastatic properties of TNBC subtype. Alternatively activated immature myeloid cells including tumor-associated macrophages (TAM), tumor-associated neutrophils (TAN), tumor-associated dendritic cells

(TADC) and myeloid derived suppressor cells (MDSC) constitute a major component of TME. However, anti-tumorigenic microenvironment is also reported and that may have clinical relevance in early TNBC patients. Therefore, our hypothesis is that myeloid cells polarize to become immunosuppressive and infiltrate tumors and pre-metastatic niches in patients with advanced disease, while patients with early TNBCs may elicit anti-tumor immune response eliminating disseminated tumor cells (DTC). The utilization of syngeneic immunocompetent mouse models has contributed to our current understanding of immunosuppressive or immunomodulatory TME. Using these models, we have demonstrated that tumor dissemination and growth at metastatic sites is facilitated by MDSC's. Emerging technologies; single cell RNA sequencing (scRNA-Seq), mass cytometry (CyTOF) or cellular indexing of transcriptomes and epitopes sequencing (CITE-Seq) has been powerful platforms for detailed characterization of tumors and TME compartments. We performed scRNA-Seq and CyTOF analyses of the myeloid cell populations of tumors and spleens from metastatic 4T1 and non-invasive EMT6 tumor-bearing mice. Tumors and spleens from 4T1 tumor-bearing mice exhibited a marked expansion of myeloid cell subsets that are characterized by the expression of immunosuppressive as well as progenitor markers. On the contrary, indicated tissues from EMT6 mice were enriched in NK cells, T and B lymphocytes and they were lacking immunosuppressive myeloid cell subsets. Furthermore, we identified a distinct differentiation pattern of immature myeloid cell subsets from neutrophil progenitors (NP) in 4T1 tumor-bearing mice. Using the murine TNBC models in syngeneic mice, we provide evidence that early TNBC tumors may elicit anti-tumor immune responses and thus the survival outcome in those patients is substantially increased after complete surgical resection of the primary tumors. Whereas immunosuppressive tumor microenvironment contributes to the poor overall survival in patients with advanced TNBCs. Therefore, identifying an anti-tumor immune signature in early TNBC patients may be utilized as a clinical biomarker before surgical intervention as well as improve the survival outcome.

#4601
Vitamin D supplementation attenuates resistance to anti-angiogenic therapy in colorectal cancer liver metastases

Miran Rada, Lucyna Krzywon, Audrey Kapelanski-Lamoureux, Stephanie Petrillo, Anthoula Lazaris, Peter Metrakos. *McGill University Health Centre, Montreal, QC, Canada*

Colorectal cancer liver metastasis (CRCLM) is one of the deadliest cancers. CRCLM tumours have two distinct histopathological growth patterns (HGPs) including desmoplastic HGP (DHGP) and replacement HGP (RHGP). The DHGP tumours are angiogenic, while their RHGP counterparts are vessel co-opting. The patients with RHGP tumours showed poor response to anti-angiogenic agents, as well as a worse prognosis. Herein, we conducted a retrospective cohort study that comprised 106 CRCLM patients to examine the effect of vitamin D supplementation on the HGPs of the tumours and the 5-year overall survival (OS). Interestingly, we found an inverse correlation between vitamin D supplementation and the presence of RHGP tumours in CRCLM patients. Additionally, the population who used vitamin D supplementation had significantly better 5-year OS. Moreover, our in vivo results suggested that vitamin D supplementation significantly improves the response of CRCLM tumours to anti-angiogenic therapy. Mechanistically, we found that vitamin D can suppress cancer cell motility, which is essential for the development of vessel co-option tumours and resistance to anti-angiogenic therapy. Collectively, this study suggests vitamin D supplementation is a promising way to attenuate resistance to anti-angiogenic therapy and improve the prognosis of CRCLM patients.

#4602

Differences in tumor vascular density between smoker and non-smoker cancer patients

Shubhangi Singh[1], Mohammad Aslam Khan[2], Elba T. Herrera[3], Seema Singh[2], Ajay P. Singh[2], Santanu Dasgupta[2]. *[1]International Studies, University of South Alabama, Mobile, AL,[2]Pathology, University of South Alabama, Mobile, AL,[3]Mitchell Cancer Institute, University of South Alabama, Mobile, AL*

Smoking is among the most significant preventable risk factors associated with cancer and other benign diseases. Cancer development is a multi-step process in which transforming cells gradually gain malignant properties

through a series of oncogenic genetic alterations. Successful cancer progression also depends on the remodeling of the surrounding stroma, which feeds the cancer cells in a host-parasite interaction. Tumor angiogenesis, the process of blood vessel formation, is an essential feature of solid tumors that ensures that they have the needed supply of food and oxygen to sustain their proliferative growth. We previously demonstrated that nicotine, an addictive component of tobacco smoke, promoted tumor angiogenesis by impacting the growth of endothelial cells. In the present work, we examined the differences in tumor vasculature between smoker and non-smoker patients to find clinical support for our laboratory findings. After searching the available tumor cases in the repository for the patient's smoking history, I selected 27 smokers (12 lung and 15 prostate adenocarcinomas) and 19 non-smokers (4 lung and 15 prostate adenocarcinomas) cases. The tissue blocks were sectioned and subjected to hematoxylin and eosin staining and immunohistochemistry using an antibody against CD31, a biomarker for endothelial cells. Following digital scanning, all slides were reviewed to identify tumor areas and $CD31^+$ tubular structures (blood vessels). We observed that lung and prostate tumor tissues from smoker patients had a significantly higher number of blood vessels than those from non-smoker patients. Thus, increased tumor vascularization appears to be a common feature of smoking cancer patients providing clinical support for a novel mechanism by which smoking may contribute to tumor pathobiology.

#4604

Effect of CDK 4/6 inhibition on anti-angiogenesis effect in gastric cancer

Sang Woo Cho[1], Woo Sun Kwon[2], Tae Soo Kim[2], Juin Park[2], Eun Seo Kim[1], Hyun Cheol Chung[3], Sun Young Rha[4]. *[1]Songdang Institute for Cancer Research, Brain Korea 21 PLUS Project for Medical Science, Yonsei University College of Medicine, Seoul, Korea, Republic of,[2]Songdang Institute for Cancer Research, Yonsei University College of Medicine, Seoul, Korea, Republic of,[3]Songdang Institute for Cancer Research, Division of Medical Oncology, Department of Internal Medicine, Yonsei Cancer Center, Yonsei University Health System, Seoul, Korea, Republic of,[4]Songdang Institute for Cancer Research, Brain Korea 21 PLUS Project for Medical Science, Division of Medical Oncology,*

Department of Internal Medicine, Yonsei Cancer Center, Yonsei University Health System, Seoul, Korea, Republic of

Angiogenesis, a hallmark of cancer, is a phenomenon in which new blood vessels are created from existing blood vessels. As the tumor grows, they secrete ligands such as vascular endothelial growth factor (VEGF). Therefore, anti-tumor effect could be achieved by preventing tumor-associated angiogenesis. In previous reports, CDK4/6 has been acknowledged to regulate VEGF transcription in addition to cell cycle regulation. There are few studies explaining the angiogenesis-related effects of CDK4/6 inhibitors in gastric cancer (GC). In this study, we aim to verify the anti-angiogenesis effect through CDK4/6 inhibition. First, we confirmed proliferation and angiogenesis in endothelial cells. Next, the change in VEGF expression induced by CDK4/6 inhibitor in GC cell lines was investigated. *In-vitro* angiogenesis research was conducted using human umbilical vein endothelial cells (HUVEC). Abemaciclib was used as a CDK4/6 inhibitor. To determine the efficacy of abemaciclib, HUVEC was treated with abemaciclib for 3 days and cell viability was assessed by CCK-8 assay. IC_{50} value was determined by the CalcuSyn software. Furthermore, tube formation assay, wound healing assay, cell cycle analysis and SA-β-gal assay were performed to explore effect of abemaciclib on HUVEC. VEGF-A expression was evaluated by ELISA. First, we identified direct anti-angiogenesis effect of abemaciclib on HUVEC. The IC_{50} value was 1.28 μM. At clinically achievable concentrations of abemaciclib (Cmax, 0.5 μM), HUVEC only showed a 20% growth inhibition. Abemaciclib did not suppress tube formation and migratory potential of HUVECs. However, abemaciclib induced a G1 arrest in HUVEC after 0.5 μM abemaciclib treatment for 24hr. To ensure whether the increase in the number of G1 phase cells is due to senescence, SA-β-gal assay was performed. The levels of SA-β-gal-positive cell staining in abemaciclib-treated group were higher than control, suggesting that abemaciclib induced cell senescence on HUVEC. While our results suggested that CDK4/6 inhibitor did not show direct anti-angiogenic effect on endothelial cells, we studied indirect anti-angiogenesis effect of abemaciclib in GC cell lines through regulation of VEGF transcription. Conditioned media of 49 GC cell lines had a wide range of VEGF secretion ranged from 0.146 to 22.676 ng/mL. (ave. 4.07 ng/mL). We have set the cut off of secreted VEGF as 10 ng/mL, at which

angiogenesis can be induced. There were four cell lines (4/49, 8.2%) whose VEGF concentrations were more than the angiogenesis-inducing VEGF concentration (10 ng/mL). Interestingly, 3 of these 4 GC cell lines demonstrated a decrease in VEGF secretion, following 0.5 μM abemaciclib treatment. In conclusion, we did not observe inhibition of angiogenesis in HUVEC. However, CDK4/6 inhibition can cause senescence in HUVEC, inhibit tumor growth, and indirectly induce anti-angiogenic effects in gastric cancer.

#4605

Chronic VEGF-C signaling exacerbates the progression of non-alcoholic steatohepatitis and hepatocarcinoma through endothelial VEGFR2 and VEGFR3

Seock-Won Youn[1], Jason W.-L. Eng[2], Bhairavi Swaminathan[1], Pamela Teneqexhi[1], Rahul Vadakath[1], Jan K. Kitajewski[1]. *[1]Department of Physiology and Biophysics, College of Medicine, University of Illinois at Chicago, Chicago, IL,[2]Division of Gastroenterology and Hepatology, Department of Medicine, University of Illinois at Chicago, Chicago, IL*

Obesity, aging, and metabolic diseases contribute to non-alcoholic fatty liver disease (NAFLD) that can progress to non-alcoholic steatohepatitis (NASH) due to ongoing inflammation and pathological angiogenesis. At present, NASH is a leading cause of cirrhosis, hepatocarcinoma cancer (HCC) and liver transplant within the United States. Pathological angiogenesis of liver sinusoidal endothelial cells (LSECs) is one of the hallmarks of liver injury that disrupt normal LSEC physiology. Therefore, strategies which target factors involved in LSEC dysregulation may improve the progression of hepatic diseases. Examination of a human tissue microarray identified increased levels of vascular endothelial growth factor-C (VEGF-C) in NASH livers compared with healthy individuals. Additionally, single nuclei RNA sequencing and immunofluorescent staining revealed that the receptors for VEGF-C, VEGFR2 and VEGFR3, are primarily expressed by the LSECs. Using murine models of NASH, we further investigated the role of VEGF-C during disease progression. Chronic over expression of VEGF-C by adeno-associated viral (AAV) infection in mice fed a western diet with carbon tetrachloride injections increased NASH progression compared with control AAV infected NASH

mice. Interestingly, overexpression of VEGF-C C156S, a variant of VEGF-C which exclusively binds to VEGFR3, resulted in significantly increased hepatic steatosis, but only minimal fibrosis. To determine whether blockade of VEGF-C signaling would delay disease progression, we administered lenvatinib, a tyrosine kinase inhibitor which primarily blocks VEGFR2 and VEGFR3 at low doses, to NASH mice. We discovered that low dose lenvatinib resulted in significantly decreased amount of fibrosis, steatosis, and tumor formation. Analysis of vehicle treated and lenvatinib treated livers by single nuclei RNA sequencing uncovered significant changes in endothelial cell genes associated with extracellular interactions and inflammation, as well as hepatocyte genes involved in lipid synthesis and metabolism. Taken together, these findings indicate that chronic VEGF-C production in NASH plays a role in promoting liver fibrosis and steatosis as well as HCC development, and that blockade of the downstream receptors for VEGF-C, VEGFR2 and VEGFR3, may be a promising therapeutic strategy to mitigate disease severity.

#4606

Heat shock proteins in immunosuppressive tumor microenvironment

Fulya Koksalar Alkan[1], Justin Wilson[1], Elayne Benson[1], Tulshi Patel[1], Virginia McEvoy[1], Nate Francois[1], Emma Nguyen[1], Hilmi Kaan Alkan[1], Ahmed Chadli[1], Jason Gestwicki[2], Hasan Korkaya[1]. *[1]Augusta University, Augusta, GA,[2]Pharmaceutical Chemistry, University of California, San Francisco, San Francisco, CA*

We previously demonstrated that upregulation of A20 in TNBC subtype in response to TNFα protects these cells from cytotoxic cell death by upregulating HSP70 protein and maintaining EMT/CSC phenotype. In contrast, luminal MCF7 or ZR75-1 cells display approximately 70% apoptosis when treated with TNFα. Overexpression of A20 in luminal cells not only protected them from TNFα-induced cytotoxicity by upregulating HSP70 and EMT/CSC phenotype, but also exhibited aggressive metastatic properties in mouse xenograft models.
We determined that TNFα-induced HSP70 upregulation in TNBC cell lines was dependent on A20 de-ubiquitinase activity that protected its degradation. Interestingly, our preliminary findings also suggested that A20 protein upregulation may be dependent on HSP70 chaperone activity. We

show significant overexpression of HSP70 and A20 proteins in 4T1 cell line when treated with TNFα or chemotherapeutic agents. However, A20 expression is significantly reduced when we block HSP70 activity in cells treated with TNFα or chemotherapeutic agents (Docetaxel-DTX or Doxorubicin-DOX). We proposed that A20 transcriptional upregulation upon TNFα stimulation leads to suppression of E3-ligase and accumulation of HSP70 which then stabilizes A20 with chaperone activity. Based on our reasoning, we performed the LIMBO chaperone binding assay which predicted A20 being the potential HSP70 client protein.
Furthermore, we show that A20/HSP70 pathway attracts tumor-infiltrating lymphocytes (TILs) while inducing the accumulation of immunosuppressive MDSCs in syngeneic mouse models. Interestingly, pulmonary DTCs as well as the immune infiltrates from 4T1 tumor-bearing mice exhibited significantly higher HSP70 expression. Therefore, targeting HSP70 will have a dual activity on tumors and MDSCs and thus it may potentiate the efficacy of immunotherapy in preclinical models of breast cancer. As previously reported, murine 4T1 tumors fail to respond to check point inhibitors. We reasoned that this may be an appropriate model to test the efficacy of HSP70 inhibitor, JG-231. Expectedly, there was no difference in tumor growth and metastasis between control and anti-PDL1 treated animals, however, combination of anti-PDL1 antibody with JG-231 and chemotherapy (cyclophosphamide-CTX) significantly reduced primary tumor growth (>10 fold) and eliminated metastasis. Collectively, our pilot experiments provide a strong rationale for testing our hypothesis and may lead to a rapid translation into the clinical utility.

#4607
TRPS1 inhibits angiogenesis in triple negative breast cancer down regulating JAG1 and TYMP genes involved in angiogenesis pathways
Liliana Guzman. *Breast Oncology, Houston Methodist Research Institute, Houston, TX*

Background**.** Triple-negative breast cancer (TNBC), the most difficult subtype to treat, is defined as estrogen receptor, HER2, and progesterone receptor negative. TNBC constitutes 10-20% of all breast cancer and has a higher rate of distal recurrence and a poorer prognosis than other breast cancer subtypes. Less than 30% of women with metastatic TNBC survive 5

years and almost all die from their disease despite adjuvant chemotherapy. Angiogenesis is a critical factor in the development of tumors and metastases in numerous cancers. Clinical trials with anti-angiogenic drugs showed to be inadequate, with moderate response rates and insignificant survival gains for patients. To understand the genetic forces involved in TNBC, we performed a transposon mutagenesis screen in Pten mutant mice that identified several candidate trunk drivers and progression genes. A major finding of our screen was the discovery and functional validation of, Trichorhinophalangeal syndrome type 1 (TRPS1), a GATA-like transcription factor, which functions as a transcriptional repressor or activator, depending on cell type, stage of development, or pathological conditions. Based on this data, we explored the role of TRPS1 in angiogenesis.
Methods and Results. Tube formation and sprouting assays were performed using overexpression and inactivation of TRPS1 in MDA-MD-231 and HCC70 cells, respectively. Interestingly, inactivation of TRPS1 expression accelerates tube formation structures compared to the vector control as well as cell branching in the sprouting assay. Overexpression of TRPS1 prevents tubing and branching formation in vitro assays. Moreover, immunohistochemistry staining of CD31 detected a reduced number of blood vessels in MDA-MB-231 tumor xenografts overexpressing TRPS1, and an increase of angiogenic vasculature in HCC70 TRPS1-shRNA tumor xenografts. In vitro and in vivo assays demonstrate the role of TRPS1 in tumor angiogenesis. Furthermore, human ChIP qPCR angiogenesis array identified 10 top candidate genes potentially regulated by TRPS1 transcription factor. Of these candidates, JAG1 and TYMP showed to have a higher fold enrichment compared to other angiogenic related genes. Finally, we validated its direct functional binding by using luciferase reporter assay, such demonstrated that TRPS1 is a direct transcriptional regulator of JAG1 and TYMP.
Conclusion. TRPS1 is a tumor suppressor involved in the mechanisms regulating tumor angiogenesis by repressing the expression of JAG1 and TYMP genes in TNBC.

Evaluating Tumor Progression via 3D and Spatial Approaches

#4611

Leveraging organotypic brain slice models to enhance adoptive cellular therapies

Alexandra Reid[1], Dan Jin[2], Bayli DiVita-Dean[2], Laura Falceto-Font[2], John Figg[2], Connor Francis[2], Catherine Flores[2]. *[1]University of Florida, Gainesville, FL,[2]Neurosurgery, University of Florida, Gainesville, FL*

Glioblastoma (GBM) is an incredibly aggressive and prevalent primary CNS tumor with dismal survival outcomes. GBM's intra-tumor heterogeneity and lack of anti-tumor immune cell infiltration have proved to be formidable challenges to the development of effective therapies. These hurdles may be overcome by garnering a better understanding of the cell-cell interactions occurring within the tumor microenvironment (TME). Accounting for the complexity and the spatial orientation of the components within the TME may offer insight into the multitiered layers of immunosuppression capitalized on by GBM tumors, thus elucidating the factors responsible for poor response to therapy and uncovering potential therapeutic targets that may offer more favorable therapeutic results for immunotherapies. Current in vitro and in vivo models, however, sorely limit our ability to probe these distinct attributes while preserving the intricate nature of the TME. To bridge this gap, we have devised a novel organotypic brain slice culture (BSC) model using tumor-bearing C57BL/6J mice, allowing us to characterize the tumor milieu in situ. We have identified infiltration of myeloid-derived suppressor cells (MDSC) and microglia polarized to the M2 anti-inflammatory phenotype within the TME. Leveraging this platform, we sought to define further the factors contributing to the dynamic impacts of GBM immunosuppression, such as the tolerogenic response in dendritic cells (DC) upon interaction with the TME. We have demonstrated outcomes similar to those seen in vivo following the introduction of DCs to tumor-bearing BSCs, further supporting the physiological relevancy of this model, and have since worked to unravel elements responsible for this response.

#4612

Microphysiological vascularized solid liver tumor model for drug and cell therapy

Jyothsna Vasudevan[1], Ragavi Vijayakumar[2], Jose Antonio Reales-Calderon[2], Maxine Sin Yee Lam[2], Jin Rong Ow[2], Joey Aw[2], Damien Tan[2],

Giulia Adriani[3], Andrea Pavesi[2]. *[1]Mechanobiology Institute, National University of Singapore (NUS), Singapore, Singapore,[2]Institute of Molecular and Cell Biology, Agency for Science, Technology and Research (A*STAR), Singapore, Singapore,[3]Singapore Immunology Network, Agency for Science, Technology and Research (A*STAR), Singapore, Singapore*

Development of efficacious therapeutic strategies against solid tumors is limited by the lack of pre-clinical models that can reliably predict treatment outcomes in patients. This is primarily because models often do not accurately reflect the complexity of the tumor microenvironment (TME). The TME consists of vasculature, stromal cells and immune cells that can promote tumor resistance or prevent targeted drug and cell therapy. Here, we developed an in vitro vascularized liver tumor model in a microfluidic device to evaluate drug delivery and immunotherapy approaches. The model consists of a tumor spheroid surrounded by a perfusable self-organized vasculature bed with physiologically relevant permeability. Sorafenib (Nexavar) efficacy was evaluated by assessing tumor spheroid viability, quantified by the loss of fluorescence signal. The presence of vasculature showed enhanced cytotoxicity, highlighting the importance of tumor-vascular interactions for testing therapeutic efficacy. Engineered immune cells (chimeric antigen receptor (CAR) T-cell and transiently expressing T-cell receptors (TCR)) were introduced into the model to demonstrate immunotherapy validation. Our results showed that the engineered immune cells were more effective at infiltrating the tumor spheroid without a vasculature but were more cytotoxic in the presence of the vasculature. By removing the cultured microtissue from the device and performing digital spatial transcriptomics on standard paraffin-embedded sections, we identified known and novel genes involved in creating a pro-tumorigenic microenvironment. This platform can be utilized to model critical features of the in vivo TME, providing better predictability of drug responses, with potential applications towards personalized medicine.

#4613

Inhibition of myosin II in triple-negative breast cancer cells limits macrophage recruitment in a 3D environment

Youngbin Cho, Ruxuan Li, Ioannis Zervantonakis. *Bioengineering, University of Pittsburgh, Pittsburgh, PA*

Among all breast cancer subtypes, triple-negative breast cancer (TNBC) exhibits the least favorable outcomes with a complex tumor microenvironment that facilitates metastatic progression. Remodeling of the extracellular matrix at the tumor invasive front is associated with increased cancer cell motility and poor outcomes. Myosin II, a key cytoskeletal regulator, plays a central role in cancer cell metastatic potential. In the clinic, high expression of myosin II in breast tumors has been associated with distant metastasis and lower survival rates. Interestingly, breast tumors overexpressing myosin II exhibited a higher density of tumor-associated macrophages and an immunosuppressive microenvironment. However, the relationship between myosin II activation in TNBC cancer cells and macrophage recruitment remains poorly understood. Here we employed a novel 3D microfluidic model of tumor-macrophage co-culture to study macrophage infiltration toward cancer cells with high spatiotemporal resolution. Using a panel of TNBC cell lines we found that high myosin II expression in cancer cells correlated with higher macrophage recruitment in a 3D matrix. Pharmacologic or genetic inhibition of myosin II reduced macrophage recruitment. Furthermore, using our microfluidic devices, we controlled the spatial distribution of cancer cells in a 3D matrix and separated the role of cancer cell-secreted paracrine factors from cancer cell-mediated matrix remodeling on macrophage recruitment. Analysis of matrix remodeling over time revealed that targeting myosin II in cancer cells limited the establishment of migratory tracks that facilitated macrophage recruitment. In sum, our studies revealed the critical role of cancer cell-driven matrix remodeling in promoting macrophage infiltration that can be therapeutically targeted to reverse the establishment of an immunosuppressive microenvironment.

#4614

Investigating lymphatic vessel remodeling and anti-tumor immunity in pancreatic cancer using tumor-on-chip and mouse models

Anna Maria Kolarzyk, Conor Loy, Renhao Lu, Iwijn De Vlaminck, Deborah Fowell, Esak Lee. *Cornell University, Ithaca, NY*

Pancreatic ductal adenocarcinoma (PDAC) remains one of the deadliest tumors in humans. PDAC has an immunosuppressive tumor

microenvironment, constituting for poor immunotherapy outcomes. Lymphatic vessels (LVs) transport leukocytes and antigens from tumor peripheries to draining lymph nodes (dLNs) for activation of anti-tumor immune responses. It is believed that impairment of the lymphatic function may result in delayed and ineffective immune activation against tumors. In this study, we created a three-dimensional (3D) tumor-on-chip model to examine phenotypical and functional changes in 3D engineered LVs, composed of human primary lymphatic endothelial cells (LECs) in co-culture with PDAC cells. Our *in vitro* studies revealed that PDAC cells induce lymphangiogenesis and tighten cell-cell junctions in LECs, forming "zipper-like" LEC junctions, compared to control LECs with "button-like" junctions. We introduced 70kDa dextran into the LV lumens and showed PDAC-induced zippering of junctions decreased vessel permeability. These results led us to hypothesize that altered LEC junctions may affect fluid drainage into the LVs *in vivo*. We inoculated PDAC cells into the mouse ear pinnae and performed whole-mount immunostaining and lymphatic drainage experiment by injecting Evans blue into the ears and measured the remained Evans blue in the ears. In the ear experiments, inoculated PDAC cells affected host LVs with originally button-like junctions to become zipper-like and impede lymphatic drainage. To identify a potential signaling pathway that may be responsible for LEC junction zippering, we used phospho-kinase arrays and discovered that PDAC cells induced LECs to increase phosphorylation of GSK3-β, JNK kinases, and enhanced the total protein level of β-catenin, implying that PDAC cells turned on the WNT signaling in LECs. In preliminary screening, we treated LECs co-cultured with PDAC cells with WNT-C59, an WNT inhibitor that blocks secretion of all WNT ligands, which resulted in decreased number of LV sprouting and less contractile actin-cytoskeleton in LECs. It is critical to know which molecules were secreted by PDAC cells and influenced the WNT signaling in LECs. With that in mind, we plan to perform mass spectrometry with PDAC-conditioned media to identify PDAC-specific secretome; and run RNA-seq with LECs isolated from mouse ears with or without PDAC to investigate molecular basis of the WNT activation in LECs and LV remodeling. Finally, we plan to examine the egress of leukocytes from primary PDAC tumor site, T cell activation in tumor-dLNs, and PDAC tumor growth with or without WNT inhibition in Kaeda mice. The identity and function of PDAC-egressed immune cells, and those which stayed

within the primary tumor will enhance our understanding of the roles of LVs in orchestrating anti-tumor immunity in PDAC.

#4615

Differential immune characteristics and anti-PD-1-induced reinvigoration capacity of tumor-infiltrating lymphocytes according to ProMisE classifier in endometrial cancer

Jung Chul Kim[1], Junsik Park[2], Yong Jae Lee[1], Sunghoon Kim[1], Sang Wun Kim[1], Jung-Yun Lee[1]. *[1]Obstetrics and Gynecology, Yonsei University College of Medicine, Seodaemun-gu, Korea, Republic of,[2]Severance Biomedical Science Institute, Yonsei University College of Medicine, Seodaemun-gu, Korea, Republic of*

Endometrial cancer (EC), one of the most common gynecological malignancies, has been gradually increasing worldwide. The Cancer Genome Atlas endometrial collaborative project discovered 4 distinct prognostic genomic subtypes, and the Proactive Molecular Risk Classifier for Endometrial Cancer (ProMisE) was developed: *POLE*-mutated, mismatch repair deficiency (MMR-D), non-specific molecular profile (NSMP), and p53-abnormal (p53abn). In the era of immunotherapy, immune checkpoint inhibitors (ICIs) become a definite management of EC, both as single agent or in combination with other targeted agents. However, the characteristics of the tumor immune microenvironment according to molecular classification in EC are not well known. This study was conducted to identify distinct immune properties of tumor infiltrating lymphocytes (TILs) according to molecular classification in EC and find optimal therapeutic targets in each molecular subtypes. We isolated peripheral blood mononuclear cells (PBMCs) and TILs from 81 patients with EC. The expression of immune checkpoint receptors and T-cell transcription factors of TILs were examined using flow cytometry. Sixty-six patients were evaluated according to the ProMisE algorithm based on sequencing for the presence of *POLE* mutations, immunohistochemistry for MMR proteins and p53 (*POLE*-mut, n=6; MMR-D, n=17; p53abn, n=20; NSMP, n=23). Tumors were categorized into one of the four molecular subtypes. TILs were *ex vivo* stimulated with anti-CD3 in the presence of anti-PD-1, and their proliferation was assessed to predict ICI-induced reinvigoration capacity of CD8 TILs. Comparing T-cell transcription factors

(TCF-1 and TOX), CD8 TILs showed higher expression of TOX, and lower expression of TCF-1. When comparing the immune characteristics of TILs according to molecular subtypes, Tregs of *POLE*-mut showed significantly lower expression of CTLA-4 and Ki-67 than that of MMR-D. In addition, CD8 TILs of MMR-D showed higher expression of immune checkpoint receptors, including PD-1, CTLA-4, and TIM-3, and lower expression of TCF-1 than those of p53abn. $CD8^+$TILs of p53abn showed significantly higher expression of CD226 than those of MMR-D. In particular, the frequency of antigen reactive $CD39^+CD103^+$CD8 T cells significantly lower in p53abn than in MMR-D. CD8 TILs of NSMP showed higher expression of TOX than those of MMR-D. In *ex vivo* T cell proliferation assay (n=49), 80.0% POLE-mut (4 of 5), 46.2% MMR-D (6 of 13), 35.7% p53abn (5 of 14) and 35.36% NSMP (6 of 17) showed enhanced proliferation of CD8 TILs upon anti-PD-1 treatment. In endometrial cancer, TILs showed distinct immune properties according to ProMisE classification. Further study is needed to develop optimal treatment targets for the p53abn and NSMP subtype, which is non-immunogenic and hardly reinvigorated by ICIs.

#4616

Automated multiplex immunofluorescence enables single cell analysis of tumor stroma

François Rivest[1], Victor de Gautard[1], Vytautas Navikas[1], Nadine Nelson[2], Bastian Nicolai[1], Joanna Kowal[1], Saska Brajkovic[1]. *[1]Lunaphore Technologies SA, Tolochenaz, Switzerland,[2]Abcam, Cambridge, United Kingdom*

Background**:** The tumor microenvironment (TME) consists of malignant cells and supporting non-malignant cellular and non-cellular components that form the tumor stroma. The tumor stroma plays an important role in tumor progression and has emerged as a modulator of anti-tumor immunity (Salmon et al., Nat Rev Cancer 2019) and responses to therapy (Hirata and Sahai, Cold Spring Harb Perspect Med 2017). As such, several therapeutic approaches have recently been developed to target stromal cells as anti-cancer treatments (Valkenburg et al., Nat Rev Clin Oncol 2018, Bejarano et al., Cancer Discov 2021). In addition, the composition of the TME has been recognized as a prognostic factor for survival in cancer patients (Pagès et

al., Oncogene 2011). Current protein-based approaches to characterize and better understand the cell composition of the tumor stroma face many limitations such as reagent availability and lengthy protocols. In this study, we identified a list of 22 markers to characterize non-tumoral immune cells, fibroblasts and endothelial cells in the TME, in a single tissue slide. We propose an approach that overcomes reagent incompatibility and opens new avenues of research of tumor stroma.
Method: Multiorgan Tumor Microarray (TMA) was interrogated with a sequential immunofluorescence (seqIF™) panel encompassing protein markers enabling characterization of TME. A 22-plex panel was created based on expanding an already established 13-plex panel (CD3, CD4, CD8, CD11c, CD20, CD45, CD56, CD68, aSMA, FoxP3, Ki67, PD1, PD-L1) by adding 9 additional antibodies (CD11b, CD14, CD31, CD47, CK, FAP, LaminB1, SIRPα, Vimentin). Hyperplex immunofluorescent staining was performed using automated staining-imaging COMET™ platform generating ome-tiff images containing 25 layers: DAPI, 2 autofluorescent and 22 marker channels. Postprocessing of images was done with HORIZON™ image analysis software.
Results: We established a panel of 22 markers that can be analyzed simultaneously on a single tissue slide despite limited variability in primary antibody species. Using seqIF™ protocol allowed the study of colocalization and co-expression of markers not compatible to study simultaneously in the traditional immunofluorescence approach. Our hyperplex data revealed distinct composition of the stromal compartment between different tumor types, highlighting high heterogeneity in the tissue composition and stromal architecture.
Conclusion: COMET™ platform enabled studying in detail TME components and highlighted heterogeneity of tumor stroma across different tissue types. SeqIF™ protocol lifted the limitation imposed by same species antibodies and allowed simultaneous interrogation of markers' expression preserving their spatial relationship.

#4617

A complete pipeline for high-plex spatial proteomic profiling and analysis on the cosmx^{tm} spatial molecular imager and atom^{tm} spatial informatics platform

Tien Phan-Everson, Zachary Lewis, Giang Ong, Yan Liang, Emily Brown, Liuliu Pan, Aster Wardhani, Mithra Korukonda, Carl Brown, Dwayne Dunaway, Edward Zhao, Dan McGuire, Sangsoon Woo, Alyssa Rosenbloom, Brian Filanoski, Rhonda Meredith, Kan Chantranuvatana, Brian Birditt, Hye Son Yi, Erin Piazza, Jason Reeves, John Lyssand, Vik Devgan, Michael Rhodes, Gary Geiss, Joseph Beechem. *NanoString Technologies, Inc., Seattle, WA*

Detecting and analyzing large numbers of proteins using whole-slide imaging is critical for a comprehensive picture of immune response to cancer. Many existing approaches for high-plex proteomics face issues around simplicity, speed, scalability, and big data analysis. Here, we present an integrated workflow from sample preparation through downstream analysis that addresses many key concerns around high plex proteomics. The CosMx Spatial Molecular Imager (SMI) and AtoMx Spatial Informatics Platform (SIP) comprise of a turnkey, end-to-end workflow that efficiently handles highly multiplex protein analysis at plex sizes exceeding 110 targets. We demonstrate an extension of our commercially available 64-plex human immuno-oncology panel to higher numbers of targets and show how the cloud computing-enabled AtoMx SIP allows flexible construction of analytic pipelines for cell typing and spatial analyses.

The CosMx protein assay uses antibodies conjugated with oligonucleotides, which are detected using universal, multi-analyte CosMx readout reagents. The CosMx Human Immuno-oncology panel was optimized to comprehensively profile lymphoid and stromal lineages within the tumor microenvironment as well as markers of cancer signaling and progression. Each CosMx SMI antibody was validated on multi-organ FFPE tissue microarrays covering prevalent solid tumor types with matched controls, and 52 human FFPE cell lines, including overexpression lines for key targets such as GITR, CD278, PD-L1, and PD-1. CosMx SMI uses a deep learning algorithm to segment whole cells and a semi-supervised algorithm to classify cell types. The AtoMx SIP provides full analysis support, including a whole-slide image viewer, and methods for performing built-in or fully customizable analyses for cell typing, ligand-receptor analysis, neighborhood analysis and spatial differential expression.

Within the cancer sample profiled, we performed in-depth single-cell proteomic profiling across different cell populations. We detected TLS,

characterized TLS maturation, and identified immune interactions with the tumor microenvironment. The CosMx SMI assay profiled the composition and spatial organization of infiltrating immune cells within and around the tumor microenvironment. We found that markers of T cell activation and exhaustion varied across the tumor landscape.
CosMx SMI is a high-plex spatial multi-omics platform that enables detection of more than 110 proteins at subcellular resolution in real-world FFPE tissues. The extensibility of the CosMx protein assay to large numbers of protein targets and our flexible, scalable bioinformatic platform provides a straightforward and robust solution for comprehensive immune phenotyping with full spatial context.
FOR RESEARCH USE ONLY. Not for use in diagnostic procedures.

#4618

Biomarkers of functionally active tertiary lymphoid structures in human breast cancer

Doïna Sofronii[1], Francine Padonou[1], Mireille Langouo[1], Noemie Thomas[1], Anais Boisson[1], Alexandre De Wind[2], Denis Larsimont[2], Ahmad Awada[3], Soizic Garaud[4], Karen Willard-Gallo[1]. *[1]Molecular Immunology Laboratory, Jules Bordet Institute, Free University of Brussels (ULB), Brussels, Belgium,[2]Department of Pathology, Jules Bordet Institute, Free University of Brussels (ULB), Brussels, Belgium,[3]Department of Medical Oncology, Jules Bordet Institute, Free University of Brussels (ULB), Brussels, Belgium,[4]B Lymphocytes, Autoimmunity and Immunotherapies, Inserm U1227, Brest, France*

The clinical relevance of tumor infiltrating lymphocytes (TIL) in breast cancer (BC) is now widely accepted and being implemented in clinical practice. Our lab previously demonstrated that 60% of BC organize some of their TIL in tertiary lymphoid structures (TLS). TLS have been detected in a wide variety of solid tumors with their prognostic value and importance in the response to immunotherapy increasingly accepted. Reliable biomarkers to identify and characterize TLS and their immune activities in tumors are needed. The specific aim of this project was to perform a comprehensive analysis across the spectrum of TLS states to identify biomarkers associated with active and inactive TLS, where the former are associated with functional anti-tumor immunity and improved responses to treatment and

long-term survival. This study analyzed FFPE tissues from 38 primary untreated HER2+ and triple negative (TN) BC patients. Patients were divided into two groups based on a TLS score evaluating CD3/CD20 and PD-1/Ki-67 dual IHC-stained tumor tissues: 1) BC containing a majority of active TLS (tumors with only active TLS have never been observed), defined by the presence of a germinal center (GC^{pos} ; $Ki\text{-}67^{+}$ follicular B cells) and 2) BC with only inactive TLS (GC^{neg} ; $Ki\text{-}67^{-}$ follicular B cells). Controls included normal breast tissues, BC without TLS and lymphoid tissues (reactive tonsils for GC^{pos} and spleens for GC^{neg} TLS). RNA extracts from microdissected tissues (N=100), including active TLS, inactive TLS and lymphoid B follicles, were sequenced. DESeq2 and CIBERSORT were employed to quantify differentially expressed genes and immune cell subpopulations, respectively. Gene Set Enrichment Analysis was used for additional data interpretation and pathway identification. Tumors from patients with active TLS were characterized by increased naïve and plasma B cell TIL compared to tumors with only inactive TLS. Preliminary analysis of the differentially expressed genes in active TLS (vs inactive TLS) revealed upregulation of key B cell differentiation, somatic hypermutation and class switch recombination genes, which paralleled their respective lymphoid controls. These gene upregulations were linked with a GC presence in active TLS. A specific set of immunoglobulin genes were also differentially expressed in active TLS. Continued analysis of the TLS data, including their cellular composition, location, maturation and functionality, along with data confirmation (RT-PCR and multiplex IHC), and assessment of their functional and clinical relevance is ongoing. Our preliminary results suggest that active B cell differentiation and Ig production contribute to TLS functionality. In lymphoid tissues, the GC plays important roles in orchestrating the molecular and cellular programs of humoral immunity. Our data suggest that active GC-containing TLS foster an immune microenvironment in BC that favors positive clinical outcomes.

#4619

Spatial analysis of the immunosuppressive tumor microenvironment in brain cancer applying a novel multiplex immunofluorescence panel

Yvonne Reiss[1], Jadranka Macas[1], François Rivest[2], Victor de Gautard[2], Saska Brajkovic[2], Bastian Nicolai[2], Tatjana Starzetz[1], Kathleen Sommer[1], Pinar Cakmak[1], Jonathan Schup[1], Jennifer H. Lun[1], Karl H. Plate[1].
[1]Institute of Neurology (Edinger Institute), Goethe University, Frankfurt, Germany,[2]Lunaphore Technologies, Tolochenaz, Switzerland

Glioblastoma (GBM) and brain metastases (BM) account for >70% of all brain cancers. The annual incidence averages to 10-17 cases per 100.000 person (~ 3 cases for GBM and 7-14 for BM), resulting in 45.000-77.000 new cases in the European Union alone. The standard of care for GBM includes maximal surgical resection followed by radiation and chemotherapy with temozolomide, whilst whole brain irradiation or surgical removal with or without chemotherapy are used for BM. In spite of therapy, the median overall survival remains < 6 months for BM, and 16 months for GBM, suggesting brain cancers as one of the most therapy-resistant tumors. Despite the emergence of novel therapeutic strategies, such as anti-angiogenic therapy, targeting myeloid cells or checkpoint immunotherapy, no significant improvement in overall survival of brain cancer patients was observed. Several studies have suggested the resistance to therapy in brain cancers is largely attributed by the presence of an immunosuppressive brain tumor microenvironment.
To investigate the spatial architecture of the tumor microenvironment in BM derived from lung and breast cancers, we employed the Lunaphore 13-plex immune-oncology (IO) Core Panel, consisting of clinically relevant IO biomarkers (CD3, CD4, CD8, CD45, FoxP3, PD1, PD-L1, CD11c, CD20, CD56, CD68, aSMA and Ki-67) for multiplex immunofluorescence (mIF) assays. These findings were then compared to isocitrate dehydrogenase-wildtype glioblastoma, which is a T-cell-poor cancer that is also characterized by an immunosuppressive tumor microenvironment. Further, the IO Core Panel was expanded with previously established antibodies targeting myeloid, blood-brain barrier and tumor cell markers in a proteomic workflow on COMET™, a fully automated, sequential immunofluorescence (seqIF™) platform.
Comprehensive mapping of the GBM microenvironment and BM confirmed previous observations obtained by bulk and single cell RNA sequencing analysis that described profound differences in the tumor microenvironment of BM versus GBM. In contrast to GBM, anti-tumor

immunity in BM was increased, whereas immunosuppressive cells remained unchanged between the two. Of note, T- and B-cells were not evenly distributed within the tumor tissue, providing an additional level of spatial information that would have been missed by bulk RNA or proteomic analyses.
Our study is the first to demonstrate a successful application of Lunaphore's IO core panel on GBM and BM samples. This highlights potential future use in the development of tools for personalized medicine for GBM and other tumor types.

#4620

Automated multiplex immunofluorescence workflow to interrogate the cellular composition of the tumor microenvironment

Vytautas Navikas, Quentin Juppet, Samuel Aubert, Benjamin Pelz, Joanna Kowal, Diego Dupouy. *Lunaphore Technologies SA, Tolochenaz, Switzerland*

Background**:** The tumor microenvironment (TME) is a constantly changing niche due to dynamic interactions between tumor cells and their surroundings. Recently, it became evident that a better understanding of the TME is needed to target the disease more accurately (Binnewies et al., Nat Med 2018; Vitale et al., Nat Med 2021). Spatial hyperplex immunofluorescence enables the visualization of cellular and non-cellular tissue components simultaneously. However, the increasing number of biomarkers detected by spatial proteomics quickly escalates the complexity of images and renders their interpretation challenging. Extracting quantitative data from images remains a challenge as it requires extensive training and experience in data analysis. Additionally, inferring cellular interactions and dependencies from spatial assays is an important milestone that needs to be overcome with image analysis approaches. Here, we present an end-to-end solution that combines automated hyperplex execution with image data extraction to study the spatial composition of TME.
Methods: Sequential hyperplex immunofluorescence was performed on COMET™ on an FFPE Breast Tissue Microarray (TMA), generating images containing 42 layers: nuclear DAPI, tissue autofluorescence, and 39 single layers for biomarkers. All layers were delivered as a single ome.tiff

file and processed using HORIZON™ image analysis software in combination with downstream statistical analysis. The tissue composition was interrogated with the use of an in-house trained nuclei detection algorithm (Schmid et al., MICCAI 2018; Weigert et al., WACV 2020), in-house developed image artifact exclusion approach, and spatial analysis based on a Squidpy workflow (Palla G. et al., Nat Meth 2022).
Results: We interrogated the composition of breast tumor tissues (n=9). Our in-house developed pipeline allows for filtering out both autofluorescent objects and segmentation artifacts based on the tissue autofluorescence and morphological features. Once the quality of segmented cell detection was assured, over 20 different cell phenotypes were identified by unsupervised Leiden clustering and visualized using UMAP dimensionality reduction method. It revealed several myeloid cell subsets highlighting their heterogeneous phenotypes including, but not limited to, immunosuppressive neutrophils and macrophages. Contrastingly, the uniform presence of T regulatory lymphocytes was detected in majority of cores and their co-occurrence with CD14+CD163+ macrophages was observed.
Conclusion: Here, we showcased an innovative automated workflow that highlights the ease of adoption of multiplex imaging to explore TME composition at single-cell resolution using simple workflow: slide in-data out. This workflow is easily transferrable to various cohorts of specimens to provide a toolset for spatial cellular dissection of the cancer milieu.

#4621

Distinct spatial and molecular maps in the tumour microenvironment of resistant melanoma patients treated with checkpoint inhibitor immunotherapy

Camelia Quek[1], Aditya Pratapa[2], Ines Pires da Silva[1], Ghamdan Al-Eryani[3], Aaron Mayer[4], Nenad Bartonicek[5], Kate Harvey[3], Oliver Braubach[2], Robyn P.M. Saw[1], Jonathan Stretch[1], Kerwin F. Shannon[1], Alexander M. Menzies[1], Richard A. Scolyer[1], Georgina V. Long[1], Alexander Swarbrick[3], James S. Wilmott[1]. *[1]Melanoma Institute Australia, Sydney, Australia,[2]Akoya Biosciences, California, CA,[3]Garvan Institute of Medical Research, Sydney, Australia,[4]Stanford University, California,*

CA,[5]Melanoma Institute Australia, Garvan Institute of Medical Research, Australia

Background: Checkpoint-based immunotherapies can achieve durable clinical responses in a variety of advanced cancers, including melanoma. However, clinical responses are not universal and there is still a substantial gap in understanding the mechanistic insights of immunotherapy resistance. This study aims to better understand patients' resistance to immune checkpoint therapies by dissecting and tracing individual tumour and immune cell clones.
Methods: Melanoma tumour dissociates and lesion matched formalin-fixed paraffin-embedded tissue samples were collected from patients with advanced melanoma receiving ipilimumab in combination with nivolumab; 2 patients were long-term responders, 2 had innate resistance and 1 acquired resistance. The molecular characteristics and spatial cellular relations associated with tumour and immune subsets in response to treatment were identified using single-cell indexing of transcriptomes and epitopes by sequencing and CODEX (CO-Detection by indEXing) multiplexed tissue imaging. Integration of spatial and molecular information was performed by combining reference-based phenotyping, Louvain clustering, and a mutual nearest neighbours-based transfer learning algorithm.
Results: Pre-treatment melanoma biopsies from 5 patients (3 responding and 2 non-responding) along with a subsequent acquired resistance biopsy from an initially responding patient were analysed. Comparisons of cellular phenotypes identified higher proportions of gamma delta T cells (1.98% versus 0.2%) and enriched memory T cell profiles (CD3E, CD44, CD45RO, CD8) in responding compared to non-responding pre-treatment biopsies. Fibroblast from non-responding lesions overexpressed stromal related cytokine, IL1A (log2 fold change (FC) = 3.3) and CXCL1 (log2 FC = 1.4), which were enrichment at the tumour margin compared to responding lesions. Comparisons of a patient's pre-treatment biopsy that initially responded to a subsequent progressing biopsy with acquired resistance had altered expression of transcript factor, ZFX (log2 FC = -1.59; adjusted p = 0.0119), and MBD2 (log2 FC = -1.5; adjusted p = 0.0225) within the patient's memory T-cells.

Conclusion: The combination of high dimensional single cell transcriptomics and spatial tissue imaging are effective tools to identify specific changes in cell phenotypes, intracellular signalling, and spatial location. This analysis identified reduced memory T cells, increased fibroblast, and altered cellular signalling were associated with resistance to immunotherapies.

#4622

Tumor microenvironment differences between lung cancer subtypes revealed by spatial transcriptomics

Matthew D. Wilkerson[1], Savannah Kounelis-Wuillaume[1], Camille Alba[2], Teri J. Franks[3], Martin L. Doughty[1], Robert L. Kortum[1], Robert F. Browning[1], Clifton L. Dalgard[1], Craig D. Shriver[1]. *[1]Uniformed Services University, Bethesda, MD,[2]Henry M. Jackson Foundation for the Advancement of Military Medicine, Bethesda, MD,[3]Joint Pathology Center, Department of Defense, Silver Spring, MD*

Lung cancer is a leading cause of cancer deaths worldwide and has complex underlying genetic drivers, subtypes and immune cell types. Molecular analysis of bulk tumors has repeatedly identified key somatic driver genes and subtypes in lung cancer. However, these key molecular strata of bulk lung tumors still contain significant heterogeneity which if characterized in finer detail may reveal new tumor microenvironment factors and lead to improved patient prognostication and therapy options. Here, we sought to compare the tumor microenvironments of lung adenocarcinoma (LUAD) and lung squamous cell carcinoma (LUSC) through spatial transcriptomics. Using four frozen lung tumors and three with replicated sections (n = 7), we sequenced spatial transcriptomes using the 10X Visium platform and illumina sequencing to measure up to 5,000 latticed-spots throughout 6.5 mm^2 of the tumor surface area. Data analysis revealed a large number of latticed-spots per tumor (median 3,486) with a large number of genes detected per median spot (tumor median 4,427). Through unsupervised clustering of spots in each tumor, we found between 8 and 10 clusters per tumor with distinct pathway activities, including multiple immune-enriched clusters per tumor (range: 3-5). Immune-enriched clusters in one LUAD tumor displayed a spatial shape consistent with tertiary lymphoid structures (TLS). Concordantly, this cluster overexpressed both B cell and T cell

pathways and as well as a TLS signature from liver cancer. Interestingly by bulk tumor RNA analysis, this TLS+ tumor was classified to be in the terminal respiratory unit expression subtype, which is an immune-mild bulk subtype. This supports that the TLS signal can be a unique property of spatial expression in lung cancer that may be unobservable by bulk tumor RNA sequencing. Then to compare global spatial heterogeneity among tumors, we calculated an index of expression spatial continuity and found LUSC tumors to have more contiguous expression patterns than LUAD tumors (mean 0.60 vs 0.54). We also quantified expression diversity across all tumor latticed-spots and found that LUSC tumors had greater values compared to LUAD tumors (mean 0.37 vs 0.27). Together, our results suggest that LUSC has a more contiguous and heterogeneous tumor expression microenvironment than LUAD. TLS are predictive of immune checkpoint inhibitor response in many other tumor types, and our results suggest that spatial transcriptomics may also identify this responsiveness in lung cancer. Future, larger cohorts of lung tumors are needed to determine recurrent spatial properties associated with patient outcome and treatment response. The views expressed in this abstract are solely of the authors and do not reflect the official policy of the Departments of Army/Navy/Air Force, Department of Defense, USUHS, HJF, or U.S. Government.

#4623

Single-cell spatial proteomic analysis of the tumor microenvironment in treatment-naive NSCLC samples with immunotherapy treatment and response data

Marie Cumberbatch[1], Geoffrey Ivison[2], Amy Lam[2], Aaron Mayer[2], Milan Bhagat[1]. *[1]TriStar Technology Group LLC, Washington DC, DC,[2]Enable Medicine, Menlo Park, CA*

The tumor microenvironment (TME) represents a complex network comprising a variety of cell types including immune, stromal, and extracellular elements in addition to malignant tumor cells. Growing evidence suggests that the spatial relationships of these components influence tumor progression and response/resistance to immunotherapeutic agents. However, the precise mechanisms driving this relationship to clinical outcomes remains poorly understood. This is in part because generating comprehensive spatial datasets has only recently been made

possible due to innovations in instrumentation, laboratory techniques, and data storage and processing. Thus, there has been little integration between various types of -omics datasets with spatial data. Here, we present a workflow for analyzing multi-omic data of the TME with the aim of providing mechanistic insights into signatures of response to immunotherapy. The workflow starts with data generation and proceeds through cell segmentation, quality filtering, phenotype assignment through unsupervised clustering, analysis of pairwise interactions and higher order multicellular structures (i.e., "neighborhoods"), and finally association with patient clinical and molecular data allowing for meaningful comparisons to be made. This analysis can be performed through the Enable Medicine Cloud Platform, a framework that facilitates the association of a multitude of data types to samples, rapid processing of multiplex images to deliver single cell spatial proteomic data, and graphical interfaces for each analysis step. To demonstrate the utility of this workflow, we generated spatial proteomic data for a tissue microarray (TMA) comprising a cohort of treatment naïve NSCLC samples (n=42) with second-line immune checkpoint inhibitor-treatment and clinical follow-up information. The spatial proteomics data was generated with the Akoya PhenoCycler-Fusion multiplexed tissue imaging platform, with an optimized panel of 51 oligonucleotide-conjugated antibodies covering a wide variety of immune, epithelial, stromal, and malignant cell markers developed by Enable Medicine. This proteomic data was then integrated with GeoMX DSP, bulk RNAseq, and clinical information using the Enable Platform. This framework for analysis allows for the comprehensive integration of both clinical and biological parameters to enable biomarker discovery and insight into signatures of response to immunotherapy. Acknowledgement: Pasteur Hospital, 30 Voie Romaine, 06000 Nice, France for NSCLC tumor samples.

#4624

Deciphering the tumor microenvironment at single-cell resolution using a workflow combining RNA transcript and protein detection with Brightplex®, a sequential chromogenic multiplex assay

Alex Trinh, Marion Olive, Aurélie Collignon, Maité Chamourin, Georgia Culley, Clemence Jaume, Vanina Leca, Assil Benchaaben, Giovanni

Bussotti, Alboukadel Kassambara, Jerome Galon, Jacques Fieschi.
Veracyte, Inc., Marseille, France

Tumor-infiltrating immune cells play an important role against cancer and are critical to control tumor growth and spread. Immunotherapy and immune checkpoint blockade, which aim to reinvigorate exhausted T cells have revolutionized cancer therapy. Despite inducing long-term response in many cancer types, these therapies remain ineffective for a majority of the patients. A better understanding of the tumor microenvironment, and in particular the characterization of immune cells and other stromal cells, along with their abundance and distribution, may help to better stratify patients and understand mechanisms of resistance to immunotherapy. Brightplex® is a chromogenic multiplex technology allowing the detection of several biomarkers on a single FFPE slide to identify and quantify complex cell populations such as T-cells expressing immune checkpoints, M1 and M2 macrophages, Treg cells and myeloid-derived suppressor cells. However, the exquisite characterization of some cell types within the tumor microenvironment or their activation status may require the identification of soluble proteins that cannot be detected by IHC. For example, the detection of secreted proteins such as cytokines or activation factors would allow one to determine the activation status of immune cells or cancer-associated fibroblasts (CAF). In that case, the detection of RNA transcripts corresponding to soluble biomarkers by In-Situ hybridization can be used as a substitute to protein detection.Here, we propose a new multiplex platform combining In Situ Hybridization (ISH) and immunohistochemistry (IHC) using Brightplex® technology. This platform allows the detection of several biomarkers that can be either RNA transcripts or proteins on a single FFPE tissue section. Thanks to that technique it is possible to: 1) detect and quantify TGFb in cancer associated fibroblasts, or IL-10 in immunosuppressive cells, 2) Quantify the level of RNA expression by individual cells, 3) assess the spatial distribution of activated cells based on complex phenotypes within the tumor or other regions of interest. This new workflow combining RNA transcript detection and proteins detection using Brightplex® is automated on Bond RX platform. Following staining and slide digitization, images are fused to create a virtual multi-channel image where cells of interest are detected by digital pathology (DP). Following cell detection, their densities and spatial distribution are obtained using R-

studio software.Integrated into an Immunogram, an analytics platform which integrates multi-omics datasets from Veracyte Biopharma Atlas, this new tool could be a powerful solution to understand the tumor landscape and predict response to immunotherapy and patient outcome.

#4625

A comprehensive guided workflow for highplex imaging, tissue segmentation, and multiplex cellular phenotyping for tumor microenvironment analysis

Brenna O'Neill[1], Smriti Kala[2], Sam Lim[2], Clinton Hupple[2], Nina Lane[2], Rasmus Norre Sorensen[1], Rasmus A. Lyngby[1], Alessandro Massaro[1], Andreas Hussing[1], Jeppe Thagaard[1], Johan Dore-Hansen[2], James Robert Mansfield[1]. *[1]Visiopharm, Horsholm, Denmark,[2]Standard BioTools, South San Francisco, CA*

The growth in cancer immunotherapy agents requires an understanding of the immune contexture of the tumor microenvironment (TME). Understanding immune contexture requires multiplex staining, imaging, and analysis to obtain multi-marker phenotypes of specific cells and analyze their biodistribution in the TME. Imaging Mass Cytometry™ (IMC) is the method of choice for single-step staining and highplex imaging of FFPE tissues. FFPE tissue is autofluorescent, which limits the utility of immunofluorescence methods. Lung and colorectal tissue (and bone, skin, etc) are highly autofluorescent, and therefore good targets for IMC. However, developments in analysis software for highplex imagery have not kept pace with imaging advances. We present a comprehensive workflow designed specifically for highplex image analysis, covering tissue segmentation, cell segmentation based on IMC DNA images, cellular phenotyping, and spatial analyses.
Lung and colorectal tissue sections with a 30-marker IMC panel of structural, tumor, stroma, immune cell, and immune activation markers were imaged (Hyperion+™, Standard BioTools). Highplex image analysis (Phenoplex™, Visiopharm) was performed as a multi-step workflow in a single software package that includes: conversion of IMC images to pyramidal format; easy visualization methods for displaying different marker subsets; a paint-to-train algorithm for tissue segmentation (into tumor, stroma, blood vessels, etc.); deep-learning-based nuclear

segmentation pre-trained on IMC DNA channels; cellular phenotyping based on thresholds based on visual assessment of positivity; spatial biodistribution metrics for cell populations; and a flexible set of outputs for downstream analysis. Tissue segmentation was used to divide the tissue into tumor, stromal, and tumor margin regions, and these regions were used to compare the immune contexture through a series of t-SNE images partitioned by spatial region.
We demonstrate that a simple analysis workflow can be used for highplex images of different tissue types by users with no programming knowledge. Visualization templates for the marker subsets and the pre-trained IMC nuclear segmentation are reusable. A new tissue segmentation algorithm for each tissue type is required, as are new thresholds for biomarker positivity. Spatial biodistribution metrics, heatmaps and partitioned t-SNE plots were generated for each tissue type with a minimum of work.
Highplex IMC imaging of lung and colorectal tumor samples is a simple and effective means of obtaining high-parameter images without interfering autofluorescence. Having a comprehensive workflow for the analysis of this complex data makes obtaining useful results from highplex images more accessible to biologists and immunologists by circumventing the requirement for expert programming for each specific application.

#4626

Spatial profiling of the tumor microenvironment in head and neck cancer identifies immune checkpoints and proteins involved in cell death signaling biomarkers of immunotherapy response

Habib Sadeghirad[1], Ning Liu[2], James Monkman[1], Chin Wee Tan[2], Caroline Cooper[3], Jeni Caldera[4], Sarah Church[5], Fabian Schneider[4], James Robert Mansfield[4], Ken O'Byrne[3], Melissa Davis[2], Brett Hughes[6], Arutha Kulasinghe[1]. *[1]The University of Queensland, Brisbane, Australia,[2]The Walter and Eliza Hall Institute, Melbourne, Australia,[3]The Princess Alexandra Hospital, Brisbane, Australia,[4]Visiopharm, Horsholm, Denmark,[5]Nanostring, Seattle, WA,[6]The Royal Brisbane and Women's Hospital, Brisbane, Australia*

Immune checkpoint inhibitors (ICIs) Pembrolizumab and Nivolumab have shown promising results in patients with recurrent or metastatic (R/M) head

and neck squamous cell carcinoma (HNSCC). Nonetheless, only up to 20% of patients may benefit from them. Next generation predictive biomarkers of response to ICI therapies are currently needed.
This retrospective study profiled pre-treatment tissue samples collected from R/M HNSCC patients (n=30) treated with Pembrolizumab or Nivolumab. Targeted spatial proteomics profiling was performed using NanoString's GeoMx® Digital Spatial Profiler (GeoMx). To develop an informed region-of-interest (ROI) selection strategy for the GeoMx, we analyzed H&E images from serial sections and performed Oncotopix® Discovery software, which considered pathology inputs and machine learning to analyze H&E imagery and 4-channel GeoMx visualization inputs. We profiled 80 proteins simultaneously using the GeoMx across modules in cell death, immune activation, immune cell typing, immuno-oncology drug target, immune profiling, PI3K/AKT signaling, and pan-tumor markers. . Next, we performed differential expression (DE) analysis of the proteins localized in the tumor and stromal compartments against response to therapy parameters of complete, partial, stable and progressive disease (according to RECIST criteria).
Four-channel GeoMx immunofluorescence images provided per-ROI cell counts (total and phenotyped based on 3 markers), and these data were used to aid in area and cell count normalization within the tumor and stromal compartments. We found that patients responsive to immunotherapy had higher expression levels of PD-L1, Bcl-2, BCLX, and BIM in the tumor, whereas VISTA, FOXP3, and CD66b were downregulated. In the stromal compartment, it was found that responders had higher expression levels of B7-H3, CD40, and SMA, but lower expression of PARP, S100B, and NY-ESO-1 in comparison to non-responders. In terms of best response analysis, patients with PR (n=5) had higher levels of PD-L1, ER-alpha, and CD68 expression, but lower levels of VISTA, CD27, and CD95/Fas in tumor regions than patients with PD (n=8). In the stroma, PD-L1, CD68, and HLA-DR were upregulated, while VISTA, BIM, and BAD were downregulated in patients with PR versus those with PD.
We found that informed ROI selection strategy aided in defining key features in the tumor microenvironment for comparative analysis across samples, and for data normalization methods. Moreover, we found that immune checkpoints and proteins involved in cell death signaling play

important roles in the immune responsive tumor microenvironment of HNSCC based on response to immunotherapy.

#4627

Immune profiling of immunotherapy and adjuvant chemotherapy pretreatment NSCLC tissues by CODEX

James Monkman[1], Afshin Moradi[1], Connor O'Leary[1], Zhenqin Wu[2], Steven Hamel[2], David Mason[3], Fabian Schneider[3], James Robert Mansfield[3], Aaron Meyer[2], Ken O'Byrne[4], Arutha Kulasinghe[1]. *[1]The University of Queensland, Brisbane, Australia,[2]Enable Medicine, Menlo Park, CA,[3]Visiopharm, Horsholm, Denmark,[4]The Princess Alexandra Hospital, Woolloongabba, Australia*

Non-small cell lung cancer (NSCLC), including adenocarcinoma and squamous cell carcinoma subtypes, is a leading cause of cancer deaths worldwide. Treatment of NSCLC has advanced from chemotherapy modalities to the use of immunotherapy, namely immune checkpoint inhibitors (ICIs) which enhance the adaptive immune response against tumour cells. Thus, while the immune cell composition of tumours and its influence on treatment outcomes is poorly understood, it likely holds the key to effective, personalized treatment regimens.

Here we profiled an adjuvant chemotherapy (n=61) as well as a second line immunotherapy (n=42) NSCLC cohort by the Phenocycler CODEX technology (highplex spatial proteomics) to investigate the association between immune composition and patient outcome. We applied a panel of 38 markers to delineate naïve, memory, cytotoxic and hyperactivated T cell states, as well as B cells, Tregs and myeloid lineage innate immune cell types. Our study sought to understand the heterogeneity of tumour-immune composition across patients and investigate the spatial neighbourhoods and clusters that these cells inhabit within TMA cores. We used Phenoplex™ software for tissue segmentation (into classes for tumor, stroma, artifacts, blood vessels, etc.), cellular segmentation, and cellular phenotyping based on thresholds for each marker, and then performed spatial analyses (distances, interactions, neighborhoods) using SpatialMap[1] to identify cellular motifs associated with clinical phenotypes.

Our study has identified spatial features associated with immune contexture linked to therapy outcome in both chemotherapy and immunotherapy

modalities. Taken together, our study demonstrates the utility of spatial proteomics to identify cellular features associated with outcome to therapy in lung cancer.

1) Trevino A, Ivison G, Hamel S, Chiou A (2022). SpatialMap: Analysis of Spatial Biology Data. R package version 0.4.57.

#4628

Profiling the tumor microenvironments of triple- and quadruple-negative breast cancers

Geetanjali Saini[1], Manali Rupji[2], Mahak Bhargava[1], Sunil Badve[3], Ritu Aneja[1]. *[1]Department of Clinical and Diagnostic Sciences, School of Health Professions, University of Alabama at Birmingham, Birmingham, AL,[2]Emory University, Atlanta, GA,[3]Department of Pathology and Laboratory Medicine, Emory University School of Medicine, Atlanta, GA*

Triple-negative breast cancer (TNBC) is a heterogeneous breast cancer subtype that lacks expression of estrogen receptor, progesterone receptor, and human epidermal growth factor receptor 2. Approximately 15%-20% of breast cancers are triple-negative. Based on expression of the androgen receptor (AR), TNBC can be categorized as AR-positive (AR+ TNBC) or AR-negative (quadruple-negative breast cancer, QNBC). Studies have reported that the loss of AR expression is associated with poor prognoses. Recent evidence suggests that QNBCs disproportionately affect women of African descent and contributes to poor overall survival. QNBC is a more aggressive disease compared to TNBC, and patients with QNBC currently have no treatment options beyond chemotherapy. Data from interrogating public databases such as TCGA indicates that QNBC is distinct from TNBC in molecular makeup, particularly in immune tumor microenvironment. Currently, QNBC is not considered distinct from the broader TNBC subtype, hence a comprehensive molecular characterization is lacking. We aim to examine differences between the TNBC and QNBC tumor microenvironments that consist of both immune and stromal components. We analyzed RNA expression data from the METABRIC (TNBC= 11, QNBC= 185) and TCGA (TNBC= 29, QNBC= 103) datasets. Based on AR transcript expression, patients with TNBC were stratified into AR-low (considered QNBC) and AR-high (deemed ‘true’ TNBC) groups. The analytical immune tools - CIBERSORTx and xCELL were used to analyze

the RNA-Seq data. CIBERSORTx can distinguish 22 mature human hematopoietic populations and provides abundance of member cell types in a mixed cell population, from gene expression data. xCELL is a gene signature-based method that can perform cell type enrichment analysis from gene
expression for 64 immune and stromal cell types. Thus, xCell can discriminate between closely related cell types. Using these immune tools, the tumor microenvironments of the TNBC and QNBC groups were compared. Correlations between individual immune and stromal components with patient survival probability were assessed. Significant differences (p-value <0.05) in several immune and stromal cell types were noted when comparing the TNBC and QNBC groups within these datasets. CIBERSORTx and xCELL yielded both unique and common sets of cell types. Notably, significant differences in the stroma score (a composite score of stromal cell types provided by xCELL) were observed between TNBC and QNBC in both the METABRIC and TCGA datasets. These immune tools are based on different methodologies and our results show that they can provide complementary information. Our data suggest that QNBC and TNBC have distinct tumor microenvironments, and that QNBC should be considered as an independent breast cancer subtype that warrants comprehensive characterization.

#4629

Heterogeneity in glioblastoma tumor microenvironment: Opportunities for new therapies

Sandra Delebecq, Adele Ponzoni, Richard Ruez, Corinne Ramos, Jonathan Stauber. *ImaBiotech, Loos, France*

Background: Glioblastoma (GBM) is the most common and aggressive form of brain tumor, characterized by a poorly accessible microenvironment that render it notoriously hard to treat. The insufficient treatment success is, in large parts, due to its tremendous molecular heterogeneity, which affects the overall prognosis and response to therapies. The significant intra- and inter-tumor microenvironment (TME) composition heterogeneity plays a crucial role in GBM progression. Mostly due to this high, multifactorial immunosuppression occurring in the microenvironment, the efficacy of immunotherapy in GBM is low. Focusing on characterizing the components

of different TMEs to evaluate their molecular and cellular component heterogeneity has a significant advantage to target group of cancer patients that would normally be resistant to immunotherapy.
Methods: Deep spatial transcriptomics profiling was performed on non-treated glioblastoma human tissue microarrays (TMA) using NanoString's *GeoMx* Digital Spatial Profiler (*DSP*). 6 tumor tissues from 6 different patients were hybridized and analyzed with the Whole Transcriptomic Atlas (WTA) panel that includes 18,000 genes. Three regions of interest (ROIs) were selected per tissue sample. All the statistical analysis were performed with GeoMx® DSP Analysis Suite. Cell deconvolution using the SpatialDecon® algorithm (Nanostring®) was then performed to estimate mixed cell type abundance in the spatially-resolved gene expression defined segments.
Results: Spatial transcriptomic analyses revealed that glioblastoma tumors varied dramatically in their global gene expression profiles and suggested the existence of differential gene expression among the tumors highlighting the inter-tumors heterogeneity of glioblastoma. Interestingly, different areas of the same tumor did not display distinct molecular profiles. Upregulation of stromal collagen genes was significantly detected in some patient specifically the fibrillar collagens type I, III and VI. Those findings indicated excessive collagen depositions in the surrounding of the tumor for some patient characteristic of tumor progression and involvement of cancer associated fibroblasts (CAFs) in the dysregulated collagen turnover leading to tumor fibrosis.
Conclusion: As a cold tumor, malignant glioma has strong immunosuppression and immune escape characteristics. The TME provides the “soil” for the survival of malignant tumors, and recent studies have highlighted a major role for cancer-associated fibroblasts (CAFs) in promoting immunotherapy resistance by excluding T cells from tumors in the TME. Here the spatial transcriptomic analyses allowed a better phenotypical stratification of the cancer patient. In some, targeting CAFs would improve the TME and enhance the efficacy of immunotherapy.

#4630
Deep Immuno-profiling of syngeneic tumor mouse models for preclinical studies

Anais Joachim[1], Emilie Maturin[1], Marielle Mello[2], Lillia Hadjem[2], Magali Grange[2], Olivier Deas[3], Ana Zarubica[1], Bernard Malissen[1], Hervé Luche[1].
[1]Immunomics, JC DISCOVERY, Marseille, France,[2]Immuno-Phenotyping Module, CIPHE, Marseille, France,[3]R&D Lab Head, Xentec, Evry, France

Identification of major cellular players involved in progression of cancer is key to success of new immunotherapies. It is however a daunting challenge due to the complex interplay between tumor cells and the immune system. Component of innate and adaptive immunity may be directed to a pro- or anti-tumor function. In order to cope with the complexity of the tumor microenvironment (TME), it is necessary to use an experimental approach characterizing the heterogeneity of cell types, the evolution of their relative proportion and their fine-tuned functional specificity. This approach should lead to the identification of new cellular biomarkers characteristics of different stages of tumor cancer progression.
To decipher the impact of immunotherapy treatments, cellular phenotyping of leukocytes infiltrating TME but also those present in peripheral organs is necessary. In order to increase our understanding in the precise mode of action of anti-PD1 treatment at the cellular level in sensitive and unsensitive syngeneic models, we investigated immunophenotypes and responses to immune checkpoint inhibitor (ICI) of several hallmark tumor models (MC38, CT26, B16F10, B16-OVA, RENCA, EMT6) in immunocompetent mouse models by flow and mass cytometry. We compared growth kinetics and profiled the immune cell composition of tumor microenvironment (TME), draining lymph node (dLN) and blood in order to establish immune-phenotypic cell signatures that correlates with treatment efficacy. Supervised, unsupervised and integrative data analysis arewere used to identify significant changes across different experimental settings. Our results indicate that each model possesses a unique tumor-immune infiltrate profile that can be modulated with immunotherapies. Overall, these studies provide an important resource of highly well-characterized syngeneic tumor model and highlight the importance of tumor immune landscape changes across models that will drive selection of the most appropriate model to test novel immunotherapeutic agents and enhance our translation of knowledge from syngeneic models to human tumors.

#4631

Multiplex IHC assay to explore regional heterogeneity of FAP and inflammatory cell density in localized prostatic adenocarcinoma

Fernanda Caramella Pereira[1], Alan K. Meeker[2], Kenneth Pienta[3], Qizhi Zheng[1], Tracy Jones[1], Srinivasan Yegnasubramanian[4], Jessica L. Hicks[1], Sujayita Roy[1], Angelo M. De Marzo[2], W. Nathaniel Brennen[3]. *[1]Department of Pathology, Johns Hopkins University School of Medicine, Baltimore, MD,[2]Departments of Pathology, Oncology, and Urology, The Sidney Kimmel Comprehensive Cancer Center at Johns Hopkins and the James Buchanan Brady Urological Research Institute., Baltimore, MD,[3]Departments of Oncology, and Urology, The Sidney Kimmel Comprehensive Cancer Center at Johns Hopkins and the James Buchanan Brady Urological Research Institute., Baltimore, MD,[4]Departments of Pathology, Oncology, and Urology, The Sidney Kimmel Comprehensive Cancer Center at Johns Hopkins and the James Buchanan Brady Urological Research Institute, Baltimore, MD*

Cancer-associated fibroblasts (CAFs) expressing FAP promote tumor growth, invasion and immune suppression. FAP is a molecular imaging target in cancer and its protease activity is a potential anti-cancer drug target. While FAP expression was associated with biochemical recurrence after prostatectomy using tissue microarrays (TMAs)(DOI:10.1158/2767-9764.CRC-21-0183), its expression has not been comprehensively correlated with morphological features of disease aggressiveness beyond grade. 48 cases of localized prostatic adenocarcinoma were used for a multiplex immunohistochemical assay that included FAP, CD45, CD163, p63 and Keratin 8. Each of these markers were individually optimized by single-plex staining and were then performed as an iterative IHC assay (PMID:35188986) and quantification was performed using the HALO image analysis platform (Indica Labs). We developed a second multiplex assay including FAP, vimentin, smooth muscle actin, desmin, CD31, S100, keratin 8 and p63. FAP IHC staining was analytically validated using a series of positive and negative cell lines. In normal appearing (non-inflamed) prostate regions, FAP expression was negative. By contrast, upregulation of FAP was observed in the stromal compartment in regions of chronic inflammation and some proliferative inflammatory atrophy (PIA) lesions. In tumor regions, only 1 case was totally negative for FAP. Except for 2 cases, in which there was focal weak tumor cell staining, all FAP

expression was present in the tumor stromal compartment (TSC). The vast majority of FAP expression was associated with Vim+/Des- fibroblasts, which at times were also positive for SMA (Vim+/Des-/SMA+), indicating they are myofibroblasts. There was very infrequent FAP expression associated with M2 macrophages, endothelial cells, nerves and vimentin-negative smooth muscle cells, indicating that the majority of FAP expression occurs in fibroblasts. Preliminary quantitative data using visual estimations of the fraction of TSC expressing FAP (range, 0-80%, mean=35.8%, median=30%, SD=23.7) was not associated with the overall GS/grade group, but was associated with non-organ confined disease. Furthermore, there was a trend towards increased FAP expression in cases showing intraductal carcinoma and large cribriform formation. Ongoing studies are in process to obtain quantitative data by image analysis and to correlate FAP expression with the presence of overall inflammatory cell density and the density of M2 macrophages. Additionally, we will characterize the cases in terms of molecular features including TMPRSS2-ERG status and PTEN genomic status. Future use of these panels will facilitate studies of associations of FAP with clinical outcome, MRI and PET imaging, response to specific treatments and to help characterize FAP as a predictor of response to emerging FAP inhibitors and FAP-targeted prodrugs.

#4632

Spatial whole transcriptome analysis of differential expression for biomarker discovery in colorectal cancer

Elim Cheung, Vidyodhaya Sundaram, Baowen Zhang, Lutong Zhang, Tong Lu. *BioChain Institute, Inc., Newark, CA*

Background**:** Colorectal cancer (CRC) is one of the leading causes of cancer death, which is frequently caused by genetic or epigenetic changes. The study of tumor microenvironment (TME) profiling may provide a better knowledge of spatial gene expression patterns of known CRC markers, visualize the cell composition and localization, and serve to aid the understanding of the mechanisms of tumor formation. BioChain Institute, Inc. is currently investigating the TME profiling of CRC through tissue-wide, whole transcriptome analysis for the ability to discover potential therapeutic targets.

Methods: BioChain's formalin-fixed paraffin-embedded (FFPE) tissue samples from 3 primary colon adenocarcinoma tumors (PT), and their matched adjacent normal tissues (PN), were used to investigate the TME. The images of Hematoxylin and Eosin (H&E)-stained tissue sections were annotated by our pathologist. The spatial whole transcriptome was analyzed using 10x Genomics Visium Spatial Gene Expression for FFPE. This assay provided about 5,000 spatially barcoded spots with mRNA-binding oligonucleotides to capture the gene expression. The integration of the imaging and sequencing data enabled a spatially resolved transcriptome of CRC heterogeneity.
Results: The annotations of both PT and PN tissue samples were found to be correlated with the spatial gene expression clustering. With the overlaying of total gene counts for each spot on the H&E-stained tissue image, about 16,000-17,000 genes were detected in each sample. The median of ~5,500 and ~1,600 genes per spot were expressed in PT and PN samples respectively. The study of gene expression levels revealed the overexpression of several well-known CRC markers (APOE, SCD, IGFBP3, TIMP1, SPARC) and the down-regulation of numerous markers (DES, CA1, KLF4) in PT samples significantly.
Conclusion: Our spatial analysis results provide insight into tumor heterogeneity, spatial organization of cells within the TME and biomarker identification. BioChain is in a unique position to facilitate researchers with a plethora of oncologic and other diseased tissue types, as well as the spatial whole transcriptome analysis. Our study enables the understanding of the TME, discovery of potential diagnostic and prognostic targets, especially for the development of personalized therapy.

#4633

Quantitative spatial profiling of NSCLC subtypes across tumor stages using 6-plex multiplex imaging technology and AI-powered phenotyping analysis

Lorcan Sherry[1], Nicole Couper[1], Bethany Remeniuk[2], Karen McClymont[1], Bei Hopkins[2], Natalie Monteiro[2], Gabriel Reines March[1], Darren Locke[2].
[1]OracleBio Ltd, Glasgow, United Kingdom,[2]Akoya Biosciences, Marlborough, MA

Non-small cell lung cancer (NSCLC) is a complex disease with varying pathological subtypes including adenocarcinomas and squamous cell carcinomas. After diagnosis, tumor staging provides important information about the extent of cancer in the body and anticipated response to treatment. NSCLC patients can have impaired immune responses within the tumor microenvironment (TME), leading to a progression of tumor growth and poorer prognosis. Accurate cell phenotyping combined with spatial profiling of the immune contexture and checkpoint expression, can provide a deeper understanding of complex cellular interactions underpinning the tumor-immune response. The aim of this study was to utilize spatial multiplexed imaging technology and associated data analysis methods to profile the immune contexture, as well as their spatial interactions with the tumor, in a set of tissue cores covering a range of NSCLC subtypes and tumor staging. Formalin-fixed paraffin-embedded (FFPE) NSCLC tissue microarrays (TMA), comprised of n=41 cores containing a range of carcinomas and pathological Tumor-Node-Metastasis (pTNM) stages (I-IV), were stained on a Leica Bond RX™ using the Akoya PhenoCode™ Signature Immuno-contexture Human Protein Panel, which includes markers for CD8, CD68, PD-1, PD-L1, FoxP3, and PanCK as a tumor indicator. Stained TMAs were scanned at 20x magnification on a PhenoImager HT multispectral imaging system. Image analysis was performed using Visiopharm software. Deep learning algorithms were applied to segment tumor and stroma regions of interest (ROI) and to accurately detect and classify specific cell phenotypes. Cell object data files *per* core were exported for spatial and neighborhood analysis using OracleBio's proprietary python-based program, PhenoXplore. Immune cell counts, phenotypes and spatial interactions were generated within tumor and stroma ROI *per* core. Data included total and negative cell phenotype counts, cell density in tumor and stroma, as well as cell distance and neighborhood spatial interactions *per* core across NSCLC subtypes and stages in the TMA set. The combination of high-quality staining provided by the PhenoCode™ panel, coupled with deep learning quantitative phenotyping and spatial pattern analysis enables detailed characterization of the complex cellular interactions, at both the functional and spatial level, within the TME of NSCLC tissue. Data generated will support a greater understanding of the complex cellular interactions that can contribute to

progression of NSCLC and may help guide future precision medicine strategies.

#4634

Identifying and analyzing tumor subtypes using custom morphology markers for NanoString® GeoMx® Digital Spatial Profiler

Jessica Runyon[1], Vijay Baichwal[2], Weston Stauffer[2], Christian Nievera[1].
[1]Canopy Biosciences, St. Louis, MO,[2]Canopy Biosciences, Hayward, CA

Molecular subtyping studies have allowed the allocation of cancer into groups based on similar molecular, morphological, and clinical characteristics. Such studies are critical to help researchers identify actionable targets for drug design and biomarkers to predict therapeutic response. Based on multi-omics data, various approaches have been used to identify and analyze tumor subtypes and their correlation with tumor immunity and immunotherapy success. The NanoString GeoMx Digital Spatial Profiler is one approach that combines morphological context with spatial transcriptomics on a single tissue specimen. A critical step in this approach involves staining with morphology markers to identify relevant regions of interest (ROIs) for analysis. Yet, widespread adoption of GeoMx DSP has revealed a significant limitation, namely that researchers base transcriptional analysis of thousands of RNA targets on the spatial information provided by only a few morphology markers. Recent efforts have greatly expanded the availability of morphology markers to facilitate cell type-specific analyses. To evaluate the ability of this technology to selectively enrich specific cell types, we developed custom morphology markers to stain non-small-cell lung cancer (NSCLC) tissue specimens of various subtypes. Focusing on squamous cell carcinoma and adenocarcinoma, we stained with P40 and TTF-1 and transcriptionally profiled cell type-specific ROIs with the Cancer Transcriptome Atlas panel. Differential gene expression analysis of the whole transcriptome was performed using GeoMx DSP Analysis Suite software. The data reveal differences in gene expression in several key cancer pathways between tumor subtypes are correlated with the presence or absence of specific cell types. The data support the use of custom morphology markers for cell type stratification in tumor subtypes, providing more meaningful gene expression analysis. Ongoing work continues to explore the utility of this

technology for cell type-specific gene expression analysis within different tumor subtypes.

#4635

Single cell definition of the immunogenic synapse between the tumorigenic schwann cells and tumor associated macrophages in Plexiform Neurofibroma

Thomas J. On, Xiyuan Zhang, Shahroze Abbas, John Shern. *Pediatric Oncology, NIH-NCI, Bethesda, MD*

Background**:** Patients with Neurofibromatosis Type 1 (NF1) frequently develop benign tumors called Plexiform neurofibromas (PN). Macrophages compose 30-50% of the total cellular composition of PNs and have previously been shown to play a critical role in the PN development and growth. This study defines components of the immunogenic synapse between the neoplastic Schwann cell and the tumor associated myeloid compartment and investigates alterations of the synapse during treatment with MEK inhibition (MEKi). The IL34-CSF1R axis is nominated as a key node in the maintenance of the tumor associated macrophages in PN.
Methods: In this work, we applied single cell RNA sequencing (scRNAseq) to human primary tumor PN samples to comprehensively evaluate tumor cellular populations and their interactions. Resulting cellular populations were compared to a single cell atlas of tumor associated immune cells taken from a panel of tumor types. Ligand and receptor interactions were informatically extracted from scRNAseq data and immunohistochemistry was used to validate scRNAseq observations. scRNAseq was also used on pre and post treatment samples taken from three patients receiving the MEKi Selumetinib. Human primary macrophage cell cultures and qPCR were used to interrogate the roles of the IL34-CSF1R signaling and MEKi in PN.
Results: scRNAseq generated data on 45101 PN myeloid cells. Integration of these cells with a publicly available tumor atlas of 11 different tumors containing a total of 52195 cells discovered correlation of cell populations between the PN as compared to other tumor types. Tumor-promoting (M2) macrophages represented the largest portion (48%) of the PN myeloid population. Receptor-ligand analysis using cellphoneDB highlighted IL34-CSF1R ($p<.0001$), TNF-TNFRSF1A ($p<.0001$) and SIRPA-CD47

(p<.0001) as significant interactions between the neoplastic Schwann cell and macrophages. IL34 and CSF1R protein expression was confirmed in human PN tumors with immunohistochemistry. scRNAseq data from NF1 patients PN tumors taken pre and post MEK inhibitor treatment, demonstrated decreased M2 macrophage gene expression of CD163(p<.001), MRC1(p<.001), TREM2(p<.001) after treatment. Finally, IL34 stimulated primary human monocytes produced macrophages with an M2-like phenotype. MEKi treatment of these macrophages resulted in increased expression of inflammatory macrophage genes CXCL9 (p<.05), CXCL10(p<.001), IDO1(p<.001).
Conclusions: PN myeloid populations contain large amounts of M2 macrophages with expression profiles consistent with TAM seen in a variety of malignant tumors. We postulate that IL34 expression by the neoplastic Schwann cell leads to expansion and maintenance of this TAM population. MEKi treatment on human PNs reduces number of macrophages in PNs and shifts macrophage gene expression towards inflammatory genes.

#4636
High-plex co-detection of RNA and protein to explore tumor-immune interactions utilizing RNAscope with Imaging Mass Cytometry
James Pemberton[1], Smriti Kala[1], Anushka Dikshit[2], Clinton Hupple[1].
[1]Standard BioTools, Markham, ON, Canada,[2]Advanced Cell Diagnostics, Inc., Newark, CA

Purpose The next breakthroughs in immuno-oncology will be driven by high-plex tools that decipher the spatial arrangement of different cell types within the tumor microenvironment (TME). Imaging Mass Cytometry™ (IMC™) is a proven tool for the study of complex cellular interactions in the TME. It utilizes CyTOF® technology for simultaneous assessment of 40-plus protein markers at subcellular resolution without spectral overlap or background autofluorescence, thus providing unprecedented insight into the organization and function of the TME. Despite this, some protein targets are challenging to include in IMC as they have very few or no commercial antibodies available. Moreover, although cellular identity can easily be deciphered through detection of protein targets, knowledge of the cell's transcriptome improves understanding of cellular function and activation

state. Here, we present a robust and reliable workflow that combines the highly sensitive and specific RNAscope™ technology for RNA detection with the multiplexing capability of IMC to visualize key RNA and protein markers in the same tumor samples.
Methods The RNAscope HiPlex v2 assay was combined with protein detection on the Hyperion+™ Imaging System to evaluate expression of both RNA and protein targets in formalin-fixed, paraffin-embedded (FFPE) tumor tissue microarray (TMA). The RNAscope assay was used with 12 target RNA marker probes and associated metal-labeled detection probes, suitable for use in IMC. The RNAscope HiPlex v2 assay workflow was followed as recommended up until applying the fluoros. Instead of using the fluoros, metal-conjugated probes were used for RNA detection. Metal-conjugated antibodies were used for protein detection in the same tissue.
Results Target protein markers identified a range of immune cells, tumor cells, stromal cells, endothelial cells, and extracellular matrix. Co-detection of RNA and protein allowed visualization of several cytokines and chemokines, such as *CXCL13, CXCL9, CXCL10, IFNγ, IL10, IL8*, and *IL1B*, enabling the identification of the cellular source of these secreted factors. Additionally, immune cell subpopulations and their activation states were visualized using marker-specific antibodies. Immune cell hubs associated with anti-tumor immune responses were detected in tumor niches across the TMA.
Conclusions Overall, combining RNAscope with protein co-detection on the IMC platform allowed simultaneous visualization of RNA and protein targets to interrogate the tumor microenvironment. The single-cell resolution offered by the RNAscope assay provides superior sensitivity for RNA detection in addition to the existing protein-detection capability of the IMC platform. This workflow can be applied to FFPE tissues to study therapeutic efficacy, stratify patients based on inflammatory signature, and study cell-cell interactions within the TME.

#4638
Integrative spatial analysis of paired IHC and H&E images identifies Foxp3 enriched tumor-infiltrating lymphocytes associated with disease-free survival in human papillomavirus (HPV)-related oropharyngeal squamous cell carcinoma

Sumanth Reddy Nakkireddy[1], Inyeop Jang[2], Minji Kim[2], Linda X. Yin[3], Michael Rivera[4], Joaquin J. Garcia MD[4], Kathleen R. Bartemes[3], David M. Routman[5], Eric J. Moore[2], Daniel J. Ma[5], Kathryn M. Van Abel[6], Tae Hyun Hwang[7]. *[1]1Department of Artificial Intelligence and Informatics, Mayo Clinic Florida, Jacksonville, FL,[2]Department of Artificial Intelligence and Informatics, Mayo Clinic Florida, Jacksonville, FL,[3]Department of Otolaryngology-Head and Neck Surgery, Mayo Clinic, Rochester, MN,[4]Department of Laboratory Medicine and Pathology, Mayo Clinic, Rochester, MN,[5]Department of Radiation Oncology, Mayo Clinic, Rochester, MN,[6]1Department of Artificial Intelligence and Informatics, Mayo Clinic, Jacksonville, FL,[7]Department of Artificial Intelligence and Informatics, Mayo Clinic, Jacksonville, FL*

Background: Recent studies support that high levels of tumor-infiltrating lymphocytes (TILs) were associated with better prognosis in HPV(+) oropharyngeal squamous cell carcinoma (OPSCC). While these studies provide a potential role for TILs as a prognostic biomarker, the analyses were relied on manual quantification performed by pathologists, resulting in inter-observer variability. Deep Learning (DL)-based whole slide hematoxylin and eosin (H&E) image analyses may overcome these challenges. However, this analysis only provides the presence of cell types without consideration for the functional roles of each cell within the tumor immune microenvironment (TME). In this work, we develop a computational pipeline to integrate paired H&E and immunohistochemistry (IHC) images to functionally characterize TILs and investigate their prognostic utility.
Methods: We analyzed 88 patients: 42 stage I, 39 stage II, and 7 stage III. Our data contain both H&E and IHCs examining FoxP3, CD3, PD-L1, CD20, etc. on serial sections of the tissue. In-house DL-based H&E analysis used to identify TILs, tumors, and stroma in each tumor, then performed registration between adjacent H&E and IHC images from the same tissue. The patients were then classified into three basic immune phenotypes: immune inflamed (IN; high TILs in the tumor region), immune excluded (EX; TILs are mostly localized in stroma), and immune desert (ID; few/no TILs) based on TIL enrichment in the TME. To functionally characterize TILs, we quantified protein expression from the adjacent IHCs.

For example, we further classified each patient into different subtypes based on enriched protein expression (e.g., FoxP3 high IN, FoxP3 low IN). We used the Kaplan-Meier method and multivariate Cox analysis to evaluate the prognostic value of different subtypes enriched with different proteins to predict disease-free survival (DFS).
Results: The IN group with 43 patients was significantly associated with good prognosis. Interestingly, further stratification of the IN subgroup based on Foxp3 quantification on TIL regions (i.e., high FoxP3 IN and low FoxP3 IN) showed that high protein expression of FoxP3 in TILs in the IN subgroup is significantly associated with a better prognosis compared to other immune subgroups (HR, 0.16; p-value, 0.003). Multivariate analysis, including other clinical covariates showed that the immune subtypes associated with high FoxP3 are independently associated with DFS. These results demonstrate that DL-based integrative IHC and H&E image analysis could be used to identify subgroups with distinct clinical outcomes. Furthermore, our results reveal unknown roles for Foxp3 expression in the TILs in HPV(+) OPSCC as a prognostic biomarker, a finding which should be evaluated in a larger cohort.

#4639

Single-cell immunoprofiling and spatial analysis of hormone receptor subtypes in HER2+ and HER2low breast tumors using multiplexed immunofluorescence

Anna Juncker-Jensen[1], David Tallman[2], Harry Nunns[1], Heather Lefebvre[2], Karen Yamamoto[1], Katharine A. Collier[2], Mark Vater[2], Ava Strahan[2], Ava Willoughby[2], Olivia Bouchard[2], Madison Kingsbury[2], Mathew Cherian[2], Ashley C. Pariser[2], Preeti K. Sudheendra[2], Bhuvaneswari Ramaswamy[2], Margaret Gatti-Mays[2], Ainura Kyshtoobayeva[1], Zaibo Li[2], Daniel G. Stover[2]. *[1]NeoGenomics, Aliso Viejo, CA,[2]The Ohio State University, Columbus, OH*

Background: Breast cancer is characterized by distinct molecular subtypes based on expression of estrogen and progesterone hormone receptors (ER and PR), and epidermal growth factor receptor 2 (HER2). To investigate presence and location of distinct immune cell populations on single cell level we utilized the multiplexed immunofluorescence (mIF) platform MultiOmyx to investigate the tumor immune microenvironment (TME) in

HER2+ breast cancer. We have built on growing data implicating distinct immunophenotypes in the breast cancer TME with breast cancer outcomes by profiling 1) prevalence; 2 location (e.g. intratumoral, stromal); 3) phenotype (e.g. activated, exhausted) of infiltrating immune cells.
Methods: We optimized a custom 26-marker MultiOmyx panel interrogating HER2 IF expression, HER2 signaling, and immune markers. This mIF platform leverages serial IF image capture to allow concurrent profiling of all 26 markers on a pathologic section at single cell resolution. We applied the 26-marker panel to a tissue microarray of 208 unique patients with matched tumor/normal tissue cores (1-4 cores/patient; total 333 tumor and 307 normal cores). HER2-positive was defined via ASCO/CAP guidelines; HER2-low was defined as HER2 immunohistochemistry (IHC) 1+/2+ but HER2 in-situ hybridization (ISH) negative.
Results: The 208 unique tumors profiled included 88.9% (185/208) HER2-positive and 11.1% (23/208) HER2-low; 62.5% (130/208) hormone receptor (HR) positive and 37.5% (78/208) HR negative. Median follow-up from diagnosis was 143 months. Among HER2-positive patients, 98.9% (n=183/185) received HER2-directed therapy in the (neo)adjuvant or metastatic setting or were diagnosed prior to FDA approval of trastuzumab for early stage disease. In sum, from 1166 regions of interest in 640 total cores, a total of 1,076,700 single cells were profiled via the 26-marker panel. Tumors categorized based on HR and HER2 reflected distinct immunophenotype. Relative to HR+HER2low, HR-HER2low tumors had a significant increase in the density of T cells (CD3) and tumor-associated macrophages (TAMs) (CD68). The increase in T cells was observed for T helper (CD3+CD4+), T regulatory (CD3+CD4+FoxP3+), as well as T cytotoxic cells (CD3+CD8+). Observed increases in pro-tumorigenic M2 TAM density (CD68+CD163+) were observed for both HR negative subtypes when compared to HR+HER2+ and HR+HER2low groups, indicating a negative correlation between M2 TAM infiltration and ER/PR status. HER2low tumors had significantly lower tumor PDL1+ than HER2+ tumors. Additionally, 18 of the 208 patients with equal distribution across the hormone-receptor subtypes underwent whole slide multiplexed analysis to perform a deeper spatial analysis.
Conclusions: In a large, clinically annotated cohort of breast cancers distinct immunophenotypes are evident among HR and HER2+ subsets.

#4640

CAF contributes to cancer progression through its immunomodulatory role within the tumor microenvironment

Muriel Antonieta Núñez[1], Oreste Corrales[1], Victoria Velasquez[1], Daniel Ernst[2], Montecinos Viviana[3], Francisco Nualart[4], María Isabel Yuseff[1], Javier Cerda-Infante[5]. *[1]Department of Cellular and Molecular Biology, Pontifical Catholic University of Chile, Santiago, Chile,[2]Institute of Science and Innovation in Medicine, University for Development, Santiago, Chile,[3]Department of Hematology-Oncology, Pontifical Catholic University of Chile, Santiago, Chile,[4]University of Concepción, Santiago, Chile,[5]Environ Spa, Santiago, Chile*

Introduction: Cancer progression and metastatic spread is modulated by the tumor microenvironment. Cancer-associated fibroblasts (CAF) are the most abundant cell type within the tumor microenvironment. Little is known about the specific mechanisms by which CAF would exert its cancer progression, through the high secretory capacity of soluble pro-tumorigenic molecules and remodeling of the extracellular matrix. Recent studies in our laboratory have shown for the first time that CAF derived from patients without metastasis express a different genetic profile than those with metastases (mCAF). This study seeks to evaluate the contribution of mCAF to tumor progression through its immunomodulatory role.
Methodology: mCAFs were obtained from patients with metastatic disease and BAF from benign patients. The fibroblasts were functionally characterized by the generation of fibroblast-derived matrices (FDM) and secretory profiles by cytokine array. CD8 T lymphocytes were obtained from healthy patients and treated with fibroblast-secretome. Markers were studied by flow cytometry: activation (CD25 and CD69) and repression (LAG3 and PD1). The migration of CD8 T lymphocytes was studied by transwell and agarose drop migration assay.
Results and conclusion: FDM of mCAF are different in their composition and organization. Furthermore, the secretome of each type of fibroblast presents a differential effect on the activation of CD8 T cells according to the markers highlighted. Regarding migration, it has been observed that the mCAF-secretome can attract lymphocytes. However, it would lead them to

apoptosis. Our results suggest that mCAF, within the tumor microenvironment, has an immunomodulatory role on CD8 T lymphocytes.
Acknowledgment: Beca Doctorado Nacional ANID 21181427

Inflammation and Tumor Progression

#4644
Modeling the effects of niche specific microenvironmental changes on patient-derived organoids
Jennifer von Schlichting, Leona Simon, Stefan Peidli, Markus Morkel, Nils Blüthgen. *Charité - Universitätsmedizin Berlin, Berlin, Germany*

Here, we present an approach to study the effects of microenvironmental changes on inter- and intratumoral heterogeneity using colorectal cancer (CRC) patient-derived organoids. We identified relevant paracrine interactions between stromal and tumor cells based on the expression of ligand-receptor pairs in single cell-RNAseq data of 12 colorectal cancer patients. Physiological relevance was tested by adding CRC stroma-derived ligands to patient-derived organoids. A systematic screening of different conditions was enabled by multiplexed mass cytometry and scRNAseq analysis. We also aimed to model the effects of a changing extracellular matrix composition, by supplementing the laminin/collagen IV rich environment with other known ECM proteins such as collagen I to identify the impact of a changing substrate on cell plasticity. We found that ECM parameters as well as niche specific paracrine factors affect proliferation, differentiation, and developmental trajectories of colorectal cancer patient-derived organoids. We hypothesize that supplementing patient-derived organoids in vitro with physiologically relevant factors and substrates may expand the phenotypic space in which organoid cells differentiate, resulting in a more versatile preclinical model system.Our data provide insights into non-genetic sources of inter- and intratumoral heterogeneity resulting in differential drug responses. Additionally, they can serve as guidelines to improve existing patient-derived colorectal cancer models and provide a feasible approach to address common limitations in organoid culture.

#4645

Identification of conditionally active antibodies that selectively block CD39 activity in the acidic tumor microenvironment

Aiping Bai, Elise Renahan, Kanam Malhotra, Thomas Thisted, F. Donelson Smith, Robert H Pierce, Edward H van der Horst. *Sensei Bio, Boston, MA*

Background CD39 expression is upregulated in the tumor microenvironment (TME), which is characterized by high levels of extracellular ATP (eATP) and low pH. CD39 catalyzes the rate-limiting degradation step of this immunostimulatory ATP, leading to a rise in immunosuppressive adenosine (ADO). CD39 displays broad expression on endothelial cells and macrophages, which represents a significant peripheral sink for CD39 targeting antibodies. Our strategy aims to circumvent this problem through delivery of pH-selective anti-CD39 blocking antibodies that will achieve a high target occupancy in the tumor, maintaining eATP and inhibiting ADO generation to enhance anti-tumor immunity.

Methods Anti-CD39 antibodies were generated through a yeast-based screening platform and characterized for efficacy of blocking CD39 activity. Cell lines (HEK293 stably overexpressing CD39, parental HEK293, $CD39^{+}$ SK-MEL28, and $CD39^{high}$ ARH77) or soluble CD39 protein were incubated with candidate antibodies. CD39 enzymatic activity was determined using CellTiter Glo 2.0 assay (Promega) and EnzCheck Phosphate Assay (Thermo Fisher).

Results Monovalent affinity of 83 candidate antibodies was measured; K_Ds ranged from $1x10^{-9}$ - $5X10^{-7}$M under both physiological (pH 7.4) and acidic (pH 6.0) conditions. All 83 antibodies bound CD39-overexpressing HEK293 cells at pH 6.0; 76 bound CD39-overexpressing HEK293 cells at pH 7.4. We identified 30 antibodies (100 nM) that block CD39 activity on HEK293-CD39 cells (threshold: > 5% inhibition) under either pH 7.4 or pH 6.0 conditions. 26 antibodies inhibit CD39 activity at pH 7.4, whereas 22 antibodies block CD39 at pH 6.0. Among these 30 antibodies, ten (at 200 nM) inhibit CD39 activity on SK-MEL28 cells (moderate CD39 expression) at both pH 7.4 and pH 6.0; 5 of these preferentially inhibit CD39 at pH 6.0 (threshold: > 7.5% inhibition). The 30 antibodies selected above were tested on ARH77 cells (high CD39 expression). Among them, 16 antibodies inhibited CD39 enzymatic activity beyond 10% at pH 6.0 (maximal inhibition: 43%) and > 6.5% at pH 7.4 (maximal inhibition: 35%). All 16 suppressed soluble CD39 activity under both pH conditions. A

set of 8 antibodies demonstrating higher efficacy of CD39 inhibition on both cell lines at pH 6.0 versus pH 7.4 were prioritized for lead optimization.
Summary and conclusions A panel of 83 antibodies were identified and characterized for inhibition of CD39 enzymatic activity at neutral and acidic pH. The 8 most promising antibodies in terms of pH-selective CD39 binding and inhibition are currently undergoing lead optimization. This pH-dependent TME targeting strategy may alleviate undesirable properties of on-target/off-tumor binding such as target-mediated drug disposition (that results in suboptimal pharmacokinetic properties) and effectively bolster the specific blocking of CD39 in the local tumor environs.

#4646
Relative contribution of tumor infiltrating B cells to the tumor microenvironment assessed using an immuno-oncology focussed multi-tumor tissue microarray
Milan Bhagat, Leorenzo Memeo, Christopher Womack, Woo Hoo Kim, Marie Cumberbatch. *TriStar Technology Group LLC, Washington DC, DC*

Although cancer immunotherapy approaches have focused primarily on driving T cell mediated immunity, attention has turned to other immune cell types within the tumor microenvironment (TME) to improve efficacy. Growing evidence supports a role for tumor-infiltrating B cells in complementing T cell-mediated immunity and contributing to the immunomodulation of cancer. Analyses of RNA sequencing data from The Cancer Genome Atlas (TCGA) have correlated high expression of B cell genes with improved patient survival in a range of cancer types. However, it is likely that effective anti-tumor immunity involves interactions between both B and T cells. To investigate the relative contribution of B cells to the overall TME across multiple tumor types simultaneously, we have examined a multi-tumor tissue microarray (TMA) comprising 29 different cancer types represented by approximately 12 unique donors per indication and duplicate 1mm cores per donor (1 from invasive margin [IM] and 1 from tumor center [TC]). Serial sections were stained by single-plex immunohistochemistry for CD20, CD3, CD4 and CD8, and immune cells enumerated by digital image analysis (CellProfiler^{TM}). Analysis of overall immune infiltration regardless of core location (IM and TC combined)

revealed tumor indications such as NSCLC, gastric, TNBC, cutaneous SCC and cervical to be most highly infiltrated, and GIST, GBM and prostate to exhibit the fewest tumor-infiltrating immune cells. B cell frequencies correlated with T cell densities for most tumor types with some notable exceptions including, for example, ER+ BC and gallbladder cancer where the proportion of B cells was higher relative to T cells, and TNBC where the converse pattern was evident. Spatial analyses revealed increased B cell frequencies in IM compared with TC, correlating with the distribution of T cells in the TME for the majority of tumor indications. However, a contrasting expression pattern was observed for ER+ BC, NSCLC SCC and cutaneous SCC where B cell frequencies were greater in TC. Clear evidence for presence of B cells in tertiary lymphoid structures (TLS) was observed for some tumor donor cores (e.g. gastric cancer). Taken together, we describe the relative distribution of B cells in the TME across multiple tumor types simultaneously. This approach demonstrates the benefits of utilizing an immuno-oncology focussed multi-tumor TMA to interrogate B cell biology and to dissect how heterogeneity of this cell population may contribute to anti-tumor immunity.

#4647

Potential of TIMP3 regulating the versican status in the colorectal cancer tumor microenvironment

Anna Field[1], Sean Kraus[1], Kristina Matkowskyj[2], Dustin Deming[3], Cheri A. Pasch[1], Wei Zhang[1]. *[1]University of Wisconsin-Madison, Madison, WI,[2]Human Pathology, University of Wisconsin-Madison, Madison, WI,[3]Hematology/Oncology, University of Wisconsin-Madison, Madison, WI*

Background: In colorectal cancer (CRC), versican (VCAN) accumulation has been found to negatively correlate with CD8+ tumor infiltrating lymphocyte (TIL) abundance and its proteolysis into versikine (Vkine) positively correlates with TIL abundance. TIMP3 has demonstrated the ability to inhibit several ADAMTS proteases able to cleave VCAN to Vkine. Here we investigate the correlation of TIMP3 accumulation in CRCs with the VCAN status and CD8+ T cell infiltration.
Methods: Matched primary and metastatic CRC samples from 156 patients who had resected oligometastatic CRC were stained for VCAN, Vkine, TIMP3, and CD8+ TILs. VCAN, Vkine, and TIMP3 were scored using an

intensity binning system ranging from 0-3+ and T cells in the epithelium were reported per high power field (HPF). Tumors were designated as high (2 or 3+) or low (0 or 1) for both VCAN and Vkine and positive (+; 1-3) or negative (0) for TIMP3. Tumors designated VCAN low and Vkine high are considered VCAN proteolytic predominant (VPP) and all other combinations are considered VCAN proteolytic weak (VPW).
Results: Across the whole dataset, 52% of cancers were VCAN high and 24% were VPP. TIMP3 was detected in 33% of cancers. The frequency of TIMP3 was similar between primary and metastatic tumors (39% and 29%, respectively). Of the VCAN high cancers, 42% were TIMP3+ whereas 61% of the TIMP3+ samples are VCAN high. Of the Vkine high cancers, 44% were TIMP3+ and 36% of VPP cancers were TIMP3+. The prevalence of the VPP phenotype was similar between the TIMP3+ and negative cancers. Additionally, among the TIMP3+ samples 68% were Vkine high versus 46% in TIMP3 negative cancers (p=0.001). VCAN proteolysis correlates with higher CD8+ TIL abundance, thus we assessed the number of CD8+ TILs in TIMP3+ and negative tumors. The TIMP3+ cancers had a median of 2 CD8+ TILs/HPF and the TIMP3 negative cancers has a median of 3 CD8+ TILs/HPF. For VPP cancers, those that were also TIMP3+ had a median of 3 CD8+ TILs/HPF compared to TIMP3 negative cancers which had a median of 6 CD8+ TILs/HPF (p=0.2).
Conclusions: TIMP3 correlates with higher levels of VCAN accumulation but does not correlate with lower levels of proteolysis. Future studies are needed to better clarify the impact of TIMP3 and other mediators in regulating VCAN accumulation and proteolysis in the tumor microenvironment.

#4648

How inherited mutations affect single cells within the tumor microenvironment in breast tumors stratified by receptor status

Dana Pueschl[1], Derek A. Oldridge[2], Jonathan Belman[1], William Chandler[1], Anupma Nayak[1], Bradley Wubbenhorst[1], John Pluta[1], Michael Feldman[1], E. John Wherry[1], Heather Thorne[3], Georgia Chenevix-Trench[4], Kathleen Cuningham Foundation Consortium for Resea kConFab[5], Susan M. Domchek[1], Katherine L. Nathanson[1]. *[1]University of Pennsylvania, Philadelphia, PA,[2]Children's Hospital of Philadelphia, Philadelphia,*

PA,[3]The Peter MacCallum Cancer Centre, Melbourne, Australia,[4]QIMR Berghofer Medical Research Institute, Brisbane, Australia,[5]kConFab, Melbourne, Australia

The tumor microenvironment (TME) plays important roles in tumor progression, therapy response and patient survival. In this comprehensive study, we performed a detailed multiomic single cell analysis of breast cancers with inherited mutations in different genes (*BRCA1*, *BRCA2*, *PALB2*, *ATM*, *CHEK2*), and wild type mutation negative (WT) patients, stratified by hormone receptor status, to understand the relationship between inherited mutation and immunogenicity. Using spatial tissue multiplexing (PhenoCycler), single cell RNAseq (10X Genomics) and bulk RNAseq, we evaluated cellular markers within the TME associated with DNA damage as well as phenotypes with tumor suppressive (M1, CD8 T cells, NK cells) or tumor promotive (M2, Treg, CAF) properties. We developed a 43-plex antibody panel and characterized eight tissue microarrays containing 443 patient samples from mutation carriers (*BRCA1*: n=142, *BRCA2*: n=118, *CHEK2*: n=2, *TP53*: n=3, *PALB2*: n=7) and WT tumors (n=171). We addressed how the TME differs in mutation carriers versus WT tumors stratified by receptor status. To further investigate immune cell function (cytolytic function, exhaustion, immune checkpoint) as well as pathways involved in immune suppression and/or promotion, we performed scRNA sequencing using isolated single cells from fresh collected BC samples (WT ER: n=3, *BRCA2* ER: n=1, *CHEK2* ER: n=1, *VUS* ER: n=1) and bulk RNA (*BRCA1*: n=17, *BRCA2*: n=9). To determine immune cell (IC) frequency, we analyzed CD45+ cells detectable in each cohort and their co-expression of markers to determine specific phenotypes. Our data suggest that within *BRCA* mutation-associated BC, there are two groups: 1) with increased tumor infiltrating lymphocytes (TILs) including CD8+ cytotoxic T cells with high cytolytic function; and 2) with decreased TILs and cytolytic function. The frequency of CD8+ T cells is significantly decreased in breast cancers with *BRCA2* mutations compared to *BRCA1*. Characterizing ER+ *CHEK2* BC reveals T cell exhaustion compared to WT ER+ BC. Furthermore, preliminary scRNA results reveal increased fibroblast markers in ER+ *CHEK2* and ER+ WT compared to ER+ *BRCA2* tumors. Interestingly, cancer associated fibroblast (CAFs) markers (*ACTA2, COL1A1, FAP, PDGFRA, PDGFRB, PDPN,*

THY1) as well as TAMs (*CCL2, CD163, CD206, CD68, IL10, LOX, PLOD2, SIGLEC1*) are increased in ER+ CHEK2 tumors compared to ER+ WT. These data could provide insights into how the TME associated with ER+ *CHEK2* mutations might be driven by CAFs and TAMs with a frequency much higher than in ER+ WT. The detection of immune suppressive (Treg, M2) and immune promotive (M1) phenotypes differs in *BRCA1* compared to *BRCA2* mutated and WT TNBC. Our findings could decipher the role of DNA repair gene mutations and their effect on cells within the TME that might influence the design of treatment options in patients with inherited mutations based on their receptor status.

#4649

Design and validation of ultrahigh-plex discovery panels for immuno-oncology and oncology

Yan He, Shannon Berry, Olive Shang, Michael McLane, Nicholas Ihley, Yi Zheng. *Akoya Biosciences, Marlborough, MA*

Introducti**on** Ultrahigh-plex single-cell spatial phenotyping is revolutionizing cancer research through deeper interrogation of cellular and protein-level co-expression, localization, and arrangements within cancer tissues. To enable in-depth characterization of the tumor microenvironment (TME), we have developed and validated pre-optimized antibody panels on cancer tissues to reveal key cell types and cellular architecture using the PhenoCycler™-Fusion system. Here, we present our methodology for the development and validation of multiplex spatial phenotyping panels for oncology and immuno-oncology.

Methods We designed panel modules such that each module answers specific biological questions about the TME and can be multiplexed together for a more comprehensive view of the structure and function of the tumor and TME. The resulting PhenoCode™ Discovery panel modules include markers that identify key immune cell types, immune activations and checkpoints, mediators of proliferation, and other hallmarks of cancer. Each antibody in the panel module was conjugated to an oligo barcode and stained on human formalin-fixed paraffin-embedded (FFPE) tissue. The slide was imaged on a PhenoCycler™-Fusion platform, where dye-labeled oligo reporters (complementary to the barcodes) are hybridized to the barcode to visualize the antibody. The results were compared serial sections

run with a 3,3'-Diaminobenzidine (DAB) chromogenic immunohistochemistry assay to ensure specificity of the antibody was retained. Antibody concentration, exposure time, and corresponding dye were further optimized, verified, and validated as a whole module using tonsil and cancer tissues based on image analysis and intensity analysis, to achieve an ultrahigh-plex detection.
Results and Conclusions In this study, we showcased the rigorous process used for development and validation of PhenoCode™ Discovery panel modules and demonstrated how they can seamlessly work together to collect more data out of one tissue sample. The introduction of these pre-optimized antibody panel modules mark a pivotal point in the evolution of ultrahigh-plex spatial phenotyping. They not only simplify experimental design and assay set up, with panels that make it easier for researchers to answer important questions with this technology, but also save precious time and resources, while reducing overall costs.

#4650
High intratumoral levels of Notch3 increase tumorigenesis and promote an immunosuppressive TME in EGFR-mutant NSCLC
Shankar Suman, Jacob Kaufman, Rajeswara Arasada, Sanjay Varikuti, Nastaran Navari, Shuxiao Guan, Joseph Amann, Mikhail Dikov, David Carbone, Regan Memmott. *The Ohio State University, Columbus, OH*

Activating mutations in the Epidermal Growth Factor Receptor (EGFR) are one of the most common driver mutations in non-small cell lung cancer (NSCLC). They are present in the tumors of ~15% of Caucasian patients and in up to 50% of Asian patients. Notch3 is a member of a family of transmembrane receptors that has been shown to increase cell proliferation and inhibit cell death and differentiation. Notch3 also promotes the formation of cancer cells with stem-like properties. Studies have shown that a high level of Notch3 in tumors is associated with poor prognosis of patients with NSCLC. However, its role in EGFR-mutant NSCLC tumorigenesis has not been specifically evaluated. We analyzed the TCGA, Moffit, and ORIEN datasets, which include tumor samples from patients with EGFR-mutant lung cancer. We found that high levels of Notch3 were associated with decreased overall survival (HR=2.0, p=0.04). Interestingly, analysis of two additional datasets derived from the phase 3 clinical trials

OAK and POPLAR showed that patients whose EGFR-mutant tumors had the highest levels of Notch3 had worse clinical outcomes when treated with immunotherapy (HR 18.6, p=4e-04) but not chemotherapy. This could suggest that Notch3 promotes EGFR-mutant lung tumorigenesis by creating an immunosuppressive tumor microenvironment (TME). To test this, we generated a novel mouse model, c/EGFR^{L858R}Notch3, that expresses tetracycline-inducible Notch3 and mutant EGFR under the control of the Clara cell-secretory protein (CCSP) promoter. CT-based imaging showed that mice whose tumors harbored high levels of Notch3 had significantly increased lung tumor burden at eight weeks. These mice also had worse overall survival (HR 2.3, p=0.04). To determine if increased Notch3 expression in tumors promotes a more immunosuppressive TME, we did immunophenotyping analysis that revealed a significant increase in regulatory T cells and a decrease in cytotoxic CD8+T cells. Furthermore, T cells in the TME expressed higher levels of markers of exhaustion, specifically, PD-1 and Tim-3. We also found that mice whose tumors had high levels of Notch3 had a greater density of immunosuppressive macrophages in the TME, which was associated with elevated levels of TNF-α. Overall, our data suggest that patients with EGFR-mutant NSCLC whose tumors harbor high levels of Notch3 may have worse clinical outcomes and response to immune checkpoint inhibitors due to Notch3 promoting an immunosuppressive TME.

#4651

Comparison of the tumor and lymph node immune microenvironment in early non-small cell lung cancer through multimodal single cell sequencing

Zhanhao Xi[1], Yusuke Koga[1], Shannon McDermott[2], Jennifer Beane[1], Sarah A. Mazzilli[1], Kei Suzuki[3], Joshua D. Campbell[1]. *[1]Computational Biomedicine, Boston University, Boston, MA,[2]Boston University, Boston, MA,[3]Department of Surgery, INOVA, Falls Church, VA*

Background/**Purpose:** Previous studies have analyzed the tumor and local immune microenvironments in lung cancers and suggest immune modulation is associated with worse clinical outcome. However, the tumor-immune microenvironment in early stage lung tumors and lymph nodes (LNs) have not been fully described. We aim to compare cell states in the

immune microenvironments between lung tumors and LNs through multi-modal profiling of the transcriptome and surface proteins.
Methods: Needle biopsy samples were taken from 10 treatment-naive early stage lung cancer patients undergoing lung cancer resections. Tissues were obtained from normal lung, lung tumor, and multiple mediastinal LNs, and processed for scRNA-seq including labeling with Total-Seq C CITE-seq panel to quantify the levels of 130 cell surface proteins. In total, 76,721 cells (4,462 normal lung; 39,019 tumor; 33,240 LN) were identified with a median of 1,673 genes and 92 protein features detected per cell. Protein expression was decontaminated through the decontX algorithm. Weighted-Nearest Neighbor analysis from the *Seurat* R package was applied to integrate the CITE-seq and RNA-seq level data for clustering cells into subpopulations.
Results: Six broad cell populations were identified including T/NK, myeloid (CD14+), B (CD19+), mast (TPSAB1+), pDC (IRF8+), and epithelial (EPCAM+) cells. Among 8 CD4+ T lymphocyte subpopulations and 11 CD8+ T lymphocyte subpopulations observed through clustering, a naïve CD4+ and a CD8+ T subpopulation (LEF1+, TCF7+) was observed respectively. These naïve T lymphocyte populations displayed increased proportions in LNs in comparison to tumors. In addition, 5 of the 8 observed CD4+ T lymphocyte populations were enriched in LNs. Immune populations enriched in LNs were largely shared and uniform across different patients. In contrast, a single CD4+ and CD8+ T lymphocyte subpopulation displayed expression of T lymphocyte exhaustion markers (TIGIT+, LAG3+, PD-1+) and were enriched in tumors. 6 of the 11 observed CD8+ T lymphocyte populations were enriched in tumor samples in comparison to LNs. Two alveolar macrophage populations (MARCO+) were enriched in normal lung tissue, in which one showed a heightened stress response.
Conclusion: Single-cell profiling reveals diversity in immune cell populations between LNs, tumor, and adjacent normal tissue in early-stage LUAD. The results suggest the composition of immune cell type is fairly consistent across LNs but more heterogeneous in the tumor and adjacent normal tissue in early-stage patients. In the future, we aim to determine if these immune subpopulations are associated with survival, recurrence, aggressiveness, and predict responses for neoadjuvant treatments, which could improve prognosis and patient quality of life.

#4652

A cellular and transcriptomic dissection of the human breast for studying mechanisms of cell and tissue function

Katelyn Del Toro[1], Rosalyn W. Sayaman[2], Kate Thi[3], Yamhilette Licon-Munoz[1], William C. Hines[1]. *[1]Biochemistry and Molecular Biology, Univ. of New Mexico School of Medicine - Albuquerque, Albuquerque, NM,[2]Department of Laboratory Medicine, University of California, San Francisco, San Francisco, CA,[3]Life Sciences Division, Lawrence Berkeley National Laboratory, Berkeley, CA*

A fundamental question in biology, central to our understanding of cancer and other pathologies, is determining how different cell types coordinate to form and maintain tissues. Recognizing the distinct features and capabilities of the cells that compose these tissues is critical. Unfortunately, the complexity of tissues often hinders our ability to distinguish between neighboring cell types and, in turn, scrutinize their transcriptomes and generate reliable and tractable cell models for studying their inherently different biologies. A lack of comprehensive methods to identify, isolate, and culture each cell type from many tissues have impeded progress. Here, we will describe such a method for the breadth of cell types composing the human breast. Furthermore, we have sequenced mRNAs from each purified population and investigated transcriptional patterns that reveal their distinguishing features. These analyses have exposed differentially expressed genes and enriched biological pathways that capture the essence of each cell type, along with transcripts that display intriguing expression patterns. These data, analytic tools, and transcriptional analyses form a rich resource whose exploration provides remarkable insights into the inner workings of the cell types composing the breast, thus furthering our understanding of the rules governing normal cell and tissue function.

#4653

Spatial architecture of tumor-infiltrating macrophagesorchestrates tumor immunity and therapeutic response

Yuanyuan Zhang, Fuduan Peng, Guangsheng Pei, Yunhe Liu, Guangchun Han, Linghua Wang. *UT MD Anderson Cancer Center, Houston, TX*

Tumor-infiltrating macrophages, a major cellular component in the tumor microenvironment (TME), have been proven to be linked with tumor progression and immunotherapy resistance. Tremendous heterogeneity has been revealed for tumor-associated macrophages (TAMs) in different cancer types, however, how these TAM subtypes are localized and interact with tissue ecosystems remains poorly understood. Here, we perform an integrative analysis of TAMs, malignant and non-malignant cells from 10 cancer types, based on single-cell RNA-seq and spatial transcriptomic data. By interrogating the spatial distributions of different TAM subtypes in situ, we reveal spatially restricted developmental, regulation, and functional heterogeneity of TAMs in TME. Different cancer types show distinct TAM subtype enrichments with specific interface architectures, which is potentially shaped by the cellular compositions and spatial niches of tumor cells. Furthermore, the compartmentalized TAM subpopulations can reflect the spatial architecture of surrounding stromal and immune cells, and thus orchestrate tumor immunity and therapeutic response. Our study demonstrates the cellular and molecular underpinnings of TAM heterogeneity and stochastic regulations of TAMs for TME architecture, tumor progression and immunotherapy responses, which will assist in the identification of possible therapeutic targets.

#4654

Differential immunomodulation following checkpoint blockade in the orthotopic ID8-luc ovarian model

Sheri Barnes, Anita Zaitouna, Lauren Kucharczyk, Scott Wise. *Laboratory Corporation of America, Ann Arbor, MI*

Syngeneic tumor models for ovarian cancer are limited in preclinical research. One of these models, ID8-luc, is established intraperitoneally with disease progression resulting in the accumulation of ascites fluid. Treatment efficacy can be determined by non-invasive bioluminescence imaging (BLI), but solid ID8-luc tumors do not form in the peritoneal cavity, making assessment of immunomodulation challenging. To this end, we have developed the ID8-luc model as a tool to investigate immuno-modulatory drug candidates by utilizing tissues in the peritoneal cavity of diseased animals for ex vivo analyses. Specifically, flow cytometry of diseased ovaries was employed to examine the effects of checkpoint inhibition on T

cell phenotypes and NK cell infiltration. To identify tumor deposits in organs from mice bearing ID8-luc disease for analysis tumor infiltrate, the model was established in untreated C57BL/6 albino mice, and ovaries, liver, peritoneal wall, pancreas, and spleen were evaluated pathologically. Progressive establishment of tumor deposits were seen in the ovaries, pancreas, and peritoneal wall of untreated mice, but not in naïve mice. Further, immune infiltration in ovaries were markedly higher compared to naïve mice. To assess immunomodulation, disease was established in a second cohort of mice, and mice were treated with anti-mPD-1, anti-mPD-L1, and anti-mCTLA-4. Disease progression was monitored by BLI, and following treatment, ovaries containing tumor deposits were collected and lymphoid infiltrate was analyzed by flow cytometry. Checkpoint blockade did not result in efficacy under the conditions tested. However, differences in T cell infiltration were notable with treatment of anti-PD-1 and anti-mPD-L1. Particularly, a marked increase of five to ten fold CD8+ and CD4+ T cells by absolute counts was seen with anti-mPD-1 and anti-mPD-L1 treatment compared to control. Further, the percentage of CD8+ T cells expressing the activation markers CD69 and ICOS as well as PD-1, TIM-3, and LAG-3 checkpoint proteins increased with anti-mPD-1 treatment. Less prominent yet similar trends in this biomarker expression were seen with anti-mPD-L1 treatment. NK and NKT infiltration also increased five to eight fold in ovaries following anti-mPD-1 treatment. Interestingly, anti-mCTLA-4 treatment did not result in any remarkable changes in infiltration or activation marker dynamics. Taken together, these findings are suggestive of a mounting immune response following PD-1 and PD-L1 blockade, but not CTLA-4 blockade, characterized by changes in the lymphocyte compartment in the ovaries. This response is seen in the absence of efficacy, suggesting the potential that this immunomodulation can be exploited in rational combination strategies with checkpoint blockade for immune-oncology drug candidates using the ID8-luc ovarian tumor model.

#4655

The prognostic significance of a 12-chemokine tertiary lymphoid structure (TLS) gene signature in uveal melanoma (UM)

Hassan Mohammed Abushukair[1], Ayah Al-Bzour[1], Andrew Knight[2], Walter J. Storkus[3], John M. Kirkwood[4], Lilit Karapetyan[5]. *[1]Jordan University of*

Science & Technology, Irbid, Jordan,[2]Department of Medicine, University of Pittsburgh Medical Center, Pittsburgh, PA,[3]Departments of Dermatology, Immunology, Pathology and Bioengineering, University of Pittsburgh Medical Center, Pittsburgh, PA,[4]Department of Medicine, Division of Hematology/Oncology, UPMC Hillman Cancer Center, Pittsburgh, PA,[5]Department of Cutaneous Oncology, H. Lee Moffitt Cancer Center & Research Institute, Tampa, FL

Introducti**on** Lymphoid aggregates are commonly associated with better prognosis and enhanced response to immune modulators in several cancers. Considering the immune-privileged status of the eye we sought to investigate the immune, genomic and prognostic significance of 12-chemokine TLS gene signature in UM patients.

Methods A previously validated 12-chemokine gene signature established in cutaneous melanoma was used (*CCL2-5, CCL8, CCL18, CCL19, CCL21, CXCL9-11, CXCL13*). Clinical, genomic and transcriptomic data was retrieved from The Cancer Genomic Atlas UM cohort (n = 80) and the GSE22138 dataset (n = 63) from the gene expression omnibus. The signature was constructed using principal component (PC) analyses based on the first PC1. Patients with a PC1 score > +4 or < -4 were considered gene expression profile (GEP) high and low, respectively. The CIBERSORT algorithm was used to estimate the immune composition in tumor tissue. Gene Set Enrichment Analysis (GSEA) was conducted using the Hallmarks gene sets. A cytotoxic T cell (CTL) score was calculated based on the coordinate expression of *CD8A, CD8B, GZMA, GZMB* and *PRF1*.

Results The 12-chemokine score was higher among epithelioid vs. spindle cell or mixed histology (mean: 7.84 vs -4.91 vs 1.22, p = 0.038) and there were no differences across different tumor sites or stages. GEP low patients had significantly better overall survival (HR: 0.10, 95% CI: 0.03-0.36, p < 0.001) and disease-free survival (HR: 0.23, 95% CI: 0.06-0.88, p = 0.031) compared to GEP high. Metastasis-free survival was not significantly different in the second cohort (0.47, 95% CI: 0.16-1.42, p = 0.182). The EIF1AX and SF3B1 driver mutations were significantly more frequent among GEP low (22.5% and 35%) compared to GEP high patients (3.7% and 7.4%). Tumor mutational burden and other driver mutations (BAP1, GNA11, GNAQ) were similar between both groups. GSEA revealed

significant enrichment of inflammatory response (IFN-α/γ, TNF-α signalling via NF-κB, IL2-STAT5, IL6-JAK-STAT3 signalling), Epithelial Mesenchymal Transition (EMT), reactive oxygen species, and angiogenesis pathways in GEP high patients. GEP low patients had lower CTL scores compared to GEP high patients (31.3 vs 11.4, $p < 0.001$). M1 macrophages, CD8+ and regulatory T cells were enriched in GEP high patients whereas CD4+ memory T cells and activated dendritic cells were more prevalent in GEP low patients.
Conclusion Uveal melanoma patients with a high GEP score had inferior survival and were enriched for inflammatory, angiogenic, and EMT pathways, while patients with a low GEP score were more likely to express prognostically favourable driver mutations (EIF1AX, SF3B1). Our results suggest a variable prognostic role of lymphoid aggregates in the setting of UM compared to other solid tumors, warranting further investigation for their differential underlying mechanisms.

#4656
Targeting macrophage PI3KGamma in aggressive prostate cancer
Kenneth M. Adusei[1], Thomas R. Nirschl[1], Alex J.-E. Lee[1], Fan Shen[1], Xiaoxu Wang[1], Jade Alvarez[1], Tamara L. Lotan[1], Judith Varner[2], Jelani Zarif[1]. *[1]Johns Hopkins University, Baltimore, MD,[2]University of California San Diego, San Diego, CA*

The phosphatidylinositol-4,5-bisphosphate 3-kinase (PI3K) family of lipid kinases play key roles in cancer biology by promoting cell motility, growth, and survival. Of the four class I PI3K isoforms, PI3Kα,β,δ,γ, the PI3Kγ isoform is primarily expressed by myeloid cells. Studies from the Varner lab have established that the macrophage lipid kinase, PI3Kγ, selectively promotes myeloid cell trafficking and immune suppressive transcription in tumor associated monocytes and macrophages, thereby inhibiting T cell recruitment, activation, and tumor eradication. We hypothesized that antagonism or deletion of PI3Kγ would induce tumor growth inhibition *in vivo* in prostate cancer (PCa) models. To test our hypothesis, we implanted syngeneic murine prostate cancer tumors (B6CaP) into global PI3Kγ knock out mice and preliminary studies show severe tumor growth inhibition. Using a publicly available single cell RNA sequencing database of metastatic PCa (mPCa) tumors from bone, we calculated regulon scores for

transcription factors C/EBPβ and NFκB which are up and down-regulated by PI3Kγ signaling in myeloid cells respectively. This analysis indicated that a notable proportion of monocytes in mPCa have active PI3Kγ signaling based on C/EBPβ activity and a lack of NFκB activity. Finally, we tested the significance of eganelisib treatment on monocytes and found that this pathway was essential for monocyte survival during macrophage differentiation and adhesion. Altogether, our proposed research delineates the mechanistic roles of PI3Kγ in the regulation of prostate cancer tumor growth and support PI3Kγ as a target to sensitize PCa to immune checkpoint inhibitors.

#4657

Topological data analysis reveals pan-cancer immune phenotypes with immune-related survival differences

Kevin A. Murgas[1], Jung H. Oh[2], Joseph O. Deasy[2], Allen R. Tannenbaum[3].
[1]Biomedical Informatics, Stony Brook University, Stony Brook, NY,[2]Medical Physics, Memorial Sloan Kettering Cancer Center, New York, NY,[3]Applied Mathematics & Statistics, Stony Brook University, Stony Brook, NY

Cancer immune phenotypes present a wide range of heterogeneity across cases, with individual tumors displaying unique patterns of infiltrating immune cell types. Deconvolutional methods allow for scoring of various immune cell types in bulk tumor RNA as a quantification of immune phenotype. Understanding how immune phenotype relates to clinical outcome remains limited. Here, we demonstrate an approach applying topological data analysis to investigate differences of immune phenotype in a pan-cancer cohort (TCGA; n=11,373 tumors). We first define an Immune Activation Score based on relative abundance of activator and suppressor immune cell types and find this score depends on cancer type and distinguishes overall survival outcomes. We then implement a robust Mapper-based algorithm to delineate clusters of immune phenotypes of tumor samples across pan-cancer and within cancer types. Our method identifies immune-activated and immune-suppressed phenotypes with distinct survival outcomes and molecular features.

#4658

Flexible multiplexed immunofluorescent panels for accelerated identification of spatial signatures for immunotherapy checkpoint investigations

Jacob Circelli, Rachel Schaefer, Oscar Perez, Linying Liu, Michael McLane, Yi Zheng. *Akoya Biosciences, Marlborough, MA*

A fundamental step in the characterization of the tumor microenvironment (TME) is the identification of the distinct immunologic phenotypes in various cancer types. The spatial arrangement of these cells and their co-expression patterns serve as an increasingly important tool for the identification of a novel class of highly predictive biomarkers for immunotherapy response knows as spatial signatures. To study the complex biological processes within the TME and develop clinically useful spatial signatures, it is imperative to take an approach that combines relevant content with flexibility, speed, and throughput. We recently introduced PhenoCode^{TM} Signature Panels that offer researchers the ability to stain for multiple biomarkers including their marker of choice at a single cell resolution on a single tissue in a scalable end-to-end automated workflow. Incorporating Akoya's novel barcoded antibody labeling chemistry, these panels enable all primary antibodies to be applied as a cocktail in a single incubation step, followed by the sequential amplified detection of each marker via Opal fluorescent dye technology. Previously, we have presented data on 3 panels that address key questions for the characterization of the TME, including whether the tumor is "hot" or "cold," the identity of the immune cells comprising the TME, the proliferative state of tumor cells and the activation state of the immune cells. Here we showcase two new PhenoCode Signature panels that allow researchers to further characterize the TME by examining immune cell exhaustion and macrophage polarization, key events that contribute to an immunosuppressive TME. In this study, staining was performed using all five PhenoCode Signature panels and DAB on the Leica BOND RX^{TM} automated stainer. Human formalin-fixed, paraffin embedded (FFPE) lung cancer tissues were stained and whole slide multispectral scans were acquired on the PhenoImager HT® platform. Image analysis was performed with a phenotyping algorithm in inForm® and staining intensities were analyzed in R using Phenoptr and PhenoptrReports. The fluorescent staining of each marker was benchmarked to the DAB staining. Each panel was proven to be both highly

accurate and reproducible. Together these five PhenoCode Signature panels provide researchers a rapid and robust method for characterizing the TME to aid the development of spatial signatures which have been shown to be highly effective at predicting therapeutic outcomes.

#4659

Depicting ONC201/Delta-24-RGD combination for the treatment of pHGGs and DMGs reveals a therapeutic benefit and a proinflammatory tumor microenvironment remodelation

Daniel de la Nava[1], Virginia Laspidea[1], Iker Ausejo-Mauleón[1], Marc García-Moure[1], Sabine Mueller[2], Javad Nazarian[2], Joshua E. Allen[3], Oren Becher[4], Juan Fueyo[5], Candelaria Gomez-Manzano[6], Ana Patiño-Garcia[1], Carl Koschmann[7], Marta M. Alonso[1]. *[1]Department of pediatrics, University of Navarra, Pamplona, Spain,[2]Department of Oncology, University Children's Hospital Zürich, Zürich, Pamplona, Switzerland,[3]Chimerix, Durham, NC,[4]Department of pediatrics, Icah School of Medicine at Mount Sinai, New York City, NY,[5]Department of Neuro-Oncology, The University of Texas MD Anderson Cancer Center, Houston, TX,[6]Department of pediatrics, University of Navarra, Houston, TX,[7]Department of pediatrics, University of Michigan, Ann Arbor, MI*

Purpose of the work: Pediatric High Grade Gliomas (pHGGs) and Diffuse Midline Gliomas (DMGs) are two of the most aggressive tumors developed during childhood. Its poor overall survival emphasizes the need of alternative treatments. ONC201, an imipiridone small molecule, and the oncolytic virus Delta-24-RGD have shown safety and effectiveness in preclinical and clinical settings for these diseases. In this work, we set to characterize the antitumor effect of these two agents combined for the treatment of pHGGs and DMGs.
Experimental procedures: A panel of human pHGG (CHLA-03-AA, SF188, SJ-GBM2), DMG (SU-DIPG IV, SF8628, TP-54, HSJD-DIPG-007, UMPED83), and murine DMG cell lines (XFM, NP-53) were used. We assessed viral replication by hexon titration, protein expression by immunoblotting/immunohistochemistry, and oxygen consumption by Seahorse analyses. Viability was measured by MTS. Mitochondrial DNA (mtDNA) were measured by qPCR. CHLA-03-AA/XFM were

orthotopically engrafted in athymic nude/Balb/c mice. For *in vivo* experiments, animals were treated with PBS/Delta-24-RGD (10^7 pfu/mice) intratumorally, followed by ONC201 oral gavage administration (125 mg/kg/twice/weekly). The tumor microenvironment immune infiltration was evaluated by flow cytometry.
Results: We checked the potential negative interaction between both agents *in vitro*. Adenovirus replication was not affected by ONC201 cotreatment, indicating the suitability of this combination. *In vitro* citotoxycity analyses showed the cotreatment is either synergistic or additive in 80% of the cells evaluated. Then, we set to characterize the mechanistic effects of the combination. Analysis of mitochondria status showed the decrease in oxygen consumption previously reported as ONC201 effect is maintained with Delta-24-RGD presence. Confirmation of higher mitochondria damage was assessed by a reduction of mtDNA in the combination. Independently, endoplasmic reticulum stress (ERS) previously described in both agents was found potentiated in cotreatment via ATF4. Altogether, these data suggest an improved response in the combination by mitochondria and ERS perturbation. *In vivo*, cotreatment led to a significant increase in the median OS (Control: 48 days; ONC201: 54.5 days; Delta-24-RGD: 62 days; Delta-24-RGD/ONC201: 95 days (P=0.0008)) in CHLA-03-AA bearing mice, leading to 20% long-term survivors, free of disease. Of importance, a reshaping of the tumor microenvironment towards a proinflammatory phenotype were described (increases of lymphoid (T and NK cells) and myeloid (macrophages, granulocytes, monocytes, denditric cells and microglia) linage.
Conclusions: Our data support the combination ONC201/Delta-24-RGD leads to a superior therapeutic effect due to the generation of a proinflammatory microenvironment in pHGG and DMGs preclinical models.

Novel Targets, Biomarkers, and Models for Cancer

#5773
A forward genetic screen identifies SIRT1 as a driver of neuroendocrine prostate cancer

Francisca Nunes de Almeida[1], Alessandro Vasciaveo[2], Min Zou[1], Matteo Di Bernardo[1], Andrea Califano[2], Cory Abate-Shen[1]. [1]*Department of*

Molecular Pharmacology and Therapeutics, Columbia University Irving Medical Center, New York, NY,[2]Department of Systems Biology, Columbia University Irving Medical Center, New York, NY

Neuroendocrine prostate cancer (NEPC) is a deadly variant of prostate cancer for which no cure is yet available. Up to 20 percent of the patients with castration resistant prostate cancer (CRPC), will progress to NEPC after treatment with standard-of-care therapies, such as abiraterone and enzalutamide, that target the androgen receptor (AR) pathway. However, the molecular mechanisms that drive the emergence of NEPC are largely unknown, contributing to a lack of treatment options for patients with NEPC. We implemented a forward genetic approach to identify novel drivers of NEPC, by using the *Sleeping Beauty* (SB) transposon-based forward genetic mutagenesis screening system in our *Pten-, Trp53*-deficient mouse model that is primed to develop NEPC at a low frequency. We generated a mouse strain (*NPp53-SB*) in which the *Nkx3.1* promoter regulates the expression of tamoxifen-inducible *Cre* specifically in the mouse prostate epithelium, resulting in transposition of the *T2Onc2* transposable element and conditional deletion of *Pten* and *Trp53* in mouse prostate epithelium. We observed an increased NEPC incidence in our *NPp53-SB* mouse model compared to control mice without the transposon *T2Onc2*, suggesting that the SB-mediated insertional mutagenesis events are driving the development of NEPC. To elucidate the genetic events that are driving the observed NEPC phenotype, we identified the common insertion sites (CISs) of the transposon insertions, which revealed a total of 330 CIS-associated genes. We further performed an integrative analysis using RNA-seq data from our SB cohort, a second mouse dataset and a metastatic CRPC patient cohort, which allowed us to identify the Master Regulator (MR) proteins that are associated with NEPC, as well as the upstream genomic events that modulate these MRs and the emergence of NEPC. Our integrative analysis identified the deacetylase Sirt1 as a candidate driver of NEPC. Using CRISPR activation (CRISPRa) technology *in vivo* we observed that SIRT1 activation induced an NEPC-like phenotype in the adenocarcinoma LNCaP cell line, while Sirt1 drug-mediated inhibition in an NEPC cell line resulted in less aggressive tumors.In summary, we have developed a *Sleeping Beauty* forward genetic screen in our mouse model of CRPC, which not only accelerates disease progression, but also increases the incidence of NEPC. Our integrative analysis identified a panel of CIS-associated genes that are likely to be functionally involved in progression to NEPC. In particular, Sirt1 was

shown to be a promising candidate, which may shed light on mechanisms that this aggressive disease uses to evade treatments and may inform the development of novel therapies.

#5774

Small cell lung cancer subtype plasticity is regulated by KDM6A

Leslie Duplaquet[1], Yixiang Li[1], Matthew A. Booker[1], Yingtian Xie[1], Radhika A. Patel[2], Deli Hong[1], Thomas Denize[3], Emily Walton[3], Yasmin N. Laimon[3], Roderick Bronson[4], Jackson Southard[1], Shuqiang Li[1], Sabina Signoretti[3], Michael Y. Tolstorukov[1], Paloma Cejas[1], Henry W. Long[1], Michael C. Haffner[2], Matthew G. Oser[1]. *[1]Dana-Farber Cancer Institute, Boston, MA,[2]Fred Hutchinson Cancer Research Center, Seattle, WA,[3]Brigham and Women's Hospital, Boston, MA,[4]Harvard Medical School, Boston, MA*

Small cell lung cancer (SCLC) is a high-grade neuroendocrine cancer that accounts for ~15% of lung cancers. While nearly all SCLCs are genetically driven by near universal loss of function (LOF) mutations in *RB1* and *TP53*; several recent studies show that there are different phenotypic SCLC molecular subtypes characterized by expression of lineage transcription factors. These include the neuroendocrine ASCL1 and NEUROD1 subtypes which together comprise ~70-80% of SCLCs. Initially subtypes were thought to be mutually exclusive, but recent evidence shows intra-tumoral subtype heterogeneity and plasticity between subtypes. A recent study found that 35-40% of human SCLCs express both ASCL1 and NEUROD1, but the mechanisms driving ASCL1 and NEUROD1 intra-tumoral heterogeneity are not well understood. My laboratory previously developed an autochthonous CRISPR-based SCLC genetically-engineered mouse model (GEMM) generated by intratracheally injecting adenoviruses encoding Cre recombinase and sgRNAs targeting *Rb1*, *Trp53*, and *Rbl2*. Cre turns on Cas9 expression and allows for CRISPR/Cas9 editing of *Rb1*, *Trp53*, and *Rbl2* in somatic cells in the lungs. The unique advantage of this model is that it allows the inclusion of sgRNAs targeting additional genes of interest in the same adenovirus. Using this CRISPR-based autochthonous SCLC GEMM approach, we studied the consequences of inactivating the epigenetic modifier KDM6A during SCLC tumorigenesis. KDM6A

functions as an H3K27 histone demethylase and also exists in the COMPASS complex with KMT2C/D to promote H3K4 mono-/di-methylation at enhancers. KDM6A along with its protein binding partner KMT2D are mutated in SCLC and KDM6A has been implicated in controlling differentiation in other lineages. Strikingly, we found that KDM6A inactivation in SCLC GEMMs induced plasticity from ASCL1 to NEUROD1 resulting in SCLC tumors that expressed both ASCL1 and NEUROD1. ATAC-sequencing showed open chromatin at the promoters of NEUROD1 and NEUROD1 target genes in KDM6A inactivated tumors. Interestingly, KDM6A inactivated tumors showed a spectrum of ASCL1 to NEUROD1 heterogeneity where some KDM6A inactivated tumors completely lost ASCL1 and solely expressed NEUROD1, some tumors expressed ASCL1 and NEUROD1 in a mutually exclusive manner, while others primarily expressed ASCL1 with very few NEUROD1 positive cells. Mechanistically, KDM6A binds and maintains ASCL1 target genes in an active chromatin state with its loss increasing H3K27me3 near both promoters and enhancers, and decreasing H3K4me1/2 at enhancers together leading to a cell state primed for ASCL1 to NEUROD1 subtype switching. This work identifies KDM6A as an epigenetic regulator that controls ASCL1 to NEUROD1 subtype plasticity and provides an autochthonous SCLC GEMM to model ASCL1 and NEUROD1 subtype heterogeneity, which is found in 35-40% of human SCLCs.

#5775

GLIS3 drives a neural-like malignant state enriched after neoadjuvant treatment in pancreatic cancer

Jimmy A. Guo[1], Jennifer Su[2], Carina Shiau[3], Ananya Jambhale[1], Annan Yang[4], Westley Wu[1], Junning Wang[4], Connor Hennessey[4], Patrick Yu[1], Brendan Parent[4], Giselle Uribe[4], Julien Dilly[4], Laleh Abbassi[4], Qijia Yu[4], Arnav Mehta[1], David Ting[3], Brian Wolpin[4], William Freed-Pastor[4], Joseph Mancias[4], Tyler Jacks[2], William L. Hwang[3], Andrew J. Aguirre[4]. *[1]Broad Institute of MIT and Harvard, Cambridge, MA,[2]MIT, Cambridge, MA,[3]Massachusetts General Hospital, Boston, MA,[4]Dana Farber, Boston, MA*

Pancreatic cancer is a challenging disease which lacks a robust precision oncology framework. Prior work has demonstrated that transcriptional subtypes in pancreatic cancer can stratify patients by response to chemotherapy and overall survival. These include classical and basal-like as the predominant subtypes in untreated disease, as well as a transdifferentiated neural-like malignant subtype enriched after standard-of-care chemotherapy. Nonetheless, our understanding of transcriptional subtypes remains critically limited by genetic and culture-based confounders in preclinical models. Furthermore, most murine pancreatic cancer models do not fully reflect the classical *vs.* basal-like divide observed in humans, preventing faithful *in vivo* investigation. Collectively, these challenges have hindered the study of and development of therapeutic strategies against these transcriptional subtypes. To enable systematic study of the classical, basal-like and neural-like subtypes, we developed isogenic KP (*Kras*$^{G12D/+}$;*Trp53*$^{FL/FL}$) organoids and leveraged CRISPR activation to endogenously overexpress state-specific transcription factors. Our data revealed that *Gata6* and dN*Trp63* drove classical and basal-like identity, respectively, supporting prior studies. Furthermore, through *in silico* approaches, we identified candidate drivers of the neural-like state, including *Glis3*, a zinc finger protein that mediates neuroendocrine fate during pancreatic development. We confirmed that *Glis3* overexpression results in neural-like transdifferentiation in cancerous organoids through RNA-seq and proteomics, and that *GLIS3* knockout abrogates neural-like identity in human cell lines. To study their malignant potential *in vivo*, we performed orthotopic transplants into murine pancreata, and observed that *Glis3* and dN*Trp63* accelerated tumor formation and progression, corresponding to clinical outcomes observed in patients. These models may therefore provide a means for *in vivo* interrogation of subtype biology and vulnerabilities. Finally, to model and predict therapeutic sensitivities, we performed *ex vivo* treatment assays with chemotherapy and emerging KRAS^{G12D} inhibitors. A selection assay showed that basal-like and neural-like organoids were starkly enriched by multi-agent chemotherapy, while classical organoids were depleted. Finally, we learned that the neural-like subtype exhibits differential sensitivity to KRAS^{G12D} inhibition through an RTK-associated mechanism. Taken together, we provide a foundational system for interrogating subtype-specific vulnerabilities in pancreatic cancer.

#5776

Advancing a screening platform with panels of patient-derived organoid models for drug discovery and development

Annamaria Rapisarda[1], Eric Jones[1], Curtis Hose[1], Erik Harris[1], Petreena S. Campbell[1], Mariaestela Ortiz[1], John Connelly[1], Nanda Mahashetty[1], Thomas Silvers[1], Zahra Davoudi[1], Penny Sellers Brady[1], Tiffany Nikirk Rohrer[1], Julie Grams[1], Karen Martin[1], Patricia Ramsey[1], Lori Bowles[1], John R. Britt[2], Ralph E. Parchment[3], Thomas S. Dexheimer[1], Beverly A. Teicher[4], James H. Doroshow[4], Nathan P. Coussens[1]. *[1]Molecular Pharmacology Laboratories, Frederick National Laboratory for Cancer Research, Frederick, MD,[2]Natural Products Support Group, Frederick National Laboratory for Cancer Research, Frederick, MD,[3]Clinical Pharmacodynamic Biomarkers Program, Frederick National Laboratory for Cancer Research, Frederick, MD,[4]Division of Cancer Treatment and Diagnosis, National Cancer Institute, Bethesda, MD*

High-throughput screening (HTS) offers the potential to rapidly evaluate the activities of anticancer single agents and combinations in many types of cell-based tumor models; however, successful translation of the findings to patients requires tumor models with high biological relevance. The National Cancer Institute's Patient-Derived Models Repository (PDMR, https://pdmr.cancer.gov) continues to develop a collection of highly characterized patient-derived organoid models representing a variety of cancer types including rare and recalcitrant malignancies and tumors from patients of diverse ancestry. More than 230 publicly available organoid models are undergoing characterization of their suitability for incorporation into HTS panels based on their recovery from cryopreservation, reproducible growth and expansion capacity, and assay performance metrics in a 384-well format with a CellTiter-Glo 3D viability endpoint. Organoid models with suitable characteristics are being screened with a library of 166 FDA-approved oncology drugs (https://dtp.cancer.gov/organization/dscb/obtaining/default.htm). Over a 7-day period, the organoids are exposed to five concentrations of each drug with a 1-log dilution series ranging from 0.01 μM to 100 μM. The concentration-response profiles of patient-derived organoids will provide

reference data for the organoid screen and will eventually include data from all approved and most investigational oncology agents (approximately 1,000 small molecules). NCI-60 cell lines were screened as monolayers in a 384-well format with a CellTiter-Glo viability endpoint after a 3-day exposure to the same oncology drug concentrations. Both monolayer and 3D tumor models were tested using a custom designed fully automated screening system and data analysis software platform. A comparison of the FDA-approved drug responses of a panel of 3D colon cancer organoids and a corresponding panel of 9 colon carcinoma NCI-60 cell lines elucidated similarities and differences attributable to the assay methodologies as well as the tumor model characteristics, such as the presence of a BRAF V600E variant or other clinically relevant genetic alterations (APC, ARID1A, BRCA2, etc.). As the characterization of PDMR organoid models for HTS continues, these pharmacological datasets will be made available as a resource for the cancer research community. This project was funded in part with federal funds from the NCI, NIH, under contract no. HHSN261201500003I.

#5777

Race as a predictive confounder in the rate of transdifferentiation and drug response in human pancreatic acinar ductal metaplasia

Corey Melissa Perkins[1], Jinmai Jiang[1], Hesam Hakimjavadi[2], Jason Brant[3], Zhongyue Zhang[3], Ji-Hyun Lee[3], David Quashie[4], Yating Mao[4], Jamel Ali[4], Sarah Kim[1], Martha Campbell-Thompson[2], Thomas Schmittgen[1].
[1]Pharmaceutics, University of Florida, Gainesville, FL,[2]Pathology, Immunology, and Laboratory Medicine, University of Florida, Gainesville, FL,[3]Biostatistics, University of Florida, Gainesville, FL,[4]Chemical & Biomedical Engineering, Florida Agricultural & Mechanical University, Tallahassee, FL

Pancreatic diseases (chronic pancreatitis, type 2 diabetes, pancreatic cancer) disproportionately affect the Black/African American (AA) community in comparison to non-White Hispanics and Whites. Acinar to ductal metaplasia (ADM), the process by which pancreatic acinar cells transdifferentiate into ductal epithelial cells, is believed to be an initiating event of pancreatic ductal adenocarcinoma. Our lab has developed a 3D organoid assay to display ADM using primary, human pancreatic acinar

cells to study the rate of transdifferentiation amongst these three different races. Preliminary data shows that the rate of ADM is occurring significantly faster ($p < 0.05$) in Blacks/AAs (White=16, Hispanic=11, Black/AA=5), which may explain the disproportionately behind the incidence and mortality rates for this race in pancreatic cancer. A sigmoid Emax function best captured the longitudinal changes in the percentage of ADM in nonlinear mixed effects modeling analysis performed in Monolix. Covariate analysis on top of the selected model demonstrated that race was the only covariate affecting the individual trajectories in the percentage of ADM. We additionally use nanoparticles to study the biomechanical properties (I.e., viscoelasticity, storage modulus) of the ADM microenvironment which shows a stiffer microenvironment in Blacks/AAs than for the other races (White=4,Hispanic=4, Black/AA=1). Furthermore, we have used a histone deacetylase (HDAC) inhibitor in reversing the process of ADM, which has consequently shown race-related outcomes, with Blacks/AAs displaying a significant chemoresistance ($p < 0.05$) to HDAC treatment (White=6,Hispanic=6, Black/AA=3) by utilizing an ADM reversal index (ADMRI). Through further analysis, the plan is to continue procuring human samples from these three races to isolate an ADM-specific biomarker in relation race and drug reversal by studying the expression/activity of pancreatic associated genes by bulk-RNA and single-cell sequencing.

#5778

Breast cancer mutations HER2^{V777L} and PIK3CA^{H1047R} activate the p21-CDK4/6 -Cyclin D1 axis driving tumorigenesis and drug resistance

Xiaoqing Cheng[1], Yirui Sun[1], Maureen Highkin[1], Nagalaxmi Vemalapally[1], Xiaohua Jin[1], Brandon Zhou[1], Julie L. Prior[1], Ashley R. Tipton[1], Shunqiang Li[1], Anton Iliuk[2], Samuel Achilefu[1], Ian S. Hagemann[1], John R. Edwards[1], Ron Bose[1]. *[1]Washington University in St. Louis, St. Louis, MO,[2]Tymora Analytical Operations, West Lafayette, IL*

In metastatic breast cancer, HER2 activating mutations frequently co-occur with mutations in the *PIK3CA*, *TP53*, or E-cadherin genes. Of these co-occurring mutations, *HER2* and *PIK3CA* mutations are the most prevalent gene pair, with approximately 40% of *HER2* mutated breast cancers also having activating mutations in *PIK3CA*. To study the effects of co-

occurring *HER2* and *PIK3CA* mutations, we bred genetically engineered mice with the (loxP-STOP-loxP) $HER2^{V777L}$; $PIK3CA^{H1047R}$ transgenes (HP mice) and studied the resulting breast cancers both *in vivo* as well as *ex vivo* using breast cancer organoids. HP mice rapidly developed invasive mammary adenocarcinoma at a median time of 2.1 weeks after adenoviral Cre injection into the mammary gland. Organoids from these breast cancers showed increased number of buddings in branching morphogenesis assay and increased migration and invasion *in vitro*. *In vivo*, HP breast cancers are resistance to the pan-HER tyrosine kinase inhibitor, neratinib, but are effectively treated by the combination of neratinib plus trastuzumab deruxtecan (T-DXd). *Ex vivo*, we found strong synergy between neratinib and T-DXd in HP organoids. Proteomic and RNA-seq analysis of HP breast cancers showed increased gene expression of *CCND1* (cyclin D1) and *CDKN1A* (which encodes p21WAF1/Cip1) and changes in cell cycle markers. An increase in p-p53, p-p27, and p-PDK1 in HP organoids was seen. The GSEA analysis showed that the mTOR pathway and the MYC target signature were significantly upregulated in the HP organoid group. As p21 stabilizes the cyclin D1-CDK4/6 complex to further activate CDK4/6, we found CDK4/6 inhibitors inhibit cell proliferation in HP mice-derived organoids. Combining neratinib with CDK4/6 inhibitors was another effective strategy for HP breast cancers with neratinib plus palbociclib showing a statistically significant reduction in mouse HP tumors as compared to either drug alone. We validated both the neratinib plus T-DXd and neratinib plus palbociclib combinations using a human breast cancer patient-derived xenograft that has HER2 and PIK3CA mutations very similar
to our transgenic mouse. This study provides valuable preclinical evidence for these drug combinations, which are being tested in phase 1 clinical trials.

#5779

A platform utilizing high-grade serous ovarian cancer organoids for prospective patient stratification in functional precision medicine

Wojciech Senkowski[1], Laura Gall-Mas[1], Matias M. Falco[2], Yilin Li[2], Kari Lavikka[2], Mette C. Kriegbaum[1], Jaana Oikkonen[2], Daria Bulanova[1], Elin J. Pietras[1], Karolin Voßgröne[1], Yan-Jun Chen[1], Erdogan P. Erkan[2], Mia K. G. Høg[3], Ida M. Larsen[3], Tarja Lamminen[4], Katja Kaipio[4], Jutta Huvila[4], Anni

Virtanen[2], Lars H. Engelholm[3], Pernille Christiansen[3], Eric Santoni Rugiu[1], Kaisa Huhtinen[4], Olli Carpén[2], Johanna Hynninen[5], Sampsa Hautaniemi[2], Anna Vähärautio[2], Krister Wennerberg[1]. *[1]University of Copenhagen, Copenhagen, Denmark,[2]University of Helsinki, Helsinki, Finland,[3]Rigshospitalet, Copenhagen, Denmark,[4]University of Turku, Turku, Finland,[5]Turku University Hospital, Turku, Finland*

High-grade serous ovarian cancer (HGSC) is the most prevalent and lethal ovarian cancer type. While HGSC usually responds well to primary treatment, most cases eventually relapse. Functional precision medicine - tailoring individualized treatments based on functional in vitro assays on patient-derived cells - has been recently employed in cancer clinical trials. Cancer organoids - three-dimensional, self-organizing, self-renewing cell cultures that recapitulate original tissue structure and function - have been applied as cellular models in these trials. However, in case of HGSC, organoid derivation has proven time consuming and inefficient, hindering their application in functional precision medicine due to a short time window, in which therapy for each patient needs to be selected.
To address this problem, we aimed to establish whether drug vulnerabilities at HGSC relapse could be predicted using organoids derived from the primary disease cells. We derived sequential organoid models from material sampled during primary treatment and at relapse. Then, for organoid pairs (primary-relapse), we performed large-scale drug response profiling of a library of 370 compounds (approved drugs or drugs in clinical development), in 384-well microplate format, alone or in combination with a standard HGSC chemotherapeutic agent carboplatin. First, we found that HGSC organoid responses to standard chemotherapeutics retrospectively correlated to observed clinical treatment outcomes. But further, for each patient we identified compounds with pronounced cytotoxicity both in the primary and in the relapsed model, amounting to 66% of all hits (7% were primary-specific and 27% relapse-specific). We then focused on identifying patient-specific hits rather than compounds displaying general toxicity in all patient models. Based on a potential clinical applicability, for three patients we selected compounds for validation in organoid outgrowth assay, with prolonged (>1 month) drug-free period post-treatment. In two patients, AZD4573, a selective CDK9 inhibitor in clinical development for hematological malignancies, at nanomolar concentrations caused

eradication of organoids when combined with carboplatin. Organoids from the third patient were vulnerable to nitazoxanide, an approved anti-helminthic agent and an inhibitor of mitochondrial oxidative phosphorylation. Importantly, the selected final hits were identified solely based on screening in organoid models from primary disease.
In summary, we here demonstrate that HGSC organoids derived from primary disease material predict a majority of patient-specific drug vulnerabilities of organoids derived from the relapsed HGSC lesions. This indicates that patient stratification in functional precision medicine for treatment of HGSC relapse could be prospectively performed at the primary disease stage.

Patient-Derived Xenograft Models

#4664
MatchR a preclinical platform of models resistant to innovative therapies

Ludovic Bigot[1], Catline Nobre[1], Francesco Facchinetti[1], Loic Poiraudeau[1], Floriane Braye[1], Jonathan Sabio[1], Naoual Mensourri[1], Olivier Deas[2], Claudio Nicotra[3], Maud Ngo-Camus[3], Lambros Tselikas[4], Jean Yves Scoazec[5], Karim Fizazi[6], Siantiago Ponce[3], Benjamin Besse[6], Luc Friboulet[1], Yohann Loriot[1]. *[1]INSERM U981 (Gustave Roussy), Villejuif, France,[2]Xentech, Evry, France,[3]Drug Development Department (DITEP), Gustave Roussy, Villejuif, France,[4]Department of Interventional Radiology, Gustave Roussy, Villejuif, France,[5]Experimental and Translational Pathology Platform, Gustave Roussy, Villejuif, France,[6]Department of Medical Oncology, Gustave Roussy, Villejuif, France*

Introduction: In the last 20 years, the advances in molecular oncology and cancer genetics allowed the identification of an increasing number of actionable oncogenic drivers and the development and clinical use of specific inhibitors. Despite these successes, it is now well established that tumour cells adapt and develop acquired resistance. It is crucial to understand these mechanisms of acquired resistance to develop overcoming therapeutic strategies. At Gustave Roussy, a prospective clinical trial MATCH-R (NCT02517892) is conducted to study the acquired resistance

mechanisms and to find new therapeutic approaches for patients. . In parallel, of genetics analysis from patients biopsies, we develop Patient Derived Xenograft (PDX) to deepen our understanding of the resistance mechanism and to investigate new therapeutic approaches.
Material and Method: Fresh tumor biopsy specimens were obtained prospectively from patients through a prospective single-institution clinical trial (MATCH-R, NCT02517892). Patient derived xenografts (PDX) in NOD Scid Gamma (NSG) mice as well as patient derived organoids from PDX (PDXO) and Patient derived cell lines were developed and characterized. Extensive molecular profiling including whole exome sequencing (WES), RNA sequencing (RNAseq) and immunohistochemistry were performed on human samples; PDX; Patient derived cells lines and PDXO.
Results and Discussion: As of November 2022, 145 PDX models have been successfully obtained from 371 biopsies (global take rate of 39%). Our focus is the development of models from different cohorts: Androgen receptor inhibitors in castration-resistant prostate cancer, (18 PDX), ALK inhibitors in lung cancers (16 PDX including 3 post brigatinib, 7 post Lorlatinib and 6 Alectinib), *EGFR* inhibitors in lung cancers (33 PDX includind 24 post osimertinib), FGFR inhibitors in urothelial carcinoma and cholangiocarcinoma (29 PDX including 14 post erdafitinib, 4 post pemigatinib, 4 post futibatinib) and KRAS inhibitors in lung cancer and pancreatic cancers (20 PDX). The PDX models recapitulate the genetics, the phenotype and the pharmacology of the original biopsies. Novel mechanisms of resistance to tyrosine kinase inhibitors (TKI) in solid tumors were identified. Adaptive treatment with novel TKI or combinatorial strategies were evaluated to restore the sensitivity in PDX (readout: mean tumor growth). These results confirmed that PDX models are crucial to study the resistance mechanism and to develop new therapeutic strategies.
Conclusion: Overall, the MATCH-R study provides a unique preclinical platform to identify resistance mechanisms to innovative therapies and to develop next generation therapeutic strategies.

#4665
Enhancing preclinical testing of agents in patient-derived pediatric solid tumor orthotopic xenografts with pharmacokinetics

Burgess B. Freeman[1], Kaley Blankenship[2], Michael A. Dyer[3], Elizabeth Stewart[2]. *[1]Preclinical Pharmacokinetics Shared Resource, St. Jude Children's Research Hospital, Memphis, TN,[2]Department of Oncology, St. Jude Children's Research Hospital, Memphis, TN,[3]Department of Developmental Neurobiology, St. Jude Children's Research Hospital, Memphis, TN*

Understanding a potential therapeutic agent's in vivo pharmacokinetics (PK) is important in translating findings from preclinical murine efficacy models to patients. In consideration of this, PK evaluations play a prominent up-front role in our pediatric solid tumor testing pipeline. The aim of such PK studies is to define an agent's PK under our experimental conditions – i.e. our mouse strain, husbandry, chow, source and lot of agent, and formulation. We ultimately relate our mouse plasma exposures to the known or anticipated exposures in humans or children, thereby deriving a clinically relevant dose (CRD). Preclinical testing of novel agents and combinations are performed simultaneously with the testing of standard of care agents using the CRD and schedule to allow for more unbiased assessment of efficacy. To date, our group has studied the PK of over 35 agents, predominantly investigational new drugs, in both normal and patient-derived orthotopically xenografted (PDOX) immuno-deficient mice. When possible, rhabdomyosarcoma and neuroblastoma PDOXs were destructively sampled over time to evaluate an agent's intra-tumor exposure. All samples were quantified using sensitive, specific, and research- or qualified-tier LC-MS/MS assays. Roughly 70% of the agents had adequate tumor penetration, approaching or exceeding concentrations in the plasma. This was unsurprising, given that many test agents had reportedly high volume of distribution (V_d) values. While most of our mouse PK exposure parameters (e.g. C_{max}, AUC) were in line with available previous reports, several agents varied appreciably, generally trending lower. We speculate that this may be due to differing study conditions, test agent physical forms, or formulations. CRD estimates were based upon unbound (when available) steady-state plasma AUC equivalencies between mice and humans for a defined clinical dosage regime. Some latitude was permitted in the recommended CRD, and being within two-fold of clinical target was generally considered acceptable. The

resultant mouse CRDs and updated PK results for studied agents will be presented, with this information also being openly available upon request and/or at http://cstn.stjude.cloud. In conclusion, we have found that PK-driven, clinically relevant dosing enhances the efficiency and rigor in our in vivo efficacy testing program. Such an approach minimizes false positive signals arising from supra-clinically relevant doses and exposures in mouse models, allowing us to focus on efficacious agents and regimens for rapid clinical translation.

#4666

PDX, mini-brain co-cultures and patient-derived tumor organoids: Preclinical models to study the prion protein in glioblastoma biology

Maria Clara da Silva Souza[1], Barbara P. Coelho[1], Camila F. L. Fernandes[1], Tiago G. Dos Santos[2], Stefan Knorst[3], Cibele Masotti[3], Maria Rita S. Passos-Bueno[4], Marilene H. Lopes[1]. *[1]Cell Biology and Developmental, Institute of Biomedical Sciences (ICB), University of Sao Paulo, Sao Paulo, Brazil,[2]International Research Center, Hospital A.C.Camargo Cancer Center, Sao Paulo, Brazil,[3]Institute of Teaching and Research Sírio-Libanês Hospital, Sao Paulo, Brazil,[4]Institute of Biosciences, University of Sao Paulo, Sao Paulo, Brazil*

Glioblastoma (GBM), supported by a subpopulation of glioblastoma stem cells (GSCs), stands among the most harmful tumors. Its invasive and aggressive behavior has been correlated with poor therapy outcomes and reduced patient survival, which remains difficult to model and treat due to its cellular and molecular heterogeneity. GSCs are responsible for the malignant features of this cancer, including increased recurrence rates and resistance to therapy. Efforts have been employed to understand the molecular and cellular mechanisms underlying GSCs biology. The cellular prion protein (PrP^C), encoded by the *PRNP* gene, is a key player in GBM biology, and our group has proposed PrP^C as a scaffold protein that integrates signaling platforms involved in GSCs maintenance. A deeper understanding of the intracellular pathways modulated by PrP^C is essential to identify novel targets for GBM treatment. We have analyzed bulk-RNA sequencing (RNA-seq) data from patient-derived xenografts (PDX) and *in vitro* preclinical experimental models. RNA-seq analyses identified

differentially expressed genes (DEGs) associated with adhesion and migration signaling pathways in PDX cells with high PRNP expression (PRNP^{-HIGH}). Morphological characterization of PDX samples with PRNP^{-HIGH} levels showed an increase in morphologically undifferentiated cell groups, that are more commonly found in younger GBM patients. Furthermore, molecular profiling using Exome data showed that groups PRNP^{-HIGH} present enhanced global patterns of gene mutations. Due to the importance of experimental models to translate basic science into clinical applications, we are establishing emerging models to study PrP^{C} function in GBM biology: glioblastoma organoids (GBO) from patient's surgically resected GBM tumors; and brain organoids derived from human-induced pluripotent stem cells. We noticed a morphological and molecular reproducibility of the cytoarchitecture of brain organoids and GBO, similar to that described in the literature, indicating consistency in 3D structures, despite the variability between patients. Furthermore, brain organoids will be co-cultured with GSCs, providing platforms for studying the interaction between tumor cells and brain parenchyma. The establishment of these models will improve our comprehension of the role of PrP^{C} in GSCs maintenance and provide additional tools to understand GBM biology and predict tumor progression and response to treatment.

#4667

Establishment of patient-derived human cell lines using PDX mouse model for intrahepatic cholangiocarcinoma

Takashi Matsumoto. *Kumamoto Univ Graduate School of Medical Sci, Kumamoto, Japan*

Background: In recent years, patient tumor transplant models (PDX models) have attracted method that can predict the effects of anticancer drugs on patients. The PDX model is a technique in which the patient's tumor tissue is directly transplanted into immunodeficient mice. Tumors can grow three-dimensionally in a living mouse, so compared to culturing in petri dishes, the situation is like the growth of tumors in the patient's body. In addition, there are reports that the efficacy of anticancer drugs in patients and the results of administration of anticancer drugs in PDX show a high concordance rate, and it is attracting attention as a model that can predict efficacy in patients. In this time, we report on the establishment of

cell lines using PDX mice for resected cases of intrahepatic cholangiocarcinoma in our hospital.
Methods: Twelve patients who underwent surgical resection between September 2019 and December 2021 were included. After resected the tumor, the tumor was transplanted into up to 10 PDX mice, and cell lines were established from the formed tumor tissue.
Results: Of the 12 cases, tumors formed in PDX mice after transplantation in 6 cases, and the median time to engraftment after the first transplantation was 133 days (75-188). Furthermore, among the 6 cases, 3 cases achieved the establishment of cell lines.Case1:moderately differentiated adenocarcinoma, tumor diameter 50mm, single, vascular invasion positive, no lymph node metastasis, Stage IIIA (UICC 8^{th})Case2:well differentiated adenocarcinoma, tumor diameter 60mm, single, vascular invasion negative, no lymph node metastasis, Stage II (UICC 8^{th})Case 3:moderately differentiated adenocarcinoma, tumor diameter 55mm, single, vascular invasion positive, no lymph node metastasis, Stage IIIA (UICC 8^{th})
Conclusion: The cell line we established this time is a case of advanced cancer, and we would like to continue to increase the number of cases and continue to establish cell lines, which will lead to future research.

#4668

***In-vitro* modeling of tumor-associated macrophages in glioblastoma**

Hasan Alrefai, Andee M. Beierle, Taylor L. Schanel, Lauren C. Nassour, Joshua C. Anderson, Patricia H. Hicks, Christopher D. Willey. *Radiation Oncology, University of Alabama at Birmingham, Birmingham, AL*

BACKGROUND**:** The Glioblastoma (GBM) tumor microenvironment (TME) is comprised of a plethora of cancerous and non-cancerous cells that contribute to GBM growth, invasion, and chemo- and radio-resistance. In-vitro models of GBM typically fail to incorporate multiple cell types. Some groups have addressed this problem by employing 3D bioprinting to incorporate macrophages, astrocytes, and other parenchymal cells in an extracellular matrix. However, these models also use serum-containing media, which has been shown to cause GBM brain-tumor initiating cells to lose their stem-like properties, and IL-4/13 polarized macrophages (M2), even though tumor-associated macrophages (TAMs) do not adhere to the traditional M2 phenotype. Taken together, these observations highlight a

critical need to develop physiologically accurate in-vitro model systems for GBM.
METHODS: THP-1 monocytes were transitioned from serum-containing RPMI 1640 to serum-free CTS™ AIM V™ SFM and TheraPEAK™ X-VIVO™-15 Serum-free Hematopoietic Cell Medium. Monocytes were stimulated towards a macrophage-like state with PMA and polarized by co-culturing them with GBM patient-derived xenograft (PDX) lines, using transwell inserts. dPCR, a cytokine array, and a phagocytosis assay were used to characterize macrophages polarized by this method relative to classically polarized resting (M0), pro-inflammatory (M1), and anti-inflammatory (M2) macrophages.
RESULTS: There was no significant difference in proliferation rates up to 48 hours for THP-1 monocytes grown in serum-free CTS AIM V or X-VIVO-15 media compared to serum-containing RPMI 1640. At 72 hours, both serum-free alternatives had slightly decreased proliferation relative to the serum-containing RPMI 1640; however, the X-VIVO-15 had higher proliferation relative to the CTS AIM V ($p<0.0001$). THP-1 macrophages polarized towards a tumor-supportive phenotype by the GBM PDX cell line, JX39P-RT, did not recapitulate the cytokine expression profile of any other polarization group. M2 macrophages had significantly higher phagocytic capacity (25%) of JX39P-RT relative to M0, M1, and TAMs (<15%, $p<0.01$).
CONCLUSIONS: We have demonstrated a serum-free method by which we can polarize macrophages towards a GBM-supportive phenotype. This high-fidelity method of modeling TAMs in GBM will aid in the development of innate immunomodulatory therapeutics that may one day enter the clinic in hopes of improving GBM outcomes.

#4669
A patient derived xenograft model for lung adenocarcinoma using Obagel®, a human derived hydrogel
Cecilia Sanchez[1], Jonathan Nakashima[2], Kristein King[2], Trivia Frazier[1].
[1]Obatala Sciences, Inc., New Orleans, LA,[2]Certis Oncology Solutions, San Diego, CA

Patient Derived Xenografts (PDXs) are valuable disease models as they preserve the tumor microenvironment's structure, providing the most

clinically relevant in vivo testing platform. Nevertheless, most of those models still use animal derived hydrogels as scaffolds for patient derived cells, reducing the potential to fully mimic the physiological microenvironment of the disease and human condition. ObaGel® is a human-derived hydrogel successfully deployed for supporting 3D cell culture, organoid, perfusion bioreactor, and/ microphysiological system development for studying obesity, type II diabetes, and various forms of related cancers. Here we are investigating the use of Obagel® in the in-vivo development of a PDX-derived culture of lung adenocarcinoma and compare its performance to currently used animal derived hydrogels. *Methods:* 3 X 10^6 CRT00295 Non-small cell lung adenocarcinoma cells in 100ul 50:50 indicated Gel in PBS per injection site; the study used 10 NOG mice per condition. *Results:* The results indicated that ObaGel® performed similarly in terms of engraftment and tumor kinetics compared to animal derived hydrogels such as Cultrex, Geltrex, and Matrigel, using a patient-derived xenograft culture of lung adenocarcinoma. *Conclusions:* Our data supports the use of a human-derived hydrogel for PDX models, ObaGel® performs equivalently to animal derived hydrogels to support tumor volume over time. The use of a human derived hydrogels as scaffolds for PDX models provide a better humanized local microenvironment for lung adenocarcinoma. Obagel® can also be adapted for use as xenografts in other tissue/disease models

#4670

True bench-to-bedside science: An international pilot study modeling hard-to-cure pediatric cancers to prioritize therapeutic intervention

Nadine Azzam[1], Nicole Melong[1], Lissandra Tuzi[1], Lisa Pinto[1], Jamie I. Fletcher[2], Alvin Kamili[2], Biljana Dumevska[2], Loretta Lau[3], Jennifer A. Chan[4], Donna L. Senger[5], Stephanie A. Grover[6], Michelle Haber[2], David Malkin[6], Jason N. Berman[1]. *[1]CHEO RI - Children's Hospital of Eastern Ontario Research Institute, Ottawa, ON, Canada,[2]Children's Cancer Institute, Sydney, Australia,[3]Sydney Children's Hospital, Sydney, Australia,[4]Arnie Charbonneau Cancer Institute, Calgary, AB, Canada,[5]Lady Davis Institute for Medical Research, Montreal, QC, Canada,[6]The Hospital for Sick Children, Toronto, ON, Canada*

There has been dramatic improvement in treatment outcomes for many pediatric cancers over the last three decades. However, for the 20% of young people with relapsed or refractory cancer, the prognosis remains grim. Canada's PRecision Oncology For Young peopLE (PROFYLE) and Australia's Zero Childhood Cancer (ZERO) programs, leverage nation-wide scientific and clinical oncology expertise to provide personalized precision medicine to children, adolescent and young adult (CAYA) cancer patients who lack treatment options. Beyond improving the lives of young cancer patients nationally, PROFYLE and ZERO have partnered to create an international pipeline for knowledge sharing and sample acquisition.
A key component of both programs is the use of mice for patient-derived xenografts (PDXs). However, long lead times for mouse PDX generation make the timely return of preclinical drug response data challenging. PROFYLE has uniquely incorporated zebrafish larval xenografts, which have the potential to provide comparable information in a clinically actionable timeframe. In a pilot study, we compared retrospective matched ZERO patient and mouse PDX therapeutic response data with prospective zebrafish larval PDX data as a proof-of-principle that drug efficacy signals were maintained across model systems. Three ZERO avatars: high-risk neuroblastoma, Ewing's sarcoma, and anaplastic large cell lymphoma were shipped from Australia to Canada and transplanted into 48h *casper* zebrafish. Following dose optimization, zebrafish PDXs were treated with targeted single and combination drug treatments by immersion therapy. Strikingly, in as little time as a week, cell proliferation rates and drug responses to single agents and combinatorial therapy in zebrafish PDXs recapitulated mouse and patient data. To expand on this pilot project, we tested additional patient samples, including multiple subtypes of sarcomas, T-cell acute lymphoblastic leukemia and an embryonal tumor with multilayered rosettes. Results further validated the practical utility of the zebrafish larval PDX model and in fact provided drug response data when mouse PDX data were unavailable. This study demonstrates the robustness and feasibility of the zebrafish larval PDX model as a preclinical tool for personalized precision therapeutic decision-making and highlights the value of international collaboration in improving outcomes of rare childhood cancers.

#4671

MAO A, MAO B inhibitors and NMI for colon cancer therapy

Shivani Soni[1], Hui Ju Tseng[2], Yan Yang[3], Goar Smbatayan[1], Unnati Hemant Shah[2], Jae Ho Lo[1], Joshua Millstein[3], Francesca Battaglin[1], Pooja Mittal[1], Lesly Torres Gonzalez[1], Wu Zhang[1], Jean Chen Shih[2], Heinz Josef Lenz[1]. *[1]Medical Oncology, USC Norris Comprehensive Cancer Center, Los Angeles, CA,[2]Department of Pharmacology and Pharmaceutical Sciences, University of Southern California, Los Angeles, CA,[3]Department of Population and Public Health Sciences, University of Southern California, Los Angeles, CA*

Background**:** Mitochondrial MAO A and MAO B isoenzymes catalyze oxidative deamination of neuroactive and vasoactive monoamines in CNS and peripheral tissues. MAO A inhibitors have been used as antidepressants; MAO B inhibitors have been used for Parkinson's disease. Recently, we and others have shown MAO inhibitors can be repurposed for cancer therapy. This study focused on the MAO inhibitors as a novel therapeutic strategy for CRC utilizing patient derived xenograft (PDX) platform which recapitulates the patient's molecular characteristics.
Methods and Results: CRC PDX models were selected from our repository based on MAO A and B expression and activity. To establish two PDX models with high or low MAO A / B activity we implanted patient's tumor samples (F0 generation) with high MAO A/B activity (MAO high) or low MAO A/B activity (MAO low) in 8 weeks NSG mice (F1 generation). F1 MAO low PDX model showed substantially slower tumor growth rates as compared to MAO high PDX model (200 days vs 65 days), suggesting the role of MAOs in CRC growth. For each PDX model trial, tumors were pooled from 6 F1 PDX mice and implanted in 30 NSG mice (F2 generation). There were five mice in each of experimental groups: one control arm (vehicle: 67% PEG 400, 33% saline) and treatment arms (i.p. for 21 days): 1. MAO A inhibitors: clorygyline: 50mg/kg; 2. Near infrared dye conjugated MAO A inhibitor (NMI): 5 mg/kg; 3. MAO B inhibitor: deprenyl 10mg/kg;4. MAO A & B inhibitor: phenelzine (30mg/kg). MAO high PDX cohort showed significant reduction in tumor volume in mice treated with MAO A inhibitors clorygyline ($p=0.009$); NMI ($p=0.053$) and MAO B inhibitor deprenyl ($p=0.022$), phenelzine ($p= 0.097$) when compared to control. Angiogenesis marker CD31 staining of tumor tissues showed significant reduction in mice treated with clorygyline and NMI.

Additionally, Ki 67 staining demonstrated considerable decrease in cell proliferation and TUNEL assay exhibited increase in apoptosis in tumor treated with clorygyline and NMI. RNA sequencing revealed 50 differentially expressed genes (DEGs) between clorygyline treated tumors and control, 171 between NMI treated and control group (padj <0.05, |fold change| >=1.5). Ingenuity Pathway Analysis showed alterations in pathways including oxidative phosphorylation, sirtuin pathway, estrogen receptor signaling, and mitochondrial dysfunction. NMI showed same efficacy with no toxicity compared to clorygyline even at 10 times lower dose in MAO high PDX model. No significant difference in tumor size was found among treatment groups in MAO low PDX cohort.
Conclusion: Our CRC PDX studies showed both MAO A and B are important for tumor growth and are potential target for therapy. Both MAO A and B inhibitors and NMI (NIR-conjugated MAO an inhibitor, clorgyline) reduced tumor growth. IHC and RNA seq data shows MAO A inhibitor and NMI has similar mechanisms, though NMI is more effective than clorygyline and also can be used for diagnosis.

#4672

In-vivo tumor implantation site exhibits differential immune response in solid tumors

Rajeev Shrimali[1], Jasmine Borroel[1], Carmen Sunico[2], Bridget Corcoran[2], Bianca Carapia[3], Rowan Prendergast[4], Jantzen Sperry[5], Jonathan Nakashima[5]. *[1]Immuno-Oncology R & D, Certis Oncology Solutions, San Diego, CA,[2]In-vitro R & D, Certis Oncology Solutions, San Diego, CA,[3]In-vivo operations, Certis Oncology Solutions, San Diego, CA,[4]Study Director, Certis Oncology Solutions, San Diego, CA,[5]Operations R & D, Certis Oncology Solutions, San Diego, CA*

Successful discovery and development of cancer targeted therapeutics depends on testing these agents in the clinically most relevant translational models. Emerging evidence highlights the importance of the local tumor microenvironment in evaluating the efficacy of new therapeutics, especially for immunotherapies. Historically, patient-derived xenograft (PDX) modeling involves subcutaneous implantation which minimally represents the actual human tumor site. Here, we use PBMC humanized PDX models to demonstrate differences in the tumor microenvironment, overall immune

response, and the pharmacological outcome, between subcutaneous and orthotopic PDX models. These findings highlight the importance of testing cancer therapeutics in the most physiologically relevant setting for greater translation into clinical success.

#4673

Therapeutic potential of polatuzumab vedotin for the treatment of diffuse large B-cell lymphoma

Hui Qi, Fuyang Wang, Bingrui Han, Xiaomin Wang, Xiangnan Qiang, Zhixiang Zhang, Qiangyang Gu. *WuXi AppTec, Shanghai, China*

Background Diffuse large B-cell lymphoma (DLBCL) is typically treated with rituximab, cyclophosphamide, doxorubicin, vincristine, and prednisone (R-CHOP). Although most patients can be cured with R-CHOP, up to one-third of them relapses with a dismal outcome in most cases. Numerous approaches have been attempted to improve the treatment outcomes with R-CHOP. Polatuzumab vedotin is an antibody-drug conjugate targeting CD79b, which is ubiquitously expressed on over 90% of B-cell NHL malignancies, including DLBCL. To determine the potential of polatuzumab vedotin as a therapeutic agent, we evaluate its potency across a series of DLBCL patient derived xenograft (PDX) models.
Method We established and characterized a series of DLBCL lymphoma PDX models. Eight DLBCL PDX models were selected for polatuzumab vedotin efficacy study, of which three are GCB DLBCL. Gene expression analysis of these lymphoma PDX models was performed using an Illumina NovaSeq 6000 system following Illumina-provided protocols for 2x150 paired-end sequencing. The expression status of CD79b on these DLBCL PDX models was also evaluated by IHC.
Conclusion Our data showed that a single dose of polatuzumab vedotin at just 2 mg/kg could reached a comparable effect with R-CHOP and no significant body weight loss was observed. Our result showed that there is no apparent correlation between polatuzumab vedotin responses (TGI) and the CD79b expression (IHC Score). Although polatuzumab vedotin demonstrated encouraging activity in the treatment of DLBCL, some of the PDX models are also resistant to polatuzumab vedotin treatment. To further investigate the molecular parameters of the relative sensitivity of polatuzumab vedotin. Gene expression profiling of those PDX models and

their sensitivity to polatuzumab vedotin were conducted, we found that the expression level of BCL-XL was correlated with reduced sensitivity to polatuzumab vedotin.

#4674

Patient-derived xenograft (PDX) and corresponding cell line models from glioblastoma for drug development, immuno-oncology and translational research

Joshua Alcaniz[1], Lars Winkler[1], Maria Stecklum[1], Hagen Wieland[2], Antje Siegert[1], Michael Becker[1], Bernadette Brzezicha[1], Wolfgang Walther[3], Jens Hoffmann[1]. *[1]EPO GmbH, Berlin, Germany,[2]PromoCell, Heidelberg, Germany,[3]Charité Universitätsmedizin, Berlin, Germany*

Background**:** Glioblastoma (GBM) is the most common malignant brain tumor in adults, with about 90% of tumors developing *de novo*. Their heterogeneity, aggressiveness and infiltrative growth limit success of current standard of care (SoC) therapy and efficacy of new therapeutic approaches. For drug development a large panel of patient-derived tumor cell models is needed to generate most comparable *in vitro* and *in vivo* platform reflecting the complex biology of glioblastoma. Glioblastoma cell lines from patient-derived xenografts (PDX) preserve many patient specific characteristics and to perform the essential steps of pre-clinical drug development from *in vitro* screening to orthotopic *in vivo* approaches under conditions, which closely resemble the clinical situation. Further, GBM PDX models are useful for immune oncology research.
Methods: A panel of 26 glioblastoma PDX models was established on immunodeficient mice (15 out of these established orthotopically). All models were characterized for drug sensitivity and molecular profile using panel and transcriptome sequencing. From these, three corresponding tumor cell lines were successfully established and characterized. Quality and identity of the models was performed by FACS and PCR analysis. Expression profile, drug sensitivity and growth behavior was determined and compared *in vitro* and after re-transplantation *in vivo* with the original PDX glioma model. In addition, we employed GBM PDX models for checkpoint-inhibitor sensitivity in humanized mouse settings.
Results: Drug testing was performed in s.c. and orthotopic models revealed, that best treatment responses in s.c. models (tumor growth

inhibition > 50%) were observed for SoC temozolomide (TMZ), irinotecan and bevacizumab. Molecular characterization identified all our models as IDH-wt (R132) with frequent mutations in PARP1, EGFR, TP53, FAT1, and within the PI3K/AKT/mTOR pathway. Their expression profiles resemble proposed *mesenchymal*, *proneural* and *classical* GBM molecular subtypes. Further, treatment of GBM PDX with ipilimumab, nivolumab or pembrozolumab generated minor growth delay.
Conclusions: In drug sensitivity screening, irinotecan or bevacizumab were identified as alternative treatment options in TMZ resistant GBM PDX models. Our data demonstrate, that the established platform of s.c. and orthotopic GBM PDX is valuable for drug development and can well be complemented by a PDX-derived cell lines for *in vitro* screens. Furthermore, these models can be used for the evaluation of new immune-oncology therapies.

#4675
Chemoresistant patient-derived xenografts to identify treatment options in breast cancer patients not responding to standard chemotherapy
Eivind Valen Egeland, Kotryna Seip, Geir Frode Øy, Eleni Skourti, Solveig J Pettersen, Siri Juell, Mads Haugland Haugen, Olav Engebraaten, Lina Prasmickaite, Gunhild M Maelandsmo. *Institute for Cancer Research, Oslo University Hospital, Oslo, Norway*

Resistance to chemotherapy is a major clinical challenge in breast cancer (BC), and patients developing resistance need treatment alternatives. In this project we utilize patient-derived xenografts (PDXs) from triple negative BC (TNBC), as these models better reflect the human tumor complexity and heterogeneity, compared to cell line-based- and transgene animal models. An in-house established orthotopically growing PDX, MAS98.12, has gained resistance to chemotherapy due to prolonged exposure to paclitaxel (MAS98.12-PR), a microtubule-targeting chemotherapeutic agent. As the resistance was obtained in animals, we also have the paclitaxel sensitive equivalent (MAS98.12-PS). By utilizing the pair of sensitive and resistant tumors we can study the corresponding mechanism evolving in patients who initially respond to chemotherapy before resistance and disease progression. This model will aid in identifying key

mechanisms of survival in the resistant tumors, and eventually in identifying targets for use as novel therapeutic opportunities in TNBC patients resistant to standard therapy. Finally, we have samples collected early and late after resistance development, allowing us to characterize mechanisms involved in stepwise progression of paclitaxel resistance. We are currently performing molecular profiling to reveal the mechanisms involved in development of resistance. Data from bulk RNAseq, immune profiling of myeloid cells, exome sequencing, secretome profiling and reverse-phase protein array (RPPA) allow for characterizing the isogenic pair of tumors on multiple levels. Preliminary observations include aberrant expression of *ABCB1*/MDR1, normally involved in translocating drugs across membranes, and previously described as a mechanism involved in pertaining resistance in tumor cells. As multiple attempts to target MDR1 itself has failed, we hypothesize that our PS and PR pair will identify vulnerable/targetable signaling axis in the resistant tumors. Additionally, both PDX models have been assessed for their sensitivity to various chemo-/targeted-drugs and their combinations, revealing alternative means of treating the resistant tumors. Altogether, the molecular profiles and the sensitivity data will give novel knowledge and treatment options for patients failing to respond to standard chemotherapy.

#4676

Deconvolution of extrinsic and intrinsic factors influencing tumor growth in solid cancer PDX models to support design, analysis and application of PDX-based pharmacology studies

Mathew Clark[1], Kanstantsin Lashuk[2], Edward McGowan[3], Julia Schueler[2].
[1]Charles River Laboratories, Inc., Wilmington, MA,[2]Charles River Laboratories, Inc., Freiburg, Germany,[3]Discovery Charles River, Chesterfield Park, United Kingdom

PDX models are one of the gold standard models in preclinical drug development. Their intra- and intertumoral heterogeneity is accepted as a model immanent feature. However, the model performance directly impacts the study design as well as the interpretation of experimental data using those models. To discriminate between intrinsic and extrinsic factors driving heterogeneous tumor growth of PDX models we investigated the model performance of >500 subcutaneously growing PDX models of solid

cancer by examining growth curves of control arms run in the framework of > 5000 independent experiments. The relative tumor volume (RTV) over time was correlated with the number of passages in mice, the respective mouse strain, and the applied control vehicle per model as well as across tumor types. The analysis of ten different colon cancer PDX models revealed statistically significant differences between RTV on a specific day across different passages in a specific model as well as across all ten models (Kruskall-Wallis test). However, neither the variance nor the doubling time of the tumor correlated with the number of passages in mice. Based on these results we extended the analysis across six different tumor types with 33 distinct models in six different mouse strains. Again, an influence of the passage number on the tumor volume on a specific experimental day was depicted. The range of mean RTV related to a specific passage were least pronounced on day 7 (71% - 1626%), most notable on day 14 (65% - 4543%) and decreasing again on day 21 (34% - 3633%). In this larger cohort a subset of data points was more similar in performance to each other than any other set. The clustering was based on performance on experimental day 7. This subset received either saline or was untreated. This demonstrates that non-saline ingredients have an evident effect on tumor progression. Due to limited size of the dataset the influence of the mouse strain was evident only on a descriptive level. Whereas the use of different nude mouse strains, such as CD1-, athymic, or NMRI nude, did not affect tumor volume over time, the use of more immunodeficient mice such as SCID, NSG or NOG led to a faster tumor growth in some of the models across different passages. In the next iteration we will analyze the full dataset overcoming current limitations due to small subsets in a specific condition. The actual aim of this project is to better understand and measure tumor heterogeneity in PDX models. Based on these analyses the output of PDX-based studies will be optimized, as we get a better understanding how extrinsic factors (mouse strain and vehicle) and intrinsic factors (passage number) influence tumor growth. In a longer perspective the ability to model tumor volume over time in a specific model will reduce the need of control animals in future experiments, thereby actively supporting the concept of 3R.

#4677

A preclinical platform of breast cancer PDX and derived cellular models as a tool for pharmacological screening and functional studies

Delphine Nicolle[1], Aurore Gorce[1], Marie Tavernier[1], Elisabetta Marangoni[2], Didier Decaudin[2], Christophe Ginestier[3], Emmanuelle Charafe-Jaufret[3], Judith Passildas[4], Nina Robin[4], Robert Clarke[5], Erwan Corcuff[6], Anaïs Joachim[7], Bernard Malissen[8], Ana Zarubica[8], Hervé Luche[8], Jean-Gabriel Judde[1], Olivier Déas[1]. *[1]XenTech SAS, Évry-Courcouronnes, France,[2]Institut Curie, Paris, France,[3]CRCM, Marseilles, France,[4]Centre Jean Perrin, Clermont-Ferrand, France,[5]University of Manchester, Manchester, United Kingdom,[6]Janvier Labs, Laval, France,[7]JC Discovery, Marseilles, France,[8]Centre d'Immunophenomique, Aix Marseille Universite, Inserm, CNRS / JC Discovery, Marseilles, France*

Despite considerable progress in understanding the biology and genetics of breast cancer, the development of effective therapies needs physiological and predictive preclinical models. In this context, breast cancer (BC) patient-derived xenograft (PDX) models have become a standard tool as they reproduce the biology of tumors of origin, in term of histology, genotype and response to chemotherapy. They have proven their relevance in the study of pathways leading to the development and progression of cancer, to the mechanisms linked to tumor resistance and to the identification of novel effective therapies. We present a preclinical platform of over 60 fully characterized BC PDX models and their *in vitro* cell derivatives for preclinical evaluation of new treatment modalities. Our platform consists of a PDX collection of 43 TNBC, 6 ER+, 4 HER2+ , 6 Luminal B models (ER+ HER2+) and 14 cellular models derived from these PDXs, representing the variety of BC. PDX models were obtained by transplantation of post-surgery tumor specimens either by grafting of tumor fragments in the interscapular region of nude mice or by injection of tumor cells into the fat pad of NOD-Scid mice. Molecular analyses were done included gene expression, gene copy number, whole exome sequencing and IHC markers staining. *In vivo* drug efficacy assays were performed with standards of care as single agent or in combinations. This PDX panel mostly reflects the molecular heterogeneity of breast cancer and reproduce accurately the molecular and drug response profile of human tumors. It provides an invaluable tool for translational research. It is widely used to

performed standard drug evaluation but also “Mouse Clinical Trials” (MCT) *in vivo* screens to provide more predictive preclinical data on single-agent or combination drug efficacy. Engrafted on highly immunodeficient mice humanized with human PBMCs or CD34+ cells, these PDX models allow bispecific T-Cell engager antibody testing or immune-checkpoint inhibitors evaluation. In addition to these PDX panel, we derived cellular models (PDXDCs) to offer a time- and cost-effective preclinical screening tool. PDXDCs were obtained from dissociated PDX tumors cultured under different media and matrix conditions. They were characterized by comparison with the parental PDX by Short Tandem Repeat (STR) profiling before performing a master bank. WES and RNASeq molecular analyses were done and *in vitro* drug sensitivity was compared with their parental PDX *in vivo* drug response. Overall, the results show that this PDXDC panel reproduced *in vitro* the *in vivo* drug response profile of the original PDXs with various therapies. This BC PDX panel and *in vitro* cell derivatives provide a powerful preclinical platform to improve our knowledge on BC biology and to rapidly evaluate response to new treatments and translate this knowledge to the clinic.

#4678

Characterization of a PDX panel covering molecular diversity of non-small cell lung cancer to accelerate the development of precision therapy

Delphine Nicolle[1], Laura Brulle-Soumare[1], Katell Mevel[1], Ludovic Bigot[2], Tala Tayoun[2], Benjamin Besse[2], Françoise Farace[2], Luc Friboulet[2], Didier Decaudin[3], Erwan Corcuff[4], Anaïs Joachim[5], Bernard Malissen[6], Ana Zarubica[6], Hervé Luche[6], Jean-Gabriel Judde[1], Olivier Deas[1]. *[1]XenTech SAS, Évry-Courcouronnes, France,[2]Gustave Roussy, Villejuif, France,[3]Institut Curie, Paris, France,[4]Janvier Labs, Laval, France,[5]JC Discovery, Marseilles, France,[6]Centre d’Immunophenomique, Aix Marseille Universite, Inserm, CNRS / JC Discovery, Marseilles, France*

Lung cancer remains the first cause of cancer-related deaths worldwide, of which Non-Small Cell Lung Cancer (NSCLC) represents more than 80% of patients with advanced disease at the time of diagnosis. NSCLC is a highly heterogenous disease, and the identification of its main actionable

oncogenic drivers (i.e. EGFR, ALK, PI3K/AKT/mTOR, RET, MET, BRAF and NTRK/ROS1) and the development of specific inhibitors against these targets has transformed therapeutic care. In addition, immune-checkpoint therapy has emerged as an indispensable treatment modality, especially for patients lacking actionable oncogenic drivers, although biomarkers for predicting response to immune-checkpoint inhibition have remained elusive. Despite these new therapeutic options, NSCLC remains a lethal disease in the majority of patients due to tumor plasticity and selection leading to frequent resistance development and disease progression. Efforts are therefore needed to identify drugs and drug combinations that can prevent or overcome these resistance pathways. Patient-Derived Xenografts (PDX) models developed in immune-compromised mice recapitulate the disease more faithfully than any other in vivo model in terms of histopathologic and genomic features. They have proven their relevance in the study of pathways leading to the development and progression of cancer, to the mechanisms linked to tumor resistance and to the identification of novel effective therapies, facilitating the translation of preclinical results in the clinical setting. We describe a platform of over 35 NSCLC PDX models covering most of the molecular diversity of the disease, that have been fully characterized at the molecular level and for their response to a panel of cytotoxic chemotherapies and targeted therapies. These NSCLC PDX models have been established in immune-deficient mice from tumor biopsies collected in treatment-naïve patients or in patients having acquired resistance following an initial objective response to a variety of targeted inhibitors (EGFRi, ALKi, ROSi, BRAFi,⋯) in the MATCH-R clinical trial. In addition, 4 PDX models were established from circulating tumor cells (CTC) isolated from the blood of advanced NSCLC patients. Finally, some of these NSCLC PDX models were established in highly immunodeficient mice humanized with human PBMCs or CD34+ cells allowing testing of efficacy of bispecific T-Cell engager antibody or immune-checkpoint inhibitors. This panel of NSCLC PDX models provides a powerful preclinical platform to improve our knowledge on the mechanisms underlying resistance to treatment and to rapidly evaluate response to new treatments and translate this knowledge to the clinic.

#4679

Molecular pathology and BTKi pharmacology of DLBCL-PDXs

Jingjing Wang[1], Yueying Wang[1], Wubin Qian[1], Jia Xue[1], Sheng Guo[1], Likun Zhang[1], Henry Qixiang Li[2]. *[1]Crown Bioscience, Inc., San Diego, CA,[2]Hanx Biopharmaceuticals Inc., Oceanside, CA*

Diffuse large B-cell lymphoma (DLBCL), the largest subtype of non-Hodgkin's lymphoma (NHL, ~40%), is a heterogeneous disease with diverse pathogenesis, represented by different subtypes/genotypes based on lymphoma related specific gene expression profiling according to cell-of-origin (COO) and/or mutation profiles, likely influencing their responses to drug treatment. Patient derived xenografts (PDXs) represent powerful experimental system to investigate heterogeneous molecular pathology, and their corresponding pharmacology of DLBCLs. We created a unique cohort of 19 PDXs representative of diverse subtypes of *de novo* DLBCL patients, along with 15 EBV transformed DLBCLs during xenografting, followed by comprehensive molecular pathological analysis, using "EBV scan", COO and LymphGen algorithm. The 19 *de novo* DLBCL-PDXs were classified into activated B cell-like (7/19 ABC, including 2 EBV^+), germinal center B-cell-like (4/19 GCB) and unclassified (8/19 including 4 EBV^+); the 15 EBV transformed DLBCL include two ABC, one GCB and 12 unclassified. The *de novo* DLBCL-PDXs were also annotated as MCD, BN2, N1, A53, ST2, and unknown genotypes. Clustering and principal component analysis (PCA) clearly separated EBV^+ DLBCL-PDXs (regardless of *de novo* DLBCL, EBV-associated, or EBV transformed DLBCLs) from the EBV^- *de novo* DLBCL-PDXs, suggesting distinct molecular pathogenesis, while no apparent difference between the two EBV^+ DLBCLs suggested the similar pathogenesis. The expanded mouse clinical trial of BTKi using drinking water administration of ibrutinib (0.16mg/ml) showed: 1) EBV^- MCD and BN2 genotype are largely sensitive, suggesting these models' dependency of chronic BCR signaling; 2) all EBV^+ DLBCLs, regardless of the origin or genotypes, are all insensitive; 3) there are some cases of EBV^- non-MCD/BN2 models being sensitive, likely due to the presence of certain related activating mutations. Molecular pathology analysis also demonstrated EBV^+ PDXs, including significantly elevated BCL2 and down-regulated BCL6, in contrast to EBV^- DLBCL-PDXs, implicating possible sensitivity to respective treatments. In summary, these observations

in PDXs, some of which are consistent with the retrospective analysis of clinical trials, can be used to help develop BTKi and other treatment for DLBCLs.

#4680

Intracranial breast cancer brain metastases (BCBM) models - stereotactic vs. intracarotid inoculation

Sigrid Cold[1], Moritz Braig[2], Trine Bjoernbo Engel[2], Maria Zeiler Alfsen[2], Maria Nikoline Baandrup Kristiansen[2], Lotte Kellemann Kristensen[2], Andreas Kjaer[3], Carsten Haagen Nielsen[2]. *[1]Department of Biomedical Sciences, University of Copenhagen, Minerva Imaging ApS & Cluster for Molecular Imaging, Oelstykke & Copenhagen, Denmark,[2]Minerva Imaging ApS, Oelstykke, Denmark,[3]Department of Clinical physiology, Nuclear Medicine and PET & Department of Biomedical Sciences, Nuclear Medicine and PET & Cluster for Molecular Imaging, Copenhagen, Denmark*

Breast cancer is the most prevalent cancer in women worldwide. 30% of breast cancer patients develops metastases at distant organs, with 10-20% of these patients developing brain metastases. The median survival time for patients with brain metastases is only 7.2 months and there is an urgent need for effective therapies. Development of novel therapies relies on good translational animal models. Subcutaneous tumors are technically easy and highly reproducible but lacks the natural tumor environment and the impact of the blood brain barrier. Breast cancer brain metastasis (BCBM) models are most often established by stereotactic intracranial inoculation. However, this leads to formation of single tumors and does not take the extravasation and seeding part of the metastatic cascade into account and resembles primary tumors to a larger extend. Intracarotid inoculation incorporates extravasation and seeding of micro metastases making it a better suited translational animal model for BCBM. A panel of intracranial BCBM was established through stereotactic and intracarotid inoculation of breast cancer cell lines with high survival and take rates (>85%). The panel included the ST941 PDX model, an estrogen receptor positive model harbouring the ESR1-Y537S mutation and exhibiting resistance to fulvestrant. The panel also included the triple negative breast cancer cell line MDA-MB-231 as well as HER2+ models. Tumor establishment and progression were

evaluated using bioluminescence and magnetic resonance imaging (MRI). Whole brain and tumors were isolated, and paraffin embedded for histological evaluation of tumor establishment, invasiveness, and infiltration. Intracranial tumor establishment was evident early after inoculation using bioluminescence imaging and tumor growth was later confirmed by MRI. Tumor growth rate were dependent on inoculation method with rapid tumor growth observed with stereotactic inoculation. While stereotactic inoculation led to single tumor establishment with defined tumor borders, intracarotid inoculation led to micro seeding with multiple foci established throughout the brain. At early timepoints, the metastases consisted of <150 cells per metastases, but at later timepoints larger metastases were formed. Tumor infiltration was more diffused in brains with multiple metastases and the blood brain barrier integrity was different when comparing the models and inoculation methods. A panel of BCBM was successfully established using both stereotactic and intracarotid inoculation. While bioluminescence allowed the earliest tumor imaging, MRI provided additional information on tumor establishment such as location, numbers, and blood brain barrier permeability. The models showed varying tumor establishment, infiltration, and marker expression. The established panel can be used as a platform for testing novel anti-cancer therapies targeting BCBM.

#4681

Human Cancer Models Initiative (HCMI): A community resource of next-generation cancer models and associated data

Eva Tonsing-Carter[1], Rachana Agarwal[2], Cindy W. Kyi[1], Julyann Perez-Mayoral[1], Conrado T. Soria[2], Jean Claude Zenklusen[1]. *[1]National Cancer Institute, Bethesda, MD,[2]Frederick National Laboratory for Cancer Research, Leidos Biomedical Research, Inc., Rockville, MD*

The Human Cancer Models Initiative (HCMI) is an international consortium founded by National Cancer Institute (NCI), Cancer Research UK, Wellcome Sanger Institute, and the foundation Hubrecht Organoid Technology. The initiative has generated patient derived Next-generation Cancer Models (NGCMs) from diverse tumor types and subtypes including rare adult and pediatric cancers as a community resource. HCMI addresses deficiencies in traditional cell lines models by collecting patients' clinical

data, as well as the genomes and transcriptomes of the parent tumor, case-matched normal tissue, and the derived next-generation cancer model. NCI's Center for Cancer Genomics (CCG) sponsors four Cancer Model Development Centers (CMDCs) who are managed by Frederick National Laboratory for Cancer Research, Leidos Biomedical Research, Inc. CCG also supports the downstream model development pipeline. The CMDCs are tasked with generating HCMI NGCMs. The model-associated clinical data are submitted to the Clinical Data Center. The models, their associated tumor, and normal samples are processed at the Biospecimen Processing Center (BPC). The nucleic acids isolated at BPC are sent to the Genomic Characterization Centers for molecular characterization. All biospecimen, clinical, and molecular characterization data are quality controlled and submitted to NCI's Genomic Data Commons (GDC) for the research community. The HCMI models and culture protocols are made available to the research community through a single third-party distributor. The HCMI Searchable Catalog (https://hcmi-searchable-catalog.nci.nih.gov/) is an online resource that allows users to query and identify available models using various data elements including clinical and molecular characterization data, including WGS, WXS, RNA-seq, and methylation array. To date, over 250 HCMI models are available to query on the Searchable Catalog and are available to the research community through the NCI designated model distributor, ATCC. These models have been derived from several cancer types including glioblastoma, colorectal, pediatric, gastroesophageal, pancreatic, and more. Biospecimen, clinical, and molecular characterization data are available for over 100 models at NCI's GDC, with additional cases released as the data completes the HCMI pipeline. Data, tools, and resources generated by CCG initiatives are made publicly available via the CCG website and GDC. The CCG website also provides available data types, data usage policies and guides to access data (https://www.cancer.gov/about-nci/organization/ccg).

#4682

PDCM Finder: an open global research platform for patient-derived cancer models

Zinaida Perova[1], Mauricio Martinez[1], Tushar Mandloi[1], Federico Lopez Gomez[1], Csaba Halmagyi[1], Alex Follette[1], Jeremy Mason[1], Steven Neuhauser[2], Dale A. Begley[2], Debra M. Krupke[2], Carol Bult[2], Helen

Parkinson[1], Tudor Groza[1], Marcelo P. Rios Almanza[1]. *[1]European Bioinformatics Institute, Hinxton, United Kingdom,[2]The Jackson Laboratory, Bar Harbor, ME*

PDCM Finder (www.cancermodels.org) is a cancer research platform that aggregates clinical, genomic and functional data from patient-derived xenografts, organoids and cell lines. Currently, the portal has over 6300 models across 13 cancer types, including rare pediatric models (17%) and models from minority ethnic backgrounds (33%), making it the largest free to consumer and open access resource of this kind. The PDCM Finder standardizes, harmonizes and integrates the complex and diverse data associated with PDCMs for the cancer community and displays over 90 million data points across a variety of data types (clinical metadata, molecular and treatment-based). PDCM Finder was launched in April 2022 and has been recently enhanced with new functionality and an updated user interface. Users can search for models of interest by either (1) exploring molecular data summaries for models of specific cancer types, or (2) using the intuitive search and faceted filtering options of the web user interface or (3) accessing resource database via REST API to run their own analysis. The data includes gene expression, gene mutation, copy number alteration, cytogenetics, patient treatment and drug dosing studies. We link external resources like publication platforms and cancer-specific annotation tools enabling exploration and prioritization of PDCM variation data (COSMIC, CIViC, OncoMX, OpenCRAVAT). PDCM Finder builds on the success of the PDX Finder resource (PMID:30535239). Critical PDCM attributes, such as diagnosis, drug names and genes, are harmonized and integrated into a cohesive ontological model based on the PDX Minimal information standard (PDX MI, PMID: 29092942). PDX MI has become established in the community for data exchange, adopted by the PDX providers, consortia and informatics tools integrating PDX data. We are driving the development of and promoting the use of descriptive standards to facilitate data interoperability and promote global sharing of models. PDCM Finder data is FAIR and underpins the generation and testing of new hypotheses in cancer mechanisms and personalized medicine development. We provide expertise and software components to support several worldwide consortia including PDXNet, PDMR and EurOPDX. PDCM Finder is freely available under an Apache 2.0 license (https://github.com/PDCMFinder). This work

is supported by NCI U24 CA204781 01, U24 CA253539, and R01 CA089713. We welcome feedback on the resource and are looking for participants for usability studies - please get in touch if interested.

#4683

Developing human Ewing sarcoma *in vitro* models to prioritise new treatments

Elizabeth A. Roundhill[1], Elton J. R. Vasconcelos[2], David R. Westhead[3], Sarah Grissenberger[4], Martin Distel[5], Susan A. Burchill[6]. *[1]University of Leeds, Leeds, United Kingdom,[2]Leeds Omics, University of Leeds, Leeds, United Kingdom,[3]Faculty of Biological Sciences, University of Leeds, Leeds, United Kingdom,[4]St. Anna Children's Cancer Research Institute, Vienna, Austria,[5]Zebrafish platform Austria for preclinical drug screening, Vienna, Austria,[6]Leeds Institute of Medical Research, University of Leeds, Leeds, United Kingdom*

Models that more accurately reflect Ewing sarcoma (ES) will enable the prioritization of novel targeted agents from bench to clinic. To date, development of an ES mouse model have been unsuccessful[1] and engraftment of human ES in mice is variable[2]. Coupled with a moral obligation to minimize the use of mammals, we have established and characterized models using patient-derived ES cultures *in vitro* and in larval zebrafish. The transcriptomes of ES cell lines and patient-derived ES cultures[3] were analyzed and compared using total RNAseq followed by DESeq2 and Gene Set Enrichment analysis. Cells in 2D, as 3D spheroids, in combination with cells of the tumor microenvironment and in larval zebrafish (*Danio rerio*) were characterized. Six cell lines clustered independently from patient-derived ES cultures (n=20), reflecting differential expression of 15,709 RNAs ($p<0.01$). Interrogation of the differentially expressed genes using Reactome, KEGG and Gene Ontology identified up regulation of genes associated with mitotic spindle and G2/M G1/S DNA damage spindle checkpoints, homologous recombination and the cell cycle in the cell lines compared to patient-derived cultures ($p<0.01$). These data are consistent with the quicker doubling time (DT) and increased sensitivity of ES cell lines to chemotherapy (actinomycin D, doxorubicin, vincristine, etoposide; DT range=19-33h, EC50 range=4-

34nM) compared to patient-derived cultures (DT range=55-197h, EC50>10μM, $p<0.05$). All patient-derived ES cultures formed spheroids of similar diameter (range 105-258μm) at 96h ($p>0.05$), although there was heterogeneity in spheroid weight (range 205-3639ng, $p<0.05$) and migration index (MI; range 30-170, $p<0.05$). Treatment with actinomycin D (1-10 μM) significantly increased spheroid diameter ($p<0.05$), whereas 4-hyperoxyifosfamide (active metabolite of ifosfamide, 7-30μM) decreased spheroid diameter ($p<0.05$). Doxorubicin did not significantly change the diameter of spheroids. When propagated in combination with mesenchymal stem cells there was a 2-fold increase in viable cell number ($p<0.0001$) compared to ES cultures alone. Patient-derived ES cultures in zebrafish were observed at the injection site (perivitelline space). Some cells were detected in circulation 3 days post injection. This is consistent with heterogeneity and the high MI of patient-derived ES cultures. The transcriptome of ES cell lines is significantly different from that of ES patient-derived cultures and is associated with increased doubling times and response to chemotherapies. This highlights the importance of developing preclinical models using patient-derived ES cultures. Patient-derived ES cultures in 2D and 3D models *in vitro* and in zebrafish may provide a reliable cost-effective preclinical pipeline. [1]Minas *et al.* 2017.Oncotarget,8(21):34141-34163.[2]Nanni *et al*. 2019.Sci Rep,9(1):12174. [3]Roundhill *et al.* 2021.Cell Oncol,44(5):1065-1085.

#4684

Genomic and transcriptomic analysis of a diffuse pleural mesothelioma patient-derived xenograft library

Triparna Sen. *Icahn School of Medicine at Mount Sinai, New York, NY*

Background: Despite recent treatment advances, malignant pleural mesothelioma (MPM) is an aggressive, recalcitrant malignancy. Currently, the histologic subtype (epithelioid/non-epithelioid/biphasic) is the primary prognostic factor; other potential biomarkers to guide therapeutic strategies remain elusive. Even with multimodality therapies, recurrence is high in early-stage disease. In the unresectable/metastatic setting, there are only two FDA-approved regimens, both in the first-line setting: cisplatin/pemetrexed and ipilimumab/nivolumab. Unfortunately, most who respond to first-line treatment experience disease progression within a year.

Therapeutic and diagnostic advances in DPM are hindered by a paucity of well-annotated preclinical models which can faithfully recapitulate the complex genomic interplay of the disease.
Methods: We established a library of patient-derived xenografts (PDX) from patients with DPM. We performed multi-omic analyses on available PDX and patient samples to deconvolute the mutational landscapes, global expression profiles, and molecular subtypes. Targeted next-generation sequencing (NGS; MSK-IMPACT), immunohistochemistry, and histologic subtyping were performed on all available samples. RNA-sequencing was performed on all available PDX samples. Clinical outcomes and treatment history were annotated for all patients. Platinum-doublet progression free survival (PFS) was determined from the start of chemotherapy until radiographic/clinical progression and grouped into $<$ or $\geq$ 6 months.
Results: The mutational landscapes of PDX models strongly correlated with paired tumor samples. There were some differences in *CDKN2A/B* mutations and relative enrichment of *NF2* with fewer *BAP1* alterations, the significance of which is being investigated. When compared by histological subtype, we observed an upregulation of genes involved in NOTCH and EMT signaling in the epithelioid models. Models derived from patients with shorter overall survival or poor response to platinum doublet had higher expression of WNT/β-catenin signaling, hedgehog pathway, and epithelial-mesenchymal transition signaling as well as downregulation of immune-activation pathways, including type I and II interferon signaling and inflammatory response pathways.
Conclusions: This library of MPM PDXs, the largest to date, effectively mimics human disease and provides unprecedented insight into the genomic, transcriptomic, and protein landscape of MPM. These PDX models will inform future clinical investigations and provide an important new preclinical resource.

Pediatric Cancer 2: Biology and Therapeutics

#3521
CCND2 promotes proliferation in *Drosha* and *DICER1* driven tumors

Claudette R. Fraire[1], Uma Obalapuram[1], Patricia D. B. Tiburcio[1], Kavita Desai[2], Kenneth S. Chen[1]. [1]*Pediatrics, UT Southwestern Medical Center,*

Dallas, TX,[2]Pediatrics, Children's Hospital of Philadelphia, Philadelphia, PA

Mutations in microRNA processing genes such as *DROSHA* and *DICER1* consist of 1.5-2% of pediatric cancers including a brain tumor called pineoblastoma. We developed a genetically engineered mouse model of Drosha- and Dicer1- driven pineal tumors. These tumors develop without microRNAs and express early pineal developmental markers. Gene set enrichment analysis revealed E2F target genes to be highly expressed in these tumors. One of the most upregulated genes in these tumors is cyclin D2 (Ccnd2). Additionally, these tumors stain positively for Rb phosphorylation. In a Wilms tumor cell line (WiT49) with Drosha knocked down, RNA sequencing revealed that *CCND2* was the most upregulated gene. Similarly, in patient-derived xenografts (PDXs) of DICER1-related tumors such as pleuropulmonary blastoma (PPB), we observed high expression of CCND2 and positive staining for Rb phosphorylation. To test the dependence of Rb phosphorylation in Drosha and Dicer tumors, we next treated a Drosha pineal tumor allograft with a CDK4/6 inhibitor, palbociclib, and observed tumor growth suppression. Additionally, treatment of *DICER1* mutant PPB PDXs with palbociclib had similar results. These experiments suggest that CDK4/6 is important for tumor proliferation in *Drosha* and *DICER1* driven cancers.

#3522

DICER1 Platform domain missense variants led to tumor susceptibility via failure of precursor miRNA binding

Dylan Pelletier, Anne-Laure Chong, Sophie Albert, Marc Fabian, William Foulkes. *Lady Davis Institute at Jewish General Hospital, Montreal, QC, Canada*

DICER1 is a key protein in the micro(mi)RNA biogenesis pathway responsible for cleaving precursor (pre)-miRNA stemloops with its RNase IIIa and IIIb domains into mature single stranded miRNAs. DICER1 syndrome is a pleiotropic tumor predisposition syndrome in which clinical manifestations are normally first seen during childhood. This genetic disorder is defined by the presence of inherited or *de novo* germline pathogenic variants (GPVs) in the *DICER1* gene. While many germline loss

of function variants fail to generate DICER1 protein, a subset of patients has germline missense variants that are predicted to produce full-length DICER1 protein that cluster in the DICER1 Platform domain, a region that plays a role in binding to the 5' phosphate of pre-miRNA stemloops. Due to the uncertainty surrounding the pathogenicity of missense variants in DICER1 syndrome, clinical actionability can be limited. To determine how Platform mutations predispose to DICER1 syndrome we characterized a number of these variants using *in vitro* pre-miRNA binding and cleavage assays. Interestingly, four of these variants displayed impaired pre-miRNA binding and processing, with three of them localizing to a hydrophobic pocket in the Platform domain. In keeping with *in vitro* results, DICER1 mutants displayed impaired miRNA processing when introduced into mesenchymal stem cells. Furthermore, we identified a second somatic hit in the RNase IIIb domain of DICER1 in thyroid nodular hyperplasia DNA from a patient affected by one of these variants. Taken together, these results identify a key region in the DICER1 protein that is essential for pre-miRNA processing and help the classification of these germline variants as pathogenic to ensure proper clinical management of affected patients. Additionally, these results provide insight on the molecular basis involved in DICER1 syndrome predisposition.

#3523

A systematic comparison of molecular features shared by H3K27-altered diffuse midline gliomas and posterior fossa A ependymomas

Matthew Pun[1], Drew Pratt[2], Patricia R. Nano[3], Piyush K. Joshi[4], Li Jiang[5], Bernhard Englinger[5], Arvind Rao[1], Marcin Cieslik[1], Arul M. Chinnaiyan[1], Kenneth Aldape[2], Stefan Pfister[4], Mariella G. Filbin[5], Aparna Bhaduri[3], Sriram Venneti[1]. *[1]University of Michigan Medical School, Ann Arbor, MI,[2]National Cancer Institute, Bethesda, MD,[3]Department of Biological Chemistry, David Geffen School of Medicine, University of California Los Angeles, Los Angeles, CA,[4]Hopp Children's Cancer Center (KiTZ) Heidelberg, Division of Pediatric Neurooncology, German Cancer Consortium (DKTK), German Cancer Research Center (DKFZ), Heidelberg, Germany,[5]Dana Farber Cancer Institute, Boston, MA*

In children, brain tumors account for the highest mortality rates of all malignancies, and in contrast to adult brain cancers, pediatric tumors often arise in infratentorial regions. Two tumors in particular, H3K27-altered diffuse midline gliomas (DMGs) and group-A posterior fossa ependymomas (PFAs) arise from structures around the fourth ventricle, and strikingly, both tumors exhibit a global decrease in the histone mark histone 3, lysine 27 tri-methylation (H3K27me3) that is associated with transcriptional repression. H3K27-altered DMGs primarily are found primarily in the pons and exhibit by lysine-to-methionine mutations at H3K27 (H3K27M). This missense mutation results in inhibition of the catalytic activity of the polycomb repressive complex 2 (PRC2) which mediates H3K27me3 deposition. PFAs are found in the lateral recess of the fourth ventricle and the cerebellum and demonstrate overexpression of EZH inhibitory protein (EZHIP). EZHIP contains a domain with striking resemblance to the mutant H3K27M histone tail and similarly blocks PRC2 activity. Although H3K27me3 levels are dramatically reduced in both areas, select genes retain H3K27me3 in both tumor types. Increasingly, data have emerged demonstrating that cases of PFAs actually harbor H3K27M mutations and cases of H3-wildtype DMGs in fact overexpress EZHIP. The neighboring origins and overlapping recurrent H3K27me3-modulating alterations observed in these two pediatric brain tumors suggest certain populations of cells in the developing hindbrain may be particularly prone to malignant transformation in the setting of PRC2 inhibition. A systematic comparison of genomic, transcriptomic, and epigenomic datasets for both tumors identified key molecular similarities between subsets of DMGs and PFAs and highlighted how developmental signatures may be preserved in tumor expression profiles. Specifically, these analyses identify shared copy-number profiles between PFAs and different subtypes of DMGs and demonstrate that the Activin A Receptor Type 1 (ACVR1), a gene with recurrent activating mutations in H3K27-altered DMGs, is overexpressed in a subset PFAs with worse survival outcomes. Additionally, interrogation of the H3K27me3 and enhancer landscapes identified critical genes with similar chromatin profiles and revealed heterogeneity in repression of H3K27me3-marked genes that correlated with patterns of inferred anatomic origins for each tumor. Moreover, one of these genes, cellular retinoic acid binding partner 1 (*CRABP1*) showed enrichment in progenitor cell types in single-cell transcriptomic datasets. Together, these analyses characterize the

common and unique molecular features of H3K27-altered DMGs and PFAs and shed light on the cellular contexts of the developing hindbrain that lead to development of each tumor.

#3524

Pharmacological characterization of pediatric brain tumor PDX models in a single mouse trial format

Eva Oswald[1], Dorothee Lenhard[1], Kanstantsin Lashuk[1], Stefan Pfister[2], Louis Stancato[3], Julia Schueler[1]. *[1]Charles River Laboratories, Inc., Freiburg, Germany,[2]DKFZ, Heidelberg, Germany,[3]Eli Lilly and Company, Indianapolis, IN*

Cancer remains the leading cause of disease-related death in children. Preclinical drug testing to identify promising treatment options for relapsed patients or those with poor prognosis is hindered by the lack of well characterized and annotated preclinical models. In the framework of the ITCCP4 consortium (www.ITCCP4.eu) our group determined the pharmacological profile of 47 orthotopically implanted pediatric brain PDX models. The panel comprised 21 high grade glioma (HGG), 13 medulloblastoma (MB), eight ependymoma (EP), three non-classified brain tumors (XT), one atypical teratoid/rhabdoid tumor (AT/RT) and one neuroblastoma (NB).. Depending on the tumor type the models were screened in an eleven or twelve arms single mouse trial study layout. Three treatment arms comprised standard of care cytotoxic compounds and radiation, whereas the other arms covered targeted therapies, mostly small molecules. Tumor load was determined using a fluorescent based in vivo imaging technology based on the lentiviral transient transduction of the PDX cells with iRFP713 prior to implantation into the brain. In addition, body weight and neurological scoring was applied to determine the overall condition of the animals. At the end of the study brain tissue was harvested and tumor load confirmed by immunohistochemistry. The mean overall survival of the orthotopic implanted animals on study was 48 days with a minimum of 7 days and a maximum of 132 days. Overall, the treatment was well tolerated in the tumor bearing animals as determined by body weight measurement. However, the combination of two cytotoxic drugs in some of the arms needed dose adjustments due to increased toxicity. Across all tumor types at least one of the cytotoxic arms improved overall survival of

the tumor bearing animals markedly: Temozolomide and Lomustine for HGG (43d and 50d, respectively vs 28d in the control arm), Lomustine and Endoxan for MB (99d and 73d, respectively vs 61d in the control arm), and Actinomycin D for EP (64d vs 52d). However, several of the targeted agents showed a distinct efficacy profile: Cobimetinib was efficacious in 50% of the HGG (47d vs 28d in the sensitive subset) and Idanasutlin in 80% of the EP models (79d in the sensitive subset vs 52d). The optical imaging signal over time confirmed tumor engraftment at the start of treatment. The most efficacious treatment arms induced growth delay or partial remission. This preclinical validation set gains even more importance using the accompanying molecular profiling data that are available not only for the PDX but also for the donor patient. Together with the breadth and depth of the still growing PDX collection, a unique preclinical platform for the development of drugs as well as companion diagnostics specifically for pediatric brain cancers is now available to the scientific community.

#3525

VGLL2-NCOA2 leverages developmental programs for pediatric sarcomagenesis

Sarah Watson[1], Collette A. LaVigne[2], Lin Xu[2], Didier Surdez[3], Joanna Cyrta[1], Delia Calderon[4], Matthew V. Cannon[5], Matthew R. Kent[5], Katherine M. Silvius[5], Jack P. Kucinski[4], Emma N. Harrison[5], Whitney Murchison[2], Dinesh Rakheja[2], Franck Tirode[6], Olivier Delattre[1], James F. Amatruda[7], Genevieve C. Kendall[5]. *[1]Paris Sciences et Lettres (PSL) Research University, Paris, France,[2]UT Southwestern Medical Center, Dallas, TX,[3]University of Zürich, Zürich, Switzerland,[4]The Ohio State University, Columbus, OH,[5]Nationwide Children's Hospital, Columbus, OH,[6]Université Claude Bernard Lyon 1, Lyon, France,[7]Children's Hospital Los Angeles, Los Angeles, CA*

Clinical sequencing efforts are rapidly identifying sarcoma gene fusions that have not been functionally validated for their transformation capacity and biological activity. An example is the new fusion of transcriptional coactivators, VGLL2-NCOA2, found in infantile rhabdomyosarcoma. To delineate VGLL2-NCOA2 tumorigenic mechanisms and identify

therapeutic vulnerabilities, we implemented a cross-species comparative oncology approach with zebrafish, mouse allograft, and patient samples. We found that in our transgenic zebrafish and mouse allograft models, VGLL2-NCOA2 is sufficient to generate mesenchymal tumors that display features of immature skeletal muscle. Zebrafish and mouse VGLL2-NCOA2 tumors are consistent with the human disease histologically and transcriptionally, and express diagnostic rhabdomyosarcoma markers. We found a shared molecular feature of these tumors was a suppression of myogenic differentiation pathways and reactivation of developmental programs. To identify impacted developmental programs, we transcriptionally clustered zebrafish VGLL2-NCOA2 tumors with the trajectory of early zebrafish development. A subset of VGLL2-NCOA2 zebrafish tumors cluster with embryonic somitogenesis and pinpoint VGLL2-NCOA2 developmental targets, including a RAS family GTPase, ARF6. In VGLL2-NCOA2 zebrafish, mouse allograft, and patient tumors, ARF6 is highly expressed and is absent from mature skeletal muscle. ARF6 knockout in our C2C12-VGLL2-NCOA2 cell culture model suppresses VGLL2-NCOA2 soft agar colony formation capacity, suggesting a genetic cooperating event in the disease. Our data indicate that VGLL2-NCOA2 is an oncogene which leverages developmental programs for tumorigenesis, and that the reactivation or persistence of ARF6 could represent a therapeutic opportunity.

#3526

The transcription factor ZEB1 shapes osteosarcoma aggressiveness by affecting tumor cell differentiation and stemness features

Caterina Cascini[1], Daniele Lecis[1], Laura Botti[1], Chiara Ratti[1], Valeria Cancila[2], Katia Scotlandi[3], Claudio Tripodo[2], Mario Paolo Colombo[1], Claudia Chiodoni[1]. *[1]Fondazione IRCCS Istituto Nazionale dei Tumori, Milan, Italy,[2]University of Palermo, Palermo, Italy,[3]IRCCS Istituto Ortopedico Rizzoli, Bologna, Italy*

Osteosarcoma (OS) is a mesenchymal bone tumor affecting mainly children and young adults, characterized by a particularly aggressive behavior, with 20% of patients showing lung micro metastasis already at diagnosis. To date, treatment options for OS are still based on multi-drug chemotherapy and prognosis for metastatic patients is dismal, making urgent the

identification of new therapies. OS is considered a differentiation disease, because of the incapability of mesenchymal stem cells or osteoblastic progenitors to proceed toward terminal differentiation. We tested the effects on OS cells of targeting ZEB1, a transcription factor known to be critical for the maintenance of mesenchymal and stemness features in cancer. We inhibited ZEB1 expression in a murine OS cell line by lentiviral vectors based on CRISPR-Cas9 technology. We firstly tested the effects of ZEB1 deficiency in vitro, evaluating OS cell stemness potential by sarcosphere forming assay and osteogenic differentiation by alkaline phosphatase (Alp) staining. Gene expression profile (GEP) comparing ZEB1 KO clones and control ones was also performed to investigate the transcriptional changes induced by ZEB1 deletion and potentially identify alternative, more easily druggable, therapeutic targets. We also investigated in vivo the effect of ZEB1 inhibition. ZEB1 KO clones showed decreased stemness potential and increased Alp staining, both features suggestive of a more differentiated phenotype. Preliminary GEP analysis showed 849 down-regulated genes and 1093 up-regulated genes in ZEB1 KO clones versus ZEB1-competent controls. Gene set enrichment analysis indicated a down-modulation of pathways related to cellular proliferation and survival such as MTORC1 signaling, MYC targets, GM2 checkpoint, E2F targets and oxidative phosphorylation in ZEB1 KO clones. In vivo we observed a reduced tumor growth in ZEB1 KO clones that were also characterized by a more differentiated morphology in comparison to controls. Interestingly, the absence of ZEB1 in tumor cells affected also the immune infiltrate, as tumors derived from ZEB1 KO clones were significantly less infiltrated by pro-tumoral CD206+ M2-like macrophages. Moreover, we observed a reduced metastatic potential in ZEB1 KO clones than controls when we inject the cells intravenously. Taken together, these results support the hypothesis of ZEB1 as a key factor in OS aggressiveness, affecting tumor cell differentiation, stemness ability and in vivo growth capability.

#3527

WNT5B drives osteosarcoma stemness, metastasis and chemoresistance

Rachel S. Perkins, Sarocha Suthon, Gustavo A. Miranda-Carboni, Susan A. Krum. *University of Tennessee Health Science Center, Memphis, TN*

Osteosarcoma is a pediatric bone cancer that has no targeted therapy and has had no treatment advances for the last three decades. Osteosarcoma frequently metastasizes to the lungs, reducing patient survival with metastatic disease to 20% after 5 years. The goal of this study is to describe the function of WNT5B and its signaling pathway in osteosarcoma stem cells, metastasis and chemoresistance and its potential as a therapeutic target. Using RNA sequencing from publicly available datasets and immunohistochemistry on tumor microarrays, we reveal that WNT5B is the most expressed WNT in osteosarcoma patients and correlates with both metastasis and survival. Osteosarcoma is thought to result from a block in differentiation, and based on WNT5B's role in inhibiting osteoblast differentiation of mesenchymal stem cells from normal bone, we hypothesized a role for WNT5B in osteosarcoma stem cells. In spheroids, we show that both protein and mRNA levels of WNT5B are enhanced in the stem cell population compared to adherent cells. We found that WNT5B upregulates the expression of the stemness gene *SOX2* and directs stemness phenotypes, such as sphere forming efficiency, proliferation and migration. We show a reduction in sphere forming efficiency with 143B-WNT5B-knockdown cells compared to parental control cells which can be rescued with re-introduction of WNT5B. Additionally, we show that WNT5B drives proliferation and migration of osteosarcoma stem cells through increasing sphere size and capability to migrate on collagen matrix. Further, WNT5B enhances osteosarcoma chemoresistance to methotrexate. Through revealing a novel role for WNT5B in osteosarcoma cancer stem cells and therapy resistance, we present the WNT5B pathway as a candidate for therapeutically targeting osteosarcoma stem cells in patients.

#3528

ALKBH5 promotes cancer growth by regulating ER homeostasis via UPR, autophagy, and mitochondrial function

Panneerdoss Subbarayalu[1], Daisy Medina[2], Pooja Yadav[1], Santosh Timilsina[1], Kunal Baxi[2], Ratna Vadlamudi[3], Yidong Chen[1], Manjeet Rao[2].
[1]Greehey Children's Cancer Research Institute, UT Health San Antonio, San Antonio, TX,[2]Greehey Children's Cancer Research Institute, UT Health San Antonio, San Antonio, TX,[3]UT Health San Antonio, San Antonio, TX

Background**:** N6-methyladenosine (m^6A) RNA methylation is a dynamic reversible epitranscriptomic modification that includes methyl transferases (writes m^6A), demethylases (erases m^6A) and reader proteins, which proofreads m^6A marks of a specific site of transcripts. Recent studies have suggested that RNA methylation affects several fundamental cellular and molecular functions including mRNA splicing, stability, export, stem cell fate, circadian rhythms, DNA repair and cell survival. The objective of this study is to establish the mechanisms by which RNA demethylase ALKBH5 (AlkB homolog 5) facilitates tumor growth and progression.
Methods: To establish the significance of RNA methylation in children's cancers, we performed siRNA screen targeting m^6A writers, erasers, and readers in osteosarcoma (OS). We used several OS cell lines including 143B, MG63, SaOS2, U2OS and multiple patient derived OS cell lines. Mechanistic studies were conducted using ALKBH5 KO and knockdown cells and by measuring the status of Autophagy and UPR associated proteins using Western blot analysis, confocal and electron microscopy.
Results: Our results revealed that depletion of ALKBH5, a demethylase that erases the m^6A mark from the target gene, altered the autophagy in OS cells. Interestingly, we found that level of LC3, which is the universal marker for autophagy, was significantly increased in OS cells. RNA seq analysis showed that depletion of ALKBH5 significantly altered several autophagy related genes in the OS cells. To better understand the molecular mechanism by which ALKBH5 regulates autophagy, we investigated the Endoplasmic Reticulum (ER) stress-induced Unfolded Protein Response (UPR) pathway, which is a known activator of autophagy. We discovered that ER stress induced UPR signaling pathway is highly activated in ALKBH5 depleted cancer cells. Further, mechanistic studies suggested that ALKBH5 promoted ER homeostasis by controlling the expression of ER lipid raft associated 1 (ERLIN1), which binds to the activated inositol 1, 4, 5,-triphosphate receptor and facilitates its degradation via ERAD to maintain calcium flux between ER and mitochondria. Using functional studies and electron microscopy, we show that ALKBH5-ERLIN1-IP3R-dependent calcium signaling modulates the activity of AMP kinase, and consequently mitochondrial biogenesis. These findings thus reveal that ALKBH5 serves an important role in maintaining ER homeostasis and cellular fitness.

Conclusion: These findings provide novel insight into how m^6A may promote cancer cell growth by regulating the crosstalk among ER signaling, UPR, autophagy, and mitochondrial function. Our study is the first to show that RNA methylation plays an important role in osteosarcoma by regulating autophagy via UPR.

#3529

EWSR1-WT1 isoform selectivity, DNA binding, and druggable targets: unpacking the biology of desmoplastic small round cell tumor

Justin W. Magrath[1], Ilon A. Goldberg[1], Alifiani B. Hartono[2], Sean B. Lee[1].
[1]Tulane University School of Medicine, New Orleans, LA,[2]Canary Center at Stanford, Palo Alto, CA

Desmoplastic small round cell tumor (DSRCT) is a rare pediatric cancer caused by the *EWSR1-WT1* fusion gene. No targeted therapies have been established and multimodal therapy is ineffective with a 5-year survival rate of 15-25%. Many questions about the biology of DSRCT remain unanswered including the critical genes regulated by the *EWSR1-WT1* fusion gene, the role of the - and +KTS fusion gene isoforms produced by alternative splicing, and the relationship between *EWSR1-WT1* binding and gene expression alterations. To address these questions, we established four doxycycline-inducible DSRCT cell lines that selectively knockdown the expression of *EWSR1-WT1*. RNA-seq analysis on these cell lines with or without *EWSR1-WT1* knockdown identified commonly altered genes and pathways. To illuminate the role of the *EWSR1-WT1* -KTS and +KTS isoforms, the -KTS, +KTS, or both isoforms were overexpressed in a mesothelial cell line, a hypothesized cell of origin for DSRCT. Remarkably, different gene expression alterations were observed between the -KTS and +KTS isoforms. While overexpression of the -KTS isoform upregulated 765 genes and downregulated 366 genes, overexpression of the +KTS isoform upregulated 203 genes and downregulated 25 genes. Gene set enrichment analysis showed *EWSR1-WT1* regulated gene signatures are recapitulated by overexpression of the -KTS isoform or both +/-KTS isoforms, but not the +KTS isoform alone, suggesting the -KTS isoform predominantly regulates gene expression in DSRCT. To interrogate the influence of direct and indirect gene regulation by *EWSR1-WT1*, ChIP-seq and CUT&RUN data were integrated into our RNA-seq analysis. Across

each of our four DSRCT cell lines, approximately 25% of *EWSR1-WT1* bound peaks led to upregulation, 10% led to downregulation, and 65% led to no gene expression alteration. *EWSR1-WT1* binding accounted for 33% of *EWSR1-WT1* commonly upregulated genes but only 4.2% of commonly downregulated genes. Upregulated *EWSR1-WT1* bound genes were more likely to be bound in the promoter or first intron and coincide with Znf263 or Hoxb4 motifs. To evaluate the functional role of *EWSR1-WT1* targets in DSRCT biology, a screen of the 24 druggable *EWSR1-WT1* targets was conducted and a number of novel and known target genes were identified as important for DSRCT survival. Current work is verifying these targets with gene knockdown and evaluating their function *in vivo*.

#3530

Mechanisms underlying Ewing sarcoma-induced osteolysis

James J. E. Williams, Joanna B. Kitlinska. *Biochemistry and Molecular Biology, Georgetown University, Washington D.C., DC*

Ewing Sarcoma (ES) is an aggressive pediatric tumor, which often arises in bones and forms osseous metastases, both of which present as osteolytic lesions. Our previous studies indicated that neuropeptide Y (NPY), which is secreted from ES tumors, stimulates tumor-induced bone degradation via its effect on macrophage recruitment and their subsequent osteoclastic differentiation. This effect was dependent on the autocrine activation of the NPY Y5 receptor (Y5R) expressed by ES cells. However, the exact mechanisms of the osteolytic activity induced by the NPY/Y5R axis remained unknown. To identify the osteolytic factors released from ES cells due to the NPY/Y5R autocrine loop activity, we used shRNA to silence NPY or Y5R in SK-ES-1 ES cells and compared concentrations of known factors involved in the regulation of bone homeostasis in their conditioned media by an antibody array. Four secreted factors were found to be significantly decreased after silencing of NPY signaling: interleukin 8 (IL-8; $p<0.005$), matrix metalloproteinase 9 (MMP-9; $p<0.05$), intercellular adhesion molecule 1 (ICAM-1; $p<0.005$), and monocyte chemoattractant protein 1 (MCP-1; $p<0.05$). Among these proteins, IL-8 and MMP-9 were selected as the main candidates for mediators of NPY-induced osteolysis. To test their role in ES-mediated stimulation of osteolysis, we co-cultured mouse RAW 264.7 cells, that represent monocyte/macrophage lineage, with

SK-ES-1 cells in the presence or absence of the MMP-9 inhibitor (JNJ-0966; 10-7M-10-5M) or anti-IL-8 neutralizing antibody (0.1-0.4µg/ml) and tested their effect on osteoclast differentiation detected by TRAP staining. Inhibiting MMP-9 activity significantly decreased osteoclastogenesis of RAW264.7 cells in dose-dependent manner, while blocking IL-8 had no significant effect on the number of formed osteoclasts. These findings implicate MMP-9 as the mediator of NPY osteolytic activity. Further studies are required to understand the exact mechanisms underlying these effects, as well as potential role of NPY-induced release of MCP-1 in macrophage recruitment to ES tumors.

#3531

Discrete extracellular matrix-secreting tumor cell subpopulations remodel the Ewing sarcoma tumor microenvironment to promote invasion

Emma D. Wrenn[1], April A. Apfelbaum[1], Shireen Ganapathi[1], Erin R. Rudzinski[2], Xuemei Deng[2], Nicolas Garcia[1], Katherine Braun[1], Trisha Lipson[3], Shruti Bhise[4], Sami B. Kanaan[4], Olivia Waltner[4], Erika Newman[5], Scott Furlan[4], Elizabeth R. Lawlor[1]. *[1]Ben Towne Center for Childhood Cancer Research, Seattle Children's Research Institute, Seattle, WA,[2]Seattle Children's Research Institute, Seattle, WA,[3]University of Washington, Seattle, WA,[4]Fred Hutchinson Cancer Center, Seattle, WA,[5]University of Michigan, Ann Arbor, MI*

Ewing sarcoma (EwS) cells exist along a neuro-mesenchymal transcriptional continuum that is largely determined by transcriptional activity of the EWS::FLI1 fusion oncoprotein. Although EWS::FLI1-low state cells are more metastatic in experimental models, the role of these cells in established EwS tumor ecosystems is unknown. Here we have leveraged multimodal single-cell sequencing, spatial transcriptomics, and immunohistochemical profiling to characterize EwS cell subpopulations in cell lines, PDX models, and patient tumors. We identify CD73 as a marker of mesenchymal-high state EwS cells and show that CD73+ tumor cells share properties of experimentally-induced EWS::FLI1-low cells including altered cytoskeletons, enhanced migration and invasion, and increased expression of EWS::FLI1-repressed genes. However, CD73+ cells retain

proliferative capacity and do not down-regulate the fusion or the EWS::FLI1-activated signature. Instead, CD73+ EwS cells selectively express a gene signature that is enriched in extracellular matrix (ECM) genes. Examination of xenograft and EwS patient biopsies confirms the existence of subpopulations of spatially and transcriptionally distinct ECM-producing tumor cells and shows them to be more prevalent in infiltrating regions. Importantly, the local tumor microenvironment (TME) surrounding these cells is rich in tumor-derived TNC, SPARC, and biglycan, ECM proteins that have been widely implicated in cancer metastatic progression. Significantly, CD73+ EwS cells also upregulate expression of ECM-sensing genes, including *ITGA5* and *ITGB1*, suggesting potential to activate autocrine feedback loops. In support of this, interrupting outside-in ECM:integrin signaling cascades, through pharmacologic inhibition of FAK or SRC pathways, strongly reduces the invasive properties of CD73+ tumor spheroids in 3D collagen. Together these studies confirm the presence and functional importance of transcriptionally distinct tumor cell subpopulations in established EwS tumor ecosystems. In particular, our data reveal that highly mesenchymal tumor cells both generate and respond to pro-metastatic ECM proteins to support invasion. Studies are ongoing to determine the role of tumor cell-derived ECM on EwS progression and treatment resistance.

#3532

Activator protein-1 (AP-1) signaling inhibits the growth of Ewing sarcoma cells in response to DNA replication stress

David Gordon, Emma Croushore, Stacia Koppenhafer, Kelli Goss, Elizabeth Geary. *Pediatrics, University of Iowa, Iowa City, IA*

Ribonucleotide reductase (RNR) is the rate-limiting enzyme in the synthesis of deoxyribonucleoside triphosphates (dNTPs) and is required for DNA replication and the repair of DNA damage. Multiple types of cancer, including Ewing sarcoma tumors, are sensitive to RNR inhibitors or a reduction in the levels of either the RRM1 or RRM2 subunits of RNR. However, the polypharmacology and off-target effects of RNR inhibitors has complicated the identification of the precise mechanisms that regulate sensitivity and resistance to this class of drugs. Consequently, we used a conditional knockout (CRISPR/Cas9) and rescue approach to target RRM1

in Ewing sarcoma cells and identified that loss of RRM1 results in upregulation of the expression of multiple members of the activator protein-1 (AP-1) transcription factor complex, including c-Jun and c-Fos. This upregulation of AP-1 is mediated, in part, by SLFN11, which is expressed at high levels in Ewing sarcoma tumor and other pediatric sarcomas. Notably, the inducible expression of c-Jun and c-Fos in Ewing sarcoma cells impairs cell growth, downregulates the expression of the stem cell factor Sox2, and upregulates markers of cellular differentiation. In addition, small-molecule inhibitors of RNR, including gemcitabine and hydroxyurea, and HDAC inhibitors, which reduce the level of the RRM1 protein, also activate this AP-1 signaling pathway in Ewing sarcoma cells. Overall, these results provide novel insight into the critical pathways activated by loss of RNR activity and the mechanisms of action of inhibitors of RNR.

#3533

Zebrafish *her3*knockout impacts developmental and rhabdomyosarcoma-related gene signatures

Matthew R. Kent[1], Delia Calderon[1], Katherine M. Silvius[1], Jack P. Kucinski[1], Collette A. LaVigne[2], Matthew V. Cannon[1], Genevieve C. Kendall[1]. *[1]Nationwide Children's Hospital, Columbus, OH,[2]UT Southwestern Medical Center, Dallas, TX*

HES3 is a basic helix-loop-helix transcription factor that regulates neural stem cell renewal during development. *HES3* overexpression is predictive of reduced overall survival in patients with fusion-positive rhabdomyosarcoma, a pediatric cancer that resembles immature and undifferentiated skeletal muscle and is most commonly driven by the fusion-oncogene *PAX3-FOXO1*. However, the mechanisms of *HES3* cooperation in *PAX3-FOXO1* driven rhabdomyosarcoma are unclear and are likely related to *her3*/*HES3's* role in neurogenesis. To investigate *HES3's* function during development, we generated a zebrafish CRISPR/Cas9 null mutation of *her3*, the zebrafish ortholog of *HES3*. Phenotypic characterization revealed that *her3* null mutation is not embryonic lethal as they are present at expected Mendelian ratios. We observed a temporary growth delay *her3* zebrafish null mutants and, rarely, eye defects in adults. Transcriptomic analysis of *her3* null mutant embryos showed early dysregulation of a known downstream target, *neurog1* and downregulation

of genes involved in organ development, such as *pctp* and *grinab*, while genes pointing toward a terminal differentiation state, such as *tmod*, are upregulated. Differentially expressed genes in *her3* null mutant embryos are enriched for HOX and SOX10 motifs, suggesting these may be key genes involved during HES3 dysregulation. Several cancer-related gene pathways are impacted, including the inhibition of matrix metalloproteinases and the tumor microenvironment pathway. To complement our zebrafish model, we are developing a double-inducible cell line model consisting of a tetracycline-inducible *HES3* and a cumate-inducible *PAX3-FOXO1* to further investigate the hypothesized cooperation between *her3/HES3* and *PAX3-FOXO1* in fusion-positive rhabdomyosarcoma. These two systems will allow us to elucidate conserved mechanisms of cooperation between *HES3* and *PAX3-FOXO1,* and identify new therapeutic opportunities for children with fusion-driven rhabdomyosarcoma.

#3534

Interrogating the immune microenvironment of a novel mouse model of fusion positive rhabdomyosarcoma

Erin E. Resch[1], Kristianne M. Oristian[2], Elizabeth Mendes[2], Corinne M. Linardic[2], Brian H. Ladle[1]. *[1]Johns Hopkins University School of Medicine, Baltimore, MD,[2]Duke University Medical Center, Durham, NC*

Immunotherapies have been largely ineffective for pediatric soft tissue sarcomas, in particular for fusion-positive rhabdomyosarcoma (FP-RMS), characterized by the PAX-FOXO1 gene fusion. We are hampered by a paucity of predictive, immune-competent mouse models of this cancer with which to develop novel and effective immune-based therapies. To overcome this barrier, we analyzed the immune microenvironment of one of the few genetically-engineered mouse models (GEMM) of FP-RMS. Briefly, this model is driven by conditional knock-in expression of *Pax3:Foxo1* at the endogenous *Pax3* locus, with or without conditional loss of MST1/2 (gene name *Stk4/3*), a Hippo pathway mediator that is modulated by PAX3-FOXO1. These two genotypes demonstrate different disease penetrance and tumor location, with mice bearing loss of MST1/2 exhibiting higher tumor penetrance and favoring head and neck disease sites. We hypothesize that these models exhibit differences in tumor-immune interactions in the microenvironment that correlate with these phenotypic differences. We aim

to characterize the immune microenvironment differences between these tumors and to establish this GEMM as a predictive, syngeneic model of FP-RMS. Tumors were generated spontaneously from a GEMM of FP-RMS. Tumors expressed PAX3-FOXO1 and either carried a conditional loss of MST1/2 (MST^{null}) or native MST1/2 (MST^{wt}). We analyzed 8 formalin-fixed, paraffin-embedded (FFPE) tumors and 2 tumor-derived cell lines from these novel models. FFPE tumor samples were analyzed via immunohistochemistry (IHC) for CD3 (T cell marker) and CD11b (myeloid cell marker) and were scored for immune cell infiltration. Overall, tumors demonstrate poor $CD3^+$ T cell infiltration with significantly higher infiltration of $CD11b^+$ myeloid cells ($p=0.0002$); this trend is also seen within the individual MST^{wt} ($p=0.0286$) and MST^{null} cohorts ($p=0.0286$). There was no significant difference in $CD3^+$ T cell or $CD11b^+$ myeloid cell density between the two genotypes. The drivers of this immune phenotype and the role of Hippo pathway signaling in mediating RMS tumor immune cell infiltration warrants further investigation. Additional ongoing studies are utilizing a spatial gene expression platform to visualize the spatially-preserved transcriptome of intact tumors to reveal potential pathways mediating the immune microenvironment.

#3536

Role of Myc family proteins in fusion-positive rhabdomyosarcoma

Bishwanath Chatterjee, Salah Boudjadi, Puspa Raj Pandey, Hana Kim, Wenyue Sun, Frederic G. Barr. *Cancer Molecular Pathology Section, Laboratory of Pathology, National Cancer Institute, Bethesda, MD*

Fusion-positive rhabdomyosarcoma (FP RMS) is an aggressive pediatric malignancy characterized by the presence of a PAX3-FOXO1 (P3F) or PAX7-FOXO1 fusion gene. Previous RNA expression studies have shown that these FP RMS tumors also express high levels of MYCN and lower levels of MYC. Our recent studies of FP RMS tumors revealed an inverse relationship between MYCN and MYC RNA expression in FP RMS tumors. Western blot studies of FP RMS cell lines and patient-derived xenograft (PDX) tumors identified tumors with high level MYCN and MYC protein expression as well as tumors with high level protein expression of either MYC or MYCN. To model the interaction of P3F with Myc family proteins in FP RMS, we generated human Dbt myoblasts with

doxycycline-inducible P3F (iP3F) with or without constitutively expressed MYCN. We previously observed that doxycycline-treated human Dbt myoblasts engineered with iP3F and constitutive MYCN expression (Dbt-MYCN-iP3F) form foci *in vitro* and rapidly form tumors *in vivo*, while doxycycline-treated Dbt myoblasts engineered with only iP3F expression (Dbt-iP3F) do not form foci *in vitro* and form tumors *in vivo* at a slower rate. Western blot and qRT-PCR analysis of the parental and tumor-derived (TD) Dbt-MYCN-iP3F lines revealed high MYCN and low MYC expression. In contrast, Dbt-iP3F parental lines express moderate levels of MYC and very low levels of MYCN whereas iP3F TD lines show increased MYC and MYCN expression, though this level of MYCN expression is considerably less than that seen in Dbt-MYCN-iP3F lines. Using CRISPR-Cas9 technology to knockdown MYCN or MYC, we found a primary dependence on MYCN in both Dbt-MYCN-iP3F parental and TD lines as indicated by loss of focus formation following MYCN knockdown while MYC knockdown does not interfere with oncogenicity. In contrast, oncogenicity in Dbt-iP3F TD lines is primarily dependent upon MYC whereas MYCN knockdown results in a modest and variable effect on oncogenicity. To elucidate the role of Myc proteins on the expression of P3F target genes, we measured expression of several transcriptional targets in these parental and TD lines by RNA sequencing and qRT-PCR. Several target genes (such as FGFR4) showed comparable upregulation by P3F in both parental and TD lines with or without constitutive MYCN expression. In contrast, a few target genes (such as FGF8) were stimulated by P3F at low levels in Dbt-iP3F parental lines and were stimulated at much higher levels in Dbt-iP3F TD lines as well as in both Dbt-MYCN-iP3F parental and TD lines. This finding indicates that some P3F target genes do not require high MYCN or MYC expression whereas other P3F target genes can only be maximally stimulated by P3F in the presence of high levels of MYCN and/or MYC. We postulate that the dependence of FP RMS on high level expression of a Myc family protein may be explained by the need to stimulate expression of one or more of the P3F target genes in this latter category.

#3537

A novel orthotopic xenograft model of spontaneous metastasis for rhabdomyosarcoma using lingual intramuscular injection

Katie E. Hebron[1], Kristine Isanogle[2], Amy James[3], Simone Difilippiantonio[3], Marielle E. Yohe[1]. *[1]NCI, National Institutes of Health (NIH), Frederick, MD,[2]Laboratory Animal Services Program, National Institutes of Health (NIH), Frederick, MD,[3]Laborator Animal Services Program, National Institutes of Health (NIH), Frederick, MD*

Rhabdomyosarcoma (RMS), a cancer characterized by the defective differentiation of skeletal muscle precursor cells, is the most common pediatric soft tissue sarcoma. Despite significant efforts to characterize the transcriptomic and genetic abnormalities of the disease, the prognosis for patients with advanced or refractory disease has remained unchanged for more than four decades. Preclinically, studies have been hampered by insufficient animal models. For example, the hindlimb orthotopic model, an injection into the gastrocnemius muscle of immunocompromised mice, produces highly encapsulated, non-invasive, non-metastatic tumors. While this model has shown a reasonable recapitulation of tumor proliferation response, investigators using this model are unable to assess the effect of their investigational treatment on local invasion or distant metastasis. Moreover, transgenic mouse models of RMS, while commonly metastatic, diverge significantly from the transcriptomic signature of human tumors. With these considerations, we hypothesized that an alternative orthotopic site, the tongue, may provide a more representative xenograft model of RMS. In a proof of principal experiment, the fusion negative RMS (FN-RMS) cell line RD was injected into the skeletal muscle of the tongue, a lingual intramuscular (LIM) injection. Tongue tumors establish in approximately 60-80% of mice injected within approximately 40 days. By histopathology, the primary tumors show evidence of local invasion. Interestingly, approximately 60% of these tumors also spread to local cervical lymph nodes, a process not observed in hindlimb orthotopic models or subcutaneous models. We expanded our investigation to include additional FN-RMS cell lines: RMS-YM, SMS-CTR, and a MEK inhibitor resistant cell line CTR-557. Mice injected with RMS-YM cells established tumors in at least 60% of mice by 75 days post injection. Additionally, enlarged local and distant lymph nodes are observed in 50% of these mice. Intriguingly, mice injected with SMS-CTR or its MEK inhibitor resistant derivative, CTR-557, frequently have tumors in both local and distant lymph nodes without evidence of a primary tongue tumor. One mouse in each group also had pulmonary metastases. Taken together, this model not only demonstrates the first orthotopic xenograft model of spontaneous metastasis for FN-RMS, it also mimics the spread of disease that is observed clinically in RMS originating in the head and neck. Ongoing and future studies include 1) generating highly metastatic human FN-RMS cell lines; 2) using spatial transcriptomics to compare the tumor microenvironment of non-metastatic hindlimb tumors and invasive and/or metastatic lingual tumors; and 3) identifying drivers of FN-RMS dissemination through transcriptomic, genome accessibility, and phospho-proteomic methods.

#3538

Endogenous HiBiT-tagging of PAX3-FOXO1 identifies potent suppressors of PAX3-FOXO1 protein levels by high-throughput screening

Yong Yean Kim[1], Robert G. Hawley[2], Mehal Churiwal[1], Teresa S. Hawley[3], Christine N. Evans[4], Raj Chari[4], David Milewski[1], Ranuka Sinniah[1], Young K. Song[1], Hsien-Chao Chou[1], Xinyu Wen[1], Ying Pang[1], Jing Wu[1], Craig J. Thomas[5], Jun S. Wei[1], Michele Ceribelli[5], Javed Khan[1]. *[1]National Cancer Institute, Bethesda, MD,[2]George Washington University, Washington, DC,[3]Research Technologies Branch, National Institute of Allergy and Infectious Diseases, Bethesda, MD,[4]Frederick National Laboratory for Cancer Research, Frederick, MD,[5]National Center for Advancing Translational Sciences, Rockville, MD*

Background: Oncogenic fusion genes are attractive therapeutic targets due to their tumor-specific expression and driver roles in cancers. PAX3-FOXO1 (P3F) is the dominant oncogenic driver of fusion-positive rhabdomyosarcoma (FP-RMS) with no targeted therapy. We developed methods to directly measure endogenous P3F protein levels amenable to high-throughput drug screens to identify suppressors of P3F.
Methods: HiBiT tag, an 11 amino acid peptide of the small fragment of NanoLuc luciferase, was inserted into the endogenous P3F using CRISPR-Cas9 in FP-RMS cell lines RH4 and SCMC. Western analysis was used for HiBiT tag validation and confirmation of P3F suppression. RNA-seq and ChIP-seq were used to assess transcriptomics and DNA binding of HiBiT-tagged P3F (P3F-HiBiT) respectively. High-throughput drug screen using Nano-Glo luciferase assay was performed using the Mechanism Interrogation PlatE (MIPE 5.0) drug library, which included

2,480 drugs with known mechanisms of action. CellTiter-Glo was used to monitor cell viability. We identified drugs that suppressed P3F by Nano-Glo without acute cytotoxicity by CellTiter-Glo at an early 24-hour timepoint. Mouse xenograft model of FP-RMS was used to investigate in vivo efficacy of top hits.
Results: We validated HiBiT tagging of P3F and not the wild-type FOXO1 by Western analysis. We showed that the HiBiT tag did not change the function of P3F by transducing human fibroblasts with P3F-HiBiT versus unmodified P3F. Gene Set Enrichment Analysis (GSEA) of RNA-seq showed that P3F-HiBiT activated the same downstream target genes as unmodified P3F. ChIP-seq using HiBiT antibody in HiBiT-tagged FP-RMS cell lines RH4 and SCMC matched the genomic locations from ChIP-seq with P3F antibody in parental RH4 and SCMC. Using a cutoff of Area Under the Curve (AUC) of CellTiter-Glo - AUC of Nano-Glo > 90, in both RH4 and SCMC, identified 182 compounds. Filtering for drugs with ≥ 3 hits for the same target identified 14 drug classes that suppressed P3F protein level including HDAC inhibitors (3), mTOR inhibitors (4), CDK inhibitors (8), and BRD4 inhibitors (3). One top hit was the CDK inhibitor TG02 (Zotiraciclib), currently in human trials. TG02 suppressed P3F protein levels by Nano-Glo and Western analysis. We confirmed induction of apoptosis by PARP cleavage in a panel of FP-RMS cell lines. GSEA analysis of RNA-seq after treatment with TG02 showed marked suppression of P3F target gene sets. TG02 also significantly delayed tumor progression of established tumors in a mouse xenograft model of FP-RMS without weight loss.
Conclusion and Future Directions:By HiBiT tagging the fusion oncogene P3F, we identified 182 compounds that suppress P3F levels of which TG02 was a top hit that also showed in vivo efficacy. Drug combination studies are currently underway to identify synergistic suppressors of P3F protein levels that can be translated into clinical trials.

#3539

Indoleamine-2,3-dioxygenase 2 (IDO-2) is expressed in hepatoblastoma cells and associated with metastatic state

Lisandro Luques[1], Ashby Kissoondoyal[1], Emily De Sousa[1], Paula Quaglietta[1], David Malkin[1], Stefano Cairo[2], Emilie Indersie[3], Reto Baertschiger[1]. *[1]Genetics & Genome Biology Program, The Hospital for Sick Children, Toronto, ON, Canada,[2]Champions Oncology Inc, Rockville, MD,[3]XenTech, Evry, France*

Hepatoblastoma (HB) is the most common pediatric primary liver malignancy and represents about 1% of all pediatric tumors. Incidence of HB has been increasing in the past 10 years. Risk stratification of HB patients is established by the extent of the liver disease, patient age, levels of serum AFP and presence of metastatic disease. Currently, treatment and prognosis of HB patients relies on chemotherapy and complete tumor resection. Unfortunately, patients with high-risk HB (metastatic, unresectable, refractory and recurrent) have dismal prognosis. The molecular mechanisms underlying the aggressiveness and metastatic potential of the tumor have not been elucidated yet. Tryptophan-2,3-dioxygenase (TDO) and indoleamine-2,3-dioxygenase 1 and 2 (IDO 1 and IDO-2) are enzymes in mammals that catabolize tryptophan to kynurenine and its activity has been related with immunoregulation and tumorigenesis. While TDO and IDO-1 have been extensively studied before the discovery of IDO-2, the role of the later in tumorigenesis is still under evaluation. Expression of IDO-2 is normally found in liver, kidney, pancreas, brain and epididymis while a dysregulated expression was reported in different types of cancer. IDO-2 activity was found to affect both the immune cells activation status and also the proliferation, migration and survival of tumor cells both *in vitro* and *in vivo*. Despite being expressed in normal liver tissues, IDO-2 expression has never been assessed in HB cells. The aim of this study was to determine if IDO-2 mRNA is expressed in HB cell lines and to determine if this expression is correlated with patient risk classification. By using real-time RT-PCR, we determined the expression of IDO-2 in commercially available HepG2 cells and in three patient derived xenograft (PDX)-derived HB cell lines (HB214, HB279, HB 303) (high risk metastatic, high-risk non metastatic and-low risk, respectively). IDO-2 is expressed in both HepG2 cells and in the 3 PDX-derived cell lines. Data analysis by using linear mixed effects modelling followed by t-tests to examine specific comparisons showed significant differences between cell lines. Expression of IDO-2 in cells from the metastatic tumor (HB214) was significantly higher than in HepG2 and cells from non-metastatic disease ($p<0.05$). In conclusion, we report here for the first time that IDO-2 is expressed in HB cells. Although further investigation should be conducted in order to understand its specific role in HB, the findings in this work suggest that IDO-2 expression might be related with clinical tumor behavior.

#3540

Reduction in cell viability of hepatoblastoma cells following inhibtion of Hsp90

Ashby Kissoondoyal[1], Emily DeSousa[1], Paula R. Quaglietta[1], Emilie Indersie[2], Stefano Cairo[3], David Malkin[1], Lisandro Luques[1], Reto M. Baertschiger[1]. *[1]Genetics and Genome Biology, SickKids, Toronto, ON, Canada,[2]XenTech, Evry, France,[3]Champions Oncology, Rockville, MD*

Background: Hepatoblastoma (HB) is the most frequent liver tumor in children. While most tumors respond well to treatment with good outcomes, there are a subgroup of refractory tumors for which novel therapies are required. Emerging literature has suggested a role of Hsp90 in HB progression. One possible mechanism hypothesizes that Hsp90 helps stabilize misfolded proteins that contribute to HB progression including β-catenin. Our study aimed to investigate if inhibition of Hsp90 would affect the cell viability of hepatoblastoma cell lines in vitro.
Methods: Commercially available HEPG2, and patient xenograft-derived hepatoblastoma cell lines (HB214, HB279, and HB303) were analyzed for differences in Hsp90 gene expression by qRTPCR as well as cell viability (n = 3 replicates for each cell line) using the MTS assay. Differences in cell viability for each cell line were further examined after treatment with a 0.1μM or 0.25μM dose of 17-AAG (an HSP90 inhibitor) for 48H. We examined gene expression and the MTS assay cell viability data using linear mixed effects modelling followed by t-tests to examine specific comparisons (significance at $p < 0.05$).
Results: Hsp90 gene expression was significantly increased in HEPG2 cells ($p < 0.001$) and in HB279 cells ($p < 0.05$), but not in HB214, or HB303 cells, compared to HUVECs control cells. Examining clinically relevant characteristics, significant improvements to model fit were found with the inclusion of sex ($p < 0.01$), β-catenin deletion status ($p < 0.01$), and a higher PRETEXT stage but not from examining if cell lines were derived from metastatic parent tumors. While we observed no significant cell line viability differences between individual HB cell lines at baseline (0μM 17-AAG treatment) or overall significant differences for treatment with either 0.1μM or 0.25μM dosages of 17-AAG, there were differences in cell viability for individual HB cell lines. We observed significant decreases in cell viability in HEPG2 cells with 0.1μM ($p < 0.05$) and 0.25μM ($p < 0.05$), as well as in HB279 cells with 0.1μM ($p < 0.05$) and 0.25μM ($p < 0.05$) 17-AAG treatments but observed no effect of 17-AAG treatment on cell viability in HB214, or HB303 cells. Similar improvements in model fit were observed with the inclusion of sex ($p < 0.01$), β-catenin deletion status ($p < 0.01$), and a higher PRETEXT stage ($p < 0.001$), but not from examining if cell lines were derived from metastatic parent tumors.
Conclusion: HB cell lines express Hsp90 at levels correlated with age, β-catenin deletion status, and risk stage. Moreover, the expression levels of Hsp90 corresponded to the sensitivity of each cell line to the Hsp90 inhibitor 17-AAG, with cells more highly expressing Hsp90 having a greater reduction in cell viability. Continuing to understand the mechanisms of Hsp90 action in HB, particularly through the previously demonstrated connection with β-catenin, may identify potential targetable therapies in the care of HB.

#3541

Tumoroid-based screening platform to test focal, chemo- and combination therapy for retinoblastoma

Irina Sinenko[1], Fabien Kuttler[2], Valentin Simeonov[3], Alexandre Moulin[4], Christina Stathopoulos[4], Gerardo Turcatti[2], Adeline Berger[4], Francis Munier[5], Paul Dyson[1]. *[1]Institute of Chemical Sciences and Engineering, Swiss Federal Institute of Technology Lausanne (EPFL), Lausanne, Switzerland,[2]Biomolecular Screening Facility, School of Life Sciences, Swiss Federal Institute of Technology Lausanne (EPFL), Lausanne, Switzerland,[3]Laboratory of Environmental Remote Sensing, Swiss Federal Institute of Technology Lausanne (EPFL), Lausanne, Switzerland,[4]Jules-Gonin Eye Hospital, Foundation Asile des Aveugles, Lausanne, Switzerland,[5]Swiss Federal Institute of Technology Lausanne (EPFL), Lausanne, Switzerland*

Current treatments for retinoblastoma, the most common intraocular malignancy, rely on a limited number of drugs repurposed from other pediatric cancer therapies. Drug toxicity and relapse of the disease necessitate new therapeutic strategies. The implementation of drug candidates in the clinic is usually followed by *in vitro* validation, which requires accurate and clinically relevant *in vitro* models. We report here a robust 3D tumoroid-based platform, for testing various clinical protocols, e.g. therapeutic agents following a single or repeated exposure, alone or in combination with focal therapy (thermotherapy). The platform, generated from the Y79 retinoblastoma cell line, consists of matrix-embedded tumoroids, which retain the key features of the disease and allow prolonged culture time. Following the optimization of growth conditions, the effect of single and repeated exposure to chemotherapeutic agents has been measured by high-throughput automated fluorescence imaging followed by quantification. The clinical conditions of chemothermotherapy have been recapitulated with a setup consisting of: an infrared diode laser (810 nm, 0.3 W) that heats the tumoroids in the presence of indocyanine green (50 μg/mL); a thermal camera to enable real-time temperature measurement; and an environment-controlled

inverted microscope to ensure physiological conditions and precise focusing of the laser. Melphalan and carboplatin, two drugs currently used to treat retinoblastoma in clinical protocols of chemotherapy and chemothermotherapy respectively, have been applied to validate the system.Tumoroid viability and size progressively decreased over 4 weeks of repeated drug exposure with melphalan, reflecting the response of retinoblastoma in advanced clinical cases. Carboplatin treatment showed an activity enhancement in the tumoroid model similar to that observed in the clinic, when combined with focal therapy, demonstrating that the platform system closely recapitulates the clinical conditions. Inversely, the thermotherapy experimental protocol designed for 2D *in vitro* cell culture and commonly used to date, i.e. an incubation temperature increased to 42 ºC for 1 h, did not show an improvement of the carboplatin cytotoxicity, confirming that our laser-based thermotherapy protocol provides a more accurate and clinically relevant drug response.
Such an approach, combining physiologically relevant *in vitro* cancer models and investigation of drugs in well-established treatment modalities, can significantly reduce the number of new drug candidates that give false-positives or overestimated efficacies when evaluated in relevant *in vivo* models. It is expected that the platform will contribute to the implementation of new therapeutic strategies to treat retinoblastoma, and could also be adapted to other diseases for which repeated drug exposure and/or chemothermotherapy is relevant.

#3542

A stem cell model dissects detrimental effects of neuroblastoma-linked chromosomal aberrations on cell differentiation during neural crest development

Ingrid M. Saldana-Guerrero[1], Luis F. Montano-Gutierrez[2], Christoph Hafemeister[2], Dylan Stavish[3], Lisa E. Shaw[4], Irfete S, Fetahu[2], Andrea Wenninger-Weinzierl[2], Caterina Sturtzel[2], Celine Souilhol[3], Sophia Tarelli[3], Mohamed R. Shoeb[2], Marie Bernkopf[2], Polyxeni Bozatzi[2], Maria Guarini[5], Eva Bozsaky[2], Michelle C. Buri[2], Eva M. Putz[2], Peter W. Andrews[6], Ivana Barbaric[3], Helen E. Bryant[7], Martin Distel[2], Sabine Taschner-Mandl[2], Matthias Farlik[4], Anestis Tsakiridis[3], Florian Halbritter[2]. *[1]Centre for Stem Cell Biology, Neuroscience Institute, & Sheffield Institute for Nucleic Acids, The University of Sheffield, Sheffield, United Kingdom,[2]St. Anna Children's Cancer Research Institute (CCRI), Vienna, Austria,[3]Centre for Stem Cell Biology & Neuroscience Institute, The University of Sheffield, Sheffield, United Kingdom,[4]Department of Dermatology, Medical University of Vienna, Vienna, Austria,[5]CeMM Research Center for Molecular Medicine of the Austrian Academy of Science, Vienna, Austria,[6]Centre for Stem Cell Biology, The University of Sheffield, Sheffield, United Kingdom,[7]Sheffield Institute for Nucleic Acids (SInFoNiA), Department of Oncology and Metabolism, The University of Sheffield, Sheffield, United Kingdom*

Early childhood malignancies are driven by sparse genetic aberrations in oncogenes that often co-occur with large copy number variants (CNVs). The combination of these mutations is thought to transform developmentally pliant embryonic cells to initiate tumorigenesis. However, the mechanistic interactions between CNVs, oncogenes, and differentiation have not been systematically studied due to several obstacles: (i) CNVs cannot be engineered efficiently yet; (ii) transient embryonic progenitors are absent in full-grown tumors; and (iii) inter-species differences in lineage specification limit the applicability of animal models.
To overcome these challenges, we used isogenic human embryonic stem cell (hESC) lines carrying gains of chromosome 17q/1q, which are prevalent in the embryonal tumor neuroblastoma (NB). We differentiated these cells toward trunk neural crest (NC) and their sympathoadrenal derivatives, the putative cells-of-origin of NB, and performed single-cell RNA sequencing and cell-biological assays at key differentiation stages. We found that CNVs impaired the specification of sympathoadrenal cell types and instead potentiated early Schwann-cell-precursor-like phenotypes. Additional overexpression of the oncogene MYCN (which is frequently amplified together with CNVs in high-risk NB tumors) exacerbated these differentiation defects, enabled tumourigenic cell proliferation, and generated cell states in vitro that transcriptionally resembled NB tumor cells. Finally, using epigenome analysis, we connected these states to a stepwise disruption of gene-regulatory networks centered on developmental transcription factors.
Together, our results chart a mechanistic route to NB tumorigenesis and provide a general framework for the CNV-driven initiation of embryonal tumors, in which CNVs ‘prime’ embryonic cells for oncogenic transformation. The tumor-like cells in our model may serve as proxies to experimentally test therapeutic interventions during tumorigenesis.

#3543

Mesenchymal stromal cells and tumor-associated macrophages modulate adrenergic to mesenchymal state switching in neuroblastoma

Meng-Hua Lee, Kevin Louault, Krinio Giannikou, Xiangming Ding, Alice Yanovsky, Jin-Seok Park, Yves A. DeClerck, Shahab Asgharzadeh. *Cancer and Blood Diseases Institute, Children's Hospital Los Angeles, Los Angeles, CA*

Neuroblastoma (NB), a common solid tumor of children, can adopt a lineage-committed adrenergic (ADRN) or an immature mesenchymal (MES) tumor cell type, which differs in phenotype, epigenetic landscape, transcription factors, and core regulatory circuitries. These cell types can spontaneously interconvert, but the mechanism remains largely unknown. Here, we hypothesize that the tumor-associated macrophages (TAM) and cancer-associated fibroblast (CAF) within the tumor microenvironment contribute to pro-tumorigenic factors production and drive switching from ADRN to MES state in neuroblastoma. We first demonstrate the ADRN and MES lineage identity of NB cell lines by Western blot and compared the control and NB cell lines co-cultured with mesenchymal stromal cells (MSC), the precursor cell of CAF, and monocyte in transwell. Initial experiments demonstrated the morphology of NB cell line CHLA255 and CHLA136 showing increased spreading area and spindle shape in TAM-CAF co-cultures compared to control cells. As compared to control cells, monocytes and MSC-CAF co-culture induced the MES lineage markers SOX9 and Notch1 of NB cell lines that had low basal SOX9 expression, with a reduction in protein levels of ADRN lineage markers PHOX2B, and GATA3. Next, single-cell RNA-sequencing was utilized to analyze the expression of TAM and CAF, and MES- and ADRN-signature genes of NB cells in NB-TAM-CAF co-cultures. Single-cell analyses of TAM-CAF co-cultured CHLA255 and CHLA136 demonstrated enrichment of MES signature over time providing clear evidence of mesenchymal differentiation of NB cells within a TME-rich environment. Pathway enrichment analyses reveal enrichment of pathways associated with extracellular matrix (ECM) deposition and epithelial to mesenchymal of TAM-CAF co-cultured NB cell lines. Our results suggested that the presence of CAF and TAM in the tumor microenvironment drives neuroblastoma ADRN: MES switch akin to that observed in epithelial: mesenchymal switch in adult tumors. ADRN-MES state switching has been shown relevant for tumor relapse and therapy resistance. Our studies point to a therapeutic vulnerability by targeting cells and pathways activated in the NB-TAM-CAF axis.

#3544

ALK signaling activity stabilizes SLC3A2 protein levels in neuroblastoma tumorigenesis

Wei-Yun Lai, Tzu-Po Chuang, Marcus Borenäs, Ruth Palmer, Bengt Hallberg. *University of Gothenburg, Gothenburg, Sweden*

Background: Neuroblastoma is the most common childhood tumor that grows in the adrenal glands or sympathetic ganglia. Approximately 10% of pediatric neuroblastoma patients harbor mutations in anaplastic lymphoma kinase (ALK). In a previous study, we identified SLC3A2 as a potential interacting partner with ALK using BioID-based *in vivo* proximity labeling. SLC3A2 is a multifunctional protein that mediates integrin-dependent signaling, acts as a trafficking chaperone for amino acid transporters, and regulates polyamine transport. No previous link to ALK signaling has been reported and the underlying mechanisms and functional consequences of a SLC3A2-ALK interaction in ALK-driven neuroblastoma are unclear.
Materials & Methods: The interaction of SLC3A2 and ALK initially detected with BioID-based *in vivo* proximity labeling was validated by immunoprecipitation. The effect of ALK signaling on SLC3A2 expression and protein stability was evaluated by quantitative PCR and immunoblotting. The functional effect of SLC3A2 on cell viability were investigated by siRNA and inhibitor treatments in both human and mouse ALK-driven neuroblastoma cells.
Results: SLC3A2 was confirmed to interact with ALK in both anti-ALK and anti-SLC3A2 antibody co-immunoprecipitations from NB1 cells (ALK-wild-type) and CLB-GE (ALK-F1174V). Moreover, this interaction was decreased by ALK inhibitor (lorlatinib) treatment. Upon ALKAL2 ligand treatment, ALK signaling increased the protein levels of SLC3A2 and this was abrogated by lorlatinib treatment in NB1 cells. Furthermore, lorlatinib treatment suppressed SLC3A2 expression and significantly affected protein stability in neuroblastoma cells with different ALK mutations including CLB-BAR (ALK exon4-11 deletion), CLB-GAR (ALK-R1275Q), and CLB-GE (ALK-F1174V) during cycloheximide chase analysis. Knockdown of SLC3A2 significantly inhibited cell growth and down-regulated the amino acid transporter SLC7A5 (LAT1) expression in CLB-GE cells (ALK-F1174V). While mono treatment of either lorlatinib (ALK TKI) or AMXT-1501 (polyamine transport inhibitor) only showed moderate effects, combinatorial treatment exhibited a synergistic effect on cell growth in ALK-driven

primary-cultured mouse neuroblastoma #9883 (Th-*MYCN*; *Alk-F1178S*) and #111 (Th-*MYCN*; *Rosa26_Alkal2*) cells.
Conclusions: SLC3A2 protein stability and its interaction with ALK is dependent on ALK signaling in an ALK-driven neuroblastoma context. The synergistic effect of combined ALK and polyamine transport inhibitors suggests a potential therapeutic option for ALK-driven neuroblastoma.

#3545
The Yes-associated protein (YAP) regulates GD2 immunotherapy response in high-risk neuroblastoma
Adeiye A. Pilgrim[1], Hunter C. Jonus[1], Andrew Ho[1], Anna Cole[2], Jenny Shim[1], Kelly C. Goldsmith[1]. *[1]Emory University School of Medicine, Atlanta, GA,[2]Emory University, Atlanta, GA*

Background Patients with the pediatric solid tumor high-risk neuroblastoma (HR NB) receive intense multimodal therapy yet 50% still relapse with chemotherapy-resistant disease. Relapsed NBs harbor increased RAS/MAPK pathway mutations and increased expression and downstream activity of the transcriptional co-regulator YAP. We have previously shown that YAP mediates resistance to chemotherapy and MEK inhibitors in RAS mutant NBs (Shim *et al., Cancer Res* 2020). Patients with relapsed NB are treated with the GD2-targeting monoclonal antibody dinutuximab in combination with chemotherapy. Given the increased expression and activity of YAP in relapsed HR NB, we posited that YAP might also play a role in GD2 immunotherapy response.
Methods/Results We stably knocked down YAP in the human derived NRAS mutant SK-N-AS NB cell line with a scrambled short hairpin (sh) control or 2 YAP-targeting shRNAs to generate 3 distinct cell lines. Dinutuximab requires antibody-dependent cellular cytotoxicity (ADCC) and we have shown that gamma delta (γδ) T cells augment dinutuximab in aggressive NB models. We exposed the shYAP1, shYAP2, and control SK-N-AS cells to γδ T cells with/ without dinutuximab. YAP knockdown sensitized both SK-N-AS shYAP cell lines to γδ T cell killing both in the presence and absence of dinutuximab. To investigate the mechanism of increased dinutuximab sensitivity, we evaluated a panel of NB cell lines (*MYCN* amplified and *MYCN* single copy) for YAP protein and GD2 cell surface expression and noted an inverse relationship. That same inverse correlation was found for GD2 and YAP gene expression in primary HR NB tumor datasets. We therefore evaluated GD2 expression following YAP knockdown in SK-N-AS and show that GD2 significantly increased on the cell surface following YAP inhibition. PRRX1 is a master transcription factor that induces a mesenchymal NB phenotype which is one of high YAP expression with very low to no GD2 surface expression. Interestingly, *PRRX1* expression increased in YAP knockdown cells yet GD2 expression also increased, suggesting YAP regulates GD2 expression more directly than PRRX1. In the GD2 biosynthesis pathway, GM3 is converted into GD3 by GD3 synthase (GD3S). GD2 synthase then catalyzes GD3 into GD2. GD3S gene (*ST8SIA1*) expression significantly increased (>100-fold) upon YAP knockdown. Furthermore, shRNA stable inhibition of GD3S in shYAP NB cells reverted the phenotype and decreased GD2 cell surface expression back to baseline. We then treated established SK-N-AS control or shYAP xenografts with an 18-day course of human γδ T cells, dinutuximab, and cyclophosphamide. Pilot results show significantly extended survival in mice harboring SK-N-AS shYAP tumors.
Conclusion These results support YAP regulation of GD2 expression through transcriptional suppression of GD3 synthase and identify YAP as a therapeutic target to augment GD2 immunotherapy responses in HR and relapsed NB.

Pediatric Cancer 3: Genomes and Novel Tumor Models

#3550
The ENL YEATS domain links leukemic stem cell frequency and enhances YEATS inhibitor sensitivity in MLL-ENL leukemias
Hsiangyu Hu[1], Nirmalya Saha[1], Yuting Yang[1], Ejaz Ahmad[1], Lauren Lachowski[1], Uttar Shrestha[1], Vidhya Premkumar[1], James P. Ropa[2], Lili Chen[1], Blaine Teahan[1], Sierrah Grigsby[1], Rolf Marschalek[3], Zaneta Nikolovska-Coleska[1], Andrew G. Muntean[1]. *[1]University of Michigan Medical School, Ann Arbor, MI,[2]Indiana University School of Medicine, Indianapolis, IN,[3]Institut für Pharmazeutische Biologie, Goethe-Universität, Frankfurt am Main, Germany*

Chromosome 11q23 translocations are present in ~10% of acute leukemia, which generate the oncogenic MLL fusion (MLL-r hereinafter) proteins and drive a subset of aggressive leukemia. Mechanistic studies of MLL-r leukemias implicated several complexes involved in RNA polymerase II-mediated transcription: the Super

Elongation Complex (SEC), the DOT1L Complex (DotCom) and the Polymerase Associated Factor 1 Complex (PAF1c). These protein complexes are dysregulated in MLL-r leukemias and amplify transcription of pro-leukemic target genes. The proteins ENL and AF9 are two common MLL fusion partners and share high homology within their N-terminal YEATS domains that function as epigenetic reader domains. Recently, the importance of the wild type ENL (but not AF9) and its epigenetic reader function has been demonstrated in acute leukemias. However, the importance of the YEATS domain in the context of MLL-ENL fusions has not been explored. In patients, we found that most MLL-ENL fusions (84.1%; N=302 patients), but not MLL-AF9 fusions, retain the YEATS domain. These findings prompted us to investigate 1) how the YEATS domain contributes to MLL-ENL leukemogenesis, 2) whether the YEATS domain affects MLL-ENL fusion protein functions, and 3) if YEATS domain presence in MLL-ENL fusion exposes a vulnerability to YEATS inhibitors. Using published YEATS epigenetic reader mutations, we found that the YEATS epigenetic reader function significantly contributes to MLL-ENL leukemogenesis. Disrupting the YEATS epigenetic reader function in MLL-ENL fusion proteins significantly impacts leukemic stem cell frequency. Using an MLL-ENL construct relevant in patients (ΔYEATS hereinafter), we discovered a subset of MLL-ENL targets with altered expression. GSEA revealed several gene signatures enriched in ΔYEATS cells, most interestingly genes downregulated in leukemic stem cells. Specifically, the MLL-ENL target *Eya1* is severely disrupted in MLL-ENL YEATS epigenetic reader mutants and ΔYEATS cells. Our mechanistic data suggest that while MLL-ENL binding at *Eya1* is impacted in ΔYEATS, YEATS epigenetic reader mutants do not significantly alter MLL-ENL and PAF1c localization. However, YEATS epigenetic reader mutations severely impact epigenetic modifications associated with active transcription, including H3K4me3, H3K9ac and H3K79me2 at the *Eya1* locus. Finally, we tested the YEATS inhibitor sensitivity in AML cell lines. We found that the cell line HB1119, which is driven by MLL-ENL fusion with an intact YEATS domain, is among the most sensitive lines to the YEATS inhibitor SGC-iMLLT. Together, our study provides the biological and mechanistic characterizations of the YEATS domain in MLL-ENL leukemias and contributes to the theoretical framework for YEATS inhibitor development in the majority of MLL-ENL patients.

#3551

Single-cell characterization of pediatric T-cell acute lymphoblastic leukemia transcriptomes

Irina Pushel, Byunggil Yoo, Daniel Louiselle, Margaret Gibson, Midhat S. Farooqi, Keith August. *Children's Mercy Kansas City, Kansas City, MO*

Pediatric T-cell acute lymphoblastic leukemia (T-ALL) is a rare cancer with a diverse set of causative genomic abnormalities. The variety and limited characterization of genomic mechanisms underlying this disease presents a unique challenge for the development of improved treatments for these patients. Using the 10x Genomics Chromium system, we have generated single-cell gene expression (scRNA) and chromatin accessibility (scATAC) data for blood and/or bone marrow samples collected at diagnosis from eight pediatric T-ALL patients. We sequenced 21,669 high-confidence cells and performed normalization and downstream analysis using the Seurat v4.0.2 package in R 4.0.3. Our data show that patient cancer cells show highly individual transcriptomes and are often characterized by combinatorial expression patterns of genes including *MEF2C*, *BCL11B*, *HOXA9*, *NKX2-1*, and *LMO2*, which have been previously implicated for their roles in various T-ALL subtypes. Additionally, we observe that each patient has a unique ratio of cancer cells with a CD4+ T-cell, CD8+ T-cell, and hematopoietic stem cell-like identity, which may be linked to treatment response and patient outcome. This dataset represents one of the first forays into exploring the biology of pediatric T-ALL at the single-cell level. Our comparative analysis of patient cancer cells reveals novel insights into the transcriptional and chromatin-related for distinct subsets of pediatric T-ALL cases, paving the way for future treatment selection and drug development to improve outcomes for these patients.

#3552

YAP-TEAD2 binding mediates therapy resistance in RAS-driven neuroblastoma

Jenny Shim[1], Andrew Ho[1], Hunter C. Jonus[1], Adeiye A. Pilgrim[1], Benjamin G. Barwick[1], Tracy T. Tang[2], Lawrence H. Boise[1], Kelly C. Goldsmith[1]. *[1]Emory University, Atlanta, GA,[2]Vivace Therapeutics, Inc, San Mateo, CA*

Background/**Objectives:** Despite intensive multimodal therapy, greater than 50% of children with high-risk neuroblastoma (HR NB) relapse with incurable disease. Next generation sequencing of primary HR NB tumors identified an increase in activating mutations in the RAS/RAF/MAPK pathway. Moreover, gene set enrichment analyses showed a significant decrease in expression of genes suppressed by the Yes-Associated Protein (YAP) at

relapse, suggesting increased YAP transcriptional repression. YAP binds with TEAD family transcription factors to regulate gene expression. We have shown that YAP promotes chemotherapy and MEK inhibitor resistance in RAS-mutated NB tumors *in vivo* by suppressing the expression of Harakiri (HRK), a BH3-only pro-apoptotic protein activated in response to tumor environmental stress such as serum starvation. Our overall objective is to elucidate how YAP represses HRK and tumor suppressor genes globally, and to enhance MEK inhibitor potency by combining MEK inhibition with agents that inhibit YAP or induce HRK to restore the tumor environmental stress response and apoptosis in RAS-mutated NB.
Design/Methods: We used publicly available databases to identify TEAD binding sites on the *HRK* gene locus in NB. To assess the global state of methylation, we treated NB cells, SK-N-AS ($NRAS^{Q61K}$ mutation, *MYCN* non-amplified) and NLF (*NF1* deletion, *MYCN* amplified), with demethylating agent azacitidine and evaluated *HRK* expression. To identify the specific TEAD (1-4) binding partner to YAP, we performed siRNA and co-immunoprecipitation studies. We further tested novel YAP-TEAD small molecule inhibitors with varying TEAD1-4 inhibition specificity in SK-N-AS and NLF cells *in vitro*.
Results: We observed that TEAD binds near *cis*-regulatory regions on the *HRK* gene locus in NB. We found that *HRK* expression is restored when SK-N-AS and NLF cells are treated with azacitidine despite *YAP* expression increasing. We also identified TEAD2 as the specific binding partner to YAP in NB and found that TEAD2 is necessary for HRK regulation. Novel YAP-TEAD small molecule inhibitors affect NB cell viability under serum-deprived conditions *in vitro*, especially the inhibitor with highest specificity against TEAD2, and affect YAP-TEAD downstream targets.
Conclusions: YAP-TEAD2 binding is essential for HRK regulation in RAS-mutated NB and thus is a logical therapeutic target to restore therapy response. Further studies are ongoing to test YAP-TEAD small molecule inhibitors in combination with MEK inhibitors and *in vivo*.

#3553
Simultaneous somatic copy number alterations and single nucleotide variants detection in paired aqueous humor and tumors from retinoblastoma eyes
Liya Xu[1], Mike J. Schmidt[2], Rishvanth K. Prakabar[2], Peter Kuhn[2], James Hicks[2], Jesse Berry[1]. *[1]Children's Hospital Los Angeles, USC - University of Southern California, Los Angeles, CA,[2]Michelson Center-CSI-Cancer, USC - University of Southern California, Los Angeles, CA*

Introduction: Retinoblastoma (Rb) is the most common childhood intraocular cancer. Tissue biopsy of Rb can cause tumor spread, so it is contraindicated. We demonstrated that aqueous humor (AH), an ocular fluid, is a high-yield liquid biopsy enabling in vivo detection of tumor-derived cell-free DNA (cfDNA) thus overcoming the contraindication of biopsy. Somatic genomic alterations, including both somatic copy number alterations (SCNAs) and single nucleotide variations (SNVs) on RB1 gene, have been able to be identified in the same clinical samples but with two separate sequencing runs. In this study, we first developed a single targeted sequencing method to identify both SCNAs and RB1 SNVs. With this method, we further investigated the degree of genomic concordance between paired tumor and AH samples from the same Rb eye.
Materials and Methods: 11 paired AH and Rb tumor samples were included in the study. cfDNA of AH and tumor DNA of enucleated Rb eyes were isolated with QIAgen commercial kits. DNAs were constructed into whole genome libraries followed by hybridization target enrichment (Agilent SureSelect). The enrichment assay covers the whole length of RB1 and MycN genes, the all-exon regions of BCOR and CREBBP genes, and a whole genome CNV backbone. Libraries were submitted to Illumina HiSeq 4000 platform for fastq data generation with 2x150bp mode. The bioinformatics pipeline was optimized to generate SCNA profiles from targeted sequencing reads, along with SNV calling.
Results: For SCNA profiles, 11/11 AH samples (100%) and 8/11 tumor samples (72.72%) have positive RB-SCNA signatures. Strong concordances were observed between AH and tumor SCNA profiles (median = 90.1%) with targeted sequencing reads. In total, 9 disease-driving RB1 SNVs were identified in 6 patients (54.5%). 7/9 (77.8%) of the variants were shared between AH and tumor samples, while the AH and tumor each contained one unique SNV. In all SNVs, the AH displayed a higher allele frequency. Notably, 4/11 samples have focal RB1 gene deletion detected with SCNA profiling, which may explain the difficulties of RB1 SNV detection in some samples. Further, one case was driven by a MYCN gene amplification with no RB1 alterations.
Conclusions: This study presented highlights the utility of a single method to call both SVNs and SCNAs in a single clinical sample, with enriched tumor information detected in AH compared with tumor. This study further strengthens the utility of AH as a liquid biopsy platform for Rb eyes.

#3554

Targeting chromatin remodeling complex in pediatric cancers

Jun Qi. *Cancer Biology, Dana-Farber Cancer Institute, Boston, MA*

Chromatin accessibility plays critical roles in maintaining normal gene regulatory programs in healthy tissue. Aberrant chromatin accessibility triggered by abnormal activity of a variety of chromatin remodeling complexes is known to activate and maintain tumor proliferation. The most widely known of these complexes is the SWI/SNF (also called BAF) complex. Studies have shown that BAF regulates chromatin accessibility in a more global manner and its long-term inhibition or functional loss may lead to non-specific downstream effects in both tumor and normal tissue. Thus, there is a need to further probe understudied complexes, such as the Imitation Switch (ISWI) family of chromatin remodelers, to find more cancer specific functions that can provide mechanistic insights that pave the way for novel therapeutic discoveries. We have examined the functions of these chromatin complex in different type of pediatric cancers to estsablish the pre-clinical rationale for potential novel pediatric cancer therapy. We discovered that fusion protein positive rhabdomyosarcoma (FP-RMS), an aggressive sub-type of RMS characterized by chromosomal translocations resulting in gene fusions between PAX3/7 and FOXO1 is highly dependent on chromatin accessibility. This aggressive subtype exhibits a significant vulnerability in its dependence on the oncogenic transcription factor PAX3-FOXO1, yet like many other TFs, PAX3-FOXO1 is currently not considered a viable therapeutic candidate. We have then carefully examined the effect of chemical inhibition and chemical degradation of BAF complex function in FP-RMS and discovered that BAF complex globally regulates chromatin accessibility, is not specifically regulating FP function. We next examined the function of other chromatin remodeling complexes that might regulate FP function specifically in FP-RMS. We identified that some of other chromatin remodeling complex, such as Nuclear Remodeling Factor (NURF) complex, a member of the ISWI chromatin remodeling complex family, interacts with a critical fusion protein, PAX3/7-FOXO1, in FP-RMS. There is limited understanding surrounding the functions of NURF complex, particularly in pediatric cancer. Here, we then studied the key functions of FP regulated by variety of chromatin remodeling complex utilizing combined chemistry and biology method to elaborate the essential functions of PAX3/7-FOXO1 fusion protein. We have developed variety of chemical strategies to target these complexes, and utilize these tool compounds to delineate the chromatin remodeling complex regulated FP functions. This study showcased our approach to advance cancer research by combining the power of chemistry, chemical biology, structural biology, computational biology and cellular biology to identify novel mechanistic understanding as well as novel therapeutic approach for pediatric cancers.

#3555

Proteomic characterization of rhabdomyosarcoma-derived extracellular vesicles reveals a fusion-positive protein signature

Paula R. Quaglietta[1], Ashby Kissoondoyal[1], Ethan Malkin[2], David Malkin[1], Reto M. Baertschiger[1]. *[1]The Hospital for Sick Children, Toronto, ON, Canada,[2]Princess Margaret Cancer Centre, Toronto, ON, Canada*

Rhabdomyosarcoma is the most common pediatric soft tissue sarcoma. Current diagnostic methods involve imaging and tissue biopsy for staging, histology and fusion status assessment. There are presently no serum biomarkers for rhabdomyosarcoma diagnosis or surveillance. Novel approaches and identification of biomarkers are warranted for minimally invasive diagnostic/surveillance techniques. Extracellular vesicles (EVs) are recognized as critical mediators of intercellular communication and the pathophysiology of carcinogenesis and metastasis. This study aimed to characterize the proteome of rhabdomyosarcoma-derived EVs and identify proteomic signatures that correlate with clinical characteristics such as histological subtype, cancer stage, age and metastasis, using patient-derived cell lines. EVs were isolated from cell culture conditioned media by differential ultracentrifugation from four rhabdomyosarcoma cell lines (RH4, RH18, RH30, RD), each in triplicate. Liquid chromatography-tandem mass spectrometry identified EV protein cargo. Proteins identified in our samples were compared to all available EV data in the Vesiclepedia database, using the FunRich software. We identified 1,527 total proteins in our rhabdomyosarcoma-derived EVs. When comparing to Vesiclepedia, 96 unique proteins were identified from our EVs that were not previously annotated in EVs within the database. Expression of these 96 proteins was further evaluated based on clinical characteristics of the tumors the cell lines were derived from. We found a four-protein signature in the EV secretome of rhabdomyosarcoma cell lines correlated with FOXO1 fusion-positive status. This signature includes proteins involved in regulating extracellular matrix organization, regulating gene expression, protein biosynthesis and translation. Rhabdomyosarcoma cells secrete EVs with unique protein cargo based on clinical characteristics of the parent tumor such as histological subtype and FOXO1

fusion status. Further validation of these secreted EV proteins in biological fluids could prove an effective liquid biopsy technique for novel diagnostic approaches or surveillance in pediatric rhabdomyosarcoma.

#3557
Stage-restricted osteoblasts specify signatures of osteosarcoma molecular subtypes
Jianning Tao, Fang Fan, Haydee Torres. *Sanford Research, South Dakota, Sioux Falls, SD*

A challenging question in osteosarcoma research is the identity of the cell of origin, and its contribution to the molecular subtypes and signatures. We examine the potential of stage restricted osteoblasts to induce fully penetrant osteosarcoma using osteoblast stage specific Cre mice to mutate Trp53. We identified three molecularly distinct subtypes of osteosarcoma induced by the same driver mutation. Our results suggest that the three subtypes arise from different subpopulations of osteoblasts. Despite histologic identity as one entry osteosarcoma, these subtypes are separable based on molecular signatures and specific signaling pathways. These studies point to the cell of origin as a determinant of osteosarcoma molecular subtypes. Our studies may provide insights for understanding osteosarcoma heterogeneity and improving treatment of the disease.

#3558
Role of FLI portion of EWS::FLI in transcription regulation via modulation of chromatin 3D landscape in Ewing sarcoma
Ariunaa Bayanjargal, Cenny Taslim, Jesse Crow, Julia Selich-Anderson, Stephen L. Lessnick. *Nationwide Children's Hospital, Columbus, OH*

Ewing sarcoma is an aggressive bone-associated tumor currently treated with dose-intense chemotherapy, radiation, and surgery and it affects adolescents and young adults. The hallmark of Ewing sarcoma is a translocated fusion transcription factor named EWS::FLI that drives the oncogenic process. We hypothesize that FLI portion of EWS::FLI containing a crucial alpha-helix plays a novel role in transcription regulation of thousands of genes by modulating chromatin looping. The hypothesis is based on recent evidences from our lab: an alpha-helix immediately downstream of DNA binding domain as an important player in regulating transcriptional activity and that EWS::FLI has a substantial role in shaping the chromatin landscape of Ewing sarcoma cells. The ***objective*** of this study is to elucidate the mechanism underlying transcriptional regulation by FLI. We utilized knockdown/rescue experiments in which EWS::FLI was depleted with shRNA and replaced with constructs containing the ETS DNA Binding Domain (DBD) alone or DBD+ (DBD and 4th alpha-helix). The binding pattern and transcriptional regulation were assessed with CUT&Tag and RNA-Seq respectively. The extent of roles each of these construct play in organization, structure, and function of chromatin are being assessed using Micro-C technique, a variation of Hi-C with improved resolution, higher signal-to-noise ratio and more information on chromatin domain boundaries and chromatin looping. The DNA binding and genomic localization of EWS::FLI was unaltered by the deletion surrounding the DNA binding domain (which contains a 4th alpha-helix) in A673 and TTC466 cells. Despite this similarity in genomic localization and binding, the transcriptional output driven by EWS::FLI was significantly diminished by the deletion. With this current study, we hope to understand if the flanking region neighboring the DNA binding domain contributes to the chromatin architecture remodeling function of EWS::FLI and whether this function could be attributed to the transcriptional output differences in the DBD and DBD+ conditions.

#3559
Understanding Ewing sarcoma cell fate
Danh Truong, Sandhya Krishnan, Alexandar Lazar, David McCall, Joseph A. Ludwig. *UT MD Anderson Cancer Center, Houston, TX*

Like several other translocation-positive sarcomas, Ewing sarcoma (ES) exists exclusively in a high-grade, undifferentiated state. We believe that the pathognomonic EWS-FLI1 fusion protein (FP) responsible for ES is intimately linked to cell fate, differentiation, and plasticity. Over the last two decades, an emerging body of research has begun the challenging task of deciphering how the FP - via its action as an aberrant transcription factor- blocks differentiation and promotes reprogramming toward a quasi-stem-like cell with features of neuroectodermal or mesenchymal stem cells. We compared ES transcriptome data to other cancers in an unsupervised comparison between the gene expression profile of cancer cells in the Cancer Cell Line Encyclopedia (CCLE) and tumor expression datasets. While ES is traditionally classified as a bone cancer, it does not cluster

near other bone cancer subtypes (e.g., osteosarcomas) or soft-tissue sarcomas. To that end, we sought to better understand how targeting the FP affected ES differentiation and lineage. Using a CRISPR knockout (CRISPR-KO) model of A673, we targeted Exon 4 of the EWSR1 protein in the n-terminus of the FP and generated a clonal pool (EWSR1 CRISPR KO). We used single-cell RNA sequencing (scRNA-seq) to identify the transcriptional changes after FP knockout (FP KO). We identified five cell clusters in the data. We observed the expression of FP target genes (EWS-FLI1 On), *PRKCB,* and *LIPI* and saw robust expression in four of the clusters suggesting normal FP expression. Conversely, FP repressed genes (EWS-FLI1 Off), *LOX* and *IGFBP3*, were elevated in cluster 2, which contained only EWSR1 CRISPR KO cells. This suggests that the FP was successfully knocked out in cluster 2 (FP EWSR1 KO). Next, we asked how the FP KO changed the lineage/fate of A673 cells. We hypothesized that loss of the FP would induce mesenchymal/fibroblastic fate in ES cells. To answer this, we used SingleR, which compares the gene expression profile of query cells to the CCLE data set, to identify the nearest cell type. Interestingly, all clusters except the FP EWSR1 KO cluster identified closely with ES and related tumors. The FP EWSR1 KO cluster, which expressed EWS-FLI1 'off' genes, did not resemble ES. Using a granular identification with cell lines, we confirmed that the highest score was A673 since these were A673 cell lines. However, the FP EWSR1 KO resulted in a phenotype unrelated to A673 and more closely resembled cell lines with fibroblastic phenotype. Our data suggest that targeting the FP significantly changed ES lineage. While the FP KO did not lead to cell death, our results suggest a novel gene regulatory network acts to sustain ES lineage. Further perturbations in this network may lead to a better understanding of ES treatment, particularly as novel EWS-FLI1-directed therapies emerge.

#3560

Understanding alternative splicing in Ewing sarcoma progression and metastasis to inform novel therapy development

Akila S. Venkataramany, Safiya Khurshid, Anthony R. Miller, Saranga Wijeratne, Pin-Yi Wang, Timothy P. Cripe, Dawn S. Chandler. *Nationwide Children's Hospital, Columbus, OH*

Introduction: Ewing sarcoma (ES) is the second most common pediatric bone cancer, and patients with metastases have five-year survival rates of <30%. Both local and metastatic ES tumors are characterized by the EWS-FLI1 chromosomal translocation, resulting in an aberrant transcription factor that increases ES cell proliferation and metastasis. EWS-FLI1 activity and ES transformation are reliant upon increased IGF-1 signaling, so initial therapies have centered on IGF-1R inhibition. However, compensatory upregulation of insulin receptor A (*IR-A*), an oncogenic spliced isoform of *IR*, provides a viable resistance mechanism to support ES growth and progression. *IR* has two spliced isoforms formed by the inclusion or exclusion of exon 11 (*IR-B* and *IR-A* respectively), and *IR-A* is differentially expressed in cancers due to its high affinity binding to IGF-II. *We hypothesize that the pathogenesis and metastatic potential of ES is driven in part by alternative splicing of IR and other key genes. Furthermore, modulation of this splicing via antisense oligonucleotides (ASOs) aided by adeno-associated viral (AAV) delivery may be a novel therapeutic avenue for ES.*

Results: We performed long-read mRNA sequencing to identify differentially spliced isoforms between the matched ES cell lines CHLA-9 and CHLA-10 (derived from a localized and metastatic ES tumor respectively). Our analysis revealed global differences in alternative splicing between CHLA-9 and CHLA-10 and identified gene isoforms in the insulin receptor/IGF signaling pathway (*IGFBP3*) that are unique to CHLA-10. Additionally, we detected both previously reported and novel isoforms for *CD99*, *RHOA*, *RACK1*, splicing factors (*PTBP1*), and eukaryotic initiation factors, among other genes.

To further understand *IR* alternative splicing, our labs have developed an *IR* ASO targeting the CUG-BP1 regulatory site upstream of exon 11, and we have previously validated its efficacy in HeLa cells transfected with an *IR* minigene and in pediatric sarcoma cell lines. In ES cell lines, we observed significant *IR-A* upregulation in a panel of ES cell lines and patient-derived xenografts derived from local and metastatic tumors, highlighting the opportunity for intervention with our ASO. To facilitate delivery, we have explored the use of AAV vectors, a clinically approved option for gene therapy, and shown successful transduction of AAV-8 over a time-course in ES cells.

Conclusions: Our results indicate that alternative splicing is differential between local and metastatic ES and produces isoforms unique to the metastatic setting. Additionally, the oncogenic *IR-A* isoform and other spliced isoforms are viable targets for ASO therapy aided by AAV delivery. By better understanding splicing in ES, we can identify targetable interactions at the transcriptional level and develop innovative therapeutics that can improve the clinical outcomes of ES patients.

#3561

Recurrent genetic alterations in epigenetic pineoblastoma subtypes

Tobias Goschzik[1], Mathias Yuan[2], Martin Mynarek[3], Elke Pfaff[4], Evelyn Dörner[1], David T. W. Jones[5], Stefan M. Pfister[6], Stefan Rutkowski[2], Torsten Pietsch[7]. *[1]Dept. of Neuropathology, University of Bonn Medical Center, Bonn, Germany,[2]Dept. of Pediatric Hematology/Oncology, University Clinics Hamburg-Eppendorf, Hamburg, Germany,[3]Dept. of Pediatric Hematology/Oncology & Mildred Scheel Cancer Career Center HaTriCS4, University Clinics Hamburg-Eppendorf, Hamburg, Germany,[4]Department of Pediatric Oncology, Hematology and Immunology & Pediatric Glioma Research Group (B360), Hopp Children's Cancer Center Heidelberg (KiTZ) & German Cancer Research Center (DKFZ), Heidelberg University Hospital, Heidelberg, Germany,[5]Pediatric Glioma Research Group (B360), Hopp Children's Cancer Center Heidelberg (KiTZ) & German Cancer Research Center (DKFZ), Heidelberg, Germany,[6]Department of Pediatric Oncology, Hematology and Immunology & Division of Pediatric Neurooncology, Hopp Children's Cancer Center Heidelberg (KiTZ) & German Cancer Research Center (DKFZ), Heidelberg University Hospital, Heidelberg, Germany,[7]Dept. of Neuropathology and DGNN Brain Tumor Reference Center, University of Bonn Medical Center, Bonn, Germany*

Introduction**:** Genome-wide methylation analyses recently revealed novel epigenetic pineoblastoma (PBL) subtypes, but so far few data are available on recurrent cytogenetic alterations due to the rarity of these neoplasms. Therefore, our aim was to shed further light onto the molecular and genetic characteristics underlying the pathogenesis of pineoblastoma subtypes.

Experimental procedures: Cytogenetic alterations of tumor samples of 60 patients with a diagnosis of PBL confirmed by reference neuropathology and methylation array profiling (450K or EPIC BeadChips (Illumina)) were analyzed by high-resolution genome-wide molecular inversion probe analysis. 52 cases could be screened for mutations by next-generation DNA panel sequencing. Survival data of 41 patients were available. All patients had surgery and older patients (≥4y) received RT followed by maintenance chemotherapy (n=37); infants (<4y) were primarily given a RT-sparing regimen that involved intensified chemotherapy dosage.

Results: Of the recently published epigenetic consensus PBL subtypes (Liu et al., 2021), our cohort consisted of 37 PBL-miRNA1 (1A, 30; 1B, 7), 17 PBL-miRNA2, 2 PBL-MYC/FOXR2, and 4 PBL-RB1 samples. PBL-miRNA subtype tumors had characteristic alterations in microRNA-processing genes; *DICER1* mutations (n=14; 4 in Grp1A / 1 in Grp1B / 9 in Grp2) were most abundant, followed by homozygous deletions of the *DROSHA* locus (n=11; 8 / 1 / 2) and *DROSHA* mutations (n=9; 3 / 3 / 3). Most frequent cytogenetic aberrations in these subtypes were chromosome (chr.) 7 gains (n=25) and chr. 14 losses (n=20, with all but one of miRNA2 cases). *DICER1* mutations were significantly associated with chr. 14 losses ($p<0.001$). 17 cases showed gains of the chromosomal arm 14q, in 6 additional cases, focal gains were found of the *OTX2* oncogene located on chr. 14q. In the miRNA subtypes we identified cases with a tetraploid phenotype (n=11; 7 / 4 / 0). Interestingly, none of the 6 patients with tetraploid tumors and survival data had relapses, while the remaining patients of the miRNA subtypes had a 5-year PFS of 72% and 5-year OS of 68% (10 of 31 with relapse/death) after a median follow-up time of 3.9 years. However, this did not reach statistical significance. A significant impact on survival could not be demonstrated for chr. 14q gains or focal *OTX2* gains. The PBL-RB1 subtype cases had homozygous *RB1* deletions (n=3) or biallelic *RB1* mutations (n=1). Focal chromosomal aberrations were frequently found in this subtype, but rarely numerical alterations.

Conclusion: The epigenetically defined PBL subtypes were characterized by distinct cytogenetic and mutational events. Although we could not demonstrate a prognostic impact of these events, this might be due to the small sample size. A possible prognostic role for a superior (e.g. tetraploidy) or inferior outcome (e.g. *OTX2* gains) need studies in larger cohorts and ideally in prospective clinical trials.

#3562

Dissecting mechanisms underlying *FOXR2*-mediated gliomagenesis in diffuse midline gliomas

Jessica W. Tsai[1], Paloma Cejas[1], Marissa Coppola[1], Dayle K. Wang[1], Smruti Patel[2], David W. Wu[3], Phonepasong Arounleut[4], Xin Wei[4], Ningxuan Zhou[1], Sudeepa Syamala[1], Frank P. B. Dubois[3], Kristine Pelton[1], Jayne Vogelzang[1], Cecilia Sousa[1], Audrey Baguette[1], Xiaolong Chen[5], Alexandra L. Condurat[1], Sarah E. Dixon-Clarke[1], Annarah Charles[1], Kevin N. Zhou[1], Sophie D. Lu[1], Elizabeth M. Gonzalez[1], Madison S. Chacon[1], Jeromy J. Digiacomo[1], Rushil Kumbhani[1], Dana Novikov[1], Maria Tsoli[6], David S. Ziegler[6], Uta Dirksen[7], Natalie Jager[8], Gnana Prakash Balasubramanian[8], Christof M. Kramm[9], Michaela Nathrath[10], Stefan Bielack[11], Suzanne J. Baker[5], Jinghui Zhang[5], James M. McFarland[3], Gad Getz[3], Francois Aguet[3], Nada Jabado[12], Olaf Witt[8], Stefan M.

Pfister[8], Keith L. Ligon[1], Volker Hovestadt[1], Claudia Kleinman[12], Henry Long[1], David T. W. Jones[8], Pratiti Bandopadhayay[1], Timothy N. Phoenix[4]. *[1]Dana-Farber Cancer Institute, Boston, MA,[2]Cincinnati Children's Hospital, Cincinnati, OH,[3]Broad Institute of MIT and Harvard, Cambridge, MA,[4]University of Cincinnati, Cincinnati, OH,[5]St. Jude Children's Research Hospital, Memphis, TN,[6]Lowy Cancer Research Centre, Sydney, Australia,[7]University Hospital Essen, Essen, Germany,[8]German Cancer Research Center, Heidelberg, Germany,[9]University Medical Center Göttingen, Gottingen, Germany,[10]Klinikum Kassel, Kassel, Germany,[11]University Hospital Stuttgart, Stuttgart, Germany,[12]McGill University, Montreal, QC, Canada*

Background: Diffuse midline gliomas (DMGs) are a universally fatal brain tumor of childhood. While histone mutations are a critical tumor initiating event, they are insufficient to drive gliomagenesis. Histone mutations co-occur with somatic alterations in other pathways including TP53, MAPK, and MYC signaling. However, the mechanisms through which these pathways are activated have not been fully elucidated.
Methods: We applied an integrative approach using transcriptomics, epigenetics, proteomics, *in vitro* cancer models, and *in vivo* mouse models to systematically evaluate how FOXR2 mediates gliomagenesis.
Results: We have recently found that a subset of DMGs aberrantly express *FOXR2*, a forkhead transcription factor. FOXR2 is both sufficient to enhance tumor formation, and necessary for *FOXR2*-expressing DMGs. While FOXR2 indeed enhances MYC protein stability, FOXR2 exerts oncogenesis through MYC-independent functions and specifically hijacks E26-transformation specific (ETS) transcriptional circuits and FOXR2 DNA-binding is highly enriched at ETS motifs. We have performed proteomic and phospho-proteomic analysis of *FOXR2*-expressing human neural stem cells to identify proteins and phospho-sites that are highly enriched in FOXR2-expressing cells.
Conclusion: Taken together, this study elucidates how FOXR2 interacts with ETS transcription factors to mediate oncogenesis, and further highlights a role for FOXR2 in activating ETS and MAPK signaling.

#3563

SWI/SNF-associated DPF1 is a unique transcriptional regulator of malignant peripheral nerve sheath tumors

Bega Murray, Xiyuan Zhang, Shahroze Abbas, Haiyan Lei, Hilda Jafarah, Jack F. Shern. *National Cancer Inst. - Bethesda Campus, Bethesda, MD*

Background**:** Malignant peripheral nerve sheath tumors (MPNST) are rare soft tissue sarcomas that are typically therapy resistant and associated with a poor prognosis. Genetic aberrations of the polycomb repressive complex 2 (PRC2) occur in up to 75% of MPNST cases. PRC2 functions antagonistically to SWI/SNF protein complexes, regulating expression of target loci in a dynamic relationship that is critical to normal cellular development and maintenance of cell identity. The consequences of PRC2 loss on chromatin state maintained by SWI/SNF in MPNST is unexplored. Therefore, this study used functional genomics to elucidate the role of SWI/SNF in MPNST.
Methods: To define the transcriptional regulatory role of SWI/SNF complexes in MPNST, SWI/SNF components were targeted via a CRISPR knock-out (KO) screen combined with a single cell RNA sequencing (RNAseq) readout. Genes of interest highlighted by this screen were further investigated using bulk CRISPR RNAseq. Phenotypic effects of the expression of these genes were studied using loss-of-function assays coupled with colony formation assays. SWI/SNF complex heterogeneity was characterized using glycerol gradient sedimentation, co-immunoprecipitation (co-IP), and mass spectrometry experiments.
Results: The investigation of SWI/SNF transcriptional regulation in MPNST highlighted the Double PHD Finger family proteins (DPF1,2,3) as regulating distinct downstream targets. Notably, *DPF1* had a unique transcriptional profile compared to other SWI/SNF components. Bulk CRISPR KO RNAseq confirmed these findings and highlighted a specific set of *DPF1* target genes including many long non-coding RNAs. The phenotypic role of DPF1 in MPNST was investigated using *in vitro* siRNA and CRISPR experiments, where DPF1 KO reduced proliferation and viability of MPNST cells in both 2D and 3D cell culture assays. Further, DPF1 was found contribute to anchorage independent cell growth of MPNST cells using soft agar assays. Glycerol gradient sedimentation assays demonstrated that DPF1 co-migrated with core components of a SWI/SNF complex known as canonical BAF (cBAF) and not the alternate GBAF and PBAF SWI/SNF complexes. These findings were further validated using co-immunoprecipitation assays where core the SWI/SNF ATPase, SMARCA4, pulled down DPF1, while components unique to the GBAF and PBAF complexes did not. An ATPase directed proteolysis targeting chimers (PROTAC) was used to therapeutically target cBAF in MPNST cells, reducing their growth and

viability. Combination treatment with standard of care chemotherapy synergistically increased the efficacy of this drug.
Conclusions: DPF1 was identified as a unique transcriptional regulator of MPNST cells and acts as a member of the cBAF SWI/SNF complex to play important phenotypic roles in this cancer type.

#3564
SNAI2 enhances oncogenesis in malignant peripheral nerve sheath tumors
Hilda Jafarah, Béga Murray, Jack Shern, Xiyuan Zhang. *NIH-NCI, Bethesda, MD*

Background: MPNSTs are highly aggressive soft tissue sarcomas. Recurrent genetic mutations have been linked to its tumorigenesis, including the loss of functional polycomb repressive complex 2 (PRC2). This results in an altered transcription landscape characterized by the global loss of methylation on histone H3 lysine 27 (H3K27me3) and increased super-enhancer (SE) -associated histone acetylation. We have previously identified SNAI2 as a core SE-driven transcription factor (TF) that is essential for the growth of MPNST. Although *SNAI2* is known to be critical for oncogenic processes, including epithelial-to-mesenchymal transition (EMT) and dedifferentiation, its role in maintaining MPNST survival through transcriptomic and epigenetic regulation has not been explored.
Methods: Using CRISPR mediated knockout (KO), we targeted the *SNAI2* DNA binding domain and confirmed KO via western blot, followed by *in vitro* phenotypic characterization, including 2D growth assays, anchorage-independent colony formation assays, and scratch assays. Additionally, an integrative analysis of *SNAI2* genomic distribution and the transcriptomic effect of its KO was performed using chromatin immunoprecipitation coupled with DNA sequencing (ChIPseq) and RNA sequencing (RNAseq). Finally, an inducible re-expression system was employed to examine the effects on the chromatin landscape with SNAI2 rescue.
Results: Genetic loss of *SNAI2* slowed the growth of MPNST cells by 50% in comparison to the control. *In vitro* tumorigenic assays revealed that SNAI2 KO diminished the cells' capacity in invasion but not in anchorage-independent cell growth. Analysis of the RNAseq results revealed that SNAI2 loss upregulated 790 genes and downregulated 1623 genes (log2fold change> 1, $p<0.01$), indicating a dominant transcriptional activation role. Gene Set Enrichment Analysis of these SNAI2-regulated genes revealed upregulation of hallmark Myc targets (normalized enrichment score (NES)=2.6, FDR=0.0), whilst genes involved in response to alpha interferon proteins were downregulated (NES=-1.87, FDR=0.002). Interestingly, genes defining EMT were upregulated (NES=1.6, FDR=0.006) in cells upon SNAI2 loss, contrasting its known repressive role in this biological process in other systems. Through integrative analysis of the RNAseq and ChIPseq data, we demonstrate SNAI2 binding to promoters of its regulated targets. Downstream targets of interest include CRELD1, a gene involved in cell adhesion, where SNAI2 KO caused loss of promoter binding and gene downregulation ($p<0.001$).
Conclusion: SNAI2 is an essential SE-driven TF in MPNST cells. Transcriptomic and genomic profiling of SNAI2 through loss- and gain-of-function experiments revealed that it is a critical TF that is involved in key biological processes. Future efforts will focus on designing methods to employ targeted degradation of this essential TF and test preclinical efficacy in treating MPNST.

#3565
Establishing a multimodal data warehousing platform to accelerate discoveries in pediatric brain tumors for the Children's Brain Tumor Network
Bailey K. Farrow, Nicholas Van Kuren, Nathan Young, Christopher Friedman, Meen Chul Kim, Alex Lubneuski, Jennifer Mason, Thinh (Bin) Nguyen, Zeinab Helili, Elizabeth Frenkel, Catherine Sullivan, Ariana Familiar, Yuankun Zhu, Mateusz Koptyra, Tatiana Patton, Jena Lilly, Phillip B. Storm, Adam Resnick, Allison P. Heath. *Children's Hospital of Philadelphia, Philadelphia, PA*

Brain tumors are the leading cause of disease-related death in children and young adults ages 0-19 in largely populated countries such as the United States. In one year alone, 4,000 children and young adults will be diagnosed with a brain or central nervous system tumor in the United States. Brain tumors are complex and difficult to treat in growing children, with current treatments oftentimes causing significant and lifelong side effects. Furthermore, there have only been five drugs in the last 20 years approved by the FDA to treat pediatric brain tumors. Founded in 2011, the Children's Brain Tumor Network (CBTN) is focused on accelerating the pace of translational research, the discovery of new treatments, and informing precision medicine for children diagnosed with brain tumors. CBTN comprises 32 member institutions/hospitals having over 4700 patient subjects

enrolled, spanning 30+ brain tumor diagnoses, over 66,000 biobanked samples and 150 preclinical models. Longitudinal clinical data is also collected for every subject that is enrolled in the observational protocol. Through large scale data generation efforts funded by the NCI and foundational support, CBTN has whole genome, RNA-seq and other molecular characterization for over half of the enrolled patient population. Additionally, efforts have been underway to collect all pathology and radiology imaging and reporting for the subjects. With sequencing being done by multiple vendors, imaging protocols being different across multiple hospitals, and complex clinical treatment and longitudinal follow up data being translated from EHR systems, CBTN has created a rich, but complex, data landscape that is the largest of its kind in the world. In order to accelerate the process of going from data to cures, the data needs to be centralized, organized, and easily distributable. To do this, CBTN has built a first of its kind data workflow that acts as the inventory system for its various data assets. Using a modern data stack including dbt, PostgresSQL, Meltano and AWS, combined with utilization of FHIR as an interchange standard, data from multiple disparate sources such as REDcap, EHR systems, and PAC systems flow in near “real-time” to be utilized as integrated data resources.
The result of this modern, multimodal, and multi-institutional warehouse allows CBTN to distribute data quickly and accurately to translational researchers around the world and contribute data to key research efforts such as AACR Project Genie, Kids First Data Resource Center, NCI Childhood Cancer Data Initiative, and the NCI’s Open Targets Platform.

#3566

Expansion of the Pediatric Brain Tumor Atlas: Children's Brain Tumor Network, Kids First Data Resource and Childhood Cancer Data Initiative Open Science effort

Mateusz P. Koptyra[1], Komal Rahti[1], Yuankun Zhu[1], Bailey Farrow[1], Daniel Miller[1], Adam Kraya[1], Yiran Guo[1], Peter Madsen[1], Nicholas Van Kuren[1], Xiaoyan Huang[1], Miguel A. Brown[1], Jennifer L. Mason[1], Meen Chul Kim[1], Allison P. Heath[1], Brian M. Ennis[1], Bo Zhang[1], Jena V. Lilly[1], Jo Lynne Rokita[1], Christopher Friedman[1], Ximena P. Cuellar[1], Catherine A. Sullivan[1], Noel Coleman[1], Trang Duros[1], Thinh Q. Nguyen[1], Emmett C. Drake[1], Zeinab Helili[1], Beth A. Frenkel[1], Gerri R. Trooskin[1], Ariana Familiar[1], Karthik Viswanathan[1], Christopher M. Beck[1], Madison L. Hollawell[1], Valerie P. Baubet[1], Cassie Kline[2], Mariarita Santi[3], Tatiana S. Patton[1], Stephanie Stefankiewicz[1], Arya Kamnaa[1], Ryan A. Velasco[1], Dani Cardona[1], Phillip J. B. Storm[1], Adam C. Resnick[1], o/b/o Children's Brain Tumor Network[1]. *[1]Division of Neurosurgery, Center for Data Driven Discoveries in Biomedicine, Children's Hospital of Philadelphia, Philadelphia, PA,[2]Division of Oncology, Children's Hospital of Philadelphia, Philadelphia, PA,[3]Department of Pathology And Laboratory Medicine, Children's Hospital of Philadelphia, Philadelphia, PA*

Pediatric central nervous system (CNS) cancers are the leading disease-related cause of death in children and there is urgent need for curative therapeutic strategies for these tumors. To address the urgency, Children’s Brain Tumor Network (CBTN) has advanced an open science model to accelerate the research discovery for pediatric brain tumors. In first phase of Open Pediatric Brain Tumor Atlas (OpenPBTA) effort CBTN together with Pacific Pediatric Neuro-Oncology Consortium (PNOC) with support of Gabriella Miller Kids First Data Resource Center (KFDRC) created and comprehensively characterized over 1000 clinically annotated pediatric brain tumors.
In the second phase of the OpenPBTA effort, through resource awards and collaboration across KFDRC, the NCI Childhood Cancer Data Initiative (CCDI), NCI’s Clinical Proteomic Tumor Analysis Consortium (CPTAC), NCI Center for Cancer Research and additional partnered institutions and foundations, CBTN has expanded OpenPBTA to support high throughput molecular characterization for an additional 1900 pediatric brain tumor patients and their families. This includes the processing and characterization of over 8000 specimens across >50 brain tumor diagnoses. The cohort expansion builds on >1000 previously characterized samples with a portfolio of multimodal data including whole genome sequencing, RNA sequencing, miRNA sequencing, methylation sequencing, proteomics, lipidomics and/or metabolomics. Molecular data is linked to patient longitudinal clinical data, imaging data (MRIs and radiology reports), histology slide images, and pathology reports. To inform novel discovery and clinical implementation of genomic approaches for diagnostic/therapeutic purposes, the data is deposited the cloud-based research environment of the NCI’s CCDI and the KFDRC to provide near real-time integration, dissemination, processing, and sharing of associated petabyte-scale harmonized data. The approach leverages the DRC platform’s cloud-based computational environment in CAVATICA. Processed annotations are facilitated via CAVATICA-enabled shareable pipelines and can be explored through PedcBioPortal, a data visualization/analysis application further integrating additional public and deposited datasets. This expansion phase of OpenPBTA is released with no embargo period and provides one of the largest deeply characterized cohorts of pediatric brain

tumor samples and associated clinical data for >3000 pediatric brain tumor patients. CBTN's open-science, rapid-release model aims to advance novel biomarkers and therapeutic exploratory research, supporting new clinical trial development and accelerated discovery on behalf of changing the outcome for kids with brain tumors.

#3567

Cancer-epigenetic mouse models for medulloblastoma

Shilpa S. Dhar, Ali S. Rizvi, Lauren Reed, Calena Brown, Min Gyu Lee. *UT MD Anderson Cancer Center, Houston, TX*

Medulloblastoma (MB) is the most common childhood brain tumors (up to 20% of all childhood brain tumors) and occurs mainly in children (<15 years old. MB is located in the cerebellum in the brain and can spread to the spine or to other parts of brain. Because MB growth is very fast, MB is categorized as a type of high-grade malignant primary tumors. MB development is often associated with the dysregulation of signaling pathways, such as the wingless (WNT) and sonic hedgehog (SHH). Methylated histone H3 lysine 4 (H3K4) is a major methylation mark. Trimethyl H3K4 (H3K4me3) occupies as much as 75% of all human gene promoters. We previously reported that the H3K4 methyltransferase KMT2D (also called MLL4, MLL2, and ALR; a transcriptional coactivator, is required for neuronal differentiation of human neuron-lineage NT2/D1 stem cells. Interestingly, our analysis of several databases has shown that *Kmt2d* is the most frequently mutated epigenetic modifier (8%–10%) in medulloblastoma (MB). Recently, we showed that brain-specific knockout of *Kmt2d* alone induces spontaneous MB in mice. *Kmt2d* loss highly upregulated several oncogenic signaling programs and downregulated tumor suppressive genes. In this study, we sought to determine whether *Kmt2d* loss cooperates with another oncogenic event in MB genesis. Particularly, *PTCH* (also known as *PTCH1*) is one of the most frequently mutated genes in MB, and *KMT2D* is known to be a shared driver gene mutation in MB. For these reasons, we examined the effect of *Kmt2d* loss on of $Ptch^{+/-}$-driven MB genesis. A heterozygous loss of *Kmt2d* increased the incidence and progression of $Ptch^{+/-}$-driven MB genesis. We have shown that *Kmt2d* loss reduces epigenomic signals for super-enhancers/enhancers and broad H3K4me3 in 4-month-old cerebella. In addition, we determine the effect of heterozygous Kmt2d loss on cell proliferation by comparing the Nes-Cre $Kmt2d^{fl/+}$ $Ptch^{+/-}$ (KP) cerebella to $Ptch^{+/-}$ cerebella at 2- & 4-month-old time points using IHC staining of Ki-67 (a proliferation marker). MB's from KP mice showed two different mechanisms by activating oncogenic cellular signaling kinases (e.g., phospho [p]-AKT and p-p38) levels as well as MYCN signaling pathway. Our transcriptomic analysis revealed several tumor suppressive and transcriptional corepressor genes to be downregulated such as *Ncor2* and *Dnmt3a*. We found *Ncor2* depletion in Ptch-/+ neurospheres shows upregulation of similar oncogenic genes as in KP mice tumors. *Kmt2d* loss reduced cerebellar granule cell differentiation. Our analysis for oncogenic kinases may provide a basis for a novel MB treatment plan involving the use of cellular kinase inhibitors. As KMT2D is among the most often mutated genes in human MBs, this mouse model may be useful for future preclinical therapeutic experiments for the treatment of MB patients. KMT2D in medulloblastoma genesis using mouse models will provide epigenetic and mechanistic insights into how heterozygous KMT2D loss promotes medulloblastoma.

#3568

Developing pediatric glioblastoma microtumors with a three-dimensional bioprinter

Andee M. Beierle, Taylor L. Schanel, Hasan Alrefai, Joshua C. Anderson, Patricia H. Hicks, Lauren C. Nassour, Christopher D. Willey. *University of Alabama at Birmingham, Birmingham, AL*

Background:Glioblastoma multiforme is one of the most devastating forms of brain cancer seen in children. Children diagnosed with high-grade gliomas have poor prognosis, and there remains a need for improvement in the standard of care. In order to improve the standard of care for this condition, it is necessary to develop *in vitro* models which better recapitulate the nature of the tumors. Three-dimensional bioprinting has proven to be an effective technique in creating microtumors using adult glioblastoma cell lines but remains unexplored in pediatric glioblastoma. As such, we sought to develop a protocol which would allow for the creation of three-dimensionally bioprinted microtumors using patient-derived pediatric glioblastoma cells.
Methods:A Bio X three-dimensional bioprinter (Cellink) was utilized to create the microtumor constructs. The composition of the bioink was modified through varying concentrations of sodium alginate and gelatin, or gelatin-methacrylate (Gel-MA). The microtumor size and volume was optimized through the variation of extrusion time, nozzle pressure, and both nozzle and print bed temperature. The crosslinking technique was also optimized through the utilization of 2% calcium chloride for varying exposure times, and also a 405-nm light (for Gel-MA bioink) at varied light intensity, length of time of application to, and distance from, the printed structure.

Bioprinted pediatric XD456 brain tumor initiating cell constructs were treated with both chemotherapeutics and radiation to determine the model's capacity to respond to treatment. PamStation 12 (PamGene Inc.) Kinomic data and RNA-seq (Illumina) data were generated for the constructs. Imaging was performed using Cytation 5 imager (Agilent).
Results:Fluorescent microscopy with Calcein AM and Sytox™ Orange (ThermoFisher), along with viability assessments via CellTiter-Glo®, demonstrated expected cytotoxic effects after exposure to 10 μM Cisplatin. Additionally, PamStation 12 Kinomic and RNA-seq data indicated a difference in kinomic signaling between the bioprinted constructs as compared to the XD456 cells cultured as neurospheres.
Conclusions:The utilization of a three-dimensional bioprinter allows for the creation of microtumors using patient-derived pediatric glioblastoma cells. Future studies will investigate the microtumors' capacity as a drug screening model. The model will also be developed to further recapitulate the native tumor microenvironment of pediatric glioblastoma.

#3569
An animal model of GLI2-amplified medulloblastoma
Yanxin Pei. *Children's National, Washington, DC*

Medulloblastoma (MB) is the most common malignant brain tumor affecting children. Among the known subtypes of MB, *GLI2*-amplified SHH-MB associated with P53 mutations has the worst prognosis, and a 5-year survival rate of less than 30%. Moreover, *GLI2*-amplified MBs are non-responsive to SMO inhibitors, the only targeted treatment option available for SHH-MB. To address this treatment gap, there is an urgent need to identify novel potential therapeutic targets, an effort that requires better understanding of key cellular and molecular mechanisms underlying *GLI2*-amplified MB. To that end, we generated a mouse model of *GLI2*-amplified MB and identified *GL12* as the critical driver of tumorigenesis, and granule cell progenitors (GCPs) as the cells of tumor origin. We further found that *GLI2* specifically drives embryonic, but not neonatal, $Math1^+$ GCPs to form SHH-MB tumors. An scRNA-seq analysis revealed MAPK pathway activation specifically in embryonic $Math1^+$ GCPs. The MAPK pathway was activated in mouse and human *GLI2*-driven MB tumors, and a MEK/ERK inhibitor significantly inhibited *GLI2*-driven MB *in vivo*. Based on these findings, we hypothesize that *GLI2*-driven MB originates from a specific population of $Math1^+$ GCPs during a discrete temporal interval in cerebellar development, and that targeting MAPK/MEK/ERK pathway components represents a novel approach to treatment of *GLI2*-amplified MB.

#3570
Preservation of cellular heterogeneity in 3D and 2D cultures of pediatric solid tumors
Justina D. McEvoy, Melody Allensworth, Mariajose Franco, Natalie McDonald, Brittney Gordon, Anand Patel, Elizabeth Stewart, Michael Dyer. *St. Jude Children's Research Hospital, Memphis, TN*

Over the past 10 years, we have developed and characterized over 280 orthotopic patient derived xenografts (O-PDXs) representing 23 different types of pediatric solid tumors. The O-PDXs have undergone comprehensive characterization including genomics, transcriptomics, epigenomics, histologic review and analysis of cellular heterogeneity. All data, tissue samples and cryopreserved O-PDXs are freely available with no obligation to collaborate through the Childhood Solid Tumor Network (CSTN) at www.stjude.org/CSTN/. While these in vivo models are useful for preclinical testing of drugs and immunotherapy, researchers are limited by throughput, expense and expertise. High throughput ex vivo culture systems that more faithfully recapitulate the cellular heterogeneity and arrested differentiation in the patient tumors are urgently needed to test new drug combinations. Solid tumor cell lines have undergone extensive selection and adaptation in culture, and most have lost the cellular heterogeneity found in patient tumors. In order to overcome this barrier in the field, we have developed a 3D-to-2D workflow. Previous attempts to produce 2D ex vivo cultures from patient tumors or O-PDXs have had limited success because most cells die upon initial plating, they are difficult to cryopreserve for future studies and they lose key cell populations found in the patient tumors. Our new workflow was designed to overcome two sources of stress when adapting patient tumors or O-PDXs to culture. The first source of stress is transitioning from the in vivo environment to ex vivo in culture medium. The second source of stress is the transition from extensive 3D cell-cell contacts in vivo to a more limited cell-cell contact ex vivo. To overcome these two sources of stress, we adapted cultures to 2D in a stepwise manner. First, we dissociate O-PDX tumors into single cell suspension and then rapidly re-aggregate them in 3D spheres for ex vivo culture. After the spheres have grown for 7 days, they are transitioned to 2D by seeding cells in culture dishes coated with extracellular matrix components. Importantly, the

3D and 2D cultures preserve the cellular heterogeneity of the O-PDX and patient tumor and they can be cryopreserved. When injected back into immunocompromised mice, they recapitulate the molecular and cellular features of the original tumors. We have shown that the 3D and 2D cultures can be genetically manipulated using lentiviral vectors and can be used for high-throughput drug screening. Matched 3D and 2D cryovials are now available to the international biomedical research community for rhabdomyosarcoma through the CSTN. Neuroblastoma, osteosarcoma, Ewing sarcoma and retinoblastoma are expected to be available in late 2023. We anticipate this will accelerate the testing of oncology drugs for pediatric solid tumors in response to the RACE act through the PIVOT program.

#3571

The ITCC-P4 sustainable platform of fully characterized PDXs supports the preclinical proof-of-concept drug testing of high-risk pediatric tumor models

Aniello Federico[1], Apurva Gopisetty[2], Didier Surdez[3], Yasmine Iddir[3], Alexandra Saint-Charles[3], Justyna Wierzbinska[4], Andreas Schlicker[4], Richard Volckmann[5], Danny Zwijnenburg[5], Sara Colombetti[6], Olaf Heidenreich[7], Fatima Iradier[8], Heinrich Kovar[9], Jan-Henning Klusmann[10], Klaus-Michael Debatin[11], Simon Bomken[12], Christina Guttke[13], Maureen M. Hattersley[14], Frédéric Colland[15], Ashley Strougo[16], María José Guillén[17], Louis Chesler[18], Chris Jones[19], Maria Eugénia Marques da Costa[20], Katia Scotlandi[21], Massimo Moro[22], Beat Schäfer[23], Marco Wachtel[23], Johannes Gojo[24], Walter Berger[24], Ángel Montero Carcaboso[25], Dennis Gürgen[26], Jens Hoffmann[26], Emilie Indersie[27], Stefano Cairo[27], Julia Schueler[28], Nicole Huebener[29], Johannes H. Schulte[29], Jan J. Molenaar[7], Birgit Geoerger[20], David J. Shields[30], Hubert N. Caron[31], Gilles Vassal[20], Lou F. Stancato[32], Lou F. Stancato[32], Stefan M. Pfister[2], Natalie Jäger[2], Jan Koster[5], Marcel Kool[2], Gudrun Schleiermacher[3]. *[1]Division of Pediatric Neurooncology, Hopp Children's Cancer Center (KiTZ), Heidelberg, Germany,[2]Hopp Children's Cancer Center (KiTZ), Heidelberg, Germany,[3]INSERM U830, Équipe Labellisée LNCC, Genetics and Biology of Pediatric Cancers, PSL Research University, SIREDO Oncology Centre, Institut Curie Research Centre, Paris, France,[4]Pharmaceuticals, Research and Development, Bayer AG, Berlin, Germany,[5]Center for Experimental and Molecular Medicine, Amsterdam University Medical Centers, Amsterdam, Netherlands,[6]Hofmann-la Roche, Zurich, Switzerland,[7]Princess Máxima Center for Pediatric Oncology, Utrecht, Netherlands,[8]Eli Lilly and Company, Lilly SAU, Alcobendas, Spain,[9]Children's Cancer Research Institute, St Anna Kinderkrebsforschung, Vienna, Austria,[10]Department of Pediatrics, Martin-Luther-University Halle-Wittenberg, Halle, Germany,[11]Department of Pediatrics and Adolescent Medicine, Ulm University Medical Center, Ulm, Germany,[12]Translational and Clinical Research Institute, Newcastle University and The Great North Children's Hospital, Newcastle upon Tyne, United Kingdom,[13]Janssen Research & Development, LLC, Spring House, PA,[14]AstraZeneca R&D, Waltham, MA,[15]Institut de Recherches Servier, Croissy-sur-Seine, France,[16]Sanofi, R&D, Amsterdam, Netherlands,[17]PharmaMar S.A., Madrid, Spain,[18]Centre for Paediatric Oncology Experimental Medicine, The Institute of Cancer Research, London, United Kingdom,[19]Division of Molecular Pathology, Institute of Cancer Research, London, United Kingdom,[20]Department of Pediatric and Adolescent Oncology, Gustave Roussy Cancer Campus, INSERM U1015, Université Paris-Saclay, Villejuif, France,[21]IRCCS—Istituto Ortopedico Rizzoli, Experimental Oncology Laboratory, Bologna, Italy,[22]Fondazione IRCCS Istituto Tumori di Milano, Milan, Italy,[23]Department of Oncology, University Children's Hospital, Children's Research Center, Zurich, Switzerland,[24]Department of Pediatrics and Adolescent Medicine, Comprehensive Center for Pediatrics, Medical University of Vienna, Vienna, Austria,[25]Institut de Recerca Sant Joan de Deu, Barcelona, Spain,[26]Experimental Pharmacology and Oncology Berlin-Buch GmbH, Berlin, Germany,[27]XenTech, 4 rue Pierre Fontaine, Evry-Courcouronnes, France,[28]Charles River Germany, Freiburg, Germany,[29]Department of Pediatric Oncology and Hematology, Charité – Universitätsmedizin Berlin, Berlin, Germany,[30]Pfizer Centers for Therapeutic Innovation, Pfizer Inc, New York, NY,[31]Hoffman-La Roche, Basel, Switzerland, Switzerland,[32]Eli Lilly and Company, Indianapolis, IN*

Cancer represents a leading cause of death by disease in childhood. Pediatric tumors exhibit a high intertumoral heterogeneity, as different tumor types and subtypes have emerged with peculiar molecular and clinical features; however, compared to cancer in adults, pediatric tumors are rare and mostly present with lower mutational burden. The lack of specific therapeutic options represents the main current challenge; systematic, multi-disciplinary approaches are required to accelerate drug development and ultimately to find cures for all children with cancer. The EU funded "Innovative Therapies for Children with Cancer--Pediatric Preclinical Proof-of-Concept Project"

(ITCC-P4; www.itccp4.eu) consortium consists of a public-private partnership including academic and industrial partners with the goal of developing a large-scale platform comprising >400 patient-derived xenograft (PDX) models representing high-risk pediatric cancers. Currently, this collection of PDX models includes the most common types of pediatric tumors, such as leukemia (n=28), bone and soft-tissue sarcomas (n=154), CNS tumors (n=96) and neuroblastomas (n=38), as well as other rare childhood cancers, such as hepatoblastomas (n=20) and malignant rhabdoid tumors (n=18); PDX models have been generated either from primary (n=206) or relapse (n=118) disease. In order to: a) investigate the biology of the pediatric PDX models in a high-throughput and systematic fashion, b) assess whether they accurately reflect the molecular features of the corresponding primary tumor and, c) identify potential new suitable biomarkers, we performed a comprehensive molecular characterization (whole-exome and low-coverage whole-genome sequencing; DNA methylation profiling; RNAseq and gene expression profiling) of the PDX models, as well as their matching human tumors and germline samples. These data contributed to the stratification of the PDX models based on their mutational status and emerging molecular vulnerabilities to inform *in vivo* drug testing in all these PDX models. This proof-of-concept drug testing has been conducted defining, for each group of models, a panel of single compounds (SOC n=3; novel targeted therapies, n=6) or combinations (with each other or with chemo- or radiotherapy). All processed molecular and drug-testing data are collected in the consortium´s centralized data repository (https://r2.amc.nl) allowing data downstream analysis, visualization and interpretation. Taken together, the ITCC-P4 sustainable platform represents a validated and powerful tool to investigate the biology of pediatric cancer based on the establishment, characterization and preclinical testing of pediatric cancer PDX models, ultimately envisaged to contribute the development of innovative therapeutic options for childhood cancer patients.

#3572

Genomic profiling of subcutaneous patient derived xenograft models of solid childhood cancer

Funan He[1], Abhik M. Bandyopadhyay[1], Laura Klesse[2], Anna Rogojina[1], Erin Butler[2], Taylor Hartshorne[2], Trevor Holland[1], Luz Perez Prado[1], Anne-Marie Langevan[3], Allison C. Grimes[3], Chatchawin Assanasen[3], Zhao Lai[1], Yi Zou[1], Dias Kurmashev[1], Lin Xu[4], Yang Xie[4], Yidong Chen[1], Xiaojing Wang[1], Gail E. Tomlinson[1], Stephen X. Skapek[2], Raushan T. Kurmasheva[1], Peter J. Houghton[1], Siyuan Zheng[1]. *[1]Greehey Children's Cancer Research Institute, University of Texas Health Science Center, San Antonio, TX,[2]Department of Pediatrics, Division of Hematology/Oncology, University of Texas Southwestern Medical Center, Dallas, TX,[3]Department of Pediatrics, Division of Pediatric Hematology Oncology, University of Texas Health Science Center, San Antonio, TX,[4]Harold C. Simmons Comprehensive Cancer Center, University of Texas Southwestern Medical Center, Dallas, TX*

Background: Cancer causes significant mortality and morbidity in children. Current therapies are effective but can cause long-term health problems for patients. Development of new therapies relies on faithful preclinical models. Patient-derived xenografts (PDXs) are an important tool for pre-clinical testing in childhood cancer research. It remains incompletely understood how well genomically PDXs recapitulate primary patient tumors (PTs), particularly in rare cancers.
Method: To characterize the fidelity of early passage subcutaneous PDXs derived from pediatric solid tumors, we established 70 early passage PDX models from 16 cancer types. The cohort comprises some very rare cancers such as hepatoblastoma (n=13), germ cell tumor (n=10), osteosarcoma (n=13), and Wilms tumor (n=14). We performed low pass whole genome, exome, and RNA sequencing on these PDXs, their matched PTs and germline samples when materials were available.
Result: Overall, we observed low somatic mutation rates in these tumors; however, prior chemotherapy was associated with higher mutation rate. Of the 25 PT/PDX pairs, 20 showed high mutation similarity. The five pairs with low mutation similarity showed evidence of clonal selection. We observed high genomic instability in osteosarcoma. Consistently, more fusions were identified in this cancer type. PTs and PDXs showed high similarity in the copy number pattern, including both broad and focal events. GISTIC analysis identified recurrently amplified or deleted genes including *MYC*, *CCNE1*, *TP53*, *PTEN*, and *BCL2*. On the transcriptional level, though PTs and PDXs were generally similar, their expression is more reflective of tissue of origin. We identified fusions that are characteristic of the cancer type such as *BCOR-CCND3* in an Ewing like sarcoma. We also identified an NTRK fusion in an osteosarcoma. In summary, we show that PDXs generally recapitulate PTs in mutations, copy number changes, and expression. The dataset represents a valuable resource for future preclinical and mechanistic studies.

PET, MRI, and CT Imaging

#3576

Molecular imaging of CD8 infiltration following combination immunotherapy in preclinical glioblastoma

Carlos A. Gallegos[1], Yun Lu[2], Alessandro Mascioni[3], Fang Jia[3], Jennifer C. Clements[4], Patrick N. Song[2], Shannon E. Lynch[2], Jason M. Warram[5], James M. Markert[4], Anna Sorace[1]. *[1]Biomedical Engineering, University of Alabama at Birmingham, Birmingham, AL,[2]Biomedical Sciences, University of Alabama at Birmingham, Birmingham, AL,[3]Imaginab Inc, Inglewood, CA,[4]Neurosurgery, University of Alabama at Birmingham, Birmingham, AL,[5]Otolaryngology, University of Alabama at Birmingham, Birmingham, AL*

Background: Novel immune-promoting therapeutics for glioblastoma multiforme (GBM), such as oncolytic herpes simplex viruses (oHSV) and immune checkpoint inhibitors (ICI), have the potential to improve overall survival and lead to long-term remission, however their clinical benefit remains inconsistent. Under standard of care imaging, assessment of immunotherapeutic response can be limited by apparent radiological tumor progression associated with treatment-induced inflammation and immune infiltration. This has led to a need for better understanding of immune cell dynamics and immunotherapy response in GBM. The objective of this study is to evaluate changes in $CD8^+$ infiltration and its relation to therapy response, through positron emission tomography (PET) imaging, in preclinical GBM.

Methods: GSC005-luc orthotopic GBM models (n= 40) were treated with saline, M002 oHSV, anti-PD1 or combination immunotherapy following three weeks of tumor growth. One-week post-treatment, [^{89}Zr]-CD8 PET imaging was performed and biologically validated through *ex vivo* PET, autoradiography and staining for H&E and CD8 immunohistochemistry (IHC). Further, longitudinal changes in CD8 infiltration were evaluated via [^{89}Zr]-CD8 PET imaging one- and three-weeks post-immunotherapy with responses monitored every three days via bioluminescence imaging (BLI). Statistical analysis involved one-way ANOVA and unpaired T-test, with $p<0.05$ considered significant.

Results: Linear correlations were seen between *in vivo* PET signal and *ex vivo* uptake ($r=0.61$, $p<0.01$), autoradiography ($r=0.46$, $p<0.01$), and IHC tumor $CD8^+$ cell density ($r=0.55$, $p<0.01$) one-week post-treatment. Immunotherapy efficacy, defined by decreased BLI signal, resembled clinical findings as only a subset of mice exhibited long-term positive response measured by BLI signal decrease (n=9/24). Response classification revealed increased $CD8^+$ cell tumor localization, as measured by peak standardized uptake value (SUV_{peak}) tumor to background ratio (TBR), in non-responders ($p<0.01$) and decreased heterogeneity in signal distribution in responders ($p<0.05$) relative to controls early in the course of therapy.

Conclusions: Early CD8 infiltration and uptake distribution from CD8-PET imaging provides potential imaging metrics of therapeutic response to oHSV immunotherapy in GBM. Development of these immune-focused imaging approaches for the assessment of positive immunotherapeutic effects in GBM is beneficial for the better understanding of immune cell dynamics and their relation to clinical outcomes.

#3577

A first assessment of CD8-PET/CT with ^{89}Zr-Crefmirlimab as predictive biomarker for response to standard of care immunotherapy in patients with solid tumors

guillaume potdevin[1], Isabelle Ayx[1], Laura Dillon[2], Emilie Mahieu[1], Hadassah Sade[1], Günter Schmidt[1]. *[1]Computational Pathology Munich / Translation Medicine, AstraZeneca Oncology, Munich, Germany,[2]Parthenon Therapeutics, Boston, MA*

Background: Elevated levels of CD8+ tumor-infiltrating lymphocytes are associated with response to immunotherapy (IoT)[1] in many indications. While immunohistochemistry (IHC) has been the method of choice to evaluate CD8+ tumor infiltration level, the utility of the CD8-PET/CT imaging method offers an attractive non-invasive alternative to biopsies, with the potential to account for both intra-patient tumor heterogeneity and lesion-specific response.

Methods: Using the data from ImaginAb's phase II trial[2], we predict response to standard of care (SOC) IoT in patients with advanced solid malignancies. Solely based on CD8-PET/CT scan data, the novel method scores each identifiable lesion by using its volume as measured in the CT data, and mean CD8-PET uptake values before and 4 to 6 weeks after treatment start. All lesion scores are aggregated to compute the patient score, to be subsequently compared to the best standard RECIST evaluation. This methodology was defined and developed using data from 14 patients, and later evaluated using the whole cohort of 40 patients.

Results: Despite the multiplicity of indications and SOC IoT in the patient cohort, the computed scores significantly identify and stratify responders (Complete or Partial Response, mean score = -0.78, 10 subjects) from non-responders (Stable or Progressive Disease, mean score = 0.088, 25 subjects): two sample t-test value = 5.378, p-value = 1e-05. RECIST evaluations remain too preliminary to report for 4 subjects. Furthermore, CD8-PET outcomes are available much earlier (median 35 days, median best of RECIST 105 days), which may facilitate important therapy decisions. In addition, the discriminative power between the response groups is reduced when restricting the method to either of the infiltration or lesion size measurements. This result highlights the complementarity of the two measurements.
Conclusions: CD8-PET offers new non-invasive opportunities in the early discrimination of responders and non-responders to IoT as well as visualization of the heterogeneity of tumor responses to IoT, supporting its use pre-IoT and early on IoT for adult solid tumors.
Acknowledgement: All the data used in this study come from clinical study [2]. These data were acquired and discussed within the frame of a pre-competitive collaboration between AstraZeneca, Takeda, Pfizer and imaginAb. We want to thank the respective parties for fruitful discussions which helped us refine our analysis methodology.
References: [1] Li F, et al. The association between CD8+ tumor-infiltrating lymphocytes and the clinical outcome of cancer immunotherapy: A systematic review and meta-analysis. EClinicalMedicine. 2021 Sep 16;41:101134. doi: 10.1016/j.eclinm.2021.101134. PMID: 34585125; PMCID: PMC8452798. [2] ClinicalTrials.gov Id: NCT03802123
https://clinicaltrials.gov/ct2/show/NCT03802123

#3578

Using a novel [^{68}Ga]-radiolabeled peptide to detect cell surface expression of calreticulin in pancreatic adenocarcinoma

Rachael Guenter[1], Maxwell Ducharme[2], Brendon Herring[1], Tejeshwar C. Rao[3], Odalyz Montes[2], Tyler McCaw[1], Herbert Chen[1], Suzanne E. Lapi[2], Benjamin Larimer[2], J. Bart Rose[1]. *[1]Surgery, University of Alabama at Birmingham, Birmingham, AL,[2]Radiology, University of Alabama at Birmingham, Birmingham, AL,[3]Cell, Developmental and Integrative Biology, University of Alabama at Birmingham, Birmingham, AL*

Background**:** Pancreatic ductal adenocarcinoma (PDAC) is the 3rd leading cause of cancer related death with a 5-year survival rate at 11%. New systemic therapies for patients with PDAC are desperately needed. Upregulation or exposure of a new protein on the tumor cell surface can serve as a therapeutic or diagnostic target. Here, we highlight our recently developed strategy to induce localization of the reticular protein calreticulin (CALR) to the cell surface in PDAC cells and its subsequent detection using a novel radiolabeled peptide.
Methods: Surface translocation of CALR was detected by flow cytometry, western blot, and total internal reflection fluorescence (TIRF) microscopy in PDAC cells treated with either doxorubicin or gemcitabine. The radionuclide-binding chelator 'DOTA' was covalently linked to a CALR-specific peptide 'KLGFFKR' and then labeled with ^{68}Ga. Samples were analyzed on HPLC with an average radiolabeling efficiency of 93%. Mice bearing Panc02 allografts were treated with doxorubicin for 24h, injected with ~3 MBq (5 μg) of radiopeptide, and sacrificed after 1 hour to determine biodistribution.
Results: Using flow cytometry, we found that treating PDAC cells with doxorubicin or gemcitabine increased both the total number and the median fluorescence intensity of surface staining for live cells expressing CALR. When membrane proteins were isolated from PDAC cells treated with doxorubicin at various time points, a peak in surface CALR protein was detected at 30 minutes with persistent expression lasting for 24 hours. TIRF microscopy showed that Panc02 cells treated with doxorubicin had approximately a 2-fold higher surface CALR expression as detected by enhanced membrane fluorescence compared to controls. *In vivo*, our novel [^{68}Ga]-CALR peptide showed rapid clearance through the kidneys with no significant uptake in vital organs (n=4). In Panc02 allograft-bearing mice treated intratumorally with either vehicle or doxorubicin, biodistribution analysis after radiopeptide injection showed a significant increase in radiopeptide uptake in the treated tumors (n=6, $p < 0.05$).
Conclusions: CALR is translocated to the cell surface in PDAC cells, where it can subsequently be targeted by a novel radiopeptide agent. Future studies are needed to determine if induced CALR can be targeted for therapeutic effect.

#3579

Assessment of target-mediated biodistribution of an ^{89}Zr labeled PD-L1/4-1BB bispecific Mabcalin protein

Claudia A. J. van Winkel[1], Xiaoyu Fan[2], Danique Giesen[2], Glenn Gauderat[3], Lucia Pattarini[4], Thomas Jaquin[5], Anissa Barakat[3], Anne-Marie De La Bigne[3], Marleen Richter[5], Nicole Andersen[5], Julie Legrand[3], Helene Lelièvre[3], Elisabeth G. E. de Vries[1], Aizea Morales-Kastresana[5], Marjolijn N. Lub-de Hooge[6]. *[1]Medical Oncology, University Medical Center Groningen, Groningen, Netherlands,[2]Nuclear Medicine and Molecular Imaging, University Medical Center Groningen, Groningen, Netherlands,[3]Institut de Recherches Internationales Servier Oncology R&D Unit, Suresnes, France,[4]Center for Therapeutic Innovation Oncology, Institut de Recherches Servier, Croissy-sur-Seine, France,[5]Pieris Pharmaceuticals, Hallbergmoos, Germany,[6]Clinical Pharmacy and Pharmacology, University Medical Center Groningen, Groningen, Netherlands*

Background: PRS-344/S095012 is a novel 4-1BB (CD137) and programmed death-ligand 1 (PD-L1) bispecific antibody-Anticalin® fusion protein (Mabcalin™ protein) designed to cluster 4-1BB on activated T cells exclusively in the presence of PD-L1 expressing cells. We aimed to study PRS-344/S095012 in vivo biodistribution and pharmacokinetics with ^{89}Zr-positron emission tomography (PET) at a dose with antitumoral activity in mice and evaluate the contribution of each targeting arm.
Methods: PRS-344/S095012 lacks cross-reactivity to murine 4-1BB and PD-L1. To explore the PRS-344/S095012 biodistribution in a humanized 4-1BB knock-in mouse model, we synthesized the surrogate ^{89}Zr-Atezo-J10 with the same 4-1BB building block and cross-reactivity to murine PD-L1. Humanized 4-1BB knock-in C57BL/6J (h4-1BB KI B6) and C57BL/6J (B6) mice (n=4-6 per group) were subcutaneously engrafted with murine wildtype MC38 colon adenocarcinoma cells. Tumors were grown to a minimum of ≥50 mm^3 (average 163 mm^3) before tracer injection. Mice received intravenously 30 µg (2.5 MBq) of ^{89}Zr-PRS-344/S095012 or ^{89}Zr-Atezo-J10 supplemented with PRS-344/S095012 or Atezo-J10 up to 10 mg/kg. Four mice groups were formed to distinguish between bispecific (Atezo-J10 in h4-1BB KI B6), monospecific PD-L1 (Atezo-J10 in B6), monospecific 4-1BB (PRS-344/S095012 in h4-1BB KI B6), and isotype (PRS-344/S095012 in B6) binding up to 4 days post-injection (pi). In addition, a fifth group (5 MBq ^{89}Zr-Atezo-J10) was studied to visualize the bispecific biodistribution up to 7 days pi. At days 1, 2, 4, or 2, 4, 7 pi, mice underwent serial PET imaging to obtain mean and maximum standardized uptake (SUVmean/max) and retro-orbital blood sampling, followed by ex vivo biodistribution.
Results: PET imaging showed ^{89}Zr-Atezo-J10 specific tumor accumulation with higher tumor-to-blood ratios of respectively 2.2-, 2.6-, and 2.4-fold ($p<0.01$) at 4 days pi compared to monospecific binding of PD-L1, 4-1BB, and isotype. The ex vivo biodistribution demonstrated the same trend with respectively 4.2-, 5.5-, and 6.8-fold ($p<0.01$) increase in tumor-to-blood uptake for ^{89}Zr-Atezo-J10 versus monospecific binding of PD-L1, 4-1BB, and isotype. ^{89}Zr-Atezo-J10 spleen uptake was comparable (ns) with monospecific binding of PD-L1 but elevated ($p<0.01$) compared to 4-1BB or isotype distribution. The uptake in lymph nodes (axillary, cervical, tumor-draining, and mesenteric) did not differ between the groups.
Conclusion: ^{89}Zr-Atezo-J10 specific accumulation in PD-L1 expressing tumors is due to both PD-L1 and 4-1BB binding and is higher than with PD-L1 and 4-1BB mono-targeting. This preclinical study supports the clinical evaluation of ^{89}Zr-PRS-344/S095012's whole-body distribution and the development of tumor-specific 4-1BB targeting bispecifics.

#3580

Noninvasive immuno-PET imaging of CD8+T cell behavior in tumor bearing mice models treated with SAR444245

Sebastion d'Heilly[1], Fabrice Tirode[1], Maxime Gaulin[1], Dudzicki Anne[1], Guillaume Bluet[1], Stéphane Guerif[1], Francis Descamps[2], Peter Casteels[2], Xiangming Li[3], Rui Wang[3], Robin Meng[3], Erwan Jouannot[1]. *[1]Sanofi, Vitry-sur-Seine, France,[2]Sanofi, Ghent, Belgium,[3]Sanofi, Cambridge, MA*

SAR444245 (formerly THOR-707) is a site-specific pegylated recombinant human IL-2 molecule which blocks IL-2R alpha-binding while retains near-native affinity for beta/gamma IL-2 receptor subunits. SAR444245 reduces B16-F10 tumor proliferation in C57BL/6 mice and induces a short transient migration of CD8+ T and NK cells from peripheral blood to lymphoid organs before a strong proliferation (Ptacin et al, Nat Commun 2021). Here we report CD8+ T cells imaging post SAR444245 as monotherapy in naive and tumor bearing mice using nuclear imaging. An anti-murine CD8+ PET probe was injected in mice 24 hours post SAR444245 administration and nuclear imaging was performed at different times over 6 days. In C57BL/6 naive and in poorly immunogenic B16-F10 tumor bearing animals, images reveal a decreased Standardized Uptake Value (SUV) within blood in treated animals at 3mg/kg compared to control ones. In parallel, blood SUV Ratio (SUVR) increases within spleen, lymph

nodes and thymus after SAR444245 injection compared to control mice. On tumor site, a stronger SUVR is measured at 144 hours post injection in SAR444245 treated group than in the control group. A dose escalation ranging from 1 to 6 mg/kg of SAR444245 was performed in highly immunogenic CT26 tumor bearing animal. Blood SUV decreases in the treated groups compared to the control group. In lymphoid organs, all SUVR increase at 144 hours post injection in the treated groups compared to the control one. In CT26 tumors, a slight increase of the SUVR is observed for groups treated at 3 and 6 mg/kg. In parallel, a pronounced reduction of tumor growth is observed in the treated group at 6mg/kg. These studies non-invasively confirm the mode of action of SAR444245 with a rapid relocation of CD8+ T cells from peripheral blood to lymphoid organs and tumor site.

#3581

Differentiation of niraparib and olaparib brain penetration in healthy rhesus macaque monkeys

Mark Reid Groseclose[1], Jeremy Barry[1], Yongle Pang[1], Jennifer Deutsch[1], Shannon Berry[1], Elaina McCormick[1], David K. Lim[1], Hoang Tran[1], Sean Maguire[1], Hasan Alsaid[1], Amine Aziez[2], Elaine Paul[3], Keyur Gada[4]. *[1]GSK, Collegeville, PA,[2]GSK, Basel, Switzerland,[3]GSK, Raleigh, NC,[4]GSK, Waltham, MA*

Purpose: There remains an unmet need to provide effective treatment therapy for patients with primary and metastatic brain tumors; lack of drug penetration across the blood brain barrier (BBB) is a key factor. Synthetic lethality is an attractive mechanism in treating brain tumors post radiotherapy. Here we investigate the brain penetration of niraparib and olaparib in healthy monkeys to understand the potential of each to cross the intact BBB.

Experimental Procedures: Four healthy male Rhesus macaque monkeys were dosed daily via oral gavage for five days with either niraparib (n=2; 6 mg/kg) or olaparib (n=2; 10 mg/kg). Pre-dose blood was collected daily and terminal blood, cerebrospinal fluid (CSF), and brain tissue was collected at necropsy. Coronal brain sections were analyzed by matrix-assisted laser desorption/ionization (MALDI) imaging mass spectrometry (IMS) to quantitatively assess the tissue distribution of the dosed compounds. Blood, CSF, and bulk homogenate of brain tissue were analyzed by LC-MS bioanalysis.

Summary of Data: Greater brain penetration was observed for niraparib when compared to olaparib in healthy Rhesus macaque monkeys following five days oral administration. The unbound brain-to-plasma partition coefficient ($K_{p,uu,brain}$) was 15x higher for niraparib compared to olaparib. Quantitative MALDI IMS of coronal brain sections from monkeys administered niraparib showed consistent concentrations distributed throughout the brain parenchyma. Olaparib was not detected by MALDI IMS in any of the coronal brain sections collected from the monkeys administered olaparib. Similar plasma and CSF concentrations were observed between the monkey's administered niraparib vs olaparib, highlighting the unique ability of niraparib to cross the intact BBB of monkeys and distribute throughout the brain.

Conclusions: Niraparib showed markedly higher brain penetration than olaparib in healthy Rhesus macaque monkeys demonstrating enhanced ability to cross intact BBB.

Summary of Quantification Results Displayed as Total Conc. with Adjusted Free Conc. in Parentheses

Compound	Animal	LC-MS Pre-Dose Plasma Days 1-5 (ng/mL)	LC-MS Pre-Dose Plasma Days 1-5 (ng/mL)	LC-MS Terminal CSF (ng/mL)	LC-MS Bulk Brain Homogenate (ng/g)	MALDI IMS Brain Section Average (ng/g)	Kp,uu Brain/Plasma	Mean Kp, uu Brain/Plasma
Niraparib	Monkey 1	BLQ, 28 (10), 49 (18), 59 (22), 72 (26)	84 (31)	9	378 (14)	283 (10)	0.45	0.30
Niraparib	Monkey 2	BLQ, 58 (21), 87 (32), 74 (27), 66 (24)	436 (160)	25	797 (29)	684 (25)	0.16	
Olaparib	Monkey 3	BLQ, 27 (8), 26 (8), 33 (10), 33 (10)	322 (99)	13	12 (2)	BLQ	0.02	0.02
Olaparib	Monkey	BLQ, 51	254 (78)	6	11 (2)	BLQ	0.03	

	4	(16), 17 (5), 53 (16), 45 (14)						

#3582

Differentiation of niraparib and olaparib brain penetration in a mouse brain metastatic tumor model

Mark Reid Groseclose[1], Jeremy Barry[1], Tinamarie Skedzielewski[1], Gerald McDermott[1], Chakravarthi Balabhadrapatruni[1], Bill Benson[1], Yongle Pang[1], David K. Lim[1], Hoang Tran[1], Mike Ringenberg[1], Keyur Gada[2], Amine Aziez[3], Elaine Paul[4], Hasan Alsaid[1]. *[1]GSK, Collegeville, PA,[2]GSK, Waltham, MA,[3]GSK, Basel, Switzerland,[4]GSK, Raleigh, NC*

Purpose: There remains an unmet need to provide effective treatment therapy for patients with primary and metastatic brain tumors; lack of drug penetration across the blood brain barrier (BBB) is a key factor. Synthetic lethality remains an attractive mechanism in treating brain tumors post radiotherapy. Here, we evaluated brain penetration and distribution of niraparib and olaparib in a mouse brain tumor model.

Experimental: Female mice (CrTac:NCr-Foxn1nu; 6 w/o) received 2.5E5 luciferase transfected human breast cancer line (MDA 231-BRM2-831) via intracardiac injection. Mice were imaged twice/week using bioluminescence imaging (BLI) to monitor tumor growth. On day 35, mice with brain metastases (BM) were treated via oral gavage once daily for 5 days with either niraparib (35 mg/kg, n=4 BM, n=3 control), olaparib (50 mg/kg, n=3 BM, n=3 control), or vehicle (n=3 control). Terminal blood samples and brains were collected 2 hr post final dose. Serial tissue sections were collected for MALDI-IMS, H&E and IHC staining from 5 distinct horizontal planes in the brain. Tissue collected between each imaging plane was homogenized for LC-MS bioanalysis.

Summary of Data: In vivo BLI imaging was used to identify mice with BM and tumor presence was confirmed ex vivo using IHC. Quantitative MALDI IMS of coronal brain sections collected from mice administered niraparib showed consistent concentrations distributed throughout the brain parenchyma with locally higher concentrations detected from tumor regions. Table 1 summarizes the LC-MS bioanalysis concentrations in plasma and bulk brain homogenates and brain section concentrations detected by MALDI IMS. The estimated mean unbound brain-to-plasma partition coefficient ($K_{p,uu,brain}$) was 3.0x and 5.6x higher for niraparib compared to olaparib in control and BM mice, respectively.

Conclusions: Herein, we demonstrated that niraparib has a higher brain penetration and distribution compared to olaparib in both control mice and mice with BM.

Summary of Quantification Results Displayed as Total Conc. with Adjusted Free Conc. in Parentheses

Compound	Group	Terminal Plasma Mean (ng/mL)	LC-MS Bulk Brain Homogenate Mean (ng/g)	MALDI IMS Brain Section Mean (ng/g)	$K_{p,uu\ Brain}$
Niraparib	Control	3847 (769)	658 (111)	532 (89)	0.18
Niraparib	BM	2535 (507)	543 (91)	473 (80)	0.14
Niraparib	Vehicle	BLQ	BLQ		
Olaparib	Control	226 (68)	6 (2)	BLQ	0.06
Olaparib	BM	119 (36)	5 (2)	BLQ	0.03
Olaparib	Vehicle	BLQ	BLQ		

#3583

Novel MRI contrast system using halloysite nanotubes embedded with iron-platinum nanoparticles for the regulation of the CHST11 expression for cancer treatment

Ming-Hsien Chan[1], Chien-Hsiu Li[1], Yu-Chan Chang[2], Michael Hsiao[1]. *[1]Academia Sinica - Genomics Research Center, Taipei, Taiwan,[2]Department of Biomedical Imaging and Radiological Sciences, National Yang MingChiao Tung University, Taipei, Taiwan*

Topic: TB Tumor Biology (TB03) *In Vivo* Imaging.
Multifunctional nanocomposites have been a popular research target in recent years. This research aims to produce magnetic nanocomposites with high saturation magnetization (Ms) and good biocompatibility to improve the disadvantage of iron-oxide was easy decomposition in the biological environment and overcome the unclear contrast problem of T2-weighted magnetic resonance imaging (MRI) of lung adenocarcinoma. In order to fit the suitable size of iron-based nanoparticles embedded into the halloysite nanotubes (HNT), the iron-platinum (FePt) nanoparticles were chosen as the MRI's core materials. The FePt@HNT nanocomposites have low toxicity, and superparamagnetism is expected to be used in biomedical therapy and magnetic separation for disease treatment and environmental protection. Lung adenocarcinoma cancer cells grow *in situ,* usually invade, and are frequently recurrent after treatment. Since CHST11-mediated gene regulation may serve as a possible means of reducing tyrosine kinase inhibitor (TKI)-induced mitotic cell death, CHST11 modulation of integrin signaling may help lung cancer cells enhance their resistance to gefitinib. To enable the FePt@HNT nanocomposite to be effective in treating lung tumors, we designed miRNAs that inhibit CHST11 expression in an attempt to diagnose lung adenocarcinoma concurrently for treatment.
Keywords: Magnetic resonance imaging, halloysite nanotubes, FePt nanoparticles, CHST11, Lung adenocarcinoma
References
1. Zhou T, Jia L, Luo YF, Xu J, Chen RH, Ge ZJ*, et al.* Multifunctional nanocomposite based on halloysite nanotubes for efficient luminescent bioimaging and magnetic resonance imaging. Int. J. Nanomed. 2016;11:4765-76.
2. Abdullayev E, Joshi A, Wei WB, Zhao YF, Lvov Y. Enlargement of Halloysite Clay Nanotube Lumen by Selective Etching of Aluminum Oxide. ACS Nano 2012;6:7216-26.

#3584
Early and non-invasive detection of radiation-induced cardiotoxicity in pre-clinical and clinical models
Taylor-Jade Higgins, Jayesh Sharma, Elizabeth R. Zhang-Velten, Sarah Elliott, Junjie Ma, Jun Chen, Gabriele Schiattarella, Chantal Vidal, Nan Jiang, Daniel Daou, Joseph Hill, Thomas Gillette, Craig Malloy, Vlad Zaha, Jae Mo Park, Prasanna Alluri. *UT Southwestern Medical Center, Dallas, TX*

Background**:** Nearly half of all patients receive radiation therapy as a component of their cancer care. Despite the efficacy of radiation therapy as a cancer treatment, cardiotoxicity is a major concern in patients receiving chest radiotherapy. There are currently no standardized approaches for early detection of radiation-induced cardiotoxicity as a stage that offers potential for early intervention. In this study, we employ hyperpolarized ^{13}C-pyruvate magnetic resonance spectroscopy to non-invasively characterize early metabolic changes in the heart in response to radiation.
Methods: We established a pre-clinical model of radiation induced heart disease (RIHD) by performing whole heart irradiation (8Gy x 5) in rats. Echocardiography was used characterize mechanical changes in the heart following radiation. To non-invasively detect myocardial mitochondrial dysfunction following cardiac irradiation *in vivo*, we employed hyperpolarized ^{13}C- pyruvate magnetic resonance spectroscopy (MRS) to track the fate of pyruvate, an intermediate of glucose metabolism, as it is metabolized in the heart. Hyperpolarized ^{13}C- pyruvate MRS was also employed in a patient who received thoracic radiation for treatment of thymoma to non-invasively study changes in glucose metabolism in response to radiation.
Results: We identified evidence of early cardiac mitochondrial dysfunction prior to onset of mechanical changes in the heart. Following cardiac irradiation, due to mitochondrial dysfunction, pyruvate was preferentially metabolized to lactate in the cytoplasm (as opposed to bicarbonate in the mitochondria in non-irradiated hearts). The ratio of products of ^{13}C- pyruvate metabolism in the mitochondria and cytoplasm as ascertained by hyperpolarized ^{13}C- pyruvate MRS served as a biomarker for metabolic dysfunction in the heart both in a pre-clinical rat model and in a patient who received thoracic radiation.
Conclusions: We have developed a non-invasive approach for detection of cardiac mitochondrial dysfunction, which may serve as a biomarker for early detection of radiation-induced cardiotoxicity, and shown feasibility in a human patient. Clinical adoption of this approach may enable early identification of patients who are at high risk for future cardiac complications and may benefit from mitigation strategies.

#3585

Probing the relationship between renal carcinoma perfusion, hypoxia, and metabolism during response to VEGFR inhibition and at resistance

Qianhui Dou, Patricia Coutinho de Souza, Xiaoen Wang, Aaron K. Grant, Leo L. Tsai. *Radiology, Beth Israel Deaconess Medical Center, Boston, MA*

Clear cell renal cell carcinoma (ccRCC) is the most common primary kidney cancer. VEGF-receptor tyrosine kinase inhibitors remain a second-line or concurrent (with immunotherapy) treatment option for advanced RCC, but resistance inevitably occurs. There remains a need for biomarkers predictive of response to VEGFR targeting. Anti-VEGFR therapy-induced hypoxia can result in changes to both tumor metabolism and vascularization that contribute to the aggressiveness of treatment-resistant tumors. In this study we used *in vivo* hyperpolarized ^{13}C-tert-butanol, a freely-diffusible novel MRI tracer that provides high-SNR tissue perfusion mapping, and hyperpolarized ^{13}C pyruvate MRI, which enables real-time investigation of glycolytic lactate production, to understand the evolution of RCC perfusion and metabolism in response to VEGFR targeting, while correlating to histologic measures of tumor proliferation (Ki67) and vascularization (CD34). A498, a human ccRCC cell line, was implanted subcutaneously into 12-week-old nude mice. When tumors reached 15mm, the mice were placed into three arms, untreated (UT), sunitinib sensitive (SS), and sunitinib resistant (SR). SS mice were treated with sunitinib (25 mg/kg via gavage) then the mice were imaged with MRI at 48 hours. SR mice were treated with sunitinib daily until 2mm of re-growth was detected, then MRI was performed. UT mice were imaged when tumors reached 20mm. Pimonidazole infusion immediately after MRI, then the tumors were harvested. Histology included Ki67, CD34, and pimonidazole (hypoxia) staining. Ki67 expression was greater in the UT group compared to SS (37.56±5.21 vs 26.23±3.78, p=0.004), but not compared to SR (37.56±5.21 vs 34.32±1.12, p=0.93). The UT group demonstrated greater vascularization with CD-34 vessel counting than SS (UT 6.70±1.81 vs. SS 2.39±1.16, p=0.002), while vascularization was increased in SR compared to SS (SR 3.82±1.81 vs SS 2.39±1.16, p=0.05). Ki67 expression was positively correlated with CD34 expression. MR-measured tumor perfusion of the SS group was greater than UT (0.0086±0.0056 vs 0.0035±0.0026, p=0.0001) and SR (0.0086±0.0056 vs 0.0043±0.0033, p=0.0003). Tumor lactate production in the SS group was lower than UT (0.752±0.268 vs 0.609±0.188, p=0.04) and SR (0.752±0.268 vs 0.593±0.246, p=0.006). However, tumor perfusion was negatively correlated with lactate production ratio only in the SR group. Untreated and sunitinib-resistent RCC tumors are associated with increased perfusion and vascularity, and decreased lactate production. An inverse relationship between lactate production and perfusion in SR may be attributable to vascular normalization. Analysis of the spatial relationship between tumor metabolism and perfusion will further yield additional detail on the interplay between hypoxia and metabolism.

#3586

In vivo targeted detection and imaging of ovarian cancer by SPMR and MRI using anti-folate receptor functionalized iron oxide nanoparticles

Marie Zhang, Kathirvel Kandasamy, Yamitha Perera, Dan Inglese, Eric Smith-Nguyen. *Imagion Biosystems, Inc., San Diego, CA*

Ovarian cancer is the second most common and most deadly gynecological cancer in women. Early and accurate detection is crucial in improving survival rate and quality of life of patients. Folate receptor alpha (FRα) is a folate transporter that has been reported to be overexpressed in approximately 90% of ovarian cancer, which makes it a suitable molecular target to use in developing tumor imaging methods. Iron oxide nanoparticles (NPs) have been used in a variety of cancer detection/imaging applications. Here we show that anti-FRα targeted superparamagnetic iron oxide nanoparticles (SPION) can be used for *in vivo* detection by two different imaging methods. Superparamagnetic Relaxometry (SPMR) is a highly sensitive *in vivo* detection technology that is able to differentiate the magnetic signature of nanoparticles bound to tumor cells from unbound nanoparticles. Same targeted SPIONs accumulated in tumor are able to provide molecular magnetic resonance imaging (MRI) contrast as well. Our results have shown that the anti-FRα NPs can distinguish high and low FRα expression cell lines, such as KB and A549, respectively in an *in vitro* cell based assay by SPMR, demonstrating good sensitivity, specificity and selectivity. *In vivo* study using xenograph model with KB and A549 cells implanted subcutaneously on the flank region of female athymic nude mice demonstrated higher level tumor accumulation of anti-FRα NPs in KB tumor compared to A549 tumor, measurable by *ex vivo* tumor detection using SPMR. Using a PEG NPs (without the target ligand) as control for the mice study have shown that minimum nanoparticle tumor accumulated were observed, demonstrating the specificity of the nanoparticles *in vivo*. Organ distribution study indicated that anti-FRα NPs mostly accumulated in liver and spleen as these nanoparticles were cleared through these two organs.

Other organs such as brain, heart, lung, kidney didn't show appreciable accumulation. The repeat of same type of xenograph mice model used in the SPMR study is currently under the way using MRI as an alternative *in vivo* detection method with images taken pre- and post- dosing of the nanoparticles. Based on the specificity and sufficient accumulation of nanoparticles demonstrated in the SPMR study, it is expected that MRI will show similar performance with additional anatomical information.Our anti-FRα NPs provided targeted and specific delivery to cancerous tissue and generated measurable signal by SPMR. Furthermore, demonstration of these anti-FRα NPs generating tumor specific contrast in MRI is currently under the way. These studies lay the groundwork for use of bio-safe magnetic particles as a detection and contrast agent for early ovarian cancer detection with improved accuracy to minimize the needs of invasive biopsies/surgery as well as potential utility for monitoring therapy response or recurrence.

#3587

High resolution microCT to analyze the 3D morphology of microcalcifications in benign breast disease and breast cancer biopsy tissues

Sarah E. Schrup[1], Thomas de Bel[2], Tanya Hoskin[3], Teresa Allers[4], Stacey Winham[3], Derek Radisky[5], Laura Pacheco-Spann[6], Lisa Seymour[4], Amy Degnim[4], Mark Sherman[6]. *[1]Mayo Clinic Alix School of Medicine, Rochester, MN,[2]Radboud University Medical Center, Nijemegen, Netherlands,[3]Department of Quantitative Health Sciences, Mayo Clinic, Rochester, MN,[4]Department of Surgery, Mayo Clinic, Rochester, MN,[5]Department of Cancer Biology, Mayo Clinic, Jacksonville, FL,[6]Department of Quantitative Health Sciences, Mayo Clinic, Jacksonville, FL*

Introduction**:** We used micro-computed tomography (microCT), a high-resolution imaging option, to detect and characterize microcalcifications (MCs) in three dimensions within pathology blocks of benign and malignant breast tissues.

Methods: A set of 44 formalin-fixed, paraffin-embedded breast tissue blocks were assessed from n=22 women at two time points: benign breast biopsy and subsequent DCIS or DCIS with invasive disease breast cancer. Blocks were scanned using the Bruker Skyscan 1276 microCT at a resolution of 10 µm. SkyScan analysis CTAn software was utilized to prepare and analyze morphological parameters and multiple MCs contained within each block were averaged. Paired morphological parameters were compared between the benign and subsequent cancer samples within women using Wilcoxon signed-rank tests.

Results: Median age of patients was 53 years (range 37-77 years) at initial benign biopsy and developed breast cancer at median of 5.6 years (range: 2.3-12.8 years) later. The initial benign biopsies were for proliferative disease without atypia in the majority (59%), while 23% had non-proliferative lesions and 18% atypical hyperplasia. The average structural model index was consistent with a near rod-like shape (median 2.99, range: 2.71-3.29). Paired comparisons between benign and cancer blocks showed that the average surface area of MCs was significantly higher in the cancer samples (p=0.0467), as was the average volume of MCs (p=0.0298) (Table 1).

Conclusions: Preliminarily, we demonstrate that microCT of routinely prepared pathology blocks of breast tissues may be useful in characterizing the 3-D morphometry of MCs with suggestive differences in benign and cancer tissues. Given that MCs are a sentinel radiologic marker of DCIS but are common in benign breast disease, developing improved approaches for classifying MCs may have value in breast cancer screening and management.

Table 1: Comparison of MC parameters in biopsy tissues (IQR = Interquartile Range).

	Benign sample from women who later developed breast cancer (N=22)	Breast cancer after prior benign sample (N=22)	Paired Differences (Cancer – Benign) (N=22)	Wilcoxon signed-rank p value
Number of Objects (Median (IQR))	43.5 (14, 789)	69.5 (33, 289)	-6 (-139, 67)	0.6830
Average Surface Area (mm^2)(Median (IQR))	0.0225 (0.0134, 0.0393)	0.0342 (0.0185, 0.0656)	0.0113 (-0.0027, 0.0322)	0.0467
Average Volume (mm^3) (Median (IQR))	0.0003 (0.0001, 0.0007)	0.0007 (0.0003, 0.0022)	0.0003 (0.000002, 0.0020)	0.0298
Average Surface Area/Volume (mm^{-1}) (Median (IQR))	214.92 (162.25, 328.39)	199.55 (151.89, 230.52)	-20.85 (-86.05, 27.04)	0.1433

Average Structural Thickness (mm)(Median (IQR))	0.0341(0.0196, 0.0446)	0.0395 (0.0336, 0.0505)	0.0074 (-0.0062, 0.0153)	0.1173
Average Structural Model Index (Median (IQR))	2.9758 (2.8465, 3.1175)	3.0026 (2.9281, 3.0927)	0.0075 (-0.1073, 0.1381)	0.7656

#3588

Multiplex proteomics profiling with the imaging mass cytometry (IMC) identifies immune cell phenotypes associated with high NOS2/COX2 expression in ER- negative and TNBC patients

Milind Pore[1], Lisa Ridnour[2], Paul Mallory[1], Ashley Cardamone[1], Stephen Lockett[1], William Bocik[1], David Wink[2]. *[1]Cancer Research Technology Program, Frederick National Laboratory for Cancer Research, Frederick, MD,[2]Center for Cancer Research, National Cancer Institute, Frederick, MD*

Elevated expression of Inducible Nitric oxide Synthase-2 (NOS2) occurs during acute and chronic inflammation and wound healing processes however, it is also a predictor of bad prognosis in aggressive ER-negative tumors. Overexpression of NOS2 correlates with other prognostic biomarkers making it a unique multifunctional oncoprotein. Cyclooxygenase-2 (COX2) is another enzyme associated with cancer inflammation and is overexpressed in >50% of breast cancers. In our previous studies, we have shown that NOS2/COX2 co-expression is a strong predictor of poor clinical outcome and promotes $CD8^+$ T cell exclusion from tumor epithelia in Triple-negative breast cancers (TNBC). This observation was further explored using multiplexing proteomics technologies. Imaging Mass Cytometry (IMC) has revolutionized tumor microenvironment research by allowing the interrogation of over 35 protein markers simultaneously for the elucidation of the spatial distribution of immune and tumor cells at sub-cellular resolution. Herein, we used multiplex capability IMC to explore the interactions of immune and tumor cell counterparts in ER-negative and TNBC tumors. We employed Formalin-fixed paraffin-embedded (FFPE) tissue from 26 ER-negative and TNBC samples from a clinical cohort of African American breast cancer patients in the Baltimore MD area. We developed a panel of 15 protein metal-labeled antibody markers including antibodies targeting NOS2, COX2, T cells (CD45, CD3, CD4, CD8,) endothelium (CD31), monocytes (CD14), macrophages (CD68), basal markers (α-SMA), cancer stem cells (CD44v6), cancer cells (Pan-CK, B7H4, Cadherin), and serine proteases (granzyme B) secreted by T cells or Natural Killer (NK) cells. Single section slides of 4 µm size were stained with the cocktail of metal-labeled antibodies. Multiple regions of interest (ROIs) representing the tumor and immune cells compartments and tumor-facing stromal cell areas were ablated with the Hyperion Imaging system. The data analysis was performed by the Bodenmiller lab pipeline and VisioPharm software packages. Our preliminary data suggest that patient tumors with high or low NOS2/COX2 expression showed variable levels of CD68 positive macrophage population and T cells. We are currently analyzing the remaining data to understand the cell phenotypes associated with the immunosuppressive and immune-rich clinical samples and performing neighborhood analysis of tumor cells to immune cells and vessels.

#3589

The use of a novel orthotopic xenograft model of fusion negative rhabdomyosarcoma to study the effect of ASAP1 on tumor progression and metastasis

Sarah M. Hammoudeh, Yeap Ng, Mukesh P. Yadav, Roberto Weigert, Paul A. Randazzo. *Laboratory of Cellular and Molecular Biology, Center for Cancer (CCR) Research, National Institutes of Health (NIH), National Cancer Institute (NCI), Bethesda, MD*

ASAP1 is a multidomain ADP-ribosylation factor (Arf) GTPase-activating protein (GAP) involved in the regulation of the actin cytoskeleton, focal adhesions dynamics and receptor tyrosine kinases trafficking. ASAP1 expression levels correlate with progression of solid tumors (e.g. breast, colorectal, pancreatic, ovarian, gastric, and prostate cancer). The first evidence for a role of ASAP1 in cancer progression was the discovery that the amplification of ASAP1 gene on chromosome 8 correlates with poor prognosis in uveal melanoma. A similar amplification of chromosome 8 has been reported in ~72% of fusion negative rhabdomyosarcoma (FN-RMS) tumors, suggesting a potential role for ASAP1 signaling in the progression of FN-RMS. To determine the function of ASAP1 in tumor growth, invasion and metastasis, we used a tongue orthotopic xenograft of FN-RMS which recapitulates physiologically relevant tumor progression and metastasis to lymph nodes and lungs, two of the

common metastatic sites in patients. Using intravital microscopy, we observed that injected FN-RMS cells formed elongated structures and exhibited dynamic branching, which might represent local invasion. H&E stained of fixed tissue revealed invasion into the tongue and local metastasis. Metastases to the regional lymph nodes, lower mandible and lungs were also observed. Using this system, we are now able to determine effect of knocking down and knocking out ASAP1 on the progression of the xenografts, including invasion in real time and metastasis.

#3590

Targeted detection of ovarian cancer using functionalized iron oxide nanoparticles

Marie Zhang, eric Smith-Nguyen. *Imagion Biosystems, Inc., San Diego, CA*

SuperParaMagnetic Relaxometry (SPMR) is a highly sensitive detection technology that can differentiate the magnetic signature of nanoparticles (NP) bound to tumor cells from unbound nanoparticles. Nanoparticles that reach and bind to the target cells are measurable by superconducting quantum interference device (SQUID) magnetometers (MRX instrument developed in house), while unbound nanoparticles such as those freely circulating in the bloodstream are not detected and bone and normal tissue do not produce any magnetic signal. We have developed a protocol to produce high precision 25nm$\pm$1nm (<7% dispersion) Fe_3O_4 nanoparticle core. These core nanoparticles are coated by a polymer shell functionalized with carboxylate groups. Antibody are then conjugated on the surface providing molecular targeting capabilities and PEG is also attached to the surface to reduce opsonization. In previous studies, we have demonstrated that when conjugated with anti-HER2 antibody such as Herceptin, these nanoparticles exhibited great specificity and selectivity towards HER2+ tumor cells in vitro and in vivo. In current studies, we expanded our nanoparticles applications to other type of cancers, such as ovarian cancer.

The CA125 is a tissue-specific antigen expressed in ovarian cancer. It is associated with greater than 80% of epithelial ovarian neoplasms. OC125, a murine monoclonal antibody, reacts with glycosylation-dependent antigens present exclusively in the cleaved portion of the molecule. OC125 antibody is conjugated to our nanoparticles using the same strategy developed for Herceptin nanoparticles. Each nanoparticle contains one to three OC125 antibody molecules covalently attached to the surface based on ELISA analysis. Our results have shown that OC125-NP can distinguish CA125+ and CA125- cell lines, OVCAR3 and HeyA8 respectively. Positive signal can be competed out by pre-incubation with free OC125 antibody and negative cell line produce undetectable SPMR signal, demonstrating good sensitivity, specificity and selectivity.

Antigen glypican-1 (GPC1) is a proteoglycan located on cell surface composed of a membrane-associated protein core anchored to the cytoplasmic membrane. GPC1 may play a functional role in the control of cell division and growth regulation. The expression of GPC1 has been found to be elevated in many cancer cells, including ovarian. Applying the same conjugation strategy developed for Herceptin NP, humanized anti-GPC1 antibody is conjugated to the nanoparticles with minor modification. GPC1-NP generate appreciable signal using SKOV3 cell line (GPC1+ ovarian cell lines) and the signal can be competed out by the presence of excess free GPC1 antibody. Together, these results suggest that in additional to breast cancer application, our antibody functionalized nanoparticle system can be developed for other targeted cancer detection, such as ovarian cancer.

#3591

Does the metastatic immunoenvironment determine poor immunotherapy responses?

Nicole D. Barth[1], Floris J. van Dalen[2], Camille Duran[1], Utsa Karmakar[3], Lorena Mendive-Tapia[3], Takanori Kitamura[4], Martjin Verdoes[2], John S. Condeelis[1], Maja Oktay[1], Marc Vendrell[3], Valerie Brunton[5], David Entenberg[1]. *[1]Albert Einstein College of Medicine, New York, NY,[2]Dept. Tumor Immunology and Institute for Chemical Immunology, Radboud Institute for Molecular Life Sciences, Radboud University Medical Center, Radbound, Netherlands,[3]Centre for Inflammation Research, Queen's Medical Research Institute, The University of Edinburgh, Edinburgh, United Kingdom,[4]MRC Centre for Reproductive Health, Queen's Medical Research Institute, University of Edinburgh, Edinburgh, United Kingdom,[5]Cancer Research UK Edinburgh Centre, Institute for Genetics & Cancer Research, United Kingdom, Edinburgh, United Kingdom*

Despite new treatments, cancer remains the second leading cause of death worldwide with breast cancer being the most common type. Of these deaths, the majority are due to the formation of distant metastases. While new immunotherapies have shown some success in primary tumors, their efficacy in combating metastases has been lacking. Thus we aim to investigate the hypothesis that immune responses at the metastatic site contribute to limitations of current therapies.Within the last decade, new microscopy technologies now enable real-time

visualization of immune responses at primary and secondary sites. Here, we present use of these microscope technologies, along with the development of novel probes to detect apoptotic cancer cells, to investigate the success of checkpoint inhibitors in the primary and secondary sites. We validate, in multiple in vitro and in vivo assays (including intravital imaging), that fluorescent cyclic amphipathic peptide probes specifically label cells undergoing therapy-induced cancer death. In addition, we introduce a newly developed fluorescent, enzyme-activatable, chemokine-conjugate capable of targeting defined macrophage subsets in live tumors. This chemokine-conjugate exploits the high expression of chemokine receptors (e.g. CCR2) and the activity of cysteine cathepsins in tumor associated macrophages to selectively target and eradicate them without affecting other macrophages or immune cells (e.g., neutrophils, T cells, B cells). This research will help to elucidate the role of combination therapy on the metastatic foci and will provide the first insights into the benefit and limitations of combination therapy on secondary site immune responses.

Regulation of Invasion and Migration

#3595

Epigenetic driven IL32 expression contributes to a JNK related cell stress response in breast cancer stem cells to promote cellular invasion

Megan A. Wilson[1], Elayne M. Benson[2], Emma Gray[1], Paige Cairns[1], Maria Ouzounova[3], Hasan Korkaya[4], Austin Y. Shull[1]. *[1]Biology, Presbyterian College, Clinton, SC,[2]Augusta University, Augusta, GA,[3]University of Lyon, Lyon, France,[4]Georgia Cancer Center, Augusta University, Augusta, GA*

Metastatic potential in basal-like breast cancers typically correspond with increased enrichment of EpCAM-/CD49f- cancer stem cells (CSC). With this premise in mind, it is important to better understand the mechanistic driver of these cell populations and their distinctive potential to interact with the tumor microenvironment (TME) for cancer promotion. Previous work from our lab has compared the 450K DNA methylation profile of EpCAM-/CD49f- poor breast cancer cell lines to that of EpCAM-/CD49f- enriched breast cancer cell lines and found the IL32 promoter to be hypomethylated in EpCAM-/CD49f- enriched cell lines, a result which corresponded basal-like patient samples in TCGA. By identifying IL32 being differentially regulated in CSC-enriched cell lines, we further sought to characterize IL32's role in breast cancer aggressiveness. We first were able to identify several overarching mechanisms altered in siIL32 treated SUM15PT cells by RNAseq differential expression analysis (FDR p-value <0.01). Most notable from our RNAseq results was the significant enrichment of upregulated pathways involved in extracellular matrix (ECM) organization as well as significant enrichment of downregulated pathways involved in cellular and replicative stress responses. Particular examples of transcripts differentially expressed between control and siIL32-treated SUM159PT cells included *COL6A1*, *ITGB3*, and *CD24* that were upregulated as well as *NQO1*, *HMOX1*, and *CXCL2/CXCL3* that were downregulated. Furthermore, IL32 suppression decreased SUM159PT invasion in both an ECM-matrix cell invasion assay and a chick CAM xenograft/angiogenesis model. From our RNAseq results, we then performed a multi-pathway protein phosphorylation array to determine whether any key signaling events were affected by siIL32 knockdown in SUM159PT cells. Based on this approach, we were able observe a significant decrease in phosphorylated JNK and phosphorylated NFKB in siL32-treated cells when compared to control, both of which are well-established events that can coordinate both cell stress responses and cellular invasion. Collectively, our results reflect the notion that differential IL32 expression by promoter hypomethylation in breast CSCs plays a role to mitigating intracellular stress and subsequently allowing for breast cancer cell invasion and metastasis.

#3596

EMG1 is an rRNA-modifying protein that contributes to breast cancer progression

Amr R. Elhamamsy, Heba A. Alsheikh, Rajeev S. Samant, Lalita A. Shevde. *Pathology, O'Neal Comprehensive Cancer Center at UAB, Birmingham, AL*

The ribosome, a multi-subunit RNA-protein complex, is essential for translation in all cells. Variation in ribosome composition and characteristics has been observed between cell types and under different metabolic conditions; this phenomenon is referred to as "ribosome heterogeneity." Ribosome heterogeneity has been linked to carcinogenesis and cancer progression. One of the major layers of ribosome heterogeneity is the diverse rRNA modifications. To study the impact of rRNA modifications on cancer, we performed a systematic literature search and identified 22 rRNA modifying proteins (RRMPs) that are involved in mediating different modifications of rRNA. We next examined the RRMPs' expression levels and frequency of mutation in different cancer types, with

a focus on breast cancer. We see that most malignancies show alterations in RRMPs' expression levels and frequent mutations. Our analysis of gene expression patterns and clinical outcomes in breast cancer has shown that several RRPMs are strongly linked to an aggressive phenotype and a poor prognosis. Our analysis also revealed that EMG1, a N1-specific psuedouridine methyltransferase, is a RRMP with potential roles in cancer progression and metastasis. Our findings pave the way for further research into the role of RRMPs in different cancers as well as the development of therapies that specifically target RRMPs involved in cancer progression.

#3597

SUV420H2-mediated regulation of collective invasion in triple-negative breast cancer

Emily Campbell Whitt[1], Laura M. McLane[2], Paula M. Vertino[2]. *[1]Cell Biology of Disease Graduate Program, University of Rochester Medical Center, Rochester, NY,[2]Department of Biomedical Genetics, University of Rochester Medical Center, Rochester, NY*

Breast cancer is the second most common cancer in women and metastasis is the leading cause of breast cancer-related mortality. While the factors leading to metastasis remain poorly understood, epigenetic changes in the cancer cell are likely strongly associated with the shift from primary tumor to metastasis. There are several breast cancer subtypes, the most aggressive of which is triple-negative breast cancer which is difficult to treat in part because it is prone to metastasis. In the early stages of metastasis, cells from the primary tumor invade the surrounding tissue before breaking away and seeding metastases. In some cases, tumor cells invade as clusters of cells that migrate as a group and maintain their cell-cell contacts through a process known as collective invasion. These clusters of collectively invading cells have been shown to seed circulating tumor cell clusters that are more efficient at forming metastases than single tumor cells. SUV420H2 is a histone methyltransferase that trimethylates histone H4 lysine 20 (H4K20me3), an epigenetic mark associated with transcriptional repression. Triple-negative breast cancer has lower levels of SUV420H2 and H4K20me3 levels than more luminal subtypes. Our lab and others have found that downregulation or inhibition of SUV420H2 promotes increased plasticity in the epithelial-to-mesenchymal transition, a transcriptional program associated with cancer metastasis. Our objective was to use a three-dimensional tumor spheroid system to determine the role of SUV420H2 and H4K20me3 on breast cancer invasion. We found that in immortalized non-tumorigenic breast cells grown as spheroids in an extracellular matrix, knockdown of SUV420H2 promotes invasion. Treatment of triple-negative breast cancer spheroids with an inhibitor of SUV420H2 (A196) also leads to an increase in invasion, as well as a shift in invasive phenotype from one where cells invade as single cells to a one where cells invade as collective chains emanating from the central spheroid. This suggests that reduced levels of SUV420H2 and the associated changes in histone marks and transcriptional programming in triple-negative breast cancer promote a phenotypic shift from single cell to collective invasion and may be one factor contributing to the increased metastatic potential of this subtype. Future studies will focus on characterizing the effects of SUV420H2 loss on gene and protein expression as well as chromatin in invading cells in tumor spheroids.

#3598

Cooperative NF-KappaB and Notch1 signaling promotes a macrophage-mediated metastatic phenotype in breast cancer

Camille L. Duran[1], George S. Karagiannis[2], Xiaoming Chen[1], Ved P. Sharma[3], David Entenberg[1], John S. Condeelis[4], Maja H. Oktay[1]. *[1]Pathology, Albert Einstein College of Medicine, Bronx, NY,[2]Microbiology and Immunology, Albert Einstein College of Medicine, Bronx, NY,[3]Bio-Imaging Resource Center, Rockefeller University, New York, NY,[4]Cell Biology, Albert Einstein College of Medicine, Bronx, NY*

Metastasis is a multistep process that leads to the formation of clinically detectable tumor foci at distant organs and, frequently, to patient demise. Only a subpopulation of breast cancer cells within the primary tumor can disseminate systemically and cause metastasis. To disseminate, cancer cells must express MenaINV, an isoform of the actin-regulatory protein, Mena, encoded by the *ENAH* gene that endows tumor cells with transendothelial migration activity allowing them to enter and exit the blood circulation. We have previously demonstrated that MenaINV mRNA and protein expression is induced in cancer cells by macrophage contact. Here, we report on the discovery of the precise mechanism by which macrophages induce MenaINV expression in tumor cells. We examined the promoter of the human and mouse *ENAH* gene and discovered a conserved NF-κB transcription factor binding site. Using live imaging of an NF-κB activity reporter and staining of fixed tissues from mouse and human breast cancer we further determined that, for maximal induction of MenaINV in cancer cells, NF-κB needs

to cooperate with the Notch1 signaling pathway. Mechanistically, Notch1 signaling does not directly increase MenaINV expression, but instead enhances and sustains NF-κB signaling through retention of p65, an NF-κB transcription factor, in the nucleus of tumor cells, leading to increased MenaINV expression. In mice, these signals are augmented following chemotherapy treatment and abrogated upon macrophage depletion. Targeting Notch1 signaling *in vivo* decreased NF-κB signaling and MenaINV expression in the primary tumor and decreased metastasis. Altogether, these data uncover mechanistic targets for blocking MenaINV induction that should be explored clinically to decrease cancer cell dissemination and improve survival of patients with metastatic disease.

#3599

Molecular characterization of mouse colorectal cancer cell lines with high potential of peritoneal metastasis

Haruki Mori[1], Hisanori Isomura[2], Shuang Zhou[2], Taisuke Kajino[2], Yuichi Abe[2], Takashi Kinoshita[2], Seiji Natsume[2], Yusuke Sato[2], Akira Ouchi[2], Toru Miyake[1], Waki Hosoda[2], Koji Komori[2], Yasuhiro Shimizu[2], Masaji Tani[1], Ayumu Taguchi[2]. *[1]Department of Surgery, Shiga University of Medical Science, Otsu, Japan,[2]Aichi Cancer Center, Nagoya, Japan*

Background: Peritoneal metastasis occurs in approximately 7% of colorectal cancer (CRC) patients and is associated with worse prognosis compared to non-peritoneal metastasis. In CRC patients with peritoneal metastasis, administration of systemic chemotherapy only slightly improves overall survival. Therefore, a better understanding of the biology of peritoneal metastasis and the development of new molecular therapeutics for CRC patients with peritoneal metastasis are urgently needed.
Materials and Methods: CT26 mouse CRC cell lines with low metastatic potentials (CT26-N5) and high metastatic potentials to peritoneum (CT26-P6) were established after several rounds of in vivo selection by orthotopic transplantation of CT26 cells into the syngeneic BALB/c mice. Transcriptomic and proteomic analyses were conducted on CT26-N5 and CT26-P6 cells.
Results: Orthotopic transplantation of CT26-P6 cells exhibited significantly increased peritoneal metastasis compared to CT26-N5 cells, while growth of primary tumors was not different between these CT26 sublines. In addition, CT26-P6 cells had higher cell migration and invasion potential in vitro than CT26-N5 cells. Integrated analyses of transcriptome and proteome resulted in identification of molecular signatures associated with peritoneal metastasis. An actin-binding protein Advillin, encoded by the Avil gene, was markedly increased at both mRNA and protein levels in CT26-P6 cells compared to CT26-N5 cells. Knockdown of Avil using siRNA or shRNA in CT26-P6 cells significantly reduced cell migration and invasion in vitro and occurrence of peritoneal metastasis in vivo. Gene Set Enrichment Analysis on transcriptome datasets from CT26-P6 cells and CT26-N5 cells identified interferon gamma response as the most significantly enriched pathway in CT26-cells. In addition, Immunoprecipitation coupled with LC-MS/MS identified potential interaction between Avil and a molecule X that regulates epithelial-mesenchymal transition in CRC. Consistent with the findings in mouse CT26 cells, AVIL knockdown in CRC patient-derived cells (PDCs) suppressed cell migration and invasion in vitro. While AVIL expression was induced by interferon gamma in CRC PDCs, JAK inhibitors, Momelotinib and Ruxolitinib, significantly reduced interferon gamma-induced AVIL expression, suggesting regulation of AVIL by interferon gamma.
Conclusion: Molecular characterization of mouse colorectal cancer cell lines with different metastatic potential identified AVIL as a potential therapeutic target in CRC patients with peritoneal metastasis. Regulation of AVIL expression by interferon gamma may suggest functional relevance of tumor immune microenvironment in the development of peritoneal metastasis in CRC.

#3600

MET-mediated STING activation regulates EMT and NF-KB pathway in non-small cell lung cancer

Seungchan Mun[1], Bogyeong Han[2], HyunKyung Ahn[1], Jaemoon Koh[2], Sehui Kim[2], DooHyun Chung[2], YoonKyung Jeon[2]. *[1]Seoul National University College of Medicine, Seoul, Korea, Republic of,[2]Pathology, Seoul National University College of Medicine, Seoul, Korea, Republic of*

The cyclic GAMP-AMP synthase (cGAS)-stimulator of interferon genes (STING) pathway is known to have anti-tumor activity by activating the innate immune response against cytosolic double-stranded DNA (dsDNA). The regulating mechanism of STING remains unclear, and a pro-tumorigenic effect of STING pathway was recently reported. In this study, we investigated the expression of STING by MET and a novel role of the STING pathway in non-small cell lung cancer (NSCLC). The Cancer Genome Atlas (TCGA) and Cancer Cell Line Encyclopedia

(CCLE) analysis showed that cGAS/STING pathway is enriched and STING expression is higher in MET-overexpressing tumors. Western blot for NSCLC cells and immunohistochemistry for NSCLC tumor tissues showed positive correlation between MET and STING expression in NSCLC cells. MET-overexpression and a MET agonist (HGF) treatment increased STING expression and CXCL10 and IFNβ expression and secretion, whereas MET-knockdown and a MET inhibitor (capmatinib) treatment decreased STING expression in NSCLC cells. In MET-positive and STING-positive cells, a STING agonist (poly-dAdT and diABZI) treatment led to increased activation of STING signaling pathway. In EBC-1 cells, MET knockdown decreased STING expression and STING-agonist-induced STING-pathway activation and cytokine production. To further investigate the role STING in NSCLC, EBC-1 cells were transfected with STING siRNA and submitted to RNS-seq. Gene set enrichment analysis revealed that several pathways were affected by STING expression. Epithelial-mesenchymal transition (EMT) and TNFα-signaling via NF-κB signaling were significantly downregulated in STING-knockdowned cells. In vitro experiments using EBC-1 cells, STING overexpression increased SLUG and TWIST1 expression and migration of cells, whereas STING knockdown decreased SLUG and TWIST1 expression and migration of cells. In summary, this study demonstrated that MET and STING expression were positively correlated with each other in NSCLC and MET overexpression increased STING expression and subsequent activation upon STING agonist stimulation. In addition, STING contributed to EMT in NSCLC.

#3601

Tumor MK2 signaling regulates cell migration and invasion in head and neck squamous cell carcinoma

Dakota D. D. Okwuone[1], Deri Morgan[1], Hannah M. Smith[1], Grace Millington[1], Kiersten L. Berggren[2], Christopher E. Lominska[1], Sufi M. Thomas[1], Gregory N. Gan[1]. *[1]University of Kansas Medical Center, Kansas City, KS,[2]The University of New Mexico Comprehensive Cancer Center, Albuquerque, NM*

Poor 5-year overall survival in head and neck cancer (HNC) can be attributed to high rates of locoregional and distant metastasis. We have previously demonstrated that high phosphorylation/activation of MAPK-activated protein kinase 2 (MK2), a stress-activated kinase directly downstream of p38 MAPK, in head and neck squamous cell carcinoma (HNSCC) is associated with worse overall survival and inhibition of the MK2 pathway enhances in vivo HNSCC radiosensitivity. Our prior work also demonstrates that radiotherapy-induced epithelial-to-mesenchymal transition (EMT) gene expression can be suppressed in cells when MK2 is inhibited. Several studies have shown that EMT plays a prominent role in HNSCC tumor invasion, treatment resistance, and locoregional metastases to lymph nodes. In this study, we investigate the impact of MK2 activity on HNSCC tumor progression by examining its contribution to cancer cell morphology. We used lentiviral-shRNA and the CRISPR-Cas9 system to knock down/out the MK2 gene in multiple human and murine HNSCC cell lines. We measured tumor cell migration and invasion in both classic 2D in vitro culture as well as with 3D spheroids. We performed unbiased analysis via RNAseq in human HNSCC cell lines comparing MK2 shRNA vs scramble cell lines. Substantial gene and pathway alterations were examined using a combination of immunoblot and RT-qPCR. Our data shows knocking down/out MK2 in HNSCC cells significantly diminishes cell migration and invasion in 2D and 3D in vitro culture assays. RNAseq analysis demonstrated loss of MK2 leads to a significant increase in many cell adhesion molecules, including E-cadherin, and a decrease in N-cadherin, suggesting a shift from mesenchymal to more epithelial phenotype. Furthermore, we note expression of multiple matrix metalloproteinases and EMT markers (i.e., Snail) are substantially reduced in MK2 shRNA and KO cell lines. These results indicate that the MK2 pathway is involved in HNSCC motility and invasion. We also observe the loss of MK2 contributes to a shift in the epithelial:mesenchymal ratio potentially by suppressing cancer EMT plasticity. All in all, this study provides evidence suggesting tumor MK2 activation mediates HNC progression.

#3602

The metastasis-suppressive function of intracellular galectin-3 in melanoma

Norhan B. B. Mohammed, Charles J. Dimitroff. *Translational Medicine, Florida International University, Miami, FL*

Melanoma is a relatively rare skin cancer. However, it accounts for most of all skin cancer-related deaths worldwide. Once melanoma spreads to distant sites, it confers a poor prognosis characterized by resistance to therapy and high mortality rate. Hence, a favorable clinical outcome is strongly correlated with early diagnosis. Despite the ongoing research to identify novel diagnostic, prognostic, and therapeutic targets for metastatic melanoma (MM), a reliable serum marker to predict whether melanoma is vulnerable to metastasize or has already metastasized is still lacking. Galectin-3 (Gal-3), a ß-galactoside-binding protein, is widely expressed by many

human epithelial and immune cells. High extracellular Gal-3 expression levels have been reported to be positively correlated with late-stage disease in melanoma patients, where it is theorized to bind surface glycosylated proteins to promote melanoma cell invasion and metastasis. Gal-3 is also expressed intracellularly where it participates in the regulation of many biological processes. However, intrinsic Gal-3 levels within the melanoma cell and its relationship to melanoma progression is still poorly understood. Using The Cancer Genome Atlas (TCGA) database, we analyzed the Gal-3 expression profiles of 471 tumor samples obtained from melanoma patients. To our surprise, TCGA data analysis has shown significantly higher expression of Gal-3 in primary melanoma samples compared to metastatic melanoma. We hypothesize that intracellular Gal-3 potentially negatively regulates primary melanoma progression to metastatic disease. Using several human melanoma cell lines silenced for Gal-3 expression, we investigated the corresponding malignancy-associated activities of these cells. Our results revealed that Gal-3 silencing in melanoma cells potentiated melanoma migration, invasion, and colony formation, compared with mock controls, suggesting that intracellular Gal-3 could interfere with melanoma metastatic activity. Moreover, loss of Gal-3 boosted the activation of the PI3K/AKT and MAPK signaling pathways and upregulated nuclear factor of activated T cells (NFAT1) expression and its pro-metastatic downstream target genes. Importantly, this study illuminates the apparent opposing roles of Gal-3 in melanoma progression, with intracellular Gal-3 potentially serving as a metastasis-suppressive molecule. Moreover, these studies reveal the potential of analyzing melanoma cell-intrinsic levels of Gal-3 to better predict metastatic potential and clinical outcome in melanoma patients.

#3604

Epithelial Caveolin-1 regulates lung metastasis in advanced stages of breast cancer

Dhirendra Pratap Singh[1], Rashmi Pathak[2], Abhishek Pandit[3], Philip J. Ebenezer[4], Nithya Jambunathan[1], Sanjay Kumar[5], Alexander Du Plooy[4], Joseph Francis[3], Mary E. White[6]. *[1]Cardiovascular Medicine, Indiana University Health Methodist Hospital, Indianapolis, IN,[2]Biological Sciences, Pennington Biomedical Research Center, Louisiana State University, Baton Rouge, LA,[3]Comparative Biomedical Science, Louisiana State University, Baton Rouge, LA,[4]Louisiana State University, Baton Rouge, LA,[5]Biological Sciences, Louisiana State University, Baton Rouge, LA,[6]Department of Pathology and Population Medicine, Midwestern University, Baton Rouge, AZ*

Organotypic metastasis is a well-orchestrated sequence of events that takes place in tumors. The interplay between secretory factors from the primary tumor and the microenvironment of a distant organ determines the fate of metastasis. A significant concern in effective triple-negative breast cancer (TNBC) treatment is lung metastasis. Caveolin-1 (Cav-1), a lipid raft protein, is an important component of the metastatic interplay and is reported to be upregulated in the advanced metastatic stage of breast cancer. Although Cav-1 has been shown to have oncogenic potential, its role in TNBC lung metastasis is not fully understood. Our data illustrates, knocking out Cav-1 in the 4T1 cells (a mouse breast cancer cell line) affects cell morphology, extracellular vesicle formation, and MMP release in vitro. Furthermore, a wound healing/ cell migration assay showed reduced migration in Cav-1 KO 4T1 cells when compared to control 4T1 cells, and these findings were validated using Cav-1 siRNA. For investigating the metastatic role, we injected Cav-1 KO 4T1 and control 4T1 cells into the mammary fat pad of female BALB/c mice, a syngeneic mouse model of triple-negative breast cancer. We found no evidence of lung metastasis in Cav-1 KO 4T1 injected mice when compared to control 4T1 injected mice. This was further supported by mRNA profiling of the tumor. We observed 21 epithelial cell migration genes that are differentially expressed in Cav-1 KO tumors when compared to WT tumors. Correlation analysis from Breast Cancer Gene-Expression Miner v4.8 (bc-GenExMiner), a human database, showed a significant correlation between Cav-1 expression and several of the 21 epithelial cell migration genes, along with integrin 3 alpha (ITGα3). Interestingly, in silico protein docking predicted an interaction between Cav-1 and ITGα3, which was later confirmed by co-immunoprecipitation. The role of ITGα3 in metastasis was further corroborated by cell migration assay, which was affected when siRNA was used to silence ITGα3 gene expression. Collectively, these findings provide evidence that Cav-1 KO, along with ITGa3, plays an important role in distant lung metastasis in the 4T1 tumor-induced mice model.

#3605

Peroxiredoxin IV promotes prostate cancer malignancy through the activation of NF-kB signaling

Na Ding, Hong Jiang, Pratik Thapa, Yanning Hao, Aziza Alshahrani, Vivek Rangnekar, Xiaoqi Liu, Qiou Wei. *University of Kentucky, Lexington, KY*

Background: The peroxiredoxin (Prx) family of proteins functions as major cellular antioxidants to maintain redox homeostasis as well as mediate oxidative signaling in both physiological and pathological conditions. Our previous studies show that Prx4 is highly expressed in prostate cancer and promotes tumor growth *in vitro* and *in vivo*. But how Prx4 contributes to prostate cancer cell invasion and metastasis remains to be elucidated. The purpose of this study is to understand the oncogenic signaling pathways that are mediated by Prx4 in prostate cancer cells. Methods: Bioinformatic analysis of existing database were used to examine the expression of Prx4 in primary and metastatic prostate cancer samples. CRISPR/Cas9 technique was used to establish Prx4 knockout in cultured human prostate cancer cell lines. Matrigel invasion assays were performed to evaluate cell migration and invasion. RNAseq was performed to examine the differences of gene expression between control and Prx4KO cells. Gene Set Enrichment Analysis (GSEA) and Gene Oncology (GO) enrichment analysis were performed using RNAseq results. RT-PCR and immunoblotting were used to validate findings from RNAseq and enrichment analysis. Results: Compared with normal prostate, transcript levels of *PRDX4* are found to be upregulated in specimens of patients with prostate cancer, and those with bone metastasis show even higher levels. Knockout of Prx4 in cultured human prostate cancer cells leads to significantly reduced ability of cell migration and invasion. Gene expression profiling reveals that loss of Prx4 leads to the upregulation of epithelial as well as downregulation of mesenchymal markers, and multiple signaling pathway changes including the inhibition of cellular response to inflammatory factors such as tumor necrosis factors and interleukins. These changes are also associated with variety of cellular activities such as wound healing, interferon signaling, and antigen processing & presentation. Among known target genes downstream of NF-κB signaling, E-cadherin, vimentin and matrix metalloproteinase 14 (MMP14) were found to be significantly affected by the loss of Prx4. Therefore, Prx4 plays a critical role in human prostate cancer cell malignancy through regulation of intracellular cell signaling pathways. Conclusions: A combination of bioinformatic, cellular and molecular methods reveals that Prx4 plays a critical role in promoting prostate cancer metastasis. Prx4 is a potential therapeutic target to reduce prostate cancer metastasis.

#3606

HDAC8-mediated inhibition of EP300 drives a neural crest-like transcriptional state that increases melanoma brain metastasis

Michael Emmons[1], Richard Bennett[2], alberto riva[2], Chao Zhang[1], Robert Macaulay[1], Daphne Dupéré-Richér[2], Bin Fang[1], John Koomen[1], Jiannong Li[1], Ann Chen[1], Edward Seto[3], Jonathan Licht[2], Keiran Smalley[1]. *[1]Moffitt Cancer Center, Tampa, FL,[2]University of Florida, Gainesville, FL,[3]George Washington University, Washington DC, DC*

Melanomas are heterogeneous and adopt multiple transcriptional states that can confer an invasive phenotype and resistance to therapy. Little is known about the epigenetic drivers of these cell states, limiting our ability to regulate melanoma heterogeneity and tumor progression. Here we identify stress-induced HDAC8 activity as the driver of a neural crest stem cell (NCSC)-like transcriptional state that increased the formation of melanoma brain metastases (MBM). Exposure of melanocytes and melanoma cells to multiple different stresses led to HDAC8 activation, a switch to a NCSC gene expression signature and the adoption of an amoeboid, invasive phenotype. This cell state enhanced the survival of melanoma cells under shear stress conditions and increased the formation of metastases in the brain. Single cell RNA-seq analyses showed that HDAC8 expression was correlated with the NCSC cell state in clinical MBM specimens. ATAC-Seq and ChIP-Seq analysis showed HDAC8 to alter chromatin structure by increasing H3K27ac and accessibility at c-Jun binding sites without changing global histone acetylation. The increased accessibility of Jun binding sites was paralleled by decreased H3K27ac and accessibility at MITF binding sites and loss of melanoma-lineage gene expression. Mass spectrometry-based acetylomics demonstrated that HDAC8 deacetylated the histone acetyltransferase (HAT) EP300 leading to its enzymatic inactivation. This, in turn, led to an increased binding of EP300 to Jun-transcriptional sites and decreased binding to MITF-transcriptional sites. Increased expression of EP300 decreased invasion and increased the sensitivity of melanoma cells to multiple stresses while inhibition of EP300 function increased invasion and resistance to stress. We identified HDAC8 as a novel mediator of transcriptional co-factor inactivation and chromatin accessibility that increases MBM development.

#3607

RNA-binding proteins are essential for EGF-induced fibronectin expression and metastasis of head and neck squamous cell carcinoma

Ting-Wei Chang[1], Wen-Chang Chang[2], Ben-Kuen Chen[3]. *[1]Institute of Basic Medical Sciences, College of Medicine, National Cheng Kung University, Tainan, Taiwan,[2]Graduate Institute of Medical Sciences, College of Medicine, Taipei Medical University, Taipei, Taiwan,[3]Department of Pharmacology, College of Medicine, National Cheng Kung University, Tainan, Taiwan*

There is a higher expression level of epidermal growth factor receptor (EGFR) in up to 90% of advanced head and neck squamous cell carcinoma (HNSCC) tissue than in normal surrounding tissues. However, the precise mechanism involved in modulating EGF-associated metastasis in HNSCC remains unclear. In this study, we reveal that the concurrent expression of EGFR and fibronectin (FN1) was highly associated with the stages of HNSCC progression. EGF-induced fibronectin/integrin axis enhanced tumor-endothelial cell interaction and increased endothelial permeability, conferred HNSCC cell metastasis. Mechanistically, we found that ERK and NF-κB pathway activation was essential for EGF-induced fibronectin expression. In addition, EGF-enhanced mRNA stability of fibronectin occurred through the 5' untranslated region (5'-UTR) of the gene and was mediated by nucleolin (NCL) and hnRNPA2/B1, which were also involved in the regulation of epithelial-mesenchymal transition gene expression. Intriguingly, the *in vivo* study showed that depletion of NCL, hnRNPA2/B1, and inhibition of the fibronectin/integrin axis significantly inhibited EGF-promoted HNSCC metastasis in the lung. Our data suggests that the nucleolin/ hnRNPA2/B1-regulated fibronectin is essential for EGF-induced tumor-endothelial cell interactions to enhance HNSCC cell metastasis.

#3608

MLL1 regulates cytokine-driven cell migration and metastasis

Praful R. Nair[1], Ludmila Danilova[2], Estibaliz Gómez-de-Mariscal[3], Dongjoo Kim[4], Rong Fan[4], Arrate Muñoz-Barrutia[3], Elana Fertig[2], Denis Wirtz[1]. *[1]Johns Hopkins University, Baltimore, MD,[2]Johns Hopkins School of Medicine, Baltimore, MD,[3]Universidad Carlos III de Madrid, Madrid, Spain,[4]Yale University, New Haven, CT*

Cell migration, particularly in three-dimensional (3D) environments, is a critical requirement for metastasis - the spread of cancer cells from a primary tumor to distant sites. Despite causing the vast majority of cancer-related deaths, targeting metastasis remains challenging clinically. Cancer cell migration can be triggered and maintained by elevated levels of cytokines, which are presumed to be predominantly secreted by immune cells in the tumor microenvironment. However, recent work has highlighted the importance and impact of cytokine production by cancer cells themselves. While the signaling cascades that regulate cell migration have been studied extensively, the epigenetic regulation of cell migration is still poorly understood. MLL1 is a histone methyltransferase, which along with its scaffold protein Menin, is integral to methylation at the histone 3 lysine 4 (H3K4) site. Here, we show that the MLL1-Menin interaction is essential for the migration of cancer cells and that the disruption of this interaction impairs cell migration and metastasis. MLL1 depletion reduces 3D cell migration *in vitro* and led to lesser metastatic burden and prolonged survival *in vivo*. Reduced lung metastatic burden was observed even after accounting for the difference in the growth rate of primary tumors. Mechanistically, MLL1-Menin interaction controls actin filament assembly via the IL-6/pSTAT3/Arp3 axis and acto-myosin contractility via the TGF-β1/Gli2/ROCK1/2/pMLC2 axis, which together regulate dynamic protrusion generation and 3D cell migration. MLL1-Menin inhibition also decreases cell proliferation by inhibiting mitosis and cell cycle-related pathways. MLL1 depletion decreases primary tumor growth, metastatic spread, and metastatic outgrowth in mouse models of triple-negative breast cancer (TNBC), thus improving survival. When comparing metastatic burden at a threshold tumor size, rather than at a timepoint, MLL1 depletion still lowered metastatic burden. Combining an MLL1-Menin inhibitor with Paclitaxel, a standard TNBC chemotherapeutic, abrogated tumor growth and metastasis in a syngeneic TNBC mouse model. Overall, our studies show that MLL1 is an epigenetic regulator of 3D cancer cell migration, which exerts its effects by controlling the production of the key cytokines IL-6 and TGF-β1. Our *in vivo* studies demonstrate the potential of targeting the MLL1-Menin interaction in metastasis prevention and its potential to be combined with currently administered chemotherapeutics.

#3609

Interaction of interleukin-6/8/18 with prostate cancer cell secreted growth factors are crucial for osteoblast proliferation and differentiation

Aaron Jeshua Todman, Wishrawana S. Ratnayake, Luke Lajmi, Sloan Breedy, Kirpal Bisht, Mildred Acevedo-Duncan. *University of South Florida, Tampa, FL*

There is currently no effective therapy for bone metastatic prostate cancer, which is the main cause of mortality in people with prostate cancer. Poor prognosis of bone metastasis has limitations in current therapeutics mainly due to the complexity of microenvironment. Our focus was on the interactions between prostate cancer cells and the bone microenvironment, including osteoclasts and osteoblasts in regard to growth factors and cytokines, as the bone microenvironment plays a significant role in this process. The present study shows the downstream effects of Stavudine (KB-S); a known antiviral compound along with 5-fluoro-1-((1R,4R)-4-((tetrahydro-2H-pyran-2-yl)oxy)cyclopent-2-en-1-yl)pyrimidine-2,4(1H,3H)-dione (KB-G) and 1-((1R,4R)-4-hydroxycyclopent-2-en-1-yl)-5-methylpyrimidine-2,4(1H,3H)-dione (KB-H) on bone metastatic prostate cancer. Effects of KB-G/H and S on HEK-293 control cells were determined as moderate under tested conditions. A series of KB-G/H and S (10, 25, 50, 75 and 100 μM) was given for a 4-day period (with 24 h intervals) and the prostate cancer cell population was determined at the end of the 4-day treatment period. Preliminary results indicated that all 3 compounds significantly decreased DU-145 and PC-3 cell population compared to the effects on HEK-293 cells. Results suggested that all 3 compounds can decrease the prostate cancer cell progression by enhancing apoptosis. Our data also suggested that all 3 compounds downregulated interleukin (IL)-18, IL-8, IL-6 and C-X-C motif ligand-1(CXCL-1) in prostate cancer cells (PC-3 and DU-145). A human osteoblast cell line (hFOB 1.19) is being used to study the effect of cytokines in relation to transforming growth factor β (TGFβ), insulin-like growth factor (IGF) and platelet-derived growth factor (PDGF) that are secreted by prostate cancer cells. *In-vitro* migration/ invasion assays, immunoprecipitation (IP), immunofluorescence microscope, cytokine profile array, real time qPCR and Western blot techniques are being used in this study to further analyze role of cytokines and growth factors on osteoblast differentiation. Our

preliminary results suggest that all 3 compounds can be used to disrupt the main steps of prostate cancer bone metastasis. Results suggested that KB-G/H and S can be targeted to develop customized, tailored therapies for bone metastatic prostate cancer which merit further research.

#3610

Prenylated PALM2 promotes the migration of esophageal squamous cancer cells through activating ezrin

Danxia Deng, Chengyu Li, Zhenyuan Zheng, Bing Wen, Liandi Liao, Enmin Li, Liyan Xu. *Shantou University Medical College, Shantou, China*

Proteins containing a CAAX motif at the C-terminus can occur prenylation modification and regulate the localization and activity of a series of key regulatory proteins, including RAS superfamily members, heterotrimeric G proteins, nuclear lamina protein, and several protein kinases and phosphatases. However, studies of prenylated proteins in esophageal cancer are limited. Here, we found that paralemmin-2 (PALM2), a potential prenylated protein, was up-regulated and associated with a poor prognosis of patients, through research on large-scale proteomic data of esophageal cancer in our laboratory. The low throughput verification also showed that the expression of PALM2 in esophageal cancer tissues was higher than that in their paired normal esophageal epithelial tissues, and it was generally expressed in the membrane and cytoplasm of esophageal squamous cancer cells (ESCC). PALM2 interacted with the two subunits of farnesyl transferase (FTase), FNTA and FNTB. The FTase inhibitor weakened the membranous location of PALM2 and mutation in the CAAX motif of PALM2 ($PALM2^{C408S}$) impaired its membranous localization, indicating PALM was prenylated by FTase. Overexpressed PALM2 promoted the migration of cancer cells, whereas $PALM2^{C408S}$ lost this ability. Mechanistically, PALM2 interacted with the N-terminal FERM domain of ezrin of Ezrin/Radixin/Moesin (ERM) family dependent on its prenylation. The mutagenesis indicated that lysine residues K253/K254/K262/K263 in ezrin's FERM domain and cysteine residue C408 in PALM2's CAAX motif were important for their interaction and ezrin activation. The knockout of ezrin prevented enhanced cancer cell migration by PALM2 overexpression. PALM2, depending on its prenylation, made ezrin get more membranous

distribution and increased the phosphorylation of ezrin Y146 site. In summary, prenylated PALM2 promoted the migration of cancer cells through activating ezrin. (This work was supported by the National Natural Science Foundation of China (82173034, 81172264), and Innovative Team Grant of Guangdong Department of Education (2021KCXTD005)).

#3611

PAUF induces migration of human pancreatic cancer cells exclusively via the TLR4/MyD88/NF-κB signaling pathway

Fen Jiang[1], So Eun Youn[1], Da Eun Hong[1], Tae Heung Kang[1], Hye Yun Won[1], Yun Yong Park[1], Sang Seok Koh[2]. *[1]Innovative Discovery Center, Prestige Biopharma Korea, Busan, Korea, Republic of,[2]Department of Biomedical Sciences, Dong-A University, Busan, Korea, Republic of*

Background**:** Pancreatic adenocarcinoma up-regulated factor (PAUF) is a cancer-secreted protein which is overexpressed on pancreatic cancer (PC) cells and promotes tumor growth in an autocrine way. However, the receptor of PAUF on PC cells has yet to be identified. Meanwhile, it is known that PAUF, as a tumor microenvironment (TME) modulator, plays a role in immune evasion and suppression through toll-like receptors notably TLR4 which are mainly expressed on immune cells. Previous studies show that TLR4 is also highly expressed in PC tumor tissues, compared to normal tissues, and activation of TLR4 signaling pathway induces the migration and invasion of PC cells.

Objective: This study aimed to investigate if TLR4 expressed on cancer cells can act as a receptor for PAUF to mediate its tumor promoting effects.

Methods and Results: We tested the TLR4 expression in six PC cell lines and one normal pancreatic cell line. And confirmed that TLR4 is expressed in all PC cell lines at variable levels, but not in the normal pancreatic cell line.Next, we found that a chemical TLR4-specific inhibitor TAK-242 significantly reduced the migration of PC cells with high TLR4 expression (BxPC-3), but it did not impact the migration of PC cells with low TLR4 expression (Panc-1). This experiment suggests that some endogenous ligands of TLR4 may have mediated PC cell migration.Using TLR4 overexpressed and knockout PC cell lines, we showed that treatment with recombinant PAUF increased the migration and invasion of TLR4 overexpressed PC cells, but not in the TLR4 knockout cells. Likewise,

treatment of anti-PAUF antibody reduced the migration and invasion of TLR4 overexpressed PC cells, but not in the TLR4 knockout cells. These results shows that PAUF's migration and invasion promoting effects of PC cells is TLR4 dependent.To further understand the molecular mechanism of PAUF-induced metastasis (migration/invasion)-promoting effects via TLR4, we conducted a series of in vitro studies including immunoprecipitation (IP), western blot analysis, flow cytometry, and luciferase reporter assay. We demonstrated that PAUF activates TLR4/MyD88 signaling pathway, but not TLR4/TRIF pathway.
Conclusions: In conclusion, for the first time this study demonstrates that TLR4 expressed on PC cell surfaces functions as a receptor of PAUF to mediate its metastasis-promoting effects, which are exclusively through the MyD88/NF-κB signaling pathway. This study also suggests TLR4 as a potential biomarker for identification of optimal patients, and a new therapeutic target to treat PC. Anti-PAUF antibody used in this study is currently evaluated by clinical trials in France, Spain, and US FDA.

#3612
KAT8/SIRT7-medicated fascin-K41 acetylation/deacetylation regulates tumor metastasis
Da-Jia Li[1], Yin-Wei Cheng[2], Li-Yan Xu[2], En-Min Li[1]. *[1]Department of Biochemistry and Molecular Biology, The Key Laboratory of Molecular Biology for High Cancer Incidence Coastal Chaoshan Area, Shantou, China,[2]Guangdong Provincial Key Laboratory of Infectious Diseases and Molecular Immunopathology, Institute of Oncologic Pathology, Cancer Research Center, Shantou University Medical College, Shantou, China*

Background: Although it is not expressed in the normal differentiated epithelial tissue of adult animals, fascin is highly expressed in a variety of cancers, including esophageal cancer, working as an important oncogenic protein. fascin promotes migration and invasion of cancer cells by binding F-actin to promote the formation of filopodia and invadopodia. However, it is not clear how exactly the function of fascin is systematically regulated in cancer cells. There are three regions on the surface of fascin protein that are significantly rich in positively charged lysine and arginine. These regions are now thought to be potential F-actin binding sites. We hypothesize that cancer cells may regulate the function of fascin by post-translational

modifications of key amino acids in these three regions, especially by acetylation. Based on this, this study aims to identify acetyltransferases that regulate the acetylation of fascin in esophageal cancer cells and reveal the effect of acetylation on the function of fascin.
Results: 1) Co-IP, pull-down, and immunofluorescence results showed that KAT8 interact with fascin and co-localize in esophageal cancer cells. 2) Mass spectrometry identification of the products of acetylation in vitro revealed that KAT8 acetylates fascin at K41 and K241. By means of Ack41-fascin specific antibodies, further analysis proved that KAT8 acetylated fascin K41. 3) Co-IP and immunofluorescence results showed that SIRT7 interact with fascin and co-localize in esophageal cancer cells, moreover, treatment of cells with SIRT7-specific inhibitor significantly increased the level of AcK41-fascin, and however, overexpressing SIRT7 reduces the level of AcK41-fascin. 4) Immunohistochemical results showed that the level of AcK41-fascin was lower in esophageal cancer tissues of patients with lymph node metastasis; Analysis of overall survival and tumor-free survival curves showed that patients with high levels of AcK41-fascin had a better prognosis. 5) Cell wound healing and transwell assay showed that fascin K41 residue mimics acetylation inhibit the movement and invasion of esophageal cancer cells. 6) Furthermore, in vitro F-actin binding assays showed that mutations mimicing acetylation of K41 inhibited the activity of fascin bunding F-actin. 7) Immunofluorescence assay showed that fascin K41 residue mimics acetylation inhibited fascin's ability to promote filopodia and invadopodia formation in esophageal cancer cells.
Conclusions: 1) KAT8 is an acetyltransferase that catalyzes fascin K41 acetylation in esophageal cancer cells, while SIRT7 decides to catalyze AcK41-fascin deacetylation. 2) SIRT7-mediated deacetylation of AcK41-fascin promotes the formation of filopodia and invadopodia, which promotes the invasion and metastasis of esophageal cancer cells. (This work was supported by grants from the National Natural Science Foundation of China (No.81872372 and 81902469))

#3613
Effect of thrombomodulin and plasminogen interaction on melanoma spheroid invasion

Thi Kim Ngan Ngo, Hua-Lin Wu, Cheng-Hsiang Kuo, Ting-Yuan Tu.
National Cheng Kung University, Tainan, Taiwan

Background: Thrombomodulin (TM), a transmembrane glycoprotein that acts as a plasminogen (Plg) receptor, has been found as a potential molecular and prognostic marker that impacts the spread of various cancers, including malignant melanoma. A previous study showed that TM plays a vital function in angiogenesis activity [1] but its role in the malignant melanoma invasion is unclear. Here, we investigate the role of TM-Plg by using melanoma spheroid (MS) embedded in an extracellular matrix (ECM) modeled to understand how TM-Plg affects the progression of MS invasion.
Methods: In this work, A2058 (A2058-GFP and A2058-TMGFP) and MeWo (siC and siTM) MS with different TM expressions were formed, harvested, and embedded in type I collagen gel for invasion assay. TM and Plg expression were determined by western blot. The surface of A2058 MS was observed by SEM imaging. Human Plg, MMPs, and Plg inhibitors, tranexamic acid (TXA) and epsilon-aminocaproic acid (ε-ACA), were utilized to investigate the effect of TM on the plasmin system. Immunofluorescence of TM and F-actin were validated.
Results: When the two cell lines expressed with TM, the formed MS invaded to the surrounding matrix more distinctively than that of the TM-silencing ones, with a 2.5-fold difference in the ratio invasive area change. Upon placing the two A2058-TMGFP MS in the vicinity of each other within the ECM, they showed a strong interaction with an observed distance between the two MS from 50 μm to 280 μm. Immunofluorescence of TMGFP assessed the role of TM in MS invasion and interaction in ECM. Microvilli structures were found on the surface of A2058-TMGFP cells that may help the cell have more cellular processes such as adhesion, signal transduction, and metabolic activities. Furthermore, TXA, ε-ACA, and MMP inhibitors inhibited the invasion of A2058-TMGFP MSs in a dose-dependent manner. Human Plg stimulated invasion in TM-expressing MSs while no effect on non-TM MSs. The results suggested that the human Plg only significantly increased the MS invasion with the presence of TM.
Conclusion: We concluded that with the presence of TM, the MS invasion and interaction become stronger than MS without TM expression. Moreover, TM enhances MS invasion in the 3D model via interacting Plg. This study provides evidence for the development of TM antagonists in the

future to analyze the drug's potential as an anti-metastasis treatment.[1] P. K. Chen *et al.*, “Thrombomodulin functions as a plasminogen receptor to modulate angiogenesis,” *FASEB J.*, vol. 27, no. 11, pp. 4520-4531, 2013, doi: 10.1096/fj.13-227561.

#3614

3D model to study migration and invasion of lung cancer

Melina Hardt, Kurt Zatloukal, Helmut H. Popper. *Medical University of Graz, Graz, Austria*

Background: In 2D cell cultures, migration of tumor cells is characterized by epithelial-to-mesenchymal transition (EMT), whereby tumor cells loose epithelial and express mesenchymal markers and very often change into a spindle cell phenotype. In contrast to 2D cultures, in 3D cultures tumor cells do not lose their differentiation. Small cell lung cancer usually moves as single cells or in small clusters, squamous cell and adenocarcinomas preferentially move in large clusters of cells. In tissue specimen, all of these carcinomas migrate in a hybrid EMT, not loosing their cytokeratin and E-cadherin expression. In AC and SCC also polarity and specification do occur, as some tumor cells act as leaders, providing orientation for the followers. However, 3D culture system might better depict real migration and come closer to the *in vivo* system as 2D cell culture systems.
Material and Method: A 3D bioprinter (TissueLabs^{R}) was used to spot an alveolar-mimicking lung-specific matrix on cell culture wells. Microscopic channels out of pluronics^{R} are created within the matrix. Pluronics is removed by cooling, leaving empty channels within the protein matrix. These channels can be filled with different interleukins, such as IL23, which will direct migration of the tumor cells. Cultured cell lines from an adenocarcinoma (A549) and small cell carcinoma (NCI-H82) are layered on top of the matrix and migration into the matrix is studied using different time points.
Results and Discussion: A matrix simulating an alveolar structure was created with Matrigel^{R}. The A549 cells were seeded on the matrix and grown for 2,5, 10, and 14 days. The cells formed cell clusters on the matrix and after one week started to invade the matrix in cell complexes. By immunohistochemistry we could show, that the A549 cells retained their epithelial differentiation. The H82 cells showed a different behavior. They

did not form large clusters, but started to invade in small groups. The use of the bioprinter enabled us not only to create a 3D tumor culture system to simulate the *in vivo* conditions but also to create matrix structures for studying invasion and migration and to stimulate carcinoma cells with migration-activating substances.

#3615

Targeting tumor-brain crosstalk in invasive brain metastases

Caitlyn Mourcos[1], Sarah M. Maritan[1], Matthew G. Annis[2], Georgia Kruck[2], Alexander Nowakowski[2], Anna-Maria Lazaratos[2], Kevin Petrecca[3], Peter Siegel[2]. *[1]Division of Experimental Medicine, Goodman Cancer Institute, McGill University, Montreal, QC, Canada,[2]Faculty of Medicine and Health Sciences, Goodman Cancer Institute, McGill University, Montreal, QC, Canada,[3]Department of Neurology and Neurosurgery, McGill University, Montreal Neurological Institute and Hospital, Montreal, QC, Canada*

Background**:** An estimated 20-40% of cancer patients develop brain metastases (BrM), mostly those affected by lung cancer, breast cancer or melanoma. Unfortunately, these patients suffer from poor outcomes and diminished quality of life. Few BrM treatment options beyond local therapy exist and this is often a short-term solution as 60% of resected BrM recur within 1 year. Our group discovered that patient prognosis is linked to BrM invasiveness, with highly invasive (HI) BrM more likely to recur, compared to minimally invasive (MI) BrM. This has presented us the opportunity to investigate exploitable biological mechanisms driving HI BrM. For instance, invasive signaling can be driven by microenvironmental proteins such as growth and immunological factors (cytokines) secreted by surrounding brain or cancer cells, through inter-cellular or self-feeding autocrine loops.

Hypothesis: Considering the influence of secreted factors on cancer invasion and the brain microenvironment, I hypothesize that secretory profiling of BrM and brain parenchymal cells will be mechanistically insightful and help identify potential targetable drivers of BrM invasion.

Results: To identify BrM invasion-related tumor- and brain-derived factors, I performed human- and mouse-specific high throughput Enzyme-Linked Immunosorbent Assay (ELISA)-based screens on conditioned media from mouse brain slices harboring intracranial MI or HI BrM patient-derived

xenografts (PDX). This secretome screen reveals distinct MI and HI secretory profiles for melanoma, breast cancer and lung cancer BrMs and several HI BrM-derived factors of interest have been identified. Such factors are important to investigate as possible drivers of invasiveness in BrM through functional studies.
Conclusion: BrM patients currently face a bleak prognosis, with few treatment options and a median survival of only 8-16 months. Considering the clinical availability of targeted therapies including inhibitors for growth factor-binding tyrosine kinases, antibody-drug conjugates, and immunotherapy, this project will help elucidate the cancer-brain crosstalk which may be exploited therapeutically with existing drugs in patients with frequently recurring HI BrM. ADDIN

#3616
Investigating proto-oncogene PBF-induced cell migration and invasion
Merve Kocbiyik, Selvambigai Manivannan, Ling Zha, Katie Brookes, Martin L Read, Chris J McCabe, Vicki E Smith. *University of Birmingham (UK), Birmingham, United Kingdom*

The proto-oncogene pituitary tumor transforming gene binding factor (PTTG1IP/PBF) is overexpressed in multiple tumors and associated with tumor progression. PBF mediates several tumorigenic processes, including cell motility, whereby it potently induces cancer cell migration and invasion. PBF is phosphorylated by Src kinase at Y174 and mutation of this residue (Y174A) renders PBF unable to induce cell invasion, suggesting that phosphorylation mediates the stimulation of cancer cell motility by PBF. This study aimed to further elucidate the mechanism of PBF-induced cell motility. PBF-Y174 is also the key residue in a YXXΦ endocytosis motif. Both PBF phosphorylation and endocytosis were found to be essential for PBF-induced cell motility as mutants which disrupted either process were unable to stimulate thyroid and breast cancer cell migration and invasion. To elucidate molecular events downstream of PBF overexpression, phosphoproteomic and RNA-Seq analyses of normal thyroid cells (Nthy-ori 3-1) with stable PBF overexpression were performed and showed an enrichment in molecules involved in cell adhesion and cytoskeleton organisation. These findings prompted further investigation into a physiological role for PBF in cell motility. We utilised a novel Pbf

knockout ($Pbf^{-/-}$) mouse model generated through CRISPR/Cas9-mediated deletion of Pbf exon 4 in C57BL/6N mice to determine the impact of Pbf deletion on cellular mechanisms. Mouse embryonic fibroblasts (MEFs) were isolated at embryonic day 13.5 and used as primary cultures. $Pbf^{-/-}$ MEFs showed a significant reduction in migration and invasion compared with wild-type ($Pbf^{+/+}$) MEFs. Interestingly, the loss of one functional copy of Pbf in heterozygote MEFs ($Pbf^{+/-}$) resulted in an intermediate decrease in motility suggesting a gene-dosage effect. Initial immunofluorescent studies of $Pbf^{-/-}$ MEFs suggest alterations in focal adhesions (FAs). In $Pbf^{+/+}$ MEFs focal adhesion kinase (FAK) and paxillin staining highlighted FA structures that were normally elongated and aligned with actin stress fibers. In contrast, $Pbf^{-/-}$ MEFs demonstrated a significant reduction in FAK and paxillin staining with smaller, punctate and more radially distributed FAs. These studies demonstrate a physiological role for PBF in cell adhesion and migration and further elucidate the mechanism by which PBF induces cell motility in tumor progression.

#3617

Investigating a role for PIKfyve in cell migration and invasion of clear cell renal cell carcinoma

Jolène Cormier, Sandra Turcotte. *Chemistry and Biochemistry, Université de Moncton, Moncton, NB, Canada*

Introduction. Clear cell renal cell carcinoma (ccRCC) is the most frequent type of kidney cancer. These highly vascularized tumors are characterized by mutations that inactivate the von Hippel-Lindau (VHL) tumor suppressor gene. About 30 % of patients present metastasis at diagnosis and 30-40% of patients with localized tumors relapse after surgery. Unfortunately, metastatic ccRCC remains incurable and are resistant to standard therapies. Our studies demonstrated that ccRCC with a loss of VHL can be targeted using a small molecule named STF-62247. This molecule blocks the autophagic flux causing enlargement of endolysosomes leading to cell death. More recently, we identified the lipid kinase PIKfyve as a target of STF-62247. A central complex assuring the functionality of the lysosome is formed by the lipid kinase PIKfyve, the scaffold protein ArPIKfyve (Vac14), and the phosphatase **S**ac3 (Fig4). Interestingly,

PIKfyve has shown to play a role in cell migration but the mechanisms are not well understood.
Objectives. Our project aims to i) assess a role for PIKfyve in ccRCC migration/invasion, ii) evaluate the potential of PIKfyve inhibitors on angiogenesis, and iii) assess the effect of PIKfyve inhibitors or genetic knockdown of PIKfyve, Vac14 or Fig4 on tumor growth *in vivo*.
Methods and Results. PIKfyve, Vac14 and Fig4 gene expression were modified using CRISPR/Cas9 (Cr) or the SMARTvector^{TM} Inducible Lentiviral shRNA system. qRT-PCR and western blot validated our models. Results obtained in Cr.PIKfyve and Cr.Vac14 indicated that loss of Vac14 decreased survival of VHL-deficient ccRCC. Moreover, our recent results show that migration measured by wound healing assay is reduced in CRISPR cells compared to control. To investigate a role for PIKfyve in angiogenesis, tube formation assay was performed in treated cells with PIKfyve inhibitors. Our results indicated a reduction in tube formation in STF-62247 and apilimod treated cells. Furthermore, we will use the proteome profiler human angiogenesis array to identify angiogenic proteins linked to PIKfyve activity.
Conclusion. Understanding how PIKfyve is involved in the process of angiogenesis would play a major role in the knowledge for new targeted therapies inkidney cancer.

#3618
The role of endothelial ACKR1 in triple-negative breast cancer metastasis
Samuel Tanner Roach, Chinwe Ewenighi-Amankwah, J. Dufraine, L.A. Naiche, Jan K. Kitajewski. *Department of Physiology and Biophysics, University of Illinois at Chicago, Chicago, IL*

Metastasis is the most common cause of breast cancer mortality. Of the breast cancer subtypes, triple-negative breast cancer (TNBC) is the deadliest due to its increased likelihood to metastasize. Tumor cell extravasation is a critical step of metastasis and allows circulating tumor cells to exit the vasculature and seed distant tissues. Clear understanding of the major regulators of tumor cell extravasation will provide insights into the progression of TNBC metastasis. One potential regulator of TNBC cell extravasation is ACKR1. In many contexts, ACKR1 expression is required

in endothelial cells (EC) for leukocyte extravasation. Endothelial ACKR1 binds CXCL2, a promigratory chemokine, and localizes it to EC junctions to guide neutrophils through leukocyte extravasation. CXCL2 expression in TNBC cells is also necessary for tumor cell extravasation from lung microvasculature and for tumor metastasis. Our preliminary data show that ACKR1 is required in at least one stromal cell type for TNBC metastasis from the primary tumor to the lung. These data suggest that endothelial ACKR1-CXCL2 interactions may mediate tumor cell extravasation in TNBC metastasis. Therefore, we hypothesize that endothelial ACKR1 promotes metastasis via retention of CXCL2 at EC junctions, increasing tumor cell chemotaxis and extravasation. To address this hypothesis, we will examine the in vivo significance of endothelial ACKR1 expression using our validated ACKR1 endothelial cell-specific knockout mouse model. We will test the requirement for endothelial ACKR1 for metastasis of orthotopically implanted TNBC tumors to distant sites in the lung and for extravasation of circulating tumor cells into lung tissue. We will determine which steps of extravasation require ACKR1 by evaluating ACKR1-low and ACKR1-overexpressing ECs using an Ibidi flow co-culture system that recapitulates the shear stress conditions of pulmonary microvasculature. We will examine whether these steps are dependent on CXCL2 by introducing CXCL2-neutralizing antibodies to the Ibidi flow system and observing their effects on each extravasation step. Our proposed studies will establish the role of endothelial ACKR1 in TNBC metastatic progression and determine the specific steps of tumor cell extravasation in which endothelial ACKR1 and CXCL2 function. Understanding these processes may guide development of ACKR1 as a prognostic marker for metastasis and can provide mechanistic insight into candidate chemokine and chemokine receptor inhibitors under evaluation for treatment of breast cancer.

#3619

EP4 promoted cell migration via mitochondrial biogenesis in oral cancer cells

Soichiro Ishikawa[1], Masanari Umemura[2], Rina Nakakaji[2], Akane Nagasako[2], Kagemichi Nagao[2], Yuto Mizuno[1], Fumina Suzuki[1], Kohei Osawa[1], Mitomu Kioi[3], Kenji Mitsudo[3], Yoshihiro Ishikawa[2].
[1]Cardiovascular Research Institute (CVRI), Department of Oral and Maxillofacial Surgery, Yokohama City Univ. School of Medicine, Yokohama,

Japan,[2]Cardiovascular Research Institute (CVRI), Yokohama City Univ. School of Medicine, Yokohama, Japan,[3]Department of Oral and Maxillofacial Surgery, Yokohama City Univ. School of Medicine, Yokohama, Japan

Introduction: Lymph node metastasis caused by migration of oral cancer cells is an important prognostic factor. We previously reported that EP4, a prostaglandin E_2 (PGE_2) receptor, regulates the cell migration in oral cancer cells via Ca^{2+} signaling. However, how Ca^{2+} signaling regulates cell migration remains unclear. The intracellular Ca^{2+} regulates a variety of signaling pathways, either directly or by forming complexes with proteins such as calmodulin (CaM), and then phosphorylates calcium/calmodulin-dependent protein kinase kinase 2 (CaMKK2). Furthermore, Ca^{2+} signaling is directly or indirectly involved in cancer cell proliferation and migration. Therefore, we hypothesized that EP4 regulates the cell migration via CaMKK2 and its downstream signaling in oral cancer.
Materials and Methods: Human gingival fibroblasts, HGnF and Human tongue squamous cell carcinoma cell lines, HSC-3 were used. EP4 agonist (ONO-AE1-437) and CaMKK2 inhibitor (STO-609) were used. HSC-3 cells were transduced with CaMKK2 shRNA, and scramble control shRNA using lentivirus. The protein expressions were evaluated by western blotting. The intracellular calcium concentrations were measured using Fura-2, the Fluorescent Ca^{2+} Indicator. The cell migration ability was evaluated by scratch assay. Immunocytochemistry was performed to evaluate the lamellipodium. The mRNA transcriptions of the mitochondrial associated genes were evaluated by real-time qPCR. The intracellular adenosine triphosphate (ATP) production and the reactive oxygen species (ROS) production were also evaluated by luciferase activity assay and DCFH-DA staining.
Results: EP4 protein expression of HSC-3 cells was higher than that of HGnF cells (n=4, $p<0.001$). EP4 agonist rapidly increased the intracellular calcium in HSC-3 cells but not in HGnF cells (n=4, $p<0.001$). EP4 agonist also promoted the cell migration and increased the lamellipodia formation in HSC-3 cells (n=3, $p<0.001$). Furthermore, EP4 agonist promoted the phosphorylation of CaMKK2 and AMP-activated protein kinase (AMPK) (n=4, $p<0.001$). In contrast, CaMKK2 inhibitor and CaMKK2 knockdown

suppressed EP4-stimulated cell migration and AMPK phosphorylation (n=4, $p<0.001$). Furthermore, EP4 agonist increased the expression of the transcriptional coactivator PGC1-α, mtDNA and mitochondrial transcription factor A (TFAM) (n=4, $p<0.01$). Furthermore, EP4 agonist increased the intracellular ATP production and the ROS production (n=6, $p<0.01$). Taken together, EP4 regulated the mitochondrial biogenesis via CaMKK2 and AMPK, and promoted the cell migration in oral cancer. Conclusion: EP4/CaMKK2/AMPK pathway is a novel signal transduction in oral cancer and may be a new target for oral cancer therapy.

#3620

N-myristoylation inhibition reduces angiogenesis and cancer cell migration

Rony Pain[1], Erwan Beauchamp[2], Katia Carmine-Simmen[3], Jay Gamma[4], Rebecca Reif[1], Abul Azad[4], Allan Murray[4], John Lewis[3], Luc Berthiaume[1].
[1]Department of Cell Biology, University of Alberta, Edmonton, AB, Canada,[2]Pacylex Pharmaceuticals Inc., Edmonton, AB, Canada,[3]Department of Oncology, University of Alberta, Edmonton, AB, Canada,[4]Department of Medicine, University of Alberta, Edmonton, AB, Canada

Myristoylation is the modification of proteins by the 14-carbon fatty acid myristate. In humans, two N-myristoyltransferases (NMT1 and NMT2) catalyze myristate transfer onto >200 proteins to regulate membrane binding and signal transduction. The pan-NMT inhibitor PCLX-001 has been in phase I clinical trials over a year for the treatment of lymphoma and advanced solid malignancies. Lack of myristoylation promotes the degradation of numerous normally myristoylated proteins like the proto-oncogenic Src family kinases (SFKs). SFKs like Src and Lyn are essential for downstream signaling of Vascular Endothelial Growth Factor (VEGF) and Epidermal Growth Factor (EGF) receptor tyrosine kinases. Thus, SFKs are critical for angiogenesis and cell motility. Angiogenesis is essential for tumor growth and dissemination of cancer cells to distal locations. VEGF-induced angiogenesis requires Src activation, suggesting that PCLX-001 may have antiangiogenic properties. SFKs also promote cell migration/metastasis, the leading cause of cancer-associated mortality. Lyn SFK knockdown was shown to reduce breast cancer migration and

neighbouring tissue invasion, suggesting that PCLX-001 may also inhibit cell migration/metastasis. We investigated the antiangiogenic properties of PCLX-001 *in vitro* using HUVEC umbilical cord cells. PCLX-001 treatment significantly reduced HUVEC sprouting and tube-formation to levels lower than two FDA-approved angiogenesis inhibitors Sorafenib and Sunitinib. PCLX-001 also significantly reduced neo-vascularisation *in vivo* at lower concentrations than these two drugs using a chicken chorioallantoic membrane model, demonstrating the high potential of myristoylation inhibitors to reduce angiogenesis. We then validated our observations *in vivo* using a HT-1376 bladder mouse xenograft model. Tumors from mice treated for 28 days at increasing PCLX-001 concentrations showed significant reduction of Src, Lyn, and VEGF receptor protein levels as measured by immunohistochemistry, further validating PCLX-001 effect *in vivo*. We hypothesize that PCLX-001 acts downstream of VEGF/ EGF receptors by inducing degradation of un-myristoylated SFKs. We confirmed this by knocking down NMT1 or treating breast cancer cells with PCLX-001 and found that both significantly reduced SFK protein levels. In a wound-healing assay using PCLX-001, we observed significant dose-dependent cell migration inhibition. PCLX-001 also dose-dependently reduced migration and invasion in transwell migration/invasion assays, indicating that myristoylation is required for optimal migration and potentially cancer cell metastasis. Overall, by lowering SFK levels, PCLX-001 reduces angiogenesis, cell migration/invasion, and thus potentially cancer metastasis. Reducing these classical cancer hallmarks in malignant cells may benefit a wide array of cancer patients and ultimately improve cancer treatment outcomes.

#3621

Identification of podocalyxin-positive tumor buds in pancreatic ductal adenocarcinoma: Implications for solid tumor collective invasion

Erin M. Bell, Steve E. Kalloger, Pamela M. Dean, Janel L. Kopp, Kelly M. McNagny, Calvin D. Roskelley. *University of British Columbia, Vancouver, BC, Canada*

High expression of the single-pass transmembrane sialomucin, podocalyxin, has been shown to predict poor disease outcome in a number of solid tumor

types, including pancreatic ductal adenocarcinoma (PDAC) (Taniuchi et al., 2016). In addition to the classical TMN staging measures of disease progression (tumor size, lymph node involvement, and distant metastasis) local invasion at the primary tumor site is a valuable indicator of solid tumor progression. Local invasion has been observed histologically as tumor buds, defined by the presence of small cohesive clusters of tumor cells in the invasive tumor-stromal interface. To date, tumor budding has been characterized as an indicator of poor prognostic outcome in colorectal carcinoma (CRC), pancreatic ductal adenocarcinoma (PDAC), invasive ductal breast carcinoma (IDC), lung adenocarcinoma (LUA), stomach and esophageal carcinomas, oral squamous cell carcinoma, periampullary adenocarcinoma, and head and neck squamous cell carcinoma (HNSCC). Our group has previously modelled tumor budding experimentally using the MCF7 human breast cancer cell line (Graves et al., 2016). We showed that forced over-expression of podocalyxin was a driver of local collective invasion and tumor budding *in vitro* and *in vivo*. Because podocalyxin is highly expressed in PDAC we sought to determine if its expression was involved in the process of tumor budding in this tumor context as well. We assessed large format histological sections from a cohort of patient PDAC tumors and identified high podocalyxin expression in tumor buds. Further, we generated podocalyxin-null MiaPaCa2 PDAC cell lines and demonstrated that podocalyxin-expression is required for collective invasion in 3D culture conditions. We are currently evaluating *in vivo* xenograft tumor models with these podocalyxin-expressing and podocalyxin-null MiaPaCa2 cells to determine whether changes in 3D culture invasion are representative of tumor budding in this model. Expression of podocalyxin by tumor buds provides rationale to support investigation into the impact of therapeutically targeting these invasive cells.

#3622

Characterizing the metastatic potential and clonal dynamics of invasive subpopulations in TNBC cells in response to chemotherapy

Carolina De Santiago, Amy Brock. *University of Texas at Austin, Austin, TX*

Triple negative breast cancer (TNBC) is one of the deadliest forms of breast cancer and is characterized by its high rates of metastasis, significant intra-tumor heterogeneity and lack of hormonal treatments. Through utilization of a novel genetic cell tracking technology, ClonMapper, we identify and characterize the origins of invasive subpopulations.
Genetic barcodes are stably integrated into HCC1806 cells to generate starting parental populations of ~1000 unique barcoded cells. Invasive barcoded subpopulations were selected by migration through transwell assays for 24 hours and then collected for expansion. Clonal abundance sequencing across all replicates showed a >8-fold decrease in the number of unique barcodes. Similarity was quantified using the Bray-Curtis and Cosine similarity indexes. 5 out of 8 replicates shared the same lineages, where more than 50% of the replicates were composed of the same 9 unique barcodes thus indicating the pre-existence of invasive clones. Following cell subpopulation isolation, we observed that isolated subpopulations display faster growth rates than parental populations. A scratch assay verified that the 5 similar invasive subpopulations displayed elevated migration rates in this 2D migration format (invasive populations vs parental population, n= 6). Separate transwell assays also confirmed the 3-dimensional migration rates of isolated subpopulations.
Parental HCC1806 and invasive subpopulations were treated with doxorubicin, cisplatin, paclitaxel and 5-flourouracil (5-FU) at their respective LD50 for 48 hours then allowed to recover to confluency before assessment by scratch assay. We observed that paclitaxel significantly decreased the migration rate, but that both doxorubicin and 5-FU resistant cells had a significantly higher migration rate (chemoresistant populations vs parental population, n=5) indicating that these drugs select for more migratory populations. Future studies will elucidate whether invasive clones are pre-existing or de novo and determine the effect of chemotherapeutics on these populations.

#3623
MIEN1 promoter ablation provides novel evidence for colorectal cancer genome editing-based therapeutics
Payal Ranade, Rucha Trivedi, Jamboor K. Vishwanatha. *University of North Texas Health Science Ctr., Fort Worth, TX*

Colorectal cancer (CRC) is one of the leading causes of cancer associated mortalities worldwide. It starts with hyperproliferation of epithelial cells forming a polyp & is characterized by four stages, where stages 3 & 4 are associated with acquisition of metastasis. Chemotherapy majorly focuses on attenuating symptoms with no promising cure. Hence, studying the underlying mechanism of CRC progression & identifying novel therapeutic targets is critical for early diagnosis & treatment. The process of metastasis involves a complex interplay of signaling pathways, where various proteins play crucial roles. One such important protein that aids the process of migration is Migration & Invasion ENhancer 1 (MIEN1). In CRC, MIEN1 expression is predominantly upregulated in cancerous tissue in comparison to normal colorectal tissue, which is closely associated with invasive behavior. But the exact mechanism involved in the process of metastasis is yet unexplored. It is established that MIEN1 overexpression is a result of 17q12 chromosomal amplification, & such dysregulated expression is linked to the trans-regulation of its minimal promoter region. Therefore, we aim to investigate the effect of MIEN1 promoter ablation on CRC migration properties. CRISPR-Cas9 gene editing technology was used for deleting MIEN1 promoter region in the CRC cell line HT29. RNA seq & bioinformatics tools were employed to assess the transcriptomic consequences of genome-editing. Several DEGs discerned by RNA seq analysis were involved in different biological processes & molecular pathways such as cell adhesion, migration, invasion, & angiogenesis. Out of these the genes vital to CRC biogenesis were evaluated at both RNA & protein levels. Additionally, we analyzed the effect of MIEN1 knock-out on CRC metastatic potential using functional assays such as wound healing, Matrigel invasion, hanging drop cell - cell adhesion, & found that migration potential of HT29 cells was significantly reduced in absence of MIEN1 protein. We also successfully demonstrated that MIEN1 deletion disrupts the cytoskeletal rearrangement by affecting F-actin reorganization using phalloidin staining. Confocal staining of different proteins participating in actin cytoskeleton rearrangement such as paxillin, FAK, MIEN1 gave us an insight about the role of MIEN1 in mediating phosphorylation of FAK at different phosphorylation sites such as Tyr 397 & 925. Immunoblotting analysis of an array of proteins further confirmed the role of MIEN1 in actin cytoskeleton dynamics. Taken together, our results prove that MIEN1 is involved in different signaling pathways responsible for CRC migration

& its deletion leads to perturbation of several biological processes especially the actin cytoskeleton rearrangement, involved in metastasis. Hence, targeting MIEN1 would be a potentially effective therapeutic strategy for CRC patients.

Signaling Pathways That Impact the Tumor Microenvironment

#3627
Inhibition of tumor cell-autonomous p38 MAPK suppresses IL1α-mediated inflammatory tumor-stromal crosstalk in pancreatic adenocarcinoma

Samara Singh, Austin R. Dosch, Siddharth Mehra, Iago de Castro Silva, Anna Bianchi, Vanessa Tonin Garrido, Zhiqun Zhou, Haleh Amirian, Edmond W. Box, Jashodeep Datta, Nagaraj Nagathihalli, Nipun B. Merchant. *Surgery, University of Miami Miller School of Medicine, Miami, FL*

Introduction: Pancreatic ductal adenocarcinoma (PDAC) continues to face major therapeutic challenges due to its innate and acquired chemoresistance. Oncogenic, activating *KRAS* mutations facilitate extensive cytokine-mediated crosstalk between tumor cells and the fibrotic stroma, producing a pro-inflammatory and immunosuppressive tumor microenvironment (TME). We have identified interleukin-1α (IL1α), downstream of KRAS, as a critical mediator of the inflammatory response due to its pleiotropic effects on cancer-associated fibroblast (CAF) activation and immune evasion. However, the regulatory mechanisms of IL1α expression remain incompletely understood. We identified p38 stress-associated MAPK α (p38α) as a central, KRAS-driven regulatory pathway involved in IL1α production within PDAC tumor cells.
Methods: Differential gene expression analyses were performed on patient data from The Cancer Genome Atlas (TCGA) was queried for overactive pathways downstream *KRAS* in "high-*IL1A*" PDAC cases. Inhibition of p38α was achieved pharmacologically with pexmetinib and genetically with an shRNA lentiviral system in human and murine PDAC cell lines. ChIP-qPCR and co-immunoprecipitation were performed on a human PDAC cell line with and without p38α inhibition. Single-cell RNA sequencing (scRNA-seq) and flow cytometry were performed on tumors from a PDAC

murine model, *Ptf1a*$^{Cre/+}$; *LSL-Kras*$^{G12D/+}$; *Tgfbr2*$^{flox/flox}$ (PKT), treated with or without pexmetinib. PKT mice were treated daily with pexmetinib, gemcitabine and paclitaxel chemotherapy, or combination therapy for downstream analysis and survival studies.
Results: Both pharmacologic and genetic inhibition of p38α significantly reduced *IL1A* transcription and protein levels in human and murine PDAC tumor cell lines. Furthermore, p38α inhibition reduced binding of Sp1 and NF-κB to the *IL1A* promoter and prevented IL1α-mediated polarization of inflammatory CAFs *in vitro*. In PKT mice, p38α inhibition reduced tumor cell-specific *Il1a* and inflammatory CAF gene signatures by scRNA-seq, and favorably altered the infiltrating immune populations by flow cytometry. Lastly, pexmetinib with chemotherapy significantly reduced tumor burden and improved overall survival in a PDAC murine model.
Conclusions: These findings provide a new therapeutic opportunity to target the p38α MAPK pathway for suppression of IL1α-mediated stromal activation and combination with chemotherapy to overcome therapeutic resistance by modulating the stromal and immune microenvironment in PDAC.

#3628
RAC1 aberrations in head and neck cancer affect immune microenvironments
Helen Hoi Yin Chan[1], Yuchen Liu[1], Hoi Lam Ngan[1], Vivian Wai Yan Lui[2].
[1]Chinese University of Hong Kong (CUHK), Hong Kong, Hong Kong,[2]Department of Medicine, Medical College of Georgia, Georgia Cancer Center, Augusta University, GA

RAC1 is a Rho GTPase well-identified as an oncogene overexpressed in various cancer types. *RAC1* amplification or gain account for ~40% of head and neck squamous cell carcinoma (HNSCC) while mutation of *RAC1* occurs at ~3% according to TCGA-HNSCC cohort. HNSCC patients with *RAC1* aberrations, including *RAC1* mutations and amplification or gain, are associated with poor overall and disease-free survival in HNSCC. Significantly higher tumor mutational burden is observed in *RAC1*-mutated group (p=0.0336) or in *RAC1*-amplified/gain group (p=0.0109) vs. wildtype patients in TCGA-HNSCC cohort. As increases in TMB are often associated with immune cell infiltration in cancers, we hypothesized that

RAC1 aberrations impact the tumor immune microenvironment (TIME) of HNSCC, potentially contributing to disease progression.PD-L1 (CD274) is an important immunosuppressive immune checkpoint molecule expressed in tumor cells. Here, we first reported that ectopic overexpression of *RAC1* p.P29S and p.A159V mutations in a human HNSCC cell line (PECAPJ41 clone D2, ATCC, USA) could cause upregulation of PD-L1 at both mRNA (by RNA-seq) and protein levels (by Western blotting), first demonstrating a direct effect of *RAC1* mutations on potential HNSCC TIME modulation via PD-L1. Furthermore, by tumor immune estimation resources (TIMER) analysis, we found that *RAC1*-mutated tumors have significantly higher level of neutrophils immune infiltration of 38.63% (p=0.027) compared to the wildtype tumors. From the CIBERSORTx analysis, M2 Macrophages was significantly increased by 40.42% in *RAC1*-mutated tumors vs wildtype in the TCGA-HNSCC cohort (p=0.031). We also validated this finding by immunofluorescent staining of PD-L1 and M2 Macrophages in immunocompetent mouse HNSCC xenografts models expressing *RAC1* p.P29S and p.A159V mutations as compared to controls.
Our in silico, in vitro and in vivo findings first uncover an important role of *RAC1* aberrations in HNSCC TIME immunosuppression by regulating PD-L1 expression, neutrophil and M2 macrophages infiltrations. Clinical activities of PD-L1 inhibitors in *RAC1*-mutated HNSCC patients worth future investigations.
Acknowledgement: This research is funded by the General Research Fund (Ref. No.:14168517) and the Research Impact Fund (Ref. No.: R4015-19) from the Research Grants Council in Hong Kong. VWYL is supported by Start-up Fund, Georgia Cancer Center, Medical College of Georgia at Augusta University.

#3629

Calcium signalling and the breast cancer microenvironment

Alice H. L. Bong[1], Krystyna A. Gieniec[2], Francisco Sadras[1], Mélanie Robitaille[1], Sarah J. Roberts-Thomson[1], Felicity M. Davis[3], Gregory R. Monteith[1]. *[1]School of Pharmacy, The University of Queensland, Brisbane, Australia,[2]School of Medical Sciences, The University of New South Wales, Sydney, Australia,[3]Department of Biomedicine, Aarhus University, Aarhus, Denmark*

Calcium is a key regulator of a variety of pathways important in breast cancer progression, including those involved in cell proliferation and invasiveness. Calcium signaling is implicated in processes relevant to the breast cancer tumor microenvironment and altered calcium influx is a feature of cancer associated fibroblasts. In these studies, simultaneous use of genetically encoded calcium indicators with distinct fluorescence spectral properties (GCaMP6m or JRCaMP1b), were used to explore the cross-talk between breast cancer cells and fibroblasts via calcium signaling and changes in different cellular compartments. HMF3S human fibroblast cells co-cultured with breast cancer cells expressing GCaMP6m or JRCaMP1b were assessed in 2D and 3D co-culture using automated epi-fluorescence or confocal microscopy. Mitochondrial calcium levels were assessed using targeted GCaMP6m (2mtGCaMP6m) in HMF3S cells expressing JRCaMP1b. Results showed distinct spatial and temporal changes in free calcium levels between both fibroblasts and breast cancer cells and the mitochondria and cytosol during activation. These methodological advances provide an opportunity to better understand calcium signaling in cancer associated fibroblasts. These techniques will also help identify the calcium channels and pumps that could be targeted to manipulate the breast cancer tumor microenvironment to inhibit pathways important in breast cancer progression.

#3630

TrkA+ sensory neurons modulate macrophage phenotype in osteosarcoma

Qizhi Qin, Sowmya Ramesh Ramesh, Thomas L. Clemens, Aaron W. James. *Johns Hopkins University School of Medicine, Baltimore, MD*

Introduction: Osteosarcoma (OS) is the most common primary malignancy of the skeleton, and inordinately affects young adults. Despite improved outcomes with current multimodal care, the prognosis for patients with metastatic disease is grim. Peripheral neural regulation of cancer growth has long been suggested by clinical observations in pancreatic and prostate cancers. Prior reports suggest peripheral nerve sprouting in osteosarcoma, but the functional roles of sensory nerves in osteosarcoma are unknown. Here, the role of $TrkA^{+}$ sensory nerves in OS disease progression was assayed.

Methods: All experiments were conducted under IACUC approval at Johns Hopkins University. $TrkA^{F592A}$ mice which are homozygous for a phenylalanine-to-alanine point mutation in exon 12 of *Ntrk1* gene were crossbred with NOD scid mice ($TrkA^{F592A}$/Scid). TrkA inhibition was performed by 1NMPP1 treatment. *In vivo* tumor growth was examined using a periosteal xenograft model. 1 million human 143B-luc OS cells were injected. Analysis was performed using serial measurements of tumor size and IVIS imaging. Nerve distribution and macrophage polarization within the tumor microenvironment was documented using immunostaining for Beta III Tubulin (TUBB3), CD86, CD206 and F4/80.
Results: Inhibition of TrkA led to a significant reduction in $Tubb3^{+}$ nerves (88.4%) within and around the OS xenografts. In addition, tumors within $TrkA^{F592A}$/Scid animals demonstrated slower growth, including a 51.5% reduction in tumor size and 60.0% reduction in IVIS luciferase activity at 4 wks. Histologic examination showed a reduction in macrophage infiltration and reprogramming of macrophages from an M2-like to M1-like phenotype in tumors with chemical denervation. Remarkably, this was associated with a reduction in Ki67 proliferative index (80.1%) and CD31 immunofluorescent staining (60.8%) within the tumors. Overall survival of mice with TrkA inhibition was significantly prolonged (p=0.0003). Retrograde tracing identified the sensory nerve fibers innervating the periosteum originated from L3-L5 lumbar DRGs and RNA seq identified OS-derived neurotrophins and axon guidance molecules.
Discussion: Disruption of $TrkA^{+}$ nerves significantly mitigates OS disease progression in a mouse xenograft model, including a significant improved overall survival. These findings are associated with a reduction of macrophage infiltration and macrophage re-polarization. Ongoing studies are examining the molecular mechanisms that mediate nerve-to-macrophage interaction in peripheral nerves and DRG neurons using a combination of sequencing approaches.
Significance/Clinical Relevance: Sensory neurons positively regulate osteosarcoma growth and disease progression. Use of chemical or microsurgical approaches to denervate tumors may represent a future adjunctive therapy to both improve pain and prognosis in high grade bone sarcomas.

#3631

Infiltrating Bruton's tyrosine kinase expressed B cells effects on prostate cancer metastasis

Crystal Byrd, Geou- Yarh Liou. *Clark Atlanta University, Atlanta, GA*

Prostate cancer is the most common type of cancer found in senior males and is the 2nd leading cause of cancer death in American males. Although prostate cancer grows slowly within the prostate glands, because of a lack of efficient treatments at the appropriate timing, cancer cells eventually become aggressive and metastatic. The progression of cancer is supported by many factors, such as signals received from surrounding cells, like B cells and other effector cells. B cells play a role as a part of the adaptive immune system to produce antibodies. To become mature B cells, they rely on activation of a non-receptor kinase, Bruton's Tyrosine Kinase (BTK). Preliminary data from our lab showed that in the prostate cancer tissues, more infiltrated B cells expressing BTK were present nearby the prostate cancer cells. Upon this finding, we hypothesize that BTK expressed B cells will support the survival of prostate cancer cells through BTK signaling. In this study, we will overexpress BTK in B cells to study the proliferation and migration of prostate cancer cells through a co-culture system. Our findings will show an increase in migration of prostate cancer cells when cultured with BTK expressed B cells. In the future, we will validate the importance of BTK in regulating prostate cancer migration and invasion; and identify their mechanisms. Our overall findings from this project would reveal key elements of the signaling pathways of BTK expressed B cells to promote prostate cancer migration.

#3633

Exploring a novel crosstalk between hyluronan/CD44 and ErbB-2 pathways in resistance to ErbB-2-targeted therapies in breast cancer.

Santiago Madera, Valentina C. Bulian, Sharon S. Merin, María F. Mercogliano, Roxana Schillaci, Rosalia I. Cordo Russo. *Instituto de Biología y Medicina Experimental (IBYME), CONICET, Buenos Aires, Argentina*

The tumor microenvironment component hyaluronan (HA) induces tumor progression through the interaction with its cell surface receptor CD44. Accumulation of HA is associated with poor prognosis and resistance to the

anti-ErbB-2 agent trastuzumab (TZ) in breast cancer (BC). ErbB-2 receptor is overexpressed in 15-20% of BC patients (ErbB-2+) and constitutes an important therapeutic target. Despite the clinical efficiency of therapies targeting ErbB-2, resistance to these drugs remains a major issue. In addition to its membrane function, ErbB-2 migrates to the nucleus (NErbB-2) where it acts as a transcription factor (TF) or as a coactivator of TF, modulating proliferation, metastasis, and resistance to anti-ErbB-2 therapies in BC. CD44 has also been found in the nucleus (NCD44). Although crosstalk between HA/CD44 and ErbB-2 pathways has been reported, how their molecular interactions mediate TZ resistance remains poorly known. Our *in silico* studies showed that TZ-resistant cells express higher CD44 levels than TZ-sensitive ones. We previously reported that stimulation with the ErbBs ligand heregulin (HRG) induces NErbB-2 translocation, acquired-TZ resistance and proliferation in the TZ-sensitive SK-BR-3 cell line. Here, we found that HRG also increased CD44 mRNA expression in SK-BR-3 cells. Then, we explored the role of HA in modulating CD44 and ErbB-2 nuclear localization in BC cells. Immunofluorescence and confocal microscopy studies showed that stimulation with exogenous HA induced nuclear translocation of ErbB-2 in T47D cells. Interestingly, we found constitutive presence of CD44 and ErbB-2 protein in nuclear lysates of JIMT-1 cells, a *de novo* TZ-resistant BC model. HA stimuli further enhanced this nuclear localization. Contrarily, treatment with the chemical inhibitor of HA synthesis 4-methylumbelliferone (4MU) decreased not only HA levels but also NErbB-2 in JIMT-1 cells. Furthermore, 4MU inhibited the proliferation of two TZ-resistant cell lines, JIMT-1 and MDA-MB-453, in a dose-dependent manner. 4MU also inhibited HRG-induced proliferation in SK-BR-3 cells. Even more, wound-healing assays showed that 4MU inhibited migration of JIMT-1 cells. This inhibition was similar to the one observed when ErbB-2 was excluded from the nucleus via transfection with the hErbB-2ΔNLS mutant. In summary, we reveal that HA induces CD44 and ErbB-2 nuclear localization in BC cells, suggesting a novel crosstalk between HA/CD44 and ErbB-2 pathways. These findings also highlight the blockade of HA synthesis with 4MU as a novel therapeutic strategy in TZ-resistant BC.

#3634

Overexpression of PLK1 activates IL4/JAK/STAT6 signaling in prostatic tumor-microenvironment

Ruixin Wang, Xiaoqi Liu. *University of Kentucky, Lexington, KY*

The correlation between PLK1 expressions with prostate cancer (PCa) stages was identified by analyzing the transcriptome profile of PLK1 in patients from the Cancer Genome Atlas (TCGA) database, and scoring the protein expression in a clinical tissue microarray (TMA) cohort. Integrating our prostate-specific PLK1 knock-in mouse model, we established an oncogenic role for PLK1 in PCa progression. To elucidate the underlying mechanism, we investigated the impact of PLK1 overexpression on prostatic tumor microenvironment (TME) *in vivo*. In addition, *in vitro* co-culture systems with both epithelial cells and macrophages were designed to uncover the regulatory function of PLK1 in macrophage polarization. We found that PLK1 induces phosphorylation of JAK3, activates the JAK/STAT6 pathway in cancer cells, and increases the secretion of IL4, which enables macrophage polarization towards the M2 phenotype in TME —ultimately accelerating PCa development. Finally, pharmaceutical inhibition of STAT6 signaling significantly reverses the PLK1-mediated M2 polarization and, subsequently, inhibits the progression of PCa. Our findings provide clinical and pre-clinical evidence to characterize the role of PLK1 in promoting PCa and novel insights into the regulatory mechanism of PLK1 in the TME. We also provide strong support for the clinical potential of targeting STAT6 for advanced PCa therapy.

#3635

TBK1 inhibition potentiates the efficacy of AXL-targeted therapy by modulating tumor microenvironment in aggressive breast cancers

Lan Phi[1], Takashi Semba[1], Ngu V. Trinh[1], Fang Zou[1], Jason M. Foulks[2], Steven L. Warner[2], Savitri Krishnamurthy[3], James P. Long[4], James M. Reuben[5], Jennifer M. Rosenbluth[6], Debu Tripathy[1], Naoto T. Ueno[1], Xiaoping Wang[1]. *[1]Breast Medical Oncology, UT MD Anderson Cancer Center, Houston, TX,[2]Sumitomo Pharma Oncology, Inc., Lehi, UT,[3]Pathology, UT MD Anderson Cancer Center, Houston, TX,[4]Biostatistics, UT MD Anderson Cancer Center, Houston, TX,[5]Hematopathology, UT MD Anderson Cancer Center, Houston,*

TX,[6]Department of Medicine, University of California San Francisco, San Francisco, CA

Introduction: Triple-negative and inflammatory breast cancer (TNBC and IBC) are the most aggressive breast cancer subtypes. Novel actionable targets and complementary therapies are critically needed. AXL, a receptor tyrosine kinase, drives pleiotropic phenotypes of TNBC and IBC aggressiveness. Targeting AXL reduces IBC tumor growth *in vivo* and inhibits polarization of M2 macrophages. To identify novel tumor microenvironment (TME) targets to enhance the efficacy of AXL-targeted therapy, we conducted a synthetic lethal kinome siRNA screening. We identified TBK1 as a candidate to synergize with AXL growth inhibition. TBK1 is a serine/threonine protein kinase that regulates innate, adaptive responses and antitumor immune responses. We hypothesized that inhibition of TBK1 enhances the antitumor effect of AXL-targeted therapy in aggressive breast cancers.
Methods: We used knockdown, knockout (KO) and inhibitors to suppress AXL and TBK1 pathways and tested the synergistic effect of targeting AXL and TBK1 on the growth of human SUM149 and BCX010 IBC cells, and HS578T TNBC cells *in vitro*. To determine the synergistic effect of targeting both pathways *in vivo*, we inoculated control or TBK1 KO murine TNBC 4T1.2 cells into BALB/c mice. We assessed the activity of AXL inhibitor TP-0903 in reducing tumor growth. Using multicolor flow cytometry, we studied the effects of targeting AXL and TBK1 on the TME. We tested the activity of TP-0903 combined with a TBK1 inhibitor in another TNBC mouse model, E0771. We used RNA-sequencing and real-time PCR/Western blot to determine the molecular mechanisms of how TBK1 inhibition synergizes AXL-targeted therapy in these cancers.
Results: Compared with AXL or TBK1 suppression alone, genomic or pharmacologic suppression of AXL and TBK1 significantly reduced the growth of SUM149, BCX010, and HST578T cells *in vitro*. In both 4T1.2 and E0771 syngeneic mouse models, TP-0903 was more active in reducing tumor growth in TBK1-inhibited tumors than in control tumors. Tumors with TBK1 inhibition and treated with TP-0903 had a significantly higher population of cytotoxic T cells than control tumors. Depletion of CD8+ T cells blocked the synergistic effect of targeting AXL and TBK1 pathways on reducing tumor growth, suggesting that cytotoxic T cells contributed to

the anti-tumor synergy of targeting AXL and TBK1. Mechanistically, TBK1 induced M2 macrophage migration via IRF3-regulated CCL5 secretion in SUM149 and HS578T cells, and AXL KO attenuated the polarization and migration of M2 macrophages by inhibiting the CCR5/CCL5 axis. Conclusions: Targeting TBK1 enhances the efficacy of AXL-targeted therapy in aggressive breast cancer by suppressing the paracrine effect of CCR5/CCL5 axis. This combination represents a novel and effective therapy modulating the TME of aggressive breast cancer, which warrants further investigation in the clinical setting.

#3636

Liver endothelium secreted LRG1 promotes metastatic colorectal cancer growth through the HER3/RSK/EIF4B AXIS

Moeez Ghani Rathore[1], Michelle Wright[1], Wei Huang[2], Derek Taylor[3], Yamu Li[1], Jordan Winter[1], Zhenghe Wang[1], John Greenwood[4], Stephen Moss[4], Rui Wang[1]. *[1]Case Western Reserve University School of Medicine, Cleveland, OH,[2]Pharmacology, Case Western Reserve University School of Medicine, Cleveland, OH,[3]Department of Biochemistry, Case Western Reserve University School of Medicine, Cleveland, OH,[4]University College London, London, United Kingdom*

Background: 25% of patients diagnosed with colorectal cancer (CRC) have liver metastasis at presentation, and ~80% of all metastatic CRC are developed in the liver. We previously reported that liver endothelial cells (ECs), a key component of the liver microenvironment, secrete LRG1 to promote CRC growth via activating human epidermal growth factor receptor (ERbB3, also known as HER3). However, we found that LRG1-induced HER3 activation is distinct from the canonical neuregulin 1 (NRG1)-induced HER3 pathway. The present study further validated LRG1 as a new HER3 ligand for promoting mCRC growth and elucidated the novel downstream signaling pathway induced by LRG1-HER3.
Methods: We first measured the binding affinity between HER3 and LRG1 by Biolayer interferometry (BLI). We then used *in vitro* and *in vivo* xenograft approaches to determine the effect of LRG1 monoclonal antibody (15C4) on HER3 activation and CRC growth. To further determine the role of LRG1 in promoting CRC growth in the liver, we used murine CRC cells in a syngeneic orthotropic liver injection model to establish CRC allografts

in the liver of $LRG1^{-/-}$ mice with systemic LRG1 knockout and wild-type siblings ($LRG1^{+/+}$). We also performed unbiased phospho-MS analysis and subsequent validations to determine the downstream signaling pathway activated by LRG1-HER3.
Results: We identified that LRG1 binds to HER3 with the affinity at ~100nM. The LRG1 antibody 15C4 completely attenuated LRG1-induced HER3 activation and *in vitro* and xenograft growth *in vivo*. Moreover, $LRG1^{-/-}$ mice with CRC allografts in the liver had 2 times longer overall survival than tumor-bearing $LRG1^{+/+}$ mice. Lastly, unbiased -omics analysis identified eIF4-protein synthesis is significantly activated by LRG1. With target-specific inhibitors, we further determined that LRG1-HER3 activates the PI3K-PDK1-RSK1/3-eIF4 axis independent of AKT.
Conclusions: We identified LRG1 as a novel HER3 ligand and demonstrated that the liver microenvironment-derived LRG1 plays a key oncogenic role in mCRC, by activating a novel RSK-eIF4 survival pathway. Our findings highlighted the potential of blocking LRG1-HER3 and involved downstream pathways for treating patients with mCRC.

#3637

Extracellular matrix drives high-grade breast cancer immune suppression down-modulating PD-1 on Treg cells via the IL-23/SATB1 axis

Giovanna Talarico[1], Mara Lecchi[2], Massimo Costanza[3], Claudia Chiodoni[2], Vera Cappelletti[2], Paolo Verderio[2], Massimo Di Nicola[2], Francesco Bertolini[1], Mario Paolo Colombo[2], Sabina Sangaletti[2]. *[1]European Institute of Oncology, Milan, Italy,[2]IRCCS Istituto Nazionale dei Tumori, Milan, Italy,[3]Fondazione IRCCS Istituto Neurologico Carlo Besta, Milan, Italy*

The pathological grade defines tumor aggressiveness and, indeed, high-grade breast cancer (HGBC), regardless of molecular findings, is characterized by a very aggressive clinical course and a poor prognosis in spite of the availability of chemotherapy regimens and specific-targeted agents. Both the cellular and the extracellular compartments of the tumor microenvironment (TME) can contribute to the evolution of BC by immune escape and immune suppression processes. In this context, structural and extracellular components of the TME, namely the extracellular matrix

(ECM), has been shown to contribute to many aspects of tumor progression, exerting important regulatory functions on tumor cells. The relevance of the ECM in cancer progression is strengthened by study showing that the ECM composition is a prognostic factor able to identify patients subgroups endowed with a different clinical outcome according to the distinct enrichment in ECM genes leading to four specific ECM signatures (ECM 1-4). Among the different ECM-related signatures, only the ECM3 signature - characterizing about 35 % of HGBC - identifies the most aggressive tumors with epithelial mesenchymal transition (EMT) features, poor prognosis, T-cell exclusion and an increased infiltration of myeloid-derived suppressor cells (MDSCs). To evaluate whether local immune suppressive features of ECM3+ tumors can be intercepted in the peripheral blood (PB), to represent a potential biomarker for this subset of tumors, we collected consecutive HGBC patients that included 22 ECM3+ and 30 ECM3- and performed a multiparametric flow cytometry analysis. We found PD-1^{neg} Treg being correlated to ECM3 patients and through ad hoc mouse BC models, we provided the mechanisms through which SPARC, a key functional gene of the ECM3 signature, was responsible for the down-modulation of PD-1 on Treg, positively affecting their suppressive activity. By sustaining the release of IL-23, SPARC promotes SATB1 expression that repress PD-1. Notably, fluvastatin treatment in vivo decreased the expression of SATB1 in treated Treg cells, a result paralleled by an increased expression of PD-1 on Treg cells. Our data extend the regulatory activity of the extracellular matrix and SPARC, which are large characterized for myeloid cells, to regulatory T-cells also offering new possible targets for the treatment of high-grade breast tumors.

#3638

Integrated single-cell and spatial analysis reveal the mechanism of KRAS^{G12C} inhibitor AMG510 in HSC-humanized NOG-EXL model

Panpan Wang, Huacheng He, Jingjing Wang, Ting Ni, Dan Lu, Qiangqiang Fan, Wenting Shi, Qingyang Gu, Qiyao Zhang. *Oncology & Immunology Unit, WuXi Biology, WuXi AppTec, Shanghai, China*

Background: Intra-tumor heterogeneity is one of the biggest challenges in cancer treatment today. Current single-cell RNA sequencing technologies itself could enable the exploration of gene expression heterogeneity at the

single cell level, but they cannot require the morphological information within the tumor, nor the protein profiles of individual cells. Spatial transcriptomics (ST) is an in situ RNA capturing technique which preserved the spatial information of histological tissue section, and CITE-Seq is a method to preform scRNA sequencing along with acquiring protein information on a single cell level. Combining CITE-Seq and ST together can enable us to understand the roles of specific cell subpopulations and their interactions in tumor microenvironment at RNA, protein and spatial level at the same time. KRAS is the most frequently mutated oncogene in human cancer, and AMG510 is a small covalent specific $KRAS^{G12C}$ inhibitors by blocking KRAS in its GDP-bound state, which leads to the regression of tumors and improved the anti-tumor efficacy. But the intrinsic mechanism of AMG510 in $KRAS^{G12C}$ mutant non-small cell lung cancer (NSCLC) is not fully understood. Therefore, we develop a multi-omics method to find the mechanism of $KRAS^{G12C}$ inhibitor AMG510 in NSCLC.
Material and Method: We established a NSCLC HSC-humanized NOG-EXL model, treated it with vehicle and AMG510, and collected 3 tumor tissues from each group. Samples were processed and cDNA library of CITE-seq were constructed based on the protocol of TotalSeq-B Human Universal Cocktail (BioLegend) and Single Cell 3' Reagent Kits v3.1 (10x Genomics). Spatial sample preparation and cDNA library generation was carried out following the user guide of Visium FFPE Spatial Gene Expression Reagent Kits (10X Genomics). All the final libraries were sequenced by NovaSeq platform. After obtained feature-cell/spot matrix, data preprocessing and analysis were performed in R environment. Cell components in the tumor microenvironment were annotated by a cross-validated multi-approaches using CITE-seq data. And ST data were further analyzed by integrating CITE-seq data.
Results: Using a multi-omics analysis system, firstly, we constructed a single-cell transcriptomic atlas of NSCLC tumor microenvironment; and then explored the characterization of cell-type infiltration. Furthermore, CITE-seq and ST datasets were integrated to assess the spatial organization of infiltrated immune cells and tumor cells. We found how AMG510 affected tumor microenvironment and enhanced the checkpoint pathways. The results in return proved the reliability of the multi-omics system, which enables us to explore how drugs treat cancer by affecting its microenvironment in multiple levels.

Summary: We established a multi-omics analysis system and explored the mechanism of the $KRAS^{G12C}$ inhibitor AMG510 against the NSCLC.

#3639

Impact of KRAS oncogenic signaling in tumorigenesis and immune evasion driven by extracellular vesicles (EVs)

Zulaida M. Soto Vargas, David C. Arteaga, Ikjot S. Sohal, Humna Hasan, Andrea L. Kasinski. *Biology, Purdue University, West Lafayette, IN*

Mutations in Kristen rat sarcoma homolog (KRAS) occur in about 25% of cancers, making this protein one of the most frequently altered genes in cancer. KRAS mutations are not only associated with poor patient survival, but also with increased tumor aggressiveness and metastasis. Tumor development and metastasis are impacted by intercellular communication. Key mediators of cell-to-cell communication include vesicles secreted by cells, also known as extracellular vesicles (EVs). EVs released by cancer cells can mediate malignant transformation of non-cancerous cells as well as influence pre-metastatic niche formation. Conversely, inhibiting the secretion and release of EVs by cancer cells decreases tumor growth and metastasis. However, the mechanisms through which EVs drive tumorigenesis in KRAS mutant tumors are still understudied. Our lab recently reported that EVs from lung cancer cells drive invasion of non-tumorigenic lung epithelial cells. Here, we found that KRAS oncogenic signaling in the donor cells contributes to the EV-driven migration and invasion of non-tumorigenic lung epithelial cells. Previous studies have demonstrated that KRAS signaling drives immune evasion and promotes an "immune cold" tumor microenvironment. Our preliminary studies showed that EVs derived from $Kras^{G12C}$ lung cancer cells (H358) inhibit T cell proliferation and that blocking $KRAS^{G12C}$ signaling, using ARS-1620 ($Kras^{G12C}$ inhibitor), impairs EV-driven T cell immunosuppression. We performed a comprehensive proteomic comparison between EVs isolated from H358 treated with ARS-1620 and those isolated from cells treated with DMSO (vehicle) and identified proteins involved in migration and invasion, such as LAMB-3, to be downregulated in EVs isolated from ARS-1620 treated cells. Ongoing studies aim to pinpoint the detailed mechanisms by which cancer cells utilize mutant KRAS signaling to promote loading of

oncogenic cargo into EVs, and the resulting contributions to tumorigenesis and immune evasion.

#3641

Loss of Smad4 induces SPP1 secretion and immunosuppressive myeloid cell formation in pancreatic ductal adenocarcinoma

Gilbert Z. Murimwa[1], Francesca Rossi[2], Henry K. Fleming[2], Zeynep Yazgan[2], Dina Alzhanova[2], Huocong Huang[3], Rolf A. Brekken[3]. *[1]Surgery, UT Southwestern Medical Center, Dallas, TX,[2]Hamon Center for Therapeutic Oncology Research, UT Southwestern Medical Center, Dallas, TX,[3]Surgery, Hamon Center for Therapeutic Oncology Research, UT Southwestern Medical Center, Dallas, TX*

Up to 50% of pancreatic ductal adenocarcinomas (PDA) harbor mutations in canonical TGFß pathway genes such as *SMAD4* and *TGFBR2*. *SMAD4* mutations have been shown to drive resistance to chemotherapy, metastasis, and margin positivity following surgical resection. To characterize the unique tumor microenvironment of *SMAD4* mutant PDA, we developed isogenic, orthotopic mouse models using CRISPR mediated knockout of *Smad4* in a cell line derived from *KPfC* ($Kras^{LSL\text{-}G12D}$;$Trp53^{fl/fl}$;$Pdx1^{Cre}$) mice, a genetically engineered mouse model of pancreatic cancer. To characterize the alteration of the secretome caused by the loss of *Smad4*, we performed proteomic analysis with conditioned media collected from *Smad4* wildtype and mutant cancer cell clones. Interestingly, the loss of *Smad4* resulted in the production of neuroendocrine related factors. In addition, gene ontology analysis with the secretome suggested that these factors were associated with neuronal processes. These data indicate that loss of *Smad4* in PDA cancer cells may lead to a neuroendocrine signature change. In particular, we found one of the most up-regulated secreted factors in the mutant cells was SPP1, which has been shown to promote tumor progression by affecting cancer cell stemness and macrophage polarization. To validate the proteomic results, we established orthotopic models with *Smad4* wildtype and mutant clones. We found that loss of *Smad4* resulted in larger tumor growth. Moreover, immunohistochemistry showed a significant up-regulation of SPP1 in the cancer cells of *Smad4* mutant tumors. To further profile the alteration of immune landscape, we stained for markers of myeloid cells and lymphocytes. We found that

Smad4 mutant tumors had an immunosuppressive microenvironment characterized by increased M2 macrophage, neutrophil and MDSC infiltration. Altogether, our study suggests that loss of SMAD4 in PDA may induce a neuroendocrine signature with increased SPP1 secretion in cancer cells. The production of this unique cancer cell secretome may result in a microenvironment marked by immunosuppressive myeloid cells.

#3642

SPHK1 mediated regulation of antitumor immunity in ovarian cancer

Prachi Gupta, Sudhir Kumar, Ishaque Pulikkal Kadamberi, Sonam Mittal, Jasmine George, Anjali Geethadevi, Pradeep Chaluvally-Raghavan, Sunila Pradeep. *Medical College of Wisconsin, Wauwatosa, WI*

Introduction: Sphingosine kinase 1 (SPHK1) is an enzyme that helps to synthesize biolipid sphingosine-1-phosphate (S1P). We showed extracellular vesicles facilitate an increased accumulation of S1P in the ovarian tumor microenvironment (TME). S1P enhances the exhaustion of CD8 T cells, thus downregulating anti-tumor immunity. Furthermore, we also found less ovarian tumor burden in SPHK1$^{-/-}$ mice compared to WT mice. Based on our preliminary data, we hypothesized that the SPHK1 depleted tumor microenvironment increases the infiltration of the immune cells and its activity downregulates the tumor progression.
Methods: SPHK1 global knockout mice and WT C57BL/6 mice were used in the study. Tumor cells (ID8 P53$^{-/-}$ BRCA$^{-/-}$) were injected, and tumor progression was studied. Immunophenotyping was performed by flow cytometry on ascites and tumor samples. Activation of CD8 T cells, B cells, and dentritic cells were studied by flow cytometry. Bulk RNA sequencing was performed on SPHK1$^{-/-}$ and WT tumors.
Results: SPHK1$^{-/-}$ mice showed regression in tumor growth in multiple tumor models. Tumor tissues from SPHK1$^{-/-}$ mice enhanced infiltration of CD4 and CD8 T cells, B cells, and dentritic cells compared to WT mice. Furthermore, infiltrated immune cells were active in SPHK1$^{-/-}$ mice. Bulk RNA sequencing also showed enhanced immune response in SPHK1$^{-/-}$ tumors compared to WT tumors.
Conclusion: SPHK1$^{-/-}$ environment decreased the tumor growth by enhancing the infiltration and activation of immune cells. We are currently

focusing on identifying the immune cells which are critical players in this process. We will further implement these findings in human immune cells for clinical benefits for ovarian cancer patients.

#3643

PTEN/STAT3 pathway in cancer-associated fibroblasts in pancreatic cancer

Samaneh Saberi, Sudarshana Sharma, Cameron Bumbleburg, Julia E. Lefler, Michael C. Ostrowski. *Department of Biochemistry & Molecular Biology, Medical University of South Carolina (MUSC), Hollings Cancer Center, Charleston, SC*

This study aims to test the hypothesis that direct interactions and auto-regulatory loop between PTEN and STAT3 in cancer-associated fibroblasts (CAFs) contribute to an immunosuppressive tumor microenvironment in pancreatic ductal carcinoma (PDAC). Pancreatic cancer accounts for almost as many deaths as cases because of its poor prognosis. Many studies have led to the paradigm that stromal elements contribute to pancreatic tumor growth. Cancer-associated fibroblasts (CAFs) are a primary cell type in the desmoplastic stroma in PDAC, and targeting them to improve PDAC treatment is thought to be a promising strategy, however; studies have shown both tumor-promoting and tumor-limiting activities associated with PDAC CAFs. Phosphatase and tensin homolog deleted on chromosome 10 (PTEN) is one of the most well-described tumor suppressor genes and can regulate essential transcription factors in stromal fibroblasts. On the other hand, STAT3 signaling in pancreatic CAFs contributes to the immunosuppressive and fibrotic stroma observed with disease progression. In this study, we used novel, dual recombinase mouse models of PDAC, with Kras and p53 mutations engineered in the pancreatic epithelium (Flp-based) and Stat3 deleted in a subpopulation of CAFS (Cre). CAFs isolated from these mice were used to probe PTEN-STAT3 interaction in vitro using the Proximity Ligation Assay (PLA) and by ChIP-seq using an RNA seq. Mouse and Human pancreatic tumor samples were analyzed and quantified using multiplex-immunofluorescence and multispectral imaging. In the mouse genetic model, we found PTEN downregulated in ~80% of CAFs, consistent with previous work from our group that demonstrated PTEN loss in 25% of PDAC patient samples. At the same time, pY705-STAT3 was

activated in CAFs, and deletion of STAT3 in CAFs correlated with increased survival, decreased M2-like macrophages, and increased T-cell infiltration. STAT3 ablation in CAFS resulted in the re-expression of PTEN in CAFS, implying an autoregulatory loop. PLA on CAFs isolated revealed that IL6 treatment resulted in the transfer of a STAT3-PTEN protein complex into the nucleus ChIP-seq on CAFs with PTEN STAT3 antibodies revealed a significant overlap in PTEN and STAT3 occupation of gene promoters. This result is consistent with *in silico* analysis on the PTEN and STAT3 ChIP-Seq data in human cell lines. ChIP-Seq data is being interacted with RNA data to identify essential target genes. Human PDAC tissue microarrays are stained with pSTAT3, PTEN, CD3, and CD8.Our study suggests an autoregulatory look between PTEN and STAT3 in PDAC CAFs. PTEN may suppress specific STAT3 target genes through direct interactions with chromatin. Alternatively, PTEN/STAT3 complexes may target CAF genes that suppress tumor growth or activate anti-tumor immune responses. These investigations could identify potential targets in CAFs for restoring the anti-tumor immune responses in PDAC.

#3644

Targeting the CD51/TGF-beta pathway: a potential innovative cancer immunotherapy in T-cell lymphomas

Jérôme Giustiniani[1], Anne Marie-Cardine[2], Sadjia Belkhelouat[1], Martine Bagot[2], Armand Bensussan[2], Nicolas Ortonne[1], Adèle De Masson[2]. *[1]TEAM "NEUROFIBROMATOSIS AND LYMPHOMA ONCOGENESIS ", INSERM U955 (IMRB)-Hôpital Henri Mondor, Créteil, France,[2]Oncodermatology and therapies, INSERM U976 HIPI- Hôpital Saint Louis, Paris, France*

T-cell lymphomas are a heterogeneous group of malignancies involving T lymphocytes and generally characterized by a poor prognosis. Among them, cutaneous T-cell lymphomas (CTCL) involve primarily the skin. The most frequent CTCL are mycosis fungoides and Sézary syndrome (SS) (1). There is no cure for advanced-stage CTCL, the remissions are generally rare and short, and the overall survival is around 5 years with an impaired quality of life. Thus, the development of new treatments inducing longstanding responses in CTCL is a major unmet need (2).
Because Sézary cells express several Treg markers as PD-1, ICOS, CD39 or CCR8 (3), we analyzed the expression of CD51, the αV integrin, which is

expressed with the β8 integrin on Treg cells (4). CD51 is involved in the production of active form of TGF-β, a cytokine with immunosuppressive properties that promotes tumor escape. Thus, targeting the αVβ8 integrin with a specific antibody has been shown to inhibit TGF-β activation while not inhibiting cell adhesion (5)**.**

Our results revealed that CD51 is significantly overexpressed in circulating lymphocytes from SS patients as compared to healthy individuals. Interestingly, CD51 is not associated with the β8 integrin but with CD29 (β1 integrin), and CD61 (β3 integrin) in some patients.CD51/CD29 and/or CD51/CD61 heterodimers appear as potential therapeutic targets in T-cell lymphoma, which may be associated with the production of active TGF-β. Targeting these heterodimers with specific antibodies to prevent the release of active TGF-β could improve patient's antitumor immune response. They could also represent depleting targets through NK or CAR-T cells activities as shown in diffuse intrinsic pontine glioma and glioblastoma for CD51/CD61 heterodimer (6).

1. Dobos G, et al. Epidemiology of Cutaneous T-Cell Lymphomas: A Systematic Review and Meta-Analysis of 16,953 Patients. Cancers. 11 oct 2020;12(10).2. Scarisbrick JJ, et al. The changing therapeutic landscape, burden of disease, and unmet needs in patients with cutaneous T-cell lymphoma. Br J Haematol. févr 2021;192(4).3. Giustiniani J, et al. CCR8 is a new therapeutic target in cutaneous T-cell lymphomas. Blood Adv. 2022 Feb 24.4. Stockis J, et al. Blocking immunosuppression by human Tregs in vivo with antibodies targeting integrin αVβ8. Proc Natl Acad Sci U S A 2017 Nov 21;114(47).5. Tsui P, et al. The TGF-β inhibitory activity of antibody 37E1B5 depends on its H-CDR2 glycan. mAbs. janv 2017;9(1):104-13.6. Cobb D, de Rossi J, Liu L, An E, Lee D. Targeting of the alphav beta3 integrin complex by CAR-T cells leads to rapid regression of diffuse intrinsic pontine glioma and glioblastoma J Immunother Cancer 2022.

#3645

OSM-induced LOXL2 expression hinges on upregulation of c-Myc and promotes tumor growth and metastasis, IL-1beta plays synergistic role in LOXL2 expression

Simion Dinca, Cody Wolf, Laura Bond, Cheryl Jorcyk. *Biomolecular Sciences, Boise State University, Boise, ID*

Ductal carcinoma is the most commonly diagnosed breast cancer in women, the presence of metastases drops patient five-year survival from 95% to an abysmal 27%. This makes studying the mechanisms that promote metastasis of critical importance. Research shows that the extracellular matrix (ECM) of the tumor microenvironment (TME) plays an important role in invasive ductal carcinoma (IDC) progression and metastasis. Specifically; the density, stiffness, and orientation of collagen I fibers in the stroma all impact IDC motility, invasion, and metastasis. Lysyl oxidase-like 2 (LOXL2) is a secreted enzymatic protein that is implicit in ECM remodeling. By catalyzing an oxidative reaction in peptidyl lysine/ hydroxylysine present on collagen I fibers, LOXL2 initiates crosslinking of the fibers. Our previous publication demonstrates that interleukin-6-related pro-inflammatory cytokine signaling, specifically oncostatin M (OSM), led to the overexpression and secretion of the LOXL2 enzyme. This increased the metastatic potential of IDC cells by promoting the crosslinking and alignment of collagen I fibers, which in turn led to increased invasion in 3D collagen I matrices. Thus, we hypothesize that OSM-induced LOXL2 expression, secretion, and subsequent collagen I fiber crosslinking and alignment, leads to an increase in IDC metastasis. *In vivo* studies utilizing nude athymic mice injected with either MCF7-Luc-EV control or MCF7-Luc-OSM overexpressing cells were performed in conjunction with LOXL2 inhibition using specially designed chow containing either LOXL2 SMI or control. Further analysis of OSM signaling pathways was performed in MCF7 and MDA-MB-468 IDC cells to determine mechanism for OSM induction of LOXL2. Our studies demonstrate that canonical OSM signaling pathways (pERK, pSTAT3, and pAKT) all contribute to LOXL2 expression in MCF7 cells suggesting a possible mediator protein we identified as c-Myc. Furthermore, OSM-induced LOXL2 played a significant role in OSM promoted tumor growth and metastasis as LOXL2 inhibition led to decreased tumor size and far less metastatic lesions. We also analyzed and confirmed a synergistic interaction between OSM and interleukin-1beta (IL-1β) in LOXL2 expression. These results confirm the significance of LOXL2 expression in OSM promoted metastasis and suggests LOXL2 would be an important target for future breast cancer therapies, specifically in patients with elevated levels of OSM. Furthermore, the synergistic interaction between OSM and IL-1β in LOXL2

expression suggests that patients with high levels of both cytokines are at even greater risk of metastasis, making these great markers for determining at risk IDC patients.

#3646

New functional role of tamoxifen in breast cancer immunomodulation: role of RACK7 in activation of type I interferon signaling and CEACAM1/TIM-3-dependent immunosuppression

Marvin A. E. Aberin[1], Yu-Ling (Pony) Lee[2], Xin-Guo Hsu[3], Chen-Yang Shen[4], Yao-Ming Chang[4], Kun-Yuan Lin[2], Chandan Guha[5], Shu-Ping Wang[4]. *[1]Taiwan International Graduate Program in Molecular Medicine, Academia Sinica and National Yang Ming Chiao Tung University, Taipei City, Taiwan,[2]Pharmacology Discovery Services Ltd., New Taipei City, Taiwan,[3]Graduate Institute of Life Sciences, National Defense Medical Center, Taipei City, Taiwan,[4]Institute of Biomedical Sciences, Academia Sinica, Taipei City, Taiwan,[5]Department of Radiation Oncology, Albert Einstein College of Medicine, Bronx, NY*

Despite advancements of immunotherapy against various cancers, breast cancer still retains poor response to immune checkpoint blockade (ICB) therapy. Therefore, the identification of promising target or new strategy to enhance ICB therapy in breast cancer is crucial. Here, we uncover that the DNA-damaging potential of tamoxifen (TAM) can shape the unfavorable but ready-to-fire tumor immune microenvironment in breast cancer. We discover that a long-term TAM administration unexpectedly induces JAK/STAT signaling and Type I interferon (IFN)-stimulated gene expression to promote T-cell infiltration. Furthermore, TAM also induces the expression of CEACAM1, which acts as an alternative T-cell inhibitory ligand *via* binding to TIM-3, a "checkpoint" receptor expressed on $CD4^+$ and $CD8^+$ T cells. The chromatin ''reader'' RACK7/ZMYND8, which functions as a transcriptional repressor of IFN-stimulated gene (ISG) and a critical factor in DNA repair, is found to be downregulated upon tamoxifen exposure and involved in the tamoxifen-mediated cellular modulation. We demonstrate that TAM in conjunction with RACK7-knockdown (KD) triggers robust upregulation of ISGs and CEACAM1 in both estrogen receptor-positive (ER+) and triple negative breast cancer (TNBC) cells.

This immunomodulatory effect lead by loss of RACK7 is specific to TAM treatment, and is not observed when combined with other endocrine therapeutics. TAM combined with RACK7-KD promotes mitochondrial DNA damage, which leads to accumulation of cytosolic DNA and subsequent activation of the cGAS/STING pathway. The murine breast orthotopic models with TS/A, EO771 and 4T1 cells further demonstrate that TAM-mediated immunomodulatory in conjunction with RACK7-KD evokes cytokine/chemokine secretion and further induces T-cell infiltration into tumor microenvironment. However, the tumor killing effect is limited due to promotion of T-cell exhaustion from CEACAM1-TIM-3 interaction between tumor and T cells. Thus, our study indicates that targeting CEACAM1-TIM-3 interaction is crucial for TAM-mediated tumor immune response. This brings promising therapeutic approach with TAM by combining RACK7-KD with blockage to CEACAM1-TIM-3 interaction in breast cancer. The resistance of tamoxifen treatment may be overcome, and RACK7 may serve as both a therapeutic target and a biomarker to enable ICB therapy.

#3647

Anti-tumor actions of neutrophils are mediated via STAT5 inhibition

Sanjana Rajgopal[1], Massar Alsamraae[2], Diane Costanzo-Garvey[2], Leah Cook[2]. *[1]Genetics, Cell Biology & Anatomy, University of Nebraska Medical Center, Omaha, NE,[2]Pathology & Microbiology, University of Nebraska Medical Center, Omaha, NE*

The overall patient survival rate drops dramatically when localized prostate cancer (PCa) progresses to bone metastatic prostate cancer (BM-PCa). The treatment for BM-PCa is limited to palliative therapy, and it is currently incurable. Neutrophils are the most prevalent immune cell in the bone, and we have found that PCa enhances their recruitment and infiltration into the prostate tumor-bone microenvironment of patients with BM-PCa. Additionally, we observed that bone marrow neutrophils directly induce apoptosis of PCa cells both in vitro and in vivo and that this is mediated by the inhibition of STAT5, a transcription factor that promotes PCa progression. Moreover, STAT5 has also been found to contribute to the development of resistance to standard care androgen deprivation therapy. Neutrophils specifically target and kill only cells that express STAT5, as

stable knockdown of STAT5 in BM-PCa cells makes them resistant to neutrophil-mediated cytotoxicity, while the overexpression of STAT5 in STAT5-negative PCa cells, which are generally resistant to killing by neutrophils, sensitizes them to neutrophil-mediated killing. Furthermore, transcriptomic analyses derived from the STAT5 knockdown and STAT5 overexpressing cells suggest that STAT5 expression in PCa induces pro-inflammatory signaling and that neutrophil-mediated cytotoxicity may be exerted via STAT5-induced IL-1 and/or IL-6. Preliminary data in our laboratory show that STAT5-induced production of IL-1 by PCa cells leads to their death by neutrophils, as knocking out the IL-1 receptor on neutrophils reduces their cytotoxic potential against STAT5-positive PCa cells. Interestingly, in addition to killing BM-PCa cells, we have demonstrated that bone marrow-derived neutrophils are also capable of killing pancreatic cancer cells. Further delineation of the role of neutrophils in STAT5 signaling in BM-PCa growth holds promise for enhancing neutrophil cytotoxicity in the bone which could lead to novel therapeutic options for bone metastatic prostate cancer.

#3648

MSU-42011, alone and in combination with selumetinib, reduces pERK levels in NF1 cancer cells and decreases *CCL2* expression in THP-1 macrophages

Pei-Yu Hung, Lizbeth Lockwood, Karen T. Liby. *Michigan State University, East Lansing, MI*

Neurofibromatosis type 1 (NF1) is a common genetic disease that predisposes approximately 50% of affected individuals to develop plexiform neurofibromas (PNFs), which can progress to highly aggressive malignant peripheral nerve sheath tumors (MPNSTs) in approximately 10% of patients. NF1 is caused by mutations in the tumor suppressor gene *NF1,* which encodes for neurofibromin, a negative regulator of RAS activity. Selumetinib, a specific inhibitor of MEK1/2, is the only FDA-approved drug for NF1-associated PNFs. However, the anti-tumor effects of selumetinib are limited in MPNSTs and have dose-limiting side effects. Deficiency of the *NF1* gene not only promotes tumorigenesis but also has broad effects on the immune cells and cytokine signaling driven by hyperactive RAS signaling. Because macrophages account for almost half

of cells in NF1 lesions and their infiltration highly correlates with disease progression, we hypothesized that targeting tumor-promoting immune cells could be an alternative approach for NF1 treatment. The novel retinoid X receptor (RXR) agonist MSU-42011 reduces tumor growth in experimental Kras-driven cancers by decreasing pERK expression, reducing tumor-promoting immune cells like $CD206^{+}$ macrophages and regulatory T cells, and increasing activated cytotoxic T cells. Here, we tested MSU-42011 and selumetinib, either alone or in combination, to evaluate their efficacy against NF1 cancer cells and macrophages using monoculture and conditioned media (CM) treatments. Treatment with 200 nM MSU-40211, 50 nM selumetinib, and the combination for 3 hours reduced pERK protein levels by approximately 40%, 70% and 90%, respectively vs. untreated controls. Treatment for 72 hours with selumetinib and the combination reduced the viability of PNF cells in a dose-dependent manner. Moreover, CM from human PNF cells increased monocyte chemoattractant *CCL2 (*C-C motif chemokine ligand 2) mRNA expression in human THP1 monocytes and THP1 macrophages differentiated by PMA. Notably, MSU-42011 and selumetinib alone similarly inhibited *CCL2* mRNA expression by 25% in THP1 macrophages stimulated with CM from PNF cells, and the inhibition of *CCL2* mRNA expression was enhanced to 50% with combination treatment. Taken together, our data suggest that MSU-42011 should be tested in relevant preclinical models of NF1.

#3649

Elucidating the role of CXCR4-CXCL12 in the tumor microenvironment of ER+ breast cancer samples using the Akoya PhenoCycler-Fusion System

Julien Tessier[1], Amir Bayegan[1], Dinesh Bangari[2], Joon Sang Lee[1], Lily Pao[3], Robert Rowlands[4], Donald Jackson[1], Angela Hadjipanayis[1].
[1]Precision Oncology, Sanofi, Cambridge, MA,[2]Global Discovery Pathology, Sanofi, Cambridge, MA,[3]Oncology Research, Sanofi, Cambridge, MA,[4]Kymab, Large Molecules Research Platform, Sanofi, Cambridge, MA

The aim of this work is to elucidate the role of the CXCR4-CXCL12 axis in ER+ breast cancer with spatial proteomics profiling. The CXCR4-CXCL12 signaling pathway has emerged as an axis of interest in cancer

tumorigenesis [1,2,3]. Current clinical trials aim to increase immune cell inflammation in solid tumors by blocking this pathway. Our analysis of bulk-RNAseq revealed ER+ breast cancer has high gene expression levels of CXCL12 transcripts, making it a potential tumor indication to investigate. We spatially characterized 20 ER+ breast cancer FFPE samples by developing a 13-plex antibody panel for the Akoya PhenoCycler®-Fusion system. This panel was designed to identify immune cells (CD45, CD3e, CD4, CD8, FoxP3, CD68), stromal cells (FAP, SMA, Podoplanin, S100A4), tumor and epithelial cells (PanCK) as well as the signaling duo (CXCR4, CXCL12). We performed cell segmentation on the multiplex immunofluorescence images, and quantified marker intensity in each cell. Phenotypes were manually identified after normalization, integration, and clustering of over 10+ million cells across 20 samples. Overall, the composition of tumor and immune cells varies significantly between patients showing the heterogeneity of their microenvironments. We observed CD8 T-cell exclusion in tumors associated with infiltration of fibroblasts (FAP+, SMA+, PDPN+) that do not express CXCL12. Instead, the CXCL12 signal is highly correlated with PanCK in all samples suggesting that either tumor cells are producing the chemokine or are being "coated" with the CXCL12 produced by fibroblasts. We also identify at least three known CXCR4+ immunosuppressive populations (fibroblasts, macrophages and Tregs) in the tumors which are known to be recruited via CXCR4-CXCL12 signaling[4,5]. This immunosuppressive tumor micro-environment (TME) results in the CD8 T-cell exclusion we observe in our samples as well as mentioned in multiple studies[1,6]. In summary, these results show the exclusion of cytotoxic T cells in the TME and the intricate relationship between tumor cells and immunosuppressive cells through the CXCR4-CXCL12 axis. This study shows the benefits of the Akoya platform compared to conventional IHC as well as the power of spatial phenotyping to study the TME immune biology for development of therapeutic strategies.

References: [1] Wang Z et al., 2022; doi:10.1073/pnas.2119463119 [2] Bockorny B et al., 2020; doi:10.1038/s41591-020-0880-x [3] Biasci D et al., 2020; doi:10.1073/pnas.2013644117 [4] Raschioni C et al., 2018; doi:10.1155/2018/501867 [5] Costa A et al., 2018;

doi:10.1016/j.ccell.2018.01.011 [6] Chen IX et al., 2019;
doi:10.1073/pnas.1815515116

#3650

STAT1 suppresses KRAS-driven lung adenocarcinoma depending on the tumor microenvironment

Christoph Trenk[1], Rebecca Sagmeister[1], Jaqueline Horvath[1], Monika Homolya[1], Andreea Corina Luca[1], Robert Eferl[2], Herwig Moll[1], Emilio Casanova[1]. *[1]Center for Physiology and Pharmacology, Medical University of Vienna, Wien, Austria,[2]Center for Cancer Research, Medical University of Vienna, Wien, Austria*

Lung cancer is responsible for the majority of cancer-related deaths worldwide. Within this severe disease lung adenocarcinoma (LUAD) belongs to the most common form of lung cancer. LUAD is highly correlated with KRAS mutations. Although, the first KRAS inhibitors entered into clinics recently, therapy resistance arises. Since KRAS-mutant LUAD is an inflammation driven disease, we focus on the JAK-STAT pathway as an alternative target. Preliminary data suggests that human KRAS-mutant LUAD is correlated to enriched JAK-STAT signaling, as well as STAT1 upregulation. Accordingly, we aimed to explore the tumorigenic functions of STAT1 in this form of lung cancer. Genetically engineered C57BL6/N mice which develop autochthonous KRAS-driven and P53-deficient LUAD proficient (KP) and deficient for STAT1 (KPS) were used. In a second mouse model expression of ovalbumin was induced in tumor cells, mimicking a neoantigen to increase immune infiltration in the presence (KPO) or absence of STAT1 (KPOS). Kaplan-Meyer analysis was performed to assess the overall survival. Tumor burden, as well as immune infiltration was analyzed in lungs 6 and 10 weeks after tumor induction via H&E, IHC and IF staining. Furthermore, the lung fluid was collected by bronchoalveolar lavage and used to profile inflammatory cytokines. Deletion of STAT1 reduced the survival in KRAS-driven LUAD mice only when ovalbumin was expressed. Tumor burden and tumor grades were increased in tumors lacking STAT1 at 6 and 10 weeks after tumor initiation. Surprisingly, although tumors of KPOS mice showed a decreased infiltration by T cells and CD4 T cells, CD8 T cell infiltration did not change, suggesting a tumor suppressive function of STAT1 via T cell

exhaustion. Moreover, the macrophage attracting cytokine CCL9 secretion was upregulated and the number of tumor infiltrating, immunosuppressive macrophages was increased in KPOS mice. This data implicates a tumor suppressive function of STAT1 by secretion of cytokines that can recruit suppressive myeloid immune cells to the TME leading to CD4 T cell exclusion and CD8 T cell exhaustion. Further studies are needed on the changes in the immune infiltrating cells to explain the mechanism behind these intriguing findings.

#3651

The role of caspase-1 in basal-like breast cancer and the tumor microenvironment

Wanda Marini[1], Weiyue Zheng[1], Kiichi Murakami[1], Pamela S. Ohashi[2], Michael Reedijk[3]. *[1]Princess Margaret Cancer Centre, University Health Network, Toronto, ON, Canada,[2]Department of Immunology, University of Toronto, Princess Margaret Cancer Centre, University Health Network, Toronto, ON, Canada,[3]Department of Surgical Oncology, University of Toronto, Princess Margaret Cancer Centre, University Health Network, Toronto, ON, Canada*

Introduction: Breast cancer is the most common malignancy in women world-wide. Basal-like breast cancer (BLBC) is an aggressive subtype with poor prognosis for which there are no known targeted therapies. Understanding what drives complex cell-cell interactions within the tumor microenvironment (TME) is critical to developing new strategies. BLBC has previously been shown to have high expression of the inflammatory cytokine IL1β, which then promotes the recruitment of pro-tumoral tumor-associated macrophages (TAMs) to the TME. Here we report that BLBC is uniquely capable of IL1β secretion due to elevated expression of caspase-1, a key component of the inflammasome required for IL1β maturation.
Methods: Using publicly available gene expression data sets, the association between caspase-1, breast cancer subtype and estrogen receptor (ER) co-expression was examined. These associations were further assessed *in vitro* by exposing luminal (T47D/MCF7) or BLBC (MDA-MB231) cell lines to siER knockdown or ER overexpression. Using both a CRISPR/Cas9 generated caspase-1 knockout (KO) BLBC mouse line as well as pharmacological inhibition with the caspase-1 inhibitor VX-765, the effect

of caspase-1 on tumor growth was studied in syngeneic immunocompetent mice. Immune infiltrates were assessed via flow cytometry of the excised murine tumors as well as immunohistochemistry. To prove these results were IL1β specific, caspase-1 KO tumor allografts containing self-cleaving IL1β were used for comparison. Finally, to determine potential synergy between caspase-1 and immune checkpoint inhibition, wild type and caspase-1 KO allografts were simultaneously treated with anti-PD1 immunotherapy. Tumor growth and immune infiltrates were analyzed between the treatment groups as stated above.
Results: Caspase-1 was found to be associated with the basal-like subtype and have an inverse relationship with ER expression. *In vitro*, inhibition of ER increased caspase-1 expression, whereas ER overexpression decreased caspase-1. Caspase-1 KO or pharmacological inhibition resulted in a significant decrease in tumor growth and TAM infiltration, and these findings were rescued back to wild type levels with the addition of a self-cleaving IL1β. Finally, caspase-1 inhibition reversed resistance to anti-PD1 immunotherapy in murine allografts, resulting in significant deceleration of tumor growth when used in combination.
Summary: The lack of ER in BLBC promotes caspase-1 expression, allowing IL1β maturation, macrophage recruitment and tumor progression. Genetic or pharmacologic inhibition of caspase-1 inhibits TAM recruitment and reverses resistance to immune checkpoint inhibition in BLBC.
Conclusions: Our data provides new insights into the biology of BLBC and identifies the combination of caspase-1/IL1β inhibition and immunotherapy as a novel therapeutic strategy to combat this disease.

#3652
Circular RNAs repress interferon responses in the sarcoma cells and promote sarcoma growth by forging a pro-tumorigenic immune microenvironment
Jlenia Guarnerio. *Cedars-Sinai Medical Center, Los Angeles, CA*

Circular RNAs (CircRNA) arise from events of non-conventional splicing in which the 3'-tail of an exon back-splices and joins the 5'-head of the upstream exon. Because of their structural conformation, these RNAs are incredibly stable in the cellular space, where they can regulate tumor-associated and anti-immunogenic pathways. Although circRNAs have been

profiled in many tumors, their functional contribution to cancer progression is still poorly understood. In the current study, we profiled the most abundant circRNAs expressed in Soft-tissue sarcomas (STS) and characterized them functionally and mechanistically. Surgery and chemotherapy are the standard treatments for STS, but the 5-year survival rate is still below 20% for the advanced cases. Response to immunotherapies, such as immune checkpoint inhibitors, is also marginal for STS, likely because sarcoma cells are not sufficiently immunogenic to recruit a high volume of cytotoxic T cells. To implement discoveries on STS, we recently generated novel immunocompetent STS mouse models and characterized the sarcoma-elicited mechanisms to block immune-recruitment. Interestingly, we observed that two circRNAs, circCsnk1g3, and circAnkib1, promote sarcoma growth by shaping a pro-tumorigenic microenvironment, possibly due to their capabilities to regulate tumor-promoting elements extrinsic to the sarcoma cells. More specifically, we observed that circCsnk1g3 and circAnkib1 control the expression of interferon-related genes and pro-inflammatory factors in the sarcoma cells, thus directing immune cell recruitment into the tumor mass and hence their activation. Mechanistically, we observed that circRNAs might repress pro-inflammatory elements by buffering activation of the pathways mediated by RIG-I, the cytosolic viral RNA sensor. The current findings suggest that targeting
specific circRNAs could augment the efficacy of sarcoma immune response to mainstay therapies.

#3653

Oncostatin m receptor signaling reprograms tumor microenvironment for chemoresistance

Anjali Geethadevi[1], Shirng-Wern Tsaih[2], Ajay Nair[3], Zhiqiang Ku[4], Ishaque Pulikkal Kadamberi[2], Deepak Parashar[2], Prachi Gupta[2], Sudhir Kumar[2], Jasmine George[2], Sonam Mittal[1], William Bradley[1], Robert F. Schwabe[3], Zhiqiang An[4], Ningyan Zhang[4], Sunila Pradeep[2], Pradeep Chaluvally Raghavan[2]. *[1]Obstetrics and Gynecology, Medical College of Wisconsin, Milwaukee, WI,[2]Department of Obstetrics and Gynecology, MCW Cancer Center, Medical College of Wisconsin, Milwaukee, WI,[3]Department of Medicine, Institute of Human Nutrition, Columbia University, New York,*

NY,[4]Texas Therapeutics Institute, Brown Foundation Institute of Molecular Medicine, The University of Texas Health Science Center, Houston, TX

Introducti**on:** High-grade serous ovarian carcinoma (HGSOC) is the most lethal gynecological malignancy and accounts for ~70% of tumor recurrences after standard chemotherapy and immunotherapy. Ovarian tumor microenvironment (TME) is undeniably complex which presents considerable challenge in understanding the immunotherapy treatment responses. Our previous study has revealed that Oncostatin M receptor (OSMR) is highly expressed in ovarian cancer cells and cancer associated fibroblasts (CAFs), whereas its ligand OSM is predominantly expressed in tumor associated macrophages (TAMs). This study aims to investigate how the OSM-OSMR paracrine signaling between tumor cells, CAFs and TAMs reprograms the TME to influence therapeutic responses in ovarian cancer.
Methods: We employed a 3D-3-cell co-culture method *in vitro* to understand how OSM/OSMR signaling modulates the interactions between ovarian cancer cells, CAFs and TAMs, that can impact therapy response of cisplatin resistant cancer cells in the ovarian TME. We performed RNA sequencing to study the differential gene signatures of each cell component in a 3-cell co-culture with their monolayer counterparts. This system was also challenged with chemotherapy-cisplatin and immunotherapy such as our newly developed anti-OSMR monoclonal antibodies to assess the therapy response of each cell component.
Results: Using single-cell and single-nuclear RNA seq dataset analyses of 17 human HGSOC patient ascites, we found that CAFs and TAMs are the predominant stromal or immune cell population enriched in ovarian cancer tissues. Using immunofluorescence, we identified that enrichment of CAFs along with extracellular matrix proteins surrounding tumor cells as an indication of heavily desmoplastic tumors. Using tumor-infiltrating immune cells dataset-TIMER, we found that high OSMR in cancer cells or CAFs along with high OSM in TAMs are associated with poor survival in ovarian cancer patients. Further, RNA sequencing data of 3-cell coculture models revealed an invasive, desmoplastic and immune-suppressive gene signature compared to independent culture conditions. Notably, CAFs and ovarian cancer cells co-cultured with TAMs exhibited an improved activation of JAK/STAT3 and PI3K-AKT oncogenic pathways for chemoresistance in ovarian cancer cells.

Conclusions: Our preliminary findings uncovered a potential mechanism of action of OSM-OSMR signaling in reprogramming ovarian cancer cells and stromal fibroblasts in ovarian cancer TME. Importantly, we highlight the importance of crosstalk between CAFs, ovarian cancer cells and TAMs for harnessing OSM/OSMR signaling for chemoresistance in cancer cells. Our findings also demonstrated the potential of anti-OSMR antibody therapy to target cancer cells and CAFs in the tumor microenvironment for abrogating desmoplasia; thus, improving chemosensitivity.

#3654

Olaparib combined with entinostat exerts differential effects on tumor-associated macrophages in tumors compared to ascites in syngeneic HR-proficient murine models of ovarian cancer

Vijayalaxmi G. Gupta[1], Tyler Woodard[1], Simona Miceska[1], Bisiyao Fashemi[1], Sangappa Chadchan[1], Wendy Zhang[1], Katherine Roby[2], Andrew Wilson[3], Fiona Yull[4], Marta Crispens[3], Sumanta Naik[1], Asya Smimov[1], Christina Stallings[1], Dineo Khabele[1]. *[1]University of Washington, School of Medicine, St. Louis, MO,[2]University of Kansas Medical Center, Kansas City, KS,[3]Vanderbilt University Medical Center, Nashville, TN,[4]Vanderbilt University, Nashville, TN*

Poly ADP ribose inhibitors (PARPi) are most effective in ovarian cancer tumors with homologous recombination (HR) deficiency. Our group has shown that histone deacetylase inhibitors (HDACi) sensitize HR proficient ovarian cancer cells to PARPi. Our current efforts are directed towards understanding how this therapeutic regimen alters tumor-associated macrophages (TAMs) in murine models of high grade serous ovarian cancer. To investigate the effects of Ola combined with Ent, we used HR-proficient ID8 P53 wild-type and ID8 $P53^{-/-}$ syngeneic murine models. Mice were randomized into 4 groups: control, Ola, Ent and Ola+Ent. Mice (Ent and Ola+Ent) were pre-treated with 15 mg/kg entinostat or vehicle (Ola and Ola+Ent) for one week via oral gavage and then treated with vehicle/Ent/Ola (100 mg/kg)/ Ola+Ent for two weeks. Mice were sacrificed 24 h after the last dose to harvest tumors and ascites. Tumors were processed for histology to determine cell proliferation (Ki67) and immune cell markers (CCL2, M1 and M2-like macrophages). Ascites fluid was

processed for flow cytometric analysis of immune cells. Tumors from parental ID8 P53 wild type mice showed significantly lower cell proliferation marker Ki67 ($P \leq 0.05$), higher anti-tumorigenic M1-like CCL2 ($P \leq 0.05$), and lower pro-tumorigenic M2-like mannose receptor ($P \leq 0.05$) in Ent and Ola+Ent groups compared to vehicle and Ola. Ascites showed no significant change in anti-tumorigenic M1-like macrophages, but significantly increased pro-tumorigenic M2-like macrophages ($P \leq 0.005$). ID8 $P53^{-/-}$ mice tumors showed significantly lower Ki-67 ($P \leq 0.05$) in Ola+Ent group compared to vehicle and mono-treatments. Ascites showed no significant change in total macrophage or pro-tumorigenic M2-like macrophages, but a significant decrease in anti-tumorigenic M1-like macrophages in Ent and Ola+Ent groups compared to vehicle. To summarize, in HR proficient ID8 P53 wildtype and ID8 $P53^{-/-}$ syngeneic mouse models, Ola and Ent treatment exerted anti-tumorigenic effects in tumors but potentially pro-tumorigenic effects in ascites. In conclusion, concomitant targeting of tumor TAMs and ascites TAMs may be a therapeutic regimen to investigate in the future.

#3655

Exploring the role of FasL in the ovarian cancer tumor microenvironment

Grace Keegan[1], Hilary Kenny[2], Agnes Bilecz[3], Ricardo Lastra[4], Ernst Lengyel[2]. *[1]University of Chicago, Chicago, IL,[2]Department of Ob/Gyn, University of Chicago, Chicago, IL,[3]Department of Pathology, University of Chicago, Chicago, IL,[4]Pathology, University of Chicago, Chicago, IL*

Introduction: High-grade serous ovarian cancer (OvCa) remains the deadliest gynecologic cancer in the United States because it often presents at an advanced stage when the disease is incurable. Despite the impressive clinical success of cancer immunotherapy in patients with lung cancer and melanoma, it is largely ineffective in OvCa patients. Resistance to cancer immunotherapy is mediated by the apoptosis of T-cells, which can be prevented by blocking Fas ligand (FasL), a death gene. However, little is known about the expression and function of FasL in OvCa. Therefore, the aims of this study were to identify the cells in the OvCa tumor microenvironment that produce and secrete FasL, and to delineate the

functional role of FasL in T-cell apoptosis within the OvCa tumor microenvironment.
Methods: FasL protein localization and levels were evaluated in OvCa tumors by immunohistochemistry (IHC) using a FasL antibody on tissue microarrays (TMAs) containing primary and matching metastases from 72 OvCa patients. In-situ hybridization (ISH) using a FasL specific probe was performed on omental OvCa tumors from pre- (n=12) and post-chemotherapy (n=12) patients to localize FasL mRNA. To define the role of OvCa and endothelial cell derived FasL on T cell apoptosis, co-culture experiments were completed. First, FasL was knocked down with a FasL siRNA or neutralized with a FasL antibody in OvCa (OVCAR8 and OVCAR5) cells or endothelial (HUVEC) cells. Next, the OvCa or endothelial cells were co-cultured with primary human blood mononuclear cell-derived T cells. Subsequently, the level of FasL secreted was measured using a FasL specific enzyme-linked immunoassay, and early (4h; cleaved-caspase 3) and late (24h; TUNEL assay) T cell apoptosis were analyzed by flow cytometry.
Results: FasL protein and mRNA are present in OvCa and endothelial cells in the tumor microenvironment of OvCa patients. Higher levels of FasL are detected in the endothelial cells when compared to the OvCa cells in these OvCa tumors. These results were confirmed in vitro as primary human endothelial cells secrete higher levels of FasL when compared to the OVCAR8 and OVCAR5 ovarian cancer cell lines. Functionally, both OvCa and endothelial cells stimulate early and late apoptosis in primary human blood mononuclear cell-derived T cells after a four hour co-culture. Knockdown or neutralization of FasL significantly inhibits the ability of OvCa or endothelial cells to induce early and late T cell apoptosis. In summary, FasL is localized to OvCa and endothelial cells in the OvCa tumor microenvironment, and both OvCa and endothelial cell derived FasL induce T cell apoptosis.
Discussion: These findings indicate that blocking FasL may be an effective approach for reducing T-cell apoptosis and improving cancer immunotherapy response in OvCa patients.

#3656
A multi-scale approach to quantitatively evaluate the SMAD signaling pathway

Ernest Heimsath[1], Lisa Arvidson[2], Reginaldo Prioli[2], Antony Wood[2].
[1]Agilent Technologies, Inc., Santa Clara, CA,[2]Cell Signaling Technology, Inc., Danvers, MA

Angiogenesis and cell proliferation are fundamental biological processes whose pathologic states represent two hallmarks of cancer. Central to controlling both processes is the TGF-β/BMP signaling pathway, for which the SMAD proteins serve as major downstream effector molecules. Upon ligand-binding, TGF-β or BMP type I/II receptor heterotetramers phosphorylate receptor-regulated SMADs (R-SMADs). TGF-β-receptor binding leads to SMAD2/3 phosphorylation, whereas BMP-receptor binding induces phosphorylation of SMADs 1/5/8. Phosphorylated SMADs (pSMADs) then form a complex with the co-SMAD SMAD4 at which point they undergo nuclear translocation, where they function as transcriptional modulators of target genes. The magnitude of SMAD phosphorylation and functional output (e.g., stimulated angiogenesis or attenuated cell proliferation) depends on both the ligand concentration, as well as the duration of exposure. In this study, we quantitatively evaluate the phosphorylation states of R-SMADs, as well as their downstream biological effects at three different biological scales: 1) biochemical, 2) cellular, and 3) tissue/3D models. At the biochemical level, the temporal and dose-dependent phosphorylation of R-SMADs in response to growth factor stimulation can be quantified using a quantitative ELISA approach. Growth factor stimulation can be quantified at the cellular level by high content imaging of SMAD phosphorylation and nuclear translocation, while simultaneously monitoring cell proliferation rates. Lastly, high-resolution confocal imaging can be employed to observe developmental consequences of phospho-SMAD signaling using a HUVEC-based 3D angiogenesis model system.
For Research Use Only. Not for use in diagnostic procedures.

Single Cell and Spatial Considerations of the Tumor Microenvironment

#4688
Comprehensive analysis of natural killer cell-associated markers using MultiOmyx™ immunofluorescence assay

Erinn A. Parnell, Jiong Fei, Harry Nunns, Eric Leones, Elaine Yeung, Blair Russell, Flora Sahafi, Qingyan Au. *NeoGenomics, Aliso Veijo, CA*

As a promising alternative platform for cellular immunotherapy, natural killer cells (NK) have recently gained attention as an important type of innate immune regulatory cell. NK cell immunotherapy approaches have been translated into clinical applications, and clinical trials of NK cell infusion in patients with hematological malignancies (HM) and solid tumors have thus far yielded many encouraging clinical results. Understanding the pattern of NK expression and the relationship to different states of NK cells may have direct relevance for immune responses in cancer. Approaches capable of simultaneously detecting NK cells with detailed information on NK differentiation state, however, remain limited. In this study, we used MultiOmyx hyperplexed immunofluorescence (IF) assay to classify and characterize the spatial arrangement of NK cell markers in a pan-cancer cohort including 9 tissue microarrays (TMAs) from breast, head and neck, prostrate, colon, bladder, lung, kidney, ovarian and melanoma indications. The panel includes CD3, CD4, CD8, CD16, CD45, CD56, CD57, CD137, FoxP3, Granzyme B, HLA-E, NKG2A, NKP46 and tumor segmentation marker. The panel enables the detection of NK cells expressing CD56 and/or NKP46 in the 9 different tumor indications. We also studied the expression of activating and inhibiting receptors, such as CD16 and NKG2A, in NK cell population. The active cytotoxic subsets of mature NK cells were evaluated using co-expression of NK cell surface markers with CD57 and the cytotoxic molecule expression in NK cells was assessed using co-expression with Granzyme B. Using proprietary deep-learning-based image analysis, we were able to quantify the densities of these different NK cell population and study the prevalence of these NK cells in different cancer indications included in this study. Many strategies have been developed for exploiting NK-mediated anti-tumor activities. CAR-NK cell therapy and antibodies that directly target NK cell inhibitory receptors such as NKG2A and TIGIT, are currently being evaluated in the clinical trials. The MultiOmyx NK cell panel reported in this study enables the comprehensive profiling of the NK population and can provide greater understanding of NK cell biology during cancer progression. The panel can be further used to explore the efficacy of the NK cell-based immune therapy.

#4691

Spatially resolved transcriptomics deconvolutes histological prognostic subgroups in patients with colorectal cancer and synchronous liver metastases

Colin S. Wood, Kathryn A. F. Pennel, Holly Leslie, Assya Legrini, Andrew J. Cameron, Paul Horgan, Joanne Edwards, Colin W. Steele, Nigel B. Jamieson. *Institute of Cancer Sciences, University of Glasgow, Glasgow, United Kingdom*

Patients demonstrating strong immune responses to primary colorectal cancer (CRC) have a survival benefit following surgery, while those with predominantly stromal microenvironments do poorly. Biomarkers to identify patients with colorectal cancer liver metastases (CRLM) who have good prognosis following surgery for oligometastatic disease remain elusive. The aim of this study was to determine the practical application of a simple histological assessment of immune cell infiltration and stromal content in predicting outcome following synchronous resection of primary CRC and CRLM, and to interrogate the underlying functional biology that drives disease progression. Patients undergoing synchronous resection of primary CRC and CRLM underwent detailed histological assessment, panel genomic and bulk transcriptomic assessment, immunohistochemistry (IHC) and GeoMx Spatial Transcriptomics (ST) analysis. Integration with genomic features, pathway enrichment analysis and immune deconvolution were performed. High-immune metastases were associated with improved cancer specific survival (HR, 0.36, P=0.01). Bulk transcriptomic analysis was confounded by stromal content but ST demonstrated that the invasive edge of the metastases of long-term survivors was characterized by adaptive immune cell populations enriched for Type II Interferon signaling (NES=-2.05 P.Adj<0.005) and MHC-Class II Antigen Presentation (NES=-2.09 P.Adj<0.005). In contrast, patients with poor prognosis demonstrated increased abundance of regulatory T-cells and neutrophils with enrichment of Notch (NES=2.2 P.Adj=0.022) and TGF-β (NES=2.2 P.Adj=0.02) signaling pathways at the metastatic tumor center. In summary, histological assessment can stratify outcome in patients undergoing synchronous resection of CRLM and ST analysis has revealed significant

intra-tumoral and inter-lesional heterogeneity with underlying transcriptomic programs identified in driving each phenotype.

#4692

Comparison of interassay similarity and cellular deconvolution in spatial transcriptomics data using Visum CytAssist

Mario G. Rosasco[1], Chi-Sing Ho[1], Tianyou Luo[2], Michelle M. Stein[1], Luca Lonini[1], Martin C. Stumpe[1], Jagadish Venkataraman[1], Sonal Khare[1], Ameen A. Salahudeen[1]. *[1]Tempus, Chicago, IL,[2]UNC Chapel Hill, Chapel Hill, NC*

Next-generation sequencing (NGS) of bulk cell populations is a useful and ubiquitous tool for the molecular characterization of clinical tumor samples. Bulk NGS reveals transcript abundance within a tumor sample and can further infer cell populations via deconvolution algorithms (PMID:31570899). However, it can't ascribe the cellular context for a given gene's expression or elucidate the spatial organization of tumor microenvironments. These additional features are critical to our understanding of tumor biology and are key to the development of immuno-oncology therapeutics. Spatial Transcriptomics (ST) is an emerging technology that characterizes gene expression within the spatial context of tissue. ST data can be generated directly from archival formalin fixed paraffin embedded samples, enabling the study of spatial gene expression in real-world clinical settings.

We have studied a dataset comprising 6 samples from non-small cell lung cancer (NSCLC) patients and 1 core needle biopsy from a tumor of unknown origin. We used the 10X Visium CytAssist platform to generate ST data and additionally generated paired bulk RNAseq data. To test the interassay reliability of CytAssist on archival FFPE tissue sections, we compared ST results across 3 sample preparation conditions. We further studied the state of the tumor microenvironment by applying state-of-the-art computational approaches to deconvolve immune cell populations and produce super-resolution ST maps, validated using multiplex immunofluorescence (IF) via CODEX (PMID:30078711).

We find key quality control metrics and spatial biomarkers are consistent across all 3 sample preparation conditions. When comparing deconvolution results between bulk and spatially-resolved methods we observe modest

correlations for many cell types despite differences in sample preparation, supporting the idea that bulk and spatial samples contain complementary transcriptomic information. However, within samples, we find many of the correlations observed in bulk do not show strong spatial correlation. These comparisons indicate the importance of considering spatial context when studying the tumor immune microenvironment. Finally, we find an agreement between super-resolution ST and multiplex IF across key spatial biomarkers.
These results demonstrate clinical archival FFPE samples yield high interassay reliability via the CytAssist platform. Results were consistent through 3 different H&E staining protocols and findings were consistent when superresolution deconvolution was utilized which further strongly correlated with high-resolution multiplex IF. Our findings demonstrate the feasibility and translational utility of ST to discover spatial signatures and the cellular context in retrospective clinical cohorts to empower discovery and translational efforts in precision oncology and therapeutic development.

#4694

Single-cell analysis of glioblastoma immune contexture identifies a subset of activated and memory tumor-reactive CD8+ TILs and a Treg signature contributing to TIL irreversible dysfunction

Irene Sambruni, Silvia Musio, Natalia Di Ianni, Martina Maffezzini, Monica Patanè, Marica Eoli, Antonio Silvani, Bianca Pollo, Francesco DiMeco, Serena Pellegatta. *IRCCS Istituto Neurologico Carlo Besta, Milan, Italy*

Despite the first classification of glioblastoma (GBM) as an immunologically “cold” tumor, evidence suggests that this cancer type is susceptible to T-cell infiltration, providing a glimmer of hope for developing effective immunotherapy approaches. However, whether the “exhausted” phenotype of tumor-infiltrating lymphocytes (TILs) and the immunosuppressive signaling in the GBM microenvironment (ME) can be therapeutically reprogrammed to unlock the anticancer potential of the immune system remains to be elucidated. We performed a histological analysis of GBM specimens collected pre-therapy from 24 newly-diagnosed GBM patients treated with dendritic cell (DC)-immunotherapy as part of the DENDR1 clinical trial (NCT04801147). Our preliminary results suggest

an association between the distribution and density of CD8+ TIL subsets and patients' responses to immunotherapy. TIL spatial patterns revealed either an immune-excluded or an immune-infiltrated scenario with either scattered or widespread TILs. A widespread CD8+ TIL pattern was significantly correlated with a better response to immunotherapy. It was also observed that the frequency of CD8+ TILs was significantly increased at recurrence compared to their primary tumors, suggesting that these patients are more likely to benefit from CD8+ T cell antitumor immunity. In light of these observations, we have hypothesized that tumor-reactive (TR) TILs isolated from GBM can be used as direct personalized treatment mediators exerting an effective antitumor activity with low side effects per se. TR-TILs were isolated from GBM surgical material using CD137 as a key marker, and successfully expanded from 50% of patients' GBM showing specific reactivity against autologous tumor cells. For the remaining cases, TR-TILs failed to expand, suggesting terminal dysfunction. Single-cell sequencing of the transcriptome was performed on the immune contexture after CD137+ TILs enrichment revealing the presence of a specific signature related to exhausted, cytotoxic, and memory state. A gene signature highly upregulated in regulatory T cells (Treg) was related to a more immune-suppressive ME. Flow cytometry analysis on immune contexture confirmed the presence of FoxP3+ CD4+ T cells, expressing CD137 can be enriched and persist, dysregulating the expansion of TR-TILs during the early stage in culture. Our preliminary findings indicate that a high frequency of Treg can be investigated as a negative predictive indicator of ex-vivo expansion of TR-TILs, which should be taken into consideration when planning a personalized TIL therapy.

#4695

Expansion of the extracellular proximity labeling (ePL) technique to novel matrisome targets

Joshua Rich, Sadeechya Gurung, Sukhbir Kaur, David Roberts, William Stetler-Stevenson, David Peeney. *National Cancer Institute, Bethesda, MD*

The extracellular matrix (ECM) is a complex and dynamic meshwork of extracellular macromolecules that plays a key role in cancer progression and metastasis. The matrisome encompasses the genes encoding ECM and

ECM-associated secretory proteins, and elucidating the protein-protein interactions (PPIs) of the matrisome is a promising area of study in the quest for a better understanding of cancer pathology and therapeutics. Proximity labeling, a powerful technique for investigating protein interactomes based on enzyme-fusion constructs and affinity chromatography, has considerable potential in detailing the protein-protein interactions of the matrisome. We have recently had success in developing a proximity labeling approach based on fusion constructs containing the biotinylating enzymes BioID2 and TurboID. We apply this approach to gain new insights into the interactome of the matrisome protein tissue inhibitor of metalloproteinase 2 (TIMP2), a protein found to have antitumorigenic potential. At present, we seek to expand this approach to other ECM protein targets, including tissue inhibitor of metalloproteinase 3 (TIMP3) and thrombospondin-1 (THBS-1). TIMP3 has been shown to possess anti-tumor properties, with loss of TIMP3 function associated with poor prognosis in multiple cancers. THBS-1 is a large (129 kDa) ECM protein that is relatively promiscuous with diverse functions in the tumor microenvironment. Expression of THBS-1 is frequently lost during oncogenesis, and such loss is associated with poor prognosis in some cancers. We describe how ePL can be expanded to these matrisome targets in different cellular systems (adherent vs. suspension) and show that ePL assays can be performed with stable and transient transgene expression. We show that ePL is a suitable method for studying PPIs in novel matrisome targets and expect to apply the technique to further targets in the near future.

#4696

Characterizing CD39 and CD73 cell subtypes in the tumor microenvironment using MultiOmyx

Courtney Todorov, Kevin Gallagher, Juliana Wortman, Harry Nunns, Erinn Parnell, Eric Leones, Elaine Yeung, Blair Russell, Flora Sahafi, Qingyan Au. *NeoGenomics, Aliso Viejo, CA*

CD39 and CD73 are membrane bound enzymes that function together to convert extracellular adenosine 5’-triphospate (ATP)/adenosine diphosphate (ADP) into adenosine. CD39 first catalyzes ATP/ADP into adenosine monophosphate (AMP), which is then converted by CD73 into adenosine.

Accumulation of extracellular adenosine creates an immunosuppressive tumor environment and facilitates tumor growth and metastasis. Conversely, the presence of ATP promotes a pro-inflammatory, tumor-suppressive environment. Suppression of CD73/CD39 activity and reduction of extracellular adenosine has been shown to support an antitumor immune response. Therefore, the targeting of CD73 and CD39, both individually as well as in combination with immune checkpoint inhibitors for biomarkers such as PD-1 and CTLA-4, is an emerging strategy for cancer therapeutics. CD73/CD39 have been described in multiple cell types, including tumor cells, fibroblasts, endothelial cells, tumor infiltrating lymphocytes (TILs), myeloid cells, and natural killer (NK) cells. While known to be expressed on multiple cell types, the spatial characterization of CD39 and CD73 in the tumor microenvironment (TME) is still poorly understood. Characterizing the diversity of active CD73 and CD39 populations in the tumor environment will help improve development of targeted therapies for cancer treatment. The multiplex immunofluorescence (mIF) platform MultiOmyx will be used to define the distinct populations of cells expressing CD73 and/or CD39 in the TME. MuliOmyx is a proprietary mIF platform for the visualization and characterization of up to 60 protein biomarkers in a single FFPE section. Herein we report the design and use of a novel panel of commercially-available antibodies broad enough to characterize CD39 and CD73 subpopulations in the TME of a variety of tumor indications including lung, prostate, and colon cancer. Using this panel in combination with proprietary deep-learning based image analysis, CD39 and CD73 positive cells can be characterized into different immune and TME subtypes. Understanding of the variety and phenotype of CD39 and CD73 expressing cells in the TME is crucial to define the populations being targeted by therapies for cancer treatment.

#4698

Reproducibility in spatial biology: reducing variables to improve the reliability of insight generation

Lisa Arvidson[1], Reginaldo Prioli[1], Samuel Jensen[1], James B. Hoying[2], Michael W. Golway[2], Michael J. Smith[3], Katie O. White[3], Richard A. Heil-Chapdelaine[3], Chi-Chou Huang[3], Tuan H. Phan[3], Hideki Sasaki[3], Melinda Angus-Hill[3]. *[1]Cell Signaling Technology, Danvers, MA,[2]Advanced*

Solutions Life Sciences, Manchester, NH,[3]Leica Microsystems, Bellevue, WA

There is an ongoing crisis in reproducibility in scientific studies, and studies in spatial biology are no exception. Cell DIVETM Multiplex imaging solution (Leica Microsystems) provides reliable workflow solutions to minimize variability from study to study. Cell DIVE allows probing and imaging of dozens of biomarkers on a whole tissue section with an iterative staining and dye inactivation workflow. At its core, Cell DIVE is designed to provide methods reproducibility, from tissue preparation, antigen retrieval, and sample imaging and slide storage. Cell DIVE is designed to work with directly conjugated primary antibodies, another source of variability. However, conjugated antibodies from Cell Signaling Technology (CST) are rigorously validated using stringent acceptance criteria to reduce variability. In addition, the use of recombinant antibodies, the consistent conjugate brightness and antibody degree-of-labeling reduce lot to lot variability, ensuring reliable conjugated antibodies for spatial biology studies. High resolution imaging results are obtained by consistent round to round imaging, consistent calibration and corrections, and reduction of human error using the BAB 200 liquid handling solution (Advanced Solutions Life Sciences). We present here, an iterative biomarker study using adjacent tissue sections probed with distinct lots of CST antibody panels, imaged in temporally separated batches using a Cell DIVE imager fitted with a BAB200 liquid handler. Following robust analysis (segmentation, phenotyping and statistical analysis), we report the reproducibility findings across parameters. Methods and results reproducibility in spatial biology is essential for reliable insight generation, giving confidence in the quality of future studies aimed at improving patient outcomes.

#4699

Pan-cancer single-cell analysis reveals the interactions of *SPP1+MMP12+* macrophages with metastasis-initiating cells that drives metastasis

Baifeng Zhang, Dora Lai-wan Kwong, Xin-Yuan Guan. *Department of Clinical Oncology, The University of Hong Kong, Hong Kong, Hong Kong*

Advanced understanding of cancer immunology has contributed to a significant decline in cancer deaths in the past few decades. However, there are still vast majority of patients with no effective response for current immunotherapy drugs because of some innate immune cells, particularly macrophages and neutrophils, promoting all steps of malignant progression to metastasis. Therefore, the development of new strategies against these pro-metastatic non-tumor components in the tumor microenvironment is in need. Tumor-associated macrophage (TAMs), as the critical component of tumor microenvironment (TME), display diverse and even opposing function phenotypes, but without systematic investigation on their ubiquitous characteristics across different cancer types. Here, we perform pan-cancer analysis on 92 samples across 6 solid cancer types to profile the TME of normal, primary tumor, metastatic lymph node and distant metastasis at single-cell resolution, illustrating the commonalities/plasticity of heterogenous TAMs. We uncover 21 distinct subtypes of TAMs with varying abundance and biological function in different tissue microenvironment, providing evidence for the plasticity of TAMs. In particular, the enrichment of *SPP1+MMP12+* macrophages in the TME of lymph node metastasis, likely interacting with metastasis-initiating cells (MICs), is associated with promoting malignant progression to metastasis and survival stratifications. Multi-color immunofluorescence (mIF) staining for relevant markers is being performed in mouse models and clinical samples for comprehensive validation. Our study comprehensively describes the characteristics and dynamics of TAMs and highlights their heterogeneity and plasticity depending on their surrounding microenvironment.

#4700

Spatial analysis of the immune microenvironment and tumor cell transition in sarcomatoid renal cell carcinoma

Allison May[1], Claire Williams[2], Stephanie The[1], Sean Kim[2], Nathan Schurman[2], Greg Shelley[1], Tyler Robinson[1], Simpa Salami[1], Rohit Mehra[1], Aaron Udager[1], Evan Keller[1]. *[1]University of Michigan, Ann Arbor, MI,[2]NanoString, Seattle, WA*

Background: Sarcomatoid renal cell carcinoma (sRCC) is thought to arise by epithelial to mesenchymal transition (EMT) of the parental tumor in

diverse RCC including clear cell RCC (ccRCC). sRCC is also known to be highly immunogenic and also express high levels of inflammatory pathway genes. Cells undergoing EMT and immune cells can have reciprocal feedback on each other; however, the role of such crosstalk in sRCC is unknown. Here, we use single cell spatial transcriptomics to evaluate the heterogeneity of EMT within sRCC in correlation with the immune microenvironment and in-vitro studies to explore mechanisms of crosstalk.
Methods: A sRCC nephrectomy specimen was subjected to single cell spatial transcriptomics of 1000 mRNA targets (NanoString CosMX). Semi-supervised clustering was performed and cell types were assigned by reference to single cell RNAseq data and then mapped spatially. Differential gene expression and cell to cell distance analysis was performed. In-vitro assays included treatment of 786-O and Caki-1 ccRCC lines with recombinant SPP1 and protein and mRNA analysis.
Results: Histopathologic evaluation revealed a ccRCC zone, a transition zone (tz) between the ccRCC and sRCC in which the ccRCC cells gained an increased mesenchymal morphology, and a well-developed sRCC zone. Transcriptomic data revealed four distinct tumor cell populations: a ccRCC, a tzRCC, and two sRCC populations. Importantly, a subset of the histologically-categorized ccRCC had a tzRCC transcriptional signature, demonstrating this signature is identifiable prior to development of morphologic features of sRCC. FZD4, a factor that may function in preventing EMT, was uniquely expressed on ccRCC and lost in tzRCC and sRCC cells. CCL20, a promoter of macrophage recruitment, was highly expressed in tzRCC. Distance analysis showed macrophages were highly spatially correlated with tzRCC and sRCC cells. Macrophages near tzRCC differentially expressed SPP1. In-vitro treatment of ccRCC cells with recombinant SPP1 led to induction of EMT and further upregulation of CCL20 expression.
Conclusion: We report a unique tumor cell population characterized by ccRCC morphology but harboring a transcriptome suggestive of progression towards sRCC. This provides rationale for the development of a novel molecular signature to subclassify ccRCC. We identified FZD4, CCL20 and SPP1 as key genes in the transition of ccRCC to sRCC which may mediate crosstalk between RCC cells and macrophages, with potential for therapeutic targets.

#4701

Spatial resolution of tumor and immune cell lineages in the hypoxic microenvironment of pancreatic ductal adenocarcinoma (PDAC)

Lisa Arvidson[1], Reginaldo Prioli[1], Samuel Jensen[1], Michael J. Smith[2], Katie O. White[2], Richard A. Heil-Chapdelaine[2], Chi-Chou Huang[2], Tuan H. Phan[2], Hideki Sasaki[2], Melinda L. Angus-Hill[2]. *[1]Cell Signaling Technology, Danvers, MA,[2]Leica Microsystems, Bellevue, WA*

Understanding how the tumor microenvironment (TME) evolves during tumorigenesis and therapeutic response is crucial to developing personalized treatments with the goal of improving cancer therapy. With robust and comprehensive multiplexed imaging technologies, immune biomarker antibodies can be used to interrogate immune cell lineages and structures. When combined with specific oncology biomarker antibodies, this approach can capture the immune response within the TME in a variety of neoplasms. The Cell DIVE^{TM} Multiplex Imaging Solution allows probing and imaging of dozens of biomarkers on a whole single tissue section using an iterative staining and dye inactivation workflow. The broad portfolio of robust IHC-validated antibodies from Cell Signaling Technology (CST) enables the detection of key proteins in the TME, allowing immune cell detection and phenotyping in tissue. Here, we demonstrate multiplexed Cell DIVE imaging using a novel CST panel to probe pancreatic ductal adenocarcinoma (PDAC). These biomarker antibodies define the immune cell landscape in the hypoxic tumor. Development of the antibody panel required minimal optimization, enabled the identification of complex cell types and revealed their cell-to-cell interactions within the tumor microenvironment. The availability of cell type specific biomarkers, combined with the ability to interrogate using multiplexed tissue imaging, provides unprecedented and novel insights and spatial resolution of immune cell populations with many cell types in the TME.

#4703

Applying spatial omics and computational integrative analyses to study drug responses and cancer immune cell interactions

Xiao Tan[1], Andrew Causer[1], Tuan Quang Anh Vo[1], Ning Ma[2], Bassem Ben Cheikh[2], Laura Genovesi[1], Jazmina Gonzalez-Cruz[1], Quan Nguyen[1], Oliver Braubach[2]. *[1]University of Queensland, Brisbane, Australia,[2]Akoya Biosciences, Marlborough, MA*

Cancer responses to drug treatment are highly heterogeneous. We postulate that spatial determinants in the tumour play a critical role in cancer therapy outcomes. Here, we will present two spatial transcriptomics studies on spatial responses to immunotherapy and chemotherapy.

Immune checkpoint inhibitors (ICI) are used to treat recurrent metastatic oropharyngeal squamous cell carcinomas (OPSCC). Unfortunately, less than 30% of patients benefit from this therapy. Thus, we performed spatial transcriptomics (ST) and *in-situ* multiprotein detection (PhenoCycler-Fusion) on tissue isolated from a patient diagnosed with metastatic OPSCC. The patient's primary oral tumour responded to chemo-radio therapy, followed by nivolumab ICI. However, new soft pallet OPSCCs resurged. Subsequent pembrolizumab combined with lenvatinib (VEGFR inhibitor) treatment had an initial effect, butnew recurrent oral tumours re-emerged suggesting drug resistance. Using ST, we observed high expression of drug resistance genes such as *SNAI2*, *SOX4* and *NDRG1* consistent with the disease aggressive behaviour. Although, *PD-1/PD-L1* expression was not observed, we identified 13 over-expressed druggable targets (*i.e.*, *EGFR, TF, VEGF*) and >10 experimental targets. To rank each drug's potential success, we measured the co-expression of each target ligand-receptor pair (L/R), reducing the candidates to 4 pathways (TF/TFRC> VEGFA/NRP1> PGF/NRP1> TGFB1/VASN>VEGFA/GPC1). Furthermore, TF/TFRC and VEGFA/NRP1 expected downstream genes were differentially over-expressed where positive LR signal was detected.

Similarly, we used ST to define the cellular diversity within a sonic hedgehog (SHH) patient-derived model of Medulloblastoma (MB) and identified how cells specific to a transcriptional state or spatial location are pivotal in responses to treatment with the CDK4/6 inhibitor, Palbociclib. We distinguished neoplastic and non-neoplastic cells within tumours and from the surrounding cerebellar tissue, further refining pathological annotation. We identified a regional response to Palbociclib, with reduced proliferation and induced neuronal differentiation in both treated tumours. Additionally, we resolved at cellular resolution a distinct tumour "interface"

where the tumour cells contacted neighbouring mouse brain tissue, consisting of abundant astrocytes and microglia, and continued to proliferate despite Palbociclib treatment.
Our data highlight the power of a spatial multi-omics approach to characterise the response of a tumour to targeted therapy and provide further insights into the molecular and cellular basis underlying the response and resistance to cancer therapies.

#4704

Characterizing and developing the clinical grade next generation sequencing based gut microbiome assay with the bioinformatics solution

Danyi Wang[1], Brajendra Kumar[2], Aaron Tenney[3], Ravi Kiron[4], Yang Liu[3], Fei Zhong[3], Juergen Scheuenpflug[5], Zheng Feng[1]. *[1]EMD Serono, Billerica, MA,[2]Sigma-Aldrich Chemicals Pvt. Ltd, Bangalore, India,[3]MilliporeSigma, St. Louis, MO,[4]EMD Serono, San Jose, CA,[5]Merck KGaA, Darmstadt, Germany*

Background: It has been recognized that gut microbiome has impact on the cancer immunotherapy efficacy and Cancer Microbiome-Immune Axis is reported. Also, it is important to discover and identify clinically translatable predictive biomarker in gut microbiome to inform the treatment selections. Multiple pre-analytical and analytical steps & factors including the sample collection, DNA extraction, library preparation, sequencing and bioinformatics analysis are associated with the microbiome data interpretation as well as its potential clinical application. 16S amplicon-sequencing coupled with bioinformatics approach for advance analysis provides end-to-end solution. It is therefore essential to develop a clinical-grade assay for targeting & characterization of taxa at genus and species level microbes in stool samples, which is designed as two-phase approach: firstly, identification the optimal sample preparation reagents using pre-mixed bacteria and healthy donor stool samples coupled with proprietary bioinformatics solution; secondly, exploratory analysis of patient samples.
Methods: Healthy stool samples (n = 30, gender ratio 1:1, 10 from US west coast, 10 from US mid-west, 10 from US east coast) were extracted across extraction kits (kit A, B and C). Following isolation, bacterial 16S rRNA amplicons were generated and sequenced using a 2x300 bp paired-end

configuration on the Illumina MiSeq. FASTQ files were analyzed using the Sigma-Aldrich® M-CAMP™ web platform[1].
Results: We previously compared 5 kits using ATCC® microbiome standards (MSA 2002 and MSA 2003). Kit A, B & C were identified as high yield DNA with the similar relative abundance of microbial family. In current study, we performed the taxonomical classification, diversity analysis and comparative analysis of 16S amplicon-seq using 30 healthy stool samples. The beta diversity showed all 3 kits clustered closely together which indicated the relative abundance of microbial families were similar across the extraction kits. The Weighted Unifrac showed significant difference among the kits (P = 0.046). Kit C species abundance is significantly difference than that of Kit A & Kit B (Pairwise Permanova P = 0.027 (Kit A vs C); P = 0.017 (Kit B vs C); P = 0.991 (Kit A vs B)). Relative frequency-based group-sample level composition at phylum and species level show high level similarity.
Conclusion: The comprehensive qualification approaches including the analytically optimized extraction condition and post-analytically implement the bioinformatics solution assures the characterization of microbiota for enabling biomarker driven precision oncology. Analytical performance assessment using colorectal cancer patients' samples is ongoing for further exploring its potential clinical utilities.

#4705

Profiling of immune cell components and soluble factors in ovarian cancer ascites highlights impaired immune environment

Assia Chaibi[1], Coriolan Lebreton[2], Dominique Bodet[3], Jean-Philippe Guegan[1], Guillaume Babin[2], Antoine Italiano[2], Alban Bessede[1], Imane Nafia[1]. *[1]Explicyte Immuno-Oncology, Bordeaux, France,[2]Medical Oncology, Institut Bergonie, Bordeaux, France,[3]ImmuSmol, Bordeaux, France*

Background: It's now increasingly recognized that ovarian cancer (OC) ascites play a significant role in OC progression - behavior of tumor cells is influenced by the nature of their surrounding microenvironment. Thus, characterization of ascites composition is essential to understand how this milieu affects tumor progression and particularly the immunosuppressive

pathways that would underlie immune response dysfunctions and, in turn, how biological ascites effects can be influenced by that composition.
Methods: Ascites samples were collected from advanced OC patients. Through respective multiplexed approaches of flow cytometry-based marker expression analysis and quantitation of mediators, immune context was profiled by investigating immune cell composition and levels of a plethora of soluble factors, including cytokines/chemokines, and metabolic pathways of some amino acids known to be involved in immunosuppression. Furthermore, ascites fluids were functionally screened for their biological effects on healthy monocytes, either undifferentiated or undergoing M1 polarization.
Results: Unlike healthy PBMCs, OC ascites were mostly "enriched" in regulatory/immunosuppressive immune cell subsets including T and myeloid populations. Also, T cells were shown to highly express immune checkpoints such as PD1 in T cells and TIGIT in Tregs. Intriguingly, a high CD4/CD8 ratio was seen. Also, CD163+ tumor-associated macrophages were shown to express CSF1R, CCR8 and CCR2, and to even display a mixed phenotype since also expressing Arg1, CD80, and iNOS. On acellular fractions, most ascites demonstrated elevated CCL18, IL6, LIF, VEGF, and CCL2 levels, and low IL2, IL4, and IL17 levels. Interestingly, unlike healthy plasmas, these ascites appeared to harbor a metabolically-immunosuppressive profile characterized by high glutaminolysis and tryptophan (Trp) degradation in kynurenine (Kyn). Functionally, we demonstrated that not only ascites basically polarized monocytes into M2 macrophages, but even antagonized with their M1 polarization to ultimately tilt to M2 status.
Conclusions: Taken together, our data show that ascites fluids most favorable to the M2 phenotype were associated with high LIF, VEGF, IL6, CCL2, and CCL18 levels, and with elevated Kyn to Trp ratios - Kyn levels being strongly higher than in healthy plasmas. Our results thus highlight a peculiar altered environment of OC ascites where a mixture of suppressive cells and signaling factors mediate extracellular cues leading to immune cell activity dysfunction. Altogether, these translational findings highlight OC ascites as a valuable tool to understand the mechanisms of suppression and develop predictive profiles, and to provide new insights for the identification of new targets and development of targeted-therapies.

#4706

Multispectral immunofluorescence analysis of the olfactory neuroblastoma tumor immune microenvironment reveals macrophage and polymorphonuclear leukocyte stroma localization and tumor parenchyma exclusion

Riley Larkin[1], Diana Lopez[1], Yvette Robbins[2], Wiem Lassoued[3], Gary Gallia[4], Clint T. Allen[2], Nyall R. London[1]. *[1]Sinonasal and Skull Base Tumor Section, NIH/NCI, Bethesda, MD,[2]Section on Translational Tumor Immunology, NIH/NCI, Bethesda, MD,[3]Tumor Immune Microenvironment Laboratory, Genitourinary Malignancy Branch, NIH/NCI, Bethesda, MD,[4]Neurosurgery, Johns Hopkins, Baltimore, MD*

Background**:** Olfactory neuroblastoma (ONB), also known as esthesioneuroblastoma, is a rare malignancy of the nasal cavity and anterior skull base. Multispectral immunofluorescence (mxIF), allows for comprehensive evaluation of tumor immune cell spatial relationships and thorough characterization of the tumor immune microenvironment (TIME). The objective of this study was to comprehensively define the ONB myeloid cell TIME with mxIF.

Methods: A tissue microarray including 47 clinically annotated human ONB samples was obtained, in addition to IRB approval, from our tertiary care hospital. A myeloid specific panel was validated in ONB tissue as well as controls. The panel stained for CD15, CD68, CD11b, CD14, HLA-DR, synaptophysin, and DAPI. Phenotypes of interest included $CD11b^{+}/CD15^{+}/CD14^{-}/HLA\text{-}DR^{low/-}$ polymorphonuclear leukocytes (PMNs), $CD11b^{+}/CD14^{+}/CD15^{-}/HLA\text{-}DR^{low/-}$ monocytes, and $CD68^{+}$ Pan Macrophages. HALO image analysis v3.4 was used to objectively quantify immune cell spatial relationships. A retrospective chart review was performed from these clinically annotated specimens with collection of patient demographics, stage, Hyams grade, dural infiltration status, and outcomes.

Results: Three samples were excluded based on too little available tissue for meaningful analysis. Of the remaining 44, 38 were primary and 6 were recurrent tumors. PMNs, monocytes, and macrophages are present in the TIME of ONB at 22 cells per mm^2, 2.0 cells per mm^2, and 34 cells per mm^2 respectively. Increased PMN and macrophage cell densities were noted in

the stroma when compared to the tumor parenchyma (28 cells per mm^2 vs 14 cells per mm^2, $p<0.0001$ and 46 cells per mm^2 vs 21 cells per mm^2, $p<0.0001$). A similar trend was seen in monocytes (3.5 cells per mm^2 vs 0.80 cells per mm^2, $p=0.0588$) but it did not reach statistical significance. When we compared by Kadish Stage, higher stage (C/D) had more tumor infiltrating PMNs than low stage (A/B) (median of 1.3 cells per mm^2 vs median 0 cells per mm^2, $p=0.0011$). No further differences in cell distributions were noted when comparing for Hyams grade, stage, dural infiltration, recurrent disease, or other clinical factors. Nearest neighbor analysis demonstrates that macrophages are closer to tumor cells than PMNs or monocytes (19.68 μm vs 27.78 μm, $p<0.0001$, and 25.77 μm, $p=0.0026$, respectively).
Conclusion: This study is the first to comprehensively define the ONB myeloid TIME using mxIF. Our study demonstrates the ONB TIME contains abundant myeloid populations. As these cells have been shown to be immunosuppressive, thereby fostering tumor cell escape and host evasion, in other human malignancies we posit they play a similar role in ONB. The functional study of myeloid populations in ONB, and whether they represent targets for therapeutic intervention, is warranted.

#4707
LED photobleaching-based multiplex 3D microscopy of the tumor microenvironment
Jingtian Zheng[1], Evan Phillips[1], Yi-Chien Wu[1], Steve Seung-Young Lee[1], Vytautas Bindokas[2]. *[1]University of Illinois at Chicago, Chicago, IL,[2]The University of Chicago, Chicago, IL*

Multiplexing in immunofluorescence imaging is important for the spatial profiling of cells and molecules in tumor tissue samples. Cyclic immunofluorescence (IF) methods using oxidants (e.g. hydrogen peroxide) and enzymes (e.g. DNase) localize a great number of cellular makers and proteins in a tissue section while repeating a process of IF staining, imaging, and fluorescence deactivation. However, the repeated use of chemicals and enzymes might cause artifacts in tissue and cell morphologies. Furthermore, these methods are restricted to thin tissue sections (~5 μm thick) which are inappropriate to provide comprehensive

structural information on tissue samples. Although reconstruction of two-dimensional (2D) images from serial tissue sections can provide a certain volumetric tissue image, it takes a huge amount of time and effort. Here we introduce a three-dimensional (3D) multiplex IF imaging method using LED photobleaching. We built high-power LED illuminators with 100W warm (emission wavelength: 480-700 nm), green (430-520 nm), and red (600- 680 nm) LED chips, which can efficiently bleach a broad or selected wavelength of fluorescence signals in tissue samples. We integrated this LED photobleaching with the Transparent Tissue Tomography (T3) protocol and created a 3D cyclic IF method involving tissue macrosectioning (400 μm), three-color IF staining, D-fructose-based tissue clearing, 3D confocal fluorescence microscopy, LED photobleaching, tissue washing, and three-color IF staining for other biomarkers, and repeating the process. By applying this method to mouse mammary tumor tissues, we could perform 8-plex fluorescence microscopy for visualizing cell nuclei (DAPI), vascular (CD31, SMA) and structural (ER-TR7) cells, immune cells (CD3, CD8, CD45), and cancer cells (CK8) in the tumor macrosections in 3D at tissue and cellular resolution. To validate the method as an evaluation tool for immunotherapy, we treated the mouse mammary tumor with a STING agonist (DMAXX) intratumorally and collected the tumor tissue 1 day after the treatment, and processed it for the 3D cyclic IF protocol. The quantitative multiplex image data showed immune-driven-cancer eradication and high tumor infiltration of a large number of CD3+CD8+CD45+ cytotoxic T cells. We also examined that Red and Green LED illumination can selectively bleach fluorophores in tissues, which would be useful for patterning fluorescence in tissue as well as studying fluorescent drug-cell interaction in a tissue. In summary, this chemical and enzyme-free 3D cyclic IF imaging method will be a powerful tissue assay tool to provide comprehensive spatial information of tissue (tumor) samples including cell types, cellular and molecular location, and their 3D organization in a tissue sample.

#4708

Application of spatially resolved transcriptomics to screen multiple tumor biospecimens using tissue microarrays

Syrus Mohabbat[1], Hardeep Singh[1], Stephen R. Williams[2], Lauren M M. Gutgesell[3], David J. Sukovich[3], Govinda M. Kamath[2], Hanyoup Kim[4],

Amanda Janesick[5], Robert Shelansky[2], Ghezal Beliakoff[5], Augusto M. Tentori[4], Albert Kim[1], Cedric R. Uytingco[1], Sarah Taylor[5]. *[1]Cell Biology, 10X Genomics, Pleasanton, CA,[2]Computational Biology, 10X Genomics, Pleasanton, CA,[3]Molecular Biology, 10X Genomics, Pleasanton, CA,[4]Microfluidics, 10X Genomics, Pleasanton, CA,[5]Applications, 10X Genomics, Pleasanton, CA*

The tumor microenvironment is composed of highly heterogeneous structures and cell types that dynamically influence and communicate with each other. Although examination of singular biospecimens is sufficient for diagnostic purposes, it is inadequate and cost prohibitive when scaling for complex and overarching studies. Thus, high density multi-tumor tissue microarrays (TMAs) have been a practical and effective solution for high-throughput molecular analysis of tissues. Introduced more than a decade ago, TMAs have been instrumental in the recent study of tumor biology, the development of diagnostic tests, the establishment of quality control, and the investigation and identification of oncological biomarkers. Here, we demonstrate the pairing of the 10x Genomics Visium Cytassist Spatial Gene Expression Solution and Xenium In-Situ Platform on multi-tumor TMAs to screen for common biomarkers among a cohort of samples. Spatial transcriptomics technology has proven valuable in mapping the whole transcriptome with spatial context (Visium), whereas In Situ (Xenium) enables high-throughput cellular characterization at single-cell resolution. With the addition of our CytAssist platform, we expand on the pre-existing standard Visium solution by facilitating the retrieval of RNA transcriptomic information from tissues placed on standard or archival slides. On the other hand, the novel Xenium platform compliments whole transcriptome Visium data by unlocking the potential to assign transcripts to a particular cell with spatial context and subcellular resolution. The combination of spatial transcriptomics and targeted in situ data with FFPE TMAs promotes a high-throughput method to accelerate the uncovering of molecular signatures suitable to understanding the tumor microenvironment. We showcase the ability to spatially and comprehensively resolve individual oncogene and tumor suppressor genes associated with multiple tumors from a cohort of cancer patients and from multiple different tumor samples. In addition, these markers are mapped back to distinct morphological features within each tissue core, and use differential gene expression data to identify

distinct cell types throughout the different patient tissues. By combining the throughput of TMA samples and depth of the Visium and Xenium platforms, the strategy enables greater insights into cell-type specifics while also expanding the spectrum of biospecimen types that can be analyzed.

#4709

Spatial whole transcriptome profiling of human normal liver and HCC uncovers unique insights into metabolic zonation

Yan Liang[1], Nan Wang[2], Xia Li[2], Liang Zhang[1], Megan Vandenberg[1], Andy Nam[1], Charlie Glaser[1], Kathy Ton[1], Zhiyong Ding[2], Joseph Beechem[1].
[1]NanoString Technologies, Inc., Seattle, WA,[2]Fynn Biotechnologies, Jinan, China

Understanding the physiology and functions of the liver and cancer requires knowing transcriptional patterns driving biological activities within the functional structures of the tissue, especially the zonated features of the liver metabolic networks. Using the powerful and unique capabilities of GeoMx® Digital Spatial Profiler (DSP) with the Whole Transcriptome Atlas (WTA) panel to resolve functional units within FFPE tissues *in situ*, here we report the spatial analysis of whole transcriptomes across three micro-dissected zones (pericentral zone 3, intermediate zone 2 and periportal zone 1) of human normal liver and HCC. We also report the whole transcriptome expression data from Kupffer cells, portal traits and interlobular bile ducts from four normal liver samples and HCC. 500 - 3000 genes were detected from functional groups within each histological structure. In the liver functional units, 1000 - 2500 genes were detected in zone 1, 2 and 3 separately. By comparing the whole transcriptome profiles of zone 1 and zone 3, we have found 32 differentially expressed targets (fold change > 1.5, p value < 0.05) which showed a gradient expression pattern along the porto-central axis. The expression patterns of *CYP1A2, CYP2E1*, *CYP3A4 and ALDOB* matched well with their respective patterns of protein expression (Human Protein Atlas), recapitulating the well-studied distribution of functional activities along the porto-central axis. Moreover, by combining with Gene Set Enrichment Analysis (GSEA), we have found important pathways involved in metabolisms in either the pericentral area or the periportal area. Pathways including biological oxidations (*CYP1A2, CYP2E1*, *CYP3A4, ADH1A,* and *ADH1B*) and lipids metabolism (*AKR1C1*,

AKR1C2, and *SLCO1B3*) showed high enrichment in zone 3 and decreased towards zone 1. In contrast, pathways including platelet degranulation (*FGA*, *FGB*, *FGG*), glucose metabolism (*ALDOB* and *PCK1*) and amino acids metabolism (*HAL*, *SDS*, *NNMT*, and *GLS2*) showed high enrichment in zone 1 and decreased towards zone 3. In conclusion, our WTA data has revealed clear metabolic zonation in the liver along the porto-central axis. GeoMx technology with WTA is a powerful tool to investigate the underlying mechanisms of liver metabolism, regeneration, and tissue structure. It can be further utilized to study the whole transcriptomic differences in normal and diseased tissue.
FOR RESEARCH USE ONLY. Not for use in diagnostic procedures.

#4710

Novel 3D cytotoxicity assay to assess the impact of chimeric antigen receptor (CAR) domain design on the tumor infiltration and cytotoxicity efficacy of CAR T-cell therapies for solid tumors

Adrian Johnston[1], Zeqi Wan[1], Tina Chen[1], Yeongseo Lim[1], Cameron Lee[1], Wenxuan Du[1], Jude Philip[2], Denis Wirtz[1]. *[1]Institute for NanoBiotechnology, Johns Hopkins University, Baltimore, MD,[2]Biomedical Engineering, Johns Hopkins University, Baltimore, MD*

CAR T-cell therapy is a popular topic of discussion in and out of the scientific community. Already with multiple therapies FDA-approved for certain blood cancers, focus has rightly shifted toward FDA approval for solid tumor indications. Yet, advancing past clinical trials to FDA approval has yet to occur and has proved challenging. Of course, multiple factors are at play as to why, but we aim to use-in house expertise to elucidate one, namely CAR T-cell tumor infiltration and tissue migration and surveillance efficacy. Migration is a central parameter ignored in traditional 2D cytotoxicity assays, but there is no tumor cell killing by T cells if there is no T cell migration. We developed a novel first-of-its-kind organoid-based 3D cytotoxicity assay using multicompartment organoids and the most abundant extracellular matrix protein in human organs, collagen. We suspend solid tumor organoids in the center of CAR T-cell/collagen gel mixtures that are solidified then imaged in intervals in the span of two weeks by live-cell time-lapse reflection/fluorescence confocal microscopy, after which standard luciferase-based readouts of quantitative specific lysis

is determined. Our assay allows high-resolution tracking of CAR T-cell 3D movements through collagen fibers surrounding solid tumor organoids to determine their random and directional migration as well as their surveillance and infiltration of solid tumor organoids. We will describe the differences between currently in clinical trial mesothelin-specific CAR T-cell therapies that differ in their scFv, hinge, transmembrane, and costimulatory domains; and comparing alongside the traditional 2D luciferase-based cytotoxicity assay, we will underline how 3D migration and infiltration around and into mesothelin-expressing ovarian cancer cell organoids allow the determination of CAR T-cell therapy efficacy of different CAR T clones in a lab's arsenal for a given solid tumor through migration, infiltration, and subsequent cytotoxic capacity that is absent in traditional 2D cytotoxicity assays. CAR T-cell therapy vector design and cloning can thus be tuned for optimal migration and infiltration using our novel 3D cytotoxicity assay.

#4712

Spatial biology of tumor-stroma assembloids reveals that nothing is lost, nothing is created, everything is reorganized

Gina Bouchard[1], Irene Li[2], Weiruo Zhang[2], Sylvia Plevritis[2]. *[1]Stanford University School of Medicine, Stanford, CA,[2]Biomedical Data Science, Stanford University School of Medicine, Stanford, CA*

A close association between active fibroblastic foci (desmoplasia) and distant metastasis in the lung adenocarcinoma (LUAD) has been established decades ago and yet, the pro- and anti-tumor properties of cancer-associated fibroblasts (CAFs) are still being resolved in the hope of preventing LUAD progression. To better understand the role of stromal cells in progression, there is a growing interest in 3D patient-derived models for their translational and throughput advantages. In parallel, the emergence of multiplexed spatial biology platforms is advancing translational oncology forward by providing a more global understanding of the tumor microenvironment (TME). Despite the enthusiasm for these new technologies, there are no study showing the applicability and significance of using multiplexed spatial biology to characterized 3D patient-derived models. Here, we modeled spatial heterogeneity by assembling EGFR mutated patient-derived organoids (PDOs) with fibroblasts harvested from

the tumor edge (tumor-adjacent fibroblasts; TAFs) or tumor core (tumor core fibroblasts; TCFs) referred here as tumor-stroma *assembloids*. Using these assembloids, we generated an extensive dataset with CODEX imaging technology and used a quantitative approach to dissect tumor-stroma crosstalk. Our results show that TAFs expressing the myofibroblast marker aSMA were strictly found at the periphery of the hydrogel dome containing the assembloid, while aSMA- fibroblasts were found strictly in the center. In contrast, we did not observe a similar spatial organization in TCF assembloids. Next, we used CELESTA, an unsupervised machine learning algorithm that uses prior knowledge of the cell expression and spatial information to dissect cell heterogeneity, then performed co-localization analyses. We also leveraged the EGFR mutation status of the PDOs and observed the protective effect of the fibroblasts from erlotinib. Both assembloid conditions showed drastically different tumor-stroma spatial changes including gains and losses of colocalizations even though erlotinib did not significantly change the subpopulation fractions, cell heterogeneity, nor cell density. The top tumor-stroma colocalization pairs that persisted after erlotinib involved either myofibroblasts and PanCK-Vim+MUC1+ cancer cells or were found in the center of the assembloids, shielded by a stromal barrier of myofibroblasts. Taken together, our results show that the assembloids undergo drastic spatial reorganization following erlotinib treatment even though subpopulation fractions and cell heterogeneity remain unchanged. This study provided new insights on tumor-stroma crosstalk in the LUAD and motivates the use 3D patient-derived models coupled with multiplex imaging to answer complex spatial biology questions.

Spatial Considerations of the 3D Tumor Microenvironment

#5782
The dynamic immune behavior of primary and metastatic tumors of ovarian cancer

Elaine Stur[1], Fuduan Peng[1], Pang-ning Teng[2], Emine Bayraktar[1], Min Hu[1], Sara Corvigno[1], David J. Brown[3], Sanghoon Lee[1], Kathleen N. Moore[3], Nicholas W. Bateman[2], Kathleen M. Darcy[2], George L. Maxwell[2], Thomas Conrads[2], Nicole Fleming[1], Nicholas Navin[1], Linghua Wang[1], Anil K.

Sood[1]. *[1]The University of Texas, MD Anderson Cancer Center, Houston, TX,[2]Uniformed Services University of the Health Sciences, Bethesda, MD,[3]Stephenson Cancer Center at the University of Oklahoma Health Sciences Center/Sarah Cannon Research Institute, Oklahoma City, OK*

Background: Despite advances in cancer diagnosis and therapy, high-grade serous ovarian cancer (HGSC) is often diagnosed when spread to multiple intraperitoneal areas; it is prone to metastasize to adipose-rich tissues such as the omentum. To gain a deeper understanding of the molecular determinants of the HGSC milieu, we carried out a single-cell analysis of primary and metastatic tumors of HGSC. Thus, our aim is to identify molecular mechanisms that lead to immunosuppressive mechanisms of HGSC in primary and metastatic tumors of HGSC.
Methods: Fresh HGSC surgical samples from 19 patients were collected right after surgery, dissociated, and then frozen. For single-cells analysis, cells were sorted by a viability dye and CD45+/- populations followed by Single cell 10X 3'v3 protocol (10X Genomics) and sequenced using the NovaSeq6000 S2 sequencer. Cell Ranger toolkit v3.1.0 (10x Genomics) was applied for data processing, followed by further downstream analysis using multiple packages from R Package Seurat.
Results: To elucidate the cellular heterogeneity of HGSC, we analyzed 100,480 cells, including epithelial, lymphoid, and myeloid populations; these were identified and represented across all patients. We explored the epithelial compartment further, including a total of 21,144 cells. Given the importance of metastatic lesions for the treatment and outcome of patients with HGSC, we examined expression programs among primary and omentum tumors as well treated and untreated tumors. The major differences between primary and omental metastatic tumors included enrichment of EMT pathways and angiogenesis, as well as a decrease in the IFNα and IFNγ response in the omentum. IFNα and IFNγ response pathways were also upregulated in primary treated (P-NACT) tumors, when compared with primary untreated (P-UT) tumors. To explore the immune compartment, we clustered the immune cells across patients in 28 sub-clusters, including 19 sub-clusters of T-cells and Natural Killer cells. Altogether, the immune infiltration on P-UT indicated an immune infiltrate environment and the composition of P-UT was highly enriched in lymphoid cells with a late stage of differentiation. This finding was also demonstrated

by the analysis of T cell trajectories, with a clear definition that CD8 and CD4 cells from P-UT tumors are in a late/ final and exhausted stage of differentiation, while post-NACT tumors (independent of tissue type) are in early stages (naïve/ central memory). The measurement of a dysfunctional score showed that P-UT tumors have the highest scores, indicating a potential increase in tumor reactivity in P-UT tumors.
Conclusions: Collectively, these data indicate that HGSC primary and omentum tumors are very distinct niches for immune cells, with primary being much more dysfunctional than omentum tissue, which could indicate that the application of immunotherapies would have different impacts in variable niches of HGSC.

#5783

Integration of AI-powered digital pathology and imaging mass cytometry to identify relevant features of the tumor microenvironment

Alessandra Rigamonti[1], Marika Viatore[2], Rebecca Polidori[1], Marco Erreni[3], Maria Fumagalli[3], Daoud Rahal[4], Massimo Locati[1], Alberto Mantovani[3], Federica Marchesi[1]. *[1]University of Milan-Humanitas Research Hospital, Milan, Italy,[2]Humanitas Research Hospital, Milan, Italy,[3]Humanitas Research Hospital, Pieve Emanuele, Italy,[4]Humanitas Research Hospital, Rozzano, Italy*

Digital pathology coupled to artificial intelligence (AI)-powered approaches are receiving great attention in the oncoimmunology field, as their adoption holds promise to improve current diagnostic workflows and potentiate the analytic outputs. In this work, we aimed at combining different histopathological approaches and AI-aided analytic tools to analyze the ecosystem of tumor tissues. By deploying AI-powered standard H&E and high-dimensional imaging-mass cytometry (IMC) to FFPE tissue samples, we could extract quantitative and standardized features that couldn’t have been easily identified and integrated by eye. One tissue microarray (TMA) slide containing 108 spots of NSCLC specimens (both adenocarcinoma and squamous carcinoma) was stained with H&E and scanned through the Axio Scan.Z1 (ZEISS) to generate high-quality virtual images. A deep learning algorithm was trained and applied to H&E images to identify tumor cells. The consecutive tissue section was stained with metal-labeled antibodies and processed through the Hyperion workflow (StandardBiotools), allowing

quantitative detection of a panel of 23 markers related to tumor cells (Pan-cytokeratin), tissue architecture (aSMA, Vimentin, CD31, Collagen I, nuclei), CD45+ immune cells, comprehensive of myeloid cells (CD68, CD14, CD16, CD163, CD63, CCR4), lymphoid cells (CD3, CD4, CD8, FOXP3, CD20) and immune activation (S100A8, HLA-DR, Granzyme-B, KI67, Arginase-1). Data were exported as MCD files, visualized using the MCD viewer and further analyzed with the Qupath software. Cell segmentation was performed by the CellProfiler and Ilastik softwares and main cell populations were identified by a supervised approach through Cytomap. On H&E images, we generated a classifier of tumor heterogeneity, by exploring the spatial localization of tumor cells with the K-function summary statistic, which analyzes the distribution of tumor cells as a function of their distance. The resulting K-score value was then used to classify each tumor spot as diffuse, poorly clustered or highly clustered. Multiparametric computational analysis of the IMC images allowed to grasp immune and stromal classifiers, including frequency of immune cell populations in the tumor nests versus fibrotic stroma and immune cell interactions. In conclusion, AI-powered analysis of H&E slides is a robust approach that can improve manual scoring and unlock tissue relevant features opening to new diagnostic possibilities. Meanwhile, the analysis of the immune ecosystem by multiparametric imaging mass cytometry allows investigating spatial patterns and cell interactions at single-cell level. Integration of these approaches is feasible and allows the identification of tumor patient profiles with clinical relevance.

#5784

Spatial clustering reveals immune hub interaction with reservoir of stem-like CD8 T cells and predicts immunotherapy response in lung cancer patients

Jonathan Chen[1], Linda Nieman[2], Maxwell Spurrell[2], Justin Gainor[2], Nir Hacohen[1]. *[1]Broad Institute, Cambridge, MA,[2]Massachusetts General Hospital, Boston, MA*

Background**:** Immunologic tumor control involves coordination of multiple cell types, but the organization of these interactions in human tumors is poorly understood. We recently reported that immunogenic tumors contain spatially-localized multicellular immunity hubs characterized by expression

of interferon-stimulated genes, including *CXCL10/CXCL11* (T cell attracting chemokines), and the presence of *IFNG*+ T cells. This suggested a positive feedback loop where T cell-derived IFNγ stimulates production of CXCR3 ligands, thereby attracting more T cells. However, we did not know (1) whether these hubs predict response to immunotherapy and (2) how hubs intersect with the various CD8 T cell states which play central roles in anti-tumor immunity.

Methods: To understand the composition of this immunity hub and its potential association with immunotherapy response, we performed multiplex RNA FISH to visualize hub components in NSCLC tissue from 68 patients prior to PD1-blockade. Cells were segmented and phenotyped automatically. We additionally imaged serial sections with a second panel for markers of CD8 T cell state. We then computationally registered sequential images, integrating our panels. To identify hubs in an unbiased manner, we employed kmeans clustering.

Results: We found that the presence of the immunity hub is predictive of subsequent response to PD1-blockade. Image registration revealed that hubs are enriched for CD8 T cells in multiple states, confirming their role as key sites of anti-tumor T cell activity. Furthermore, immunity hubs in responders contained more activated CD8 T cells and *IFNG*+ cells than those in nonresponders. To determine how hub heterogeneity may influence hub functions, we subclustered hubs by phenotypic composition. This analysis uncovered a ‘hybrid hub’ subclass that spatially overlaps with structures containing stem-like TCF7+ CD8 T cells, resembling the interfollicular zone of lymph nodes. The presence of a single hybrid hub was strongly associated with RECIST response ($p = 0.0005$), found in 85% of responders and only 24% of non-responders. Hybrid hubs also showed a striking association with patient PFS ($p = 0.0014$). Using ultra-highplex RNA ISH technologies, we further explored the hybrid hubs and found they are enriched in macrophages that express CXCR3 ligands.

Conclusions: Our study provides insight into the multicellular networks that underlie anti-tumor immunity. Immunity hubs are predictive of response to immunotherapy in human lung cancer and organize intratumoral CD8 T cell activity. Moreover, hybrid hubs may represent an active intratumoral niche for tumor-specific stem-like T cells that sustain anti-tumor immunity. These multicellular networks are excellent candidates for biomarker development and targets for immunotherapy.

#5785

A pan-cancer single-cell tumor micro-environment atlas predictive of immunotherapy response

Francesca Lodi[1], Sam Vanmassenhove[1], Elena Donders[2], Pierre Van Mol[2], Amelie Franken[1], Sarah Cappuyns[3], Ayse Bassez[1], Siel Olbrecht[4], Liselore Loverix[4], Michel Bila[5], Hanne Vos[6], Joanna Pozniak[7], Kevin Punie[8], Diether Lambrechts[1]. *[1]Laboratory for Translational Genetics, Department of Human Genetics, KU Leuven, Leuven, Belgium, VIB-KU Leuven Center for Cancer Biology, Leuven, Belgium,[2]Department of Pneumology, University Hospitals Leuven, Leuven, Belgium, VIB-KU Leuven Center for Cancer Biology, Leuven, Belgium,[3]Digestive Oncology, Department of Gastroenterology, University Hospitals Leuven, Leuven, Belgium, VIB-KU Leuven Center for Cancer Biology, Leuven, Belgium,[4]Department of Oncology, Laboratory of Gynaecologic Oncology, KU Leuven, Leuven, Belgium, VIB-KU Leuven Center for Cancer Biology, Leuven, Belgium,[5]Department of Oncology, UZ Leuven - KU Leuven Laboratory of Experimental Oncology, Leuven, Belgium, VIB-KU Leuven Center for Cancer Biology, Leuven, Belgium,[6]Department of Surgical Oncology, University Hospitals Leuven, KU Leuven, Leuven, Belgium, Leuven, Belgium,[7]Laboratory for Molecular Cancer Biology, Department of Oncology, KU Leuven, Leuven, Belgium, VIB-KU Leuven Center for Cancer Biology, Leuven, Belgium,[8]Department of General Medical Oncology, University Hospitals Leuven, KU Leuven, Leuven, Belgium, Leuven, Belgium*

The tumor microenvironment (TME) shapes response to immune checkpoint blockade (ICB). Several pan-cancer single-cell RNA-sequencing (scRNA-seq) analyses have reported how TME heterogeneity profoundly differs between cancer types. These studies mainly focused on one cell type (e.g., T-cells) and combined different technologies and bioinformatics pipelines with data being collected from both published and newly generated datasets. A comprehensive pan-cancer scRNA-seq map of the TME involving all cell types is therefore still lacking.
We obtained scRNA-seq (10x Genomics) on 234 fresh tissue samples from 161 treatment-naïve patients. Samples were collected from 9 cancer types

and subjected to a uniform in-house optimized protocol of tissue dissociation, sequencing and bioinformatics analysis. Abundancies of cell types and subtypes were correlated with each other and a tumor-reactive T-cell signature.
From 683,184 high-quality single cells, we identified 9 cell types and 71 subtypes of T-cells, B-cells, dendritic cells (DCs), monocytes/macrophages and endothelial-cells (ECs), shared between cancer types. *PDCD1* (PD1) was expressed by differentiated T-cells subtypes (e.g., $CD8^+$ exhausted and $CD4^+$ T-helper-1 subclusters), while *CD274* and *PDCD1LG* (PDL-1/PDL-2) were mainly expressed by regulatory B-cells, immune-regulatory DCs, $CXCL10^+$ and $CCL2^+$ monocyte-derived macrophages as well as inflammatory ECs. Pairwise analyses showed positive correlations between PD1-expressing T-cell subclusters, $CD4^+$ T-regulatory cells, plasma B-cells (plasmablasts, IgA and IgG plasma cells), immune-regulatory DCs, $CXCL10^+$ and $CCL2^+$ macrophages and lymphatic ECs. On the other hand, negative correlations were observed with naïve T- and B-cells, conventional DC2 (cDC2), monocytes, $CX3CR1^+$ macrophages, as well as arterial and capillary ECs. When ranking individual tumors based on a tumor-reactive T-cell signature, we found reactive tumors to correlate with positively interacting subtypes, while they anti-correlated with subclusters negatively interacting with PD1-expressing differentiated T-cells. Upon deconvolution of bulk RNA-seq data using gene signatures derived from each subcluster, these correlations were replicated in TCGA datasets across cancers. These signature scores correlated with tumor mutation burden (TMB) and other immunological features, while they were also predictive of response in clinical trials involving ICB.
We provide insights into the TME complexity at unprecedented level, identifying numerous subclusters enriched in immune-reactive (hot) or -suppressive (cold) tumors across cancer types. We validate these observations in TCGA by deconvolution of bulk RNA-seq data, and show that already pre-treatment several TME subclusters predict response to ICB.

#5786
Spatial relationships in the tumor microenvironment predict response to immune checkpoint inhibitors in urothelial and head and neck cancer

Alberto Gil-Jimenez[1], Nick van Dijk[1], Yoni Lubeck[2], Maurits L. van Montfoort[1], Dennis Peters[2], Erik Hooijberg[2], Annegien Broeks[3], Joris L. Vos[4], Charlotte L. Zuur[4], Bas van Rhijn[5], Daniel J. Vis[1], Michiel S. van der Heijden[6], Lodewyk F. A. Wessels[1]. *[1]Department of Molecular Carcinogenesis, The Netherlands Cancer Institute, Amsterdam, Netherlands,[2]Department of Pathology, The Netherlands Cancer Institute, Amsterdam, Netherlands,[3]Core Facility Molecular Pathology & Biobanking, The Netherlands Cancer Institute, Amsterdam, Netherlands,[4]Department of Head and Neck Surgery and Oncology, The Netherlands Cancer Institute, Amsterdam, Netherlands,[5]Department of Urology, The Netherlands Cancer Institute, Amsterdam, Netherlands,[6]Department of Molecular Carcinogenesis, Department of Medical Oncology, The Netherlands Cancer Institute, Amsterdam, Netherlands*

Background: Immune checkpoint inhibitors (ICI) can achieve remarkable clinical responses in urothelial cancer (UC). However, it remains unclear which aspects of the tumor microenvironment (TME) determine a patient's response. The TME is usually characterized by immune cell density, which ignores cells' spatial relationships relative to each other.
Methods: Using multiplex immunofluorescence data (PanCK, CD20, CD68, CD3, CD8, and FoxP3 antibody panel) of 24 pre-ICI UC transurethral resections retrieved from the NABUCCO trial (NCT03387761), we spatially profiled cancer cells, macrophages, B-cells, and distinct T-cell populations. We first quantified the TME immune cell densities at the tumor and stroma tissue compartments. We then quantified the TME spatial relationships with a novel approach based on fitting a Weibull function to the first nearest neighbor (1-NN) distance distribution, allowing us to uniquely summarize spatial relationships with two parameters (Weibull approach). We compared this approach to conventional techniques (G-functions) that rely upon a predefined distance threshold. We performed a simulation study to identify sources of variation in the spatial relationship parameters. Lastly, we associated the TME parameters with ICI (ipilimumab + nivolumab) response.
Results: Unlike the Weibull approach, the G-function quantifications manifested a variable effect size and statistical power in association studies

because of its distance threshold dependence. We found that variation in density affected the spatial relationship metrics of rare cell types (i.e., B-cells) but not of abundant cell types (i.e., cancer cells). The spatial relationship metrics from the Weibull approach outperformed immune cell density in ICI response prediction. Specifically, immune cell density did not discriminate between ICI response groups (FDR>10%). In contrast, the spatial relationship between either $CD8^+$ T-cells or macrophages to their closest cancer cell did associate with response to ICI (FDR=1%). Furthermore, non-responding tumors were characterized by $CD8^+$ T-cells close to B-cells (FDR=9%). Importantly, we validated the association between proximity and response from $CD8^+$ T-cells to cancer cells (FDR=1%) and from macrophages to cancer cells (FDR=1%) using data from 25 pre-ICI head and neck squamous cell carcinoma tumors from the IMCISION trial (NCT03003637, arm B, ipilimumab + nivolumab). Conclusion: We created a framework to quantify, study, interpret and analyze spatial relationships in the TME and illustrated its superior clinical relevance compared to density metrics for predicting ICI treatment response. Our findings emphasize the importance of spatial relationships in the TME for response and suggest that proximity between either macrophages or $CD8^+$ T-cells to cancer cells are candidate biomarkers for ICI response.

#5787

Modelling the spatial heterogeneity of CD45-positive tumor infiltrating lymphocytes in early-stage, estrogen receptor-positive breast cancer

Zak Kinsella[1], Anna Blümel[1], Mairi Lucas[1], Andreas Lindner[1], Claudia A. Gonzalez[2], Arman Rahman[2], Joanna Fay[3], Tony O'Grady[3], Verena Murphy[4], John Crown[5], Cathy Kelly[6], William Gallagher[7], Darran O'Connor[1]. *[1]Royal College of Surgeons in Ireland, Dublin, Ireland,[2]Cancer Biology Therapeutics, University College Dublin, Dublin, Ireland,[3]Beaumont Hospital, Dublin, Ireland,[4]Cancer Trials Ireland, Dublin, Ireland,[5]St Vincent's Hospital, Dublin, Ireland,[6]St James' Hospital, Dublin, Ireland,[7]University College Dublin, Dublin, Ireland*

The frequency of lymphocytes infiltrating tumors is a known prognostic in estrogen receptor (ER) negative cancers. ER+ disease is putatively believed

to be immune cold, however, there exists a subset of ER+ tumors with high immune infiltrate and with a significant spatial heterogeneity. The clinic impact of such infiltrate - especially between the Oncotype Dx Recurrence Score risk categories - remains unclear. Moreover, the distribution of tumor and stromal tissues, while noted as significantly heterogenous, is still ill-defined and not yet clinically used prognostically, despite evidence to support its utility. Using a cohort (n=450) of serial sections taken from early-stage, ER+/HER2- breast tumors of the Irish arm of the TAILORx clinical trial, we aimed to investigate the tumor architecture and spatial distribution of tumor immune infiltrate and proliferating tumor cells using digital image analysis. Antibodies against Ki67 (proliferation marker) and CD45 (leukocyte common antigen), and a routine Haematoxylin and Eosin stain were applied to serial sections of 450 full-face tumors via chromogenic immunohistochemistry, as outlined previously [1]. Digital image analysis was performed using open-source software, QuPath [2]. Pixel classifiers were trained and validated against an expert pathologist in order to define observed lymphocytes as tumor or stromal-infiltrating, and to establish a classifier to quantify the tumor-stroma ratio (TSR) and infiltrating tumor area. Distances of CD45-positive cells from tumor were computed, along with autocorrelation statistics [3,4] of CD45 and Ki67 hotspots; firstly in order to quantify spatial heterogeneity, and secondly to examine whether Ki67 as a component gene in the Oncotype Dx assay has a foundation in tumor biology or is being confounded by potentially Ki67-positive lymphocytes. Subdividing by Oncotype Dx risk categories, no significant difference in TSR was observed ($p=0.09799$), neither for intermediary risk patients receiving hormone therapy alone or in combination with chemotherapy ($p=0.3873$). While there was an observed trend overall ($p=0.092$), no significance was found for recurrence between intermediary risk subcategories (HT alone: $p=0.393$, HT+CT: $p=0.288$). However, in the cohort as a whole, median TSR was 0.3215 (range 0 - 5.023), with statistically significant differences in recurrence risk observed (cohort high v low by median TSR. HR: 6.356, 95CI: 2.263-17.84, $p<0.0001$).

#5788

Single-cell and spatial transcriptomic mapping of human renal cell carcinoma brain metastases uncovers actionable immune-resistance

targets

Elshad Hasanov[1], Truong Nguyen Anh Lam[1], Jerome Lin[1], Patrick K. Reville[1], Merve Hasanov[1], Anna K. Casasent[1], David Shih[2], Sahin Hanalioglu[3], Mehmet Asim Bilen[4], Omar Alhalabi[1], Berrin Babaoglu[3], Baylar Baylarov[3], Adeboye O. Osunkoya[4], Lisa M. Norberg[1], Joy Gumin[1], Tuan M. Tran[1], Jianzhuo Li[1], Anh G. Hoang[1], Haidee D. Chancoco[1], Brittany C. Parker Kerrigan[1], Erika J. Thompson[1], Betty YS Kim[1], Dima Suki[1], Melike Mut[5], Figen Soylemezoglu[3], Giannicola Genovese[1], Kadir C. Akdemir[1], Hussain A. Tawbi[1], Nizar M. Tannir[1], Florencia McAllister[1], Michael A. Davies[1], Padmanee Sharma[1], Jason Huse[1], Frederick Lang[1], Nicholas Navin[1], Eric Jonasch[1]. *[1]The University of Texas MD Anderson Cancer Center, Houston, TX,[2]School of Biomedical Sciences, The University of Hong Kong, Hong Kong,[3]Hacettepe University Faculty of Medicine, Ankara, Turkey,[4]Emory University School of Medicine, Atlanta, GA,[5]University of Virginia, Charlottesville, VA*

Introduction: The discovery of immune checkpoint inhibitors has revolutionized metastatic renal cell carcinoma (RCC) treatment. However, in patients with RCC brain metastases, response rates are low and survival outcomes poor. To understand the tumor microenvironmental differences between primary kidney tumors, extracranial metastases, and brain metastases, we developed a detailed single-cell atlas of RCC brain metastases along with their matched extracranial and primary tumors.
Methods: We performed single-nucleus RNA-seq on 27 samples (nearly 200,000 cells) from RCC patients; samples included 14 brain metastases, 8 matched primary kidney tumors, and 5 matched extracranial metastases. We performed multiplex IHC to validate selected transcriptomic findings. We used Nanostring CosMx 960-plex RNA spatial molecular imaging technique on selected samples to validate cellular interactions in a spatial context.
Results: We established a multi-tissue single-cell atlas of RCC brain metastases by identifying 9 major and 37 minor malignant, immune, and stromal cell clusters. Brain metastases had higher neuronal and glial cells interacting with immune and tumor cells. Brain metastasis tumor cells were also transcriptomically reprogrammed to adapt to the brain microenvironment through enrichment of MYC targets, MTORC1

signaling, epithelial-mesenchymal transition, fatty-acid metabolism, oxidative phosphorylation, and reactive oxygen species pathways. Moreover, cell-to-cell communication and downstream target gene expression analyses showed that brain metastasis tumor cells expressed ligands and receptors that induce tumor cell proliferation in both autocrine and paracrine fashions. Among T-cell populations, we found fewer proliferating cytotoxic T lymphocytes in the brain than in other sites. Moreover, T cells in brain metastases expressed higher levels of several targetable inhibitory checkpoints than did extracranial metastases. In addition, we found that naïve/memory T cells in brain metastases were a favorable prognostic marker for overall survival after craniotomy. Our characterization of myeloid cell populations across the 3 disease sites found fewer dendritic cells and monocytes in the brain compared to other sites. Macrophages in brain metastases more highly expressed an M2 immunosuppressive gene signature than did those in primary RCC tumors. Conclusion: Our findings from the largest single-cell atlas of RCC brain metastases with matched primary and extracranial metastases suggest several unique targetable, immunosuppressive biological mechanisms in the brain microenvironment. These results provide a foundation for a deeper understanding of RCC brain metastasis biology and can serve as a resource for the scientific community to further explore therapeutically targetable tumor and immune-related mechanisms.

Stem Cells and the Microenvironment

#3659
RAS drivesmalignancy through stem cell crosstalk with the microenvironment

Shaopeng Yuan. *The Rockefeller University, New York, NY*

Squamous cell carcinomas (SCCs) are triggered by marked elevation of RAS/MAPK signaling and progression from benign papilloma to invasive malignancy. At tumor-stromal interfaces, a subset of tumor-initiating progenitors, the cancer stem cells (CSCs), obtain increased resistance to chemo and immunotherapy along this path. The distribution and changes in CSCs during progression from a benign state to invasive SCC remain elusive. Here, we show that following $HRAS^{G12V}$ activation, CSCs rewire

their gene expression program and trigger a self-propelling, aberrant signaling crosstalk with their tissue microenvironment that drives their malignant progression. Surprisingly, the non-genetic, dynamic cascade of intercellular exchanges involves downstream pathways often mutated in advanced metastatic SCCs with high mutational burden. Coupling our clonal skin $HRAS^{G12V}$ model with single-cell transcriptomics, chromatin-landscaping, lentiviral reporters and lineage-tracing, we show that aberrant crosstalk between CSCs and their microenvironment triggers angiogenesis and TGFβ-signaling, creating conditions ripe for hijacking leptin and leptin receptor (LEPR)-signaling, which in turn launches downstream PI3K-AKT-mTOR signaling at the benign-malignant transition. By functionally interrogating each step in this pathway, we unravel how dynamic temporal crosstalk with the microenvironment and orchestrated by the stem cells (SCs) profoundly fuels this path to malignancy. These new insights suggest broad implications for cancer therapeutics.

#3660

Bone mechanics influence cancer stem cell formation in osteosarcoma

Zunaira Shoaib[1], Aleczandria S. Tiffany[2], Brendan Harley[2], Joseph Irudayaraj[3], Timothy M. Fan[1]. *[1]Pathobiology, University of Illinois at Urbana-Champaign, Urbana-Champaign, IL,[2]Chemical and Biomolecular Engineering, University of Illinois at Urbana-Champaign, Urbana-Champaign, IL,[3]Bioengineering, University of Illinois at Urbana-Champaign, Urbana-Champaign, IL*

Osteosarcoma (OS) is the most common primary tumor of bone and is characterized by rapid bone remodeling accompanied by structural and mechanical heterogeneity across the tumor. Chemoresistance and recurrence of OS can be attributed to a subpopulation of OS cells known as cancer stem-like cells (OS-CSCs). It can be hypothesized that tumor niches possessing distinct structural and mechanical properties could be harboring different OS cell populations, and certain niches might be more conducive for OS-CSCs formation and maintenance.
To evaluate the presence of OS-CSCs, mineralized collagen scaffolds mimicking heterogenous bone niches with distinct structural and mechanical properties were fabricated by changing collagen content and pore alignment and were cultured with the highly metastatic human OS cell

line 143B. Scaffolds with 47% collagen by weight but different pore alignment were chosen for further analysis because they possessed different stiffness and topographical properties. Cytoskeletal changes, epigenetic changes, chemoresistance and chemoresistance-related pathways, and the levels of stemness genes were assessed in the 3D scaffold cultures.
A consistent trend of OS-CSC phenotype was observed in the cell population grown in the softer bone niches (12 kPa) with aligned pores as compared to stiffer niche (31 kPa) with non-aligned pores. The cell population growing in softer, aligned scaffolds had a significantly higher expression of stemness genes (OCT4, NANOG, SOX2, ALDH1A1) and drug efflux gene ABCB1 and increased chemoresistance to doxorubicin and cisplatin. Epigenetic changes associated with cisplatin resistance in OS such as a decrease in methyl transferase EZH2 accompanied by the upregulation of LIF/Notch and PRKCA pathways was observed in cells grown in softer, aligned niches. Fluorescent imaging of actin organization showed rounder cells in the aligned niche indicative of the CSC phenotype, and stretched, elongated cells in the non-aligned niche indicative of a differentiated phenotype.
Our study showed that the mechanical and structural properties of bone niches influence the formation of distinct OS cell populations. A softer niche with an aligned structure is more conducive for maintaining OS-CSCs.

#3661

Extracellular vesicle derived from neural stem cells as potential vehicles of genetic information to modulate glioblastoma biology

João Pedro Alves de Araújo[1], Lilian Cruz[2], Maria Clara da Silva Souza[1], Mariana Brandão Prado[1], Rodrigo Nunes Alves[1], Bárbara Paranhos Coelho[1], Samuel Ribeiro Soares[1], Camila Félix de Lima Fernandes[3], Marilene Hohmuth Lopes[1]. *[1]Department of Cell and Developmental Biology, Institute of Biomedical Sciences (ICB), University of São Paulo, São Paulo - SP, Brazil,[2]Vertex Pharmaceuticals, Cambridge, Massachusetts, United States of America (USA), Cambridge, MA,[3]University of Cologne (UoC), Cologne, Germany*

Glioblastoma (GBM) is a deadly brain tumor and its high aggressiveness is partly due to a subpopulation of tumor stem cells known as glioblastoma

stem-like cells (GSCs). GBM establishes crosstalk with non-tumoral cells, mediated mainly by extracellular vesicles (EVs) and the interaction between GSCs and neural stem cells (NSCs) from the subventricular zone may influence GBM biology. Literature data suggests that cellular communication is an important process for GSCs stemness maintenance, and some authors consider NSCs as a possible cell of origin for GSCs. However, the specific effects that neural stem cells-derived extracellular vesicles (NSCs-EVs) promote in GSCs are still uncertain. Previous data from our group demonstrated specific groups of microRNAs (hsa-miR -137, -216a-5p, -216b-5p, 217), enriched in NSCs-EVs in contrast to intracellular compartments, suggesting these molecules are being produced for secretion. Our study aims to evaluate the role of the miRs contained in NSCs-EVs in GSCs biology. Human induced pluripotent stem cells (hiPSC) were differentiated into NSCs. NSCs were characterized by western blotting and immunofluorescence by the expression of neural commitment markers, such as nestin and β-III-tubulin. NSCs-EVs were isolated from NSCs' culture media with a commercial kit and analyzed by NTA (nanosight) for EVs size profiling and western blotting to detect specific markers, such as Alix, CD63, and HSP90. In a first approach, we analyzed the effects played by those miRs through predictive online tools. We identified target genes related to stemness (NANOG, SOX2, KLF4), oncogenesis (KRAS, CDC42, CDK6) and metabolism (CAMK2A), besides the Wnt and Notch signaling pathways. The online predictions also identified transcriptional factors related to vasculogenesis and self-renewal, key processes for GSCs activity. We will expose GSCs to NSCs-EVs and evaluate the expression of neural and stemness markers. In a future step, the GSCs previously exposed to NSCs-EVs will be treated with temozolomide, and viability assays will be performed. Additionally, we intend to modulate the four miRs identified and evaluate if they act as effector molecules of NSCs-EVs. Our data corroborate with our initial hypothesis that NSCs-EVs may act as important signalling modes in GSCs activity and consequently in GBM biology. Supported by FAPESP:22/08106-1.

#3664

Mechanism for bone marrow failure differs between acute myeloid and lymphoid leukemia

Ryan Matthew Bertoli[1], Peter D. Aplan[2], Yang Jo Chung[2]. *[1]NIH-NCI, Bethesda, MD,[2]Center for Cancer Research, NIH-NCI, Bethesda, MD*

Acute lymphoid leukemia (ALL) and acute myeloid leukemia (AML) are aggressive forms of blood cancer that impair normal hematopoiesis and are typically associated with bone marrow (BM) failure, reflected by peripheral blood pancytopenia. While BM failure is thought to be mediated by the loss of hematopoietic stem and progenitor cells (HSPCs) due to leukemic expansion, with leukemic cells "crowding out" normal HSPCs, the mechanisms underlying this process remain unclear. To elucidate these mechanisms, we examined the effects of AML or ALL on residual normal or wild type (WT) hematopoiesis. The 961C cell line is an AML cell line derived from a NUP98-PH23 (NP23) transgenic mouse, and the T259 cell line is a B cell precursor ALL (BCP ALL) cell line also derived from an NP23 mouse. AML and BCP ALL were generated by transplantation of 961C or T259 cell lines into congenic recipients without cytotoxic conditioning. The use of congenic mice allowed engraftment of immunocompetent mice, and the lack of cytotoxic conditioning prevented damage to the BM microenvironment. Mice with AML demonstrated severe anemia, thrombocytopenia, and depletion of HSPCs, along with a marked reduction of total BM cellularity (WT + AML cells), suggesting that BM suppression was not due to a physical "crowding" mechanism. Instead, BM suppression in the absence of BM replacement with myeloblasts suggested that hematopoiesis may be inhibited by a factor secreted by the AML blasts. The inflammatory cytokines TNF-A and IL-6 were markedly increased in the peripheral blood of mice with AML, suggesting these were candidates for a factor responsible for decreased cellularity and pancytopenia. In contrast, mice with BCP ALL demonstrated normal hemoglobin and leukocyte counts, even with significant ALL engraftment. The loss of WT hematopoietic cells in the BM was equivalent to the gain of leukemic cells in the BM, and the total number of leukemic cells in mice with BCP ALL was 14-fold higher than the number of leukemic cells in mice with AML. Of note, the spleen of mice with BCP ALL displayed a 100x increase in WT HSPCs compared to non-transplanted mice with healthy BM. These findings suggest that BCP ALL depletes WT HSPCs in the BM through a physical expansion mechanism. WT splenic HSPCs from mice with AML were shown to have normal

numbers of functional hematopoietic stem cells via a limiting dilution assay. In addition, WT HSPCs harvested from mice with BCP ALL generated similar numbers and types of colonies in vitro compared to WT HSPC harvested from non-leukemic mice. Both experiments suggest that neither BCP ALL nor AML induced a permanent change in the functionality of WT HSPCs. In conclusion, our results suggest that AML induces BM failure independent of leukemic burden, possibly via a secreted cytokine, whereas BCP ALL induces BM failure through physical expansion that replaces WT HSPCS with leukemic cells.

#3665

Umbilical cord blood endothelial progenitor cell-derived extracellular vesicles control important endothelial cell functions

Sawssen Ben Fraj[1], Sina Naserian[2], Bileyle Lorenzini[2], Sylvie Goulinet[2], Philippe Mauduit[2], Georges Uzan[2], Houda Haouas[1]. *[1]of Biological and Chemical engineering, National Institute of Applied Sciences and Technology (INSAT) Carthage University, LR18ES40, Inflammation, environment and signalization pathologies, Tunis, Tunisia,[2]INSERM UMR-S-MD 1197, Hopital Paul Brousse, Villejuif, France*

Background: Circulating endothelial progenitor cells (EPCs) play a pivotal role in vascular regeneration and the repair of diseases in which angiogenesis is required, including ischemia and tissue transplantation. Although they are a potentially valuable cell therapy tool, their clinical use remains limited due to suboptimal storage conditions and especially, immune rejection. Even if these cells have been shown to be tolerated by the immune system, their *in vivo* long-term effects still remain to be elucidated. EPC-derived extracellular vesicles (EPC-EVs) may be an attractive alternative to EPCs given their key role in cell-cell communication and expression of the same parental markers. In this study, we investigated the regenerative effects of umbilical cord blood EPC-EVs on EPCs *in vitro.*

Methods: EPCs were obtained from human umbilical cord blood (CB) and characterized by flow cytometry. After amplification, EPCs were cultured in a medium containing an EVs-depleted serum (EV-free medium). Then the conditioned medium was used to isolate the EVs with Tangential Flow Filtration (TFF). The EVs were characterized by a series of tests defining

their size, number, and protein content. The regenerative effects of EPC-EVs on endothelial cells were investigated by analyzing cell migration, wound healing, and tube formation. We also analyzed the effect of EPC-EVs on endothelial cell inflammation and NO production.
Results: We showed that adding different doses of EPC-EVs on EPCs does not alter the basal expression of the endothelial cell markers CD31, CD144, and KDR, nor change their proliferative potential and NO production level. Furthermore, we demonstrated that
EPC-EVs, when used at a higher than physiologic dose, create a mild inflammatory condition that activates EPCs and boosts their regenerative features like migration and tube formation functions.
Conclusions: Our results reveal for the first time that EPC-EVs, when used at a high dose, could enhance EPC regenerative functions without altering their endothelial identity.

#3666

A human skeletal muscle stem/myotube model reveals multiple signaling targets of cancer secretome in skeletal muscle

Ruizhong Wang[1], Brijesh Kumar[1], Poornima Bhat-Nakshatri[1], Aditi Sanjay Khatpe[1], Michael P. Murphy[2], Kristen E. Wanczyk[2], Emma H. Doud[3], Amber L. Mosley[1], Yunlong Liu[1], Duojiao Chen[1], Ed Simpson[1], Hongyu Gao[1], Harikrishna Nakshatri[2]. *[1]Surgery, Indiana University School of Medicine, Indianapolis, IN,[2]Surgery, Indiana University School of Medicine, VA Roudebush Medical Center, Indianapolis, IN,[3]Indiana University School of Medicine, Indianapolis, IN*

Skeletal muscle dysfunction due to the effects of cancer secretome is observed in multiple cancer types and extreme dysfunction is manifested as cachexia. Major preclinical studies on cancer-associated muscle defects utilized mouse models or mouse C2C12 mouse myoblast cell line for *in vitro* studies. Because of species specificity of certain cytokines/chemokines in the secretome, a human model system is required to fully comprehend the effects of cancer secretome on skeletal muscle. Here, we report a simple method to establish skeletal muscle stem cell line (hMuSC), which can be differentiated into myotubes. Using single nuclei ATAC-seq (snATAC-seq) and RNA-seq (snRNA-seq), we document chromatin accessibility and transcriptomic changes associated with

hMuSCs to myotube transition. Cancer cell line derived factors accelerated stem to myotube differentiation with accompanying changes including an increase in PAX7+/MyoD+ myogenic progenitor cells. Among the pathways activated by cancer-derived factors include inflammatory pathway involving CXCL8 (also called IL-8), glucocorticoid receptor (GR) pathway, and wound healing pathway. Furthermore, cancer-derived factors significantly altered splicing machinery in hMuSCs. Additionally, AKT and p53 pathways that function in metabolic/survival pathways of the skeletal muscle were adversely affected when hMuSCs were exposed to cancer cell-derived factors. Cancer-derived factors increased the expression levels of previously known cachexia-associated genes such as MT-2, ZIP14, and PDK4. Thus, the model system not only recapitulates results of previous mouse studies but also provides much needed human model system that can easily be adapted for large scale studies to explore the epigenomic changes during hMuSC differentiation and to screen for drugs that restore skeletal muscle function in various diseases.

Wednesday, April 19, 2023

BIOINFORMATICS / COMPUTATIONAL BIOLOGY / SYSTEMS BIOLOGY / CONVERGENT SCIENCE

Bioinformatics Applications in Cancer Biology 3

#6535
Identification of coding and non-coding genes associated with survival outcomes in uterine cancer

Enrique I. Ramos[1], Axel M. Hidalgo[1], Ken Y. Lin[2], Shrikanth S. Gadad[1].
[1]Molecular and Translational Medicine, Texas Tech Univ. Health Sciences Ctr. El Paso, El Paso, TX,[2]Department of Obstetrics & Gynecology and Women's Health, Albert Einstein College of Medicine Montefiore Medical Center, Bronx, NY

Endometrial (or uterine) cancer is the most commonly diagnosed cancer in the female reproductive system and it disproportionately affects Black women, who are twice as likely to die from the disease than White women. In this study, we focused on the molecular characterization of copy-number high (CN-high) molecular subclassification of uterine cancer tumors, which includes most serous and serous-like endometroid tumors. These poorly characterized subcategories account for less than 10% of all uterine cancers but are responsible for over 80% of the mortality in uterine cancers and occur more commonly in Black women.We leveraged publicly available Pan-Cancer Atlas data to perform differential gene expression analyses between control and cancer samples in the Black and White CN-high groups with the aim of identifying relevant genes that could play a role in the aggressiveness of this cancer. We then performed survival analysis using the genes of interest using Kaplan-Meier estimators to ascertain the gene-specific survival outcomes.In the significantly upregulated subset of genes, we found that the high expression of the candidate gene was associated with higher survival in both White patients (p=0.046), and Black patients (p=0.021). Additionally, the expression levels of one of the noncoding genes were associated with differential survival between the groups, with low expression being associated with higher survival in White patients (p=0.0045), and high expression associated with higher survival in Black patients (p=0.018). This differential association of survival was also observed in one of the most downregulated genes in both groups, with low expression predicting higher survival in white patients (p=0.004), and Black patient survival is associated

with high expression (p=0.0082). We also identified novel non-coding genes that predicted different survival outcomes in both groups, with high expression predicting better survival in Black patients and low expression predicting better survival in White patients (p=0.048 and p=0.039, respectively). These results showcase the identification of both coding and noncoding potential genomic targets that are associated with clinical outcomes in the aggressive CN-high molecular subtype of uterine cancer. These targets merit further characterization and experimental validation to elucidate their molecular roles in the progression of endometrial cancer.

Acknowledgments S.S.G. is a CPRIT scholar in cancer research and is supported by a First-time Faculty Recruitment Award from the Cancer Prevention and Research Institute of Texas (CPRIT; RR170020). S.S.G. is also supported by a) the Lizanell and Colbert Coldwell Foundation, b) The Edward N. and Margaret G. Marsh Foundation, and c) the American Cancer Society.

#6537

Single cell transcriptomics uncovers cellular and molecular differences in PBMCs of responders and non-responders to the MUC1 cancer vaccine given in the preventative setting

Daniel Y. Yuan[1], Michelle L. McKeague[2], Matthew T. Dracz[2], Olivera J. Finn[2], Panayiotis V. Benos[3]. *[1]Computational and Systems Biology, University of Pittsburgh, Pittsburgh, PA,[2]Immunology, University of Pittsburgh, Pittsburgh, PA,[3]Epidemiology, University of Florida, Gainesville, FL*

Introduction: A single arm trial (NCT007773097) and a double-blind, placebo controlled randomized trial (NCT02134925) were conducted in patients with newly diagnosed advanced colonic adenomas to test the safety and immunogenicity of the MUC1 antigen vaccine and its potential to prevent new adenoma formation. These are the first trials of a non-viral cancer vaccine administered in the absence of cancer. In both trials, the vaccine was safe and strongly immunogenic in 43% and 25% of participants (Responders), respectively. The lack of robust response in a significant number of participants suggested, for the first time, that even in a premalignant setting, the immune system may have already been exposed to regulatory influences that, in the case of the vaccine, determine who does and who does not respond. We hypothesized that there could be molecular and cellular differences in the immune competence between vaccine responders and non-responders, and that they could be identified by studying their pre-vaccination peripheral blood mononuclear cells (PBMCs).

Methods: The two MUC1 vaccine trials are described in https://doi.org/10.1101/2022.10.05.22280474 and https://doi.org/10.1158%2F1940-6207.CAPR-12-0275. We performed single cell RNA-sequencing (scRNAseq) on banked pre-vaccination PBMCs from 16 Responders and 16 Non-Responders, determined by anti-MUC1 IgG response. Using differential gene expression (DGE), pathway enrichment, and network estimation analyses, we identified specific cell types, genes, and pathways that differ between responders and non-responders.
Results: Pre-vaccination PBMCs from Responders contained a significantly higher percentage of CD4+ naive T cells, while Non-Responders showed significantly higher percentage of CD8+ T effector memory (TEM) cells and a higher percentage of CD16+ monocytes. DGE and gene interaction network analysis showed a higher level of expression of T cell activation genes, such as Fos and Jun, in the CD4+ naive T cells in Responders. Further network analysis showed that these genes were directly connected to response. We also found pre-vaccination specific gene ontology (GO) pathways for translational and transcriptional activity enriched in all cell types in Responders compared to Non-Responders.
Conclusion: Our analyses identified candidate biomarkers that are predictive of a preventative cancer vaccine response. Thus, our results can be used for patient selection for vaccine administration. Furthermore, we identified cell type differences and transcriptional pathways that provide information of possible mechanisms of vaccine response.

#6538

Development and refinement of functional gene expression signatures as a computational tool for comprehensive characterization of transcriptomic data

Elena Ocheredko, Nadezhda Lukashevich, Maria Savchenko, Sofia Kust, Syune Ambaryan, Dmitry Tabakov, Maria Sorokina, Linda Balabanian, Kushal Suryamohan, Anastasiya Zotova, Nathan Fowler, Aleksander Bagaev.
BostonGene, Corp., Waltham, MA

Functional gene expression signatures (FGES) are widely used as biomarkers in cancer diagnostics as descriptive and predictive models for treatment selection. Since FGES scores are based solely on gene expression profiles, they can be applied to data from bulk and single-cell RNA-seq or gene expression microarrays. However, FGES development and implementation has several challenges including technical limitations of calculating FGES scores based on

ranked gene expressions such as background noise and gene cross-correlations and difficulty in assessing the biological relevance of FGES. Here, we developed an FGES validation pipeline that addressed these limitations by examining publicly available and internally-developed FGES.
The pipeline was developed by applying a modified single-sample gene set enrichment analysis (ssGSEA) to a manually curated database of more than 50,000 RNA-Seq samples, including sorted cells, cell lines, and tumor and normal tissue biopsies. We defined technical and biological criteria to validate signature quality: 1) single gene expression noise distribution minimum is greater than zero; 2) cross-correlation of genes comprising a signature is positive; 3) specificity, whereby a FGES differentiates a group of interest and has a minimal overlap with other unrelated signatures and molecular pathways; 4) generalizability, requiring FGES score to differentiate a group of interest across datasets of different origin, cell type, or diagnosis.
We tested these criteria on FGES that describe cellular processes such as epithelial-mesenchymal transition (EMT) and senescence as well as FGES that can delineate cell types such as macrophages. We were able to better distinguish 12 different cell types using the corresponding cell type-specific FGES with significantly higher ssGSEA scores (p-adj ≤ 0.00004 in 99.9% cases) than 911 analogous MSigDB gene signatures. Our EMT FGES, tuned specifically for melanoma, exhibited higher precision than the MSigDB Hallmark EMT gene set ($p < 0.001$) for predicting histological pigment scores. The senescence FGES also accurately distinguished senescent from non-senescent cells in datasets of differing cell origin and data acquisition methods, demonstrating signature generalizability. Finally, using macrophage-describing FGES, we showed that specificity of a publicly available gene set can be significantly improved (p-adj = 0.00001) by tuning it according to the aforementioned criteria.
Taken together, our proposed workflow enables better assessment of the technical quality and biological adequacy of FGES for their further use in transcriptomic analyses and computational models of complex biological processes and tumorigenesis.

#6539

Application of optical genome mapping to identify samples with homologous recombination deficiency

Andy Wing Chun Pang[1], Kelsea Chang[1], Nikhil Sahajpal[2], Daniel Saul[1], Ravindra Kolhe[3], Alka Chaubey[1], Alex Hastie[1]. *[1]Bionano Genomics, San Diego, CA,[2]Greenwood Genetics Center, Greenwood, SC,[3]Augusta University, Augusta, GA*

Certain cancer treatments, such as the poly (ADP-ribos) polymerase (PARP) inhibitors, have been shown to be effective in killing cancer cells exhibiting genome instability signatures indicative of homologous recombination deficiency (HRD). Hence, these signatures are used as biomarkers to inform treatment decisions and prognosis. There are three measurements of HRD signatures commonly employed: loss of heterozygosity (HRD-LOH), telomeric allelic imbalance (TAI) and large-scale state transition (LST). It has been shown that combining all three scores can better determine the HRD phenotype, leading to a higher clinical impact. Yet current HRD signature tests, used to estimate HRD, have low negative predictive value, and one possible reason is that current genomic technologies lack sensitivity to capture the full extent of somatic genomic rearrangements. Here, optical genome mapping (OGM) was used to detect large structural variants (SVs) and calculate a HRD score. OGM captures high molecular weight DNA to call SVs by aligning these molecules to the public reference genome. OGM can comprehensively detect insertions and deletions >5kbp, inversions, interchromosomal translocations, plus large interstitial copy number variation (CNV) and aneusomies. Subsequently, an automated script was developed to compute the HRD score, which is the summation of the three HRD signatures: HRD-LOH, the number of regions with a loss >15 Mbp but shorter than the whole chromosome; TAI, the number of regions of gain and loss >10Mbp that extend to a subtelomere but do not cross the centromere; and LST, the number of chromosomal breakpoints whose SV size >10Mb but not the whole chromosome. We applied this script on 20 samples of solid tumors and myeloid neoplasms, and the automated scores are concordant with expertly curated scores, confirming the validity of the calculation. We believe that OGM data combined with this automated analysis of HRD signatures is much more sensitive and accurate for detection of HRD signatures and that this will enable more precise prediction of drug response for multiple tumor types.

#6540

Multiscale protein networks: de novo aberrant protein interactions and oncogenic regulators in seven cancer types

Won Min Song, Abdulkadir Elmas, Richard Farias, Peng Xu, Xianxiao Zhou, Benjamin Hopkins, Kuan-lin Huang, Bin Zhang. *Icahn School of Medicine at Mount Sinai, New York, NY*

We conducted integrative proteomic network analyses of 687 cases across 7 cancer types including breast cancer (115 tumor samples), clear cell renal carcinoma (100 tumor samples), colorectal cancer (91 tumor samples), hepatocellular carcinoma (101 tumor samples), lung adenocarcinoma (104 tumor samples), stomach adenocarcinoma (80 tumor samples), and uterine corpus endometrial carcinoma (96 tumor samples). Using Multi-scale embedded gene co-expression network analysis (MEGENA), we constructed co-expression protein network for each cancer type, and interrogated the network topology and co-expressed protein modules. For each cancer type, we identified disease-associated pathways as co-expressed protein modules enriched for differentially expressed proteins in tumor. Comparing with respective cancer transcriptome network models, this systematically revealed proteome-specific cancer subnetworks associated with heme metabolism, DNA repair, spliceosome, oxidative phosphorylation and KRAS oncogenic signaling pahways in several cancer types. Cross-cancer comparison identified highly preserved protein modules showing robust pan-cancer interactions and identified endoplasmic reticulum-associated degradation (ERAD) and N-acetyltransferase activity as the central functional axes. Then, we utilized these network models to predict pan-cancer protein network regulators in the up-stream of disease-associated pathways. The predicted pan-cancer regulators were experimentally validated by loss-of-function to confer anti-tumor effects in diverse cancer types: lung (H847), colon (HCT116), fetal kidney (HEK293T) and breast (MDA-MB-231) cancer cells. Overall, the study was designed to provide tractable network models of cancer proteome, and unlock the further potentials to understand oncogenic regulators and mechanisms in different cancer types.

#6541

Geometry of gene expression network reveals potential novel indicator in Ewing sarcoma

Rena Elkin[1], Jung Hun Oh[1], Filemon Dela Cruz[1], Larry Norton[1], Joseph O. Deasy[1], Andrew L. Kung[1], Allen R. Tannenbaum[2]. *[1]Memorial Sloan Kettering Cancer Center, New York, NY,[2]Stony Brook University, Stony Brook, NY*

Oncogenic driver mutations in different pediatric sarcoma subtypes have been identified but may not be druggable. In general, identifying novel therapeutic targets and biomarkers for response remains a major challenge. We hypothesize that considering the structure of the interaction network in which the genes operate as a system is crucial for understanding a gene's role. We propose to use the protein interaction network geometry to characterize the shape of network

architecture and identify key aspects of direct and indirect cooperation pertaining to the cancer network and prognosis using geometrical methods.
We model gene networks as weighted graphs where edges indicate protein-level interactions and edge weights estimate the strength of the interaction. The Human Protein Reference Database was used to define the gene network topology. RNA-Seq data from pediatric sarcoma tissues extracted from patients treated at MSK (n=12 Ewing sarcoma; n=29 osteosarcoma; n=20 desmoplastic small round cell tumor) was employed to prescribe correlation-based weights to create pediatric sarcoma subtype-specific weighted graphs. The geometry of the weighted gene networks was computed via a discrete notion of Ricci curvature. Intuitively, the curvature provides a measure of feedback (triangles) in the network. Positive curvature reflects robust communication and ease of information transfer, while negative curvature reflects bridge-like architecture or bottlenecks of information flow. We utilized a dynamic (multi-scale) notion of curvature to quantify the functional associations between genes, computed as a function of scale between diffusion processes initially localized on each node (i.e., gene). The curvature becomes more positive on edges between communal genes and more negative on bridge-like edges between communities, until reaching the critical scale. Curvature therefore, as we demonstrate, partitions the cancer networks into functionally associated communities.
Community detection by removing bridge-edges, determined as edges with negative curvature at the critical scale, revealed sarcoma subtype-specific preferential gene associations. In particular, we agnostically found the *EWSR1-FLI1* association in a cluster that was unique to the Ewing sarcoma network. Interestingly, we found *ETV6* in the same community as the characteristic Ewing sarcoma *EWSR1-FLI1* feature, suggesting a novel implication of *ETV6* in Ewing sarcoma. These results suggest that persisting communities found by leveraging the cancer network geometry may identify potential mechanisms of drug resistance and actionable therapeutic targets.

#6542
Detection of androgen receptor splice variants from clinical sequencing
Suhyun Hwangbo, Sungyoung Lee, Sheehyun Kim, Hongseok Yun. *Seoul National University Hospital, Seoul, Korea, Republic of*

Androgen receptor (*AR*) splice variants (*AR*-Vs) have been widely studied on its important role in prostate cancer (PC) progression. In particular, *AR*-Vs lacking ligand binding domains, such as *AR* splice variant 7 (*AR*-v7) that links exon 3 and cryptic exon 3 or *AR* variant that losses exons 5 to 7 (AR^{v567es}), have been

demonstrated as one of the resistant mechanisms to androgen deprivation therapy in PC. Despite its clinical importance, the current algorithms to detect fusions such as TopHat-Fusion have limitation to detect intra-chromosomal rearrangements including *AR*-Vs. In this respect, we propose a novel approach to identify *AR*-Vs from targeted RNA sequencing (RNA-seq) dataset. In short, our two-step approach first gathers soft-clipped or divided reads that are adjacent to the splicing sites of *AR*-Vs and then yields the number of splitting reads that support the existence of *AR*-Vs. Next, the algorithm selects the paired-end reads whose one side and the other side are mapped to the preceding and following exons, respectively. The final number of spanning reads are calculated following to the removal of low-quality reads. We validated the proposed approach using two large-scale, independent RNA-seq datasets of PC samples: 34 samples from Seoul National University Hospital (SNUH) and 558 samples from The Cancer Genome Atlas (TCGA) dataset. Overall, our approach successfully identified samples with putative *AR*-Vs, including *AR*-v7 and AR^{v567es}. In addition, our approach successfully detected *AR*-v7 with reliable number of supporting reads, from the RNA-seq dataset of *AR*-v7-expressing cell line. Finally, statistical analyses of 34 SNUH PC patients suggested potential detection threshold in clinical sequencing settings (at least 10 split reads and 1% proportion). In the SNUH dataset, The *AR*-v7 positive group, which included 6 patients (17.1%) with values above the threshold, had higher *AR*-v7 expression levels than the negative group (p=4.8E-04). The similar pattern was also found in the analysis of TCGA dataset. Owing to its flexibility, we also confirmed that the developed approach can be used to detection of other *AR*-Vs, including *AR*-v3 and AR^{v567es}. We expect that the further in-depth analyses including larger samples and clinical outcomes can discover clinical applicability of *AR*-Vs.

#6543

Comparative analysis of immune landscape according to EGFR mutation and tumor PD-L1 proportion scores in non-small cell lung cancer at single cell resolution

YoungJoon Park, Su-Jin Choi, Jii Bum Lee, Dong Kwon Kim, Sun Min Lim, Seong Gu Heo, Ke Jia Qi, Byoung Chul Cho, Kyoung-Ho Pyo. *Yonsei University College of Medicine, Seoul, Korea, Republic of*

Introduction: In EGFR-mutant non-small cell lung cancer (NSCLC), the efficacy of immune checkpoint blockade (ICB) is limited with higher incidence of toxicity profiles. EGFR-mutant NSCLC is associated with immune suppressive microenvironment, including lower programmed death-ligand 1

(PD-L1), tumor mutational burden (TMB), and tumor-infiltrating $CD8^+$ T lymphocytes. However, tumors expressing high levels of PD-L1 show improved and durable clinical benefit in immunotherapy. In addition, Understanding the dynamics of tumor microenvironment may elucidate immune response in terms of immune composition, and help overcome resistance to immune checkpoint inhibitors. Here, we demonstrate that conventional type 1 dendritic cells (cDC1s) is one of the key tumor microenvironment, resulting in priming of $CD8^+$ T cells and production of chemokines, such as CXCL9/CXCL10 and cytokines that augment anti-tumor immunity.

Methods: A total of 31 surgical samples of NSCLC, including EGFR wild and mutant NSCLC of stages I-III, and 16 normal lung tissue samples were collected. PD-L1 expression in EGFR wild type was categorized into tumor proportion score (TPS) of < 50% and ≥ 50% using immunohistochemistry (IHC). Single cell RNA sequencing was performed with the Scanpy toolkit on the retrospective cohorts of normal (n=16), EGFR mutant (n=14, L858R=6, E19Del=8), EGFR wild TPS ≥ 50% (n=10), and TPS < 50% (n=7).

Results: We observed that an overall tumor specific immune response occurred in EGFR wild-type TPS ≥ 50% compared with others. *XCL1*$^+$ innate-like T cells, which act as an orchestra of tumor specific immune response, were found. These cells had high expression of *FCER1G* and *IL2RB*, a receptor for IL-15, However, expression of *CD8A/B*, *CD4* and *FCGR3A* was low. Interestingly, in these innate-like T cells, the expression of *ITGAE*, which interacts with E-cadherin in cancer cells, and *CD81*, which interacts with CD3 and enhances immunological synapse, was observed in EGFR wild TPS ≥ 50%. According to these results, *XCR1*$^+$ cDC1s were enriched in EGFR wild-type TPS ≥ 50%. *CXCL9*/*CXCL10*, which recruits $CXCR3^+$ effector T cells which are primed at the lymph node, was highly expressed in activated DCs at EGFR wild TPS ≥ 50%. $CD8^+$ T cells were significantly enriched in EGFR wild-type TPS ≥ 50%. These cells also expressed *IFNG* and *FLT3LG*, which maintain the function of intra-tumoral dendritic cells (DCs), and were also up-regulated in EGFR wild-type TPS ≥ 50%. Among them, exhausted $CD8^+$ T cells expressing *PDCD1* were observed in EGFR wild TPS ≥ 50%, and these cells also expressed *ITGAE* and *CD81*. In addition, these cells also showed high expression of *CXCR3*, a receptor for CXCL9/CXCL10 which were expressed in the activated DCs.

Conclusion: cDC1s-mediated tumor specific immune response occurred in patients with EGFR wild TPS ≥ 50%, which could be an important mechanism to predict anti-PD-1 response.

#6544

Identification of epigenetic regulatory networks associated with the basal-like breast cancer subtype

Larissa Miyuki Okano[1], Alexandre Luiz Korte de Azevedo[2], Tamyres Mingorance Carvalho[2], Fernanda Brandão Berti[1], Luciane Regina Cavalli[1].
[1]Instituto de Pesquisa Pele Pequeno Principe, Curitiba, Brazil,[2]Genetics Department, Universidade Federal do Paraná, Curitiba, Brazil

Purpose: Basal-like breast cancer (BLBC) is a biologically aggressive and molecular heterogeneous breast cancer subtype that confers to the patient´s poor prognosis. The crosstalk of epigenetic regulators, such as methylation events and microRNA (miRNA) deregulation, drives breast cancer progression and modulates aggressive tumor phenotypes. However, few studies have specifically characterized the epigenetic regulatory networks of genome-wide DNA methylation-based modifications, miRNAs and transcription factors (TF) expression in BLBC. Therefore, the main objective of this study was to identify and correlate the DNA methylation profiles and the transcriptional expression of miRNAs and TFs of the BLBC subtype.
Methods: To achieve our goal, a comprehensive computational pipeline using the R language was used. First, the transcriptional expression profiles and DNA methylation data of BLBC and non-tumor samples were downloaded from The Cancer Genome Atlas (TCGA). Then, the ELMER package was used to determine the differentially methylated distal probes between these two groups, identifying gene-probes pairs that can be regulated by un/methylated regions that affect the function of TFs. The different expressed (DE) miRNAs were identified using the DESeq2 package. To determine the regulatory pairs (gene, miRNA and TF interactions) the multiMiR, miRWalk, ENCODE, and hTFtarget were used and the regulatory networks were identified by the FANMOD algorithm. Finally, pathway enrichment analysis (PEA) was conducted using the Reactome database and microT-CDS (Diana Tools mirPath v.3).
Results: A total of 147 and 199 pairs of gene-probes were identified in hypermethylation and hypomethylation analyses, respectively. Fifty genes and 59 regulatory TFs whose expression was associated with DNA methylation were selected, including members of the E2F (E2Fs) and Krüppel-like factor (KLFs) family. Eleven DE miRNAs, out of the 51 identified, were selected based on their interaction with genes and TFs. These pairs of miRNAs, TF, and genes generated three types of feed-forward loops (FFLs): coherent FFLs, mediated by miRNAs; incoherent FFLs, mediated by TFs; and compost FFLs, mediated by TF and miRNAs. Finally, the PEA analysis showed 51 pathways in which miRNAs, genes, or TFs may interact, including pathways related to DNA repair,

cell cycle, pathways in cancer, as well as the defective binding of RB1 mutants to E2F1, and the ErbB signaling pathway.
Conclusion: Our findings demonstrated the epigenetic regulation of methylation patterns and miRNA expression and their impact on the expression of TFs that may exert critical roles in the BLBC. The functional analysis of these regulatory networks in well-established BLBC models, targeting the signaling pathways identified, can determine whether they modulate the BLBC phenotype and can be used as potential clinical targets.

#6545

Investigating secondary findings in a pediatric cancer cohort: preliminary findings

Safa Majeed[1], Stephenie Prokopec[2], Brianne Laverty[1], Vallijah Subasri[1], Michael Taylor[3], Yvonne Bombard[4], Trevor Pugh[2], Adam Shlien[1], Anita Villani[3], David Malkin[3]. *[1]Genetics and Genome Biology, Hospital for Sick Children, Toronto, ON, Canada,[2]Princess Margaret Cancer Centre, University Health Network, Toronto, ON, Canada,[3]Hospital for Sick Children, Toronto, ON, Canada,[4]Genomics Health Services Research Program, Li Ka Shing Knowledge Institute, St. Michael's Hospital, Toronto, ON, Canada*

Purpose: An expected outcome following germline genome sequencing in oncology is the discovery of 'secondary findings' (SFs). SFs comprise pathogenic(P)/likely P (LP) germline variants in cancer genes not typically associated with the presenting cancer, in addition to germline variants of uncertain significance (VUS) to the patient's cancer. Due to the rarity of childhood cancers and a dearth of studies analyzing SFs, many pediatric SFs are categorized as VUS without clinical interpretation. Interpreting SFs poses significant challenges: VUSs and other SFs are frequently not included in clinical molecular reports, and even when reported (often through research), their clinical utility and long-term impact on patient health are unclear. However, we know VUSs can have clinical importance because some VUSs, when investigated thoroughly, have been reclassified as pathogenic predictors of significant health conditions in children. We hypothesize that an in-depth characterization of the landscape of germline SFs/VUSs across a diverse pediatric cancer cohort will reveal new roles of these genes and mutations in pediatric cancers.
Methods: To explore germline SFs in pediatric cancer patients, we analyzed germline whole-genome sequencing (WGS) data for patients with rare, relapsed, refractory, and metastatic childhood cancers enrolled in the SickKids Cancer

Sequencing Program (KiCS). We developed a custom analysis pipeline to identify germline single-nucleotide variants and indels deemed SFs, auto-classify their pathogenicity (ex. P, LP, or VUS) using CharGer, filter for PanCanAtlas-indicated cancer predisposition genes, and sort the remaining variants by cancer and non-cancer associations.
Results: The KiCS cohort (n = 511) encompassed over 133 different tumor types; the median age of participants was 14 years (SD = 10.27) and 55% of patients were male. Ongoing work in our lab will catalogue the frequency and distribution of SFs in KiCS and analyze germline variants by subgroup (gene, tumor subtype, stage, demographics, gene function). We will also compare SF prevalence in KiCS to the general population using the gnomAD dataset. Results from preliminary analyses of this cohort will be presented.
Significance: SFs/VUSs are under-utilized in cancer management. This work advances the holistic understanding of germline genomics in pediatric oncology and the roles of SFs in disease. Future studies will evaluate SFs by patient ancestry and validate cancer associations through the evaluation of allelic imbalance/loss of heterozygosity in matched tumor genomes.

#6546

Peritoneal microenvironment promotes appendiceal adenocarcinoma tumor formation in PDX models

Vinay K. Pattalachinti[1], Ichiaki Ito[1], Saikat Chowdhury[1], Abdelrahman Yousef[1], Yue Gu[1], Keith F. Fournier[2], John P. Shen[1]. *[1]Gastrointestinal Medical Oncology, UT MD Anderson Cancer Center, Houston, TX,[2]Surgical Oncology, UT MD Anderson Cancer Center, Houston, TX*

Background: Few preclinical models of appendiceal adenocarcinomas (AAs) exist. Orthotopic patient-derived xenografts (PDXs) better recapitulate the original tumor microenvironment. Therefore, we hypothesized that AA patient tumors should grow more successfully in orthotopic PDXs compared to standard flank implanted PDXs.
Methods: After obtaining informed consent, tumor samples were obtained from 16 patients with AA undergoing surgical resection at MD Anderson Cancer Center. Tumors were implanted in both the flank and peritoneum of NSG mice; from each patient, at least 6 mice (n≥3 IP, n≥3 flank) were implanted with an approximately 0.5 cm^3 tumor. Mice were assessed after 6 months for tumor formation.
Whole transcriptomic RNAseq was performed on tumor samples taken from either the flank (n=3) or peritoneum (n=3) of two poorly differentiated (grade 3)

patient tumors. The R package DESeq2 was used to conduct differential gene expression analysis comparing IP to Flank PDXs, controlling for the specific patient tumor. Finally, Gene Set Enrichment Analysis (GSEA) with the hallmark gene sets from MSigDB was implemented to study the relative up/down-regulation patterns of gene sets in each PDX cohort.
Results: Tumor formation rate, regardless of grade, was greater in IP vs. flank implantation (31.4% vs 11.7%). Higher grade was associated with higher average tumor formation rates (IP—G1: 13.3%, G2: 33.8%, G3: 44.5%; Flank—G1: 0%, G2: 0%, G3: 31.2%).
GSEA identified that cell proliferation and energy metabolism gene sets were significantly enriched in IP tumors relative to flank: E2F Targets, G2M Checkpoint, Oxidative Phosphorylation, MYC Targets V1, MYC Targets V2, and DNA Repair (NES = 2.91, 2.62, 2.60, 2.31, 1.61, 1.82, respectively; FDR q-val $\leq$ 0.01 for all). Meanwhile, gene sets associated with tumor environmental stress were enriched in flank tumors: Angiogenesis, Hypoxia, and TGF-β Signaling (NES = -2.00, -1.73, -1.62, respectively; FDR q-val $\leq$ 0.01 for all). Epithelial Mesenchymal Transition and TNF-α signaling via NF-κB were also enriched in flank tumors (NES = -2.28, -2.20; FDR q-val < 0.01).
Conclusions: The peritoneal microenvironment promotes growth of appendiceal tumors in PDXs, with higher-grade being associated with greater tumor formation rate. GSEA also suggests that AAs preferentially grow in the peritoneal microenvironment in association with greater activation of cellular proliferation and energy metabolism pathways and lower activation of tumor environmental stress pathways.

#6547
Features of the TCR repertoire associate with patient's clinical and molecular characteristics in acute myeloid leukemia
Mateusz Pospiech, Mukund Tamizharasan, Yu-Chun Wei, Advaith M. S. Kumar, Mimi Lou, Joshua Milstein, Houda Alachkar. *USC - University of Southern California, Los Angeles, CA*

Allogeneic hematopoietic stem cell transplant (allo-HSCT) remains the most effective strategy for high risk patients with acute myeloid leukemia (AML). Leukemia specific neoantigens when presented by the major histocompatibility complexes (MHCs) are recognized by the T cell receptors (TCR) triggering the graft versus leukemia effect. Unique TCR signature is generated by a complex rearrangement process of an array of variable (V), diversity (D), and joining (J) exons to form a functional receptor with complementary determining regions 3

responsible for the interaction between the TCR and the peptide-MHC. The generated TCR repertoire undergoes dynamic changes with the onset and progression of leukemia and with the course of treatment.
To better understand how the TCR repertoire impacts disease progression and patient's clinical outcome, we leveraged RNA-seq data from The Cancer Genome Atlas (TCGA) to extract the TCR sequences using TRUST4 and MIXCR and examined the association between features of the TCR repertoire in patients with AML and their clinical and molecular characteristics. Data were analyzed by normalizing the number of unique clones to the number of total RNA-seq reads specific for each sample and one minus peripheral blood blast percentage.
Both TRUST4 and MIXCR data showed a strong correlation between the number of unique clones for TCRA and TCRB per patient ($r=0.944$, $p<0.001$ for TRUST4, $r=0.941$, $p<0.001$ for MIXCR). Only 1389 TCRA clones (28.9%; TRUST4: 3450, MIXCR: 2747) and 1327 TCRB (31.3%; TRUST4: 3986, MIXCR: 1584) unique clonotypes were shared by the two computational tools. Nevertheless, we were able to identify the majority of the known TRAV and TRBV segments. Our analysis shows that the normalized number of unique TCRA and TCRB clones were lower in patients carrying FLT3 mutations (TRUST4: TCRA: $p=0.013$; TCRB: $p=0.058$; MIXCR: TCRA: $p=0.043$; TCRB: $p=0.030$), and higher in patients carrying IDH1 mutations (TRUST4: TCRA: $p=0.037$; TCRB: $p=0.038$; MIXCR: TCRA: $p=0.037$; TCRB: $p=0.002$) compared with patients carrying the wild type gene. No significant difference was observed for DNMT3A, NPM1, TET2, RUNX1, CEBPA IDH2, NRAS, WT1 and TP53 compared with wild type. Although the normalized number of unique TCR clones was not significantly associated with patient's overall survival, we found that patients that shared TCRB clones with any other patients had a trend toward an improved overall survival compared with patients that did not share any TCRB clones with other patients (median OS: 32.3 vs 16 months, $p=0.068$).
Despite the limitations of low TCR gene coverage associated with RNAseq data and the small sample size, we were able to find associations between TCR repertoire and clinical and molecular features in patients with AML using two different computational tools. This study further supports the need for TCR-Seq analyses to provide the depth needed to characterize the TCR repertoire in patients with AML.

#6548

Bioinformatic characterization of dendritic and T cell subpopulations in the tumor microenvironment across different cancer types by single-cell RNA-Seq analysis

Yamil D. Mahmoud[1], Natalia Rego[2], Marcela Vilarino[3], Florencia Veigas[1], Maria R. Girotti[1], Juan M. Perez Saez[1], Gabriel A. Rabinovich[1], Marcelo Hill[3].
[1]Laboratorio de Glicomedicina, IBYME, Buenos Aires, Argentina,[2]Bioinformatics Unit, Institut Pasteur de Montevideo, Montevideo, Uruguay,[3]Laboratory of Immunoregulation and Inflammation, Institut Pasteur de Montevideo, Montevideo, Uruguay

Although the development of single-cell RNAseq (scRNAseq) has improved the knowledge of the tumor microenvironment (TME), there is not a clear understanding of specific cell subtypes, markers that define these cell populations, nor the interaction between them. Previously, we showed that inflammasome activation is correlated with antitumor responses triggered by immune checkpoint blockade (ICB). This highlights a central role for TMEM176B, mostly expressed in myeloid cells, that impairs the recruitment of cytotoxic immune cells in the TME by inhibiting NLRP3 inflammasome activation. Still, the roles of the different subsets of myeloid and T cells in the TME and to what extent they are connected remain controversial. Here, we used scRNAseq data from human tumors to identify and characterize cDC2, Th17 and exhausted $CD8^+$ T cell subpopulations in cancer. Five scRNAseq data sets of melanoma, basal cell carcinoma, breast, lung, colorectal, and ovary cancer patients were integrated, accounting for 382,019 immune cells in total. We applied and compared different bioinformatic tools for scRNASeq data normalization and data sets integration to find conserved immune cell populations across samples, data sets, and cancer types. Then, we evaluated different parameters using well-established methods for clustering and cell type classification to identify subtypes of DCs and T cells in the integrated data. We combined automatic methods with manual analysis of cluster markers to improve robustness and confidence in the cell populations identified. Three clusters of cDC2 were defined and characterized using different scRNAseq analysis tools for pathway enrichment analysis and transcription factors (TF) activation prediction. We found a subset of inflammatory cDC2 with high gene expression of *IL1B* and *NLRP3*, in contrast with another cluster characterized by high expression of *TMEM176B* and *CD14*. A third cluster showed an intermediate transcriptomic profile. The $TMEM176B^+$ $CD14^+$ cluster was characterized by the activation of JAK-STAT and hypoxia pathways, and the TF FOXL2, ETS2, and ESR2. The $NLRP3^+$ $IL1B^+$ cluster showed more activation

of MAPK, Trail, and PI3K pathways, and the TF CEBPE. Moreover, the activation of TNFα and NFkB signaling pathways was found in both clusters. In addition, a conserved population of Th17 cells in the integrated data was observed. Th17 cells were heterogeneous, making the subpopulations and transcriptome signature difficult to define. Further analysis is being performed to identify Th17 subsets and their potential interactions with the cDC2 subclusters. A robust identification and characterization of these immune cell subsets will build towards our understanding of the interactions between these subpopulations triggered by inflammasome activation within the TME and the mechanisms behind ICB response.

#6549

Investigating the effects of density and frequency-dependent selection on subpopulations of cancer cells defined by copy number

Thomas A. Veith[1], Andrew Schultz[1], Noemi Andor[1], Saeed Alahmari[2]. *[1]Moffitt Cancer Center, Tampa, FL,[2]Najran University, Najran, Saudi Arabia*

Intratumoral heterogeneity is a major obstacle for many cancer therapies. Treatment modalities which target a particular phenotype select for cells with different phenotypes. For example, chemotherapy which targets fast-dividing cells may select for a tumor composed of slower-dividing cells which cannot be effectively targeted by the drug. We hypothesize that subpopulations (SPs) of cells defined by somatic copy number alterations (sCNAs) differ in how quickly they divide and how well they can compete at high population densities. Additionally, we expect that sCNA-defined SPs affect the fitness of one another through cooperative (e.g., exchange of growth factors) and competitive (resource depletion) interactions. To test these hypotheses and compare the relative effects of (i) density and (ii) frequency-dependent selection on tumor evolution, we have developed two mathematical models integrated with experimental and computational techniques. In both models, we evaluate the growth dynamics of cancer cell SPs defined by sCNAs detected in single cell RNA/DNA-sequencing data from 4 gastric cancer cell lines (HGC-27, KATOIII, NUGC-4, SNU-16). To investigate the effects of density dependent selection (i), we start by growing the cell lines in our lab in order to infer growth rate (r) and carrying capacity (K). Next, linear models are built correlating pathway expression levels with r/K values. We tested 50 KEGG pathways previously identified as differentially expressed between r and K-selected cells as transcriptomic biomarkers of growth parameters. The best fitting models are then used to infer SP-specific r/K values. For growth, we found r as a function of the KEGG pathway ‘RNA Polymerase’

(R^2 = 0.9636, p-val=0.0019). For carrying capacity, we used 'Pathways in Cancer' (R^2 = 0.7898, p-val=0.0629). In each cell line, an r/K tradeoff existed between at least one pair of SPs, suggesting sCNAs indeed have effect on r/K parameters. For frequency-dependent selection (ii), we use an inverse game theory algorithm which takes SP frequencies over time as input and outputs a parameterization for the replicator equation to recapitulate detected frequencies and predict future growth. The algorithm uses a penalized least squares method that takes the error to be the difference between replicator equation output and SP frequency input. SP growth over time can then be modeled with the replicator equation to characterize conditions for co-existence or dominance. These approaches reveal the dynamics of heterogeneous tumor growth, and make it possible to compare the relative influence of different selective pressures. We can examine how the growth of a tumor would change with the elimination of a given SP. This greater understanding can contribute to a better design of evolution-based therapies that avoid, or at least delay, the evolution of resistance to treatment.

#6551

HiTAIC: Hierarchical tumor artificial intelligence classifier traces tissue of origin and tumor type in primary and metastasized tumors using DNA methylation data

Ze Zhang[1], Brock Christensen[2], Lucas Salas[2]. *[1]Dartmouth Geisel School of Medicine, Hanover, NH,[2]Dartmouth Geisel School of Medicine, Lebanon, NH*

Background: Human cancers are heterogenous by their cell composition and origination site. Cancer metastasis generates the conundrum of the unknown origin of migrated tumor cells. Tracing tissue of origin and tumor type in primary and metastasized cancer is vital for clinical significance. Researchers have demonstrated the high performance of DNA methylation-based machine learning models tracing the tissue origin of tumor cells. However, previous models were devised based on tissue site instead of tumor type, generating potential problems of indistinguishable tumor subtypes from the same site, e.g., esophageal squamous cell carcinoma versus esophageal adenocarcinoma. Methods: we employed a novel tumor-type-specific hierarchical model using DNA methylation data to develop a multilayer perceptron model (MLP) to trace tumor tissue of origin and subtype. DNA methylation data on 7735 tumor samples from 27 cancer types were downloaded from GEO and TCGA to develop tumor-type-specific libraries. The discovery data set was split into 80% training and 20 % testing. The tumor classifier hierarchy was established with

two layers for 27 cancer types. In each layer of the hierarchy, the MLP model was trained using the selected cancer-type discriminatory CpGs. HiTAIC was established based on the four hierarchical MLP models. To validate HiTAIC, we applied the model to the external validation data sets computing stratified and overall precision, recall, and f1-score to evaluate the performance. Next, we applied the model to the application data sets and used stratified and overall precision, recall, and f1-score to evaluate model performance in metastasized cancers.
Results: We observed high accuracy of HiTAIC's performance in primary cancer tracing with 99% accuracy and 99% weighted average F1-score in the testing dataset. We observed 93% accuracy and 93% weighted average F1-score for external validation across 25 cancer types. In metastasized cancer, HiTAIC demonstrated 96% accuracy and 98% weighted average F1-score across five cancer types with six different metastatic locations. HiTAIC traces tumor tissue of origin and cancer subtype with high accuracy in primary and metastasized cancer.
Conclusion: We developed HiTAIC, a DNA methylation-based classifier, to trace tissue of origin and tumor type in primary and metastasized tumors. The model's capability to trace the tumor origin and subtype with high resolution and accuracy promises potential clinical use in identifying cancer of unknown origin. HiTAIC can be easily deployed in a web-based application, transforming computational sophistication into a user-friendly public tool.

#6552

ZEB1-AS1 lncRNA prevents ZEB1 suppression and leads to tumor progression in undifferentiated AML subtype

Stefano Percio[1], Daniela Magliulo[2], Silvia Martini[1], Sandro Pasquali[1], Rosa Bernardi[2]. *[1]DRAST, Fondazione IRCCS - Istituto Nazionale dei Tumori di Milano, Milano, Italy,[2]DRAST, San Raffaele Scientific Institute, Milano, Italy*

The zinc finger E-box binding homeobox 1 (ZEB1) transcription factor is a master regulator of the epithelial to mesenchymal transition (EMT). In solid tumors, its overexpression induces EMT, which activates cellular motility and is also associated with the maintenance of stem cell properties, driving tumor progression and metastasis. A double-negative feed-forward loop circuit has been described where, to promote EMT, ZEB1 suppresses the expression of *miR-200* family members, which in turn inhibits its activity. Albeit recent evidence highlighted the existence of EMT processes also in hematological malignancies, the role of ZEB1 is not completely defined yet. Hence, this study aims to

characterize ZEB1 behavior in acute myeloid leukemia (AML). To this purpose, we retrieved and analyzed RNA-Seq data from public repositories to evaluate the expression levels of the main EMT master regulator genes in normal and malignant hematopoietic cells. We observed a heterogeneous expression of these genes among AML morphological subtypes (from M0 to M5) defined by the French-American-British (FAB) classification system. Specifically, *TWIST1* has the highest expression value in M3 and *ZEB2* in M5, as already observed in published studies, while *ZEB1* has the highest expression in M0, which significantly decreases until M5. To evaluate the ZEB1 transcriptional program, we performed a gene set enrichment analysis of hallmark signatures based on gene-wise correlation with *ZEB1* among FABs that revealed the up-regulation of EMT in the M0 subtype. Moreover, the highest value of correlation was found between *ZEB1* and its antisense lncRNA (*ZEB1-AS1*). This trait emerged as peculiar to AML both with respect to other cancer types and normal hematopoietic cells. Since ZEB1 orchestrates its transcriptional program by inhibiting the activity of specific miRNAs, we selected putative candidates that may take part in this circuit in AML by calculating their bimodality distribution, which reflects the toggle switch behavior typical of the double-negative feed-forward loop. We identified *miR-425-5p*, which was coherently down-regulated in M0 with respect to other FABs, and *miR-151-3p* which was surprisingly up-regulated. Specifically, the simultaneous up-regulation in the M0 subtype of *miR-151-3p* and its target *ZEB1* is inconsistent with the toggle switch behavior of the circuit. Thus, we hypothesized that *miR-151-3p* is not able to inhibit *ZEB1* expression in M0 due to the presence of *ZEB1-AS1*, which is supposed to disrupt the circuit mechanism protecting *ZEB1* from miRNA-mediated inhibition. This hypothesis is also supported by the fact that all target genes of *miR-151-3p* were significantly up-regulated. A better comprehension of this regulatory circuit could allow identifying aberrant epigenetic mechanisms during leukemic development and discriminating of the different AML subtypes.

#6553

The development of homologous recombination repair deficiency (HRD) score methodology using WES data and its application in patient-derived xenograft models

Jixin Wang[1], Krista Kinneer[2], Wenyan Zhong[1], Zhongwu Lai[1]. *[1]Oncology Data Science, AstraZeneca in Cambridge, Gaithersburg, MD,[2]Translational Medicine, AstraZeneca in Cambridge, Gaithersburg, MD*

Homologous recombination repair deficiency (HRD) and mutations in genes involved with homologous recombination repair (HRR) are associated with sensitivity to platinum-based chemotherapy, topoisomerase 1 inhibitors and inhibitors targeting DNA repair pathway. Use of the Myriad HRD test for HRD determination in preclinical models is not feasible globally. To address this challenge, we developed an approach to generate HRD scores from whole exome sequencing (WES) data and applied it to assess HRD status in patient-derived xenograft (PDX) models.

We used python package CNVkit for segmentation and gene-level/allele-specific copy number calling with customized settings according to CNVkit documentation. The reference was constructed using the WES BED file and hg38 reference genome when there are no paired control samples available. Next R package scarHRD was used to determine the HRD score that is the sum of loss of heterozygosity (LOH), telomere allele imbalances (TAI), and large fragment migrations (LST). The method was applied to the WES of 25 Xentech triple negative breast cancer (TNBC) PDX models to derive HRD scores. The samples were also separately profiled using Myriad's MyChoice CDx assay. The two scores showed moderate correlation with Pearson r = 0.56. However, when n = 6 PDX models with low coverages (average depth <100x) were excluded, the Pearson r improved to r = 0.76. We also found that the absolute value of HRD score calculated by CNVkit/scarHRD is lower than that of Myriad HRD score. Furthermore, we evaluated the genomic landscape in this cohort of TNBC PDX models for the selected genes of HRR pathway (BRCA1, BRCA2, ATM, BRIP1, PALB2, RAD51C, BARD1, CDK12, CHEK1/2, FANCL, RAD51B, RAD51D, RAD54L). Sixteen models found to carry HRR mutations, with ATM and BRCA1 mutations being the most common ones, being found in 9 and 5 of 25 models, respectively. Although HRRm positive (HRRm+) models have higher HRD score for both Myriad HRD score and HRD score generated with CNVkit/scarHRD approach, the association between HRR (HRRm+/HRRm-) and Myriad HRD (HRD+/HRD- defined by HRD threshold of 42) is not statistically significant (Fisher's exact test p value = 0.1998, odds ratio=3.5), likely due to small cohort sizes.

These results suggest that combination of CNVkit and scarHRD for HRD score calculation may be an alternative approach for HRD identification in preclinical PDX models.

#6554

Prediction of MET amplification from H&E images in non small cell lung cancer using self-supervised deep learning and its role in clinical trial

enrollment

Chaitanya Parmar[1], Oscar M. Carrasco-Zevallos[2], Joshua C. Curtin[2], Darshana Govind[3], Bing Xia[4], S. Martin Shreeve[1], Songbai Wang[2], Timothy Jatkoe[2], Patricia Raciti[1], Levon Demirdjian[1], Joel Greshock[2], Kristopher Standish[1], Stephen S.F. Yip[5]. *[1]Janssen R&D, US, San Diego, CA,[2]Janssen R&D, US, New Jersey, NJ,[3]Janssen R&D, US, San Francisco, CA,[4]Janssen R&D, US, New jersey, NJ,[5]Janssen R&D, US, Boston, MA*

Objective: DNA amplifications of the cMET locus (METamp) are rare (1-6%) in non-small cell lung cancer (NSCLC). The ability to efficiently identify patients with METamp could accelerate development of cMET-targeting therapies by identifying patients for enrollment efficiently. We developed a self-supervised deep learning algorithm (SSDL) to predict METamp status using H&E stained whole slide images (WSI).

Methods:Three datasets (CD_{train}, CD_{NGS}, CD_{FISH}) consisting of data from 1,436 advanced NSCLC patients (1 slide/pt) were used to develop an SSDL algorithm to predict METamp status. The METamp+ status across datasets was standardized for CD_{train} (n=788, METamp+ Prevalence=15%), CD_{NGS} (n=186, 19 positive, 167 negative, Prev=10%) as harboring ≥5 copies of the gene using NGS(Next Generation Sequencing) and for CD_{FISH} (n=462, 36 positive, 426 negative, Prev=8%) as MET CN gain to centromere 7 ratio (CEN) ≥2.5. The datasets were divided into a discovery set (CD_{train}) for training and held-out test sets (CD_{NGS}, CD_{FISH}) for validation. To improve robustness of SSDL, we first pre-trained ResNet34 with Simple Contrastive Learning, using >25k WSIs from diverse sources. During the training phase, 4-fold cross validation was applied on CD_{train}. The first 3-layers of ResNet34 were frozen while the final layer and an attention-based aggregation system were trained for METamp prediction. The performance was assessed using sensitivity, specificity, AUC, positive predictive value (PPV), and negative predictive value (NPV) on the test sets. Predictions from the model were binarized using two separate thresholds selected from CD_{train}, resulting in a High-Sensitivity model ($SSDL_{Sens}$ = 90% Sensitivity) and High-Specificity model ($SSDL_{Spec}$ = 90% Specificity). Each model's potential impact on patient enrollment is presented below.

Results: The trained SSDL models achieved an average cross-validation AUC of 0.77±0.04 across folds. The final trained model with the highest cross-validated AUC was chosen for METamp status prediction on the test sets. The selected model maintained predictive performance on CD_{NGS} (AUC=0.82) and CD_{FISH}

(AUC=0.75) test sets. The $SSDL_{Spec}$ model had a PPV more than twice the baseline prevalence in both CD_{NGS} (PPV=27%), and CD_{FISH} (PPV=29%), providing a significant enrichment in METamp+ patients. The $SSDL_{Sens}$ model correctly classified ~55% of METamp– in CD_{NGS} and CD_{FISH} with NPV of ≥97%. These results suggest a potential reduction in genetic screening by 50% while maintaining high sensitivity.
Conclusions: The SSDL model robustly predicted METamp status in independent patient cohorts, regardless of METamp definitions (i.e., by NGS or FISH). We demonstrate the ability to classify patients with high sensitivity or specificity, which can help reduce genetic testing or surface potentially eligible patients for trials, respectively.

#6555
Integrated bioinformatics analysis identified ASNS and DDIT3 as the therapeutic target in castration resistance prostate cancer
Ae Ryang Jung, Sun Shin, U-Syn Ha, Mee Young Kim, Sung-Hoo Hong, Ji Youl Lee, Sae Woong Kim, Yeun-Jun Chung, Yong Hyun Park. *Catholic University of Korea, Seoul, Korea, Republic of*

Background: Many studies have demonstrated the mechanisms of progression to castration-resistant prostate cancer (CRPC) and novel strategies for the treatment of CRPC. Despite these advances, the molecular mechanism underlying the progression to CRPC remain unclear, and no effective treatments for CRPC are currently available. Here, we characterized the pathways and key genes involved in the progression to CRPC to gain insight into the mechanisms and potential therapeutic targets of CRPC.
Methods: Bicalutamide-resistant prostate cancer cells derived from LNCaP was generated and named Bical R. RNA sequencing was used to identify differentially expressed genes (DEGs) between LNCaP and Bical R. DAVID and Clue GO were used to perform functional enrichment analysis, and the Cytohubba plug-in Cytoscape was used to identify hub genes associated with progression to CRPC. To validate the expression of hub genes, we performed qRT-PCR and western blot analyses. Further validation was performed using GEO microarray (GSE 32269 and GSE28403). To elucidate the clinical usefulness of these genes, we assessed the disease-free survival of patients with prostate cancer from The Cancer Genome Atlas (TCGA) database.
Results: In total, 631 DEGs (302 upregulated genes and 329 downregulated genes) were identified, and Kyoto Encyclopedia of Genes and Genomes pathways were analyzed based on DAVID and Clue GO. We found that the

PI3K-Akt and MAPK signaling pathways are of great significance for investigating the mechanism of CRPC progression. Hub genes from protein-protein interaction network of upregulated DEGs (AGT, ASNS, ATF3, ATF4, DDIT3, EFNA5, and VEGFA) were identified. Among the hub genes, ASNS and DDIT3 were markedly up-regulated in CRPC cell lines and CRPC tissues, respectively. Additionally, patients with high expression of ASNS and DDIT3 showed worse disease-free survival in TCGA database.
Conclusion: Our study revealed that the PI3K-Akt and MAPK signaling pathways may be important in the mechanism of CRPC progression, and ASNS and DDIT3 may be associated with progression to CRPC. These results may contribute to the development of potential therapeutic targets and mechanisms underlying the progression to CRPC to improve clinical efficacy for CRPC treatment.
Acknowledgements: This work was supported by the National Research Foundation of Korea(NRF) grant funded by the Korea government(MSIT) (No. 2022R1A2C2003513).

#6556
A gene signature of DNA damage response pathway is predictive of patient clinical outcomes and is associated with tumor immune microenvironment of lung adenocarcinoma
Xiaoli Zhang, Junran Zhang. *The Ohio State University, Columbus, OH*

DNA damage response (DDR) is crucial to prevent the accumulation of DNA lesions that can lead to genomic instability and promote tumorigenesis. Dysregulation of DDR pathways also provides therapeutic opportunities for new cancer therapy. Given that lung cancer displays a high level of genetic mutation and genomic instability, a comprehensive understanding of the dysregulation of DDR genes in lung cancer, especially non-small cell lung cancer (NSCLC) which accounts for 85% of all lung cancer cases, will be critical for identifying new genes contributing to tumorigenesis and novel targets for lung cancer therapy.
The goal of this study is to identify novel targets for lung cancer treatment through a comprehensive analysis of DDR genes and its association with patient survival, genomic mutation/instability, tumor immune microenvironment (TIME), and tumor proliferation ability. To this end, we have comprehensively characterized the expression of 276 DDR genes using the Cancer Genome Atlas (TCGA) and other publicly available data of lung adenocarcinoma (LUAD), the most common NSCLC. We found that 36 out of 276 DDR genes are

dysregulated with majority being upregulated in tumors and are associated with patient overall survival (OS) and progression free survival (PFS) based on the TCGA LUAD cohort. A gene expression signature, i.e., DDR gene expression dysregulation score (DDRDS), was constructed based on the geometric mean of the differentially expressed genes that were also associated with patient OS. Patients with a higher DDRDS showed significantly worse OS and PFS, more advanced tumor stage, a higher tumor mutational burden (TMB), neoantigen load, and homologous recombination deficiency (HRD) score. In addition, tumors with higher DDRDS displayed an increase in CD4+ activated memory T-cells, CD8+ T- cells, M0 and M1 macrophage, and NK cells, but a decrease in B cells, CD4+ resting memory T-cells, monocytes, and dendritic cells in TIME. Further, these tumors also showed a higher expression of immune check point molecules PD1 and PD-L1. Lastly, gene set enrichment analysis demonstrated that these tumors had significantly increased nuclear division, DNA replication, chromosome segregation, and cell cycles, reflecting the aggressiveness of the disease. Hence, despite the previous studies demonstrating that mutation and deletion defects in DDR genes are frequent in tumors, we found that the dysregulated DDR genes are mainly upregulated, and DDRDS based on the dysregulated expression of DDR genes is associated with the alteration in TMB/HRD/TIME, tumor aggressiveness, and ultimately patient outcomes. These results suggested that patients with a higher tumor DDRDS are associated with poor prognosis but might benefit from immune checkpoint blockade-associated immunotherapy.

#6557

A 6-microbial signature risk score for overall survival prediction in hepatocellular carcinoma: a machine learning approach

Nour N. Al-Bzour[1], Ayah N. Al-Bzour[2]. *[1]Jordan University of Science & Technology, Irbid, Jordan,[2]Faculty of Medicine, Jordan University of Science & Technology, Irbid, Jordan*

Introduction: Hepatocellular carcinoma (HCC) is a severe type of cancer associated with high malignancy and poor prognosis. To reach a better prognosis, several factors affecting HCC patients must be considered. In this study, we aim to investigate the relationship between gut microbiota with the survival of HCC patients, and to build a machine learning (ML) prognostic model based on microbiome signatures.
Methods: Microbial and survival data for HCC patients from The Cancer Genome Atlas Program (TCGA) were obtained using the cBioportal database.

The microbiome signatures were screened for prognostic effect using the univariate cox regression. The significant microbial signatures were fitted into the Least Absolute Selection and Shrinkage Operator - Cox (LASSO-Cox) model to reduce multicollinearity. Signatures with non-zero LASSO coefficients were screened for independent effect in the multivariate cox regression analysis. Results: A total of 1407 microbial signatures were downloaded from TCGA dataset. 63 prognostic microbial signatures were identified using the univariate cox. A total of 30 prognostic microbial signatures were screened out using LASSO and further evaluated using independent effect to obtain microbiome risk score. Six microbial signatures were identified as independent prognostic markers including: Marichromatium (HR: 1.26; 95%CI: [0.01-1.56]), p=0.038), Paraclostridium (HR: 1.45; 95%CI:[1.15-1.82], p=0.002), Pseudorhodoferax (HR: 1.20; 95%CI:[1.01-1.43], p=0.037), Chitinimonas (HR: 1.47 95%CI: [1.10-1.97], p=0.009), Marinobacter (HR: 0.79; 95%CI: [0.65-0.97], p=0.022), Desulfovermiculus (HR: 1.44; 95%CI: [1.16-1.78, p=0.001]). Kaplan-Meier survival plot showed better overall survival (OS) in the low-risk group compared to the high-risk group (median OS: 83.6 vs. 41.8; log-rank p-value <0.0001). Conclusion: Our results show that the gut microbiota is significantly associated with HCC prognosis, in which 5 of them were associated with poorer prognosis and one was associated with better survival. These microbial signatures provide a potential prognostic marker for HCC survival.

#6558

Defining differentiation States in well-differentiated and de-differentiated liposarcoma

Danh Truong, Hannah C. Beird, Chia-Chin Wu, Sandhya Krishnan, Davis Ingram, Alexander Lazar, Emily Keung, Christina Roland, Wantong Yao, Robert Benjamin, Neeta Somaiah, Barry W. Feig, Joseph A. Ludwig. *UT MD Anderson Cancer Center, Houston, TX*

Among the many sarcoma subtypes, high-grade tumors that have failed to differentiate or undergone dedifferentiation strongly correlate with metastatic potential and poor clinical outcomes. To examine the factors that regulate cell fate, lineage plasticity, and tumor grade, we focused on two common liposarcoma variants, dedifferentiated liposarcoma (DDLS) and well-differentiated liposarcomas (WDLS), that exist at both ends of the differentiation spectrum. Since tumor grading using histology is highly subjective due to widespread tumor heterogeneity, we hypothesized that an sc/snRNA-seq-based approach would be more accurate. To determine if candidate therapies modulate

differentiation, we developed a quantitative metric of differentiation using scRNA-seq. The resulting mesenchymal tissue landscape (MTL) is akin to a Waddington landscape but optimized to distinguish DDLS from WDLS. After prospectively obtaining tumors from seven chemo-naïve patients, we performed scRNA-seq on three DDLS and five WDLS specimens, totaling 59,917 cells. Classical markers were used to identify cell types. Since no pre-existing liposarcoma training sets existed, malignant cells were identified by copy number variation (CNV) inferred from the scRNA-seq data. Overexpression of MDM2, CDK4, and HMGA2, known markers of LS, were positive in clusters classified by SingleR as fibroblasts, adipocytes, and myocyte - the mesenchymal subpopulation. We also inferred CNVs and found expected amplifications in 12q13-15 in the mesenchymal subpopulation. Next, we measured cell differentiation by CytoTRACE. A subcluster of malignant fibroblast-like cells positive for MDM2 and CDK4 was the most de-differentiated. Conversely, cells labeled as adipocytes and endothelial cells were the most differentiated cells. Mapping WDLS and DDLS onto the MTL demonstrated that WDLS had more mature cells than DDLS. Surprisingly, while the pathology-assigned diagnosis falls into just two categories, our approach identified a wide range of liposarcoma cells spanning the full spectrum of possible differentiation states. Though follow-on studies are needed, our data suggest that quantitative differentiation metrics can identify malignant cells in transit from a DDLS-to-WDLS state, or possibly the reverse, whereby cells undergo dedifferentiation. Both phenomena are suspected clinically, given the frequent co-existence of WDLS and DDLS in the same tumors, and the noted emergence of DDLS from WDLS diagnosed years earlier. Summarizing our key findings, we measured the degree of differentiation in liposarcoma cells as a precursor to ongoing studies aimed at understanding the molecular mechanisms that underpin LS plasticity and differentiation. Ultimately, we aim to identify the genes and pathways linked to cell fate and discover novel biologically targeted therapies capable of pushing DDLS toward a less aggressive, slower-growing state.

#6559

Model constructed by ferroptosis-related genes and m6A genes predicts the sensitivity to different drug treatments

Tao Han[1], Mengyuan Liu[2]. *[1]The First Hospital of China Medical University, Beijing, China,[2]ChosenMed Technology Co. Ltd, Beijing, China*

Background: Immune checkpoint blockade (ICB) therapies exhibit distinct response in hepatocellular carcinoma (HCC) patients, therefore biomarkers to

screen beneficial patients remains an urgent need in clinical practice. Ferroptosis, an unique form of programmed cell death (PCD), has been implicated in the carcinogenesis and considered as one of the underlying mechanism of targeted and chemotherapeutic therapies in HCC. N6-methyladenosine (m6A), the most dominant form of RNA post-transcriptional modification, has been reported to regulat cancer-associated genes, including ferroptosis-related genes.
Methods: Differentially expressed genes (DEGs) between tumor and normal tissues were screened from TCGA-LIHC dataset. The overlap of DEGs and ferroptosis-related genes (FRGs) resulted in a set of 51 genes. These genes together with 22 m6A-related genes were next subjected to univariate Cox regression for their association with survival. In total, 35 genes showed significant association with survival in this analysis, and they were then used to construct the regression model by Lasso-Cox regression analysis. We then validated the performance of the signature derived from the model in TCGA-LIHC and an external dataset (GSE14520). The signature was also examined for their association with immune-related characters, and their performance in predicting drug response using datasets of immunotherapy cohort studies and cellular experimental studies.
Results: We constructed this prognosis model by expression level of four genes (G6PD, YTHDF1, STMN1, and SLC7A11). Patients with a high-risk score of the signature have a shortened survival time, and the signature is an independent predictor of the prognosis. We also found that the difference between the risk score before and after ICB treatment was significantly associated with sensitivity to the treatment: an increase in the risk score after the treatment correlated with an adverse response. Using the in vitro cellular experimental dataset, we detected a positive association between the risk score and the sensitivity to 5-fluorouracil and sorafenib.
Conclusion: The prognosis signature constructed by four ferroptosis- and m6A-related genes exhibited promising predictive value for OS of HCC patients. The signature could also indicate the sensitivity for different kinds of clinical treatment. A higher risk score indicated a higher resistance for immunotherapy but a higher sensitivity for chemotherapy and RTKs inhibitor. The results of this study not only help to improve the clinical practice of HCC, but also provide new insights into unveiling the underlying mechanisms of tumorigenesis and progression.

#6560
Identification of distinct patterns in diffuse large B-cell lymphoma through alternative splicing analysis

Sanyeowool An[1], Youngil Koh[2], Sung-Soo Yoon[2]. *[1]Seoul National University, Seoul, Korea, Republic of,[2]Seoul National University Hospital, Seoul, Korea, Republic of*

Background Aberrant splicing in cancer cells contributes to cellular proliferation, escape from cell death, growth inhibition, invasion and metastasis, and immune escape. Diffuse large B-cell lymphoma (DLBCL) is the most common type of non-Hodgkin lymphoma, but the effect of AS on its pathogenesis has not been fully elucidated, so it is essential to find out DLBCL-specific splicing patterns and their potential as treatment targets.
Material and Method RNA-Seq dataset from DLBCL patients was retrieved from The Cancer Genome Atlas (TCGA) DLBCL (N=48) and Pan-cancer Analysis of Whole Genomes (PCAWG) DLBC (N=7) were used as the cancer group. In order to identify spliced genes that are significantly different from normal tissue, RNA-Seq data of normal lymphoid tissue produced in two studies of E-MTAB-513 (N=1) and E-MTAB-1733 (N=13) from the BioStudies were downloaded. Sequence reads were aligned to the GRCh38 reference genome using STAR aligner.
Results 5,470 genes identified as differentially spliced compared to normal in both rMATS and MAJIQ tools were studied. After sorting the AS events of these genes in order of highest average PSI value, events with an average PSI value of 0.7 or more in the top 2/3 samples and events with an average PSI value of 0.3 or less in the bottom 2/3 samples are selected. 8 exons of 7 genes were involved in Exon skipping (ES) events, 6 exons of 5 genes were involved in mutually exclusive exon (MXE) events, and an exon of a gene was involved in alternative 5' splice site (A5SS) Among these genes, exons 6 and 7 in *CD53* showed high PSI values between exons 4 and 9. The average PSI values for exons 6 and 7 of *CD53* in DLBCL were 0.923855 and 0.89096, respectively, which were significantly higher than the Normal group ($p<0.05$). *CD53* mediates *IL-7R* signaling and plays a role in the regulation of normal B-cell development. As a gene coding for cell surface protein, it is involved in various immune systems in T-cell and B-cell surfaces. In healthy tissue, transcripts that skip exon 5 and have a junction between exon 4 and exon 6 or 7 are not yet known and should be further studied. In addition, *SLAMF8*, which has an exon with a PSI value specific to DLBCL, is also involved lymphocyte activation and regulates B-cell receptor signaling.
Conclusion These DLBCL-specific patterns of selective exon usage are expected to be potential targets for cancer immunotherapy.

#6561

Specific binding mode of RNA binding protetin FAM120A to lncRNA

Kenichiro Kawai. *Nagoya University, Nagoya, Japan*

Long noncoding RNAs (lncRNAs) are defined as transcripts >200 nucleotides in length with no protein-coding potential. LncRNAs play diverse roles in regulating gene transcription, post-transcription, translation, and epigenetic modification through interaction with RNA binding proteins (RBPs). Here, we analyzed binding motif of a RBP, family with sequence similarity 120A (FAM120A), which is highly expressed in multiple cancer types and associated with poor prognosis. To investigate FAM120A interacting RNAs genome-wide, we conducted cross-linking immunoprecipitation combined with deep sequencing (CLIP-seq) using an anti-FAM120A antibody in osteosarcoma cell line, U2OS. We identified 37,151 FAM120A-binding clusters by a peak detection algorithm. Up to 92% of these clusters were found within about 5,700 mRNAs, with the highest enrichment at 3'-UTRs. Interestingly, other clusters located within 959 lncRNAs, with peaks at 5’ and 3’ end. Fold enrichment analysis of CLIP reads in comparison with input reads revealed that FAM120A binds more preferentially to lncRNA than mRNA (median fold enrichments, 4.81 (lncRNA) versus 4.41 (mRNA), $P<0.001$, Mann-Whitney *U* test). Motif analysis using the HOMER algorithm showed that FAM120A enriched sequence motifs in 3’ of mRNAs, 5’ and 3’ of lncRNAs were completely distinct. These results suggest that FAM120A may exhibit a motif-dependent selective binding to lncRNA in cancer cells. Given that RBPs bind to RNA molecules immediately after their transcription on chromatin, FAM120A may also selectively recognize RNA species and classify lncRNA and mRNA at the transcriptional stage. Since lncRNAs play pivotal roles in cancers FAM120A may exert oncogenic effects by the post-transcriptional regulation of a certain set of lncRNAs.

#6562

Comparative analysis of blood-based tumor fraction estimation in 300 cancer patients

Chao Dai, Tiantian Zheng, Xiaoxi Dong, Wei Mo, Xiaohong Wang, Shujun Luo, Kemin Zhou, Shidong Jia, Pan Du. *Predicine Inc, Hayward, CA*

Introduction Tumor fraction (TF) in cell-free DNA is an important known biomarker for monitoring treatment response and disease progression. cfDNA TF is usually estimated by variant allele frequency (VAF) of somatic mutations or copy number variation (CNV). cfDNA assays provide high VAF detection

sensitivity by using deep sequencing depth based on target panels, which often makes TF underestimated due to limited panel gene coverage. Also because the interference of copy number changes and lack of matched normal, the VAF estimation is often inaccurate. On the other hand, although CNV based TF estimation does not require matched normal samples, it has lower detection sensitivity and underestimates cfDNA TF for patients without copy number changes. Importantly, tumor heterogeneity exists in many clinical cancer patient samples, where tumor DNA has complex subclone structures, which makes accurate TF estimation even more challenging.
Methods Here we performed comprehensive concordance study of cfDNA TF estimation, by applying both PredicineWES+ (20,000x sequencing depth in boosted cancer-related genes and 2,500x depth in rest exome regions) and PredicineCNB (LP-WGS with 3× sequencing depth) on more than 300 plasma samples from cancer patients. Using a proprietary algorithm, we calculated TF by integrating PredicineWES+ derived VAFs and PredicineCNB derived CNVs for each sample, where tumor subcloning was taken into the consideration. We implemented proprietary EM algorithm to infer subclone populations, where CNV has high concordance with TF in each subclone.
Results Our study showed that CNV-based TF estimation is highly concordance with VAF-based TF from PredicineWES+ (correlation coefficient > 0.8) when TF is >5%. For clinical samples with < 5% TF inferred from PredicineCNB, we used VAF-based TF. We developed an integrated TF estimation methodology by leveraging molecular insights derived from PredicineWES+ and PredicineCNB, and further performed clinical evaluation study using 50 longitudinal plasma samples from prostate cancer patients that are under different cancer stages or therapies. Our results demonstrated that the integrated TF estimation shows a positive correlation with therapy response and disease stage revealed by CT scan. Finally, serial analysis of plasma cfDNA demonstrated an increase in ctDNA TF and cancer variants, preceding evidence of radiographic and clinical disease progression in many patients.
Conclusion We conducted a comprehensive concordance study to infer cfDNA TF using PredicineWES+ and PredicineCNB in more than 300 patient samples. Our study demonstrated its clinical utility where the integrated TF analysis may provide a more robust and accurate estimation of disease burden in cancer patients.

#6563
Glioma stem cell index recapitulates grade, IDH mutation status and correlates with survival of glioma patients

Renan L. S. Simões, Maycon Marção, Tathiane M. Malta. *School of Pharmaceutical Sciences, University of São Paulo, Ribeirão Preto, Brazil*

Adult diffuse gliomas are heterogeneous and the most common primary brain tumors. Gliomas have high tissue invasion, proliferation and therapeutic resistance potential. Although much knowledge has been recently gained regarding glioma biology and evolution, many questions are still open, such as which is the cell of origin, what are its characteristics and how the tumor propagation occurs. The cancer stem cell (CSC) model proposes a population of cells with high self-renew capacity and capable of propagating the tumor with more differentiated cells, generating intratumoral heterogeneity. Based on the CSC model, our work aims to integrate the most advanced techniques available such as scRNAseq and machine learning models to estimate the enrichment of glioma stem cells (GSCs) in tumors, by defining a GSC-Stemness Index (GSCsi). To build the prediction model, we used public scRNA-seq data from glioblastoma (GBM)-enriched GSCs. We used the standard Seurat pipeline for quality control, normalization and downstream analysis. The GSC single cell data was used to train a prediction model using the One Class Logistic Regression (OCLR) algorithm. Several models were tested, including overdispersed genes, differentially expressed genes between GSCs and the whole tumor, GSCs from each patient individually and a model with all GSCs. The prediction models were applied to gene expression data from TCGA, GLASS, and publicly available scRNA-seq data from different glioma subtypes. The model built with all the GSCs and all genes showed the best performance, being able to identify with higher indices grade 4 gliomas and IDHwt in the TCGA and GLASS data. Survival analysis resulted in a hazard ratio greater than 20, indicating a high correlation between increased GSCsi and poor prognosis. By applying the model to scRNA-seq data from gliomas, clusters of high GSCsi were identified. We can partially conclude that the GSCsi obtained with the model is capable of identifying grade 4 gliomas and IDHwt and we are performing analyzes with the genes with the highest correlation (positive and negative) with the GSCsi in the TCGA and GLASS data. The analysis of these genes together with genes differentially expressed in the high GSCsi clusters in scRNA-seq data can elucidate pathways responsible for the therapeutic resistance and propagation of gliomas, in addition to proposing theories about the cell of origin and potential therapeutic targets to improve the diagnosis and treatment of these patients.

#6564

Biomarker discovery in triple negative breast cancer using RNA-sequencing analysis

Jenna B. Poulsen, Mauri E. Dobbs, Naomi Rapier-Sharman, Brett E. Pickett.
Brigham Young University, Provo, UT

Breast cancer is the most common form of cancer, and afflicted over 2.2 million people in 2020. The sheer volume of patients who suffer from breast cancer warrants continued research and discovery efforts to improve treatment options. Triple negative breast cancer (TNBC) affects 10-15% of breast cancer patients. Unlike other forms of breast cancer, TNBC does not have estrogen or progesterone receptors and makes little to none of the HER2 protein. Due to the lack of these biomarkers that are typical treatment targets for other kinds of breast cancers, the hormone therapies and drugs that target other breast cancers are often ineffective against TNBC. This leaves chemotherapy and radiation therapy as the main treatment options. Although chemotherapy and radiation have treatment benefits, the recurrence rate after treatment is around 40%. Furthermore, these treatment options are very detrimental to the body, resulting in a weaker patient and a necessary recovery time between treatments. In this study, we analyzed publicly available RNA-sequencing (RNA-seq) data to identify the upregulated and downregulated transcriptional mechanism(s) that play a role in TNBC compared to healthy breast tissue. The analysis of the RNA-seq data was completed with the Automated Reproducible Modular Workflow for Preprocessing and Differential Analysis of RNA-seq Data (ARMOR), which trims, maps, and quantifies the mRNA sequencing reads to the human transcriptome for each read. The ARMOR program identified more than 12,000 differentially expressed genes between TNBC and healthy breast tissue samples. We then applied an artificial intelligence-based classification method, a random forest algorithm, to identify new biomarkers that best differentiate TNBC cells from healthy cells. These specific transcriptional biomarkers for TNBC could potentially be used as diagnostic biomarkers or as therapeutic targets. We anticipate that this data may expand the treatment options for TNBC.

Databases, Platforms, and Tools

#6568

Extended support for model organisms: The next frontier for the molecular signatures database

Anthony S. Castanza[1], Jill M. Recla[2], David Eby[1], Alexander T. Wenzel[1], Helga Thorvaldsdottir[3], Carol J. Bult[2], Jill P. Mesirov[1]. [1]*Department of Medicine,*

University of California, San Diego, La Jolla, CA,[2]The Jackson Laboratory for Mammalian Genomics, Bar Harbor, ME,[3]Broad Institute of MIT and Harvard, Cambridge, MA

In 2005, we introduced the Gene Set Enrichment Analysis (GSEA) method to enable the identification and estimation of significance of activated biological pathways and processes in molecular data. Serving a community of over 300,000 registered users, and contributing scientific analysis to more than 30,000 publications, GSEA has become ubiquitous in gene expression analysis and particularly in cancer research. The power of GSEA relies, in a large part, on the Molecular Signatures Database (MSigDB) that provides tens of thousands of expertly curated and annotated gene sets representing cellular processes, canonical pathways, response signatures, etc., derived from prior studies, public data, and curated pathway databases. Here we describe an important recent addition to the GSEA/MSigDB resource.

Historically, the GSEA-MSigDB resource has focused specifically on human data, offering guidance and support for analysis of model organism data through limited provision of orthology mapping files. In recognition of the importance of the mouse as a model organism for cancer research, we recently significantly expanded our support for mouse data in two ways.

(1) We introduced Mouse MSigDB with a total of about 15,000 sets that are provided in the native mouse gene symbol space and are derived from published mouse datasets and mouse-focused resources. This allows GSEA analysis of mouse datasets without the need for orthology conversion.

(2) For investigators who wish to use MSigDB's human gene sets to analyze mouse data, or vice versa, we also implemented a new procedure for orthology mapping gene identifiers in an input dataset to match the identifiers of the gene sets. The new mapping considers the particular requirements of gene set enrichment analysis, and incorporates high confidence gene ortholog data from the Alliance of Genome Resources and ortholog-match refinement utilizing Ensembl's ortholog datasets.

Together, these new additions offer a substantial step forward for making mouse a first-class citizen of the GSEA-MSigDB ecosystem. The new Mouse MSigDB, and the full GSEA-MSigDB resource, is available at gsea-msigdb.org.

#6569

ClinGen Somatic and CIViC collaborate to comprehensively evaluate somatic variants in cancer

Jason Saliba[1], Arpad Danos[1], Kilannin Krysiak[1], Adam Coffman[1], Susanna Kiwala[1], Joshua McMichael[1], Cameron J. Grisdale[2], Ian King[3], Shamini Selvarajah[3], Xinjie Xu[4], Rashmi Kanagal-Shamanna[5], Laveniya Satgunaseelan[6], David Meredith[7], Mark Evans[8], Charles G. Mullighan[9], Yassmine Akkari[10], Gordana Raca[11], Angshumoy Roy[12], Alex H. Wagner[10], Ramaswamy Govindan[1], Obi L. Griffith[1], Malachi Griffith[1], on behalf of the ClinGen Somatic Clinical Domain Working Group. *[1]Washington University School of Medicine, St. Louis, MO,[2]BC Cancer, Vancouver, BC, Canada,[3]University Health Network and University of Toronto, Toronto, ON, Canada,[4]Mayo Clinic, Rochester, MN,[5]The University of Texas MD Anderson Cancer Center, St. Louis, MO,[6]Royal Prince Alfred Hospital, Sydney, Australia,[7]Dana-Farber Cancer Institute and Harvard Medical School, Boston, MA,[8]Caris Life Sciences, Phoenix, AZ,[9]St. Jude Children's Research Hospital, Memphis, TN,[10]Nationwide Children's Hospital, Columbus, OH,[11]Children's Hospital Los Angeles, Los Angeles, CA,[12]Baylor College of Medicine, Houston, TX*

The comprehensive evaluation of somatic variants in cancer requires consensus interpretation of their potential clinical significance (diagnosis, prognosis, and treatment response) and oncogenicity. To aid precision medicine through public interpretations, a multifaceted collaborative effort is required to bring together a community, structured guidance, and a public platform. The over 200 multi-disciplinary experts in the Clinical Genome Resource (ClinGen) Somatic Cancer Clinical Domain Working Group (CDWG) provide a community that develops data curation guidelines and standards and curates evidence to determine the clinical significance and oncogenicity of somatic alterations in cancer. The Somatic CDWG established the Pediatric Cancer, Hematological Cancer, and Solid Tumor Taskforces to facilitate membership growth and targeted curation projects. Within these Taskforces, Somatic Cancer Variant Curation Expert Panels (SC-VCEPs) are developed through a 4-step approval process adapted from ClinGen germline VCEP procedures. Five SC-VCEPs (NTRK-fusions, FGFR variants, FLT3 variants, Histone H3 variants, and BCR::ABL1-like B-ALL alterations) are working through the approval process and one (Established Significance) is in the planning stage. SC-VCEPs tailor AMP/ASCO/CAP [PMID:27993330] and ClinGen/CGC/VICC Oncogenicity [PMID:35101336] guidelines, or create new classification guidance to aid granular assessment of their genomic alterations of interest.
The Clinical Interpretations of Variants in Cancer (CIViC) knowledgebase provides the public platform for the Taskforces and SC-VCEPs to display their

high-quality somatic cancer variant interpretations. These groups curate evidence from published literature and create Assertions summarizing evidence collected. These Assertions are further disseminated through other resources like ClinVar and the Variant Interpretation for Cancer Consortium (VICC) MetaKB. CIViC supports the application of AMP/ASCO/CAP tiering and levels for clinical significance Assertions. CIViC recently created Oncogenic Assertions, which supports the application of ClinGen/CGC/VICC codes. Three SC-VCEPs (FGFR, FLT3, and Histone H3) are tailoring the ClinGen/CGC/VICC Oncogenicity guidelines to their specific genes and CIViC will enable their ClinGen-approved, modified codes to be applied directly to their Oncogenic Assertions. Also, two SC-VCEPs (NTRK and BCR::ABL1-like) are developing fusion specific oncogenicity classification guidelines, which will be applied to their fusion specific CIViC Oncogenic Assertions. ClinGen Somatic groups have generated 695 CIViC Evidence Items and 33 Assertions from over 400 published papers. These numbers will continue to grow along with the development of more SC-VCEPs. ClinGen Somatic and CIViC foster collaboration, innovation, and most importantly the advancement of precision medicine.

#6570

Integrative pan-cancer genomic and transcriptomic analyses of refractory metastatic cancer

Yoann Pradat[1], Julien Viot[2], Konstantin Gunbin[2], Andrey Yurchenko[2], Luigi Cerbone[2], Marc Deloger[2], Guillaume Grisay[2], Loic Verlingue[2], Véronique Scott[2], Ismael Padioleau[2], Leonardo Panunzi[2], Stefan Michiels[2], Antoine Hollebecque[2], Gerome Jules-Clément[2], Laura Mezquita[2], Antoine Lainé[1], Yohann Loriot[2], Benjamin Besse[2], Luc Friboulet[2], Fabrice André[2], Paul-Henry Cournède[1], Daniel Gautheret[1], Sergey Nikolaev[2]. *[1]Université Paris-Saclay, Gif-Sur-Yvette, France,[2]Gustave Roussy, Villejuif, France*

Metastatic relapse after treatment is the primary cause of cancer morbidity and mortality. While genetic mechanisms of primary tumors and, to a lesser extent, metastatic cancers have been studied in large cohorts, refractory metastatic tumors are not yet sufficiently characterized. Markers of aggressiveness and resistance that molecular profiling can extract from these tumors have yet to be identified and incorporated into clinical care. In this study, we present a pan-cancer cohort of 1,031 metastatic tumors (which we refer to as META-PRISM) that are resistant to at least one systemic therapy or with no approved treatment options. We retrieved the complete clinical history of patients and performed whole-exome (n=571) and transcriptome sequencing (n=947) for this cohort.

The prevalence of detected cancer biomarkers was assessed and compared to an external cohort of primary tumors. In the META-PRISM cohort, we observed an increase in (i) whole-genome duplication frequency, (ii) tumor mutational burden, (iii) germline cancer-predisposing variants, and (iv) somatic alterations in cancer genes, including KRAS, EGFR, CCND1, MYC, and TP53, as compared to the tumor type-matched primary tumors. The most extensive increase in genomic variation at metastatic stage was observed in prostate bladder, and pancreatic cancer types. We also identified enrichment of standard-of-care resistance biomarkers in most cancer types. However, only 9.3% of tumors harbored at least one such biomarker, indicating that the current understanding of resistance mechanisms remains insufficient. Our cohort demonstrated a significantly improved 6-month survival prediction from models incorporating molecular markers over models with only clinical markers for breast cancer patients and to a lesser extent for other studied tumor types. Overall, our data establish a unique resource for investigating treatment resistance mechanisms and performing predictive analyses in cancer.

#6571

Mammonc-DB: A web based user-friendly tool for comprehensive multi-omics data analysis in breast cancer

Santhosh Kumar Karthikeyan[1], Darshan S. Chandrashekar[1], Upender Manne[2], Chad Creighton[3], Zhaohui S. Qin[4], Sidharth Kumar[5], Sooryanaraya Varambally[2].
[1]University of Alabama at Birmingham, Birmingham, AL,[2]Department of Pathology, University of Alabama at Birmingham, Birmingham, AL,[3]Bioinformatics, Baylor College of Medicine, Ann Arbor, MI,[4]Biostatistics and Bioinformatics, Emory University, Atlanta, GA,[5]Department of Computer Science, University of Alabama at Birmingham, Birmingham, AL

Breast cancer (BC) accounted for 15% cancer related death among women, in the United States last year. It is a highly heterogeneous and complex diseases with multiple molecular events occurring during cancer initiation and progression. It is important to unravel the heterogeneity of breast cancer and the molecular events to develop diagnostic biomarkers and targeted therapies. There is need for comprehensive and user-friendly tool for the utilization of available breast cancer data including metastatic and treatment response data. We have earlier created a highly used pan-cancer proteogenomic portal called UALCAN (ualcan.path.uab.edu). Based on the current unmet need for comprehensive BC data analysis and visualization resource, we developed an integrated proteo-genomicbreast cancer data analysis portal, called Mammonc-DB

(http://resource.path.uab.edu/MammOnc-ge.html)**.** For Mammonc-DB, we collected data from public repositories like NCBI Gene Expression Omnibus (GEO), The Cancer Genome Atlas (TCGA) for collecting and analysis of genomics and epigenetics data, and, PRIDE, and, ProteomeXchange for proteomics data. We procured and processed multi-omics studies related to normal, primary, and metastatic human breast cancer data with other clinical information available, for different clinical models. We also collected and analyzed different therapy, and treatment studies that are currently employed in treating BC patients. Mammonc-DB has user friendly interface that aid breast cancer researchers and clinicians in, a) allows users to identify potential biomarkers in breast cancer, b) accessing publicly available breast cancer multi-omics data, c) Visualizing the expression pattern of gene or protein of interest with clinical feature stratification in each dataset among others This resource serves as a one-stop resource to study gene expression (protein-coding and non-coding) analysis along with epigenetic regulation, and protein expression patterns in BC. With this platform, we tend to create global user base that will accelerate discovery of biomarkers in BC that might be involved in diagnosis, therapeutic target identification and treatments of breast cancer.

#6572

A lung cancer cell line explorer

Ling Cai, Luc Girard, Ralph DeBerardinis, Guanghua Xiao, John Minna, Yang Xie. *UT Southwestern Medical Center, Dallas, TX*

Over 300 lung cancer cell lines have been established in the past few decades with clinical annotations. Efforts from multiple institutions comprehensively profiled these cell lines for their genetic and epigenetic variations, gene and protein expression, metabolism, and functional liabilities. These data provide an unprecedented opportunity to accelerate lung cancer research. We developed a lung cancer cell line explorer at https://lccl.shinyapps.io/LCCL/ integrating over 35 datasets. We also incorporated engineered features such as pathway enrichment scores from copy number-denoised transcriptomic data and neuroendocrine scores. Our web application allows users to 1) query and download the processed datasets, 2) assess data reproducibility across studies, 3) review genomic abnormalities, 4) perform ad hoc bivariate analyses with the option to add filtering or coloring by a third feature, 5) generate heatmaps and correlation maps, 6) perform global association test to screen for significant association between a feature of interest and all features from a dataset of interest, and 7) upload their own datasets to be analyzed in conjunction with our

in-house datasets. In summary, this online tool will greatly facilitate the utilization of high-dimensional datasets that characterize lung cancer cell lines.

#6573

Drug Combo: A unique resource for efficient phase 1 trial design with manually curated MTD and DLT

Lei Wang, Shijun Zhang, Lai Wei, Yuxi Zhu, Dwight Owen, Lang Li. *The Ohio State University College of Medicine, Columbus, OH*

Background: With prior preclinical and clinical knowledge, an effective and efficient cancer drug combinatory trial design could be expected, which will significantly accelerate the translation. However, our internal survey results suggested that some knowledge and data sources were underused or underestimated by researchers. One primary reason is that knowledge of drug combinations is scattered in many distinct databases. Moreover, some essential information, such as MTD and DLT was missed in current databases. Drug Combo (https://drugcombo.shinyapps.io/DrugCombo/) is the first knowledge base that integrates drug toxicity and PK data that may help design an efficient Phase I trial. It is a unique informatics resource that manually curated MTD and DLT are well organized in the knowledgebase.
Methods: Drug Combo integrates various publicly available PK and toxicity knowledge for individual drugs and drug combinations (Table 1). More importantly, it is the unique knowledgebase with MTD and DLT. An expert team manually curated MTD and DLT data from publicly available publications. Some standard healthcare terminologies, e.g., Rx-Norm and MedDRA were applied for concept normalization at the back end. We implemented a User-Centered Design process in the user interface (UI).The UI layout will be simple, consistent, purposeful, comprehensive, easy to navigate and informative with readable or scannable typography. A summary view was provided to inform users of some essential information, e.g., MTD, and Overlapping toxicities. The user can find the details in the “Detail Tab”.
Results: Currently, Drug Combo integrates pharmacological, pharmacokinetics, and toxicity data. Especially, MTD and DLT data from more than 1,600 published Phase I trials results are exclusive in Drug Combo.
Conclusions: Drug Combo is the first knowledge base that provides expert-curated MTD and DLT information. It could help design an effective and efficient drug combination phase 1 trial.

Current knowledge type in Drug Combo	
Type	Source

Drug Names	DrugBank, RxNorm
Target	DrugBank, Manual curation
Associated Condition	RxNorm, Drug Labels
PK profiles	DrugBank
Adverse Drug Event	Drug Label, FAERS
MTD	Manual curation
DLT	Manual curation
DDI	DrugBank, Manual curation

#6574

Systematic analysis of the predictive gene expression signatures of immunotherapies across multiple cancer types using IOSig

Samuel Coleman[1], Caroline Wheeler[2], Rebecca Hoyd[2], Louis Denko[2], Ching-Nung Lin[1], Muhammad Z. H. Fadlullah[1], Siwen Hu-Lieskovan[1], Christine Chung[3], Ahmad A. Tarhini[3], Daniel Spakowicz[2], Aik Choon Tan[1]. *[1]University of Utah Huntsman Cancer Institute, Salt Lake City, UT,[2]Ohio State University Wexner Medical Center, Columbus, OH,[3]Moffitt Cancer Center, Tampa, FL*

Immune checkpoint inhibitors (ICI) have provided durable responses in a subset of patients in multiple solid tumor types. However, developing robust and reproducible predictive gene signatures for ICIs remains a challenge partly due to the lack of systematic comparisons across a large pan-cancer transcriptomics compendia. We recently developed Immuno-Oncology Signatures Explorer (IOSig), a user-friendly web tool, to allow users to query and explore predictive biomarkers from a large collection of pan-cancer patient samples treated with ICIs (> 2500 patient samples from 40 studies). Here, we investigated six solid tumors: kidney, melanoma, bladder, head and neck squamous cell, gastrointestinal, and non-small cell lung cancers tissue-based RNA-seq datasets in IOSig. The 2175 samples, from 45 cohorts, were Z-normalized with the genes from each signature being averaged to assign a sample a single score per signature. Area Under the Receiver Operating Characteristic (AUROC) curve was used to summarize the gene signatures' ability to predict response to ICIs. We focus on the top 10 predictive gene signatures for each cancer type. There were 22 unique gene signatures from the top 10 of the six cancer types. Overall, 17 signatures were predictive in GI, NSCLC, melanoma and HNSCC. Many of these signatures were enriched in immune activation and inflammatory signatures. Conversely, the MYC, DNA damage repair, and proliferation

signatures are only predictive in bladder cancer. No predictive signatures were associated with kidney cancer. Interestingly, the immune activation signatures were highly predictive in the GI cancer cohorts in our study, as the cohorts were enriched with patients having high tumor mutational burdens and microsatellite instability. In summary, we used IOSig to analyze the predictive ability of previously published gene signatures across 6 cancer types. Some of these signatures warrant further investigation in a cancer-specific manner.

A table showing the AUROC value of the 22 selected gene signatures in each cancer type.

Signature	Melanoma	Bladder	Kidney	NSCLC	HNSC	GI Cancer	Average
Chemokines	0.657	0.563	0.526	0.721	0.657	0.870	0.665
TIP Hot	0.657	0.571	0.544	0.737	0.592	0.866	0.661
ifng18	0.674	0.557	0.584	0.680	0.589	0.871	0.659
Ipi_Neo	0.660	0.567	0.563	0.675	0.602	0.859	0.654
Rooney	0.669	0.569	0.568	0.661	0.646	0.797	0.652
Chaurio	0.670	0.572	0.570	0.679	0.570	0.834	0.649
ifng6	0.655	0.593	0.553	0.627	0.635	0.823	0.648
ifng-effector	0.672	0.566	0.567	0.686	0.564	0.830	0.648
Roh	0.661	0.551	0.565	0.697	0.548	0.856	0.646
NRS	0.649	0.512	0.588	0.687	0.605	0.818	0.643
effector_t	0.679	0.567	0.579	0.670	0.524	0.835	0.642
impres	0.619	0.516	0.577	0.706	0.555	0.847	0.637
mMDSC	0.643	0.524	0.558	0.706	0.557	0.797	0.631
Ock	0.640	0.563	0.586	0.579	0.578	0.827	0.629
Davoli	0.665	0.546	0.569	0.655	0.514	0.822	0.629
MHC_1	0.644	0.593	0.550	0.574	0.553	0.806	0.620
MHC_2	0.661	0.533	0.554	0.659	0.437	0.802	0.608
gMDSC	0.582	0.477	0.526	0.706	0.458	0.695	0.574
DNA_damage_repair	0.432	0.598	0.555	0.383	0.499	0.361	0.471
Proliferation	0.434	0.655	0.530				

0.370	0.420	0.372	0.463				
Mitoscore	0.422	0.588	0.374	0.418	0.580	0.312	0.449
MYC	0.367	0.607	0.503	0.381	0.482	0.303	0.441

#6575

LinkedOmicsKB: A web portal to explore pan-cancer molecular and phenotype associations

Sara R. Savage, Yuxing Liao, Yongchao Dou, Zhiao Shi, Xinpei Yi, Wen Jiang, Jonathan T. Lei, Bing Zhang. *Lester and Sue Smith Breast Center, Baylor College of Medicine, Houston, TX*

Pan-cancer multi-omics data produced from integrated genomic, epigenomic, transcriptomic, proteomic, and post-translational modification (PTM) profiling of a wide variety of cancer types holds great potential for understanding cancer biology and generating therapeutic hypotheses. To realize this potential and make analysis and visualization of these complex and interconnected data easily accessible to cancer biologists and clinicians, we have developed a web portal, LinkedOmicsKB. The web portal provides access to a harmonized proteogenomic dataset of over 1000 patient samples covering 10 cancer cohorts from the Clinical Proteomic Tumor Analysis Consortium (CPTAC). We calculated associations between methylation, copy number variation (CNV), RNA, protein, and phosphosite data for each gene and further correlated the proteogenomics data with clinical and computed molecular phenotypes. All results are stored in a MongoDB database and visualizations are provided for exploring pan-cancer multi-omics relationships as well as individual statistics. We demonstrate the utility of LinkedOmicsKB to provide insights into clinical phenotypes, somatic mutations, and understudied genes. In the pan-cancer CPTAC data, overall survival was correlated with proteins involved in protein hydroxylation, including PLOD1 and PLOD2. Additionally, two phosphorylation sites on the tumor suppressor MIG-6 were associated with worse survival. These sites were also associated with hypoxia, MAPK, and EGFR pathway activity scores, suggesting a relationship between the signaling in these pathways and cancer prognosis. STK17B is an understudied kinase that regulates apoptosis. We found STK17B was

upregulated in 6 cancer types at the protein level but only two at the RNA level. The protein abundance of STK17B was highly associated with immune scores and JAK/STAT signaling, supporting a role for STK17B in the immune response. We identified 3 phosphorylation sites on STK17B, which were associated with EGF pathway activity scores and immune-related scores. LinkedOmicsKB is a valuable tool that can be used to generate biological and clinical insights into any gene, phosphosite, mutation, or phenotype.

#6576

Gabriella Miller Kids First Data Resource Center (KFDRC): Empowering discovery across germline and somatic variation in pediatric cancer

David Higgins[1], Jean-Philippe Thibert[2], Michele Mattioni[3], Jack DiGiovanna[3], Robert L. Grossman[4], Bailey K. Farrow[1], Eric Wenger[1], Samuel Volchenboum[4], Robert J. Carroll[5], Melissa A. Haendel[6], Deanne M. Taylor[1], Yuankun Zhu[1], Vincent Ferretti[2], Adam C. Resnick[1], Allison P. Heath[1]. *[1]Children's Hospital of Philadelphia, Philadelphia, PA,[2]CHU Sainte-Justine, Montreal, QC, Canada,[3]Seven Bridges Genomics, Boston, MA,[4]University of Chicago, Chicago, IL,[5]Vanderbilt University Medical Center, Nashville, TN,[6]University of Colorado Anschutz Medical Campus, Denver, CO*

The Gabriella Miller Kids First Pediatric Research Program (Kids First) has enabled genomic and transcriptomic characterization across a multitude of pediatric diseases at an unprecedented scale. This includes both pediatric cancer cohorts and structure birth defect cohorts, as co-occurrences of these suggest a shared context of developmental biology alterations. Making this quantity of data findable, accessible, interoperable and reusable (FAIR) to researchers around the world has been enabled via the Gabriella Miller Kids First Data Resource Center (KFDRC). Twenty-six Kids First studies are released on the Kids First Data Resource Portal, representing more than 21,000 participants and more than 1.25 PB of data, with additional datasets being released yearly. Additionally, via a partnership between NCI Childhood Cancer Data Initiative and Kids First, large studies currently

undergoing sequencing on childhood sarcomas and brain tumors will also be made available via the KFDRC.
The KFDRC Portal (https://portal.kidsfirstdrc.org/) provides an interactive cohort building interface as well as powerful search capabilities across 61 billion germline variants in real-time. The somatic variants are made available on the open-access PedcBioPortal (https://pedcbioportal.kidsfirstdrc.org/). Search features include leveraging ontologies to enable different granularity across studies to be cross-querable. The use of these ontologies enable semantic interoperability, while also leveraging FHIR as an interoperable standard for exchange of clinical and other relevant metadata. GA4GH DRS and Passport services via Gen3 and NIH's Researcher Authentication Service (RAS) enable streamlined access to controlled access data within researchers' cloud platform of choice, including CAVATICA (https://cavatica.org) which is directly integrated with the KFDRC Portal.
The KFDRC is part of the NIH Cloud-Based Platform Interoperability efforts, which includes the NCI Cancer Research Data Commons. This enables discovery and analysis across combined cancer datasets and data modalities and further potential for the cross analysis between cancers and structural birth defects to accelerate the discovery process to ultimately lead to improved knowledge and outcomes for childhood cancer and more generally pediatric disease from genetic causes.

#6577

CARMEN: A pan-HLA and pan-cancer proteogenomic database on antigen presentation to support cancer immunotherapy

Ashwin Adrian Kallor[1], Michał Waleron[1], Georges Bedran[1], Patrícia Eugénio[2], Catia Pesquita[2], Daniel Faria[2], Fabio Massimo Zanzotto[3], Christophe Battail[4], Ajitha Rajan[5], Javier Alfaro[1]. *[1]Intercollegiate Faculty of Biotechnology & Medicine (IFB), International Center for Cancer Vaccine Science, University of Gdansk, Gdansk, Poland,[2]LASIGE, Faculdade de Ciências, Universidade de Lisboa, Lisboa, Portugal,[3]Dipartimento di Ingegneria dell'Impresa (DII), University of Rome Tor Vergata, Rome, Italy,[4]French Alternative Energies and Atomic Energy Commission (CEA), Grenoble, France,[5]School of Informatics, University of Edinburgh, Edinburgh, United Kingdom*

Cancer immunotherapy has greatly improved the quality of life of cancer patients and it hinges on the discovery of novel cancer antigens that could be targeted to improve disease outcomes. The creation of databases such as IEDB, SysteMHC, TANTIGEN, caAtlas, HLA Ligand Atlas, Cancer Antigenic Peptide Database, SPENCER and IEAtlas support the immunopeptidomics community in understanding the landscape of antigen presentation. We have developed a pan-cancer, pan-HLA, and pan-tissue database containing immunopeptidomics data mapped to transcriptomic, genomic, immunological and biochemical data. The database was generated from 80 different publicly available immunopeptidomics mass spectrometry datasets collected between 2015-2022 (76 cancer and 4 normal datasets), covering 15 different types of cancers and 152 different HLA-I alleles. The peptides contained in our database were obtained by a combination of closed, open and de novo searches using an in-house developed computational pipeline. Following rigorous false discovery rate estimation at 1% and a second-round search to eliminate any false signals that may not have been detected in the previous round of FDR estimation, we obtained a list of 11.2 million peptide-HLA combinations comprising both coding and non-coding regions of the genome as well as bacterial peptides. These peptides have been mapped to chromosomal coordinates to facilitate adoption by the genomics community of this useful resource on antigen presentation. Pathway/biochemical analysis of each peptide was performed using the rWikiPathways package. Finally, mutations associated with each peptide were annotated using COSMIC and dbSNP resources. Our database includes a FAIR knowledge graph which contextualizes and enriches the data to enable clinicians to take effective therapeutic decisions on the appropriate form of treatment for cancer immunotherapy with the case study of clear cell renal cell carcinoma (ccRCC). We will continue to expand our database with new data over the next two years and expand the scope of its applications to facilitate uptake by the larger scientific community.

#6578

reVUE: repository for variants with unexpected effects

Ino de Bruijn[1], Aditi Gopalan[2], Xiang Li[1], Hongxin Zhang[1], Onur Sumer[1], Thomas Y. Cong[3], Tona Gonzalez[4], Madelaine Rangel[5], Nikolaus Schultz[1],

Debyani Chakravarty[1]. *[1]Memorial Sloan Kettering Cancer Center, New York, NY,[2]Graduate School of Medical Sciences, Weill Cornell Medicine, New York, NY,[3]Ossining High School, New York, NY,[4]Harvey Mudd College, Claremont, CA,[5]Cornell University, Ithaca, NY*

Clinical sequencing of tumor samples is now a component of routine cancer care used to identify predictive biomarkers of drug response, refine patient cancer diagnoses, assess heritable cancer risk, or inform patient prognosis. Most genomic alterations are accurately annotated with tools such as the Variant Effect Predictor (VEP) that infer the effects of these alterations on the mRNA and protein by following basic rules of transcription, mRNA post-transcriptional processing, and translation. However, some genomic variants are not as easily captured by these rules, which can cause inappropriate or unclear annotation of the protein effect. For example, a variant that alters an existing splice site or creates a new one can activate or inactivate the protein. Similarly, specific mutations in the non-coding promoter region of a gene may de-regulate gene expression (e.g., TERT promoter mutations). In some instances, these so-called variants with unexpected effects (VUE) may have therapeutic implications. For example, while ~2-3% of GIST tumors harbor KIT exon 11 deletions that extend into the non-coding intron between exons 10 and 11 and are shown to cause in-frame deletions, they are typically misclassified as inactivating splice site mutations, precluding patients with tumors harboring these mutations from receiving standard care imatinib.

Thus, while many VUEs are functionally characterized and documented in the literature, there are no resources to systematically identify, curate and store these events such that they can be correctly annotated in routine clinical sequencing leading to suboptimal treatment decisions.

To address this unmet clinical need, we built a novel bioinformatic resource, the Repository for Variants with Unexpected Effects (reVUE - cancerrevue.org). The reVUE resource consists of (1) an intuitive website listing curated VUEs with their observed effects as demonstrated by functional characterization in peer-reviewed literature and (2) an application programming interface (API) for programmatic annotation of variants. We built reVUE as a crowd-sourced resource to enable contributions of VUEs to the repository from the clinical and scientific communities. Both the software and data are openly available. Our goal is to enable clinical

bioinformatic pipelines to accurately annotate all DNA mutations, including those with unanticipated protein coding effects, some of which can have therapeutic implications.

#6579

Accelerating de-identification of images with cloud services to support data sharing in cancer research

Benjamin P. Kopchick[1], Laura K. Opsahl-Ong[1], Qinyan Pan[2], Michael W. Rutherford[3], Ulrike Wagner[4], Bhavani S. Singh[1], Scott Gustafson[2], Fred W. Prior[3], David A. Clunie[5], Juergen A. Klenk[6], Keyvan Farahani[7].
[1]Biomedical Data Science, Deloitte Consulting LLP, Arlington, VA,[2]Ellumen, Inc., Silver Spring, MD,[3]Biomedical Informatics, University of Arkansas for Medical Sciences, Little Rock, AR,[4]Bioinformatics and Computational Sciences, Frederick National Laboratory for Cancer Research, Frederick, MD,[5]PixelMed Publishing, Bangor, PA,[6]Health Data & AI, Deloitte Consulting LLP, Arlington, VA,[7]Center for Biomedical Informatics and Information Technology, National Cancer Institute, Bethesda, MD

Purpose: De-identification of cancer imaging data is vitally important for data sharing and the advancement of research, however it is a time consuming and complex process that limits access to new cancer data sets such as those shared through NCI's Imaging Data Commons (IDC), built on the Google Cloud Platform (GCP). Our research demonstrates how this process can be automated using GCP-native services.
Methods: We configured the Medical Image De-Identification (MIDI) pipeline to automate de-identification of cancer imaging data. De-identification is performed using an alpha release of GCP's Healthcare API which was configured to scrub all Protected Health Information (PHI) from both Digital Imaging and Communications in Medicine (DICOM) headers and burnt-in text in pixel data. A dataset containing 216 patients and 23,921 images was prepared to test the de-identification algorithm by placing synthetic PHI in both DICOM headers and pixel data. The synthetic data matched real data seen during curation at The Cancer Imaging Archive (TCIA) and included data difficult for an algorithm to detect. Accuracy of the MIDI pipeline was measured against TCIA's standard tools and

procedures for de-identification. Measures included correct detection of all PHI data and correct action taken (e.g., remove, encrypt, or otherwise obscure). Throughput was also measured.
Results: Throughput was measured at 22.0 images per second over 10 runs. The MIDI pipeline's accuracy for DICOM headers was 98.7%, accurately detecting dates, addresses, phone numbers, unique identifiers, names, and other common PHI. The most common PHI failed to remove were special cases that included uncommon names or names with symbols, dates in string data types that were mistaken for other IDs, patient IDs, and abbreviated institution names. Private Creator data elements were consistently failed to be retained. These errors were due to options not currently available, and algorithms not trained on specific PHI, such as abbreviated institution names. UIDs were correctly replaced. PHI burnt-in the pixel data was successfully detected and removed, with one false positive.
Conclusion: We demonstrate the current capability and performance of automated cancer image de-identification. Our results show that while full automation is within grasp, a semi-automated pipeline is now feasible. A human expert in the loop can be used for final verification. This will lead to a much-needed acceleration of image de-identification, to handle the rapidly growing volume of data and provide rapid timely access in support of cancer research. Future work will focus on including pre- and post-processing tools to aid the human expert in the loop, such as identifying and flagging questionable images for manual review. These tools will also be used to catch the errors mentioned in results.

#6580

A machine learning-based pipeline and web server ImmuneMirror for neoantigen prediction

Wei Dai[1], Gulam Sarwar Chuwdhury[1], Yunshan Guo[1], Zhonghua Liu[2].
[1]The University of Hong Kong, Hong Kong, Hong Kong,[2]Columbia University, New York, NY

Background: Gastrointestinal tract (GIT) cancer is a group of cancers that affect the digestive system. It has become a leading cause of cancer mortality worldwide. However, the clinical outcome for advanced-stage patients with cancer metastasis after conventional treatment remains poor.

Although cancer immunotherapy has attracted much attention for the treatment of these deadly cancers as a single agent or in combination with chemotherapy, the objective response rate to this treatment remains low and most of the responsive patients only have a partial response. Accumulating evidence suggests that multiple mechanisms are involved in the resistance to cancer immunotherapy.

Methods: To facilitate the identification of the cancer patients who most likely respond to immunotherapy, we developed a stand-alone open-source ImmuneMirror pipeline with graphical analysis results for evaluating the selected features including tumor mutation burden, microsatellite instability (MSI) status, HLA typing, predicted neoantigen load and the top-ranked neoantigens with T cell immunogenicity as well as the expression of innate anti-PD1 resistance (IPRES) gene signature. We incorporated a machine-learning model for neoantigen prediction and prioritization in ImmuneMirror and established a web server. The model was trained and tested using the known neopeptides with T cell immunogenicity collected from 19 published studies, and combined neoantigen-relevant features: agretopicity, foreignness, hydrophobicity, binding stability, peptide processing, and transportation scores.

Results: The accuracy of neoantigen prediction accuracy of ImmuneMirror model is 0.87. We utilized ImmuneMirror to analyze 805 normal-tumor paired samples in GIT cancers including esophageal squamous cell carcinoma (ESCC), colorectal cancer (CRC) and hepatocellular carcinoma (HCC). Elevated neoantigen load was correlated with good clinical outcomes in ESCC. Interestingly, we identified a subgroup of MSI-H CRC with relatively low neoantigen loads for MHC Class I and Class II, respectively, though the tumor mutation burdens of this subset of patients were comparable with other MSI-H CRC. Our result suggests this subset of patients may not respond well to immunotherapy. In addition, the neopeptide YMCNSSCMG<u>V</u> derived from the TP53 hotpot mutation G245V mutation restricted by HLA-A02 was identified as the actional target in the ESCC patient by ImmuneMirror and confirmed by the experimental validation.

Conclusions: These results showed the reliability and effectiveness of ImmuneMirror for evaluating the relevant features and predicting putative neoantigens.

Acknowledgments: We acknowledge the support from Health Medical Research Fund (Grant No. 07182016) from the Research Fund Secretariat of Health Bureau in Hong Kong.

#6581

SLKB: Synthetic lethality knowledge base for gene combination double knockout experiments

Birkan Gökbağ[1], Shan Tang[2], Kunjie Fan[1], Lijun Cheng[1], Lang Li[1].
[1]Department of Biomedical Informatics, The Ohio State University College of Medicine, Columbus, OH,[2]The Ohio State University College of Pharmacy, Columbus, OH

Introduction: Synthetic lethality (SL) of two genes is defined that a cell loses its viability if both genes lost their functions, but it remains viable if losing only one gene. Because of the emerging CRISPR-cas9 technology, a number of cancer cells were screened in gene combination double knockout (CDKO) experiments. These CDKO experiments have been effective in identifying SL gene pairs as potential combination targets in treating cancer. The existing SL database, SynLethDB v2.0, attempted to integrate SL experiments and data, but has several knowledge gaps: (1) missing all non-SL gene pairs; (2) inaccurate cell line annotations; (3) incomprehensive coverage of CDKO experiments; (4) deviation from originally reported SL scores, and most importantly (5) ignoring the difference among various SL calculation methods, including sequence mapping, sequence count processing, sample normalization, background control normalization, and SL score calculation.
Methods: SL knowledge base (SLKB) is developed. It includes SL data from 11 published CDKO experiments in 22 cell lines. Between SLKB and SynLethDB, their cell line data and positive/negative SL gene pair data collected from CDKO experiments were compared. Five SL calculation methods are compared: median SL score with and without background control normalization (Median-B/NB), similarly sgRNA-Derived B/NB, Horlbeck-Score, GEMINI, and MAGeCK-based SL score (MAGeCK-Score). We compared their overall overlapping and pairwise overlapping among top 10% SL gene pairs.
Results:

- For human SL, SynLethDB only included two CDKO experiments, 189 SL gene pairs, and 0 non-SL gene pairs. Our SLKB has 11 CDKO experiments, 22 cell lines, 16,044 SL gene pairs, and 264,444 non-SL gene pairs..
- Among top 10% SL gene pairs from five SL calculation methods, only 0.05% are overlapping.
- In pairwise overlapping analysis, Median-B/NB Score has the highest averaging pairwise overlapping with the other four methods, 26.82%. GEMINI has the lowest average pairwise overlapping with the other methods, 5.11%. The averaging overlapping rates for MAGeCK-Score, sgRNA-Derived B/NB Score, and Horlbeck-Score are 24.52%, 18.50%, and 9.89% respectively.

Conclusion: SLKB is a much more comprehensive SL database than SynLethDB in CDKO experiment data integration and includes original scorings. There is a significant amount of difference between five SL calculation methods and their SL scores. All five SL scores can be queried and ranked in SLKB. SLKB also documents sufficient technical details of these five methods, allowing users to review and choose proper methods for their data analysis and presentation.

#6582

A path to sustainability for the National Cancer Institute's Cancer Research Data Commons

Juergen A. Klenk[1], Angela Maggio[1], Bhavani S. Singh[1], Erin N. Byrne[1], Erika Kim[2], Tanja M. Davidsen[2]. *[1]Deloitte Consulting LLC, Arlington, VA,[2]Center for Biomedical Informatics and Information Technology, National Cancer Institute, Rockville, MD*

Purpose: The volume of data produced by the biomedical research community continues to grow rapidly. Efficient collection, curation, and sharing of these data are expected to enable researchers to synthesize larger datasets and apply novel methods to discover new patterns for diagnosis, treatment, and care of disease. Consequently, data platforms that support these functionalities have become an important instrument for the biomedical research community. The National Cancer Institute’s (NCI’s) Cancer Research Data Commons (CRDC) is a data platform for the cancer research community that provides cloud-based, secure storage and analytic

tools for cancer data, including genomics, proteomics, imaging, and clinical trial data. CRDC has been funded by multiple sources, including the Beau Biden Cancer Moonshot program. Achieving long-term sustainability of the CRDC program is the focus of our study.
Methods: We applied a Financial Operations (FinOps) framework to map all costs to functionalities provided by the CRDC, including processes such as data intake, storage, compute, user support, and project management. We established a comprehensive financial baseline for the operations of the CRDC, identified opportunities for optimization across multiple dimensions (people, processes, technology), projected future costs based on trends for cancer data, and evaluated sustainability under defined funding scenarios.
Results: We identified 15 recommendations for optimization of the CRDC, including automation and centralization of core services (e.g., intake, curation, indexing), optimization of storage (e.g., compression, archiving), and harmonization of common services across the CRDC components (e.g., common architecture, governance). If implemented, we could demonstrate that these recommendations offer a path to long-term sustainability of the CRDC program under a variety of funding scenarios.
Conclusion: Data platforms such as the CRDC will see rapid increases in operational costs due to the growing data volumes and demand from researchers. Optimizing governance and operational frameworks will result in efficiency gains that can ensure long-term sustainability. Taking these steps will be critical to provide the necessary infrastructure to advance the field of data-driven biomedical research.

#6584

Potential carcinogenic effects of electronic nicotine delivery systems through epigenetic reprogramming in oral, brain, and lung stem cells

Akilah Shepard[1], Oneilia Yearde[1], Juan Sanchez[2], Ryan Amador[2], Gabriel Xirinachs[2], Erika Hernandez[2], Elizabeth Corrales[2], Swarnava Das[3], Marco Ruiz[4], Madhumita Das[2], Rose M. Stiffin[1], Marilyn Sherman[1], Alessandra Manzon[1], Ayivi Huisso[1], Jayanta K. Das[1]. *[1]Florida Memorial University, Miami, FL,[2]Miami Dade College, Miami, FL,[3]Miami Coral Park Senior High School, Miami, FL,[4]Baptist Health Medical Group, Miami, FL*

Recent scientific studies exhibited that the electronic nicotine delivery systems (ENDS) aerosols comprise numerous carcinogens namely

propylene glycol, diacetyl, formaldehyde, acetaldehyde, crotonaldehyde (2-butenal), acetone, acetyl propionyl (2,3-pentanedione), acrolein, nicotine, arsenic, cadmium and radioisotopes, such as Polonium-210 and lead-210. However, there was no such investigation for clarifying the mechanism of carcinogenic effects and epigenetic reprogramming of human oral, brain, and lung stem cells. In this study, we investigated the carcinogenic effects of ENDS aerosols, and the mechanism of epigenetic reprogramming using the Comparative Toxico-genomics Database (CTD), NIH Toxicology Data Network (TOXNET), the database of the National Institute of Environmental Health Sciences (NIEHS), AACR Genomics Evidence Neoplasia Information Exchange (GENIE) database, and other bioinformatics databases. We found from CTD analysis that the chemical gene interactions showed approximately 3% of genes highly expressed by propylene glycol and diacetyl from a total of 98 genes. The AACR GENIE database analysis showed EGFR, is associated with gliomas (191 clinical data, DFCI glioma cohort), found among 98 genes regulated by propylene glycol and diacetyl. The CTD analysis also exhibited the chemical gene interactions of highly expressed 9 common genes (with miR140 by propylene glycol, and formaldehyde from a total of 3983 genes; 5 common genes by propylene glycol, acetaldehyde, from a total of 275 genes; 1 common gene by propylene glycol, crotonaldehyde (2-butenal), from a total of 227 genes; 7 common genes by propylene glycol, acrolein from total 2185 genes; 18 common genes by propylene glycol, and nicotine from total 1244 genes; 11 common genes by propylene glycol, and arsenic from total 4983 genes; 9 common genes with HDAC4, CD86, miR21 by propylene glycol, and cadmium from total 5242 genes. The ENDs aerosols contain Polonium-210 and lead-210 (concentration; 13 ± 2 Bq/kg), which have been reported as Group 1 human carcinogens and emit alpha particles. We found that alpha particles caused DNA lesions, and gene mutations in human oral, brain, and lung stem cells and resulted in long-term chromosomal instability in primary human T lymphocytes by analyzing recent works of literature. The epigenetic mechanisms of histone modifications and these potential carcinogens have been revealed by the database of NIH Roadmap Epigenomics Mapping Consortium and our analysis discovered that Mitogen-activated protein kinase 1(MAPK1) is epigenetically reprogrammed with close interaction of teen genes. Therefore, it is important to find the actual epigenetic mechanism of transcriptional

regulation by these potential carcinogens on oral, lung, and brain stem cells, and our current study revealed this important relationship.

#6585

OncoKB, MSK's precision oncology knowledge base

Sarah P. Suehnholz, Moriah Nissan, Hongxin Zhang, Ritika Kundra, Calvin Lu, Amanda Dhaneshwar, Nicole Fernandez, Stephanie Carrero, Maria E. Arcila, Marc Ladanyi, Michael F. Berger, Aijazuddin Syed, Rose Brannon, Ross Levine, Ahmet Dogan, Ezra Rosen, Alexander Drilon, David B. Solit, Nikolaus Schultz, Debyani Chakravarty. *Memorial Sloan Kettering Cancer Center, New York, NY*

OncoKB, Memorial Sloan Kettering Cancer Center's (MSK) precision oncology knowledge base (www.oncokb.org), is an FDA-recognized* somatic variant database that contains information about the oncogenic effect and clinical implications of genomic alterations in cancer. Since its 2016 public release, OncoKB has grown to include annotation for >5,770 alterations in ~700 cancer-associated genes. OncoKB data is integrated into the cBioPortal for Cancer Genomics and used to annotate >12,000 MSK patient sequencing reports annually, encompassing both solid tumor and hematological malignancies. Users in academic, commercial and hospital settings outside MSK can programmatically access OncoKB data via its web API with an OncoKB license, which is free for academic research. To date, users from ~ 1400 institutions across >70 countries have licensed access to OncoKB annotations. The OncoKB Therapeutic (Tx) Levels of Evidence assign tumor-type specific clinical actionability to individual mutational events based on data supporting whether an alteration is predictive of response to matched targeted therapies. To date, OncoKB includes 44 Level 1 genes (included in the FDA drug label), 23 Level 2 genes (included in professional guidelines), 33 Level 3A genes (predictive of drug response in well-powered clinical studies), 27 Level 4 genes (predictive of drug response based on compelling biological evidence), and 11 R1/R2 resistance genes. In 2022, several major content additions were made to OncoKB based on key shifts in the precision oncology landscape. For example, OncoKB included 2 new tumor-agnostic FDA drug approvals, dabrafenib + trametinib and selpercatinib for BRAF V600E and RET fusion-positive solid tumors respectively (Level 1), capturing 5 tumor-

agnostic FDA drug approvals to date. OncoKB promoted ERBB2 oncogenic mutations and FGFR1 fusions to Level 1 following their inclusion as patient eligibility criteria in FDA drug labels for trastuzumab deruxtecan (NSCLC) and pemigatinib (myeloid/lymphoid neoplasms) respectively. NCCN guidelines for uterine sarcoma and pancreatic cancer listed PARP-inhibition for BRCA-mutant disease, making them Level 2 in these indications. Lastly, previously considered undruggable targets, TP53 Y220C and KRAS G12D, were included in OncoKB based on compelling evidence demonstrating response to allele-targeting drugs, PC14586 and RMC-6263, respectively. In sum, 7 novel clinically actionable biomarkers (Levels 1-4) and 11 follow-on precision oncology therapies for existing leveled biomarkers were added to OncoKB in 2022. Current OncoKB efforts are focused on prioritized high-volume cancer gene curation for annotation of whole exome/genome data, annotation of germline alterations and development of a clinical trials matching system. *FDA recognition of OncoKB is partial and limited to the information clearly marked on www.oncokb.org.

#6586

Updates to UALCAN, a comprehensive cancer proteogenomic data analysis platform for discovery research

Darshan Shimoga Chandrashekar[1], Sooryanarayana Varambally[2], Santhosh Kumar Karthikeyan[2], Praveen Kumar Korla[2], Henalben Patel[2], Mohammad Athar[3], Upender Manne[2], George J. Netto[2], Ahmedur Rahman Shovon[4], Sidharth Kumar[5], Zhaohui S. Qin[6], Chad J. Crieghton[7]. *[1]University of Alabama at Birmingham, Birmingham, AL,[2]Pathology, University of Alabama at Birmingham, Birmingham, AL,[3]Dermatology, University of Alabama at Birmingham, Birmingham, AL,[4]Computer Science, University of Alabama at Birmingham, Birmingham, AL,[5]Computer science, University of Alabama at Birmingham, Birmingham, AL,[6]Department of Biostatistics and Bioinformatics, Emory University, Atlanta, GA,[7]Baylor College of Medicine, Houston, TX*

Background: Recent advances in high throughput technologies and initiation of multiple consortium driven projects have led to generation of high volume of molecular data related to thousands of cancer patients.

These high throughput data are extremely useful for novel biomarker identification, therapeutic target identification in tumor subclasses and allows numerous hypothesis driven cancer research projects. However, the sheer volume of data and diverse data formats presents tremendous challenge for researchers with no programming experience to access and analyze comprehensively. These factors prompted us to develop **UALCAN** (University of ALabama CANcer portal, Yes! You All Can) for comprehensive cancer data analysis in a user-friendly manner. UALCAN enables cancer researchers/clinicians in tumor subgroup based gene expression, protein expression and survival analyses. UALCAN is extremely popular among cancer researchers round the world with well over a "MILLION" site visits and cited over 3400 times in research articles. UALCAN integrates The Cancer Genome Atlas (TCGA) and Clinical Proteomic Tumor Analysis Consortium (CPTAC), as well as gene expression data from Children Brain Tumor Tissue Consortium (CBTTC). Users can also analyze non-coding RNA (miRNA and lncRNA) expression data from The Cancer Genome Atlas (TCGA) and the epigenetic data though the promoter DNA methylation analysis form the TCGA data. **Results:** UALCAN now enables user to study expression profile of ~10000 proteins in 14 CPTAC cancers and expression pattern and survival impact of 20,500 protein-coding, ~17,000 lncRNA and 1800 miRNA in 33 TCGA cancers. It also facilitates analysis of gene expression pattern in pediatric brain cancer. User-friendly graphical user interface of UALCAN facilitates a) analyzing protein/non-coding RNA expression in tumor subgroups based on race, stage, age and molecular types; b) identifying top differentially expressed lncRNA/miRNA in specific cancer subtype; c) listing potential gene targets of non-coding RNA; d) performing pan-cancer analysis and e) determining impact of gene expression on patient's overall survival. **Conclusions:** UALCAN is freely available at http://ualcan.path.uab.edu (Google: UALCAN) This dynamic data portal provides constant updates that empower cancer researchers in studying gene and protein level expression and identifying tumor subgroup specific non-coding RNA biomarkers. UALCAN serves a one-stop platform for access, study, analyze and leverage large cancer datasets.

#6587

Method to increase performance of genome-wide association study using imputation for Asian ancestry

GangPyo Ryu[1], Youngil Koh[2], Sung-soo Yoon[2]. *[1]Seoul National University, Seoul, Korea, Republic of,[2]Department of Internal Medicine, Division of Hematology and Medical Oncology, Seoul National University Hospital, Seoul, Korea, Republic of*

The emergence of the large-scale public genomic database facilitates genome-wide association study. An unprecedented number of samples emerged, which enable elucidate valid genetic inferences and contribute to finding novel associations for various phenotypes including cancer. However, most of the genome data is from European-based ancestry, which leads to the disparity in study for relatively minor ethnic groups including Asian. Meanwhile, among public genomic database, TOPMed consortium consists of ~180k participants, over 60% of the 180k samples are of predominantly non-European ancestry, and Asian ancestry consisted of 8 % in total. In addition, 1000 Genomes Project(1KG) contains 2,504 individuals from 26 populations and has sequenced 698 samples in addition. These projects serve as a reference to impute missing variants to improve association power for Genome-Wide Association Study (GWAS) subsequently. We compared the imputation results using those reference panels.Korean Genome Project (Korea1K), including 1094 whole genomes are public datasets consisting of only Korean (East Asian) origin. On GRCh38, Korea1K variants consisting of 59,463,566 variants in total, 99.6% with MAF <1% rare variant, only 35.7% of those rare variants passed from GATK Best Practice VQSR filter. With Korea1K data, we have downsampled the result into the exonic level, imputed with reference panels, and seen the consequences for which reference panel shows the best performances. Using 1KG as a reference, we could identify novel rare variants only in 0.1 to 0.38 fold of filtered rare variant in 1KG phase3 and 1KG phase3 30X respectively. On the other hand, TOPMed imputation resulted in rare variants over 1.65 fold increase. With well-imputed variants R^2 over 0.8, all three reference database showed poor conservation which only 0.009 % of rare variant are rescued. The reference panel we commonly use are large but required to have more diversity in a Asian rare variant perspective. Despite increase of the Asian fraction in the public genomic database, our result suggests that the number of reference Asian samples are

still low to perform association study. In conclusion, our finding highlights both the utility and limitation of the imputation reference panel for Asian ancestry. Novel variants filled by imputation are promising for adding power to various association studies.

#6588

Systems biology-based drug repositioning and biomarker discovery for Thai liver fluke-associated cholangiocarcinoma

Supawan Jamnongsong[1], Patipark Kueanjinda[2], Piyathida Tawornparcha[1], Kulthida Vaeteewoottacharn[3], Seiji Okada[4], Siwanon Jirawatnotai[1], Ananya Pongpaibul[5], Krittiya Korphaisarn[6], Somponnat Sampattavanich[1].
[1]Department of Pharmacology, Faculty of Medicine Siriraj Hospital, Mahidol University, Bangkok, Thailand,[2]Department of Microbiology, Faculty of Medicine, Chulalongkorn University, Bangkok, Thailand,[3]Department of Biochemistry, Faculty of Medicine, Khon Kaen University, Khon Kaen, Thailand,[4]Division of Hematopoiesis, Joint Research Center for Human Retrovirus Infection, Kumamoto University, Kumamoto, Japan,[5]Department of Pathology, Faculty of Medicine Siriraj Hospital, Mahidol University, Bangkok, Thailand,[6]Division of Medical Oncology, Department of Medicine, Faculty of Medicine Siriraj Hospital, Mahidol University, Bangkok, Thailand

Our group has recently reported the successful use of comprehensive drug response and pan-omic profiling for identifying repurposable drug shortlists in Asian cholangiocarcinoma. We also developed the CCA45 gene-expression signature that could accurately predict the prognosis of CCA patients, especially those with Asian ethnic backgrounds. To further explore therapeutic candidates and potential resistance mechanisms, we have established CCA1 cell lines resistant to their subgroup-specific drug candidates: MEK and SRC inhibitors. Reverse-phase protein arrays (RPPA)-based proteomic profiling revealed upregulation of cell cycle, apoptosis, MAPK, and mTOR-related proteins in both MEKi- and SRCi-resistant cells. Src pathway activity was found to be more significantly reduced in SRCi-resistant cells. We identified CDK4/6 inhibitors as the second-line therapeutic candidates for MEK inhibitor-resistant cells by systematic drug screening. SRCi-resistant cells unexpectedly developed

cross-resistance to MEK inhibitors and showed sensitivity to only a few CDK4/6 inhibitors. These data are beneficial for the clinical translation of our proposed drug candidates for Asian CCA, preparing the alternate regimens after drug resistance. We also adopted the DSP-based spatial transcriptomic platform to compare the tumor microenvironment between chemotherapy-sensitive and chemotherapy-resistant CCA patients. While the CTA panel showed consistent patterns of normalized gene expression to those of the WTA panel, the CTA panel can only measure 17 of the 45 genes required for our CCA45 signature. Out of these 17 genes, *ITGB4*, *FGFR3*, *VEGFC*, *NOTCH1*, and *RRAD* showed significant gene expression changes with reducing tumor percentage. The microenvironment of gemcitabine/cisplatin responder (R) non-responder (NR) exhibited negative regulation of ERK1/2 and MAPK, high WNT pathway activity, and high tumor-infiltrating lymphocyte (TIL). In contrast, the microenvironment of the non-responder (NR) subgroup showed high neutrophil-related activity, high NFκB, high Treg, and the exhausted immune phenotype. Overall, our study contributes toward realizing the precision medicine concept for CCA patients.

#6590

Undergraduate e-mentoring in cancer research: The ACE scholars program

Cristina Baciu, Compton Zachary, Carlo Maley. *Arizona State Univ. Biodesign Institute, Tempe, AZ*

Only 1 in 4 undergraduate college students report having had access to mentoring while in college. To create community and training opportunities for a diverse body of undergraduate students (incl. online students) interested in cancer research, we developed a well-rounded e-mentoring program that incorporates alternated sessions of scientific mentoring (i.e., design a study, create a poster) and professional development (i.e., graduate school strategy and applications, networking). The theoretical background of our program derives from project and team-based learning, which state that students tend to learn better and be more engaged when working hands-on on a given project, in teams. Our teams are led by experienced undergraduate researchers, which enables them to gain leadership experience before applying to graduate school.

We implemented this e-mentoring program in a research center at a large southwestern public university, where 43 undergraduate research assistants were mentored via Zoom during the Spring of 2022. At the end of the semester, we administered a survey to assess program effectiveness and collect student feedback. 31 students took the survey, which revealed that during Spring 2022, 25% of students were responsible for the care of children or other family member(s), 47% worked part-time and 22% worked full-time, and 56% of students encountered personal and/or professional challenges. Furthermore, we measured program effectiveness using the College Student Mentoring Scale, a comprehensive tool that measures students' perceived psychological and emotional support, degree and career support, academic knowledge support, and role modeling they received during their time in the program. Findings indicate that 82% of students felt they received psychological and emotional support and degree and career support while in the program. Moreover, 96.3% of students indicated that they felt they received academic knowledge support and benefited from role modeling while in the ACE Scholars Program. Additionally, 85% of students agreed or strongly agreed that the ACE Scholars Program, with its research experience and career and professional development components, has helped them be prepared for their future endeavors. Overall, 86% of the students indicated that they were extremely satisfied with the ACE Scholars Program. We will discuss the implications of this program and its findings for the practice of e-mentoring undergraduate students who are interested in cancer research.

#6591

A universal atlas of cellular and oncogenic phenotypes

Corey Weistuch[1], Kevin Murgas[2], Ken Dill[2], Larry Norton[1], Joseph Deasy[1], Allen Tannenbaum[2]. *[1]Memorial Sloan Kettering Cancer Center, New York, NY,[2]Stony Brook University, Stony Brook, NY*

Tumors and healthy tissues exhibit gene expression variability in many of the same pathways. We propose that these commonalities result from a performance trade-off between universal cellular phenotypes; each phenotype is defined by an orthogonal gene expression profile identified using unsupervised dimensionality reduction. Using two publicly available RNA-seq datasets (n=54 normal tissues; n=1504 cancer cell lines), we show

that both healthy and cancerous cells occupy a trade-off between five canonical phenotypes: OxPhos, Warburg, Fibroblastic, Immune, and Growth. Each cell is assigned a phenotype score that, as we demonstrate, predicts differential drug sensitivities and mutational signatures, even among cancers of the same tissue type. Since these phenotype scores are defined using only healthy tissues, they can be generally applied to other diseases as well.

#6592

An AI platform for vascular and fibrosis analysis of pathology images

Yawen Zheng, Likun Zhang, Dawei Wang, Sheng Gao. *Crown Bioscience Inc, Suzhou, China*

Introduction: Changes in the number of blood vessels and the proportion of fibrosis regions in xenograft tumors are key indicators for efficacy of oncology drugs, which currently are assessed mainly by human visual examination that is time-consuming, inaccurate and biased because only part of a pathology image is checked. We developed an online AI platform that integrates machine learning algorithms in Computer Vision to quickly and automatically obtain accurate and comprehensive information on blood vessels and fibrosis regions from a whole pathology image.
Methods: In a stained pathology image, blood vessels are stained with a different color than other components (e. g. connective tissues, tumor cells, background), so we can directly locate pixels representing them. They also have different topological structures, so we can outline and count the contours of vessels. To count the number of vessels more precisely and reduce the interference of noise, we keep a contour only if it intersects with some located pixels and the number of pixels in the intersection exceeds an adjustable threshold. The fibrosis regions are identified by color contrast since they are stained with a distinct and easily recognizable color. The algorithms were implemented using the OpenCV package.
Results: Our AI platform automatically annotates blood vessels and fibrosis regions in pathology images, and generates reports in excel format to report the number and total area of blood vessels, the area and ratio of fibrosis regions, and execution time. It demonstrates superior performance to standard pathology software.

Integrative Spatial and Temporal Multi-omics of Cancer

#6596

Genomic and proteome analysis using preoperative cell free DNA and extracellular vesicles of lung cancer patients

Hayato Koba, Hideharu Kimura, Seiji Yano. *Kanazawa Univ. Hospital, Kanazawa, Japan*

Background: The detection of circulating cell free DNA (cfDNA) has been examined as a predictor of postoperative recurrence and survival in lung cancer patients. Extracellular vesicles (EVs) have potent for searching a new target to cancers.
Objective: To analyze the association between cfDNA/EVs and prognosis after lung cancer surgery.
Methods: We retrospectively examined patient background, disease-free survival, overall survival, and preoperative cfDNA in lung cancer patients who underwent surgery at Kanazawa University Hospital between January 2017 and May 2020, in whom preoperative chemotherapy was not administered. We extracted cfDNA from 4 ml plasma within 7 days before surgery and measured its concentration. EVs were extracted from 500 μl serum via Tim4 protein. Proteins included in EVs were analyzed by mass spectrometry.
Results: 285 patients were included, 179 males and 106 females, median age 71(36-88) years, and 8 patients had SCLC. EGFRm- positive lung cancer was included in 93 cases (32.6%). The pStage0/l/ll/lll/lV of NSCLC was 7/187/42/36/6 respectively, and the pStagel/ll/lll of SCLC was 4/1/3 respectively. The mDFS of NSCLC was 14.6 (7.8-29.7)/21.5 (8.5-NA) months in pStage lll/lV, respectively. mOS was 53.3 (28.7-NA) months in pStage lll and was not achieved in other stages. The mDFS of SCLC was 19.8 (1.9-NA)/NA/5.7 (1.9-NA) months in pStage l/ll/lll, respectively. mOS was NA/NA/9.3 (9.3-NA) months, respectively. cfDNA was detected in 283 (99.2%) patients, with a concentration of 4.7 (0-60.0) ng/μl. The correlation coefficient between cfDNA concentration and DFS/OS in NSCLC was -0.023 (P=0.70)/-0.014 (P=0.81). The correlation coefficient between cfDNA concentration and DFS/OS for SCLC was -0.86 (P=0.024)/-0.89 (P=0.012). No recurrence was observed in patients in whom cfDNA was not detected.EVs were detectable from pre-operative serum samples, and

the proteins included in these were different, whether disease was recurrent or not.
Conclusion: The cfDNA concentration did not correlate with DFS/OS in post-operative NSCLC, whereas it correlated negatively with DFS/OS in SCLC. In the presentation, we will further discuss about the concrete genetic alterations and protein expression, based on the cfDNA sequencing and proteomics analysis.

#6597

A multi-omics classifier achieves high sensitivity and specificity for pancreatic ductal adenocarcinoma in a case-control study of 146 subjects

John Blume, Ghristine Bundalian, Jessica Chan, Connie Chao-Shern, Jinlyung Choi, Rea Cuaresma, Kevin Dai, Sara N. Golmaei, Jun Heok Jang, Manoj Khadka, Ehdieh Khaledian, Thidar Khin, Yuya Kodama, Ajinkya Kokate, Joon-Yong Lee, Manway Liu, Hoda Malekpour, Megan Mora, Nithya Mudaliar, Preethi Prasad, Madhuvanthi Ramaiah, Saividya Ramaswamy, Peter Spiro, Kavya Swaminathan, Dijana Vitko, James Yee, Brian Young, Susan Zhang, Chinmay Belthangady, Bruce Wilcox, Brian Koh, Philip Ma. *Prognomiq Inc, San Mateo, CA*

Pancreatic ductal adenocarcinoma (PDAC) is currently the 3rd leading cause of cancer-related deaths in the US. Although the all-stage 5-year survival rate is ~10%, early-stage 5-year survival is markedly superior and in excess of 40%. Hence, early detection of PDAC via blood-based liquid biopsies holds promise to reduce morbidity and mortality. PrognomiQ's multi-omics platform performs deep and unbiased molecular profiling of blood samples to detect proteins, metabolites, lipids, mRNA, miRNA, cfDNA fragmentation and copy-number, and CpG methylation. Here we report results from training and validation of a classifier on a subset of that multi-omic data with the potential to enable the development of high sensitivity and specificity tests for early detection of PDAC.We conducted a case-control study comprising 146 subjects across 16 clinical sites, including 63 pathology-confirmed, untreated PDAC cases (12 stage I, 8 stage II, 4 stage III, 36 stage IV, and 3 stage unknown) and 83 age- and gender- matched controls without any known cancer. For each subject, venous blood samples including plasma were collected. Unbiased LCMS was used to detect and

quantify proteins, and targeted, multiplexed MRM-LCMS assays were used for both metabolites and lipids. After data processing, we detected 54,114 proteomic features, 898 lipids, and 373 metabolites. 445 proteomic features, 170 lipids, and 37 metabolites were found to be significantly different as determined by Bonferroni-corrected Wilcoxon tests with FWER $\leq$ 0.05. For classification, the dataset was split into training (37 cases and 37 controls) and validation (26 cases and 46 controls) sets, with control for collection site and date, age, and gender. XGBoost models were constructed for each analyte class using ten repeats of 10-fold cross-validation. To improve specificity to PDAC, all proteomic features which mapped to GOBP terms associated with acute-phase response, inflammation, and immune response were excluded prior to training. The best-performing hyperparameters were used for a final model built on the full training set and then used for inference on the validation set. At 99% specificity, the proteomic classifier had sensitivities of 77%, 57%, and 88% for Stages 1-4, Stages 1-2, and Stages 3-4, respectively, estimated by bootstrap re-sampling of the validation results. Metabolomics had sensitivities of 81%, 71%, and 88%. Lipidomics had sensitivities of 65%, 71%, and 65%. A joint, multi-omic model was constructed by averaging the scaled probabilities of all models. This joint model improved performance at 99% specificity with sensitivities of 92%, 86%, and 94%, highlighting the synergy of multi-omics data, particularly phenotypically related omics such as those described here. Multi-omic classifiers such as these can serve as the foundation for blood-based liquid biopsies for the early detection of PDAC.

#6598

The development of a tumor-agnostic liquid biopsy assay for minimal residual disease detection and monitoring in cancers

Giancarlo Bonora, Hang Dong, Chao Dai, Binggang Xiang, Billie Gould, Tiantian Zhen, Wei Mo, Xiaohong Wang, Kemin Zhou, Shidong Jia, Shujun Luo, Pan Du. *Predicine, Inc., Hayward, CA*

Purpose

Non-invasive liquid biopsy (LBx) based assays hold great promise for early cancer diagnosis and disease progression monitoring. Personalized baseline tissue-informed minimal residual disease (MRD) monitoring exhibits a particularly high detection sensitivity in many studies, however, baseline

samples (especially tissue biopsies) are often difficult to acquire in a clinical setting, and the personalized panel design and tracking creates operation complexities.

Methods

We developed PredicineALERT^{TM}, a baseline-agnostic MRD LBx assay that measures methylation and mutational variants associated with cancers. At its core lies the PredicineEPIC^{TM} DNA methylation assay with the advantage of low DNA damage and low input amount. Tumor burden is assessed by detecting abnormally methylated DNA fragments with high sensitivity using the Predicine DeepSea bioinformatics analysis pipeline. PredicineALERT^{TM} provides integrated methylation and mutational profiling, as well as copy number variation (CNV) profiling.

Results

The PredicineALERT^{TM} assay was tested using longitudinal LBx samples (blood, urine, CSF) from patients with mCRPC, CRC, NSCLC, breast, liver, kidney, prostate, and bladder cancers. The PredicineALERT^{TM} assay demonstrates highly-sensitive MRD detection and quatification capability (LOD < 0.01%) using 2.5 - 15ng input cfDNA. It has the ability to identify unique cancer biomarker signatures, and robustly detect MRD ctDNA dynamics during treatment. By leveraging genome-wide fragment-level DNA methylation, PredicineALERT^{TM} measures molecular response and MRD in targeted therapy, immunotherapy and chemotherapy. A strong concordance was observed in the pattern of tumor burden as ascertained by CNV and methylation analyses, respectively.

Conclusion

We developed PredicinceALERT^{TM}, a baseline agnostic, multidimensional MRD LBx assay without the need for baseline samples and personalized panel design. It integrates DNA methylation, mutation, and copy number changes for detecting MRD from genome-scale data without relying on target selection before library generation.

#6599

Neomer and fragmentation profiles of cell-free DNA with low-pass whole genome sequencing to predict prostate cancer biopsy outcomes

Fei Liu[1], Kaoqing Peng[2], Rui Chen[3], Mingzhao Li[2], Tao Zeng[4], Yan Zhao[4], Ming Wang[2], Hongxing Liu[2], Jianhao Wu[2], Min Wu[5], Haimeng Tang[5], Hua

Bao[5], Xue Wu[5], Yang Shao[5], Di Gu[2], Shancheng Ren[6]. *[1]Department of Urology, National Cancer Center/National Clinical Research Center for Cancer/Cancer Hospital, Chinese Academy of Medical Sciences and Peking Union Medical College, Beijing, China,[2]Department of Urology; Guangdong Key Laboratory of Urology, The First Affiliated Hospital of Guangzhou Medical University, Guangzhou, China,[3]Department of Urology, Shanghai Changhai Hospital, Shanghai, China,[4]Department of Urology, The First Affiliated Hospital of Guangzhou Medical University, Guangzhou, China,[5]Geneseeq Research Institute, Nanjing Geneseeq Technology Inc., Nanjing, China,[6]Department of Urology, Shanghai Changzheng Hospital, Shanghai, China*

Prostate cancer is one of the most common types of cancer in men. Current prostate-specific antigen (PSA)-based diagnostic strategy for prostate cancer may frequently cause overdiagnosis. In this study, we prospectively recruited 380 individuals, including 167 with pathologically confirmed prostate cancer, 127 with negative prostate biopsy results, and 86 assessed healthy cohort with no need for biopsy. We collected a plasma sample from each participant, performed whole-genome sequencing, and profiled cell-free DNA (cfDNA) neomer and fragmentation characteristics. We then developed a machine learning model using these cfDNA profiles to predict prostate cancer biopsy outcomes. Our results showed that this assay could achieve high accuracy (Accuracy: 85.3%, AUROC: 0.919, 95% CI: 0.892 - 0.946) in repeated 5-fold cross validations. Patients with negative biopsy results had higher prediction scores than healthy individuals ($P < 2.2X10^{-16}$), making them less distinguishable from prostate cancer patients (AUROC: 0.878, 95% CI: 0.837 - 0.918 vs. AUROC: 0.980, 95% CI: 0.963 - 0.997). We further combined this cfDNA-based assay with the PSA testing and constructed an ensemble model. The classification performance was further improved in the ensemble model, showing AUROC metrics of 0.951 (95% CI: 0.932 - 0.969) between cancer and non-cancer, 0.919 (95% CI: 0.889 - 0.949) between cancer and negative biopsy, and 0.998 (95% CI: 0.994 - 1.000) between cancer and healthy individuals. At a sensitivity of 90.4%, the ensemble assay accurately identified 85.4% of non-cancerous conditions, including 76.4% of negative biopsy patients and 98.8% of healthy individuals. We concluded that our cfDNA fragmentation and

neomer-based assay could be incorporated into the PSA-based predicting system for prostate cancer to increase the accuracy and reduce the overdiagnosis.

#6600

The nRichDX ® revolution sample prep system enables recovery of more amplifiable copies and more cancer fraction detection from cfDNA as evaluated on the MassARRAY ® System

Nafiseh Jafari[1], Mayer Saidian[1], Darryl Irwin[2]. *[1]nRichDX, Irvine, CA,[2]Agena Bioscience, San Diego, CA*

Introduction Liquid biopsies utilize cell-free DNA (cfDNA) in blood plasma or urine across various applications, including cancer detection, treatment selection, and treatment/minimal residual disease monitoring. Higher amplifiable copies recovered from liquid biopsies can lead to better cancer detection and monitoring. In this study, we evaluated the recovery of cfDNA amplifiable copies and circulating tumor DNA (ctDNA) dynamics using the nRichDX extraction method, which can extract cfDNA from a broad range of biological fluids (1mL - 20mL). cfDNA quality and ctDNA dynamics were assessed using Liquid IQ and UltraSEEK on the MassARRAY System.

Methods Whole blood from healthy donors was collected in K2EDTA tubes, and plasma was isolated and then pooled in preparation for cfDNA extraction. Plasma aliquots at 5mL (6) and 20mL (6) were extracted using the Revolution Max20 cfDNA Extraction Kit. (12) replicate samples were extracted using QiAmp Circulating Nucleic Acid Kit. Half of the samples were spiked with a cfDNA standard containing a KRAS p.G12V mutation. The quantity and quality of extracted cfDNA were determined using the Liquid IQ panel on the MassARRAY system, which measures amplifiable cfDNA copies, high/low molecular weight dynamics, white blood cell (WBC) contamination along with a molecular barcode for sample matching. Recovery and frequency of the spiked ctDNA standard were performed with the UltraSEEK Lung V2 Panel, capable of detecting variants as low as 0.1% allele frequency.

Results This study compared the amplifiable copies recovered from cfDNA extracted using the nRichDX and Qiagen kit. The amplifiable copies for the nRichDX and Qiagen methods, respectively, were: 5mL non-spiked

517+/-36 Vs. 398+/-17, 5mL spiked 946+/-99 Vs. 732+/-73; 20mL non-spiked 1526+/-26 Vs. 1071+/-55 and 20mL spiked 3004+/-278 Vs. 1777+/-207. All results were statistically different by conventional criteria, evaluated by a two-tailed t-test. Other cfDNA quality characteristics, such as low/high molecular weight DNA and WBC contamination, were concordant between the 2 methods. The spiked KRAS mutation was recovered consistently by both methods with a mutation frequency (5.3+/-0.3) and mutation significance z-score (296+/-19).
Conclusion The nRichDX Revolution System extracts cfDNA and ctDNA with consistently high yields. Two sample T-Test analysis shows that nRichDX, at all levels, performed significantly better than Qiagen at $p < 0.05$. The results demonstrate the capability of the nRichDX system to recover more amplifiable copies with consistent cfDNA quality and ctDNA frequency and hence offer the opportunity to increase the sensitivity of detecting lower frequency mutations in cfDNA and a wider variety of biomarkers.

#6601
Analytical validation of a robust integrated genomic and epigenomic liquid biopsy for biomarker discovery, therapy selection, and response monitoring
Tingting Jiang, Indira Wu, Yvonne Kim, Nageswara Alla, Giao Tran, Dustin Ma, Forum Shah, Jun Zhao, Sai Chen, Sante Gnerre, Melis Hazar, Hao Wang, Catalin Barbacioru, Karen Ryall, Ankit Jambusaria, Anupam Chakravarthy, Anthony Zunino, Theresa Pham, Farsheed Ghadiri, Evan Diehl, Benjamin Morck, Arancha Sanchez, Rochelle Dayan, XianXian Liu, Jeffrey Werbin, Jill Lai, Brett Kennedy, Ross Eppler, Justin Odegaard, Han-Yu Chuang, Helmy Eltoukhy. *Bioinformatics, Guardant Health, Palo Alto, CA*

Background: Despite its revolutionary impact, cancer genomics alone provides little information on tumor phenotype or functional state, which are governed by epigenetic mechanisms, notably methylation of regulatory regions. Tumor and host epigenetic methylation signatures reflect not only tumor phenotype, such as histology, prognosis, protein expression, and functional sub-type, but also that of the tumor microenvironment and the patient, including immune status, therapy-related adverse events,

comorbidities, and disease location. Epigenetic markers also provide more sensitive and precise measures of tumor burden, opening up applications for longitudinal therapy response and monitoring. Here we report the initial validation of GuardantINFINITY, a liquid biopsy assay combining genomic information from >800 genes with characterization of the blood-quiet regulatory methylome, both at single-molecule sensitivity from a single tube of peripheral blood.
Methods: Analytical performance was assessed using 594 cancer patient cfDNA, cell line, and cancer-free donor samples at 5-30ng cfDNA input.
Results: Reportable ranges established for SNVs were ≥0.04% variant allele fraction (VAF), ≥0.04% for indels, ≥0.06% for fusions, ≥2.12 copies for amplifications (CNAs), <1.7 copies for copy loss. Observed 95% limits of detection (LoD) were 0.282% for SNVs across all genes (0.2% for oncogenic hotspots), 0.397% for non-homopolymeric indels, 0.05% for fusions, 2.5 copies for CNAs, 16.3% VAF or 1.84 copies for gene deletions, 7.3 copies for viral (HPV, EBV) detection, and 0.06% for MSI-H. For promoter and sample-level methylation, LoDs were 0.06% and 0.05% tumor fraction, respectively. cfDNA cancer samples demonstrated 100% accuracy for SNVs and Indels above 0.5% VAF and 100% for CNAs and fusions across the reportable range. The analytical false positive rate per base was 6.84e-6 for SNVs, 3.42e-6 for indels, and 0 for CNAs and fusions, with positive predictive values of 97.5% for SNVs, 98% for indels, and 100% for CNAs above 2.5 copies and all tested fusions.
Conclusions: GuardantINFINITY is a patient-care-ready liquid biopsy capable of integrated genomic and epigenomic analysis of all solid tumors at single-molecule sensitivity. In addition to traditional genotyping compatible with Guardant360 for more content, the technology's demonstrated LoD showed the potential for ultra-sensitive ctDNA detection for MRD and recurrence surveillance, tumor fraction quantitation for therapy monitoring, oncogenic virus detection, immunogenotyping, epigenotyping, and tumor phenotype characterization, representing a new standard in biomarker discovery.

#6602
Refining liquid biopsy: generating more information from cell free DNA

Fabio Puddu, Casper K. Lumby, Nick Harding, David J. Morley, Jamie Scotcher, Robert Crawford, Jens Füllgrabe, Walraj S. Gosal, Shirong Yu, Daniel Brudzewsky, Jane Haywood, Andrada Tomoni, Philippa Burns, Joanna D. Holbrook, Paidi Creed. *Cambridge Epigenetix Limited - CEGX, Cambridge, United Kingdom*

Liquid biopsy for profiling of cell free DNA (cfDNA) in blood holds huge promise to transform how we experience and manage cancer by early detection and identification of residual disease and subtype. However, a standard blood draw yields an average of only 10 ng of cfDNA, of which DNA derived from the tumor is a small minority. Therefore, we are faced with a dilemma when utilizing the limited sample to obtain maximum information. Genetic sequencing provides information on actionable somatic mutations but detection of a few loci in a minority of the sample is challenging. Modified cytosine profiles of cancer are differential from non-cancer at many more loci and so provide a stronger signal. Moreover, they can be used to distinguish tissue-of-origin of the tumor. However, methods such as bisulfite sequencing, EM-seq and TAPS sacrifice genetic information (namely C->T mutations, which are the most common mutation in cancer) to measure modified cytosine. Genetic and modified cytosine data together have been shown to be more powerful for the detection of early cancer than either alone. Here we present a technology, which sequences at base resolution the complete genetic sequence integrated with modified cytosine from low nanogram amounts of cfDNA. It consists of (i) a single pre-sequencing workflow, which creates a copy of the original DNA and performs enzymatic base conversions which discriminate genetic and epigenetic states and (ii) post-sequencing data processing which resolves the resultant sequencing data to an information-rich 16-state code and derives genetic variants integrated with modified cytosine levels, within easy-to-use software. It is, in principle, compatible with any sequencing methodology and is shown here optimized for the Illumina fleet. In cfDNA we show accuracy of modC measurement is higher than that of bisulfite sequencing and EM-seq; and the accuracy of genetic sequencing is higher than that of Illumina alone. Accuracy of measurement is extremely important for liquid biopsy where tumor DNA is in the minority and observed in a small number of reads. We demonstrate the impact of varying base calling error rate on limit of detection for rare alleles in cfDNA

samples. Further we show derivation of cfDNA fragment characteristics and that this is produced in combination with genetic and modC information. This further increases the signal available from cfDNA in only one workflow. We suggest this method will help advance the field of liquid biopsy towards its promise.

#6603

BRCA1 promoter methylation in sporadic breast cancer patients detected by liquid biopsy

Jennifer Yen[1], Sai Chen[2], Colby Jenkins[1], Brooke Overstreet[1], Yu Fu[3], Jun Zhao[1], Tingting Jiang[2], Leylah Drusbosky[1], Stephen Pettitt[4], Michael Dorschner[3], Lauren Lawrence[1], Han-Yu Chuang[1], Andrew Tutt[4]. *[1]Guardant Health, Palo Alto, CA,[2]Guardant Health, San Diego, CA,[3]Guardant Health, Seattle, WA,[4]The Institute of Cancer Research, London, United Kingdom*

Background: *BRCA1* promoter methylation (PM) is an early initiating event in cancer, occurring in 3 to 65.2% of all breast tumors, and 30 to 65% of triple negative tumors. *BRCA1* PM has been associated with defective homologous recombination repair (HRR), early onset of breast and ovarian cancer, and improved clinical response to adjuvant chemotherapy. Historically, there has been no diagnostic assay that comprehensively evaluates both *BRCA1* PM and genomic alterations in cell-free circulating tumor DNA (ctDNA). Here, we describe the novel detection of *BRCA1* PM and genomic alterations in a cohort of patients with breast cancer using GuardantINFINITY, a liquid biopsy assay interrogating 800+ genes and genome-wide methylation detection.

Method: We assessed for *BRCA1* PM in ctDNA from 274 patients with late-stage breast cancer. Genomic sequencing of 800+ genes and PM profiling of 398 genes was performed by GuardantINFINITY. The positive calling threshold for PM was established by comparing cell-free DNA derived from patients with cancer and cancer-free donors. The limit of detection (LoD) was determined through *in silico* and experimental titrations of ctDNA from clinical samples and cell lines with known gene PM into the plasma of cancer-free donors.

Results: Among the 274 patients with advanced breast cancer, 8 (2.9%) had germline pathogenic mutations in *BRCA1, BRCA2, or ATM. BRCA1* PM was detected in 11/274 (4.0%) patients at the predefined threshold of >99%

specificity. *BRCA1* PM detection in this cohort was 8.9% (8/90) when excluding samples with low tumor shedding (<1% epigenomic tumor fraction in cfDNA). Among the 11 patients with *BRCA1* PM detected in ctDNA, one had a co-occurring somatic *BRCA1* nonsense variant (p.S361*); none of the remaining patients with *BRCA1* PM had another HRR-related mutation detected in cfDNA. Among patients without *BRCA1* PM detected, pathogenic somatic alterations were detected in *BRCA2, ATM,* and *CHEK2* in 25 (9.4%) patients. *In silico* simulations using clinical samples with *BRCA1* PM indicated an LoD of 0.0408%. *BRCA1* PM was not detected in 3210 individual and mixed cancer-free clinical samples, indicating a high specificity for *BRCA1* PM calls.
Conclusion: GuardantINFINITY, a plasma-based diagnostic assay, detected both *BRCA1* PM and genomic alterations in this unspecified advanced breast cancer cohort. The *BRCA1* PM
detection rates of 4.0-8.9% are consistent with values previously reported in the literature. As *BRCA1* PM has important prognostic and therapeutic implications for the management of breast (as well as ovarian) cancers, additional studies are warranted to further describe the PM patterns across breast cancer subtypes and how these patterns both influence and are influenced by disease evolution and therapeutic response. Liquid biopsy thus serves as a suitable method to noninvasively identify and monitor changes in both genomics and epigenomics.

#6604

Analytical development and validation of a personalized hybrid capture based assay for high sensitivity monitoring minimal residual disease (MRD)

Xiaoqiang Wang, Lei Ye, Chao Zhang, Wanglong Deng, Yongjie Wei, Jing Chen, Xuan Tang, Xiaoxuan Wang, Chao Song, Qing Xu, Yong Ren. *State Key Laboratory of Translational Medicine and Innovative Drug Development, Jiangsu Simcere Diagnostics Co., Ltd., Nanjing, China*

Introduction: 5-30% of patients with early-stage cancer relapse, even though most patients had undergone radical surgery. There is increasing evidence that circulating tumor DNA (ctDNA) minimal residual disease (MRD) predicts relapse following treatment for solid tumors. However, liquid biopsy analyses are challenged by the very low concentrations of

ctDNA in blood samples. Existing ctDNA methods lack the sensitivity needed for detecting minimal residual disease (MRD) following therapy. Here, we describe a tumor-informed personalized hybrid capture based method using next-generation sequencing (NGS) to highly sensitive and specific detect MRD and predict recurrence in plasma cell-free DNA. To validate the performance of the assay, we present a technical validation study on DNA from cancer cell line material, including lung cancer cell line, reference material, Onco gDNA reference standard and wild type gDNA reference standard.
Method: The performance of the assay was assessed using samples from Onco gDNA reference standard and lung cancer cell line. To estimate number of monitoring single nucleotide variants (SNVs) at input volume of 20-80ng, Onco gDNA reference standard was diluted into 8 concentrations (10, 20, 30, 40, 50, 60, 150 and 750 ppm with a variant allele frequency [VAF] range of 0.001% to 0.075%).To estimate limit of detection (LoD) of the assay at input volume of 20ng and 40ng, lung cancer cell line was diluted into 5 concentrations (10, 20, 40, 80 and 160 ppm with a variant allele frequency [VAF] range of 0.001% to 0.016%).10 samples were performed for each concentration, as well as 10 negative reference samples. Personalized panel was performed using ultradeep (100,000X) NGS with customized 55 or 60 SNVs.
Result: Validation results of Onco gDNA reference standard: using 40 variants, sensitivity of input volume of 20ng and 40ng are 95% and 98% at 40 ppm, with a specificity of 100%, respectively. Using 40 variants, sensitivity of input volume of 60ng are 95% at 20 ppm, with a specificity of 100%. Using 50 variants, sensitivity of input volume of 60ng are 70% at 10 ppm, with a specificity of 100%. Validation results of lung cancer cell line: using 40 variants, sensitivity of input volume of 20ng and 40ng are 98% and 100% at 50 ppm, with a specificity of 100%, respectively.
Conclusion: The assay was validated by sequentially diluting of lung cancer cell line and Onco gDNA reference standard. With input volume of 20ng, sensitivity of the assay is 95% at 40ppm when monitoring 40 variants, while with input volume of 60ng the LoD reached as low as 10 ppm with sensitivity of 70% when monitoring 50 variants. The assay demonstrates high sensitivity, while maintaining specificity above 99%.

#6605

Automated isolation and identification of circulating rare cells from blood samples using a label-free rare cell isolation platform - the Genesis System with Celselect Slide technology

Yoon-Tae Kang[1], Errile Pusod[1], Ally Crudgington[1], Abiodun Bodunrin[2], Nick Bosio[1], Susana Chan[1], David Coe[1], Michelle Racey[3]. *[1]Bio-Rad Laboratories, Ann Arbor, MI,[2]Bio-Rad Laboratories, Pleasanton, CA,[3]Bio-Rad Laboratories, Boulder, CO*

Introduction: Isolation and identification of circulating tumor cells (CTCs) offers a promising non-invasive diagnostic tool for cancer research, but significant technical hurdles have made practical application challenging. Recent studies have shown that CTCs undergo cellular changes, such as an epithelial-mesenchymal transition (EMT), with disease progression and metastasis, implying the heterogeneity of the tumor cell population in circulation. Systems for CTC isolation are often limited by a requirement for epithelial markers or separate systems for identification of CTCs. As such, an automated platform that successfully isolates both epithelial and mesenchymal cells and enables identification of cells is necessary for successful study of CTCs. The Genesis System from Bio-Rad™ Laboratories, Inc. isolates rare CTCs based on size and deformability. It also enables users to identify isolated cells through use of an on-slide immunofluorescence (IF) staining workflow, which minimizes sample manipulation and potential sample loss.

Methods: In order to achieve high-throughput label-free CTC isolation, the Genesis System uses Celselect Slides™. Each slide contains 56,400 individual microchambers to capture CTCs while maintaining viability. This Celselect Slide technology can be used for either enrichment or enumeration protocols. For this study, enumeration protocols were performed to capture and identify CTCs using on-slide IF staining. Enrichment protocols were utilized to capture, enrich, and retrieve CTCs for downstream applications. The performance was evaluated using a breast cancer cell line, MCF-7, spiked into whole blood from healthy donors.

Results: The slide isolated 83.95 ± 10.25% of spiked cancer cells in blood samples at a concentration of 10-250 cells/ml. During the CTC enrichment procedure, 99.92% of blood cells were eliminated. Afterwards, 70% of the isolated CTCs were successfully released from the slide and over 92% of the released cells remained viable.

Discussion and Conclusion: We present a fully automated platform to isolate and identify CTCs using on-slide immunofluorescence staining, which minimizes inevitable cell loss during the workflow. Captured cells can be retrieved for downstream applications to facilitate discovery of unknown CTC functions and their clinical relevance in cancer research. The wide range of possible downstream applications include Droplet Digital™ PCR, quantitative PCR, western blot assays, bulk/single-cell genomics, cell culture, fluorescence in situ hybridization, and RNA-Seq. Additionally, the design of the system is amenable to other biofluids which may be utilized for liquid biopsies. The Genesis System with Celselect Slide technology offers a powerful diagnostic tool to monitor disease progression and personalized treatment.

#6606

Biomarker discovery in non-small-cell lung cancer enabled by deep multi-omics profiling of proteins, metabolites, transcripts, and genes in blood

Jinlyung Choi, Ajinkya Kokate, Ehdieh Khaledian, Manway Liu, Preethi Prasad, John Blume, Jessica Chan, Rea Cuaresma, Kevin Dai, Manoj Khadka, Thidar Khin, Yuya Kodama, Joon-Yong Lee, Hoda Malekpour, Megan Mora, Nithya Mudaliar, Sara Nouri Golmaei, Madhuvanthi Ramaiah, Saividya Ramaswamy, Peter Spiro, Dijana Vitko, Kavya Swaminathan, James Yee, Brian Young, Chinmay Belthangady, Bruce Wilcox, Brian Koh, Philip Ma. *Prognomiq Inc, San Mateo, CA*

Lung cancer is the leading cause of cancer-related deaths in the United States, with estimates of 236,740 new cases and 118,830 deaths in 2022 secondary to the disease. Blood-based liquid biopsies hold promise to reduce morbidity and mortality from lung cancer by enabling early detection to downstage disease at diagnosis, theragnostic identification of patients most likely to be helped or harmed by therapy, monitoring of therapeutic efficacy, and detection of residual disease. PrognomiQ's multi-omics platform comprehensively profiles proteins, metabolites, lipids, mRNA, and cfDNA in blood samples which can be used for the development of liquid biopsy tests with high sensitivity and specificity for lung cancer. We conducted a case-control study comprising 1031 subjects: 361 subjects with untreated non-small-cell lung cancer (NSCLC) and 670

matched controls which included 340 subjects with salient pulmonary and gastrointestinal co-morbidities. Blood samples from each subject were processed to provide 7 different `omics readouts. LCMS was used to detect and quantify proteins, metabolites, and lipids. In addition, cfDNA and mRNA were assayed using next-generation sequencing. cfDNA reads were analyzed to estimate fragment-lengths, copy-number variation, and CpG site methylation. All molecular data were normalized using standard methods specific to each assay. Univariate analyses of cases vs controls were performed to identify differentially abundant features on all available samples per assay. We detected 9,868 proteins, 605 lipids, 329 metabolites, and 109,070 mRNA transcripts. Of these, 3,098 proteins, 210 lipids, 57 metabolites, and 30,236 mRNA transcripts were significantly different (FWER < 0.05) in cases versus controls. Gene set enrichment analysis on statistically significant transcripts and proteins identified multiple gene-ontology terms associated with cancer including the Wnt signaling process and IgA immunoglobulin complex, respectively. From cfDNA data, we identified 234 non-contiguous genomic regions associated with the fragment-length disorder, 4,790 with copy-number variation, and 74 differentially methylated genomic regions spanning 184 CpG sites (FWER < 0.05). With the premise that deviations from copy number neutrality are more likely to indicate a tumor contribution, we then focused our examination on those differentially expressed proteins that overlap with differentially expressed mRNA transcripts as well as CNV genomic regions. We identified 52 protein coding genes including E-cadherin (associated with EMT) and related binding proteins such as RAB11B, CAPZB, EPS15, FLNB, MYH9, STK24 and YWHAE. Ongoing machine-learning-based classifier training to distinguish between cancer and non-cancer can serve as the basis for the development of high-sensitivity liquid-biopsy tests for lung cancer.

#6607

Dried blood spot (DBS) sample analysis for drug and metabolomic profiling in oncology clinical trials: Cost-effective decentralized sampling modality for precision oncology

Kelli Goodman, Megan R. Showalter, Anne M. Evans, Matthew W. Mitchell, Rangaprasad Sarangarajan. *Metabolon, Inc., Morrisville, NC*

The COVID19 pandemic accelerated opportunities for innovation within the decentralization process of clinical trials with opportunities for implementation of patient-centric workflows for efficiency and cost-reduction. Decentralized sample collection, particularly whole blood using dried blood spots (DBS) provides the ideal mechanism for patient driven sample collection with ease of access to sample generation, drug level assessments and metabolomic prMegofiling, providing longitudinal real-time measure of drug specific pharmacodynamic readout for safety and efficacy. In this study, we report the development of a protocol for the capture and comprehensive profiling of metabolomics using dried blood spots from a cohort of 49 healthy volunteer donors. Using liquid chromatography combined with mass spectrometric (UPLC-MS/MS) methods an untargeted metabolomic approach resulted in the identification of >800 biochemicals of which a significant subset was found to be presented in corresponding matched plasma (from whole blood) samples. The biochemicals identified from the DBS samples included metabolites that were part of the lipid, amino acid, nucleotide, peptide, cofactors, carbohydrate and energy super pathways. A significant number of metabolites identified in the DBS samples were xenobiotics including those representing the biotransformation products of drugs. The overall metabolite profiles were analyzed for precision and accuracy of measure, variability in performance and dynamic range to establish benchmarks for evaluation. An additional cohort with a longitudinal sampling as part of the protocol provided the reproducibility of the analytic method for inter-day variability of metabolite performance over time. Although metabolomic profiles varied between individuals from a population perspective, there was minimal variation observed within individuals when samples were profiled longitudinally over several weeks. Thus, the protocols for DBS collection and the corresponding capture of a large set of metabolites with reproducible performance provides an opportunity for its implementation in oncological clinical trials as part of a de-centralized clinical trial solution.

#6608

High-sensitivity detection of specific ultra low-frequency somatic mutations for minimal residual disease monitoring

Tong Liu, Michael Bocek, Patrick Cherry, Shawn Gorda, Jean Challacombe, Derek Murphy, Esteban Toro. *Twist Bioscience, South San*

Francisco, CA

Minimal/Molecular residual disease (MRD) refers to the small number of tumor cells which may remain within a patient after therapeutic intervention. The detection of these remnants and monitoring of their abundance is a promising prognostic marker to identify individuals at risk of recurrence or in need of adjuvant therapy. Due to the low abundance of ctDNA present in samples obtained during remission, MRD assays need to be highly sensitive. In addition, each individual will have a different set of somatic variants, requiring personalized solutions for detection. Therefore, personalized NGS assays with high sensitivity and specificity are needed for MRD diagnostics.

To address this need and empower accurate assessments of MRD, Twist Bioscience has developed the MRD Rapid 500 Panels. This product enables customers to design, manufacture and ship fully personalized MRD panels (up to 500 targets) in as little as six days.

To demonstrate the detection sensitivity of Twist Rapid 500 MRD panels, we designed five custom MRD panels which specifically target somatic variants found in Breast, Lung, CRC, Melanoma and Renal Cell Carcinoma. Each of these MRD panels were designed to include 197 targets, with 3-5 variants per tissue origin and a selection of passenger mutations. To create the sample set, we blended synthetic variant sequences with fragmented cell line gDNA (NA12878) to form a contrived specimen which approximates the profile cell-free and circulating tumor DNA. Five frequency levels were created with average VAFs of 0% (WT), 0.01%, 0.05%, 0.1% and 2%. Libraries were prepared with UMI adapters and target enrichment was performed using the MRD panels.

With a sequencing depth of 80,000x, variant calling results revealed that an average of 20 SNV targets can be detected with confidence in the 0.01% VAF samples for each MRD panel, clearly distinguishable from the WT control samples. In addition to demonstrating the accuracy of variant calling, we showcase the utility of targeting a large number of variants for the detection of an MRD signature at very low levels (e.g. 0.01% VAF).

In summary, the performance of the Twist MRD Rapid 500 Panels showed high detection sensitivity of ultra low-frequency somatic mutations while maintaining high specificity for the purposes of MRD monitoring.

For Research Use Only. Not for use in diagnostic procedures.

#6609

Detection of rare mutations, copy number variation, and DNA methylation in the same template DNA molecules

Yuxuan Wang, Christopher Douville, Joshua Cohen, Chetan Bettegowda, Nick Papadopoulos, Ken Kinzler, Bert Vogelstein. *Johns Hopkins, Baltimore, MD*

The analysis of cell-free DNA (cfDNA) from plasma offers great promise for the earlier detection of cancer. At present, changes in DNA sequence, methylation, or copy number are the most sensitive ways to detect the presence of cancer. To increase the sensitivity of such assays, it would be useful to be able evaluate the same template molecules for all these changes. Here we report an approach, called MethylSaferSeqS, that achieves this goal, and can be applied to any standard library preparation method suitable for massively parallel sequencing. The innovative step was to copy both strands of each DNA-barcoded molecule with a primer that allows the subsequent separation of the original strands (retaining their 5-methylcytosine residues) from the copied strands (in which the 5-methylcytosine residues are replaced with unmodified cytosine residues). The original and copied strands are queried for epigenetic and genetic alterations, respectively. We applied this approach to plasma from 265 individuals, including 198 with cancers of the pancreas, ovary, lung or colon, and found the expected patterns of mutations, copy number alterations, and methylation. Furthermore, we could determine which original template DNA molecules were methylated and/or mutated. MethylSaferSeqS should be useful for addressing a variety of questions relating genetics and epigenetics in the future.

#6610

Increasing blood volumes to detect minimal residual disease in neoadjuvant-treated early breast cancer patients

Alfonso Alba-Bernal[1], Ana Godoy-Ortiz[1], María Emilia Domínguez-Recio[1], Begoña Jimenez-Rodriguez[1], María Elena Quirós-Ortega[1], Esperanza López-López[1], Guillermo Carbajosa-Antona[2], Jesús Peralta-Linero[3], Luis Vicioso[2], Estefanía Bellagarza-García[3], Guadalupe Dolores Garrido-Ruiz[4], Cynthia Robles-Podadera[1], Alicia Garrido-Aranda[1], María

Dunia Roldán-Díaz[1], Jesús Velasco-Suelto[1], Rocío Lavado-Valenzuela[1], Martina Álvarez[2], Nuria Ribelles[1], Javier Pascual[1], Emilio Alba[2], Iñaki Comino-Méndez[1]. *[1]Biomedical Research Institute of Málaga, Málaga, Spain,[2]University Of Málaga, Málaga, Spain,[3]Unidad de Gestión Clínica Intercentros de Oncología Médica, Hospitales Universitarios Regional y Virgen de la Victoria, Málaga, Spain,[4]Radiology Department, Hospital Clínico Universitario Virgen de la Victoria de Málaga, Málaga, Spain*

Breast cancer (BC) is the most frequent neoplasia affecting women worldwide normally detected at early stages. In this regard, early diagnosis drastically decreases mortality, however, around 20% of these patients will later relapse. This is mainly caused by undetectable molecular residual disease (MRD) not eliminated by standard primary treatments. Therefore, it is crucial to detect the after-treatment MRD to stratify the patients by their risk of relapse. Liquid biopsies have emerged as non-invasive method to obtain information about tumors and improve clinical cancer management. Regarding this, much has been hypothesized about utilizing high blood volumes to overcome the necessity of complex and resource-intensive next generation sequencing (NGS) methodologies to detect highly diluted blood tumor components in localized cancers. Herein, we employed a combined analysis of circulating tumor DNA (ctDNA) and circulating tumor cells (CTCs) together with high blood volumes and single-assay droplet digital PCR (ddPCR) to detect MRD with ultra-high sensitivity. We prospectively assayed 124 samples extracted at baseline, post-neoadjuvant therapy (NAT), post-surgery and a follow-up on a six-monthly basis. A median of 76.40 mL of blood to detect CTCs and 40 mL of plasma to detect ctDNA per patient from 19 BC women were used in this study. ddPCR assays were performed with a median of 14 partitions per determination to detect ctDNA and 12 partitions for CTCs. Overall, ctDNA, CTCs and ctDNA and/or CTCs were detected in 84.21%, 66.66% and 89.47% respectively in the pre-treatment blood samples. MRD (ctDNA and/or CTCs) was detected in 73.68% of the after NAT blood samples. On the other hand, it was detected in 46.66% and 70.00% of the post-surgery and follow-up samples respectively. Post-NAT MRD was detected in 57.14% (4/7) and 83.33% (10/12) of patients with and without pathological complete response pCR respectively. To note, the discordant patients achieving pCR in tissue with detectable MRD in blood were high-risk BC. Importantly, in one of the two patients without pCR and

no MRD detected, not enough sample were available to complete the analysis. The other discordant patient presented a localized disease with residual cancer burden value of 1 and no lymph nodes affected. In 1 out of 19 (5.26%) patient clinically relapsed with a positive MRD detection 6 months earlier. Applying this methodology, we observed a sensitivity of 0.004% in ctDNA detection and 0.224 CTCs per mL of blood. Overall, this novel methodology greatly improves sensitivity for ctDNA and CTCs detection in treatment-naïve early BC. In addition, MRD was successfully detected in post-treatment samples antedating clinical relapse by 6 months in one patient. This prospective study is potentially demonstrating that using high blood volumes and a single-assay ddPCR is a cost-effective strategy to monitor localized BC and predict relapses.

#6611

Harnessing the power of multiomics from a single sample to explore tumor heterogeneity and advancing immuno-oncology research

Bhagyashree S. Birla, Andrea O'Hara, Elizabeth Louie, Ben Niu, Haythem Latif, Vanessa Tumilasci, Yang Han, Yongjun Fan, David Corney, Pranay Vishwanath, Wei Wang, Alfredo Staffa, Ilaria DeVito, Laure Turner, Chris Mozdzierz, Peter Nowacki, Ginger Zhou. *Azenta, Life Sciences, South Plainfield, NJ*

The omics era has greatly expanded the repertoire of approaches available for researchers and clinicians to unravel the complexity behind cancer onset in humans: Next Generation Sequencing (NGS) approaches can characterize genomes, epigenomes, transcriptomes and proteomes of patient samples. Advanced DNA barcoding and automated microfluidics can take this to the next level, enabling multiomic characterization of single cells. Peripheral blood mononuclear cells (PBMCs) offer a window into the immune system that, when combined with these omics tools, can provide an insight into immune cells mediating anti-tumor responses in cancer patients. Here we detail a workflow using a single blood draw to rapidly produce a diverse set of multiomics results including genomics, epigenomics, transcriptomics and proteomics. This starts with automated sample handling and processing of the primary blood draw to ensure high viability and yield of PBMCs, along with simultaneous plasma separation and collection. These samples are then aliquoted and simultaneously processed for

automated and semi-automated whole exome sequencing, single-cell RNA sequencing, methylation sequencing and Olink proteomics assay. Germline and somatic mutations can be detected using whole exome or whole genome sequencing with deep coverage, whereas methylation, ATAC or ChIP sequencing can be used for epigenetic characterization of the same sample. While bulk expression offers a high-level transcriptomics profile, single-cell transcriptomics facilitates detection of gene expression changes in each individual cell type, allowing for analysis of rare cell types including circulating tumor cells. Olink proteomic assays can be utilized for both biomarker discovery and validation, with highly targeted or broad-spectrum panels. With this robust workflow and advanced robotics for sample handling and processing to minimize potential batch effects, all these datatypes can be produced within days of primary sample collection using minimal sample amounts. High throughput integrative omics workflows, as described here, are useful in gaining a multidimensional view of cancer and advance immunotherapies by characterizing immune cell modulation in tumor progression, and can be expanded for use in tumor/normal analysis, evaluation of metastases and exploration of tumor microenvironment.

#6612

Data-driven hallmarks of cancer as a new paradigm for precision medicine: multi-omics and functional profiling in acute myeloid leukemia

Tom Erkers[1], Nona Struyf[1], Tojo James[1], Francesco Marabita[1], Mattias Vesterlund[1], Nghia Vu[1], Cornelia Arnroth[1], Albin Österroos[2], Anna Bohlin[1], Sofia Bengtzén[1], Matthias Stahl[1], Rozbeh Jafari[1], Lukas Orre[1], Yudi Pawitan[1], Brinton Seashore-Ludlow[1], Janne Lehtiö[1], Sören Lehmann[2], Päivi Östling[1], Olli Kallioniemi[1]. *[1]Karolinska Institutet, Stockholm, Sweden,[2]Uppsala University, Uppsala, Sweden*

The cancer hallmark concept defines biological properties that play a key role in cancer development and progression. The hallmarks reflect generic properties across all cancer types, and are not directly quantifiable nor applicable in cancer diagnostics. Here, we applied a data-driven approach to identify quantifiable hallmarks to be used as a basis for precision cancer medicine (PCM) in Acute Myeloid Leukemia (AML).

We applied deep exome, transcriptome, DNA methylation and proteome profiling as well as ex-vivo functional testing of 525 drugs to 118 AML patient samples. Unsupervised multi-omic dimensionality reduction defined 11 independent axes of biological variability that we interpreted to reflect data-driven hallmarks (DDHM) of AML. Each DDHM integrates and ranks different data types and features, pinpointing those molecular features that were most informative for each hallmark. We calculated values for the 11 DDHM for each patient, constructing a DDHM-based precision medicine approach for AML diagnosis and therapy assignment.

Most DDHMs were driven by other data types than genomics. For several DDHMs, different cytogenetic and mutational drivers converge on the same hallmarks and specific drug vulnerabilities. We also see how DDHM predictors of poor prognosis and high-risk AML are distinct from those that dictate specific drug response vulnerabilities.

DDHM 2 reflected the cell differentiation path leading towards resistance to BH3 mimetics, ACK-inhibitors, and anthracyclines, and sensitivity to MEK inhibitors and TLR8 agonists. DDHM 2 derived a strong impact from protein expression of GATA2, MLLT11, DNMT3B and from RNA expression of WT1 and SOX4 as well as from multiple markers of different monocytic subtypes. DDHM 5 depicted cell cycle regulation and the Megakaryocytic-erythrocyte progenitor cell state that was enriched in AML patients with antecedent hematological disease. Interestingly, DDHM5 was linked to the sensitivity to purine analogs and vinca alkaloids. Moreover, DDHMs 1 and 8 captured clinical risk groups, prognosis, and responsiveness to hypomethylating agents. These DDHMs also revealed the phenotypic and functional biology that distinguished patients with high versus low FLT3-ITD mutant allele frequency.

Validation of the DDHMs is realized through profiling and analysis of prospective AML samples, AML cell lines and previously published datasets.

In summary, we present a data-driven approach for defining hallmarks in AML. The application of the DDHMs in AML provides a new paradigm for PCM and an opportunity for combinatorial therapeutic targeting. Each patient is characterized by a combination of independent and potentially druggable hallmarks, as opposed to traditional stratification in PCM, where each patient is assigned to one specific subgroup defined by genetic or other biomarkers.

#6613

Label-free multimodal multiphoton microscopy for predicting DNA damage response in patient derived non-small cell lung cancer organoids

Terrence T. Roh[1], Aneesh Alex[1], Janet E. Sorrells[2], Prasanna Chandramouleeswaran[1], Marina Marjanovic[2], Steve R. Hood[3], BanuPriya Sridharan[1], Stephen A. Boppart[2]. *[1]GSK, Collegeville, PA,[2]Bioengineering, University of Illinois Urbana-Champaign, Champaign, IL,[3]GSK, Stevenage, United Kingdom*

Background: DNA damage response (DDR) is a fundamental mechanism for evaluating efficacy of cancer therapeutics, many of which target DNA or associated processes (e.g., etoposide: inhibits DNA synthesis, cisplatin: crosslinks DNA). Current techniques to evaluate DDR rely on immunostaining for gamma H2AX foci (γH2AX), which is an indicator of DNA double-strand break formation. While γH2AX immunostaining can provide a snapshot of DDR in fixed cellular and tissue samples, this method is technically cumbersome as: 1) temporal monitoring of DDR requires timepoint replicates; 2) extensive assay development efforts for 3D samples such as organoids, and 3) protocols for γH2AX immunostaining and its evaluation are time-consuming. The goal of this project is to reduce overall burden on assay duration and development in NSCLC organoids by leveraging label-free multiphoton imaging.
Method: To predict DDR in 3D organoid samples, label-free multimodal multiphoton techniques such as simultaneous label-free autofluorescence multiharmonic (SLAM) imaging can provide intracellular information based on endogenous contrast mechanisms. SLAM makes use of a single laser to excite autofluorescence in multiple cellular components including FAD and NAD(P)H, enabling the calculation of the optical redox ratio, which estimates the equilibrium of electron donating versus accepting species in cells. Moreover, label-free, multiphoton systems enable imaging of live samples without the need to add labels or generate sacrificial samples and have improved image acquisition in 3D space over conventional confocal microscopy. Using SLAM, we propose to predict DDR in non-small cell lung cancer (NSCLC) organoids. NSCLC organoids

recapitulate histological and genetic features of their derived patient tissue, retaining tumor variability.
Results: Predictive modeling via gradient boost regressor between handcrafted SLAM image features and γH2AX immunostained images on weakly-paired images confirmed strong correlation between SLAM image features and γH2AX speckles/nuclei. Across multiple patient derived NSCLC organoid lines and multiple DNA targeting chemotherapeutics, the optical redox ratio was demonstrated to robustly predict DDR.
Conclusion: Label-free imaging via SLAM can be used to predict DDR in live 3D NSCLC organoids with minimal sample handling and without the need to add labelled reporters, enabling quicker and less technically involved DDR assaying.

#6614

Spatial transcriptomic driven mechanistic model to investigate and predict pathogenesis of oligodendroglioma

Sandhya Prabhakaran[1], Heyrim Cho[2], Maximilian Strobl[3], Russell Rockne[4], Alexander R. A. Anderson[3]. *[1]Integrated Mathematical Oncology, H. Lee Moffitt Cancer Center and Research Institute, Tampa, FL,[2]University of California Riverside, California, CA,[3]H. Lee Moffitt Cancer Center and Research Institute, Tampa, FL,[4]City of Hope, California, CA*

Rationale: Oligodendrogliomas represent the second most common glioma in adults after glioblastoma. Recent studies conjecture that oligodendrocyte progenitor cells (OPCs) are precursors for glioma. The etiology of OPC derived oligodendrogliomas, the corresponding genetic program and genetic aberrations, and the underlying mechanisms leading to the pathogenesis of oligodendroglioma is yet to be explored. We hypothesize that genetic mechanisms mediating oligodendrogenesis (the process of OPCs maturing to oligodendrocytes (OL)) are temporally and spatially coordinated. In this study, we spearhead a comprehensive computational framework that utilizes a) Machine learning (ML) to interpret spatial transcriptomic (ST) images of a normal whole mouse brain dataset obtained from Vizgen's MERFISH Mouse Brain Receptor Map and b) mathematical modeling to perturb the cellular mechanisms in the normal brain to understand the abnormalities leading to the pathogenesis of oligodendroglioma.

Methods: Using ML for clustering and trajectory inference, we create a comprehensive spatial catalog of cell types. The cell types are validated using canonical genes from the scRNAseq mouse brain data from CZI Biohub's Tabula Muris Consortium. From the cell types, we extract potential OL pseudotime differentiation (from immature to mature OLs) trajectories. These trajectories are used to develop a phenotype structured partial differentiation equation (PDE) model of oligodendrogenesis. This can be used to simulate both spatial and phenotypic interactions, differentiation status, and the pathogenesis of oligodendroglioma by mathematically perturbing the process of cellular proliferation and differentiation using genes known to cause oligodendroglioma: PDGFRA, OLIG1, MAS1.
Results: We mathematically perturb cell differentiation lineages in normal oligodendrogenesis to simulate, and predict the effects of perturbation and how this leads to abnormal (cancer aiding) cell states. Our PDE simulations reinforce that OPC proliferation and OL differentiation occur more in the white matter in the normal mouse brain, and further postulate that OPC and OL differentiation occur more in gray matter in malignant mouse brains.
Conclusions: Our study is one of the earliest attempts to integrate qualitative and scalable ML techniques with quantitative and interpretable mathematical modeling at the cellular, omics, and organ level using ST imaging and sequencing data. We develop and calibrate PDE mathematical models for robustly simulating, predicting, and studying the effects of perturbation from sparse, noisy single cell spatial measurements to forecast abnormal behavior in OLs based on spatial and (pseudo)temporal changes. In future work, we will apply our framework to jointly perturb differentiation trajectories of multiple cell types to understand their cumulative effects in tumor progression.

#6615

Novel digital pathology tools for exploring role of myeloid cells in modulating next generation immunotherapies

Richard Van Krieken[1], Lisa Adams[1], Beiru Chen[2], Emmanuel Pacia[1], Naveen Dakappagari[2], Brian Bourke-Martin[3], Jennifer Bordeaux[1]. *[1]Digital Pathology, Navigate BioPharma, Carlsbad, CA,[2]Navigate BioPharma, Carlsbad, CA,[3]Data Science, Navigate BioPharma, Carlsbad, CA*

Purpose: Deeper understanding of the immune landscape in tumor microenvironments is critical for creation of next generation immunotherapies (I-O). While significant investments were made to understand the role of T-cells, the contribution of myeloid cells in limiting the effectiveness of I-O therapies is not well understood primarily due to limitations posed by conventional immunohistochemistry (IHC) analysis that typically provides information on a single target. We developed a clinical grade multiplex fluorescence IHC (mFIHC) assay to simultaneously evaluate different subsets of myeloid cells (e.g., M1, M2 and MDSC) as well as PD-L1 receptors associated with these subsets as the latter is known to have profound positive impact on patients treated with PD-1 blockers *(Liu et al., CCR, 2019)*. In addition, we developed an algorithm to identify the microenvironment using imaging datasets from AQUA® (Automated Quantitative Analysis) and HALO to understand the spatial relationship between tumor cells and myeloid cell subsets as well as immune checkpoint (IC) expression. mFIHC combined with hypothesis driven spatial profiling algorithms (e.g., AQUA Technology) were found to provide superior predictors of I-O therapies in a systematic meta-analysis of over 8000 patients treated with PD1/L1 pathway blockers (*Lu et al., JAMA Oncol 2019)*. Furthermore, spatial profiling by AQUA has proven to robustly identify powerful biomarker predictors (PD1/PDL1) in melanoma (*Johnson et al., CCR, 2018*). Implementation of mFIHC coupled with robust image analysis may provide great insight into immune surveillance, mechanisms of resistance and patient stratification.
Study Design: We designed a novel mFIHC assay (CD68, CD163, HLA-DR, IDO-1, PD-L1, PanMel-CK) and evaluated various myeloid and tumor cell types on tissue sections (e.g., non-small cell lung cancer, gastric carcinoma, breast carcinoma, and renal cell carcinoma). Following the initial evaluation, the mFIHC assay was validated for clinical trial application using automated staining (Leica Bond RX) and imaging (PhenoImager HT). We conducted image analysis using AQUA and HALO technologies.
Results: Analysis of samples by AQUA and HALO revealed unique myeloid microenvironments in the examined tissue types. Microenvironment data from AQUA and HALO were assessed by analyzing enrichment of macrophage phenotypes in areas dense with

checkpoint markers. Our analysis revealed unique myeloid cell clusters in the assessed tumor microenvironments.
Conclusion: We anticipate this hypothesis driven clinical trial grade mFIHC assay design combined with novel analyses algorithms will aid in the better understanding of the immunomodulatory effects of myeloid cells in several cancer types and the development of next generation I-O therapies.

#6616
Development of a high-throughput image processing pipeline for multiplex immunofluorescence whole slide images at scale
Waleed Tahir, Emma Krause, Jin Li, Howard Mak, Mohammad Mirzadeh, Kevin Rose, Judy Shen, Vignesh Valaboju, Guillaume Chhor, Joseph Lee, Jun Zhang, Jacqueline Brosnan-Cashman, Michael G. Drage, Justin Lee, Carlee Hemphill, Saumya Pant, Robert Egger. *PathAI, Inc., Boston, MA*

Background. Fluorescent imaging technologies now allow for multiplex immunofluorescence (mIF) for up to 100 targets on a single slide. However, the ability to quantitatively analyze the resulting data, especially on whole-slide images (WSI), is limited by scalability and reproducibility. Currently available platforms for segmenting cancer cells and nuclei involve segmentation algorithms that are hand-tuned on individual fields of view, making these methods subjective and difficult to replicate. To this end, we sought to develop an end-to-end workflow for WSI mIF data in cancer, from raw images to cell-level features, using state-of-the-art deep learning models for tissue, cell, and nuclei segmentation.
Methods. mIF was performed using the Akoya 6-plex Lung IO panel (CD8, FoxP3, CD68, PD-1, PD-L1, and pan-cytokeratin) with a DAPI counterstain on clinical NSCLC specimens obtained from commercial sources (N=41). Slides were scanned using the Akoya PhenoImager HT. To remove bleed-through between different fluorophores, mIF WSIs were linearly unmixed based on a reference single-stain matrix, generated by selecting pure stain regions in mIF images. Convolutional neural network models previously trained on hematoxylin and eosin (H&E) images for 1) artifact detection, 2) tissue region identification, and 3) nucleus detection and segmentation were then deployed on mIF images that were converted to RGB images using a synthetic H&E transformation. Cell segmentation models were developed and implemented for each marker assessed. For

each demixed channel representing a single antibody signal, expert annotations were used to train deep learning models for cell detection and segmentation. Finally, segmentation results from separate channels were aggregated based on spatial colocalization to identify cells and cell phenotypes.
Results. We developed a pipeline for mIF image analysis at scale. After unmixing, conversion of an mIF image to a synthetic H&E image allowed for 1) removal of artifact regions, 2) detection of cancer and stroma using tissue segmentation, and 3) nuclei segmentation. Nuclear segmentation using this approach improved upon a widely used commercial segmentation platform when compared to manual expert annotations (Dice scores = 0.85 and 0.52, respectively). Finally, using state-of-the-art instance segmentation models allows a novel approach to cell phenotyping compared to currently available platforms, allowing positive identification of cells lacking a nuclear signal in the sectioned plane (e.g. large cytokeratin-positive cells).
Conclusions. We developed a robust workflow to accurately segment cells and nuclei from mIF WSIs at scale. Improving the scalability and reproducibility of complex mIF image analysis may help improve the adoption of this approach for biomarker development and incorporation into clinical trial workflows in oncology.

#6617
Gleason score 6 often coexists with Gleason score 7 adenocarcinoma within 3D z-levels of a prostate biopsy
Xavier Farré[1], Vanessa Roybal[2], Can Koyuncu[3], Sarah Chow[2], Hongyi Huang[2], Alan Aberdeen[4], Andrew Janowczyk[3], Anant Madabhushi[3], Lawrence D. True[2], Jonathan T. C. Liu[2]. *[1]Public Health Agency of Catalonia, Lleida, Spain,[2]University of Washington, Seattle, WA,[3]Emory University, Atlanta, GA,[4]Ground Truth Labs, Oxford, United Kingdom*

Background: Primary prostate cancer is diagnosed by biopsy. However, biopsies sample only a limited amount of the prostate gland. Many studies report that GS6 cancer at biopsy is often upgraded in the radical prostatectomy. Undergrading results from sampling limitations of the biopsy - both of the prostate and of tissue within the biopsy. Since pathological diagnosis is based on 4 micron thick sections of 1 mm thick biopsies, only 0.4% of the biopsy is analyzed. We hypothesize that the

evaluation of a biopsy in 3D results in variable Gleason scores or even no cancer in certain z-levels. Here, we examined 3D pathology image datasets of Gleason score 7 (GS7) biopsies using a web-based image viewing platform to determine if they underdiagnose and/or undergrade cancer when examined by conventional 2D slide-based histology.
Methods: We used a custom-developed 3D open-top light-sheet (OTLS) microscope, not yet available for clinical use, to study all z-levels of a prostate biopsy. The patient cohort used in this study came from the Canary TMA study. 105 prostate biopsies were non-destructively digitized in 3D with at least 500 z-levels per biopsy (at a spacing of ~1 micron per level). Samples were stained with fluorescence analogs of H&E. The image datasets were false colored to mímic conventional H&E histology. A pathologist reviewed the images using a web-based image platform and gave overall Gleason scores (OGS) based examing all z-levels within a biopsy. Six z-levels (1, 100, 200, 300, 400 and 500) were selected for 2D Gleason scoring.
Results: 63 images had a OGS of 3+4 and 42 a OGS 4+3. We found presence of GS6 (Gleason grade 3 glands only) in some z-levels: 32 cases (50.8%) with OGS 3+4 and 4 cases (9.5%) with OGS 4+3. When we only studied the 6 selected z-levels, we found z-levels with no cancer in 4 cases (6.3%) of OGS 3+4 and 2 cases (4.8%) in OGS 4+3. In addition, we found z-levels with limited number of glands. We reported these levels as Atypical Small Acinar Proliferation (ASAP) in 2 cases (3.2%) with OGS 3+4 and 3 cases (7.1%) with OGS 4+3. Examining all z-levels enabled unambiguous grading of biopies containing z-levels with ASAP and tangential sections.
Conclusion: We describe the frequent coexistence of GS6 z-levels within a OGS7 3D prostate biopsy. This finding supports prior observations that finding of GS6 prostate cancer in a 2D-based sections of prostate cancer does not rule out a higher Gleason grade areas in other parts of the prostate nor in other levels of each biopsy. We also show that availability of 3D levels eases the interpretation of ASAP glands and tangential sections.

#6618

Longitudinal, multimodal profiling of metastatic ER+ breast cancer on CDK4/6 inhibitor therapy

Allison L. Creason[1], Julian Egger[1], Cameron Watson[1], Shamilene Sivagnanam[1], Jia-Ren Lin[2], Koei Chin[1], Peter K. Sorger[2], Lisa M.

Coussens[1], Zahi I. Mitri[1], Joe W. Gray[1], Gordon B. Mills[1], Jeremy Goecks[1].
[1]Knight Cancer Institute, Oregon Health & Science University, Portland, OR,[2]Harvard Ludwig Cancer Center and Laboratory of Systems Pharmacology,Harvard Medical School, Boston, MA

Introduction: Use of CDK4/6 inhibitors (CDK4/6i) in combination with endocrine therapy has transformed treatment and greatly improved outcome for ER+ breast cancer (BC) patients. However, many BC patients eventually progress on therapy. To understand how ER+ metastatic BC (mBC) tumors become refractory to CDK4/6i, we have created a multimodal, longitudinal tumor atlas to investigate tumor mechanisms of therapeutic resistance, as part of the NCI Cancer Moonshot Human Tumor Atlas Network. By deeply profiling individual patients, we identified a wide variety of putative tumor intrinsic and extrinsic mechanisms of resistance to CDK4/6i.
Methods: mBC ER+ patients (n=5) enrolled in the Knight Cancer Institute SMMART Trials program underwent biopsies before treatment and on progression with combination CDK4/6i and endocrine therapy. Biopsies were profiled using: clinical imaging, bulk genomics (WES), transcriptomics (RNAseq), and proteomics (RPPA), multiplex tissue imaging (mIHC, cycIF), single-cell genomics (scDNAseq) and epigenomics (sci-ATAC-seq).
Results: Upon progression, patients displayed dysregulated tumor-intrinsic activity via upregulation of gene expression in cell cyclins and kinases as well as genomic copy loss of regulatory factors, such as Rb. On-progression biopsies exhibited increased expression and pathway activity of IL-Jak-Stat and Interferon signaling and changes in tumor microenvironment immune cell composition, including elevated immune cytotoxicity; however, a subset of CD8 T cells expressed LAG3, Tbet, and TIM3, indicating signs of immune activation trending toward exhaustion. Patients also exhibited increased M2 Macrophage and T regulatory cell infiltration, suggesting compensatory feedback to dampen immune activity. Analysis of spatial organization identified cellular neighborhoods recurring across all samples with changes after therapy observed primarily in neighborhoods associated with epithelial-stromal density and immune reactivity/suppression.
Conclusion: Findings from this mBC ER+ cohort highlight heterogenous molecular and cellular changes that occur after treatment with a CDK4/6i.

We observed multiple tumor intrinsic and extrinsic factors, including modulation of proliferation in neoplastic cells and tumor microenvironment composition, that are suggested to play a role in acquired resistance. We hypothesize a set of patients that initially respond to CDK4/6i therapy may initially display immune activation, but the sustained activation and long-term exposure to therapy may lead to chronic inflammation and immunosuppression. These observations suggest combining CDK4/6i therapy with immunotherapy may provide benefit. We also observed recurrent spatial cellular patterns that recapitulate known biological structures in these tissues; future work will explore association of spatial organization with therapeutic response.

#6619

Virtual staining enabled combined morphological and spatial transcriptomic analysis of individual malignant B cells and local tumor microenvironments

Michael E. Kallen[1], Alyssa Rosenbloom[2], Zihang Fang[3], Raymond Kozikowski[3], Yair Rivenson[3], Kevin de Haan[3], Serge Alexanian[4], Mark Conner[2], Daniel Newhouse[2], Felicia New[2], Yan Liang[2], Kyla Teplitz[2], Joachim Schmid[2], Jaemyeong Jung[2]. *[1]University of Maryland School of Medicine, Baltimore, MD,[2]Nanostring Technologies, Seattle, WA,[3]PictorLabs, Los Angeles, CA,[4]PictorLab, Los Angeles, CA*

B-cell lymphomas, commonly classified by histological presentation and B-cell lineage, are in fact heterogeneous diseases with respect to gene expression and tumor microenvironment. Certain lymphomas, such as Hodgkin and T-cell rich B-cell lymphoma, may contain fewer than 1% malignant cells in a largely inflammatory background. These rare malignant cells have unique interactions with local tumor microenvironments (TME), in some cases driving distinct gene expression patterns for individual B-cells. This presents a challenging fundamental biology landscape, which can create uncertainty in directing patient care or developing new therapies. The lack of tools allowing subtyping of malignant B-cells while simultaneously preserving the context of local TMEs and providing deep spatial transcriptomic sequencing further complicates analysis.
Here we have developed an integrated, single-slide workflow of virtual H&E staining using the inherent tissue autofluorescence (PictorLabs, Los

Angeles, CA) of formalin-fixed, paraffin embedded lymphoma tissue sections on the GeoMx® Digital Spatial Profiler (Nanostring, Seattle, WA) combined with spatial expression analysis of 1,800 genes using the Cancer Transcriptome Atlas (CTA) panel. The H&E virtual staining allows for the assessment of B-cell lymphoma subtypes, identification and phenotyping of malignant B-cells and the immediately proximal (within 30μm) TME regions by a certified pathologist. These regions of interest (ROI) are spatially profiled for transcriptional expression determined by NGS sequencing of the RNA target specific DNA oligo tags.
We benchmarked our system by analyzing four lymphoma cases: Nodular sclerosis classical Hodgkin, Nodular lymphocyte-predominant Hodgkin, T-cell/histiocyte rich large B-cell, and Diffuse large B-cell lymphomas. Using virtual H&E staining on the GeoMx Digital Spatial Profiler platform, a pathologist correctly identified the diagnosis and subtype based on the morphology. Regions of inflammatory B- and T-cells could be distinguished from lymphoma cells on virtual staining, allowing subset segregation for digital transcriptional expression profiling with the GeoMx CTA panel. Additionally, background TME more distant to B-cell lymphoma as well as regions of high T-cell infiltration were selected for profiling. Analysis of the ROIs revealed distinct transcriptional profiles of malignant B-cells (including cell-of-origin signature), the signaling contributions of local TMEs (versus non-adjacent regions) and confirmed that the expression patterns are further influenced by the presence of T-cell infiltration.

#6620

Identification of crosstalk signaling between brain-tumor niche and reactive human cytomegalovirus in brain metastases

Xin Wang, Puri Akshjot, Kun Han, Amna Irfan, Liliana Guzman, Wei Qian, Roberto Rosato, Hong Zhao, Jenny Chang, Stephen Wong. *Houston Methodist Hospital, Houston, TX*

Purpose: Human cytomegalovirus (HCMV) is a common neurotropic herpes virus although its DNA was confirmed highly prevalent in various peripheral cancers. HCMV is also a major cause of neuropathology in immune-compromised patients. Since HCMV reactivation frequently causes encephalopathy during chemotherapy or radiation therapy in brain

tumor patients, understanding the brain niche-HCMV crosstalk signaling may pinpoint effective strategies in managing brain metastases.
Methods: We collected nine pairs of primary breast and brain metastatic tumor samples from our institution and analyzed their RNA-Seq data. Pairwise differential gene expression analysis and gene set enrichment analysis (GSEA) were conducted. TCGA-BRCA (n=1,222) dataset was used for clinical and immune-infiltration correlation analysis. GSE12276 (n=204) dataset was used for brain-metastasis free survival correlation. Immunohistochemistry staining of HCMV was conducted on sixteen primary breast and brain metastatic tumor sections and an 86-core tissue microarray (TMA) of human brain metastasis tissue. CCCExplorer software was used to explore molecular crosstalk signaling between the secretome proteins from HCMV-infected cells and brain metastatic niche cells.
Results: *Reactome Human cytomegalovirus (HCMV) early and late events* was the top enriched pathway for the 371 brain metastasis up-regulated genes while *Reactome IL4 and IL5 signaling* was the top enriched pathway for the 2,153 primary breast tumor up-regulated genes. Among the 371 brain metastasis up-regulated genes, 287 genes are also up-regulated in primary breast cancer *vs.* normal breast in the TCGA 1222 cohort ($P<0.05$). High expression of 19 out of the 287 genes are significantly associated with poor brain metastasis-free survival in the GSE12276 cohort (Logrank $P<0.05$). We further identified that elevated expression of 12 out of the 19 genes are consistently associated with Th2 cell activation and NK cell deactivation in the TCGA 1,222 cohort, for which immunosuppressive Th2 cells are defined by secretion of IL4 and IL5 signature cytokines. Immunoreactive HCMV reactivation proteins were examined in the paired breast tumor and brain metastatic specimens, and most of the TMA tumors. Preventive treatment of an anti-HCMV drug, ganciclovir, by suppressing viral DNA replication inhibited tumor colonization in the mouse brains of the two HCMV-positive PDX models. Several HCMV cell-entry co-receptors are highly expressed in brain metastatic niche. Furthermore, from the secretome of HCMV-infected cells, we identified 89 paired receptors that potentially regulate niche cell behaviors.
Conclusions: Our systemic analysis revealed a causal relationship between HCMV reactivation and brain metastatic outgrowth. Targeting the key brain-tumor niche-HCMV crosstalk signaling may benefit the management of brain metastases.

#6621

Simulating the distortion of clonal fractions in ctDNA due to spatially heterogenous selection

Thomas W. Rachman, Oana Carja, Russell Schwartz. *Computational Biology, Carnegie Mellon University, Pittsburgh, PA*

Time-series circulating tumor DNA (ctDNA) sequencing has the potential to reveal emerging variants in the tissue in real time, and there is now substantial evidence that it can detect tumor growth and treatment-resistant mutations long before growth is visible. However, the reliability of ctDNA for profiling the primary tumor may be compromised by spatial heterogeneity in the tumor genetics, for example due to selective effects of differential drug penetration, immune infiltration, and oxygenation. We explore the influence of spatial factors on tumor genetics through a lattice-based branching process model of solid tumor evolution and ctDNA shedding with the goal of understanding where spatially variable selection pressure could lead to a significant difference between the clonal fractions in the blood and the tissue. The lattice model divides space into regions with different growth rates which result in different rates of driver mutation accumulation. The effects of regional differences in selection cause different apoptosis rates to correlate with the location of expanding driver clones. Using these rates to simulate ctDNA shedding, our model found that clones fit enough to invade a hostile region are temporarily amplified in the blood compared to their tissue frequency by as much as 300% for a limited window of time before the population expands further and the clonal fraction in the blood returns to close agreement with tissue. The results suggest evolutionary contexts in which liquid biopsy might provide highly biased estimates of tumor state, but also shows how this effect might be exploited to provide more sensitive detection of clonal expansion with implications for blood-based detection of recurrence and metastasis.

#6622

Developing spatial molecular correlates of response to immunotherapy in kidney cancer

Kathryn Beckermann[1], Scott Haake[1], Alex Nesta[2], Michael Caponegro[2], N R Nirmala[2], Anupama Reddy[2]. *[1]Vanderbilt University Medical Center,*

Nashville, TN,[2]Vindhya Data Science, Morrisville, NC

Immunotherapy has emerged as a promising new therapy for kidney cancer with durable clinical responses in a subset of the patients. However, discovery of biomarkers that predict patient response to immunotherapy has thus far been unsuccessful. Diverse sets of biomarkers have been proposed, (e.g., PD-L1 immunohistochemistry, tumor mutation burden, gene expression signatures), but have failed to validate in clinical studies. There is an urgent need to identify predictive biomarkers for selecting kidney cancer patients most likely to respond to immunotherapy.Spatial biology technologies provide molecular data at single cell resolution along with spatial coordinates in patient's tumor slides. We hypothesized that the presence of immune cell types and their spatial 2-D patterns in a histology image could potentially predict response to immunotherapy. For this project we are using Tissue Microarray (TMAs). We are using two cohorts of data: (Dataset-1) 70 clear cell renal cell carcinoma (CCRCC) patients treated with checkpoint inhibitors, and (Dataset-2) 180 patients, early stage papillary RCC (PRCC) cohort. Dataset-1 was assayed using CosMx (Nanostring technologies) for a RNA panel of 980 immune-related genes. Dataset-2 was assayed with PhenoCycler (Akoya Biosciences) for a 31 marker protein panel with immune-related genes. We have developed methodology and novel algorithms to process both the datasets and to identify spatial phenotypes. Our pipelines include QC, normalization, dimensionality reduction and clustering. For annotation of cell types, we used as reference single cell datasets from RCC to identify tumor-type specific cell types. These cell types were mapped back to their spatial coordinates and visualized. We verified the annotations based on visual checks of their cellular morphology and organization. Next, we identified cellular neighborhoods around each cell and identified spatial clusters. We also performed a network-based analysis to identify additional spatial patterns. We performed correlation analysis with clinical phenotypes and identified spatial clusters of immune cell subtypes located in proximity of cancer cells to be associated with response to therapy.

#6623
Spatial organization of tumor-infiltrating lymphocytes (TILs) is prognostic for survival in triple negative breast cancer (TNBC)

Sahil H. Patel[1], Germán Corredor[2], Rachel Yoder[3], Cristian Barrera[2], Miluska Castillo[4], Luis Bernabe[4], Joshua Staley[3], Shane Stecklein[3], Satish E. Viswanath[1], Carlos A. Castaneda[4], Priyanka Sharma[5], Anant Madabhushi[2]. *[1]Case Western Reserve University, Cleveland, OH,[2]Emory University, Atlanta, GA,[3]The University of Kansas Cancer Center, Westwood, KS,[4]Instituto Nacional de Enfermedades Neoplásicas, Lima, Peru,[5]University of Kansas Medical Center, Westwood, KS*

Introduction: TILs quantification is a predictor of response to neoadjuvant chemotherapy and prognostic for long term outcomes in TNBC. TILs are typically quantified using standard hematoxylin/eosin (H&E) slides manually by trained pathologists; limitations include interobserver variability and need for cutoffs that aid in clinical decision making. Computational approaches utilizing H&E slides have potential to improve reproducibility and refine predictive/prognostic utility by evaluation of additional metrics beyond quantification.
Methods: H&E whole slide images digitized at 20x magnification from patients with stage I-III TNBC (ER/PR ≤10%, HER2 negative) treated with neo/adjuvant chemotherapy at two institutions were utilized. All cell nuclei were automatically segmented using a deep learning model (Hover-Net) and classified as TIL or non-TIL based on morphological features. Features related to TIL density, spatial distribution, and morphological features were extracted. The top 3 features determined by least absolute shrinkage and selection operator were used to train a Cox proportional hazards regression model (SpaTILs) that assigned a recurrence free survival (RFS) event risk score to each patient. First quartile risk score in the training cohort was used as a cutoff for SpaTILs high vs low risk. Model performance for prediction of RFS and overall survival (OS) was evaluated in the testing cohort by Kaplan Meier method, with SpaTILs high vs low risk groups compared by log rank test and Cox regression analysis.
Results: In the training cohort (n=26) and testing cohort (n=62), median age was 51 and 53 years, 77% and 36% were node positive, and 81% and 45% received neoadjuvant chemotherapy, respectively. Median follow up in testing and training cohorts was 2.3 and 6.8 y, respectively. In the testing cohort, 31% and 69% of patients were categorized as SpaTILs high and low risk, respectively. Baseline characteristics were not significantly different

between SpaTILs high and low risk patients. In the SpaTILs high and low risk groups, 5y RFS was 53% and 90%, respectively (HR 4.85 [95% CI: 1.62-14.52], p=0.002) and 5y OS was 78% and 98%, respectively (HR 13.91 [95% CI 1.67-115.66], p=0.001). SpaTIL high risk remained a significant predictor for RFS and OS after adjusting for T stage and nodal status: HR 7.25 (95% CI 2.14-24.39), p=0.001 for RFS; HR 4.80 (95% CI 1.31-131.06), p=0.028 for OS.
Conclusion: The computational model based on TILs density, spatial, and morphological features (SpaTILs) was independently prognostic for RFS and OS in early stage TNBC. This model is being validated in larger TNBC cohorts and warrants prospective evaluation in clinical trials.

#6624

3D assessment of the lung cancer microenvironment using multi-resolution open-top light-sheet microscopy

Alexandra Alvarsson[1], Carl Storey[1], Brandy Olin Pope[1], Caleb Stoltzfus[1], Robert Vierkant[2], Jessica Tufariello[3], Aaron Bungum[4], Julia Naso[5], Cheuk Ki Chan[5], Eric Edell[6], Christopher Hartley[5], Janani Reisenauer[7], Nicholas Reder[1]. *[1]Alpenglow Biosciences, Inc., Seattle, WA,[2]Mayo Clinic, Rochester, MN,[3]BioPharma Diagnostics, Mayo Clinic, Rochester, MN,[4]Pulmonary and Critical Care Medicine and Thoracic Surgery, Mayo Clinic, Rochester, MN,[5]Laboratory Medicine and Pathology, Mayo Clinic, Rochester, MN,[6]Pulmonary Medicine, Mayo Clinic, Rochester, MN,[7]Pulmonary Medicine and Thoracic Surgery, Mayo Clinic, Rochester, MN*

Background: Non-small cell lung cancer (NSCLC) tissue is a valuable resource for diagnosis, treatment planning, and drug development. Current 2D histopathological techniques introduce under-sampling error (i.e., a single 5 um section represents 0.5% of a 1 mm thick biopsy), interobserver variability, and fail to capture the biology contained within the entire tissue sample. We have developed a suite of technologies to stain, chemically clarify, image, visualize, and analyze entire intact NSCLC tissue samples.
Methods: Human NSCLC tissue, stored frozen in OCT, was fixed in 4% paraformaldehyde, stained with nuclear (TOPRO-3) and general protein (Eosin) fluorescent dyes, and optically cleared using a modified iDISCO protocol with ethyl cinnamate as the refractive index matching solution.

Whole, intact tissue samples, roughly 1-5mm3 in volume, were imaged at 2 microns/pixel resolution with an open-top light-sheet microscope (3Di, Alpenglow Biosciences). Smaller regions of interest (ROIs) with key pathologic features were reimaged at higher resolution, 0.17 microns/pixel, to reveal subnuclear features and for cell typing. Visualization was performed using Aivia software.
Results: NSCLC tissue samples were successfully imaged in 3D. Low resolution images (2 microns/pixel) were obtained within 4-31 minutes, depending on the tissue volume. The 3D distribution of cancer cells, immune cells, vessels, and fibrosis varied substantially throughout the volume of the tissue. Recognizable histologic features, including nests of tumor cells surrounded by vasculature and immune cells, were readily visualized. Squamous and adenocarcinoma with its subtypes (solid, acinar, lepidic, and micropapillary) morphologies were recognizable in 2D optical sections of the 3D datasets. Imaging quality degraded in tissue deeper than 1 mm due to light scattering.
Conclusion: We assessed intact NSCLC tissue samples measuring up to 5 mm3 using our custom light-sheet microscope and tissue clearing techniques. This novel method enables us to visualize key features of NSCLC such as the tumor interfaces, tertiary lymphoid structures, vessels and fibrosis in the entire tissue sample, preventing under sampling error, and potentially enabling new biologic insights. Next steps include segmentation and quantification of key tissue structures such as tumor volume, immune cell distribution, and fibrosis / immune cell exclusion. This proof-of-concept study provides motivation for further investigation into the significance of 3D tissue features in NSCLC tissue samples.

#6625

Mathematical modeling of single-cell data reveals the key role of stochasticity - not fitness - in determining the clonal origins of relapse in childhood leukemia

Virginia Turati[1], Javier Herrero[2], Mark Robertson-Tessi[1], Tariq Enver[2], Andriy Marusyk[1], Alexander RA Anderson[1]. *[1]H. Lee Moffitt Cancer Center, Tampa, FL,[2]University College London, London, United Kingdom*

Acute lymphoblastic leukemia (cALL) is the most common pediatric cancer, and since up to 20% of children relapse after initially responding to

chemotherapy treatment, the largest cause of cancer-related childhood deaths in the western world. With the idea that dissecting the evolutionary population dynamics leading to relapse would help explain treatment failure from a mechanistic standpoint, several studies have performed comparisons of genetic heterogeneity at diagnosis and relapse. These showed that as many as 70% of relapses are dominated by a single diagnostic subclone or one of its evolutionary progeny; leading to the prevailing view that treatment selection in cALL primarily operates at the genotype level. However, a crucial caveat of these studies is their reliance, due primarily to technical and economic constraints, on very limited data timepoints. While the dynamics linking said timepoints are often interpreted based on simple intuition. To overcome this sparse data challenge and reconstruct the entire spatial and temporal evolutionary trajectories of individual cALL cells from diagnosis to relapse, we have integrated experimental data with an *in silico* model. Single-cell WGS and RNAseq data were obtained from primary and xenografted leukemic cells before and after chemotherapy. These were then used to parameterize an agent-based mathematical model allowing tracking of the genotype and evolving phenotype of individual cells over time. When short treatment courses akin to those we delivered *in vivo* were used, the *in silico* model closely recapitulated the experimental results. Since cALL treatment lasts several years, it cannot be entirely modelled in vivo. Due to the rarity of post-treatment residual cells and the lack of universal cell surface markers to isolate them, direct analysis of clinical samples is also challenging. However, based on the initial treatment data, our calibrated model provided a unique opportunity to simulate longer remission-relapse dynamics of several leukemias. Mechanistic analysis of the collected data showed that, strikingly, in most cases, clonal dominance at relapse results from stochastic sweeps rather than deterministic differences in clonal fitness. Indeed, independent treatment of the same leukemia with an identical drug regimen more frequently ended with a considerably different clonal landscape (either polyclonal disease or a different dominant clone) than with the same outcome initially observed. Rather than genotype differences, the size of residual disease and a founder effect linked to the stochastic exit, post-treatment, of individual cells from quiescence were the key determinants of the relapse genetic landscape. Altogether, our data highlight the misinterpretation risk associated with snapshot analysis and might inform promising alternative treatment schedules.

CLINICAL RESEARCH EXCLUDING TRIALS

Immune Checkpoints

#6629

Genomic and immunophenotypic landscape of acquired resistance to PD-(L)1 blockade in non-small cell lung cancer

Biagio Ricciuti[1], Giuseppe Lamberti[1], Sreekar Puchala[2], Navin Mahadevan[3], Joao Alessi[1], Xinan Wang[4], Yvonne Li[2], Federica Pecci[1], Alessandro Di Federico[1], Malini Gandhi[1], Adriana Barrichello[1], Victor Vaz[1], Andy Pangilinan[1], Danielle Haradon[1], Elinton Lee[1], Hersh Gupta[2], Mizuki Nishino[5], Andrew Cherniack[2], Scott Rodig[6], Lynette Sholl[1], Renato Umeton[7], MArk M. Awad[1]. *[1]Lowe Center for Thoracic Oncology, Dana-Farber Cancer Institute, Boston, MA,[2]Informatics and Analytics, Dana-Farber Cancer Institute, Boston, MA,[3]Dana-Farber Cancer Institute, Boston, MA,[4]Biostatistics, Harvard Medical School, Boston, MA,[5]Lowe Center for Thoracic Oncology, Brigham and Women's Hospital, Department of Radiology, MA,[6]Lowe Center for Thoracic Oncology, Brigham and Women's Hospital, Department of Pathology, MA,[7]Department of Informatics and Analytics, Dana-Farber Cancer Institute, Boston, MA*

Background: Despite immune checkpoint inhibition (ICI) has extended survival in patients (pts) with non-small cell lung cancer (NSCLC), acquired resistance to ICI develops after an initial clinical benefit. However, the mechanisms underlying the development of acquired resistance to ICI in NSCLC are largely unknown.
Methods: Tumor genomic profiling, immune cell subsets assessment from standard haematoxylin/eosin (H&E) stained slides using machine learning, multiplexed immunofluorescence (CD8, PD1, PD-L1, Foxp3, CK7), and HLA-I immunohistochemistry (IHC) were performed on matched pre and post ICI tumor biopsies from pts with NSCLC treated with ICI at the Dana-Farber Cancer Institute who developed acquired resistance to ICI.
Results: Among 1823 pts with advanced NSCLC who received ICI, 80 developed acquired resistance to treatment and had matched pre- and post-

ICI tissue samples for correlative analysis. Putative resistance mutations were identified in 27.3% of cases. The most common acquired loss-of-function mutations included *STK11* (9.1%), *B2M* (6.5%), *NF1/2* (5.2%), *SMARCA4* (5.2%), *APC* (3.9%), *KEAP1* (2.6%), and *JAK1* (2.6%). In addition, acquired activating mutations were found in *PI3KCA* (3.9%) and *SOS1* (1.3%). In examining copy number variations (CNVs), we identified acquired CNVs in 49.3% (38/77) of ICI-resistant samples, including heterozygous loss of *B2M* (23.4%), *STK11* (16.8%), *SMARCA4* (16.9%), *KEAP1* (15.6%), *PTEN* (10.4%), *CDKN2A*/B (9.1%) and *PD-L1*/*PD-L2* genes (9.1%), among others. Importantly, we also noted acquired homozygous deletions in *CDKN2A*/B (9.1%), *PD-L1*/*PD-L2* (1.3%) and *JAK2* (1.3%), and amplification in *MDM2* (5.2%), *KRAS* (3.9%) and *MYC* (2.6%), at the time of resistance to ICI. Among 16 cases with pre- and post-ICI H&E stained slides, digital pathology analysis showed a significant decrease in the density of intratumoral lymphocytes in ICI-resistant tumor samples compared to pre-ICI samples (88 vs 36 cells/mm^2, P=0.03). Consistently, among 6 pts with pre- and post-ICI multiplexed immunofluorescence we observed a significant decrease in CD8+ PD1+ T cells in ICI-resistant vs pre-ICI tumor samples (24 vs 10 cells/mm^2, P=0.01). Among pts with tissue available for HLA-I IHC (N=9), we found a significant decrease in HLA-I expression by H-score at the time of acquired resistance (300 vs 260, P=0.03). In control cohorts of pts with pre- and post-chemotherapy (CT) (N=32) or targeted therapies (TT) (N=89) tumor genomic profiling no acquired mutations in *STK11*, *KEAP1, B2M, JAK1, APC, SOS1* were detected. Similarly, intervening chemotherapy and targeted therapies were not associated with changes in lymphocytes density and HLA-I expression.

Conclusion: Mechanisms of acquired resistance to ICI are heterogenous, including both genomic and immunophenotypic factors. New therapeutic strategies are required to delay and overcome ICI resistance in pts with NSCLC.

#6630

Flow cytometry immunophenotyping using commercial antibodies to maximize detection of PD-1 in immuno-oncology (I-O) clinical studies with anti-PD-1 check point inhibitors

Venkat Mohanram, Ming Yang, Angelina Bisconte, Deborah Phippard.
Precision for Medicine, Frederick, MD

Precision for Medicine's translational biomarker expertise supports global clinical trials with flow cytometry. A biomarker strategy which includes flow cytometry to generate pharmacokinetic/pharmacodynamic (PK/PD) models for rational design of dose escalation and expansion of clinical studies, may need to consider concomitant drugs for checkpoint inhibition like Pembrolizumab.

Precision has optimized the use of commercial anti-PD-1 and anti-IgG4 reagents to detect both free PD-1 and/or Pembro-bound PD-1 when patients are on study with a new molecular entity as either a monotherapy or in combination with concomitant checkpoint inhibitors. For I-O studies conventional efficacy endpoints combined with flow biomarker driven surrogate endpoints enhance therapeutic decisions for determining mechanism of action and biological response when incorporated in early-phase clinical studies. Precision developed and qualified a flow immunophenotyping assay to quantify PD-1 on CD4+ and CD8+ T cells using a commercial PD-1 clone (PD1.3.1.3) and an anti-IgG4. This enabled detection of both free and drug bound PD-1 receptor. We compared detection of PD-1 in PHA stimulated healthy donors treated with saturating Pembrolizumab or no drug treatment. There was not a significant difference observed in PD-1 quantification in the presence or absence of Pembrolizumab, which demonstrated that our approach was able to accurately measure total PD-1 whether free or bound. As Pembrolizumab was titrated from the saturating concentration there was a dose-dependent decrease in detection of PD-1. We have used this assay to detect PD-1 with several new I-O therapies that combined standard anti-PD-1 checkpoint inhibitors, and in these clinical studies for advanced and rare solid tumor indications, we observed an average of 20-40% increase in PD-1 compared to no drug treatment.

Immuno-oncology clinical trials which incorporate checkpoint inhibitors like either PD-1 or PD-L1, the availability of commercial reagents are key considerations to detect these receptors when designing a sensitive, selective, and accurate biomarker assay.

#6631

Association between poliovirus receptor (PVR) expression in tumor and exclusion of immune cells expressing T cell immunoreceptor with Ig and ITIM domain (TIGIT) from tumor area

Sara A. Moore, Julie Cheung, Aram B. Cholanians, June Clements, Jessica L. Baumann, Tsu-Shuen Tsao. *Roche, Tucson, AZ*

Context: TIGIT has grown to be an increasingly important target for immunotherapy of cancer. However, it is unclear if there is an association between abundance of TIGIT expressing immune cells in tumor microenvironment and effectiveness of TIGIT-based intervention. This study utilizes an exploratory novel duplex immunohistochemical (IHC) assay to assess if the distribution patterns and/or the abundance of TIGIT-positive immune cells are related to the expression levels of TIGIT's receptor PVR in tumor.
Methods: Individual formalin-fixed, paraffin-embedded surgical resections and tissue microarray cores of 75 cervical, 84 esophageal, 79 non-small cell lung , and 81 small cell lung carcinoma specimens were stained using a duplex chromogenic IHC assay that detects PVR and TIGIT sequentially on a single slide. The slides were examined for (1) overall intensity and percentage of tumor staining positive for PVR, (2) percentage of tumor area occupied by TIGIT-expressing immune cells, and (3) distribution pattern of TIGIT-positive cells. For each specimen, overall PVR intensity was multiplied by percentage of tumor positive for PVR to generate the PVR Expression Score.
Results: PVR and TIGIT staining at any intensity was widely observed in all four tumor types ranging from 91% to 100% of specimens positive for PVR and 77% to 100% of specimens positive for TIGIT. Little to no differences in the average percentages of PVR tumor positivity or TIGIT tumor area positivity were found among the four tumor types. However, individual tumor specimens differed widely in these two parameters. Among all 319 tumor specimens evaluated, the percentages of tumor expressing PVR at any intensity ranged from 0 to 100% with approximately 1/3 of the specimens having less than 50% and 3% showing no PVR expression. Percentages of tumor area occupied by TIGIT-positive cells ranged from 0% to 30% with approximately 40% of the specimens having less than 1%. Distribution patterns of TIGIT-expressing cells in each specimen was classified as peritumoral, intratumoral, or mixed. Specimens

classified as peritumoral exhibited higher PVR Expression Scores than those classified as intratumoral. Specimens classified as having a mixed TIGIT-positive cell distribution pattern had an average PVR Expression Score that was intermediate between specimens having intratumoral and peritumoral TIGIT distribution patterns. Interestingly, no correlation was found between tumor PVR Expression Scores and abundance of TIGIT expressing cells in tumor area.
Conclusion: The correlation between high tumor PVR expression levels and peritumoral distribution patterns of TIGIT-positive cells suggests PVR/TIGIT signaling pathway activation status could be important in infiltration of T cells into tumor parenchyma.

#6632

Simultaneous comparison of response to two different anti-PD1 drugs in the same patient using a human tumor histo-culture platform

Satish Sankaran[1], Biswajit Das[1], Kowshik Jaganathan[1], Gowri Shankar K[1], Jayaprakash C[2], Ganesh MS[3], Amritha Prabha[3], Vijay Pillai[4], Syamkumar V[1], Chandan Bhowal[1], Rajashekar M[1], Oliyarasi M[1], Ritu Malhotra[1], Govindraj K[1], Nandini Pal Basak[1]. *[1]Farcast Biosciences, Bangalore, India,[2]DBR & SK Superspeciality Hospital, Tirupati, India,[3]Vydehi Multi Specialty Hospital, Bangalore, India,[4]Mazumdar Shaw Medical Centre, Bangalore, India*

Based on preclinical and clinical study data, anti-programmed cell death protein 1 (PD-1) drugs Pembrolizumab (P), and Nivolumab (N) have been considered equivalent in terms of response efficacy. Both the antibodies have IgG4 backbone but vary considerably in terms of the PD-1 epitopes they bind to.. Given that there is almost no overlap between the PD-1 binding sites there is a definite possibility of nuanced drug-dependent differences in patient response to treatment. These differences would not be possible to discern unless the same patient with the same tumor microenvironment were evaluated with both drugs simultaneously. We attempted to address this question using the near native Farcast^{TM} TruTumor histoculture platform. Fresh surgically resected Head and Neck squamous Cell Carcinoma (HNSCC) samples (n=8) along with matched blood were collected from consented patients. The tumor sample was

processed to generate explants that were distributed into arms. These arms were treated in culture with P (32.9 µg/ml) or N (132 µg/ml) for 72 hours. The response was characterized using histopathology, cytokine release and flow cytometry. T-cell re-invigoration was assessed by evaluating Interferon gamma release while a decrease in tumor content and/or increase in cleaved Caspase expression was correlated with tumor cytotoxicity Pre-treatment cytokine levels across control and both treatment arms were equivalent (z-score <1.5) across all samples. Additionally, when treated with the same drugs in duplicate arms similar tumor cytotoxic response was observed in the replicate arms (n=1). These data established arm equivalence. Post treatment with N or P, 6 out of 8 samples exhibited a T-cells reinvigoration phenotype. Of the remaining 2 samples, one exhibited tumor cytotoxicity with both treatments while the other showed tumor cytotoxicity only on N treatment. We evaluated the 6 samples that exhibited T-cell re-invigoration response further to understand the subtle differences in response to either N or P. While the response trends were similar for both drugs, the rate of response, as evaluated by significant increase in cleaved caspase-3 or decrease in tumor content, seem to be different in 3 samples. These 3 samples responded better with P compared to N.In this study, we broadly observed equivalent response to both the drugs with some patient samples responding slightly better to one over the other. Further studies are required to tease out the molecular reasons for these nuanced differences in response to these two anti-PD1 treatments. The FarcastTM TruTumor platform provides the unique opportunity to make personalized choice of the drug treatment that might provide best response in a patient.

#6633

T regulatory cell subsets in colorectal cancer: friends or foes

Eyad Elkord. *University of Nizwa, Nizwa, Oman*

T cells in the tumor microenvironment (TME) have diverse roles in anti-tumor immunity. Different T cell subsets may have opposing roles in tumor progression, especially in inflammatory cancers such as colorectal cancer (CRC). In different series of studies, we performed extensive characterization and critical analyses of T regulatory cell (Treg)-related markers and key inhibitory immune checkpoints (ICs) in $CD4^+$ and $CD8^+$ T cell subsets in the TME and periphery of CRC patients. We found a

significant increase in levels of $CD4^+FoxP3^+Helios^+$ T cells, which represent potentially highly immunosuppressive Tregs, in the TME. Additionally, tumor-infiltrating $CD4^+$ T cells upregulated PD-1, CTLA-4, TIM-3 and LAG-3 immune checkpoints. CTLA-4, TIM-3, and LAG-3 were mainly co-expressed on $FoxP3^+Helios^+$ Tregs in the TME. Additionally, we found that FoxP3 expression and ICs including PD-1, CTLA-4, TIM-3, and LAG-3 were significantly upregulated in tumor-infiltrating $CD8^+$ T cells. We then investigated associations between different tumor-infiltrating $CD4^+$ and $CD8^+$ T cell subpopulations and disease-free survival (DFS). Interestingly, a high frequency of circulating $CD4^+FoxP3^+$ Tregs was associated with poorer DFS, while higher frequency of these cells in the TME was associated with better DFS. Additionally, high frequencies of circulating $CD4^+FoxP3^+Helios^+$ Tregs and tumor-infiltrating $CD4^+FoxP3^-Helios^-$ T cells were associated with poorer DFS. Moreover, a high frequency of $CD4^+FoxP3^+Helios^-PD\text{-}1^+$ Tregs in circulation was associated with worse DFS. In contrast, high frequencies of $CD4^+TIM\text{-}3^+$ T cells, $FoxP3^+Helios^+TIM\text{-}3^+$ Tregs, and $FoxP3^-Helios^+TIM\text{-}3^+$ $CD4^+$ T cells in circulation were associated with longer DFS. Additionally, we found that high levels of certain circulating $CD8^+$ T cell subsets ($TIM\text{-}3^+$, $FoxP3^-Helios^-TIM\text{-}3^+$ and $FoxP3^-Helios^+TIM\text{-}3^+$ cells) were associated with longer DFS. In the TME, elevated levels of $CD25^+$ and $TIM\text{-}3^+$ $CD8^+$ T cells, and $FoxP3^+Helios^-TIM\text{-}3^+$ $CD8^+$ Tregs were associated with better DFS. These data show that circulating and tumor-infiltrating immune checkpoint-expressing $CD4^+$ and $CD8^+$ Treg/T cell subsets play different roles in disease prognoses, and certain subsets could serve as independent predictive biomarkers in CRC patients.

#6634

Digital and spacial characterization of PD-L1 expression and IVD assay performance in the immune landscape of head and neck squamous cell carcinoma: A multimodal approach

Clara Troccoli, Lauren Matelski, Adam Beharry, Vanessa Ly, Morgan Wambaugh, Melanie Amen, Will Paces, Geoffrey Metcalf, Roberto Gianani, Tom Turi. *Flagship Biosciences, Broomfield, CO*

The anti-PD-L1 antibody (22C3) is used as a companion diagnostic for successful checkpoint inhibitor therapy in head and neck squamous cell carcinoma. The positive predictive value of this assay, however, is less than ideal as a high PD-L1 score does not necessarily associate with a good response, and a good response may be seen with a low or negative PD-L1 score. In principle, this could be due to lack of accuracy and/or precision of the assay, as well as biological factors, such as variable expression across tumor cells and interacting immune cells. In this study, we describe a digital image analysis algorithm to address assay-related problems and improve both accuracy and precision, as well as improve identification of PD-L1 expression in differing cell populations of the tumor microenvironment. In addition, we propose a panel of assays that in aggregate might reveal inherent heterogeneity among cases with similar PD-L1 score and thus provide vital context underlying the efficacy of checkpoint inhibitors in the clinic. Here we show that applying novel machine-learning based digital image analysis to multiplex assays together with digital scoring of PD-L1 provides an accurate and precise assessment of the real-world tumor milieu that we hypothesize will help establish the immunophenotypes that inform therapeutic efficacy of checkpoint inhibitors. We have additionally interrogated whether expression of PD-L1 in these groups are consistent with known molecular patterns assayed using novel methodologies, such as high-plex digital spatial transcriptomics through the nanoString GeoMx Digital Spatial Profiler (DSP) platform and assessed the ability of the different digital platforms to provide concordant data relating to real-world expression patterns of PD-L1 and associated biomarkers. Thus, our results point to the importance of robust methodologies, used in combination, to evaluate complex tumor immune landscapes and the advantages of digital analyses to provide accurate and precise clinical contexts for better patient outcomes.

#6635

Lipid and glycolipid antigen presentation faults as a mechanism of resistance to immune checkpoint therapy in poorly immunogenic melanomas

Carlos Rogerio Figueiredo. *Faculty of Medicine / Medical Immune Oncology Research Group, University of Turku, Turku, Finland*

Introduction: Cold tumors are characterized by lacking infiltration of antitumor T cells. These tumors are universally refractory to immune checkpoint therapies (ICT). While poor T cell infiltration has been partly ascribed to low tumor mutational burden (TMB), TMB doesn't necessarily exclude immunogenic responses nor ensure a response to ICT. Mechanisms of T cell exclusion in tumors with sufficient TMB may be caused by molecular failure of the antigen processing and presentation (APP), which impacts T cell generation. It was previously described that loss of heterozygosity (LOH) of an essential component of the MHC class I molecule, the beta-2-microglobulin (B2M), is associated with low antigen presentation, tumor T cell infiltration, and ICT resistance in melanoma. Here we provide further insight into APP and ICT response in melanoma.
Methods: Transcriptomic analysis and visualization of genomic data from the GDC-TCGA skin cutaneous melanoma (SKCM) study were performed using the Xena platform. Four anti-PD1 metastatic melanoma cohorts were normalized with transcripts per million units. STRING protein-protein interaction analysis was performed in the human database with 11 nodes and 39 edges. Nanostring transcriptomic data from metastatic uveal melanoma (mUM) was revisited from our previous publications for *Spearman's* correlational and group analysis of APP signatures amongst ICT responders and non-responders.
Results: In an expanded analysis of 4 normalized anti-PD1 treated metastatic melanoma cohorts (n=272), we confirmed that transcriptomic levels of *B2M* are significantly reduced in non-responders. Moreover, STRING protein-protein interaction analysis of B2M revealed CD1D as a potential molecular partner of B2M. We, therefore, observed that *CD1D* transcriptomic expression is not only reduced in anti-PD1 poor responders but is a survival prognosticator in primary tumors from the GDC-TCGA study. Interestingly, *CD1D* expression is also significantly reduced in poorly immunogenic mUM tumors, a cancer type regarded as universally refractory to ICT.
Conclusions: These findings suggest that APP faults in ICT-resistant tumors are not restricted to faults in peptide presentation to T lymphocytes (via B2M) but may also impact the presentation of tumor-associated lipid and glycolipid antigens via CD1d, which can impact antitumor responses of natural killer T cells (NKT). Adjuvant therapies that restore MHC-I and CD1d-mediated antigen presentation may unleash the response to ICT via

NKT. Understanding CD1d expression faults locally and systemically may provide valuable prognostication information likely to impact how cancer is treated by optimally selecting patients for ICT and validating novel therapeutic targets for immunotherapy development.

#6636

Metformin suppresses tumor immune evasion through downregulation of PD-L1 expression in cancer cells and PD-1 expression in NK cells and T cells

Su Hwan Park, Jong-Ho Lee. *Dong-A University, Busan, Korea, Republic of*

Up-regulation of programmed cell death 1 (PD-1) receptor on T cells and its ligand (PD-L1) on cancer cells is reported in various tumor microenvironment, and the interaction between PD-L1 and PD-1 inhibits the cytotoxic activity of NK cells and T cells, allowing cancer cells to evade immune destruction. Extensive studies suggested that metformin, the most widely used first-line drug for treatment of type 2 diabetes, had a potential efficacy of enhancing anti-tumor immune response. However, the detail mechanisms underlying the efficacy are unknown. Here, we showed that metformin decreases AKT-mediated β-catenin S552 phosphorylation and β-catenin transactivation in an AMPK activation-dependent manner, resulting in reduced *CD274* transcription in cancer cells. In the cocultures of cancer cells with NK cells or T cells, cancer cells induced PD-1 protein stability and expression in the NK cells and T cells, these PD-1 upregulation was also observed in infiltrated NK cells and T cells *in vivo* mouse tumors. Metformin reduced the half-life and expression of PD-1 in an AMPK activation-dependent manner *in vitro* and *in vivo*. These inhibitory roles of metformin in PD-L1 expression in cancer cells and in cancer cell-induced PD-1 expression in NK cells and T cells led to ameliorated the cancer cell-reduced cytotoxic activity of NK cells and T cells and inhibited tumor growth *in vivo* models. These findings suggest that metformin may act as both PD-L1 and PD-1 blockades within tumor microenvironment, providing a mechanistic insight for the efficacy of metformin to improve immunotherapy in human cancer.

#6637

Transcriptomic biomarkers of immunotherapy response in solid tumors

Balazs Gyorffy, Szonja Anna Kovacs, János Tibor Fekete. *Research Centre for Natural Sciences, Budapest, Hungary*

Background. Immune-checkpoint inhibitors can be administered in multiple solid tumor types. Currently available biomarkers, like the expression of PD-L1 or tumor mutational burden, miss a significant proportion of patients who could benefit from the therapy. Our goal was to set up a database consisting of both gene expression and clinical response data and to uncover the most significant biomarkers of response to anti-PD-1, anti-PD-L1, and anti-CTLA-4 immunotherapies.
Methods. The GEO repository was screened to identify datasets with simultaneously available transcriptomic and clinical response data across different solid tumor types. The screening focused on studies involving the administration of nivolumab (anti-PD-1), pembrolizumab (anti-PD-1), atezolizumab (anti-PD-L1), durvalumab (anti-PD-L1), and ipilimumab (anti-CTLA-4). Mann-Whitney U-test and receiver operating characteristic analysis were performed across all genes to identify features related to therapy response. False discovery rate was computed to correct for multiple hypothesis testing.
Results. The database that we established consists of 1,439 unique tumor samples from nineteen datasets with gastric-, lung-, esophageal-, head, neck-, and urothelial cancers, and malignant melanoma. The strongest upregulated candidates linked to resistance in anti-PD-1 treated tumors were PRXL2A (AUC=0.771), ODR4 (AUC=0.734), and RBM15B (AUC=0.734). The most robust hits in the anti-PD-L1 treated cohort were NOTCH3 (AUC=0.639), NECTIN1 (AUC=0.631) and ITGAV (AUC=0.63). In the anti-CTLA-4 treatment cohort C5orf24 (AUC=0.76) was the most promising candidate. We have also established a portal for additional analysis and ranking of further biomarker candidates by extending our previously established ROC plotter. The immunotherapy-treated transcriptomic database is accessible at the website www.rocplot.com/immune.
Discussion. An integrated database and an online platform were set up to validate potential biomarkers of immunotherapy response in a sizeable cohort of cancer samples from multiple tumor types. By using the direction

of expression change as a filter, we have identified the most promising biomarker candidates.

#6638

Pulsed electric fields combined with anti-PD1 prolongs survival and triggers an adaptive immune response in an IO-non-responsive orthotopic mouse model

Ebtesam Nafie[1], Mukta Wagh[1], Chiara Pastori[1], Mo Trikha[2], Robert Neal[1]. *[1]Immuno-oncology, Galvanize Therapeutics Inc, San Carlos, CA,[2]Immunology, Apple Tree Partners, San Fransisco, CA*

Background: Although anti-PD1 therapy is standard of care in multiple tumor types, unmet need remains for those non-responsive to immunotherapy. Pulsed Electric Field (PEF) treatment may alter the tumor micro-environment, converting an immune "cold" tumor into an immune "hot" tumor, triggering an adaptive immune response and abscopal effect. We evaluated PEF in combination with anti-PD1 in a highly aggressive orthotopic triple negative breast tumor mouse model.

Methods: Murine mammary 4T1 cells ($2x10^5$) non-responsive to anti-PD1 therapy were orthotopically implanted in mammary fat of 48 female Balb/C mice. Once tumors were established (5 mm diameter), mice were randomized into six groups: Sham+IgG controls, aPD-1-only, PEF (1X), PEF (2X), aPD-1 + PEF (1X), and aPD-1 + PEF (2X). Groups 4 and 6 received two PEF treatments, five days apart. Anti-PD1 and isotype matched control IgG was administered (200 ug, intraperitoneal) weekly, starting 3 days after PEF treatment. Tumor volumes were recorded 3x/week and standard survival analyses were conducted per IACUC protocol. In the cohort of tumors collected 30 days after PEF, flow cytometry (FC) evaluated T-cell immune infiltrates and associated markers. Blood was collected at different time points to evaluate systemic immunological response. Tumor-specific cytotoxic lymphocytes (CTL) were isolated from tumor-infiltrating and circulating lymphocytes by gp70 MHC tetramer formation assay.

Results: Single PEF reduced tumor growth compared to IgG and aPD-1-only groups by 65% and 62%, respectively. Double PEF treatment reduced tumor growth by 74% and prolonged survival. FC demonstrated circulating helper T-cells and CTL frequency was increased two weeks post-PEF compared to the control group. The tetramer detected substantial increases in antigen-specific T-cell populations in both single and double PEF treatment groups. PEF groups had significant tumor and spleen infiltration of CD8 and CD4 T-cells, including increased tetramer levels. Anti-PD1-only animals showed no meaningful reductions in tumor growth, prolonged survival, or significant changes in CD8, CD4 T cells or in the tetramer assay.

Conclusions: PEF treatments prior to initiation of anti-PD1 in orthotopic 4T1 mouse model triggers a tumor-specific adaptive immune response in an immune "cold" tumor model, irrespective of anti-PD-1 therapy. PEF increases circulating and tumor-infiltrating T-cells and antigen-specific T-cells, with these effects observed after a single or two treatments with PEF. Collectively, our results demonstrate that PEF treatment prior to initiation of anti-PD1 treatment can reduce tumor growth, prolong survival, and activate an adaptive immune response in an immune "cold" tumor. These findings suggest that PEF treatment merits further evaluation in IO-non-responsive cancer patients.

#6639

Preclinical characterization and clinical biomarker studies with RP3, a novel oncolytic immunotherapy expressing a fusogenic protein, a human anti-CTLA-4 antibody, hCD40L and h4-1BBL

Praveen K. Bommareddy[1], Kevin Harrington[2], Victoria Roulstone[2], Joan Kyula[2], Aaron Clack[1], Linta Kuncheria[1], Sylwia Jones[1], Robert Coffin[1]. *[1]Replimune, Inc., Woburn, MA,[2]The Institute of Cancer Research and The Royal Marsden NHS Foundation Trust, London, United Kingdom*

Introduction: RP3, a tumor-directed oncolytic immunotherapy (TDOI), is a selectively replication-competent HSV-1 that contains the codon-optimized sequence for the fusogenic GALV-GP-R- protein, an anti-CTLA-4 antibody-like molecule, CD40L, and 4-1BBL. The expression of GALV-GP-R- potentiates immunogenic tumor cell death through the induction of cell-to-cell fusion. CD40L enhances dendritic cell and macrophage activation and 4-1BBL promotes CD8+ T-cell activation and co-stimulation. The anti-CTLA-4 antibody-like molecule blocks the interaction of CTLA-4 with its ligands B7.1 and B7.2, further enhancing T cell activation. RP3 is currently being assessed in a Phase 1 clinical trial with or without nivolumab in patients with advanced solid tumors (NCT04735978).

Methods: CD1 nude mice with A375 melanoma xenograft tumors (Group 1) were treated with a single intratumoral injection of $1x10^7$ PFU/mL of RP3. Tumors and blood samples were collected 3 days later, and immunohistochemistry (IHC) was performed to detect CD40L, 4-1BBL and HSV-1. For anti-CTLA-4 detection, two doses of 10^7 PFU/mL of RP3 were injected intratumorally into C57BL/6 mice bearing 4434 murine

$BRAF^{V600E}$ mutant melanoma tumors (Group 2). Tumors and blood samples were collected at 3, 6, 9, 12 and 15-days post-dosing and anti-CTLA-4 ELISA was performed. For clinical biomarker studies, tumor biopsies were collected pre- and post-RP3 treatment. CD8 and PD-L1 were characterized by IHC, and gene expression analysis (GEA) was performed. TCR analysis was also performed using PBMCs.
Results: IHC analysis from Group 1 confirmed abundant and widespread expression of CD40-L and 4-1BBL, which were detected alongside with HSV-1 antigen. In the blood samples collected from Group 2, robust levels of anti-CTLA-4 antibody were detected, which stayed in detectable range up to 15 days after the 2nd RP3 injection. IHC analysis of patient tumor samples demonstrated a marked increase in CD8 T cells and PD-L1 expression. GEA of patient tumor biopsies demonstrated increased levels of genes associated with innate and adaptive immune activation and genes previously reported to be associated with responsiveness to anti-PD1 therapy. TCR sequencing of PBMCs and multiplex IHC analysis are ongoing and updated results will be presented.
Conclusion: Preclinical experiments from mice models confirmed the robust expression of CD40-L, 4-1BBL and anti-CTLA-4 in RP3-injected tumors. Biomarker studies from patients demonstrate increases in CD8-T cell infiltration and PD-L1 expression post RP3 +/- nivolumab treatment, including increases in the expression of genes associated with response to anti-PD-1 therapy. These data indicate the potential for broad utility of RP3 in a range of tumor types, including in tumors that are not sensitive to PD-1 blockade.

#6641
ATG-031, a first-in-class humanized anti-CD24 antibody, demonstrates potent *in vivo* efficacy and repolarizes tumor-associated macrophages in the TME
Peng Chen[1], Min Deng[1], Yun Liu[1], Jiamei Luo[1], Linjie Tian[2], Jay Mei[3], Bo Shan[3], Bing Hou[3]. *[1]Antengene Corporation Limited, Shanghai, China,[2]Antengene Biotech LLC, Doylestown, PA,[3]Antengene Corporation, Shaoxing, China*

Background: Tumor microenvironment (TME) is shaped by not only cancer cells but also a variety of resident and infiltrating cells, including stromal fibroblasts, endothelial cells and immune cells like tumor-associated macrophages (TAM) and lymphocytes (Roghayyeh et al., 2020). Most TAMs are considered as the M2 subtype with pro-tumor/anti-inflammation effects. CD24 is a small, highly glycosylated cell adhesion protein and was reported to be the dominant innate immune checkpoint in ovarian cancer and breast cancer, and acts as a novel "don't eat me" target . CD24 is over-expressed on tumor cells and can help them avoid being engulfed by macrophages through its interaction with Siglec-10 expressed by TAM. ATG-031 is a humanized anti-CD24 monoclonal antibody that binds to CD24 with high affinity and specificity and blocks the interaction of CD24 with Siglec-10 on macrophages, enhancing macrophage-mediated phagocytosis of tumor cells. In this study, we evaluated the *in vivo* efficacy of ATG-031 and explored its pharmacodynamic effects.
Methods: C57BL/6J mice were inoculated with wild-type (WT) MC38 cells on the left flank and MC38 cells that express human CD24 (MC38-hCD24) on the right flank. When the average tumor volume reached 120 to 140 mm^3 for MC38-hCD24, mice were treated with vehicle control (PBS) or ATG-031 at 3 mg/kg intravenously twice a week for four doses. A group of mice inoculated with only MC38 tumor cells was set as the control and treated with ATG-031 by the same way. Tumor volume was measured twice a week to evaluate the efficacy of ATG-031. Tumor samples were isolated at the endpoint of this efficacy study, and a multiplex IHC staining was performed to evaluate the change of tumor-infiltrating immune cells in response to ATG-031.
Results: ATG-031 treatment significantly inhibited the tumor growth of MC38-hCD24 on the right flank of mice with a tumor growth inhibition (TGI) of 60.52%. Interestingly, although the WT MC38 tumor on the left flank did not express the antigen, human CD24, ATG-031 still demonstrated efficacy in controlling the tumor growth with a TGI of 21.17%. Without the co-inoculation of MC38-hCD24, ATG-031 did not affect the WT MC38 tumor growth in the control group. Multiplex IHC staining revealed that the proportion of M1 macrophage increased in response to ATG-031 treatment, not only in MC38-hCD24 tumors but also in WT MC38 tumors on the left flank.
Conclusions: ATG-031, a first-in-class anti-CD24 antibody, demonstrated potent anti-tumor activity *in vivo*, re-polarizing M2-like TAM to anti-tumor M1 subtype in the TME and induced systemic anti-tumor immunity. A clinical study to investigate the safety and efficacy of ATG-031 in cancer patients is being developed.

#6642
Rapid tissue donation identifies LAG3 as a potential therapeutic target for ALK fusion positive lung cancer
Hilal Ozakinci, Gina Nazario, Karina Colossi Furlan, Dung-Tsa Chen, Trevor Rose, Matthew B. Schabath, Eric B. Haura, Bruna Pellini, Amer Beg, Theresa A. Boyle. *Moffitt Cancer Center, Tampa, FL*

Introduction: The rapid tissue donation (RTD) program provides post-therapy primary and metastatic tumor tissue samples at the time of death for the study of resistance mechanisms and the tumor microenvironment to inform therapeutic opportunities. NCCN guidelines (NCCN v5.2022) recommend against PD-1/PD-L1 inhibitor monotherapy in the second-line setting for *ALK* fusion+ non-small cell lung cancer (NSCLC) due to lack of efficacy, irrespective of tumoral PD-L1 expression. We observed high LAG3 protein expression by multiplex immunofluorescence (mIF) in postmortem *ALK* fusion-positive tumor tissue samples from 3 RTD donors who were treated with ALK inhibitors. Further studies are recommended to investigate the therapeutic potential of LAG3 inhibitors in this patient population.
Case Series: Of the 38 patients with lung cancer tissue collected by RTD, 3 patients had *ALK* fusion and were treated with ALK inhibitors. Despite the initial response, all 3 patients succumbed to the disease. Tissue samples were collected from primary and multiple metastatic sites after death. Immune checkpoint markers, including LAG3, were quantitated via multiplex immunofluorescence staining, and genomic analyses were performed.
Results: Analysis of two tissue microarrays comprised of 130 tumor cores from multiple tissue sites of the first 10 NSCLC RTD donors revealed that 66% of tumor cores had >1% LAG3 expression in CD3+ T cells. Among the three patients with *ALK* fusion-positive NSCLC, 83% (5 of 6 cores), 85% (6 of 7 cores), and 100% (18 of 18 cores) of the tissue cores had >1% LAG3 expression in T cells. The median LAG3 expression in T cells measured by mIF was 1.8% in 99 tumor cores from the *ALK* fusion-negative study cohort versus 7.3% in the 31 cores from the *ALK* fusion-positive subset (p=0.004). Postmortem genomic analyses revealed an *ALK* p.L1196M resistance mutation in the first patient and an *AGK-BRAF* fusion in the 2nd patient. No known ALK-TKI resistance mutations were detected in the 3rd patient.
Discussion: High-quality post-therapy tumor samples collected by the RTD program enable the investigation of genomic and potential immune-related resistance mechanisms. Such studies can inform potential targets for drug development and the study of new therapies to overcome treatment resistance. Our observation of high LAG3 expression in 3 RTD donors with *ALK* fusion-positive NSCLC suggests the need for further studies to explore the potential for LAG3 inhibitors in patients with NSCLC whose tumors develop resistance to ALK inhibitors.

#6643
Immune checkpoint reporter cell lines based on the protein profiling of ATCC cell lines for cancer immunotherapy drug screening
Hyeyoun Chang, Kevin Tyo, John Foulke, Luping Chen, Zhizhan Gu, Fang Tian. *ATCC, Gaithersburg, MD*

The success of immune checkpoint inhibitors in the treatment of various types of cancers and their continued growth in the market have driven burgeoning interests in developing more drugs in this category. However, the intrinsic complexity of the immunological models and the variable drug responses among different cancer types have become the most prominent challenges. To facilitate large scale research projects and drug discovery of immune checkpoint inhibitors, we conducted a comprehensive protein profiling of ATCC's vast portfolio of human tumor and immune cell lines for several established and novel immune checkpoint molecules. Based on this protein profiling data, we generated immune checkpoint reporter cancer cell lines with high expression of endogenous immune checkpoint molecule ligands (PD-L1, CD155, and B7-H3). The reporter system contains a gamma interferon activation site (GAS)-response element upstream of the luciferase gene, preventing luciferase expression when the immune checkpoint molecule ligand binds to its corresponding receptor that suppresses T cell-mediated antitumor activity. In the presence of a relevant immune checkpoint inhibitor, a luciferase expression-based bioluminescent signal is produced, which can be readily detected and quantitated to evaluate the efficacy, potency, and dynamics of the inhibitor. Our data showed that the bioluminescence in the reporter cancer cells increased approximately 100-250 folds in a dose-dependent manner in response to interferon gamma stimulation, which mimics the signaling from activated CD8+ cytotoxic T cells. The bioluminescence increased approximately 50-100 folds in response to CD8+ primary T cell-conditioned media stimulation. In particular, we observed up to 5-fold increase in luciferase signal from our PD-L1 reporter cell line in response to co-culture with CD8+ primary T cells in the presence of an anti-PD-L1 blocking antibody in a dose-dependent manner. The luciferase expression and endogenous immune checkpoint molecule ligand expression were well maintained after the cell lines had reached >30 population doubling level. These results highlight the robustness and responsiveness of the reporter system for the assessment of T cell-mediated immune responses triggered by checkpoint inhibitors. These immune checkpoint reporter cancer cell lines yield exceptional in vitro and ex vivo assay sensitivity and reproducibility, while simplify the complex immunological model by providing physiologically relevant

expression of immune checkpoint molecule ligands, in comparison to similar assays with an artificial checkpoint ligand overexpression system.

#6644

Investigating the effect of immune checkpoint inhibitors (ICI) on ovarian function in young patients with melanoma

Ashley Hickman[1], Katherine Smith[1], Zaraq Khan[2], Elizabeth Ann Enninga[3], Yulian Zhao[2], Elizabeth Cathcart-Rake[1], Haidong Dong[4], Lisa Kottschade[1], Svetomir Markovic[1], Heather Montane[1], Anastasios Dimou[1], Yiyi Yan[5]. *[1]Mayo Clinic Medical Oncology, Rochester, MN,[2]Mayo Clinic Obstetrics and Gynecology, Rochester, MN,[3]Mayo Clinic Research Services, Rochester, MN,[4]Mayo Clinic Urology, Rochester, MN,[5]Mayo Clinic Medical Oncology, Jacksonville, FL*

Immune related adverse events (irAEs) from immune checkpoint inhibitors (ICIs) are well documented for nearly every organ system, except for the reproductive system. Mouse models have demonstrated that ICIs can decrease ovarian follicular reserve and impair oocyte maturation, which may have implications for fertility (PMID: 36008687). There are no studies investigating the effect of ICIs on fertility in humans. We sought to evaluate ovarian function in women treated with ICIs compared to untreated women by evaluating non-invasive surrogate markers of ovarian reserve, anti-müllerian hormone (AMH) and antral follicle counts (AFC). We enrolled women 18 - 40 years old diagnosed with stage III or IV melanoma. Participants underwent phlebotomy for AMH levels and a pelvic ultrasound to assess AFC. The medical record was retrospectively reviewed to obtain data on patient characteristics, treatments, and outcomes. A total of 14 patients with stage IIIA - IV melanoma participated. Six patients received ICI treatment before AMH and AFC testing while 8 had no prior ICI exposure. The ICI group ages ranged from 22-40 years with a median age of 31 years. The untreated group ages ranged from 25-39 years with a median age of 32 years. The time between starting an ICI and enrolling in the study ranged from 28 - 351 days. ICI regimens included ipilimumab/nivolumab, nivolumab, pembrolizumab, and atezolizumab (on a clinical trial). Four of these six patients experienced an irAE during their course, including: dermatitis, hepatitis, colitis, thyroid dysfunction, and adrenal insufficiency. Median AMH levels were lower for patients treated with ICIs (2.9 vs 4.0 ng/mL), as was median AFC (22.5 vs 23.5 ng/mL). Only three patients' clinicians discussed fertility preservation. None of the patients underwent fertility preservation. Our study found lower AMH and AFC in women with melanoma who were treated with an ICI compared to untreated women. Although AMH and AFC are surrogate markers for ovarian reserve and fertility, and our study is a small cohort, these early results suggest that ICIs may impact ovarian function. Age is less likely to be a confounding factor as the median age of the treated group was younger than the untreated group. While these results are preliminary, when considered in conjunction with recent pre-clinical data showing changes within the ovaries after ICI treatment, fertility consultation should be considered for young women prior to ICI initiation. We are investigating associations between AMH, AFC, age, ICI exposure, and future pregnancies in an ongoing prospective study.

#6645

A systematic approach for detection of tumor genomic alterations which alter the immune microenvironment

Raven Vella, Emily L. Hoskins, Julie W. Reeser, Michele R. Wing, Eric Samorodnitsky, Anoosha Paruchuri, Amy Smith, Leah Stein, Thuy Dao, Zachary Risch, Sameek Roychowdhury. *The Ohio State University, Hilliard, OH*

Objectives: Leveraging whole exome and transcriptome data from large cancer datasets, we sought to develop a computational approach to nominate candidate genomic alterations that are associated with hot or cold tumor. We anticipate this tool will identify candidate novel drug targets and biomarkers for immunotherapy in cancer. Methods: The user selects a gene of interest (GOI) as input for the pipeline. The pipeline searches TCGA (The Cancer Genome Atlas) mutation and structural variant outputs to collect hits in the gene of interest. Each sample with an alteration in the GOI is annotated with the alteration's predicted biological function (loss-of-function or LOF vs gain-of-function or GOF) using gene set enrichment analysis and pathway analysis from RNA sequencing. After annotating by sample, the alterations themselves are scored and recorded. Next, Quantiseq and Trust4 are employed to estimate features of the immune microenvironment in both the LOF and GOF samples. These results along with cancer type distributions, genomic position maps, and oncoplots are delivered to the user for further investigation. We are creating an online application to provide these results to the public. Simultaneously, a command line tool is being developed for application to any data source.

Results: We will present findings for the pipeline using positive controls including genomic alterations in ADAR, MTAP, IDH1, and CD274 (PD-L1). Preliminarily, we identified candidate GOF mutations (n=81) in PD-L1 that have inflamed tumor immune microenvironments like those of samples with known GOF structural variations in PD-L1. These samples have an overall "hot" immune microenvironment with significantly ($p<.05$) increased M1 macrophages, increased expression of IFN-gamma, and decreased M2 macrophages.
Conclusion: Currently there are no systematic approaches to interrogate individual genomic alterations and their association with an altered immune microenvironment. Our approach is pragmatic for any gene of interest, can be applied to any database, and identifies clinically actionable targets. This approach will identify heretofore unstudied connections between genomic alterations and immune microenvironment and support personalized drug development strategies in immuno-oncology.

#6646

Inhibition of HuR/CD147/IL-6 axis enhances anti-PD1 immunotherapy response in cancer

Qi Zhang, Lauren Dandreo, Xiaoqing Wu, Liang Xu. *Molecular Biosciences, University of Kansas, Lawrence, KS*

Immune checkpoint blockade (ICB) targeting PD-1/PD-L1 has emerged as a revolutionizing treatment modality for multiple cancers. However, durable remission and objective response rates with ICB monotherapy remain low. Several immune resistance mechanisms have been revealed and used to develop combinational therapy. In consideration of the durable and impressive responses observed in 'hot' tumors, it will be valuable to make an endeavor to elucidate the tumor evasion mechanisms. Despite the well-established mechanisms in immunotherapy resistance, our study uncovered a new mechanism of tumor immune evasion through the RNA-binding protein HuR/CD147 axis. The RNA-binding protein Hu antigen R (HuR) is overexpressed in a variety of cancers and promotes tumorigenesis by interacting with a subset of oncogenic mRNAs. The tumor-associated antigen CD147, a highly glycosylated transmembrane immunoglobulin, is widely and specifically expressed in multiple malignancies. We phenotypically observed the downregulation of CD147 in HuR-deficient cells and elucidated that HuR regulates *CD147* mRNA via binding to the AU-rich elements of its 3' UTR. The direct binding of HuR to *CD147* mRNA in multiple types of cells was validated by Ribonucleoprotein immunoprecipitation (RNP-IP) and RNA pulldown assay. These data together clarify HuR is engaged in *CD147* post-transcription regulation. KH-39 is a HuR-specific small molecule inhibitor, which disrupts the HuR function by competing for the binding site with its target mRNAs. KH-39 treatment reduced CD147 level in a time-/dose-dependent manner. We also tested the anti-tumor action of HuR small molecular inhibitor KH-39 in tumor proliferation, clonogenicity, cell death, cytokine secretion, and *in vivo* tumor growth. The cytokine array assay indicated multiple immune-related cytokines changed after HuR inhibition and CD147 knockdown, including IL-6, which is proven to act as an immunomodulating agent in the tumor microenvironment. These data demonstrated the potential mechanism of overcoming immunoresistance by inhibiting the HuR/CD147/IL-6 axis. To test the combination strategy using HuR inhibitor and anti-PD-1 antibody in vivo, we established the EMT6 orthotopic mouse breast cancer model. A combination of HuR inhibitor KH-39 and anti-PD-1 antibody enhanced the anti-PD1 immunotherapy response and prolonged survival compared to the single agent group. Taken together, we preliminarily explored the HuR/CD147/IL-6 axis in tumor immune evasion, which might be a promising therapeutic target to overcome immune evasion and improve immunotherapy response in cancer. This finding may have reference significance for clinical cancer therapy.

#6647

Dostarlimab shows dose-dependent immune activation of the tumor microenvironment in a patient-derived NSCLC explant model similar to pembrolizumab

Jessica Perrin[1], Frank Wippich[1], Valeriia Sherina[2], Dmytro Dvornikov[1], Katharina Lupar[1], Murad M. Melhem[2], Patrick Hanafin[2], Jeremy Waight[2], Jong Yu[2], Sapna Yadavilli[2], Daniel Poeckel[1], Giovanna Bergamini[1]. *[1]Cellzome, GSK, Heidelberg, Germany,[2]GSK, Upper Providence, PA*

The ability to more faithfully mimic the tumor microenvironment (TME) of cancer patients offers a wide range of possibilities for non-clinical evaluation of anti-cancer therapeutics, including guidance for patient selection, dose, and combinations. We have established a patient-derived tumor explant (PDE) model to monitor immune activation within a structurally preserved TME, following *ex vivo* incubation with immune check point inhibitors (ICI). When testing anti-PD-1 agents, such as dostarlimab and pembrolizumab, in a cohort of NSCLC explants from stage I-III treatment-naïve patients, we observed that approximately half demonstrate release of inflammatory cytokines after two days incubation. Interestingly, responsive tumors presented with a high level of PD-L1

expression (high TPS), had elevated TMB, and were highly infiltrated by CD8+ T cells at baseline, in line with tumor baseline characteristics predictive of clinical response to anti-PD-1. When testing a dose-range of dostarlimab and pembrolizumab comparable potencies were observed when measuring cytokine release after treatment of the NSCLC explants. In conclusion, we describe here an *in vitro* patient-derived NSCLC model that mirrors the heterogeneity of patients' response for anti-PD-1 agents observed in clinical settings, representing a valuable tool for comparative analysis of novel ICI assets and combinations, such as the CD226 axis members. Importantly, this system is also amenable to extensive multi-omics and genetics-based analyses, providing the opportunity to better identify predictive or pharmacodynamic characteristics within patient tumors.

#6648

Prediction of anti-PD-1 efficacy based on immune marker densities and their spatial distribution in colorectal cancer

Bahar Saberzadeh-Ardestani[1], Rondell P. Graham[2], Qian Shi[3], Eze Ahanonu[4], Sara McMahon[4], Crystal Williams[4], Antony Hubbard[4], Wenjun Zhang[4], Andrea Muranyi[4], Dongyao Yan[4], Kandavel Shanmugam[4], Frank A. Sinicrope[5]. *[1]Gastrointestinal Research Unit, Mayo Clinic, Rochester, MN,[2]Pathology, Mayo Clinic, Rochester, MN,[3]Quantitative Health Science, Mayo Clinic, Rochester, MN,[4]Roche Tissue Diagnostics, Tucson, AZ,[5]Oncology and Gastrointestinal Research Unit, Mayo Clinic, Rochester, MN*

Background: Immune checkpoint inhibitors (ICIs) have revolutionized the treatment of patients with deficient DNA mismatch repair (d-MMR) metastatic colorectal cancer (CRC), yet less than half of patients receive clinical benefit. We hypothesized that immune contexture including spatial distribution of cells expressing immune molecules in the tumor microenvironment may predict immunotherapy outcome. Methods: Primary CRC tissues from consecutive patients with d-MMR metastatic CRC (N=33) were treated with anti-PD-1 antibodies at Mayo Clinic Comprehensive Cancer Center (2015-2018). Tumors were stained for PD-L1, PD-1, CD8, CD3, CD68, LAG3, TGFβR2, MHC-I, CD14, B2M, DAPI and pan-cytokeratin in 5 compartments (overall tumor, tumor epithelia, tumor stroma, peritumor inside vs outside) by multiplex immunofluorescence with digital image analysis. Features computed within each image analysis region included positive cell density, fraction of positive cell types, intensity of positive cells, and spatial distribution between distinct cell types (distances measured using image analysis software). Prior to model fitting, feature selection was performed using regularized Cox regression with LASSO. Regularization parameter was chosen based on 5-fold cross validation. A Cox proportional hazards model was fitted to predict patient progression-free survival (PFS).
Results: Among patients with d-MMR CRCs, 16/33 (48.4%) were female, 10 received first-line ICI therapy, and 23 had received $\geq$ 1 prior chemotherapy regimen. Median age was 61.6 years (IQR of 49.4, 73.7). Eight patients (24.2%) harbored $BRAF^{V600E}$, 9 (27.2%) had mutant KRAS, and median PFS was 22.2 months (95% CI: 11.8, NR) with 20 events. PD-L1 was expressed in tumor cells, $CD68^+$ macrophages, and $CD3^+$ T lymphocytes. PD-1 expression on $CD8^+$ T lymphocytes was also observed. By univariate analysis, only cell-cell distance readouts achieved statistical significance. Multivariable feature selection identified the mean number of $PD\text{-}1^+$ cells within 10 microns of a $PD\text{-}L1^+$ cell in the overall tumor as the strongest predictor of anti-PD-1 efficacy, and was significantly associated with PFS (HR=0.87, 95% CI: 0.79-0.95, $p< 0.001$). In contrast, the ratio of $PD\text{-}1^+/PD\text{-}L1^+$ cells was not predictive of treatment efficacy ($p= 0.47$), thereby underscoring the importance of spatial distribution for PFS prediction.
Conclusion: The mean number of $PD\text{-}1^+$ cells in proximity to $PD\text{-}L1^+$ cells in tumors was a predictive biomarker of anti-PD-1 efficacy. Confirmatory studies are warranted.

#6649

Prevalence and spatial interplay of mononuclear phagocyte and lymphocyte subpopulations in 49 carcinoma entities in respect to its TIM3, PD-1, PD-L1 and CTLA-4 expression using BLEACH&STAIN

Zhihao Huang, Nicolaus F. Debatin, Elena Bady, Jan H. Mueller, Tim Mandelkow, Magalie C. J. Lurati, Ronald Simon, David Dum, Guido Sauter, Franziska Büscheck, Doris Hoeflmayer, Sören Weidemann, Claudia Hube-Magg, Till Clauditz, Maximilian Lennartz, Eike Burandt, Niclas C. Blessin. *University Medical Center Hamburg-Eppendorf, Hamburg, Germany*

Background: A combination of different immune-checkpoint-inhibitors (ICIs) have shown remarkable success in several tumor entities. However, the likelihood of positive response to ICIs is poor in most tumor entities and recent evidence suggests that the quantity and the expression level of immune checkpoints such as TIM3, CTLA-4,

PD-1 of tumor infiltrating lymphocytes (TILs) influences the likelihood of response to immune checkpoint inhibitors.
Design: To assess the density and spatial interplay of 42 immune checkpoint expressing leukocyte subpopulations in 6031 tumor samples from 49 carcinoma (sub)entities two different types of tissue microarrays (0.6 mm and 4 mm in diameter) were stained with 21 antibodies using our BLEACH&STAIN multiplex fluorescence immunohistochemistry approach. A deep learning-based framework comprising two different convolutional neuronal networks (U-Net and DeepLabv3+) was used for image analysis.
Results: We found that the mean overall fraction of TIM3, PD-1, PD-L1 and CTLA-4 expression on M1, M2 macrophages, cD11c$^+$ dendritic cells, CD8$^+$ cytotoxic T-cells, CD4$^+$ T-helper cells, FOXP3$^+$ Tregs and CD20$^+$ B-cells, ranged from 10% (sum of the fractions of immune checkpoint expression) in small cell carcinomas of the prostate up to 123 % in squamous cell carcinoma of the lung. Tumor types approved for checkpoint inhibitor therapy, including adenocarcinomas of the lung (121 %), small cell carcinoma of the lung (74%), malignant melanoma (59 %), and clear cell renal cell cancer (49%) were all ranking among the upper half of our list of mean fractions of overall immune checkpoint expression. Spatial analysis and the shift in immune cell compositions revealed that in most carcinoma (sub)entities, the overall immune cell density and fraction of immune checkpoint expression of individual patients occasionally exceeded the average immune cell density and fraction of tumors for which checkpoint inhibitors have been approved.
Conclusion: These data support the concept that among most carcinoma entities at least some individual patients may benefit from treatment with immune checkpoint inhibitors.

#6650
Cell-based assay to support development and characterization of new drugs in immuno-oncology
Mohammad Haque, Safnas Abdul Salam, Shawn McGinley, Haiching Ma, jianghong Wu. *Reaction Biology Corporation, Malvern, PA*

The years since 2009 have seen tremendous progress in unlocking the curative potential of the immune system for the treatment of cancer. Much of that revolution in immuno-oncology has been fueled by the clinical success of immune checkpoint inhibitors, targeting cytokines, antibody dependent cell cytotoxicity and complement dependent cytotoxicity via the T cell activation. Reaction biology has established state-of-art high throughput screening procedures for measuring the ability of new Biologics or compounds to activate T cells. Antibody Dependent Cell Cytotoxicity (ADCC), T cell activation assay (NFAT), immune checkpoint inhibitor assay (PD-1/PD-L1 blockade bioassay), cytokines activation assay and Complement Dependent Cytotoxicity (CDC) are commonly used for drug discovery industry. ADCC is a desirable mechanism for killing target cells using antibody-based drugs. T cell activation assay can be used for the discovery and development of novel biologics and cell therapies aimed at inducing, strengthening and/or engineering T cell response. Blocking of immune inhibitory receptors by their respective ligands on an adjacent cell inhibits TCR mediated proliferation, transcriptional activation and cytokines production. Biologics or compounds designed for measuring the stimulatory or inhibitory function of cytokines are promising in the field of immune oncology. Reaction Biology developed biochemical assays for PD-1/PD-L1, CTLA4/CD80 and CTLA4/CD86 to screen immune checkpoint inhibitors. All of these screening procedures and experimental methods will help to identify new therapeutic biologics or compounds for drug discovery in immune-oncology field.

#6651
MoA-based potency bioassays for immunotherapy programs targeting the TIGIT/CD112R/CD96 axis
Steven Edenson, Jamison Grailer, Denise Garvin, Frank Fan, Jim Harnett, Mei Cong. *Promega, Madison, WI*

Immune checkpoint (IC) receptors play critical roles in maintaining immune homeostasis and have emerged as proven therapeutic targets for the treatment of various cancers and autoimmune disorders. Monoclonal antibodies (mAbs) designed to block immune inhibitory receptors PD-1 and CTLA-4 have shown unprecedented efficacy in cancer treatment. This led to rapid expansion of mAb discovery programs to many more IC receptors including members of the T cell immunoreceptor with Ig and ITIM domains (TIGIT) - CD112R - CD96 Axis. TIGIT binds to its ligands CD155 (PVR) and CD112 (PVRL2) while CD112R (PVRIG) binds to CD112 and CD96 (TACTILE) binds to CD155. Binding of TIGIT/CD112R to CD155/CD112 inhibits the co-stimulatory activity of the paired receptor CD226. Human CD96 can have co-stimulatory or co-inhibitory activity based on the cell type and context. Thus, therapeutic targeting of this axis can modulate T cell and NK cell activation and unleash anti-cancer immunity. One of the bottlenecks of immunotherapy mAb development is the lack of quantitative and reproducible

bioassays for functional analysis and potency determination. Existing methods rely heavily on primary immune cells, which is labor- and cost-intensive and highly variable. To address this need, we developed a panel of cell-based reporter bioassays that can quantitatively measure the potencies of mAbs targeting TIGIT/CD155, TIGIT/CD112, CD112R/CD112, and CD96/CD155. Owing to the clinical combination of TIGIT blockade with PD-1/PD-L1 blockade, we further developed a potency bioassay for bispecific antibodies simultaneously targeting TIGIT and PD-1/PD-L1. These bioassays each consist of an engineered T effector cell line that expresses T cell receptors and IC receptors of interest, and an engineered artificial antigen presenting cells (aAPC) expressing the cor
responding ligands for the IC receptors. The T effector cell lines also express a luciferase reporter driven by a promoter specifically responding to TCR activation which can be inhibited by signaling from the IC receptors. Additionally, we developed bioassays that can measure potencies of agonist or antagonist mAbs targeting CD226. These bioassays are designed to reflect the mechanisms of action for the drug candidates designed for each IC receptor and the assay signals are specific. Most are prequalified according to ICH guidelines and show the precision, accuracy and linearity required for cGMP environments. Therefore, these MoA-based bioassays can serve as valuable tools for early drug discovery, potency determination and stability studies throughout the development of mAbs targeting the TIGIT/CD112R/CD96 axis.

#6652

Overcoming immune resistance in DNA mismatch repair deficient tumors

Guillaume Mestrallet. *Icahn School of Medicine at Mount Sinai, New York, NY*

Patients with Lynch Syndrome, an inherited mismatch repair deficiency, have an increased risk for developing microsatellite unstable (MSI-H) cancers. Our team recently identified shared immunogenic frameshift peptides in patient tumors that can be targets of T cell surveillance and preventative MSI-H cancer vaccines. We hypothesize that in Lynch Syndrome some premalignant lesions are capable of evading immune surveillance from cytotoxic T lymphocytes due to immune checkpoint expression and immunosuppression from tumor, myeloid and stromal cell populations. Immune checkpoint blockade (ICB) showed promising results in the treatment of MSI-H tumors and are being evaluated in the adjuvant setting of patients with Lynch syndrome post surgical resection. However, a significant percentage of advanced MSI-H tumors resist ICB suggesting evolving mechanisms of immune resistance. We will use a MSI-H in vivo mouse model and additionally develop 3D spheroids cocultured with immune cells to characterize the underlying immune resistance mechanisms. The MSI-H mouse model will first be applied to identify shared frameshifts in MSI-H tumors by WES to develop vaccination approaches preventing tumor growth. Then, we will quantify MSI-H tumor growth and immune infiltration in the MSI-H mouse model, with or without ICB. We will analyze the presence of immunosuppressive pathways and myeloid subsets in high growth resisting tumors by immunohistochemistry, scRNAseq, spatial transcriptomics and flow cytometry. In addition, we will perform short-term in vitro spheroid-splenic cell co-cultures to better characterize the early immune resistance mechanisms. We will also perform these spheroid-immune cell co-cultures using the immune cells taken from mice after vaccination or ICB to identify the early myeloid immune resistance mechanisms. Overall, the identification of shared immune frameshifts in MSI-H tumors will allow developing peptide vaccination approaches to prevent tumor growth. Further, the identification of myeloid resistance pathways will guide therapeutic strategies against tumor resisting to ICB and/or vaccination.

#6653

Analysis of selective response of anti-PD-L1 treatment in huPBMC-NCG mice reconstituted with different donors

Tingting Gu[1], Weiwei Yu[1], Hongyan Sun[1], Fang Zhu[1], Huiyi Wang[1], Mengting Wang[1], Shuai Li[1], Jianming Xu[1], Santi Suryani Chen[2], Zhiying Li[2], Mark Wade Moore[2], Cunxiang Ju[1], Hongyu Wang[1], Jing Zhao[1], Xiang Gao[1].
[1]Gempharmatech Co., Ltd., Nanjing, China,[2]GemPharmatech LLC., La Jolla, CA

Despite the success of programmed death ligand 1 (PD-L1) and programmed death 1 (PD-1) blockage as cancer therapies, the overall clinical response rates are still unsatisfying, with only a 25% response rate in most cancers. The underlying mechanisms of non-responsiveness towards anti-PD-L1 treatment have been extensively studied and associated with many factors, including PD1/PD-L1 expression level, tumor mutation burden, IFN signaling, loss of MHC-I, tumor microenvironment (immune infiltration, suppressive immune system), and so on. Immunodeficient mice such as the NSG and NCG are commonly used to study the efficacy of cancer immunotherapies. These mice, reconstituted with either human PBMC or HSC, act as an avatar to provide a

window of the potential agent efficacy at the preclinical level. However, due to the challenge of obtaining an HSC/PBMC donor, and often cost and time can also be a limiting factor, many studies only use 2-5 human donors. Here we present data demonstrating the significant variation observed between donor-to-donor, highlighting the importance of testing multiple donors.
We reconstituted immune system and tumor tissue humanized mouse models using peripheral blood mononuclear cells (PBMCs), and cell line-derived xenografts (CDX) in severe immunodeficiency NCG mice. Anti-tumor efficacy of anti-PD-L1 (Tecentriq) in huPBMC-NCG mice engrafted with several tumor cells including MDA-MB-231, HCC827, NUGC4, and some other CDX cell lines was tested in our system. In the cases of MDA-MB-231, HCC827, and NUGC4, different donors were enrolled in the same study, and tumor growth inhibition measured by tumor volume (TGI_{TV}) of 3% to 52.40% (MDA-MB-231), 5% to 33% (HCC827) and 4.75% to 20.74% (NUGC4) were observed. Especially, In the case of MDA-MB-231, 6 donors were enrolled in this study at the same time. About 40% of immune infiltration was first observed in tumors. High expression of PD1 on immune cells and PDL1 on tumor cells were also detected from different donors simultaneously. Although the similar immune infiltration and PD1/PDL1 expression, the TGI_{TV} of 6 donors varied between 3% and 52.40%, suggesting the donor-dependent response to anti-PD-L1 treatment, which is similar to the clinical trials.
Our data showed diverse in vivo responses when multiple human PBMC donors were used for preclinical agent evaluation. While unsurprising, it showed the critical need to include various human PBMC donors when an agent is in preclinical status because the donors' immune profile may dictate the study's outcome. This can be divided into two parts, on the one hand, donor screening for favorable efficacy response donors in advance is an alternative approach to ensure the positive efficacy of anti-PDL1 blockade relative therapy. On the other hand, the low-efficacy response donors also can be candidates for anti-PD1/PDL1 combination therapy.

#6654

Association PD-L1 overexpression with immune checkpoint inhibitor effect in triple-negative breast cancer

A Young Park[1], Ju Hee Kim[2], Sangen Lee[1], Hong Kyu Kim[2], Han-Byoel Lee[3], Wonshick Han[3]. *[1]Seoul National University Graduate School, Seoul, Korea, Republic of,[2]Seoul National University Hospital, Seoul, Korea, Republic of,[3]Seoul National University College of Medicine, Seoul, Korea, Republic of*

Background: Recently, studies on the antitumor effects of PD-L1 inhibitors have gained importance in difficult to treat solid tumors. In particular, the expression of PD-L1 could be an important factor in evaluating the possibility of immunotherapy in triple-negative breast cancer where targeted therapy is not possible and the prognosis is poor. Accordingly, this study investigated the effect of PD-L1 overexpression on the immune checkpoint inhibitor effect in triple-negative breast cancer.
Method: The relationship between T stage and N stage according to PD-L1 mRNA expression was analyzed in the TCGA and METABRIC datasets of breast cancer. To evaluate the role of PD-L1, PD-L1-overexpressing breast cancer cell lines for *in vitro* and *in vivo* experiments were established.
Result: Using TCGA and METABRIC datasets, we found that PD-L1 showed the highest expression in breast cancer of the basal subtype, but the correlation between T stage and N stage according to PD-L1 expression was not statistically significant. To determine the functional importance of PD-L1 in breast cancer, we established 4T1-PD-L1-overexpressing breast cancer cell lines. We observed that the overexpression of PD-L1 promoted cell proliferation, migration, and invasion. In the orthotopic tumor mouse model, PD-L1 showed no significant difference in tumor growth compared to the control group, but anti-PD-L1 treatment showed a significant antitumor effect.
Conclusion: We confirmed that overexpression of PD-L1 in an orthotopic breast cancer model did not induce increased tumor growth. Above all, it was confirmed that a high PD-L1 level enhances the antitumor effect of immune checkpoint inhibitors. Our findings show that the expression level of PD-L1 in breast cancer has a significant effect on the immune checkpoint inhibitor effect. We need to further investigate the role of PD-L1 in breast cancer.

#6655

A real world analysis: Impact of clinical trial eligibility criteria on clinical outcomes among patients with advanced non-small cell lung cancer (aNSCLC) receiving second line (2L) immune checkpoint inhibitor (ICI) therapy

Hina Mohammed[1], Miso Kim[2], Mahder Teka[1], Monika Izano[1], Frank Wolf[1], Thomas Brown[1]. *[1]Syapse, San Francisco, CA,[2]Seoul National University Hospital, Seoul, Korea, Republic of*

Background. Clinical trials (CT) include patients (pts) satisfying eligibility criteria including normal organ function and low comorbidity. Real-world outcomes for pts with aNSCLC receiving ICIs in 2L were compared based on whether pts met CT eligibility criteria.
Methods. 2L- associated outcomes were compared between pts with aNSCLC diagnosed between 04/01/2015 - 12/31/2020 in US community health systems that fulfilled or failed to fulfill CT eligibility criteria. CT-eligible (CTE) pts had at 2L: performance status of 0-1; normal renal, hepatic, and bone marrow function; no evidence of Hepatitis B or C, HIV, rheumatic diseases, or interstitial lung disease. Pts were CT-ineligible (CTI) if they failed to meet one or more of these criteria. Follow-up spanned 2L start to the first of: outcome of interest, death, or study end on 06/30/2021. Outcomes were evaluated in pts receiving ICI monotherapy (monotherapy) or ICI + chemotherapy (combination).
Results. Of the 505 pts in this analysis, 81% and 19% received monotherapy and combination, respectively; 19% of pts were CTE (76% monotherapy, 24% combination, **Table)**. Overall, in ICI subgroups among monotherapy pts, pembrolizumab-treated pts had longer OS and TTNT; time to treatment discontinuation (TTD) was less variable across subgroups. CTE pts in the monotherapy group had longer OS, shorter TTNT, and similar TTD compared to CTI. Among combination pts, CTE had similar OS and TTD, but shorter TTNT compared to CTI.
Conclusions. CTE pts appear to have longer survival than CTI pts with aNSCLC receiving ICI monotherapy, but not among pts receiving combination. TTNT was longer for CTI pts in both groups. In addition to CTE pts, some CTI pts appear to benefit from 2L ICI therapy.

Time-to-event outcomes (months), median (95% CI) in the study cohort

	Monotherapy (N = 412)	Monotherapy (N = 412)	Monotherapy (N = 412)	Monotherapy (N = 412)	Combination (N = 93)	Combination (N = 93)	Combination (N = 93)	Co (N
	N (%)	OS	TTNT	TTD	N (%)	OS	TTNT	TT
Atezolizumab	37 (9%)	7 (3-16)	9 (7-NA)	2 (1-3)	9 (10%)	6 (5-NA)	NA (5-NA)	2 (
Nivolumab	234 (57%)	14 (9-18)	20 (15-NA)	2 (2-3)	9 (10%)	36 (6-NA)	23 (6-NA)	5 (
Pembrolizumab	138 (34%)	20 (16-28)	NA (31-NA)	2 (1-3)	75 (80%)	12 (8-NA)	20 (15-NA)	1 (
Overall	-	15 (13-18)	23 (18-NA)	2 (2-2)	-	11 (7-NA)	20 (10-NA)	2 (
Trial-Eligible (all regimens)	72 (18%)	20 (12-NA)	19 (10-NA)	2 (2-3)	23 (25%)	11 (5-NA)	10 (7-NA)	3 (
Trial-Ineligible(all regimens)	292 (70%)	13 (8-16)	26 (18-NA)	2 (2-2)	64 (69%)	11 (7-NA)	20 (9-NA)	2 (
Unknown Trial Eligibility	47 (12%)	-	-	-	6 (6%)	-	-	-

#6656
Expression pattern and clinicopathological implication of B7 family immune checkpoints, VTCN1 and HHLA2, in non-small cell lung cancer
Sojung Lim[1], Jaemoon Koh[1], Seung Geun Song[1], Jeemin Yim[1], Bogyeong Han[1], Young A Kim[2], Doo Hyun Chung[1], Yoon Kyung Jeon[1]. *[1]Pathology, Seoul National University College of Medicine, Seoul, Korea, Republic of,[2]Pathology, Seoul Metropolitan Government Boramae Hospital, Seoul, Korea, Republic of*

Background: Efforts are needed to discover novel immunotherapeutic targets in non-responders of current immunotherapies. VTCN1 (B7-H4/B7x/B7S1) and HHLA2 (B7-H7/B7y) are B7 family co-inhibitory molecules reported to be expressed in PD-L1-negative or *EGFR*-mutant lung adenocarcinoma (LUAD). To elucidate the clinicopathological implications of these two immune checkpoints, we checked their detailed expression patterns including intratumoral heterogeneity.
Methods: VTCN1 and HHLA2 expression were evaluated in public single-cell RNA sequencing (scRNAseq) and The Cancer Genome Atlas (TCGA) dataset. Their immunohistochemistry (IHC) was performed on tissue microarrays of 413 LUAD and 382 lung squamous cell carcinoma (LUSC) specimens. Intratumoral heterogeneity was evaluated by IHC on representative sections of 59 surgically resected LUAD and 49 LUSC specimens.

Results: In LUAD scRNAseq, VTCN1 and HHLA2 were predominantly expressed on epithelial cells and were not co-expressed with PD-L1. However, IHC showed their expression in both tumor and immune cells. In TCGA analysis, there was a negative correlation between VTCN1 and PD-L1 (LUAD, r = -0.094, $p = 0.033$; LUSC, r = -0.227, $p < 0.001$). VTCN1 and HHLA2 showed positive correlations in both TCGA (LUAD, r = 0.211, $p < 0.001$; LUSC, r = 0.182, $p < 0.001$) and IHC analysis (LUAD, $p < 0.001$; LUSC, $p = 0.016$). They were more frequently expressed in *EGFR*-mutant LUAD (52.9% vs. 40.3%, $p = 0.015$ for VTCN1 in *EGFR*-mutant vs. wildtype; 59.8% vs. 40.5%, $p < 0.001$ for HHLA2). $CD8^+$ T-cell infiltration was significantly higher in VTCN1- or HHLA2-positive *EGFR*-mutant LUAD, but there was no significant relationship in *EGFR*-wildtype. In 60% of cases expressing both VTCN1 and HHLA2, the two showed spatially concordant expression (15 out of 24 LUAD; 3 out of 6 LUSC). However, VTCN1 and PD-L1 showed concordant expression in 37.2% of cases expressing both (6 out of 16 LUAD; 10 out of 27 LUSC). HHLA2 expression was associated with better overall survival in LUSC, but there was no significant difference in survival according to VTCN1 expression.
Conclusions: VTCN1 and HHLA2 are frequently co-expressed in PD-L1-negative NSCLC, especially *EGFR*-mutant LUAD rich in $CD8^+$ T-cells and can serve as potential novel immunotherapeutic targets.

#6657

Phase I trial of first-in-class anti-PVR mAb NTX1088: Restoration of DNAM1 expression as MOA for enhanced antitumor immunity

Anas Atieh[1], Akram Obiedat[1], Alon Vitenshtein[1], Guy Cinamon[1], Keren Paz[1], Tihana lenac[2], Paola Kucan[2], Marija Mazor[2], Ofer Mandelboim[3], Stipan Jonji[2], Pini Tsukerman[1]. *[1]Nectin Therapeutics, Ltd., Jerusalem, Israel,[2]MEDRI, Rijeka, Croatia,[3]HUJI, Jerusalem, Israel*

NTX1088, a first-in-class anti-PVR (CD155) monoclonal antibody (mAb), is currently evaluated in a Phase 1, open-label, multi-center study (NCT05378425), initiated at MD Anderson Cancer center. Study objectives are safety, dose-finding, and efficacy with focus on pharmacokinetics, pharmacodynamics, and biomarker discovery. NTX1088 will be investigated as a single agent and combined with the anti-PD1 mAb, pembrolizumab (Keytruda) in patients with locally advanced and metastatic solid malignancies.NTX1088 is a humanized, IgG4-S228P mAb that binds PVR with sub-nM affinity and blocks all known interacting receptors with a single nM EC_{50}. PVR, is a membranal protein, highly upregulated on tumor cells, across multiple cancer types. PVR expression has been associated with worse patient outcomes, due to its role in immune suppression. PVR's impact on immune cells is mediated through interaction with the key stimulatory receptor, DNAM1 (CD226), on T and NK cells, leading to internalization and degradation of DNAM1. Additionally, PVR is the ligand for the inhibitory immune checkpoint receptors, TIGIT, CD96 and KIR2DL5A. Blocking PVR by NTX1088, therefore, has a multi-faceted immune-stimulating role, through restoration of DNAM1 expression and its immune activation function, while simultaneously neutralizing TIGIT, CD96 and KIR2DL5A inhibitory signals in immune cells. Importantly, DNAM1 downmodulation was recently identified as a key resistance mechanism to approved immune checkpoint inhibitors (ICIs), and its restoration by NTX1088 is a novel MoA, not demonstrated by other therapies.In vitro, as a monotherapy, NTX1088 significantly increased immune cell activation, and was superior to TIGIT, CD112R, and PD1 antibody blockade, leading to greater immune-mediated tumor cell killing, IFNγ secretion, and CD137 induction. Importantly, only NTX1088 was able to restore DNAM1 to the surface of immune cells in all experimental settings. Synergy was observed when NTX1088 was combined with PD1 blockers, or with the anti-CD112R mAb, NTX2R13, in line with the restoration of DNAM1 expression.Numerous humanized murine xenograft models were investigated. NTX1088 exhibited robust tumor growth inhibition as a standalone and in combination with PD1 blockade. Syngeneic models of $PVR^{K.O}$ resulted in complete immune-mediated tumor regression, including hard to treat colorectal tumors. In conclusion, PVR blockade by NTX1088 has a remarkable pre-clinical efficacy, suggesting a potential clinical breakthrough, based on the ability of simultaneously overcome multiple tumor escape mechanisms. First-in-human (FIH) trial is currently ongoing and biomarker data is analyzed to assess clinical impact of the drug and prepare for patient stratification.

#6658

Prevalence of PD-L1 expression and its correlation with tumor biomarkers in the Chinese muscle invasive urothelial bladder carcinoma patients

Yu Fan[1], Tao Dai[2], Dahong Zhang[3], Hongqian Guo[4], Fangjian Zhou[5], Benkang Shi[6], Shaogang Wang[7], Zhigang Ji[8], Chunxi Wang[9], Xudong Yao[10], Qiang Wei[11], Nanhui Chen[12], Jinchun Xing[13], Jinjian Yang[14], Chuize Kong[15], Jian Huang[16], Dingwei Ye[17], Liqun Zhou[1]. *[1]Department of Urology, Peking University First Hospital, Beijing,*

China,[2]Department of Urology, The Affiliated Cancer Hospital of Xiangya School of Medicine, Central South University and Hunan Cancer Hospital, Changsha, China,[3]Department of Urology, Zhejiang Provincial People's Hospital, Hangzhou, China,[4]Department of Urology, Drum Tower Hospital, Medical School of Nanjing University, Institute of Urology, Nanjing University, Nanjing, China,[5]Department of Urology, Sun Yat-sen University Cancer Center, Guangzhou, China,[6]Department of Urology, Qilu Hospital, Cheeloo College of Medicine, Shandong University, Jinan, China,[7]Department of Urology, Tongji Hospital of Tongji Medical College, Huazhong University of Science and Technology, Wuhan, China,[8]Department of Urology, Peking Union Medical College Hospital, Chinese Academy of Science, Beijing, China,[9]Department of Urology, First Hospital of Jilin University, Jilin, China,[10]Department of Urology, Shanghai Tenth People's Hospital, Tongji University School of Medicine, Shanghai, China,[11]Department of Urology, Institute of Urology, West China Hospital, Sichuan University, Shanghai, China,[12]Department of Urology, Meizhou People's Hospital, Meizhou, China,[13]Department of Urology Surgery, The First Affiliated Hospital of Xiamen University, Xiamen, China,[14]Department of Urology, The First Affiliated Hospital of Zhengzhou University, Zhengzhou, China,[15]Department of Urology, The First Hospital of China Medical University, Shenyang, China,[16]Department of Urology, Sun Yat-sen Memorial Hospital, Sun Yat-sen University, Guangzhou, China,[17]Department of Urology, Fudan University Shanghai Cancer Center, Shanghai, China

The association of programmed cell death-ligand 1 (PD-L1) expression with the activity of immune checkpoint inhibitor therapy setting has encouraged us to study the prevalence of PD-L1 in muscle invasive urothelial bladder cancer (MIUBC) patients. Since, the prevalence of PD-L1 expression and its prognostic role in MIUBC is unclear in China, we conducted a multi-center, prospective, epidemiological study to investigate prevalence of high PD-L1 expression and its correlation with other exploratory biomarkers including CD8+ T cells and tumor mutation burden (TMB) in Chinese MIUBC patients (NCT03433924). The study enrolled newly diagnosed, untreated MIUBC patients from 17 hospitals in China. High PD-L1 expression by Ventana PD-L1 [SP263] assay was defined as 1) ≥25% tumor cell (TC) + or 2) tumor associated immune cell (IC) area >1%: ≥25% IC+; 3) IC area=1%: 100% IC+. The primary outcome was prevalence of high PD-L1 expression; secondary outcome was PD-L1 expression profile in TC or IC in patients. An exploratory study was conducted to investigate the percentage of patients with high infiltration of CD8+ T cells and elevated TMB using immunohistochemistry and next generation sequencing, respectively. High CD8+ and TMB status was considered if it refers to > median value (3%) and >10 mut/Mb, respectively. Association of PD-L1 expression with demographic and baseline characteristics was evaluated by logistic regression model while PD-L1 with tumor biomarkers were evaluated by spearman's rank correlation coefficient. Overall, 248 MIUBC patients were enrolled and 229 patients with PD-L1 data were included. High PD-L1 expression was observed in 52.4% patients. High PD-L1 expression was positive in 59 (25.8%) patients of TC and 82 (35.8%) patients of IC. CD8+ T cell and TMB showed high expression in 44.5% and 54.1% patients, respectively, with mean TMB of 14.14 mut/Mb. The exploratory analysis showed no significant association of PD-L1 expression with age, gender, primary tumor site, metastatic disease, regional lymph node, tobacco use or AJCC stage. Further a weak and positive correlation was observed between percentage of TC with membrane PD-L1 positivity and CD8+ T cells (0.34, 95%Cl, 0.22 - 0.45, $p<0.001$), IC with membrane PD-L1 positivity and CD8+ T cells (0.44, 95%Cl, 0.33 - 0.54, $p<0.001$), TC with membrane PD-L1 positivity and TMB (0.05, 95%Cl, -0.08 - 0.19, $p=0.441$), IC with membrane PD-L1 positivity and TMB (0.16, 95%Cl, 0.02 - 0.29, $p=0.020$). In conclusion, our study showed high prevalence of PD-L1 expression in patients with MIUBC along with their weak, positive correlation with CD8+ T cells and TMB. These findings are consistent with other studies that show that PD-L1 and TMB stand as the most robust predictive biomarkers, but may be uncorrelated. With subsequent follow-up time, the effect of biomarkers on survival will be assessed in future study.

Immune Monitoring and Responses to Therapy

#6662

Studying immune responses against human endogenous retroviruses in immune checkpoint blockade-treated lung adenocarcinoma

Khaled Sanber[1], Sydney Connor[1], Steven Vensko[2], Christopher Cherry[1], Zhen Zeng[1], Drew Pardoll[1], Patrick Forde[1], Benjamin Vincent[2], Kellie Smith[1]. *[1]Sidney Kimmel Comprehensive Cancer Center, Bloomberg-Kimmel Institute for Cancer Immunotherapy at Johns Hopkins University, Baltimore, MD,[2]Lineberger Comprehensive Cancer Center, University of North Carolina at Chapel Hill, Chapel Hill, NC*

Background: Clinical response to immune checkpoint blockade (ICB) is predicated upon the existence of tumor-reactive T cells, but their precise targets remain poorly defined. Some patients with low tumor mutational burden (TMB) lung adenocarcinoma (LUAD) derive clinical benefit from ICB, suggesting that non-mutated antigens may serve as T cell targets. Human endogenous retroviruses (hERVs) can be differentially expressed in malignant cells due to epigenetic dysregulation and can be targeted by T cells. We hypothesize that the detection of T cell responses against hERVs correlates with a favorable clinical response to ICB in LUAD.
Methods: Tumor tissues from patients with Stage I-III LUAD who underwent upfront surgical resection were enzymatically digested. Viable $CD45^{-}EPCAM^{+}$ cells were sorted. Total RNA was extracted and RNA sequencing was performed. The hervQUANT workflow was used to bioinformatically identify differentially-expressed, open reading frame (ORF)-encoding hERV transcripts. Publicly available RNAseq datasets derived from human medullary thymic epithelial cells (mTECs) and normal tissues were queried to exclude hERV transcripts expressed in these tissues. Overlapping peptide libraries (OPLs) spanning the shared hERV ORFs were synthesized and used in Functional Expansion of Specific T Cells (FEST) assays to detect hERV-specific T cell clones in the peripheral blood of a cohort of patients who met these criteria: (1) had advanced/metastatic LUAD, (2) were treated with ICB, (3) had peripheral blood mononuclear cells isolated at 4-8 weeks post-initiation of ICB and (4) had formal radiographic assessment of response to ICB.
Results: We identified 41 differentially-expressed, ORF-encoding hERV transcripts that were shared by ≥4 (out of 11) $CD45^{-}EPCAM^{+}$ LUAD samples. OPLs covering hERV ORFs with mean expression of ≥ 3 CPM in $CD45^{-}EPCAM^{+}$ LUAD cells and <3 CPM in mTECs were synthesized. Low expression in normal tissues was also confirmed (<3 CPM). A total of 318 patients were screened and 30 patients (22 radiographic responders and 8 non-responders) met the inclusion criteria. The median age was 66.5 years for responders and 58 years for non-responders. The median PD-L1 TPS was 72.5% and 70%, respectively. The median TMB was 8 and 2.55, respectively. FEST assays utilizing hERV OPLs revealed 4 potential hERV-reactive T cell clonotypes in the peripheral blood of 2 patients with LUAD treated with ICB. Studies are ongoing to validate and characterize these clonotypes. Testing of the remainder of the selected patient cohort is also ongoing.
Conclusions: Potential hERV-reactive T cell clonotypes are detectable in ICB-treated patients with LUAD. Correlation with clinical response to ICB will be evaluated upon validation of these clonotypes, but these results are promising findings in the ongoing efforts to identify immunogenic sources of non-mutated antigens in cancer.

#6663

Immunostimulatory gene therapy targeting CD40/4-1BB in combination with chemotherapy induces an inflammatory gene profile in tumors from patients with advanced disease

Jessica Wenthe[1], Emma Eriksson[2], Sedigheh Naseri[1], Linda Sandin[3], Amanda Hahn[1], Sandra Irenaeus[1], Anders Sundin[1], Justyna Leja-Jarblad[3], Gustav Ullenhag[1], Tanja Lövgren[1], Angelica Loskog[2]. *[1]Uppsala University, Uppsala, Sweden,[2]Uppsala University/Lokon Pharma AB, Uppsala, Sweden,[3]Lokon Pharma AB, Uppsala, Sweden*

In the LOKON002 phase I/II clinical trial (NCT03225989), therapy with LOAd703 (delolimogene mupadenorepvec) is investigated in combination with gemcitabine-based chemotherapy in patients with advanced cancer. LOAd703 is an immunostimulatory gene therapy utilizing an oncolytic adenovirus that is engineered to express two transgenes (trimerized membrane-bound CD40L (TMZ-CD40L) and 4-1BBL), which are key players in the induction of an anti-tumor immune response. Herein, we present the preliminary immunological evaluation of the first 27 patients enrolled in the trial. The primary tumor was pancreatic cancer (n=16), colorectal cancer (n=5), ovarian cancer (n=3) or biliary cancer (n=3). Patients received a maximum of eight intratumoral LOAd703 treatments, given biweekly, and chemotherapy was administered at the same time according to standard protocol. Matched tumor biopsies from the injected tumor lesion were taken at baseline and after six LOAd703 treatments, and analyzed for gene expression with nCounter® PanCancer Immune Profiling Panel from NanoString (n=12; 7 patients analyzed so far). Blood samples were collected for isolation of serum samples and peripheral blood mononuclear cells, and these were analyzed with multiplex assays (Meso Scale Diagnostics) (n=15) and flow cytometry (n=27), respectively. Preliminary results indicate that after treatment, most tumors displayed a strong inflammatory profile with an upregulation of gene profiles, which have been shown to predict responses to immune checkpoint inhibitor therapy (T cell inflamed profile (Ayers et al.) & T effector and IFNγ associated profile (Fehrenbacher et al.)). We also noted an upregulation of genes connected to dendritic cell activation and antigen presentation (MHC class I and II, CD80, CD86, TAP1/2), as well as adenoviral-response genes. Moreover, we observed systemic treatment effects after three LOAd703 treatments, as shown by an increase in serum levels

of pro-inflammatory cytokines and chemokines (IFNγ, IL-15, CXCL10, CCL2, IL-8, IL-6), as well as an increased percentage of CD8+ effector memory T cells (CD45RA-CCR7-) and PD-1+ CD8+ T cells in the blood. The fractions of natural killer (NK) cells (CD14-CD3-CD56+CD16+) and M2-like macrophages (CD11b+CD163+) were reduced in the blood at that time point. In conclusion, LOAd703 therapy in combination with chemotherapy generated an inflamed tumor microenvironment in tumors that are normally seen as immunologically "cold". Hence, LOAd703 may be able to prime tumors for immune checkpoint inhibitors or other immunotherapies, such as adoptive T or NK cell transfer.

#6664

Comprehensive immunoprofiling of peripheral blood reveals five conserved immunotypes with implications for immunotherapy in cancer patients

Daniiar Dyikanov, Iris Wang, Tatiana Vasileva, Polina Shpudeiko, Polina Turova, Arseniy A. Sokolov, Olga Golubeva, Evgenii Tikhonov, Anna Kamysheva, Ilya Krauz, Mary Abdou, Madison Chasse, Tori Conroy, Nicholas R. Merriam, Boris Shpak, Anastasia Radko, Anastasiia Kilina, Lira Nigmatullina, Linda Balabanian, Christopher J. H. Davitt, Alexander A. Ryabykh, Olga Kudryashova, Cagdas Tazearslan, Ravshan Ataullakhanov, Alexander Bagaev, Aleksandr Zaitsev, Nathan Fowler, Michael F. Goldberg. *BostonGene, Corp., Waltham, MA*

Recent advances in immunotherapy demonstrate the need to further understand the characteristics of an individual cancer patient's immune system and how it influences responses to cancer treatment. Here, we developed an immunoprofiling platform to evaluate the features in the blood of cancer patients to test the hypothesis that peripheral immune cell heterogeneity could be used to stratify these patients into different categories or immunotypes to monitor disease progression and treatment response.
To that end, we established a unique diagnostic immunoprofiling assay and analytical framework based on the analysis of leukocytes in the peripheral blood using multiparameter flow cytometry. Supervised manual gating of flow cytometry data from a cohort of 50 healthy donors identified 415 cell types and immune activation states that were used to train and later independently validate machine learning models to automatically identify immune cell subsets from raw cytometry data. By applying this tool to peripheral blood samples from a mixed cohort of 299 healthy donors and 323 cancer patients, we developed a machine-learning classification model that can differentiate between these two groups with 93% accuracy. This model was further refined using spectral clustering with bootstrapping, revealing 5 clusters, or immunotypes, characterized by specific physiological immune profiles: (1) Myeloid-derived suppressor/NK cell, (2) Terminally-differentiated $CD8^+$ T cells, (3) Mixed $CD4^+$ T helper cells, (4) $CD4^+$ Th1 & $CD8^+$ T cell memory, and (5) Naive T and B lymphocytes. Interestingly, very few healthy donors could be found in clusters 1 and 2 but were assigned most frequently to cluster 5. Matched RNA-seq was used to further validate these profiles using the cellular deconvolution algorithm, Kassandra, and differential gene expression analysis revealed immunotype-specific signatures that are consistent with immune response potential. Patients in the terminally-differentiated $CD8^+$ T cell cluster had a narrower range of HLA-types than the other clusters, and TCR repertoire analysis indicated significantly increased clonality and reduced clonotype diversity. Within this cluster there was a high degree of overlap between TCR sequences in the peripheral blood and the tumor, indicating a relationship between peripheral blood immunotype and tumor infiltration. Altogether, the establishment of these immunotypes using peripheral blood immunoprofiling represents a promising signature that can be used to identify and stratify cancer patients that will benefit from immune-based therapies.

#6665

A spatiotemporal cell atlas of human gastric malignancy reveals mechanisms underlying metastasis and immunotherapy response

Yikai Luo[1], Muxing Kang[2], Wei Liu[3], Shiping Jiao[4], Lie Wang[2], Jian Chen[2], Han Liang[3]. *[1]UT MD Anderson Cancer Center, Houston, TX,[2]Zhejiang University School of Medicine, Hangzhou, China,[3]Department of Bioinformatics and Computational Biology, UT MD Anderson Cancer Center, Houston, TX,[4]The Affiliated Hospital of Nanjing University Medical School, Nanjing, China*

Cellular heterogeneity in the tumor immune microenvironment (TIME) of gastric cancer (GC) is progressively molded in pre- and early-malignant lesions and has a profound impact on disease progression and responses to therapeutics, in particular those based on immune checkpoint blockade (ICB). To date, no study has been conducted to characterize the single-cell kinetics of tumor-infiltrating immune populations in gastric cancer

patients treated with ICB. Here, we generated for the first time single-cell RNA sequencing (scRNA-seq) and TCR sequencing (scTCR-seq) profiles of ICB-treated primary GC tumors, as well as liver and ovary metastases. When integrated with public scRNA-seq datasets, our data capture a full trajectory of GC malignancy comprising more than 300,000 cells derived from 73 samples. We further performed bulk TCR-seq, cytometry by time of flight (CyTOF), and multiplex immunofluorescence (mxIF) on independent GC samples to orthogonally validate the key observations from the scRNA-seq cohort and unbiasedly search for more in-depth and spatial-relationship-focused features of ICB-responsive immune populations. Built upon this multi-omic atlas of GC cell states, we identified remarkable transformation of the abundance and clonal dynamics of distinct immune populations and their population-specific transcriptional programs. Most importantly, we observed the rejuvenation of exhausted CD8+ T cells induced by anti-PD-1 treatment, which is associated with the enhanced immunogenicity of gastric cancer cells. In addition, we found the enrichment of NK-like terminally differentiated CD8+ T cells in metastases independent of migration destinations. Our single-cell ICB-perturbed spatiotemporal GC landscape reveals how neoadjuvant checkpoint blockade induces local and systemic tumor immunity. As a cellular and molecular reference, it also enables high-resolution interpretation of future single-cell omics data in gastric cancer that may be masked by de novo analysis.

#6666

Multispectral imaging to detect immune phenotypes in pre and post therapy breast cancer patient specimens

Bhavika Patel, Stephanie Allen, Brenna Dennison, Jacob Stapleton, Roni Archuleta, Mary Lou Rath, Navi Mehra, Sameer S. Talwalkar. *Lanterne Dx, Broomfield, CO*

The immune microenvironment is an important component in cancer therapy. Immune cells can encourage tumor growth, leading to disease progression. A high number of immune cells may be predictive of disease prognosis and response to therapies. Therefore, understanding the immune cell phenotypes present within cancerous tissue can be valuable in developing strategies that aid in the treatment of cancer. In this study, we analyzed pre-and post-therapy samples from breast cancer patients, treated with neoadjuvant chemotherapy, using a 6-plex immunofluorescence assay which included clinically relevant immuno-oncology biomarkers (FoxP3, PD-L1, PanCK, CD4, CD8 and CD163). This assay was developed and optimized in-house prior to testing the cohort. Endpoints for this analysis were characterization of the tumor microenvironment and analysis of the individual immune cell subsets pre and post treatment. Staining was completed on the Leica Bond RX autostainer (Leica Biosystems) and slides were scanned using the PhenoImager™ Fusion (Akoya Biosciences). Using Visiopharm® software, the multiplex phenotyping module was used to analyze the high dimensional human tissue and cell phenotypes were detected using artificial intelligence. Qualitative and quantitative results revealed a change in immune cell phenotypes between pre- and post-therapy samples. These included an increase in intra-tumoral and stromal T cells, no significant difference in PD-L1 positive cells, and an increase in the FOXP3 positive T cells in post-treatment samples. Our data provides insights into the development and application of multispectral imaging for characterization of tumor microenvironment and its dynamics before and after treatment in breast cancer. This can be applied to other cancer types and can aid in making treatment decisions.

#6667

Pan-cancer assessment of tumour and peripheral T-cell receptor repertoire dynamics in patients treated with immune checkpoint inhibitors

Shirin Soleimani[1], Ben X. Wang[2], Stephanie Pedersen[2], Jenna Eagles[2], Jacob Brick[2], Marcus O. Butler[3], Scott V. Bratman[2], Lillian L. Siu[3], Pamela S. Ohashi[2], Trevor J. Pugh[2]. *[1]Medical Biophysics, University of Toronto, Toronto, ON, Canada,[2]Princess Margaret Cancer Centre, Toronto, ON, Canada,[3]Division of Medical Oncology and Haematology, Princess Margaret Cancer Centre, Toronto, ON, Canada*

Introduction: Clinical benefit from Immune Checkpoint Blockade (ICB) is a function of local T-cell specificity for tumor-associated antigens. However, overcoming local T-cell dysfunction necessitates systemic immunity engagement. Therefore, studying the dynamics of both local and peripheral T-cell repertoires in response to ICB is required to identify features of T-cell repertoires associated with pathological response.
Methods: We conducted TCRβ-sequencing on tumor-residing T-cells (n=59), Peripheral Blood Mononuclear Cells (PBMCs) (n=306) and cell-free DNA (cfDNA) (n=73) from pre- and multiple on-ICB timepoints collected from patients enrolled in the pan-cancer INvestigator-initiated Phase II Study of Pembrolizumab Immunological Response Evaluation (INSPIRE; NCT02644369) trial. To assess specificity-agnostic shifts in TCR repertoires, we

first compared TCR diversity and clonal expansion in longitudinal tumor and PBMC samples. Then, to temporally track the specificity-associated features of local and systemic TCR repertoires, we leveraged a Graph Neural Network (GNN) model that took in unique TCRβ chains as nodes. The connectivity between the nodes was defined by multi-relational edges that represented VJ-gene usage and GLIPHII-identified (Grouping Lymphocyte Interactions by Paratope Hotspots) specificities derived from a compendium of TCR sequences with empirically confirmed specificities. **Results:** While absolute diversity and clonal expansion values in baseline tumor (n=33) were not associated with response to ICB, changes in these values were informative between pre- and on-ICB tumors. All patients (n=4) with low baseline tumor TCR diversity and lack of clonotypic re-structuring in tumor TCR repertoire on-ICB had either progressive or short-term stable disease. Furthermore, pairwise comparison of pre- and on-ICB tumors for each patient (n=17) revealed that all the patients, irrespective of their pathological response, experienced emergence of new TCR clonotypes (i.e., clonal replacement) in response to ICB, suggesting only a minority of these TCRs might consist of tumor-associated clonotypes. Patients with clinical benefit also had higher degree of GLIPHII-identified clustering at baseline tumor, highlighting the role of both specificity-agnostic and specificity-centric TCR analysis in determining the response to ICB. Analysis of TCR sequences in blood plasma found cfDNA contains a small number of TCR sequences (median 32, range 12-89) enriched for TCRs found in matched tumor tissues, suggesting that cfDNA TCR repertoire may provide an indirect measurement of tumor-residing T-cells.
Conclusions: TCR diversity and functional clonal annotation are emerging biomarkers of ICB response and cfDNA TCR repertoire can potentially be exploited for clinical diagnostics and monitoring.

#6668

Immune infiltrate co-occurrence and neoantigen similarity are prognostic factors in early stage NSCLC

Martina M. Sykora[1], Jason Pugh[2], Bailiang Li[2], Finn O. Mildner[1], Hubert Hackl[3], Arno Amann[1], Fabienne I. Nocera[1], Rachel M. Pyke[2], Lee McDaniel[2], Charles W. Abbott[2], Sean M. Boyle[2], Richard O. Chen[2], Dominik Wolf[1], Sieghart Sopper[1], Gabriele Gamerith[1]. *[1]Internal Medicine V, Hematology and Oncology, Medical University of Innsbruck, Innsbruck, Austria,[2]Personalis Inc, Menlo Park, CA,[3]Medical University of Innsbruck, Innsbruck, Austria*

The prevalence of early-stage non-small cell lung cancer (NSCLC) with curative treatment options is expected to increase with recent implementation of annual screening programs. Predictors and molecular drivers of disease relapse, especially the role of intra-tumoral immune dysfunction, remains unclear but critical for the refinement of therapeutic decisions. By leveraging a comprehensive individual portrait of each patient's immune system potential novel mechanisms associated with tumor relapse in early-stage NSCLC may be identified. We profiled 11 non-relapsed (at least 2 year FU) lung adenocarcinoma patients and 11 covariate-matched (gender, age, stage) relapsed patients, who underwent curative treatment in stage IA-IIIB disease. We used NeXT Summit^{TM} for variant and CNA calling, gene expression quantification, neoantigen prediction, HLA profiling (typing, mutation, and loss of heterozygosity), T-cell receptor and tumor microenvironment (TME) profiling. Neoantigen peptide sequences were subjected to further filtering and clustering based on between-patient similarity scores, with the goal of identifying shared clusters of relapse-associated neoantigens in each possible pair of patients. Differential network analyses were applied to the TME composition estimates to investigate relapse-associated patterns of cellular co-occurrence and interaction. When considering neoantigens selected on the basis of similarity, we found that those belonging to non-relapsed patients had significantly lower HLA binding rank (17.8 points) compared to that of relapsed patients ($P=0.02$), indicating weaker binding for relapsed cases. Clustering of both the most similar and frequently shared neoantigens correlated with relapse ($P < 0.002$). In the TME, we observed differential immune cell co-occurrence associated with relapse status, such as Tregs are positively correlated with B and CD4 T cells only in relapsed patients (Pearson's $R=0.7$ and 0.74, both $P<0.02$ vs. $R=0.18$ and 0.35, both $P>0.2$ in non-relapsed patients), indicating suppressive anti-tumor immunity. Relapsed patients did not share significant enrichment of mutations in any biological pathway. Surprisingly, mutation purity (less mutations than expected by chance) was observed in relapsed patients, suggesting selective killing and escape. In this pilot cohort, we used an integrated platform to broadly characterize both the tumor and immune system, enabling identification of relapse-associated neoantigens that may share universal features which enhance HLA binding. Relapses in early-stage LUAD patients were associated with neoantigens with lower immunogenicity and an immunosuppressive TME. These findings demonstrate that deeper profiling of shared neoantigen features has the potential to become an early biomarker of relapse, informing patient therapy selection and surveillance.

#6669

Antigen features are associated with response and survival after neoadjuvant chemo-immunotherapy for muscle-invasive bladder cancer

Wolfgang Beckabir, Steven Vensko, Alec Wilkinson, Gatphan Atassi, Mi Zhou, Kenneth Fowler, Leah Flick, Hsing-Hui Wang, Mark Woodcock, Karen McKinnon, Jonathan Serody, Tracy Rose, Matthew Milowsky, William Kim, Benjamin Vincent. *UNC-Chapel Hill, Chapel Hill, NC*

In the Phase II LCCC1520 trial, neoadjuvant chemo-immunotherapy (pembrolizumab with gemcitabine plus cisplatin) induced response in 22 of 39 muscle-invasive bladder cancer patients[1]. In this correlative analysis, we identify molecular features associated with response and survival. Associations of molecular subtype, TMB, and antigen presentation and immune checkpoint gene expression with response and survival were evaluated pre-and post-treatment. Neoantigens were predicted in 4 immuno-oncology data sets (LCCC1520, IMvigor210 cohorts 1[2] and 2[3], and Hugo[4]) using Landscape of Effective Neoantigens Software[5]. Effective neoantigen count (ENC) was calculated by binning predicted neoantigens by expression, binding affinity, binding stability, and tumor PD-1 and PD-L1 expression, then identifying the bin in which neoantigen count was most strongly associated with response in the discovery set. Using elastic net modeling with 10-fold cross-validation, survival was predicted from immune gene signature expression, clinical variables, TMB and ENC. Response was associated with pre-treatment molecular subtype and immune checkpoint expression. Pre-treatment ENC was associated with response in Hugo (discovery set, p = 0.020) and the three validation sets (p = 0.011, 0.042, 0.049). The final elastic net model (Cox P-H p = 5.6e-5) predicted survival significantly better than TMB (p = 0.055) or ENC (p = 0.141) alone. Post-treatment antigen presentation gene expression was associated with survival among non-responders. We identify pre-and post-treatment features associated with response and survival in the LCCC1520 trial and propose that tumor antigen presentation is a major driver of neoadjuvant chemo-immunotherapy outcomes. *[1] Rose JCO 2022 [2] Balar Lancet 2017 [3] Mariathasan Nature 2018 [4] Hugo Cell 2016 [5] Vensko bioRxiv 2022*

#6670

Association between circulating CD4 memory T cell levels and severe immune-related adverse events in melanoma patients treated with immune checkpoint blockade

Abul Usmani[1], Noah Earland[1], Wubing Zhang[2], Peter K. Harris[1], Antonietta Bacchiocchi[3], Aishwarya Nene[3], David Y. Chen[1], Mario Sznol[3], Ruth Halaban[3], Aaron M. Newman[2], Aadel A. Chaudhuri[1]. *[1]Washington University in St. Louis, St. Louis, MO,[2]Stanford University, Stanford, CA,[3]Yale University School of Medicine, New Haven, CT*

Introduction: Severe immune-related adverse events (irAEs) occur in up to 60% of melanoma patients treated with immune checkpoint inhibitors (ICIs), causing substantial treatment-related morbidity and in the most severe cases, death. There is no clinical assay to predict who will develop severe ICI-induced irAEs and who will not. Using single-cell profiling assays applied to a retrospective melanoma cohort treated with ICIs, we recently showed that higher baseline levels of circulating CD4 effector memory T (TEM) cells were associated with severe irAE development, independent of the affected organ system (Lozano et al. *Nature Medicine*, 2022). As part of a prospective validation study of 100 melanoma patients, here we report our initial findings on the first 24 patients accrued to date.

Methods: We prospectively collected pre-ICI blood from 24 metastatic melanoma patients from two academic medical centers from February 2021 onward. Peripheral blood was collected pre-treatment on the day of immunotherapy (cycle 1 day 1). We then isolated peripheral blood mononuclear cells (PBMCs) and applied mass cytometry by time of flight (CyTOF) to profile 38 leukocyte markers including markers specific to CD4 TEM cells. Cellular subpopulations were quantified using Cytobank v9. Patients underwent routine medical oncology follow-up during and after ICI treatment including grading of irAEs using the Common Terminology Criteria for Adverse Events v5.

Results: Median follow-up time after pre-ICI blood collection was 9.1 months (range 2.6-18.5). Fifteen (63%) patients received combination (anti-PD1 / anti-CTLA4) ICIs while the remainder received anti-PD1 monotherapy. Eight patients developed severe (grade 3+) irAEs at a median of 8.5 weeks (range 4-21) after treatment initiation, including 4 who developed life-threatening (grade 4) irAEs. Severe and life-threatening irAE development spanned 9 separate organ systems, most commonly gastrointestinal, dermatological, and hepatic. Using CyTOF, we found that circulating CD4 TEM cells were more abundant in patients who developed severe irAEs compared to those who did not ($P = 0.01$; AUC = 0.81), irrespective of the involved organ systems. Moreover, median-

splitting the patient cohort into two groups based on pretreatment CD4 TEM levels revealed that patients with low CD4 TEMs had significantly longer freedom from severe irAE than those with high CD4 TEMs (not reached vs. 4.6 months; $P = 0.013$; HR = 6.7). There was no significant difference in pretreatment CD4 TEM levels between patients with and without durable clinical benefit to ICIs ($P = 0.75$).
Conclusion: Circulating CD4 TEM levels measured by CyTOF were associated with severe irAE development, independent of response status, in patients with advanced melanoma. These findings could form the basis for pretreatment ICI risk stratification in the future.

#6671
Simplifying high-parameter phenotypic and functional characterization of cancer immune cells
Deeqa Mahamed, Michael Cohen, Stephen Li, Lauren Tracey, Huihui Yao, Christina Loh, Leslie Fung. *Standard BioTools, Markham, ON, Canada*

Interrogating immune cell composition and function in patients with cancer is critical for making disease prognoses, monitoring clinical efficacy of tumor immunotherapies, identifying novel therapeutic targets, and discovering predictive biomarkers of disease. Both the adaptive and innate arms of the immune system play important roles in generating pro- or anti-tumor milieus. In particular, natural killer (NK) cells are gaining increasing attention as potential cell-based therapies in immuno-oncology, including in adoptive transfer of chimeric antigen receptor (CAR) and iPSC-derived NK cells or off-the-shelf NK cell lines to target multiple myeloma. Since NK cells can also indirectly impact CAR T cell or antibody-based immunotherapies, characterizing these cells using optimized and reproducible assays is critical. CyTOF® is a high-plex flow cytometry technology that exploits metal-isotope-tagged antibodies to probe cellular phenotypes and functions. In contrast to fluorescence-based conventional and spectral flow cytometry, CyTOF experimental workflows are streamlined as autofluorescence is not an issue and signal spillover is minimal, allowing rapid design and application of 40-plus-marker panels. To expand on the increasing clinical and preclinical utility of the 30-marker Maxpar® Direct™ Immune Profiling Assay™ (Maxpar Direct Assay), we developed nine add-on Expansion Panels for deeper phenotyping of specific cell types and activation states, including panels designed to characterize *ex vivo* and activated myeloid cells, T cells, and NK cells. Peripheral blood mononuclear cells from healthy donors and donors with multiple myeloma were stimulated *in vitro*, then stained in the 30-antibody Maxpar Direct Assay tube with the NK Cell Expansion Panel (CD181, NKp30, NKp46, PD-1, NKG2A, ICOS, and TIGIT) or the T Cell Panel 3 (OX40, TIGIT, CD69, PD-1, Tim-3, ICOS, and 4-1BB) as drop-in antibodies. Surface staining was followed by intracellular staining with the Basic Activation Expansion Panel antibodies (IL-2, TNFα, IFNγ, perforin, granzyme B) after cell fixation and permeabilization. Anti-CD107a was added during stimulation to measure degranulation. Samples were acquired on a CyTOF XT™ instrument in automated batch acquisition mode. Automated analysis was performed with Maxpar Pathsetter™ software to enumerate immune cell types and quantify marker expression. In addition to the 37 populations identified by Pathsetter with the base Maxpar Direct Assay, the new Expansion Panels allowed deeper profiling of NK and T cells, while the Basic Activation Panel revealed their cytokine responsiveness and cytotoxic potential. Thus, the optimized single-tube Maxpar Direct Assay is a powerful tool that can be further expanded and customized with predefined panels or antibodies to comprehensively study immune cells in health and disease.
For Research Use Only. Not for use in diagnostic procedures.

#6673
Simultaneous detection of IGH VDJ rearrangements and JH translocations via Ring-Seq, a novel multiplex PCR technology for targeted sequencing of translocations with novel gene partners or breakpoints
Shannon Owens, Katherine Fichter, Richard Que, Sabrina Shore, Timothy Looney. *Singular Genomics, San Diego, CA*

Introduction: Next-generation sequencing (NGS) of B cell receptor rearrangements is a leading method for clonality assessment and measurable residual disease (MRD) monitoring of B cell malignancies. Current methods rely upon multiplex PCR (mPCR) amplification of rearranged IGH, IGK or IGL loci via variable and joining gene targeting primers followed by NGS to assess rearrangements. Limitations include a need for reflex testing owing to somatic hypermutation (SHM) mediated loss of sensitivity and an inability to detect clinically relevant translocations of the IGH locus. Here we apply Ring-Seq, a novel technology for the targeted detection gene fusions with unknown partners, to simultaneously detect IGH VDJ rearrangements and translocations in a single

reaction. We demonstrate detection of clinically relevant translocations and VDJ rearrangements from highly degraded gDNA.
Methods: The method begins with a highly efficient circularization of DNA fragments followed by a multiplex inverse PCR of joining genes that preferentially amplifies breakpoint junction containing templates. Amplicon libraries are sequenced on the G4 platform and analyzed to detect translocations and VDJ rearrangements. We pooled gDNA from reference cell lines harboring marker IGH VDJ rearrangements and BCL1/2-JH translocations. Pooled reference gDNA was spiked into a background of healthy donor PBL gDNA to evaluate performance over a range of marker frequencies. To simulate performance with degraded materials, gDNA input was fragmented to ~200bp by sonication prior to analysis.
Results: BCL1-JH and BCL2-JH translocations and marker IGH VDJ rearrangements were detected from 50ng pooled reference gDNA. Translocations and marker VDJ rearrangements were also detected in 50ng samples consisting of reference gDNA spiked at 10% and 1% frequency into a background of healthy donor PBL gDNA. Sequencing of healthy donor PBL gDNA yielded IGH repertoire features that were highly concordant with results obtained from BIOMED-2 mPCR analysis of the same samples.
Conclusions: We have applied Ring-Seq to enable the simultaneous detection of B cell receptor rearrangements and JH translocations relevant to the diagnosis of MCL and FL while minimizing loss of sensitivity owing to SHM. Traditional mPCR often fails to detect JH translocations owing to variation in the breakpoint region. Consequently, suspected MCL and FL diagnostic samples are assessed for translocations by FISH, while separate material is submitted for NGS-based VDJ clonality analysis via traditional mPCR. Ring-Seq may streamline this process by consolidating separate tests into a single rapid NGS assay for the G4 platform. Looking ahead, we envision broad applicability of the technology to mPCR-based variant detection.

#6675

Integration of associations of immune profiles in peripheral blood and tumor microenvironment with bladder cancer outcomes

Ji-Qing Chen[1], Lucas A. Salas[1], John K. Wiencke[2], Devin C. Koestler[3], Annette M. Molinaro[2], Angeline S. Andrew[4], John D. Seigne[5], Margaret R. Karagas[1], Karl T. Kelsey[6], Brock C. Christensen[1]. *[1]Epidemiology, Dartmouth College, Hanover, NH,[2]Neurological Surgery, University of California San Francisco, San Francisco, CA,[3]Biostatistics & Data Science, University of Kansas Medical Center, Kansas City, KS,[4]Neurology, Dartmouth College, Hanover, NH,[5]Surgery, Dartmouth College, Hanover, NH,[6]Epidemiology and Pathology and Laboratory Medicine, Brown University, Providence, RI*

Immune cell profiles in peripheral blood have been associated with bladder cancer outcomes, however, their association with response to immunotherapy and the tumor microenvironment is a major unresolved issue. Although tumor growth can be attenuated via the activation of tumor-infiltrating effector T cells, the relationship between tumor infiltration and immune activation remains unclear. This study explored the interaction between bladder cancer outcomes and immune profiles within peripheral blood and a tumor microenvironment (TME) based on DNA methylation profiles. Peripheral blood and the matched tumor FFPE DNA methylation profiles of 60 non-muscle-invasive bladder cancer (NMIBC) and 12 muscle-invasive bladder cancer (MIBC) patients. Cell-type deconvolution approaches were applied to estimate 12 peripheral immune cell-type proportions and 17 cell-type proportions within TME. We found a positive correlation between dendritic cell proportions in the TME with peripheral CD8T memory cell proportions ($r = 0.35$, $P = 0.003$) and a negative correlation between dendritic cell proportions in the TME with peripheral regulatory T cell proportions ($r = -0.28$, $P = 0.021$). In addition, monocyte cell proportions in TME had a positive correlation with peripheral B memory ($r = 0.37$, $P = 0.002$) and CD8T memory cell proportions ($r = 0.43$, $P = 0.0002$). To investigate associations of bladder cancer outcomes with immune cell profiles, using Cox proportional hazard models, we observed an association between the fraction of dendritic cells and the hazard of death (HR = 1.27, 95% CI = 1.06-1.53). Further, a high endothelial cell proportion was significantly associated with an increased hazard of death and tumor recurrence (HR = 1.06, 95% CI = 1.01-1.13) in TME. In addition, the peripheral neutrophil-to-lymphocyte ratio (HR = 1.49, 95% CI = 1.01-2.22), monocyte (HR = 1.17, 95% CI = 1.05-1.31), neutrophil (HR = 1.04, 95% CI = 1.01-1.07), and basophil (HR = 1.35, 95% CI = 1.01-1.81) cell proportions were associated with an increased hazard of death and tumor recurrence. Our results integrated the information on bladder cancer outcomes and cell profiles in TME and peripheral blood, providing biomarkers for estimating bladder cancer prognosis using genome-scale DNA methylation measures.

#6676

Exploratory biomarker analyses in phase 1 study of regorafenib, ipilimumab, and nivolumab (RIN) in chemotherapy resistant microsatellite stable (MSS) metastatic colorectal cancer (mCRC)

Jian Ye[1], Chongkai Wang[2], Colt Egelston[1], Weihua Guo[1], Peter P. Lee[1], Marwan Fakih[2]. *[1]Beckman Research Institute of the City of Hope, Duarte, CA,[2]City of Hope National Medical Center, Duarte, CA*

Background: We recently reported an objective response rate of 36.4% in a phase I trial of RIN in MSS mCRC patients without liver metastases, while no response was noted in patients with liver metastases. Here we characterized kinetics in local and systemic immune responses associated with clinical outcomes, liver metastasis, and immune related toxicity during RIN treatment.
Methods: Patients with chemotherapy-resistant MSS mCRC received RIN at (R) at 80 mg QD x 21 days in 4-week(w) cycle, (I) at 1mg/kg Q6w and (N) at 240 mg Q 2w (n=29). Needle biopsies were collected at baseline (n=8) and 4 weeks (n=6) after treatment. Blood samples were collected at baseline (n=29), 4 weeks (n=29) and 8 weeks (n=25) after treatment. Alterations in the tumor microenvironment (TME) were characterized by RNA sequencing. We analyzed the immune cell composition and activities in the blood, including 90 subpopulations of leukocytes and 29 activation/suppression/proliferation markers, with high-dimensional spectral flow cytometry.
Results: The clinical responses are positively correlated with the induction of local anti-tumor immunity. Patients with better clinical outcomes exhibited higher levels of lymphocyte infiltration, chemokine production, and antigen-presentation potential in the local TME following one cycle of RIN treatment. The duration of progression-free survival (PFS) was correlated with a higher baseline STING signal in the TME. In the peripheral blood, the responders have more circulating CD4 T cells, B cells, and cDC1, while expressing lower immune activation markers, especially in T cells with type 1 immunity at baseline. At 4 weeks, immune activation and proliferation markers were higher in responders than non-responders. Interestingly, immune effectors (non-Tregs, $CD45RA^-$ CD8 T cells, NKT cells, and M1 monocytes) in the blood were proportionally reduced in responders at 4 weeks, coincident with their enrichment in the local TME. We also compared peripheral immune signatures between patients with and without liver metastases, liver metastases (n=7) were associated with a significantly lower ratio of CD4/CD8 T cells in the blood, a phenomenon of immunosenescence, both at baseline and after RIN treatment. Lastly, the occurrence of immune-related toxicities was closely correlated with the induction of immune activities in both acellular and cellular components in the circulation.
Conclusions: Clinical benefit of RIN was correlated to more robust immune activation of the TME and peripheral blood following one cycle of treatment. A higher baseline STING signal in the TME was associated with longer PFS. Liver metastasis was associated with a lower ratio of peripheral CD4/CD8 T cells which may contribute to the resistance to immunotherapy in those patients.

#6677

Preliminary immune correlatives from BCA101 trial show favorable modulation of tumor immune microenvironment

Patrick H. Lizotte[1], Paul Paik[2], Liviu Niculescu[3], Seng-Lai H. Tan[3], David Bohr[3], Elham Gharakhani[3], Ralf Reiners[3], Rachel Salazar[3], Avanish Varshney[3], Shiv Ram Krishn[4], Pradip Nair[4], Cloud Paweletz[1]. *[1]Dana-Farber Cancer Institute, Boston, MA,[2]Memorial Sloan Kettering Cancer Center, New York, NY,[3]Bicara Therapeutics, Cambridge, MA,[4]Syngene International Limited Biocon, Bangalore, India*

Background: BCA101 is a bispecific antibody targeting EGFR and TGF-β. TGF-β pathway activation is a hallmark of human immune-excluded tumors, and TGF-β expression is associated with resistance to anti-PD-1 blockade. Neutralization of TGF-β removes an immunosuppressive signal that drives accumulation and polarization of myeloid-derived suppressor cells (MDSCs) and tumor-associated macrophages (TAMs) in solid tumors, while EGFR inhibition targets tumor cell-intrinsic oncogenic signaling. Co-targeting of EGFR and TGF-β directly impacts tumor progression while enhancing the immunogenicity of tumors.
Methods: Patients with multiple solid tumor types (CRC, pancreatic, HNSCC, SqNSCLC, and others) were treated with escalating doses of either single agent BCA101 or in combination with anti-PD-1 (pembrolizumab) enrolled on NCT04429542 trial. We performed a variety of immune correlatives on pre- and on-treatment tumor biopsies, including Nanostring-based transcriptomic profiling and IHC for immunophenotypic markers, as well as multiparametric flow cytometric profiling of circulating PBMCs.
Results: Our preliminary evidence suggests that neutralization of TGF-β positively alters the systemic immune state (PBMCs) and tumor immune phenotype (mRNA, IHC). Circulating HLA-DR+ monocytes were significantly

increased in on-treatment PBMC samples relative to screening. Pathway analysis of on-treatment tumor biopsies revealed enhanced costimulatory signaling, cytokine and chemokine signaling, immune infiltration, and interferon signaling. Top differentially regulated genes in on-treatment biopsies included CCL21, CXCL9, CXCL11, and CXCL13, which recruit T and NK cells. HDAC11, which negative regulates type-I interferon signaling, was significantly reduced in on-treatment biopsies. Notably, two patients with EGFR-amplified squamous non-small cell lung cancer, who both progressed on first-line immunotherapy treatment, were treated with BCA101 at 1250 mg and 1500 mg qw and achieved a partial response (ongoing for 10 months at the time of the data cutoff) and a prolonged stable disease for 11 months, respectively. They exhibited increased CD8+ T cell infiltration and a reduction in TAMs following treatment.
Conclusions: Increased abundance of circulating HLA-DR+ monocytes following treatment indicated polarization towards a more positive, Th1-like systemic immune state. We observed enhanced immunogenicity of tumors as assessed by a targeted IO transcriptomic analysis. The results of the pathway analysis were supported by IHC on post-treatment biopsies from a subsequent cohort showing enhanced CD8+ T cell infiltration and stable, or reduced expression of TAM marker CD163. These results indicate that neutralization of TGF-β induces a more permissive tumor immune microenvironment.

Liquid Biopsies: Circulating Nucleic Acids and Circulating Tumor Cells 5

#6681
XNA increases assay sensitivity in sanger sequencing, qPCR, NGS and CRISPR mutant screening
Wei Liu, Robert Brown, Andrew Fu, Shuo Shen, Michael Sha, Aiguo Zhang. *DiaCarta, Pleasanton, CA*

The proprietary XNA (xeno nucleic acid) technology has wide applications in sensitive detection of rare mutations in different genomic platforms. These target-specific DNA oligo analogs increase assay sensitivity by blocking the polymerase-dependent amplification of wildtype sequence so only amplification of the mutant sequence occurs. Here we show that the XNA technology helps enrich rare somatic mutations in different human specimen types such as FFPE and plasma samples, using technology platforms such as Sanger sequencing, TaqMan qPCR, and NGS. XNA increases assay sensitivity to 0.1% for Sanger sequencing and qPCR. For NGS, XNA allows detection of the mutant sequence at a lower sequencing depth, thus combining XNA technology with NGS for MRD (molecular residual disease) detection could improve cancer management. In addition, We also show CRISPR mutant screening using a target-specific XNA in a SYBR Green qPCR assay. XNA can be used for rapid CRISPR mutant screening for DNA from pool or individual clones generated from gene editing experiments. In summary, XNA technology is a powerful tool when combined with existing genomic mutation detection platforms to screen for rare somatic mutations and for rapid CRISPR mutant screening. The technology is customizable as a service for easy integration with current technology platforms and applications.

#6682
A patient-specific, tumor-informed, circulating tumor DNA (ctDNA)-based minimal residual disease (MRD) assay in surgical patients with biliary tract cancer
Tianqiang Song, Qiang Wu, Yunlong Cui, Huikai Li, Wei Zhang, Feng Fang, Qingqing Xiong. *Tianjin Medical University Cancer Institute and Hospital, Tianjin, China*

Background: Biliary tract cancer (BTC) refers to malignancies arising from the bile ducts, gallbladder, and ampulla of Vater. ctDNA-based MRD testing has shown promise in identifying surgical patients at high risk of recurrence, although there is a paucity of evidence on its utility in BTC. In this study, we prospectively evaluated the performance of Burning Rock Patient-specific pROgnostic and Potential tHErapeutic marker Tracking (brPROPHET), a patient-specific, tumor-informed MRD assay.
Methods: Surgical specimens and two serial blood biopsies (before and approximately 4 weeks after surgery) were collected. The brPROPHET MRD assay (Burning Rock Biotech, China) uses whole exome sequencing for detecting patient-specific somatic alterations from tumor tissues and for blood a personalized panel designed to target up to 50 variants. For head-to-head comparison, the samples were also subjected to a tumor-informed, fixed-panel assay using 520- and 168-gene panels respectively for tumor and blood samples.
Results: A total of 17 patients were analyzed. Most were men (11, 64.7%), had extrahepatic cholangiocarcinomas (13, 76.5%), or stage II disease (15, 88.2%). Median age was 64 years (range 57-68). Disease-free survival (DFS) was available for 14 patients at a median follow-up of 11.5 months (range 6.5-16.0). Baseline and postoperative ctDNA positivity rates were 64.7% (11/17) and 11.8% (2/17) with brPROPHET and 17.7% (3/17) and 5.8% (1/17)

with the fixed-panel assay using 520- and 168-gene panels. Moreover, of the 3 patients who have relapsed, 1 was postoperatively ctDNA-positive by both assays and 1 only by brPROPHET. These findings suggested superior technical sensitivity of patient-specific over fixed-panel approach in detecting tumor-associated aberrations, and this advantage could translate into more sensitive identification of surgical BTC patients at high risk of recurrence. Furthermore, ctDNA positivity determined brPROPHET by was significantly associated with shorter DFS (log-rank p = 0.003), while that by fixed-panel was not (log-rank p = 0.113), suggesting a stronger association between the patient-specific approach with clinical outcomes. brPROPHET-derived postoperative ctDNA positivity also showed higher negative predictive value (91.7% vs 84.6%) and accuracy (92.9% vs 85.7%) in predicting recurrence. Together, these results supported a better performance of brPROPHET than the fixed panel approach for MRD detection.
Conclusions: This prospective study demonstrated the clinical performance of brPROPHET, a patient-specific tumor-informed ctDNA-based MRD test for surgical patients with BTC. Compared with the fixed-panel approach using 520- and 168-gene panels respectively for tumor and blood samples, brPROPHET yields higher sensitivity, accuracy, and negative predictive value in predicting relapse.

#6683
Genetic alterations of circulating tumor DNA in advanced pancreatic cancer patients receiving 5-fluorouracil based chemotherapy
SooBeen Heo[1], Sunhwa Park[1], Jung Won Chun[1], Yun-Hee Kim[1], Jun-Kyu Kang[2], Hwang-Phill Kim[2], Sang Myung Woo[1], Sun-Young Kong[1]. *[1]National Cancer Center, Goyang, Korea, Republic of,[2]IMBdx, Seoul, Korea, Republic of*

Background: Pancreatic cancer remains one of the most devastating malignancies due to lack of target therapeutic options for advanced disease. Liquid biopsy which analyzes tumor-related biomarkers in blood, has emerged as an innovative technology. The aim of this study was to identify circulating tumor DNA (ctDNA) mutations in pancreatic adenocarcinoma(PDAC) patients using multi-gene panels.
Methods: Total of 45 patients (27 male, median age 63 years) blood samples were obtained at baseline then follow-up after 2 months samples were acquired in 16 patients at National Cancer Center, Korea from November 2021 to April 2022. CtDNA were analyzed by next-generation-sequencing (NGS) panel of 118 genes and the varient allele frequency (VAF) of detected genes were analyzed. Then the association between outcomes of 5FU treated response and survival (overall survival and progression-free survival; OS and PFS) and VAF reduction at follow-up were analyzed.
Results: Total of 35 genes with 114 genetic alterations were detected and frequent mutations were as follows: KRAS (29.9%), TP53 (14.9%), GNAS(4.4%), SMAD4(4.4%), AR(3.5%), RNF434(3.5%), ATM(3.5%), BRCA2(2.6%) and PIK3CA(2.6%). The mean VAF level considering all pathogenic variants of 45 patients was 8.9%(range, 0 - 87.2) including 8 patients who were not detected ctDNA mutations in baseline, and the mean VAF was 4.2% (0 - 50.0) at follow-up in 16 patients. With association of clinical response, patients with partial response (PR) and stable disease (SD) were decreased VAF from 11% at baseline to 10% after 2 months, and three (60%) of patients showed clearance of ctDNA. Progressive disease (PD) patients were also decreased VAF 67% after 2 months, however, clearance of ctDNA was only observed in one patient (12.5%). Reduction of ctDNA more than 50% were associated with longer survival as PFS (> 50% reduction groups vs. no reduction group; 5 vs. 3 months, p value=0.903, OS (undefined vs. 6 months, p value =0.180).
Conclusions: This study showed most common mutation was KRAS with several other mutations of ctDNA in PDAC, and outcomes represented association with ctDNA.

#6684
Detection of PD-L1, HER2 and EGFR on circulating tumor cells in carcinoma patients
Jayant Khandare[1], Atul Bharde[1], Sreeja Jayant[1], Gourishankar Aland[1], Meghana Garbhe[1], Sayali Gosavi[1], Apoorva Janorkar[1], Purva Tikekar[1], Mrunmayi Patil[1], Vikas Jadhav[1], Ganesh Khutale[1], Amrut Ashturkar[1], Aravindan Vasudevan[1], Kumar Prabhash[2], Nirmal Raut[3], Pankaj Chaturvedi[4]. *[1]Actorius Innovation and Research USA and India, Pune, India,[2]Tata Memorial Hospital, Mumbai, India,[3]Bhaktivedanta Hospital And Research Institute, Mumbai, India,[4]Tata Memorial Hospital, Tata Memorial Hospital, Mumbai, India*

Background: Small molecular inhibitors and immunotherapy has emerged as a novel alternative treatment regime for a variety of epithelial cancers. Large number of clinical trials are in progress to gauge efficacy of tyrosine

kinase inhibitors or immune checkpoint inhibitors against actionable targets such as receptor tyrosine kinases and program death ligand 1 (PD-L1). Although highly effective, the outcome of PD-L1 based ICI or TKI against RTKs is vitally contingent on the presence of PD-L1 or RTK expression on circulating tumor cells. We report validation of CTCs with PD-L1, HER2 and EGFR expression in different epithelial cancers.
Methods: We retrospectively evaluated 134 carcinoma patients blood for presence of CTCs expressing PD-L1, HER2 or EGFR markers respect. 45 % patients had lung cancer, while 25 % and 20 % were presented with breast and GI and CRC malignancies. Remaining were gallbladder, ovarian, prostate, and head and neck cancers. CTCs were isolated from DCGI approved OncoDiscover platform with immunomagnetic targeting of EpCAM. CTCs were confirmed with expression of CK18, absence of CD45 and presence of DAPI nucleus. Presence/absence of biomarkers was determined using fluorescence imaging. Expression of PD-L1, HER2 or EGFR was detected by fluorescence microscopy using fluorescently labelled anti PD-L1, HER2 or EGFR antibodies respect. Based on fluorescence intensity CTCs were binned as PD-L1, HER2 or EGFR negative for no detectable fluorescence signal or weakly or strongly positive based on low or high fluorescence signal.
Results: Among the evaluated cohort, 51% of CTCs showed presence of PD-L1 expression. While 63% showed HER2 positive CTCs (breast cancer). 20% from the PD-L1 positive population showed stronger PD-L1 expression. 78% of CTCs from lung cancer patients showed presence of detectable PD-L1 signal, while 66% breast, GI and CRC patients showed CTCs with PD-L1 expression. CTCs from HNC and gall bladder cancer patients showed low PD-L1 expression (25% and 50% respect.). Among CTCs originating from different cancer types, breast cancer CTCs showed higher mean expression of PD-L1 compared to CTCs from CRC patients. A clear subset of CTCs for PD-L1 and Her2 expression was observed in lung and breast cancer patients respect, suggesting the heterogeneity in expression or presence of different subclones within the same tumor type. CTCs evaluated for EGFR expression, 50% showed presence of detectable EGFR compared to the cut-off signal.
Conclusions: CTC can be used as a real-time surrogate for molecular profiling of PD-L1, HER2 and EGFR expression. These CTC cell surface markers offer alternative for immunotherapy or targeted therapies decisions in a adenocarcinomas.

#6685
Targeted liquid biopsy mutation profiling and genome-wide cfDNA copy-number landscape in 3000 samples from six major cancer indications
Billie Gould, Lu Tan, Chao Dai, Tiantian Zheng, Wei Mo, Xianghong Wang, Michael Sneddon, Shidong Jia, Kemin Zhou, Pan Du. *Predicine Inc., Hayward, CA*

Introduction. PredicineCARE is a CLIA-certified targeted next-generation sequencing (NGS) assay that provides comprehensive, non-invasive genomic profiling of circulating tumor DNA (ctDNA) in blood and urine. Here we present liquid biopsy mutational profiles and genome-wide cell-free DNA (cfDNA) copy-number burden levels for historical cancer cohorts analyzed with PredicineCARE. We include a total of 3,147 samples from six major cancer indications: prostate (n=1681), lung (n=630), breast (n=300), colorectal (n=217), pancreatic (n=190), and bladder (n=129).
Methods. PredicineCARE employs a 152 targeted gene panel covering all major guideline-recommended alterations for patient care and clinical drug development including targeted therapies and immunotherapies. The assay detects single nucleotide variants (SNVs), small insertions and deletions, gene-level copy number loss/gain, and targeted re-arrangements/fusions. Concurrent low-pass whole-genome sequencing (without the need for additional sample volume) is performed to measure blood-based genome-wide copy-number burden (bCNB) and tumor fraction, providing important complementary molecular insights to variant detection.
Results. We present data from a representative cohort of blood and urine samples processed at Predicine lab in Hayward California (n=3,147). Sequencing was performed using a minimum of 5 ng total cfDNA input from 1-5 mL of plasma or 20-40mL of urine, at one or more clinical timepoints per patient. Samples were sequenced at ~20,000X target panel coverage and the majority also had ~2.5X low-pass whole genome sequencing. Using the Predicine in-house DeepSea bioinformatics pipeline, we report variants as low as 0.05% allele frequency and estimate genome-wide CNVs and bCNB from low-pass data. We compare the mutational and CNV profiles of important genes in each liquid biopsy cancer cohort to variants reported in solid tumor tissues from several large public data sets including Project GENIE (n=71,817 patients) and 136 additional study programs including TCGA (n=38,619 patients, www.cBioPortal.org).
Conclusion. PredicineCARE is a highly sensitive and robust assay for detecting cancer variants in blood and urine. The cfDNA mutation profiles are mostly consistent with public tissue datasets. A small but significant portion of the detected ctDNA variants have been shown to be important for treatment selection or are currently

being tested for targeted drug development. Increased bCNB provides a useful measure to monitor treatment response and disease progression. PredicineCARE has been CE-marked and received breakthrough device designation from FDA. A harmonized PredicineCARE assay is available in the US and China to support patient testing in the clinic, global clinical trials and CDx development.

#6686

Tumor suppressor miRNA-665 based serum biomarker for detecting pancreatobiliary cancer

Shuichi Mitsunaga[1], Makoto Ueno[2], Masahiro Tsuda[3], Takamichi Kuwahara[4], Yukiko Takayama[5], Keiji Hanada[6], Hitoshi Yoshida[7], Kenji Takahashi[8], Kohei Nakata[9], Hideaki Iwama[10], Masafumi Ikeda[11], Satoshi Kobayashi[2], Ikuya Miki[3], Kazuo Hara[4], Ryota Higuchi[12], Akinori Shimizu[6], Tomohiro Nomoto[7], Hidetaka Iwamoto[8], Masafumi Nakamura[9], Etsuro Hatano[10], Hiroko Sudo[13], Satoko Takizawa[13], Atsushi Ochiai[14]. *[1]Division of Biomarker Research, Exploratory Oncology Research and Clinical Trial Center, National Cancer Center, Kashiwa, Japan,[2]Department of Gastroenterology, Kanagawa Cancer Center, Yokohama, Japan,[3]Department of Gastroenterological Oncology, Hyogo Cancer Center, Akashi, Japan,[4]Department of Gastroenterology, Aichi Cancer Center, Nagoya, Japan,[5]Department of Gastroenterology, Tokyo Women's Medical University, Tokyo, Japan,[6]Department of Gastroenterology, Onomichi General Hospital, Onomichi, Japan,[7]Department of Medicine, Division of Gastroenterology, Showa University School of Medicine, Tokyo, Japan,[8]Department of Medicine, Asahikawa Medical University, Asahikawa, Japan,[9]Department of Surgery and Oncology, Graduate School of Medical Sciences, Kyushu University, Fukuoka, Japan,[10]Department of Gastroenterological Surgery, Hyogo College of Medicine, Nishinomiya, Japan,[11]Department of Hepatobiliary and Pancreatic Oncology, National Cancer Center Hospital East, Kashiwa, Japan,[12]Department of Surgery, Institute of Gastroenterology, Tokyo Women's Medical University, Tokyo, Japan,[13]Toray Industries, Inc., Kamakura, Japan,[14]Research Institute for Biomedical Sciences, Tokyo University of Science, Noda, Japan*

Background: MicroRNA-665 (miR-665), an intracellular inhibitor of pancreatic cancer (PC) cells, might be a potential biomarker to detect pancreatobiliary cancer (PBca). We sought to determine the diagnostic ability of miR-665 as a serum biomarker for PBca, and to explore the role of miR-665 in PC.
Methods: This multicenter study enrolled patients with treatment-naïve PBca and healthy participants. PBca-related serum miRNAs were determined using weighted co-expression network analysis of a comprehensive serum miRNA microarray dataset in an exploratory cohort. Using various combinations of PBca-related serum miRNAs, Fisher's linear discriminant analyses provided miRNA signatures to discriminate PBca from healthy controls. MiRNA signatures with a sensitivity/specificity (SN/SP) of ≥80/80% and high AUC in comparison with the AUC of CA19-9 were defined as the diagnostic miRNA signature in exploratory, validation and independent validation cohorts, whose accuracy was confirmed by 5-fold cross validation. Biology of the diagnostic miRNAs was evaluated using biopsy samples from liver metastasis of PC patients and human PC cells.
Results: We analyzed 496 of 1487 enrolled subjects (150 healthy and 134 PBca, 50 healthy and 47 PBca, and 50 healthy and 46 PBca subjects in the exploratory, validation and independent validation cohorts, respectively). Among miRNA signatures from 82 PBca-related miRNAs, a five serum miRNA combination containing miR-665 was identified as the diagnostic miRNA signature in all three cohorts. SN/SP and AUC in the validation and independent validation cohorts were 92/88% and 0.95 (CA19-9: 81/92% and 0.94) and 87/80% and 0.91 (CA19-9: 80/98% and 0.87), respectively. In sub-population analysis for detecting 48 resectable PCs, the discriminative ability of the diagnostic miRNA signature plus CA19-9 (SN/SP: 90/78%) was superior in sensitivity to that of CA19-9 alone (60/94%). In seven PC patients with liver metastasis, high expression of intratumor miR-665 tended to correlate with high serum miR-665 level ($r = 0.56$) and low expression of intratumor phospho-Erk expression ($r = 0.57$). Transfection of miR-665 to a human PC cell led to cell growth suppression.
Conclusions: This study identified the diagnostic ability of a tumor suppressor miR-665-based serum miRNA signature for PBca. For detecting resectable PC, a miR-665-based serum miRNA signature plus CA19-9 is a superior biomarker to CA19-9 alone.

#6687

Prevalence of four major gene mutation classes in a survey of ctDNA recovery from early and advanced stage NSCLC

Claire Gould, Leisa Jackson, Colin Cochran, Audrey Audetat, Brittany D'Alessio, Amanda Weaver, Janice Riley, Gary A. Pestano. *Biodesix, Inc., Boulder, CO*

Introduction: Circulating tumor DNA (ctDNA) has emerged as a powerful biomarker with many applications in oncology including early and late-stage disease prognosis and in treatment decision making. Liquid biopsies have become critical in non-small cell lung cancer (NSCLC) given the patient risks associated with biopsies. It is well established that circulating nucleic acid levels representative of all solid tumors are increased in advanced stages of the disease. Less well characterized is the status of cfDNA levels in the earliest stages of solid tumor progression. We used validated methods for quantitative fluorometry and a high sensitivity amplicon based NGS method to survey cfDNA recovery and prevalence for the four major mutation classes (copy number amplifications (CNAs), single nucleotide variations (SNVs), fusions, and insertions/deletions (INDELs)) from patients previously diagnosed with NSCLC.
Methods: Cell-free nucleic acid was extracted from 1,139 late-stage and 185 early-stage NSCLC plasma specimens. cfDNA was quantified using fluorometry, and the 52 gene GeneStrat NGS Test was used for the detection of CNAs, SNVs, fusions and INDELs. We evaluated cfDNA concentration (normalized to plasma input volume), quantity in circulation, and the prevalence of the four classes of mutations in early-stage (I-IIIA) versus late-stage (IIIB-IV) NSCLC.
Results: We observed significantly lower average concentrations of cf nucleic acids in plasma recovered from early versus late-stage NSCLC specimens (early-stage: 13.7 ng/mL; range (3.14, 118.65); n = 185; late-stage: 18.3 ng/mL; range (0.67, 187.2); n =1,139; p=0.00176). We also evaluated total cfDNA recovered for the sample set and observed significantly lower average measurements for early-stage specimens versus late-stage (early-stage: 101.4 ng; range (18.38, 652.6); n=185; late-stage: 140.5 ng; range (9.802, 1534); n=1,139; p=0.00692). We do note that there were overlaps at the low end of the ranges. Also significant was the finding that all mutation classes were more prevalent in late versus early-stage NSCLC. Specifically, 56 of 58 CNAs (96.6%); 737 of 805 SNVs (91.6%); 42 of 43 INDELs (97.3%) and 12 fusions (100%) were associated with late-stage specimens.
Conclusion: In this observational study cohort, cfDNA yields were significantly higher in late-stage NSCLC patients compared to early-stage. We also observed significantly more and varied mutations in plasma from late-stage patients. These initial findings need to be extended to additional cancers and refined by stage at diagnosis. We are currently expanding our study to include additional technologies and panels to assess ctDNA mutations especially for the early-stage patients. Quantitative cfDNA data may be of utility in diagnosis, monitoring and recurrence of cancer.

#6688
Development of a liquid biopsy cfDNA assay for detection of multiple HPV types in cervical neoplasias
Johanna Herbst[1], Vanessa Vohl[1], Maroje Krajina[2], Katharina Prieske[3], Anna Jaeger[3], Markus Leffers[1], Leticia Oliveira-Ferrer[3], Yvonne Goy[4], Klaus Pantel[1], Alexander Sartori[2], Caren Vollmert[2], Linn Wölber[3], Katharina Effenberger[1], Harriet Wikman[1]. *[1]Tumor Biology, University Medical Center Hamburg-Eppendorf, Hamburg, Germany,[2]Agena Bioscience GmbH, Hamburg, Germany,[3]Gynecology, University Medical Center Hamburg-Eppendorf, Hamburg, Germany,[4]Radiology, University Medical Center Hamburg-Eppendorf, Hamburg, Germany*

Background: Over 95% of cervical cancers and their precancerous lesions are caused by human papillomavirus (HPV). Molecular screening approaches for HPV detection are gaining promising data over cytologic analysis. Similarly, liquid biopsy-based approaches are becoming a powerful tool for cancer detection and monitoring.
Materials and Methods: An HPV panel detecting 24 HPV types was developed suitable for liquid biopsy approaches. Here, HPV measurement was performed with an iPLEX multiplex PCR-based workflow combined with mass spectrometry-based analysis (MassARRAY System, Agena Bioscience). The assay was validated on HPV positive plasmid controls and cell lines. Furthermore, 52 cervical smear samples from HSIL positive women and 40 cfDNA samples (peripheral blood) from cervical cancer patients were screened using this approach.
Results: According to already published ring trial results, the HPV types HPV6, 11, 16, 18, 31, 33, 35, 39, 45, 51, 52, 58 and 59 were considered proficient with the required detection level of 50 and 5 international units (IU)/5 µl for HPV 16 and 18, and 500 and 50 HPV genome equivalents (GE)/5µl for the other HPV types (Arroyo Mühr et al., 2022). Further analyses showed a sensitivity of 0.03% for HPV16 and 0.33% HPV18 and 0.33% for the other tested HPV types. HPV DNA was detected in 94% of (49/52) smear samples analyzed. 86.5% were found positive for at least one of the high-risk HPV (hrHPV) types in the study cohort. Two of the three HPV negative samples were truly negative according to clinical data. In 15 samples, multiple HPV types were found, with positivity in up to five different HPV types. For smear samples a sensitivity of 98.14% and a positive predictive value of 0.98 (49/50) were thus obtained. The overall agreement between the MassARRAY and Seegene (from clinical records) HPV tests was 97.2% (κ=0.84). 27 of 40 (67.5%) cfDNA cervical cancer samples were tested positive for any

HPV type. The distribution of HPV types showed most infections being due to hrHPV (25/27 plasma HPV positive). HPV positive samples were found in all FIGO stages, with 56.5% positivity in FIGO stage I and 87.5% in FIGO stage III and IV.
Conclusions: The HPV assay showed reliable results for detecting a large number of HPV types in a multiplex mass spectrometry-based assay. A high sensitivity was achieved for both, cervical smear samples of HSIL patients as well as cfDNA from blood samples of cervical cancer patients.

#6689

Whole genome cell-free tumor DNA mutational signatures from blood for early detection of recurrence of low stage lung adenocarcinoma

Ivy Tran[1], Alejandro Vargas[1], Reid Wilkins[1], Isabella Pizzillo[1], Kenneth Tokoro[2], Danielle Afterman[3], Tomer Lauterman[3], Maja Kuzman[4], Santiago Gonzalez[4], Dunja Glavas[4], James Smadbeck[4], Dillon Maloney[4], Jurica Levatic[4], Samuel Phillips[4], Sunil Deochand[4], Michael Yahalom[4], Ryan Ptashkin[4], Iman Tavassoly[4], Zohar Donenhirsh[3], Eric White[4], Ravi Kandasamy[4], Ury Alon[3], Paz Polak[4], Boris Oklander[3], Asaf Zviran[4], Matija Snuderl[1], Harvey I. Pass[2]. *[1]Pathology, NYU Langone Health, New York, NY,[2]Department of Cardiothoracic Surgery, NYU Langone Health, New York, NY,[3]C2i Genomics, Haifa, Israel,[4]C2i Genomics, New York, NY*

Introduction: Lung cancer remains the leading cause of cancer-related deaths. Surgery is the best option for early lung cancer, and the role of adjuvant therapy remains controversial. Liquid biopsy offers a noninvasive approach to monitor cancer burden. Targeted sequencing of circulating cell free tumor DNA (ctDNA) in blood has shown success for diagnosis; however, low tumor burden and dynamic evolution of low stage disease is challenging for targeted panels. Thus, we hypothesized that a whole genome sequencing (WGS)-derived patient specific mutational signature from a matched tumor-normal WGS can provide sensitive and specific approach to detect mutations and copy numbers in ctDNA for monitoring of lung adenocarcinoma patients.
Methods: We successfully profiled 50 Stage 1 or 2 lung adenocarcinomas. ctDNA was extracted from 1-2 mL of plasma, tumor DNA was extracted from pathology tissue and normal germline DNA from the white blood cells. WGS using was performed on matched tumor and normal DNA, and ctDNA extracted from plasma. WGS coverage was 40x for matched tumor-normal and 20x for ctDNA. We derived a personalized mutational pattern for each tumor and used an AI-based error suppression model for quantification and ultra-sensitive detection of ctDNA in plasma samples. A patient-specific personalized genome-wide compendium of somatic mutations and copy numbers was established and ctDNA tested at 3 to 18 available time points during the therapy or follow up. A personalized mutational signature for detection ctDNA from WGS was quantified and the ctDNA Tumor Fraction (TF) was compared to the clinical status and time to recurrence.
Results: Tumor specific signatures were derived from matched tumor-normal samples with >5% tumor purity and <30% duplications rate. Out of all patients, 33 patients showed no recurrence and 12 recurred. Tumor-specific signatures detected the presence of the tumor signature in plasma with TF as low as 10^{-5}. Based on positive minimal residual disease in plasma, the recurrence prediction sensitivity was 0.75 and specificity 0.82, with positive predictive value of 0.6 and negative predictive value 0.9. WGS ctDNA predicted recurrence with a median lead time of 508 days before clinical/imaging recurrence. In one case we were able to identify the second primary by deconvoluting known and novel ctDNA mutations. ctDNA mutational profiles enabled identification of smoking mutational signature matching clinical history, and APOBEC and ageing signatures as well as tumor mutational burden.
Conclusions: Patient-specific WGS tumor signature from plasma derived ctDNA enables specific and ultrasensitive tracking of minimal residual disease in low stage lung adenocarcinoma patients. Molecularly positive status can be used to predict recurrence and identify patients with clinical low stage disease that may benefit from adjuvant therapy.

#6690

Monitoring response and resistance to EGFR inhibition with circulating tumor DNA in a non-small cell lung cancer patient-derived xenograft

Long H. Do, Raffaella Pippa, Warren Andrews, Yuan Chien, Jantzen Sperry, Jonathan Nakashima. *Certis Oncology Solutions, San Diego, CA*

Circulating tumor DNA (ctDNA) has been shown as a clinically relevant biomarker for non-invasive monitoring of therapy response, disease burden and disease progression in cancer patients. Patient-derived xenografts (PDX) are

essential translational models used for evaluating therapeutic response and identifying novel biomarkers, but analysis of ctDNA in these models remains understudied. Here, we report the use of ctDNA for the monitoring of therapeutic response and secondary resistance of a Non-Small Cell Lung Cancer PDX treated with EGFR inhibitors. We demonstrate measurable ctDNA changes correlate with disease burden and therapeutic response. Altogether, the isolation of ctDNA from PDX models is a robust methodology for interrogating therapeutic efficacy, response, and resistance in a preclinical setting that can be translated as a viable biomarker for non-invasive monitoring in patients.

#6691

Paired comparison of routine molecular screening of patient samples with advanced non-small cell lung cancer in circulating cell-free DNA using OncoBEAM™ EGFR V2, targeted next-generation sequencing Plasma-SeqSensei™ Solid Cancer IVD Kit and custom-validated NGS assay

David Barthelemy[1], Emmanuel Grolleau[1], Gaelle Lescuyer[1], Florence Geiguer[1], Arnaud Gauthier[1], Julie Balandier[1], Margaux Raffin[1], Claire Bardel[1], Bruno Bouyssounouse[2], Claire Rodriguez-Lafrasse[1], Sébastien Couraud[1], Anne-Sophie Wozny[1], Lea Payen-Gay[1]. *[1]Centre Hospitalier Lyon Sud - HCL, Pierre Benite, France,[2]Inovotion, Grenoble, France*

Background: Noninvasive genotyping using plasma cell-free DNA (cfDNA) has the potential to obviate the need for some invasive biopsies in cancer patients. We sought to validate an ultra-deep plasma Next-Generation Sequencing (NGS) assay for patients with Non-Small-Cell Lung Cancers (NSCLC) for detecting Minimal Residual Disease (MRD) following curative-intent NSCLC treatment or EGFR detection at an early stage.
Patients and Methods: We carried out targeted NGS using the Plasma-SeqSensei™ Solid Cancer IVD Kit on cfDNA extracted from plasma. Somatic alterations were filtered, removing somatic mutations attributable to clonal hematopoiesis. Sensitivity and specificity for plasma detection of known oncogenic drivers were calculated. In a subset of cases, validation was carried out using an orthogonal OncoBEAM™ EGFR V2 assay, as well as with a custom-validated NGS assay.
Results: In comparison with the OncoBEAM™ EGFR V2 kit, we observed a 75% concordance with the Plasma-SeqSensei™ Solid Cancer IVD Kit. The 25% genomic discordances were respectively observed in 5%, 7% and 13% linked to the limit of coverage of the OncoBEAM™ EGFR V2 kit, the limit of EGFR sensitivity of the Plasma-SeqSensei™ Solid Cancer IVD Kit and the larger *KRAS, PIK3CA, BRAF* coverage of the Plasma-SeqSensei™ Solid Cancer IVD Kit. In comparison with the custom-validated NGS assay, we observed a 68% concordance with the Plasma-SeqSensei™ Solid Cancer IVD Kit. The 32% genomic discordances were respectively observed in 5%, 11% and 16% linked to the limit of coverage of the Plasma-SeqSensei™ Solid Cancer IVD Kit, the limit of covered sensitivity of the custom-validated NGS assay and the additional oncodrivers analysis only covered by the custom-validated NGS assay. Benefitting from the higher coverage from targetable *BRAF, KRAS, PIK3CA* targetable alterations, the plasma targeted NGS Plasma-SeqSensei™ Solid Cancer IVD Kit showed 13% additional discordances with the Plasma OncoBEAM™ EGFR V2 kit. Most of these additional somatic alterations were cross-validated in our orthogonal custom-validated NGS assay, used in the routine management of patients. The custom-validated NGS assay sensitivity is determined for MAF at 1%, explaining the limit of sensitivity with the Plasma-SeqSensei™ Solid Cancer IVD Kit.
Conclusions: Plasma-SeqSensei™ Solid Cancer IVD Kit resulted in *de novo* detection of targetable oncogenic drivers and resistance mechanisms in patients with NSCLC, including when tissue biopsies were inadequate for genotyping with high sensitivity and accuracy for low and high cfDNA inputs.

#6692

Identification of circulating tumor cells based on machine learning

Jae Hyuk Lee[1], Sung Ho Park[2], Jihoon Kang[2], Jihyun Lee[1], Soee Kim[1], Jungwon Kim[1], Young Woong Sohn[1], Jong Kil Lee[1]. *[1]CytoGen, Inc., Seoul, Korea, Republic of,[2]Tech University of Korea, Siheung-si, Korea, Republic of*

Circulating tumor cells (CTC) are tumor cells that have shed into the bloodstream from primary tumor and circulate in the blood. CTC could provide better understanding of tumor metastasis and show the possibility as promising biomarker for early detection of cancer, cancer prognosis, noninvasive monitoring of treatment response, and personalized medicine. However, the isolation and characterization has been a major technological challenge due to their rareness among the massive blood cells. CytoGen's Smart BiopsyTM CTC platform

comprised of CTC isolator, IF (Immunofluorescence) Stainer, and Cell Image Analyzer is a unique and competitive technology platform for the isolation and analysis of CTC from blood. Intact live CTC could be isolated gravity-based filtration via high-density micro-porous (HDM) chip with minimized cellular damage and high retrieval rate. For the more accurate and quick analysis of CTC after isolation with Smart BiopsyTM CTC platform, we are developing the analysis method of CTC identification using machine learning technologies. Preliminary results of machine learning showed the accurate separation of CTC and PBMC (peripheral blood mononuclear cells) based on the specific markers of them. CTC identification based on machine learning technologies might be reliable analysis method and give secure information of CTC.

#6693

Stability of urinary cell-free DNA and detection of T790M variant

Carolin Münch[1], Saikal Shamkeeva[1], Mitja Heinemann[1], Berend Isermann[1], Sabine Kasimir-Bauer[2], Bahriye Aktas[1], Ivonne Nel[1]. *[1]University of Leipzig, Leipzig, Germany,[2]University Hospital Essen, Essen, Germany*

Background: The so-called “liquid biopsy” has become a powerful tool for cancer research in the recent years, with circulating cell-free DNA (cfDNA) that originates from tumors as one of the most promising analytes. In contrast to plasma derived cfDNA, only a few studies were performed investigating urinary cfDNA. One reason might be quick degradation and hence relatively low concentrations of urinary cfDNA. This study focused on examining the stability of cfDNA in urine using different ways of preservation under various storage conditions.
Methodology: To mimic patient samples, a pool of healthy male and female urine donors was spiked with a synthetic cfDNA reference standard (fragment size 170 bp) containing the T790M mutation in the EGFR gene and preserved with three different buffers and no buffer over four different storage periods (0; 4; 12; 24 h) at room temperature vs. fridge. Preservatives used were the Urinary Analyte Stabilizer (UAS, Novosanis), the Urine Conditioning Buffer (UCB, Zymo) and a self-prepared buffer called “AlloU”. The cfDNA was extracted with the QIAamp MinElute ccfDNA Mini Kit (Qiagen) and the concentration measured with the Qubit™ 4 fluorometer (Thermo Fisher Scientific). Droplet digital PCR (ddPCR) was used for detection and quantification of the T790M mutation (Bio-Rad)
Results: From the model samples with no preservation buffer, almost no spiked cfDNA could be recovered and the T790M variant could not be detected using ddPCR, indicating that without preservation cfDNA was degraded below the detection limit by the nucleases present in urine. The most effective stabilizing buffer over all storage periods and at room as well as fridge temperature was the UAS, resulting in accurate detection of the T790M variant using ddPCR.
Conclusion: From a technical point of view, urinary cfDNA might be useful for non-invasive disease monitoring when the samples are stabilized and stored adequately during clinical routine.

#6694

Evaluation of a multi-omics approach to molecular residual disease detection

Alanna Chan, Martin You, Oliver Limbo, Billyana Tsevtanova, Gerald Dodson, Brenda Curiel, Karma Farhat, Samantha Scott, Archana Ramesh, Jacquelyn Hennek, Viacheslav Katerov, Michael Kaiser, Hatim Allawi, Brady P. Culver, Michael Reshatoff, Jorge Garces, Gina Costa. *Exact Sciences, San Diego, CA*

Introduction: Advancements in DNA sequence detection technology and assay design have enabled molecular residual disease (MRD) assays to detect cancer earlier and with greater sensitivity. In Tumor-Informed (TI) strategies, mutations from the tumor are used to define a set of patient-specific markers that are tracked in the blood as circulating tumor DNA (ctDNA). Whereas tumor-naïve (TN) approaches do not require prior genomic information from the tumor and instead employ a fixed panel of marker(s). Methylated DNA Markers (MDMs) can be used to distinguish cancer from non-cancer and can be found in plasma. We have developed a proprietary TN MRD platform for colorectal cancer (CRC) capable of measuring as few as 1-5 strands of MDM target. Additionally, we are actively developing a TI MRD assay platform. Here we describe the evaluation of both TI and TN approaches for the detection of circulating tumor DNA (ctDNA) in blood across all stages of colorectal cancer and explore the complementarity of these two approaches in the context of MRD monitoring. Procedures: A 20-sample cohort of paired tumor/normal and pre-surgery plasma specimens from stage I (6/20), stage II (7/20), stage III (6/20), and stage IV (1/20) CRC patients and 20 demographically matched non-cancer controls were acquired for our study. All cancer plasma samples were collected prior to tumor resection. Neat and diluted plasma samples were tested for the presence of ctDNA containing short variants specifically derived from the corresponding primary tumor and for a pre-defined set of MDMs and protein cancer biomarkers. Tumor-specific short variants were characterized by whole exome sequencing of the primary tumors. MDMs were detected from bisulfite converted cfDNA by Target Enrichment Long probe Quantitative Amplified Signal (TELQAS) for 35 MDMs. A cancer detection classifier for the TN assay was trained and validated using a separate cohort of non-cancer and CRC plasma samples and employed for this study. Protein was detected by high throughput ELISA.Results: Tumor sequencing of the 20 CRC samples identified between 122 and 7146 (median = 230) somatic mutations per tumor sample.

The combination of features from TI and TN assays achieved 95% accuracy, demonstrating an improvement over either assay in isolation. Indeed, 5 “positive” calls were made for cancer samples for which only one of the two methods met pre-defined RUO thresholds for ctDNA detection. Comparison of median variant allele fraction from the TI assay with median percent methylation of CRC markers for these CRC samples had a Pearson’s correlation of 0.967. Conclusion: TI and TN assays show high concordance in cancer detection, but also complement each other. Additionally, ctDNA quantifications produced from TI and TN assays are linearly correlated. The combination of data from both assays can be used to further differentiate cancer samples from non-cancer samples.

#6695

Utility of circulating tumor DNA in breast cancer clinical research and practice: systematic review and meta-analysis

Xuezheng Sun[1], Nicholas Ballew[2], Linda Kalilani[1], Kelesitse Phiri[3], Kelly Bell[2], Alexander Slowly[4], Magdalena Zajac[4], Erin Hofstatter[5], Angela Silvestro[5], Zebin Wang[6], Jeanne Schilder[2]. *[1]GSK, Research Triangle Park, NC,[2]GSK, Philadelphia, PA,[3]GSK, Collegeville, PA,[4]GSK, London, United Kingdom,[5]GSK, Waltham, MA,[6]GSK (at the time the analysis was conducted), Waltham, MA*

Background: Circulating tumor DNA (ctDNA) has been increasingly used in the clinical care of patients with cancer. This systematic review summarizes current data on the utility of ctDNA in breast cancer clinical research and practice and provides insights for integrating ctDNA into drug development and patient treatment.
Methods: The Embase database was used to identify original clinical research articles of ctDNA in breast cancer published from 2015 to 2020. ctDNA clinical utilities were reviewed and summarized, focusing on 3 areas: early diagnosis, prognostication, and monitoring disease progression/treatment response. Associations of ctDNA with disease-free survival (DFS) and overall survival (OS) were estimated in the embedded meta-analysis. Pooled estimates were calculated using fixed-effect or random-effect models depending on study heterogeneity.
Results: After screening and review, 72 articles were included. ctDNA studies have increased in recent years, with 59.7% of included articles

published in 2019 or 2020. Overall, 61.1% of the studies were in patients with advanced stage/metastatic cancer; 45.8% were restricted to patients with specific cancer subtypes. ctDNA was minimally used in diagnosis; it was predominantly used in clinical outcome prediction with differences by stage. In patients with early-stage disease, the meta-analyses found that overall ctDNA detection/positivity was associated with shorter DFS (n=697; HR, 5.37; 95% CI, 2.94-9.80) and OS (n=238; HR, 4.60; 95% CI, 2.56-8.26). Specific gene mutations in ctDNA were mainly assessed in patients with advanced/metastatic disease, with mutations of *ERBB*, *ESR1*, and *TP53* linked to shorter DFS in the meta-analyses (P<0.05). Moreover, current studies provided evidence that ctDNA reflects the dynamics of breast tumors in the patient treatment journey, acting as a biomarker to monitor tumor evolution and drug resistance.
Conclusions: Recent studies demonstrate ctDNA application in breast cancer prognostication/monitoring, suggesting an important role in patient stratification, molecular relapse identification, and personalized treatment. Large, multicenter clinical trials and real-world longitudinal data sets are needed to validate findings and to address challenges related to ctDNA to improve clinical utility and to integrate ctDNA testing into clinical practice and drug development.

#6696

Genomic alterations associated with early-onset and late-onset colorectal cancer

Eric M. Lander[1], Samuel Rivero-Hinojosa[2], Vasily N. Aushev[2], Jesús Izaguirre-Carbonell[2], Adham Jurdi[2], Minetta C. Liu[2], Cathy Eng[1].
[1]Department of Medicine, Vanderbilt University Medical Center, Nashville, TN,[2]Natera, Inc., Austin, TX

Background: The causes of the rising incidence of early-onset colorectal cancer (EOCRC), defined as CRC in patients aged <50, remain unknown. In this study, we evaluated tumor genomic differences in patients with EOCRC versus late-onset CRC (LOCRC, age >60).
Methods: The international cohort included 13,262 patients diagnosed with stages I-III colon or rectal cancer who had ctDNA testing using a personalized and tumor-informed multiplex PCR assay (Signatera™ 16-plex bespoke mPCR NGS assay), from which whole-exome sequencing

(WES) on the surgically resected tumor was performed. Tumor mutational burden (TMB) and microsatellite instability (MSI) status were derived from WES analysis. The prevalence of gene-wide mutations, pathogenic gene variants, and mutations in known oncogenic pathways was compared between EOCRC and LOCRC groups, stratified by TMB and MSI status. Fisher's exact test was used to test significance between the groups and p-values were adjusted using the FDR method for multiple test correction.
Results: A total of 3,093 patients with EOCRC (70.8% colon, 27.4% rectal, 1.9% unknown) and 10,169 patients with LOCRC (79.9% colon, 18.3% rectal, 1.7% unknown) were included, where 9.0%/37.3%/53.7% were AJCC stages I, II, and III, respectively. Early-onset patients compared to late-onset patients had fewer cases of stage II CRC (30.7% vs. 39.3%, $p<0.01$) and more cases of stage III CRC (60.9% vs 51.6%, $p<0.01$). Adjusted by stage, patients with EOCRC were less likely to be MSI-H compared to patients with LOCRC (10% vs. 17%, $p<0.01$), or have high tumor mutational burden (TMB-H) (15% vs. 19%, $p<0.01$). Genes of the Hippo, NOTCH, WNT, and RTK-RAS oncogenic pathways were less commonly mutated in the EOCRC cohort ($p<0.01$). The BRAF V600E mutation was less prevalent in the EOCRC group (3% vs. 15%, $p<0.01$), regardless of TMB and MSI status. In the TMB-low/MSS group, TP53 mutations were more common in EOCRC (8% vs. 5%, $p<0.01$), but APC gene mutations were less common in EOCRC (56% vs. 66%, $p<0.01$). When comparing EOCRC and LOCRC in the TMB-H/MSI-H group, BRAF V600E (4% vs. 60%), RNF43 G659V (16% vs. 45%), and WNT1 G619A (6% vs. 20%) mutations were less prevalent in EOCRC ($p<0.01$ for all mutations); however, patients with EOCRC had more mutations in PIK3CA H1047R (22% vs. 9%), APC R1468* (11% vs. 3%), and KRAS A146T (7% vs. 2%) gene variants ($p<0.01$ for all mutations). In the TMB-H/MSS group, EOCRC patients were more likely to have driver mutations in the PI3K pathway (74% vs. 56%, $p<0.01$). Further, POLE P286R mutations were more common in TMB-H/MSS patients with EOCRC compared to LOCRC (38% vs. 13%, $p<0.01$), whereas ACVR2A K437R was less common (11% vs. 30%, $p<0.01$).
Conclusion: Patients with LOCRC were more likely to have pathogenic gene variants and mutations in established pathways of CRC carcinogenesis. Tumors in EOCRC cases harbored unique genomic

alterations that varied between the TMB-low/MSS, TMB-H/MSI-H, and TMB-H/MSS subpopulations.

#6697

Deep learning algorithm for cancer detection using multimodal characteristics of whole methylome sequencing of cf-DNA

Juntae Park[1], Minjung Kim[1], Sook Ryun Park[2], Ki-Byung Song[3], Eunsung Jun[3], Dongryul Oh[4], Jeong-Won Lee[5], Young Sik Park[6], Ki-Won Song[7], Jeong-Sik Byeon[8], Bo Hyun Kim[9], Chang-Seok Ki[1], Eunhae Cho[1]. *[1]GC Genome, Yongin, Korea, Republic of,[2]Asan Medical Center, Seoul, Korea, Republic of,[3]Department of Surgery, Asan Medical Center, Seoul, Korea, Republic of,[4]4.Department of Radiation Oncology, Samsung Medical Center, Seoul, Korea, Republic of,[5]Department of Obstetrics and Gynecology, Samsung Medical Center, Seoul, Korea, Republic of,[6]Department of Internal Medicine, Seoul National University Hospital, Seoul, Korea, Republic of,[7]Department of Surgery, Song, Asan Medical Center, Korea, Republic of,[8]Department of Gastroenterology, Asan Medical Center, Seoul, Korea, Republic of,[9]Center for Liver and Pancreatobiliary Cancer, National Cancer Center, Goyang, Korea, Republic of*

Background Various cell-free DNA (cfDNA) features including methylation and genomic profiles have been investigated for their potential use in early cancer detection. We developed deep learning models based the data generated by the enzymatic conversion based whole methylome sequencing of cfDNA.

Methods Cell-free whole genome Enzymatic Methyl sequencing(cfWEMseq) data were generated from 198 cancer patients (stage I: 11%, II: 17%, III: 22%, IV: 20%, unknown: 31%) and 69 healthy controls. The cancer types were consisted of breast (n=31), liver (n=24), esophageal (n=38), pancreatic (n=30), colon (n=34), ovarian (n=18), and lung (n=23). Sequence data was produced on average of 200 million reads using Novaseq 6000 (Illumina). For model training and evaluation, data partitioning was stratified by cancer type, and 5-fold cross validation was used. Coverage and methylation beta values were calculated by binning at fixed size of 100K, 1M, and 5M base and variable size from Topologically Associated Domains (TAD). Genome Coverage (GC), Genome Methylation

Beta values (GMB), and Mutation Signature (MS) features were trained using a one-dimensional convolutional neural network (1D-CNN). The performance of the model was evaluated by measuring the average value of the results measured in each test set of 5 fold.
Results We tested the cancer detection performance of various feature combinations using all data from cfWEMseq (n=267). Regardless of the bin size, the GMB single model achieved higher performance than the GC single model. The best-performing model is the ensemble model of GMB (100k bin) and MS. The cancer detection performance of this ensemble model reached an accuracy 96% (CI: 93.6% to 98.1%), AUC 0.99 (CI: 0.97 to 1.0) and sensitivity 98.0% (CI: 92.4% to 99.5%) with a specificity of 90%.
Conclusions These results provide an opportunity for higher accuracies by integrating methylation information and genomic data using cfWEMseq.
This research was supported through the National Research Foundation (NRF) funded by the Ministry of Science and ICT (2020M2D9A3094213).

#6698

Combinatorial genomic and epigenomic cell-free DNA analysis of high-risk metastatic castration resistant prostate cancer reveals prognostic liquid biopsy signatures

Irfan Alahi[1], Pradeep S. Chauhan[1], Alexander L. Shiang[1], Jace Webster[1], Ha X. Dang[1], Lilli Greiner[1], Breanna yang[1], Elisa M. Ledet[2], Ramandeep K. Babbra[3], Wenjia Feng[1], Peter K. Harris[1], Ellen B. Jaeger[2], Patrick J. Miller[2], Sydney A. Caputo[2], Giordano Cittolin Santos[1], Oliver Sartor[2], Russell K. Pachynski[1], Christopher A. Maher[1], Aadel A. Chaudhuri[1].
[1]Washington University in St. Louis, Saint Louis, MO,[2]Tulane University School of Medicine, New Orleans, LA,[3]Wilmot Institute Cancer Center, University of Rochester Medical Center, Rochester, NY

Background: Androgen receptor signaling inhibitors (ARSI) such abiraterone and enzalutamide have significantly improved clinical outcomes in metastatic castrate-resistant prostate cancer (mCRPC) patients. However, patients with genomic alterations in the androgen receptor (*AR*) and its enhancer region do not respond well and acquire resistance to these inhibitors. Here, we applied our previously developed cell-free DNA

(cfDNA) liquid biopsy assay (EnhanceAR-Seq) to detect these high-risk mCRPC patients prior to the administration of first-line AR-directed therapy and correlated with survival. We also interrogated the plasma methylome to identify differentially methylated regions (DMRs) across these high-risk patients. **Methodology**: We applied EnhanceAR-Seq to plasma cfDNA isolated from 99 mCRPC patients enrolled from two institutions (n=52 Tulane; n=47 WashU). Plasma samples were collected prior to ARSI initiation (n=63) or during treatment (n=36). We also performed Enzymatic Methyl-seq in pre-treatment plasma from 43 patients. We split these 43 patients into cell-free genomically high-risk and low-risk groups using our EnhanceAR-seq results, and conducted DMR analysis using metilene. To identify significant DMRs, we performed multiple hypothesis testing and required $q<0.05$ using the Benjamini-Hochberg procedure, and further required at least 5 CpGs per DMR. **Results**: EnhanceAR-Seq detected *AR*/enhancer alterations in 35% of all plasma samples. Cell-free *AR*/enhancer detection was highly prognostic (PFS HR=2.80, p=0.0002; OS HR=2.6, p=0.01). When considering only pre-treatment plasma, *AR*/enhancer alterations detected in 44% (28/63) of samples correlated significantly with worse PFS (HR=2.21, p=0.009) and OS (HR=2.60, p=0.02). *AR*/enhancer alterations detected in 19% (7/36) of samples collected during ARSI were also associated with worse PFS (HR=15.6, p=0.0002) and OS (HR=8.09, p=0.05). Plasma methylome analysis revealed that for cell-free genomically high-risk mCRPC patients (based on *AR*/enhancer alterations detected in cfDNA), significantly hypomethylated DMRs were found in the *AR* promoter, upstream *AR* enhancer, and in *AR*-associated genes including *FOXP1* and *FOLH1*. Significantly hypomethylated DMRs were also observed in DNA damage repair and cell cycle genes including *MSH6*, *MSH3*, *FANCD2*, *CDK12* and *RAD51B*. Hypermethylated DMRs were seen in tumor suppressor genes including *ZBTB16*, *BRCA2*, *WT1* and *GNAS*. **Conclusions***: AR*/enhancer alterations detected in plasma cfDNA predicted inferior survival in mCRPC patients. Cell-free genomically high-risk mCRPC patients could be distinguished from low-risk patients based on distinct methylation signatures.

#6699

What are the characteristics of mutations to use as targets in tumor-informed ctDNA analysis?

Marijana Nesic, Mads H. Rasmussen, Tenna V. Henriksen, Christina Demuth, Amanda Frydendahl, Iver Nordentoft, Lars Dyrskjøt, Claus L. Andersen. *Aarhus University, Århus, Denmark*

Introduction: Tumor-informed, mutation-based approaches for the detection of circulating tumor DNA (ctDNA) are among the most common and widely used ctDNA detection approaches. To identify the mutations to be used as ctDNA targets, tumor tissue is often mutation-profiled using broad panel sequencing strategies. Optimally, the strategy for mutation profiling should enable assessment of clonality and copy number of the identified mutations. Hereby, it will be possible to rank the mutations and select those that are clonal and present in multiple copies per cancer cell. Theoretically, this should increase the ctDNA detection likelihood. However, there is no consensus on how best to identify and select the targets. Here, we propose a bioinformatic pipeline for an easy and robust selection of target mutations for ctDNA detection from tumor whole-exome sequencing (WES) profiles.

Methods: The pipeline consists of Mutect2 and PureCN, which were both applied to paired tumor and normal WES profiles. The output from the pipeline is a list of somatic mutations, each with estimated measures of clonality, in the form of a cancer cell fraction (CCF), and multiplicity (local mutation copy number). Mutations with CCF above 0.9 were considered clonal. The performance of the pipeline was assessed using matched WES and ctDNA data from 98 colorectal cancer (CRC) and 30 bladder cancer patients. For CRC patients, 1-5 mutations per patient within a pre-defined CRC panel were used as ctDNA targets, while an average of 41 selected mutations per patient were used for bladder cancer patients. The performance measure was the mutation detection rate in pre-operative plasma samples, stratified for clonality (CCF), multiplicity, and the combination of CCF and multiplicity.

Results: For CRC patients, 51% of mutations with CCF > 0.9 were detected compared to only 17% when CCF < 0.9 (p= 4.3e-09). In bladder cancer patients 21% of mutations with CCF > 0.9 were detected compared to 2 % when CCF < 0.9 (p=1.2e-09). For CRC patients the ctDNA detection rate was 58% when mutation multiplicity was higher than 1 and 31% when

multiplicity was 1 (p= 9.175e-06). For bladder cancer, the same numbers were 22% and 16% (p=4.635e-03). Mutations with CCF > 0.9 and multiplicity >1 had significantly increased ctDNA detection rate compared with mutations with CCF < 0.9 and multiplicity 1, in both CRC (p= 1.486e-09) and bladder cancer (p=1.077e-09).
Conclusion: The CCF and multiplicity measures provided by the pipeline are highly useful when selecting ctDNA targets. By selecting mutations with CCF> 0.9 and multiplicity >1 the likelihood of detecting ctDNA in plasma cfDNA is significantly improved.

#6700
Characterizing circulating tumor DNA release kinetics and fragment length in a chemotherapy resistant model of esophageal adenocarcinoma
Alexandra Bartolomucci[1], Sarah Tadhg Ferrier[1], Thupten Tsering[1], Xin Su[1], Jonathan Cools-Lartigue[2], Julia V. Burnier[1]. *[1]McGill University Health Centre Research Institute, Montreal, QC, Canada,[2]McGill University Health Centre, Montreal, QC, Canada*

Background: While the incidence of esophageal adenocarcinoma (EAC) is rapidly increasing, the 5-year survival rate of this disease remains poor at less than 25%, with a substantial number of patients exhibiting inherent or acquired resistance to chemotherapy. Circulating tumor DNA (ctDNA) isolated from liquid biopsies of EAC patients holds clinical biomarker potential in this disease, but our understanding of how chemotherapy affects ctDNA release remains limited.
Methods: In order to study the impact of cancer treatment on ctDNA emission *in vitro*, we first sought to establish a chemo-resistant model of EAC. As such, the EAC cell line OE19 was exposed to discontinuous cisplatin treatments for three months in order to establish drug resistance. Following this, established chemo-resistant OE19 cells and parental (chemo-sensitive) OE19 cells were exposed to five daily cisplatin treatments, and cell culture supernatant was collected every day throughout treatment. ctDNA was subsequently isolated from cell culture supernatant and quantified by Qubit fluorometer dsDNA HS assay. ctDNA quantities were additionally assessed by droplet digital PCR (ddPCR) assay using primers and probes targeting the *TP53* N310K mutation in the OE19 cell

line. Finally, ctDNA fragment lengths were analyzed using the Agilent Bioanalyzer 2100.
Results: A chemo-resistant model of the OE19 cell line was established, as exemplified by marked morphological changes in the cells and significantly increased cell viability determined by CCK8 assay after 48-hour treatments of various doses of cisplatin ($p<0.05$). ctDNA levels, as measured by both Qubit fluorometer and mutant copies detected by ddPCR assay, increased after chemotherapy treatment for both chemo-sensitive and resistant cells. Notably, ctDNA emission was higher with larger amounts cell death, with chemo-sensitive cells emitting significantly higher levels of ctDNA compared to chemo-resistant cells throughout treatment ($p<0.05$). Fragmentomics analysis revealed ctDNA peaks corresponding to apoptosis (~167 bp) and necrosis (~10,000 bp). Moreover, chemotherapy treatment caused a shift in average fragment size, with larger fragments being observed during chemotherapy treatment in both chemo-sensitive and resistant cells.
Conclusion: This study reveals that *in vitro* cancer models can be used to successfully study ctDNA emission during pre-clinical drug analyses. ctDNA release was found to be correlated to cytotoxicity and cell death, providing us with valuable insight into how clinical liquid biopsy data should be interpreted. Finally, fragment size analysis of ctDNA reveals a potential novel biomarker for treatment response in cancer patients.

#6701

6-color Crystal Digital PCR for the high-plex detection of 10 *ESR1* mutations in breast cancer

Stavroula Smilkou[1], Aliki Ntzifa[1], Dimitra Stergiopoulou[1], Quentin Blache[2], Myrtille Remy[2], Cecile Jovelet[2], Allison Mallory[2], Evi Lianidou[1].
[1]University of Athens, Athens, Greece,[2]Stilla Technologies, Villejuif, France

Introduction. *ESR1* mutations have emerged as a key mechanism of resistance to endocrine therapy in estrogen-receptor-positive (ER+) breast cancer, thus detection of *ESR1* mutations is crucial to monitor during patient treatment. We evaluated a novel 12plex breast cancer assay for the detection of 10 *ESR1* mutations and *AKT1* E17K in plasma cell-free DNA (cfDNA) using 6-color Crystal Digital PCR™ (naica® system, Stilla Technologies, France). We further compared the results with our previously

reported *ESR1* NAPA assay for D538G, Y537S, Y537C and Y537N mutations (Stergiopoulou et al, Cancers, 2021).
Patients and Methods. Using the 6-color Crystal Digital PCR™ breast cancer 12plex assay, we analyzed 35 plasma cfDNA samples from ER+ breast cancer patients and 10 plasma cfDNA from healthy donors (HD). We also analyzed the same cfDNA samples using the *ESR1* NAPA assay.
Results. The Stilla 6-color breast cancer assay revealed in 5/35 (14,3%) ER+ cfDNA samples the *AKT1*_E17K and *ESR1* D538G mutations. *ESR1* D538G was detected in 4/35 ER+ cfDNA samples with the *ESR1* NAPA assay. Direct comparison between Crystal Digital PCR™ and the *ESR1* NAPA assay revealed a high concordance (97.1%) for 34/35 samples tested, for the detection of the D538G mutation, and with a higher sensitivity for the Stilla 6-color breast cancer assay. The *ESR1* mutations Y537S, Y537C and Y537N were not detected by either method in any of the plasma-cfDNA samples. No *AKT1* E17K or *ESR1* mutations were detected in cfDNA from HD plasma.
Conclusions. The naica® system 12plex *ESR1* assay is quantitative, highly sensitive and easy to perform using plasma-cfDNA samples. The use of highly multiplexed Crystal Digital PCR™ shows great promise for clinical utility for ER+ breast cancer patient monitoring.
Key words: Circulating tumor DNA; Crystal Digital PCR™, *ESR1* mutations; liquid biopsy; mutation monitoring, 6-color multiplexing;

#6702
The clinical characteristics and outcomes of NSCLC patients with genomic alterations detected by blood-based NGS ctDNA assay
Hsin-Yi Wang[1], Chao-Chi Ho[2], Yen-Ting Lin[3], Wei-Yu Liao[2], Chung-Yu Chen[1], Jin-Yuan Shih[2], Chong-Jen Yu[2]. *[1]National Taiwan University Hospital, Yun-lin Branch, Yunlin, Taiwan,[2]National Taiwan University Hospital, Taipei, Taiwan,[3]National Taiwan University Cancer Centre, Taipei, Taiwan*

Background: The Blood First Assay Screening Trial (BFAST) (NCT03178552) is a prospective study screening for actionable genetic alterations using NGS of ctDNA among patients with treatment-naive advanced or metastatic NSCLC. We aimed to perform a more systematic

investigation of genomic alterations in Asia/Taiwan NSCLC patients through the BFAST database at NTUH.
Materials and Methods: There was a total of 269 patients enrolled and receiving FoundationOne Liquid Companion Diagnostic (F1LCDx) assay at cancer diagnosis between Feb, 2019 and Mar, 2022 in NTUH. The concordance of tissue-based genetic testing in the real-life clinical setting and the blood-based NGS testing in the clinical trial were analyzed. The co-occurrence of genomic alterations detected with blood-based NGS ctDNA assay were also interpreted.
Results: A total of 206 patients (76.5%) detected driver mutations. Tissue-based genetic testing in the real-life clinical setting missed driver mutations in 67 (24.9%) patients with a sensitivity of 67.32%. Liquid NGS detected 38 (14%) patients with RET, KRAS, Met or ErbB2 mutations which were beyond the scope of current genetic testing in the clinical settings. Also, the F1LCDx assay detected more uncommon EGFR mutations than the Roche Cobas EGFR Mutation Test V2 ($P < 0.0001$). Thirty-four (12.6%) patients had non-detected results in the F1LCDx assay which produced a sensitivity of 83.41%. By multivariate analysis, the predictors associated with discordant blood-based NGS ctDNA results were T stage (odds ratio [OR] 0.35, 95% confidence interval [CI] 0.15-0.79, $p = 0.012$) and M stage (OR 0.21, 95% CI 0.09-0.49, $p < 0.0001$). The most common co-occurring mutations in the blood-based NGS ctDNA assay were TP53, DNMT3A, TET2, PIK3CA and CTNNB1. Among the EGFR mutant population, first-generation compared to third-generation TKI use (hazard ratio [HR] = 0.43, 95% CI 0.22-0.85, P=0.02) and co-occurring genomic alterations in TET2 (HR = 2.35, 95% CI 1.15-3.48, P=0.02) were associated with shorter progression free survival of EGFR TKIs treatment in multivariate analysis. Disease stage was the only factor associated with overall survival in the EGFR mutant population.
Conclusion: NGS ctDNA analysis provided a more comprehensive genetic testing than conventional single gene testing kits. The lower stage which could imply lower or lack of ctDNA shedding into the blood was associated with a discordant result of the blood-based NGS ctDNA assay. Co-occurring mutations might have an impact on the treatment duration of EGFR-TKI.

#6703

Objective qualification of cell-free DNA by applying the cfDNA quality metric

Annika Dorn. *Agilent Technologies, Inc., Waldbronn, Germany*

Next Generation Sequencing (NGS) of cell-free DNA (cfDNA) has the potential to reveal new biomarkers for various conditions. Despite the establishment of low input library protocols, library preparation of cfDNA samples remains a challenge due to restricted amount of starting material and variable size distribution of cfDNA fragments. The yield and quality of cfDNA can vary and a lot of care is required to obtain appropriate cfDNA starting material for downstream applications. Further, cfDNA samples may contain high molecular weight (HMW) DNA that can negatively affect library yield and sequencing quality. Therefore, quality control of cfDNA starting material is essential to ensure the success of downstream experiments. The Agilent Tapestation system with the Cell-free DNA ScreenTape Assay is based on automated electrophoresis and thereby offers an objective and reliable qualification of cfDNA samples by applying the %cfDNA quality score. By comparing different samples with varying total DNA yield and HMW contamination, the additional level of information gained by the %cfDNA score is highlighted. While other QC methods might miss critical information on HMW DNA contamination, this could result in flawed yield estimations, ultimately threatening the successful outcome of downstream experiments. Therefore, accurate quantification of cfDNA starting material, taking also HMW DNA contamination into account is essential for NGS library preparation and generating reliable NGS results.

#6704

A digital-PCR primer/probe library for pan-cancer ctDNA monitoring established from public databases for somatic mutations

Hayato Hiraki, Akiko Yashima-Abo, Takeshi Iwaya, Satoshi S. Nishizuka. *Iwate Medical Univ., Iwate, Japan*

Background: Circulating tumor DNA (ctDNA), a new class of tumor marker, has been demonstrated the clinical validity of: 1) early relapse prediction, 2) therapeutic efficacy evaluation, and 3) relapse-free corroboration in the context of cancer treatment. Variant allele frequencies

(VAFs) of ctDNA were under 0.1% even in most advanced cancer patients. Since the detection limit of next-generation sequencing (NGS) is above 1%, higher sensitivity is needed for sensitive ctDNA monitoring. Digital PCR (dPCR) offers excellent sensitivity at an affordable cost compared with NGS. A mutation-specific primer/probe (P/P) is required for the dPCR assay, but a limited number of P/Ps are commercially available.
Materials and Methods: To provide essential probes for the rapid monitoring of sensitive ctDNA, we developed an off-the-shelf (OTS) dPCR P/P library (OTS-Probes) that includes probes that can detect >1,000 mutations found in human cancer. The majority of the mutations to be detected by these P/P sets have been selected using an originally developed statistical scoring from hot spot mutations reported in the Catalogue of Somatic Mutations in Cancer (COSMIC) database. To evaluate the coverage of OTS-Probes in human cancer specimens, the Cancer Genome Atlas (TCGA) and the Center for Cancer Genomics and Advanced Therapeutics (C-CAT) datasets were used. TCGA is an international landmark cancer genomic program in the U.S., and C-CAT is a Japanese cancer genome profiling database.
Results: At least one mutation was matched to the OTS-Probes for ctDNA monitoring in lung, colorectum, stomach, liver, pancreas, breast, uterus, and prostate from TCGA and C-CAT cancer specimens, reflecting 63% and 77% of corresponding tumor types, respectively. The mutation coverage of the OTS-Probes tends to be lower in TCGA than in C-CAT, partially due to the fact that information about the *TERT* promoter mutation is absent in TCGA. We found that some *ARID1A* deletion mutations that have a high count in COSMIC were not observed in either the TCGA or the C-CAT database. We also analyzed the coverage of the OTS-Probes in different organs and driver genes. Currently, more than 250 P/P sets have been designed, synthesized, and validated with human tumor DNA or synthesized DNA fragments. Importantly, nearly 98% of P/P sets work with the same PCR condition. With our proprietary oligo synthesis method with modified bases, only a small percentage of P/P sets required optimization of the annealing temperature.
Conclusion: We developed a dPCR P/P library called OTS-Probes. Our analysis suggests that 60-80% of cancer patients could immediately apply at least one P/P set for sensitive ctDNA monitoring by dPCR. A quarter of the P/P library has already been validated by tumor DNA or synthesized DNA

fragments. OTS-Probes is a great tool for ctDNA- related studies and for clinical use when a higher sensitivity than NGS can offer is required.

#6705

Molecular detection of circulating cancer cells with cancer stem cell or mesenchymal characteristics in esophageal squamous cell carcinoma

Zhen Tan, Josephine Mun-Yee Ko, Valen Zhuoyou Yu, Hoi Yan Ng, Simon Law, Maria Li Lung. *The University of Hong Kong, Hong Kong, China*

Esophageal squamous cell carcinoma (ESCC) is a clinically challenging disease that requires a multidisciplinary approach. Unfortunately, the scarcity of ESCC genomic data hinders the understanding of ESCC biology, disease progression and rational therapy design. Circulating tumor cells (CTCs), which are shed from the primary and metastatic tumors and then circulate within the peripheral vasculature, reflect the existing tumor heterogeneity. Here, we utilized the non-biased size-based CTC enrichment strategy in combination with the real-time RT-PCR to molecularly characterize the CTCs with cancer stem cell (CSC) or mesenchymal properties in ESCC. Comprehensive data from ESCC cell lines, mouse ESCC xenograft models and clinical ESCC peripheral blood samples emphasize the importance of *TWIST1* (Twist Family BHLH Transcription Factor 1) in ESCC progression. Gain-of-function and loss-of-function analyses demonstrate that TWIST1 promotes cell migration, invasion and colony formation in ESCC cells. Moreover, positive TWIST1 expression is responsible for the chemoresistance of ESCC cells to Cisplatin and is correlated with poor overall survival in ESCC patients. In addition, we show that TWIST1 promotes malignant potential, including tumor growth, invasion and chemoresistance via the TWIST1-TGFBI-ZEB1 signaling pathway in ESCC. Meanwhile, the TWIST1-TGFBI-ZEB1 signaling pathway confers immunosuppressive conditions to the tumor microenvironment, which in turn contributes to EMT to promote tumor progression. Collectively, these findings indicate that TWIST1 has a novel role in ESCC carcinogenesis by regulating tumorigenicity and cancer stem cell properties that may be useful as a prognostic monitoring biomarker and a promising therapeutic target in clinical ESCC treatment.

#6706

Co-culture of circulating tumor cells (CTCs)-derived 3D organoids and autologous cytotoxic CD8+ T cells: A new functional precision oncology platform

Lanlan Zhou, Leiqing Zhang, Lindsey Carlsen, Kelsey E. Huntington, Vida Tajiknia, Andrew George, Arielle De La Cruz, Arunasalam Navaraj, Praveen Srinivasan, Maximilian Schwermann, Benedito A. Carneiro, Wafik S. El-Deiry. *Pathology and Laboratory Medicine, Legorreta Cancer Center at Brown University, Providence, RI*

Greater than 10 million patients succumb to cancer each year. Cancer metastasis is responsible for more than 90% of all cancer-associated deaths due to treatment resistance and increased tumor burden. As a seed for metastases, circulating tumor cells (CTCs) present a new dimension and horizon for clinical doctors in diagnosis, prognosis prediction, treatment monitoring, disease mechanism, and drug development. CTCs could gradually replace tissue biopsies which are painful and may be difficult to obtain depending on tumor location. CTC isolation is feasible after minimally invasive liquid biopsy and provides the basis for a multitude of *ex vivo* and *in vivo* studies including establishment of CTCs-derived 2D and 3D cultures. Organoids are miniscule models of tissues that grow in a 3D semisolid extracellular matrix medium with specific growth factors supplied. CTCs-derived 3D organoids play a vital role in precision oncology because they can preserve tumor heterogeneity, imitate the tumor microenvironment (TME), mimic cancer hypoxia in the TME, and maintain cancer and metastasis phenotypes. Cytotoxic $CD8^+$ T cells are the most powerful effectors in the anticancer immune response. We hypothesized that co-culture of CTCs-derived 3D organoids and autologous cytotoxic $CD8^+$ T cells could maximize patient-relevance of laboratory assessment of cancer-treatment immune-system interactions to facilitate precision oncology practice. TellBio's novel TellDx CTC technology allows for isolation of viable and intact CTCs in liquid biopsies, regardless of cancer type. Unlabeled CTCs were cultured in growth factor reduced Matrigel with organoid culture WENRAS medium. Magnetic beads labeled white blood cells (WBCs) were cultured with T cell culture medium - WBCs and magnetic beads usually separate in three days - cytotoxic $CD8^+$ T cells were isolated with the EasySep™ Human $CD8^+$ T Cell Isolation Kit. CTCs-derived 3D organoids and autologous cytotoxic $CD8^+$ T cells were co-

cultured with or without different drug treatments - cytotoxicity was measured with CellTiterGlo® 3D Cell Viability Assay and imaging, and further mechanistic studies were feasible. Our co-culture platform enables us to utilize a patient's peripheral blood or pleural effusions to create a patient-specific, *in vivo*-like TME and immune microenvironment to model and assess *ex vivo* responses to investigational and FDA-cleared cancer therapies, and potentially provide oncologists with insights to improve clinical outcomes.

#6707

Optimization of miRNA isolation from plasma biopsies of proton therapy prostate cancer patients

Johnny I. Velasquez[1], Andrew Bass[2], Moein Rajaei[3], Curtic Bryant[4], Nancy Mendenhall[4], Luisel Ricks-Santi[5]. *[1]Florida-California Cancer Research Education and Engagement Health Equity Center (CaRE2 Center), Gainesville, FL,[2]University of Florida, Gainesville, FL,[3]Department of Pharmacotherapy and Translational Research, College of Pharmacy, University of Florida, Gainesville, FL,[4]University of Florida Health Proton Therapy Institute, Jacksonville, FL,[5]Cancer Center, University of Florida, Gainesville, FL*

Introduction: Radiotherapy (RT) is a treatment option for men with Prostate Cancer (PCa). While minimizing damage to proximal healthy tissue, RT can still result in severe toxicities. Studies have shown that exposure to ionizing radiation leads to changes of miRNA expression at the cellular level, making cells more radioresistant or radiosensitive which could result in toxicity, recurrence, and metastatic spread. Importantly, RT induced miRNA changes have been found to be associated with RT response in clinical contexts and may serve as diagnostic tools to assess PCa risk stratification that inform precision medicine approaches. However, miRNAs have not been assessed in patients treated with proton therapy (PT), a type of particle-based RT which purports improved dose distribution and reduced toxicity. This is attributed to the proton’s unique ability to deposit most of its energy at a narrow bragg peak with minimal energy deposition beyond the peak, into surrounding organs. Because miRNAs are ubiquitous in the human body, they are stable in many environments including the bloodstream and are becoming attractive biomarkers of treatment response,

including RT. Still, blood-derived biomarkers for diagnosis, prognosis, and therapy response is an emerging field and there remains a lack of standardization and normalization of sample preparation and protocol for isolating human derived miRNA from plasma. The objective is to optimize RNA isolation procedures so that it is achievable to accurately identify miRNA biomarkers in PCa patients undergoing PT.
Methods: The results of 2 RNA isolation kits were compared. To assess the effectiveness of each optimization strategy performed, a number of metrics were used to quantitate and determine the quality of the RNA: fluorometry (Qubit 2.0 and 4.0), spectrophotometry (nano-drop), and qRT-PCR amplification (Taqman).
Results: Fluorometry methods were not sensitive enough for RNA quantification for either kit. Of the two RNA isolation kits, Kit A outperformed Kit B in every metric output when 100 uL of plasma was initially used. Furthermore, amelioration of metric output was observed when the original starting plasma amount of 100 uL was increased to 200 uL in Kit A. Nanodrop quantities ranged from 8.85 - 32.65 ng/uL and -72.82 - 4.98 ng/uL using Kit A and Kit B, respectively. The quality (260/280 ratios) ranged from -7.65 - 3.17 and -41.65 - 6.13 for Kit A and Kit B, respectively. Taqman amplification was achieved for both kits.
Conclusions: Although total RNA isolation was effectively performed, there is a need for properly optimizing miRNA detection in these blood-based biopsies. Enhancing miRNA detection to determine treatment outcomes may result in miRNA's becoming a powerful predictive biomarker. The goal is to utilize miRNAs as a diagnostic tool for real time monitoring of individualized therapy response, detecting developing metastases, and predicting relapse.

#6709

Utility of RNA sequencing for transcriptome analysis of small extracellular vesicles derived from blood sera of colorectal cancer patients

Tana Machackova[1], Petra Vychytilova-Faltejskova[1], Marie Madrzyk[1], Karolina Trachtova[1], Marketa Pavlikova[1], Jan Kotoucek[2], Jana Halamkova[3], Dagmar Al Tukmachi[1], Jiri Sana[1], Petra Pokorna[1], Milana Sachlova[3], Ondrej Slaby[4]. *[1]Molecular Medicine, Central European Institute of Technology, Brno, Czech Republic,[2]Pharmacology and Toxicology,*

Veterinary Research Institute, Brno, Czech Republic,[3]Comprehensive Cancer Care, Masaryk Memorial Cancer Institute, Brno, Czech Republic,[4]Biology, Masaryk University, Faculty of Medicine, Brno, Czech Republic

Introduction: Currently used molecular diagnostic tests for colorectal cancer (CRC) are underperforming and more sensitive, non-invasive biomarkers are needed. Long non-coding RNAs (lncRNA) and microRNA (miRNA) have shown potential as diagnostic biomarkers. Unfortunately, the identification of non-coding RNA circulating biomarkers in blood serum is significantly burdened by abundant RNA specimens from disrupted blood cells. Recently, small extracellular vesicles (sEVs) emerged as potential reservoirs of clinically relevant biomarkers, including lncRNAs and miRNAs. In theory, sEVs protect RNAs from degradation and might serve as a source of intact RNA for further analyses. However, there is a lack of evidence supporting the superior quality of RNA extracted from sEVs over RNA from whole blood serum. This study aimed to analyze the RNA content of blood serum and the sEVs derived from the blood serum of CRC patients and healthy controls using RNA sequencing. Moreover, small RNA sequencing was used to evaluate the difference in miRNA profiles of sEVs and corresponding blood sera of CRC patients and healthy controls.
Methods: Spin-column chromatography (Exiqon), precipitation-based method (Norgen), and size-exclusion chromatography (iZON) were used to extract sEVs from blood sera. The concentration of sEVs was measured by dynamic light scattering (DLS), the size was evaluated by electron microscopy (EM), and sEV-specific content was analyzed by western blot and qRT-PCR. RNA was extracted using the column-based method. Next-generation sequencing (NGS) analyses of blood serum and sEVs extracted from blood serum included samples from 10 CRC patients and 10 healthy controls for RNAseq, and 5 CRC patients and 5 healthy controls for small RNAseq. Differential expression analysis was carried out in R using DESeq2 package.
Results: DLS and EM showed that size-exclusion chromatography yielded the purest population of sEVs characterized according to ISEV recommendations. Extraction of sEVs and subsequent RNA extraction and sequencing library preparation from ultra-low input samples were optimized. Over 30k different RNAs were identified in the sEVs derived

from blood sera of CRC patients and healthy controls, including lncRNAs, miRNAs, and protein-coding RNAs. A detailed comparison of the transcriptome of blood sera and corresponding sEVs is a part of the poster. **Conclusion:** sEVs could serve as a source of RNA biomarkers; however, proper characterization and optimal methodology are necessary.
This work was supported by the Ministry of Health of the Czech Republic grant No. NU20-03-00127, by The project National Institute for Cancer Research (Programme EXCELES, ID Project No. LX22NPO5102) - Funded by the European Union - Next Generation EU, by the project BBMRI-CZ, nr. LM2018125, and in co-operation with CEMCOF, CEITEC MU (CIISB) supported by MEYS CR, LM2018127.

Preclinical Therapies and Clinical Observations in Pediatric Oncology

#6713
Myc-regulated miR17, 20a modulate RANK expression in osteosarcoma

Bikesh Kumar Nirala[1], Lyazat Kurenbekova[1], Tajhal Patel[1], Ryan Lane Shuck[1], Atreyi Dasgupta[1], Nino Carlo Rainusso[1], Jason T. Yustein[2]. *[1]Texas Children's Hospital Cancer & Hematology Ctr., Houston, TX,[2]Pediatrics, Emory University School of Medicine, Atlanta, GA*

Osteosarcoma (OS) is the most common primary bone tumor in children and adolescents. Approximately 25-30% of these tumors carry amplification of chromosome 8q24, which harbors the oncogene c-Myc, and correlates with a poor prognosis in patients with OS. To understand the mechanisms that underlie the ability of Myc to alter both the tumor and its surrounding tumor immune microenvironment (TiME), we generated and molecularly characterized an osteoblast-specific Cre-Lox-Stop-Lox;(LSL)-c-MycT58A;p53f/+ knockin genetically engineered mouse model (GEMM). Phenotypically, the Myc knockin-GEMM had rapid tumor development with a high incidence of metastasis. Myc-dependent gene signature in our murine model demonstrated significant homology to the human Myc-amplified OS.Interestingly, we noticed a significant reduction in the osteoclast (OCL) cell population in the Myc knockin OS tumor compared to the p53-driven. We found the expression of RANK was significantly downregulated in the Myc knockin tumor compared to the Non-knockin

p53 heterozygous tumors. The RANK/RANKL pathway is vital in OCL maturation and bone modeling/remodeling. To understand the involvement of Myc in RANK regulation, we used murine-derived OS cell lines and transiently knocked down of Myc expression using siRNA. We observed a significant upregulation in RANK expression after Myc knockdown. To decipher the molecular mechanism behind the Myc-dependent regulation of RANK expression in OS, we looked into the Myc-mediated microRNAs. Myc regulates the expression of several microRNAs, including the polycistronic miR-17-92 cluster. The expression of miR17-5p and Mir20a-5p was significantly higher in the GEMM tumor tissue samples isolated from the Myc knockin compared to the p53-driven. Further, we validated the Myc-dependent regulation of miR-17-5p/20a-5p expression using transient knockdown of Myc in mouse Myc knockin-derived cell lines. To examine the role of miR17-5p/20a-5p on the RANK regulation, we performed both gain and loss-of-function studies using microRNA-17/20a mimics and inhibitors. After the treatment with miR-17-5p/20a-5p inhibitors, the expression of RANK was significantly upregulated whereas in
the case of miR17/20a mimics reversed these effects and led to a downregulation of RANK expression. We established that miR-17-5p/20a-5p is causally responsible for at least part of the mechanism by which Myc regulates the RANK expression in OS.We concluded that the Myc-regulated miR17/20a modulates the RANK expression that is involved in the OCL cell population regulation and function in the OS.

#6714

ALCAM promotes neuroblastoma proliferation, migration, and immune evasion

Jarrett Lindsay, Minu Samanta, Nathan Kendsersky, Jonathan Gaither, Molly Christie, Kyabeth Torres-Rodriguez, Catherine Wingrove, John M. Maris. *Children's Hospital of Philadelphia, Philadelphia, PA*

BACKGROUND: Neuroblastoma is a cancer arising from the developing sympathetic nervous system. Less than half of children diagnosed with high-risk neuroblastoma survive five years. Two transcriptional subpopulations have been identified: aggressive, chemotherapy-sensitive adrenergic (ADRN) and indolent, chemotherapy-resistant mesenchymal

(MES). ALCAM is a cell adhesion molecule that is overexpressed in neuroblastoma. ALCAM is a cancer stem cell marker in colorectal and small cell lung cancer and promotes bone metastasis in prostate cancer. ALCAM also interacts with the CD6 receptor on T cells, which facilitates adhesion in the immunological synapse and inhibits T cell activation.
METHODS: We characterized ALCAM expression in 24 neuroblastoma cell lines using immunoblotting. We investigated ALCAM expression in ADRN and MES neuroblastoma using RNA-sequencing data from two patient datasets. Next, we developed doxycycline (dox)-inducible ALCAM depletion cell lines using CRISPR inhibition (CRISPRi) in three high-ALCAM cell lines with relevant oncogenic aberrations. Using the Incucyte® SX5 Live-Cell Analysis System, we interrogated the effects of ALCAM depletion on proliferation and scratch wound migration. To determine the mechanism of ALCAM overexpression, we leveraged ChIP-sequencing data for MYC and MYCN in 9 cell lines. We probed the effects of the MYC(N)-MAX disrupter MYCi975 on ALCAM expression using immunoblotting. To investigate the effects of the ALCAM-CD6 interaction on T cells, we stimulated CD4+ and CD8+ T cells with CD3/28 antibodies in the presence or absence of recombinant ALCAM and measured activation by ELISA for IFN-γ, and TNF-α and flow cytometry for CD69 expression.
RESULTS: ALCAM is highly expressed in most neuroblastoma primary tumors and cell lines. ALCAM mRNA expression is higher in the ADRN subpopulation ($p \leq 0.0045$), although both ADRN and MES tumors and cell lines express high levels of ALCAM. Dox-inducible CRISPRi mediated robust ALCAM depletion in all three cell lines, and ALCAM knockdown significantly delayed proliferation ($p \leq 0.0025$) and impaired scratch wound migration. ChIP-sequencing showed robust MYC(N) peaks at the ALCAM promoter, and treatment with IC_{50} concentrations (3.5 - 9.0 μM) of MYCi975 depleted MYC(N) and ALCAM. Activation of CD4+ and CD8+ T cells in the presence of recombinant ALCAM mediated dose-dependent reduction in expression of T cell activation marker CD69 after 3 days and inhibited IFN-γ and TNF-α release.
CONCLUSIONS: ALCAM is overexpressed in neuroblastoma and its expression is driven, at least in part, by MYC(N). ALCAM is a mediator of cellular proliferation and migration and may contribute to immune evasion by inhibiting T cell activation. Ongoing *in vivo* studies will characterize the

effects of ALCAM depletion on tumor growth and metastasis. We propose ALCAM is a tractable immunotherapy target through multi-specific antibodies or the ALCAM-CD6 interaction.

#6715

CLIC1 and CLIC4 ion channels as bioelectric targets for tumor treating fields in pediatric high-grade glioma

Michaela Griffin, Paul Smith, Raheela Khan, Surajit Basu, Stuart James Smith. *University of Nottingham, Nottingham, United Kingdom*

Background: High Grade Glioma is a lethal brain cancer with an average survival of 14 months. Due to the scarcity of effective treatment, and aggressive nature of the tumor, pediatric High Grade Glioma (pHGG) forms a leading cause of CNS cancer-related death in children. Optune™ is a non-invasive therapy that uses alternating electric fields - coined Tumor Treating Fields (TTFields) - to disrupt cancer cell division. Increasing evidence shows that ion channels not only regulate electrical signaling of excitable cells, but also play a crucial role in the development and progression of brain tumors. Ion channels are essential in cell cycle control, invasion and migration of cancer cells and therefore present as valuable therapeutic targets.
Methods: CLIC channel expression patterns were identified via multivariate analysis of in-house and publicly available data sets and RNA sequencing of in-house patient tissues. siRNA depletion of CLIC1 and CLIC4 was assessed using cell cycle, clonogenic, migration and proliferation assays, alone and concomitant with TTFields and or CLIC channel inhibitors, IAA94 or metformin. Whole transcriptome gene expression analysis (Human Clariom™ Array) of pHGG cells treated with TTFields was carried out. Whole cell and cell attached patch clamp protocols were used to assess ion channel activity in pHGG and normal astrocytes.
Results: Clinical correlation determined that CLIC4 and CLIC1 deficiency was associated with increased overall survival ($p=<0.03$), with siRNA depletion propagating a reduction in the proliferation, migration and invasion of pHGG cell lines associated with cell cycle arrest. Furthermore, CLIC1 and CLIC4 deficiency exacerbated the killing capacity of TTFields, reducing clonogenic and proliferative capabilities. Concomitant application of either IAA94 or metformin, and TTFields increased the sensitivity of

cells to TTFields. Whole transcriptome gene expression analysis of pHGG cell lines treated with TTFields and found that cells treated with TTFields exhibited a down-regulation in CLIC1 and CLIC4 compared to untreated cells. Furthermore, neurophysiological patch clamp experiments revealed increasingly depolarized membrane potential readings in pHGG cell lines compared to normal astrocytes, with unique ion channel activity (including chloride channel function) observed and the potential for further pharmacological exploitation.
Conclusions: These data provide rationale that genetic, electrical, and pharmacological manipulation of ion channels can reduce the capacity of childhood brain tumors to proliferate and invade. CLIC channels may be a suitable target to enhance the treatment efficacy of TTFields and help optimize this non-invasive therapy in pediatric HGG patients.

#6716

Preclinical evaluation of nano-liposomal irinotecan in pediatric solid tumor patient-derived xenografts

Elizabeth Stewart[1], Kaley Blankenship[1], Burgess Freeman[2], Sara Federico[1], Michael Dyer[3]. *[1]Oncology, St. Jude Children's Research Hospital, Memphis, TN,[2]Preclinical PK Shared Resource, St. Jude Children's Research Hospital, Memphis, TN,[3]Developmental Neurobiology, St. Jude Children's Research Hospital, Memphis, TN*

Background: Pediatric solid tumors are rare and the use of well characterized preclinical models can be a helpful tool to prioritize novel drug combinations and formulations which are challenging to test in a limited patient population. Irinotecan (IRN) has shown efficacy in diverse pediatric cancers where children are often treated on an extended low-dose schedule rather than a single large dose commonly used in adults. The use of nano-liposomal irinotecan (nal-IRI) is a promising strategy as 95% of the drug remains encapsulated during systemic exposure while maintaining prolonged exposure in the tumor. Adult clinical trials have shown reduced side effects without compromising efficacy but nal-IRI has had limited use thus far in pediatric cancers.
Methods: Orthotopic xenograft models of Ewing sarcoma (EWS, 4 models) and rhabdomyosarcoma (RMS, 2 models) were generated by injecting luciferase labeled cells into the femur and hind-leg muscle of nude mice

respectively. Pharmacokinetic (PK) studies on normal and tumor-bearing mice were performed for both nal-IRI and standard IRN to determine matched human AUC-guided dosing and schedule of chemotherapy agents. Mice were randomized to single agent and relevant combinations of nal-IRI with PARP inhibitors and temozolomide (EWS) and with vincristine and temozolomide (RMS) and compared to the same regimens using standard IRN. Therapy was given on a clinically relevant schedule with each course consisting of 21 days and tumor response was measured weekly using bioluminescence.
Results: PK studies showed that plasma levels of the active metabolite of IRN (SN-38) drop quickly for both standard IRN and nal-IRI single dosed mice while the levels of SN-38 were maintained in the tumor for several days using the nal-IRI formulation. In all 6 models tested, nal-IRI combinations were as or more effective when compared to regimens using standard IRN. No significant toxicity was seen in mice treated with nal-IRI combinations.
Conclusions: The substitution of nal-IRI for standard IRN remains a promising strategy in pediatrics with the potential to reduce side effects as well as hospital visits due to the dosing schedule with nal-IRI given once per cycle where standard IRN is often given for 5 or 10 days in children. Our preclinical PK data confirmed the liposomal formulation resulted in sustained SN-38 levels in the tumor and efficacy was maintained or improved in pediatric cancer models. The combination of nal-IRI with temozolomide and talazoparib is now being tested in a multi-center randomized phase I/II trial for children with relapsed solid tumors and this data supports consideration for use in other pediatric cancer trials both in the upfront and relapse setting.

#6717

Extracellular vesicles in diagnostic retinoblastoma aqueous humor correlate with disease stage and clinical outcome: a pilot study

Sarah Pike[1], Chen-Ching Peng[1], Paolo Neviani[2], Jesse L. Berry[1], Liya Xu[1].
[1]The Vision Center, Children's Hospital Los Angeles, Los Angeles, CA,[2]Extracellular Vesicle Core, Children's Hospital Los Angeles, Los Angeles, CA

Introduction: Retinoblastoma (RB), a pediatric retinal malignancy, is unique in that it cannot be biopsied, impeding biomarker discovery. Aqueous humor (AH) is an ocular fluid that is an established source of tumor information, serving as a surrogate liquid biopsy. Extracellular vesicles (EVs) are promising biomarker candidates, and were recently established in RB AH. EVs are membrane-enclosed secretory vesicles carrying bioactive molecular information, which can be phenotyped using validated tetraspanin protein markers. Currently, relationships between EVs and RB clinical features are unknown, but establishing such relationships is necessary to determine the utility of EVs as RB biomarkers. Methods: We quantified and phenotyped EVs in 37 AH samples from 18 RB eyes with varying International Intraocular Retinoblastoma Classification (IIRC) stages and explored clinical correlations. Samples were collected from 10 eyes at diagnosis (DX) and 27 eyes during treatment (Tx). By outcome, 6 DX eyes were enucleated and 4 were salvaged. DX samples were collected from one A, one B, six D and two E eyes by IIRC group. 10μL of unprocessed AH underwent Single Particle-Interferometric Reflectance Imaging Sensor (SP-IRIS) (Exoview R100) analysis for fluorescent-based particle count and immunophenotyping of tetraspanin expression (CD63/81/9). Counts were converted to percentages. Statistics were done with Mann-Whitney U, ANOVA, and Tukey's tests. Results: Samples from DX eyes (n=10) contained a higher number of EVs than samples from Tx eyes (n=27) (1.68 x 107 ± 4.28 x 107 per mL vs. 2.10x 106 ± 1.33 x 106 per mL) by SP-IRIS analysis. By percentage, DX samples were enriched with CD63/81+ EVs ($P<0.001$) while Tx samples had more homogenous mono-CD63+ dominant EV populations ($P=0.007$). Enrichment of CD63/81+ EVs was significantly higher in enucleated AH (n=6) than salvaged AH (n=4) when compared by count ($P=0.038$) and marginally higher when compared by percentage ($P=0.067$). The CD9/81+ EV population percentage was significant in salvaged eyes ($P=0.01$). By IIRC, CD63/81+ EVs were most abundant in Group E eyes (n= 2) when compared to Group D eyes (n=6) by count ($P<0.001$), and when compared to Group A+B eyes (n=2) by count ($P=0.01$) and percentage ($P=0.019$). Group A+B eyes had a larger percentage of CD9/81+ EVs than did Group E eyes ($P=0.043$). Conclusions: EV quantity in RB AH decreases with treatment, and phenotypic expression profiles vary by treatment status and clinical outcome. TheCD63/81+ EV subpopulation is higher in eyes with advanced

Group E disease and those requiring enucleation, while the CD9/81+ subpopulation is higher in eyes with less advanced Group A+B disease and those salvaged with treatment. Our data suggests that EV phenotypes correlate with RB clinical features, and further research into these subpopulations offers the prospect of establishing critical RB biomarkers.

#6718

Exploiting metabolic vulnerabilities of pediatric rhabdomyosarcoma with novelnicotinamide phosphoribosyltransferase (NAMPT) inhibitor OT-82

Grace McKay-Corkum[1], Victor J. Collins[1], Choh Yeung[1], Takeshi Ito[2], Sameer H. Issaq[2], Arnulfo Mendoza[1], Kazutoshi Yamamoto[3], Murali Cherukuri[3], Len Neckers[2], Christine M. Heske[1]. *[1]Pediatric Oncology Branch, National Cancer Institute, Bethesda, MD,[2]Urologic Oncology Branch, National Cancer Institute, Bethesda, MD,[3]Radiation Biology Branch, National Cancer Institute, Bethesda, MD*

Purpose: A hallmark of cancer cells is altered metabolism. Therapeutically, these alterations may be exploited by targeting metabolic vulnerabilities specific to cancer cells. Efficient production of NAD through the NAD salvage pathway is one such potential vulnerability, as some tumor cells demonstrate a high need for rapid NAD turnover. Nicotinamide phosphoribosyltransferase (NAMPT) is the pharmacologically targetable rate-limiting enzyme in this pathway. We report on the effect of targeting NAMPT in models of pediatric rhabdomyosarcoma (RMS), a cancer for which novel therapeutics remain an unmet need.
Experimental Procedures: The relative sensitivity of RMS cell lines to NAMPT inhibitors was first compared to NAMPT inhibitor sensitivity of other cancer cell lines using viability assays. A panel of ten molecularly diverse RMS cell lines was used for the remainder of the evaluations. *In vitro* activity of NAMPT inhibition was evaluated using assays of proliferation and cell death. Measurements of NAD and functional assessment of NAD-dependent processes, such as glucose metabolism, were used to study the mechanistic activity of NAMPT inhibition in these models. *In vivo* studies included assessments of toxicity, efficacy, and mechanism of action of a clinical NAMPT inhibitor, OT-82, in four orthotopic RMS models.

Results: RMS cells showed striking sensitivity to NAMPT inhibition with IC-50 values in the low nanomolar range. *In vitro,* NAMPT inhibition resulted in NAD depletion and impaired cellular proliferation. Effects on glucose metabolism included decreases in glycolytic activity and glycolytic capacity in all cell lines tested, as well as decreased oxidative phosphorylation in a subset of cell lines. The majority of cell lines exhibited ATP depletion and irreversible necrotic cell death. Apoptotic cell death was not observed. *In vivo*, the effects of OT-82 treatment delivered on the human clinical schedule replicated those seen *in vitro,* including loss of glycolytic activity as measured using hyperpolarized ^{13}C MRI spectroscopy. In all four xenograft models, complete tumor regressions were observed at multiple doses and with minimal toxicity.
Conclusions: NAMPT inhibition with OT-82 was highly effective in decreasing RMS proliferation and impairing glucose metabolism both *in vitro* and *in vivo*. Given these results, there is a critical need for further clinical study of this class of agents for RMS.

#6720
Using proteasome inhibition to hyperactivate the integrated stress response in aggressive pediatric brain tumors
Orlandi Valencia Novak, Tyler Findlay, Jeffrey Rubens, Charles Eberhart, Eric H. Raabe. *Johns Hopkins University School of Medicine, Baltimore, MD*

H3K27-altered diffuse midline glioma (DMG) and atypical teratoid/rhabdoid tumor (AT/RT) are aggressive pediatric brain tumors with dismal outcomes. DMG and AT/RT have increased baseline activation of the integrated stress response (ISR), an evolutionarily conserved system that enables cells to tolerate various forms of stress. This activation is manifested by elevated levels of ATF4 and NRF2 in DMG and AT/RT, respectively. Transient or low-level expression of these transcription factors protect cells from stress, while sustained, high-level activation leads to cell death. Ixazomib is an orally bioavailable proteasome inhibitor that causes endoplasmic reticulum stress, which is a major upstream activator of the ISR. We hypothesized that the high baseline level of ATF4 in DMG and NRF2 in AT/RT would make these tumors susceptible to ISR activators such as ixazomib. After determining the IC50 of ixazomib, DMG and

AT/RT cell lines (JHH-DIPG1, JHH-DIPG16A, and CHLA06) were treated with increasing concentrations of the drug. Cleaved caspase 3 immunofluorescence showed a significant increase of apoptosis in all cell lines (JHH-DIPG16A and CHLA06 $p<0.0001$, JHH-DIPG1 $p=0.0008$ by ANOVA). Additionally, western blots for cleaved PARP and phospho-Rb expression detected induction of apoptosis and suppression of cell proliferation in JHH-DIPG1 treated with ixazomib. We are currently testing ixazomib in combination with idarubicin, a brain-penetrant anthracycline, and gemcitabine, a brain-penetrant nucleoside analog. Synergy testing in CHLA06 showed an overall zero-interaction-potency (ZIP) synergy score of 23.464 with inhibitory concentrations of ixazomib and idarubicin in the low nanomolar range (scores of 10 or above indicate synergy). Similarly, ixazomib and gemcitabine synergized to suppress CHLA06 growth and induce apoptosis (67% Annexin V+ cells in combination compared to 14 and 24% Annexin V+ with single agent treatment). In the future, we will determine if ixazomib selectively kills DMG and AT/RT while sparing normal cells in iPSC brain organoids. We will also test ixazomib singly and in combination with traditional chemotherapy in orthotopic xenografts of AT/RT. These results suggest that ixazomib, especially in combination with idarubicin, gemcitabine or other ISR activators, has the potential to serve as an effective therapy for aggressive pediatric brain tumors.

#6721

β3-adrenergic receptor correlates with tumor growth and progression in neuroblastoma

Alessia Boaretto, Gennaro Bruno, Nicoletta Nastasi, Claudio Favre, Maura Calvani. *Meyer Children's Hospital Florence, Firenze, Italy*

Neuroblastoma (NB) is a heterogeneous, often aggressive, extracranial tumor and the most common malignancy to be diagnosed in the first year of life. It has been already demonstrated that the specific antagonism of the β3-adrenergic receptor (β3-AR) on NB tumor cells affects tumor growth. To confirm the results obtained with the pharmacological approach on the crucial role played by the β3-AR receptor in influencing different pro-tumoral signaling pathways, here we investigated the effect of CRISPR/Cas9-mediated knock-out of β3-AR gene (ADRB3) on human NB cell line BE(2)-C *in vitro* and *in vivo*. Inoculation of BE(2)-C β3-AR$^{-/-}$ cells

in athymic nude mice (NU(N-Cr)-Foxn1nu) showed a strong reduction of NB tumor growth compared to wild type cells, and in some cases β3-AR knock-out tumor cells failed in producing a tumor mass. RNA Sequencing on these tumor masses showed alterations of signaling pathways related to various tumor mechanisms, such as proliferation, cell motility and cell differentiation. Furthermore, we evaluated by flow cytometry the expression of β3-AR in circulating tumor cells (CTCs) from NB patients with different degrees of disease. Following depletion with anti-CD45 magnetic beads, tumor cells were identified through the expression of specific tumor markers, CD56 and GD2. Results showed that a high expression of β3-AR correlates with poor prognosis, characterized by metastatic or recurrent tumors, compared to patients with a favorable clinical outcome that instead show a low expression of β3-AR. Overall, our results demonstrate the β3-AR involvement in supporting NB tumor growth and suggest a possible role in regulating the metastatic potential of this tumor.

#6722

RNAScope *in situ* hybridization as a novel approach for the spatiotemporal assessment of RD3 mRNA expression in neuroblastoma

Dinesh Babu Somasundaram[1], Sheeja Aravindan[2], Zhongxin Yu[1], Ashley Baker[1], Natarajan Aravindan[1]. *[1]University of Oklahoma Health Sciences Center, Oklahoma City, OK,[2]OU Health Stephenson Cancer Center, Oklahoma City, OK*

Our recent investigations unveiled the transcriptional and translational loss of Retinal degeneration Protein 3 in neuroblastomas (NB) when compared to the healthy adult and fetal tissues. Further, our preclinical studies with patient derived cellular systems and mouse model of high-risk NB (HR-NB) demonstrated that RD3 loss orchestrates disease progression. More importantly, we defined the therapy pressure driven acquired loss of RD3 in neuroblastomas, its crucial function in the evolution of progressive disease (PD), and further defined the prognostic and predictive significance of RD3 loss in NB. In this study, we investigated the use of RNAScope as a sensitive and specific method for the evaluation of spatiotemporal RD3 transcriptional loss in NB. We investigated the expression of RD3 mRNA in FFPE NB (n = 100) tissues utilizing RNAScope with custom archived RD3

specific probes comparing it with the matched RD3 protein (IHC) expression patterns. With positive (PPIB) and negative (DapB) controls in place, our results displayed definite and specific RD3 mRNA expression in NB. We observed a statistically significant association of RD3 mRNA loss to the disease progression and poor clinical outcomes. Further, we observed significant correlation to the loss of RD3 transcription to the evolution of progressive disease. More importantly, the expression gradients of RD3 mRNA observed with RNAScope assay (compared in terms of no treatment vs progressive disease, primary vs metastatic disease, relapsed vs no relapse, favorable to unfavorable disease) illustrate the concordance with the RD3 IHC outcomes. Our results provide a reference basis for better RD3 mRNA readouts in NB, and more importantly identify the technically sound, adaptable (high throughput/single event, manual/automatic) RNAScope *in situ* hybridization assay as an alternate approach to detect spatiotemporal expression of RD3 mRNA. Together, the results provide a new, descriptive, and efficient platform, RNAScope for assessing spatiotemporal RD3 mRNA expression that could better inform disease prognosis and therapy response in children with NB.
Funding: This work was partially or in full, funded by Department of Defense DoD-CA210339 and Oklahoma Center for the Advancement of Science and Technology, OCAST-HR19-045.

#6723

Application of in vitro drug screening of circulating tumor cells in pediatric glioma therapy

Yen-Lin Liu[1], Yin-Ju Chen[2], Shu-Huey Chen[3], Yu-Mei Liao[4], Wu Shih-Pei[5], Yi-Hsuan Chen[1], Wan-Ling Ho[1], Liang-Yi Juo[1], Chia-Yau Chang[1], Jinn-Li Wang[6], Min-Yu Su[7], Pei-Chin Lin[4], Shih-Chung Wang[8], James S. Miser[9], Tai-Tong Wong[10], Yuan-Hung Wu[11], Peng Yuan Wang[12], Thierry Burnouf[2], Jeng-Fong Chiou[13], Long-Sheng Lu[13]. *[1]Departments of Pediatrics, Taipei Medical University Hospital, Taipei, Taiwan,[2]Graduate Institute of Biomedical Materials & Tissue Engineering, Taipei Medical University, Taipei, Taiwan,[3]Departments of Pediatrics, Taipei Medical University-Shuang Ho Hospital, New Taipei, Taiwan,[4]Division of Pediatric Hematology/Oncology, Kaohsiung Medical University Hospital, Kaohsiung, Taiwan,[5]CancerFree Biotech Ltd., Taipei, Taiwan,[6]Departments*

of Pediatrics, Taipei Municipal Wanfang Hospital, New Taipei, Taiwan,[7]Department of Pediatrics, China Medial University Children's Hospital, Taichung, Taiwan,[8]Division of Pediatric Hematology/Oncology, Changhua Christian Children's Hospital, Changhua, Taiwan,[9]Taipei Cancer Center, Taipei Medical University, Taipei, Taiwan,[10]Pediatric Neurosurgery, Taipei Medical University Hospital, Taipei, Taiwan,[11]Division of Radiation Oncology, Department of Oncology, Taipei Veterans General Hospital, Taipei, Taiwan,[12]Key Laboratory of Alzheimer's Disease of Zhejiang Province, Institute of Aging, Wenzhou Medical University, Zhejiang, China,[13]Radiation Oncology, Taipei Medical University Hospital, Taipei, Taiwan

Twenty-one gliomas in patients aged 0-21 years were evaluated for drug sensitivity by *ex vivo* expanded circulating tumor cells (CTC). The results were correlated with clinical outcomes. Venous blood samples were obtained prior to drug treatment. Peripheral blood mononuclear cells were processed in a 3D cell culture system (EVA Select™, Cancer Free Biotech Ltd., Taipei, Taiwan) and cultured for 3 weeks. Expanded CTCs were successfully cultured into organoids from 18 out of 21 patients and were analyzed for ATP abundance. Staining with CD45, a marker for blood cells, and pancytokeratin, a marker for keratinocytes, was performed on the cultured cells. Staining of GFAP, a marker of glioma cells, was performed in a subset of samples. These cells were then tested in cytotoxicity assays in triplicate with a panel of chemotherapeutic and targeted agents at clinically relevant concentrations. The surviving fraction was normalized to a buffer-only control. Based on the percentage of cell viability, the agent was chosen for clinical treatment. Comparing the results among low-grade glioma (LGG; $n = 6$), diffuse midline glioma (DMG; $n = 4$), and high-grade glioma (HGG, $n = 8$; including glioblastoma multiforme [GBM; $n = 5$]), the mean surviving fraction to temozolomide was similarly high across the three tumor types (LGG *vs*. DMG *vs*. HGG = 57.5% *vs*. 50.6% *vs*. 49.5%, respectively). 6 of 6 patients in the LGG group showed CTC sensitivity to at least one chemotherapeutic agent tested. The clinical response of patients treated with selected agents was evaluated with the RANO criteria at 6 months after initiation of treatment. Among the 24 agents tested with clinical correlation, the CTC surviving fraction after exposure to the agent

was significantly higher in patients who had progressive disease within 6 months (n = 11; 68%) *vs*. in patients with no progression at 6 months (n = 13; 39%; P = 0.039). Treating CTCs with histone deacetylase inhibitors *in vitro* resulted in a consistently lower surviving fraction (15.1% ± 12.0%) for DMG and HGG/GBM; however, clinical correlation was not available. The 1 patient with clinical correlation with HGG had a 34.9% surviving fraction to a Tyrosine kinase inhibitor (TKI) *in vitro* and showed a 42.9% shrinkage at 6 months after treatment with the TKI. The expansion of CTCs in patients with relapsed/refractory pediatric gliomas provides the ability to test drug sensitivity of patient-derived organoids. Our data suggest a correlation between the *ex vivo* drug sensitivity of CTCs and clinical response.

#6725

Targeting urea cycle dysfunction to prevent and treat osteosarcoma

Rachel Offenbacher[1], Paul Ciero[2], David Loeb[1]. *[1]The Children's Hospital at Montefiore, Bronx, NY,[2]Albert Einstein College of Medicine, Bronx, NY*

Introduction: Osteosarcoma (OS) is the most common primary malignant bone tumor in adolescents and young adults. Intensive multimodal treatment cures almost 75% of patients who present with localized disease; however, only 25% of patients who present with metastases become long term survivors, and those who suffer a metastatic relapse are almost never cured. Polyamine metabolism and signaling play important roles in multiple cancers but have not previously been studied in osteosarcoma. D, L-alpha-difluoromethylornithine (DFMO) is an irreversible inhibitor of ornithine decarboxylase (ODC), the initial, rate-limiting enzyme within the polyamine biosynthetic pathway, and has been studied in a number of different cancers as either a therapeutic or a chemopreventive agent. We investigated the role of polyamines in OS proliferation and metastasis and whether blocking the polyamine synthetic pathway with DFMO had therapeutic potential in the treatment of OS.
Methods: We evaluated proliferation, apoptosis, clonogenic growth and the ability to grow under nonadherent conditions in vitro using established OS lines. To investigate the effect of DFMO on tumor growth in vivo, we implanted fragments of patient derived xenograft into the tibias of NOD/SCID/IL-2Rγ null mice. Upon confirmation of tumor growth, mice

were randomized to either receive drinking water or drinking water supplemented with 2% DFMO. A third cohort of mice received water supplemented with 2% DFMO only after hindlimb amputation.
Results: DFMO has a profound effect on the proliferation of OS cell lines in vitro. Utilizing caspase assays, we determined that DFMO does not induce apoptosis, but is cytostatic and inhibits proliferation. We found that DFMO prevents the clonogenic growth of 3 different OS cell lines in soft agar and prevents spheroid formation under non-adherent conditions. Interestingly, once established, spheroidss were not disrupted by the addition of DFMO. In vivo, administration of 2% DFMO after hindlimb amputation decreased local recurrence and limited metastasis ($p=0.02$).
Conclusion: DFMO inhibits proliferation and clonogenic growth in vitro, and decreases distant metastasis in vivo. Since pediatric dosing and safety data are already established, our findings are readily translatable to clinical trials.

#6726
Effectiveness of irinotecan plus trabectedin in a desmoplastic small round cell tumor patient-derived xenograft
Valentina Zuco, Sandro Pasquali, Monica Tortoreto, Stefano Percio, Valentina Doldi, Marta Barisella, Paola Collini, Gianpaolo Dagrada, Silvia Brich, Patrizia Gasparini, Marco Fiore, Michela Casanova, Anna Maria Frezza, Alessandro Gronchi, Silvia Stacchiotti, Andrea Ferrari, Nadia Zaffaroni. *Fondazione IRCCS Istituto Nazionale dei Tumori, Milano, Italy*

Desmoplastic small round cell tumor (DSRCT) is a ultra-rare pediatric scarcoma with poor overall survival. This tumor is dependent on the continued expression and activity of its pathognomonic molecular lesion, the EWS-WT1 transcription factor. DSRCT is often treated with multimodal approach of chemotherapy, surgery, and radiotherapy. Given the rarity of the disease, there have not been clinical studies to establish an effective therapeutic regimen. Indeed, the development of fully characterized preclinical models, able to reproduce the molecular characteristics of clinical tumors, appears instrumental for testing novel therapeutic strategies and accelerating the translation of preclinical findings to the clinical practice. In this study we exploited a novel DSRCT patient-derived xenograft (PDX), which reproduces histomorphological, genomic

(CNV) and transcriptomic characteristics of the paired clinical tumor, to comparatively assess the activity of cytotoxic and targeted anticancer agents. Anti-tumor effect was moderate for single-agent doxorubicin, pazopanib and larotrectenib [maximum tumor volume inhibition (max TVI): 55-66%], trabectedin had a higher effect (max TVI: 82%) while irinotecan and eribulin almost complete inhibited tumor growth (max TVI: 96% and 98%, respectively). Interestingly, combination of irinotecan with either eribulin or trabectedin resulted in complete responses which were maintained until the end of the experiment for irinotecan + trabectedin. The trabectedin + irinotecan combination markedly reduced the expression of anti-apoptotic proteins and caused caspase-3 cleavage, consistent with an apoptotic response, and also induced the accumulation of phospho-RIP1 (Ser166) and phospho-RIP3 (Ser227), indicating the occurrence of necroptosis, a type of programmed cell death with necrotic morphology. In line with these findings, transcriptomic profile analysis of ex-vivo tumor samples obtained from mice exposed to trabectedin ± irinotecan revealed a reduced expression of the biological pathways related to apoptosis and cell proliferation in tumor exposed to the drug combination. Mechanistically, we found that these effects were mediated, at least in part, by the down-regulation of EWS-WT1 chimeric protein and its downstream targets, as assessed by PCR and western blotting. Overall, this study emphasizes the importance of patient-derived pre-clinical models to explore new treatments in DSRCT and fosters clinical investigation in the activity of irinotecan plus trabectedin, providing a step forward for developing more effective trabectedin-based combinations for DSRCT to be tested in clinical trials.

#6727

Therapeutic targeting of BET bromodomain proteins increases DNA damage and potentiates salvage therapy in osteosarcoma xenografts derived from patients with replication stress signatures

Niknam Riyahi, Pankita H. Pandya, Barbara J. Bailey, Erika A. Dobrota, Courtney Young, Harlan E. Shannon, Farinaz Barghi, Rada Malko, Khadijeh Bijangi-Vishehsaraei, Melissa A. Trowbridge, Kathy Coy, Felicia M. Kennedy, Anthony L. Sinn, Steve Angus, Michael J. Ferguson, M. Reza Saadatzadeh, Karen E. Pollok. *Indiana University School of Medicine, Indianapolis, IN*

Osteosarcoma (OS) is an aggressive cancer of the bone with high metastatic potential in pediatric as well as adolescent and young adults. The survival rate for metastatic and relapsed OS patients is <30% and there is currently no effective standardized salvage therapy. Lack of efficacy is attributed to genetic complexity present in OS that is partly due to moderate levels of replication stress (RS). While high levels of RS can induce cell death, moderate RS levels may cause genomic instability that contributes to OS progression. Therefore, induction of RS to high levels that cause cell death could be a promising therapeutic strategy. Bromodomain and extra-terminal domain [BET proteins (BRD2,3, and 4)] are a family of epigenetic readers that not only regulate gene expression networks, but also regulate DNA replication and RS. Thus, we tested the hypothesis that BET inhibition will potentiate the efficacy of salvage therapy through exacerbation of RS in xenograft models of aggressive OS. The effect of the bivalent BET inhibitor (BETi), AZD5153, as a single agent and in combination with cytotoxic agents such as topotecan and ifosfamide was evaluated. Combination index and Bliss independence analyses demonstrated additive to synergistic cell growth inhibition in OS cell lines upon treatment with clinically relevant concentrations of AZD5153+ topotecan/ifosfamide. Treatment with PROTAC ARV825 that degrades BET proteins, resulted in similar growth inhibitory effects. Significant increase in PARP cleavage was observed following AZD5153+topotecan treatment compared to single agent, indicating enhancement of apoptosis. In addition, western blot and comet assays showed that BETi+topotecan induces its effect, at least partly, through increased DNA damage and RS *in vitro*. *In vivo* efficacy and safety studies focused on patient-derived xenografts (PDXs) of naive and pre-treated OS that harbor RS signatures. AZD5153 as a single agent significantly suppressed tumor growth in both naïve (PDX96) and pretreated (TT2) OS PDX models compared to vehicle ($p<0.05$, Two-way ANOVA; Holm-Sidak). Anti-tumor effect correlated with increased γ-H2AX following AZD5153 exposure in PDX, indicative of increased RS. Moreover, RNA-seq analysis integrated with kinome profiling data from BETi-treated PDX exhibited deregulation of factors involved in RS. Combination treatments of BETi+topotecan/ifosfamide indicated that AZD5153 potentiated the anti-cancer effect of salvage therapy in TT2 OS PDX, was well tolerated, and increased the probability of survival in mice. Efficacy in an OS RS+ metastatic lesion model is in progress. These data

collectively suggest that BET inhibition as a single agent and in combination with low-dose salvage therapy holds promise as novel treatment strategies for inducing RS-mediated cell death in aggressive OS.

#6728

Osteosarcoma patient-derived xenografts derived from naive and pretreated metastatic patients with high-risk CDK4/6 hyperactivation signatures are sensitive to dual inhibition of CDK4/6 and PI3K/mTOR

Farinaz Barghi[1], M. Reza Saadatzadeh[2], Erika Dobrota[3], Rada Malko[1], Barbara J Bailey[2], Courtney Young[4], Harlan E. Shannon[4], Ryli Justice[4], Niknam Riyahi[4], Khadijeh Bijangi-Vishehsaraei[5], Melissa Trowbridge[6], Kathy Coy[6], Felicia M Kennedy[6], Anthony L Sinn[6], Amber Mosley[7], Steve Angus[4], Michael J. Ferguson[8], Pankita H. Pandya[5], Karen E. Pollok[1].
[1]Indiana University School of Medicine, Department of Medical and Molecular Genetics, Indianapolis, IN,[2]Indiana University School of Medicine, .Herman B Wells Center for Pediatric Research, Indianapolis, IN,[3]Indiana University School of Medicine, Herman B Wells Center for Pediatric Research, IUSM, Indianapolis, IN,[4]Indiana University School of Medicine, Herman B Wells Center for Pediatric Research, Indianapolis, IN,[5]Indiana University School of Medicine, Department of Pediatrics, Hematology/Oncology, Indianapolis, IN,[6]Indiana University School of Medicine, In Vivo Therapeutics Core, Indiana University Melvin and Bren Simon Comprehensive Cancer Center, Indianapolis, IN,[7]Indiana University School of Medicine, Indianapolis, IN,[8]Indiana University School of Medicine, Department of Pediatrics, Indianapolis, IN

Precision genomics studies have demonstrated hyperactivation of cyclin-dependent kinases 4 and 6 (CDK4/6) as a top actionable marker in children, as well as adolescents and young adults (AYA) with osteosarcoma (OS). CDK4/6 binds to cyclin D resulting in a complex that mediates RB phosphorylation leading to cell cycle progression. Preclinical modeling approaches are critical for identification of tumor adaptive responses to CDK4/6 inhibitors (CDK4/6i) as well as validation of alternative or combination therapies. Although CDK4/6i are clinically well-validated, cytostatic effects make combination treatments essential. Moreover, concomitant dysregulation of CDK4/6 and PI3K/mTOR pathways are

observed in aggressive OS. Multiple positive feedback loops between these pathways exacerbate the hyperactivation of CDK4/6 and PI3K/mTOR signaling. Thus, we hypothesize that dual inhibition of CDK4/6 and PI3K/mTOR will be efficacious in RB+ OS PDXs. In this study, OS PDX models TT2-77 (pretreated patient) and HT96 (treatment-naïve patient) with molecular signatures indicative of therapeutic sensitivity to palbociclib (RB+, CDKN2A null, CCND3 amplified) were treated long-term with CDK4/6i (palbociclib) (50 mg/kg), PI3K/mTOR inhibitor (PI3K/mTORi; voxtalisib) (50 mg/kg) or combination palbociclib+voxtalisib. In both PDXs, growth was significantly reduced in single-agent and combination groups compared to vehicle ($p<0.05$, two-way ANOVA). Importantly, combination palbociclib + voxtalisib was more efficacious than single-agents following prolonged treatment and well tolerated based on histological analyses. Kinome profiling analysis of long-term treated HT96 PDX demonstrated that compared to single agents, dual inhibition of CDK4/6+PI3K/mTOR significantly decreased PI3K pathway activity, including downregulation of Pik3ca, mTOR, and the G2 to M transition regulator CDK1 (-log10[p] ≥1.3). OS metastatic lesion 143B model indicated increased survival based on body scoring criteria in combo versus single agent. In RB+ OS cell lines and TT2-77 xenoline, palbociclib+voxtalisib caused additive-to-synergistic cell growth inhibition, G1 arrest, and minimal apoptosis at clinically relevant doses. Increased activity of senescence biomarker beta-galactosidase indicated that inhibition of CDK4/6 but not PI3K/mTOR induced significant levels of senescence in OS cells. Mechanistic siRNA RB studies indicated CDK4/6i effect was partially dependent on RB status. These data provide evidence that combination palbociclib+voxtalisib therapy is safe, efficacious, and increases CDK4/6i efficiency in both pretreated and naive PDX models of OS. These studies provide rationale for earlier therapeutic intervention in pediatric and AYA OS patients with CDK4/6 hyperactivation signatures.

#6729

Urea cycle metabolism is disturbed in Fibrolamellar carcinoma

Mahsa Shirani[1], Solomon Levin[1], Michael D. Tomasini[1], James Knox[2], Bassem Shebl[1], David Requena[1], Jackson Clark[1], Søren Heissel[3], Hanan Alwaseem[3], Rodrigo Surjan[4], Ron Lahasky[5], Henrik Molina[3], Barbara Lyons[1], Rachael D. Migler[6], Philip Coffino[1], Sanford M. Simon[1].

[1]Laboratory of Cellular Biophysics, Rockefeller University, New York, NY,[2]Rockefeller University, New York, NY,[3]Proteomics Resource Center, Rockefeller University, New York, NY,[4]General Surgery Division, Surgery Department, Hospital Nove de Julho, São Paulo, Brazil,[5]Lahasky Medical Clinic, Abbeville, LA,[6]The Fibrolamellar Registry, New York, NY

In fibrolamellar hepatocellular carcinoma (FLC), hyperammonemic encephalopathy is a common occurrence and occasionally causes death. Using mass spectrometry, we quantitatively analyzed the proteomes of FLC patient's tumor and adjacent normal, to find pathways that are changed in FLC. These data identified multiple proteins that were altered in the proteome, among these, enzymes involved in metabolism of ammonia. These results were confirmed with immunofluorescence demonstrating that these alterations occur in all tumor cells. These results suggest that FLC cells have defects in the two primary ammonia detoxification pathways in the liver, which are responsible for detoxification of 70% of the ammonia in the body: 1) consumption of ammonia by glutamine synthetase (GLUL), and 2) addition of ammonia by ornithine carbamoyltransferase (OTC) to the urea cycle. Additionally, they also generate extra ammonia because of upregulation of glutaminase (GLS). This was tested with a targeted metabolomics of the reactants and products of these enzymes. The results were consistent with both a loss of the two pathways for consumption of ammonia activation of a pathway for generating ammonia. This production of ammonia is consistent with the observation that surgical resection of fibrolamellar reduces the ammonia in patients. All FLC patients with hyperammonemic encephalopathy and documented urine test results showed increased urinary orotic acid, evidence of blockage of the OTC pathway. This study implies that hyperammonemic encephalopathy in FLC may require alternatives to commonly used therapies.

#6730

Preclinical testing of lestaurtinib (CEP701) as a single and combination agent for the treatment of Ewing sarcoma

Samet Dayi[1], Christiane Schaefer[1], Anne Albers[2], Kiruthiga Balusamy[2], Marc Hotfilder[2], Maximilian Kerkhoff[1], Leonhard Koch[1], Hatice Önder[1], Claudia Rössig[2], Uta Dirksen[1], Stefan K. Zöllner[1]. *[1]Pediatrics III,*

University Hospital Essen, Essen, Germany,[2]Pediatric Hematology and Oncology, University Hospital Münster, Münster, Germany

Background: Multimodality treatment of Ewing sarcoma (EwS), a highly malignant bone and soft tissue tumor, provides a cure in most patients, but in the metastatic stage the prognosis remains bleak; new systemically effective therapeutic options are urgently needed. The multikinase inhibitor lestaurtinib (CEP701) is an orphan drug that has been clinically studied in various carcinomas, refractory neuroblastoma, and acute myeloid leukemia, but has not yet established itself as a standard therapy.
Methods: We performed an in vitro screening of 142 compounds with different mechanisms of action at two different concentrations and measured cell viability 120 hours after the first of two days of treatment. Lestaurtinib was further tested as a lead compound in various cell biology assays in a group of EwS cell lines genetically representing clinically predominant tumor characteristics.
Results: Lestaurtinib was among the 21 of 142 (14.8%) compounds tested that were sensitive, i.e., reduced cell viability to below 20% at 1 μM and/or 10 μM in at least four of five EwS cell lines tested. In an expanded group of six other EwS cell lines, 72 hours of treatment with lestaurtinib resulted in significantly reduced cell growth compared to human mesenchymal stem cells. In several colony formation assays, a significant reduction in the number or size of colonies was observed, both when treatment occurred prior to colony growth and when colonies that had already formed were treated. Lestaurtinib induced apoptosis with a significant increase in PI+/FTIC+-driven cells, significantly promoted anoikis, and prevented cell migration by FACS, low adherence flow cytometry analysis, and scratch assays, respectively. Cell cycle analyses by FACS showed significant G_2-M cell cycle arrest after 24 hours of treatment. Lestaurtinib also displayed a synergistic cytotoxic effect with doxorubicin, an established agent for the treatment of EwS, and exhibited a favorable dose-reduction index in all EwS cell lines tested. Notably, treatment with lestaurtinib significantly reduced doxorubicin dose at high efficacy levels (Fa 0.97) and low combination index values.
Conclusion: Our results highlight the *in vitro* efficacy of lestaurtinib in EwS and warrant further testing in an *in vivo*model as a single agent and in combination with doxorubicin.

#6731

Gut microbiome associated with the psychoneurological symptom cluster among children with solid tumors receiving chemotherapy

Jinbing Bai[1], Melissa Martin[2], Kathryn S. Sutton[1], Christie Powell[2], Thomas Olson[1], Hye In Noh[1], Maria C. Swartz[3], Deborah Watkins Bruner[1].
[1]Emory University, Atlanta, GA,[2]Children's Healthcare of Atlanta, Atlanta, GA,[3]University of Texas MD Anderson Cancer Center, Houston, TX

Background: Children with cancer (CWC) receiving chemotherapy (chemo) report significant suffering from a cluster of psychoneurological symptoms (PNS), including pain, fatigue, anxiety, depression, and cognitive dysfunction. Continuous or severe PNS reduce a child's quality of life. Chemo can disturb the gut microbiome (GM), which is associated with PNS based on the gut-brain axis. This study aimed to examine associations of GM with PNS and the PNS cluster in CWC undergoing chemo.
Methods: An observational prospective study was conducted in 21 CWC enrolled from Children's Healthcare of Atlanta. Children with at least 1 cycle of chemo were consented pre-cycle 2 chemo (T1) and followed at the end of chemo (T2). At T1, parents reported children's demographics; at T1 and T2, PNS (pain, fatigue, anxiety, depression, cognitive dysfunction) were reported by children by the Pediatric PROMIS scales and fecal specimens were collected for GM. T-score of the PROMIS scales was computed; an average of T-scores of the five PNS was computed for the PNS cluster. T-score >50 indicates a significant symptom or symptom cluster. 16S rRNA V4 gene from fecal specimens was sequenced for GM. QIIME 2 was used to examine associations of α- and β-diversity with PNS. Linear discriminant analysis effect size identified microbial taxa associated with each PNS and the PNS cluster.
Results: We analyzed 21 CWC with a mean age of 13 years, 67% male, and 67% white. Children at T2 had higher fatigue (54% vs. 43%), cognitive dysfunction (69% vs. 43%), depressive symptoms (23% vs. 19%), and multiple PNS (62% vs. 48%), but lower pain interference (31% vs. 38%) and anxiety (23% vs. 38%) than those at T1. No association was found for α-diversity at T1; higher α-diversity was associated with lower cognitive dysfunction (Faith's phylogenetic diversity, p=0.04) and anxiety (Pielou's_e, p=0.08) at T2; β-diversity (Jaccard distance) showed the GM

dissimilarities by levels of pain interference (moderate vs. severe, p=0.02) and levels of anxiety (mild vs. moderate, p=0.07). After controlling for study timepoint, children with low pain interference had an enriched *Bacteroides*; those with low fatigue had enriched *Bacteroides* and *Turicibacter*; those with normal cognitive function had enriched *Parasutterella, UBA1819, NK4A214, Sellimonas*, and *Ruminococcaceae*. Children without the PNS cluster had enriched *Bacteroides, while* those with the PNS cluster had enriched *Enterobacteriaceae*. Children without multiple PNS had enriched *UCG_003*.
Conclusions: Children with low PNS showed a higher α-diversity and a higher abundance of taxa involved in nutrition and vitamin metabolism (eg, *Bacteroides*), reducing inflammation (eg, *Turicibacter*), and producing short chain fatty acids (eg, *Ruminococcaceae*). These findings provide potential solutions to treat PNS. Further work is needed to corroborate these associations in CWC.

#6732

Identifying novel combination therapies for Ewing sarcoma

Maria Ana Isabel C. De Los Santos[1], Anne-Florence Blandin[1], Alejandra E. Aguilar[1], Matthew Hall[2], Min Shen[2], Ya-Qin Zhang[2], Brian D. Crompton[1].
[1]Dana-Farber Cancer Institute, Boston, MA,[2]National Center for Advancing Translational Sciences, Bethesda, MD

Ewing sarcoma is the second most common pediatric bone cancer in children and young adults. The standard of care therapy consists of chemotherapy, surgery, and radiation. Despite therapeutic advances, metastatic and relapsed Ewing sarcoma have poor outcomes. This is partially because transcription factors, such as the Ewing sarcoma oncoprotein *EWS-FLI1,* are difficult targets for the development of small molecules. Novel synergistic combination treatments are needed, and drug repurposing efforts can fast track potential therapies into clinical trials. To identify synergistic anti-Ewing combinations of targeted cancer agents, we conducted an initial library screen of 26 tyrosine kinase inhibitors, cell cycle inhibitors, and chemotherapies on two Ewing cell lines. While the screening results revealed multiple synergistic combinations of tyrosine kinase inhibitors and cell cycle inhibitors, we focused our follow-up validation studies on combinations that met at least one of the following

criteria: 1) agents that exhibited additivity when combined with VEGFR inhibitors, a class of agents already shown to having clinical efficacy in Ewing sarcoma and 2) combinations involving approved FDA drugs that could be rapidly translated into early phase trials for patients with Ewing sarcoma. Efficacy of selected synergistic combinations were then tested in vitro on a larger collection of Ewing cell lines. Based on these results, two combinations, one with a VEGFR inhibitor and one combination of FDA approved agents, was tested in an aggressive Ewing sarcoma xenograft mouse model for efficacy and impact on survival. We demonstrated that the combination of ribociclib, a CDK 4/6 inhibitor, and regorafenib, a VEGFR inhibitor, exhibited additivity and synergy in Ewing cell lines. Xenografted mice treated with this combination had significantly impaired tumor proliferation in a subcutaneous tumor model and prolonged survival (median 35 days) compared to mice treated with vehicle (median 28 days) or single-agent therapy. Similarly, cell lines treated with copanlisib, a PI3K inhibitor, and ribociclib, two FDA-approved drugs, synergistically inhibited cell line viability in vitro and impaired xenograft proliferation in vivo. This combination also significantly improved survival (median 48 days) in a mouse xenograft compared to treatment with vehicle (median 27 days) or either drug alone. This work demonstrates that CDK 4/6 inhibitors show synergistic activity with both VEGFR inhibitors and PI3K inhibitors in Ewing Sarcoma by impairing the growth of cultured Ewing cells and improving the survival of mice with Ewing sarcoma. We believe that pre-clinical validation of novel approved drug combinations in Ewing sarcoma will accelerate the development of early phase trials for patients with relapsed refractory disease, a group of patients greatly in need of new therapeutic opportunities.

#6733

Targeting Sp1 in Ewing sarcoma: a multi-approach method for the utilization of mithramycin

Christoffer Lambring, Riyaz Basha, Umesh Sankpal. *University of North Texas Health Science Ctr., Fort Worth, TX*

Purpose: Ewing Sarcoma (ES) is a bone and soft tissue cancer affecting young adults and children. Localized ES presents with a 5-year survival rate of 70%, while metastatic cases range from 15-30%. Our laboratory

investigates combination treatments using less toxic agents to induce sensitization to chemotherapy in ES. The anti-cancer activity of an antineoplastic antibiotic, Mithramycin (Mit), against ES cells has been shown. Mit inhibits Specificity protein 1 (Sp1) a marker associated with aggressive cancer cell growth and resistance to chemo/radiation therapies. However, its mechanistic effects on other oncogenic proteins have yet to be elucidated in ES. The purpose of this study is to evaluate the effectiveness of Mit and combination with other chemotherapeutic agents, Etoposide and Vincristine, to inhibit ES cell growth and assess the effect on cancer related proteins regulated by Sp1. Future studies will expand upon Mithramycin's mechanism of action in Ewing Sarcoma utilizing RNA sequencing and computational methods.
Methods: Anti-proliferative activity of Mit and/or Vincristine and Etoposide against ES cell lines, TC205 and CHLA10, was evaluated using CellTiterGlo kit. Dose curves and IC50 values were determined by Sigma-Plot software. The expression of Sp1 and survivin was determined by Western blot analysis. Cell lines were obtained from Children's Oncology Group. The specific type of drug effect of the combination treatments were determined by analyzing the combination index obtained via Calcusyn software. Nude mice were injected with TC-205 cells and treated over two weeks with either Mit (1mg/kg per week) and/or Etoposide (5mg/kg per week) and tumor volume was compared. Protein models were obtained from RCSB PDB and homology tests were performed in the Swiss-model workspace.
Results: Mit significantly decreased ES cell line viability and tumor volume in nude mice. Mit showed the ability to reduce the expression of Sp1 and offered differing effects on survivin expression, indicative of anti-apoptotic mechanisms being implemented in the ES cell lines. IC50 values of both chemotherapeutics and Mit were decreased by nearly 50% when used in combination and this effect was mirrored in further decreases in Sp1 expression. Synergistic drug responses were shown in the combination of Mit with both Vincristine and Etoposide. Sp1 and survivin protein models were established and homology verification using Ramachandran plots and QMEAN Z-scores indicated quality protein models for further computational studies.
Conclusions: Mit may effectively sensitize ES cells and improve the response of chemotherapy while lowering necessary effective dosages.

Studies to understand the mechanism of action of Mit on Sp1, survivin, and other proteins involved in Ewing Sarcomagenesis are underway. This study is partially supported by a grant from the Cancer Prevention and Research Institute of Texas (Award#: RP210046)

#6734

Identification of the novel *TENM3-ALK* fusion in an AYA case with *ALK* rearranged neuroblastoma

Mitsuteru Hiwatari[1], Masafumi Seki[2], Ryosuke Matsuno[3], Kenichi Yoshida[4], Takeshi Nagasawa[2], Aiko Sato-Otsubo[2], Shohei Yamamoto[5], Motohiro Kato[2], Kentaro Watanabe[2], Masahiro Sekiguchi[2], Satoru Miyano[6], Seishi Ogawa[4], Junko Takita[7]. *[1]Pediatrics, Teikyo University School of Medicine, Tokyo, Japan,[2]Pediatrics, University of Tokyo, Tokyo, Japan,[3]Pediatrics, Kansai Medical University, Osaka, Japan,[4]Pathology and Tumor Biology, Kyoto University, Kyoto, Japan,[5]Pediatrics, Tokai University School of Medicine, Isehara, Japan,[6]Tokyo Medical and Dental University, M&D Data Science Center, Tokyo, Japan,[7]Pediatrics, Kyoto University, Kyoto, Japan*

Neuroblastoma is the most common extracranial solid tumor that occurs in childhood and the most common cancer in infancy. Fewer than 5% of neuroblastomas occur in adolescents and young adults (AYAs), for whom the disease has an indolent and fatal course. Chen et al. previously reported that missense mutations in the protein- tyrosine kinase domain of *anaplastic lymphoma kinase* (*ALK*) occur in approximately 10% of cases of sporadic neuroblastoma, and these missense mutations result in the activation of the ALK protein kinase domain, which plays a key role in the tumorigenic process as seen in ALK fusion proteins. Since the initial discovery of the NPM-ALK fusion protein in human anaplastic lymphoma cell lines, more than 24 different ALK fusion proteins have been discovered in various malignancies. Till date, ALK-containing chimeric proteins have not been reported in neuroblastoma. In this study, a translocation within chromosome 2p and 4q was found to bring about the formation of an in-frame fusion gene that was composed of portions of the *teneurin transmembrane protein 3* (*TENM3*) gene and *ALK* gene in tumor cells from an AYA patient with neuroblastoma. The patient was 19-year-old female diagnosed with stage 4

neuroblastoma (unfavorable histology, poorly differentiated subtype, MYCN DNA not amplified). Computed tomography revealed a mass in the left adrenal gland with bone, spine, liver, and lung metastasis. *ALK* rearrangement was confirmed via FISH analysis. Crizotinib resulted in no disease progression for 5 months, except for metastatic spinal disease, but it did not exhibit high efficacy compared with its effects against lymphoma and lung cancer. This 5′ in-frame fusion partner gene in neuroblastoma has not yet been identified, and its role is not well-known in oncogenesis. We generated the cell line with the expression of the full length *TENM3-ALK* cDNA in NIH-3T3 cells led to the formation of a fusion protein. A cell-based evaluation of this predicted ALK protein variant revealed activation of downstream targets-STAT3, AKT and ERK- and ALK inhibitors, crizotinib or lorlatinib, treatment inhibited the growth of xenograft tumors with stable TENM3-ALK expression. We determined whether TENM3-ALK affects transformation and proliferation using a soft agar colony formation assay. As expected, the cells that expressed an empty vector and wild type ALK line did not produce a considerable number of colonies, whereas TENM3-ALK transfected cells showed anchorage-independent growth, resulting in the production of a higher number of colonies .The evidence for the role of ALK receptor signaling in stimulating neuroblastoma tumor cell growth and the demonstrated *in vitro* and *in vivo* efficacy of the ALK selective inhibitors in this study provide biological and clinical justification for the further exploration of this combination and testing in patients with recurrent or refractory neuroblastoma.

#6735

Identifying the role of novel driver TREX subcomplex in medulloblastoma growth and progression

Shahad M. Abdulsahib, Santosh Timilsina, Manjeet Rao. *UT Health Science Center at San Antonio, San Antonio, TX*

Background: Medulloblastoma (MB) is the most common malignant brain cancer in children. Despite the progress made in treating MB, the 5-year survival rate for high-risk tumors remains poor and risk of recurrence within 2 years of treatment is still high. Almost all MB deaths are attributed to leptomeningeal dissemination (LMD) as MB spreads exclusively through cerebrospinal fluid (CSF) to spinal and intracranial leptomeninges.

Unfortunately, patients who do survive have reduced quality of life because of the highly toxic side effects of radiation and chemotherapy. *Those facts underline the importance of identifying new drivers of medulloblastoma and understanding the mechanism by which those drivers may promote medulloblastoma.* Towards that goal, I aim to identify novel drivers of MB and characterize novel therapies for treating (LMD-MB). Using an unbiased genome-wide screen, we discovered THO complex as one of the highly differentially expressed genes that may provide survival advantage to MB cells. THO is a subcomplex of the TREX complex, is known to couple mRNA transcription, processing and nuclear export associated with spliced mRNA.

Methods: Recent work in our lab utilizing various genomes and proteomics identified THO complex as a possible target. Transfection agents were used to knockdown part of the TREX subcomplex expression in several MB cells. Western blot and qPCR verified the knockdown. The cell viability was measured using Cell Titer Glo, and cell proliferation was evaluated with an IncuCyte. Cells were seeded at a low density and cultured until colonies formed then were fixed and stained with crystal violet. In addition, cells were seeded in a serum-free medium and allowed to migrate to complete media before being fixed and stained. Flow cytometry was used to examine cells for apoptosis and cell cycle. For apoptosis, cells were stained with propidium iodide (PI) and Annexin FTIC, and for the cell cycle, cells were stained and followed by PI.

Results: The Cancer Dependency Map (Dep-Map) meta-analysis revealed that MB strongly depends on The TREX subcomplex. Significantly, increased THO complex expression was associated with a worse overall survival rate in MB patients. Our findings indicated that part of the TREX subcomplex depletion decreased MB cell survival in the short- and long-term proliferation, migration, and invasion. Furthermore, part of TREX subcomplex depletion promoted apoptosis in MB cells. I propose that THO complex may be a new driver of MB and that strategies aiming to reduce part of TREX subcomplex levels and activity might benefit MB patients.

Conclusion: TREX subcomplex parts depletion has been demonstrated to reduce MB cells in vitro in various experiments. Future research, including CRISPR-CAS9-based knockout models, single-cell sequencing, and metabolomics, will further elucidate the mechanism(s) and utility of the TREX subcomplex axis in LMD-MB.

#6736

Suppression of antigen presentation is a hallmark of pediatric rhabdomyosarcoma

David Milewski, Meijie Tian, Yong Kim, Jun Wei, Javed Khan. *National Cancer Inst. - Bethesda Campus, Bethesda, MD*

Background: Rhabdomyosarcoma (RMS) is the most common soft tissue tumor in children and young adults, accounting for approximately 350-400 new cases annually in the US. These tumors are diagnosed based on their expression of skeletal muscle lineage markers. Clinical trials testing conventional immunotherapies such as cancer vaccines or immune checkpoint blockade (ICB) therapy have found no activity in RMS, although the root causes of failure are largely unexplored. A recent study by our group found that RMS tumors have a lack of immune infiltrate, consistent with previous reports. However, we made an unexpected observation that RMS tumors had a near absence of antigen processing and presentation (APP) gene expression, a key requisite for anti-tumor CD8+ T lymphocytes. In this study, we investigate the root causes of the lack of APP in RMS and evaluate implications for immunotherapy.
Methods: Publicly available DNA sequencing datasets were used to evaluate APP gene mutations in RMS tumor samples. RNAseq from reporter iPSC cell lines demarcating specific stages of skeletal muscle differentiation were used to evaluate APP gene expression during myogenesis. Surface MHC class I expression was evaluated using flow cytometry against a panel of pediatric sarcoma cell lines. RMS PDX and cell line APP protein levels were measured by western blot. Stimulation of APP in RMS cell lines was tested using IFNγ or sub-cytotoxic doses of different epigenetic therapeutics (DNMTi, HDACi, EZH2i) before analyzing surface MHC class I expression by flow cytometry.
Results: RNAseq analysis of the differentiation states across the normal human skeletal muscle lineage revealed a myoblastic cell state which transiently downregulates the APP pathway. RNA expression of *HLA-A,B,C* genes were lower in RMS than any other pediatric extracranial solid tumor histology studied. RMS cell lines and PDX models also displayed low APP pathway gene expression by western blot and flow cytometry, with *FOXO1* fusion positive RMS having a near absence of expression. RMS tumor

exome sequencing data from RMS patients showed a lack of enrichment of APP gene mutations. Instead, we found that APP could be induced in nearly all samples tested using IFNγ or epigenetic stimulation with Decitabine, Entinostat, or Tazemetostat.
Conclusions: We uncovered a previously unappreciated lack of antigen presentation in RMS which phenocopies myoblasts in normal skeletal muscle development. The downregulation of MHC class I antigen presentation is not due to APP pathway mutations but rather a partially reversible downregulation mirroring this specific stage of normal skeletal muscle development. Our findings suggest that pharmacological reversal of the APP pathway downregulation may enhance immunotherapies targeting MHC class I antigens in RMS.

#6737

Exposure-response and age subgroup analyses to support body-weight (BW) dosing of brentuximab vedotin (BV) in newly diagnosed high-risk classical Hodgkin lymphoma (cHL) in children and young adults (aged 2-21 years [y]): A randomized children's oncology group phase 3 trial (AHOD1331)

Zufei Zhang[1], Daping Zhang[1], Wenchuan Guo[2], Keenan Fenton[2], Sujata Narayanan[3], Shweta Jain[3], Joy Jiang[4], Sharon M. Castellino[5], Kara M. Kelly[6], Peter D. Cole[7], Frank G. Keller[5], Amit Garg[8], Yen Lin Chia[8].
[1]Quantitative Pharmacology and Disposition, Seagen Inc., Bothell, WA,[2]Biometrics, Seagen Inc., Bothell, WA,[3]Clinical Development, Seagen Inc., Bothell, WA,[4]Safety Evaluation & Risk Management, Seagen Inc., Bothell, WA,[5]Emory University School of Medicine, Atlanta, GA,[6]Roswell Park Comprehensive Cancer Center, University at Buffalo Jacobs School of Medicine and Biomedical Sciences, Buffalo, NY,[7]Rutgers Cancer Institute of New Jersey, New Brunswick, NJ,[8]Quantitative Pharmacology and Disposition, Seagen Inc., San Francisco, CA

Introduction: High-risk cHL in pediatric patients (pts) is typically treated with chemotherapy and radiation. BV, an antibody-drug conjugate (ADC) directed to CD30, is approved in six adult indications including cHL and in children with previously untreated high-risk cHL. In AHOD1331, BV was incorporated into the standard chemotherapy backbone treatment regimen

of doxorubicin (Adriamycin®), bleomycin, vincristine, etoposide, prednisone & cyclophosphamide (ABVE-PC) for cHL to replace bleomycin and its expectant toxicity. BV-AVEPC treatment resulted in a statistically significant improvement in efficacy compared to ABVE-PC; safety profiles were comparable. We sought to examine the exposure-response (E-R) relationships in this pediatric population.
Methods: Pts in the BV-AVEPC arm received 1.8 mg/kg BV (max: 180 mg) every 3 weeks (Q3W) for a max of 5 cycles. Pharmacokinetics (PK) evaluation focused on pts aged <13 y (n=26), as lower BV exposure was previously reported in pts with lower BW. Age and BW subgroup analyses were conducted on the primary efficacy endpoint, event-free survival (EFS); key secondary efficacy endpoints included early response rate (ERR) and key AEs of interest: peripheral neuropathy (PN) and neutropenia. E-R was evaluated in the PK population.
Results: In all, 593 pts (aged 2 to 21 y) with previously untreated high-risk cHL (Ann Arbor Stage IIB with bulk/IIIB/IVA/IVB) were randomized to ≥1 cycle of ABVE-PC (n=297) or BV-AVEPC (n=296). Compared to adults, BW dosing provided similar BV exposure in pts aged 12 to <18 y (median: 54 kg) but numerically lower ADC exposure (31%) in pts aged 2 to <12 y due to their lower BW (median: 21 kg). However, EFS was comparable between pts aged 2 to <12 y and 12 to <18 y in the BV-AVEPC arm (EFS rate at 36 mo: 96.2% [91.1-100%] vs. 92.0% [88.5-95.7%]). Similarly, in the exploratory E-R no trends were observed for ERR.
Similar PN rates (Grade [Gr] ≥3: 5.8% vs 6.4%) and neutrophil count decrease (Gr ≥3: 53.8% vs 48.6.%) with BV-AVEPC were observed between pts aged <12 y and 12 to <18 y. There were no apparent trends in neutropenia across BW groups but slightly elevated PN in pts with BW ≥70 kg (Gr ≥3: 11.3% vs ≤8.2%). Overall, there was no consistent evidence that PN and neutropenia were exposure or age-driven in this pediatric population.
Conclusions: Consistent efficacy was observed in pediatric pts in the BV-AVEPC arm across age groups despite lower exposure in pts 2 to <12 y, with no evidence of exposure-driven PN and neutropenia. For pediatric pts with previously untreated cHL,1.8 mg/kg Q3W BV + AVEPC ≤5 cycles demonstrated a favorable risk-benefit profile. These data support the 1.8 mg/kg Q3W BV dosage and do not indicate a need for dose adjustment by age or BW subgroups. ZZ and DZ contributed equally.

Retrospective Clinical Analyses 2

#6741

Number of prescription drugs and overall survival in metastatic castrate resistant prostate cancer

Martin W. Schoen[1], Carley Pickett[1], Daniel B. Eaton[2], Brendan T. Heiden[3], Su-Hsin Chang[3], Yan Yan[3], Melanie P. Subramanian[3], Varun Puri[3]. *[1]Saint Louis University, Saint Louis, MO,[2]VA St. Louis Healthcare System, Saint Louis, MO,[3]Washington University in St. Louis, Saint Louis, MO*

Background: Assessment of comorbid diseases is essential to clinical research and may risk-stratify patients for adverse events and death. Total number of prescription medications and drug classes could be an easy-to-use tool for estimating patient risk independent of established methods such as the Charlson Comorbidity Index (CCI) that is created from administrative data. Additionally, clinicians have access to prescription medication lists, facilitating assessment of comorbidities in clinical settings.
Methods: Retrospective observational study of US Veterans treated for metastatic castrate resistant prostate cancer in the Veterans Health Administration who received treatment with abiraterone or enzalutamide between May 2011-June 2, 2017. We determined number of unique drugs and anatomic therapeutic chemical (ATC) drug classes prescribed in the year prior up to 14 days before initiation of treatment. Multivariable logistic regression and Cox proportional hazard modeling was used to assess the association between number of drugs with all-cause 90-day mortality and overall survival (OS) while accounting for important covariates including age, CCI, body-mass index, prostate specific antigen, race, prior docetaxel, hemoglobin, albumin, bilirubin, and creatinine.
Results: Among 11,021 Veterans, a median (IQR) of 11 (6,18) unique medications and 10 (5,15) unique ATC medication classes were filled in the year prior to treatment. The median age was 75 years with median CCI of 3 and 2,550 were black (23.1%). Increasing age was associated with increased CCI across age strata with mean CCI of 3.7 in age <70, 4.2 in age 70-79, and 4.3 in age 80+ ($p<0.001$). Increased age was associated with decreased number of unique medicines with mean 14.7 in age <70, 12.7 in age 70-79, and 11.2 in age 80+ ($p<0.001$). Black race was associated with

increased mean number of medications compared to white race (15.5 vs. 12.0, $p<0.001$). After adjusting for relevant patient, tumor, and treatment factors, the number of medications and drug classes were each independently associated with increased 90-day mortality with adjusted OR (95% CI) of 1.021 (1.011,1.030) and 1.024 (1.012,1.036) respectively. Both number of medications and number of classes were also associated with decreased OS with adjusted Hazard Ratio of 1.015 (1.013,1.018) and 1.018 (1.014,1.021) respectively. Within subgroups of patients with comparable CCI, increased number of medications was associated with increased risk of death.
Conclusion: The number of prescription medications and drug classes are independently associated with short- and long-term outcomes in patients undergoing treatment for metastatic castrate resistant prostate cancer, even after accounting for important covariates including age and CCI. Assessment of patient medications may provide a simple, yet reliable tool to assess comorbidities, risk of adverse events, and death.

#6742

Genomic profiling and sites of metastasis in non-small cell lung cancer (NSCLC)

Kok Hoe Chan, Ji Lin, Arthi Sridhar, Syed H. Jafri. *Internal Medicine, The University of Texas Health Science Center at Houston, Houston, TX*

Introduction: Molecular genotyping of metastatic NSCLC adenocarcinoma subtypes using next generation sequencing (NGS) is currently the standard practice. However, there is limited data on the biological predisposition to site of metastasis in patients with NSCLC based on their molecular profiling. We sought to identify any association between metastatic site and molecular profile in NSCLC patients.
Method: This is a retrospective analysis conducted at UTHealth Houston/Memorial Hermann Cancer Center from January 2014 to June 2022. Clinical characteristics, pathology, NGS panel reports, and imaging were retrieved and reviewed. The χ^2 test was used for categorical variables. Continuous variables were compared using Kruskal-Wallis one-way analysis of variance. Progression-free survival (PFS) and overall survival (OS) were analyzed using the Kaplan-Meier test.

Results: After excluding patients who did not have complete clinical data, a total of 143 patients were included, and their NGS panels analyzed. Median age was 65 years, with an equal number of men (n=71) and women (n=72). The most common histology was adenocarcinoma (81.8%), followed by squamous cell cancer (11.9%) and large cell carcinoma (3.5%). At least one genetic mutation was discovered in 100 patients. Mutations with a targetable drug were found in 86 patients, and many patients had >1 genetic mutation. The most common mutations were TP53 (25.2%), EGFR (24.5%), KRAS/NRAS (20.3%), and CDKN2A/2B (7.7%). Patients with any mutation were significantly more likely to have metastatic disease to the brain (57% vs 37%, p=0.03), but there was no difference in metastatic disease to bone (34% vs 26%, p=0.32). Patients without a discoverable mutation were significantly more likely to have metastatic disease to other sites (e.g., adrenal gland, liver; 91% vs 66%, p=0.002). There was no difference in PFS or OS between those with versus without mutations. Median PFS was significantly longer in patients with EGFR mutation than those with KRAS/NRAS or TP53 mutations (36 vs 16.2 vs 11.9 months, p=0.03). Median OS for patients with EGFR mutation was not reached and was significantly longer than in patients with TP53 (28.7 months) or KRAS/NRAS (26 months) mutations (p=0.003).Patients with PDL-1 >1% or TP53 were significantly more likely to have metastatic disease to organs other than bone or brain (p=0.047 and p=0.023, respectively). There was also no difference between rates of brain and bone metastasis with regards to mutational profile.
Conclusion: Metastatic lung cancer patients with discoverable mutations on NGS are more likely to have metastatic disease to the brain. PDL-1 expression and TP53 mutation tend to lead to disease metastatic to organs other than brain or bone. Patients with EGFR mutations, despite having a great propensity to brain metastasis, have significantly better PFS and OS than patients with KRAS/NRAS and TP53 mutations, likely due to targeted therapy options.

#6743
Clinical outcomes with pembrolizumab-based therapies in relapsed/refractory NSCLC after definitive chemoradiation and durvalumab

Lukas Delasos, Wei Wei, Khaled A. Hassan, Nathan Pennell, Pradnya Patil, James Stevenson. *The Cleveland Clinic, Taussig Cancer Institute, Cleveland, OH*

Background: More than 50% of patients (pts) with unresectable non-small cell lung cancer (NSCLC) experience relapsed/refractory (R/R) disease within 2 years of starting chemoradiation (CRT) and durvalumab. Based on current national guidelines, these patients are offered treatment for metastatic disease as definitive therapy is no longer feasible. Immunotherapy +/- chemotherapy is typically initiated if a driver-oncogene is absent. The addition of programmed cell death protein-1 (PD-1) antibody pembrolizumab to chemo has resulted in improved progression-free survival (PFS) (8.8 vs 4.9 mos) and overall survival (OS) (69.2% vs 49.4% 12-mos OS) compared to chemotherapy alone. Although this treatment strategy has been incorporated for R/R NSCLC, there remains a paucity of data regarding its efficacy within this population. Here we present clinical outcomes data with pembrolizumab-based regimens for R/R NSCLC following definitive CRT and durvalumab.
Methods: This was a retrospective analysis of pts treated between January 2016 to November 2022 at the Cleveland Clinic Foundation in Cleveland, OH. Eligibility criteria included pts age ≥ 18 years with unresectable NSCLC who had received definitive CRT and durvalumab consolidation followed by pembrolizumab for R/R disease. The primary objective was to estimate OS and PFS in this distinct cohort and to compare these findings to historical outcomes. Secondary objective was to compare OS and PFS between specific groups including age, sex, smoking history, combined chemo, histology, *KRAS*-mutation, and PD-L1 expression. OS and PFS were estimated by Kaplan-Meier method and compared using log rank test.
Results: 62 pts were identified, of whom 50 met full eligibility criteria and were included for data analysis. Median follow-up time was 11.3 months (0.7 - 38.2 mos). Median OS was 10.6 months (95% CI; 7.9 mos - NA) with a 1-year OS rate of 48% (95% CI; 35 - 67%). Median PFS was 6.1 months (95% CI; 4.8 - 9.9 mos) with a 1-year PFS rate of 26% (95% CI; 16-45%). Current smokers had significantly better median OS and PFS rates as compared to former smokers (NA vs 10.5 and 9.9 vs 6.0 mos, respectively; P = 0.036 and 0.028). An OS benefit in pts who received chemo with pembrolizumab (median OS 12.9 vs 6.0 mos) was noted but was not

statistically significant. No other statistically significant difference was detected.
Conclusion: Patients with R/R NSCLC after definitive CRT and durvalumab consolidation represent a distinct cohort with apparent inferior outcomes as compared to those with *de novo* stage IV disease when treated with pembrolizumab-based therapies. Although improved survival was observed with the addition of chemo to pembrolizumab, further investigation is warranted to optimize treatment strategies for this patient population. Given the limited sample size of our analysis, larger studies with matched real-world treatment cohorts are planned.

#6744

Cell-free DNA detection of alterations in the MAPK pathway in metastatic hormone receptor positive breast cancer: A multi-institutional analysis of incidence and clinical outcomes

Arielle J. Medford[1], Andrzej Niemierko[2], Whitney L. Hensing[3], Andrew A. Davis[3], Katherine Clifton[3], Jennifer C. Keenan[4], Lesli Kiedrowski[5], Ami N. Shah[6], Lorenzo Gerratana[7], Massimo Cristofanilli[8], Aditya Bardia[2].
[1]Hematology/Oncology, Massachusetts General Hospital, Harvard Medical School, Broad Institute, Boston, MA,[2]Hematology/Oncology, Massachusetts General Hospital, Harvard Medical School, Boston, MA,[3]Hematology/Oncology, Washington University in St Louis, St Louis, MO,[4]Hematology/Oncology, Massachusetts General Hospital, Boston, MA,[5]Guardant Inc, Palo Alto, CA,[6]Hematology/Oncology, Northwestern University, Chicago, IL,[7]Hematology/Oncology, Centro di Riferimento Oncologico, Aviano, Italy,[8]Hematology/Oncology, Weill Cornell Medicine, New York, NY

Background Alterations in the MAPK pathway are known mechanisms for tumorigenesis in multiple solid tumors. While not major drivers in early breast cancers, activating MAPK pathway alterations have been invoked as potential resistance mechanisms in advanced hormone receptor positive (HR+) breast cancer. While MAPK pathway mutations are believed to be relatively rare in breast cancer, the accessibility of cell-free DNA (cfDNA) analysis allows for evaluation of their prevalence, co-occurring mutations, and associated clinical outcomes. In this study, we evaluated the incidence

of MAPK pathway alterations and impact on clinical outcomes among patients with metastatic breast cancer (MBC).
Methods Plasma was collected in patients with HR+ MBC at the Massachusetts General Hospital and Washington University in St. Louis, and cfDNA was analyzed via the Guardant 360 assay, a 74-gene next generation sequencing panel. The impact of MAPK pathway alterations on progression-free survival (PFS) and overall survival (OS) was analyzed using multivariable Cox regression analysis, adjusting for age, number of prior therapies, visceral metastases, de novo metastases, and *PIK3CA* alterations. PFS and OS were evaluated in the overall study population, as well as in subgroups that received endocrine therapy + CDK4/6 inhibitor, endocrine monotherapy and chemotherapy.
Results Out of 647 HR+ MBC patients, 103 (16%) had non-synonymous mutations in the MAPK pathway detected in cfDNA. Median age was similar (61.9 and 60.7) in MAPK-altered and non-altered patients, respectively. Both groups had received a median of 2 prior lines of therapy (p=0.08). MAPK pathway alterations included *NF1* (n = 45, 7.0%), *KRAS* (n = 22, 3.4%), *BRAF* (n = 22, 3.4%), *MAPK1* (n = 8, 1.2%), *MAP2K1* (n = 6, 0.9%), *NRAS* (n = 5, 0.8%), *RAF1* (n = 5, 0.8%), *HRAS* (n = 4, 0.6%), *ARAF* (n = 4, 0.6%), *MAP2K2* (n = 4, 0.6%), *RIT1* (n = 3, 0.5%), and *MAPK3* (n = 2, 0.3%). Mutant allele fractions ranged from 0.03 to 26. Co-alterations in *PIK3CA* occurred in 49% (n = 51), *TP53* in 41% (n = 42), and *ESR1* in 27% (n = 28). In multivariable analysis, patients with MAPK-altered HR+ MBC had significantly poorer median PFS, 7.6 months vs 11.5 months (HR: 1.6; p = 0.005; 95% CI: 1.2-2.2). There was no statistically significant impact on outcomes when stratifying by treatment type.
Conclusions MAPK pathway alterations are associated with a significantly poorer PFS among patients with HR+ MBC. Further research is needed to independently validate these observations and evaluate the impact of genotype-directed therapy targeting MAPK-altered, HR+ MBC.

#6745
Prognostic indicators and outcomes of hepatocellular carcinoma (HCC) in an Appalachian population
Michelle Hartzell[1], Gary Monroe[1], Jon Shakesprere[1], Sijin Wen[2], J. Wallis Marsh[3], Jacob Fuqua[4], Robert Grammer[5], Beau Toskich[6], Midhun Malla[4].
[1]Medicine, West Virginia Univ. School of Medicine, Morgantown,

WV,[2]Epidemiology and Biostatistics, West Virginia University Health Science Center, Morgantown, WV,[3]Surgery, West Virginia Univ. School of Medicine, Morgantown, WV,[4]West Virginia University Cancer Institute, Morgantown, WV,[5]Radiology, West Virginia Univ. School of Medicine, Morgantown, WV,[6]Division of Vascular/Interventional Radiology, Mayo Clinic, Jacksonville, FL

Introduction: The development of hepatocellular carcinoma (HCC) is associated with underlying chronic liver disease from viral hepatitis or nonviral etiologies, such as nonalcoholic fatty liver disease (NAFLD) and alcoholic liver disease. An area of current research interest is the relationship between etiology of chronic liver disease in HCC patients and the response to specific treatment modalities. The purpose of this study is to identify prognostic indicators and compare survival outcomes among HCC patients within an Appalachian patient population.
Methods: A single-institution, retrospective chart review was conducted for all patients diagnosed with HCC between August 2009 and March 2017 at West Virginia University Hospital. Patient demographics, tumor characteristics, laboratory data and treatment information were obtained from the electronic medical record (EMR). Survival analyses were performed using Kaplan-Meier method and multivariable Cox regression analysis.
Results: The study sample (n=100) had a mean age of 62 years and was comprised of 82% males and 18% females. Nonviral etiologies of chronic liver disease were predominant (55%) over chronic viral hepatitis (45%). Significant adverse prognostic indicators of overall survival (OS) were Child-Pugh class C and tumor size >5 cm at diagnosis ($p<0.0001$, log-rank test). Patients who received liver-directed therapy (LDT) or liver resection had greater OS compared to those not treated with either modality (15.5 vs. 2.0 months, $p<0.0001$). Liver ablation or resection as initial modes of treatment had greater OS compared to those who initially received transarterial chemoembolization (TACE) or transarterial radioembolization (TARE) (17.2 vs 14.9 months, $p<0.05$). Patients who received TACE or TARE (n=60) as initial treatment had characteristics of advanced disease, with 45% having a tumor greater than 5 cm in size and 77% having multifocal unilobar or bilobar tumors. Among all patients who received LDT or resection, post-treatment albumin-bilirubin grade (ALBI) of 1 or 2

correlated with greater OS than grade 3 (22.5 vs 6.2 months, $p<0.0001$). In the multivariate Cox analysis, tumor size, Child-Pugh class and mode of initial treatment (resection/ablation vs. TACE/TARE) were independent predictors of OS ($p<0.05$).
Conclusions: Treatment with LDT or liver resection correlated with greater overall survival in this predominantly nonviral cohort of HCC patients. Post-treatment ALBI grade correlated with overall survival and may have prognostic value in guiding clinical management. Mode of initial treatment was a predictor of overall survival, but further studies are needed to compare tumor characteristics between groups. Research is ongoing to evaluate the relationship between chronic liver disease etiology and survival among HCC patients treated with LDT, immunotherapy or a combination of both.

#6746
Academic facility is associated with improved survival in patients with leiomyosarcoma: a national cancer database analysis
Steven Stanley, Marco Braaten, Peter Silberstein. *Creighton University School of Medicine, Omaha, NE*

Background: Leiomyosarcoma is a malignant sarcoma of smooth muscle that comprises 10-20% of all sarcomas with a predilection to the uterus and peritoneum. [1] Prior studies have shown treatment at Academic facilities is associated with improved outcomes in cancer treatment.[2] The objective of this study was to investigate the effect of treatment at an Academic facility on overall survival in patients with leiomyosarcoma.
Methods: The National Cancer Database (NCDB) was used to identify patients with leiomyosarcoma from 2004-2019 using the ICD-O-3 histology codes 8900 and 8901. Facility types used were assigned by the Commission on Cancer Accreditation program. Categorical Academic and Non-Academic variables were created. Data was analyzed using SPSS with a statistical significance of $\alpha = 0.05$.
Results: Of the 7950 patients included in this study, 3122 were treated at Academic facilities with a median survival of 77.6 months compared to 61.0 months for patients treated at a Non-Academic facility, which was statistically significant on long-rank testing ($p<0.001$). Compared to patients treated at Non-Academic facilities, patients at Academic facilities

experienced delay in the average surgical initiation time (p<0.001), however, they were more likely to have surgery (88.1% vs. 74.1%; p<0.001), have no residual tumor margins on resection, (63.4% vs. 53.3%; p<0.001) and receive adjuvant chemotherapy (15.2% vs. 12.4%; p<0.001). Academic facility patients also had a younger mean age and were more likely to come from highest median income quartile (36.9% vs. 33.2; p<0.001).
Conclusions: Patients with leiomyosarcoma treated at Academic facilities experienced improved survival compared with patients with the same disease treated at Non-Academic facilities. These patients experienced higher rates of surgery, adjuvant therapy and wider excisional margins. It is possible that treatment discrepancies and/or differences in surgical technique vary by facility type and contribute to the observed differences in survival.
Citations-1. Devaud, N., et al. (2022). Leiomyosarcoma: Current Clinical Management and Future Horizons. *Surgical oncology clinics of North America*, *31*(3), 527-546. https://doi.org/10.1016/j.soc.2022.03.0112. Gootee, J., Silberstein, P., et al. (2020). Important prognostic factors in leiomyosarcoma survival: a National Cancer Database (NCDB) analysis. *Clinical & translational oncology : official publication of the Federation of Spanish Oncology Societies and of the National Cancer Institute of Mexico*, *22*(6), 860-869. https://doi.org/10.1007/s12094-019-02196-7

#6747

Sites of metastases prior to systemic treatment influence progression patterns and survival in stage IV melanoma patients

Ismael A. Vergara[1], Serigne N. Lo[2], Isabel Li[2], Alexander M. Menzies[3], Matteo S. Carlino[4], Richard A. Scolyer[5], Georgina V. Long[6], Ines Pires da Silva[7]. *[1]Melanoma Institute Australia, Charles Perkins Centre, The University of Sydney, Camperdown, Australia,[2]Melanoma Institute Australia, The University of Sydney, Sydney, Australia,[3]Melanoma Institute Australia, The University of Sydney, Royal North Shore and Mater Hospitals, Sydney, Australia,[4]Melanoma Institute Australia, The University of Sydney, Blacktown Hospital, Crown Princess Mary Cancer Centre, Camperdown, Australia,[5]Melanoma Institute Australia, Charles Perkins Centre, The University of Sydney, , Royal Prince Alfred Hospital and NSW*

Health Pathology, Sydney, Australia,[6]Melanoma Institute Australia, Charles Perkins Centre, The University of Sydney, Royal North Shore and Mater Hospitals, Sydney, Australia,[7]Melanoma Institute Australia, Charles Perkins Centre, The University of Sydney, Blacktown Hospital, Sydney, Australia

Background: Different metastatic sites have distinct response rates to immune checkpoint inhibitors (ICI), suggesting that anatomical locations play a role in treatment response and survival. This project investigated the impact that sites of metastases present at baseline - *ie.* before starting treatment - have on the anatomical patterns of progression and their association with survival in patients (pts) exposed to ICI and BRAF/MEK inhibitors (BRAF/MEKi) as first line treatment.
Methods: We curated the progression history of distant metastases of 568 stage IV pts; 352 pts had first line treatment with antiPD1 +/- antiCTLA4, and 216 pts had first line BRAF/MEKi. We sought to investigate the association between sites of metastases at baseline and (a) sites of progression in pts who failed first line anti-PD1 vs first line BRAF/MEKi, (b) sites of progression in pts who failed first line anti-PD1 with innate vs acquired resistance, and (c) survival of all pts, from time of first line treatment to last follow-up.
Results: Using a sophisticated mathematical graph representation of anatomical disease progression, we unveiled sites of metastases at baseline that impacted where new sites of metastases developed on treatment failure. In pts with brain metastasis at baseline, pts who failed anti-PD1 had higher progression in the brain compared to BRAF/MEKi progressors (68.1% in anti-PD1 progressors vs 62.5% in BRAF/MEKi progressors). In contrast, the opposite trend was observed in the progression to the brain in pts with no brain metastasis at baseline, which was lower in anti-PD1 progressors compared to BRAF/MEKi progressors (20.6% in anti-PD1 progressors vs 32.6% in BRAF/MEKi progressors).Within pts who failed anti-PD1, pts with innate resistance (n=95) had a higher rate of progression in the brain (42.1%) compared to pts with acquired (n=36) resistance (25%). Among pts with innate resistance who had brain metastasis at baseline (n=36), 80.6% progressed in the brain. In contrast, among pts with innate resistance without brain metastasis at baseline (n=59), only 18.6% progressed to the brain.Sites of metastases at baseline also had an impact on the survival of

pts. In BRAF/MEKi pts, brain metastasis at baseline was not associated with survival (log-rank p-value=0.6). In contrast, anti-PD1 pts with brain metastasis at baseline had worst survival (2-yr survival 56%) compared to pts without brain metastasis at baseline (2-yr survival 73%, log-rank p-value=0.005).
Utilisation of this graph representation for the development of a time-dependent predictor of brain metastases will be presented.
Further associations of metastatic sites of disease at baseline with progression and survival will be discussed.
Conclusions: Different sites of metastases at baseline have a distinct effect on the progression patterns and survival of pts who received BRAF/MEKi or anti-PD1 as first line treatment.

#6749
Histiocytic sarcoma descriptors and clinicopathologic determinants of survival: Analysis of a pooled database
Dinesh Keerty, Philip A. Haddad. *LSUHSC-S, Feist-Weiller Cancer Center/Overton Brooks VAMC, Shreveport, LA*

Background Histiocytic sarcoma (HS) is an aggressive, rare malignant neoplasm of cells with histiocytic differentiation. It can occur de novo or develop in the context of other malignant disorders. HS can present as disseminated or localized lesions in the skin, lymphatics, gastrointestinal tract, central nervous system, or other organs. Little is known about factors that impact HS clinical outcomes. We conducted this pooled database analysis to delineate key clinicopathological characteristics, prognostic indicators, and treatment modalities that affect survival in this rare histiocytic entity.
Methods To study the demographic characteristics, molecular and immunohistochemical signatures, therapeutic interventions, survival, and prognostic factors, we compiled a pooled database of 146 cases of HS. Kaplan-Meier survival curves were constructed. Cox proportional hazards model and Log-rank tests were used to assess the influence of demographic and clinicopathologic factors on overall survival (OS).
Results A total of 146 patients with confirmed HS were identified. The median age was 52, with bimodal peaks between 14-28 and 56-70 years. There was a male preponderance with M:F of 1.3. Primary sites of

involvement were CNS (21%), GI(16%), soft tissues (12%), H&N and bones (9% each), skin (8%), liver (7%), spleen (5%), lung (4%), and breast (1%). Lymphadenopathy and bone marrow (BM) were involved in 21% and 42%, respectively. Constitutional symptoms were present in 6%. The median size of the HS tumor was 4.45cm. The median OS of the whole group was 16 months. Age younger than 55 had better median OS (NR vs. 6 months, p=0.038). The primary site of involvement also impacted the median OS, where soft tissues and visceral disease had longer OS than those with CNS and spleno-lymphatic disease (60 vs. 7 vs. 6 months, p=0.03). Stage 1 disease had better median OS than stages 2-4 (p=0.06). Furthermore, unifocal had better median OS than multifocal/multicentric disease (60 vs. 9 months, p=0.007). The presence of inflammatory background positively impacted OS (p=0.01). Compared to no treatment, localized therapies such as surgery (S) and radiation therapy (RT), and systemic combination chemotherapy (CT) were statistically superior, with a median OS of 1, 204, and 21 months, respectively (p=0.003). With HS not amenable to complete resection, CT and CT+S were superior to RT+S (15 vs. 60 vs. 7 months, p=0.008). While BM involvement and size >10 cm were associated with worse OS, the latter did not reach statistical significance. There was no difference in median OS with respect to sex. **Conclusion** This study presents updated clinicopathologic data from a pooled cohort of patients with HS. It identifies age, the primary site of the disease, stage and extent of the disease, the inflammatory background status, and treatment approach as key determinants of OS.

#6750

Primary effusion lymphoma descriptors and clinicopathologic determinants of survival: Analysis of a pooled database

Supriya Gupta, Christopher Graham, Philip A. Haddad. *LSUHSC-S, Feist-Weiller Cancer Center/Overton Brooks VAMC, Shreveport, LA*

Background Primary effusion lymphoma (PEL) is a rare and aggressive type of B-cell non-Hodgkin lymphoma presenting primarily as lymphomatous effusions in body cavities and less often as solid extracavitary masses. It is typically associated with human herpesvirus 8 (HHV8) infection and occasionally with Epstein-Barr virus (EBV) co-infection. It is commonly seen in immunocompromised states, such as

human immunodeficiency virus (HIV) infection, organ transplantation, immunosuppressive therapy, or advanced age. Due to our limited understanding of this disease, we conducted this pooled database analysis to delineate key clinicopathological characteristics, prognostic indicators, and treatment modalities that affect survival in this rare and unique lymphoma subtype.
Methods To study the demographic characteristics, molecular and immunohistochemical signatures, therapeutic interventions, survival, and prognostic factors, we compiled a pooled database of 303 cases of PEL. All cases with an unequivocal expression of CD19 and CD20 expression were excluded. Kaplan-Meier survival curves were constructed. Cox proportional hazards model and Log-rank tests were used to assess the influence of demographic and clinicopathologic factors on overall survival (OS).
Result A total of 304 patients with confirmed PEL were identified. The median age was 49, with a peak incidence between 42 and 56 years. There was a male preponderance with M:F of 10. The majority (71%) was associated with HIV infection, with a median CD4 count of 108. Sixty-eight percent were cavitary with the pleural, pericardial, and peritoneal cavities involved in 56%, 20%, and 30%. The median duration of symptoms before diagnosis was 1.5 months. Patients presented with constitutional symptoms, hepatosplenomegaly, lymphadenopathy, and bone marrow involvement in 31%, 10%, 20%, and 16%. The median OS of the whole group was 6.5 months. Presentation with constitutional symptoms ($p=0.026$), extracavitary/solid tumors ($p=0.03$), and normal platelet counts ($p=0.04$) were associated with better median OS. Cavitary disease with effusions restricted to the thoracic cavity had also better median OS ($p<0.0001$). PEL occurrence in the context of immunosuppression due to transplantation had poor median OS ($p=0.004$). While having Kaposi sarcoma tended to impact OS negatively ($p=0.08$), Castleman's disease did not. Compared to no treatment, combination chemotherapy alone, chemotherapy with anti-retroviral therapy, and stem cell transplant were statistically superior with a median OS of 1.5, 8, 30, and 16 months, respectively ($p<0.0001$).
Conclusion This study presents updated clinicopathologic data from a pooled cohort of patients with PEL. It identifies the type of clinical setting contributing to immunodeficiency, disease presentation, the primary location of cavitary disease, and treatment approach as key determinants of OS.

#6751

Provisional prognostic score for primary effusion lymphoma

Philip A. Haddad, Supriya Gupta, Christopher Graham. *LSUHSC-S, Feist-Weiller Cancer Center/Overton Brooks VAMC, Shreveport, LA*

Background Primary effusion lymphoma (PEL) is a rare and aggressive type of B-cell non-Hodgkin lymphoma presenting primarily as lymphomatous effusions in body cavities and less often as solid extracavitary masses. It is typically associated with human herpesvirus 8 (HHV8) infection and occasionally with Epstein-Barr virus (EBV) co-infection. It is commonly seen in immunocompromised states, such as human immunodeficiency virus (HIV) infection, organ transplantation, immunosuppressive therapy, or advanced age. Survival remains poor, and an optimal regimen has yet to be identified. However, the disease presents a diverse spectrum of survival outcomes. We conducted this study to develop a provisional PEL prognostic score (PPS) for this rare disease.
Methods We used our constructed PEL database, which contains retrospective data on 302 cases. Such data included demographics such as sex, age, and race. It also included disease presentation symptoms, duration of symptoms before diagnosis, site(s) of the disease, blood counts, coexisting comorbidities, disease immunohistochemical and molecular phenotype, types of treatment, and survival outcomes. Of the 302 cases, only 238 had complete survival and outcomes data, the sample chosen for this study. Cox proportional-hazards model and Log-rank tests were used to assess the influence of clinicopathologic factors on overall survival (OS). Due to the relatively small training cohort, we included factors that statistically impacted OS and those that numerically trended that way.
Results The median OS of the cohort was 6.5 months. The following dichotomous variables were identified as impactful prognostic factors in this cohort: the absence of constitutional symptoms (5 vs. 18 months), cavitary effusion disease (6 vs. 66 months), peritoneal cavity disease (3.5 vs. 11 months), transplant context (4 vs. 7 months), male sex (6 vs. 40 months), and detectable HHV8 viremia (7 vs. 66 months). A prognostic model was devised using these variables to identify different levels of risk. Each variable was assigned a score of 1 when present, except for peritoneal cavity disease and transplant context, which were assigned 2 points as they

had the highest hazard ratio of all the other variables. In this exploratory cohort, low risk was assigned a score of 0-1, intermediate risk a score of 2-3, and high risk a score of 4-8. This prognostic score system led to our cohort's most optimal risk discriminatory model, where low, intermediate, and high risk had a median OS of 66, 28, and 4 months, respectively ($p<0.0001$).
Conclusion This PPS is a promising new tool for risk-stratifying patients with PEL. However, it still needs prospective validation.

#6752
Patient (pt) characteristics, diagnostic journey, and cancer enrichment among pts with nonspecific signs and/or symptoms (s/sx) in the US community oncology setting: a real-world retrospective study
Christopher Benton[1], Ding He[2], Karen Todoroff[2], Marie V. Coignet[3], Ying Luan[3], Kathryn N. Kurtzman[3], Ira Zackon[4]. *[1]Rocky Mountain Cancer Centers, Englewood, CO,[2]Ontada, The Woodlands, TX,[3]GRAIL, LLC, a subsidiary of Illumina, Inc., currently held separate from Illumina, Inc. under the terms of the Interim Measures Order of the European Commission dated 29 October 2021, Menlo Park, CA,[4]New York Oncology Hematology, Albany, NY*

Of the >1.6 million people diagnosed with cancer in the US each year, >60% are diagnosed after symptomatic presentation, including nonspecific s/sx. These nonspecific s/sx may cause pts to undergo unnecessary diagnostic evaluation while the possibility of cancer and search for its origin is explored, causing delayed treatment and poor outcomes. Additionally, pts who do not have cancer are often subjected to various undirected/misdirected procedures due to initial cancer suspicion. Our objective was to examine pt characteristics, diagnostic journey, and cancer incidence of pts with nonspecific s/sx within The US Oncology Network. This retrospective observational cohort study included pts aged ≥40 with ≥1 of the following nonspecific s/sx in their problem list at their first visit within The US Oncology Network (index date) during the identification period from 1/1/2016 to 12/31/2020: anemia, venous thromboembolism, general malaise, weight loss, nonspecific abdominal symptoms, new and unexplained breathlessness, unexplained worsening pain, and abnormal lab test results. Pts were excluded if diagnosed with any cancer (except basal

cell carcinoma and squamous cell carcinoma skin cancer) within 3 years prior to or on index date. Pts were followed longitudinally with data from electronic health records for initial cancer diagnosis (dx), death, end of study observation period, or 12 months, whichever occurred first. Demographic and clinical characteristics were assessed descriptively. 103,984 pts were identified. The median age was 65.7, 64% were female, 65% were White, 41% were obese, 47% were never smokers, and 48% were from a southern practice region. 6,774/103,984 pts (7%) were diagnosed with cancer and 6,537/6,774 (97%) with 1 primary cancer: 3,825/6,537 (59%) were diagnosed with a hematologic malignancy and 2,712/6,537 (41%) with a solid tumor cancer. Among pts diagnosed with primary solid tumors, 31% had gastrointestinal, 15% genitourinary, 15% respiratory, 13% breast, and 11% gynecologic cancer. Among pts diagnosed with cancer, median time to cancer dx after being referred to secondary care within The US Oncology Network with nonspecific s/sx was >5 wks (solid: >7 wks; hematologic: >4 wks); by 17 and 34 wks, 75% and 90% of pts received a cancer dx, respectively.
Within this population of pts most frequently presenting with nonspecific hematologic s/sx and subsequent cancer dx, 40% were diagnosed with solid tumor cancers within 1 year. This speaks to the unmet need for more tools such as a multi-cancer detection test that could aid in detection of multiple cancers and faster diagnostic resolution of nonspecific s/sx. Given the impact of delayed cancer dx and timely treatment on outcomes, such a test could potentially substantially improve cancer care and diagnostic evaluations.

#6753

Non-HIV cryptococcal patients with hematological malignancies: A retrospective analysis of a ten-year study from a Peruvian oncologic center

Kelly Meza, Luis E. Cuellar. *Instituto Nacional de Enfermedades Neoplasicas, Lima, Peru*

Background Globally, cryptococcal infection has become a public health challenge. However, relatively little is known about cryptococcal infection in people with hematological disorders.

Methods We developed a retrospective cohort study that includes hematological patients who had cryptococcosis infection seen in the Instituto Nacional de Enfermedades Neoplasicas between 2007 and 2017.
Results During the 11-year study period, a total of 21 cases of cryptococcosis (incidence rate of 13,4 per 1000 hematological malignancies). The time of diagnosis of cryptococcosis since hematologic malignancy diagnosis was 42 (18-161) days. Non-Hodgkin lymphoma (NHL) was the most frequent malignancy (47.6%), followed by leukemias (23.8%), multiple myeloma in (19.1%), and HL (9.5%). Three cases of adult T-cell leukemia/lymphoma associated with HTLV-1 infection were identified in the NHL. Cryptococcemia was the most frequent diagnosis (85.7%) followed by pulmonary (52.4%) and CNS (38.1%) involvement. Regarding clinical presentation, f ever was the most common symptom in meningeal cryptococcosis (76.2%) and dyspnea in pulmonary cryptococcosis (61.9%). The use of immunosuppressant chemotherapy within a month before the diagnosis of cryptococcosis was the most common risk factor. The main characteristics between patients with cryptococcosis and type of neoplasms (NHL vs other hematological neoplasms) such as age at admission, site of presentation of cryptococcosis, and lymphocyte count at admission were different significantly between these groups. In the NHL group, there was less involvement of the lungs. Overall survival (OS) in 15 and 120 days were 70% (95%CI: 0.43-0.86) and 51% (95%CI: 0.26-0.72), respectively. OS for patients with NHL was 57% at 15 days (95% CI: 0.17-0.83) and 42% at 120 days (95%CI:0.09-0.73). OS for other hematological malignancies was 90% at 15 days (95%CI:0.47-0.98) and 60% at 120 days (95%CI: 0.25-0.82).
Conclusions CNS cryptococcal infection was more frequent in patients with NHL.

#6754

Clinical characteristics, real-world treatment patterns, and clinical outcomes among patients with previously treated metastatic or unresectable EGFR-mutated non-small cell lung cancer in the United States

Jyoti D. Patel[1], Jie Meng[2], Sudarshan Phani[3], Aaron Crowley[4], Summera Zhou[4], Maribel Salas[3], Yoko Tanaka[3], Hoa Le[3], Jeffrey Anderson[4], Karen L. Reckamp[5]. *[1]Northwestern University, Chicago, IL,[2]Daiichi Sankyo*

Europe GmbH, München, Germany,[3]Daiichi Sankyo, Basking Ridge, NJ,[4]Genesis Research, Hoboken, NJ,[5]Cedars-Sinai Medical Center, Los Angeles, CA

Background: A consensus on preferred treatment for patients with EGFR-mutated (EGFRm) advanced or metastatic non-small-cell lung cancer (a/mNSCLC) who have progressed on osimertinib and platinum-based chemotherapy (PBC) has yet to be established. The study objectives were to describe patient characteristics and treatment patterns in this context and assess corresponding clinical outcomes in the US real-world setting.
Methods: This study was a retrospective analysis of data sourced from Flatiron's de-identified database, which included electronic health records and curated cancer data from approximately 280 US cancer clinics (~800 US sites of care). The index line of therapy (LOT) was defined as initiation of a new treatment regimen after osimertinib and PBC. Adults were eligible for inclusion if they: 1) were diagnosed with a/mNSCLC on or after January 1, 2011; 2) had evidence of an activating EGFR mutation (exon 19 or L858R); 3) initiated a new LOT between November 13, 2015, and June 30, 2021, after treatment with osimertinib and PBC. Treatment regimens in the index LOT were summarized, and real-world overall survival (rwOS, defined as the time from initiation of index LOT to death) and real-world progression-free survival (rwPFS, defined as the time from initiation of index LOT to disease progression or death) were assessed.
Results: Among 273 study patients included, the majority were ≥65 years (57%), female (67%), Caucasian (65%; Asian, 17%; Black or African American, 6%), with no history of smoking (58%), performance status 0-1 (82%), and >2 prior LOT (64%). Median follow-up duration was 7.3 months. Index treatment regimens were classified as tyrosine kinase inhibitor (TKI) monotherapy (15%) or TKI in combination with non-immuno-oncologic agents (12%), non-platinum-based chemotherapy (23%), immuno-oncologic monotherapy (17%) or combination therapy (15%), PBC (12%), a regimen containing a clinical study drug (4%), or other NSCLC therapy (1%). Deaths occurred in 203 patients (74%) during follow-up; median rwOS was 8.6 months (95% confidence interval [CI], 7.4-9.8). Real-world progression occurred in 235 patients (86%); median rwPFS was 3.3 months (95% CI, 2.8-4.4).

Conclusions: For patients with EGFRm a/mNSCLC, third-generation EGFR TKIs such as osimertinib can provide disease control, however progression is common. After disease progression, chemotherapy is often the next treatment of choice. Results of this real-world study show that treatment patterns after EGFR TKI and PBC are highly variable and suggest poor clinical outcomes, highlighting the need for more efficacious treatments among patients with previously treated a/mNSCLC.

#6755

The impact of renin-angiotensin system inhibitors on survival outcomes of pancreatic adenocarcinoma patients

Kuan-Yu Tseng, Cheng-Wei Chou. *Taichung Veterans General Hospital, Taichung, Taiwan*

Introduction Pancreatic adenocarcinoma (PDAC) is a highly aggressive malignancy with significant morbidity and mortality. RAS (renin-angiotensin system) inhibitors have been used for hypertension, and the potential role of using RAS inhibitors in pancreatic adenocarcinoma have been investigated in pre-clinical models by enhancing drug delivery and reducing hypoxia. However, the clinical benefit of RAS inhibitors in pancreatic cancer patients was still unclear.
Methods We retrospectively investigated the impact of RAS inhibitors on survival outcomes of pancreatic adenocarcinoma patients in Taichung Veterans General Hospital between January 2014 and July 2021. Patients with histologically proven pancreatic adenocarcinoma were included in the study. Clinical feature with drugs exposure and survival outcome were analyzed.
Results A total of 384 pancreatic cancer patients were analyzed. Among them, 70 patients had concurrent use of RAS inhibitors and 314 patients had no concurrent medication use. Among patients with RAS inhibitors use, the diagnosed age was significantly older (70.0 vs. 68.0, $p = 0.023$), and a higher proportion of hypertension (100.0% vs. 51.0%, $p < 0.0001$), chronic kidney disease (27.5% vs. 9.1%, $p < 0.0001$), and diabetes (64.3% vs 39.5%, $p < 0.0001$) than those without RAS inhibitors use. The 12-month progression-free survival were 22.9% and 13.7% in the RAS inhibitors and control group ($p = 0.008$), respectively. The Overall survival was not significantly different in the both groups ($p = 0.356$). In the multivariate

analysis, the use of RAS inhibitors had a significantly better progression-free survival outcome (Hazard ratio = 0.025, CI:0.52-0.96). The advanced disease status, poor ECOG performance status and the elevated level of CA19-9 were correlated with poor progression-free survival.
Conclusion In our study, although higher percentage of existed comorbidities in the RAS inhibitor group, we demonstrated that the use of RAS inhibitors among pancreatic cancer patients might provide a better progression-free survival outcome. Further prospective study and investigation are warranted.

#6756

Ramucirumab plus paclitaxel as second-line treatment in patients with advanced gastric cancer who previously treated with first-line nivolumab plus chemotherapy

Youngkyung Jeon, Sun Young Jeong, Jaeyeon Jang, Ye Ji Jung, Daeho Choi, Joohyun Hong, Seung Tae Kim, Won ki Kang, Jeeyun Lee. *Division of Hematology-Oncology, Department of Medicine, Samsung Medical Center, Seoul, Korea, Republic of*

Background: For human epidermal growth factor receptor 2 (HER2)-negative advanced gastric cancer (AGC), a combination of fluoropyrimidines and platinum agents was the standard first-line treatment. After the failure of the first-line therapy, ramucirumab plus paclitaxel was the standard second-line treatment. In the CheckMate 649 study, nivolumab plus chemotherapy has been considered a new standard first-line treatment in previously untreated AGC. However, the role of ramucirumab plus paclitaxel as 2nd line after the failure of nivolumab plus chemotherapy is not confirmed.
Methods: We analyzed AGC patients with ramucirumab plus paclitaxel as second-line therapy, who failed the nivolumab plus chemotherapy (capecitabine plus oxaliplatin (XELOX) or 5-fluorouracil plus oxaliplatin (FOLFOX)) as frontline therapy at Samsung Medical Center, South Korea.
Results: Under the routine clinical practice, 23 AGC patients, who progressed after first-line chemotherapy with nivolumab plus chemotherapy, were treated with ramucirumab plus paclitaxel between Dec 2021 to Sep 2022. The median age was 56 (range, 24-76), and 18 (78.3%) patients received nivolumab plus XELOX, while 5 (21.7%) patients

received nivolumab plus FOLFOX. The overall response rate (ORR) to ramucirumab plus paclitaxel was 10.0% (2 of PR) and the disease control rate was 55.0%. At the median follow-up of 4.5 months, the median progression-free survival (PFS) from second-line ramucirumab plus paclitaxel commencement was 2.7 months (95% confidence interval (CI), 1.7-3.7); 6.9 months (95% CI, not calculated) in the first nivolumab plus chemotherapy responders(n=7), and 2.3 months (95% CI, 1.6-3.0) in non-responders(n=15) (p=0.232). At the time of data cutoff, 6 patients continued to receive ramucirumab plus paclitaxel and the median OS was 6.3 months (95% CI, 4.9-7.7).
Conclusions: This analysis showed that ramucirumab plus paclitaxel as 2nd line therapy was not sufficient in AGC patients after the failure for nivolumab plus chemotherapy. The new innovative 2nd line therapy might be needed in AGC patients after nivolumab plus chemotherapy.

#6757

Identification of predictive factors for early relapse in patients with unresectable stage III NSCLC receiving consolidation durvalumab after concurrent chemoradiation

Chang Dong Yeo[1], Hye Seon Kang[2], In Kyoung Kim[1], Sang Haak Lee[1], Jin Woo Kim[3]. *[1]St. Mary's Hospital, The Catholic University of Korea, Seoul, Korea, Republic of,[2]St. Mary's Hospital, The Catholic University of Korea, Bucheon, Korea, Republic of,[3]St. Mary's Hospital, The Catholic University of Korea, Uijeongbu, Korea, Republic of*

Background: Patients with locally advanced, unresectable, non-small cell lung cancer (NSCLC) receiving definitive concurrent chemoradiation (CCRT) benefit from durvalumab consolidation therapy. However, predictive factors for early relapse during durvalumab maintenance were not identified.
Patients and Methods: The present study used the lung cancer cohort of the Catholic Medical Centers at the Catholic University of Korea from 2018 to 2021. In all, 51 NSCLC patients that were treated with durvalumab consolidation therapy after definitive CCRT. Early relapse was considered if it occurred within 6 months of starting initial durvalumab therapy.
Results: During study period, 15 (29.4%) relapsed among 51 included patients. Median time from initial therapy of durvalumab to progression

was 107.73 ± 47.69 days in early relapse group. In mutivariate analysis, younger age (HR 0.713, 95% CI 0.572-0.888, *P*=0.003), higher pack years (HR 1.311, 95% CI 1.109-1.549, *P*=0.001), non-COPD (HR 0.030, 95% CI 0.001-0.677, *P*=0.027), anemia (HR 23.30, 95% CI 2.030-267.48, *P*=0.011) and stage IIIC (vs. stage IIIA) (HR 17.890, 95% CI 1.997-160.243, *P*=0.010) were independent predictive factors for early relapse during durvalumab consolidation therapy.
Conclusion: Younger age, higher pack years, non-COPD, anemia and stage IIIC were independent predictive factors for early relapse during durvalumab consolidation therapy in patients with unresectable stage III NSCLC after definitive CCRT. Careful patient selection and clinical attention are needed for high-risk individuals.

Spatial Proteomics and Transcriptomics 2

#6762

Tumor immune microenvironment &genomic features of non-small cell lung carcinomas in patients with HIV (PWH)

Shruti Desai[1], Kishu Ranjan[1], Syim Salahuddin[2], Ramsey Yusuf[2], Jianlei Gu[3], Daiwei Tang[3], Yong Kong[3], Barani Kumar Rajendran[1], Hongyu Zhao[3], Yuval Kluger[1], Sarah Goldberg[2], Brinda Emu[2], Kurt Alex Schalper[1].
[1]Department of Pathology, Yale University School of Medicine, New Haven, CT,[2]Department of Internal Medicine, Yale University School of Medicine, New Haven, CT,[3]Department of Biostatistics, Yale University School of Medicine, New Haven, CT

Introduction: Lung cancer is the leading cause of cancer-related death among PWH with a relative risk that is over 3-fold higher compared to the uninfected population. In addition, HIV-infected patients with non-small cell lung cancer (NSCLC) have a significantly worse prognosis. The determinants for these associations remain uncertain.
Methods: We investigated the immune contexture of 18 primary NSCLCs from PWH and 19 clinicopathologically matched NSCLCs from HIV-negative cases represented in tissue microarrays using 37-plex Imaging Mass Cytometry (IMC) panels including cell phenotype markers (CK,CD4,CD8,CD20,CD45RO,CD25,etc), immunomodulatory targets (PD-L1,PD-L2,B7-H3,B7-H4,B2M,etc) and DNA damage response/repair

(DDR) indicators (γH2AX, RAD51,BRCA1,53BP1,etc). The samples were analyzed using single-cell tissue segmentation and spatial analysis. A subset of cases was also studied using whole exome DNA sequencing (WES) and mRNA sequencing (RNAseq).
Results: NSCLCs from PWH showed comparable levels of tumor infiltrating lymphocytes (TILs) relative to HIV-negative cases with a trend towards a lower CD4+/CD8+ cell ratio. However, CD4+ and CD8+ TILs in PWH showed higher levels of markers associated with T-cell activation and dysfunction including GZB, CD25, Ki-67, PD-1, LAG-3, and TIM-3 than non-HIV tumors. The epithelial tumor cells in HIV-associated cases showed higher levels of the immunomodulatory ligands PD-L1, CD47, B7-H4 and VISTA; and altered levels of the DDR markers γH2AX, BRCA1 and 53BP1 relative to the non-HIV controls. Differences were also seen in tumor-associated macrophages consistent with an immune regulatory environment. The spatial analysis of tumor and immune cells revealed a distinct topographic distribution of these cells in HIV-associated malignancies. WES analysis showed a higher nonsynonymous tumor mutational burden in HIV-associated tumors (400 vs 202 mean mutations/exome) with increased predicted HLA class-I neoantigens and a numerically higher immunoediting score than the non-HIV group. Exploratory analysis identified enrichment in RYR2 and KIAA1671 gene mutations in HIV-associated malignancies. RNAseq revealed distinct mRNA expression profiles of HIV-positive and negative NSCLCs with a fraction of transcripts showing differential expression associated with tumor suppressor functions, interleukin signaling and DDR.
Conclusion: NSCLCs in PWH display profound immunological and genomic alterations suggesting defective immunosurveillance. Our study reveals novel characteristics of HIV-associated NSCLC with possible clinical implications for this growing and understudied population.

#6763
Spatial profiling of cancer-associated fibroblasts in non-small cell lung cancer
Yunhe Liu, Guangchun Han, Enyu Dai, Guangsheng Pei, Jiahui Jiang, Humam Kadara, Linghua Wang. *UT MD Anderson Cancer Center, Houston, TX*

Cancer-associated fibroblast (CAF) is an unique component of the tumor microenviroment (TME). CAFs heterogeneous have been identified by recent single-cell studies. However, their spatial distribution, orgnization patterns and neighbors remain incompletely understood. Deep profiling of CAFs in tissue context may provides new insights into improved understanding of their functions and identify targets for the development of CAF-targeted therapies.We obtained the open-source CosMx SMI dataset generated on 8 tissue sections from 5 non-small-cell lung cancer (NSCLC) tissues *(He, S. et al. Nat Biotechnol. 2022)*. We extracted the cells' spatial locations and transcriptome data for subsequent analyses. Quanlity filtering, data normalization, batch correction and clustering analysis was performed by Seurat package. Cell type was defined based on canonical immune markers and curated gene sets. In addition, we applied NMF clustering approach to define the spatial subtypes of CAFs based on the composition of neighboring cells. After that, Four spatial subtypes of CAFs were defined, exhibiting distinct spatial distribution patterns and compositions of neiboring cells, including CAFs that are clustered with tumor cells, CAFs localized within stromal, CAFs co-localized with B cells and T cells within the tertiary lymphoid structures, and CAFs localized within myeloid-enriched areas. Notably, we observed an intimate link between their spatial location and tarnscriptioanl states, i.e., these different spatial CAF subtypes showed clearly distinct expression profiles, may suggest their heterogeneous functions in the tumor microenviroment. For example, tumor-enriched CAFs showed high expression of contractile (e.g., *ACTA2, TAGLN*) and extracellular matrix (*COL1A1*) related genes, resembling myofibroblast (myCAFs), whereas the TLS-niches CAFs showed high expression of genes involved in antigen presentation such as major histocompatibility complex class II molecules and CD74, suggesting their antigen presentation function and were identified as apCAFs. Consistently, we observed high expression of inflammation related genes such as interleukin and PDGFRA in the myeloid-enriched CAFs suggesting an inflammatory phenotype (iCAFs). In addition, these CAFs in different spatial subtypes showed differential expression of molecular pathways

regulating stress and inflammation response, likely reflecting their complex interactions with other components of the tunmor microenvironment. We also included single-cell RNA sequencing (scRNA-seq) and spatially resolved whole transcriptomics datasets for cross validation of our novel discoveries in additional cohorts.In summary, by applying a novel approach to classify CAFs in the spatial context, this study provided novel insights into an improved understanding of the phenotypic and functional heterogeneity of CAFs in the tunmor microenvironment of NSCLC.

#6764

Multi-parametric comparison of scRNA-seq with CITE-seq and ultrahigh-plex spatial phenotyping of proteins in FFPE head and neck tumor biopsies: An opportunity to generate uniquely comprehensive multi-omic single cell datasets to investigate the tumor microenvironment.

Aditya Pratapa[1], Shawn M. Jensen[2], Niyati Jhaveri[1], Yoshinobu Koguchi[2], Venkatesh Rajamanickam[2], Brady Bernard[2], Tanisha Christie[2], Brian Piening[2], Rom S. Leidner[2], Oliver Braubach[1], Bernard A. Fox[2]. *[1]Discovery Applications, Akoya Biosciences, Marlborough, MA,[2]Providence Cancer Institute, Earle A. Chiles Research Institute, Portland, OR*

Single cell RNA-seq (scRNA-seq) performed on cell suspensions isolated from tumor biopsies provides substantial insights into the transcriptional state of the cells in the tumor microenvironment (TME). Complementing this work with multi-omic Cellular Indexing of Transcriptomes and Epitopes (CITE-seq), which adds barcoded antibodies to label the surface of isolated cells, allows us to additionally characterize surface proteins. While information gleaned from these studies is dramatically expanding our understanding of the evolving immune response and tumor-immune interactions, it lacks an appreciation of the many spatial relationships that are present within the TME. Spatial phenotyping with the power of single cell resolution and whole slide imaging provides a valuable tool for identifying the cellular architecture and organization of spatial neighborhoods that perform critical roles in tumor progression, resistance, and clinical responses. Here, we explore bioinformatic strategies aimed at combining scRNA-seq and CITE-seq data with single-cell spatial protein data obtained with the PhenoCycler-Fusion (PCF) imaging platform. To this

end, we performed whole-slide spatial phenotyping with an ultrahigh-plex PCF panel on FFPE human head and neck tumors. The same biopsies were also enzymatically digested and subjected to CITE-seq and scRNA-seq analysis. The combined multi-omic, single cell dataset provides a uniquely comprehensive account of the cellular states, functional significance and spatial neighborhoods that govern the TME. This study represents a novel approach to integrate high dimensional data from bulk tissue and single-cell spatial technologies to provide deeper insights into tumor biology and, in turn, to develop more informed strategies for combination immunotherapy trials and improved patient outcomes.

#6765

Spatial insights into tumor immune evasion illuminated with 1000-plex RNA profiling with CosMx Spatial Molecular Imager

Claire Williams, Jason W. Reeves, Patrick Danaher, Shanshan He, Sean Kim, Michael Patrick, Julian Preciado, Mark Gregory, Zach Reitz, Justin Jenkins, Rachel Liu, Sarah Murphy, Christine Kang, Byron Hartman, Vikram Devgan, Michael Rhodes, Joseph Beechem. *NanoString Technologies, Inc., Seattle, WA*

Patient response to immunotherapy has been revolutionary but remains limited due to the inability to convert excluded or cold tumors into ones which would be permissive to therapeutic intervention. To treat patients that evade immune therapy, comprehensive understanding of their tumor microenvironment (TME) is needed. To date, most profiling efforts have lacked the ability to capture high-plex ‘omics data while retaining the spatial architecture of the TME. We developed the CosMx™ Spatial Molecular Imager (SMI) for analyzing formalin-fixed paraffin-embedded (FFPE) or fresh-frozen (FF) tissue and capturing the expression of over 1000 RNA targets simultaneously with subcellular resolution from a single histopathology slide. We profiled a cohort of 16 slides with CosMx using the Human Universal Cell Characterization (UCC) Panel across a range of solid tumors. This cohort represents a diverse array of patients which include both infiltrated and excluded tumors. We included technical replicates for 5 of the samples to better understand reproducibility of the assay. We were able to characterize over 4.5 million cells and detected on average over 80% of the panel per patient and assigning more than 95% of

the transcripts profiled to unique cells across these samples. We were able to robustly identify more than 20 cell types by integrating our data with previous single-cell sequencing projects from the human cell atlas. We demonstrate robust delineation of critical immune cell populations from across lymphoid and myeloid lineages, as well as stromal cell populations inclusive of cell types frequently missed using dissociated cell sequencing, such as vascular endothelium associated with immune cell migration into the tumor bed. We leveraged 450+ genes from our panel dedicated to cell lineage, cell-cell interaction, and ligand-receptor signaling to identify unique interactions occurring at different scales between the tumor and the TME. We find that diverse mechanisms of immune evasion can be captured, and a clear role for cell types such as SPP1+ Macrophages emerges in multiple cancer types. Utilizing the CosMx platform to profile tissues allows for robust resolution of critical immunogenic signaling cascades and cellular interactions that are necessary to truly understand the tumor architecture. By maintaining the tissue structure, we can directly measure cellular interactions and capture cells commonly missed during dissociative studies. With this new platform, we are better poised than ever to truly understand the molecular mechanisms that drive tumor response to intervention. FOR RESEARCH USE ONLY. Not for use in diagnostic procedures

#6766

Pan-cancer characterization of tumor-immune interactions using spatially resolved transcriptomics

Guangsheng Pei[1], Jingjing Wu[1], Enyu Dai[1], Yunhe Liu[1], Guangchun Han[1], Jian Hu[2], Fuduan Peng[1], Kyung S. Cho[1], Jiahui Jiang[1], Daiwei Zhang[2], Ansam F. Sinjab[1], Boyu Zhang[1], Shumei Song[1], Junya Fujimoto[1], Luisa M. Solis Soto[1], Anirban Maitra[1], Jaffer Ajani[1], Mingyao Li[2], Humam Kadara[1], Linghua Wang[1]. *[1]UT MD Anderson Cancer Center, Houston, TX,[2]University of Pennsylvania, Philadelphia, PA*

The development of immunotherapy drugs, such as immune checkpoint inhibitors (ICIs) has changed the environment of cancer treatment tremendously by providing efficacious therapeutic options for many cancer patients. However, only a minority of patients experience durable clinical benefit and increasing evidence has linked the efficacy of ICIs to tumor cell

heterogeneity, the complex tumor immune microenvironment and their interactions, which remains poorly understood, particularly in the tissue context. Recent advances in spatially resolved transcriptomics (SRT) has provided great opportunity to better understand spatial tumor-immune interactions. In this study, we obtained public and in-house SRT data on a total of 136 tissue sections across 11 different cancer types, representing to date, the largest collection of SRT on human cancer. Sample and spot-level quality filters were applied, batch effects were assessed and properly handled. High-quality SRT data were pre-processed uniformly to comprehensively interrogate the spatial heterogeneity and architectures of the 3 major compartments (malignant, stroma, and immune) as well as relationships among them. Transcriptome data was integrated with region- and/or spot-level annotations from pathologists. For regions enriched with malignant cells, we inferred somatic copy number alterations, clonal structure of tumor cells, and profiled the transcriptional hallmarks of intra-tumor heterogeneity (ITH) including a number of curated gene sets and meta-programs, and systematically characterized tumor cell heterogeneity under the spatial modality. We observed a great variation in aneuploidy levels and transcriptome profiles within and across patients and cancer types and notably in molecular processes regulating tumor cell responses to stress, hypoxia and interferon signals and other key processes such as epithelial-mesenchymal transition. In addition, we performed cell-type deconvolution analysis using available tools including RCTD and cell2location, based on expression of curated cell-type specific gene signatures, we inferred levels of immune infiltration in each tissue section in both tumor core and invasive edges, and classified tumors into “cold”, “warm”, “hot”, and “mixed” immune phenotypes. We further quantified the abundance and spatial distribution of stromal cells and key TME structures such as tertiary lymphoid structures and lympho-myeloid aggregates, as well as their spatial neighbors with oncogenic features which revealed multiple interesting interplay patterns. Together, this study provide novel insights into our improved understanding of spatial tumor heterogeneity and tumor-immune interactions and revealed potential exploitable targets, and great resource for the community.

#6767

Cancer-associated fibroblasts promote T-cell exclusion and resistance to immunotherapy in non-small cell lung cancer with tertiary lymphoid structures

Florent Peyraud[1], Jean-Philippe Guegan[2], Christophe Rey[2], Oren Ngouala[2], Ophélie Odin[2], Emma Clot[1], Lucile Vanhersecke[1], Maxime Brunet[1], Thomas Grellety[3], Marie Del Castillo[4], Sylvestre Le Moulec[5], François Le Loarer[1], Alban Bessede[2], Antoine Italiano[1]. *[1]Institute Bergonié, Bordeaux, France,[2]Explicyte, Bordeaux, France,[3]Centre Hospitalier de la Côte Basque, Bayonne, France,[4]Atlantic Pathologie, Saint Pierre d'Irube, France,[5]Clinique Marzet, Pau, France*

Background: We and others have reported the major role of mature tertiary lymphoid structures (TLS) in the efficacy of PD-L1 blockade in NSCLC. The objective response rate (ORR) to inhibition of PD1/PDL1 used as single agents observed in TLS-positive NSCLC is similar to ORRs observed in all-comers NSCLC treated with a combination of immune checkpoint inhibitor (ICI) and chemotherapy. However, a substantial proportion of patients with TLS-positive NSCLC did not display clinical benefit. The aim of our study was to identify the determinants of response to ICI in TLS-positive NSCLC.

Methods: We spatially profiled the expression of >18,000 protein-coding genes across six patients with mature TLS-positive NSCLC (three with objective response and three with progressive disease as the best response) using the GeoMx whole-transcriptome atlas (WTA) assay. Using two consecutive slides stained with CD3/CD20 and CD45/PanCK markers, a first set of regions of interest (ROIs) selected the TLS (CD3+/CD20+) as an entire area of illumination (AOIs). A second set of ROIs was selected outside the TLS region and further segmented into 'tumor' (PanCK+/CD45-) versus 'stroma' (PanCK-/CD45+) AOIs. To further validate our findings, we performed multiplex immunofluorescence (mIF) on 70 mature TLS-positive NSCLC tumors.

Results: Comparative transcriptomic analysis of TLS between non-responders and responders revealed upregulation in responders of CCL21 which plays a crucial role in T cell recruitment, and of IGHM indicating the presence of unswitched B cells. Outside of TLS, in the stromal compartment, the most significantly differentially expressed genes between

responders and non-responders were those belonging to a subset of cancer associated fibroblasts (CAFs) expressing both FAP and αSMA markers, and recently described as linked to more inflammatory activated immune cells and involved in T cell exclusion in NSCLC. We then used FFPE tissue mIF to histologically profile CAF subset composition and spatial distribution of T cells in a cohort of 70 mature TLS-positive NSCLC. In tumor lesions enriched in FAP+αSMA+ CAFs, the tumor-to-stroma ratio of infiltrating CD8+ cells was significantly lower, consistent with a decreased infiltrating CD8+ T cell density in the tumor. Strikingly, ORR and survival of patients with mature TLS NSCCLC enriched in FAP+αSMA+ CAFs were significantly lower than those of patients with low abundance of CAFs. Conclusions: We report here the first study investigating the mechanisms of resistance to immunotherapy in TLS-positive tumors. Our analysis of human tumor samples suggests a crucial role of FAP+αSMA+ CAFs in excluding T cells and in driving resistance to immune checkpoint inhibition in mature TLS-positive NSCLC. The development of novel CAF-targeting strategies may be particularly relevant in this subset of tumors.

#6768

The potential predictive role of spatial phenotyping in non-small cell lung cancer

Ning Ma[1], Aditya Pratapa[1], James Monkman[2], Ken O'Byrne[3], Oliver Braubach[1], Arutha Kulasinghe[2]. *[1]Akoya Biosciences, Menlo Park, CA,[2]University of Queensland, Brisbane, Australia,[3]Princess Alexandra Hospital, Brisbane, CA*

Background Lung cancers are the leading cause of cancer-related deaths with a 5-year-survival of only ~20%. Whilst immunotherapies have led to durable and prolonged survival, only a subset of patients remain responsive. Additional biomarkers are thus needed to better predict if patients will respond or develop resistance against immune checkpoint inhibitor (ICI) therapies. Spatial phenotyping of the tumor microenvironment (TME) is now recognized as a proxy for ICI therapy outcomes. Our study employs an end-to-end spatial biology strategy to survey non-small-cell lung cancer (NSCLC) tissues for new biomarkers that could guide immunotherapy treatments.

Methods We phenotyped pre-treatment biopsies from non-small-cell lung cancer (NSCLC) patients treated with single-agent Nivolumab. We first performed 57-plex whole-slide Single Cell Spatial Phenotyping on the PhenoCycler®-Fusion platform. Next, we developed the spatial analysis of a larger NSCLC cohort using customizable PhenoCode Signature Panels (PSP) for high-throughput immune profile (CD3/CD8/CD20/CD68/PanCK + CD4 add-in) and immuno-contexture (CD8/CD68/PD-L1/FoxP3/PanCK + PD-1 add-in) imaging. The PSP panel content combines the barcode-based antibody chemistry from the PhenoCycler platform with the signal amplification of Opal chemistry from the PhenoImager platform. PSP panels were profiled across n=27 NSCLC biopsies and provided a wider breadth of tissue profiling.
Results Our whole-slide single-cell spatial phenotyping analyses revealed high phenotypic diversity in the TME of patients responsive and resistant to ICI therapy. However, higher-throughput analyses of the same tissues using targeted PSP panels revealed no significant differences in quantities of immune cell lineages, including T-cells and macrophages. On the contrary, we discovered multiple quantifiable and statistically significant spatial signatures that appear to be predictive of treatment benefit, which confirms the potential biomarker value of spatial associations in patient tissues.
Conclusions This study amounts to a uniquely comprehensive Single Cell Spatial Phenotyping analysis of pre-treatment NSCLC biopsies from a single-agent Nivolumab study. Our data catalogue the diversity in the immune microenvironment of NSCLC but highlighted that immune cell quantification is insufficient to stratify patient cohorts. Single-cell spatial phenotyping, on the other hand, promises to reveal new biomarkers that may aid in better stratification of patients in pre-treatment evaluations.

#6769
Precise spatial multiplexing of protein biomarkers for immune profiling in tissue samples with chip cytometry
Karen Kwarta, Thomas Campbell, Adam Northcutt, Spencer Schwarz.
Canopy Biosciences, St. Louis, MO

Immunohistochemistry is the most widely used diagnostic technique in tissue pathology. However, IHC is associated with several limitations including the labeling of just a few markers per tissue section and limited

quantification of cell populations. As a result of plex limitations, key insights about tumor biology are missed, which could be important for advancing our understanding of tumor biology and ultimately improving patient outcomes. Chip Cytometry is a novel image-based platform for precise spatial multiplexing that addresses these challenges by combining iterative immuno-fluorescent staining with high-dynamic range imaging to facilitate quantitative phenotyping with single-cell resolution. The platform enables simultaneous detection of dozens of markers on a single tissue section and enables accurate quantification of protein expression levels necessary to deeply profile single cells, understand interactions between key immune cells, and identify topographic biomarkers. Here we demonstrate how standard FCS files are generated from multichannel OME TIFF images, enabling identification of cellular phenotypes via flow cytometry-like hierarchical gating. Quantification of results reveal precise expression levels for each marker in the assay in each individual cell in the sample, while maintaining spatial information about each cell. Chip Cytometry has the potential to advance precision medicine in immuno-oncology and inform the discovery of novel biomarkers by enabling quantitative analysis of cellular phenotypes in the spatial context. The Chip Cytometry platform enables simultaneous detection of multiple protein markers on a single tissue section for deep immune cell profiling in the tumor microenvironment. Combined with the single-cell spatial information, such data sets provide an opportunity for the discovery of new complex multiplexed biomarker signatures to inform therapeutic development.

#6770

Spatial characterization of immune microenvironment from early onset metastatic colorectal cancer (EOmCRC) showed a dual prognostic role for IDO1 expression

Raghavendar Thyagaraja Nagaraju[1], Jakub Franczak[1], Markus Möhler[2], Elisa Fontana[3], Anne Giraut[4], Lieve Dirix[4], Jose Casas-Martin[4], Beatrice Borelli[5], Florian Lordick[6], Elizabeth Smith[7], Sabine Tejpar[8], Gunnar Folprecht[9], Jorge Barriuso[1]. *[1]Division of Cancer sciences, University of Manchester, Manchester, United Kingdom,[2]Mainz-University Medical Center, Mainz, Germany,[3]Sarah Cannon Research UK, London, United*

Kingdom,[4]Headquarters, EORTC, Brussels, Belgium,[5]Azienda Ospedaliera Universitaria Pisana, Pisa, Italy,[6]Universitaetsklinikum Leipzig UCCL-Krebszentrum, Leipzig, Germany,[7]Royal Marsden Hospital, London, United Kingdom,[8]Digestive Oncology Unit, University Hospital Gasthuisberg, Leuven, Belgium,[9]Medical Department I, University Cancer Center, University Hospital Carl Gustav Carus, Dresden, Germany

Background: Epidemiological studies demonstrate that the incidence of CRC in young adults is continually rising in both Europe and the USA. The differences between the spatial distribution of immune related markers (IRM) and their prognostic role in EOmCRC compared to late onset (LOmCRC) remains to be elucidated.
Methods: Forty paraffin embedded formalin fixed unstained sections from patients (pts) diagnosed with either EOmCRC (≤45) or (≥50) LOmCRC, matched for chemotherapy (chx) and molecular features, all with microsatellite stable disease were included. All tissue samples were obtained from pts enrolled in SPECTAcolor (EORTC-40CRC-GITCG) platform trial. The expression of IRM was studied using the GeoMX Digital Spatial Profiler (DSP). Fifty-seven IRMs were used and three morphology markers (MMs) anti-CD45, pan-cytokeratin and SYTO 13. Three 300 μm regions of interest (ROIs) were selected within the core of the tumour and further 3 ROIs within the active margin of the tumour. Each ROI was segmented based on MMs to obtain a tumour microenvironment (TME) and a tumour (T) mask. The analysis used the GeoMX DSP Advanced Analysis Suite software, R and IBM SPSS. Control for multiple comparisons use a false discovery rate (FDR) threshold of 0.05.
Results: Samples from 40 pts were collected; 19 (47.5%) were EOmCRCs; 16 (40%) were female; 23 (57.5%) with pathological stage IV. The majority being, 23 (57.5%) grade ≥ 2, left sided 26 (65%), oxaliplatin based first line chx 23 (57.5%). Ten (25%) were KRAS mutant (mt), 1 (2.5%) NRAS mt and 1 (2.5%) BRAF mt. The median overall (OS) and progression free survival (PFS) for the entire cohort was 36.6 months (m) 95%CI (33.5 - 39.7) and 11.7 m (8.1 - 15.3), respectively.The <0.05 FDR differential expression analysis based on tissue segmentation uncovered 9 hits when comparing the TME between different age groups and 2 hits when comparing T segments, all overexpressed in LOmCRC. Indoleamine 2,3-dioxygenase 1 (IDO1) was differentially overexpressed in TME (adjusted

p=0.043) and T (adjusted p=0.042) for LOmCRC.In the EOmCRC group IDO1 relative high expression in T was an independent marker associated with worse survival outcomes after multivariate cox regression corrected for the rest of significant markers (MVCC) for OS, HR: $7.01*10^5$ 95%CI ($9.08*10^5$-$5.41*10^{10}$), p=0.003 and PFS, HR:$7.7*10^5$ 95%CI (1.96-$30.3*10^6$), p=0.029. However, interestingly high IDO1 in TME was an independent marker associated with better OS, HR: 0.02 95%CI (0.01-0.46), p=0.015.
Conclusion: Differential expression analysis of IRMs found IDO1 as differentially expressed in both segments (T and TME). Furthermore, high IDO1 expression seemed to have a dual prognostic role depending on the segment analysed, showing worse OS when found in the tumour but better OS when found in tumour microenvironment for early onset mCRC.

#6771
Interrogating the tumor-immune landscape with a novel automated RNAscope™ assay for multiplexed detection of RNA and protein
Anushka Dikshit, Sayantani Basak, Vasudha Murlidhar, Ge-Ah Kim, Julia Yu, Sonali Deshpande, Li-Chong Wang, Maithreyan Srinivasan. *Bio-Techne Corporation, Newark, CA*

Understanding tissue heterogeneity is critical for elucidating cell-cell interactions with important implications in immuno-oncology, inflammation, and neuroscience. Tissue heterogeneity poses immense challenges to understanding underlying molecular mechanisms using techniques such as qRT-PCR or bulk sequencing. While single-cell RNA sequencing can provide information about precise cellular composition of tissues, data analysis can be cumbersome and spatial context is lost. With single-cell spatial platforms such as RNAscope, target gene and protein expression can be visualized to characterize cell types and tissue neighborhoods. Here, we demonstrate a novel method for the simultaneous detection of RNA and protein using a modified co-detection assay. This novel co-detection assay enables visualization of a combination of up to 12 RNA and/or protein targets on the same sample. We used a set of antibodies targeting key immune and tumor cell markers- PD1, CD3, CD4, CD8, CD68, FOXP3 and KRT17, along with RNA biomarkers to interrogate the tumor microenvironment (TME) in human FFPE tumor samples. Using a

combination of RNA and protein targets, we characterized different cell types such as T cells, macrophages, and tumor cells in the TME. We also developed a novel method for visualizing intercellular interactions between PD1 and PD-L1, offering insights into popular checkpoint mechanisms that are targeted for therapeutic intervention in cancer treatment. The assay offers a powerful technique for visualizing target RNA biomarkers in specific cell-types identified by cell-marker protein expression. This is a valuable tool for multi-omic analysis and accurate interrogation of complex tissues to obtain insights into novel biomarkers and therapeutic targets.

#6772

Powerful background reduction in fluorescent tissue stains with an improved proximity-based technology for detection of protein-protein interactions

Hampus Elofsson, Doroteya Raykova, Agata Zieba Wicher. *Navinci Diagnostics AB, Uppsala, Sweden*

Immunofluorescent staining of tissues via *in situ* proximity ligation assay (isPLA) is now a well-established tool for highly sensitive detection of protein-protein interactions and their localization. It finds versatile applications in basic research, understanding of cellular processes, visualization of tissue architecture, and identification of biomarkers, among others. However, standard IF and isPLA techniques alike may suffer from high background. Tissues are particularly affected by background problems caused by autofluorescence and tissue infiltration of various cell types (e.g., immune, endothelial) where the fluorescently labelled oligos used for detection in isPLA may bind unspecifically. To address this, we developed a next generation isPLA-based technology for fluorescent detection of protein interactions in FFPE and fresh frozen human and mouse tissues, called NaveniFlex Tissue. In contrast to previously available protocols, it can visualize signal that would otherwise be obscured by background, thereby increasing sensitivity. Here, we compare the ability of NaveniFlex Tissue and similar commercial kits to detect the interaction between low abundance proteins Podocalyxin and Ezrin in the glomeruli of healthy kidney and in breast cancer, where co-expression is a prognostic marker for increased metastatic potential. While other kits generate high background which masks isPLA signal entirely, NaveniFlex Tissue dramatically reduces

cell-based background and visualizes the interaction in its specific localization. Furthermore, in a TMA staining for the Mucin 16/Mesothelin interaction, our method successfully demonstrates strong and clear signal in stage III ovarian cancer. Moreover, it sensitively detects even low abundance interaction in a stage Ia tumor. In contrast, a different commercial kit detects significantly less interactions in the stage III tumor, while in the lower grade tumor it does not generate signals above background level. Therefore, NaveniFlex Tissue improves detection in tissues with varying disease progression, thus adding information and prognostic value to the staining. Taken together, our data illustrate that NaveniFlex Tissue outperforms current isPLA-based techniques by efficiently reducing background, which improves visualization of signal and signal-to-noise ratios in various healthy and diseased tissues.

#6773

Spatial dynamics of cytotoxic T lymphocyte exhaustion in reactive and tumoral tissue

Maxim De Schepper[1], Asier Antoranz[2], Nikolina Dubroja[2], Giuseppe Floris[2], Frederik De Smet[2], Francesca Bosisio[2]. *[1]Laboratory for translational breast cancer research, Department of Oncology, KU Leuven, Leuven, Belgium,[2]Translational Cell and Tissue Research, Department of Imaging and Pathology, KU Leuven, Leuven, Belgium*

Background The study of cytotoxic T-lymphocytes (Tcy) has shown increased attention from the scientific community in the last years because of their predictive role in anti-cancer therapy with specific interest in immune check point blocking therapy. However, most of these studies have used bulk or dissociation-based single-cell technologies to draw their biological insights. Lately, new spatial -omics technologies are increasing our knowledge on this population by adding the spatial location of these cells in-situ in the native structure of the tissue. In this study, we have compared the activation of Tcy in reactive and cancerous conditions at single cell level and in the micro-anatomical context of the tissue.
Experimental procedures One tissue micro array slide containing: reactive tonsil, inflammatory liver disease, breast cancer, glioblastoma and melanoma was stained using the COMET™ instrument (Lunaphore Technologies SA) for a multiplex panel of 20 markers. The derived

multiplexed images were analyzed using the DISSCOVERY software platform developed by the MILAN Unit at KU Leuven (Belgium). 12/20 markers were specifically aimed at identifying the main cell populations in the tissue (CD11b, CD163, CD20, CD3, CD31, CD4, CD56, CD68, CD8, CK, FOXP3, S100) while the remaining 8 markers were aimed at adding functional information on immune cell types of interest (CD69, HLA-DR, Ki67, LAG3, OX40, PD-1, PD-L1, TIM3).
Results The general activation levels of the Tcy in the reactive conditions were higher than in the three cancer subtypes. When looking at Tcy activation as a function of the distance from the vascular structures (identified via CD31+ endothelial cells), we observed an orderly distribution of activated Tcy around CD31+ endothelial cells with a gradient of increasing exhaustion levels with increasing distance from the vessel in the reactive conditions. In the cancer samples, on the contrary, a patchy disorderly organized pattern of exhausted and activated Tcy was observed around the vessels.
Conclusion The spatial location of inflammatory cells plays a critical role to understand their functional behavior and thanks to technological progress it is now possible to start doing this at scale. The study of the dynamics of exhaustion of Tcy in the tissue will help clarify the interplay between cancer cells and immune environment. These results will be crucial to better select patients who may benefit the most of immune check point blockade.

#6774

The development of a spatial metabolic map of immunotherapy sensitive and resistant cutaneous skin carcinoma

Niyati Jhaveri[1], Dmytro Klymyshyn[1], Bassem B. Cheikh[1], James Monkman[2], Dan Winkowski[3], James Mansfield[3], Subham Basu[4], Michael Prater[4], Nadine Nelson[4], Gabrielle Belz[2], Oliver Braubach[1], Arutha Kulasinghe[2]. *[1]Akoya Biosciences, Menlo Park, CA,[2]The University of Queensland, Brisbane, Australia,[3]Visiopharm A/S, Horsholm, Denmark,[4]Abcam, Cambridge, United Kingdom*

Background: Cutaneous squamous cell carcinoma (cSCC) is the second most common skin cancer and represents a major global health burden. Approximately 50% of cSCC patients develop primary resistance and 20% will develop secondary resistance to immune checkpoint inhibitors (ICI).

There are limited biomarkers that reflect the tumor dynamics predictive of response to ICI therapy, and therefore we need to explore new biomarkers that can better understand the cSCC tumor microenvironment (TME).
Methods: Our retrospective study profiled pre-treatment cutaneous skin cancer tissues from patients with immunotherapy sensitive and resistant diseases. In this exploratory study, we designed a high-dimensional > 50-plex antibody panel identifying cell lineages, activation states, and immune checkpoints. In addition, we deployed a combination of antibodies for a novel multiplexed metabolic readout, to enhance our *in situ* profiling beyond well-known TME targets. Whole-slide spatial phenotyping was conducted on the PhenoCycler-Fusion spatial biology platform. Highplex image analysis was performed using Phenoplex (Visiopharm), including tissue segmentation and cellular phenotyping. Here, we used a deep learning approach to discriminate tumor regions and margins based on their morphology. Spatial analyses including phenotypic composition, cell-to-cell localization, and cellular neighborhoods were performed and compared to clinicopathological findings and responses to ICI therapy.
Results: We have profiled the TME of cSCC via ultrahigh-plex, single-cell spatial analyses of whole tissues. Our data have revealed unique cell phenotype compositions and metabolic states within the TME of different patient cohorts. Areas of metabolic activity were visualized and compartmentalized to determine spatial distributions of inherent sensitivity and resistance to ICI therapy. Additionally, a comparison of the phenotypic expression patterns between immunotherapy sensitive and resistant cohorts in the tumor, stromal and margin regions showed relevant differences in the immune content. Taken together, this high-dimensional imaging approach of the cSCC TME has revealed new tissue insights.
Conclusion: There is a need to understand the contexture of the cSCC immune microenvironment. Here we identify distinct cellular phenotypic compositions and metabolic states in tissues from immune-competent and immunocompromised cSCC. We thereby confirm biological differences in tissue composition and cellular interactions between these tissues and provide putative new biomarkers for cSCC patient stratification.

#6775
Combination of spatial transcriptomics and multiplex IHC as valuable multi-omics tool for biomarker discovery

Nicole Kerstedt, Monika Schoeppler, Bita Motamedi-Baniassad, Antonia Hirt, Julia Ploetzky, Mirja Kastein, Laura Thoms, Malik Khenkhar, Hartmut Juhl, Kerstin A. David. *Indivumed, Hamburg, Germany*

Colorectal cancer (CRC) is one of the most common cancers worldwide and shows heterogenous molecular subtypes making personalized medicine as well as identifying new targets highly important to provide individual patients with the most appropriate treatment.
To gain more insight into the visualization of potential molecules or pathways for targeting CRC we used a multi-omics approach for the simultaneous analysis of gene and protein expression within a sample. In this study we combined fluorescent multiplex immunohistochemistry (mIHC) for the detection of proteins (4-plex panel) with the Visium Spatial Transcriptomics technology (10x Genomics) that enables the detection of the whole transcriptome in the histological context.
A formalin-fixed paraffin-embedded (FFPE) tumor tissue sample from a patient diagnosed with CRC was selected according to our quality standards. For this multi-omics approach, serial sections were prepared. The first section was used for fluorescent mIHC staining visualizing the protein expression of Ki67 (proliferation marker), p53 and p21 (both tumor suppressor genes). The second section was stained for hematoxylin and eosin (H&E) to evaluate the tissue morphology. On the third section the Visium FFPE Spatial Gene Expression workflow was applied, and gene expression patterns were analyzed by using the software Space Ranger and Loupe Browser.
Our data showed on the one hand a good correlation of protein and gene expression of Ki67, p53 and p21 within the analyzed sample and on the other hand a clear difference of expression patterns between tumor cell areas and regions with corresponding normal mucosa cells. Moreover, by comparing Spatial Transcriptomics gene expression patterns of tumor cell and corresponding normal mucosa cell areas, we also identified genes that were linked to other cancer types and/or are still only poorly described in cancer, especially for CRC. Corresponding protein expression will be verified by chromogenic IHC in the next steps.
The combination of fluorescent mIHC and Spatial Transcriptomics has been shown to be a valuable approach not only to visualize already described relations as proof of principle, but more importantly to enable the discovery

of new biomarkers or pathways predominantly linked to colorectal tumor tissue that may serve as new targets for cancer treatment.

#6776

Spatial transcriptomics of response to tepotinib treatment in a patient with NSCLC

Manon A. Simard[1], Felix Geist[1], Carlos Cabrera[2], Santiago Viteri[2], Joachim Albers[1], Michael Zuehlsdorf[1], Niki Karachaliou[1]. *[1]Research Unit Oncology, Merck KGaA, Darmstadt, Germany,[2]UOMI Cancer Center, Barcelona, Spain*

Background: While cancer therapies are becoming increasingly more targeted, our understanding of the genomic changes occurring during these treatments is lacking. Moreover, the tumoral heterogeneity and its spatial distribution remain important obstacles in predicting tumor evolution and treatment responses. In recent years, genomic spatial profiling techniques have shed light on this complexity by detecting gene expression changes in heterogenous tumor regions and their microenvironment over the course of treatment.
Methods: Tepotinib is a highly selective and potent MET class Ib inhibitor, approved for the treatment of patients with NSCLC with *MET* exon 14 skipping alterations. To detect genomic changes during neoadjuvant treatment with tepotinib, a GeoMx® digital spatial profiler (DSP; Nanostring Technologies) analysis was conducted in paired baseline and on-treatment patient samples. GeoMx® DSP was performed by selecting regions of interest with nuclear, TTF-1, CD3 and CD33 morphology markers followed by next-generation sequencing (NGS) using the Cancer Transcriptome Atlas RNA panel (>1,800 cancer-related genes).
Results: Following a poor response to chemotherapy, neoadjuvant tepotinib treatment was initiated in a 54-year-old female, never-smoker with NSCLC harboring a *MET* exon 14 alteration. Owing to a good response to tepotinib, surgical resection of the tumor was decided by the tumor board given the downgrading (from IIIB to IA1) and resulting in a major pathological response. This resection allowed spatial transcriptomics to be compared to a baseline biopsy from the same patient. MET signaling inhibition by tepotinib treatment increased immune cell infiltration in the tumor microenvironment compared to the baseline sample. This enhanced tumoral

immune cell density was shown by the fluorescent morphology markers and confirmed through spatial deconvolution of the NGS results. It was further characterized by the significantly altered gene expression levels between the two samples. Gene ontology (GO) assessment of the differentially expressed genes revealed GO terms associated with tumorigenesis in the basal sample, such as cell mobility and motility, vascular epithelial growth factor production and cell communication. In turn, the tepotinib-treated tissue mainly exhibited tumor-clearing characteristics, including antigen processing and presentation through major histocompatibility complex classes I & II, T cell-mediated toxicity, and granulocyte and leukocyte activation.
Conclusion: This is the first spatial genomic characterization of the effect of tepotinib on the tumor and its microenvironment in a patient with NSCLC over time. Results from this case report highlight the impact of MET inhibition by tepotinib on the tumor immune microenvironment, likely enabling the recruitment of antigen-presenting cells for tumor clearance, while reducing the expression of tumor-promoting genes.

#6777

Digital Spatial Profiler highlights a T and B cells inflamed tumor microenvironment in brain metastases derived from melanoma vs. non-melanoma solid tumors

Alberto Mendoza-Valderrey[1], Daria M. Kessler[2], Ethan Dettmann[3], Xinmin Li[4], Sierra Thompson[5], Steven E. Kolker[5], Kim A. Margolin[6], Maria L. Ascierto[1]. *[1]Translational Cancer Immunology and Immunotherapy, Saint John's Cancer Institute, Providence Saint John's Health Center; Rosalie and Harold Rae Brown Cancer Immunotherapy Research Program; Borstein Family Melanoma Program, Santa Monica, CA,[2]Bioinformatic Department, Saint John's Cancer Institute, Providence Saint John's Health Center, Santa Monica, CA,[3]Translational Cancer Immunology and Immunotherapy, Saint John's Cancer Institute, Providence Saint John's Health Center, Santa Monica, CA,[4]Technology Center for Genomics and Bioinformatics, UCLA, Los Angeles, CA,[5]Dermatopathology Section, Saint John's Cancer Institute, Providence Saint John's Health Center, Santa Monica, CA,[6]Melanoma Program, Saint John's Cancer Institute,*

Providence Saint John's Health Center; Borstein Family Melanoma Program, Santa Monica, CA

Introduction**:** Systemic immunotherapies (IO) have recently shown activity in melanoma and non-small cell lung cancer metastatic to the brain, but minimal activity in the treatment of other brain metastases. Further, only a limited percentage of melanoma or lung cancer (MBM/NSCLC)-brain metastasis (BrMs) patients respond to IO. The aim of this study is to explore the differences in the tumor microenvironment (TME) among BrMs from different tumor types including melanoma, NSCLC, breast, and renal cell carcinoma (RCC).
Methods: Formalin-fixed paraffin-embedded (FFPE) tumor from 13 MBM and 43 non-MBM [18 NSCLC-BrMs, 20 breast-BrMs and 5 Renal RCC-BrMs] and primary tissue from 7 melanoma, 4 NSCLC and 3 breast cases were identified. RNA was isolated from tumor regions and subjected to whole gene expression profiling (GEP) by RNA-seq. Microenvironment Cell-Populations counter method estimated the abundance of immune and stromal infiltrated cell subpopulations. Inter- and intra-tumor heterogeneity was evaluated in selected regions of interest using a 59-plex immune related protein panel assessed by GeoMx Digital Spatial Profiling (DSP) technology.
Results: Whole GEP revealed 3650 transcripts differentially expressed between MBM and non-MBM (False Discovery Rate, FDR, ≤0.01). MBM showed increased expression of genes involved in B cell function, cytolytic activity associated with CD8 and NK cells and complement signaling (*C1QA*/*B*/*C*). Conversely, overexpression of genes involved in epithelial signaling, cell adhesion and neurovascular coupling was observed in non MBM vs MBM. Spatial protein profiling revealed in the TME of MBM vs non-MBM, an increased expression ($p < 0.1$, $FC > 1.5$) of the tumor antigen MART-1, together with a higher infiltration of CD8+ cytotoxic cells ($CD8^+$, $41BB^+$), antigen presenting cells (HLA-DR^+, $B2M^+$, $CD40^+$) and cells involved in the formation of tertiary lymphoid structures ($CD20^+$, $CD11c^+$). Conversely, increased infiltration of Tregs ($CD25^+$, $CD127^+$), neutrophils ($CD66b^+$) and epithelial cells ($EpCAM^+$, $PanCK^+$) was observed in non-MBM vs MBM. Interestingly, $LAG3^+$and PD-$L2^+$cells were also observed to be more enriched in non-MBM vs MBM. GEP in primary tumors (FDR≤0.01) showed limited immune-related signals but revealed

overexpression of genes associated with NK cells functions and immune chemoattraction (*CCL18*/*20*, *CXCL2*/*5*/*17*) to be overexpressed in PM vs other primary tumors.
Conclusion: TME interrogation at molecular and protein levels has shown that MBM are more immune infiltrated than brain metastases derived from non-melanoma solid tumors. Particularly, a cytotoxic and B cells - enriched TME was observed in MBM vs brain metastases derived from NSCLC, breast and RCC. These findings will be validated in larger cohorts and incorporated in therapeutic investigations.

#6778
Spatial analysis of genomic signatures on colorectal cancer pathogenesis using the GeoMx® Digital Spatial Profiler
Xiang Li[1], Qinqin Zha[1], Brigitte Lovell[2], Jane Reed[2], Anna Juncker-Jensen[1], Tricia Peters[2], Lakshmi Chandramohan[2]. *[1]NeoGenomics, Aliso Viejo, CA,[2]NeoGenomics, Houston, CA*

Background: The development of colorectal cancer (CRC) is a complex process, involving multiple sequential molecular aberrations that contribute to disease progression. Understanding the immunopathogenesis of CRC particularly within the spatial context of tumor microenvironment (TME) may elucidate the genomic and biological changes to improve patient prognosis for adjuvant therapies and identifying potential drug targets. However, this can be challenging, as genomic signatures from sub-cellular populations and varying levels of immune cell infiltration in TME may be lost in bulk sequencing. In this study, we used the NanoString GeoMx® Digital Spatial Profiler (DSP) to spatially select epithelial, proximal stromal and distal stromal regions of TMEs on a total of 10 FFPE samples (5 colon cancer patients and 5 healthy donor samples) and profiled up to 1,800 genes included in the Cancer Transcriptome Atlas (CTA) panel.
Methods: Selection of regions of interest (ROI) were guided by pathology assessment of H&E images and fluorescent markers (CD45, PanCK, Syto13). Tumor and stroma (proximal and distal) regions were profiled through geometric ROI selection in PanCK+ (epithelial) and CD45+ (stromal/immune) enriched areas respectively, followed by collection of indexed oligonucleotides and sequencing on NextSeq 550 Illumina instrument. Differential expression and pathways enrichment analyses was

performed using R BioConductor package DESeq2 and DSP GeoMx analysis suite. A subset of samples were tested for bulk RNA expression using PanCancer IO360 panel on NanoString nCounter Flex system and data analyzed using nSolver software 3.0 and TIS algorithm App.
Results: The CTA panel is designed to profile the global immune response and all aspects of tumor microenvironment biology. From differential gene expression analysis of epithelial and distal/proximal stromal ROIs, we have identified biomarkers such as SOX9, IRAK2 and NLRP3 that are specifically upregulated in CRC samples compared to the healthy cohort. Comprehensive pathways analysis revealed an over activation of NF-kB signaling, extracellular matrix organization and interferon signaling pathways in the CRC cohort. Suppression of the NF-kB signaling pathway is a potential therapeutic approach in the treatment of colon cancer.
Conclusion: With this spatial study using GeoMx CTA panel, we have highlighted key genes and pathways involved in CRC in order to provide a much-needed understanding of the underlying mechanisms as well as immune signatures in the development of colon cancer.

#6779

Spatial and single-nucleus transcriptomics of human glioblastoma

Yue Hao[1], Angela Baker[1], Brian Hilbush[2], Marcos Otero[2], Chris Streck[2], Karen L. Fink[3], George J. Snipes[3], Bruce E. Mickey[3], Michael Berens[1].
[1]Cancer and Cell Biology Division, TGen (The Translational Genomics Research Institute), Phoenix, AZ,[2]Veranome Biosystems LLC, Mountain View, CA,[3]Baylor Scott & White Medical Center, Dallas, TX

Glioblastoma (GBM) multiforme is the most aggressive type of brain cancer. These lethal brain tumors are characterized by the inter- and intra-tumor molecular heterogeneity and diverse cell plasticity. We sought to interrogate the immune landscape of GBM, tease out the distinct biological and therapeutic niches in GBM and to understand how the tumor microenvironments mediated the heterogeneity of GBM. We have collected six human GBM samples for spatial profiling and single-nucleus RNA sequencing. Multiple sets of spatial gene panels were designed to capture the cell identities (cancer stem cells, astrocytes, oligodendrocytes, microglia, macrophages, endothelial cells, etc.) and the spatially-resolved expression patterns of genes indicative of different functional states. We

also aim to find altered neurovascular units by examining the spatial correlation between cells that highly express angiogenesis markers such as VEGFA with tumor-associated macrophages, which could be recruited to the angiogenic niche by GBM tumor cells. From the spatial RNA dataset of the first two samples, we observed close proximity of tumor-associated macrophages and endothelial cells that form the microvasculature. Our preliminary results from the single-nucleus RNA sequencing and spatial transcriptomics of two samples shed light on the complex cell landscape and the dynamic interaction between tumor cells and infiltrating or resident immune cells in the GBM tumor tissue.

#6780

Characterization of immunological heterogeneity in the tumor microenvironment by integrated analyses using single cell RNAseq, spatial RNAseq and multiplex IHC

Seul Lee[1], Jae-Hwan Kim[2], Kwangmin Na[2], Seung Min Yang[2], Dong Kwon Kim[1], Sujeong Baek[3], Seong-san Kang[4], Yu Jin Han[2], Chun-Bong Synn[1], Mi hyun Kim[2], Heekyung Han[2], Young Taek Kim[2], Sungwoo Lee[4], Youngseon Byeon[2], Young Seob Kim[2], Ji Yun Lee[5], Jii Bum Lee[5], Chang Gon Kim[5], Min Hee Hong[5], Sun Min Lim[5], Kyoung-Ho Pyo[2], Byoung Chul Cho[5]. *[1]Brain Korea 21 PLUS Project for Medical Science, Yonsei University College of Medicine, Seoul, Korea, Republic of,[2]Severance Biomedical Science Institute, Yonsei University College of Medicine, Seoul, Korea, Republic of,[3]Severance Biomedical Science Institute, Yonsei University College of Medicine, Seoul, Korea, Seoul, Korea, Republic of,[4]JEUK Institute for Cancer Research, JEUK Co., Ltd, Gumi-city, Korea, Republic of,[5]Division of Medical Oncology, Department of Internal Medicine and Yonsei Cancer Center, Severance Hospital, Yonsei University College of Medicine, Seoul, Korea, Republic of*

Heterogeneity in resistant to immunotherapies of tumor microenvironment (TME) has been implicated in immunotherapies to cause immune evasion or drug resistance. This study was conducted to explore the heterogeneity of TME through multiplex IHC, spatial and RNA sequencing analysis. We selected a sample from a lung adenocarcinoma patient without EGFR-activating mutation and expressing 30% of PD-L1. For quantitative analysis

by multiplex IHC, various markers including CD4, CD8, FoxP3, granzyme B, CD20 and pan-cytokeratin were stained with 7 different fluorescence dyes, which was imaged with Vectra Polaris (Akoya). For scRNAseq and spatial RNAseq, we used 5' chromium library kit (10X Genomics) to make library construction. Integrated raw data was generated using Cell ranger, Seurat pipeline and Azimuth package. The tumor area was divided into 16 clusters in which we selected 2 clusters based on CD3/45 expression. There was a noticeable distinction between the two clusters which were defined as the 'High' region ($CD45^{high}CD3^{high}$ cluster) and the 'Low' region ($CD45^{low}CD3^{low}$ cluster). By multiplex IHC, percentage of $CD8^{+}$T cells was higher in the 'High' region than in the 'Low' region (8.5% vs. 0.8%, respectively). Subsequent analysis of two clusters using spatial and single cell RNA seq, the 'Low' region was characterized by increased hypoxia-associated gene expressions including HIF1A, HIF3A and VEGFA. Various immune cells were abundant in the 'High' region and CD45 expression level was 11-fold higher in the 'High' region compared to the 'Low' region. Cytokine/chemokine network analysis via spatial RNAseq revealed that gene expression of tumor necrosis factor (TNF) family-associated factors increased in the 'High' region compared to the 'Low' region (TNF, FAS, TRAIL, RANKL and CD40), which is well-known to promotes apoptosis, programmed cell death, or necrosis of certain cancer. Additionally, the 'High' region also had elevated levels of the PD-1/PD-L1, CD155, CD122/TIGIT, Siglec10/CD24, LAG3/LAGLS3, and CD47/CD172a axes, suggesting active immune responses. Intriguingly, combined analyses showed that 'High' region showed enhanced level of *CD44* expression as the leading-edged gene, which suggests the metastatic potential of tumor cells. Furthermore, scRNA analysis confirmed that *CD44* expression was mainly higher in macrophages, suggesting that tumor-associated macrophages partially affected tumor cell metastasis in the 'High' region. Our finding suggests that understanding the intratumoral immunological heterogeneity of lung adenocarcinoma can help to study the mechanism of tumor heterogeneity by integrated spatial RNAseq and scRNAseq analyses. This type of technique could be applied to understand complex networks of anti-tumor immune activities, drug resistance mechanisms and immunotherapeutic response of cancer.

#6781

Spatial omics using spatially-resolved laser-activated cell sorting for cancer biomarker discovery

Amos C. Lee, Sumin Lee, Sunghoon Kwon. *Seoul National University, Seoul, Korea, Republic of*

Cancer is spatially heterogeneous in terms of genetic molecules. Revealing genomic, epigenomic, transcriptomic, and epitranscriptomic features that are unique to the malignant cell populations within cancer lead to cancer biomarker discoveries that can be translated into diagnostic or therapeutic tools. Here, we introduce spatially-resolved laser-activated cell sorting (SLACS) technology coupled to next generation sequencing and mass spectrometry that analyzes genetic molecules from regions of interest within spatial context. Specifically, we demonstrate application of SLACS in various cancers such as breast cancer, glioblastoma, glioma, meningioma, multiple myeloma, and leukemia. Examples of discovering cancer biomarker and their mechanism of action within spatial context are also provided. Specifically, we describe Select-seq which isolates the regions of interest as small as single cells from the immunofluorescence stained tissue and obtains the full-length transcriptome data. We demonstrated Select-seq on tumor tissue section from triple negative breast cancer patient who have received neoadjuvant chemotherapy. Select-seq produced full-length spatial transcriptome data, with which we analyzed the transcriptomic and epitranscriptomic features including alternative splicing variant, complementarity-determining region analysis of B cells, and even adenosine-to-inosine base editing. We were also able to analyze the immune- and stem-cell-like microniches, in which the complex mechanisms behind ferroptosis inhibition might suggest therapeutic options for the TNBC patients. Bridging spatial technologies to omics technologies, the discovery of specific markers within spatial context will provide insights into the next generation diagnostics and cancer therapeutics such as cancer vaccines.

#6782

Spatial transcriptomics of serous tubal intraepithelial carcinoma and its putative precursor lesions

Rahul Krishnan[1], Lisa Schweizer[2], Agnes Bilecz[1], Aasa Shimizu[1], Rachelle Mendoza[3], Diane Yamada[1], Ricardo Lastra[3], Matthias Mann[2], Ernst

Lengyel[1]. [1]*Gynecologic Oncology, Obstetrics & Gynecology, The University of Chicago, Chicago, IL,*[2]*Max Planck Institute of Biochemistry, Munich, Germany,*[3]*Pathology, The University of Chicago, Chicago, IL*

Background: Increasing evidence over the past two decades has implicated serous tubal intraepithelial carcinoma (STIC) of the fallopian tube (FT) epithelium as the putative precursor lesion for high-grade serous ovarian cancer (HGSC). Additional atypical lesions of the FT known as p53 signature lesions and serous tubal intraepithelial lesions (STIL) have been proposed as early precursors in the carcinogenic sequence based on morphology, histochemical and genetic studies. Little however is known about the molecular events that drive FT epithelial cells to transform into HGSC.Methods: To elucidate the molecular changes that underlie the progression from p53 signature to STIL to STIC, we performed spatial transcriptomics on formalin-fixed paraffin embedded (FFPE) tissue sections using the Nanostring GeoMx Whole Transcriptome Atlas panel (18,000 protein-encoding gene panel). Our study cohort consisted of 16 representative cases (3 p53 signature cases, 3 STIL cases, 3 STIC lesions, and 7 STIC cases with matched HGSC).Results: We characterized gene expression to a depth of over 9400 genes in these rare precursor cell populations. Our analysis demonstrated that by gene expression profiles, p53 signatures and STIL lesions bear close resemblance to normal FT secretory cells compared to FT ciliated cells or even STIC and invasive HGSC. We identify for the first time, several pathways altered in expression between normal fallopian tube epithelium and early p53 signature lesions including those related to signaling pathways (Trop-2), Wnt pathway (LGR5), identifying new pathways observed in the progression from normal FT cells to precursor intraepithelial lesion. Our data show that STIC lesions bear significant similarities to invasive HGSC by gene expression, especially compared to the earlier precursor lesions (p53 signature and STIL). We observed several alterations in cell-adhesion(EGR1) and signaling pathways, transcription factors (Trop-2) and metabolism that mark the transition from STIC to HGSC, representing possible mechanisms by which these intraepithelial lesions transform into disseminated invasive disease. Conclusion: Our data profile HGSC precursor lesions in high-depth with characterization of over 9400 genes providing new insight into the molecular alterations that characterize these intraepithelial lesions. Our

future direction is to pair transcriptomics data with our established spatial proteomics platform (Deep Visual Proteomics) to measure matched spatial protein expression in our cohort.

Vaccines

#6785

Dendritic cell/myeloma fusion vaccine with lenalidomide maintenance following autologous hematopoietic cell transplant induced T cell activation and expansion

Giulia Cheloni[1], Dimitra Karagkouni[2], Daniela Torres[1], David J. Chung[3], Nina Shah[4], Natalie S. Callander[5], Thinle Chodon[6], Yvonne Efebera[7], Nancy Geller[8], Peiman Hematti[9], Hillard Lazarus[10], Ehsan Malek[11], Philip L. McCarthy[12], Ajay K. Nooka[13], Jacalyn Rosenblatt[1], Aaron P. Rapoport[14], Robert J. Soiffer[15], Dina Stroopinsky[1], Edmund K. Waller[13], Marcelo C. Pasquini[16], Ioannis Vlachos[2], David Avigan[1].

[1]Hematology/Oncology, Beth Israel Deaconess Medical Center, Harvard Medical School, Boston, MA,[2]Pathology, Beth Israel Deaconess Medical Center, Harvard Medical School, Boston, MA,[3]Medicine, Memorial Sloan Kettering Cancer Center, New York, NY,[4]University of California, San Francisco, CA,[5]University of Wisconsin, Madison, WI,[6]Roswell Park, Buffalo, NY,[7]Internal Medicine, The Ohio State University Comprehensive Cancer Center, Columbus, OH,[8]National Institutes of Health, Bethesda, MD,[9]Hematology/Oncology, University of Wisconsin School of Medicine & Public Health, Madison, WI,[10]Adult Hematologic Malignancies & Stem Cell Transplant Section, University Hospitals Cleveland Medical Center, Shaker Heights, OH,[11]Adult Hematologic Malignancies & Stem Cell Transplant Section, Seidman Cancer Center, University Hospitals Cleveland Medical Center, Cleveland, OH,[12]Medicine, Roswell Park Cancer Institute, Buffalo, NY,[13]Winship Cancer Institute, Emory University, Atlanta, GA,[14]Hematology/Oncology, University of Maryland Greenebaum Comprehensive Cancer Center, Baltimore, MD,[15]Dana-Farber Cancer Institute, Harvard Medical School, Boston, MA,[16]Medical College of Wisconsin, Milwaukee, WI

Introduction: Multiple myeloma (MM), a clonal disorder of terminally differentiated plasma cells, is the second most common hematologic malignancy with ~57.9% 5-year survival rate. Current MM therapies are not curative and in most patients MM relapse. Aiming to restore antitumor immunity and counteract MM evolution, we have developed a personalized dendritic(DC)/MM cell fusion vaccine, whereby several tumor antigens are presented in the context of DC mediated co-stimulation. BMT CTN 1401 is a multicenter randomized phase II clinical trial (NCT02728102) evaluating the efficacy of the DC/MM vaccine combined with lenalidomide maintenance (Len) after autoHCT. 203 patients were enrolled from 18 centers. **Aim:** To evaluate the impact of the DC/MM vaccine on the establishment of anti-MM immune response we profiled the peripheral blood (PB) immune landscape at the single-cell level, with particular focus on the T cell compartment.
Method: We performed single-cell immunoprofiling (gene expression + V(D)J sequencing) on 40 patients (3xDC/MM vaccine/Len/GM-CSF: N=20; Len/GM-CSF: N=10; Len: N=10). 160 PB mononuclear cells (PBMC) samples were collected at enrollment, prior to Len, after 1 and 3 vaccines and were processed using the 10x Genomics single cell 5' assay. Here we present the analysis relative to 52 PBMC samples from 13 vaccinated patients included in the initial study cohort. The remaining 108 PBMC samples have already been subjected to single-cell immunoprofiling and the analysis is ongoing.
Results: 309,423 cells passed quality-check identifying 47 cell populations, corresponding to 20 major compartments. The T cell compartment (146,373 cells) was divided into 14 different cell populations including activated CD8, CD4, and NKT cells that exhibited a gradual increase during the course of the study. Relatively, TCR sequencing demonstrated a recovery of T cell clonal diversity and a progressive rise in the frequency of expanded clonotypes within the activated CD4 and cytotoxic T cell populations after vaccination. Consistently, we observed a progressively raised number of shared TCR clonotypes within the activated CD8 and CD4 T cell subsets. The identification of common epitope/paratope hotspots among the expanded clonotypes and the different patients revealed a higher proportion of shared TCR clonotype groups across patients after vaccination compared to the early post-transplant period, predominantly after 3 vaccinations.

Conclusions: Assessment of PBMC samples from 13 vaccinated patients provided a detailed picture of the PBMC landscape. The constant T cell expansion in patients following vaccination coupled with the shared paratope/epitope hotspots and TCR signatures among patients indicated the TCR cross-reactivity and suggested for the establishment of an anti-MM immune response.

#6786

NT-I7 as an adjuvant to DNA neoantigen vaccination enhances and prolongs neoantigen-specific anti-tumor immunity

Michael Y. Chen[1], Ina Chen[1], Suangson Supabphol[1], Alexandra A. Wolfarth[2], Sara F. Martinez[2], Byung Ha Lee[2], Lijin Li[1], Xiuli Zhang[1], Peter S. Goedgebuure[1], William E. Gillanders[1]. *[1]Surgery, Washington University School of Medicine in St. Louis, St. Louis, MO,[2]NeoImmuneTech, Inc., Rockville, MD*

Background: IL-7 is an essential cytokine in the development and maintenance of antigen-specific T cells. NT-I7 (efineptakin alfa; NeoImmuneTech, Inc, Rockville, MD), is a long acting IL-7 composed of recombinant human IL-7 (rhIL-7) fused to a hybrid Fc antibody platform that has significantly improved *in vivo* stability and half-life compared to rhIL-7. DNA cancer neoantigen vaccines are a promising personalized cancer immunotherapy capable of generating strong anti-tumor immunity, but limited by a short-lived neoantigen-specific T cell response. We hypothesize NT-I7 as an adjuvant to a DNA neoantigen vaccine will enhance the magnitude and duration of neoantigen-specific anti-tumor immunity.

Methods: C57BL/6 mice were vaccinated with DNA vaccine encoding neoantigens present in E0771 murine breast cancer model on days 0, 3, and 6. NT-I7 (5 mg/kg) was administered intravenously on day 4 or 13 during T cell expansion or contraction phase respectively. Primary T cell responses to neoantigens were assessed by IFN-γ ELISPOT. Tumor protection was evaluated by inoculating mice with 5×10^5 E0771 cells subcutaneously after receiving DNA vaccine with or without NT-I7. Duration of neoantigen-specific CD8 T cell immunity was determined by *in vivo* CFSE killing assay.

Results: NT-I7 administered during the T cell contraction phase following the DNA vaccine increases the magnitude of neoantigen-specific T cell responses on day 20 compared to DNA vaccine alone. DNA vaccination and NT-I7 alone prior to tumor inoculation confers partial protection against tumor growth compared to control while DNA + NT-I7 during contraction phase rejects 100% of tumors. Compared to DNA vaccine alone, DNA vaccine + NT-I7 during contraction phase induces greater neoantigen-specific killing on day 41 (34.6% vs. 11.97%, p=0.03).
Conclusion: NT-I7 as an adjuvant to a DNA neoantigen vaccine increases the magnitude and duration of neoantigen-specific anti-tumor immunity in a murine model. Clinical application of NT-I7 may help overcome immunologic shortcomings of current neoantigen vaccines.

#6787
Vaccinia virus harboring TRAIL (vTRAIL) for in vivo lung cancer therapy
So Young Yoo. *Pusan National University, Busan, Korea, Republic of*

While oncolytic virotherapy has shown promising results for uncured patients with cancer, its effects on lung cancer remain unclear. Lung cancer is mostly unlikely to respond to conventional anticancer drug, therefore, oncolytic virotherapy can be the best option. Herein, we evaluated the anti-cancer activity of the previously developed three oncolytic vaccinia viruses encoding TNF-related apoptosis-inducing ligand (TRAIL), angiopoietin 1 (Ang1) and both genes, especially on killing lung cancer (LC). In this study, we confirmed that our engineered vaccinia viruses showed overall higher anti-cancer activity on lung cancer cells, compared to WT. Vaccinia virus engineered with both Ang1 and TRAIL (vTRAN) showed the highest oncolytic activity and selectivity in vitro (WT < vTRAIL < vAng1 < vTRAN). However, In vivo LLC1 murine lung cancer syngeneic model showed highest attenuated tumor growth when vTRAIL was treated (WT < vAng1 < vTRAN < vTRAIL), which was in accordance with $CD8^{high}$ $PD1^{low}$ expression levels in the tissues. It concludes that engineered vaccinia virus harboring TRAIL (vTRAIL) is the promising therapeutic option for in vivo lung cancer therapy.

#6788

hNIS imaging data from a first-in-human trial of the oncolytic virus CF33-hNIS-antiPD-L1 in patients with triple negative breast cancer

Jamie Green Rand[1], Dave Yamauchi[1], Shyambabu Chaurasiya[1], Jianying Zhang[1], Raju Pillai[1], Colt Egelston[1], Jonathan Kessler[1], Badri Modi[1], Leslie Chong[2], Amanda Seiz[2], Giovanni Selvaggi[2], Nick Ede[2], Mireya Murga[1], Norma Martinez[1], Wichanee Borisuthirattana[1], Hans Meisen[1], Susan Yost[1], James Waisman[1], Daphne Stewart[1], Joanne Mortimer[1], Yuman Fong[1], Yuan Yuan[3]. *[1]City of Hope Comprehensive Cancer Center, Duarte, CA,[2]Imugene Limited, Sydney, Australia,[3]Cedars-Sinai Medical Center, Los Angeles, CA*

Background: CF33-hNIS-anti-PD-L1 is a novel chimeric orthopoxvirus shown to have anti-cancer activity in triple negative breast cancer (TNBC) xenografts. For clinical tracking of the oncolytic virus (OV), human sodium iodide symporter (hNIS) transgene was inserted into the virus. hNIS gene expression allows cells to take up iodine and be visible by non-invasive imaging techniques. Animal studies showed that tumor cells infected with CF33-hNIS-anti-PD-L1 express functional hNIS and are visible by single-photon emission computed tomography (SPECT) or positron emission tomography (PET). The current report describes imaging results from an ongoing first-in-human trial.

Methods: This is a phase I, single center, single arm clinical trial evaluating the safety and tolerability of CF33-hNIS-anti-PD-L1 intratumoral (IT) injections in patients with metastatic TNBC. Key eligibility criteria include patients with unresectable or metastatic TNBC; progressed on at least 2 prior chemotherapies; ECOG 0-2; RECIST 1.1 measurable disease; and at least one tumor amenable to repeated IT injections. Eligible patients receive CF33-hNIS-anti-PD-L1 IT at 1 of 8 assigned dose levels (from 1×10^5 PFU to 3×10^8 PFU) on Days 1 and 15 of each 28-day cycle for a total of 3 cycles of treatment. The primary objective is to evaluate the safety and tolerability of CF33-hNIS-anti-PD-L1. Secondary objectives are to determine optimal biological dose, recommended phase II dose, and response rates. Exploratory objectives include assessing feasibility of non-invasive hNIS imaging as a method of tracking viral infection and replication. SPECT whole body imaging was performed at Cycle 1 Day 8 (C1D8).

Results: From October 2021 to October 2022, 8 patients were enrolled in this ongoing study and received at least 1 dose of CF33-hNIS-anti-PD-L1 injection at one of the first 3 dose levels (1 x 10^5, 3 x 10^5, or 1 x 10^6 PFU). All 8 patients underwent SPECT imaging at C1D8 with 6/8 patients (75%) having uptake at the site of injection on the SPECT imaging study. Four of 4 patients (100%) with injection sites at metastatic subcutaneous nodules, intramuscular masses, or axillary lymph nodes and 2/4 patients (50%) with injection sites at matted dermal metastatic lesions had uptake on SPECT. Conclusion: SPECT imaging successfully showed enhancement at the injected lesions in 75% of patients treated with CF33-hNIS-anti-PD-L1, even at current low doses, suggesting local viral replication and hNIS expression. Further analysis will evaluate the correlation of SPECT imaging results with pathologic immune cell infiltrate, viral staining, and tumor response. This is the first known report of hNIS-based imaging to track oncolytic poxvirus replication in humans and gives promise that this technology may be used for noninvasive tracking of systemically administered OV and other therapies.

#6789

The oncolytic virus VET3-TGI both blocks TGF-beta signaling and activates type 2 IFN responses, resulting in potent therapeutic responses in multiple mouse models

Ravikumar Muthuswamy, Steve Thorne. *Immunology, Kalivir Immunotherapeutics LLC, Pittsburgh, PA*

Background: TGFB1 mediated immune resistance is one of the major mechanisms of immune suppression utilized across multiple tumor types. Immune resistance imparted by TGFB1 is mediated through its pleiotropic effects on vasculature, fibrogenesis and regulatory/effector immune cells within the tumor microenvironment. Blockade of TGFB1 (TGFBi) will likely improve response to immunotherapy. IL-12 is a cytokine that through IFNg induction, promotes type 1 inflammatory response, M1 macrophages and effector CD8 T cell response. Combining TGFB1 blockade with IL-12 may maximize therapeutic benefits through simultaneously reducing immunosuppression and enhancing anti-tumor immune response. Current studies have developed a vaccinia-based immunotherapy, combining enhanced systemic virus delivery to CXCR3 ligand rich tumors and locally

expressed IL-12 and TGFBi within the tumor microenvironment, for efficient control of multiple tumor models.
Methods: An oncolytic vaccinia virus expressing CXCR3, IL-12 and a TGFB1 antagonizing mini-monomer was constructed (VET3-TGI) and the expression and function of the transgenes were confirmed. Using *in vivo* mouse RENCA, EMT-6 and MC38 tumor models, the functionality and therapeutic efficacy of VET-TGI were tested with comparison to control virus. Post-mortem analysis was used to analyze the impact of VET3-TGI on immune/stromal/endothelial milieu of the tumors and to determine toxicity profile.
Results: VET3-TGI infected cells expressed CXCR3 and showed enhanced migration to CXCR3 ligands *in vitro* and improved systemic delivery to tumors expressing CXCR3 ligands *in vivo*, even in the face of pre-existing anti-viral immunity. IL-12 expression and TGFBi blockade of TGFB1 mediated suppression of CD8 T cell proliferation were confirmed *in vitro*. *In vivo* mouse studies using EMT6, RENCA and MC38 tumor models demonstrated potent therapeutic activity, including 100% CRs, even at doses several logs below equivalent clinical doses and in multiple models. Mechanism of activity studies suggested that the therapeutic efficacy of VET3-TGI is associated with considerable modification of the tumor microenvironment. In addition, preliminary toxicity studies demonstrated the safety of VET3-TGI in mouse models.
Conclusions: VET3-TGI demonstrated an ability to reduce immunosuppression and dramatically enhance antitumor immune response leading to safe and potent therapeutic activity in multiple mouse tumor models. This data led to the selection of VET3-TGI as our lead clinical candidate. A human version of the virus is currently undergoing clinical manufacture and toxicology testing.

#6790
The peptide vaccine revived in cancer immunotherpay: a novel peptide vaccine platform for effective cancer immunotherpay
Dongho Kim, SeungHwan Lee. *NA Vaccine Institute, Seoul, Korea, Republic of*

The production of tumor-specific T cells is essential for cancer immunotherapy. Due to the low cost and ease of CMC, peptide vaccines

have been suggested as effective immunotherapy for cancer. A variety of peptide vaccines have been designed and tested in clinical trials for decades. However, most clinical trials of peptide vaccines have failed for several reasons. Poor stability of peptides, use of inappropriate adjuvants, lack of co-delivery of peptides and adjuvants, and immunosuppression by the tumor microenvironment. We tried to solve the problems that lead to failure and developed effective platform technologies for them. The first problem was the choice of vaccine adjuvants. Poly IC and its derivatives are known to induce antigen-specific Th1 and CTL responses. Since Th1-type immunity is essential for the elimination of intracellular pathogens or tumors, they may be suitable as the adjuvant for peptide vaccines. Despite several limitations of poly IC and its derivatives, such as high heterogeneity, inconsistent activity, poor stability, and unpredictable in vivo kinetics, they still serve as major adjuvants in numerous clinical trials. A novel and defined TLR3 agonist called NexaVant (NVT) was developed as an alternative to them. NVT induces a stronger anti-cancer efficacy compared to the known TLR agonists through multiple advantages of homogeneity, stability, and quantitative in vivo kinetics. Second, the stability of peptides was dramatically improved by a peptide/adjuvant complex formation. When a cationic peptide domain is introduced into the epitope together with an epitope processing domain, the peptide and adjuvant can form a nanocomplex by a simple charge interaction. And this complex improves the stability of the peptide which leads to improvement of the T cell immunity. Third, suppression of T cell immunity in cancer was mitigated by Treg modulation in the presence of a known chemotherapeutic drug. When this combination therapy of the vaccine and chemical was applied to various animal models, a strong anticancer effect was obtained by increasing T cell immunity and suppressing Treg. The same therapeutic effect was shown in several terminal stage tumor models with strong T cell memory regardless of whether the epitope was self or foreign originated.

#6791

Inovative *in vivo* (i*n ovo*) CAM model to predict efficacy and mode of action of a new antitumor vaccine stc-1010 on human colorectal adenocarcinoma

Yan Wang[1], Arnaud Peyronnier[1], Benoit Pinteur[2], Lionel Chalus[2], Corinne Tortorelli[2], Paul Bravetti[2], Jean Viallet[1], François Ghiringhelli[3], Philippe

Fornies[1]. *[1]Inovotion, La Tronche, France,[2]Brenus Pharma, Issoire, France,[3]Team Inserm 1231 TIRECs « Therapies and Immune REsponse in CancerS », Inserm, Dijon, France*

BACKGROUND: Colorectal cancer (CRC) is the second-most deadly cancer. Therapeutic resistance to immuno-oncology drives the need for new treatments. Stimulated tumor cell (STC) vaccine (Brenus Pharma) is composed of selected tumor cell lines, stimulated to overexpress tumor-associated or tumor-specific antigens and neoantigens including resistance factors. Haptenization of these proteins forms an immunogenic complex which stimulate the immune system to recognize and target the patient's tumor cells expressing same resistance factors. We report *in vivo* results of STC-1010 vaccine, on human CRC adenocarcinoma from HT29 cell using chorioallantoic membrane (CAM) assay developed by Inovotion in immune reactive model.
METHODS: This study was carried out in 2 steps: Firstly, three batches of naïve chicken embryos were stimulated by injections of STC1010 at Embryo Development Day (EDD) 11 and EDD13. At EDD18 of each batch, chicken peripheral blood mononuclear cells (PBMCs) were collected and used as anti-tumor reagent to treat respectively, at EDD 11, EDD 13 and EDD16 chicken embryos xenografted with HT29 cells. Activation of PBMCs was evaluated by IL2 and IL12 secretion quantified by ELISA. At EDD18, i.e., 9 days post-graft, *in ovo* anti-tumor efficacy was evaluated by tumor weight, metastatic invasion (qPCR analysis of human Alu sequence in lower CAM) and quantification of tumor-infiltrating by CD8, CD4, IFN-gamma, Perforin and TNF-alpha.
RESULTS: Compared to negative control, STC-1010 vaccine induced: 1) significant increase of IL-12 and IL-2 secretion in peripheric blood during the generation of all three batches of PBMCs, confirming previous results (IL-12: +52%, p=0.0003 ; IL-2: +482%, p=0.0033); 2) a significant expression of IFN-gamma in tumor (+130,83%, p=0.0185); 3) a tendency to increase infiltrating cells: CD4+: +79,2%, CD8+: +29,4% , Perforin: +105,5%, TNFα : +78,63% confirmed by immunohistochemistry and translated into 4) a significant increase of tumor necrosis (p = 0.0267); and 5) a tendency of metastasis regression (-49%); with 6) no embryonic toxicity/mortality (daily evaluation of embryonic viability) induced by STC-1010.

CONCLUSION: This *in ovo* study confirms efficacy of the STC-1010 observed in previous CRC syngeneic models and gives more insight about STC mechanism of action with the activation and maturation of dendritic cells, induction of CD8+ and LTh1 against tumor as the main driver of the response, all without toxicity. Inovotion's CAM model could be used for indication screening and as a pre-proof-of-concept before syngeneic model study.

#6792

Targeting immunosuppressive adenosine to enhance vaccinia virus renal cancer oncolysis *in vivo*

Valery A. Chavez[1], Floritza Bustamante[1], Carolina Merchan-Mendes[2], Shannon Saigh[3], Patricia Guevara[3], Eric Wieder[4], Jaime Merchan[5].
[1]Hematology, Univ. of Miami Sylvester Comprehensive Cancer Ctr., Miami, FL,[2]Miami Dade Colege, Miami, FL,[3]Flow Cytometry Facility, Univ. of Miami Sylvester Comprehensive Cancer Ctr., Miami, FL,[4]Cellular Therapy, Univ. of Miami Sylvester Comprehensive Cancer Ctr., Miami, FL,[5]Medical Oncology, Univ. of Miami Sylvester Comprehensive Cancer Ctr., Miami, FL

Background: The oncolytic vaccinia virus (VV) is a promising biotherapy undergoing clinical development in human cancer, including renal cell carcinoma (RCC). While VV induces potent tumor oncolysis and immunomodulation, clinical experience has shown that OV therapy alone leads to limited benefit. Moreover, OVs and checkpoint inhibitor combinations, do not significantly improve clinical responses, underscoring the need to identify new tumor microenvironment targets to overcome OV resistance in vivo. The adenosine pathway is a biologically and clinically relevant target in RCC and is associated with adaptive resistance to immunotherapy. The objectives of this study are to characterize the role of the adenosine axis in tumor escape mechanisms to vaccinia virus in RCC, and to determine the efficacy of novel OV-immunotherapy combinations targeting adenosine.
Methods: The in vitro oncolytic effects of JX-594 and mJX-594 (oncolytic VVs expressing human or murine GMCSF, respectively) in human (786-0, ACHN, CAKi-1, UOK262) and murine (RENCA) renal cancer cell lines were assessed. Proteomic analysis of 786-0 lysates treated with JX-594 was performed for mechanistic studies. The effects of JX-594 and mJX 594 on

CD73 and CD39 expression were determined in human and murine RCC. In vivo antitumor effects of mJX-594 alone, and in combination with A2AR, A2BR and Dual Adenosine receptor inhibition was determined in the RENCA model in immunocompetent mice.
Results: Potent in vitro oncolysis and efficient viral replication were observed in human and murine RCC cells after infection with vaccinia virus. VV oncolysis was associated with significant modulation of proliferation, survival, and ER stress pathways, as determined by functional proteomics. JX-594 and mJX-594 treatment induced increased expression of CD39 and CD73 in RCC cell lines and in renal tumors in vivo. While no significant enhancement of vaccinia oncolysis was observed with combinations with A2AR and A2BR inhibitors *in vitro*, a significant improvement on *in vivo* tumor control and survival were observed when mJX594 given intravenously was combined with A2AR and A2BR inhibitors (triplet), at a higher degree than single agents or doublets (mJX-594 in combination with single A2AR or A2BR inhibitors). Characterization of treatment mediated changes in immune signatures (nanostring) is underway and will be presented at the meeting.
Conclusion: Vaccinia virus potently induces in vitro oncolysis in RCC cell lines, while also increasing expression of adenosine rate limiting enzymes in vitro and in vivo, which could explain tumor escape to oncolytic VV. MJX-594 combination with A2AR and A2BR inhibition safely and significantly improves renal cancer oncolysis and tumor control in vivo. Our studies uncover a novel, translationally relevant strategy to improve OV efficacy in vivo, in RCC and other cancers.

#6793

***In vivo* effects and molecular mechanisms of Minnelide mediated enhancement of measles virus oncolysis in human colorectal cancer**

Valery A. Chavez[1], Floritza Bustamante[1], Carolina Merchan-Mendes[2], Ashok Saluja[3], Jaime Merchan[4]. *[1]Hematology, Univ. of Miami Sylvester Comprehensive Cancer Ctr., Miami, FL,[2]Miami Dade College, Miami, FL,[3]Department of Biochemistry & Molecular Biology, Univ. of Miami Sylvester Comprehensive Cancer Ctr., Miami, FL,[4]Medical Oncology, Univ. of Miami Sylvester Comprehensive Cancer Ctr., Miami, FL*

Background: The development of novel biotherapies for metastatic colorectal cancer (CRC), a fatal disease when advanced, is an urgent medical need. Oncolytic viruses (OVs) are novel cancer biotherapies, and the oncolytic measles virus (MV) has demonstrated safety and antitumor activity in early clinical studies. Triptolide (TRP), a diterpenoid epoxide extracted from the thunder god vine, and Minnelide (MN), its water-soluble compound, are novel agents associated with potent antitumor, anti-proliferative, pro-apoptotic, antiangiogenic, and ER stress inducing effects. The objectives of this study are to characterize the in vitro and in vivo effects and molecular mechanisms of measles virotherapy in combination with TRP and MN in CRC.
Methods: The in vitro effects of TRP, MV-GFP (Edmonston strain of Measles virus expressing eGFP), MV-CD46-muPA (dual targeted MV against the murine uPA receptor and human CD46), or virus-triptolide combinations on tumor cell cytotoxicity were assessed on HT-29, HCT116 and SW620 CRC cells. Molecular and mechanistic characterization of TRP's effects alone and combination with MV in HT29 cells was analyzed by the Reverse Phase Protein Array (RPPA) and validated by western blot analysis. In vivo effects (tumor progression and survival) of MN alone and in combination with MV vectors using different treatment schemes were assessed in HT-29 tumor bearing NSG mice, and tumor correlative studies were performed.
Results: MV and TRP had single agent antitumor activity against human CRC cell lines. MV-TRP combinations were associated with increased in vitro cytotoxicity compared to single agent treatments. Functional proteomics analysis showed that TRP-MV combinations were associated with inhibition of survival and proliferation pathways, such as AKT, ERK, inhibition of HSP70 as well as induction of autophagy, at a higher level than each agent alone. In vivo, both a 7-days MN treatment and a 21-days MN treatment significantly improved long term tumor control and significantly improved survival, compared to each agent alone. Tumor studies showed that MN increased MV tumor deposition, as well as enhancement in apoptosis and inhibition of proliferation. Molecular characterization of oncogenic pathways modulated by MV-Minnelide combinations (Nanostring) are underway and will be presented at the meeting.

Conclusions: Our results demonstrated that, in human CRC xenografts, Minnelide safely and significantly enhances measles virus oncolysis in vivo, leading to improved antitumor effects and prolonged survival. These effects were associated with enhanced antiproliferative and pro-apoptotic effects with the MV-Minnelide combination, suggesting in vivo synergy. Studies characterizing the molecular mechanisms of in vivo synergy and assessing this promising combination in immunocompetent CRC models are underway.

#6794

SETD2 loss in renal cell carcinoma generates peptides from aberrantly translated retained introns

Marya T. Kozinova[1], Alexander Metz[1], Robert Uzzo[2], Janusz Franco-Barraza[1], Michael Slifker[1], Jessica Peskin[2], Angel Fernández Sanromán[3], Samra Turajlic[3], Edna Cukierman[1], Phillip Phillip Abbosh[1]. *[1]Fox Chase Cancer Center, Philadelphia, PA,[2]Penn State University, Philadelphia, PA,[3]Francis Crick Institute, London, United Kingdom*

Introduction: SETD2, a histone H3-K36 trimethyltransferase, is necessary for regulation of proper intron splicing. SETD2 is frequently inactivated in kidney cancer. We hypothesized that SETD2 deficiency would cause aberrant translation of retained introns (ATaRI) that could serve as potential immunotherapeutic targets in *SETD2*-mutant states.

Methods and Results: We detected increased presence of retained introns in *SETD2*-mutant vs WT tumors in two publicly available renal cell carcinoma RNA-seq data sets. We hypothesized that if intronic sequences translated into proteins, accumulation of misfolded proteins would activate the Unfolded Protein Response (UPR). The UPR pathway was strongly transcriptionally enriched as measured by GSEA, as were several immunotherapy-relevant pathways, suggesting that tumors are inflamed, possibly related to the antigenic nature of translated introns. To investigate this further, we generated Setd2-isogenic mouse renal cancer cells using CRISPR in the RENCA cell line. RNAseq followed by GSEA confirmed upregulation of UPR pathway transcriptional signature in the Setd2-null condition, supporting our observation in human tumors. Indicators of UPR activation such as cleavage of ATF6 and increase in ATF4 and Xbp1 levels in Setd2 deficient vs. unedited RENCA cells, as well as nuclear

translocation of ATF6 in *SETD2*-mutant human kidney cancer samples validates these findings. We then measured the presence of ATaRI-derived peptides in *Setd2*-mutant RENCA cells using mass spectrometry, detecting 47 such peptides. Using publicly available proteomics data from one human data set, we preliminarily identified peptides translated from 151 introns that are retained in *SETD*2-mutant cases. Applying netMHCpan to both the human and murine data, we found that detectable ATaRI peptides were predicted to generate multiple 10-amino acid-long peptides which strongly bind to the 8 murine MHC or to the 20 most common human HLA receptors. We propose that these presentable peptides might activate an immune response to SETD2-mutant renal cell carcinoma.
Conclusions: We identified intron retention which may cause activation of the UPR as a feature of *SETD2*-mutant kidney cancer. ATaRI peptides are detectable and should be presented to the adaptive immune system. These features may represent a new therapeutic vulnerability for exploitation as a rationale for personalized medicine.

#6796

PoxSTG, a novel chimeric poxvirus with improved oncolytic potency

Philippe Erbs, Annie Findeli, Johann Foloppe, Juliette Kempf, Isabelle Farine, Baptiste Moreau, Julie Hortelano, Christelle Pichon, Jules Deforges, Eric Quemeneur. *Transgene S.A., Illkirch Graffenstaden, France*

Oncolytic virus (OV) therapy has emerged as a promising approach for cancer treatment with the potential to be less toxic and more efficient than classic cancer therapies. Various types of OVs in clinical development, including Vaccinia virus (VACV)-derived OVs, have shown good safety profiles, but limited therapeutic efficacy as monotherapy in some cancer models. Many different methods have been employed to improve the oncolytic potency of OVs. We used a directed evolution process, pooling multiple species of orthopoxviruses to generate chimeric poxviruses with increased oncolytic properties. Through selective pressure by successive passages on human tumor cells, a new chimeric oncolytic poxvirus, named PoxSTG, was derived. The chimeric viral genome contains, in addition to sequences from several strains of Vaccinia virus, sequences of Rabbitpox virus and Cowpox virus. Compared with its parental viruses, PoxSTG has demonstrated superior oncolytic characteristics, and was notably attenuated

in normal primary cells. PoxSTG has superior secretion of extracellular-enveloped virus (EEV) compared to all parental strains inducing higher dissemination of the virus into the tumors and more resistance to neutralization. PoxSTG was saved and showed potent antitumor effects in several syngeneic and xenograft mouse models of cancers. Furthermore, PoxSTG exerted low-dose antitumor effects in virus-injected and non-virus-injected distant tumors in a CRC xenograft model, demonstrating strong virus spread to distant tumors. All these data demonstrate the potential of PoxSTG as a novel therapeutic agent for cancer treatment.

#6797

Oncolytic virotherapy with non-human viruses to improve anti-myeloma effect

Valentina Marchica[1], Rosanna Vescovini[1], Valentina Franceschi[2], Paola Storti[1], Nicolas Thomas Iannozzi[1], Vincenzo Raimondi[1], Oxana Longu[1], Jessica Burroughs Garcia[3], Denise Toscani[1], Anna Benedetta Dalla Palma[3], Gaetano Donofrio[2], Nicola Giuliani[1]. *[1]Department of Medicine and Surgery, University of Parma, Parma, Italy,[2]Department of Medical-Veterinary Science, University of Parma, Parma, Italy,[3]Department of Hematology, Azienda Ospedaliero-Universitaria di Parma, Parma, Italy*

Multiple myeloma (MM) is an incurable hematological malignancy characterized by remission and relapse with drugs resistance. Therefore, new therapeutic approaches are needed. Oncolytic viruses (OVs) represent a new strategy to augment the spectrum of cancer therapeutics. Several studies reported that, in MM, the OVs act through tumor-specific oncolysis and generation of an antitumor immune response. The main viruses that have been tested for MM setting are human viruses, this approach is highly restricted by pre-existing anti-virus humoral immunity that neutralize the anti-tumor effect of OVs. Recently, our group have demonstrated for the first time the role of a bovine virus, non-pathogen for the human, Bovine Viral Diarrhea Virus (BVDV) in direct MM cell killing suggesting its possible use as alternative strategy in MM oncolytic virotherapy. The aim of this study was to increase the bovine oncolytic viruses's spectrum for anti-MM treatment investigating the role of another bovine virus, Bovine Herpes Virus type 1 (BoHV-1), in the direct effect on MM cells. Firstly, after virus preparation, we treated human MM cell lines (HMCLs) for 24,

48 and 72 hours with BoHV-1 at 1 and 2 multiplicity of infection (MOI). We showed a significant increase of cell mortality, checked by flow cytometry analysis, already after 48 hours of infection in JJN3 (BoHV-1 1 MOI *vs* untreated $p< 0.001$; BoHV-1 2 MOI *vs* untreated $p< 0.001$) and in MM1.S (BoHV-1 1 MOI *vs* untreated $p= 0.025$; BoHV-1 2 MOI *vs* untreated $p= 0.002$). Interestingly, the cytotoxic effect of BoHV-1 treatment in HMCLs was associated by a significant increased expression of apoptotic markers as Apo2.7, evaluated by flow cytometry (JJN3 at 48 hours: BoHV-1 1 MOI *vs* untreated $p= 0.007$; BoHV-1 2 MOI *vs* untreated $p= 0.001$. MM1.S at 48 hours: BoHV-1 1 MOI *vs* untreated $p< 0.001$; BoHV-1 2 MOI *vs* untreated $p< 0.001$). Subsequently, we infected bone marrow mononuclear cells (BMMNCs) obtained from MM patients with BohV-1 for 48 and 72 hours. Already after 48 hours of infection, we found that MM cells had significantly increased cell mortality in BoHV-1-treated BMMNCs compared with untreated conditions. Overall, our data indicate that BoHV-1, as BVDV, was able to exert a direct anti-tumor effect on both HMCLs and primary cells from MM patients. In addition, data from ongoing studies will characterize the role of immune microenvironment in bovine oncolytic virotherapy. Focusing on monocytes, NK cells and CD8+ T cells we will explore a possible bovine virus-induced immune response to enhance anti-MM virotherapy. This study will highlight the possible use of non-human OVs as new anti-MM strategy.

#6798

CD8α+ dendritic cells potentiate the antitumor and immune activities against murine ovarian cancers

Shin-Wha Lee[1], Dasol Oh[1], Hyunah Lee[2], Kyung-Won Lee[3], Min-Je Kim[3], Sung Wan Kang[3], Young-Jae Lee[1], HyunSoo Kim[2], Yong-Man Kim[1].
[1]Obstetrics and Gynecology, Asan Medical Center, University of Ulsan College of Medicine, Seoul, Korea, Republic of,[2]Pharmicell Co. Inc., Seongnam, Korea, Republic of,[3]Asan Institute for Life Sciences, Seoul, Korea, Republic of

Objectives: Dendritic cell (DC) based immunotherapies have been shown to be a potential treatment option for various cancers; however, the exact strategies in ovarian cancer remain unknown. This study aimed to evaluate the effectiveness of mouse CD8α+ dendritic cells (DCs), corresponding to

human CD141+ DCs, derived from bone marrow (BM) hematopoietic stem cells (HSCs) in a syngeneic and orthotopic mouse ovarian cancer model.
Methods: Stem-DCs from HSCs and Mono-DCs from monocytes were generated from the bone marrow mononuclear cells (BM-MNCs) of C57BL/6 mice in condition of pulsing with ID8 tumor cell lysates. C57BL/6 mice were intraperitoneally injected with 5×10^6 ID8 cells. They were treated with vehicle, low/medium/high dose pulsed Stem-DCs, Mono-DCs, and unpulsed Stem-DCs. At 8 to 9 weeks, the treated mice were sacrificed, and tumor responses and immune responses, such as lymphocyte proliferation and cytokine secretion, were analyzed.
Results: Mono-DCs and Stem-DCs were characterized by CD11c+CD80+CD86+ and CD8α+Clec9a+ expression, respectively. They were confirmed by the secretion of immunostimulatory cytokines, such as interleukin (IL)-12 and interferon (IFN)-γ, and T cell proliferation was observed after maturation. Despite a lower dose compared with Mono-DCs, mice treated with pulsed Stem-DCs showed a reduced amount of ascitic fluid and lower body weights compared with those of vehicle treated mice ($P = 0.0021$ and $P = 0.0092$, respectively). These mice treated with pulsed Stem-DCs appeared to have fewer tumor implants which were usually confined in the epithelium of ovaries, diaphragm and peritoneum. All mice injected with DCs demonstrated longer survival than the vehicle group ($P = 0.0187$), especially the medium/high dose pulsed Stem-DC treatment groups. Moreover, these favorable tumor responses were associated with a low proportion of myeloid-derived suppressor cells (MDSCs) and regulatory T cells, high IL-12 and IFN-γ levels, and accumulation of several tumor-infiltrating lymphocytes.
Conclusions: We demonstrated that mouse CD8α+ DCs derived from BM HSCs could decrease tumor progression and enhance antitumor immune responses against murine ovarian cancer. Further studies are necessary to develop potent DC vaccines using human CD141+ DCs.

#6799

A porous silicon particle based particulate anti-cancer vaccine for immunotherapy

Junhua Mai, Yongbin Liu, Dongfang Yu, Haifa Shen. *Houston Methodist Research Institute, Houston, TX*

Background: Anti-cancer vaccine is a widely-studied strategy that activates innate and adaptive host immunity via its adjuvant components and tumor antigens against cancer. Unfortunately, its response rate in clinical trials was not promising. On the vaccine part, sufficient stimulation of strong and long-lasting local and systemic immunity and efficient promotion of intratumoral infiltration of cytotoxic T lymphocytes are among the critical issues determining the therapeutic efficacy of cancer vaccines in addition to the innate features of tumor. Our project aims to develop a porous silicon particle based particulate vaccine against cancer, and investigate the therapeutic mechanism and combinational effects with current first-line strategies.
Method: We first screened the combinations of ligands of Toll-like receptors (TLRs) expressing on antigen presenting cells (APCs) and selected the most powerful combo for immune stimulation. We then loaded the identified adjuvants in addition to antigen peptides to produce vaccine particles. Stimulation and licensing of APCs were tested in vitro, and its therapeutic efficacies were evaluated on multiple orthotopic and systemic metastasis cancer murine models of breast and colon cancers. Furthermore, we investigated the vaccine's synergistic effects and impacts on tumor microenviroment (TME) with an immunogenic chemotherapeutic oxaliplatin on a CT26 colon cancer model.
Result: According to the adjuvant screening assays, we identified a capable combination of CpG1826 (CpG) and 2'3'-cGAMP (cGAMP), which extensively stimulated the activation, maturation and type-I interferon secretion of APCs. A μGCVax formulation composed by these two adjuvants and antigen peptides was then applied on primary and metastatic HER2+ breast cancer TUBO bearing mice. μGCVax potently promoted the activation and lymph node migration of $CD8^+$ and $CD103^+$ dendritic cells in vivo. Distal metastatic tumor nodules in all different tissues vanished after two vaccinations. Functional cure of cancer and extension of animal survival were achieved. Moreover, oxaliplatin treatment on colon cancer caused immunogenic cell death and generated an immune favorable TME in a subcutaneous CT26 colon cancer model. The combination of μGCVax with the oxaliplatin effectively blocked the progression of large tumor mass. We finally revealed that the reprogramming of TME and the promotion of efficacy were mostly achieved from diminishing myeloid-derived suppressor cells (MDSCs) in tumor.

Conclusion: μGCVax is an effective and board-spectrum formulation for cancer immunotherapy. It effectively induces APC activation and licensing, and stimulates the innate and adaptive immunity against multiple cancers. The combination with oxaliplatin further promotes the therapeutic efficacy of μGCVax by decreasing tumor MDSCs.

#6800

Unique autologous cancer vaccine comprised of irradiated whole tumor cells and MBTA (rWTC-MBTA) triggers antitumor immune response to prevent metastasis

Juan Ye[1], Herui Wang[1], Mitchell Sun[1], Ondrej Uher[1], Mark R. Gilbert[1], Karel Pacak[1], Zhengping Zhuang[1], Rogelio Medina[2], Samik Chakraborty[3], Jan Zenka[4]. *[1]National Institutes of Health (NIH), Bethesda, MD,[2]Northwestern Memorial Hospital, Chicago, IL,[3]NE1 Inc, New York, NY,[4]University of South Bohemia, České Budějovice, Czech Republic*

Despite the advances made in cancer treatment over the past decades, one statistic has remained unchanged: metastatic cancer accounts for 90 percent of annual cancer deaths in the United States. Our group previously demonstrated that an autologous whole tumor cell vaccine (rWTC-MBTA: irradiated autologous whole tumor cells pulsed with Mannan-BAM, TLR ligands, and anti-CD40 antibody) had a potent anti-tumor immune response and prolonged survival in a mouse colon carcinoma model. To investigate whether rWTC-MBTA would work in “cold” tumor models, we evaluated the vaccine’s effect on preventing and treating tumor metastasis in 4T1 breast tumors. Our data showed that vaccinated mice could significantly prevent lung metastasis in both intravenous injection and mammary pad subcutaneous implantation animal models. Further, we used another metastasis model that more closely mimics clinical practice by resecting the primary tumor after metastasis development. The data showed that vaccinated mice could prevent tumor recurrence, increase T-cell infiltration in the metastatic tumor, and prolong the survival curve. The mechanistic investigation by immunophenotyping revealed that rWTC-MBTA vaccination induced both effector memory ($CD44^+CD62L^-$) and center memory ($CD44^+CD62L^+$) T cells as well as increased overall $CD4^+$ and $CD8^+$ T-cell count while depletion experiments demonstrated that $CD8^+$ T

cells were required for vaccine efficacy. Isolated splenocytes co-cultured with 4T1 cells showed rWTC-MBTA significantly increased T-cell mediated cytotoxicity through TNF-a and IFN-γ in $CD107a^{+}CD4^{+}$ T cells and Granzyme B and IFN-γ in $CD107a^{+}CD8^{+}$ T cells. In all experiments, vaccination exerted negligible systemic toxicity. Collectively, our study demonstrates that the rWTC-MBTA vaccine is a safe and promising therapeutic option to prevent and treat tumor metastasis by triggering an antitumor immune response.

EXPERIMENTAL AND MOLECULAR THERAPEUTICS

Apoptosis and Growth Factor Receptors as Therapeutic Targets

#6121

UCP2 inhibitor eradicates cancer stem-like population in trastuzumab-resistant HER2-positive breast cancer

Minsu Park, Soeun Park, Juyeon Seo, Dongmi Ko, Seongjae Kim, Yong Koo Kang, Kee Dal Nam, So Ra Seuk, Tae-Min Cho, Eunsun Jung, Yoon-Jae Kim, Ji Young Kim, Jae Hong Seo. *Korea University Guro Hospital, Seoul, Korea, Republic of*

Purpose: Uncoupling protein 2 (UCP2) is a member of the mitochondrial anion carrier protein family that plays an important role in stabilizing the inner mitochondrial membrane potential (MMP, ΔΨm) and controlling reactive oxygen species (ROS) production. A selective UCP2 inhibitor, genipin is known to elicit cytotoxicity in several cancers, however, its effects on cancer stem cells (CSCs)-like properties and trastuzumab resistance in HER2-positive breast cancer cells have not been fully elucidated. In the present study, we sought to investigate the mechanism of action of genipin responsible for the induction of apoptosis and its effects on CSC-like features, expression of HER family member and trastuzumab resistance in HER2-positive breast cancer cells *in vitro* and *in vivo*.
Experimental Designs: The effects of genipin on trastuzuamb-sensitive [BT474 and SKBR3] and trastuzumab-resistant [JIMT-1 and MDA-MB-453] HER2-positive breast cancer cell lines *in vitro* were evaluated for cell viability, Sub-G1, ROS, MMP, ALDH1 activity, CD44+/CD24- subpopulation and mammosphere formation. To confirm the physiological

relevance of our *in vitro* observations, we explored the impact of genipin on tumor growth and angiogenesis and expression of p95HER2 and ALDH1A1 in trastuzumab-resistant xenograft model *in vivo*.
Results: HER2-positive breast cancer cells harbored a higher level of UCP2, when compared to their counterparts. Genipin significantly downregulated UCP2 and mitochondrial dysfunction coinciding with increased ROS generation and disruption of MMP. These phenomena were accompanied with upregulation of the Bax/Bcl-2 ratio and activation of caspase-3 and caspase-7. Genipin treatment led to significant reduction in levels of truncated p95HER2, p-HER2, p-HER3 and p-Akt levels in both trastuzumab-sensitive and -resistant lines. Marked decline of CD44 and ALDH1A1 expression by genipin treatment was associated with attenuation of mammosphere-forming ability. UCP2 level is predominantly upregulated in CSC-enriched populations, while its knockdown significantly suppressed CSC-like characteristics concomitant with decreased ALDH1A1 and CD44 expression as well as impairment of ALDH1 activity. Genipin administration significantly retarded tumor growth and angiogenesis in trastuzumab-resistant JIMT-1 xenograft tumors. The antitumor effect occurred concomitantly with a decrease in Ki-67 proliferating index and enhancement of apoptosis. Furthermore, individuals receiving genipin exhibited markedly lower levels of p95HER2, full-length p185HER2, CD44 and ALDH1A1 expression compared to their control counterparts.
Conclusion: To our knowledge, our findings are the first reported instance of genipin-induced suppression of CSC-like properties and HER2/HER3/Akt axis, implying that genipin treatment may have application in addressing trastuzumab resistance.

#6122
Targeting mutant p53 and KRAS for novel pancreatic cancer therapy by combination treatment of simvastatin and imipridones
Xiaobing Tian, Wafik S. Deiry. *Brown University, Providence, RI*

KRAS mutation is found in 95% pancreatic ductal adenocarcinoma (PDAC). TP53 is altered in 70% of patients with PDAC that co-occur with KRAS mutations. Enhanced de novo cholesterol biosynthesis is a hallmark of cancer cells. P53 inhibits the mevalonate pathway to mediate tumor repression. p53 mutations drive de novo cholesterol pathway activation and

are required for the proliferation of KRAS-mutant cancers. Inhibition of the mevalonate pathway leads to feedback activation of SREBP-2, which restores mevalonate pathway and leads to re-activation of KRAS and restoration of mutant p53 GOF. Imipridones induced ATF4 through the action of mitochondria protease ClpP. Simvastatin triggers ATF4 activation through inhibition of mevalonate pathway. We hypothesize that combined treatment with imipridones can overcome the resistance to simvastatin by two different mechanisms: (1) Imipridones inhibit oxidative phosphorylation through ClpP hyperactivation and result in AMPK activation. AMPK phosphorylates and inhibits SREBP-2 transcriptional function, which blocks the feedback activation of SREBP-2. (2) Enhanced ATF4 and CHOP induction through different pathways leads to cancer cell death. We also expect that the combined treatment through sustained induction of ATF4 and CHOP can sensitize cancer cells to imipridone treatment.

Mouse and human PDAC cell lines (KPCY, HPAF-II, and PANC-1) with p53 and KRAS mutations were used to test the effects of combination treatment of simvastatin and imipridones. The combined treatments synergistically inhibited the proliferation of p53 and KRAS co-mutant cell lines. For example, the synergy scores of simvastatin and ONC201 combination are 75 (KPCY), 15 (HPAF-II), and 14 (PANC-1). Enhanced cell death is consistent with sustained and enhanced induction of ATF4 and CHOP compared to single drug treatment alone. Imipridones activated AMPK in the tested PDAC cell lines. Imipridones potently inhibit AKT and ERK1/2 activation at 72-hour time point, which might also contribute to block above mentioned feedback activation of KRAS. We also observed that cell lines with a structural mutant of p53 are more sensitive to the combination treatments than a cell line with a DNA-contact mutant of p53, which is consistent with the fact that simvastatin treatment leads to degradation of structural p53 mutants. Surprisingly, our data indicated that simvastatin potently inhibits kinase WEE1 and leads to CDK1 dephosphorylation and activation, which has not been reported before. Together, our data is consistent with publications that p53 mutated cancer cell lines are sensitive to statin treatments. In short, combination treatment may overcome simvastatin resistance and/or imipridone resistance by modulating ATF4/CHOP and SREBP-2 activity.

#6123

Characterization of the synergistic tumor cytotoxicity of agonistic DR5 IgM antibody IGM-8444 with chemotherapeutic agents

Beatrice T. Wang, Thomas J. Matthew, Poonam Yakkundi, Miho Oyasu, Mélanie Desbois, Susan E. Calhoun, Ling Wang, Tasnim Kothambawala, Devinder K. Ubhi, Marvin S. Peterson, Eric W. Humke, Maya F. Kotturi, Bruce A. Keyt, Angus M. Sinclair. *IGM Biosciences, Inc., Mountain View, CA*

Death receptor 5 (DR5) is a tumor necrosis factor receptor (TNF) superfamily member that requires multimerization to activate the extrinsic apoptotic pathway and is broadly expressed on solid and hematologic cancers. IGM-8444 is a multivalent IgM DR5 agonist that efficiently multimerizes DR5 to induce tumor cell apoptosis while maintaining a favorable in vitro and in vivo safety profile. The universal mechanism of apoptotic cell death and the safety profile of IGM-8444 makes it an attractive combination partner with standard of care treatment regimens. Here we describe the characterization of single agent and combinatorial cytotoxicity with different classes of chemotherapeutic agents. IGM-8444 was first evaluated as a monotherapy across a panel of human solid tumor cell lines in vitro and xenograft tumor models in vivo. IGM-8444 responses ranged from highly sensitive to resistant. In a sensitive Colo205 model IGM-8444 additionally showed rapid intratumoral pharmacodynamic (PD) activity, inducing maximal caspase-3 cleavage at 6 hours post-dose. Next a panel of solid tumor (including colorectal, gastric, non-small cell lung cancer, and pancreatic) cell lines were selected to evaluate IGM-8444 in combination with standard of care chemotherapeutic agents. Synergistic cytotoxicity was observed when IGM-8444 was used in combination with certain classes of chemotherapeutic agents including topoisomerase inhibitors, microtubule inhibitors, nucleoside analogs, and platinum-based agents. Enhanced anti-tumor activity was also observed in xenograft mouse models where IGM-8444 was dosed in combination with these classes of chemotherapeutic compounds. Mechanistically, this synergistic combinatorial cytotoxicity may be explained by the reported increase in DR5 expression on tumor cells following treatment with many of these classes of chemotherapeutic agents. In summary, IGM-8444 shows in vitro cytotoxicity and in vivo PD and anti-tumor efficacy responses in preclinical

models, with enhanced activity in combination with several classes of chemotherapies reported to upregulate DR5 expression. IGM-8444 combination with FOLFIRI standard of care is currently under evaluation in a Phase 1 study in patients with metastatic colorectal cancer (NCT04553692).

#6124

Recombinant apurinic/apyrimidinic endonuclease-1/redox factor-1 plus acetylsalicylic acid combination therapy inhibits tumorigenesis in an orthotopic xenograft murine model of triple-negative breast cancer

Yu Ran Lee, Hee Kyoung Joo, Eun-Ok Lee, Sungmin Kim, Hao Jin, Yeon Hee Choi, Eun Ju Choi, Byeong Hwa Jeon. *College of Medicine, Chungnam National University, Daejeon, Korea, Republic of*

Triple-negative breast cancer (TNBC) is characterized with hormone receptor negative and frequently exhibits inherently aggressive clinical behavior, resulting in poor prognoses. TNBCs are highly heterogenic, leading to obstacles in identifying new therapeutic targets and performing targeted therapy. Apurinic/apyrimidinic endonuclease 1/redox factor-1 (APE1/Ref-1), a multifunctional protein, is mainly involved in DNA repair and redox regulation; it is upregulated in various cancers and is extracellularly secreted because of hyperacetylation. We previously reported that hyperacetylation induced APE1/Ref-1 release causes apoptosis in TNBCs. In the current study, we aimed to assess the therapeutic efficacy of combination treatment involving recombinant human APE1/Ref-1 (rhAPE1/Ref-1) plus acetylsalicylic acid (ASA) in TNBC xenograft mice. ASA co-treatment was used to induce and lasting acetylation of rhAPE1/Ref-1. For in vivo analysis, we constructed an orthotopic xenograft in vivo model of TNBC by using MDA-MB-231 cells. We performed combination therapy involving intravenous injection of purified rhAPE1/Ref-1 (1 mg/kg) and oral administration of ASA (20 mg/kg) thrice a week for 6 weeks in TNBC xenograft mice. This rhAPE1/Ref-1 plus ASA combination therapy inhibited tumor formation and growth, without damaging liver or kidney tissue, and decreased plasma levels of the cancer marker CEA and breast cancer-specific markers CA27-29 and CA15-3 in the TNBC xenograft mice. The TNBC group, which underwent combination therapy, had more apoptotic cells and greater inflammatory

cell infiltration in tumor tissues than the vehicle group did. Additionally, in tumor tissue of TNBC with combination therapy exhibits increased apoptosis following upregulation of Bax, cleaved-caspase-3, and cleaved-PARP. Thus, we found that rhAPE1/Ref-1 plus ASA combination therapy enhanced antitumor effects in TNBCs via inflammatory cell infiltration and apoptosis signaling pathways. Our findings indicate the therapeutic potential of rhAPE1/Ref-1 plus ASA combination therapy for TNBC.

#6125

Induction and modulation of apoptosis in pancreatic ductal carcinoma PANC-1 cells by Chinese medicinal herbs *Scutellaria barbata* and *Oldenlandia diffusa*

MinSeo Kang[1], Allana Benjamin[2], Christine Choi[2], Rekha Isaac[3], Sarah Wolf[2], Jasmine Cha[2], Elim Choi[2], Jessica Yi[2], Padma T. Uppala[4], Ryan Hayes[5], Brian Yuen Yau Wong[6]. *[1]Mathematics, Andrews University, Berrien Springs, MI,[2]Biology, Andrews University, Berrien Springs, MI,[3]Biochemistry, Andrews University, Berrien Springs, MI,[4]Public Health, Nutrition & Wellness, Andrews University, Berrien Springs, MI,[5]Chemistry, Andrews University, Berrien Springs, MI,[6]Andrews University, Berrien Springs, MI*

Pancreatic cancer is a devastating disease with a poor prognosis. It is usually symptom-free during development and is advanced by the time of diagnosis. PANC-1 is a pancreatic ductal carcinoma cell derived from a 56-year-old male with adenocarcinoma in the head of the pancreas and metastasized to the duodenal wall. Apoptosis is a controlled program cell death process that the body uses to combat cancer development. *Scutellaria barbata* (SB) has been used in traditional Chinese medicine for treating liver, lung, and rectal cancers. SB and *Oldenlanida diffusa* (OD) are included in most of the herbal cancer treatment formulas in Taiwan hospitals. We previously showed that aqueous extracts of SB and OD selectively induced apoptosis in colon HCT 116 cancer cells but not in colon CCD 841 CoN normal epithelial cells by modulating the pro-apoptotic and anti-apoptotic proteins. These two herbs also effectively modulated apoptosis in MDA-MB-157 and 93B breast cancer cells. Green synthesis of gold nanoparticles (AuNPs) of SB demonstrated effective

anticancer activity against this PANC-1 cell. This study used the green/red/blue fluorescent Apoptosis /Necrosis Detection Kit and the Human Apoptosis Antibody Array - Membrane [43 Targets] Test (Abcam). Our fluorescent apoptosis data showed that a 2-hour treatment with 1.5 mg and 3.0 mg aqueous extract of SB and OD induced a statistically significant percentage of apoptosis in PANC-1 cells (SB: 57.5 ± 2.5%, 68.0 ± 0.0% > 11.5% ± 3.5%, $p < 0.05$; OD: 62.0 ± 9.0%, 67.0 ± 11.0%> 11.5% ± 3.5%, $p < 0.05$) as compared to the negative control respectively. Similar results were obtained with the 4-hour incubation period (SB: 73.5 ± 0.5%, 72.0 ± 2.0% > 18.2% ± 2.0%, $p < 0.05$; OD: 59.0 ± 1.0%, 73.5 ± 13.5%> 18.2% ± 2.0%, $p < 0.05$). From the antibody array-membrane experiments, modulation of various apoptosis markers by SB and OD such as the pro-apoptotic proteins Bid, Bim, Bad, Bax, p27, and p53 as compared to the negative controls were observed; and regulation of anti-apoptotic proteins Bcl-2, FasL, IGF-I, and p21 were also revealed. These results suggest that SB and OD contain phytochemicals that induce apoptosis in pancreatic ductal carcinoma PANC-1 cells via the modulation of various apoptotic protein productions. Further study of their specific modulation effects of apoptosis is warranted to reveal their potential chemopreventive and therapeutic properties against pancreatic and other cancers.

#6126

Antitumor effect of Iso-mukaadial acetate in MCF-7 human cancer xenograft models

Portia Raphela-Choma[1], Lesetja R. Motadi[2], Mpho S. Choene[2]. *[1]University of Johannesburg, Johannesburg, South Africa,[2]Biochemistry, University of Johannesburg, Johannesburg, South Africa*

Antitumor drugs used today have shown significant efficacy and are derived from natural products such as plants. Iso-mukaadial acetate has previously been shown to possess anticancer properties by inducing apoptosis. The purpose of this study was to investigate the therapeutic effect of Iso-mukaadial acetate in the breast cancer xenograft mice model. Female athymic mice were used and were inoculated with breast cancer cells subcutaneously after culturing. Group one served as a negative control group (no treatments) and group two positive control group (cisplatin) which was administered intravenously. Iso-mukaadial acetate treatment was

administered orally to group three(100 mg/kg) and group four (500 mg/kg). Blood was collected (70 μL) from the tail vein on day zero, day seven and day 14. Tumor regression was measured, and a pharmacokinetic study was conducted. Estimation of Serum Parameters for Hepatic and Renal Indices were examined using an Automated Chemistry Analyzer. Histopathological analysis was conducted to evaluate morphological changes before and after treatment under a light microscope. Tumor shrinkage was observed after treatment. In conclusion, Iso-mukaadial acetate inhibited tumor progression in breast cancer athymic mice without major side effects.

#6127

MDM2 inhibition in combination with MEK inhibition in pre-clinical models of lung adenocarcinomas with *MDM2* amplification

Arielle Elkrief[1], Vladimir Markov[1], Álvaro Quintanal-Villalonga[1], Rebecca Caeser[1], Pawel Sobczuk[1], Emily Cheng[1], Alexander Drilon[1], Gregory J. Riely[1], William W. Lockwood[2], Elisa de Stanchina[1], Charles M. Rudin[1], Igor Odintsov[1], Romel Somwar[1]. *[1]Memorial Sloan Kettering Cancer Center, New York City, NY,[2]University of British Columbia, Vancouver, BC, Canada*

The eventual development of resistance to single-agent targeted therapies in lung adenocarcinomas (LUAD) is inevitable, and new strategies are needed. We hypothesize that combination therapies aimed at a known driver and a distinct targetable alteration could prolong time on oral targeted therapy. In an analysis of 7636 patients with LUAD who underwent MSK-IMPACT large panel NGS testing, 5.5% (416/7636) harbored *MDM2* amplification (*MDM2*amp), a known mechanism of TP53 inactivation. *MDM2*amp was over-represented among tumors with alterations in *MET*ex14 (34.4%, $p<0.001$), *EGFR* (10%, $p<0.001$), *RET* (11%, $p<0.05$), and *ALK* (9.9%, $p<0.002$). The small molecule MDM2 inhibitor milademetan (mila) caused growth inhibition as a single-agent in *MDM2*amp patient-derived cell lines with concurrent kinase alterations including ECLC5-GLx (*MDM2*amp/*TRIM33::RET*/*TP53* wildtype (WT)) and LUAD12c (*MDM2*amp/*MET*ex14/*KRAS*^{G12S}/*TP53* WT). Mila also caused growth inhibition in a cell line with *KRAS*^{G12C} and WT *TP53* without *MDM2*amp (SW1573 (*KRAS*^{G12C}/*TP53*^{WT})), but not in cell lines with *TP53* mutations

(LUAD-002AS1 (*KIF5B::RET/TP53*^{P128fs}*, H1792 (KRAS*^{G12C}*/TP53 splice site mut*)). Treatment of ECLC5-GLx and LUAD12c with mila resulted in restoration of ERK phosphorylation, confirming a previous report of ERK activation upon MDM2 inhibition. At 48 hours, ERK phosphorylation was suppressed by concurrent mila and MEK inhibition using trametinib (tram). In contrast, ERK phosphorylation was not suppressed by concurrent mila and KIF5B::RET inhibition using selpercatinib (in ECLC5-GLx) or MET inhibition using capmatinib (in LUAD12c). The combination of mila+tram was synergistic in slowing growth of ECLC5-GLx, LUAD12c, and SW1573 cells, and increased expression of pro-apoptotic proteins PUMA and BIM, beyond that achieved by either agent alone. In ECLC5-GLx, mila+tram also caused increased apoptotic cells measured by Annexin-V compared to either agent alone (combination $p<0.01$ compared to mila, $p<0.001$ compared to tram). In *vivo*, combination mila+tram was more effective than mila or tram alone in ECLC5-GLx ($p<0.0001$ and $p<0.0001$, respectively), LX-285 (*EGFR*ex19del/*MDM2*amp) ($p<0.0001$ and $p<0.0001$, respectively), and L-13BS1 (model resistant to capmatinib) (*MET*ex14/*MDM2*amp) ($p<0.05$ and $p<0.0001$, respectively). These results suggest that combined MDM2/MEK inhibition is effective in patient-derived LUAD models harboring *MDM2*amp. This combination, potentially applicable to LUADs with a wide variety of oncogenic driver mutations and kinase fusions will be investigated as part of a phase 1/2 clinical trial.

#6128

Deubiquitinating enzyme Inhibitor PR-619 inducesendoplasmic reticulum stress-related apoptosisin human chondrosarcoma

Kuan-Lin Kuo, Chen-Hsun Hsu, Shih-Ming Liao, Kuo-Yuan Huang.
National Taiwan University Hospital, Taipei, Taiwan

It is reported that PR-619 is a deubiquitination enzyme inhibitor that can exert anti-tumor effects on a variety of malignancies. We conducted this study to explore the antitumor effects of PR-619 on chondrosarcoma in vitro and in vivo by using two different classes of human chondrosarcoma cell lines SW-11353 and JJ012. To determine these effects, we measured cell viability (MTT), apoptosis (detection of Annexin V-FITC labeling using flow cytometry) and western blot to evaluate molecules associated with apoptosis and cell stress. In addition, we used a nude mouse xenograft

mouse model to determine the effect of PR-619 on tumor growth. As our data revealed, in addition to inducing BAD and activating Capase-7, Caspase-8, and PARP, PR-619 also has a dose-effect that induces cytotoxicity, proliferation restriction, and apoptosis in these human chondrosarcoma cells. PR-619 has also been found to activate endoplasmic reticulum pressure-related molecules (caspase-4 and CHOP) and other stress responses (activation of JNK and c-Jun). We conclusively demonstrated the ability of PR-619 to inhibit tumor growth while achieving minimal general toxicity in a developed xenograft mouse model of chondrosarcoma. Therefore, we conclude that PR-619 exacts an antitumor effect in conjunction with cellular and endoplasmic reticulum pressure in human chondrosarcoma. These findings suggest that PR-619 may provide a novel therapeutic strategy for chondrosarcoma.

#6129

The proapoptotic peptide PEP-010 is efficient on several models of different tumor origins and it can be monitored by pharmacodynamic biomarker candidates in clinical practice

Rayan Farhat[1], Laura Dadon[1], F. Nemati[2], A. Rebollo[3], D. Decaudin[2], Joelle Wiels[4], Catherine Brenner[4], Diego Germini[1]. *[1]PEP-Therapy, Paris, France,[2]Translational Research Department, Laboratory of Preclinical Investigation, PSL University, Paris, France,[3]Unité de Technologies Chimiques et Biologiques pour la Santé, Paris, France,[4]CNRS UMR9018, Villejuif, France*

In cancer cells, the proapoptotic proteins caspase-9 and PP2A interaction prevents them to play their role in apoptosis. PEP-010, a drug candidate developed by PEP-Therapy, a French Biotech company, is a proapoptotic peptide targeting and disrupting this interaction leading to restoration of the apoptotic cascade. PEP-010 is an innovative bifunctional peptide. It penetrates into cells thanks to its cell penetrating part and specifically disrupts the caspase-9/PP2A interaction thanks to its interfering part. PEP-010 is currently in Phase I a/b multicenter clinical trial for the treatment of advanced solid tumors.To the aim of screening different potential therapeutic targets, to investigate the molecular mechanism-of-action of PEP-010 and to identify potential pharmacodynamic biomarkers, we have tested PEP-010 efficacy on several cell models of different tumor origins.

By the Annexin V/Propidium Iodide staining and flow cytometry analysis, we found that PEP-010 induces apoptosis in most of the tested models. One possible mechanism-of-action is an involvement of the PP2A which, once released by PEP-010, could regulate expression and/or activity of different intracellular factors leading to caspases activation and cell death.The identification of the major molecular features involved in PEP-010 mechanism-of-action, were instrumental to identify different pharmacodynamic biomarker candidates (e.g. active caspase-3). Hence, such biomarkers could be useful in clinical practice to monitor the effect of PEP-010 at molecular level. We have compared specific features related to the mechanism-of-action of PEP-010 in sensitive (MDA-MB-231, IGROV1) and not sensitive cell models of different tumor origins and in tissue sections derived from Patient-Derived Xenografts models of breast cancer treated or not with PEP-010. Widely used techniques as immunofluorescent staining and immunohistochemistry were employed, making these results easily transferable in clinical routine.Taken together, our pre-clinical data showed the potential of PEP-010 as an anti-cancer peptide on a wide variety of malignancies and enabled the identification of pharmacodynamic biomarker candidates, important to ease the clinical development.

#6130

Cancer sensitivity to therapy is constrained by apoptosis regulation in cells of origin

Cameron Fraser[1], Xingping Qin[1], Kenichi Shimada[2], Johan Spetz[1], Mary Heather Florido[1], Rumani Singh[1], Stacey Yu[1], Adam Presser[1], Zintis Inde[1], Gaurav Joshi[1], Jennifer Guerriero[3], Francisco Sanchez-Rivera[4], Alison Karst[5], Omar Lopez[6], Chendi Li[7], Peter Winter[4], Ying Yue[2], Peter Sorger[2], Jingwei Cheng[8], Izidore Lossos[9], Aaron Hata[7], Ronny Drapkin[10], Adam Palmer[11], James Decaprio[8], Manisha Thakuria[3], Charles Yoon[3], Ursula Matulonis[8], Matthew Meyerson[8], Elizabeth Stover[8], Diana Cardona[6], Kris Wood[6], Shayna Sarosiek[8], David Kirsch[6], Joseph Mancias[8], Andrew Cherniack[12], Anthony Letai[8], Kristopher Sarosiek[1]. *[1]Harvard School of Public Health, Boston, MA,[2]Harvard Medical School, Boston, MA,[3]Brigham and Women's Hospital, Boston, MA,[4]Massachusetts Institute of Technology, Boston, MA,[5]Gilead Sciences, Seattle, WA,[6]Duke University,*

Durham, NC,[7]Massachusetts General Hospital, Boston, MA,[8]Dana-Farber Cancer Institute, Boston, MA,[9]University of Miami Miller School of Medicine, Miami, FL,[10]University of Pennsylvania Perelman School of Medicine, Philadelphia, PA,[11]University of North Carolina at Chapel Hill, Chapel Hill, NC,[12]Broad Institute of Harvard and MIT, Cambridge, MA

Many chemotherapeutic agents target cellular components or processes that are present in all cancers, yet clinical responses to these agents vary greatly between cancer types and even patient age - the basis for these broad-scale differences are unclear. The vast majority of targeted and cytotoxic cancer therapies including ionizing radiation produce pro-apoptotic signaling in exposed cells, suggesting that the mitochondrial apoptosis sensitivity of cancer cells could act as a central signaling “node” to broadly impact therapy outcomes. To test this, we used BH3 profiling and complementary chemosensitivity assays to analyze hundreds of primary cancer specimens across twelve major cancer types. We find that cancers with typically favorable outcomes including certain hematologic malignancies, testicular cancer, and some pediatric cancers contain mitochondria that are highly primed for apoptosis, which renders them hypersensitive to cytotoxic as well as targeted agents and radiation therapy. Priming levels in many epithelial cancers including ovarian cancer and non-small cell lung cancer are highly heterogeneous, mirroring their variability in clinical outcomes. Finally, many tumor types that are typically chemoresistant including adult soft tissue sarcomas, hepatocellular carcinoma and pancreatic cancer are almost completely resistant to pro-apoptotic signaling. By analyzing in vitro and in vivo pancreatic, ovarian, hepatocellular and sarcoma tumorigenesis models, we find that apoptotic priming generally increases during neoplastic transformation, in part due to consistent upregulation of pro-apoptotic proteins BAX and BAK. However, the level of apoptotic priming in cancer cells is constrained by the baseline apoptosis sensitivity of normal cells prior to transformation. Remarkably, we find that apoptotic priming is dynamically regulated by cell lineage and differentiation state but can also be modulated by oncogenes. For instance, Myc activation typically increases apoptotic priming while activation of mutant Ras signaling decreases it - these changes in priming alter the chemosensitivity of cancer cells. Finally, we use inducible mouse tumor models to demonstrate that neoplastic transformation of cells from developmentally immature tissues

yields pediatric tumors that are more primed for apoptosis than equivalent tumors arising in adults. This difference in priming causes pediatric tumors to be more sensitive to front-line therapies and BH3 mimetics targeting pro-survival BCL-2 family proteins in vitro and in vivo. Thus, lineage-determined regulation of apoptosis prior to and during neoplastic transformation leads to broad-scale differences in cancer cell chemosensitivity and can be exploited therapeutically by targeting BCL-2 family proteins.

#6131

Extracellular vesicles containing p53 of xenogeneic origin as a therapeutic strategy

Alex Tendler[1], Gil Shalev[1], Harel Kasuto[1], Lana Volokh[1], Albina Lin[1], Yevgeny Tendler[1], David Sidransky[2]. *[1]ExoProTher Medical, Haifa, Israel,[2]Israel Biotech Fund, Rehovot, Israel*

Introduction: It was recently discovered that extracellular vesicles (EVs) containing p53 are actively secreted by corneal epithelial cells into the corneal extracellular space and tear film. These EVs are re-captured by neighboring epithelial cells and play a pivotal role in local anti-cancer defense because the corneal epithelium (As an immuno-privileged tissue site), lacks classic critical pathways of innate and adaptive immunity. We took advantage of the local corneal mechanism of anti-cancer defense to develop a novel therapeutic approach based on EVs delivery of WT p53 protein to tumors. In order to avoid the inhibition of newly delivered WT p53 through the known dominant negative effect of mutant p53, we utilized p53 containing EVs produced by corneal epithelial cells of chicken origin. The C-terminal domain responsible for oligomerization is sufficiently diverse between chicken and human p53 to preventing suppression of the delivered WT p53.
Methods: The functional consequences of chicken tissue derived p53 containing EVs in human malignancies was assessed in vitro in variety of p53 mutated panels through the Annexin/PI potency assay, cell cycle arrest assessment, cell counting and IncuCyte. Confirmation of the p53 driven mechanism of action (MoA) was achieved using RT-PCR of p53 downstream responsive genes such as p21, YPEL3, BAX and PIDD. In

vivo testing was performed using the Colo320 DM human colon cancer xenograft model in nude mice.
Results: Following treatment with avian p53 containing EVs multiple tested human malignant cell lines exhibited cell cycle arrest and/or massive apoptosis within 24h. Transcription levels of the YPEL3 and BAX genes were increased significantly in human LN18 cells (p53 mut GBM) post treatment. Moreover transcription levels of the YPEL3 and PIDD genes were increased significantly in human HCT116 p53wt cells (p53 WT colorectal carcinoma) while BAX and PIDD genes are increased significantly in human HCT116 p53ko cells (p53 KO colorectal carcinoma) after treatment. In vivo results showed significant inhibition of growth in Colo320DM xenografts with further histopathological findings of reduced proliferation (Ki-67) and increased apoptosis (TUNEL) in treated group.
Conclusions: Upregulation of key p53 responsive genes is direct evidence of p53-driven response in human cancer cells triggered by p53-containing avian EVs. Further functional evidence of activity was observed through documented apoptosis and cell cycle arrest in multiple cell lines and in-vivo model. Additional relevant in-vivo models are being treated and assessed for tumor growth inhibition and functional p53 downstream activity. These preliminary preclinical results show promise for this novel therapeutic concept in targeting a hallmark genetic alteration that poses a major challenge in human cancer therapy.

#6132

Impact of treatment with agents targeting different members of HER family, CDKs and downstream cell signaling molecules on growth and migration of stomach cancer cells.

Tina Al-Janaby[1], Narmin Nahi[1], Said A. Khelwatty[1], Alan Seddon[1], Izhar Bagwan[2], Helmout Modjtahedi[1]. *[1]School of Life Science, Pharmacy and Chemistry, Kingston University London, Kingston upon Thames, United Kingdom,[2]Berkshire Surrey Pathology Services, Royal Surrey County Hospital, Guildford, United Kingdom*

Stomach cancer ranks fifth and fourth for the incidence and mortality rate for cancer worldwide, respectively. In recent years, several inhibitors with specificity to one or more members of human epidermal growth factor receptor (HER) family have been approved for the treatment of patients

with different cancer types. Of these, only the anti-HER2 monoclonal antibody (mAb) Herceptin/trastuzumab and the antibody-drug conjugate trastuzumab deruxtecan has been approved for the treatment of patients with stomach cancer. However, the duration of response may be short in many patients and with tumor heterogeneity being one contributing factor. In this study, we investigated the effect of various types of targeted agents on the growth *in vitro* of a panel of human stomach cancer cells (HSCCLs) and the impact of stomach cancer proliferation rate on the anti-tumor activities of these agents. Moreover, we investigated the cell surface expression of the HER family members, other biomarkers such as C-Met, Alk-7 and cancer stem cell makers CD44 and CD133 by flow cytometry and the effect various targeted agents on tumor migration using Incucyte. Of the 18 agents examined, the CDK 1/2/5/9 inhibitor dinaciclib was the most effective and inhibited the growth of all human HSCCLs at IC50 values between 1nM to 9nM. Of various HER inhibitors, the irreversible pan-HER family inhibitors (e.g., afatinib) were more effective than the reversible dual EGFR/HER2 TKI lapatinib and the EGFR specific TKI erlotinib in inhibiting the growth of HSCCLs. Interestingly, the HER-2 overexpressing cells lines NCI-N87 (Mean Fluorescence Intensity =596) was most sensitive to the HER inhibitors. Of agents targeting different downstream cell signaling molecules, dasatinib targeting Ab1/Src/C-Kit, trametinib targeting MERK1/2 and miransertib targeting AKT1/2/3 inhibited growth of majority of HSCCLs and with the IC50 values ranging from 2nM to 7uM. Interestingly, many of these agents were more effective in inhibiting the growth of HSCCLs when proliferating at slower rate. Of the agent examined, neratinib, afatinib, dinacicilib, dasatinib, stattic and miransertib also inhibited the migration of stomach cancer cells. Finally, treatment with a combination of afatinib with dinaciclib, capmatinib, dasatinib, stattic, ponatinib or miransertib resulted in synergistic and additive growth inhibition of stomach cancer cells. As stomach cancer cells are heterogenous in nature, our results support further research on the therapeutic potential of the CDK dinaciclib in combination with a pan-HER inhibitor in stomach cancer.

#6133

Growth response and migration of brain cancer cell lines to treatment with agents targeting different members of the HER family, CDKs and

other signalling pathways

Ermira Mulliqi[1], Said A. Khelwatty[1], Anna L. Morgan[1], Keyoumars Ashkan[2], Helmout Modjtahedi[1]. *[1]School of Life Science Pharmacy and Chemistry, Kingston Univ. London, Kingston upon Thames, United Kingdom,[2]Department of Neurosurgery,, Kings College Hospital, London, United Kingdom*

Glioblastoma (GB) is one of the most frequent primary brain tumors in adults with an extremely poor prognosis and a very high demand for novel therapies. Poor prognosis has been linked to its complex biology, tumor heterogeneity and an increased activation of signaling pathways through various growth factor receptors signaling pathway. In particular, aberrant expression and activation of epidermal growth factor receptor (EGFR) expression has been found to be common in patients with GBM. However, no EGFR inhibitor has yet been approved for the treatment of patients with brain tumor and there is currently no comprehensive study of all members of the HER family in the progression brain tumors. The aim of this study was to investigate the role of all members of the HER family (EGFR, HER2 HER3 and HER4), other growth factor receptors (e.g., C-MET) and downstream cell signaling pathways in the growth of a panel of human brain cancer cell lines (HBCCLs) and response to therapeutic interventions. Using Sulforhodamine B colorimetric assay, the growth response of four HBCCLs to treatment with 18 agents targeting different members of the HER family and other growth receptors (e.g. C-met/ALK 7, PDGFRs, FGFRs, C-kit), cyclin dependent kinases inhibitors (e.g. CDKs 1/2/5/9, CDK4/6) and downstream signaling molecules (e.g. STAT3, Src, Abl) was examined. We determined the expression level of all members of the HER family in brain cancer cells by flow cytometry and Western blot and the effect of these agents on migration of brain cancer cells were determined using Incucyte. Of the targeted agents examined, the CDK 1/2/5/9 inhibitor dinaciclib was the most potent and inhibited growth for all four HBCCLs with an IC50 below 10nM. Of the HER inhibitors, neratinib and afatinib were more effective than erlotinib and lapatinib and inhibiting the growth of all HBCCLs at IC50 values below 700nM and 1.9 μM, respectively. Treatment with Src/Abl/c-kit inhibitor dasatinib, STAT3 inhibitor static, Abl/PDGFRα/VEGFR2/FGFR1 inhibitor Ponatinib and the TRK/ROS/ALK inhibitor entrecitinb also inhibited the growth of HBCCLs

with IC50 value ranging from 0.06 - 2.96 μM, 1 - 3.8μM, 0.19- 0.42 μM and 2.85- 3.47μM, respectively. Interestingly, these agents were more effective in inhibiting growth of HBCCLs when proliferating at a slower rate. In addition to inhibiting the proliferation of HBCCLs, treatment with neratinib, dinaciclib, dasatanib, static and trametinib inhibited the migration of brain tumor cells. Finally, treatment with neratinib in combination with Palbociclib, AZD4547, trametinib and miransertib inhibited the growth of HBCCLs synergistically. Taken together, our results support further investigation on the therapeutic potential of irreversible pan HER in combination with the CDK inhibitor dinaciclib and other targeted agents in brain cancer.

#6134

Exploiting the oncogenic state of colorectal cancer for therapeutic development

Felipe de Sousa e Melo. *Genentech, Inc., South San Francisco, CA*

Over the past two decades, only incremental progresses have been made in the therapeutic management of colorectal cancer (CRC). This is in part attributed to the fact that the Wnt pathway, the oncogenic pathway that initiates the transformation of CRC and sustains tumor maintenance, has been largely undruggable. While most efforts targeting Wnt signaling have revolved around interfering with Wnt target genes that regulate cell growth, we turned our attention to a subset of genes encoding for negative regulators of the pathway. Of particular interest are the cell-surface E3 ubiquitin ligases, ring finger protein 43 (RNF43) and ZNRF3, two known negative regulators of Wnt signaling that promote the turnover of Wnt receptors Frizzled/low-density lipoprotein receptor-related proteins (FZD/LRPs) via ubiquitination-mediated degradation. Given their exposed extracellular domains (ECDs), we set out to explore whether this intrinsic cellular degradative machinery could be repurposed for an antibody-based targeted protein degradation platform. More specifically, we have devised a technology that exploits the elevated expression of ZNRF3 and RNF43 in colon cancer by generating bispecific antibodies that can tether these E3 ubiquitin ligases to a variety of cell surface receptors to promote tumor receptor degradation. Most notably, these antibody degraders are highly active in vivo and can degrade receptors in a tumor specific manner while

sparing normal tissues. This platform, that we have been dubbed Proteolysis Targeting Antibodies (PROTABs) describes a strategy for the rapid development of potent, bioavailable and tissue-selective degraders of cell-surface proteins.

#6135

Dynamics of ligand-induced epidermal growth factor receptor internalization in cancer cell lines

Mandy W. E. Smeets, Eef F. P. Smits, Janneke J. T. M. Melis, Dimitri Pappaioannou, Guido J. R. Zaman. *Oncolines B.V., Oss, Netherlands*

Antibody-drug conjugates (ADCs), comprised of cancer cell-specific antibodies linked to cytotoxic drugs, represent an innovative and promising class of anticancer agents. Due to its amplified expression in various tumor types, the epidermal growth factor receptor (EGFR) presents an attractive target for ADC therapy, and three anti-EGFR ADCs are currently studied in clinical trials. As ADCs depend on receptor internalization for intracellular release of drugs in the targeted cancer cells, studying the dynamics of receptor internalization can aid in their development and optimization. We studied the internalization of EGFR induced by its ligand EGF, as a mimic of ADCs, in cell lines with different surface receptor densities.
BxPC-3 (pancreas) and RT-112 (bladder) cancer cells were seeded in 6-well plates and allowed to adhere for 24 hours. Cells were serum-starved overnight, followed by stimulation with 150 ng/mL EGF for 2, 4, 6, 24 and 48 hours. Internalization was studied by quantification of the number of surface-expressed receptors using flow cytometry with Quantibrite PE beads and EGFR-PE antibody. Moreover, incorporation of the ligand-receptor complex into acidic endo-lysosomes was studied using EGF conjugated to the fluorescent pH sensor pHrodo™ Green. Total EGFR and EGFR phosphorylation levels were assessed by western blot analysis. RNA was isolated and converted into cDNA to perform TaqMan qPCR.
Unstimulated BxPC-3 cells showed higher numbers of EGFR per cell compared to unstimulated RT-112 cells. Since high receptor expression is key for some ADCs to induce effective endocytosis, this may indicate BxPC-3 cells as a more attractive model to study EGFR internalization.
Stimulation with EGF induced a strong decrease in surface receptor density for both BxPC-3 and RT-112 cells during the first two hours, suggesting

receptor internalization. Accordingly, treatment of BxPC-3 cells with pHrodo™ Green EGF demonstrated the incorporation of ligand-receptor complexes into endo-lysosomes. During following hours, the cell surface expression of EGFR remained stable, whereas it partially recovered after 24 to 48 hours. In contrast, the lysosomal incorporation of EGF-EGFR complexes was not decreased at 24 or 48 hours, suggesting that the increase in surface EGFR may be due to *de novo* protein synthesis rather than recycling. No increase of EGFR mRNA was, however, detected. Finally, increased phosphorylation of EGFR was observed after two to six hours of stimulation, whereas total EGFR levels were highest in unstimulated and 24- or 48-hour-stimulated cells, which is in concordance with the flow cytometry data.
In conclusion, both BxPC-3 and RT-112 cells show dynamic changes in EGFR internalization upon EGF stimulation, despite differences in EGFR expression levels. These cell lines can therefore successfully be used for internalization studies, which may contribute to future ADC development.

Cell Death Pathways and Treatment / Molecular Classification of Tumors for Diagnostics, Prognostics, and Therapeutic Outcomes

#6139
Clinical implication of EZH2 inhibitors in hepatocellular carcinoma
Bo Hwa Sohn[1], Sung Hwan Lee[2], Yun Seong Jeong[1], Ju-Seog Lee[1].
[1]Systems Biology, UT MD Anderson Cancer Center, Houston, TX,[2]Surgery, CHA Bundang Medical Center, Seongnam, Korea, Republic of

Background & Aim: Aberrant upregulation of EZH2 is frequently observed in hepatocellular carcinoma (HCC) and significantly associated with poor prognosis of HCC patients. While EZH2 inhibitors (EZH2i) are recently approved for treatment of lymphoma and sarcoma, their antitumor effect alone is not optimally efficacious against solid tumors like HCC. Ferroptosis is a newly discovered nonapoptotic type of cell death characterized by the iron-dependent accumulation of lipid hydroperoxides in cell membrane to lethal levels. Owing to anti-cancer effects of ferroptosis, many oncogenes are known to suppress ferroptosis. However, their mechanisms in HCC are currently unknown. We aim to uncover a novel mechanism for EZH2-mediated resistance to ferroptosis in HCC.

Methods: Multi-step analyses were performed with genomic data from mouse models (*Ezh1*/*2* KO), cancer cell lines treated with EZH2i GSK126, and primary tumors including HCC to identify genetic networks or signaling/metabolic pathways associated with EZH2 in cancer cells. Functional connection of identified networks or pathways from the prediction analyses was tested in cell line models with various molecular biology approaches including western blots, colony forming assay, overexpression and/or depletion of genes of interest.
Results: Gene network analysis predicted that ferroptosis pathway is inhibited by EZH2. Interestingly, lipid biosynthesis is also identified as an inhibited metabolic pathway by EZH2. Since polyunsaturated fatty acid (PUFA) is essential for executing ferroptosis, we hypothesize that EZH2 suppresses ferroptosis by inhibiting synthesis of PUFA. HCC cells with high EZH2 expression have higher IC50 values to erastin, a ferroptosis inducer, than those with low EZH2 expression. Moreover, inhibition or depletion of EZH2 sensitize HCC cells to erastin-induced ferroptotic cell death, strongly suggesting that EZH2 accounts for resistance to ferroptosis. Mechanistically, EZH2 increases H3K27me3 methylation near PUFA gene promoters, leading to suppression of PUFA gene expression and subsequently low cellular PUFA level. Most interestingly, treatment of EZH2i significantly sensitized HCC cells with high EZH2 expression to erastin-induced ferroptosis, suggesting potential therapeutic opportunity for treatment of HCC patients with high EZH2 expression.
Conclusion: EZH2 is a novel suppressor of ferroptosis by negatively regulating lipid metabolism. Thus, our study provides scientific evidence for developing a novel therapeutic strategy for treatment of HCC patients with co-treatment of ferroptosis inducers and EZH2 inhibitors.

#6140

Caspase-3 mediated cleavage of GSDME enhances the antitumor efficacy of HER2-targeted therapy in HER2-positive gastric cancer

Qiuyun Luo, Zengfei Xia, Jing Yang, Wentao Pan, Fan Luo, Jiaxin Cao, Yuting Sun, Liqiong Yang, Lin Zhang, Miaozhen Qiu, Dajun Yang. *Sun Yat-Sen University Cancer Center, Guangzhou, China*

Background: Gasdermin E (GSDME) is one of the gasdermin family proteins, which induces a new type of programmed cell death - pyroptosis

after cleavage by caspase-3. Previous researches have shown that the overexpression of GSDMB, another gasdermin family protein, is associated with poor prognosis in HER2 breast cancer and attributed to HER2-targeted therapy resistance through mediating protective autophagy. However, the role of GSDME in the anti-HER2 treatment of HER2-positive gastric cancer remains unclear. In this study, we sought to explore the function of GSDME in response to anti-HER2 treatment of HER2-positive gastric cancer and investigate the combination treatment strategies.
Methods: GSDME overexpressed vector and siRNA interference were applied to evaluate the function of GSDME in HER2-positive gastric cancer. The correlation between the expression of GSDME and survival in HER2-positive and negative gastric cancer was analyzed in the Kaplan Meier plotter database. Flow cytometry, LDH release assay and western blotting were used to determine apoptosis and pyroptosis. Moreover, the phospho-tyrosine kinase array was applied to explore the synergistic mechanism of combination therapy. GSDME overexpressed NCI-N87 xenograft model was established to evaluate the synergistic antitumor effect in vivo.
Results: We found that anti-HER2 agents upregulated the expression level of GSDME in a dose- and time-dependent manner. The bioinformatics analysis showed that a higher level of GSDME was correlated with poor overall survival both in HER2-negative and HER2-positive gastric cancer. We further demonstrated that GSDME upregulation in response to anti-HER2 treatment is associated with anti-HER2 therapy resistance. In order to validate whether cleavage of GSDME may render the cancer cells more sensitive to anti-HER2 agents, we applied a novel BCL-2/BCL-XL dual target inhibitor APG-1252 to test the combination antitumor effect with anti-HER2 agents. We found that APG-1252 could enhance the antitumor effect of lapatinib by promoting cell apoptosis and pyroptosis. Mechanistically, the combination treatment synergistically inhibited the phosphorylation of AKT/GSK-3β, subsequently inducing depolarization of the mitochondrial membrane and caspase-3-dependent cleavage of GSDME, which consequently triggered cell apoptosis and pyroptosis. Finally, in the HER2-positive GC cells xenotransplantation models, both lapatinib and APG-1252 monotherapy could delay tumor growth, while the combination therapy significantly suppressed tumor growth.

Conclusions: Taken together, our data indicated that anti-HER2 agents could upregulate the expression of GSDME, and the combination of lapatinib and APG-1252 showed a synergistic antitumor effect against HER2-positive gastric cancer through inducing caspase-3/GSDME mediated apoptosis and pyroptosis.

#6141

Mechanisms by which Mito-lonidamine inhibits *EGFR* mutant lung cancer

Katherine M. Weh[1], Connor Howard[1], Yun Zhang[1], Jean-Jack Riethoven[2], Jennifer Clarke[2], Gang Cheng[3], Balaraman Kalyanaraman[3], Ming You[4], Laura Kresty[1]. *[1]University of Michigan, Ann Arbor, MI,[2]University of Nebraska-Lincoln, Lincoln, NE,[3]Medical College of Wisconsin, Milwaukee, WI,[4]Houston Methodist, Houston, TX*

Lung cancer remains the leading cause of cancer mortality. Efficacious targeted therapy options are urgently needed for lung cancer prevention and treatment. Epidermal growth factor receptor (EGFR) mutant lung cancer represents about 15% of lung cancer cases generally occurring in patients with minimal to no smoking history and with higher prevalence in females. Linkages to environmental exposures have been postulated. Our group synthesized Mito-lonidamine (Mito-LND), a mitochondrial targeted analog of lonidamine which inhibits aerobic glycolysis in cancer cells. We previously identified that Mito-LND induces mitophagy in *KRAS* mutant lung cells and inhibits lung tumorigenesis and brain metastasis *in vivo*. Yet, the cancer inhibitory capacity of Mito-LND in *EGFR* mutant lung cancer has not been investigated. Viability staining assessed Mito-LND induced cell death in *EGFR* mutant cell lines PC9 (parent) and PC9BrM3 (brain metastatic). Transcriptomic profiling was conducted following Mito-LND treatment and results analyzed in Metacore to assess molecular changes. Deconvolution analysis interrogated alterations in immune cell populations. To discern cell death mechanisms, we evaluated FDA-approved inhibitors for autophagy (chloroquine, CQ), mitophagy/apoptosis (cyclosporin A, CsA) and necrosis (Ponatinib) in *EGFR* mutant cell lines using viability assays with Mito-LND treatment. In PC9 cells, the IC50 for Mito-LND at 24h and 48h was 1.5μM and 0.5μM, respectively and in PC9BrM3 cells at 24h and 48h was 1.5μM and 0.7μM, respectively. These data support that

EGFR mutant cell lines are >2-fold more sensitive to Mito-LND induced cell death compared to *KRAS* mutant lung cell lines H2030 and H2030BrM3. Transcriptomic profiling results show that Mito-LND treatment upregulated pathway maps linked to heat shock protein and HIF-1A signaling in both PC9 and PC9BrM3 cells. Process networks linked to unfolded protein response, response to hypoxia and oxidative stress, apoptosis and the immune response were upregulated with Mito-LND treatment. Deconvolution analysis revealed monocytes and macrophages were upregulated in Mito-LND treated *EGFR* mutant cell lines, with CD8+ T cells increased in PC9BrM3 cells and regulatory T cells increased in PC9 cells. Last, CsA significantly inhibited Mito-LND induced cell death in both cell lines, while CQ had no effect suggesting blocking apoptosis, but not late autophagy inhibits cell death induction in EGFR mutant cell lines. Further, necrosis inhibition with Ponatinib synergistically increased Mito-LND induced cell death in *EGFR* mutant cell lines. These results begin to define the cancer inhibitory mechanisms of Mito-LND in *EGFR* mutant lung cancer cells which appear to differ from those observed in *KRAS* mutant lung cancer cells. Future directions include dissecting apoptotic and necrosis driven Mito-LND induced cell death using additional pharmacological inhibitors and genetic approaches.

#6142

Inhibition of both MAPK and AKT pathways overcomes resistance of NRAS-mutant melanoma stem cells to apoptosis

Ryyan Alobaidi, Nusrat Islam, Yanjun R. Zhang, Mathew M. Shamo, Samuel Allsup, Cynthia M. Simbulan-Rosenthal, Dean S. Rosenthal.
Biochemistry and Molecular & Cellular Biology, Georgetown Univ. School of Medicine, Washington, DC

Malignant melanoma is a lethal skin cancer containing melanoma-initiating cells (MIC) implicated in tumorigenesis, invasion, and drug resistance, and characterized by elevated expression of stem cell markers, such as CD133. We have shown that siRNA knockdown of CD133 enhanced apoptosis induced by the MEK inhibitor trametinib in melanoma cells. The current study investigates the underlying mechanisms of CD133's anti-apoptotic activity in patient-derived BAKP melanoma, harboring the difficult-to-treat $NRAS^{Q61K}$ driver mutation, after either CRISPR-Cas9 CD133 knockout or

Dox-inducible expression of CD133. CD133 knockout in BAKP cells increased trametinib-induced apoptosis by reducing anti-apoptotic BCL-xL, p-AKT, and p-BAD and increasing pro-apoptotic BAX. Conversely, Dox-induced CD133 expression diminished apoptosis in trametinib-treated cells, coincident with elevated pro-survival p-AKT, p-BAD, BCL-2, and BCL-xL and decreased activation of BAX and caspases-3 and -9. Inhibition of MEK with trametinib, in combination with pan-AKT inhibitor capivasertib (AZD5363) in BAKP cells with either CD133 overexpression or knockout *in vitro* reduced cell survival as measured by XTT, FACS analysis and colony formation assays. Further, *in vivo* studies with nude mice xenografted with Dox-inducible BAKP melanoma cells, showed significantly decreased tumor growth after xenografted mice were treated with trametinib alone or in combination with AZD5363. CD133 may therefore activate a survival pathway where (1) increased AKT phosphorylation and activation induces (2) BAD phosphorylation and inactivation, (3) decreases BAX activation, and (4) reduces caspases-3 and -9 activity and caspase-mediated PARP cleavage, leading to apoptosis suppression and drug resistance in melanoma. Targeting nodes of the AKT and MAPK survival pathways with both trametinib and AZD5363 highlights the potential for combination therapies for NRAS-mutant melanoma stem cells for the development of more effective treatments for patients with high-risk melanoma.

#6143

Novel multiplexed assays of ferroptosis, pyroptosis and necroptosis biomarkers for translational studies

William G. Herrick[1], Jeevan Govindharajulu[1], Ralph E. Parchment[1], James H. Doroshow[2], Apurva K. Srivastava[1]. *[1]Applied and Developmental Research Directorate, Frederick National Laboratory for Cancer Research, Frederick, MD,[2]Division of Cancer Treatment and Diagnosis, National Cancer Institute, Bethesda, MD*

Background: The recent discovery that multiple chemo- and immuno-therapies activate non-apoptotic cell death pathways such as necroptosis, pyroptosis, and ferroptosis in cancer cells has necessitated development of pharmacodynamic biomarker assays to study their novel mechanisms of action. We describe the development, analytical validation, and proof-of-

concept demonstration of assays for potential biomarkers of ferroptosis, pyroptosis and necroptosis pathways to support anti-cancer drug development.
Methods: We developed multiplex sandwich immunoassays on the Luminex platform to quantify transferrin receptor (TfR), glutathione peroxidase 4 (GPx4), active caspase-3, cleaved and full-length gasdermins D and E (GSDMD, GSDME), MLKL oligomers, and MLKL heterodimers with RIPK1 and RIPK3. Novel antibodies to gasdermin cleavage neoepitopes were generated and their specificity validated with knockout (GSDMD) or non-expressing (GSDME) cell lines. We utilized well-established in vitro cancer cell line models (NCI-H522, THP-1, MV411, MB231, HT29) and inducers/inhibitors of pyroptosis, necroptosis and ferroptosis to test for expected directional changes of biomarker modulation.
Results: Analytical validity of the measurements is demonstrated with acceptable reproducibility, precision, dilutional linearity, dilutional recovery, spike recovery, sample freeze-thaw and temperature stability. The fitness-for-purpose of the assays is demonstrated by increased cleavage of GSDME, loss of full-length GSDME, and activation of caspase-3 in NCI-H522 cells treated with doxorubicin; similarly, cleavage of GSDMD and loss of full-length GSDMD is shown in THP-1 cells primed with LPS and treated with nigericin, and in MV-4-11 cells treated with val-boroPro. HT29 cells treated with ZVAD + birinapant + TNFα were used to demonstrate increased MLKL oligomerization or heterodimer formation with RIPK1/RIPK3. Modulation of ferroptosis biomarkers TfR and GPx4 (SU-DHL-5, MDA-MB-231) in response to imidazole ketone erastin (IKE) or RSL3 was cell line-dependent. Studies are underway to validate modulation of select ferroptosis biomarkers using orthogonal LC-MS methods.
Conclusions: We describe development and translational readiness of novel multiplex assays to interrogate drugs inducing ferroptosis, pyroptosis and necroptosis cell death pathways. Our data demonstrate utility of biomarkers of pyroptosis and necroptosis, whereas biomarkers of ferroptosis require further appraisal. In vivo pharmacodynamic studies of pyroptosis, ferroptosis and necroptosis inducers are ongoing to verify assay fitness-for-purpose with tumor biopsy specimens. This project was funded with federal funds from the NCI, NIH, under contract no. HHSN261201500003I.

#6144

Polyploidization enables initial survival of chemotherapy but a progressively increased susceptibility to ferroptosis

Luke Loftus. *Johns Hopkins University School of Medicine, Baltimore, MD*

Once cancer has metastasized it remains incurable owing to evolved resistance to nearly all systemic therapies. Classical views of therapeutic resistance include tumor heterogeneity and genetic instability, but our group and others have identified an unappreciated cancer cell phenotype, the polyaneuploid cancer cell (PACC) state, that provides an alternative model. The PACC state is induced upon exposure to a variety of applied stressors, including multiple different classes of chemotherapy, and is characterized by polyploidization of the aneuploid cancer genome. We have shown that this polyploidization is accomplished through endocycling that leads to an enlarged cell size with increased transcriptomic and protein content, higher oxidative buffer capacity, and increased autophagy. We have demonstrated that PACCs are present in a variety of cell lines, arise in response to multiple stressors *in vitro,* and are resistant to subsequent treatment with several classes of chemotherapy. Thus, we hypothesize that the PACC state is driving therapeutic resistance to current treatment regimens. Elimination of this overlooked phenotype is critical for sustained anticancer therapy response. Cancer cells, including those in the PACC state, control canonical cell cycle and cell death programs to evade apoptosis from external stressors including chemotherapy, highlighting an opportunity to leverage cell cycle-independent death pathways as an alternative therapeutic strategy[1]. Ferroptosis is a cell cycle agnostic immunogenic form of cell death that is an ideal pathway for elimination of cells in the PACC state. Characterization of ROS levels, glutathione content, labile iron homeostasis, and lipid content indicate that cells in the PACC state have a mounting susceptibility to ferroptosis. Our data suggests that cells in the PACC state keep ferroptosis in check through elevated levels of reduced glutathione and proficient redox activity, including turn over of GPX4, the sole enzyme counteracting lipid peroxidation. Direct inhibition of GPX4 is highly toxic to cells in the PACC state, particularly at later timepoints post therapy removal when the immediate stress response is largely resolved. These studies will directly lead to development of a therapeutic strategy specifically targeting the PACC state with the intention of eliminating cancer resistance.

[1]Loftus, L.V.; Amend, S.R.; Pienta, K.J. Interplay between Cell Death and Cell Proliferation Reveals New Strategies for Cancer Therapy. *Int. J. Mol. Sci.* **2022**, *23*, 4723. https://doi.org/10.3390/ijms23094723

#6145

Alternative splicing of GSDMB modulates killer lymphocyte-triggered pyroptosis

Qing Kong[1], Shiyu Xia[2], Xingxin Pan[3], Kaixiong Ye[4], Zhouyihan Li[5], Haoyan Li[5], Nidhi Sahni[5], S. Stephen Yi[3], Xing Liu[6], Hao Wu[7], Judy Lieberman[7], Zhibin Zhang[5]. *[1]Department of Immunology, UT MD Anderson Cancer Center, Houston, TX,[2]California Institute of Technology, Pasadena, CA,[3]The University of Texas at Austin, Austin, TX,[4]University of Georgia, Athens, GA,[5]UT MD Anderson Cancer Center, Houston, TX,[6]Institut Pasteur of Shanghai, Shanghai, China,[7]Boston Children's Hospital, Boston, MA*

Killer lymphocyte-mediated tumor cell killing is a vital and final step of anti-tumor protective immunity. Killer cells, including cytotoxic CD8 T cells and Natural Killer (NK) cells, deliver granzymes (Gzm) into target cells, which normally activates noninflammatory cell death, but becomes inflammatory when target cells express the gasdermin (GSDM) proteins responsible for pyroptosis. GzmA and GzmB cleave and activate GSDMB and GSDME, respectively. However, the role of GSDMB in anti-tumor immunity is unclear - GSDMB pore formation is controversial and GSDMB expression has been linked to both anti- and pro-tumor functions. Here we found that GSDMB splicing variants are functionally distinct. Cleaved N-terminal (NT) fragments of isoforms 3 and 4 caused pyroptosis, but isoforms 1, 2 and 5, which deleted or modified exon 6, did not. Structural analysis based on AlphaFold predictions and the cryoEM structures of GSDMA3 and GSDMD showed that pore formation required the formation of a functional stabilizing belt structural element near the C-terminus of the cleaved N-terminal fragment, which was disrupted in the non-cytotoxic alternatively spliced isoforms. NK attack of GSDMB3-expressing cells caused pyroptosis, but GSDMB4 cells died mostly by apoptosis, and GSDMB1/2 cells died only by apoptosis. GSDMB4 partially resisted NK cell-triggered cleavage, suggesting that only GSDMB3 is fully functional.

GSDMB1-3 were the most abundant isoforms in tested cells and were similarly induced by IFNγ and a chemotherapy drug methotrexate. Expression of cytotoxic GSDMB3/4, but not GSDMB1/2, was associated with better outcome in bladder and cervical cancer, suggesting GSDMB-mediated pyroptosis was protective in those tumors. Our study uncovers a novel role of alternative splicing in modulating caner-associated pyroptosis, and suggests that tumors may manipulate GSDMB splicing to avoid pyroptosis. Thus, modulating GSDMB splicing to increase cytotoxic GSDMB variants but suppress non-cytotoxic GSDMB isoforms could improve anti-tumor immunity and have therapeutic utility.

#6146

Tumor suppressor p73 primes extrinsic apoptosis via transcriptional activation of DR5 and c-FLIP

Shengliang Zhang, Wafik S. El-Deiry. *Pathology and Laboratory Medicine, Brown University, Providence, RI*

The tumor suppressor p73 is a member of p53 family. p73 transcriptionally activates p53-targeted genes involved in cell cycle regulation and apoptosis. It is well known that p73 induces cellular apoptosis via the intrinsic apoptotic pathway upon cellular stresses. However, the role of p73 in extrinsic apoptosis is poorly studied. We observed cell cycle arrested at the G1 phase in cells infected with a p73-expressing recombinant adenovirus (Ad-p73). We observed that overexpression of p73 upregulated c-FLIP at the protein level, in addition to DR5 and p21. c-FLIP is an anti-apoptotic factor that inhibits caspase 8/10 activation, thus blocking extrinsic pathway apoptosis. We demonstrated that c-FLIP is a transcriptional target of p73 based on our observations that: 1) p73 increases c-FLIP at mRNA level, 2) p73 binds to the c-FLIP promoter and 3) p73 enhances c-FLIP promoter-driven luciferase expression. We sought to explore whether the upregulation of c-FLIP prevents extrinsic apoptosis in cancer cells following p73 activation. To address this question, p73 was overexpressed in cells by adenovirus infection and c-FLIP was knocked down by siRNA. Overexpression of p73 induced cellular apoptosis in the cells with knockdown of c-FLIP and this effect was blocked by knockdown of caspase 8. Our results suggest that p73 induces extrinsic apoptosis when c-FLIP is depleted in cancer cells. We further found that the knockdown of DR5

inhibited p73-induced apoptosis in c-FLIP-deficient cancer cells. By contrast, PUMA knockdown did not block p73-induced apoptosis. Our results suggest that DR5 is required for cell extrinsic apoptosis in c-FLIP-deficient cancer cells upon p73 activation. p21 is the cyclin dependent kinase inhibitor that leads to cell cycle arrest at the G1/S phase. Knockdown of p21 enhanced cleaved-caspase 8 and cleaved-PARP in c-FLIP-depleted cancer cells treated with Ad-p73. Our results, taken together, suggest that the p73 primes extrinsic apoptosis via DR5 and the priming level appears to be titrated at the level of c-FLIP. Upregulation of c-FLIP decreases the priming level, resulting in cells converting to cell cycle arrest and survival via p21 whereas reduction of c-FLIP leads the primed cancer cells to undergo extrinsic apoptosis upon p73 treatment in cancer cells. Our discovery of p73 transcriptional upregulation of c-FLIP provides a rationale for depleting c-FLIP to improve antitumor efficacy of p73-targeting cancer therapy.

#6147

MCL1 inhibitor PRT1419 demonstrates anti-tumor activity in PBRM1-altered clear cell renal cancer and synergizes with standard of care agents

Norman Fultang, Brian Vidal, Ashley M. Schwab, Alexander Grego, Stephanie Rodgers, Diane Heiser, Kris Vaddi, Neha Bhagwat, Peggy Scherle. *Prelude Therapeutics, Wilmington, DE*

Induced myeloid leukemia cell differentiation protein (MCL1) is a member of the B-cell lymphoma-2 (BCL2) family of apoptosis regulators, which plays a critical role in maintaining cellular homeostasis and promoting cancer cell survival. Increased expression of MCL1 in various cancers has been associated with poor prognosis and resistance to chemotherapeutic and targeted agents. We previously described PRT1419, a novel, potent, selective MCL1 inhibitor that demonstrates anti-tumor efficacy in various preclinical models of solid and hematologic malignancies. PRT1419 is currently under evaluation in Phase I clinical trials in patients with relapsed/refractory hematologic malignancies and advanced solid tumors. To identify novel biomarkers that might predict sensitivity to MCL1 inhibition, we conducted a gene essentiality analysis using publicly available human cancer cell line gene dependency data generated from

genome-wide CRISPR/Cas9 cell viability screens. We observed that clear cell renal cancer (ccRCC) cell lines with deleterious alterations in *PBRM1* (*Polybromo 1*) displayed a strong dependency on *MCL1*. PBRM1, also known as BAF180, is a chromatin-targeting subunit of mammalian pBAF (SWI/SNF-B) complexes. PBRM1 is frequently altered in various human cancers but it has a particularly high alteration rate in ccRCC with ~40% of tumors harboring damaging PBRM1 alterations. We had previously described alterations in other mammalian SWI/SNF factors as biomarkers of MCL1 inhibitor sensitivity.We observed potent inhibition of tumor growth as well as induction of apoptosis by PRT1419 in various preclinical models of PBRM1-mutant ccRCC but not in PBRM1-WT tumor models. Depletion of PBRM1 via RNAi in PBRM1-WT ccRCC induced sensitivity to PRT1419. Mechanistically, PBRM1 depletion coincided with increased expression of pro-apoptotic factors, priming PBRM1-loss cells for caspase-mediated cell death following MCL1 inhibition. Increased MCL1 activity has previously been described as a resistance mechanism to Sunitinib and Everolimus, two approved targeted agents for ccRCC. To investigate if MCL1 inhibition could potentiate the anti-tumor effects of these agents, we evaluated PRT1419 in combination with Sunitinib or Everolimus in PBRM1-loss ccRCC. PRT1419 synergized with both Sunitinib and Everolimus in inhibiting tumor growth in various models. Taken together, these findings suggest PBRM1 loss is associated with sensitivity to MCL1 inhibition in ccRCC and provide rationale for the evaluation of PRT1419 for the treatment for PBRM1-deficient ccRCC

#6148

Disulfide isomerases AGR2, ERp44, and PDIA1 maintain death receptor 5 in an auto-inhibited, monomeric form

Brian K. Law[1], Mary E. Law[1], Elham Yaaghubi[1], Amanda Ghilardi[1], Brad J. Davis[1], Renan Ferreira[1], Samantha Eggleston[1], Jade Nguyen[1], Grace Alexandrow[1], Jin Koh[1], Sixue Chen[1], Chi-Wu Chiang[2], Coy Heldermon[1], Peter Norgaard[3], Ronald K. Castallano[1], Zaafir M. Dulloo[1]. *[1]University of Florida, Gainesville, FL,[2]National Cheng Kung University, Tainan, Taiwan,[3]Copenhagen University Hospital, Herlev, Denmark*

Previous studies indicated that compounds termed Disulfide bond Disrupting Agents (DDAs) exhibit anti-cancer activity that is associated

with downregulation of EGFR/HER1, HER2, and HER3, and activation of Death Receptors 4 and 5 (DR4/5). DDA-induced HER1-3 downregulation is preceded by disulfide-mediated oligomerization. In contrast, DDA-mediated DR4/5 oligomerization results in DR5 upregulation, and activation of DR4/5 pro-apoptotic signaling through Caspases 8 and 3. However, the precise mechanisms by which altered disulfide bonding stabilizes and activates DR5 are unknown. A recent report indicated that the extracellular domain of DR5 acts in an auto-inhibitory manner to prevent DR5 oligomerization and pro-apoptotic signaling in the absence of its ligand, TRAIL. A subsequent paper showed that the DR5 auto-inhibitory domain is a positive patch consisting of three basic residues. Importantly, the structure of the auto-inhibitory loop is formed by two disulfide bonds. We hypothesize that DDAs disrupt the disulfide bonds that make up the auto-inhibitory loop, resulting in DR5 oligomerization, and activation of Caspase 8/3-driven apoptosis in a TRAIL-independent manner. Due to their novel mechanisms of action, DDAs may overcome the pharmacological liabilities that have limited the efficacy of TRAIL analogs and DR5 agonist antibodies. Another unanswered question is how precisely DDAs alter DR5 and EGFR disulfide bonding. The direct targets of DDA action were revealed through affinity purification studies with biotinylated-DDA analogs. These studies identified the protein disulfide isomerases AGR2, ERp44, and PDIA1 as DDA target proteins, explaining how DDAs alter DR5 and EGFR disulfide bonding patterns. Consistent with this interpretation, knockdown of AGR2 or ERp44, or expression of catalytically null AGR2 or ERp44 mutants, mimicked DDAs in inducing disulfide-mediated DR5 oligomerization and Caspase 8 activation. Together, these results demonstrate a fundamentally novel, ligand-independent mechanism for activation of DR5 through DDA-mediated inhibition of the PDIs AGR2, ERp44, and PDIA1. Significantly, DDAs are the first identified active site inhibitors of AGR2 and ERp44.

#6149

STAT3 activation promotes invasiveness and cancer stemness in lung cancer

Sai Fung Yeung, Sze Man Chan, Chun Ho Law, Hoi Yin Chan, Kwok Wing Tsui. *School of Biomedical Science, The Chinese University of Hong Kong, Shatin, NT, Hong Kong*

Lung cancer is the leading cause of cancer-related death worldwide, featuring a high incidence and low 5-year survival rate. Nearly 40% of patients are diagnosed with metastatic disease when they are first presented to the clinic. However, drug intervention targeting established metastatic tumors remains challenging, a better understanding of therapeutically exploitable mechanisms is urgently needed. This present study aims to explore novel therapeutic intervention against metastatic lung cancer. To understand the tumor-cell-intrinsic pathway that drives metastatic progression, we generated a highly invasive subline of lung cancer cell - A549 (ATCC, USA) by serial selections for Matrigel-coated transwells. The invasive subline A549-i3 shows about 5 times higher invasion potential than the parental cell line A549-Par ($p<0.05$, Student t-test). Colony-formation Assay and suspension growth in ultra-low attachment plates were used to measure the 2D proliferation ability and anoikis resistance, albeit with no difference. The differential efficacies between A549-Par and A549-i3 against multiple pathway inhibitors were screened using MTT assay *in vitro*. Notably, A549-i3 is more sensitive towards napabucasin (STAT3 inhibitor) and tipifarnib (FTase inhibitor) when compared with A549-Par, suggesting their potency in targeting cancer stemness and addicted oncogenic driver. Furthermore, napabucasin reduced the migration and invasion abilities of A549-i3 to similar extent as their parent counterpart. Overall, our preliminary data identified STAT3 as a potential therapeutic vulnerability in highly invasive cancer cells. Future work will be focused on identifying pathways responsible to sensitize highly invasive NSCLC cells toward STAT3 inhibition using multiomics approach. This project was supported by the Research Impact Fund (Ref. No.: R4015-19) from the Research Grants Council in Hong Kong.

#6150

AZD0466, a dual BCL-2/XL targeting nanomedicine, is active in small cell lung cancer models

Courtney L. Andersen[1], Giulia Fabbri[1], David Jenkins[1], Zumla Cader[2], Shringi Sharma[3], Areya Tabatabai[1], Srividya Balachander[1], Jordan Roebuck[4], Melanie Galvin[4], Kathryn Simpson[4], Caroline Dive[4], Jordi Rodon Ahnert[5], Jamal Saeh[1]. *[1]AstraZeneca, Waltham, MA,[2]AstraZeneca, Cambridge, United Kingdom,[3]AstraZeneca, South San Francisco,*

CA,[4]CRUK Manchester Institute, Manchester, United Kingdom,[5]MD Anderson Cancer Center, Houston, TX

Small cell lung cancer (SCLC) is an aggressive malignancy with critical need for new therapies. While currently treated as a single disease, SCLC is heterogenous, comprised of several transcriptional subtypes. Each of these subtypes has distinct drivers and may warrant unique therapeutic targets. Two potential therapeutic targets for SCLC are the pro-survival proteins BCL-2 and BCL-XL. BCL-2 is overexpressed in ASCL1 (A) and POUF3 (P) subtypes of SCLC. We therefore sought to evaluate efficacy of the dual BCL-2/XL inhibitor AZD0466 in SCLC models and to determine whether transcriptional subtype would predict response. AZD0466 is a novel drug-dendrimer conjugate. The active moiety, AZD4320, is a potent dual inhibitor of BCL-2 and BCL-XL. AZD4320 is covalently conjugated to a 5th-generation PEGylated poly-lysine dendrimer through a hydrolytically labile linker to make AZD0466. AZD0466 has been optimized to deliver efficacy while mitigating potential Cmax-driven on-target toxicities of AZD4320. AZD4320 was active (IC50 $\leq$0.1 μM) in 9/27 SCLC cell lines. AZD4320 in vitro sensitivity was enriched in cell lines that represented A and P subtypes of SCLC compared to NEUROD1 and YAP1 subtypes. We next profiled AZD0466 in a panel of SCLC patient-derived models: 14 patient-derived xenografts and 10 circulating tumor cell-derived xenografts. AZD0466 monotherapy dosed weekly IV was active in 12/24 SCLC xenografts, driving regressions in 8 models. AZD0466 drove efficacy and cleaved caspase-3 induction in a dose-dependent manner. Similar to in vitro, AZD0466 in vivo efficacy was enriched in subtype-A, driving responses in 10/14 ASCL1 models (7 regression, 3 stable disease). AZD0466 response also correlated strongly with BCL-2 mRNA expression ($P<0.0001$). AZD0466 outperformed the selective BCL-2 inhibitor venetoclax in 6/10 models. Notably, AZD0466 was active in models resistant to platinum/etoposide chemotherapy, the standard-of-care for SCLC. Together, these data suggest BCL-2/XL inhibition has therapeutic potential in SCLC. AZD0466 is in clinical development. The first-in-human study treated 9 patients with advanced solid tumors (NCT04214093) at doses from 50-200mg, all of which were well-tolerated. The BOR was SD observed in 3 patients (100mg) with 1 patient receiving treatment for 5.5 months. AZD0466 is now under evaluation in patients with hematologic

malignancies (NCT04865419 and NCT05205161). AZD0466 has been dosed in 33 patients up to 2400mg. No DLTs have been reported to date. Initial clinical activity has been observed through reduction of bone marrow blasts following AZD0466 treatment. AZD0466 exhibits linear PK, consistent across solid tumor and leukemia patients. The doses tested are in line with preclinical studies in SCLC.

#6151

Loss of GPR54 inhibits tumor growth by suppressing AKT/DDC signaling pathway in KRAS-mutant non-small cell lung cancer

Seo Yeon Lee, Yu-Jeong Choi, Hyun-Ha Hwang, Sooyeon Kang, Kangwook Lee, Seong-Gyu Ko. *Kyung Hee University, Seoul, Korea, Republic of*

Therapeutic targeting of KRAS-mutant lung cancers has remained a challenge. There are increasing evidence that KISS1/GPR54 signaling pathway is associated with the development of various cancer. Although KISS1 and GPR54 are expressed in the lung, their biological role in the lung tumorigenesis remains unclear. In this study, using the genetically engineered mouse models, we have identified that loss of Gpr54 inhibited Kras-driven lung tumorigenesis by suppressing pathways in oncogenesis such as the MAPK and AKT pathways and inducing apoptosis. Similarly, genomic inhibition of GPR54 suppressed cell proliferation, decreased ERK and AKT signaling pathway, and increased apoptotic cell death in NSCLC cells. RNA-sequencing analysis revealed that DDC expression and glycolysis gene sets were significantly changed in Gpr54 deficient mice. Interestingly, HIF-1α expression is regulated by GPR54/AKT/DDC signaling pathway in NSCLC cells, leading to glycolytic change. Genomic inhibition of DDC suppressed cell proliferation and enhanced apoptotic cell death in NSCLC cell lines. Also, pharmacological inhibition of GPR54 and DDC lower glucose consumption and lactate production in NSCLC cell lines. Taken together, we demonstrate GPR54, as a potential therapeutic target, suggesting a new strategy to cure for lung cancer patients.

#6152

Exploiting ferroptosis in mutant BAP1 uveal melanoma

Camille J. Cunanan. *Pharmacology and Physiology, MCBG, Drexel University College of Medicine, Philadelphia, PA, PA*

Uveal melanoma (UM) arises from melanocytes of the uveal tract in the eye and is the most common intraocular malignancy in adults. Primary UM lesions often harbor mutations in G-proteins, GNAQ or GNA11, and are successfully treated by radiotherapy or enucleation. However, 50% of patients develop metastases. Of these metastatic UM (MUM) patients, 80%develop metastases to the liver, an effect strongly correlated with the loss of function of BAP1,a nuclear deubiquitinase. BAP1-mutant MUMs are less responsive to conventional treatments, such as chemotherapy and immune checkpoint inhibitors, with 50% of these patients having an overall survival of only 1 year. We propose that the unique metabolic intermediates found in liver microenvironment may dictate MUM tropism, aggressiveness, and poor therapeutic response. Here, using a combination of *in vitro* and *ex vivo* liver slice cultures, we found that the liver microenvironment induces gene expression alterations consistent with limiting the toxicity of reactive oxygen species (ROS). Importantly, we note that mutant BAP1 UM displayed improved ROS detoxification compared to its wildtype counterparts. Furthermore, publicly available datasets suggest patients with mutant BAP1 UM, the subset of patients with liver metastases, have corresponding ROS detoxification gene expression patterns. These findings suggest that the liver microenvironment and BAP1 loss directs MUM to mitigate ROS-associated toxicity. This compensatory mechanism may be therapeutically exploited and pair well as a combination treatment with the recently approved bispecific agent, Tebentafusp, to selectively target liver MUM.

#6153

Triple negative breast cancer targeted by Ophiobolin A: Epithelial-mesenchymal transition take the lead

Santhalakshmi Ranganathan[1], Alexander Kornienko[2], Antonio Evidente[3], Daniel Romo[4], Joseph Taube[1]. *[1]Baylor University - Department of Biology, Waco, TX,[2]Department of Chemistry and Biochemistry, Texas State University, San Marcos, TX,[3]Department of Chemical Sciences, University of Naples Federico II, Complesso Universitario Monte Sant'Angelo, Naples, Italy,[4]Department of Chemistry and Biochemistry, Baylor University, Waco, TX*

Triple negative breast cancer (TNBC) has fewer treatment options than other types of invasive breastcancer. Moreover, Epithelial to Mesenchymal Transition (EMT) helps enrichment of cancer stem cells(CSCs) which promotes resistance to chemotherapy. Ophiobolin A (OpA), a drug like small molecule wasrecently found to have anti-CSC properties. Our current study investigated the cell death mechanism(s)induced by OpA in various breast cancer cell lines with respect to epithelial-mesenchymal transition(EMT).The mechanism of cell death elicited by OpA was analyzed by applying inhibitors for specific pathwaysincluding apoptosis, necroptosis and paraptosis and by analyzing markers of cell death using flowcytometry and western blotting. HMLE(R) and HMLE(R)-Twist cell lines were used to assay the role of EMT.The formation of necrosomes was analyzed with exogeneous expression of RIPK3 tagged with greenfluorescence protein (GFP) in HeLa cell line which lacks endogenous RIPK3 expression. The necrosomeformation was identified by formation of puncta using confocal microscopy. Immune compromised SCIDmice were used to analyze the effect of OpA *In vivo*.The data obtained in the present study indicates that OpA has an increased anticancer effect in TNBCcompared to the estrogen receptor (ER) positive breast cancer cells. Cells having undergone EMT wereshown to have more sensitivity towards OpA when compared to -uninduced cell lines, which is sensitiveto Necrostatin-1, an inhibitor of necroptosis. OpA also diminished the $CD44^{hi}/CD24^{lo}$ population in TNBCcells. However, apoptosis and paraptosis inhibitors failed to rescue cell death which clearly confirms thatOpA induces necroptosis cell death pathway in EMT undergone cells. An increased phosphorylation ofRIPK, a necroptosis protein marker, was observed on OpA treatment compared to the control. OpAtreatment significantly increased puncta TNBC compared to the untreated control cells, furtherconfirming the necroptotic cell death in TNBC. OpA treatment showed a significant tumor regression intumor bearing SCID mice. All together our findings identify that OpA induce necroptosis in EMT-enrichedTNBC. The study further needs an in-depth analysis of involvement of EMT in necroptotic cell death inTNBC.**Key words: Triple-negative breast cancer, EMT, Ophiobolin A, Necroptosis, cell deathmechanism**

#6154

Imipramine induces apoptosis and inhibits metastasis via suppression of EGFR signaling pathway in bladder cancer

Tsai Lin Lo[1], Jai-Jen Tsai[2], Fei-Ting Hsu[1], Yuan Chang[3]. *[1]Department of Biological Science and Technology, China Medicial University, Taichung, Taiwan,[2]Division of Gastroenterology, Department of Medicine, Taipei Veterans General Hospital, Yuanshan/Su'ao Branch, Su'ao, Taiwan,[3]Department of Medical Imaging, Taipei Medical University-Shuang Ho Hospital, Ministry of Health and Welfare, New Taipei City, Taipei, Taiwan*

Bladder cancer (BC) is one of the most common malignant diseases of the urinary system, with poor prognosis and high recurrence and metastasis rate. Recent literatures suggested that BC patients have proportionately worse depression and mental health, as well as being at increased risk of suicidal death when compared to the general population, while relatively sane BC patients have a 2.2 times higher mortality rate, which means that depression can make BC worse. Imipramine is a tricyclic antidepressant, was used to treat neuropathic pain, nocturnal enuresis, and depression. Recently, imipramine has been reported to owns anti-tumor efficacy in various type of cancer. However, the effects and underlying mechanisms of imipramine on BC is remaining unclear. First, we indicated that imipramine may induce cytotoxicity of BC by MTT assay. Flow cytometry also showed that imipramine may trigger the loss of mitochondrial membrane potential, the accumulation of oxidative stress (ROS), and the activation of cleaved-caspase-3, -8 and -9. Our western blotting assay and immunofluorescence translocation staining also verified that imipramine markedly inhibited BC progression by inhibiting both EGFR/AKT/NFKB and EGFR/ERK/NKB signaling pathways. Furthermore, transwell and wound healing assay indicated that imipramine effectively reduced the metastatic ability of BC. In addition, the anti-tumor effect of imipramine was also validated by MB49 bearing animal model. Most importantly biochemistry level and pathology was not affected by imipramine. In conclusion, imipramine may not only suppressed BC progression by inactivation of EGFR/AKT/NFKB and EGFR/ERK/NFKB signaling pathways and induction of apoptosis pathways. These results suggested that imipramine has the opportunity to be a new therapeutic strategy for BC patients.

#6155

Lurbinectedin exhibits combinatorial activity with BCL2/BCL2L1 inhibitors *in vitro* and *in vivo* by modulation of MCL1 expression

Kedar S. Vaidya, Aparna Gupta, Robert Hauptschein, Robin C. Humphreys.
Jazz Pharmaceuticals, Palo Alto, CA

Lurbinectedin (Zepzelca) is a marine-derived anti-tumor agent currently approved for metastatic small cell lung cancer (SCLC). Lurbinectedin has been previously shown to exert its anti-tumor effect by binding to the minor groove of DNA and inhibition of nucleotide excision repair. In addition, lurbinectedin inhibits transcription by inducing degradation of RNA polymerase II. While these activities hint towards a general mechanism, specific molecular targets for lurbinectedin remain obscure. We demonstrate that *in vitro*, Lurbinectedin specifically induced downregulation of MCL1 protein, a member of the BCL2 family of pro-survival proteins, in a dose- (0-30 nM) and time-dependent manner (0-24 h) by Western analysis. Expression of other pro-survival proteins BCL2 and BCL2L1 were not affected. The downregulation of MCL1 was consistent in all nine tumor cell lines tested regardless of indication. Increased activity or expression of MCL1 is a known compensatory mechanism to offset loss of BCL2 or BCL2L1. We therefore hypothesized that lurbinectedin induced MCL1 loss, along with inhibition of the pro-survival proteins BCL2 and BCL2L1 would lead to an enhancement in cell killing. Consistent with the dominant pro-survival role of BCL2 in SCLC, the combination of lurbinectedin with a specific BCL2 inhibitor (venetoclax) *in vitro* induced synergistic cytotoxicity (measured by Bliss Sum analysis) in a panel of small cell lung cancer lines. In solid tumor lines other than SCLC, the combination of lurbinectedin with a specific BCL2L1 inhibitor (A-1331852) was also synergistic. Correspondingly *in vivo*, enhancement in the efficacy of lurbinectedin was observed in combination with venetoclax in SCLC models, while in solid tumor models other than SCLC the combination with a specific BCL2L1 inhibitor enhanced efficacy. Collectively, these data identify MCL1 as a specific lurbinectedin target and suggest that combinations that target other pro-survival proteins may represent a viable strategy to enhance the anti-tumor activity of lurbinectedin.

#6156

MALT1 protease inhibition overcomes BTK inhibitor resistance and shows synergistic activity with venetoclax in models of B cell lymphoma and leukemia

Joshua P. Plotnik[1], Raghuveer S. Mali[2], Velitchka Bontcheva[1], Colleen Dowell[1], Jun Chen[2], Adam E. Richardson[1], Ryan A. McClure[1], Paul Jung[1], Lan Pham[2], Andrew J. Souers[1], Jonathan A. Meulbroek[1], William N. Pappano[1]. *[1]Oncology Discovery Research, AbbVie, North Chicago, IL,[2]Oncology Discovery Research, AbbVie, South San Francisco, CA*

Introduction: Specific B cell malignancies, including CLL and the aggressive non-GCB subtype of DLBCL, are driven by constitutive activation of the B cell receptor (BCR) pathway and the transcription factor NF-κB. Pharmacological inhibition of MALT1 protease, a key mediator of the BCR/NF-κB signal transduction pathway, may therefore provide an attractive treatment option for patients with these cancers. Further, as combination therapy is often required for the treatment of aggressive B cell malignancies, the identification of therapies that synergistically combine with MALT1 inhibitors could afford additional and promising treatment options.

Experimental Procedures: A highly potent and orally bioavailable MALT1 protease inhibitor (ABBV-MALT1) was used to test the hypothesis that MALT1 inhibition will abrogate the proliferation of preclinical models of B cell malignancies in vitro and in vivo. Tumors treated with ABBV-MALT1 were subjected to transcriptomic and functional proteomic assays to elucidate molecular mechanisms of action and rational combination partners.

Results: Mechanistic studies reveal that ABBV-MALT1 effectively inhibits signal transduction of the BCR pathway and reduces NF-κB gene activation in non-GCB DLBCL cell lines resulting in cell cycle arrest and diminished viability. In vivo, oral administration of this compound demonstrates robust tumor growth inhibition in several models of B cell tumors, including non-GCB DLBCL models that are resistant to Bruton's tyrosine kinase (BTK) inhibitors. NF-κB target genes include the pro-survival family members BCL-X_L and BCL2-A1, which aid in regulation of the intrinsic apoptosis pathway. As ABBV-MALT1-induced inhibition of the NF-κB pathway resulted in downregulation of these genes, we hypothesized that the

associated tumor models would become increasingly dependent on the pro-survival family member BCL-2. To test this hypothesis, combination studies of ABBV-MALT1 and the selective BCL-2 inhibitor venetoclax were performed in both cell line and patient-derived xenograft models of DLBCL. Herein we show that concomitant administration of ABBV-MALT1 and venetoclax results in dramatic antitumor activity in all models tested in vivo. This efficacy also translates to primary patient CLL cells in vitro where the combination confers greater levels of apoptosis compared to either agent alone.
Conclusion: ABBV-MALT1 demonstrates robust single agent anti-tumor activity in malignant B cell models that are resistant to BTK inhibitors. Moreover, combination of ABBV-MALT1 with the BCL-2 inhibitor venetoclax shows synergistic cell killing of B cell tumors in vitro and dramatic tumor regression in vivo. Together, these data indicate that MALT1 inhibition may overcome BTK inhibitor resistance and combine with venetoclax to effectively treat patients with B cell malignancies.

#6157
USP7 is a promising therapeutic target for neuroblastoma
Christophe Le Clorennec[1], Karen Lee[2], Peter Zage[3]. *[1]UCSD Moores Cancer Center, La Jolla, CA,[2]Hematology/Oncology, Rady Children's Hospital, San Diego, CA,[3]Pediatrics, UCSD Moores Cancer Center, La Jolla, CA*

Background: The ubiquitin-proteasome system (UPS) plays an essential role in post-translational modification of proteins to maintain proteostasis. Ubiquitination of target protein is coordinated by different enzymes, which add and link ubiquitin to each other in specific ways that determine the fate of the protein for to be degraded or to be included into protein complex to induce signaling pathways. Ubiquitination is further regulated by deubiquitinases, which remove ubiquitin and rescue target protein from being degraded or diverted from it signaling role. UPS dysregulation has been linked to many human diseases, including cancer. Ubiquitin-specific protease 7 (USP7) is a deubiquitinase that plays a critical role in immune response, tumor suppression and DNA repair. USP7 overexpression has been associated with tumor aggressiveness in a variety of tumors, including in neuroblastoma (NB). Therefore, USP7 is a potential therapeutic target for

NB. Some new specific USP7 inhibitors are highly potent and selective and have demonstrated significant antitumor activity in preclinical models of adult cancer. We hypothesize that inhibition of USP7 alone or in combination with epigenetic drugs like HDAC inhibitors will be more effective against NB tumor growth. To evaluate the efficacy of USP7 inhibition with specific USP7 inhibitors alone or with combination with epigenetic drugs like HDAC inhibitors (Saha) or chemotherapy against NB tumor growth, NB cell lines were treated with increasing concentrations of USP7 inhibitors alone or in combination with chemotherapy or with HDAC inhibitors. Cell proliferation was measured using continuous live cell imaging and cell viability using AlamarBlue assay. Apoptosis was measured by caspase cleavage using Caspase 3/7 apoptosis assay as well as by PARP cleavage by Western Blotting (WB). Changes in various proteins were measured by WB and co-immunoprecipitation were performed to analyze the ubiquitin status of specific protein targets regulated by USP7. Pharmacologic inhibition of USP7 resulted in significant decreases in both cell proliferation and cell viability *in vitro* only in p*53* wild-type NB cell lines. There was no correlation seen between *MYCN* amplification status and treatment response. USP7 inhibition induced apoptosis as well as necroptosis with dose-dependent increase. Treatment with USP7 inhibitors led to decrease p53 ubiquitination leading increased of p53 protein expression in all sensitive cell lines tested and decreased MYCN protein level in *MYCN*-amplified cell lines. EZH2, which is a predominant target of USP7 is significantly downregulated with increasing dose of USP7 inhibitors. In addition, the combination of USP7 inhibitors with chemotherapy commonly used in NB or with combination with HDAC inhibitors showed enhanced efficacy. Our data suggests that USP7 inhibition may be a promising therapeutic strategy for children with high-risk and relapsed neuroblastoma.

#6158

BGB-24714, a novel oral IAP antagonist, displayed significant anti-tumor activities in preclinical models as a monotherapy and in combination with paclitaxel

Jie Li[1], Nan Hu[2], Yilu Zhang[2], Xiaolong Yang[2], Minjuan Deng[2], Wenfeng Gong[2], Longbo Yin[2], Yong Liu[2], Yajuan Gao[2], Wei Wei[2], Xing Wang[2], Xinyi Liang[2], Yanwen Ma[2], Xuxing Sang[2], Chang Liu[2], Jingyuan Wang[2],

Qianqian Lu[2], Fengtao Song[2], Xi Yuan[2], Yibing Wang[1], Jing Li[2], Wei Jin[2], Xuesong Liu[2], Xiaomin Song[2]. *[1]BeiGene Ltd., Shanghai, China,[2]BeiGene Ltd., Beijing, China*

Background: Evasion of apoptosis is identified as one of the essential hallmarks of cancer and upregulation of inhibitor of apoptosis proteins (IAPs) is one of the mechanisms by which tumor cells evade apoptosis. An oral SMAC mimetic and antagonist of cellular IAP1 (cIAP1) and X-linked IAP (XIAP), BGB-24714, is currently investigated in a phase 1a/1b oncology trial in patients with advanced or metastatic solid tumors (NCT05381909). Here, we evaluated the anti-tumor activity of BGB-24714 as a single agent or in combination with paclitaxel in preclinical models. Results: BGB-24714 effectively inhibited cIAP1 by inducing its degradation in MDA-MB-231 cells, with an EC50 of 2.5 nM. BGB-24714 also potently antagonized the inhibitory interaction of XIAP with caspase-9 and induced caspase-9 autoactivation in MDA-MB-231 cells, with an EC50 of 23 nM. In a total of 25 breast cancer cell lines treated with TNFα, BGB-24714 potently inhibited the in vitro proliferation of 5 breast cancer cells with EC50 < 100 nM. In pharmacodynamics studies, single dose administration of BGB-24714 significantly induced degradation of cIAP1 and antagonism of the XIAP: Smac interaction in the MDA-MB-231 xenograft model in a dose dependent manner. Using the same model, BGB-24714 exhibited dose-dependent anti-tumor activities as a single agent. The tumor growth inhibition rates were 30%, 52% and 73% in low to high dosage treatment groups. Furthermore, BGB-24714 at medium dosage level demonstrated synergized anti-tumor activity in HCC1806 xenograft model when used in combination with paclitaxel. In intermittent dosing study, BGB-24714 with the intermittent dosing schedule demonstrated significant but slightly less effective anti-tumor activity than the continuous dosing schedule. In summary, BGB-24714, as a novel oral IAP antagonist, showing significant anti-tumor activities in preclinical models, which is promising and warrants the testing of the compound in human.

#6160

Targeting RNA N^6-methyladenosine methyltransferase, METTL3 activates p53 and apoptosis pathways in osteosarcoma cells

Seungjae Shin[1], Yumi Oh[2], Yoojin Yang[1], Sung-Yup Cho[1]. *[1]Biomedical Sciences, Seoul National University College of Medicine, Seoul, Korea, Republic of,[2]Medical Research Center, Genomic Medicine Institute, Seoul National University College of Medicine, Seoul, Korea, Republic of*

Osteosarcoma (OS) is a malignant tumor which is mesenchymal origin from bone stroma. The 5-year overall survival of localized OS is approximately 70%, however patients who have metastasis to other organs, mostly lung, have a poor 5-year survival rate, approximately 20%. Recently, oncogenic role of Methyltransferase-like 3 (METTL3), which is the only catalytic subunit of RNA N^6-Methyladenosine methyltransferase complex, has been suggested, but its mechanism in OS is still unclear. To elucidate the roles of METTL3 in OS, we generated METTL3 knock-out U2OS osteosarcoma cell lines by CRISPR knock-out system. Knock-out of METTL3 decreased cell proliferation on U2OS cells, which was assessed by WST-1 assay and manual cell counting assay. Also, RNA-sequencing was conducted in METTL3 wild type and knock-out cell lines. Gene set enrichment analysis (GSEA) revealed that gene sets of 'Programmed cell death' in gene ontology (GO) category, 'p53 pathway' and 'Apoptosis' in HALLMARK gene sets, and 'p53 signaling pathway' and 'Apoptosis' in KEGG pathway were enriched in METTL3 knock-out cells. To validate the result of GSEA in our METTL3 knock-out cells, mRNA and protein levels of GADD45A and CDKN1A, which are downstream targets of p53, and BAX and BAK, which are apoptosis-related molecules induced by p53, were detected by real-time PCR and western blot, respectively, and these genes were upregulated in METTL3 knock out cell lines. Collectively, these results suggest that inhibition of METTL3 is potential therapeutic targets against OS by activating p53 and apoptosis pathways.

#6161

Targeting endogenous and therapy-induced dependence on BCL-X_L in high grade serous ovarian carcinoma

Lissah Johnson[1], Xingping Qin[1], Cameron Fraser[1], Elizabeth Stover[2], Yang Yang[3], Daohong Zhou[4], Bo Rueda[5], Kristopher Sarosiek[1]. *[1]John B. Little Center for Radiation Sciences, Harvard T.H. Chan School of Public Health, Boston, MA,[2]Division of Gynecologic Oncology, Dana-Farber Cancer*

Institute, Boston, MA,[3]College of Pharmacy, University of Florida, Gainesville, FL,[4]Department of Biochemistry and Structural Biology, Long School of Medicine, University of Texas Health San Antonio, San Antonio, TX,[5]Division of Gynecologic Oncology, Department of Obstetrics and Gynecology, Vincent Center for Reproductive Biology, Massachusetts General Hospital, Boston, MA

Though most patients diagnosed with high-grade serous ovarian carcinoma (HGSOC) have favorable initial responses to therapy, approximately 80% will experience tumor recurrence and develop chemoresistant disease. This highlights the urgent need for more effective therapeutic strategies and a better understanding of the mechanisms that drive therapy resistance. Altered expression of BCL-2 family proteins that control the intrinsic apoptosis pathway is a prominent mechanism by which tumor cells can develop therapy resistance. Therefore, we sought to elucidate how changes in apoptotic regulation may contribute to chemoresistance in HGSOC in order to uncover potential opportunities for improving treatment outcomes. We used well-established HGSOC cell lines and human primary tumors to measure sensitivity to inhibitors of pro-survival BCL-2 family proteins as single agents and in combination with the front-line ovarian cancer chemotherapy drugs carboplatin and paclitaxel. Based on BH3 profiling, flow cytometry-based cell death analysis and colony formation assays, we found that HGSOC cells are particularly sensitive to BCL-X_L inhibitors including the first-generation BH3 mimetics ABT-263 and A1331852 as well as novel proteolysis-targeting chimeras (PROTACs) that degrade BCL-X_L. Clinical use of first-generation BCL-X_L inhibitors has been hampered by thrombocytopenia resulting from platelet dependence on BCL-X_L for survival. PROTACs have been developed to avoid this toxicity by degrading BCL-X_L using the VHL E3 ligase, which is expressed at very low levels in platelets. We tested BCL-X_L targeting in vivo using HGSOC xenografts in immunocompromised mice and found these tumors to be highly sensitive to BCL-X_L inhibitors as single agents and in combination with chemotherapeutic agents. BCL-X_L inhibitors reduced xenograft tumor growth and prolonged overall mouse survival. Importantly, thrombocytopenia was observed with in vivo use of first-generation BCL-

X_L inhibitors but not with use of BCL-X_L targeting PROTACs. Transcriptional profiling demonstrated that expression levels of pro-apoptotic BAX and BAK, which initiate apoptosis by causing mitochondrial outer membrane permeabilization, increase during ovarian tumorigenesis, as do levels of BCL-X_L. These changes are consistent with the increased BCL-X_L dependence evident in HGSOC cells. We also detected BCL-X_L dependence in ovarian cancer tumorigenesis models utilizing human fallopian tube secretory epithelial cells, the putative cell of origin for HGSOC. Overall, we find that BCL-X_L inhibitors, especially PROTACs, can safely enhance the chemosensitivity of HGSOC cells in vitro and in vivo and may therefore prevent tumor recurrence in women diagnosed with this disease.

#6162

High resolution detection of HER2 copy number variation in admixed breast cancer cell lines and HER2+ FFPE donor tissue using a digital PCR multigene reference panel

Tyler Landrith[1], Samantha Smith[1], Jennifer Chan[1], Mari Christensen[1], Yu Chuan Tai[1], Megan Gonzales[1], William Yee[1], Nicolas Newton[1], Wouter Pattje[2], Patrick Bogard[1], Wei Yang[1]. *[1]Roche Diagnostics Solutions, Inc, Pleasanton, CA,[2]Roche Diagnostics International AG, Rotkreuz, Switzerland*

The measurement of *HER2* (*ERBB2*) gene amplification guides both the prognosis and treatment of breast cancer, as amplification correlates with worse outcomes and the recommendation for anti-*HER2* treatment. Digital PCR (dPCR) can serve as a useful tool for the direct quantification of copy number variants (CNV) in this gene, without the need for calibration standards as required for qPCR, or labor-intensive histological techniques such as FISH. Furthermore, increasing the number of available partitions in a digital PCR reaction can yield substantial gains in precision, thus offering the potential for ultra-high resolution discrimination of copy number changes. In this study, we evaluated the utility of a multiplex dPCR assay for the high-resolution detection of HER2 copy number variation in clinically relevant samples. The precision achievable by digital PCR correlates with the number of partitions, and the resolution of small CNV

differences greatly relies on high precision. We utilized a dPCR setup with ~100,000 physical partitions per reaction, which allowed for a theoretical precision (relative confidence) of 1%, assuming optimal input and template. Five single-plex primer and probe sets, published by the National Institute of Standards and Technology, were assembled and optimized into a multiplex configuration. The final 5-plex consisted of four reference genes and *HER2* as the target of interest. The accuracy and precision of the optimized five-plex assay was tested in nine breast cancer cell lines with established *HER2* amplification ratios, ranging from 1.3 to 70 fold. The assay demonstrated the precise and accurate measurement of the *HER2* amplification ratio across all nine cell lines over a wide dynamic range of sample input. Along with increasing the reaction partition number, the use of multiple reference genes also improved the precision of the *HER2* amplification ratio measurement and avoided inaccurate copy number calls due to outlier references. The resolution of the assay was evaluated using admixed samples simulating low tumor fraction. A minimum of a 1.03 fold difference (3% difference from wild type) was detected with statistical significance. Assay concordance was evaluated against IHC-characterized HER2+ FFPE donor tissue with concordant FISH/CISH results. The assay demonstrated robust performance in clinically relevant sample types, supporting further investigation of dPCR as a complementary or even alternative diagnostic approach to current methods.

#6163

Fusion landscape in acute leukemias: A submerged world of not routinely characterized transcripts

Anna Ferrari[1], Silvia Vitali[2], Eugenio Fonzi[3], Andrea Ghelli Luserna Di Rora[1], Chiara Domizio[1], Cristina Papayannidis[4], Maria Teresa Bochicchio[1], Giovanni Marconi[5], Daniele Dall'Olio[2], Michela Tebaldi[3], Michela Rondoni[6], Barbara Giannini[7], Fabio Giglio[8], Crescenza Pasciolla[9], Monica Fumagalli[10], Sara Galimberti[11], Gastone Castellani[2], Daniel Remondini[2], Giorgia Simonetti[1], Giovanni Martinelli[12]. *[1]Biosciences Laboratory, Istituto Scientifico Romagnolo per lo Studio e la Cura dei Tumori (IRST) - IRCCS, Meldola, Italy,[2]Dipartimento di Fisica e Astronomia, INFN, Università di Bologna, Bologna, Italy,[3]Unit of Biostatistics and Clinical Trials, Istituto Scientifico Romagnolo per lo Studio e la Cura dei Tumori (IRST) - IRCCS,*

Meldola, Italy,[4]IRCCS Azienda Ospedaliero-Universitaria di Bologna, Istituto di Ematologia "Seràgnoli" Bologna, Bologna, Italy,[5]Hematology Unit, Istituto Scientifico Romagnolo per lo Studio e la Cura dei Tumori (IRST) - IRCCS, Meldola, Italy,[6]Hematology Unit & Romagna Transplant Network, Ravenna Hospital, Ravenna, Italy,[7]Laboratorio Unico- AUSL della Romagna Pievesestina di Cesena (FC), Cesena, Italy,[8]Hematology and Bone Marrow Transplantation Unit, IRCCS San Raffaele Scientific Institute,, Milan, Italy,[9]Hematology and Bone Marrow Transplantation Unit, Istituto Oncologico IRCCS "Giovanni Paolo II", Bari, Italy,[10]Hematology Unit, Ospedale San Gerardo, Monza, Italy,[11]Hematology Unit, AOUP Santa Chiara, Pisa, Italy,[12]Scientific Directorate, Istituto Scientifico Romagnolo per lo Studio e la Cura dei Tumori (IRST) - IRCCS, Meldola, Italy

Background: Fusions (Fs) are major molecular biological abnormalities in acute leukemias (ALs), and all well-known Fs in leukemias are founder variations are routinely used as molecular markers for the diagnosis, classification, risk stratification, and targeted therapy but there is a considerable part of ALs that are not screened for other known/unknown transcripts. For example in B-Other B Acute Lymphoblastic Leukemia (B-ALL) [Ph**-/-/-;** negative for t(9;22)*;* t(1;19); t(4;11); 61% of adult B-ALL], many chimeric genes have been identified leading to a refined classification of B-ALL and to, in some cases, tailored therapies. At this point, a RNA-seq approach is needed but challenging for many aspects, among them a not standardized and very heterogeneous F data analysis.
Aims: We developed and validated our integrated pipeline in order to assess targetable biomarkers and to better classify patients (pts).
Methods: we performed 1385 gene RNAseq (Illumina) of 224 adult AL samples (112 Ph-/-/-, 41 Ph+, 6 t(1;19), 16 T-LBL/T-ALL and 49 AML). Starting from Ph-/-/-, we developed a combined 4 tool analysis that is further implemented with a filtering strategy with a specific ALs fusion literature filter (Patent PCTEP2021-065692 and 749 ALL Fs database copyright) (Fig.1A). We validate our strategy using: RT-PCR, FISH SNP Arrays; MLPA and total RNA-seq.
Results: From 3022 candidate Fs, we retained 160 of them (5.3%; excluding WHO canonical Fs) not otherwise detected, in 120 pts with a

high Fs rate in T-LBL/T-ALL, Ph-/-/- and Ph+ (62.5%, 62.2% and 61% respectively) denoting that ALs are not deeply characterized (Fig 1B). The lower rate was found in AML (26.5%), but we were able to identify new *ETV6* rearrangement (r) and a FISH cryptic F in a 46,XY pt (*TBL1XR1-MECOM*). We validated 98 Fs that have been already reported in the literature and 43 novel F transcripts. We obtained a validation rate of 81%. The majority of fused samples (65.2%) had only one detectable F while a smaller group was characterized by multiple Fs. Many of these Fs were previously described in B/T-ALL and AML (e.g. *KMT2A-MLLT1, ABL1/2-RCSD1, IGH-MYC, NUP214-SET, ETV6-MECOM*). In our bigger sub-cohort (Ph-/-/-), 44 Fs out of 109 (40.3%) were never been reported in Ph-ALL cases. In 15 Ph-like pts, we identified and validate 11 new transcripts. Ph-/-/- F detection help to sub-classify our fused pts in Ph-/-/- subgroups (ZNF384r-11.8%; Ph-like-19.1%; DUX4r- 4.4%; HLFr, MLLr and BCL2/MYC in 2.9%; MEF2Dr-1.5%).
Conclusions: we identified pivotal transcripts in all ALs and an unexpected high rate of secondary Fs in adult ALs subgroups (52.4%) that are not characterized with conventional diagnostic methods. The use of an NGS approach and a powerful pipeline permit us to detect Fs useful for a better classification, prognostic identification (e.g. *TBL1XR1-MECOM)* and in some cases to find targetable Fs (e.g. *ABL1-2/RCSD1, NUMA1-CSF1R, ZMYM2-FLT3*). Supported by: L3P2505.

#6164

NF-κB and NRF2 signaling pathways affect prognosis in HPV-associated head and neck cancer

Aditi Kothari[1], Travis Parke Schrank[2], Wendell Gray Yarbrough[3], Natalia Isaeva[3]. *[1]University of North Carolina at Chapel Hill, Durham, NC,[2]Otolaryngology, University of North Carolina at Chapel Hill, Chapel Hill, NC,[3]University of North Carolina at Chapel Hill, Chapel Hill, NC*

Incidence of HPV associated head and neck squamous cell carcinoma (HNSCC) is on the rise, displaying a significantly favorable prognosis and overall better survival as compared to HPV negative HNSCC. Intense radiotherapy is the primary medical care leading to treatment associated morbidity in patients, thereby generating a need for de-intensification strategies. Biomarkers that can identify patients with less aggressive tumors

as candidates for de-escalation therapy would revolutionize treatment. We applied an unbiased approach (weighted gene correlation network analysis (WGCNA)) that allows detection of autocorrelated gene sets on 3 independent cohorts of HPV+ HNSCC and created 22 consensus transcriptional modules by selecting genes that grouped together in WGCNA analyses from all 3 cohorts. Interestingly, only 1 module intrinsically divided HPV+ HNSCC into 2 subtypes, displaying different mutational profiles, mutational signatures, HPV gene expression patterns, HPV integration status, and patient survival. Gene set enrichment analysis revealed that this module was enriched in NF-kB genes and strongly associated with NF-κB signaling, confirming our prior findings that defined HPV+ HNSCC subtypes by presence or absence of NF-kB regulators, *TRAF3* or *CYLD* defects and by the NF-κB activity classifier. Our studies show that *NF-* κ*B* -driven intrinsic tumor characteristics contribute to increased sensitivity of *NF-* κ*B* active HPV+ head and neck tumors to radiation, providing patients survival benefits. Indeed, *TRAF3* or *CYLD* deletion activated NF-kB and dramatically increased radiation sensitivity of HPV+ head and neck cancer cells. In line with our RNA seq analysis, we found that activation of NF-κB via TRAF3/CYLD deletion significantly correlated with marked downregulation of NRF2 activity and reduced nuclear localization in in HPV+ HNSCC cells. Interestingly, *TRAF3* CRISPR KO cells had lower NRF2 protein levels that were restored by MG132 treatment, indicating an involvement of KEAP1/CUL3 mediated proteasomal degradation of NRF2. In summary, our data unveils a unique relation between *NF-κB* pathway and radiosensitivity in HPV+ HNSCC. The distinct biological characteristics that separate patients into two subclasses associated with favorable prognosis could serve as a biomarker for personalized therapy.

#6165

Identification of biomarkers of early onset colorectal cancer from transciptome and whole genome data

Yejin Ha[1], Yun-Jae Shin[2], Ka Hee Tak[1], Jong-Lyul Park[2], Jeong-Hwan Kim[2], Jong Lyul Lee[1], Seon-Young Kim[2], Chan Wook Kim[1]. *[1]Asan Medical Center, Seoul, Korea, Republic of,[2]Korea Research Institute of Bioscience and Biotechnology, Daejeon, Korea, Republic of*

Colorectal cancer (CRC) is not only the third most commonly occurred cancer worldwide, but it is the leading cause of cancer deaths in 2018. However, the overall incidence of CRC and death from CRC has declined since 1998, the case of early-onset CRC (EOCRC) defined as CRC diagnosed under age 50 has been increasing. Including the etiology of EOCRC, the reasons underlying this upward trend are not well understood. Moreover, some suggested that EOCRC patients have difficulty in early diagnosis compared to late-onset colorectal cancer (LOCRC). For this reason, EOCRC patients tend to be diagnosed at advanced stages. In addition to the clinical feature, EOCRC tumors have different features in pathology and molecularity compared with LOCRC tumors. With these distinct characteristics of EOCRC, there is necessary to characterize EOCRC compared to LOCRC patients. In this study, patients under 50 years (from hereon referred to as ‘‘early-onset’’) and over 70 (‘‘late-onset’’) were considered for comparison. Whole transcriptome sequencing (WTS) for profiling gene expression and whole genome sequencing for mutations were carried out with tumor tissues of early-onset (n=49) and late-onset (n=50) CRC patients. Subsequently, we performed bioinformatic analysis to identify genomic and transcriptomic features. For the precise selection of differentially expressed genes, we selected constantly differentially expressed genes (DEG) in TCGA COAD and READ data. Genes up-regulated in both data set were CPS1, CCL19, CHGB, GLDC, WASF3, RPL39L and MAP9. The down-regulated were PRSS33, ANPEP, DKK4 and NTS. To identify whether CMS classification had different feature in each type if age onset was different, we classified CMS subtypes using transcriptome data. The ratio of each CMS subtypes both early and late-onset group had no significant difference. In terms of somatic mutations reported for driving colorectal cancer, three genes (ATM, BCL9L, NF1) had significantly mutated in early-onset group. Moreover, Non-synonymous mutation frequency had no significant difference while total mutation frequency had significantly difference between early and late-onset group. Lastly, Mutational signature had difference in both groups, assuming that the early-onset group had been through different event attributing to mutational changes. Although these findings should be further validated by detailed functional experiments, our genomic and transcriptomic analysis provide additional insights into understanding of young CRC patients.

#6166

TBL1, a multifunctional transcriptional regulator, is highly expressed in osteosarcoma and correlates with activated beta catenin

Kimberly R. Holloway[1], Taku Yamamichi[2], Bikesh Nirala[2], Nino Rainusso[2], Jason T. Yustein[2], Stephen Horrigan[1]. *[1]Iterion Therapeutics, Houston, TX,[2]Dept. of Pediatrics, Texas Children's Cancer Center/Baylor College of Medicine, Houston, TX*

Background: Osteosarcoma (OS) is the most common primary bone cancer in children and adolescents. Two-thirds of OS patients are cured through chemotherapy and tumor resection. However, survival rates have plateaued over the past 30 years, especially for patients with relapsed and/or metastatic disease, with overall long-term outcomes of less than 30%. Transducin beta-like protein 1 (TBL1) protects beta-catenin from nuclear degradation and mediates Wnt targeted transcription by forming a TBL1-beta-catenin complex. Overexpression of TBL1 and nuclear beta-catenin are positively correlated to adverse clinicopathological features and poor prognosis for osteosarcoma patients. Functional experiments reveal that down-regulation of TBL1 and nuclear beta-catenin activity inhibit proliferation, migration, and invasion of osteosarcoma cells. The objective of this study was to determine TBL1 levels within a panel of OS patient-derived xenograft (PDX) tumors.
Methods: TBL1 and beta-catenin protein levels were measured via western blot and immunohistochemistry in OS samples. We examined protein levels in OS PDX cell lines collected at distinct clinical stages of metastatic OS and OS primary tumor samples. TBL1, total beta-catenin, and activated beta-catenin levels were measured by immunohistochemical (IHC) staining in tissue microarray (TMA) derived from patient derived xenograft (PDX) tumor and clinical samples. Each tumor sample were formalin fixed, paraffin embedded, and spotted in triplicate on the TMA.
Results: Beta-catenin and TBL1 protein were detected in OS samples, and we found higher TBL1 protein levels in cells derived from advanced disease stages. Assessment of TBL1 protein was expanded to OS tissue microarray where TBL1, total beta-catenin, and active beta-catenin were independently stained in a TMA. TBL1, total beta-catenin, and activated beta-catenin were present in 100% of OS PDX cores. Finally, a majority of

OS cores were shown to have high expression for both TBL1 and active beta-catenin.
Conclusion: Elevated TBL1 levels have been associated with metastatic disease and poor survival. We have measured TBL1 and activated beta-catenin protein levels in a variety of osteosarcoma samples and identified a large percentage of osteosarcoma that co-express both proteins. These results indicate that metastatic OS represents a TBL1 enriched patient population and is a candidate for therapeutics that target TBL1.

#6167

Targeting TBL1 with tegavivint promotes anti-tumor and immunomodulatory responses in preclinical models of hepatocellular carcinoma

Kimberly R. Holloway[1], Thomas Drake[2], Thomas Bird[2], Stephen Horrigan[1]. *[1]Iterion Therapeutics, Houston, TX,[2]CRUK Beatson Institute, Liver Disease and Regeneration Laboratory, Glasgow, United Kingdom*

Background: Hepatocellular cancer (HCC) is the 3rd leading cause of death worldwide with approximately 30% of patients possessing a beta-catenin activating mutation. Despite recent progress in combination with VEGF inhibition, resistance to immune checkpoint inhibitors (ICI) still occurs in a majority of HCC patients. Recent studies suggest that activated beta-catenin regulates both tumor metabolism and immune microenvironment in CTNNB1-mutated HCCs. Transducin beta-like protein 1 (TBL1) is necessary for canonical Wnt -regulated gene transcription by binding nuclear beta-catenin, which prevents its nuclear degradation and promotes recruitment to Wnt-target gene promoters. The TBL1 inhibitor, tegavivint, disrupts the TBL1-beta-catenin complex and inhibits beta catenin signaling. This study measures TBL1 levels and determines tegavivint response within preclinical models of HCC.
Methods: Tegavivint cytotoxicity (GI_{50}) was determined in an HCC cell line panel. Tegavivint activity was measured in a syngeneic mouse model of HCC. Tumors were collected for FACS analysis of cell subpopulations of interest from the vehicle and tegavivint group at study termination. Efficacy and tolerability were measured and evaluated by tumor growth curve and body weight change in treatment groups. Liver and tumor tissue were collected at study termination. TBL1 levels were measured in HCC cells

and mouse tumors via western blot and immunohistochemical (IHC) staining.
Results: Tegavivint sensitivity was measured in a of HCC cell line panel resulting in GI_{50} values ranging from 0.03 μM - 0.20 μM. Correlation between cell sensitivity and activating beta-catenin mutational status was identified and further characterized by measurement of active beta-catenin and TBL1 expression in cell lysates. In an HCC syngeneic mouse model with reported elevated levels of beta-catenin, tegavivint significantly inhibited tumor growth in comparison to vehicle control and demonstrated a significant change in PD-1+ CD3+ and PD-1+ CD4+ subpopulations. TBL1 and active beta-catenin levels were also characterized in tumor mouse tissue relative to tegavivint response.
Conclusion: Tegavivint monotherapy demonstrated antitumor activity in a range of HCC preclinical models. In vitro studies show correlation between tegavivint potency and beta-catenin mutation. In a syngeneic HCC mouse model with elevated beta-catenin, tegavivint reduces tumor growth and induces an activated T-cell subpopulation. We are currently characterizing potential biomarkers of TBL1/beta-catenin activity to identify HCC patient populations that will be most responsive to tegavivint in a clinical setting.

#6168

Implementation and adoption of a web tool to support precision diagnostic and treatment decisions for patient with myelodysplastic syndromes

Elsa Bernard[1], Juan E. Arango Ossa[1], Heinz Tuechler[2], Peter L. Greenberg[3], Robert P. Hasserjian[4], Yasuhito Nannya[5], Sean M. Devlin[6], Maria Creignou[7], Philippe Pinel[1], Lily Monier[1], Juan S. Medina-Martinez[1], Dylan Domenico[1], Martin Jädersten[8], Ulrich Germing[9], Guillermo Sanz[10], Arjan A. van de Loosdrecht[11], Olivier Kosmider[12], Matilde Y. Follo[13], Felicitas Thol[14], Lurdes Zamora[15], Ronald F. Pinheiro[16], Andrea Pellagatti[17], Detlef Haase[18], Pierre Fenaux[19], Monika Belickova[20], Michael R. Savona[21], Virginia M. Klimek[22], Fabio P. S. Santos[23], Jacqueline Boultwood[17], Ioannis Kotsianidis[24], Valeria Santini[25], Francesc Solé[26], Uwe Platzbecker[27], Michael Heuser[14], Peter Valent[28], Kazuma Ohyashiki[29], Carlo Finelli[30], Maria Teresa Voso[31], Lee-Yung Shih[32], Michaela Fontenay[12], Joop H. Jansen[33], José Cervera[34], Norbert Gattermann[9],

Benjamin L. Ebert[35], Rafael Bejar[36], Luca Malcovati[37], Mario Cazzola[37], Seishi Ogawa[38], Eva Hellström-Lindberg[39], Elli Papaemmanuil[1].
[1]Computational Oncology Service, Department of Epidemiology and Biostatistics, Memorial Sloan Kettering Cancer Center, New York, NY,[2]Institute of Science and Technology Austria, Klosterneuburg, Austria,[3]Stanford University Cancer Institute, Stanford, CA,[4]Department of Pathology, Massachusetts General Hospital, Boston, MA,[5]Department of Pathology and Tumor Biology, Kyoto University, Kyoto, Japan,[6]Department of Epidemiology and Biostatistics, Memorial Sloan Kettering Cancer Center, New York, NY,[7]Department of Medicine Huddinge, Center for Hematology and Regenerative Medicine,, Karolinska Institutet, Karolinska University Hospital, Stockholm, Sweden,[8]Department of Medicine Huddinge, Center for Hematology and Regenerative Medicine, Karolinska Institutet, Karolinska University Hospital, Stockholm, Sweden,[9]Department of Hematology, Oncology and Clinical Immunology, Heinrich Heine University, Düsseldorf, Germany,[10]Deparment of Hematology, Hospital Universitario y Politécnico La Fe, Valencia, Spain and CIBERONC, Instituto de Salud Carlos III, Madrid, Spain,[11]Department of Hematology, Amsterdam University Medical Center, Vrije University Medical Center, Amsterdam, Netherlands,[12]Department of Hematology, Assistance Publique-Hôpitaux de Paris, Hôpital Cochin and Université de Paris, Université Paris Descartes, Paris, France,[13]Cellular Signaling Laboratory, Human Anatomy Section, Department of Biomedical & Neuromotor Sciences, University of Bologna, Bologna, Italy,[14]Department of Hematology, Hemostasis, Oncology and Stem Cell Transplantation, Hannover Medical School, Hannover, Germany,[15]Hematology Department, Hospital Germans Trias i Pujol, Institut Català d'Oncologia, Josep Carreras Leukaemia Research Institute, Barcelona, Spain,[16]Drug Research and Development Center, Federal University of Ceara, Ceara, Brazil,[17]Nuffield Division of Clinical Laboratory Sciences, Radcliffe Department of Medicine, University of Oxford and Oxford BRC Haematology Theme, Oxford, United Kingdom,[18]INDIGHO Laboratories. Clinics of Hematology and Medical Oncology, University Medical Center, Göttingen, Germany,[19]Department of Hematology, Hôpital St Louis, Paris University, Paris, France,[20]Department of Genomics, Institute of

Hematology and Blood Transfusion, Prague, Czech Republic,[21]Department of Medicine, Vanderbilt-Ingram Cancer Center, Vanderbilt University School of Medicine, Nashville, TN,[22]Leukemia Service, Department of Medicine, Memorial Sloan Kettering Cancer Center, New York, NY,[23]Oncology-Hematology Center, Hospital Israelita Albert Einstein, Sao Paulo, Brazil,[24]Department of Hematology, Democritus University of Thrace Medical School, Alexandroupolis, Greece,[25]Myelodysplastic syndromes Unit, Department of Experimental and Clinical Medicine, Hematology, Azienda Ospedaliero Universitaria Careggi, University of Florence, Florence, Italy,[26]Myelodysplastic Syndromes Group, Institut de Recerca contra la Leucèmia Josep Carreras, Barcelona, Spain,[27]Medical Clinic and Policlinic 1, Hematology and Cellular Therapy, University of Leipzig, Leipzig, Germany,[28]Department of Internal Medicine I, Division of Hematology and Hemostaseology, Ludwig Boltzmann Institute for Hematology and Oncology, Medical University of Vienna, Vienna, Austria,[29]Tokyo Medical University, Tokyo, Japan,[30]Institute of Hematology "Seràgnoli", Istituti di Ricovero e Cura a Carattere Scientifico Azienda Ospedaliero-Universitaria di Bologna, Bologna, Italy,[31]MDS Cooperative Group GROM-L, Department of Biomedicine and Prevention, Tor Vergata University, Rome, Italy,[32]School of Medicine, Chang Gung Memorial Hospital at Linkou, Chang Gung University, Taoyuan, Taiwan,[33]Laboratory Hematology, Department of Laboratory Medicine, Radboud University Medical Centre, Nijmegen, Netherlands,[34]Department of Hematology and Genetics Unit, University Hospital La Fe, Valencia, Spain,[35]Department of Medical Oncology and Howard Hughes Medical Institute, Dana-Farber Cancer Center, Boston, MA,[36]University of California San Diego Moores Cancer Center, La Jolla, CA,[37]Fondazione Istituto di Ricovero e Cura a Carattere Scientifico Policlinico San Matteo, University of Pavia, Pavia, Italy,[38]Institute for the Advanced Study of Human Biology, Kyoto University, Kyoto, Japan,[39]Department of Medicine Huddinge, Center for Hematology and Regenerative Medicine, Karolinska Institutet, Karolinska University Hospital, Stockholm, Sweden

Despite a detailed understanding of the genes mutated in myelodysplastic syndromes (MDS), diagnostic and treatment decisions for patients with MDS rely primarily on clinical and cytogenetic variables as considered by

the Revised International Prognostic Scoring System (IPSS-R). Here we describe the recently developed Molecular IPSS (IPSS-M), a clinico-genomic risk stratification system that considers clinical, cytogenetic and genetic parameters; the implementation of a web portal to facilitate its adoption, a strategy to handle missing variables, and the worldwide utilization of the web calculator as a clinical support tool.

The IPSS-M was trained on 2,957 clinically annotated diagnostic MDS samples profiled for mutations in 156 driver genes. To maximize the clinical applicability of the IPSS-M and account for missing genetic data (i.e genes missing from a sequencing panel), we implemented a strategy to calculate a risk score under three scenarios: best, worst and average. Last, we developed an online calculator as a standalone single-page web application using VueJs, and D3Js for the interactive visualizations, deployed through a CI/CD pipeline on AWS, where collection of anonymous usage analytics allows to track adoption and usability of the new proposed model.

The model incorporates clinical, morphological, genetic variables informed by cytogenetics and constructed from the presence of oncogenic mutations in 31 genes. It delivers a unique risk score for each individual patient, as well as an assignment to one of six IPSS-M risk strata. Compared to the IPSS-R the IPSS-M re-stratified 46% of MDS patients. The model was validated in an external dataset of 754 MDS patients. We released an open-access IPSS-M web calculator available at https://mds-risk-model.com. By specifying the patient clinical and molecular profiles, the tool returns the patient-specific IPSS-M risk score and category, and the probability estimates over time for three clinical endpoints, i.e. leukemia free survival (LFS), overall survival, and incidence of leukemic transformation. Since its launch in June 2022, the calculator has been used by >6000 users in >75 countries, reaching a daily average of 100 users per day. Risks have been calculated for >45,000 patient profiles. 99.28% of the sessions initiated reach an IPSS-M score, suggesting that the calculator is intuitive and easy to use.

We trained and validated the IPSS-M on 3,711 patients, a patient tailored risk stratification tool for patients with MDS that considers clinical, morphological and genetic variables inclusive of cytogenetics and mutations in one of 31 genes. The development of a web based tool was instrumental to the global dissemination of the model, enabling non-expert

users to leverage the power of molecular biomarkers in risk stratification for patients with MDS.

DNA Damage Response

#6172

Characterization of a novel series of highly selective PARP1 inhibitors

Phillip M. Cowley, Barry E. McGuinness, Gillian M. Campbell, Alan Wise.
Duke Street Bio Limited, London, United Kingdom

First-generation PARP1 inhibitors have provided significant therapeutic benefit to patients whose tumors exhibit homologous repair deficiencies, including BRCA mutations, however their use has been associated with hematological toxicities that have restricted their application, particularly in combination with standard-of-care chemotherapy. All four FDA-approved PARP1 inhibitors are largely non-selective for the closely related enzyme PARP2, inhibition of which has been shown to drive hematotoxicity. Hence, the development of second-generation molecules highly selective for PARP1 over PARP2 offers a significant opportunity to 1) dramatically enhance therapeutic index, 2) enable additional precision medicine / combination approaches with chemotherapy, radiotherapy, immunotherapy and targeted agents and 3) expand the addressable patient population to those whose tumors harbor additional DDR defects. Utilizing X-ray crystallography and structure-based drug design, we describe the characterization of a novel chemical series of highly selective PARP1 inhibitors. These molecules demonstrate high potency in multiple biochemical and cell-based assays, including viability and colony forming unit read-outs in BRCA-deficient cancer cells, whilst sparing isogenically-paired BRCA wild-type cells and non-transformed primary cell lines. The molecules are potent PARP1-DNA trappers and exhibit high affinity, high selectivity and prolonged residence time in biophysical surface plasmon resonance (SPR) binding assays. The molecules also demonstrate exceptionally high selectivity for PARP1 over PARP2, and across the mono and polyPARP family, using a cell-based NanoBRET target engagement assay. This chemical series generally exhibits highly desirable physico-chemical and in vitro ADME properties, coupled with an excellent in vitro safety profile, which translate to high oral bioavailability and low clearance

in rodent PK studies. Lead molecules yield deep and durable anti-tumor efficacy in a BRCA1m MDA-MB-436 breast cancer xenograft model with responses continuing after cessation of treatment. Percent tumor regression and post-dose tumor control was superior to olaparib at $1/10^{th}$ of the dose. Importantly, our molecules demonstrate prolonged tumor residence time and a markedly superior tumor:plasma ratio compared to competitor PARP1-selective inhibitors. Taken together, these data predict low therapeutic dosing with the potential to demonstrate improved efficacy and tolerability compared to marketed PARP inhibitors. In summary, we describe the characterization of novel potent and selective PARP1 inhibitors. These molecules demonstrate excellent in vitro ADMET and in vivo PK, coupled with profound anti-tumor efficacy and tumor-targeting properties in a genetically-defined mouse model, supporting their progression into clinical studies.

#6173

AKT1 prevents aberrant R-loops accumulation via regulating DHX9 and suppresses transcription-replication collision in PARP inhibitor-resistant ovarian cancer

Tzu-Ting Huang[1], Chih-Yuan Chiang[2], Jayakumar R. Nair[1], Chi-Ting Shih[1], Kelli Wilson[2], Ken Chih-Chien Cheng[2], Jung-Min Lee[1]. *[1]National Cancer Institute, Bethesda, MD,[2]National Center for Advancing Translational Sciences, Rockville, MD*

Background: Acquired resistance to PARP inhibitors (PARPis) is a pressing problem in high-grade serous ovarian cancer (HGSC), highlighting the development of novel therapeutic options. To address this unmet need, we conducted high-throughput drug combination screens in PARPi-resistant HGSC cells using ATR inhibitor (ATRi), given that ATR/CHK1 signaling activation is one of the main mechanisms of PARPi resistance. In the screens, PI3K/AKT pathway inhibitors were synergistic with ATRi. Mechanistically, ATR signaling plays a major role in R-loop dynamics and replication stress (RS) response pathways, but the role of AKT is unclear. Here, we aim to investigate AKT's role in R-loop-mediated RS in PARPi-resistant HGSC cells. We also hypothesize that AKT inhibitor (AKTi) would augment ATRi-induced R-loop formation by reducing the expression of helicases.

Methods: We used PARPi-resistant variants and parental PEO1 as a negative control. ATRi (ceralasertib) and AKTi (capivasertib) were used for further mechanistic studies. Induction of RS, DNA double-strand break, and R-loop were evaluated using immunofluorescence staining for markers pRPA, γH2AX, and S9.6, respectively. We measured multiple nuclear helicases and *in situ* DHX9-R-loop interaction by western blot and proximity ligation assay. DHX9-AKT1 interaction was confirmed by co-immunoprecipitation. All data were repeated in triplicate, analyzed using one-way ANOVA test, and shown as mean ± SD. $P < 0.05$ was considered statistically significant.
Results: The ATRi and AKTi combination induced greater RS, as evidenced by a 1.7-12.0-fold increase in pRPA+/γH2AX+ population relative to each drug alone. Adding AKTi to ATRi significantly increased R-loops compared to monotherapy alone (signal intensity 14-19 x 10^5 vs. 9.9-14.6 x 10^5, $P < 0.001$), suggesting that AKT also contributes to R-loop dissolution. Moreover, the combination showed a higher percentage of cells with γH2AX and R-loops relative to monotherapy (54.7-75.4% vs. 33.3-49.0%, $P < 0.001$) in the presence of pan-caspase inhibitor, indicating the increased DNA damage is unlikely caused by increased apoptosis but by R-loop accumulation. Also, AKTi addition to ATRi significantly reduced the nuclear DHX9 among other helicases. Moreover, we found that AKT1 directly binds with DHX9 via its kinase domain and couples with DHX9 to resolve R-loops.
Conclusion: Our data suggest ATRi and AKTi combination could be a new therapeutic combination in HGSC with PARPi resistance. Mechanistically, our data reveal a previously unknown direct role of AKT1 and its interaction with DHX9 in R-loop resolution besides ATR.

#6174
ATX-101, a peptide drug targeting PCNA, enhances the effect of gemcitabine in liposarcoma and leiomyosarcoma
Elgilda Musi, Tahir Sheikh, Matthew Ingham, Sminu Bose, Gary K. Schwartz. *Columbia University Irving Medical Center, New York, NY*

Soft tissue sarcomas are heterogeneous mesenchymal neoplasms and account for 1% of all cancers in adults. Over 50 sarcomas subtypes have been classified and many have very limited treatment options which include

surgery, chemotherapy and radiation. Two of the most common sarcomas are liposarcoma and leiomyosarcoma which are often treated with chemotherapies such as doxorubicin, dacarbazine and gemcitabine with low response rates. There is now more than ever an urgent need for new therapies for sarcoma. PCNA (Proliferating Cell Nuclear Antigen) is considered to be a key regulator of DNA and cell cycle control. In addition, it has been implicated to have roles in metabolism, cellular signaling and some immunological functions. PCNA forms complexes with proteins bearing a novel PCNA-interacting Peptide Motif called APIM (AlkB homolog 2 PCNA Interacting Motif). This binding usually occurs during stress responses such as those achieved during cancer therapy or cancer development. By preventing stress proteins from repairing or defending themselves, cancer therapies can be made more effective. We examined the in vitro effects of ATX-101, a PCNA-APIM protein interaction blocking peptide, on liposarcoma cell lines LS141, DDLS, SW872, 93T449 and 94T778 and leiomyosarcoma cell lines SK-LMS, SK-UT1 and SK-UT-1B. Cell survival, as measured by cell proliferation assays, indicated IC50s of 7.5-15μM with ATX-101. Enhanced combination effects with ATX-101 and chemotherapies such as doxorubicin, irinotecan and gemcitabine were also observed by proliferation assay. Synergism, with ATX-101 and gemcitabine, was indicated with SynergyFinder analysis. Cell cycle changes exhibited increases of S and G2 phases when treated with ATX-101 and gemcitabine. This correlated with increase of cell cycle proteins, cyclin B1 and cyclin A2. Western blot observations included increase of apoptotic marker, cleaved caspase 3, and DNA damage marker, pH2A.X. In addition, immunofluorescence assay showed increasing pH2A.X with ATX-101 and gemcitabine. In vivo studies revealed ATX-101 enhanced gemcitabine decrease of tumor volume in leiomyosarcoma cell line xenograft, SK-UT1. Tumor target inhibition by western blot showed increased pH2A.X and cleaved PARP along with decreased RAD51 API protein with combination treatment. Taken these observations and results, there is strong evidence of combining gemcitabine with ATX-101 in liposarcoma and leiomyosarcoma.

#6175

CDK8 inhibition potentiates the efficacy of niraparib in homologous recombination proficient cancer cell lines

Karen A. Simon-Crevatis[1], Shailesh R. Metkar[1], Justin T. Hardcastle[1], Keith Jansson[2], Usman Shabon[2], Rajarshi Choudhury[2], Euan A. Stronach[3], Kevin G. Coleman[1], Asli Muvaffak[1]. *[1]Synthetic Lethality Research Unit, GlaxoSmithKline LLC, Cambridge, MA,[2]Genomic Sciences, GlaxoSmithKline LLC, Collegeville, PA,[3]Genomic Sciences, GlaxoSmithKline LLC, Stevenage, United Kingdom*

While cyclin dependent kinases (CDKs) were originally implicated in cell cycle regulation, several CDKs including CDK7, CDK8, and CDK9 play critical roles in transcription through regulation of RNA polymerase II (Pol II) activity. In addition to expected phosphosite targets associated with DNA-binding transcription factors, chromatin regulators, or other known regulators of pol II activity, a phospho-proteomics study on a CDK8/19 inhibitor (Cortistatin A) also identified DNA replication and repair proteins, i.e., namely BRCA1 and MDC1, as substrates for CDK8. RVU120, a first in-class CDK8/19 inhibitor in phase I clinical trial demonstrated preclinical efficacy in acute myeloid leukemia PDX models. A robust relationship has also been observed between the exposure to RVU120 and inhibition of pSTAT5, a pharmacodynamic marker, in solid tumor indications in a recent clinical trial. Additionally, preclinical data suggested RVU120 reduced expression of genes related to interferon-related DNA damage signature (IRDS) suggesting a potential role of CDK8 in DNA repair signaling. CDK8 loss was identified as a synthetic lethal hit in two internal, orthogonal screens that surveyed targets which can synergize with niraparib inhibition. Niraparib inhibits PARP enzymatic activity and promotes PARP trapping on ssDNA breaks which lead to replication stress-induced dsDNA breaks that require BRCA-dependent homologous recombination repair (HRR). Combination with other therapeutic agents is anticipated to improve the efficacy of niraparib in HR proficient (HRP) and BRCA1/2.WT tumors. This work describes our proof-of-concept data from in vitro validation of combination synergy response of RVU120 with niraparib in a panel of 129 HRR.WT and HRR mutant cancer cell lines across ovarian, breast, lung, and colorectal cancer indications. Our results indicated that the niraparib+RVU120 combination was synergistic, and a strong synergy response, i.e., a SS (Synergy Score) ≥ 5 was detected by Loewe modelling across the entire surface of the combination matrix in ~26% of Horizon Discovery OncoSignature™ panel cell lines that were largely resistant to

niraparib monotherapy. The study findings indicated the potential of CDK8/19 inhibitors to enhance niraparib activity in both HRR.WT and HRR mutant populations. The potential benefit of CDK8/19i+niraparib combination will be further explored in PARPi-resistant models. Molecular studies are underway to explore potential biomarkers associated with synergy response, and to analyze the downstream effects on DNA Damage Response.

#6176

Enhancing treatment efficacy of glioblastoma cell lines by adding tumor treating fields (TTFields) to temozolomide and lomustine

Hila Fishman, Roni Monin, Eyal Dor-On, Adi Haber, Moshe Giladi, Uri Weinberg, Yoram Palti. *Novocure Ltd, Haifa, Israel*

Background: Tumor Treating Fields (TTFields) are electric fields that disrupt cellular processes critical for cancer cell viability and tumor progression, ultimately leading to cell death. Concurrent maintenance temozolomide (TMZ) with TTFields was approved by the FDA in 2014 for treatment of patients with newly diagnosed glioblastoma (ndGBM). Recently, the addition of lomustine (CCNU) to TMZ demonstrated clinical benefit in ndGBM patients. The aim of the current study was to examine in GBM cells the effect of TTFields concurrent with TMZ and CCNU.
Methods: Human GBM cell lines (U-87 MG, LN229, U118, and LN18) with various MGMT expression levels were treated with TTFields (intensity of 0.83 V/cm RMS; frequency of 200 kHz) using the inovitro system. Effectiveness of TTFields concomitant with TMZ and/or CCNU was tested by measuring cell count and colony formation. Levels of DNA repair proteins in control and TTFields-treated cells were measured using Western blot.
Results: The cell lines displayed different sensitivity to TMZ, in accordance with their MGMT expression level, but showed a comparable response to TTFields. TTFields concomitant with TMZ displayed an additive effect on cell numbers, irrespective of MGMT expression levels. The effect of TTFields concomitant with CCNU was additive in cell lines expressing MGMT, whereas it trended toward synergy in cell lines not expressing MGMT. Application of TTFields to the cells downregulated expression of proteins from the Fanconi Anemia-BRCA pathway for DNA repair.

TTFields concurrent with both TMZ and CCNU provided higher efficacy relative to TMZ plus CCNU or TTFields apart.
Conclusions: Efficacy of TMZ and CCNU may be enhanced by TTFields, with synergism seen for the latter case in cells with limited MGMT expression. The BRCAness state induced by TTFields rationalizes these outcomes, as DNA damage induced by CCNU requires the BRCA pathway for repair, especially in the absence of MGMT. The results suggest a potential benefit for concomitant TTFields with the TMZ/CCNU combination in ndGBM.

#6177

ATRN-119 and ATRN-W1051: Novel and potentially well tolerated ATR and WEE1 inhibitors for targeted cancer treatment

Joseph Vacca[1], Stephen Rocca[2], Justin Frye[2], Steven J. Schnell[2], Molly Hansbarger[2], Gregory Korbel[2], Fiona Simpkins[3], Eric J. Brown[3], Oren Gilad[2]. *[1]Aprea Therapeutics, Dolyestown, PA,[2]Aprea Therapeutics, Doylestown, PA,[3]Perelman School of Medicine, University of Pennsylvania, Philadelphia, PA*

Previous studies have demonstrated the promise of ATR and WEE1 inhibitors (ATRi and WEE1i) as cancer treatments. Inhibition of these DNA replication checkpoint kinases disrupts normal DNA synthesis and causes replication fork collapse, and these effects are accentuated by numerous cancer-associated mutations. However, a key limitation to this approach in clinical trials has been the occurrence of adverse hematological effects, including anemia, neutropenia, and thrombocytopenia. Herein, we describe two novel inhibitors, ATRN-119 (ATRi) and ATRN-W1051 (WEE1i), that exhibit increased target selectivity that potentially decreases these dose-limiting toxicities. ATRN-119, the first macrocyclic ATRi to enter clinical trials, is highly specific for inhibition of ATR relative to other phosphatidylinositol kinase-related kinases (PIKKs), such as ATM, DNA-PK, and MTOR. This specificity correlates with increased tolerability, which permits continuous dosing in animal models. Importantly, dose scheduling of ATRN-119 that suppresses tumor growth in xenograft mouse models of colon, pancreatic, and prostate cancers causes no appreciable loss of body weight or hematologic toxicity (anemia, neutropenia or thrombocytopenia). Daily dosing is also tolerated in combination with

PARP inhibition, which causes significant tumor reduction in a BRCA2-defient PDX model of high-grade serous ovarian cancer. These findings have led a biomarker-driven Phase I clinical trial of ATRN-119 with daily dosing for ovarian and other cancers (Simpkins, PI). To potentially reduce the toxicity of WEE1i, a new potent and selective WEE1 inhibitor, ATRN-W1051, was developed. *In vitro*, ATRN-W1051 inhibits WEE1 with an IC50 of 2.2 nM and limits the proliferation of ovarian cancer cell lines in the 100 nM to 200 nM range. Importantly, ATRN-W1051 exhibits low off-target inhibition of the PLK family of kinases (PLK1, PLK2 and PLK3), which are substantially inhibited by the leading WEE1i in the clinic (AZD1775 and ZN-c3)[1]. In addition, ATRN-W1051 also has potentially favorable pharmacokinetic properties that permits 3-8 times lower dosing than AZD1775 or ZN-c3 to achieve similar exposure (AUC_{0-24}) levels[2]. Notably, daily oral dosing of ATRN-W1051 is well tolerated in mice and suppresses the growth of CCNE1-amplified HGSOC xenografted tumors. These preclinical data suggest that ATRN-W1051 may be a potential therapeutic candidate for CCNE1-overexpressing HGSOC. Together, ATRN-119 and ATRN-W1051 provide promising alternative DNA replication checkpoint inhibitors for the treatment of a variety of cancers.

#6178

A novel second-generation nano-fluoropyrimidine to treat metastatic colorectal cancer and overcome 5-fluorouracil resistance

Naresh Sah[1], Pamela Luna[1], Chinnadurai Mani[1], William Gmeiner[2], Komaraiah Palle[1]. *[1]Cell Biology and Biochemistry, Texas Tech University Health Sciences Center, Lubbock, TX,[2]Department of Cancer Biology, Wake Forest University School of Medicine, Winston-Salem, NC*

Colorectal cancer (CRC) is the 3rd leading cause of cancer-related mortality. The mortality associated with colon cancer results notably from metastatic disease (mCRC), with a 5-year survival rate for patients with stage IV CRC being < 14%. Despite extensive efforts towards developing personalized therapies, limited success has been achieved and chemotherapeutic regimens that include the fluoropyrimidine (FP) drug 5-fluorouracil (5-FU) are central to patient management. While using 5-FU-based regimens such as FOLFOX and FOLFIRI in combination with biologics confer a survival

benefit, their ineffectiveness at promoting long-term survival in a substantial fraction of mCRC patients and associated toxicities limits their use. This underscores the pressing need to develop improved FP drugs. To overcome the limitations of 5-FU that include resistance due to elevated expression of thymidylate synthase (TS) and inefficient anabolic metabolism to FdUMP, the TS-inhibitory/active metabolite, we are developing FP polymers consisting of single-stranded DNA with FdUMP (only active metabolite) as the repeating nucleotide unit. Our therapeutic objective is to initiate a Phase I clinical trial with a new 2nd generation nanoscale FP polymer (CF10) that demonstrates promising anticancer effects in several preclinical models and significantly lower systemic toxicity. We observed that CF10 displayed significantly higher anti-tumor activity than 5-FU in flank and syngeneic tumor models. Additionally, CF10 treatment improved survival (84.5 days *vs* 32 days; $P < 0.0001$) relative to 5-FU in an orthotopic HCT-116-*luc* colorectal cancer mice model that spontaneously metastasized to the liver. Interestingly, a reduction in metastatic tumor burden in the CF10 treatment group led us to hypothesize that CF10 could inhibit the TS-mediated EMT phenotype and pro-metastatic activities in colorectal cancer cells (CRCs). This was supported by increased vimentin, decreased E-cadherin expression, and increased cell migration and invasion in TS-overexpressing CRC cells ("Tet-on" system). Alkaline comet assay, immunofluorescence imaging, and immunoblot identified significantly higher replication stress with CF10 treatment than 5-FU in mouse, rat, and human-established CRC cell lines and primary CRC cells. Strikingly, we also discovered that CF10 attenuates the growth of TS-overexpressing primary colonoids. In conclusion, CF10 induces increased replication stress compared to a similar concentration of conventional drugs. Our findings suggest the significance of elevated TS in CRC metastatic progression and 5-FU resistance and demonstrate that CF10 may be effective at inhibiting CRC metastatic progression. CF10 may be a successful candidate for early-phase clinical trials to treat mCRC.

#6179

Comparative study of Polθ helicase and polymerase inhibitor biochemical and cellular potency

Johanna K. Ahlskog[1], Antti Pohjakallio[2], Ralf Paul[1], Martin Augustin[3], Elisabeth Schneider[3], Sakshi Johri[3], Tuomas Tervahauta[2], Hans-Georg

Beisel[1], Lars Neumann[3], Julia Lindqvist[1], Anu Moilanen[1]. *[1]Orion Corporation, Turku, Finland,[2]Orion Corporation, Espoo, Finland,[3]Proteros Biostructures GmbH, Martinsried, Germany*

Background: DNA Polymerase θ (Polθ) is active in Theta-mediated end joining (TMEJ), a repair pathway that utilizes resected 3' ends and micro-homology sequences to repair double strand breaks. Polθ contains an N-terminal helicase domain and a C-terminal polymerase domain. The helicase domain facilitates stripping of RPA/RAD51 from single stranded DNA and is involved in DNA-end recognition, and micro-homology search and pairing. The polymerase domain performs DNA synthesis following micro-homology pairing. Lack of Polθ is synthetic lethal in homologous recombination deficient (HRD) cells. In this study, we utilized existing small molecule inhibitors targeting either helicase or polymerase domain of Polθ, to assess their translational potential in HRD *in vitro* cancer cell models.
Methods: Small molecules inhibiting either the helicase or polymerase activity of Polθ were studied with biochemical and cellular assays. For the biochemical studies, recombinant helicase or polymerase domains were purified. The helicase activity of Polθ was analyzed using ADP-Glo and the polymerase activity by primer extension assay. Binding assays confirmed inhibitor binding to recombinant proteins. To study inhibitor efficacy in cellular models, we probed cell viability of BRCA2-deficient cell lines.
Results: Both helicase and polymerase inhibitors showed good potency in inhibiting Polθ enzymatic activity in ATPase or primer extension assays, respectively, with IC50 values in low-nanomolar range. However, the viability of BRCA2-deficient cell lines was not significantly affected after treatment with either helicase or polymerase inhibitors. The measured compound properties (stability, efflux, solubility) did not explain the lack of efficacy in cellular viability assays. Combining Polθ inhibitor treatment with ionizing radiation led to a modest enhancement of radiation-induced decrease in cell viability.
Conclusions: Recently, significant advances have been made in Polθ inhibitor development prompted by the synthetic lethal interaction between Polθ and HRD discovered in several screening efforts. Both helicase and polymerase inhibitors are highly potent in biochemical assays. However, without exogenous genotoxic stress, the potential of Polθ inhibitors as

therapeutic target may not be reached *in vitro.* Additional studies are required to understand the translational gap between biochemical and biological read-outs.

#6180

Antitumor activity of the ATR inhibitor Elimusertib in patient-derived xenograft models with DNA damage response pathway alterations

Kaushik Varadarajan[1], Christian X. C. Pico[1], Kurt Evans[1], Maria G. Raso[1], Yasmeen Rizvi[1], Xiaofeng Zheng[1], Timothy P. Diperi[2], Bailiang Wang[1], Stephen Scott[1], Ming Zhao[1], Argun Akcakanat[1], Antje M. Wengner[3], Timothy A. Yap[1], Funda Meric-Bernstam[1]. *[1]UT MD Anderson Cancer Center, Houston, TX,[2]Cedars Sinai Medical Center, Los Angeles, CA,[3]Bayer AG, Berlin, Germany*

Introduction: The ataxia telangiectasia and RAD3-related (ATR) kinase is a key component of the DNA damage response (DDR) and functions in conjunction with ataxia telangiectasia mutated (ATM). ATM loss or functional deficiency may enhance reliance on ATR signaling. Preclinical and clinical studies have pointed to a potential synthetic lethality of ATR inhibition and ATM loss. In this study, we sought to further elaborate potential candidates for ATR inhibition by testing the anti-tumor effect of elimusertib (BAY 1895344) in patient-derived tumor xenograft (PDX) models with DDR alterations including ATM loss.

Methods: Patient derived xenograft (PDX) models were implanted into athymic nu/nu mice. Once tumors reached an appropriate size of approximately 200-400mm^3 treatments were started. Mice were randomized (N= 3-8) to different treatment arms for assessment of anti-tumor activity of elimusertib as monotherapy and in combination therapy with copanlisib. Monotherapy treatment was performed with 20 mg/kg and 40 mg/kg doses, applied twice daily for 3 days with 4 days treatment break (BID 3 days on/4 days off). Efficacy read-out was either Event-Free Survival (EFS-2), defined as time for doubling of tumor volume relative to baseline, or response based on RECIST criteria:(partial response [PR]= >30% decrease, stable disease [SD]= between 20% increase and 30% decrease, and progressive disease [PD]= >20% increase). For assessment of pharmacodynamic effects, tumors were harvested 10 days after treatment

start and analyzed by immunohistochemistry (IHC) and RPPA (Reverse Phase Proteomics Array).
Results: Elimusertib was tested in 21 PDX models with various DDR alterations. Of those 11 showed a statistically significant prolongation of event free survival compared to control. In 4 PDX models elimusertib reached a partial response (PR), and another 4 models showed stable disease (SD). Amongst the 5 models with ATM protein Ioss (IHC), one was PR and another one SD. In 3 of 5 PARP inhibitor resistant there was statistically significant prolongation of EFS upon elimusertib treatment vs control. We found an increase in DNA damage in tumors, as indicated by increased level of YH2AX (on IHC and RPPA). We also detected an increase in PI3K/mTOR pathway signaling as determined by p-MTOR and pS6 (RPPA) in 2 of 4 models (PR and PD model) with different sensitivity to ATRi and PARPi alone. We tested the combination of elimusertib with the PI3K inhibitor copanlisib achieved a statistically significant increase of EFS compared to monotherapy in 3 of 11 models tested.
Conclusion ATR inhibition shows potent monotherapy activity in selected PDX models that harbor DDR defects, including models with intrinsic and acquired PARPi resistance. Further work is needed to identify markers predicting sensitivity or resistance that providing rationale for synergistic combination therapies.

#6181
Dynamic changes in monocyte and reticulocyte counts predict mechanism-based anemia development and recovery during ATR inhibitor treatment in phase I/II trials
Natalie Y. L. Ngoi, Heather Y. Lin, Ecaterina Dumbrava, Siqing Fu, Daniel D. Karp, Aung Naing, Shubham Pant, Sarina A. Piha-Paul, Jordi Rodon, Vivek Subbiah, Apostolia M. Tsimberidou, Erick Campbell, Samuel Urrutia, David S. Hong, Funda Meric-Bernstam, Ying Yuan, Timothy A. Yap. *UT MD Anderson Cancer Center, Houston, TX*

Introduction: Clinical trials are exploring ATR inhibitors (ATRi) in genomically selected contexts. However, dose-dependent anemia has limited the therapeutic index of this class. We hypothesized that monocytes and reticulocytes are more vulnerable to ATRi due to their lack of base excision repair and high levels of oxidative stress, respectively. We sought

to examine the kinetics of decline and recovery of red blood cell (RBC) and reticulocyte indices, in relation to hemoglobin (Hb), in the first 28 days after ATRi initiation.
Methods: We retrospectively retrieved peripheral blood cell indices from complete blood count (CBC) reports of patients (pts) pre- and during treatment with an oral ATRi on phase I/II trials at our center. Pts received ATRi monotherapy or in combination with a PARP inhibitor (ATRi+PARPi) in dose-escalation and expansion cohorts, which included ATRi at potentially toxic doses. We applied linear mixed effect models to evaluate the joint evolution of Hb and other RBC or reticulocyte indices over time via bivariate analysis. A random intercept was included in the model to account for the longitudinal nature of the data and a variance component option for the covariance structure was specified to model a different variance component for each index of interest. To assess if Hb decline was preceded by decline in the index of interest from baseline, piecewise regression models were used to estimate break points, defined as the time point where the fitted functions intersect, of each index. Log transformed data with a base of 2, were noted to have more symmetric distributions, and were used in the analyses. The time variable assessed was days from cycle 1 day 1 of ATRi. A two-sided p value <0.05 was considered statistically significant.
Results: 35,007 indices from 1,843 CBC of 119 pts treated with an ATRi from 10/2017 to 1/2022 were analyzed. 110 (92.4%) pts received ATRi, 9 (7.6%) received ATRi+PARPi. Monocytes (-0.120 vs -0.022, $p <0.0001$) and reticulocytes (-0.140 vs -0.022, $p <0.0001$) declined at a faster rate compared with Hb. Time to monocyte and reticulocyte nadir after ATRi initiation was 8.9 and 5.8 days, respectively, while time to Hb nadir was 19.5 days. Conversely, RBC (-0.020 vs -0.023, $p=0.410$), MCV (-0.002 vs -0.022, $p <0.0001$) and MCH (-0.001 vs -0.022, $p<0.0001$) declined at a slower rate than Hb. Time to RBC, MCV and MCH nadir after ATRi initiation was 26.3, 18.7 and 15.0 days, respectively. After reaching their individual index nadir, monocytes (0.004 vs 0.001, $p <0.0001$) and reticulocytes (0.005 vs 0.0005, $p <0.0001$) increased more quickly than Hb.
Conclusions: Charting the kinetics of CBC index evolution in relation to Hb identified peripheral monocytes and reticulocytes as relevant blood indices that herald Hb decline. Our findings may inform patient monitoring strategies to mitigate hematologic toxicity on future ATRi trials.

#6182

Tumor treating fields (TTFields) concomitant with PARP inhibitors or carboplatin for treatment of ovarian cancer cell lines

Antonia Martinez-Conde, Hila Ene, Roni Frechtel-Gerzi, Eyal Dor-On, Adi Haber, Moshe Giladi, Uri Weinberg, Yoram Palti. *Novocure Ltd, Haifa, Israel*

Purpose/Objectives: Ovarian cancer continues to be the leading cause of death among gynecological malignancies. Platinum-based chemotherapy is recommended after surgery for most patients with ovarian cancer; and PARP inhibitors (PARPi) are suggested as maintenance therapy. Both therapies induce DNA damage that require the proper activity of the Fanconi Anemia (FA)- BRCA pathway for its resolution, and hence are most beneficial in cancers with a BRCA mutation. However, 75% of patients with ovarian cancer do not harbor BRCA mutations, and thus may experience limited benefit from these treatments. TTFields are electric fields that disrupt cellular processes critical for cancer cell viability and tumor progression, ultimately leading to cancer cell death. Recently, TTFields have been shown to induce a state of BRCAness in various cancer types, and to be effective in ovarian cancer pre-clinical models. The objective of the current study was to examine the effect of TTFields concomitant with carboplatin or PARPi on ovarian cancer cell lines.
Materials/Methods: A2780 (BRCA wild type) and OVCAR3 (BRCA mutated) ovarian carcinoma cells were treated with TTFields (72 h, 1 V/cm RMS, 200 kHz), alone or with concomitant application of carboplatin or the PARP inhibitors olaparib or niraparib. Efficacy was examined via measurements of cell count, colony formation, and induction of apoptosis. The overall effect was calculated by multiplying cell count with colony formation.
Results: Application of TTFields to A2780 or OVCAR3 cells resulted in reduced cell count, increased overall effect, and elevated apoptosis. Carboplatin, olaparib, and niraparib each displayed dose dependent effects in both cell lines, with higher sensitivity demonstrated in the BRCA mutated cells. Concomitant application of TTFields with any of these drugs displayed a synergistic interaction in the BRCA wild type A2780 cells and an additive effect in the BRCA mutant OVCAR-3 cells.

Conclusions: The data suggest potential benefits for TTFields concomitant with platinum-based chemotherapy and PARPi in ovarian cancer, even in the absence of background BRCA mutations, in accordance with the BRCAness state induced by TTFields. As such, TTFields may enhance the efficacy of treatment for ovarian cancer in both the adjuvant and maintenance settings.

#6183

PARP inhibitors preferentially sensitize splicing factor mutant myeloid neoplasms

Dang Hai Nguyen[1], Sayantani Sinha[2], Zhiyan Silvia Liu[3], Maxwell Henry Bannister[3], Erica Arriaga-Gomez[2], Axia Song[2], Dawei Zong[3], Martina Sarchi[4], Victor Corral[3], Wannasiri Chiraphapphaiboon[3], Jennifer Yoo[3], Matthew McMahon[3], Cassandra Leibson[3], Derek L. Stirewalt[5], H. Joachim Deeg[5], Sumit Rai[6], Matthew Walter[7], Timothy A. Graubert[6], Sergei Doulatov[4], Stanley C. Lee[2]. *[1]Department of Pharmacology, The Masonic Cancer Center, University of Minnesota, Minneapolis, MN,[2]Fred Hutchinson Cancer Center, Seattle, WA,[3]Department of Pharmacology, University of Minnesota, Minneapolis, MN,[4]Division of Hematology, Department of Medicine, University of Washington, Seattle, WA,[5]Clinical Research Division, Fred Hutchinson Cancer Center, Seattle, WA,[6]Massachusetts General Hospital Cancer Center, Charlestown, MA,[7]Division of Oncology, Department of Internal Medicine, Washington University School of Medicine, St Louis, MO*

Somatic heterozygous mutations in genes encoding for RNA splicing factors (SF) *SRSF2*, *U2AF1*, and *SF3B1* are frequently mutated in patients with hematologic malignancies, representing a unique genetic vulnerability for targeted therapy. In the current study, we performed a focused drug screen with inhibitors targeting different DNA damage response and DNA metabolic pathways to identify novel therapeutic vulnerabilities generated by SF mutations. We generated a murine leukemia model by overexpressing the MLL-AF9 fusion oncogene on an $Srsf2^{P95H/+}$ background, a mutational combination that is found in ~10% of *MLL*-rearranged leukemias. We surprisingly found that MLL-AF9 $Srsf2^{P95H/+}$ mutant leukemias are sensitive to inhibitors targeting ADP-ribosyltransferases (PARP). PARP

inhibitor sensitivity was also observed in isogenic murine MLL-AF9 *U2af1*$^{s34/+}$ cells compared to MLL-AF9 *U2af1*$^{+/+}$ cells. Second, murine Srsf2^{P95H} leukemias showed improved prolonged survival when treated with olaparib (PARPi) compared to vehicle treatment *in vivo*. Third, human primary AML patient samples that harbor SF mutations are sensitive to PARPi compared to non-SF mutant samples. These data highlight that both *SRSF2*^{P95H} and *U2AF1*^{S34F} mutations create a common vulnerability that is dependent on PARP activity for survival. To evaluate PARP activity, we used isogenic K562 leukemia cells expressing *SRSF2*^{P95H} and *U2AF1*^{S34F} mutations from their endogenous loci and monitored ADP-ribosylation (ADPr) levels, a marker of PARP activity. Both SRSF2^{P95H} and U2AF1^{S34F} cells exhibited elevated levels of ADPr compared to wildtype cells in a PARP1- dependent manner. PARPi preferentially induced DNA damage and cell death in SF mutant cells. Surprisingly, we found that SRSF2^{P95H} and U2AF1^{S34F} cells are not defective in homologous recombination repair. Instead, the increased PARP1-mediated ADPr in SF-mutant cells is caused by accumulated R loops, a group of transcription intermediates containing RNA:DNA hybrids and displaced single-stranded DNA. To determine whether PARPi sensitivity is due to R-loop accumulation, we overexpressed RNase H1, an enzyme that specifically cleaves the RNA moiety within RNA:DNA hybrids in U2AF1^{S34F} cells. Overexpression of RNase H1 significantly reduced ADPr levels and suppressed the PARPi-induced U2AF1^{S34F} cell growth inhibition. Collectively, these results suggest that spliceosome mutants induce R-loop accumulation and elicit an R-loop-associated PARP1 response to promote cell survival. In summary, our data establish a previously unknown link between R-loop-induced PARP1 response and RNA splicing perturbation and provide a mechanistic rationale to evaluate the clinical efficacy of PARP inhibitors in spliceosome-mutant malignancies. Furthermore, our study highlights a new therapeutic potential of targeting the R-loop tolerance pathways caused by different spliceosome gene mutations.

#6184

Pre-clinical study of SYX3759, a novel PARG inhibitor for the treatment of homologous recombination deficient malignancies

Xuzhen Tang, Yaqi Cui, Lanqiao Zhang, Huihui Jin, Zeqiong Xu, Hu He, Chongxun Ge, Song Liu, Xiaochun Yu, Song Shi. *SynRx Therapeutics, Hangzhou, China*

Although PARP inhibitors (PARPi) are very successful on the treatment of BRCA-mutant cancer, the tumor spectrum targeted by PARPi is quite narrow. Interestingly, Poly(ADP-ribose) Glycohydrolase (aka PARG), the major dePARylation enzyme, has emerged as a promising therapeutic target for cancer treatment. Here, we have developed a cell membrane permeable PARG inhibitor with subnanomolar IC_{50}. SYX3759 directly binds to the catalytic domain of PARG and induces significant accumulation of PARylation at DNA lesions, where it traps numerous DNA repair factors, such as XRCC1. Compared to PARPi, such as Olaparib, SYX3759 shows selective and potent cytotoxicity on a broader spectrum of homologous recombination deficient (HRD) tumors both in vitro and in vivo. Moreover, SYX3759 is well tolerated at the highest dose tested without obvious adverse effect on hematopoiesis. Collectively, SYX3759 is a potent PARG inhibitor both in vitro and in vivo warranting future clinical trials for the treatment of HRD cancers and beyond.

#6185

Debio 0123 is a selective WEE1 inhibitor that effectively penetrates the brain and demonstrates anti-tumor activity in preclinical models of glioblastoma

Luke Piggott, Noemie Luong, Frederic Massiere, Annett Kunze, Christophe Chardonnens, Anne Vaslin. *Translational Medicine, Debiopharm International S.A., Lausanne, Switzerland*

Background: Glioblastoma (GBM) is one of the most aggressive and hard-to-treat cancers with a 5-year survival rate of 5.8%, in part due to the presence of the blood brain barrier (BBB) that prevents most therapeutics from reaching the tumors at efficacious concentrations. Debio 0123 is a WEE1 inhibitor that has previously shown significant preclinical efficacy in combination with DNA damaging agents or radiotherapy and is currently being investigated in phase 1 clinical studies either as a monotherapy or in combination with carboplatin. Herein we present data that demonstrates Debio 0123 effectively penetrates in to the brain and subsequently leads to

anti-tumor activity in GBM models both in vitro and in vivo as a monotherapy or in combination with standard-of-care therapies (SOC).
Methods: Radio- and chemo-sensitizing effects of Debio 0123 were evaluated in GBM cell lines in vitro using standard clonogenic assays or cytotoxicity assays. In vivo, distribution and bioanalysis studies were performed to determine the amount of Debio 0123 present in the different parts of the brain and intracranially implanted tumors. Efficacy of Debio 0123 as monotherapy or in combination with the SOC, temozolomide (TMZ), was further assessed in vivo in U87MG-luc intracranial or subcutaneous xenograft models.
Results: In vitro, Debio 0123 in combination with radiation enhanced cell death in GBM cell lines and reduced TMZ IC50 in primary GBM cell lines. In vivo studies demonstrated substantial Debio 0123 brain penetration in mice, rats and monkeys, with mean brain-to-plasma concentration ratios of ~0.6 and 1.52 and 4, respectively. Furthermore, a mean tumor-to-plasma ratio of 0.62 was determined in orthotopically implanted brain tumors in mice. In efficacy studies, Debio 0123 administered at 30 or 60mg/kg every day for 28 days displayed significant anti-tumor activity in a GBM xenograft model U87-MG implanted in immunodeficient mice either subcutaneously, with up to 57.5% tumor growth inhibition, or orthotopically in the brain, with up to 73.7% tumor growth inhibition. Finally, efficacy of Debio 0123 in combination with TMZ was also assessed in intracranially transplanted U87-MG tumors. Here, TMZ was highly active, however, the combination of Debio 0123 and TMZ resulted in significantly enhanced anti-tumor activity leading to sustained complete regressions in 75% of animals for up to 100 days and was well tolerated throughout the 28-day treatment.
Conclusion: These results demonstrate that following oral administration, Debio 0123 effectively crosses the BBB, has significant efficacy as a monotherapy and improves response to standard-of-care chemo or radiotherapy in preclinical models. Collectively, these data highlight Debio 0123 as a promising candidate for further clinical development in GBM patients that may provide improved response to SOC therapy.

#6186
Patient-derived tumor organoids with p53 mutations, and not wild-type p53, demonstrate synergistic sensitivity to treatment with

temozolomide in combination with talazoparib PARP inhibitor

Florencia P. Madorsky Rowdo[1], Gu Xiao[2], Melissa B. Davis[1], Laura Martin[1], Olivier Elemento[1], Jill Bargonetti[2]. *[1]Weill Cornell Medicine, New York, NY,[2]Biological Sciences Hunter College, City University of New York, New York, NY*

Mutations in the *TP53* gene can be found in more than 50% of tumors. We recently showed in 2D breast cancer cell lines that mutant p53 (mtp53) proteins tightly associate with replicating DNA, chromatin and Poly (ADP-ribose) polymerase (PARP) protein. In addition, missense mtp53 R273H causes an increase in the chromatin association of replication proteins including PARP, and mini-chromosome maintenance complex 2-7 (MCM2-7). The expression of mtp53 R273H enhances overall MCM2 levels, promotes cell proliferation, and improves the synergistic cytotoxicity of treatment with the alkylating agent temozolomide in combination with the PARP inhibitor (PARPi) talazoparib. Currently, PARPis are indicated for patients that present BRCA1/2 mutations, but there might be patients with other alterations associated with DNA damage repair that could benefit from PARPi treatment; this includes expression of mtp53. Patient-derived Tumor Organoids (PDTO) are 3D culture models that retain cell-cell and cell-matrix interactions and are shown to reproduce drug responses observed in patients. Here, we evaluated the sensitivity of wild-type BRCA1/2 breast and lung PDTO with either mtp53 or wild-type p53 (wtp53) to the combination of DNA damaging agent temozolomide plus the PARPi talazoparib. First, we tested the sensitivity of the organoids to talazoparib and temozolomide individually. To determine if there was synergy between the two treatments, the organoids were treated with an inhibitor matrix to evaluate multiple combinatorial concentrations. Three breast cancer and two lung cancer PDTO with mtp53 presented synergistic cytotoxicity of the combination treatment. Two breast organoid lines with wtp53 showed no synergistic interaction between the two drugs, and the same was observed in a wtp53 lung organoid line. We analyzed wtp53 and mtp53 PDTO cell extracts by western blot to assess the activation of downstream p53 effectors and DNA damage markers after treatment with temozolomide and/or talazoparib. Combination of talazoparib and temozolomide induced higher DNA double-strand breaks in mtp53 organoids as shown by increased gamma-H2AX expression. The results

obtained demonstrated that in mtp53 PDTO synergism is achieved with combined talazoparib-temozolomide treatment supporting the idea that tumors expressing mtp53 may be potential candidates for this combination PARPi treatment.

#6187

The combination of Trifluridine/Tipiracil and a WEE1 inhibitor is an effective and tolerable candidate strategy against ESCC

Hoang Trang Nguyen Vu, Osamu Kikuchi, Tomoki Saito, Yukie Nakai, Tomomi Ida, Yuki Kondo, Shigeki Kataoka, Yosuke Mitani, Shinya Ohashi, Manabu Muto. *Therapeutic Oncology, Kyoto Univ. Graduate School of Medicine, Kyoto, Japan*

Background: Recently we reported that trifluridine (FTD)/ Tipiracil (TPI) is tolerable for unresectable Esophageal squamous cell carcinoma (ESCC) patients although the anti-tumor effect was modest (Mori Y, et al. Esophagus 2022). Therefore, we aimed at developing a combination therapy with FTD/TPI with another small molecule to achieve better efficacy against ESCC. CHK1 inhibitor was considered to be the candidate, because combination treatment with FTD/TPI and prexasertib showed potent antitumor effects in p53-mutant ESCC cells through the synthetic lethality (Ohashi S, et al. Mol Cancer Ther 2020); however, CHK1 inhibitors are not clinically available for further clinical development. Here we explored the concept of synthetic lethality with CHK1 perturbation to the whole ATR-CHK1-WEE1 pathway, especially to the downward WEE1 which directly targets a cell cycle regulator CDK1. The aim of this study is to elucidate the efficacy of the combination of a WEE1 inhibitor (WEE1i) MK1775 with FTD/TPI in ESCC.
Methods: ESCC cells (TE-8 and TE-11) are used for *in vitro* assay, with compounds including FTD, MK1775 (WEE1i). Mitosis assay (flowcytometry with phospho-Histone H3 [p-hH3] antibody), cell viability assay (WST-1 and clonogenic assays), cytotoxicity assay (CytoTox-Glo assay), and western blotting (double-strand DNA break [γ-H2AX], DDR activity [phospho-CHK1], and CDK1 activity [phospho-Tyr15-CDK1]) were performed. Antitumor effects and tolerability were observed *in vivo* with TE-8 xenograft model with nu/nu nude mice.

Results: FTD induced activation of CHK1 and inhibition of CDK1 sequentially in ESCC cells. FTD also decreased the proportion of p-hH3 positive cells in mitosis assay. Combination treatment with WEE1i and FTD had activated CDK1, increased p-hH3 positive cells, and induced γ-H2AX. The WST-1 cell viability assay showed significant sensitizing effect of WEE1i to FTD in ESCC cells. The cytotoxicity assay also revealed the significant increase of dead cells by the combination treatment ($p = 0.003$). Furthermore, we confirmed the combination treatment significantly suppressed xenografted tumor growth (-86%) without major adverse events *in vivo* (two-way ANOVA and Tukey post-hoc analyses: FTD/TPI vs. control, $P < 0.05$; MK1775 vs. control, $P < 0.05$, without significant interaction between the FTD/TPI treatment and MK1775 treatment). Conclusion: FTD/TPI and WEE1i combination showed potent cytotoxicity, and is considered as a candidate treatment strategy against ESCC.

#6188

Exportin 1 inhibition synergizes with lurbinectedin by altering the response to DNA damage in neuroendocrine lung tumors

Esther Redin Resano[1], Charles Rudin[2], Alvaro Quintanal-Villalonga[1].
[1]Memorial Sloan Kettering Cancer Center, New York, NY,[2]Memorial Sloan Kettering Cancer Center/Weill Cornell Graduate School of Medical Sciences, New York, NY

Background: Neuroendocrine lung cancer carcinomas (Lung NECs), which include large cell neuroendocrine carcinomas (LCNECs) and small cell lung cancer (SCLC) tumors, are particularly aggressive lung neoplasms with limited clinical therapeutic options. Patients with lung NECs are treated with platinum-based chemotherapy as the first line of treatment, but they promptly develop resistance. Lurbinectedin has recently been approved by the FDA as a second-line treatment for SCLC due to its efficacy in metastatic chemorelapsed SCLC patients. However, there is still a large percentage of SCLC patients who do not respond to lurbinectedin and the overall survival of those who benefit from it remains very low (<6 months). Previous work from our group had shown that exportin-1 (XPO1) was a driver of chemoresistance in SCLC and its inhibition with selinexor resentitized to first- and second-line chemotherapies in naïve and chemorelapsed SCLC patients derived xenografts, respectively. Importantly,

selinexor is an FDA-approved drug for the treatment of relapsed multiple myeloma and is currently undergoing clinical testing in multiple solid tumors.
Methods: We performed synergy proliferation assays *in vitro*. DNA damage/repair pathways were analyzed by western blotting. Cell cycle and apoptosis were analyzed by flow cytometry.
Results: We explored the cytotoxic capacity of the combination of lurbinectedin with selinexor in cell linesfrom both SCLC (N=2) and LCNECs (N=3) in synergy *in vitro* assays. Selinexor strongly synergized with lurbinectedin in both SCLC and LCNEC settings and induced a potent increase in the DNA damage marker γ-H2A, reflective of increased DNA damage induced by the combination treatment. Mechanistically, this combination altered DNA damage and DNA repair mechanisms by decreasing CHK1 and CHK2 protein levels in short-term treatments, suggestive of the impairment of DNA response. Additionally, selinexor reduced the expression of MLH, a key regulator of DNA mismatch repair in monotherapy and in combination with lurbinectedin. Consistent with these results, selinexor in combination with lurbinectedin also induced a significant increase in apoptotic cells and promoted cell cycle arrest.
Conclusions: These data indicates that inhibition of exportin 1 with selinexor in combination with lurbinectedin is a promising therapeutic strategy in lung NECs. Subsequent *In vivo* testing in patient-derived xenograft to study efficacy and toxicity of this combination will provide preclinical rationale for clinically exploring this combination in patients with lung NECs who have failed chemotherapy regimen.

#6189
Targeting DNA damage responsive pathways in cancer therapy
Junjie Chen. *Experimental Radiation Oncology, UT MD Anderson Cancer Center, Houston, TX*

DNA double strand breaks (DSBs) result in activation of several key DNA damage response (DDR) kinases including ATM, ATR, and DNA-PK. These protein kinases not only promote DNA damage-induced checkpoint control, but also facilitate DSB repair in humans. Thus, these DDR kinases have become promising drug targets for cancer therapy. However, the benefits of targeting DDR kinases remain to be realized, in part due to the

lack of predictive biomarkers. By undertaking CRISPR screens with inhibitors targeting key DDR kinases, we obtained a global and unbiased view of genetic interactions with DDR inhibition. Additionally, we compared the synergistic effects of combining different DDR inhibitors and found that an ATM inhibitor plus a PARP inhibitor induced dramatic levels of cell death, probably through promoting apoptosis. Our results provide a better understanding of DDR pathways, which may facilitate the use of these DDR-targeting agents in cancer therapy. Moreover, To provide comprehensive and unbiased perspective of DDR signaling pathways, we performed 30 fluorescence-activated cell sorting-based genome-wide CRISPR screens with antibodies recognizing distinct endogenous DNA damage-signaling proteins to identify new regulators involved in DNA damage response (DDR). We discovered that proteasome-mediated processing is an early and prerequisite event for cells to trigger camptothecin- and etoposide-induced DDR signaling. Furthermore, we identified PRMT1 and PRMT5 as new modulators that regulate ATM protein level. Moreover, we discovered that GNB1L is a master regulator of DDR signaling via its role as a co-chaperone for PIKK proteins. Collectively, these screens offer a rich resource for further investigation of DDR, which may provide insight into strategies of targeting these DDR pathways to improve therapeutic outcomes.

#6190

Polymerase theta inhibition activates the cGAS-STING pathway and cooperates with immune checkpoint blockade in BRCA-deficient cancers

Jeffrey Patterson-Fortin[1], Heta Jadhav[1], Constantia Pantelidou[1], Tin Phan[1], Carter Grochala[1], Anita K. Mehta[2], Jennifer L. Guerriero[2], Gerburg M. Wulf[3], Brian M. Wolpin[1], Ben Z. Stanger[4], Andrew J. Aguirre[1], James M. Cleary[1], Alan D. D'Andrea[1], Geoffrey I. Shapiro[1]. *[1]Dana-Farber Cancer Institute, Boston, MA,[2]Department of Surgical Oncology, Brigham and Women's Hospital, Boston, MA,[3]Hematology and Oncology, Beth Israel Deaconess Medical Center, Boston, MA,[4]University of Pennsylvania, Philadelphia, PA*

Cancers deficient in homologous recombination (HR) repair secondary to mutations in genes such as *BRCA1* or *BRCA2*, are dependent on alternative DNA damage response (DDR) pathways to maintain genomic integrity, rendering them susceptible to synthetic lethal targeting of these pathways. Recently, inhibitors of polymerase theta (POLθ, encoded by *POLQ*), the critical enzyme in microhomology-mediated end-joining (MMEJ), have been shown to be synthetic lethal with HR repair deficiency (*Zhou et al. Nature Cancer 2021*). Both HR and MMEJ require nucleolytic DNA end-resection to allow for DSB repair, and we have previously shown that MMEJ acts as a barrier to DNA end-resection at DSBs (*Patterson-Fortin et al. Cancer Research 2022*). Given the synthetic lethality between HR and MMEJ leads to unrestrained DNA end-resection generating chromosomal abnormalities and the release of nuclear DNA into the cytoplasm, we hypothesized that POLθ inhibition in HR-deficient cancers would activate the cGAS/STING innate immune response pathway and facilitate immunotherapy. To investigate the interactions of POLθ inhibition with the immune microenvironment in HR-deficient cancers, we used human cell lines and genetically modified mouse models representative of BRCA1-deficient triple-negative breast cancer (TNBC) and BRCA2-deficient pancreatic ductal adenocarcinoma (PDAC). Genetic or pharmacological inhibition of POLθ using novobiocin, a first-in-class inhibitor of the POLθ ATPase domain, induced significantly increased cytosolic dsDNA contained in micronuclei. This free DNA was sensed by the cytosolic DNA sensor cyclic GMP-AMP (cGAMP) synthetase (cGAS), increasing synthesis of cGAMP, in HR-deficient tumor cells but not in HR-proficient tumor cells. Increased cGAMP bound to and activated stimulator of interferon genes (STING), triggering phosphorylation of TBK1 and ultimately of IRF3. Activation of the cGAS/STING pathway by POLθ inhibition drove the expression of type I interferon response elements, including PD-L1. Depletion of *STING* by siRNA or by CRISPR abrogated this pro-inflammatory signaling and abolished the anti-tumor efficacy of novobiocin-mediated POLθ inhibition. Pharmacologic inhibition of POLθ enhanced Granzyme B+ CD8+ T-cell tumor infiltration. Importantly, antibody-mediated depletion of CD8+ T-cell severely compromised the anti-tumor efficacy of novobiocin-mediated POLθ inhibition, whereas anti-tumor activity of POLθ inhibition was augmented with the addition of either anti-PD-1 or anti-CTLA-4 antibodies. These results demonstrate that

POLθ inhibition in HR-deficient cancers mediates a pro-inflammatory response in HR-deficient TNBC or PDAC tumor microenvironments, and that immune checkpoint blockade inhibition enhances the therapeutic efficacy of POLθ inhibition.

#6191

Temozolomide-associated DNA damage processes related to glioblastoma-immune interactions

Elizabeth Y. Choe, Forest M. White. *Biological Engineering, Massachusetts Institute of Technology, Cambridge, MA*

How do cancer cells convert an external perturbation into an interaction with the immune system? The processes associated with antigen presentation remain largely unknown, especially in cancer cells responding to treatment. These intracellular changes may be critical in cancers where immunotherapies need significant optimization, such as glioblastoma. Glioblastoma is also a particularly relevant cancer to characterize the cellular response to perturbations, since all patients currently receive temozolomide, an alkylating agent, regardless of their prognosis.

We used mass spectrometry methods to quantify temozolomide-associated changes to the repertoire of peptides presented on MHC class I molecules in vitro over time, as well as the associated changes that occur in DNA damage signaling and protein synthesis. We treated U87-MG cells with temozolomide and directly profiled the peptide-MHC repertoire, ATM/ATR kinase substrate phosphorylation, and newly-synthesized proteins via isotopically labeled and non-canonical amino acid-tagged proteins after 24, 48, and 72 hours.

These proteomics approaches identified several MHC-peptides, including phosphorylated peptides, whose presentation changes over time after treatment with temozolomide. We also found that the temporal dynamics of the DNA damage response mirrored that of immunopeptidome remodeling. Additionally, temozolomide alters translation at these time points, with newly-synthesized proteins reflecting internal cell stress processes.

These findings suggest potential treatment-associated antigens against which to design vaccines as well as particular signaling nodes that could be modulated with combination therapies to improve presentation of these peptides.

#6192

MSI2 regulates DNA damage response signaling and tumor progression in murine NSCLC

Igor Bychkov[1], Alexander Deneka[2], Iuliia Topchu[1], Rajendra P. Pangeni[1], Christopher Lengner[3], Evgeny Izumchenko[4], Jyoti Patel[1], John Karanicolas[2], Petr Makhov[2], Yanis Boumber[1]. *[1]Northwestern University - Chicago, Chicago, IL,[2]Fox Chase Cancer Center, Philadelphia, PA,[3]University of Pennsylvania, Philadelphia, PA,[4]University of Chicago, Chicago, IL*

Lung cancer is one of the most frequently diagnosed cancers and is the leading cause of cancer-related death worldwide, accounting for >2.2 million of new cancer diagnoses and 1.8 million cancer-related deaths in 2020. Non-small cell lung cancer (NSCLC) is the most common type of lung cancer, including adenocarcinomas and squamous cell carcinomas. Many lung adenocarcinomas have activating driver mutations in *KRAS* (~32% tumors), often co-occurring with mutations inactivating the *TP53* tumor suppressor. Expression of the RNA-binding protein Musashi-2 (MSI2) MSI2 regulates target mRNA translation, and its expression is progressively elevated along with tumor stage in lung cancers. We previously showed that MSI2 actively promotes lung cancer growth, invasion, and metastasis, in part through promoting expression and activity of the TGFβR1/SMAD3 and EGFR signaling cascades. We now find that genetic *MSI2* deficiency in a murine lung tumor model, $Kras^{mut}/Trp53^{KO}/Msi2^{KO}$ (KPM2) decreases both the total tumor number and tumor burden in comparison to control $Kras^{mut}/Trp53^{KO}$ (KP) mice. Using a panel of KPM2 and KP cell lines we established from tumors from these mice, we found KPM2 cell lines demonstrate a significant decrease in proliferation compared to KP cell lines. Interestingly, reverse phase protein array (RPPA) comparison analysis of KPM2 and KP cell lines showed that MSI2 strongly and positively regulates expression of Ataxia-Telangiectasia Mutated (ATM) protein, with lower levels observed in KPM2 cells. The ATM serine/threonine protein kinase is a key transducer of DDR signaling in cases of double-strand breaks; ATM activation causes G1/S cell cycle arrest, contributes to efficiency of DNA repair, and triggers apoptosis in

cases of repair failure. Notably, KPM2 cells showed significantly higher levels of γH2AX, suggesting inefficient DDR. Finally, untreated or cisplatin-treated KPM2 cells demonstrated G2/M arrest and had increased level of apoptosis as demonstrated by increase in caspase 3 cleavage, consistent with ATM loss and compensatory activation of Ataxia-telangiectasia and Rad3-related protein (ATR). Taken together, our data suggests that one of the consequences of MSI2 upregulation in NSCLC includes maintenance of an efficient DDR. Targeting MSI2 and its downstream signaling would be of therapeutic interest.

#6194

A bifunctional inhibitor of PARP and HDAC enzymes with activity in Ewing sarcoma 3D spheroid and metastasis models

Sarah Truong[1], Louise Ramos[1], Beibei Zhai[1], Jay Joshi[1], Fariba Ghaidi[1], Michael M. Lizardo[2], Taras Shyp[2], John Langlands[3], Dennis Brown[3], Jeffrey Bacha[3], Poul Sorensen[4], Wang Shen[3], Mads Daugaard[4]. *[1]Vancouver Prostate Centre, Vancouver, BC, Canada,[2]British Columbia Cancer Research Centre, Vancouver, BC, Canada,[3]Rakovina Therapeutics, Vancouver, BC, Canada,[4]University of British Columbia, Vancouver, BC, Canada*

Introduction: Poly(ADP-ribose) polymerase (PARP) plays a major role in DNA repair and PARP inhibitors (PARPi) have shown promise in pre-clinical studies for the treatment of Ewing sarcoma (ES). While a clinical trial using olaparib as a single agent failed to show significant response against ES, combination therapies with PARPi have emerged as an area of interest. Deacetylation of histones, controlled by histone deacetylases (HDACs) is a key regulatory event in DNA repair and inhibition of HDACs has been shown to reduce ES tumor growth *in vitro* and *in vivo*. PARP inhibition combined with HDAC inhibition has demonstrated enhanced efficacy in pre-clinical studies in various tumor indications, and a clinical trial of olaparib and vorinostat combination therapy against metastatic breast cancer is currently ongoing. However, combination therapies can be limited in clinical utility due to overlapping toxicities and different pharmacokinetic profiles. Here, we report the efficacy of a novel bifunctional small-molecule compound, kt-3283, designed to have both PARP and HDAC inhibitory activities.

Materials and methods: PARP1 and PARP2 activity were measured using Trevigen Universal Colorimetric PARP Assay Kit, BPS Bioscience PARP2 Colorimetric PARP2 Assay Kit, and PARylation assay. HDAC activity was measured using HeLa cell nuclear extracts and a fluorogenic peptide-based biochemical assay. Cell survival EC_{50}s were determined using live cell imaging with an Incucyte® S3 system and CellTiter Glo viability assay. Cell cycle analysis was performed by flow cytometry with propidium iodide staining. DNA damage was investigated by western blot, immunofluorescence, and comet assay. Spheroid assays were performed using the Incucyte® S3 spheroid analysis module and inhibition of metastases was assessed in a PUMA ES mouse model.
Results and discussion: Kt-3283 showed potent inhibition of PARP1/2 activity and PAR synthesis with IC_{50} values comparable to olaparib. Kt-3283 also showed inhibition of HDACs with an IC_{50} value in the low μM range. Cell survival EC_{50} values for the compound were also superior to those of olaparib and vorinostat in ES cell lines. Cell cycle and DNA damage analyses indicated S/G2/M cell cycle arrest and strong DNA damage upon treatment with kt-3283 at lower concentration range compared to olaparib and vorinostat. This compound also exhibited potent inhibition of 3D spheroid growth of ES cells with low μM EC_{50} values, and inhibited metastatic growth in a PUMA mouse model.
Conclusion: Kt-3283 shows potent inhibition of PARP1/2 and HDAC activities. It induces S and G2/M cell cycle arrest and DNA damage, and inhibits 3D spheroid growth and metastatic potential of ES cells. Further investigation of this bifunctional single-molecule inhibitor may offer a novel treatment opportunity for ES and other solid tumors with limited responses to PARPi.

#6195

Assessing replication stress as an actionable therapeutic opportunity in chordoma

Nindo Punturi[1], Lee Dolat[1], Wendy Leung[2], Joan Levy[1], Lee Zou[2], Daniel M. Freed[1], Gregory M. Cote[2]. *[1]Chordoma Foundation, Durham, NC,[2]Massachusetts General Hospital, Charlestown, MA*

Chordoma is a rare bone cancer with a high rate of disease recurrence and no approved systemic therapies. Tumor profiling studies indicate a significant number of chordomas are characterized by alterations in SWI/SNF chromatin remodeling and DNA damage repair genes, which have been associated with replication stress in other cancer types. We demonstrate here that preclinical chordoma models exhibit a replication stress phenotype and dependence on ATR activity. To assess the effect of ATR inhibition on cell viability, a panel of chordoma cell lines were treated with the ATR inhibitor elimusertib (BAY 1895344). In a subset of cell lines, elimusertib inhibited viability with low-nanomolar IC50 values. Upon treatment with the ATR inhibitor ceralasertib (AZD6738), DNA fiber assays revealed a mild decrease in replication fork speed and a significant increase in fork asymmetry in cells sensitive to ATR inhibitor, suggesting possible fork stalling or collapse in response to ATR inhibition. To assess genomic instability as a consequence of ATR inactivation and fork stalling or collapse, alkaline and neutral comet assays were performed to determine the presence of genome-wide ssDNA and/or dsDNA breaks, respectively. In a panel of chordoma PDX models, striking differential sensitivity to ATR inhibition was observed. In sensitive models, elimusertib (50 mg/kg, po, bidx3) promoted 85-90% tumor growth inhibition, in contrast to resistant models, where elimusertib treatment had no effect on tumor growth. Moreover, PDX models sensitive to ATR inhibition were sensitive to other therapies that exacerbate replication stress; for example, gemcitabine promoted multiple complete responses in a pediatric chordoma PDX model. Coupled with preclinical efficacy data, genomic and transcriptomic sequencing of differentially-sensitive chordoma models provided insight into the molecular factors associated with the replication stress phenotype in chordoma - illuminating potential biomarkers for patient selection. Finally, we explore various combination therapies and show that combining elimusertib with cisplatin or gemcitabine synergistically inhibits the viability of chordoma cell lines. Collectively, our data indicate that a subset of chordomas are characterized by intrinsic replication stress that can be therapeutically exploited by inhibiting ATR.

DNA Repair / Molecular Classification of Tumors for Diagnostics, Prognostics, and Therapeutic Outcomes / Others

#6199

Proteasome inhibitors induce DNA damage and mitotic catastrophe in acute lymphoblastic leukemia via autophagy-mediated degradation of WEE1

Chun-fung Sin, Rahman Ud Din, Anan Jiao, Kei-ching Yuen. *Department of Pathology, The University of Hong Kong, Hong Kong, Hong Kong*

Acute lymphoblastic leukemia (ALL) is an aggressive hematolymphoid malignancy and the prognosis is poor in adults with long-term survival of only 30% due to the high prevalence of high-risk subtypes. Therefore, there is an urgent need to develop novel treatment for ALL. Carfilzomib is a second-generation proteasome inhibitor which is more potent than its first-generation counterpart, bortezomib, with an excellent activity against bortezomib-resistant plasma cell myeloma. However, pre-clinical and clinical studies of carfilzomib in ALL are limited. Targeting DNA damage and mitotic defects of cancer cell is a major treatment strategy of cancer. WEE1 kinase prevents mitosis of cells with unrepaired DNA through inhibiting cyclin B. Pharmacological inhibition of WEE1 was effective in treating T-ALL with induction of DNA damage. Thus, targeting WEE1 kinase is an attractive approach of novel therapy in ALL. However, there are no studies to evaluate the mechanism of action of carfilzomib in ALL, especially in the aspect of DNA damage and mitotic catastrophe. Moreover, the role of WEE1 modulation by carfilzomib and its underlying mechanism has not been studied in ALL. In view of these unmet clinical needs and research gap, we conducted the study with the aims: 1). To show that carfilzomib induces DNA damage and mitotic catastrophe; 2). To show that carfilzomib induces WEE1 downregulation and delineate underlying mechanisms. ALL cell lines representing a spectrum of high-risk ALL including TOM-1, SEM, LOUCY, CCRF-CEM, KE-37 and PEER were treated with various doses of carfilzomib. Cell viability was reduced, and percentage of apoptotic cells was increased in a time and dose-dependent manner, measured by trypan blue assay and flow cytometry analysis by annexin V/PI staining respectively, upon treating with carfilzomib for 24 & 72 hours. Comet assay showed evidence of DNA damage after treating with carfilzomib for 24 hours. Fluorescence microscopy also demonstrated evidence of mitotic catastrophe upon treating with carfilzomib. Western blot analysis showed downregulation of WEE1 upon treatment of carfilzomib

for 24 hours, with evidence of autophagy induction as shown by western blot analysis of LC3-1 and LC3-II. Quantitative PCR showed the upregulation of ER-stress related gene, CHOP while the mRNA level of WEE1 remained unchanged. Co-treatment of carfilzomib with autophagy inhibitor, bafilomycin A1, reversed the process of WEE1 downregulation. Herein, we proved that carfilzomib induced DNA damage and mitotic catastrophe with WEE1 downregulation. Moreover, carfilzomib trigger autophagy-mediated degradation of WEE1 in ALL via induction of ER-stress. The findings provide mechanistic insights of carfilzomib in ALL and rationalize the introduction of novel approach of combination treatment of carfilzomib with other DNA damaging agents.

#6200

PARP1 hyperactivation by the decoy oligodeoxynucleotide OX425 mediates DNA repair abrogation and unleashes the anti-tumor immune response

Vlada Zakharova[1], Claudia Galassi[2], Chloé Doizelet[1], Vincent Hayes[1], Lorenzo Galluzzi[2], Wael Jdey[1]. *[1]Onxeo S.A., Paris, France,[2]Weill Cornell Medical College, New York, NY*

Background: Poly (ADP-ribose) polymerase inhibitors (PARPis) lead to synthetic lethality when used in cancers with homologous recombination deficiency (HRD). However, the development of resistance to PARPis is a recurrent problem thus limits the duration of response and hence the clinical utility of these agents. Here, we describe the antineoplastic and immunomodulatory effects of OX425, a first-in-class oligodeoxynucleotide that operates as a PARP1 decoy, resulting in constitutive PARP1 hyperactivation and consequent exhaustion of the DNA damage response.
Methods: OX425-induced PARP trapping, hyperactivation and cell cytotoxicity were examined *in vitro* in HRD and homologous recombination proficient (HRP) human cancer cells, as well as in non-transformed cell lines. DNA repair efficacy was monitored by analyzing repair protein recruitment to damage sites. OX425 effects on the innate and adaptive immune responses were assessed by following STING activation and T-cell mediated anti-tumor cytotoxicity. RNAseq analysis in HRP/HRD tumor cells treated with OX425 or PARP inhibitors was employed to uncover the molecular mechanisms underlying OX425 effects. The

anticancer efficacy of OX425 was assessed *in vivo* in different HRD and HRP tumor models. OX425-induced PARP activation and tumor infiltration by immune cells were analyzed by flow cytometry.
Results: At odds with conventional PARP inhibitors, OX425 bound to and hyperactivated PARP1 with high affinity in a dose-dependent manner, resulting in elevated cytotoxicity to multiple cancer cells (breast, ovarian, prostate, colon, hematological, endometrial cancers) irrespective of HR status. Interestingly, long-term treatment with OX425 did not show any mutagenicity compared to PARPi. The activity of OX425 was specific to tumor cells, as no significant effect on cell viability was observed for normal cells, at odds with PARP inhibitors. In line with *in vitro* results, OX425 mediated considerable anticancer effects *in vivo*. Moreover, OX425 triggered activation of the STING pathway and CCL5 secretion in the EMT6 mouse mammary carcinoma model. The anticancer effect of OX425 was coupled with tumor-targeting T cell responses. In MPA/DMBA-driven mammary tumors, OX425 mediated considerable anticancer effects in monotherapy and synergistic effects in combination with PD1 inhibition. Moreover, OX425 treatment significantly delayed acquired resistance to olaparib in *BRCA1* mutated MDA-MB-436 cell-derived xenografts.
Conclusions: Our results provide preclinical rationale for using OX425 to trigger DNA damage exhaustion and STING activation in cancer cells and initiate inflammatory responses that can be actioned by immune checkpoint inhibitors in patients bearing HRD or HRP tumors

#6201
Identification of SP-002, a highly selective USP1 inhibitor effectively inhibits HRD tumor growth and displays low hematotoxicity risk
Feng Zhou[1], Zhengtao Li[2], Lei Zhou[3], Wei Zhu[4], Jiyan Zhang[5], Wenqing Yang[1], Liting Xue[1], Xiaokang Qin[6], Ping Chen[6], Renhong Tang[1]. *[1]State Key Laboratory of Translational Medicine and Innovative Drug Development, Jiangsu Simcere Pharmaceutical Co. Ltd., Nanjing, China,[2]State Key Laboratory of Translational Medicine and Innovative Drug Development, Hainan Sparkle Therapeutics Co., Ltd., Hainan, China,[3]Jiangsu Simcere Pharmaceutical Co. Ltd., Nanjing, China,[4]Hainan Sparkle Therapeutics Co., Ltd., Hainan, China,[5]Jiangsu Simcere Pharmaceutical Co. Ltd., Hainan, China,[6]Simcere Pharmaceutical Co. Ltd., Hainan, China*

Tumors with homologous repair deficiencies (HRD) are sensitive to agents interrupting DNA repair. The deubiquitinase USP1 involves in the DNA damage response by translesion synthesis and Fanconi anemia pathway. And the synthetic lethality of USP1 and HRD is well reported. Moreover, deficiency of USP1 or its downstream pathway leads to hypersensitivity of HRD tumors to PARP inhibition. In addition, target-related hematotoxicity is widely observed in serval DNA Damage Response (DDR) pathway inhibitors, including PARP and ATR inhibitors, which limits the combination therapy. Here, we reported SP-002, a highly selective USP1 inhibitor, displayed monotherapy potential and combination activity with PARP inhibitor in HRD cancers. In the biochemical assay, SP-002 strongly inhibited USP1 enzyme with IC_{50} of 15.7 nM, and potently inhibited proliferation of *BRCA1*-mutant MDA-MB-436 breast cell (GI50, 47.4 nM). SP-002 demonstrated synergistic anti-proliferation effects in combination of olaparib, a PARP inhibitor, in MDA-MB-436 cells. And further results revealed that the combination significantly enhances the DNA damage burden and cells apoptosis. Moreover, synergistic activities of SP-002 and olaparib also were observed in a panel of HRD cell lines, such as UWB1.289, Capan-1, MDA-MB-453 and NCI-H292. In a human hematopoietic stem cells based *in vitro* hematotoxicity assay, SP-002 showed no significant inhibition on lineage-specific (myeloid, erythroid, and megakaryocytic) cell differentiation and survival. In comparison, positive controls, 5-fluorouracil and olaparib significantly attenuated those primary cells both on differentiation and survival, which was consistent with the hematological toxicity observed in human. Oral administration of SP-002 led to completely tumor growth inhibition in MDA-MB-436 xenograft model, and combination of SP-002 and olaparib resulted in tumor regression. In conclusion, SP-002, a selective and potent USP1 inhibitor without significant hematotoxicity, that demonstrated excellent efficacy on treatment of HRD cancers.

#6202

6-Phosphofructo-2-kinase in regulating DNA damage and repair in EGFR-driven lung cancer

Nadiia Lypova, Lilibeth Lanceta, Susan Dougherty, Jason Chesney, Yoannis Imbert-Fernandez. *Medical Oncology, James Graham Brown Cancer*

Center, University of Louisville, Louisville, KY

Activating mutations of epidermal growth factor receptor (mutEGFR) are established drivers of lung tumor development, aggressiveness, and resistance to targeted therapies. While targeting mutEGFR with small-molecule tyrosine kinase inhibitors (EGFR-TKIs) dramatically improved progression-free survival in patients with non-small cell lung cancers (NSCLCs), intrinsic or acquired resistance to TKI therapy limits the duration of an effective response to TKIs. Alteration in DNA damage response (DDR) plays a vital role in genomic stability and cancer progression and helps cells to escape apoptosis, limiting the efficacy of targeted therapies.

Interestingly, lung cancer cells exposed to EGFR-TKIs demonstrate attenuated glycolytic flux - one of the major providers of precursors for *de novo* nucleotide synthesis. A key regulator of glycolysis is the enzyme 6-phosphofructo-2-kinase (PFKFB3). PFKFB3 synthesizes fructose 2,6-bisphosphate (F2,6BP), which is a potent allosteric activator of the glycolytic rate-limiting enzyme, 6-phosphofructo-1-kinase (PFK1). Accordingly, F2,6BP controls flux throughout the entire glycolytic pathway. In preliminary studies, we provide evidence that PFKFB3 plays multiple roles in regulating the efficacy of DDR in lung cancer cells exposed to EGFR-TKIs. We show that PFKFB3 is required for EGFR-driven glucose metabolism, which provides a list of intermediates utilized in nucleotide synthesis. PFKFB3 regulates the expression of ribonucleotide reductase small subunit M2 (RRM2) of the ribonucleotide reductase (RNR), which is important for *de novo* onsite synthesis of deoxynucleotide triphosphate (dNTP) during DNA replication and repair. Moreover, a PFKFB3 inhibitor, PFK-158, increases oxidative stress in mutEGFR lung cancer cell lines and, as a result, promotes DNA damage. Importantly, we found that PFKFB3 plays an important role in the chromatin binding of scaffold proteins regulating the assembly of DNA repair complex.

Our studies suggest that PFKFB3 plays an important role in DDR and provide a clear rationale to propose the use of PFKFB3 inhibitors in combination with EGFR inhibitors to increase the efficiency and/or overcome resistance to EGFR-TKIs.

#6203

CTC1-STN1-TEN1 (CST) complex-independent roles for STN1 in DNA double-strand break repair in pancreatic ductal adenocarcinoma

Changxian Shen[1], Linlin Yang[1], Sergio Corrales-Guerrero[2], Sindhu Nair[1], Terence Williams[1]. *[1]City of Hope National Medical Center, Duarte, CA,[2]College of Medicine, The Ohio State University, Columbus, OH*

KRAS mutation occurs in 90-95% of pancreatic ductal adenocarcinoma (PDAC) and is a driver of PDAC; however, the underlying molecular mechanisms by which *KRAS* mutation maintains survival and promotes progression of PDAC need further refinement. We herein report that *KRAS* mutations increase *STN1* (also named *OBFC1*) expression leading to enhanced repair of DNA double strand breaks (DSBs) in PDAC. Analysis of The Cancer Genome Atlas databases reveal that *STN1* is significantly upregulated in PDAC tissue and, is associated with *KRAS* mutation and poor survival. Silencing *KRAS* or pharmacologic inhibition of KRAS signaling decreased *STN1* expression in PDAC cells. Canonically, STN1 forms a CST (CTC1-STN1-TEN1) complex, which is important for telomere duplication and maintenance. Intriguingly, siRNA-mediated depletion of STN1 (but not CTC1 or TEN1) sensitized PDAC cells to ionizing radiation and chemotherapy as assessed by radiation clonogenic assay and alamarBlue assay, respectively. Consistently, immunoblotting and immunofluorescence analyses of γH2AX (marker of DNA damage) demonstrated that depletion of STN1 (but not CTC1 or TEN1) resulted in DNA damage. To explore the underlying molecular mechanisms, we performed proteomic analysis and found that STN1 physically interacts with many proteins important for DNA repair, replication and cell cycle progression. Of note, we revealed unreported interactions of STN1 with ATM, ATR and DNA-PKcs, key components of DNA damage response signaling. Furthermore, homologous recombination and non-homologous end joining repair reporter assays demonstrated that STN1 silencing reduced both homologous recombination and non-homologous end joining repair of DSBs in U2OS and PDAC cells. Moreover, flow cytometry and immunofluorescence analyses showed that knockdown of STN1 by siRNA impaired cell cycle arrest at S and G2/M phases which was accompanied with mitotic catastrophe in response to ionizing radiation. Our findings have revealed novel CST complex-independent roles for STN1 in DSB repair

and suggest STN1 is a novel biomarker for PDAC as well as potentially other cancers.

#6204

DNA-PK inhibition augment the cancer specific cytotoxicity of mitotic MTH1 inhibitor OXC-101

Akhilesh Nagesh Danda[1], Helge Gad[1], Martin Scobie[1], Laura Martínez-López[2], Nuria Pastor Carrillo[2], Manuel Luis Orta[2], Thomas Helleday[1], Ulrika warpman berglund[1], Kumar Sanjiv[1]. *[1]Oncology-Pathology, Karolinska Institutet, Stockholm, Sweden,[2]Department of biology, University of Sevilla, Sevilla, Spain*

DNA-dependent protein kinase (DNA-PK) plays an important role in the repair of DNA double-strand breaks via the non-homologous end joining (NHEJ) pathway. In addition to its role in the NHEJ pathway, DNA-PK is also known to have an emerging role in cell cycle progression and mitosis. Some studies have shown that depletion or inhibition of DNA-PK inhibitors leads to a delay in the transition from metaphase to anaphase. The mitotic MTH1 inhibitor OXC-101(TH1579, karonudib) is a dual inhibitor that both targets MTH1 and disrupts tubulin polymerization in cancer cells, causing DNA damage and mitotic catastrophe in cancer cells. Based on the involvement of DNA-PK in mitosis, we hypothesized that depletion/inhibition of DNA-PK might enhance the DNA damage and mitotic catastrophic effect of OXC-101.To test our hypothesis, we performed an in vitro drug combination experiment using the DNA-PK inhibitor nedisertib with OXC-101 in non-small cell lung carcinoma NSCLC (H460,A549), uveal melanoma (MP -38, MP -41 and MP46), osteosarcoma (U2OS) and) and neuroblastoma (IMR32, Kelly, SKNFI) cancer cell lines and non-cancerous foreskin fibroblasts(VH-10, BjhTERT). We found cancer-specific synergistic drug interactions between nedisertib and OXC-101. Combined treatment of nedisertib and OXC-101 to H460 and MP46 increased expression of s10H3 (mitotic marker) and the apoptosis marker (cPARP) compared with single treatment. However, there was no additional increase in expression of the DNA damage markerγH2AX with combined treatment. We also performed annexin V staining by FACS on MP38 andMP48 cells and observed a significant increase in the apoptotic population with combination treatment compared

with single treatment. Imaging live cells, we observed a significant delay or arrest in the mitotic phase followed by death of cancer cells in mitosis in response to combination treatment, whereas cells treated individually with nedisertib or OXC-101 continued to proliferate and progress to the next phase of the cell cycle. These data suggest that the DNA-PK inhibitor may enhance the cytotoxic effect of OXC-101specifically in cancer cells. In addition, we will conduct an in-depth mechanistic study of how depletion/inhibition of DNA-PK enhances the cytotoxicity of OXC-101 and validate the drug combination in an appropriate preclinical mouse model.

#6205

Visualizing dynamics of long non-coding RNA TUG1 in live glioblastoma cells

Ayaka Minematsu. *Nagoya University, Nagoya, Japan*

Long non-coding RNAs (lncRNAs) are transcripts longer than 200 nucleotides that are not translated into proteins. lncRNA TUG1 (taurine upregulated gene 1) is highly expressed in various cancers, including glioblastoma. Previously we found that TUG1 is an essential molecule for cancer cells to cope with excessive replication stress in the S phase. Albeit its importance to cell cycle-related function, how it is dynamically regulated during the cell cycle is entirely unknown. Here, we established a system visualizing endogenous TUG1 molecules in live cells. TUG1 was tagged with stem-loop motifs recognized by a specific binding protein fused with GFP. We tracked TUG1 RNA by the GFP signal for 22 hours in T98G glioblastoma cells and found that the expression started from the later G1 phase. When cells were treated with Hydroxy Urea, a chemical that interferes with replication and increases replication stress, the expression of TUG1 was further upregulated in the S phase within 20 mins. We also observed some TUG1 molecules accumulated in several nuclear locations. It may indicate that TUG1 assembles to protect damaged DNA loci efficiently. Our results suggest that the expression of TUG1 is regulated in a cell cycle-dependent manner and is strongly connected with its function of TUG1. The current live-cell imaging system could help further discover the critical roles of TUG1 in cancer cells.

#6206

Combined inhibition of AXL and ATR enhances replication stress, cell death and immune response in small cell lung cancer

Kavya Ramkumar, C. Allison Stewart, Azusa Tanimoto, Qi Wang, Yuanxin Xi, Benjamin B. Morris, Runsheng Wang, Li Shen, Robert J. Cardnell, Jing Wang, Carl M. Gay, Lauren A. Byers. *UT MD Anderson Cancer Center, Houston, TX*

Small cell lung cancer (SCLC) is an aggressive neuroendocrine lung tumor. Despite high initial responses to frontline chemo-immunotherapy, therapeutic resistance develops rapidly. There are limited treatment options in the relapsed setting, where the prognosis remains dismal. SCLC tumors experience continuous and high levels of replication stress (RS) due to ubiquitous loss of key cell cycle checkpoints, *RB1* and *TP53*. Frequent amplification and high expression of the transcription factor *cMYC* further contribute to increased RS. Thus, high levels of RS expose a potential SCLC vulnerability and provide a therapeutic opportunity. Our group and others have shown that AXL, a TAM family receptor tyrosine kinase that is highly expressed in mesenchymal tumors, mediates resistance to chemotherapy, radiation and targeted therapies in SCLC, non-small cell lung cancer and other cancers, through its role in driving epithelial to mesenchymal transition (EMT). More recently, a novel role for AXL in DNA damage repair and tolerance has emerged. Therefore, we hypothesize that AXL targeting may be a potential therapeutic approach in SCLC. We first investigated the transcriptomic expression profile of *AXL* in SCLC clinical cohorts. *AXL*-high tumors were seen in a subset of treatment-naïve SCLC tumors, frequently among, but not limited to, the inflamed SCLC subtype. *AXL* expression was also seen in many relapsed SCLC tumors. As expected, tumors with high *AXL* expression also expressed several mesenchymal genes and higher EMT scores. Interestingly, among the treatment-naïve SCLC tumors, *AXL* expression was inversely correlated with a RS signature (rho=-0.54, $p<0.001$). Next, we tested the effects of AXL inhibition in SCLC *in vitro* and *in vivo* models. In a panel of 30 SCLC cell lines, bemcentinib, a selective AXL inhibitor in clinical trials for various advanced solid tumors, exhibited a range of antiproliferative activity, with IC_{50} values ranging from 41 nM to 10 μM (median IC_{50} 3.1 μM). Bemcentinib also significantly delayed tumor growth in *in vivo* SCLC models. Biomarkers associated with sensitivity to bemcentinib in SCLC cell

lines included markers of RS (cMYC, replication stress score) and DNA damage response (phospho CHK1^{S345}, phospho CHK2^{T68}). Bemcentinib also induced RS, indicated by the activation of ATR/CHK1-mediated RS response pathway, and DNA damage, and the combination with an ATR inhibitor (ceralasertib) showed a greater than additive effect. In a syngeneic model of SCLC, the combination of bemcentinib, ceralasertib and an anti-PDL1 antibody induced significant tumor regression. Together, these promising findings demonstrate that AXL inhibition may be an effective strategy to target the RS vulnerability common in SCLC.

#6208

Targeting DNA polymerase theta and ATM leads to synergistic killing of mantle cell lymphoma cells

Jithma Prasad Abeykoon[1], Shuhei Asada[2], Kalindi Parmar[2], Xiaosheng Wu[1], Thomas Witzig[1], Geoffrey Shapiro[2], Alan D. D'Andrea[2]. *[1]Mayo Clinic, Rochester, MN,[2]Dana-Farber Cancer Institute, Boston, MA*

Introduction: Rapid cell proliferation requires intact and faithful DNA damage repair mechanisms. DNA polymerase theta (POLQ) plays a key role in repairing DNA double-strand breaks through the microhomology-mediated end-joining (MMEJ), which is one of the three main pathways involved in repairing replication-induced double-strand breaks. Limited data have suggested that concurrent depletion of POLQ and ataxia-telangiectasia mutated (ATM) could be embryonic lethal. Hence, this phenomenon has the potential to be exploited for therapeutic benefit in cancers where ATM mutations are commonly seen. Mantle cell lymphoma (MCL) is a non-Hodgkin lymphoma marked by (11;14) translocation with ATM alterations seen in 40-50% of patients. There is an unmet need to find novel therapeutic strategies, especially in relapsed and/or refractory (R/R) MCL. Here, we investigated whether targeting POLQ and ATM could be a potential therapeutic strategy in MCL.
Methods: *In vitro* studies were conducted by using MCL cell lines. CRISPR-Cas9 system was used to genetically deplete POLQ and ATM genes and sgRNAs co-expressing fluorescence markers were used to track the cell population with respective genotypes over time. Cell viability was assessed by CellTiter-Glo assay and flow cytometry. All cell lines were profiled for ATM expression and activity. A p-value of < 0.05 was

considered statistically significant. The combination index of <1 was defined as synergistic.
Results: CRISPR-Cas9-mediated depletion of POLQ significantly decreased cell proliferation in multiple MCL cell lines. In particular, Granta-519, which possesses a single copy of kinase-dead ATM that is reduced in expression, was most sensitive to POLQ depletion. Concurrent genetic depletion of ATM and POLQ resulted in a synergistic antiproliferative effect in ATM-proficient MCL cell lines. Subsequently, this cellular phenotype caused by the genetic intervention was recapitulated by using two POLQ inhibitors (novobiocin and ART558) and an ATM inhibitor (AZD0156). *In vitro*, single-agent treatment with novobiocin or ART558 caused a significant cytotoxic effect at physiologically relevant concentrations in ATM-deficient cells and co-treatment of novobiocin or ART558 with AZD0156 was synergistic in killing ATM-proficient MCL cells. Importantly, POLQ inhibitors significantly decreased the cell viability of MCIR1, which is an ibrutinib-resistant MCL cell line. Mechanistically, novobiocin or ART558 treatment induced gH2AX and cleaved PARP upregulation, which was further enhanced by ATM depletion, suggesting that co-inhibition of POLQ and ATM caused apoptosis due to the accumulation of unrepaired DNA damage.
Conclusion: POLQ is a promising target in MCL, especially in ATM-deficient setting. In ATM-proficient MCL, targeting ATM and POLQ is synergistic. Our data has the potential to uncover novel biomarker-driven drug therapy of POLQ inhibitors in R/R MCL.

#6209
O6-methylguanine as the junction of MGMT and PARP1-mediated repair pathways
Jodie D. Cropper, Dauren S. Alimbetov, Kevin T. G. Brown, Andrew Robles, Rostislav I. Likhotvorik, James T. Guerra, Yidong Chen, Youngho Kwon, Raushan T. Kurmasheva. *Greehey Children's Cancer Research Institute, San Antonio, TX*

Temozolomide is the first-choice DNA alkylating agent and has been commonly used in oncology over the last several decades. The cytotoxicity that temozolomide elicits through the methylation of guanine and adenine residues often becomes the limiting factor in effective treatment. Despite

growing evidence of dysregulated alkylating DNA damage repair as a driving force of genome instability leading to cancer, neurological diseases, and premature aging, little is currently known about the coordinated role of PARP1 and MGMT (O6-methylguanine methyltransferase) enzymes in the repair of temozolomide-induced methylated DNA lesions. A major PARP1 function in DNA damage is facilitation of repair of the methylated DNA lesions, N6-methyladenine and N7-methylguanine, via base excision repair (BER); while MGMT restores guanine in O6-methylguanine (O6meG), the most cytotoxic adduct, by a one-step catalysis. It is generally thought that BER and MGMT represent two distinct mechanisms for removing DNA damage induced by alkylating agents; however, using a number of advanced cell-free and cell-based approaches, we provided evidence for direct (DNA-independent) and indirect (through PARylation) interaction between PARP1 and MGMT and demonstrated a functional crosstalk between these repair pathways. Particularly, O6meG repair activity is increased once PARP1 PARylates MGMT. Further, longer (more clinically relevant) exposure to temozolomide induced stronger MGMT PARylation in cells, indicating that the PARP1-MGMT interaction is important for enhanced O6meG repair and cell survival. As PARP1-MGMT complex forms in a variety of cancer cell types, our findings have strong implications for the development of an effective cancer therapy for cells dependent on PARP1 and MGMT mediated DNA repair.

#6210

Combination of M1774 and niraparib can overcome ATR and PARP inhibitor resistance in BRCA1 mutated ovarian cancer models

Jie Hao[1], Arindam Bose[2], Golbahar Sadatrezaei[2], David B. Martignetti[2], Yuqing Jiao[2], Alexandre André B. A. da Costa[2], Jean-Bernard Lazaro[2], Bose Kochupurakkal[2], Huy Nguyen[2], Kalindi Parmar[2], Alan D. D'Andrea[2], Geoffrey I. Shapiro[1]. *[1]Medical Oncology, Dana-Farber Cancer Institute, Boston, MA,[2]Radiation Oncology, Dana-Farber Cancer Institute, Boston, MA*

PARP inhibitors are being used in maintenance treatment of *BRCA*-mutated high-grade serous ovarian cancer (HGSOC). However, *de novo* and acquired resistance to PARP inhibitors, resulting from restoration of homologous recombination repair or stabilization of replication forks, is a

pressing clinical problem. ATR inhibitors are known to reverse both of these mechanisms of PARP inhibitor resistance and are currently in clinical development. In this study, we assessed the activity of a novel ATR inhibitor, M1774, as a monotherapy and in combination with PARP inhibition in HGSOC preclinical models. M1774 exhibited single-agent activity across a panel of ovarian cancer cell lines with induction of DNA damage. We used a panel of *BRCA1*-mutated patient-derived xenograft (PDX) models of HGSOC with acquired PARP inhibitor resistance and identified two M1774-sensitive models and one M1774-resistant model. M1774 monotherapy demonstrated anti-tumor activity in mice bearing sensitive PDX models of HGSOC with PARP inhibitor resistance. In the M1774-sensitive models, the combination of M1774 and niraparib augmented the degree and durability of response compared with M1774 monotherapy. The combination of M1774 and niraparib also demonstrated synergistic anti-tumor activity in the M1774-resistant model, indicating that the combination could overcome monotherapy resistant to either agent. We also generated organoid cultures from these PDX models. Treatment of the organoid models with M1774, niraparib or the combination faithfully recapitulated the anti-tumor activities seen in vivo. Mechanistically, M1774-resistant organoid cultures demonstrated stable replication forks and an absence of replication stress. The combination of M1774 with niraparib resulted in destabilization of the replication forks. In contrast, M1774-sensitive organoids exhibited unstable replication forks, which were further destabilized by the niraparib combination. In addition, the sensitive models demonstrated higher basal levels of replication stress, as detected by increased levels of phospho-RPA. Collectively, these results indicate that the combination of M1774 and niraparib can overcome PARP inhibitor resistance and ATR inhibitor resistance in *BRCA1*-mutant ovarian cancer PDX models and demonstrate the utility of organoid cultures for discerning mechanisms of resistance and strategies to restore drug sensitivity. Combined M1774-mediated ATR inhibition and PARP inhibition may be a promising therapeutic strategy for the treatment of ovarian cancer.

#6211
Development and validation of a novel sSTRIDE-MMR functional assay to study the efficiency of MMR inhibitors

Kamil Solarczyk, Karolina Uznańska, Olga Wójcikowska, Maja Białecka, Agnieszka Waligórska, Szymon Koman, Magdalena Kordon-Kiszala.
intoDNA, Kraków, Poland

Mismatch repair (MMR) is considered to be one of the fundamental pathways that guards genome stability and mutations in genes encoding for crucial MMR proteins have been shown to promote cancer initiation. On the other hand, inactivation of MMR components in cancer cells leads to increased neoantigen formation and in consequence, exposes the tumor to the immune system. Therapeutic strategies aiming at inhibiting MMR are thus under development, yet methods reporting on the status of MMR are lacking. We report here the development, optimization and validation of a first MMR-specific functional assay. The assay, which is based on the STRIDE platform technology, detects DNA nicks localized in close proximity to PMS2 protein and can thus be utilized as a direct reporter of inhibition of PSM2 itself or upstream acting proteins. The optimization phase of assay development was performed in U2OS cells. First, in untreated cells we have shown that the sSTRIDE-MMR signals constitute ca. 10-15% of total single-strand DNA breaks foci detected by the classic sSTRIDE assay variant. In a series of technical negative controls we have then shown that the number of false-positive foci never exceeds 10% of the total number of signals, with as little as 2% for the isotype controls. The assay was further validated in HAP1 wild-type and PMS2-KO isogenic cell line pair. As expected, the number of sSTRIDE-MMR foci in the PMS2-KO cell line was significantly lower than in wild-type cells and additionally, no response to the treatment with 6TG, a known inducer of MMR, was detected in PMS2 null cells. Finally, the assay was used to verify the efficiency of first-in-class small-molecule MMR inhibitors. After treatment with the compounds, the number of detected sSTRIDE-MMR foci was significantly lower when compared to the number of foci in untreated cells. In conclusion, we show here that sSTRIDE-MMR is an assay characterized by high specificity, low false positives rate and a high-dynamic range. We believe that sSTRIDE-MMR can prove to be a very useful cell-based solution to study the efficiency of MMR inhibitors.

#6212

Inhibition of ATM-dependent checkpoint control and DNA double-strand break repair enhances the efficacy of ATR inhibitors

Audrey Turchick[1], Astrid Zimmermann[2], Li-Ya Chiu[1], Heike Dahmen[2], Brian Elenbaas[1], Frank T. Zenke[1], Andree Blaukat[2], Lyubomir T. Vassilev[1]. *[1]Research Unit Oncology, EMD Serono, Billerica, MA,[2]Research Unit Oncology, Merck KGaA, Darmstadt, Germany*

Ataxia telangiectasia and Rad3 related (ATR) and ataxia telangiectasia mutated (ATM) protein kinases play key roles in the DNA damage response (DDR) by responding to replication stress and double-strand DNA breaks respectively to pause the cell cycle and promote DNA repair. ATR kinase inhibition in cancer cells disrupts cell cycle control and causes unrepaired DNA lesions and cytotoxicity. Accordingly, several ATR inhibitors (ATRi) are in clinical development as monotherapies and in combination with DNA damaging chemotherapies and poly(ADP-ribose) polymerase (PARP) inhibitors. Here we show that while treatment of cancer cells with an ATRi inhibits the ATR pathway, it simultaneously activates the ATM signaling pathway as shown by increased levels of p-ATM, p-CHK2, p-KAP1 and p-p53. In p53 wild-type cancer cells, ATR inhibition causes an ATM-mediated G1 cell cycle arrest which diminishes the DNA lesions and cytotoxic effects of ATR inhibition. Combination of an ATRi with a selective ATM inhibitor (ATMi) synergistically potentiated efficacy in cancer cells *in vitro* and increased efficacy *in vivo* at doses that did not show overt toxicities. In a panel of patient-derived xenograft (PDX) models of triple-negative breast cancer treated with an ATRi/ATMi combination, substantial improvement in efficacy was observed. Thus, activation of the ATM pathway by an ATRi acts as a compensatory resistance pathway for ATR inhibition. These results suggest a novel and efficacious combination approach for cancer therapy by dual inhibition of these two key DDR kinases.

#6213

Disruption of XPF function by HPV promotes alternative end joining and sensitivity to cisplatin in HNSCC

Qi Liu[1], Nan Zuo[1], Lin Ma[2], Lanlan Wei[3]. *[1]Shenzhen Bay Laboratory, Shenzhen, China,[2]Department of Stomatology, General Hospital, Shenzhen*

University, Shenzhen, China,[3]The Second Affiliated Hospital of Southern University of Science and Technology, Shenzhen, China

Human papillomavirus (HPV) positive head and neck squamous cell carcinoma (HNSCC) usually show a tremendous better clinical outcome compared to their HPV-negative counterparts. Although the HPV associated survival advantage is partially explained by the enhanced cisplatin sensitivity in HNSCC (Clin Ca Res 2018, 24(23): 6001), the underlying mechanisms are still poorly elucidated. Cisplatin causes DNA interstrand crosslinks (ICLs) that requires Fanconi anemia (FA) pathway for DNA repair. Consistently, our study showed that HPV-positive HNSCC cells exhibited a FA defective cellular phenotype. In clonogenic cell survival assay, 1h treatment with 5μM cisplatin eliminated approximately 56.7% more HPV-positive HNSCC cells than HPV-negative ones. Furthermore, HPV-positive cells treated with cisplatin showed prolonged G2/M cell cycle arrest and more 53BP1 foci, indicating profound deficiency in repairing ICLs. Consistent with these findings, increased aberrant chromosome formation was observed in HPV-positive cells following Mitomycin C treatment. In order to reveal the mechanism, we further interrogated HPV-labeled HNSCC samples in TCGA database, and identified XPF, an endonuclease protein in FA pathway, was downregulated in HPV-positive HNSCC. Further analysis of cellular and clinical samples confirmed that both mRNA and protein expressions of XPF were significantly lower in HPV-positive HNSCC ($P<0.001$). To test the importance of XPF in HPV-induced cisplatin sensitivity, we performed a cell viability assay, and found that knock-down of XPF increased the effects of cisplatin on HPV-negative HNSCC by 39.54% (± 4.42%), while no significant change was observed in HPV-positive HNSCC ($P>0.05$). Notably, inhibition of XPF function by a small molecule inhibitor recapitulated the effect of HPV, resulted in enhanced error-prone DNA repair with alternative end-joining (alt-EJ). In a probe-based ddPCR assay, XPF inhibition increased 32.02% (± 5.80%, $P<0.001$) alt-EJ events in HPV-negative HNSCC cells, while little difference was detected in HPV-positive cells. Thus, we speculated that combined inhibition of XPF and alt-EJ may improve clinical outcome in the difficult-to-treat, HPV-negative HNSCC, which worth further research efforts.

#6214

FANCA promotes transcription-coupled homologous recombination by catalyzing R-loops formation

Fang Li. *University of Miami Miller School of Medicine, Miami, FL*

R loops arise from hybridization of RNA transcripts with template DNA during transcription, which are not only cause DNA damage in certain contexts as cancer hallmarks but also be important regulators of cellular processes. Recent findings revealed that DNA double-strand breaks (DSBs) elicit RNA-DNA hybrid formation. The RNA moiety of the R-loop displays an extraordinary potential to regulate multiple steps of homologous recombination (HR) by substituting for the double-stranded DNA (dsDNA) substrate on which DSB repair processes naturally occur. Here, we use the Damage At RNA Transcription assay to reveal colocalization of FANCA with R-loops in a highly transcribed genomic locus upon DNA damage. We further demonstrate FANCA participates in forming R-loops in the initial DSBs repair stage and assists in removing R-loops later. Besides, we find that highly purified human FANCA anneals synthetic single-stranded RNA (ssRNA) and ssDNA species to R-loops and binds R-loop substrates with high affinity, preferring guanine-rich sequences in vitro. Importantly, we illustrate that FANCA promotes HR efficiency via catalyzation of DNA: RNA hybrids at DSBs sites. Finally, a series of RNA and R-loop substrates are found to stimulate ID2 monoubiquitination, with activity corresponding to remove transient R- loops in later HR stage. In summary, our results support a mechanism whereby FANCA promotes the formation of temporary R-loops by annealing ssRNA and ssDNA species at DSBs in transcribed regions, thereby stimulating HR.

#6215

Peposertib, a DNA-PK inhibitor, enhances the antitumor efficacy of anthracyclines in triple-negative breast cancer models in vitro and in vivo

Steffie Revia[1], Christian Sirrenberg[1], Antonia Schach[1], Astrid Zimmermann[1], Frank T. Zenke[2], Joachim Albers[1]. *[1]Merck Healthcare KGaA, Darmstadt, Germany,[2]EMD Serono, Billerica, MA*

Background: Triple-negative breast cancer (TNBC) is the most lethal breast cancer subtype, exhibiting poor response rates toward current chemotherapy regimens and lacking additional effective treatment options. Approximately 30% of patients with TNBC respond well to anthracycline/taxane-based standard-of-care chemotherapy regimens. However, remaining patients demonstrate limited improvements in clinical outcomes, highlighting the critical need for effective strategies to improve anthracycline/taxane-based chemotherapy (1, 2). DNA-dependent protein kinase (DNA-PK), a member of the phosphoinositide 3-kinase-related kinase protein family, promotes nonhomologous end joining (NHEJ) as part of the DNA damage response. Peposertib is a potent, selective, and orally bioavailable DNA-PK inhibitor that strongly potentiates the antitumor effects of ionizing radiation and DNA double-strand break-inducing agents, including anthracyclines, in preclinical models. Here we report the synergistic antitumor effects of peposertib combined with topoisomerase II (TOPO II) inhibitors, particularly anthracyclines, in TNBC models in vitro and in vivo.
Methodology: Combinations of peposertib with TOPO II inhibitors were evaluated in TNBC cell lines by viability assays, immunoblotting, and flow cytometry. Gene expression analysis was performed using the nCounter PanCancer pathways panel and results were confirmed by quantitative polymerase chain reaction (qPCR). In vivo efficacy was assessed in cell-line derived and patient-derived xenograft models.
Results: When administered in combination with doxorubicin, epirubicin, and etoposide, peposertib exhibited synergistic antiproliferative activity in TNBC cell lines in vitro. The downstream analysis of pharmacodynamic biomarkers revealed induction of NHEJ mediated repair upon TOPO II inhibitor treatment and provided mechanistic insights into the synergistic antitumor effects of peposertib combined with TOPO II inhibitors. Furthermore, this combination treatment induced ataxia telangiectasia mutated (ATM)-dependent compensatory signaling and inflammatory responses, potentially creating a proinflammatory tumor microenvironment. To evaluate whether peposertib enhanced the antitumor effects of TOPO II inhibitors in vivo, we established a well-tolerated preclinical treatment schedule for the combined use of peposertib and pegylated liposomal doxorubicin, which was capable of achieving tumor regression in patient- and cell line-derived xenograft models of TNBC.

Conclusion: Our findings suggest that cotreatment with the DNA-PK inhibitor peposertib can enhance the efficacy of anthracycline/TOPO II-based chemotherapies. *This work was supported by the healthcare business of Merck KGaA, Darmstadt, Germany (CrossRef Funder ID: 10.13039/100009945).*
1) Davison C et al. NPJ Breast Cancer. 2021;7(1):38.
2) Bianchini G et al. Nat Rev Clin Oncol. 2016;13(11):674-690.

#6216

Pre-ribosomal RNA mediates HR repair via the BRCA1/BARD1 complex

Duo Wu[1], Huang huang[1], Tenglong Chen[1], Xiaochen Gai[1], Song Liu[2], Hu He[2], Song Shi[2], Xiaochun Yu[1]. *[1]Westlake University, Hang Zhou Shi, China,[2]SynRx Therapeutics, Hang Zhou Shi, China*

The BRCA1/BARD1 complex plays a key role in DNA double-stand break (DSB) repair in both somatic cells and germ cells. However, the underlying molecular mechanism by which this complex mediates DSB repair remains elusive. Here, we show that the recruitment of the BRCA1/BARD1 complex to the unsynapsed axis of the XY body in male germ cells is mediated by pre-rRNA. Similarly, the BRCA1/BARD1 complex associates with pre-rRNA in somatic cells, which targets the BRCA1/BARD1 complex to DSBs. The interactions between the BRCT domains of the BRCA1/BARD1 complex and pre-rRNA induces liquid-liquid phase separations, which may be the molecular basis of DSB-induced nuclear foci formation of the BRCA1/BARD1 complex. Pre-rRNA also mediates BRCA1-dependent homologous recombination (HR). Cancer-associated mutations in the BRCT domains of BRCA1 and BARD1 abolish the interaction with pre-rRNA. We developed novel RNA pol I inhibitors to suppress pre-rRNA biogenesis, which not only abolished HR repair but also sensitized tumor cells to PARP inhibitor treatment. Collectively, this study reveals that pre-rRNA is a functional partner of the BRCA1/BARD1 complex in the DSB repair. It is also a potential therapeutic target for cancer therapy.

#6217

Inhibiting ataxia-telangiectasia mutated and RAD3-related (ATR) by BAY 1895344 overcomes chemoresistance to oxaliplatin and promotes synergistic anti-tumor effect in pancreatic cancer

Hye Won Shon[1], Jung Won Chun[2], Jeong Eun Gong[2], Mi Rim Lee[1], Yu-Sun Lee[2], Sumin Kang[1], Sunshin Kim[2], Sang Myung Woo[2], In Rae Cho[3], Woo Hyun Paik[3], Woo Jin Lee[2], Ji Kon Ryu[3], Yong-Tae Kim[3], Sang Hyub Lee[3], Yun-Hee Kim[2]. *[1]National Cancer Center Graduate School of Cancer Science and Policy, Goyang, Korea, Republic of,[2]Research Institute and Hospital, National Cancer Center, Goyang, Korea, Republic of,[3]Department of Internal Medicine and Liver Research Institute, Seoul National University Hospital, Seoul National University College of Medicine, Seoul, Korea, Republic of*

Pancreatic Ductal Adenocarcinoma (PDAC) is a highly aggressive disease with a poor prognosis and a limited response to most of the treatments. Despite a platinum-based drug such as oxaliplatin or cisplatin is one of the most effective chemotherapy drugs for PDAC, resistance to it is a major limiting factor in PDAC treatment, indicating an urgent need for new approaches. Recently, targeting major DNA damage response (DDR) regulators such as ATM (Ataxia-telangiectasia mutated) or ATR (Ataxia telangiectasia mutated and Rad3-related) kinase has shown therapeutic potential in cancer treatment. This shows that it may be possible to enhance the responsiveness of platinum medicines via a DDR inhibition strategy. The most recently developed ATR inhibitor with the greatest potency, BAY 1895344, showed an anti-proliferative effect in clinical trials. Here, we aimed to evaluate the effect of ATR inhibition using BAY 1895344 on responsiveness to oxaliplatin in pancreatic cancer, for the first time. CFPAC-1 and Capan-2 are selected among six kinds of pancreatic cancer cell lines as oxaliplatin-sensitive and -resistant cells, respectively. According to BRAID analysis, combining the BAY 1895344 and oxaliplatin resulted in strong synergistic effects in both cell lines, particularly in Capan-2. The synergism is also confirmed in all four organoids derived from PDAC patients. We found that p-Chk1, coordinating DDR and cell cycle checkpoint, was considerably suppressed by the combined treatments, which was associated with elevated γ-H2AX intensity, cell cycle arrest and apoptosis. Moreover, we investigated the in vivo synergistic anti-tumor efficacy of combination therapy using a tumor-

bearing nude mice model with CFPAC-1 and Capan-2 cells, demonstrating a substantial reduction of tumor growth in combination therapy when compared to single treatment. In conclusion, ATR inhibition enhanced the anticancer effect of oxaliplatin, and this combined therapeutic strategy may be effective in overcoming chemo-resistance in PDAC. (This study is supported by National Cancer Center, Republic of Korea (No. 2212470, 2010330))

#6218

NKX3.1 immunohistochemistry and methylome profiling in mesenchymal chondrosarcoma: additional diagnostic value for a well defined disease?

Salome Glauser[1], Baptiste Ameline[1], Vanghelita Andrei[1], Dorothee Harder[2], Chantal Pauli[3], Marcel Trautmann[4], Wolfgang Hartmann[4], Daniel Baumhoer[1]. *[1]Bone Tumour Reference Centre, Institute of Medical Genetics and Pathology, University Hospital Basel, Basel, Switzerland,[2]Department of Radiology, University Hospital Basel, Basel, Switzerland,[3]Department of Pathology and Molecular Pathology, University Hospital Zurich, Zurich, Switzerland,[4]Gerhard-Domagk-Institute of Pathology, University Hospital Munster, Munster, Germany*

Background: Mesenchymal chondrosarcoma (MCS) is a high-grade sarcoma characterized by a biphasic histological appearance. However, more often than not, only the poorly differentiated component is present on a biopsy, thus more entities enter the differential diagnosis. Since the small cell component is morphologically non-specific, the differential diagnoses are broad, such as Ewing sarcoma, rhabdomyosarcoma, poorly differentiated synovial sarcoma small cell carcinoma, lymphoma and also melanoma. Morevoer, although the *HEY1::NCOA2* gene fusion is present in almost all MCS, some studies have shown alternative alterations in the absence of the *HEY1::NCOA2* fusion, suggesting genomic heterogeneity in at least a small subset of MCS. Thus, new diagnostic aids would be helpful to confirm the diagnosis. While most of the immunohistochemical profile overlaps between these tumours, NKX3.1 was recently proposed as a useful diagnostic marker for MCS. Furthermore, studies using DNA-methylation profiling show that MCS forms a distinct methylation cluster. The aim of this study is to evaluate the utility of these new diagnostic tools.

Methods: Slides from 45 samples with MCS were stained with NKX3.1 antibody (EP356, Cell Marque, Roche) and were also investigated by methylome analysis (Mehylation Epic BeadChips, Illumina). Depending on tissue availability, the cases were subjected to *HEY1::NCOA2* gene fusion testing.
Results: The methylation profile showed a distinct cluster for mesenchymal chondrosarcoma, in line with the previous studies. Moreover, these findings were reproduced even when submitting tissue solely from one component, either the cellular or the cartilaginous one. In addition, the copy number profile derived from the methylome analysis proves its utility in distinguishing MCS from its mimics. On the other hand, only 32.6% of cases were positive for NKX3.1. Four samples initially diagnosed as MCS were histologically re-evaluated due to an atypical methylome profile, a high amount of CNV and/or lack of validation of the gene fusion. Methylation profiling led to the re-classification of three cases, whereas the fourth sample could not be further classified.
Conclusions: We conclude that the methylation analysis, along with the copy number profile, are reliable tools in terms of diagnosing MCS. On the contrary, the immunomarker NKX3.1 shows contradicting results, proving itself as an unreliable marker in this setting.

#6219
Endogenous human retroviruses in epithelial ovarian cancers: An exploratory analysis
Jill Alldredge[1], Vinay Kumar[2], Brook Sanders[1], Farahnaz Rahmatpanah[2].
[1]University of Colorado Anschutz Medical Campus, Aurora, CO,[2]University of California, Irvine, Orange, CA

Objectives: Endogenous human retroviruses (ERVs) are remnants of exogenous retroviruses that gained access to germline cells allowing integration into the human genome. Emerging data suggest that some ERVs may become activated allowing epigenetic alterations through DNA methylation or histone modification, which can further alter gene regulation. This may serve as a targeted therapeutic opportunity in modulating oncogenesis, through aberrant oncogene activation or tumor suppressor gene inactivation. This is an emerging area of exploration in ovarian cancer.

Methods: We applied our ERV mapping tools (1) to RNA-seq data from 24 female patients with ovarian, fallopian tube, or primary peritoneal cancers to investigate expression of ~550,000 ERV elements from the Human Endogenous Retrovirus database (HERVd) (2, 3). Univariate Cox regression models were constructed with normalized ERV expression data and the most significantly differentially expressed ERVs were then filtered using a penalized Lasso-Cox proportional-hazards model. ERV expression, alongside the available clinical data (including age, histotypes, and tumor stage) were provided as inputs and linear predictors generated by the model separated samples into either high or low risk categories. We identified a panel of 15 predictive ERVs and these risk evaluations allowed for Kaplan-Meier analyses of survival by clinical parameters alone versus combined with ERV signature. We also performed a secondary analysis of platinum resistant ovarian cancers using RNA-seq data (GSE102118) to investigate the effect of demethylating agent guadecitabine on ERV expression (n=9) (4).

Results: Exploratory analyses of ERVs demonstrated significantly different expression between histologies (clear cell, mucinous, endometrioid, high grade serous) and FIGO disease stage. In our prognostic model, Kaplan-Meier survival analysis using only clinical parameters resulted in a significance level of 0.0013, however the supplemented model combining the 15-ERV panel and the clinical data discriminated the two risk groups for time to recurrence at a much higher significance level of $p = 7.076 \times 10^{-8}$. Included in the 15 ERV panel are HERVK, HERV3, and several putative ERV promoters including LTR12, LTR7, LTR3 and LTR4 (5). In our secondary analysis of platinum-resistant patients, the ERV transcripts were compared for each patient pre- and post-guadecitabine treatment and there were several ERVs with risk-predictive values induced in patients receiving guadecitabine including LTR7, LTR12 and HERVK.

Conclusions: In summary, ERV RNA expression in ovarian cancer is significantly different between histologies and disease stages. The ability to successfully classify patients as either high-risk or low-risk for disease progression is of considerable value for patient management and ERVs may improve prognostication and guide future therapeutic targeting.

#6220

Development of a mutation profiling NGS assay to facilitate clinical decisions in hematologic malignancies.

Grant Hogg[1], Tong Liu[1], Helen Cao[1], Adib Shafi[1], Ashraf Shabaneh[1], John Howitt[2], Amanda Williamson[2], Rachel Dango[2], Xiaojun Guan[3], Heidi Hoffmann[4], Michael Mooney[5], John Pruitt[2], Scott Parker[2], Stan Letovsky[4], Li Cai[2], Eric A. Severson[2], Shakti Ramkissoon[2], Anjen Chenn[2], Marcia Eisenberg[6], Eyad Almasri[1], Taylor Jensen[5]. *[1]Oncology, Labcorp, San Diego, CA,[2]Labcorp, Durham, NC,[3]Labcorp, San Diego, CA,[4]Labcorp, Westborough, MA,[5]Oncology, Labcorp, Durham, NC,[6]Labcorp, Burlington, NC*

Introduction: Accurate diagnosis, prognosis and treatment of hematologic disorders from both myeloid and lymphoid origin requires assessing somatic mutation status in an increasingly large number of genes. Here we present the results of the assay development and validation of a targeted next generation sequencing panel which provides full exon sequencing of 141 genes associated with myeloid and lymphoid malignancies, as well as the ability to detect clinically relevant copy number alterations (CNAs) and certain sub-gene level CNAs.

Methods: Based on review of clinical guidelines, 141 genes including 72 myeloid and 84 lymphoid associated genes were selected. The assay interrogates all coding exons of the 141 genes to detect single nucleotide variants (SNVs) and insertions/deletions (indels). The assay also identifies CNAs in 16 genes, *FLT3* internal tandem duplicates (ITDs), and select non-coding pathogenic variants. The custom hybrid capture-based assay utilizes genomic libraries created from 250 ng gDNA extracted from peripheral blood or bone marrow followed by sequencing on Illumina sequencers. Concordance studies were performed on clinical samples previously assessed using an orthogonal NGS-based laboratory developed test for SNVs/Indels or digital multiplexed ligation-dependent probe amplification for CNAs. In addition, analytical sensitivity was assessed using cell line dilution series and specificity by reference samples from Genome in a Bottle (GIAB). Small indels were defined as <25bp while long indels are ≥ 25bp.

Results: Interim estimates of positive percentage agreement (PPA) and specificity have been determined for SNV/Indels, *FLT3*-ITDs, and CNVs,

with further testing ongoing. PPA of SNVs was 100% (218/218 SNVs; n = 134 samples). PPA was also 100% for both small indels (21/21; n = 14 samples) and long indels (6/6; n = 6 samples). A dilution series of 8 positive clinical samples at 4 different dilutions showed SNV and small indel detection of 100% at allele frequency (AF) ≥ 3%. Long indel detection was 87.5% at AF ≥ 5%. *FLT3*-ITD was evaluated with 2 cell line samples at 5 different dilutions with 100% detection at AF ≥ 5%. PPA of CNAs were 95.7% (157/164) in 46 clinical samples. CNA detection was also evaluated with 8 cell line samples at 4 different dilutions showing 92.3% detection at a copy number ratio threshold ± 0.15. A preliminary estimate of specificity was determined using 4 replicates of the GIAB sample, NA12878, and was >99.99% for SNVs and small indels (n=6.9 x 10^5). Finally, a model for gender classification was created using a training cohort of 70 clinical samples. The performance was evaluated on a test set of 144 clinical samples with 100% PPA (144/144).
Conclusions: Taken together, these data demonstrate that the developed NGS assay is a sensitive, specific, and accurate assay with high clinical utility to inform treatment decision making in hematologic malignancies.

#6221
Support for targeted therapy selection in triple negative breast cancer patients using aberrant signal transduction pathway activity profiles
Diederick M. Keizer, Yvonne J. W. Wesseling, Dianne A. M. van Strijp, Saskia M. J. Vermeer, Eveline C. A. den Biezen. *InnoSIGN B.V., Eindhoven, Netherlands*

Introduction: Success of therapeutic interventions largely rely on the pathological and biological characteristics of the tumor and varies due to the heterogeneous nature of breast cancers. Triple negative breast cancers (TNBC) stain IHC negative for both hormone receptors (ER, PR) and HER-2. TNBC is usually treated with chemotherapy because of absence of any molecular target. This study is initiated to characterize TNBC based on a new methodology that measures and quantifies signal transduction pathways (STPs) activities to reveal potential tumor-driving STPs in TNBC and create new options for targeted therapy.
Method: Using the mRNA-based OncoSIGNal pathway activity profiling PCR test (InnoSIGN) STP activities of 7 pathways (AR, ER, PI3K, MAPK,

HH, TGFβ and Notch) in 39 samples from normal breast tissue and 12 TNBC patients were quantified and expressed on a scale from 0-100. Normal healthy breast tissue was obtained from breast reduction surgery and areas where epithelial cells content was at least 50% were annotated and harvested for mRNA isolation and STP analyses. The normal STP activity is representing the normal physiological activity and is used as reference value. Aberrant high pathway activity in a patient tumor sample was concluded when this score was higher than twice the standard deviation above the mean of normal breast tissue STP activity.
Results: STP thresholds for interpretation of high aberrant activity were determined from 39 normal breast samples. Using these thresholds, STP activities in 12 TNBC samples were analyzed. In these TNBC samples, MAPK was in 75%, HH in 67%, PI3K in 58%, and AR, Notch and TGFβ were in 17% of the cases above the thresholds. In 50% of the cases a combination of MAPK and HH or a combination of PI3K and HH were found above thresholds. In 42% of the cases MAPK in combination with PI3K were above thresholds. Increased activity of AR was never observed in combination with increased HH activity.
Conclusion: By using the OncoSIGNal test high aberrant STP activities could be determined in TNBC patient samples. Results show that different pathways are aberrantly active, depending on the patient sample, which opens the opportunity for personalized targeted treatment of individual TNBC patients.
Next steps: The TNBC data set will be extended to further profile the STP activity in relation to different clinical outcomes and to investigate new opportunities for targeted therapies.

#6222

Clinical impact of p53 and AXL immunostaining on the efficacy of immune checkpoint inhibitor-based therapy after osimertinib treatment in patients with epidermal growth factor mutant non-small cell lung cancer

Kenji Morimoto, Tadaaki Yamada, Shinsaku Tokuda, Koichi Takayama.
Pulmonary Medicine, Kyoto Prefectural University of Medicine, Kyoto, Japan

Background: Current evidence indicates that immune checkpoint inhibitors (ICIs) have a limited efficacy in patients with lung cancer harboring epidermal growth factor receptor (*EGFR*) mutations. However, there is a lack of data on the efficacy of ICIs after osimertinib treatment, and the predictors of ICI efficacy are unclear.
Methods: We retrospectively assessed consecutive patients with *EGFR*-mutant NSCLC who received ICI-based therapy after osimertinib treatment at 10 institutions in Japan, between March 2016 and March 2021. Immunohistochemical staining was used to evaluate the expression of p53 and AXL. The deletions of exon 19 and the exon 21 L858R point mutation in *EGFR* were defined as common mutations; other mutations were defined as uncommon mutations.
Results: A total of 36 patients with advanced or recurrent *EGFR*-mutant NSCLC were analyzed. In multivariate analysis, p53 expression in tumors was an independent predictor of PFS after ICI-based therapy ($p = 0.002$). In patients with common *EGFR* mutations, high AXL expression was a predictor of shorter PFS and overall survival after ICI-based therapy (log-rank test; $p = 0.04$ and $p = 0.02$, respectively).
Conclusion: The levels of p53 in pretreatment tumors may be a predictor of ICI-based therapy outcomes in patients with *EGFR*-mutant NSCLC after osimertinib treatment. High levels of AXL in tumors may also be a predictor of ICI-based therapy outcomes, specifically for patients with common *EGFR* mutations. Further prospective large-scale investigations on the predictors of ICI efficacy following osimertinib treatment are warranted.

#6223
Evaluating peroxiredoxins 1-6 and their potential as prognostic biomarkers for uterine corpus endometrial carcinoma
Lauren Lambros, Vien Sturm, Calli A. Davison-Versagli. *Biology, Saint Mary's College, Notre Dame, IN*

Introduction: Uterine corpus endometrial carcinoma (UCEC) is one of the most commonly diagnosed cancers in women in the United States, where the death rate continues to climb by 1.9% every year due to poor prognostic and therapeutic methodologies. Recently, altered expression patterns of peroxiredoxins (PRDX) (1-6), a family of antioxidant enzymes comprised of six known isoforms, has been connected to overall outcome in many

cancers. While recent studies have begun to unravel the potential of PRDXs as prognostic biomarkers in other cancers, PRDX expression patterns and their use as prognostic biomarkers in UCEC have yet to be explored. This study aimed to determine the value of PRDX1-6 as potential prognostic biomarkers for UCEC patients.
Methods: To determine the impacts of PRDX1-6 expression on overall survival (OS) and relapse-free survival (RFS), UCEC samples (n=543) from the TCGA database available on the Pan-Cancer RNA seq platform on Kaplan-Meier Plotter (KM plotter) were utilized. The patient cohort was split into groups according to high PRDX expression status and low PRDX expression status using the autoselect best cutoff function in KM plotter where all possible cutoff values between the lower and upper quartiles of PRDX expression were computed. The best-performing threshold was used as the cutoff and data was plotted in a Kaplan-Meier plot. Hazard ratio (HR), 95% confidence interval (95% CI), and log-rank P value were calculated using the KM plotter platform. For molecular analyses, a total of 507 UCEC samples obtained from the PanCancer Atlas on the cBioportal platform were analyzed for PRDX1-6 copy number alterations (CNAs), and mRNA expression Z-scores relative to all samples were used to evaluate the association between CNAs and transcriptional levels of PRDXs.
Results: Favorable OS associated with high PRDX2 (P=0.044, HR=0.65, 95% CI: 0.43-0.99) and high PRDX4 (P=0.01, HR=0.56, 95% CI: 0.36-0.88) mRNA levels. High PRDX2 (P=0.029, HR=0.56, 95% CI: 0.33-0.95) and high PRDX3 (P=0.034, HR=0.56, 95% CI:
0.33-0.96) expression in UCEC tumor samples correlated with favorable RFS. Shallow deletions were identified in PRDX2 (9.8%), PRDX3 (9.6%), and PRDX4 (14%) of the UCEC samples analyzed in cBioportal. Compared to diploid cells, shallow deletions in PRDX2 and PRDX3 correlated with decreased PRDX2 ($P=1.33 \times 10^{-12}$) and PRDX3 ($P=8.17 \times 10^{-13}$) mRNA levels, respectively. High expression of PRDX6 correlated with unfavorable OS (P=0.0021, HR=1.9, 95% CI: 1.25-2.88) and unfavorable RFS ($P= 4.3 \times 10^{-5}$, HR=2.88, 95% CI: 1.69-4.88). Notably, 41.2% of UCEC patients displayed PRDX6 copy number gain that correlated with increased PRDX6 mRNA levels ($P= 8.69 \times 10^{-24}$) compared to diploid cells.
Conclusion: High PRDX2, PRDX3, and PRDX4 expression could serve as favorable UCEC prognostic biomarkers, while high PRDX6 expression may be a novel unfavorable prognostic biomarker.

#6224

Exploring the integration of CMS subtyping and other omics in colorectal cancer classification and its reflection in stool miRNome and metagenome for non-invasive precision medicine

Amedeo Gagliardi[1], Giulia Francesca[1], Giulio Ferrero[2], Sonia Tarallo[1], Giulia Piaggeschi[1], Antonio Francavilla[1], Carla Di Battista[1], Enrico Berrino[3], Caterina Marchiò[3], Francesca Cordero[4], Barbara Pardini[1], Alessio Naccarati[1]. *[1]Italian Institute for Genomic Medicine (IIGM), Candiolo, Italy,[2]Department of Clinical and Biological Sciences, University of Turin, Turin, Italy,[3]Candiolo Cancer Institute, FPO-IRCCS, Candiolo, Italy,[4]Department of Computer Science, University of Turin, Turin, Italy*

Background: The Consensus Molecular Subtypes (CMS) is a subtyping system used for colorectal cancer (CRC) to facilitate traditional tumor classification and clinical translation. Relying on RNA-seq data, the system classifies patients into four molecular subtypes (CMS 1-4). Each subtype is enriched with several mutations, but no genetic aberrations are peculiar to a single CMS. A more in-depth characterization of each subtype's genomic and epigenomic background by integrating different omics may help in refining this classification, including the missing assignment of a subgroup of tumors. The possible translation of this improved classification to surrogate tissues, such as stool, has never been investigated.
Aims: We aim to comprehensively characterize the CMS by the integrative analysis of target genomic sequencing, RNA-Seq, small RNA-Seq, and immune infiltrate profiling data of a cohort of CRC patients. These data will be used to identify integrative CMS-specific signatures and to characterize those tumors not assigned to any CMS. In addition, differences in stool miRNome and metagenomic profiles will be explored to identify potential specific signatures characterizing each subtype.
Methods: Tumor tissue and adjacent mucosa were collected from 87 CRC patients and preserved in RNA later. mRNA and other non-coding RNA expression levels were evaluated with ribosomal depleted RNA-seq and small RNA-seq. Tumors were assigned to a CMS subtype using the CMScaller algorithm and genomically characterized with the TruSight Oncology 500 (TSO500) cancer panel. Differential expression analyses were performed using the DESeq2 package for the R software to identify

CMS-specific expression signatures. Small RNA-seq and shotgun metagenomic analyses were performed on stool samples collected from the same patients.
Preliminary Results: Tumors were assigned to CMS1 (n=9), CMS2 (n=24), CMS3 (n=26), and CMS4 (n=22), except for six samples. Differential expression analyses between paired tumor samples and adjacent mucosa within each CMS revealed 1096 differentially expressed genes in CMS1, 4218 in CMS2, 27 in CMS3 and 190 in CMS4.From the genomic point of view, CMS3 cases showed 384 unique missense variants, while CMS1 included almost all samples with microsatellite instability. Small RNA-seq on the same tissue sample identified 380 dysregulated miRNAs (215 up and 165 downregulated) in the tumor compared to adjacent mucosa.
Conclusions: A more in-depth CMS subtyping by integrating different omics analyses could help refine this classification system. Moreover, the possible CMS reflection in stool miRNome and metagenomic could shed new light on the host gut-microbiota interactions and allow a non-invasive classification applicable for a routine personalized clinical management of CRC.

#6225

SERPINB3 promotes the aggressive basal-like/squamous subtype and correlates with poor prognosis in pancreatic ductal adenocarcinoma through metabolic reprogramming

Yuuki Ohara[1], Wei Tang[1], Liu Huaitian[1], Shouhui Yang[1], Peijun He[1], Helen Cawley[1], Paloma Valenzuela[1], Lin Zhang[1], Jochen Gaedcke[2], B. Michael Ghadimi[2], Matthias M. Gaida[3], Frank Bergmann[3], H. Richard Alexander[4], Nader Hanna[5], Stefan Ambs[1], S. Perwez Hussain[1]. *[1]National Cancer Institute, Laboratory of Human Carcinogenesis, National Institutes of Health, Bethesda, MD,[2]Department of General, Visceral and Pediatric Surgery, University Medical Center Göttingen, Göttingen, Germany,[3]Institute of Pathology, University Hospital Heidelberg, Heidelberg, Germany,[4]Rutgers Cancer Institute of New Jersey, New Brunswick, NJ,[5]Division of General & Oncologic Surgery, University of Maryland School of Medicine, Baltimore, MD*

In this study, we aimed to find genes with a key function in the development of molecular subtypes in pancreatic ductal adenocarcinoma (PDAC). Through transcriptome analysis, we discovered that the endogenous serine/cysteine proteinase inhibitor SERPINB3 (squamous cell carcinoma antigen 1, SCCA1) was distinctively upregulated in the basal-like/squamous subtype, known as an aggressive subtype, and this upregulation associated with decreased patient survival in both a test (N=123) and a validation cohort (N=84). In additional investigations of the tumor metabolome and transcriptome using PDAC patient tumors and cell lines, SERPINB3 and the basal-like/squamous subtype showed a robust relationship with upregulated levels of amino acids (e.g., hydroxyproline) whereas SERPINB3 promoted a gene signature indicative of the basal-like/squamous subtype. Additional mechanistic studies revealed that SERPINB3 and hydroxyproline promoted the migration/invasion of PDAC cells. Moreover, SERPINB3 also promoted metastasis in an orthotopic mouse model of PDAC through stromal factors that increased tumor microvessel density. To conclude, inhibiting SERPINB3 function may attenuate disease progression of the basal-like/squamous subtype in PDAC through changes to the tumor stroma and tumor metabolism.

#6226

Therapeutic vulnerability of *MTAP*-deleted nasopharyngeal carcinoma by MAT2A inhibitors

YUK-Yu Chan[1], Chi-Man Tsang[1], Grace T.Y. Chung[1], Ka-Fai To[1], Yi Zhang[2], Xiaodong Zhang[2], Jun Tang[2], Kwok Wai Lo[1]. *[1]Department of Anatomical & Cellular Pathology, The Chinese University of Hong Kong, Hong Kong, Hong Kong,[2]ScinnoHub Pharmaceutical Co., Ltd., Chengdu, China*

Introduction: EBV-associated nasopharyngeal carcinoma (NPC) is a distinct type of head and neck cancer that is prevalence in southern China and Southeast Asia. While radiotherapy or concurrent chemo-radiotherapy are efficient for the patients with early disease, more than 60% of NPC patients are diagnosed at an advanced stage and frequently develop local failure and distant metastases. The lack of druggable targets is a challenge for controlling this common cancer. By whole-genome sequencing and FISH analysis, we have defined the frequent homozygous deletion of 9p21.3 in

NPC. The loss of *MTAP* that encodes methylthioadenosine phosphorylase on this region was found in 32% and 34% of primary and recurrent NPC respectively, indicating vulnerability to targeted-therapies for MAT2A/PRMT5 axis.
Methods: The preclinical efficacy of MAT2A inhibitors, FIDAS-5 and BT115386 was elucidated in a panel of *MTAP*-deleted EBV-positive NPC cell lines and patient-derived xenografts. *In vitro* and *in vivo* growth inhibition of NPC cells by these compounds were determined. In addition to the suppression of PRMT5 activity, the effects of MAT2A inhibitor treatment on activating p53 pathway, inducing EBV lytic genes and modulating expression of proteins involved in cellular differentiation, apoptosis and lipogenesis in NPC were accessed.
Results: *In vitro* study has revealed that treatment of the MAT2A inhibitors markedly reduced PRMT5 activity and cell growth in all MTAP-deleted NPCs. Compared to the MTAP-wild type NPC cells, the MTAP-deleted cells, either with wild type or mutated *TP53*, showed heightened sensitivity (>9 fold more sensitive) to the MAT2A inhibition by FIDAS-5 and BT115386. The potent *in vivo* growth inhibitory effect of BT115386 were observed in the *MTAP*-deleted xenografts, but not in that with wild type *MTAP*. In the *MTAP*-deleted NPC treated with MAT2A inhibitors, activation of p53 pathway and induction of BAX apoptotic protein were consistently found. The treatment also promoted differentiation, suppressed stemness transcription factors and inhibited lipogenesis. Notably, the MAT2A inhibitors also disrupted EBV latency in the *MTAP*-deleted NPC, induction of multiple EBV lytic genes including *BZLF1* and *BMRF1* were demonstrated.
Conclusion: Selective sensitivity of *MTAP*-deleted NPC to the treatment of MAT2A inhibitors including FIDAS-5 and BT115386 was demonstrated. To facility its growth inhibitory effects, the compounds targeted PRMT5 activity, subsequently modulated multiple cellular mechanisms and induced EBV lytic reactivation. The potent antitumor effect of BT115386 was demonstrated in the *in vivo* MTAP-deleted NPC mouse models. The findings warrant future assessments of *MAT2A* inhibitors in clinical studies for NPC, which might well impact a large subset of patients.
Acknowledgment: Acknowledgment: The work was supported by Hong Kong RGC funding (GRF:14101721 and AoE/M-401/20) and HMRF grant (#09203176)

#6227

Tumor cell heterogeneity may cause treatment failure of GPA33-targeted therapy in colorectal cancer

Teresa Börding, Tobias Janik, Markus Morkel, Christine Sers, David Horst.
Charité - Universitätsmedizin Berlin, Berlin, Germany

Purpose: Glycoprotein A33 (GPA33) is a membrane protein almost exclusively expressed in intestinal epithelia and in more than 95% of colorectal cancers (CRCs). This renders GPA33 a promising antigen for targeted therapy, but trials did not meet pre-specified response rates. We investigated intratumoral heterogeneity as a reason for low treatment efficacy, GPA33 regulation and the potential for pharmacological induction of GPA33 expression *in vitro* and *in vivo* to enhance treatment response.
Methods: We assessed intratumoral heterogeneity of GPA33 in tissue specimens of 223 stage II CRCs using immunohistochemistry and immunofluorescence, and obtained scRNAseq transcriptomic analysis from 12 primary CRCs. We then manipulated WNT and PPARγ signaling pathways and transcription factor expression in colon cancer cells using specific inhibitors, siRNAs or inducible dominant negative TCF4 (dnTCF4), and analyzed the effects on GPA33 protein and RNA expression. Furthermore, we investigated the effects of WNT inhibition on GPA33 *in vivo* in NOD/SCID xenografts. Additionally, we developed anti-GPA33 CAR-T cells and measured their activation after co-cultivation with colon cancer cells using flow cytometry.
Results: In the CRC cohort we found that GPA33 expressing cells had a differentiated phenotype and low WNT activity. GPA33-negative subpopulations were located at the infiltrative tumor edge and showed increased nuclear β-catenin. Downregulation of WNT pathway activity using inhibitors, siRNAs or inducible dominant negative TCF4 (dnTCF4), as well as activation of PPARγ signaling induced GPA33 expression *in vitro*. Forced expression of dnTCF4 also enhanced GPA33 expression *in vivo* in previously GPA33-negative tumor cell subpopulations in colon cancer xenografts. siRNA mediated knockdown of CDX1 and KLF4, two transcription factors that were previously implicated in GPA33 regulation, only moderately reduced GPA33 expression levels *in vitro*. Anti-GPA33

CAR-T cells activated in response to co-culture with GPA33-expressing CRC cells *in vitro*.
Conclusion: Our analysis highlights a heterogenous expression of GPA33 *in vivo* as a limiting factor for anti-GPA33 therapy. WNT inhibition or PPARγ activation induced GPA33 expression *in vitro* and *in vivo*. Depletion of CDX1 and KLF4 had moderate effects on GPA33 only, indicating a complex regulation in colon cancer. We suggest that pharmacological induction of GPA33 expression may increase the efficacy of anti-GPA33 targeted therapy in patients with CRC.

DNA-reactive Agents, HDAC and Methyltransferase Inhibitors, and Tubulin Agents

#6231
Activation of GCN2 by HC-7366 results in significant antitumor efficacy as monotherapy and in combination with multiple standard of care agents in various solid cancer models

Feven Tameire[1], Paulina Wojnarowicz[1], Crissy Dudgeon[1], Sho Fujisawa[1], Sharon Huang[1], Owen B. Reilly[1], Nicholas Collette[1], Jeremy Drees[1], Kathryn Bieging-Rolett[1], Takashi O. Kangas[1], Weiyu Zhang[1], Maria Fumagalli[1], Iman Dewji[1], Yunfang Li[1], Anissa SH Chan[1], Xiaohong Qiu[1], Ben Harrison[1], Ashley LaCayo[1], Ricardo A. Cordova[2], Kirk A. Staschke[2], Alan C. Rigby[1], Savithri Ramurthy[1], Eric S. Lightcap[1], David Surguladze[1], Nandita Bose[1]. *[1]HiberCell, New York, NY,[2]Department of Biochemistry and Molecular Biology, Indiana University School of Medicine, Indiana University Melvin and Bren Simon Comprehensive Cancer Center, Indianapolis, IN*

The integrated stress response (ISR) is an adaptive signaling pathway that cells utilize to respond to a wide range of extrinsic and intrinsic stresses, which are important for tumorigenesis. Activation of ISR is suggested to play a dual role in cell fate decisions. While the ISR promotes survival, prolonged activation of ISR induces apoptosis. We are developing HC-7366, a first-in-class, first-in-human GCN2 activator, and are currently evaluating it in a phase 1 clinical trial in solid tumors (NCT05121948). In

this study, we present the characterization of the antitumor effects of HC-7366 in solid tumors.
In vivo efficacy studies using HC-7366 montherapy showed significant tumor growth inhibition (TGI%) in preclinical cancer models of colorectal (78-95%), head and neck (33% regression), sarcoma (80%) and prostate (65%). HC-7366 activated the ISR in tumors from treated mice as evidenced by induction of the ATF4 target genes ASNS and PSAT1. Additionally, HC-7366 induced the proapoptotic protein PUMA and reduced HIF1α and HIF2α levels. Furthermore, HC-7366 showed significant benefit in colorectal models when combined with DC101 (anti-VEGFR2 antibody), 5-fluorouracil (chemotherapy), alpelisib (PI3Kα inhibitor), or trametinib (MEK1/2 inhibitor). Using GCN2 CRISPR-knockout cells, we confirmed that the HC-7366 mediated reduction of cell growth and induction of ISR markers was dependent on GCN2. We performed multi-omics analyses to further understand the mechanism of action. Metabolomics analysis of tumors treated with HC-7366 revealed that HC-7366 altered several metabolites involved in amino acid metabolism, oxidative stress, the urea cycle, and pyrimidine biosynthesis. Additionally, proteomics analysis showed that HC-7366 significantly reduced proteins involved in oxidative phosphorylation. Analysis of the transcriptome in tumors from treated mice demonstrated that HC-7366 reduced the activity of HIF and E2F1-driven transcription, including expression of metaphase-anaphase transition genes, consistent with decreased Ki67 staining in tumors. ATF4 and JUN transcriptional activity was enhanced with HC-7366 treatment consistent with activation of ISR. Collectively, our *in vitro* and *in vivo* results demonstrate that HC-7366 is a potent GCN2 activator with strong antitumor activity across multiple solid tumor models as a monotherapy or in combination with standard of care agents.

#6232

Ulipristal acetate, a selective progesterone receptor modulator, induces cell death via inhibition of STAT3/CCL2 signaling pathway in uterine sarcoma

Jae Ryoung Hwang[1], Young-Jae Cho[1], Ji-Yoon Ryu[1], Ju-Yeon Choi[1], Jung-Joo Choi[2], Jeong-Won Lee[2]. [1]*Sungkyunkwan University School of*

Medicine, Seoul, Korea, Republic of,[2]Samsung Medical Center, Seoul, Korea, Republic of

Purpose: Ulipristal acetate (UPA) is used for the treatment of uterine leiomyoma as a selective progesterone receptor modulator. Until now, there has been no experimental research on the effect of UPA on uterine sarcoma. In this study, we examined the efficacy of UPA in uterine sarcoma with *in vitro* and *in vivo* animal models.
Experimental Design: The cytotoxicity of UPA was determined in uterine sarcoma cell lines (MES-SA, SK-UT-1, and SK-LMS-1) by MTT and caspase-3 activity assays. A migration assay was done using a Transwell chamber, and MMP-2 was measured with its specific ELISA kit. Apoptotic genes and signaling pathways affected by UPA were analyzed by complementary DNA (cDNA) microarray of uterine sarcoma cell lines and western blot, respectively. The *in vivo* efficacy of UPA was examined in uterine sarcoma cell line- and patient-derived xenograft mice models.
Results: UPA inhibited cell growth and increased apoptosis in cell lines including uterine sarcoma (MES-SA) and leiomyosarcoma (SK-UT-1 and SK-LMS-1) in a dose-dependent manner. UPA also inhibited cell migration and the expression of MMP-2. cDNA microarray analysis revealed that CCL2 was commonly down-regulated by UPA in investigated cell lines. The UPA-mediated inhibition of CCL2 expression was confirmed by ELISA. The phosphorylation and the total expression of STAT3, downstream from the CCL2 signaling pathway, was also inhibited by UPA. We also found that UPA reduced cell growth and increased caspase-3 activity in primary culture cells from leiomyosarcoma patient-derived xenografts (PDX-C). Moreover, we found that STAT3/CCL2 inhibition by UPA was independent of the expression of progesterone receptor. *In vivo* studies with MES-SA and SK-UT-1 cell line-derived xenografts and a PDX model with leiomyosarcoma demonstrated that UPA significantly decreased tumor growth.
Conclusions: UPA had significant anti-tumor effects in uterine sarcoma through the STAT3/CCL2 signaling pathway and might be a potential therapeutic agent to treat this disease.

#6233

Omacetaxine reduces c-MYC expression and demonstrates antitumor effects in osteosarcoma

Kristen B. Farrell, Douglas H. Thamm. *Colorado State University, Fort Collins, CO*

Omacetaxine mepesuccinate (OMX), also known as homoharringtonine, is a protein translation inhibitor approved for use in chronic myeloid leukemia. Recent studies suggest OMX may be effective against other cancer types with high rates of protein translation, and may be successful against protein targets that are difficult to inhibit by reducing their translation rates. Using both canine and human osteosarcoma (OS) cell lines, we have investigated the efficacy of OMX against osteosarcoma and expression of c-MYC. OMX provides significant growth inhibition of OS cells with IC_{50} values in the low nanomolar range. OMX also reduces migration and invasion capabilities of OS cells. Strikingly, we observed reduction in levels of c-MYC protein in most canine and human OS cell lines after OMX exposure. This reduction was both dose and time dependent. We also investigated the efficacy of OMX against OS in an orthotopic mouse OS model. OMX is a promising candidate for treatment of OS in both dogs and humans, and potentially additional cancers dependent on c-MYC.

#6234

Targeting integrin alpha V beta 5 heterodimer stability using a novel small molecular inhibitor for tumor suppression

Nicole Mattson, Kazuya Miyashita, Anthony Chan, Lu Yang, Sheela Pangeni Pokharel, Wei Liu, Mingli Li, Qiao Liu, Xiaobao Xu, Priyanka Singh, Leisi Zhang, Mingye Feng, Chun-Wei Chen. *Systems Biology, Beckman Research Institute of The City of Hope, Monrovia, CA*

Integrins have long been sought as therapeutic targets in cancer, but there are no FDA approved drugs to target this gene family. Since integrins require the dimerization between an alpha and beta subunit to function, we developed a CRISPR library targeting all 26 alpha and beta subunits to identify which pair is the most important. We found a strong correlation between ITGAV and ITGB5 (Integrin Beta 5), which form a known heterodimer, in solid tumors. CRISPR targeting either ITGAV or ITGB5 led

to attenuated cell proliferation with increased cell cycle stalling and apoptosis. As the more essential partner, we designed a CRISPR tiling scan targeting the entire coding region of ITGAV and determine the essential nature of each amino acid. We found a sub-domain within the beta propeller to be important for ITGAV function, the CRISPR identified pocket (CIP). Genetic targeting of this pocket disrupted the ability to detect the heterodimer signal of ITGAV-ITGB5 by a specific antibody. Furthermore, we confirmed that essential amino acids within the CIP responsible for the heterodimer stability by the NanoBRET energy transfer system. Knowing the role of the CIP in heterodimer stability we searched for a small molecule to bind in the CIP to phenocopy our genetic findings. A combined *in-silico* and *in-vitro* high throughput drug screen started tested compounds for cell killing and disruption of the ITGAV-ITGB5 heterodimer. "Compound 2" (cpd_2) showed both strong cell killing and dissociation of the heterodimer. Disruption was measured by detection by flow cytometry and through the NanoBRET system. Cpd_2's binding was confirmed with thermal shift studies with purified ITGAV beta propeller, validating that this compound is behaving and binding as we expect at the CIP. Next, we sought to understand how the ITGAV-ITGB5 heterodimer controls cancer cell survival. From the Dependency Map Public database (DepMap) we found that Rac1 dependency is significantly correlated only with ITGAV and ITGB5. We hypothesized that this meant that ITGAV-ITGB5 regulated Rac1 activity. Loss of Rac1 phenocopies knock out of ITGAV or ITGB5 and loss of either Rac1 or ITGAV led to dysregulation of the actin cytoskeleton, a known downstream feature of Rac1. A constitutively Rac1 (CA_Rac1) rescues the effects of targeting of ITGAV or treatment with cpd_2. Altogether this data suggests that ITGAV-ITGB5 signals to Rac1 and that attenuation of their function can be reversed by an active Rac1 In summary, our study highlights a novel strategy of targeting the integrin heterodimer ITGAV-ITGB5 with a small molecule binding to a novel subdomain, CIP, of ITGAV. The CIP is responsible for the heterodimer stability of ITGAV and ITGB5. Disruption of this heterodimer led to the dysregulation of Rac1 and destabilization of the actin cytoskeleton. This mechanism highlights a novel strategy for targeting integrins as a therapeutic target in cancer.

#6235

Discovery of novel HDAC6 inhibitors that enhance proteasomal activity to boost antigen presentation and trigger anti-myeloma T-cell immunity

Priyanka S. Rana[1], James Ignatz-Hoover[2], James J. Driscoll[2]. *[1]Hematology and Oncology, Case Western Reserve University, Cleveland, OH,[2]University Hospitals - Seidman Cancer Center, Cleveland, OH*

Transformative success of cancer immunotherapy has revolutionized cancer treatment and can induce long lasting responses in patients with cancers from a wide range of histologies. However, only a fraction of patients respond to immunotherapy and cancer cells escape immunosurveillance through molecular mechanisms that remain elusive. Proteasomes play a central role in the immune response by generating peptides from intracellular antigens which are presented on the cell surface for recognition by $CD8^+$ cytotoxic T lymphocytes (CTLs). Malignant cells employ strategies to downregulate antigen presentation and impair CTL-mediated tumor recognition and lysis. Recently, we discovered that HDAC6-specific inhibitors increased intracellular proteasome activity and the generation of antigenic class I MHC peptides. However, current HDAC6 inhibitors have pharmacologic liabilities that limit efficacy, e.g., low potency and solubility, poor pharmacokinetic properties and potential genotoxicity. Therefore, we performed a cell-based, high-throughput screen (HTS) of 9,600 HDAC-specific compounds to identify novel compounds that increased proteasomal activity in myeloma cells. We identified 8 hits that increased proteasomal activity at least two-fold. Importantly, two novel molecules identified in the HTS increased proteasome activity more potently and more rapidly than the HDAC6-specific inhibitors Tubastatin-A and ACY-1215 (Ricolinostat) with comparatively low cytotoxicity. Proteasomes degrade chicken ovalbumin (Ova) to generate the immunodominant antigen SIINFEKL presented at the cell surface complexed with the MHC-class I molecule H-$2K^b$. Treatment of tumor cells with Tubastatin-A and ACY-1215 increased levels of the MHC-class I-SIINFEKL complex by ~3-fold. Tumor cells were pretreated with Tubastatin-A and ACY-1215 and then co-cultured with CTLs that had been genetically-engineered to express a SIINFEKL-restricted T-cell receptor (TCR). Pre-treatment of lymphoma or multiple myeloma cells with novel HDAC6 inhibitors also increased tumor lysis by CTLs that expressed the SIINFEKL-restricted TCR by 2-fold.

Taken together, our results support repositioning pharmacologics that inhibit HDAC6 to activate proteasomal generation of antigenic peptides and boost antigen presentation as cancer immunotherapeutics.

#6236

Stellettin B induces apoptosis and autophagy in human bladder cancer RT112 cells

Mei-Chuan Chen, Chun-Han Chang. *Taipei Medical University, Taipei, Taiwan*

Bladder cancer is one of the most prevalent cancers worldwide. Although most of the patients have good prognosis and good life expectancy with standard treatments, recurrence rate and five-year survival rate have not been significantly improved in patients with bladder cancer, demonstrating there is an urgent need for development of a novel therapeutic strategy for the treatment of bladder cancer. Stellettin B (SP-2), a triterpene isolated from marine sponge *Jaspis stellifera ,* suppresses cell viability in bladder cancer RT112 cells without severe toxicity toward normal uroepithelial SV-HUC-1 cells. Our results showed that SP-2 induces accumulation of cells at subG1 phase in parallel with increase of early apoptotic cells via annexin V/PI staining and activation of cell apoptotic death proteins. Moreover, non-cytotoxic concentrations of SP-2 induces LC3-II formation and p62 downregulation to activate autophagy in RT112 cells, suggesting autophagy may play a role in SP-2 -induced cell death. Inhibition of autophagy by pharmacological inhibitors (3-MA and chloroquine) or ATG5 knockout protects stellettin B-induced apoptosis and cell viability suppression, indicating SP-2 induces autophagy to promotes cell death. Taken together, stellettin B may be a promising therapeutic agent for bladder cancer treatment.

#6237

Small molecule screen identifies pyrimethamine as an inhibitor of NRF2-driven esophageal hyperplasia

chorlada Paiboonrungruang. *North Carolina Central University, Durham, NC*

Objective: NRF2 is a master transcription factor that regulates the stress response. NRF2 is frequently mutated and activated in human esophageal squamous cell carcinoma (ESCC), which drives resistance to chemotherapy and radiation therapy. Therefore, a great need exists for NRF2 inhibitors for targeted therapy of $NRF2^{high}$ ESCC.
Design: We performed high-throughput screening of two compound libraries from which hit compounds were further validated in human ESCC cells and a genetically modified mouse model. Mechanism of action of one compound was explored by biochemical assays.
Results: Using high-throughput screening of two small molecule compound libraries, we identified 11 hit compounds as potential NRF2 inhibitors with minimal cytotoxicity at specified concentrations. We then validated two of these compounds, pyrimethamine and mitoxantrone, by demonstrating their dose- and time-dependent inhibitory effects on the expression of NRF2 and its target genes in two $NRF2^{Mut}$ human ESCC cells (KYSE70 and KYSE180). RNAseq and qPCR confirmed the suppression of global NRF2 signaling by these two compounds. Mechanistically, pyrimethamine reduced NRF2 half-life by promoting NRF2 ubiquitination and degradation in KYSE70 and KYSE180 cells. Expression of an $Nrf2^{E79Q}$ allele in mouse esophageal epithelium (*Sox2CreER;LSL-*$Nrf2^{E79Q/+}$) resulted in an $NRF2^{high}$ phenotype, which included squamous hyperplasia, hyperkeratinization, and hyperactive glycolysis. Treatment with pyrimethamine (30mg/kg/day, *p.o.*) suppressed the $NRF2^{high}$ esophageal phenotype with no observed toxicity.
Conclusion: We have identified and validated pyrimethamine as an NRF2 inhibitor that may be rapidly tested in the clinic as a radiation and chemotherapy sensitizer for $NRF2^{high}$ ESCC.

#6238
ABM-2752, a potent and selective HPK1 inhibitor with excellent efficacies as a single agent or in combination with a PD-1 antibody
Chen Chen, Charles Huang, Min Xu, Xiuquan Chen, Xiaobing Lv, Chen Yang, lanjiao Zhao, YouQin Chen, jizhi li, li zhao. *ABM Therapeutics, San Diego, CA*

Hematopoietic Progenitor Kinase 1 (HPK1, MAP4K1) is predominantly expressed in hematopoietic cells and is a negative immune regulator of T-cell and B-cell activation through phosphorylating adaptors. Loss of HPK1 kinase function suppresses tumor growth in preclinical tumor models, and therapeutic co-blockade of HPK1 kinase and PD-1 enhances anti-tumor responses. Therefore inhibition of HPK1 is an attractive approach for the immunotherapy of cancers. ABM-2752 has a unique chemical structure that was potent on the HPK1, and selective over other MAP4K family members. It showed dose-dependent inhibition of SLP-76 phosphorylation and induction of IL-2, with good ADME and animal PK properties. In vivo efficacy was demonstrated in murine colorectal MC38 and CT26 syngeneic models as a single agent, enhanced by aPD-1. Treatment of ABM-2752 in these two models also improved animal overall survival. Other efficacy studies in murine melanoma B16F10 model and glioblastoma GL261 orthotopic model showed good efficacy and safety, demonstrating its good brain penetration in animals. Preliminary tox studies indicated a good safety window. Based on these preclinical results we plan to file IND in 2023.

#6239

PM534 is a novel microtubule-destabilizing agent with high affinity and potent antineoplastic properties

Maria Ángela Oliva[1], Beatriz Álvarez-Bernad[2], Daniel Lucena-Agell[1], Marta Martínez Diez[3], María José Guillén[4], Gema Santamaría Nuñez[3], María José Muñoz-Alonso[3], Eva M. Garrido-Martin[3], Pablo Avilés[5], Carmen Cuevas[6], J. Fernando Díaz[7]. *[1]Structure, Function and Pharmacology of Cytoskeleton, Centro de Investigaciones Biológicas CSIC, Madrid, Spain,[2]Structure, Function and Pharmacology of Cytoskeleton, Centro de Investigaciones Biologicas CSIC, Madrid, Spain,[3]Cell Biology and Mechanism of Action, Pharma Mar, S.A., Madrid, Spain,[4]Pharmacology, Pharma Mar, S.A., Madrid, Spain,[5]Pharmacology and Toxicology, Pharma Mar, S.A., Madrid, Spain,[6]Research and Development, Pharma Mar, S.A., Madrid, Spain,[7]Structure, function and pharmacology of cytoskeleton, Centro de Investigaciones Biológicas, Madrid, Spain*

Background: Microtubule targeting compounds are a successful class of anticancer agents in the clinic. Although highly potent, the currently approved antitumor agents targeting tubulin present some drawbacks such as the development of acquired resistances, which remain an obstacle for an effective prolonged anticancer treatment. In this work, we present a novel microtubule destabilizing agent with an optimized interaction for the colchicine site and a novel mechanism of action which confers it a high affinity binding for tubulin.
Methods and Results: We have determined the X-ray crystallographic structure of the complex T_2R-TTL with PM534 at a resolution of 2.45 Å. We unequivocally found PM534 ligand density at the intra-dimer interface between α and β tubulin of both tubulin dimers (the colchicine domain) within the complex. The colchicine domain of tubulin can be divided into three zones: a central pocket and two accessories. Whereas other colchicine site-ligands only bind to two of the zones, we found that PM534 binds extensively along the three zones, making multiple contacts with β-tubulin N terminal domain, central hinge helix, and the intermediate domain. PM534 interaction did not affect the overall curved conformation of tubulin and its mechanism of action consists on precluding the curve-to-straight conformational transition required for tubulin to assemble intro microtubules and thus, to perform its cellular functions. In competition assays we found that the compound displaces a bona fide high-affinity colchicine-probe with a binding affinity of 5.1 ± 0.3 x10^7 M^{-1} at 25ºC. Moreover, PM534 shows potent antineoplastic activity *in vitro*, with GI_{50} values in the low nanomolar range, observed in different human tumor cancer cell lines. An *in vivo* Proof of the Concept (PoC) was performed in athymic *nu/nu* mice bearing H460 (NSCLC) tumors that were treated (intravenous, on days 0, 7, 14) with different doses (ranging from 0.75 mg/kg to 2.5 mg/kg) of PM534. Results demonstrated strong, dose-related PM534-induced antitumor activity in this *in vivo* model.
Conclusions: The mechanism of action of PM534 involves an optimized interaction with the colchicine site, which is reflected in its high affinity for the substrate, being this the ultimate reason for the observed cellular activity. Additionally, PM534 presents a potent antitumor activity *in vitro* that was translated into a clear positive *in vivo* PoC that resulted in strong antitumor effect.

#6240

The potent quadruplex-binding compound QN-302 shows anti-tumor activity as a monotherapy in an orthotopic *in vivo* model of pancreatic cancer

Nicole Williams[1], Danielle Santos[1], Jenny Worthington[1], Ahmed Ahmed[2], Tariq Arshad[3], Stephen Neidle[2]. *[1]Axis Bioservices, Coleraine, United Kingdom,[2]University College London (UCL), London, United Kingdom,[3]Qualigen Therapeutics Inc, San Diego, CA*

The compound QN-302, a tetra-substituted naphthalene diimide derivative has single-digit nM anti-proliferative activity in a panel of human pancreatic cancer (PDAC) cell lines (Ahmed et al., ACS Med Chem Lett, 2020, 11, 1634-1644). It has significant anti-tumor activity in the MIA-PACA2 xenograft model for PDAC and in the genetic KPC model. We now report that this compound also shows significant mono-therapy anti-tumor activity in an orthotopic model for PDAC. Female athymic nude mice bearing orthotopically implanted pancreatic BxPC-3 cells were dosed with 1 x weekly IV QN-302 at 0.5 and 1.0 mg/kg, over a period of 21 days. A separate group of mice was treated with Gemcitabine twice weekly IV during this period, at a dosage of 15 mg/kg. Blood samples from animals were collected on a weekly basis and were used to detect and quantify circulating tumor DNA as a method of following treatment efficacy. In line with previous studies QN-302 was well-tolerated at 0.5 and 1.0 mg/kg with no adverse effects on animal health or behavior noted during the study. Circulating tumor DNA levels were significantly less than vehicle controls in gemcitabine-treated animals from day 7 and QN-302 (1.0 mg/kg) treated animals from day 14 of treatment. Survival was significantly increased in gemcitabine and QN-302 (1.0 mg/kg) QW treatment groups. Statistically significant efficacy was observed in gemcitabine and QN-302 (1.0 mg/kg) treated animals. Examination of blood chemistry and biochemistry of treated animals did not indicate any adverse effects due to QN-302. This orthotopic model is the 4th *in vivo* study in a pancreatic cancer model showing anti-tumor activity for QN-302, further confirming the potential of this compound for human disease. QN-302 is currently in an advanced stage of pre-IND development by Qualigen Inc.

#6241

LP-184, an acylfulvene class small molecule therapeutic, is synthetically lethal in DNA damage repair deficient cancers

Aditya Kulkarni, Jianli Zhou, Neha Biyani, Kishor Bhatia, Panna Sharma.
Lantern Pharma Inc., Dallas, TX

As many as one third of solid tumors (ovarian, breast, pancreatic, prostate cancers) harbor deficiency in some DNA Damage Repair (DDR) pathways. Such cancers become dependent on alternative DDR pathways to maintain genome integrity, making them selectively vulnerable to DDR inhibitors. The concept of synthetic lethality has been successfully applied to develop strategies to treat subsets of such tumors. Clinically, PARP inhibitors (PARPi) have been successful particularly in Homologous Recombination Deficiency (HRD) cancers. Other agents have also been designed to target these DDR deficiencies in cancer cells and have potential to be clinically beneficial. LP-184 is a next generation acylfulvene prodrug metabolized to an active compound by prostaglandin reductase 1 (PTGR1) that is often elevated in multiple tumors. LP-184-induced DNA lesions are likely repaired by the Nucleotide Excision Repair (NER) and Homologous Repair (HR) pathways. Reduced activities of multiple DDR-related pathways in solid tumor models correlated with increased sensitivities to LP-184 as indicated by Gene Set Enrichment Analysis. Chinese Hamster Ovary cells with NER mutations (ERCC1/2/6) were at least 4 fold more sensitive to LP-184 relative to otherwise isogenic parental cells. ERCC2 or BRCA2 depletion enhanced LP-184 sensitivity 5-8X in a metastatic prostate cancer cell line. LP-184 showed ~120 fold higher potency (IC50 77 nM) compared to Olaparib in HRD prostate cancer organoid model LuCaP 96 (BRCA2/ CHEK2 inactivating mutations). Across 14 patient-derived pancreatic, lung and prostate tumor models harboring HR mutations (BRCA1/2, CHEK1/2, ATM/ATR, PALB2, PARP1/2, RAD51, FANCA/B), LP-184 showed ex vivo IC50s in the range of 30-300 nM, whereas Olaparib IC50s ranged from 1700-6900 nM. LP-184 treatment resulted in complete tumor regression (107-141% TGI) in 10/10 HR deficient triple negative breast cancer PDX models of which 7/10 were resistant Olaparib/ Niraparib and to Doxorubicin/ Cyclophosphamide. LP-184 treatment resulted in complete and durable tumor regression in HRD (BRCA1/ATR mutant) pancreatic cancer PDX models (112-140% TGI). In the ovarian cancer cell line OVCAR3 having HRD/NERD phenotype, LP-184 IC50 was 13 nM,

Olaparib IC50 was 145 nM and their combination Bliss Synergy Score was 16 indicating synergy. LP-184 is synthetic lethal resulting from its abilities to cause unresolvable DNA damage if tumor cells express high PTGR1 and are deficient in NER/HR genes. Unlike PARPi, LP-184 has striking activity in both NERD as well as HRD cancers. These strong data have prompted the development of a soon to be launched clinical trial to translate the broad preclinical anticancer activity of LP-184 in solid tumors with HR/NER pathway defects, such as pancreatic, prostate, ovarian and breast cancers.

#6242

Inhibition of BIRC5/survivin by LQZ-7I inhibits neuroblastoma growth while hemizygosity of *BIRC5* does not: implications for therapy of neuroblastoma

Carmen Dorneburg[1], Celimene Galliger[1], Voker Rasche[2], Andre Lechel[3], Thomas F. E. Barth[3], Klaus-Michael Debatin[1], Christian Beltinger[1].
[1]University Children's Hospital, Ulm, Germany,[2]Experimental Cardiovascular MRI, University Medical Center Ulm, Ulm, Germany,[3]Innere Medizin, University Medical Center Ulm, Ulm, Germany

Overexpression of survivin, a crucial regulator of the mitotic spindle checkpoint, is associated with poor prognosis in neuroblastoma (NB). Transcriptional inhibitors of survivin have been tested in clinical trials. However, results have been disappointing. We thus investigated the small molecules LQZ-7I and S12 that inhibit dimerization of survivin protein and compared their growth-inhibiting efficacy with that of markedly decreased survivin expression in a novel transgenic NB mouse. Mice hemizygous for *BIRC5* were crossed with TH-MYCN mice to generate BIRC5$^{+/-}$/MYCN$^{tg/+}$ mice. NB incidence, growth and retransplantation capacity were assessed. In vitro, LQZ-7I and S12 were used to inhibit survivin protein interactions and the effects on proliferation and cell cycle of NB cells were investigated. *BIRC5* hemizygous mice developed NB although mRNA and protein expression of survivin was markedly decreased. Surprisingly, incidence and latency of the NB that developed in the BIRC5$^{+/-}$/MYCN$^{tg/+}$ mice did not differ from the NB in the TH-MYCN mice, and tumor growth and survival of the mice was not affected. In stark contrast, the survivin interaction inhibitors LQZ-7I and S12 abolished anchorage-independent growth and proliferation of NB cell lines. Reduced growth of NB cells resulted from

defects in mitosis induced by LQZ-7I or S12 or. LQZ-7I was the more efficient inhibitor of NB cells while S12 was not able to reduce tumor growth in a xenograft model. Taken together, these results support the notion that inhibiting survivin interaction is more efficacious in NB than inhibiting survivin transcription.

#6243

The novel antitubulin agent PM534 exhibits potent antitumoral and antiangiogenic properties in vitro and in vivo

Marta Martínez Diez[1], María José Muñoz-Alonso[1], Gema Santamaría Nuñez[1], María José Guillén[2], María Ángela Oliva[3], Eva Maria Garrido-Martin[1], Pablo Avilés[4], J. Fernando Díaz[3], Carmen Cuevas[5]. *[1]Cell Biology and Mechanism of Action, Pharma Mar, S.A., Madrid, Spain,[2]Pharmacology, Pharma Mar, S.A., Madrid, Spain,[3]Structure, function and pharmacology of cytoskeleton, Centro de Investigaciones Biológicas CSIC, Madrid, Spain,[4]Pharmacology and Toxicology, Pharma Mar, S.A., Madrid, Spain,[5]Research and Development, Pharma Mar, S.A., Madrid, Spain*

Background: Microtubule targeting agents have demonstrated to be very effective antitumoral drugs. The development of novel anti-tubulin agents with more efficient mechanisms of action presents several challenges due to their poor solubility, troublesome synthesis or purification, and toxicities. In this work, we present the novel anti-tubulin agent PM534, a synthetic small molecule that shows efficient antitumoral and antiangiogenic properties *in vitro* and *in vivo*.

Methods and Results: PM534 exhibits a potent antitumor activity *in vitro* with a mean GI_{50} value in the low nanomolar range in several different human cancer cell lines. Washout *in vitro* experiments show irreversible cellular effects after 1h in contact with the compound, compelling the cells to apoptotic cell death likely due to PM534 induced disorganization of the tubulin cytoskeleton. PM534 inhibits migration and invasion of tumor cells *in vitro*, and arrests the cell cycle in the G2/M phase, forcing them to apoptosis. In addition, PM534 presents potent antiangiogenic effects *in vitro*, robustly inhibiting endothelial cells proliferation and migration, and the formation of angiotubes. The *in vivo* antitumor activity of PM534 was

characterized in human-derived tumors xenografted in athymic *nu/nu* mice, namely breast (MDA-MB-231), and pancreas (Mia-Paca-2). PM534 was intravenously administered once per week for three consecutive weeks at 5.0 mg/kg. *In vivo* PM534-induced antitumor activity (vs. placebo) was seen in MDA-MB-231 (T/C, 0.3% on Day 28; TV, $p<0.0001$) and Mia-Paca-2 (21.3% on Day 21; TV, $p<0.0001$). Also, PM534 treatment increased with statistical significance (vs. placebo) the median survival time of mice bearing MDA-MB-231 (82 vs. 33 days; $p<0.0001$) and Mia-Paca-2 (51 vs. 30 days; $p=0.0008$). Of note, complete tumor remissions were observed in 2/10 (lasting 11 days and 161 days, each), and 10/10 (lasting 45 days in 9/10 and 140 days in 1/10) PM534-treated animals bearing Mia-Paca-2 and MDA-MB-231 and tumors, respectively.
Conclusions: Based on *in vitro* activity against different human tumor cell lines, *in vivo* activity in xenografted human tumors, as well as on its anti-angiogenic properties, the safety, pharmacology and preliminary antitumor activity of PM534 will be evaluated in a first-in-human clinical trial to be conducted in patients with advanced solid tumors.

#6244

Design, synthesis, and structure-activity relationships of substituted pyrido[3,2-*d*]pyrimidines as microtubule targeting agents and anti-cancer agents

Yesha Vijaykumar Shah[1], Ruoli Bai[2], Ernest Hamel[2], Aleem Gangjee[1].
[1]Medicinal Chemistry, Duquesne University School of Pharmacy, Pittsburgh, PA,[2]Frederick National Laboratory for Cancer Research, National Cancer Institute, Frederick, MD

Microtubules (MTs) are composed of *αβ*-tubulin heterodimers and are essential components of the cellular cytoskeleton involved in critical cellular functions, including mitosis, cell migration and signaling, intracellular trafficking, and angiogenesis. Microtubule targeting agents (MTAs) are highly successful chemotherapeutic agents because they target MT dynamics and interfere with MT-dependent cellular processes. The clinical efficacy of MTAs is limited by multidrug resistance due to expression of the P-glycoprotein (Pgp) drug efflux pump or increased expression of *β*III-tubulin. This necessitates the development of novel MTAs effective against cell lines expressing these forms of drug resistance,

which could offer potential advantages in patients who fail to respond to current MTAs, such as paclitaxel. Previously, we reported colchicine site (CS) binding compound **1** with a pyrido[3,2-*d*]pyrimidine scaffold and a 2-H substitution and *N*4-4'-methoxyaniline substitution inhibited colchicine binding and tubulin assembly (87% inhibition at 5 μM and IC_{50} = 1.3 μM, respectively). Compounds **2-9** were designed with a 2-CH_3 substitution to evaluate the structure-activity relationships at the 4-position by using conformational restriction and isosteric replacements. Compounds **2-9** were synthesized, and the biological evaluation showed that compounds **2-9** inhibited tubulin assembly (**7**, IC_{50} = 0.72 μM) and binding of colchicine to tubulin (**7**, 97% inhibition at 5 μM, 81% at 0.5 μM). Compound **7** was found to be highly potent in the MCF-7 breast cancer cell line with an IC_{50} of 2.5 nM which was ~3.5-fold better than combretastatin-A4 (CA4). Compound **7** inhibited the growth of the human ovarian cancer cell line OVCAR-8 with an IC_{50} = 3.0 nM. For the Pgp overexpressing cell line NCI/ADR-RES, **7** was equally potent (IC_{50} = 3.0 nM), whereas paclitaxel was almost inactive (IC_{50} = 1,500 nM). Thus, we have identified 2-CH_3 substituted pyrido[3,2-*d*]pyrimidines as a novel structural scaffold for inhibition of tubulin assembly and colchicine binding that have potent cytotoxic activity against the breast cancer cell line MCF-7 and against both the parental ovarian cancer cell line OVCAR-8 and its derivative Pgp overexpressing cell line NCI/ADR-RES. These compounds thus merit further study as potential cancer chemotherapeutic agents.

#6245

Selective HDAC6 inhibition by ITF3756 modifies the landscape of gene and protein expression in human monocytes: Possible identification of a specific biomarker signature

Chiara Ripamonti, Valeria Spadotto, Monica Forino, Christian Steinkuhler, Gianluca Fossati. *Italfarmaco S.p.A., Cinisello Balsamo, Italy*

Histone deacetylase 6 (HDAC6) modulates tumor immunogenicity through several pathways, such as the control of PD-L1 expression on tumor and on lymphoid cells. Thus, HDAC6 is a potential pharmacological target for cancer treatment. In humans, HDAC6 inhibition can be monitored by measuring the ratio between tubulin and histone acetylation. However, the

identification of biomarkers to be used as a signature for patient stratification that correlates with the treatment efficacy is missing. Since we have previously demonstrated that the activity of the selective HDAC6 inhibitor ITF3756 on myeloid cells plays a role in the antitumor immune response in the TME, we reasoned that an ITF3756-specific signature could be identified in unstimulated monocytes treated with the compound. Monocytes were purified from healthy donors, treated with ITF3756 and RNAseq and proteomic analyses were performed. Gene Ontology analysis shows that ITF3756 has a widespread effect on monocyte transcriptome and proteome. We observed the down-modulation of genes and proteins involved in inflammatory pathways and in transcription regulation. Up-regulation of neutrophil-mediated immunity, metabolic pathways and protein phosphorylation was also identified. Focusing on genes that could be relevant in the tumor context, we selected a panel of genes from the most up- (SCL27A1, ANXA6 and IRF6) and down-modulated (CD84, RANK, CXCL2, CXCL3, STAB-1, CD163, PD-L1, CD206 and ADA). Interestingly, we found among the downmodulated genes markers of M2 macrophages, genes related to the tumor associated macrophages, and STAB-1, whose targeting is currently in clinical trials for cancer immunotherapy. Peripheral Blood Mononuclear Cells (PBMCs) could be a less expensive starting material for biomarker identification to be collected during a clinical trial when compared to purified monocytes. Thus, to ascertain whether the regulation by ITF3756 of our selected genes was detectable also in PBMCs we performed gene expression analysis after ITF3756 treatment and we confirmed that all selected genes were reproducibly modulated. Surface protein expression of M2 macrophages biomarkers in our panel, were determined by flow cytometry and all of them were significantly modulated in PBMCs. These data show how our approach successfully led both to the identification of a biomarker signature that could be used in clinical trials to monitor the pharmacodynamic effect of ITF3756, and to the discovery of previously unknown targets of HDAC6 inhibition.

#6246

The MTA-cooperative PRMT5 inhibitor AM-9747 exhibits robust antitumor activity in combination with clinically relevant chemotherapies and targeted agents in MTAP null tumor models

Katherine Slemmons, Brian Belmontes, Siyuan Liu, Jodi Moriguchi, Antonia Policheni, Paul E. Hughes. *Discovery Research, Amgen Inc., Thousand Oaks, CA*

Homozygous deletion of chr9p21, containing genes *CDKN2A* and *MTAP*, occurs in about 15% of cancers. MTAP loss, a key enzyme in the methionine and adenine salvage pathways, leads to the accumulation of its substrate MTA. MTA competes with the methyl donor SAM for binding to type II arginine methyltransferase PRMT5, placing PRMT5 in a hypomorphic state and vulnerable to further PRMT5 inhibition. MTA-cooperative PRMT5 inhibitors are an emerging class of therapeutics targeting MTAP null tumors. AMG 193, currently in Phase 1 trials, and its representative analog AM-9747 have broad spectrum activity in MTAP null tumor models across hematologic and solid tumor indications. Mechanistically, AM-9747 induces DNA damage, shown by increased phosphorylated H2AX, resulting in cell cycle arrest and senescence. Exploration of clinically relevant therapeutic combinations with standard of care (SOC) chemotherapies or targeted agents that could potentiate this DNA damage or target orthogonal pathways is a rational therapeutic approach. Here, we evaluated AM-9747 in combination with SOC chemotherapies and assessed synergy using the Chou-Talalay Method to generate Combination Index (CI) scores. SOC agents representing a variety of mechanisms of action (paclitaxel, carboplatin, gemcitabine, pemetrexed, irinotecan, 5-FU) were evaluated and results ranged from strongly synergistic ($CI<0.3$) to additive ($CI=1$) in a panel of non-small cell lung carcinoma (NSCLC) and pancreatic cancer cell lines. The SOC combinations augmented AM-9747 induced DNA damage resulting in increased cell cycle arrest and nuclear count assays confirmed the synergistic antiproliferative effects of the combinations. Combinations of AM-9747 and one strongly synergistic agent (carboplatin) and one moderately synergistic agent (paclitaxel) were evaluated in H292 NSCLC xenografts. Significant reductions in tumor burden compared to single agent treatments were observed with AM-9747 + paclitaxel (67% TGI) and AM-9747 + carboplatin (82% TGI). Additionally, roughly 2-3% of NSCLC tumors harbor both *MTAP* loss and a KRAS G12C mutation. To target both pathways we combined the FDA-approved KRAS G12C inhibitor sotorasib with AM-9747 and observed synergy ($CI<0.6$) in MIAPACA2 cells.

Nuclear counts confirmed a greater cell growth inhibition in the combination and immunoblots confirmed on target inhibition of both pathways. Combination treatment of AM-9747 and sotorasib in LU99 NSCLC xenografts resulted in significant tumor regression compared to each single agent with 10/10 mice tumor free. This combination is being tested in additional MTAP null KRAS G12C mutant models. Overall, our data suggests that combining MTA-cooperative inhibitor AM-9747 with SOC or clinically relevant targeted agents is a compelling therapeutic strategy for the treatment of *MTAP* null cancers.

#6247

Lurbinectedin shows potent activity in all four molecular subtypes of small cell lung cancer (SCLC) and POU2F3 and SLFN11 are biomarkers for a better response

Marta Martínez Diez[1], Gema Santamaría Nuñez[1], María José Guillén[2], Daniel Rueda[3], Eva Maria Garrido-Martin[1], Pablo Avilés[4], Carmen Cuevas[5]. *[1]Cell Biology and Mechanism of Action, Pharma Mar, S.A., Madrid, Spain,[2]Pharmacology, Pharma Mar, S.A., Madrid, Spain,[3]Biomarkers and Translational Studies, Pharma Mar, S.A., Madrid, Spain,[4]Pharmacology and Toxicology, Pharma Mar, S.A., Madrid, Spain,[5]Research and Development, Pharma Mar, S.A., Madrid, Spain*

Background - SCLC is the most aggressive lung cancer type and with the worst prognosis. There are four molecular subtypes based on the high expression of distinct transcription factors and with different therapeutic vulnerabilities. However, all share transcriptional addiction as pathogenic mechanism. Lurbinectedin is a novel oncogenic transcription inhibitor, approved in the United States and other countries for the treatment of adult patients with metastatic SCLC with disease progression on or after platinum-based chemotherapy. The aim of this study was to analyze the activity of lurbinectedin in the different SCLC molecular subtypes and to investigate new biomarkers of response.
Methods and Results - We have characterized a panel of 20 SCLC human cell lines based on the expression of ASCL1, NEUROD1, YAP1 and POU2F3, where lurbinectedin yielded a mean IC_{50} value of 6.52 nM, which is considerable greater than the activity exerted by topotecan, irinotecan,

carboplatin, etoposide, olaparib, alisertib and navitoclax (IC_{50} 100 μM-100 nM). Lurbinectedin potency is high in the four molecular subtypes, with IC_{50} values of 4.1, 14.9, 7.2, and 0.2 nM for SCLC-A, -N, -I and -P, respectively. However, high expression of POU2F3 correlated with better responses. In fact, mean IC_{50} was 0.28 nM for $POU2F3^{high}$ cells versus 12.1 nM for all $POU2F3^{low}$ cells (p=0.0443). Additionally, basal SLFN11 levels were evaluated, observing that $SLFN11^{high}$ cells responded better to lurbinectedin, with IC_{50} values of 1.1 nM versus 11.8 nM for $SLFN11^{low}$ (p=0.05). Likewise, lurbinectedin treatment induced greater antitumor activity in $SLFN11^{high}$ tumor-bearing mice (H526: T/C, 18% on day 11) than in $SLFN11^{low}$ tumor-bearing mice (H82: T/C, 65% on day 7) after intravenous treatment at 0.18 mg/kg (on days 0, 7 and 14). Finally, SLFN11 expression was evaluated by IHC in FFPE tumor samples from SCLC patients participating in a multicenter phase II clinical trial in advanced solid tumors (NCT02454972), which allowed lurbinectedin accelerated approval in this indication by FDA. Patients with higher expression of SLFN11 had a slightly better overall survival (OS at 6 months: 68.4% (<15%, N=20) vs. 98.7% (≥15%, N=20) p=0.0261)), especially in the refractory/resistant subgroup (OS at 6 months: 33.3% (<15%, N=9) vs. 100.0% (≥15%, N=6) p<0.0001).
Conclusions - Lurbinectedin is highly effective in all molecular subtypes of SCLC *in vitro* and *in vivo*, with IC_{50} values at least two logs more potent than for other antitumoral agents and its activity is even greater in tumors with high POU2F3 expression and/or high SLFN11 expression.

#6248

Inhibiting β-catenin in AML by targeting DDX5

WEI NI[1], Swati Garg[1], Fen Zhu[1], Ellen L. Weisberg[1], Basudev Chowdhury[1], Martin Sattler[1], Amulya Jakkani[1], Suiyang Liu[1], Dana M. Sanchez[1], Lizi Wu[2], Richard M. Stone[1], Matthew S. Davids[1], James D. Griffin[1]. *[1]Medical Oncology, DFCI/Harvard Medical School, Boston, MA,[2]Molecular Genetics & Microbiology, University of Florida, Gainesville, FL*

Despite the use of high-dose chemotherapy and HSCT, less than 70% of adult AML patients enter complete remission and most patients relapse in less than two years. These poor outcomes have motivated intensive searches for effective and safe targeted agents. Asp-Glu-Ala-Asp (DEAD)-box protein DDX5 was found to be highly expressed in several solid cancers. DDX5, especially its phosphorylated form at Y593, has been reported to promote β-catenin cytoplasm-to-nucleus shuttling and subsequently facilitate the transcriptional activities of the β-catenin/T-cell factor (TCF) complex leading to enhanced expression of genes that are critical for growth, including *MYC* and *CCND1*. Knockdown of *DDX5* has also been reported to reduce the growth of AML cells, indicating that DDX5 is a potential therapeutic target in AML. However, it remains unknown whether the growth dependence of AML on DDX5 is mainly mediated by β-catenin signaling. Importantly, drugs that selectively target DDX5 have not been tested in AML. In this study, we first analyzed the TCGA AML dataset and found that *DDX5* gene is significantly overexpressed in the AML cohort compared to normal bone marrow samples. High *DDX5* expression is associated with worse overall survival in AML patients. Moreover, *DDX5* correlates with *CTNNB1* which encodes β-catenin, at transcript levels. We further found that DDX5 is constitutively phosphorylated at Y593 and predominantly present in the nucleus of 10 AML cell lines tested. These results indicate the clinical relevance of DDX5 whose functional impact may link to β-catenin signaling in AML. We then determined the therapeutic efficacy of targeting DDX5 in human AML using RX-5902, a quinoxalinyl-piperazine compound. RX-5902 was previously shown to interfere with the interaction between phosphorylated DDX5 and β-catenin, inhibiting β-catenin signaling in some solid tumors. We found that RX-5902 attenuated phosphorylation of DDX5 at Y593, led to accumulation of β-catenin in the cytoplasm and consequently downregulated c-MYC in human AML cells within 24 hours. Treatment with RX-5902 dramatically increased cellular ROS level, induced cleaved-caspase3 mediated apoptosis and eventually inhibited cell growth of most human AML cell lines and primary AML cells in culture. These results mirrored what we observed following DDX5 depletion by shRNAs in AML cell lines. Also, dosing of RX-5902 *in vivo* significantly suppressed the growth of AML xenotransplants in immunocompromised mice and prolonged survival. Finally, we performed dynamic BH3 profiling and showed that RX-5902

increased apoptotic priming and BCL-2 dependence in AML cells. Therefore, we reasoned that simultaneous targeting DDX5 and BCL-2 may improve the therapeutic efficacy in AML. Indeed, concurrent treatment using RX-5902 and Venetoclax, a BCL-2 inhibitor, synergistically induced apoptosis in AML cells. Collectively, therapeutic targeting of DDX5 may be a novel and effective approach in AML and warrants further study.

#6249

Low Bcl-2 is a robust biomarker of sensitivity to nab-paclitaxel in Ewing sarcoma

Guillem Pascual-Pasto, Claudia Resa-Pares, Angel M. Carcaboso. *Hospital Sant Joan de Déu Barcelona, Barcelona, Spain*

Nanoparticle albumin-bound paclitaxel (nab-paclitaxel) shows potent preclinical anticancer activity in pediatric solid tumors such as Ewing sarcoma, rhabdomyosarcoma and neuroblastoma, but responses in clinical trials have been modest. In this work, we aimed to discover a rational biomarker-based approach to select the right candidate patients for this treatment. We assessed the efficacy of nab-paclitaxel in 27 patient-derived xenografts (PDX), including 14 Ewing sarcomas, five rhabdomyosarcomas and several other pediatric solid tumors. Response rate (partial or complete response) was remarkable in rhabdomyosarcomas (four of five) and Ewing sarcomas (four of 14). We addressed several predictive factors of response to nab-paclitaxel such as the expression of the secreted protein acidic and rich in cysteine (SPARC), chromosomal stability of cancer cells and expression of antiapoptotic members of the B-cell lymphoma-2 (Bcl-2) family of proteins such as Bcl-2, Bcl-xL, Bcl-W and Mcl-1. Protein (immunoblotting) and gene expression of SPARC correlated positively, while immunoblotting and immunohistochemistry expression of Bcl-2 correlated negatively with the efficacy of nab-paclitaxel in Ewing sarcoma PDX. The negative correlation of Bcl-2 immunoblotting signal and activity was especially robust ($r = 0.8352$; $P = 0.0007$; Pearson correlation). Consequently, we evaluated pharmacological strategies to inhibit Bcl-2 during nab-paclitaxel treatment. We observed that the Bcl-2 inhibitor venetoclax improved the activity of nab-paclitaxel in highly resistant Bcl-2-expressing Ewing sarcoma PDX. Overall, our results suggest that low Bcl-2 expression could be used to select patients with Ewing sarcoma sensitive to

nab-paclitaxel, and Bcl-2 inhibitors could improve the activity of this drug in Bcl-2-expressing Ewing sarcoma.

#6251

High expression level of GSK3β in basal triple negative breast cancer: Effects of the HDAC inhibitor, vorinostat

Beverly D. Lyn-Cook, Fatemeh Nouri Emamzaden, Beverly Word, George Hammons. *FDA-NCTR (National Center for Toxicological Research), Little Rock, AR*

High expression levels of glycogen synthases kinase 3 beta (GSK3β) have been correlated with poor prognosis in triple negative breast cancer (TNBC) patients. GSK3β is a multifaceted kinase and is a key regulator of a number of cellular processes. It is known to function as a positive regulator of epithelial-mesenchymal transition (EMT). Usually, cells that undergo EMT are known to acquire stem cell properties and these cells have properties that are known to be resistant to chemotherapies. Inhibition of GSK3β has been shown to decrease markers of EMT and reduce cancer stem cells. High levels of GSK3β were found in the basal-2 subtype of triple negative breast cancer cells, HCC1806. Histone deacetylases (HDACs) are expressed at high levels in some cancers, including TNBC. In this study, vorinostat, a histone deacetylase inhibitor, was shown to down regulate GSK3 expression in HCC1806 cells at both the gene and protein level using qPCR and western blots. Furthermore, cancer stem cells (CSC) cell markers CD44/CD24 using flow cytometry and immunostaining were significantly decreased. Previous studies published from our laboratory have shown vorinostat's ability to decrease TNBC cells invasion compacity, as well as cell growth. This study suggests that targeting GSK3β may be a potential therapeutic target for certain subtypes of TNBC. Triple negative breast cancer remains one of the most aggressive breast cancers, often having a high mortality rate in younger women.

#6252

HDAC inhibition increases Ewing sarcoma sensitivity to chemotherapy

Kaitlyn H. Smith, Chloe Sholler, Divya Gandra, Kimberly McKinney, Karl Dykema, Abhinav Nagulapally, Erin Trovillion. *Atrium Health, Charlotte, NC*

Purpose: The survival rate of those with Ewing sarcoma (ES) has seen very little improvement over the past several decades and remains dismal for those with recurrent or metastatic disease. Current treatment for Ewing sarcoma includes a combination of cytotoxic chemotherapeutic agents and local control with radiation and/or surgery. The purpose of this study is to identify currently available targeted agents which may be combined with chemotherapy for use in Ewing sarcoma to improve patient outcomes.
Methods: Novel targeted approaches for the treatment of ES were identified using RNA sequencing performed on ES patient tumors with bioinformatic analysis of gene expression. HDAC inhibitors were tested on patient cell lines at escalating doses and cell viability was assessed with CellTiter-Glo 2.0 and analyzed with GraphPad Prism to determine the IC50. Cells were treated with Panobinostat for 12 and 24 hours and RNA sequencing was performed. Cell cycle analysis was performed using Incucyte® Cell Cycle Lentivirus Reagent and analyzed using an Incucyte® S3. At 24- and 48-hours western blot analysis was performed to evaluate the effect on cell cycle and apoptosis. Combination studies with standard chemotherapy were performed and viability was assessed with CellTiter-Glo 2.0. At 24 hours of treatment with a combination of doxorubicin and HDAC inhibition western blot analysis was performed to evaluate changes in DNA damage and repair.
Results: RNA analysis identified HDAC2 as a potential therapeutic target. The pan-HDAC inhibitors, Panobinostat and Belinostat, and the HDAC1/2 inhibitor, Romidepsin, were cytotoxic to all Ewing sarcoma cell lines tested with clinically relevant IC50s. Mechanistically, pathways involved in cell cycle progression and DNA repair were repressed by Panobinostat as shown by RNA sequencing and western blotting (Cyclin D1, pRb, CHK1). Additionally, cell cycle analysis has shown a G1 arrest in response to HDAC inhibition. HDAC inhibitors significantly decrease cell viability when combined with standard chemotherapy (upfront and relapse therapy) compared to that of chemotherapy alone. When combined with doxorubicin, CHK1 and CHK2 were significantly decreased and pH2AX was significantly increased indicating an accumulation of DNA damage.
Conclusion: This work highlights that combining HDAC inhibitors with standard of care chemotherapy may be an effective treatment and improve outcomes for Ewing sarcoma patients. Future studies of HDAC inhibitors

combined with chemotherapy drugs will aim to determine efficacy in xenograft models.

#6253

SP-3164, a novel molecular glue degrader with activity in preclinical models of multiple myeloma

Aundrietta D. Duncan[1], Daniela Y. Santiesteban[2], Nadeem Q. Mirza[2], Steve Horrigan[2], Sheila DeWitt[2], Vincent Jacques[2], P. Leif Bergsagel[3]. *[1]Salarius Pharmaceuticals, Inc, Houston, TX,[2]Salarius Pharmaceuticals, Houston, TX,[3]Mayo Clinic, Phoenix, AZ*

Multiple myeloma (MM) makes up approximately 10% of all hematologic malignancies, with increasing incidence worldwide. Though treatment options for newly diagnosed patients have evolved in recent years, they are not curative, and relapse is common with 2,500-3,000 relapsed or refractory (R/R) MM US patients seeking novel treatments, annually. Cereblon (CRBN)-binding Ikaros and Aiolos (I/A) protein degraders (i.e., lenalidomide (LEN) and pomalidomide (POM)) have had great success in treating MM. However, due to the unstable chiral nature of the CRBN-binding moiety, common to these molecules, many exist as racemic mixtures (1:1 mixture of interconverting (*R*)- and (*S*)-enantiomers). A growing body of evidence suggests that the (*S*)- enantiomer is the active anticancer species, while the (*R*)-enantiomer is inactive and potentially results in undesired activity. The ability to stabilize the active (*S*)-enantiomer represents a potential strategy to improve therapeutic outcomes. We are developing SP-3164, the deuterium-stabilized (*S*)-enantiomer of avadomide (AVA), an I/A-degrading molecular glue which has been studied in over 400 patients, demonstrating safety and activity in hematologic diseases. Our *in vitro* data demonstrate that SP-3164 more potently and rapidly degrades the cancer-promoting transcription factors, I/A, compared to LEN, POM, and AVA, while the stabilized (*R*)-enantiomer, SP-3165, neither binds CRBN nor degrades I/A. In preliminary *in vivo* studies, SP-3164 elicited significant tumor growth inhibition (TGI). Here, we investigate the activity of SP-3164 in MM, compared to established treatment regimens.

SP-3164's potential to degrade Aiolos in MM.1S cells was compared to SP-3165, AVA, and POM. SP-3164 rapidly and robustly degraded Aiolos in a

time- and dose-dependent manner, more potently than AVA and POM, while SP-3165 demonstrated minimal Aiolos degradation. To investigate the effect of SP-3164 on cell survival, we treated NCI-H929 cells with SP-3164 (0.1 μM, 1 μM, and 10 μM) and SP-3165 (1 μM) and assessed apoptosis by flow cytometry. SP-3164 induced dose-dependent early and late apoptosis after 72 hours, while SP-3165 showed no induction of apoptosis. SP-3164's *in vivo* activity was assessed and compared to SP-3165, LEN, and POM in an NCI-H929 mouse xenograft model. SP-3164 showed significant TGI as a single agent while SP-3165 seemed to support tumor growth. LEN and POM demonstrated minimal TGI. When combined with dexamethasone (DEX), SP-3164 had improved TGI compared to the combination of POM+DEX.
These preclinical data demonstrate that SP-3164 is a potent CRBN-binding molecular glue with the ability to rapidly degrade cancer-promoting transcription factors and induce apoptosis *in vitro*. *In vivo*, SP-3164 has superior single agent and combination activity compared to approved molecular glues. These data support the continued development as a novel therapy in MM.

#6254

The discovery and preclinical characterization of the SAM-competitive PRMT5 inhibitor UCT-000445

Martina S. J. McDermott[1], Neil A. O'Brien[1], Brendan O'Boyle[2], Michael Bartberger[2], Oliver C. Losón[2], Kevin Chau[1], Ella Schwab[1], Jenny Hong[1], Jiaying Zhou[1], Chuhong Hu[1], Tong Luo[1], Raul Ayala[1], John Glasby[1], Brian M. Stoltz[3], Dennis J. Slamon[1]. *[1]UCLA, Los Angeles, CA,[2]1200 Pharma, Culver City, CA,[3]California Institute of Technology, Pasadena, CA*

Protein arginine methyltransferase 5 (PRMT5) is a methyltransferase enzyme that symmetrically dimethylates arginine residues of histones, transcription elongation factors, translation regulators, and transcription factors like p53. It also regulates the activity of MAPK and PI3K signaling through methylation and activation of various receptor tyrosine kinases. As such, it has epigenetic effects that may be therapeutic in oncology. Successful clinical development of PRMT5 inhibitors will depend on upon utilizing this unique inhibitor modality and identifying those cancers with sensitivity to PRMT5 inhibition. By evaluating the potency and efficacy of

several SAM-competitive, substrate-competitive, and MTA-cooperative PRMT5 inhibitors using a large (n>500), diverse panel of human cancer cell lines, we determined that the SAM-competitive inhibitor modality offers the best therapeutic potential thanks to its larger therapeutic window *in vitro*. This screening approach also identified several solid tumor histologies that were extremely sensitive to PRMT5 inhibition. Using our proprietary chemistry and by screening through the panel of human cancer cell lines, we identified UCT-000445, a SAM-competitive PRMT5 inhibitor with high selectivity over PRMT9 and good pharmacokinetic properties. Moreover, efficacy UCT-000445 is achieved regardless of *MTAP* gene status in histologies outside of hematological malignancies and including colon. UCT-000445 potently inhibits tumor growth in multiple human xenograft models of cancers, including but not limited to colon and lung cancers. The responses observed are durable upon cessation of treatment. Marked combined efficacy was also observed with standard of care treatment in these cancer types. UCT-000445 was well tolerated in vivo and using a CD-1 nude mouse model we found that while reticulocyte proliferation (a surrogate marker for bone marrow cytopenias) is abrogated by continuous treatment with UCT-000445, the use of intermittent dosing schedules overcomes this effect, while yielding equivalent efficacy. Our data with UCT-000445 indicate that SAM-competitive PRMT5 inhibitors may represent a novel and compelling therapeutic strategy for the treatment of multiple solid tumors.

#6255

Anti-proliferative effect of two copper complexes against medulloblastoma cells

Hope Korshie Fiadjoe[1], Christoffer Lambring[1], Umesh T. Sankpal[1], Duaa Alajroush[2], Alvin A. Holder[2], Riyaz Basha[1]. *[1]Microbiology, Immunology and genetics, University of North Texas Health Science Ctr., Fort Worth, TX,[2]Old Dominion University, Norfolk, VA*

Background and Purpose: Copper is a crucial structural component for many significant enzymes, as well as a key catalytic co-factor in redox processes. The flexible Cu(I/II) redox behavior facilitates the formation of copper complexes that are more potent and less toxic. The anticancer activity of several agents can be enhanced by forming copper complexes.

The purpose of this study is to evaluate the anti-proliferative effects of two copper (II) complexes, copper-tolfenamic acid (Cu-TA) and copper thiosemicarbazone (Cu-acetylethTSC or CuTSC) against medulloblastoma (MB). MB is a cancer of the cerebellum which is associated with frequent relapse and drug resistance with the current treatments. It necessitates the development of alternative strategies. The anti-cancer activity of Cu-TA was evaluated in laboratory testing in some cancer models, but it has not been studied in MB. CuTSC against colorectal cancer, leukemia and breast cancer has been studied but it has not in MB.
Methods: TA and TSC were complexed with Cu and Cu-TA and CuTSC complexes were characterized through colorimetric/mass spectrometric analyses. Cancer cells and cardiomyocytes were cultured using standard protocols and cell viability was measured using Cell Titer-Glo kit (Promega). Protein expression was determined by Western blot analysis.
Experiments/Results: CuTA and CuTSC complexes showed proper characterization and stability during the testing period. Cardiomyocytes (H9C2) and human cancer cell lines representing breast, Ewing sarcoma and MB were screened for anti-proliferative activity of these two Cu complexes. While, cell viability was inhibited in all cancer cell lines, MB cell lines (DAOY and D283) showed higher efficacy while H9C2 cell viability was not affected. To understand the underlying mechanism of action, the effect of Cu-TA was assessed on the expression of c-PARP, Specificity protein 1 (Sp1) and an antiapoptotic protein, survivin. Western blot results revealed a clear decrease in the expression of both Sp1 and survivin and upregulation of c-PARP.
Discussion/Conclusion: Both Cu-TA and CuTSC treatments result in a dose-time dependent anti-proliferative activity against cancer cells but not affecting non-malignant cardiomyocyte cells. Cu-TA can inhibit Sp1 and survivin and increase PARP cleavage suggesting the effect on Sp1-regulated oncogenes and an induction of apoptotic pathways. The studies to establish crossing of Blood Brain Barrier and further understand the underling mechanisms of these two Cu complexes in single and combination treatment alongside chemotherapeutic agents are currently under investigation.

#6256

Inhibition of class IIa HDACs potentiates MYC inhibitor-driven cytotoxicity by inducing MYC depletion and oxidative stress in non-small cell lung cancer

Jina Park, Ying-Yu Chen, Jennie Cao, Michelle Vaz, Ray-Whay C. Yen, Stephen B. Baylin, Michael J. Topper. *Johns Hopkins, Baltimore, MD*

Lung cancer is the most common cause of cancer mortality worldwide and non-small cell lung cancer (NSCLC) accounts for approximately 85% of all lung cancers. Dysregulation and/or overexpression of MYC are widely implicated in NSCLC, which suggests that MYC may be a promising therapeutic target for the treatment of NSCLC. Recently, two direct MYC inhibiting agents with improved *in vivo* efficacy and tolerability, MYCi975 and Omomyc, have been developed. To define new drug strategies that could potentiate the therapeutic effects of MYC inhibitors, transcriptome datasets from MYCi975 and Omomyc studies were reanalyzed. These data revealed the induction of two class IIa histone deacetylases (HDACs), HDAC5 and HDAC9, upon MYC inhibition. Importantly, class IIa HDACs are involved in cancer proliferation, aggressiveness, and prognosis. In addition, novel agents that selectively inhibit class IIa HDACs have demonstrated promising anti-tumor efficacy; thus, suggesting potential therapeutic benefits from dual targeting of MYC and class IIa HDACs. We assessed the treatment efficacy of MYCi plus class IIa HDACi across 18 NSCLC cell lines, 10 of which demonstrated substantial reduction of cell viability upon combination treatment. Querying of driver mutation spectra associated with differential drug response in our cell line panel defined that EGFR mutant cell lines exhibited resistance, while STK11 or Ras mutant cell lines were sensitive to our drug paradigm. Gene set enrichment analysis comparing the transcriptomes of sensitive versus resistant cell lines revealed that MYC Targets, Oxidative Phosphorylation, and Reactive Oxygen Species (ROS) pathways were activated in combination treatment responsive cell lines. RNA sequencing on treated cell lines identified large-scale transcriptional shifts facilitated by combination treatment, including suppression of MYC, cell cycle, and mitochondrial pathways. Furthermore, G1/S arrest and elevated mitochondrial ROS levels in combination drug-treated cells were confirmed using flow cytometry. Concordant with the role of MYC as a key cell cycle regulator, MYC protein levels were decreased in the combination treatment group as compared to the vehicle or

mono-treatment groups. Importantly, both MYC overexpression and ROS scavenger treatment partially rescued the reduction of cell viability by combination treatment, suggesting both MYC depletion and ROS elevation as contributors to therapeutic efficacy driven by combination treatment. Expanding these studies to *in vivo* models, we discern that combination MYC and class IIa HDAC inhibition significantly reduced tumor burden in a patient-derived xenograft model of human NSCLC. In summary, we define here a novel drug paradigm combining MYC and class IIa HDAC inhibitors, which potentiates anti-tumor efficacy in NSCLC via MYC depletion and oxidative stress.

#6257

Developing HDAC inhibitors as immunomodulators

Sean Colligan, Li Shen, Christopher Rupert, Jonathan Bard, Roberto Pili.
University at Buffalo, Buffalo, NY

Immune checkpoint inhibitors (ICIs) are standard of care for several solid tumor types, including renal cell carcinoma (RCC). However, the clinical success of these therapies is dampened by the fact that the majority of patients demonstrate either inherent resistance to treatment or develop secondary resistance following an initial response. One key mechanism of tumor-driven ICI resistance is the generation and recruitment of suppressive immune cell types, including regulatory T cells (Tregs) and myeloid-derived suppressor cells (MDSCs), which coordinate to suppress anti-tumor T cell responses. Thus, there is a critical need for the development of novel combination strategies aimed at mitigating the presence and function of suppressive immune cells to improve the efficacy of ICIs in the clinic. Our laboratory has previously demonstrated that histone deacetylase inhibition (HDACi) is associated with a decrease in both the number and function of tumor-infiltrating Tregs and MDSCs in the RENCA tumor model. Thus, the overall goal of these studies both preclinically and clinically is to investigate the impact of the immunomodulatory effects of HDACi in combination with ICI therapy, with the overall hypothesis that HDACi will improve the efficacy of anti-PD1 therapy in RCC. Our pre-clinical data support this hypothesis by demonstrating increased tumor control and survival in RENCA tumor-bearing mice when treated with a combination of anti-PD1 and HDACi compared to single agent therapy. These increases

were also associated with an increase in the activation state of anti-tumor immune cells, as demonstrated by increased surface expression of MHC Class II molecules on macrophages and a decrease in phenotypically defined monocytic MDSCs. ATACseq and RNAseq data generated from combination-treated animals also outline a gene expression signature associated with both myeloid and T cell activation. Interestingly, our clinical studies also afforded us the opportunity to investigate potential biomarkers associated with responder status, which will allow us to better predict patient outcomes and administer therapies accordingly. Accumulating evidence from two independent clinical trials run by our group suggests that high levels of suppressive $CD11b^{+}HLA\text{-}DR^{lo}$ MDSCs at baseline in the peripheral blood is associated with lack of clinical response to the combination of HDACi and ICI. Overall, these data support the rationale for the combination of ICI and HDACi in the clinic, and provide a potentially useful biomarker through which we can predict the success of combination therapy.

#6258

The discovery and preclinical characterization of the potent covalent $KRAS^{G12C}$ inhibitor UCT-001024

Tristin E. Rose[1], Brendan M. O'Boyle[1], Justin A. Hilf[l], Emma L. Baker-Tripp[1], Zhengao Feng[1], Kevin Yang[1], Michael D. Bartberger[1], Oliver C. Losón[1], Neil A. O'Brien[2], Martina S. J. McDermott[2], Naeimeh Kamranpour[2], Weiping Jia[2], Tong Luo[2], Raul Ayala[2], John Glasby[2], Brian M. Stoltz[3], Dennis J. Slamon[2]. *[1]1200 Pharma, Culver City, CA,[2]UCLA, Los Angeles, CA,[3]California Institute of Technology, Pasadena, CA*

Small molecule inhibitors of $KRAS^{G12C}$ have garnered substantial interest as a targeted therapy for lung, colon and pancreatic cancers bearing this mutation. Data from multiple clinical programs have shown strong efficacy in lung tumors but diminished and differential efficacy for other tumor sites including lung-derived brain metastases. We undertook a series of *in vitro* and *in vivo* studies to evaluate clinically staged $KRAS^{G12C}$ inhibitors in an effort to elucidate pharmacological factors underlying these clinical differences and identified potency, permeability/efflux, and clearance as impediments to efficacy, particularly in the context of brain metastases.

Adagrasib is reportedly efficacious in patients with brain metastases. Our preclinical experimentation suggests that distinguished potency and pharmacokinetics are critical to therapeutic benefit, particularly in the context of brain metastases. Using both structure- and ligand-based design approaches, we identified a development candidate UCT-001024, which is a covalent $KRAS^{G12C}$ inhibitor that demonstrates superior target-engagement kinetics and cellular potency *in vitro*. UCT-001024 also demonstrates improved plasma and whole brain unbound clearance, and *in vivo* potency in ectopic xenograft models and a brain-tropic NSCLC metastasis model relative to adagrasib. Additionally, UCT-001024 shows a favorable DDI profile and ion channel safety in an *in vitro* iPSC-derived cardiomyocyte cardiac proarrhythmia assay.

#6259

Novel inhibitors of StAR related lipid transfer protein 5 inhibitors target plasma membrane lipid raft growth signaling

Shoja Hajira, Chetna Sharon, Daniel RodriguezAgudo, Rio Boothelllo, Glenn Kellogg, Gregorio Gil, William Pandak, Bhaumik B. Patel. *Virginia Commonwealth University, Richmond, VA*

Background: Treatment of colorectal cancer (CRC) presents a major challenge due to chemotherapeutic resistance and recurrence, which are attributed to the presence of cancer stem cells (CSCs). Cholesterol metabolism is a critical regulator of CSCs. Lipid Rafts are cholesterol-rich microdomains in the plasma membrane (PM) that anchor various growth receptors tyrosine kinases (RTKs). STARD5 is a novel protein that helps transport cholesterol from the endoplasmic reticulum to the PM. We have identified specific small molecule inhibitors of the STARD5 which disrupt the lipid rafts, resulting in the inhibition of growth signaling pathways.
Methods and Results: In-silico modeling studies using STARD5 crystal structure revealed 8 putative inhibitors (SD5i (A-H)). In vitro binding studies to determine secondary structural changes using circular dichroism spectroscopy revealed SD5iA and SD5iB as excellent STARD5 ligands. Both SD5iA and SD5iB caused a potent inhibition (IC_{50} 0.3 -18 μM) of CSC-enriched 3D spheroids in 9 CRC cell lines representative of 3 consensus molecular subtypes. However, SD5iA but not SD5iB showed toxicity towards normal murine intestinal organoids at effective doses

against CRC CSCs. Also, SD5iB enhanced cytotoxicity by oxaliplatin and panitumumab against CRC CSCs in HT-29 spheroids. Hence, SD5iB was advanced into in vivo studies. SD5iB caused no discernible toxicity in doses as high as 100 mg/kg in NCr nude mice at gross, serum chemistry, organ viability, or intestinal stem cell level (organoid formation). Subsequently, we generated s.c. xenograft using dual CSC marker sorted HT-29 cells and enriched them further with chemotherapy (5-fluorouracil and oxaliplatin weekly x 3) treatment followed by randomization to vehicle or SD5iB (100mg/kg i.p. 3/wk x 3 wks.). We observed xenograft growth inhibition and LGR5 expression in SD5iB-treated animals compared to vehicle controls. Mechanistically, we observed a decrease in free accessible PM cholesterol by SD5i measured by fluorescently tagged cholesterol-binding bacterial protein fALOD4 in HT-29 cells. Moreover, lipid raft staining (cholera toxin B staining) was significantly reduced in SD5iB-treated HT-29 cells compared to vehicle control using immunofluorescence. Further, lipid raft isolation was done by sucrose gradient ultracentrifugation to study the changes in the phosphorylation of RTKs SD5iB treatment in HT-29 spheroids resulted in decreased phosphorylation of EGFR, IGF1Rβ, and FGFR1 in isolated lipid rafts. Consequently, we observed a robust inhibition of ERK1/2 activation following SD5iB treatment compared to vehicle control.
Conclusion: SD5i shows anti-CSC activity by targeting lipid-raft-driven growth factor signaling. Hence, STARD5 inhibitors represent a novel class of targeted therapy that will enhance the efficacy of FDA-approved therapies in CRC.

Epigenetics

#6263
Lysine-specific histone demethylase 1A (KDM1A/LSD1) inhibition attenuates DNA double-strand break repair and augments efficacy of temozolomide in glioblastoma

Salvador Alejo[1], Bridgitte Palacios[1], Prabhakar Pitta Venkata[1], He Yi[1], Wenjing Li[2], Jessica Johnson[1], Sridharan Jayamohan[1], Weixing Zhao[2], Siyuan Zheng[3], Takayoshi Suzuki[4], Rajeshwar R. Tekmal[1], Andrew Brenner[3], Ratna K. Vadlamudi[1], Gangadhara R. Sareddy[1]. *[1]Obstetrics & Gynecology, UT Health Science Center at San Antonio, San Antonio,*

TX,[2]Biochemistry & Structural Biology, UT Health Science Center at San Antonio, San Antonio, TX,[3]UT Health Science Center at San Antonio, San Antonio, TX,[4]The Institute of Scientific and Industrial Research, Osaka University, Osaka, Japan

Background: Glioblastoma (GBM) patients face a dismal prognosis, with median survival of ~15 months and 5-year survival rate of 6.8%. Standard of care includes surgical resection, external beam radiation therapy, and adjuvant chemotherapy with temozolomide (TMZ). Unfortunately, all GBM patients succumb to their disease. Glioma stem cells (GSCs), a GBM subpopulation, possess enhanced DNA repair that contributes to chemoradiotherapy resistance. The epigenetic modifier lysine-specific histone demethylase 1A (KDM1A/LSD1) is overexpressed in GBM and emerging studies show KDM1A is implicated in DNA damage response. This study aims to determine the significance of KDM1A to promote DNA repair in GSCs. We hypothesize KDM1A inhibition augments therapeutic efficacy of TMZ via attenuation of DNA repair pathways.
Methods: Patient-derived GSCs were obtained via IRB-approved protocol from patient samples at UT Health San Antonio. KDM1A knockdown and knockout cells were generated by transduction of validated KDM1A-specific shRNA or gRNA, respectively. Brain bioavailability of KDM1A inhibitor NCD38 was established using LS-MS/MS. Effect of combination KDM1A knockdown or inhibition with TMZ was studied using cell viability, neurosphere, and self-renewal assays. Mechanistic studies were conducted using CUT&Tag-seq, RNA-seq, immunofluorescence, comet, Western blotting, RT-qPCR, homologous recombination (HR), and non-homologous end-joining (NHEJ) reporter assays. *In vivo* efficacy of KDM1A knockdown or inhibitor alongside TMZ was determined using orthotopic murine GBM models.
Results: GBM patient data sets showed KDM1A is elevated in recurrent GBM versus primary tumors. KDM1A knockdown, knockout, or pharmacological inhibition increased efficacy of TMZ in reducing cell viability and self-renewal of GSCs. Pharmacokinetic studies demonstrated KDM1A inhibitor NCD38 is readily brain penetrable. CUT&Tag-seq studies showed KDM1A is enriched at the promoters of DNA repair genes. RNA-seq studies confirmed that KDM1A inhibition reduced expression of DNA repair-related genes. RT-qPCR and Western blotting validated

downregulation of DNA double-strand break repair genes. Knockdown, knockout, or inhibition of KDM1A attenuated HR and NHEJ-mediated DNA repair capacity. Immunofluorescence and comet assay demonstrated increased TMZ-mediated DNA damage in NCD38-treated GSCs. Importantly, KDM1A knockdown or inhibition enhanced efficacy of TMZ and significantly improved survival of mice bearing orthotopic GBM tumors.
Conclusions: Our results provide compelling evidence KDM1A is essential for DNA repair in GSCs and KDM1A inhibition sensitizes GBM to TMZ via attenuation of DNA repair pathways. These findings suggest combination therapy of KDM1A inhibitor NCD38 with TMZ is a potential novel therapeutic strategy to improve GBM outcomes.

#6264
NUV-868, a novel BD2-selective BET inhibitor, in combination with enzalutamide or olaparib, inhibits growth of solid tumor xenografts
Hitisha Patel, Jennifer Hertzog, Laura Heller, Spandana Vootukuri, Yan Zhang, Chris Miller, Gary Hattersley. *Nuvation Bio, Inc., New York, NY*

The bromodomain and extraterminal domain (BET) family of proteins play a vital role in gene transcription, making it an attractive therapeutic target for cancer. BET inhibitors can also combine with many anticancer agents to enhance activity. The bromodomains of the BET protein, BD1 and BD2, have unique functions and inhibiting either domain can result in differential responses. To date, non-selective BET inhibitors have failed during early clinical development due to significant on-target toxicity and limited benefit; however, selectively targeting specific bromodomains may result in a more favorable benefit/risk profile. NUV-868 is a novel and highly selective BD2 inhibitor of the BET protein family with ~1500-fold selectivity for BRD4-BD2 relative to BRD4-BD1. Herein, we describe NUV-868 and its activity in multiple in vitro and in vivo solid tumor models. Target engagement, selectivity of bromodomain inhibition, and regulation of BET-mediated gene expression were examined. Additionally, the antitumor activity of NUV-868 in combination with enzalutamide or olaparib was studied in tumor xenograft models of prostate, breast, and pancreatic cancer. NUV-868 demonstrated high selectivity for BD2 and regulated expression of several BET target genes. NUV-868 in combination

with enzalutamide inhibited growth of several prostate cancer cell line- and patient-derived xenografts. NUV-868 in combination with olaparib inhibited tumor growth in models of breast, ovarian and pancreatic cancer. Our preclinical data demonstrate that NUV-868, a BD2-selective BET inhibitor, inhibits growth of tumor xenografts in combination with enzalutamide or olaparib and provides rationale for examination of these combinations in the clinic. An ongoing, phase 1 clinical study (NCT05252390) is evaluating NUV-868 as a monotherapy and in combination with olaparib or enzalutamide in patients with advanced solid tumors.

#6266

Group 3 medulloblastoma transcriptional networks are selectively sensitive to EP300 and CBP bromodomain inhibition

Noha Ahmed Mohammed Ahmed Shendy. *St. Jude Children's Research Hospital, Memphis, TN*

EP300/CBP are paralogous, multidomain histone acetyltransferases (HATs) that regulate gene expression by establishing enhancer and promoter marks on histone proteins. While EP300 and CBP proteins bind and regulate genes broadly across the genome, they also function to promote the expression of tumor-selective oncogenes such as the transcription factor *c-MYC*. This activity makes these proteins attractive targets for preclinical therapeutic development. EP300/CBP proteins contain highly homologous domains, including catalytic HAT domains and bromodomains (BRDs) that mediate physical binding of EP300/CBP to acetylated proteins. Importantly, however, the relative contribution of these distinct domains to tumor cell proliferation remains unresolved. To identify the relative contribution of the EP300/CBP BRD and HAT domains, we used a chemical strategy. We performed a cell viability-based high-throughput screen of the potent EP300/CBP BRD- or HAT-specific inhibitor, CCS1477 or A-485 on 454 barcoded cancer cell lines representing 31 distinct cancer types. These data revealed that the proliferation of most tumor cell lines regardless of the type of cancer were equally affected by targeting either domain of EP300/CBP. Intriguingly, Group 3 medulloblastoma (G3MB) cell lines were the most sensitive to EP300/CBP BRD inhibition, compared to HAT inhibition. Since G3MB cells are highly sensitive to BRD4 inhibition, we conducted a

bromoscan analysis of the phase 1 compound CCS1477, which revealed high selectivity for EP300/CBP (K_d~4-5nM), with limited off-target effects on BRD4 (K_d~250nM) or other bromodomain-containing proteins. To validate that the effects on G3MB were primarily due to inhibition of EP300/CBP, we performed biotinylated CCS1477 pulldown assays in G3MB neurosphere cultures using *in vitro* relevant dosing of CCS1477, which demonstrated selective pulldown of EP300 and CBP, but not BRD4. Further, crystallographic studies of the EP300, CBP and BRD4 bromodomains in complex with CCS1477 demonstrated that the selectivity for the EP300/CBP BRD was critically dependent on interactions between the difluorophenyl group of CCS1477 and amino acid side chains in the BRD of EP300/CBP. In contrast, the analogous sidechains of BRD4 were unable to coordinate efficient binding of CCS1477. Mechanistically, treatment of MB cells with CCS1477, but not A-485 or the BRD4 inhibitor JQ1, caused rapid early loss of mRNA expression of specific G3MB dependency networks including the driver oncogene c-*MYC*. These studies identify a selective role for the EP300/CBP bromodomain in maintaining genetic dependency networks in G3MB cells and provide new chemical approaches to disrupting malignant transcription in Group 3 medulloblastoma.

#6267

A novel and potent EZH1/2 dual inhibitor, HM97662 demonstrates antitumor activity in T-cell lymphoma

Jooyun Byun, Seung Hyun Jung, Yu-Yon Kim, Miyoung Lee, Gunwoo Lee, Heesun Moon, Eun Young Lee, Junghwa Park, Seon Yeong Han, Young Gil Ahn, Young Hoon Kim, Kwee Hyun Suh. *Hanmi Pharmaceutical Co., Ltd., Seoul, Korea, Republic of*

Chromatin remodeling is a crucial process for transcriptional regulation, of which dysregulation is often observed in various human cancers. The enhancer of zeste homology 2 (EZH2) and its homolog EZH1 are catalytic subunits of polycomb repressive complex 2 (PRC2), which trimethylate histone H3 at lysine 27 (H3K27me3) to repress transcription of its target genes.

Although methlytransferase activity of PRC2 is mainly contributed by EZH2, EZH1 also conducts a compensatory role to maintain tri-methylation

of H3K27. EZH1 also directly binds to chromatin and modulates its condensation. Recent studies have suggested that EZH1 as well as EZH2 played a critical role in T-cell lymphoma such as ATL/L and PTCL, which had high innate EZH1 and increased EZH2 expression upon acquisition of their malignancy. Consequently, dual inhibition of EZH1/2 might induce higher expression of downstream tumor suppressor genes than blocking EZH2 alone, expecting greater activity as an anti-cancer therapy.
Herein, we presented a novel and potent EZH1/2 dual inhibitor, HM97662, which simultaneously inhibited the methyltransferase activity of both EZH1 and EZH2 with 2.1 and 16 nM of IC_{50}, respectively. Surface plasmon resonance (SPR) assay verified that HM97662 had great binding affinity on EZH1-EED-SUZ12 complex as well as EZH2-EED-SUZ12 complex than competitors. HM97662 also showed broad and strong antiproliferative activity against various T-cell lymphoma cell lines. Representatively in HH cells, HM97662 not only suppressed global tri-methylation of H3K27, but also dose-dependently increased protein expression levels that modulate cell cycle or cancer cell apoptosis. HM97662 exhibited increment of CDKN1A (p21) proteins involved in cell cycle arrest and induced protein levels of cleaved caspase-3 as well as PARP. Additionally, resulting induction of apoptosis by HM97662 in HH cells was confirmed by TUNEL staining. Mechanistically, HM97662 increased mRNA expression of several target genes inducing cell cycle arrest and apoptosis in gene panel assay performed in HH cells. Two cell cycle repressor, CDKN2A (p16) and CDKN1C (p57), and a pro-apoptotic marker, BTG-2, were dose-dependently increased by HM97662. We further conducted chromatin accessibility assay and identified that the chromatin structures of them were loosened and highly transcribed after the treatment of HM97662.
Based our *in vitro* pharmacology data, we evaluated an antitumor activity of HM97662 in EZH1/2 co-expressed HuT-102 T-cell lymphoma cell mouse xenograft model, and daily oral dosing of HM97662 showed potent tumor growth inhibition.
In conclusion, the present studies demonstrated that HM97662 has promising prospective for the treatment of patients with T-cell lymphoma. Given that the necessity of new treatment options on T-cell lymphoma, it is urgent to assess the effectiveness of HM97662 in further clinical trials.

#6268

TT125-802 is a potent and highly selective CBP/p300 bromodomain inhibitor for the treatment of castration resistant prostate cancer and haematological malignancies

Sara Laudato, Dorothea Gruber, Thomas Bohnacker, Martin Schwill, Charles-Henry Fabritius, Raquel Herrador, Katrin Westritschnig, Thushara Pattupara, Vikram Ayinampudi, Stefanie Flückiger-Mangual. *TOLREMO Therapeutics AG, Muttenz, Switzerland*

The paralogous lysine acetyltransferases CREB-binding protein (CBP) and p300 are key epigenetic regulators involved in diverse signaling pathways in cancer. The bromodomain (BRD) of CBP/p300 serves as an acetyl-lysine "reader" that allows CBP/p300 to bind chromatin at acetylated histone and non-histone proteins leading to the regulation of gene transcription. Indeed, CBP/p300 are critical co-activators of nuclear receptors, including the androgen receptor (AR) in castration resistant prostate cancer (CRPC). Thus, inhibition of CBP and p300 is an emerging therapeutic strategy to block the transactivation activity of the AR in CRPC. In addition, inhibition of the CBP/p300 BRD has been described as a potential therapeutic strategy to treat multiple myeloma (MM) through transcriptional suppression of interferon regulatory factor 4 (IRF4) and concomitant repression of its target genes MYC and MYB.

TT125-802 is a highly selective and potent, oral small molecule inhibitor of the BRD of CBP/p300. In a BROMOscan assay against a panel of 40 BRD-containing proteins, TT125-802 revealed the unique selectivity to the BRD of CBP/p300 with a minimal off-target binding to all other BRDs, including BET proteins.TT125-802 shows selective anti-proliferative activity in AR-dependent prostate cancer cell lines (22Rv-1, C4-2, and LNCaP) and inhibits AR target gene expression (KLK2, KLK3, TMPRSS2, and MYC) in a dose-dependent manner (IC50 of 2 to 33 nM). AR-negative prostate cancer cell lines (DU-145 and PC-3) are insensitive to TT125-802 in vitro, pointing to an AR-selective mode of action. In an *in vivo* model of CRPC, TT125-802 inhibited tumor growth when administered orally to human C4-2 xenograft-bearing mice. Daily dosing of TT125-802 was well tolerated with stable bodyweights and platelet counts. In addition, preclinical studies in CRPC patient-derived xenograft (PDX)-bearing mice showed that the combination treatment of TT125-802 and enzalutamide had a synergistic effect on tumor growth inhibition compared to single agent treatments.

TT125-802 reduced mRNA expression of the AR-target genes in tumor samples and decreased plasma PSA levels compared to enzalutamide alone, and the combination reduced levels even further. In a preclinical model of MM (OPM2), TT125-802 had a dose-dependent effect on tumor growth, inducing tumor regressions at the highest dose. Target genes such as MYC, MYB, and IRF4 were potently downregulated in tumors. We conclude that TT125-802 is a novel, highly selective inhibitor of the BRD of CBP/P300. It has therapeutic potential as monotherapy in prostate cancer and multiple myeloma and in combination with next-generation AR inhibitors for patients with lethal prostate cancer. A FIH study of TT125-802 in cancer patients is on track to start in 2023.

#6269

JBI-778, a novel brain-penetrant small molecule PRMT5 inhibitor for treatment of cancer

Dhanalakshmi Sivanandhan[1], Chandru Gajendran[1], Naveen Sadhu M[2], Zainuddin Mohammed[1], Ramachandraiah Gosu[3], Divsha Sher[4], Shahar Mansur[4], Dinorah Friedmann-Morvinski[4], Sridharan Rajagopal[2], Luca Rastelli[5]. *[1]Discovery Biology, Jubilant Therapeutics Inc, Bedminster, NJ,[2]Discovery Chemistry, Jubilant Therapeutics Inc, Bedminster, NJ,[3]Protein Chemistry, Jubilant Therapeutics Inc, Bedminster, NJ,[4]Sagol School of Neuroscience, Department of Biochemistry and Molecular Biology, Tel Aviv University, Tel Aviv, Israel,[5]Chief Scientific Officer, Jubilant Therapeutics Inc, Bedminster, NJ*

Introduction: Protein arginine methyltransferases (PRMTs) transfer a methyl group from the cofactor S-adenosyl-L-methionine (SAM) to the arginine of a substrate protein [(1,2)]. PRMT5 is a type II protein arginine methyltransferase that catalyzes the symmetrical dimethylation. PRMT5 drives transcriptional suppression of cell cycle control and tumor suppressor genes by hypermethylating promoter histones H3R8 and H4R3. Recently, dysregulation of the splicing machinery has been identified to be one of the therapeutic vulnerabilities for PRMT5 inhibition in multiple cancers. Therefore, inhibitors selectively targeting PRMT5 could be of high clinical value in cancers with defects in spliceosome machinery. In this regard, we

are developing a series of novel substrate competitive PRMT5 inhibitors to target brain cancer and solid tumors with brain metastasis.
Methods: Structure based drug design was used to identify novel PRMT5 inhibitors. To assess *in vitro* potency, flash plate assay was used. Cell based activity was assessed by measuring the symmetrical dimethylation of SmD3, intron retention and long-term cell proliferation assays. Tumor growth inhibition was measured in orthotopic glioblastoma models in mice.
Results: Our lead PRMT5 inhibitor JBI-778 had a strong in vitro potency against PRMT5 where the EC_{50} was ~5 nM and a similar cellular potency (< 10 nM) in inhibiting symmetric dimethylation of arginine. JBI-778 showed a strong anti-proliferative activity in select Neuroblastoma, Medulloblastoma, NSCLC, and glioma cell lines where the IC_{50}s ranged from 27 to 700 nM. Of note, NSCLC cell lines with mutation in the spliceosome protein RBM10 appeared to be more sensitive to JBI-778 treatment, which is consistent with enhanced retention of introns that are reported to be PRMT5 substrates including ATM, POLD and PNISR. JBI-778 showed an excellent oral bioavailability with a very high and sustained brain exposure in rodents. In U87-MG human GBM orthotopic model, oral administration of the JBI-778 resulted in strong and dose dependent efficacy with complete (~95 %) tumor growth inhibition and regression in few mice and translated into significant survival advantage. In 005 mouse GBM orthotopic model that mimics human GBM, JBI-778 showed a strong tumor growth inhibition and significantly extended survival (40 in control vs 58 days in 778 treated, $p<0.05$). IND-enabling GLP toxicology studies conducted in rodent and non-rodent species did not detect anemia or thrombocytopenia even at higher than efficacious concentrations.
Conclusion: PRMT5 inhibitor JBI-778 is able to penetrate the brain in all animal species tested and it is highly efficacious in orthotopic glioma models. Its differentiated mechanism makes it a potential option for the treatment of gliomas and brain metastasis with a focus on patients with spliceosome mutations. IND application for JBI-778 has been approved by FDA and a FIH trial is being planned.

#6270
Combination therapy with selective SMARCA2 (BRM) degraders for treatment of SMARCA4 (BRG1)-deficient cancers

Michael Hulse, Margot Elkins, Jessica Burtell, Komali Vykuntam, Philip Pitis, Liang Lu, Kris Vaddi, Andrew Combs, Koichi Ito, Peggy Scherle.
Prelude Therapeutics, Wilmington, DE

SMARCA2 (BRM) and SMARCA4 (BRG1) are mutually exclusive core catalytic subunits of the SWI/SNF complexes and use their ATPase domain to regulate the composition of nucleosomes. Between 4-5% of Non-Small Cell Lung Cancer (NSCLC) patients harbor SMARCA4 damaging mutations or SMARCA4 homo-deletions, resulting in loss of SMARCA4 protein expression. These SMARCA4-deleted cancer cells are predicted to be highly dependent on the paralog gene SMARCA2 for their survival. Therefore, targeting SMARCA2 in SMARCA4-deleted cancers using selective SMARCA2 degraders induces synthetic lethality while sparing SMARCA4 wild type normal cells. Although the treatment of lung cancer has improved considerably in recent years with the development of immune checkpoint inhibitors (ICIs) and specific $KRAS^{G12C}$ covalent inhibitors, $KRAS^{G12C}$ mutations significantly co-occur in 15-17% of SMARCA4-deleted NSCLC patients and have also been shown to correlate with a worse clinical outcome. The co-occurrence of $KRAS^{G12C}$/SMARCA4-deletion mutations in NSCLC led us to investigate whether combining our selective SMARCA2 degraders with $KRAS^{G12C}$ or other MAPK pathway inhibitors would demonstrate synergistic effects. To test this hypothesis, we treated SMARCA4 damaging/low expression $KRAS^{G12C}$ mutant cell lines with our SMARCA2 degraders and several $KRAS^{G12C}$ inhibitors, in addition to SHP2 and MEK inhibitors. Robust synergy was observed with these combinations, suggesting that targeting SMARCA2 together with agents that inhibit distinct nodes of the MAPK pathway in patients with SMARCA4-deleted cancer may be a promising therapeutic strategy. To further understand the mechanisms underpinning the synergy between our SMARCA2 degraders and $KRAS^{G12C}$/MAPK pathway inhibitors, we conducted RNA-seq and found unique transcriptional signatures in the synergistic combinations relative to those of either agent alone. We are currently testing if this *in vitro* synergy with our SMARCA2 degraders extends to *in vivo* combination efficacy in CDX and PDX models. Furthermore, early data suggested that SMARCA4 deletion may indicate poor outcomes of ICIs in lung cancer patients. Interestingly, our

SMARCA2 degraders promote the antigen presentation pathway and induce pro-inflammatory cytokine expression in SMARCA4-deleted cancer cells. We are currently investigating combinations of our SMARCA2 degraders with ICIs using syngeneic mouse models and human ex-vivo approaches. In summary, our preclinical data suggest that potent and selective SMARCA2 targeted degraders may potentially improve patient outcomes when combined with therapeutic agents targeting the RAS/MAPK pathway and/or ICIs in SMARCA4-deleted cancers. The combination of SMARCA2 degraders with standard of care agents warrants further investigation as a potential novel, effective, and highly targeted combination approach.

#6271

Discovery of BR1733 for the treatment of SWI/SNF deficient or highly vascularized solid tumor

Xinghao Wang, Shichao Ma, Min (Bella) Xie, Lele Wang, Yajun Wang, Song Zhang, Sheng Chen, Lynette Zhang, Yongqi Zhou, Mengxi Zhao, Dandan Li, Guobin Li, Xiao Fan, Hailong Zhang. *Blueray Biopharma, Shanghai, Shanghai, China*

Polycomb repressive complex 2 (PRC2) catalyze the writing of H3K27me3 epigenetic marker and suppresses the expression of genes including tumor suppressors. Activation mutation of EZH2, the catalytic subunit of the PRC2 complex, drives the progression of tumors such as DLBCL. The embryonic ectoderm development (EED) protein acts as the scaffolding and H3K27me3-binding subunit of PRC2 and is essential for its activity. We have developed potent, selective, and orally bioavailable EED inhibitor BR1733. BR1733 blocks the interaction between EED and H3K27me3, and inhibits catalytic activity of PRC2. BR1733 showed superior PK profile across species and exhibited tumor growth inhibition against several B cell lymphoma CDX models. Indication expansion studies demonstrated that BR1733 could inhibit solid tumors with SWI/SNF loss-of-function mutation only when both CDKN2A and TET1 are expressed. BR1733 also inhibited tumor angiogenesis and showed tumor growth inhibition in several CDX models of highly vascularized solid tumors such as HCC and RCC. BR1733 is currently in Phase I clinical trials.

#6272

AZ-PRMT5i-1: A potent MTAP-selective PRMT5 inhibitor with pharmacodynamic and monotherapy anti-tumor activity in MTAP-deleted tumours

James T. Lynch[1], Shaun Moore[1], Ivan Del Barco Barrantes[1], Lauren Bradshaw[1], Chris Chambers[1], Ted Hong[2], Sophie Cooke[1], Jelena Urosevic[1], Mercedes Vazquez-Chantada[3], James M. Smith[4], Anna Cronin[5], Benedicte Recolin[5], Sonja Gill[5], Susan Critchlow[1], Ho Man Chan[6], Emma Dean[7]. *[1]Bioscience, Oncology R&D, AstraZeneca, Cambridge, United Kingdom,[2]Early Data Science, Oncology R&D, AstraZeneca, Boston, MA,[3]Discovery Sciences, BioPharmaceuticals R&D, AstraZeneca, Cambridge, United Kingdom,[4]Chemistry, Oncology R&D, AstraZeneca, Cambridge, United Kingdom,[5]Clinical Pharmacology and Safety Sciences, Oncology R&D, AstraZeneca, Cambridge, United Kingdom,[6]Bioscience, Oncology R&D, AstraZeneca, Boston, MA,[7]Projects, Oncology R&D, AstraZeneca, Cambridge, United Kingdom*

Background: PRMT5 is an epigenetic enzyme that catalyzes symmetric dimethylation of arginine substrates (SDMA), regulating multiple cell processes. The PRMT5-MTAP collateral vulnerability describes the accumulation of the metabolite methylthioadenosine (MTA) in tumor cells (as a result of the deletion of the *MTAP* gene), which acts as a natural endogenous partial inhibitor of PRMT5. This provides an opportunity to selectively inhibit PRMT5 in *MTAP* deleted tumors, which occurs in ~15% of all cancers. First generation PRMT5 inhibitors, which cannot discriminate between MTAP-proficient normal cells and MTAP-deficient tumor cells, have a narrow therapeutic index which may limit clinical efficacy due to on-target toxicity. MTAP-selective PRMT5 inhibitors spare MTAP-proficient normal cells, improving therapeutic index and clinical efficacy. We have developed a novel MTAP-selective PRMT5 inhibitor, AZ-PRMT5i-1, that selectively targets MTAP-deficient tumors and spares MTAP-proficient tissue.
Methods: In vitro activity of AZ-PRMT5i-1 was profiled using six MTAP isogenic cell lines, as well as in a panel of 300 cancer cell lines. In vivo efficacy was assessed using three MTAP deleted models and hematological toxicity was addressed using a 3D human bone marrow model.

Results: Using a *MTAP* CRISPR KO isogenic pair we demonstrate potent inhibition of SDMA in MTAP-null tumors with a 54-fold margin over the MTAP wildtype (WT) counterpart. MTAP differential activity was maintained in proliferation assays across a number of MTAP isogenic cell lines and in a panel of 300 cancer cell lines. AZ-PRMT5i-1 demonstrates strong dose dependent efficacy across *MTAP* deleted xenograft and PDX models of gastric and lung origin, where greater than 80% of tumor growth inhibition was detected, with no apparent toxicity. In addition, corresponding dose-dependent inhibition of SDMA is observed in the treated tumors. In an *in vitro* 28-day 3D human bone marrow model, AZ-PRMT5i-1 has reduced toxicity in erythroid and megakaryocyte cell lineages, compared to a first generation PRMT5 inhibitor.
Conclusion: Overall, these studies demonstrate that AZ-PRMT5i-1 is a potent PRMT5 inhibitor demonstrating MTAP selectivity and anti-tumor activity in *in vitro* and *in vivo* pre-clinical models.

#6273

CTS3157, a novel MTA-cooperative PRMT5 inhibitor for targeting *MTAP*-deleted human tumors

Long Wang[1], Yilin Liu[1], Hui Shi[1], Yuanyuan Liu[1], Qiugeng Ouyang[1], Jiannan Guo[1], Yiqin Wang[2], Youzhen Wang[1], Guoliang Xu[2], Yuan Mi[1], Haiping Wu[1]. *[1]CytosinLab Therapeutics Co., Ltd., Shanghai, China,[2]Shanghai Institute of Biochemistry and Cell Biology, Center for Excellence in Molecular Cell Science, Chinese Academy of Sciences, Shanghai, China*

MTAP deletion is common in about 15% of all human cancers and coincides with the deletion of tumor suppressor locus containing *CDKN2A/B*. Methylthioadenosine (MTA), the substrate of MTAP, accumulates as a result of *MTAP* deletion. Increased levels of MTA result in partial inhibition of the PRMT5 enzyme by competing with S-adenosylmethionine (SAM, the methyl donor for PRMT5 substrate) due to structural similarity. Cancer cell lines with *MTAP*-deletion exhibit profound sensitivity to PRMT5 inhibition, suggesting *MTAP*^{null}-selective PRMT5 inhibitors have the potential to treat patients with MTAP deficiency (Kryukov *et al*., 2016). We identified CTS3157 as an orally bioavailable small molecule MTA-cooperative PRMT5 inhibitor that binds to PRMT5-MTA complex and

inhibits PRMT5 enzymatic activity. Cell-based assays revealed that CTS3157 demonstrated potent PRMT5 inhibition as evidenced by suppression of symmetric dimethylarginine (SDMA) and cell growth inhibitory activity for *MTAP*-deleted cell lines over isogenic *MTAP*^{WT} cell lines. Moreover, CTS3157 series compounds exhibited strong cell growth inhibition in a diverse panel of *MTAP*^{null} human tumor cell lines across several lineages. *In vivo*, CTS3157 demonstrated potent antitumor response after once-daily oral administration in *MTAP*-deleted xenograft models. The anti-tumor activity is correlated with PRMT5 modulation as measured by reduced SDMA levels. At molecular level, PRMT5 inhibition by CTS3157 resulted in massive RNA splicing defects and differentially expressed genes involving key cellular activities in *MTAP*^{null} cells. In summary, *MTAP*^{null}-selective PRMT5 inhibitor CTS3157 showed strong and durable antitumor responses *in vitro* and *in vivo* in *MTAP*-deleted tumors across diverse lineages. CTS3157 is an effective and promising therapeutics against *MTAP*-deleted tumors.

#6274

Preclinical characterization of the BET inhibitor, INCB057643, in combination with ruxolitinib for treatment of myeloproliferative neoplasms (MPN)

Michelle Pusey[1], Gaurang Trivedi[1], Bob Collins[1], Nina Zolotarjova[1], Pat Feldman[1], Monica Bomber[2], Jacob Ellis[2], Kristy Stengel[3], Cynthia Timmers[1], Hamza Celik[1], Matt Stubbs[1], Jeff Jackson[1], Scott Hiebert[2], Susan Wee[1], Sunkyu Kim[1]. *[1]Incyte Research Institute, Wilmington, DE,[2]Vanderbilt University, Nashville, TN,[3]Albert Einstein College of Medicine, Bronx, NY*

Patients with MPNs share common characteristics including overproduction of myeloid cells and chronic inflammation. In MPNs, bromodomain and extra-terminal (BET) proteins can bind to acetylated chromatin to regulate the activity of transcription factors such as NF-kB, leading to overproduction of inflammatory cytokines. Dysregulation of transcriptional gene expression can drive disease defining characteristics, therefore, targeting BET proteins could be an attractive therapeutic approach. In preclinical models, BET inhibitors decreased inflammatory cytokine

production and restored hematopoietic cell differentiation. Combination of BET inhibitors with the JAK1/2 inhibitor, ruxolitinib, resulted in further reduction in cytokine production and bone marrow fibrosis (Kleppe M. *Cancer Cell* 2018). Here, we investigate a novel, orally bioavailable BET inhibitor, INCB057643, for the treatment of MPN in combination with ruxolitinib. INCB057643 is a potent and selective inhibitor of the BET family. In binding assays, INCB057643 selectively inhibited both BRD4 bromodomains, BD1 and BD2, with IC_{50} values of 39 nM and 6 nM, respectively. INCB057643 comparably inhibited both NF-kB reporter activity and *MYC* protein levels. Nascent transcript analysis on the JAK2 V617F-mutant cell line SET2 showed decreased transcription of genes linked to inflammation, alone and in combination with ruxolitinib. These data suggest that INCB057643 and ruxolitinib can be used in combination to effectively suppress the pathogenic gene program driving chronic inflammation. Functionally, INCB057643 inhibited proliferation of SET2 cells at nanomolar concentrations. In a SET2 xenograft model, combination of INCB057643 and ruxolitinib potently inhibited tumor growth. Similarly, in the MPLW515L-driven MPN mouse model, INCB057643 in combination with ruxolitinib resulted in a greater reduction in spleen volume, compared to that achieved with single agent treatment. Meso scale discovery assays on MPN-patient-derived $CD34^+$ cells and whole blood using INCB057643 showed inhibition of NF-kB-mediated production of cytokines such as IL-8. In addition, flow cytometry-based analysis on MPN-patient-derived $CD34^+$ cells showed that INCB057643 in combination with ruxolitinib decreased pathogenic megakaryopoiesis, and increased terminal erythroid differentiation. Our data demonstrate that the combination of the BET inhibitor, INCB057643, with ruxolitinib can restore normal hematopoietic differentiation, reduce inflammatory gene expression, and inhibit pathogenic cell differentiation in preclinical models of MPN. INCB057643 is currently being evaluated in clinical studies as monotherapy and in combination with ruxolitinib in patients with MPN.
Acknowledgments: Michelle Pusey and Gaurang Trivedi contributed equally to this study.

#6275
DW91170: A novel potent EZH1/2 dual inhibitor for lymphoma treatment

Doc-Gyun Jeong, Woon Heo, DongHyuk Shin, Yeonkyung Oh, Sangho Lee, Seongsu Jeong, Whuijung Park, Jiyoung Woo, Chanseok Jeon, Subin Kim, Jaekyung Lim, Yun-Ha Hwang. *Dong Wha Pharm, Yongin, Korea, Republic of*

EZH2(Enhancer of zeste homolog2) is a catalytic subunit of PRC2 (polycomb repressive complex 2) for chromatin remodeling through methyl transfer activity. Previous studies have reported correlation between EZH2 and cancer progression with overexpression and mutations in various cancers. EZH1, homolog of EZH2, also has been known to role in development and progression of cancers by complementarily replacing EZH2. In recent researches, EZH1/2 dual inhibition showed global epigenetic modification on histone methylation and acetylation. Also, cancers associated with change in epigenetic factors such as mutations in subunit of SWI/SNF responded on EZH1/2 dual inhibition. Therefore, EZH1/2 dual inhibition is expected to be an effective strategy for cancer treatment. Herein, we present a novel potent EZH1/2 dual inhibitor, DW91170, as a promising candidate for treatment of lymphoma with improved anti-cancer activity. DW91170 selectively inhibited EZH1 and EZH2 enzyme activity. DW91170 brought about histone modification by reducing tri-methylation and enhancing acetylation of H3K27, which increased expression of target genes and cell cycle arrest was confirmed by treatment of DW91170. DW91170 showed effective tumor growth inhibition in two types of EZH2 hot spot mutation models. In Pfeiffer (A677 mutation) and WSU-DLCL2 (Y641 mutation) CDX models, DW91170 showed improved tumor regression activity with no significant abnormal signs such as weight loss. In order to verify the potential of DW91170 in R/R-lymphoma patients, the anti-cancer effect was evaluated in Rituximab-resistant cell line and R/R-DLBCL patient-derived PDX model. As a result, DW91170 efficiently inhibited Rituximab-resistant cell proliferation and suppressed tumor growth in R/R-DLBCL PDX model more significantly compared to other EZH inhibitors. Moreover, DW91170 has a good absorption profile that works in a physiological condition. Taken together, we demonstrated that DW91170, a dual epigenetic regulator of EZH1 and EZH2, showed great anti-tumor activities in various lymphoma cell lines and animal models such as CDX and PDX. We are currently

trying to expand indication into solid tumor to find a targetable population in clinical trials.

#6276

SKL27969, an oral selective PRMT5 inhibitor, sensitizes the effect of DNA-damaging agents in preclinical models of multiple solid tumors

Mijin Moon[1], Yongje Shin[1], Soyoung Ki[1], Jungtae Na[1], Ho Yeon Lee[1], Ilkyoo Koh[1], Beomjin Hong[1], Jiyeon Yun[1], Janice Laramy[2], Vijaykumar Vashi[2], Sook-Kyung Park[1]. *[1]SK Biopharmaceuticals Co., Ltd., Seongnam-si, Korea, Republic of,[2]SK Life Science, Inc., Paramus, NJ*

Background: Protein arginine methyltransferase 5 (PRMT5) is overexpressed in various human malignancies and induces epigenetic and post-translational changes, which have a significant impact on cell growth, proliferation, apoptosis, and DNA damage repair. SKL27969 is a potent and selective brain-penetrating PRMT5 inhibitor demonstrating antitumor activity in the preclinical models of glioblastoma (GBM) and non-small cell lung cancer (NSCLC) and triple-negative breast cancer (TNBC) brain metastasis models. In this study, we evaluated the antitumor activity of SKL27969 alone or in combination with DNA-damaging agents in various cancer models.

Methods: Cell cycle analysis, apoptosis, proliferation, and invasion assays were conducted to determine *in vitro* profiles of SKL27969. *In vivo* efficacy of SKL27969 was evaluated in human cancer cell line-derived xenograft (CDX) or patient-derived xenograft (PDX) models. Immunohistochemistry and RNA-sequencing analysis in tumor samples from animal models were conducted to confirm the *in vivo* mechanism of action (MoA). *In vitro* synergistic effects of SKL27969 with combination partner drugs were analyzed using Combenefit software.

Results: SKL27969 exhibits strong anti-proliferative effect by inducing cell cycle arrest and apoptosis and also inhibits invasion of cancer cells. An evaluation of SKL27969 in a panel of over 100 cancer cell lines revealed a broad spectrum of anti-proliferative activity in various cancer types, and an especially more sensitive response in cell lines harboring genetic alterations in the mitotic DNA damage checkpoint, DNA repair, or RNA processing pathways. Administration of SKL27969 demonstrated significant tumor growth inhibition, with a decrease in tumor symmetric dimethylarginine

(SDMA) in NSCLC and TNBC subcutaneous xenograft models. Transcriptome and immunohistochemical analysis of SKL27969-treated tumors revealed that the cell cycle checkpoint pathways and DNA damage repair genes were downregulated, supporting the rationale for combination treatment with DNA-damaging agents such as chemotherapeutic agents. Robust antitumor effects were observed after treatment with SKL27969 in combination with paclitaxel or gemcitabine in NSCLC PDX or pancreatic cancer CDX models. Further *ex vivo* studies to confirm the *in vivo* MoA of this synergism, and *in vivo* combination studies of SKL27969 with standard chemotherapeutic agents in other solid cancer CDX models, are ongoing. **Conclusion:** This is the first preclinical study that suggests the therapeutic potential of SKL27969 in combination with currently approved DNA-damaging agents, and supports further clinical investigation of SKL27969's role in improving the therapeutic benefit of standard therapies.

#6277

Selective and orally bioavailable SMARCA2 targeted degraders induce synthetic lethality in SMARCA4- deficient solid tumor

Koichi Ito, Artem Shvartsbart, Joseph Rager, Anjana Agarwal, Michael Hulse, Komali Vykuntam, Min Wang, Justin Kurian, Miles Cowart, Joy Cote, Monisha Sivakumar, Jack Carter, Jessica Burtell, Alex Grego, Andrew Moore, Neha Bhagwat, Stefan Ruepp, Tom Emme, Liang Lu, Philip Pitis, Corey Basch, Klare Bersch, Song Mei, Raul Leal, John Rose, Danielle Roth, Ganfeng Cao, Kris Vaddi, Sandy Geeganage, Bruce Ruggeri, Andrew Combs, Peggy Scherle. *Prelude Therapeutics, Wilmington, DE*

Targeted protein degradation (TPD) is an emerging therapeutic modality with the potential to target previously undruggable targets. However, it has been more challenging to identify orally bioavailable TPD molecules due to the physicochemical properties of the large molecules and narrow structure-activity relationship (SAR) compared to conventional small molecule inhibitors. In the present study, we identified orally active TPD molecules that selectively and potently degrade SMARCA2 protein and induce synthetic lethality in SMARCA4-deficient cancer cells. SMARCA2 (BRM) and SMARCA4 (BRG1) are the two mutually exclusive catalytic core subunits of SWI/SNF complexes that play an important role in controlling gene expression by remodeling chromatin. The complexes are mutated in

more than 20% of human cancers and subsets of solid tumors lose expression of SMARCA4 protein due to damaging mutations or gene deletion. The SMARCA4-deficient cancer cells are highly dependent on the paralog gene SMARCA2 for their survival and thus SMARCA2 has been suggested as an attractive therapeutic target for patients with SMARCA4-deficient cancers. We have recently identified SMARCA2 selective degraders that demonstrate oral bioavailability in mice with favorable pharmacokinetic properties, and acceptable DMPK and safety profiles in rodent studies. These SMARCA2 degraders show 50 to 300-fold DC_{50} selectivity for SMARCA2 over SMARCA4 in our cellular assays. When pre-treated with a proteasome inhibitor or neddylation inhibitor, the degradation of SMARCA2 was rescued, confirming that the degradation is mediated by the ubiquitin-proteasome-dependent pathway. These TPD molecules inhibit only SMARCA4-deficient cancer cell proliferation (NCI-H838, NCI-H1693, HT1080 SMARCA4 KO) with IC_{50} values ranging from 3-10 nM, but not SMARCA4 WT cells (Calu-6, NCI-H520, HT1080 WT). Oral administration of our SMARCA2 degraders resulted in significant tumor growth inhibition of SMARCA4-deficient lung cancer xenografts at well tolerated doses. The treated tumor tissues show robust SMARCA2 protein reduction for more than 72h post dosing, consistent with the SMARCA2 degradation kinetics-based pharmacodynamic prediction model. In summary, our orally bioavailable SMARCA2 degraders induce synthetic lethality in SMARCA4-deficient cancers *in vitro* and *in vivo*. Efforts to further evaluate these compounds in additional models and in combination with other agents are ongoing.

#6278

Combination therapeutic strategy with type I PRMT inhibition in cancer treatment

Hui Shi, Xingnian Fu, Yilin Liu, Qiugeng Ouyang, Meng Wang, Jiaxin Huang, Long Wang, Youzhen Wang, Yuan Mi, Haiping Wu. *Cytosinlab Therapeutics Co., Ltd., Shanghai, China*

Type I protein arginine methyltransferases (PRMTs) are highly expressed and associated in various tumors. Targeting PRMTs as an epigenetic modulation could be valuable for treating cancer when combined with other therapies. We identified a series of orally bioavailable small molecule type I

PRMT inhibitors with demonstrated single and combination anti-tumor efficacy in a variety of scenarios or models. Firstly, mutations of RNA splicing factors (SFs) commonly occur in hematologic malignancies and a variety of solid tumors, resulting in vulnerability to further disruption of the spliceosome. Inhibiting symmetric or asymmetric dimethylation of arginine could alter the RNA-binding specificity of the SFs and lead to the preferential killing of SF-mutant leukemias over wild-type counterparts (Fong *et al*., 2019). Therefore, targeting type I protein arginine methyltransferases (PRMTs) and PRMT5 concomitantly could minimize the compensatory effects and synergistically enhance antitumor activity. We validated the synergistic effects and mechanisms of combined treatment with a type I PRMT inhibitor and a PRMT5 inhibitor (JNJ-64619178, GSK3326595/EPZ015938 or an in-house PRMT5i) using cell-based assays and *in vivo* studies. Secondly, Methionine Adenosyltransferase 2A (MAT2A) inhibition decreases formation of S-adenosylmethionine (SAM), the cofactor of PRMTs, could in turn sensitize cancer cells to type I PRMT inhibition. *In vitro* and *in vivo* studies revealed that inhibitors of type I PRMT and MAT2A (AG-270) dosing combination indeed exhibited stronger anti-cancer activity than mono-treatment. Thirdly, the arginine methylation of receptor tyrosine kinases (RTKs) mediated by type I PRMT could increase the therapeutic sensitivity to RTK inhibitors like FLT3i. PRMT1 overexpression may contribute to AML stem/progenitor cells survival possibly through FLT3-ITD methylation, which may lead to enhanced activation of downstream signaling for cell survival and impact the regulation of self-renewal genes in leukemic initiating cells (LIC) (He *et al*, 2018). Hence, the combination treatment of FLT3 and type I PRMT inhibitors may provide a broader therapeutic benefit on *FLT3* mutated and/or overexpressed Acute Myeloid Leukemia (AML). *In vitro*, strong combination synergy was observed with a remarkable induction of cell death. *In vivo*, the combination of type I PRMT inhibitor with different FLT3 inhibitors (Gilteritinib, Midostaurin, or CTS2016) led to deeper antitumor responses in a variety of *FLT3-ITD* AML models. Taken together, these findings support the co-administration of type I PRMT inhibitor with various therapies including epigenetic reprogramming, cancer metabolism modulation, or targeted therapies for receptor tyrosine kinases, which could benefit cancer patients as a promising therapeutic strategy.

#6279

CTS2190, a next-generation epigenetic inhibitor for targeting type I PRMT deregulated human tumors

Hui Shi[1], Xingnian Fu[1], Qiugeng Ouyang[1], Jiaxin Huang[1], Yiqin Wang[2], Youzhen Wang[1], Guoliang Xu[2], Yuan Mi[1], Haiping Wu[1]. *[1]CytosinLab Therapeutics, Shanghai, China,[2]Shanghai Institute of Biochemistry and Cell Biology, Center for Excellence in Molecular Cell Science, Chinese Academy of Sciences, Shanghai, China*

Methylation of arginine residues by protein arginine methyltransferases (PRMTs) is involved in the regulation of fundamental cellular processes. Type I PRMTs are frequently overexpressed in a variety of human cancers and associated with poor prognosis. Knockout (KO) of *Prmt1* in mice results in decreased asymmetric dimethylarginine (ADMA) on cellular proteins, together with increased monomethylarginine (MMA) and symmetric dimethylarginine (SDMA) (Dhar *et al*., 2013). A structure-based drug discovery effort led to the identification of CTS2190 that showed single-digit nanomolar enzymatic inhibitory activity on type I PRMTs. Here, we report the development and preclinical characterization of CTS2190, a potent, orally bioavailable small molecule type I PRMT inhibitor. CTS2190 demonstrated strong cellular proliferation inhibitory activity in a large, diverse panel of human hematological and solid tumor cell lines across several lineages. *In vivo*, oral CTS2190 administration once daily resulted in tumor regression in a variety of xenograft (both CDX and PDX) models across different lineages with good tolerance. The anti-tumor activity was dose-dependent and correlated with the inhibition of type I PRMT activity as measured by decrease in ADMA and increase in MMA. In summary, CTS2190 is a promising type I PRMT inhibitor and clinical trial is underway to explore the proof-of-concept anti-tumor benefit for patients.

#6281

OTX-015 inhibits proliferation and migration in *ARID1A*-mutated bladder cancer

Ryan M. Kemper[1], Manfred Meng[1], Jeffrey S. Damrauer[2], William Y. Kim[2], Daniel J. Crona[1]. *[1]Pharmacotherapy and Experimental Therapeutics,*

UNC Eshelman School of Pharmacy, Chapel Hill, NC,[2]Lineberger Comprehensive Cancer Center, Chapel Hill, NC

Background: ARID1A mutations (*ARID1A*^{mut}) occur in up to 30% of metastatic bladder cancers (mBC) and have been associated with poorer response to standard treatments and shorter overall survival. We previously identified bromodomain and extraterminal (BET) protein inhibition as a potential treatment paradigm for mBC, with particular potency of BET inhibitors (BETi) in cells lines containing *ARID1A* inactivating mutations (*ARID1A*^{mut}). BETi prevents BET protein bromodomains from interacting with acetylated histone lysine tails and promoting transcription of multiple oncogenes. Our previous data shows that treatment with the pan-BETi OTX-015 reduces *ARID1B* expression, and significantly reduces both gene and protein expression of *RAD51*/RAD51 in *ARID1A*^{mut} cells compared to *ARID1A* wild type (*ARID1A*^{WT}), suggesting impaired DNA damage repair function. Here we evaluate the phenotypic effects of BETi on proliferation and migration in preclinical models of BC.
Methods: To evaluate OTX-015-induced changes to gene expression, 5637 (*ARID1A*^{WT}) and HT1197 (*ARID1A*^{mut}) cells were treated with 1 μM OTX-015 for 48-h. RNA was extracted and sent to Novogene for bulk RNA-seq. Differential expression was quantified using DESeq2, and gene enrichment was analyzed using GSEA. 5637 and HT1197 cells were treated with 1 or 5 μM OTX-015 for 48-h, and colony forming potential was assessed by crystal violet staining after 10 days. Cells were treated with the same treatment schema as above, and a wound-healing assay evaluated wound closure over 48-h. Differences in the percent area of wells covered with colonies and relative wound closure were assessed by FIJI v.2.9.1.
Results: BET inhibition of *ARID1A*^{mut} HT1197 cells lead to a significant decrease in the pathway enrichment for G2/M checkpoint (NES=-2.78, q<0.0001) and E2F target (NES-2.61, q<0.0001) genes. Conversely, BET inhibition of *ARID1A*^{WT} 5637 cells, lead to more muted response (G2/M: NES=-1.31; q=0.08, and E2F: NES=-1.53; q=0.02). After 1 μM OTX-015, cell cycle pathway targets were significantly impacted in *ARID1A*^{mut} HT1197 cells (P=0.0002), but not in *ARID1A*^{WT} 5637 cells (P=0.47). Results from our *in vitro* phenotypic data confirmed that OTX-015 significantly reduced proliferation and migration in HT1197 cells. After 1

μM OTX-015, 5637 colonies covered only 2% less area than 0.1% DMSO treated control colonies (n=3, *P*=0.99), and wounds were fully healed at 48-h (n=3, *P*=0.99). Conversely, HT1197 treated cells covered 96% less area (n=3, *P*<0.0001), and maintained a 38% larger wound size at 48-h (n=3, *P*=0.008), when compared to 0.1% DMSO treated colonies.
Conclusions: These preliminary data highlight how OTX-015 potently inhibits proliferation and migration in *ARID1A*^{mut} cells. These data will be confirmed in isogenic cell lines harboring inactivating *ARID1A* mutations, and support future mechanistic exploration (e.g., BETi-mediated cell cycle dysregulation) in *ARID1A*^{mut} bladder cancer.

#6282
EP102: Pharmacological inhibition of METTL3 arrests tumor progression and prolongs survival in CDX and PDX models of AML
Graeme Fraser, Catherine Sorlet, Nicolas Parmentier, Elodie Brunel, Anne-France Hartiel, Killian Oukoloff, Guillaume Dutheuil. *EPICS Therapeutics, Gosselies, Belgium*

METTL3 is the RNA methyltransferase predominantly responsible for the addition of N-6-methyladenosine (m6A), the most abundant modification to mRNA. The prevalence of m6A and the activity and expression of METTL3 have been linked to the appearance and progression of acute myeloid leukemia (AML)1. EPICS has discovered and optimized a small molecule inhibitor of METTL3 ("M3i"). M3i was shown to inhibit the enzymatic activity of METTL3 (IC50 = 2 nM, SPA assay) and inhibit the presence of intracellular m6A in a cell-based assay (IC50 = 8 nM, Calu6). The anti-proliferative effects of METTL3 was demonstrated in a spheroid model (NCIH-560, IC50 = 100 nM) as well as cell viability assays in various AML (Kasumi-1, IC50 = 30 nM; LEXF 41283, IC50 = 46 nM; MV-4-11, IC50 = 248 nM) and solid tumor (Calu6, IC50= 6 nM; Caov3, IC50 = 27 nM) cell lines. In vivo efficacy was evaluated in a disseminated xenograft model using established systemic MV-4-11-Luc-mCh-Puro2 in female NSG mice where M3i (30 mg/kg, i.p., QDx31 days) significantly ($p<0.01$, relative to vehicle control) inhibited cancer progression as measured by in-life imaging in addition to flow cytometry of hCD45+ cells in bone marrow, blood and spleen; M3i had minimal effects on hematopoiesis in this model with no significant changes in RBCs, WBCs

and neutrophils, but an increase in platelets (measured by IDEXX). In an orthotopic, patient-derived xenograft model of AML (LEXF 41283, intratibial implantation, female NSG mice), M3i (30 mg/kg, i.p., QDx91 days) significantly prolonged survival ($p<0.01$, relative to vehicle control) with a commensurate absence of hCD45+ cells following compound treatment. These results confirm that the pharmacological inhibition of METTL3 is a viable strategy for the treatment of AML and support the additional exploration of the role of METTL3 inhibitors in alternate blood cancers as well as solid tumors.

#6283

Evaluating the potency of a first-in-class covalent antagonist of the H3K9me3 reader protein MPP8 in bladder cancer

Stephany Gonzalez Tineo[1], Ryan M. Kemper[1], Surya K. Tripathi[1], Peter H. Buttery[2], William Y. Kim[3], Lindsey I. James[2], Daniel J. Crona[1].
[1]Pharmacotherapy and Experimental Thrapeutics, UNC Eshelman School of Pharmacy, Chapel Hill, NC,[2]Chemical Biology and Medicinal Chemistry, UNC Eshelman School of Pharmacy, Chapel Hill, NC,[3]Division of Oncology, Department of Medicine, UNC Lineberger Comprehensive Cancer Center, Chapel Hill, NC

Background: Bladder cancer (BC) is a common and deadly disease, and despite recent treatment advances, metastatic BC (mBC) remains incurable. Mutations in genes that encode epigenetic/chromatin modifier proteins are common in mBC, with >90% of tumors harboring at least one inactivating mutation. The epigenetic reader protein MPP8 recognizes the histone-3-lysine-9-trimethyl (H3K9me3) region of target gene promoters, and recruits transcription factors associated with cell proliferation and metastasis. UNC7713 was developed as a covalent antagonist to disrupt MPP8 binding to H3K9me3. Here, we explored whether UNC7713 potently inhibits cell proliferation, migration, and viability in preclinical models of BC.
Methods: 5637 cells were treated with ascending concentrations of UNC7713 (0.1 nM-100 μM), negative control compound UNC7716, or 0.1% DMSO negative control. Cell viability was measured using CellTiter-Glo™ after 48 h and 96h incubations. IC_{50} values were calculated using a four-parameter non-linear regression model in GraphPad. Cells were

stained with Annexin V and propidium iodide (PI) to evaluate apoptosis versus necrosis signaling by flow cytometry after 48 h incubation of UNC7713. Flow cytometry experiments were performed on a Thermo Attune NxT, and data were analyzed using FlowJo. 5637 cells were grown in a monolayer, treated with UNC7713 (25 nM-100 nM), and then subjected to a wound healing assay to evaluate cell migration after 48 h. To evaluate effects on cell proliferation, 5637 cells were treated with four doses of UNC7713 (25 nM-100 nM), and colony formation was evaluated after 10 days using crystal violet and analyzed by Fiji. For wound healing, images were captured by an Olympus IX83 inverted microscope and analyzed by Fiji.
Results: UNC7713 achieved submicromolar potency for reduction of cell viability in 5637 cells and was nearly 200x more potent than UNC7716 at 48 h (IC_{50}: 0.28 μM vs. 56.03 μM). Potency was also maintained at 96 h (0.18 μM). Concentrations of UNC7713 as low as 75 nM caused over 2.5x greater apoptotic signaling than 20 μM UNC7716 after 48 h (18.5% vs. 7.3% Annexin V and PI positive cells). Next, cells treated with UNC7713 did not migrate to initiate wound closure, but instead caused cell death, increasing the size of the initial wound. Cells treated with UNC7713 at concentrations as low as 50 nM caused dramatic wound expansion compared to 0.1% DMSO and 20 μM UNC7716 (70% wound expansion for UNC7713 vs. 100% wound closure for both controls). Last, after 10 days >90% fewer colonies were detected in cells treated with UNC7713 (25 nM-100 nM) when compared to 20 μM UNC7716 and 0.1% DMSO controls.
Conclusions: These preliminary data support further inquiry into the role of *MPP8* in BC. Future studies will focus on identifying molecular mechanisms that underlie UNC7713's ability to inhibit cell proliferation, migration, and viability in preclinical models of BC.

#6284
SUV420H1 as a novel target in HPV-negative head and neck squamous cell carcinoma
Arfa Moshiri[1], Hui Cheng[2], Sohyoung Kim[3], Vassiliki Saloura[1]. *[1]Thoracic and GI Malignancies Branch, National Cancer Institute, Bethesda, MD,[2]Bioinformatics and Biostatistics Collaboration Core, National Institute on Deafness and Other Communication Disorders, Bethesda,*

MD,[3]Laboratory of Receptor Biology and Gene Expression, National Cancer Institute, Bethesda, MD

Human Papilloma Virus (HPV)-negative head and neck squamous cell carcinoma (HNSCC) is the sixth most common cancer type in the world and its outcomes are mostly unchanged for the past few decades, especially for HPV-negative HNSCC. The TCGA recently revealed a plethora of genetic alterations in chromatin modifiers in HPV-negative HNSCC, including protein lysine methyltransferases which methylate lysine residues on histone tails and regulate gene expression. One of these enzymes, SUV420H1, is known to trimethylate H4K20 and is recurrently amplified in approximately 6% of HPV-negative HNSCC tumors (TCGA). It has also been found to be significantly overexpressed in multiple HNSCC cell lines compared with normal keratinocytes. This study aims to investigate whether SUV420H1 has oncogenic activity and could be a novel therapeutic target in HPV-negative HNSCC. To evaluate the effect of SUV420H1 depletion on HPV-negative HNSCC cell lines, siRNA-mediated knockdown was performed in four SUV420H1 overexpressing HPV-negative HNSCC cell lines, and MTT assays showed significantly reduced cell viability by approximately 80-90% after 12 days of siRNA treatment. Colony formation assays, cell cycle analysis and apoptosis assays are ongoing, and these assays are planned in SUV420H1 CRISPR KO cell lines. Gene Set Enrichment Analysis in 434 HPV-negative HNSCC tumors (TCGA) showed significant enrichment of immune signatures, EMT, cell cycle and apoptosis pathways. Ongoing experiments aim to investigate the effects of SUV420H1 knockdown on the global histone methylome, and to identify direct downstream targets of SUV420H1 through combined genome-wide mapping of SUV420H1 using CUT&RUN assays and RNA-seq in HPV-negative HNSCC cell lines. Syngeneic and xenograft mouse models are also planned to evaluate the effect of SUV420H1 depletion on flank tumor growth in vivo. These studies may elucidate the oncogenic effects and mechanisms of SUV420H1, and may provide evidence to support SUV420H1 as a potential novel target in the treatment of HPV-negative HNSCC tumors with SUV420H1 amplification or overexpression.

#6285

Preclinical efficacy of CDK7 inhibitor-based combinations in cellular models of advanced myeloproliferative neoplasms (MPN)

Christopher P. Mill, Warren C. Fiskus, Christine E. Birdwell, John A. Davis, Kaberi Das, Kapil N. Bhalla. *UT MD Anderson Cancer Center, Houston, TX*

Advanced MPN are characterized by driver mutations in JAK2, c-MPL or calreticulin (CALR) gene, with hyperactive JAK-STAT5/3 and NFkB signaling. Co-occurrence of mutations in chromatin/transcriptional regulators, including DNMT3A, TET2, ASXL1, EZH2, SRSF2, RUNX1 and TP53, creates the dysregulated transcriptome, which is responsible for the increased growth, survival and therapy-refractoriness in MPN blastic phase (BP). Treatment with JAK inhibitors (JAKis), e.g., ruxolitinib, venetoclax and hypomethylating agents are ineffective in improving survival in MPN-BP. CDK7 is the crucial catalytic component of the general transcript initiation factors TFIIH, which is recruited to the transcription start-sites along with RNA-pol II (RNAP2) to initiate transcription. Complexed with cyclin H, CDK7 phosphorylates CDK1, 2, 4 and 6, as well as serine 5 and 7 in the C terminal domain (CTD) of RNAP2, thus facilitating transcript initiation. CDK7 also phosphorylates CDK9, which in turn phosphorylates serine 2 of the CTD of RNAP2, and phosphorylates and inactivates the negative elongation factors, thus enabling productive mRNA transcript elongation of growth and survival promoting oncogenes. In MPN-BP, these include RUNX1, Bcl-xL, MCL1, CDK4/6, PIM1 and MYC. CRISPR-gRNA dependency-screen (DepMap) demonstrated that CDK7 is a dependency in the Advanced-AML cell lines, SET2 and HEL cells. Present studies demonstrate that treatment with ATP-competitive, covalent CDK7 inhibitors (CDK7i) SY-1365, and its clinical grade counterpart SY-5609, dose-dependently inhibits cell cycle, growth and induces lethality in SET2 and HEL as well as patient-derived (PD), CD34+ MPN-sAML cells. ChIP-Seq analysis showed that SY-1365 treatment caused log2 fold-reduction in p-Ser2-RNAP2 occupancy on the DNA of MYC, PIM1 and MCL1 genes in HEL cells. RNA-Seq analysis showed that SY1365 treatment caused negative enrichment of gene-sets of MYC and E2F targets, as well as inflammatory response, IL6-JAK-STAT3 and mTORC1 signaling. SY-1365 treatment also dose-dependently depleted protein expressions of p-Ser5 RNAP2, p-Ser2 RNAP2, c-Myc, c-Myb,

RUNX1, PU.1, MCL1 and Bcl-xL, while inducing cleavage of PARP protein. As compared to the parental JAKi-sensitive, in vitro generated JAKi-persister/resistant (P/R) SET2/RuxP cells were significantly more sensitive to SY-1365-induced apoptosis. Co-treatment with CDK7i and ruxolitinib or the BET inhibitor OTX015 was synergistically lethal in PD MPN-BP cells (n=7). In an aggressive xenograft model of HEL-GFP/Luc cells in NSG mice, compared to the vehicle control, monotherapy with SY5609 significantly reduced the MPN sAML burden and improved survival of the NSG mice without causing host toxicity. These findings demonstrate promising activity and support the rationale to further evaluate the in vivo efficacy of CDK7i-based combinations against advanced MPN.

#6286

Targeting Polycomb Repressive Complex 1 with small-molecule inhibitors as a potential therapeutic approach to combat leukemia

Miranda L. Simes[1], Yiwu Yao[1], Se Ra Park[1], Trupta Purohit[1], Hongzhi Miao[1], Xiaotian Zhang[1], Weijiang Ying[2], Felicia Gray[3], Shirish Shukla[4], Qingjie Zhao[1], Caroline Nikolaidis[5], Alyssa Winkler[1], Jolanta Grembecka[1], Tomasz Cierpicki[1]. *[1]University of Michigan, Ann Arbor, MI,[2]Penrose TherapeuTx, Plymouth, MI,[3]Schrodinger, Portland, OR,[4]The Janssen Pharmaceutical Companies of Johnson & Johnson, Spring House, PA,[5]Wayne State University School of Medicine, Detroit, MI*

Background: Polycomb repressive complex 1 (PRC1) is an epigenetic regulatory complex that monoubiquitinates lysine 119 on histone H2A, resulting in the repression of target genes. The canonical core of PRC1 responsible for its E3 ligase activity is a heterodimeric unit comprised of RING1B and BMI1. Emerging data implicates RING1B in various cancers and highlights the importance of PRC1 function in the maintenance and proliferation of leukemic stem cells. Studies demonstrate that loss of PRC1 activity through *RING1B* knockdown impairs leukemic stem cell proliferation, causes leukemic stem cell differentiation, and enhances survival in MLL-AF9 mouse models. Therefore, development of potent small molecules targeting the activity of PRC1 might offer a new approach for generating new therapeutics for leukemia.

Results: Here, we report the discovery and development of the first-in-class small-molecule inhibitors directly binding to RING1B in PRC1. We

performed an NMR-based fragment screen against RING1B-BMI1, identifying fragment hit, RB-1, with low-millimolar binding affinity. RB-1 was extensively optimized into a class of inhibitors with considerably enhanced binding affinity to the low-nanomolar range. These inhibitors have been shown to diminish the H2A ubiquitination activity of PRC1 E3 ligase cores. Structural studies revealed that our PRC1 inhibitors bind directly to the RING domain of RING1B and ultimately block the protein-protein interaction between RING1B and the nucleosome. In leukemic cell lines and primary AML samples, PRC1 inhibitor treatment elicits an anti-proliferative effect on cell growth and displays on-target action seen by the reduction of the H2A ubiquitination mark. Additionally, small-molecule inhibition of PRC1 results in the induction of cellular differentiation of leukemic cells, as well as apoptosis. Gene expression analysis in leukemic cells treated with our PRC1 inhibitors reveals upregulation of multiple genes that are repressed by PRC1, which is also supported by the displacement of PRC1 from chromatin assessed by CHIP-seq studies. Furthermore, our PRC1 inhibitors are active *in vivo* in mouse models of leukemia, demonstrating reduction of leukemia progression upon treatment. **Conclusions:** We developed first-in class inhibitors directly targeting the E3 ligase core of PRC1. Treatment with our PRC1 inhibitors in leukemic cells elicit an anti-proliferative effect, blocks ubiquitination of H2A, and results in the de-repression of many genes repressed by PRC1. Additionally, our PRC1 inhibitors elicit an anti-proliferative effect on leukemia progression *in vivo*, demonstrating the traction for developing anti-leukemia therapeutics that inhibit PRC1.

#6287

Selective CBP degradation shows superior potency and differentiated biological activity compared to small molecule inhibitors

Laura La Bonte, Darshan Sappal. *Foghorn Therapeutics, Cambridge, MA*

CREB binding protein (CBP) and E1A binding protein (p300) are paralog histone acetyltransferases involved in many cellular processes via their activity as transcription factor co-activators. Dysregulation of one or both proteins has been implicated in a variety of cancers, and functional genomic screens have exhibited a bidirectional synthetic lethal relationship between the two genes in many cancer indications. Due to the high homology

between CBP and p300, identification of selective chemical matter that specifically and directly targets CBP has proven challenging. Small molecule inhibitors (SMIs) targeting the HAT or bromodomain of CBP/p300 have been developed, however these agents are not selective for either paralog and inhibit both proteins equally, potentially limiting their clinical application. Herein, we describe the biological activity of selective, potent CBP degraders and show differentiation from SMIs.

#6288
Discovery and characterization of potent, selective CBP degraders
Laura La Bonte, Darshan Sappal. *Foghorn Therapeutics, Cambridge, MA*

CREB binding protein (CBP) and E1A binding protein (p300) are paralog histone acetyltransferases involved in many cellular processes via their activity as transcription factor co-activators. Dysregulation of one or both proteins has been implicated in a variety of cancers. Due to the high homology between CBP and p300, identification of selective chemical matter that specifically and directly targets CBP has proven challenging. Here, we describe a potent, highly selective CBP heterobifunctional degrader with selective biological activity in CBP dependent cancer lines.

#6289
Enhancer reprogramming by novel SMARCA2 degrading PROTACs underlies therapeutic utility in SMARCA4 mutant tumors
Sasi Kotagiri, Nicholas Blazanin, Yuanxin Xi, Jing Wang, Yonathan Lissanu. *UT MD Anderson Cancer Ctr., Houston, TX*

Lung cancer is the top cause of cancer mortality. Despite recent advances, the majority of patients with lung cancer still lack effective therapeutic options, underscoring the dire need for additional treatment approaches. Genomic studies have identified frequent mutations in subunits of the SWI/SNF chromatin remodeling complex including *SMARCA4* and *ARID1A* in non-small cell lung cancer with a frequency of up to 33% in advanced stage disease, making it the most frequently mutated complex in lung cancer. Recent reports, as well as our own data, have identified the paralogue *SMARCA2* to be synthetic lethal to *SMARCA4* suggesting SMARCA2 is a valuable therapeutic target. However, the discovery of

selective inhibitors of SMARCA2 has been challenging. To overcome this hurdle, we have utilized iterative structure-activity relationship (SAR) studies to develop novel, potent and selective SMARCA2 degrading small molecules based on proteolysis targeting chimera (PROTAC) technology. We demonstrated that YD23, our lead SMARCA2 PROTAC, potently and selectively induces degradation of SMARCA2. Mechanistically, we demonstrated that YD23 reduces chromatin accessibility only in *SMARCA4*-deficient cells with profoundly decreased chromatin accessibility at enhancer regions. Gene expression profiling and pathway analysis indicated that core cell cycle genes were downregulated by YD23 and is consistent with reduced chromatin accessibility at their regulatory regions. Furthermore, integrative analysis of RNA-seq and ATAC-seq revealed a strong correlation between gene expression and enhancer accessibility changes by YD23. In particular, we identified the mitotic regulator NEDD9 as a critical target in enhancers that are strongly reduced by YD23 in SMARCA4-deficient lung cancer cells. In conclusion, our study provides a promising chemical probe for studying the synthetic lethal interaction between SMARCA2 and SMARCA4, dissect the chromatin and epigenetic landscape alterations and lay the foundation for future preclinical and clinical development of SMARCA2 degraders as therapeutics.

#6290

Characterizing antitumor responses to EXS-74539, a novel, reversible LSD1 inhibitor with potential in small-cell lung cancer

Andrew Payne, Manisha Naik, Simon Richards, Victor Sebastian Perez, Maria Dominguez. *Exscientia, Oxford, United Kingdom*

Background: Lysine demethylase 1 (LSD1) is a potentially important target in oncology due to its role in demethylating histones and suppressing expression of genes required for cellular differentiation. In small-cell lung cancer (SCLC), high LSD1 expression is associated with suppressed differentiation pathways. Although selective LSD1 compounds are in clinical development, understanding of the molecular markers of tumor sensitivity to inhibition of LSD1 inhibition is incomplete.Methods: We report on the pharmacological characterization of EXS-74539, a potent, selective and reversible LSD1 inhibitor. We assessed EXS-74539 efficacy in in vitro and in vivo SCLC cell line models, encompassing the four

molecular subtypes of SCLC tumor cells previously proposed (Rudin et al, 2019), based on differential expression of key transcription regulators, ASCL1, NEUROD1, POU2F3 and YAP1. Results: In vitro, EXS-74539 demonstrated similar anti-proliferative activity against both neuroendocrine (NCI-H1417 and NCI-H69, ASCL1 sub-type) and non-neuroendocrine (NCI-H526: POU2F3) SCLC cell lines, with IC50 values of 28, 12 and 11 nM, respectively. In vitro exposure of these cell lines to EXS-74539 led to concentration-dependent alterations in differentiation-associated genes. However, in vivo, significant differences in antitumor growth response upon LSD1 inhibition were observed between the cell lines; NCI-H69 tumor growth was unaffected following treatment with EXS-74539 and an irreversible LSD1 inhibitor at dose regimens which were efficacious in the NCI-H1417 and NCI-H5126 models. We describe in vitro and in vivo gene expression correlations associated with LSD1 sensitivity. Conclusions: The reversible LSD1 inhibitor, EXS-74539, is a potent inhibitor of SCLC cell line proliferation and shows in vivo efficacy. Characterizing SCLC cell line sensitivity in vitro and in vivo identified gene signatures that may have use as markers of sensitivity, which we are currently characterizing and validating in human SCLC patient samples.Rudin et al., Nat Rev Cancer, 2019

Growth Factor Receptors as Therapeutic Targets

#6294

CXCR5 is a very promising drug target for the development of antibody-drug conjugates to treat patients with lymphoma

Tibor Schomber[1], Beatrix Stelte-Ludwig[1], Amy J. Johnson[2], Oliver von Ahsen[3], Christoph Schatz[4], Raquel Izumi[2], Ahmed Hamdy[2], Hans-Georg Lerchen[1]. *[1]Vincerx Pharma, Monheim, Germany,[2]Vincerx Pharma, Palo Alto, CA,[3]Nuvisan ICB, Berlin, Germany,[4]Bayer AG, Berlin, Germany*

Introduction: The chemokine receptor CXCR5 is highly expressed in tumor cells from different lymphoma types and represents a viable drug target for the development of antibody-drug conjugates (ADC) to treat patients with lymphoma.
Methods: Immunohistochemistry of human tissues of different lymphoma types were stained using antibodies against human CXCR5, CD20, CD70

and CD79b. Slides were examined by a pathologist and scored for expression. CXCR5 expression on tumor cell lines was analyzed by flow cytometry. Cell surface receptor density was analyzed by Quantibrite ™ PE-beads. Evaluation of antibody internalization was performed using the Operetta High Content Imaging System. NOD/SCID mice were transplanted subcutaneously with lymphoma patient-derived (PDX) tumor specimens and treated with 2mg/kg or 10mg/kg VIP924 CXCR5-ADC or isotype control.
Results: CXCR5 reveals very low to no expression in most tissues except for lymph nodes. Expression of CXCR5 and other B-cell targets like CD19, CD20, CD70 and CD79b was analyzed on patient-derived tumor samples. High expression of CXCR5 was found on naïve and previously treated diffuse large B-cell lymphoma (DLBCL), follicular lymphoma (FL), mantle cell lymphoma (MCL), and chronic lymphocytic leukemia (CLL) samples. Based on these results, we developed a CXCR5 targeted ADC with a novel, highly potent kinesin spindle protein inhibitor (KSPi) payload linked via a legumain-cleavable linker (VIP924). To compare the performance of KSPi ADCs, the same effector chemistry was attached to antibodies against other B-cell targets and tested in cytotoxicity assays in various cell lines. CXCR5-targeted ADC demonstrates significantly higher activity compared to the other ADCs tested except for the CD79b ADC with equal potency. VIP924 was then tested in vivo in different PDX tumor mouse models with different levels of CXCR5 expression. In the LY2264 and HBL-1 DLBCL models, we obtained a tumor growth inhibition of 68% and 100% respectively compared to isotype control. The median survival time for the isotype control group was 29 days and median survival time for the mice treated with 10mg/kg VIP924 could not be determined as all mice survived until the end of the study (Day 37). No effect on body weight or any adverse effects in the VIP924 treated mice were observed.
Conclusions: CXCR5 is a highly attractive target in hematological malignancies such as DLBCL, MCL, and FL due to high protein expression and almost no expression in healthy tissues. CXCR5-targeting ADC with KSPi payload showed high potency and superiority to other B-cell-targeted ADCs in vitro on a broad range of lymphoma cell lines. VIP924 with a novel legumain-cleavable linker showed activity in in vivo PDX models from lymphoma patients. Due to the high CXCR5 expression found in

relapsed DLBCL patients, VIP924 may bring promising new treatment options for previously treated patients with lymphoma.

#6295

Belzupacap sarotalocan, an investigational virus-like drug conjugate, preferentially binds cancer cell glycosaminoglycans associated with the epithelial to mesenchymal transition

Nathan R. Fons[1], Rhonda C. Kines[2], John T. Schiller[1]. *[1]National Cancer Institute, NIH, Bethesda, MD,[2]Aura Biosciences, Boston, MA*

Human papillomaviruses (HPVs) are non-enveloped, double-stranded DNA viruses that utilize modified glycosaminogycans (GAGs) such as heparan sulfate proteoglycans, within the epidermal basement membrane as initial attachment factors prior to cell entry and infection. Similarly modified GAGs are also commonly found on the surface of tumor cells, enabling HPV capsids with tumor-selective binding properties. Belzupacap sarotalocan (bel-sar, formerly AU-011), is a virus-like drug conjugate composed of an HPV virus-like particle (VLP) conjugated to a cytotoxic payload (phthalocyanine dye) which upon light activation, causes rapid immunogenic tumor necrosis of bound tumor cells in vivo and has the potential to induce long-term anti-tumor immunity. Bel-sar has been shown to bind to and kill a wide variety of tumor types in preclinical models and is entering a Phase 3 clinical trial for the treatment of early-stage choroidal melanoma. To investigate the precise GAG modifications as well as the overall genetic signature which mediates the binding specificity of bel-sar, a large, multi-tumor type binding screen of bel-sar on 124 cancer cell lines was performed in vitro, where we identified a strong relationship between drug binding and pathways involved in the epithelial to mesenchymal transition (EMT). Additionally, through dose escalation treatments, HeLa subclones were generated which fail to bind and are resistant to the cytotoxic effects of bel-sar. Gene expression profiling and biochemical characterization of these resistant HeLa cell lines demonstrated a strong reduction in the expression of GAGs and a marked down-regulation of TGF-β signaling, ultimately resulting in the induction of a mesenchymal to epithelial transition (MET). Furthermore, gene-gene correlation studies showed that a variety of GAG biosynthesis genes are associated with TGF-β signaling and EMT progression, and that these genes are important

determinates of bel-sar binding. Overall, these data suggest that the binding of bel-sar and HPV VLPs is strongly dependent on the expression and modification of GAGs that occurs during the EMT process. As many cancers, especially metastatic tumors, are thought to undergo at least partial EMT, these data provide mechanistic insights into the tumor-targeting ability of HPV VLP-conjugates such as bel-sar and suggest possible applications for such therapies across a wide variety of other tumor types.

#6296

Preclinical study of a novel anti-CLEC12A antibody-drug conjugate with a glucuronide-protected pyrrolobenzodiazepine payload

Jinwon Jung[1], Juhee Kim[1], Bora Lee[1], Jung A Kwon[1], Suyoun Lee[1], Byeongmin Yoo[1], Minji Ko[1], Ilhwan Ryu[1], Donghoon Yeom[1], Kyoungjae Lee[1], Jaehyun Eom[1], Hanbyul Lee[1], Jinhyung Ahn[1], Eunsil Sung[1], Weonkyoo You[1], Sang Hoon Lee[1], Myeong Joo Kim[2], Keon Woo Kwon[2], Hyun Joo Bae[2], Yun-Hee Park[2], Ho Young Song[2], Chul-Woong Chung[2].
[1]ABL Bio, Inc., Sungnam-si, Korea, Republic of,[2]LegoChem Bioscience, Inc., Daejeon, Korea, Republic of

C-type lectin domain family 12 member A (CLEC12A, CLL-1) is a single-pass transmembrane protein of 265 amino acids that is found on monocytes and AML blasts. We have created and characterized antibody-drug conjugates (ADCs) based on a humanized CLEC12A specific antibody to determine whether CLEC12A may be exploited as a therapeutic target for AML. The payload is a proprietary PBD prodrug with a beta-glucuronide trigger, and the linker-payload was conjugated through farnesyltransferase-mediated functionalization. The ADC demonstrated sub-nM cytotoxicity in vitro against several CLEC12A-positive cell lines including HL-60 and PL21. Leu234Ala/Leu235Ala (LALA) mutations were employed to reduce Fc gamma receptor binding and to avoid on-target toxicity. The LALA mutation-bearing ADC displayed a nearly 50-fold decrease in cytotoxicity towards CD34+ hematopoietic stem cells. Its potency was reduced but still sufficient with IC50 values of 61 pM and 15 pM against HL60 and PL21, respectively. Regardless of LALA mutation, the ADCs demonstrated potent antitumor activities with a complete regression at a dose of 0.5 mpk against a subcutaneous HL-60 SCID mouse xenograft model. When the LALA-mutated ADC was tested against a disseminated NSGA mouse model of

HL-60-luc, all treated animals survived without clinical symptoms for three weeks after treatment, whereas vehicle-treated animals exhibited morbidity 19 days after treatment or 35 days after tumor implantation. The bone marrow of ADC-treated animals appeared to have nearly fully recovered, whereas that of vehicle-treated animals showed necrosis or tumor growth. In cynomolgus monkeys, the LALA-mutated ADC had a half-life of 82 hours at a dose of 0.2 mpk, and target-mediated drug disposition appeared weak or negligible. Our preclinical studies have shown that CLEC12A targeting ADC can be used as a therapeutics for treating AML.

#6297

Rationale for the development of a differentiated Trop2 ADC

Satyajit K. Mitra[1], William Monteith[1], Mary Do[2], Greg Tuffy[3], Scott Savage[4], Jeffrey Kang[2], Mastewal Abuhay[1], Teodora Losic[2], Sanjeevani Ghone[1], William E. Haskins[1], Vasu Jammalamadaka[5], Sanjeev Satyal[6].
[1]Peak Bio Inc., Palo Alto, CA,[2]Dren Bio Inc., Foster City, CA,[3]3T Biosciences, South San Francisco, CA,[4]Neuron23 Inc., South San Francisco, CA,[5]Aarvik Therapeutics Inc., Hayward, CA,[6]Monterey Bio, New York, NY

Background: Trophoblast antigen 2 (Trop2) or Tumor-Associated Calcium Signal Transducer 2 (TACSTD2) is a transmembrane glycoprotein that is overexpressed in several solid tumor cancers. Antibody drug conjugate (ADC) targeting of Trop2 has been clinically validated. The Trop2 ADC Trodelvy® (also known as Sacituzumab govitecan/ IMMU-132) is approved for therapy of TNBC and urothelial cancer, and Datopotamab DXd (DS-1062) is currently being tested in NSCLC.
Peak Bio's Thailanstatin suite of immunomodulatory linker-toxins (L-Ts) is a set of 7 related molecules with distinct ADC features that have been extensively characterized *in vitro* and *in vivo* as Her2 ADCs and is being used as a platform to generate a pipeline of potentially differentiated ADCs (AACR; Cancer Res 2021;81(13_Suppl):Abstract nr 1832).
Results: M2.8 is a fully humanized Peak Bio antibody (Ab) that targets human Trop2 (hTrop2) with high binding affinity [K_d (M)= 8.97^{-09}]. M2.8 was optimized for binding affinity and humanization relative to its parent M2.1 [K_d (M)= 1.78^{-08}], and, both M2.1 and M2.8, display species-

specificity for the human and cynomolgus monkey Trop2 proteins. When bound to hTrop2-positive cell lines, M2.1 and M2.8 can rapidly internalize and deliver an ADC payload.
To identify the optimal release for therapeutic efficacy, we conjugated our family of L-Ts with hRS7 at a comparable drug-to-antibody ratio (DAR) of 4. Maximal tumor growth inhibition (TGI) was associated with the Trop2 ADCs that were conjugated *via* amine coupling to lysine residues using non-cleavable L-T L22, later renamed PH1.
To determine the effect of antibody on TGI efficacy, different doses, and DARs of M2.1 PH1 ADC were compared to PH1 ADCs made from other Trop2 Abs. At low dose levels, M2.1 PH1 ADCs exhibited comparable TGI with hRS7 PH1, TINA PH1, and T6-16 PH1 ADCs, but exhibited significantly greater TGI than hRS7 SN38 (IMMU-132), suggesting that payload potency, rather than epitope, was important in targeting Trop2. The results also suggested that a PH1 DAR of 4 was sufficient to obtain 90% TGI with multiple anti-Trop2 Abs.
M2.1 PH1 ADC was safely tolerated by cynomolgus monkeys at 3 and 6 mg/kg Q3W x 3 doses with mild-to-moderate changes in liver enzymes and platelets that reversed to baseline within 7-10 days of administration of each dose.
The optimized M2.8 PH1 DAR4 ADCs killed Trop2-positive cell lines with single-digit nanomolar potency, while exhibiting low off-target cytotoxicity *vs* normal human skin fibroblasts and Trop2-negative cell lines *in vitro*.
M2.8 PH1 ADC regressed all 200mm^3 sized NCI-N87 tumors and 50% of these tumors exhibited long-term regression for 5 months.
Conclusion: The target validation studies suggest that Trop2 PH1 ADCs were sufficiently differentiated in areas of preclinical efficacy and well tolerated in a toxicologically relevant host.

#6298

A novel topoisomerase I inhibitor based anti-ICAM-1 antibody drug conjugate for the treatment of hematologic malignancies and solid tumors

Oi Kwan Wong, David Jackson, Lei Shi, Qi Fei, Xiaocheng Chen, Leonard Post. *Virtuoso Therapeutics, Inc., San Mateo, CA*

Intercellular Cell Adhesion Molecule 1 (ICAM-1, CD54) is a type I transmembrane protein and a member of the immunoglobulin superfamily. ICAM-1 is involved in many key processes such as cell-cell interactions, signal transduction and leukocytes trans-endothelial migration. ICAM-1 is constitutively present at low levels on healthy tissues but highly expressed in some lymphoma, myeloma and some types of solid tumors including melanoma, non-small cell lung cancers and liver cancers. Previous attempt to target ICAM-1 with a monoclonal antibody bersanlimab (BI505, BioInvent) showed that it was well-tolerated but with limited clinical efficacy. To improve the effectiveness of targeting ICAM-1, we developed a novel ICAM-1 antibody drug conjugate (ADC). The ICAM-1 ADC is comprised of a humanized anti-ICAM-1 hIgG1 antibody conjugated to a novel topoisomerase I inhibitor through a cleavable linker at a drug-to-antibody ratio (DAR) of about 8. The antibody moiety of the ADC targets a unique epitope on ICAM-1 which is far from its ligand binding domain. Potent *in vitro* cytotoxicity of ICAM-1 ADC, with nanomolar to sub-nanomolar EC50, was observed on a panel of hematologic and solid tumor cell lines. In preclinical studies, one or two doses of ICAM-1 ADC at 5-6 mg/kg were generally sufficient to induce tumor regression in multiple cell line-derived xenograft models, including those of lung and liver cancers. In all models tested so far, the novel topoisomerase I inhibitor conjugated ICAM-1 ADC is at least as efficacious as the same ICAM-1 antibody conjugated to the benchmark topoisomerase I inhibitor linker payload deruxtecan (ICAM-1-DXd). Furthermore, in a repeat dose exploratory non-human primate safety study, the benchmark conjugate ICAM-1-DXd (DAR 8) was well-tolerated at 41 mg/kg, the highest dose tested. In conclusion, ICAM-1 is an attractive target for topoisomerase I inhibitor based ADC and warrants further investigation.

#6299

ZB131 antibody-drug conjugates induce potent antitumor activity

Samantha M. Perez[1], Brian P. Murphy[1], Danielle B. Heckert[1], Sarah Hall[1], Abby L. Colvin[1], Molly F. Owens[1], Ben R. Verfurth[1], Julien Dimastromatteo[2], Jiang He[3], Reid B. Adams[4], Yelena Kovtun[1], Lindsey T. Brinton[1], Kimberly A. Kelly[1]. *[1]ZielBio, Inc., Charlottesville, VA,[2]Department of Biomedical Engineering, University of Virginia, Charlottesville, VA,[3]Department of Radiology and Medical Imaging,*

University of Virginia, Charlottesville, VA,[4]Department of Surgery, University of Virginia, Charlottesville, VA

Antibody-drug conjugates (ADCs) have become increasingly adopted clinically, with 13 drugs FDA-approved and over 100 under clinical development. Despite this momentum and major advances in payload and linker technology, ADCs are limited by off-cancer target-mediated toxicities incurred by currently available targets. In contrast to genomic and proteomic strategies, our unique drug discovery approach accounts for a disease's native context. This led to the identification of cancer-specific plectin (CSP) as not only overexpressed in malignant tissue compared to healthy, but exclusively present on the surface of cancer cells and absent in normal or pre-malignant tissue. A Phase 0 imaging trial (Biodistribution of Novel Imaging for Resectable Pancreatic Cancer - NCT01962909) evaluating a radiolabeled CSP-targeted peptide has revealed that CSP is bioavailable and abundant, with over a million CSP molecules per cancer cell in pancreatic cancer. Previously, we generated ZB131, a humanized monoclonal antibody that targets CSP. ZB131 demonstrated potent monotherapy efficacy in pancreatic, ovarian, and bile duct preclinical cancer models, indications that have high CSP expression and are being evaluated in a first-in-human Phase 1/2 clinical trial (NCT05074472). Here, we show that CSP is an ideal target for an ADC: it is abundantly and selectively expressed in many indications, bioavailable, and its inhibition is predicted to synergize with FDA-approved payloads. ZB131 binds specifically to CSP, rapidly internalizes, displays linear pharmacokinetics in pre-clinical models, and demonstrates a strong safety profile. We describe the development of two ZB131 ADCs, ZB131-MMAE (monomethyl auristatin E) and ZB131-DXd (Deruxtecan), with drug-to-antibody ratios of 3 – 4 and 7 – 8, respectively. After binding, both ADCs are rapidly and specifically internalized by CSP-positive cells resulting in drug payload release and enhancing cancer cell death compared to ZB131 alone. Moreover, we characterize cytotoxic activity in high and low CSP cell lines to evaluate ADC activity in relation to CSP abundance. In preclinical xenograft models, ZB131-ADC enhanced tumor regression compared to controls at clinically relevant doses. Furthermore, anti-huIgG staining revealed selective target engagement by ZB131-ADC. Taken together, these

data show that ZB131-ADCs demonstrate potent antitumor activity and support their evaluation in a Phase 1 clinical trial.

#6300
Therapeutic potential of EO-3021/SYSA1801, a Claudin18.2 antibody-drug conjugate, for the treatment of CLDN18.2-expressing cancers

Mo Dan[1], Xiwu Hui[2], Yancui Wang[1], Can Yuan[2], Thomas O'Hare[3], Valerie Malyvanh Jansen[3], Shawn M. Leland[3], Yang Zhang[1], David Dornan[3], Xiaoyan Wang[1]. *[1]CSPC Zhongqi Pharmaceutical Technology (Shijiazhuang) Co., Ltd., Shijiazhuang, China,[2]CSPC Megalith Biopharmaceutical Co., Ltd., Shijiazhuang, China,[3]Elevation Oncology, Inc., New York, NY*

Background: Claudin18.2 (CLDN18.2), a tight junction protein normally expressed only on gastric mucosa, is overexpressed in gastric, pancreatic, esophageal, ovarian, lung and other solid tumors. Unlike in normal tissue, CLDN18.2 is exposed on epithelial surfaces in malignancy. There are no approved targeted therapies for CLDN18.2-expressing cancers. An antibody-drug conjugate (ADC) composed of a monoclonal antibody (mAb) targeting CLDN18.2 with a monomethyl auristatin E (MMAE) payload site-specifically conjugated via a cleavable linker at a drug-antibody ratio (DAR) of 2, EO-3021/SYSA1801, was developed to target CLDN18.2-expressing cancer cells, minimize toxicities and maximize therapeutic index.
Methods: HEK293-CLDN18.2 cells were used to evaluate CLDN18.2-dependent EO-3021 endocytosis, MMAE payload release, inhibition of proliferation and antibody dependent cellular cytotoxicity (ADCC). Cell cycle distribution and caspase-3/7 activity were measured 24 hours after treating BxPC3-CLDN18.2 pancreatic cells with EO-3021 or the unconjugated antibody, EO-3021 mAb. Inhibition of proliferation by EO-3021 was measured on cell lines ectopically expressing medium to high CLDN18.2 and on cell lines with endogenous low to medium CLDN18.2 expression. Xenograft studies evaluating tumor growth inhibition by EO-3021, EO3021 mAb, and cisplatin or gemcitabine were done in gastric (NUGC4; NUGC4-CLDN18.2), pancreatic (Patu8988S; BxPC3-CLDN18.2), and lung (NCI-H460) cancer models.
Results: EO-3021 binding to cancer cells, endocytosis, MMAE release, and inhibition of proliferation were dependent on CLDN18.2 expression. EO-3021 (EC_{50}: 172 ng/ml) and EO-3021 mAb (EC_{50}: 130 ng/ml) demonstrated similar levels of ADCC. EO-3021 but not EO-3021 mAb promoted G2/M cell cycle arrest and apoptosis and exhibited potent activity across cell lines with low, medium, and high CLDN18.2 expression (IC_{50}:

7-456 ng/mL). EO-3021 induced tumor regressions with a single dose across low, medium, and high CLDN18.2-expressing in vivo models derived from pancreatic (2-10 mg/kg), gastric (0.5-10 mg/kg), and lung cancers (4 mg/kg), respectively. In contrast, standard of care (SOC) chemotherapies and EO-3021 mAb did not induce tumor regressions across in vivo models.
Conclusions: EO-3021 demonstrated profound *in vivo* antitumor activity and outperformed SOC in gastric, pancreatic, and lung cancer models. Results from *in vitro* and *in vivo* studies highlight the promising therapeutic potential of EO-3021/SYSA1801 for patients with CLDN18.2-expressing cancers. A Phase 1 study is ongoing to evaluate the safety, tolerability, pharmacokinetics and preliminary anti-tumor activity of SYSA1801 in patients with CLDN18.2 positive advanced solid tumors (NCT05009966).

#6301

Post-translational modifications regulate sensitivity to Polatuzumab Vedotin in DLBCL

Sean R. Corcoran[1], Louis M. Staudt[2], Daniel Hodson[1]. *[1]University of Cambridge UK, Cambridge, United Kingdom,[2]Lymphoid Malignancies Branch, National Cancer Institute, NIH, Bethesda, MD*

Diffuse Large B-Cell Lymphoma (DLBCL) is an aggressive malignancy of which one-third of diagnosed patients ultimately relapse and die. New treatment paradigms for relapsed-refractory patients are needed. Most DLBCL tumors are reliant on signaling through their cell surface B-cell receptor (BCR) mediated by ITAMs on CD79A and CD79B to drive anti-apoptotic NF-kB and PI3 kinase signaling. In order to understand how surface BCR is regulated, we performed whole genome CRISPR screens in 9 DLBCL cell lines in which we sorted for high and low surface CD79B or added the CD79B targeted antibody-drug conjugate Polatuzumab-Vedotin (POLA-V). Strikingly, independent of genetic or cell of origin subtype, sgRNAs encoding the entire N-linked glycosylation pathway and specific sugar modification by addition of galactose and sialic acid were found to be enriched in high CD79B fractions and depleted in POLA-V treated samples compared to control. Further testing showed that removing sialic acid by treating with a small molecule inhibitor of sialic acid, genetic perturbation of golgi sugar transporters SLC35A1 and SLC35A2, or the a2,6

sialyltransferase ST6GAL1 resulted in more surface CD79B antibody binding with no significant change in CD79B protein abundance. The specificity of the effect of sialic acid loss on POLA antibody binding was confirmed by removing cell surface sialic acid with exogenous sialidase and observing increased binding of POLA, but not other therapeutic antibodies like Rituximab or CD19 FMC-63. Loss of SLC35A1, SLC35A2, and ST6GAL1 synergized with POLA-V but not the drug conjugate MMAE alone, showing a BCR dependent mechanism of sialic acid loss on POLA-V sensitization. In a further cell of origin subtype analysis of the germinal center B-cell (GCB) DLBCL cell lines, loss of the E3 ligase KLHL6 was found to synergize with POLA-V. Importantly, KLHL6 is heavily mutated across all germinal center derived malignancies, is more highly expressed in germinal center B-cells than other members of the B-cell lineage, and plays an unknown role in the development of autoimmune diseases. Further work will give evidence for the target of KLHL6 mediated ubiquitination and will show how this gene can drive lymphoma and autoimmune disease development in the germinal center.

#6302

Identification of OASEP1 as a biomarker and therapeutic target for oral cancer

Atsushi Takano[1], Yoshihiro Yoshitake[2], Masahiro Shinohara[2], Yataro Daigo[3]. *[1]University of Tokyo, Tokyo, Japan,[2]Kumamoto University, Kumamoto, Japan,[3]Shiga University of Medical Science, Otsu, Shiga, Japan*

This study aims to identify new biomarkers and therapeutic targets for oral cancer. Our strategies are as follows: i) Identification of overexpressed genes in oral cancers by gene expression array analysis, ii) Validation of clinicopathologic significance of their protein expression by tissue microarray, iii) Examination of their growth effect on cancer cell by siRNAs. We identified a secreted protein, OASEP1 (oral cancer-associated serum protein 1) as a candidate. Immunohistochemical staining showed that OASEP1 protein expression was observed in 120 (75.4%) of 159 oral cancers that had undergone curative surgery. High level of OASEP1 expression was associated with poor prognosis for oral cancer patients (P = 0.0054, by log-rank test). Multivariate analysis revealed that strong

OASEP1 expression was an independent prognostic factor. Suppression of OASEP1 expression by siRNA significantly inhibited the growth of *oral cancer* cell lines through apoptosis as detected by apoptosis assays and time lapse imaging. Transient OASEP1 overexpression significantly enhanced the growth of oral cancer cells. In addition, knock down of OASEP1 receptor by siRNAs also significantly inhibited the growth of oral cancer cells. Addition of OASEP1 protein significantly increased the growth of oral cancer cells in a dose dependent manner, suggesting that the interaction between OASEP1 and its receptor regulated the growth of oral cancer cells. Microarray analysis coupled with siRNAs for OASEP1 demonstrated various OASEP1-related oncogenic pathways in oral cancer cells. Our data suggest that OASEP1 is a possible prognostic biomarker and therapeutic target for *oral cancer.*

#6304

Preclinical development of a next generation antibody drug conjugate (ADC) targeting B7-H3 for treatment of solid tumors

Jian Xu[1], Qing Zong[2], Wei Wang[2], Qigang Liu[2], Sasha Stann[1], Jiaqiang Cai[2]. *[1]MediLink Therapeutics USA, INC., Cambridge, MA,[2]MediLink Therapeutics (Suzhou) Co., Ltd., Suzhou, China*

B7-H3 (CD276), an immune checkpoint member of the B7/CD28 family, is widely expressed in multiple cancers and is associated with poor prognosis. YL201 is a novel B7-H3-targeting antibody-drug conjugate (ADC) and built on MediLink's tumor microenvironment activable linker-payload platform (TMALIN platform). This ADC is comprised of an anti-B7-H3 human monoclonal antibody conjugated to a novel topoisomerase 1 inhibitor *via* a protease-cleavable linker.

The novel linker-payload and site-specific conjugation of YL201 results in a homogeneous and more hydrophilic ADC. In addition, the binding specificity, affinity and avidity of antibodies show no impact after conjugation. *In vitro*, upon binding to B7-H3, the antigen-ADC complexes are internalized to lysosomal vesicles releasing the toxic payload, whose cytotoxic features drive cell cycle arrest, apoptosis, elevation of PARP/caspase 7 expression, as well as cell death and bystander effect. In preclinical studies, YL201 is effective in causing tumor regressions in both cell line- and patient-derived xenograft (CDX and PDX) mouse models at

doses that are well tolerated. The *in vivo* pharmacokinetics in monkeys showed that YL201 is deemed as 'highly stable' in circulation. Safety evaluations demonstrated acceptable safety profile and no off-target toxicity in monkeys. These non-clinical data suggest the stability of linker in circulation but efficiently release the payload in tumors, and eventually, expanded the therapeutic window.
Taken together, preclinical data suggest that YL201 could be a promising treatment strategy for B7-H3 positive cancer patients.

#6305

Bispecific claudin 18.2 and GPRC5D antibodies with potent cell-killing activity for cancer therapeutics

Ileine Sanchez, Hayley Roth, Brad Screnci, David Tucker, Nick Molino, Trevor Barnes, Paige Murphy, Kyle Guldner, Tim Phillips, Kristen Shema, Thomas Charpentier, Alyssa Cunningham, Janae Latta, Breanna Tyrell, Meghan Pitts, Carmen Navia, Charles Azuelos, Anna Lobley, Jawhara Karam, Valerie Fiers, Daniela Reyes, Kate Slovik, Alison Snyder, Marianne Assogba, Kai-Ti Chang, Riley Payne, Kyle Doolan, Ross Chambers, Joe Rucker, Benjamin Doranz. *Integral Molecular, Philadelphia, PA*

Tumor-associated antigens with little or no expression in healthy tissue are attractive targets for anti-tumor modalities including T cell-engaging bispecific antibodies. CLDN18.2 is a transmembrane adhesion protein undetectable in most healthy adult tissues but highly expressed in gastric, pancreatic, esophageal, and lung cancers. GPRC5D is a G protein-coupled receptor that is absent from most healthy tissues except for hair follicles but expressed on multiple myeloma cells. Both CLND18.2 and GPRC5D are novel oncology targets with no clinically approved therapies against them. Using our discovery platform tailored to complex transmembrane proteins, we have developed bispecific antibodies with the ability to potently kill CLDN18.2-positive or GPRC5D-positive cells. Multipass membrane proteins are valuable therapeutic targets in oncology and other disease areas but are largely inaccessible as antibody targets due to their poor expression, membrane-dependent structure, small extracellular regions, and poor immunogenicity due to sequence conservation. We developed an antibody discovery platform (MPS) that specifically addresses each of these challenges. This platform utilizes advanced immunization techniques

including DNA, mRNA, and Lipoparticles (virus-like particles). It also employs chickens as an evolutionarily divergent host species for robust immune responses against conserved targets. Antibodies raised in chickens are directly humanized prior to isolation, reducing the need for downstream engineering. In two separate campaigns, we immunized chickens with CLDN18.2 and GPRC5D and obtained high-titer immune responses. We were successful in isolating high-affinity antibodies specific to each of these targets. Our CLDN18.2 antibodies showed specificity for their target and did not bind the closely related splice variant CLND18.1, which is highly expressed in healthy lung tissue. Additionally, the antibodies showed no binding to ~6,000 other proteins that were screened using a Membrane Proteome Array. A subset of antibodies from both discovery programs were configured as bispecific molecules using a CD3-targeting arm to bring tumor cells into close proximity with cytotoxic T cells that mediate cell killing. The panels of molecules encompassed multiple bispecific formats bearing different stoichiometries, geometries, and sizes to enable identification of lead molecules with favorable activities and safety profiles. Both CLDN18.2 and GPRC5D bispecifics showed potent T cell-mediated cytotoxicity with picomolar potency. They also showed good cytokine release and developability profiles. GPRC5D x CD3 and CLDN18.2 x CD3 bispecifics hold promise as potent and safe therapeutics for different cancer types.

#6306

Pharmacological deuteration of SCID mice using the water-isotopologue deuterium oxide (D_2O) inhibits tumor growth in bioluminescent models of human malignant melanoma and pancreatic ductal adenocarcinoma

Jana Jandova[1], Jean-Philippe Galons[2], David L. Dettman[3], Georg T. Wondrak[1]. *[1]Pharmacology and Toxicology, R Ken Coit College of Pharmacy and UA Cancer Center, The University of Arizona, Tucson, AZ,[2]Department of Medical Imaging, The University of Arizona, Tucson, AZ,[3]Department of Geosciences, The University of Arizona, Tucson, AZ*

Since its initial discovery as a natural isotopologue of dihydrogen oxide (^1H_2O), extensive research has focused on the biophysical, biochemical,

and pharmacological effects of deuterated water [^2H_2O (D_2O, also referred to as 'heavy water')]. Here, using diverse panels of cultured human malignant melanoma and pancreatic ductal adenocarcinoma (PDAC) cells we have profiled (*i*) D_2O-induced phenotypic anti-proliferative and apoptogenic effects, (*ii*) redox- and proteotoxicity-directed stress response gene expression, and (*iii*) phosphoprotein-signaling related to endoplasmic reticulum (ER) and MAP-kinase stress response pathways. Differential RT-qPCR array analysis revealed early modulation of stress response gene expression elicited by D_2O (90%; ≤6 h) confirmed by independent RT-qPCR analysis. Immunoblot-analysis revealed rapid (≤ 6 h) onset of D_2O-induced MAP-kinase signaling (p-JNK) together with ER stress response upregulation (p-eIF2α, ATF4, XBP1s, DDIT3/CHOP) attributable to deuteration-induced alteration of hydrogen bonding triggering proteotoxic stress. Next, we tested the chemotherapeutic efficacy of D_2O-based drinking water supplementation in bioluminescent murine models of malignancy (A375-luc melanoma and BxPC-3-luc orthotopic PDAC xenografts in SCID mice). Time course of systemic deuteration (30% D_2O in drinking water fed continuously for up to 21 days) was established using time-resolved whole-body proton magnetic resonance imaging (MRI) and isotope-ratio mass spectrometry (IR-MS)-based plasma (D/H)-analysis. In both models, D_2O supplementation significantly suppressed tumor growth and metastasis with downregulated expression of PCNA/Ki67 while increasing tumor levels of DDIT3/CHOP, HO-1, and p-eIF2α. Taken together, these data demonstrate for the first time that pharmacological induction of systemic deuteration by oral administration of D_2O, associated with induction of cellular ER stress, reduces tumor burden and metastasis in murine models of human malignant melanoma and PDAC.

#6307

A novel pegylated bispecific antibody-drug conjugate (P-BsADCpb-adc) targeting cancers co-expressing PD-L1 and CD47

Shumin Liu, Weidong Lyu, Shuqiang Yin, Yang Lei, Qiudong Zhuo, Liling Zheng, Bin Sun, Shuangyu Tan, Lidong Jiang, Teng Zhang, Bo Gao, Rui Xu, Dechang Huang, Yong Li, Zibin Wu, David Wu, Yvonne (Yu) Wen.
Shenzhen Enduring Biotech, Ltd., Shenzhen, China

ADCs have demonstrated improved efficacy and target selectivity comparing to the non-specific small molecule cytotoxicity drugs in cancer treatment. Yet, in solid tumor therapies, effort for further improvement of efficacy and safety has been hindered by the poor tumor penetration of conventional IgG based ADC, low internalization efficiency, undesired efflux of ADC from tumor cells, narrow therapeutic window due to the on-target/off tumor and Fc induced toxicity, etc. To address those issues, we previously reported that the compound JY201, a Polyethylene Glycol (PEG)-based bispecific ADC (P-BsADC) targeting two epitopes of Her2, demonstrated advantages in tumor penetration, internalization efficiency, lysosome trafficking, no Fc related toxicity, and better efficacy in tumor inhibition than transtuzumab deruxtecan (Ds-8201). In this study, we reveal another novel pegylated P-BsADC (JY207) formed by site-specific conjugation of a bispecific single chain fusion protein targeting PD-L1 and CD47 with PEG-MMAE (a pegylated cytotoxic payload MMAE). As expected, the compound JY207 retains all the advantages that JY201 possesses. Furthermore, JY207 does not bind to human red blood cells, but preferentially binds to CD47/PD-L1 double positive tumor cells, thus reduces the possibility of on-target toxicities. In vitro cytotoxicity studies showed that JY207 has strong potencies in CD47/PD-L1 double positive tumor cells, while showing almost no killing effect to CD47 or PD-L1 single positive tumor cells. In CDX models and a PDX model of transplanted tumor tissues from lung cancer patients, the compound demonstrated excellent tumor inhibition at low doses. In an in vitro plasma stability test, JY207 displays high stability in cynomolgus monkey and human serums. Preliminary repeated-dosing toxicological study has found the maximum tolerated dose of JY207 in CD47/PD-L1 double transgenic mice is 50mg/kg. In vivo pharmacokinetics and toxicological studies of JY207 are being conducted in cynomolgus monkeys and are expected to show desirable results. All those findings in this study warrant JY207 as a promising candidate for the clinical development for patients with CD47/PD-L1 double positive cancers.

#6308

Preclinical development of ABBV-319: a CD19-targeting glucocorticoid receptor modulator (GRM) agonist antibody-drug conjugate (ADC) for the treatment of B-cell malignancies

Chewei Anderson Chang[1], Ethan Emberley[1], Aloma L. D'Souza[1], Weilong Zhao[1], Cormac Cosgrove[2], Axel Hernandez Jr[3], Anatol Oleksijew[2], Paul Ellis[2], Luis Rodriguez[2], Gail Bukofzer[2], David Peetz[2], Wissam Assaily[1], Raghuveer Singh Mali[1], Wei Liu[1], Danqing Xu[1], Gregory K. Potts[2], Shaun McLoughlin[2], Kimberley McCarthy[3], Zhaomei Zhang[1], Jos Campbell[1], Isabella Sturdevant[1], Gloria Zhang[1], Tyler Curran[1], Jon D. Williams[2], Erwin Boghaert[2], Milan Bruncko[2], Christopher C. Marvin[2], Adrian Hobson[3], Michael Mcpherson[3], Tamar Uziel[2], Marybeth Pysz[1], Xi Zhao[1], Alex Bankovich[1], Kevin J. Freise[2], Susan Morgan-Lappe[2], James W. Purcell[1]. *[1]AbbVie Bay Area, South San Francisco, CA,[2]AbbVie Inc., North Chicago, IL,[3]AbbVie Bioresearch Center, Worcester, MA*

Introduction: Glucocorticoids are key components of standard-of-care treatment regimens (*e.g.*, R-CHOP, Hyper-CVAD) for several B-cell malignancies. However, prolonged systemic glucocorticoid treatment results in glucocorticoid-associated adverse events and acquired resistance that limit its therapeutic potential. ABBV-319 is a novel CD19-targeting ADC engineered to reduce glucocorticoid-associated toxicity observed with systemic glucocorticoids while possessing three distinct mechanisms of action (MoA) to increase efficacy: 1) antibody-mediated delivery of GRM to activate glucocorticoid receptor (GR) induced cell death in cancer cells, 2) inhibition of CD19 signaling, and 3) enhanced Fc-mediated cancer cell killing via afucosylation of the antibody backbone.
Results: We identified a GRM agonist that is 15 and 150 times more potent at driving GR transcriptional activation and cell death compared to clinical glucocorticoids dexamethasone and prednisolone, respectively. The conjugation of GRM agonist as the payload on ABBV-319 enables potent GRM-driven anti-cancer activity against malignant B-cell lines *in vitro* as well as in cell-line and patient derived xenograft (CDX and PDX) models *in vivo*. Remarkably, a single-dose of ABBV-319 induced sustained tumor regression and enhanced anti-tumor activity compared to repeat dosing of systemic glucocorticoids (*e.g.,* prednisolone) at its maximum tolerated dose in mice. The CD19 monoclonal antibody (mAb) also reduced proliferation of a subset of B-cell malignant cell lines through inhibition of the PI3K/AKT pathway. Moreover, afucosylation of the CD19 mAb in ABBV-319 enhanced Fc-mediated antibody-dependent cellular cytotoxicity

(ADCC), and this activity was maintained after conjugation with GRM payloads. ABBV-319 bound similarly to both V158 (high-affinity) and F158 (low-affinity) FcγRIIIa allotypes and mediated potent ADCC in co-culture assays with human peripheral blood mononuclear cells (PBMCs). Notably, ABBV-319 displayed superior efficacy compared to afucosylated CD19 mAb in human CD34+ hematopoietic stem cell-engrafted NSG-Tg(Hu-IL15) mice, demonstrating that the three MoA (GR-driven cell death, CD19 signaling inhibition, and ADCC) collectively contribute to anti-tumor activity *in vivo*. ABBV-319 also displayed on-target depletion of normal human B-cells but did not affect peripheral NK cell counts in mice. Furthermore, CITE-seq profiling revealed that ABBV-319 treatment of human PBMCs activated GRM-induced signature genes restricted to B-cells, demonstrating the specificity of CD19-mediated delivery of GRM. Conclusion: ABBV-319 has potent anti-tumor activity from three distinct MoA and exhibits safety improvements compared to systemic glucocorticoids, supporting its recent progression into Phase I clinical trial.

#6309

Anti-tumor efficacy of SI-B001, a novel EGFR×HER3 bispecific antibody, against EGFR-driven epithelial tumors alone or in combination with paclitaxel and carboplatin

Blair Renshaw[1], Jahan Salar Khalili[1], Sa Xiao[2], Yi Zhu[2]. *[1]SystImmune Inc., Redmond, WA,[2]Sichuan Baili Pharmaceutical Co., Ltd., Chengdu, China*

EGFR is a member of the human epidermal growth factor receptor (ErbB) family with tyrosine kinase activity. Evidence indicates that EGFR is involved in the pathogenesis and progression of human carcinoma of different types. HER3 is a unique pseudokinase receptor of the ErbB family and known to mediate resistance to EGFR-targeting therapies. Therefore, we created SI-B001, an EGFR×HER3 bispecific antibody, which can bind EGFR×EGFR homodimers and EGFR×HER3 heterodimer to block their downstream pathways. We performed non-clinical studies to investigate *in vitro* and *in vivo* anti-tumor effects.
In vitro, the inhibition of tumor cell growth by SI-B001 was stronger than cetuximab and duligotuzumab in FaDu (mRNA expression levels of $EGFR^{high}/HER3^{high}/NRG1^{medium}$). Importantly, testing with the cell line Oka-c-1 (mRNA expression levels of $EGFR^{high}/HER3^{high}/NRG1^{low}$),

showed that NRG1 supplementation did not change the potency of cetuximab. However, SI-B001 showed much stronger potency than cetuximab and duligotuzumab under conditions of NRG1 supplementation. This result indicates that the functionality of the bi-specific SI-B001 is competitive against a HER3 natural ligand and capable to act against cancer with HER3 ligand mediated resistance to cetuximab.
In vivo, single agent SI-B001 exhibited superior anti-tumor activity to cetuximab in the FaDu xenograft model. Meanwhile, SI-B001 in combination with paclitaxel and carboplatin led to a significant synergistic antitumor effect, which was stronger than the combination of cetuximab + paclitaxel + carboplatin. Compared to chemotherapy alone in this model, which could result in weight loss and treatment related mortality, no serious weight loss or deaths occurred in the single agent SI-B001 and the combination of SI-B001 with chemotherapy.
These results suggest that SI-B001 alone and in combination with chemotherapy can exhibit favorable safety and robust anti-tumor activity. Currently, 6 phase II clinical trials of SI-B001, either alone or in combination with chemotherapy, have been conducted in different epithelial carcinomas. These studies have shown a potential break-through activity in NSCLC and HNSCC with a very good safety profile.

#6310

Phylogenetic conservation of primate Trop-2 underscores favorable pharmacokinetics and lack of toxicity of the cancer-selective Hu2G10 anti-Trop-2

Saverio Alberti[1], Martina Ceci[2], Ludovica Pantalone[2], Marco Trerotola[2], Emanuela Guerra[2]. *[1]University of Messina, Messina, Italy,[2]University of Chieti-Pescara, Chieti, Italy*

Trop-2 is a transmembrane signal transducer that activates growth-signaling networks that converge on Akt, ERK, Cyclin D1, NFkB (1). We discovered that Trop-2 cleavage by ADAM10 is an activator switch of cancer growth and metastatic diffusion (2) and exposes novel target epitopes that are inaccessible in the unprocessed wtTrop-2. The Hu2G10 mAb selectively binds these epitopes with an affinity that is ≈10,000-fold higher than for the unprocessed molecule. To validate a reliable model for Hu2G10 binding *in vivo,* we explored Trop-2 phylogenetic conservation in primates. *Pan*

troglodites (chimpanzee), *Papio anubis* (baboon), *Macaca mulatta/fascicularis* (Rhesus/Cynomolgous), *Callithrix jaccus* (marmoset) *TROP2/TACSTD2* sequences were compared. The only difference between *Pan troglodytes* and human Trop-2 is one additional leucine in the Pan leader peptide, making the mature Trop-2 identical to that in man. The *Macaca mulatta/fascicularis* Trop-2 sequences are 97% identical, 100% similar to the human sequence. Three-dimensional modeling revealed polymorphic residues usage versus activation-driven structural rearrangement of Trop-2. COS-7 and HEK-293 cells transfected with individual primate Trop-2 showed efficient recognition by Hu2G10 in all tested species. Immunohistochemistry analysis of normal Macaca tissues showed Trop-2 expression patterns essentially corresponding to the human ones. IV injected Hu2G10 at doses of 5 to 10 mg/kg was well tolerated by Cynomolgous monkeys. No neurological, respiratory, digestive and urinary adverse effects were observed, and no body-weight loss occurred during the 28-day observation. No alterations of blood monocyte, neutrophil and basophil counts nor significant changes in biochemical parameters were detected. A pharmacokinetic (PK), study was carried out. Serum concentration of Hu2G10 was determined using anti-idiotypic antibody-based ELISA assays. At the higher dosing of 10 mg/kg Hu2G10 serum values reached a peak 2-hour after the injection (13281±4686 ng/ml). The concentration of Hu2G10 then diminished gradually, and reached baseline levels on day 21. The serum concentration peak of 5 mg/kg Hu2G10 was 5759±1729 ng/ml, and reached baseline levels on day 14. Thus, Hu2G10 is stable in plasma, and is detectable in the circulation up to three weeks after the infusion ($t_{1/2}$=6.5 days). Taken together, these findings validate primate models as reliable for assessing Hu2G10 *in vivo* toxicity and PK. The lack of toxicity and favorable PK parameters candidate the cancer specific Hu2G10 as first-in-class anti-Trop-2 mAb. (1) Guerra E. *et al.*, Oncogene 41:1795-1808 (2022).(2) Trerotola M. *et al.*, Neoplasia 23: 415-428 (2021).

#6311

ABBV-400: An ADC delivering a novel topoisomerase 1 inhibitor to c-Met-positive solid tumors

Regina M. Reilly[1], Cheng Ji[1], Ryan P. Matuszak[1], Mark G. Anderson[1], Lora Tucker[1], Nadezda Klunder[1], Adelyn L. Zelaya Lazo[1], Erwin R. Boghaert[1], Marybeth A. Pysz[2], Aloma D'Souza[2], Laura Kreckler[3], Milan Bruncko[4],

Brittney J. Mills[5], Matthew Ravn[6], George Doherty[1], Kevin J. Freise[7], Andrew C. Phillips[1]. *[1]Oncology Discovery Research, AbbVie Inc., North Chicago, IL,[2]Oncology Discovery Research, AbbVie Inc., South San Francisco, CA,[3]Global Preclinical Safety, AbbVie Inc., North Chicago, IL,[4]Drug Discovery Science & Technology, AbbVie Inc., North Chicago, IL,[5]Drug Product Development, AbbVie Inc., North Chicago, IL,[6]Process Research & Development, AbbVie Inc., North Chicago, IL,[7]Oncology Early Development, AbbVie Inc., North Chicago, IL*

Antibody-drug conjugate (ADC) technology is founded on the premise that antigen-mediated payload delivery selectively targets tumor cells and spares normal tissue. While approval of several ADCs has proven this to be a successful therapeutic approach, there remain opportunities to generate optimized ADCs with tailored selection of antigen matched with payload highly active in the target indication. To this end, ABBV-400 has been developed as an ADC that targets c-Met and topoisomerase-1 (Top1), both of which are overexpressed in solid tumors. The antibody is directed to the cell surface tyrosine kinase receptor, c-Met, a key driver of tumor cell growth and development of resistance to EGFR-targeted and other targeted therapeutics. Supporting this, Teliso-V, a c-Met-targeted ADC with MMAE payload, has been granted Breakthrough Therapy Designation in non-small cell lung cancer (NSCLC). To extend activity of a c-Met-targeted ADC to patients with tumors expressing lower c-Met levels and to indications, such as colorectal cancer (CRC), where MMAE-based ADCs have not been effective, a novel topoisomerase-1 inhibitor linker-drug was developed. Screening over 400 linker-drugs identified a unique, potent Top1 inhibitor with a cleavable valine-alanine linker and stable bromoacetamide attachment designed to minimize systemic payload release. Preclinically ABBV-400 exhibits favorable pharmacokinetics, anti-proliferative activity in vitro, and compelling efficacy in NSCLC, gastroesophageal, and CRC xenograft models. Furthermore, ABBV-400 is well tolerated by cynomolgus monkeys with bone marrow and gastrointestinal tract toxicities common to other Top1 inhibitors. This pairing of a novel linker-drug and an antibody with demonstrated clinical activity provides an exciting opportunity to treat patients with c-Met expression in indications sensitive to Top1 inhibition.

ABBV-400 has progressed through dose escalation, and dose expansion is currently ongoing in a Phase 1 FIH clinical study (NCT05029882).
All authors were employees of AbbVie during this research. The design, study conduct, and financial support for this research were provided by AbbVie. AbbVie participated in the interpretation of data, review, and approval of the publication

#6312

Targeting HSPG is more efficient than using soluble heparin for interfering with cancer cell adhesion and migration

Lorenzo Depau, Elisabetta Mandarini, Jlenia Brunetti, Marta Zanchi, Chiara Falciani, Luisa Bracci. *University of Siena, Siena, Italy*

Given the relevance of heparan sulfate proteoglycans (HSPG) and of heparin binding ligands in the regulation of cancer cell adhesion, migration and invasiveness, drugs that may interfere with HSPG functions have been studied for decades for their possible use in oncology. In this view heparin analogues have been tested for their effectiveness not only in cancer associated thromboembolism but also for their potential effects on cancer growth and metastasis. Despite a number of promising preclinical results and clinical hypothesis, many different clinical trials on the use of heparin analogues in different cancers reported no significant benefits in tumor progression and overall survival, indicating that using heparin as a soluble decoy for the many HSPG ligands does not appear to be the best possible approach (1,2). Taking advantage of the tetra-branched peptide NT4, which is a specific ligand of HSPG sulfated glycosaminoglycan (GAG) chains (3, 4), we tested the effectiveness of targeting cell membrane HSPG, as a potential alternative approach for interfering with HSPG functions in cancer cell invasiveness. We had demonstrated that NT4 can either inhibit or increase oriented migration in respectively PANC-1 pancreas adenocarcinoma and TE671 rhabdomyosarcoma human cancer cells, indicating a crucial but diverse role of HSPGs in oriented cell migration in different cancer cells.NT4 and heparin were here compared for their effect on adhesion and migration of different cancer cell lines on extracellular matrix (ECM) supports, as well as for their effect on proliferation and in vitro invasiveness of the same cell lines. We found that inhibition of cancer cells adhesion to ECM proteins by NT4 varies in different cancer cell lines,

ranging from 90% inhibition to as low as 20%, whereas heparin has no effect. Analogous results were obtained when testing cancer cell migration. NT4 inhibited migration and in vitro invasiveness of different human cancer cell lines, with the sole exception of TE671 cells. Heparin did not modify cell migration in any of the tested cancer cell lines. NT4 had no effect on cell proliferation, whereas, notably, heparin resulted to stimulate cell proliferation in some cancer cell lines. Differently from using heparin as an unspecific soluble decoy, targeting HSPG with well-defined ligands can result in an efficient tumor-specific treatment. Nevertheless, as for most cancer cellular targets, a detailed definition of cellular mechanisms and a related personalized approach is mandatory.

1) Schünemann HJ et al. Lancet Haematol. 2020;7(10):e746. 2) Posch F et al. ibid:e703. 3) Brunetti J et al. Sci. Rep. 2016,6,27174. 4) Depau L et al. J Med Chem 2020;63(24):15997.

#6313

IND-enabling studies for GrB-Fc-IT4: *in vivo* efficacy, pharmacokinetics, schedule optimization and maximum tolerated dose

Ana Alvarez-Cienfuegos, Lawrence H. Cheung, Khalid A. Mohamedali, Mihai Gagea, Michael G. Rosenblum. *UT MD Anderson Cancer Center, Houston, TX*

Fn14 (fibroblast growth factor-inducible 14) is the only known receptor of TWEAK (tumor necrosis factor-related weak inducer of apoptosis). The binding of TWEAK to Fn14 activates several intracellular signal transduction cascades that lead to cell death, proliferation, migration, or survival depending on the cellular contexts. Several studies have shown that Fn14 is upregulated in many solid tumors when compared with healthy tissues. The activation of TWEAK/Fn14 signaling increases the proliferation, invasion, and migration of tumor cells. Moreover, angiogenesis, pro-inflammatory cytokine expression, and epithelial-mesenchymal transitions are promoted upon TWEAK/Fn14 activation. Therefore, Fn14 is considered a potential therapeutic target, and attempts to generate targeted therapeutics have achieved limited success in pre-clinical and clinical trials. We generated a completely human fusion protein, GrB-Fc-IT4, consisting of the IT4 scFv antibody targeting the Fn14 receptor and the serine protease granzyme B (GrB) as the cytotoxic payload.

Comprehensive mechanism of action studies showed that GrB-Fc-IT4 effectively induced cell death *in vitro* against a broad selection of tumor types with high specificity. The intracellular pathway included rapid, irreversible activation of the caspase cascade and independent mitochondrial depolarization leading to intense apoptotic cellular damage. Pharmacokinetic studies in mice showed that GrB-Fc-IT4 cleared bi-exponentially from plasma with a rapid initial clearance ($t_{½}\alpha$ = 0.36 hours) followed by a prolonged terminal-phase plasma half-life ($t_{1/2}\beta$ = 35 hours), similar to that of IgGs. Based on our PK study, we compared the *in vivo* antitumor efficacy of GrB-Fc-IT4 against A549 (NSCLC) tumors, using two different dosing schedules (QODx5 vs QWx5). Tumor efficacy showed a clear dose and schedule dependence. Mice bearing A549 tumors treated with 32 mg/kg/dose (QOWx5) exhibited complete tumor growth inhibition (7/10 tumors regressed) with 3/10 tumors showing no growth up to 50 days after the last dose. Thus, GrB-Fc-IT4 displays impressive *in vitro* and *in vivo* cytotoxic effects. Even though GrB-Fc-IT4 cross-reacts with the murine Fn14 antigen, maximum tolerated dose studies in mice have confirmed that GrB-Fc-IT4 is a safe product, as mice treated with the drug up to 500 mg/kg showed no evidence of toxicity (changes in respiration, rough hair coat, unusual behavior or hunched posture). Taking in consideration these results we estimate that the therapeutic index for this class of drug is higher than four. Our data suggest that GrB-Fc-IT4 is a novel antitumor agent with a unique mechanism of action compared to all other therapeutic agents. The exceptionally safe and effective profile of this drug makes it an ideal candidate for advancing to clinical trials. Research conducted, in part, by the Clayton Foundation for Research.

#6314

Novel granzyme B-based fusion constructs targeting FRα on liquid and solid tumors

Ana Alvarez-Cienfuegos[1], Lawrence H. Cheung[1], Khalid A. Mohamedali[1], Natalia Baran[1], Marina Konopleva[2], Michael G. Rosenblum[1]. *[1]UT MD Anderson Cancer Center, Houston, TX,[2]Albert Einstein College of Medicine, Bronx, NY*

Folate receptor α (FRα) has been an attractive therapeutic target for many decades because it is highly overexpressed on several solid tumors and demonstrates low or restricted distribution on healthy tissues. Additionally, high expression of FRα has been associated with tumor progression and thus poor prognosis of cancer patients. Therefore, utilizing FRα to effectively locate tumor cells for targeted therapy using antibody drug conjugates, small molecule drug conjugates, radioimmunoconjugates or chimeric antigen receptor T cells, has been extensively investigated. Although some of the mentioned targeted therapies have shown promising preclinical results, their clinical utility has been limited due to associated toxicities in healthy tissues. We generated two new fusion constructs targeting FRα and containing active human granzyme B (GrB) as the cytotoxic payload. We used as binding domains two different scFvs targeting the FRα from antibodies previously used in clinical trials. These human scFvs (mov003 and mov018) were fused to the human serine protease GrB through an engineered human IgG heavy-chain fragment (designated as Fc) which contains a dimerization domain for longer half-life. The cytotoxicity of the constructs against a panel of cell lines expressing various levels of FRα showed a specific cytotoxic effect with an IC_{50} in the low nanomolar range (5-100 nM), particularly exhibiting very low IC_{50} values against breast and ovarian cell lines. FRα negative cells demonstrated IC_{50} levels in the micromolar range. Immunofluorescence studies demonstrated that the fusion constructs targeting FRα are efficiently internalized and effectively delivered the active serine protease to the cytosol. *In vitro* stability assays over 96 hours showed that both constructs are highly stable in mouse serum. Additionally, recent publications suggested that FRα is significantly associated with acute myeloid leukemia (AML) and might serve as a therapeutic target. We assessed the cytotoxic efficacy of GrB-based constructs on a panel of FRα+ AML cell lines and have found that these cell lines were very sensitive (IC_{50} in the low nanomolar range). Furthermore, evaluation of GrB fusion efficacy in two AML cell lines resistant to Bcl-2 inhibitor Venetoclax showed IC_{50}s to be similar or lower than their parental cell lines. These results, therefore, demonstrate no cross-resistance to GrB. The safe and effective profile of these drugs together with their unique mechanism of action makes them ideal candidates for advancing pre-clinical development and may offer a

potential new strategy for treatment of solid tumors and particularly Venetoclax relapsed AML patients, ineligible for intensive chemotherapy. *In vivo* efficacy studies to compare the two constructs are warranted and will help to identify the optimal therapeutic for further clinical consideration. Research conducted, in part, by the Clayton Foundation for Research.

#6315

Human granzyme B fusions targeting VEGFR on tumor cells and activated vasculature

Khalid A. Mohamedali, Lawrence H. Cheung, Ana Alvarez-Cienfuegos, Walter N. Hittelman, Michael G. Rosenblum. *UT MD Anderson Cancer Center, Houston, TX*

$VEGF_{121}$ is a naturally-occurring splice variant that binds to VEGF receptors R-1 and R-2, which are over-expressed on the endothelium of tumor vasculature but not normal vasculature, as well as several tumor cells. While anti-VEGF therapy is a key therapeutic in several cancer treatment regimens, none of the current therapeutics (bevacizumab, VEGF-trap, tyrosine kinase inhibitors) are directly cytotoxic against tumor cells. The serine protease Granzyme B (GrB) is a key effector in immune-mediated cell killing by inducing apoptosis through both caspase-dependent and -independent mechanisms. We previously reported the development and characterization of a fusion protein composed of GrB and $VEGF_{121}$ (GrB/$VEGF_{121}$). Here, we report on GrB-Fc-$VEGF_{121}$, a fusion protein that incorporates a human IgG heavy chain Fc fragment for dimerization which increases the molecular weight and improves *in vivo* circulation and targeting potential. GrB-Fc-$VEGF_{121}$ was expressed in HEK-293E cells under serum-free conditions and purified from the conditioned medium with a final yield of approximately 40 mg/L. The enzymatic activity of GrB in GrB-Fc-$VEGF_{121}$ was comparable to that of commercially available human GrB. *In vitro* studies of GrB-Fc-$VEGF_{121}$ showed cytotoxicity in the nanomolar range against tumor and endothelial cell lines expressing high levels of VEGFR-1 or VEGFR-2. Receptor-negative cells demonstrated IC_{50} levels in the high micromolar range. Immunofluorescence and confocal microscopy demonstrated that GrB-Fc-$VEGF_{121}$ readily

internalized into VEGFR-2+ tumor cells and endothelial cells within 2 hours of treatment while untargeted GrB did not internalize, suggesting internalization was receptor-mediated. Treatment of VEGFR-2+ endothelial and tumor cells at the IC_{50} dose resulted in >50% cell death via apoptosis and/or necrosis within 48 h. *Ex vivo* serum stability of GrB-Fc-$VEGF_{121}$ indicated a gradual protein loss of GrB-Fc-$VEGF_{121}$, with an overall stability of about 50% over 96 hours. No toxicity was observed in BALB/c mice treated with a total 475 mg/kg given IP every other day over 5 doses, indicating that the maximum tolerated dose of GrB-Fc-$VEGF_{121}$ exceeds this dose level. *In vivo* efficacy studies in an OVCAR8 tumor xenograft model with GrB-Fc-$VEGF_{121}$ (100 mg/kg over 5 doses) resulted in significant growth inhibition of established tumors compared to vehicle controls. We observed a significant decrease in the number of CD31+ blood vessels and Ki-67+ proliferating tumor cells in treated tumors compared to controls. Thus, GrB-Fc-$VEGF_{121}$ has significant anti-tumor effects *in vivo* with virtually no toxicity against normal tissues at doses 4-5 times higher than therapeutic levels. This tumor- and vascular-targeting agent appears to have significant potential as a new class of targeted therapeutic agents with a unique mechanism of action. Research conducted, in part, by the Clayton Foundation for Research.

#6316

In vitro and in vivo studies of human granzyme B fusion constructs targeting mesothelin

Khalid A. Mohamedali[1], Lawrence H. Cheung[1], Louis R. DePalatis[2], Claire Thuning-Roberson[2], Michael G. Rosenblum[1]. *[1]Experimental Therapeutics, M.D. Anderson Cancer Center, Houston, TX,[2]H2Biologics, Inc, Shrewsbury, MA*

Mesothelin is highly expressed on tumor cells and promotes tumor growth and drug resistance. Pancreatic, ovarian, mesothelioma, and lung cancers highly express mesothelin and are cancers of unmet needs with ≤16% relative 5-year survival using standard of care. When delivered to tumor cells by immune effector cells, granzyme B (GrB) is a highly cytotoxic serine protease which induces apoptosis through both caspase-dependent and -independent mechanisms. We developed a fusion protein (GrB-Fc-

SD1) composed of human GrB and containing SD1, a novel human single-domain antibody that uniquely targets Region III of the glycoprotein, mesothelin. The SD1 and GrB domains are connected by a human IgG heavy chain fragment which enables dimerization. Thus, the increase in total construct molecular weight leads to an increased *in vivo* circulation time and anti-tumor efficacy. GrB-Fc-SD1 was transiently expressed in HEK-293E cells under serum-free conditions and purified to homogeneity to a final yield of approximately 5 mg/L. Anti-GrB western blot analysis confirmed the expression of GrB-Fc-SD1 exclusively as a dimer. Comparison of GrB-Fc-SD1 with its expected molecular weight suggests significant glycosylation when produced in HEK-293E cells. The enzymatic activity of granzyme B in GrB-Fc-SD1 was comparable to that of commercially available human granzyme B. *In vitro* cytotoxicity against a limited panel of lung, pancreatic and ovarian cancer cell lines expressing surface mesothelin indicate cytotoxicity in the nanomolar range, while cytotoxicity against mesothelin-negative cells was at micromolar levels. GrB-Fc-SD1 bound specifically to mesothelin extra-cellular domain compared to a non-specific control, as determined by ELISA. Biacore analysis confirmed binding with a dissociation constant between 10^{-7} to 10^{-8} M. These data warrant continued investigation of the protein as a therapeutic candidate. Accordingly, *ex vivo* serum stability studies are underway. In addition, screening of an expanded panel of tumor cell lines for *in vitro* cytotoxicity is currently in progress and will be reported. *In vivo* efficacy studies against nude mice bearing Capan-2 xenograft models are currently underway and will also be reported. Research supported by H2Biologics. Research conducted, in part, by the Clayton Foundation for Research.

#6317

Targeting cell-surface CEA with a novel human fusion construct delivers the serine protease granzyme B to solid tumor cells

Khalid A. Mohamedali, Ana Alvarez-Cienfuegos, Lawrence H. Cheung, Walter N. Hittelman, Michael G. Rosenblum. *UT MD Anderson Cancer Center, Houston, TX*

Cancer treatment has improved in the past decades due to advances in targeted therapies and surgical techniques. Immunotherapy, for example,

has greatly improved outcomes for people with several types of cancer that typically have a poor prognosis. However, the response rate depends on the type of cancer being treated, with an average response rate between 20 to 50%. Thus, novel approaches to overcome such therapeutic challenges are warranted. Emerging therapies include fusion proteins and immunoconjugates that deliver a cytotoxic payload to the tumor cell with more specificity and potentially less avenues for resistance than exerted by the antibody or toxin alone. Carcinoembryonic antigen (CEA) is a cell surface protein normally found at low levels in adult tissues but over-expressed in a high percentage of solid tumors including colon and rectum, lung, prostate, ovary, thyroid, or liver. Thus, oncologic therapies against CEA may promote anti-tumor activity while sparing off-target toxicity to unaffected normal tissue. Our newly developed construct, designated GrB-Fc-huMFE, is a completely human fusion protein that contains the single-chain variable fragment huMFE antibody recognizing a juxta-membrane epitope of CEA remaining after proteolytic cleavage of CEA from the cell surface. The construct rapidly internalized into target cells resulting in granzyme B (GrB)-mediated mitochondrial depolarization and irreversible activation of both apoptotic and necrotic cascade mechanisms of cell death. *In vitro* cytotoxicity of GrB-Fc-huMFE against an initial subset of CEA+ tumor cell lines demonstrated cytotoxicity in the nanomolar range, compared to micromolar IC_{50} cytotoxicity against CEA-negative cell lines. Significantly, GrB-Fc-huMFE cytotoxicity *in vitro* was unaffected by exogenously-added CEA extracellular domain at doses up to 1000 µg/ml, suggesting that the construct is not competitively absorbed by soluble CEA proteolytically released by tumors and present in the circulation of patients. An *in vivo* efficacy study against established CEA+ (A-549) tumors in nude mice resulted in significant growth inhibition compared to vehicle controls (1200 mm^3 vs <40 mm^3). Complete tumor regression was observed in 7/10 tumors in mice treated (IP) with doses of 100 mg/kg of GrB-Fc-huMFE in a Q3Dx5 dose administration schedule. Mouse weight was unaffected in both treated and control groups for the duration of the study, suggesting no apparent toxicity of the construct. Pharmacokinetic, stability and *in vitro* tests against a broader panel of tumor cell lines are ongoing and will be reported. Altogether, GrB-Fc-huMFE appears to have significant potential in targeting a large category of CEA-expressing solid tumors and is a promising candidate for further pre-clinical and eventual clinical

development. Research conducted, in part, by the Clayton Foundation for Research.

#6318

Preclinical characterization of ARX305, a next-generation anti-CD70 antibody drug conjugate for the treatment of CD70-expressing cancers

Lillian Skidmore[1], Jingjing Zhu[2], David Mills[1], Ting Jin[2], Suqin Li[2], Keith Tatsukawa[1], Nick A. Knudsen[1], Liying Gong[2], Jay Nelson[1], Kari Cox[1], Amha G. Hewet[1], Jianing Wang[1], Tim Buss[1], Feng Tian[1], Gang Xia[2], Shawn Zhang[1]. *[1]Ambrx Biopharma Inc., La Jolla, CA,[2]NovoCodex Biopharmaceuticals, Inc., Shaoxing, China*

CD70 has emerged as an attractive tumor target with its over-expression in multiple solid and hematological cancers, yet tightly controlled and limited expression in normal cells. In the last decade, multiple anti-CD70 antibody drug conjugates (ADCs) have been developed, but most, if not all, of these ADC programs have been discontinued. Using an expanded genetic code to create Engineered Precision Biologics (EPBs), Ambrx has developed ARX305, a CD70-targeted next-generation antibody drug conjugate (ADC) to potentially overcome the challenges associated with earlier ADCs and treat patients with cancers over-expressing CD70. ARX305 is comprised of a proprietary, high-affinity, humanized anti-CD70 antibody stably and site-specifically conjugated to AS269, a potent microtubule inhibitor. After binding to CD70 expressed on target tumor cells, ARX305 internalizes and releases the cytotoxic payload pAF-AS269 which inhibits cellular proliferation. In vitro testing across a panel of solid and liquid tumor cell lines showed ARX305 elicited highly potent and specific cell killing across multiple tumor types with medium to high CD70 expression levels. In multiple in vivo CD70-expressing xenograft or disseminated models, ARX305 induced significant tumor growth inhibition or regression whereas unconjugated antibody exhibited poor activity. ARX305 utilizes stable oxime conjugation chemistry, a non-cleavable PEG linker, and a membrane-impermeable payload to minimize premature payload release in circulation and associated off-target toxicity. These properties of ARX305 result in high serum stability, with rodent pharmacokinetic studies confirming a similar exposure profile of ARX305 compared to unconjugated antibody and a long serum half-life. Repeat dose toxicokinetic studies in cynomolgus

monkeys demonstrated ARX305 was tolerated at exposures well above therapeutic exposures in mouse pharmacology studies, indicating a wide therapeutic index. In summary, the highly potent anti-tumor activity in multiple tumor types and wide therapeutic index of ARX305 support clinical evaluation of this next generation anti-CD70 ADC. ARX305 is currently in a Phase 1 dose escalation study in China, and the IND in the United States is open.

#6319

Mechanism of anti-EGFR antibody endostatin fusion protein action on inhibition of vasculogenic mimicry and tumor cell motility in triple negative breast cancer

Ankita Sankar[1], Hava Gil Henn[2], Hyun Mi Cho[1], Dania Nassar[2], Sundaram Ramakrishnan[1], Yu Zhang[1], Christian Elledge[1], Seung Uon Shin[1], Joseph Rosenblatt[1]. *[1]University of Miami Miller School of Medicine, Miami, FL,[2]Bar Ilan University, Azrieli Faculty of Medicine, Tzfat, Israel*

Triple Negative Breast Cancer (TNBC) is an aggressive subtype of breast cancer with high metastatic potential and increased morbidity and mortality. Although expression of and signaling by the epidermal growth factor receptor (EGFR) is commonly seen in TNBC, anti-EGFR antibodies such as Cetuximab have had limited therapeutic efficacy, used alone or in combination with chemotherapy.

Primary TNBC tumor growth and metastases require supporting vasculature, which develops through a combination of endothelial angiogenesis and vasculogenic mimicry (VM). VM is frequently seen in TNBC and is associated with aggressive metastatic behavior. We previously developed αEGFR-E-P125A, an antibody-endostatin fusion protein, linking an anti-EGFR antibody to a mutated version of the anti-angiogenic protein endostatin (E-P125A). αEGFR-E-P125A delivers a dimeric E-P125A payload which inhibits TNBC angiogenesis and VM *in vitro* and *in vivo*, and markedly decreases metastasis in multiple TNBC xenograft models. To study changes in the transcriptome following induction of VM and inhibition of VM with αEGFR-E-P125A, RNA-seq was conducted on MDA-MB-231-4175 TNBC cells grown in a 2D monolayer and compared to TNBC cells undergoing VM when plated in matrigel. A second comparison was made between TNBC cells undergoing VM and TNBC

cells in which VM was inhibited by treatment with αEGFR-E-P125A. Differential gene expression analysis and gene set enrichment analysis (GSEA), were used to define pathways which were inversely regulated during the induction of VM on matrigel and inhibition of VM with αEGFR-E-P125A.
Gene set enrichment analysis demonstrated that αEGFR-E-P125A treatment significantly downregulated genes in the JAK-STAT and angiogenesis signaling pathways. Phospho-array analysis demonstrated decreased EGFR phosphorylation at Y1069 in addition to decreased phosphorylation of FAK Y397 and STAT3 Y705 sites downstream of α5β1 integrin. Since inhibition of EGFR signaling alone did not inhibit VM, and endostatin is a known ligand of α5β1 integrin, we focused on effects of αEGFR-E-P125A on inhibition of α5β1 integrin/FAK signaling pathway. Independent siRNA knockdowns of α5 integrin and FAK in MDA-MB-231-4175 cells confirmed that downregulation of α5 integrin/FAK signaling inhibited VM *in vitro*.
αEGFR-E-P125A additionally prevented EGF-induced EGFR phosphorylation and fibronectin-induced FAK phosphorylation by α5β1 integrin. Treatment of TNBC cells with αEGFR-E-P125A reduced total α5 integrin protein levels and decreased co-localization of EGFR and α5β1 integrin receptors. These results indicate that αEGFR-E-P125A suppressed both EGFR and α5β1 integrin signaling. Simultaneous inhibition of EGFR and α5β1integrin signaling by αEGFR-E-P125A fusion is a promising approach to inhibition of TNBC growth and metastases.

#6320

CUSP06/AMT-707, a new CDH6-targeting antibody-drug conjugate, demonstrates potent antitumor activity in preclinical models

Wei Lu[1], Jing Shi[2], Shu-Hui Liu[2], Nicole Covino[1], Xun Meng[2], Eric D. Slosberg[1]. *[1]OnCusp Therapeutics, Inc., New York, NY,[2]Multitude Therapeutics Inc., Shanghai, China*

Cadherin-6 (CDH6), also known as K-cadherin, is a type II classic cadherin molecule that plays an important role in the embryonic development of the kidney, but has very limited expression in adult tissues. It is overexpressed in several human malignancies, primarily in ovarian, renal, but also (to a lesser degree) gastric, thyroid, cholangiocarcinoma and other tumor types.

The characteristics of limited expression in normal tissues, high expression in tumor tissues, and rapid internalization upon antibody binding makes CDH6 a well-suited Antibody-drug Conjugate (ADC) target. We developed a novel CDH6-targeting ADC, CUSP06, consisting of a proprietary humanized antibody selective for CDH6, a protease cleavable linker, and an exatecan payload, with a drug-to-antibody ratio (DAR) of 8. CUSP06 selectively bound to cell surface CDH6 and was efficiently internalized into CDH6 positive ovarian and renal cancer cells. CUSP06 exhibited strong antiproliferative activity against several CDH6 positive cancer cell lines *in vitro*. Furthermore, compared to a DXd-based ADC, a exatecan-based ADC demonstrated improved bystander effect. Treatment with CUSP06 resulted in tumor regression in several CDH6 positive cell line derived xenograft (CDX) models, including PA-1, OVCAR3, and 786-O. In addition, CUSP06 demonstrated potent antitumor activity with tumor regression observed in two CDH6 low and high expressing patient derived xenograft (PDX) models. The preclinical activity of CUSP06 against CDH6-expressing tumors provide compelling support for the clinical development of CUSP06 in CDH6-expressing human cancers. CUSP06 is currently in IND-enabling studies. CUSP06 showed an expected toxicity profile consistent with it's exatecan payload in the ongoing pilot toxicology studies. We plan to initiate a Phase 1 first-in-human clinical trial in the 2nd half of 2023.

#6321

HMPL-453, a highly selective inhibitor of fibroblast growth factor receptors 1, 2, and 3, displays potent activity in FGFR-altered tumor models

Jia Hu, Jun Ni, Longxian Jiao, Jinghong Zhou, Shiming Fan, Renxiang Tang, Wei Zhang, Xuelei Ge, Qihang Zhang, Juntao Yu, Ying Yu, Dongxia Shi, Min Cheng, Weifang Xue, Sumei Xia, Zeyu Zhong, Jian Wang, Yang Sai, Weiguo Qing, Guangxiu Dai, Yongxin Ren, Michael Shi, Weiguo Su.
HUTCHMED Limited, Shanghai, China

Background: Fibroblast growth factors (FGFs) and their receptors (FGFRs) regulate numerous cellular processes. Dysregulation of FGFR signaling due to receptor fusion, mutation or amplification is observed across multiple cancer types, making activated FGFRs an important therapeutic target.

Herein, we present the preclinical characterization of HMPL-453, a highly potent and selective inhibitor of FGFR1, 2, and 3, discovered and being currently developed in phase II clinical trial (NCT04353375) by HUTCHMED.
Methods: Kinase activity was measured by Transcreener™ Fluorescence Polarization assay or Z'-LYTE kinase assay. *In vitro* anti-proliferation activity was measured by CellTiter-Glo luminescent or CCK-8 assay. The effect of HMPL-453 on FGFR signaling pathway was detected by western blot. Multiple tumor models with FGFR alteration were applied in Nu/Nu nude mice to determine anti-tumor efficacy of 453 as a single agent. A model in immune-competent BALB/c mice inoculated with the constructed NIH/3T3 cells carrying FGFR2-AHCYL1 fusion was chosen to investigate the combination effect of HMPL-453 with anti-PD-1 antibody.
Results: HMPL-453 potently inhibited the tyrosine kinase activities of recombinant FGFR 1, 2, and 3 *in vitro* (IC_{50} values of 6, 4, and 6 nM, respectively) with weaker activity against FGFR4 (IC_{50} = 425 nM). HMPL-453 selectively inhibited proliferation of tumor cell lines with dysregulated FGFR signaling (GI_{50}s: 3~105 nM) compared with cell lines lacking FGFR aberrations (GI_{50}s > 1.5 μM). HMPL-453 demonstrated strong inhibition of phosphorylation of FGFR and downstream protein in tumor cell lines harboring FGFR2 fusion. Oral administration of HMPL-453 could induce time- and dose-dependent inhibition of phosphorylation of FGFR and resulted in remarkable and dose-dependent anti-tumor activity in multiple FGFR-altered tumor models. HMPL-453 at the dose of 50 mg/kg/day could induce tumor regression in most tumor models tested. Moreover, HMPL-453 significantly improved anti-tumor activity of anti-PD-1 antibody in a FGFR2 fusion model by priming the immune environment.
Conclusion: HMPL-453 is a highly potent and selective inhibitor of FGFR 1, 2, and 3 with strong activity against FGFR-deregulated tumors in preclinical models, supporting continued investigation in patients with FGFR alterations (such as fusion and mutation) either as a single agent or in combination with PD-1 blockade.

IMMUNOLOGY

Anticancer Immunotherapeutics

#6325

A novel EGFR x MUC1 bispecific antibody-drug conjugate, BSA01, targets MUC1 transmembrane cleavage products and improves tumor selectivity

Yifu Zhang, Chenzhang Shang, Anqi Wang, Jia Zhang, Yuji Liu, Hao Li, Xiaopeng Li, Gao An, Li Hui, Frank An, Yi Yang. *Biocytogen Pharmaceuticals (Beijing) Co., Ltd, Beijing, China*

Epidermal growth factor receptor (EGFR) and mucin 1 (MUC1) are tumor-associated antigens that are highly co-expressed in esophageal squamous cell carcinomas, non-small cell lung cancers (NSCLC), and triple negative breast cancers, among others. MUC1, a glycoprotein essential for the formation of the epithelial mucous barrier, is hypoglycosylated and dimerizes with EGFR, a potent oncoprotein, in transformed cells. Dual-targeting of both tumor-associated antigens (TAAs) represents a promising therapeutic strategy to treat common malignancies. We generated a fully human anti-EGFR/MUC1 bispecific antibody-drug conjugate (BSA01) from RenLite® humanized, common light chain mice. BSA01 is conjugated with Monomethyl auristatin E (MMAE). BSA01 targets the extracellular domain of MUC1-C (C-terminal domain of MUC1), which is the membrane-bound MUC1 cleavage product that remains after MUC1 is cleaved, providing more access to the tumor antigen *in situ*. In addition, we generated affinity and internalization optimized binders targeting EGFR that increases the tumor selectivity, to avoid potential skin toxicity due to ubiquitous basal EGFR expression. Internalization assays demonstrate that the anti-EGFR/MUC1 bispecific antibody used to generate BSA01 was endocytosed in tumor cells co-expressing EGFR/MUC1 more efficiently than mono- or bivalent antibodies targeting EGFR or MUC1 alone. When conjugated with payload, BSA01 also exhibited strong anti-tumor efficacy *in vitro* against gastric, NSCLC and pancreatic cancer cell lines. Moreover, BSA01 showed similar activity *in vivo*, effectively inhibiting tumor growth in multiple cell-derived xenograft and patient-derived xenograft models. These results suggest that BSA01 has great clinical potential for treating tumors co-expressing EGFR and MUC1.

#6326

Discovery & preclinical evaluation of BPB-101: A novel triple functional bi-specific antibody targeting GARP-TGFβ complex/SLC, free TGF-β and PD-L1

Wenxin Xu, Jieying Xu, Deyu Xu, Hongjie Cheng, Li Zhang, Huan Zheng, Siyuan Ye, Mengshi Jiang, Jiabing Wang, Lieming Ding. *Betta Pharmaceuticals Co.,Ltd, Hangzhou, China*

Background: Recent studies on tumor microenvironment (TME) have been conferred considerable attention, especially the transforming growth factor-β (TGF-β) signal axis and the PD-L1/PD-1 signal axis. TGF-β is a crucial enforcer in promoting tumor cells angiogenesis, plasticity, fibrosis, and in regulating immune homeostasis and tolerance. The TGF-β signaling controls innate and adaptive immunity in TME by inhibiting the activity of natural killer (NK) cells and effector T cells, while promoting the expansion of regulatory T cells (Tregs). Many studies have revealed that free TGF-β mainly released from glycoprotein A repetitions predominant (GARP)-TGFβ complex at the surface of activated Tregs, B, NK, and tumor cells. Existing antibodies or fusion proteins targeting TGF-β cannot simultaneously block the TGF-β releasing and naturalized free TGF-β in TME, thus limiting the anti-tumor effect. Herein, we designed a bi-specific antibody named as BPB-101 with triple functions: specifically target GARP-TGFβ complex and/or small latent complex (SLC), free TGF-β, and PD-L1. BPB-101 can stop tumor expansion and recruitment, and may enhance the immune effector cells to eliminate the tumor.

Methods: An anti-GARP mAb was discovered using a hybridoma platform and selected for binding with GARP-TGFβ complex/SLC and free TGF-β. An anti-PD-L1 nAb was screened out by VHH library and optimized in tumor-bearing mice. After humanizing, these two antibodies were successfully assembled to form a unique bi-specific antibody, BPB-101. The binding affinity of BPB-101 to GARP-TGFβ complex/SLC, free TGF-β and PD-L1 was determined by ELISA, FACS and SPR/BLI. Report gene assay was utilized to detect the blocking activity of BPB-101. The TGF-β secretion from activated Tregs was also analyzed. Finally, the anti-tumor efficacy of BPB-101 was assessed with a transgenic mouse model (B6-hLRRC32). To address the biosafety risks, the nonclinical safety profile was also evaluated in cynomolgus monkeys.

Results and Conclusion: BPB-101 is a high-affinity antibody aims to reverse immunosuppressive TME by triple-targeting functions. The blocking ability of TGF-β in not only latent form but also free form makes our BPB-101 distinct from M7824, any other existing anti-TGF-β mAbs and anti-GARP mAbs. In a MC38-hPD-L1 tumor-bearing B6-hLRRC32 model, BPB-101 showed significant tumor growth inhibition of 93 % at the dose of 5 mg/kg ($p<0.001$), showing superior efficacy to monoclonal antibody alone or in combination with anti-PD-L1 nAb. In addition, BPB-101 showed durable responsiveness and a splendid safety profile with manageable adverse events. These striking results support the clinical development potential of our trifunctional agent as a monotherapy and in combination with other immunotherapies.

#6327

Intratumoral administration of ultra high-concentration nitric oxide (UNO) is more efficacious than anti-PD1 therapy in 4T1 tumor-bearing mice

Yana Epshtein[1], Matan Goldshtein[1], Selena Chaisson[2], Jedidiah Monson[2], Matt Johnson[2], Amir Avniel[3], Steve Lisi[4], Hila Confino[1]. *[1]Beyond Cancer, Rehovot, Israel,[2]Beyond Cancer, Atlanta, GA,[3]Beyond Air, Ltd., Rehovot, Israel,[4]Beyond Air, Inc., Garden City, NY*

Background: For the majority of metastatic triple-negative breast cancer (mTNBC) patients, chemotherapy is the standard first-line treatment, however, outcomes in this population are poor. A monoclonal antibody against the immune checkpoint inhibitor anti-programmed death 1 (PD-1) also has antitumor activity in patients with mTNBC. Previously, we reported that delivering ultra-high concentrations of nitric oxide (UNO) to mouse colon tumors stimulated innate and adaptive immune responses leading to the rejection of secondarily-induced tumors. Moreover, adding an anti-PD-1 antibody to UNO treatment resulted in primary tumor regression in 53% of the mice, the rejection of a distant tumors in all mice, and prolonged survival compared to control and anti-PD-1 arms. In this *in vivo* study, we investigated the ability of UNO to improve the efficacy of anti-PD-1 antibody treatment in the aggressive mouse breast cancer model, 4T1. Methods: We tested two treatment protocols: 4T1 mice tumors were treated with either a single dose of UNO and anti-PD-1 or a repeated dose of UNO

and anti-PD-1. In the single dose design, 4T1 tumors were treated with a single administration of UNO combined with Anti-PD1 administration starting one day after UNO treatment (n=9-10 mice per group). In the repeated dosing design, 4T1 tumors were treated with UNO twice combined with Anti-PD-1 administration starting on the first UNO treatment day (n=8 mice per group). • UNO treatment regimen: 50,000 ppm, 10 minutes, flow rate ~0.2 liters per minute • Anti-PD1 treatment regimen: 10 mg/kg antibody was administered every 3 days for a total of 5 treatments.
Results (UNO Single Dose): The primary tumors of 4T1 tumor-bearing mice were 13.2% smaller in the combined single-dose UNO group compared to anti-PD-1 alone 15 days post-UNO treatment.
Results (UNO Repeated Dosing): The primary tumors of 4T1 tumor-bearing mice were 25.2% smaller in the combined repeated dose UNO group compared to the anti-PD-1 alone group 16 days after the first UNO treatment.
Conclusion: Treating 4T1 tumors with single and repeated doses of UNO improved outcomes compared to anti-PD-1 alone. This suggests that local short-term treatment with UNO can serve as a treatment option for cancer patients with tumors that are not amenable to immune checkpoint inhibitor treatment.

#6328

An off-the-shelf Twin BiTE combination therapy controls heterogenous glioblastoma and shapes immune response

Filippo Rossignoli, Paulo Borges, Rebecca Lumia, Khalid Shah. *Harvard Medical School/Brigham and Women's Hospital, Boston, MA*

Glioblastoma (GBM) is the most common primary brain tumor in adults, characterized by a median survival of 12-14 months with less than 10% of patients surviving at least 2 years from diagnosis. The discovery of tumor-associated antigens (TAAs) has permitted development of a new array of therapeutic strategies that selectively target GBM and spare normal cells of the CNS. In this study we used an alternative off-the-shelf approach to activate the immune system and direct it against the tumor, taking into account antigen heterogeneity and TME immune suppression without the need of engineering the patient’s immune cells. We generated TAA-targeting Bispecific T-cell Engagers (BiTEs) and engineered adult stem

cells to secrete twin BiTEs (T-BiTE-SC). The approach was tested in combination with in naïve T cells on established and primary patient-derived cell lines expressing various levels of the target antigens. Moreover, to further support the therapeutic action of T cells, and combat immune-suppressive microenvironment and exhaustion, we combined our T-BiTE SC with an immune-stimulating cytokine. We show the efficacy of the individual BiTEs against different primary and established tumor cell lines. Moreover, the T-BiTE-SC, significantly controlled the growth of a tumor expressing heterogeneous levels of the targeted antigens. The immune stimulation reduced T cell exhaustion and consolidated a Th1 phenotype. Altogether our study demonstrated the feasibility and efficacy of an off-the-shelf immunotherapy, based on BiTEs simultaneously targeting tumor heterogeneity without the need for direct engineering of the immune cells.

#6329

Preclinical study of CD19 detection methods using monoclonal antibodies post tafasitamab treatment

Kristina M. Ilieva[1], Markus Eberl[1], Jan Jaehrling[1], Carmen Ginzel[1], Britta Voland[1], Michaela Zankl[1], Andrea Polzer[1], Derek Blair[1], Rainer Boxhammer[1], Liang-Chuan Wang[2], Diana Alvarez Arias[2], Christina Heitmüller[1]. *[1]MorphoSys AG, Munich, Germany,[2]Incyte Corporation, Wilmington, DE*

Introduction Tafasitamab (TAFA), an Fc-enhanced antibody immunotherapy against CD19 received accelerated/conditional approval in relapsed or refractory diffuse large B cell lymphoma (R/R DLBCL) in combination with lenalidomide. Several other CD19 targeting therapies including CAR Ts are now available for R/R DLBCL treatment warranting evaluation of potential therapeutic sequencing strategies. In this context, CD19 expression status may be assessed on patient samples post TAFA treatment. However, methods for detecting CD19 using monoclonal antibodies (mAbs) following TAFA treatment are not standardized which may lead to data misinterpretations including confusion of CD19 epitope masking with CD19 loss or downregulation.
Aim This study evaluated various CD19 detection methods following TAFA treatment using comprehensive panels of available flow cytometry

(FC) and immunohistochemistry (IHC) anti-CD19 mAbs, routinely used in laboratory practice.
Methods FC and IHC competition assays were used on TAFA pre-treated CD19+ cell lines to differentiate non-competing from competing mAbs, the latter resulting in epitope masking by TAFA. Bound TAFA was removed from CD19+ cells using an acidic dissociation protocol. Antibody affinities for CD19 were determined using Surface Plasmon Resonance (SPR) or Bio-Layer Interferometry (BLI).
Results All but one of the 8 mAbs tested in FC competed with TAFA and their affinities for CD19 were shown to be lower than that of TAFA. The non-competing clone OTI3B10, reported to recognize a linear epitope of CD19 (1), bound to only one of three tested CD19+ cell lines, which rendered it unsuitable for reliable FC detection of CD19. In contrast, several clones could detect CD19 on TAFA pre-treated samples using IHC. To circumvent TAFA masking in FC, we successfully unmasked CD19 via acidic dissociation and similar CD19 levels on TAFA pre-treated as on untreated cells could be subsequently detected by a competing CD19 antibody (HIB19).
Conclusion Our study provides an overview of commonly used mAb tools for CD19 detection post TAFA treatment, some of which may be used in routine clinical practice. Our findings reveal that CD19 expression post TAFA could be detected by IHC but lack of TAFA non-competing anti-CD19 antibodies for FC poses a risk of mistaking CD19 masking by TAFA with CD19 loss or downregulation. Prior acidic dissociation is critical in the staining protocol to avoid data misinterpretations.
1. Klesmith et al, 2019, Biochem.

#6330

Countering antidrug antibodies to programmed cell death-1 blockade in mouse *Pten*-null prostate cancer

Marco A. De Velasco[1], Yurie Kura[1], Noriko Sako[1], Naomi Ando[1], Kazutoshi Fujita[1], Mitsuhisa Nishimoto[1], Kazuko Sakai[1], Kazuhiro Yoshimura[1], Masahiro Nozawa[1], Scott A. Hammond[2], Simon J. Dovedi[3], Barry R. Davies[3], Kazuto Nishio[1], Hirotsugu Uemura[1]. *[1]Kindai University School of Medicine, Osaka-Sayama, Japan,[2]AstraZeneca, Gaithersburg, MD,[3]AstraZeneca, Cambridge, United Kingdom*

Therapeutic biologics have the potential to elicit immune responses that results in the development anti-drug antibodies (ADAs). ADAs that develop after immune checkpoint blockade (ICB) limit their therapeutic efficacy and increase the risk of adverse events. Mitigating ADAs would improve the efficacy of antibody-based therapeutics and identifying reliable biomarkers would allow for rational, evidence-based criteria for tailoring treatments. However, detecting ADAs is challenging and data regarding their biology and means to counter this phenomenon are limited. Here, we examined the development of ADAs to anti-programmed cell death-1 (PD-L1) monoclonal antibodies in a mouse model *Pten/Trp53*-null (DKO) prostate cancer and countered their negative effect with systemic administration of a JAK1/2 inhibitor. Like human prostate cancer, adding PD-L1 ICB to androgen deprivation therapy has failed to produce a therapeutic effect in DKO cancer model. Our analysis showed that tumor-bearing DKO mice have increased levels of peripheral dendritic cells (pDC) of which >80% exhibited high levels of PD-L1. Given this finding, we developed a system to monitor the development of ADAs against two murine anti-PD-L1 (aPD-L1) monoclonal antibodies clone 80 and 10F9.G2. Pharmacodynamic studies showed that a single-dose administration of the blocking antibodies effectively neutralized PD-L1 in pDC that lasted for four days. Chronic (twice/week) dosing of the aPD-L1 antibodies strongly neutralized PD-L1 in pDCs, but the efficacy waned after 22 days. Using crossover approach, consisting of clone 10F9.G2 dosing for two weeks followed by clone 80, extended PD-L1 blockade in pDCs to 36 days, but did not improve antitumor activity. Blocking STAT3 signaling with the JAK1/2 inhibitor AZD1480 restored PD-L1 blockade in pDCs and was associated with improved reduction of tumor burden. Further analysis showed improved neutralization of PD-L1 in cancer cells and tumor infiltrating immune cells in mice treated with AZD1480. These effects were associated with greater T and NK cell reactivity in tumors. Our study shows that the presence of ADAs is associated with lack of antitumor responses to ant-PD-L1 blockade in a preclinical model of prostate cancer and provides additional data that will improve our understanding of ADAs against immune checkpoint inhibitors. This study also offers an approach to monitor ADA development and a platform to investigate novel approaches to target ADAs.

#6331

The anti-tumor activity of HSP-90 therapeutic cancer vaccine (AST-021p) combine with TLR2/3 agonist in a MMTV-neu transgenic model

JinHo Kang[1], Jee Hyun Choi[1], Min Ji Seo[2], Eunjung Jung[3], Byung cheol Ahn[3], Jinback Lim[1], Hyo-Hyun Park[1], Hyunwon Shin[2], Eunkyo Joung[2], Hun Jung[2], Kyong Hwa Park[4]. *[1]Aston Research Institute, Hanam, Korea, Republic of,[2]Aston Sci. Inc., Seoul, Korea, Republic of,[3]R&D Center, CHA Vaccine Institute, Seoul, Korea, Republic of,[4]Department of Internal Medicine, Korea University College of Medicine, Korea, Korea, Republic of*

Background: AST-021p, which is derived from HLA class II binding epitopes of human HSP90 protein, is an investigational therapeutic cancer vaccine for the malignant neoplasms. AST-021p is designed to demonstrate the immunologic efficacy by activating antigen-specific CD4+ Th1 cell in humans. Due to their ability to link the innate with the adaptive immune response, Toll-like receptor (TLR) agonists are highly promising as adjuvants in vaccines against life-threatening and complex diseases such as cancer, AIDS and malaria. In this study, AST-021p was investigated to evaluate the immunogenicity and tumor growth inhibitory effect under the condition of combining with various immune adjuvants derived from TLR agonists, using in-vivo model.

Methods: Three different agonists of TLR (TLR-4, TLR-2/3, TLR-7/8) were assigned to investigate the immunogenicity in each group (4 FVB/N mice/group, total 4 groups). AST-021p was intradermally injected 3 times with different TLR-agonists and the immunogenicity was assessed from mouse splenocyte by HSP90-specific IFN-γ ELISpot method. We also examined the efficacy of AST-021p and selected TLR-agonist in MMTV/neu Tg mice (4 mice/group, conducted twice and A total 8 mice was assigned to each group). The combination of AST-021p and TLR-2/3 agonist (AST-021p plus TLR-2/3 agonist) was injected 3 times every 10 days to mice followed by inoculated mouse mammary cancer cell line. The tumor volume change and immunogenicity were evaluated.

Results: The most effective TLR-agonist as a potent immune adjuvant was a TLR-2/3 agonist (L-pampoTM, supplied by CHA Vaccine Institute). AST-021p (100 μg) plus TLR-2/3 agonist significantly improved immunogenicity by increasing HSP-90 epitope-specific T cells up to 130±10 per $1x10^5$ spleen cell of FVB/N mice (P<0.001). AST-021p plus

TLR-2/3 agonist also showed higher tumor growth inhibitory effect (170±108 mm^3) on post-implantation 35^{th} day by suppressing mouse mammary cancer cell line ($5x10^5$)-derived tumor growth, compared with a TLR-2/3 agonist alone (1031±450 mm^3).
Conclusions: Combination regimen of AST-021p and TLR-2/3 agonist (as immune adjuvant) demonstrated significant immunogenicity and tumor prevention effect in in-vivo study. These data supported the clinical study of AST-021p combined with TLR-2/3 agonist as active immune adjuvant in certain tumor types, and phase 1/2 clinical program would be expected to be initiated.

#6332

A humanized anti-cd40 antibody with anti-tumor pharmacological activity and cynomolgus monkey safety

Zhenyu Li, Lili Zhao, Guimin Zhang, Bin Li, Zhong Liu, Guangyan Li, Zhongsong Zhu. *National Engineering Laboratory of High Level Expression In Mammalian Cells, Lunan Pharmaceutical Group Co. Ltd., Linyi, China*

LNF1901 is a humanized CD40 agonistic antibody. LNF1901 can bind to CD40 protein of human(EC50=23.6ng/mL) and monkey(EC50=23.5ng/mL), but cannot bind to CD40 protein of rat and mouse. LNF1901 had strong activation effect on DC cells(EC50=0.04ug/mL) and had strong ADCC and CDC effects. AT a dose of 20mg/kg, the TGI_{TW} of LNF1901 was 59.9% in Female NPG mice were inoculated with Raji/CIK/DC subcutaneous transplanted tumor model. Following intravenous infusion of LNF1901 at doses of 6, 30, or 150 mg/kg to cynomolgus monkeys weekly for 4 weeks, the highest non-severely toxic dose (HNSTD) was considered to be 150 mg/kg.LNF1901 had demonstrated manageable safety and promising antitumor activity in vivo and in vitro tests.

#6333

Repurposing NSAIDs for chemo-immunotherapy: mechanisms beyond COX inhibition

Ogacheko D. Okoko[1], Md Y. Gazi[2], Xin Wang[2], Caitlin Brandle[2], Mercy Kehinde-Ige[2], Gary A. Piazza[3], Huidong Shi[2], Gang Zhou[2]. *[1]Molecular Medicine, Augusta University, Augusta, GA,[2]Georgia Cancer Center, Augusta University, Augusta, GA,[3]Department of Drug Discovery and Development, Auburn University, Auburn, AL*

It has been well-established that some nonsteroidal anti-inflammatory drugs (NSAIDs) have antitumor activities. The beneficial effects of these NSAIDs are mainly attributed to their ability to inhibit the production and activity of cyclooxygenases (COX1 and COX2) and prostaglandin (PGE2), which are known to promote tumor progression, angiogenesis, metastasis and immunosuppression. We recently reported that administration of indomethacin, a prototypical NSAID, can enhance the antitumor efficacy of adoptive T cell therapy in animal models. However, currently adoptive T cell therapy as a treatment option is only suitable for selected patients with certain types of cancer. Here, we set out to explore the utility of indomethacin in a chemo-immunotherapy setting that is readily applicable to a wide range of cancers. Cyclophosphamide (CTX) is a widely used antineoplastic chemotherapeutic agent with immunostimulatory activities when used at low-medium doses. We show that indomethacin had no impact on tumor growth but can significantly enhance the antitumor effect of CTX in multiple mouse tumor models. The beneficial effect of indomethacin was diminished in immunodeficient mice or CD8 T cell-depleted wild-type mice, indicating the requirement for the host immunity. Furthermore, the CTX and indomethacin regimen can sensitize tumors to anti-PD1 immunotherapy. scRNAseq analysis of tumor samples revealed the impact of indomethacin on the tumor microenvironment. Our data also indicate that the immunopotentiating effect of indomethacin can be independent of PGE2 inhibition, and involves the TRAIL-DR5 axis in promoting tumor regression. Other potential mechanisms, including modulation of chronic interferon signaling in tumor cells, have also been investigated. Altogether, our study sheds light on the multiple mechanisms underlying indomethacin's beneficial effects, and highlights the potential of NSAID administration as a readily applicable and cost-effective approach to augment the efficacy of chemo-immunotherapy.

#6334

VBI-002, a CD47xICAM-1 bispecific antibody for the treatment of hepatocellular carcinoma, melanoma and non-small cell lung cancers

Oi Kwan Wong, Xinhua Wang, Leonard Post, Xiaocheng Chen. *Virtuoso Therapeutics, Inc., San Mateo, CA*

Intercellular Cell Adhesion Molecule 1 (ICAM-1, CD54) is a type I transmembrane protein and a member of the immunoglobulin superfamily. ICAM-1 is involved in many key processes such as cell-cell interactions, signal transduction and leukocytes trans-endothelial migration. ICAM-1 is constitutively present at low levels on healthy tissues but highly expressed in some hematological cancers and solid tumors, making it an attractive tumor target.

VBI-002 is a novel human IgG1 based CD47xICAM-1 bispecific antibody with excellent safety profile and potent single agent activities in xenograft models of lymphoma, multiple myeloma and some solid tumors (Cancer Res 2022;82(12_Suppl):Abstract nr 3430). The bispecific design allows VBI-002 to selectively block CD47/SIRPα binding in tumor cells with high ICAM-1 expression. In contrast to the benchmark CD47 monoclonal antibody, VBI-002 exhibits minimal red blood cell binding and does not cause hemagglutination. In non-human primate (NHP) safety study, four weekly doses of 60 mg/kg VBI-002 were well-tolerated with only mild and reversible reduction in hemoglobin and platelets.

Here we further investigate the anti-tumor activities of VBI-002 in solid tumors. Gene expression analysis suggested that ICAM-1 is highly expressed in non-small cell lung cancers (NSCLC), melanoma and a subset of hepatocellular carcinoma. Flow cytometry studies confirmed the frequent co-expression of ICAM-1 and CD47 in these tumors. VBI-002 has potent ICAM-1 dependent SIRPα blocking, antibody-dependent cellular phagocytosis and antibody-dependent cellular cytotoxicity activities against cell lines of NSCLC, hepatocellular carcinoma, and melanoma. Furthermore, *in vivo* efficacy studies demonstrated that VBI-002 has potent single agent activities in cell line derived xenograft (CDX) models of NSCLC, hepatocellular carcinoma, and melanoma. Weekly dose of 20 mg/kg VBI-002 is sufficient to stop tumor growth or drive tumor regression in most models. Notably, VBI-002 is highly effective against NSCLC CDX models carrying Kras mutation and it synergizes with paclitaxel to provide additional anti-tumor activity. In conclusion, VBI-002 is a versatile novel

CD47xICAM-1 bispecific antibody with potent single agent activity in various solid tumors and combined well with standard of care chemotherapies for added activity. Thus, VBI-002 warrants clinical evaluations as a single agent and in combination with standard of care chemotherapies.

#6335

Developing anti-IL-22 therapeutics for inflammation and cancer

Christina Wheeler[1], Jian Chen[1], Cathy Chang[1], Gerhard Frey[1], Haizhen Liu[1], Jing Wang[1], Kathryn Woodard[1], Solmarie Joyner[1], Wei Zhou[1], William J. Boyle[2], Jay M. Short[2]. *[1]R&D, BioAtla, Inc., San Diego, CA,[2]BioAtla, Inc., San Diego, CA*

Chronic inflammation facilitates the development of cancer, age-related, inflammatory autoimmune and other diseases. Proinflammatory cytokines play a central role in this pathogenic process by driving activation of NF-ƙB, STAT3 and other signaling cascades. IL-22 is an inflammatory cytokine involved in the pathology of autoimmune diseases such as psoriasis, atopic dermatitis, and ulcerative colitis. IL-22 has also been shown to promote epithelial cell proliferation, stemness and tumorigenesis in cancer. Recent studies demonstrated that neutralization of IL-22 reduced dysplasia and tumor development in preclinical models. To date, there has not been a clear application for anti-IL-22 therapy for autoimmune diseases and cancer, likely due to identifying the right disease indication and to their low potency and low efficacy. Thus, there remains an opportunity to explore the potential of more potent anti-IL-22 therapeutics. Using BioAtla's proprietary antibody discovery and engineering platforms, we have generated humanized anti-IL-22 antibodies with high affinities to human, cynomolgus and mouse IL-22. *In vitro* data demonstrated that our anti-IL-22 antibodies inhibited IL-22-induced p-STAT3, CXCL-1 and IL-10 activities. In addition, our antibodies showed a 10-fold increased binding activity to human IL-22 compared to Fezakinumab, which was previously developed by Pfizer for the treatment of autoimmune diseases. BioAtla's high affinity anti-IL-22 antibodies were shown to be more potent relative to Fezakinumab using multiple *in vitro* assays. To test the functions of our antibodies *in vivo*, we also established mouse models to determine anti-IL22 efficacy. More specifically, to study whether targeting IL-22 in an

inflammation-induced tumor microenvironment reduces tumor occurrence, we developed an inflammation-driven sporadic colitis-associated colorectal cancer mouse model for ongoing cancer studies that will be discussed. In addition, we evaluated our anti-IL22 antibodies in an imiquimod-induced psoriasiform skin inflammation mouse model. The mice treated with potent anti-IL-22 antibodies had significantly reduced skin lesions, including erythema, scales, and skin thickness compared to isotype antibody-treated mice. Q-PCR analysis of the mouse skin demonstrated that treatment with our anti-IL-22 antibody led to significantly decreased RNA levels of the imiquimod-induced inflammatory marker CXCL3. Thus, the enhanced anti-IL-22 therapy is a promising strategy for targeting anti-inflammation in autoimmune diseases, such as psoriasis and atopic dermatitis, and inflammatory cancers, including colorectal cancer. In conclusion, the development of a potent, species cross reactive anti-IL-22 antibody using BioAtla's antibody discovery and engineering platforms addresses the challenges of anti-IL-22 therapeutics and allows for translational studies in relevant animal efficacy and safety models.

#6336

Heterodimeric Fc-fused IL12 shows potent antitumor activity and low toxicity

Yang Huang[1], Wenting Liu[2], Dayan Zhang[2], Pengfei Zhou[2], Weiming Zhou[2], Xiaoli Zeng[2], Qun Zhao[2], Liangwei Li[3], Guodong Shen[4], Liansheng Cheng[2]. *[1]Georgetown Lombardi Comprehensive Cancer Ctr., Atlanta, GA,[2]Hefei Hankemab Biotechnology Co., LTD, Hefei, China,[3]Georgia State University, Atlanta, GA,[4]The First Affiliated Hospital of University of Science and Technology of China, Hefei, China*

Background: Interleukin-12 (IL12) is a heterodimeric pro-inflammatory cytokine (70 kDa) composed of two different polypeptide chains: an α-chain (p35 subunit) and a β-chain (p40 subunit). IL12 could induce the proliferation and cytotoxicity of T and NK cell and production of interferon-γ (IFN-γ), promote the differentiation of T helper 1 (TH1) cells and regulate innate resistance and adaptive immunity. However, the clinical efficacy of IL12 has been hindered for its high dose-related toxicities and short serum half-life. Here we have developed a heterodimeric Fc-fused

IL12, HK054-V, with reduced potency to improve tolerability and prolong half-life.
Methods: We assessed the binding, bioactivity, anti-tumor efficacy and safety of HK054-V. The binding ability of IL12-Fc lead variants to activated PBMCs was analyzed by flow cytometry. The bioactivity of HK054-V was determined by assessing the activated T-cell proliferation and IFN-γ production in human PBMCs, and STAT-4 phosphorylation in a reporter gene assay. A murine surrogate, mHK054-V, was engineered to mimic HK054-V to evaluate the antitumor efficacy in MC38 and CT26 syngeneic tumor mouse models. Cytokine release assay was conducted by incubating HK054-V with peripheral blood mononuclear cells (PBMCs) from healthy donors. The safety profiles and pharmacokinetic (PK) behavior of HK054-V were characterized in non-tumor-bearing Balb/c mice.
Results: HK054-V is a heterodimeric Fc-fused IL12, which was designed with reduced potency. HK054-V was observed to stimulate the proliferation of activated T cells and NK cells and induce production of IFN-γ in a dose-dependent manner. HK054-V could activate pSTAT4 signal in luciferase reporter gene assay and showed up to 100-fold reduction of potency compared to wild-type IL12-Fc. Human IL12 is inactive in mice, so in vivo anti-tumor activity was assessed by a murine surrogate, mHK054-V. mHK054-V demonstrated anti-tumor efficacy in syngeneic mouse models and was better tolerated than WT mIL12-Fc. Furthermore, mHK054-V has improved PK and therapeutic index in mice.
Conclusion: These data demonstrate that HK054-V, a heterodimeric Fc-fused IL12 with reduced potency, retain strong anti-tumor efficacy with a favorable tolerability profile, which may provide a practical alternative to the systemic administration of IL12 for antitumor therapy.

#6337

Tri-specific CD3 x HER2 x HER2 antibodies in 1:2 format recognizing two different epitopes on HER2 demonstrate selective activity on human cancer cells with high HER2 expression

Jie Zhang, Xiaoqing Wang, Zhenhao Zhou. *Chimagen Biosciences, Shanghai, China*

Human epidermal growth factor receptor 2 (HER2) is a membrane tyrosine kinase that was found to be amplified and overexpressed in various human cancers including breast cancer. Monoclonal antibodies targeting HER2 such as trastuzumab and pertuzumab provide good therapeutic benefits in patients with high HER2 expression tumors, however, not all patients respond to the treatment, and many suffer recurrence. There is still a large unmet need for targeted therapies to treat HER2 high expression tumors. T cell engaging antibodies that direct T cells to kill cancer cells by simultaneously binding to CD3 on T cells and tumor-associated antigens (TAA) on cancer cells have emerged as a promising new approach. Such therapeutics are potent, but safe use of them depends on selectivity of the TAA engaged. Though HER2 is highly overexpressed in ~ 20% of breast cancer, expression of HER2 is not restricted to cancer cells and present at low level in normal tissues. The capability of selectively targeting cancer cells over HER2 low expressing normal tissues is critical to the safety of CD3 x HER2 antibodies. It is noteworthy to mention that unlike antibody-drug conjugate (ADC) therapeutics, CD3 x HER2 antibodies might not be a good approach to target HER2 low/neg expression tumors due to the difference in mechanism of action.

CMG6A19 is a 150 kD IgG-like tri-specific CD3 x HER2 x HER2 T cell-engaging antibody generated on Chimagen's TRIAD platform. It is capable of simultaneously recognizing and binding to two different epitopes on HER2 proteins. Multiple human cell lines with different levels of HER2 expression were used as targets in the antibody-mediated hPBMC killing assays in vitro and in vivo, among which SK-BR-3, KPL-4 and BT474 have high HER2 expression as seen in HER2 positive cancers, HT55 and JIMT1 have medium level of HER2 expression, and PC3 and MCF7 have HER2 expression level that is close to in normal tissues. Conventional 1:1 IgG-like CD3 x HER2 bispecific antibodies were used as control. Results showed that CMG6A19 demonstrated higher tumor inhibition effect compared to control antibodies in SK-BR-3/KPL-4/BT474 models, meanwhile remarkably weaker effect in PC3/MCF7 models suggesting better safety in HER2 low expressing tissues. This selectivity of reactivity towards HER2 high expressing cells is likely due to the unique orientation of the antibody which allows better T cell activation when antigen abundance is high. Preliminary preclinical study in cynomolgus monkeys

suggested that the antibody was well tolerated in monkeys at the dosage of 20 mpk and had a half-life that is comparable to conventional antibodies. CD3 x HER2 x HER2 tri-specific antibodies selectively showed potent anti-tumor activity on HER2 high expressing cells and good safety on HER2 low expressing cells. Current findings warrant further development in human.

#6338

Development of a novel MSLN×4-1BB bispecific antibody

Liangwei Li[1], Dayan Zhang[2], Guodong Shen[3], Wenting Liu[2], Xiaoli Zeng[2], Lingling Wu[2], Qun Zhao[2], Weiming Zhou[2], Yang Huang[1], Liansheng Cheng[2]. *[1]Georgia State University, Atlanta, GA,[2]Hefei Hankemab Biotechnology Co., LTD, Hefei, China,[3]The First Affiliated Hospital of University of Science and Technology of China, Hefei, China*

Background: 4-1BB (CD137) is not only expressed on the surface of activated T cells and NK cells, but also a marker for Treg cells. Mesothelin (MSLN) is a ~71 kDa cell surface glycoprotein that is rarely expressed in normal tissues but overexpressed in many types of tumors. The fastest progress of MSLN-targeted therapy is in clinical phase II currently, including antibodies, ADCs, immunotoxins, vaccines and CAR-T. Here, we developed a bispecific antibody (bsAb) targeting both MSLN and 4-1BB with an intact Fc fragment from human IgG1. It can simultaneously exert the cytotoxic effect of CD8+T cells and and NK cells on tumor cells expressing MSLN to achieve better antitumor efficacy.
Methods: Firstly, two bsAbs with IgG-scFv format were constructed with IgG1 and IgG4, named as HK013-G1 and HK013-G4 respectively. Secondly, we evaluated the binding activities of two candidates to tumor cells with different MSLN expression levels and their effects on 4-1BB+ cell activation mediated by MSLN-crosslinking. Subsequently, the cell-killing abilities of NK and cytotoxic T cells induced by bsAbs were quantified. Finally, we compared the ability of bsAbs to inhibit tumor growth in vivo and their effects on intratumoral CD8+T cells and Tregs. The capacity of bsAb candidates to induce liver toxicity was investigated simultaneously in these immunocompetent mice. Moreover, to further confirm the safety of HK013-G1, the risk of cytokine release storm (CRS) and activation of 4-1BB signal mediated by Fc receptors (FcRs), which are

responsible for the potential side effects of 4-1BB mAbs were also evaluated.
Results: HK013-G1 is able to bind different MSLN-expressing cancer cells and bridge MSLN+ cells and 4-1BB+ cells. In luciferase reporter assay, the bsAb-induced 4-1BB activation is dependent on expression level of MSLN. While incubated with CD8+T cells, HK013-G1 increased IFN-γ production only in the presence of MSLN+ cells. Furthermore, HK013-G1 could exert its affects via both NK cell and activated PBMC. In MC38-hMSLN tumor models, HK013-G1 showed a more significant growth inhibition effect than HK013-G4, and did not show detectable liver damage. In addition, HK013-G1 could enhance the antitumor effect of anti-PD-1 in CT26-hMSLN tumor models. Also, HK013-G1 was shown no stronger ability to inducing CRS and activating 4-1BB signal in the presence of FcRs than HK013-G4 and parent anti-4-1BB mAb in vitro.
Conclusions: HK013-G1, a MSLN×4-1BB bsAb with human IgG1 Fc fragment prevents tumor development by killing tumor cells directly via effector functions mediated by NK and cytotoxic T cells. These results show that this bsAb has the potential to develop into a new clinical therapy for cancer types with high-level MSLN expression.

#6339

BCA101, a novel tumor-targeted bifunctional fusion antibody simultaneously inhibiting EGFR and TGF-β signaling with potential for durable tumor growth inhibition

Srinivas Reddy Boreddy[1], Reshmi Nair[1], Prashant Kumar Pandey[2], Anshu Kuriakose[2], Arindam Banerjee[1], Chaitali Dey[2], Madhukara A R[1], Bhadravathi Marigowda Shivakumar[1], Hanumant Kulkarni[2], Milind Sagar[2], Prashantha Kumar M. V[2], Shiv Ram Krishn[2], Jaya Bhatnagar[1], Moni Abhram Kuriakose[3], Ram Bhupal Reddy[3], Amritha Suresh[3], Praveen Reddy Moole[4], Usha Bughani[1], Seng-Lai Tan[1], Pradip Nair[1], Rachel Salazar[1]. *[1]Bicara Therapeutics Inc., Boston, MA,[2]Discovery Biology, Syngene International Ltd, Bengaluru, India,[3]Integrated Head and Neck Oncology Program, MSCTR, Mazumdar Shaw Medical Foundation, Bengaluru, India,[4]Biocon Biologics Limited, Bengaluru, India*

Introduction: The suboptimal clinical efficacy EGFR-targeting therapeutics is attributed to both tumor intrinsic and tumor microenvironment (TME) derived acquired (extrinsic) resistance mechanisms. Intrinsic factors include activation of other receptor tyrosine kinases and key extrinsic resistance mechanism include the enhanced secretion of immunosuppressive factors such as IL-10 and TGF-β1. Here, we describe a first-in-class bifunctional monoclonal antibody fusion designed to simultaneously target EGFR and sequester TGF-β in the TME.
Experimental Procedures: Functional activity of BCA101 was evaluated in multiple in vitro assays such as ELISA, inhibition of proliferation, antibody-dependent cellular toxicity, SMAD-reporter assay. Neutralization of TGF-β by BCA101 was demonstrated by epithelial-to-mesenchymal transition and tumor cell/immune cell co-culture assays. BCA101 tumor targeting was evaluated in a whole animal imaging study and efficacy studies were performed in nude xenograft models while combination studies with immune checkpoint inhibitors were performed in B16-EGFR syngeneic models.
Results: BCA101 is an anti-EGFR IgG1 monoclonal antibody linked to an extracellular domain of human TGF-βRII. The TGF-β "trap" fused to light chain in BCA101 did not sterically interfere with its ability to bind EGFR, inhibit cell proliferation, or mediate antibody-dependent cellular cytotoxicity *in vitro.* BCA101 increased production of proinflammatory cytokines and key markers associated with T and NK cell activation, while suppressing VEGF secretion. Additionally, BCA101 inhibited differentiation of naïve $CD4^+$ T cells to inducible T-regulatory (iTreg) cells when compared to cetuximab. *In vivo*, biodistribution studies showed that BCA101 localized to tumor tissues in xenograft mouse models, with comparable kinetics as cetuximab. TGF-β in tumors was neutralized to about 90% in animals dosed with 10 mg/kg of BCA101 compared to 54% in animals dosed with equimolar TGF-βRII-Fc. BCA101 had longer tumor tissue retention compared to cetuximab, further confirming improved tumor localization. In patient-derived xenograft mouse models of head and neck squamous cell carcinoma, BCA101 showed durable response post dose cessation as compared to cetuximab. In FaDu xenografts, BCA101 displayed early and durable response to cetuximab/cetuximab plus TGF-βRII-Fc combination. The combination of BCA101 and anti-PD1 antibody improved tumor inhibition in both B16-hEGFR expressing syngeneic

mouse and in humanized HuNOG-EXL mice bearing human PC-3 xenograft models.
Conclusion: These results support clinical development of BCA101, either as a monotherapy or in combination with immune checkpoint therapy.

#6340
Preclinical development of a monoclonal antibody targeting CD24 as cancer immunotherapy
Wenzhi Tian, Song Li, Dianze Chen, Dandan Liu, Huiqin Guo, Chunmei Yang, Li Zhang, Wei Zhang, Xiaoping Tu, Liang Peng, Gui Zhao, Ruliang Zhang, Fan Zhang, Frank X. Gan. *ImmuneOnco Biopharmaceuticals (Shanghai) Inc., Shanghai, China*

CD24 is a novel immune checkpoint that suppresses activation of macrophages, natural killer (NK) cells, T cells and B cells by binding to inhibitory receptor Siglec-10. CD24 is highly expressed on cancers of genitourinary (GU) and gastrointestinal (GI) systems, breast, and lung. High expression of CD24 is also known to be associated with poor prognosis for many types of cancers including breast, lung, GU and GI systems, bone, skin and brain. Mouse models of breast and lung cancer in literature revealed that CD24 attenuation in vivo leads to tumor inhibition and prolonged survival. To address the limited (~25%) overall response rate (ORR) of approved PD-1 / PD-L1 antibodies for solid tumors, we developed IMM47, an IgG1 antibody that differentially targets phagocytosis and cytotoxicity onto CD24-expressing cancer cells. At doses between 3 mg/kg to 10mg/kg, IMM47 significantly reduced tumor volume in a MC38 mouse model of colon cancer. Mice treated with 10mg/kg IMM47 produced tumor-specific immune response that prevented growth of re-inoculation of colon cancer cells. Further mechanism of action studies showed that IMM47 selectively and differentially increased M1 spleen macrophages quantity to 7-10 folds higher in that induced by PBS control. In contrast, IMM47 only increased M2 spleen macrophages to less than 1.5 folds higher than induced by PBS control. Expression of MHC II in M1 macrophages was also increased in IMM47-treated mice, suggesting significant activation and antigen presentation by macrophages. Our data has also confirmed that IMM47 specifically binds to and induces ADCC (antibody-dependent cellular cytotoxicity) ,ADCP (antibody-dependent

cellular phagocytosis), and CDC (complement-dependent cytotoxicity) against a variety of cancer cells. Taken together, our data show that targeting CD24 on tumor cells using our IMM47 antibody may serve as potent immunotherapy for multiple cancer indications.

#6341

Preclinical development of a monoclonal antibody targeting CD70 as cancer immunotherapy

Wenzhi Tian, Song Li, Dianze Chen, Dandan Liu, Huiqin Guo, Chunmei Yang, Li Zhang, Wei Zhang, Xiaoping Tu, Liang Peng, Gui Zhao, Ruliang Zhang, Fan Zhang, Frank X. Gan. *ImmuneOnco Biopharmaceuticals (Shanghai) Inc., Shanghai, China*

CD70 is a novel immune checkpoint highly expressed on cancers of kidney, blood and lymphoid tissues, mesothelium and gastrointestinal system. High expression of CD70 is a prognostic marker for poor survival in patients with ovarian carcinoma, pancreatic cancer and mesothelioma, etc. Several CD70 antibodies are under early stages of clinical trials for oncology indications. We have developed IMM40H, a humanized IgG1 antibody that differentially induces phagocytosis and cytotoxicity in CD70-expressing cancer cells. Results of in vitro study have demonstrated that, in comparison with cusatuzumab, IMM40H possesses better CD70 binding (kD= 3.22E-11M) and functional inhibition ability, as well as more potent activities of ADCC (antibody-dependent cellular cytotoxicity, EC50 = 0.5 -2.0ng/ml) and CDC (complement-dependent cytotoxicity, EC50 = 170 ng/mL) against certain cancer cells. IMM40H also induces strong ADCP (antibody-dependent cellular phagocytosis) activity (EC50 = 0.02nM). At doses between 0.3 mg/kg to 10mg/kg, IMM40H significantly reduced tumor volume in mouse models of multiple myeloma, lymphoma and kidney cancer. Notably, in a U266 multiple myeloma model, IMM40H, at the dose of 0.3 mg/kg, completely inhibited tumor growth in a way that therapeutic effects appeared significantly earlier than that of cusatuzumab at a higher dose of 1 mg/kg. Therapeutic effects of IMM40H at the dose of 3 mg/kg also appeared earlier than that of bortezomib at the dose of 0.5 mg/kg. Interestingly, combination of IMM40H and IMM01 (a SIRPα-IgG1 Fc fusion protein targeting CD47) generated significant therapeutic synergy in models of A498 kidney cancer and Raji lymphoma. Importantly, maximum

tolerated dose of IMM40H exceeds 100 mg/kg (IV, single dose) in cynomolgus monkeys and no significant adverse reaction was observed at a dose range of 3 to 30 mg/kg (IV, QW, 5 times) in monkeys. Taken together, our data show that targeting CD70 on tumor cells using IMM40H antibody may serve as a potent immunotherapy for multiple cancer indications. IND of IMM40H has been approved in China and US. This antibody is now in a phase 1 study in patients with advanced malignancies expressing CD70.

#6342

Preclinical safety & pharmacokinetics of AFVT-2101, a tetravalent FRα x CD16A bispecific innate cell engager for the treatment of solid tumors

Wendy Luo[1], Eric J. Gaukel[1], Janice A. Lansita[2], Stephen M. Laczko[1], Peter Sandy[3], Daniel J. O'Shannessy[4], Sudhir Penugonda[1], Bhavik Manocha[1], Daniel E. Patterson[1], Izabela Kozłowska[5], Séverine Sarlang[5], Stefan Knackmuss[5], Daniela Penston[5], Uwe Reusch[5], Zoë Johnson[3].
[1]Roivant Sciences, Inc., New York, NY,[2]ToxAlliance, Kennett Square, PA,[3]Affivant Sciences GmbH, Basel, Switzerland,[4]TMDx Consulting LLC, Schwenksville, PA,[5]Affimed GmbH, Heidelberg, Germany

AFVT-2101 is a novel bispecific innate immune cell engager in development to treat solid tumors. It is comprised of bivalent folate receptor alpha (FRα) and CD16A (FcγRIIIA) binding domains with a silenced IgG1 Fc region. AFVT-2101 is engineered to exert potent and selective immune-mediated antitumor activity with minimal off-tumor toxicity by promoting NK cell and macrophage engagement of FRα-positive tumors.
A comprehensive package of IND-enabling studies is currently in progress to support the preclinical safety profile of AFVT-2101. In agreement with target sequence homology, binding affinity of AFVT-2101 against human and cynomolgus monkey FRα and CD16A is highly similar, confirming non-human primate (NHP, specifically cynomolgus monkey) as the only pharmacologically relevant preclinical safety model. The toxicology program includes tissue cross-reactivity assessment against a panel of human and cynomolgus cryosections, single- and repeat-dose range finding (DRF) non-GLP studies and a 4-week IND-enabling GLP study with 4-week recovery period in NHPs.

In a single-dose study AFVT-2101 demonstrated non-linear pharmacokinetics when administered as a 2-h IV infusion to male NHPs where the mean C_{max} (85.1 and 1620 µg/mL) and AUC_{168hr} (3,430 and 97,000 µg.h/mL) at 3 and 30 mg/kg, respectively, increased supra-proportionally with respect to dose, consistent with target-mediated drug disposition. Half-life was 103-155 h across doses.
A DRF study was conducted to characterize toxicity, identify target organs, determine toxicokinetics (TK), immunogenicity (anti-drug antibodies, ADA), and to inform the dose selection of the subsequent 4-week study. AFVT-2101 was administered once-weekly to female NHPs via 2-h IV infusion for a total of 4 doses. Mean C_{max} (1120, 3320, 7190 µg/mL) and AUC_{168hr} (83,600, 209,000, 592,000 µg.h/mL) at 30, 75, and 150 mg/kg, respectively, increased in a generally dose-proportional manner with a trend for modest accumulation (<2-fold) upon repeated administration with a half-life of 80-230 h. Exposure did not appear to be impacted by any treatment-emergent ADA. AFVT-2101 was well-tolerated with no test article-related adverse effects on clinical observations, bodyweight, clinical chemistry, hematology, coagulation, anatomic pathology, or immunotoxicity parameters. The no observed adverse effect level (NOAEL) was determined to be 150 mg/kg under the conditions of the study.
The safety profile is being further evaluated in an ongoing pivotal 4-week GLP study incorporating standard toxicology endpoints, safety pharmacology (CNS, CV, and respiratory), gross and anatomic pathology, as well as cytokine, immunophenotyping, receptor occupancy, TK, and ADA analyses.
In conclusion, AFVT-2101 is well-tolerated in NHPs with a pharmacokinetic and safety profile consistent with its intended clinical application.

#6343

7E1, a novel blocking antibody targeting human anti-Müllerian-hormone-receptor II (AMHRII), elicits potent anti-tumor activity *in vivo*

Yongfei Yang[1], Huilin Li[1], Hao Li[1], Yue Yan[1], Jianhui Li[1], Qingcong Lin[1], Huijun Yin[2], Xiangshan Zhou[2], Miao Zhang[2], Kunbao Wu[2], Leqiao Sun[2],

Shan Zhong[2]. *[1]Biocytogen Pharmaceuticals (Beijing) Co., Ltd., Beijing, China,[2]China Resources Biopharmaceutical, Beijing, China*

Anti-Müllerian hormone (AMH), is a TGF-β family autocrine hormone and cognate ligand for the type II AMH receptor (AMHR2). AMH signaling through AMHR2 plays an important role in fetal sexual development by inducing Müllerian duct regression in males. AMHR2 is aberrantly expressed in various human malignancies, including colon, testis, gastric, and ovarian cancers. Functionally, AMH has complex effects on cell cycle regulation; at physiological concentrations it promotes survival and chemoresistance of cell lines, whereas at supraphysiological concentrations it inhibits tumor cell viability. Like other TGF-β family members, binding of its target receptor effects changes in gene expression through activation of intracellular SMAD, NF-κB, and Akt signaling. We developed a fully human anti-AMHR2 monoclonal antibody, 7E1, from RenMab™ mice, which contain the full human immunoglobulin variable domain. 7E1 was found to contain a distinct binding epitope associated with efficient inhibition of AMH binding and signaling. 7E1 also displayed a better ADCC effect than the reference AMHR2 antibody. The *in vivo* half-life of 7E1 in AMHR2- and FcRn-humanized mice exceeded the reference antibody as well and is in a desirable range from a development perspective. To evaluate the safety and efficacy of 7E1 *in vivo*, we established syngeneic murine tumor models in AMHR2-humanized mice. We found that 7E1 monotherapy significantly inhibited tumor growth in a dose-dependent manner. Moreover, 7E1 was well tolerated in mice, and no adverse effects were observed even at extremely high doses (e.g. 100 mg/kg). Taken together, these data demonstrate that 7E1 is a novel anti-human AMHR2 blocking antibody with desirable pharmacokinetic and pharmacodynamic properties. 7E1 may potentially find broad application for a range of cancer indications in which AMH signaling is implicated.

#6344

Recombinant Immunotoxin exhibited targeted killing of Trop2 overexpressing tumour cells lines

Dennis Makafui Dogbey, Sizalobuhle Masuku, Stefan Barth. *Integrative Biomedical Sciences, University of Cape Town, Rondebosch, South Africa*

Introduction: The high prevalence of cervical cancer remains a global challenge particularly in developing countries where its therapy is principally by chemoradiation marked by severe toxicities. Antibody-based therapy targeting specific overexpressed surface antigen has proven as a promising strategy. Tumor-associated calcium signal transducer 2 (Trop2), also known as epithelial glycoprotein-1 antigen, is a membrane protein found in epithelial tissues involved in cellular signalling, migration, proliferation, and differentiation in normal cells. Its overexpression is validated in several tumor types including basal, squamous and adenocarcinomas of the cervix, breast, colon, and gastrointestinal tracts. Due to its differential overexpression, Trop2 is a viable therapeutic marker whereby a recombinant immunotoxin composed of a single chain variable antibody fragment (scFv) armed with Pseudomonas exotoxin A (Anti-Trop2-ETA) may be delivered for targeted killing of such tumors.
Methods: Plasmids encoding Anti-Trop2-ETA were designed in silico by fusion of anti-Trop2 single chain variable fragment (scFv) antibody to the N-terminus of Pseudomonas exotoxin A and then cloned into an pMT backbone. Expression was performed in BL21 E. Coli cells under osmotic stress and then Anti-Trop2-ETA was purified by IMAC via an N-terminus encoded polyhistidine tag. Purified fractions were structurally characterized by SDS PAGE gel and immunoblotting to confirm the presence of the Anti-Trop2-ETA protein to be used for treatment of tumor cell lines. Trop2 expression cervical cancer and breast tumor cell lines were confirmed, and cells were treated with Anti-Trop2-ETA.
Results: Dose dependent killing by Anti-Trop2-ETA was observed in the Trop2 expressing tumor cell lines. IC50 values were significantly lower for Trop2 expressing cells as compared to control cells lacking Trop2 expression.
Conclusion: Here, we demonstrated antigen specific killing of Trop2 overexpressing tumor cells in vitro. Targeted deployment of recombinant immunotoxin to specifically engage and kill Trop2 positive cells is a potential approach for cancer therapeutics. As such, the ability of the rIT to specifically target and kill Trop2 expressing tumors is an important initial finding towards the possibility of antigen-dependent elimination of Trop2 expressing cancer cells. Ongoing evaluations are aimed at antigen dependent biological activity as well as pharmacokinetics of the rIT in tumor bearing in vivo models.

#6345

Non-clinical pharmacology of HX009, a novel FIC PD1xCD47 BsAb

Faming Zhang, Hang Ke, Feiyu Peng, Cen Chen, Lei Zhang, Henry Qixiang Li. *Hanx Bio, Hangzhou, China*

Immune checkpoint inhibitors (ICIs) have been widely tested as cancer therapeutics but with respective limitations such as marginal activity and/or poor safety profiles. It is possible that some of these limitations could be overcome by specially engineered molecules, *e.g*. bi-functional agents. Here we report a novel rationally designed bi-specific antibody (BsAb) targeting both PD1 and CD47, HX009, in order to improve both efficacy and safety over the two respective single-targeting ICIs. HX009 features IgG4 and 2x2 symmetric format, but with specifically weakened CD47 binding affinity. We performed a comprehensive preclinical pharmacology characterization of HX009 to test our hypothesis by confirming its candidacy as a novel first-in-class biologic for cancer therapy. The affinity constant (KD) of the HX009 binding to PD1 was determined to $3.96x10^{-11}$ M, while $5.06x10^{-9}$ M for binding to CD47, significantly reduced affinity as compared to the binding to PD1 and the binding between native SIRPα and CD47. HX009 has little binding to red blood cell (RBC) and platelets so to minimize hematological toxicity that usually associated with CD47 targeting. The antibody injectable formulation caused little cytokine release from PBMC (CRS or cytokine storm). HX009 cross-species binds to cynomolgus monkey PD1 and CD47 receptors, with the similar affinity as with the counterparts of human, but not to those of rodents. Cynomolgus monkey was thus chosen to investigate non-clinical pharmacokinetic (PK) and toxicology profiles of HX009. The intravenous (IV) infusion PK study revealed that HX009 is largely distributed within vasculature, with terminal half-life ($T_{1/2}$) around 50hr and dose proportional exposure. Repeat dosing caused no accumulation. The production of antidrug antibody (ADA) were observed in the dosed animals, as expected for administration into different species, which impacted PK parameters of repeated dosing. The IV single dose toxicology study revealed the maximal tolerated dose (MTD) of 150mg/kg with 14-day observation, while the maximum non-severely toxic dose (HNSTD) was determined to be 15 mg/kg in the repeated dose study after once weekly dose for 4 consecutive weeks (5 times total). The main

drug related toxicities observed seemed to be related to CD47 targeting as expected. Strong antitumor activity was also confirmed in in several preclinical cancer models, including humanized syngeneic models. In summary, the desired PK and safety profiles of HX009, along with anti-tumor activity, supporting further clinical development. Currently, HX009 is under clinical investigation (ClinicalTrials.gov Identifier: NCT05189093).

#6346

Discovery of HX011, a novel OX40 mAb, for potential cancer immunotherapy

Hang Ke, Faming Zhang, Jialin Li, Feiyu Peng, Cen Chen, Henry Qixiang Li. *Hanx Bio, Hangzhou, China*

OX40, tumor necrosis factor receptor superfamily member 4, is an immune co-stimulatory receptor, together with its ligand OX40L, forming OX40-OX40L trimer-trimer complex between the surface of T-cells (OX40) and APCs/NKs (OX40L). OX40 expresses constitutively on T_{reg} as well as on conventional T_{eff}, particularly within TME. OX40/OX40L interactions directly triggers conventional T cell activation via NF-*k*B1 pathway and inhibits bcl-x and survivin to prevent apoptosis; and it also downregulates FoxP3/CTLA4, thus T_{reg} function. OX40 agonistic antibodies have also been shown to activate tumor immunity and increase anti-tumor activity in preclinical models. Here we report that we identified/constructed a novel OX40-agonistic humanized IgG1 monoclonal antibody (mAb), HX011, with high affinity through hybridoma technology. HX011 was subsequently confirmed of the similar binding properties and functions as the original mouse mAb clone, 9C12: 1) binding to human OX40 (EC_{50} ~0.012 nM; 2) similar function binding in the reporter assay (EC_{50} ~6.6 nM); but 3) has little blockade of the OX40L binding to OX40. In another word, HX011 is similar to BMS-986178 for the first two assays, but contrastingly different for the third assay. Non-competing with OX40L may actually maximize T-cell activation, a potential advantage over a competing antibody. *In vivo* pharmacology modeling of HX011 in the humanized syngeneic CRC model, MC38, where syngeneic C57BL/6 mouse mice were knocked in with huOX40 (“HuGEMM-OX40”), demonstrated strong anti-tumor

activity (TGI ~100% at 1 mg/kg, twice weekly). HX011 is being further investigated as a potential new immunotherapy for the treatment of cancers.

#6347

Preliminary results of an exploratory phase I clinical trial of anchored canine interleukin-12 (cANK-101) in dogs with advanced oral malignant melanoma

Matheus Moreno Passos Barbosa[1], Angel J. Lopez[1], Rachel Uyehara[1], Rebecca L. Kamerer[1], Michael Schmidt[2], Sailaja Battula[2], Howard L. Kaufman[2], Timothy M. Fan[1]. *[1]Veterinary Clinical Medicine, University of Illinois Urbana-Champaign, Urbana, IL,[2]Ankyra Therapeutics, Boston, MA*

Background*:* Malignant melanoma is the most common form of oral cancer in canines with a median survival of 3 months for dogs with stage III or IV disease. Currently, there are limited effective systemic treatment options for these patients with advanced disease. We have developed an anchored immunotherapy approach in which canine interleukin-12 is stably linked to aluminum hydroxide (cANK-101). The anchored IL-12 forms a stable, functional depot of IL-12 and is expected to increase therapeutic responses with limited systemic toxicity. We report the preliminary results of an exploratory Phase I study of cANK-101 in dogs with advanced melanoma.

Methods*:* The clinical study was approved by the University of Illinois IACUC, conducted at the College of Veterinary Medicine, and all pet owners provided written informed consent. The primary objective of the trial was to determine the safety and tolerability of cANK-101 in dogs with advanced melanoma. A standard 3+3 dose-escalation design was used with three dose levels (1, 3, and 10 µg/kg) cANK-101 given by intratumoral injection every three weeks for 4 cycles. In the absence of overt clinical progression, dogs were allowed to receive a second course of four cycles. Dogs were monitored for adverse events via VCOG-CTCAE and clinical responses were measured using RECISTv1.1. Serum was collected for pharmacokinetic (PK) and immunogenicity analyses. In addition, serial tumor biopsy and lymph node cytology were performed. Serum cytokines were assayed via ELISA while immunophenotyping of PBMC and lymph node aspirates were assessed by flow cytometry. Tumor-infiltrating lymphocyte (TIL) analysis was performed by immunohistochemistry (IHC)

and gene expression profiling (Nanostring). Descriptive statistics were used for analyses.
Results*:* As of November 16, 2022, 8 dogs have been enrolled and all dogs remain on treatment. Thirteen adverse events have been reported in 6 dogs, all being grade 1. However, only two are considered related to the study drug (tumor site inflammation and pain). Treatment was associated with increases in serum IFNγ and IL-10, as well as increases in peripheral $CD4^+$ T and $CD21^+$ T cells. Additional data on PK analyses, anti-drug antibody levels, gene expression, and clinical responses will be presented.
Conclusions*:* Thus far, cANK-101 appears to be safe and tolerable in dogs with advanced melanoma. Data from this trial will help inform human clinical trials and may represent a new therapeutic option for dogs with advanced melanoma and perhaps other solid tumors. Our experience further suggests that companion animal trials could serve as relevant translational models for early immuno-oncology drug development.

#6348

ABN202 (αEGFR-interferon-β mutein), a potent antibody-cytokine fusion protein for the treatment of EGFR-positive non-small cell lung cancer

Heegeon Park[1], Saehyung Lee[1], Hayeon Park[1], Sunghyun Hong[1], Jaemun Kim[1], Sungyoul Hong[2], Ji-hyun Park[3], Young Kee Shin[3], Jun Young Choi[1], Na Young Kim[1]. *[1]ABION INC., Seoul, Korea, Republic of,[2]College of Pharmacy and Research Institute of Pharmaceutical Sciences, Seoul National University, Seoul, Korea, Republic of,[3]Graduate School of Convergence Science and Technology, Seoul National University, Seoul, Korea, Republic of*

ABN202 is an antibody-cytokine fusion protein consisting of interferon-β mutein (ABN102) molecularly fused to a anti-EGFR monoclonal antibody that recognizes the EGFR expressed on various types of cancer cells. In previous studies, we developed ABN102, a bio-better version of recombinant human interferon-β with hyperglycosylation via site-directed mutagenesis to improve stability, productivity, and pharmacokinetics properties. An addition of glycosylation at the N25 residue of ABN102 is expected to reduce the peripheral toxicity of ABN202, as it can shield the IFNAR2 binding interface. In this study, the binding ability and biological

activity of ABN202 was evaluated *in vitro* models. ABN202 downregulates the EGFR protein expression and reduces EGFR phosphorylation by degrading target proteins via internalization in the EGFR-positive NSCLC cell line. In addition, we also determined the direct and indirect anti-cancer activity of ABN202 *in preclinical models*. Taken together, we suggest that ABN202 has potent anti-cancer activities, via direct cytotoxicity in EGFR-positive tumors and indirectly activating immune cells through Type I IFN signaling. we conclude ABN202 is a promising drug candidate for patients with EGFR-positive NSCLC.

#6350

Monoclonal antibody against BST2 isoform: potential tool for diagnostic and cancer therapy

Laura C. Bover[1], Ahmed Muhsin[2], Long T. Vien[3], Felipe Amaya Manzanares[3], Zhuang Wu[3], Janis D. Johnson[3], Diego Castro Reyes[1], Myrthala Moreno-Smith[3], Estefania Labanca[4], Irene Sorin[5], Silvia Saucedo[5], Silvina Gazzaniga[6], Alicia I. Bravo[5]. *[1]Genomics Medicine/ Immunology, UT MD Anderson Cancer Center, Houston, TX,[2]Center for Epigenetics & Disease Prevention - Institute of Biosciences and Technology, Texas A&M, Houston, TX,[3]Immunology, UT MD Anderson Cancer Center, Houston, TX,[4]Department of Genitourinary Medical Oncology, UT MD Anderson Cancer Center, Houston, TX,[5]Servicio de Patologia, Hospital HIGA Eva Peron, San Martin - Provincia de Buenos Aires, Argentina,[6]Química Biológica, Facultad de Ciencias Exactas y Naturales - Universidad de Buenos Aires, Buenos Aires, Argentina*

BST2, a raft-associated type II transmembrane protein, functions as a restriction factor and inhibits HIV release by cross-linking virions onto infected cell surfaces. It also engages ILT7, a specific inhibitory receptor on plasmacytoid dendritic cells, which are associated with poor prognosis when infiltrate patients' breast tumors. Two groups have identified BST2 isoforms of different lengths, generated by post-transcriptional modification. Based on these findings and our work on protein interaction of ILT7-BST2, we hypothesized that the expression of BST2 isoforms differed in normal and cancer tissues. To demonstrate that, we generated and characterized anti-long BST2 isoform monoclonal antibodies (mAbs).

Results were compared with our previously developed mAb anti-BST2 full length molecule, 26F8, that recognizes a common epitope to all BST2 isoforms. By comparing the amino acid sequences of different isoforms of BST2, we identified a region of 24 residues on the extracellular domain of BST2, restricted to its long isoform. We then generated mAbs by hybridoma technology, immunizing BALB/c mice with the 24 mers peptide-KLH conjugated. Screening and positive selection of several clones were performed following our lab SOP. One of the mAbs, LA5, was selected based on positive ELISA against the immunogen and FACS staining of recombinant HEK293 cells expressing full-length BST2 protein. Pharmacokinetic determined using OCTET platform, revealed a KD of $4.61+/- 0.074 \times 10^{-9}$ M for LA5. Epitope mapping of LA5 on BST2 overlapping peptides, confirmed specific recognition of full-length BST2 protein and the peptide used as immunogen. LA5 heavy and light chains were sequenced and analysis was performed by IgBlast and IMGTV. Binding of LA5 and 26F8 to the myeloma cell lines MM1 (B-lymphoblast) and U266 (B-lymphocyte) by flow cytometry, indicated 97-100% positive cells with both mAbs, with higher MFI values observed for clone 26F8: 5.8 and 1.8-fold-increase in MM1 and U266 cells respectively. IHC on formalin-fixed paraffin embedded tissues of human ductal breast carcinoma, revealed that LA5 staining was able to identify infiltrating carcinoma cells but not the normal surrounding acinar cells. In contrast, 26F8 staining did not discriminate between BST2+ malignant and surrounding normal acinar cells. Currently, we are analyzing a panel of >105 breast cancer tissue samples of different molecular classifications. Initial data revealed a high-level of expression of BST2 (by 26F8) on the epithelial area of the tumors, lower in the TME (tumor microenvironment-infiltrating immune cells) and almost negative expression in the surrounding fibroblasts rich stroma. Evaluation of IHC staining by LA5 is being processed and yet to be established. These IHC findings indicate a potential diagnostic value of LA5 to distinct between tumor and normal cells in patients' specimens. Treatment prospects may arise during the process.

#6351

Reversal of dysfunctional CIK cells after the exposure to resistant cholangiocarcinoma cells through chemical perturbation of resistant

gene signature

Adisak Wongkajornsilp, Khin Su Su Htwe, Porncheera Chusorn, Sunisa Duangsa-ard, Kanda Kasetsinsombat, Nathawadee Sawatpiboon.
Pharmacology, Mahidol University Faculty of Medicine, Bangkok, Thailand

Clinical trials on cholangiocarcinoma revealed differential sensitivity to cytolytic action of allogeneic cytokine-induced killer (CIK) cells. Different metastatic foci in the same individual could also display different sensitivity. The differential sensitivity of separate lines of cultured cholangiocarcinoma cells could be demonstrated based on the evaluation of GR50. Allogeneic CIK cell or $CD3^+CD56^+$ subset was co-cultured with nine cell lines at E:T ratio of 20:1 for 48 h. The tumor cells were categorized into 2 groups based on the obtained GR50. This resulted in 4 sensitive cell lines and 5 resistant cell lines. The cholangiocarcinoma cell-exposed CIK cell and $CD3^+CD56^+$ subset displayed defective anti-tumor cytotoxicity upon subsequent experiment. RNAseq analysis revealed 261 genes upregulated in sensitive cell lines and 665 genes upregulated in resistant cell lines. The top 50 resistant genes were evaluated for their linked signal transduction and protein interaction network. Based on the interaction network, a list of chemicals that could interrupt the stipulated network were selected. They were assayed for their synergistic activity with dysfunctional CIK cell or $CD3^+CD56^+$ subset for cytolysis of resistant tumor cells.

#6352

Combination treatment with recombinant murine IL-12 and anti-PD-1 antibody enhanced anti-tumor efficacy through the activation of cytotoxic T cell response

Yeng-Jey Yang[1], Pei-Yi Tsou[1], Shiuh-Dih Chou[1], Meng-Na Lee[1], San-Chi Chen[2]. *[1]Libo Pharma Corporation, Taipei, Taiwan,[2]Department of Oncology, Taipei Veterans General Hospital, Taipei, Taiwan*

Introduction:Immune checkpoint inhibitors (ICIs) are widely used in cancer therapy. Among them, anti-PD-1 antibodies are the most used and have been approved by FDA for the treatment of many types of cancer (1). In our previous studies, combination of anti-PD-1 antibody with IL-12

demonstrated significant synergistic effect on tumor growth inhibition. The elevation of IFN-γ mRNA expression suggested the potential roles of CD8 T cells and NK cells in this process. In this study, we used two syngeneic mice tumor models to investigate the mechanisms of synergistic effect by the combination of IL-12 and anti-PD-1 antibody.
Methods: We used syngeneic mice tumor models with mice cancer cell lines CT-26 and MC-38. The mice inoculated with tumor cells and were treated until tumors grew to 100 mm^3. The mice were divided into three groups to receive the treatment, including rmIL-12 alone, anti-PD1-antibody alone, and the combination of rmIL-12 and anti-PD1-antibody (BIW x 3 weeks). At the end of the study, the mice were sacrificed and tumor resection and splenectomy were performed. The tumor infiltrating lymphocyte subpopulations within the tumor microenvironment were analyzed by flow cytometry and gene expression profile by RNA Seq.
Results: The combination of rmIL-12 and anti-PD-1 antibody significantly inhibited tumor growth compared to the treatment with rmIL-12 and anti-PD-1 antibody alone. The combination group demonstrated more $CD8^+$ T cell in the tumor microenvironment via flow cytometry. In addition, RNA Seq showed the combination group increased $CD8^+$ T cells, NK cells, and Th1 populations. The levels of cytotoxicity related genes (IFN-γ, Granzyme B, Perforin) were also higher in combination group.
Conclusion: Combination of rmIL-12 and anti-PD-1 antibody increased immune cells infiltration in the tumor microenvironment and enhanced anti-tumor response suggesting the potential of this combination for cancer treatment.
Citation:(1). Watson, G.A. et al. (2020) “Novel strategies in immune checkpoint inhibitor drug development: How far are we from the paradigm shift?,” British Journal of Clinical Pharmacology, 86(9), pp. 1753-1768. https://doi.org/10.1111/bcp.14355.

#6353

Combination of poly-γ-glutamic acid with anti PD-L1 blockade leads to improved anti-tumor activity in murine models

Jae-Pyung Jang, Jae Chul Choi, Kyung-Soo Hahm, Do Young Lee, Young-Chul Park. *BL Corporation, Gyeonggi-do, Korea, Republic of*

Immune checkpoint inhibitors(ICIs) have been shown to be key role in cancer therapy. Especially, antibodies targeting programmed cell death ligand1(PD-L1) promoted T cells to activate immune response against cancer cells. However, the current ICIs still have insignificant to motivate effective antitumor immunity by blocking PD-1/PD-L1 pathway and the regulatory network of PD-L1 by cytokines in the tumor microenvironment remains to be uncovered. Previously, we have reported the anti-cancer effects of combination treatment with a natural product, poly-γ-glutamic acid(γ-PGA), and PD-1 blockade. Now, we showed that combination therapy with anti PD-L1 and γ-PGA overcome the limits of ICIs and enhance anticancer effect in murine melanoma(B16F10). In vivo efficacy studies were performed by intraperitoneal injection of antibody targeting PD-L1 and oral administration of γ-PGA in C57BL/6 model transplanted with B16F10 melanoma cell. Systemic changes in immunophenotype were measured by tumor volume size and survival rate. The splenocytes were isolated from mice and the populations of myeloid-driven suppressor cells(MDSCs) and CD4/CD8 T cells were analyzed by FACS. Combination therapy with γ-PGA and anti PD-L1 blockade showed dramatically more suppressive tumor growth and enhanced long-term survival rate than other monotherapic treatment. In addition, γ-PGA was shown to play a role in the immune modulation of tumor microenvironment by activation of T cells and inhibition of MDSCs so as to prevent tumors from immune escape. Therefore, we suggest that γ-PGA can promote ICI-mediated antitumor responses by the transformation of "cold tumors" into “hot tumors”

#6354

A new tumor-bearing humanized mouse model to evaluate the efficacy of bispecific T cell engager and monoclonal checkpoint antibodies

Li-Chin Yao[1], Danying Cai[1], Destanie Rose[1], Guoxiang Yang[1], Mingshan Cheng[1], Michael A. Brehm[2], Dale L. Greiner[2], Leonard D. Shultz[3], James G. Keck[1]. *[1]The Jackson Laboratory-West, Sacramento, CA,[2]University of Massachusetts Medical School, Worcester, MA,[3]The Jackson Laboratory, Bar Harbor, ME*

T cell-based immunotherapies such as bispecific T- cell engagers (BiTE) and checkpoint inhibitors (CIs) have been developed rapidly for cancer treatment, but each has their own limitations in the clinic. Combination

therapies are an emerging approach in ongoing clinical trials to enhance the drug efficacy of monotherapy. Here we described a new preclinical animal model using immunodeficient NSG™-SGM3-IL15 mice engrafted with human CD34+ hematopoietic stem cells (HSC) to evaluate the combination treatment of EGFRXCD3 BiTE and two CIs (anti-PD-1 pembrolizumab and anti-PD-L1 avelumab). NSG™-SGM3-IL15 mice, which were created by crossing NSG™-SGM3 with NSG™-IL15, develop a more complete humane immune system after HSC engraftment. Humanized NSG™-IL15 mice have a higher peripheral NK cell frequency, and NK cells are functional with ADCC activity when compared to NSG™ (Aryee et al., 2022 FASEB). Here we show that humanized NSG™-SGM3-IL15 mice show improved human CD33+ myeloid progenitor cells and near physiological levels of NK cells and Tregs in peripheral blood when compared to humanized NSG™-SGM3. Triple negative breast cancer MDA-MB-453 cell line is PD-L1 positive, expresses low levels of EGFR and has a low baseline tumor immune cell infiltration in xenograft using humanized NSG™ mice. Previously we have shown BiTE efficacy on this tumor model. Here tumor-bearing humanized NSG™-SGM3-IL15 mice from two donors were used to evaluate the efficacy and immune responses from the BiTE treatment in combination with CIs. For donor 0348, monotherapy BiTE and avelumab didn't result in significant tumor growth reduction when compared to PBS control whereas the combination treatment significantly reduced tumor growth. BiTE treatment alone resulted in a significant increase in CD3+ T cell infiltration into tumor and higher frequency of CD69+ CD4 T and CD8 T cells. PD-1 expression on the tumor infiltrating lymphocytes and PD-L1 expression on tumor cells increased significantly. BiTE and avelumab combination treatment further increased human CD45+ and CD3+ T cell infiltrations with activated T cell phenotypes in tumor. For the second donor 0313, BiTE alone or in combination with the CIs didn't show anti-tumor growth activity. Flow cytometry analysis showed that the immune response to BiTE treatment was less pronounced in this donor, especially there were little change in lymphocyte infiltration and CD4+ T cell population in tumor. In this study, we demonstrated donor-dependent response to combination treatment of BiTE and avelumab and found that the responding donor showed an increase in T cell infiltration and activation in tumor after the treatment. The data suggested beneficial effects from inhibition of PD-1/PD-L1 axis

when used in combination with an immunotherapy targeting tumor antigen. The potential involvement of NK cells in this combination therapy remained to be examined.

Immune Checkpoints

#6357
Generation of a mutant SIRPa fusion protein with highly-improved affinity and favorable safety profile

Yingying Hu, Yayuan Fu, Lei Liu, Wenjing Li, Liting Xue, Zhiyong Yu, Yun Zhang, Meijuan Gao, Yixin Tan, Fudong Wang, Yadan Wu, Jie Li, Zhenzhen Li, Feng Zhou, Wenqing Yang, Zhuoxiao Cao, Renhong Tang.
Jiangsu Simcere Pharmaceuticals Co. Ltd, Nanjing, China

Background/Purpose: CD47 has been validated to be expressed on various tumor types including acute myeloid leukemia, myelodysplastic syndrome and other hematologic or solid tumors. As primary 'don't eat me' signal, high expression of CD47 on tumor cells interacts with SIRPα negatively regulating the phagocytosis level. However, poor safety profile as well as insufficient combinatory effect remain to be the issues limiting the clinical outcomes of CD47-targeting molecules. Herein, we used rational design strategies to generate SCR9168 with potent affinity improvement, and maintained favorable safety profiles in different animal species, including cynomolgus monkeys.
Procedures: Mutagenesis was introduced to the residues critical for CD47/SIRPα binding interface. Affinity was measured by SPR analysis. *In vitro* activities were determined by biochemical- or cell-based binding, blocking and antibody-dependent cellular phagocytosis (ADCP) assays. The efficacy *in vivo* was assessed with the OE19 xenograft model. Pharmacokinetics (PK) and safety were monitored in both mice and cynomolgus monkeys.
Results: The affinity of SCR9168 achieves 178 pM for human CD47 which is nearly 50-fold increase in comparison with wild-type SIRPα. Enhanced affinity has also been confirmed in binding to OE19 or DLD1 cell lines, as well as in blocking human SIRPα binding to Raji cells. SCR9168 remains strong binding potency to monkey, mouse or rat CD47 which allows the PK and safety assessment using these animal species. The combined effects of

SCR9168 and multiple therapeutic antibodies targeting tumor-associated antigens (TAAs) have been evaluated with ADCP assays using human monocyte-derived macrophages. SCR9168 markedly increases the ratio of phagocytic cells combining with antibodies, such as cetuximab. However, due to the inert function of Fc fragment, no phagocytosis of red blood cells or platelets was caused after the incubation *in vitro*. In addition, SCR9168 treatment in combination with trastuzumab leads to significantly improved suppression of tumor growth in a dose-dependent manner. Moreover, administration of two doses at day 1 and day 11 in cynomolgus monkeys results in no toxicity events related to SCR9168 based on the data from hematological analysis.
Conclusion: SCR9168 demonstrates the best-in-class potential among SIRPα mutein molecules. It elicits improved and dose-dependent efficacy in phagocytosis or tumor suppression combining with therapeutic antibodies, such as trastuzumab or cetuximab. Favorable safety profile with no phagocytosis of RBC or platelets *in vitro* as well as no hematological toxicity observation in cynomolgus monkeys allows broader dose range exploration in early clinical phase. SCR9168 is currently in development stage and IND enabling will be expected in the end of 2023.

#6358

CLEC-1 inhibitory myeloid checkpoint blockade enhances antitumor responses and tumor phagocytosis by macrophages

Vanessa Gauttier[1], Irène Baccelli[1], Marion Drouin[1], Isabelle Girault[1], Sabrina Pengam[1], Emmanuelle Wilhelm[1], Javier Saenz[2], Julien Taurelle[1], Emmanuel Mérieau[2], Bérangère Evrard[2], Caroline Mary[1], Géraldine Teppaz[1], Ariane Desselle[1], Virginie Thépénier[1], Nicolas Poirier[1], Elise Chiffoleau[2]. *[1]OSE Immunotherapeutics, Nantes, France,[2]Nantes Université, CHU Nantes, INSERM, Center for Research in Transplantation and Translational Immunology, UMR 1064, F-44000 Nantes, France, Nantes, France*

Myeloid cells represent the most abundant immune component of the tumor microenvironment, where they often assume immunosuppressive roles. Therefore, developing therapeutic strategies reinvigorating immunosuppressive myeloid cell subsets is of raising interest in oncology. We have identified CLEC-1, a member of the C-type lectin receptor (CLR)

family as being expressed by myeloid cells, especially by conventional type one dendritic cells (cDC1), and by tumor-associated macrophages (TAM). However, the role of CLEC-1 in myeloid function and its mechanism of action remained to be fully elucidated. Here, we investigated the effect of CLEC-1 blockade, either by genetic deletion or by antibody targeting, on myeloid function and anti-tumor response. First, we observed that CLEC-1 genetic deletion significantly increases the survival of syngeneic tumor-bearing mice in the Hepa1.6 orthotopic model of hepatocarcinoma, as well as in the AK-7 orthotopic model of mesothelioma. Moreover, the synergy with chemotherapy treatment (cyclophosphamide, gemcitabine) in the MC38 model of colon adenocarcinoma in *Clec1a* deficient animals significantly enhanced complete responses. Eventually, cured mice developed a robust memory antitumor immune response against the tumor. Next, we generated anti-human CLEC-1 monoclonal antibodies (mAbs) as well as CLEC-1 humanized mice. We found that CLEC-1 targeting through mAb treatment was able to prolong mouse survival as efficiently as by CLEC-1 genetic deletion in MC38 and Hepa1.6 models. CLEC-1 blockade by genetic deletion or by different mAbs treatment profoundly impacted the tumor microenvironment: we observed an increase in the frequency of invigorated dendritic cells (DCs) and macrophages, activated and memory T cells, while frequencies of immunosuppressive myeloid cells and PD1-expressing T cells largely decreased. Mechanistically, the *in vivo* phagocytosis of tumor cells (Hepa1.6 and MCA101) by macrophages was enhanced in CLEC-1 deficient animals compared to WT animals. Altogether, our results demonstrate that CLEC-1 acts as a novel immune checkpoint in myeloid cells and highlight its high potential as a target for innovative immunotherapy in oncology.

#6359

Structural insights into Siglec-15 reveal glycosylation dependency for interaction with T cells through integrin CD11b

Maria Pia Lenza[1], Leire Egia-Mendikute[1], Asier Antoñana-Vildosola[1], Cátia O. Soares[2], Francisco Corzana[3], Iker Oyenarte[1], Filipa Marcelo[2], Jesús Jiménez-Barbero[1], June Ereño-Orbea[1], Asis Palazon[1]. *[1]CIC bioGUNE, Derio, Spain,[2]Universidade NOVA de Lisboa, Lisbon, Portugal,[3]Universidad de La Rioja, Logroño, Spain*

Sialic acid-binding Ig-like lectin 15 (Siglec-15) is emerging as an immune modulator and target for cancer immunotherapy. However, limited knowledge regarding the mechanism of action, structure and binding partners on T cells restrains the development of drug candidates that unleash its full therapeutic potential. Here, we solve the crystal structure of Siglec-15 and delineate its binding epitope by co-crystallization with an anti-Siglec-15 blocking antibody. Saturation transfer-difference (STD) nuclear magnetic resonance (NMR) spectroscopy assisted with molecular dynamic simulations revealed the binding mode of Siglec-15 to the cancer-associated sialyl-Tn (sTn) glycoform. Binding of Siglec-15 to T cells, which lack sTn expression, depends on the presence of sialic acid. We identified the leukocyte integrin CD11b as a binding partner of Siglec-15 on human T cells. Collectively, these data provide an integrative understanding of the structural features of Siglec-15 and underscore glycosylation as an additional layer of control of T cell responses.

#6361

A preclinical model of acquired anti-PD-1 resistance is responsive to SEA-TGT, an effector-function enhanced anti-TIGIT monoclonal antibody

David R. Gruber, Weiping Zeng, Bob Thurman, Brian P. O'Connor, Shyra J. Gardai, Alyson J. Smith. *Seagen, Bothell, WA*

Immune checkpoint inhibitors, including monoclonal antibodies targeting the PD-1/PD-L1 axis, induce robust antitumor immunity in a subset of patients with various cancers. Despite continued success of these therapies, some patients experience limited efficacy owing to clinically complex and unresolved mechanisms of primary and acquired immunotherapy resistance. To begin to understand the mechanisms of acquired resistance to anti-PD-1 blockade, we developed a syngeneic murine CT26 colorectal tumor model that is resistant to anti-PD-1 therapy. To achieve this, CT26 tumors were subjected to successive rounds of increasing levels of anti-PD-1 therapy. When tumors grew out, they were cultured in vitro and then re-implanted and re-treated for three rounds until PD-1 resistance was achieved. To characterize the underlying drivers of acquired resistance across the generation of the model, wild type and anti-PD-1 resistant tumors and cultured cell lines were evaluated by flow cytometric immunophenotyping

and RNA-sequencing analysis. To assess how observed changes in the tumor microenvironment impact response to various therapeutics, the resistant tumors were treated with anti-PD-1 therapy or SEA-TGT, a nonfucosylated anti-TIGIT mAb with enhanced Fc-function that drives activity through multiple modes of action. As expected, treatment with anti-PD-1 monotherapy was ineffective, however, treatment with SEA-TGT demonstrated potent anti-tumor activity. These data are consistent with responsiveness to anti-TIGIT agents in other in vivo models of PD-1 resistance and/or PD-1 refractory response, indicating that the factors driving resistance to anti-PD-1 therapy can be different than those driving response to other known checkpoint molecules such as TIGIT. Thus, investigational agents such as SEA-TGT may have the potential to be efficacious in tumors that are primary or secondarily resistant to anti-PD-1 therapy. We have initiated a phase 1 study (NCT04254107) evaluating the safety, tolerability, and activity of SEA-TGT monotherapy and in combination with anti-PD-1 therapy in patients with advanced malignancies.

#6362

Overcoming resistance to immunotherapy due to loss of antigen presentation

Brian C. Miller[1], Yacine Choutri[2], Rose Al Abosy[3], Amy Huang[4], Emily K. Cox[1], Matthew P. Zimmerman[1], Wan Lin Chong[1], Katherine J. Vietor[1], Jenna Collier[4], Sarah A. Weiss[4], Debattama Sen[5], W. Nicholas Haining[6], Arlene H. Sharpe[4]. *[1]University of North Carolina at Chapel Hill, Chapel Hill, NC,[2]University of Toronto, Toronto, ON, Canada,[3]Boston Medical Center, Boston, MA,[4]Harvard Medical School, Boston, MA,[5]Massachusetts General Hospital, Boston, MA,[6]Arsenal Biosciences, San Francisco, CA*

Resistance to immune checkpoint inhibitors represents a major therapeutic challenge, as only 40% of patients with melanoma (and less with other tumor types) have a long-term response to anti-PD-1 therapy. Resistance can arise because of somatic mutations in cancer cells that allow evasion of T cell-mediated killing. One commonly acquired resistance mutation in melanoma, loss of beta-2 microglobulin (B2m), prevents T cell killing by hiding cancer cells from CD8+ T cell recognition. To understand the failed

immune response against resistant tumors, we used single-cell RNA-seq to characterize tumor-infiltrating immune cells in antigen presentation-deficient human melanoma biopsies and CRISPR-modified mouse melanoma tumors. Our data demonstrate an increase in immunosuppressive M2-like macrophages and absence of CD8+ T cells in B2m-null tumors. To overcome this resistance, we treated tumor-bearing mice with CD40 agonist antibody, which promotes differentiation of macrophages towards a pro-inflammatory phenotype and increases dendritic cell priming of CD8+ T cells. Treatment with CD40 agonist reduced tumor growth and improved tumor clearance in B2m-null melanoma and colorectal cancer models. To determine how CD40 agonist treatment works, we depleted different immune populations from the tumor microenvironment. We hypothesized that by depleting M2 macrophages, CD40 agonist treatment would remove an immunosuppressive brake to allow natural killer (NK) cells to kill tumor cells lacking MHC expression. To our surprise, NK cells were not required for the efficacy of CD40 agonist. Instead CD8+ T cells were required, even though the CD8+ T cells cannot directly recognize the tumor cells. scRNA-seq identified a transcriptionally unique state of CD8+ T cells that is recruited to the tumor microenvironment after CD40 agonist treatment. These CD8+ T cells produce IFNγ, which is required for the efficacy of CD40 agonist treatment. These data demonstrate that CD8+ T cells, a key mediator of anti-tumor immunity, can still be recruited to control tumors deficient in antigen presentation. More broadly, they suggest that strategies to activate CD8+ T cells may be effective even in the context of acquired resistance to checkpoint inhibitor therapy.

#6363

Short-term exposure of cancer cells to ultra-high concentrations nitric oxide induces PDL-1 upregulation

Yana Epshtein[1], Matan Goldshtein[1], Selena Chaisson[2], Jedidiah Monson[2], Matt Johnson[2], Amir Avniel[3], Steve Lisi[4], Hila Confino[1]. *[1]Beyond Cancer, Rehovot, Israel,[2]Beyond Cancer, Atlanta, GA,[3]Beyond Air, Ltd., Rehovot, Israel,[4]Beyond Air Inc, Garden City, NY*

Background: We have previously shown that treating mouse colon carcinoma (CT26) tumor-bearing mice with ultra-high concentrations of nitric oxide (UNO) upregulates innate and adaptive immune cells both

locally and systemically. As immune-checkpoint molecules, such as the PD-L1 receptor PD-1, are expressed on immune cells, our group assessed the potential synergy of UNO and an anti-PD-1 antibody for treating tumors *in vivo*. Indeed, primary tumors regressed in 53% of the CT26 tumor-bearing mice treated with UNO and anti-PD-1. Moreover, these mice were primary and distant tumor-free and survived 100 days post-treatment. In the current study, we assessed PD-L1 expression levels on cancer cells *in vitro* following short-term exposure to UNO.
Methods: CT26 cells were exposed to 25,000 - 100,000 ppm NO for 10 - 60 seconds. The percentage of PD-L1-expressing cells was assessed by flow cytometry analysis.
Results: 1. Exposing CT26 cells to 100,000 ppm NO for 10 seconds upregulated PD-L1 expression. 85.1% of cells, which are still viable or at early apoptosis, expressed PD-L1 compared to 71% of untreated cells ($p<0.0001$). Exposure of CT26 cells to 25,000 ppm or 50,000 ppm NO for 10 seconds did not change the level of PD-L1 expression significantly. 2. Exposure to 100,000 ppm NO for 30 seconds further increased the percentage of cells expressing PD-L1 to 96.7% ($p<0.0001$ compared to untreated cells). For this duration, lower concentrations of NO also increased PD-L1-expression in viable early apoptotic CT26 cells to 82.8% - 92.3% when treated with 25,000 ppm or 50,000 ppm NO, respectively. 3. Finally, a 60 second exposure of CT26 cells to 25,000 ppm, 50,000 ppm, or 100,000 ppm NO resulted in the highest percentage of PD-L1 expressing cells. Approximately 95% of all viable or early apoptotic CT26 cells express PD-L1 under all NO conditions. This finding is significant compared to 71% of cells in the control arm that express PD-L1 ($p<0.0001$).
Conclusion: Short-term exposure (10 - 60 seconds) to UNO upregulates PD-L1 expression on cancer cells in an NO concentration-dependent and exposure-dependent process. A 10-second exposure to 100,000 ppm NO is sufficient to significantly induce PDL-1 expression. Therefore, NO therapy can potentially be combined with anti-PD-L1 antibody treatment to improve therapeutic outcomes.

#6365
TRIM21 is a novel endogenous partner of the inhibitory myeloid checkpoint CLEC-1 involved in tumor antigen cross-presentation

Irene Baccelli[1], Vanessa Gauttier[1], Marion Drouin[1], Caroline Mary[1], Isabelle Girault[1], Emmanuelle Wilhelm[1], Sabrina Pengam[1], Géraldine Teppaz[1], Julien Taurelle[1], Ariane Desselle[1], Virginie Thepenier[1], Nicolas Poirier[1], Elise Chiffoleau[2]. *[1]OSE Immunotherapeutics, Nantes, France,[2]Nantes Université, CHU Nantes, INSERM, Center for Research in Transplantation and Translational Immunology, UMR 1064, Nantes, France*

Myeloid cells represent the most abundant immune component of the tumor microenvironment, where they often assume immunosuppressive roles. Therefore, understanding the mechanisms regulating the immunosuppressive activity of myeloid cells is of major interest in oncology. We have identified CLEC-1, a member of the C-type lectin receptor (CLR) family, as a myeloid cell-driven brake for anti-tumor T cell response in different murine models, including mesothelioma, hepatocellular and colorectal carcinomas. However, the molecular mechanism underlying the immunomodulatory role of CLEC-1 remained to be fully elucidated. Here, using both murine and human cells, we identified and characterized a novel endogenous ligand for CLEC-1, shedding new light on CLEC-1 driven inhibitory myeloid checkpoint activity. First, using single cell RNA sequencing, we confirmed that CLEC-1 is expressed by human myeloid cells, especially by conventional type-one dendritic cells and by tumor-associated macrophages. Using an Fc-fusion human CLEC-1 protein (huCLEC-1) as a bait for potential endogenous ligands, we observed both in human and murine cells that huCLEC-1 binds specifically to stressed or dying cells following programmed necrosis, for instance after X-ray or chemotherapy treatments. CLEC-1 interaction with its ligand expressed by necrotic cells was able to activate the NFAT promoter in a CLEC-1-CD3zeta NFAT reporter cell line *in vitro*; furthermore, CLEC-1 ligand targeting *via* Fc-CLEC-1 treatment *in vivo* extended the overall survival of chemotherapy-treated mc38-colorectal cancer bearing mice, altogether demonstrating the functional relevance of CLEC-1 interaction with its ligand. Immunoprecipitation of proteins bound to huCLEC-1 subsequently enabled the identification of TRIM21, an intra-cellular Fc receptor and E3 ubiquitin ligase as a novel interaction partner for CLEC-1. Direct interaction between recombinant TRIM21 and CLEC-1 human proteins was subsequently confirmed by ELISA and Biacore affinity

analysis. TRIM21 was indeed detected at the cell surface of necrotic cells following genotoxic treatments *in vitro* in several human cancer cell lines and, interestingly, high TRIM21 expression was predictive of worse overall survival in patients with hepatocellular carcinoma, pancreatic cancer, or glioma. Mechanistically, we demonstrated that CLEC-1 genetic deletion in mice enhances the capacity of dendritic cells to cross-present tumor antigens, a process known to be regulated by TRIM21 through its E3 ubiquitin ligase activity. Antagonist anti-CLEC-1 or anti-TRIM21 antibodies are therefore being evaluated to further confirm the involvement of the newly identified CLEC-1 interaction with TRIM21 in the regulation of CLEC-1's function as an inhibitory myeloid checkpoint. Altogether our data highlight the CLEC-1/TRIM21 axis as a new target for cancer immunotherapy.

#6366

NB002, a novel therapeutic antibody targeting unique epitope on TIM-3 presenting potent antitumor activity

Yu Zhang[1], Jinyu Dong[1], Binbin Wang[1], Jie Ni[1], Dong Wang[1], Liegang Shao[1], Meiguang Xiong[1], Ting Wang[1], Florencia McAllister[2], Xin Dong[1].
[1]NeoLogics Bioscience Co. Ltd., Suzhou, China,[2]Clinical Cancer Prevention, The University of Texas MD Anderson Cancer Center, Houston, TX

Antibody-based Immune checkpoint inhibitor (ICI) therapies targeting cytotoxic T lymphocyte antigen-4 (CTLA-4) or programmed death receptor-1 (PD-1) have significantly improved clinical outcomes in cancer treatment. Nonetheless, a large portion of the population has limited benefit from these ICI treatments due to lack of efficacy, resistance and intolerance. T-cell immunoglobulin and mucin domain containing-3 (TIM-3) has been proposed as a target for cancer immunotherapy. It is an inhibitory receptor modulating immune tolerance, and its expression has been broadly reported to be closely correlated to T cell exhaustion and pessimistic prognosis. Besides negatively modulating T cell status, TIM-3 is also expressed on natural killer (NK) cells, dendritic cells (DCs), macrophages and regulates immune responses bridging innate immunity and adaptive immunity. NB002 is a novel humanized Fc-engineered IgG1κ antibody, developed via NeologicsBio's integrated target validation & antibody screening Tier-A

platform. It has been characterized in a serial of function and efficacy studies and completed IND-enabling preclinical development. NB002 binds to human TIM3 with high affinity in the low nanomolar range and antagonize the TIM-3 pathway effectively in reporter cell and primary cell assays. NB002 increased the secretion of IFN-γ by activated PBMC cells and enhanced activation and killing activity of NK cells. Moreover, it exhibited a distinctive activity of restoring myeloid cells and enhancing antigen presentation and processing during anti-tumor immune responses, and superior efficacy in multiple humanized mouse models of cancer as monotherapy regimen. Importantly, X-ray crystallography demonstrated that NB002 recognized a unique epitope on TIM-3 and was confirmed by epitope binning assay and structural alignment. These data could potentially explain novel features of NB002, restoring both acquired and innate immunity which could lead cold tumor to hot tumor.In summary, these data showed that NB002 is a potent anti-TIM-3 antibody with pre-clinical properties. A phase 1 study is planned and patients with advanced metastatic solid tumors will be recruited.

#6367

BSI-507, a first-in-class bispecific antibody targeting PD1 and PVRIG for cancer immunotherapy

Zeyu Peng[1], Xiaodong F. Liu[2], Hongyan Li[1], Wenwen Dai[1], Jinyu Liu[1], Xiaoyao Hao[1], Shukai Xia[1], Qun Lv[1], Hugh M. Davis[2], Mingjiu Chen[1], Mark Z. Ma[1]. *[1]Biosion, Inc., Nanjing, China,[2]Biosion USA, Inc., Newark, DE*

Introduction: Despite the success of anti-PD1/PDL1 therapies, only a small fraction of patients benefit from these checkpoint inhibitors (CPIs). Novel approaches to improve outcomes for patients who are resistant to current CPIs are needed. PVRIG is expressed on $CD4^+$ and $CD8^+$ T cells, NKT and NK cells. PVRIG binds with high affinity with its ligand PVRL2, which is expressed on tumor cells and some myeloid cells. The PVRIG-PVRL2 axis exerts an inhibitory effect on the cytotoxic activity of lymphocytes. Bispecific antibodies that exhibit dual blockade of PD1 and PVRIG provide a promising strategy to enhance anti-tumor immune response.

Methods: An anti-PD1 mAb was identified from PD1 KO mice immunized with PD1-ECD-Fc and screened by our proprietary H^3 (High-throughput, High-content and High-efficiency) platform. An anti-PVRIG mAb was identified from rats immunized with recombinant PVRIG-ECD-Fc and screened by the H^3 platform. Both anti-PD1 and anti-PVRIG antibodies were humanized, and the anti-PD1 scFv was fused to the N-terminus of the heavy chain of the anti-PD1 antibody via a flexible linker. The binding activities and affinities were evaluated by ELISA, FACS and SPR, and the ligand blocking activities were measured by ELISA and FACS. Cell-based reporter assays were used to evaluate the functions of the anti-PD1 and anti-PVRIG mAbs alone and the bispecific antibody. In addition, the activity of the bispecific antibody to reverse PD1 and PVRIG mediated suppression of CMV $pp65_{495\text{-}503}$ antigen specific $CD8^+$ T-cell cytotoxicity was evaluated.
Results: BSI-507, an anti-PD1xanti-PVRIG bispecific antibody demonstrated comparable activity to the parental anti-PD1 antibody regarding PD1 binding and PD1/PDL1 blocking. It also exhibited comparable activity to the parental anti-PVRIG antibody in PVRIG binding and PVRIG/PVRL2 blocking. Based on cell-based reporter assays, BSI-507 was able to reverse either PD1 or PVRIG mediated T-cell suppression and exhibited comparable potency to the parental antibodies. BSI-507 was also able to show enhanced reversal of both PD1 and PVRIG mediated T-cell suppression, much better than anti-PD1 or anti-PVRIG alone. In addition, BSI-507 showed the ability to reverse PD1 and PVRIG mediated suppression of CMV $pp65_{495\text{-}503}$ antigen specific $CD8^+$ T-cell cytotoxicity, stronger than either the anti-PD1 or anti-PVRIG monoclonal antibody.
Summary: BSI-507 is a first-in-class anti-PD1xanti-PVRIG bispecific antibody for dual blockade of PD-1 and PVRIG pathways to enhance reversal of T cell inhibition. BSI-507 demonstrates favorable biophysical and functional characteristics, supporting the initiation of development activities including manufacturing and IND-enabling studies.

#6368

Preclinical pharmacology and safety studies of ZG005: an anti-PD-1/TIGIT bispecific mAb in a phase I clinical trial for advanced tumors

Bing Zhu[1], Tongcheng Dai[1], Ruifeng Liu[1], Alfonso Suarez[2], Tyler Liban[2], Bin Zhang[1], Margaret Karow[2], Jackie Sheng[2], Zelin Sheng[1], Binhua Lv[1].

[1]Suzhou Zelgen Biopharmaceuticals Co., Ltd., Shanghai, China,[2]Gensun Biopharma, Inc., Newbury Park, CA

ZG005 is a humanized anti-PD-1/TIGIT bispecific antibody that effectively blocks the binding between PD-1 and TIGIT, on immune cells, with their specific ligands PD-L1 and PVR, on tumors. As a dual blockade of PD-1/TIGIT immune checkpoints, ZG005 exhibits sustained occupancy to both targets and inhibits their pathways specifically and simultaneously, leading to synergistic effects and boosting the ability of the immune system in killing tumor cells. With high binding affinities, ZG005 elicits the activation of T cells and NK cells resulting in increased release of cytokines and the depletion of Tregs, independent of ADCC activities. ZG005 utilizes the IgG4 isotype to avoid the potential negative impact of effector function and target-crosslinking that has been reported for anti-TIGIT therapeutics using IgG1 isotype. *In vivo* animal studies indicate that ZG005 has potent and dose-dependent anti-tumor efficacies in syngeneic models using CT26 and MC38 colon tumors in humanized PD-1/TIGIT dKIs mice. In these models, the whole blood and TIL analyses confirmed increases in $CD8^+$ and NK cells but reduction of Treg cell levels after ZG005 treatments. The combination of ZG005 with chemotherapeutic-reagents, cisplatin and donafenib, enhanced their anti-tumor efficacies. Toxicity and safety pharmacology studies with weekly repeat doses for four weeks in cynomolgus monkeys, indicate that ZG005 is well tolerated. Over the dose range 20-180 mg/kg, there were no obvious toxic or adverse effects, and the HNSTD and NOAEL values were 180 mg/kg and 60 mg/kg, respectively. PK/TK analyses indicate a prolonged ZG005 receptor occupancy over 80%, consistent with *in vitro* binding results that are attribute to the S228P mutation in the IgG4 hinge region to prevent Fab exchange and enhance stability. The IND application of ZG005 has been approved by both FDA and NMPA, and the molecule is currently in phase I clinical trials for advanced solid tumors at escalated dosing of 0.3~20 mg/kg, Q3W, via *i.v.* administration.

#6369

Modulation of tumor microenvironment with TIM-3 blockade improves survival in diffuse midline glioma models

Iker Ausejo-Mauleon[1], Sara Labiano[1], Virginia Laspidea[1], Daniel de la Nava[1], Oren Becher[2], Mariella G Filbin[3], Fernando Pastor[4], Marta M Alonso[1]. *[1]Department of Pediatrics, Clinica Universidad de Navarra, Pamplona, Spain,[2]Jack Martin Fund Division of Pediatric Hematology-oncology, Mount Sinai, New York, NY,[3]Department of Pediatric Oncology, Dana-Farber Boston Children's Cancer and Blood Disorders Center, Boston, MA,[4]Molecular Therapeutics Program, Center for Applied Medical Research, Pamplona, Spain*

Purpose of Study: Diffuse midline glioma (DMG) is an aggressive brain tumor and the leading cause of pediatric death caused by cancer. Despite great strides in the understanding of this disease, survival is still dismal. One of the objectives of our lab is to modulate the tumor microenvironment (TME) towards a proinflammatory phenotype to render these tumors amenable to immunotherapy. TIM-3 is a member of the TIM family of immunoregulatory proteins expressed on multiple immune cell types, including T-cells, NK, myeloid populations, and microglia, regulating adaptive and innate immunity. Therefore, the aim of this project is to study the antitumor effect of the anti-TIM-3 monoclonal antibody and its effect on the DMG tumor microenvironment. Experimental Procedures: TIM-3 expression in DMG patients was analyzed using total mRNA sequencing data and single-cell RNAseq data. To perform all the experiments, DIPG murine cell lines were used (NP53 and XFM). For in vivo experiments, cells were injected into the pons of mice using a screw-guided system. The antibody was administered intracranially (25μg) with the same system and two times intraperitoneally (10mg/kg) 3, 7, and 11 days after the cell implantation respectively. Tumor immune populations, chemokines, and cytokines were analyzed by flow cytometry.
Results: In silico assessment of TIM-3 expression in DMG mRNA and single-cell datasets showed a robust expression of this gene mainly in microglia and macrophages uncovering this molecule as a potential target in DMGs. In vivo studies showed that TIM-3 blockade with an antibody significantly increased the overall survival of two DMG immunocompetent orthotopic models, led to long-term survivors (50%), and showed immune memory. TIM-3 inhibition resulted in significant increase in the number and proliferative state of microglia, NK, and CD8+ cells and higher levels of IFNγ, GrzB and TNFα corresponding to NK and T-cell activate phenotypes.

Interestingly, there was a decrease in the Treg population, which caused an increase in the pro-inflammatory CD8/Treg ratio. Chemokine studies demonstrated an augmentation of CCL5, CCL2 chemotactic chemokines, and CXCL10, IL-1β and IFN-γ pro-inflammatory cytokines in the tumor microenvironment of treated mice. Additionally, DCs, CD4+, and CD8+ cells were increased in treated draining lymph nodes and of functional significance, expressed higher amounts of pro-inflammatory cytokines than in control mice. Interestingly, the depletion NK, CD4 and CD8 immune populations did not completely abrogate the treatment efficacy. However, microglia and macrophages depletion with an anti-CSF1R resulted in a total loss of efficacy indicating a critical role of these populations in the effect of TIM-3 blockade.
Conclusions: These data uncover TIM-3 as a potential target for the treatment of DMG and its role as an immune regulator of the DMG tumor microenvironment.

#6370
Cell-based luminescent reporter bioassays for immunotherapies targeting macrophage effector functions
Jonathan Mitchell, Julia Gilden, Jim Hartnett, Pete Stecha, Gopal B. Krishnan, Frank Fan, Mei Cong, Jamison Grailer. *Promega, Madison, WI*

Macrophages play a key role in the elimination of cancer via phagocytosis and presentation of tumor antigens to T cells. Antibody-dependent cellular phagocytosis (ADCP), mediated by macrophages and other myeloid cells, is an important mechanism-of-action (MoA) for antibody-based cancer immunotherapies. Therapeutic strategies that enhance ADCP and other macrophage effector functions can augment direct tumor destruction and enable anti-tumor immunity. ADCP is initiated by binding of antibody Fc domains to Fc gamma receptors (FcgRs), and FcgR crosslinking results in signal transduction that drives inflammatory cytokine production and phagocytosis. Simultaneously, macrophage effector functions are regulated by immune checkpoints. Blockade of these immune checkpoints (e.g., SIRPa, ILT4), or agonists of activation pathways (e.g., TLR receptors) can enhance macrophage effector functions. Current assays to measure macrophage function are tedious, low throughput, and highly variable. Here, we present a suite of cell-based luminescent reporter bioassays to

measure macrophage effector functions: 1) A monocytic cell background was used to measure ADCP via endogenous expression of multiple FcgRs and integration of a FcgR-activation dependent luminescent reporter. 2) Direct detection of cellular phagocytosis can be measured using the HiBiT split luciferase system. 3) Modulation of macrophage-expressed immune checkpoints can be determined using cell-based reporter bioassays for SIRPa/CD47 and ILT4/HLA-G. 4) Activation of TLRs 1, 2, 4, 5 and 6 can be measured using a TLR reporter bioassay. These bioassays are robust, easy-to-use, and are pre-qualified according to ICH guidelines. Together, these novel reporter bioassays provide a robust, high-throughput toolbox to facilitate discovery and development of immunotherapies targeting macrophage effector functions.

#6371

Identification of a *lymphocyte activation gene-3*-binding peptides using phage displayed-peptide libraries for cancer immunotherapy

Seok-Min Lee, Byungheon Lee. *Kyungpook National Univ. School of Med, Daegu, Korea, Republic of*

Treatment with immune checkpoint blockades against CTLA-4, PD-1, and PD-L1 is currently giving improved results to many cancer patients. Nevertheless, a significant proportion of cancer patients treated with immune checkpoint blockades are still largely unsatisfied with the benefits of these drugs. One of the reasons is that cancer cells also use other immune checkpoints such as lymphocyte activation gene-3 (LAG-3), T cell immunoreceptor with Ig and ITIM domains, and T-cell immunoglobulin and mucin-domain containing-3. In this study, we screened phage displayed-peptide libraries for peptides that selectively bind to LAG-3. After five rounds of screening, we selected a candidate peptide and named it LAG3Pep. LAG3Pep preferentially bound to human LAG-3-transfected HEK 293T cells over mock-transfected cells and phorbol myristate acetate/ionomycin/chloroquine-stimulated Jurkat T cells over unstimulated cells. LAG3Pep also bound to splenocytes isolated from tumor-bearing mice, suggesting the reactivity across human and mouse LAG-3. Pull-down assay of human recombinant LAG-3 protein using biotin-labeled LAG3Pep yielded a protein band of LAG-3. LAG3Pep showed a high-affinity binding to the LAG-3 protein in SPR assays. Pre-treatment of a LAG-3-blocking

antibody competed the binding of LAG3Pep to stimulated Jurkat T cells. LAG3Pep inhibited the binding of the LAG-3 protein to THP-1 cells expressing HLA-DR, a well-known LAG-3 ligand. In addition, treatment of T-cells with LAG3Pep in combination with a PD-L1-blocking antibody recovered the secretion of IL-2 by T-cells which was suppressed by FGL-1, another ligand of LAG-3, secreted from HepG2 tumor cells in co-culture. Intravenous administration of LAG3Pep in combination with a PD-L1-blocking peptide showed an anti-tumor growth activity in the MC38 syngeneic mouse colon tumor model. These results show that LAG3Pep acts as LAG-3 blockade and, in combination with a PD-L1-blockade, could be a promising tool for cancer immunotherapy.

#6372

In situ detection of various activated immune checkpoints via next-generation proximity ligation assays in tumor tissue

Desirée Edén, Ka I Au Ieong, Naomi Cook, Doroteya Raykova, Agata Zieba Wicher. *Navinci Diagnostics AB, Uppsala, Sweden*

Immune checkpoints (ICs), which are inhibitory signaling pathways that can down-modulate the immune responses of T cells, are pivotal in peripheral tissues and for maintaining immune self-tolerance. Among the many molecularly defined IC proteins, some of the most studied ones are CTLA-4 and its binding partners important for early T-cell co-inhibition, along with the PD-1/PD-L1 axis proteins that carry out late co-inhibitory signals. Notably, in addition to antigen presenting and other immune cells, many tumors also express CTLA-4 and PD-L1, which facilitate tumor evasion from the immune system. The inhibition of these IC proteins has revolutionized the field of cancer therapy, but its efficiency has been limited to a poorly defined subset of patients. Patient outcomes are likely to have a stronger correlation to high levels of PD-1/PD-L1 interaction and other hallmarks of pathway activation, such as PD-1 phosphorylation and recruitment of SHP-2, than to the overexpression of a single IC protein alone. To improve the predictive value of tissue staining, we created an immuno-oncology line of ultrasensitive kits based on proximity ligation, which detect the activation of multiple ICs. Naveni™ PD1/PD-L1 is a tool for direct visualization of the interaction between PD-1 and PD-L1, and has been verified in various FFPE tumor tissues. Naveni™ pY PD1 sensitively

detects PD1 phosphorylation, which is the first step in the PD-1/PD-L1 inhibitory pathway activation. To study the subsequent recruitment of SHP-2 to the activated PD-1 receptor, which is crucial in immune cells but dispensable when the pathway is activated between two tumor cells, one can use the upcoming Naveni™ PD1/SHP-2 kit. Furthermore, we are developing assays to observe the competing interactions of CTLA-4 and CD28 with their binding partners CD80 and CD86, the interplay of which is pivotal for the initiation of early co-inhibition. All kits can be used on consecutive tissue sections to obtain a comprehensive picture of tumor IC pathway activation, which may not always correspond to CTLA-4, PD-1 or PD-L1 overexpression. While these kits have a chromogenic readout applicable to brightfield microscopy, we also have preliminary data on a PD-1/PD-L1 assay with a fluorescent readout thanks to which it can also be multiplexed. The multiplex feature generates an immune profile which may help improve immunotherapeutic strategies. The Naveni™ assays can be applied in basic research to elucidate the interplay of IC axes and downstream molecules, in pre-clinical and clinical research to compare stainings with the existing IHC assays and evaluate the potential prognostic value of interaction detection, and in pharma, aiding the development of new drugs or bispecific antibodies.

#6373

P-selectin glycoprotein ligand-1 modulates the functions of human T cells and macrophages in vitro

Jun Guan[1], Sundee Dees[2], Tony Chadderton[3], Alejandro Amador Arjona[1].
[1]Applied Technology Group, Incyte Research Institute, Wilmington, DE,[2]Biotherapeutics Research Group, Incyte Research Institute, Wilmington, DE,[3]Pharmacology Group, Incyte Research Institute, Wilmington, DE

P-selectin glycoprotein ligand-1 (PSGL-1) is a type I transmembrane protein expressed on the surface of most hematopoietic cells. PSGL-1 can engage multiple ligands (e.g., selectins, VISTA, Siglec-5, versican, CCL19, and CCL21). Apart from being a key adhesion molecule involved in immune cell trafficking, PSGL-1 has been shown to function as a negative immune checkpoint receptor in both T cells and macrophages. PSGL-1 is highly expressed in tumor-infiltrating T cells (TILs) and in tumor-associated macrophages (TAMs) in the tumor microenvironment (TME). PSGL-1 signaling in TILs induces development of T-cell exhaustion and, in TAMs, it promotes immunosuppressive activity of macrophages. In the TME, PSGL-1 is also highly expressed on the surface of myeloid-derived suppressor cells, regulatory T cells, and some types of cancer cells. We hypothesized that PSGL-1 may also act as a ligand to modulate the effector functions of human T cells and macrophages in the TME. In the present study, flow cytometry analysis showed that monocytes and granulocytes had a higher PSGL-1 expression than $CD4^+$ and $CD8^+$ T cells isolated from normal human blood cells. To mimic the cell-expressing PSGL-1, a recombinant human PSGL-1-Fc protein (rhPSGL-1-Fc, R&D Systems) was coated onto 96-well plates overnight. Human peripheral blood mononuclear cells (PBMCs), purified human $CD4^+$ T cells, or $CD8^+$ T cells were cultured in the PSGL-1-coated plates for 3 days in the presence of anti-CD3 antibody. In some experiments, a commercial tool PSGL-1 monoclonal antibody (mAb) with the ability to block PSGL-1/P-selectin interaction was added into the culture system. Cytokine secretion in the culture supernatants was measured using Meso Scale Discovery assays. Similar experiments were also conducted with commercially supplied human M1 and M2 macrophages. The results demonstrated that plate-bound rhPSGL-1-Fc dose-dependently inhibited IFN-γ, IL-2, and TNF-α cytokine production in

human PBMCs, $CD4^+$ T cells, and in $CD8^+$ T cells following T-cell receptor stimulation. The tool PSGL-1 mAb was able to partially rescue the suppression of cytokine production. Plate-bound rhPSGL-1-Fc also inhibited TNF-α secretion from human M1 macrophage, and the PSGL-1 mAb significantly enhanced TNF-α production in both human M1 and M2 macrophages treated with plate-bound PSGL-1-Fc. Together, these data indicate that PSGL-1 expressed on immune cells in TME may act as both an inhibitory ligand and receptor to impact on T-cell and macrophage function.

Acknowledgements: Thanks to Patrick Mayes and Ricardo Macarron for scientific input and thanks to Qian Wang Yao and Lynn Leffet for technical assistance.

Trial Registration: N/A

Ethics Approval: N/A

#6374

The role of myeloid cell-expressed PVRL2 in high-grade serous ovarian cancer

Kosuke Murakami, Hirofumi Ando, Michele Doucet, William Huang, Sudipto Ganguly. *The Bloomberg~Kimmel Institute for Cancer Immunotherapy, Johns Hopkins University, Baltimore, MD*

Ovarian cancer (OC) is the fifth leading cause of cancer death in women in the United States. Standard of care (surgical resection and platinum-based chemotherapy) has limited survival benefit for patients with advanced disease. Since 3 of every 4 patients are diagnosed with stage III-IV disease, novel therapeutic approaches are needed to improve survival. In trials with PD1/PD-L1 blockers, patients with OC had modest responses, highlighting an unmet need for effective immunotherapies. Our group has shown the PVRL2-PVRIG node in the DNAM-1 axis suppresses CD8 T cell effector function in syngeneic tumors as well as patient-derived ovarian tumors. This study aims to determine the requirement of tumor- vs myeloid cell-derived PVRL2 for driving immune suppression in OC.Taqman qPCR was conducted for PVRL2, PVR and PD-L1 mRNA expressions of classically activated (M1), and alternatively activated (M2) macrophages from wild-type and $PVRL2^{-/-}$ mice. In our syngeneic OC model, ID8-Vegf-Defb29 (50,000 cells/ovary) were surgically implanted in the ovarian bursa and

monitored for disease progression. These studies were performed in (1) PVRL2$^{-/-}$ mice vs. wild type mice and (2) PVRL2$^{-/-}$ -> Wild-type vs. wild-type -> wild-type bone marrow chimeras. PVRL2$^{-/-}$ ID8-Vegf-Defb29 clones were generated by CRISPR-Cas9, validated for absence of off-target edits by whole exome sequencing and implanted in wild-type and PVRL2$^{-/-}$ mice. Multiplex immunofluorescence (mIF) of PanCK/CD8-CD68-PVRL2/PVR was performed on archived HGSOC tissue from patients treated at Johns Hopkins Hospital. CITE-seq was performed on viable TILs from 6 treatment-naïve and 4 neoadjuvant chemotherapy-treated patients.PVR transcripts were elevated in PVRL2$^{-/-}$ M1 (3.77-fold, p=0.04) and M2 (2.61-fold, p=0.003) macrophages compared to wild type. The expression of PD-L1 was increased in M2 macrophages of PVRL2-/- mice compared to wild-type mice (Mean ratio: 2.28, p=0.04). PVRL2$^{-/-}$ mice and PVRL2 bone marrow chimeras had significantly improved survival compared to their respective control cohorts. Tumors derived from PVRL2$^{-/-}$ ID8-Vegf-Defb29 clones grew slowly in PVRL2$^{-/-}$ mice compared to wild-type mice. PVRL2 and PVR were highly expressed in human HGSOC, and the prognosis was worse for patients with high PVRL2 expression. In mIF, PVRL2 was expressed not only on tumor cells but also on CD68-positive cells. In CITE-seq, PVRL2 and PVR were strongly expressed in macrophage and dendritic cell clusters.The enhanced expression of PVR and PD-L1 in PVRL2$^{-/-}$ M1 and M2 macrophages suggests compensatory activation of co-inhibitory signaling pathways. PVRL2 deficiency selectively in hematopoietically-reconstituted immune cells (primarily myeloid cells) and not in tumor cells conferred a significant survival benefit in our syngeneic OC model. Taken together, blockade of the PVRL2-PVRIG axis in conjunction with PD-1/L1 inhibition may be an effective modality in OC.

#6375

Transcriptomic signatures in melanoma lymph node metastasis that relate to immune oncology treatment

Matias A. Bustos[1], Shodai Mizuno[2], Suyeon Ryu[3], Dave S. B. Hoon[4].
[1]Providence Saint John's Health Center, Santa Monica, CA,[2]Translational Molecular Medicine, Providence Saint John's Health Center, Santa Monica, CA,[3]Genome Sequencing Center, Providence Saint John's Health Center,

Santa Monica, CA,[4]Translational Molecular Medicine and Genome Sequencing Center, Providence Saint John's Health Center, Santa Monica, CA

Background: Frequently, patients with primary cutaneous melanoma develop regional lymph node metastasis (LNM). The outcomes in melanoma patients with LNM can be poor, depending on clinicopathological features including the size and the number of the LNM. Newer immunotherapies including immune checkpoint inhibitors (ICI) have significantly improved outcomes in metastatic melanoma patients, and when tumors respond to ICI the durable responses are noteworthy. The aim of the current study is to identify transcriptomics changes in immune-related genes in LNM that correlate to outcomes in melanoma patients receiving adjuvant ICI therapy.
Methods: The analysis were performed in formalin-fixed paraffin-embedded (FFPE) sections from LNM positive (LNM(+); n=17) and LNM negative (LNM(-); n=8) of patients who received surgery at SJHC. For each tissue, a single section was processed and analyzed for 2,002 genes using the direct (mRNA extraction-free) transcriptomic assay of the HTG EdgeSeq AutoImmune Panel (HTG-AI). The HTG-AI transcriptomic normalized data were compared between both groups. For verification of gene signatures, publicly available RNA-seq datasets were obtained from patients with clinical outcomes receiving anti-PD-1. All biostatistical analysis were performed using HTG Reveal and/or GraphPad Prism software.
Results: Comparisons between melanoma LNM(+) and LNM(-) samples showed 229 DEGs (Log2fold-change <-2; >2 FDR<0.01), with 213 genes upregulated and 16 downregulated. Pathway analyses using Reactome indicated that the DEGs in LNM(+) were associated with cytokine, interferon (IFN), and chemokine signaling, as well as signaling by receptor tyrosine kinases (FDR<0.0001). The chemokines *CXCL8*, *CXCL2*, and *CXCL10* were significantly upregulated in LNM(+) (p<0.001). LNM(+) showed significantly higher levels of IFN signaling mediators (*STAT1*, *STAT2*, *IFI6*, *IFI30, IFI44*) compared to LNM(-) specimens (p<0.001). Also, LNM(+) showed a significant increase in *CD276* (B7-H3) levels (p<0.001). Then, we correlated the mRNA levels of IFN signaling (*STAT1*, *STAT2*, *IFI6*, *IFI30*, and *IFI44*) obtained from samples before anti-PD-1

therapy (Nivolumab or Pembrolizumab) to overall survival (OS). Of clinical importance, patients with elevated levels of the IFN signaling genes showed better OS for patients receiving adjuvant anti-PD-1 (HR=0.6, CI=0.42-0.86, Log-rank test, p=0.0044).
Conclusions: We identified a distinctive transcriptomic profile in LNM(+). Several genes were upregulated and associated with specific pathways. Using publicly available data, we demonstrated that *STAT1*, *STAT2*, *IFI6*, *IFI30*, and *IFI44* gene signature correlated with improved OS for patients receiving adjuvant ICI treatment. The *STAT1*, *STAT2*, *IFI6*, *IFI30*, and *IFI44* genes may represent new biomarkers to assess in biopsies of patients that will receive adjuvant or neoadjuvant ICI therapies.

#6376
Discovery and preclinical characterization of dual antagonist antibodies targeting both LILRB1 and LILRB2 that enhance innate and adaptive anti-cancer immune responses
Meghan Zuck, Myriam Bouchlaka, Huyen Dinh, Kevin Green, Francisco Zapata, Ramya Chandrasekaran, Tatyana Pisarenko, Lauren Loh, Gajendra S. Naika, Meilyn Sylvestre, Jacob Heit, Raymond Fox, Darbie Whitman, Tom Graddis, Kamal D. Puri, Peter Probst. *OncoResponse, Inc., Seattle, WA*

Background: One cause for the failure of checkpoint inhibitors is the immunosuppressive nature of the tumor microenvironment. LILRB1 (ILT2) and LILRB2 (ILT4) are ITIM-containing inhibitory receptors that recognize HLA Class 1 and nonclassical ligands (e.g., HLA-A, HLA-G, etc.). LILRB1 is expressed on myeloid cells and subsets of B, NK, and T cells, while LILRB2 expression is mostly restricted to myeloid cells. Interaction of LILRB1 and LILRB2 receptors with HLA ligands promotes an inhibitory milieu that prevents T cells from attacking cancer cells. The distinct pattern of expression and function of these lymphoid and myeloid checkpoints suggests complementary targeting approaches for cancer immunotherapy. Dual blockade of LILRB1 and LILRB2 receptors by a single antibody that restores both innate and adaptive immune responses is a promising strategy to enhance efficacy of checkpoint inhibitors.
Methods: Dual LILRB1 and LILRB2 targeting antibodies were cloned from B cells derived from rabbits immunized with human LILRB2 recombinant protein, and subsequently humanized. Antibodies were evaluated for

binding to human LILRB1 and LILRB2 proteins. Dual targeting antibodies were evaluated in a panel of functional and phenotypic assays. Selected antibodies were further tested for efficacy in a humanized NSG-SGM3 tumor model.
Results: Dual antibodies were selected based on binding to recombinant human LILRB1 and LILRB2 protein, as well as blocking of HLA-G binding. These antibodies demonstrated binding to cells expressing LILRB1 and LILRB2, with no appreciable binding to other family members. Lead antibodies demonstrated activity in functional cell-based assays modeling LILRB1- or LILRB2-mediated immunosuppression. Dual antibodies also enhanced IFN-γ production by LPS-stimulated human PBMC. Selected clones restored T-cell function from M2c macrophage-mediated suppression in coculture with $CD8^+$ T cell, and enhanced the tumoricidal activity of NK cells. Importantly, the lead antibody demonstrated in vivo efficacy with significant tumor growth inhibition and tumor regression in an SK-MEL-5 tumor model in humanized NSG-SGM3 mice.
Conclusions: We have identified dual antagonist antibodies targeting both LILRB1 and LILRB2 antibodies that restore both innate and adaptive immune responses. Additionally, dual antibodies restored $CD8^+$ T cell activation from macrophage-mediated suppression and enhanced NK cell cytotoxic activity. These data provide a strong rationale for further development of dual antibodies as an anti-cancer immunotherapy.

#6377

A translatable tumor-killing platform with robust sensitivity towards immune checkpoint inhibitor targeted therapeutics

Marie Carkill, Kaitlin Mitchell, Lauren Kelsey, Jezrom Self-Fordham, Nunan Robert, Louise Brackenbury. *Charles River Laboratories, Inc., Bristol, United Kingdom*

The cancer treatment landscape has transformed following the clinical success of early immune checkpoint inhibitors (ICI) which demonstrate the remarkable power of harnessing the immune system to treat a variety of metastatic cancers. Despite the success of Pembrolizumab, Nivolumab and Atezolizumab, the programmed cell death protein-1 (PD1)-programmed death ligand-1/2 (PD-L1/L2) pathway remains a tractable target for many drug discovery programs, particularly for bi-specific or combinational

therapies. The PD1 - PD-L1/L2 pathway is important in protecting the host from uncontrolled immune responses, but can be hijacked by tumors, rendering them resistant to immune attack. Antibodies which antagonize this pathway potentiate T-cell mediated tumor destruction yet do not show efficacy in all patients or guarantee long-term protection, in part due to tumor-associated ICI-resistance mechanisms. There is a distinct need to develop novel ICI therapeutics and robust, complex co-culture platforms to better predict clinical efficacy. Here we outline a series of translationally relevant co-culture assays using Pembrolizumab as a benchmark therapeutic alongside other ICI. PD-1 expression levels are known to be low on resting T cells, as indeed are many checkpoint receptors, and so to enhance the therapeutic window, CD3+T cells from healthy human donors were polyclonally stimulated before addition to SK-OV-3 target cell cultures. The SK-OV-3 tumor line was stably transduced with NucLight Red (NLR) to allow co-localization of the caspase 3/7 signal to tumor cells. Autologous, mature monocyte-derived dendritic cells (moDC), expressing high levels of PD-L1/PD-L2 were added into tri-cultures in a 2D tumor killing assay. Tumor killing kinetics were quantified via live cell imaging using an Incucyte S3. Although Pembrolizumab enhanced immune-mediated direct (pre-stimulated) T cell killing, the therapeutic window increased in the presence of autologous moDC. Using a modified 3D (tumor spheroid) format over a longer time course, Pembrolizumab was also shown to enhance PBMC-mediated killing and the ability of moDC to enhance this effect further was determined. In recent years, the development and implementation of combinatorial approaches has resulted in significant improvements in patient responsiveness and disease outcomes for various cancers. Here, we describe a suite of tumor killing assays which can be adapted to multiple tumor or therapeutic targets, with a focus on immune involvement. ICI are shown to work robustly and efficacy tracks expression of the relevant checkpoint receptors, making this a powerful format in which to test combination therapies or novel ICI.

#6378

An *in vitro* human CD8 T cell exhaustion model for the functional screening of immune checkpoint inhibitors

Roberto Carrio[1], Margot Cucchetti[2], Mikielia Devonish[1], Louis Poisson[1], Mihaela Babiceanu[1], Andrew Kettring[1], Yingchun Liu[3], Donald Jackson[3],

Evan Gomes[1], Jeremy Baudhuin[2], Donald R. Drake[1], Valeria Fantin[4], Anthony Byers[1], Ingrid Sassoon[2]. *[1]Sanofi, Orlando, FL,[2]Sanofi, Vitry-sur-Seine, France,[3]Sanofi, Boston, MA,[4]Sanofi, San Franciso, CA*

T cell exhaustion is a state of dysfunction that frequently occurs during chronic infections and cancer due to persistent antigen stimulation and inflammation. It is defined by poor effector function, sustained expression of inhibitory receptors, and a transcriptional state distinct from that of functional effector or memory T cells. In this state, cells remain in the local environment but lack effector functions necessary to combat the tumor or infection. In the current study, we developed an *in vitro* human antigen-specific CD8 T cell exhaustion model to evaluate the ability of immune checkpoint inhibitors to restore functionality to exhausted T cells. Using the fully human, autologous MIMIC (**M**odular **IM**mune **I**n vitro **C**onstruct) effector CD8 T cell assay as a framework, we assessed the effect of antigen dose, timing, and frequency of repeated antigen stimulation with antiviral HLA Class I-restricted peptides to drive the development of Ag-specific CD8 T cells toward an exhausted state. Epitope-specific CD8 T cell responses were monitored by HLA class I-restricted pentamers and establishment of an exhausted profile was evaluated by increased expression of inhibitory co-stimulatory receptors and decreased intracellular expression of antiviral effector cytokine via flow cytometry relative to functional Ag-specific CD8 T cells from the same donor. Repeated antigen exposure led to decreased production of IFN-γ and TNF-α and increased expression of inhibitory co-stimulation markers on antigen-specific CD8 T cells. After establishment of an exhausted phenotype, treatment with various immune checkpoint inhibitor molecules restored functionality to Ag-specific CD8 T cells upon an additional antigen re-stimulation. Moreover, here using this model we characterized distinct transcriptomic signatures of functional and exhausted MIMIC CD8 T cells. Development of an in vitro human viral antigen-specific CD8 T cell exhaustion model with characteristic features of dysfunctional CD8 T cells as observed *in vivo* and the ability to restore effector function by treatment with immune checkpoint inhibitors, provides a platform to assess the effectiveness of therapeutic mono-specific or bi-specific “checkpoint blockade” antibody candidates and, in general, the potential to evaluate a myriad of immunotherapeutic approaches for cancer treatment.

#6380

Ultrasensitive detection of circulating human PD-1 and PD-L1 using Single Molecule Counting (SMC) technology

Laila Faramarzi, Wen-Rong Lie, Rick Wiese, Jared Fiske. *MilliporeSigma, St. Louis, MO*

Immune checkpoint proteins are key regulators of the immune system and potential drug targets for cancer immunotherapy. Cancer immunotherapy targeting immune checkpoint, like programmed cell death protein-1 (PD-1) and programmed cell death ligand 1 (PD-L1) inhibitors has shown treatment efficacy for a broad spectrum of human cancers. Immune checkpoint molecules PD-1 and PD-L1 are expressed on the cell surface of immune cells and tumor cells. Recent studies have also reported these immune checkpoint proteins may undergo alternative splicing or proteolytic cleavage to produce soluble checkpoint proteins. Multiple molecular forms of soluble PD-1 (sPD-1) and PD-L1 (sPD-L1) are detectable in patient sera of multiple types of cancer, and these soluble checkpoint proteins have been reported as putative liquid biopsy biomarkers in the diagnosis and prognosis of oncological disease. Though the clinical significance of circulating soluble immune checkpoint protein profiles as predictive biomarkers has yet to be fully explored and validated, we have committed to develop better and more reliable bioassays to further this research. With that, we have developed 2 Luminex-based multiplex immunoassays for simultaneous quantitation of 48 immune checkpoint proteins, including PD-1 and PD-L1, for patient sera and tumor lysate samples. Here we report the development of 2 novel Single Molecule Counting (SMC) technology-based ultrasensitive single-plex immune checkpoint immunoassays for the detection of sPD-L1 and sPD-1 in human serum and plasma samples. Comparative studies demonstrate these SMC ultrasensitive assays possesses at least 10-100-fold higher sensitivity as compared with the Luminex-based immunoassays. Using these novel ultrasensitive assays, we have validated the detection of significant increases in sPD-L1 and sPD-1 in cancer serum samples as compared with the levels in healthy controls. We have also applied these high sensitivity assays to measure human PD-L1 and PD-1 biomarkers in other sample types including urine, tumor lysates and exosomes. In conclusion, we envision that these PD-1 and PD-L1 SMC

assays may overcome a major limitation in biomarker utility and enable the ultrasensitive detection of sPD-1 and sPD-L1 in liquid biopsy and blood biomarker research.

#6381

Quantitative multiplex analysis of soluble and cellular immune checkpoint proteins in response to interferon gamma across multiple murine tumor models

Wen-Rong Lie[1], Ryan Bucktrout[2], Sanjukta Chakraborty[2], Andrea Orlando[2], Inna Serganova[2], Christine Kornmeier[1], James Hoberg[1], Roberta Zappasodi[2]. *[1]MilliporeSigma, St. Louis, MO,[2]Joan & Sanford I. Weill Medical College of Cornell University, New York, NY*

Immune checkpoint proteins are key regulators of the immune system and drug targets of cancer immunotherapy. Immune checkpoint molecules have been found on the cell surface of various tumor cells and immune cells as immune activating or inhibitory receptors and ligands. Recent studies have shown these immune checkpoint proteins can undergo alternative splicing or proteolytic cleavage leading to soluble isoforms. IFNγ is a pleiotropic and multifunctional cytokine commonly released by cytotoxic immune cells. IFNγ production can be enhanced in response to immunotherapy and further modulates the expression of immune checkpoints in the tumor microenvironment. To better understand the immune checkpoint signatures in tumors, we developed a 28-plex mouse checkpoint protein multiplex immunoassay for quantitative analysis of soluble (secreted) and cellular immune checkpoint proteins. Using this immunoassay, we tested 16 mouse cell lines of tumor (n=13) and normal tissues as control (n=3): 2 melanomas (B16F10, YUMM1.7), 3 mammary carcinoma (4T1, NT5, AT-3), 1 lung carcinoma (LLC), 1 prostate cancer (MycCaP), 1 fibrosarcoma (MCA205), 1 ovarian cancer (ID8), 1 bladder cancer (MB49), 1 glioma (CT-2A), 2 blood cancer (RAW, EL4), 1 dendritic cells (DC2.4), 1 myoblast cells (C2C12), and 1 endothelial cells (bEnd.3). We analyzed changes in immune checkpoint protein expression and secretion in these cell lines cultured in normal conditions or upon exposure to IFNγ to reflect an immune inflamed microenvironment. Cells were cultured in 96-well plate, 100 mm, or 150 mm Petri dishes, and treated with either 10 ng/ml or 100 ng/mL mouse IFNγ. Cell culture supernatants and cell lysates were harvested after 6h,

12h, or 24h incubation with IFNγ and processed for multiplex Luminex bead-based immunoassay. The soluble and cellular checkpoint proteins most substantially modulated by IFNγ treatment in these cell lines included: CD137, BTLA, HVEM, PD-L1. The tumor-specific signature of cellular and soluble checkpoint proteins and its response to IFNγ may have implications in the tumor microenvironment and in the outcome to immunotherapy.

#6382

Activation of transcription factors, p65 and NFATc1, mediated by WNT5a, induces up-regulation of novel immune checkpoint CNTN4 expression

Mi Young Cha, Bu-Nam Jeon, Hyeokgu Kang, Kyung Mi Park, Hansoo Park. *Genome & Company, Sungnam-si, Gyeonggi-do, Korea, Republic of*

We previously confirmed that contactin 4 (CNTN4) is highly expressed in the various human tumor tissues and inhibits mouse and human T cell activity by suppressing a cascade of signaling processes associated with T cell activation through binding with amyloid precursor protein (APP) of T cells. However, the molecular mechanism for the expression of CNTN4 in tumors has yet to be elucidated. So, we investigated whether oncogenic ligands regulate the expression of CNTN4 through *CNTN4* promoter (-2,000 bp ~ + 100 bp)-based reporter gene assays in HEK293 cells using oncogenic ligands. Here, we identified that WNT5a significantly increased the expression of CNTN4 in a dose-dependent manner. Furthermore, the treatment of the WNT5a ligand in the human colorectal cancer cell line SW480, which expresses CNTN4 at a low level, increased the expression of CNTN4. In addition, CNTN4 expression was decreased when the WNT5a antagonist (Box5, a WNT5a-derived N-butyloxycarbonyl hexapeptide) was treated in the human osteosarcoma cell line U2OS expressing CNTN4 endogenously. The changes in the expression of CNTN4 were observed by RT-PCR and FACS. Treatment of the WNT5a ligand or WNT5a antagonist changed the transcriptional expression of CNTN4 in each cell line and affected the cell surface expression of CNTN4. Since WNT5a ultimately increases the activity of transcription factors such as NFATc1 or p65 to increase the transcriptional expression of the target gene, we further investigated the effect of NFATc1 or p65 on the expression of CNTN4. We

found that NFATc1 or p65 binds to the promoter of CNTN4 and increases the expression of transcription. Moreover, it was recently reported that anti-PD-1-refractory melanoma exhibits elevated WNT ligand signaling activity, especially upregulated WNT7b and WNT5a in the WNT ligands. Following this background, the expression level of CNTN4 can be increased in the refractory environment to immunotherapy induced by elevated WNT signaling. Therefore, we constructed B16F10 murine melanoma cells overexpressing WNT5a (B16F10/WNT5a) to assess the anti-tumor efficacy by administering GENA-104A16, the anti-CNTN4 humanized monoclonal antibody, in the syngeneic mice model with increased expression of CNTN4 induced by WNT5a, and *in vivo* efficacy by treatment of GENA-104A16 is under assessment in the B16F10/WNT5a syngeneic mice model. Through the investigation, we expect to support the rationale and strategy for a combination therapy approach of GENA-104A16 for non-responding patients to immunotherapy.

#6384

ATG-034, an LILRB4 antagonist antibody, reinvigorates dendritic cells and prevents tumor progression

Ao Sun[1], Enlin Zheng[1], Huili Cao[1], Mengshi Cao[2], Suya Bai[2], Peng Chen[1], Linjie Tian[3], Jay Mei[1], Bo Shan[4], Bing Hou[4]. *[1]Antengene Corporation, Shanghai, China,[2]Antengene (Hangzhou) Biologics, Hangzhou, China,[3]Antengene Biotech LLC, Doylestown, PA, China,[4]Antengene Corporation, Shaoxing, China*

Background: Dendritic cells (DCs) are vital for initiating antigen-specific T cell-dependent antitumor immune responses. However, emerging evidence reveals that local DCs within the tumor microenvironment (TME) are tolerized to facilitate immune evasion. Reprogramming of DCs is recognized as a promising strategy for tumor immunotherapy. Leukocyte immunoglobulin-like receptor B4 (LILRB4) is an inhibitory receptor belonging to the LILR family which is mainly expressed on normal myeloid cells and myeloid-derived malignant cells. It is upregulated on tolerogenic DCs (tolDCs), which exhibit low expression levels of costimulatory molecules and resistance to DC maturation. Targeting LILRB4 to reprogram tolDCs has been reported to be a promising strategy for cancer

treatment. Here we report the preclinical development of an LILRB4 antagonist antibody, ATG-034.
Method: The protein-based and cell-based binding affinity of ATG-034 were measured using SPR, ELISA and FACS analysis. Fc receptor (FcR) stimulation assay was used to evaluate the ability of ATG-034 to block the interaction of LILRB4 with its ligand fibronectin. ATG-034-mediated enhancement of antigen presentation and co-stimulation ability of DCs was determined by FACS analysis for the change of surface expression of HLA-DR, HLA-ABC, CD86, and CD206. The mixed lymphocyte reaction (MLR) assay was used to assess the immunomodulatory potential of ATG-034. The *in vivo* antitumor efficacy of ATG-034 was evaluated in a radiation therapy-resistant murine Lewis lung carcinoma (LLC) syngeneic model.
Results: ATG-034 binds to LILRB4 protein with a single-digit nM affinity. It potently reversed the fibronectin-mediated inhibition of FcR-driven TNF-α cytokine production. TolDCs were reprogrammed by ATG-034 to immunogenic DCs with significant upregulation of the expression of HLA-DR, HLA-ABC, CD86 and downregulation of the expression of CD206. Furthermore, ATG-034 remarkably reinvigorated tolDCs for priming T cell activation with noticeable upregulation of the expression of CD25 and the secretion of IFN-γ, enhancing antitumor immunity. In addition, 10 mg/kg ATG-034 significantly inhibited the LLC tumor growth *in vivo* with a TGI of 40.28%, while a benchmark antibody only demonstrated a 24.43% TGI.
Conclusion: Our data show that ATG-034 reprograms tolDC, enhancing anti-tumor immunity, and demonstrates potent *in vivo* anti-tumor efficacy. Therefore, ATG-034 may be a promising strategy for the treatment of cancer.

Immune Mechanisms Mediated by Other Therapies

#6388
High dose acetaminophen with n-acetylcysteine rescue inhibits M2 polarization of tumor associated macrophages.

Alexander Neuwelt, Allyn Bryan, Won Lee, Pavani Pingali, Howard Li, Bhaumik Patel. *Veterans Affairs, Richmond, VA*

Background: High dose acetaminophen (AAP) with n-acetylcysteine (NAC) rescue is among the few treatments that has shown a signal of activity in phase I trials (21% response rate, 3/14 assessable patients) without achieving dose limiting toxicity that has not progressed to evaluation in later line studies. We have previously shown that high dose AAP selectively depletes glutathione in the liver but not the tumor, suggesting that NAC, the FDA-approved antidote for AAP toxicity and a glutathione precursor, may selectively rescue the normal liver but not the tumor from high dose AAP. While the anti-tumor effects of AAP/NAC appear to not be mediated by glutathione depletion and free radical injury, the mechanism of anti-tumor effects of AAP/NAC has not been definitively characterized.
Methods: In vitro the effects of Vehicle, AAP, or AAP/NAC was evaluated on bone marrow derived macrophages polarized to M2 and M1 phenotypes using IL-4 or IFN/LPS, respectively. Tumor cell viability was assessed with MTT assay. Effects of AAP on IL-4/STAT6 (M2) or IFN/LPS/STAT1 (M1) signaling, and downstream gene and protein expression was studied. In vivo, effects of AAP/NAC on tumor size and tumor associated macrophage polarization were characterized in orthotopic triple negative breast tumor models 4T1 and EF43.fgf4 using cytokine elisa of tumor lysate and flow cytometry.
Results: NAC reversed AAP toxicity in the normal liver but did not reverse AAP cytotoxicity against tumor cells in vitro. AAP/NAC selectively inhibited IL-4-induced STAT6 phosphorylation but not IFN/LPS-induced STAT1 phosphorylation. Downstream, AAP/NAC inhibited IL-4 induction of M2-associated genes (such as CCL24, YM1 and arginase) and proteins (arginase, PD-L2, and CD206). However, AAP/NAC did not inhibit IFN/LPS induction of M1-associated genes (IL-6, TNF, IL-12) and proteins (INOS, PD-L1, MHC I, and CD64). In vivo, AAP/NAC inhibited tumor growth in EF43.fgf4 and 4T1 triple negative breast tumors. Flow cytometry of tumor associated macrophages revealed that AAP/NAC selectively inhibited M2 but not M1 polarization. ELISA of tumor lysate demonstrated relatively stable expression of IFN gamma but markedly suppressed expression of IL-10 in the tumor immune microenvironment.
Conclusion: Our study is the first to show that at high doses AAP/NAC has profound effects on the tumor immune microenvironment that may facilitate immune-mediated inhibition of tumor growth.

#6389

Differential role of CD8 cells and CD4 cells in anti-tumor immunity triggered by tumor cell apoptosis using HSVtk/GCV system

Sho Umegaki, Hidekazu Shirota, Tomoyuki Iwasaki, Yuki Kasahara, Chikashi Ishioka. *Medical Oncology, Tohoku University Hospital, Sendai, Japan*

Immune cells can recognize tumor antigens and elicit an adaptive immune response, potentially resulting in tumor regression. Drug-induced dead tumor cells have been reported to enhance anti-tumor immunity, but results are conflicting, possibly due to the immunosuppressive effects of the cytotoxic drugs. To investigate whether apoptotic tumor cells trigger anti-tumor immunity independent of anti-cancer treatment, local immune responses were evaluated after direct induction of tumor cell apoptosis using a herpes simplex virus thymidine kinase (HSV-tk)/ganciclovir (GCV) system. The inflammatory cytokines IFNγ and IL-12β and anti-inflammatory factor PD-1 and TGFβ1 were upregulated at the tumor site after apoptosis induction. HSV-tk/GCV-induced tumor cell apoptosis resulted in suppression of tumor growth in vivo and promoted the infiltration of CD8 and CD4 T lymphocytes in tumor. To explore the role of T cells after induction of tumor cell death, GCV was administered together with anti-CD8 or anti-CD4 depleting antibodies to syngeneic HSV-tk transfected tumor-bearing mice. CD8 T cell depletion abrogated the anti-tumor efficacy of GCV, indicating that tumor regression was mainly dependent on CD8 T cells. This anti-tumor immunity was enhanced by anti-PD-1 antibody injection. On the contrary, CD4 T cell depletion further inhibited tumor growth than GCV alone, suggesting the potential role of CD4 T cells in suppressive tumor immunity. To elucidate this immunological mechanism, tumor tissues were evaluated after tumor cell apoptosis and CD4 T cell depletion. Foxp3, a regulatory T cell marker, was decreased after CD4 T cell depletion. In addition, Arg1, a marker of immunosuppressive myeloid cells, was significantly downregulated, which was expressed on tumor-associated macrophages (TAMs) and monocytic myeloid-derived suppressor cells (mMDSCs). Collectively, these findings indicate that tumor cell apoptosis accelerates CD8 T cell-dependent anti-tumor immunity and CD4 T cell-mediated Arg1 production from TAMs and mMDSCs.

#6390

N17350 is an emerging therapeutic modality that selectively kills cancer cells and stimulates anti-tumor immunity

Ravindra Gujar[1], Chang Cui[1], Lilibet Valdovinos[1], Christine Lee[1], Arezoo Arjmand[1], Nicole Grigaitis[1], Asna Khalid[1], Catherine A. Reardon[2], Kelly Q. Schoenfelt[2], Sonia Feau[1], Chris Twitty[1], Lev Becker[1]. *[1]Onchilles Pharma, Inc., San Diego, CA,[2]University of Chicago, Chicago, IL*

INTRODUCTION: Cancer is a disease driven by variable genetic mutations. Overcoming this variability while sparing normal cells has stymied broad-acting therapy development. Our innate immune system evolved to clear genetically diverse pathogens and limit host toxicity, raising the possibility that it can produce similar effects in cancer. Previous studies showed that neutrophil elastase (ELANE) - a neutrophil-derived serine protease - killed a wide range of cancer cells without harming non-cancer cells by cleaving CD95, the FAS receptor (Cui et al.,Cell, 2021). ELANE attenuated primary tumor growth and produced a CD8+T cell-mediated abscopal effect to attack metastases. Here we leveraged this ELANE-mediated pathway to produce an optimized N17350 biologic and tested its effects on tumor development, both as a monotherapy and in combination with checkpoint inhibitors. Our findings underscore the viability of N17350 as a new therapeutic modality leveraging innate immunity.

METHODS: Anti-cancer effects of N17350 were examined in vitro and in vivo and compared with standard of care (SoC) agents. For in vitro studies, cells were treated with N17350 and viability was quantified by calcein-AM and immunogenic cell death (ICD) markers. Cancer/non-cancer cells included human/murine cell lines and primary cells isolated from healthy donors and ovarian cancer patients. We further tested the ability of cancer cells to develop resistance to N17350 and FAS-L. For in vivo studies, a single dose of N17350 was delivered intratumorally into CT26 (colon) and 4T1 (metastatic breast) tumors. Effects on primary and metastatic tumor growth, immunology, and survival were assessed in comparison to SoC agents (oxaliplatin, cyclophosphamide) or in combination with a checkpoint inhibitor (anti-CTLA4).

RESULTS: N17350 killed and induced ICD markers in all cancer cell types tested without harming non-cancer cells, while SoC agents were similarly toxic to both cell types. Repeatedly killing E0771 cancer cells with N17350 did not produce resistance, which was observed with a FAS-L that targets CD95 via a distinct mechanism. A single intra-tumoral dose of N17350 produced durable effects in the 4T1 and CT26 models (CT26:75%-100% tumor-free). N17350 induced a robust innate/adaptive immune profile, abscopal effect to limit 4T1 lung metastasis, and synergized with anti-CTLA4 in cold (4T1) and hot (CT26) tumors. Finally, N17350 showed markedly improved efficacy over SoC agents in both models.
CONCLUSIONS: Taken together, our data suggest that N17350 selectively kills cancer cells, produces complete responses in a subset of mice, induces favorable innate and adaptive immunology, and combines with checkpoint inhibitors in cold and hot tumors. Its ability to escape resistance, produce abscopal effects, and outperform SoC chemotherapies warrants further studies of this unique therapeutic modality in a clinical setting.

#6391

Development of a novel strategy for cancer immunotherapy based on tumor immunogenicity improvement by HLA-drug interaction

Takeshi Susukida[1], So-ichiro Sasaki[1], Tomohiro Shirayanagi[2], Shigeki Aoki[2], Kousei Ito[2], Yoshihiro Hayakawa[1]. *[1]University of Toyama, Toyama, Japan,[2]Chiba University, Chiba, Japan*

[Purpose] Tumors with low T cell infiltrates (poor immunogenicity) display lower probability of clinical response to immune checkpoint inhibitors. To achieve higher immunotherapy efficacy, it is imperative to establish a novel strategy for improving immunogenicity. Abacavir (ABC), an anti-HIV drug, binds to the specific allele of human leukocyte antigen (HLA-B*57:01) and activate $CD8^+$ T cells by presenting altered abnormal peptides. In this study, we considered the immune interaction between ABC and HLA-B*57:01 improving immunogenicity in poorly immunogenic tumors leading to a potent anti-cancer effect.
[Methods] Mice were inoculated subcutaneously with tumor cells into the right flanks and interperitoneally treated with either ABC 5 mg or vehicle (water) for consecutive 9 days (B16F10) or 13 days (3LL) after tumor inoculation. Each tumor size was measured using vernier calipers on every

2 days. Activation, proliferation, and IFN-γ secretion of tumor infiltrating $CD8^+$ T cells were analyzed by FACS.
[Results and Discussion] ABC treatment showed significant tumor growth inhibition associated with $CD8^+$ T cell infiltration into tumor in mice inoculated with HLA-B*57:01 expressing B16F10 melanoma or Lewis lung carcinoma (3LL) cells, but neither in HLA-B*57:03 (negative allele)-expressing nor control tumors inoculated mice. Moreover, the tumor infiltrating $CD8^+$ T cell were immune-activated and proliferated, with secreting IFN-γ. In contrast, ABC-induced anti-tumor effect was abrogated in $CD8^+$ T cell-depleted mice, IFN-γ KO mice, and CXCR3-blocked mice. The combination therapy with anti-PD-1 antibody treatment induced better inhibition of tumor growth than ABC monotherapy in HLA-B*57:01 expressing B16F10 inoculated mice. These results suggested that ABC/HLA-B*57:01 interaction could improve tumor immunogenicity associated with $CD8^+$ T cell-mediated anti-tumor effect in poorly immunogenic tumors. This finding lays a foundation to develop a novel drug-induced cancer immunotherapy targeting immune resistant tumors.

#6392

Combination of pulsed electric field, immunotherapy and cisplatin significantly prolongs survival in an orthotopic breast cancer mouse model

Chiara Pastori[1], Mukta Wagh[1], Ebtesam Nafie[1], Fatima Murad[1], Mohit Trikha[2], Robert Neal[1]. *[1]Galvanize Therapeutics Inc, San Carlos, CA,[2]Apple Tree Partners, New York, NY*

Introduction: Pulsed Electric Field (PEF) therapy is a novel approach to treat cancer by providing focal tumor ablation while sparing sensitive structures within the tumor micro-environment. Previous studies have demonstrated that PEF induces immunogenic cell death by activating inflammatory signaling pathways and stimulation of antigen presenting cells withing the tumor micro-environment. PEF ablation provides a tumor focused *in situ* vaccination strategy that combines with checkpoint blockade. We hypothesized that PEF ablation should synergize with chemotherapy and anti-PD1 in a model where checkpoint inhibitors are inactive.

Experimental Design: To test this hypothesis, we utilized a highly aggressive syngeneic orthotopic triple negative breast cancer 4T1 mouse model that is non-responsive to anti-PD1 and only marginally responsive to cisplatin to determine if this combination treatment could prolong survival. Thirty-two Balb/c mice were inoculated in the mammary fat pad with 200,000 4T1 cells. Once tumors were established (5mm in diameter), animals were randomized to the following groups: (A) Sham/IgG control (n=8; needle inserted but no PEF), (B) PEF only (n=8), (C) cisplatin + anti-PD-1 (n=8) and (D) PEF + cisplatin + anti PD-1 (n=8). Tumors in groups B and D were treated once with PEF. Anti-PD1 and isotype matched control IgG was administered once per week (200μg, i.p injections) starting on the day of PEF (Group D) for four weeks. Cisplatin was administered (2mg/kg, i.v) once per week for four weeks starting on the day of PEF (d=0) for four weeks. All the mammary fat pad tumors were resected when they achieved a tumor volume of ~200 mm^3 to recapitulate post-resection metastatic relapse (See Schematic 1).
Results and Conclusions: All mice in the Sham-control IgG group needed to be euthanized by day 43 due to metastases in multiple organs including lungs, bones, liver and brain. All mice in the cisplatin + anti PD-1 group had to be euthanized by day 74. Interestingly, all groups that were treated with PEF survived much longer. On day 90, 28% of mice in the PEF alone group were alive and 43% were alive in the PEF + anti-PD1 + Cisplatin (see Figure 1). The rank-log p-value for the Kaplan-Meier survival curve was statistically significant.
In conclusion, our results demonstrate that PEF treatment in combination with anti-PD1 and Cisplatin significantly prolongs survival in a highly aggressive triple negative breast tumor mouse model that is non-responsive to immunotherapy. These findings support evaluation of PEF in cancer patients that are receiving combination of checkpoint blockade and chemotherapy.

#6395

Atovaquone promotes release of damage-associated molecular patterns from epithelial ovarian cancer cells

Mayra A. Betancourt Ponce[1], Nicha Boonpattrawong[1], Sejal Sharma[1], Jenny Gumperz[2], Manish Patankar[1], Lisa Barroilhet[1]. [1]*University of*

Wisconsin Carbone Cancer Center, Madison, WI,[2]University of Wisconsin, Madison, WI

Epithelial ovarian cancer (EOC) is the deadliest gynecologic cancer in the United States. Most patients are diagnosed with EOC at advanced stages and have limited treatment options. Developing new therapies that are effective against localized and disseminated disease is imperative. Unfortunately, clinical trials evaluating immunotherapies in EOC have not been consistently effective. Preclinical data have shown that neoadjuvant chemotherapy can help increase antigen presentation and T cell infiltration, as well as decrease immunosuppressive effectors, suggesting that combining cytotoxic chemotherapy with immunotherapies can be a powerful approach to potentiate antitumor responses in EOC. However, studies looking at the combination of immunotherapies with carboplatin and paclitaxel, which are the mainstay chemotherapies for EOC, have not improved progression-free survival rates. We propose a novel combination approach using the well-tolerated, FDA-approved, oxidative phosphorylation (OXPHOS) inhibitor atovaquone as a sensitizer to cellular immunotherapies for EOC. OXPHOS inhibition leads to oxidative stress, which in turn leads to DNA and protein damage, activation of stress response pathways, and ultimately cell death. During cell injury and death, Damage-Associated Molecular Patterns (DAMPs) can be released into the extracellular environments, activate the innate immune system, and lead to immunogenic cell death. We have previously shown that atovaquone leads to increased reactive oxygen species levels and DNA damage. Thus, we hypothesized that atovaquone treatment would lead to release of DAMPs, including HMGB1 and TFAM, from EOC cells. Following treatment with atovaquone, we collected the supernatant of EOC cell cultures at different timepoints and measured HMGB1 and TFAM concentrations via enzyme-linked immunosorbent assays (ELISAs). We observed that both HMGB1 and TFAM concentrations were elevated at 24 and 48 hours following atovaquone treatment. This suggests that atovaquone can facilitate immune detection and attack by promoting DAMPs release. When DAMPs are released into the extracellular environment, they are recognized by innate immune cells, which become activated to produce pro-inflammatory cytokines and increase antigen presentation to T cells. Given our results showing increased release of DAMPs following exposure to atovaquone,

we are developing an in vitro culture system to study immune cell responses to atovaquone-treated EOC cells. We are also monitoring transcriptomic responses of EOC cells treated with atovaquone to identify changes in expression of DAMPs and other immune-activating pathways through RNA sequencing. Our ultimate goal is to test T cell recognition and responses toward atovaquone-treated EOC cells with the intention of utilizing this chemotherapeutic agent as an adjunct to immunotherapeutic efforts for EOC.

#6396

BET inhibition alleviates T-cell dysfunction in chronic lymphocytic leukemia

Audrey L. Smith[1], Alexandria P. Eiken[1], Sydney A. Skupa[1], Christopher R. D'Angelo[2], Avyakta Kallam[2], Matthew A. Lunning[2], Gregory Bociek[2], Julie M. Vose[2], Ben Powell[3], Gideon Bollag[4], Dalia El-Gamal[1]. *[1]Eppley Institute for Research in Cancer and Allied Diseases, University of Nebraska Medical Center, Omaha, NE,[2]Division of Hematology and Oncology, University of Nebraska Medical Center, Omaha, NE,[3]Plexxikon Inc., South San Francisco, CA,[4]Opna Bio, LLC, South San Francisco, CA*

Background: The chronic lymphocytic leukemia (CLL) tumor microenvironment (TME) is laden with hyporesponsive T-cells that permit disease persistence. Yet, redundant TME immunosuppressive mechanisms and epigenetic maintenance of T-cell exhaustion limit the efficacy of T-cell targeted therapies in CLL. Bromodomain and extra-terminal (BET) proteins regulate key pathways contributing to CLL pathogenesis and TME interactions, including T-cell function and differentiation. We hypothesize that blocking BET protein function can reverse T-cell exhaustion to yield durable tumor elimination in CLL.
Methods: WT C57BL/6 mice were engrafted with Eμ-TCL1 spleen-derived lymphocytes, then treated daily with the novel pan-BET inhibitor, OPN-51107 (OPN5; 20mg/kg PO) for up to 4 weeks. Splenic gene expression was evaluated with the NanoString PanCancer iO360 panel. T-cell differentiation status, immune inhibitory receptor (IR) expression, proliferation (72 h ex vivo α-CD3/α-CD28 stimulation), and cytokine production (6 h ex vivo PMA/ionomycin stimulation) was measured via flow cytometry. CLL patient and healthy donor PBMCs were used for

validation studies and to assess T-cell transcription factor (TF) expression via flow cytometry. Evaluation of BRD4 occupancy at select T-cell TFs via ChIP qPCR is ongoing.
Results: OPN5 significantly increased cytotoxic cell signatures and reduced exhaustion-associated cell signatures in leukemic mice through inhibition of T-cell exhaustion signaling, as well as activation of Th1, natural killer cell, and IL-7 signaling pathways. Correspondingly, T-cells from OPN5-treated mice demonstrated greater ex vivo proliferative capacity and effector response to stimuli. A greater proportion of CD8+ T-cells from OPN5-treated mice were classified as naïve, and OPN5 significantly reduced KLRG1 expression on antigen-experienced CD8+ T-cells. Importantly, OPN5 curtailed IR co-expression (PD-1, PD-L1, VISTA, CD244, CD160, and LAG3) on splenic T-cells. These findings were confirmed with primary CLL cells ex vivo. OPN5 also impaired expression of terminal differentiation-associated TFs in CLL patient-derived T-cells, enriching for a TCF1+ progenitor T-cell population. While BTK inhibitors are known to similarly improve T-cell function in CLL, ibrutinib treatment was inadequate to revert CLL T-cell terminal differentiation. Future ATAC-sequencing analysis will inform how BET inhibition alleviates exhaustion-associated chromatin organization in CLL T-cells.
Conclusion: BET inhibition dismantles immunosuppressive mechanisms in the CLL TME, alleviating CLL-induced T-cell dysfunction and terminal differentiation. These findings suggest that BET inhibition may be a useful component of combination strategies for the treatment of CLL to yield lasting anti-cancer immune memory and prevent relapsed/refractory disease.

#6397

Eribulin acts as an immune adjuvant to enhance the antitumor efficacy of STING agonists in triple-negative breast cancer models

Leila Takahashi-Ruiz, Charles S. Fermaintt, Nancy Wilkinson, Peter Y. Chan, Susan L. Mooberry, April L. Risinger. *Pharmacology, UT Health Science Center at San Antonio, San Antonio, TX*

Triple-negative breast cancer (TNBC) is a heterogenous subtype of breast cancer lacking effective targeted treatment options. However, TNBC typically has a higher mutational burden and greater degree of

immunogenicity than other breast tumors, making immunotherapy a viable strategy for effective treatment. Strategies to improve the response of TNBC patients to immunotherapy include the upregulation of the cGAS-STING innate immune sensing pathway and STING agonists are in clinical development. We previously showed that eribulin, a microtubule destabilizer used in the treatment of TNBC, functions as an indirect STING agonist because it promotes the release of mitochondrial DNA into the cytoplasm. In separate studies, we demonstrated that eribulin also significantly enhances type I interferon expression induced by STING agonists through a second TBK1-dependent mechanism downstream of STING activation. Both mechanisms of eribulin-mediated activation of interferon expression occur in immune and TNBC cells and are shared with other microtubule destabilizers but not with the microtubule stabilizer paclitaxel. Our current studies demonstrate the in vivo immunological effects of the microtubule destabilizer eribulin with the STING agonist ADU-S100 that lead to a significant decrease in tumor growth in the spontaneous MMTV-PyVT mammary tumor model upon combination treatment. The immunostimulatory effects of eribulin with or without concurrent administration of a STING agonist were determined in the spleen, tumor draining lymph nodes, and tumors with distinct effects observed in the activation of innate and adaptive responses. We further demonstrate the immunological and antitumor efficacy of combinations of eribulin and ADU-S100 in the syngeneic 4T1 model that is resistant to the antimitotic effects of eribulin as a single agent. Even in the absence of direct antimitotic effects on the tumor, eribulin was sufficient to promote activation of $CD4^+CD25^-$ effector T-cells in the spleen and lymph nodes specifically in tumored animals but not untumored controls. Additionally, eribulin was able to promote a similar increase in the activation of $CD4^+$ effector T-cells even in untumored animals when administered in combination with a STING agonist. Together, these data contribute to accumulating evidence that there are important mechanistic differences between the microtubule targeted chemotherapeutics currently used in the treatment of TNBC that could inform on their more rational use in the clinic as single agents or as chemotherapeutic backbones in combination with targeted therapy, including immunotherapeutics. More specifically, our data demonstrate that eribulin can act as an immune adjuvant to promote STING

signaling and T-cell activation in multiple in vivo TNBC models in addition to its well established anti-mitotic effects to enhance antitumor efficacy.

#6398
Targeting ENPP1 to boost anti-tumor immunity during PARP inhibition
Jie Li, Charlotte Mason, Kay Hanggi, Vincent Luca, Brian Ruffell. *H. Lee Moffitt Cancer Center, Tampa, FL*

Homologous recombination (HR) deficiency confers sensitivity to poly (ADP-ribose) polymerase inhibitors (PARPi), which have been approved for use in ovarian and triple negative breast cancers (TNBC) carrying loss-of-function mutations in HR pathway genes, most commonly *BRCA1/2*. Preclinical studies in BRCA1-deficient tumor models have demonstrated that the immune compartment is required for PARPi efficacy through the ability of PARPi to cause micronuclei formation and activate cGAS in tumors cells. The production of the 2'3'-cGAMP secondary intermediate stimulates STING in neighboring tumor-infiltrating immune cells to promote an anti-tumor response. Despite this evidence of immune stimulation, PARPi does not extend overall survival in TNBC patients, suggesting that immune suppression remains a significant barrier for efficacy. Here we sought to evaluate the role of ectonucleotide pyrophosphatase/phosphodiesterase 1(ENPP1), a type II transmembrane glycoprotein that hydrolyzes extracellular 2'3'-cGAMP. We generated *Brca1*/*Pten*/*Trp53*-deficient TNBC cell lines from a genetically engineered mouse model and found that these expressed higher levels of ENPP1 than *Brca1*-proficient TNBC and non-TNBC cell lines. Knocking out *Enpp1* via CRISPR/Cas9 increased 2'3'-cGAMP production during Niraparib treatment but did not affect cellular proliferation *in vitro*. Critically, knocking out *Enpp1* significantly reduced the growth of orthotopic *Brca1*-deficient tumors, with no change in growth observed for orthotopic E0771 or PyMT models, suggesting an important role for ENPP1 in HR-deficient tumors. Therapeutic dosing of Niraparib further reduced the growth of *Enpp1* knockout tumors in a manner that was dependent upon host STING and correlated with higher $CD8^+$ T cell infiltration and effector function. These findings demonstrate that ENPP1 suppresses anti-tumor immunity in *Brca1*-deficient tumors, suggesting that blocking the enzymatic activity of

ENPP1 may provide therapeutic benefits during PARPi treatment for TNBC patients.

#6399

Hyperthermic intrathoracic chemotherapy (HITOC) improves malignant pleural mesothelioma control through a tumor specific cytotoxic immune response

Yameng Hao[1], Aspasia Gkasti[1], Louis-Emmanuel Chriqui[2], Damien Marie[2], Michel Gonzalez[2], Thorsten Krueger[2], Solange Peters[2], Paul J. Dyson[1], Etienne Meylan[3], Johanna Joyce[4], Sabrina Cavin[2], Jean Y. Perentes[2]. *[1]École Polytechnique Fédérale de Lausanne, Lausanne, Switzerland,[2]CHUV Lausanne University Hospital, Lausanne, Switzerland,[3]Université libre de Bruxelles, Bruxelles, Belgium,[4]University of Lausanne, Lausanne, Switzerland*

Introduction: The management of malignant pleural mesothelioma (MPM) remains challenging with poor patient survival. Local therapies such as hyperthermic intrathoracic cisplatin (HITOC) have shown good tumor control in selected patients. HITOC was shown to increase MPM drug exposure while limiting systemic side effects but alternative mechanisms for HITOC are still lacking. Here, we hypothesized that HITOC induces an immune response directed against MPM which decreases cancer related mortality.

Methods: We implanted AB12-luc MPM cells in the pleural cavity of BALB/c mice. A chemotherapy perfusion circuit was downsized to administer cisplatin (80mg/m^2 equivalent dose) in the thoracic cavity at normo (37°C, ITOC) or hyperthermic (39°C, HITOC) conditions for 30 minutes. Tumor growth (visualized by bioluminescence) and mouse survival were then assessed. We determined tumor platinum content and distribution by inductively coupled plasma mass spectrometry (ICP-MS) and by laser ablation ICP-MS (LA-ICP-MS) respectively. We also questioned the impact of (H)ITOC on the MPM immune microenvironment (innate and adaptive immune cells, activity and checkpoint expression) by 16-colour flow cytometry and immunohistochemistry. Finally, tumor response to (H)ITOC was assessed in BALB/c athymic mice implanted with AB12-luc cells.

Results: MPM tumor control and mouse survival were significantly improved by HITOC compared to controls (ITOC, saline 37 and 39°C). Tumor platinum content was significantly higher in HITOC compared to ITOC but was majorly located at the surface of tumors. HITOC enhanced MPM infiltration by $CD8^+$Granzyme B^+ T-cells and decreased the levels of $MCHII^-/CD80^-$ (M2-like) macrophages compared to controls at day 7. Interestingly, immune checkpoint expression of PD1 and CTLA4 was significantly enhanced in $CD8^+$ lymphocytes in HITOC treated MPM compared to controls at day 7. Finally, the lack of T lymphocytes (BALB/c athymic mice) abrogated the impact of HITOC on MPM control and mouse survival.
Conclusion: HITOC improves MPM control through a T lymphocyte immune mediated response. The enhanced immune checkpoint (PD1/CTLA4) expression in $CD8^+$ lymphocytes opens perspectives for the combination of HITOC with immune checkpoint inhibitors.

#6400
Synergistic combination of NCX 4040 and napabucasin induces immunogenic activation via upregulation of mitochondrial oxidative stress and STAT3 inhibition in cadmium transformed and metastatic prostate cancer cells
Nishtha Pathak, Gnanasekar Munirathinam. *Biomedical Sciences, University of Illinois College of Medicine (Rockford), Rockford, IL*

Despite recent diagnostic and therapeutic advances, prostate cancer (PCa) poses a significant burden on men's health and quality of life, retaining the second highest incidence rate after lung cancer. The combinatorial therapy approach has emerged as a useful treatment option for various types of cancer to target tumor heterogeneity and overcome the limitations of existing treatment modalities. Here, we explored the combination of NCX 4040, a nitric oxide-releasing aspirin derivative and Napabucasin, a recently developed STAT3 and cancer stemness inhibitor as a potential treatment for PCa. Two cellular models were used namely BPH-Cd, a cadmium-transformed carcinogenic cell line and DU145, a brain metastatic PCa cell line. Cell viability assay indicated reduced cell viability in both cell lines in a dose-dependent manner and more so in combination as opposed to individual treatments, with an IC_{50} of 5 μM for NCX 4040 and 250 nM for

Napabucasin. Notably, treatment with catalase prevented the synergistic activity of NCX 4040 and Napabucasin in reducing the viability of these cells. This suggested that NCX 4040 and Napabucasin might be inducing oxidative stress related cellular death. In addition, the combination of NCX 4040 and Napabucasin robustly impeded the *in-vitro* tumorigenic potential in both cell lines in colony formation assay and decreased the size of spheroids with increasing doses in *in-vitro* 3D spheroid assay in BPH-Cd. Western blot analysis revealed that in addition to the downregulation of STAT3, NCX 4040 and Napabucasin treatment showed upregulation in cGAS-STING immunogenic activation pathway related markers (pSTING, cGAS, pTBK1 in DU145 and STING, TBK1 in BPH-Cd). This data demonstrated that combination drug treatment might be inducing cell death via immunogenic activation. Additional markers related to this pathway are being tested in both cellular models. Interestingly, thioredoxin (TRX)-interacting protein was highly upregulated in both cell lines following combination treatment indicating that the synergistic effects are mediated via targeting TRX-regulated cellular redox signaling. Subsequently, TRX and thioredoxin reductase 1 were also downregulated in both cell lines. Furthermore, confocal imaging analysis indicated that NCX 4040 and Napabucasin together might be causing DNA damage and mitochondrial stress as DNA release was clearly evident. Flow cytometric analysis demonstrated that the drug combination shows a synergistic effect in producing excess mitochondrial and cellular ROS, causing apoptosis and in inducing cell cycle arrest in both BPH-Cd and DU145 cells. Taken together, our study demonstrates that NCX 4040 and Napabucasin in combination could be a potential anti-PCa therapy which warrants further evaluation for its clinical application.

#6401

HMGB1 release predicts chemotherapy combinatorial efficacy with TIM-3 blockade

Alexis Onimus, Jessica Mandula, Paulo Rodriguez, Brian Ruffell.
Immunology, H. Lee Moffitt Cancer Center, Tampa, FL

We have recently shown that TIM-3 blockade promotes response to paclitaxel chemotherapy in preclinical breast cancer models through its ability to suppress uptake of HMGB1-DNA complexes by dendritic cells.

However, it remains unclear why paclitaxel is necessary for response to TIM-3 blockade. Here we demonstrate that the taxanes paclitaxel and docetaxel induce the loss of HMGB1 from breast cancer cells *in vitro* and *in vivo*. Interestingly, this does not occur through loss of cellular integrity, but rather through an active secretion process involving ADP-ribosylation of HMGB1 by PARP1. PARP1 was activated by docetaxel treatment, as measured by detection of its cleaved form in the cytoplasm, and HMGB1 release was prevented by the use of the PARP inhibitor niraparib. Both PARP1 activation and ADP-ribosylation of HMGB1 were dependent upon the activity of TLR4, a known receptor for paclitaxel, as demonstrated with CRISPR/Cas9-generated knockout cells and TLR4 inhibitors. However, TLR4 stimulation alone was insufficient to induce HMGB1 release. By understanding how taxanes promote the release of HMGB1 we may be able to develop biomarkers for the selection of patients most likely to respond to the combination of chemotherapy and immunotherapy with TIM-3 blocking antibodies.

#6402

The effects of cytotoxic chemotherapy on colorectal cancer immunogenicity

Pietro Paolo Vitiello[1], Rosaria Chilà[2], Giuseppe Rospo[3], Gaia Grasso[3], Giovanni Crisafulli[2], Alice Bartolini[4], Vito Amodio[2], Federica Di Nicolantonio[3], Giovanni Germano[3], Alberto Bardelli[1]. *[1]Università degli Studi di Torino; IFOM - AIRC Institute of Molecular Oncology ETS, Milan, Italy,[2]IFOM - AIRC Istitute of Molecular Oncology - ETS, Milan, Italy,[3]Università degli Studi di Torino, Torino, Italy,[4]Candiolo Cancer Center, Candiolo (Torino), Italy*

Introduction: Immunotherapy based on PD1/PDL1 and/or CTLA4 blocking antibodies has shown efficacy in the molecular subgroup of colorectal cancers (CRCs) characterized by deficient mismatch repair (MMRd). This feature, present in only 4-5% of metastatic CRCs, causes a significant increase of tumor mutational burden (TMB) and tumor neoantigens, ultimately leading to immune rejection. On the other hand, for the majority of MMR proficient (MMRp) CRCs, cytotoxic chemotherapy ± targeted agents still constitute the mainstay of the treatment. Interestingly, even though it is known that cytotoxic agents induce mutations, their

immunogenic potential is still not fully understood. The aim of this work is to systematically investigate the immunogenicity of chemotherapy-induced mutations in CRC.
Methods: We performed a two-step experiment: first, murine CRC models were exposed to chemotherapy agents in an immune-free context (priming phase) and then challenged in immune-deficient and -proficient contexts (editing phase). Chemotherapy agents included the commonly used cytotoxic drugs 5-fluorouracil (5FU), oxaliplatin, SN38 (the active metabolite of irinotecan), cisplatin, and temozolomide, used as single drugs or combinations, in a pulsatile schedule using weekly 'cycles' (2 days on/5 days off) in order to mimic drug exposure in clinical settings. Whole exome sequencing (WES) was performed at baseline, and after both the priming and the editing phases.
Results and discussion: WES analysis showed that cisplatin-based treatment is associated with the highest increase in TMB and predicted neoantigens when compared to 5FU-based combinations. Multiple mutational processes contribute to the accumulation of mutations upon exposure to chemotherapy, as revealed by analysis of mutational signatures. A statistically significant growth delay and increased survival was reported for tumors primed with cisplatin/temozolomide and 5FU/Oxaliplatin/SN38 (FOLFOXIRI) combinations compared to unprimed tumors in immunocompetent but not in immunodeficient mice, suggesting the active involvement of the immune system in controlling tumor growth. Sequencing data of residual (escaped) tumors at the end of the editing phase revealed a preferential loss of mutations etiologically linked to chemotherapy in the immunocompetent models, pinpointing an active immune-editing of chemotherapy-induced mutations.
Conclusions: Cisplatin/temozolomide and FOLFOXIRI treatment effectively prime murine CRC models for subsequent immune rejection. These results suggest that the anticancer effect of chemotherapy treatment may be in part mediated by the immune-editing of chemotherapy-induced mutant cancer subclones.

#6403
A self-replicating RNA precision medicine approach to overcoming resistance to endocrine therapy in ER+BC

Zelanna Goldberg[1], Christian Maine[2], Gabrielle P. Dailey[3], Christine Domingo[2], Gaelle Picarda[2], Hunter Little[2], Annie Chou[2], Jessica Sparks[2], Darina Spasova[2], Shigeki Miyake-Stoner[2], Zachary C. Hartman[3], Christopher A. Rabiola[3], Erika J. Crosby[3], Herbert K. Lyerly[3], Nathaniel Wang[4], Parinaz Aliahmad[2]. *[1]Clinical Development, Replicate Bioscience, San Diego, CA,[2]Research, Replicate Bioscience, San Diego, CA,[3]Department of Surgery, Duke University, Durham, NC,[4]Replicate Bioscience, San Diego, CA*

Drug resistance remains the major driving factor behind the clinical failure of targeted therapeutics. Current oncology precision medicine approaches rely on targeting known acquired resistance mutations, such as EGFR T790M or ALK/ROS mutations in NSCLC with 2nd and 3rd generation molecules designed to overcome or prevent resistance. These next generation targeted therapeutic approaches have increasingly long and complex drug development timelines and burdensome toxicities from off target effects (e.g. wild-type receptor targeting) or drug-drug interactions (DDI). The toxicities limit tolerability, compliance and combinability of different targeted therapeutics. RNA-based immunotherapy approaches offer an increasingly attractive alternative to next generation small molecule targeted therapeutics approaches: (1) RNA-based approaches only require a known acquired resistance sequence, (2) drug development timelines, cost and complexity can be meaningfully condensed, and (3) multiple acquired resistance mutations can be targeted with the same candidate. RBI-1000 is a candidate using a novel type of self-replicating RNA (srRNA) to generate robust immunity directed against acquired resistance mutations that develop in ER+ breast cancer (ER+ BC) in response to endocrine therapy. RBI-1000 includes on-target mutations within the estrogen receptor ligand binding domain, and bypass mutations either in the form of activating mutations in the PI3K kinase domain or amplifications of HER2/HER3. Here, we demonstrate that this srRNA encapsulated in a lipid nanoparticle primes polyfunctional CD4 and CD8 T cells leading to tumor growth inhibition and improved survival in a mouse model expressing the targeted acquired resistance mutation. Priming of T cells against acquired mutations is also confirmed in human HLA-transgenic mice. The immune cell-mediated elimination of clones expressing the acquired resistance mutations is

predicted to prolong endocrine control of ER+BC, in an analogous manner to small molecule or monoclonal antibody targeted therapies, but with a more favorable dosing and adverse event profile due to precise immunologic targeting and no DDI.

#6404

Clinical scenario of immune checkpoint inhibitor treatment in metastatic nasopharyngeal carcinoma

Cheng-Lung Hsu, Yung-Chia Kuo. *Chang Gung Memorial Hospital - Linkou branch, Taoyuan, Taiwan*

Advanced in local treatment technology and early detection methodology, distant metastasis became a critical issue in Nasopharyngeal carcinoma (NPC). Recently, cancer immunotherapy especially immune checkpoint inhibitors (ICIs) including anti-programmed death-1 (PD-1) and PD-1 ligand (PD-L1) monoclonal antibodies (Mabs) had a rapid progress in cancer patient management. We try to clarify the clinical scenario of immune-related parameters in metastatic NPC. We had check 81 metastatic tissue PD-L1 expression without ICI treatment from the tissue bank of CGMH, Linkou, during 2005~2019. Using anti-PD-L1 antibody, 22C3 Dako, tumor proportional score (TPS) was positive in 43.2% (35/81) checked tissue and combine positive score (CPS) was positive in 58.0% (47/81) tissue respectively. For overall survival (OS) combined with PD-L1 expression in metastatic tissue analysis, positive CPS but not TPS correlated with longer survival with statistical significance (TPS: >0% vs =0%, median survival, 24m vs 22.5m, p=0.615186; CPS: >0% vs =0%, median survival, 28m vs 16m, p=0.003709). Retrospectively analysis of metastatic NPC treatment of combination of chemotherapy, ICIs, and local treatment in our institute in the past 6 years, total 40 patients was enrolled with median overall survival of 34.1 months. Objective response rate by RECIST criteria for immunotherapy-based regimen was 75% (CR:40%; PR:35%) and disease control rate was 85%. According to response by RECIST criteria, median overall survival were 34.1 months vs. 16.7 months respectively for responders and non-responders. With pre-treated NLR as cutoff value of 1.6, difference of median overall survival between two groups (responder vs nonresponder) was statistically significant (p=0.021). We also found that lower median post-treatment NLR in responders than in

non-responders (1.4 vs. 3.2, p=0.013). Using rapid lymphocyte amplification protocol via IL-2 stimulation, the PBMC from most of the patient received ICIs treatment can be amplified 1~10 folds and positively correlated with total lymphocyte count. Through flowcytometry analysis, we found these amplified PBMC was lymphocyte dominant and rich in CD8+. We also found these amplified PBMC can kill the NPC EBV-positive cell line and xenograft in vitro and in vivo. These results demonstrated that combination of chemotherapy, ICIs, and local treatment will benefit metastatic NPC patients.

#6406

Radiation and STING activation limit tumor development and modulate the immune environment via distinct mechanisms

Kay Shigemori[1], Yanyan Jiang[1], Bruno Beernaert[1], Anderson J. Ryan[1], Eileen E. Parkes[2]. *[1]Oncology, University of Oxford, Oxford, United Kingdom,[2]Oncology, Centre for Immuno-Oncology, University of Oxford, Oxford, United Kingdom*

Carcinogen-induced lung cancer in A/J mice is an established model of tumor initiation and development. The impact of radiation, immune response, and STING pathway activation on tumor development in this model is not well understood. In this study, we examined the effect of radiation and the STING agonist, DMXAA (Vadimezan), on the development of urethane-induced lung cancer.A/J mice were treated with urethane (i.p.) to induce the development of lung tumors. Three days after urethane treatment, mice received 13 Gy thorax radiation treatment (RT)/ mock RT, DMXAA (20 mg/kg i.p.)/ vehicle, or a combination treatment (n = 5). Mice were euthanized after 6 hours to 7 days after treatment to assess early events in the lung with RNA-sequencing and flow cytometry, or 5 months after treatment to assess tumor growth and long-term changes to the immune microenvironment with multiplex immunofluorescence.Mice treated with urethane followed by RT had fewer lung surface tumors ($p < 0.01$) and reduced tumor area ($p = 0.0732$) compared to their mock RT controls. In parallel, mice that received urethane pre-treatment and RT had high numbers of tertiary lymphoid structures (TLSs; these contained T-cells, B-cells, MHCII+ APCs and CXCL13) compared to the mock RT control mice ($p < 0.001$). Analysis of immune cell contents of the TLS

revealed a notable increase in CD4, CD8 and regulatory T-cells in the RT condition (with urethane pretreatment). Important early events in the lung following RT of urethane pre-treated mice included a transient increase in type I and type II interferons, CD4 and CD8 T-cell infiltration ($p < 0.001$) and a strong downregulation of cell cycle events. In contrast to these findings, DMXAA treatment after urethane resulted in fewer tumors ($p < 0.05$), but larger tumors compared to the vehicle-treated group. An increase in immune cells was observed in the lung, however, without clear structures that resembled TLSs. Early events following DMXAA treatment with urethane pre-treatment included dampened levels of type I IFN and TNF-α in circulation and a decrease in T-cell infiltration into the lungs. Interestingly, RT and DMXAA combination treatment (with urethane pre-treatment) drove a synergistic anti-tumor effect, further reducing tumor numbers compared to the RT or DMXAA controls 5 months after treatment.RT and STING agonist treatment of pre-neoplastic lesions have differential impacts on tumor growth in the A/J mouse model, and work synergistically when combined. The different outcomes of RT and DMXAA on tumor growth may be driven by their distinctive mechanism of action on immune responses and capacities to form TLSs. These findings may have future implications for strategies for the early treatment of lung and other cancers, and they suggest that immune responses, including modulation of the STING pathway, may be an important aspect of early tumor development that could be targeted therapeutically.

#6407

Radionuclide-specific effects of ^{90}Y-,^{177}Lu-, or^{225}Ac-NM600 targeted radionuclide therapy on tumor immunomodulation and enhanced immunotherapy response in syngeneic murine tumors

Thanh Phuong T. Nguyen[1], Caroline P. Kerr[1], Joseph J. Grudzinski[2], Carolina A. Ferreira[3], Julia Sheehan-Klenk[1], Ohyun Kwon[3], Maria Powers[1], Paul A. Clark[1], Raghava N. Sriramaneni[1], Reinier Hernandez[3], Bryan Bednarz[3], Jamey P. Weichert[2], Zachary S. Morris[1]. *[1]Human Oncology, University of Wisconsin - Madison, Madison, WI,[2]Radiology, University of Wisconsin - Madison, Madison, WI,[3]Medical Physics, University of Wisconsin - Madison, Madison, WI*

Background: Targeted radionuclide therapy (TRT) delivers radiation treatment systemically to tumor sites via a therapeutic radionuclide-linked tumor-selective targeting vector. NM600 is an alkylphosphocholine analog selectively taken up and retained in murine and human tumor cells. We previously showed that low dose radiation delivery with ^{90}Y-NM600 improves tumor response to immune checkpoint inhibitors (ICIs). Understanding the effect of different radionuclide physical properties (emission type, linear energy transfer (LET), half-life, and tissue range) on immunomodulation of metastatic cancers may guide therapy development. Here, we evaluated the type 1 interferon (IFN1) response elicited by ^{90}Y-, ^{177}Lu-, and ^{225}Ac-NM600 in an immunologically cold syngeneic murine tumor model, B78 melanoma. We hypothesized that the unique physical properties of radionuclides will differentially impact immunomodulation by TRT.
Methods: Mice bearing B78 WT or *Tmem173* -/- CRISPR deletion B78 (STING KO) tumors were randomized to receive 1.5 Gy external beam radiation (EBRT), an equivalent tumor dose of ^{90}Y-, ^{177}Lu-, or ^{225}Ac-NM600 determined by the Monte Carlo-based RAPID platform, or no radiation on day 1. Tumors were harvested on days 4, 7, and 10 for RT-qPCR. Mice bearing two B78 WT or *Tmem173* -/- CRISPR deletion B78 (STING KO) tumors were randomized to receive 4 Gy external beam radiation therapy (EBRT), an equivalent tumor dose of ^{90}Y- or ^{177}Lu-NM600, 0.5 μCi ^{225}Ac-NM600, or no radiation +/- dual ICI (anti-CTLA4 and anti-PDL1). Mice were monitored for tumor growth and survival following these treatments.
Results: Both EBRT and TRT upregulated expression of IFN1 response-associated genes (*Ifnβ1, Mx1*) in B78 WT tumors. Only TRT induced upregulation of *Ifnβ1* and *Mx1* in STING KO B78 tumors. *Ddx58*, which encodes RIG-I, integral to an alternative IFN1 pathway, was upregulated in both B78 WT and STING KO tumors following ^{225}Ac-NM600, but not other treatments. TRT in B78 STING KO tumors had earlier expression of IFN1 response-associated genes than B78 WT, ^{225}Ac-NM600 in combination with dual ICI improved overall survival over ^{90}Y- or ^{177}Lu-NM600 + ICI and ^{225}Ac-NM600 monotherapy.
Conclusions: The distinct physical properties of TRT radiation, γ, β or α, affect the timing, magnitude, and molecular pathways leading to this IFN1

response. Understanding TRT effects on the tumor microenvironment may optimize TRT and immunotherapy.

#6408

Anti-tumor immunity evolved by novel titanium peroxide nanoparticles (TiOxNPs) as a radiosensitizer and PD-1 blockade

Yoshiko Fujita[1], Hikaru Kubota[1], Chiaki Ogino[2], Ryohei Sasaki[1]. *[1]Division of Radiation Oncology, Kobe University Graduate School of Medicine, Kobe, Japan,[2]Department of Chemical Science and Engineering, Kobe University Graduate School of Engineering, Kobe, Japan*

Abstract: Release and presentation of tumor antigens are the preconditions of cellular immune response. Radiotherapy have been reported to release endogenous tumor antigens and enhanced the adjuvanticity from dying cancer cells via endoplasmic reticulum (ER) stress, known as immunogenic cell death. We developed a novel radiotherapy using radiosensitizer (TiOxNPs) that could drive effective anti-tumor responses. The TiOxNPs were robustly radiation-induced reactive oxygen species (ROS) generation. This burst therapy could enhance to release and presentation of endogenous tumor antigens, subsequently cross-presentation of antigens by Dendritic cells (DCs) for T-cell activation in secondary lymphoid organs (SLO).
Methods: B16-F10 murine melanoma cells ($5x10^5$) were subcutaneously injected into the right flank of C57BL/6J respectively. Mice were divided into five treatment groups: 1) untreated; 2) XRT; 3) XRT+ TiOxNPs; 4) XRT+anti-PD-1Ab; and 5) XRT+ TiOxNPs +anti-PD-1Ab. B16-F10 tumors were intratumorally injected with TiOxNPs (8mg/kg) on days 10 and received 5Gy or 10Gy X-ray radiation approximately 1 hour after the injection. Anti-PD-1 antibody (200μg) intraperitoneally administered to the mice on the first day of X-ray irradiation, days 13 and 16. The tumor volume were assessed every 2-3 days after treatment. Mice were sacrificed after days 17 and isolated spleen and tumor.
Results: TiOxNPs acted as a potent radiosensitizer, which enhanced cytotoxic ROS-mediated cell death. This combination effect could not only a local treatment that directly kills cancer cells but also could enhance the adjuvanticity from dying cancer cells by DAMPs, and significantly upregulate expression of MHC class I on tumor cells. Treatment of B16-F10 melanoma tumor model with burst therapy resulted in tumor shrinkage

and extended overall survival. Burst therapy facilitated the recruitment and maturation of DCs into SLO, and improved antigen presentation to naive T cells. Infiltration into the tumor site of CTL were correlated with increasing of migration DCs into SLO.
Conclusion: A novel radiotherapy combining with TiOxNPs played an important role in release of endogenous tumor antigens and DAMPs. The upregulation of MHC class I expression on tumor cells after X-ray irradiation facilitated the recognition of the tumor cells by T cells, leading to significantly enhanced antitumor immune response compared to exisiting immunoradiotherapy. This novel nanoparticles exposed to X-ray irradiation could trigger of antigen-specific immune responses and transform a tumor into a site for activation of antitumor immune response.

#6409

Non-redundant mechanisms of immune resistance to radiotherapy converge on innate immunity

Anthony T. Nguyen[1], Tahir B. Dar[1], Jolene Viramontes[1], Satchel Stevens[1], Julie K. Jang[1], Emily Y. Ko[1], Diana J. Lu[1], Eric M. Chung[1], Samuel C. Zhang[1], Katelyn M. Atkins[1], Mitchell Kamrava[1], Howard M. Sandler[1], Jlenia Guarnerio[1], Simon Knott[2], Zachary S. Zumsteg[1], David M. Underhill[2], Stephen L. Shiao[1]. *[1]Department of Radiation Oncology, Cedars-Sinai Medical Center, Los Angeles, CA,[2]Department of Biomedical Sciences, Cedars-Sinai Medical Center, Los Angeles, CA*

Multiple studies have demonstrated synergy between immune checkpoint blockade (ICB) and radiotherapy (RT) in preclinical murine models; however, randomized trials of RT/ICB have been inconsistent in patients with solid tumors. To better understand this discordance, we hypothesized that there are non-redundant inhibitory immune pathways that restrain the efficacy of RT beyond T-cell oriented immune checkpoints. To this end, we performed scRNA-seq and CITE-seq analysis of the EO771 syngeneic murine model of breast cancer to characterize the immune landscape following RT±ICB. We found that ICB reprograms the immune response to RT by shifting tumor-associated macrophages (TAMs) from a lipid-associated phenotype (APOE, FABP5) to an M1-like interferon-stimulated state (CXCL10, ISG15). However, ICB also promoted the late recruitment of intratumoral neutrophils, which drive resistance to RT in other contexts.

To evaluate whether neutrophils may be limiting antitumor immunity to RT/ICB, we depleted intratumoral neutrophils using two separate antibodies, anti-Ly6G and anti-Gr-1. Compared to RT/ICB alone, both neutrophil depletion strategies enhanced tumor control and prolonged survival in advanced EO771 tumors ($P<0.001$). Given that indiscriminate neutrophil depletion is not a viable therapeutic strategy, we tested alternative immune targeting approaches to alter the TAM response to RT/ICB. By scRNA-seq, we found that RT strongly upregulated several innate immune checkpoints on TAMs (e.g., SIRPα, SLAMF3/7, LRP1). Accordingly, we disrupted the SIRPα-CD47 interaction with anti-CD47 antibodies and characterized the impact on response to RT/ICB. Anti-CD47 significantly improved tumor regression and survival when combined with RT/ICB ($P<0.001$). We then used scRNA-seq and CITE-seq to understand why disruption of SIRPα-CD47 improved antitumor responses to RT/ICB. We found that anti-CD47 depleted an entire cluster of chronically inflamed TAMs, expressing pro-inflammatory markers (IL1A, NOS2) and chemokines (CCL3, CXCL1/2/3). Furthermore, anti-CD47 reduced the recruitment of intratumoral neutrophils and depleted a cluster of pathologically activated neutrophils (PMNs), termed myeloid-derived suppressor cells (PMN-MDSCs), expressing WFDC17, PTGS2, S100A8/9. Lastly, anti-CD47 enhanced the recruitment of tumor-infiltrating lymphocytes including central memory $TCF7^+$ T cells and $CD19^+$ B cells. By inference and analysis of cell-cell communication (CellChat), we found that anti-CD47 strengthened the interactions between myeloid cells and T cells compared to RT/ICB alone. Collectively, our data indicate that innate immune cells, in particular neutrophils and chronically inflamed TAMs, promote resistance to RT/ICB in the EO771 model. These data suggest that inhibition of CD47-SIRPα is a promising therapeutic strategy to overcoming immune resistance through the elimination of PMN-MDSCs.

#6410

Deciphering the role of MyD88 signaling pathway in regulating type I IFN-mediated responses to radiation therapy in solid tumors

Aanchal Preet Kaur, Terry R. Medler, Tiffany C. Blair, Alejandro F. Alice, Megan R. Ball, Alexa K. Dowdell, Brian D. Piening, Marka R. Crittenden, Michael J. Gough. *Earle A. Chiles Research Institute, Providence Cancer Institute, Portland, OR*

The balance of innate signaling through adaptor proteins such as MyD88 and TRIF is critical in directing the pattern of inflammatory responses following exposure to endogenous adjuvants. While innate stimuli can cause inflammation that supports adaptive immunity, cancer myeloid cells can be pre-polarized such that the same inflammatory signals cause myeloid cells to suppress adaptive immune responses. We aim to investigate the signals regulating type I IFN secretion by innate immune cells in tumors in order to improve type I IFN secretion, activation of innate immune cells, direct macrophage polarization and improve CD8+ T cell mediated anti-tumor immunity. To better understand the role of MyD88-mediated signaling in driving response to innate adjuvants released following RT in solid tumors, we developed MyD88 conditional knockout mouse models. MyD88 was deleted specifically in CD11c expressing dendritic cells (DC), Lck expressing T cells, or Lyz2 expressing myeloid cells that include macrophages, monocytes and granulocytes. Mice bearing pancreatic tumors (Panc02-SIY or PK5L1940) were randomized to no treatment or 16 Gy CT-guided RT and followed for treatment responses. Lyz2-Cre/MyD88$^{fl/fl}$ mice demonstrated improved responses to RT in pancreatic tumors as compared to control MyD88$^{fl/fl}$ mice, or Lck-Cre mice. The improved responses in Lyz2-Cre/MyD88$^{fl/fl}$ mice were shown to be dependent on CD8+ T cells as well as on type I IFN signaling. To analyze mechanisms of response, tumors were digested into a single cell suspension and CD45+ cells were isolated for single cell sequencing three days post-RT. Lyz2-Cre/MyD88$^{fl/fl}$ mice showed diminished Th1 and Th2-type T cells and had a higher M1/TAM ratio compared to MyD88$^{fl/fl}$ mice. Loss of MyD88 in myeloid cells resulted in increased activation of IFN-dependent transcriptional responses in multiple immune cell populations in the tumor. To model responses ex vivo, bone marrow-derived macrophages (BMDMs) were activated with lipopolysaccharide (LPS) or a synthetic cyclic dinucleotide (CDA) for analysis of cytokine secretion in either monolayer or 3D spheroid culture conditions. BMDM derived from Lyz2-Cre/MyD88$^{fl/fl}$ cultured as a monolayer showed significantly altered secretion of TNF-α, IL-10 and IL-6 on activation with LPS as compared to controls. Preliminary data obtained from 3D spheroid culture systems demonstrated that 3D interactions between cancer cells and macrophages resulted in a significant increase in BMDM co-stimulatory phenotype following activation with innate stimuli

compared to 2D cultures. These data suggest that conventional innate signaling through MyD88 in myeloid populations suppresses IFN production and adaptive immune control of irradiated tumors. 3D cultures are an effective tool to study cellular interactions ex vivo and screen novel interventions prior to in vivo translation.

Immunotherapy Strategies and Mechanisms

#6414
Concomitant anti-tumor immunity and checkpoint blockade responses are restored by depletion of CD62L expressing cells

Brianna Burke[1], Lourdes Plaza-Rojas[2], Cynthia Perez[1], Elena Kostenko[2], Anna Austin[2], Justin Boucher[2], Kushal Prajapati[1], Michael Delos Reyes[1], Christine Chung[2], Jose-Alejandro Guevara-Patino[3]. *[1]Loyola University Chicago, Maywood, IL,[2]H. Lee Moffitt Cancer Center, Tampa, FL,[3]Immunology, H. Lee Moffitt Cancer Center, Tampa, FL*

Studies have shown the importance of CD62L in leukocyte trafficking. However, the significance of CD62L-expressing cells in concomitant anti-tumor immunity has not been investigated. Using a model of post-surgical tumor immunity, we show that in vivo depletion of CD62L-expressing cells before or immediately after surgical tumor resection enabled the development of anti-tumor concomitant responses against poorly immunogenic B16 (melanoma) or MTE-Ras (head & neck cancer) tumor cells. Anti-CD62L mAb administration depleted the cellular immune components that express CD62L, including NK, NKT, Mo, Ma, B, and T cells. Within the T cell compartment, naïve T cells (CD44lo CD62Lhi), effector (CD44hi CD62Llo), memory (CD44hi CD62Lhi) and regulatory T cells (Treg, CD4 CD25 Foxp3) were also depleted, while effector CD62L-negative T cells were spared in the TDLN. Tumor immunity did not occur in the absence of a primary tumor (sham surgery group) or after CD8 depletion. Whereas anti-CTLA-4 or anti-PD-1 mAbs failed as monotherapies, their administration during CD62L depletion restored their anti-tumor properties. The unified global gene expression analysis of the TDLN shows the significant enrichment of biological processes involved in the CD8 T cell effector phase, IL-2/IL-15, TNF-α, IFN-γ, IFN-α, IL-6, responses, mitotic cell division, glycolysis, and acetylation. Also, genes

related to Treg responses were downregulated. These data point to a process in which depletion of CD62L cells in tumor-bearing hosts transforms the TDLN into a highly active immunological site in which tumor-reactive effector CD8 T cells (CD62L-negative) actively divide in the absence of Treg, accompanied by a cytokine response, glucose consumption, and acetylation of transcriptional factors and histones. These results identify an unrecognized role of CD62L-expressing cells in regulating concomitant anti-tumor immunity and restoring anti-tumor responses by checkpoint blockade inhibitors. Our study provides a new framework that could help understand how anti-tumor responses are limited.

#6415

CD25-targeted aptamer-drug conjugate (CD25-ApDC) depletes and blocks regulatory T cells selectivel

Daekyun Lee, Ju-hyung Kang, Inu Song. *Aptamer Sciences Inc., Seongnam-si, Korea, Republic of*

Background: Regulatory T cells (Tregs) have a strong immunosuppressive function, inhibit anti-tumor immunity, and promote the occurrence and development of tumors. In addition, a high infiltration of Treg cells is associated with poor survival in various types of cancer. Since CD25 is highly expressed on Treg cells, it is a potential target protein for Treg depletion.
Methods: The binding affinity(Kd) of CD25 aptamer to rhCD25 protein was calculated through bio-layer interferometry(BLI). The cell binding of Cy5-labelled CD25 aptamer was detected by flow cytometry, and the internalization was visualized by confocal microscopy. The cell internalization rate was determined using the MFI value of flow cytometry. Competitive ELISA, western blot, and qPCR were performed to investigate the effect of CD25 aptamer on CD25/IL-2 binding. In vitro cytotoxicity of prototype-ApDC was determined by CCK-8 assay. Moreover, CD25-dependent cytotoxicity of prototype-ApDC was evaluated by Karpas299(Treg-like):HuT78(Teff-like) 1:1 co-culture model using FACS analysis.
Results: CD25 aptamer binds human CD25 protein with 4.64nM affinity. CD25 aptamer showed selective binding and internalization to CD25-positive Karpas299 and had no interaction with CD25-negative Daudi. The

internalization half-time of CD25 aptamer in karpas299 was determined to 9.9 min (95% CI 8.2~12.6min). Interestingly, CD25 aptamer was identified as IL-2R antagonist by evaluating competitive ELISA and the level of phosphor-STAT5 and downstream mRNA expression of TGF-beta. The IC50 value of prototype-ApDC was 24nM to Karpas299 while >1uM to Daudi. These results show that prototype-ApDC has selective cytotoxicity against CD25-expressing cells. Furthermore, in a study of an in vitro co-culture model mimicking the Treg-rich intratumoral T cell environment, prototype-ApDC treatment induced CD25-specific depletion resulting in escalating the ratio of HuT89/Karpas299 with increasing exposure time. Conclusions: Our CD25-targeted aptamer and its drug-conjugated ApDC have demonstrated the selective blocking of IL-2R-STAT5 signaling and induction of CD25-positive cell-specific depletion, respectively. Moreover, in the co-culture system of the Treg-like and Teff-like cells, CD25-ApDC also proved its cytotoxic selectivity. Therefore, one potential strategy in cancer patients is to use CD25-ApDC with excellent tumor permeability as an anticancer agent with a mechanism of Treg cell depletion through specific targeting of CD25 overexpressed in tumor-infiltrating Treg cells.

#6416

Statins inhibit onco-dimerization of 4Ig-B7-H3

Margie Nicole Sutton[1], Sarah E. Glazer[2], Riccardo Muzzioli[1], Ping Yang[1], Seth T. Gammon[1], David Piwnica-Worms[1]. *[1]UT MD Anderson Cancer Center, Houston, TX,[2]Oregon Health Science University, Portland, OR*

B7-H3 (*CD276*) is a member of the B7 family of immune regulators, but unlike the immune checkpoint targets that have revolutionized cancer therapy, blockade has resulted in mixed outcomes. B7-H3 has 2Ig and 4Ig isoforms, has no known direct ligand, and many of the physiological functions remain elusive. While protein expression of B7-H3 is differentially expressed on many solid tumors and correlates with poor survival, mechanisms of how B7-H3 elicits a pro-tumorigenic phenotype are still poorly understood, significantly hampering therapeutic efforts for targeting. Using a facile, recombinase-enhanced split-luciferase reporter, we visualized 4Ig-B7-H3 homodimerization in live U2OS cells by bioluminescence imaging and confirmed 4Ig-B7-H3 dimerization using a second non-invasive imaging technique: fluorescence lifetime imaging

microscopy (FLIM) where 4Ig-B7-H3 was exogenously re-expressed following knockout of *CD276* in HeLa cervical cancer cells. Homodimerization of 4Ig-B7-H3 correlated with enhanced clonogenic cell growth in HeLa, SKOv3, MDA-MB-231, and U2OS cells and tumor growth *in vivo* for several models. This phenotype was reversed following knockout of B7-H3 and rescued upon lentiviral re-expression. By RPPA and phospho-kinase array analysis, increases in PI3K/AKT signaling, Jak/Stat pathway, and modulators of HIF1α and NF-κβ pathways were observed with B7-H3 expression and homodimerization ($p<0.05$), all which are known to support increased oncogenic functions, such as increased glycolysis, increased survival and proliferation, as well as cytokine modulation and immune evasion. Next, capitalizing on our bioluminescence-based reporter of 4Ig-B7-H3 homodimerization, we performed a high-throughput small molecule screen with a 5,362 Bioactive compound library to identify modulators of 4Ig-B7-H3 dimerization. Notably, our HTS identified several HMG-CoA reductase inhibitors (statins) as significant inhibitors of B7-H3 dimerization ($p<0.01$). Treatment with 1 μM mevastatin or atorvastatin calcium inhibited clonogenic growth of HeLa cervical, SKOv3 ovarian and MDA-MB-231 breast cancer cells, which all endogenously express B7-H3. *In vivo*, treatment with 10 mg/kg of atorvastatin calcium reduced tumor growth and increased mouse survival ($p=0.035$) of SKOv3-ip tumors and produced functional cures (15-30%) of HeLa or MDA-MB-231 xenografts in nude mice in a B7-H3 tumor expression-dependent manner, proven through knockout and rescue experiments in live cells and animals. Thus, in the context of studies to dissect the tumor-intrinsic mechanism(s) of B7-H3 biochemical functions and activation, we identified a novel, dimerization-dependent oncogenic role for 4Ig-B7-H3 that increased oncogenic intracellular signaling activation and was modulated by statin treatment. This may provide a molecular mechanism for the statin-mediated immune modulation and enhanced cancer survival clinically reported for several tumor types.

#6417

Deciphering aberrant STING pathway and exploring oncolytic viruses therapy in low grade serous ovarian carcinoma

Almira Zhantuyakova[1], Dawn Cochrane[1], Gian Negri[2], Sandra E. Spencer Miko[2], Taha Azad[3], Jutta Huvila[4], Marta Llaurado Fernandez[5], Mark

Carey[5], Gregg B. Morin[2], John Bell[3], David Huntsman[6]. *[1]Molecular Oncology, BC Cancer Research Centre, Vancouver, BC, Canada,[2]Canada's Michael Smith Genome Sciences Centre, BC Cancer Research Centre, Vancouver, BC, Canada,[3]Department of Biochemistry, University of Ottawa, Ottawa, ON, Canada,[4]University of Turko, Turko, Finland,[5]Department of Obstetrics and Gynecology, University of British Columbia, Vancouver, BC, Canada,[6]Department of Pathology and Laboratory Medicine, University of British Columbia, Vancouver, BC, Canada*

There are two serous ovarian cancer histotypes, low and high grade (LGSOC and HGSOC), which are distinct clinical and biological entities. LGSOC is a rare histotype with a relatively stable genome, while HGSC is more common and genomically unstable. Somewhat surprisingly LGSOC expresses high levels of the stimulator of the interferon genes (STING). The STING pathway recognizes cytoplasmic double-stranded DNA and mounts innate cellular immunity through interferon-beta type I production. Our objective is to investigate the aberrant STING signaling in LGSOC and test the effectiveness of oncolytic viruses against LGSOC. We used immunohistochemistry on tissue microarrays (TMAs) to assess STING protein expression in different ovarian cancer histotypes. Whole proteome analysis was applied to identify differentially expressed proteins in LGSOC and HGSOC patient samples (both n=9). Further, a semi-targeted proteomics approach was used to evaluate the expression levels of the STING pathway-related proteins in LGSOC, HGSOC, and LGSOC precursor tumors (each subtype, n=20). To evaluate the key transcription, phosphorylation, and translocation events in STING signaling, we treated LGSOC cell lines with an agonist (dsDNA90) and performed qPCR, immunoblotting, and immunofluorescence experiments, respectively. We tested the viability of the LGSOC cell lines in response to Vaccinia Virus (VV), and Vesicular Stomatitis Virus (VSV) based oncolytic vectors with or without immunostimulatory transgenes. Our results show that STING protein levels were consistently higher in LGSOC TMAs relative to other histotypes. Proteomics analysis showed that the half of the 16 most differentially expressed proteins were the effectors of STING signaling with unexpectedly lower expression in LGSOC, suggesting that despite the robust levels of STING in LGSOC tumors, the pathway is not fully active.

Attenuated STING translocation and expression of IFNB1 and other cytokines in LGSOC cell lines confirm the aberrancy in the STING pathway. Semi-targeted proteomics revealed the considerable overexpression of STIM1 in LGSOC patient tumors, which has previously been shown to sequester STING in the endoplasmic reticulum. The treatment with VV and VSV oncolytic viruses significantly reduced the proliferation of LGSOC cell lines. In summary, we find attenuated STING signaling in LGSOC, possibly due to overexpression of STIM1 preventing STING translocation. Although oncolytic viruses show promising results in LGSOC cell lines, more research is needed to determine the optimal treatment strategy, testing oncolytic viruses expressing various transgenes and combination therapies.

#6418

xWU-NK-101 as salvage therapy post immune checkpoint blockade (ICB)

Tom A. Leedom[1], Barbara Muz[1], Jaykumar Vadakekolathu[2], John J. Muth[1], Xiao-Hua Li[1], Gregory Watson[1], Kristaan Magee[1], Ryan P. Sullivan[1], Melissa Berrien-Elliott[3], Todd Fenigher[3], Sergio Rutella[2], Matthew L. Cooper[1], Ayman Kabakibi[1], Jan K. Davidson-Moncada[1]. *[1]Wugen, St Louis, MO,[2]John VanGeest Cancer Research Centre, Nottingham Trent University, Nottingham, United Kingdom,[3]Washington University, Saint Louis, MO*

ICB therapy has transformed cancer treatment; durable responses in difficult-to-treat cancers have been observed. Despite this most patients (pts) don't respond to ICB (primary resistance), and many pts who initially respond eventually relapse (acquired resistance). Primary resistance is associated with tumor cell extrinsic factors, e.g., the immunosuppressive nature of the tumor microenvironment (TME), while acquired resistance is associated with tumor intrinsic factors, e.g., downregulation of MHC1, preventing T cell recognition. Treatments to overcome ICB resistance are necessary. WU-NK-101 is a PBMC-derived, cytokine-reprogrammed, expanded, and cryopreserved off-the-shelf memory NK cell product. WU-NK-101 cells capture the memory-like NK cell biology of cytokine-induced memory-like (CIML) NK cells, exhibiting enhanced cytotoxicity, metabolic fitness/flexibility, and resistance to TME immunosuppression (Muth *et al.* EHA 2022; Rutella *et al.* ESMO 2022). Bone marrow biopsies, collected

from R/R AML pts who received CIML-NK cells (NCT01898793), were interrogated using immune gene expression (GE) profiling and spatially resolved proteomics (IO360® panel, n = 740 genes, and GeoMx® DSP; NanoString Technologies). Higher T-cell infiltration was noted post CIML-NK. CIBERSORT deconvoluted GE data inferred higher abundance of macrophages, γδT cells and activated dendritic cells on day 28 post-treatment. GE signatures showed downregulation of NFIL3 and FAM30A (log2 fold-change <1.0; $p<0.05$) post CIML-NK. TIDE algorithm modelling indicated that lower expression of NFIL3 and FAM30A correlated with high CTL infiltration and improved outcomes in many TCGA tumors (Jiang *et al.* Nat. Med. 2018). Hence, CIML-NK treatment led to modifications in the TME towards a more T-cell amenable environment. Deleting *MHC1* on NALM6 cells significantly improved WU-NK-101 killing compared to WT ($p<0.0001$), highlighting one mechanism whereby WU-NK-101 overcomes acquired ICB resistance. In transwell assays, co-incubation of tumor cells with WU-NK-101 in the lower chamber led to dose dependent killing; in the upper chamber (tumor cells alone), viability was preserved but a dose-dependent increase of MHC1/PDL1 expression was noted. Similar results were observed using cell-free conditioned media from WU-NK-101 cytotoxicity assays, suggesting that soluble factors released from WU-NK-101 augment MHC1/PDL1 expression. Treatment of tumor cells with IFNγ alone led to similar increases in MHC1/PDL1 expression. Importantly, *in vivo* experiments revealed that residual tumor cells post WU-NK-101 treatment exhibited higher levels of MHC1/PDL1. Overall, these data highlight a further mechanism through which WU-NK-101 overcomes acquired ICB resistance. In summary, WU-NK-101 has the potential to reverse primary and acquired mechanisms of ICB resistance. A Phase 1b clinical trial of WU-NK-101 as salvage therapy post-ICB is in development.

#6420

Harnessing immune responses in prostate MMRd tumors treated with immune checkpoint blockade

Marcel Arias Badia, Zenghua Fan, Yee May Lwin, PeiXi Chen, Aahir Srinath, Lawrence Fong. *UCSF Helen Diller Family Comprehensive Cancer Ctr., San Francisco, CA*

There is increasing evidence correlating tumor mutational burden with response to immunotherapy in many different types of cancer. Some tumors show high microsatellite instability (MSI-H) as a consequence of the loss of function of mismatch repair (MMR) genes, which would resolve DNA damage in normal conditions. MSH2 plays a critical role in MMR, and several studies have identified mutations in MSH2 as key drivers of MSI in tumors**.** In preclinical mouse models, MMR deficiency and high microsatellite instability have been previously shown to translate into higher sensitivity to anti-PD-1 treatment. Despite the advances led by the recent tumor-agnostic approval of checkpoint inhibitors for highly mutated tumors, response rates among MMR-deficient (MMRd) tumors in humans are variable, and the mechanisms behind such heterogeneity are still poorly understood. We successfully knocked out the MSH2 gene in the murine prostate adenocarcinoma TRAMP-C2 cell line by CRISPR gene editing. By sequential passaging, we generated a MSH2-KO subclonal population that presents MSI and MMR deficiency, validated by increased tumor mutational burden (TMB) observed by exome sequencing. In studies where we challenged immunodeficient and immunocompetent mice with MMR-proficient (MMRp) and MMRd tumors, the latter showed increase immunogenicity, which led us to interrogate and better characterize such immune responses in the context of immune checkpoint blockade by anti-PD-1.In our studies, MMRd tumor-infiltrating T cells presented significantly enhanced effector and cytotoxic profiles, which likely led to improved tumor control with or without anti-PD-1. We observed an intriguingly lower frequency of SPAS-1 (a well-known TRAMP-C2 immunodominant epitope) antigen-specific T cells in the tumor-reactive fraction of MMRd infiltrates compared to MMRp, which prompted us to interrogate tumor-infiltrate gene expression, TCR repertoire and the potential expansion of multiple antigen-reactive subsets against MMRd tumors in successful immune responses by single cell RNA sequencing and functional *ex vivo* studies. We also interrogated TCR repertoire data from patients harboring MMRd tumors to add translatability to our findings in mice.Our results constitute a relevant addition to the understanding of immune responses in MMRd tumors and the potential features that could be exploited to improve response rates in immunotherapeutic strategies targeting such malignancies.

#6421

Molecular profiles and single cell analysis identify immunogenic pancreatic ductal adenocarcinoma (iPDAC)

Wungki Park, Catherine O'Connor, Shigeaki Umeda, Roshan Sharma, Yingjie Zhu, Elias-Ramzey Karnoub, Anna Varghese, Kevin C. Soares, Alejandro Jimemez, Asli Yavas, Kenneth H. Yu, Balachandran P. Vinod, Joanne F. Chou, Danny N. Khalil, Kelsen David, Hulya Sahin Ozkan, Olca Basturk, Marinela Capanu, Tal Nawy, Michael F. Berger, Ghassan K. Abou-Alfa, Jorge S. Reis-Filho, Ronan Chaligne, Nadeem Riaz, Dana Pe'er, Christine Iacobuzio-Donahue, Eileen M. O'Reilly. *Memorial Sloan Kettering Cancer Center, New York, NY*

Most pancreatic ductal adenocarcinomas (PDAC) are lethal and resistant to immunotherapy. Thus, identifying the immunogenic subgroup (iPDAC) and therapeutic targets can save lives. Herein, we present molecular features of iPDAC. 3 cohorts (A, B, C) from 288 patients whose sequenced tumors (MSK-IMPACT) were classified by homologous recombination deficiency groups. MSI-H were excluded. Survival, tumor mutation burden, genomic instability score, and enriched pathways for each cohort are included in Table 1. Patients in A (BRCA1/2/PALB2) had longer survivals vs B/C. 61 samples were selected for bulk RNAseq analysis for A vs C. Gene Ontology was enriched for upregulated humoral, T cell, and neutrophil immunity. CIBERSORT suggested higher infiltration of gamma delta T (Tgd) cells (p=0.039) and neutrophils (p=0.012), but lower Treg (p=0.001). Multidimensional insights in cellular components of cancer, immune, stroma, and neural genes were obtained by single nuclear RNA (snRNAseq) analysis from 30 biopsies for A vs C. 10x Genomics Chromium platform for library and Scanpy for computational analysis after Cell Ranger pipelines were used. 61,868 nuclei were profiled from 18 (13 baseline and 5 matched longitudinal) samples after quality evaluation. UMAP accurately clustered cells from each patient. Long-term survivors (LTS) had heterogenous baseline immune cell infiltrates of plasma cells, neutrophils, and CD8 (+) cytotoxic T cells. In matched samples of LTS, evolution of more prominent CD8 (+) T cells, macrophage, plasma cell, and neutrophil were observed. Single nucleus T-Cell Receptor sequencing for clonal trajectory inference will be done to determine the associated single cell

molecular features contributing to iPDAC and identify novel targets for future intervention.

Table 1

Cohort (Total: N=288)	A: core HRD (BRCA1/2/PALB2)	B: non-core HRD (ATM, BARD1, BLM, CHEK2, RAD50, RAD51C, RTEL1, MUTYH)	C: others without HR-gene alterations
Number (%)	48 (16.6)	19 (6.5)	221 (76)
Median overall survival (95% confidence Interval)	33 months (3.6-64)	16 (11- not reached)	16 (14-18)
Tumor Mutation Burden (TMB)	4.4	3.5	3.9
Genomic Instability Score (GIS, HRD score)	26	12	13
Gene Ongology term, enrichment score, adjusted p-value	Adaptive immune response, GO:0002250, 0.49, 1.69e-10	Not included	Reference to cohort A
	Humoral immune response, GO:0006959, 0.58, 1.67e-9		
	T cell activation, GO:0042110, 0.44, 2.75e-8		
	Neutrophil chemotaxis, GO:0030593, 0.73, 4.3e-10		

#6422

Combined TGFβ/PD-L1 blockade enhances systemic antitumor immunity in head and neck cancer

Magdalena Rainey, Marco Craveiro, Yvette Robbins, Cem Sievers, Clint T. Allen. *Head and Neck Section, National Cancer Institute, National Institutes of Health, Bethesda, MD*

Head and neck squamous cell carcinoma (HNSCC) unrelated to human papillomavirus (HPV) confers poor prognosis, with half of patients experiencing disease relapse in advanced stages. Response rates to traditional immunotherapies are low and novel approaches such as the bifunctional fusion protein Bintrafusp alfa (BA) that concurrently blocks PD-L1 signaling and neutralizes TGFβ are actively under investigation. Our group showed that when HNSCC patients received neoadjuvant BA therapy, it reversed exhaustion of tumor-infiltrating lymphocytes (TILs) by promoting antigen-mediated signaling. Additionally, we observed that BA promoted recirculation of TILs into peripheral blood possibly through decreased expression of the TGF-β-driven tissue-retention marker CD103. We hypothesize that addition of TGFβ neutralization to PD-L1 blockade can enhance systemic anti-tumor immunity compared to PD-L1 blockade alone. We assessed immune responses to BA in wild-type mice bearing established mouse oral cancer (MOC)-1 tumors that were randomized into the following groups: 1) vehicle; 2) anti-PD-L1 antibody (Avelumab); 3) TGFβ neutralizing construct with a mutated PD-L1 antibody (BA-M); 4) TGFβ neutralizing construct with a functional PD-L1 antibody (BA). Additionally, since our previous data suggests that BA responsiveness depends on CD8 T cell activity, we included two extra groups 5) CD8 depleting antibody alone or 6) in combination with BA. Three days after

completing treatment, MOC-1 tumor cells were injected into the contralateral flank and engraftment and progression of secondary challenge tumors was analyzed. Primary tumor progression was significantly inhibited by BA and to a lesser extent avelumab compared to control or BA-M. Engraftment or progression of secondary challenge tumors was significantly inhibited by BA and to a lesser extent avelumab compared to control or BA-M. The growth inhibitory effects of BA were abrogated by CD8 depletion in both the primary and challenge tumors. Flow cytometry analysis of tissue collected on day 7 post-tumor challenge showed that BA-mediated clearance of the tumors was associated with a proportional increase of $CD4^+$ and $CD8^+$ TILs. We also observed that the frequency of CD103 expression among $CD4^+$ TILs was reduced both in the primary and challenge tumors. Although TGFβ neutralization alone fails to induce anti-tumor immunity, the addition of TGFβ neutralization to PD-L1 blockade provides greater control of primary tumor growth and protection from engraftment of a challenge tumor compared to PD-L1 blockade alone. Through adoptive transfer of tumor-specific T cell receptor-engineered T cells, ongoing experiments aim to determine if TGFβ-driven CD103 expression is required for T cell tumor residency and if neutralization of TGFβ in the setting of PD-L1 immune checkpoint blockade allows for recirculation of tumor-specific T cells into the periphery.

#6423

Targeting an autophagy regulator augments antitumor immunity and immunotherapy

Yi Bao, Yuanyuan Qiao, Arul Chinnaiyan. *University of Michigan, Ann Arbor, MI*

Immunotherapy has strikingly changed the landscape of cancer treatment, yet many patients fail to respond to the therapy exhibiting primary resistance. Accumulating evidence has supported that autophagy inhibition may sensitize tumor to immunotherapy. Here, we found that pharmaceutical or genetic inhibition of an autophagy regulator induces MHC class I surface expression in cancer cells. In a co-culture of OT1 $CD8^+$ T cells and ovalbumin-expressing cancer cells, inhibition of the regulator enhances $CD8^+$ T cell killing and increases functional and proliferative $CD8^+$ T cells. Concordantly, genetic depletion or inhibition of the regulator elevates MHC

class I in tumor cells, reduces tumor growth, and increases intratumoral functional $CD8^+$ T cells in syngeneic mouse models. Furthermore, we found that inhibition of the regulator sensitizes syngeneic tumors to anti-PD1 therapy. Collectively, inhibition of this autophagy regulator augments antitumor immunity and immunotherapy via inducing MHC class I surface expression in cancer cells.

#6424

Immune characteristics and anti-PD-1-induced reinvigoration capacity of tumor-infiltrating lymphocytes in ovarian clear cell carcinoma relative to high-grade serous ovarian carcinoma

Junsik Park, Yong Jae Lee, Jung Chul Kim, Jung-Yun Lee. *Yonsei University College of Medicine, Seoul, Korea, Republic of*

Recent clinical trials have demonstrated the potential efficacy of immune checkpoint inhibitors (ICIs) for ovarian clear cell carcinoma (OCCC). However, little is known about the immune characteristics of OCCC. In this study, we aimed to investigate the distinct immune characteristics of tumor-infiltrating lymphocytes (TILs) in OCCC to high-grade serous ovarian carcinoma (HGSOC). We isolated peripheral blood mononuclear cells (PBMCs) and TILs from patients with epithelial ovarian cancer. The expression of immune checkpoint receptors and T-cell transcription factors of TILs in OCCC (n=26) and HGSOC patients (n=44) were accessed using flow cytometry. TILs were *ex vivo* stimulated with anti-CD3 in the presence of anti-PD-1 and/or anti-CTLA-4, and their proliferation was assessed to predict response to ICIs. CD8 TILs and tumor-infiltrating regulatory T cells (Tregs) exhibited higher expression of immune checkpoint receptors, including PD-1, CTLA-4, and 4-1BB, compared to PBMCs. Tregs were more infiltrated in advanced/recurrent stage than early stage OCCC. However, immune characteristics of CD8 TILs and Tregs were not significantly different regardless of stage. When we compared the characteristics of TILs in OCCC (n=26) with those in HGSOC (n=44), the expression of PD-1 on CD8 TILs was significantly lower in OCCC than in HGSOC. The frequencies of $PD\text{-}1^{high}CD8$ TILs and $PD\text{-}1^+TOX^+CD8$ TILs were also lower in OCCC than HGSOC. In *ex vivo* assay (n=19), 9 cases responded to anti-PD-1 in terms of enhanced proliferation capacity of CD8 TILs. In addition, when anti-CTLA-4 was added to anti-PD-1, an additional

increase in proliferation of CD8 TILs was observed in patients who responded to anti-PD-1. Responders to anti-PD-1 had significantly lower frequencies of effector Tregs in the TILs than non-responders. Overall, CD8 TIL in OCCC was found to be less exhausted than HGSOC in terms of PD-1 and TOX expressions. Tumor-infiltrating Tregs affected on reinvigoration ability of CD8 TILs upon ICIs treatment in OCCC. This study provides the rationale and evidence for establishing the optimal strategies for ICIs treatment in patients with OCCC.

#6425

Functional roles of enhancers in immune microenvironment & immunotherapy response

Kunal Rai[1], Mayinuer Maitituoheti[2], Alvin Shi[3], Ming Tang[2], Li-Lun Ho[4], Firas Youssef Kreidieh[5], Christopher Terranova[2], Kyriakitsa Galani[3], Emily Z. Keung[6], Caitlin A. Creasy[5], Manrong Wu[2], Jiajia Chen[7], Nana Chen[8], Anand K. Singh[2], Apoorvi Chaudhri[2], Nazanin E. Anvar[2], Giuseppe Tarrantino[7], Jiekun Yang[9], Sharmistha Sarkar[2], Shan Jiang[1], Jared Malke[6], Lauren Haydu[5], Elizabeth Burton[5], Michael A. Davies[5], Jeffrey E. Gershenwald[5], Patrick Hwu[5], Alexander Lazar[2], Jaime H. Cheah[10], Christian K. Soule[10], Stuart S. Levine[10], Chantale Bernatchez[5], Srinivas V. Saladi[11], David Liu[7], Hussein Tawbi[5], Jennifer Wargo[2], Genevieve M. Boland[12], Manolis Kellis[9]. *[1]UT MD Anderson Cancer Center, Houston, TX,[2]Genomic Medicine, UT MD Anderson Cancer Center, Houston, TX,[3]Massachusetts Institute of Technology, Boston, MA,[4]Massachusetts Institute of Techology, Boston, MA,[5]Melanoma Medical Oncology, UT MD Anderson Cancer Center, Houston, TX,[6]Surgical Oncology, UT MD Anderson Cancer Center, Houston, TX,[7]Dana-Farber Cancer Institute, Harvard Medical School, Boston, MA,[8]Otolaryngology Head and Neck Surgery, Massachusetts Eye and Ear Infirmary, Harvard Medical School, Broad Institute of Harvard and MIT, Boston, MA,[9]Computer Science, Massachusetts Institute of Technology, Boston, MA,[10]Koch Institute for Integrative Cancer Research at MIT, Cambridge, MA,[11]Otolaryngology Head and Neck Surgery, Massachusetts Eye and Ear Infirmary, Harvard Medical School, Broad Institute of Harvard and MIT, Cambridge, MA,[12]Surgery, Massachusetts General Hospital, Boston, MA*

Immune checkpoint blockade (ICB) therapy has improved long-term survival for patients with advanced melanoma. However, there is critical need to identify potential biomarkers of response and actionable strategies to improve response rates. Through generation and analysis of over 200 chromatin modification maps for ICB-treated melanoma patient samples, melanoma cells and T cells, we identified significant enrichment of active enhancer states in non-responders at baseline. Enhancer mapping by bulk ChIP-Seq or single cell ATAC-Seq methods in two independent cohorts of ICB-treated melanoma samples identified an enhancer signature that predicted response to anti-PD-1 therapy. The activated non-responder enhancers marked a group of key regulators of several pathways in melanoma cells (including c-MET, TGFβ, EMT and AKT) that are known to mediate resistance to ICB therapy. In addition, several checkpoint receptors were alternatively activated by aberrant enhancers in T cells. Unbiased CRISPRi screening in melanoma cells and T cells identified novel functional enhancers, such as one upstream of c-MET, that mediate ICB response or T cell mediated killing. Finally, inhibition of enhancers and repression of these pathways using bromodomain inhibitors along with anti-PD-1 therapy significantly decreased melanoma tumor burden and increased T-cell infiltration. Epigenomic experiments identified a signature of 107 genes that could be used as pharmacodynamic marker for BET inhibitor response. Together, these findings identify enhancer upregulation as a key mechanism of adaptive resistance to ICB response, a potential enhancer-based biomarker of resistance to anti-PD-1 and enhancer blockade in combination with ICB as a potential strategy to improve responses.

#6427

Selective-HDAC inhibitor relieves the suppressive immune microenvironment in the brain to impede breast cancer brain metastasis

Shao-Ping Yang[1], Yimin Duan[2], Xiangliang Yuan[2], Lin Zhang[2], Patrick Zhang[2], Dihua Yu[2]. *[1]The University of Texas MD Anderson Cancer Center, UT Health Houston Graduate School of Biomedical Sciences, Houston, TX,[2]Molecular and Cellular Oncology, The University of Texas MD Anderson Cancer Center, Houston, TX*

Brain metastasis (BrM) incidence is rising due to longer survival resulted from better systemic control of cancer, counting for approximately 20% of patients with cancers. Major cancer types, including lung, breast, and skin cancers, have a high rate to develop BrM with a 1-year survival rate of less than 20% for symptomatic patients. The overall response rate for immune checkpoint inhibitors (ICI) is merely 10-30% in patients with neurological symptoms. Developing novel combinatorial therapeutic strategies based on mechanistic understanding is urgently needed to further improve the efficacy of current immunotherapies in BrM patients. We recently found that BrMs in patients frequently have severe MHC-I loss. BrM patients' scRNA-seq data from available datasets show that MHC-I expression level is negatively correlated with HDAC level in breast cancer brain metastasis. On the other hand, HDAC inhibitors (HDACi) are epigenetic modulators which have been indicated to recover MHC-I expression loss that contributes to immune invasion. HDACi has been indicated to enhance ICI efficacy in primary tumors by reprogramming the tumor microenvironment (TME). However, the immunomodulatory effect of HDACi is unclear in the unique brain immune microenvironment (BrIME), which is characterized as immunosuppressive. Here, we report that although the selective-HDACi Entinostat has a relatively poor blood-brain barrier (BBB) penetration compared to pan-HDACi Panobinostat, Entinostat induced a comparable level of histone acetylation in the brain to that of Panobinostat. Furthermore, combinatorial treatment consisting of HDACi Entinostat/Panobinostat and anti-PD1 reduced BrM outgrowth of EO771 mammary tumor cell-induced BrM in synergetic mouse model. We explored the impact of HDACi on cell surface MHC-I expression by flow cytometry. Entinostat restored MHC-I expression levels on both brain-seeking human and murine breast and lung cancer cell lines, indicating a general epigenetic regulation on MHC-I expression by inhibition of HDACs. To dissect the impact of HDACi on the BrIME, immune profiling of BrM was performed by mass cytometry (CyTOF). Notably, Entinostat induced a dramatic increment of a specific antigen-presenting cell (APC) cluster in BrM-bearing BrIME with increased ratio of M1 proinflammatory macrophages: M2 tumor-associated macrophages (TAMs) and decreased Tregs. Our results suggest that Entinostat can upregulate MHC-I for more effective antigen presentation and enhance anti-tumor immunity in BrIME.

#6428

Targeting SMARCAL1 as a therapeutic strategy to enhance cGAS/STING signaling in gastric cancer

Po-Yen Hsu[1], Yu-Ming Chuang[1], Shu-Hui LIN[2], Yu-Ting Lee[3], Yin-Chen Chen[1], Enders K.W. Ng[4], Kun-Tu YEH[2], Alfred S.L. Cheng[5], Michael W.Y. Chan[1]. *[1]Department Biomedical Sciences, National Chung Cheng Univ., Chiayi County, Taiwan,[2]Department of Surgical Pathology, Changhua Christian Hospital, Changhua, Taiwan,[3]Divsion of Hematology & Oncology, Department of Medicine, Ditmanson Medical Foundation Chiayi Christian Hospital, Chiayi County, Taiwan,[4]Deptartment of Surgery, The Chinese University of Hong Kong, Hong Kong, Hong Kong,[5]School of Biomedical Sciences, The Chinese University of Hong Kong, Hong Kong, Hong Kong*

Gastric cancer is one of the leading causes of cancer death in Eastern Asia. Although immunotherapy, such as immune checkpoint blockade, is an emerging therapeutic strategy against gastric cancer, only a fraction of cancer patients show a therapeutic response. Therefore, developing a novel therapeutic strategy to turn a “cold” tumor into a “hot” tumor is considered a crucial issue in cancer treatment. By methylomic analysis, we found that SMARCAL1 is one of the STAT3 targets which might be regulated by STAT3-mediated promoter methylation. Moreover, an inverse correlation between SMARCAL1 promoter methylation and expression was observed in the TCGA online database and in our cell lines experiment. Bisulfite pyrosequencing also showed a significant hypomethylation of SMARCAL1 compared to gastritis and adjacent normal in our in-house cohort (gastritis n=15; IM n=13; cancer n=58). More importantly, SMARCAL1 knockdown showed increased sensitivity of gastric cancer cell lines to DNA-damaging agents and increase the expression of cGAS and its downstream target, IFNB1. Therefore, in this study, we propose SMARCAL1 as a therapeutic target for improving the efficiency of immunotherapy by enhancing the cGAS/STING signaling pathway.

#6429

A surrogate to the anti-IL1RAP antibody nadunolimab induces tumor microenvironment changes to the metastatic lung and reduces

metastatic lesions in mouse models of metastatic cancer

Elin Jaensson Gyllenbäck, Camilla Rydberg Millrud, Petter Skoog, Caitríona Grönberg, David Liberg. *Cantargia AB, Lund, Sweden*

Interleukin-1 Receptor Accessory Protein (IL1RAP) is a coreceptor for the IL-1 receptor (IL1R1) and is required for IL-1α and IL-1β signaling. IL1RAP is expressed in the tumor microenvironment (TME); on cancer cells, stromal cells and on infiltrating immune cells in several types of cancers, including non-small cell lung cancer (NSCLC), pancreatic cancer (PDAC), triple-negative breast cancer (TNBC) and in metastatic lesions. Nadunolimab (CAN04) is a fully humanized ADCC-enhanced IgG1 antibody targeting IL1RAP and blocking both IL-1α and IL-1β signaling, currently evaluated in combination with chemotherapy in phase I/II clinical trials in NSCLC and PDAC (NCT03267316) and in TNBC (NCT05181462). Interim efficacy data are available for PDAC and NSCLC and are stronger than expected from chemotherapy alone based on historical controls; in a total of 73 PDAC patients, median iPFS is 7.2 months and median OS 12.7 months, while in a total of 30 NSCLC patients, a response rate of 53% is achieved, resulting in median PFS of 6.8 months. Microenvironmental IL1RAP-dependent IL-1 signaling contributes to tumorigenesis, tumor invasiveness and an immune-suppressive TME, partly driven by infiltration and induction of myeloid-derived suppressor cells (MDSCs). We have thus used the MDSC-rich 4T1 murine mammary tumor TNBC model to study metastatic lesions and TME modulation in 4T1 metastatic lungs upon treatment with a mouse surrogate antibody to nadunolimab. Infiltration of gMDSC/Ly6G$^+$ cells was very prominent in metastatic lungs from mice with orthotopically implanted 4T1 breast cancer cells compared to lungs from naive mice. Interestingly, infiltrating Ly6G$^+$ cells from metastatic lungs had a distinctly upregulated IL1RAP expression compared to Ly6G$^+$ cells from naïve lungs. Treatment with the nadunolimab surrogate antibody significantly reduced the number of lung metastases and induced prominent changes in the lung microenvironment where nanostring analysis showed global changes in adhesion and migration-related genes, as well as genes associated with cell activation. The effect on metastasis was not confined to the 4T1 model since a reduction of metastatic tumor cells after treatment with the mouse surrogate antibody was also observed in the murine B16-F10-luc i.v. model. Together

these data indicate that targeting IL1RAP is an effective way to modulate the TME and counteract the suppressive environment in metastatic tissue, and ultimately may reduce the potential for metastatic tumors in cancer patients.

#6430

Single-cell transcriptomic and epigenomic landscapes of innate and adaptive immune cells in metastatic melanoma treated with immunotherapy

Jiekun Yang[1], Doris Fu[1], Kyriakitsa Galani[1], Li-Lun Ho[1], Emily J. Robitschek[2], Dennie T. Frederick[3], Sandeep K. Yadav[4], Wentao Deng[4], Anand K. Singh[4], Kelly P. Burke[2], Cassia Wang[1], Tatyana Sharova[3], David Liu[2], Kunal Rai[4], Genevieve M. Boland[3], Manolis Kellis[1]. *[1]MIT, Cambridge, MA,[2]Dana-Farber Cancer Institute, Boston, MA,[3]Massachusetts General Hospital, Boston, MA,[4]University of Texas MD Anderson Cancer Center, Houston, TX*

Immune checkpoint inhibitors (ICIs) have revolutionized the care for cancer and extended survival for advanced cancer patients. While ICIs have shown astonishing clinical benefits, less than 50% of patients experience a durable response. To find better biomarkers for ICI response and understand the diverse cellular players in the tumor microenvironment (TME), we performed single-cell RNA sequencing (scRNA; 222,351 cells; 39 samples), single-nucleus transposase-accessible chromatin sequencing (scATAC; 45,478 cells; 15 samples), and bulk RNA sequencing (39 samples) on a metastatic melanoma cohort with rich phenotypic and molecular data. In ICI resistant tumors, we revealed how cell-adhesion and ribosomal activity changes in adaptive immune cells can reflect tumor-level therapeutic failure. We characterized T cell diversity in the TME and discovered an early activated state and a terminally exhausted state. Among the innate immune cells, we detected a mature dendritic cell (DC) state as a strong prognostic predictor of progression-free survival associated with ICI treatment. We studied its differentiation trajectory, transcriptome signatures, epigenome landscape and interactome with T-cells, in comparison to conventional dendritic cell types 1 and 2. We also showed that CRISPR deactivation of the enhancers induced by the mature DC state compromised DCs' antigen-presentation capabilities and their interactions with antigen-

specific T-cells. Lastly, we identified genes and functional modules associated with ICI response (e.g. cell-adhesion) and resistance (e.g. oxidative phosphorylation). Given their functional roles in strengthening immune response to cancer, the molecular and cellular mediators discovered here can help predict ICI regimen efficacy, guide therapeutic development and drug combinations, and pave the path to targeted therapies with long-term effects and new immunotherapies.

#6431

Targeting Rab7-mediated STING degradation to amplify therapeutic STING agonism in TNBC

Yuqing Zhang[1], Jessica L. Ritter[2], Tran C. Thai[1], Deborah A. Dillon[3], David A. Barbie[1], Thanh U. Barbie[4]. *[1]Medical Oncology, Dana-Farber Cancer Institute, Boston, MA,[2]Homology Medicines, Inc, Bedford, MA,[3]Pathology, Brigham and Women's Hospital, Boston, MA,[4]Dana-Farber Cancer Institute; Brigham and Women's Hospital, Boston, MA*

STING (Stimulator of interferon genes), encoded by *TMEM173*, is a critical regulator of the innate immune response to cytoplasmic double stranded DNA in cancer and is actively being pursued as a target for cancer immunotherapy. STING agonist analogues of 2'-3'cGAMP, the cyclic dinucleotide that directly activates STING downstream of cyclic-GAMP synthase, have entered phase 1 clinical trials for triple negative breast cancers (TNBC). Recently, we have identified tumor cell Phosphatase and tensin homolog (PTEN) inactivation as a precision-based context in which to apply STING agonists. Mechanistically, PTEN null TNBCs maintain Ras-related protein Rab-7a (Rab7) in an inactive state and therefore trafficking of STING to the lysosome is impaired and cells are rendered hypersensitive to STING agonism. Tissue microarray analysis reveals high STING expression in PTEN null TNBCs. Consistently, PTEN null TNBC cell lines were hyper-responsive to STING agonists with increased downstream production of IRF3 targets including CXCL10. In contrast, PTEN wild-type cells exhibit low STING expression and modest sensitivity to STING agonism. As such, although a significant proportion of TNBCs are PTEN null, we sought to broaden these findings to PTEN wild-type TNBCs by genetically and pharmacologically mimicking the PTEN null state by Rab7 knockout and use of a novel selective Rab7 inhibitor,

CID1067700. Indeed, using the PTEN wild-type TNBC cell line, MDA-MB-231, we found that PTEN deletion robustly increased STING protein expression. Rab7 CRISPR-Cas9 knockout or treatment of MDA-MB-231 cells with CID1067700 and the STING agonist (ADU-S100) impaired trafficking of STING for lysosomal degradation, upregulated T cell chemokines, and enhanced growth inhibition. Next, to model the potential *in vivo* implications for immune cell recruitment and function, we used a 3D microfluidic T-cell migration assay. We found that the enhanced CXCL10 levels resulting from addition of CID1067700 to MDA-MB-231 cells led to T-cell recruitment to the tumor spheroids. Taken together, our study identifies PTEN null status as a specific genomic context in TNBC that has exquisite sensitivity to STING agonist therapy and combination with Rab7 inhibition could amplify therapeutic STING agonism in PTEN wild-type TNBCs.

#6432

Glutamine antagonist prodrug JHU083 reprograms immunosuppressive tumor-associated macrophages (TAMs) to drive tumor immunity in urologic cancers

Monali Praharaj[1], Fan Shen[1], Alex J. Lee[1], Liang Zhao[1], Thomas Nirschl[1], Xiaoxu Wang[1], Debebe Theodros[1], Alok K. Singh[2], Raekwon A. Williams[1], Laura A. Sena[1], Elizabeth A. Thompson[1], Ada Tam[1], Srinivasan Yegnasubramanian[1], Edward J. Pearce[1], Robert D. Leone[1], Jesse Alt[1], Rana Rais[1], Barbara S. Slusher[1], Andrew M. Pardoll[1], Jonathan D. Powell[1], Jelani C. Zarif[1]. *[1]Johns Hopkins University School of Medicine, Baltimore, MD,[2]University of Pennsylvania, Philadelphia, PA*

Tumor metabolism is emerging as a regulator of immune mediated anti-tumor responses. Previously, we reported increased immunosuppressive tumor-associated macrophages (TAMs) infiltration with disease progression in prostate adenocarcinoma (PCa).[1] Glutamine metabolism has been implicated in metastatic castration resistant prostate cancer (mCRPC)[2]. To harness the potent anti-tumor effects of 6-Diazo-5-oxo-L-norleucine (DON), which targets glutamine utilizing enzymes and to mitigate known significant toxicities, we here use a novel pro-drug moiety, i.e., JHU083. We hypothesize that JHU083 will enhance anti-tumor immunity by

simultaneously targeting TAMs and cancer cells.Using scRNA-seq dataset from mCRPC patients, we investigated the importance of glutamine metabolism in TAMs in the tumors.[3] Enriched expression of glutamine utilizing enzymes was observed in TAMs in the metastasized tumor tissue relative to benign. We used JHU083 to treat two urological syngeneic immunogenic mouse tumor models *in vivo*; B6CaP (PCa) and MB49 (bladder cancer). JHU083 showed significant tumor regression in both models. Using *in vivo* depletion of CD4 or CD8 T cells or adoptively transferring *in-vivo* JHU083 treated TAMs in TME, we established a direct anti-tumor role of TAMs. Moreover, to characterize the effect of JHU083 on TAMs transcriptional & translational signatures and metabolite flux *in vivo*, we used scRNA-sequencing and bulk RNA sequencing at two different time points, multi-parameter flow cytometry and targeted LC-MS/MS metabolic profiling. Clustering of the transcriptional signatures at both time points using UMAP dimensionality reduction classified 6 discreet differentially expressed clusters of TAMs. It elutes to an overall induction of TNF signaling and increased proliferation in the TAM sub-clusters. Strikingly, this was observed translationally as well. Moreover, translationally in the TME at a later timepoint, an increase of glycolytic transporter and enzyme, i.e., Glut1 and Hexokinase II was also observed. The overall impact of this on the metabolome, specifically glycolytic pathway changes in the sorted TAMs, remains to be elucidated. Lastly, we assessed in-vivo the functional phagocytosis of TAMs with flow cytometry and IF microscopy. JHU083-treated TAMs showed significantly increased phagocytic activity, providing direct evidence of functional reprogramming. Conclusions: We found that JHU083 reprograms TAMs from an immunosuppressive to an inflammatory state which we show has a direct anti-tumor effect. These macrophages convert to a highly proliferative and glycolytic state, have increased TNF production which might be resulting in improved phagocytic activity against tumor cells. As urologic cancers are heavily infiltrated with immunosuppressive TAMs, JHU083 is an excellent preclinical candidate.

#6433

A novel bacterial strain, CJRB-101, induces anti-cancer effects by repolarization of M2 to CXCL9 and CXCL10 dual expressing M1 macrophages in humanized non-small cell lung cancer mice models

Arim Min[1], Chun-bong Synn[2], Seong-san Kang[3], Bo-eun Kwon[1], Junwon Yang[1], Hyunkyung Park[1], Jieun Im[1], Hyunjeong Kim[1], Sujeong Beak[4], Dong Kwon Kim[2], Jii Bum Lee[5], Hyeonseok Oh[1], Seung Min Yang[4], Yu Jin Han[4], Mi hyun Kim[4], Heekyung Han[4], Kwangmin Na[4], Young Taek Kim[4], Sungwoo Lee[3], Mi Ran Yun[6], Jae Hwan Kim[4], Youngseon Byeon[4], Young Seob Kim[4], Ji Yun Lee[5], Chang Gon Kim[5], Min Hee Hong[5], Sun Min Lim[5], Kyoung-Ho Pyo[6], Byoung Chul Cho[5]. *[1]CJ Bioscience Inc., Suwon, Korea, Republic of,[2]College of Medicine, Brain Korea 21 PLUS Project for Medical Science, Yonsei University, Seoul, Korea, Republic of,[3]JEUK Institute for Cancer Research, JEUK Co., Ltd., Gumi, Korea, Republic of,[4]Severance Biomedical Science Institute, Yonsei University College of Medicine, Seoul, Korea, Republic of,[5]Division of Medical Oncology, Department of Internal Medicine, Yonsei Cancer Center, Severance Hospital, Yonsei University College of Medicine, Seoul, Korea, Republic of,[6]Yonsei New Il Han Institute for Integrative Lung Cancer Research, Yonsei University College of Medicine, Seoul, Korea, Republic of*

Backgrounds: Live biotherapeutic products (LBPs) emerged as potential therapeutics to overcome the limitation of ICIs. This research shows that CJRB-101, a novel bacterial strain, can improve anti-tumor effects in synergy with pembrolizumab in non-small cell lung cancer (NSCLC).
Objectives and Methods: Tumors from NSCLC patients (anti-PD-1 refractory and resistant) were transplanted into Hu-CD34-NSG to establish humanized patient-derived xenograft (PDX) mice models. Five models (YHIM-2003, 2004, 2009, 2010 and 2014) were treated with CJRB-101 at low ($5x10^7$ CFU) or high (10^9 CFU) doses, or with pembrolizumab (10 mg/kg, i.p., Q5D) or in combination. Tumor growth inhibition (TGI) rate was measured. Tumor microenvironment (TME) was analyzed using multiplex IHC, flow cytometry and single cell RNA sequencing. *Ex-vivo* assays were performed to validate in silico findings.
Results: Tumor in PDX models was unresponsive to pembrolizumab alone, however, in combination with CJRB-101 effectively suppressed tumor growth. The synergy was highlighted in YHIM-2009 where TGI was 10-fold higher (56%) than pembrolizumab group (5%). Immune profiling revealed that macrophages may be responsible for the anti-tumor effects of CJRB-101. IHC showed significantly increased antigen presenting

specialized DCs ($CD16^+CD68^-CD11c^+$) and granzyme B^+ $CD8^+$ T cells in the tumor by CJRB-101 compared to pembrolizumab ($p<0.01$). This suggested that CJRB-101 induced infiltration of cytotoxic CD8 T cells into the tumor nest by enhancing antigen presenting machinery. Trajectory analysis showed that CJRB-101 induced repolarization of M2 to M1 macrophages, characterized by high expression of CXCL9/10. $CXCL9^+/10^+$ M1 macrophages were comparatively more abundant in the combination group (23.11%) than the pembrolizumab group (0.91%). CXCL9/CXCL10 expression in macrophages was higher in the CJRB-101 group compared to the pembrolizumab group ($p<0.0001$). The combination group (10.84%) had a higher relative abundance of $CD8^+$ T cells compared to the pembrolizumab group (1.58%) and higher IFNγ expression in $CD8^+$ T cells compared to the pembrolizumab group ($p=0.0152$), suggesting that CJRB-101 repolarized macrophages and recruited active $CD8^+$ T cells. Co-culture assays using bone marrow-derived macrophages validated that CJRB-101 drove differentiation towards $F4/80^+$ or MHC II^+ expressing M1 macrophage ($p<0.0001$) and repolarized existing M2 ($CD206^+$) to M1 ($p=0.0002$).
Conclusion: Combination treatment of CJRB-101 with anti-PD-1 showed synergistic anti-tumor effects via repolarization of M2 to M1 macrophages, leading to activation of $CD8^+$ T cells in TME. Especially, $CXCL9^+/10^+$ M1 macrophage playing a key role in TGI induced by CJRB-101 in NSCLC models. Findings from this study provided rationale for clinical investigation of CJRB-101.

#6434

A precision probiotic therapeutic promotes a more efficacious type I immune response and limits breast cancer growth in mice

Denise L. Cecil[1], Erin Rodmaker[1], Susan Strenk[2], Lauren Corulli[1], David N. Fredricks[2], Mary L. Disis[1]. *[1]University of Washington, Seattle, WA,[2]Fred Hutchinson Cancer Center, Seattle, WA*

High levels of Type I T-cells are needed to eradicate breast cancer. Few cancers induce Type I immunity except those that contain a high mutational burden. The majority of solid tumor patients develop a Type II immune response to commonly recognized tumor antigens, which are aberrantly

expressed non-mutated tumor associated proteins. We found that within the amino acid sequence of non-mutated tumor associated antigens are class II binding epitopes that preferentially elicit a T-helper 1 interferon-gamma (g) or an IL-10 T-helper-2 response. We have identified high levels of IL-10 secreting T-cells present in the peripheral blood of both humans and mice, specific for non-mutated tumor antigens, which share significant sequence homologies with bacterial organisms found in the human gut microbiome. These lymphocytes, cross-reactive for both bacterial and tumor antigens (BAC-TA), are enriched for memory T-cells. In mice, the BAC-TA cross-reactive T-cells traffic to tumors and accelerate cancer growth. We have identified a selected number of bacterial species that are most commonly associated with numerous TA homologies (bacteria^{high}) and certain species that are rarely homologous to any TA sequences (bacteria^{low}). We hypothesized that bacteria^{low} species can safely be enriched in the gut microbiome. TgMMTV-neu mice, a transgenic model of luminal B murine mammary cancer, pre-treated with vancomycin and metronidazole in the drinking water, received six weekly oral treatments of 10^9 CFU of a combination of *Lactobacillus acidophilus* and *Ruminococcus albus*, both bacteria^{low} species. Metagenomic sequencing of stool examined one week after the last treatment revealed a mean 28% increase in *R. albus* (p=0.07) and a mean 38% increase in *L. acidophilus* (p=0.08) as compared to untreated stool. The increase in these two bacteria^{low} species corresponded with ≥30% reduction of 10 bacteria^{high} species. This oral treatment regimen also inhibited the growth of a syngeneic ectopic tumor by 36% (p=0.002). Enriching the microbiome with these bacteria^{low} species also enhanced the immunogenicity of a previously reported non-efficacious whole protein vaccine. Immunization with a full-length plasmid-DNA based vaccine targeting IGFBP-2 demonstrated no IFN-g response in control mice (p=0.012). However, after mice were treated with *L. acidophilus/R. albus*, the full-length vaccine significantly induced IFN-g secretion (p=0.02). These data provide preliminary evidence that reduction of bacteria^{high} species can inhibit tumor growth and augment immune responses, providing a basis for using a precision probiotic for the treatment of cancer. Future studies will address whether modulating bacteria^{high} species in the gut reduces BAC-TA T-cells in the blood.

#6435

BCG008, a human Siglec-15 blocking antibody, displays potent anti-tumor activity in Siglec-15-humanized mice

Yongfei Yang[1], Aidong Qu[2], Fengping Yao[1], Pan Song[1], Hongyuan Liang[2], Maopeng Tian[1], Fang Yang[1], Zhaoxue Yu[1], Xu Zhou[2], Xiuling Li[2].
[1]Biocytogen Pharmaceuticals (Beijing) Co., Ltd., Beijing, China,[2]Shanghai Institute of Biological Products Co., Ltd, Shanghai, China

Sialic acid-binding Ig-like lectin 15, or Siglec-15, is identified as a critical immune suppressor. Siglec-15 expression is normally limited to certain myeloid cells, but it can be upregulated in a variety of tumors and on tumor-infiltrating myeloid cells. Siglec-15 significantly inhibits antigen-specific T cell responses both *in vitro* and *in vivo*. Conversely, genetic ablation of Siglec-15 promotes anti-tumor responses. Therefore, a Siglec-15-targeting blocking antibody could represent a novel class of anti-tumor immunotherapy. BCG008, a fully human monoclonal antibody antagonist of Siglec-15, was generated from RenMab™ mice, which contain the entire human immunoglobulin variable domain. Compared to a reference Siglec-15 blocking antibody (5G12), BCG008 exhibited higher affinity for human and cynomolgus monkey Siglec-15 and targeted distinct binding epitopes. In *in vitro* studies, BCG008 significantly abrogated Siglec-15-mediated T cell suppression in a dose-dependent manner, as measured by $CD4^+$ and $CD8^+$ T cell proliferation. Subsequently, the efficacy and safety of BCG008 was evaluated in syngeneic tumor models in Siglec15-humanized mice. BCG008 monotherapy significantly inhibited tumor growth, and the effect of the tumor inhibition was potentiated when administered in combination with other immune-checkpoint inhibitors, including anti-PD-L1 antibodies. In safety evaluation, BCG008 was well-tolerated in the tumor-bearing mice; no adverse effects were observed even at high doses (e.g. 30 mg/kg). Taken together, these results demonstrate that BCG008 is a novel anti-human Siglec-15 blocking antibody with favorable efficacy and safety profiles that can provide potential benefits for future cancer immunotherapy.

#6436

1C3, a novel non-blocking anti-human TNFR2 antibody, promotes effector T cell responses and demonstrates potent anti-tumor activity

Yongfei Yang[1], Shuzhen Cao[1], Wenjiao Zhang[1], Jing Zhang[1], Zhe Shao[2], Xueyuan Jiang[1], Qingya Duan[1], Maopeng Tian[1], Sen Mei[1], Zhaoxue Yu[1].
[1]Biocytogen Pharmaceuticals (Beijing) Co., Ltd., Beijing, China,[2]Dragonboat Biopharmaceutical, Shanghai, China

Regulatory T cells (Tregs) are a subset of immunosuppressive $CD4^+$ T lymphocytes which can inhibit effector T cell activity in the tumor microenvironment (TME) and promote tumor growth. Depletion of Tregs is a promising immunotherapy strategy for treatment of cancers. Tumor necrosis factor receptor-2 (TNFR2) is highly expressed on both Tregs and many kinds of tumor cells, making it a potential candidate for tumor-targeted antibody therapy. A fully human, non-blocking agonist antibody to TNFR2, 1C3, was generated from RenMab™ mice, which contain the full human immunoglobulin variable domain. 1C3 was selected from a large panel of antibody candidates after unbiased, high-throughput efficacy screening conducted in syngeneic tumor mouse models established in humanized TNFR2 mice. *In vitro*, 1C3 effectively promoted proliferation of cytotoxic T cells. Subsequently, the *in vivo* anti-tumor efficacy and safety of 1C3 was evaluated in syngeneic tumor mouse models expressing human TNFR2. The results demonstrated that 1C3 monotherapy significantly inhibited tumor growth in a dose-dependent manner. In combination with anti-human PD-1 or PD-L1 antibodies, 1C3 also greatly potentiated anti-tumor responses compared to monotherapy of each agent. Analysis of tumor-infiltrating lymphocytes (TIL) demonstrated that 1C3 treatment significantly increased the ratio of effector T cells to Tregs in the TME. Moreover, 1C3 was well tolerated in mice, and no adverse effects were observed even at high doses (e.g. 100 mg/kg). In conclusion, these data demonstrate that 1C3 is a novel anti-human TNFR2 non-blocking agonist antibody with effective anti-tumor efficacy and favorable safety. 1C3 may exert these effects by regulating Treg and effector T cell activities.

#6437

Development of therapeutic vaccines against ovarian cancer

Leslie Hesnard, Catherine Thériault, Maxime Cahuzac, Chantal Durette, Krystel Vincent, Marie-Pierre Hardy, Gabriel Ouellet Lavallée, Joël Lanoix, Pierre Thibault, Claude Perreault. *IRIC Université de Montréal, Montreal, QC, Canada*

Epithelial ovarian cancer (EOC) has a devastating impact on the health of women and has not significantly benefited from advances in immunotherapy mainly because of the lack of well-defined actionable antigen targets. It is therefore essential to discover tumor-specific antigens (TSAs) that are specific to ovarian cancer, shared by a significant proportion of patients and capable of being targeted by the immune system. Using a groundbreaking method, we have previously identified 91 aberrantly expressed TSAs (aeTSAs), 18% of which were shared by at least 80% of the TCGA cohort (The Cancer Genome Atlas). These TSAs originate from unmutated non-exonic genomic sequences and their expression results from cancer-specific epigenetic changes. In the present study, our goal was to evaluate the immunogenicity of these aeTSAs. To do so, 49/91 antigenswere selected based on their presentation by high-frequency HLA allotypes (9 alleles included) and their expression in a large proportion of EOCs patients. Using functional *in vitro* expansion of naive CD8 T cells by co-culture with TSA-pulsed dendritic cells (DC) followed by CDR3 TCR sequencing, we first assessed the ability of aeTSAs in stimulating the immune system. Notably, 98% of our antigens were able to significantly expand CD8 T cell clonotypes, indicating that their repertoires are available for vaccination. In addition, tetramer staining of CD8 T cell populations after culture with TSA-pulsed DCs revealed that 32% of our aeTSAs tested (13/40) could expand specific CD8 T cells at levels that are detectable by flow cytometry. When selecting an optimal vaccination strategy, DC vaccines are particularly attractive. Using mass spectrometry to measure the abundance of TSAs presented at the cell surface, we next compared two modalities for engineering TSA-based DC vaccines: synthetic peptide pulsing vs TSA-encoding RNA minigenes transfection. Our preliminary results show that synthetic peptide pulsing leads to higher amounts of peptides presented at the surface of the dendritic cells compared to RNA minigenes electroporation. Moreover, we show a direct correlation between the abundance of peptides detected by MS immediately after pulsing on DCs and their predicted binding affinity. This correlation is not maintained with time (24h after pulsing), suggesting that the detection of peptides 24h post-pulsing is linked to the stability of peptide-MHC complexes rather than peptide binding affinity. In conclusion, we show that aeTSAs are attractive targets for EOC immunotherapy, as most of them can

expand sizeable populations of CD8 T cells. We also reveal that direct pulsing of aeTSAs on DCs leads to better peptide presentation than RNA minigene transfection. These results are of capital importance, as optimal TSA presentation by DCs leads to stronger anti-tumor responses. We believe that our approach could have a significant impact on immunotherapy of EOC, and eventually of other cancer types.

#6438

Next-generation pan-cancer immunotherapy with patient-derived APC

Zhen Bian, Lei Shi, Yuan Liu, harry Stylli. *Georgia Institute of Technology, Atlanta, GA*

Harnessing phagocytic antigen presenting cells (APC) and tumor neoantigen-specific T cells represent the ultimate power of immunotherapy against cancer. The promises of phagocytic APCs lie in their abilities of not only initiating phagocytosis towards cancer cells (to “eat off” tumor) but also, through immunogenic antigen presentation, activating neoantigen-specific Tcells that systemically and durably eliminate cancer cells, as well as the establishment of a long-lasting cellular and hormonal immunity that prevents tumor recurrence. However, the efforts of developing APCs -based therapy have been hindered by the current lack of technology that robustly produce APCs from cancer patients, as none of the traditional methods for differentiating DC or macrophage APCs are effective for cancer patients. Through a proprietary process, we have created a unique reagent combo that enables robust differentiation of cancer patients’ peripheral monocytes (cMo) to be potent APC, termed κAPC. κAPC display a unique gene expression profile, separating from classical DC or macrophage, and profound proinflammatory phenotype with enhanced phagocytic capability and elevated immunogenic antigen presentation machinery. In both in vitro and in vivo settings, κAPC demonstrate direct uptake of tumor antigens and presentation to T cells, the latter leading to activation and large expansion of multi-targeting, polyclonal tumor-specific CD4 and CD8 T populations -termed NeoT- from circulating and tumor-infiltrating lymphocytes. Theexpanded CD8 NeoT are highly tumoricidal and once adoptively transferred in vivo, potently eliminated late-stage metastatic solid tumors, whereas CD4 NeoT contribute to immune memory and repolarize a proinflammatory TME favorable for tumor elimination.

Key words: κAPC, NeoT, NeoT adoptive cell therapy, κAPC-based cancer vaccine, combination therapies

#6439

Actin remodeling, inhibitory ligand polarization and small vesicle recruitment hinder effective anti-tumor immunity by shaping the tumor cell side of the immune synapse

Andrea Michela Biolato[1], Liza Filali[2], Céline Hoffmann[1], Felix Kleine-Borgmann[2], Elena Ockfen[1], Max Krecke[1], Michel Mittelbronn[3], Clément Thomas[1]. *[1]Department of Cancer Research (DOCR), Luxembourg Institute of Health, Luxembourg, Luxembourg,[2]Luxembourg Institute of Health, Luxembourg, Luxembourg,[3]National Center of Pathology (NCP), Laboratoire Nationale de Santé (LNS), Dudelange, Luxembourg*

Cancer immune evasion is a major obstacle to effective anticancer immunotherapies. Recently, we unveiled a mechanism crucial in cancer escape from natural killer (NK)-mediated killing. The identified process is characterized by a rapid and massive accumulation of actin filaments at the cancer cell side of the immunological synapse (IS). We termed this process “actin response” (AR) and discovered that its inhibition is sufficient to restore cancer cell susceptibility to NK-mediated killing in vitro. Importantly, the AR is conserved across a wide range of malignancies, highlighting the broad translational potential of targeting this pathway. In this study, we investigated the molecular mechanisms underlying AR-mediated cancer cell immune evasion. Cancer-NK cell conjugates were analyzed by imaging flow cytometry (IFC) to investigate the polarization of inhibitory and activating ligands to the cancer cell side of the IS relative to the AR. We found that the AR is associated with and necessary for polarization of several inhibitory ligands. For instance, HLA-A,-B,-C molecules, which act as potent inhibitors of NK cells, were 2-fold increased at the IS of cancer cells with an AR when compared to cancer cells without an AR. Using confocal microscopy, we found that such polarization of inhibitory molecules is associated with the loss of MTOC and lytic granule polarization in conjugated human primary NK cells. In addition, correlative light and electron microscopy analysis revealed the presence of small vesicles (100 nm in size) and multivesicular bodies (MVBs) in the synaptic region of cancer cells with an AR. Quantification of vesicle markers at the

IFC revealed a significant enrichment of CD63+/CD9+/CD81+ vesicles in the synaptic region of cancer cells with an AR. Interestingly, ultrastructure analysis showed that the AR is largely made of long actin-rich protrusions projecting into and altering the morphology of the synaptic cleft. Moreover, these protrusions were decorated with inhibitory molecules, such as PD-L1, and CD63. We identified a novel, highly conserved immune escape mechanism that exploits the fast remodeling of the actin cytoskeleton in cancer cells to induce the polarization of inhibitory ligands along with small tumor vesicles towards the IS. These findings suggest that actin remodeling in tumor cells at the IS actively promotes immune evasion. Further insights on the molecular and cellular mechanisms underpinning this pathway, such as the identification of selective targeting of linker proteins between the actin cytoskeleton and inhibitory ligands or small vesicles, represent a promising therapeutic strategy to improve the efficacy of anticancer immunotherapies. Nevertheless, additional research is needed in order to evaluate the translational potential of targeting the AR in a clinical setting.

#6440

Targeting TCTP reverses the multi-malignant phenotypes of immune-refractory tumor cells

Hyo-Jung Lee, Tae Woo Kim. *Korea University, Seoul, Korea, Republic of*

Cancer immunotherapy, particularly T cell-mediated therapy such as immune checkpoint blockade (ICB) and adoptive T cell transfer (ACT), has emerged as a potentially powerful approach to cancer treatment. However, immunotherapeutic resistance limits its clinical success by disrupting one or more steps of the cancer immunity cycle. In addition, multi-malignant phenotypes of immune-refractory tumor cells are also one of the major causes result poor prognosis of patients. Therefore, identifying the immune-resistance and multi-malignant factor, which not only can be targeted by clinically available medicines it can also be a prognostic marker, is needed ideally. Here, we identified TCTP as a novel factor conferring multi-malignant phenotypes of immune-refractory tumor cells. We discovered a crucial role of TCTP at the crossroads between multi-malignant tumor cells and the anti-cancer immunity system by demonstrating that $TCTP^{high}$ tumor cells enriched by immune selection pressure drive immune-refractory phenotypes. Importantly, the levels of TCTP within the tumors significantly

correlated with the clinical outcome of anti-PD-L1 therapy, which demonstrate TCTP as a prognostic marker in the case of clinical trials. Furthermore, targeting TCTP by clinical available drug enhanced the response to T cell-mediated therapy including ICB and ACT. Thus, our findings emphasize that TCTP could be a both a valid target a prognostic marker providing a framework for patient selection to apply combined therapy of T cell-mediated therapy with TCTP-targeting agents.

#6442

Role of TWEAK-Fn14 axis in driving immunosuppression in glioblastoma multiforme

Angad Beniwal[1], Ryan Eghlimi[1], Kenneth D. Alexander[2], Mylan R. Blomquist[1], Nhan Tran[1]. *[1]Mayo Clinic College of Medicine and Science, Scottsdale, AZ,[2]University of Kentucky, Lexington, KY*

Cellular heterogeneity within glioblastoma multiforme (GBM) is a key driver of resistance to standard-of-care therapeutic approaches such as DNA damage (temozolomide, TMZ), angiogenesis inhibition (Bevacizumab, BM), radiation necrosis, and surgical resection. As such, understanding and targeting heterogeneous tumor-associated populations is a critical aim of ongoing GBM research. Central nervous system (CNS) resident microglia constitute significant percentages of primary GBM samples, often up to 50% of bulk tumor. Additionally, glioblastoma-associated microglia have been implicated in intra-tumoral immunosuppression, and are thus a key barrier to successful implementation of immunotherapies that seek to enhance T-cell mediated anti-tumoral cytotoxicity. As such, insight into targetable pathways that upregulate immunosuppressive cytokines within GBM-associated microglia is necessary for overcoming immuno-therapeutic failure. Here, we identify expression of the cytokine TWEAK (TNFSF12) and its receptor Fn14 (TNFRSF12A) within the myeloid compartment of primary GBM samples via scRNA-seq. Furthermore, we demonstrate TWEAK-mediated reprogramming of GBM-associated microglia towards an immunosuppressive phenotype capable of inhibiting CD8+ T cell activation and proliferation. These findings unveil a potent, targetable axis of immunosuppression within GBM and are thus an exciting step towards enhancing efficacy of existing T-cell based anti-cancer strategies for GBM patients.

MOLECULAR/CELLULAR BIOLOGY AND GENETICS

Cyclin-dependent Kinases and Cyclin-dependent Kinase Inhibitors

#5972

CDK1 bridges NF-kB and b-catenin signaling in response to H. pylori infection in gastric tumorigenesis

Marwah M. Al-Mathkour, Shoumin Zhu, Longlong Cao, Shayan Khalafi, Zheng Chen, Julio Poveda, Dunfa Peng, Heng Lu, Mohammed Soutto, Tianling Hu, Oliver McDonalnd, Alexander Zaika, Wael El-Rifai. *Surgery, University of Miami Miller School of Medicine, Miami, FL*

Background: Cell cycle dysregulation is a hallmark of cancer, resulting in unregulated cell proliferation and, eventually, tumor development. Cyclin-dependent kinase 1 (CDK1) is a cell cycle regulatory protein that is involved in cell cycle maintenance. CDK1 has been discovered to be substantially elevated in a several tumors and is linked to poor overall and relapse-free survival. The aim of this study is to understand the regulation role of *Helicobacter Pylori* infection and inflammation on CDK1 expression in gastric cancer.
Methods: Using TCGA data and our integrated comprehensive gene expression analysis, we found a significant overexpression of CDK1 in gastric cancer human and mouse tissues. We detected overexpression of CDK1 in human and mouse gastric glands in response to *H. pylori* infection. Our data demonstrated that *H. pylori* infection induced phosphorylation (S536) and activation of NF-kB in vitro and in vivo. Furthermore, *H. pylori* infection and TNF-α treatment increased the CDK1 mRNA and protein levels in gastric cancer cell lines. Using the ChIP assay, we detected direct biding of NF-κB on the CDK1 promoter regulating its transcription. CDK1 promoted activation of the β-catenin signaling pathway. Using the pTOP/pFOP luciferase reporter assays, as a measure of β-catenin/TCF transcription activity, we confirmed CDK1-dependent activation of β-catenin in response to *H. pylori* infection. Pharmacologic and genetic inhibition of CDK1 reversed these effects and decreased number and size of gastric tumors organoid from mouse and human.

Conclusion: Our findings demonstrate NF-kB-mediated induction of CDK1 expression in response to *H. pylori* infection with subsequent activation of tumorigenic β-catenin signaling. This novel regulatory link between infection, CDK1, and β-catenin suggests the importance of considering CDK1 inhibitors in gastric cancer.

#5973

The brain penetrant CDK4/6 Inhibitor, PRT3645, is highly effective in combination with other targeted therapies in preclinical models of NSCLC, CRC, and HER2-positive breast cancer

Yue Zou[1], Srijita Dhar[1], Kirsten Gallagher[1], Andrew Buesking[2], Sarah Pawley[2], Ryan Holmes[2], Xiaowei Wu[2], Katarina Rohlfing[2], Min Wang[2], Joseph Rager[2], Tom Emm[2], Stefan Ruepp[2], Miles Cowart[2], Jing Ni[3], Jean Zhao[3], Bruce Ruggeri[2], Andrew Combs[2], Kris Vaddi[2], Sandy Geeganage[2], Ashish Juvekar[4], Sang Hyun Lee[2], Peggy Scherle[2]. *[1]Biology, Prelude Therapeutics Inc., Wilmington, DE,[2]Prelude Therapeutics Inc., Wilmington, DE,[3]Dana-Farber Cancer Institute, Boston, MA,[4]Modifi Bio, New Haven, CT*

Cell cycle deregulation is a hallmark of cancer and the hyperactivation and overexpression of CDKs are often drivers of cancer pathogenesis. Cyclin-dependent kinase 4 and 6 (CDK4)/(CDK6) are critical mediators of cellular transition into S phase and important for the initiation, growth, and survival of many cancers. Activated CDK4/CDK6 complexes phosphorylate Rb1, reduce their binding affinities and release Rb1-containing transcription repressor complexes from E2F transcription factors, resulting in activation of E2F controlled cell cycle genes and progression of the cell cycle. At present three CDK4/CDK6 inhibitors are approved for the treatment of ER+/HER2- breast cancer, and are being explored in other cancer indications as well. Previously we described a novel brain penetrant CDK4/CDK6 inhibitor, PRT3645, that exhibits single digit nanomolar biochemical potency against CDK4/CDK6 and >2000-fold selectivity against CDK1, CDK2 and CDK9. PRT3645 inhibits cellular phosphorylation of Rb and exhibits a protein binding-adjusted cellular IC50 of <300 nM. PRT3645 exhibits favorable in-vitro safety pharmacology and ADME properties, including increased brain penetration, and demonstrates

oral bioavailability across rodents, dog, and non-human primates. In addition to robust monotherapy activity observed in preclinical models of ER+/HER2- breast cancer, we explored the activity of PRT3645 in other tumor types as well as in combination with other targeted therapies. In NSCLC, PRT3645 treatment resulted in significant inhibition of cell lines that harbor activation of the RAS/MEK/ERK pathway in proliferation assays and demonstrated comparable high synergy scores when combined with clinically approved covalent KRAS G12C inhibitors. In-vivo, oral PRT3645 was well tolerated and induced anti-tumor efficacy in two KRAS G12C mutant xenograft models that harbor the CDKN2A (p16) deletion. Anti-tumor efficacy was further improved when PRT3645 was combined with KRAS/MEK inhibitors in xenograft models and the combination therapy was well tolerated. In addition, we explored combinations of PRT3645 with a brain penetrant receptor tyrosine kinase inhibitor (TKI), an approved treatment for patients with advanced HER2+ breast cancer, including patients with brain metastases. In a HER2+ orthotopic human breast cancer brain metastasis model, PRT3645 was highly efficacious in combination with HER2 kinase inhibition and enhanced median survival significantly. In summary, PRT3645 demonstrates an excellent balance of potency, selectivity, PK parameters across species and brain penetrance. In preclinical studies, PRT3645 was highly efficacious when combined with KRAS/MEK inhibitors, and with a brain penetrant HER2 receptor TKI, both in-vitro and in-vivo. PRT3645 has advanced into Phase 1 clinical trials (*NCT05538572*).

#5974

Synergistic activity of the CDK4/6 antagonist narazaciclib (ON123300) with irreversible BTK inhibition in ibrutinib-resistant mantle cell lymphoma

Nuria Profitos-Peleja[1], Marcelo L. Ribeiro[1], Adar Makovski Silverstein[2], Stephen Cosenza[2], Gaël Roué[1]. *[1]Lymphoma Translational lab, Josep Carreras Leukaemia Research Institute, Badalona, Spain,[2]Onconova Therapeutics, Newtown, PA*

Bruton tyrosine kinase inhibitors (BTKi) have transformed the therapeutic landscape of B-cell lymphoma including the aggressive mantle cell lymphoma (MCL) subtype, although primary and acquired resistance is

frequently observed. Interestingly, preliminary results have suggested that the second-generation, orally bioavailable and clinical-stage CDK4/6 inhibitor, ON123300 (narazaciclib), may be effective in preclinical models of BTKi-resistant MCL. We compared the efficacy and safety of ON123300 vs the approved CDK inhibitors palbociclib, abemaciclib or ribociclib, in association with various BTKi, in a panel of 10 MCL cell lines with distinct sensitivity to the first-in-class BTKi, ibrutinib, or the second generation acalabrutinib. We evaluated the effects of these combinations by CellTiter-Glo proliferation assay, FACS-mediated analysis of cell cycle and apoptosis, RT-PCR and western blot. Efficacy and safety of ON123300 in vivo was evaluated in a chicken embryo chorioallantoic membrane (CAM) xenograft model of MCL. We observed that ON123300 exhibited a significant antitumor activity in MCL cell lines independently of their sensitivity to ibrutinib, with IC50 at 72h ranging from 0.7 to 7.1μM (mean: 3.61±2.1μM), while it achieved a 32% tumor growth inhibition, with no detectable toxicity, in the CAM-MCL model. In vitro, ON123300 demonstrated a superior activity than palbociclib and ribociclib, and a similar effect that abemaciclib. Interestingly, ON123300 exhibited an antitumor activity comparable to ibrutinib but was more effective than acalabrutinib. ON123300 single agent treatment repressed several positive regulators of the G2/M cell cycle phase and triggered the accumulation of the CDK inhibitors p21, p16, and phospho-p27, with the consequent loss of phospho-Histone H3 and phospho-CDK2. Accordingly, ON123300 treatment evoked a 20-35% increase in G1 cell cycle fraction at 24h, which preceded the ignition of mitochondrial apoptosis. When combined with ibrutinib, rather than with acalabrutinib, ON123300 exhibited a significant antitumor activity with synergistic combination indexes in both BTK-sensitive and BTK-resistant cell lines. This phenomenon was associated with a slight but constant (+10-15%) augmentation of G1 blockade, histone H3/CDK2 dephosphorylation and p27/p16 accumulation in cells exposed to ibrutinib-ON123300 combination, with no detectable potentiation of apoptosis. In conclusion, ON123300 is safe and effective as single agent in preclinical models of MCL, including BTKi-resistant cases. Due to its complete distinct MoA from BTKi involving the direct modulation of cell cycle, ON123300, but not abemaciclib or palbociclib, can achieve significant synergistic activity in combination with ibrutinib, and in lower extent with acalabrutinib, especially in BTKi-resistant MCL cases.

#5975

Discovery of mechanisms that modulate the hippo pathway and CDK6 expression in CDK4/6 inhibitor resistant breast cancer cells

Chung-Jen Yu[1], Yong-Ji Zhuang[1], Ting-Yi Lin[1], Ta-Chung Chao[2], Chun-Yu Liu[2], Ling-Ming Tseng[2], Jiun-I Lai[1]. *[1]National Yang-Ming Chiao Tung University, taipei, Taiwan,[2]Taipei Veterans General Hospital, taipei, Taiwan*

Hormone positive (HR+) breast cancer is the most common subtype in this population. The current standard of care in advanced HR+ breast cancer includes endocrine therapy (tamoxifen, aromatase inhibitors, etc) and CDK4/6 inhibitors. CDK4/6 inhibitors significantly prolong survival and is now the general accepted choice of drug in first line. Despite the enormous clinical benefit, there remains a substantial portion of patients who ultimately develop resistance against CDK4/6 inhibitors. Many mechanisms have been proposed for CDK4/6 inhibitor resistant, including upregulation of CDK4, CDK6, Cyclin E, and others. Recently studies have linked the hippo pathway to CDK6 upregulation and resulting in CDK4/6 inhibitor resistance. We have set up a kinase library screen for kinase inhibitors that downregulate CDK6 amplification and further assess for reversal of resistance. We discovered staurosporine and the PI3K inhibitor PIK-75 as small molecules that potently downregulate CDK6 expression in breast cancer cells. We further confirmed that these compounds reverse the resistance towards CDK4/6 inhibitors in CDK6 amplification cells. By kinase profiling combined with a small hairpin RNA (shRNA) screen, we discovered the mechanisms that resulted in CDK6 downregulation and modulation of the hippo pathway to reverse the CDK4/6 inhibitor resistance. Our discovery has implications for therapeutic development in this group of patients posing a huge unmet need.

#5977

Evaluation of the potential combination regimens for q901, a clinical stage selective cdk7 inhibitor, as a DNA damage repair inhibitor

Donghoon Yu[1], Yeejin Jeon[1], YoonJi Lee[1], Seung-Joo Lee[1], Jaeseung Kim[1], Hyerim Jung[2], Tae-Kyung Kim[2], Kiyean Nam[1]. *[1]Qurient Co. Ltd., Seongnam-si, Korea, Republic of,[2]Department of Life Sciences, Pohang University of Science and Technology, Pohang, Korea, Republic of*

Background; Q901 is an extremely selective CDK7 inhibitor with potent single agent activity in the multiple in vivo tumor models including small cell lung cancer, cholangiocarcinoma, colon cancer, pancreatic cancer, hormone receptor positive breast cancer, castrate-resistant prostate cancer, and ovarian cancer. Q901 is currently in Phase 1/2 clinical trial for patients with selected advanced solid tumors (ClinicalTrials.gov: NCT05394103). In the preclinical models, Q901 treatment induces DNA damage response (DDR) impairment markers, particularly ones involved in the double-strand break repair mechanisms. This opens up broad range of possibilities for new combination regimen that could benefit from the accumulated DNA damages caused by Q901 treatment.
Methods: Various combinations have been tested to evaluate potential clinical regimens in multiple solid tumor models. Two different BRCA wild-type ovarian cancer A2780 and OVCAR3 models, an estrogen receptor positive MCF7 breast cancer model, or a syngeneic RENCA mouse renal cancer model was tested with Q901 in combination with poly ADP-ribose polymerase (PARP) inhibitor, selective estrogen receptor degrader (SERD), an estrogen receptor (ER) PROTAC degrader, or an anti-PD-1 antibody, respectively.
Results: In the A2780 model, the PARPi alone group showed 15% TGI (tumor growth inhibition), but significant tumor regression (104% TGI) was observed in the Q901 and PARPi combination. In the OVCAR3 model, the Q901 and PARPi combination group showed 105% TGI, whereas the PARPi alone group showed 38% TGI. In the MCF7 model, SERD alone showed 64% TGI and Q901 combination with SERD showed 94% TGI. Remarkable tumor regression (111% TGI) was observed in the MCF7 model combining ER PROTAC and Q901, whereas ER PROTAC alone group showed 55% TGI. In the RENCA model, the anti-PD-1 antibody alone group showed 13.2% TGI and the combination of Q901 and anti-PD-1 antibody showed 66% TGI. In summary, these preclinical model studies demonstrated significant additive/synergistic effects of the Q901 combination on tumor growth inhibition.
Conclusion: The non-clinical data demonstrate that Q901 not only has a potential as a single agent,but can also be used in combination with other therapeutic strategies to develop next-generation cancer therapeutics to potentially address unmet medical needs.

#5978

Cyclin dependent kinase 9 inhibitor AZD4573 induces cell death through DNA damage accumulation in breast cancer cells *in vitro*

Minyoung Lee[1], So Hyeon Kim[1], Sujin Ham[1], Hae Min Hwang[1], Youlim Noh[1], Yu-Jin Kim[1], Ahrum Min[1], Jinyong Kim[2], Dae-Won Lee[2], Kyung-Hun Lee[2], Seock-Ah Im[2]. *[1]Cancer Research Institute, Seoul National University, Seoul, Korea, Republic of,[2]Department of Internal Medicine, Seoul National University College of Medicine, Seoul, Korea, Republic of*

Background: Cyclin dependent kinase 9 (CDK9) regulates progression of RNA polymerase II through phosphorylation. Inhibition of CDK9 induces transcription-replication conflicts (T-R conflicts), leading to replication stress. AZD4573, a highly selective CDK9 inhibitor, showed anti-tumor effects in acute myeloid leukemia *in vitro* and *in vivo*. Recently it is being evaluated in phase 2 clinical trial (NCT04630756). However, the anti-tumor effect of AZD4573 is unknown in breast cancer. Thus, we investigated the anti-tumor effect of AZD4573 in breast cancer cells and explored the underlying mechanism.

Methods: To evaluate the antitumor effect *in vitro*, MTT assays were preformed using increasing concentration of AZD4573 (doses range : 0-100 nM). The IC_{50} values were calculated using Sigma Plot software. Cell cycle analysis was performed using flow cytometry analysis. The expression of signal transduction molecules was determined using quantitative PCR, western blotting, and immunofluorescence. Apoptotic cell death was verified by annexin-V assay. DNA strand breaks and repair efficacy were evaluated through alkaline comet assay. siRNA knock-down system was used to confirm the action mechanism.

Results: SK-BR-3, HCC70, HCC1937 and ZR-75-1 were sensitive to AZD4573 with IC_{50} ranging from 9.16-25.81 nM, whereas T47D and HCC1428 were less-sensitive (IC_{50} >100 nM), as assessed by MTT assay. After treatment of AZD4573, sensitive and less-sensitive cells showed increased T-R conflicts in 10 minutes. T-R conflicts were maintained in SK-BR-3, HCC70, HCC1937 and ZR-75-1 for 3 hours, but T-R conflicts disappeared immediately in T47D and HCC1428 cells. Moreover, expression of γ-H2AX, cleaved PARP and cleaved caspase-3 was increased, indicating the induction of apoptosis in sensitive cells. Contrary to these results, γ-H2AX induction and apoptosis were not observed in T47D and

HCC1428 cells. siRNA knock-down of CDK9 in HCC1937 resulted in an increase of T-R conflicts, γ-H2AX, with induction of PARP cleavage and caspase-3 cleavage.
Conclusion: AZD4573 induced T-R conflicts and subsequent DNA damage. Accumulation of DNA damage caused caspase-3-dependent apoptotic cell death in sensitive breast cancer cells. However, less-sensitive breast cancer cells resolved T-R conflicts immediately and maintained genomic stability. These data suggest that AZD4573 induced significant anti-tumor effects by apoptotic cell death through accumulation of DNA damage, following T-R conflicts.

#5979

TY-0540, a highly potent CDK2/4/6 inhibitor, attenuates acquired resistance against CDK4/6 inhibition

Meihua Li[1], Chengshan Niu[2], Mingtao Chen[2], Kaige Ji[2], Hui Xu[1], Shengli Dong[1], Yan Zhang[2], Qinguo Meng[2], Yuge Dou[2], Yijun Wang[1], Rui Wu[1], Yian Tu[1], Chao Zhou[1], Apeng Liang[1], Huan Wang[3], Rongzhen Ni[3], Aishen Gong[3], Hui Su[3], Mingyu Jiang[3], Feng Xing[3], Shaoqing Chen[3], Xiugui Chen[3], Jun Li[1], Yusheng Wu[1]. *[1]TYK Medicines, Inc., Huzhou, China,[2]TYK Medicines, Inc., Zhengzhou, China,[3]TYK Medicines, Inc., Shanghai, China*

The introduction of cyclin-dependent kinase (CDK) 4 and 6 dual inhibitors significantly improves the progression-free survival of patients with ER+/HER2- advanced or metastatic breast cancer. A large cohort of patients, however, eventually relapse to CDK4/6 therapy. To further empower the CDK therapy, simultaneous targeting of CDK2, CDK4, and CDK6 has been proposed as a new strategy based on the finding that abnormal activation of CDK2/CyclinE1 due to CCNE1 gene amplification is determined the key resistant mechanism to CDK4/6 inhibition. Here we present preclinical data of TY-0540, a novel CDK2/4/6 inhibitor for the treatment of breast cancer that is resistant to CDK4/6 inhibition. TY-0540 demonstrates high selectivity against CDK2, CDK4, and CDK6 compared to that of CDK1, CDK7, and CDK9 in a CDK panel screening. *In vitro* cell proliferation data shows that tumor cell lines OVCAR3 and HCC1806, both bearing CCNE1 amplification, are highly sensitive to TY-0540 treatment. To test the effectiveness of the clinical candidate compound on CDK4/6i resistance models, two Palbociclib resistant cell populations (T47D-R,

HCC1428-R) were in-house generated via gradient exposure of the cells to Palbociclib. As expected, TY-0540 potently inhibits T47D-R and HCC1428-R cell proliferation whereas Palbociclib only confers mild interruption to cell proliferation. TY-0540 abolishes Rb phosphorylation at all its three phosphorylation sites and down-regulates E2F1, FOXM1, and c-Myc expression levels in the model cell line OVCAR3. Meanwhile, cell cycle analysis suggests the occurrence of strong G1 arrest at 24 hours after TY-0540 treatment. Consistent with the *in vitro* results, TY-0540 treatment confers extraordinary in vivo efficacy with a spectrum of tumor CDX mouse models and PDX models in mice. To examine the *in vivo* effectiveness of TY-0540 over resistance models to CDK4/6 inhibition, we developed Palbociclib-resistant MCF7 tumor model (Palbociclib-R-MCF7) through a combination of *in vitro* and *in vivo* evolution of the cells under the selection pressure of Palbociclib. In agreement with its mode of action, TY-0540 is able to suppress Palbociclib-R-MCF7 tumor growth and maintain tumor size at stable disease status. Taken together, we have identified a potent CDK2/4/6 inhibitor which may grant new therapeutic opportunities for cancer patients who relapse or refractory to CDK4/6 signaling blockage therapy. #Meihua Li and Chengshan Niu contributed equally to this work. *Jun Li, Meihua Li and Chengshan Niu are the correspondent authors.

#5980

Identification of CDK15 activating cyclins by a recombinant co-expression approach

Daniel Mueller, Constance Ketterer, Diane Kraemer, Carolin Heidemann-Dinger, Lena Pilgermayer, Thomas Weber, Andreas Gericke, Frank Totzke, Michael H. G. Kubbutat. *Reaction Biology Europe GmbH, Freiburg im Breisgau, Germany*

Cyclin dependent kinases (CDK) form a family of 20 different CDKs with an additional 6 CDK-like proteins. Members of this family have been shown to be involved in the regulation of many critical cellular processes, including the regulation of cell cycle progression, gene transcription and neuronal function. Deregulated CDK activity has been observed frequently in human cancer and other diseases. Enzymatic kinase activity of CDKs has been found to depend on the formation of complexes with regulatory

proteins of the Cyclin family and requires in some cases the presence of additional complex partners, like MAT1 for CDK7/Cyclin H. To date, at least 15 different Cyclins have been described. For some CDKs it has been shown that they can also be activated by binding to proteins distinct from classical Cyclins. However, even while the 20 canonical CDKs share significant structural homology, they regulate very different functions of cell growth and development, partially due to their inherent substrate specificity but also regulated by their respective Cyclin partners. During the past 30 years several CDKs have been subject to extensive study resulting in a multitude of publications. This includes specifically CDK1, CDK2 and CDK4/6 and to a lesser extend CDK7 and CDK9. Other CDKs have been studied much less extensively and consequently the accumulated knowledge about their biological function and regulation is very limited. CDK15 (also known as PFTK2 or ALS2CR7) is one of these understudied members of the CDK family, with less than 20 publications in PubMed and the search term "CDK15" in contrast to more than 8600 hits for "CDK2". Its biological function is largely obscure even while evidence was presented that CDK15 is involved in the regulation of breast and colorectal cancer. Comparable to all other members of the CDK family, recombinantly overexpressed purified CDK15 does not exhibit detectable in-vitro activity and to date no Cyclin or other activating complex partner for CDK15 has been published. Since CDK inhibitors have been in the focus of interest at least since the approval of the first candidate (Palbociclib) for the treatment of ER+/HER+ breast cancer, testing the selectivity of other drug candidates within the complete group of CDKs is critically important to avoid unwanted off-target effects and toxicity. In order to enable in-vitro activity studies with CDK15 we evaluated different CDK15 constructs in combination with a comprehensive panel of different Cyclins using the baculo virus expression system. CDK15 and the respective Cyclins were co-expressed in insect cells, purified by affinity chromatography and tested for in-vitro activity using a panel of generic, broad-spectrum protein kinase substrates. We will present data on the identification of CDK15 activating Cyclins and the biochemical characterization of the in-vitro kinase activity of such CDK15/Cyclin complexes including a panel of kinase inhibitors.

#5981

TY-2699a is a highly potent CDK7 inhibitor to abolish dysfunctional tumor cell cycle for clinical development

Shengli Dong[1], Apeng Liang[1], Jian Zhu[1], Huan Wang[2], Meihua Li[1], Kai Wang[1], Rongzhen Ni[2], Haoyun Li[1], Yundi Cao[1], Linglin Xiao[1], Hongqiang Li[1], Yian Tu[1], Chao Zhou[1], Aishen Gong[2], Shuyi Xu[1], Hui Su[2], Chengshan Niu[3], Mingyu Jiang[2], Feng Xing[2], Xiugui Chen[2], Shaoqing Chen[2], Jun Li[1], Yusheng Wu[1]. *[1]TYK Medicines, Inc., Huzhou, China,[2]TYK Medicines, Inc., Shanghai, China,[3]TYK Medicines, Inc., Zhengzhou, China*

Cell cycle dysregulation is a hallmark of cancer and represents tremendous opportunities for clinical blockage in cancer therapy. Currently, trilaciclib, palbociclib, ribociclib, and abemaciclib that bear dual specificities against CDK4 and CDK6 have been approved for clinical usage, and more CDK4/6 targeted agents are actively under clinical evaluations, among which, TY-302, a novel CDK4/6 inhibitor being developed by TYK Medicines, is under Phase II trial (NCT04433494). To further drive the potential of pharmacological regulation of cancer cell cycle, here we report a novel CDK7 kinase inhibitor TY-2699a towards clinical investigation in 2023. CDK7 is a kinase at the core of transcription and also functions in regulating cell cycle progression. CDK7 overexpression has been identified in a wide spectrum of tumor tissues including triple negative breast cancer (TNBC), ovarian carcinoma (OC), small cell lung cancer (SCLC), and pancreatic cancer, and has been correlated to poor prognosis in the diseases. These malignant pathological profiles make CDK7 a pivotal target for the development of novel cancer therapy. Several CDK7 targeted agents, such as SY-5609 and Samuraciclib (CT7001), are under development. TYK Medicines is also committed to provide novel yet safe CDK7 kinase inhibitor. Our data show that TY-2699a potently inhibits the kinase activity of CDK7 in the form of CDK7/Cyclin H/MAT1 kinase complex (IC_{50} 9.5 nM) with high selectivity compared to that with CDK1/Cyclin A2, CDK2/Cyclin E1, CDK4/Cyclin D1, and CDK6/Cyclin D1. The screening of a panel of cancer cell lines revealed strong anti-cell proliferation activities of TY-2699a compared to that of the reference compound, and the phenotypic findings are underscored by TY-2699a-dependent cell cycle disruption. Our data demonstrate that TY-2699a triggers G2 cell cycle arrest, and induces apoptosis in tested cancer cells (HCC70, and MDA-MB-

468), but not in hTERT-immortalized normal cell (RPE-hTERT). *In vivo* studies show that TY-2699a confers significant efficacies in tested CDX mouse models of HCC70 (TNBC), OVCAR3 (OC), and MV-4-11(AML) in a dose-dependent manner. To further validate the anti-tumor activity of the agent, BR5010, a TNBC PDX model was employed to assess the response to TY-2699a treatment. Our data show that the efficacy of TY-2699a at 3 mg/kg, bid × 21 days was similar to that of the reference compound CT7001 at 100 mg/kg, qd × 21 days, and the efficacy of TY-2699a at 6 mg/kg, bid × 21 days was significantly better than that of CT7001 at 100 mg/kg, qd × 21 days in BR5010 mouse model. In summary, we report that TY-2699a is a highly selective and potent CDK7 kinase inhibitor with an acceptable toxicity profile within the therapeutic window. TY-2699a is planned to be advanced for clinical evaluation in 2023. # Shengli Dong and Apeng Liang contributed equally to this work. * Jun Li, Shengli Dong and Apeng Liang are the correspondent authors.

#5982

A potent and selective CDK8 inhibitor ABM-3249 with excellent efficacies in multiple in vivo cancer models

Chen Chen, Charles Huang, Min Xu, Xiuquan Chen, Xiaobing Lv, Chen Yang, Lanjiao Zhao, YouQin Chen, Jizhi Li, Li Zhao. *ABM Therapeutics, San Diego, CA*

CDK8 is a member of the CDK family in which belongs to the serine/threonine protein kinase. It binds with cyclin C to regulate the transcription. By modulation of various gene expression programs, CDK8 associated with the mediator complex to sustain proliferation and viability of cancer cells. CDK8 has been identified as an important factor in cancer occurrence and development. It also involves in the regulation of cancer cell stress response to radiotherapy and chemotherapy, assists tumor cell invasion, metastasis and drug resistance. Therefore inhibition of CDK8 is regarded as a promising target for cancer therapy. ABM-3249 was discovered as a potent and selective CDK8 inhibitor with a novel chemical structure. It inhibited CDK8 kinase activity in biochemical assay and cellular binding assay, with IC_{50} values of 1.4 nM and 19nM respectively. ABM-3249 displayed good kinase selectivity: <50% inhibition on all other CDK family members at 1uM. Consistently, ABM-3249 reduced STAT1-

S727 phosphorylation with an IC_{50} of less than 100nM. ABM-3249 showed good ADME properties with high oral bioavailability (~90%) in rodents. In efficacy studies, ABM-3249 exhibited excellent anti-tumor activities in multiple in vivo models. In an AML MV4-11 xenograft model at 25mpk oral dosing ABM-3249 achieved complete remission in all mice within 17 days and no tumor recurrence within one month after drug withdrawal. ABM-3249 showed good efficacies as a single agent, as well as a synergetic effect with anti-PD1 combination in a murine colon cancer MC38 model. It also showed an efficacy in a murine colon cancer B16F10 metastasis model. In addition, ABM-3249 displayed a good safety margin in a preliminary tox screen in rodents.

#5983

The secretome produced by senescent gastric cancer cells can lead to different paracrine effects depending on the status of autophagy

Claudio A. Valenzuela[1], Danitza Rebolledo[1], Angel Cayo[1], Whitney Venturini[1], Raúl Segovia[1], Rodrigo Moore-Carrasco[2], Nelson Brown[1].
[1]Center for Medical Research, Medical School, Universidad de Talca, Talca, Chile,[2]Faculty of Health Sciences, Universidad de Talca, Talca, Chile

Introduction: The initial transition from a proliferative to a senescent state is accompanied by a reduction in the activity of the cyclin-cyclin-dependent kinase (CDK) complexes, which in turn could be explained by the activation of the p53-$p21^{CIP1/WAF1}$ and/or $p16^{INK4a}$-pRB signaling pathways. As overexpression of D-type cyclins is commonly observed in gastric cancer cells, the use of CDK4/6 inhibitors could represent a viable alternative for gastric cancer treatment. Nonetheless, senescent cell can synthesize and secrete a plethora of bioactive molecules (a feature known as the senescence-associated secretory phenotype, SASP) with the potential of modifying the tumor microenvironment in ways that could be therapeutically deleterious. Among processes that are upregulated in most senescent cells, autophagy has received great attention during the last years. So far, however, the role of autophagy in the modulation of SASPs has yet to be clarified. Previous work from our lab has revealed an increased autophagic flux in gastric cancer cell lines undergoing drug-induced

senescence, suggesting a regulatory role in the implementation of this modality of cellular senescence. More specifically, the secretory phenotype of senescent gastric cancer cells seems to depend on the autophagy status. Materials and Methods: In order to determine the role of autophagy in the modulation of the SASP, cellular senescence was pharmacologically triggered in gastric cancer cell lines (AGS, MKN-45) through inhibition of CDK4/6 activity (0.5-1.0 μM of Palbociclib for 48 and 96 hours), with or without the concomitant inhibition of autophagy by either genetic (knocking down ATG5) or pharmacologic (treatment with 0.5 μM of Spautin-1) approaches. The expression of factors secreted by senescent cells under different experimental conditions was analyzed from conditioned media; and the same conditioned media were used in assays aimed to assess migration, invasion, and cell proliferation of non-senescent cells.
Results and Discussion: Inhibition of autophagy in senescent cells led to a downregulation in the expression of proinflammatory molecules that were overexpressed in autophagy-proficient senescent cells (MIF, IL-8, IL1β). Unlike conditioned media derived from AGS cells, conditioned media derived from senescent MKN-45 cells that were rendered deficient in autophagy enhanced the invasive capabilities of non-senescent cells. Our results suggest that autophagy modulates the expression of SASP components and, by so doing, affects the behavior of neighboring non-senescent cells. Interestingly, these effects were also influenced by the genetic status of gastric cancer cells. This work was supported by Fondecyt ANID 11201182

#5984

CDK9 inhibition as a potential therapeutic strategy in Ewing sarcoma

Yuta Matsumura, Richard E. Heinz, Curtis A. Allred, Adam Siddiqui, Jason M. Foulks, Steven L. Warner. *Sumitomo Pharma Oncology, Inc., Lehi, UT*

Ewing sarcoma (EWS) is the second most common bone and soft tissue sarcoma in children and adolescents and accounts for approximately 2% of all childhood cancer diagnoses. EWS is a highly aggressive cancer: the overall 5-year survival rate for localized and metastatic EWS are 67 and 38%, respectively. Each year, approximately 200 children and adolescents in the United States are diagnosed with EWS. Genetically, nearly all EWS

have chromosomal translocations in which a member of the FET gene family is fused with an ETS transcription factor, with 85% of cases being EWSR1-FLI1. Cyclin-dependent kinase 9 (CDK9) is a serine/threonine protein kinase involved in transcription elongation through phosphorylation and activation of RNA polymerase II (RPB1) and increases the levels of key oncogenic genes like myeloid cell leukemia-1 (MCL-1) and c-Myc, which are reported to be involved in chemoresistance. CDK9 may be a viable target in transcriptionally addicted cancers including EWS driven by oncogenic fusion genes like EWSR1-FLI1. TP-1287 is an investigational orally delivered phosphate pro-drug of alvocidib, a potent CDK9 inhibitor. We hypothesized that alvocidib, the pharmaceutically active form of TP-1287, may show activity in EWS cells as a single agent and in combination with standard of care agents. Alvocidib demonstrated the suppression of downstream targets of CDK9 including c-Myc in EWS cell lines after 6-hr treatment. In cell viability assays using CellTiter-Glo, alvocidib resulted in IC_{50} values of 68 - 125 nM in EWS cell lines after 3-day treatment and 27 - 160 nM in EWS cells from patient derived xenograft (PDX) models, after 6-day treatment. MCL-1 amplified EWS cells were observed significantly more sensitive to alvocidib than MCL-1 diploid EWS cells in the EWS cells from PDX models ($p=0.004$). Further bioinformatic analysis to predict alvocidib sensitivity is currently underway. Alvocidib demonstrated an additive inhibitory response in combination with topotecan, phosphoramide mustard, a biologically active metabolite of cyclophosphamide, and palifosfamide, a biologically active metabolite of ifosfamide, in EWS cell lines after 3-day treatment. Alvocidib treatment showed reduction of RAD51 which is involved in DNA damage response (DDR), suggesting the activity of alvocidib on DDR may contribute to this additive response. In an *in vivo* preclinical study using the A-673 model, TP-1287 (2.5 mg/kg, QD) showed tumor growth inhibition (TGI). *In vivo* combination studies with standard of care agents using EWS xenograft models are currently ongoing. In summary, alvocidib has shown activity inhibiting the growth of EWS cells as a single agent and an additive response in combination with EWS standard of care agents in EWS cell lines. TP-1287 may be a potential therapeutic option for the current regimen in EWS. TP-1287 is being investigated for solid tumors including EWS (clinicaltrials.gov, NCT03604783).

#5985

Cyclin dependent kinase 9 (CDK9) inhibition increased efficacy of programmed cell death protein 1 (PD-1) blockade for hepatocellular carcinoma (HCC) through decreasing programmed death-ligand 1 (PD-L1) expression

Ching-Tso Chen[1], Yu-Yun Shao[2], Hung-Wei Hsu[3], Rita R. Wo[3], Han-Yu Wang[3], Ann-Lii Cheng[3], Chih-Hung Hsu[3]. *[1]Department of Oncology, National Taiwan University Hospital Hsin-Chu Branch, Hsinchu, Taiwan,[2]National Taiwan University, Taipei City, Taiwan,[3]Department of Oncology, National Taiwan University Hospital, Taipei City, Taiwan*

Background: PD-1 blockade has been approved as treatment for advanced HCC. We previously demonstrated the efficacy of CDK9 inhibition in reducing the expression of inducible proteins and as a treatment for HCC (Shao et al. Oncology 2022). We thus examined the influence of CDK9 inhibition on the expression of PD-L1 in HCC and the potential of improving the efficacy of PD-1 blockade with the combination of CDK9 inhibitors.

Methods: We first examined the influence of specific CDK9 inhibitors, AZD4573 and atuveciclib, on interferon-γ (IFN-γ) induced PD-L1 expression of human HCC cell lines HuH7 and Hep3B. Overexpression of CDK9 and siRNA to CDK9 were used to confirm the findings. Similar experiments were repeated in the mouse HCC cell line BNL. To test the in vivo efficacy, we orthotopically implanted BNL cells in the subcapsular area of BALB/c mice, which were then treated with vehicle, CDK9 inhibitors, anti-PD-L1 antibodies, or their combination. To compare with tumor sizes, all mice were sacrificed after 14 days of treatment. To compare survival, the mice were only sacrificed if they met the criteria of animal euthanasia.

Results: Both HuH7 and Hep3B cells had minimal PD-L1 expression, which however could be induced using IFN-γ. AZD4573 and atuveciclib decreased the IFN-γ induced PD-L1 expression of HuH7 and Hep3B cells in a dose dependent manner. The flow cytometry results confirmed that membrane PD-L1 expression was also decreased by CDK9 inhibition. Overexpression of CDK9 decreased the influence of these CDK9 inhibitors on PD-L1 expression. CDK9 knockdown using siRNA reduced the IFN-γ induced PD-L1 expression. AZD4573 and atuveciclib also reduce the PD-

L1 expression in BNL cell lines. In the orthotopic animal model, the tumors of the sacrificed mice were significantly smaller in mice treated with atuveciclib and an anti-PD-L1 antibody than mice treatment with either alone. The survival of mice treated with the combination was also longer than mice treated with each therapy alone.
Conclusion: We demonstrated that CDK9 inhibition could reduce the IFN-γ induced PD-L1 expression of HCC cells. Combination of CDK9 inhibitors and anti-PD-L1 antibodies was more effective than either therapy alone.

#5987

Differential targets engaged by narazaciclib in comparison to the approved CDK4/6 inhibitors contribute to enhanced inhibition of tumor cell growth

Petros Kechagioglou[1], Camille Dupont[1], Hajime Yurugi[1], Ute Distler[1], Stefan Tenzer[1], Alexey Chernobrovkin[2], Kristina Riegel[1], Juliane Mooz[1], Mahil Lambert[3], Volker Dötsch[3], Stephen Cosenza[4], Steven M. Fruchtman[5], Krishnaraj Rajalingam[1]. *[1]University Medical Center of the Johannes Gutenberg University Mainz, Mainz, Germany,[2]3Pelagobio Bioscience, Solna, Sweden,[3]Goethe University, Frankfurt, Germany,[4]Onconova Therapeutics Inc, Newtown, PA,[5]Onconova Therapeutics Inc, Newton, PA*

CDK4/6 inhibitors are clinically approved for the treatment of HR+, HER2- metastatic breast cancer by reinstating the G1/S checkpoint in tumor cells. Despite clinical benefit, safety concerns such as neutropenia and diarrhea, and disease progression, raises a critical need to identify novel therapeutic strategies. Narazaciclib (ON123300), novel CDK4/6i, designed to enhance efficacy and safety by its multi-targeted kinase inhibitor activity at low nM concentrations against CDK4/6, ARK5, CSF1R, and c-Kit. Narazaciclib is in Ph I trials; NCT04739293 and CXHL1900340; studying different administration regimens. Since several oncogenic signaling pathways are affected, we examined the efficacy of ON123300 in various breast cancer cell lines, and consolidate its mechanism of action by identifying the other targets engaged by ON123300. To identify direct and secondary targets engaged by narazaciclib and palbociclib, proteome wide Cellular Thermal Shift Assay (CETSA) was performed. To investigate narazaciclib's effect

on signaling pathways, Integrative Inferred Kinase Activity (INKA) was performed. Bioinformatics analysis explored the potential clinical effect of the identified targets. Molecular docking simulations investigated the potential interactions of narazaciclib to engage the new targets compared to other CDK4/6i. Both CETSA and INKA analysis revealed more potential targets engaged by narazaciclib compared to palbociclib in both MDA-MB-231 lysates and intact cells such as BUB1, CHEK1, AURKA, GSK3α and GSK3β. In TNBC patients with BUB1 overexpression bioinformatics analysis indicates a low survival correlation. Docking data showed a higher affinity of narazaciclib with BUB1 compared to palbociclib and abemaciclib. A stronger induction of apoptosis and senescence was detected in narazaciclib treated MMTV-PYMT cells, a murine mammary carcinoma model, compared to the other CDK4/6i, while narazaciclib enhanced CCL5 and CXCL10 mRNA levels. Reduction of PD-L1 protein levels and a promoting effect on the H2D1 and B2M mRNA levels was perceived in narazaciclib treated PYMT cells. Lastly, inhibition of autophagy, both at the early and late stages, may sensitize cancer cells to narazaciclib and induce irreversible cell proliferation inhibition, providing a novel therapeutic approach. Our data unveiled the differential targets engaged by narazaciclib in comparison to palbociblib. Narazaciclib treatment led to BUB1 protein degradation, overexpression of which is associated with poor prognosis in TNBC. Combination of narazaciclib with autophagy inhibitors sensitized several breast cancer cells to cell death. Narazaciclib treatment may promote antitumor immunity by influencing the expression of various immune modulators in the tumor cells which needs to be further validated in preclinical animal models; and ultimately in the clinic.

#5988

A non-canonical CDK9 complex mediates endocycling in polyaneuploid cancer cell (PACC) state

Cheng-fan Lee, Michael Loycano, Luke LOFTUS, Laurie Kostecka, Melvin Li, Sarah Amend, Kenneth Pienta. *Cancer Ecology Center, The Brady Urological Institute,, Johns Hopkins University School of Medicine, Baltimore, MD*

Once prostate cancer has spread from its primary site, treatment is limited to systemically administered therapy. While tumors initially respond to

these therapies, eventually, all therapies fail, and the tumor recurs. Ours and others' recent studies have shown the presence of a universal mechanism of resistance: accession of the polyaneuploid cancer cell (PACC) state. The PolyAneuploid Transition (PAT) is initiated when a cancer cell is subjected to external stress, including therapy (we have tested three classes of chemotherapy and radiation), and accesses an alternative non-mitotic cell cycle known as endocycling, resulting in a greater-than-G2 polyploidization of the aneuploid genome (polyaneuploidy). While in this pro-survival PACC state, we have shown that cells are resistant to all forms of cytotoxic therapy. Initial RNA sequencing of cells that have accessed the PACC state in response to multiple classes of chemotherapy, including docetaxel and cisplatin, demonstrate a remodeled transcriptional profile that is distinct from control cultures. We hypothesize that accession of the resistance-mediating PACC state requires transcriptional remodeling. Our data show that cells in the PACC state had increased overall transcriptional activity. The multi protein complex pTEFB (positive transcription elongation factor) is a critical driver of RNA Polymerase II function and is composed of multiple subunits, including CDK9, a cyclin regulatory subunit, and a transcription factor. CDK9 phosphorylation was significantly elevated during accession and persistence in the PACC state. Genetic inhibitionof CDK9 by siRNA led to decreased expression of cyclin A which plays a role in S phase, both in the mitoticcycle and in the PACC endocycle. Interestingly, despite increased CDK9 levels, known CDK9 pTEFb complex members cyclin T1 and BRD4 were both decreased in cells in the PACC state. We treated cancer cells induced to enter the PACC state upon exposure to cisplatin with pharmaceutical inhibitors of CDK9, Flavopiridol and Fadraciclib. Combination of CDK9 inhibition with chemotherapy showed a suppressive effect on the PACC population. Our findings therefore suggest that a non-canonical CDK9 complex could be critical role for the endocycling to access and maintain the PACC state and represents a therapeutic candidate to eliminate the resistance-mediating PACC state.

#5989

Targeting RRM2 & cell cycle for breast cancer treatment

Nahid Sultana[1], Howard L. Elford[2], Jesika S. Faridi[1]. *[1]University of the Pacific, Stockton, CA,[2]Molecules for Health Inc., Stockton, CA*

Endocrine treatment is an effective first-line therapy for targeting ER positive, HER2 negative breast cancer. But success is limited by development of acquired resistance due to long-term therapy. Cyclin D1 and cyclin dependent kinase 4/6 (CDK4/6) complex causes phosphorylation and subsequent inactivation of retinoblastoma (Rb) tumor suppressor protein which promotes progression of the cell cycle from G1 to S phase. This observation led the development of the first CDK4/6 inhibitor palbociclib (Ibrance; Pfizer) which induces cell cycle arrest at G1 phase in cancer cells. Owing to intrinsic and acquired drug resistance development, success is limited despite promising clinical outcomes. This situation necessitates the development of potential combination strategies to overcome drug resistance. Ribonucleotide reductase (RR) is a rate limiting enzyme in DNA synthesis consisting of two subunits RRM1 and RRM2. Didox inhibits ribonucleotide reductase subunit 2 (RRM2) which ultimately blocks DNA synthesis. Combination of didox with palbociclib is a potential strategy to target ER positive and ER negative/triple negative breast cancer. Previously, we have shown that didox (DDX) can significantly halt malignant breast cancer cell division in combination with the anthracycline drug doxorubicin by targeting RRM2, mutant p53 and NFkB regulatory proteins. Recently, we confirmed that didox in combination with palbociclib significantly lowers ER positive and ER negative breast cancer and their palbociclib resistant counterparts' growth compared to no treatment or palbociclib treatment. We also confirmed that ER positive MCF7 and ER negative MDA-MB-468 parental breast cancer cells IC50 of palbociclib drug is lower than their palbociclib resistant counterparts. Here, we are reporting that didox decreases cell cycle proteins alone or in combination with palbociclib in ER positive MCF7 and ER negative MDA-MB-468 parental and palbociclib resistant breast cancer cells. This finding opens a novel approach for targeting both ER positive as well as ER negative breast cancer treatment. We are also reporting that didox treatment modulates cyclin D1 (CCND1) and RRM2 expression in MCF7 and MDA-MB-468 breast cancer along with their palbociclib resistant counterparts. Additionally, we observed that didox alone or in combination with palbociclib alters the cell cycle of MCF7 and MDA-MB-468 parental and palbociclib resistant breast cancer cells. Our data presents a novel and promising approach for the treatment of ER positive and ER negative breast

cancer that involves inhibition of RRM2 and cell cycle that merits further clinical investigation in animal and human models.

#5990

Druggable CRISPR/Cas9 screen identifies Cyclin E1 (CCNE1) as a key mediator of sensitivity to CDK4/6 inhibition in non-small cell lung cancer (NSCLC)

Matthew Bott, Maria Skamagki, Nelson Salgado, Francisco Sanchez-Rivera, Scott Lowe. *Memorial Sloan Kettering Cancer Center, New York, NY*

Objective: CDK4/6 inhibition has become an important treatment option in some epithelial malignancies but its utility in the setting of NSCLC remains limited. While CDK4-based monotherapy has been generally ineffective, combinatorial regimens have shown promise. Here we sought to perform an unbiased assessment of potential combinatorial strategies in pre-clinical models of NSCLC.
Methods: We performed a CRISPR/Cas9 screen in two NSCLC cell lines (A549 and H2030) in the presence and absence of the CDK4/6 inhibitor Palbociclib and identified guide RNAs that selectively depleted in the setting of drug treatment. We subsequently performed validation and mechanistic experiments as described. CDK4 and CDK2 activity was assessed using a fluorescent reporter system.
Results: Palbociclib-sensitizing screen hits include MAPK1 (ERK2), AKT1, MAP3K2 (MEKK2), PIK3CA, MAPK14 (p38a), AKT3, PORCN, LGR4, CDK1, CDK9, and AURKB . Screen results were compared with a previously published Palbociclib sensitizing screen and shared hits were identified. Of these, CCNE1 was the highest scoring hit suggesting relevance across histologies. Interestingly, several screen hits such as ERK2, PIK3CA, VCP and ELAVL1 have reported roles in CCNE1 transcription or post-translational stabilization suggesting a central role for CCNE1 in determining drug sensitivity. Western blot analyses demonstrate that CCNE1 is rapidly upregulated following Palbociclib exposure in a panel of NSCLC cell lines and immunofluorescence shows strong post-treatment CCNE1 expression in human A549 xenografts *in vivo*. CDK2/4 fluorescent reporter assays show partial restoration of CDK2 activity within 48 hours of Palbociclib treatment. Genetic validation experiments using

dox-inducible shRNA constructs targeting CCNE1 show that CCNE1 knockdown sensitizes cells to Palbociclib treatment and enhances senescence induction. Pharmacologic and genetic co-inhibition of CDK2 improves Palbociclib efficacy yet such co-inhibition further elevates CCNE1 levels and CDK2 suppression remains incomplete based the fluorescence reporting system. Furthermore, knockdown of CCNE1 in conjunction with CDK2/4/6 inhibition shows improved growth inhibition compared to drug treatment alone. Based on this data, we hypothesize that targeting signaling pathways upstream of CCNE1 transcription or those which affect CCNE1 stabilization and turnover may be more efficacious than combined CDK inhibition.
Conclusion: CCNE1 is a critical mediator of sensitivity to CDK4/6 inhibition and Palbociclib treatment results in rapid compensatory increases in CCNE1 levels. Despite drug treatment, NSCLC cells retain CDK2 activity which is only partially inhibited by combined CDK 2/4/6 inhibition. Screen results suggest several potential approaches for co-targeting of CCNE1 to enhance drug sensitivity.

#5991

Development and characterization of a novel CDK4/6 inhibitor for the treatment of CDK4/6 dependent cancers

Neil A. O'Brien[1], Martina S. J. McDermott[1], Brendan M. O'Boyle[2], Justin A. Hilf[2], Oliver Loson[2], Kevin Chau[1], Weiping Jia[1], Naeimeh Kamranpour[1], Tong Luo[1], Raul Ayala[1], Shawnt Issakhanian[1], John A. Glaspy[1], Brian M. Stoltz[3], Dennis J. Slamon[1]. *[1]UCLA - University of California Los Angeles, Los Angeles, CA,[2]1200 Pharma, Culver City, CA,[3]Division of Chemistry and Chemical Engineering, California Institute of Technology, Pasadena, CA*

CDK4/6 inhibitors give clinical benefit in the treatment of metastatic ER+/HER2- breast cancer (mBC) in combination with endocrine therapy. Although this class of inhibitor has been extensively studied in several other cancer types, CDK4/6 inhibitors have not been approved as a treatment for outside of ER+/HER2- cancer. We evaluated the clinically approved CDK4/6 inhibitors, palbociclib, ribociclib and abemaciclib—in a 500+ cell line screening platform and identified several cancers outside of breast that may have subpopulations that are sensitive to CDK4/6 inhibitors. Kinome

and KiNativ analyses helped identify differences in sensitivity/selectivity that we observed between each CDK4/6 inhibitor. Comprehensive molecular profiling of the cell lines at baseline allowed us to screen for potential associations with sensitivity to these compounds. These analyses identified potential biomarkers of sensitivity in non-small cell lung carcinoma (NSCLC) and colorectal cancer (CRC) that will later be evaluated in human clinical studies. Having thoroughly studied the CDK4/6 class and discovered new opportunities for clinical development, we set out to develop a CDK4/6 inhibitor that would have the best properties of the two distinguished class members. Using our proprietary chemistry, we developed UCT-03-008, a potent CDK4/6 small molecular inhibitor with a pharmacology known to enhance therapeutic benefit in mBC. Pharmacokinetic properties of UCT-03-008 are improved over those of other CDK4/6 inhibitors. UCT-03-008 has activity in preclinical models as a monotherapy and yields *in vivo* efficacy in multiple cancer models outside of ER+/HER2- breast cancer, including CRC and NSCLC. In summary, UCT-03-008 is a CDK4/6 inhibitor with optimized pharmacological properties. Clinical development of this compound will be guided by the biomarker hypotheses developed here. We are currently enrolling patients for treatment with UCT-03-008 in a Phase 1 clinical trial of advanced solid tumors (NCT05103046).

#5992

Cells rapidly adapt to CDK2 inhibitors via plasticity of the CDK2/4/6-Rb-E2F axis

Mansi Arora[1], Justin Moser[2], Timothy E. Hoffman[3], Lotte P. Watts[3], Mingwei Min[4], Monica Musteanu[5], Yao Rong[3], Jordan Schneider[6], C. Ryland Ill[3], Varuna Nangia[3], Manuel Sanclemente[7], John Lapek[8], Lisa Nguyen[9], Sherry Niessen[8], Stephen Dann[9], Todd van Arsdale[10], Mariano Barbacid[7], Nichol Miller[11], Sabrina L. Spencer[3]. *[1]Cyteir Therapeutics, Lexington, MA,[2]Lumicks, Waltham, MA,[3]University of Colorado Boulder, Boulder, CO,[4]Guangzhou Laboratory, Guangzhou, China,[5]Complutense University of Madrid, Madrid, Spain,[6]Josh.ai, Denver, CO,[7]Spanish National Cancer Research Centre, Madrid, Spain,[8]Belharra Therapeutics, San Diego, CA,[9]Genesis Therapeutics, San Francisco, CA,[10]Pfizer*

Worldwide Research & Development, San Diego, CA,[11]Kinnate BioPharma, San Diego, CA

CDK2 is a core cell-cycle enzyme that phosphorylates a variety of substrates to drive progression through the cell cycle. CDK2 is hyperactivated in multiple cancers and is therefore an attractive therapeutic target. Here, application of a novel small molecule CDK2/4/6 inhibitor, PF-06873600, enabled in-depth interrogation of CDK2 substrate phosphorylation, cell-cycle progression, and drug adaptation in preclinical models. CDK2-specific inhibition leads to rapid loss of substrate phosphorylation, but unexpectedly, CDK2 substrate phosphorylation rebounds within several hours. Whereas CDK1 is known to compensate for loss of CDK2 in Cdk2-/- mice, here we demonstrate an early dependence on CDK4/6 activity. CDK2 inhibition reveals latent CDK4/6 activity throughout S phase that backstops the proliferative program by maintaining Rb1 hyperphosphorylation, active E2F transcription, and Cyclin A2 expression, enabling re-activation of CDK2. Our results augment our understanding of CDK plasticity and indicate that co-inhibition of CDK2 and CDK4/6 is required to suppress adaptation to CDK2 inhibitors.

#5993

Dissecting the role of CDK4 in liposarcoma

Silvia Vanni[1], Graziana Gallo[2], Valentina Fausti[3], Giacomo Miserocchi[1], Chiara Liverani[1], Chiara Spadazzi[1], Claudia Cocchi[1], Chiara Calabrese[1], Giovanni De Luca[2], Massimo Bassi[4], Manlio Gessaroli[4], Angelo Campobassi[4], Federica Pieri[5], Giorgio Ercolani[6], Davide Cavaliere[6], Lorena Gurrieri[3], Nada Riva[3], Giovanni Martinelli[7], Laura Mercatali[1], Alessandro De Vita[1]. *[1]Ostencology Unit, Biosciences Laboratory, IRCCS Istituto Romagnolo Per Lo Studio Dei Tumori (IRST) "Dino Amadori", Meldola (FC), Italy,[2]Pathology Unit, Bufalini Hospital, Cesena (FC), Italy,[3]Clinical and Experimental Oncology, Immunotherapy, Rare Cancers and Biological Resource Center, IRCCS Istituto Romagnolo Per Lo Studio Dei Tumori (IRST) "Dino Amadori", Meldola (FC), Italy,[4]Maxillofacial Surgery Unit, Bufalini Hospital, Cesena (FC), Italy,[5]Pathology Unit, Morgagni-Pierantoni Hospital, Forlì (FC), Italy,[6]General and Oncologic Surgery, Morgagni-Pierantoni Hospital, Forlì (FC), Italy,[7]Scientific Directorate,*

IRCCS Istituto Romagnolo Per Lo Studio Dei Tumori (IRST) "Dino Amadori", Meldola (FC), Italy

Background: Liposarcoma (LPS) encompass one of most common soft tissue sarcoma (STS) histological subtypes accounting for 15% of all cases. They can be divided into four entities including atypical lipomatous tumor or well-differentiated LPS (ALT/WDLPS), dedifferentiated LPS (DDLPS), myxoid LPS (MLPS) and pleomorphic LPS (PLS). Their heterogeneity is reflected in their morphology, molecular landscape, prognosis and clinical behavior. Current treatment options for localized disease include surgery, (neo)adjuvant radiotherapy and chemotherapy; for the metastatic setting chemotherapy represents the cornerstone but its role needs to be elucidated. The unavailability of predictive biomarkers makes the management of these mesenchymal diseases even more challenging. Recent evidences have shed light on the key role of cyclin-dependent kinase 4 (CDK4) in cancer cells proliferation.
Methods: This study involved 21 adult patients affected by liposarcoma (n= 5 ALT/WDLPS and n= 16 DDLPS). IHC analyses of CDK4 and MDM2 were performed on FFPE surgically resected specimens by experienced sarcoma pathologists. Moreover, a patient-derived DDLPS cell line was established and pharmacological profiling was performed. Next, standard and innovative drugs currently used for LPS management were assessed in both 2D and 3D culture systems. Finally*, in silico* analyses based on public repositories on STS were carried out including 260 sarcoma patients.
Results: IHC results highlighted an higher expression of CDK4 and MDM2 biomarkers in DDLPS compared to ALT/WDLSP. Moreover, although CDK4 and MDM2 are codified by the same genomic region, their expression did not correlate (e.g. 100% of CDK4 and 2% of MDM2 in the same patient). Therefore we hypothesized that even exhibiting a low MDM2 expression, a patient could benefit from CDK4 inhibition. Furthermore, our data showed that in DDLPS cases CDK4 expression ranged from 90% to 100% in spermatic cord, skin and abdomen while it ranged from 5% to 50% in the retroperitoneum. The above observations prompted us to hypothesize a correlation of CDK4 expression with specific anatomical sites. Moreover, pharmacological profiling showed a synergistic effect exerted by sequential treatment with palbociclib and some chemotherapeutics including trabectedin, dacarbazine, eribulin and

lenvatinib. Indeed we observed a 10% increase in cell proliferation inhibition compared to standard treatment. In addition, *in silico* analyses revealed the role of CDK4 as negative prognostic biomarker for PFS and OS in STS.
Conclusions: Our study highlighted the promising role of CDK4 in the management of LPS patients. In particular, we pointed out encouraging results of sequential treatment combining CDK4 inhibitor palbociclib and chemotherapy. Furthermore, preliminary analyses highlighted the involvement of this biomarker as a potential prognostic tool for STS.

#5994

INX-315, a potent and selective CDK2 inhibitor, demonstrates robust antitumor activity in *CCNE1*-amplified cancers

Alec G. Trub[1], John E. Bisi[1], Catherine Dietrich[2], Michael Taylor[2], Jay C. Strum[1], Shom Goel[2], Patrick J. Roberts[1]. *[1]R&D, Incyclix Bio, Durham, NC,[2]The Sir Peter MacCallum Department of Oncology, Peter MacCallum Cancer Centrer, Melbourne, Australia*

Cyclin-dependent kinases (CDK) are a family of serine/threonine kinases that heterodimerize with regulatory subunits called cyclins to drive cell cycle progression. Uncontrolled cellular proliferation is a hallmark of cancer commonly driven by dysregulated kinase activity of specific CDK family members, including cyclin-dependent kinase 2 (CDK2). Aberrant CDK2 activity most frequently occurs through amplification of CCNE1 and/or overexpression of its protein product cyclin E1, which is a canonical binding partner of CDK2. Overexpression of cyclin E1 is observed in many solid tumors including in patients with high grade serous ovarian cancer (HGSOC), gastric cancer, and ER-positive breast cancer patients whose tumors have progressed on a prior CDK4/6 inhibitor regimen. Selective inhibition of CDK2 is thus a compelling therapeutic approach to regain cell cycle control. Here, we report preclinical data supporting the development of INX-315 for patients with cancers in which proliferation is CDK2-dependent. INX-315 is a potent inhibitor of CDK2/cyclin E (0.6 nM biochemical IC50) with high selectivity over other CDK family members in both biochemical and intracellular NanoBRET assays. In CCNE1-amplified human ovarian and gastric cancer cell lines, INX-315 potently inhibited Rb phosphorylation, induced a G1 cell cycle arrest, and inhibited proliferation.

INX-315 also showed potent anti-proliferative activity in luminal breast cancer cell lines that had been cultured in CDK4/6 inhibitor (+/- anti-estrogen therapy) for prolonged periods to the point of developing drug resistance. While these cell lines did not readily respond to either CDK4/6 or CDK2 inhibition alone, combination treatment again suppressed Rb phosphorylation, accompanied by G1 arrest and a senescent-like phenotype. Lastly, in CCNE1-amplified xenograft models of ovarian and gastric carcinomas, INX-315 inhibited Rb-phosphorylation and induced tumor regression. These data demonstrate INX-315 to be a potent and selective CDK2 inhibitor that may benefit patients with CDK2/cyclin E driven cancers.

DNA Methylation Changes in Cancer

#5999

Comparative and integrative analysis of transcriptomic and epigenome wide DNA methylation changes in African American prostate cancer

Bernard Kwabi-Addo[1], Somiranjan Ghosh[2], Chad Creighton[3], Michael Ittmann[3]. *[1]Biochemistry and Molecular Biology, Howard University, Washington, DC,[2]Biology, Howard University, Washington, DC,[3]Baylor College of Medicine, Houston, TX*

African American (AA) men have the highest incidence and mortality rate from Prostate cancer (PCa) than any other racial/ethnic group. To understand this racial disparity, molecular features of different types, including gene expression, DNA methylation and other genomic alterations, must be carried out in tumor samples from these 2 populations. To date, PCa genomic studies have largely under-represented tumor samples from AA men due to lack of inclusion of significant numbers in such studies. In this study we carried out genome-wide DNA methylation analysis in 63 clinically annotated fresh-frozen PCa and 50 normal prostate tissues from AA men using the Illumina Infunium 850K Human Methylation EPIC BeadChip array. mRNA expression database from a sub-set of the AA biospecimen were used to assess correlation of transcriptome and epigenomic datasets. Using bioinformatic analysis to integrate a comprehensive set of genomic datasets we identified probesets that were significant ($p<0.01$) and differentially methylated in AA PCa compared to

normal prostate tissues and were significant ($p<0.01$) and inversely correlated with AA mRNA expression. GO analysis in this AA cohort showed significant differential methylation that were mostly hypermethylated genes with corresponding down-regulated mRNA expression for top genes associated with biological pathways in hemidesmosome assembly, mammary gland development, epidermis development, hormone biosynthetic process and cell communication. On the other hand, few significant differential top hypomethylated genes and corresponding up-regulated mRNA expression were identified in biological pathways of negative regulation of macrophage differentiation, cAMP-dependent protein kinase inhibitor activity, protein destabilization, transcription corepressor activity and fatty acid biosynthetic process. Furthermore, we identified significant and differential methylated genes in our AA PCa cohort that were associated with PCa progression when compared to the TCGA EA and AA dataset. These genes were *AMIGO*3, *IER*3, *UPB*1, *GRM*7, *TFAP*2C, *TOX*2, *PLSCR*2, *ZNF*292, *ESR*2, *MIXL*1, *BOLL* and *FGF*6. Overall, IPA of differential methylated promoter region are genes enriched for network involved in sex-steroid hormonal signals and tumor microenvironment signaling pathways. **Our integrative analysis provides new candidate genes associated with prostate cancer progression in AA men as potential targets for** improving prostate cancer treatment and addressing the racial disparity problem.

#6000

Distinct HOX gene family DNA methylation profiles in histologically normal skin dependent on dermoscopic pattern of adjacent nevi

Meghan E. Muse[1], Helmut Schaider[2], Harald Oey[2], H. Peter Soyer[2], Brock C. Christensen[1], Mitchell S. Stark[2]. *[1]Department of Epidemiology, Geisel School of Medicine at Dartmouth, Hanover, NH,[2]Frazer Institute, University of Queensland, Brisbane, Australia*

Melanoma may arise within a pre-existing nevus, but commonly forms in the skin adjacent to nevi. We have performed global DNA methylation profiling using the Illumina EPIC array (>800K loci) of 32 dermoscopically ('globular' vs 'non-globular' pattern) and histopathologically classified nevi, together with matching adjacent perilesional skin, and discovered that methylation patterns can accurately decompose the proportion of cell types

present in the tissue. In this study, we sought to assess whether there are differences in the DNA methylation profiles of histologically normal skin samples that surround nevi, independent of cellular composition. Among the 739,270 CpG loci included in the analysis, there were a total of 8,200 CpG loci identified as significantly differentially methylated ($Q < 0.05$) in 'globular skin' vs 'non-globular skin' adjusted for age, sex, and the estimated relative proportions of epithelial cells, fibroblasts, and melanocytes in each sample. After imposing a more stringent threshold (M value of ≥ 0.5) a total 816 CpG loci were found to be DM, with 696 loci identified as significantly hypermethylated, and 120 loci significantly hypomethylated ($Q < 0.05$ and $\Delta M > 0.5$) in 'globular' vs 'non-globular' skin. Mapping of the DM ($Q < 0.05$ and $|\Delta M| < 0.5$) CpG loci to their respective genes revealed that eight of the top 20 DM genes, by proportion of differentially methylated loci, were positioned in proximity to suggest regulation of members of the HOX gene family. We next assessed the differential gene expression of the eight DM HOX genes in the perilesional skin as well as the matching adjacent nevus. After adjusting for age, sex, and sample cellular composition, none of the assessed HOX genes demonstrated statistically significant ($P \leq 0.05$) differential expression in the nevi, however, 'non-globular skin' demonstrated a statistically significant ($P < 0.05$) increase in the expression of five of the eight *HOX* genes relative to 'globular skin'. Importantly, this increased gene expression corresponds to the methylation status of the DM loci. HOX genes are known to be involved in limb and axial development as well as the positioning of dermal fibroblasts. Moreover, melanocytes from different anatomic positions have distinct transcriptional profiles and the anatomical position of melanocytes plays a key role in determining whether genetic alterations will subsequently drive melanoma formation. This positioning of melanoma subtypes (cutaneous vs acral) was recently shown to be related to interaction of specific *HOX* genes with site-specific oncogenic alterations. The distinct *HOX* gene family members we have revealed, differ to those related to melanoma development and positioning, as such we propose that these may contribute to the positioning of acquired melanocytic nevi, and in combination with common somatic alterations in *BRAF*, may contribute to nevus formation.

#6001

Epigenetic regulation of BARD1 confers resistance to anti-VEGF therapy in ovarian cancer

Emine Bayraktar[1], Cristian Rodriguez-Aguayo[1], Sudhir Kumar[2], Elaine Stur[1], Lingegowda S. Mangala[1], Stephen Baylin[3], Gabriel Lopez-Berestein[1], Sunila Pradeep[2], Anil K. Sood[1]. *[1]UT MD Anderson Cancer Center, Houston, TX,[2]Medical College of Wisconsin, Milwaukee, WI,[3]Johns Hopkins University, Baltimore, MD*

Introduction: Vascular endothelial growth factor (VEGF) is a key promoter of angiogenesis and disease progression in epithelial ovarian cancer (OC). Bevacizumab, a humanized anti-VEGF monoclonal antibody, is approved for treatment of patients with ovarian and other cancers. Despite the wide use of anti-VEGF therapy for cancer treatment, most patients develop resistant disease. Therefore, new combinations/strategies are needed to reduce adaptive resistance to anti-VEGF antibody (AVA) therapy. Our aim is to determine the potential role of epigenetic changes in AVA-adaptive resistance. We identified and characterized epigenetic changes in BARD1, a tumor suppressor, at the emergence of AVA resistance.
Methods: To define epigenetic changes during AVA therapy induced resistance, we performed series of in vitro (methylation array, RNA sequencing) and in vivo (orthotopic OC (PDX-MDA-OVCA1, immunocompetent-IG10, and immunocompromised-SKOV3) and fibrosarcoma-HT1080, an inherently VEGF resistant model) experiments. The biological effects of DNA methylation agent (5`-Azacytidine; 5`-Aza) with B20 (murine anti-VEGF antibody) treatment were subsequently tested using in vivo models.
Results: To determine whether 5`-Aza can enhance the efficacy of AVA therapy and overcome resistance to AVA in OC, we established AVA-resistant SKOV3 model. In AVA-resistant mice treated with B20 + 5`-Aza, there was a statistically significant reduction in tumor weight ($p=0.03$). Next, we performed a Human 450k methylation and mRNA arrays from xenografts of SKOV3 tumors. Based on both analyses, we demonstrated that BARD1 was one of the top candidate which was highly expressed ($p=0.02$) and less methylated ($p<0.05$) in the combination of B20 and 5`-Aza group compared to B20 alone. Our data also showed that BARD1 expression was restored in the combination therapy. The sequential treatment with 5`-Aza reverted the resistance towards the AVA therapy in

SKOV3 model. Furthermore, the combination of B20 and 5`-Aza significantly decreased tumor weight in SKOV3 ($p=0.005$), IG10 ($p<0.05$), MDA-OVCA1 ($p=0.01$), and HT1080 ($p<0.05$). BARD1 expression levels were substantially increased in combination therapy compared to the B20 alone group (>4-fold, $p=0.006$). Tumor weight and BARD1 expression were inversely correlated. To determine the biological significance of BARD1, we knockdown BARD1 using Tet-inducible shRNA system. Our data showed a significant reduction in tumor weight in the BARD1 knockdown group in SKOV3 model ($p=0.021$). RNA-sequencing of BARD1 knockdown showed an enrichment of the angiogenesis pathway. Moreover, BARD1 expression levels were decreased in hypoxic conditions both in vitro and in vivo.
Conclusion: Our findings indicate a previously unrecognized role for BARD1 in mediating resistance to AVA therapy. Use of epigenetic drugs to control the expression of tumor suppressor genes may enhance the efficacy of AVA therapy in OC.

#6002

Characterizing dynamic landscape of DNA methylation in ovarian high-grade serous carcinoma

Alexandra Lahtinen[1], Giovanni Marchi[1], Daria Afenteva[1], Susanna Holmström[1], Kaisa Huhtinen[2], Anni Virtanen[1], Johanna Hynninen[2], Antti Häkkinen[1], Sampsa Hautaniemi[1]. *[1]University of Helsinki, Helsinki, Finland,[2]University of Turku, Turku, Finland*

Dysregulated DNA methylation (DNAm) is a hallmark of all cancer types, though the precise role of these aberrations in tumor progression and treatment response remains elusive. Advances in whole-genome bisulfite sequencing (WGBS) have enabled profiling methylomes at full resolution and stimulated interest to explore dynamics of DNAm across tumor sites and cancer treatment. A major challenge in the analysis of patient data is that a surgically removed tumor sample represents a mixture of cancer cells and microenvironment, and that the insights on DNAm changes are intertwined due to mixed effects from patient epigenomic background, tissue context, and treatment pressure. By using a computational approach, these effects can be decomposed into patient background, tissue site, and treatment phase specific changes, and controlled for natural

microenvironment variation. retion, and action, as well as in several oncogenic signaling cascades. The analysis of the tissue profiles indicated that the progression of HGSC from the tissues-of-origin to the metastatic deposits is accompanied by drastic changes in DNAm profiles. Thus, when comparing ovaries and peritoneum, intra-abdominal tissues mesentery and omentum featured prominent change of promoter DNAm: loss in 10% and gain in 20% of genes. Interestingly, the genes with aberrant DNAm included ABC transporters implicated in pumping drugs across the cell membrane, as well as the members of MAPK and PI3K signaling cascades. The joint analysis of both treatment and tissue contributions suggests that the overall modest effect of NACT is further reduced in metastases, mediated via DNAm changes in genes involved in multidrug resistance.

#6003

Study of secondary epimutations in *cis* of the promoter in germline tumor suppressor genes as a cause of hereditary breast and ovarian cancer

Miguel Ruiz De La Cruz[1], Héctor Martínez Gregorio[2], Clara Estela Díaz Velásquez[2], Aldo Hugo De La Cruz Montoya[3], Fidel de la Cruz Hernández-Hernández[4], Felipe Vaca Paniagua[2]. *[1]Infectómica y Patogénesis Molecular, Centro de Investigación y de Estudios Avanzados IPN (CINVESTAV-IPN), México City, Mexico,[2]Laboratorio Nacional en Salud, Diagnóstico Molecular y Efecto Ambiental en Enfermedades Crónico-Degenerativas, FES-Iztacala UNAM, México City, Mexico,[3]Unidad de Biomedicina, Facultad de Estudios Superiores Iztacala UNAM, Tlalnepantla de Baz, Mexico,[4]Infectómica y Patogénesis Molecular, Centro de Investigación y de Estudios Avanzados IPN (CINVESTAV-IPN), México CIty, Mexico*

Cancer is a multifactorial and highly heterogeneous disease. Breast cancer (BC) is the main malignant neoplasm in women and has the highest incidence and mortality rates worldwide. About 10% of all BC cases are hereditary and its most common form is Hereditary Breast and Ovarian Cancer Syndrome (HBOC).In a study conducted by our research group in a cohort of 300 Mexican women with HBOC using a panel of 143 genes of susceptibility to different types of cancer (Quezada-Urban et al., 2018), we found that 74% of patients were negative for variants in the coding regions and only 15% of patients had at least one pathogenic variant in 18 different

genes. In several types of hereditary cancer syndromes, it has been shown that germline genetic alterations such as single nucleotide variations, and indels in *cis* of the promoter region of tumor suppressor genes modify the methylation pattern and cause epigenetic silencing and the concomitant somatic loss of heterozygosity. These events are known as secondary *cis* epimutations and represent an alternative mechanism of molecular pathogenesis in patients with hereditary cancer syndromes. In this work we are investigating in germline gDNA the methylation profile in the promoter region of 18 tumor suppressor genes in 231 patients negative for pathogenic variants and 156 matched controls by using direct bisulfite massive parallel sequencing. So far, we have extracted gDNA and treated with sodium bisulfite from all patient and control samples. From the converted gDNA, we amplified the promoter region of the 18 study genes by PCR (9,675 endpoint PCR products). We have prepared a total of 387 genomic libraries from which we perform massive sequencing and bioinformatic analysis of 229 patients, 74 controls and 2 positive controls. Currently, we have found 4 patients with promoter hypermethylation in the *RAD51C*, *POLH*, *EPCAM*, and *BRCA1* genes that can be generated by a secondary *cis* epimutation. We have found statistically significant differences in the methylation levels of the promoter regions of the *BRCA1/2, PMS2, FANCI, MLH1, PALB2, POLH, ERCC3, ATM, MSH2, BRIP1,* and *EPCAM* genes in patients compared with controls. This result suggests that low level basal methylation marks could be potential biomarkers of HBOC pathogenesis. Interestingly, our studies indicate that hypermethylation at the promoter of *MSH2, PALB2, BRIP1,* and *EPCAM* are associated with HBOC risk, and that specific hypermethylation at the CpG sites of *MSH2* and *PALB2* (cg47630224 and cg23652916, respectively), could be potential biomarkers in HBOC risk. Lastly, according to preliminary *in silico* results, the co-occurrence of site-specific hypermethylation in *MSH2* and *PALB2* is possibly due to the absence of interaction of the common transcription factor SP4 in a GC-box site. These findings expand our vision of the genetic and epigenetic mechanisms of susceptibility to this disease.

#6004

DNA methylation diagnostics for upper urinary tract urothelial carcinoma using newly developed high-performance liquid chromatography

Mao Fujimoto[1], Eri Arai[1], Takuya Kikushima[2], Naotaka Nishiyama[2], Tomofumi Nakamura[3], Yuriko Yamada[3], Hiroaki Taira[3], Takuya Yotani[3], Hiroshi Kitamura[2], Yae Kanai[1]. *[1]Keio University School of Medicine, Tokyo, Japan,[2]Graduate School of Medicine, The University of Toyama, Toyama, Japan,[3]Sekisui Medical Co., Ltd., Ryugasaki, Japan*

Backgrounds: For diagnosis of upper urinary tract urothelial carcinoma (UTUC), conventional ureteroscopic examinations are invasive, and selective urine cytology has insufficient sensitivity. We have developed a new anion-exchange column for high-performance liquid chromatography (HPLC) with electrostatic and hydrophobic properties. Both cytosine and thymine, corresponding to methylated and unmethylated cytosine after bisulfite modification, respectively, are captured by electrostatic interaction and then discriminated from each other by their hydrophobic interactions. This method is expected to be very suitable for quantification of DNA methylation levels of cancer cells in urine samples with contamination of various cell lineages.
Purpose: The aim of this study was to establish a less invasive and more accurate method for UTUC diagnosis based on DNA methylation quantification by our newly developed HPLC.
Methods: Urine samples were collected by urinary catheterization during surgery for 218 urological cancer patients. Our previous studies have identified 4 CpG sites showing differences in DNA methylation levels between non-cancerous urothelium and UTUC based on genome-wide DNA methylation analysis using tissue specimens. In the present study, DNA methylation levels of these marker CpG sites were quantified by HPLC using the urine samples.
Results: The thresholds have been set for the retention time by HPLC and the area under the chromatogram. Diagnostic criteria have been established to distinguish cases with current UTUC from non-urothelial cancer cases, bladder cancer cases and post-urothelial cancer treatment cases by combining marker CpG sites. The sensitivity and specificity were 90.9% and 87.0% respectively.
Conclusions: Since HPLC-based DNA methylation diagnostic system was able to discriminate UTUC cells from blood cells and other contaminating cells in urine samples, application of our criteria will ultimately allow non-invasive diagnosis of UTUC in the clinical setting. It may be possible to at

least partially replace highly invasive procedures such as ureteroscopy and to enable early initiation of treatment for UTUC resulting in improved prognosis.

#6005

Promoter methylation occurs at high frequencies regardless of mutation status of tumor-associated genes in oral malignancies

Masanobu Abe[1], Kazuto Hoshi[1], Toshikazu Ushijima[2]. *[1]Graduate School of Medicine and Faculty of Medicine, The University of Tokyo, Tokyo, Japan,[2]Division of Epigenomics, National Cancer Center Research Institute, Tokyo, Japan, Tokyo, Japan*

Background: Genetic and epigenetic alterations are both important in tumorigenesis. However, their association in oral carcinogenesis has not been fully investigated yet. In this study, we analyzed somatic mutations of tumor-related genes and promoter methylation of tumor-suppressor genes (TSGs) in oral malignancies/premalignancies, and analyzed their association.
Materials and Methods: 39 oral squamous cell carcinomas (OSCCs) and 2 oral epithelial dysplasias (OEDs) were obtained as fresh-frozen?. Somatic mutations of 46 tumor-related genes, 13 TSGs and 33 oncogenes, were analyzed by targeted next-generation sequencing (NGS). Promoter methylation of five TSG: (*p16/INK4A*, *CMTM3*, *EGFLAM*, *NKX2-3,* and *RBP4*) were determined by methylation-specific PCR (MSP).
Results: Somatic mutations of tumor-related genes were observed in 63.4% of 41 OSCCs/OEDs. Particularly, mutations of *p53* and *PIK3CA* were observed 39.0% and 31.7%, respectively, of the 41 OSCCs/OEDs. Promoter methylation of *p16/INK4A*, *CMTM3*, *NKX2-3*, *RBP4*, *and EGFLAM* were observed in 34.1%, 48.8%, 41.5%, 68.3%, and 36.6%, respectively, of the 41 OSCCs/OEDs. No differences in the frequency of promoter methylation of the five genes were observed between tumors with and without somatic mutations of *p53* and *PIK3CA*.
Conclusions: Promoter methylation was observed at high frequencies regardless of mutation status of *p53* and *PIK3CA* in OSCCs/OEDs. Oral tumorigenesis appears to be difficult to be explained solely by genetic events indicating involvement of epigenetic events.

#6006

RNA m6A methylation relay the oncogenic flow from DNA methylationto gene expression of ANKRD13B

JingRong Weng, JinXin Lin, YuMo Xie, GuanNan Tang, LiangLiang Bai, JinHua Chen, ZengHong Huang, ZhuoKai Zhuang, ShaoYong Peng, Heng Wang, GaoPo Xu, Yu Zhang, XiaoXia Liu, MeiJin Huang, YanXin Luo, XiaoLin Wang, Huichuan Yu. *The Sixth Affiliated Hospital of Sun Yat-sen University, Guangzhou, China*

Background: Colorectal cancer (CRC) is one of the most common causes of cancer-related death in the world. More comprehensive studies of key molecular alterations in CRC progression were urgent. DNA methylation promotes tumor progression. However, the mechanism of the ANKRD13 gene methylation that drives colorectal cancer evolution remains largely unknown. This was the first study focused on the role of ANKRD13 and the hypermethylated mechanisms in colorectal cancer.
Methods: Chi-Square tests were utilized to the comparison of the baseline characteristics of patients with hypomethylation ANKRD13B and hypermethylated ANKRD13B. Kaplan-Meier analysis were used to estimate the difference of overall survival between the two groups patients. The methylation level of ANKRD13B was quantified by qMSP in colorectal cancer, normal colon epitheliums and colorectal adenoma tissues. CRISPR/dCas9-DNMT3A and CRISPR/dCas9-TET1-CD methylation editing tools were applied to enable targeted and specific CpG methylation at the CpG loci near stop codon of ANKRD13B. Transwell-migrated assay, wound scratch assay and colony formation assay were preformed to ascertain the abilities of viability, migration and invasion in the editing CRC cell lines. The methylated RNA immunoprecipitation (MeRIP) assays, chromatin immunoprecipitation (ChIP) assays and 5-AZA treatment assays were performed combined with qPCR to quantify the m6A levels of ANKRD13B mRNA following hypermethylated-editing.
Results: Here, we identified a novel oncogenic gene, ANKRD13B, encoding ankyrin repeat domain 13B. This gene was frequently hypermethylated in CpG islands surrounding the stop codon region of colorectal cancer. This hypermethylation was associated with poor clinical outcomes in patients diagnosed with colorectal cancer. Compared with normal tissue (4.2%), this type of epigenetic alteration upregulated

ANKRD13B expression in both adenoma (73.0%) and adenoma cancer tissues (83.3%) (P< 0.0001), and it also promoted colorectal cancer cell growth, invasion, and migration. Demethylation treatment can reduce the ANKRD13B expression and the growth, migration, and invasion of the cancer cell. Moreover, we found that the aberrant ANKRD13B methylated surrounding the stop codon, and it can promote RNA N6-methyladenosine methylation modification, suggesting that aberrant DNA 5mC methylation promotes ANKRD13B expression and tumor progression in an RNA m6A-dependent manner.
Conclusions: In summary, our findings illustrated that ANKRD13B is an oncogenic gene of colorectal cancer that is commonly methylated and overexpressed in colorectal cancer whose function in the pathogenesis of colorectal cancer depends on RNA m6A-dependent manner. Aberrant DNA 5mC methylation promotes ANKRD13B expression and tumor progression in an RNA m6A-dependent Manner.
Key words: ANKRD13B, DNA methylation, Epigenetic regulation, Colorectal cancer

#6007

p16 epimutation modulates the tumor microenvironment and promotes malignancy of *Apc*-mutant colon cancer

Li Yang[1], Xiaomin Chen[1], Christy Lee[2], Jiejun Shi[3], Emily B. Lawrence[1], Lanjing Zhang[4], Yumei Li[1], Nan Gao[5], Sung Yun Jung[1], Chad J. Creighton[1], Jingyi Jessica Li[2], Ya Cui[3], Sumimasa Arimura[1], Wei Li[3], Lanlan Shen[1]. *[1]Baylor College of Medicine, Houston, TX,[2]University of California, Los Angeles, CA,[3]University of California, Irvine, CA,[4]Rutgers University, Piscataway, NJ,[5]Rutgers University, Newark, NJ*

Methylation of the *p16* promoter resulting in mitotically stable gene silencing—known as p16 epimutation—is the most common epigenetic event in human colorectal cancer (CRC) and is also common in normal-appearing colonic mucosa of aging individuals. However, the functional role of *p16* epimutation in CRC carcinogenesis is not completely understood. Here, using a mouse model of engineered *p16* promoter hypermethylation, we show that *p16* epimutation cooperates with mutant *Apc* to promote colon cancer development. Mice carrying combined *Apc* mutation and *p16* epimutation display significantly shortened survival and

increased tumor growth compared to those with *Apc* mutation only. Moreover, colon tumors from these animals express increased levels of programmed death-ligand 1 (*Pdl1*). Single-cell RNA sequencing (scRNA-seq) analysis further revealed the presence of dysfunctional cytotoxic $CD8^+$ T cells together with $Foxp3^+$ Tregs and γδT17 cells, which promote an immunosuppressive tumor microenvironment (TME). Lastly, we show that a combined therapy using an inhibitor of DNA methylation and a PD-L1 immune checkpoint inhibitor is more effective for improving survival in tumor-bearing mice than anti-PD-L1 treatment alone. These findings provide a mechanistic rationale for targeted epigenetic and immunotherapy in CRC patients, with the potential to improve colon cancer treatment.

#6008

Antibody validation for clinical pharmacodynamic assay reveals cross-reactivity of commercial DNMT3B clones

Gabriel J. Benton[1], Manisha Mohandoss[1], James H. Doroshow[2], Ralph E. Parchment[1], Katherine V. Ferry-Galow[1]. *[1]Clinical Pharmacodynamic Biomarkers Program, Frederick National Laboratory for Cancer Research, Frederick, MD,[2]Division of Cancer Treatment and Diagnosis, National Cancer Institute, Bethesda, MD*

Cooperativity between the maintenance DNA methyltransferase, DNMT1, and *de novo* methyltransferases, DNMT3A and 3B, is essential for proper maintenance and integrity of the methylome, and deregulation of these enzymes and associated transcriptional silencing of multiple genes has been shown in many types of cancer. Two DNA methyltransferase inhibitors are currently in clinical use with several others undergoing clinical evaluation, and the pharmacodynamic response of DNMT enzymes is a crucial aspect of understanding therapeutic effects in preclinical studies and clinical trials. Vigorous fit-for-purpose validation of research-grade reagents and the application of effective quality control testing procedures to assess lot-to-lot variability (and reject unacceptable lots) are essential to assure robust and reproducible pharmacodynamic assay performance. During the antibody validation process for the DNMT3B enzyme target, two commercial monoclonal antibody clones were found to exhibit significant cross-reactivity to another cellular protein and inappropriate subcellular localization via immunohistochemistry (IHC) , including diffuse

cytoplasmic staining and significant staining in a DNMT3B knock out (KO) cell line. Two other commercial monoclonal antibody clones showed the expected nuclear expression in the HCT116 parental cell line and lack of staining in the DNMT KO cells. Further evaluation via western blot revealed that the cross-reacting antibodies detected a band of the approximate expected molecular weight (MW) of DNMT3B but of a protein that was expressed equivalently in the parental and DNMT3B KO cell line pair, whereas the two other antibody clones only detected a significant band of correct MW in the parental but not the KO cell line. These results suggest that some commercial antibody clones are binding to a protein other than DNMT3B and that they are unsuitable for use with IHC and western blot to evaluate subcellular localization and expression levels of DNMT3B protein. We presume that these non-specific antibody clones were chosen for commercial development based on target screening via Western blot that did not include evaluation of a validated DNMT3B knock out cell line, as is not uncommon for research-grade antibody clones. This data highlights the critical importance of thorough fit-for-purpose validation and quality control for crucial reagents used for pharmacodynamic biomarker studies. Funded by NCI Contract No HHSN261200800001E

#6009

An end-to-end workflow for improved methylation detection

Lydia Bonar, Kristin Butcher, Michael Bocek, Holly Corbitt, Bryan Hoglund, Cibelle Nassif, Patrick Cherry, Derek Murphy, Jean Challacombe, Esteban Toro. *Twist Bioscience, South San Francisco, CA*

Introduction: DNA methylation at CpG nucleotide sites in eukaryotes is a key epigenetic mark that can help regulate gene expression. Specific changes in CpG methylation occur in many human cancers, making them a promising biomarker for early cancer detection. However, existing assays can be costly, lack specificity to regions of interest and often provide only semi-quantitative estimates of the methylation fraction. Here, we present a targeted methylome panel to decrease costs associated with next generation sequencing (NGS), methylation controls to calibrate quantitative assays and UMIs for accurate deduplication in low-diversity samples.
Experimental Procedures: Genomic DNA (gDNA) was prepared for sequencing using the Twist Methylation Detection System consisting of

enzymatic methylation conversion and hybrid capture using the Twist Human Methylome Panel. Twist's synthetic CpG methylation level controls were spiked-in to gDNA and taken through the Twist Methylation Detection System to demonstrate their utility in calibrating methylation assays. Additionally, libraries were generated using cell free DNA (cfDNA) and either conventional or UMI-containing adapters to investigate the impact on quantitative detection and total unique coverage.
Results: Using the Twist Human Methylome Panel at 150x raw coverage achieves uniform coverage with low off-bait Picard metrics. 6.59 million CpG sites were detected using a minimum depth of 10X. Target capture with the Human Methylome Panel allows for informative CpG calling of up to 82 samples on a single Illumina Novaseq S4 flowcell, compared to 3 samples per flowcell with a tradition whole-genome bisulfite sequencing (WGBS) assay. The Twist CpG methylation specific controls are constructed of 48 unique contrived sequences that contain a total of 8 different levels of methylation, ranging from 100% to 0%. Including these controls allows for quantitation of methylation levels in the experimental samples and qualification of the enzymatic conversion process.
Conclusions: Our study leverages the Twist methylation detection portfolio to interrogate genome-wide methylation patterns for various applications. In combination, these tools can be used to design cost effective end-to-end assays.
**For Research Use Only. Not for use in diagnostic procedures.*

#6010
Targeting *p16* epimutation during lung cancer progression for anticancer therapy
Xiaomin Chen[1], Emily Brisnna Lawrence[1], Leah Farmer[1], Li Yang[1], Robert Craig Perry[1], David Joel Sequeira[1], Lanjing Zhang[2], Lanlan Shen[1]. *[1]USDA Children's Nutrition Research Center, Baylor College of Medicine, Houston, TX,[2]Department of Pathology, Princeton Medical Center, Plainsboro, NJ*

Background: Whole-genome DNA methylation profiling revealed that epimutation (gene silencing associated with alteration in DNA methylation) is common in human lung cancer, but it remains unclear whether the aberrant DNA methylation is a cause or a consequence of tumorigenesis.

Furthermore, different from genetic mutations, which are irreversible, epigenetic mutation is reversible and could be restored to normal status. The potential reversibility of epimutation presents new therapeutic opportunities for cancer treatment.
Methods and Results: We utilized an epigenetically engineered mouse cancer model in which the expression of *p16* (also known as Cyclin-dependent kinase inhibitor 2A) is silenced by accumulating DNA methylation at the promoter region ($p16^{meth}$). To investigate whether *p16* epimutation functionally contributes to the lung cancer initiation and progression, we obtained Cre recombinase inducible $K\text{-}ras^{+/LSL\text{-}G12D}$ mice from the Jackson Laboratory and crossed them with $p16^{meth}$ mice to produce $K\text{-}ras^{+/LSL\text{-}G12D}; p16^{meth/meth}$ mice (with combined *K-ras* mutation and *p16* epimutation). These mice have been maintained on the C57BL/6J background. We administered $5x10^7$ pfu of adenovirus-Cre (Ad5-CMV-Cre) to mice at 20 weeks (wk) of age through intranasal instillation to activate oncogenic *K-ras*. We monitored the lung tumor development at 6, 8, 12, and 16 wk post-infection. Remarkably, as early as 6 wk post-infection, we found substantially increased tumor numbers and sizes in the $K\text{-}ras^{+/LSL\text{-}G12D}; p16^{meth/meth}$ mice compared with the $K\text{-}ras^{+/LSL\text{-}G12D}$ mice (n=4 per group). Histopathological analyses confirmed the tumor progression to adenocarcinoma. Interestingly, the $K\text{-}ras^{+/LSL\text{-}G12D}; p16^{meth/meth}$ lung tumors exhibited distinct papillary and intraluminal growth patterns, which were not observed in mice with *K-ras* mutation alone. In addition, to investigate the therapeutic effects of reversing *p16* epimutation, we generated MEFs from these mice and compared the efficiency of *p16* reactivation by either a standard hypomethylating agent 5-Aza-2'-Deoxycytidine (DAC) or a first-in-class reversible DNMT1-selective inhibitor GSK3685032. We found that GSK3685032 induced *p16* demethylation more effectively than DAC. Treatment of GSK3685032 at 1.5μM for 6 days resulted in robust *p16* hypomethylation (58% loss) and three-fold increase in gene expression.
Conclusion: Our study validates that *p16* epimutation functionally contributes to lung cancer initiation and provides an ideal *in vivo* preclinical platform for testing epigenetic therapeutic strategies

#6011

Methylation profiling reveals the role of PRC2 in regulating DNA methylome changes in malignant peripheral nerve sheath tumors

Christopher M. Stehn, Minu Bhunia, Kyle B. Williams, Alex T. Larsson, David A. Largaespada. *University of Minnesota, Minneapolis, MN*

Neurofibromatosis type 1 (NF1) syndrome is an autosomal dominant cancer predisposition syndrome defined by germline deletion of one *NF1* allele. Somatic loss of heterozygosity in the remaining *NF1* allele in Schwann lineage cells gives rise to benign tumors known as plexiform neurofibromas. These tumors have a high risk of developing into cancerous lesions known as malignant peripheral nerve sheath tumors (MPNST) through the sequential deletion of *CDKN2A/B* followed by recurrent mutations in *SUZ12* or *EED,* constituting the inactivation of polycomb repressor complex 2 (PRC2). PRC2 is a transcriptional repressor complex involved in the silencing of several genes throughout cell development and differentiation. Loss of this complex leads to a depletion in trimethylation marks on Histone H3 Lysine 27 (H3K27me3) and the subsequent gain of acetylation marks on the same lysine residue (H3K27Ac). However, full range of epigenetic consequences of these events are currently not well characterized, especially with respect to MPNST formation and development. The Largaespada lab has developed Schwann cell lines engineered to harbor deletions in *NF1* and either *SUZ12* or *EED* and assayed the methylation status of 850,000 CpG sites using the EPIC array. The resulting methylation profiles reveal a large degree of change in promoter methylation between cell lines with and without PRC2 inactivation. These changes, however, appear to be inconsistent. To further understand this phenomenon, I have analyzed differential methylation patterns between lines with *SUZ12/EED* deletions on top of *NF1* deletion compared to those with *NF1* deletion alone. Pathway analysis of genes whose promoters are differentially methylated upon PRC2 reveals a bias towards developmental modules such as morphogenesis and neuronal differentiation, suggesting that DNA methylation is a mechanism by which PRC2 loss promotes stemness in Schwann lineage cells prior to MPNST formation. Additionally, differentially methylated regions were overlapped with functional non-coding elements in the genome to understand potential ripple effects in the epigenome. These findings underline the importance of DNA methylation in contributing to tumor formation and define unique

functions by which PRC2 specifically leverages diverse methylation states to drive malignant transformation in Schwann lineage cells.

#6012

Comparison of pre-analytical methods for DNA methylation analysis of cfDNA

Miljana Tanic[1], Oluwadunni Emiloju[2], Pawan Dhami[2], Stephan Beck[2].
[1]Institute for Oncology and Radiology of Serbia, Belgrade, Serbia,[2]UCL Cancer Institute, London, United Kingdom

Liquid biopsies in the form of cell-free circulating tumor DNA (ctDNA) isolated from blood plasma or serum have shown great promise to be used as minimally-invasive markers in cancer patients providing an insight into the composition of both primary tumor and metastases, and an opportunity to assess clonal dynamics throughout the course of disease. CtDNA carries not only tumor- specific changes in its sequence but also distinctive epigenetic marks, namely DNA methylation patterns similar to the patterns in the primary tumor. Deregulation of tissue-specific DNA methylation patterns is an early event in carcinogenesis holding great promise to be exploited for early detection of cancer. However, in contrast to mutation detection, targeted DNA methylation sequencing of cfDNA remains a challenge due to low concentration and heavy fragmentation. The limiting step in detection of any analyte is the recovery of the DNA molecules. The pre-analytical steps in the DNA methylation detection pipeline include extraction of cfDNA molecules and their conversion using sodium bisulfite. Bisulfite conversion is a harsh chemical reaction that induces further fragmentation and degradation of already scarce cfDNA. In this study we compared commercial methods for cfDNA extraction and for bisulfite conversion to evaluate the yield, degradation and procedural loss. We compared five commercial kits for cfDNA extraction from blood plasma, three column-based (Qiagen's QIAamp Circulating nucleic acids kit, Norgen's Plasma/Serum Cell-Free Circulating DNA Purification and Macherey-Nagel's NucleoSpin® Plasma XS) and two based on magnetic beads cleanup (Bioo Scientific's Next Prep magnetic Cell-Free Circulating DNA isolation kitand Applied Biosystems' Magmax Cell-Free Circulating DNA isolation kit. The kits used for bisulfite conversion were Zymo EZ DNA Methylation Lightning with column based purification and with

magnetic beads purification, Zymo EZ DNA Methylation Direct with column based purification and with magnetic bead purification, Qiagen Epitect Fast DNA Bisulfite and Diagenode Premium Bisulfite kits. Same samples were processed by each of the kits, Sample degradation was determined using Agilent Bioanalyzer dsDNA kit. Yield was evaluated by Picogreen, absolute qPCR for single-copy gene and for contamination of gDNA by a B-cell specific assay, while procedural loss was determined based on the recovery of a synthetic spike-in.

#6013

DNA methylation-based inflammation score is associated with hepatocellular carcinoma among people living with HIV

Kyeezu Kim[1], Yinan Zheng[1], Claudia Hawkins[1], Edith Okeke[2], Olufunmilayo Lesi[3], Yishu Qu[1], Lewis R. Roberts[4], Demirkan Gursel[1], Fatimah B. Abdulkareem[3], Alani Akanmu[5], Godwin Imade[2], Jian-Jun Wei[1], Masha Kocherginsky[1], Kwang-Youn Kim[1], Wasiu L. Adeyemo[3], Firas Wehbe[1], Chad J. Achenbach[1], Atiene Sagay[2], Folasade T. Ogunsola[3], Robert L. Murphy[1], Lifang Hou[1]. *[1]Northwest University, Chicago, IL,[2]University of Jos, Jos, Nigeria,[3]University of Lagos, Lagos, Nigeria,[4]Mayo Clinic, Rochester, MN,[5]Lagos University Teaching Hospital and College of Medicine, Lagos, Nigeria*

Background: Hepatocellular carcinoma (HCC) is the second leading cause of cancer-related deaths worldwide. In countries with high human immunodeficiency virus (HIV) prevalence, such as Nigeria, HIV-associated HCC causes a great health burden due to its early onset, late diagnosis, and poorer prognosis. HIV infection is involved in inflammation of the liver, which may determine an increased risk of hepatocyte neoplastic transformation. Inflammation-related DNA methylation signatures obtained in liquid biopsy, such as circulating cell-free DNA (ccfDNA) extracted from serum/plasma are promising minimally-invasive biomarkers that may inform HCC among people living with HIV.
Methods: A total of 289 Nigerian participants with information on ccfDNA and other covariates were included. Participants were classified into three groups by their HCC/HIV status: 1) HCC+/HIV+ (n=28); 2) HCC-/HIV+ (n=185); and 3) HCC+/HIV- (n=76). We constructed ccfDNA methylation

inflammation scores using 49 CpGs previously linked to circulating C-reactive protein (CRP) concentrations, and higher scores represented elevated CRP concentrations with lower methylation levels. To compare the ccfDNA methylation inflammation score across the groups, we performed multivariable logistic regression analyses adjusting for age, sex, alcohol consumption, smoking status, body mass index, study sites, and technical variables.
Results: Participants with HCC+/HIV+ presented the highest ccfDNA methylation inflammation scores (mean=-0.03, standard deviation [SD] =0.01). Participants with HCC-/HIV+ presented the lowest scores (mean=-0.05, SD=0.01). In the multivariable logistic regressions, one SD increase of inflammation score was associated with 2.5 times higher odds of having HCC among HIV-infected participants (HCC+/HIV+ vs. HCC+/HIV-; OR=2.56, 95% CI=1.39-4.73, P=0.002). No evidence was found for the association between the inflammation score and HIV status among HCC patients (HCC+/HIV+ vs. HCC+/HIV-; OR=1.00, 95% CI=0.59-1.70, P=0.991). In the secondary analysis comparing HCC+ vs. HCC- adjusting for HIV status, one SD increase of inflammation score was associated with 3.2 times higher odds of having HCC (OR=3.22, 95% CI=1.39-7.46, P=0.006).
Conclusions: We observed that ccfDNA methylation inflammation score is associated with HCC status among people with HIV. Our findings suggest that ccfDNA methylation-based inflammatory profiles may serve as a potential biomarker for early detection and risk stratification of HCC in resource-constrained countries with a high prevalence of HIV.

#6014

Cancer risk diagnosis by epimutation burden: a multicenter prospective study

Harumi Yamada[1], Masahiro Maeda[2], Seiichiro Abe[3], Taichi Shimazu[4], Takayuki Ando[5], Kazunari Murakami[6], Shinji Tanaka[7], Takao Maekita[8], Osamu Inatomi[9], Ken Sugimoto[10], Tetsuro Kawagoe[11], Nobutake Yamamichi[12], Toshikazu Ushijima[13]. *[1]Department of Epigenomics, Hoshi University, Tokyo, Japan,[2]Center for Epigenetics, Johns Hopkins School of Medicine, Baltimore, MD,[3]Division of Science and Technology for Endoscopy, National Cancer Center Hospital, Tokyo, Japan,[4]Division of*

Prevention, Center for Public Health Science, National Cancer Center, Tokyo, Japan,[5]Third Department of Internal Medicine, University of Toyama, Toyama, Japan,[6]Department of Gastroenterology, Oita University, Oita, Japan,[7]Department of General Internal Medicine, Hiroshima University Hospital, Hiroshima, Japan,[8]Second Department of Internal Medicine, Wakayama Medical University, Wakayama, Japan,[9]Division of Digestive Endoscopy, Shiga University of Medical Science, Shiga, Japan,[10]Center for Clinical Research, Hamamatsu University Hospital, Shizuoka, Japan,[11]Department of Gastroenterology, Nippon Medical School, Tokyo, Japan,[12]Center for Epidemiology and Preventive Medicine, The University of Tokyo Hospital, Tokyo, Japan,[13]President, Hoshi University, Tokyo, Japan

Aberrant DNA methylation, induced by aging and accelerated by chronic inflammation, accumulates in normal tissue. Accumulation of DNA methylation in multiple genes, namely epimutation burden, is closely associated with cancer risk. Indeed, we demonstrated that the measurement of the methylation level of a marker gene in normal tissue is useful for cancer risk prediction of metachronous cancers, by a multicenter prospective study with gastric cancer patients (Asada, Gut, 64:388, 2015 : Maeda, Gut, 66:1721, 2017). In this study, we attempted to predict the risk of primary gastric cancer by performing a new multicenter prospective study. We recruited 1,880 healthy people, after *Helicobacter pylori* eradication, with a clinically high risk of gastric cancer. Biopsy specimens were obtained from the antrum and body, and the methylation level of *RIMS1*, which is a preselected epigenomic risk marker for this study, was measured in 1,757 participants. The participants are annually being followed-up to detect primary gastric cancer, for 5-8 years. Currently, the median follow-up is 4.05 years, and 27 people have developed primary gastric cancers (as of September 2022). The results of statistical analysis are being determined. This study will establish the clinical utility of a cancer risk diagnosis by epimutation burden in normal tissue, and is promising for application in various inflammation-associated cancers.

#6015

Methylation synthetic lethality: *CHFR* methylation and KRAS inhibition in gastric cancers

Hideyuki Takeshima[1], Takahiro Ebata[1], Yumi Furuichi[1], Satoshi Yamashita[2], Toshikazu Ushijima[1]. *[1]Department of Epigenomics, Institute for Advanced Life Sciences, Hoshi University, Tokyo, Japan,[2]Department of Life Engineering, Faculty of Engineering, Maebashi Institute of Technology, Maebashi, Japan*

Synthetic lethality is a promising therapeutic strategy, but the number of founder mutations is limited. In contrast, DNA methylation is frequently present in many types of cancers, and can be a potential target for a synthetic lethality. So far, *BRCA1* methylation with a PARP inhibitor is known as a synthetic lethality [Kawachi *et al*., Breast Cancer Res Treat, 181:323-329, 2020]. In this study, we aimed to identify a novel methylation synthetic lethal combination in gastric cancers. Founder methylation was searched for in 8,008 genes with putative promoter CpG islands (CGIs), and 137 genes which were 1) heavily methylated and 2) frequently methylated in primary gastric cancers (10 or more of 50 cases) were selected. The association analysis between DNA methylation and gene expression showed that 10 of 137 genes were completely silenced in gastric cancer cell lines with methylation of their promoter CGIs, but were expressed in those without. Among these 10 genes, we focused on *CHFR*, a known tumor-suppressor gene in gastrointestinal cancers, and genes lethal for *CHFR* methylation were screened for using the sgRNA screening database (The Cancer Dependency Map, DepMap). Comparison of gene dependencies of 17,645 genes between four cell lines with *CHFR* methylation and 12 cell lines without revealed that knockout of *KRAS* reduced cell growth specifically in cell lines with methylation. This synthetic lethality could be experimentally confirmed in two cell lines with *CHFR* methylation, AGS and 44As3, and three cell lines without, HSC41, HSC42, and MKN74. These cell lines included those not used in the screening, validating the usefulness of the combination. These results showed that gastric cancers with *CHFR* methylation were sensitive to KRAS inhibition, and that methylation synthetic lethality is a promising therapeutic strategy.

#6016

A comprehensive analysis of gut microbiome mediated epigenetic regulation of intestinal stem cells

Robert Craig Peery[1], Jiejun Shi[2], Leah Farmer[3], Li Yang[3], Emily Lawrence[3], Yumei Li[4], Wei Li[2], Lanlan Shen[5]. *[1]USDA Children's Nutrition Research Center, Baylor College of Medicine, Houston, TX,[2]University of California Irvine, Irvine, CA,[3] USDA Children's Nutrition Research Center, Baylor College of Medicine, Houston, TX,[4]Baylor College of Medicine, Houston, TX,[5]Pediatrics, USDA Children's Nutrition Research Center, Baylor College of Medicine, Houston, TX*

Background: Gut microbial colonization, represents a critical time period for establishing the overall health of an individual. The intestine is a highly dynamic tissue with high turnover of intestinal epithelial cells throughout the life span of an individual making intestinal stem cells (ISCs) critical for normal gut homeostasis. Currently, there exists a lack of knowledge in how the gut microbiota regulates DNA methylation to influence the behavior of these ISCs. Aberrant DNA methylation is now documented to be critical in the disease pathogenesis of intestinal disorders such as colorectal cancer, thus understanding how the gut microbiome influences DNA methylation and ISCs is fundamental for improving human health.
Methods: We utilized the Lgr5-GFP mouse model in which endogenous GFP expression is driven by the bonafide intestinal stem cell marker Lgr5. These mice were maintained under two different housing conditions, conventional and germ free. We collected mice under the two conditions and performed dissociation of the colon and small intestine epithelial cells using EDTA dissociation. We then analyzed cell populations using flow cytometry, and collected two cell populations: the differentiated cell population (EpiCam +, GFP -) and intestinal stem cell population (EpiCam +, GFP +). To perform a genome wide comprehensive DNA methylation analysis we performed Whole Genome Bisulfite Sequencing (WGBS) which included both stem cell and differentiated cell populations of females and males at the two age groups points (postnatal day 21 (p21) and p100).
Results: There was no significant difference in CpG methylation at the global level between the two housing conditions. Next, we analyzed age matched samples from germ free and conventional mice to determine if there are differentially methylated regions (DMRs) associated with the presence of intestinal microbiota. We have identified DMRs that are

maintained in germ free stem cells from p21 to p100 compared to conventional mice, as well as DMRs in the differentiated cell population at both ages. Interestingly in our analysis several genes displayed robust hypomethylation of control mice versus germ free mice at the p100 time point in both the stem cell and differentiated cell populations. One such gene, Ifitm3, has been heavily associated with chronic inflammation in the colonic epithelium and a poor risk factor for colonic cancer (Li D et. Al, Clin Cancer Res. 2011). We validated Ifitm3 methylation and expression changes between cohorts using pyrosequencing and RT-PCR respectively. Conclusions: This comprehensive analysis has yielded top candidate genes for studying functional consequences of DNA methylation changes that have been previously linked to severe patient diseases including cancer.

#6017

Exposure-related DNA methylation and gene expression changes in mammary glands of Sprague Dawley rats treated with lorcaserin

Volodymyr P. Tryndyak[1], Rose A. Willett[1], Todd Bourcier[2], Frederick A. Beland[1], Igor P. Pogribny[1]. *[1]FDA National Center for Toxicological Research, Jefferson, AR,[2]FDA Center for Drug Evaluation and Research, Silver Spring, MD*

The development of cancer in humans is caused by irreversible modifications of the genome through genetic or epigenetic alterations resulting in the acquisition of multiple heritable abnormal cellular phenotypes. We have investigated DNA methylation and gene expression alterations in mammary glands of Sprague Dawley rats induced by treatment with the weight-loss drug lorcaserin, a drug that increased the cancer incidence in a human clinical trial (CAMELLIA-TIMI 61) and in rats. Female Sprague Dawley rats received lorcaserin by gavage 7 days/week for 12 weeks, at doses previously used in a 2-year rodent cancer bioassay (0, 30, and 100 mg/kg bw/day). DNA methylation changes were investigated in mammary glands, a target organ for lorcaserin carcinogenicity in rats, by reduced representation bisulfite sequencing. Gene expression changes were analyzed by RNA sequencing. Lorcaserin exposure resulted in dose-dependent DNA methylation alterations in the mammary glands, as evidenced by the presence of 1832 and 2352 significantly differentially methylated CpG (dmCpG) sites in the 30 and

100 mg/kg bw/day treatment groups, respectively, as compared to the control group, among which 593 sites were hypomethylated or hypermethylated in common. Similar to DNA methylation changes, lorcaserin treatment resulted in dose-dependent changes in gene expression. Pathway enrichment analysis of the dmCpG-containing genes demonstrated a strong representation of genes associated with cell morphology, cellular function and maintenance, and cellular growth and proliferation. Analysis of dmCpG sites indicated an increase in the number of hypermethylated sites compared to the number of hypomethylated sites in both 30 (1.9 fold) and 100 (2.6 fold) mg/kg bw/day treatment groups. Furthermore, while the number of hypomethylated CpG sites did not differ between treatment groups, the number of hypermethylated CpG sites in rats treated with 100 mg/kg bw/day of lorcaserin was 1.4 times greater than in rats treated with 30 mg/kg bw/day. By combining the analysis of differentially expressed genes and dmCpG sites, we identified 13 genes (11 hypermethylated and 2 hypomethylated) the expression of which was inversely correlated with DNA methylation in the mammary glands of rats treated with 100 mg/kg bw/day of lorcaserin. We also identified 41 hypermethylated and 17 hypomethylated genes containing more than two dmCpG sites. In summary, we have demonstrated that lorcaserin induces extensive DNA methylation and transcriptomic changes in mammary glands at early preneoplastic stages of lorcaserin-induced rat carcinogenesis. These findings suggest the importance of these non-genotoxic alterations in the carcinogenicity of lorcaserin.

#6018

Sequencing of 5-hydroxymethylcytosine to single base resolution

Daniel J. Evanich, V. K. Chaithanya Ponnaluri, Vaishnavi Panchapakesa, Ariel Erijman, Matthew A. Campbell, Nan Dai, Bradley W. Langhorst, Romualdas Vaisvila, Louise Williams. *New England Biolabs, Inc., Ipswich, MA*

DNA methylation is an epigenetic regulator of gene expression with important functions in development and diseases such as cancer. The modified cytosines, 5-methylcytosine (5mC) and 5-hydroxymethylcytosine (5hmC) are identified using Illumina sequencing. Libraries are generated using either NEBNext® EM-seq™, an enzyme-based workflow, or by using

sodium bisulfite conversion. These methods, however, cannot differentiate between 5mC and 5hmC. Distinguishing these modifications is important as there is increased interest in 5hmCs role in regulating gene expression. Methods currently exist to enable discrimination of 5mC and 5hmC, for example, oxBS-seq and TAB-seq. These methods still rely upon sodium bisulfite conversion and have reduced data quality due to fragmentation and loss of DNA. Here we describe an enzymatic method that enables specific detection of 5hmC. 5hmC is detected using two enzymatic steps. Firstly, 5hmCs are glucosylated, which protects them from subsequent deamination by APOBEC. In contrast, cytosines and 5mCs are deaminated resulting in their conversion to uracil and thymine, respectively. During Illumina sequencing deaminated cytosine and 5mC are read as thymine and the glucosylated 5hmC are read as cytosine. Subtractive analysis of 5hmC data from EM-seq data, which detects both 5mC and 5hmC, permits the identification of individual 5mC and 5hmC sites. 5hmC data were generated for inputs of 0.1 ng to 200 ng DNA isolated from E14 mouse embryonic stem cells and human brain. The 5hmC libraries had similar characteristics to EM-seq libraries, including expected insert sizes due to intact DNA molecules, low duplication rates and minimal GC bias. T4147 phage DNA was used as an internal control, as all cytosines are 5-hydroxymethylated, with 98-99% of cytosines identified as 5hmC. 5mC and 5hmC levels were also profiled during E14 cell differentiation for 10 days. Interestingly, 5hmC levels decreased whereas 5mC levels increased particularly during the first five days of differentiation. LC-MS/MS quantification of this same DNA mirrored the changes observed by sequencing. The ability to discriminate between 5mC and 5hmC will provide key insights into the role of these cytosine modifications in development and disease.

#6019

Characteristics and impactof DNA methylationon prognosis in hepatitis B virus-related follicular lymphoma

Jianli Ma[1], Yuwei Deng[2], Huilai Zhang[3], Xiaosan Zhang[4], Lihong Liu[5], Xianhuo Wang[3], Hongtao Song[6], Zirong Zhang[7], Caili Liu[7], Qingyuan Zhang[2], Jinming Yu[1]. *[1]Radiation Oncology, Shandong University Cancer Center, Jinan, China,[2]Medical Oncology, Harbin Medical University Cancer Hospital, Harbin, China,[3]Lymphoma, Tianjin Medical University Cancer Institute and Hospital, Tianjin, China,[4]Medical Oncology, Henan*

Cancer Hospital, Zhengzhou, China,[5]Hematology, the Fourth Hospital of Hebei Medical University, Shijiazhuang, China,[6]Pathology, Harbin Medical University Cancer Hospital, Harbin, China,[7]Hematology, The Fourth Hospital of Hebei Medical University, Shijiazhuang, China

Hepatitis B virus (HBV) infection (surface antigen positive, HBsAg+) has been linked to the increased risk and poor prognosis for B-cell lymphoma. Here, we aimed to discover distinctive potential factors to influence the prognosis in HBV-associated follicular lymphoma (FL). Retrospective investigation from multiple clinical centers showed that patients with HBsAg+ FL were featured with a higher incidence of disease progression within 24 months (POD24, *P*=0.031), shorter progression-free survival (PFS, *P* = 0.004) and overall survival (OS, *P* = 0.039). The patients with high HBV-DNA load (>10^5 copies/mL) had worse PFS (*P* <0.001) and OS (*P* = 0.007). Methylation detection identified that POD24 in HBsAg+ FL were contributed by pro-tumoral methylated *KMT2A*, *EP300-AS1,* and *ARID1B*. The majority of MHC I class molecular retained hypermethylated status with silencing expression to promote immune escape and progression in HBsAg+ FL. Hypermethylated *TNFRSF1A* significantly contributed to prevent the POD24 of HBsAg+ FL, whereas hypermethylated *LTA* promoted progression. Regarding the unsatisfactory prognosis guidance based on FLIPI in patients with HBsAg+ FL, we proposed new scoring combined with HBV-related clinical parameters, contributed gene methylation and FLIPI to define a high-risk group with worse prognosis than FLIPI in our study (mean OS, 67.7 vs 69.8). It exhibited good performances in internal cohort and external validation cohort from other three clinical centers. Taken together, chronic HBV infection may affect methylation of the immune-related genes to promote progression in FL. The combination of clinical features and genes methylation with FLIPI could provide a better prognostic model for HBV-related FL.

Univariable and multivariable Cox regression analysis with respect to progression-free survival of c

	Univariate analysis			Multivariate analysis		
	HR	95%CI	P value	HR	95%CI	P value

Age(>60 vs ≤60)	1.457	0.963-2.205	0.073*	1.608	1.037-2.493	0.034
Sex(male vs female)	0.876	0.578-1.325	0.529			
Grade(3A va 1-2)	1.315	0.847-2.042	0.221			
Ann Arbor stage(III/IV vs I/II)	0.852	0.526-1.379	0.513			
Number of extranodal sites≥5	0.732	0.483-1.110	0.141			
B symptoms	1.679	1.028-2.741	0.036*	2.023	1.142-3.584	0.016
BM involvement	0.690	0.383-1.244	0.215			
High FLIPI risk	3.081	1.740-5.454	<0.001*	1.972	1.023-3.803	0.043
Elevated LDH level	1.317	0.829-2.092	0.242			
Serum albumin <3.5 g/dL	2.633	1.315-5.270	0.004*	1.465	0.649-3.309	0.358
ALC <1000 /μL	1.581	0.641-3.898	0.316			
HBsAg positivity	1.850	1.209-2.833	0.004*	1.184	0.705-1.991	0.523
HBeAg positivity	1.668	0.768-3.623				
High HBV-DNA load(>10^5 copies/mL)	4.110	2.360-7.160	<0.001*	3.774	1.958-7.278	<0.001
Treatment (BR vs R-CHOP)	1.261	0.752-2.113	0.379			

#6021

Genetic and epigenetic features OF *KMT2D*, *CREBBP*, *ATM*, *TSC2* and *GNAS* in uterine leyomiosarcomas

Laura G. dos Anjos[1], Daniela Bizinelli[2], Katia C. Carvalho[3]. *[1]Obstetrics and Gynecology, University of São Paulo, Faculty of Medicine, São Paulo, Brazil,[2]International Research Center (CIPE), São Paulo, Brazil,[3]University of São Paulo, Faculty of Medicine, São Paulo, Brazil*

Background: Uterine leiomyosarcoma (LMS) comprises 60% to 70% of the uterine sarcoma (US). These tumors present high rates of recurrence and metastasis, and the patients' survival rates are very low (20% in five years). It is known that somatic mutations and modifications in the DNA methylation levels are associated with several types of neoplasms. Previously, our group identified missense and loss of function mutations in *KMT2D*, *CREBBP*, *ATM*, *TSC2*, and *GNAS,* using a genetic screening method in LMS samples. Based on these results, we decided to investigate whether a genetic and epigenetic crosstalk could help to understand the biological processes involved in the LMS origin, development, and pathogenesis. The present study aimed to evaluate the *KMT2D*, *CREBBP*, *ATM*, *TSC2* and *GNAS* gene expression profile in LMS cell line, and their methylation levels in formalin-fixed and paraffin-embedded (FFPE) patients´ samples.

Methods: We selected 15 LMS - FFPE samples obtained via surgical procedures performed between 2012 and 2019 at the Instituto do Cancer do Estado de São Paulo (ICESP). Genomic DNA was extracted using the QIAamp DNA FFPE Tissue Kit and we evaluated methylation levels using the Illumina Infinium Methylation EPIC BeadChip system 850k, including samples treated with bisulfite-treated DNA. Leiomyoma (LM) (THESCs CRL-4003) and LMS (SK-UT-1) cell lines were cultivated for gene expression analysis. Cells were growth for 24, 48, 72, and 96 hours, and the total RNA was extracted by TRIzol. High-Capacity cDNA Reverse Transcription Kit was used for cDNA synthesis and for gene expression evaluation, real-time PCR reactions were performed using TaqMan Universal PCR Master Mix and inventoried TaqMan probes.

Results: *KMT2D* and *TSC2* showed increased expression in LMS compared to LM (cut-off $\leq$ -2 and $\geq$ 2 for down and upregulation, respectively), with higher expression in 24 hours of *KMT2D* [Fold Regulation (FR): 2.77] and *TSC2* (FR: 2.58). In contrast, *CREBBP* was downregulated, with lowest

expression in 72 hours (FR: -6.57). *ATM* was upregulated at 24, 48 with higher expression in 72 hours (FR: 2.32), and *GNAS* was downregulated, with lowest expression in 96 hours (FR: -4.31). Moreover, the methylation analyzes showed an expressive hypomethylation in LMS samples, compared to myometrium, for *KMT2D* (β value: 0.45; p= 0.004); *CREBBP* (β value: 0.51 $p < 0.0001$); *ATM* (β value: 0.47 $p < 0.0001$); *TSC2* (β value: 0.53 $p < 0.0001$) and *GNAS* (β value: 0.41 $p < 0.0001$). In conclusion, our study showed that potentially pathogenic mutations may be associated with an aberrant hypomethylation profile, as well as increased expression of *KMT2D*, *TSC2*, *ATM* and loss expression of *CREBBP* and *GNAS* in LMS. The interconnection of these genetic and epigenetic events is essential for understanding the complex biology of these tumors, in addition to enabling identification of biomarkers.

#6022

The importance of DNA methylation to breast cancer cell phenotype and its role in the anticancer activity of withaferin-A

Andrew Brane, Trygve O. Tollefsbol. *University of Alabama at Birmingham, Birmingham, AL*

Breast Cancer (BC) is a widespread malignancy that affects the lives of millions of women each year. Prevention of BC through administration of epigenetically active dietary phytochemicals has received increased interest in recent years due to its relatively low cost, few side effects and potential to reduce the financial and healthcare burdens associated with BC. Many phytochemicals' anticancer functions are thought to arise from their effects on the epigenome, although the relative importance of specific genes' epigenetic states remain unclear. To elucidate this, we utilized human BC cell lines in combination with CRISPR-dCas technology tied to methylation modifiers to explore the importance of gene specific DNA methylation to cancer cell phenotype in both naïve BC cells and BC cells treated with the phytochemical Withaferin A (WA). We found that demethylation of promoters of the tumor suppressors *p21* and *p53* results in increased gene expression, while methylation of the promoter of the oncogene *CCND1* results in decreased in gene expression. Additionally, changes to biological processes were associated with tumor suppressor promoter methylation state, including increases in cell cycle arrest for a demethylated *p21*

promoter and decreases in cell viability for a demethylated *p53* promoter. We also found that downregulation of *p21* through targeting DNMT3A to its promoter was able to ablate the anticancer function of WA in both MDA-MB-231 and MCF-7 cells. Taken together, these results highlight the potential importance of DNA methylation changes for cancer cell phenotype and a possible mechanism of action for the phytochemical WA in BC prevention.

#6023

Plasma methylome landscape across the spectrum of prostate cancer progression, and differentially methylated region (DMR) based biomarkers of hormonal therapy failure in metastatic hormone-sensitive prostate cancer

Manish Kohli[1], Jodie Wong[2], Yijun Tian[3], Amir Bitaraf[3], Claire Hanson[1], Matt Larsen[1], Jennifer Lloyd[1], Julia Batten[1], Neeraj Agarwal[1], Umang Swami[1], Benjamin Maughan[1], Sumati Gupta[1], Jonathan Tward[1].
[1]University of Utah Huntsman Cancer Institute, Salt Lake City, UT,[2]Moffit Cancer Institute, Tampa, FL,[3]Moffitt Cancer Institute, Tampa, FL

Background: DNA silencing of gene expression can affect tumorigenesis, treatment outcomes and prognosis. Epigenetic silencing of tumor suppressor genes in prostate cancer detected in plasma at different stages of progression and its effect on clinical outcomes has not been determined. In a cohort study across different stages of prostate cancer (PC) progression, we performed plasma cell-free DNA (cfDNA)-based epigenomic profiling for determining the landscape of methylation and Differentially Methylated Region (DMR) classifiers and the potential impact on clinical outcomes in metastatic hormone-sensitive prostate cancer (mHSPC) state.
Methods: Plasma was collected prospectively in a longitudinal cohort study of 108 PC patients (pts) of which 24 had non-metastatic Local PC; 28 had mHSPC; 56 had mCRPC. cfDNA was used for enzymatic methylation sequencing (EM-seq) of a targeted panel of genes (N=441) implicated in prostate cancer biology. Methylation status at CpG islands of these genes were examined using Twist targeted cfDNA methylation assay. The Bismark program was used for methylation calls. Temporal trends of differentially methylated regions (DMRs) were identified in different states of progression by comparing the methylation status of target genes in

localized PC, mHSPC and mCRPC states using a False Discovery Rate (FDR-q-value) of 0.2 or less. DMRs uniquely associated with mHSPC state were identified and determination of genes with DMRs in pts experiencing early failure of androgen deprivation therapy (ADT)-based therapies was performed. Early failure was defined as progression on ADT within 12 months.
Results: We identified 304/441 genes that were differentially methylated between localized PC and advanced PC (mHSPC and mCRPC) (FDR<0.2), of which 237 genes differed between mHSPC and mCRPC ($p<0.05$) states. mHSPC pts were serially profiles before and after 3 months of ADT-based therapies. All 28 pts experienced a PSA response at 3-months and 112/237 genes showed significant change in methylation status in these serial samples taken before/after 3 months of ADT-based therapies. The median follow up of the cohort was 18 months (range 10-24). 6/28 mHSPC pts experienced early ADT failure (<12 months; median 10 months). 8/112 genes were significantly associated with early failures and included DMRs in *RB1, FOXA1, SOX11. GSC, ALDH1L1, SCGB3A1, FLT4*, and *PTPRN2.*
Conclusions. A targeted cfDNA plasma liquid-biopsy based epigenomic profiling of PC cancer related genes was able to capture significant differences in DMRs across different states of cancer progression. Candidate differentially expressed CpG methylome gene biomarkers detected in plasma also identified biomarkers associated with early ADT-based treatment failure in mHSPC.

#6024

Precancerous nature of intestinal metaplasia with accelerated DNA methylation along with altered epigenomic landscape

Chihiro Takeuchi[1], Satoshi Yamashita[2], Yu-Yu Liu[1], Hideyuki Takeshima[1], Toshikazu Ushijima[1]. *[1]Department of Epigenomics, Hoshi University, Tokyo, Japan,[2]Department of Biotechnology, Maebashi Institute of Technology, Gunma, Japan*

Objective. The presence of intestinal metaplasia (IM) is a risk factor for gastric cancer. However, it is still controversial whether IM itself is a precancerous or paracancerous lesion. Here, we aimed to explore the precancerous nature of IM in terms of epigenetic alterations.

Design. Genome-wide DNA methylation analysis was conducted by EPIC BeadArray using IM and non-IM crypts isolated by Alcian blue staining. Organoid establishment, ChIP-seq for H3K27ac, and single-cell ATAC-seq were conducted using IM mucosa. *NOS2* was induced using a Tet-on gene expression system in normal cells.
Results. IM crypts had a methylation profile unique from that of non-IM crypts, showing extensive DNA hypermethylation in promoter regions with CpG islands, including those of tumor suppressor genes. Also, the IM-specific methylation profile was carried into a fraction of gastric cancers (GC), and the frequency of the IM-type GCs was higher than the fraction of IM cells in the adjacent mucosa, indicating that IM cells have a higher chance of developing into cancer cells than non-IM cells. Moreover, the patients with IM-type GCs showed better overall survival than those without, and IM-type GCs showed good response to chemotherapy. As for the mechanism of accelerated methylation induction, IM organoids had remarkably high endogenous *NOS2* expression, and *NOS2* induction in normal cells was shown to accelerate aberrant DNA methylation by increasing DNMT activity. IM mucosa underwent dynamic enhancer reprogramming, including the regions involved in abnormal *NOS2* expression. Single-cell ATAC-seq also showed *NOS2* open chromatin in IM cells but not in gastric cells, and frequent closed chromatin of tumor-suppressor genes in IM cells. *NOS2* expression in IM-derived organoids was up-regulated by IL-17A, a cytokine secreted by extracellular bacterial infection.
Conclusions. IM cells were considered to have a strong precancerous nature with an increased chance of converting into cancer cells in terms of the specific methylation profile and the accelerated DNA methylation induction due to abnormal *NOS2* expression.

Metabolism and Metabolomics of Cancer

#6028
Cancer-selective metabolic vulnerabilities in MYC-amplified medulloblastoma
William Gwynne. *Surgery, McMaster University, Hamilton, ON, Canada*

[Background] Medulloblastoma (MB) is the most frequently diagnosed malignant pediatric brain tumor. Multiple integrated genomic analyses have been used to stratify MB into four molecular subgroups, each unique in its gene expression profile, clinical characteristics, and prognosis. *MYC*-driven group 3 MB (G3MB) tumors are poorly understood entities, defined by metastasis down the leptomeninges, disease recurrence and particularly poor survival. *There is hence an urgent need for a more thorough molecular understanding of G3MB, particularly at recurrence, in order to develop more effective therapeutic modalities that will improve the durability of remission.*
[Methods] We previously developed a therapy-adapted mouse model of G3MB disease progression from xenoengraftment through treatment-induced minimal residual disease until eventual relapse in the brain and spine compartments. Temporal transcriptomic profiling of tumor tissue at each stage revealed an enrichment of several metabolic pathways at recurrence. Here we mapped further functional insight into the G3MB metabologenomic landscape by performing a genome-wide loss-of-function CRISPR-Cas9 genetic screen in patient-derived G3MB cells, which we cross-referenced with screens performed in human neural stem cells (NSCs), the proposed cell- of-origin for G3MB.
[Results] By examining G3MB context-specific gene ontologies, we discovered differential essentiality of several metabolic processes exclusively in G3MB. In tandem, mass spectrometry-based global metabolomic profiling shows dysregulation of several metabolic pathways in in G3MB tumor cells in comparison to NSC, including the enrichment of *de novo* pyrimidine biosynthesis and depletion of salvage pyrimidine intermediates. We investigated a lead hit from our screen, DHODH (dihydroorotate dehydrogenase), which facilitates *de novo* pyrimidine biosynthesis. Our data demonstrate that genetic or pharmacological inhibition of DHODH selectively targets G3MB brain tumor initiating cell (BTIC) activity while sparing normal NSC, by disrupting hallmark MYC activity. We further show that MYC-amplified G3MB tumors harbor subgroup-specific transcriptomic signatures that delineate enrichment of *de novo* pyrimidine biosynthesis.
[Significance] Despite clear evidence favoring an altered metabolic landscape in *MYC*-driven cancers, there have been only a few reports into the role of metabolic reprogramming in *MYC*-amplified G3MB. Given the

paucity of treatment options for patients with recurrent G3MB, this study has the potential for a significant impact on the field of pediatric oncology. Translation of therapies that target unique metabolic vulnerabilities exclusive to G3MB may lead to more durable cures and radical improvements in quality of life for survivors.

#6029

Multi-omic landscape of squamous cell lung cancer

Paul Stewart[1], Ashley Lui[2], Eric Welsh[2], Dalia Ercan[2], Vanessa Rubio[2], Hayley Ackerman[2], Guohui Li[3], Bin Fang[2], Steven Eschrich[2], John Koomen[2], Elsa Flores[2], Eric Haura[2], Gina DeNicola[2]. *[1]Biostatistics and Bioinformatics, Moffitt Cancer Center, Tampa, FL,[2]Moffitt Cancer Center, Tampa, FL,[3]Zymergen, Emeryville, CA*

Patients with squamous cell lung cancer (SCC) have high unmet medical need. Knowledge of these tumors is limited, and a lack of targetable genomic drivers means patients have few treatment options. To provide a detailed analysis on the influence of genomic alterations to proteome-level changes in SCC, we previously integrated DNA copy number, somatic mutations, RNA-sequencing, and expression proteomics in a cohort of 108 SCC patients. A major finding was identification of three proteomic subtypes, two of which made up the majority (87%) of tumors: the "Inflamed" subtype was enriched for B-cell rich tertiary lymphoid structures (TLS), and the "Redox" subtype was enriched for redox pathways and NFE2L2/KEAP1 alterations but had significantly less immune infiltration. We hypothesized these proteomic subtypes would give rise to distinct metabolic signatures. Therefore, we performed untargeted metabolomics on 87 tumors from the same cohort using chromatographic separation on a HILIC column, followed by analysis on a Q Exactive HF mass spectrometer. This analysis yielded 7,344 features corresponding to 7,072 unannotated metabolites and 272 identified metabolites. Glutathione, a key redox metabolite, was anticorrelated with immune score (R = -0.44, padj = 0.004) calculated from our transcriptomic data with the ESTIMATE algorithm, and glutathione was elevated in the Redox proteomic subtype (0.58 log2 ratio, padj = 9.87E-04). Consensus clustering was next used to identify novel metabolomic subtypes of SCC. Surprisingly, none of the five metabolomic subtypes we identified corresponded to proteomic subtype or

NFE2L2/KEAP1 alteration (Fisher's Exact test p-values > 0.05). The fifth subtype had 332 metabolites (26 identified) differentially expressed (> 1.5 fold-change, padj < 0.05) with ascorbate and aldarate metabolism as the top enriched pathway (padj = 3.36E-04). Interestingly, this fifth metabolomic subtype had significantly higher DNp63-alpha (p = 2.40E-05), a primary transcript of delta-N p63 that is known to promote non-small cell lung cancer. Ongoing integrative analyses across omic types will determine how p53, p63, and p73 transcripts influence these metabolomic subtypes, how these transcripts relate to the poor immune infiltration in some SCC tumors, and if these transcripts relate to novel metabolic vulnerabilities in SCC.

#6031

KYNU upregulation is a prominent feature of NRF2-activated cancers and is associated with tumor immunosuppression and poor prognosis

Ricardo A. Leon Letelier, Ali H. Abdel Sater, Yihui Chen, Ranran Wu, Jennifer B. Dennison, Soyoung Park, Ehsan Irajizad, Hiroyuki Katayama, Jody Vykoukal, Samir Hanash, Edwin J. Ostrin, Johannes F. Fahrmann.
Clinical Cancer Prevention, The University of Texas MD Anderson Cancer Center, Houston, TX

Activation of the nuclear factor erythroid 2-related factor 2 (NRF2) pathway, either through gain-of-function mutations in the NRF2 encoding gene *NFE2L2* or through loss-of-function of its suppressor, Kelch-like ECH-associated protein 1 (*KEAP1*), is a frequent manifestation in various malignancies. NRF2 activation exerts pro-tumoral effects in part by altering cancer cell metabolism. We previously reported a novel mechanism of NRF2 tumoral immune suppression through selective upregulation of the tryptophan metabolizing enzyme kynureninase (KYNU) in lung adenocarcinoma. In the current study, we explored the Pan-Cancer relevance of NRF2-mediated KYNU upregulation. We analyzed the gene expression dataset for 9,801 tumors representing 32 cancer types in The Cancer Genome Atlas (TCGA). Elevated KYNU expression levels paralleled increased gene-based signatures of NRF2-activation and was strongly associated with an immunosuppressive tumor microenvironment, marked by high expression of gene-based signatures of Tregs as well as immune checkpoint blockade-related genes CD274 (PDL-1), PDCD1 (PD-1), and CTLA4, regardless of cancer type. Cox proportional hazard models

further revealed that increased tumoral KYNU gene expression was prognostic for poor overall survival in several cancer types, including thymoma, acute myeloid leukemia, low grade glioma, kidney renal papillary cell carcinoma, gastric adenocarcinoma, and pancreatic ductal adenocarcinoma (PDAC). Using PDAC as a model system, we confirmed that siRNA-mediated knockdown of NRF2 reduces KYNU mRNA expression, whereas activation of *NFE2L2* (the encoding gene for NRF2) through either small molecule agonists or siRNA-mediated knockdown of *KEAP1* upregulated KYNU. Metabolomic analyses of conditioned media from PDAC cell lines revealed elevated levels of KYNU-derived anthranilate, confirming KYNU as enzymatically functional. Collectively, our findings highlight the multi-cancer relevance of the NRF2-KYNU axis and of tumoral KYNU as a prognostic marker of poor overall survival associated with immunosuppression.

#6032

Exploiting metabolic vulnerabilities of ovarian cancer with upregulated succinate dehydrogenase

Lin Wang, Magdalena Bulicz, Patryk Mucha, Michael Kinter, Atul Pranay, Timothy M. Griffin, Benjamin F. Miller, Magdalena Bieniasz. *Aging and Metabolism, Oklahoma Medical Research Foundation, Oklahoma City, OK*

Ovarian cancer remains the deadliest of all gynecologic malignancies nationwide due to limited therapeutic options and chemotherapy resistance. The response to chemotherapy is substantially influenced by the high metabolic flexibility of ovarian cancer cells, which allows the cells to reprogram their metabolism and survive the treatment. Better understanding mechanisms regulating ovarian tumor metabolism could be exploited to develop new improved therapies. Our work demonstrated that the upregulation of mitochondrial enzyme succinate dehydrogenase (SDHA) is particularly prevalent (~20% of patients) in ovarian carcinoma and contributes to high energy tumor metabolism and cell survival. We observed that SDHA overexpressing ovarian cancer cells showed improved ability to survive and generate colonies in anchorage-independent conditions, which is an important feature of ovarian tumor cells surviving and spreading in peritoneal fluid (ascites). Proteomics data revealed that the SDHA overexpressing tumor cells showed reduced levels of proteins promoting

anaerobic glycolysis (LDHA and HIF1α), and increased levels of mitochondrial pyruvate carrier (MPC) proteins. In addition, our tracer-based metabolomics data revealed that the elevated SDHA stimulates glutaminolysis by increasing mitochondrial glutamine supply fueling the TCA cycle with essential metabolites. We also demonstrated that the overexpression of SDHA is associated with a significant increase of OXPHOS and ATP production rate. Further, we reasoned that the SDHA overexpressing tumor cells could be particularly vulnerable to drugs disrupting glucose and/or glutamine metabolism. We performed a drug screening and identified an anti-metabolic compound shikonin known to disrupt glucose and amino acid metabolism. In *in vitro* studies, shikonin exhibited a profound anti-tumor efficacy and selectivity towards SDHA overexpressing tumor cells superior to that observed with chemotherapy. Importantly, our *in vivo* study validated the *in vitro* observations, and showed that shikonin is highly effective in suppressing SDHA overexpressing patient-derived tumor growth. In summary, the unique metabolic state of ovarian cancer associated with SDHA amplification could be successfully targetable offering a potential new treatment strategy for ovarian cancer patients.

#6033

RA123, a new GLS1 allosteric inhibitor demonstrates *in vitro* and *in vivo* activity in multiple myeloma models

Christophe Henry[1], Dimitri Gorge-Bernat[1], Pascal Pannier[1], Isabelle Meaux[1], Jane Cheng[2], Fangxian Sun[2], Olivier Pasquier[1], Philippe Lienard[1], Erwan Jouannot[1], Thierry Gouyon[1], Geneviève Estenne-Bouhtou[1], Bailin Zhang[2], Bérangère Thiers[1], Laurent Debussche[1], David Machnik[1]. *[1]Sanofi, Vitry-sur-Seine, France,[2]Sanofi, Cambridge, MA*

The conditional essential amino acid glutamine is utilized by tumors to sustain bioenergetic requirements in a nutrient-poor microenvironment. Based on this specific tumor need, efforts have been made to target the glutamine metabolism using glutaminase inhibitors. In this study, we present in vitro and in vivo studies demonstrating activities and target engagement of a new specific GLS1 allosteric inhibitor (RA123). In vitro, RA123 was tested in imid-resistant, CD38 low RPMI8226 multiple myeloma cell line using the ATP Cell titer Glo assay over a 72h treatment

period. In vivo, RA123 was tested in mice xenografted with RPMI8226 multiple myeloma cell line. Compound was given at three different under a BID (twice a day) regimen. Tumor growth under treatment was monitored by caliper measurement for 20 days. A terminal PK/PD study on the same model was setup measuring impact of the drug on the glutamine and glutamate tumor content post 24 hours after the last administration. Over the same period, PK measurements were planned to document drug exposure in the plasma and in the tumor. Finally, in a stand-alone study, target engagement was documented using imaging modality. [18F]FSPG PET radiotracer was used to visualize and quantify impact of RA123 on tumor (RPMI8226) glutamate pool. RA123 was given at three doses under a BID regimen. Treatment was administered for 3 days, and PET signal was recorded at baseline and at end of day 3. In vitro study demonstrated that RA123 was able to induce cell killing of RPMI8226 after 72 hours of treatment. These data translated in vivo by a dose-dependent effect on cell growth. In a terminal PK/PD study, RA123 confirmed a dose-dependent impact on glutamine and glutamate tumor levels which correlated with both plasma and tumor exposure. Further confirmation of target engagement was observed with reduced PET uptake post- RA123 treatment at the three doses tested. In conclusion, this study demonstrated that RA123, a new specific GLS1 allosteric inhibitor was able to impact multiple myeloma tumor cell growth both in vitro and in vivo. This effect was associated with reduced glutamate pools and accumulation of glutamine levels within the tumor cells.

#6034

Detection of potassium channel (KCN) gene expression, often multiple and pH sensitive, in cancer genomic landscapes, as low to mid level genes of interest, suggests potassium transmembrane flow may enable proton efflux in a Goldilocks manner

Marie E. Beckner. *Kent State University, Willoughby Hills, OH*

A reversed pH gradient across cell membranes underlies multiple malignant features, including invasiveness. Extracellular low pH activates metalloproteases and intracellular high pH activates ATP citrate lyase, inactivates caspases, etc. Hydrogen ions attracted to inner membrane fixed anions are putatively displaced by potassium ion flow through membrane

channels. Altered expression of potassium channel (KCN) genes sensitive to pH in invasive brain tumors (Beckner, Proc AACR, A3039, 2022) and 2 mutated KCN genes (1 pH sensitive) in U87 glioblastoma cells (Clark MJ et al, PLOS Genet 2010, e1000832) led to this investigation. Published studies with altered expression or mutations in KCN genes qualifying them as genes of interest (GOI) were compared. Both study types included breast, lung, gastrointestinal, brain, bone marrow, liver, melanocytic malignancies, and 8 others were in either. At least 1 figure (heatmap, Venn diagram, phylogenetic tree, etc.) or table (not Supplemental) had 1 or more KCN genes in a group of GOI. Average numbers of GOI with 95% CI for 23 expression and 14 mutation studies were 38.5 ± 0.4 and 28.4 ± 0.4. No KCN GOI was further examined in the studies. Expression was according to tumor types, inhibitors, siRNAs, regulators of pathways, transcription factors, location, etc. Mutations were single nucleotide polymorphisms, insertions, deletions, fusions, etc. Tissue from surgery, organoids, xenografts, cell lines, stem cells, etc. were analyzed. Of 27 KCN GOI in expression studies, 2/3 were detected with other KCN GOI. For 12 mutated KCN genes there were no other KCN genes mutated in the same study. In expression studies, 8 (34.8%) had multiple KCN GOI, differing from mutation studies, p=0.015, Fishers Exact. In expression studies, 8 found pH sensitive KCN GOI including KCNK1 (2X), K3, K5, K6, K12, K15 (2X), and KCNJ16. In mutation studies, KCNK9 was the only one found. The most frequently mutated KCN subfamily was KCNJ, KCNJ5 (2X) and KCNJ12 (2X). All expression studies included at least 1 repeat GOI (KCN or other). APOE, RET, and RTN1 were each GOI 3 times. Additionally, 40 expressed GOI (including 6 KCN GOI) were found 2X. A small cell lung cancer study had 6 repeats (30%) in 20 GOI (ASCL1, BCL2, KCNA1, RET, SCN3A, and SOX2). KCN gene multiplicity, often pH sensitive members, among low to mid level GOI consistent with a Goldilocks' level of expression, and repeated association with cancer genes supports a pH related measured/regulated role for potassium channels in malignancy. Mainly inward (and some outward for recirculation) potassium transmembrane flows in tumor cells potentially compete with hydrogen ions attracted to inner membrane anions to promote proton efflux by displacement with subsequent reversed pH gradients that aid invasion, cell survival, etc.

#6035

Glutaminase inhibitors block metabolic switch in prostate cancer and prevents anti-androgen treatment resistance

Hirak Subhra Basu[1], Meredith Spradlin[2], Tian Weihua[1], Jose Enriquez[1], Pratip Bhattacharya[1], Livia Eberlin[3]. *[1]UT MD Anderson Cancer Center, Houston, TX,[2]Department of Surgery, Baylor College of Medicine, Houston, TX,[3]Baylor College of Medicine, Houston, TX*

Background: All prostate cancers first manifest as androgen dependent tumors and most patients are initially treated with surgery or radiation. About 30% of these patients return to clinic with recurrent prostate cancer that initially responds to androgen ablation therapy (ADT). Unfortunately, almost all of them fail ADT and develop castrate resistant disease (CRPC) that responds poorly to most cancer therapies and progress to often lethal metastatic CRPC (mCRPC). There are accumulating evidence that at a certain state of progression of hormone sensitive prostate cancer (HSPC) to CRPC, prostate cancer cells adopt to androgen signaling axis targeted therapy (ASI) by switching their metabolism from glycolysis to mitochondrial oxidative phosphorylation (OXPHOS). High OXPHOS activity induces mitochondrial dysfunction, autophagy, cancer invasion, and metastasis. A mitochondrial enzyme glutaminase (GLS) produces L-glutamate from L-glutamine. L-glutamate is utilized in mitochondrial metabolism for energy production through TCA cycle. GLS inhibitors CB-839 and IACS-6274 are being clinically developed for treatment of various human malignancies. We have shown that growth of prostate cancer patient derived xenografts (PDX) is markedly inhibited by a combination treatment of a clinically used ASI enzalutamide (ENZA) followed by a GLS inhibitor. Methods: We followed the growth of one HSPC and two CRPC PDX tumors in mice and collected tumor tissues and circulating human tumor cells (CTC) from mouse blood samples at sacrifice. We used super resolution STED confocal microscopy to image mitochondria in the tissue samples and in the CTCs, desorption ionization mass spectrometry (DESI-MS) imaging of multiple metabolites in the tissue samples as well as hyperpolarized MRI (HP-MRI) of the xenografted tumors to follow the changes in cellular central carbon metabolism *in vivo*.

Results: We observed that growth of PDXs developing ENZA resistance is markedly inhibited when ENZA is followed by adding GLS inhibitors with a concomitant reduction in OXPHOS activity. In addition, the *ex vivo* and *in vivo* methods introduced to monitor tumor metabolic activities can be easily translated into clinic to monitor the metabolic status of the tumors for early detection of resistance development and as a pharmacodynamic marker for metabolic inhibitor therapy.
Conclusion: GLS inhibitors added to ASI could be effective against CRPC and mCRPC developing resistance to ASI treatment.

#6036

Functional antibodies against multi span transmembrane proteins - revisiting the Warburg effect in cancer cells

Siret Tahk[1], Kai Virumäe[1], Paule Hermet[1], Korneelia Anton[1], Maiken Abel[1], Denis Belitškin[1], Luciano Galdieri[2], Steven Garner[2], Jillian Krings[2], Kaleb Collver[2], Emily Hoehn[2], Brendan Lahm[2], Kaitlyne Powers[2], Tuuli Käämbre[3], Alastair J. King[2], Francisca Neethling[2], Anu Planken[1], Mart Ustav[1], Andres Männik[1], Mart Ustav[1]. *[1]Icosagen Cell Factory OU, Tartu maakond, Estonia,[2]Eurofins Discovery, St Charles, MO,[3]Chemical Biology Laboratory, National Institute of Chemical Physics and Biophysics, Tallinn, Estonia*

Background: Alterations in tumor cell metabolism are one of the central processes guiding cancer progression. The increased glucose dependence of cancer cells, also known as the Warburg effect, opens the possibility to therapeutically target the glycolytic pathway and challenge the metabolic needs of tumor cells. We generated 24 monoclonal antibodies targeting the main glucose transporter on cancer cells - SLC2A1 (GLUT1). We evaluated the ability of the antibodies to affect cancer cell fitness alone and in combination with OXPHOS inhibitors to find clinically applicable therapeutics targeting tumor metabolism.
Methods: Immunization, discovery and isolation of monoclonal antibodies against SLC2A1 protein was conducted using HybriFree technology using $SLC2A1^{+}$ virus like particle (VLP)-based immunization strategy (Kivi, et al., BMC Biotechnology, 2016). Antibodies were functionally characterized by 2-deoxyglucose uptake interference assay and sensitivity to antibody

single and combination treatments were evaluated in various tumor cell lines. Metabolomics and oxygen consumption rates were examined as mechanistic endpoints for tumor cell lines and primary tumor samples.
Results: The anti-SLC2A1 antibodies specifically bind to SLC2A1 with low nanomolar EC50 values and not to other glucose transporters. Antibody clones with functional properties inhibit glucose uptake leading to reduced metabolic activity and growth inhibition in a subset of cancer cell lines. A drastic cell proliferation inhibition is moreover observed in combination of anti-SLC2A1 antibodies and OXPHOS inhibitors metformin, phenformin or IACS-010759 in 2D cultures of colon, breast and pancreatic cancer cell lines. The inhibition of metabolic activity was further confirmed in an *ex vivo* primary patient tissue samples highlighting the putative translational applicability of our antibodies.
Conclusions: This is the first study to provide highly specific antibodies bocking the function of SLC2A1 transporter and demonstrate the proof of principle for inhibiting complex muti-pass membrane transporters with antibody therapeutics. While the developed anti-SLC2A1 antibodies could be efficacious in some indications as single agents, appreciable clinical activity could be obtained by the combined use with OXPHOS inhibitors.

#6037

Identification of collateral lethal targets in cancers using integrated machine learning and flux analysis platform for personalized metabolic therapy

Abhinav Achreja[1], Jin Heon Jeon[1], Mark Slayton[1], Tao Yu[2], Olamide Animasahun[1], Minal Nenwani[1], Fulei Wuchu[1], Anjali Mittal[1], Xiongbin Lu[2], Sofia D. Merajver[1], Deepak Nagrath[1]. *[1]University of Michigan, Ann Arbor, MI,[2]Indiana University, Bloomington, IN*

Chromosomal alterations that occur frequently in cancers confer selective advantages for tumor progression by deleting tumor-suppressing genes or amplifying oncogenic drivers. However, the collateral effect of these, i.e., deletion of essential genes or upregulation of metabolic regulators, exposes cancers to biological pressures by suppressing essential metabolic pathways. Cancer cells rely on paralogous metabolic pathways to compensate for this loss of function, which in turn opens the door to exploit metabolic vulnerabilities arising as a direct consequence of chromosomal

alterations. These pathways are collateral lethal (CL) targets and offer a unique precision medicine approach for metabolic therapeutics. We have developed an integrated machine learning and systems biology platform, collateral lethal gene identification via metabolic fluxes (CLIM) to identify metabolic targets across multiple cancers. Results: In ovarian cancers with 19p13.3 deletion, a loss of Complex III subunit-encoding gene UQCR11 occurs, leading to suppressed electron transport chain (ETC) activity. CLIM predicted that MTHFD2 acts noncanonically to oxidize NADH to NAD^+ to compensate for reduced NAD^+ recycling via the ETC. We demonstrate selective death of ETC deficient ovarian cancers by targeting MTHFD2 and provide mechanistic validation of oxidative MTHFD2 flux. We observed significant shrinkage of ovarian tumors with ETC deficiency upon MTHFD2 knockdown in mouse models. In triple negative breast cancers (TNBC), we discovered a chromosomal amplification leading to reprogramming of the serine biosynthesis pathway. CLIM predicts a target in the tryptophan metabolism. Methods: Patients are stratified using machine learning to identify tumors with distinct chromosomal alterations. Multiobjective metabolic flux analysis is employed to predict CL pathways in curated genome-scale metabolic models. Validation of metabolic rewiring predicted by CLIM were examined using 3-^{2}H-glucose, 4-^{2}H-glucose and 2,3,3-^{2}H-serine to probe the one carbon metabolism. Oxidative MTHFD2 flux was quantified using innovative combinatorial tracer study with ^{2}H-formate and 4-^{2}H-glucose. We utilized gain- and loss-of-function assays in multiple cell-lines to show utility of the predicted CL targets in TNBCs with chromosomal amplifications. Conclusion: Our integrated platform successfully identifies CL gene pairs to decipher novel metabolic targets specific to chromosomal alterations across many cancer types. Importantly, targets identified by CLIM are based on quantitative flux analysis. This approach reveals functional connection between CL pairs, thereby providing a mechanistic understanding of emerging lethality. This is critical in developing therapeutic interventions that selectively target cancer cells, with minimal off-target or side effects.

#6038

KDM2B regulates Serine-Glycine-One Carbon (SGOC) metabolism by targeting the SGOC enzyme genes via a combination of direct and indirect epigenetic mechanisms

Evangelia Chavdoula[1], Vollter Anastas[1], Allesandro La Ferlita[1], Julian Aldana[1], Giuseppe Carota[2], Mariarita Spampinato[2], Sameer Parashar[1], Ilaria Cosentini[3], Burak Soysal[1], Giovanni Nigita[1], Michael Freitas[1], Philip Tsichlis[1]. *[1]The Ohio State University College of Medicine, Columbus, OH,[2]Department of Biomedical and Biotechnological Sciences, University of Catania, Catania, Italy,[3]Department of Clinical and Experimental Medicine, Bioinformatics Unit, University of Catania, Catania, Catania, Italy*

Our earlier studies had shown that overexpression of the JmjC domain histone demethylase KDM2B renders mouse embryo fibroblasts (MEFs) resistant to oxidative stress due to the role of KDM2B in the regulation of antioxidant mechanisms. Here we present evidence that the knockdown of KDM2B in basal-like breast cancer cell lines results in a decrease of Glutathione (GSH) levels, a secondary increase of intracellular ROS levels and in enhanced sensitivity to deubiquitinase inhibitors. The expression of the Glutamate-Cystine antiporter, the Glutamate-Cysteine Ligase GCLC/GCLM and the Glutathione Peroxidase GPX4, all of which regulate GSH abundance was not affected. To address the mechanism of the GSH regulation we carried out RNA-Seq, quantitative proteomics and metabolomics analyses in shKDM2B- and empty vector-transduced MDA-MB-231 cells. The results showed that the KD of KDM2B causes major shifts in metabolism and that one of the metabolic pathways whose activity depends on KDM2B is the SGOC pathway, which has a major role in GSH biosynthesis. Experiments in cultured cells confirmed the importance of KDM2B in the regulation of this pathway and they also showed that the inhibition of the pathway via the KD of KDM2B is partly responsible for the shKDM2B-induced inhibition of cell proliferation in culture and in xenograft experiments in NSG mice. More important, the transcriptomic signature of the SGOC pathway correlates with the expression of KDM2B in basal like mammary adenocarcinomas in the TCGA database. The genes encoding the majority of the enzymes in the SGOC pathway are known to be regulated by MYC and ATF4 and our data show that both MYC and ATF4 are under the regulatory control of KDM2B. ATAC-Seq and ChIP-Seq experiments in shKDM2B and control MDA-MB-231 cells also showed that KDM2B binds the promoter region of not only MYC and ATF4, but also of the genes encoding the SGOC enzymes and that it

regulates chromatin accessibility and the abundance of H3K4me3/H3K27Ac active histone marks in these promoters. Overall, our data indicate that KDM2B regulates the SGOC pathway by targeting MYC and ATF4 and by making the promoters of the genes encoding the SGOC enzymes accessible to these regulators. Overall, our data provide new evidence on SGOC regulation, and identify novel KDM2B-dependent metabolic vulnerabilities in basal like breast cancer.

#6039

ELOVL5 affects prostate cancer cell proliferation and modulates the AR pathway

Silvia D. Rodrigues[1], Caroline Ribeiro[1], Isadora Teixeira[1], Hubert Pakula[1], Giuseppe N. Fanelli[2], Fabio Socciarelli[1], Lisa Butler[3], Johannes Swinnen[4], Massimo Loda[1]. *[1]Pathology and Lab Medicine, Weill Cornell Medicine, New York, NY,[2]University of Pisa, Pisa, Italy,[3]University of Adelaide, Adelaide, Australia,[4]University of Leuven, Leuven, Belgium*

Prostate cancer (PCa) is characterized by alterations in lipid metabolism, exemplified by increased rates of *de novo* lipogenesis and elongation by fatty acid elongase enzymes known as ELOVLs (elongation of very long chain fatty acids). We have previously shown that the ELOVL family members ELOVL2, 5, and 7 are Androgen Receptor (AR)-regulated proteins; and that ELOVL5 is overexpressed in both primary and castration-resistant prostate cancer. To confirm the role of ELOVL5 activity in prostate carcinogenesis, we generated genetically engineered mouse models (GEMM) with deletion of *Elovl5*, validated by immunohistochemistry, in combination with the overexpression of c-Myc, an oncogene known to affect lipid metabolism in cancer cells. As expected, we observed alterations in the lipid profile of the murine prostate with the partial deletion of *Elovl5*, as determined by a significant reduction in levels of phosphatidylcholine (PC) and phosphatidylethanolamine (PE) with long-chain fatty acids (22 carbons) and increased levels of PE with short-chain fatty acids (14 carbons), suggesting an overall shortening on acyl chains of the most common phospholipid species. Interestingly, we also observed that the heterozygous deletion of *Elovl5* reduced the expression levels of the AR on the anterior lobe of the murine prostate, in comparison to tissue from *Elovl5* wild type mice. Preliminary data also indicates a modulation in

prostate volume when *Elovl5* is genetically deleted in comparison to tissue from wild type mice. Heterozygous *Elovl5* deletion did not affect healthy tissue.To explore biological effects, we generated a 3D organoid line derived from the prostate of mice with homozygous deletion of *Elovl5* and overexpression of c-Myc. We found that *Elovl5 knock-out* decreased organoid diameter and proliferation of c-Myc-driven cells compared to *Elovl5 WT*. This effect was potentiated when organoids were treated with Enzalutamide, suggesting that targeting *Elovl5* may sensitize prostate cells to anti-androgen therapy.Our findings suggest lipid elongation via ELOVL5 as a potential therapeutic target for PCa.

#6040

The CHST11-CP-iron axis contributes to NSCLC stemness

Li-Jie Li[1], Wei-Min Chang[2], Michael Hsiao[1]. *[1]Genomics Research Center, Academia Sinica, Taipei, Taiwan,[2]School of Oral Hygiene, College of Oral Medicine, Taipei Medical University, Taipei, Taiwan*

The emerging advances in cancer therapies have changed the landscape for the treatment, but there are limited treatments options for advanced non-small-cell lung cancer (NSCLC). Cancer stem cell-induced chemoresistance and tumor metastasis accounts for treatment failure and recurrence in NSCLC. Additionally, the up-regulated glycosaminoglycan-chondroitin sulfate (CS) biosynthesis pathway contributes to the mesenchymal state of lung cancer and related to unfavorable prognosis. Previously, we found carbohydrate sulfotransferase 11 (CHST11), a key CS biosynthetic enzyme, was associated with tumor progression and metastasis in NSCLC as well as lung fibrosis. Furthermore, ceruloplasmin (CP) acted as a downstream effector of CHST11 through interferon-γ signaling pathway stimulation and increased NSCLC metastatic features. However, the linkage between metabolic dysregulation and NSCLC stemness remains unclear. Here, we found not only overexpression of CHST11 but also CS-A treatment, the metabolite of CHST11, promoted NSCLC tumor sphere formation, the expression of cancer stemness markers, and transcriptional activities of stemness-related pathways. Iron was a necessary ion in upregulating cancer stemness properties such as tumor-initiation, metastasis and chemoresistance. We found both CHST11 and iron enhanced NSCLC tumorigenesis. Moreover, iron chelation disrupted CHST11-CP axis

induced-stemness. The combination of iron chelator with chemotherapies showed the synergistic effect on antitumor as well as anti-cancer stemness and further promoted apoptosis. Our findings implicate that the CHST11-CP-iron axis facilitates tumor progression and cancer stemness in NSCLC. A regimen that combines an iron chelator and chemotherapies targeting cancer stem cells will benefit for not only preventing NSCLC tumorigenesis but cancer recurrence.

#6041

Investigating metabolic dependencies of group 3 medulloblastoma

Derek Dang[1], Kyle S. Smith[2], Pooja Panwalkar[3], John McKolay[3], Olamide Animasahun[4], Abhinav Achreja[4], Deepak Nagrath[4], Paul A. Northcott[2], Sriram Venneti[3]. *[1]University of Michigan, Ann Arbor, MI,[2]Department of Developmental Neurobiology, St Jude Children's Research Hospital, Memphis, TN,[3]Department of Pathology, University of Michigan, Ann Arbor, MI,[4]Department of Biochemical Engineering, University of Michigan, Ann Arbor, MI*

Medulloblastomas (MB) are the most common pediatric brain malignancy. Transcriptomic, genomic, and epigenomic insights have stratified these tumors into four distinct subtypes: SHH, WNT, Group 3 and Group 4. Of the four subtypes, Group 3 tumors bear the worst prognosis. Each MB subtype is distinguished by their unique transcriptome profile and epigenetic landscape. Metabolic reprogramming is a hallmark of cancer and allows cells to actively promote the utilization of nutrients to support their uncontrolled proliferation. We identified distinct transcriptional metabolic profiles in medulloblastomas. We found that Group 3 MB show upregulation of key anabolic pathways. We then cross-referenced these data from comprehensive single-cell RNA sequencing profiles of cerebellar developmental niches. We found that Group 3 MB exhibits metabolic signature similar that of early progenitors, rhombic lip progenitors, and cerebellar ventricular zone derivatives. Finally, we identify DLAT, the E2 subunit of the pyruvate dehydrogenase complex, as a uniquely upregulated gene in Group 3 MB. Knockdown of DLAT inhibited tumor growth in-vitro and in-vivo suggesting a potential targets for future therapeutic regimens.

#6042

Targeting metabolic vulnerabilities in MET-driven lung cancer brain metastases

Kasey R. Cargill[1], Sanja Dacic[2], Riyue Bao[1], Bharathri Sivakama[1], Eric S. Goetzman[1], Steven J. Mullett[1], Stacy G. Wendell[1], Sameer Agnihotri[1], Laura P. Stabile[1], Timothy F. Burns[1]. *[1]University of Pittsburgh, Pittsburgh, PA,[2]Yale School of Medicine, New Haven, CT*

Non-small cell lung cancer (NSCLC) has the highest incidence of brain metastases (BM) with almost 40% of lung cancer patients developing BM throughout the course of their disease. The presence of BM portends an extremely poor prognosis even when extracranial disease is controlled and remains a major clinical problem. To date, there are no BM-specific targeted therapies available. MET is a receptor tyrosine kinase that, upon binding hepatocyte growth factor (HGF), mediates proliferation, epithelial-mesenchymal transition, invasion, angiogenesis and metastasis. The MET pathway has emerged as a targetable oncogenic driver of NSCLC BM; however, almost half of patients with *MET* alterations fail to respond to MET tyrosine kinase inhibitors (TKIs). Interestingly, we identified a significant enrichment of *MET* amplification in lung adenocarcinoma (LUAD) BM (16%) compared to primary LUAD (3%) or liver metastases (5%). Subsequent RNA-sequencing and Gene Set Enrichment Analysis of *MET*-amplified and non-*MET* amplified LUAD BM identified many dysregulated pathways including those involved in cellular metabolism. In contrast to previous reports in melanoma which found that oxidative phosphorylation was the dominant metabolic pathway in BM, we found that genes involved in glycolysis and glutamine catabolism were increased in the high MET expressing cell lines compared to low MET expressing cell lines. We confirmed glycolytic pathway up-regulation by evaluating the activity of hexokinase 1 and 2 (HK1, HK2), glutaminase (GLS), and lactate dehydrogenase (LDHA) in a *MET*-amplified metastatic line (H1993) compared to a *MET* wild-type NSCLC cell line (H2073) derived from the same patient. Further, bioenergetic analysis revealed that H1993 cells were more metabolically active, generated higher levels of ATP, and exhibited increased glycolysis compared to H2073 cells. The enhanced metabolic activity of H1993 cells increased their susceptibility to glucose deprivation and metabolic inhibitors, supporting that metabolic reprogramming is important for MET-driven disease. Additionally, untargeted metabolomics

of *MET* amplified compared to non-*MET* amplified cells identified alterations in numerous amino acid catabolism pathways, including glutathione biosynthesis among other novel pathways. Treatment with the MET TKI capmatinib similarly reduced glycolysis-associated gene expression, oxygen consumption, extracellular acidification, and amino acid catabolism generating a metabolic phenotype more comparable to non-*MET* amplified NSCLC. Together, our data show *MET*-amplified NSCLC BM undergo metabolic reprogramming, which can be inhibited to suppress tumor growth. Current and future experiments are exploring whether we can specifically target *MET* altered BM with glycolytic inhibitors.

#6043

Manipulation of mitochondrial metabolism, through SIRT3 agonists, in a novel immunoreactive melanoma organoids model

Azza M. El-derby[1], Nadeem Wajih[1], Jack Arbiser[2], Konstantinous Votanopoulos[3], Shay Soker[4]. *[1]Wake Forest Institute for Regenerative Medicine, Wake Forest School of Medicine, Winston-Salem, NC,[2]Department of Dermatology, Winship Cancer Institute, Emory University School of Medicine, Atlanta, GA,[3]Department of Surgery, Wake Forest Baptist Health, Wake Forest Comprehensive Cancer Center, Wake Forest School of Medicine, Winston-Salem, NC,[4]Department of Surgery, Wake Forest Baptist Health, Wake Forest University, Wake Forest Institute for Regenerative Medicine, Wake Forest Comprehensive Cancer Center, Wake Forest School of Medicine, Winston-Salem, NC*

The interplay between tumor cell metabolism and immune cells in the tumor microenvironment has emerged as a determinant factor in cancer progression and treatment. Sirtuin 3 (SIRT3) is a mitochondrial deacetylase that modulates ROS levels and governs many enzymes that regulate mitochondrial metabolism and homeostasis. SIRT3 has a dual role in cancer; it is regarded as an oncogene and tumor suppressor gene simultaneously. It has tumor-promoting action via keeping ROS levels low and favoring cell proliferation; on the contrary, it can trigger cell death under stress conditions by modulating tumor cell glycolysis. Recent data suggest a role for SIRT3 in cancer immunology with PD-L1 levels are found to be inversely associated with SIRT3 level in cervical cancer, and CD8+ T cells from SIRT3 knockout donor mice exhibited low GVHD in

recipients. In this study, we explored the potential role of SIRT3 agonists in sensitizing the immunoreactivity of melanoma cells in a novel immunoreactive melanoma organoids model. We used the B16-F10 melanoma cell line spheroids to determine the effects of SIRT3 agonists on cellular viability, using an ATP assay. Validation of SIRT3 expression was determined via Western blot. Non-toxic amounts of SIRT3 agonists were also applied to melanoma organoids prepared from patient-derived metastatic melanoma from a lymph node. Preliminary results revealed a significant decrease in the viability of the organoids treated with R-propranolol (20μM) and Imipramine blue (0.25μM) agonists. We further investigated the effect of SIRT3 agonists R-propranolol and Imipramine blue on immunotherapy targeting PD-1, Pembrolizumab (100 nM) and Nivolumab (100 nM), and CTLA-4 inhibitor Ipilimumab (100 nM). We found a limited effect of Pembrolizumab and Nivolumab. Anti-tumor cytotoxicity was markedly increased in combination of Imipramine blue with Pembrolizumab and R-propranolol with Nivolumab. We propose that these effects are mediated through the activation of the endogenous immune cells and/or via the regulation of the PD-L1 and NKD2 ligand expression levels in the melanoma cells to become more sensitized to immune cells. Further studies will aim to validate these results in immunoreactive organoids from both mice and human patients. Our studies will shed light on the immune and metabolic axes and the use of specific agonists to develop new immune therapy treatment strategies for melanoma.

#6044

Identification and molecular characterization of cancer cells survived under glucose starvation

Elimelech Nesher[1], Bar Levi[2], Hadas Levy[2], Raichel Cohen-Harazi[2], Igor Koman[2]. *[1]Ariel University, Ari'el, Israel,[2]Molecular Biology, Ariel University, Ari'el, Israel*

Tumors are heterogeneous, consisting of different cell subpopulations to allow tumor survival in variable conditions. We observed the survival of a small percentage of HCT116 cells under glucose starvation. We hypothesized that these cells represent a previously undescribed subpopulation able to adjust their metabolism in the absence of glucose. Here we aimed to characterize the metabolic and molecular properties

allowing these cells to survive. We propagated individual clones from HCT116 cells and further analyzed a single clone descendants were able to survive glucose starvation. Biochemical and molecular analyses were performed under standard glucose conditions, under glucose starvation during adaptation period, and under glucose starvation after resumption of proliferation. Metabolic analysis by Seahorse revealed that surviving cells completely shifted their metabolism from glycolysis to oxidative phosphorylation. LC-MS metabolomics analysis revealed that during senescence-like adaptation the cells accumulate metabolites required for NAD synthesis. FAD, a co-factor involved in the TCA cycle, was not found in the dormant cells, while higher levels of carnosine, essential for ROS elimination, were observed. The metabolic shift toward enhanced oxidative phosphorylation was accompanied by increased production of ROS leading to DNA damage, reflected in an upregulation of the genes NUPR, ST6GAL1, and EGRF as observed by RNAseq. Cells that resumed proliferation were also characterized by enhanced expression of DNA damage repair genes and upregulated subunits of ATP-synthase, a key enzyme in oxidative phosphorylation. We suggest that cells predisposed to effective DNA repair have more time and capabilities to adjust their metabolism and to survive.

#6045

Role of PP2A methylation on methionine dependence of cancer

Anna Andronicos, Da-Wei Lin, Yi-Chen Su, Mari Ishak Gabra, Mei Kong, Peter Kaiser. *University of California, Irvine, Irvine, CA*

Dependence on exogenous methionine is a well-known, but poorly understood cancer-specific metabolic requirement. Although most cancer cells can convert homocysteine to methionine, they are unable to grow when methionine depleted media is supplemented with homocysteine. In contrast, non-tumorigenic cells proliferate well in homocysteine media. Previous work from our laboratory has shown that cancer cells cultured in homocysteine medium increase metabolic flux towards the transsulfuration pathway, away from S-adenosylmethionine (SAM) synthesis resulting in overall reduced methylation potential. We have shown that methionine sensing occurs independently of the mTOR pathway, which is known to link amino acid abundance and cell growth. Instead, our results suggest that

Protein Phosphatase 2A (PP2A) methylation is sensitive to changes in the SAM/SAH ratio. Reduced PP2A methylation correlates with reduced cell proliferation in homocysteine medium. Furthermore, overexpression of the PP2A demethylase Pme1 forcibly reduces PP2A methylation and induces methionine dependence in cells that normally proliferate in homocysteine medium. These findings suggest a model that links methionine metabolism to cell cycle progression via regulation of PP2A methylation. Here we use quantitative proteomics to define changes in B-subunit binding to PP2A during methionine starvation to investigate the molecular mechanism of this methionine dependence seen in cancer.

#6046

Enhanced *Acod1* expression in cancer cells promotes immune evasion

James H. Schofield[1], Joseph Longo[2], Sean Murphy[1], Ryan Sheldon[2], Mark A. Hawk[1], Emma Albano[1], Russell G. Jones[2], Xin Lu[1], Zachary T. Schafer[1]. *[1]University of Notre Dame, Notre Dame, IN,[2]Van Andel Research Institute, Grand Rapids, MI*

The monoclonal antibody αPD-1 used in immune checkpoint blockade (ICB) therapy has made a substantial impact in clinical outcomes for melanoma, lung, and breast cancer patients. Despite the success of ICB in these contexts, such strategies are not universally effective due to unresponsiveness or development of resistance by the malignant cells. Poor understanding of the molecular mechanisms leading to ICB resistance is a crucial barrier to more effective ICB. Recent studies have demonstrated that the metabolic milieu of the tumor microenvironment (TME) can modulate the anti-tumor immune response. However, the specific mechanisms by which the secretion of cancer cell metabolites into the TME impacts the efficacy of ICB in unresponsive tumors remains poorly understood. To better characterize the factors that influence ICB, we utilized a murine model (*Smad4$^{-/-}$/Pten$^{-/-}$/Trp53$^{-/-}$)* of castration-resistant prostate cancer (CRPC) that is responsive to αPD-1. Serial culture and passage of residual tumor cells following exposure to αPD-1 treatment into new recipient mice allowed us to develop an ICB-insensitive CRPC cell line. Unbiased metabolic analysis revealed that the αPD-1 resistant cells produced elevated levels of itaconate, a metabolite whose biological functions in epithelial cells remain poorly characterized. Consistent with this finding, the resistant

cells display increased expression of aconitate decarboxylase 1 (*Acod1*), the enzyme responsible for itaconate production. Additionally, we have identified established human epithelial cancer cell lines which express high levels of *ACOD1*. Interestingly, conditioned media (CM) from the *Acod1*-high cell lines, but not the *Acod1*-low lines, restricts the proliferation and activation of naïve CD8+ T cells *in vitro*. CRISPR-mediated *Acod1* reduction in the αPD-1 insensitive cells (Acod1KO) produces CM which promotes increased naïve CD8+ T proliferation and activation, suggesting a link between Acod1 abundance in cancer cells and the activity of cytotoxic T cells. Furthermore, Acod1KO tumors have increased CD8+ tumor infiltrating lymphocytes (TILs) and increased sensitivity towards αPD-1 ICB *in vivo*. Taken together, these data suggest that cancer cell intrinsic ACOD1 abundance may be predictive of ICB efficacy.

#6047

ZFTA-RELA fusion aberrantly drives glutamine metabolism in lethal pediatric ependymomas

Siva Kumar Natarajan[1], James Haggerty-Skeans[2], Joanna Lum[2], Pranav Narayanan[2], Stefan Sweha[2], Sushanth Sunil[2], Pooja Panwalkar[2], Jill Bayliss[2], Peter Sajjakulnukit[2], Derek Dang[1], Abhinav Achreja[3], Deepak Nagrath[3], Costas Lyssiotis[2], Sriram Venneti[1]. *[1]Pathology, University of Michigan Medical School, Ann Arbor, MI,[2]University of Michigan Medical School, Ann Arbor, MI,[3]Biomedical Engineering, University of Michigan Medical School, Ann Arbor, MI*

Ependymomas are fatal brain malignancies with very few treatment options. More than 70% of supratentorial (ST) ependymomas harbor fusions of the zinc-finger containing, chromatin modifier ZFTA and the transcriptional activator of NF-κB signaling, RELA. Oncogene-driven metabolic reprogramming is a fundamental hallmark of cancer that enables sustained tumor proliferation. ZFTA-RELA fusion protein is essential for tumorigenesis and our goal is to determine how it drives metabolism in ST-ependymomas. To address this, we developed an *in vitro* isogenic system by expressing the ZFTA-RELA fusion protein in immortalized mouse neural stem cells (ZFTA-RELA^{FUS}). Using this system, we show that these tumor cells selectively upregulate expression of the glutamine transporter

(SLC1A5), glutaminase (GLS), and many downstream enzymes in the glutamine metabolic pathway. Therefore, we hypothesized that the ZFTA-RELA fusion drives glutamine metabolism in ST-ependymomas. We further demonstrate that ZFTA-RELA^{FUS} tumor cells utilize glutamine to maintain redox homeostasis and show marked cell death upon its withdrawal. Moreover, JHU-083, a specific pharmacologic inhibitor of glutaminase, killed ZFTA-RELA^{FUS} tumor cells *in vitro* and *in vivo*. To summarize, our results suggest that the ZFTA-RELA fusion expressing tumor cells exhibit strong glutamine dependence, and targeting it has significant therapeutic relevance.

#6048
OGT/CDK5/ACSS2 axis regulates breast cancer brain metastatic growth
Emily Esquea, Lorela Ciraku, Giang Le Ming, Mauricio Reginato. *Drexel University College of Medicine, Philadelphia, PA*

Brain metastases (BMs) in breast cancer patients is considered an end-stage event, with no effective drug treatment and a median survival after diagnosis measured in months. Currently, there are no effective drug treatment for BM patients, thus there is an urgent need to develop novel treatment strategies. Breast cancers that metastasize to the brain must adapt to lack of lipid availability in the brain environment and are highly dependent on fatty acid synthesis for growth and survival. However, the signaling pathways that regulate precursors of fatty acid synthesis and lipid metabolism in breast cancer brain metastatic (BCBM) tumors are not known. Here, we show that BCBM cells can generate acetyl-CoA, a major metabolite feeding lipid biosynthesis, via phosphorylation of acetyl-CoA synthetase 2 (ACSS2) by the cyclin-dependent kinse-5 (CDK5) regulated by the nutrient sensor O-GlcNAc transferase (OGT). Breast cancer cells selected to metastasize to the brain contain higher levels of O-GlcNAcylation, OGT. and ACSS2-Ser267 phosphorylation compared to parental cells, and we show that human breast cancer brain metastatic patient samples contain elevated ACSS2-Ser-267 levels. Additionally, overexpression of the OGT, CDK5, or ACSS2-S267D phospho-mimetic mutant confers a growth advantage of breast cancer cells in the brain *in vivo.* Importantly, we show that ACSS2 is required for breast cancer growth

in the brain but not in the mammary fat pad. Pharmacologically targeting the CDK5 or ACSS2 with respective small molecule inhibitors reduces tumor growth in orthotopic *ex vivo* brain slice model. These results suggest a crucial role for OGT/CDK5/ACSS2 signaling axis to regulate lipid metabolism in BCBM cells and identify CDK5 and ACSS2 as novel therapeutic targets for treatment of breast cancer brain metastatic growth.

#6049

Exogenous serine promotes cancer stem cells in oral squamous cell carcinoma

Stacy Ann Jankowski, Nina C. Hardy, Maria A. Kukuruzinska. *Molecular & Translational Medicine, Boston Univ. Chobanian & Avedisian School of Medicine, Boston, MA*

Cancer development and progression is associated with metabolic reprogramming of tumor cells required to meet their proliferative, bioenergetic and survival challenges. Some metabolites, including a non-essential amino acid, serine, have been shown to play a role in tumorigenesis by promoting aggressive cell states, such as cancer stem cells (CSCs). Previous studies from our laboratory showed that the nuclear branch of the Wnt/β-catenin signaling pathway, the β-catenin/CBP/MLL1 axis, enhanced CSC states during oral squamous cell carcinoma (OSCC) evolution through H3K4 trimethylation (H3K4me3) and epigenetic remodeling of the chromatin landscape. Given that metabolism has also been shown to modulate cell plasticity via epigenomic modifications, we have aimed to decode the relationship between serine synthesis and cell identity in OSCC.

We have shown that under serine starvation conditions, OSCC cells upregulate steady-state mRNA and protein levels of serine synthesis pathway enzymes. The latter is associated with an increase in the by-product, alpha-ketoglutarate (αKG), a co-substrate for nuclear αKG-dependent dioxygenases, which demethylate histone marker H3K27me3 and de-repress differentiation-associated genes. Furthermore, increased production of αKG is associated with downregulation of the β-catenin/CBP/ML11 complex and CSC-associated H3K4me3.

In this study, we used human OSCC cell lines CAL27 and HSC3, derived from a primary tongue tumor and a metastatic site, respectively. Each cell

line was cultured in either complete medium or serine starvation medium. Serine starvation conditions led to a downregulation of H3K27me3 along with H3K4me3, promoting a switch from cancer stem cell to differentiation-enhancing chromatin landscape. The observed changes in cell plasticity were further investigated through tumorsphere formation, a surrogate assay for cancer stem cells. We found that OSCC CAL27 and HSC3 cells readily formed tumorspheres replete with stem cell markers BMI1, KRT14 and SOX2, under non-adhesive conditions when grown in complete media, supporting our findings that utilization of exogenous serine enables OSCC cells to maintain stemness. Our findings suggest that a switch from exogenous serine uptake to the endogenous serine biosynthesis promotes OSCC cell differentiation concomitant with the loss of CSC identity.

#6050

Analysis of diverse metabolic pathways using bioluminescent cell-based assays

Donna Leippe, Natasha Karassina, Mike Valley, Kayla Sylvester, Jolanta Vidugiriene. *Research and Development, Promega Corporation, Madison, WI*

Cellular energy metabolism is a complex system of many interconnected metabolic pathways that govern both cell health and function. Cancer cells are adept at quickly switching between metabolic pathways to adapt to nutrient limitations in the environment, enhancing their growth advantages while negatively impacting other cells in the tumor microenvironment such as immune cells. To facilitate metabolic characterization of cancer cells, we developed assays for detection of metabolites involved in key pathways, such as glycolysis and glutaminolysis, using a bioluminescent NADH detection technology coupled to specific dehydrogenases. We have now extended these assays to include metabolites involved in glycogen, lipid, ketone body and amino acid metabolism, as well as intermediates in the TCA cycle such as malate, isocitrate, and 2-hydroxyglutarate. A second core bioluminescent hydrogen peroxide detection system was also used to develop an assay for pyruvate. Here we describe the use of these assays to measure metabolite levels in cell lysates and cell culture media collected from cancer cell lines plated in 96- or 384-well plates and in 2D or 3D

cultures. Changes in metabolite levels were monitored in response to altered media composition and drug treatments. Levels were also compared between different cell lines. In comparative studies of glioblastoma cell lines, 2-hydroxyglutarate production was higher in cells expressing mutant isocitrate dehydrogenase. By reconfiguring the NADH detection technology to measure cellular enzyme activity rather than metabolite levels, we were able to detect activity of dehydrogenases that participate in the glycolysis pathway, the TCA cycle, and pentose phosphate pathway. Assays for cellular malate dehydrogenase, isocitrate dehydrogenase and other dehydrogenase enzymes were sensitive, requiring ≤ 400 lysed cells per assay. The expanded collection of bioluminescent assays provides a way to quickly characterize the metabolic states and behaviors of cancer cells to help identify pathways that may present therapeutic targets.

#6051

Dissecting unique metabolic vulnerabilities in triple-negative breast cancer metastasis

Divya Ramchandani[1], Liron Yoffe[1], Arshdeep Singh[1], Linda Vahdat[2], Vivek Mittal[1]. *[1]Weill Cornell Medicine, New York, NY,[2]Dartmouth Cancer Center, Lebanon, NH*

Introduction. Triple-negative breast cancer (TNBC) exhibits the worst outcome due to an aggressive clinical course, high rates of metastasis, and therapeutic resistance. Lack of effective FDA approved anti-metastatic targeted therapies has generated an unmet medical need for developing effective novel treatments. Targeting metastatic seeding and colonization remains a therapeutic challenge. Only recently, attention has been drawn to the idea that cancer cells selectively and dynamically adapt their metabolism along the changing microenvironments of the metastatic cascade. However, the precise nature of the metabolic reprograming *in vivo* is poorly understood and constitutes a major barrier in formulating a rationally designed therapeutic approach. Using a genetic lineage tracing approach, we identified a discrete subpopulation of highly metastatic SOX2/OCT4+ cells within primary tumors that exhibit enhanced invasion and metastasis, increased self-renewal, higher chromosomal instability, and marked resistance to chemotherapy. We posited that this lineage tracing

system may allow assessment of precise metabolic alterations as a function of tumor progression directly *in vivo*.
Methods and data. Transcriptomic analysis of sorted cellular fractions from progressing primary TNBC tumor identified metabolic heterogeneities between metastatic SOX2/OCT4+ and the SOX2/OCT4- counterparts. SOX2/OCT4+ metastatic cells exhibited elevated levels of mitochondrial respiration (OXPHOS) and fatty acid (FA) metabolism; a finding supported by proteomic analysis. Using a combination of CRISPR knockout of key pathway genes, seahorse metabolic flux analysis, metabolomics, and stable isotope tracing, we provide evidence for increased dependence of the metastatic SOX2/OCT4+ population on these unique metabolic adaptions. Importantly, we have identified upstream regulators of these pathways and demonstrate impact of both genetic and pharmacological inhibition of the metabolic regulatory networks on metastasis *in vivo*.
Conclusion. By identifying metabolic adaptations unique to the metastatic compartment of the primary tumor, we provide evidence for using clinical grade pharmacological inhibitors including metformin, tetrathiomolybdate and FA pathway inhibitors like TVB-2640 and BMS-303141, as an anti-metastatic approach in TNBC. This knowledge of metabolic remodeling could therefore be employed as a next-generation therapeutic approach for high-risk TNBC patients.

#6052
Metabolic consequences of casein kinase 2α inhibition in lymphoid leukemia
Diwakar Bastihalli Tukaramrao[1], Arati Sharma[2], Dhimant Desai[2], Sinisa Dovat[1]. *[1]Department of Pediatrics, Penn State College of Medicine, Hershey, PA,[2]Department of Pharmacology, Penn State College of Medicine, Hershey, PA*

Overexpression of casein kinase 2α (CK2α) is a common feature in lymphoid leukemias. Constitutively active CK2α can disable transcriptional activity of lymphoid transcription factors like IKAROS that act as metabolic gatekeeper and limit the energy supply needed for oncogenic transformation of B cells. Our studies have shown that pharmacological inhibition of CK2α can restore the transcriptional activity of IKAROS and ablate leukemia. However, the role of CK2α in glucose metabolism has not

been fully studied in B and T acute lymphoblastic leukemia (ALL). Therefore, in the present study we explored the metabolic alterations induced by the pharmacological inhibition of CK2α in B and T ALL. We studied the effect of CK2α inhibition using a specific inhibitor - CX4945 on cell proliferation, glucose utilization, lactate production, and intracellular ATP levels using established methods in human B-ALL (NALM6) cell line. Effect of CX4945 on glycolysis was studied using the Seahorse cell analyzer in human B (NALM6 and 697) and T (MOLT4 and 697) ALL cell lines. Metabolomics study was undertaken to analyze differential metabolite profiling in NALM6 cells treated with CX4945 compared to vehicle using LC-MS/MS based methods. Results showed that CX4945 induced apoptotic cell death in ALL cell lines with IC50 concentrations ranging between 4-10 μM. CX4945 treatment significantly affected the glucose consumption in NALM6 cells. Similarly, substantial decrease in intracellular ATP and lactate levels compared to vehicle was recorded. CK2α inhibition significantly decreased the glycolytic activity in B- and T-ALL cell lines. It was observed that glycolytic reserves were significantly decreased in 697 (3-fold), MOLT4 (4-fold), CEM (3-fold) cells incubated with CX4945 in comparison to vehicle. The principal component analysis from metabolomics study showed a clear separation between CX4945 and vehicle-treated NAML6 cells. Sixty-four statistically significant, differentially expressed metabolites were recorded in the study. Analyte classes included TCA cycle intermediates, nucleic acids and their precursors as well as glycolysis intermediates that were significantly affected by CK2α inhibition. In conclusion, our study shows that selective inhibition of CK2α by CX4945 caused energy deficiency and cell death in ALL cell lines. CK2 inhibition targeted the key energy dependent pathway by rendering ALL cells inefficient in utilizing glucose and operating glycolysis for generation of cellular energy. These results offer a new mechanistic understanding of CK2α inhibition mediated ablation of ALL.

#6053

Sulfation is required for prostate cancer xenograft tumor formation but is dispensable for cell viability*in vitro*

Ko-Chien Chen[1], Yonhong Liu[1], Chenchu Lin[1], Er-Yen (Nick) Yen[1], Francesca Citron[1], Xingdi Ma[1], Tan Lin[1], Philip Lorenzi[2], Florian Muller[3], Ronald DePinho[1]. *[1]UT MD Anderson Cancer Center, Houston,*

TX,[2]Department of Bioinformatics and Computational Biology, UT MD Anderson Cancer Center, Houston, TX,[3]Sporos Bioventures, Houston, TX

Sulfation of proteins, carbohydrates, lipids, and xenobiotics is an essential post-translational modification (PTM) process thought to play critical roles in diverse biological processes ranging from detoxification, cell signaling, and extracellular matrix architecture, to immune modulation. Sulfation is accomplished by the universal sulfate donor, PAPS (3'-Phosphoadenosine-5'-phosphosulfate), which is synthesized by bifunctional enzymes PAPSS1 and PAPSS2 (PAPS synthases). The PAPSS2 gene situates near PTEN and is frequently deleted with PTEN across cancer types. Approximately 20% of prostate cancer patients exhibit loss of PTEN, and ~50% of these cases also sustain a loss of PAPSS2. However, the loss of PAPSS2 appears to be tolerated and possibly compensated by its functionally redundant paralogue, PAPSS1, located on chromosome 4q24. The functional redundancy between PAPSS1 and PAPSS2 suggests that these two genes may be collateral lethality pair provided that sulfation is essential for cancer cell viability. Thus, we hypothesize that targeting PAPSS1 in PTEN/PAPSS2-null prostate cancer can generate cancer-specific vulnerabilities while leaving normal cells undisturbed. To assess this possibility, knockdown and knockout of PAPSS1 in cell lines of PAPSS2-null and PAPSS2-wildtype background were generated to characterize cell viability *in vitro* and tumor formation *in vivo*. PAPS and APS, an intermediary product of the sulfation pathway, are measured to verify that no alternative pathways for sulfate donors exist and that the co-extinction of PAPSS1/2 eliminates all avenues of generating sulfate donors. Combined extinction of PAPSS1/2 across multiple cancer cell lines was shown to be tolerated *in vitro*, and recurrent changes in morphology were observed. Loss of sulfation verified by the disappearance of sulfotyrosine and mass spectrometry measurements of PAPS and APS are pending. Our *In vitro results* surprisingly indicate that a major PTM, like sulfation is entirely dispensable for cancer cell viability under normal culture conditions. However, PAPSS1/2-null cell lines demonstrated a profound delay in tumor formation and prolonged survival, suggesting that sulfation may be required for stromal and innate immune modulation.

#6054

Weight specific effects of hyaluronic acid on glioblastoma's energy metabolism and bio-molecular content

Ashwin A. Bale[1], Brendan Harley[1], Rohit Bhargava[2]. *[1]Department of Chemical and Biomolecular Engineering, University of Illinois at Urbana-Champaign, Urbana, IL,[2]Department of Bioengineering, University of Illinois at Urbana-Champaign, Urbana, IL*

Glioblastoma (GBM) is one of the deadliest forms of brain cancer with inter and intra tumor heterogeneity and altered cell metabolism pathways. Developing multi-dimensional *in vitro* platforms can help explore different tumor micro-environments and can thus offer therapeutic opportunities. For a molecular-level understanding, non-destructive and label-free imaging techniques combined with *in vitro* tumor models offer discovery and automation potential for targeted studies. Here, we use the Fourier Transform Infrared (FTIR) spectroscopic imaging technique to profile biomolecular behavior of U87-MG GBM cell lines in a 2D culture in varied metabolic and tumor micro-environment conditions. As a micro-environmental cue, we chose to vary different molecular weights of hyaluronic acid (HA), a key component of brain's extra-cellular matrix (ECM) and known to significantly influence cell-behavior. U87-MG cell lines were cultured for 72 hours in a DMEM supplemented with combinations of (i) glucose concentration: absent (0 mM), normal (5.5 mM) and elevated (25 mM) and (ii) molecular weights of 2 μg/ml HA: low (10 kDa)-LMW, medium (60 kDa)-MMW and high (500 kDa)-HMW. Fixed cells at different timepoints were imaged with FTIR and stained for HA-specific CD44 and RHAMM markers. Supernatant media was analyzed for metabolite expressions with LC/MS. FTIR study revealed that the Phosphate I/Amide II and Amide I/Amide II IR absorbance ratios were significantly influenced in the presence of 500 kDa HA. Visible differences in the phosphate (~1080 cm^{-1}) and lipid (~2936 cm^{-1}) intensities indicated signs of DNA breakages and changes in oxidative stress levels. Areas under the peaks representing α-helix (decrease) and β-sheet (increase) proteins revealed signs of protein denaturation in HMW HA cultures. These cultures also revealed elevated RHAMM expressions while the CD44 expression remained relatively unchanged. Metabolic profiling with LC/MS revealed an increase in metabolites like choline, histidine, and creatine, for cells cultured in the 0 mM glucose and HMW HA. Ornithine and Methionine

remained relatively unaffected by the HA weight but showed some dependence on changing glucose levels. Proline and Tyrosine majorly showed HA weight-specific variations. Overall, this preliminary study has shown the impact of glucose and HA weight-specific effects on the biomolecular content and metabolic profiles of cancer cells. Most of the altered metabolite expressions seen are known to be involved in the Arginine-biosynthesis pathway which suggests a possible alteration in the same in response to environmental glucose and weight-specific HA levels. Further studies would involve the use of multi-dimensional hydrogel-cell models to assess variations in a more bio-mimetic surrounding. Highlighting altered metabolic pathways could help present novel therapeutic targets for future.

#6055

Polyaneuploid cancer cells are metabolically active and utilize lipid droplets to survive toxic stress

Laurie Gayle Kostecka, Anne Le, Sarah Amend, Kenneth J. Pienta. *Johns Hopkins University School of Medicine, Baltimore, MD*

Over 30,000 men in the U.S. die from metastatic prostate cancer each year. Metastatic cancer remains incurable as a population of cancer cells within a tumor are resistant to all known therapies. Despite decades of research, the source of therapeutic resistance is still unknown. We have identified the polyaneuploid cancer cell (PACC) state as a chemo-resistant cell state that is associated with therapeutic resistance. Cells in the PACC state are large in size, have high genomic content, and represent the majority cell state following high dose chemotherapy *in vitro*. While the PACC state has been documented in patient samples of many cancer types, including prostate cancer where it is associated with progression, the survival mechanisms that enable the PACC state remain largely undefined. We discovered that cells in the PACC state are highly metabolically active and contain a higher number of lipid droplets (LDs) than the non-polyploid parental cells they are derived from. LDs act as central anti-lipotoxic organelles and sequestration of toxic moieties into LDs allows for lower lipotoxicity in cells and higher chances of survival and future proliferation. Higher levels of LDs are associated with increased tumor aggressiveness and chemotherapy resistance. We found that PLIN1 (an exclusive LD surface protein), and

DGAT1 (an enzyme that catalyzes the generation of TAG, which is the main component of LDs) are expressed at higher levels in the tumors of prostate cancer patients with lower disease-free survival and higher Gleason score. This indicates that aggressive prostate cancer is most likely associated with high levels of LDs. We hypothesize that cells entering the PACC state survive chemotherapeutic stress by having an elevated metabolism and sequestering toxic lipids into LDs to enhance cell survival. Metabolomic and lipidomic data demonstrate that PACCs have a highly active TCA cycle and higher overall lipids in multiple classes compared to the parental cells they are derived from. Additionally, utilizing flow cytometry and imaging, we found that LDs form in cells accessing the PACC state as early as three hours post chemotherapy treatment, suggesting a crucial role for avoiding lipotoxicity. We also observed low levels of HSL (a rate limiting enzyme in lipolysis) in the PACC state indicating that after PACCs form LDs they do not immediately break them down, another possible mechanism of avoiding lipotoxicity. We have shown this in four cancer cell lines from two tumor types (Prostate cancer: PC3, DU145, and LNCaP. Breast cancer: MDA-MB-231) with three classes of chemotherapies (cisplatin, docetaxel, etoposide), proving the observed phenotype is not specific to any one cell line, tumor type, or drug class. Our future work will focus on inhibiting lipid droplet formation *in vivo* and *in vitro* to increase cellular lipotoxicity in the PACC state to induce cancer cell death.

#6056

A nested case-control study of untargeted plasma metabolomics and lung cancer risk among never-smoking women in the prospective Shanghai Women's Health Study

Mohammad L. Rahman[1], Xiao-Ou Shu[2], Douglas Walker[3], Dean P. Jones[4], Wei Hu[1], Bu-tian Ji[1], Batel Blechter[1], Jason YY Wong[1], Qiuyin Cai[2], Gong Yang[2], Tu-Tang Gao[5], Wei Zheng[2], Nathaniel Rothman[1], Qing Lan[1].
[1]Division of Cancer Epidemiology and Genetics, National Cancer Institute, Rockville, MD,[2]Division of Epidemiology, Vanderbilt University School of Medicine, Nashville, TN,[3]Division of Environmental Health, Emory University School of Public Health, Atlanta, GA,[4]Medicine, Emory

University, Atlanta, GA,[5]Epidemiology, Shanghai Cancer Institute, Shanghai, China

Background: The etiology of lung cancer among never-smokers is unclear despite 15% of cases in men and 53% in women worldwide are not smoking-related. Metabolomics provides a snapshot of dynamic biochemical activities, including those found to be driving tumor formation and progression. This study used untargeted metabolomics with network analysis to agnostically identify network modules and independent metabolites in pre-diagnostic blood samples among never-smokers to further understand the pathogenesis of lung cancer.
Methods: Within the prospective Shanghai Women's Health Study, we conducted a nested case-control study of 395 never-smoking incident lung cancer cases and 395 never-smoking controls matched on age. We performed liquid chromatography high-resolution mass spectrometry to quantify 20,348 unique metabolic features in plasma. Because metabolic features are expected to be highly correlated and more likely to be involved in biological processes as a network of intertwined features than individually, we agnostically constructed 28 network modules using a weighted correlation network analysis approach. The associations between metabolite network modules and individual metabolites with lung cancer were assessed using conditional logistic regression models, adjusting for age, body mass index, and exposure to environmental tobacco smoke. We accounted for multiple testing using a false discovery rate (FDR) < 0.20.
Results: We identified a network module of 122 metabolic features enriched in lysophosphatidylethanolamines that was associated with all lung cancer combined ($p = 0.001$, FDR = 0.028) and lung adenocarcinoma ($p = 0.002$, FDR = 0.056) and another network module of 440 metabolic features that was associated with lung adenocarcinoma ($p = 0.014$, FDR = 0.196). Metabolic features were enriched in pathways associated with cell growth and proliferation, including oxidative stress, bile acid biosynthesis, and metabolism of nucleic acids, carbohydrates, and amino acids, including 1-carbon compounds.
Conclusions: Our prospective study suggests that untargeted plasma metabolomics in pre-diagnostic samples could provide new insights into the etiology of lung cancer in never-smokers. Replication and further characterization of these associations are warranted.

#6057

Association of liver cancer and chronic liver disease with urinary glyphosate and its metabolites in Thailand

Daxesh P. Patel[1], Benjarath Pupacdi[2], Siritida Rabibhadana[2], Leila Toulabi[1], Majda Haznadar[1], Bhavik Dalal[1], Mohammed Khan[1], Joshua Stone[1], Vajarabhongsa Bhudhisawasdi[2], Nirush Lertprasertsuke[3], Anon Chotirosniramit[3], Chawalit Pairojkul[4], Chirayu U. Auewarakul[5], Thaniya Sricharunrat[6], Kannika Phornphutkul[7], Suleeporn Sangrajrang[8], Anuradha Budhu[1], Chulabhorn Mahidol[2], Xin W. Wang[1], Frank J. Gonzalez[1], Mathuros Ruchirawat[9], Christopher A. Loffredo[10], Curtis C. Harris[1], TIGER-LC Consortium. *[1]NIH-NCI, Bethesda, MD,[2]Chulabhorn Research Institute, Bangkok, Thailand,[3]Chiang Mai University, Chiang Mai, Thailand,[4]Khon Kaen University, Khon Kaen, Thailand,[5]Chulabhorn Royal Academy, Princess Srisavangavadhana College of Medicine, Bangkok, Thailand,[6]Chulabhorn Royal Academy, Chulabhorn Hospital, Bangkok, Thailand,[7]Rajavej Hospital, Chiang Mai, Thailand,[8]National Cancer Institute, Bangkok, Thailand,[9], Office of Higher Education Commission, Ministry of Education, Center of Excellence on Environmental Health and Toxicology, Bangkok, Thailand,[10]Georgetown University Medical Center, Washington, DC, MD*

Background: Glyphosate, the primary weed-killing ingredient in Roundup®, is the most widely used herbicide worldwide. The World Health Organization's International Agency for Research on Cancer (IARC) Monographs Program classified glyphosate is a probable human carcinogen (Group 2A), capable of causing human cancer under some circumstances. Methods: We analyzed urine specimens from 848 sequential patients with liver cancer and matched non-cancer controls from five different regional hospitals in Thailand. Gas chromatography electrospray ionization mass spectrometry (GC-ESI/MS) technique was used to measure glyphosate and its metabolites aminomethylphosphonic acid (AMPA) and phosphoric acid (PPA) to study their levels in hepatocellular carcinoma (HCC), intrahepatic cholangiocarcinoma (CCA), and chronic liver disease (CLD) in comparison to matched population controls.

Findings: Significantly higher levels of glyphosate were found in CLD patients compared to cancer cases and population controls, while significantly elevated levels of both AMPA and PPA were observed in HCC and CLD patients. Glyphosate and its metabolites were also detected at low to moderately high levels in convenience samples of food products and drinking water.
Interpretation: These results raise concern about the potential role of glyphosate in chronic human liver disease and cancer.

Multi-omics Tumor Profiling

#6062
Viral genome structure correlates with patterns of somatic alteration in human papillomavirus associated head and neck squamous cell carcinoma
Jeremiah Ray Holt[1], Xiaobei Zhao[1], Hyo Young Choi[2], Paul Little[3], Angela L. Mazul[4], Benjamin Wahle[4], Vonn Walter[5], Jose P. Zevallos[6], David Neil Hayes[1]. *[1]Medicine - Hematology/Oncology, University of Tennessee Health Science Center, Memphis, TN,[2]Preventive Medicine, University of Tennessee Health Science Center, Memphis, TN,[3]Public Health Sciences Division, Biostatistics Program, Fred Hutchinson Cancer Research Center, Seattle, WA,[4]Otolaryngology—Head & Neck Surgery, Washington University School of Medicine, St. Louis, MO,[5]Public Health Sciences, Penn State College of Medicine, Hershey, PA,[6]Otolaryngology, University of Pittsburgh, Pittsburgh, PA*

Integration of viral DNA into the host genome has been implicated in human papillomavirus (HPV) associated tumorigenesis, and studies in HPV associated head and neck squamous cell carcinoma (HNSCC) attempting to classify viral integration status have reported associations among HPV status, viral load, and overall survival. However, few genomic studies have correlated HPV structure with commonly occurring somatic mutations in HNSCC. Here, we conducted hybrid-capture DNA sequencing using a panel of over 800 cancer related genomic targets, as well as probes specific for the full HPV16 and HPV18 genomes, in a novel cohort of 525 HNSCC cases. Paired reads were aligned to a human reference containing complete

viral genomes, including all high-risk HPV types, which allowed for robust identification of HPV(+) tumors and specific HPV type. Variant calling and filtering, followed by pathway analysis of significantly mutated genes, defined the catalog of somatic driver alterations in HNSCC. Viral genome structure, integration status, and viral load were determined via initial copy number analysis of HPV-specific reads, followed by identification of viral/human breakpoints and indels with variant calling algorithms. Manual review was required in some cases due to variability in read coverage and alignment to HPV genome. We identified 252 HPV(+) tumors, the majority of which were HPV16 (n=228, 90%). Analysis of HPV16(+) tumors revealed five classes with variable viral loads: pure episome (EPI, n=54), episomal rearranged (EPI-R, n=51), episomal chimeric (EPI-C, n=22), integrated (INT, n=92), and integrated deleted (INT-A, n=12). Integrated tumors had at least one integration event (INT) and a few exhibited recurrent deletions in the viral genome (INT-A). Episomal samples had either complete HPV genomes (EPI), circular genomes with one or more indels (EPI-R), or circular genomes with HPV and human DNA (EPI-C). Interestingly, PIK3CA, the most frequently mutated gene in HPV(+) HNSCC, was mutated at a higher frequency in all integrated samples compared to all episomal types (44% vs 23%, p=0.005). We also noticed more deleterious mutations in innate immunity genes (HLA-A/B, B2M, TRAF3, BIRC3) in the episomal samples (16% vs 8%), which may allow cells with intact HPV genomes to evade anti-viral immune responses. Additionally, mutations in oxidative stress response genes that lead to the constitutive activation of NRF2 (NFE2L2, CUL3, KEAP1) were more frequent in integrated samples (11% vs 4%), which could confer radiotherapy resistance and a worse prognosis. Overall, using DNA sequencing and integrative genomic analysis in the largest cohort of HPV(+) HNSCC to date, we developed a novel classification method based on viral genome structure which associates with host somatic alterations that may contribute to variable outcomes in HNSCCs.

#6063

Genomic characterization of non-small cell lung cancer (NSCLC) brain metastasis (BM) patients identifies novel alterations associated with tropisms and disease progression

Henry Walch[1], Anna Skakodub[1], Kathryn R. Tringale[1], Harish N. Vasudevan[2], Jordan Eichholz[1], Daniel W. Kelly[1], Emily Lebow[1], Nelson S. Moss[1], Kenny Kwok Hei Yu[1], Bob T. Li[1], Boris Mueller[1], Atif Khan[1], Yao Yu[1], Simon Powell[1], Jorge S. Reis-Filho[1], Brandon S. Imber[1], Pedram Razavi[1], Daniel R. Gomez[1], Nikolaus Schultz[1], Luke R. G. Pike[1].
[1]Memorial Sloan Kettering Cancer Center, New York, NY,[2]University of California San Francisco, San Francisco, CA

Intro: Half of all patients with NSCLC develop BM during their clinical course. While modern NSCLC-directed agents yield excellent systemic response, most patients require focal BM treatment. Prior reports of BM genomics have been limited by low numbers and a lack of matched specimens. Here, we report the largest cohort to date of molecularly-profiled NSCLC BM samples with comprehensive clinical follow-up.
Methods: Clinical data and outcomes for 244 patients with NSCLC and resected BM were identified. Samples were assessed using MSK-IMPACT, a custom tumor-normal next generation sequencing assay. 51 (20.9%) patients had matched primary site tissue, and 44 (18%) patients had matched tissue from another metastatic site or CSF. Genomic alterations were filtered for driver variants using OncoKB. Publicly available genomic data for NSCLC primary samples was used for comparison against the primary samples from our BM cohort.
Results: The most frequently altered genes in BM tumors were *TP53* (72%), *CDKN2A* (34%), *KRAS* (31%), *KEAP1* (26%), and *EGFR* (21%). *CDKN2A* was more frequently altered in BM samples compared to NSCLC primary lesions (34% vs 14%, $p = 0.003$). Additionally, cell cycle pathway alterations were enriched in BM (56% vs 31%, $p = 0.002$). BM samples also had a significantly higher fraction of genome altered (FGA) relative to primary samples ($p < 0.0001$). We then compared primary samples from BM patients against primary samples from metastatic NSCLC patients without BM and primary samples from non-metastatic NSCLC patients. We found an enrichment of alterations in *TP53* (68.6% vs 27.7%, $p < 0.0001$), *NKX2-1* (11.4% vs 1.7%, $p = 0.006$), *SMARCA4* (11.4% vs 2.1%, $p = 0.01$), *RB1* (11.4% vs 1.7%, $p = 0.006$), and *FOXA1* (11.4% vs 0.9%, $p = 0.001$) in the primary samples from BM patients compared to non-metastatic patients. Next, we grouped patients based on CNS progression patterns and found that *EGFR* alterations were enriched in patients with leptomeningeal

progression when compared to patients without progression (42% vs 18%, p = 0.03).
Conclusions: In our cohort of molecularly-profiled NSCLC BM, we found an enrichment of cell cycle pathway alterations and a higher FGA in BMs compared to their primary tumor controls. Additionally, several genes were enriched in the primary tissue of patients that developed BM compared to primary tissue from non-metastatic patients. *EGFR* alterations were enriched in patients who develop leptomeningeal disease (LMD). Our work herein characterizes the genomic profiles of NSCLC patients with BM and identifies specific genes enriched in the primary tissue of BM patients compared to primary tissue from both non-BM metastatic patients and non-metastatic patients. Finally, our finding that *EGFR* alterations were enriched in patients with LMD suggests specific biologic underpinnings driving patterns of CNS progression.

#6064

Patient-partnered research enables germline characterization of angiosarcoma predisposition genes

Hoyin Chu[1], Marissa Hollyer[1], Seunghun Han[2], Sabrina Y. Camp[1], Riaz Gillani[3], Eliezer Van Allen[1], Nikhil Wagle[1], Corrie A. Painter[4], Saud H. AlDubayan[1]. *[1]Medical Oncology, Dana-Farber Cancer Institute, Boston, MA,[2]Harvard Medical School, Boston, MA,[3]Pediatric Oncology, Dana-Farber Cancer Institute, Boston, MA,[4]Cancer Program, Broad Institute, Cambridge, MA*

Background: Angiosarcoma (ASC) represents 1-2% of soft tissue sarcomas. Due to its rarity, to date, no large-scale studies have been done to systematically identify ASC-predisposition genes and the broader landscape of pathogenic germline variants in patients with ASC remains unclear.
Methods: Through the Angiosarcoma Project, an ongoing patient-partnered research approach that allows patients living anywhere in the U.S. or Canada with angiosarcoma to participate through a website, blood and saliva samples were collected from more than 300 patients and whole-exome-sequencing was performed. Machine-learning frameworks were used to identify germline short variants (SNPs, indels) and rare germline copy number variants (CNVs). The pathogenicity of variants in 107 curated cancer-predisposition and sarcoma-related genes were evaluated according

to the ACMG guidelines. A short-variant-based gene-burden analysis was then performed using 223 unrelated ASC patients and 4557 ancestry-matched unrelated cancer-free controls.
Results: In total, 38 patients (17.04%) carried at least one pathogenic short variant, including 37 carrying germline heterozygous pathogenic variants in POT1 (9, 4.04%), BRCA2 (3, 1.35%), CHEK2 (3, 1.35%), MUTYH (3, 1.35%), BRCA1 (2, 0.90%), PRF1 (2, 0.90%), ERCC3 (1, 0.45%), TP53 (2, 0.90%), ATM (1, 0.45%), TSHR (1, 0.45%), TSC2 (1, 0.45%), SDHA (1, 0.45%), SBDS (1, 0.45%), MSH6 (1, 0.45%), MITF (1, 0.45%), MET (1, 0.45%), LZTR1 (1, 0.45%), FH (1, 0.45%), ERCC2 (1, 0.45%), XPC (1, 0.45%). In addition, one patient harbored pathogenic short variants in both BRCA1 and ERCC3. In the 8 unique CNVs detected in 10 (4.55%) patients, 6 were classified as pathogenic including 3 heterozygous duplications overlapping MSH2, LZTR1, SMARCB1, and 3 heterozygous deletions overlapping NF1, MSH2, and WRN. Two unique heterozygous duplications met VUS criteria including one overlapping ERCC2 and one overlapping SMARCB1. In a comparison between ASC patients and cancer-free controls of predominantly European ancestry, we found ASC patients tobe 40 times more likely to carry a pathogenic variant in POT1 (OR: 42.91, CI: [15.40-174.08], $q < 0.001$, $p < 0.001$), while TP53 was nominally significant (OR: 7.37, CI: [1.19 - 41.13], $p = 0.037$).
Conclusion: We confirmed prior observations of POT1 being responsible for ASC and called for attention to investigate the effect of germline CNVs in ASC. Overall, the elucidation of various germline elements associated with ASC risk highlighted the value and importance of patient-partnered research, particularly for rare cancers, and the analysis support using germline testing of patients for more precise clinical management.

#6065

Patterns of dysregulated coding and noncoding gene expression in high-grade serous ovarian carcinomas

Brett M. Reid[1], Ann Chen[1], Zhihua Chen[1], Florian A. Karreth[1], Peter Kanetsky[1], Jennifer B. Permuth[1], Ozlen Saglam[2], Jamie Teer[1], Xiaoqing Yu[1], Simon Gayther[1], Ellen Goode[3], Paul Pharoah[4], Thomas A. Sellers[5], Kate Lawrenson[4]. *[1]Moffitt Cancer Center, Tampa, FL,[2]Oregon Health and Science University, Portland, OR,[3]Mayo Clinic, Rochester, MN,[4]Cedars-Sinai, Los Angeles, CA,[5]TAS Consulting, Portland, OR*

Purpose: Identifying dysregulated gene expression in ovarian cancers has been limited by a deficit of available normal tissues. Here, we generated the largest set of high-grade serous ovarian cancer (HGSOC) tumors with normal precursor tissues for transcriptome analyses.
Methods: We performed RNA sequencing on 220 primary HGSOCs and 116 benign epithelia (micro-dissected fallopian tube, ovarian surface, and inclusion cysts), and combined samples with 428 HGSOCs from TCGA, 60 HGSOCs from a prior study, and 180 bulk ovary tissues from GTEx. Raw reads were processed with a uniform bioinformatic and quality control pipeline; combined data were batch corrected. We tested for differences in median normalized CPM expression values using the Wilcoxon rank sum test with >2-fold change and a false discovery rate <1% considered statistically significant. We also conducted weighted gene co-expression network analysis in each tissue type. The hypergeometric test was used for enrichment of differentially expressed genes (DEGs) and gene ontologies within modules.
Results: Transcriptomes comprised 27,700 expressed genes (8,202 lncRNAs) across 706 HGSOCs, 180 bulk ovary, and 88 ovarian epithelia tissues. Most (~90%) genes were expressed in all tissues; 5% each showed HGSOC- or normal tissue-specific expression and ≥50% were lncRNA. Comparing HGSOCs to ovarian epithelia and to bulk ovary identified 11,804 DEGs with 4,522 lncRNAs (DElncRNA) of which ~50% were tissue-specific. DEGs included *MUC16* and multiple GWAS/TWAS implicated susceptibility genes including *RAD51*, *BRIP1*, *BNC2*, *TIPARP-AS1*, *PRC1*, *KANSL1*, *ANKLE1*, *CHMP4C*, *ESRP2*, and *CCNE1*. The most highly expressed DElncRNA in HGSOC were upregulated *RMRP* ($P=1.4x10^{-39}$), *SNHG1* ($P=3.0x10^{-27}$), and *HAGLR* ($P=2.0x10^{-24}$) at the *HOXD* risk locus. The highest expressed DElncRNA in precursor tissues was the HGSOC-downregulated *MEG3* ($P=1.7x10^{-67}$). DEGs were enriched in HGSOC co-expression modules associated with immune response, cell motility/localization, cell cycle regulation, angiogenesis, reproductive development, transcriptional regulation, and metabolic processes. Tissue-specific DElncRNA tended toward upregulation compared to ovarian epithelia with enriched modules associated with cell cycle regulation (hub=*BUB1B;* top DElncRNA *TRPM2-AS*, $P=1.5x10^{-38}$); and toward downregulation compared to bulk ovary with enriched modules associated

with chemokine signaling/response (hub= *GADD45B*, top DElncRNA *RP11-87P3.1*, P=1.7x10^{-113}).
Conclusion: HGSOC-dysregulated lncRNA expression revealed tissue-specific differences that highlight unique biological pathways in precursor epithelia and the ovarian microenvironment that contribute to HGSOC pathogenesis. Our results provide additional evidence to support previously nominated risk genes. Integration with eQTL and GWAS are underway to further elucidate novel HGSOC susceptibility genes.

#6066
Genomic analysis of end-stage renal disease
Kosuke Ieiri[1], Nobuyuki Kakiuchi[1], Tomonori Hirano[1], Tomomi Nishimura[1], Koichi Watanabe[1], Hiroko Tanaka[2], Satoru Miyano[2], Dai Takamatsu[3], Keisuke Monji[3], Eiji Kashiwagi[3], Masaki Shiota[3], Junichi Inokuchi[3], Masatoshi Eto[3], Seishi Ogawa[1]. *[1]Kyoto Univ. Graduate School of Medicine, Kyoto, Japan,[2]Department of Integrated Analytics, M&D Data Science Center, Tokyo Medical and Dental University, Tokyo, Japan,[3]Department of Urology, Graduate School of Medical Science, Kyushu University, Fukuoka, Japan*

Background: Chronic kidney disease is frequently associated with persistent inflammation, which results in fibrosis in the stroma, a reduced number of renal tubules, the formation of multiple cystic lesions, ultimately terminating in renal failure and hemodialysis. Given the high incidence of renal cell carcinoma (RCC) in hemodialysis patients, suggesting a relationship between tissue remodeling by chronic inflammation and carcinogenesis. However, little is known about the genetic background of cancer development from remaining tubules and cystic lesions in hemodialysis patients.
Method: We enrolled 5 patients under hemodialysis who were accompanied by acquired cystic kidney disease and underwent radical nephrectomy for RCC. Surgical specimens were fixed with alcohol-based solution and paraffin-embedded, and after H&E staining, subjected to laser capture microdissection (LCM) to collect remaining tubules and cysts containing approximately 200 cells. DNA was extracted and analyzed for somatic mutations and copy number alteration by whole-exome sequencing.

Result: In total, we collected 161 LCM samples, including 118 from proximal tubules, 17 from collecting ducts, and 26 from cysts. Median variant allele frequencies of detected mutations were 0.237 in proximal tubules, 0.133 in collecting duct, and 0.381 in cysts, indicating larger clonal expansion in proximal tubules and cysts than in collecting ducts. Proximal tubules and cysts contained recurrent mutations in *FAT1* (11% and 8%, respectively), *STAG2* (5% and 8%), and *PTEN* (3% and 4%), whereas no recurrent driver mutations were identified in collecting ducts. In copy number analysis, 26% of proximal tubules, 35% of collecting ducts, and 80% of cysts had copy number alterations. Of note, samples from cysts had more copy number alterations compared to remaining tubules (on average, 2.3 vs. 1.1). Proximal tubules had recurrent copy number gains of chromosomes 3, 7, 10, 18, and 20, and loss of chromosome 22 and samples from collecting ducts showed gains of chromosome 7 and loss of chromosome 18. In cysts, gains of chromosomes 2, 3, 7, 10, 12, and 16 and loss of chromosomes 15, 16, 21, and 22 were frequently observed. Copy number profile in cysts was similar to that of papillary RCC and acquired cystic disease-associated RCC.
Conclusion: In the end-stage cystic kidney, proximal tubules and cysts showed an enrichment of driver mutations commonly found in papillary RCC and RCC with acquired cystic disease, reflecting the fact that the incidence of these two types of RCC increases as the duration of dialysis becomes longer. In addition, clear cell RCC drivers, such as *VHL* mutation and loss of chromosome 3, were not observed, possibly explaining the rare occurrence of clear cell RCC in hemodialysis patients. Since cysts had more frequent copy number alterations than remaining tubules, cysts in the end-stage kidney might be precursor lesions of RCC.

#6067

Characterizing the landscape of rare structural variant events in newly diagnosed multiple myeloma

Monika Chojnacka[1], Benjamin Diamond[1], Bachisio Ziccheddu[1], Even Rustad[2], Kylee Maclachlan[3], Marios Papadimitriou[1], Eileen Boyle[4], Patrick Blaney[4], Saad Usmani[3], Gareth Morgan[4], Ola Landgren[1], Francesco Maura[1]. *[1]Myeloma Division, Sylvester Comprehensive Cancer Center, University of Miami, Miami, FL,[2]Institute for Cancer Research, Oslo University Hospital, Oslo, Norway,[3]Myeloma Service, Department of*

Medicine, Memorial Sloan Kettering Cancer Center, New York, NY,[4]Myeloma Research Program, Perlmutter Cancer Center, NYU Langone, New York, NY

Background: Structural variants (SV) are known to play a critical role in the pathogenesis of multiple cancer types. Using whole genome sequencing (WGS), we recently characterized the SV landscape of 752 newly diagnosed multiple myeloma (MM) patients, identifying 68 SV hotspots and 152 recurrent copy number aberrations (CNA; Rustad et al. Blood Cancer Discovery 2020). Despite comprehensive annotation, more than half of SVs were not linked to any known MM genomic driver. The biological impact of these SV events, here defined as rare SV, occurring in 93% (702/752) of patients, is unknown.
Methods: To study the biological impact of rare SVs, we interrogated WGS (n=752) and RNAseq (n=591) in the CoMMpass trial. Recurrent SVs identified by involvement in canonical Ig translocations, recurrent CNAs, or SV hotspots were excluded. All SVs within an event must not involve a recurrent region to be defined rare. To determine SV class-specific gene relationships, breakpoint enrichment was compared against a permuted background model for each SV class and gene expression direction, up to 1 Mb. Genes were considered affected if expression was above a gene specific outlier Z-score of +/- 2. Lastly, we modeled breakpoint density to the nearest MM superenhancer up to 10 MB, and compared to permuted background rates.
Results: Of the total 8,942 SVs, 4,959 (55%) were identified as rare. 201 (34%) patients had at least 1 enriched rare SV event associated with gene expression outliers. Amongst over-expressed gene outliers, rare templated insertions and duplications were enriched within the gene body and up to 1 MB away. Rare inversions were enriched in genes 100kb and 1MB away, and rare translocations were associated with outliers 1 MB away. Amongst under-expressed gene outliers, rare complex SVs were enriched within the gene body, while deletion SVs were enriched in the gene body and up to 1 MB away. Rare duplications, translocations and templated insertions were enriched up to 1 MB of superenhancers. Rare templated insertions were significantly enriched against the background model ($p < 0.001$, Fisher Exact). Overall, 82% (104/126) of gene outliers affected by rare templated insertions were associated with superenhancers, (95 over-expressed, e.g.

IRF6 and 9 under-expressed), 54% (130/237) by rare translocations, (105 overexpressed, e.g. *FAM46A* and 25 under-expressed), and 55% (96/172) by rare duplication events, (93 overexpressed, e.g. *MAPK13*, and 7 under-expressed). In addition, among the 853 outlier genes affected by enriched rare SVs, at least 15 are involved with B-cell development, suggesting a potential driver role in myeloma pathogenesis.
Conclusion: In summary, leveraging WGS and RNA-seq of clinical samples, we demonstrate that rare SVs are frequently associated with aberrant gene expression, expanding our understanding of their potential role in heterogenous clinical response in patients diagnosed with MM.

#6068
Methylomic, transcriptomic and immune profiles of high grade serous ovarian cancer among Black and non-Hispanic White women
Hao Huang[1], Russell Keathley[1], Ping Xie[1], JianJun Wei[2], Ernst Lengyel[3], Bin Zhang[1], Daniela Matei[1]. *[1]Department of Medicine; Hematology/Oncology Division, Feinberg School of Medicine, Northwestern University, Chicago, IL,[2]Department of Pathology, Feinberg School of Medicine, Northwestern University, Chicago, IL,[3]Department of Obstetrics and Gynecology/Section of Gynecologic Oncology, University of Chicago, Chicago, IL*

Background: Ovarian cancer (OC) is the most lethal gynecological malignancy. There remains a significant difference in outcomes among black women, whose mortality/incidence ratio is 0.68 - the highest among all ethnic groups. Little is known about racially-defined biological key determinants of OC disparity. We recently characterized transcriptomic and methylomic profiles of high grade serous ovarian tumors (HGSOC) from black vs. non-Hispanic white women (NHW) to understand the observed disparity in survival.
Methods: Nucleic acids were extracted from treatment-naïve HGSOC specimens (30 black and 26 NHW) and used for DNA methylation (EPIC array) and RNA-sequencing. Differential expression was performed using EBseq; pathway enrichment was performed using Enrichr. TIMER was used to deconvolute immune cell infiltration based on RNA-seq results, and multiplex immunohistochemistry (mIHC) was used for validation. Top

differentially expressed genes (DEGs) were validated by qRT-PCR and studied functionally.
Results: 191 and 825 genes were up- and down-regulated, respectively, in HGSOC tumors from black vs. NHW women (FDR-adjusted p-value < 0.10). Significantly enriched pathways among these DEGs included multiple classes of *GPCRs - Class A, Monoamine GPCRs, and Peptide GPCRs*. Among DEGs, calmodulin like-5 gene *CALML5,* involved in GPCR signaling, was significantly downregulated in tumors from black patients (0.086 fold-change). *CALML5* downregulation in tumors from black vs. NHW women was validated by qRT-PCR. *CALML5* knockdown by using shRNA disrupted colony and tumor sphere formation ($p<0.05$). Analysis using TIMER predicted that $CD8^+$ and $CD4^+$ memory-resting T-cells were enriched in tumors from black patients. mIHC validated increased infiltration by $CD3^+CD4^+$ and $CD4^+FOXP3^+$ lymphocytes in humors from black women, as well as increased expression of PD-L1, supporting an immunosuppressive phenotype. Global, modest hypermethylation was discovered in tumors from black vs. NHW patients: 47 CpGs were hypermethylated (FDR-adjusted p-value < 0.10) and 19 regions were differentially methylated between the two groups.
Conclusions: We identified significant transcriptomic and modest methylation differences in HGSOC tumors from black and NHW patients. Pathway enrichment within GPCR-signaling was observed and an immunosuppressive phenotype was identified. Further exploration of the contribution of these differences to clinical outcomes and treatment response in black women is needed.

#6069

Genomic and transcriptomic characterization of medullary thyroid cancer

Seong Eun Lee[1], Seongyeol Park[2], Shinae Yi[1], Joonoh Lim[2], Na Rae Choi[1], JungHak Kwak[3], June-Young Koh[2], Boram Yi[2], Jaemo Koo[2], Jae Won Chang[4], Young Seok Ju[2], Bon Seok Koo[4], Jin Man Kim[5], Young Joo Park[6], Minho Shong[7], Eun Kyung Lee[8], Jae Kyung Won[9], Yea Eun Kang[7], Kyu Eun Lee[3]. *[1]Chungnam National University, College of Medicine, Daejeon, Korea, Republic of,[2]GENOME INSIGHT THECNOLOGY Inc, Daejeon, Korea, Republic of,[3]Department of Surgery, Seoul National University*

Hospital & College of Medicine, Seoul, Korea, Republic of,[4]Department of Otolaryngology-Head and Neck Surgery, Chungnam National University, College of Medicine, Daejeon, Korea, Republic of,[5]Department of Pathology, Chungnam National University, College of Medicine, Daejeon, Korea, Republic of,[6]Department of Internal Medicine, Seoul National University Hospital & College of Medicine, Seoul, Korea, Republic of,[7]Department of Internal Medicine, Chungnam National University, College of Medicine, Daejeon, Korea, Republic of,[8]Department of Internal Medicine, National Cancer Center, Goyang, Korea, Republic of,[9]Department of Pathology, Seoul National University Hospital & College of Medicine, Seoul, Korea, Republic of

Medullary thyroid carcinoma (MTC) is a rare thyroid malignancy derived from the parafollicular C cells of thyroid gland. It features relatively aggressive biologic behavior among thyroid cancers, but its genomic landscape has not yet been fully explored. Here, we conducted multi-omics data (whole genome sequencing (WGS), and bulk (bulk RNA-seq) or single nucleus RNA sequencing (snRNA-seq)) on MTC, and found genetic characteristics of MTC and a new gene signature predicting aggressiveness of tumors. WGS was performed for 35 pairs of tumor specimens and normal thyroid tissues from 30 patients. And bulk RNA-seq for 59 samples (20 normal thyroid tissues, 26 primary MTCs, 9 recurred lymph nodes, and 4 metastatic lymph nodes) and snRNA-seq for 3 primary MTCs, and 2 recurred/metastatic lymph nodes were also performed. In WGS results, we verified driver mutations, including RET, RAS, and BRAF. Four patients were classified as germline RET mutations based on familial history. Somatic RET M918T mutations were occurred in 8 patients, 9 patients were observed other RET mutations. Also, we observed other somatic mutations such as HRAS and BRAF. Seven patients occurred somatic HRAS mutations (Q61L, Q61R, G13R, A11 and G15), and somatic BRAF mutations (G469A, K601E) were observed in two patients. We found broad-level copy-number alterations in ~50% of patients, and we also found a patient who shows whole-genome duplication. The copy-number alteration was associated with aggressive phenotype in MTC. In addition, we found complex rearrangements such as microhomology-mediated break-induced replication in five patients. Interestingly, we found intra-tumoral heterogeneity of several genes related to C cell differentiation through

snRNA-seq analysis by comparing clusters of tumor cells. Using the genes, we calculated the C cell differentiation score of the samples with bulk RNA-seq by GSVA algorithm. This score was related to poor clinical characteristics such as recurrence. In conclusion, multi-omics profiling of MTC reveals that copy number alterations and C cell differentiation status are the important biomarkers for cancer aggressiveness.

#6070

Comprehensive real-world-data based molecular profiling and mapping of non-squamous NSCLC patients to immune-checkpoint-inhibitor biomarkers

Andreas Kloetgen[1], Danyi Wang[2], Anna Coenen-Stass[1], Ioannis Gounaris[3], Julia F. Hopkins[4], Giuseppe Locatelli[1], Juergen Scheuenpflug[1], Zheng Feng[2]. *[1]Merck Healthcare KGaA, Darmstadt, Germany,[2]EMD Serono Research and Development Institute, Inc., Billerica, MA,[3]EMD Serono, Feltham, United Kingdom,[4]Foundation Medicine, Inc., Cambridge, MA*

Purpose: Non-squamous non-small cell lung cancer (nsqNSCLC) patients without detectable actionable alterations in EGFR, ALK, or ROS1, have a diverse genetic background. These patients are eligible to and usually receive untargeted, first line immune checkpoint inhibitors (ICI) and/or chemotherapy with heterogeneous outcomes. To identify potential predictive biomarkers for the stratification of nsqNSCLC patients without actionable genetic alterations, a comprehensive molecular profiling of this subpopulation was performed using the Foundation Medicine genomic database.
Methods: Molecular profiles from 53,119 nsqNSCLC patients were analyzed using the FoundationInsights^{TM} web platform. After the patients with known and likely functional short variants for EGFR and fusions for ALK and ROS1 were excluded, the prevalences for commonly altered genes were determined. Pathway analysis was conducted with Metascape. Statistical significance and enrichment in PD-L1 and tumor mutation burden (TMB) biomarker overlap with altered genes was calculated using a fisher exact test against an alteration negative cohort.
Results: nsqNSCLC patients without actionable genetic alterations can be described as a heterogenous population with different genetic alterations. We found a total of 103 genes with an individual, minimal prevalence of

>1% to be the major descriptors that collectively were found in most patients of the nsqNSCLC subpopulation. These genes relate to pathways involved in cell cycle, cell proliferation, response to growth factors or chromatin organization. Out of the most frequently altered genes, we identified those that are associated with PD-L1 or TMB high status for which ICI treatment is most effective in nsqNSCLC.
Conclusions: The results supported the lack of a general association with high PD-L1 and high TMB calls for biomarker informed treatment options for nsqNSCLC patients. We reported a subpopulation of nsqNSCLC patients that can be described by certain genetic alteration, of which some were associated with ICI-related biomarkers for which patients might benefit from a future precision oncology approach utilizing combined targeted and ICI treatment.

#6071

Whole-exome RNA sequencing of metastatic synovial sarcomas reveals heterogeneous transcriptomic profile and targetable co-alterations: Cohort study from the French Sarcoma Group

Helene Vanacker[1], Mehdi Brahmi[1], Yannick Le Meitour[2], Julien Bollard[2], Valery Attignon[3], Alexandra Meurgey[4], Myriam Jean-Denis[5], Laurie Tonon[3], Shibani Pokras[6], Erika Klohe[7], Michael Nathenson[8], Kristin Blouch[9], Ioanna Eleftheriadou[10], Jean-Yves Blay[1], Franck Tirode[2], Armelle Dufresne[1]. *[1]Medical Oncology Department, UNICANCER Centre Léon Bérard, Lyon, France,[2]CITI department, Centre de Recherche contre le Cancer de Lyon (CRCL), Lyon, France,[3]Department Of Clinical Research And Innovation, UNICANCER Centre Léon Bérard, Lyon, France,[4]Bio-pathology platform, UNICANCER Centre Léon Bérard, Lyon, France,[5]Department Of Translational Research And Innovation, UNICANCER Centre Léon Bérard, Lyon, France,[6]Oncology Cell & Gene Therapy, Global Medical, GSK, Collegeville, PA,[7]Oncology Experimental Medicine Unit, GSK, Collegeville, PA,[8]Oncology Cell & Gene Therapy, GlaxoSmithKline, Collegeville, PA,[9]Oncology Clinical Development, GlaxoSmithKline, Collegeville, PA,[10]Oncology Experimental Medicine Unit, GlaxoSmithKline, Collegeville, PA*

Introduction: Synovial Sarcoma (SS) is a rare and aggressive disease that predominantly occurs in young adult. SS are characterized by a pathognomonic t(X:18) translocation leading SS18: SSX1/2/4 fusion. Small studies (n<100) described molecular background beyond this fusion in patients and the transcriptomic profile of SS remains poorly known. The aim of our study is to provide a large cohort analyzing transcriptomic and co-alterations to better understand and treat SS.
Methods: We present a clinico-biological cohort study including all adult patients with histologically confirmed diagnosis of afvanced SS from January 2000, registered in the French Sarcoma database (NETSARC+) and with available formalin-fixed paraffin embedded (FFPE) archival tumor samples and clinical data. FFPE tumor samples were analyzed by dedicated whole-exome RNA-sequencing (WERS) to assess transcriptomic, small nucleotide variation (SNV) and fusions.
Results: 122 patients (133 samples) met the study criteria, including 11 patients with paired primary-metastatic tumor samples. Clinical characteristics (age, sex, tumor grade, primary and metastasis site distribution) were consistent with expected SS population. The SS18:SSX1/2/4 fusion was found in all patient (90% by WERS and if negative, by FISH). Unsupervised analyses of transcriptomic data by principal component analyses, hierarchical sample clustering or UMAP revealed heterogeneity in gene expression. Clinical factors (age, sex, grade, tumor type, complete response to treatment, survival) did not correlate with transcriptomic profiles. Immune cell analyses confirmed a low infiltration of immune cells, notably poor in CD8+ T cells. Cancer testis antigens such as NYESO-1, MAGE-A4 were both expressed with a heterogeneous co-expression of other CTAs across samples. In the 11 primary-metastatic paired- samples, no gene pathway was found differentially expressed between primary and metastatic samples cohort with the exception of lung tissue specific genes. Comparing chemotherapy-naïve versus pre-treated samples did not identify differential expression of specific genes across samples. Single Nucleotide Variant analyses was reliable on 84% FFPE samples and revealed an overall low Tumor Mutational Burden with some samples harboring canonical oncogene pathogenic mutations of BTK, RAS, NF1, RB1 as well as in DNA repair pathway(15% spanning over ATM ATR,CHK2, BRCA1/2 PALB2 CHK2, FANCM, RAD51), PI3K pathways (PI3KCA E545K) and other poorly described in SS.

Conclusion: Investigating the largest cohort of metastatic SS by whole-exome RNA-sequencing, revealed Synovial Sarcoma, usually classified as “simple genomic sarcoma” is a translocation-related sarcoma harboring heterogeneous transcriptomic and numerous SNV co-alterations including targetable mutations.

#6072

Chromosomal aneuploidy, whole-genome doubling and mutational signatures in NCI PDMR models

Li Chen[1], Biswajit Das[1], Ting-Chia Chang[1], Yvonne A. Evrard[1], Chris A. Karlovich[1], Alyssa Chapman[1], Brandie Fullmer[1], Ashley Hayes[1], Ruth Thornton[1], Nikitha Nair[1], Shahanawaz Jiwani[1], Lindsay Dutko[1], Kelly Benauer[1], Gloryvee Rivera[1], Corinne Camalier[1], John Carter[1], Suzanne Borgel[1], Tiffanie Miner[1], Chelsea McGlynn[1], Justine Mills[1], Shannon Uzelac[1], Tia Shearer[1], Lauren Hicks[1], Michelle Norris[1], Carley Border[1], Sergio Alcoser[2], Thomas Walsh[1], Michael Mullendore[1], Michelle Eugeni[2], Dianne Newton[1], Melinda G. Hollingshead[2], P. Mickey Williams[1], James H. Doroshow[3]. *[1]Frederick National Laboratory for Cancer Research, Frederick, MD,[2]National Cancer Institute at Frederick, Frederick, MD,[3]Division of Cancer Treatment and Diagnosis, National Cancer Institute, Bethesda, MD*

Introduction: Structural variants (SVs) are a unique class of mutations which have certain therapeutic implications for the tumor. Certain SVs, such as chromosomal aneuploidy, whole-genome doubling (WGD), have specific therapeutic implications. The underlying cellular processes present in the tumor are reflected in mutational signatures. Here, we describe the landscape of chromosomal aneuploidy, WGD and mutational signatures in the National Cancer Institute’s Patient-Derived Models Repository (NCI PDMR) to facilitate the investigation of their roles in therapeutic responses of the preclinical models.

Method: Chromosome arm-level aneuploidy was called by scoring at the individual arm level if >90% of the arm copy number (CN) was gained/lost based on whole-exome sequencing (WES) data. Aneuploidy score was defined as number of arms with aneuploidy. WGD was determined by derived allelic specific CN, purity and ploidy from tumor/normal matched

samples and permutation test. Mutational signatures (COSMIC v3) including single base substitutions (SBS), doublet base substitutions (DBS), small insertions and deletions (ID) and CN signatures were derived using SigProfiler for specimens with somatic mutations and CNs.
Results: A large fraction (85%) of patient-derived xenograft (PDX) models (N=755) have at least one arm -level aneuploidy. Certain chromosomes and arms (7, 8, 17p and 18) are more frequently aneuploid, which might be biased due to the overrepresentation of gastrointestinal cancer in the cohort. Histology specific differences were observed in the frequency of arm level aneuploidies. For example, synovial sarcoma (SYNS) and endometrioid carcinoma (UEC) have much lower level of aneuploidy than non-small cell lung cancer (NSCLC) or clear cell renal carcinoma (ccRCC) models. 61% of PDX models (N=277) have WGD, in which certain histologies have more WGD [NSCLC: 81%, head and neck squamous cell carcinomas (HNSCC): 71%] than others. Samples having WGD have a higher degree of aneuploidy and chromosomal instability. WGD and aneuploidy remain stable along the passages in 78% PDX models. Intra-model heterogeneity of WGD was observed due to lineage difference. Mutational signatures (SBS6,15,20) indicating concurrent DNA polymerase epsilon (*POLE*) mutation and defective DNA mismatch repair were highly enriched in microsatellite instability-high models ($p<0.01$, Fisher's exact test). Among 30 PDX models where the patients had known platinum-based chemotherapy history, 40% of them had an identifiable platinum chemotherapy treatment signature (SBS31 or DBS5). Chromothripsis associated amplification signature (CN8) was enriched in models with WGD ($p<0.05$).
Conclusion: We have characterized chromosomal aneuploidy, WGD and mutational signatures in NCI PDMR models. The models with SVs can be utilized in preclinical drug studies to understand their role in therapeutic response in patients.

#6073

Distinct subtype of multiple myeloma revealed by whole genome and transcriptome sequencing

Sheehyun Kim[1], Hyundong Yoon[2], Youngil Koh[1], Sung-Soo Yoon[1]. *[1]Seoul National University Hospital, Seoul, Korea, Republic of,[2]Seoul National University Cancer Research Institute, Seoul, Korea, Republic of*

Background: Advanced sequencing technologies have contributed to identifying genomic and transcriptomic features of various types of tumors. Despite several sequencing data from multiple myeloma (MM) being generated, understanding various properties of MM remained insufficient.
Methods: The patients confirmed with MM by bone marrow examination were analyzed in the study. Myeloma cells were enriched from the bone marrow aspirates of the patients using CD138. Whole genome sequencing (WGS) and whole transcriptome sequencing (WTS) were performed for isolated myeloma cells. Mutational signatures were analyzed using somatic mutations detected by WGS.
Results: A total of 37 MM patients (median age 67) were enrolled in this study. WGS revealed somatic mutations of an average of 8872 single nucleotide variants (SNVs) and 934 insertions and deletions (Indels) from the patients, respectively. By the analysis of structural variants, 7 chromothripsis and 4 chromoplexy patients were identified. Mutational signature analysis showed that single base substitution (SBS) 9 signature largely varied between patients. SBS9 signature high patients were mostly diagnosed with non-IgG/non-IgA heavy chain and lambda light chain type myeloma. Notably, IgD myeloma patients were solely detected in the SBS9 signature high group compared to the low group ($p = 0.001$). Gene expression patterns obtained from WTS were well-divided into SBS9 signature high and low groups, and analysis of differentially expressed genes (DEG) between SBS9 signature high and low groups implied IgD myeloma features including high expression of *IGHD*. As a validation test, we tried mutational signature analysis on whole exome sequencing (WES) data of 784 MM patients from the MMRF database. Of the 38 patients with more than 500 exonic mutations, only the SBS9 signature high group had IgD myeloma candidates, whereas the SBS9 signature low group had no IgD myeloma candidate ($p = 0.014$).
Conclusions: DNA and RNA sequencing of myeloma patients could classify specific subtypes of disease categories. Further study for SBS 9 signature high and IgD myeloma is needed to discover the underlying mechanism of distinct features and to find out their clinical implication.

#6074
Germline and somatic genomic profiling of urothelial carcinoma

Bing-Jian Feng[1], Wendy Kohlmann[2], David A. Nix[2], Aaron Atkinson[2], Kenneth M. Boucher[2], Courtney Carroll[1], Jill Kolesar[3], Eric A. Singer[4], Stephen B. Edge[5], Kamal Sahu[2], Alejandro Sanchez[2], Mikaela Larson[2], Michelle L. Churchman[6], Laura Graham[7], John D. Carpten[8], Yousef Zakharia[9], Lindsey Byrne[10], Rohit K. Jain[11], Kenneth G. Nepple[9], Ahmad Shabsigh[10], Jad Chahoud[12], Sumati Gupta[2]. *[1]University of Utah, Salt Lake City, UT,[2]Huntsman Cancer Institute, Salt Lake City, UT,[3]University of Kentucky, Lexington, KY,[4]Rutgers Cancer Institute of New Jersey, New Brunswick, NJ,[5]Roswell Park Comprehensive Cancer Center, Buffalo, NY,[6]M2Gen, Tampa, FL,[7]University of Colorado, Aurora, CO,[8]University of Southern California, Los Angeles, CA,[9]University of Iowa, Iowa City, IA,[10]Ohio State University Comprehensive Cancer Center, Columbus, OH,[11]Moffitt Cancer Center, Tampa, FL,[12]Moffit Cancer Center, Tampa, FL*

Urothelial carcinoma (UC) presents most frequently as bladder cancer and is the most common cancer of the urinary system in the United States. UC relapse and progression are common and impose a significant negative impact on the lives of patients and healthcare resources. To elucidate the biological mechanisms of UC and find novel biomarkers, we analyzed the clinical and genomic data in the Oncology Research Information Exchange Network (ORIEN). We conducted gene-based and gene-set based association tests on rare germline variants comparing the exome sequencing of 336 UC patients and genome sequencing of 366 healthy controls (42 unrelated individuals from the Centre d'Etudes du Polymorphisme Humain [CEPH] families and 324 from the University of Utah Heritage 1000 [H1K] Projects). The analysis of loss-of-function (LoF) variants revealed that the forkhead box (FOX) J2 gene set was significantly associated with UC at the genome-wide level (Bonferroni-corrected p-value=0.01). Genes in this gene set contain a motif that matches the FOXJ2 transcription factor binding site. Firth-penalized Cox proportional hazard regression on overall survival identified LoF variants in genes down-regulated in naive CD8 T cells to be associated with worse prognosis (Bonferroni-corrected p-value=0.032, hazard ratio=28.2, and 95% confidence interval 6.66 to 119.0). In exome sequencing of tumor tissues, we searched for driver genes and pathways by testing for higher variant allelic fractions than the genome average. The tests yielded eleven genes with genome-wide significance (**Table 1**). By

gene set analysis using the MSigDB Hallmark database, significant pathways included the P53 pathway ($p<2x10^{-16}$), Wnt beta-catenin signaling ($p<2x10^{-16}$), E2F targets ($p=8x10^{-13}$), PI3K/AKT/mTOR signaling ($4x10^{-7}$), and apoptosis ($p=9x10^{-7}$). These results reveal the germline predisposition variants and somatic oncogenic drivers in UC and suggest immune evasion as a contributing factor for poor clinical outcomes in UC patients.

Table 1: Genes with high allelic fractions

Gene	**P-value**	**Number of Variants**
TP53	$<2x10^{-16}$	203
RB1	$2.42x10^{-16}$	67
ELF3	$2.06x10^{-7}$	38
TSC1	$4.05x10^{-7}$	32
KMT2D	$7.59x10^{-7}$	91
ZFP36L1	$8.80x10^{-7}$	33
CDKN1A	$2.47x10^{-6}$	40
FGFR3	$1.11x10^{-5}$	37
ARID1A	$1.28x10^{-5}$	62
SMARCA4	$1.53x10^{-5}$	17
PIK3CA	$2.00x10^{-5}$	53

#6075

Comprehensive genomic characterization of early-stage bladder cancer from 438 patients by whole genome- and exome sequencing

Frederik Prip[1], Philippe Lamy[1], Iver Nordentoft[1], Sia Viborg Lindskrog[1], Trine Strandgaard[1], Karin Birkenkamp-Demtröder[1], Gregers G. Hermann[2], Astrid C. Petersen[3], Veronika Bahlinger[4], Marc-Oliver Grimm[5], Marcus Horstmann[6], Karin Mogensen[7], Roman Nawroth[8], Ulrika Segersten[9], Danijel Sikic[10], Kim E. M van Kessel[11], Tobias Maurer[12], Tatjana Simic[13], Arndt Hartmann[4], Ellen C. C. Zwarthoff[11], Per-Uno Malmström[9], Torben Steiniche[14], Jørgen Bjerggaard Jensen[15], Núria Malats[16], Francisco X. Real[17], Lars Dyrskjøt[1]. *[1]Department of Molecular Medicine, Aarhus*

University, Aarhus, Denmark,[2]Department of Urology, Herlev Hospital, Copenhagen University, Copenhagen, Denmark,[3]Department of Pathology, Aalborg University Hospital, Aalborg, Denmark,[4]Institute of Pathology, University Hospital Erlangen, Friedrich-Alexander-University Erlangen-Nuremberg, Erlangen, Germany,[5]Department of Urology, Jena University Hospital, Jena, Germany,[6]Department of Urology, University of Duisburg-Essen, Essen, Germany,[7]Department of Urology, Herlev Hospital, Copenhagen, Denmark,[8]Department of Urology, Technical University of Munich, Klinikum rechts der Isar, Munich, Germany,[9]Department of Surgical Sciences, Uppsala University, Uppsala, Sweden,[10]Department of Urology and Pediatric Urology, University Hospital Erlangen, Friedrich-Alexander-University Erlangen-Nuremberg, Erlangen, Germany,[11]Department of Pathology, Erasmus MC Cancer Institute, Erasmus University Medical Center, Rotterdam, Netherlands,[12]Department of Urology and Martini-Klinik, University of Hamburg-Eppendorf, Hamburg, Germany,[13]Faculty of Medicine, University of Belgrade, Institute of Medical and Clinical Biochemistry, Belgrade, Serbia,[14]Department of Pathology, Aarhus University, Aarhus, Denmark,[15]Department of Urology, Aarhus University, Aarhus, Denmark,[16]Spanish National Cancer Research Center (CNIO) and CIBERONC, Genetic and Molecular Epidemiology Group, Madrid, Spain,[17]Spanish National Cancer Research Center (CNIO) and CIBERONC, Epithelial Carcinogenesis Group, Madrid, Spain

Background: The genomic landscape of cancer is complex and includes mutations and copy number alterations (CNAs) that affect several cancer related pathways and drive tumor evolution. Non-muscle-invasive bladder cancers (NMIBC) are largely orphan for integrative genomic studies. Large studies are needed to delineate the genomic complexity and heterogeneity of NMIBC.

Methods: A total of 438 patients with NMIBC were analyzed, 296 of which were part of the UROMOL cohort (PMID: 27321955). The median follow-up was 5 years. The progression rate was 13% (n= 56). Whole exome sequencing (WES) was performed on DNA from tumor (~150x) and matched germline samples to call somatic mutations. Additionally, shallow whole genome sequencing (sWGS; ~2x) was performed on DNA from 362 of the tumors to quantify CNAs. RNA-sequencing was available for 414 of

the samples, and tumors were classified according to the UROMOL2021 transcriptomic classes. We identified significantly mutated genes by mutsigCV and significantly amplified or deleted regions by GISTIC2.
Results: The median tumor mutation burden (TMB) was 3.7/Mb. TMB was not associated with progression (p=0.28). A total of 61 genes were significantly mutated in the cohort, the most frequent being *FGFR3* (61%), *KDM6A* (44%) and *KMT2D* (38%). Mutations in *EP300* and *RHOB* were significantly associated with an increased risk of progression after adjusting for grade and stage (p=0.040 and 0.044, respectively). Several mutations showed a strong transcriptomic class dependent occurrence: mutations in *RB1, TP53, ERCC2* and *ERBB2* were enriched in the aggressive class 2a, *FGFR3* and *STAG2* in class 1 and class 3, and *KMT2C* and *KMT2D* in class 3.
Genome doubling was identified in 15% of the tumors. These tumors were enriched in the aggressive classes 2a and 2b and were associated with increased risk of progression (p=0.0049). In addition, we observed several significantly altered genomic regions, the most significant being deletions in 9p21.3 (*CDKN2A & CDKN2B*, 64%), 2q37.1 (*GIGYF2 & EIF4E2*, 28%) and amplification in 11q13.3 (*CCND1*, 9%). Class 2a tumors were enriched for genomic alterations in most of the significant regions. 9p21.3 was the only region with frequent homozygous losses (22%). High-level gains were prognostic of progression, independently of ploidy, stage and grade, for several regions, including 4p16.3 (*FGFR3*, p=0.00013), 17q23.2(*TBX2*, p=0.0004) and 8p11.23(*ZNF703, p*=0.011). In addition, we observed an enrichment of uniparental disomy in 4p16.3 (*FGFR3*, 8%).
Conclusion: Here we investigated the landscape of DNA alterations in NMIBC in a large patient cohort of NMIBC samples with paired transcriptomic data and detailed clinical follow-up. We identified several novel genomic alterations; specifically, we showed that 15% of the tumors had genome doublings, and we identified a complex underlying copy number landscape of the region containing *FGFR3*.

#6076
Compartment-specific multiomic characterisation of ovarian carcinosarcoma
Robert L. Hollis, Ailsa Oswald, Lorna J. Stillie, Ian Croy, Michael Churchman, Charlie Gourley, C. Simon Herrington. *University of*

Edinburgh, Edinburgh, United Kingdom

Background: Ovarian carcinosarcoma (OCS) is the most aggressive ovarian cancer type. Risk of relapse and death is high across all patient groups, including those diagnosed at early stage. OCS is biphasic, comprising both carcinomatous and sarcomatous populations, leading to its historic consideration alongside true sarcomas. However, we now recognize that OCS in fact represent metaplastic carcinomas, with the sarcomatous component having undergone complete epithelial to mesenchymal transition (EMT) from carcinoma. Detailed understanding of shared and compartment-specific OCS biology has the potential to identify therapeutic opportunities to improve patient survival.
Methods: We recently curated the largest pathologically-confirmed OCS cohort to date. Here, we perform compartment-specific profiling of 12 cases by mRNA sequencing, whole exome sequencing, microRNA (miRNA) profiling and quantification of tumor-infiltrating lymphocytes. These data paint a detailed picture of shared and compartment-specific biology between matched carcinomatous and sarcomatous compartments.
Results: The sarcomatous compartments harbored significantly fewer infiltrating CD8+ cells (P=0.006), with a significantly lower CD8+:CD3+ cell ratio compared to the carcinomatous components (P=0.002). In 11 of 12 cases, identical *TP53* mutations were identified in both cell populations; the remaining case was *TP53* wild-type in both compartments. Paired analysis of mRNA sequencing identified 1477 significantly differentially expressed transcripts at FDR<0.01. The sarcomatous compartments demonstrated significantly higher MAPK activity, as determined by the MPAS transcriptomic score (P=0.042). Principal component analysis and unsupervised hierarchical clustering of miRNA expression grouped samples by compartment (carcinomatous versus sarcomatous), rather than by patient, suggesting global differences in the miRNA landscape. Paired analysis identified 131 significantly differentially expressed miRNAs between the two populations (FDR<0.01). Significantly enriched miRNA gene targets were identified using The MiRNA Enrichment Analysis and Annotation Tool (miEAA), identifying key EMT-associated gene targets, including *SIRT1*, *PRDM16*, *ZEB1*, *ZEB2* and TGFB signaling components, among other biological processes.

Conclusions: Carcinomatous and sarcomatous compartments of OCS demonstrate marked differences in transcriptomic profiles, immune engagement and miRNA expression patterns. Identification of shared *TP53* mutations between compartments supports the notion that OCS represent metaplastic carcinomas. Shared biological events represent opportunities for targeted interventions that may be efficacious against both cell populations, while compartment-specific biological events allude to mechanisms by which the carcinomatous population undergoes EMT to form the sarcomatous compartment.

#6077

Comprehensive multi-omic characterization of genetic changes associated with sinonasal squamous cell carcinoma progression

Alka Singh[1], Nikita Babushkin[2], Michael Korzinkin[3], Viktoria Sarkisova[3], Vasudha Mishra[1], Ari Rosenberg[1], Mark Lingen[4], Justin Bishop[5], Alex Zhavoronkov[3], Nyall London[6], Nishant Agrawal[7], Xuanyao Liu[2], Evgeny Izumchenko[1]. *[1]Medicine, Section of Hematology and Oncology, University of Chicago, Chicago, IL,[2]Medicine, Section of Section of Genetic Medicine, University of Chicago, Chicago, IL,[3]InSilico Medicine, Pak Shek Kok, Hong Kong,[4]Pathology, University of Chicago, Chicago, IL,[5]University of Texas Southwestern, Dallas, TX,[6]Otolaryngology - Head and Neck Surgery, Johns Hopkins University, Baltimore, MD,[7]Surgery, Otolaryngology-Head and Neck Surgery, University of Chicago, Chicago, IL*

Approximately 50-80% of sinonasal tract cancers are sinonasal squamous cell carcinoma (SNSCC), a rare malignancy which occur in the nasal cavity and maxillary sinus. These lesions possess a propensity for local invasion into adjacent structures including the skull base, brain, and orbit. Owing to relatively mild symptoms during early stages, which resemble benign sinonasal disease, most patients are already in clinically advanced stages when diagnosed. Therefore, despite improvements in endoscopic surgical approaches, radiotherapy and imaging techniques, the 5-year overall survival for advanced SNSCC patients remains poor (~40%).
Inverted sinonasal papilloma (IP) is a locally aggressive, benign epithelial neoplasm arising in the paranasal sinuses which has a high recurrence rate and transforms to SNSCC in 10%-25% of cases. As some IP evolve to

malignant neoplasms, it has been presumed that they represent an intermediate step in SNSCC progression. However, the current tools for detecting altered epithelial cells, such as clinical examination and histological characteristics, have limited prognostic value for predicting which IP will progress to malignancy, and the link between IP and invasive disease remains unclear.
Activating mutations in EGFR and PIK3CA genes as well as loss-of-function mutations in TP53 have been reported in a few very small cohorts of IP and SNSCC lesions, suggesting their role in IP pathogenesis and progression to invasive malignancy. Other observed alterations potentially associated with malignant transition include KRAS mutations, loss of heterozygosity (LOH) at the 9p21 locus (containing p16INK4a), mismatch repair genes deficiency, amplification of FGFR1 and SOX2 genes, as well as NFκB, COX2 and HOXA9 overexpression. While these studies provide a snapshot of molecular changes in SNSCC, genetic alterations critical to the development of SNSCC are poorly understood, and the exact mechanism underlying malignant transformation remains unknown.
In this study we have used PandaOmic, a multi-omic data analysis and visualization algorithm, to perform a first comprehensive integrative analysis of WES, mitochondrial sequencing and transcriptomic data obtained from 11 IP lesions, matched invasive SNSCC tumors and histologically normal paranasal sinus epithelium collected from the same patients. Our analysis reveals heterogeneous mutational patterns, gene expression changes and signaling pathways features associated with SNSCC pathogenesis, and provides crucial insights that may aid in the development of novel means of prevention, diagnosis, and treatment of this rare, aggressive and poorly characterized malignancy.

#6079
Comprehensive characterization of FBXW7 mutational and clinicopathological profiles in human colorectal cancers
Hanlin Chen, Hua Bao, Haimeng Tang, Xue Wu, Yang Shao. *Nanjing Geneseeq Technology Inc., Nanjing, China*

Background: FBXW7 is a critical tumor suppressor gene of human colorectal cancers (CRC). However, the comprehensive profiling of FBXW7 in CRC is largely underrepresented in current studies. Herein, we

present molecular profiling of FBXW7 in human CRC cohorts and clinical outcomes.
Methods: 7626 colorectal cancer patients were retrospectively enrolled. Comprehensive genomic profiling was performed on formalin-fixed paraffin-embedded (FFPE) or fresh tumor samples using a next-generation sequencing (NGS) panel covering 425 cancer-related genes, and matching plasma samples were sequenced to exclude germline mutations. The patients' microsatellite instability (MSI) score, tumor mutation burden (TMB), and chromosomal instability (CIN) score were measured. 3541 colorectal cancer patients in the MSK MetTropism cohort with survival data were analyzed for survival outcomes and risk factors. Survival analyses were performed using the Kaplan-Meier method. 263 patients in the TCGA COAD cohort with RNA sequencing data were analyzed for immune cell infiltration and gene set enrichment analysis (GSEA). P values in multiple comparisons were FDR (false discovery rate) adjusted. Tests with P values or FDR less than 0.05 were considered statistically significant.
Results: The cohort had a median age of 59 (20-93), with 60.45% male patients. The median TMB of the cohort was 7.78 muts/Mb (1.11-655.56). There were 1227 (16.1%, >12 muts/Mb) hypermutated and 187 (2.5%, >100 muts/Mb) ultrahypermutated tumor-carrying patients. Within the cohort, a total of 7442 (97.6%) patients had identifiable microsatellite status, of which 548 (7.4%) were MSI. The FBXW7 mutation carrying rate was 17.9% (1365). Compared to FBXW7 wild type (WT) patients, FBXW7 mutated patients had higher TMB ($P < 0.001$), higher MSI score ($P < 0.001$), and lower CIN score ($P < 0.001$). In the MSK cohort, 500 (14.1%) patients with FBXW7 mutations showed better overall survival (HR: 0.67; 95%CI: 0.55-0.80, $P < 0.001$). The most mutated sites of FBXW7 were R505C (54), R465H (47), R465C (44). Among them, R465C showed worse OS in multivariate cox analysis when compared with other FBXW7 mutations (HR: 1.6; 95%CI: 1.13-3.1, $P = 0.015$), and when compared with all other mutations (HR: 1.87; 95%CI: 0.99-2.5, $P = 0.053$). In the immune cell infiltration analysis using the TCGA COAD cohort, patients with FBXW7 mutations displayed higher M1 macrophage ($P = 0.014$), CD8+ T cell ($P = 0.008$), and regulatory T cell ($P = 0.011$) infiltration rates. In the GSEA analysis, in MSI patients, 11 hallmark gene sets are significant enriched in FBXW7 mutated patients, including interferon gamma response (FDR = 0.031), allograft rejection (FDR = 0.026), etc.

Conclusions: Comprehensive profiling of FBXW7 in colorectal patients revealed that FBXW7 mutations were associated with better OS, except the FBXW7 R465C mutation was identified as an indicator for worse OS.

#6080

Comprehensive profiling of pathogenic/likely pathogenic large genomic rearrangements in pan cancer samples

Haimeng Tang, Hua Bao, Xue Wu, Yang Shao. *Nanjing Geneseeq Technology Inc., Nanjing, China*

Background: Correlations between large genomic rearrangements (LGRs) and cancer types beyond breast or ovarian cancer have not been sufficiently profiled, likely due to the highly inefficient methods of detecting these types of mutations.
Methods: This study utilized next-generation sequencing (NGS) to analyze and classify the germline LGR mutation profile in 17,025 cancer patients across 22 cancer types. We characterize novel LGRs based on predicted pathogenicity and take a closer look at genes that acquire both germline and somatic mutations within our samples. Detection method was validated using ddPCR assay of commonly investigated LGR genes.
Results: In total, 15,659 samples from across 22 cancer types were retained for analysis after filtering. We observed that, in our cohort, the cancer type with the highest proportion of LGRs are ovarian cancer (4.7%), renal cell carcinoma (2.5%), breast cancer (2%), glioma (1.8%), and thyroid carcinoma (1.8%). Annotation of detected germline variants revealed several genes containing novel LGRs including *MSH2*, *FANCA*, and *PMS2*. We observed co-mutational events between LGR in *MSH2* and somatic mutations in *BRCA2, KTM2B, KDM5A, CHD8*, and *HNF1A*. Furthermore, our analysis shows that samples with pathogenic and likely pathogenic germline LGR mutations tended to also have higher mutational burden, chromosomal instability, and microsatellite instability ratio compared to other samples with non-LGR germline mutations.
Conclusion: In this study, we demonstrated the prevalence of LGRs beyond that of *BRCA1/2* and *RB1* in breast and ovarian cancer. Our profiles of these pathogenic/likely pathogenic alterations can potentially fuel further investigations and highlight new understanding of LGRs in multiple cancer types.

Proportion of samples with large genomic rearrangements in each cancer type

Cancer Type	Germline Non-LRG P/LP proportion (%)	Germline Non-LRG P/LP proportion (%)	
Ovarian cancer (OC)	22.4	22.4	
Breast cancer (BC)	16.2	16.2	
Prostate (PRAD)	13	13	
Endometrial	13.4	13.4	
Glioma	11.7	11.7	
Pancreatic (PC)	11.3	11.3	
Neuroendocrine (NEN)	8.5	8.5	
Sarcoma	9.5	9.5	
Colorectal cancer (CRC)	9.7	9.7	
Thyroid (THCA)	8	8	
Hepatocellular carcinoma (HPC)	9.1	9.1	
Gastrointestinal stromal tumor (GIST)	9.5	9.5	
Gastric cancer (GC)	8.2	8.2	
Renal cell carcinoma (RCC)	9.3	9.3	
Cervical cancer	10.2	10.2	
Lung cancer	8.2	8.2	
Esophageal cancer	9.2	9.2	
Bladder cancer (BLCA)	8.8	8.8	
Leukemia	3.9	3.9	
Head and neck cancers (HNC)	6.7	6.7	
Lymphoma	1.2	4.8	4.8

Melanoma	0.5	4.8	4.8
Pan-Cancer	1	9.1	9.1
P/LP: Pathogenic/Likely pathogenic			
LGR: Large genomic rearrangement			

#6081
Integrative genomic analysis of primary prostate tumors and corresponding lymph node metastases
Carlos S. Moreno, Cynthia L. Winham, Emma R. Klein, Yijian Huang, David M. Schuster, Martin G. Sanda, Adeboye O. Osunkoya. *Emory University, Atlanta, GA*

Background: Prostate cancer (PCa) is a highly heterogeneous disease, and mortality is mainly due to metastases. However, the molecular underpinnings that lead to the initial steps of metastasis have not been well characterized. We have performed integrative whole exome sequencing and transcriptome analysis of primary prostate tumor foci and corresponding lymph node metastases (LNM).
Design: Primary tumor foci (PTF) and LNM from 40 patients with high-risk PCa were analyzed by RNAseq. Two or more PTF and all available LNM greater than 0.4cm were subjected to sequencing. Of these 40 patients, 17 (42.5%) had LNM and 23 (57.5%) had benign LNs. A total of 155 tissue samples (97 PTF, 39 benign LNs, and 19 LNM) were sequenced and mapped to the human transcriptome with STAR mapper after QC trimming and removal of adapter sequences using TrimGalore. Differentially expressed genes between PTF, LNM, and benign LNs were identified using DESeq2, and gene set enrichment analysis was performed using WebGestalt. WES data was analyzed using GATK pipelines including Mutect2.
Results: A median of 57 million paired-end reads were obtained per sample, with a median of 10 million total readcounts per sample across the transcriptome, and 39,021 transcripts were detected in at least 5% of

samples. Comparing PTF to LNM, 6203 transcripts were differentially expressed (p-adj < 0.01). PTF were enriched relative to LNM in gene sets associated with Wnt signaling, hormone signaling, Hippo signaling, *KRAS* signaling, and the epithelial to mesenchymal transition. Comparing PTF from metastatic patients to non-metastatic patients, 1265 transcripts were differentially expressed (p-adj < 0.01). PTF from metastatic patients were enriched in gene sets associated with cell cycle progression, oxidative phosphorylation, ER stress, fatty acid metabolism, and DNA repair. LNM gene sets were enriched in endoplasmic reticulum (ER) stress and oxidative phosphorylation. The top 500 upregulated genes in malignant tissues were significantly enriched in genes related to androgen and estrogen signaling as expected. We also identified a set of 193 genes whose expression was significantly increased in primary tumor over benign LNs and in LNM over primary tumors. This gene set was significantly enriched in genes related to oxidative phosphorylation and included oncogenes such as *PIK3CB, NCOA2*, and *SCHLAP1.* Integrative RNAseq analyses with WES will be discussed.
Conclusions: Signaling pathways associated with ER stress, oxidative phosphorylation, metabolism, and cell cycle progression are prominent in LNM of aggressive PCa. *PIK3CB, NCOA2,* and *SCHLAP1* expression are significantly increased in LNM.

#6082

Assessing difference in the tumor and immune microenvironment of BRCA1/2 mutated versus BRCA wild type high grade serous ovarian cancers

Jing Qian[1], Lynda D. Roman[2], Seeta Rajpara[1], Monica Neuman[2], Varun Khetan[2], David W. Craig[1], Joseph Carlson[3], John D. Carpten[1].
[1]Translational Genomics, Keck School of Medicine, University of Southern California, Los Angeles, CA,[2]Department of Obstetrics and Gynecology, Keck School of Medicine, University of Southern California, Los Angeles, CA,[3]Department of Pathology, Keck School of Medicine, University of Southern California, Los Angeles, CA

Ovarian cancer (OvCa) is the deadliest gynecological malignancy in the United States. Surgery and chemotherapy are the primary treatments for

OvCa, but 80% of late-stage OvCa patients experience chemo-resistant recurrence, which necessitates the development of new treatment strategies. The genomic diversity within a tumor and the interactions among various cell types within its microenvironment are considered key factors contributing to therapeutic efficacy. Specifically, women who harbor germline BRCA1 or BRCA2 mutations are at increased risk of developing high grade serous ovarian cancer (HGSC). To understand the genomic consequences, including somatic alterations, associated with defective DNA repair, tumor DNA and RNA was isolated from fresh frozen OCT embedded sections from 15 HGSC patients with BRCA1/2 mutation and 10 without any alterations in the BRCA genes (BRCA-wt). Whole exome sequencing (WES) and total RNA-seq was performed to determine the association of homologous recombination (HR) DNA repair gene defects with tumor mutation burden (TMB), neoantigen load (NL), and immunological assessment of tumor microenvironment. TMB was calculated from mutation rates of somatic WES. Germline exome analysis was used to validate inherited BRCA mutations. To identify the somatic mutations, somatic single nucleotide variants and InDels were detected using Strelka. TP53 mutations were most common with several other genes showing only modest mutation frequency. Mutation signatures were also detected with maftools and compared to the COSMIC mutational signature database. BRCA-mutated samples displayed a unique mutational signature associated with defects in HR DNA repair pathway. We also observed heterogeneity in copy number variation profiles amongst cases, as determined by the tool Sequenza. Furthermore, gene set enrichment analysis indicated differential enrichment of P53 pathway, MAPK pathway, and PTEN pathway, in addition to numerous pathways related to immune cell signaling and immune response. RNA-seq data was analyzed with CIBERSORTx and revealed different proportions of 22 immune effector cell types that accompany tumor cells within the HGSC microenvironment. Additional analyses are underway, including measuring differences in NL in BRCA-mutated versus BRCA-wt cases. This work will represent a significant advancement in our fundamental knowledge regarding the complexities of the TME and effective immunological responses in OvCa.

#6083

Extensive epigenetic and transcriptomic donor-specific differences observed in iPSC derived allogenic NK (iNK) cells

Rohith Srivas, Snehal Nariya, Melissa Rojsza, Barry A. Morse, Ohad Manor, Rupesh Amin, Luis Borges. *Century Therapeutics, Seattle, WA*

Several autologous CAR-T cell therapies have been approved for the treatment of B cell lymphomas and leukemias and a number of trials are in progress to investigate the use of allogeneic, donor derived CAR-T and CAR-NK cell therapies for multiple tumor indications. However, sourcing cell donors, editing cells and generating large batches of clinical grade allogeneic CAR-T and CAR-NK can be challenging. To overcome these difficulties, we are developing NK and T cell-based therapies derived from induced pluripotent stem cells (iPSCs). iPSCs have the capacity to be genetically engineered, enabling precise edits that can enhance the function of cell therapies, and indefinitely expanded in culture, allowing for the production of highly uniform master cell banks. Yet, an open question of this system is the extent to which the donors' genetic background shapes the phenotype of the iPSC-derived NK and T cells. To answer this question, we measured the genome-wide landscape of chromatin accessibility and gene expression in iNK cells generated from multiple donors. Donor background was linked to significant changes in chromatin accessibility (~30% of regions tested) and expression (~15% genes). We found accessibility changes at binding sites for transcription factors regulating various aspects of NK cell function, including differentiation (GATA2, EOMES, and ETS1), activation (AP-1, T-bet), and cytokine production (STAT3, STAT5), indicating that the donor background could impact the functionality of iPSC-derived NK cells. In particular, we noted that iNK cells derived from one donor, which had decreased effector functions compared to other cell lines, showed increased accessibility at BACH2 binding sites, a key negative regulator of NK cell function. iNK cells derived from this donor also showed an increase in expression of genes linked to NK cell differentiation and cell development, and a decrease in genes involved in cell cycle, cell proliferation, and inflammatory response pathways. Taken together, these data indicate the importance of assessing the impact of donor background on iPSC derived cell therapies through a variety of functional and genomic assays.

#6084

The Osteosarcoma and Leiomyosarcoma Count Me In Projects of the Cancer Moonshot funded PE-CGS Network directly engage patient participants in genomics research

Katherine A. Janeway[1], Suzanne George[1], Corrie Painter[2], Carrie Cibulskis[2], Taylor Cusher[2], Jordan Doucette[2], Elana Anastasio[2], Benjamin Zola[2], Ashley Mathews[2], Evelina Ceca[1], Maeve Smart[1], Beena Thomas[2], Jason Hornick[3], Alanna Church[4], Lorena Lazo De La Vega[1], Jill Stopfer[1], Sidney Benich[1], Ellen Sukharevsky[1], Sarah Winnicki[2], Brendan Reardon[1], Brian Crompton[1], Priscilla Merriam[1], Adrian Marino-Enriquez[3], Diane Diehl[2], Eliezer VanAllen[1], Judy Garber[1], Gad Getz[2], Stacey Gabriel[2], Timothy Rebbeck[1], Jennifer Mack[1], Nikhil Wagle[1]. *[1]Dana-Farber Cancer Institute, Boston, MA,[2]Broad Institute, Cambridge, MA,[3]Brigham and Women's Hospital, Boston, MA,[4]Boston Children's Hospital, Boston, MA*

Osteosarcoma (OS) and Leiomyosarcoma (LMS) are sarcomas with complex genomes for which there has been limited progress in identifying new treatments and improving outcomes. Slow progress in OS and LMS is partially due to insufficient characterization of the genomic landscape. Generating large genomic datasets in OS and LMS is challenging because of the rarity of these sarcomas and recruitment barriers such as care fragmentation between institutions and specialties. The OS and LMS Project research studies aim to: 1) establish a network of engaged pediatric and adult participants with OS and LMS who will co-create a shared database of clinical, genomic, molecular, and patient reported data to enable research; 2) define the clinicogenomic landscape of OS and LMS; and 3) optimize the approach to direct patient engagement in cancer research. Count Me In, a research initiative with prior success in angiosarcoma, working with patients and advocates created websites (OSProject.org and LMSProject.org) where patients register and consent to participation. Within two months of launching, 233 patients age 6-79 from 149 Institutions have consented. Blood and saliva are collected from consented participants, tumor samples are obtained from pathology departments and medical records are requested from treating hospitals. WES and WGS of tumor and normal, and RNASeq of tumor is performed. ctDNA is obtained and sequenced. Results are shared with patient, advocacy, physician and

research communities in several ways. Individual participants receive a shared learning report describing the somatic variants identified in their tumor from paired tumor-normal WES and are offered genetic counseling and clinical germline testing. Registered participants receive updates via email and Project websites. There are regular pre-publication data releases to the genomic data commons and to cBioPortal. A physician engagement committee meets regularly to discuss clinical insights and conundrums from shared learning reports and germline testing. Patient accrual over the next 3 years is anticipated to result in sequencing of 750 tumor-normal pairs and 500 ctDNA samples.

#6085

Molecular profile by next generation sequencing in papillary thyroid carcinoma, Colombian Cohort at Fundacion Santa fe de Bogota University Hospital

Paula Rodriguez[1], Sebastián González[2], Sergio Cruz[1], Yesith Juez[3], David Becerra[4], Margarita Baldión[1], Sandra Perdomo[5], Angela Beltran[5], Jose Hakim[6], Deyanira Gonzales[7]. *[1]Pathology Department, Fundación Santa Fe de Bogotá Univ. Hosp., Bogotá, Colombia, Colombia,[2]Pathology Department, Fundación Santa Fe de Bogotá Univ. Hosp., Bogotá, Colombia,[3]Facultad de Ingeniería, Universidad de los Andes, Bogotá, Colombia, Colombia,[4]Pathology Department, Universidad Nacional de Colombia, Bogotá, Colombia, Colombia,[5]Faculty of Medicine, Universidad el Bosque, Bogotá, Colombia, Colombia,[6]Head and Neck Surgery, Fundación Santa Fe de Bogotá Univ. Hosp., Bogotá, Colombia, Colombia,[7]Endocrine Division, Fundación Santa Fe de Bogotá Univ. Hosp., Bogotá, Colombia, Colombia*

Objective/ aim: To describe the main molecular alterations in a Colombian Cohort of patients diagnosed with Papillary Thyroid Carcinoma (PTC) at Fundacion Santa Fe de Bogota University Hospital between 1993 and 2011 Methods: A total of 231 surgically intervened patients at our institution and diagnosed with PTC with available paraffin blocks were analysed. DNA and RNA extraction was performed from FFPE samples using Quick-DNA & RNA FFPE MiniPrep Kit (Zymo Research). Next Generation Sequencing analysis was performed using SOPHiA Solid Tumor Solutions Kit

(SOPHiA GENETICS, Saint Sulpice, Suiza) , which detects 42 DNA genes and 137 fusion genes with the platform MiSeq System (Illlumina, San Diego, California). Data underwent QA and QC and variants were analysed through Sophia commercial pipeline for somatic aberrations.
Results: Among 231 patients, 82% were women, average age 45 +/- 13 y-o, 97% from Colombia, with institutional pathologic diagnosis of PTC. The most frequent histological subtypes were Classic PTG (33%), Follicular Infiltrative (29%) and Tall cell (23%). Identification of clinically relevant molecular alterations was done (see table 1). The most frequent SNV mutations were BRAF-V600E (72%), TP53 (9%) and IDH1-R132H (8%). The most frequent insertions or deletions (INDELS) were found in KIT (75%). We identified 8 fusion genes (most frequent were RET-CCD6 and ETV6-NTRK3). Interestingly, we detected 3 MSI positive cases.
Conclusions: PTC molecular profile by NGS can allow us to improve molecular understanding of the disease and identify possible prognostic factors and treatment targets.

Table 1. Molecular alterations detected by next-generation sequencing in Papillary carcinoma			
Molecular alterations	Gene	n	%
INDEL (n=20)	KIT	15	75,0
	NRAS	1	5,0
	PTPN11	1	5,0
	TP53	3	15
SNV (n=226)	BRAF	163	72,1
	FGFR1	1	0,4
	HRAS	2	0,9
	IDH1	19	8,4
	KIT	2	0,9
	KRAS	2	0,9
	NRAS	9	4,0
	PDGFRA	1	0,4
	PIK3CA	3	1,3
	SMAD4	4	1,8
	TP53	20	8,8
Fusion genes (n=6)	CCDC6-RET	2	25,0
	ETV6-NTRK3	2	25,0
	GOLGB1-TACC3	1	12,5
	MYH14-BICC1	2	25,0
	GOPC-RET	1	12,5
MSI (n=231)	MSI-L	3	1,3
	Negative	228	98,7

#6086

PALB2 germline mutations in a large cohort Middle Eastern breast-ovarian cancer patients

Rong Bu, Abdul K. Sira, Sandeep Kumar Parvathareddy, Kaleem Iqbal, Saud Azam, Zeeshan Qadri, Maha Al-Rasheed, Wael Haqawi, Mark Diaz, Ingrid G. Victoria, Khawla S. Al-Kuraya. *Human Cancer Genomic*

Research, King Faisal Specialist Hospital & Research Centre, Riyadh, Saudi Arabia

Background: The *PALB2* gene encoding protein is involved in the homologous recombination repair pathway and plays an important role in maintaining genomic integrity. *PALB2* heterozygous pathological variants (PV) or likely pathogenic variants (LPV) are associated with increased risk of breast and ovarian cancer. However, the prevalence and clinicopathological association of *PALB2* germline PV/LPV in Middle Eastern breast and ovarian cancers is not fully identified.
Purpose: We retrospectively screened a cohort of 918 cancer patients (791 breast cancer and 127 ovarian cancer) from Saudi Arabia using targeted capture-based next generation sequencing (NGS) method for *PALB2* germline variants regardless the family history of these patients or the presence of other hereditary cancer susceptibility genes mutations. Clinicopathological criteria were also fully analyzed.
Results: Five heterozygous PVs or LPVs were identified in six cases, accounting for 0.65% (6/918) of entire cohort. Two cases (33.3%) harbored PVs and four cases (66.7%) carried LPVs. Four PVs/LPVs (80%) were frameshift along with one novel splicing LPV (c.2835-1 C>A). One recurrent LPV (c.3425delT) was identified in two cases. All six affected carriers have breast cancer diagnosis with median age of 39.5 years (range 34-49 years). Only two cases (33%) have documented family history of cancer. Breast cancer phenotype was invasive ductal unilateral cancer in all cases with 66.7% of hormone receptor positive and 16% of triple negative tumors.
Conclusion: Germline PVs/LPVs in the *PALB2* gene were observed in low frequency of 0.65% in Saudi breast and/or ovarian cancer. Our study confirms one recurrent LPV and one novel LPV in Saudi breast cancer patients.

#6087

Mutation and co-mutation landscape of*ERBB2* alterations in advanced NSCLC

Lingzhi Hong[1], Leylah Drusbosky[2], Yinyi Wang[3], Yuanyuan Xiong[4], Rongrong Chen[4], Simon Heeke[1], Monique B. Nilsson[1], Jianjun Zhang[1], John V. Heymach[1], Xiuning Le[1]. *[1]The University of Texas MD Anderson*

Cancer Center, Houston, TX,[2]Guardant Health, Redwood City, CA,[3]Peking Union Medical College Hospital, Beijing, China,[4]Geneplus-Beijing Institute, Beijing, China

Background: *ERBB2* (*HER2*) insertions and point mutations are oncogenic drivers in non-small cell lung cancer (NSCLC) and now has approved targeted therapy for this patient population. Here, we present the landscape of *ERBB2* genetic alterations (alts) and co-mutations, and the comparison between ERBB2 and EGFR exon 20 insertions in NSCLC.
Methods: Two large retrospective cohorts were analyzed. In the Geneplus (China) cohort, 1,281 newly diagnosed NSCLC patients (pts) harboring *ERBB2* alt were analyzed based on tissue and/or ctDNA. In the Guardant360 (Guardant Health, Redwood City, USA) cohort, 1719 ctDNA profiles of newly diagnosed NSCLC samples harboring *ERBB2* alts were evaluated, with clonal alterations defined as those with ≥50% ratio of the maximum somatic variant allele fraction.
Results: In the Geneplus cohort of 1,281 pts with *ERBB2* alts, 55% were female with a median age of 58 years. *ERBB2* mutations or insertions were identified in 930 pts, *ERBB2* amplification(amp)-only in 351 pts, with mutation and co-amp at 7.5%. Most common alterations were in the tyrosine kinase domain exon 20 (85%), with Y772_A775dupYVMA to be the most frequent (57.4%), followed by G776delinsVC/LC/VV/IC (10.6%), and S310X (10.4%). *EBRR2*-mutation NSCLC were frequently having PDL1<1% (63%) and low TMB (mean 3.5). *TP53* and *EGFR* were most frequent co-mutations. *CDK12* amp was frequently co-occurring with *ERBB2* amp as both were located to Chr17q12. In the Guardant360 cohort, 54% were female with a median age of 70 years. 634 had COSMIC/OncoKB annotated oncogenic mutations. Similar to Geneplus, Y772_A775dupYVMA (39.4%), S310F (10.7%), G776delinsVC/LC/VV (9.7%) were the most common alterations. Using Y772/G776/G778 insertion as the control, a clonality cut-off of 50% had a positive prediction value of 87.5%. When this clonality cut-off was applied to all the other variants of unknown significance (VUS), 335 (19%) samples had clonal mutations with S335 (n=9), D277Y (n=6), R499W (n=4), and G222C (n=4) being most frequent. Comparison between ERBB2 Exon20 (n=370) to EGFR (ERBB1) exon20 insertions (n=323) showed a different distribution of patterns with greater heterogeneity in EGFR exon20 insertions.

Conclusion: In two large independent cohorts, Chinese and Western, *ERBB2* mutation and co-mutation patterns were similar. *ERBB2* exon 20 insertions/mutations were dominant at over 80% with Y772_A775dupYVMA being the most common driver mutation; *TP53* and *EGFR* were the most frequently co-occurred genes. *ERBB2* mutation lung cancers had low TMB and PDL1, as expected in female dominant lung adenocarcinomas, similar to EGFR exon 20 NSCLC. Clonal VUSs may represent a novel subset of mutations to functionally characterize.

#6088

Charting new cancer dependencies with patient derived organoids

James V. Neiswender[1], Lisa Brenan[1], Tate Bertea[1], Jimmy Guo[2], Ashley Anderson[1], Megan Wong[1], Zoe Posner[1], Kevin Kapner[2], Connor Hennessey[2], Sarah Wie[1], Isabella Boyle[1], Barbara De Kegel[1], Joshua Dempster[1], Yuen-Yi (Moony) Tseng[1], David Root[1], Andrew Aguirre[2], Francisca Vazquez[1]. *[1]Broad Institute, Cambridge, MA,[2]Dana Farber Cancer Institute, Boston, MA*

The number of patients benefiting from precision cancer medicine (PCM) is very limited. The Cancer Dependency Map Initiative aims to dramatically accelerate PCM by systematically identifying the landscape of cancer vulnerabilities across all tumors. Genome-wide knockout screens have been performed in over 1000 cancer cell lines, but these have been sourced from historically derived models, leaving many cancers underrepresented. Advances have been made in model derivation by growing cells in 3D formats, such as organoids or spheroids. These models present an opportunity to screen new cancer types, but come with challenges that require a new pipeline. Here, we present a set of screens using a genome wide CAS12 library in organoid tumor models representing novel subtypes of pancreatic, esophageal, and gastric cancer, along with treatment-resistant breast, ovarian, and prostate cancer organoids. We show that genome-wide screening of these models is feasible and can be achieved with quality comparable to 2D cell lines. Our work uncovered a set of novel dependencies associated with cell-ECM interactions that have not previously been identified in 2D models. Our methods provide a framework for screening future patient derived 3D culture models and discovering vulnerabilities in new tumor types.

#6089

Identification of novel YAP/TAZ pathway regulators in the triple-negative breast cancer cell line MDA-MB231 using single-cell CRISPR screening

Mareike Berlak[1], Zuzanna Makowska[1], Filippos Klironomos[1], Julia Kuehnlenz[2], Atanas Kamburov[2], Andreas Steffen[2], Martin Lange[3], Barbara Nicke[3], Ralf Lesche[1], Peter Staller[1], Charlotte Kopitz[3], Jan Naujoks[1].
[1]Functional Genomics, NUVISAN ICB GmbH, Berlin, Germany,[2]Bayer AG, Berlin, Germany,[3]NUVISAN ICB GmbH, Berlin, Germany

The Hippo signaling cascade is a major pathway that integrates a broad spectrum of mechanosensory signals at the plasma membrane and regulates response via control of cell proliferation, self-renewal, differentiation, and apoptosis. Dysregulation of this pathway has been observed across a range of cancer types and results in an altered activity of its primary downstream effectors, the oncogenic transcription factors YAP/TAZ. For example, both germline and somatic loss-of-function mutations in the tumor suppressor gene *NF2,* a component of Hippo, induce hyperactivation of YAP/TAZ, transcriptional changes and ultimately result in tumor growth. The Hippo signaling pathway is an attractive target for drug discovery efforts, however, it is highly complex and still incompletely understood. Hence it is indispensable to get a deeper insight into the Hippo - YAP/TAZ signaling axis. To this end, we performed a genome-wide CRISPR knockout screen in the triple-negative breast cancer (TNBC) cell line MDA-MB231 ($NF2^{LOF}$) expressing a YAP/TAZ reporter construct. We identified both negative and positive regulators of YAP/TAZ in breast cancer cells. In a second step, screening hits were further characterized in a focused single-cell CRISPR screen (Perturb-Seq), aiming at better understanding of the effects on YAP/TAZ activity regulation and downstream effects on gene expression. Here we present the technical details of our screening approaches and the results of perturbing known and novel regulators of YAP/TAZ on single cell level. We discuss the use of Perturb-Seq in the initial validation of hits from genome-wide screens and provide data that may serve as a basis for future drug discovery efforts, seeking for novel and effective treatments for triple-negative breast cancers and other malignancies with Hippo pathway alterations.

Targeting DNA Damage Response and Novel Pathways

#6093

IDE161, a potential first-in-class clinical candidate PARG inhibitor, selectively targets homologous-recombination-deficient and PARP inhibitor resistant breast and ovarian tumors

Monah Abed, Diana Muñoz, Vidya Seshadri, Steve Federowicz, Arjun A. Rao, Deepthi Bhupathi, Marya Liimatta, Rita Ousterhout, Firoz Jaipuri, Claire Neilan, Mark Lackner, Mike White, Zineb Mounir. *Ideaya Biosciences, South San Francisco, CA*

Poly (ADP-ribose) polymerase inhibitors (PARPi) were the first clinically approved drugs designed to exploit synthetic lethality. Despite initial responses, patients harboring homologous recombination (HR) alterations that receive PARPi develop treatment resistance, which has generated a need for additional therapies targeting homologous recombination deficient (HRD) tumors. Poly (ADP-Ribose) glycohydrolase (PARG) plays a key role in the resolution of PARP1/2-dependent DNA damage repair through hydrolysis of Poly (ADP-ribose) (PAR) chains and consequent release of DNA repair protein complexes from chromatin. In culture, the accumulation of PAR chains in the absence of a functional PARG enzyme causes delayed repair of DNA breaks resulting in increased sensitivity to alkylating agents and ionizing radiation. Notably, some HRD cell models have shown differential sensitivity to PARGi vs PARPi, suggesting that PARGi may overcome some PARPi resistance mechanisms. The ability of PARGi to exacerbate replication deficiencies nominates it as a potential therapeutic target for a broad range of cancer types with genomic instability. IDE161 is an orally bioavailable small molecule inhibitor of PARG. Biochemical and cellular assays demonstrate that IDE161 is a potent inhibitor of PAR chain hydrolysis and has anti-proliferative activity in breast and ovarian HRD cancer cell lines with both inherent and acquired PARPi resistance. IDE161 anti-proliferative effects were associated with induction of mitotic arrest and activation of the DNA damage response pathway, suggesting the position of PARG in the DNA repair cycle remains essential in the context of some PARPi resistance mechanisms. Furthermore, profiling of IDE161 across a panel of 264 molecularly

characterized cancer cell lines indicated that PARGi may show benefit beyond HRD and in indications other than ovarian and breast. Nonclinical studies in cell line and patient derived xenograft models of breast, ovarian, and gastric tumor types harboring defects in the HR pathway demonstrated anti-tumor activity in response to IDE161. Consistent with *in vitro* findings, we observed IDE161 antitumor activity in PARPi resistant xenograft models. Moreover, studies in cell lines, tumors and tissues revealed that dose and time-dependent accumulation of PAR chains serves as a robust proximal pharmacodynamic biomarker indicative of PARG target engagement. IDE161 is a novel targeted therapy that exploits the synthetic lethal relationship between PARG and genomic instability, thus leading to selective anti-proliferative effects in tumors harboring defects in the HR pathway.

#6094

Longitudinal analysis of PARP inhibitor and platinum resistance in *BRCA1/2m* breast cancer using liquid biopsy

Elizabeth Harvey-Jones[1], Maya Raghunandan[1], Luisa Robbez-Masson[1], Alaguthurai Thanussuyah[2], Roberta Liccardo[2], Arielle Yablonovitch[3], Mingyang Cai[3], Leylah Drusbosky[3], Michael Dorschner[3], Lorena Magraner Pardo[1], Rebecca Marlow[1], Asha Konde[1], Jennifer Trendell[2], John Alexander[1], Syed Haider[1], Chris Starling[1], Ioannis Roxanis[1], Jennifer Yen[3], Stephen J. Pettitt[1], Christopher J. Lord[1], Andrew N. J. Tutt[1]. *[1]Breast Cancer Now Toby Robins Research Centre, The Institute of Cancer Research, London, London, United Kingdom,[2]Breast Cancer Now Research Unit, King's College London, London, United Kingdom,[3]Guardant Health Inc., Redwood City, CA*

Background: Assessing how clinical resistance to PARP inhibitors develops has been challenging, due to the lack of coverage of potential resistance genes in sequencing panels and biopsies being subject to spatial heterogeneity. We studied the development of PARPi and/or platinum resistant disease using both tissue and a novel liquid biopsy assay, in patients treated for BRCA1/2-mutated metastatic breast cancer (BRCA1/2m mBC).

Approach: A cohort of 35 mBC patients with germline or somatic *BRCA1*/*2* mutations were identified as having developed PARPi or platinum resistant disease. Tumour biopsies were analysed by exome and transcriptome sequencing whereas ctDNA isolated from plasma sampled across the pre-treatment, response and eventual progression journey were analysed using the Guardant INFINITY platform equipped to detect mutations in >800 genes, and genome wide methylation, including promoter methylation in 398 cancer-related genes. Somatic mutations or regions of methylation that were associated with resistance were identified, including *BRCA1/2* reversion mutations. Somatic mutations with the potential to cause PARPi resistance were annotated using CRISPR screen data and other functional analyses describing genes that alter PARPi synthetic lethality.
Results: The most common resistance mechanism was BRCA1/2 reversion mutation (51%; n=8 *BRCA1*m patients*, n*=10 *BRCA2*m patients). Most reversions (77%) occurred via deletions (*BRCA1*, 70%; *BRCA2,* 79%) and exhibited microhomology use at junctions (> 80% for both *BRCA1* and *BRCA2*). In 14 patients, multiple concurrent reversion mutations were detected with VAFs ranging from 0.1-40% for *BRCA1* and 0.05-18% for *BRCA2*. Changes in VAF over time indicated that different reversions in the same patient may impart different fitness advantages in the face of treatment. Loss-of-function mutations in the 53BP1-Shieldin pathway were identified in two *BRCA1*m patients, and VUS mutations in the pathway were seen in two further patients. In some patients, reversion mutations co-occurred with either 53BP1-Shieldin pathway mutations or with replication fork stability mutations (*PAXIP1* in *BRCA2*m patients) - indicating concurrent but mechanistically distinct forms of resistance develop in the same patient. We isolated a PDX model from one patient that exhibits resistance via both BRCA1 reversion and loss of 53BP1, allowing this phenomenon to be modelled in more detail. We also detected *BRCA1* methylation in ctDNA in a patient with a somatic rearrangement in *BRCA1*.
Conclusions: Liquid biopsy profiling of PARPi-resistance breast cancer patients indicates that many patients develop multiple reversion mutations, and that alterations in the 53BP1-Shieldin pathway are present but less frequent. The co-occurrence of 53BP1-Shieldin pathway mutations and reversion mutations suggests parallel mechanisms of resistance can operate in the same patient.

#6095

A DNA damaging agent affects *BRCA2* exon 3-skipping

Jordan R. Werner[1], Hiba Siddiqui[1], Ethan Castillo[2], Mohammed Ansari[1], James D. Fackenthal[1]. *[1]Biological Sciences, Benedictine University, Lisle, IL,[2]Biology, Elmhurst University, Elmhurst, IL*

Introduction: *BRCA2* is a tumor suppressor that participates in DNA repair. Inherited pathogenic mutations in *BRCA2* are associated with a 38%-84% risk for breast cancer and a 16.5%-27% risk for ovarian cancer. *BRCA2* exon 3, which encodes a binding site for the interacting proteins EMSY and PALB2, is frequently skipped during alternative splicing events, often due to spliceogenic mutations, but also for as yet uncharacterized environmental conditions. A genomic deletion that results in complete allelic loss of exon 3 has been shown to be pathogenic, yet sequence variants that result in increased frequency of exon 3-skipping have been shown to be non-pathogenic. Thus, the allele-specific ability of *BRCA2* to contribute to DNA repair is affected by the level of exon 3-skipping. In this study we explore the effects of the topoisomerase inhibitor doxorubicin on the frequency of *BRCA2* exon 3-skipping. Isoform-specific end-point RT-PCR shows that doxorubicin increases the frequency of *BRCA2* exon 3-skipping in the breast cancer cell line MCF7 at concentrations below those required for promoting apoptosis.

Methods: MCF7 cells were treated with doxorubicin according to standard protocols. IC_{50} levels of doxorubicin were determined using a crystal violet assay. Flow cytometry was performed using standard protocols. RNA was prepared using Qiagen reagents and amplified with Invitrogen One-Step RT-PCR reagents. Isoform-specific RT-PCR primers were designed to amplify the full-length region surrounding *BRCA2* exon 3 independently from the region left by an exon-skipping event (Δ3). RT-PCR products were visualized using agarose gel electrophoresis.

Results and Conclusion: Results suggest that doxorubicin increases the level of *BRCA2* exon 3-skipping in MCF7 at concentrations below those required for promoting apoptosis. This suggests doxorubicin may compromise the DNA repair functions of *BRCA2* and other alternatively spliced mRNAs, which may contribute to the therapeutic benefits and/or toxicity of the drug.

#6096

BRCA1-BARD1 ubiquitylates histones for genome maintenance

Wenjing Li[1], Samuel R. Witus[2], Meiling Wang[1], Peter S. Brzovic[2], Rachel E. Klevit[2], Weixing Zhao[1]. *[1]UT Health Science Center at San Antonio, San Antonio, TX,[2]Department of Biochemistry, University of Washington, Seattle, WA*

Background: Breast cancer type 1 susceptibility protein (BRCA1) is a tumor suppressor gene involved in DNA double strand break repair with well-known cancer implications. BRCA1 heterodimerizes with BRCA1 associated Ring domain 1 (BARD1) to form a complex with DNA binding and ubiquitin E3 ligase function capable of interacting with proteins of diverse biological processes, most notably homology-directed DNA repair. During DNA repair, BRCA1-BARD1 directly interfaces with nucleosomes and transfers mono ubiquitin (Ub) to lysine residues on the C-terminal tail of histone H2A. Although truncation of the enzymatic BRCA1-BARD1 RING-RING domain retains H2A ubiquitylating activity, full-length BRCA1-BARD1 binds more tightly with nucleosomes and displays higher H2A-Ub activity. However, the molecular basis and biological significance for this enhanced nucleosome binding and H2A-Ub activity is uncharacterized.

Methods: Full length BRCA1-BARD1 or truncated mutants and histones were purified from E. coli. or insect cells. Nucleosomes were assembled for *in vitro* ubiquitylation reaction and binding assays. To determine the biological significance, mammalian cell lines that stably express wild type or mutant forms of BARD1 were established for cellular fractionation, foci analysis, and clonogenic survival studies alongside various DNA damage agents.

Results: Our results show multiple interaction sites exist between BRCA1-BARD1 and nucleosomes which allow high-affinity chromatin binding and promote increased histone H2A ubiquitylation activity. Multivalent BARD1-nucleosome interactions, namely those using strong binding motifs located in the intrinsically disordered region (IDR) of BARD1, and the weak “kiss” interaction mediated by the RING domains of both BRCA1 and BARD1, are essential for H2A ubiquitylation by BRCA1-BARD1. Further, we isolated two types of specific histone binding and/or ubiquitylation-defective mutants of BARD1: a BARD1-IDR mutant with

disrupted nucleosome binding withe retained H2A ubiquitylation ability, and a RING mutant that solely impairs H2A ubiquitylation. In both cases, we demonstrate that these mutants are hypersensitive to DNA damage agents, including polyADP-ribose polymerase (PARP) inhibitors, and demonstrate reduced capacity of BARD1 to associate with chromatin and foci formation owing to attenuated repair capacity.
Conclusion: Our studies provide convincing evidence BRCA1-BARD1 interacts with nucleosomes and ubiquitylates histones via its E3 ligase activity. Further, it plays a critical role in DNA damage response and repair that contributes to genome stability, which when disrupted sensitizes them to DNA damage agents. Our results open new avenues towards understanding whether and how these mutations in BRCA1-BARD1 affect its tumor suppression functions and their implications clinically, ultimately with the goal to translate these findings for the benefit of cancer patients.

#6097

Determination of *BRCA2* deletion status by copy number estimation using next generation sequencing to predict prognosis of clinically localized prostate cancer

Makoto Sumitomo[1], Takuhisa Nukaya[1], Eiji Sugihara[1], Mayu Takeda[1], Sachio Nohara[2], Shigeki Tanishima[2], Masashi Takenaka[3], Kenji Zennami[3], Kiyoshi Takahara[3], Ryoichi Shiroki[3], Hideyuki Saya[1]. *[1]Fujita Cancer Center, Fujita Health University, Toyoake, Japan,[2]Department of Bio Informatics, Communication Engineering Center, Electronic System Business Group, Mitsubishi Electric Software Corp., Tokyo, Japan,[3]Department of Urology, Fujita Health University, Toyoake, Japan*

The significance of *BRCA* alterations has been implicated in the development of metastatic castration-resistant prostate cancer (PC). On the other hand, the details of the frequency and significance of *BRCA* alterations in localized PC remain unknown. In this study, we investigated the frequency and clinical significance of *BRCA* alterations in localized PCs using an in-house next-generation sequencer (NGS) system. NGS analyses revealed that the *BRCA2* CN decreased in 17 patients (13.5%) and the *BRCA1* CN in six (4.8%). NGS-based CN values were shown to be highly correlated with droplet digital PCR-based CN values. Tissue-specific BRCA expression investigated using the Human Protein Atlas showed that

the decreased CN of BRCA2, but not BRCA1, is responsible for the decreased BRCA activity in PC. Ten of the 22 patients with decreased *BRCA2* CN were presumed to have somatic heterozygous deletion. There were no observed associations between the heterozygous deletion of *BRCA2* and various clinicopathological parameters. Furthermore, three of 10 patients developed biochemical recurrence within 3 months after surgery. Multivariate analyses revealed that the initial prostate-specific antigen levels and *BRCA2* CN were independent factors for biochemical recurrence. Our results suggest that a decrease in *BRCA2* CN may be used as a biomarker for predicting recurrence after surgery in localized PC. Early screening for somatic alterations in *BRCA2* using NGS may help to broadly predict the risk of PC progression.

#6098

Genome wide CRISPR screen reveals genetic vulnerabilities of next generation PARP1 inhibitor AZD5305

Ling Yin[1], Junjie Chen[2]. *[1]Experimental radiation oncology, The University of Texas MD Anderson Cancer Center, Houston, TX,[2]Experimental Radiation Oncology, The University of Texas MD Anderson Cancer Center, Houston, TX*

The first-generation PARP inhibitors (PARPi) olaparib, niraparib, talazoparib and rucaparib have been clinically approved for several cancers, like breast, ovarian and prostate, especially in BRCA-mutant tumors which are of homologous recombination repair (HRR)-deficiency. All PARPi both target PARP1 and PARP2, causing cancer cell deaths deficient in HRR. However, only inhibition of PARP1 is required for synthetic lethality in HRR-deficient cells. AZD5305 is a highly selective PARP1 inhibitor which has been used in clinical trials. In this study, we used the Toronto Knock Out Library version 3 (TKOv3), which contains 70948 gRNAs targeting 18,053 protein-coding genes to perform whole-genome CRISPR-Cas9 screens with three isogenic cell lines 293A, MCF10A, and Hela to uncover known and new high-confidence genes synthetic lethal interacted with AZD5305. MAGeCK and Drug Z were used to analyze the results and genes were ranked according to their drugZ scores. We identify that in all three cell lines, PARP1 was in the top hit in positive selection which proves the AZD5305 indeed a PARP1 inhibitor. Moreover, through a

comprehensive and comparative analysis with the screen results of first generation PARPi olaparib, we reveal known and new essential genes which are proved to be a common mechanism for synthetic lethality. We identify the gene AUNIP (Aurora Kinase A and Ninein Interacting Protein), in the top hit from AZD5305 screen but not in olaparib screen, suggesting that AUNIP may be an additional target for synthetic lethality with PARP1 loss. Taken together, this screen reveals the potential molecular genes related with PARP1 inhibitor that can be further explored targeted and combined cancer therapy.

#6100

The Fanconi Anemia pathway protein complex FANCI/FANCD2 couples the DNA damage response to R-loop regulation through SRSF1-mediated mRNA export

Anne Olazabal-Herrero[1], Fengshan Liang[2], Arijit Dutta[3], Yuxin Huang[4], Zhuobin Liang[5], Abhishek Gupta[2], Yaqun Teng[6], Li Lan[6], Xiaoyong Chen[2], Huadong Pei[1], Manoj Pillai[2], Patrick Sung[3], Gary Kupfer[1]. *[1]Oncology, Georgetown University, Washington, DC,[2]Yale University, New Haven, CT,[3]University of Texas Health Science Center at San Antonio, San Antonio, TX,[4]Department of Biochemistry and Structural Biology, University of Texas Health Science Center at San Antonio, San Antonio, TX,[5]Shenzhen Bay Laboratory, Shenzhen, China,[6]Harvard Medical School, Boston, MA*

Background: Fanconi Anemia (FA) is a rare genetic disease characterized by bone marrow failure and cancer susceptibility. FA gene mutations are also widespread somatically in non-FA cancer patients. While the FA pathway participates in DNA repair, it is also linked to R-loop metabolism and regulation. R-loops are co-transcriptional RNA:DNA hybrids that form as a result of replication-transcription collisions that are enhanced due to DNA damage, but their aberrant formation drives genomic instability and is an endogenous source of genotoxicity. However, the interplay between FA proteins, DNA repair, and R-loops remains mechanistically ill-defined. Disturbance of mRNA processing, export, and splicing has also been linked to R-loop-mediated genomic instability. The splicing factor SRSF1 participates in mRNA export through the Nuclear Export Factor 1 (NXF1).

Aberrant splicing factors expression has been linked to R-loops, cancer, and myelodysplastic syndrome (MDS), which clinically resembles FA. In the present study, we study the coupling of the DNA damage response to the prevention of pathogenic R-loops via mRNA export regulation through the FA pathway and SRSF1.
Methods: Cells: FA-D2 mutant, corrected, and ubiquitin-dead mutant; HeLa. siRNA transfections to reduce SRSF1 and FANCD2 protein levels. Cell survival assays against DNA damaging agents. In vitro immunoprecipitation and ubiquitination assays using purified SRSF1 and ID2. DART assay, S9.6 immunofluorescence, and S9.6 slot-blot to measure R loops in cells. Immunoprecipitation of mRNPs used to detect mature mRNA-bound ribonucleoproteins. RNA FISH to measure mRNA export.
Results: In this study, we provide strong evidence that the FA pathway coordinates the prevention of R-loop formation and subsequent genomic instability through its interaction with splicing factors via regulation of mRNA export. First, we demonstrate that knockdown of SRSF1, which is known to result in increased R-loops, also is associated with diminished activation of the FA pathway. Second, the central FA complex ID2 binds to SRSF1 in cells and in recombinant protein assays. Further, we demonstrate that SRSF1 activates the FA pathway by binding ID2 and stimulates its monoubiquitination in an RNA-dependent fashion. This activity is associated with co-localization in cells at transcriptional-DNA damage inducible R loops. In turn, FANCD2 monoubiquitination proves crucial for the assembly of the SRSF1-NXF1 nuclear export complex and mRNA export. Importantly, cancer-associated SRSF1 mutants fail to interact with FANCD2, leading to inefficient FANCD2 monoubiquitination, decreased mRNA export and R-loops accumulation.
Conclusion: Our findings uncover a novel mechanism of FANCD2 and SRSF1 in the prevention of R-loop formation via coupling of mRNA export to the DNA damage response, thus preventing genomic instability.

#6101

PUM3 is a novel R-loop regulator and is essential for efficient DNA damage repair

Chenyu Lin[1], Jian Ouyang[2], Robert Wine[3], Chen Qiu[3], Jason Williams[3], Traci M. T. Hall[3], Lee Zou[2], Wayne Miles[1]. *[1]The Ohio State University College of Medicine, Columbus, OH,[2]Massachusetts General Hospital*

Cancer Center, Charlestown, MA,[3]National Institute of Environmental Health Sciences, Research Triangle Park, NC

R-loops have important roles in regulating transcription and genome integrity. To identify novel proteins that function to modulate DNA damage repair, we screened a library of CRISPR-engineered RNA binding protein knock-out cells. From this analysis, we found that a poorly characterized protein, PUM3, is important DNA damage repair and that PUM3-deficient cells were very sensitive the chemotoxic agents. We show that under normal conditions, PUM3 is localized to the nucleolus and nucleus, where it binds to R-loops and modulates transcription. In this setting, PUM3 functions to suppress/resolve R-loops and that *PUM3*$^{-/-}$ cells have elevated R-loop levels. Following DNA damage, PUM3 is rapidly re-localized from the nucleolus to sites of DNA damage in the nucleus by members of the DDX/DHX family of RNA-helicases. Using small molecule inhibitors and quantitative assays, we find that PUM3 functions in homologous recombination (HR) mediated DNA repair and that *PUM3*$^{-/-}$ cells have significantly reduced HR-efficiency. PUM3 function at sites of DNA breaks are not affected by transcription or R-loops, implicating PUM3 as functioning after DNA resection during DNA repair. Analysis of TCGA patient data shows that PUM3 levels correlate with Cisplatin resistance and patient outcome. Collectively, our data shows that PUM3 is a previously unknown regulator of R-loops and DNA damage repair that has an important role in chemotherapy sensitivity in cancer patients.

#6102

Targeting BARD1 slows PDAC growth in vitro and in vivo and sensitizes cells to DNA damaging agents

Sohum Patel, Anoohya Arkala, Avinoam Nevler, Carolyn Coats, Charles J. Yeo, Aditi Jain. *Thomas Jefferson University, Philadelphia, PA*

Pancreatic ductal adenocarcinoma (PDAC) is the most prevalent malignant neoplasm of the pancreas, responsible for over 90% of pancreatic cancer cases. Despite recent therapeutic advances, the five-year overall survival rate for PDAC is only 11% and therapies remain limited. It is now known that deficiency in DNA damage repair (DDR) renders PDAC cells vulnerable to certain DNA damage agents, for example, poly (ADP-ribose)

polymerase inhibitors (PARPi). Most of the DDR genes mutated in PDAC are crucial for the proper functioning of the homologous recombination repair (HRR) pathway, and loss-of-function alterations in DDR genes sensitize cells to DNA-damaging agents. Since this treatment strategy is currently limited to 5-10% of PDAC cases with known mutations in the DDR genes, it underscores a dire need to understand new therapeutic avenues and expand the PDAC patient population that could benefit from this therapeutic approach. We have recently published that BARD1 (BRCA1- Associated- Ring- Domain- 1), an obligate binding partner of BRCA1, is upregulated in PDAC cells exposed to PARPi/platinums. We found that transient inhibition of BARD1 rendered PDAC cells extremely sensitive to olaparib (PARPi)/oxaliplatin (platinum), and enhanced DNA damage. Based on these results, we created two genetic models of BARD1 inhibition and utilized these model systems to investigate if loss of BARD1 chemo-sensitizes PDAC cells to other PARPis and DNA damage agents. Doxycycline inducible shRNA and BARD1 CRISPR KO models were created to inhibit gene expression of BARD1 in PDAC cells. We first characterized these model systems to confirm the loss of BARD1 protein and mRNA expression by western blot and qRT-PCR analyses. Using colony formation and Pico green cell survival assays, we found that inhibiting BARD1 resulted in slower growth of pancreatic cancer cells in vitro. Moreover, expression of several cell cycle genes from G2-M phase was significantly decreased ($p=0.05$). These studies were recapitulated in a mouse xenograft subcutaneous model, where BARD1 KO and WT PDAC cells were injected subcutaneously and tumor growth was analyzed over 25-30 days. Kaplan-Meier curves were calculated and plotted using Log-rank test. We found that inhibiting BARD1 significantly ($p=0.026$) delayed formation of PDAC tumors in vivo. Next, we analyzed the efficacies of various DNA damaging agents when BARD1 was inhibited. Silencing or CRISPR KO of BARD1 enhanced efficacy of mitomycin C, irinotecan, as well as other PARPis, which are currently in clinical trials (rucaparib, veliparib) in vitro and lowered their IC50s. These results indicate that targeting BARD1 has the potential to benefit patients in terms of novel or improved treatments. Our ongoing and future studies will expand on these findings to understand BARD1-mediated pathway and evaluate sensitivity of multiple DNA damage agents by screening a library of > 250 compounds.

#6103

Genomic instability delays cell death in PDAC after simultaneous double strand breaks

Selina Shiqing K. Teh[1], Eitan Halper-Stromberg[1], Laura Morsberger[1], Kirsten Bowland[1], Alexis Bennett[1], Robert B. Scharpf[2], Ying S. Zou[1], James R. Eshleman[1]. *[1]Department of Pathology, Johns Hopkins University School of Medicine, Baltimore, MD,[2]Department of Oncology, Johns Hopkins University School of Medicine, Baltimore, MD*

Apoptosis, the main cell death mechanism triggered by double strand breaks (DSBs), occurs as quickly as 2-3 hours, or 6-24 hours *in vivo*. However, when we transduced Cas9-expressing pancreatic cancer (PC) cell lines with multi-target sgRNAs, in which each sgRNA contains 2-16 target sites in the human genome, we found that most of the reduction in sgRNA tag counts did not occur in the first 7 days post transduction, but rather occurred between days 7 and 21. We demonstrated that CRISPR-Cas9 scission occurs over the course of days in our PC cells and peaked at days 3-5, consistent with another recent observation. Thus, we hypothesized that the mechanism of cell death was likely not due to DNA damage response pathways that were immediately and directly triggered by the multiple scission events, but rather was caused by a slower process. To test this, we treated the Cas9-expressing TS0111 PC cell line with a 14-target sgRNA and performed cytogenetic analysis on cells harvested from 0-21 days after transduction at 3-4 day intervals using a chromosome breakage assay. We observed various karyotypic abnormalities, such as formations of ring, dicentric, and tricentric chromosomes. These abnormalities accumulated over time and peaked at day 14, except for the chromatid and chromosome breaks in which the frequency was maintained through day 21, suggesting ongoing occurrence of breakage events. Analysis of breakpoints on dicentric and tricentric chromosomes showed that although breakpoints at sgRNA targeted regions predominated at early time points and decreased over time, non-targeted regions increased and peaked at day 14. A break-apart FISH assay was also implemented to confirm that these structural variants (SVs) were a direct result of CRISPR-Cas9 cuts, in which the number of cells with abnormal FISH patterns increased over time and also peaked at day 14. Additionally, we performed bioinformatics analyses on

the whole genome sequencing data of surviving colonies post treatment of multi-target sgRNAs to identify novel SVs. We found that novel SVs increased as a function of the number of sgRNA target sites, and majority of the SVs were found at non-targeted sites, consistent with ongoing genomic instability. Interestingly, we found that cells responded to the 14-cutter by becoming polyploid, manifesting as extremely large nuclei or multinucleated giant cells. XY FISH showed that polyploidy peaked at day 10 and decreased by day 21. Finally, we assayed for apoptosis, which increased on days 7 and 14 but decreased by day 21. We concluded that cytotoxicity occurred following the induction of multiple DSBs that resulted in ongoing chromosomal rearrangements and polyploidization, ultimately leading to cell death via apoptosis and possibly other mechanisms.

#6104

Prognostic and therapeutic impact of a homologous recombination repair protein TONSL in cancer stem cells

Hani Lee[1], SeokGyeong Choi[1], Sojung Ha[1], Sukjoon Yoon[2], Woo-Young Kim[1]. *[1]Sookmyung Women's University, College of Pharmacy, Yongsan Gu, Korea, Republic of,[2]Sookmyung Women's University, Department of Biological Sciences, Seoul, Korea, Republic of*

Previously, we found that an important homologous recombination repair protein ‘Tonsoku Like, DNA Repair Protein’ (TONSL) might be required for glioblastoma cancer stem cell (CSC). In this study, we further investigated the role of TONSL in CSC from several cancer cell lines from different tissues. We also analyzed the clinical data available from the public databases to find the clinical impact of TONSL. The higher expression of TONSL is associated with the worse prognosis of lung and gastric cancer. Interestingly, in breast cancer, while its higher expression is also the negative prognostic marker of the luminal A and HER2 positive cancers, that is rather the positive prognostic marker for luminal B and basal cancers. TONSL expression is higher in all 4 subtypes of breast cancer, and ovarian cancer than the corresponding normal tissues. The knockdown of TONSL in an ovarian cancer cell line, OVCAR8, results in the increase of G2/M cells and apoptotic cells in the bulk cultured population while increase also the senescence cells only in the CSC

population leading to the severe loss of CSC population. TONSL and the close binding partner in homologous recombination repair (HRR), MMS22L, both were essential for the CSC growth but the bulk cultured cells could survive without those two in a colon cancer cell line, HCT15 suggesting the importance of HRR in colon CSC. Indeed, gemcitabine treatment induced DNA breaks showed a synergistic cytotoxicity with those two HRR factors knockdown in the CSC only. These results suggest that the TONSL and MMS2L mediated HRR is essential for the CSC and while most of bulk cultured cancer cells circumvent the HRR deficit. Collectively, these data showed that the CSCs ultimately depend on the HRR process which requires TONSL and, therefore, CSC population may be more vulnerable to HRR targeting therapeutic approaches.

#6105

Unravelling the mechanistic basis of chromoplexy, a mutational process driving early cancer genome evolution

Nataliia Serbyn[1], Myrthe M. Smit[1], Vimathi S. Gummalla[2], Gregory J. Brunette[1], David S. Pellman[3]. *[1]Pediatric Oncology, Dana-Farber Cancer Institute, Boston, MA,[2]Dana-Farber Cancer Institute, Boston, MA,[3]Pediatric Oncology, Dana-Farber Cancer Institute / Harvard Medical School / Howard Hughes Medical Institute, Boston, MA*

Genome evolution can happen gradually or via bursts of rearrangements. Chromoplexy is an example of a process driving rapid genome evolution. This mutational signature is detected in ~18% of human cancers (PCAWG Consortium, 2020) and is frequently observed in prostate adenocarcinoma, lymphoid malignancies, and thyroid adenocarcinoma. Chromoplexy is inferred to happen as one catastrophic event that generates copy-neutral chains of translocations involving multiple chromosomes (Baca *et al*., 2013). Existing studies of chromoplexy monitor the outcome of massive cancer genome reorganization, thus early molecular events leading to catastrophic chromosome rearrangements remain elusive. In this work, we aimed to recapitulate molecular mechanisms underlying chromoplexy. For this, we set out to establish a cell line model and use fluorescence-based reporter systems to enrich for and allow isolation of cells containing signatures of chromoplexy. We additionally address whether colocalization of multiple double-strand breaks, for example in transcription hubs or

abnormal nuclear structures, might stimulate chained inter- and intra-chromosomal translocations typical for chromoplexy. If successful, this work will provide a mechanistic understanding of an important mutational process driving rapid genome evolution in cancer, congenital disease, and potentially organismal evolution.

#6106

Epigenetic-miRNA regulatory circuit confers ovarian cancer chemoresistance through RAD18-mediated DNA damage tolerance and repair signaling

Tasmin Rahman Omy[1], Chinnadurai Mani[2], Komaraiah Palle[2], Mark Reedy[3]. *[1]Texas Tech University Health Sciences Center, Lubbock, TX,[2]Cell Biology and Biochemistry, Texas Tech University Health Sciences Center, Lubbock, TX,[3]Obstetrics and Gynecology, Texas Tech University Health Sciences Center, Lubbock, TX*

Epithelial ovarian cancer (EOC) is the deadliest gynecological malignancy. This cancer typically is not detected, 70-80% of patients, until an advanced stage (stage III-IV). The standard of care OC entails complete surgical resection of all visible abdominal-pelvic tumors, followed by platinum-based chemotherapy combined with a taxane. New recommendations for patients responding to adjuvant therapy is to include a PARP inhibitor with or without bevacizumab for maintenance therapy. Despite initial responses, the majority of stage 3 & 4 more than 70% of OC patients experience recurrent disease. Frequently, individuals become resistant to these treatments. This dreadful circumstance highlights the pressing need to identify the molecular mechanisms underlying the disease's aggressive nature upon recurrence and the development of treatment resistance. Several genetic and epigenetic factors have been linked to the reprogramming of tumor cells by controlling the pattern of transcriptional and post-transcriptional gene expression. Particularly, the miRNA-mediated regulatory circuit plays a significant role in tumor progression and therapeutic responses. Our analysis of miRNA expression signature in human ovarian cancer cell line panel showed little to no expression of miR221_5p and a corresponding increase in DNA damage response and repair gene RAD18 expression. RAD18 plays a critical role in cellular DNA damage tolerance and repair activity against chemotherapeutics,

including platinum drugs. Similarly, loss of miRNA221_5p is associated with aggressive tumor cell growth, stemness, chemoresistance to platinum drugs, and poor prognosis in several cancers. Based on this information, we have hypothesized that miR221_5p regulates RAD18-mediated DNA damage tolerance and repair and may offer novel therapeutic intervention to overcome EOC chemoresistance. Our experimental data confers that miR221_5p post-transcriptionally regulates RAD18 by binding to its 3'-UTR region and restores OC cell sensitivity to platinum drugs. Mechanistically, our results demonstrate that miRNA221_5p epigenetically regulates RAD18-mediated DNA damage tolerance and homologous recombination repair and could be a novel therapeutic to overcome OC chemoresistance. Collectively, our studies identify a novel chemotherapy-induced epigenetic modulator in OC therapeutic resistance and offer novel miRNA 221-5p-mediated therapeutic intervention for the treatment of chemoresistant OC and to prevent disease recurrence.

#6107

Novel roles for AMBRA1 in regulating DNA double-strand breaks

Yuning Jiang[1], Tarek Abbas[2]. *[1]Radiation Oncology, University of Virginia, Charlottesville, VA,[2]University of Virginia, Charlottesville, VA*

AMBRA1 (Activating Molecule in Beclin-1-Regulated Autophagy) is a tumor suppressor protein whose expression is downregulated in several human malignancies. AMBRA1 was recently found to function as a substrate receptor for the cullin-4-based ubiquitin ligase ($CRL4^{AMBRA1}$) that promotes the ubiquitin-dependent proteolysis of D-type cyclins (cyclin D1, D2 and D3); this serves to guard against premature S-phase entry and replication stress, providing a potential mechanism for its tumor suppressive activity. Cyclin D1 protein, which is stabilized, along with cyclin D2 and D3, in AMBRA1-deficient cells, has been shown to promote homologous recombination (HR) repair of DNA double-strand breaks (DSBs), suggesting that AMBRA1 may be additionally involved in the repair of DSBs. Using our recently published CRISPR-Cas9-based dual fluorescent reporter assay system, we show that while the loss of AMBRA1 increased D-type cyclins and Rb hyperphosphorylation as expected, it did, surprisingly, inhibit HR-mediated repair and stimulated error-free non-homologous end-joining (NHEJ), and that both of these new activities are

independent of cyclin D1 or RB1. High-throughput sequencing of DSB repair junctions confirm these results and shows significant depletion of indels with reduction in microhomology-mediated end-joining in AMBRA1-deficient cells, suggesting that AMBRA1 plays a role in promoting resection at DSBs. In support of this hypothesis, we found that the loss of AMBRA1 reduces RAD51 recruitment to DSBs in cells exposed to ionizing radiation. Consistent with its role in promoting HR, we found that AMBRA1-deficient cells are significantly more sensitive to PARP inhibitors compared to AMBRA1-proficient cells. In summary, we show that AMBRA1 is a novel regulator of DSBs, and that its downregulation in cancer cells and tumors render cancer cells susceptible to inhibition by PARP inhibitors.

#6108

Novel functional dSTRIDE-HR assays to report on the status of homologous recombination repair in cancer cells

Kamil Solarczyk, Agnieszka Waligórska, Karolina Uznańska, Zsombor Prucsi, Olga Wójcikowska, Ewelina Matuszyk, Magdalena Bartyńska, Agata Kitlińska, Aleksandra Bober, Franek Sierpowski, Maja Białecka, Monika Jarosz, Malgorzata Szczygiel, Szymon Koman, Karolina Korpanty, Lukasz Beben, Lukasz Bandzarewicz, Przemyslaw Stachura, Magdalena Kordon-Kiszala. *intoDNA, Kraków, Poland*

Since the early days of the synthetic lethality concept in DNA Damage Response the status of homologous recombination (HR) repair in cancer cells have been the focus of attention of researchers and clinicians. While different approaches exist, such as the RAD51 immunofluorescence (IF) or HRD genomic assays, functional biomarkers that can assess HR proficiency are missing. We report here the development, optimization and validation of two complementary, HR-specific functional assays. The assays, which are based on the STRIDE platform technology, detect double-strand DNA breaks localized in close proximity to RPA or RAD51 proteins. The optimization phase of assay development was performed in U2OS cells. First, repeatability (intra-run variation) and reproducibility (inter-run variation) of the assays were measured in untreated cells. Then, a series of technical negative controls was performed which have shown that the number of false-positive readouts is below 10% of the total number of

signals. Finally, treatment of cells with compounds known to induce double-strand DNA breaks (etoposide and cisplatin) resulted in statistically significant increase in the number of detected dSTRIDE-RAD51 and dSTRIDE-RPA foci when compared to untreated controls. The assays were further validated in NCI-H661 (BRCA2 wild-type) and NCI-H169 (BRCA2 KO) cell line pair. The cells were treated with two concentrations of etoposide and the readouts from dSTRIDE, detecting the total pool of DSBs and dSTRIDE-HR assays were compared. In NCI-H661 cells, treatment with etoposide resulted in an increase in the number of double-strand breaks detected by dSTRIDE and as expected, more DSBs were formed after treatment with the higher concentration. dSTRIDE-HR assays confirmed that approximately 15% and 10% of these DSBs contain RPA and RAD51 proteins, respectively. In NCI-H169 cells etoposide produced a stronger reaction with even more DSBs detected by dSTRIDE, but importantly, no increase in the number of dSTRIDE-RAD51 foci was observed. dSTRIDE-RPA foci increased after treatment hinting that this step of HR remains unperturbed. Interestingly, the number of dSTRIDE-RAD51 foci in untreated cells was comparable between the two cell lines. In conclusion, we show here that two newly developed dSTRIDE-HR assays are well validated and can be successfully applied to report on the status of homologous recombination repair in different cell models.

#6109

Multi-site evaluation of novel BRCA1/2 reference materials including large genomic rearrangements

Dana Ruminski Lowe, Benedicta Forson, Maria Cowen, Matthew G. Butler, Yves Konigshofer, Melissa Berenger, Krystyna Nahlik, Dianren Xia, Catherine Huang, Russell Garlick, Bharathi Anekella. *LGC Clinical Diagnostics, Gaithersburg, MD*

Mutations in the tumor suppressor BRCA1 and BRCA2 genes can cause cell damage that significantly increases the risk of developing breast, ovarian, prostate, and pancreatic cancers. Large genomic rearrangements (LGRs) are defined as deletions, duplications or insertions; often involving a significant portion of an exon. Usually pathogenic, they have been reported to account for up to 27% of the BRCA1 and 5% of BRCA2 disease-causing mutations with a strong founder effect accounting for about

1/3 of all cancer diagnoses in some populations. Accurate detection of a BRCA1/2 pathogenic variants has immense impact on clinical management of disease including eligibility for PARP inhibitor therapy. However, these LGRs are frequently missed by PCR-based methods and NGS assays that do not detect partial or complete exon losses or gains. Given the difficulty in detecting LGRs, there is a need for improvement of BRCA1/2 testing algorithms including reference materials that incorporate challenging LGRs to support NGS assays that analyze for these mutations.

Biosynthetic DNA constructs bearing clinically relevant BRCA1/2 variants including deletions up to 500 bp spanning 2 exons and duplications up to 170 bp, were mixed with purified genomic DNA from the GM24385 human reference cell line at 10% and 50% variant allele frequency (VAF) to represent somatic and inherited BRCA disease states, respectively. The same variants were engineered into GM24385 cells at the desired VAF (>5%) and the cells were formalin fixed and paraffin embedded using a proprietary method to mimic preserved tumor biopsies. In both materials, VAF was measured using digital PCR. The prepared purified gDNA and FFPE materials were sent to multiple clinical laboratories and analyzed using various NGS assays to assess variant detection performance and ensure that the product was compatible with clinical testing workflows. Digital PCR confirmed the presence of all 20 BRCA1 and BRCA2 variants within a 20% range of the target VAF in the purified gDNA material and between 11-23% in FFPE. NGS results were variable but confirmed the presence of most variants. A few variants were detected at very low levels but reported as not detected by the bioinformatic software due to limit of detection.

We have successfully developed a reference material to support both BRCA1 and BRCA2 inherited and somatic genetic testing, providing laboratories and assay developers with a tool to challenge and optimize their assay's detection and quantitation of pathogenic variants by NGS. Provided as full process in FFPE format or in purified gDNA, these reference materials include 11 challenging LGRs, which are useful in evaluating the ability of different NGS platforms to detect such variants. This study has highlighted the need for reference materials that contain these challenging genomic alterations to improve genetic testing and ultimately, support PARP inhibitor treatment selection.

#6110

Multi-site evaluation of FFPE homologous recombination deficiency reference materials

Dana Ruminski Lowe, Robert M. Whiting, Matthew G. Butler, Yves Konigshofer, Catherine Huang, Indira Chivukula, Krystyna Nahlik, Dianren Xia, Russell Garlick, Bharathi Anekella. *LGC Clinical Diagnostics, Gaithersburg, MD*

Homologous recombination deficiency (HRD) arises when defects in DNA repair pathways occur, leading to genomic instability. HRD status is an emerging therapeutic biomarker; NGS assays that measure it can be used to stratify ovarian and breast cancer patients and determine eligibility for clinical trials, and PARP inhibitor- and platinum-based therapies. Seraseq FFPE HRD reference materials were developed to cover a range of genomic instability scores (GIS) to help NGS HRD assay validation and development. Here we discuss a multi-site evaluation across various platforms of our high-positive, low-positive, and negative HRD reference materials.

Tumor cell lines were characterized by sequencing and evaluated in collaboration with several IVD partners. Three breast cancer cell lines (along with their SNP-matched normal cell lines) were selected based on their GIS. Tumor cells were blended with their SNP-matched normal cells to achieve ~65% tumor content. Biosynthetic DNA containing mutations in homologous recombination repair (HRR) genes (ATM, BRIP1, RAD51C, RAD51D) were added to the high-positive and negative reference materials targeted at >5% variant allele frequency (VAF) and measured by digital PCR. Formalin fixed paraffin embedded (FFPE) blocks were made and each block was tested for yield per curl using both the Qiagen QIAamp DNA FFPE Tissue Kit and the Maxwell RSC DNA FFPE Kit for extraction and Qubit dsDNA HS kit for concentration analysis. DNA quality was assessed using an Agilent gDNA ScreenTape Assay for the TapeStation. Whole genome shotgun sequencing was performed on extracted DNA using LGC NxSeq AmpFREE Low DNA Library Kit and Roche KAPA UDI adapters and Illumina NextSeq 2000 P1 flow cell. HRD status was evaluated by external collaborators with multiple NGS and microarray assays, including the Illumina TSO500 HRD RUO assay, the SOPHiA DDM HRD Solution and the OncoScan CNV Array.

A breast cancer cell line with a GIS of ~75 was selected as the HRD high-positive reference material, a second breast cancer cell line with a GIS of ~60 was selected as HRD low-positive, and a third breast cancer cell line with a GIS of ~30 was selected as HRD negative. Representative DNA yields per 10-micron section (determined using the HRD positive FFPE curls extracted by Qiagen QIAamp method) were 165 ± 28 ng/curl. Digital PCR confirmed the presence of the 8 HRR mutations (in 4 genes) at levels >5% VAF. GIS varied for each material across assays, but HRD status was consistent, confirming the wide applicability of the new reference materials. We have developed the Seraseq HRD reference materials to meet the needs of laboratories looking to analyze HRD in cancer patient samples. These reference materials facilitate standardization and quality control in HRD testing by clinical labs for current and new PARP inhibitor treatment stratification in expanded patient populations that may include those with WT BRCA1/2 genes.

#6111

Design of a small molecule screening assay to detect DNA trapping of PARP1/2

Kasia Zientara-Rytter, Veronique T. Baron, Junguk Park, Pavel Shashkin, Henry Zhu. *BPS Bioscience, San Diego, CA*

Poly(ADP-ribose) polymerase (PARP) inhibitors are currently used in the clinic for the treatment of tumors with a defective DNA damage response (DDR). When PARP1 or PARP2 binds damaged DNA, it adds poly(ADP-ribose) chains to its own backbone and to other DDR proteins, which recruits and activates them. PARylated PARP1/2 next detaches from the DNA so that the other PARylated proteins can initiate the repair process. It has been observed that some PARP inhibitors prevent PARP1/2 from dissociating the DNA. The continuous presence of PARP at the site of damage prevents repair and blocks replication, leading to cell death. Therefore, drugs that trap PARP1/2 to the DNA tend to be significantly more cytotoxic than other PARP inhibitors, which is highly desirable. This study describes the design and optimization of novel PARPtrap assays to specifically assess the ability of a drug to trap PARP onto DNA. The assay is based on principles of fluorescence polarization and uses fluorescently labeled DNA probes that are excited by polarized light and emit light with a

degree of polarization that is proportional to the rate of molecular rotation. The free DNA probes that rotate fast have low fluorescence polarization (FP), but high FP when are bound to PARP1 or PARP2. When NAD+ is added, the PARylated enzymes detach from the probe, reducing FP levels. If a PARP inhibitor is added, the inhibitor's trapping ability increases FP in a dose-dependent manner.Proof-of-principle titration of known PARP-trapping inhibitors (Talazoparib, AZD305, Olaparib and Veliparib) was performed to validate the assay. We observed that:i)The known relative trapping efficacies of Talazoparib, Olaparib and Veliparib were similar to known relative efficacies. ii)Talazoparib, Olaparib and Veliparib had similar trapping efficacy against PARP1 and PARP2, as measured by their EC_{50}, whereas AZD305 was 1,000 times more efficient at trapping PARP1 than it was PARP2, demonstrating selectivity between PARP1 and PARP2.iii)AZD305 displayed as efficient DNA trapping activity toward PARP1 as best-in-class Talazoparib. In summary, we have designed an innovative PARPtrap assay designed for the high throughput screening of small molecule libraries to specifically identify or compare inhibitors that are capable of trapping PARP1 and/or PARP2 onto DNA.

#6112

Automated scoring to assess RAD51-mediated homologous recombination in patient-derived tumor organoids of ovarian cancers

Lucie Thorel[1], Pierre-Marie Morice[1], Nicolas Elie[2], Louis-Bastien Weiswald[1], Romane Florent[1], Florence Giffard[1], Margaux Jacobs[1], Agathe Ricou[3], Raphaël Leman[3], Guillaume Babin[4], Jean-François Lebrun[4], Sandrine Martin[4], Mélanie Briand[1], Benoit Goudergues[1], Bernard Lambert[1], Cécile Blanc-Fournier[5], Dominique Vaur[3], Benoit Plancoulaine[2], Laurent Poulain[1]. *[1]Normandy University, UNICAEN, INSERM U1086 ANTICIPE (Interdisciplinary Research Unit for Cancers Prevention and Treatment), BioTICLA lab. (Biology and Innovative Therapeutics for Ovarian Cancers), Caen, France,[2]Normandie University, UNICAEN, SF Normandy Oncology, US PLATON, VIRTUAL'HIS Platform, Caen, France,[3]UNICANCER, Comprehensive Cancer Center François Baclesse, Department of Cancer Biology and Genetics, Caen, France,[4]UNICANCER, Comprehensive Cancer Center François Baclesse, Department of*

Gynecological Surgery, Caen, France,[5]UNICANCER, Comprehensive Cancer Center François Baclesse, Department of Pathology, Caen, France

Extensive trials of PARP inhibitors (PARPi) have shown that they improve progression-free survival in patients with various cancers, including ovarian cancers. This improvement is marked in patients carrying *BRCA* mutations, and in Homologous Recombination Deficiency (HRD) subgroups. To date, identifying patients eligible for PARPi has been a challenge for scientific and clinical teams using next-generation sequencing (NGS) analysis and the persistence of genomic scars in tumors after restoration of proficient HR or epigenetic changes is a limitation of NGS. Functional assays could be used to improve the profiling of HR status and faithfully identify HRD tumors. The Repair Capacity Test assesses the formation of RAD51 foci in proliferating cells after irradiation and can be used on fresh primary cancer tissues irradiated *ex vivo* as well as on Patient-Derived Tumor Organoids (PDTO). However, RAD51 foci scoring is often performed manually without any possibility for the standardization of techniques. By contrast, recent progress in whole slide imaging referring to scan a complete microscope slide and creating a single high-resolution digital file, could represent an opportunity for automatizing the evaluation of HR. The purpose of this translational study was to develop an automated tool for scoring RAD51-mediated homologous recombination, to use this tool on ovarian PDTO and to compare the result to the sensitivity to olaparib (PARPi), determined by direct exposure of PDTO to the drug. We show that immunofluorescence of RAD51 foci can be automatically detected and quantified in Cyclin A2 positive nuclei in all the cells of each PDTO slice thus offering a new opportunity for the routine management and standardization of HR assessment in PDTO that goes beyond the widely used manual estimation. Finally, this automated scoring will be optimized to directly assess HR on tumor slices to make the Repair Capacity Test a highly relevant functional precision oncology tool to identify patients who will benefit from PARPi.

#6113

Predictive value of HRD testing on the response to PARP inhibitors in ovarian cancer preclinical models

Giulia Dellavedova, Alessandra Decio, Laura Formenti, Luca Porcu, Carmen Ghilardi, Raffaella Giavazzi, Maria Rosa Bani. *Istituto di Ricerche Farmacologiche Mario Negri IRCCS, Milano, Italy*

Since the introduction of Poly(ADP-ribose)polymerase inhibitors (PARPi) in the clinical practice, the search of biomarkers to distinguish homologous recombination defective tumors, eligible for PARPi therapy, has become a priority.Along with testing for BRCA mutations, commercially available tests, such as MyChoice® assay (Myriad Genetics), exploit scores calculated from genomic scarring patterns. Platinum sensitivity is also considered a surrogate marker of PARPi efficacy. However, the prognostic accuracy remains a challenge because these tests can only infer homologous recombination functionality but not directly measure it. Moreover, the association between platinum and PARPi response is imperfect since not all platinum-sensitive patients benefit from PARPi and PARPi response has been observed in platinum-resistant cancers. A panel of 20 high-grade serous ovarian carcinoma patient-derived xenografts (OC-PDXs) were molecularly and pharmacologically characterized to assess predictive markers of response to PARPi therapy. Genomic DNA and total RNA were sequenced searching for BRCA1/2 alterations or sent to Myriad Genetics to obtain HRD scores. Absolute BRCA1 mRNA expression was measured by RT-qPCR. OC-PDXs growing subcutaneously or orthotopically in nude mice were treated with the PARPi olaparib or platinum to test drug sensitivity. The molecular analyses revealed that nearly 90% (17/20) of OC-PDXs are TP53 mutated, thus reflecting the clinical scenario. 50% (10/20) of OC-PDXs harbor mutations in BRCA1/2 genes, while 10% (2/20) lack BRCA1 mRNA expression. MyChoice® assay showed that 65% (13/20) of OC-PDXs score higher than 42, which is the currently used threshold to classify HRD-positive tumors. Correlation analysis confirmed that the HRD score is highly associated with the presence of mutations in BRCA1/2 genes. Preclinical testing showed that 50% of OC-PDXs are sensitive to olaparib. Notably, in 20% of cases the therapeutic response was incorrectly predicted considering either BRCA1/2 mutations or HRD score. 30% of platinum-sensitive OC-PDXs were not responsive to olaparib, confirming that platinum sensitivity not always correlate with response to PARPi. Our results show that tumor genotype and HRD score are strongly associated. Further analyses are required to improve the predictive value of currently

used tests to select patients who will benefit the most from PARPi treatment while sparing toxicities in patients that are unlikely to respond.

#6114

Race-associated base excision repair defects alter the DNA damage landscape in prostate cancer

Kaveri Goel[1], Kimiko Krieger[2], Manoj Sonavane[1], Arun Sreekumar[2], Natalie R. Gassman[1]. *[1]Pharmacology and Toxicology, University of Alabama at Birmingham, Birmingham, AL,[2]Department of Molecular and Cell Biology, Baylor College of Medicine, Houston, TX*

Prostate cancer is the most diagnosed cancer among men in the United States. African American men are diagnosed with and succumb to prostate cancer at higher rates than other demographic groups. However, the biological drivers contributing to poorer outcomes in African American men compared to European American men with prostate cancer are still poorly defined. One understudied area is DNA repair defects, which drive genomic instability in cancers. Defects in homologous recombination are often at the forefront of repair defects examined and exploited for therapeutic intervention. However, defects in other DNA repair pathways may contribute to poor disease outcomes and chemoresistance. We demonstrated that defects in the base excision repair (BER) pathway contribute to chemoresistance and alter growth in breast cancer. Others have also shown chemoresistant effects from dysregulated BER protein expression in gastric, colorectal, and ovarian cancers. Examination of the TCGA database show dysregulation of key BER protein like X-ray cross complementing protein 1 (XRCC1) and DNA polymerase β (POLβ) are common across several cancers. Therefore, we decided to explore DNA damage and repair defects in prostate cancer to explore if altered DNA repair contributes to poorer outcomes in African American men. To measure DNA repair defects in formalin-fixed paraffin-embedded (FFPE) tissues, we employed a novel assay, Repair Assisted Damage Detection (RADD), which measures DNA lesions within the tissues. RADD fluorescently tags DNA lesions for quantification and is compatible with immunohistochemistry detection of DNA repair or other proteins of interest. Using the tissue microarrays, we used RADD to discover that prostate tumors from African American patients have more uracil and

pyrimidine lesions, elevated uracil DNA glycosylase (UNG) levels, and reduced XRCC1 levels than European American tumors, which indicate defects in the BER pathway. In addition, these men had higher uracil monophosphate (UMP) and lower expression of folate cycle metabolites, suggesting that metabolic rewiring may also contribute to the dysregulation of BER. Defects in the BER pathway may offer new therapeutic opportunities for African American prostate cancer patients. These defects may be targeted by therapeutics which pressure the BER pathways. This work demonstrates that functional detection of DNA repair defects through RADD offers new insight into race-specific DNA repair defects offering new molecular targets or therapeutic strategies to reduce racial disparities in prostate cancer.

#6115

Comprehensive DNA repair landscape analysis reveals novel small cell lung cancer biology

Benjamin B. Morris[1], Barzin Nabet[2], David Shames[2], Simon Heeke[1], Carl M. Gay[1], Jing Wang[1], Jianjun Zhang[1], John V. Heymach[1], Lauren A. Byers[1]. *[1]Thoracic/Head and Neck Medical Oncology, UT MD Anderson Cancer Center, Houston, TX,[2]Department of Oncology Biomarker Development, Genentech Inc., South San Francisco, CA*

Background: Small cell lung cancer (SCLC) is the most lethal form of lung cancer. The five-year overall survival rate for SCLC patients is only ~7%, a statistic that has not improved for decades. Compared to non-small cell lung cancers, SCLCs highly express DNA repair proteins. Despite this acknowledgement, a comprehensive analysis of the DNA repair machinery within SCLC has not been completed. This study was performed to study the SCLC DNA repair landscape.
Methods: We applied a novel DNA repair analysis method to IMPOWER133 (n = 271) and MD Anderson GEMINI (n = 85) clinical SCLC datasets. This single-sample weighted expression (ssWE) method uses transcriptomic data to assess regulation of ten single-strand break repair, double-strand break repair, translesion synthesis, and damage sensing pathways within individual tumors. Importantly, this method considers all pathway effectors and applies a scaling factor to capture effector essentiality to repair completion. Unsupervised k-means clustering

was used to group samples following ssWE analysis. Chi-square tests were used to test for significant enrichment patterns between DNA repair and established SCLC transcription factor (TF) subtypes assignments. Results: Unsupervised clustering demonstrated that IMPOWER133 and GEMINI SCLCs were robustly split into three clusters as defined by their DNA repair phenotypes (DNA Damage Response (DDR) High, Intermediate, Low). We found that expression of DNA damage responsive transcription factors (E2F1, MYBL2, FOXM1) and the intra-S and G2/M checkpoint machinery significantly increased across DDR clusters (High>Intermediate>Low). Also, we found that SCLC TF subtypes showed statistically significant enrichment patterns across DDR clusters (IMPOWER133, MDACC X^2 $p<0.001$). Most notably, inflamed SCLC (SCLC-I) were significantly under-represented in the DDR High cluster. Given this, we hypothesized that DDR Low tumors exhibited a more "inflamed" phenotype. To test this hypothesis, we isolated ASCL1+ SCLC (SCLC-A) tumors, which are considered "immune cold" compared to other subtypes, stratified them by their DDR status, and analyzed expression patterns of key immune genes. Strikingly, we found that splitting treatment naïve SCLC-A tumors by their DDR status identified tumors that appeared more "inflamed" (DDR Low). DDR Low SCLC-A showed increased expression of MHC Class I and inflammatory cytokine genes. Conversely, DDR High SCLC-A tumors exhibited an immune evasive profile. Conclusions: We provide the first evidence that SCLCs exhibit a spectrum of DNA repair machinery and cell cycle checkpoint pathway expression within TF subtypes. Additionally, we find that DDR status may be a key determinant of "inflamed" biology in treatment naïve SCLC-A—the predominant form of SCLC—independent of the SCLC-I subtype. Moving forward, our results have important implications for SCLC treatment and clinical trial design.

#6116

Ablation of mitotic checkpoint kinase BUB1 sensitizes lung adenocarcinoma to different classes of chemotherapy, radiation, and chemo-radiation

Shivani Thoidingjam[1], Sushmitha Sriramulu[1], Farzan Siddiqui[1], Benjamin Movsas[1], Shirish Gadgeel[2], Shyam Nyati[1]. *[1]Department of Radiation*

Oncology, Henry Ford Health System, Detroit, MI,[2]Department of Medical Oncology, Henry Ford Health System, Detroit, MI

Lung cancer causes the most cancer associated deaths worldwide. About 80 percent patients with inoperable non-small cell lung cancer (NSCLC) develop local recurrence and about 60 percent distant metastasis. NSCLC subtype, lung adenocarcinoma (LUAD) accounts for about 40% of all lung cancers. Recently, targeted therapy with chemotherapy combination has shown to enhance the pathologic complete response rate in a subgroup of NSCLC patients, but most patients do not benefit from therapy due to development of resistance. Thus, identifying molecular drivers of primary and adaptive chemotherapy resistance that can be effectively targeted represents a critical unmet clinical need. Here we aim to evaluate BUB1 (a mitotic checkpoint kinase) as a viable molecular target for increasing the effectiveness of radiotherapy and chemotherapy in LUAD. Bioinformatic analyses were conducted to evaluate BUB1 expression across lung cancer and normal tissues. BUB1 was found to be overexpressed in LUAD compared to normal tissues and BUB1 expression also correlated with cancer stage and tumor grade. LUAD cell lines A549, H1975 and H2030 were used to study the effect of BUB1 inhibition on chemo-radiosensitization. MTT cell proliferation and clonogenic cell survival studies were conducted with pharmacological (BAY1816032) and genomic (CRISPR) BUB1 ablation in combination with Platinum (Cisplatin), Taxol (Paclitaxel) or a PARP inhibitor (Olaparib) without/with radiation. BUB1 inhibition showed cytotoxicity in LUAD cell lines at micromolar concentration and enhanced the radiation mediated cell killing at nanomolar concentration. Moreover, BUB1 inhibition sensitized LUAD cell lines to Cisplatin, Paclitaxel and Olaparib in double or triple chemotherapy combinations. Additionally, BUB1 inhibition significantly increased LUAD cell death when combined with different classes of chemotherapies with radiation (chemo-radiation). Our preliminary mechanistic studies revealed prolonged presence of γH2AX foci, an indicator of DNA double stand breaks. BLRR DNA damage reporter assay indicated that the non-homologous end joining (NHEJ) pathway was inhibited upon BUB1 ablation. Detailed mechanistic studies combining BUB1 ablation with chemo-radiation are underway to delineate signaling cascades involved in BUB1 driven chemo-radiation sensitization. Our data provides evidence

that BUB1 inhibition sensitizes lung adenocarcinoma to radiotherapy, different classes of chemotherapy and chemo-radiation through DNA-double strand break repair pathways and provides rationale for clinical trials that combine BUB1 inhibition with chemo-radiation in NSCLC.

#6117

Dose, dose rate, and linear energy transfer influence tumor immunologic and DNA damage response following alpha- and beta-emitting radionuclides

Julia Sheehan-Klenk[1], Caroline P. Kerr[1], Thanh P. T. Nguyen[1], Joseph J. Grudzinski[2], David Adam[3], Maria Powers[1], Raghava N. Sriramaneni[1], Paul A. Clark[1], Reinier Hernandez[3], Bryan Bednarz[3], Jamey P. Weichert[2], Zachary S. Morris[1]. *[1]Human Oncology, University of Wisconsin School of Medicine and Public Health, Madison, WI,[2]Radiology, University of Wisconsin School of Medicine and Public Health, Madison, WI,[3]Medical Physics, University of Wisconsin School of Medicine and Public Health, Madison, WI*

Background: The low response rate to immunotherapies in poorly immunogenic cancers highlights the potential for combination therapies that propagate an anti-tumor response in metastatic settings. Targeted radionuclide therapy (TRT) can deliver radiation to metastatic tumor sites. In preclinical studies, combining low dose TRT with immune checkpoint blockade augments the anti-tumor immune response, promoting the immune susceptibility of metastatic disease sites. Radionuclides differ in their physical properties such as emission type, linear energy transfer (LET), half-life, and tissue range. In this study, clinically relevant α- and β-emitting radionuclides (^{225}Ac, ^{90}Y, ^{177}Lu) were compared in vitro in MOC2 head and neck squamous cell carcinoma and B78 melanoma. We hypothesized that the unique physical properties of radionuclides would differentially impact the quantity and accumulation over time of double stranded DNA breaks, mirroring the timing of effects on tumor cell immune susceptibility markers.
Methods: MOC2 or B78 cells were grown in culture and treated with external beam radiation (EBRT), or culture media containing ^{90}Y, ^{177}Lu, or ^{225}Ac delivering continuous radiation at activity levels using GEANT4

Monte Carlo to deliver 12 Gy (MOC2) and 4 Gy (B78) to the cell monolayer. Cells were harvested, and cDNA was isolated for RT-qPCR one, three, and seven days after the start of irradiation. Additional cells treated in this manner were fixed and stained with DAPI/γ-H2AX antibody for confocal microscopy at the same timepoints. γ-H2AX foci/cell were quantified manually using ImageJ.
Results: γ-H2AX foci counts/cell increased significantly and accumulated over time following treatment with ^{225}Ac, but not with ^{90}Y or ^{177}Lu. EBRT, ^{90}Y, and ^{225}Ac, but not ^{177}Lu, upregulated expression of immune response associated genes (*Fas*, *Pdl1*, *Mhc1*) compared to non-irradiated controls. In cells treated with EBRT every 24h at doses mimicking the interval dose delivered by continuous exponential decay of ^{90}Y and ^{225}Ac, but not ^{177}Lu, the time course and magnitude of *Fas* and *Pdl1* expression phenocopied that of these radionuclides.
Conclusions: DNA damage accumulation and the timing of immunomodulation are modified by the dose, dose-rate, and LET of radiation emitted from a given radionuclide. Understanding the effects of radionuclide therapies on cancer cell immunogenicity could enable rational design of clinical trials that investigate the integration of TRT and immunotherapies into the clinical care of patients with metastatic cancers.

POPULATION SCIENCES

Diet, Alcohol, Tobacco Use, and Other Lifestyle Factors

#6447
Carotenoid and tocopherol intake in relation to pancreatic cancer risk in a population-based case-control study
Bronson Dokmanovich[1], Hao fan[2], Yunpeng Yu[1], Kristin Anderson[3], Jianjun Zhang[1]. *[1]Indiana University, Indianapolis, IN,[2]Indiana University, Bloomington, IN,[3]University of Minnesota, Minneapolis, MN*

Pancreatic cancer is the third leading cause of cancer-related death in the U.S. and has a 5-year relative survival rate of only 11.5%. The etiology of pancreatic cancer is not well understood, with cigarette smoking, type 2 diabetes, and chronic pancreatitis as the only well-established risk factors. Therefore, it is critical to identify modifiable risk factors for primary

prevention. Persistent oxidative stress and resultant oxidative damage can lead to accumulated mutations in oncogenes and tumor suppressor genes and subsequent carcinogenesis of the pancreas. Carotenoids are abundant in fruits and vegetables, while tocopherols are rich in oilseeds and nuts. Both carotenoids and tocopherols have antioxidant functions. Thus, it is possible that high intake of these bioactive compounds can reduce risk of pancreatic cancer. The present study sought to investigate this question in a case-control study conducted during 1994-1998 in Minnesota. Cases (n=150), aged 20 years or older, were ascertained from all hospitals in the metropolitan area of the Twin Cities and the Mayo Clinic; from the latter, only cases residing in the Upper Midwest of the US were recruited. Controls (n=459) were randomly selected from the general population and frequency matched to cases by age (within 5 years) and sex. Intake of carotenoids and tocopherols from diet and supplements was estimated from a validated food frequency questionnaire. Odds ratios (OR) and 95% confidence intervals (95% CI) were calculated using unconditional logistic regression. As lutein and zeaxanthin are isomers that have identical chemical formulas, they are combined into a single variable in the analysis. All dietary variables were adjusted for energy intake with the residual method prior to data analysis. After adjustment for age, sex, race, education, physical activity, cigarette smoking, and alcohol consumption, intake of lutein and zeaxanthin was associated with a significantly reduced risk of pancreatic cancer [OR (95% CI) for quartile 4 (median: 4972 μg/day) vs. quartile 1 (median: 976 μg/day): 0.39 (0.19-0.79); p-trend: 0.06]. This inverse association became slightly weaker but remained statistically significant after additional adjustment for intake of energy, fat, and fiber. No significant associations were observed for intake of α-carotene, β-carotene, lycopene, β-cryptoxanthin, α-tocopherol, β-tocopherol, and δ-tocopherol, although a higher intake of all these nutrients except α-tocopherol and δ-tocopherol tended to confer a lower risk. Our study shows that there is a significant, beneficial effect of lutein and zeaxanthin intake on pancreatic cancer risk, although it may be a chance finding due to multiple comparisons. More epidemiologic studies are warranted to further elucidate the roles of carotenoids and tocopherols in the etiology and prevention of pancreatic cancer.

#6448

Processed, red, and white meat consumption and breast composition in a prospective cohort study of Chilean girls

Claire E. Kim[1], Audrey J. Gaskins[2], Camila Corvalan[3], Ana Pereira[3], John Shepherd[4], Karin B. Michels[5]. *[1]Epidemiology, Harvard T.H. Chan School of Public Health, Boston, MA,[2]Epidemiology, Rollins School of Public Health, Emory University, Atlanta, GA,[3]Institute of Nutrition and Food Technology, University of Chile, Santiago, Chile,[4]Epidemiology and Population Sciences in the Pacific Program, University of Hawaii Cancer Center, Honolulu, HI,[5]Epidemiology, Fielding School of Public Health, Los Angeles, CA*

Meat consumption has been associated with risk of breast cancer. However, the association between different types of meat (processed and unprocessed red, and white) intake during childhood and breast density has not been explored. This prospective study included 290 Chilean girls from the Growth and Obesity Cohort Study. Diet was assessed every 6 months with a 24-hour recall. Dual-energy X-ray absorptiometry was used to assess breast density (absolute fibroglandular volume (FGV)) and percent breast density (FGV/total breast volume, %FGV) at Tanner Breast Staging 4 (B4). Multivariable linear regression models were adjusted for total calorie intake, age at B4, sugar sweetened beverage intake, vegetable intake, TV watching after school, highest maternal education level, BMI z-score, and height. Substitution analysis was assessed using white meat in replacement of processed and unprocessed red meat. There was no association between total, processed and unprocessed red, or white meat intake and %FGV and absolute FGV. In the estimated substitution analyses, we observed a slightly lower breast density when processed or unprocessed red meat was replaced with white meat; however, effect estimates were modest and imprecise. For example, substituting 1 serving of unprocessed white meat for 1 serving of processed or unprocessed red meat was associated -4.1 cm^3 (95% CI -10.3, 2.2) and -4.5 cm^3 (95% CI -10.3, 1.3) lower absolute FGV, respectively. In this cohort of Chilean girls, there was little association between total or specific types of meat intake and breast density.

Substitution analysis of different types of meat and average breast density at Tanner stage 4

	Beta	Confidence	P

	coefficient	interval	value
Absolute FGV (cm^3)			
Substituting 1 serving of unprocessed white meat for 1 serving of unprocessed red meat	-4.1	(-10.3, 2.2)	0.21
Substituting 1 serving of unprocessed white meat for 1 serving of processed red meat	-4.5	(-10.3, 1.3)	0.13
Percentage FGV (%)			
Substituting 1 serving of unprocessed white meat for 1 serving of unprocessed red meat	-2.5	(-5.9, 0.8)	0.14
Substituting 1 serving of unprocessed white meat for 1 serving of processed red meat	-2.8	(-5.8, 0.3)	0.08

#6449

Association between dietary one-carbon metabolism-related nutrients and the risk of colorectal cancer: Findings from the Singapore Chinese Health Study

Yen Thi-Hai Pham[1], Aizhen Jin[2], Renwei Wang[1], Woon-Puay Koh[2], Jian-Min Yuan[1], Hung N. Luu[1]. *[1]UPMC Hillman Cancer Center, University of Pittsburgh Medical Center, Pittsburgh, PA,[2]Yong Loo Lin School of Medicine, National University of Singapore, Singapore, Singapore*

Background. Colorectal cancer (CRC) is a commonly diagnosed subtype of cancer with a high mortality rate. One-carbon metabolism is a set of complex pathways, responsible for providing methyl group for DNA synthesis, repair and methylation. Adequate DNA methylation maintains chromosome stability and prevents gene disruption. Diet is a major source for key substrates and co-factors (i.e., vitamin B6, choline and folate) involved in one-carbon metabolism. A majority of epidemiologic studies that have evaluated one-carbon metabolism-related nutrients in relation to CRC risk have focused on the potential role of folate only. Due to the involvement of multiple nutrients and the complexity of one-carbon metabolism pathways, a comprehensive assessment of the nutrients involved and their associations with CRC risk is needed. The purpose of the current analysis was therefore to evaluate the association between one-

carbon metabolism-related nutrients with the risk of developing CRC using the Singapore Chinese Health Study (SCHS).
Methods. The SCHS is an on-going population-based prospective cohort study that includes 61,321 Chinese men and women in Singapore who were 45-74 years of age at baseline. A 165-item semi-quantitative food frequency questionnaire was used to obtain information of dietary intake. Cox proportional hazard regression models were used to estimate the hazard ratios (HRs) and respective 95% confidence intervals (CIs) for CRC associated with one-carbon metabolism-related nutrients, including thiamine, riboflavin, niacin, vitamin B6, folate acid, vitamin B12, choline, methionine, and betaine, adjusting for potential confounders.
Results. After an average of 17.5 years of follow-up, 2,140 participants developed CRC. An inverse association between folate acid and colon cancer. The HRs and respective 95% CIs for quarters 2, 3 and 4 vs. quarter 1 (the lowest quartile) was 0.98 (0.84-1.14), 0.93 (0.79-1.10) and 0.80 (0.64-0.98) (P_{trend}=0.04). Similar pattern was observed between folate acid intake and colon cancer risk among never smokers (HR_{Q4vsQ1}=0.67, 95% CI: 0.51-0.86; P_{trend}=0.005). No association was found between other one-carbon metabolism-related nutrients and the risk of colorectal cancer
Conclusions. In a large on-going prospective cohort study of more than 61,000 Chinese Singaporeans, we found inverse associations between dietary folate acid and the risk of colon cancer. This association was more obvious among never smokers. Our findings provide critical implication for primary prevention and control of colorectal cancer.

#6450
Fatty acid intake as potential risk factor of colorectal cancer: A multicenter case control study in Iran
Monireh Sadat Seyyedsalehi[1], Paolo Boffetta[1], Kazem Zendehdel[2].
[1]Department of Medical and Surgical Sciences, University of Bologna, Bologna, Italy,[2]Cancer Research Center, Cancer Institute, Tehran University of Medical Sciences, Tehran, Iran, Islamic Republic of

A higher risk of colorectal cancer (CRC) has been associated with high animal fat intake, but not vegetable fat. To date, limited data provides the quantification of the effect exerted by fatty acids (FAs) on CRC overall and

by anatomical sub-sites. This study aims to look at associations between some FAs intakes [cholesterol, total fat, total saturated fatty acids (SFAs), total monounsaturated fatty acids (MUFAs), total polyunsaturated fatty acids (PUFAs), total trans fatty acids (TFAs), oleic acid, myristic acid, total ruminant (rTFAs) and industrial fatty acids (iTFAs), eliadic acid (EA), conjugated linoleic acid (CLA), and CRC risk in a large case-control study (IROPICAN) in Iran . We analyzed 865 CRC cases (434 in colon, 404 in rectum, and 27 with unknown subsite) and 3,206 controls from seven provinces of Iran. Detailed information was collected by trained interviewers using validated lifestyle and food frequency questionnaires (FFQ). The different types of total and individual FAs intake were categorized into quartiles of intake. The odds ratios (OR) and 95% confidence intervals (CI) for the association between CRC them were calculated using multivariate logistic regression models by adjusting for the potential confounders. Furthermore, analyses were stratified by age (under and over 50) and also, we repeated the analyses for CRC subsites. There was a statistically significant positive association between CRC and high intake (quartile 4) compared to the low intake (quartile) of dietary total fat (OR=1.77, 95% CI=1.32-2.38), cholesterol (OR=1.58, 95% CI=1.22-2.05), total TFAs (OR=1.31, 95% CI=1.02-1.68), TFAs (OR=1.73, 95% CI=1.12-2.68), EA(OR=2.69, 95% CI=1.46-4.93), and SM (OR=1.45, 95% CI=1.00-2.09), as well as an inverse association with high intake of dietary rTFAs (OR=0.60, 95% CI=0.39-0.93), CLAs (OR=0.34, 95% CI=0.19- 0.60). Stratified analyses by age indicated that there was a statistically significant association between CRC and total fat intake [OR =1.30, 95% CI =1.16-1.46, p=0.006 for the interaction], cholesterol intake [OR =1.22, 95% CI=1.11-1.35, p=0.019 for the interaction], and iTFA intake [OR =1.31, 95% CI=1.06-1.62, p=0.02 for the interaction] after 50 years old. The results of our study indicate that decreasing fat consumption, particularly from industrial and animal sources, may reduce the risk of CRC.

#6451

Dietary medium-chain fatty acids and risk of incident colorectal cancer in a predominantly low-income population: a report from the Southern Community Cohort Study (SCCS)

Lei Fan[1], Xiangzhu Zhu[1], Qingxia Chen[2], Xiang Huang[1], Mark D. Steinwandel[3], Martha Shrubsole[1], Qi Dai[1]. *[1]Vanderbilt University Medical*

Center, Nashville, TN,[2]Department of Biostatistics, Vanderbilt University, Nashville, TN,[3]International Epidemiology Field Station, Rockville, MD

Purpose: Previous studies have investigated medium-chain fatty acids (MCFAs) as a part of saturated fat intake and risk of colorectal cancer (CRC). However, unlike long-chain saturated fatty acids, MCFAs possess many unique properties, including inhibition of pro-carcinogenic bacteria, biofilm formation, and induction of apoptosis. Further, C12:0 has been consistently shown *in vitro* to exhibit the most potent anti-microbial properties in a dose-dependent manner compared to other MCFAs. Black Americans have the highest CRC incidence and mortality across all racial subgroups in the US. In a predominantly low-income population, we aimed to examine whether dietary intake of MCFAs is associated with a reduced risk of CRC overall and among racial subgroups.
Methods: The daily intake of total energy and individual nutrients, including MCFAs, was derived from a food frequency questionnaire. Multivariable-adjusted Cox regression was used to assess the associations between dietary intake of MCFAs and the risk of incident CRC during the 13.75-year follow up after adjustment for confounders.
Results: Among 71,599 eligible participants, 868 incident CRC cases were identified (622 Blacks, 220 Whites and 26 other racial groups). High intake of C12:0 was significantly associated with a reduced risk of CRC only in White participants in a dose-response manner (for highest VS lowest quartile: HR, 0.37; 95% CI, 0.17 to 0.80; *P* for trend =0.0068). This protective association primarily appeared in White participants at high risk of CRC, such as those aged 50 years or older, overweight or obese, ever smokers, or living in a neighborhood with greater deprivation. On the other hand, we did not find a significant association in Black participants (HR, 0.87; 95% CI, 0.59 to 1.27); *P* for trend =0.72). However, there was a marginal linear association in Black participants with the lowest deprivation index while the association disappeared among Black participants with higher deprivation index. Finally, we found from the NHANES 2005-2016, a representative sample of the US general population, that Black Americans had the lowest intake of MCFAs across all racial subgroups and, overall, intakes of MCFAs decreased with reducing poverty-income ratio. No associations were found between intakes of C6:0, C8:0, or C10:0 and the risk of incident CRC overall or within the racial group.

Conclusion: In this predominantly low-income population, increasing dietary C12:0 intake was associated with a substantially reduced risk of CRC only among White participants, but not in Black participants. This racial difference in associations may be because Black Americans consumed the lowest levels of MCFAs in all racial groups while a much higher proportion of Black participants had lactose intolerance and a lower proportion of them consumed lactose-free fermented foods.

#6452

A plasma metabolomic signature of healthy lifestyles and risk of colorectal cancer in the UK Biobank

Fangcheng Yuan, Danxia Yu, Wanqing Wen, Wei Zheng. *Division of Epidemiology, Vanderbilt University Medical Center, Nashville, TN*

Background: Lifestyle factors contribute to the etiology of colorectal cancer (CRC). We aimed to derive a metabolomic signature of adherence to healthy lifestyles and examine its association with CRC risk.
Methods: In the analysis, we included 98,898 UK Biobank participants with 168 metabolomic biomarkers measured by nuclear magnetic resonance spectroscopy from baseline plasma samples. A healthy lifestyle score (HLS) was derived from 8 lifestyle factors according to the American Cancer Society (ACS) guidelines. We applied elastic net regularized regressions to identify a metabolomic signature from 130 biomarkers. Cox proportional hazard models were used to estimate hazard ratios (HRs) and 95% confidence intervals (CIs) for the association of metabolomic signature with CRC risk after adjusting for known confounders.
Results: During a median follow-up time of 8.2 years, 818 incident primary CRC cases were identified after participants were enrolled for more than two years. We observed a strong partial correlation between the metabolomic signature and HLS (r = 0.34), as well as waist-to-hip ratio, sedentary time, red and processed meat intake, and tobacco smoking aspects of the HLS (r = 0.14-0.33). A higher HLS was characterized by a signature of increased levels of linoleic acid, total cholines, and polyunsaturated fatty acids and decreased levels of omega-6 fatty acids, phospholipids in intermediate-density lipoprotein, and phosphatidylcholines. The metabolomic signature showed a significantly inverse association with CRC risk (HR = 0.84; 95% CI = 0.80-0.89 per

standard deviation increment). The significantly inverse associations were observed irrespective of sex, educational attainment, and CRC subsite. Stronger associations were seen among participants aged between 50 and 60 years at study enrollment, and those diagnosed with CRC at 60 years old or later.
Conclusion: We identified a metabolomic signature characterizing adherence to the ACS guidelines and showed that the signature was inversely associated with CRC risk.

#6453

Lifestyle and environmental factors in relation to colorectal cancer risk and survival by colibactin tumor mutational signature status

Claire Elizabeth Thomas[1], Peter Georgeson[2], Conghui Qu[1], Robert S. Steinfelder[1], Daniel D. Buchanan[2], Mark A. Jenkins[3], Andrea Gsur[4], Jane C. Figueiredo[5], Polly A. Newcomb[1], Peter T. Campbell[6], Christina Newton[7], Caroline Y. Um[8], Lisa Boardman[9], Victor Moreno[10], Jenny Chang-Claude[11], Michael Hoffmeister[11], Marc J. Gunter[12], Andrew T. Chan[13], Shuji Ogino[14], Ellen L. Goode[15], Brigid Lynch[16], Yohannes A. Melaku[17], Steven Gallinger[18], Sonja I. Berndt[19], Wen-Yi Huang[19], Ulrike Peters[1], Amanda I. Phipps[1]. *[1]Fred Hutchinson Cancer Center, Seattle, WA,[2]Colorectal Oncogenomics Group, Department of Clinical Pathology, The University of Melbourne, Parkville, Australia,[3]The University of Melbourne, Parkville, Australia,[4]Center for Cancer Research, Medical University of Vienna, Vienna, Austria,[5]Cedars-Sinai Medical Center, Los Angeles, CA,[6]Department of Epidemiology and Population Health, Albert Einstein College of Medicine, Bronx, NY,[7]Department of Population Science, American Cancer Society, Atlanta, GA,[8]Behavioral and Epidemiology Research Group, American Cancer Society, Atlanta, GA,[9]Mayo Clinic, Rochester, MN,[10]Catalan Institute of Oncology-IDIBELL, L'Hospitalet de Llobregat, Barcelona, Spain,[11]German Cancer Research Center (DKFZ), Heidelberg, Germany,[12]Nutrition and Metabolism Section, International Agency for Research on Cancer, World Health Organization, Lyon, France,[13]Division of Gastroenterology, Massachusetts General Hospital and Harvard Medical School, Boston, MA,[14]Program in MPE Molecular Pathological Epidemiology, Harvard*

Medical School, Boston, MA,[15]Department of Health Science Research, Division of Epidemiology, Mayo Clinic, Rochester, MN,[16]Cancer Epidemiology Division, Cancer Council Victoria, Melbourne, Australia,[17]Flinders Health and Medical Research Institute, Adelaide Institute for Sleep Health, Flinders University, Adelaide, Australia,[18]Lunenfeld Tanenbaum Research Institute, Mount Sinai Hospital, University of Toronto, Toronto, ON, Canada,[19]Division of Cancer Epidemiology and Genetics, National Cancer Institute, National Institutes of Health, Bethesda, MD

Background: The genotoxin colibactin, produced by *Escherichia coli* containing the *pks* island, is associated with a tumor single base substitution (SBS) mutational signature SBS88. It is unknown whether lifestyle and environmental factors related to gut dysbiosis impact colorectal cancer (CRC) risk and survival differently by colibactin signature status.
Methods: Utilizing the resources of the Genetic Epidemiology of Colorectal cancer Consortium and Colon Cancer Family Registry (GECCO-CCFR), a consortium including both case-control and cohort study designs, SBS88 tumor mutational signature was measured in 4308 CRC cases who were microsatellite stable (MSS) and had at least five somatic single nucleotide variants for signature decomposition. Associations of 13 lifestyle and environmental factors with CRC risk by colibactin signature status were assessed using logistic and multinomial regression; associations with CRC survival were assessed using Cox proportional hazards regression.
Results: 392 (9%) of the 4308 MSS tumors were positive for SBS88. Having a BMI ≥30 kg/m^2 (versus a BMI 18.5-24.9 kg/m^2) was strongly associated with worse CRC-specific survival among those with the SBS88 signature, but not among those with SBS88 negative CRC [further adjusted hazard ratio (HR) = 3.40 95% confidence interval (CI) 1.47, 7.84, and HR = 0.97 95% CI 0.78, 1.21, respectively, *P* for heterogeneity = 0.066]. Associations of fruit intake with CRC *risk* may be differential by SBS88 status. In minimally adjusted models, those in the highest quartile of fruit intake (versus the first quartile) had 0.53 (95% CI 0.37, 0.76) times the risk of SBS88 positive CRC, as opposed to 0.75 (95% CI 0.66, 0.85) times the risk of SBS88 negative CRC (*P* for heterogeneity = 0.047). Among cohort studies specifically, associations between CRC risk and BMI, alcohol, and

fruit intake also differed by SBS88 status (*P* for heterogeneity ranging 0.02-0.05).
Conclusions: Higher BMI may be associated with worse CRC-specific survival among those with SBS88 positive tumors. BMI, alcohol, and dietary factors may be differentially associated with CRC risk based on SBS88 status.

#6454

Metabolic obesity phenotype and risk of obesity-related cancers in the women's health initiative

Prasoona Karra[1], Maci Winn[2], Garnet Anderson[3], Benjamin Haaland[2], Aladdin H. Shadyab[4], Marian Neuhouser[3], Rebecca Seguin-Fowler[5], Cynthia A. Thomson[6], Mace Coday[7], Jean Wactawski-Wende[8], Marcia L. Stefanick[9], Xiaochen Zhang[10], Ting-Yuan David Cheng[11], Shama Karanth[11], Yangbo Sun[7], Nazmus Saquib[12], Margaret Pichado[13], Su Yon Jung[14], Fred Tabung[10], Scott A. Summers[1], William L. Holland[1], Thunder Jalili[1], Marc Gunter[15], Sheetal Hardikar[2], Mary C. Playdon[1]. *[1]Department of Nutrition and Integrative Physiology, University of Utah, Salt Lake City, UT,[2]Department of Population Health Sciences, University of Utah, Salt Lake City, UT,[3]Fred Hutchinson Cancer Research Center, Seattle, WA,[4]University of California, San Diego, CA,[5]Texas A&M University, College Station, TX,[6]The University of Arizona, Tucson, AZ,[7]University of Tennessee Health Science Center, Memphis, TN,[8]University at Buffalo, Buffalo, NY,[9]Stanford Prevention Research Center, Stanford, CA,[10]The Ohio State University, Columbus, OH,[11]University of Florida, Gainesville, FL,[12]Sulaiman AlRajhi University, Kingdom of Saudi Arabia, Saudi Arabia,[13]Yale University, Chevy Chase, MD,[14]University of California, Los Angeles, CA,[15]Nutrition and Metabolism Branch, International Agency for Research on Cancer, Lyon, France*

Introduction: Body mass index (BMI) may misclassify obesity-related cancer (ORC) risk since metabolic dysfunction can exist at any BMI. We measured the association of metabolic dysfunction, independent of BMI with risk of ORC.
Methods: Study included 60% white and 34% black Women's Health Initiative participants with available baseline cardiovascular disease

biomarkers. Metabolic obesity phenotypes were classified as normal weight with no metabolic dysfunction (NWNMD), normal weight with metabolic dysfunction (NWMD), overweight/ obese with no metabolic dysfunction (OONMD) and overweight/ obese with metabolic dysfunction (OOMD) when defined by Wildman and ATP III criteria. We performed a Cox proportional hazards regression with death as a competing risk adjusting for confounders.
Results: Defining by Wildman and ATP III criteria, 17.0%, 6.5%, 31.0%, 45.0%; and 22.2%, 2.4%, 41% and 35% were NWNMD, NWMD, OONMD and OOMD respectively. The risk of all ORC combined was elevated among NWMD (HR 1.12, 95% CI: 0.90-1.39), OONMD (HR 1.15, 95% CI: 1.00-1.32) and OOMD (HR 1.35, 95% CI: 1.18-1.54) when compared to NWNMD using Wildman criteria. Results were similar when defined by ATP III, hs-CRP and HOMA-IR. When stratified by cancer type, NWMD were at increased risk of colorectal cancer when compared to NWNMD (HR 1.70, 95% CI: 1.02-2.82). Individuals who were overweight/obese were at increased risk of cancer for all cancer types though the effect estimates were lower among OONMD phenotype.
Conclusions: NWMD and OOMD individuals are at increased risk of all ORC combined, independent of BMI status when compared to individuals with NWNMD.

#6456

Association of dietary inflammatory and insulinemic potential with risk of liver cancer and chronic liver disease mortality

Xinyuan Zhang[1], Longgang Zhao[2], Cami Christopher[3], Fred K. Tabung[4], Wei Bao[5], David O. Garcia[6], Marian L. Neuhouser[7], Aladdin H. Shadyab[8], Nazmus Saquib[9], Lesley Tinker[7], Xuehong Zhang[1]. *[1]Channing Division of Network Medicine, Harvard Medical School/Brigham and Women's Hospital, Boston, MA,[2]Epidemiology and Biostatistics, Arnold School of Public Health, University of South Carolina, Columbia, SC,[3]Nutrition, Harvard T. H. Chan School of Public Health, Boston, MA,[4]Internal Medicine, The Ohio State University College of Medicine, Columbus, OH,[5]Division of Life Sciences and Medicine, University of Science and Technology of China, Institute of Public Health, Hefei, China,[6]Health Promotion Sciences, Mel & Enid Zuckerman College of Public Health,*

University of Arizona, Tucson, AZ,[7]Division of Public Health Sciences, Fred Hutchinson Cancer Center, Seattle, WA,[8]Herbert Wertheim School of Public Health and Human Longevity Science, Univeristy of California, San Diego, La Jolla, CA,[9]Clinical Sciences, College of Medicine, Sulaiman AlRajhi University, Al Bukayriyah, Saudi Arabia

Background: Increasing burdens of liver cancer and chronic liver disease (CLD) urge investigation of modifiable risk factors for primary prevention. Despite strong experimental evidence showing the role of chronic insulin resistance/hyperinsulinemia and inflammation in liver cancer and CLD, whether the insulinemic and inflammatory potential of diet are independently associated with higher risk of these outcomes requires further investigation.
Methods: We conducted a prospective cohort study among 78,356 postmenopausal women in the Women's Health Initiative Observational Study. Two validated dietary indices that predict circulating C-peptide or biomarkers of inflammation, namely, the empirical dietary index for hyperinsulinemia (EDIH) and the empirical dietary inflammation pattern (EDIP), were estimated from a food frequency questionnaire. Incident cases of liver cancer and CLD mortality were ascertained via review of medical records and linkage to national registries. Multivariable hazard ratios (HRs) with 95% confidence intervals (CIs) were calculated using Cox proportional hazard models, adjusted for age, diabetes, body mass index (BMI), and other covariates.
Results: During a median 22.1 years of follow-up, we documented 176 primary liver cancer cases and 156 CLD mortality cases. The EDIH was positively associated with incident liver cancer risk ($HR_{Quartile4\ vs.\ Quartile1}$ = 1.70; 95% CI: 1.03, 2.81; p-trend = 0.03) and CLD mortality risk ($HR_{Q4\ vs.\ Q1}$ = 2.75; 95% CI: 1.54, 4.93; p-trend = 0.01) in the multivariable adjusted model, including diabetes and BMI as covariates. The EDIP was also positively associated with liver cancer ($HR_{Q4\ vs.\ Q1}$ = 1.93; 95% CI: 1.21, 3.09; p-trend <0.001) and CLD mortality risk ($HR_{Q4\ vs.\ Q1}$ = 2.09; 95% CI: 1.24, 3.52; p-trend <0.001) in the multivariable adjusted model. The estimates remained significant and robust in sensitivity analyses, after exclusion of cases in the first 2 years of follow-up or with liver disease history. There was no additive effect between the two dietary indices.

Further analyses of individual food groups and liver outcomes indicated positive associations with refined grains, processed meat, butter, and eggs, and inverse associations with coffee, poultry, green leafy vegetables, and dark yellow vegetables.
Conclusions: Dietary insulinemic and inflammatory potential were independently associated with higher risk of liver cancer and CLD mortality in US postmenopausal women. Monitoring dietary patterns to reduce chronic hyperinsulinemia and inflammation may contribute to the primary prevention of liver cancer and CLD mortality.

#6457
Blood magnesium level is associated with liver cancer risk in a prospective cohort of liver cirrhosis patients
Xinyuan Zhang[1], Longgang Zhao[2], Tao Hou[3], Michelle Lai[4], Qi Dai[5], Xuehong Zhang[1]. *[1]Channing Division of Network Medicine, Harvard Medical School/Brigham and Women's Hospital, Boston, MA,[2]Epidemiology and Biostatistics, Arnold School of Public Health, University of South Carolina, Columbia, SC,[3]Epidemiology, Harvard T. H. Chan School of Public Health, Boston, MA,[4]Division of Gastroenterology and Hepatology, Beth Israel Deaconess Medical Center, Boston, MA,[5]Medicine, Vanderbilt University Medical Center, Nashville, TN*

Background: Previous studies showed that higher magnesium intake was linked to a lower risk of liver cancer. However, the relationship between blood magnesium level and the risk of liver cancer has not been fully established, especially among cirrhosis patients where magnesium deficiency commonly occurred. To address this knowledge gap, we have established a prospective cohort of patients with liver cirrhosis based on real-world, electronic health record data.
Methods: In the Mass General Brigham Biobank, a biorepository of consented patients, we established a prospective cohort by identifying liver cirrhosis patients using the International Classification of Diseases 9th and 10th version codes (ICD-9: 571.2, 571.5, and 571.6; ICD-10: K70.3, K74.3-6). We excluded patients with liver cancer history or without blood magnesium assessment at the time of cirrhosis diagnosis (baseline). We identified subsequent incident liver cancer (ICD-9: 155; ICD-10: C22) and

levels of liver function biomarkers assessed at each hospital visit, including alanine transaminase (ALT), aspartate aminotransferase (AST), and alkaline phosphatase (ALP). We used Cox regression models to generate ratios (HRs) with 95% confidence intervals (CIs) for developing liver cancer according to quartiles (Qs) of baseline blood magnesium levels, adjusting for age, sex, race, smoking status, alcohol intake, physical activity, body mass index, diabetes, ALT, and hepatitis B/C infection. We used generalized estimating equation (GEE) models to estimate the associations between baseline blood magnesium levels and repeated measurements of liver function biomarkers after cirrhosis diagnosis.
Results: We included 1257 liver cirrhosis patients (median age at diagnosis 59.5 years; 36% female; 87% white) with magnesium levels measured at baseline. During a median follow-up period of 3.55 (range: 0.1-12) years from liver cirrhosis diagnosis, 106 developed liver cancer. In multivariable-adjusted Cox models, higher baseline blood magnesium (Q4: ≥2.10 mg/dL vs. Q1: <1.80 mg/dL) was associated with a lower risk of liver cancer ($HR_{Q4\ vs.\ Q1}$ = 0.57; 95% CI: 0.33, 0.99; p-trend =0.03). Results remained similar in 1-year lagged analysis. In multivariable-adjusted GEE models, higher magnesium was associated with a slower change of ALT ($coefficient_{Q4\ vs.\ Q1}$ = -7.09; 95% CI: -12.6, -1.62) and AST ($coefficient_{Q4\ vs.\ Q1}$ = -8.06; 95% CI: -13.9, -2.25).
Conclusions: In a prospective cohort of high-risk population with liver cirrhosis, higher blood magnesium was associated with a lower risk of developing liver cancer and a slower change of biomarkers suggestive of liver function. Magnesium is implicated in liver carcinogenesis and progression, therefore monitoring and maintaining blood magnesium could be important to delay the progression from cirrhosis to cancer.

#6458
Maternal and paternal alcohol exposures program higher incidence of hepatocellular carcinoma in offspring
Alison Basel, Sanat S. Bhadsavle, Kara N. Thomas, Katherine N. Zimmel, Alexis N. Roach, Matthew Gaytan, Grace Parkey, Michael C. Golding.
Texas A&M University, College Station, TX

Environmental exposures during development are known to influence adult health and disease. Specifically, early developmental exposures have been

shown to increase susceptibility to cancer in adults through epigenetic mechanisms. Alcohol is a potent environmental carcinogen and teratogen, causing a wide range of health problems across the life course of an individual. Current literature examining early life exposures solely focuses on maternal exposures despite recent efforts to recognize paternal epigenetic contributions. Thus, we investigated the influence of preconception paternal, maternal, and dual parental alcohol exposures on offspring's predisposition to develop liver disease and hepatocellular carcinoma (HCC). We hypothesized that dual-parental alcohol exposure would exacerbate the incidence of liver cancer in adult offspring.
Using an established mouse model, we exposed male and female adult C57BL/6J mice to control (0% EtOH) or alcohol (10% EtOH) preconception treatments. Next, we randomly assigned pups from each treatment to either a single injection of Diethylnitrosamine (DEN; 25mg/kg) to promote liver tumors, or saline control. Finally, we sacrificed offspring on postnatal day 182 and collected organs and blood for enzyme analysis. DEN-treated males display an increased liver-to-body weight ratio compared to saline males while also exhibiting lower body weight. The male progeny from the dual-parental treatment group exhibited a significant increase in tumor incidence and burden in DEN-treated males, exceeding those measured for the maternal and paternal treatments. Further, offspring from the dual-parental group had high levels of alanine transaminase (ALT) and aspartate transaminase (AST) compared to the other treatment groups. Oil Red-O and Sirius Red staining of liver sections revealed increased hepatic steatosis and fibrosis in DEN males compared to saline males. Again, the dual-parental exposed offspring exhibited the most aberrant phenotype. Blind scoring of H&E-stained liver sections identified increases in steatosis, fibrosis, and HCC lesions, with the highest scores emerging in DEN-treated dual-parental offspring.
These findings demonstrate that preconception paternal and gestational maternal alcohol exposures program a predisposition to adult-onset chronic diseases including alcoholic fatty liver disease, hepatic fibrosis, and HCC. These experiments not only confirm our hypothesis that dual-parental exposed offspring exhibit an exacerbated hepatic abnormality phenotype, but also highlight the importance of both maternal and paternal environmental exposures on disease risk in offspring. While the negative effects of maternal alcohol consumption have been well established, our

novel finding that paternal alcohol exposure also promotes hepatocellular carcinoma in offspring has potentially profound clinical implications.

#6459

Developed and persistent dyslipidemia is associated with increased risk of gastric cancer in a prospective study

Dan Huang, Woo-Kyoung Shin, Katherine De la Torre, Sukhong Min, Aesun Shin, Jong-Koo Lee, Hyung-Ho Kim, Daehee Kang. *Seoul National University, Seoul, Korea, Republic of*

Background: Increasing evidence suggests that metabolic disorders are a risk factor for gastric cancer. However, there is a lack of evidence on whether changes and persistence of metabolic disorders affect the subsequent gastric cancer occurrence. Therefore, this study aimed to evaluate the effects of changes or persistence in metabolic syndrome and its components' status on the incidence of gastric cancer among Korean population.
Methods: This study comprised 59,671 individuals from the Health Examinees Study who had baseline surveys from 2004 to 2012 and repeated measurements from 2012 to 2016; and were followed up until 2018. Metabolic syndrome and its components were defined according to the National Cholesterol Education Program Adult Treatment Panel III and modified based on Korean population criteria. Participants were categorized into free, developed, recovered, and persistent metabolic syndrome and its components. We estimated hazard ratios (HRs) and 95% confidence intervals (CIs) for gastric cancer incidence using multivariable cox proportional hazard models with age as a time scale.
Results: During the mean follow-up of 9.4 years, 312 subjects were newly diagnosed with gastric cancer. Compared with the metabolic syndrome-free group, the persistent group had a higher incidence of gastric cancer (HR 1.37, 95% CI 1.02-1.84). Among individual components, the developed-high triglycerides group had the highest gastric cancer incidence (HR 1.52, 95% CI 1.12-2.05), followed by the persistent group (HR 1.40, 95% CI 1.04-1.90) compared to the free group. The low HDL-cholesterol persistent group (HR 1.45, 95% CI 1.08-1.93) showed a higher incidence than in the free group. In the subgroup analysis, we found association between high triglycerides developed and gastric cancer in men, while for women, the

associations were significant between high triglycerides and low HDL-cholesterol persistent groups and gastric cancer incidence.
Conclusions: In this prospective cohort study, we found that developed or persistent dyslipidemia, assessed as abnormal triglycerides and low HDL-cholesterol, were associated with an increased incidence of gastric cancer. These findings suggest that effective management of dyslipidemia may reduce gastric cancer risk.
Keywords: Gastric cancer, Dyslipidemia, Metabolic syndrome, Prospective cohort

#6460

Smoking initiation at young age increases risk of gastric cancer among Korean men

Hwi-Won Lee[1], Woo-Kyoung Shin[1], Dan Huang[2], Katherine De la Torre[1], Jae Jeong Yang[1], Minkyo Song[1], Aesun Shin[1], Kyoung-Mu Lee[3], Hyuk-Joon Lee[4], Jong-koo Lee[5], Daehee Kang[1]. *[1]Preventive Medicine, SNU Medicine, Seoul, Korea, Republic of,[2]SNU Medicine, Seoul, Korea, Republic of,[3]Environment Health, Korea National Open University, Seoul, Korea, Republic of,[4]Surgery, SNU Medicine, Seoul, Korea, Republic of,[5]Family Medicine, SNU Medicine, Seoul, Korea, Republic of*

Objective: Early initiation of smoking is associated with adverse health outcomes. This study aimed to investigate the association of various smoking-related factors with the risk of gastric cancer in a population with a high incidence rate of gastric cancer.
Method: From 2004 to 2013, Korean adults 40-69 years of age were enrolled in the large-scale prospective cohort, the Health Examinees-Gem study. Incident gastric cancer cases were identified until December 31, 2017, through linkage to the Korea Central Cancer Registry. Participants' information regarding socio-demographics, smoking-related factors, and other lifestyle factors was obtained via self-reported questionnaires. Cox proportional hazards models were used to estimate hazard ratios (HR) and 95% confidence intervals (CI) for gastric cancer risk associated with smoking-related factors such as smoking duration, amount, pack-years, and age of smoking initiation.

Results: Among 44,207 men included in the final analysis, 565 gastric cancer cases were identified during a mean (±SD) follow-up period of 8.6 (±2.0) years. Compared to non-smokers, current smokers who smoked for more than 35 years (HR 1.44, 95% CI 1.06-1.96) or with ≥30 pack-years of smoking (HR 1.40, 95% CI 1.05-1.87) were positively associated with gastric cancer. These associations were shown to be significant with increasing smoking years (*p* trend 0.019) and pack-years (0.016) as well. Compared to non-smokers, current smokers who initiated smoking at a younger age, before or at 20 years, were at a higher risk of gastric cancer (HR 1.46, 95% CI 1.10-1.93). No significant associations were observed among former smokers. When stratified by smoking duration, increased risk of gastric cancer was observed among those who smoked for more than 25 years in the younger smoking initiation age group (≤20 years; HR 1.50, 95% CI 1.15-1.94). In terms of smoking intensity, those who smoked less than 20 cigarettes or 1 pack a day showed an increased risk of gastric cancer in the younger smoking initiation age group that began smoking before or at 20 years of age (HR 1.78, 95% CI 1.30-2.44).
Conclusion: Our findings suggest that earlier initiation of smoking is associated with a greater risk of gastric cancer. Among those who began smoking early, longer duration is an important factor, but increased gastric cancer risk was also observed among those who smoked moderate amount on a daily basis. Thus, measures to manage and control onset age of cigarette smoking among teenagers may be considered when taking actions against the health burden of gastric cancer.

#6461

Excess risk due to smoking and modifying effect of quitting on bladder cancer incidence: the multiethnic cohort

David Bogumil[1], Victoria Cortessis[1], Daniel Stram[1], Veronica W. Setiawan[1], Christopher Haiman[1], Loic Le Marchand[2], Gertraud Maskarinec[2]. *[1]Population and Public Health Sciences, USC - University of Southern California, Los Angeles, CA,[2]Epidemiology Program, UH - University of Hawaii Cancer Center, Honolulu, HI*

Background: Smoking is an established risk factor for urothelial cancer of the bladder (BC), attributed to over 50% of cases among men, however associations outside of European-descent populations are infrequently

reported. Further, absolute risk of BC by smoking history has not yet been reported. Characterizing these associations will identify value of smoking cessation across non-European ancestry populations.
Methods: We estimated the association between pack-years, years quit, and BC among 181,231 Multiethnic Cohort Study participants from five major racial/ethnic groups (African Americans [AA], European Americans [EA], Japanese Americans [JA], Latinos [LA], Native Hawaiians [NH]) 45-75 years old at enrollment (1993-1996). Smoking history was assessed by self-report at cohort entry and on a follow-up survey (2003-2008). Associations were estimated using an excess relative risk model to distinguish between variables that affect baseline risk and variables (e.g. years quit) that only affect excess risk due to smoking, while adjusting for sex, age, race/ethnicity, diabetes, body mass index, and cigarettes smoked per day. BC cases were identified through SEER cancer registries to 2017. We tested for heterogeneity of smoking variables by race/ethnicity and estimated incidence across age, race-ethnicity, pack-years, and years quit.
Results: Over a mean 19 years of follow-up, 1,914 BC cases were identified. Age-standardized incidence rates of BC were highest among EA (51/100,000) and lowest among LA (24/100,000). Never smokers were most common among JA and LA (51%) and least common in other racial/ethnic groups (39-40%). In the full study sample, 50 pack-years smoked was associated with BC (HR=3.2 95% CI 2.7, 3.6). The association was heterogeneous by race/ethnicity ($p=0.02$) and statistically significant within each racial/ethnic group ($p<0.05$), except NH ($p=0.07$). Associations were strongest among EA (HR=4.0), followed by AA (HR=3.6), JA (HR=2.7), LA (HR=2.6), and NH (HR=2.4). There was no statistically significant heterogeneity of smoking cessation ($p=0.08$) or cigarettes smoked per day ($p=0.82$) by race/ethnicity. Each year quit resulted in a less than 1% decrease in the excess relative risk from smoking ($p=0.12$). The absolute risk models showed highest incidence at age 70 among EA current smokers (176/100,000) and lowest among AA never smokers (27/100,000). At age 70, current smokers across all ethnic groups had lower risk than EA who quit at age 45.
Conclusion: Pack-years smoked is significantly associated with BC risk. EA and AA groups experience the greatest excess relative risk from smoking and NH the lowest. Reduction in excess relative risk following smoking cessation is weak, meaning the cumulative effect of pack-years

smoked on BC risk cannot easily be attenuated with quitting. This contrasts with the risk reduction seen for lung and pancreatic cancer.

#6462

Cigarette smoking reduction and lung cancer risk in the Alpha-Tocopherol, Beta-Carotene Cancer Prevention Study

Daniela S. Gutiérrez-Torres, Sungduk Kim, Paul Albert, Demetrius Albanes, Stephanie J. Weinstein, Maki Inoue-Choi, Neal D. Freedman.
Division of Cancer Epidemiology and Genetics, National Cancer Institute, Rockville, MD

Background. Cigarette smoking is a leading cancer risk factor. In addition to quitting smoking, reducing the number of cigarettes/day may decrease risk of lung cancer compared with continuing to smoke more heavily. However, few cohort studies have longitudinal assessments of cigarette use. **Methods**. We examined the association of changes in smoking status (trying to quit, not smoking at this time, and still smoking) and changes in cigarettes/day with subsequent incidence of lung cancer in 24,613 Finnish male participants of the Alpha-Tocopherol, Beta-Carotene Cancer Prevention (ATBC) Study, a cancer prevention trial of vitamin supplements that collected serial assessments of cigarette use. At baseline (1985-1988), all participants were current smokers 50-69 years old who smoked 5+ cigarettes/day. During the five-to-eight year intervention period, men were asked at 4-month intervals about changes in their smoking use since their last visit. We obtained individual estimates of the proportion of follow-up time (% of time) in each of the three smoking statuses, the transition probabilities between statuses and intercepts and slopes for the number of cigarettes/day. We then examined associations between changes in smoking and in cigarettes/day and subsequent incidence of lung cancer occurring between the end of the trial (April 30, 1993) and December 31, 2012. Using Cox regression, we modeled lung cancer risk ratios (RRs) and 95% confidence intervals (95%CI) associated with changes in smoking (% of time and number of cigarettes/day) relative to individuals who smoked 20 cigarettes/day across all the study visits. Models were additionally adjusted for age at the end of the trial, ATBC intervention group, education, and age at smoking initiation. **Results**. Overall, 3013 lung cancers were diagnosed during follow-up. The risk of lung cancer was lower among participants

who reduced their smoking intensity by 5 or 10 cigarettes/day [RR=0.80(95%CI:0.71,0.89) and RR=0.64(95%CI:0.51,0.81), respectively]. RRs were further decreased among participants who also smoked at only 50% of study visits [-5 cigarettes/day RR=0.71(95%CI:0.57, 0.90) and -10 cigarettes/day RR=0.46(95%CI:0.44, 0.74)]. Individuals with the lowest risk were those who stopped smoking early at follow-up and continued to not smoke over the intervention period. For example, an individual who began the study smoking 15 cigarettes/day, stop smoking at 4 months and remained not smoking had a RR=0.24(95%CI: 0.11, 0.50). **Conclusion**: Even in the absence of cessation, smokers may meaningfully lower their lung cancer risk by reducing the number of cigarettes they smoke per day and the proportion of time they smoke. Yet, the lowest risk was observed among smokers who quit completely.

#6463

Persistence of smoking mutational signatures in the non-small cell lung cancer genome

Colin R. Lindsay[1], Pantelis Nicola[2], Andreas Gruber[3], Kate Brown[2], Mathew Carter[2], Helen Adderley[1], Shereen Rafee[2], Anna Moss[4], Andrew Wallace[5], George Burghel[5], Helene Schlecht[5], Katie Baker[2], Sharzad Moghadam[6], Jane Rogan[6], Jamie Weaver[1], Angeliki Malliri[7], William Newman[5], Fiona Blackhall[1], David Wedge[1], Genomics England. *[1]Division of Cancer Sciences, The University of Manchester, Manchester, United Kingdom,[2]The Christie NHS Foundation Trust, Manchester, United Kingdom,[3]The University of Konstanz, Konstanz, Germany,[4]Division of Cancer Sciences, The Christie NHS Foundation Trust, Manchester, United Kingdom,[5]Manchester Centre for Genomic Medicine, Manchester, United Kingdom,[6]Manchester Cancer Research Centre Biobank, Manchester, United Kingdom,[7]Cancer Research UK Manchester Institute, Manchester, United Kingdom*

Mutational signatures offer insights into cancer etiology. Smoking tobacco is associated with three signatures involving single base substitutions (SBS4), double base substitutions (DBS2) and insertions/deletions (ID3). Combining mutational signatures with clinical data allows examination of

temporal and quantitative aspects of carcinogenic exposures. We analyzed 132 non-small cell lung carcinoma (NSCLC) whole genomes, sequenced through the 100,000 Genomes Project (Genomics England), with paired clinical data available for 130/132 (98.5%). Clinical data included smoking status, duration, pack-years (py), and duration of smoking cessation. The majority were "ever-smokers" (ex-smokers: 90/130, 69.2%; current smokers: 32/130, 24.6%) and 120/122 (98.4%) had at least one smoking signature. DBS2 was the most sensitive signature for ever-smokers (118/122, 96.7%), although SBS4 was the optimal signature for diagnosing smoking-related NSCLCs (SBS4 positive likelihood ratio 7.15). An absence of ID3 best identified true never smoker NSCLCs (ID3 negative likelihood ratio 0.08). Ever-smokers had a higher tumor mutational burden (TMB) than never smokers (median 8.25 mutations/Mb vs 1.18 mutations/Mb, $p = <0.0001$), while TMB positively correlated with smoking pack-years ($p = 0.044$). Following smoking cessation, the median length of discontinuation was 11 years before a smoking-related NSCLC was diagnosed and, in some cases, smoking signatures persisted for up to 50 years prior to NSCLC diagnosis. To complement existing epidemiological data, 40 pack years was estimated as a critical cut-off for minimizing ongoing NSCLC risk. Prolonged smoking cessation did not reduce TMB ($p = 0.055$) or SBS4 mutations ($p = 0.11$), although this did produce lower DBS2 counts ($p = 0.0067$). Further signatures observed included SBS92 (previously seen in the bladder urothelium of ever-smokers) and a novel signature hypothesized to be linked to DNA mismatch repair deficiencies. NSCLCs from two patients with prior platinum chemo-radiotherapy harbored signatures of both chemotherapy- and radiotherapy-induced damage in their recurrent biopsy sample. These results highlight the importance of paired sequencing and clinical data, revealing that smoking-induced DNA damage can have long-lived effects, and strengthening health guidance of abstinence from smoking at the earliest possibility.

#6464

Antidepressant use and lung cancer risk and mortality: A meta-analysis of observational studies

Eunkyung Lee[1], David Li[1], Yongho Park[2], Alice Rodriguez-Fuguet[2], Xiaochuan Wang[3], Wen Cai Zhang[2]. *[1]Health Sciences, University of Central Florida, Orlando, FL,[2]College of Medicine, University of Central*

Florida, Orlando, FL,[3]School of Social Work, University of Central Florida, Orlando, FL

Objectives: Recent preclinical studies suggested potential anticancer effects of antidepressant (AD) use in multiple cancers, but the effect on lung cancer in human studies remains unclear. This meta-analysis examined the effect of AD use on lung cancer incidence and mortality.

Methods: Web of Science, Medline, CINAHL, and PsycINFO databases were searched to identify eligible studies published by June 2022. We conducted a meta-analysis using a random effects model to estimate pooled risk ratio (RR) and 95% confidence interval (CI) for comparing those with AD use and non-use. Heterogeneity was examined using Cochran's Q test and inconsistency I^2 statistics. The methodological quality of selected studies was assessed using the Newcastle-Ottawa Scale for observational studies.
Results: The meta-analysis, including 11 publications involving 1913172 participants, showed that AD use significantly increased lung cancer risk by 11% (RR= 1.11; 95% CI= 1.01, 1.22; I^2= 74.3%; n= 6); however, all-cause mortality was not affected by AD use (RR= 1.05; 95% CI= 0.68, 1.58; I^2= 90.1%; n= 4) while lung cancer-specific mortality could be reduced by 32% from one study. Subgroup analysis showed that serotonin and norepinephrine reuptake inhibitors (SNRIs) were associated with an increased lung cancer risk (RR= 1.38; 95% CI= 1.07, 1.78), but selective serotonin reuptake inhibitors (RR= 1.05; 95% CI=0.91, 1.21) and tricyclic antidepressants (RR= 1.09; 95% CI=0.95, 1.26) were not. In addition, variations in the definition of AD use could be the source of heterogeneity of observed effects. The quality of selected studies was good (n= 5) to fair (n= 6).
Conclusions: Evidence suggests that AD use was associated with an elevated risk of lung cancer but not with all-cause mortality. More research is needed to precisely estimate the effect of AD use on lung cancer-specific mortality. (Funding: University of Central Florida Center for Behavioral Health Research and Training; Registration: PROSPERO; registration number: CRD42022350719)

#6465
Associations of early menopause and hormone therapy with lung health and mortality among female never and ever smokers from the Prostate, Lung, Colorectal and Ovarian Cancer Screening Trial
Tessa Flores, Xiaochun Gai, Yiliang Zhu, Kimberly Leslie, Shuguang Leng. *University of New Mexico Health Sciences Ctr., Albuquerque, NM*

Our previous study using the Lovelace Smokers cohort identified early natural menopause (i.e., age at menopause<45 yr), which is a biomarker of ovarian aging, as a risk factor for lung disease and mortality among female smokers. However, most of the associations reported in female smokers with natural menopause were not observed in those with surgical menopause, (a mixed group of subjects with bilateral oophorectomy or hysterectomy without bilateral oophorectomy). Females with bilateral oophorectomy lose ovarian estrogen and progesterone production, while females with hysterectomy, +/- unilateral oophorectomy, maintain some of this hormone production. We hypothesize that associations between early menopause, lung health and mortality will vary based on type of menopause. Among 69,071 females from the Prostate, Lung, Colorectal and Ovarian (PLCO) Cancer Screening Trial, early menopause rates were 8.7%, 44.1%, and 72.8% in never smokers versus 12.1%, 51.6%, and 78.0% in ever smokers with natural, bilateral oophorectomy, or hysterectomy without bilateral oophorectomy, respectively. We analyzed the associations of early menopause and hormone therapy with lung health (physician diagnosed emphysema and chronic bronchitis and lung cancer incidence) and mortality (all-cause and cause-specific) outcomes by smoking status and menopause types. The most consistent associations were observed for all-cause mortality: 1) Except in never smokers who received hysterectomy only, early menopause was associated with higher all-cause mortality regardless of smoking status 2) hormone therapy was associated with lower all-cause mortality in all groups and the longer the use, the more beneficial the outcome; 3) the magnitude of this association was strongest in those who underwent bilateral oophorectomy. Furthermore, in ethnic disparity analysis, all-cause mortality was affected by early menopause to a lesser degree in non-Hispanic black ever smokers and there was increased benefit from hormone therapy in non-Hispanic black never smokers. Overall, we identified further evidence supporting early menopause as a risk factor for lung health and mortality and hormone therapy as being beneficial regardless of smoking status or menopause type. Our results support the "shorter lifetime estrogen exposure in early menopause" hypothesis and the clinical importance of hormone therapy beyond withdrawal symptom coping.
Supported by National Cancer Institute (NCI) grant P30 CA118100. The authors thank the NCI for access to NCI's data collected by the PLCO Cancer Screening Trial (the Cancer Data Access System Project Number PLCO-981).

#6468

Association of food groups and dietary pattern with breast cancer risk: A systematic review and meta-analysis

Jialei Fu[1], Woo-Kyoung Shin[2], Dan Huang[2], Sukhong Min[2], Li-Juan Tan[1], Hyein Jung[1], Khongorzul Ganbat[1], Jiwon Jeong[1], Seok-Jae Oh[1], Bayarmaa Nasan Ulzii[1], Daehee Kang[1], Sangah Shin[1]. *[1]Chung-Ang University, Anseong, Korea, Republic of,[2]Seoul National University, Seoul, Korea, Republic of*

We conducted a systematic review and meta-analysis of current evidence for the association between food groups, dietary patterns, and breast cancer risk among the Asian population. This systematic review and meta-analysis followed the Preferred Reporting Items for Systematic Reviews and Meta-analyses (PRISMA) guidelines. We performed a systematic literature search up to November 2022 in English in the PubMed, Web of Science, Embase, and Cochrane databases. Risk ratios (RRs) with 95% confidence intervals (CIs) were extracted as effect sizes. Publication bias was estimated by the funnel plot method. We collected the data from 15 cohort studies and 30 case-control studies meeting the search criteria. The meta-analysis found that fruit and vegetable consumption was associated with a 27% and 35% lower risk of breast cancer, respectively [RR = 0.73 (0.56, 0.96); RR = 0.65 (0.47, 0.90)]. By contrast, no significance was found between meat, soy food, and green tea consumption and breast cancer risk ($P > 0.05$). However, soy protein and isoflavone intake could lower breast cancer risk by 35% and 32%, respectively [RR = 0.65 (0.51, 0.83); RR = 0.68 (0.55, 0.82)]. As for dietary pattern, higher adherence to a healthy dietary pattern and healthy eating index was associated with a 38% and 62% reduction in breast cancer risk, respectively [RR = 0.62 (0.44, 0.88; RR = 0.38 (0.22, 0.67)], while high adherence to an unhealthy dietary pattern was associated with a 44% increased risk [RR = 1.44 (1.06, 1.96)]. Considering alcohol consumption, a 75% increased risk of breast cancer was found [RR= 1.75 (1.33, 2.30)]. The present meta-analysis found that high intakes of fruit, vegetable, soy protein, and soy isoflavone significantly reduced the risk of breast cancer, while high intake of alcohol had a significantly increased risk. Meat, soy food, and green tea consumption were not significantly associated with breast cancer risk. Considering dietary patterns, higher adherence to a healthy eating index and a healthy dietary pattern may reduce breast cancer risk. Conversely, adherence to unhealthy dietary patterns may increase breast cancer risk. However, further studies are needed to confirm the associations between dietary patterns and breast cancer in the Asian population. This research was supported by the National Research Foundation of Korea (NRF) grant funded by the Korea government (MSIT) (No.2022R1F1A1074279). MSIT: Ministry of Science and ICT.

#6469

Associations between serum iron levels and breast cancer tumor size

Ann Von Holle[1], Rachel L. Thompson[2], Katie M. O'Brien[3], Dale P. Sandler[3], Clarice R. Weinberg[1]. *[1]Biostatistics and Computational Biology, NIH-NIEHS (National Institute of Environmental Health Sciences), Durham, NC,[2]Environmental and Planetary Health Sciences, CUNY Graduate School of Public Health & Health Policy, New York, NY,[3]Epidemiology, NIH-NIEHS (National Institute of Environmental Health Sciences), Durham, NC*

Background: Iron metabolism is disrupted in cancer cells, with well-established associations between increased iron availability and cancer growth. Excess iron can be toxic, and animal models have demonstrated that excess iron promotes tumor growth, whereas iron deficiency reduces or slows tumor growth. Few observational studies have assessed associations between serum iron levels and human tumor characteristics. The objective of this study is to estimate the associations between serum iron levels and tumor size at diagnosis in breast cancer cases from The Sister Study, a large prospective cohort based in the United States. Methods: Data are from a case-cohort sample of the Sister Study selected in 2016 to study serum iron levels. Of the 3,007 invasive or ductal carcinoma in situ cases included, we used the 2,494 incident breast cancer cases with information on tumor size and iron levels. Serum iron (mcg/dL), ferritin (mcg/dL), and percent transferrin saturation were measured in samples collected at baseline (median time from collection to diagnosis 4.6 years). Prior to modeling, we applied a natural log transformation to the largest tumor size and ferritin levels. To estimate the associations between body iron levels and tumor size, we used Spearman's rank correlation and linear regression models adjusting for body mass index and age at study entry. If there

were multiple tumor measures for one person, we selected the largest tumor size. Sensitivity analyses included: 1) restricting analyses to diagnoses more than 6 months after or less than 4 years after baseline iron measures, 2) excluding women who reported taking iron supplements, and 3) stratifying analyses by tumor subtypes.
Results: Associations between all three serum iron levels and tumor size were close to the null, indicating no evidence of an association between iron and tumor size. Spearman's rank correlations were all close to zero. Adjusted regression slopes (95% confidence interval) were -0.0005 (-0.0010, 0.0005) for serum iron, -0.0163 (-0.055, 0.022) for ferritin, and -0.0009 (-0.004, 0.0021) for percent transferrin saturation. Results from the sensitivity analyses did not substantively differ from our primary findings.
Conclusions: We did not find evidence to support the hypothesis of a positive association between breast cancer tumor size at the time of diagnosis and serum iron levels. The conflicting evidence between this study and previous research in animal models suggests that iron in the human tumor microenvironment may operate independently of circulating iron or body iron stores.

#6470

Coffee and tea consumption, coffee-related metabolites, and breast cancer risk in US Women

Andrea Romanos-Nanclares[1], Oana A. Zeleznik[1], Mingyang Song[2], Walter C. Willett[3], Rulla M. Tamimi[4], Wendy Y. Chen[5], Michelle D. Holmes[6], Jae Hee Kang[1], A. Heather Eliassen[7]. *[1]Harvard Medical School/Brigham and Women's Hospital, Boston, MA,[2]Massachusetts General Hospital and Harvard Medical School, Boston, MA,[3]Nutrition and Epidemiology, Harvard Medical School/Brigham and Women's Hospital and Harvard T.H. Chan School of Public Health, Boston, MA,[4]Department of Population Health Sciences, Weill Cornell Medicine, New York, NY,[5]Department of Medical Oncology, Dana-Farber Cancer Institute, Boston, MA,[6]Harvard Medical School/Brigham and Women's Hospital and Harvard T.H. Chan School of Public Health, Boston, MA,[7]Nutrition, Harvard Medical School/Brigham and Women's Hospital and Harvard T.H. Chan School of Public Health, Boston, MA*

Background: Coffee intake may protect against breast cancer; however, previous studies have been inconsistent and potential underlying mechanisms remain unclear. We aimed to 1) examine the association between total coffee, tea, and caffeine intake and breast cancer risk and 2) identify plasma metabolites associated with coffee intake and examine these metabolites in relation to breast cancer risk.
Methods: Data on breast cancer risk factors were collected from questionnaires administered biennially and at the time of blood collections (Nurses' Health study, NHS, distant collection: 1989-1990, recent collection: 2000-2002; NHSII, 1996-1999). We evaluated the association between total coffee (caffeinated and decaffeinated), tea consumption and caffeine intake and breast cancer risk in the full cohort using Cox regression models. Leveraging dietary and metabolomic data, we identified and validated plasma metabolites associated with coffee intake in 2,033 women from the NHSII breast cancer sub-study. We then evaluated the prospective association of all prior (PMID: 32788283) and new coffee-related metabolites with breast cancer risk in a nested case-control study using conditional logistic regression models.
Results: We documented 10,060 cases of invasive breast cancer during 3,901,211 person-years of follow-up. In pooled, multivariable-adjusted models, compared to never consumers (0 cups/d), women consuming ≥6 cups/d of total coffee were at lower risk of invasive breast cancer (HR, 0.91; 95% CI, 0.82, 1.00; P-trend<0.01). Stratified analysis showed a significant effect modification by BMI (P-interaction=0.03). Compared to never consumers, drinking ≥6 cups of coffee per day was inversely associated with risk of invasive breast cancer among lean women (HR, 0.83; 95% CI, 0.72, 0.97) but not among overweight or obese women. Moreover, a lower risk of ER-negative breast cancer was observed with total coffee ($HR_{\geq 6 \text{ cups/d vs. } 0 \text{ cups/day}}$ 0.75; 95% CI, 0.59, 0.95; P-trend=0.01) and decaffeinated coffee consumption ($HR_{\geq 4 \text{ cups/d vs. o cups/day}}$ 0.66; 95% CI, 0.45, 0.95; P-trend=0.01). Among the 31 studied metabolites, no single metabolite was associated with breast cancer risk. Associations were generally consistent between ER-positive and ER-negative breast cancer, although trigonelline seemed to be suggestively stronger for ER-negative (OR, 95% CI, 0.87, 0.75-1.01; P-value=0.061). Furthermore, 1,7-dimethyluric acid, some cholesterol esters (C18:1 CE, C18:2 CE and C20:4 CE) and trigonelline, all positively associated with coffee, were indicative of an inverse association with breast cancer risk among lean women.

Conclusions: Coffee consumption was associated with lower breast cancer risk, particularly among lean women and ER-negative breast cancer. Some metabolites that might explain some of the observed inverse associations. Nonetheless, these results merit further exploration.

#6471

Tattooing and risk of hematologic cancer: A population-based case-control study in Utah

Rachel D. McCarty[1], Britton Trabert[1], Morgan M. Millar[1], Benjamin Haaland[1], Laurie Grieshober[1], Mollie Barnard[2], Lindsay Collin[1], Jeffrey A. Gilreath[1], Paul J. Shami[1], Jennifer A. Doherty[1]. *[1]University of Utah, Salt Lake City, UT,[2]Boston University Chobanian & Avedisian School of Medicine, Boston, MA*

Background: Tattooing is increasing in popularity throughout western countries and is seen in approximately 32% of the United States. However, little is known about long-term health effects of tattooing. Some tattoo inks contain carcinogens, which can interact with solar radiation to produce potentially toxic compounds. Tattoo inks can also migrate to the lymphatic system and produce inflammatory and immune responses. In this study, we evaluated whether tattooing exposures were associated with risk of hematologic malignancies.
Methods: This population-based case-control study included 656 cases of hematologic malignancies (156 myeloid neoplasms and 500 lymphomas), ages 19-79 years, who were diagnosed between July 2019 and December 2021, and identified through the Utah Cancer Registry using rapid case ascertainment. Controls were selected from ~19,000 adult Utah residents who participated in the 2020 Utah Behavioral Risk Factor Surveillance System (BRFSS) statewide survey and frequency matched to cases in a 3:1 ratio on age, sex, race, and ethnicity. Telephone surveys collected data on number of tattoo sessions, number of large tattoos, age at first tattoo, and relevant covariates. We fit binary logistic regression models for general hematologic malignancies and multinomial logistic regression models for myeloid neoplasms and lymphomas, to calculate odds ratios (ORs) and 95% confidence intervals (CIs) for each tattoo variable, adjusted for age, sex, race, ethnicity, education level, past cancer diagnosis (yes/no), and ever smoker (yes/no).
Results: There was no strong evidence that ever having received a tattoo versus never having received a tattoo was associated with risk of overall hematologic cancers (OR=1.01, 95% CI: [0.96-1.07]), myeloid neoplasms (1.12 [0.59-2.13]), or lymphomas (1.07 [0.77-1.49]). However, having three or more large tattoos, compared with never having received a tattoo, was suggestively associated with an increased risk of overall hematologic cancers (1.33 [0.69-2.47]). The effect estimate was strongest among myeloid neoplasms (1.73 [0.54-5.50]). Compared with never having received a tattoo, receiving a first tattoo before age 20 was associated with an elevated risk of myeloid neoplasms (2.00 [0.91-4.38]), and receiving a first tattoo at age 20 or older was associated with an elevated risk of lymphoma (1.24 [0.84-1.83]), though the estimates were imprecise.
Conclusion: We observed a potential association between having several large tattoos and risk of hematologic cancers, particularly myeloid neoplasms. The risk of myeloid neoplasms appeared to be strongest among individuals receiving tattoos at young age. If confirmed, these findings could inform public health messaging about the safety of tattoos.

#6472

Self-reported knowledge of Δ9-tetrahydrocannabinol (THC) and cannabidiol (CBD) potency in cannabis products among cancer patients and survivors: Results from a survey of cannabis consumers at an NCI-designated cancer center

Michelle Goulette[1], Nicolas J. Schlienz[1], Amy Case[1], Eric Hansen[1], Rebecca L. Ashare[2], Maciej Goniewicz[1], Maansi Bansal-Travers[1], Andrew Hyland[1], Danielle M. Smith[1]. *[1]Roswell Park Comprehensive Cancer Center, Buffalo, NY,[2]State University of New York at Buffalo, Buffalo, NY*

Background: Cannabis use may introduce risks and/or benefits to cancer patient treatment and survivorship, depending on product type, composition and nature of its use. Δ9-tetrahydrocannabinol (THC) and cannabidiol (CBD) are two primary cannabinoids that elicit therapeutic effects, but only THC has abuse potential, highlighting the importance of patient knowledge of cannabinoid potency in patient-provider interactions and provider risk-benefit assessments. This study aims to understand factors associated with

knowledge of THC or CBD potency in cannabis products among a sample of cancer patients and survivors who consumed cannabis since diagnosis.
Methods: Data were analyzed from a random sample of cancer patients and survivors using cannabis (n=343) and completed an anonymous, mixed-mode survey at Roswell Park. Survey questions asked about modes of use post-cancer diagnosis including smoking (joints/bongs/pipes/blunts), vaping (e-cigarettes/other vaping device), eating cannabis (foods/drinks), and taking orally (pills/tinctures/sublingually), and knowledge of cannabinoid potency was defined as knowing THC or CBD (mg or %) against no knowledge. Chi-square and separate multivariable logistic regression analyses for the most prevalent modes of cannabis use (smoking and eating) were examined to determine factors associated with knowledge of THC and CBD potency. Models controlled for acquisition source (informal; unlicensed seller vs formal; licensed seller), cannabis use instruction source (informal; personal vs formal; healthcare professional), current use status, and educational attainment.
Results: Prevalence of cannabis use following cancer diagnosis was 26.5% (20.9% among patients in active treatment; 29.2% among survivors). Among consumers, eating cannabis foods/drinking cannabis beverages was the most prevalent mode of delivery (58.6%), followed by smoking cannabis in joints (52.8%), vaping (30.3%), and taking oral pills, tinctures, or sublingually (29.2%). Overall, 27.2% had knowledge of THC and CBD potency of the products that they consumed. Those who smoked cannabis had the lowest rates (7.8% & 3.9%) followed by those eating cannabis foods/drinks (15.0% & 7.0%). Controlling for other factors, knowledge of THC and CBD potency showed significant associations with cannabis acquisition source, cannabis use instruction source, and current use status.
Conclusions: Overall, cancer patients and survivors who use cannabis have low levels of knowledge of THC and CBD potency. These data reinforce the need for provider awareness. Relying on patient self-report of THC and CBD potency is unlikely to provide key information that providers require to assess risks and benefits of cannabis use in relation to cancer symptom management.

#6473
Association of sun-seeking behaviors with indoor tanning habit in US females
Bojung Seo[1], Eunyoung Cho[2], Abrar A. Qureshi[2], Jiali Han[1]. *[1]Department of Epidemiology, Richard M. Fairbanks School of Public Health, Indiana University, Indianapolis, IN,[2]Department of Dermatology, Alpert Medical School of Brown University, Providence, RI*

Introduction: Frequent exposure to ultraviolet in early life has more detrimental and long-term effects on skin than in adulthood. Teenagers with strong sun-seeking behaviors are more likely to use an indoor tanning bed than those who seek less sun, probably due to addictive component of ultraviolet exposure. We aimed to examine the associations between sun exposure behaviors and average annual indoor tanning usage frequency during high school/college in US females.
Methods: In this cross-sectional study, we included a total of 76,122 US females who answered the average annual frequency of indoor tanning during high school/college from the Nurses' Health Study II, a large prospective cohort of US female nurses. We adjusted for age, daily number of cigarettes, number of alcohol drinks, strenuous sports frequency, hair color, family history of melanoma, chronic disease history, and mole numbers.
Results: In multivariable-adjusted multinomial logistic regression models, we demonstrated positive and dose response associations between sun exposure behaviors and annual times of indoor tanning bed usage. Specifically, teenagers who spent daily outdoors in a swimsuit (adjusted odds ratio [aOR], 95% confidence interval [CI] for daily vs. <1/week: 3.17, 1.63-6.15) were more likely to use indoor tanning beds. High school students and undergraduates who spent ≥5hours/week outdoors in direct sunlight during daytime also showed more usage of indoor tanning beds (aOR, 95% CI for ≥5hours vs. <1/week: 2.01, 1.06-3.79). Teenagers who had ≥10 sunburns that blistered also tended to more frequently use indoor tanning beds (aOR, 95% CI for ≥10 vs. Never: 2.32, 1.41-3.82).
Conclusions and Relevance: Teenagers who more spent outdoors in a swimsuit or in direct sunlight during daytime, or got more sunburns tended to use indoor tanning more frequently than those who did not. These findings provide evidence that teenagers with strong sun-seeking behaviors have excessive exposure to ultraviolet through indoor tanning.

Table 1. aORs (95% CIs) on the association between sun-exposure behaviors and tanning bed use habit

	None	1-2			3-11			≥12		
	N	**N**	**Age-adjusted model**	**Multivariable-adjusted model**	**N**	**Age-adjusted model**	**Multivariable-adjusted model**	**N**	**Age-adjusted model**	**Multivariable-adjusted model**
Average weekly time spent outdoors in a swimsuit as a teenager										
<1	7,650	202	1.00	1.00	127	1.00	1.00	51	1.00	1.00
1	5,891	223	1.35 (1.11-1.64)	1.25 (0.88-1.78)	154	1.46 (1.15-1.85)	1.26 (0.80-1.97)	48	1.10(0.74-1.63)	1.70 (0.77-3.73)
2	10,057	425	1.46 (1.23-1.73)	1.32 (0.97-1.79)	314	1.66 (1.34-2.04)	1.32 (0.89-1.96)	103	1.29 (0.92-1.81)	1.47 (0.71-3.02)
Several	28,395	1,490	1.75 (1.51-2.04)	1.40 (1.07-1.85)	1,253	2.26 (1.88-2.72)	1.81 (1.28-2.57)	551	2.34 (1.75-3.12)	2.80 (1.47-5.31)
Daily	9,761	535	1.80 (1.53-2.13)	1.36 (1.01-1.84)	497	2.55 (2.10-3.11)	1.91 (1.32-2.76)	263	3.18 (2.35-4.30)	3.17 (1.63-6.15)
Average percentage of time of wearing sunscreen at the pool or beach as a teenager										
100%	858	33	1.00	1.00	17	1.00	1.00	16	1.00	1.00
75%	2,430	122	1.22 (0.82-1.81)	0.94 (0.44-2.00)	86	1.63 (0.96-2.77)	3.12 (0.93-10.49)	41	0.81 (0.45-1.45)	4.96 (0.64-38.39)
50%	5,986	298	1.23 (0.85-1.78)	1.10 (0.56-2.17)	254	2.00 (1.22-3.29)	3.20 (1.00-10.29)	96	0.79 (0.46-1.36)	3.63 (0.49-27.04)
25%	13,617	829	1.55 (1.09-2.22)	1.20 (0.63-2.31)	629	2.28 (1.40-3.72)	3.06 (0.97-9.71)	253	0.98 (0.59-1.63)	4.26 (0.59-30.91)
0%	37,946	1,588	1.25 (0.88-1.78)	1.12 (0.59-2.13)	1,351	2.21 (1.36-3.58)	3.12 (0.99-9.82)	605	1.15 (0.70-1.91)	4.72 (0.65-34.01)
Average weekly hours spent outdoors in direct sunlight in the middle of the day during high school/college										
<1	4,900	136	1.00	1.00	71	1.00	1.00	32	1.00	1.00
2-4	22,416	965	1.44 (1.20-1.72)	1.19 (0.87-1.62)	618	1.71 (1.34-2.19)	1.29 (0.83-2.00)	211	1.25 (0.86-1.82)	0.94 (0.48-1.85)
≥5	40,863	2,133	1.65 (1.38-1.97)	1.20 (0.89-1.62)	1,940	2.74 (2.16-3.49)	2.07 (1.35-3.15)	911	2.70 (1.89-3.85)	2.01 (1.06-3.79)
The number of severe sunburns which blistered between ages 15-20										
Never	22,970	856	1.00	1.00	735	1.00	1.00	318	1.00	1.00
1-2	26,939	1,393	1.38 (1.27-1.51)	1.40 (1.20-1.63)	1,106	1.28 (1.16-1.40)	1.33 (1.12-1.58)	470	1.25 (1.08-1.45)	1.43 (1.11-1.85)
3-4	11,837	637	1.47	1.53 (1.27-	475	1.29	1.36 (1.10-	199	1.26	1.23 (0.89-

			(1.33-1.64)	1.84)		(1.15-1.45)	1.68)		(1.06-1.51)	1.70)
5-9	5,190	265	1.42 (1.23-1.63)	1.54 (1.21-1.96)	242	1.53 (1.32-1.78)	1.52 (1.17-1.98)	116	1.73 (1.39-2.15)	1.88 (1.30-2.74)
≥10	1,747	94	1.50 (1.20-1.87)	1.55 (1.08-2.23)	87	1.64 (1.31-2.07)	1.36 (0.90-2.06)	59	2.64 (1.98-3.50)	2.32 (1.41-3.82)

#6474

Stress-related sick leave and subsequent cancer risk: A Swedish national register study of 516 678 cancer cases

Sai San Moon Lu[1], Jenny Hadrévi[2], Lisbeth Slunga Järvholm[2], Florentin Späth[1], Richard Palmqvist[3], Tommy Olsson[2], Sophia Harlid[1], Bethany van Guelpen[1]. *[1]Department of Radiation Sciences, Oncology Unit, Umeå University, Umeå, Sweden,[2]Department of Public Health and Clinical Medicine, Umeå University, Umeå, Sweden,[3]Department of Medical Biosciences, Umeå University, Umeå, Sweden*

Background: Despite previous studies investigating psychological stress in relation to cancer risk, no consensus has been reached as to whether stress is a modifiable risk factor for cancer. This study aims to investigate whether sick leave due to psychological stress can affect the risk of developing cancer.
Method: This is a matched case-control study using Swedish nation-wide register data (study period 2005-2018). The main exposure is stress-related sick leave defined as registered sick leave due to psychological stress with the diagnosis codes of F43 (International Classification of Diseases codes: ICD) and its subclassifications and hereafter referred to as stress leave. For each primary cancer case (except non-melanoma skin cancer), up to five cancer-free controls were matched based on sex, age and county. Conditional logistic regression, conditioned on matching factors and adjusting for socioeconomic factors, was used to calculate odds ratios (ORs) with 95% confidence intervals (CIs). For subgroup analyses by specific tumor sites, Bonferroni-corrected significance level of 0.002 (alpha value divided by the number of tumor sites = 0.05/24) was also applied.
Results: The study comprised 516 678 cancer cases and 2 357 433 matched controls. Stress leave of any duration, was associated with a modestly increased risk of cancer, with the highest risk observed for 1-30 days of leave, vs no leave during follow-up (adjusted OR 1.05, 95% CI 1.02-1.09). In subgroup analyses by tumor sites, stress leave was associated with an increased risk of prostate cancer (adjusted OR for >90 days vs no stress leave 1.10, 95% CI 1.01-1.20) and cervix cancer (adjusted $OR_{>90\ days\ vs\ no\ leave}$ 1.11, 95% CI 1.05-1.17). For lung cancer, an inverse risk relationship was found (adjusted $OR_{>90\ days\ vs\ no\ leave}$ 0.88, 95% CI 0.77-0.99). For other tumor sites, associations were generally null or had wide confidence intervals. After applying a Bonferroni-corrected significance level, the association was still significant for cervical cancer. Further examination by sex, specific types of psychological stress and cancer groups based on established etiology (tobacco use, obesity, alcohol consumption and gastric hyperacidity) showed a clear exposure-response trend in men and pronounced associations for exhaustion disorder (ICD code: F43.8A) and tobacco-related cancers. In a post-hoc analysis, the association for other HPV-related cancers was similar to that for cervical cancer but not statistically significant.
Conclusion: In this register study covering the entire Swedish population, we found that stress-related sick leave was associated with modestly higher risk of cancer, particularly the risk of cervical cancer. Potential higher risk of prostate cancer and lower risk of lung cancer were observed, though these associations were not statistically significant after controlling for multiple testing.

#6475

Compatibility of chatbot-based mobile and paper-based FFQs in participants with colorectal or gastric cancer screening

Eui Yeon Lim[1], Yun Jeong Lim[2], Sang Hoon Kim[2], Woongsup Kim[3], Jung Eun Lee[1]. *[1]Food and Nutrition, College of Human Ecology, Seoul National University, Seoul, Korea, Republic of,[2]Internal Medicine, Dongguk University Ilsan Hospital, Dongguk University College of Medicine, Goyang, Korea, Republic of,[3]Information Communication Engineering, Dongguk University, Seoul, Korea, Republic of*

Background: The food frequency questionnaire (FFQ) is the most commonly used method to assess the usual diet of groups and individuals. Paper or electronic FFQ consists of frequencies and portion sizes of foods and beverages. We developed a chatbot-based mobile FFQ, by embedding the validated FFQs in KakaoTalk, Korea's most popular mobile messenger. We examined the compatibility of the paper and chatbot-based mobile FFQs in participants who underwent cancer screening endoscopy.
Method: A total of 50 men and 45 women aged 24 to 79 were recruited from Dongguk University Ilsan Hospital between April and August 2022. Participants underwent gastroscopy or colonoscopy for cancer screening. They completed both the paper and chatbot-based mobile FFQs. Log-transformed intakes of energy and nutrients were compared using the Pearson correlation coefficient. We also calculated the Cohen's Kappa coefficients and evaluated Bland-Altman plots and the percent agreement from cross-classification to assess the compatibility.
Results: The Pearson correlation coefficients of energy and energy-adjusted nutrients ranged from 0.74 (niacin) to 0.90 (vitamin A), and the median of coefficients was 0.85. Cohen's kappa coefficient ranged from 0.56 (sodium) to 0.75 (n-6 fatty acid). In the Bland-Altman plots, most data were located between the lower and upper limits of agreement. The percentages of participants classified into the same and adjacent quartiles were between 88% and 98% for energy-adjusted nutrients.
Conclusions: Our study suggests a good compatibility of paper and chatbot-based mobile FFQs. The chatbot-based mobile FFQ may provide comparable intake rankings and be used to evaluate the association between dietary intake and disease risk in longitudinal studies.

Novel Factors Associated with Cancer Mortality

#6480

Mortality in patients with monoclonal gammopathy of undetermined significance: an analysis of National Health and Nutrition Examination Survey

Mengmeng Ji[1], John Huber[1], Mei Wang[1], Yi-Hsuan Shih[1], Yao-Chi Yu[1], Lawrence Liu[2], Theodore Thomas[3], Martin W. Schoen[3], Kristen M. Sanfilippo[1], Graham A. Colditz[1], Shi-Yi Wang[4], Su-Hsin Chang[1].
[1]Washington University in St. Louis, Saint Louis, MO,[2]City of Hope Comprehensive Cancer Center, Duarte, CA,[3]St. Louis Veterans Affairs Medical Center, Saint Louis, MO,[4]Yale University, New Heaven, CT

Introduction: Monoclonal gammopathy of undetermined significance (MGUS) is an asymptomatic premalignant plasma cell disorder with an annual risk of ~1% of progression to more advanced diseases, including multiple myeloma (MM). Few studies reported mortality risk in patients with MGUS, among which the diagnosis of MGUS was typically incidental due to unrelated symptoms or laboratory abnormalities. This study aims to compare the survival of MGUS patients with the U.S. general population using a nationally representative screening-based survey.
Methods: Data were obtained from the third National Health and Nutrition Examination Survey (NHANES III) 1988-1994 and continuous NHANES 1999-2004, with follow-up all-cause mortality data through December 31, 2019. Participants were screened for MGUS by protein electrophoresis, immunofixation, and kappa and lambda free light chain assays in serum. Multivariable Cox-proportional regressions were performed, adjusting for demographic characteristics (age, gender, race/ethnicity, education, income, body mass index [BMI]), health behaviors (smoking, physical activity), baseline medical conditions (hypertension, diabetes, osteoporosis, myocardial infarction, stroke, congestive heart failure, coronary heart disease, peripheral vascular disease [PVD], arthritis, liver diseases, chronic obstructive pulmonary disease, renal diseases, cancer), and survey year. We also tested the interaction between race/ethnicity and MGUS diagnosis in the fully adjusted model. The NHANES complex sampling design was accounted for in all analyses to obtain population estimates.

Results: The prevalence of MGUS among the U.S. population aged 50 years or older was 2.5% in 1988-1994 (sample size n=6,557; population size N=56,136,480) and 2.3% in 1999-2004 (n=5,847; N=68,835,295). MGUS patients were older and more likely to have PVD (13.1% vs. 7.7%, p = 0.03). No evidence was found showing a difference in gender distribution, education, income, BMI, and other comorbidities between the two populations. In NHANES 1999-2004, MGUS was associated with an increased risk of death (Hazard ratios [HR] 1.20, 95% CI: 1.02-1.41, p = 0.03) compared to the general population. NHANES III also showed a trend toward increased risk of mortality (HR 1.15, 95% CI: 0.89-1.48, p = 0.27). No interaction between race/ethnicity and MGUS diagnosis was found. It was notable that PVD was associated with an increased risk of death (HR 1.67, 95% CI: 1.43-1.94, p < 0.001).
Conclusion: In the large cohort of NHANES participants, MGUS was associated with an increased risk of mortality. MGUS is typically viewed as a "benign" condition that has the potential to progress to cancer. These findings suggest that there may be alternate health implications to a diagnosis of MGUS. Future studies should focus on the causes of death in this population and the role of MGUS.

#6481
Systematic review of the literature: tertiary prevention in leukemia patients
Nikita Manyak, Su Yon Jung. *UCLA - University of California Los Angeles, Los Angeles, CA*

Background: After conducting a thorough search, we found a lack of published literature review about the tertiary prevention of patients with leukemias and discussion about their prognosis. We thus searched related publications in the last decade and wrote an extensive literature review on the topic.
Method: We conducted an extensive search for electronic database via MEDLINE and PubMed. Using the key terms "progression-free survival (PFS) leukemia" and restricting the search to "English language" for the last decade, we initially found 1,083 published papers on the related topic. On the basis of review, we collected necessary data and extracted some recommendations for treatment of leukemia patients.
Results: Standard treatments such as Daunorubicin, Doxorubicin, or Asparaginase for leukemias in children, adolescents, and young adults (ages 18 to 24) were associated with high rates of relapse and other complications within 5 years post-treatment. Of note, Blinatumomab and Ibrutinib-Rituximab showed higher success rates of PFS and overall survival compared to other chemotherapy treatments. Two-year disease free survival was 39.0% for patients with intensive chemotherapy while it was 54.4% for patients given the anticancer drugs. In addition, two-year overall survival was relatively worse (58.4%) in patients treated with chemotherapy compared with those with other treatments (71.3%). In comparison, radiotherapy has been used for patients who relapsed after remission and found to be more successful in the long run in preventing another relapse and leading to higher rates of overall survival. For example, patients previously experienced a 78% response rate to the treatment received cranial radiation; compared to the survival rate (11.3%) of patients who were not treated with the radiation, they experienced higher four-year survival rates (77.7%). For most pediatric leukemias, allogenic stem cell therapies have been the most effective treatment with a higher rate of remission. However, after this treatment, a majority of the patients relapsed soon after and were unable to continue fighting the disease, resulting in death. Of note, during the past 10 years, some immunotherapies have been discovered and reported more effective than traditional chemo/radiotherapies and allogenic/autologous stem cell treatments. In particular, Tisagenlecleucel, a chimeric antigen receptor (CAR) T-cell therapy, has been approved to treat pediatric leukemias when they have relapsed after initial or tertiary remission. Their 5 or 10 year survival rate after this treatment was over 50%.
Conclusion: Among the standard treatments that have been studied during a decade for leukemia in children and adolescents, CAR T-cell immunotherapy appears to be the most effective after patient relapse. More research for the immunotherapies on different populations with diverse age groups is requested on a tertiary prevention perspective.

#6482
CLDN18.2 expression is associated with clinicopathological features and prognosis of Chinese patients with digestive system cancers: a retrospective analysis
Chong XiaoYi[1], Changsong Qi[1], Jifang Gong[1], Miao Zhang[1], Mingyang Ma[1], keren Jia[1], Ting Zhou[1], Li Jian[1], Zhi Peng[1], Jun Xiao[2], Xiaohui Peng[2], Zhen Liu[1], Zonghai Li[2], Xiaotian Zhang[1], Lin Shen[1]. *[1]Peking*

University Cancer Hospital, Beijing, China,[2]CARsgen Therapeutics Co., Ltd., Shanghai, China

Importance: CLDN18.2 was a promising therapeutic target in solid tumors, whereas the clinicopathological features of Chinese CLDN18.2-positive cancer patients were rarely elucidated.
Objective: This study aimed to explore the association between CLDN18.2 expression and clinicopathological features of Chinese patients with CLDN18.2-positive digestive system cancers.
Methods: This retrospective study included digestive system cancer patients from June 2019 to April 2021 who were screened for two clinical trials of CT041 (an anti-CLDN18.2 CAR-T cell, NCT03874897, and NCT04581473), which were initiated at our center.
Results: A total of 875 digestive system cancer patients were included. CLDN18.2 expression was observed in 73.1% GC patients, 61.8% pancreatic cancer (PC) patients, 10.6% colorectal cancer (CRC) patients, and 65.6% biliary tract carcinoma (BTC) patients. In GC, CLDN18.2 expression was associated with age, sex, and Lauren phenotype (all P<0.01). CLDN18.2-positive GC patients had a higher incidence of uterine adnexa metastasis (6.4% vs. 20.8%, P<0.001), and a lower incidence of liver metastasis (22.2% vs. 35.7%, P<0.001). In PC, CLDN18.2-positive cases had a higher proportion of tumors with moderate/high differentiation (46.1% vs. 19.0%, P<0.001), compared with CLDN18.2-negative patients. Additionally, compared with CLDN18.2-negative patients, the proportion of right colon cancer was higher in CLDN18.2-positive patients (40% vs. 18.1%, P=0.028).
Conclusions: The results of this study suggested that CLDN18.2-positive tumors had unique clinicopathological features, which provided a theoretical basis for the treatment of CLDN18.2 positive tumors.

#6483

The association between food deserts, food swamps, and obesity-related cancer mortality in the United States: the new epidemic

Malcolm Bevel, Meng-Han Tsai, April Parham, Sydney Andrzejak, Samantha R. Jones, Justin X. Moore.
Medicine, Augusta University, Augusta, GA

Background: Obesity-related cancers account for 40% of all cancers in the United States (U.S.). Healthy food consumption is a modifiable factor shown to reduce obesity-related cancer mortality, but residing in geographical areas with poor access to grocery stores/farmer's markets (food deserts) or higher access to fast-food/convenience stores (food swamps) reduces healthy food access and has been severely understudied.
Methods: We conducted an ecological study utilizing 2010 - 2020 data from the U.S. Department of Agriculture Food Environment Atlas and Center for Disease Control and Prevention mortality. 3,041 U.S. counties with complete information on food environment scores and obesity-related cancer mortality data were included. Food swamp score was calculated as the ratio of fast-food and convenience stores to grocery stores and farmer's markets. Obesity-related cancer (based on the International Agency for Research on Cancer evidence between obesity and 13 types of cancer) mortality rates were categorized as high (≥71.8 per 100,000) versus low (<71.8 per 100,000) per county. We performed an age-adjusted multivariable polytomous logistic regression for the association between food desert scores, food swamp scores, and obesity-related cancer mortality rates.
Results: Counties with high obesity-related cancer mortality rates had higher percentage of NH-black population (3.30 vs 1.80), persons older than 65 years (15.7 vs 15.4), poverty rates (19.0 vs 14.4), adult obesity rates (33.0 vs 32.1), and adult diabetes rates (12.5 vs 10.7) when compared to counties with low obesity-related cancer mortality (p-value < 0.0001; Table 1). We observed 77% increased odds of having high obesity-related cancer mortality rates among U.S. counties with high food swamp scores (adjusted odds ratio [AOR] = 1.77; 95% CI: 1.43 - 2.18). A positive dose-response relationship between three levels of food desert and food swamp scores and obesity-related cancer mortality was also observed (p-value <0.0001).
Conclusions and Relevance: Policymakers, funding agencies, and community stakeholders should implement sustainable approaches at combating obesity and establishing healthier accessible food such as creating more walkable neighborhoods and community gardens.

#6484

Impact of time between last childbirth and diagnosis of early-onset breast cancer on survival in germline *BRCA1/2* carriers

Zhenzhen Zhang[1], Shangyuan Ye[1], D Gareth Evans[2], Pepper Schedin[1]. *[1]Knight Cancer Institute, Oregon Health & Science University, Portland, OR,[2]The University of Manchester, Manchester, United Kingdom*

INTRODUCTION: Young women diagnosed with breast cancer in close proximity to childbirth have increased risk of mortality compared to nulliparous women, and the postpartum period has been identified as a risk window for breast cancer metastasis. BRCA1/2 germline mutation carriers have a high risk of developing breast cancer at young age, yet it is unknown if recent childbirth is a poor prognostic risk factor for BRCA1/2 carriers. Here we assessed whether time between last childbirth and breast cancer diagnosis impacted survival among early-onset BRCA1/2 breast cancer patients. METHODS: The study population includes 903 female BRCA1/2 mutation carriers diagnosed with stage I-III breast cancer at ≤45 years of age between 1950 and 2021 in the UK. The primary outcome of this study is all-cause mortality. The primary exposures were no prior childbirth (n=224), or time between last childbirth and breast cancer diagnosis grouped as 0-<5 years (n=228), 5-<10 years (n=191), or ≥10 years since last childbirth (n=260). Cox proportional hazards regression was applied to identify factors associated with risk of 20-year mortality. RESULTS: Breast cancer diagnosed 5-<10 years after last childbirth was associated with an elevated risk for mortality [HR=1.56 (95% CI, 1.05-2.30)] compared to nulliparous cases after adjusting for patient age and tumor stage. Across groups, nulliparous women had the best prognosis, suggesting parity may increase risk of death in BRCA1/2 carriers. ER-negative cancers were the dominant tumor type across all groups: 54.8% (nulliparous), 52.6% [postpartum breast cancer (PPBC) <5], 58.4% (PPBC 5-<10), and 54.0% (≥10). ER-negative cases were more prevalent among BRCA1 carriers (77%) compared to BRCA2 carriers (24%). In stratified analyses by either ER or BRCA status, increased mortality in the PPBC 5-<10 group was significant for ER-negative cases [HR=3.12 (95% CI, 1.22-7.97)] and BRCA1 carriers [HR=2.03 (95% CI, 1.15-3.58)], compared to nulliparous groups. For ER-positive cases, 71% of cases were BRCA2 carriers, and the most significant postpartum interval among ER-positive cases was observed in the 0-<5 group [HR=2.35 (95% CI, 1.02-5.42)]. No association was observed for BRCA2 carriers with PPBC 0-<5 vs nulliparous groups [HR=1.26 (95% CI, 0.73-2.16)].CONCLUSION: Results suggest that BRCA1/2 breast cancer patients are at increased risk for all-cause mortality if diagnosed within 10 years of childbirth. For ER-positive disease, poorest prognosis occurs within 0-5 years postpartum, consistent with promotion of existing sub-clinical tumors. For BRCA2 carriers, the association between postpartum diagnosis and mortality is weak. For ER-negative disease, similar to BRCA1 carriers, poorest prognosis occurs 5-10 years postpartum, suggesting an interaction between BRCA1 and parity may result in increased tumor initiation.

#6485

Oxidative phosphorylation-associated radiomic feature and survival of women with serous ovarian cancer

Christelle Colin-Leitzinger, Jaileene Perez-Morales, Steven Eschrich, Jamie K. Teer, Sweta Sinha, Melissa J. McGettigan, Daniel K. Jeong, Olya Stringfield, Mahmoud A. Abdalah, Natarajan Raghunand, Robert J. Gillies, Jing-Yi Chern, Matthew Schabath, Lauren Cole Peres. *H. Lee Moffitt Cancer Center, Tampa, FL*

Novel biomarkers that can be utilized for clinical decision support to improve patient outcomes are critically needed for ovarian cancer. At present, there are no standard of care biomarkers to inform the first-line treatment regimen (neoadjuvant chemotherapy vs. upfront surgical debulking) best suited for each patient or which patients are at the highest risk of recurrence. To address this unmet need, we identified pre-treatment computed tomography (CT) image-based radiomic features predictive of outcomes and primary treatment response among 298 women diagnosed with serous ovarian cancer from 2008 to 2019. A decision tree analysis identified a single volumetric feature, region of interest (ROI) volume center of mass (CoM) in the X direction, as the most informative radiomic feature that stratified patients with upfront surgery into high- and low-risk groups for overall survival. The high-risk group consists of patients with higher values of the radiomic feature. In the training (N=91) and test (N=91) cohorts of women treated with upfront surgery, high-risk patients had worse survival compared to low-risk patients (HR=2.01, 95% CI=1.07, 3.77 and HR=2.23, 95% CI=1.19, 4.17, respectively). This radiomic feature was not associated with survival among women

treated with neoadjuvant chemotherapy (N=116; HR=1.23, 95% CI=0.73, 2.07). To reveal potential underlying biology of this radiomic feature, we performed RNAseq gene expression profiling on 47 formalin-fixed paraffin-embedded tumor specimens and correlated gene expression with the radiomic feature using DESeq2 from RSEM estimates. Dichotomized analysis (high- vs. low-risk) yielded 7 significant genes and continuous analysis yielded 15 significant genes (adjusted $p<0.05$), with both approaches identifying *AKT2* and *PSMC4*. Gene set enrichment analysis (GSEA) was used to identify enriched gene sets from continuous associations using the MSigDB Hallmarks pathways (adjusted $p<0.05$). GSEA identified the oxidative phosphorylation (OXPHOS) pathway as one of the gene sets most negatively associated with the predictive radiomic feature (Hallmark Normalized Enrichment Score=-2.28, adjusted $p<0.001$). We derived a PCA-based gene signature from significantly associated OXPHOS genes ($p<0.01$) resulting in a negative correlation with the radiomic feature ($R=-0.65$, $p<0.001$). Prior studies have shown that high OXPHOS ovarian tumors are associated with an increased response to conventional chemotherapy, suggesting that OXPHOS may be a key pathway for chemoresistance in ovarian cancer. In summary, we identified an OXPHOS-associated radiomic feature predictive of survival among women with serous ovarian cancer treated with upfront surgery. Further research is needed to elucidate the biologic and mechanistic underpinnings of the identified radiomic feature and to validate these findings in a larger cohort of women with ovarian cancer.

#6486

Single nucleotide polymorphisms that predict serum cholesterol as a prostate cancer prognostic factor - a Mendelian randomization study

Sebastian Boele[1], Aino Siltari[1], Paavo Raittinen[2], Johanna Schleutker[3], Kimmo Taari[4], Kirsi Talala[5], Teuvo Tammela[1], Anssi Auvinen[6], Teemu J. Murtola[1]. *[1]Faculty of medicine and health technology, Tampere University, Tampere, Finland,[2]Oriola, Helsinki, Finland,[3]Turku University, Turku, Finland,[4]Urology, Helsinki University Hospital, Helsinki, Finland,[5]Finnish Cancer Registry, Helsinki, Finland,[6]Faculty of social sciences, Tampere University, Tampere, Finland*

Introduction: Intracellular cholesterol metabolism plays an important role in prostate cancer progression and emergence of treatment resistance. However, it remains unclear whether serum cholesterol and lipoproteins are associated with prostate cancer outcomes. Studies on serum cholesterol and cancer are often confounded by lifestyle factors such as diet and obesity. A possible solution is to use instrumental variables, such as SNPs predicting serum cholesterol. According to the Mendelian randomization theory, germline SNP distribution is unaffected by confounding variables such as diet and lifestyle factors. **Objective**: To estimate whether SNPs that predict serum cholesterol and lipoproteins also predict mortality among a cohort of men with prostate cancer. **Methods**: Our study cohort consisted of 3,241 men diagnosed with prostate cancer between 1996-2015, using data collected by the Finnish Randomized Study of Screening for Prostate Cancer. Blood samples were genotyped by PRACTICAL consortium. A UCSC genome browser was utilized for selecting 85 SNPs in lipid metabolism-associated genes. Dates and causes of deaths between 1996-2015 were obtained from the Statistics Finland's statistics on causes of death. Information on serum cholesterol and lipoprotein measurements were obtained from a regional laboratory database.Scores predicting serum cholesterol, LDL, HDL and triglyceride level by SNP genotype were created using linear regression and lasso regression. Risk of prostate cancer death and overall mortality by level of the SNP risk score were evaluated with multivariable-adjusted Cox regression. Follow-up started at prostate cancer diagnosis and continued until death, emigration or common closing date of Dec 31, 2015.**Results:** SNP score predicting total cholesterol stratified prostate cancer patients both for disease-specific (HR 1.27, 95% CI 0.49-3.28 for highest tertile vs. lowest) and overall survival (HR 1.43, 95% CI 0.94-2.20, p for trend = 0.077), albeit statistical significance was not reached. Similar survival differences were observed for SNP score predicting triglyceride level, but not for scores predicting LDL or HDL.**Conclusions:** SNPs predicting serum cholesterol and triglycerides are likely prognostic factors for survival of prostate cancer patients. This suggest serum cholesterol and lipoproteins areimportant in prostate cancer progression.

Total cholesterol SNP scoreProstate-cancer specific survival
Overall survival

#6487

Association between telomere length and overall survival in lung cancer patients: a mendelian randomization study

Ting Zhai, David C. Christiani, Zachary D. Nagel. *Harvard T.H. Chan School of Public Health, Boston, MA*

Background: An association between chronological age and poor lung cancer survival is well established, but it is unclear whether accelerated biological aging may also predispose lung cancer patients to worse survival outcomes. While telomere shortening in blood cells is a biomarker of aging, its relationship to lung cancer prognosis remains unclear due to limited sample size, confounding, and reverse causation from observational studies. As telomere length could be a precursor of worse prognosis, a causal inference method is needed to clarify the role of telomere length in predicting lung cancer outcomes.
Methods: A Mendelian Randomization study for the causal relationship between telomere length and overall survival in lung cancer was carried out. We searched the GWAS catalog for single-nucleotide polymorphisms (SNPs) associated with telomere length and collected effect estimates for the association between each SNP and telomere length from the literature. The summary data for all SNPs were acquired by analyzing their associations with overall survival of lung cancer patients in the Boston Lung Cancer Study (BLCS) and through Cox proportional hazards regression. The effect size of telomere length on overall survival was calculated and compared through several weighting methods including inverse-variance weighting (IVW) and MR-Egger.
Results: A total of 16 SNPs were identified as the genetic instruments for telomere length. 1798 lung cancer patients from BLCS provided survival data with a median follow-up of 33 months. Surprisingly, a non-significant *positive* trend was observed for the association between telomere length and overall survival across the weighting methods (IVW: HR 1.718, 95%CI 0.849 - 3.476; MR-Egger: HR 2.347, 95%CI 0.592 - 9.309). Further analysis is ongoing to incorporate more patients and genetic instruments for additional markers of biological aging in the BLCS to explore the source of heterogeneity (I^2= 98.1%) in the present study and gain more power for detecting the underlying relationship between telomere length and overall survival in lung cancer.
Conclusion: A positive trend between telomere length and risk of death in lung cancer patients is consistent with previous reports of an association between increased cancer risk and longer telomere length, but is seemingly at odds with an established link between chronological age and poor lung cancer prognosis. Since markers of biological aging are strongly correlated with chronological age, we conclude that a more robust assessment of biological age will be needed to clarify the causal relationship between telomere length and lung cancer prognosis.

#6488

Correlation of availability of primary care physicians and colorectal cancer-related mortality in the United States: Do racial disparities exist?

Udhayvir S. Grewal[1], Shiva J. Gaddam[2], Manik Aggarwal[3], Subhash C. Garikipati[4], Prabhat Kumar[5], Naomi Fei[1]. *[1]University of Iowa Holden Comprehensive Cancer Center, Iowa City, IA,[2]Hematology and Oncology, LSU Health Sciences Center, Shreveport, LA,[3]Gastroenterology and Hematology, Mayo Clinic, Rochester, MN,[4]Carillion Clinic, Roanoke, VA,[5]Internal Medicine, Cleveland Clinic Fairview, Cleveland, OH*

Introduction: Colorectal cancer (CRC) is the second leading cause of cancer death in the United States (US). Primary care physicians (PCP) are critical towards a successful CRC screening program. However, the impact of availability of PCP on CRC-related mortality is not well studied.
Materials and Methods: We extracted data on crude incidence and mortality rates of CRC among all 50 states and District of Columbia (D.C.) from the Center for Disease Control (CDC) WONDER database for the year 2019. Data on number of actively practicing PCPs in all 50 states and D.C. for the year 2020 were obtained from Association of American Medical Colleges (AAMC) State Physician Workforce Data Report. The correlation between the ratio of number of PCPs per CRC case with age-adjusted mortality rate (AAMR) for CRC was studied by state and within White and African American (AA) populations from 2017-2019. Pearson's co-efficient was used to study correlations and T-test was used for comparing independent samples. Statistical analysis was performed using VassarStats.

Results: The median AAMR for CRC from 2017-2019 in the US was 13.2 (IQR 11,15.4) per 100,000 population. AAMR for CRC was significantly higher among AA versus White populations (t=5.79, p<0.001). The national median PCP per CRC case ratio was 2.14 (IQR 1.46, 2.82). Higher state-wide PCP per CRC case ratio correlated with lower state CRC-related mortality (r=-0.36, p=0.011). PCP per CRC case ratio was significantly lower among AA as compared to White populations (t=-15.95, p<0.0001). Higher PCP per CRC case ratio correlated with lower CRC-related mortality among both White (r=-0.64, p<0.0001) and AA (r=-0.57, p=0.0002) populations. Using Fisher r-to-z transformation, we found no significant difference between the correlation of PCP per CRC case ratio with CRC-related mortality in White versus AA populations (z=-0.51, p=0.61).
Conclusion: Results of this study suggest that greater availability of primary care physicians correlates with lower CRC-related mortality. AA have a significantly higher AAMR for CRC with a lower PCP per CRC case ratio. This may indicate a lower access to primary care among AA populations with CRC. Our results underscore the need to expand access to primary care among AA populations with the goal of minimizing disparities in CRC-related mortality.

#6489

Marital status, living arrangement, and overall survival among individuals with advanced prostate cancer in the IRONMAN cohort

Naiyu Chen[1], Colleen B. McGrath[1], Caroline I. Ericsson[1], Jane B. Vaselkiv[1], Michelle O. Sodipo[1], Emily M. Rencsok[1], Konrad H. Stopsack[2], Daniel J. George[3], Karen A. Autio[4], Dana E. Rathkopf[4], Kathryn L. Penney[5], Lorelei A. Mucci[1]. *[1]Epidemiology, Harvard T.H. Chan School of Public Health, Boston, MA,[2]Clinical and Translational Epidemiology Unit, Massachusetts General Hospital and Harvard Medical School, Boston, MA,[3]Duke Cancer Institute, Durham, NC,[4]Memorial Sloan Kettering Cancer Center, New York, NY,[5]Medicine, Brigham and Women's Hospital and Harvard Medical School, Boston, MA*

Background: More than 100,000 individuals in the United States are survivors of advanced prostate cancer, defined as metastatic hormone sensitive (mHSPC) or castration resistant prostate cancer (CRPC). This growing, vulnerable population could be uniquely susceptible or responsive to factors that are associated with overall survival. We investigated the associations of marital status and living arrangements with overall survival among individuals with advanced prostate cancer in the International Registry for Men with Advanced Prostate Cancer (IRONMAN).
Methods: We included 2,347 men (ages 40-96 years, median 70 years) with advanced prostate cancer recruited between 2017 and October 2022. Cox proportional hazards models estimated adjusted hazard ratios (adjusted HR) and 95% confidence intervals (CI) for the associations between marital status (married vs. not married), living arrangement (living alone vs. not living alone) and all-cause mortality, mutually adjusting for marital status and living arrangement and potential confounders (disease state [mHSPC vs. CRPC], country of enrollment, age at enrollment, race, education, employment status, smoking status, family history of prostate cancer, prostate specific antigen level at enrollment, and Gleason score). We conducted stratified analyses by disease state (mHSPC vs. CRPC), age (<70 vs. ≥70 years), and country of enrollment (North America vs. others).
Results: This study included 1524 (65%) participants with mHSPC and 809 (35%) with CRPC. 1690 (77%) were married and 338 (16%) lived alone. Over the follow-up period (maximum: 52 months, median: 6 months, IQR: 13 months), we observed 451 deaths, with 313 deaths among married individuals and 59 deaths among those who lived alone. Overall, married individuals had better survival compared to those not married (adjusted HR: 0.52; 95% CI 0.35, 0.78), while those living alone had better survival compared to those not living alone (adjusted HR: 0.48; 95% CI: 0.29, 0.80). The protective association between being married and survival is stronger among those with mHSPC (adjusted HR: 0.42; 95% CI: 0.24, 0.71) compared to those with CRPC (adjusted HR: 0.72; 95% CI: 0.35, 1.49) and stronger among those with ages 70 or older (adjusted HR: 0.43; 95% CI: 0.25, 0.74) compared to those younger than 70 (adjusted HR: 0.71; 95% CI: 0.36, 1.43).
Conclusion: Being married was associated with better survival among advanced prostate cancer survivors. While living alone was also associated with better survival, this finding should be interpreted with caution as there may be residual confounding by socioeconomic status or physical functioning.

#6490

Post-diagnosis statin use and survival among head and neck cancer patients: A cohort study in the US military health system

Jie Lin, Craig D. Shriver, kangmin Zhu. *Uniformed Services University, Bethesda, MD*

Head and neck squamous cell carcinoma (HNSCC) arises from the mucosal lining of the aerodigestive tract. Statin is a class of commonly prescribed medications used for treatment of high cholesterol. Studies have shown that statin exhibits anticancer effects, and the use of statin is associated with improved survival of common cancers, such as prostate, breast and colorectal cancers. However, few research has been conducted on statin use in relation to the survival of HNSCC. This study assessed whether statin use after HNSCC diagnosis is associated with overall survival among patients with HNSCC in the U.S. military health system (MHS). The MHS provides universal health care to its beneficiaries with no or little out-of-pocket cost, thus a study in the MHS reduces the effects of prescription drug access related to patients' insurance coverage, race and socio-economic status. This study included 1,842 adult patients (18 or older) with histologically confirmed HNSCC identified from the MilCanEpi database which contains information from the Department of Defense's Central Cancer Registry (CCR) and the Military Health System Data Repository (MDR). Patients were diagnosed between January 1, 2002 and December 31, 2014 and followed up through December 31, 2015. Statin use was extracted from the MDR pharmacy data containing prescription records from all sources. Among the 1,842 patients, 389 patients used statin after HNSCC diagnosis. Time-dependent multivariate Cox proportional hazards models were used to assess the relationship between post-diagnosis statin use and overall survival, reducing the potential effects of immortal time bias. Statistical adjustment was made for covariables including age, sex, race, Hispanic ethnicity, active-duty status, history of cardiovascular diseases, Charlson comorbidity index, baseline statin use, tumor site, tumor stage and cancer treatments. Increased post-diagnosis cumulative use of statin (per one-year of use) conferred a significant improved survival with adjusted hazard ratio (HR) of 0.70 (95% CI=0.55 to 0.90). When analysis was stratified by status of statin use prior to HNSCC diagnosis, the HRs were 0.36 (95% CI=0.19-0.69) and 0.81 (95% CI=0.59-1.11) for those who used and did not use it before the diagnosis, respectively. While the numbers of patients for each group of this stratified analysis were not large, our study suggest that prolonged duration of Statinuse may be associated with improved survival among HNSCC patients. Future research with a larger number of patients is warranted.

Disclaimer: The contents of this publication are the sole responsibility of the authors and do not necessarily reflect the views, opinions, or policies of the USUHS, HJF, the DoD or the Departments of the Army, Navy, or Air Force. Mention of trade names, commercial products, or organizations does not imply endorsement by the U.S. Government.

#6491

Temporal changes in circulating sex hormones and aromatase activity and associations with lung cancer survival in postmenopausal women

Yingya Zhao[1], Xiao-Ou Shu[1], Yu-Tang Gao[2], Mark M. Kushnir[3], Qiuyin Cai[1], Hui Cai[1], Qing Lan[4], Nathaniel Rothman[4], Wei Zheng[1], Gong Yang[1]. *[1]Vanderbilt University Medical Center, Nashville, TN,[2]Shanghai Jiaotong University School of Medicine, Shanghai, China,[3]ARUP Institute for Clinical and Experimental Pathology, Salt Lake City, UT,[4]National Cancer Institute, Bethesda, MD*

Background: Exogenous sex hormone supplements had been associated with increased lung cancer mortality in a large clinical trial. No study to date has evaluated temporal trajectories of circulating sex hormones and aromatase activity and their associations with lung cancer survival.

Objective: To characterize temporal changes in prediagnostic levels of circulating sex hormones and aromatase activity and to evaluate their associations with overall survival in lung cancer patients.

Methods: Included in the analysis were 385 incident lung cancer patients identified in a large prospective cohort among postmenopausal women who had never used cigarette products nor exogenous sex hormone supplements. Concentrations of sex hormones were quantitated using LC-MS/MS assays in prediagnostic plasma samples. The product-substrate molar ratio of estrone to androstenedione was used as an index of

aromatase activity (IAA). A multivariable Cox model with restricted cubic spline functions was used to calculate hazard ratio (HR) for overall survival.
Results: Of 385 patients with lung cancer, 308 died during a median follow-up of 18.1 years. Initial analyses in all patients showed that higher levels of circulating estrone and IAA and lower levels of androstenedione and testosterone were associated with poorer overall survival after adjusting for nonclinical covariates. In analyses restricted to those with clinical data (n=281), stronger associations were found after further adjustment for tumor stage and treatment regimens. Compared with patients at the median level of IAA, adjusted HRs (95% CI) for total mortality in those at the 30^{th}, 70^{th}, 90^{th} and 95^{th} percentiles were 0.98 (0.84-1.13), 1.05 (0.94-1.16), 1.28 (1.06-1.54), and 1.64 (1.27-2.12), respectively, with *P*-overall < 0.001. A similar positive association was observed for estrone. In contrast, inverse associations were seen for androgens. For example, compared with the median level of testosterone, HRs (95% CI) for those at the 5^{th}, 10^{th}, 30^{th}, 70^{th} percentiles were 2.10 (1.43-3.09), 1.69 (1.29-2.23), 1.45 (1.19-1.76), and 0.86 (0.78-0.94), respectively, with *P*-overall = 0.001. Further, we found that circulating levels of sex hormones changed during disease progression. The closer the hormone measurement to cancer diagnosis the higher the IAA and estrone levels (*P*-overall < 0.001 for both), and the temporal change plateaued 10 years before cancer diagnosis (*P*-nonlinearity < 0.001 for both). An opposite temporal pattern was found for testosterone. Moreover, the significant association between sex hormones and lung cancer survival was only observed when sex hormones were measured within 10 years before diagnosis.
Conclusions: Findings from our study, for the first time, demonstrate temporal changes in circulating sex hormones and their associations with lung cancer survival in postmenopausal women.

#6492
Body mass index characterization of patients undergoing neoadjuvant chemotherapy for breast cancer: Correlation with survival
Sangeetha Prabhakaran[1], Vernon S. Pankratz[2], Christopher F. McNicoll[3], Jacklyn M. Nemunaitis[2], Nadja Falk[4], Jain Zhou[4]. *[1]University of New Mexico, Albuquerque, Mexico,[2]University of New Mexico/UNM Comprehensive Cancer Center, Albuquerque, NM,[3]Kaiser Permanente Anaheim and Irvine Medical Centers, Anaheim, CA,[4]University of New Mexico, Albuquerque, NM*

Background: The significance of body mass index (BMI) on treatment outcomes of neoadjuvant chemotherapy for breast cancer and impact on overall survival is not well understood. We reviewed our single institution data on BMI of patients who underwent curative intent neoadjuvant chemotherapy for breast cancer.
Methods: An IRB-approved retrospective review identified demographics (including BMI), disease presentation, response to treatment, and outcomes. ER and PR status were categorized as low positive (1-9%), positive (≥ 10%) and negative. Treatment response was noted as percent residual cellularity(complete 0%, almost complete < 10%, good 10-30%, moderate >30-80% and poor >80%) in the surgical specimen. Cox proportional hazards models were used to assess relationships with overall survival.
Results: 372 patients underwent curative-intent from 2005-2020; mean age was 51.0 years (SD=11.8); mean BMI was 28.6 (SD=6.3). Median follow-up was 4.3 years. There are significant differences in BMI among racial groups: American Indian (mean 31, SD 6.35), black (mean 30.1, SD 6.89), white (mean 28.3, SD 6.11) (p=0.001). There are significant differences in BMI between Hispanic and non-Hispanic patients: Hispanic (mean 29.6, SD 6.07), non-Hispanic (mean 27.5, SD 6.44), (p=0.001). Hormone receptor status (ER, PR, HER2 status) was not significantly associated with BMI, nor was treatment response either as complete pathologic response (p=0.52) or percent residual cellularity (p=0.98). BMI was not significantly associated in tumor shrinkage noted by changes in T stage or N stage categorizations from pre- to post-NAC. BMI was significantly associated with overall survival through interactions with ER status (p=0.01), and residual percent cellularity (p=0.02). ER- vs. ER+ risk was higher for those with low (HR, 95% CI=7.87, 2.60-23.8 at BMI=20) and moderate (HR, 95% CI=3.25, 1.68-6.33 at BMI=27.5). A five-point higher BMI was associated with a 1.6-fold higher mortality risk for those with complete percent residual cellularity (95% CI: 1.1-2.4), but this risk differential was not observed for those with good, moderate, or poor residual percent residual cellularity.

Conclusions: In our study, BMI was significantly associated with race and Hispanic ethnicity. Although there were no significant association of BMI with treatment response to neoadjuvant chemotherapy, there appears to be a significant relationship between BMI and overall patient survival, through its interactions with other prognostic factors. Future research efforts should focus on exploring reductions in BMI through modifications of diet and exercise in improving survival of breast cancer patients, particularly those with higher risk tumors.

#6493

Ethnic disparities in breast cancer survival in Guam

Grazyna Badowski[1], Rodney Teria[1], Louis Dulana[1], Cabrini Aguon[1], Lynne Wilkens[2], Yurii Shvetsov[2], Rachel Novotny[2], Rachael T. Leon Guerrero[1]. *[1]University of Guam, Mangilao, GU,[2]University of Hawai'i Cancer Center, Honolulu, HI*

Background: Breast cancer is the second leading cause of cancer-related death among women in Guam. The breast cancer mortality rate is higher in Guam than in the U.S. (27.3 vs 20.3 per 100,000 women, age-adjusted, 2013-2017 data); even though the incidence rate remains lower (86.6 vs 126.8 respectively). Guam has major ethnic disparities in breast cancer survival with CHamoru (indigenous people) and Micronesian (immigrants from other Micronesian Islands) faring much worse than other ethnic groups. The purpose of this study was to determine the survival rates of breast cancer patients in Guam and examine the effects of demographic and other mortality risk factors on breast cancer survival.
Methods: This study included 1105 women diagnosed with primary invasive breast cancer and reported to the Guam Cancer Registry from 1998-2020. Five-year and 10-year survival rates were calculated using the Kaplan-Meier method and were compared using the log-rank test across different ethnic groups: CHamoru (N = 528), Filipino (N = 336), Asian (N = 66), Micronesian (N = 51), and Caucasian (N = 71). The Cox proportional hazards regression was used to investigate the effects of age, year of diagnosis, ethnicity, breast cancer staging, and cancer treatment status on the risk of all-cause mortality.
Results: Mean age at diagnosis was 58.2 years. Significant differences in the 5-year and 10-year survival rates were found across ethnic groups. Micronesians had the lowest 5-year and 10-year survival rates (55.9% and 48.5%) followed by CHamorus (81.1% and 68.1%, respectively). All-cause mortality was higher among CHamoru (HR = 2.28, 95% CI: 1.65, 3.16) and Micronesian women (HR=5.33, 95% CI: 3.30, 8.61) compared with Filipino women after adjusting for age, year of diagnosis, staging, and cancer treatment status. All-cause mortality among White and Asian women was not statistically significantly different from that among Filipino women. Cancer staging also indicated significantly higher hazard rate for late-stage patients when compared to early-stage patients (HR = 3.62, 95% CI: 2.70, 4.85).
Conclusion: The analysis suggests significant differences in breast cancer 5-year and 10-year survival rates across different ethnic groups, with Micronesian women exhibiting the highest hazard rate among women in Guam.
Acknowledgement: This study was supported by the PIPCHE/U54 Grant (U54CA143728), a partnership between the University of Hawai'i Cancer Center and the University of Guam.

#6494

Postdiagnosis adherence to American Cancer Society cancer prevention guidelines and mortality among survivors of obesity-related cancers

Ying Wang, Christina Newton, Marjorie L. McCullough, Lauren R. Teras, Erika Rees-Punia, Caroline Um, Alpa V. Patel. *Population Science, American Cancer Society, Atlanta, GA*

Purpose: To examine the combined and individual associations of postdiagnosis body mass index (BMI), physical activity, diet quality and alcohol consumption with all-cause mortality, cardiovascular disease mortality (CVDM) and cancer-specific mortality (CSM) among survivors of obesity-related cancers.
Methods: American Cancer Society (ACS) Cancer Prevention Study-II Nutrition Cohort participants diagnosed with one of 13 invasive (but non-metastatic) obesity-related cancers between 1992 and 2003 were followed for mortality until 2018. Postdiagnosis lifestyle exposures were assessed at least one year after cancer diagnosis between 1999 and 2003. A lifestyle score ranging 0-8 was created according to adherence to the American Cancer Society (ACS) 2020 cancer prevention guidelines on BMI, physical activity, diet, and

alcohol, with a score of 8 representing optimal behaviors for cancer prevention. Associations of the overall and individual component scores with mortality were estimated using multivariable-adjusted Cox proportional hazards regression models.
Results: Among 7,945 cancer survivors, 4,862 died between 1992 and 2018. Higher ACS guideline score was associated with 6-8% lower risk of mortality per 1 point score increase (all-cause: HR: 0.94, 95% CI: 0.92-0.95; CVDM: HR:0.92, 95% CI:0.89-0.95; CSM: HR: 0.93, 95% CI 0.90-0.97) among cancer survivors. Individual scores of BMI, physical activity, and diet were inversely associated with overall mortality; however, alcohol score was positively associated with all-cause mortality, only among female survivors. Compared with participants who had low scores both before and after cancer diagnosis, those with high scores after diagnosis had lower risk of all-cause mortality, CVDM, and possibly CSM.
Conclusion: Following ACS guidelines on diet and physical activity for cancer prevention after a cancer diagnosis is associated with better survival outcomes among survivors of obesity-related cancers.

#6495

The relationship between inflammatory diet score and cancer-specific outcomes: Systematic review and meta-analysis

Eric Han[1], Eunkyung Lee[2], David Li[1], Jeanette Garcia[2], Humberto Lopez Castillo[2]. *[1]University of Central Florida, Orlando, FL,[2]Department of Health Sciences, University of Central Florida, Orlando, FL*

Cancer remains one of the most prevalent diseases in the United States and a leading cause of death. Large prospective studies have found significant correlations between dietary intake and cancer. Chronic inflammation promotes pro-cancer inflammatory environments and nutrition can influence inflammation, with the intake of certain food items increasing inflammatory biomarkers. The objective of this research was to explore the relationship between inflammatory diet score measured by the Dietary Inflammatory index and all-cause mortality, cancer-specific mortality, and cancer recurrence among cancer survivors. Web of Science, Medline, CINHAL, and PsycINFO databases were searched to collect potentially eligible sources that focus on dietary inflammation and cancer outcomes. All sources were uploaded to Covidence software and screened by two independent blinded reviewers. The quality of the sources was assessed using the Newcastle Ottawa scale and relevant data was extracted and transferred to the Comprehensive Meta Analysis software and a random effects model was used to perform meta-analysis. Of the 1444 studies imported into the Covidence software, 13 passed all the screening stages and were included in the final analysis. Eight studies reported on pre-diagnosis diet while five others reported on post-diagnosis diet. Five studies reported on colorectal cancer, four on breast cancer, two on ovarian cancer, one on endometrial cancer and one on prostate cancer. Meta-analysis of the studies found that being in the highest postdiagnosis DII score indicating pro-inflammatory diet significantly increased the risk of all-cause death among cancer survivors by 33.5% (HR = 1.335, 95% CI = 1.049, 1.698, $n = 6$). Analysis did not show a statistically significant association between DII score and cancer mortality or recurrence (HR = 1.097, 95% CI = 0.939, 1.281, $n = 6$). Analysis by cancer subtype found a significant correlation between postdiagnosis DII score and all-cause mortality among the breast cancer survivors (HR = 1.335, 95% CI = 1.041, 1.711, $n = 3$) though there were no significant associations between DII and the outcomes of interest from the other cancer types. The meta-analysis concludes that being in the highest postdiagnosis DII score group significantly increased the risk of all-cause death among cancer survivors. This suggests that risk of all-cause mortality could be reduced for cancer survivors by consuming more anti-inflammatory food components and reducing consumption of pro-inflammatory foods. These findings also warrant more research in this field to clarify the relationship between dietary inflammation as measured by the DII and cancer outcomes, particularly cancer-specific mortality.

#6496

Exposure phenotype risk scores (E-PRS) and prostate cancer aggressiveness in the Michigan Genomics Initiative (MGI)

Xinman Zhang, Lars G. Fritsche, Bhramar Mukherjee, Alison M. Mondul. *University of Michigan, Ann Arbor, MI*

Background: Exposure phenotype risk scores (E-PRS) use genetic variation as a natural experiment to examine the causal relationship between risk or protective factors and diseases. A recent review summarized 76 studies using this approach, finding that several factors (alcohol consumption, BMI, telomere length, hormones) likely cause cancer. However, this article also highlighted the need for larger studies incorporating more, newly discovered associated, variants in the E-PRS and investigating specific cancer types vs. all cancers and cancer subtypes.
Methods: We used 21 published E-PRS that were derived from summary statistics of large genome-wide association studies using PRSCS. We evaluated 15 continuous and 6 binary E-PRS for factors that are known or hypothesized to contribute to cancer risk or progression and their association with prostate cancer aggressiveness and death. Our sample included 1784 unrelated, genotyped prostate cancer patients from the Michigan Genomics Initiative (MGI). Conditional logistic regression was used to estimate these 21 E-PRS's odds ratios (OR) and their 95% confidence intervals (CI) for high- vs. low-stage, high- vs. low-grade, and aggressive (high-stage or -grade) vs. non-aggressive (low-stage and -grade) prostate cancer. Cox regression was used to evaluate the hazard ratios (HR) and their 95% CI of prostate cancer deaths by E-PRS. Lasso and Ridge regressions were used to reduce model complexity and prevent overfitting for the final E-PRS model. All multivariable models were adjusted for age, genotyping batch, recruiting study, and genetic PCs.
Results: For high- vs. low-stage prostate cancer, we detected statistically significant associations with E-PRS for type 2 diabetes (per standard deviation (SD) change OR=0.86, 95% CI=0.77-0.97) and estimated glomerular filtration rate (eGFR) (per SD change OR=1.19, 95% CI=1.00-1.41). We also observed a suggestive inverse association with sleep apnea E-PRS. We observed no statistically significant associations for high- vs. low-grade prostate cancer, but there was a possible inverse association with the diastolic blood pressure (DBP) E-PRS. We noticed no statistically significant associations when comparing aggressive vs. non-aggressive prostate cancer; however, suggestive inverse associations with E-PRS for DBP and smoking were found. For prostate cancer death, we observed a statistically significant decreased risk of death with higher BMI E-PRS (per SD HR=0.29, 95% CI: 0.09 - 0.89). We also observed a suggestive inverse association with the eGFR E-PRS. Similar results were found in Lasso and Ridge regression.
Conclusions: Several E-PRS were significant predictors of aggressive or fatal prostate cancer. In the future, we will test significant E-PRS from this analysis to determine whether they predict aggressiveness or mortality in newly recruited MGI prostate cancer cases in 2022.

#6497
Availability of healthcare providers and its association with survival outcomes in non-Hodgkin lymphoma in the United States

Shiva Jashwanth Gaddam[1], Udhayvir Singh Grewal[2], Zara Hassan[1], Poornima Ramadas[1]. *[1]Feist Weiller Cancer Center, Shreveport, LA,[2]University of Iowa, Iowa City, IA*

Background: Survival outcome in Non-Hodgkin lymphoma (NHL) is significantly better in earlier stages, compared to advanced stages. Early identification of signs and symptoms, and prompt specialist availability and referral, are crucial for diagnosis and treatment at earlier stages. Mounting physician shortages are a growing concern, and we sought to analyze their effect on NHL mortality rates.
Methods: We extracted data on the age-adjusted mortality rate (AAMR) and crude incidence rate (CIR) of NHL for all U.S. states and the District of Columbia from the Center for Disease Control (CDC) Wide-ranging Online Data for Epidemiologic Research (WONDER) database (2017-2019). Nevada was excluded due to missing information. Data on the state-wise number of primary care physicians (PCPs) was obtained from the Association of American Medical Colleges (AAMC) state physician workforce data report (2020), and of Hematology/Oncology specialists (HOs) was gathered from the National Provider Identifier (NPI) registry (2020). The number of PCPs and HOs per each NHL incidence (PCP/CIR, HO/CIR respectively) was then calculated. Correlations were analyzed using Pearson's coefficient. Statistical analysis was performed using VassarStats.
Results: Median AAMR for NHL in the US was 5.15 (IQR 4.35, 5.95) per 100, 000 population. The median number of PCP and HO per each case of NHL incidence was 4.32 (IQR 3.43, 5.21), and 0.28 (IQR 0.1, 0.37) respectively. States with fewer PCPs per each NHL incidence had higher AAMR ($r=-0.37$, $p=0.007$). States with a lower number of HOs per each NHL incidence had higher AAMR ($r=-0.41$, $p=0.003$)
Conclusions: Based on the analysis, the availability of a lower number of PCPs and HOs per each NHL incidence is associated with increased AAMR of the disease. This data may strengthen the need for intensification of focus on decreasing the soaring physician shortages in the states, in order to help decrease the overall mortality associated with NHL.

#6498

Association of lifestyle related risk factors with multiple myeloma mortality rates in the United States

Shiva Jashwanth Gaddam[1], Udhayvir Singh Grewal[2], Himaja Kumari Avvaru[3], Poornima Ramadas[1]. *[1]Feist Weiller Cancer Center, Shreveport, LA,[2]University of Iowa, Iowa City, IA,[3]LSU Health Shreveport, Shreveport, LA*

Background: The prognosis for multiple myeloma (MM) has significantly improved over the years. Lifestyle risk factor modifications have improved the quality of life in MM patients, however, their effect on the survival outcomes in these patients remains unknown.
Methods: We extracted data on age-adjusted mortality rate (AAMR) rates of MM (per 100,000 population) for all 50 U.S. states and the District of Columbia from the Center for Disease Control (CDC) WONDER database (2015-2019). Data on risk factors such as obesity, physical activity, alcohol, tobacco abuse, and nutrition were obtained from the Behavioral Risk Factor Surveillance System (BRFSS, 2021). Florida was excluded due to missing information. Correlations were analyzed using Pearson's coefficient. Statistical analysis was performed using VassarStats.
Results: Median AAMR of MM in the US was 3.2 (IQR 2.7, 3.7) per 100,000 population. States with higher age-adjusted prevalence (AAP) percentages of obesity had higher AAMR (r=0.39, p=0.004) of MM. This association was significant in non-Hispanic white (r=0.32, p=0.021), and non-Hispanic black (r=0.31, p=0.034) subgroups as well. States with a higher AAP of adherence to recommended weekly aerobic activity had lower AAMR (r=-0.37, p=0.007). We did not identify any correlation of AAMR with AAP of binge drinking (r=-0.036, p=0.803), consumption of fruits (r=0.04, p=0.75), vegetables (r=-0.133, p=0.357), and smoking history (r=0.052, p=0.72).
Conclusions: In the current analysis, a higher prevalence of obesity and lower rates of aerobic physical activity were strongly associated with increased AAMR of MM. Our results, therefore, underscore the need for emphasis on a holistic approach in the management of MM by including lifestyle-based risk factor modification, to further improve the survival outcomes in patients with MM.

#6499

Towards a combined immunohistochemistry-based subtyping of ovarian endometrioid carcinoma

Brooke Jorgensen[1], Stacey Winham[1], Julie Cunningham[2], Sebastian Armasu[1], Chen Wang[1], Hunter Atkinson[1], Bryan McCauley[1], Linda Kelemen[3], Martin Koebel[4], Ellen Goode[1]. *[1]Department of Quantitative Health Sciences, Mayo Clinic, Rochester, MN,[2]Department of Laboratory Medicine and Pathology, Mayo Clinic, Rochester, MN,[3]Department of Quantitative Health Sciences, South Carolina Department of Health and Environmental Control, Columbia, SC,[4]Department of Pathology and Laboratory Medicine, University of Calgary, Calgary, AB, Canada*

Background: Ovarian endometrioid carcinoma (OEC) is an uncommon, understudied histotype that is distinguished from other histotypes by unique genomic features and high hormone receptor expression. There is growing interest in the biological relevance of subtyping using immunohistochemistry (IHC).

Methods: Women with primary invasive OEC diagnosed from 1989 to 2010 were retrospectively identified from the population-based Alberta Cancer Registry, Canada. Pathology slide review and IHC staining for Napsin A, TP53, and WT1 were used to reduce histologic misclassification, resulting in N=166 participants (low-stage N=138, high-stage N=28), excluding those who received neo-adjuvant chemotherapy. The following markers were stained and scored on tissue microarrays: TP53 (normal/abnormal), PMS2/MSH6 (mismatch repair proficient [MMRp]/deficient [MMRd]), PGR (loss/retained), and CTNNB1 (nuclear/cytoplasmic). Using a hierarchical decision tree by stage group (low/high), we categorized tumors as TP53 abnormal, MMRd, PGR loss, nuclear CTNNB1, and no specific immunohistochemical profile (NSIP). Distributions and five-year disease specific survival (DSS) was estimated for each group; hazard ratios (HRs) adjusted for age were estimated using Cox regression with NSIP as referent group.

Results: Among low-stage cases, five-year survival was as follows: 80% for TP53 abnormal (N=10, 7%), 87% for MMRd (N=15, 11%), 80% for PGR loss (N=10, 7%), 98% for nuclear CTNNB1 (N=63, 46%), and 95% for NSIP group (N=40, 29%). Overall, IHC group was associated with DSS among low stage cases (LRT p-value=0.006), and the group with nuclear CTNNB1 had a small but statistically significant DSS advantage

(HR=0.089, 95% CI 0.011-0.742, p=0.025). TP53 and PGR loss suggested shorter DSS than the referent NSIP group, but not statistically significantly so (HR=1.26 and 3.08, respectively). Among high-stage cases, five-year DSS was as follows: 57% for TP53 abnormal (N=7, 25%), 75% for MMRd (N=8, 29%), 33% for nuclear CTNNB1 (N=3, 11%), and 17% for NSIP (N=10, 36%). There were no high-stage cases in the PGR-loss group. Nuclear CTNNB1 group had a shorter DSS among high-stage cases, but this was not statistically significantly so (HR=1.16, p=0.85).
Conclusion: Pending replication in additional datasets, results suggest that OEC cases in nuclear CTNNB1 or NSIP IHC groups may have a favorable prognosis in which de-escalation of therapy can be considered. In addition, abnormal TP53 and loss of PGR may identify a high-risk subset of low-stage OEC.

PREVENTION / EARLY DETECTION / INTERCEPTION

Early Detection and Molecular Markers of Prevention

#6503

A case of stage IIA anal squamous cell carcinoma (SCC) diagnosed using a multi-cancer early detection (MCED) test

David A. Myers[1], Brenda Wood[2]. *[1]MDVIP, Metairie, LA,[2]GRAIL, LLC, a subsidiary of Illumina, Inc., currently held separate from Illumina, Inc. under the terms of the Interim Measures Order of the European Commission dated 29 October 2021, Menlo Park, CA*

Although some anal cancers can be detected early via screening, current screening options have limitations. A blood-based MCED test that uses a cell-free DNA-based targeted methylation assay and machine learning classifiers to detect a cancer signal and predict the cancer signal origin (CSO) is available for cancer screening. If the MCED test detects a cancer signal, the test reports ‘cancer signal detected’ with 1 or 2 CSO prediction(s). In the Circulating Cell-free Genome Atlas (CCGA) study, the top-predicted CSO was 89% accurate overall. Despite high average CSO prediction accuracy, the biological similarity among HPV-related cancers of the anogenital tract, and head and neck (H&N), may lead to CSO misclassification. An HPV-driven anal cancer case is reported to review the

diagnostic journey following a positive test result and misclassified CSO prediction. An asymptomatic 67-year-old White, non-Hispanic female (BMI: 21.6 kg/m^2) with history of HPV-associated cervical dysplasia and resultant hysterectomy >20 years prior was screened using the MCED test. She had an anoscopy 2 years prior to using the test for hemorrhoids. 11 days after a blood sample was collected for analysis, a positive test result (CSO1=Lung; CSO2=H&N) was communicated to the patient (Day 1). Chest CT w/o contrast was normal except for a small pericardial effusion (Day 2). The patient was referred to an ENT specialist for an extensive evaluation; there was no evidence of cancer found (Day 7). Repeat chest CT with and w/o contrast and with 2mm cuts was also normal except for the small pericardial effusion (Day 21). After the initial diagnostic workup ended, the possibility of HPV-driven CSO misclassification was raised, and in the context of past medical history, HPV-driven anorectal cancer was considered. The patient underwent a flex sigmoidoscopy, which revealed a 4 cm anterior distal anorectal mass consistent with cancer (Day 60). Biopsy showed invasive moderately differentiated SCC with focal keratinization and negative for lymphovascular invasion (Day 65). PET (skull base to mid-thigh) showed a 1.8 cm focus of activity in the anorectal area and no evidence of metastatic disease (Day 71). MRI of the pelvis with and w/o contrast showed a 2.7 cm anal mass with no lymph node invasion consistent with T2N0 disease (Day 72). Consultation with a radiation oncologist diagnosed the cancer as p16+, cT2N0M0 (stage IIA) SCC of the anal canal (Day 72). She was provided chemoradiation for ~1.5 months (Day 80). The most recent scans revealed no evidence of cancer (Day 364). The MCED test detected a cancer signal for an asymptomatic individual with stage IIA anal cancer. In the CCGA study, sensitivity was 75% in stage II anal cancer. Based on this case, CSO misclassification may be considered in patients with an HPV medical history. The use of this MCED test informed aggressive cancer workup and led to early detection and treatment with curative intent.

#6504

Germline genetically predicted body mass index is associated with endometrial cancer somatic transcriptomic, immune, and mutational signatures in The Cancer Genome Atlas

George Richenberg, Victoria Gray, Carina Owen, Tom Gaunt, Caroline Relton, Emma Vincent, Siddhartha Kar. *MRC Integrative Epidemiology Unit, University of Bristol, Bristol, United Kingdom*

High body mass index (BMI) is a causal risk factor for endometrial cancer but the molecular mechanisms underlying this association remain elusive. Here we sought to characterize the tumor genomic landscape of endometrial cancers that have developed on a germline genetic background of predisposition to elevated BMI. We built a polygenic score (PGS) for adult BMI in women using effect size estimates and allele information on 242 independent (r^2<0.05) variants associated with BMI at genome-wide significance (P<5x10^{-9}) in 379,501 women of European ancestry. We performed sample and germline (blood) genotype quality control and imputation into the 1000 Genomes reference panel on data from 354 endometrial cancer cases of genetically inferred European ancestry from The Cancer Genome Atlas (TCGA). We assigned each woman in this TCGA cohort her genetically predicted life-course BMI based on the BMI PGS and found this to be modestly correlated with BMI at the point of diagnosis (r^2=0.23; P=2.1x10^{-5}). Multivariable linear (default) and quasi-Poisson (for zero-inflated counts) regression models were used to test for associations between the BMI germline PGS and endometrial cancer tumor genomic, transcriptomic, proteomic, and immune traits in TCGA. All analyses were adjusted for age, stage, microsatellite status and 10 genetic principal components. Mutational signature models were also adjusted for signature accuracy. We ranked 18,458 genes based on the association between their tumor expression and the BMI PGS and performed gene set enrichment analysis to identify associations between the BMI PGS and upregulation of genes in the IL6-JAK-STAT3 signaling (false discovery rate (FDR)=8.50x10^{-7}), inflammatory response (FDR=7.03x10^{-6}), interferon gamma response (FDR=5.49x10^{-5}) and glycolysis (FDR=3.28x10^{-4}) pathways. High BMI PGS had an inverse association with endometrial tumor EGFR (FDR=0.07) protein levels of the 131 tumor proteins profiled by reverse phase protein array. Endometrial tumors that had developed on a germline background predictive of high BMI were also associated with increased infiltration of activated mast cells (FDR=9.55x10^{-3}) in our evaluation of 22 tumor immune cell infiltrates quantified by the CIBERSORT algorithm, as well as the mitotic and aging clock-like single

base substitution (SBS) signatures 1 (FDR=0.01) and 5 (FDR=0.04). The two SBS signature associations and the activated mast cell association with the BMI PGS were substantially more pronounced in the subgroup of endometrial cancers with microsatellite instability. Thus, we combined germline and somatic data using a novel approach to identify endometrial cancer tumor molecular features associated with genetically predicted higher BMI, providing precision multi-omic portraits of endometrial cancers that develop on a background of adiposity.

#6505

ColoScape test: a molecular assay to detect early-stage colorectal cancer in plasma cell-free DNA

Hiromi Tanaka, Shuo Shen, Mauro Scimia, Larry Pastor, Jonathan Li, Andrew Y. Fu, Daniel Kim, Rui Ni, Aiguo Zhang, Michael Y. Sha.
DiaCarta Inc, Pleasanton, CA

Colorectal cancer (CRC) is the second most common cause of cancer deaths when men and women are combined in the U.S. Early detection in the precancerous stage is key to reducing the CRC morbidity and mortality rates. Thus, there is a critical need for a cost-effective, time-efficient, and convenient clinical tool for early CRC detection. We have developed a multiplex qPCR assay (ColoScape™) to detect CRC-associated genetic and epigenetic changes from liquid biopsy samples (i.e., cell-free DNA) using our proprietary QClamp® XNA technology. The QClamp® XNA technology is very unique and enables the ColoScape™ assay to selectively amplify the mutant and methylated DNA target sequences by using a synthetic DNA analog XNA (Xenonucleic Acid). This study demonstrates the analytical performance for detecting low-abundant mutated and methylated gene copies, as well as assess the clinical performance using plasma cell-free DNA samples from patients with CRC or advanced adenomas (≥1 cm) and from individuals with normal colonoscopies. The Coloscape™ test is currently designed to detect mutations in 8 genes with 61 mutations and 7 methylated markers. The test consists of two parts: (i) the detection of mutations in 8 genes (*APC*, *KRAS*, *BRAF*, *TP53*, *CTNNB1*, *NRAS*, *SMAD4*, and *PIK3CA*) and (ii) the detection of 7 methylation targeted genes. For the assay analytical performance, the ColoScape™ test shows that XNA effectively suppressed the wild-type background

amplifications and led to amplify mutation and methylation target sequences dominantly, providing a high level of analytical sensitivity and specificity. The ColoScape^{TM} test is highly reproducible with intra- and inter-assay coefficient of variation of <10% and the cross-reactivity within the assay was limited and negligible. The results for the assay analytical sensitivity indicated that each target could be detected between 0.1% and 0.5% variant allele frequency in 10 ng cfDNA. The preliminary assay clinical specificity and sensitivity were 100% (95% CI: 91.3-100%) and 86% (95% CI: 66-95%) respectively for CRC and 91% specificity (95% CI: 75%-98%) and 60% sensitivity (95% CI: 17%-93%) for advanced adenomas. In summary, the ColoScape test utilizing the XNA-based technology provides high sensitivity and high specificity to CRC and advanced adenomas with a great potential to be used as an early screening test.

#6506

Early colorectal cancer detection with a spectroscopic liquid biopsy

James M. Cameron[1], Georgios Antoniou[1], Paul M. Brennan[2], Justin J. A. Conn[1], Sharon King[3], Rose G. McHardy[1], Susan Moug[4], Jennifer Nobes[3], David S. Palmer[1], Alexandra Sala[1], Benjamin R. Smith[1], Judith Strachan[5], Craig Mowat[6], Matthew J. Baker[1]. *[1]Dxcover Ltd., Glasgow, United Kingdom,[2]Centre for Clinical Brain Sciences, University of Edinburgh, Edinburgh, United Kingdom,[3]School of Medicine, University of Dundee, Dundee, United Kingdom,[4]Royal Alexandra Hospital, Greater Glasgow and Clyde NHS and Golden Jubilee National Hospital, Glasgow, United Kingdom,[5]Department of Blood Sciences, Ninewells Hospital and Medical School, Dundee, United Kingdom,[6]Department of Gastroenterology, University of Dundee, Dundee, United Kingdom*

Background: Early detection of cancer is vital to improve patient survival, since earlier diagnosis and treatment maximizes the opportunity to combat or control disease progression. Specifically for colorectal cancer (CRC), the average 5-survival rate after diagnosis decreases from 91% in early-stage CRC, to as low as 15% for stage IV CRC. Furthermore, the rapid detection and subsequent removal of pre-cancerous adenomas - e.g., advanced adenomas (AA) - can improve survival rates of affected patients. Current

stool-based tests, such as FIT and FIT-DNA, have poor AA sensitivities of 24% and 42%, and specificities of 95% and 87%, respectively. Recent research into liquid biopsies have shown some promise, however tests based on tumor-derived biomarkers alone have limited sensitivity, especially in early-stage disease.
Methods: We initially applied the Dxcover® Cancer Liquid Biopsy for use as a multi-cancer early detection (MCED) test. The test uses Fourier transform infrared (FTIR) spectroscopy and machine learning algorithms to build a classifier of the resultant spectral profiles to detect cancer, and can be fine-tuned to maximize either sensitivity or specificity depending on the requirements of specific international healthcare systems. Additionally, we have analyzed a retrospective cohort of serum samples comprising 100 CRC, 99 advanced adenomas removed by surgical resection and 97 colonoscopy screening controls.
Results: The CRC classifier from the discovery MCED dataset reported an area under the receiver operating characteristic curve (AUROC) value of 0.91, with 74% sensitivity and 91% specificity when differentiating CRC and non-cancer, which surpasses the targets set by the Centers for Medicare & Medicaid Services (CMS) for coverage of CRC tests. When tuned for higher sensitivity, the model produced 97% sensitivity (49% specificity), and when tailored for greater specificity (97%) the sensitivity was 47%. In this study, we have progressed these findings to examine the ability of the technology to differentiate patients with CRC, AA and colonoscopy controls.
Conclusions: Cancer treatment is more effective when given earlier and this low-cost strategy can facilitate the requisite earlier diagnosis. A rapid blood test that sensitive to AA and early-stage CRC could improve patient prognosis and ultimately reduce mortality.

#6507

E3 ubiquitin-protein ligase, tetratricopeptide repeat domain 3 (TTC3), H4 clustered histone 5 (H4C5), and epithelial cell adhesion molecule (EpCAM) are novel urine-enriched liquid biopsy biomarkers to detect prostate cancer in men

Ranjan Joseph Perera[1], Marcio Moschovas Moschovas[2], Roshane Perera[2], Bongyong Lee[3], Alexandra Miller[4], Ernest K. Amankwah[1], Rudramani Pokhrel[3], Christian Pavlovich[3], Guru Sonpavde[5], Vipul Patel[2]. *[1]Johns*

Hopkins University School of Medicine, Baltimore, MD,[2]Global Robotics Institute, Advent Health, Celebration, FL,[3]Oncology, Johns Hopkins University School of Medicine, Baltimore, MD,[4]Johns Hopkins All Children's Hospital, St. Petersburg, FL,[5]Cancer Instittute, Advent Health, Orlando, FL

Background: Prostate Cancer (PCa) is one of the leading causes of cancer deaths among American men; however, the estimated number of diagnoses represents a small fraction of disease-related biopsies performed yearly. Although the Prostate-Specific Antigen (PSA) test is widely used for screening, several advisory groups recommend against using PSA because of its suboptimal performance. Thus, there is an *urgent unmet* need for novel and more accurate diagnostic biomarkers for PCa detection and to differentiate aggressive cancer from its indolent form.
Methods: In our study, we used voided urine (50ml) from pre and post-prostatectomy men with PCa and urine from normal healthy men as control. We isolated RNA from exfoliated cells and debris shed into urine and performed RNA-sequencing using the Illumina Next-seq 550 platform. Advanced computational and machine-learning approaches were employed to identify candidate biomarkers in men with PCa. We examined the TCGA database to validate the PCa-specific expression of the identified RNA in tumor tissues. Two RNA markers were further tested by qPCR, and one urinary soluble protein marker was measured by immunoassays.
Results: Our study included 106 men with PCa and 88 control men. We identified and validated the presence of ≥1 RNA markers (TTC3, H4C5) and a protein marker (EpCAM) in urine as potential candidate biomarkers for PCa detection. We tested and developed these markers using qPCR for TTC3, H4C5, and ELISA assay for EpCAM with higher specificity and sensitivity (Table 1). Our results outperformed known urinary markers, PCA3 and SPDEF (Figure 1). TTC3, H4C5, and EpCAM markers diminished to low or undetectable levels in post-prostatectomy compared to pre-prostatectomy men with PCa. shRNA knockdown of TTC3 and EpCAM in androgen-sensitive and insensitive cells induced biological changes, suggesting their relevance to Prostate Cancer.
Conclusions: We report a highly accurate panel of 3 urine-based biomarkers that detect PCa consisting of EpCAM (protein) and TTC3 and H4C5

(RNA). To identify the advantage of using individual or combinatorial markers is an ongoing study in our laboratory.

#6508

Eclipse, an automated CRISPR platform for the large-scale generation of cell models

Peter Deng, Matthew Rowe, Anna King, Dana Sailor, Antinea Chair, Montse Morell, Andreia G. Sommer, Kevin Holden. *Synthego, Redwood City, CA*

Major advances in gene editing using CRISPR have improved accessibility for the creation of disease relevant *in vitro* models, allowing researchers to readily interrogate oncogenic driver mutations and elucidate novel targets to overcome challenges within cancer research such as drug resistance. Despite this, the rapid generation of disease relevant cell lines at the scale needed for successful and efficient therapeutic development remains challenging in part due to the sheer number of potential oncogenic driver mutations and cancer targets along with using traditional manual approaches. Specific challenges include: the efficient generation of gene knockouts and corresponding loss of protein; efficient knock-in of gene tags and single nucleotide variants; and controlling the zygosity of these genetic outcomes. To address these limitations, we describe the use of our automated, high throughput CRISPR editing platform, ECLIPSE, for the rapid generation of cell models such as immortalized cells and induced pluripotent stem cells. We leveraged our chemically modified synthetic sgRNAs, optimized nucleofection methods, and automated pipelines for the generation of CRISPR-edited cells at various scales to address the needs of researchers. This scale ranges from individual edited cell clones for drug target validation to the generation of hundreds of knockout cell pools in a ready-to-assay arrayed format for gene target identification in drug screening. The utilization of automated systems such as the ECLIPSE platform are critical catalysts for the rapid generation of engineered cell lines at relevant scales to address the challenges of cancer research.

#6509

Panel of CD-34, CD-105 & vimentin in immunohistochemical & histomorphometric analysis for prognostic evaluation of oral

potentially malignant lesions

Saravanan SP. *Kalinga Institute of Industrial Technology (KIIT), Bhubaneswar, India*

Introduction: The Angiogenic Theory, proposed by Folkman in 1971, is one of the most widely recognized ideas in carcinogenesis, which is a complicated and dynamic process. This emphasized the fact that tumor growth occurs at a certain density of new blood vessels during angiogenesis. However, whereas many of vascular markers are well understood in established oral malignancies, their relevance in oral premalignant lesions remains unknown.

Materials and Methods: Prospectively, 54 patients with potentially oral malignant lesions (POML) were observed for three years. These patient's paraffin blocks were subjected to immunohistochemical and histomorphometric examination with CD34 and CD105 (Endoglin), as well as qualitative analysis with Vimentin. All patients provided written informed consent to subject the blocks to immunohistochemical analysis, as well as the necessity of 3 monthly visits up to 3 years follow up to assess the malignant transformation potential. In case of clinical suspicion, a repeat biopsy was performed to rule out malignancy.

Results: With a sample size of 54, the clinical and histological parameters were evaluated using the paired 't' test, validating the underlying normality assumption. During the three-year follow-up period, 52% (n=28/54) of the total patients developed oral malignancies. The most commonly detected was Oral Squamous Cell Carcinoma with the most common site being Gingivo-Buccal Sulcus area. The microvessel
density was dramatically boosted in premalignant stage samples utilizing CD34 and CD105. In PMOL, the mean Vascular Caliber (VC) using CD 34 and CD 105 (μm^2) was 7.7 ± 1.9 μm^2 and 7.1 ± 1.4 μm^2, respectively. The mean VC - CD 34 and CD105 did not differ statistically (P-value>0.05). More than 50% of individuals with malignant transformation have shown increased vimentin expression in connective tissue of the premalignant stage samples (P-value0.001).

Conclusion: The use of CD 34 and CD105 markers to assess micro vessel density and vessel morphometry was found to be useful in predicting the malignant transformation potential of POML. The combination of these two markers, coupled with Vimentin, was proven to be a successful IHC

PANEL for predicting the malignant transformation potential of oral premalignant lesions well in advance of 1.5 ± 2.5 years. In diagnosed cancer patients, increased CD105 expression was also associated with lymph node metastases. As a result, CD34, Endoglin, and Vimentin are proposed as IHC Panel Markers to determine the prognosis of potentially malignant oral lesions.

#6510

REM-DREAMing: Low-cost digital microfluidic analysis of DNA methylation heterogeneity for enhanced, liquid biopsy-based detection of early-stage lung cancer

Yang Zhao[1], Christine M. O'Keefe[1], James G. Herman[2], Thomas R. Pisanic[1], Tza-Huei Wang[1]. *[1]Johns Hopkins University, Baltimore, MD,[2]University of Pittsburgh, Pittsburgh, PA*

We report the results of a study exploring the ability to exploit molecular heterogeneity in DNA methylation for improving the performance of liquid biopsy-based screening for early-stage (I & II) non-small cell lung cancer (NSCLC). Annual low-dose CT (LDCT) screening is currently recommended for adults aged 50 or older who are at high-risk of developing lung cancer. While this approach has resulted in improvements in survival, the false positive rate of lung nodules detection by LDCT remains over 95%, leading to unnecessary invasive follow-up procedures and further points to the need for new, complementary methods to improve diagnostics performance and reduce patient risk. DNA methylation biomarkers have demonstrated considerable potential as tumor-specific biomarkers for blood-based detection of early-stage NSCLC. Nonetheless, cell-free DNA (cfDNA) assessment techniques, such as methylation-specific PCR (MSP) or bisulfite sequencing, have limited sensitivity to assess epigenetic heterogeneity of rare epiallelic variants in a cost-effective manner. Here we reported a new platform, named REM-DREAMing (Ratiometric-Encoded Multiplex Discrimination of Rare EpiAlleles by Melt), which provides a simple, low-cost solution for multiplexed assessment of loci-specific DNA methylation heterogeneity at single molecule sensitivity. The microfluidic nanoarray contains four independent but identical 10,040 nanowell modules. Methylation biomarkers are differentiated by a ratiometric fluorescence scheme and the assessment of

individual epiallele species of each locus are achieved through digitization in the nanoarray and precise high-resolution melt (HRM) analysis. In this study, we explore the potential utility of REM-DREAMing as a complementary assay for improving LDCT screening of NSCLC by testing a cohort of 48 clinical samples (28 cancer and 20 control samples) of low-volume liquid biopsy specimens from patients with CT-scan indeterminant pulmonary nodules. A machine learning algorithm incorporating logistic regression models with leave-one-out cross validation was developed to identify a proper methylation density threshold of each biomarker in the panel. Evaluation of the receiver operation characteristic (ROC) curve yielded an area under the curve (AUC) of 0.97 (95% CI, 0.94-1) with 93% sensitivity at 95% specificity for the REM-DREAMing assay, compared with 93% sensitivity at 62% specificity achieved using a traditional, MSP-based approach. These results suggest that the assessment of intermolecular epigenetic heterogeneity can provide superior clinical performance for cfDNA methylation and noninvasive detection of early-stage NSCLC, in particular. Our results warrant further investigation in a larger sample cohort to validate its utility for improving routine screening of NSCLC in high-risk populations.

#6511

Optimizing an *in vitro* toolbox to interrogate pancreatic tumorigenesis from a patient-derived intraductal papillary mucinous neoplasm sample

Raymond M. Paranal, Julie Schlanz, Maria A. Trujillo, Nicholas J. Roberts, Laura D. Wood. *Johns Hopkins University School of Medicine, Baltimore, MD*

Pancreatic Ductal Adenocarcinoma (PDAC) is a lethal disease with a five-year survival rate of 11%. PDAC develops from pancreatic precursor lesions, including intraductal papillary mucinous neoplasm (IPMN); studying these lesions is important to understand the multi-step process of pancreatic tumorigenesis. Development of model systems and associated tools is a critical step that is 1) scientifically necessary to understand IPMN biology and 2) clinically important for improving patient outcome. To date, only one patient-derived IPMN cell line that grows in a monolayer has been reported, illustrating the challenges of growing precancerous cells in this

format. While protocols have previously been established to generate patient-derived IPMN models, the majority of these cell-based models utilize 3D organoids. To date, no study has successfully converted patient-derived IPMN organoids into 2D culture. Converting these cellular models to propagate and divide in a monolayer allows us to expand our *in vitro* toolbox to perform experimental methods that are less efficient or not practical in 3D culture. In this study, we optimized the conversion of a high-grade IPMN patient-derived organoid model into a monolayer culture. We considered conditions that could recapitulate an extracellular matrix as well as growth factors and/or inhibitors that could promote IPMN cell growth. In total, we tested 15 different conditions and were able to successfully culture the human high-grade IPMN cells in a monolayer culture for up to 5 passages (~1 month). Additionally, while human IPMN cellular models exists, genetic modification of these *in vitro* models has not been reported. Such approaches allow direct interrogation of the role of specific genes in premalignant pancreatic tumorigenesis. In this study, we report successful transduction of IPMN cells via lentivirus. By first converting the organoid into a monolayer culture, transducing them in 2D, and then converting them back into 3D culture as spheroids, we were able to successfully express EGFP into our IPMN cellular model. In summary, we optimized culture conditions to temporarily grow a patient derived 3D IPMN model in a 2D monolayer form, genetically modified this IPMN cell line model, and successfully converted it back into a 3D spheroid. These protocols have potential to be replicated in other IPMN models and can provide further insight into overall IPMN biology and pancreatic tumorigenesis.

#6512

Label-free autofluorescence imaging reveals different metabolic responses to adverse growth conditions between normal and breast cancer cells lines

Katherine Junkins[1], Angel Perez Martinez[2], Margaret Rodgers[1], Shelley A. Phelan[1], Min Xu[2]. *[1]Biology, Fairfield University, Fairfield, CT,[2]Physics & Astronomy, Hunter College and the Graduate Center of CUNY, New York, NY*

Cancer cells are metabolically distinct from normal cells, and can adapt differently to adverse growth conditions. We sought to compare normal

MCF10A and Ras-transformed MCF10AT cells under various conditions (regular growth media, doxorubicin-treatment, and glucose-deprived media) by imaging endogenous cellular FAD and NADH fluorescence and comparing it to proliferation rates (measured by MTS assay) and chromatin structure (measured by Hoescht staining).

Under normal growth conditions, MCF10AT cells displayed similar levels of FAD and higher levels of mitochondrial NADH than MCF10A cells. Elevated NADH in MCF10AT cells seems to reflect the preference for anaerobic glycolysis rather than oxidative phosphorylation (the so-called Warburg effect). Our MTS data showed that doxorubicin treatment did not significantly affect MCF10AT cell proliferation but led to a modest reduction in cell proliferation in the normal cell line. Likewise, in MCF10AT cells, doxorubicin treatment led to an increase in FAD and a decrease in NADH. Conversely, in MCF10A cells, doxorubicin led to a decrease in FAD levels and an increase in mitochondrial NADH. These results suggest that the cancer line may be switching to oxidative phosphorylation to resist doxorubicin-induced toxicity, while the normal cells reduce oxidative phosphorylation with growth inhibition.

In contrast to the doxorubicin response, glucose deprivation produced significant growth inhibition and cell death in MCF10AT cells while having a modest growth-inhibitory effect on the normal line. Interestingly, low glucose decreased FAD and mitochondrial NADH in MCF10AT cells, suggesting that both aerobic and anaerobic respiration was reduced and consistent with the marked reduction in observed cell viability. In contrast, MCF10A cells showed a slight decrease in FAD and an increase in NADH, suggesting a decrease in oxidative phosphorylation consistent with the modest growth inhibition observed.

Finally, MCF10ATs displayed higher levels of Hoechst staining than MCF10A cells, consistent with a higher proportion of condensed chromatin observed in cancer cells. In addition, we found a larger increase in Hoechst staining in MCF10AT cells in response to both doxorubicin and low glucose, as compared to MCF10A cells. This data suggests that the chromatin state of the two lines is also differentially affected by these treatments.

In conclusion, label-free measurement of autofluorescence of cellular FAD and mitochondrial NADH reveals the different metabolic and chromatin responses to adverse growth conditions between cancer and non-cancer

cells. These differences are associated with the different proliferation rates and may have important clinical implications for cancer risk stratification.

#6513

Single cell and spatial profiling reveal molecular and immune evolution from precancers to invasive lung adenocarcinomas in genetic and carcinogen-induced mouse models

Bo Zhu[1], Jian-Rong Li[2], Hong Chen[1], Pingjun Chen[1], Junya Fujimoto[1], Yanhua Tian[1], Muhammad Aminu[1], Chenyang Li[1], Lingzhi Hong[1], Alexandre Reuben[1], Edwin Roger Parra Cuentas[1], Ou Shi[1], Monique Nilsson[1], Alissa Poteete[1], Shawna Hubert[1], Khaja Khan[1], Wei Lu[1], Daniel Kraushaar[2], Xingzhi Song[1], Jianhua Zhang[1], Don Gibbons[1], Luisa Solis Soto[1], Ignacio Wistuba[1], Jia Wu[1], John Heymach[1], Chao Cheng[2], Jianjun Zhang[1]. *[1]UT MD Anderson Cancer Center, Houston, TX,[2]Baylor College of Medicine, Houston, TX*

Introduction: An improved understanding of early lung carcinogenesis may facilitate development of novel diagnostic, screening, and prevention strategies to decrease lung cancer mortality. We have previously led a series of studies on the molecular and immune landscape of lung adenocarcinoma (LUAD) precursors. However, resected human specimens only provide molecular snapshots. Here, we sought to establish and characterize human-relevant murine lung precancer models to depict molecular evolution during early lung carcinogenesis and to provide novel insights for lung cancer interception.

Methods: We have established 3 genetically engineered mouse models (GEMMs) (K: *Kras*$^{\text{LSL-G12D/+}}$, KP: *Kras*$^{\text{LSL-G12D/+}}$/*Trp53*$^{\text{R172H/+}}$, KL: *Kras*$^{\text{LSL-G12D/+}}$/*Lkb1*$^{\text{fl/fl}}$) and 2 carcinogen-induced models (CITMs) (UWT: Urethane in wild type mice, URG: Urethane in Rag2$^{-/-}$ mice). Lung tissues were serially collected at multiple time points after induction and subjected to whole exome sequencing (WES), single cell RNA sequencing (scRNA-seq), spatial transcriptomics (Visium), and imaging mass cytometry (IMC).

Results: Pathological review of specimens from 252 mice revealed normal lung, precancers and LUAD at different timepoints mirroring the evolution of human LUAD. Overall, the tumor burden was significantly higher in GEMMs than CITMs ($p<0.05$). Tumor mutation burden progressively

increased with progression from precancers to LUADs across all models. scRNA-seq demonstrated a progressive decrease of $CD4^+$ T cell, $CD8^+$ T cell, NK cell, and B cell infiltration in all models except the B/T cell-deficient WRG model; and a progressive increase of neutrophils (in KL model) and macrophages (in K, KP, UWT and URG models) along with progression of precancers. These findings were confirmed by spatial Visium and IMC profiling. Infiltration of T cells, B cells and NK cells inside tumors was not different between GEMMs (K, KP, KL) and CITMs (UWT). However, UWT showed significantly higher density of immune cells at the peritumor regions ($P<0.05$). Compared to the immune-competent UWT model, the B/T-cell deficient URG model showed similar progression and tumor burden at early phases, but rapid progression and larger tumor burden in the later phases. URG had no mature B/T cells but significantly higher NK cell infiltration than UWT ($p<0.05$).
Conclusion: We have established 5 murine carcinogen-dependent and -independent precancer models, morphologically resembling human LUAD and its precursors. Although progressive immunosuppression along with progression of lung precancers is universal across all models, the evolution patterns and the molecular/immune features underlying immunosuppression vary in different models, particularly between CITMs and GEMMs. These models may be valuable assets for studying early lung carcinogenesis and lung cancer interception.

#6514

Liquid biopsy for lung cancer based on extracellular vesicles

Juan P. Hinestrosa[1], Harmeet Dhani[1], Jean M. Lewis[1], Gregor K. Schroeder[1], Heath I. Balcer[1], Razelle Kurzrock[2], Paul Billings[1]. *[1]Biological Dynamics, Inc., San Diego, CA,[2]Medical College of Wisconsin, Milwaukee, WI*

Background Liquid biopsy approaches for lung cancer are becoming increasingly common for diagnosis, prognosis, and management of the disease. Of the Approximately 236K new lung cancer cases that will be diagnosed in 2023, over 70% of those will be regional or distant with diminished chances of curative resection. Therefore, highly sensitive and specific approaches for early detection are key for mortality reduction. Extracellular vesicles (EVs), a new class of blood-based cell-free

biomarker, can be informative for the diagnosis of lung cancer at its earliest stages.
Methods A case-control cohort of blood plasma samples from 146 pathologically confirmed lung cancer cases (stage I = 90, II = 42, III = 14; median age = 63 yrs.) and 491 controls (median age = 58 yrs) was used in this study. EVs were isolated using a proprietary technology and the EV protein cargo was analyzed via immunoassay. A machine learning engine was employed to determine the most informative biomarkers and algorithm for differentiation between cases and controls in a detection setting.
Results Using a stratified cross-validation approach, we found a biomarker signature that yielded an AUC of 0.966 (95% CI: 0.949 - 0.979) with an overall sensitivity of 91.1% (CI: 85.4% - 94.7%) at a specificity of 91.0% (CI: 88.2% - 93.3%). By stage, the following sensitivities were obtained: stage I: 92.2%, stage II: 88.1%, stage III: 92.8%. The algorithm developed includes 13 EV-protein biomarkers using the adaptive boosted tree methodology.
Conclusions Our pilot study demonstrates utility of a blood-based approach that can detect lung cancer at early stages, when treatment can be more effective. By combining multiple EV protein signatures, it is possible to achieve high sensitivity and specificity. Independently collected cohorts including confounding conditions, such as benign lung nodules and COPD, are being evaluated for validation purposes to improve performance in clinical settings.

#6515
Pancreatic ductal adenocarcinoma (PDAC) early detection
Juan P. Hinestrosa[1], Harmeet Dhani[1], Gregor Schroeder[1], Jean M. Lewis[1], Heath I. Balcer[1], Razelle Kurzrock[2], Dove Keith[3], Rosalie Sears[4], Paul Billings[1]. *[1]Biological Dynamics, Inc., San Diego, CA,[2]Medical College of Wisconsin, Milwaukee, WI,[3]Oregon Health and Sciences University, Portland, OR,[4]Oregon Health Sciences University, Portland, OR*

Introduction Pancreatic ductal adenocarcinoma (PDAC) is the most common form of pancreatic cancer and is one of the deadliest cancer in the U.S., with a 5-year survival rate of just 11%. It is expected that ~62,000 new cases will be diagnosed in the US in 2023 and >70% of those will be at the regional or distant state, when curative resection is no longer an option.

It is imperative that tools enabling early disease detection (stages I and II) are developed to improve patient survival outcomes. Here, we report the results of a study on the utility of extracellular vesicles (EVs) for early PDAC detection.

Methods Our case-control training set was comprised of 75 pathologically confirmed PDAC cases (Stage I = 31, Stage II = 44) and 640 controls (including 11 subjects with pancreatitis) for EV biomarker and algorithm selection via machine learning. EVs from plasma were isolated using a proprietary technology, then EV-bound proteins of interest were analyzed via an immunoassay. A second independently collected cohort of 20 confirmed PDAC cases (Stage I = 10, Stage II = 10) and 27 controls (including 9 patients newly diagnosed with diabetes) was used for validation.

Results The machine learning analysis using EV-isolated proteins generated a signature that utilized 8 different biomarkers, with an AUC of 0.989 (95% CI: 0.980 - 0.998) in the training set and an AUC of 0.987 (CI: 0.964 - 1.000) in the validation set. For the validation set, the sensitivity was 95% (CI: 76.4% - 99.1%) and the specificity was 92.6% (CI: 76.6% - 97.9%), with 10 out of 10 stage I cases and 9 out of 10 stage II cases correctly classified.

Conclusions The ability to alter the future outcomes of PDAC patients will be predicated on development of a new generation of early-detection biomarkers and technologies. The use of EV protein signatures, a new class of cell-free biomarker, permits detection at high sensitivity and specificity, as demonstrated for the independently collected validation cohort. Studies aimed to assess this test for high-risk patients (family history of PDAC, known germline mutations, precursor lesions, hereditary pancreatitis, new onset diabetes will continue towards the establishment of real-world evidence.

#6516

Comparison study between a ketogenic diet and a high-fat diet on pancreatic cancer incidence in mice

Tarek Bacha[1], Natalia Cortez Penso[2], Maria Rodriguez[1], Brian Hong[1], Gerardo Mackenzie[1]. *[1]UC Davis, Davis, CA,[2]University of Turin, Turin, Italy*

Pancreatic Ductal Adenocarcinoma (PDAC) remains among the most lethal cancers. PDAC can take up to 15-20 years to develop from the occurrence of the first initiating mutational event, which opens the opportunity for intervention and prevention strategies. In particular, nutritional interventions could provide an avenue to prevent or slow down pancreatic carcinogenesis, since certain diets such as high-fat diets (HFD) have shown to promote it. On the other hand, ketogenic diets (KD), characterized by a high fat and very low carbohydrate content, have gained attention for their anti-tumor and anti-inflammatory potential. However, the role of a KD in the onset and progression of PDAC is still unknown. In this project, we investigated the impact of both a HFD and a KD on late-stage pancreatic carcinogenesis. For this purpose, we used an animal model of pancreatic cancer carrying a pancreas-specific oncogenic $KRAS^{G12D}$ mutation [*LSL-*$KRAS^{G12D}$*; P48+/Cre;* (KC mice)]. On average, KC mice develop PDAC at 12-15 months of age, so they are a valuable tool to study late-stage carcinogenesis. We hypothesized that a HFD would accelerate PDAC progression while a KD would slow it down. To test our hypothesis, 6 months-old male and female KC mice (n=18/group) were randomized and fed, either a control diet (CD), a HFD, or a KD for 6 months and then euthanized at 12-months of age to evaluate pancreatic cancer incidence and progression. At 12-months of age, HFD-fed mice had significantly higher body weight compared to the other two groups. Moreover, KD-fed mice had significantly higher levels of blood ketone bodies, with lower levels of glucose and serum insulin levels, when compared to KC mice fed a HFD. However, after 6 months on the diets, no significant differences in pancreas weight nor in PDAC incidence were observed across all diet groups. Of note, male KC mice experienced double the PDAC incidence rates (55%) than female KC mice (27%), irrespectively of the group. In addition, no significant differences among the groups were observed in RAS/RAF/ERK and PI3K/AKT/mTOR pathways, known to be associated with cancer proliferation. In summary, despite the improvement in insulin and increases in ketone bodies, consumption of a strict KD failed to improve late-stage pancreatic carcinogenesis in mice.

#6518

Time course genomic characterization reveals progressive accumulation of mutations during tumor development in a Lynch

syndrome mouse model

Yurong Song[1], Shaneen Baxter[1], Lisheng Dai[1], Chelsea Sanders[1], Holli Loomans-Kropp[2], Brandon Somerville[1], Ryan N. Baugher[1], Stephanie D. Mellott[1], Todd B. Young[1], Heidi E. Lawhorn[1], Teri M. Plona[1], Bingfang Xu[1], Lei Wei[3], Qiang Hu[3], Song Liu[3], Alan Hutson[3], Baktiar Karim[1], Simone Difilippantonio[1], Ligia Pinto[1], Matthias Kloor[4], Steven M. Lipkin[5], Shizuko Sei[6], Robert H. Shoemaker[6]. *[1]Frederick National Laboratory for Cancer Research, Frederick, MD,[2]The Ohio State University, Columbus, OH,[3]Roswell Park Comprehensive Cancer Center, Buffalo, NY,[4]University of Heidelberg, Heidelberg, Germany,[5]Weill Cornell Medicine, New York, NY,[6]Division of Cancer Prevention, Bethesda, MD*

DNA mismatch repair (MMR) genes (e.g., *MLH1, MSH2, MSH6, PMS2*, and *EPCAM*) play an important role in maintaining genomic stability during DNA replication and recombination. Deficiency in MMR resulting from mutations in these genes leads to mutations in microsatellite regions throughout the genome (microsatellite instability; MSI) and in cancer driver oncogenes or tumor suppressor genes, which accumulate over time and eventually lead to cancer formation. Monoallelic germline mutation in MMR genes causes Lynch syndrome (LS). Among LS-related cancer types, the lifetime risk for colorectal cancer (CRC) is the highest (~80%). Frameshift mutations (FSMs) in coding microsatellites produce neoantigens, which have been shown to elicit immune responses. It was thus postulated that they can serve as vaccine targets. To develop a prophylactic vaccine and prevention strategy for this high-risk population, we characterized a LS mouse model (*Msh2$^{LoxP/LoxP}$;Villin-Cre*) to determine whether these mice recapitulate the human LS oncogenic process. We found that tumor development was already notable at 7-8 months of age and median survival was 11.5 months. Histopathological analysis showed that tumors were adenoma or adenocarcinoma mixed with mucinous features. Using a targeted sequencing approach, a panel of FSMs in mononucleotide regions were identified in both tumors and histologically normal mucosa, suggesting that Msh2 deletion and FSMs were not sufficient for tumor development. In addition, *Apc, Ctnnb*, and *Trp53* mutations were also observed with low frequency in organoids derived from these tumors, indicating that other driver mutations may be required for tumor initiation

and progression, and most FSMs detected in tumors and mucosa were probably passenger mutations. To determine if fecal samples can be used to monitor the FSM load, fecal DNA from different time points was sequenced. We found that FSMs can be detected at 1month of age although the number of FSMs was relatively low compared to that from older mice, indicating that FSMs accumulate over time. MSI detection via fragment analysis confirmed that these tumors were MSI-H. Interestingly, mucosa and fecal samples from a time course study showed progressive increase in microsatellite instability, suggesting the possibility of using MSI score for disease monitoring. Our preliminary data indicates that combined fecal FSM status and MSI score can be potentially used as a biomarker to monitor the tumor development and disease progression for LS colorectal cancer.

Funded by the National Cancer Institute, National Institutes of Health, under Contract No. HHSN261201500003I

#6519

Haploinsufficiency for BRCA2 leads to common fragile site instability in human mammary epithelial cells

Mihriban Karaayvaz, Kavya Vipparthi, Antony Caputo. *Genomic Medicine Institute, Cleveland Clinic Lerner Research Institute, Cleveland, OH*

Individuals with germline heterozygous mutations of breast cancer susceptibility genes *BRCA1* or *BRCA2* have a 50 to 80% lifetime risk of developing breast cancer, yet the mechanisms of these cancers remain largely unknown. There is growing evidence that *BRCA1* and *BRCA2* heterozygosity confer haploinsufficiency in normal human mammary epithelial cells for their multiple known functions. Haploinsufficiency for *BRCA1* leads to defects in differentiation, replication stress response, premature senescence and genomic instability in human mammary epithelial cells. Deficiencies in error-free DNA damage repair has been observed in genetically engineered cells as well as primary human mammary epithelial cells carrying *BRCA1* heterozygous mutations. There is relatively less research on understanding the role of haploinsufficiency for *BRCA2* in human mammary epithelial cells. It has been reported that haploinsufficiency for *BRCA2* leads to genomic instability via unscheduled R-loops. We previously showed that accumulation of sub-chromosomal

copy number variations (CNVs) and replication stress-induced DNA damage, together with attenuated checkpoint and apoptotic responses, constitute a haplo-insufficient phenotype in mammary epithelial cells of *BRCA2* mutation carrier patients. Common fragile sites (CFS) are found in all individuals and represent a normal component of chromosome structure. Numerous studies have shown that CFSs are prone to deletions and rearrangements in many cancers, a situation referred as CFS instability. Importantly, Fanconi Anemia/BRCA pathway has been previously reported to have a role in regulating CFS instability. In this study, we further explored a link between *BRCA2* haploinsufficiency and CFS instability. We induced replication stress with DNA polymerase inhibitor aphidicolin (APH) treatment in control and BRCA2- deficient human mammary epithelial cells. We then performed DAPI banding to map and score the cytogenic lesions in metaphase spreads cells, in the absence or presence of APH treatment. Our results demonstrated that BRCA2- deficient human mammary epithelial cells showed increased frequency of CFS regions such as FRA18B. Correspondingly, BRCA2-deficient cells exhibited a failure to activate CHK1, a central coordinator of the response to replication stress and DNA damage, in response to APH treatment, despite normal levels of total CHK1 protein. ATR/CHK1 pathway is a major regulator of CFS stability. Thus, our results provide support for *BRCA2* haploinsufficiency leading to CFS instability in human mammary epithelial cells. These studies will yield unanticipated opportunities for improved risk assessment and prevention strategies in high-risk patients.

#6520

Combination of serum human satellite RNA and miR-21 levels as a biomarker for diagnosis of pancreatic cancer

Takahiro Seimiya, Takahiro Kishikawa, Mtoyuki Otsuka, Mitsuhiro Fujishiro. *University of Tokyo, Tokyo, Japan*

Pancreatic ductal adenocarcinoma (PDAC) has a poor prognosis due to the difficulty of its diagnosis. Because human satellite II (HSATII) RNA, a satellite repeat RNA, is highly and specifically expressed in human PDAC, the serum HSATII RNA level may be a biomarker for diagnosis of PDAC. To measure the serum HSATII RNA level with high sensitivity and reproducibility, we previously developed a convenient method, tandem

repeat amplification by nuclease protection (TRAP) combined with droplet digital PCR (ddPCR). Here, we refined the original method by simultaneously measuring the serum miR-21 level to enhance the detection of PDAC. A total of 135 patients were enrolled in this study, including 65 patients with pancreatic cancer and 70 healthy controls. We developed the PDAC-Index as a combination of the HSATII RNA and miR-21 levels to discriminate PDAC from healthy controls. The PDAC-Index demonstrated good diagnostic performance (AUC: 0.92 (95% CI: 0.86-0.99); sensitivity: 0.94; specificity: 0.85) which was significantly better than HSATII RNA alone (AUC: 0.92 vs 0.82, p=0.004) . Importantly, the PDAC-index was elevated in an early-stage PDAC case that was negative for CA19-9. The PDAC-index also discriminated PDAC from chronic pancreatitis and intraductal papillary mucinous neoplasm more accurately than CA19-9. These results suggest that the PDAC-Index may be a promising biomarker for diagnosis of PDAC.

#6521

Subtype-specific molecular signatures of field cancerization in patients with sporadic breast cancer

Anjana Bhardwaj[1], Zhenlin Ju[2], Constance Albarracin[1], Celestine Trinidad[3], Preethi Gunaratne[4], Jing Wang[2], Randa El-Zein[5], Isabelle Bedrosian[1]. *[1]UT MD Anderson Cancer Center, Houston, TX,[2]Department of Bioinformatics and Computational Biology, UT MD Anderson Cancer Center, Houston, TX,[3]University of Santo Tomas Hospital Benavides Cancer Institute, Manilla, Philippines,[4]University of Houston, Houston, TX,[5]Houston Methodist Research Institute, Houston, TX*

Background: We have previously shown the presence of molecular field cancerization in patients with sporadic breast cancer. Given the heterogeneity of breast cancer, we hypothesized that such field cancerization is likely to be subtype-specific.
Methods: RNA exome sequencing was performed on 360 samples obtained from 75 breast cancer patients undergoing mastectomy; 25 cases were selected from each subtype: hormone receptor (HR) positive, Her2 positive, triple negative (TN) breast cancer. Four sites were sampled from each patient: primary tumor (A), adjacent normal parenchyma within 2cm of the tumor (B), 2 separate, histologically normal sites at least 2cm away from

the tumor (C &D) or, if available, tissue from the unaffected contralateral breast (E). Normal breast tissue (N) from cancer-free controls was obtained from reduction mammoplasty. Tumor-associated genes (TAGs) were identified by comparison of primary tumor to tissue from cancer free controls. We estimated tumor content that was shared across samples B-E by applying deconvolutional analysis to the tumor associated genes, to calculate indices that ranged from 0, indicating normal, to 1, indicating tumor. Molecular field-associated genes and pathways were identified by Spearman's correlation coefficient analysis between the differential genes/pathways and ISTC.

Results: Across all subtypes, the proportion of tumor content present in the histologically normal breast tissue samples (samples B, C, D, E) obtained from cancer patients ranged from 80% in tissue adjacent to the tumor to approximately 50% in tissue obtained from the contralateral breast. We found over 600 deregulated genes to constitute the molecular field across all of the 3 major subtypes tested ($Her2^{+}$, HR, and TNBC), of which approximately 20% were shared in the molecular field of all 3 subtypes of breast cancer. Among the 664 genes noted to be part of the molecular field in TNBC, 23.8% were unique to this subtype. In contrast, only 13% of the genes that constituted the field cancerization in the Her2 and HR+ subtypes were subtype-specific. PIP3-AKT, TCR signaling, and DNA synthesis were among the top pathways specifically activated in the molecular field of the Her2+ subtype of breast cancer. The molecular field of HR+ breast cancer was uniquely characterized by upregulation in the mitotic cell cycle, G1- S transition, and RB pathway. The field of cancerization in the TNBC subtype showed an upregulation in MEK-MAPK, mTOR, and JNK-JUN-TAK1 pathways.

Conclusions: Our study suggests the presence of a breast cancer molecular field effect that extends beyond the adjacent normal breast tissue and includes the entire mammary gland. A substantial proportion of this field cancerization is subtype specific with uniquely deregulated pathways within each subtype. These findings provide new opportunities for developing subtype-specific chemoprevention strategies.

#6522

Improved detection of low frequency mutations in ovarian and endometrial cancers by utilizing a highly accurate sequencing platform

Jiannis Ragoussis[1], Nairi Pezeshkian[2], Lucy Gilbert[1]. *[1]McGill University, Quebec, QC, Canada,[2]Pacific Biosciences, Menlo Park, CA*

Ovarian and endometrial cancers come within the top-4 for incident cancers as well as deaths in North American women. Cure rates have not improved in 30 years as high-grade subtypes continue to be diagnosed in Stage III/IV. Attempts at early diagnosis have failed because high-grade cancer cells exfoliate and metastasize while the primary cancer is small and undetectable by existing tests based on imaging and blood-based tumour markers.DOvEEgene (Detecting Ovarian and Endometrial cancers Early using genomics) is a genomic uterine pap test developed by a McGill team to screen and detect these cancers while they are confined to the gynecologic organs and curable by surgery. The test identifies pathogenic somatic mutations in uterine brush samples A high sensitivity error-reducing capture technology (DOvEEgene-SureSelectHS) utilizing duplex sequencing interrogates the exons of 23 genes involved in the development of sporadic and hereditary ovarian and endometrial cancers. We apply a combination of germline gene panel testing on saliva samples with deep duplex sequencing to detect somatic mutations at <0.1% VAF, interrogation of microsatellite loci for instability and low coverage WGS for copy number analysis of uterine brush samples. Currently, DOvEEgene is the only test that can discriminate ovarian and endometrial cancers in peri- and postmenopausal women from benign gynecologic diseases common in that age group. This is important because pathogenic somatic driver mutations are also associated with increasing age and benign disease. DOvEEgene incorporates a deep machine-learning derived classifier that can discriminate the mutational signature of these cancers from benign disease aiming for a sensitivity of 70% and a specificity of 100% in a population with high background mutational burden. Here we tested the Onso system, a highly accurate sequencing technology from PacBio in order to potentially increase sensitivity while driving down sequencing costs by reducing required sequencing depth vs the current NGS standard. We sequenced 15 duplex Illumina sequencing libraries produced using the DovEE assay at PE 100bp mode and compared Onso data in non- duplex sequencing mode as well as duplex sequencing mode to the original duplex sequencing method. Here, we present this comparison and highlight the

benefits of high accuracy sequencing for the detection of very low frequency (<0.1%) somatic mutations.

#6523

A case of stage I HPV-mediated oropharyngeal squamous cell carcinoma (SCC) diagnosed using a multi-cancer early detection (MCED) test

Janet Vittone[1], Julia Feygin[2], Jason Carey[2]. *[1]Mayo Clinic, Rochester, MN,[2]GRAIL, LLC, a subsidiary of Illumina, Inc., currently held separate from Illumina, Inc. under the terms of the Interim Measures Order of the European Commission dated 29 October 2021, Menlo Park, CA*

There are no routine screening tests for head and neck (H&N) cancers, which account for approximately 4% of all cancers in the US. Risk factors for oropharyngeal cancer include smoking and human papillomavirus (HPV) infection. An MCED test that uses a cell-free DNA-based targeted methylation assay and machine learning classifiers to detect a shared cancer signal and predict the cancer signal origin (CSO) is available as a complement to existing single-cancer screening tests. If a cancer signal is detected, the positive result is reported with 1 or 2 CSO prediction(s). We report here a tonsil cancer case detected using an MCED test and review the CSO-guided diagnostic journey. An asymptomatic 74-year-old White male (BMI: 29.9 kg/m^2) with history of chronic lymphocytic leukemia (CLL; Rai stage 0; 13q, CD38, and ZAP-70 negative; no treatment was needed) 17 years prior and papillary thyroid cancer (stage IVa; pT3N1bM0; thyroidectomy and radiation therapy; no recurrence) 8 years prior was screened using the MCED test. Patient had an elevated PSA level (9-10 ng/mL) and was a nonsmoker. Fifteen days after a blood sample was collected for analysis, a positive test result (CSO prediction=H&N) was communicated to the patient (Day 1). PET showed abnormal uptake in the right tonsil (Day 28). The patient was referred for an ENT consult and underwent a right lymph node biopsy (Day 54). The biopsy showed invasive moderately differentiated SCC, non-keratinizing, forming a 3x2.1x1.2 cm mass (Day 57). Patient underwent right tonsillectomy (the surgical margins were negative for invasive or in situ carcinoma) and lymph node dissection (Day 57). The cancer was diagnosed as HPV-mediated p16+, pT2, pN1, cM0 (stage I) SCC of the oropharynx (Day 57). No

chemotherapy or radiation was required due to the early stage of detection. The patient will follow-up with ENT and radiation oncology. The MCED test detected a cancer signal and predicted an accurate CSO for an asymptomatic individual with stage I HPV-mediated oropharyngeal SCC. Notably, despite a history of CLL and an elevated PSA level, the test accurately predicted CSO leading to a directed workup diagnosing asymptomatic cancer in less than 2 months, while the cancer was still at stage I. In the case-control Circulating Cell-free Genome Atlas study, the MCED test sensitivity to detect a cancer signal was 63% in stage I H&N cancer. The use of this MCED test led to detection of cancer in a patient with CLL history and treatment (surgery without complications and without chemotherapy or radiation) with curative intent.

#6524

Single-cell transcriptomic analysis reveals immune landscape in the malignant transformation of normal lung to lung adenocarcinoma in genetic murine models

Hong Chen[1], Bo Zhu[1], Junya Fujimoto[1], Yanhua Tian[1], Jian-Rong Li[2], Pingjun Chen[1], Alexandre Reuben[1], Monique B. Nilsson[1], Xiuning Le[1], Alissa Poteete[1], Shawna M. Hubert[1], Don L. Gibbons[1], Ignacio I. Wistuba[1], Jia Wu[1], Chao Cheng[2], John V. Heymach[1], Jianjun Zhang[1]. *[1]The University of Texas MD Anderson Cancer Center, Houston, TX,[2]Baylor College of Medicine, Houston, TX*

Background: Our understanding of the initiation and progression of lung precancers is rudimentary, which has impeded advance for lung cancer prevention and interception. Although human specimens are the gold standard to study human cancer biology, lung precancer specimens designated for research are often very limited. Furthermore, human specimens are not amendable for preclinical intervention studies. We sought to establish and characterize human-relevant murine lung precancer models to study evolution of lung precancers and to provide insights for lung cancer interception.

Methods: We established two mouse models, KrasG12D (a genetically engineered mouse model with KrasG12D activating mutation) and CITMs (a carcinogen urethane-induced model) in the same 129S4 background. We performed single-cell transcriptome sequencing of lung tissues collected at

5 time points after induction for each model to characterize the dynamics of immune response along with the initiation and progression of lung adenocarcinoma.
Results: A total of 82,198 immune cells were analyzed and 23 immune cell subpopulations were identified. The results demonstrated dynamic changes of immune cell compositions and cell states along with the evolution from normal lung to lung precancers, and to lung adenocarcinomas in both models. CD4+ effector T cells, CD4+ regulatory T cells, mucosal associated invariant T cells (MAIT) and macrophages progressively increased during tumor progression, in contrast to progressively decreasing naive CD4+ T cells, naive CD8+ T cells and naive B cells. In contrast to CITMs, KrasG12D model harbors a clear decrease in conventional dendritic cells (cDCs) and activated B cells, but significantly more neutrophils (Wilcoxon test, $P < 0.01$).
Conclusion: These data provide a temporal atlas of lung cancer evolution during early lung carcinogenesis and a resource for interception preclinical study. Our results revealed progressive immunosuppression along with progression of lung precancers in both genetic and carcinogen-induced models, but the immune features underlying immunosuppression may be different.

#6525
Colon cancer screening and treatment with engineered probiotics
Candice R. Gurbatri[1], Georgette Radford[2], Jongwon Im[1], Courtney Coker[1], Nicholas Arpaia[1], Susan L. Woods[2], Daniel L. Worthley[3], Tal Danino[1].
[1]Columbia University, New York, NY,[2]Adelaide Medical School, Adelaide, Australia,[3]South Australian Health and Medical Research Institute, Adelaide, Australia

Bioengineered probiotics enable new opportunities to improve colorectal cancer (CRC) screening, prevention and treatment strategies. Here, we demonstrate selective colonization of CRC tumors with the orally-delivered probiotic *E. coli Nissle 1917* (EcN) in genetically-engineered and orthotopic murine models of CRC, and human CRC patients. We subsequently engineer EcN to produce screening and therapeutic molecules, resulting in non-invasive detection of precursor CRC lesions and reduction of tumor burden through local induction of robust anti-tumor immunity.

#6526

Investigation levels of trace elements in breast cancer types using laser spectroscopic techniques

Ola Sayed Ahmed[1], hisham imam[2]. *[1]National Cancer Institute, Cairo University, Cairo, Egypt,[2]National laser Institute, Cairo University, Cairo, Egypt*

Breast cancer (BC) is the 2nd leading cause of death from cancer in women. Women have a lifetime risk of breast cancer of around 31%, which makes it the first most common malignancy in women .Diagnosing cancer and classifying its types is a complex process that relies heavily on sample analysis. Early detection of cancer diseases is one of the important and main factors in determining treatment and saving many patients before the disease worsens and reaches dangerous stages. Alterations in the levels of trace elements have been observed in breast cancer (BC) patients. However, the relationships between these alterations and the metabolic and clinical consequences of BC are unknown. The aim of the present work is to study in vitro possibilities and the effectiveness of introducing an efficient optical spectroscopic technique such as LIBS for the identification types of breast cancer, as well as determining the disease grade and severity. The ultimate goal of this work is to investigate the concentrations of several trace elements in BC patients, and their relationships with the molecular subtypes of tumors. The atomic transition of the neutral element lines of Fe, Al, Na, Ca, K, V, Co and Pb was chosen to determine the trace element levels of four breast cancer types. We found that the measured average level of trace elements can differentiate between different types of breast cancer.

#6527

Fusion genes as novel putative biomarkers for head and neck squamous cell carcinomas

Yabdiel A. Ramos Valerio[1], Hannah C. Van Wyk[2], Esther Peterson Peguero[3], Josué Pérez Santiago[1]. *[1]Cancer Biology, UPR - Comprehensive Cancer Center, San Juan, PR,[2]Epidemiology, University of Michigan School of Public Health, Ann Arbor, MI,[3]Natural Sciences, UPR - Rio Piedras, San Juan, PR*

Head and neck squamous cell carcinomas (HNSCC) are highly aggressive types of cancers with a complex molecular etiology of disease and consequently result in delayed clinical detection, poor prognosis, and limited treatment strategies. Fusion genes, a hallmark of cancer, may be targeted for early identification and treatment of HNSCC; however, studies characterizing fusion genes in HNSCC remain limited. Oral Human Papillomavirus (HPV) infection is a major cause of HNSCC and can also promote the acquisition of fusion genes due to the genomic instability induced by its integration. Here, we retrieved RNA-sequencing data from 36 HNSCC tumors (18 HPV+ and 18 HPV-, GEO Accession: GSE74956) to identify fusion genes using the STAR fusion algorithm in each sample. Statistical analyses were performed in R statistical software. A total of 10 fusion genes were identified in at least 4 of the samples regardless of HPV status. We identified 3 fusion genes that were present in at least 4 of the HPV+ tumors: PMS2P9-CCDC146, MACC1-AC005062.1, AC096711.2-RPL7AP28, and one solely present in HPV- tumors: CTSC-RAB38. The remaining 6 fusion genes were present in both HPV+ and HPV- tumors: TVP23C-CDRT4, AC009271.1-LINC01905, MIR205HG-AOPEP, SEPTIN7P2-PSPH, KRT5-KRT84, KANSL1-ARL17A. While 4 of the identified fusion genes had been previously associated with cancer, there were 6 novel identified fusion genes, in which one or both partner genes have been associated with different cancers. Additionally, the identified fusion genes may be a product of transcription read-through of neighbor genes. The fusion genes associated with HPV infection might explain biological disparities in HPV+ versus HPV- HNSCC and may be targets for the prevention and diagnosis of HNSCC. Future studies need to determine the functional impact of the identified fusion genes in HPV+ tumors.

#6528

HPV status and epigenetic profiling of saliva from a cancer-free population

Ana Paula Muterle Varela[1], Dieila Giomo De Lima[2], Laura Palmieri[2], Juliana Comerlato[1], Fernando Hayashi Sant'Anna[1], Isabel C Bandeira[1], Marina Bessel[1], Pedro Isaacsson Velho[1], Eliana M. Wendland[1], Mariana Brait[2]. *[1]Hospital Moinhos de Vento, Porto Alegre, Brazil,[2]Johns Hopkins University School of Medicine, Baltimore, MD*

Identifying environmental factors and their relationship with epigenetic alterations is essential for understanding cancer, a leading cause of death. Currently, cancer screening and early detection development efforts are ongoing and epigenetics-based tests are one of the top choices as strategies. The understanding of how these alterations behave in cancer-free (CF) populations with well annotated data is essential. We randomly selected 601 saliva specimens from two Brazilian countrywide epidemiological studies POP-Brazil and SMESH. Extracted DNAs were sodium bisulfite converted and analyzed by Quantitative Methylation-Specific PCR (QMSP). Five genes previously reported as DNA methylation prone in cancer were selected (*ITGA4*, *EDRNB*, *PAX5, p16, CCNA1*). All participants were interviewed and provided sociodemographic and sexual behavior information as well as genital (gn) and oral biological samples. Variables were categorized and Fisher's exact test was performed using SAS 9.4.Surprisingly, methylation in 3 cancer associated genes showed considerable frequencies in this CF group. DNA methylation was observed for *EDNRB* in 75/601 samples (12.5%), *PAX5* in 55/601 (9.2%), and *ITGA4* in 20/601 (3.3%). 12 samples displayed concomitant methylation on 2 of these 3 genes. *p16* and *CCNA1* methylation were only present in 1 sample each. Preliminary analyses suggest that specific genes methylation are observed with the presence of low (LR) and high-risk (HR) HPV types. *EDNRB* methylation groups with the presence of HR HPV type 16, 31, 39, 51, 58 and 59 from gn samples and LR types 6 and 42. *ITGA4* methylation and HR HPV types 16 and 59 were detected in oral samples, and types 52, 56 and 68 in gn samples, as well as LR HPV types 40 and 42. In people with early onset of smoking, *EDNRB* and *PAX5* seem to be more frequently methylated. The positivity of *PAX5* was higher in participants who smoke, use alcohol and presented a positive diagnosis of syphilis and/or HIV. *PAX5* methylation was more frequent in HR HPV 33, 58, 68 and 62 and LR type 6. Further analyses are ongoing. Our study shows methylation in cancer related genes in a CF population. The variables collected include some proven cancer risk factors and others still unknown, thus lead us to uncover directions to identify main cancer related players in a Brazilian population. The presence of cancer related alterations may indicate premalignant stages, exposure and lifestyle consequences, both at the same time or separately. In our pilot analysis, different types of HPV seem to correlate with epigenetic changes, this could bring attention to less studied HPV types and their role

in carcinogenesis. Additional analyses of the current data and larger prospective, population-based studies, assessing the use of salivary DNA methylation in cancer-free and cancer groups of subjects are needed to explore the current findings and dissect the potential of saliva as a means of tracking cancer related changes.

#6529

Early life liver proteomic signature and minerals mitigation of liver injury

Isabelle Harber, Shannon D. McClintock, Randall N. Knibbs, James Varani, Muhammad N. Aslam. *University of Michigan Medical School, Ann Arbor, MI*

Background and Aims: Previous long-term murine (12- and 18-month) studies in C57BL/6 mice have demonstrated the beneficial role of Aquamin, a red marine algae-derived multi-mineral supplement containing calcium, magnesium, and 72 additional trace elements, in inhibiting liver tumor formation in mice on high-fat, Western-style diet (HFWD). Liver tumor incidence in mice on HFWD was decreased to 12% with the addition of Aquamin supplementation compared with 48% in the HFWD mice. Similarly, in mice on the low-fat diet, tumor incidence was only 16% and Aquamin further reduced it to 4%. Recently, we assessed the safety and tolerability of Aquamin in human subjects in a 90-day interventional trial and there was no evidence of potential liver harm, measured by liver enzymes. A short-term (16-week) mouse study was carried out to investigate early protein changes in the liver that may play a role in liver tumorigenesis and how Aquamin can interfere with that signature.
Methods: Male MS-NASH mice were maintained on a HFWD for 16 weeks with and without red algae-derived minerals. A cohort of C57BL/6 mice maintained on a standard chow (low-fat diet) was used as a control. At the end of the in-life portion of the study, body weight, liver weight, liver enzyme levels and liver histology were assessed. Samples obtained from individual livers were subjected to Tandem Mass Tag labeling and quantitative proteomics mass spectrometry.
Results: As expected, no tumors were observed at 16 weeks. Mice on the HFWD demonstrated multiple protein changes associated with dysregulated fat and carbohydrate metabolism, lipotoxicity and oxidative stress. In mice

receiving Aquamin-supplementation along with the HFWD, there was reduced liver toxicity as evidenced by a decrease in levels of several cytochrome P450 enzymes and other oxidant-generating moieties. Additionally, multiple keratins, which provide cytoskeletal support were elevated. Phosphate and tensin homolog (PTEN), a tumor suppressor, was upregulated with Aquamin. There was an upregulation of several pathways implicated in tumor suppressor activity, notably *keratinization*, *hedgehog signaling in the off-state*, and *regulation of PTEN stability and activity*. *Conclusions:* The proteomic expression of the livers of HFWD mice in this short-term study explains early protein changes that may contribute to liver cancer and the potential mechanisms by which dietary minerals may mitigate such down-stream effects.

#6530

Preferential low frequency allele enrichment with lower sequencing depth requirement using KAPA HyperPETE specialized primer designs

Florence K. Crary-Dooley, Liu Xi, Ruben van der Merwe, Nitya M. Furtado, Jingchuan Li, Junyan Lin, Manuel Ochoa, Brian Godwin. *Roche Diagnostics, Pleasanton, CA*

Background: The presence of circulating tumor DNA (ctDNA) can be used for minimal residual disease (MRD) monitoring and guide adjuvant therapy decisions. However, even when present, total ctDNA could be less than 0.01% of cell free DNA (cfDNA). Sequencing such low mutation frequency can be costly due to high sequencing read depth and accuracy requirements. The ability to enrich for low-abundance variants could improve detection performance and greatly lower sequencing cost by reducing the sequencing depth required.
Purpose: The KAPA HyperPETE (Primer Extension Target Enrichment) workflow employs primer extension reactions to specifically capture and release target library molecules for sequencing, detects all major somatic variant types (SNV, InDel, CNV, MSI status, and novel fusion transcript partners) and could be leveraged to specifically target certain alleles. In this study, we assessed the variant enrichment capabilities of the KAPA HyperPETE workflow.

Methods: Variant specific primers were designed to 8 low allele frequency single nucleotide variants (SNVs) in mixed cell line samples (NA12878 and NA24143, two Epstein-Barr virus transformed B cell female cell lines, with variant allele frequency (VAF) 1%, 0.5%, and 0.1%). Variant enrichment primers were used alongside a 37kb panel in the KAPA HyperPETE workflow. Additional optimizations and a study enriching all low allele frequency SNVs* in SeraCare ctDNA Mutation Mix v2 reference samples (VAF 1%, 0.5%, and 0.125%) are planned.

Results: The preliminary results exhibited a median of 249×, 159×, and 86.5× enrichment of the targeted variants compared to the expected VAFs of 0.1%, 0.5%, and 1%, respectively. All 8 targeted variants were detected at 100K, 150K, and 550K read pairs per variant for VAF 1%, 0.5%, and 0.1%, respectively. Results from further optimizations and the study using SeraCare ctDNA samples will be shared at the AACR meeting.

Conclusion: Preferential enrichment of specific variants down to 0.1% can be achieved using the KAPA HyperPETE Workflow. Utilizing primers designed for variant enrichment, we simultaneously enriched multiple variants and demonstrated the potential to minimize required sequencing. The KAPA HyperPETE workflow can be a powerful, cost-effective tool for detecting low frequency mutations in MRD research applications.

KAPA HYPERPETE is For Research Use Only. Not for use in diagnostic procedures. KAPA HYPERPETE is a trademark of Roche.

*Except GNA11 (COSM52969) due to stretches of polybase. Seraseq ctDNA Mutation Mix v2 gene list available on SeraCare website.

#6531

Point of care test for cervical cancer screening

Samrin Farouk Idris Habbani[1], Sayeh Jalali Dowlatshahi[2], Monisha Elumalai[2], Scott Charles Bolton[2], Lucy Teberh Tecle[2], Pankti Rajesh Thakkar[2], Jacqueline C Linnes[2], Sulma I Mohammed[1]. *[1]Comparative Pathobiology, Purdue University, West Lafayette, IN,[2]Biomedical Engineering, Purdue University, West Lafayette, IN*

Cervical cancer is a lethal gynecological malignancy and the fourth most common cancer among women. Most high-grade cervical pre-cancers and cancer cases are linked to infection with high-risk human papillomaviruses

(HPV). There is an inequity between high-income countries (HICs) and low- and middle-income countries (LMICs) in cervical cancer burden; according to the World Health Organization, the estimated mortality rate of cervical cancer is 342,000 women worldwide in 2020, and 90% of these women reside in low- and middle-income nations where the human papillomavirus vaccine is unavailable and access to early detection testing are either unavailable or too expensive. This study aims to develop a simple and affordable point-of-care test based on four critical biomarkers for screening high-risk pre-cancer and invasive cervical cancer in collaboration with the biomedical engineering department. A cervical cancer swab will be used in the test. The swab will be placed on a paper-based device that looks for four protein biomarkers critical for the progression of noninvasive cervical cancer into invasive cervical cancer by combining two approaches using proteomics and lateral flow immunochromatography technology. We have validated the markers' expression in cervical cancer and precancerous tissues. The four markers were expressed in squamous cell carcinoma, glassy cell carcinoma, adenocarcinoma, clear cell carcinoma cancer tissues, and the high-grade cervical intraepithelial neoplasia. This point-of-care test will be affordable and implementable, especially in low and middle-income countries.

TUMOR BIOLOGY

Cancer Stem Cells and Therapeutic Resistance

#5791

Autophagy & PIM1 kinase inhibition in breast cancer stem cells & bulk cancer cells attenuates breast cancer & metastasis

Kanakaraju Manupati[1], Mingang Hao[2], Michael Haas[2], Syn Kok Yeo[1], Jun-Lin Guan[1]. *[1]University of Cincinnati, Cincinnati, OH,[2]Department of Cancer Biology, University of Cincinnati, Cincinnati, OH*

Autophagy is a self-degradation process, it is essential for growth of heterogenous of breast cancer cells. Breast tumor heterogeneity majorly comprises bulk cancer cells & cancer stem cells (CSCs). Targeting either CSCs or cancer cells could lead to interconversion between these cells due to EMT/MET transitions. Therefore, it is important to identify a common

molecular targets & its mechanism of regulation in these populations for improvement of breast cancer therapy. Here, we utilized a PCR based screen & identified NUMA1 downregulation in FIP200 KO (autophagy gene) cells of three major breast cancer subtypes, FF99 (luminal), N418 (Her2+) & BF3M (basal). Further, NUMA1 KO in these cells reduced tumor formation & CSCs indicating the role of NUMA1 on regulation of CSCs. Therefore, we sorted breast CSCs, $ALDH^{+}$ and $CD29^{hi}$ $CD61^{+}$ from WT & NUMA1 KO cells, tail-vein injected nude mice depicted reduced metastatic potential with NUMA1 KO than WT CSCs. Mechanistically, NUMA1 regulation by PIM1 kinase was observed in CSCs but not in bulk cancer cells. Cell viability assays revealed that combination treatment of autophagy & PIM1 inhibitor showed higher efficacy against cancer cells of three breast cancer subtypes than individual treatments alone. Finally, the combination treatment of autophagy inhibitor, Lys05 & PIM1 inhibitor, SMI-4a reduced tumor formation & metastasis of breast cancer. Human tissue microarray results depicted high expression of NUMA1 & PIM1 in different breast cancer subtypes than non- tumor tissues. Our study demonstrated that inhibition of autophagy & PIM1 in bulk cancer cells & CSCs showed attenuation of tumor formation & metastasis, suggesting this combination treatment serves as an important therapeutic approach for treating breast cancer.

#5792

The novel therapeutic diiminoquinone exhibits anticancer effects on human prostate cancer cells in 2D and 3D in vitro models

Amani Yehya, Alissar Monzer, Kevork Wakimian, Fatima Ghamlouche, Nour Saheb, Ayman Tawil, Hala Gali-Muhtasib, Deborah Mukherji, Albert El-Hajj, Wassim G. Abou-Kheir. *American University of Beirut, Beirut, Lebanon*

Aim: To investigate the anticancer potential of the novel quinone DIQ on prostate cancer (PCa) cells in two-dimensional (2D) and three-dimensional (3D) *in vitro*.

Methods: The anti-proliferative effect of DIQ on PC3 and DU145 PCa cell lines was determined *in vitro* by using 3-(4,5 dimethylthiazol-2-yl)-2,5-diphenyltetrazolium bromide (MTT) and trypan blue exclusion assays. In addition, the potency of DIQ was tested on the formation and size of PCa

cell-derived prostatospheres and organoids grown in a specialized 3D-culture system. Also, 3D organoids were established from fresh tissue samples representing different stages of PCa obtained from consented patients who underwent radical prostatectomy at the American University of Beirut Medical Center (AUBMC) according to appropriate Institutional Review Board (IRB) approval guidelines. This model was used to assess DIQ
individualized tumor response on organoids growth and the effect was evaluated by quantifying the number of organoids formed (OFC) and calculating the average size (diameters).
Results: Our results showed that DIQ significantly attenuated cell proliferation and viability in PC3 and DU145 PCa cell lines. DIQ also reduced the formation ability and size of PC3 and DU145 prostatospheres and organoids at sub-toxic doses of 1 μM. Potently, DIQ displayed a significant decrease in both the count and the size of the different patient-derived organoids as compared to their respective control.
Conclusion: This study provides promising clues for the use of the novel anticancer therapeutic DIQ in targeting CSCs, findings that may have promising therapeutic implications for PCa patients.

#5793

Met confers radioresistance-associated aggressiveness through enhancing PLXDC2-mediated cancer stem cell plasticity

Fanghui Chen[1], Liwei Lang[2], Chloe Shay[1], Georgia Chen[1], Nabil Saba[1], Yong Teng[1]. *[1]Emory University, Atlanta, GA,[2]Augusta University, Augusta, GA*

The development of radioresistance in head and neck squamous cell carcinoma (HNSCC) remains a significant problem in cancer treatment, contributing to the lack of improvement in survival trends in the past decades. One of the clinical challenges is that radioresistance often promotes tumor aggressiveness. However, the underlying mechanisms and molecular determinants are largely unknown. We report here that radioresistance-associated HNSCC aggressiveness is effectively exacerbated by c-Met but can be suppressed by its genetic knockdown and pharmacological inactivation. Through unbiased RNAseq data, we further uncovered that the resulting upregulation of c-Met signaling increases the

expression of PLXDC2. a critical gene associated with the tumor microenvironment. Mechanistically, PLXDC2 is upregulated in radioresistant HNSCC cells through c-Met mediated activation of ERK1/2-ELK1 signaling cascade. Most importantly, PLXDC2 modulates cancer cell plasticity by inducing epithelial-mesenchymal transition (EMT) and the emergence of cancer stem cell (CSC) subpopulation. Additionally, depletion of PLXDC2 overcomes c-Met-mediated radioresistance by reversing the EMT progress and blunting the self-renewal capacity of CSCs. Therapeutically, a combination of the c-Met selective inhibitor SU11274 with radiation remarkably induces tumor shrinkage and constrains tumor metastasis to lymph nodes in vivo. Our study is novel in being the first to explore the role and mechanism of the c-Met-PLXDC2 axis in radioresistance-associated HNSCC aggressiveness and the first to our knowledge to evaluate how to take advantage of blocking this signaling to overcome radioresistance in preclinical mouse models of HNSCC.

#5794

Targeting CD133$^+$/CD90$^+$ liver cancer stem cells by piperlongumine: A novel strategy for liver cancer treatment

Basma A. Abdelaziz[1], Omayma M. Sadek[2], Ahmed S. Sultan[2]. *[1]Basic Sciences / Biochemistry, Pharos University in Alexandria / Alexandria University, Alexandria, Egypt,[2]Biochemistry, Alexandria University, Alexandria, Egypt*

Liver cancer is an aggressive malignant disease. It's the most common cancer worldwide and the leading cause of cancer death. Because of the atypical early symptoms of liver cancer, the majority of liver cancer patients are diagnosed with advanced-cancer stage, decreasing the chance of resection and resulting in a poor survival rate. Liver cancer stem cells (LCSCs) are a small subpopulation inside the tumor bulk, characterized by the maintenance of self-renewal and pluripotency. Thus, LCSCs are responsible for cancer initiation, metastasis, relapse, and chemoresistance. Elucidating LCSC characteristics and disclosing their regulatory mechanism might facilitate the development of prognostic, diagnostic, and therapeutic approaches to improve the clinical management of liver cancer. Piperlongumine (PL) an active biological pyridine alkaloid has anti-angiogenic, anti-diabetic, and anti-bacterial activities. The present study

aimed to isolate highly tumorigenic and aggressive subpopulation of LCSCs ($CD133^+/CD90^+$) from primary tumors and different cell lines and investigate the effect of (PL), a novel targeting therapy, on LCSCs proliferation. The isolated LCSCs were treated with different concentrations of PL and its effect was examined by cell viability, cell morphological changes, western blot, caspase-3 activity, apoptotic induction, and clonogenic formation. By using Immunocytochemistry (ICC) analysis, the localization of nuclear and cytoplasmic Aldehyde dehydrogenase (ALDH6A1) was detected. PL inhibited the viability of $CD133^+/CD90^+$LCSC-sub-popupation and caused morphological changes after 48 hours while enhancing the pre-apoptotic signals and caspase-3 activity. In addition, PL decreased the colonies' formation ability compared to control group. Furthermore, PL suppressed the protein expression levels of ALDH6A1, Notch-1, β-catenin, ERK1/2, and Cyclin-D1 in the dose and time-dependent manners. Besides, PL decreased the localization and intensity of nuclear and cytoplasmic ALDH6A1 compared to the control group, indicating that PL decreased the proliferation and stemness markers of LCSCs. Overall, Piperlongumine as a novel targeting therapy has an important role in targeting $CD133^+/CD90^+$ LCSCs sub-population proliferation.

#5795

Leukemic stem cells confer ferroptosis resistance in aggressive blood cancer

Nunki Hassan, Hangyu Yi, Lucie Gaspard-Boulinc, Jenny Wang. *School of Medical Sciences, Faculty of Medicine and Health, University of Sydney, Sydney, Australia*

Acute myeloid leukemia (AML) is an aggressive blood cancer with limited therapeutic options against leukemic stem cells (LSCs), resulting in poor clinical outcomes for decades. We have demonstrated the clinical importance of aberrant activation of RSPO3/β-catenin pathway in a subset of poor prognosis AML (*Cancer Cell,* 38:263-278, 2020) and its ability to sustain low levels of reactive oxygen species (ROS), a critical characteristic of human LSCs. This current study has extended our recent finding, and for the first time linked the pathway activation to ferroptosis resistance, a new drug resistance mechanism in cancer therapy. Our single-cell multiomics

data in patient-derived xenograft mouse models of relapsed AML showed that the pathway activation in human LSCs led to upregulation of 43 differentially expressed genes associated with iron detoxification (e.g., FTH1) and ROS sensing/detoxification (e.g., PRDX1), two key features of ferroptosis resistance. Consistent with this observation, we found that AML patient specimens with favourable outcomes, which are independent of RSPO3 pathway, were sensitive to RSL3 treatment leading to increased cell death associated with elevated levels of intracellular ROS and iron. In contrast, AML patient specimens with poor clinical outcomes, which critically depend on RSPO3 pathway activation for survival and maintenance of myeloid undifferentiated state, revealed resistance to ferroptosis inducers (e.g., RSL3). Intriguingly, we found that anti-RSPO3 antibody, a clinical-grade drug that inhibits AML LSCs by blocking the interaction of RSPO3 with its receptor, sensitizes human LSCs to RSL3 treatment, leading to reduced cell viability. Overall, this study is the first to demonstrate the role of ferroptosis resistance in human LSCs and provides an opportunity to develop precision combination therapy by concurrently targeting self-renewal and ferroptosis resistance to improve therapeutic outcomes for patients with poor-risk AML.

#5797

NTX301, a novel DNA hypomethylating agent, targets lipid metabolism in ovarian cancer

Yinu Wang, Xiaolei Situ, Horacio Cardenas, Daniela Matei, Ellie Siu, Sayedabdulrazzaq A. Alhunayan. *Northwestern University - Chicago, Chicago, IL*

Background: DNA methylation causes the silencing of tumor suppressor and differentiation-associated genes being linked to chemoresistance and stemness. Previous studies demonstrated that hypomethylating agents (HMA) re-sensitize ovarian cancer (OC) cells to chemotherapy, however, translation to the clinic has been slow. NTX 301 (PinotBio) is a novel, highly potent, and orally bioavailable HMA, in early clinical development. Methods: We assessed the anti-tumor effects of NTX301 in OC models and studied the underlying molecular mechanisms by using cell proliferation, stemness, and ferroptosis assays, RNA sequencing, and validation.

Results: OC cells (SKOV3, IC_{50}=5.089nM; OVCAR5 IC_{50}=3.664nM) were highly sensitive to NTX301 ($p<0.05$) compared to immortalized fallopian tube epithelial cells (FT-190) (IC_{50}=103.3nM). Treatment with NTX301 induced significant downregulation of the DNA methyltransferases (DNMTs) 1-3 expression in SKOV3 and OVCAR5 cells compared with decitabine ($p<0.05$). Treatment with low dose NTX301 (100nM) induced significant transcriptomic reprogramming with 15,000 differentially expressed genes (DEGs) compared to DMSO ($p<0.05$). Among the NTX301 down-regulated DEGs, Gene Ontology (GO) enrichment analysis identified pathways related to the *regulation of alcohol, cholesterol, and fatty acid biosynthetic process and* molecular functions related to *aldehyde dehydrogenase (ALDH) and oxidoreductase activity*, known features of cancer stem cells (CSCs). Indeed, treatment with low dose NTX301 (100nM) reduced the ALDH(+) cell population and expression of stemness-associated transcription factors (Oct4 and Sox2). Additionally, stearoyl-Coenzyme A desaturase 1 (SCD), a key enzyme that regulates unsaturated fatty acid homeostasis in the lipogenesis process was found among the top DEGs downregulated in response to NTX3 (fold change=9.36, *FDR*<0.05). As blockade of SCD had been shown to induce ferroptosis, oxidized lipids levels were measured by C11-BODIPY staining. NTX301 treatment increased the levels of oxidized lipids compared to DMSO and this was blunted by deferoxamine, indicating that NTX301 promoted cell death via ferroptosis. NTX301-induced ferroptosis was successfully rescued by the addition of oleic acid (200μM) into the culture medium, supporting that it was mediated through SCD depletion. *In vivo*, monotherapy with NTX301 (0.5mg/kg), significantly inhibited subcutaneous OC xenograft tumor growth ($p<0.05$). Decreased SCD levels and increased oxidized lipids were recorded in NTX301-treated xenografts.
Conclusions: NTX301 is a potent HMA active in OC models. Our findings point to a new mechanism by which epigenetic blockade disrupts lipid homeostasis and promotes cancer cell death.

#5798

Ex vivo culturing of primary AML cells facilitates the study of developmental therapeutics

Satyam Patel[1], Upendarrao Golla[2], Arati Sharma[3], David Claxton[2]. *[1]Penn State College of Medicine, Hershey, PA,[2]Department of Medicine, Penn*

State College of Medicine, Hershey, PA,[3]Department of Pharmacology, Penn State College of Medicine, Hershey, PA

Studies with acute myeloid leukemia (AML) cell lines have limited potential as they tend to acquire mutations, thus, do not represent typical leukemias found in patients. Ex vivo culturing of primary human AML patient cells is therefore of interest; however, the long-term culture of these cells has been limited by rapid differentiation and loss of clonogenicity. Previously, different growth factors and stromal cells were implicated in the short-term culturing of primary cells. Thus, we aimed to evaluate culture conditions using a cytokine cocktail, allowing long-term expansion and phenotypic maintenance of primary AML cells in vitro. Different culture conditions were constituted by combination of cytokines (SCF, FLT-3L, TPO, IL-6, IL-3, GCSF, GM-CSF) and small molecules (SR1, UM729) in serum-free StemSpan SFEM media. The ability of different growth mediums to support the expansion and clonogenicity of 6 primary AML cells (collected from blood/bone marrow) over two weeks was assessed using cell counts and colony formation assays. Additionally, cell surface markers (hCD34, hCD45, hCD123, hCD117) were assessed by flow cytometry during the culture period. All tested cultured conditions exhibited successful cell proliferation (4-6-fold expansion) and survival of primary AML cells over two weeks of culture. In addition, the growth media successfully supported 3.5-fold CD34+ stem cell expansion. Growth mediums with early-acting cytokines (SCF, FLT-3L, TPO, and IL-6) and small molecules resulted in phenotypic maintenance of cell surface markers (CD34, CD123) and secondary clonogenicity of primary AML cells over the culture period. The addition of late-acting cytokines (IL-3, GCSF, and GM-CSF) showed a higher growth rate but negatively affected the cell surface markers and clonogenicity. Secondary colony counts (day-9 culture) showed a significant positive correlation with CD34 expression levels. Thus, CD34 levels could serve as a potential surrogate marker for the clonogenicity of primary AML cells. Furthermore, we tested the engraftment ability of two primary AML cells grown in 3 of our promising culture conditions (Day 4, Day 8) in xenograft mice. Flow cytometry analysis on peripheral blood and tissues (spleen and bone marrow) from xenograft mice showed successful engraftment of primary cells cultured for 8 days. On an application note, the optimal condition from our results was

used to study the effects of ceramide nanoliposomes (CNL) in AML patient cells. Interestingly, the AML patient cells treated for two weeks with IC15 and IC30 doses of CNL led to cell cycle arrest, reduced CD34 expression, and clonogenicity relative to control cells. The CNL findings from primary cells are different from that of cell lines cultured under the same conditions. Thus, our optimal growth conditions may facilitate researchers to understand AML biology and study various therapeutics under development using primary AML cells.

#5799

SPINK1-induced tumor plasticity provides a therapeutic window for chemotherapy in hepatocellular carcinoma

Ki-Fong Man[1], Lei Zhou[1], Ying-Tung Lam[1], Jun Yu[2], Jing-Ping Yun[3], Xin-Yuan Guan[4], Ming Liu[5], Stephanie Ma[1]. *[1]School of Biomedical Sciences, The University of Hong Kong, Hong Kong, Hong Kong,[2]The Chinese University of Hong Kong, Hong Kong, Hong Kong,[3]Pathology, Sun Yat-Sen University Cancer Centre, Guangzhou, China,[4]Clinical Oncology, The University of Hong Kong, Hong Kong, Hong Kong,[5]School of Basic Medical Sciences, Guangzhou Medical University, Guangzhou, China*

Intratumor molecular heterogeneity of hepatocellular carcinoma (HCC) is partly attributed to the presence of cancer stem cells (CSCs), which we now know represents a critical root of tumor recurrence and chemotherapy resistance. CD133 is known to represent an important functional marker of liver CSCs. We have demonstrated CD133 to enrich following chemotherapy treatment, while CD133/Prom1-depletion would enhance sensitivity of HCC tumors to chemotherapy. Yet unfortunately, CD133 is not specific to HCC, but is also expressed in normal regenerating liver. Identifying critical factors expressed specifically in liver CD133+ CSCs, but not in liver normal CD133+ stem/progenitor cells may offer important therapeutic opportunities overcoming chemoresistance in HCC. RNA-seq profiling comparing sorted CD133+ and CD133- subsets of normal regenerating liver induced by DDC diet and HCC induced by either N-nitrosodiethylamine (DEN)/carbon tetrachloride (CCl_4) or hydrodynamic tail vein injection of oncogenic plasmids AKT and NRAS identified Serine Peptidase Inhibitor Kazal Type I (SPINK1) to be distinctly expressed in the

HCC CD133+ subpopulation but not in normal regenerating liver CD133+ subpopulation. SPINK1 overexpression in HCC clinical samples is correlated with a poor prognosis. Expression of SPINK1 increased during early liver progenitor development, peaked during the premature hepatocyte stage, decreased during hepatocyte maturation and increased progressively from well-differentiated to poorly differentiated HCCs. Enhanced transcriptional activity of SPINK1 was mediated by promoter binding of the epithelial cell-specific transcription factor ELF3, which like CD133, were both increased following chemotherapy treatment. SPINK1 inhibition by lentiviral-based knockdown or a specific monoclonal antibody (mAb) mitigated tumor initiation, self-renewal and chemoresistance. Mechanistically, secretory SPINK1 bound to epidermal growth factor receptor (EGFR) activating MEK/ERK signaling and consequently promoting the formation of CDK4/6-cyclin D1 complex to phosphorylate Rb and release E2F2, allowing the cells to overcome G1/S checkpoint promoting cell cycle progression as well as transcribing stemness, oncogenic dedifferentiation and chemoresistance-related genes. Collectively, our findings suggest SPINK1 to play a critical role in hepatocarcinogenesis and that SPINK1 mAb may represent a novel therapeutic option for the treatment of HCC, targeting at the CD133+ CSC tumor roots and overcoming chemoresistance.

#5800

Anti-metastatic potential of pitavastatin in triple-negative breast cancer via targeting breast cancer stem-like properties and STAT3 signaling

Dongmi Ko, Juyeon Seo, Seongjae Kim, Soeun Park, Minsu Park, Kee Dal Nam, Yong koo Kang, Sora Seock, Eunsun Jung, Yoon-Jae Kim, Jaeyoun Park, Ji Young Kim, Jae Hong Seo. *Korea University Guro Hospital, Seoul, Korea, Republic of*

Triple-negative breast cancer (TNBC) is the most deadly and aggressive phenotype, with a higher rate of metastatic recurrence. TNBC does yet have a suitable treatment option other than cytotoxic anticancer drugs. Although pitavastatin has been shown to exert anti-proliferative effects and cytotoxicity in various types of cancer cells, the precise mechanisms underlying pitavastatin’s anti-cancer effects in TNBC have not been fully

elucidated. We sought to investigate the mechanism of pitavastatin-induced apoptosis and its effects on cancer stem cell (CSC)-like characteristics in TNBC. Exposure to pitavastatin induced mitochondria-mediated apoptotic cell death in BT549 and 4T1 cells. Mitochondrial dysfunction was accompanied with a robust production of reactive oxygen species (ROS) and collapse of mitochondrial membrane potential (MMP), resulting in subsequent activation of caspase-3/-7 and PARP cleavage. Pitavastatin effectively suppressed CSC-like properties in TNBC via targeting CD44+/CD24- and CD49f+/CD24- phenotypes, as well as impediment of mammosphere formation *in vitro*. This phenomenon was accompanied with dysregulation of STAT3 survival pathway, concomitant with significant downregulation of cyclin D1, survivin and vimentin. Pitavastatin effectively targets both the proliferating TNBC tumor cells and CSCs via the dysregulation of STAT3 and suppression of CSC-like properties, markedly reducing angiogenesis and tumor growth, coinciding with decreased Ki-67 expression. It is noteworthy that pitavastatin considerably suppressed metastasis, coinciding with significant reduction of MMP-2, MMP-9 and VEGF in the circulating blood of mice. Our findings highlight that pitavastatin may be potentially effective for the treatment of metastatic TNBC.

#5801

Inhibition of muscarinic acetylcholine receptors in glioma stem cells blocks tumor progression

Sumyuktha V. Anand[1], Min K. Lee[1], Alexander G. Skorput[1], Isabella B. Fox[2], Alison L. Young[1], Brock C. Christensen[1], Allan Gulledge[1], Matthew C. Havrda[1]. *[1]Dartmouth Geisel School of Medicine, Lebanon, NH,[2]Dartmouth College, Hanover, NH*

Primary gliomas arising within the brain are the deadliest form of brain cancer and account for 78% of all malignant brain tumors. Glioma patients have a 5 percent five-year survival rate and drug-resistant tumors often recur following surgical resection and treatment with radiation and/or chemotherapy. The cancer stem cell hypothesis suggests the presence of a subset of undifferentiated cells, namely glioma stem cells (GSCs), in the heterogenous tumor mass responsible for disease progression. Understanding mechanisms responsible for maintaining GSCs and

developing strategies to deplete the GSC population could improve glioma treatment and prognosis. Some GSCs are similar to oligodendrocyte precursor cells (OPCs), which are observed in neural development and the adult brain. OPCs are prone to malignant transformation and are believed to be a cell of origin for glioma. Recent findings indicate that the well-characterized neurotransmitter acetylcholine (ACh) maintains the primitive state of normal OPCs via muscarinic ACh receptors (mAChRs) preventing maturation and cell cycle exit. We hypothesized that cholinergic signaling may also maintain the primitive state of OPC-like GSCs. We analyzed publicly available single nuclei RNASeq data of patient glioblastoma samples and observed high expression of *CHRM3*, encoding the M3 mAChR, in OPC-like cells of the proneural subtype of glioma. Studies in mouse OPC-like GSCs confirmed high levels of *CHRM3* expression and demonstrated that ACh generated voltage changes and rapid (< 1 second) increases in cytosolic calcium from internal calcium stores. Exposure to a brain permeant FDA-approved anti-muscarinic drug targeting M3mAChR suppressed proliferation, evoked calcium release, and the activation of intracellular second messengers PKC and ERK. Pharmacologic inhibition of mAChRs in established patient derived glioma grafts prevented re-initiation of tumors in subsequent host animals compared with vehicle treated tumors. These studies suggest that the cholinergic microenvironment maintains GSCs in a manner similar to normal OPCs and provides a platform for repositioning available small molecule mAChR antagonists for treatment of glioma.

#5802

The impact of tumor-treating fields on cancer stem-like cells isolated from the sub-ventricular zone of glioblastoma patients

Yamhilette Licon Munoz[1], Rachel B. Sidebottom[1], Frank J. Martinez[1], Samantha Varela[2], Christian A. Bowers[3], Sara G.M. Piccirillo[1]. *[1]Cell Biology and Physiology, University of New Mexico Health Sciences Center, Albuquerque, NM,[2]University of New Mexico School of Medicine, Albuquerque, NM,[3]University of New Mexico Hospital, Albuquerque, NM*

Treatment of glioblastoma (GBM) is challenging due to its heterogeneous nature, invasive potential and poor response to standard of care treatments. As a result, GBM inevitably recurs and only approximately 9% of patients

survive 5 years post-diagnosis. Areas of residual disease represent the source of the recurrent tumor that is fatal for GBM patients. However, targeting the residual disease is not offered as part of the standard of care because these areas are difficult to identify and, to date, they have not been characterized during disease progression. Our laboratory was the first to identify and characterize residual disease in the sub-ventricular zone (SVZ) of the lateral ventricles of GBM patients. Specifically, we found that in the majority of GBM patients the SVZ is a reservoir of tumor cells that promote therapeutic resistance and seed the recurrent tumor. Specifically, our work revealed that in 65% of the cases the SVZ contains treatment-resistant cancer stem-like cells (CSCs), thus investigating residual disease in this area may hold the key to developing a valid therapeutic target for many patients. In this study, we are examining the impact of Tumor-Treating Fields (TTFields) on treatment-resistant CSCs isolated from the SVZ of GBM patients using molecular techniques, such as single-cell transcriptomics and functional phenotyping analysis. To date, we have isolated and characterized 12 CSCs. These cells are maintained in conditions that preserve the molecular profile of the original patient tumor, thus representing *bona fide* models to study the impact of TTFields on GBM residual disease. We observed that: (i) CSCs show heterogeneous patterns of response to the alkylating agent Temozolomide (100 μM) and radiation (10 Gy), that mimic the standard of care for GBM patients, (ii) their treatment response is independent of the MGMT promoter methylation status and (iii) the proliferation of CSCs resistant to Temozolomide and radiation is significantly inhibited by TTFields when cells are exposed for 48 hours to the optimized frequency for GBM (200 kHz). Altogether, these findings point to the effectiveness of TTFields following Temozolomide and radiation and set the foundation for the single-cell transcriptomic and functional analysis to elucidate the mechanisms whereby TTFields impact the proliferation of CSCs in the SVZ of GBM patients. In the long run, the results of this work will allow the identification of SVZ-specific targets for the development of novel and more effective treatments for GBM patients.

#5804
Targeting methyl donor synthesis inhibits platinum-induced enrichment of ovarian cancer stem cells

Shu Zhang, Tara X. Metcalfe, Christiane A. Hassel, Heather M. O'Hagan, Kenneth P. Nephew. *Indiana University Bloomington, Bloomington, IN*

Ovarian cancer (OC) is one of the deadliest gynecologic cancers in US. Platinum (Pt)-based chemotherapy can reprogram cancer cells to ovarian cancer stem cells (OCSCs) and contribute to incurable recurrence. We have previously shown that Pt-containing drugs, e.g., cisplatin, enrich for OCSCs and Pt-induced alterations in DNA methylation enhanced OCSC malignant properties. CSCs have been shown to be dependent on methionine (Met) in many cancers, and in the current study, we investigated the role of Met and the interplay between methylation and Met metabolism in OCSC enrichment. In high grade serous ovarian cancer cell lines (OVCAR5, OVCAR3), cisplatin treatment (IC50, 16hr) increased ($p<0.01$) the percentage of cells that were positive for aldehyde dehydrogenase (ALDH+ cells), a known OCSCs marker. Cisplatin treatment also increased ($p<0.05$) the whole cell level of 5-methylcytosine, indicating Pt-induced methylation changes. In addition, Met metabolism was altered by cisplatin, demonstrated by decreased ($p<0.01$) level of Met derivative, S-adenosyl-methionine (SAM), and increased ($p<0.01$) expression of Met utilization enzyme, methionine adenosyltransferase 2A (MAT2A). To investigate a possible role of Met metabolism in Pt-induced enrichment of OCSCs, OVCAR5 cells were cultured in complete or Met-depleted (Met-) media, treated with cisplatin or vehicle and examined for CSC properties, including ALDH+ cells and the ability to form spheroids under low-attachment conditions. Met depletion blocked ($p<0.01$) both the Pt-induced increase of ALDH+ cells and spheroid formation. Both Met- only and Met- in combination with cisplatin activated p38, determined by increased phosphorylated p38, which may have responded to Met depletion and promoted cell cycle arrest. In addition, MAT2A expression was higher ($p<0.01$) in ALDH+ compared to ALDH- OC cells. MAT2A inhibitor FIDAS-5 combined with cisplatin blocked the Pt-induced increase in ALDH+ cells ($p<0.01$), demonstrating a requirement for Met utilization in Pt-induced OCSC enrichment. As MAT2A is a therapeutic target in cancer, MAT2A inhibition could represent a therapeutic approach for inhibiting CSC in ovarian cancer. We are further investigating the mechanism of MAT2A-mediated inhibition on Pt-induced OCSCs enrichment by examining the OC methylome and cell cycle arrest.

#5805

Ebastine targets cancer stem cell-like properties and metastasis in triple-negative breast cancer by binding focal adhesion kinase

Juyeon Seo, Minsu Park, Dongmi Ko, Seongjae Kim, Soeun Park, Kee Dal Nam, Yong Koo Kang, So Ra Seuk, Jaeyoun Park, Eunsun Jung, Yoon-Jae Kim, Ji Young Kim, Jae Hong Seo. *Korea University Guro Hospital, Seoul, Korea, Republic of*

Triple-negative breast cancer (TNBC) exhibits an aggressive behavior associated with poor prognosis due to the absence of established molecular targets. Focal adhesion kinase (FAK) is a major determinant and participates in the acquisition of migration and invasion, as well as the maintenance of breast cancer stem cell (BCSC)-like traits in TNBC. We sought to investigate the effect of ebastine, a second-generation antihistamine on apoptosis, FAK activation, BCSC subpopulations and metastasis in TNBC in vitro and in vivo. TCGA dataset analysis revealed that mRNA levels of FAK were highly expressed in TNBC compared to other breast cancer subtypes. We found that ebastine binds to the tyrosine kinase domain of FAK, which blocks phosphorylation at the Y397 and Y576/577 residues and subsequent inactivation of SRC. Ebastine-induced apoptosis was associated with attenuation of JAK2/STAT3 and MEK/ERK signaling in TNBC cells. Kinetic analysis revealed a concentration-dependent impairment of cell migration in the presence of ebastine in MDA-MB-231 and 4T1 cells *in vitro*. Ebastine targets BCSC-like cell populations as evidenced by a sharp decline in the expression of the BCSC markers ALDH1, CD44 and CD49f and suppression of mammosphere-forming capacity. Ebastine administration led to a significant reduction in the growth ebastine of BCSC-enriched 4T1 mammospheres orthotopically injected into the mammary glands of Balb/c mice. Ebastine administration significantly impeded angiogenesis and distant metastasis while reducing MMP-2/-9 levels in circulating blood in vivo. Importantly, biochemical analysis in mice serum showed that ebastine had no effect on liver and kidney function. Our findings suggest that EBA may be an effective therapeutic repositioning candidate for the simultaneous targeting of multiple survival signaling pathways for the treatment of molecularly

heterogeneous TNBC. Further investigation of ebastine as an anti-metastatic agent for the treatment of TNBC is warranted.

#5806

Kinase library screening identifies IGF-1R/PI3K/AKT axis as a crucial pathway for survival of intrahepatic cholangiocarcinoma cells with stemness characteristics

Chotirat Rattanasinchai[1], Chidchanok Chornkrathok[2], Donlaporn Sriphan[2], Panida Navasumrit[1], Mathuros Ruchirawat[1]. *[1]Environmental Toxicology Laboratory, Chulabhorn Research Institute, Bangkok, Thailand,[2]Chemical Carcinogenesis, Chulabhorn Research Institute, Bangkok, Thailand*

Intrahepatic cholangiocarcinoma (iCCA) is a subtype of biliary malignancy that arises along the peripheral bile duct epithelium. Given its limited and inefficacious treatment options, the mortality rate of iCCA remains high and thus a novel therapeutic strategy is urgently needed. The concept of cancer stem cells (CSCs) explains a subpopulation of cancer cells that possesses self-renewal and differentiation capacities. These CSCs become the culprit for cancer metastasis, cancer recurrence and chemotherapeutic resistance, making them promising targets for cancer treatment. The propose of this study is to identify the signaling pathways crucial for the survival of iCCA with stemness characteristics. Gene expression analysis on a dataset of Thai iCCA patients (n=91) showed that iCCA tumors are enriched in the Adult Stem Cell (ASC) signature which are the shared characteristics among the epithelial-derived cancer with stemness characteristics. Although iCCA cells exhibit some degree of enrichment in stem cells markers when compared with cholangiocyte cells, further upregulation of stem cell-related genes, *e.g. Nanog, Oct3/4, Sox2, and Sox9*, were found in iCCA cells grown as 3D tumorspheres. A kinase inhibitor screening library was then performed on iCCA tumorspheres. Our initial screening demonstrated that 11 out of the top 50 kinase inhibitors that effectively decrease viability of iCCA tumorspheres belongs to the insulin-like growth factor-1 receptor (IGF-1R)/phosphoinositide-3-kinase (PI3K)/protein kinase B (PKB/AKT) axis. Additionally, these inhibitors increase cell apoptosis, judged by the caspase 3/7 activity, within iCCA tumorspheres. Conversely, IGF-1 treatment which is sufficient to induce activation of IGF-1R and AKT also enhances cell viability and decrease cell

apoptosis in iCCA. Taken together, our data demonstrate that IGF-1R/PI3K/AKT axis is crucial for survival of iCCA cells with stemness characteristics and this pathway could be a potential therapeutic target in iCCA.

#5807

mTOR regulates stem cells of glioblastoma by altering the self-renewal and proliferation

Olivia Gellerson, Julie Bree, Mohan Das, George Kleinman, Chirag Gandhi, Meena Jhanwar-Uniyal. *Department of Neurosurgery New York Medical College/WMC, Valhalla, NY*

The mechanistic target of rapamycin (mTOR: aka mammalian target of rapamycin), a serine/ threonine kinase, functions by forming two multiprotein complexes termed mTORC1 and mTORC2. Glioblastoma (GBM) is a malignant and lethal brain tumor that remains incurable partly due to the existence of untreatable cancer stem cells (CSC). The pathogenesis of GBM is largely due to the loss of the tumor suppressor gene PTEN, which is implicated in the aberrant activation of the mTOR pathway. The major cause of tumor recurrence, growth, and invasion is the presence of a unique population of CSC. Resistance to conventional therapies appears to be caused by both extensive genetic abnormalities and dysregulation of the transcription landscape. Consequently, CSCs have emerged as targets of interest in new treatment paradigms. Evidence suggests that inhibition of the mTOR pathway can also be applied to target CSCs. In this study, we explored the role of the mTOR pathway in the regulation of stem cells of GBM. GBM stem cells were treated with various inhibitors of canonical PI3K/AKT/mTOR pathways such as rapamycin (mTORC1 inhibitor), PP242 (ATP binding mTORC1/2 inhibitor), LY294002 (PI3K inhibitor), and MAPK inhibitor, U0126. We previously demonstrated the presence of CSC in the peritumor area of GBM. A significant number of GBM tumors expressed stem cell marker nestin and activated mTOR (pmTORSer2448), with most tumor cells co-expressing both markers. The expression of stem cell marker NANOG was suppressed following rapamycin treatment, while U0126 induced translocation of NANOG from the nucleus to the cytoplasm. The neurospheres were disrupted following rapamycin and LY294002 treatments. Rapamycin or

PP242 treatments given with differentiating agent All-trans-retinoic acid reduced stem cell proliferation. Treatment with novel small molecule dual inhibitors of mTORC1/2 demonstrated that Torin1 and Torin2 suppressed the proliferation of GBM CSC, while XL388 was less effective. Torin1 and XL388 delay the process of self-renewal as compared to controls, whereas Torin2 halted the self-renewal of GBM CSC. Additionally, Torin2 was able to eradicate tumor cells. Torin2 effectively targeted CSCs of GBM by halting self-renewal and inhibiting cell proliferation, underscoring the use of Torin2 in the treatment of GBM.

#5808

Integrin-linked kinase regulates Wnt transcriptional activity in platinum resistant ovarian cancer stem cells

Rula Atwani, Virginie Lazar, George Earl Sandusky, Salvatore Condello.
Indiana University School of Medicine, Indianapolis, IN

Ovarian cancer (OC) is the most lethal gynecological cancer, characterized by chemo-resistance and fatal tumor recurrence after primary treatment. The metastatic progression is mediated by exfoliation of tumor cells into the peritoneal cavity, the formation of compact OC spheroids, and their implantation onto the overlying peritoneal surface. Spheroid formation is promoted by a change of cell adhesion properties, enhanced secretion of extracellular matrix (ECM) components, such as fibronectin (FN), that stiffen the tumor stroma, promote the aberrant activation of integrins, and recruit the adaptor protein integrin-linked kinase (ILK). ILK drives cytoskeletal assembly and modulates key processes, including survival, invasion, and stemness. However, the functional role of ILK in chemoresistance of ovarian cancer stem cells (OCSCs) remains incompletely understood. We tested the hypothesis that the formation of FN-integrin complexes at the cell membrane promotes survival of OCSCs and supports OC spheroid formation by activating ILK and downstream oncogenic signaling. In OCSCs compared with non-CSC, ILK, FN, and integrin β1 *m*RNA expression levels were increased ($P<0.001$) and further enriched in OC spheroids compared with monolayers ($P<0.01$). ILK blockade with the specific inhibitor cpd-22 suppressed spheroid proliferation and tumor initiating capacity in xenograft mouse model. Furthermore, key oncogenic signaling pathways, in particular decreased β-

catenin signaling essential to sustaining cancer cell stemness, were altered in OC spheroids treated with cpd-22. Of the genes examined, expression of Wnt receptor Frizzled 7 (Fzd7) was the mostly highly downregulated in OC spheroids treated with cpd-22, indicating a direct correlation between ILK activation and Wnt signaling. By using co-immunoprecipitation and proximity ligation assay, we demonstrated that ILK co-localizes with Fzd7 in OC spheroids. Mechanistically, treatment of OC spheroids with the combination of carboplatin and ILK-Fzd7 blockade decreased β-catenin signaling, inhibited phospho-Akt at Ser473 and increased levels of cleaved-caspase-3 compared to single agent alone, resulting in apoptosis. By regulating β-catenin signaling, Fzd7 expression and ILK activation are essential for OCSCs survival. Targeting Fzd7-ILK clusters may represent a new therapeutic approach to eradicate OCSC and ultimately improve patient outcomes.

#5809

Tracking cancer stem cell expression of pancreatic and ampullary cancer organoids in response to chemotherapy

Eleanor Riedl[1], Austin Stram[1], MD Shahadat Hossan[1], Ethan S. Lin[1], Luke Koeppel[1], Jamie Warner[1], Sam Lubner[1], Stephanie McGregor[2], Wei Zhang[2], Jeremy Kratz[1]. *[1]Department of Medicine, University of Wisconsin - Madison, Madison, WI,[2]Department of Pathology and Laboratory Medicine, University of Wisconsin - Madison, Madison, WI*

Background: Cancer stem cells (CSCs) have been described to confer resistance and aggressive disease biology in pancreatic ductal adenocarcinoma (PDAC) and ampullary carcinoma (AMPC). Patient derived cancer organoids (PCOs) are an important model of PDAC that maintain the molecular features of advanced disease and have been shown to predict drug response. This study aimed to determine the dynamics of CSC expression on the oligoclonal culture growth of three independent PCOs models.

Methods: PCOs were assayed using low volume 10μL microformat in 96 well design (Ibidi, Inc). PCOs were treated with physiologic FOLFIRINOX or gemcitabine + nab-paclitaxel (nab-pac) including single agent controls. Response was assayed by growth using timecourse data from 0h to 72h using high content imaging (Cytation 5). At 72h, the PCOs were stained

using four distinct CSC markers (CD44, CD133, CD117, and EpCAM). Images were aligned using thresholded root mean standard deviation of 75μm and tracked for normalized change in longest diameter. At 72h, CSC markers were tracked using % area positive from brightfield region of interest. Response was tracked by effect size Glass's Delta (GΔ) defined as the difference between the mean of media control and treatment group normalized to standard deviation of media control.
Results: PCOs maintained nuclear atypia and high nuclear-chromatin ratios consistent with matured xenografts. AMPC1 showed similar sensitivity with growth arrest by PCO Δ diameter for gem + nab-pac (mean = +2.2%, GΔ = 1.29) and FOLFIRINOX (mean = 0.0%, GΔ = 1.33). AMPC1 had CSC enrichment for CD44 after treatment with nab-pac (GΔ = 0.93), CD133 expression after treatment with gem + nab-pac (GΔ = 0.75), CD117 after treatment with nab-pac treatment (GΔ = 0.80), and EpCAM after treatment with gem + nab-pac (GΔ = 0.78). In AMPC1, interquartile analysis revealed increased CSC expression conferred reduced growth for CD133 (+72% v. 37%, $p<0.005$) and CD117 (+81% v. +25%, $p<0.005$). Normalized Δ diameter across PDAC PCOs revealed PDAC1 had reduced sensitivity to gem + nab-pac (mean = +16.0%, GΔ = 1.2) vs. PDAC2 (Mean = 2.1%, GΔ = 1.65). PDAC1 had CSC enrichment with increased % area of CD44+ after treatment with gem + nab-pac (GΔ = 1.13). In PDAC2, interquartile analysis revealed increased CSC expression conferred decreased growth rate for CD133 (+65% v. +36%, $p< 0.005$) and CD117 (+75% v. +38%, $p<0.005$).
Conclusions: PDAC and AMPC PCOs reveal oligoclonal expression of CSC markers within a population. Increased CSC expression for CD133 and CD117 within a population consistently revealed decreased growth within an organoid population. CSC expression (CD44, CD133, CD117, and EpCAM) was found to be enriched under therapeutic challenge with gem and nab-pac containing chemotherapy. This work supports the oligoclonal and dynamic nature of CSCs for pancreaticobiliary cancers in response to therapeutic challenge.

#5810
The effects of retinoid agents and retinoic acid receptor genotype on proliferation, differentiation, and stem cells in colorectal cancer

Victoria Oluwajuwon Hunsu[1], Caroline O. B. Facey[2], Bruce M. Boman[1].
[1]Department of Biological Sciences, University of Delaware, Newark, DE,[2]Center for Translational Cancer Research, Helen F Graham Cancer Center, Newark, DE

Understanding how to therapeutically target colonic stem cells (SCs) is important because SC overpopulation drives CRC growth and development. Our *goal* is to therapeutically sensitize cancer SCs (CSCs) to differentiation-inducing effects of retinoid agents against CRC. We found that ALDH specifically marks normal and malignant colonic SCs and that retinoic acid (RA) signaling mainly occurs in colonic ALDH+ SCs. That RA signaling occurs through ALDH+ SCs was derived from finding that RA receptors and RA signaling components are selectively expressed in ALDH+ SCs. Indeed, All-*trans*retinoic acid (ATRA) is a highly effective treatment for leukemia (APL) which has a *RARA* translocation. We conjecture that response of solid tumors to RA agents depends on RA pathway genotype. Our bioinformatics analysis shows mutations often occur in RA receptors in human CRCs. Therefore, we *hypothesize* that the ability of RA agents and RA metabolism blocking agents to induce differentiation of CSCs depends on RA pathway genotype.
Methods: The ability of RA agents (ATRA, 13-*cis* retinoic acid, 9-*cis* retinoic acid) and RA metabolism blocking agents (Liarozole, Talarozole) to inhibit proliferation and induce differentiation of CRC cells was evaluated. Nanostring Profiling was used to measure effects of agents on mRNA expression of various markers.
Results: Our results show that RA pathway genotype affects the response of RA agents in CRC cell lines. HCT116 and SW480 cells, which have RA receptor mutations, displayed resistance to ATRA. In contrast, HT29 cells that have wild-type RA receptors are sensitive to ATRA. All three cell lines however showed similar responses to the CYP26A1 inhibitor Liarozole. This finding indicates that regardless of RA receptor mutations, inhibition of ATRA metabolism will increase intracellular RA levels. Nanostring profiling analysis shows ATRA treatment of HT29 cells increases expression of *RARA*,*CYP26A1* (ATRA metabolizing enzyme), & *KRT20* (differentiation marker), and decreases expression of CSC markers *LGR5* & *ALDH1A1*. Moreover, ATRA treatment of both CRC cell lines decreases

ALDH+ cell population size. These findings show upregulated RA signaling can increase differentiation and decrease CSC numbers in CRC. **Discussion** Our findings indicate that colon SCs are regulated by RA signaling mechanisms and dysregulation of RA signaling contributes to the SC overpopulation that drives CRC growth. Thus, therapeutically sensitizing CSCs to differentiation-inducing effects of RA agents should provide insight into design of new SC-targeted therapies for CRC.

#5811

Epigenetic regulation of chromosomal instability in triple-negative breast cancer

Yang Bai[1], Albert Agustinus[2], Cem Meydan[1], Dylan R. McNally[1], Shira Yomtoubian[1], Liron Yoffe[1], Ari M. Melnick[1], Samuel Bakhoum[2], Vivek Mittal[1]. *[1]Weill Cornell Medicine, New York, NY,[2]Memorial Sloan Kettering, New York, NY*

Metastasis is the leading cause of cancer-related death among women with breast cancer. Chromosomal instability (CIN) has emerged as a hallmark of triple-negative breast cancer (TNBC) as it has recently been shown to promote metastasis. However, the underlying molecular mechanisms by which CIN drives metastasis are not completely understood. We have identified a discrete population of highly metastatic SOX2/OCT4+ cells expressing elevated levels of epigenetic regulator EZH2 associated with increased CIN in both human and mouse TNBC. EZH2 histone methyl transferase (HMT) is the catalytic subunit of the Polycomb repressive complex 2 (PRC2), represses target genes through trimethylation of Histone 3 at lysine 27 (H3K27me3). Importantly, genetic and pharmacologic inhibition of EZH2 lead to reduction of CIN and impaired metastasis. These findings led to the hypothesis that EZH2-mediated CIN constitutes a novel mechanism of metastasis regulation. To directly demonstrate epigenetic regulation of CIN, we used genome wide-Cleavage Under Targets and Release Using Nuclease (CUT&RUN) in parallel with RNA-seq. Gene set enrichment of EZH2-repressed target genes directly implicated the spindle formation pathway network. The central core of this network comprised of tankyrase (TNKS), a multifunctional poly (ADP-ribose) polymerase (PARP) previously implicated in DNA repair, telomere function and centrosome maturation. ChIP-PCR confirmed that EZH2 directly binds to

the TNKS promoter, and CRISPR knockout of TNKS abrogated the ability of EZH2 inhibition in suppressing CIN, consistent with pharmacological inhibition of TNKS. More specifically, dysregulation of TNKS by EZH2 in OCT4/SOX2+ cells lead to increased numbers of centrosomes and multipolar mitosis. To directly demonstrate the role of aberrant H3K27me3 in regulating chromosomal segregation during mitosis, we used dCas9-EZH2 or dCas9-EZH2 catalytically dead mutant together with chromosome-specific CRISPR guides to ectopically enhance H3K27 trimethylation at the pericentromeric region of specific chromosomes. Ectopic deposition of EZH2 at pericentromeric regions lead to increased CIN.
Conceptually, our work provides an unappreciated link between epigenetic regulation and CIN which have been hitherto studied in isolation. From a clinical perspective, demonstrating epigenetic regulation of CIN has opened the possibility for the development of first CIN suppressive therapeutic strategies targeting TNBC metastasis.

Cell Adhesion and Cell Signaling in Cancer and Drug Resistance

#5815
Nucleus positioning and composition dictate the invasion performance of E-cadherin mutant cells
Joana Figueiredo[1], Joana Pereira[1], Rui M. Ferreira[1], Luísa Carvalho[1], Margarida Gonçalves[1], Soraia Melo[1], Patrícia Carneiro[1], Parry Guilford[2], Eurico Morais-de-Sá[1], Raquel Seruca[1]. *[1]Institute for Research and Innovation in Health (i3S), University of Porto, Porto, Portugal,[2]Department of Biochemistry, University of Otago, Otago, New Zealand*

Introduction: Cell invasion is a critical step for tumor progression and dissemination into neighboring and distant tissues, which constitute the foremost cause of cancer mortality. Loss of the cell-cell adhesion molecule E-cadherin occurs in 70% of carcinomas and is widely described as an initiating event in the invasion process. Recently, data has emerged demonstrating that this milestone phenomenon is accompanied by an abnormal affair between cancer cells and the extracellular matrix (ECM). In fact, cancer cells display increased plasticity and a remarkable ability to

overcome the fibrous structure of the ECM. Since the nucleus is the largest and stiffest organelle in the cell, we hypothesize that it represents a major determinant of cell reshaping and spreading capacity. Our main aim is thus to dissect the mechanisms through which the nucleus supports invasion of cancer cells.
Material and Methods: To determine alterations in nuclear composition and architecture that are distinctive of cells with E-cadherin impairment, we have used cell lines and *Drosophila* strains expressing either wild-type E-cadherin or the Y755C variant identified in Hereditary Diffuse Gastric Cancer (HDGC) patients. Nuclear morphological features and migratory rates were assessed by fluorescent markers coupled with confocal microscopy and advanced bioimaging techniques. The molecular profile of nuclei envelope from E-cadherin mutant and wild-type cells was subsequently investigated by implementation of a proteomic workflow, encompassing cellular fractionation and processing through high-resolution Mass Spectrometry (LC-MS).
Results: We have shown that the Y755C E-cadherin mutation induces evident changes in nuclear morphology, and an increased migration performance of border cells in *Drosophila*. In particular, detailed quantitative measurements revealed differences in nuclear area, mean intensity, perimeter, solidity and relative position to basal surface of E-cadherin mutant cells, when compared with those expressing the wild-type protein. Further, proteomic analysis of enriched nuclear fractions disclosed that the composition of the nuclear envelope from E-cadherin mutant cells is significantly different from that of the wild-type counterparts. Differentially abundant molecules include proteins relevant for spatial and structural integrity of the nucleus.
Conclusion: Overall, this work provides evidence that cells with E-cadherin loss of function activate a specific mechanotransduction program that imposes nuclear remodeling at physical and biochemical levels, endowing cells with a pro-invasive signature.

#5816

Tensin1 tension sensor reveals novel features associated with actomyosin, focal adhesion dynamics, and mechanosensitivity

Yoon-Kwan Jang[1], Jung-Soo Suh[1], Gyuho Choi[1], Sanghyun Ahn[1], Ki Seok Han[1], EunHye Kim[1], Yerim Lee[1], Xiaoqi Hu[1], Eunbae Hwang[2], Tae-Jin

Kim[2]. [1]*Department of Integrated Biological Science, Pusan National University, Pusan, Korea, Republic of,*[2]*Department of Biological Sciences, Pusan National University, Pusan, Korea, Republic of*

Cellular responses to mechanical stimuli play an imperative role in the regulation of physiological and pathological functions. Unlike other integrin-mediated adhesion proteins, the force transmission mechanism of tensin1 is not well understood. In this study, we describe the development and visualization of a tensin1 tension sensor. A signal from this sensor indicates that tensin1 is under greater tension at peripheral adhesions than at central adhesions, and that it is controlled by actomyosin in fibroblasts. In a bidirectional manner, tension in tensin1 is regulated by focal adhesion kinase (FAK) activity. Our findings demonstrate that tensin1 is capable of sensing the extracellular matrix through alterations in the tension it receives from the extracellular matrix. Furthermore, tensin1 depletion increases the tension of talin1, but the absence of talin1 decreases the tension applied to tensin1. These results indicate that tensin1 is complementary and dependent on the tension received by talin1. Overall, our data, together with the prognosis following tensin1 expression in colorectal and urothelial cancer, elucidate the tension-receiving function of tensin1 and highlight the necessity of tensin1-mediated mechanotransduction studies.

#5817

LKB1 overcomes RAS pathway-mediated loss of epithelial integrity

Topi A. Tervonen[1], Shishir M. Pant[1], Johanna Englund[1], Juha Klefström[2]. [1]*University of Helsinki, Helsinki, Finland,*[2]*University of Helsinki and Finnish Cancer Institute and FICAN South Helsinki University Hospital, Helsinki, Finland*

Oncogenic RAS pathway disassembles cell-cell and cell-basement membrane junctions, thus promoting epithelial cell motility and invasion. To find tumor proteomic changes responsible for the disrupting effects of RAS on epithelial integrity, we explored cBioportal cell line proteomics data across all cancer types for correlations between oncogenic KRAS or HRAS mutations and possible regulators of epithelial integrity. We found inverse correlation between these RAS mutations and tumor suppressor LKB1 protein levels in a cohort where LKB1 was not inactivated by a

mutation. Furthermore, LKB1 protein levels were also positively correlated with NF2 protein (a negative regulator of RAS) in human breast tumors and inversely correlated with c-RAF (RAS effector) activating phosphorylation at serine 338 in breast cancer cell lines. We sought to functionally clarify the relationship between RAS pathway and LKB1, finding that an ectopic constitutive or inducible expression of $HRAS^{V12}$ downregulates LKB1 protein in mammary epithelial MCF10A cells and HMEC-hTERT cells. Furthermore, RAS-mutant MCF10A cells regained LKB1 protein levels upon treatment with MEK/ERK inhibitors. We establish that the RAS-mediated downregulation of LKB1 protein occurs through proteasomal activity. LKB1 reconstituted MCF10A-$HRAS^{V12}$ (RAS-LKB1) cells displayed restored desmoplakin, γ-catenin and E-cadherin pericellular immunostaining pattern in monolayer cultures, suggesting restoration of desmosomes and adherence junctions. We also cultured RAS-LKB1 cells in 3D egg-white and observe restoration of E-cadherin, γ-catenin, α6-integrin, and laminin-332, indicating a rescue of epithelial integrity in 3D context. Our findings suggest that LKB1 rescues mutant RAS-mediated disruption of cell-cell and cell-basement membrane junctions and general epithelial integrity. Our current aim is to define how LKB1 suppresses RAS mediated disruption of breast epithelial integrity, that is expected to shed new light into early stages of tumor invasion and uncover novel therapeutic opportunities via restoration of LKB1.

#5818

Cadherin complexes recruit PIWIL2 to suppress pro-tumorigenic transformation

Alyssa Risner[1], Joyce Nair-Menon[1], Vamsi Gangaraju[2], Antonis Kourtidis[1].
[1]Regenerative Medicine, The Medical University of South Carolina (MUSC), Charleston, SC,[2]Biochemistry and Molecular Biology, The Medical University of South Carolina (MUSC), Charleston, SC

Recent studies have shown that genomic instability, oncogene expression, and high mutation rates in more than 50% of tumors can be attributed to increased transposon activity. Transposons, also called transposable elements (TEs), are parasitic mobile DNA elements that make up 45% of the human genome and can cause DNA damage and gene mutations. The reasons for increased TE activity in somatic tumors are currently unknown.

TE RNA transcripts are targeted for degradation by PIWI ribonucleases, which are members of the Argonaute superfamily of proteins, through regulation of small RNAs called piRNAs (PIWI-interacting RNAs). Although the function of the PIWI-piRNA pathway has been extensively studied in the germline, there is little understanding about the presence or functionality of the pathway in somatic tissues. We have evidence of a novel interaction of the adherens junctions of well-differentiated epithelial cells with PIWIL2 (PIWI-like RNA-Mediated Gene Silencing 2), a key catalytic component of the PIWI-piRNA complex. Through immunofluorescence staining, confocal microscopy, and co-immunoprecipitation studies, we found co-localization and association of PIWIL2, as well as of other key members of the PIWI complex, such as PIWIL4 and TDRD1, with E-cadherin and p120 catenin at adherens junctions of well-differentiated breast and colon epithelial cells, whereas this association is lost in cancer cells and patient tissues. Adherens junction disruption results in mis-localization of PIWIL2, PIWIL4, and TDRD1 from the adherens junctions and their accumulation either to the cytoplasm or to the nucleus. E-cadherin depletion particularly results in increased expression of the LINE1 transposon, which is the most abundant transposon in human cells, and in increased levels of γ-H2AX, an indicator of DNA damage. Our working hypothesis is that cadherin junctions of well-differentiated epithelial cells recruit and regulate the PIWIL2 complex to suppress transposon activity. Since both loss of junctional integrity and increased transposon activity are universal events in cancer, this study has the potential to deepen our understanding of the role of the PIWI-transposon pathway in somatic tumorigenesis.

#5819

Src inhibitor suppresses rab11 mediated collective cell migration in colon cancer cells

Yi-Wen Lu, Xiang-Ling Hou, Hui Min Koo, Wei-Ting Chao. *Tunghai University, Taichung, Taiwan*

Collective cell migration has been demonstrated the importance in cancer metastasis. Instead of single cell migration, collective cell migration requires E-cadherin for the cohort cell migration. Rab11 the recycling vesicle protein plays the key role in E-cadherin dynamics and mediates

collective cell migration. In this study, Src was hypothesized to regulate Rab11 mediated collective cell migration. Our results demonstrated Src inhibitor Dasatinib has less toxicity in HT-29 colon cancer cells, instead, the cell morphology was turned aggregated. The immunofluorescence image also showed E-cadherin polarity was lost after Dasatinib treatment and increased the potential of cell-cell contact inhibition. In transwell assay, Rab11 was found colocalized with E-cadherin in collective migrated cells. Dasatinib treatment can suppress collective cell migration and decrease the interaction of Rab11 and E-cadherin. This study demonstrated the important role of Src in Rab11 mediated collective cell migration through E-cadherin dynamics in colon cancer.

#5820

Chloroquine inhibited Rab11 mediated E-cadherin transport in collective colon cell migration in Dasatinib resistant cells

Xiang-Ling Hou, Hui Min Koo, Chia-Wen Lin, Chien-Chi Huang, Yu-Chi Tseng, Kai-Yu Tseng, Wei-Ting Chao. *Tunghai University, Taichung City, Taiwan*

In has been demonstrated epithelial mesenchymal transition (EMT) is related to E-cadherin expression level. Recently, studies have been demonstrated the collective cancer cell migration which expresses high E-cadherin is a powerful mechanism of metastasis. Therefore, the role of E-cadherin in cancer metastasis is still not clear. Endocytosis was shown to regulate E-cadherin turnover on the membrane and the function of lysosome is also associated with cell vesicle trafficking. The past studies indicated Src can regulate vesicle trafficking. In this study, HT29 colon cancer cells were treated with Src inhibitor, Dasatinib (DST), to investigate the role of lysosome in regulating E-cadherin dynamics through vesicle trafficking in collective cell migration. In the result, the recycling protein Rab11 and lysosome marker Lamp1 were found localized with E-cadherin in the cell-cell contacts, however, Dasatinib sensitive (DSTS) cells showed less colocalization of Rab11 with E-cadherin. When cells were treated with lysosome inhibitor chloroquine, Rab11 were accumulated in the cell-cell contacts and reduced collective cell migration in Dasatinib resistant (DSTR) cells. These results suggest lysosome inhibition can suppress Rab11 mediated vesicle trafficking of E-cadherin transport for collective cell

migration, and chloroquine has therapeutic potential in colon cancer treatment.

#5821

Synergism of FAK and ROS1 inhibitors in the treatment of *CDH1*-deficient cancers mediated by FAK-YAP-TRX signaling

Jiaming Gao[1], Yunying Yao[1], Zaiqi Wang[2], Baoyuan Zhang[1], Ruibao Ren[1].
[1]Ruijin Hospital Affiliated to Shanghai Jiao Tong University School of Medicine, Shanghai, China,[2]InxMed (Shanghai) Co., Ltd, Shanghai, China, Shanghai, China

CDH1 deficiency is common in triple negative breast cancer and diffuse gastric cancer patients, both of which lack effective therapeutics. Although inhibiting ROS1 function results in synthetic lethality in *CDH1*-deficient cancers, adaptive resistance limits their potential clinical benefits. Hyperactive focal adhesion kinase (FAK) signaling contributes to adaptive drug resistance, and FAK inhibitors are partially effective against *CDH1*–deficient cancers. Thus, co-treatment with ROS1 and FAK inhibitors may provide stronger anti-cancer effects by targeting *CDH1* deficiency and potentially overcome drug resistance. Here, we evaluated the effects and mechanisms of combined treatment with FAK inhibitor IN10018 and ROS1 inhibitors. Cell-based assays and *in vivo* animal experiments revealed that FAK and ROS1 inhibitor combination treatment showed stronger anti-cancer effects than either monotherapy. ROS1 inhibitors induced FAK-YAP-TRX signaling, decreasing oxidative stress–related DNA damage, and consequently reducing its anti-cancer effects. However, the combination treatment suppressed the aberrant FAK-YAP-TRX signaling, reinforcing the cytotoxicity of ROS1 inhibitor towards cancer cells. This mechanism of action was confirmed by inhibiting the activity of FAK-YAP-TRX downstream signaling molecules and by pretreatment with oxidative stress scavengers. These findings support the co-administration of FAK and ROS1 inhibitors as a therapeutic strategy in *CDH1*-deficient triple negative breast cancer and diffuse gastric cancer patients and support further clinical testing of this combination regimen.

#5822

YAP inhibition via targeting MAP3K3-dependent lysosomal degradation pathway overcomes BRAF and CDK4/6 inhibitor resistance

Won-Ji Ryu[1], Sanghyun Park[2], Tae Yeong Kim[1], Yumi Hwang[1], Hyun Ju Han[1], Jeong Dong Lee[1], Gun Min Kim[3], Joohyuk Sohn[3], Sang Kyum Kim[1], Joon Kim[4], Min Hwan Kim[3]. *[1]Yonsei University Health System, Seoul, Korea, Republic of,[2]Department of Dermatology, Chonnam National University Medical School, Gwangju, Korea, Republic of,[3]Department of Internal Medicine, Yonsei University Health System, Seoul, Korea, Republic of,[4]Korea Advanced Institute of Science and Technology (KAIST), Daejeon, Korea, Republic of*

The Hippo-yes-associated protein (YAP) signaling pathway activation underlies the resistance to a wide range of molecularly targeted anti-cancer agents. However, strategies to block YAP activity in cancer by promoting YAP degradation have been largely unsuccessful despite rigorous investigations into canonical Hippo-YAP regulatory mechanisms. Here, we report a novel mechanism of YAP stability regulation by MAP3K3 independently of LATS-mediated proteasomal degradation. We observed that MAP3K3 depletion significantly reduced YAP protein levels in both normal and malignant cells, and mass spectrometry analysis revealed that MAP3K3 phosphorylates YAP at its serine 405 residue. MAP3K3-mediated serine 405 YAP phosphorylation polarizes YAP interaction with BTRC while hindering its interaction with FBXW7, collectively preventing both proteasomal degradation and the p62-mediated lysosomal degradation of YAP. We investigated the role of this mechanism in overcoming anti-cancer resistance and observed robust YAP activation in CDK4/6 inhibitor-resistant luminal breast cancer cells. Genetic and pharmacological MAP3K3 inhibition suppressed YAP-induced drug resistance. Moreover, increased MAP3K3 expression supported the pro-survival activity of YAP in BRAF inhibitor-resistant melanoma cells, and MAP3K3 depletion downregulated YAP-dependent cell cycle gene signatures. Accordingly, the combination of vemurafenib and ponatinib was effective in reducing the survival of BRAF inhibitor-resistant melanoma cells. Collectively, our study identified a novel phosphorylation-mediated YAP stability regulation mechanism and underscored MAP3K3 inhibition as a promising strategy to

overcome BRAF and CDK4/6 inhibitor resistance by directly promoting YAP degradation.

#5823

Uncovering the mechanisms of matrix metalloproteinase-3 (MMP-3) in the cisplatin resistance of ovarian cancer

Mariela Rivera-Serrano[1], Pablo E. Vivas-Mejia[2]. *[1]Biology, University of Puerto Rico Rio Piedras Campus, San Juan, PR,[2]Biochemistry, University of Puerto Rico Medical Sciences Campus, San Juan, PR*

Seventy percent of women with ovarian cancer will develop chemotherapy-resistance to cisplatin. Regardless of the advancements in technology, mortality rates for ovarian cancer have declined only slightly in the last forty years, reiterating the need to generate novel treatment options targeting cisplatin resistance. In RNA-seq and microarrays experiments we observed that Matrix-metalloproteinase-3 (MMP3) was highly abundant in cisplatin-resistant when compared to cisplatin-sensitive cells. MMP3 is a member of the matrix metalloproteinases (MMPs) family of proteolytic enzymes, involved in the degradation of proteins in the extracellular matrix (ECM). Deregulation of MMPs alters the extracellular matrix and contributes to proliferation, invasion, and metastasis of cancerous cells. A typical MMP structure consists of a pro-domain, a catalytic, and a hemopexin domain. The catalytic domain is responsible for MMPs proteolytic activity, while the hemopexin domain contributes to substrate and ligand specificity. Inhibitors targeting the catalytic domain of MMPs were unsuccessful in clinical trials due to a lack of selectivity and specificity. When we used a chemical inhibitor, we did not observe reduced cell-proliferation or invasiveness. However, MMP3-targeted small interference RNA (siRNA) was able to reduce cell proliferation and invasive capabilities in cisplatin resistant ovarian cancer cells. Additionally, MMP3-targeted siRNA significantly reduced the sensitivity of ovarian cancer cells to cisplatin treatment. Cisplatin also increased MMP3 mRNA levels in ovarian cancer mice models and human cell lines. This evidence suggests that the MMP3 levels correlate with the sensitivity of ovarian cancer cells to cisplatin treatment. We hypothesize that the hemopexin domain will bind to proteins promoting cisplatin-resistance. We validated our expression profile studies at mRNA and protein levels via western blot,

ELISA and qRT-PCR. Additionally, survival analysis using the Kaplan-Meier plotter database showed that ovarian cancer patients with low MMP3 levels live longer than patients with higher MMP3 levels. Furthermore, when we measured MMP3 activity, we observed decreased activity in cisplatin-resistant versus cisplatin-sensitive cells. Taken together, these data suggest that other domains of MMP3 (i.e., hemopexin domain) may have a function in the cisplatin resistance of ovarian cancer cells.

#5824

Human ovarian cancer cell seeding density as a mechanism of cisplatin resistance associated with expression of anti-apoptotic and autophagy proteins

Thomas W. Brown, Ujwal Punyamurtula, Wafik S. El-Deiry. *Brown University, Providence, RI*

Drug effects may vary depending on cancer cell density. We investigated discrepancies in phenotypes for high density and low-density cultured cancer cells and elucidated relevant variables that influence them. We assessed chemosensitivity as a function of tumor cell density by plating TOV-21G and OVMANA ovarian cancer cell lines in 96-well plates at various seeding densities per well and treated them with various concentrations of cisplatin. CellTiterGlo assays were performed at 72 hours of treatment to determine cisplatin dose response curves. We used ethidium homodimer fluorescence staining and imaging to quantify extent of cell death at differing cell densities of TOV-21G and OVMANA cells treated with cisplatin for 48 and 72hours in 48-well plates. We performed western blot analyses of apoptotic and autophagy proteins from TOV-21G and OVMANA cells that were seeded at high and low cell densities in 24-wellplates. TOV-21G and OVMANA cells plated at higher cell seeding densities displayed less cisplatin sensitivity than TOV-21G and OVMANA cells plated at lower seeding densities, as shown by cisplatin dose response curves. Ethidium homodimer staining of TOV-21G and OVMANA cells treated with cisplatin revealed that cells seeded at lower densities experience a greater amount of cell death that cells seeded at higher densities. Western blot analyses showed that high density TOV-21G cells may express greater amounts of BCL2 and c-FLIP and lower amounts of p62 and NOXA compared to low density cells when normalized for protein

expression. Similarly, high density OVMANA cells express greater amounts of c-FLIP andBCL2 and lower amounts of NOXA compared to low density cells when normalized for protein expression. Our experiments reveal that human ovarian cancer cells display different phenotypic changes depending on cell density, causing higher density cells to require increased cisplatin to achieve the same level of effect seen in lower density cells. Ovarian cancer cell resistance to cisplatin is associated with alterations in autophagy and anti-apoptotic protein expression at high cell seeding density. These alterations may also affect chemosensitivity *in vivo* in settings of differential tumor density, such as single circulating tumor cells compared to clumps of tumor cells, and other settings, such as metastasis.

#5825

TM4SF19 regulates oxidative stress-dependent YAP transcription in HNSCC

Eunbie Shin, Joon Kim. *KAIST, Daejeon, Korea, Republic of*

Head-and-neck squamous cell carcinoma (HNSCC), which arises from epithelial cells in mucosal surfaces of the upper aerodigestive tract, is the sixth leading cancer worldwide with 40-50% mortality rates. YAP is a transcriptional regulator that plays important roles in cancer cell proliferation and survival. HNSCC shows the highest levels of YAP gene expression among various types of human cancers. However, the molecular mechanisms explaining upregulation of YAP expression in HNSCC are poorly understood. Excessive consumption of tobacco and alcohol are classical risk factors of HNSCC. Tobacco and alcohol generates metabolites that increase reactive oxygen species (ROS) to abnormally high levels. It is not known whether YAP expression and function are interlinked with the oxidative stress response in HNSCC. Here, we aimed to elucidate the mechanism of YAP upregulation involved in the progression of HNSCC under conditions of oxidative stress. To identify candidates for YAP expression regulators in HNSCC, we analyzed whole-genome siRNA library screening data and TCGA genomics data. We performed loss-of-function and gain-of-function experiments to elucidate the molecular mechanism of TM4SF19, which is the top candidate for mediating transcriptional regulation of YAP in HNSCC. TM4SF19 is one of the transmembrane 4 L six family proteins that have topological similarities to

tetraspanins, but little is known about its biological function. We found TM4SF19 controls the expression of YAP gene by regulating GABPβ1, a subunit of the GABP transcription factor complex, which is known to bind and activate YAP gene promoter. We observed that the depletion of TM4SF19 reduced GAPBPβ1, thereby decreasing the transcriptional activity of GABP complex. Importantly, we observed that TM4SF19 was dimerized in response to oxidative stress and consequently mediates the upregulation of YAP transcription by ROS elevation. We further show that TM4SF19 knockdown significantly reduces key characteristics of malignant cells, such as active proliferation and migration. Our results suggest that TM4SF19 is not only a novel transcriptional regulator of YAP but also a strong therapeutic target to suppress the oncogenic activity of YAP, and also provide new clue to understand HNSCC tumorigenesis involving YAP and oxidative stress.

Crosstalk between Cancer Cells, Immune Cells, and Fibroblasts

#5828

Distinct immunosuppressive tumor microenvironment modulates small cell lung carcinoma neuroendocrine phenotypic plasticity and heterogeneity

Parth Anil Desai[1], Nobuyuki Takahashi[2], Yingying Cao[1], Christopher Schultz[1], Darryl Nousome[1], Desiree Tillo[1], Lakshya Chauhan[3], Mayank tandon[1], Rajesh kumar Bhardwaj[1], Delphine Lissa[1], Vinodh Rajapakse[1], Suresh kumar[1], Yang Zhang[1], Elmeskini Rajaa[1], Donna Butcher[1], Linda Scuito[1], Jingjing Gong[4], Brett Schroder[1], Andrew Warner[1], Samantha Nichols[1], Jordan Kimberly[5], Alejandro Schaffer[1], Mohit kumar Jolly[3], Stephen Hewitt[1], Anish Thomas[1]. *[1]National Institutes of Health, Rockville, MD,[2]Center Hospital, National Center for Global Health and Medicine, Tokyo, Japan,[3]IISC, Bangalore, India,[4]Nanostring, Seattle, WA,[5]University of Colorado-Anschutz Campus, Boulder, CO*

Small cell lung carcinoma (SCLC) is prototypical of cancers with exceptional chemoresistance, and metastatic capabilities fueled by remarkable heterogeneity. The cell-extrinsic factors that govern SCLC heterogeneity are poorly understood especially since non-genetic

mechanisms are thought to be major contributors to its intratumoral heterogeneity and plasticity. In order to answer the above question, we sought to inquire about the role of tumor microenvironment (TME) in SCLC heterogeneity which is challenged universally by a lack of patient-derived adequate tumor biopsies. Leveraging large tumor sampling performed at rapid autopsies done on 10 different patients who died from SCLC metastatic disease, we developed a multi-omics approach involving spatial transcriptomics (ST) (Whole transcriptomic atlas), bulk whole genome sequencing, and multiplex immunofluorescence (IF) and standard immunohistochemistry (IHC) to better characterize spatially proximate tumor (36 segments), TME (32 segments) and 4 normal segments. Genomically, SCLC characteristic alterations like TP53 (70%) and RB1 (80%) inactivation and MYC (50%)/MYCL (80%) were evident. ST profiling reveals three distinct tumor subtypes corresponding to the known high-Neuroendocrine (NE) and low-NE SCLC subtypes as well as a novel hybrid-NE state with multiple elevated cancer hallmark capabilities and morphological evidence of nesting and budding. High-NE and hybrid-NE subtypes appear to be driven by ASCL1 and the low-NE subtype resembles the SCLC- inflamed subtype. ST profiling of proximate TMEs reveals similar heterogeneity that is closely linked with SCLC-NE heterogeneity at inter-patient and intra-tumoral levels with distinct features and cellular compositions. Specifically, low-NE TME is marked by increased pro and anti-tumor features including B cells, NK cells, M1-macrophages, and evidence of more checkpoint molecules. High-NE TMEs are predominated by a distinct absence of adaptive immune cells and a strong presence of M2 macrophages. Most strikingly the hybrid-NE TME shows a significant enrichment of immunosuppressive cancer-associated fibroblasts with the absence of T and other adaptive immune cells confirmed using IHC and IF. Next, we attempt to narrow down the fibroblast growth factor receptor (FGF) axis as one of the unique TME-driven factor(s) that could groom non-NE features in SCLC fueling their plasticity and heterogeneity. Subsequently using various SCLC cell lines, we demonstrate that in-vitro modulation of FGFR in SCLC may constrain their plasticity by downregulation of NOTCH signaling, MYC, and its downstream effector REST. We describe the remarkable phenotypic heterogeneity of SCLC tumor and TME and demonstrate their interlinking as well as potential

translational avenues of leveraging the cellular crosstalk in order to constrain SCLC heterogeneity.

#5829

Differential expression of PD-L1 and PD-L2 is associated with M2 tumor-associated macrophages and tumor differentiation in non-small cell lung cancer

Ryota Sumitomo[1], Cheng-long Huang[2], Hiroshi Date[1]. *[1]Thoracic Surgery, Kyoto Univ. Graduate School of Medicine, Kyoto, Japan,[2]Thoracic Surgery, Kitano Hospital, Tazuke Kofukai Medical Research Institute, Osaka, Japan*

Objectives: To improve the treatment strategy of immune-checkpoint inhibitors for non-small cell lung cancer (NSCLC), a comprehensive analysis of programmed death-ligand (PD-L)1 and PD-L2 expression is clinically important. The expression of PD-L1 and PD-L2 on tumor cells (TCs) and tumor-infiltrating immune cells (ICs) was investigated with respect to M2 tumor-associated macrophages (TAMs), which are key components of the tumor microenvironment.
Methods: We performed immunohistochemical studies to evaluate the M2 TAM distribution by CD163 staining, PD-L1 expression on TCs and ICs by the Ventana SP263 assay, and PD-L2 expression on TCs and ICs, using the Ventana BenchMark GX system, in 175 patients with resected NSCLC.
Results: M2 TAM density revealed high levels of variation among the 175 tumor tissues (mean ± standard deviation (SD), 382.5 ± 381.9 cells per mm^2). The percentage of PD-L1-positive TCs and PD-L1-positive ICs varied greatly among the 175 tumor tissues (mean ± SD; 15.6 ± 27.0% and 9.4 ± 10.9%, respectively). In addition, the percentage of PD-L2-positive TCs and PD-L2-positive ICs also ranged widely among the 175 tumor tissues (mean ± SD, 14.6 ± 22.9% and 12.5 ± 18.4%, respectively). M2 TAM density was significantly associated with the expression of PD-L1 on TCs and ICs ($P < 0.0001$ and $P < 0.0001$, respectively). M2 TAM density was also significantly associated with the expression of PD-L2 on TCs and ICs ($P = 0.0452$ and $P = 0.0125$, respectively). The percentage of PD-L1-positive TCs was significantly correlated with the percentage of PD-L1-positive ICs ($r = 0.396$; $P < 0.0001$). In addition, the percentage of PD-L2-positive TCs also was significantly correlated with the percentage of PD-L2-positive ICs ($r = 0.488$; $P < 0.0001$). However, there was no correlation

between the percentage of PD-L1-positive TCs and the percentage of PD-L2-positive TCs (r = 0.019; P = 0.8049). Meanwhile, tumor differentiation was significantly associated with PD-L1 expression on TCs and ICs (P = 0.0002 and P < 0.0001, respectively). By contrast, tumor differentiation was inversely associated with PD-L2 expression on TCs and ICs (P = 0.0260 and P = 0.0326, respectively).
Conclusions: PD-L1 and PD-L2 expression on TCs and ICs was associated with M2 TAMs in NSCLC, although there was no correlation between PD-L1 and PD-L2 expression on TCs. The combined evaluation of PD-L1 and PD-L2 expression could be clinically important in the treatment strategy of immune-checkpoint inhibitors in patients with NSCLC. In particular, the evaluation of PD-L2 expression may be necessary for patients with PD-L1-negative NSCLC.

#5830

Presence of androgens improves efficacy of PD1 blockade

María Elena Vargas-Delgado[1], Lara Meier[1], Jonas Waizenegger[1], Julia Oberbauer[2], Nikolaus Berenbrok[1], Janik Engelmann[3], Victoria Gensch[1], Franziska Heilmann[2], Jochim Reinert[4], Kristoffer Riecken[5], Boris Fehse[5], Hannelore Lotter[6], Dorothee Schwinge[7], Christoph Schramm[7], Hans-Willi Mittruecker[8], Isabel Ben-Batalla*[1], Sonja Loges* (*equal contribution)[1].
[1]DKFZ-Hector Cancer Institute, University Medical Center Mannheim; German Cancer Research Center; University Hospital Mannheim, Medical Faculty Mannheim, University Heidelberg, University Medical Center Hamburg-Eppendorf, Heidelberg, Germany,[2]2) Division of Personalized Medical Oncology, 3) Department of Personalized Oncology, DKFZ-Hector Cancer Institute, University Medical Center Mannheim; German Cancer Research Center; University Hospital Mannheim, Medical Faculty Mannheim, University Heidelberg, Heidelberg, Germany,[3]Department of Oncology, Hematology and Bone Marrow Transplantation with section Pneumology, Hubertus Wald Comprehensive Cancer Center, University Medical Center Hamburg-Eppendorf; DKFZ-Hector Cancer Institute, University Medical Center Mannheim, Hamburg, Germany,[4]Department of Oncology, Hematology and Bone Marrow Transplantation with section Pneumology, Hubertus Wald Comprehensive Cancer Center Hamburg, University Medical Center Hamburg-Eppendorf, Hamburg,

Germany,[5]Research Department Cell and Gene Therapy, Department of Stem Cell Transplantation, University Medical Center Hamburg-Eppendorf, Hamburg, Germany,[6]Department of Molecular Biology and Immunology, Bernhard Nocht Institute for Tropical Medicine, Hamburg, Germany,[7]Department of Medicine, University Medical Center Hamburg-Eppendorf, Hamburg, Germany,[8]Department of Immunology, University Medical Center Hamburg-Eppendorf, Hamburg, Germany

Immune therapies have revolutionized the treatment of cancer, however, until now only a minority of patients derive long-term benefit. Notably, despite widely reported significant differences between the immune system of males and females, there continues to exist a knowledge gap regarding sex disparities in anti-cancer immune responses. Recent meta-analyses indicate that immune checkpoint blockade (ICB) treatment has higher efficacy in male patients compared to females, regardless of the cancer type. To investigate the mechanisms underlying these sex-specific differences we utilized the syngeneic colorectal cancer model MC38 because it mirrors the clinical situation yielding responding and non-responding mice. Therefore, we inoculated tumor cells subcutaneously (s.c.) into male and female mice, and treated them with either IgG2a control Ab or anti-PD1 Ab. When analyzing the tumor response to anti-PD1 treatment we observed significant sex-biased growth kinetics upon ICB favoring males. To asses a potential role of androgens in impacting observed sex differences to ICB response *in vivo*, we performed surgical androgen deprivation therapy (orchiectomy) in male mice, as well as sham-surgery in male and female mice as control. After a recovery period, we proceeded with s.c. cell injection and ICB treatment as previously described. Sham male mice showed a very high response rate to anti-PD1 (92%) compared to sham females (58%), but more importantly, testosterone suppression by surgical androgen deprivation therapy led to a lower response rate of castrated mice (71%). To further confirm whether the presence of testosterone was beneficial for ICB response, we implanted s.c. sham or testosterone pumps into male and female mice and proceeded as before. Males with sham pumps showed a very high response rate to anti-PD1 (90%) compared to females with sham pumps (50%), while testosterone supplementation in females led to enhanced response rate (85%). Overall, this demonstrated that regardless of biological sex,

presence of testosterone is sufficient to positively impact ICB therapy outcome. Furthermore, immunophenotyping analysis by flow cytometry showed that females supplemented with testosterone and treated with anti-PD1 had significantly increased intratumoral stem-like $CD8^+TCF1^+PD1^+$ T cells compared to sham females. Additionally, these findings also correlated with enhanced intratumoral terminal differentiated effector $CD8^+TCF1^-PD1^+$ T cells in both sham males and females supplemented with testosterone, compared to sham females. In summary, androgens can modulate anti-cancer immune responses by contributing to a more sustained anti-tumor $CD8^+$ T cell response and consequently better responses upon treatment with anti-PD1. These findings are in concordance with male cancer patients responding better to ICB and warrant therapy escalation in female patients.

#5831

CD200R signaling contributes to unfavorable tumor microenvironment through regulating production of chemokines by tumor associated macrophages

Cho-Hao Lin[1], Fatemeh Talebian[1], Yang Li[2], Jianmin Zhu[1], Bolin Zhao[2], Jin-Qing Liu[1], Sujit Basu[1], Xueling Pan[2], Xi Chen[2], Pearlly Yan[2], William E. Carson[2], Gang Xin[2], Haitao Wen[2], Ruoning Wang[2], Zihai Li[2], Qin Ma[2], Xue-Feng Bai[1]. *[1]Pathology, The Ohio State University, Columbus, OH,[2]The Ohio State University, Columbus, OH*

CD200 is overexpressed in human solid tumors such as neuroblastoma and melanoma and is considered as an immune checkpoint molecule for dampening cancer immunity. However, how CD200 affects tumor microenvironment (TME) and host immunity is incompletely understood. In the present study, we evaluated the role of the CD200-CD200R pathway in TME using loss-of-function $CD200R^{-/-}$ mice, along with two clinically relevant, CD200-positive murine tumor models: the mouse neuroblastoma NB9464D and melanoma Yummer1.7. We found that comparing with the wild type mice, $CD200R^{-/-}$ mice were significantly more potent in rejecting these $CD200^{+}$ tumors. Transcriptome analysis by single cell RNA sequencing demonstrated that tumors from $CD200R^{-/-}$ mice had more infiltration of $CD45^{+}$ immune cells, including $CD4^{+}$ and $CD8^{+}$ T cells, and NK cells but less infiltration of neutrophils. Antibody depletion experiments revealed that immune effectors including $CD8^{+}$ T cells and NK cells in combination, are crucial in inhibiting tumor growth in $CD200R^{-/-}$ mice. Mechanistically, we found that CD200R signaling differentially regulates the expression of chemokines in tumor-associated macrophages (TAMs). In the absence of CD200R, TAMs up-regulate CCL24 and CCL8 and down-regulate CXCL3, CXCL2, and CCL3 via activation of ERK and/or p38 MAP kinases. Increased expression of CCL24 in CD200R-deficient tumors resulted in increased infiltration of eosinophils, which also contributes to anti-tumor activity. Overall, we conclude that CD200R-mediated signaling, via interaction with CD200 on tumor cells, contributes to unfavorable TME primarily through chemokine-dependent recruitment of immune suppressive neutrophils and exclusion of anti-cancer immune

effectors. Our study has significant implications in developing CD200-targeted immunotherapy of solid tumors.

#5832

Integrinα5 mediates the direct heterocellular interaction between cancer cells and cancer-associated fibroblasts and promotes peritoneal metastasis of diffuse-type gastric carcinoma

Hideki Yamaguchi, Shingo Miyamoto, Yoshiko Nagano, Makoto Miyazaki, Yuko Nagamura. *Department of Cancer Cell Research, Sasaki Institute, Sasaki Foundation, Tokyo, Japan*

Diffuse-type gastric carcinoma (DGC) is an aggressive subtype of gastric cancer characterized by rapid infiltrative growth and frequent peritoneal metastasis. Peritoneal metastasis is the main cause of poor prognosis and decreased quality of life for patients with DGC. Histologically, DGC tumor lesions are associated with massive fibrotic stroma caused by the extensive proliferation of cancer-associated fibroblasts (CAFs). Peritoneally metastasized tumors of DGC are also accompanied by abundant fibrotic stroma and CAFs. CAFs are known to promote the progression of DGC by enhancing the growth, invasion, and dissemination of tumor cells. Previously, we reported that the direct heterocellular interaction between cancer cells and CAFs is necessary for the invasion and peritoneal metastasis of DGC. In this study, we aimed to identify and target the molecules that mediate such direct heterocellular interaction. Monoclonal antibodies (mAbs) against intact DGC cells were generated and subjected to high-throughput screening to obtain mAbs that block the adhesion of DGC cells to CAFs. As a result, several such inhibitory mAbs were obtained. Immunoprecipitation and mass spectrometry revealed that all mAbs recognized integrin α5 complexed with integrin β1. Blocking integrin α5 in DGC cells abrogated the adhesion of DGC cells to CAFs. Similarly, blocking fibronectin, a ligand of integrin α5β1, deposited on CAFs blocked the heterocellular adhesion. Furthermore, administration of mAbs or knockout of integrin α5 in DGC cells suppressed their invasion led by CAFs in vitro and peritoneal metastasis in a mouse xenograft model. Analysis of the public database revealed that integrin α5 and fibronectin were highly expressed in DGC. In addition, integrin α5 and fibronectin expression levels were correlated with worse overall survival in DGC

patients. Taken together, these results show that integrin α5 mediates the heterotypic cancer cell-CAF interaction during peritoneal metastasis of DGC and may thus be a promising therapeutic target.

#5833

Crosstalk between cancer-associated fibroblasts and CD8 T cells leads to improved T cell activation in head and neck cancer

Diana Graves[1], Aleksandar Obradovic[2], Henry Schares[1], Michael Korrer[3], Brian Bachmann[1], Young Kim[4], Ben Park[1], Paula Hurley[1]. *[1]Vanderbilt University, Nashville, TN,[2]Columbia University, New York City, NY,[3]Elephas Biosciences, Madison, WI,[4]Regeneron Pharmaceutical, Tarrytown, NY*

Cancer-associated fibroblasts (CAFs) have been shown to modulate immune responses in the tumor microenvironment (TME), however, the extensive heterogeneity of these cells has precluded rigorous understanding of their immunoregulatory role in the head and neck TME. To gain a better understanding of the relationship between CAFs and the immune environment in head and neck cancer, we leveraged protein activity inference tools to analyze single-cell RNA sequencing of advanced-stage head and neck squamous cell carcinoma (HNSCC) patients pre- and post-treatment with the αPD-1 therapy, nivolumab. From this analysis, we identified a novel CAF population predictive of patient response to αPD-1 therapy. Utilizing *in vitro* co-culture assays with primary human CD8 T cells, we discovered that this novel CAF population was able to elicit features associated with enhanced CD8 T cell function, namely the reduction of PD-1+TIM-3+ exhaustive phenotypes and induction of CD103+NKG2A+ tissue-resident memory phenotypes and cytotoxicity. Due to their unique ability to stimulate T cells in this manner, we termed this novel CAF population T cell-stimulating CAFs (tsCAFs). In efforts to elucidate the mechanism behind this pro-inflammatory function, we determined that tsCAFs secrete a heat-sensitive small molecule/s in order to alter CD8 T cell behavior. However, tsCAFs will only secrete this factor in the presence of activated T cells demonstrating crosstalk between T cells and CAFs in the head and neck TME. This pro-inflammatory crosstalk between CAFs and T cells represents a novel finding that further contributes to the idea of immunoregulatory pleiotropy among CAFs.

Accordingly, our findings highlight the functional importance of distinct CAF subsets in modulating the immunoregulatory milieu of human HNSCC and warrant more extensive characterization of CAF-T cell interactions in human squamous cell carcinoma.

#5834

The pro-tumoral function of cancer-associated mesothelial cells

Maeva Chauvin. *Massachusetts General Hospital / Harvard Medical School, Boston, MA*

Cancer-associated mesothelial cells have emerged as significant contributors to the tumor microenvironment, influencing tumor growth and immune evasion. Mesothelial cells are the first point of contact with ovarian cancer cells during peritoneal spread. Peritoneal mesothelial cells also play an essential role in immune surveillance. However, the mechanism by which cancer and mesothelial cells within the tumor microenvironment coordinate growth and immune evasion remains poorly understood. To study the role of mesothelial cells in the tumor microenvironment, we have recently generated novel syngeneic mouse models of high-grade serous ovarian cancer, which were derived from Fallopian tube epithelium, and bear human-relevant mutational genotypes. Analysis of one such model (CCNE1 amplified) using single-cell transcriptomics in omental metastases revealed specific expression of the anti-Mullerian hormone type II receptor (Amhr2) in cancer-associated mesothelial cells, whereas normal omental mesothelium does not express Amhr2. Co-culture of cancer cells with normal omental mesothelial cells induces AMHR2 expression along with a pro-tumorigenic cancer-associated mesothelial cell phenotype. Overexpression of AMHR2 in a human immortalized mesothelial cell line significantly modulated the expression of genes involved in immune response pathways, remodeling of extra-cellular matrix, and secretion of growth factors by RNAseq and qPCR. Furthermore, we showed that anti-Mullerian hormone (AMH) (the ligand of AMHR2), is secreted by ovarian cancer cells and further downregulates the chemoattractant cytokines secreted by CAMCs, thus promoting immunosuppression within the tumor. Finally, implantation of ovarian cancer cells in syngeneic Amhr2$^{-/-}$ hosts results in tumors that grow significantly slower than those implanted in wild-type hosts. Together these data suggest AMHR2 is a specific marker of

CAMCs, whose expression is necessary for the reprogramming of mesothelial cells into CAMCs. The AMH-AMHR2 axis mediates paracrine signaling between cancer cells and CAMCs within the tumor microenvironment to promote tumor growth and immune evasion. These results suggest that AMHR2 could be a highly specific target to enhance immunotherapies in ovarian cancer.

#5835

Targeting discoidin domain receptor 1 (DDR1) reverses glioma immune suppression by remodeling collagen fiber architecture

Syed M. Faisal, Andrea Comba, Maria L. Varela, Anna E. Argento, Emily Brumley, Molly E. J. West, Santiago Haase, Anzar A. Mujeeb, Clifford Abel, Marcus N. Barissi, Jarred E. Clewner, Brooklyn Stack, Grace A. Abbud, Maria G. Castro, Pedro R. Lowenstein. *Neurosurgery, University of Michigan Medical School, Ann Arbor, MI*

Glioblastoma (GBM) is the most aggressive and immunosuppressive form of brain tumor, and its treatment remains a large, unmet medical need. Recently, we introduced oncostreams to refer to dynamic multicellular neuropathological structures that facilitate glioma cell growth and invasion into the normal brain. Moreover, we have shown that targeting Col1α1 within gliomas eradicates oncostreams and prolongs median survival in two genetic murine models. However, the signaling that collagen utilizes to maintain the glioma tumor microenvironment is still unknown. Our RNA-seq data show that collagen receptor DDR1 is overexpressed in genetically engineered glioma mouse models (GEMMs) including NPA (NRAS/shp53/shATRX), NPD (NRAS/shp53/PDGFβ), and NPAI (NRAS/shp53/shATRX/ $IDH1^{R132H}$) compared to healthy mouse brain tissue. We discovered that pharmacological inhibition of DDR1 radio-sensitized gliomas *in vitro* and dismantled oncostreams *ex vivo,* imaged with time-lapse confocal microscopy. GEMMs of DDR1 knockdown (NRAS/shp53/shATRX/shDDR1) using the Sleeping Beauty transposase system significantly increased median survival. This suggests that gliomas employ DDR1 mediated mechanisms to promote the immunosuppressive TME and thus stimulate tumor growth. Inhibition of DDR1 within gliomas enhanced intratumoral infiltration of $CD45^+$, and $CD3^+$ immune cells at the tumor core and invasive tumor border and prolonged median survival in

GEMMs of glioma. We postulate that glioma DDR1 blocks immune-surveillance by enhancing collagen fiber alignment, which we assessed using collagen-specific second-harmonic generation microscopy. In human datasets such as CGGA and TCGA, DDR1 expression negatively correlates with PTPRC (CD45) gene expression. Furthermore, our results show that DDR1 inhibition suppresses oncostream formation, impairs glioma cell proliferation ($PCNA^+$) and remodeled the tumor microenvironment by lowering $Iba1^+$ glioma-associated microglia. We propose that DDR1 inhibition within glioma cells reprograms the TME to an immune-stimulatory state with enhanced radio-sensitivity. Targeting the DDR1 collagen receptor is a novel and highly promising avenue for GBM therapeutics.

#5836

Non-invasive quantification of fibroblast activation protein (FAP) cleaved type III collagen in serum reflects FAP activity and has biomarker potential in non-small cell lung cancer

Rasmus Sund Pedersen, Jeppe Thorlacius-Ussing, Nicholas Willumsen, Morten A. Karsdal. *Nordic Bioscience, Herlev, Denmark*

Introduction: Fibroblast activation protein (FAP) is an established cancer associated fibroblast (CAF) marker. FAP is highly expressed in the cancer stroma and is a predictor of poor survival for patients with non-small cell lung cancer (NSCLC). For this reason, it is being explored as a potential drug target. FAP has broad proteolytic activity and can directly promote multiple aspects of tumor progression. The aim of this study was to develop a tool to non-invasively measure FAP activity and validate its potential as a non-invasive biomarker in NSCLC.
Methods: An ELISA, named C3F, was developed to reflect proteolytic activity of FAP by quantifying FAP-mediated cleavage of type III collagen in serum. To confirm that C3F reflects proteolytic activity of FAP, type III collagen was assayed after incubation with and without FAP. C3F was measured in serum samples from healthy controls (n = 26) and patients with NSCLC: adenocarcinoma (AD) (n = 26) and squamous cell carcinoma (SCC) (n = 14). An ELISA quantifying matrix metalloprotease degraded type III collagen (C3M) was used for measuring the same serum samples

and compared to C3F using spearman correlation test and area under receiver operating characteristic curves (AUROCs).
Results: A C3F signal only appeared after FAP cleavage of type III collagen, supporting that C3F reflects FAP proteolytic activity. Compared to healthy controls, C3F was significantly elevated in serum from patients with SCC ($p = 0.0004$, AUROC = 0.86), but not AD ($p = 0.21$, AUROC = 0.66). C3F was also significantly elevated in SCC compared to AD ($p = 0.030$, AUROC = 0.77). In comparison, C3M was significantly elevated in serum from both SCC and AD compared to healthy controls ($p < 0.0001$, AUROC = 0.93 and $p < 0.0001$, AUROC = 0.92, respectively), but no difference was seen between SSC and AD ($p > 0.99$, AUROC = 0.56). Only a moderate correlation was seen between C3M and C3F ($r = 0.58$, $p < 0.0001$).
Conclusion: FAP activity can be non-invasively quantified in serum by assaying FAP cleaved type III collagen (C3F). C3F shows promise as a cancer biomarker in NSCLC with potential for discriminating between NSCLC subtypes. As C3F reflects FAP activity, it is potentially a more suitable (or complementary) biomarker for anti-FAP drug development and prediction of anti-FAP treatment response compared to methods that asses the presence of FAP.

#5838
Cancer-associated fibroblasts drive spheroid formation and pleural dissemination in non-small cell lung cancer
Masayoshi Ohki, Naoki Matsuda, Ken Suzawa, Tomohiro Habu, Mao Yoshikawa, Kazuma Iwata, Yin Min Thu, Kazuhiko Shien, Hiromasa Yamamoto, Shinichi Toyooka. *General Thoracic Surgery and Breast and Endocrinological Surgery, Okayama University Graduate School of Medicine, Dentistry and Pharmaceutical Sciences, Okayama, Japan*

Introduction: Cancer-associated fibroblasts (CAFs) play an important role in cancer progression and malignant transformation by interacting with cancer cells in the tumor microenvironment. Pleural dissemination of non-small cell lung cancer (NSCLC) is a condition in which cancer cells directly spread from the primary tumor site into the extrapulmonary thoracic cavity and colonize the pleura. However, not all free detached cancer cells can survive under anchorage-independent conditions in thoracic cavity, and

some important factors are assumed to be involved in the formation of pleural dissemination. In this study, we investigated the role of CAFs in the formation of pleural dissemination in NSCLC.
Methods: Using in vitro co-culture models, conditioned medium, and in vivo xenograft models, we investigated CAF-induced phenotypic changes in lung cancer cell: proliferative ability, invasive ability, anchorage-independent growth ability, cell adhesion to extracellular matrix, and tumorigenicity in thoracic cavity. Next, we performed RNA sequencing analysis using 3D co-culture models of cancer cells and CAFs to explore a molecule that contributes to the formation of pleural dissemination, and then verified it using in vitro and in vivo mice models of pleural dissemination.
Results: Cancer cells showed enhanced migration, anchorage-independent growth, adhesion, and invasion ability by co-culture with CAFs. In 3D co-culture model of cancer cells and CAFs, even cancer cells which did not form spheroid by themselves acquired the ability of spheroid formation surrounding the CAF core, suggesting that the interactions with CAFs promote spheroid formation. Inoculation of cancer cells together with CAFs into mouse thoracic cavity developed pleural dissemination more efficiently than inoculation of cancer cells alone. RNA sequencing analysis revealed that co-culture with CAFs upregulated the expression of Cellular Communication Network Factor 1 (CCN1), a matricellular protein, in cancer cells. We then verified that ectopically CCN1-overexpressing lung cancer cell lines increased migration and adhesion ability in vitro, and tumorigenicity in thoracic cavity in mouse pleural dissemination model.
Conclusions: CAFs promote development of pleural dissemination via driving spheroid formation and upregulating CCN1 expression in NSCLC.

#5839

Novel stroma-derived prostate cancer subtypes are associated with risk of clinical progression

Martin Rasmussen[1], Jacob Fredsøe[1], Paul V. Salachan[1], Marcus P. L. Blanke[1], Benedicte P. Ulhøi[2], Michael Borre[3], Karina D. Sørensen[1].
[1]Department of Clinical Medicine, Aarhus University, Aarhus, Denmark,[2]Department of Pathology, Aarhus University, Aarhus, Denmark,[3]Department of Urology, Aarhus University, Aarhus, Denmark

The tumor microenvironment influences prostate cancer aggressiveness, and by focusing on how different changes to the microenvironment can affect the cancer, we aimed to identify novel stromal subtypes in localized prostate cancer (LPC), characterize these subtypes, and utilize subtypes to increase accuracy in prostate cancer risk stratification. Subtype identification was conducted using non-negative matrix factorization with consensus clustering on a stroma-specific expression signature in RNA sequencing data. A discovery cohort (127 LPC patients) and two independent validation cohorts (406 LPC & 126 LPC patients) were used for subtype identification. All three cohorts were subsequently used for subtype characterization and prognostic evaluation. Identified subtypes were characterized by evaluation of clinical characteristics, by gene set enrichment analysis, and by cell-type deconvolution analysis. Survival differences between subtypes were assessed using Kaplan-Meier and univariate Cox regression analyses with biochemical recurrence (BCR) as endpoint. Lastly, a high-risk stromal subtype was investigated for its ability to improve risk stratification for intermediate risk prostate cancer using hazard ratio changes from univariate Cox regression analysis. We identified three stromal subtypes (S1-S3) in prostate cancer. Of these, subtype S3 showed characteristics of a highly reactive stromal environment with significantly (adj. $p < 0.05$) decreased cell polarity and stroma related functions, significantly (adj. $p < 0.05$) reduced fibroblast infiltration, and a significantly (adj. $p < 0.05$) increased immune cells infiltration compared to the other subtypes. Survival analysis also revealed significant ($p < 0.05$) association of S3 with BCR in all three cohorts (HR = 3.2, 2.1, and 3.4 in cohorts 1, 2 and 3 respectively). Lastly, S3 significantly ($p < 0.05$) improved the risk prediction for patients with intermediate recurrence risk according to the clinical nomogram CAPRA-S (cohort 1, delta HR = 1.4; cohort 2, delta HR = 2.3; cohort 3, delta HR = 4.2). In conclusion, by focusing on the stromal alteration in prostate cancer, this study sheds new light on the influence of tumor microenvironment on LPC aggressiveness. A stromal subtype characterized by dysregulated stromal functions and changes in stroma and immune cells infiltration predicted adverse outcome in patients with a high prognostic ambiguity. This utilization of stromal information to improve risk assessment for clinically intermediate risk PC indicates a potential use in future evaluation of PC aggressiveness.

#5840

Normal fibroblasts, cancer-associated fibroblasts, and their senescent counterparts exert varying effects on tumorigenic potential and ABT-263 sensitivity of gastric cancer cells

Francesca R. Di Cristofano, Shengliang Zhang, Kelsey E. Huntington, Wafik S. El-Deiry. *Legorreta Cancer Center at Brown University, Providence, RI*

It has become increasingly apparent that cancer is not a tumor cell-centric disease. Elements of the tumor microenvironment (TME), including fibroblasts and senescent cells, have been shown to contribute to tumor cell proliferation, metastasis, and therapy resistance, and are therefore major contributors to disease progression. However, this has been complicated by accumulating evidence suggesting that the function of fibroblasts is heterogeneous, with normal fibroblasts (NFs) and cancer-associated fibroblasts (CAFs) both promoting or suppressing tumorigenesis and drug sensitivity within different contexts. Moreover, although senescent fibroblasts have been shown to accelerate tumor growth and contribute to therapy resistance, whether phenotypic differences exist between different senescent fibroblasts remains poorly understood. It is clear that additional work must be done to unravel the precise mechanisms by which NFs, CAFs, and their senescent counterparts interact within the tumor microenvironment to modulate tumor cell growth and sensitivity to therapy. Here, we show different NF and CAF lines exert varying effects on AGS gastric cancer cells. We found that when AGS cells are co-cultured with IMR90 lung fibroblasts, they form fewer and smaller colonies (total colony area = 5.14E3 pixels^2) than when cultured alone (total colony area = 2.57E4 pixels^2). On the other hand, colony formation ability is enhanced when AGS cells are co-cultured with GF1 primary gastric fibroblasts (total colony area = 3.56E4 pixels^2), and to a greater extent when cultured with CK4520 (total colony area = 4.59E4 pixels^2) and CK8612 (total colony area = 4.88E4 pixels^2) primary gastric CAFs. We next sought to determine whether these cells modulate AGS sensitivity to ABT-263, a BH3 mimetic that activates the intrinsic apoptotic pathway by targeting and inhibiting Bcl-2 and Bcl-xl. We treated AGS cells with ABT-263 with or without the addition of fibroblast-conditioned medium. We showed that IMR90 cells sensitize AGS cells to ABT-263, with an IC50 shift from 109 nM to 54 nM

in AGS cells treated with IMR90-conditioned medium. On the other hand, AGS cells were more resistant to ABT-263 when treated with GF1, CK4520, or CK8612-conditioned medium, with IC50s of 270 nM, 520 nM, and 540 nM, respectively. Ongoing efforts involve expanding these experiments to senescent fibroblasts and conducting cytokine profiles to begin investigating the mechanisms underlying these phenotypes. These results contribute to our understanding of tumorigenesis and drug resistance.

#5841

Exploring the role of versican in immune exclusion within triple negative breast cancer

Priyanka Hirani[1], Kimberly M. Alonge[2], Daniel J. Pennington[3], Pedro R. Cutillas[1], Thomas N. Wight[4], Oliver M. T. Pearce[1]. *[1]Cancer Research UK Barts Centre, London, United Kingdom,[2]University of Washington Medicine Diabetes Institute, Seattle, WA,[3]Blizard Institute, London, United Kingdom,[4]Benaroya Research Institute, Seattle, WA*

Immunotherapy has found limited success in solid tumors such as triple negative breast cancer (TNBC). The poor response can be attributed to the presence of the extracellular matrix (ECM) that can act biochemically or physically to interfere with cytotoxic T cell migration, leading to a limitation in tumor cell killing. Through previous work on deconstructing this matrix and outlining the spatial arrangement of proteins, we were able to identify versican as a key protein in T cell location. Versican is a chondroitin sulfate proteoglycan and has multiple functions in the ECM due to its ability to bind many ECM components. Using immunohistochemistry in this study, we analyzed the localization of CD8+ T cells within human TNBC tissues to classify them as inflamed ($tumor^{hi}$, $stroma^{hi}$), desert ($tumor^{lo}$, $stroma^{lo}$) or immune excluded ($tumor^{lo}$, $stroma^{hi}$). From the analysis of 26 tissues, nearly half were classified as immune excluded with most of the CD8+ T cells restricted to the stroma, whilst only a quarter were inflamed. When comparing this to versican accumulation we noticed that immune excluded tissues have significantly higher levels of versican in the tumor epithelium compared to inflamed tissues where versican is mostly found within the stroma. To investigate the function of versican's structure,

we carried out transwell migration assays using versican enriched protein treated with or without chondroitinase ABC and showed that the chondroitin sulfates attached to versican's peptide backbone are an important factor towards T cell trafficking with a reduction in migration following chondroitinase ABC treatment. Comparison of versican levels to chondroitin sulfate via immunohistochemistry showed a positive correlation within inflamed tissues, however no correlation was observed in immune excluded tissues. Versican isoforms expression in TNBC tissues and cell lines was examined with qRT-PCR which showed that within all tissues and cell lines the V0 and V1 isoform are the highest expressed out of the 5 isoforms. Overall, in this work, we have found that versican is differentially expressed in excluded tissues in comparison to inflamed tissues. With chondroitin sulfate shown to play a major role in immune cell trafficking, understanding how it differs between inflamed and excluded tumors can help identify potential targets to improve immunotherapy response.

#5842

Determining the tumor supportive and inhibitory capabilities of cancer associated fibroblast subpopulations in central nervous system metastasis

Thomas Simon[1], David N. Buckley[1], Gerald C. Gooden[1], Ben Y. Tew[1], Gabriel Zada[2], Bodour Salhia[3]. *[1]Department of Translational Genomics, Keck School of Medicine, USC - University of Southern California, Los Angeles, CA,[2]Department of Neurosurgery, Keck School of Medicine/USC Norris Comprehensive Cancer Center, USC - University of Southern California, Los Angeles, CA,[3]Department of Translational Genomics, Keck School of Medicine/USC Norris Comprehensive Cancer Center, USC - University of Southern California, Los Angeles, CA*

Central nervous metastases (CM) are surrounded by a complex tumor microenvironment (TME) comprised of a meshwork of extracellular matrix (ECM) proteins and an assemblage of cell types including cancer-associated fibroblasts (CAFs). We have previously shown that patient-derived CM CAFs can either support or inhibit tumor growth *in vivo*, suggesting that CM CAFs comprise a heterogenous subgroup of cells. Accordingly, we recently reported, based on literature in other cancer types, that CAFs can be categorized into four main subpopulations: 'desmoplastic', 'immune',

‘contractile’ and ‘aggressive’. The purpose of our study is to identify different CAF subpopulations in the TME of CM and determine their impact on CM growth. To do this, we performed single cell RNA sequencing (scRNA-seq) on 10 CM patient tissues and 8 patient-derived CM CAF cell lines established in our lab. ScRNA-seq analysis of tumor tissues revealed that desmoplastic, immune, contractile, and aggressive CAF subpopulations are also present in the TME of CM. In addition, scRNA-seq showed that CM CAF cell lines were mainly comprised of the desmoplastic and aggressive CAF subpopulations. These two subpopulations showed differential expression of the newly described tumor inhibitory CAF marker Immunoglobulin Superfamily Containing Leucine Rich Repeat (ISLR) and classic tumor supportive CAF marker Actin Alpha 2, Smooth Muscle (ACTA2, α-SMA), with desmoplastic CAFs showing $ISLR^{high}/\alpha\text{-}SMA^{low}$ expression while aggressive CAFs were associated with $ISLR^{low}/\alpha\text{-}SMA^{high}$ expression. Next, we used fluorescence activated cell sorting (FACS) based on the expression of ISLR on the cell surface to enrich and expand the $ISLR^{high}/\alpha\text{-}SMA^{low}$ desmoplastic CAF and the $ISLR^{low}/\alpha\text{-}SMA^{high}$ aggressive CM CAF subpopulations. Reciprocal expression of α-SMA and ISLR was confirmed by western blot and immunofluorescence after FACS. Additionally, co-culture experiments showed that $ISLR^{high}/\alpha\text{-}SMA^{low}$ CM CAFs inhibit CM cell proliferation. In summary, our data show that there are several molecularly defined subpopulations of CAFs in the TME of CM that can act to either inhibit or promote CM tumor growth *in vitro* and *in vivo*. Our results support that the desmoplastic CM CAFs characterized by $ISLR^{high}/\alpha\text{-}SMA^{low}$ can inhibit tumor growth. Overall, the present study improves our understanding of the CM TME, which ultimately will help establish new strategies to harness the cancer restraining capabilities of tumor inhibitory CAFs in order to improve outcomes for patients with CM.

#5843

miR-224 activates cancer-associated fibroblasts to promote cancer cell invasion in lung tumor microenvironment

Seonyeong Oh, Inyoung Cheon, Young-Ho Ahn. *Ewha Womans University, Seoul, Korea, Republic of*

Cancer-associated fibroblasts (CAFs) promote EMT (epithelial-mesenchymal transition), invasion, and metastasis of cancer cells in the tumor microenvironment. To identify microRNAs (miRNAs) associated with the reprogramming of normal lung fibroblasts (LFs) into CAFs, global miRNA expression was profiled in LFs and CAFs through Nanostring nCounter. miR-224 was one of the increased miRNAs in CAFs, and its expression was higher in tumors than in normal tissues in dbDEMC and TCGA_lung adenocarcinoma data. miR-224 levels were then checked by qRT-PCR in paraffine-embedded tumor samples from patients with lung adenocarcinoma. Kaplan-Meier survival analysis showed that high miR-224 expression was related to poor survival. These data show that lung cancer progression is promoted by miR-224. To discover the roles of increased miR-224 in CAFs, miR-224 was overexpressed by lentiviral infection in LFs. LF_miR-224 overexpression enhanced the expression of CAF activation markers including *Fap, S100a4,* and *Vim*. In spheroid invasion assay using co-culture of LFs and cancer cells, as an experimental model of the tumor microenvironment, LF_miR-224 promoted invasion of lung cancer cells compared with control LFs. In transwell migration assay, LF_miR-224 stimulated migration of lung cancer cells more than control LFs. Collectively, these results indicate that CAFs reprogrammed by miR-224 promote the migration and invasion of lung cancer cells.

#5844

Fibroblasts play an immunoregulatory role in lung cancer through exosome secretion and by controlling extracellular matrix composition

Giulia Bertolini, Elvira Pantano, Giuliana Pollaci, Federica Facchinetti, Ugo Pastorino, Gabriella Sozzi, Luca Roz*. Fondazione IRCCS Istituto Nazionale dei Tumori, Milan, Italy*

Introduction: Cancer associated fibroblasts (CAF) are increasingly recognized as central players in the regulation of the tumor immune microenvironment. In lung cancer however little is known about specific fibroblast subpopulations or mechanisms subtending their immunoregulatory potential. We previously identified the nuclear transporter XPO1 as a master controller of lung fibroblast protumorigenic potential. Here we evaluated the potential of fibroblasts to modulate interactions between immune and cancer cells.

Material and Methods: Cultures of primary lung fibroblasts isolated from tissues resected during lung cancer surgery were characterized by multiparametric flow-cytometry and used for experiments with lung cancer cells and monocytes. Co-cultures, conditioned media and decellularized extracellular matrices deposited by fibroblasts (dECM) were employed to investigate different modes of interactions. Modulation of stemness and EMT properties were evaluated by flow cytometry and Real-Time PCR. Co-injection of dECM and lung cancer cell lines were performed in immunocompromised mice and heterotypic tumors were evaluated for their growth, local microenvironments and disseminating potential.
Results and Discussions: Using fibroblast cultures form both cancer and normal lung tissue we detected protumorigenic potential also in cultures form normal lungs, in line with presence of classical activation markers (alpha-SMA, FAP). Bioactivity of fibroblasts include the ability to induce EMT and modulate stemness potential (increase of CD133+ cancer stem cells and CD133+/CXCR4+ metastasis initiating cells). Interestingly dECM displayed similar potential compared to co-cultures. Exosomes isolated from both CAF and normal fibroblasts also showed potential to induce conversion of normal monocytes into myeloid derived suppressor cells. In co-injection experiments, dECM from pro-tumorigenic fibroblasts regulated the local immune microenvironment of ensuing tumors inducing generation of a stroma with high content of COL1A and COL6A3, reducing the infiltration from NK cells and increasing neutrophil content, thereby favoring dissemination of cancer cells to distant organs. Pharmacological inhibition of fibroblast activation through compounds targeting XPO1 activity was able to reduce these effects and counteract fibroblast protumorigenic action.
Conclusion: Fibroblasts play a regulatory role in tumor stroma and dissection of their activities could pave the way for rationale development of treatments to reverse immunosuppressive microenvironments.

#5845

Periostin secreted by cancer-associated fibroblasts promotes cancer progression and drug resistance in non-small cell lung cancer

Mao Yoshikawa, Fumiaki Takatsu, Ken Suzawa, Tomohiro Habu, Ohki Masayoshi, Kazuma Iwata, Naoki Matsuda, Yin Min Thu, Kazuhiko Shien, Hiromasa Yamamoto, Shinichi Toyooka. *Okayama University Graduate*

School of Medicine, Dentistry and Pharmaceutical Sciences, Okayama, Japan

Background: Cancer-associated fibroblasts (CAFs) are key players in the tumor microenvironment (TME) due to their abundance in most solid tumors and active crosstalk with cancer cells, and promote the initiation of tumor formation, tumor growth, angiogenesis, metastasis, and therapeutic resistance. In this study, we sought to identify effective therapeutic targets in CAFs for non-small cell lung cancer (NSCLC).
Experimental Design: We established fibroblast cell lines from the cancerous and non-cancerous parts of surgical lung specimens from patients with NSCLC and evaluated the differences in behaviors towards NSCLC cells using in vitro co-culture models, conditioned medium, and in vivo xenograft mouse models. Next, RNA sequencing analysis was performed to investigate the differentially expressed genes between normal fibroblasts (NFs) and CAFs, and we then verified the biological activity of the identified molecule on NSCLC cells in vitro and in vivo mouse model.
Results: Cancer cells showed enhanced cell proliferation, migration, and drug resistance by co-culture with CAFs or CAF-derived conditioned medium. RNA sequencing analysis revealed that CAFs showed higher expressions of POSTN, a matricellular protein, than NFs. Single-cell RNA sequencing data of NSCLC from public database confirmed that POSTN-positive fibroblasts were highly enriched in lung tumor tissues but rarely observed in normal lung tissues, suggesting CAF-specific POSTN expression in lung cancer. Recombinant POSTN increased cell proliferation via NSCLC cells' ERK pathway activation and induced epithelial-mesenchymal transition (EMT), which improved migration in vitro. In addition, POSTN knockdown in CAFs suppressed these effects, and in vivo experiments demonstrated that the POSTN knockdown improved the sensitivity of EGFR-mutant NSCLC cells for Osimertinib treatment.
Conclusion: Our results showed that CAF-derived POSTN is involved in tumor growth, migration, EMT induction, and drug resistance in NSCLC. Targeting CAF-secreted POSTN in TME could be a potential therapeutic strategy for NSCLC.

#5847

The splanchnic mesenchyme is the main tissue origin of fibroblasts in the pancreas during homeostasis and tumorigenesis

Lu Han[1], Yongxia Wu[1], Kun Fang[2], Sean Sweeney[1], Ulyss Roesner[1], Melodie Parrish[1], Khushbu Patel[1], Tom Walter[1], Julia Piermattei[1], Anthony Trimboli[2], Julia Lefler[1], Cynthia Timmers[1], Xue-Zhong Yu[1], Victor Jin[2], Michael Zimmermann[2], Angela Mathison[2], Raul Urrutia[2], Michael Ostrowski[1], Gustavo Leone[2]. *[1]The Medical University of South Carolina (MUSC), Charleston, SC,[2]Medical College of Wisconsin, Milwaukee, WI*

In pancreatic ductal adenocarcinoma (PDAC), cancer associated fibroblasts (CAFs) play critical and complex roles in the tumor microenvironment. CAFs are also a major cell type in the desmoplastic stroma in PDAC and may account for half of the entire tumor tissue. Multiple subtypes of CAFs have been suggested, but the tissue origin(s) of CAF subtypes are unknown and genetic tools to robustly target them *in vivo* are lacking. Here we aimed to examine three potential tissue sources of CAFs: the pancreatic epithelium (through epithelium-to-mesenchyme transition), the bone marrow (through circulation), and the pancreatic mesenchyme or tissue resident fibroblasts (TRFs) in the normal pancreas (through proliferation). We utilized a genetically engineered mouse model of PDAC, where *Kras* and *p53* mutations were engineered in the pancreatic epithelium using an *Flp-Frt* system. To determine whether the pancreatic epithelium gives rise to CAFs, we permanently labeled the pancreatic epithelium with a GFP reporter and traced their cell descendants by GFP expression. Despite robust GFP labeling of the epithelium, GFP expression was rarely identified in CAFs. To determine whether the bone marrow gives rise to CAFs, we transplanted donor bone marrow carrying a ubiquitously expressed GFP reporter to GFP-negative recipient mice. We found that minimal proportion of pancreatic CAFs were tagged with GFP. Lastly, to determine whether pancreatic TRFs give rise to CAFs, we used an inducible *CreER-LoxP* system to allow for permanent Tomato labeling in TRF progenitors, the splanchnic mesenchyme, during mid-gestation. Lineage tracing in PDAC showed that the vast majority of CAFs were labeled with Tomato expression, suggesting their splanchnic origin. Furthermore, certain splanchnic gene expression signatures persisted in subsets of CAFs in both the PDAC mouse model and human patient samples. Deletion of one of the splanchnic genes, *Gata6*, in CAFs resulted in increased tumor burden in the

pancreas, suggesting a tumor-restraining role of Gata6 in CAFs. In summary, we found that the pancreatic epithelium and bone marrow contributes to a minimal proportion of CAFs in PDAC. Meanwhile, pancreatic TRFs are derived from the splanchnic mesenchyme during fetal development and they expand to contribute to the vast majority of CAFs in PDAC. Moreover, the persistence of splanchnic signature defines subtypes of CAFs, with a potential tumor-suppressing function. This study provides genetic approaches to robustly target CAFs *in vivo,* and novel insights into CAF origin, heterogeneity and function in PDAC.

#5848

Identification of mechanosensitive cancer associated fibroblasts in pancreatic cancer

Weikun Xiao[1], Chae-Young Eun[1], Weian Zhao[2], Reginald Hill[1]. *[1]Lawrence J. Ellison Institute for Transformative Medicine, Los Angeles, CA,[2]Department of Biomedical Engineering and Department of Pharmaceutical Sciences, Chao Family Comprehensive Cancer Center, Irvine, CA*

The purpose of this study is to investigate whether a subpopulation of cancer associated fibroblasts (CAFs) are responsible for mechanosensation-mediated chemoresistance in pancreatic adenocarcinoma (PDAC). PDAC is one of the most lethal types of cancer with few effective treatments. The abundant stromal cells and the stiff desmoplastic microenvironment constitute more than 90% of the primary tumor bulk. However, there are few easily tunable models to recapitulate this stiff microenvironment. To address this issue, we have developed a Matrigel-based, orthogonally tunable 3-dimensional (3D) culture system to co-culture mouse derived PDAC organoids and host-matching cancer-associated fibroblasts (CAFs). Using this biomimetic model and a mechano-sensation-dependent reporter, we have identified a unique subpopulation of CAFs responsible for mechano-sensing the fibrotic matrix and facilitating CAF-mediated chemoresistance. Moreover, these mechanosensitive CAFs (mecCAFs) respond to increased stiffness through YAP-mediated pathways. Our results also demonstrate how ECM stiffness affects chemoresistance via the hypersecretion CAF-derived exosomes. Moving forward, therapies

designed to interrupt the function of mecCAFs could be utilized to overcome matrix-mediated chemoresistance in PDAC.

#5849

SMAD3 in tumor associated fibroblasts drives enhanced fibroblast accumulation in lung adenocarcinoma through increased migration

Natalia Isabel Diaz Valdivia[1], Yago Juste Lanas[2], Alejandro Llorente[1], Rafael Ikemori[1], Alejandro Bernardo[1], Noemi Reguart[3], Jose M. Garcia Aznar[2], Jordi Alcaraz[1]. *[1]Unit of Biophysics and Bioengineering, Universitat de Barcelona, Barcelona, Spain,[2]Multiscale in Mechanical and Biological Engineering Group, University of Zaragoza, Zaragoza, Spain,[3]Medical Oncology, Hospital Clinic, Barcelona, Spain*

Lung cancer is characterized by a stiff fibrotic microenvironment rich in activated/pro-fibrotic tumor-associated fibroblasts (TAFs). We previously reported a larger accumulation of TAFs in lung adenocarcinoma (ADC) compared to lung squamous cell carcinoma (SCC), the two most frequent lung cancer subtypes. However, the underlying mechanisms remain elusive. TAF accumulation is largely contributed by the proliferation and/or migration of resident fibroblasts. Moreover, we recently showed that SMAD3 is epigenetically repressed in SCC-TAFs compared to ADC-TAFs owing to an excessive exposure to cigarette smoke particles, which elicited a compensatory increase in its closely related homolog SMAD2 in SCC-TAFs. However, it remains unknown whether the differential SMAD2/3 expression between ADC- and SCC-TAFs contributes to the larger accumulation of TAFs in ADC. To address this question, we knocked-down SMAD2 or SMAD3 in control pulmonary fibroblasts by shRNA and used them as ADC-like or SCC-like models. To assess proliferation, we examined cell number density and found that shSMAD2 (ADC-like) fibroblasts exhibited a significantly lower number density in basal conditions compared to shSMAD3 (SCC-like) fibroblasts, which was confirmed in TAFs. In the presence of TGF-β1, number density increased and attained similar values in shSMAD2 and shSMAD3 fibroblasts as well as in ADC- and SCC-TAFs. To assess fibroblast migration, we used a microfluidic device to quantify biophysical descriptors of protrusions and subsequent migration within a 3D collagen culture. Notably, both protrusions and migration descriptors were increased in basal conditions

selectively in shSMAD2 (ADC-like) fibroblasts concomitantly with Erk1/2 hyperactivation This enhanced migration was abrogated by TGF-β1 as well as by the MEK inhibitor Trametinib. In contrast, high SMAD2 fibroblasts were poorly responsive to TGF-β1 and Trametinib, exhibiting impaired migration in all conditions. Consistent results were observed in ADC-TAFs upon knocking-down SMAD3 as well as using the Transwell migration Boyden assay, thereby revealing that the enhanced migration in high SMAD3 conditions as in shSMAD2 and ADC-TAFs is caused by an intrinsic migratory priming. These results reveal that altered SMAD2/3 expression provide growth and migration advantages only in the absence of TGF-β1, although in opposing directions, since growth advantage was observed in high SMAD2 conditions (as in SCC), whereas migration advantage was found in high SMAD3 conditions (as in ADC). These findings strongly support that the larger TAF accumulation in ADC occurs at early stages (under low TGF-β1) and is driven by the enhanced migration of ADC-TAFs due to their high SMAD3 and Erk1/2 activation. Moreover, our results encourage the therapeutic use of MEK inhibitors in ADC-TAFs but not SCC-TAFs.

#5850

Development and characterization of patient-derived pancreatic fibroblasts to study CAF heterogeneity

Nidhi V. Dwivedi, Shailendra K. Gautam, Satya Rachagani, Ramakanth C. Venkata, Vipin Dalal, Maneesh Jain, Surinder K. Batra. *BMB, University of Nebraska Medical Center, OMAHA, NE*

Pancreatic ductal adenocarcinoma (PDAC) has complex tumor microenvironment (TME), characterized by phenotypically and functionally heterogenous cancer-associated fibroblasts (CAFs). Different CAF subtypes have been identified that evidently contribute to desmoplasia, immunosuppression, and therapy response variably. The lack of models to study their plasticity and heterogeneity reproducibly poses a major limitation. We, thus, describe the development and characterization of a panel of immortalized patient-derived pancreatic fibroblasts (iPDPFs), studying their impact on PDAC cell lines *in vitro* and *in vivo*.
Method: We developed six iPDPF lines using human telomerase reverse transcriptase (hTERT) from cancer-adjacent normal pancreas (9-26-NP),

chronic pancreatitis (CPP1), and PDAC CAFs (9-17-P, 10-15-P, 10-03-P, & 10-32-P). Immunoblotting, bulk-RNAseq, and qPCR were performed for their molecular characterization. Functional characterization was done *in vitro* using collagen contraction assay and co-culture studies with COLO357. The impact of iPDPFs on the tumor cell behavior *in vivo* was studied by their co-implantation with COLO357 in athymic nude mice.
Results: The iPDPFs exhibited variable expression of activation, inflammatory, and ECM markers indicative of heterogeneity across the panel. While CAFs expressed high levels of αSMA (alpha-smooth muscle actin) and fibroblast-specific protein-1 (FSP1), the expression of these markers was low in 9-26 NP & CPP-1. Also, the iPDPFs variably expressed TGFβ, PDGFRβ, VDR, COL1A, and small GTPases. High expression of inflammatory markers was observed in 9-26 NP, CPP-1, & 10-32-P suggesting their iCAF type while 9-17-P, 10-03-P, and 10-15-P were of myCAF type. These observations were recapitulated in the transcriptomic analysis. Interestingly, the marker expression changed with passage suggesting existence of plasticity in the iPDPFs. 9-17-P induced highest collagen contraction (47.9%) while 10-15-P induced the least contraction (25.89%). Co-culture of iPDPFs with COLO357 enhanced the expression of ROCK-1. *In vivo*, iPDPFs resulted in stroma-rich tumors; however, the extent of stroma and growth rate were variable across iPDPF lines and implantation sites. 9-17-P xenograft tumors exhibited the highest percent αSMA (14.5%), and FSP1 (30.7%) positive cells. Limited analysis showed that iPDPF co-implanted tumors exhibited variable vascularity and ECM composition suggesting that the heterogeneity observed *in vitro* was manifested *in vivo*.
Conclusion: Overall, the iPDPFs recapitulate pancreatic fibroblasts heterogeneity, reflecting the overlapping nature of CAF subtypes. Also, the iPDPFs are functionally variable and plastic *in vitro*. Importantly, these fibroblasts exert variable effects on the tumor cells *in vivo*. The iPDPFs can thus serve as a useful model to reproducibly study CAF heterogeneity and plasticity in PDAC.

#5851
Cancer associated fibroblast crosstalk through VEGF increases tumor cell proliferation in human pancreatic ductal adenocarcinoma

Samantha Guinn, Joseph Tandurella, Jignasha Patel, Richard Burkhart, Jacquelyn Zimmerman, Elizabeth Jaffee. *Johns Hopkins Medicine, Baltimore, MD*

Introduction: Pancreatic ductal adenocarcinoma (PDAC) is a classically heterogeneous tumor for which tumor cells comprise less than 40% of the total tumor mass. To better understand mechanisms of intercellular interactions driving tumor response or resistance to chemotherapy, it is crucial to account for the complex tumor microenvironment (TME). Cancer associated fibroblasts (CAFs) have been implicated as key drivers supporting mechanisms that both promote and restrain tumor growth. Using our model system that investigates interactions between CAFs and cancer cells, we show a novel intercellular interaction through VEGF signaling that drives proliferation.
Methods: We interrogate intracellular crosstalk in the PDAC TME using a novel 3-dimensional (3D), patient-matched coculture system of patient-derived organoids (PDO) and CAFs, obtained from patients undergoing surgical resection. Molecular characterization is performed by profiling with a 1200 analyte multiplex ELISA screen, multiparameter flow cytometry, bulk RNA sequencing of CAF and PDO cocultures, imaging mass cytometry (IMC) on patient samples, and qPCR.
Results: Secretome profiling of 7 patient-derived CAF lines demonstrated patient-specific heterogeneity in proteins such as: FGF-12, FGF3, and CD79a. Common CAF-derived signaling proteins with the potential to regulate intercellular crosstalk that were seen across all samples include CRP, IL-6R, R-Spondin and others. To better understand how factors change with intercellular interactions, we set up direct CAF-PDO cocultures over 4 days to identify global transcriptional changes using bulk RNAseq. Phenotypically, coculture drives gene expression changes in both PDO subtype (basal vs classical) and CAF subtype (prevalence of iCAFs vs myCAFs). We used these transcriptome data to identify pathways modulated by CAF-PDO crosstalk. Profiling coculture supernatant, we identified upregulation in VEGF secretion. In tandem, when we investigate cellular surface marker changes, we see upregulation of VEGFR2 on the surface of CAFs by flow cytometry. This interaction is accompanied by an increase in PDO proliferation seen in the coculture conditions. Ongoing

experiments aim to investigate the impact of this relationship spatially using matched patient tissue.
Conclusions: Interactions between cancer cells and CAFs compound the complexity of the biology of the TME and contribute to poor patient outcomes; therefore, we have put forth a model that better represents these interactions through patient matched PDO - CAF cocultures. Using this model, we demonstrate a novel interaction through VEGF that enhances tumor cell proliferation. We introduce a targeted approach to investigating the complex biology of the TME to inform the mechanisms driving cancer biology in individual patients that can also be used to develop novel therapeutic targets.

#5852

Vimentin content associated with shear wave speed in hepatocellular carcinoma: Non-invasive identification of more aggressive tumor phenotypes.

Andrea C. Cortes[1], Kiyoyuki Minamiguchi,[1], Patricia L. Da Costa Lopez[1], Simone Anfossi,[2], Williams Malea L[1], Maria S. Stenkamp[3], Rony Avritscher[1], Natalie W. Fowlkes[4]. *[1]Interventional Radiology, The University of Texas MD Anderson Cancer Center, Houston, TX,[2]SAnfossi@mdanderson.org, The University of Texas MD Anderson Cancer Center, Houston, TX,[3]Experimental Radiation Onc, The University of Texas MD Anderson Cancer Center, Houston, TX,[4]Veterinary Medicine & Surgery, The University of Texas MD Anderson Cancer Center, Houston, TX*

Tumor stromal heterogeneity can negatively impact immune surveillance and treatment outcomes. Current cross-sectional imaging tools rely solely on tumor size and perfusion to monitor therapy and fail to characterize tumor biomechanics. Shear-wave elastography has emerged as a non-invasive technique that can quantify stromal elasticity. The goal of the present study is to characterize the molecular underpinnings associated with shear wave elastography measurements in liver cancer. To this end, rat hepatoma cell line McA-RH7777 stably expressing green fluorescent protein genes (fluc/GFP) were implanted in the left liver lobe of Buffalo rats. Three weeks after tumor implantation, adequate tumor size was verified by B-mode ultrasound. A 7-color panel was developed to assess the

percentage of vimentin, α-smooth muscle actin, IBA-1, S100A4, TGF-β, and glial fibrillary acidic protein (GFAP) in tumor sections. Shear wave elastography data was used to stratify tumor nodules as stiff or soft according to the mean value of the shear wave (3.05 versus 2,26 m/s). Our results showed two distinct tumor phenotypes. Stiffer tumors, as determined by higher shear wave speed measurements on ultrasound, were characterized by higher percentages of vimentin-positive cells, low S100A4 and IBA-1 macrophages expressing TGF-b, and intermediate expression of IBA-1 macrophages and GFAP cells. Slow shear wave speed, characteristic of softer tumors, displayed the opposite phenotype (two-factor ANOVA; $P \leq 0.001$). The most remarkable difference between stiffness phenotypes was the percentage of cells expressing vimentin, with a mean percentage in stiffer tumors of 26.54 compared with 13.68% in softer tumors ($P < 0.003$). Our results indicate that high expression of vimentin is highly correlated with increased shear wave speeds. Given the association between vimentin expression and epithelial-mesenchymal transition a marker of aggressive characteristics of tumor cells (increased migration and invasion), our findings suggest that longitudinal quantification of shear wave speed can be useful to assess functional changes in the stromal component and identify more aggressive tumor phenotypes with a higher likelihood of metastatic potential.

#5854

Suppression of phosphorylated focal adhesion kinase+ (pFAK+) fibroblasts and C-X-C chemokine receptor type 4 (CXCR4) expressing granulocytes is associated with exceptional clinical outcomes in pancreatic ductal adenocarcinoma (PDAC)

John Davelaar, Anser A. Abbas, Angela Minasyan, Omer H. M. Elmadbouh, Natalie Moshayedi, Brent Larson, Nicholas Nissen, Simon Lo, Srinivas Gaddam, Kambiz Kosari, Jun Gong, Andrew Hendifar, Stephen Pandol, Arsen Osipov. *Cedars-Sinai Medical Center, Los Angeles, CA*

Background: PDAC is an aggressive and treatment-refractory cancer due to its desmoplastic and immunosuppressive tumor microenvironment (TME). Overexpression of pFAK, a master regulator of the TME, and CXCR4, a receptor involved immunosuppression and tumor progression, are associated with poorer outcomes in PDAC. Exceptional responders, broadly

defined by extended survival and durable treatment responses, represent a rare subset in PDAC. We hypothesize that the immune and stromal signatures of exceptional responders vary significantly from non-exceptional responders, specifically exhibiting decreased p-FAK and CXCR4 expression and decreased immunosuppressive myeloid phenotypes in the TME.
Methods: We performed correlative quantitative analysis of multiplex immunohistochemistry (mIHC) employing 40 biomarkers on stage I/II PDAC, surgically resected formalin-fixed paraffin-embedded tissues from 9 non-exceptional responders and 11 exceptional responders. Exceptional responders were selected based on degree and duration of disease-free survival or overall survival more than double the historical matched medians. mIHC and image cytometry were used to distinguish and quantify total immune cell populations and colocalize biomarker expression across each distinct cell type. Cell populations and expression levels were compared using unpaired T-tests.
Results: Exceptional responders showed significantly decreased overall pFAK expression ($p=0.02$) and overall CXCR4 expression ($p=0.04$). In exceptional responders, pFAK expression and CXCR4 expression were significantly decreased in immunosuppressive $CD66b^+$ granulocytes ($p=0.01$, $p=0.03$, respectively) and in tumor associated macrophages ($p=0.01$, $p=0.006$, respectively). While not significant, exceptional responders demonstrated a marked decrease in immunosuppressive $pFAK^+$ fibroblasts ($p=0.12$) when compared to non-exceptional responders. No change was seen in the $CD8^+$ T cell infiltration between groups; however, a trend was observed towards an increased proportion of granzyme B^+ $CD3^+$ $CD8^+$ cytotoxic lymphocytes ($p=0.57$) in exceptional responders.
Conclusion: Exceptional responders selected in this preliminary study have significantly lower FAK and CXCR4 expression and markedly reduced populations of immunosuppressive FAK^+ and $CXCR4^+$ myeloid cells. Suppression of pFAK and CXCR4 in fibroblasts and granulocytes, respectively are associated with exceptional clinical outcomes. Future expanded research comparing the distinct TME and genetic signatures of exceptional responders to non-exceptional is warranted.

#5855

Spatial transcriptomics deciphers the cellular society of advanced colorectal cancer

Masahiro Hashimoto[1], Yuki Ozato[2], Yusuke Nakano[1], Tadashi Abe[1], Yuichi Hisamastu[1], Takeo Toshima[1], Yusuke Yonemura[1], Mamoru Uemura[2], Takaaki Masuda[1], Hirofumi Yamamoto[2], Masaki Mori[3], Hidetoshi Eguchi[2], Yuichiro Doki[2], Koshi Mimori[1]. *[1]Department of Surgery, Beppu Hosipital, Kyusyu University, Beppu, Japan,[2]Department of Gastroenterological Surgery, Osaka University, Graduate School of Medicine, Suita, Japan,[3]Tokai University, School of Medicine, Isehara, Japan*

Introduction: In recent years, single-cell RNA sequencing (scRNA-seq) and high-dimensional spatial transcriptomics (ST-seq) have contributed significantly to our understanding of the tumor microenvironment (TME) in many cancers. This is essential for understanding the tumor-stromal crosstalk. Thus, integrating scRNA-seq data with ST-seq data will facilitate understanding intercellular communication in TMEs.
Material and Method: We performed and combined ST-seq in CRC with public scRNA-seq. And, immunohistochemistry (IHC) (HLA-G, CD68, and SPP1) was performed on 20 CRC surgical specimens collected in our hospital. To verify this, we knocked out H2-M3 (HLA-G in humans) in mouse CRC cell lines (MC-38 cells) using the CRISPR/Cas9 system and examined H2-M3 KO tumor volume in xenograft mouse models.
Results: We identified co-localized cells with CRC cells at the invasive front and those in the center based on the spatial distribution estimated by an analytical pipeline, Cell2location. At the invasive front, CRC cells co-localized more frequently with SPP1+ macrophages than other cells. To dissect the molecular machinery and cell types inducing SPP1+ macrophages, we found ligand activity by another pipeline, NicheNet. The prominent signal to SPP1+ macrophages was mediated by several ligand-receptor pairs including HLA-G- immunoglobulin-like transcript (ILT)2/ILT4. Next, we disclosed the effect on CD8+ cells, and SPP1+ macrophages secrete IL-10 suppressing the immune activity of CD8+ T cells. And the ratio of HLA-G-positive cancer cells was predominantly higher in areas with more SPP1+ macrophages by IHC in CRC. In vivo analysis, H2-M3 KO reduced CRC tumor volume and tumor tissue from H2-M3 KO cells exhibited higher SPP1 and CD68 staining compared with wild type cells.

Conclusion: SPP1+ macrophages and cancer cells secreting high levels of HLA-G may represent targets to improve the prognosis of patients with CRC. Further analysis is currently underway with a focus on early-stage cancer in carcinoma in adenoma.

Immunotherapy and Cellular Interactions in the Tumor Microenvironment

#5860
ZEB1-driven reconstruction of the hyaluronan network establishes a pro-metastatic microenvironment in lung adenocarcinoma.

Sieun Lee[1], Jihye Park[1], Eun Ju Kim[1], Sungsoo Park[2], Jonathan M. Kurie[3], Young-Ho Ahn[1]. *[1]Ewha Womans University, Seoul, Korea, Republic of,[2]Deargen, Inc., Daejeon, Korea, Republic of,[3]University of Texas MD Anderson Cancer Center, Houston, TX*

Hyaluronan, one of the major components of the extracellular matrix (ECM), surrounds and protects neighboring cells from diverse stresses. Hyaluronan promotes epithelial-to-mesenchymal transition (EMT) and metastasis in various epithelial cancers. However, the mechanism by which the hyaluronan network built up by cancer cells regulates cancer progression and metastasis in the tumor microenvironment has not been elucidated in detail. In this study, ITIH2, a hyaluronan-binding protein that participates in building a hyaluronan network, was confirmed to be secreted from mesenchymal-like lung cancer cells when co-cultured with cancer-associated fibroblasts. ITIH2 was transcriptionally upregulated by ZEB1, an EMT-inducing transcription factor. Hyaluronic acid synthase-2 (HAS2) was also up-regulated by ZEB1, and the expression of HAS2 and ZEB1 showed a positive correlation in the TCGA database. In addition, ZEB1 controlled alternative splicing and isoform expression of CD44, a hyaluronan receptor. Interestingly, ITIH2 knockdown and 4-methylumbelliferone (4-MU), a HAS inhibitor, reduced the formation of hyaluronan cables and inhibited the migration and invasion of lung cancer cells. Likewise, when lung cancer cells were treated with “Compound S,” an ITIH2 inhibitor predicted by a deep learning-based drug-target interaction algorithm, the formation of hyaluronan cables and cell migration were suppressed. In addition, the ITIH2 inhibitor prevented the growth of metastatic tumors in an orthotopic

lung cancer mouse model. Collectively, the EMT signal controlled by ZEB1 establishes the pro-metastatic hyaluronan network in the tumor microenvironment, suggesting a novel strategy for targeting the hyaluronan network to suppress lung cancer progression and metastasis.

#5861

Tumor cell-intrinsic factors promoting fibrotic tumor microenvironment in gastric cancer

Takashi Semba[1], Yiling Tong[1], Feng Wei[1], Atsuko Yonemura[1], Tadahito Yasuda[1], Tomoyuki Uchihara[1], Huaito Wang[1], Hideo Baba[2], Takatsugu Ishimoto[1]. *[1]Gastrointestinal cancer biology, International Research Institute of Medical Sciences, Kumamoto University, Kumamoto, Japan,[2]Department of Gastroenterological Surgery, Graduate School of Medical Sciences, Kumamoto University, Kumamoto, Japan*

Background: Gastric cancer (GC) is one of the leading causes of death in the world. Evidence has shown over the past decade that cancer-associated fibroblasts (CAFs) play essential roles in various types of cancers, including GC, such as tumorigenesis, therapy resistance, and immunosuppression, which contribute to the progress of tumors. Although GC tumors are known to be enriched with stroma, the molecular mechanisms of how GC tumors foster the fibrotic milieu is still largely unknown. Here we analyzed a large-scale genomic and transcriptomic dataset of GC to identify GC tumor cell-intrinsic factors for developing fibroblast-rich microenvironments.
Methods: We analyzed GC patient samples with gene expression data and copy number variation profiles from the Asian Cancer Research Group (ACRG) (N = 271). The microenvironment cell populations-counter (MCP-counter) method was used for transcriptome deconvolution to estimate the population of fibroblasts and immune cells in GC tumors. Genes with q value < 0.05 and fold change > 1.5 were defined as differentially expressed genes (DEGs) and identified using the Subio Platform. The copy number amplified genes found in more than 3% of the samples were selected as amplified genes. Pathway and process enrichment analysis and protein-protein interaction analysis were performed using Metascape.
Results: We analyzed MCP-counter outputs and observed a fibroblast-enriched population with few infiltrations of anti-tumor immune cells, such as CD8 T cells and cytotoxic T cells in GC patients, suggesting the

immunosuppressive role of CAFs in the GC tumor. By analyzing 933 DEGs upregulated in fibroblast-high patients, we found 96 genes with frequent copy number amplification that were not listed on the curated stroma and extracellular matrix-related genes and thus potentially tumor cell-intrinsic genes correlated with the abundance of the stroma. Pathway and protein-interaction analyses revealed that G protein-coupled receptor (GPCR) signaling pathway was enriched in these genes, including *HTR2A*, *AGTR1*, *FZD1*, *CALCRL*, and *NBEA* with strong correlations between fibroblast score (Spearman's $r > 0.55$), implying that these signaling in GC tumor cells contribute to promoting fibroblast-enriched microenvironment. Conclusions: Bioinformatic analyses of a publicly available genomic and transcriptomic dataset revealed a fibroblast-rich and immune-excluded population in GC patients. Several GPCR signaling in tumor cells were strongly correlated with fibroblast abundance in tumors, and these signaling pathways have potential roles in promoting the stroma-rich GC microenvironment.

#5862

ABCB5 knockdown suppresses tumor-intrinsic expression of immune checkpoint regulators PD-1 and PD-L1 in hepatocellular carcinoma (HCC)

Chun Philip Yeung[1], Brian J. Wilson[2], Yuzuru Sasamoto[3], Ana Maria Waaga-Gasser[4], Svetlana Karpova[5], Qin Guo[5], Natasha Y. Frank[5], Markus H. Frank[6]. *[1]Medical Sciences, Harvard Medical School, Boston, MA,[2]Transplant Research Program, Boston Children's Hospital, Boston, MA,[3]Ophthalmology, Boston University School of Medicine, Boston, MA,[4]Medicine, Brigham and Women's Hospital, Boston, MA,[5]Genetics, Harvard Medical School, Boston, MA,[6]Dermatology, Harvard Medical School, Boston, MA*

ATP-binding cassette member B5 (ABCB5) identifies cancer-initiating cells (CICs) in multiple malignancies, including malignant melanoma, colorectal cancer, glioblastoma, and hepatocellular carcinoma (HCC). In human melanoma, ABCB5-positive CIC subpopulations have been shown to preferentially express the immune checkpoint molecules PD-1 and PD-L1, and tumor-intrinsic PD-1 receptor functions have been found to promote

tumor growth, even in mice lacking adaptive immunity. In HCC, where ABCB5 mediates CIC chemoresistance, PD-1 expression has also recently been identified. However, whether ABCB5 regulates tumor-intrinsic PD-1 expression in HCC or other malignancies is currently unknown. Here, we employed RNA interference in Hep G2 HCC cells with high endogenous ABCB5 expression to study the potential role of ABCB5 in regulating PD-1 expression, utilizing the ABCB5 shRNA target sequence GCTGGAAAGATAGCAACTGAA for ABCB5 knockdown (KD) as described previously. Endogenous ABCB5 levels in ABCB5-KD cells were successfully reduced by 92.8% compared to controls. Investigation of the effects of ABCB5-KD on tumor-intrinsic immune checkpoint molecule expression and on expression of the HCC-CIC marker GRN revealed that ABCB5-KD significantly reduced PD-1 expression by 98.0%, and PD-L1 expression by 62.8% compared to controls. Expression of GRN was also significantly reduced in ABCB5-KD cells by 78.8% compared to controls, suggesting ABCB5 KD-dependent loss of CIC phenotype. Injection of ABCB5-KD cells in NSG mice showed 32.3% reduction in tumor size at endpoint (6 weeks) compared to controls (728.7 ± 199.3mm^3 vs 1076.0 ± 450.9 mm^3, mean ± SD; $p<0.005$, repeated measures ANOVA) and 8.53% reduction in tumor weight at endpoint (0.47 ± 0.21g vs 0.51 ± 0.21g, mean ± SD). These results provide initial evidence in an HCC cell line model system that ABCB5 functionally regulates tumor-intrinsic PD-1 and PD-L1 expression. They therefore suggest that ABCB5 blockade represents a novel therapeutic strategy for targeted inhibition of pro-tumorigenic tumor-intrinsic PD-1/PD-L1 expression, with important additional implications for immune checkpoint-targeted cancer immunotherapy.

#5863

Blockade of tumor glucocorticoid production inhibits Treg function and tumor growth

Shizuka Otsuka[1], Matthew D. Taves[2], Kaitlynn M. Donahue[1], Jonathan D. Ashwell[1]. *[1]NIH-NCI, Bethesda, MD,[2]Department of Neurobiology & Behavior, Cornell University, Ithaca, NY*

Glucocorticoids (GCs) are steroid hormones with potent immunosuppressive properties. GCs are primary produced from cholesterol in the adrenals via the *de novo* synthetic pathway. In some tissues, however,

there is also a recycling pathway in which the enzyme 11β-HSD1 generates GCs from the inactive metabolites dehydrocorticosterone (rodent) or cortisone (human). Here we find that multiple tumor types produce GCs via 11β-HSD1 *in vitro* and *in vivo*. We used CRISPR/Cas9 technology to knock out *Hsd11b1* in GC-producing tumor cell lines and found that lack of 11β-HSD1 in B16 melanoma, Panc02 pancreatic adenocarcinoma, and MC38 colon carcinoma lines reduced their growth *in vivo*. Reduced tumor growth corresponded with increased expression of the activation marker CD44 and production of the effector cytokines IFNγ and TNFα by tumor-infiltrating $CD8^+$ T cells (TILs). Rather than directly suppressing effector cell function, recent findings have suggested that GCs instead act primarily by activating Treg cells, and that these Treg are responsible for inhibition of effector cell function. Consistent with this, we found that tumor-derived GCs upregulate Treg expression of miRNA-342, which downregulates the mTOR component Rictor and activates Treg activity. A role of tumor-derived GCs in enhancing Treg function was demonstrated by inoculating tumor cells into mice with Treg-specific glucocorticoid receptor deficiency ($GR^{Foxp3Cre}$ mice). Notably, growth of tumors was reduced in $GR^{Foxp3Cre}$ mice, along with increased $CD8^+$ TIL activation. Importantly, pharmacologic inhibition of 11β-HSD1 reduced WT tumor growth to the same degree as knockout of 11β-HSD1, and rendered immunotherapy-resistant tumors susceptible to inhibition with anti-PD-1 antibodies. Given that 11β-HSD1 expression is upregulated in many human tumors, these data suggest that its inhibition, which has been accomplished in a number of phase 3 clinical trials for other indications and is well-tolerated, may be beneficial in their treatment.

#5864

An angiogenic target of immune exclusion with checkpoint blockade in melanoma

Saba Tabasum[1], Dinesh Thapa[1], Anita Giobbie-Hurder[1], Jason L. Weirather[1], Xinqi Wu[1], Marco Campisi[2], Xiaoyun Li[1], Jingjing Li[1], Michael P. Manos[1], David A. Barbie[1], F. Stephen Hodi[1]. *[1]Medical Oncology, Dana-Farber Cancer Institute, Boston, MA,[2]Dana-Farber Cancer Institute, Boston, MA*

With the development of immune checkpoint blockade to treat a variety of malignancies, better predictive biomarkers as well as new targets to further improve anti-tumor immunity remains a need. Our understanding of the role of angiogenesis in immune regulation continues to improve, and combinations of anti-angiogenesis and immune checkpoint blockade demonstrate improved clinical efficacy, as well as mechanisms for improved immune cell trafficking. Tumor biopsies from a phase I study with 46 advanced melanoma patients treated with Ipilimumab and Bevacizumab combination (Ipi-Bev) therapy, revealed activated endothelium accompanied by lymphocyte infiltration. To discover possible targets involved in the observed clinical benefit, a serological screen was performed using human protein arrays with post-treatment plasma samples of long-term patients with clinical benefit to Ipi-Bev therapy (Wu et. al., 2017; Hodi et. al., 2014). EDIL3 (EGF Like Repeats and Discoidin Domains 3), a pro-angiogenic extracellular matrix protein, was identified. Humoral responses against EDIL3 were associated with favorable clinical outcomes including improved response rates *(p=0.003)* and overall survival *(p=0.03)* to Ipi-Bev therapy. The anti-EDIL3 response was also observed to be significantly *(p=0.03)* related to Ipi-Bev treatment when compared with patients treated with Ipilimumab alone, anti-PD1 therapy alone, or the combination of Ipilimumab and Nivolumab in a combined analysis. Transcriptome analyses of TCGA SKCM (n=469) and BMS Checkmate 064 trial (n=90) related upregulated EDIL3 expression with enrichment of EMT, TGFβ signaling in fibroblasts, and angiogenesis signatures. Interestingly, TIDE analysis demonstrated a role for EDIL3 in T cell exclusion and immunosuppressive cancer-associated fibroblasts (CAFs) as its source in the tumor microenvironment. EDIL3 was also predicted as a biomarker of non-response to immune checkpoint blockade treatment. *In vitro* studies confirmed the upregulation of EDIL3 expression and secretion by patient-derived CAFs along with its role in modulating TGFβ1 mediated EMT. Mechanistically, EDIL3 was found to interfere with leukocyte-endothelial interactions by disturbing LFA-1/ICAM1 mediated adhesion and inhibited T cell transmigration in 2-D and microfluidic 3-D coculture studies with patient-derived tumor endothelial cells. Our findings suggest that the humoral response against EDIL3 may serve as one of the underlying mechanisms involved in effectuating an excluded to an inflamed phenotype observed in responders of checkpoint blockade treatment. This

study develops EDIL3 as a potential target to enhance cytotoxic immune responses and improve the outcomes of combination immune therapy. Studies are ongoing for targeted inhibition of EDIL3 with implications for therapeutic application to promote anti-tumor immunity.

#5865

Combinatorial activity of amivantamab and pembrolizumab in head and neck squamous cell carcinoma and lung squamous cell carcinoma expressing wild-type EGFR and MET

Sun Min Lim[1], Chun-Bong Synn[1], Seong-san Kang[2], DongKwon Kim[1], Soo-Hwan Lee[2], Sujeong Baek[1], Seung Min Yang[3], Yu Jin Han[3], Mi hyun Kim[3], Heekyung Han[1], Kwangmin Na[1], Young Taek Kim[1], Sungwoo Lee[2], Mi Ran Yun[4], Jae Hwan Kim[1], Youngseon Byeon[1], Young Seob Kim[1], Jii Bum Lee[5], Ji Yun Lee[5], Chang Gon Kim[5], Min Hee Hong[5], Kyoung-Ho Pyo[4], Joshua Curtin[6], Bharvin Patel[6], Isabelle Bergiers[7]. *[1]Yonsei University College of Medicine, Seoul, Korea, Republic of,[2]JEUK Institute for Cancer Research, Seoul, Korea, Republic of,[3]Severance Biomedical Science Institute, Yonsei University College of Medicine, Seoul, Korea, Republic of,[4]Yonsei New Il Han Institute for Integrative Lung Cancer Research, Seoul, Korea, Republic of,[5]Division of Medical Oncology, Department of Internal Medicine, Yonsei Cancer Center, Severance Hospital, Yonsei University College of Medicine, Seoul, Korea, Republic of,[6]Janssen R&D, Spring House, PA,[7]Janssen R&D, Beerse, Belgium*

Introduction: Unmet needs exist for immunotherapy targeting PD-1/PD-L1 in head and neck squamous cell carcinoma (HNSCC) and lung squamous cell carcinoma (LUSC) due to its suboptimal response. Amivantamab, a bispecific antibody targeting epidermal growth factor receptor (*EGFR*) and c-Met, has been demonstrated to induce antibody-dependent cytotoxicity and trogocytosis in tumor cells. We hypothesized that combination of amivantamab with pembrolizumab may synergistically enhance antitumor immunity. In this study, we present comprehensive immunomodulatory and synergistic antitumor efficacy of amivantamab and pembrolizumab in humanized HNSCC and LUSC mice models.
Methods: EGFR and MET-expressing tumors from a HNSCC and a LUSC patient were transplanted into Hu-CD34-NSG to establish humanized

patient-derived xenograft (PDX) models. Tumor-bearing PDXs were treated with vehicle, pembrolizumab (10mpk, Q5D, n=10), amivantamab (10mpk, BIW, n=10), or a combination of pembrolizumab and amivantamab (n=10). Analysis of immune modulatory responses within the tumor microenvironment (TME) using multiplexed IHC, flow cytometry, and single cell RNA sequencing was performed.
Results: Combination of amivantamab and pembrolizumab showed a significant reduction of tumor volume ($p<0.001$) compared to vehicle or single treatment in both models. Additionally, significantly longer survival was observed for combination treated compared to the vehicle treated groups ($p<0.0001$). Multispectral imaging of tumor indicated that granzyme B-producing $CD8^+$ T cells were significantly increased within the tumor in the combination group ($p<0.01$). Further analysis of T cell subsets suggested that central memory type $CD8^+$ T cells were increased upon combination treatment. This group also demonstrated significantly higher CEA-tetramer positive $CD8^+$ T cells in the tumor ($p<0.01$), suggesting that cytotoxic T cells recognizing tumor specific antigens enhanced antitumor immune response. Single cell RNA sequencing analysis of HNSCC showed that an $EGFR^{high}MET^{high}$ cluster was enriched in the TME after pembrolizumab treatment. This subcluster had elevated glycolysis and lactic acid pathway-related genes compared to $EGFR^{low}MET^{low}$ cluster. Lactate transporter, MCT4 (SLC16A3) and LDHA genes were dramatically increased in the $EGFR^{high}MET^{high}$ cluster. Elevated lactic acid pathway may lead to immune evasion in the tumor, dampening the activity of pembrolizumab. Interestingly, combination treatment with amivantamab could reduce $EGFR^{high}MET^{high}$ cluster, and could effectively control tumor *via* creating favorable immune TME.
Conclusion: Our study demonstrated combinatorial benefits of amivantamab and pembrolizumab by effectively remodeling TME, providing a preclinical rationale to clinically combine amivantamab and PD-1 blockade treatments.

#5866

Mavorixafor enhances apoptosis of tumor cells treated with ibrutinib or venetoclax in diffuse large B-cell lymphoma, follicular lymphoma, mantle cell lymphoma, and chronic lymphocytic leukemia

Tom Kruitwagen[1], Thalia Martins Rebelo[1], Barbara Maierhofer[2], Gerwin Heller[3], Halenya Monticelli[2], Arthur G. Taveras[4], Chi Nguyen[2]. *[1]Former Employee at X4 Pharmaceuticals (Austria) GmbH, Vienna, Austria,[2]X4 Pharmaceuticals (Austria) GmbH, Vienna, Austria,[3]Department of Medicine, Division of Oncology, Medical University of Vienna, Vienna, Austria,[4]X4 Pharmaceuticals, Inc., Boston, MA*

Despite advances in therapies for B-cell lymphoma, patients may still develop resistance and often relapse. Contributing factors may include interactions between lymphoma cells (LCs) or leukemia cells and bone marrow microenvironment (BMM). Overexpression of $CXCR4^{WT}$ and its ligand CXCL12 promote LC-BMM interactions, contributing to disease severity in lymphomas or leukemia such as diffuse large B-cell lymphoma (DLBCL), chronic lymphocytic leukemia (CLL), follicular lymphoma (FL), and mantle cell lymphoma (MCL). Mavorixafor is an investigational oral CXCR4 antagonist being evaluated in combination with the Bruton tyrosine kinase (BTK) inhibitor ibrutinib in patients with Waldenström's macroglobulinemia (WM). In preclinical models of $MYD88^{L265P}$ $CXCR4^{WT}$ WM, mavorixafor restored sensitivity of WM cells to B-cell-targeted therapies in coculture of WM cells and bone marrow stromal cells (BMSCs); however, the effects of mavorixafor on other lymphomas with $CXCR4^{WT}$ have not been evaluated. We report the effects of mavorixafor alone or in combination with B-cell─targeted therapies on LCs in an *in vitro* preclinical model and assess the role of BMM in the pathogenesis of B-cell lymphomas in an *in vitro* coculture model of LCs and BMSCs. Bioinformatic analysis of publicly available gene expression datasets GSE11318 and GSE32918 showed patients with DLBCL and $CXCR4^{hi}$ have significantly inferior survival probability compared with those with $CXCR4^{low}$ ($P<.001$ and $P<.05$, respectively). *In vitro* studies assessing effects of targeting CXCR4 with mavorixafor showed apoptosis of $CXCR4^{+}$ LCs *OCILY19* (DLBCL), *MEC1* (CLL), *MINO* (MCL), and *DOHH2* (FL) cells increased by ≈10%─60%. The apoptosis of LCs was further enhanced by ≈5%─60% when treated with mavorixafor in combination with ibrutinib or venetoclax compared to ibrutinib or venetoclax alone. Coculture of LCs with BMSCs reduced the sensitivity of LCs to apoptosis-inducing effects of ibrutinib and venetoclax. Combining mavorixafor with ibrutinib or

venetoclax restored sensitivity of LCs to apoptosis-inducing effects of the tested B-cell–targeted inhibitors. Mavorixafor also inhibited migration of LCs toward CXCL12, suggesting prevention of the homing of LCs to protective niche. Overall, our findings suggest the contribution of *CXCR4*^{WT} to pathogenicity of LCs. This is the first *in vitro* study to show that reduced sensitivity of LCs against B-cell-targeted therapies conferred by BMSCs can be overcome by inhibition of the CXCL12-CXCR4 axis with mavorixafor. Our study provides supporting evidence for further exploration of mavorixafor alone or in combination with other B-cell-targeted therapies in the treatment of lymphomas and leukemias. Further studies using additional LC lines and/or primary patient cells are warranted to support these findings.

#5867

Multimodal analysis of glioblastoma identifies the additional function of CXCL12 for modulating GBM resistance and immunosuppressive microenvironment

Chan-Chuan Liu[1], Chia-Hung Chien[2], Wen-Bin Yang[3], Jian-Ying Chuang[4], Kwang-Yu Chang[5]. *[1]National Institute of Cancer Research, National Health Research Institutes, Tainan City, Taiwan,[2]National Institute of Cancer Research; School of Medicine, National Health Research Institutes; I-Shou University, Tainan City, Taiwan,[3]TMU Research Center of Neuroscience, Taipei Medical University, Taipei City, Taiwan,[4]TMU Research Center of Neuroscience, the Ph.D. Program for Neural Regenerative Medicine, College of, Taipei Medical University, Taipei City, Taiwan,[5]National Institute of Cancer Research; Department of Oncology, National Cheng Kung University Hospit, National Health Research Institutes; National Cheng Kung University, Tainan City, Taiwan*

Glioblastoma (GBM), a WHO Grade IV glioma, is the most common and aggressive primary brain tumor. Despite the standard of care consisting of surgery removal following radio- and chemo- therapy, the prognosis of GBM patients remain dismal. The interplay between GBM cells and its microenvironment contributes to maintaining the cancer stemness, developing resistance, and forming immunosuppression. GBM-associated macrophages (GAMs) are recruited to the GBM microenvironment by

cytokines/chemokines. Conversely, GAMs may promote GBM progression. Therefore, we hypothesized that GBM cells modulated immune microenvironment via macrophage activation. We integrated the bulk RNA sequencing (seq.) of the paired primary-recurrent GBM specimens, single-cell RNA seq., and *in vitro* validation to investigate the hypothesis. The bulk RNA seq. of the paired primary-recurrent GBM specimens indicated that recurrent GBM enhanced the neuroinflammation pathway. Among the components, we found that CXCL12, also known as stromal cell-derived factor 1 was accumulated during GBM progression and up-regulated in temozolomide (TMZ)-resistant GBM cells. On the other hand, the newly CXCL12 receptor CXCR7 may act as a scavenger for CXCL12 during developing TMZ resistance in GBM. The bulk RNA sequencing seq. from primary-recurrent GBM specimens showed the decrement of CXCR7. Single-cell RNA seq. of GBM patients' specimens indicated CXCR7 dominantly expressed in GBM cells other than normal neural and immune cells. Developing TMZ resistance in GBM cell lines down-regulated CXCR7 expression. Furthermore, silencing CXCR7 attenuated TMZ cytotoxicity while combining CXCR7 agonists (Plerixafor, VUF11207, and TC14012) and TMZ enhanced TMZ cytotoxicity. Otherwise, the GBM-associated CXCL12 activated M0 macrophages into GAMs by facilitating macrophage proliferation and inducing pro-tumor factors, including interleukine (IL)-1β and its receptors, IL-6, MMP9, and immune checkpoint PD-L1. Mechanistically, GBM-associated CXCL12 upregulated PD-L1 in GAMs via NF-κB. Accordingly, by multimodal analysis, CXCL12 was identified with the additional role in regulating resistance in GBM cells and GBM microenvironment. Also, re-activating CXCR7 may overcome the resistance to TMZ and immune checkpoint blockade therapy. Combination of CXCR7 activation with current therapy and immunotherapy may be an effective strategy for improving the prognosis of primary GBM patients.

#5868

Uncovering key microenvironmental features for immunotherapy response at the subclonal level in pancreatic cancer

Er-Yen Yen, I-Lin Ho, Chieh-Yuan Li, Charles Dyke, Shan Jiang, Francesca Citron, Sergio Attanasio, Rutvi Shah, Ko-Chien Chen, Giulio Draetta, Andrea Viale. *MD Anderson Cancer Center, Houston, TX*

The lack of suitable experimental approaches to investigate and model functional heterogeneity in vivo has had a profound negative impact on our understanding of how heterogeneity affects the response to immunotherapy. To bridge this technological gap, we leverage a new platform that visualizes the spatial architecture of subclones and microenvironments. To study heterogeneous populations of cells and their clonal dynamics in vivo, we performed barcode lineage tracing with next-generation sequencing analysis. It allows a quantitative evaluation of the spatial distribution and temporal clonal dynamic in vivo with multiple pharmacological perturbations, such as immune checkpoint blockade (ICB). We found that treatment with a PD1 inhibitor, despite a limited effect on tumor volume, induced dramatic changes in tumor clonal architecture. Furthermore, we revealed that subclones from well-defined geographical domains in vivo share differential behavior upon immune checkpoint blockade (ICB). By visualizing 40 different markers with multiplexed staining technology, we further identified that the microenvironment also exhibits a high level of spatial heterogeneity. Therefore, we coupled spatial barcode sequencing with high-content imaging and revealed the differential microenvironment feature of sensitive and resistant clones. We will further explore the mechanisms of immune evasion at the subclonal level. Through isolation and deep characterization of clonal lineages endowed with a distinct ability to engage the immune response, we hope to identify new vulnerabilities to overcome resistance to ICB.

#5869

The concordant disruption of B7/CD28 immune regulators predicts the prognosis of oral carcinoma

Sih-Rou Chang. *National Yang Ming Chiao Tung University, Taipei, Taiwan*

Immune-escape is a critical factor determining the survival of malignancies including oral squamous cell carcinoma (OSCC). The immune escape of cancer cells may be driven by B7/CD28 family members and others on the tumor cells that form ligand-inhibitory receptor complexes with immune cells. Since the family members of B7/CD28 can functionally compensate, the concomitant disruption of multiple B7/CD28 family members in OSCC pathogenesis remains elusive. RNAseq performed on OSCC and paired oral mucosa retrieved the transcriptome of OSCC, and algorithms signified the

general alterations of T cell population and the increase of macrophage population in tumors relative to controls. Upregulation of CD80, CD86, PD-L1, PD-L2, CD276 and CTLA4, and downregulation of L-ICOS in OSCC relative to normal mucosa was noted. In addition, there was a high concordance in the expression profile across the dysregulated regulators. The co-upregulation of CD276 and CTLA4 was associated with the decrease of T helper and NK cell population, and the increase of Treg and myeloid dendritic cell population. Interestingly, tumors harboring higher PD-L1 and/or PD-L2 expression accompany with lower ICOS or PD1 expression exhibited worse prognosis. In combination with these immunity features in primary tumors, the survival of patients with lymph node metastasis was further worsened. In the isografic models of murine OSCC cell lines, the decrease of CD4+T population in the lymph node and increase of myeloid dendritic cell population in the spleen were induced in the host mice. Many miRNAs are involved in the modulation of immune escape for malignancies. With the treatment of inhibitors against oncogenic miRNAs which enabled the OSCC suppression, the inhibitors of miR-146a and miR-211 also resulted in the down-regulation in the protein expression of multiple B7/CD28 members. This study concludes the eminent co-disruption of B7/CD28 members in OSCC tumors, which would confound the patient survival. The efficacy of miRNA inhibitors in abrogating oncogenicity and B7/CD28 members could be a therapeutic strategy.

#5870

T-cell factor-4 variants regulate PD-L1 expression in liver cancer cells

Hironori Koga[1], Yasuko Imamura[1], Toshimitsu Tanaka[1], Hideki Iwamoto[1], Toru Nakamura[1], Atsutaka Masuda[1], Takahiko Sakaue[1], Hiroyuki Suzuki[1], Hirohisa Yano[2], Takumi Kawaguchi[1]. *[1]Kurume Univ. School of Medicine, Kurume, Japan,[2]Pathology, Kurume Univ. School of Medicine, Kurume, Japan*

Background: We previously identified 14 isoforms of T-cell factor (TCF)-4, a key transcriptional factor in the Wnt signaling pathway, from human hepatocellular carcinoma (HCC) cell lines (Exp Cell Res 2011). The TCF-4J and K pair has been characterized based on the presence (K) or absence (J) of a conserved SxxSS motif at the head of exon 9. TCF-4J-overexpressing HCC cells (J cells) exhibited high tumorigenic potential in

contrast to TCF-4K-overexpressing cells (K cells) (PLoS ONE 2012); however, resistance to anti-cancer agents was more prominent in K cells than J cells. Another analysis demonstrated that loss of exon 4 increased resistance to chemotherapeutic agents and induced epithelial-mesenchymal transition (EMT) (Liver Int 2013). EMT and the expression of programmed cell death 1-ligand 1 (PD-L1) is closely associated with each other, and our preliminary study revealed that EMT was regulated by TCF-4 variants, suggesting possible involvement of the variants in the regulation of PD-L1 expression. In general, PD-L1 is known to be upregulated by hypoxia-inducible factor-1α (HIF-1α) under hypoxic conditions. Therefore, if the TCF-4 variants regulate PD-L1 expression under normoxia, it would be a unique mechanism bridging the Wnt signaling pathway and the tumor immune microenvironment (TIME).
Aim: To assess whether or not the TCF-4 variants regulate the expression of PD-L1 in cancer cells under normoxia.
Methods: HAK-1A, a well-differentiated HCC cell line (Hepatology 1993), was used in this study. TCF-4K mutants (S269A, S272A, and S273A) were prepared with the conversion of serine (S) in the SxxSS motif to alanine (A) by site-directed mutagenesis. HAK-1A-derived stable clones overexpressing TCF-4J, K, and K-mutants (S269A, S272A, and S273A cells, respectively) were established. Empty vector-transfected mock cells (EV cells) were used as a control. Western blot analysis and real-time RT-PCR were employed to evaluate protein and mRNA expression levels, respectively.
Results: J cells and K cells expressed PD-L1 mRNA 2-fold and 4-fold of that in the EV cells, respectively. Of note, the PD-L1 expression mRNA was enhanced up to 11-fold in S269A cells, 11-fold in S272A cells, and 17-fold in S273A cells. The increased mRNA expressions were verified in protein levels.
Conclusion: PD-L1 expression was regulated by TCF-4 variants in liver cancer cells under normoxic conditions. The finding suggests that the Wnt signaling pathway fine-tunes the TIME by regulating the expression levels of PD-L1 in a HIF-1α-independent manner.

#5871
Pan-cancer myeloid cell analysis at the single cell level reveals the influence of distinct organ sites in myeloid cell phenotypes and support

targeting S100A4 to reverse immune suppression

Nourhan Abdelfattah[1], Parveen Kumar[2], Caiyi Wang[1], Jia-Shiun Leu[1], David Baskin[1], William Flynn[2], Ruli Gao[1], Kumar Pichumani[1], Omkar Ijare[1], Stephanie Wood[1], Suzanne Powell[1], David Haviland[1], Brittany Parker Kerrigan[3], Frederick Lang[3], Sujit Prabhu[3], Kristin Huntoon[3], Wen Jiang[3], Betty Kim[3], Joshy George[2], Kyuson Yun[1]. *[1]Houston Methodist Research Institute, Houston, TX,[2]The Jackson Laboratory, Farmington, CT,[3]MD Anderson, Houston, TX*

With abundant pro-tumorigenic myeloid cells and few tumoricidal tumor-infiltrating lymphocytes (<5%), GBM is representative of "immune cold" tumors. As such, many different types of immunotherapies have failed to show significant benefits for most glioma patients. Hence, a better understanding of drivers of the immune suppressive microenvironment in GBM and other immune cold tumors is urgently needed to guide future immunotherapy development and application. We recently analyzed 201,986 human glioma and immune cells from 44 tissue fragments from 18 human glioma patients, and present a comprehensive and high-resolution cellular, molecular, and spatial heterogeneity atlas of human glioma. We report an extensive spatial and molecular heterogeneity of glioma and immune cells within the same patient. In addition, we discovered that cell:cell communication between glioma:myeloid cells is considerably more robust than glioma:T-cells, indicating that myeloid cells form a communication hub *in vivo*. To gain a deeper understanding of these important immune cells, we analyzed 83,479 glioma-infiltrating myeloid cells and identified 9 molecularly distinct myeloid subtypes: 3 microglia subtypes, 3 bone marrow-derived macrophage (BMDM) subtypes, MDSCs, neutrophils, and dendritic cells. Notably, we found that five of these myeloid cell subtype gene signatures are significant predictors of glioma patient survival, independent of glioma cell mutational profiles or gene expression patterns. Leveraging our dataset, we also identified a novel immunotherapy target that is highly expressed in immune-suppressive macrophages and T cells but not in anti-tumor leukocytes: *S100A4*. We provide both *in vitro* and *in vivo* evidence that *S100a4* deletion in stromal cells is sufficient to reprogram the immune microenvironment and significantly extend the survival of two independent glioma models. To

broaden the potential impact of targeting S100A4 as a selective modulator of immune suppressive leukocytes, we compared the molecular signatures of glioma-associated myeloid cells to those from 12 other cancer types and peripheral blood myeloid cells. We found that *S100A4* expression pattern is highly consistent among all tumor types, where its expression is highest in the monocytes and MDSCs and low in most DCs and tissue-resident macrophages. Our preliminary analysis also shows that myeloid cells in gliomas are molecularly distinct from corresponding cell types in other cancers, strongly indicating the role brain microenvironment in influencing the infiltrating BMDM maturation and polarization.

#5872

Spatial immunophenotypes contribute to predict survival of triple-negative breast cancer assessed as Miller-Payne grade 4 and N0 after neoadjuvant therapy

Jianli Ma[1], Yuwei Deng[2], Dawei Chen[1], Xiaomei Li[3], Zhiyong Yu[4], Haibo Wang[5], Lei Zhong[6], Yingjie Li[7], Chengqin Wang[8], Xiaoping Zhou[2], Xiang Li[2], Qingyuan Zhang[2], Jinming Yu[1]. *[1]Radiation Oncology, Shandong University Cancer Center, Jinan, China,[2]Medical Oncology, Harbin Medical University Cancer Hospital, Harbin, China,[3]Pathology, Harbin Medical University Cancer Hospital, Harbin, China,[4]Breast Cancer Center, Shandong University Cancer Center, Jinan, China,[5]Breast Disease Center, The Affiliated Hospital of Qingdao University, Qingdao, China,[6]Breast Surgery, the Second Affiliated Hospital of Harbin Medical University, Harbin, China,[7]Pathology, the Second Affiliated Hospital of Harbin Medical University, Harbin, China,[8]Pathology, the Affiliated Hospital of Qingdao University, Qingdao, China*

Objectives Some Miller-Payne 4 and N0 patients with triple-negative breast cancer (TNBC) after neoadjuvant chemotherapy (NACT) who had better survival should avoid treatment escalation. We aimed to identify these patients based on spatial distributions of immunophenotypes at initial diagnosis.

Methods We retrospectively analyzed 272 TNBC patients with Miller-Payne grade 4/5 and N0 for tumor-infiltrating lymphocytes (TILs) in relation to clinical survival. The spatial immunophenotypes were analyzed

by multiplexed ion beam imaging by time of flight combined with proteomic. A prognostic classifier was established by the random forest algorithm.
Results The 5-year disease-free survival (DFS) was 63.8% for Miller-Payne 4 and 83.0% for Miller-Payne 5 (p=0.003), and overall survival (OS) was 71.0% and 85.5% respectively (p=0.007). High TILs were significantly associated with better DFS and OS in the Miller-Payne 4 patients (both p=0.016). Spatially, Miller-Payne 4 with good prognosis exhibited inflamed phenotype, with dominant CD8+ T cells on tumor center, few scattered CD68+ myeloid-derived cells far away from T cells, and deposit of increased lymphocyte activate molecules. Miller-Payne 4 with poor prognosis presented excluded phenotype, with few CD8+ T cells restricted to invasive margin, high density of $CD14^{+}CD68^{+}CD11c^{+}$ myeloid cells with related molecules. These spatial immunophenotypes provided a good classifier model (AUC=0.975) to identify Miller-Payne 4 patients with different prognosis. We also observed similar signatures in Miller-Payne 5.
Conclusion Spatial immunophenotypes may indicate the prognosis in TNBC assessed as Miller-Payne 4 and N0.

#5873
LDH inhibition boosts effector T cells while destabilizing regulatory T cells and improves responses to CTLA-4 blockade
Svena Verma[1], Inna Serganova[1], Lauren Dong[2], Sadna Budhu[2], Levi Mangarin[3], Roberta Zappasodi[4], Taha Merghoub[5], Jedd D. Wolchok[6].
[1]Weill Cornell Medicine, New York, NY,[2]Pharmacology, Weill Cornell Medicine, New York, NY,[3]Meyer Cancer Center, Weill Cornell Medicine, New York, NY,[4]Medicine, Weill Cornell Medicine, New York, NY,[5]Pharmacology, Meyer Cancer Center, Weill Cornell Medicine, New York, NY,[6]Meyer Cancer Center, Immunology, Weill Cornell Medicine, New York, NY

Tumor reliance on glycolysis is a hallmark of cancer and a mechanism of resistance to immunotherapy. This resistance is due to lactate-mediated immune suppression and competition for glucose between T cells and tumor cells within the tumor microenvironment. We have shown that CTLA-4 blockade is more effective in glycolysis-low tumors, or tumors

lacking functional lactate dehydrogenase A (LDH-A), primarily due to functional destabilization of regulatory T cell suppression. LDH inhibitors (LDHi) have been reported to inhibit tumor glucose uptake and slow tumor cell proliferation in pre-clinical models of cancer. However, their effect on immune cells has not been explored in depth. In addition, the optimal conditions for pharmacological inhibition of LDH in combination with immunotherapy to maximize anti-tumor immune and therapeutic responses require further investigation. At baseline, tumor cells express higher levels of *ldha* and consume more glucose than tumor-infiltrating T cells, creating a therapeutic window for tumor-specific targeting of the glycolysis pathway. In vivo, LDHi relies on the adaptive immune system and the overexpression of tumor LDH to delay B16F10 murine melanoma progression. We found that treatment with LDHi has two effects: 1) reduction of tumor cell glucose uptake and 2) increase in glucose uptake by tumor-infiltrating T cells. Thus, LDH inhibition is an effective, tumor-specific strategy to reduce tumor cell glucose uptake and increase glucose availability within the tumor microenvironment, consequently boosting tumor-infiltrating T cell glucose uptake. *In vitro,* increased glucose levels improve effector T cell killing of tumor cells while reducing regulatory T cell suppressive ability. Accordingly, inhibiting LDH in combination with CTLA-4 blockade is more effective in controlling tumor progression compared to CTLA-4 blockade alone, and that this combination promotes effector T cell infiltration and activation, while destabilizing regulatory T cell function. Additionally, we observe serum LDH and lactate levels correlate with primary tumor burden as well as tumor LDH levels. Therefore, serum LDH may serve as a biomarker for tumor burden and tumor LDH, as well as clinical response to LDHi. This study provides a comprehensive rationale for combining immune checkpoint blockade with inhibitors of glycolysis for patients with highly glycolytic cancers.

#5874

HSF1 downregulation of CCL5 reduces CD8 T cell trafficking in breast cancer

Curteisha LeeAnn Jacobs, Sakhi Shah, Wen-Cheng Lu, Richard Carpenter, Haimanti Ray, Xin Lu, Sha Cao. *Indiana University School of Medicine, Bloomington, IN*

Breast cancer is the leading cause of cancer related deaths in women. The presence of cytotoxic immune cells, specifically CD8+ T cells, in breast tumors is associated with better patient outcomes. Our goal is to understand mechanisms that regulate the infiltration of CD8+ T cells. This will in turn, improve the treatment and enhance patient overall survival. Utilizing a novel HSF1 activity gene signature, we observed that HSF1 activity was negatively associated with the presence of CD8+ T cells in breast cancer patients. Both CIBERSORT analysis of TCGA data as well as direct assessment of patient primary specimens demonstrated that patient tumors with high HSF1 activity had lower numbers of CD8+ T cells. To functionally test this relationship, HSF1 was knocked down in 4T1 breast cancer cells and grown orthotopically in BALB/c mice. Tumors with HSF1 knockdown showed lower tumor volumes and increased CD8+ T cell infiltration. We subjected the control and knockdown tumors to single- cell RNA sequencing analysis and found increased immune cell presence specifically CD8+ T cell presence in knockdown tumors. We further tested the effect of CD8+ T cells on the growth of HSF1 knockdown tumors by depleting CD8+ T cells in BALB/c mice. HSF1 knockdown tumors were significantly larger with CD8+ T cell depletion suggesting a functional role for HSF1 to inhibit CD8+ T cell infiltration and protect the tumor from immune-mediated killing. To investigate the mechanism by which HSF1 affects CD8+ T cells, we investigated whether HSF1 affects chemotactic cytokines. We found that loss of HSF1 significantly increased secretion of CCL5, a known chemoattractant for CD8+ T cells. Loss of HSF1 also increased mRNA levels of CCL5, suggesting a transcriptional effect on CCL5. To test the importance of CCL5 in the phenotype of HSF1 knockdown, a transwell migration assay was performed wherein T cells from BALB/c mice were placed in the upper chamber of a transwell chamber and the lower chamber contained conditioned medium from 4T1 cells with knockdown of HSF1 with or without knockdown of CCL5. The lower chamber was subjected to flow cytometry for CD3/CD8 to identify CD8+ T cells and we observed that loss of HSF1 increased migration of CD8+ T cells and this was ablated with additional loss of CCL5. These results suggest CCL5 is a significant mediator for the recruitment of CD8+ T cells when HSF1 is lost in cancer cells. We propose the model whereby high HSF1 activity in breast cancer cells suppresses expression and

secretion of the chemo-attractant cytokine CCL5 that ultimately leads to a decrease in CD8+ T cells in breast tumors microenvironment.

#5875

Rab37 mediates intracellular trafficking and membrane presentation of PD-1 in T cells to foster an immunosuppressive microenvironment in lung cancer

Wan-Ting Kuo[1], I-Ying Kuo[1], Shih-Ting Wu[1], Wu-Chou Su[2], Yi-Ching Wang[1]. *[1]National Cheng-Kung University, College of Medicine, Department of Pharmacology, Tainan, Taiwan,[2]National Cheng-Kung University, College of Medicine, Division of Oncology, Department of Internal Medicine, Tainan, Taiwan*

Programmed cell death protein 1 (PD-1) expressed on the surface of $CD8^+$ T cells is known as an immune checkpoint protein. High expression of PD-1 leads to T-cell dysfunction in the tumor microenvironment (TME). Our published studies show that Rab37 small GTPase-mediated vesicular trafficking of cell surface proteins and cytokines is critical in immunosuppressive TME. Here, we identify novel mechanisms of intracellular trafficking and plasma membrane presentation of PD-1 mediated by Rab37. Confocal immunofluorescence (IF) and vesicles isolation data demonstrated that PD-1 colocalized with Rab37-specific vesicles in T cells in a GTP-dependent manner. Total internal reflection fluorescence imaging, membrane fractionation, and flow cytometric analyses confirmed the dynamic trafficking and membrane presentation of PD-1 by Rab37. In addition, sucrose density gradient centrifugation and IF revealed that the level of glycosylated wild-type PD-1 in membrane compartment was more than glycosylation mutant PD-1, suggesting that glycosylation mutant PD-1 delayed in recruitment to the Rab37 vesicles and thus stalled in membrane presentation. Furthermore, T cell proliferation and activity were downregulated in *Rab37* wild-type splenocytes co-cultured with cancer cells compared to those from *Rab37* knockout mice using various T cell functional assays. Clinically, the multiplex IF-immunohistochemical assay indicated that the tumor infiltrated $Rab37^+/PD1^+/TIM\text{-}3^+/CD8^+$ exhaustion T cells were more in late staged lung cancer patients compared to those in early staged patients. Importantly, patients with $Rab37^+/PD\text{-}1^+/TIM\text{-}3^+/CD8^+$ tumor infiltrated T cells

expression profile correlated with poor overall survival. Our results provide first trafficking mode of PD-1 mediated by Rab37 small GTPase and novel evidence of the tumor promoting function of Rab37/PD-1 axis in T cells of the tumor microenvironment.

#5876

Sorafenib and Lenvatinib induce vascular responses in patient derived HCC on-Chip models

Orsola Mocellin[1], Abbie Robinson[1], Aleksandra Olczyk[1], Stephane Treillard[2], Thomas Olivier[1], Chee Ng[1], Jeroen Heijmans[3], Désiréé Goubert[1], Arthur Stok[1], Gilles van Tienderen[4], Monique Verstegen[4], Sebastian Trietsch[1], Henriëtte Lanz[1], Paul Vulto[1], Jos Joore[1], Karla S. Queiroz[3]. *[1]MIMETAS, Oegstgeest, Netherlands,[2]MIMETAS, oegstgeest, Netherlands,[3]MIMETAS, Leiden, Netherlands,[4]Erasmus MC, Rotterdam, Netherlands*

Hepatocellular carcinoma (HCC) is the most common type of liver cancer. Its incidence is increasing, and is closely related to advanced liver disease. Interactions in the HCC microenvironment between tumor cells and the associated stroma actively regulate tumor initiation, progression, metastasis, and therapy response. In the present study, we used the OrganoPlate graft to establish a co-culture system consisting of dissociated HCC tumors (HCC 1-8) and cell lines, HCC derived fibroblasts and vasculature. Cultures were prepared and validated by assessing their response to Sorafenib and Lenvatinib (72 hours). Cultures had their viability (alamar blue assay), and chemokine/cytokine levels in the supernatant (Luminex) determined. In addition, the organization of the vasculature in the tumor compartment was studied through immunostainings, confocal imaging, and subsequent morphological analyses. HCC models were characterized by a range of specific markers, tumor (albumin), endothelial (CD31 and VE-Cadherin) and stromal (aSMA) cells. CD31 immunostained cultures were imaged, and morphology changes quantified. Sorafenib and Lenvatinib induced changes in the tumor vasculature area and organization. Hereby, we present vascularized patient-derived HCC models that include relevant cellular players of the HCC microenvironment. These co-cultures are highly suitable for studying specific cell types as well as patient-specific responses. We envision that this patient derived model will evolve to

become a platform for understanding the interplay between angiogenesis, stroma and immune infiltrate in HCC.

#5877

Intratumoral lymphocyte networks harbor TCF1+ PD1+ progenitor CD8 T cells in lung cancer

Megan L. Burger[1], Giorgio Gaglia[2], Claire C. Ritch[2], Danae Rammos[2], Yang Dai[2], Grace E. Crossland[3], Sara Z. Tavana[3], Simon Warchol[4], Alex M. Jaeger[3], Santiago Naranjo[3], Shannon Coy[2], Ajit J. Nirmal[2], Robert Krueger[5], Jia-Ren Lin[2], Hanspeter Pfister[4], Peter K. Sorger[2], Tyler Jacks[3], Sandro Santagata[2]. *[1]Oregon Health and Science University, Portland, OR,[2]Laboratory of Systems Pharmacology, Harvard Medical School, Boston, MA,[3]Koch Institute, Massachusetts Institute of Technology, Cambridge, MA,[4]School of Engineering and Applied Sciences, Harvard University, Boston, MA,[5]Harvard Medical School, Boston, MA*

Cancer immunotherapies that activate cytotoxic T cell responses against tumors have been remarkably effective in some patients, but the determinants of response remain unclear. To investigate how spatial organization of T cells might influence immunotherapy response, we developed a tissue-based cyclic immunofluorescence (t-CyCIF) platform to characterize preclinical genetically engineered mouse models (GEMMs) of cancer. We optimized a 21-antibody panel delineating major myeloid and lymphoid cell subsets, that included key markers for characterizing T cell phenotypes and function. The panel was used to characterize the Kras/p53-mutant GEMM of lung adenocarcinoma, treated with anti-PD-1/anti-CTLA-4 immune checkpoint blockade (ICB) therapy or a neoantigen-targeted long-peptide vaccine. Spatial profiling by t-CyCIF identified intratumoral lymphocyte networks (“lymphonets”) as a key feature associated with a productive immune response against lung tumors. Lymphonets were predominantly composed of B cells and conventional CD4 T cells, but harbored tumor-reactive CD8 T cell populations. TCF1+ PD1+ progenitor CD8 T cells, a subset previously correlated with patient response to ICB, were almost exclusively localized to lymphonets inside tumors. Lymphonets of similar composition harboring TCF1+ PD1+ cells were also found in early-stage human lung adenocarcinomas. In response to

ICB and vaccine therapies in mice, cytotoxic CD8 T cells (Granzyme B+/Perforin+) colocalized with TCF1+ PD1+ cells in lymphonets, likely having differentiated from this progenitor pool. Notably, vaccination further induced a highly proliferative ($Ki67^{hi}$) and cytotoxic ($GranzymeB^{hi}Perforin^{hi}$) population of CD8 T cells localized outside of tumors that we posit enter tumors without passing through the intratumoral progenitor cell state. Upon becoming dysfunctional, marked by loss of Granzyme B/Perforin expression and upregulation of inhibitory receptors, CD8 T cells were excluded from lymphonets and localized predominantly to the tumor margin. Altogether, these results shed light on the spatial dynamics associated with a productive response to immunotherapies and open avenues for exploration into the function of lymphonets in supporting cytotoxic CD8 T cell responses in tumors.

#5879

Defining the cancer Immunogram using multimodal analysis to guide immunotherapy in diffuse large B cell lymphoma

Michael D. Mattie[1], Regis Perbost[2], Sarah Turcan[2], Corinne Danan[2], Frederick L. Locke[3], Sattva S. Neelapu[4], David B. Miklos[5], Caron A. Jacobson[6], Lazaros J. Lekakis[7], Yi Lin[8], Armin Ghobadi[9], Jenny J. Kim[10], Zixing Wang[11], Allen Xue[1], Simone Filosto[1], Nathalie Scholler[12], Jerome Galon[13]. *[1]Translational Medicine, Kite Pharma, a Gilead company, Santa Monica, CA,[2]Veracyte, Marseille, France,[3]Moffitt Cancer Center, Tampa, FL,[4]MD Anderson Cancer Center, Houston, TX,[5]Stanford University School of Medicine, Palo Alto, CA,[6]Dana Farber Cancer Institute, Boston, MA,[7]University of Miami Health System, Sylvester Comprehensive Cancer Center, Miami, FL,[8]Mayo Clinic, Rochester, MN,[9]Washington University School of Medicine, St. Louis, MO,[10]Clinical Development, Kite Pharma, a Gilead company, Santa Monica, CA,[11]Biostatistics, Kite Pharma, a Gilead company, Santa Monica, CA,[12]Gilead Sciences, Foster City, CA,[13]Laboratory of Integrative Cancer Immunology, INSERM, Sorbonne Universite, Universite Paris Cite, Centre de Recherche des Cordeliers, Equipe Labellisee Ligue Contre le Cancer, Paris, France*

(a) Expansion of therapeutic strategies against diffuse large B-cell lymphoma (DLBCL) offers new opportunities to fight aggressive non-

Hodgkin's lymphoma. Therapy approaches, such as R-CHOP and stem cell transplant, and CAR-T cell therapies are now available for the treatment of DLBCL. While the role of the tumor microenvironment (TME) during the therapeutic response is now recognized, the spatial organization and the communication between the diverse factors that compose the TME remains to be fully understood. In this study, we describe a new immunogram tool to help clinical researchers measure the tumor microenvironment contribution to drug efficacy or toxicity in DLBCL context.
(b) In a previous work, using a high-quality testing and innovative multimodal and integrative approach, we constructed the first Veracyte Biopharma Atlas for DLBCL lesions. Based on this knowledge and the understanding of the immune contexture of tumors, we constructed an immunogram using the scoring of clinically relevant biomarkers.Our immunogram scoring approach is composed of key features driving computational derivation of DLBCL Atlas clusters, which include immune gene signatures, immune cell phenotyping combined with spatial information, and genomic and clinical parameters.
(c) Patterns that strongly associated with CAR-T treatment response were determined. In addition, promising results have been obtained in the prediction to CAR-T toxicity related to T-regulatory cells or R-CHOP response with transcriptomic signature.
(d) Retrospective analysis of CAR-T clinical trial data and tumor biopsies highlighted the Veracyte Immunogram as a powerful tool to score the patient probability of response to CAR-T. This work provides the framework for identification of predictors of response to therapy, potential targets of interest or biomarkers that could be applied in future clinical trials.

#5880

The role of SOAT1 on $CD8^+$T cells-mediated immune response in ovarian cancer

Jiangnan He, Michelle K.Y. Siu, Runying Long, Ruiqian Zhang, Mingo M.H. Yung, Hextan Y. S. Ngan, Karen K.L. Chan. *Obstetrics and Gynecology, University of Hong Kong, The - Li Ka Shing Faculty of Medicine, Hong Kong, China*

Introduction: Sterol-O acyltransferase 1 (SOAT1) functions by converting cholesterol and acyl-CoA into cholesterol ester and coA-SH. High SOAT1 expression with its mediated tumorigenesis has been shown in multiple cancers. Studies showed that SOAT1 inhibition by its inhibitors augmented the outcome of immunotherapies, in terms of the immune checkpoint blockades, cancer vaccines, and CAR-T cells, by boosting the function of T cells. However, in order to have a better understanding of the role played by SOAT1 in the tumor microenvironment of ovarian cancer (OC) and optimize strategies of combination immunotherapy, it's necessary to detect the role of SOAT1 in OC cells on T cell-mediated immune response.
Methods: *SOAT1* knockdown was manipulated by siRNAs transfection. SOAT1 was inhibited by avasimibe and OC cells were treated in different doses of avasimibe. qPCR was performed to detect gene expressions in ovarian cancer cells. T cells, isolated and activated from healthy donors, were cocultured with SOAT1-silenced and avasimibe pre-treated OC cells and their tumor-conditioned medium (TCM). Flow cytometry analysis was used to measure cytotoxic secretory molecules of human T cells, like IFN-r, TNF-a, and Granzyme B.
Results: The downregulation of intracellular cytotoxic cytokines was shown in the T cells cocultured with SOAT1-silenced and avasimibe-pretreated OC cells or treated by their TCM, thereby impairing the cytotoxic capacity of T cells, compared to the corresponding control group. qPCR results showed that several immunosuppressive cytokines, like IL-6, IL-8, TGF- were upregulated in the SOAT1-silenced or avasimibe-treated OC cells.
Conclusion:SOAT1 inhibition in ovarian tumor cells impairs $CD8^+$ T cell cytotoxic function, to some extent, via the upregulation of immunosuppressive-related cytokines.

#5881

PERIO-01: Initial safety experience and immunologic effects of a Class C TLR9 agonist using pressure- enabled drug delivery in a phase 1 trial of hepatic arterial infusion of SD-101 +/- checkpoint inhibition in metastatic uveal melanoma

Sapna P. Patel[1], Cara Haymaker[1], Rahul A. Sheth[1], Joshua D. Kuban[1], Joshua Weintraub[2], Eric Wehrenberg-Klee[3], Paula Novelli[4], Carin Gonsalves[5], Robert Adamo[5], Virgina Honaker[1], Laura Timciuc[1], Tarin Hennegan[1], Juan C. Amador Molina[1], Dzifa Duose[1], Edwin R. Parras

Cuenta[1], Anthony Lucci[1], Salyna Meas[1], Vanessa Sarli[1], Victor G. Prieto[1], Jason LaPorte[6], Ann-Marie Hulstine[6], Ashley Moody[6], Bryan Cox[6], David Geller[4], Diwakar Davar[4], Kamaneh Montazeri[3], Marlana Orloff[5], Steven C. Katz[6], Richard Carvajal[2]. *[1]UT MD Anderson Cancer Center, Houston, TX,[2]Columbia University Irving Medical Center, New York, NY,[3]Massachusetts General Hospital, Boston, MA,[4]University of Pittsburgh Medical Center, Pittsburgh, PA,[5]Thomas Jefferson University, Philadelphia, PA,[6]TriSalus Life Sciences, Westminster, CO*

Immune checkpoint inhibitors (ICI) have demonstrated limited success in patients with metastatic uveal melanoma (MUM) with liver involvement due to an immunosuppressive tumor microenvironment (TME) driven in part by myeloid-derived suppressor cells (MDSCs). Toll-like receptor-9 agonists (TLR-9A) have improved ICI response rates in cutaneous melanoma, but delivery challenges have limited their application for MUM. Hepatic arterial infusion (HAI) of TLR-9A using a pressure-enabled drug delivery™ (PEDD™) device has the potential to enhance responsiveness to ICI by optimizing delivery to intrahepatic tumors and reprogramming the TME, including elimination of MDSCs.PERIO-01 is an open-label first-in-human Phase 1 trial of SD-101 given by HAI using a PEDD™ in MUM (NCT04935229). The study consists of dose-escalation cohorts of single agent SD-101 alone and with ICI. SD-101 is delivered over 2 cycles, with 3 weekly doses per cycle. Research blood, tumor and normal liver biopsies are collected serially for correlative studies. At data cutoff, a total of 20 patients were enrolled, with 13 in the single agent dose escalation cohort (2, 4, and 8 mg) and 7 patients with SD-101 (2 mg) + nivolumab. The median age was 65.5 years with an equal gender distribution. Only 2 patients were treatment-naïve and the median number of liver metastases was 5.1. The average number of SD-101 infusions was 5.2. One patient in the combination cohort experienced a serious adverse event related to treatment - asymptomatic Grade 3 increase in liver enzymes. PEDD™ resulted in high drug levels in the liver (up to 2,340 ng/ml at 8mg) with only transient exposure in the periphery (<4 hours) with one Grade 2 cytokine related syndrome adverse event. Dose-dependent increases in canonical TLR9-associated cytokines (IL-18, IFNγ, IP-10, and soluble CD25) was observed across the 2mg, 4mg, and 8mg single-agent dose levels. Concordant with

predicted mechanism of action, PEDD^{TM} HAI administered SD-101 resulted in decreases in liver monocytic MDSCs in 4 of 4 patients with available multiplex immunofluorescence data. NanoString analysis from three patients revealed increases in ISG15, IL-9, IFNα, and IL-2 transcripts and decreases in ARG1 and IDO transcripts, with increased scores for macrophages, activated CD8 T cells, Th1 cells, and Th1 activation. For patients who received 2mg SD-101 + ICI with available liquid biopsy data, 4 of 7 demonstrated decreases in circulating tumor cells and 3 of 5 showing ctDNA decreases after the first cycle.In this first-in-human experience, HAI of SD-101 via PEDD^{TM} was well tolerated and associated with encouraging immunologic activity. Evidence of biologic activity with 2 mg of SD-101 with nivolumab is encouraging and patients are currently enrolling at higher SD-101 dose levels + ICI.

#5882

Prevention of antibiotic-induced dysbiosis in human volunteers by DAV132 and preservation of responsiveness to anti-PD-1 demonstrated by transplantation of human feces into tumor-bearing mice

Meriem Messaoudene[1], Nathalie Saint-Lu[2], Frédérique Sablier-Gallis[2], Stéphanie Ferreira[2], Mayra Ponce[1], Clément Le Bescop[2], Thomas Loppinet[2], Tanguy Corbel[2], Céline Féger[1], Fabien Vitry[2], Antoine Andremont[2], Jean de Gunzburg[2], Bertrand Routy[1]. *[1]University of Montreal, Montreal, QC, Canada,[2]Da Volterra, Paris, France*

Background: Over the last decade, studies unraveled the cancer-immune dialogue in the setting of immune checkpoint inhibitors (ICI) and influenced by the gut microbiota. The first evidence of the key role of the microbiota in ICI modulation was observed during antibiotics (ATB) treatment, where altering the microbiota composition by ATB inhibited ICI responses. DAV132 (DAV) is an orally administered colon-targeted ATB adsorbent capsules designed to prevent ATB-induced dysbiosis. We investigated whether DAV co-administered with ATB could prevent ATB-related dysbiosis and ICI response.

Methods: 72 human healthy volunteers (HV) were randomized to receive either IV ceftazidime-avibactam (CZA) or Piperacillin tazobactam (PTZ) alone or in combination with oral DAV. CZA and PTZ plasmatic and fecal

pharmacodynamic levels were measured using HPLC-MS/MS. Microbiome was profiled with metagenomics at different timepoints. FMT experiments in germ-free mice were performed using fecal samples from HV from the trial, before (D1) or after 6 days (D6) of CZA or PTZ+/-DAV; subsequently mice were inoculated with MCA205 or B16 tumors and treated with anti-PD-1. Tumor infiltrating lymphocytes (TILs) were analyzed by flow cytometry.
Results: DAV did not impact plasmatic CZA or PTZ concentrations, but significantly reduced ceftazidime and piperacillin concentrations in feces compared to ATB groups alone. DAV significantly prevented the reduction in microbiota alpha-diversity at D6 and was associated with a rapid return to baseline microbiota. 50 and 43 metagenomics species were preserved in the CZA+DAV *vs* CZA, or PTZ-DAV vs PTZ such as *Faecalibacterium praunistzii, Alistipes Spp and Blautia obeum*. FMT in germ-free mice using feces collected at D1 exhibited a significant anti-PD-1 activity. This anti-tumor response was inhibited in two tumors models in mice transplanted with D6 feces from patients in the CZA or PTZ alone groups. Conversely, the anti-tumor response was maintained in mice transplanted with D6 feces from HV treated with CZA+DAV or PTZ+DAV groups. Flow cytometry on TILs demonstrated that CZA decreased $CD8^+$T cell and $CD8^+$/Treg ratio compared to CZA+DAV.
Conclusions: DAV prevented ATB-induced dysbiosis in HV treated with CZA or PTZ without influencing plasmatic concentrations. In avatar mice FMT from HV treated with CZA+DAV was able to preserve anti-PD-1 efficacy. These results provide rationale to launch clinical trials combining DAV in patients on ATB amenable to ICI.

#5883
Computational analysis of immune synapses in melanoma tumor microenvironment
Zichao Liu, Victor G. Wang, Jan Martinek, Ali Foroughi pour, Jie Zhou, Karolina Palucka, Jeffrey H. Chuang. *The Jackson Laboratory for Genomic Medicine, Farmington, CT*

High-resolution multiplexed tissue imaging such as imaging mass cytometry (IMC) has enabled quantitative cell characterization with preserved tissue architecture. However, the subcellular resolution

information has not been fully leveraged yet, as most analyses have focused on cellular or compartment level features. Here, we have developed a robust computational approach integrating cellular spatial and molecular features in multiplexed images to quantify immune synapses. Our approach enables computational detection of subcellular enrichment of T cell co-receptors at immune synapses, which are key regulators of T cell functions in the tumor microenvironment (TME). We quantified immune synapse strength between T cells and various antigen-presenting cells in tumor regions in one melanoma whole tissue immunofluorescence dataset and two independent melanoma IMC datasets covering 99 patients. We observed that sub-localizations of immune synapse-related molecules are highly correlated, e.g. CD3 with CD8. These co-localizations are cell type-specific, with differential behaviors in CD4+ or CD8+ T subtypes. Intra-tumoral T-cell-myeloid synapses are associated with improved T cell proliferation ($p = 2.8E-4$). In addition, we also observed that cytotoxic T cell - melanoma synapses in immune rich regions are stronger in immune checkpoint inhibition therapy responders than in non-responding patients ($p = 0.013$). Our approach enables computational resolution of spatial inter-cellular interactions within the TME, is applicable across imaging modalities, and facilities assessment of biological and clinical significance.

#5884

Targeting T regulatory cells to intercept progression from preinvasive to invasive lung adenocarcinoma using a novel KRAS-driven murine model

Mitchell Martin, Michael J. P. Crowley, Geoffrey Markowitz, Alain Borczuk, Chen Zhang, Liron Yoffe, Arshdeep Singh, Nasser K. Altorki, Vivek Mittal. *Cardiothoracic Surgery, Weill Cornell Medicine, Memorial Sloan Kettering Cancer Center, New York City, NY*

Non-small cell lung cancer is the leading cause of cancer-related death in the US and worldwide, with a 5-year survival of ~18-20%. Understanding of the biology of early lung cancer is necessary to intercept early steps of progression. Indeed, increased utility of low-dose CT guided lung cancer screens in populations at risk have begun to detect early premalignant disease; however, little is known about the underlying biology that drives progression of preinvasive lesions to invasive adenocarcinoma. Moreover,

there exists a lack of reliable animal models to assess interception strategies to target disease progression. We have developed and characterized a lung cancer cell-of-origin-specific KRAS-driven mouse model which accurately mirrors progression of human precursor lesions to invasive disease. Transcriptional analysis of preinvasive and invasive stages identified cellular and molecular alternations observed in human lesions, including upregulation of cell proliferation, extracellular matrix remodeling, and an increasingly complex immune microenvironment. Interrogation with immunofluorescence microscopy and Hyperion mass cytometry imaging showed marked reprogramming of the immune microenvironment including increased T cell infiltration and abundance of T regulatory cells (Tregs). Surprisingly, depletion of T cells impaired progression of preinvasive lesions, implicating the critical immunosuppressive roles of Tregs. Spatial transcriptomics (10X Genomics Visium) revealed unique spatial transcriptional changes in the progression from preinvasive to invasive stage disease, including specific ligand-receptor interactions highly expressed in Tregs. Genetic and pharmacological approaches using FoxP3-DTR-GFP mice and low dose cyclophosphamide have begun to define the functional role of Tregs in early premalignant disease.
This study demonstrates critical roles of immunosuppressive Tregs in driving progression of preinvasive to invasive lung cancer, and advocates for Treg targeting as a potent immunoprevention approach for patients at risk of developing lung cancer.

#5885

A pathway-centric approach to characterising tumour heterogeneity and cell diversity across multiple cancer types

Leiam Colbert, Benjamin Patterson, Cheng Yi Chen, Nicolas Fernandez, Jiang He. *R&D, Vizgen, Boston, MA*

Biological tissues are composed of heterogeneous populations intricately organized in 3D architectures, yet cell type composition and spatial organization remain largely unknown for most tissue types. Single-cell sequencing analysis provides a systematic and quantitative approach to identify cell types and determine their composition in tissues. However, the spatial organization of cells and cell-cell interactions that are critical for tissue function are lost when cells are dissociated from tissue. This is

especially important when working with the complex microenvironment of a tumour where such information is needed to fully understand patient prognosis. Complex diseases such as cancer can be better understood from the perspective of dysregulated pathways, rather than as a disease resulting from alterations of individual genes. Recently, spatially resolved, single-cell imaging platforms have provided a necessary solution to bridge the spatial information gap evident in previous transcriptomic methodologies. Vizgen's MERSCOPE platform, built on multiplexed error robust in situ hybridisation (MERFISH) technology, enables the direct profiling of the spatial organisation of intact tissue with subcellular resolution. Here, we present a Pan-Cancer approach to characterise various cancers in human clinical samples with MERSCOPE. Using a 500-gene panel that includes the canonical signalling pathways of cancer, cancer type-specific genes, key immune genes, proto-oncogenes, and tumour-suppressor genes we demonstrate MERSCOPE's ability to spatially profile gene expression across multiple tumour samples, including breast, colon, prostate, ovarian, lung, and skin cancer. To confirm the specificity and sensitivity of our pathway-focused gene panel, we assessed how tumour cell clusters in each dataset expressed different cancer type-specific markers. As expected, we found specific cancer types enriched in corresponding marker genes. To further evaluate how individual cell types in each tumour are dysregulated by cancer, we compared non-tumour cell clusters to similarly annotated clusters derived from single-cell RNA-sequencing data of normal tissue. Notably, the non-tumour cells in these datasets exhibit higher expression of stress and inflammation pathways, while immune cell clusters demonstrate higher immune activity and higher immune exhaustion compared to those in normal tissue. These results demonstrate the power of the MERSCOPE platform to generate individualised, accurate cell atlases from patient-derived tumours and to enable further insights into the relationship between genomic profiles, dysregulated pathways, and disease phenotype. Such network-centric approaches are critical for identifying genotypic causes of diseases, classifying disease subtypes, and identifying drug targets.

#5886

Targeting IDO1 and TDO2 is crucial for the modulation of immune effector in platinum resistant non-small cell lung cancer

Sydney Spector[1], Chunjing Wu[1], George Theodore[1], Jonathan Dan Nguyen[1], Emily Kim[1], Ashley Garcia[1], Niramol Savaraj[1], Diane Lim[1], Lynn Feun[2], Medhi Wangpaichitr[1]. *[1]Univ. of Miami/VA Medical Ctr., Miami, FL,[2]Univ. of Miami, Miami, FL*

The impact of non-small cell lung cancer (NSCLC) tumor metabolism on the immune microenvironment is not well understood in the context of platinum resistance. We have identified and characterized crucial metabolic differences between cisplatin-resistant (CR) and cisplatin-sensitive (CS) NSCLC cells in which CR cells possessed higher indoleamine 2,3-dioxygenase-1 (IDO1) activity as determined by an increase in extracellular kynurenine concentration *in vitro* and *in vivo*. Utilizing *in vitro* co-culture models (n=6), we showed that IDO-mediated kynurenine production from CR cells suppressed natural killer group 2 member D (NKG2D) on natural killer (NK) and CD8+ T cells, but enhanced immunosuppressive regulatory T cell (Treg) and myeloid-derived suppressor cells (MDSC) populations. Utilizing syngeneic (n=7) and humanized (n=5) mouse models, mice with CR tumors exhibited a more highly immunosuppressive environment that blocked the antitumor immune response. Inhibition of IDO1 by the selective IDO1 inhibitor epacadostat (200 mg/kg P.O. once a day for 15 days) attenuated tumor growth in these CR tumor-bearing mice. Interestingly, we found an induction of tryptophan 2,3-dioxygenase-2 (TDO2) enzyme in epacadostat-treated mice. To overcome this compensatory effect induced by IDO1 inhibition, mice were treated with a novel IDO1/TDO2 dual inhibitor (AT-0174; Antido Therapeutics Pty Ltd, Melbourne, Australia) at 170 mg/kg P.O. once a day for 15 days. Dual inhibitors suppressed tumor growth to a greater degree than IDO1 inhibitors in CR conditions, and significantly enhanced immune effector populations as well as suppressed immunosuppressive Tregs and MDSC population in CR tumors. In addition, increased expression of programmed death-ligand 1 (PD-L1) was observed in CR cells, we assessed the effects of combination treatment of AT-0174 + anti-PD1 antibody. This combined therapy produced a profound anti-tumor effect in CR tumors and extended survival in mice. Our data support an increase in the therapeutic efficacy of blocking both IDO1/TDO2 in treating CR lung cancer by enhancing tumor immune surveillance. Thus, inhibiting the kynurenine pathway may be a more suitable therapeutic approach in a subgroup of lung cancer patients who

failed platinum therapy and lead to improved outcomes in the treatment and management of NSCLC. Support by Dept. of Veterans.

Interactions Between the Microbiome, Cancer Cells, and Tumor Stromal Components

#5890

Distinct differences in microbial enrichment and diversity identified between gastric and gastroesophageal junction adenocarcinoma

Miseker Abate[1], Harrison Drebin[1], Shoji Shimada[1], Santosh Vardhana[2], Smita Sihag[3], Vivian E. Strong[1], Chad Vanderbilt[4]. *[1]Department of Surgery, Memorial Sloan Kettering Cancer Center, New York, NY,[2]Human Oncology and Pathogenesis Program, Memorial Sloan Kettering Cancer Center, New York, NY,[3]Department of Thoracic Surgery, Memorial Sloan Kettering Cancer Center, New York, NY,[4]Department of Pathology, Memorial Sloan Kettering Cancer Center, New York, NY*

Objective: The microbiome is associated with the pathogenesis and progression of disease in gastric cancer (GC). Eradication of *Helicobacter pylori* has reduced overall GC incidence, however, gastroesophageal cancer (GEJC) continues to increase. While there are oncologic differences between GEJC and GC, distinctions based on microbial profiles are unknown. In this study, we characterize differences in the microbial profiles of GEJC and GC.
Methods: 562 patients with microsatellite stable GC (n=303) and GEJC (n=259) who had an institutional Integrated Mutation Profiling of Actionable Cancer Targets assay on the primary tumor were included in the study. A validated microbiome bioinformatics pipeline that is generalizable across multiple next generation sequencing platforms was utilized to compare microbial enrichment and alpha diversity between GC and GEJC, defined by type 1-3 Siewert classification.
Results: Over 20 unique microbial species were enriched in GC when compared to GEJC, including *Helicobacter* and *Lymphocryptovirus* (Table 1). *Prevotella* had increased incidence in GEJC (OR:1.57,95%CI:1.02,2.41). Siewert type 2 and 3 GEJC had a significantly lower alpha diversity compared to GC. There was no significant difference in alpha diversity between GC and Siewert type 1 GEJC.

Conclusion: There are distinct differences in microbial enrichment and alpha diversity between GEJC and GC. *Helicobacter* and *Lymphocryptovirus*, the genus family for Epstein Bar Virus, were noted to have the highest odds ratios in the GC group. Our findings showing the reduced incidence of microbes in GEJC which are the current targets of GC screening, prevention, and therapy, have implications in evaluating optimal preventative and treatment strategies in GEJC.

Table 1. Microbes with enrichment in gastric cancer (GC) when compared to gastroesophageal cancer (GEJC)

Microbes	**OR (95% Confidence Interval)**	**p-value**
Helicobacter	85.40 (5.191, 1404.81)	0.002
Lymphocryptovirus	6.83 (2.31,20.17)	0.001
Pelagibacterium	6.01 (1.71, 21.06)	0.005
Gluconacetobacter	5.14 (1.70, 15.53)	0.004
Myxococcus	5.14 (1.70, 15.53)	0.004
Kribbella	4.48 (1.46, 13.74)	0.009
Celeribacter	3.46 (1.43, 8.37)	0.006
Halomonas	3.46 (1.43, 8.37)	0.006
Nakamurella	3.35 (1.46, 7.71)	0.004
Nitrobacter	2.91 (1.40, 6.05)	0.004
Pseudogulbenkiania	2.80 (1.30, 6.03)	0.009
Mycobacteroides	2.78 (1.33, 5.81)	0.006
Polaromonas	2.70 (1.49, 4.90)	0.001
Meiothermus	2.54 (1.41, 4.57)	0.002
Sphingopyxis	2.44 (1.33, 4.46)	0.004
Mesorhizobium	2.38 (1.32, 4.30)	0.004
Staphylococcus	2.23 (1.37, 3.62)	0.001
Thermus	2.13 (1.22, 3.70)	0.008
Mycolicibacterium	1.99 (1.29, 3.07)	0.002
Mycobacterium	1.95 (1.23, 3.08)	0.005
Lactobacillus	1.94 (1.17, 3.22)	0.01

#5891

Identification of intratumor pathogens from single-cell RNA sequencing, cellular dysfunction and immune response

Laura Bukavina[1], Mohit Sindhani[2], Henkel Valentine[1], Daniel Ranti[3], Kirtishri Mishra[4], Alexander Kutikov[1], Shilpa Gupta[5], John Sfakiano[3], Mahmoud Ghannoum[6], Mauricio Retuerto[6], Andres Correa[1], Robert Uzzo[1], Philip Abbosh[1]. *[1]Fox Chase Cancer Center, Philadelphia, PA,[2]India Institute of Technology, Delhi, India,[3]Mount Sinai, New York, NY,[4]University Hospitals Cleveland Medical Center, Cleveland, OH,[5]Cleveland Clinic, Cleveland, OH,[6]Case Western Reserve, Cleveland, OH*

Introduction: We aim to assess the transcriptomic features of the single cell level to identify intracellular pathogens in patients with high grade bladder cancer.

Methodology: CellRanger and Alevin were utilized to extract cell barcodes and unique molecular identifiers. After quality control, reads were aligned with human reference genome with Kraken2 for species level identification of bacteria. Contaminants (false positives) were removed based on higher frequencies and negative control (reference control) of 2,491 sterile cell experiments. Seuret Findmarkers, scIntegrate, and scDensity Plot were utilized to normalize the data, cluster the cells, and calculate markers in each cluster of differentially expressed genes between the two conditions. We focused our analysis on *Pseudomonas aeruginosa* due to high urogenital virulence, and immunomodulation capabilities by pattern recognition receptors and inflammasome.

Results: We identified presence of three over-represented intracellular taxa in tissue biopsies of patients with BC compared to healthy controls (after false discovery rate correction and cross validation of contaminants). Patients with history of high-grade BC demonstrated increased presence of Aeromonas (175,473 reads, 54%), Pseudomonas (75,002 reads, 26.73%), and Bacillus (15,410 reads, 5.49%) in their tissue samples, not visualized in healthy controls (counts <10). Among 8,324 cells (across 7 patients), classical CD14+ monocyte subtype was most likely to be exposed to Pseudomonas species (4150 /5069, 81.8%), followed by non-classical CD16+ monocytes (722/1040, 69.4%), and CD8+ Tcells (348/680, 51.1%).

(Figure 1A-C). Relative gene expression level between exposed and non-exposed monocytes demonstrated total 25 upregulated genes, with increased expression *GNBL21* (aka: RACK1, *log10 4.1*), *MALAT1(log10 3.7), TCEB2(log10 2.9) (increasing proliferation, migration, and reduction of cell autophagy) compared* to non-infected, and normal controls. Pseudomonas involvement of non-monocyte cells (CD8+, CD4+Th17, CD4+ naïve) was associated with disease progression (2/5 patients), as well as increased expression of *IFI6/27*(interferon alpha inducible protein 6 &27), *ITAC* (interferon inducible T cell alpha-chemoattractant). Conclusion: Altogether, our analysis depicted the distribution of intracellular bacteria not previously recognized within tumor microenvironment utilizing scRNAseq, and revealed overexpression of *RACK1* in Pseudomonas positive cells, associated with apoptosis resistance.

#5892

Microbial diversity and composition according to short-term postoperative complication status in colorectal cancer patients

Hyeree Park[1], Tung Hoang[1], Min Jung Kim[2], Ji Won Park[2], Seung-Yong Jeong[2], Aesun Shin[1]. *[1]Department of Preventive Medicine, Seoul National University College of Medicine, Seoul, Korea, Republic of,[2]Department of Surgery, Seoul National University College of Medicine, Seoul, Korea, Republic of*

Background: Previous studies have suggested the disturbance in the microbial composition followed by dysbiosis contribute to the onset of gastrointestinal malignancies, including colorectal cancer (CRC). However, the impact of microbiome on short-term postoperative complications after CRC surgery is not well investigated. This study aimed to investigate whether the gut microbial diversity and composition in CRC patients were associated with the occurrence of short-term postoperative complications. Methods: We linked the clinical data and preoperative sequencing data of fecal samples of 331 patients who underwent CRC surgery from 2017 to 2019 in Seoul National University Hospital. Short-term postoperative complications were defined as first complications that developed within 30 days of surgery. We used linear discriminant analysis (LDA) of effect size (LEfSe) in the Galaxy webserver to identify enriched bacteria in patients with and without complications. Then, we calculated microbial dysbiosis

index (MDI) by each patient and compared them according to the complication status. Wilcoxon rank sum test was conducted to compare the alpha diversity indices according to the complication event. Subgroup analyses according to types of complications were also performed: surgical procedure-related (SP) group and nonsurgical procedure-related (NSP) group.
Results: Overall, 84 patients (25%) developed short-term postoperative complications: SP group (n=39) and NSP group (n=45). From the LEfSe analysis, *Bacteroides uniformis* (LDA score: 3.64, p-value 0.04) and *Clostridium colicanis* (LDA score: 3.39, p-value 0.01) were enriched in patients who developed short-term complications, whereas *Roseburia faecis* (LDA score: 3.26, p-value 0.05), *Bifidobacterium bifidum* (LDA score: 2.98, p-value 0.03), *Faecalibacterium sp.* (LDA score: 3.12, p-value 0.02) and *Prevotella nigrescens* (LDA score: 2.87, p-value 0.05) were enriched in patients without complications. When compared with patients without complications, taxa related to class *Gammaproteobacteria*, genus *Clostridium*, species *Roseburia faecis*, and *Desulfovibrio D168* were abundant in the SP group. Alpha diversity indices were not significantly different according to the complication status or the type of complication. MDI from the enriched bacteria were significantly higher in patients with complications compared to those without complications (p-value<0.001), and MDI of the SP group were also significantly higher than that of patients free of complications (p-value 0.001).
Conclusion: Our study suggests a potential relationship between microbial composition and surgical outcome in CRC patients. No significant difference in alpha diversity was observed according to the occurrence or the type of complication. Further studies are needed to investigate the postoperative changes of microbial features.

#5893

Suppression of anti-tumor immunity by the *Fusobacterium nucleatum* protease fusolisin

Amjad Shhadeh[1], Liat Dassa[2], Jamal Fahoum[3], Nicole Haj[1], Reuven Wiener[3], Ofer Mandelboim[2], Gilad Bachrach[1]. *[1]Institute of Dental Sciences, The Hebrew University-Hadassah School of Dental Medicine, Jerusalem, Israel,[2]Department of Immunology and Cancer Research, Institute for Medical Research Israel Canada, Hebrew University-Hadassah*

Medical School, Jerusalem, Israel,[3]Department of Biochemistry and Molecular Biology, Institute for Medical Research Israel Canada (IMRIC), Faculty of Medicine, The Hebrew University Medical School, Jerusalem, Israel

Fusobacterium nucleatum is an oral pathogen associated with periodontal disease, preterm births and the exacerbation of colorectal, esophageal, pancreatic, and breast cancers. *F. nucleatum* was previously found to inhibit killing of cancer cells by natural killer (NK) cells and tumor infiltrating T cells by inducing the NK cells killing-suppressing receptors TIGIT and CEACAM1. In this study, we show that the incubation of *F. nucleatum* with primary human natural killer (NK) cells causes the cleavage of the activating receptors CD16, NKp44 and NKp46 by fusolisin. Fusolisin is a fusobacterial outer-membrane, auto-transporter, serine protease and to date the only functional protease found in *F. nucleatum*. We previously showed that fusolisin is essential for fusobacterial growth in culture. High expression of a functional recombinant fusolisin in *E. coli* was enabled using codon optimization and replacement of the fusolisin's signal peptide with that of the *E. coli* OmpA. Recombinant fusolisin was found to cleave the same NK-activating receptors degraded by *F. nucleatum*. Cleavage of these activating receptors by fusolisin inhibited NK cells activity including killing of tumor cells *in-vitro* and *in-vivo*. Our results provide a new bacterial protease-dependent mechanism in which tumors colonized by *F. nucleatum* are protected from NK cells attack by exploiting fusolisin proteolytic activity. Importantly, our previous and current results suggest that fusolisin might serve to target for tumor-colonized fusobacteria.

#5894

Changes in the gut microbiota associated with oncolytic virotherapy efficacy in a gastric cancer murine model

Natalie M. Melendez-Vazquez[1], Sagar Sohoni[2], Arie Van Wieren[2], Juan Fueyo[2], Candelaria Gomez-Manzano[2], Filipa Godoy-Vitorino[1].
[1]Department of Microbiology and Medical Zoology, University of Puerto Rico-Medical Sciences Campus, San Juan, PR,[2]Department of Neuro-Oncology, The University of Texas MD Anderson Cancer Center, Houston, TX

Gastric cancer is the third leading cause of cancer-related mortality worldwide, and current standard-of-care treatment allows for a 5-year survival rate of 20%. Newer treatments against solid tumors include an oncolytic adenovirus armed with T-cell activator OX40L, named Delta-24-RGDOX, which expresses the positive immune checkpoint OX-40L. While studies have revealed the interaction between the gut microbiome and immunotherapy agents, it's still unknown how the gut microbiome might influence viroimmunotherapy efficacy. We hypothesized that the gut microbiota plays an important role in modulating the virus-driven anti-tumor response. To test this hypothesis, immunocompetent C57BL/6 mice were subcutaneously implanted M12Luc gastric cancer cells and were administered PBS (control) or Delta-24-RGDOX by intratumoral injections. Mice fecal pellets were collected at three different time points: (1) before tumor implantation, (2) after tumor establishment, and (3) 14 days after the first dose of the treatment. Genomic DNA was isolated with the QIAGEN DNeasy Powersoil Kit from fecal pellets of cancer-bearing mice (n=60), and the V4 region of the 16S ribosomal RNA gene (prokaryotes) was sequenced using the Illumina platform. Data was deposited in QIITA for quality assessment, followed by microbial community analysis using the taxonomic reference database SILVA and the downstream platforms QIIME2 and R with a rarefaction depth of 9,187 reads per sample. We found significant differences in the gut microbiome community structure of viroimmunotherapy-treated mice compared to controls (ANOSIM p-value=0.025). No differences in gut diversity were observed, although control animals tended to show higher richness (Kruskal-Wallis p-value>0.05). Of interest, the bacterial composition of responders to the viroimmunotherapy had a decrease in Actinobacteria and an increase of Patescibacteria. Additionally, responders had higher levels of butyrate-producer bacteria such as *Ruminococcaceae* and *Clostridium sensu stricto*. These findings suggest that butyrate producers may be important in regulating host gut homeostasis associated with the clinical efficacy of Delta-24-RGDOX, suggesting possible benefits of microbiota modulation in patient survival. *This project was sponsored by a pilot award within The University of Puerto Rico/University of Texas MD Anderson Cancer Center (MDACC) Partnership for Excellence in Cancer Research Grant (2U54CA096297-16).*

#5895

Analysis of microbiome in gastric MALT lymphoma

SeungJoo Yoo[1], Dong-Yeop Shin[2], Ja Min Byun[2], Junshik Hong[2], Hongseok Yun[2], Youngil Koh[2], Sung-Soo Yoon[2]. *[1]Seoul National University, Seoul, Korea, Republic of,[2]Seoul National University Hospital, Seoul, Korea, Republic of*

Gastric MALT (mucosa-associated lymphoid tissue) lymphoma is found at a rate of 50% or more among the types of MALT lymphoma. Majority of patients with gastric MALT lymphoma are infected with *Helicobacter pylori* and also have clinical improvement with eradication therapy. However, it is unclear how *H. pylori* cause gastric MALT lymphoma. To explore it, we prospectively collected 13 patients who are newly diagnosed with gastric MALT lymphoma with *H. pylori.* We gathered samples from normal regions and lesions during endoscopy for diagnosis. Samples of lesion were harvested again after eradication of *H. pylori*. we sequenced 10 of WES (whole exome sequencing) and 13 of WTS (whole transcriptome sequencing) with these samples. With sequencing data, we aligned the sequenced reads to human reference genome (hg19) using BWA and called the variants with Mutect2. We aligned the reads and calculated TPM (Transcripts Per Million) from WTS with STAR and RSEM. We performed DEG (Differentially Expressed Genes) and GSEA (Gene Set Enrichment Analysis) for three comparison groups which are divided into normal, lesion, and after eradication. Gene fusions were detected using STAR-Fusion and Arriba with WTS. To detect potential microbiome from the samples, we used Kraken2, a taxonomic classification tool. We found that *MUC6* was mutated from all samples and some samples have mutated *MUC3A, KMT2C*, *ZNF595*, *CDC27,* etc., and two have *BIRC3-MALT1* fusion. From DEG and GSEA analysis, G protein-coupled receptor activity was activated in the group of lesion samples and suppressed in normal samples and eradication samples. Lymphocyte activation and immune response were also activated in the cancerous lesion. Kraken2 classified the reads which were not aligned to the human reference genome as reads from microbiota including *H. pylori*. The reads of *H. pylori* were more abundant in the lesion group than the other groups. According to the result of differentially expressed species analysis between the groups of lesion and eradication, the following species were also more abundant in the lesion

group; *Veillonella dispar, Helicobacter hepaticus, Helicobacter winghamensis,* etc. We analyzed genetic alterations and differentially expressed genes and also classified non-human reads as microbiome with sequencing data from gastric MALT lymphoma. Our results suggest how H.pylori infection is related to carcinogenesis of gastric MALT lymphoma.

#5896

Identification of microbial biomarkers to predict recurrence of oral squamous cell carcinoma

Wei-Ni Lyu[1], Mei-Chun Lin[2], Pei-Jen Lou[2], Liang-Chuan Lai[1], Mong-Hsun Tsai[1]. *[1]National Taiwan University, Taipei, Taiwan,[2]National Taiwan University Hospital, Taipei, Taiwan*

Introduction: Oral cancer is a fatal cancer and the sixth most common neoplasm worldwide. Over 90% of oral cancer is oral squamous cell carcinoma (OSCC). OSCC is a global health problem because of its late diagnosis and high rate of relapse and metastasis. Currently, cumulative evidence has suggested the association between oral microbiome and oral cancer. However, the correlation between the oral microbiome and OSCC recurrence remained unclear. Therefore, we investigated the OSCC patients' oral microbiota to understand the roles of oral microbiome in the recurrence of OSCC.
Materials and Methods: To evaluate the role of the oral microbiome in the recurrence of oral cancer, we compared the oral bacterial composition of tumor samples from the OSCC patients with or without recurrence based on 16S rRNA amplicon sequencing of 54 oral swab samples. Then, the structures of the oral microbiome were analyzed to establish a prediction model for the recurrence of OSCC. To identify microbial signatures capable of distinguishing recurrence from non-recurrence, the 54 tumor samples from OSCC patients were used as a training dataset. Furthermore, 46 external tumor samples from other OSCC patients were used to validate the dataset.
Results: The oral bacterial compositions differed in OSCC patients between with and without recurrence. Compared to nonrecurrence OSCC, periodontitis-related bacteria were enriched in OSCC recurrence. Functional analysis of the oral microbiome showed several functions associated with OSCC recurrence including amino acid metabolism,

carbohydrate metabolism, lipid metabolism, glucose utilization, and drug resistance. Subsequently, we established a random forest prediction model with high accuracy (accuracy = 0.963) to discriminate OSCC recurrence from the original OSCC based on five specific microbial signatures. Moreover, the prediction model achieved an accuracy of 0.761 in another independent cohort (46 OSCC patients). On the other hand, the accuracy predicted by the current clinical-used model was 0.519 with the training dataset. Thus, our novel model could improve the prediction accuracy of OSCC recurrence.
Conclusions: In this study, we elucidated the relationship between oral bacteria and the recurrence of OSCC. Moreover, we established a novel bacteria-based prediction model for the recurrence of OSCC. Thus, the present study provided a new insight and treatment strategy for the clinical prediction of OSCC recurrence.

#5898
Gut microbiota-derived metabolism of 5-fluorouracil affects drug efficacy

Despoina Chrysostomou, Mark David, James L. Alexander, Julian R. Marchesi, James M. Kinross. *Imperial College London, London, United Kingdom*

Introduction: Fluoropyrimidines are drugs currently used as a first-line treatment for colorectal cancer (CRC)[1]. The impact of gut bacteria on 5-Fluorouracil (5FU) activity remains relatively unknown. The objective of this analysis was to delineate potential bacteria-drug interactions that modify 5FU.
Methods: Tumor and tumor-adjacent healthy tissue samples from 130 colorectal adenocarcinoma patients, 55% males and 45% females, median age of 71 years old (36-91 age range), were extracted following surgical resection of the tumor. TNM classification varied across the cohort (15% pT1, 43% pT2, 35% pT3, 4% pT4). 16s rRNA gene amplicon sequencing was performed to map the microbiome composition of tumor and paired normal mucosa. 20 bacterial from the genera whose abundance changed significantly between tumor and healthy tissue were incubated with 5FU to assess drug-bacteria interactions. Ultra-performance liquid chromatography-mass spectrometry (UPLC-MS) was employed to identify changes in drug concentration (Wilcoxon spare rank test) as well as products of bacteria-driven drug metabolism. A metabolic activity-based assay was used to assess viability of a colorectal adenocarcinoma cell line (HCA46) following co-incubation with microbe-driven drug metabolites, aiming to determine significant effects on 5FU efficacy, assessed by 2-way ANOVA.
Results: *Escherichia coli* BW25113, *Bifidobacterium longum*, *Citrobacter freundii* and *Enterococcus faecalis* significantly modify 5FU *in vitro*, allowing us to conclude that bacteria can metabolise the drug *($q < 0.001$)*. *Ruminococcus gnavus* does not have the ability to metabolise the drug as no significant change in 5FU concentration was observed. Incubation of microbe-derived drug metabolites with HCA46 resulted in significant decrease in cell viability compared to incubation with 5FU only, indicating that bacteria-5FU interactions result in increase of drug efficacy (Figure 2).
Conclusion: This is the first report of 5FU metabolism by *Escherichia coli* BW25113, *Bifidobacterium longum*, *Citrobacter freundii* and *Enterococcus faecalis in vitro*. This study provides an insight into the potential of large

and small intestinal bacteria in chemically modifying chemotherapeutic agents and therefore modulating their activity.

1. Mahipal A, Grothey A. Role of biologics in first-line treatment of colorectal cancer. *J Oncol Pract*. 2016.

#5900

Tolerance to colibactin correlates with response to chemotherapeutic agents in colorectal cancer

Alberto Sogari[1], Emanuele Rovera[2], Nicole Megan Reilly[2], Simona Lamba[3], Mariangela Russo[2], Annalisa Lorenzato[1], Erika Durinikova[3], Livio Trusolino[1], Sabrina Arena[1], Manuela Donalisio[4], Federica Di Nicolantonio[1], David Lembo[4], Alberto Bardelli[5]. *[1]Department of Oncology, University of Torino - Candiolo Cancer Institute FPO-IRCCS, Candiolo, Italy,[2]University of Torino - Candiolo Cancer Institute FPO-IRCCS, Candiolo, Italy,[3]Candiolo Cancer Institute FPO-IRCCS, Candiolo, Italy,[4]Department of Clinical and Biological Sciences, University of Torino, Orbassano, Italy,[5]University of Torino; IFOM - Istituto Fondazione di Oncologia Molecolare, ETS, Candiolo, Italy*

Introduction: The bacterial genotoxin colibactin is enriched in colorectal cancer (CRC) and promotes the accumulation of mutations that drive tumorigenesis. However, systematic assessment of its impact on DNA damage response is lacking and the effect of colibactin exposure on response to other genotoxic agents (such as chemotherapy) is missing.
Materials and Methods: We implemented an *in vitro* bacteria-coculture system to assess the effect of colibactin on a representative subset of 40 molecularly and pharmacologically annotated CRC cell lines and in a panel of isogenic DDR KO cell lines we generated. We further validated our results in patient-derived organoids. Finally, we recapitulated prolonged exposure to colibactin occurring during tumorigenesis by chronically infecting sensitive cells until the emergence of a tolerant phenotype. }
Results: We found that different cell lines display specific sensitivity to colibactin's genotoxic stress: while colibactin-tolerant cells are capable to quickly and efficiently repair colibactin-induced DNA damage, sensitive cells lack this ability. Moreover, we found that homologous recombination (HR) proficiency discriminates colibactin-tolerant cells, which display

higher levels of RAD51 foci (as marker of activation of HR) compared to sensitive cells upon infection with colibactin. Screening of isogenic DDR KO cell lines revealed that genetic inactivation of the intertwined pathways of HR (through KO of *ATM*) and replication stress (RS) response (through KO of *ATRIP*) significantly sensitized cells to colibactin. In addition, we found that restoration of HR activity was sufficient to induce a colibactin-tolerant phenotype in initially sensitive cell lines. Notably, thanks to a previous effort of pharmacological characterization of CRC cell lines in our lab, we found a significant correlation between sensitivity to colibactin and irinotecan active metabolite SN38, but not oxaliplatin. We validated the same correlation in patient-derived organoids annotated for response to SN38. While colibactin, SN38 and oxaliplatin all induced RS in treated cells, we found that colibactin and SN38 showed a similar DNA damage response which involved activation of ATM. Finally, chronic re-infection of sensitive, HR-deficient CRC cells with colibactin selected a tolerant phenotype characterized by restoration of HR activity. Of translational relevance, colibactin-tolerant derivative cells acquired cross-resistance to SN38 and PARP inhibitor olaparib but not to oxaliplatin.
Conclusion: Our results shed novel insight into colibactin's genotoxic mechanism and support a model in which colibactin both promotes tumorigenesis and acts as an evolutionary bottleneck which selects HR proficient CRC cells. Furthermore, our study provides preclinical evidence on colibactin's role in promoting chemoresistance in colorectal cancer.

#5901
Microbiome and genomic profiling in rectal adenocarcinoma
David Hein, Laura Coughlin, Nicole Poulides, Andrew Koh, Nina Sanford.
University of Texas Southwestern Medical Center, Dallas, TX

Introduction: Recent studies have identified bacteria associated with colorectal cancer (CRC), with some data supporting causality in preclinical CRC models. We examined the gut microbiome composition and tumor genomic profiles in a diverse cohort of rectal cancer patients.
Methods: Twenty-two patients with newly-diagnosed, Stage II-IV rectal cancer without pathogenic germline mutations (mismatch repair genes, *MUTYH*) were included in the study. Gut microbiome profiling was performed on genomic DNA extracted from collected fecal samples (16S

rRNA sequencing, V4 region). Tumor specimens were tested for somatic and germline mutations using the Tempus xT 648-gene panel and whole transcriptome RNA sequencing, providing information on tumor mutation burden (TMB), pathogenic *KRAS* mutation status and consensus molecular subtype (CMS). We then assessed differential abundance of microbial taxa (using ANCOM-BC) between the following groups: high vs low TMB (dichotomized at median, 3.7 mut/MB), presence versus absence of pathogenic *KRAS* mutation, and CMS subtype.
Results: The median age of study subjects was 49 years (range 37-78). Racial/ethnic breakdown was as follows: 2 non-Hispanic Asian, 4 non-Hispanic Black, 5 non-Hispanic White, and 11 White Hispanic. Twelve tumors carried a pathogenic *KRAS* variant and the median TMB was 3.7 m/MB (range 0.5-8.9 m/MB). Among 20 tumors that underwent whole transcriptome RNA sequencing, 1 was categorized as CMS1, 8 CMS2, 3 CMS3, 7 CMS4, and 2 CMS undetermined. There were no statistically significant differences in gut bacteria taxa abundance by *KRAS* mutation status or among CMS subtypes. The group with greater than median TMB, however, had statistically significant enrichment of *Pepostreptococcus stomatis* (18.4 fold increase, p=0.039 after Benjamini-Hotchberg adjustment with FDR = 0.05).
Conclusions: In this pilot study, we found that CRC patients with higher TMB had an enrichment of *Peptostreptococcus stomatis*, a bacteria associated with colonic dysplasia in mouse models and enriched in CRC patients as compared to healthy controls. (PMID 28823860, 35292756) Higher TMB is a predictive biomarker for response to immunotherapy across cancer types including CRC. Since the gut microbiome is potentially modifiable, further research is needed to better elucidate the connection between microbiome and CRC carcinogenesis including specific mutation profiles, which could pave the way for microbiome-related risk reduction or therapeutic strategies in CRC.

#5903

Comparison of the tissue and gut microbiome in extrahepatic cholangiocarcinoma patients and healthy liver donors

Sora Kang[1], Jihee Kang[2], Gun-Seok Park[2], Seung-Hyun Ko[2], Jung-Hyun Park[3], Yunseon Jang[3], Ik-Chan Song[4], Hyewon Ryu[5], Seok-Hwan Kim[6].
[1]Division of Hemato-oncology, Chungnam National University Hospital,

Daejeon, Korea, Republic of,[2]AtoGen Co., Ltd., Daejeon, Korea, Republic of,[3]Translational Immunology Institute, Chungnam National University School of Medicine, Daejeon, Korea, Republic of,[4]Chungnam National University Hospital, Daejeon, Korea, Republic of,[5]Division of hemato-oncology, Chungnam National University Hospital, Daejeon, Korea, Republic of,[6]Division of Liver Transplantation and Hepatobiliary Surgery, Chungnam National University Hospital, Daejeon, Korea, Republic of

Background: Biliary tract cancer (BTC) is an aggressive malignancy associated with a poor prognosis. Most BTC patients are diagnosed at an unresectable stage; further, the efficacy of cytotoxic chemotherapy for BTC remains unsatisfactory. Recently, there is growing evidence that gut microbial dysbiosis is related to multiple diseases, including biliary disease and cancer. However, the association between tumor and gut microbiome environments and BTC, especially extrahepatic cholangiocarcinoma (EH-CCA), remains unclear. In the present study, we compared the microbiome from the tissue and stool samples of EH-CCA patients and healthy living liver donors (controls). Methods: A total of 24 people (13 EH-CCA patients and 11 healthy controls) were included. We collected fecal and swab samples, which were obtained from the EH-CCA tissues of the patients and normal gallbladder tissues of the controls during operation. The bacterial 16S rRNA gene (V3 and V4 region) was amplified using PCR and sequenced on the Illumina MiSeq platform. The QIIME 2 pipelines were used to analyze the raw data. Results: The median age of the patients and controls were 70 (range, 58-79) and 29 (range, 19-35) years, respectively. The swab samples from EH-CCA patients showed significantly lower alpha diversity than the samples from the controls ($pShannon < 0.001$). Proteobacteria was the most commonly found phylum (53%) in the EH-CCA patients; Firmicutes (79%) and Actinobacteria (13%) were the common phyla in the controls. The genera Streptococcus (25.1%), Escherichia_Shigella (16.9%), and Enterococcus (13.9%) were found in the patient samples, whereas Blautia (12%), Limosilactobacillus (12%), and Bifidobacterium (19%) were observed in the controls. The Principal Coordinate Analysis (PCoA) plot of the weighted UniFrac distances showed that the patient and control groups formed separate clusters. Among the fecal samples, Streptococcus (12.5%), bacterioides (8.2%) is most common in patients' group, whereas Blautia (13.8%) and Faecalibacterium

(11.5%) is most common in control group at the gene levels. The PCoA plot of the fecal samples showed significant differences in microbiota composition between the EH-CCA patients and healthy controls (P=0.001 by PERMANOVA). In the beta diversity analysis of all samples (swab plus fecal), the patient-swab samples formed distinct clusters, whereas the patient-fecal, control-swab, and control-fecal samples showed overlapping clusters.Conclusions: To the best of our knowledge, this study is the first that compares the microbiome of tissues and stools from EH-CCA patients and healthy controls; the EH-CCA patients and healthy controls showed different microbiota profiles. Further studies are needed to investigate the clinical implications of microbial dysbiosis in BTC and formulate novel microbiome-based treatments for BTC.

#5904

Intra-tumor microbes identified by RNAseq associated with response to immune checkpoint blockade in metastatic melanoma

Caroline E. Wheeler[1], Samuel Coleman[2], Rebecca Hoyd[1], Afaf Osman[3], Louis Denko[1], Aik Choon Tan[2], Daniel Spakowicz[1], Ahmad Tarhini[4].
[1]Department of Medical Oncology, The Ohio State University Wexner Medical Center, Columbus, OH,[2]Data Science, Huntsman Cancer Institute, Salt Lake City, UT,[3]Internal Medicine, Huntsman Cancer Institute, Salt Lake City, UT,[4]Department of Cutaneous Oncology, Moffitt Cancer Center, Tampa, FL

The tumor microbiome has recently been shown to play a key role in the context of oncogenesis, cancer immune phenotype, cancer progression and treatment outcomes in a variety of cancers. We investigated the possible associations between tumor microbiome and successful treatment outcomes with immune checkpoint blockade (ICB) in patients with metastatic melanoma.
We evaluated RNAseq from tumor samples, collected prior to the start of treatment with ICB, from 71 patients with metastatic melanoma. Samples were provided by eight members of the Oncology Research Information Exchange Network (ORIEN). Non-response was determined as change in treatment after less than 12 months. Patients maintaining the same treatment regimen for greater than 12 months were classified as responders.

We applied our custom tool, {exotic} (Exogenous sequences in Tumor and Immune Cells), to carefully identify non-human sequences within the RNAseq data. After filtering reads aligning to the human reference genome, reads were further filtered of common laboratory contaminants, taxa inversely correlated with input RNA quantity, and taxa frequently found in the negative controls of microbiome experiments. A differential abundance analysis was performed on the response groups at every taxonomic level utilizing DESeq2. We calculated expression signatures using {tmesig}, and related them to ICB response using {IOSig}.
We observed significantly enriched taxa (p-value < 0.05) with a high (>1.00) fold-difference in abundance between responders and non-responders found within the tumor RNAseq data, including *Fusobacterium nucleatum* and several viruses in responders, and *Delftia lacustris* and Fungi in non-responders. These microbes were associated with immune cell expression signatures, including Th17 cells and CD8+ T-cells.
We calculated the gene expression scores of 30 signatures with literature precedence for the ability to predict ICB treatment outcomes in melanoma. The receiver operator characteristic (ROC) curve of the random forest classification model for prediction of response to ICB using the combined expression signature scores resulted in an AUC of 0.8750. Combining expression signature scores with microbe relative abundances at the genus level improved the ability to predict ICB response (AUC = 0.8958). Combining tumor expression signatures with curated tumor microbiome relative abundances improves the performance of predictive models for treatment outcomes with ICB in melanoma.

#5905

Enterotoxigenic *Bacteroides fragilis*, a colon microbe, dysregulates polyamine catabolism to promote breast cancer progression

Deeptashree Nandi[1], Sheetal Parida[1], Sowjanya Thatikonda[1], Jackson Foley[1], Tracy Stewart[1], Cynthia L. Sears[2], Robert A. Casero[2], Dipali Sharma[2]. *[1]Oncology, Johns Hopkins University School of Medicine, Baltimore, MD,[2]Johns Hopkins University School of Medicine, Baltimore, MD*

Background: With more than 2.3 million cases worldwide, breast cancer persists as a major health burden and warrants a greater understanding of

the molecular triggers underlying this disease. Focusing on microbial dysbiosis, our lab discovered the pivotal role of the enterotoxigenic *Bacteroides fragilis* (ETBF) in promoting breast tumorigenesis through activation of key oncogenic pathways. A gap in knowledge exists regarding how microbes/microbial toxins modulate the oncogenic pathways in cancer cells. Polyamines are imperative for various physiological processes, including cell growth, survival, differentiation and apoptosis and are strongly associated with breast cancer. We questioned the involvement of polyamine pathway in mediating the oncogenic effects of microbial dysbiosis on breast cancer.

Methods: Human Her2 expressing spontaneous breast cancer model, MMTV.f.HuHer2 mice, were infected with ETBF and tumor incidence and progression were monitored for 18 months. We used qRT-PCR, western blotting, immunocytochemistry and immunohistochemistry to examine expression of key nodes of polyamine pathway. Various growth, migration and invasion assays were performed to assess carcinogenic properties in breast cancer cells. We employed a colorimetric-based assay to analyze enzymatic activities of key polyamine metabolic members. ROS generation was examined *via* DCFA staining.

Results: Our *in vivo* data showed that ETBF colonization in mice led to a considerable increase in the level of spermine oxidase (SMOX) in breast tumors, hinting at a correlation between ETBF and polyamine metabolism. Moreover, a marked rise in expression of γH2AX foci was observed in these tumors and in breast cancer cells, suggesting a critical role of ETBF in SMOX-related DNA damage. In agreement, we found SMOX upregulation in breast cancer cells. Our findings displayed a substantial increase in SMOX enzymatic activity in the presence of ETBF toxin, BFT, in breast tumor cells. BFT caused a marked rise in ROS generation of breast tumor cells, suggesting a plausible association of ETBF in SMOX-mediated oxidative stress. Interestingly, we noted a significant induction of ornithine decarboxylase (ODC) expression and activity in response to ETBF or BFT in breast cancer cells. Treatment of BFT-exposed breast cancer cells with SMOX inhibitors led to a sharp inhibition of neoplastic transformations, like cellular migration and γH2AX induction.

Conclusion: Our collated evidences suggest the existence of an important cross-talk between key polyamine metabolic enzymes and ETBF that aids in exacerbating breast tumorigenesis. Of importance, therapeutic inhibition

of SMOX dramatically impeded BFT-related breast tumorigenesis. Collectively, our results demonstrated the attractive potential of intervening the polyamine catabolic pathway for the management of breast cancer.

#5906

Gut microbiota signatures are associated with immunotherapy induced cognitive decline and neurotoxicity

Anik Banerjee[1], Christina Roland[2], Sarah Johnson[2], Nadim Ajami[2], Jennifer Wargo[2]. *[1]MD Anderson UTHealth Graduate School of Biomedicial Sciences, Houston, TX,[2]MD Anderson Cancer Center, Houston, TX*

Studies have demonstrated promising outcomes of combined immune checkpoint blockade (CICB) modulating tumor cytotoxicity via targeting cytotoxic T lymphocyte-associated antigen 4 (CTLA-4) and programmed cell death 1 (PD-1). The emergence of long-term patient management has been transformed among health care professionals as patient survival rates are increasing significantly. Despite promising advances, patient outcomes are heterogenic and are correlative to host intrinsic and extrinsic factors. Multiple reports have highlighted the negative effects of cancer treatments towards inducing cognitive impairment and neurotoxicity often referred to as “chemofog”. More recently, the gut microbiome has been increasingly recognized to regulate antitumor immunity and further distinct microbiome signatures can confer favorable outcomes in the context of CICB. Interestingly, specific microbes within the gut microbiome have been shown to regulate social behavior and cognition via the bidirectional communication along the gut-brain axis though changes in microbiota-derived metabolites and vagal afferent fibers. Insights into mechanisms of immunotherapy induced cognitive decline are warranted. Thus, we hypothesize CICB exacerbates cognitive impairment and neurotoxicity via the detrimental alterations to the gut microbiome. To address this, we profiled the gut microbiome, through 16S rRNA gene and metagenomic sequencing of fecal samples from patients (n=146) with advanced melanoma treated with CICB stratified based on severity of cognitive dissonance. Beta-diversity, incorporating weighted UniFrac distances by principal coordinate analysis (PCoA), revealed a cluster of samples from patients with cognitive impairment as compared to samples from those with minimal to absent cognitive decline. Further, taxonomical analysis showed

significant alterations in relative abundances of microbial candidates (e.g., *L. intestinalis*, *A. muciniphila*, *F. prausnitizii*, and *R. hominis*). These results suggests that CICB patients with cognitive impairments and neurotoxicity have altered microbiome signatures which may potentially exacerbate downstream neuroinflammatory signaling. Further studies investigating specific host-microbe pathways and profiling microbiota-derived metabolites which are implicated in these detrimental effects are essential for biomarker discovery and mechanistic insight.

#5907

The tumor microbiome associates with features of the tumor microenvironment, treatment outcomes, and histologies: A national collaboration of the exORIEN Consortium

Rebecca Hoyd[1], Caroline E. Wheeler[1], Samuel Coleman[2], Louis Denko[1], Carlos Chan[3], Yousef Zakharia[4], Rebecca Dodd[4], Cornelia M. Ulrich[5], Sheetal Hardikar[5], Jennifer Ose[5], Michelle Churchman[6], Ahmad Tarhini[7], Lary A. Robinson[8], Eric Singer[9], Alexandra P. Ikeguchi[10], Martin McCarter[11], Kyra Anderson[12], John Carpten[13], Gabriel Tinoco[14], Marium Hussain[1], Nicolas Denko[15], YunZhou Liu[15], Ning Jin[15], Youngchul Kim[8], Asgeir Masson[16], Naomi Fei[16], Martin Benej[17], McKenzie Kreamer[18], Dennis Dennis Grencewicz[15], Ahmed Hussein[15], Aik Choon Tan[19], Daniel Spakowicz[1]. *[1]Division of Medical Oncology, The Ohio State University Wexner Medical Center, Columbus, OH,[2]Data Science, Huntsman Cancer Institute, Salt Lake City, UT,[3]Department of Surgery, University of Iowa Carver College of Medicine, Iowa City, IA,[4]Department of Internal Medicine, University of Iowa Carver College of Medicine, Iowa City, IA,[5]Huntsman Cancer Institute, Salt Lake City, UT,[6]M2GEN, Tampa, FL,[7]Departments of Cutaneous Oncology and Immunology, Moffitt Cancer Center, Tampa, FL,[8]Moffitt Cancer Center, Tampa, FL,[9]The Cancer Institute of New Jersey, New Brunswick, NJ,[10]Department of Medicine, College of Medicine University of Oklahoma Health Sciences Center, Oklahoma City, OK,[11]University of Colorado Denver School of Medicine, Aurora, CO,[12]University of Colorado Cancer Center, Aurora, CO,[13]National Human Genome Research Institute, Bethesda, MD,[14]The Ohio State University Comprehensive Cancer Center, Columbus,*

OH,[15]Comprehensive Cancer Center, The Ohio State University Wexner Medical Center, Columbus, OH,[16]University of Iowa Carver College of Medicine, Iowa City, IA,[17]The Ohio State University Wexner Medical Center, Columbus, OH,[18]Department of Radiation Oncology, The Ohio State University Wexner Medical Center, Columbus, OH,[19]Department of Data Science, Huntsman Cancer Institute, Salt Lake city, UT

A tumor microbiome has recently been established as present in many cancer types. Further study is needed to define the scope of its role in cancer tumorigenesis, progression, and treatment outcomes. The Oncology Research Information Exchange Network (ORIEN) established a collaboration among eight member institutions to study the tumor microbiome and clinical features across several cancers. We evaluated RNAseq data from n = 2,892 tumors , including colorectal adenocarcinomas, lung adeno- and squamous cell carcinomas, pancreatic adenocarcinomas, sarcomas, melanomas, and thyroid carcinomas, using the tool {exotic}. Matched cancers from the Cancer Genome Atlas were processed by the same method (n = 2,720 samples). Clinical data, including treatment information, lab values, detailed histology, and long-term follow-up, were collected and harmonized across sites. Microbe abundances (bacteria, fungi, and viruses) were associated with clinical features and human gene expression, which was deconvolved into immune cell composition using {CIBERSORT} and {TIMEx}, and aggregated into expression signatures using {tmesig} and {IOSig}. Microbes were found in all tumors and associated with treatment outcomes for all modalities tested, including radiation in colorectal cancer, chemotherapy in pancreatic cancer, and immunotherapy in melanoma. In the case of radiation treatment in colorectal cancer, the microbes also affected outcomes in preclinical model systems and were modified by altering hypoxia levels with the drug atovaquone. Virus prevalence associated with histological subtypes in lung cancer. Similar microbes in ORIEN and TCGA tumors associated with overall survival in subtypes of sarcoma (dedifferentiated liposarcoma, leiomyosarcoma, and others). Finally, microbes associated with expression-based indicators of the tumor microenvironment across cancer types. These results suggest that the tumor microbiome may have broad clinical utility as a biomarker of treatment outcomes and as a target for rational manipulation.

#5908

Specific gut microbial community is associated with specific cancer types: A strategy for cancer detection and prevention

Ekansh Mittal[1], Andrew Oliver[2], Kenza El Alaoui[2], Carolyn Haunschild[2], Julio Avelar-Barragan[2], Laura F. Mendez Luque[2], Katrine Whiteson[2], Angela G. Fleischman[2]. *[1]Westview High School, Portland, OR,[2]University of California Irvine, Irvine, CA*

Background: Cancer is the second leading cause of death in the world. Unfortunately, survival rates for cancer patients have stayed poor for many decades. Thus, there is an unmet need to identify novel strategies for early cancer detection and prevention. Recent studies suggest that the gut microbiome including bacteria may have a role in cancer initiation and progression. These bacteria play a vital role in maintaining homeostasis in the body. An imbalance in the bacterial composition may cause diseases including cancer. This evidence led us to hypothesize that the changes in the composition of the gut microbiome can be used as a biomarker for early cancer detection. To test this hypothesis, we focused on analyzing the microbial community of colorectal and blood cancers, which have poor survival rates.

Methods and Results: To analyze the association of cancer with the microbiome, we used a published microbiome dataset of leukemic and healthy individuals that were collected by sequencing stool samples (Oliver et al., 2022). We identified that specific bacteria are either abundant, such as *Faecalibacterium* (1.17 fold), or reduced, such as *Clostridium* (0.32 fold, *p* value=0.0029), in leukemia patients compared to healthy controls. We observed similar correlations by analyzing the published colorectal cancer data (Flemer et al., 2017) in which *Prevotella* increased by 3.75 fold and *Escherichia/Shigella* increased by 4.0 fold in colorectal cancer while *Blautia* is reduced compared to healthy controls. *Faecalibacterium,* which is abundant in leukemia, is reduced in colorectal cancer. Further, we found that treatment of leukemia patients normalized the abundance of these bacteria to the level of healthy patients. To improve analysis efficiency, we applied machine learning algorithms to predict the presence of cancer in patients based on the composition of bacteria, age, gender, and symptoms. Among the tested algorithms, the decision tree and Random Forest both had very high false-negative rates, with 45.5% and 40% respectively, as well as

having low sensitivities, with 50% and 60% respectively. The support Vector Machine had a suboptimal false-negative rate of 28.6% and good sensitivity of 80%. Finally, the Neural network had a good false-negative rate of 16.7% and great sensitivity of 90%. Overall, our results suggest that different cancers have an abundance of specific bacteria that can be used as biomarkers for cancer detection.
Conclusion: We demonstrate that the increased abundance of certain bacteria in the microbiome can be used as a biomarker for cancer detection. Our data set was small for this project, but the machine learning approaches can be used to further predict cancer These are clinically relevant findings as a microbiome test would be non-invasive and easily accessible that can be performed at a routine checkup.

#5909
Characterization of the lung cancer microbiome using whole genome sequencing
John McElderry, Tongwu Zhang, Jianxin Shi, Maria Teresa Landi. *NCI Div. of Cancer Epidemiology & Genetics, Rockville, MD*

Microbiome studies have been rapidly increasing over the last decade, providing valuable insights into the commensal bacterial contribution to human physiology and disease, including human cancer. Many studies have demonstrated the important roles of the microbiome in cancer progression, anti-tumor immunity, resistance to therapies, metastasis formation, and in some rare cases even cancer development through the production of genotoxins. However, relatively few studies have analyzed the lung cancer microbiome, and both its composition and role in cancer progression are largely unknown. To characterize the microbiome of tumor and matched normal lung tissues, we performed whole-genome sequencing (WGS) in 872 never smokers using the Kraken pipeline. At the phylum level, WGS analyses of tumor and normal samples showed predominantly *Proteobacteria* and *Actinobacteria* (58% and 32%, respectively). Notably, we found overall similar microbiome composition in tumor and normal lung tissue samples. At the genus level, *Cutibacterium, Klebsiella*, *Pseudomonas, Sphingomonas, Staphylococcus, and Acinetobacter* genera were among the most abundant bacteria in tumor and normal tissues, alike, and the genera *Prevotella*, *Corynebacterium*, and *Streptococcus* were more

abundant in tumor samples compared to normal lung tissue. Comparison of alpha diversity at the genus level between tumors and normal samples showed no substantial difference. We are currently investigating whether the microbiome composition varies by lung tumor anatomical location, sex, histology, study subjects' geographical location, and immune microenvironment. We will also investigate whether the tumor microbiome composition varies in relation to important genomic features, like cancer driver genes and mutational signatures. Finally, we have 16s rRNA seq data from 771 tumor and normal lung tissues from never smokers and we will compare bacterial microbiome composition and diversity based on WGS and 16s rRNA seq for the same samples. This study, based on the largest analysis of lung microbiome to date, is poised to provide important insights into the role of commensal microbiota in shaping lung tumor development and progression.

#5910

Prospective platform to define microbiome correlates of metastasis and therapy resistance in early onset and average onset gastrointestinal cancers

Melissa A. Lumish, Asha R. Saxena, Nicholas Waters, Anqi Dai, Saskia Hartner, Teng Fei, Matthew Drescher, Jonathan Bermeo, Dorina Ismailgeci, Maggie Fox, Yelena Y. Janjigian, Luis A. Diaz, Martin R. Weiser, Jonathan Peled, Marcel van den Brink, Karuna Ganesh. *Memorial Sloan Kettering Cancer Center, New York, NY*

Background: The incidence of early onset (EO) gastrointestinal (GI) cancers prior to age 50 is rising, and the etiology is unknown. The gut microbiome may contribute to GI cancer pathogenesis, though how bacteria drive metastasis and treatment resistance is not known.
Purpose: To define the microbiome contribution to EO-GI cancers and metastasis by analyzing longitudinal samples from previously untreated patients with GI cancers.
Methods: We designed a prospective biospecimen collection platform. We selected patients with newly diagnosed, previously untreated colorectal cancer (CRC) and esophagogastric cancer (EGC). We collected stool, biopsy or surgical tissue, and peripheral blood mononuclear cells (PBMCs) at baseline prior to treatment and at each restaging scan for patients with

metastatic disease. For those with locally advanced disease, we collected samples at baseline and after each treatment phase (surgery, radiation, chemotherapy). Stool samples were analyzed using shotgun sequencing. Tissue samples were banked for further analysis. Clinical data was manually curated. Relative abundances of bacteria at the species level were compared between groups. Alpha diversity was calculated using the inverse Simpson index and compared between groups using the Wilcoxon signed-rank test. Beta diversity was analyzed using the Bray-Curtis dissimilarity matrix and compared using PERMANOVA. Multivariate association between species abundance and clinical covariates was performed using MaAsLin2 R package.
Results: We analyzed a total of 150 stool samples from 76 patients (colorectal n=53, esophagogastric n=23), including up to 6 samples from a single patient over time. Mean alpha diversity did not differ significantly by primary site or age at diagnosis in patients with CRC but was higher in stage IV compared with stage I disease (P=0.054). Beta diversity was significantly different between samples from patients with right- compared with left-sided CRC (P=0.005) but did not differ significantly by diagnosis age (<50 vs. $\geq$ 50). Among those with EGC, mean alpha diversity was not significantly different in samples from patients with esophagus or gastroesophageal junction (proximal) tumors compared with gastric (distal) tumors and did not differ significantly by age group. Beta diversity was significantly different between patients with EGC over 50 compared with those under 50 (P=0.002). When CRC baseline samples were examined, several bacterial species were associated with age <50 at diagnosis, including *Streptococcus anginosus* group (P=0.001), *Solobacterium moorei* (P=0.013), and *Firmicutes* bacterium CAG83 (P=0.016).
Conclusions/Future Directions: Microbiome composition may cluster by primary tumor site and age at diagnosis in patients with previously untreated GI cancers. Functional analysis and is ongoing and will be presented.

#5912
Bitter taste receptors link between microbiome dysbiosis and programmed cell death in oral squamous cell carcinoma
Byeong-Oh Hwang, Se-Young Park, Na-Young Song. *Yonsei University, Seoul, Korea, Republic of*

Oral squamous cell carcinoma (OSCC) is the most common type of head and neck cancers. It has been reported that the composition of the oral microbiome was shifted in OSCC patients compared to healthy subjects. In particular, *Pseudomonas aeruginosa* was enriched in the oral cavity of OSCC patients. Bitter taste receptors (taste 2 receptors, TAS2Rs), known as G protein-coupled receptors (GPCRs), can recognize quorum sensing molecules, such as N-(3-oxododecanoyl)-L-homoserine lactone (oxo-C12) secreted from *P. aeruginosa*. Based on The Cancer Genome Atlas analysis, downregulation of TAS2Rs was correlated with poor prognosis in various cancers. This prompted us to investigate the role of TAS2Rs in oral dysbiosis and cancers. Here, we found that TAS2Rs mediated both apoptosis and pyroptosis, distinct types of programmed cell death, in response to oxo-C12, in OSCC cell lines. Of note, it was blocked by knockdown of *TAS2R4, 14*, or *38*. Unexpectedly, TAS2Rs-mediated apoptosis and pyroptosis were GPCR-independent. Given our observation that the blockade of NLRP3 inflammasome attenuated oxo-C12-induced OSCC cell death, TAS2Rs seem to recruit NLRP3 inflammasome rather than G protein signaling pathway in order to mediate the programmed cell death in OSCC. Once NLRP3 is activated, caspase-8 triggered both apoptosis and pyroptosis in response to oxo-C12, supporting the role of TAS2Rs-NLRP3-caspase-8 axis. Interestingly, siRNA knockdown of *MyD88* diminished oxo-C12-induced programmed cell death, implying the possible involvement of MyD88 in the TAS2Rs-NLRP3-caspase-8 axis. Taken together, bitter taste receptors promote the programmed cell death of OSCC in response to oral dysbiosis through activation of NLRP3 inflammasome, which further supports TAS2Rs as prognostic markers in OSCC. Thus, these results will shed light on better understanding of interplay between microbiome and cancer, proposing TAS2Rs as novel therapeutic targets in oral dysbiosis-induced OSCC development.

#5913

Semi-supervised analysis of myeloid and T cell behavior in *ex vivo* ovarian tumor slices reveals changes in cell motility after treatments

Florian Laforets[1], Panoraia Kotantaki[1], Beatrice Malacrida[1], Samar Elorbany[1], Ranjit Manchanda[2], Emmanuel Donnadieu[3], Frances Balkwill[1].
[1]Cancer Research UK Barts Centre, London, United Kingdom,[2]Wolfson

Institute of Population Health, London, United Kingdom,[3]Institut Cochin, Paris, France

Cell motility is an important component of anti-tumor responses, allowing immune cells like myeloid and cytotoxic T cells to infiltrate tumors. Using *ex vivo* human and mouse high-grade serous ovarian cancer (HGSOC) tumor slices combined with time-lapse imaging, we monitored the movement of $CD8^+$ T and myeloid cells in live tumors, in real-time. To analyze the recordings and characterize immune cell movements, we developed a semi-supervised analysis, identifying four types of cell behavior: migrating, long migrating, static and wobbling. Tumor slices were maintained 24h *ex vivo*, retaining viability and cell movements. We show that *ex vivo* treatments with LPS altered $CD8^+$ T and myeloid cell behavior. *In vivo* chemotherapy reduced *ex vivo* cell movements in human and mouse tumors, and differentially affected $CD8^+$ T and myeloid cells in 60577 and HGS2 murine tumors, respectively chemo-sensitive and chemo-resistant mouse models, suggesting those cell types have different roles in the response to chemotherapy. *Ex vivo* tumor slices can extend *in vivo* mouse work to human, providing a stepping stone to translate mouse cancer studies to clinical trials.

#5914

Colorectal cancer attributes and outcomes according to *Fusobacterium nucleatum* enrichment and presence

Courtney M. Hill[1], Meredith A. J. Hullar[2], Adriana Reedy[2], Rachel Malen[2], Hamza Ammar[2], Orsalem Kahsai[2], Ningxin Ma[2], Shuji Ogino[3], Timothy Randolph[2], Polly Newcomb[2], Amanda Phipps[2]. *[1]Epidemiology, University of Washington, Seattle, WA,[2]Fred Hutchinson Cancer Center, Seattle, WA,[3]Pathology, Brigham & Women's Hospital, Harvard Medical School, Boston, MA*

Purpose: *Fusobacterium nucleatum* (*Fn*) has been associated with colorectal cancer (CRC) etiology and outcomes. However, these relationships may differ by tumor attributes. We examined whether *Fn* enrichment and presence in CRC was associated with tumor attributes and survival.

Experimental Design: We measured the abundance of *Fn* via droplet digital PCR in patient-matched CRC tumor and normal tissue samples from a subset of participants in the Puget Sound CRC Cohort (n=526). *Fn* enrichment was defined as the continuous difference in *Fn* abundance (normalized to counts of a host housekeeping gene) between patient-matched tumor and normal tissue samples. *Fn* presence in tumor was classified categorically as negative, low (*Fn* abundance >0 but <median level among those positive for *Fn*), or high (abundance ≥median). *Fn* enrichment and presence variables were examined in relation to tumor attributes (site, stage, microsatellite instability [MSI] status, CpG island methylator phenotype [CIMP] status, *BRAF* and *KRAS* mutation status), molecular subtypes, and CRC survival. Molecular subtypes were defined as: type 1 (MSI-high, CIMP-high, *BRAF*-mutated); type 2 (microsatellite stable [MSS]/MSI-low, CIMP-high, *BRAF*-mutated); type 3 (MSS/MSI-low, non-CIMP, *KRAS*-mutated); type 4 (MSS/MSI-low, non-CIMP, *BRAF*- and *KRAS*-wildtype); and type 5 (MSI-high, non-CIMP, *BRAF*- and *KRAS*-wildtype). Logistic regression was used to estimate odds ratios (OR) and 95% confidence intervals (CI) for associations of *Fn* enrichment and presence with tumor attributes, adjusted for age, sex, tumor site, and *Fn* abundance in normal tissue (*Fn* enrichment only). Cox regression was used to estimate hazard ratios (HR) and 95% CIs for the associations of *Fn* enrichment and presence with CRC survival, adjusted for age, sex, tumor site, tumor markers, and *Fn* abundance in normal tissue (*Fn* enrichment only).
Results: High *Fn* presence was negatively associated with left-sided colon and rectal tumors. While *Fn* enrichment was only significantly associated with CIMP-high status (OR 1.2; 95% CI 1.0, 1.4; p=.03), high *Fn* presence was positively associated with MSI (OR 4.9; 95% CI 2.8, 8.4; p<.001), CIMP-high (OR 3.2; 95% CI 1.8, 5.7; p<.001), and *BRAF*-mutated status (OR 3.3; 95% CI 1.8, 6.1; p<.001). *Fn* enrichment was associated with higher odds of type 2 tumor classification (OR 1.2 95% CI 1.0, 1.5; p=.03) and high *Fn* presence was associated with higher odds of type 1 (OR 5.8; 95% CI 2.3, 15.0; p<.001) and type 5 tumor classification (OR 3.4; 95% CI 1.1, 10.4; p=.03). Continuous *Fn* enrichment was independently associated with lower survival (HR 1.1; 95% CI 1.0, 1.1; p=.006) but high *Fn* presence was not (HR 1.0; 95% CI 0.6, 1.6; p=.99).

Conclusions: Our findings suggest that *Fn* enrichment and presence are associated with certain CRC tumor attributes and survival, but associations varied by how *Fn* status was defined.

#5915

Exploring the impact of microbiome in the response of combined radiation with immune checkpoint blockade in muscle invasive bladder cancer (MIBC)

Eva Michaud[1], Cynthia Faubert[2], Jose Joao Mansure[1], Irah King[2], Wassim Kassouf[1]. *[1]McGill University Health Centre Research Institute, Montréal, QC, Canada,[2]McGill Interdisciplinary Initiative in Infection and Immunity, Montréal, QC, Canada*

BACKGROUND : Radiation therapy is a promising bladder-sparing option for MIBC treatment. Yet, 30% of patients do not respond and of those, half will later die of metastasis. Combining radiation therapy with immunotherapy (CT) thus presents a worthy candidate to fulfill this unmet need. In preclinical models, improved antitumor responses when RT is combined with PD-1/ PD-L1 blockade have been described. Yet, there remains a flagrant lack of knowledge on the determinants of combination therapy success. In this context, the composition of the gut microbiome is critical in conditioning local and peripheral immunity. Recent metagenomic studies have shown the gut microbiome influences the efficacy of PD-1-based IT in epithelial tumors, melanoma, and lung cancer, to name a few. In addition, modification of the gut microbiome with oral gavage of immunogenic bacteria potentiates the activity of combined RT and anti-PD-L1 therapy. Furthermore, immune profiling shows enhanced systemic and antitumor immunity in responding patients with a favorable gut microbiome (such as enrichment in *Akkermansia muciniphila*, *Bifidobacterium* and *Faecalibacterium*). Therefore, we aim to document the role of patients' microbiome in polarizing anti-tumor immune responses to CT in order to eventually use its composition as a predicting factor of CT success. METHODS : Fecal material from responder (R, n=3) and non-responder (NR, n=3) MIBC patients was gavaged into 20 germ-free (GF) mice in two administrations one week apart. 3 weeks after the last gavage, tumor cells (MB49) were delivered subcutaneaously. Once tumors reached 0.1-0.15cm^3, mice were randomized into 4 groups : control; anti-PD-L1 alone;

RT alone; RT + anti-PD-L1. 7 days after the start of treatment, tumors were harvested, dissociated and frozen as cell suspensions for single cell immune profiling and TCR sequencing (10X Genomics). Stool were collected weekly for 16S sequencing. Correlation networks from sequencing data were built (TransNet and Microbiome R packages) and visualized using Cytoscape to show interactions between the tumor immune microenvironment and the gut microbiome in R and NR-receiving mice.
RESULTS : We show feasibility of the experimental design as well as robust engraftment of human FMT to germ-free mice in a bladder cancer tumor model. FMT from NR lessened the known beneficial effects of RT in the MB49 model compared to FMT from R. Transkingdom analysis of sc-RNA-seq and 16S show robust statistical interactions between immunosuppression and enrichment in microbes associated to poor outcome in immunotherapy.
SIGNIFICANCE : To our knowledge, this is the first study to use FMT as a modulator of response in the context of radiation therapy combinations in MIBC. Findings from this study have a strong predictive value that could be used to select patients who will benefit most from a personalized therapeutic approach.

#5916

Weight loss intervention triggered gut microbiota modulation can positively impact obesity associated endocrine therapy resistance

Sheetal Parida[1], Sumit Siddharth[1], Nethaji Muniraj[1], Zhenhui Liu[2], Ishan Barman[3], Michael Smith[1], Jenni Sheng[1], Vered Stearns[1], Janelle W. Coughlin[1], Dipali Sharma[1]. *[1]Johns Hopkins University School of Medicine, Baltimore, MD,[2]Department of Mechanical Engineering, Johns Hopkins University, Baltimore, MD,[3]2Department of Mechanical Engineering, Johns Hopkins University, Baltimore, MD*

Background: 41.9% of adult US population is obese and every 5-unit BMI increase is associated with 12 percent increase in breast cancer risk; it is an independent predictor of poor outcomes in breast cancer. Microbiome has emerged as a central regulator of obesity and we recently discovered that microbes can not only potentiate breast cancer growth and metastasis but also affect therapeutic response. We showed weight-loss by Diet/Exercise/Behavioral intervention (POWER-remote trial) exerts

favorable effects. Here, we examine molecular underpinnings of poor therapy response in obese state and explore the gut microbiome to mitigate the same.
Methods: We co-implanted lineage determined human White preAdipocytes (hWAT) with MCF7 breast cancer cells in the mammary glands of mice. Changes in tumor microenvironment and tumor cells were evaluated *ex situ* by RNA sequencing, flow cytometry, Raman spectroscopy, Quantitative phase microscopy, PCR, immunoblotting and functional assays. To inspect the gut microbiome, 16 obese breast cancer patients were subjected to weight loss intervention over 14 weeks. Gut microbiome was analyzed at baseline and post-intervention by microbial shotgun sequencing. Patients were divided into responders and non-responders based on % weight-loss.
Results: We found that human breast cancer cells co-implanted with hWAT formed more aggressive tumors compared to controls. RNA sequencing revealed significant upregulation of multiple oncogenic pathways along with robust innate immune response. Tumor dissociated cells from hWAT-MCF7 tumors showed extensive molecular reprogramming rendering them more proliferative, motile and stem-like along with dramatic physiological changes like increased intercellular lipid accumulation. hWAT-MCF7 cells attained resistance to multiple drugs including Tamoxifen, Fulvestrant, Letrozole and Palbociclib. Simultaneous targeting of multiple signaling pathways using pharmacological inhibitors is infeasible in clinical setting hence we explored the obesity-microbiome axis. Obese breast cancer patients underwent POWER-remote intervention and their gut microbiome analysis showed significant differential expression of many microbes. Based on abundance and metabolite profile, *F. prausnitzii* was selected as the candidate of interest. On treatment with *F. prausnitzii* growth media, acquired multi-drug resistance in hWAT-MCF7 cells could be reversed suggesting that increase in gut population of the bacterium could be helpful in sensitizing patients unresponsive to therapy.
Conclusion: Direct interaction between breast cancer cells and WAT rendered them resistant to multiple drugs. Metabolites produced by weight-loss-associated bacterium *F. prausnitzii* reversed adiposity-induced multi-drug resistance, hence, can potentially have therapeutic benefits in obese breast cancer patients.

#5917

Development of a medium-to-high throughput organoid-bacteria co-culture platform for the assessment of host pathogen interaction

Eider Valle-Encinas[1], Roshni Nair[1], Katerina Pisa[1], Mayke Doorn[1], Farzin Pourfarzad[1], Lani San Mateo[2], Nicole Desch[2], Prashanth Gokare[2], David Pocalyko[2], Sylvia F. Boj[1], Carla Verissimo[1]. *[1]Hubrecht Organoid Technology, Utrecht, Netherlands,[2]Janssen, Spring House, PA*

Pathogens such as colibactin-producing bacteria strains of the *Enterobacteriaceae* family are highly prevalent in the gut microbiota of colorectal cancer (CRC) patients. HUB patient derived Organoids, (HUB-Organoids™ or PDOs) are self-organized epithelial cell structures with near-physiological features, extensively used to model aspects of cancer initiation and progression. Studies conducted by Pleguezuelos-Manzanos et al. (2020) showed that repetitive cycles of colibactin-producing bacteria into the organoid lumen via microinjection, led to two co-occurring mutational signatures appearance, a single-base substitution signature (SBS-pks) and an indel signature (ID-pks), identified in a subset of CRC patients (~2% and 7%, respectively). These results highlight the relevance of organoids for modelling host-pathogen interactions and the application of these systems as *in vitro* platforms for investigating long-standing cause-correlation relationship between the presence of genotoxic pathogens and CRC development. The limited scalability of sophisticated co-culture strategies with pathogens such as microinjection has represented a bottleneck in the use of organoids as throughput screening tools in the development of preventive therapies. Thus, there is an unmet need to develop alternative co-culture systems compatible with the process of compound screening. An organoid-bacteria co-culture system compatible with medium-to-high throughput screening readouts has been developed. This co-culture system is currently tailored for the modeling of colibactin genotoxic effects in the gut epithelium, but theoretically could be extended as a discovery platform to identify targetable, novel and complex interactions between host and pathogen. Key words: colibactin, organoids, CRC, screening

#5918

Interrogating host-intratumoral microbial interactions in pancreatic cancer

Vidhi Chandra[1], Hajar Rajaei[1], Seyda Baydogan[1], Javier Gomez[1], Sammy Ferri-Borgogno[1], Anirban Maitra[1], Erick Riquelme[2], Ismet Sahin[3], Jared Burks[1], Michael Kim[1], Florencia McAllister[1]. *[1]University of Texas MD Anderson Cancer Center, Houston, TX,[2]Universidad Mayor, Santiago, Chile,[3]Texas Southern University, Houston, TX*

Cancer is increasingly becoming a rising cause of mortality worldwide. Microbiota, both within the gut and tumors, has emerged as a significant player influencing tumor growth and responses to therapies. The tumor niche provides a privileged microenvironment for microbial colonization. Recent evidence links microbiota and pancreatic tumorigenesis. Pancreatic ductal adenocarcinoma (PDAC), is an aggressive cancer surrounded by a highly immuno-suppressive tumor microenvironment (TME) which limits efficacy of most available therapies. We have previously reported that rare long-term survival in pancreatic cancer is associated with an intratumoral microbial signature which correlates with enhanced TME immunoactivation, suggestive of microbial mediated immune cell recruitment. A gut-to-tumor microbial crosstalk was also found in a human-to-mouse Fecal Microbiota Transplant (FMT) tumor model. While we have identified the vital role of microbiota in affecting tumor immunity, there is still a gap of knowledge about local microbial interactions within TME. Deeper understanding of the microbial mediated events that are triggered and follow PDAC development, which act to induce and support tumor growth, would provide us with potential novel targets that could be blocked to reverse PDAC immunosuppression and tumor growth. To interrogate the features of the pancreatic tumor microbial niche, we performed spatial co-detection of microbial and host targets to identify the cellular compartment which interacts with microbes inside the TME in clinical samples. We developed novel qualitative and quantitative imaging methodologies for evaluating crosstalk between the host and microbes. We also evaluated the effect of microbial burden on transcriptomic changes in host cells through multiple spatial sequencing approaches. Overall, we dissect the functional role of microbes in orchestrating TME organization and their effect on tumor signaling.

#5919

The significant role of HMGB1 in mesothelial cells in contributing to the mesothelioma development induced by asbestos

Joelle S. Suarez[1], Giovanni Gaudino[1], Tak W. Mak[2], Michele Carbone[1], Haining Yang[1]. *[1]University of Hawai'i Cancer Center, Honolulu, HI,[2]The Campbell Family Institute for Breast Cancer Research, Princess Margaret Cancer Center, University Health Network,, Toronto, ON, Canada*

Diffuse Malignant mesothelioma is a very aggressive cancer that is related to asbestos exposure. We found previously that following asbestos deposition in the pleura and in the peritoneum, mesothelial cells release HMGB1 that attract granulocytes and macrophages that, in turn, secrete HMGB1. It was unknown whether the primary source of HMGB1 that drives the inflammatory process caused by asbestos, which may ensue in mesothelioma, derives from the mesothelial cells exposed to asbestos or from the granulocytes and macrophages. To study separately the contribution of mesothelial cells and of the inflammatory cells to HMGB1 secretion that drives mesothelioma development, we used two tissue-specific HMGB1 knockout mouse models: (1) An inducible mesothelial conditional HMGB1 knockout ($HMGB1^{\Delta pMeso}$) mouse model, and (2) a constitutive myelomonocytic-lineage knock out ($HMGB1^{\Delta Mylc}$) mouse model. To investigate the role of HMGB1 in asbestos induced carcinogenesis *in vivo*, we conducted both short-term and long-term experiments in $HMGB1^{\Delta pMeso}$ mice and in $HMGB1^{\Delta Mylc}$ mice. For the Short-term experiment, we observed that one week following the completion of the 10-weekly crocidolite i.p. injections, all the mice in experimental and control groups showed inflammation with multiple granulomas around asbestos deposits in the various tissues and organs present in the abdomen, and diffuse mesothelial hyperplasia. However, the granulomas in $HMGB1^{\Delta pMeso}$ mice were significantly smaller compared to those found in the control WT mice. TNFα IHC stain was minimal to non-detectable in the granulomas and areas of mesothelial hyperplasia of $HMGB1^{\Delta pMeso}$ mice, compared to a strong TNFα staining in both $HMGB1^{\Delta Mylc}$ and WT mice. For the Long-term experiment, we observed that the incidence of mesothelioma was significantly lower in $HMGB1^{\Delta pMeso}$ mice compared with the 3 control groups including WT mice, $HMGB1^{F/F}$ mice and $Wt1ERT2^{Cre/+}$ control mice. Moreover,

HMGB1$^{\Delta pMeso}$ mice had a significantly longer mesothelioma-specific survival compared to all three controls. Histologically, the HMGB1$^{\Delta pMeso}$ mesotheliomas were smaller and grew largely over the surface rather than infiltrating the abdominal organs, compared to the mesotheliomas that developed in the three control groups.In summary, our findings underscore the role of HMGB1 in asbestos pathogenesis, including asbestos induced chronic inflammation and mesothelioma. Moreover, our findings elucidated the mechanisms responsible for asbestos induced inflammation and asbestos carcinogenesis, and the causal link between HMGB1, TNFα secretion and mesothelioma. Our results point to the HMGB1 secreted by mesothelial cells as the culprit and thus the ideal target to prevent the growth of mesothelioma upon asbestos exposure and during the early phases of mesothelioma growth.

Methods to Measure Clonal Evolution

#5923
The genetic landscape of metastatic breast cancer reflected in circulating tumor DNA

Stephanie Kavan. *Odense University Hospital, Odense, Denmark*

Tissue biopsies of breast tumors only provide a snapshot of the evolution of the disease and may miss potential therapeutic targets, especially in the metastatic setting. Plasma-derived cell-free tumor DNA constitutes a potential surrogate for tumor DNA obtained from tissue biopsies to potentially capture inter-and intra-tumoral heterogeneity present in metastatic breast cancer. We aimed to investigate to what extent variants identified in the primary tumor and metastases are reflected in plasma. We performed whole-exome sequencing on tumor DNA from primary and metastatic lesions and plasma-derived circulating tumor DNA of eight patients with metastatic breast cancer. Our results show that metastases most often follow parallel evolution, given the low levels of stem mutations detected between primary tumors and matched metastases and mutational events private to the primary tumor. Furthermore, we demonstrated that ctDNA mainly reflected old stem mutations shared between primary tumor and metastasis, and less often, genetic alterations found solely in primary tumor or metastasis. Lastly, clinically relevant variants, e.g., resistance

mutations detected in primary tumor and metastasis, were to some extent reflected in ctDNA, including affected genes *MET, MTOR, CDK6, PIK3CA,* and *GATA3*. However, mutations in MED*1, NCOR1,* and *NCOR2* were only found in tumor tissues. These findings support the importance of a metastatic deposit biopsy to guide treatment decisions. Together, our results have implications for future ctDNA studies. For monitoring tumor burden using ctDNA, our results suggest that truncal mutations are the best candidates, as they are highest in circulating levels. For confident tracking of subclonal mutations in ctDNA, liquid biopsies are not yet to substitute metastatic tissue biopsies and instead demonstrate support to the current gold standard.

#5924

Intratumor heterogeneity in thyroid cancer progression

Vincenzo Davide Pantina. *University of Palermo, Palermo, Italy*

Thyroid cancer (CT) is the most common endocrine organs malignancy and is classified into:well-differentiated carcinomas, characterized by favourable prognosis and sensitive to standardtreatments, and undifferentiated carcinomas (UTC), the most lethal and highly refractoryagainst current therapies. UTCs have invasive and highly metastatic phenotype. The metastaticcascade model described distant metastasis origin deriving from cancer cells that seed to lymphnode and then disseminate to distant organs. According to this, lymphadenectomy was definedas an elective therapy for TC patients. However, recent TC trials discredit the improvement inpatient outcome. We aim to unveil the mechanism underlying tumor promotion, primary tumorclonal selection and TC metastatic origin determining which specific subclone is able to colonizedistant organs.
Material and method:Thyroid carcinogenesis model was previously generated starting from human embryonic stemcells which underwent to a differentiation protocol. At day 22 of differentiation, thyroidprogenitor cells (TPCs) were engineered using CRISPR CAS-9 technology to introduce mutationin BRAFV600E/TP53R248Q and NRASQ61R /TP53R248Q gene in order to recapitulate, wheninjected in *vivo*, UTC. Double mutated TPCs were transduced with Barcode-mediated clonaltracking technology and subcutaneously/orthotopically injected in immunocompromisedmice.

Results:We trasduced D22 double-mutated TPCs using highly complex lentiviral barcode library to mapclonal architecture in serial subcutaneous xenograft and multiple metastatic sites.Immunohistochemistry analysis obtained from P1 and P3 engraftment revealed conservation ofanaplastic thyroid cancer histologic features. Moreover, tumor-derived cells were in vitrocharacterized showing that P3 retains high migratory, invasion capacity and high MMP-9expression level, compared to P1. Transcriptomic analysis of P3 versus P1 derived cells showalso a critical metabolic switch. Cell derived from P3 engraftment were used to generateorthotopic model using Barcode mediated-clonal tracking technology.
Conclusion:Given its impact on patient care, understanding the evolutionary history of anaplastic thyroidcarcinoma is critical in cancer treatment. Phylogenetic studies on the primary and metastatictumor should determine the emergence of one or more subclones, which have a crucial roleduring all the phases of tumor promotion, progression and metastatic onset. A phylogeneticanalysis performed via the barcode-mediated clonal tracking technology, will allow us to trackprimary tumor cellular clones selection and the arising progenity, determining their role in themetastatic cascade. NGS Analysis and RNA-Seq technology will define a specific primary tumor
vs metastatic signature. The identification of cellular clones enriched in the metastasis willprovide new prognostic markers for metastatic thyroid carcinoma.

#5925

Prevalence of clonal hematopoiesis in patients with monoclonal gammopathy of undetermined significance

Vianey Quaney[1], Benjamin Kroger[2], Aishwarya Sannareddy[3], Umar Khan[3], Fatma Kalkan[4], Robert H. Collins[3], Yazan F. Madanat[3], Madhuri Vusirikala[3], Yi Huang[5], Farrukh T. Awan[3], Praveen Ramakrishnan[3], Aimaz Afrough[3], Larry D. Anderson[3], Stephen S. Chung[5], Gurbakhash Kaur[3].
[1]Division of Hematology/Oncology, Department of Internal Medicine, University of Texas Southwestern Medical Center, Dallas, TX,[2]Division of Hematology and Oncology, Department of Internal Medicine, Children's Research Institute, UTsouthwestern Medical Center, Dallas, TX,[3]Hematology/oncology - Bone Marrow Transplant, Utsouthwestern

Medical Center, Dallas, TX,[4]Division of Cardiology, Department of Internal Medicine, Utsouthwestern Medical Center, Dallas, TX,[5]Division of Hematology and Oncology, Department of Internal Medicine, Children's Research Institute, Utsouthwestern Medical Center, Dallas, TX

INTRODUCTION: Clonal hematopoiesis of indeterminate potential (CHIP) is defined by the expansion of progeny derived from hematopoietic stem cells that have acquired somatic mutations at a VAF greater than 2%. CHIP manifests in 10% of patients older than 65 and is associated with an increased risk of progression to malignancies such as the MDS or AML. Although the risk factors for developing CHIP remain incompletely defined, they include prior exposure to chemotherapy and a history of smoking. Monoclonal gammopathy of undetermined significance (MGUS) is characterized by the abnormal growth of clonal plasma cells in the bone marrow and carries a risk of 1% for progression to multiple myeloma (MM) per year. Like CHIP, it becomes more prevalent with age and is associated with smoking. Additionally, patients with MM have demonstrated an increased risk for malignancies. Thus, an examination for a correlation between CHIP and MGUS promises to reveal a link between these two pre-malignant conditions. A recent study did not demonstrate such an association, but this study was performed in a very elderly population and may not be applicable to younger patients. In this study, we aim to assess the relationship between CHIP and MGUS in a population-based cohort of MGUS patients seen at UT Southwestern Medical Center.
METHODS: To evaluate an association between CHIP and MGUS, we collected bone marrow samples from 37 patients diagnosed with MGUS. We employed a hybridization capture-based next generation sequencing assay in order to detect CHIP. We identified 24 genes known to cause CHIP in adults. We also evaluated patients risk for developing MM after having been diagnosed with CHIP.
RESULTS: The mean age was 68, (range 26-92). 22 patients were white, 8 were black and 3 Hispanic/Latino. 17 patients had IgG, 7 had IgA, 3 had IgM, 3 had biclonal gammopathy and 7 light-chain MGUS. We identified 18 mutations to validate the presence of CHIP in 10 (27%) patients, with the most frequent being DNMT3A (7 patients) and TET2 (5 patients). Other common mutations noted were PPM1D (2), GND1 (1), SF3B1 (1), ASXL1 in (1), and NRAS in (1). 3 out of the 10 patients harbored 2 mutations and 1

harbored 4 mutations. History of chemotherapy (n=6) and smoking (n=14) was taken into consideration to determine the relative risk of patients with MGUS developing CHIP. We found that those who had a prior history of smoking and chemotherapy displayed a higher risk of CHIP. CONCLUSION: There was no significant association between CHIP and MM progression. Our analysis showed 1 patient with CHIP progression and 2 without CHIP progression. Because the rates of CHIP and MGUS are positively correlated with characteristics like aging and a history of smoking, we expected to see high rates of CHIP in patients within our cohort. However, our data suggests that CHIP is frequent (27%) in MGUS patients, but larger future cohorts need to be evaluated to validate this association.

#5926

High dimensional morphology analysis reveals new insights in melanoma cell heterogeneity

Evelyn Lattmann[1], Aizhan Tastanova[1], Andreja Jovic[2], Kiran Saini[2], Tiffine Pham[2], Christian Corona[2], Jeanette Mei[2], Michael Phelan[2], Stephane C. Boutet[2], Ryan Carelli[2], Kevin B. Jacobs[2], Julie Kim[2], Manisha Ray[2], Chassidy Johnson[2], Nianzhen Li[2], Mahyar Salek[2], Maddison Masaeli[2], Mitchell P. Levesque[1]. *[1]Department of Dermatology, University Hospital Zürich, Schlieren, Switzerland,[2]Deepcell Inc., Menlo Park, CA*

Melanomas are the deadliest skin cancers, in part due to cellular plasticity and heterogeneity within the tumors. These characteristics have made a deeper understanding of melanomas challenging. Classically, melanoma cells are characterized with a limited set of protein biomarkers. Gene expression signatures and mutational analysis (e.g., BRAF and NRAS genotyping) can provide a more detailed view of heterogeneity but may not translate to readily available biomarkers for functional studies. The Deepcell platform enables multi-dimensional morphology analysis and enrichment of unlabeled single cells using artificial intelligence (AI), advanced imaging, and microfluidics, enabling high resolution profiling of population heterogeneity. Label-free multi-dimensional morphology analysis may have higher resolution than a limited set of protein biomarkers, minimizes perturbation to the transcriptome, and reduces cell handling steps. We used patient-derived cell lines and dissociated biopsy

samples to train a Deepcell AI model to identify and sort for melanoma cells based on morphology alone. The model was tested on metastatic melanoma biopsies, with identification and enrichment of melanoma cells verified by various downstream assays, including scRNASeq. In addition to melanoma populations, the AI model classified various cells of the microenvironment, such as stromal cells and immune subtypes, based on morphology only. To further characterize tumor heterogeneity, we imaged >25 patient-derived melanoma cell lines representing melanocytic, mesenchymal, and intermediate phenotypic states on the Deepcell platform. Morphology analysis of these images revealed distinct clusters of cells for each phenotype, indicating that there are morphological differences associated with each state. We developed a random forest (RF) classifier to identify the top differential morphological features between the different cell lines, thereby providing a label-free means of phenotyping melanoma samples. The morphology analysis of the cell lines uncovered significant variability in pigmentation; an RF classifier distinguished between pigmented vs non-pigmented cells with >90% accuracy. Pigmentation is a hallmark of melanoma cells, and it has been associated with the melanocytic phenotype and differential drug response in vitro. However, there is not currently a robust method to profile and study pigmentation in live cells. We further investigated this observation by correlating morphological profiles, molecular, and functional information with the level of cell pigmentation. The Deepcell platform presents a new method for sorting and characterizing cellular heterogeneity using morphology, including pigmentation status. As such, multi-dimensional morphology analysis will bolster the understanding of complex melanoma states and tumor microenvironment, particularly in patient derived biopsies.

#5927

Leveraging single cell RNA profiling to uncover intra-tumor heterogeneity across cytogenetic subgroups in acute myeloid leukemia

Bofei Wang[1], Christopher Ly[1], Fatima Zahra Jelloul[1], Enes Dasdemir[1], Guilin Tang[1], Sonali Jindal[1], Yulong Chen[1], Sreyashi Basu[1], Poonam Desai[1], Pamella Borges[1], Preethi Gunaratne[2], Natalia Baran[1], Qing Deng[1], Dapeng Hao[3], Sean Post[1], Michael Green Green[1], Marina Konopleva[1], Andy Futreal[1], Padmanee Sharma[1], Hussein A. Abbas[1]. *[1]UT MD Anderson*

Cancer Center, Houston, TX,[2]University of Houston, Houston, TX,[3]Harbin Medical University, Harbin, China

Acute Myeloid Leukemia (AML) is a heterogenous disease characterized by immature blasts at different states of differentiation resulting in marked intra-tumor heterogeneity (ITH). Compared to patients with diploid cytogenetics, deletions in chromosome 7/7q (del7/7q), 5/5q (del5/5q) or double deletion (del5/5q & del 7/7q) confer worse outcomes in AML. We conducted single cell RNA (scRNA) profiling of bone marrow mononulear cells (BMMCs) from 20 newly diagnosed adult AML patients with diploid (n=7), del5/5q (n=5), del7/7q (n=5) and double deletion (n=3) to uncover ITH within each group and reveal cellular hierarchies associated with inferred copy number variations (CNV). Diffusion map analysis revealed heterogenous gene expression pattern in AML cells of del7/7q and double deletion patients, compared to diploid and del5/5q patients. CNV-based subgrouping of AML cells revealed significant enrichment of antigen presentation and immune response pathways in cells with inferred del7/7q or double deletion compared to cells without these deletions in the same patients, suggesting a heterogenous immune state in AML cells correlating with inferred genomic copy numbers. To dissect the composition of cellular hierarchies, AML cells were then projected onto an independent healthy BMMC reference (>20,000 cells) and labeled based on transcriptional similarity to healthy hematopoietic cells. AML cells from diploid patients were enriched for GMP-like and monocyte-like cells, while cells from non-diploid patients were enriched in more primitive states (HSC-like and CMP/LMPP-like). Correlating these hierarchal groups with leukemic stem cell (LSC) hierarchies revealed shared transcriptional program in LSC-like states across HSC-like, GMP-like, CLP-like and erythroid-like cells. This suggests that LSC signatures can also be expressed across AML cells and not just primitive cells. These findings were also validated in deconvolution analysis of bulk transcriptomes from three independent newly diagnosed AML cohorts (TCGA, BEAT-AML and MDACC). Spatial deconvolution of 3 patients using whole transcriptomic GeoMx revealed that primitive cells were more likely to be proximal to bone, while more differentiated states were enriched in distal region from the bone. Our findings reveal complex hierarchies in AML cells sharing the LSC expression pattern, while more

primitive cells were likely to localize to bone regions suggesting spatial migration of AML cells at time of differentiation.

#5928

Prevalence of clonal hematopoiesis in neuroendocrine tumor patients prior to lutetium 177 dotatate therapy (Lu177): A prospective trial of 36 patients

Yael Kusne[1], Terra Lasho[2], Zaid Elsabbagh[1], Abhishek Mangaonkar[2], Rachel Eiring[2], Timothy Hobday[2], Jason Starr[2], Tanios Bekaii-Saab[1], Thorvardur Halfdanarson[2], Mrinal Patnaik[2], Mohamad Sonbol[1]. *[1]Mayo Clinic Arizona, Scottsdale, AZ,[2]Mayo Clinic Rochester, Rochester, MN*

Introduction: Clonal hematopoiesis (CH) is defined by acquisition of somatic mutations in hematopoietic stem cells with potential for expansion over time. CH is influenced by exposures to chemotherapy/radiation & has been associated with therapy related myeloid neoplasms (tMN). Peptide receptor radionuclide therapy (PRRT) is a radionuclide therapy and is FDA approved for neuroendocrine tumors (NET). PRRT has been associated with a 2-10% risk of tMN, especially with prior exposure to alkylating agents. A prior study of 13 NET patients found CH prevalence of 64%. We carried out a prospective assessment of CH in NET patients prior to PRRT.
Methods: We evaluated pre-PRRT blood samples in 37 NET patients. Genomic DNA from mononuclear cells was analyzed for CH using a custom panel targeting 229 genes to a targeted depth of >1000X.
Results: After approval by Mayo Clinic IRB, 45 patients with Stage IV NET were enrolled & CH data was available for 37. Fifty-one percent of patients were female, with a median age of 68yrs (range, 34-84yrs). Types of NET included small bowel (51%), pancreatic (29%), carcinoid (8%), paraganglioma (5%), & other (5%). The median number of therapies prior to PRRT was 1 (range, 0-4) & included somatostatin analogues (SSA)-81%, alkylating agents-30%, & prior radiation-13%. Thirty-six of 37 patients had variants identified, 5 of which were presumed germline (DDX41, CDKN2B, CHEK2, POT1, ERBB2), & 17 (45.9%) had pathogenic variants meeting the operational definition of CH (DNMT3A, TET2, PPM1D, TP53, SF3B1, ASXL1). The median number of pathogenic variants per patient was 1 (range, 0-2), & 6 patients had >1. In patients >60yrs old, 46% had pathogenic variants & 3 patients with pathogenic variants (TET2, TP53,

DNMT3A) were <60 years old. The most common pathogenic variants were in epigenetic regulators, DNMT3A (37.5%) & TET2 (16.7%) with a median VAF of 2.8% (range, 0.70-50%). Eight patients (47%) with pathogenic CH had grade 1 cytopenias at baseline, compared to 10 patients (50%) without pathogenic CH. One patient had grade 3/4 cytopenia at baseline & had a missense variant in TP53 (VAF 50%) & history of exposure to anthracyclines, alkylating agents, platinum & radiation. The patient developed MDS before receiving PRRT. Pathogenic CH variants were more common in patients with previous exposure to radiation (p=0.008) or SSA (p=0.005). Two patients had PPM1D variants, both with a history of prior radiation, one with a history of prior alkylating treatment. Conclusion: To our knowledge this is the largest prospective evaluation of CH in NET. We identified CH to be present in 46% of patients & DNMT3A mutations were most common. This establishes the clonal landscape with mutations involving epigenetic regulators, DNA damage repair, transcription & splicing factors. Prospective longitudinal evaluation will evaluate the association between CH, cytopenias and tMN.

#5929

Individual organoid level analyses reveal hidden tumor molecular heterogeneity

Shirsa Udgata, Aishwarya Sunil, Katherine A. Johnson, Cheri A. Pasch, Dustin A. Deming. *University of Wisconsin-Madison, Madison, WI*

Introduction: Tumor heterogeneity is a major cause of resistance to therapies in cancer patients occurring during disease progression or secondary to therapeutic intervention due to clonal selection. Mapping tumor heterogeneity is crucial for developing therapeutics for cancer patients. Currently there are no reliable models for identifying heterogeneity *in vitro.* Patient-derived cancer organoids (PDCOs) from tissue samples of patients capture clonal and subclonal mutations. Here we use PDCOs from colorectal cancer (CRC) patients to study molecular heterogeneity across individual organoids and how the heterogeneity changes with passages.

Methods: Fresh CRC tissues from 4 patients undergoing endoscopy were obtained following consent on an IRB-approved protocol. PDCOs were cultured using Matrigel and previously published CRC organoid media.

Following maturation, individual organoids (spikes) were separated into Matrigel domes and expanded. Parent cultures from high/low passage numbers and expanded spikes were collected for next generation sequencing (NGS). A variant allele frequency (VAF) was determined for each nonsynonymous variant and considered subclonal if the VAF was between 10%-30%. Variants were annotated pathogenic or not using ClinVar.

Results: A total of 49 spikes were collected from 4 CRC PDCO lines and compared to the parent cultures using NGS. For low passage parent cultures, a median of 4 (range 3-8) subclonal alterations were identified. At high passages the number of subclonal variants decreased (median: 2 (range 2-4)). The individual organoid spikes maintained the founder (clonal) alterations and most also contained subclonal alterations, though at a lower frequency. Of those subclonal variants in the parent cultures, 31% were found in the spikes and an additional 54% found in the spikes were not identified in the parent. In a high tumor mutation burden line (MTB111), 12/17 spikes showed subclonal alterations in $APC^{A896V,\ F1515C,\ Q1544*}$ that were not present in the parent culture. Two PDCO lines (RC46A and RC46B) obtained from distinct sites of the same tumor were generated. One contained a subclonal mutation in MYC^{N26S} in the high passage parent culture and 7/9 spikes. This mutation was not present in any RC46A samples. The high passage RC46A parent culture and 2/7 spikes showed an alteration in $ARID1A^{G1037fs}$ while it was present only in a single spike of RC46B.

Conclusion: PDCOs identified subclonal alterations at the single-organoid level and are an exciting tool to study tumor heterogeneity. The spikes presented less subclonal variants than the parent but were largely not clonal. Future implications of using heterogeneity data from single organoids in therapeutic decisions are warranted.

#5930

Single day workflow for high-quality whole genome analysis of thousands of single cells

Jay A. A. West, Jeff G. Blackinton, Kyle Hukari, Joe Dahl. *BioSkryb Genomics, Durham, NC*

DNA sequencing technology provides the capability to tell the story of every cell in a heterogenous sample. ResolveDNA® generates uniform coverage of >95% of a single genome, enabling researchers to generate single-cell genomic data of unparalleled quality. Here, we report an enhancement to the ResolveDNA® workflow that increases the rate of data collection; the ability to reliably generate complete genomic information from up to 1536 cells in parallel from a single experiment. To achieve this, we have coupled a high-throughput automated process to a low volume reaction using the latest ResolveDNA® 2.5-hour chemistry. This establishes the potential for users to go from a single cell, or low-input DNA sample, to ready to sequence libraries in a single day for >3000 samples. As with earlier ResolveDNA® workflows, these reactions generate negligible amounts of contaminating and off target DNA during the reaction. A typical single-cell reaction yields ~ 85 ng of DNA. The single cell's amplified DNA product is amenable to multiple post amplification library preparation processes. We utilized both BioSkryb ResolveDNA® and Watchmaker Library Preparation kits for Illumina sequencing. We did not identify significant differences in the performance of the two products. Libraries were assessed at a depth of ~ 2million reads and determined to be of high quality, with low rates of chimeric DNA formation and less than 1% mtDNA resulting in the reaction product. A subset of samples was probed at >200 million reads, with >85% of the genome covered at 1x. Consistent with earlier ResolveDNA® workflows, the libraries were characterized with >99% precision and >80% sensitivity. The story told from a single cell's genome drives discovery and shines a light on the questions surrounding the causes of disease and cellular function. This workflow is designed to empower researchers to probe the genomic landscape of a heterogenous tissue sample.

#5931

Characterizing tumor heterogeneity through bulk and single cell analysis of patient derived bladder cancer models

Ziyu Chen[1], Xinran Tang[1], Eliyahu Havasov[2], Andrew Mcpherson[2], Carissa Chu[2], John R. Christin[3], Michael F. Berger[2], Nikolaus D. Schultz[2], Elisa de Stanchina[2], Michael M. Shen[3], Hikmat Al-Ahmadie[2], Kwanghee Kim[2], Gopa Iyer[2], David B. Solit[2]. *[1]Weill Cornell Medicine, Memorial Sloan Kettering Cancer Center, New York, NY,[2]Memorial Sloan Kettering Cancer*

Center, New York, NY,[3]Columbia University Irving Medical Center, New York, NY

Background: A major hurdle to the development of novel targeted therapies for bladder cancer is the lack of preclinical models that reflect the genomic and biological heterogeneity of this human disease. To address this deficiency, we generated and characterized a new collection of patient-derived organoid (PDO) and xenograft (PDX) models and then used these models to study the role of mutated kinases in bladder cancer pathogenesis and the potential clinical utility of HER2-targeted antibody-drug conjugates (ADC).
Material and Methods: To define the landscape of HER2 and FGFR3 alterations in bladder cancer patients, we leveraged data generated by The Cancer Genome Atlas and multiple cohort subsets of the first 50,000 cancer patients enrolled in the MSK-IMPACT prospectively sequencing cohort. We successfully generated 19 PDOs and 34 PDXs that genetically and phenotypically reflect the molecular heterogeneity of human bladder cancers. A subset of these models was further characterized using a multiplatform approach, including bulk and single-cell DNA and RNA sequencing; and employed to study HER2 oncogenic dependence and sensitivity to multiple anti-HER2 targeted agents.
Results: 16% and 24% of the patients in the prospective MSK bladder cancer cohort had oncogenic HER2 and FGFR3 alterations, respectively. HER2 alteration frequency varied significantly as a function of histology, while FGFR3 alteration were less common in all variant histologies as compared to UC, NOS. Analysis of 119 patients with paired primary/metastatic tumors noted HER2 and FGFR3 mutational discordance in over 35% and 10% respectively. Single-cell RNA seq and DNA seq analysis of 4 PDOs demonstrated high interpatient and intratumoral heterogeneity of HER2 expression and *ERBB2* copy number. Our bladder cancer PDX models also demonstrated greater sensitivity to the HER2-targeted ADC trastuzumab deruxtecan (T-DXd) than to the kinase inhibitor neratinib, consistent with clinical data in bladder cancer patients.
Conclusion: FGFR3 and HER2 are both commonly mutated in bladder cancer patients. We observed frequent discordance in HER2 mutational status between primary/metastatic pairs suggesting that the analysis of archival primary tumor tissue may fail to detect actionable genomic

alterations when present in a subset of bladder cancer patients. Multi-omic single-cell analysis demonstrated significant interpatient and intratumor heterogeneity of HER2 expression and *ERBB2* copy number gain. Preclinical evaluation of HER2-altered PDO/PDXs indicated significantly greater sensitivity to the HER2-directed ADC T-DXd compared to the HER kinase inhibitor neratinib, providing rationale for future clinical trials of HER2 ADCs in bladder cancer patients.

#5932

Clonal mapping phylogenetic and transcriptomic analysis of an M36 PDX amputation lung metastatic osteosarcoma model

Sylvester Jusu[1], Zhongting Zhang[2], Zhang Wendong[2], Zhaohui Xu[2], Michael Roth[2], Jonathan Gill[2], Richard Gorlick[2]. *[1]The University of Texas MD Anderson Cancer Center, Houston, TX,[2]Pediatrics, The University of Texas MD Anderson Cancer Center, Houston, TX*

Introduction: Osteosarcoma is a primary malignant bone tumor characterized by the production of spindle cells resulting in immature bone formation. It has been revealed that metastatic cancers including osteosarcoma have a subset of cells with different phenotypic and genetic signatures conferring advantage to drive progression and drug resistance within the intra-tumorally heterogeneous population. However, the lack of a defined in vivo model that can identify the rare genetic subpopulation and recapitulate clonal evolution has been a challenge. In this study, we used an established model to track and identify the clonal subpopulations and assess the genetic signatures that confer specific advantages selecting for uncontrolled growth, adaptation and colonization in the lungs.
Methods: We injected barcoded M36 PDX osteosarcoma cells intratibially in ten severe combined immunodeficiency disease (SCID) mice to track the clonal population/subpopulation of cells that metastasize the established primary tumors to the lungs. Limb amputation was performed on the tumor bearing leg upon detection of palpable tumor. Lung tissue was harvested post-amputation following death from metastasis or euthanasia. DNA and RNA from frozen tissues was extracted and analyzed by PCR, NGS, WES and RNA sequencing to map clonality, mutational and evolutionary profiles.

Results: Limb amputation was performed in 7 mice with all mice surviving the surgery. The mean mouse survival following amputation was 46.9 days and the longest survival was 167 days. Four (40%) of the primary tumor bearing mice had lung metastasis. A Shannon-Wiener and Jaccard similarity index show a diversity in clonal architecture between the primary tumors of all mice injected on the same day and a diversity in clonal population in both the primary tumors and their matched lung metastatic nodules. Clonal mapping further revealed 21 unique clones shared in all primary tumors examined. However, the clonal frequencies and distribution varied within each primary tumor and across the tumor samples. Interestingly, clonal frequencies increased in the lung metastatic nodules when compared to their matched primary tumors. Four distinct clones that were present in all the primary tumors were also found in all lung metastatic samples. These unique clones, here in called "seeding clones" may play an important role in the lung metastatic process.
Conclusions: We previously showed that the barcoded osteosarcoma PDX models are inter and intratumorally heterogenous both in vitro and in vivo. In the current model, we identify the multiple tumorigenic seeding clones that potentially act as drivers in the lung metastatic process. Furthermore, we show the dynamic evolutionary relationships between the clones by reconstructing a phylogenetic map of the M36 PDX tumor model.
Funding: Swim Across America, Foster Foundation and the Barbara Epstein Foundation.

#5933

Trimodal molecular analysis in single cells of a primary breast cancer cohort with ResolveOME ™ amplification

Jon S. Zawistowski[1], Isai Salas-Gonzalez[1], Tia A. Tate[1], Tatiana V. Morozova[1], Katherine Kennedy[1], Durga M. Arvapalli[1], Swetha D. Velivela[1], Jamie E. Remington[1], Josh Croteau[2], Kevin Taylor[2], Jeff G. Blackinton[1], Victor J. Weigman[1], Jeffrey R. Marks[3], Eun-Sil Shelley Hwang[4], Gary L. Harton[1], Jay A. A. West[1]. *[1]BioSkryb Genomics, Durham, NC,[2]BioLegend, San Diego, CA,[3]Surgery, Duke University Medical Center, Durham, NC,[4]Duke University Medical Center, Durham, NC*

The ResolveOME™ single-cell amplification solution unites whole-genome and full-length transcriptome information from the same cell, providing critical insight between these layers not possible when analyzed in isolation. We expand here upon the core layers of ResolveOME™ with the incorporation of BioLegend TotalSeq™ antibody oligo conjugates to investigate the expression of a panel of extracellular proteins in conjunction with the genomic and transcriptomic data.

The present study demonstrates the power of exploring all tiers of the Central Dogma of Biology in a series of experiments aimed at defining the molecular characteristics facilitating the transition from Ductal Carcinoma In Situ (DCIS) to Invasive Ductal Carcinoma (IDC), sequencing single cells from mastectomy samples from twelve patients in collaboration with Duke University Medical Center. We either enriched for ductal epithelial cells by fluorescence-activated cell sorting (FACS) or dispensed single cells agnostic to marker and relied on the full transcriptome output of ResolveOME™ to report cell identity. At the genomic level, we identified oncogenic driver mutations in *PIK3CA* (H1047R, N345K) and distinct classes of copy number loss at either or both Chr. 13 and 16q/17p, harboring *BRCA2/RB1 and TP53* tumor suppressor loci—whereby both SNV and CNV both varied in frequency within single cells of each patient and between patients of the cohort. These oncogenic mutations were nearly exclusive to biopsy cells of epithelial identity. However, intriguingly, ResolveOME™ uncovered cells of stem-like identity harboring *PIK3CA* missense mutations as well as uncovered cells still formally identified as epithelial and harboring mutant *PIK3CA* but with differential expression profiles—indicative of cells morphing cell state. Finally, the TotalSeq™ antibody panel unveiled intercellular heterogeneity and interpatient heterogeneity both in cell-surface protein phenotype of immune cells and in epithelial identity and signaling.

This ongoing study continues to catalog the three omic layers in increasing numbers of single cells and significantly expanding targeted surface-protein analysis harnessing the power of the single-cell united data to determine the “penetrance” of genomic changes in the context of cognate transcript and protein information, with the ultimate goals of defining DCIS to IDC transition factors as well as novel biomarker identification that may be exploited therapeutically.

#5934

Tracking T cell clonal dynamics across time and space in metastatic colorectal cancer

Ann-Marie Baker[1], Alison Berner[2], Tahel Ronel[2], Nick Trahearn[1], Barbara Bravi[3], John Bridgewater[4], Benny Chain[5], Trevor A. Graham[1]. *[1]Centre for Evolution and Cancer, The Institute of Cancer Research, Sutton, United Kingdom,[2]Centre for Genomics and Computational Biology, Barts Cancer Institute, Queen Mary University of London, London, United Kingdom,[3]Department of Mathematics, Imperial College, London, United Kingdom,[4]UCL Cancer Institute, University College London, London, United Kingdom,[5]Division of Infection and Immunity, University College London, London, United Kingdom*

Here we tracked T cell dynamics in 15 metastatic colorectal cancer (mCRC) patients who had multiple resections (median: 3, range: 2-7) over a period of >7 years (median: 10 years, range: 7-16 years), using a novel T cell receptor sequencing (TCRseq) method. These samples had been previously characterized for DNA and methylation alterations and gene expression, enabling an integrated analysis to determine potential cellular and molecular drivers and consequences of immune dynamics. This multi-region, multi-timepoint dataset presents a unique opportunity to study the co-evolution of mCRC and the T cell response over time, across metastatic sites and in response to therapy.

T cell antigen specificity is defined by the TCR - a highly diverse sequence that enables tracking of specific T cell expansions across time and space. TCRseq quantifies the abundance of T cell clones and maps the dynamics of the TCR repertoire, however little is known about how these are altered in different metastatic sites, and post-chemotherapy. We developed and validated a new FFPE-compatible TCRseq method and sequenced 216 longitudinal samples representing the mCRC cohort described above.

We detected a median of 348 unique TCRs per sample (range 69-9700), and revealed high levels of intra-tumor spatial heterogeneity. No significant difference was detected in the number of T cell clones or the TCR clonality between primary tumors (n=40), lung metastases (n=30) and liver metastases (n=50). Furthermore, these were not significantly different between tumor regions (n=139) and surrounding stroma (n=38). We found that compared to chemo-naïve tumors (n=36), those that had been exposed

to recent chemotherapy (n=41) had a significant increase in both the number of unique T cell clones and Simpson's evenness, likely reflecting a broad T cell response to DNA-damaging agents. After more than a year had passed without chemotherapy (n=64) these returned to pre-chemotherapy levels.
In most cases the 10 most abundant TCR sequences in the primary tumor represented 15-40% of the total repertoire. We tracked these expanded clones through metastases, identifying ubiquitous clones which persisted across metastatic sites and through therapy. We found other expanded clones which were no longer present in metastases lesions, although some of these were found to expand again in later metastases. Finally, we examined correlations with tumor genomics, finding evidence in some patients that the TCR repertoire tracks closely with tumor clones even through metastasis and chemotherapy.
In summary, this project represents the first comprehensive analysis of T cell dynamics through colorectal cancer metastasis, highlighting the changing T cell landscape post-chemotherapy and correlating the TCR repertoire with tumor genomics. Our results could have important clinical implications for mCRC immunotherapy and the design of personalized T cell-based therapy.

#5935

Phenotype profiling of tumor microenvironment in EGFR mutant lung adenocarcinoma with multi-omics data

You Won Lee[1], Eun Ji Lee[2], Seung Yeon Oh[3], Kyoung-Ho Pyo[4], Seong Gu Heo[4], YoungJoon Park[5], Su-Jin Choi[1], Kyumin Lim[6], Ju-hyeon Lee[6], Jae Hwan Kim[4], Jii Bum Lee[7], Ji Yoon Lee[8], Sun Min Lim[8], Chang Gon Kim[8], Min Hee Hong[8], Mi Ran Yun[4], Byoung Chul Cho[8]. *[1]Yonsei Biomedical Research Institute, Yonsei University College of Medicine, Seoul, Korea, Republic of,[2]Department of Biomedical Science Institute, Graduate School of Medical Science, Brain Korea 21 Project, Yonsei University College of Medicine, Seoul, Korea, Republic of,[3]Department of Biomedical Science Institute, Graduate School of Medical Science, Brain Korea 21 Project,Yonsei University College of Medicine, Seoul, Korea, Republic of,[4]Severance Biomedical Science Institute, Yonsei University College of Medicine, Seoul, Korea, Republic of,[5]Yonsei Biomedical Research*

Institute,Yonsei University College of Medicine, Seoul, Korea, Republic of,[6]JEUK Institute for Cancer Research, JEUK Co., Ltd., Gumi-City, Korea, Republic of,[7]Division of Medical Oncology, Yonsei Cancer Center, Yonsei University College of Medicine, Seoul, Korea, Republic of,[8]Division of Medical Oncology, Yonsei Cancer Center, Yonsei University College of Medicine, Seoul, Korea, Republic of

Introduction: EGFR mutations holds the major targets for drug in lung adenocarcinoma (LUAD). Despite the tremendous study of EGFR mutant (MT) LUAD, the comprehensive interpretation of the heterogeneous character of LUAD harboring EGFR MT remains a key challenge. Here, we investigated the heterogeneity of EGFR MT LUAD and explored the tumor microenvironment (TME) in EGFR MT LUAD.
Method: We performed single-cell RNA sequencing (scRNA-seq) from 135 LUAD patients which consist of normal(n=24), EGFR wild (WT)(n=18), and MT(n=93). Also, we used whole genome sequencing and bulk-RNA sequencing to validate with scRNA-seq results. From 898,648 cells, main cell types were classified. To explore the various characteristics of MT LUAD tumor cells, we used two ways: i) We re-clustered epithelial cells populating the normal, WT, and MT. ii) We re-clustered only MT epithelial cells. In each analysis, we identified the tumor character in the clusters using differential expressed genes analysis, lineage tracing, clinical information, mutation, and trajectory analysis. Also, we extracted each main cell type except epithelial cells, and identified subtypes of main cell types. Finally, we revealed the interaction of cellular components in TME.
Results: In the analysis of epithelial cells, we identified characteristics of specific EGFR MT by comparing of EGFR WT and MT tumors in clusters with similar biological features. The cluster represented by alveolar type 2 (AT2) known as initiation of LUAD was populating normal, WT, and MT. In this cluster, MT- and WT-associated pathway shared but differently significant between MT and WT in the pathway analysis. The cluster represented by proliferative is mostly comprised tumor cells and we found significantly increased the expression of MDK, CD24 in the MT of the cluster. In the analysis of only MT epithelial cells, 2 of clusters were stage-specific cluster: i) The cluster annotated as early stage cluster, ii) The cluster annotated as advanced stage cluster. Trajectory showed that there is a pseudotemporal continuum, following the stage from early stage cluster to

advanced stage cluster. Also, based on the lineage tracing, 2 of clusters revealed lineage-specific clusters: i) The cluster annotated as AT2 was enriched from early stage cells, ii) The cluster annotated as basal cell known as origin of lung squamous cell carcinoma(LUSC) was enriched from advanced stage cells. Psedotemporal ordering of these cluster revealed AT2 cluster transdifferentiate into basal cell cluster which implied the possibility of LUAD to LUSC transition by drug resistance. In the interaction of MT and WT TME, the number of signaling received epithelial cells from myeloid cells, endothelial cells, and fibroblasts as sender increased compared with the interaction of normal.
Conclusion: We shed light on the ecosystem of TME according to clinical and biological feature of tumor in EGFR mutant LUAD.

Tumor-Stromal Cell (Including Immune Cell) Interactions and Therapy Responses

#5940
Enhanced mast cell abundance is associated with the enrichment of CCR2+ cytotoxic T cells and favorable prognosis in lung adenocarcinoma.

Fan Fan[1], Xiaoming Zhang[2], Haiquan Chen[1]. *[1]Department of Thoracic Surgery, Fudan University Shanghai Cancer Center, Shanghai, China,[2]Key Laboratory of Molecular Virology and Immunology, Institute Pasteur of Shanghai, Chinese Academy of Sciences, Shanghai, China*

Mast cells constitute indispensably immunoregulatory sentinel cells in tumor microenvironment, however, their functions are poorly characterized in lung adenocarcinoma (LUAD). Here, we performed flow cytometry and single-cell RNA sequencing to comprehensively characterize LUAD infiltrating MCs. MCs exhibited remarkably functional heterogeneity and were enriched in ground-glass opacity featured LUAD (gLUAD). The MCs in gLUAD exhibited proinflammatory and chemotactic properties while the MCs in radiologically solid LUAD (sLUAD) were associated with tumor angiogenesis. MCs were an important source of CCL2 that correlated with the recruitment of CCR2+ cytotoxic T lymphocytes (CTLs), which represent a specific subcluster of pre-exhausted T cells with tissue-resident memory phenotype and enhanced cytotoxicity. Increased infiltration of

MCs-CCR2+ CTLs and their colocalization showed a strong association with favorable prognosis after surgery but were not associated with improved survival after chemotherapy. Collectively, these findings reveal a key role of MCs in LUAD and their potential crosstalk with CTLs, suggesting that targeting MCs may be a novel immunotherapeutic strategy for LUAD.

#5941

Sequencing of targeted- and immune-therapy: delineating time dependent changes in both melanoma cells and the immune microenvironment

Riyaben Patel[1], Anna Trigos[1], Nicole Haynes[1], Emily Lelliott[2], Grant McArthur[1], Karen E. Sheppard[1]. *[1]Peter MacCallum Cancer Centre, Melbourne, Australia,[2]The Walter and Eliza Hall Institute of Medical Research, Melbourne, Australia*

Targeted and immune therapies have transformed outcomes for melanoma patients, nevertheless, significant challenges remain to maximize their clinical benefit. BRAF/MEK targeted therapy (TT) is associated with very high initial response rates that are typically short-lived, while in contrast Immune Checkpoint Inhibitors (ICI) provide more durable responses but have lower initial response rates. Hence, it has been proposed that sequencing ICIs with TT would lead to a higher frequency of durable responses. However, there are many unanswered questions regarding the choice of immunotherapy, the best sequencing strategy and the mechanism leading to this synergy. To address these questions, we have optimized a syngeneic mouse melanoma model, YUMMER1.7-PV1 that is sensitive to both TT and ICIs. Importantly, this model recapitulates the known three therapeutic response phases of targeted therapies: initial response, followed by drug tolerance and then resistance. Investigation of the tumor immune microenvironment (TIME) at these three drug-induced phases, demonstrates that the immune suppressive microenvironment present during the acquired resistant phase is primed at the drug tolerance phase. Utilizing this model, we have explored the time-dependent therapy-induced changes in both tumor cells and the TIME during various TT and ICI sequencing strategies. This information will determine the optimal

sequencing strategy of targeted therapy and immunotherapy that will deliver better outcomes for melanoma patients.

#5942

Mechanism and role of neutrophil recruitment in head and neck squamous cell carcinoma

Kulsoom Ghias[1], Hina Shakeel[1], Alisalman Sheikh[1], Syed Hani Abidi[1], Kiran I. Masood[2], Saira Fatima[2], Fareena Bilwani[1]. *[1]Biological and Biomedical Sciences, Aga Khan University, Karachi, Pakistan,[2]Pathology and Laboratory Medicine, Aga Khan University, Karachi, Pakistan*

The immune system plays a pivotal role in identification and clearance of tumor cells, but can also be counterproductive and enhance tumor progression. Presence of neutrophils in solid tumors, including the sixth most common cancer globally - head and neck squamous cell carcinomas (HNSCC), is associated with poor prognosis. Pro-inflammatory cytokines regulated by NF-κB promote extravasation of neutrophils into tissue; neutrophils are polarized to anti-tumor (N1) or pro-tumor (N2) phenotype through the action of various pathways, including TGF-β. The mechanism and role of neutrophil recruitment in HNSCC were explored this study. Neutrophils isolated from adult donors were co-cultured for 5 hours with conditioned media (CM) from HNSCC cells SCC-9 and Cal-27, and stained with TNF-α, ICAM-1, CCL2, CCL5 for analysis of neutrophil phenotype by flow cytometry. TGF-β blocking antibody was used to explore the role of TGF-β in polarization of neutrophils. Canonical and non-canonical TGF-β signaling pathway activation was also investigated in these neutrophils through western blots. Using HNSCC patient samples, qPCR was performed for expression of genes involved in apoptosis, epithelial-to-mesenchymal transition, metastasis, and neutrophil function.
Following co-culture with 24-hour HNSCC CM, neutrophils begin to exhibit cell surface markers indicative of N2 phenotype, which is impacted by TGF-β blocking antibody. Neutrophils co-cultured with HNSCC CM exhibited altered expression of TGF-β mediators Smad2/3, p38 and Akt, which was abrogated with the addition of TGF-β blocking antibody indicating specificity of a TGF-β induced signaling. Gene expression analysis exhibited significantly higher expression of anti-apoptotic BCL2 and neutrophil function marker alpha defensin 1 in HNSCC patient samples

with greater neutrophil infiltration, while caspase 3 was expressed at significantly higher levels in HNSCC patient samples with low neutrophil infiltration.
HNSCC cells recruit neutrophils; evidence suggests that TGF-β pathway, which typically promotes N2 phenotype in neutrophils, is involved via canonical and non-canonical mediators including p38 and Akt. Further, HNSCC patient samples have varying levels of neutrophil infiltration and differentially express genes involved in apoptosis, EMT, metastasis and invasion, inflammation.

#5943

Plasma cell repertoire in the lung cancer tumor microenvironment

Akshay J. Patel[1], Naeem Khan[1], Alex G. Richter[1], Babu Naidu[2], Mark T. Drayson[1], Gary W. Middleton[1]. *[1]University of Birmingham, Institute of Immunology and Immunotherapy, Birmingham, United Kingdom,[2]University of Birmingham, Institute of Inflammation and Ageing, Birmingham, United Kingdom*

Background: Post-operative recurrence in lung cancer continues to pose a major clinical challenge. B cell and plasma cell presence has been shown to correlate with improved survival and lower relapse rates in solid cancers and with improved response to checkpoint blockade. The aim of this study was to identify distinct immune cell compositions in the circulation and tumor microenvironment and make correlations with clinical and disease specific outcomes.
Methods: In this study, utilizing high-dimensional deep immunophenotyping techniques (mass cytometry), multispectral immunofluorescence based imaging and bulk RNA sequencing, we explored the B cell repertoire in the circulation and tumor microenvironment in early-stage lung cancer patients undergoing radical surgical resection.
Results: We demonstrate using high-dimensional deep phenotyping, clear differences in B cell composition between the circulation and the intratumoural microenvironment. Intratumoural predominant populations include plasma cells, from $CD38^{var}$ immature to CD138+ mature cells. B cells undergoing germinal center and follicular maturation as well as class-switched memory cells were predominantly found in the circulation. Eight

key populations were significantly differentially abundant between compartments on generalized linear mixed modelling ($p<0.0001$ with BH correction). These differences were observed in an external validation set. Plasma cell infiltration existed on a phenotypic spectrum from natural regulatory suppressive cells to antibody producing effector phenotypes. The latter correlating with better outcomes. Higher B cell expression of CD138 and Ig was noted within the tumor microenvironment in patients who did not experience early relapse. Significantly higher levels of circulating ki67+ $CD27^{hi}$ $CD38^{hi}$ $CD95^{hi}$ $IL10^{int}$ plasmablasts were noted in recurrence patients ($p=0.02$). Geospatial mapping identified clusters of suppressive plasma cells localized to the tumor stroma, likely regulating entry of effector cells into the tumor nest.
Conclusions: Our data has demonstrated the unique roles of effector and suppressive B cell subsets in NSCLC and the clear difference in surrogacy between tissue compartments. The lesser infiltration of suppressive phenotypes into the tumor nest may be to prevent the subsequent infiltration of effector plasma and effector B cells into the tumor nest. This tumor line of defense would be in keeping with the observation that higher levels of suppressive B cell subsets in the circulation links to higher rates of recurrence and a higher tumor effector plasma cell infiltrate correlates with protection against recurrent disease. The ambiguous role of B cells in the tumor environment predetermines the multidirectional development of immunotherapeutic approaches, either supporting positive B cell types or inhibiting the suppressive B cell phenotypes.

#5944

Relief of chromosomal instability-induced cGAS-STING signaling sensitizes *STK11*-mutant non-small cell lung cancer to immune checkpoint blockade

Lindsay A. Caprio[1], Christy Hong[2], Amit Dipak Amin[1], Somnath Tagore[1], Johannes Melms[1], Luke Cai[1], Yiping Wang[1], Patricia Ho[1], Michael Mu[1], Hanina Hibshoosh[3], Brian Henick[1], Kwok K. Wong[4], Samuel F. Bakhoum[2], Benjamin Izar[1]. *[1]Columbia University Irving Medical Center, New York, NY,[2]Memorial Sloan Kettering Cancer Center, New York, NY,[3]Pathology and Cell Biology, Columbia University Irving Medical Center, New York, NY,[4]New York University Langone Medical Center, New York, NY*

Non-small cell lung cancers (NSCLCs) harboring deletions or inactivating mutations in *STK11* (encoding LKB1) are associated with treatment-resistance, including to immune checkpoint blockade, and poor survival, yet the underlying mechanisms are poorly understood.

Here, we combined multi-modal single-cell transcriptomics, whole-genome sequencing (WGS), and analysis of public data bases totaling >10,000 NSCLC whole-exome sequencing (WES) and when available RNA (RNA-seq) profiles of AACR GENIE, MSK IMPACT, TCGA and CPTAC, high-content imaging, and functional assays, to determine genomic and mechanistic features of *STK11*-mutant NSCLC.

Across human WES/RNA-seq data, we find that *STK11*-mutant NSCLC have a significantly higher fraction of genome altered (FGA) and score strongly for the mRNA-based *CIN70* signature compared to other NSCLC genotypes, overall indicating that these tumors have a higher degree of chromosomal instability (CIN). Using high-content imaging, we show that both human and murine STK11-mutant models have a higher rate of micronuclei and chromosome-mis-segregation events, confirming their CIN^{high} status in dynamic assays. Next, we show that tonic CIN-induced activation of cGAS-STING signaling, whose activation is typically thought of inducing type I interferon expression, results in strong suppression of anti-tumor immune signaling. Remarkably, genetic or pharmacologic suppression of cGAS, and thus depletion of the STING ligand cGAMP, results in reprogramming and re-sensitization of *STK11*-mutant models to cGAS-STING mediated type I interferon responses. Furthermore, we show that CIN promotes excessive production cGAMP in *STK11*-mutant models. We find upregulation of two ectonucleotidases (ENPP1 and CD73/*NT5E*) that hydrolyze exported cGAMP to adenosine, which may further contribute to the highly dysfunctional tumor-microenvironment observed in *STK11*-mutant tumors. Lastly, suppression of CIN through overexpression of mitotic-centromere associated kinesin (MCAK) in murine *STK11*-mutant models results in decreased tumor growth and sensitization to anti-PD1 therapy.

In summary, we define *STK11*-mutant as archetypical chromosomally form of NSCLC, provide mechanistic basis that corelates with poor clinical outcomes, and demonstrate how relief of tonic CIN-induced changes may be therapeutically leveraged.

#5945

Transcriptional analysis of TME in MC38 colon carcinoma model following checkpoint inhibition

Priyanka Singh, Dan Saims, David Draper, Sheri Barnes. *In Vitro Preclinical Oncology, Labcorp Drug Development, Ann Arbor, MI*

Colorectal cancer (CRC) is one of the most common cancers with 200,000 US cases per year. Adenocarcinoma is the most common type of CRC, making up 95 percent of all CRC cases. Checkpoint inhibitors used for CRC have shown efficacy for a specific subset of patients. MC38 is a very popular tumor model due to its characteristics as an immunologically warm tumor and response to some immunotherapies. To identify underlying factors that influence differences in treatment response, the tumor microenvironment (TME) of the MC38 model was analyzed following the treatment with anti-programmed cell death protein 1 (PD-1) and anti-cytotoxic T lymphocyte associated protein 4 (CTLA-4). The minimal tumor growth inhibition was observed in MC38 tumors treated with anti-PD-1 or anti-CTLA-4. The NanoString® nCounter system and flow cytometry were used to provide gene and cell-specific signatures of TME in response to immunomodulatory agents. NanoString® nCounter and flow cytometry analyses were complementary and demonstrated evidence of T cell recruitment and upregulation of genes associated with several immune-related pathways following treatment. Cytotoxic CD8+ T cells, CD4+ T cells, and NK cells in MC38 tumors following treatment with anti-PD-1, suggesting activation of an immune response. With treatment of anti-CTLA-4, tumors did not have demonstrable alterations to immune cell subset distribution which supports evidence that anti-CTLA-4 treatment show minimal activation of the immune system in MC38 tumors. Further, transcriptome analysis with NanoString® nCounter system revealed that the immune pathways related to signatures such as interferon signaling, cytotoxicity, antigen presentation, cytokine signaling, and chemokine signaling were upregulated with anti-PD-1 treatment compared to control or anti-CTLA-4 treatment of MC38 tumors. The transcriptome analysis also demonstrated 2-5-fold increases of interferon, cytotoxicity, cytokine, and chemokine genes such as, Gbp2, Gbp3, Irf1, Irf7, Irf8, Ifit1, Ifit2, Ifit3, Tnfsf10, Ccl2, Ccl5, Ccl7, Ccl12, Cxcl9, Cxcl10, and Cxcl11 over control

in the case of anti-PD-1 treatment. In summary, anti-PD-1 treatment increased T cell recruitment into the tumor and upregulated genes in TME. Anti-CTLA-4 treatment known to enable combination activity with anti-PD-1, but not enough to show notable monotherapy activity. Immune cell subset distribution in TME and relative gene expression are two potential types of analyses to predict anti-tumor response. These data can be used mechanistically as well as to inform rational combination strategies for checkpoint inhibitors in colon adenocarcinoma.

#5946

OBI-999, an anti-Globo H antibody drug conjugate, exhibits synergistic anti-tumor effect in combination with pembrolizumab

Chun-Chung Wang, Chi-Huan Lu, Jhih-Jie Yang, Wan-Fen Li, Ming-Tain Lai. *OBI Pharma, Inc, Taipei, Taiwan*

Background: Globo H (GH) is highly expressed in a variety of epithelial tumors with a limited expression in normal tissues rendering it a novel therapeutic target. OBI-999 is an antibody drug conjugate (ADC) consisting of a GH-specific monoclonal antibody conjugated with monomethyl auristatin E (MMAE) through a cathepsin B cleavable linker. MMAE is known to induce immunogenic cell death (ICD) which involves in the activation of cytotoxic T lymphocyte-driven adaptive immunity with long-term immunological memory.
Aim: The aim of this study was to evaluate the synergistic effects of OBI-999 + pembrolizumab on tumor growth suppression in several xenograft tumor models.
Methods: OBI-999-induced ICD was examined *in vitro* by the detection of damaging-associated molecular patterns (DAMPs) such as calreticulin (CRT), HMGB1, and ATP in incubated Globo H expressing cells. The synergistic effects with the combination of OBI-999 and pembrolizumab as well as the ICD-related immunity were assessed *in vivo* using advanced severe immunodeficient mice that were reconstituted with human peripheral blood mononuclear cells (PBMCs).
Results: Incubation of OBI-999 with high GH expression cancer cell lines (HCC-1428, NCI-N87 and NCI-H526) and mid GH expression cancer cell line (SW-480) induced the release of DAMPs including CRT, HMGB1, and ATP, in a dose- and time-dependent manner, indicating that OBI-999 is

capable of inducing ICD *in vitro*. In the high GH expression human breast cancer cell line HCC-1428 xenograft model, OBI-999+pembrolizumab exhibited significantly stronger inhibition of tumor growth compared to either OBI-999 or pembrolizumab alone. Similar synergistic effects were observed in other xenograft tumor models including gastric (NCI-N87), small cell lung (NCI-H526), and colorectal (SW-480) cancers. Analysis of tumor-infiltrating lymphocytes (TILs) in HCC-1428 humanized mice showed that OBI-999 + pembrolizumab induced populations of activated cytotoxic CD8 T-cells and mature dendritic cells. Pembrolizumab decreased PD-1 expression on CD8 and CD4 cells, and OBI-999 decreased PD-L1 expression on tumor cells, which reversed the exhausted status of immune cells and alleviated immunosuppression in the tumor microenvironment. Conclusion: We demonstrated significant synergistic effects of OBI-999 and pembrolizumab in several animal models. These synergistic effects may be attributed to the ability of OBI-999 to induce ICD, as demonstrated by the release of DAMPs *in vitro* and tumor-specific immunity *in vivo*, suggesting that OBI-999 can create a tumor microenvironment that enhances the function of pembrolizumab. The results suggest that combination therapy with OBI-999 and immune checkpoint inhibitors is warranted in human clinical studies. OBI-999 is currently in Phase 1/2 clinical trials for the treatment of advanced solid tumors with high GH expression (NCT04084366).

#5947

Tumor cells escape cell death after radiotherapy by senescence - a mechanism that can be counteracted with zinc oxide nanoparticles

Nadine Wiesmann, Rita Gieringer, Johannes Kupka, Jonas Eckrich, Sebahat Kaya, Peer Kaemmerer, Bilal Al-Nawas, Juergen Brieger. *University Medical Center Mainz, Mainz, Germany*

Radiotherapy is still an important pillar for the therapy of head and neck squamous cell carcinoma (HNSCC); however, local recurrences arise in 15-50% of patients. During radiotherapy, there is a risk that individual tumor cells survive and proliferate again after a period of dormancy. Growing evidence suggests that senescence may play a key role in this context. We investigated *in vitro* radiotherapy-induced senescence and found that quiescent tumor cells survived treatment with 16 Gy. Those cells exhibited

characteristics of senescence, yet were able to regain their proliferative capacity, and senescence was associated with radioresistance. During radiotherapy, the cells of the tumor stroma are inevitably irradiated as well. It is already known that cancer-associated fibroblasts (CAFs) can promote tumor progression. However, their contribution to the survival of senescent tumor cells after radiotherapy is unknown so far. Furthermore, the association between radiotherapy-induced senescence and recurrences raises the question of how residual, senescent tumor cells can be eliminated to prevent the development of a recurrence at an early stage. These aspects were the subject of the study presented here. To study the interaction between tumor cells and CAFs during their response to irradiation, both cell types were irradiated with 16 Gy *in vitro* individually and in co-culture. Subsequently, proliferation, cell death, morphological characteristics, and the secretome were analyzed. Additionally, we investigated whether senescent tumor cells can be targeted by treatment with zinc oxide nanoparticles. We could show that not only the tumor cells but also the CAFs go into a senescent state in response to irradiation, seen by loss of proliferation, increased senescence-associated β-galactosidase activity, and typical morphological characteristics. The secretome analysis revealed that the co-culture of tumor cells with CAFs significantly altered the repertoire of cytokines released upon irradiation, indicating intense communication between the cell types during their response to irradiation. Therefore, it is important for future studies on radiotherapy-induced senescence to include the tumor stroma as well. Finally, we demonstrated that senescent tumor cells were vulnerable to cell death induced by treatment with zinc oxide nanoparticles, which thus could potentially contribute to eliminating residual tumor cells after radiotherapy. This study revealed that radiotherapy-induced senescence in tumor cells and associated fibroblasts could well be a therapeutic problem, as senescent tumor cells are not targetable by radiotherapy anymore. In the future, zinc oxide nanoparticles may help to counteract this escape mechanism to prevent recurrences.

#5948

MAGE-A3 expression with MMR-MSH6 screening suggests MAGE-A3 as a potential target for microsatellite-stable colorectal cancer

Jina Yom[1], Rachel Gonzalez[1], Eden Zewdu[1], Aubrey Su[1], Patrick Yin[1], Bailey Gilmore[1], Dehe Kong[1], Andy Han[1], Zhaoying Guo[1], Tianli Qu[1], Zoe

Zhao[1], Eric Christenson[1], Yan Ma[1], Hailey Guo[1], Xiaomin Hu[2], Qi Ren[2], zhaohui Wu[2], Xuan Liu[1], Wei Fu[1]. *[1]OriGene Technologies, Inc., Rockville, MD,[2]OriGene Wuxi Biotechnology Co., Ltd., Binhu District, China*

Colorectal Cancer (CRC) is the second leading cause of death worldwide. Recent developments in cancer immunotherapy have obtained encouraging clinical responses, including PD-1/PD-L1 blockade therapy, although response rates vary depending on tumor type. For example, despite the lack of response by microsatellite-stable CRC, a subset of CRC with deficient mismatch repair (dMMR) and high microsatellite instability (MSI-H) responds especially well to the PD-1/PD-L1 blockade therapy. For other types of CRC which do not respond to PD-L1 therapy, new targets are being investigated. One family of targets is the cancer testis antigen MAGE-A whose expression is restricted to germline cells in normal tissue but is overexpressed in many cancer cells. In this study, immunohistochemical analysis of MAGE-A3 expression in colon cancer along with IHC screening of mismatch protein MSH6 was performed. Many of the cases in this study observed a co-expression in the tissue. In the tumors, MAGE-A3 was observed to have weak cytoplasmic expression while MSH6 had strong nuclear expression in the epithelial cells. The immune cells adjacent to the epithelial cells were also positive for MAGE-A3. This result suggests that MAGE-A3 may be a promising target for microsatellite-stable colorectal cancer immunotherapy.

#5949

Modulate TAM infiltration at cancer-immune interface by targeting at monocyte migration

Wenxuan Du[1], Adrian Johnston[1], Praful Nair[1], Jingyi Zhu[2], Khin Sandar Win[1], Bryan Zhou[1], Jude Phillip[2], Pei-Hsun Wu[3], Denis Wirtz[1]. *[1]Chemical and Biomolecular Engineering, Johns Hopkins University, Baltimore, MD,[2]Biomedical Engineering, Johns Hopkins University, Baltimore, MD,[3]Institute for NanoBioTechnology, Johns Hopkins University, Baltimore, MD*

Extensive infiltration of tumor-associated macrophages (TAMs) into the solid tumor microenvironment (TME), where they promote angiogenesis,

initiate metastasis, and tune immunosuppression, has long been proven to correlate with worse patient prognosis. Thus, much significance has been attached on either impeding TAM infiltration or reversing pro-tumoral TAMs back into phagocytic M1 phenotype. Nevertheless, while revealing underlying mechanisms of blocking TAM recruitment, widely adopted *in vitro* migration assays like Transwell, μ-slides fail to distinguish cell's random migration from chemotaxis (biased migration) and introduce 3D extracellular matrix environment. Here we present data that monocytes, as major replenishment source of TAMs, massively boost their random migration via paracrine pathway to initiate early-stage infiltration using an advanced 3D multi-compartment organoid model. In addition, before re-educated into TAMs, monocytes in the TME are capable of inducing triple negative breast cancer cells' hyper-proliferation by activating their MEK/ERK signaling pathway. This work provides evidence that TAM infiltration is driven by monocytes' random/biased migration separately and identifies a potential combinational immunotherapy targeting at monocytes instead of TAMs.

#5950

Ccr2+ monocyte derived macrophages influence trajectories of acquired therapy resistance in BRAF-mutant melanoma

Dahihm Kim, Luye An, Jiwon Moon, Andrew White. *Cornell Univ. College of Veterinary Med., Ithaca, NY*

Therapies targeting oncogene addiction have had a tremendous impact on patient care, but drug resistance continues to be problematic. One method to deal with this challenge entails extending the scope of anti-cancer treatment beyond tumor cells by additionally altering their tumor microenvironment. Understanding how the tumor microenvironment can contribute to the evolution of diverse resistance pathways could aid in the rational design of sequential treatments that enforce pressure towards a more predictable resistance trajectory. Tumor associated macrophages often support neoplastic growth and are frequently the most abundant immune cell found in tumors. Here, we used clinically relevant *in vivo* Braf-mutant melanoma models and *Ccr2-RFP; Cx3cr1-GFP* mice to track the long-term changes in tumor cells and macrophages under targeted therapy with Braf/Mek inhibitors. We assessed the dynamic evolution of the macrophage

population generated by therapy pressure-induced stress. During the onset of a drug-tolerant persister state, *Ccr2*+ macrophage infiltration rises, underscoring a prominent role at this point in melanoma evolution for development of drug-resistance. Importantly, we show that a lack of melanoma infiltrating *Ccr2*+ macrophages delays onset of resistance. In this case, rebounded tumor cells from *Ccr2* knockout recipients favor the evolution of cell-extrinsic mediated resistance mechanisms, which can be reversed when these adapted melanoma cells are relocated to a microenvironment with functional Ccr2. Conversely, Ccr2 presence promotes development of cell-intrinsic drug resistance with a stable phenotype in rebounded tumor cells. Overall, this demonstrates that the development of resistance may be manipulated and directed to improve timing and probability of relapse.

#5951

The correlation between single nucleotide polymorphism of chemokine receptor and ligand and infiltrating immune cells on tumor microenvironment of gastric cancer

Sunjoo Yoon[1], Ju Hyun Lee[1], Minsu Kang[1], Hyeon Jeong Oh[2], Jiwon Koh[2], Hye Seung Lee[2], So Hyun Kang[3], Young Suk Park[3], Keun-Wook Lee[1], Jin Won Kim[1]. *[1]Internal Medicine, Seoul National University Bundang Hospital, Seoul National University College of Medicine, Seongnam, Korea, Republic of,[2]Pathology, Seoul National University Bundang Hospital, Seoul National University College of Medicine, Seongnam, Korea, Republic of,[3]Surgery, Seoul National University Bundang Hospital, Seoul National University College of Medicine, Seongnam, Korea, Republic of*

Objective: Chemokines play roles in many normal biological processes, such as hematopoietic cell genesis and leukocyte migration and homing. Chemokines could be responsible for eliciting local accumulation of immune cells within tumor microenvironment. In this study, we examine if genetic variations in chemokine receptor and ligand are associated with infiltrations of immune cells on tumor microenvironment in gastric cancer. Methods: In 356 gastric cancer patients who received curative surgery followed by adjuvant chemotherapy, total 105 single nucleotide polymorphisms (SNP) in a chemokine ligand and chemokine receptor locus

within 16 genes (CXCR4, CXCR2, CXCR1, CX3CR1, CCR8, CCR9, CCR3, CCR2, CCR5, CCRL2, CCR6, CXCR5, CCR6, CXCR6, CCR7, DARC) were genotyped from peripheral blood sample. Total 11 immune markers such as CD3, CD4, CD8, FOXp3, CD68, CD163, L-selectin, i-NOS, ADMA17, Arginase, CD45RO were analyzed for deposition of immune cells according to SNP of chemokine receptor and ligand. Levels of immunohistochemistry staining were quantified by Image Analysis Toolbox and density of immune cells infiltration was calculated.
Results: 32 SNP locus of 8 genes (such as CXCR1, CXCR2, CCR3, CCR2, CCR5, CCRL2, CCR6. CXCR5) were selected using 25% cut-off value of minor allele frequency (MAF). Among 8 genes, CCR5 was the most relevant gene for immune cell infiltration on tumor microenvironment. Intron1-2545G>A (rs1799987) were associated with increased accumulation of CD3+, CD68+ and FOXp3+ cells compared to recessive carriers of the common allele. In CCR5 SNP that contained the common alleles of intron1-2549 G>T (rs2734648) and exon2A-2081 A>G (rs1800023), CD3+, CD4+, CD8+ and FOXp3+ cells
were infiltrated more than minor alleles.
Conclusions: The associations between infiltration of immune cells and SNP of chemokine receptor and ligand in gastric cancer were shown. Particularly, CCR5 SNP may be most relevant for correlation with infiltration of immune cells on tumor microenvironment.

#5952

Pyroptotic adipocytes contribute to chemoresistance in advanced stage ovarian cancer

Chang-Ni Lin[1], Yu-Ling Liang[1], Keng-Fu Hsu[1], Yi-Ying Wu[2]. *[1]Obstetrics and Gynecology, National Cheng Kung University Hospital, Tainan, Taiwan,[2]Graduate Institute of Clinical Medicine, National Cheng Kung University, Tainan, Taiwan*

Background: Ovarian cancer is known the gynecologic malignancy with the highest case-to-fatality ratio. Once appear metastasis, the 5 years survival rate reduce to 30-40% in these patients. Different with hematogenously metastasizing tumors, ovarian cancer cells primarily disseminate within the peritoneal cavity. Omentum, a lipid-rich tissue, is the most common metastatic site of ovarian cancer. In addition, the adipocyte-released free

fatty acid can be used by cancer cells to fuel its growth and proliferation. In this study, we attempt to clarify the regulation between metastatic ovarian cancer cell and omental adipocytes, and find a therapeutic strategy for advanced stage ovarian cancer.
Materials and Methods: A three-cell (SKOV3, 3T3L1 and THP-1) co-culture model was established to mimic in vitro tumor microenvironment of ovarian cancer omental metastasis. Flow cytometry was performed for the adipocytes survival rate with Annexin V/PI double staining. Caspase-1 activity assay was used to detect the cleavage of substrate YVAD-AFC level in adipocytes and quantified by a fluorescence microliter plate reader. The free fatty acid assay kit was used to detect free fatty acid level in condition medium and ascites. Invasion assay and MTT assay were used to validate the invasive ability and cell viability of ovarian cancer cells. Immunohistochemistry was used to CD36 staining in clinical specimens, and correlation analysis through prism 8 software. Results: We observed the adipocyte pyroptosis in 3-cell co-culture model, and the free fatty acid increased in culture medium by flow cytometry analysis, caspase-1 activity assay kit and free fatty acid assay kit. In the meantime, the invasive ability and cisplatin resistance increased in ovarian cancer cells. The free fatty acid level in ascites positive correlated with CD36 expression (r^2=0.2189, p=0.0375). Of note, combination treatment of cisplatin and sulfosuccinimidyl oleate (SSO) can reverse chemoresistance in 3-cell co-culture model. Overall, free fatty acid released form the pyroptotic adipocytes and increase invasive ability and chemoresistance in ovarian cancer cells. Block the interaction of free fatty acid and CD36 can reverse the chemoresistance in advanced ovarian cancer.
Conclusion: In this study, we demonstrated adipocytes pyroptosis can increase the free fatty acid release to the microenvironment, and then promote ovarian cancer cell invasion and increase chemoresistance. For more important, inhibition of free fatty acid and CD36 interaction can reverse the chemoresistance in the in vitro experiments. Thus, reduce the adipocytes pyroptosis may be a novel therapeutic strategy for the omentum metastatic ovarian cancer.

#5953
Reshaping the tumor microenvironment: new application of tamoxifen in triple negative breast cancer immunomodulation

Pony Yu-Ling Lee[1], Marvin A. E. Aberin[2], Chien-Chang Shen[1], Kun-Yuan Lin[1], Chao Di Chang[1], Chih-Chieh Yang[1], Shan-Yun Cheng[1], Ya Wen Hung[1], Xin-Guo Hsu[3], Shu-Ping Wang[4]. *[1]Pharmacology Discovery Services Taiwan, Ltd., New Taipei City, Taiwan,[2]Taiwan International Graduate Program in Molecular Medicine, Academia Sinica and National Yang Ming Chiao Tung University, Taipei City, Taiwan,[3]Graduate Institute of Life Sciences, National Defense Medical Center, Taipei City, Taiwan,[4]Institute of Biomedical Sciences, Academia Sinica, Taipei City, Taiwan*

Tamoxifen is a widely known estrogen receptor (ER) modulator which has been employed in adjuvant treatment of ER^+ breast cancer for over 30 years. Interestingly, clinical observations reveal that tamoxifen is capable of inducing regression of some tumors lacking ER expression whereas tamoxifen is also capable of increasing host resistance against cancer in an ER-independent mechanism. These findings suggest the immunomodulatory effects of tamoxifen may be ER-independent, but little is known about the underlying mechanism and the potential clinical implication. Recently, we identified a novel mechanism by which tamoxifen exerts its DNA-damaging potential by re-shaping the unfavorable tumor microenvironment in breast cancer. A long-term tamoxifen administration induces downregulation of the chromatin ‘‘reader’’ RACK7/ZMYND8, which acts as a suppressor of interferon-stimulated genes (ISGs, including cytokines and chemokines) and CEACAM1 in both ER^+ and triple negative breast cancer (TNBC) cells. To investigate the immunomodulatory effects of tamoxifen in conjunction with RACK7-knockdown, the orthotopic murine TNBC 4T1 model was employed to investigate tamoxifen-mediated cellular modulation in TNBC. The control and RACK7-knockdown 4T1 cells are orthotopically implanted into the mammary fat pad of female BALB/c mice. Peripheral cytokines/chemokines and high-content biomarker studies (multiplex immunoassays, flow cytometry, and single-cell RNA sequencing) are deployed to obtain insights into the mechanistic rationale behind the immunomodulatory effects of tamoxifen and/or RACK7-knockdown. The tamoxifen-mediated cellular modulation evokes cytokine/chemokine secretion and further induces T-cell infiltration into tumor area. However, tumor reduction was limited due to extensive T-cell

exhaustion from interaction of CEACAM1 and TIM-3, a “checkpoint” receptor expressed in $CD4^+$ and $CD8^+$ T cells. The expression patterns of CEACAM1 and PD-L1 in 4T1 tumor cells and that of TIM-3 and PD-1 in $CD4^+$ and $CD8^+$ T-cells correlate with intra-tumor infiltration of T-cells and tumor cell growth. Therefore, targeting the interaction between CEACAM1 and TIM-3 to overcome T-cell exhaustion is crucial for the new therapeutic role of tamoxifen treatment in TNBC breast cancer in conjugation with RACK7-knockdown. Altogether, our findings provide direct evidence to support a new therapeutic opportunity by targeting CEACAM1-TIM-3 interaction in the tamoxifen-mediated tumor immune microenvironment for improving immune checkpoint blockade therapy in breast cancer.

#5954

Germline epitopes modulate immune surveillance informing breast cancer subtypes

Kathleen Houlahan, Aziz Khan, Christina Curtis. *Stanford University, Stanford, CA*

Cancer represents a wide spectrum of molecularly and morphologically diverse diseases. Individuals with the same histopathological classification can have tumors with drastically different molecular profiles and clinical responses to treatment. It remains unclear as to when during the disease course these differences arise and why some tumors are addicted to one oncogenic pathway over another. Somatic genomic aberrations occur within the context of an individual’s germline genome, which can vary across millions of germline polymorphisms. It is unknown the extent to which germline differences influence the somatic evolution of a tumor. Interrogating 4,912 breast cancer lesions, spanning pre-invasive to metastatic disease, we demonstrate that germline variants in highly expressed and amplified genes influence somatic evolution by modulating immunoediting at early stages of tumor development. Specifically, we show that the burden of germline-derived epitopes in recurrently amplified genes selects against somatic gene amplification in pre-invasive and invasive breast cancer. As a representative example, individuals with high burden of germline-derived epitopes in *ERBB2* are significantly less likely to develop HER2+ breast cancer than ER+ or triple negative breast cancer. The same negative association between epitope burden and somatic amplification is

observed for four recurrent amplicons observed in high risk ER+ breast tumors. No association was observed between somatic amplifications and epitope burden in metastatic breast cancer suggesting a subset of tumors are able to overcome immune-mediated negative selection. Tumors that do are more aggressive and demonstrate an "immune cold" phenotype. Taken together, these data show the germline genome plays a pivotal role in dictating somatic evolution in breast cancer. Exploiting germline-mediated immunoediting may facilitate the development of blood-based biomarkers that refine risk stratification within breast cancer subtypes.

#5955

***In Silico* dissection of immune infiltrate signatures that are detected by DetermaIO, a predictor of response to immune therapy**

Brian Z. Ring[1], Catherine T. Cronister[1], Robert S. Seitz[1], Douglas T. Ross[1], Brock Schweitzer[1], David R. Gandara[2]. *[1]Oncocyte Inc., Nashville, TN,[2]UC Davis, Sacramento, CA*

Background: The composition of tumors includes not only malignant but also immune, stromal and other cell types. Understanding this dynamic tumor immune microenvironment (TIME) is important to guide treatment and develop novel therapies and markers. We have previously validated immuno-oncology gene expression signatures (DetermaIO (DTIO) and a 101-gene algorithm), that predict efficacy of checkpoint inhibitors (ICI) based on distinguishing immunomodulatory (IM), mesenchymal stem-like (MSL), and mesenchymal (M) phenotypes. In this study we used TCGA and clinical cohorts to identify immune infiltrate populations within these defined TIME spaces and their association with ICI treatment.
Methods: We derived novel human immune infiltrate signatures from a translation of murine ImmGen cell populations and a search for conserved co-expression of immune markers across multiple tumors. In total, 20 tumors from TCGA were employed for derivation and analysis encompassing 7163 unique samples. These novel signatures were compared to published immune infiltrate signatures and then their association with ICI efficacy and each other assessed in three cohorts treated with ICI therapy, IMvigor210 and an additional bladder cohort, comprising 272 and 89 patients with censored outcome results, and a melanoma cohort (N=105).

Results: The ImmGen analysis created 35 immune cell signatures and pan-tumor conserved co-expression of immune markers created eight signatures. The co-expression signatures often contained a mixed population of cell-type markers, though largely dominated by either myeloid or lymphoid markers. These signatures showed highly reproducible proportions of samples with strong expression between train and test TCGA sets. Most immune signatures had their highest representation in IM and DTIO+ tumors, however there was also consistent identification of presumptive immune infiltrate presence in MSL, M and DTIO negative cases. Two of the conserved co-expression signatures, one comprised of B-cell markers, and the other of T cell and other lymphoid markers, were associated with ICI efficacy in IMvigor210 and validated in the other "real-world" bladder cohort (B-cell: OR=0.8, p=0.022, T lymphoid: OR=0.7, p=0.005). Both signatures also had significant association with outcome in the cohort with clinical response outcomes, being strongest in patients after treatment had initiated.
Conclusions: These cell-type signatures may be identifying novel immune infiltrate populations that co-exist within the tumor immune microenvironment and are potentially predictive of ICI response. The two signatures were not independent of DTIO in either cohort, suggesting that the 27-gene algorithm DTIO largely incorporates this information. This analysis begins to dissect the complex physiology of the tumor immune microenvironment that mediates response to immune therapy.

#5956
Tumor-infiltrating neutrophil progenitors impair homologous DNA repair and promote sensitivity to PARP-inhibition
Arianna Calcinotto. *Institute of Oncology Research, Bellinzona, Switzerland*

Tumor evolution is one of the major mechanisms responsible for acquiring therapy-resistant and more aggressive cancer clones. Whether the tumor microenvironment through immune-mediated mechanisms might promote the development of more aggressive cancer types is crucial for the identification of additional therapeutical opportunities. Here, we identified a novel subset of tumor-infiltrating neutrophils, defined as tumor-associated neutrophil progenitors (NePs). These NePs are enriched in highly proliferative hormone-dependent breast cancers and impair DNA repair

capacity. Mechanistically, succinate secreted by tumor-associated NePs inhibits homologous recombination, promoting error-prone DNA repair through non-homologous end-joining regulated by PARP-1. Consequently, breast cancer cells acquire genomic instability, resulting in tumor progression and resistance to endocrine therapies. Selective inhibition of these pathways induces increased tumor cell kill in vitro and in vivo. Intra-tumor NePs score correlates with copy number alterations in highly proliferative hormone-dependent tumors from breast cancer patients. Treatment with PARP-1 inhibitors counteract the pro-tumorigenic effect of these neutrophils and reverses endocrine resistance.

#5957

Chemotherapy-induced extracellular matrix remodeling in HGSOC

Panoraia Kotantaki, Florian Laforêts, Eleni Maniati, Chiara Berlato, Anna Malliouri, Michael John Devlin, Beatrice Malacrida, Samar Elorbany, Ranjit Manchanda, Frances R. Balkwill. *Barts Cancer Institute, London, United Kingdom*

In this study we explored the effects of chemotherapy on the extracellular matrix of high-grade serous ovarian cancer metastasis (HGSOC) at structural-textural protein level and transcriptionally, in order to identify the microenvironmental features that accompany a successful response. We studied two murine orthotopic, transplantable syngeneic models of HGSOC, one that displays excellent response to carboplatin/paclitaxel (60577) and one that is resistant to treatment (HGS2)[1]. Using immunohistochemistry, we stained omental tumors from both models for the ECM components fibronectin (FN1), collagen 1A1 (COL1A1) and versican (VCAN), also using Masson's Trichrome to stain for collagen. We analyzed their abundance, textural features (Haralick features) and structure with the image analysis softwares, QuPath and TWOMBLI respectively. A compilation of 44 ECM metrics, which we named the "structure index", correlated with response to chemotherapy, as measured by reduction in omental tumor weight. In parallel, we performed RNAseq on the omental tumors, identifying clusters of genes that change over time with chemotherapy treatment of the responsive model 60577, while the chemoresistant model HGS2 displayed limited alteration of gene expression. We integrated RNAseq and ECM structure and texture data, and

showed the structure index was correlated with 144 core matrisome genes. To identify potential therapeutic targets, we then focused our study on genes that remained highly expressed in resistant tumors post chemotherapy, but were originally low or decreased with treatment in the sensitive tumors. Members of the LOX and P4HA family were found amongst these genes. We confirmed by immunohistochemical analysis that expression of LOX, LOXL2, P4HA1 and P4HA2 was downregulated by chemotherapy in the 60577 chemo-sensitive tumors while their levels remained relatively unaffected in the resistant HGS2 tumors. This study refines our understanding of the mechanisms of microenvironmental chemoresistance in HGSOC, highlighting putative therapeutic targets to increase the efficacy of platinum-based chemotherapy in ovarian cancer.

1 Maniati, E. *et al.* Mouse Ovarian Cancer Models Recapitulate the Human Tumor Microenvironment and Patient Response to Treatment. *Cell Rep* **30**, 525-540.e527, doi:10.1016/j.celrep.2019.12.034 (2020).

#5958

Analysis of MDSCs as a diagnostic and therapeutic target for gastric cancer

Suguru Yamauchi[1], Takumi Iwasawa[2], Tomoaki Ito[3], Malcom V. Brock[4], Tetsu Fukunaga[1], Hajime Orita[1], Kazunori Kato[2]. *[1]Department of Upper Gastrointestinal Surgery, Juntendo University School of Medicine, Tokyo, Japan,[2]Department of Biomedical Engineering, Faculty of Science and Engineering, Toyo University, Saitama, Japan,[3]Department of Surgery, Juntendo University Shizuoka Hospital, Shizuoka, Japan,[4]Department of Surgery, The Johns Hopkins University, Baltimore, MD*

Background: Gastric cancer (GC) is the second most common cancer in Japan in terms of incidence and the third most common in terms of deaths. The onset and progression of cancer are generally suppressed by the action of immune cells, which is an inflammatory response. MDSCs are thought to promote cancer progression and invasion by suppressing the function of immune cells, making them potential therapeutic and diagnostic targets. We measured MDSCs in GC patients and observed more monocyte-derived MDSCs in peripheral blood in advanced GC than in early GC. However, granulocyte-derived MDSCs showed no difference in GC progression when markers for classical MDSCs were used. We considered that granulocyte-

derived MDSCs were much more abundant than monocyte-derived MDSCs in peripheral blood and were involved in cancer progression. We hypothesized that we had a new granulocyte-derived marker for advanced GC that did not show differences in classical markers, but may have different functions, and aimed to identify a novel subset that may be a therapeutic and diagnostic target.
Method: For GC patients, we used heparin blood samples provided by patients who consented to Juntendo University. We analyzed the expression of various cell surface proteins against populations of $CD33^{high}$, $CD66b^{high}$, and $HLA\text{-}DR^{low}$ as classical markers of MDSCs derived from granulocytes of GC patients using FACS (Melody). MDSCs were isolated by a cell sorter and used for experiments such as RNA-Seq. Novel markers and involved cytokines were quantified in plasma components by cytometric bead array.
Result: The chemokine receptors CCR2, CCR5, CXCR4, and CXCR5 were highly expressed in MDSCs of advanced GC patients. The ability to suppress T-cell activation was also found to be stronger in MDSCs with advanced GC. In addition, IL-10 produced by MDSCs was also more abundant in the plasma of patients with advanced GC, as well as chemokines according to chemokine receptors.
Conclusion: The high expression of chemokine receptors on MDSCs in advanced GC may indicate that chemokines produced at the cancer site facilitate the migration of MDSCs. These novel subsets of MDSCs found in advanced GC suggest that they may be new therapeutic targets.

#5959

Dissecting the stromal drivers of gastroesophageal adenocarcinoma chemoresistance

Kulsum Tai[1], Sanjima Pal[1], Julie Bérubé[1], Iris Kong[1], Adam Hoffman[1], Swneke Bailey[1], Aki Kirbizakis[1], Sui Huang[2], Michael Strasser[2], David Gibbs[2], Nicholas Bertos[1], Veena Sangwan[1], Lorenzo Ferri[1]. *[1]McGill University Health Centre Research Institute, Montreal, QC, Canada,[2]Institute of Systems Biology, Seattle, WA*

Gastroesophageal adenocarcinoma (GEA) is the fastest rising cancer in North America. Over the course of five years, the survival rate is <20%, creating an urgent need for appropriate treatments against GEA. Currently, providing patients with peri-operative systemic docetaxel triplet-based

chemotherapy (DCF or FLOT) is the most effective approach to treat GEA. Despite this, for 50% of patients that do present an initial response to therapy, the tumor returns due to pre-existing or newly acquired resistance (i.e., chemoresistance) by the cancer. Researchers have shifted their focus to the tumor microenvironment (TME) as one of the factors influencing chemoresistance in patients. The TME is composed of tumor cells, immune cells and their secreted products, as well as fibroblasts. The components of the TME have been shown to interact with one another to influence tumor growth and progression. Fibroblasts are wound-healing cells that can be transformed into cancer-associated fibroblasts (CAFs) in response to stress and the release of inflammatory products. CAFs are the most abundant cells in the TME, yet their role in the chemoresponse of GEA is still unclear. Previous studies on other cancer types demonstrated that CAF expression is distinct between chemoresistant and chemo-sensitive tumors and certain CAF subpopulations may confer this resistance. This project will investigate the role of CAFs in the chemo-response of GEA using patient-derived organoids (PDOs) and CAFs from >200 GEA patients. A single-cell RNA sequencing atlas developed from >30 GEA DCF- or FLOT-treated patient samples will be used to identify CAF markers and targetable processes. CAF sub-populations will then be elucidated and correlated to tumor response. IF, FACS, and ELISA will be performed for subsequent CAF marker validation and characterization. Ex vivo drug testing with DCF or FLOT will be conducted on PDO-CAF co-cultures to recapitulate their drug response.

#5960

Identification and validation of sarcoma cellular ecosystems associated with prognosis and predictive of immunotherapy response

Ajay Subramanian[1], Neda Nemat-Gorgani[1], Timothy J. Ellis-Caleo[1], David G.P. van IJzendoorn[1], Timothy J. Sears[1], Anish Somani[1], Bogdan A. Luca[1], Maggie Y. Zhou[1], Martina Bradic[2], Ileana A. Torres[1], Eniola Oladipo[1], Christin New[1], Deborah E. Kenney[1], Raffi S. Avedian[1], Robert J. Steffner[1], Michael S. Binkley[1], David G. Mohler[1], William D. Tap[2], Sandra P. D'Angelo[2], Matt van de Rijn[1], Kristen N. Ganjoo[1], Nam Q. Bui[1], Gregory W. Charville[1], Aaron M. Newman[1], Everett J. Moding[1]. *[1]Stanford*

University, Stanford, CA,[2]Memorial Sloan Kettering Cancer Center, New York, NY

The tumor microenvironment contributes to tumorigenesis, disease progression, and response to therapy in soft tissue sarcomas (STSs). However, characterizing the malignant and stromal cells that make up STSs and correlating their abundance with clinical outcomes has proven difficult in fixed clinical specimens. We employed a machine learning framework called EcoTyper (Luca et al. Cell 2021) to identify cell type-specific transcriptional states and define tumor ecotypes consisting of co-occurring cell states from bulk transcriptomes. Analyzing 292 previously published STSs profiled by bulk RNA-sequencing (RNA-Seq), we identified 23 transcriptionally-defined sarcoma cell states in malignant, immune, and other stromal cells and validated the majority of these cell states using single cell RNA-Seq. Although sarcomas originate from mesenchymal tissues, we identified four epithelial-like sarcoma cell states and observed epithelial differentiation and expression of epithelial markers within malignant sarcoma cells across histologies. Cell states reflected known and novel cell phenotypes and many were strongly associated with patient outcomes in our RNA-Seq training cohort and an independent validation cohort of STSs profiled by microarray (n=309). By identifying co-occurring cell states across STSs, we discovered 3 sarcoma ecotypes associated with underlying genomic alterations and distinct clinical outcomes. On spatial transcriptomic analysis, we observed co-localization of cell states within the same sarcoma ecotypes and spatial aggregation of ecotypes within STSs, suggesting that sarcoma ecotypes represent distinct functional units within human sarcomas. One ecotype (sarcoma ecotype 3: SE3) defined by *CLEC5A/SPP1+* M2-like immunosuppressive macrophages and MYC/MTORC1-activated epithelial-like malignant cells was associated with inferior progression-free survival (PFS) in the RNA-Seq training cohort (P=0.01) and inferior metastasis-free survival in the microarray validation cohort (P=0.002). Remarkably, SE3 was associated with improved PFS in patients with metastatic STSs treated with ipilimumab and nivolumab (n=38, P=0.003) but not patients treated with chemotherapy. Furthermore, SE3 outperformed previously reported predictors of immunotherapy response in STSs, PD-L1 expression and tertiary lymphoid structures (TLS), for predicting response to immunotherapy (AUCs: SE3

0.87; PD-L1 0.81; TLS 0.62). Finally, SE3 similarly predicted response to immunotherapy in an independent validation cohort (n=29, AUC 0.89). In summary, our findings provide a high-resolution cell atlas of STSs to guide the development of novel therapeutic strategies. In addition, we have identified a predictive biomarker of response to immune checkpoint inhibition that may enable personalization of systemic therapy in patients with advanced STSs.

#5961

Inhibition of AURKA destabilizes glioblastoma primary cilia and sensitizes cells to tumor treating fields (TTFields) in vitro and ex vivo

Jia Tian, Julianne Mallinger, Ping Shi, Dahao Ling, Loic Deleyrolle, Min Lin, Habibeh Khoshbouei, Matthew Sarkisian. *University of Florida, Gainesville, FL*

Tumor Treating Fields (TTFields) can prolong survival of patients with glioblastoma (GBM), but GBM cells still escape this therapy requiring an urgent need for new or adjunct treatments. Recently we reported that TTFields disrupt primary cilia on GBM cells which lowers resistance to standard of care temozolomide chemotherapy. Here we asked if concomitant or sequential treatment of TTFields with other agents that interfere with GBM ciliogenesis enhance TTFields efficacy. Aurora Kinase A (AURKA) plays both a role in promoting cilia disassembly and regulating GBM growth in xenograft models. We found that within 24hr of treatment with the AURKA inhibitor, Alisertib, there was surprising and significant decrease in GBM cilia frequency across multiple GBM patient derived lines. However, similar Alisertib treatment did not affect neuronal or glial cilia frequencies in mixed primary cell cultures from mouse forebrain. Notably, overnight treatment of patient GBM biopsy ex vivo with Alisertib also resulted in reduced cilia frequency within the tumor tissue. Next, we co- or sequentially treated several different GBM patient cell lines with 24hr of 200kHz TTFields together with or followed by 250nM or 1μM Alisertib and examined the subsequent expansion of cells in vitro. We observed a significant synergistic reduction in cell proliferation compared to either treatment alone. However, this synergistic effect does not appear to be cilia-dependent as dual treatment reduction in proliferation was still observed in cell lines lacking different key cilia genes or in GBM cells that

naturally lack cilia. Considering Alisertib crosses the blood brain barrier and inhibits intracranial growth of tumors, our data warrant investigation of whether concomitant or sequential treatment of TTFields and Alisertib in vivo can further prolong survival.

#5962

NUC-7738 causes reduction of soluble and exosome-associated PD-L1 in melanoma cell lines and patients

Mustafa Elshani[1], Ying Zhang[1], Boback Kaghazchi[1], Alison L. Dickson[1], Sarah P. Blagden[2], Stefan Symeonides[3], Ruth Plummer[4], David J. Harrison[1]. *[1]University of St. Andrews, St. Andrews, United Kingdom,[2]Department of Oncology, Medical Sciences Division, University of Oxford, Oxford, United Kingdom,[3]Cancer Research UK Edinburgh Centre,, Institute of Genetics and Cancer, The University of Edinburgh, Edinburgh, United Kingdom,[4]Northern Centre for Cancer Care, Newcastle Hospitals NHS Foundation Trust,, Newcastle Hospitals NHS Foundation Trust, Freeman Hospital, Newcastle upon Tyne, United Kingdom*

Background: Immune checkpoint inhibitors (ICIs), including PD-(L)1 pathway inhibitors, are now standard of care for a variety of cancers. Characterization of PD-L1 protein has revealed multiple secreted forms; soluble (sPD-L1) and exosomal (ExoPD-L1) variants. In the tumor microenvironment these interfere with T-cell activation, facilitating tumor immune evasion. High circulating levels of sPD-L1 are correlated with advanced disease, a worse prognosis and/or poor response to ICIs. High levels of ExoPD-L1 are reported to contribute to T-cell dysfunction. NUC-7738, a ProTide transformation of 3'-deoxyadenosine (3'-dA), currently in Phase 1/2 in patients with solid tumors (NuTide:701 NCT03829254), has shown encouraging efficacy signals in several tumor types, including melanoma. This study investigates the dynamic between NUC-7738 and secreted forms of PD-L1 in a melanoma cell line and patients.
Material and Methods: A375 malignant melanoma cells were treated with NUC-7738 (10 μM) or DMSO for 6 - 72 hours. Cell supernatant was collected for sPD-L1 and ExoPD-L1 analysis and cells were measured for mRNA and metabolites. sPD-L1 mRNA and protein expression were measured in supernatant using RT-qPCR and sandwich ELISA, respectively. NUC-7738 and 3'-dATP were measured by LC-MS. ExoPD-

L1 protein levels were assessed by Jess Western analysis (normalized to CD81) and PD-L1 cell surface expression by flow cytometry. Findings were validated in patient plasma samples taken before and 24 hours after C1D1 treatment with NUC-7738 and prior to C2D1of a 14-day cycle.
Results: NUC-7738 was converted into anti-cancer metabolite 3'-dATP within 6 hours of treatment with an average concentration of 80 pmoles /10^6 cells, which was maintained for at least 24 hours and decreased by approximately 50% by 72 hours. The levels are comparable to those measured in PBMCs from patients treated with NUC-7738. NUC-7738 treatment reduced sPD-L1 mRNA expression by up to 40% and caused a time dependent decrease in sPD-L1 protein in the media supernatant by up to 3-fold. NUC-7738 also reduced ExoPD-L1 protein by 50%. NUC-7738 did not alter cell surface PD-L1 expression. Preliminary studies in serum from 4 study patients treated with NUC-7738 showed reductions in Exo-PD-L1 of ≤50% compared to pre-treatment levels.
Conclusion: NUC-7738 reduces secreted forms of PD-L1 whilst having no effect on cell surface protein levels. These *in vitro* results (melanoma cell line) were validated in the clinical setting, whereby ExoPD-L1 was reduced in plasma samples from patients treated with NUC-7738. These findings indicate that, by reducing sPD-L1 levels, NUC-7738 may have the potential to act as an immune sensitizer. We propose that NUC-7738 given in combination with PD-(L)1 pathway inhibitors may offer a promising treatment option, and are currently exploring this in patients who have experienced therapeutic resistance to ICI treatment.

#5963

Germline variant positive melanoma patients exhibit an enhanced inflammatory microenvironment

Alan Shen[1], Roshan Lodha[1], Brandon Bungo[2], Michelle Arbesman[1], Nikhil Pramod[1], Jennifer Ko[3], Brian Gastman[3], C. Marcela Diaz[3], Timothy Chan[3], Joshua Arbesman[4], Pauline Funchain[1]. *[1]Cleveland Clinic Taussig Cancer Center, Cleveland, OH,[2]Northwestern Lurie Cancer Center, Chicago, IL,[3]Cleveland Clinic Center for Immunotherapy and Precision Oncology, Cleveland, OH,[4]Department of Dermatology, Cleveland Clinic, Cleveland, OH*

Germline pathogenic variants (gPV) in cancer susceptibility genes are present in roughly 15% of all melanoma diagnoses. Prior studies note improvements in checkpoint immunotherapy responsiveness in patients with a gPV, which is associated with an increased neo-antigen load in gPV patients. We have also previously reported improvements in melanoma specific survival (MSS) in gPV patients vs non-gPV. No studies to date have examined the immune environment in gPV patients which may account for improvements in survival. In our study, melanoma patients with a personal or family history of multiple cancers were offered germline testing utilizing a commercial germline cancer sequencing panel. Enrolled patients also received a blood draw with subsequent flow cytometry to analyze the immune phenotype. In a cohort of 540 melanoma patients, 80 had a gPV. Multivariable linear regression indicated that significantly fewer polymorphonuclear myeloid derived suppressor cells (PMN-MDSC's) were noted relative to non-gPV patients when adjusting for melanoma stage at germline testing [β = -.45, 95% CI (-.76, -.15), p = .0036]. This difference was most significant in cutaneous, later stage (IIB-IV) patients, primarily stage III. We also interrogated patterns in gene signature between gPV and non-gPV patients in the TCGA PanCancer cutaneous melanoma cohort. We identified reductions in CCL27 (p = .007) and CCL1 (p = .06), genes associated with MDSC recruitment, across all stages in gPV patients, as well as reductions in ARG1 (p= .05) and S100A7 (p = .08), genes associated with PMN-MDSC's, in later stage gPV patients. Pathway differences were analyzed using gene set enrichment analysis (GSEA). Analysis of Hallmark gene sets identified significantly upregulated signatures in inflammatory response, TNF-α signaling, IFN-γ signaling, and IL-2 STAT5 signaling in late stage gPV patients. KEGG pathway analysis further identified NK cell mediated cytotoxicity and TCR signaling as significantly upregulated in late stage gPV patients. Notably, fatty acid metabolism pathways, which have been implicated in immunosuppression through MDSC suppressive function, were downregulated in gPV patients. These results suggest that gPV melanoma is associated with both a depletion of PMN-MDSC's and an upregulation of inflammatory microenvironmental genes in later stages which may explain improved outcomes.

#5964

Context-dependent induction of interferon signaling by CD11b agonists supports anti-tumor immunity in mouse models and human cancer patients

Xiuting Liu[1], Graham Hogg[1], Chong Zuo[1], John Baer[1], Varintra Lander[1], Liang Kang[1], Nicholas Borcherding[1], Brett Knolhoff[1], Robin Osterhout[2], Anna Galkin[2], Jean Bruey[2], Laura Carter[2], Cedric Mpoy[1], Julie Schwarz[1], Haeseong Park[1], Vineet Gupta[3], David DeNardo[1]. *[1]Washington University in St. Louis, Saint Louis, MO,[2]Gossamer Bio, San Diego, CA,[3]Rush University Medical Center, Chicago, IL*

Chronic activation of inflammatory pathways and suppressed interferon signaling are hallmarks of myeloid cells in immunosuppressive tumors that drive poor responsiveness to conventional and immune therapies. Previous studies have identified agonistic activation of the CD11b integrin as a potential strategy to enhance anti-tumor immunity. However, the mechanisms by which CD11b-agonism reprogram tumor immunity are poorly understood, and this may impair patient selection and identification of effective treatment combinations. Here we will use a combination of in vitro systems, animal models, and samples from first in human clinical trials of the CD11b-agonist to identify the mechanism of action of this approach and identify combinations for further testing. CD11b agonism alters tumor-associated macrophage (TAM) phenotypes by simultaneously repressing NFκB/IL1-signaling and activating interferon (IFN) gene expression. Repression of NFκB/IL-1 signaling was due to rapid degradation of p65 protein by the proteosome, contributing to suppressing myeloid cells infiltration. In contrast, CD11b agonism triggers mitochondrial dysfunction to stimulate STING-induced, STAT1-mediated interferon signaling, contributing to macrophages-augmented anti-tumor T cell immunity. Tissues from phase I clinical trials shows that CD11b agonist activates STING and STAT1 signaling in TAMs in human tumors, which is in consistent with preclinical data. Furthermore, combining CD11b agonism with cytotoxic therapies, STING agonist or TLRs agonists leads to robust anti-tumor activity in PDAC models. These studies pave the way for mechanism-based therapeutic combination strategies in cancer patients.

#5965

B2M loss of heterozygosity in melanoma is associated with increased numbers of activated NK cells and higher expression of the NK cell inhibitory ligand, HLA-G

Mildred Galvez, Katie M. Campbell, Egmidio Medina, Antoni Ribas.
UCLA, Los Angeles, CA

β2-microglobulin (B2M) is a critical subunit of antigen presenting major histocompatibility complex (MHC) class I molecules. Its genetic inactivation in tumor cells has been implicated in tumor-intrinsic immune escape and immunotherapy resistance. Currently, the impact of B2M dysregulation on tumor-immune dynamics requires furthers characterization. Using a clinical dataset of patients with melanoma treated with immune checkpoint blockade (ICB), whole-exome sequencing and bulk RNA-sequencing data from baseline tumor biopsies (n=295) were analyzed to identify somatic B2M alterations and evaluate correlative clinical outcomes, infiltrating immune cells, and gene expression patterns. No loss-of-function mutations in B2M were found; however, 50% of tumors had B2M alterations in the form of homozygous loss (n=2), loss of heterozygosity (LOH; n=56), or copy number gains (n=88). B2M LOH events were overrepresented in tumors from patients who progressed during ICB therapy compared to those who responded (34% versus 19%; Pearson chi-square test, p=0.035). Additionally, tumors with B2M LOH had lower B2M expression compared to B2M-unaltered tumors (Wilcoxon test, p=0.05). Gene set enrichment analysis revealed reduced expression of immune and inflammatory signatures in B2M-LOH tumors. Furthermore, immune cell deconvolution showed that B2M-LOH tumors had lower total immune cell counts, but greater numbers and proportions of activated natural killer (NK) cells (Wilcoxon test, numbers p=0.021, proportions p=0.032). Differential gene expression analysis revealed concordant higher expression of human leukocyte antigen G (HLA-G), an NK cell inhibitory ligand, in B2M-LOH tumors (Wilcoxon test, p=0.0035). Moreover, B2M-LOH progressive tumors had the highest median HLA-G expression and trended toward a positive correlation between increasing HLA-G expression and increasing numbers of activated NK cells (Pearson correlation, r=0.55, p=0.015). In conclusion, melanoma biopsies with B2M LOH were associated with non-response to ICB, had increased presence of activated NK cells, and demonstrated a compensatory increase in HLA-G.

These results suggest that in melanoma B2M alterations may be implicated in modulating NK cell interactions and point toward HLA-G potentially playing a role in inhibiting NK cell anti-tumor activity.

#5966

Cathepsin S mediates interleukin 7 to sculpture the tumor immunity in head and neck cancer

Yung-Chieh Chang[1], Shan-Hung Chen[2], Kwang-Yu Chang[2], Jang-Yang Chang[3]. *[1]Taipei Medical University, Taipei, Taiwan,[2]National Institute of Cancer Research, National Health Research Institutes (NHRI), Tainan, Taiwan,[3]Taipei Cancer Center, Taipei Medical University, Taipei, Taiwan*

Cathepsin S (CTSS) is a lysosomal enzyme that belongs to cysteine proteases. It is associated with progression of different types of cancer, mediating the antigen presentation, extracellular matrix degradation, angiogenesis, and metastasis. In recent studies, CTSS was suggested as a therapeutic target for cancer treatment. We found that, with a CTSS inhibitor RJW-58 treatment over tumor-bearing mouse, the serum showed an enhanced anti-tumor cytokine releasing of interleukin 7 (IL-7). In the mRNA array results of 40 pair head and neck patients' sample, we found the negative correlation between CTSS and IL-7 comparing to the normal head and neck tissue. Moreover, we also found that the level of CD8 T cell infiltration is negatively correlated with the expression of CTSS in 20 head and neck cancer patients' slides. In cell model, targeting CTSS by siRNA or RJW-58 promoted IL-7 secretion in different head and neck cancer cell lines. We demonstrated that cathepsin S decreased the secretion level of IL-7 through downregulating IL-7 receptor, a receptor that mediating IL-7 secretion, protein expression level resulting in activating lysosomal degradation pathway. Promoting cell proliferation of activated CD8 T cells was proved when CD8 T cells were treated with the condition medium from CTSS-knockdown head and neck cancer cells. In conclusion, this is the first study demonstrated that CTSS acted as a negative regulator in mediating IL-7 resulting in inducing an immune cell-suppressed microenvironment in head and neck cancer cells. (This work is supported by the NSTC grand number: MOST 110-2314-B-400-035)

#5967

Advanced patient-derived lung tumoroids to identify limiting factors for oncolytic virotherapy

Le Hélène. *Transgene S.A., Illkirch-Graffenstaden, France*

Introduction: Despite major progress in its diagnosis, and treatment, lung cancer remains one of the deadliest cancers in the world. Patient-derived tumoroids offers unique advantage to integrate patients' heterogeneity, and the diversity of resistance mechanisms in the drug discovery and development pathway. Organization of the tumor microenvironment both at the tissue, and at the molecular levels, is another critical factor that regulate drug response, in particular for immunotherapy. In this study, we have focused on oncolytic virotherapy, a promising concept that still deserves optimization. Different physiological barriers might limit the efficacy of oncolytic viruses (OVs): (i) mutations limiting viral replication and spreading, (ii) structure of the tumor tissue (basement membrane, vasculature, immune cells among other actors), (iii) physical parameters (therapeutic pressure, physical barriers), and iv) anti-viral vector response (reticulo-endothelial system, neutralizing antibodies, complement).
Purpose of the Study: Development of an advanced *in vitro* model for NSCLC that would recapitulate major physical and biological barriers to the action of Vaccinia-based oncolytic vectors. Identification of major determinants of activity, and of R&D axes for the design of improved OVs.
Experimental Approach: Lung tumor biopsies, and healthy tissues were obtained from the CRB of Strasbourg, and organoids were generated after an enzymatic treatment. Dissociated cells were mixed with exogenous microvessels derived from the adipose tissue. At day seven of the culture, patient-derived tumoroids and organoids (PDTs/PDOs) were transferred and embedded in a hydrogel mimicking the extracellular matrix. OVs were applied in fluidic to mimic intravenous perfusion, and viral properties were analyzed at 24h and 96h timepoints. Specificity was demonstrated by direct comparison of PDTs and PDOs from the same patient. Addition of circulating PBMCs after 24h of infection allowed us to analyze the interaction of OV with immune effectors.
Results: Under fluidic conditions, mimicking intravenous infusion, we could confirm infection at the periphery of the lung PDT after only one hour of perfusion. IL-6 was significantly increased compared to IL-10, TNF-α and IL-1β (seven times more than the untreated condition).

Compared to a passive diffusion mode (static conditions) infection was lower, suggesting the laminar flow and the matrix become efficacy-limiting factors. Indeed, under fluidic conditions, infection and replication were observed one day later than passive diffusion mode. The contribution of endothelial cells, and of immune cells was also characterized. Some experiments are still ongoing, and results on neutralizing antibodies will be presented in the poster.

#5968

Leukemia inhibitory factor regulates macrophage immune response in head and neck squamous cell carcinoma

Yun Hua Sui, Tzu Tung Liu, Shu Chen Liu. *National Central University, Taoyuan City, Taiwan*

The high recurrence rate of head and neck squamous cell carcinoma (HNSCC) is associated with an immune suppressive tumor microenvironment (TME). Tumor-associated macrophage (TAM)-mediated immunosuppression is a critical feature in HNSCC TME. We provide evidence demonstrating that leukemia inhibitory factor (LIF) is involved in macrophage polarization and remodeling of the HNSCC microenvironment. By interrogating the head and neck squamous cell carcinoma RNA sequencing dataset extracted from the TCGA database, we found that the levels of LIF and M2 macrophage markers (CD163, CD206, VEGF) were enhanced in tumors compared to normal counterparts. Higher LIF expression in tumors was further correlated with worse overall survival. Immunohistochemical analysis found that macrophages with higher LIF immunoreactivities were located at the periphery of HNSCC tumors. In a macrophage-cancer cell coculture system, the presence of LIF promoted the proliferation and mobility of cancer cells and induced an M2-dominant macrophage polarization. Stimulating monocyte-derived macrophages (MDMs) with LIF increased the expression of several M2 markers (CD163, CD206, CD209, and IL10) but decreased the expression of M1 markers (iNOS, CD80, and CD86). Moreover, LIF-treated macrophages exhibited little cancer cytotoxicity compared to vehicle-treated macrophages. Treating macrophages with soluble LIF receptor (sLIFR), a LIF antagonist, partly reversed the LIF-mediated M2 polarization and enhanced cytotoxicity toward cancer cells. Results of RNA-sequencing data demonstrated that LIF

suppressed antigen presentation process, type I interferon production, TNFR signaling, and molecules participating in the Hippo signaling pathway in MDMs. Mechanistic studies found that LIF might trigger M2 polarization via activating YAP1, as reflected by a reduction of p-YAP1 (S127) and an enhanced YAP1 nuclear localization in macrophages. Treating macrophages with YAP1 inhibitors (Saracatinib and Verteporfin) blocked the LIF-mediated YAP1 nuclear translocation, expression of M2 markers, and tumor-promoting effects. Our findings suggest that the presence of LIF in HNSCC promotes macrophage M2 polarization through YAP1 signaling, which assists in establishing an immune-suppressive, tumor-promoting microenvironment. The blockade of LIF-mediated effects may tailor therapeutic strategies by converting the immunosuppressive microenvironment for selected HNSCC patients.